

Moss and Adams'

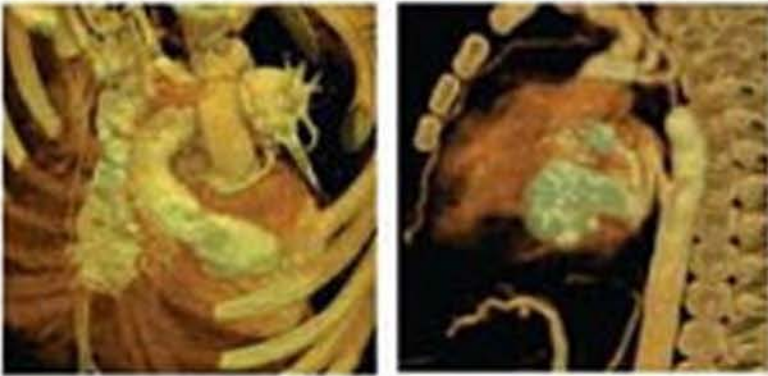
Heart Disease

In Infants, Children, and Adolescents

Including the Fetus and Young Adult

e i g h t h e d i t i o n

Includes
FREE Online
Access to Fully
Searchable Text
& Question
Bank!



Hugh D. Allen

David J. Driscoll

Robert E. Shaddy

Timothy F. Feltes

Moss and Adams' Heart Disease in Infants, Children, and Adolescents

Including the Fetus and Young Adult

EIGHTH EDITION VOLUME I

EDITORS

Hugh D. Allen, MD, FACC, FAAP, FAHA

Professor of Pediatrics (Cardiology)
Baylor College of Medicine
Staff Cardiologist
Texas Children's Hospital
Houston, Texas

David J. Driscoll, MD

Professor of Pediatrics
Division of Pediatric Cardiology
Department of Pediatric and Adolescent
Medicine
Mayo Clinic College of Medicine
Mayo Clinic Foundation
Rochester, Minnesota

Robert E. Shaddy, MD

Professor of Pediatrics
Department of Pediatrics
University of Pennsylvania Perelman
School of Medicine
Chief, Division of Pediatric Cardiology
Vice Chair, Department of Pediatrics
The Children's Hospital of Pennsylvania
Philadelphia, Pennsylvania

Timothy F. Feltes, MD

Andy Paxon Chair in Cardiology
Co-Director of the Heart Center
Chief, Pediatric Cardiology
Professor of Pediatrics
The Ohio State University
Nationwide Children's Hospital
Columbus, Ohio



Wolters Kluwer

Health

Lippincott Williams & Wilkins

Philadelphia • Baltimore • New York • London
Buenos Aires • Hong Kong • Sydney • Tokyo

Acquisitions Editor: Julie Goolsby
Product Manager: Leanne Vandetty
Production Manager: Alicia Jackson
Senior Manufacturing Manager: Benjamin Rivera
Marketing Manager: Kimberly Schonberger
Design Coordinator: Teresa Mallon
Production Service: SPi Global

© 2013 by LIPPINCOTT WILLIAMS & WILKINS, a WOLTERS KLUWER business
Two Commerce Square
2001 Market Street
Philadelphia, PA 19103 USA
LWW.com

7th Edition © 2008 by Lippincott Williams & Wilkins
6th Edition © 2001 by Lippincott Williams & Wilkins

All rights reserved. This book is protected by copyright. No part of this book may be reproduced in any form by any means, including photocopying, or utilized by any information storage and retrieval system without written permission from the copyright owner, except for brief quotations embodied in critical articles and reviews. Materials appearing in this book prepared by individuals as part of their official duties as U.S. government employees are not covered by the above-mentioned copyright.

Printed in China

Library of Congress Cataloging-in-Publication Data

Moss & Adams heart disease in infants, children, and adolescents: including the fetus and young adult / Hugh D. Allen ... [et al.]. — 8th ed.

p. ; cm.

Includes index.

ISBN 978-1-4511-1893-3 (hardback)

1. Heart—Diseases. 2. Pediatric cardiology. I. Allen, Hugh D.

RJ421.H38 2013

618.92'12—dc23

2012004155

Care has been taken to confirm the accuracy of the information presented and to describe generally accepted practices. However, the authors, editors, and publisher are not responsible for errors or omissions or for any consequences from application of the information in this book and make no warranty, expressed or implied, with respect to the currency, completeness, or accuracy of the contents of the publication. Application of the information in a particular situation remains the professional responsibility of the practitioner.

The authors, editors, and publisher have exerted every effort to ensure that drug selection and dosage set forth in this text are in accordance with current recommendations and practice at the time of publication. However, in view of ongoing research, changes in government regulations, and the constant flow of information relating to drug therapy and drug reactions, the reader is urged to check the package insert for each drug for any change in indications and dosage and for added warnings and precautions. This is particularly important when the recommended agent is a new or infrequently employed drug.

Some drugs and medical devices presented in the publication have Food and Drug Administration (FDA) clearance for limited use in restricted research settings. It is the responsibility of the health care provider to ascertain the FDA status of each drug or device planned for use in their clinical practice.

To purchase additional copies of this book, call our customer service department at (800) 638-3030 or fax orders to (301) 223-2320. International customers should call (301) 223-2300.

Visit Lippincott Williams & Wilkins on the Internet: at LWW.com. Lippincott Williams & Wilkins customer service representatives are available from 8:30 am to 6 pm, EST.

10 9 8 7 6 5 4 3 2 1

Dedication

*To my grandchildren, Christopher, Stella,
and Adam, and to my families at home as
well as at work.*

—HDA

*To my grandchildren, Brendan and
Emmaleine.*

—DJD

*To family and friends for their patience and
support.*

—RES

*Jethro got it right; life's a long song starting
with you, Mr. Johnson. But was the deal
worth it? It may be a buckdancer's choice
to travel with traffic or to take the lonely
Ventura Highway, but we always seem to
end up in Winslow Arizona. To Taj, Ste-
vie Rae, John Lee, Lightnin', Eric, and the
King himself, thanks for the tunes boys.
Pete, glad the Detours name didn't stick but
then the "lead balloon" did! And to Club
27's Jim, Jimi, and Janis, your poetry lives
on. I'm bad...I'm Nationwide!*

—TFF

CONTENTS

Contributors ix
 Preface xvii
 Acknowledgments xviii
 Tribute to Moss, Adams, & Emmanouilides xix
 The Development of Pediatric Cardiology: Historical
 Milestones <http://solution.lww.com>

VOLUME I

SECTION I:

Structure and Function of the Cardiovascular System 1

- 1 Cardiac Anatomy and Examination of Cardiac Specimens 1
 William D. Edwards and Joseph J. Maleszewski
- 2 Classification and Terminology of Cardiovascular Anomalies 32
 William D. Edwards and Joseph J. Maleszewski
- 3 Development of Myocardial Structure and Function 52
 Pamela A. Lucchesi, Kirk R. Hutchinson, Luciana Martins, and Loren E. Wold
- 4 Circulation Physiology 69
 David F. Teitel, Steven C. Cassidy, and Jeffrey R. Fineman

SECTION II:

Diagnostic and Therapeutic Methods 82

- 5 History and Physical Examination 82
 Steven C. Cassidy, Hugh D. Allen, and John R. Phillips
- 6 Exercise Screening and Sports Participation. 93
 Julie A. Brothers, Paul Stephens, Jr., and Stephen M. Paridon
- 7 Exercise Testing 118
 Paolo T. Pianosi and David J. Driscoll
- 8 Echocardiography: Basic Principles and Imaging 134
 Thomas R. Kimball and Erik C. Michelfelder
- 9 Echocardiographic Assessment of Cardiac Dimensions, Cardiac Function, and Valve Function 172
 Luc L. Mertens and Mark K. Friedberg
- 10 Magnetic Resonance Imaging. 207
 Tal Geva and Andrew J. Powell

- 11 Cardiac Computed Tomography in Children with Congenital Heart Disease 247
 Frederick R. Long and Joachim G. Eichhorn
- 12 Cardiac Catheterization and Angiography 258
 Nathaniel W. Taggart and Allison K. Cabalka
- 13 Therapeutic Cardiac Catheterization . . 288
 Ralf J. Holzer and John P. Cheatham

SECTION III:

Electrophysiology 348

- 14 Development and Functional Maturation of the Cardiac Conduction System 348
 Aleksander Sizarov, Antoon F.M. Moorman, and Arthur S. Pickoff
- 15 The Normal Electrocardiogram 372
 George F. Van Hare and Anne M. Dubin
- 16 Cardiac Channelopathies, Syncope, and Sudden Death 389
 Michael J. Ackerman
- 17 Electrophysiology Studies and Electrophysiologic Therapeutic Catheterization. 401
 J. Philip Saul and John D. Kugler
- 18 Disorders of Cardiac Rhythm and Conduction 441
 Bryan C. Cannon and Christopher S. Snyder

SECTION IV:

Pediatric Cardiac Intensive Care 473

- 19 Physiology of the Preterm and Term Infant. 473
 Timothy M. Hoffman and Stephen E. Welty
- 20 Pediatric Cardiovascular Intensive Care 483
 Dean B. Andropoulos and Anthony C. Chang
- 21 Cardiac Mechanical Support Therapies 530
 Elizabeth D. Blume, Ravi R. Thiagarajan, and Peter C. Laussen

- 22** Cardiopulmonary and Right-Left Heart Interactions 546
Andrew N. Redington
- 23** Cardiac Trauma 552
Gary A. Smith and Timothy F. Feltes

SECTION V:**From the Gene to the Neonate 560**

- 24** Molecular Determinants of Cardiac Development and Disease. 560
Deepak Srivastava and H. Scott Baldwin
- 25** Epidemiology and Prevention of Congenital Heart Defects. 577
Lorenzo D. Botto
- 26** Genetic Aspects of Congenital Heart Defects. 617
Elizabeth Goldmuntz, Melissa L. Crenshaw, and Angela E. Lin
- 27** Fetal Echocardiography and Fetal Cardiology 644
Charles S. Kleinman, Julie S. Glickstein, Ganga Krishnamurthy, and Jodie K. Votava-Smith

SECTION VI:**Congenital Cardiovascular Malformations 672****PART A: Septal Defects**

- 28** Atrial Septal Defects. 672
Ritu Sachdeva
- 29** Atrioventricular Septal Defects. 691
Frank Cetta, Luann L. Minich, Joseph J. Maleszewski, Joseph A. Dearani, and Harold MacDonald Burkhardt
- 30** Ventricular Septal Defects 713
Agustin E. Rubio and Mark B. Lewin

PART B: Arterial Abnormalities

- 31** Patent Ductus Arteriosus and Aortopulmonary Window 722
Phillip Moore and Michael M. Brook
- 32** Congenital Anomalies of the Coronary Vessels and the Aortic Root 746
D. Scott Lim and G. Paul Matherne
- 33** Aortic Arch and Vascular Anomalies 758
Paul M. Weinberg, Shobha Natarajan, and Lindsay S. Rogers
- 34** Abnormalities of the Aortic Root. 799
Matina Prapa, John Pepper, and Michael A. Gatzoulis

VOLUME II**PART C: Venous Abnormalities**

- 35** Anomalies of the Pulmonary Veins. . . 809
David W. Brown and Tal Geva
- 36** Abnormal Systemic Venous Connections 840
Tal Geva
- 37** Vascular Tumors and Anomalies 864
Ahmad I. Alomari
- 38** Tricuspid Atresia, Stenosis, Regurgitation, and Uhl's Anomaly . . . 877
Michael L. Epstein
- 39** Ebstein's Anomaly, Congenital Tricuspid Valve Regurgitation, and Dysplasia. 889
Sameh M. Said and Joseph A. Dearani
- 40** Pulmonary Stenosis 913
Lourdes R. Prieto and Larry A. Latson
- 41** Pulmonary Atresia and Intact Ventricular Septum 939
David G. Nykanen
- 42** Pulmonary Atresia and Ventricular Septal Defect 959
Patrick W. O'Leary, William D. Edwards, Paul R. Julsrud, and Harold MacDonald Burkhardt
- 43** Tetralogy of Fallot with Pulmonary Stenosis and Tetralogy of Fallot with Absent Pulmonary Valve 969
S. Lucy Roche, Steven C. Greenway, and Andrew N. Redington

PART D: Left Ventricular Inflow and Outflow Abnormalities

- 44** Truncus Arteriosus. 990
Allison K. Cabalka, William D. Edwards, and Joseph A. Dearani
- 45** Anatomical and Functional Mitral Valve Abnormalities in the Pediatric Population 1003
Andrew S. Mackie and Jeffrey F. Smallhorn
- 46** Aortic Stenosis 1023
Douglas J. Schneider and John W. Moore
- 47** Coarctation of the Aorta 1044
Robert H. Beekman, III
- 48** Hypoplastic Left Heart Syndrome . . 1061
James S. Tweddell, George M. Hoffman, Nancy S. Ghanayem, Michele A. Frommelt, Kathleen A. Mussatto, and Stuart Berger

PART E: Abnormalities of the Origin of the Great Arteries

- 49** Transposition of the Great Arteries . . . 1097
Gil Wernovsky

- 50** Congenitally Corrected Transposition of the Great Arteries (Atrioventricular and Ventriculoarterial Discordance) . . . 1147
Joseph Atallah, Jennifer M. Rutledge, and John D. Dyck

PART F: Complex Cardiac Abnormalities

- 51** Double Outlet Right Ventricle . . . 1161
Gail E. Wright, Katsuhide Maeda, Norman H. Silverman, Frank L. Hanley, and Stephen J. Roth

- 52** Univentricular Atrioventricular Connection. 1175
Michael G. Earing, Donald J. Hagler, and William D. Edwards

- 53** Cardiac Malpositions and Abnormalities of Atrial and Visceral Situs. 1195
Patrick W. O'Leary and Donald J. Hagler

SECTION VII:

Diseases of the Endocardium, Myocardium, and Pericardium 1217

- 54** Hypertrophic Cardiomyopathy . . . 1217
Barry J. Maron

- 55** Dilated Cardiomyopathy 1235
Timothy M. Olson and David P. Chan

- 56** Myocarditis 1247
Jeffrey A. Towbin, Angela Lorts, and John Lynn Jefferies

- 57** Restrictive Cardiomyopathy. 1267
Susan W. Denfield

- 58** The Heart in Muscular Dystrophies. . . 1277
Hugh D. Allen, Jerry R. Mendell, Kevin M. Flanigan, and Timothy M. Hoffman

- 59** Kawasaki Disease (Mucocutaneous Lymph Node Syndrome) 1287
Sarah D. De Ferranti and Jane W. Newburger

- 60** Rheumatic Fever and Rheumatic Heart Disease. 1303
Lloyd Y. Tani

- 61** Inflammatory Noninfectious Cardiovascular Diseases. 1331
Charles H. Spencer, Anjali Patwardhan, and Sharon L. Roble

- 62** Pericardial Diseases 1350
Jonathan N. Johnson and Frank Cetta

- 63** Infective Endocarditis and Prevention 1363
Michael Gewitz and Kathryn A. Taubert

- 64** Myocardial Ischemia 1377
Ali N. Zaidi and Curt J. Daniels

- 65** Pediatric Heart Transplantation. . . . 1384
Robert E. Shaddy and Francesco Parisi

SECTION VIII:

Pulmonary Vascular Disease 1401

- 66** Pathophysiology of Pulmonary Hypertension 1401
Marlene Rabinovitch

- 67** Clinical Management of Pediatric Pulmonary Arterial Hypertension. . . 1433
D. Dunbar Ivy

SECTION IX:

The Young Adult with Congenital Heart Disease 1463

- 68** The Adolescent and Adult with Congenital Heart Disease. . . . 1463
Ali N. Zaidi and Curt J. Daniels

- 69** Pregnancy in Young Women with Congenital Heart Disease. . . . 1494
Candice K. Silversides, Jack M. Colman, and Samuel C. Siu

SECTION X:

Other Special Problems and Issues 1509

- 70** Chest Pain in Children and Adolescents 1509
Jonathan N. Johnson and David J. Driscoll

- 71** Coronary Risk Factors in Children. . 1514
Stephen R. Daniels

- 72** Cardiac Tumors 1549
Gerald R. Marx and Adrian M. Moran

- 73** Chronic Heart Failure in Children . . 1565
Robert E. Shaddy and Lloyd Y. Tani

- 74** Neurodevelopmental Outcomes after Heart Surgery in Children . . . 1579
Caren S. Goldberg and Jane W. Newburger

- 75** Hematologic Aspects of Pediatric and Adolescent Heart Disease: Bleeding, Clotting, and Blood Component Abnormalities 1589
Therese M. Giglia and Char Witmer

76 Evaluation of Quality of Life in Children
and Adolescents with Congenital and
Acquired Heart Disease1608

Bradley S. Marino

77 Safety and Quality in the Heart
Center1622

Anthony Y. Lee, Thomas Taghon, Richard Eugene McClead, Jr.,
Terrance Davis, and Richard J. Brilli

78 Design, Execution, and Appraisal
of Clinical Trials1636

Brian W. McCrindle

79 Pharmacology1661

Michael Artman and Gregory L. Kearns

Index I-1

CONTRIBUTORS

Michael J. Ackerman, MD, PhD, FACC

Windland Smith Rice Cardiovascular
Genomics Research Professor
Professor of Medicine, Pediatrics, and
Pharmacology
Director, Long QT Syndrome/Genetic
Heart Rhythm Clinic
Director, Windland Smith Rice Sudden
Death Genomics Laboratory
Medicine, Pediatrics, and Molecular
Pharmacology and Experimental
Therapeutics
Mayo Clinic
Rochester, Minnesota

Hugh D. Allen, MD, FACC, FAAP, FAHA

Professor of Pediatrics (Cardiology)
Baylor College of Medicine
Staff Cardiologist
Texas Children's Hospital
Houston, Texas

Ahmad I. Alomari, MD, MSc

Assistant Professor
Division of Vascular and Interventional
Radiology
Children's Hospital Boston
Harvard Medical School
Boston, Massachusetts

Dean B. Andropoulos, MD

Professor of Anesthesiology
Director, Pediatric Cardiovascular
Anesthesia
Texas Children's Hospital
Houston, Texas

Michael Artman, MD

Chair
Department of Pediatrics
School of Medicine
University of Missouri–Kansas City
Joyce C. Hall Distinguished Professor
and Chair
Department of Pediatrics
Children's Mercy Hospitals and Clinics
Kansas City, Missouri

Joseph Atallah, MD CM, MSc(Epi), FRCP

Assistant Professor
Departments of Pediatrics and Public
Health Sciences
University of Alberta
Attending Staff
Departments of Pediatrics and Medicine
Stollery Children's Hospital and Univer-
sity of Alberta Hospital
Edmonton, Alberta, Canada

H. Scott Baldwin, MD

Professor of Pediatrics and Cell and
Developmental Biology
Chief, Division of Pediatric
Cardiology
Co-Director of the Pediatric Heart
Institute
Vanderbilt Children's Hospital
Nashville, Tennessee

Robert H. Beekman, III, MD

Professor
Department of Pediatric
Cardiology
University of Cincinnati College of
Medicine
Professor
Heart Institute
Cincinnati Children's Hospital Medical
Center
Cincinnati, Ohio

Stuart Berger, MD

Professor of Pediatrics
The Medical College of Wisconsin
Medical Director of the Herma Heart
Center
Children's Hospital of Wisconsin
Milwaukee, Wisconsin

Elizabeth D. Blume, MD

Associate Professor
Department of Pediatrics
Harvard Medical School
Medical Director, Heart Failure and
Transplant Program
Department of Cardiology
Children's Hospital, Boston
Boston, Massachusetts

Lorenzo D. Botto, MD

Professor of Pediatrics
Department of Pediatrics
University of Utah
Attending Physician
Division of Medical Genetics
Primary Children's Medical
Center
Salt Lake City, Utah

Richard J. Brilli, MD

Professor
Department of Pediatrics
The Ohio State University College of
Medicine
Chief Medical Officer
Hospital Administration
Nationwide Children's Hospital
Columbus, Ohio

Michael M. Brook, MD

Professor of Clinical Pediatrics
Director, Pediatric and Congenital
Echocardiography
University of California–San Francisco
Benioff Children's Hospital
San Francisco, California

Julie A. Brothers, MD

Assistant Professor
Department of Pediatrics
Perelman School of Medicine at the
University of Pennsylvania
Medical Director, Lipid Heart Clinic
Division of Cardiology
The Children's Hospital of Philadelphia
Philadelphia, Pennsylvania

David W. Brown, MD

Assistant Professor
Department of Pediatrics
Harvard Medical School
Associate
Department of Cardiology
Children's Hospital Boston
Boston, Massachusetts

Harold MacDonald Burkhardt, MD

Associate Professor of Surgery/
Cardiovascular Surgeon
Department of Cardiovascular Surgery
Mayo Clinic
Rochester, Minnesota

Allison K. Cabalka, MD, FACC, FASE, FSCAI

Associate Professor of Pediatrics
Division of Pediatric Cardiology
Mayo Clinic
Rochester, Minnesota

Bryan C. Cannon, MD

Associate Professor
Department of Pediatrics
Director
Pediatric Arrhythmia and
Pacing Service
Mayo Clinic
Rochester, Minnesota

Steven C. Cassidy, MD

Associate Professor
Department of Pediatrics
Ohio State University College of
Medicine
Director, Inpatient Services
Heart Center
Nationwide Children's Hospital
Columbus, Ohio

Frank Cetta, MD

Professor of Medicine and Pediatrics
Divisions of Pediatric Cardiology and
Cardiovascular Diseases
Chief
Division of Pediatric Cardiology
Mayo Clinic
Rochester, Minnesota

David P. Chan, MD

Professor of Clinical Pediatrics
Department of Pediatrics
University of Illinois College of
Medicine Peoria
Division Head Pediatric Cardiology
Department of Pediatrics
Children's Hospital of Illinois
Peoria, Illinois

Anthony C. Chang, MD, MBA, MPH

Medical Director
Heart Institute at Children's Hospital
of Orange County
Orange California
Associate Professor of Pediatrics
University of California, Irvine
Irvine, California

John P. Cheatham, MD, FAAP, FACC, FSCAI

Professor
Department of Pediatrics and Internal
Medicine
The Ohio State University
Co-Director, The Heart Center
Director of Cardiac Catheterization
and Interventional Therapy
Heart Center
Nationwide Children's Hospital
Columbus, Ohio

Jack M. Colman, MD, FRCPC

Professor of Medicine and Obstetrics &
Gynecology Division of Cardiology
University of Toronto
Mount Sinai Hospital and Peter Munk
Cardiac Centre/University Health
Network
Toronto Congenital Cardiac Centre for
Adults
Toronto, Ontario, Canada

Melissa L. Crenshaw, MD

Medical Director
Clinical Genetics
All Children's Hospital, a member of
Johns Hopkins Medicine
St. Petersburg, Florida

Curt J. Daniels, MD

Associate Professor
Internal Medicine and Pediatrics
Director, Columbus Ohio Adult
Congenital Heart Disease and
Pulmonary Hypertension Program
National Children's Hospital
The Ohio State University
Columbus, Ohio

Stephen R. Daniels, MD, PhD

Professor and Chairman
Department of Pediatrics
University of Colorado School of
Medicine
Pediatrician-in-Chief
L. Joseph Butterfield Chair of Pediatrics
Children's Hospital Colorado
Aurora, Colorado

Terrance Davis, MD

Professor Emeritus of Clinical Surgery
Department of Surgery
The Ohio State University
Associate CMO, Co-Medical Director
for Patient Safety
Department of Administration
Nationwide Children's Hospital
Columbus, Ohio

Sarah D. De Ferranti, MD, MPH

Assistant Professor of Pediatrics
Harvard Medical School
Director, Preventive Cardiology Clinic
Boston Children's Hospital
Boston, Massachusetts

Joseph A. Dearani, MD

Professor of Surgery
Chair, Cardiovascular Surgery
Division of Cardiovascular Surgery
Mayo Clinic
Rochester, Minnesota

Susan W. Denfield, MD

Associate Professor
Department of Pediatrics
Division of Pediatric Cardiology
Baylor College of Medicine
Texas Children's Hospital
Houston, Texas

David J. Driscoll, MD

Professor of Pediatrics
Division of Pediatric Cardiology
Department of Pediatrics
Mayo Clinic, Mayo Clinic College of
Medicine, and Mayo Foundation
Rochester, Minnesota

Anne M. Dubin, MD

Associate Professor
Department of Pediatrics
Stanford University
Director of Pediatric Arrhythmia Service
Department of Pediatric Cardiology
Lucile Packard Children's Hospital
Palo Alto, California

D. Dunbar Ivy, MD

Professor
Department of Pediatrics
University of Colorado
Chief and Selby's Chair
Director, Pediatric Pulmonary
Hypertension Program
Children's Hospital, Colorado
Aurora, Colorado

John D. Dyck, MD, FRCP(C)

Professor
Department of Pediatrics
University of Alberta
Director of Pediatric
Cardiology
Department of Pediatrics (Pediatric
Cardiology)
Stollery Children's hospital
Edmonton, Alberta, Canada

Michael G. Earing, MD

Associate Professor
Departments of Internal Medicine and
Pediatrics
Divisions of Adult Cardiovascular
Medicine and Pediatric
Cardiology
Medical College of Wisconsin
Director of the Adult Congenital Heart
Disease Program
Children's Hospital of Wisconsin
Milwaukee, Wisconsin

William D. Edwards, MD

Professor of Pathology
Laboratory Medicine and Pathology
Mayo Clinic
Rochester, Minnesota

Joachim G. Eichhorn, MD

Privatdozent
Department of Pediatrics
Ruperto Carola University
Deputy Chief
Department of Pediatric Cardiology/
Congenital Heart Disease
University Children's Hospital
Heidelberg, Germany

Michael L. Epstein, MD

Affiliate Professor
Department of Pediatrics
University of South Florida College of
Medicine
Tampa, Florida
Senior Vice President for Medical
Affairs
All Children's Hospital
St. Petersburg, Florida

Timothy F. Feltes, MD

Professor of Pediatrics
Department of Pediatrics
The Ohio State University
Chief of Cardiology, Co-Director of the
Heart Center
Nationwide Children's Hospital
Columbus, Ohio

Jeffrey R. Fineman, MD

Professor of Pediatrics
Division Chief, Critical
Care Medicine
University of California,
San Francisco
San Francisco, California

Kevin M. Flanigan, MD

Professor of Pediatrics and Neurology
Department of Pediatrics
Ohio State University
Professor
Center for Gene Therapy
Nationwide Children's Hospital
Columbus, Ohio

Mark K. Friedberg, MD

Associate Professor
Department of Pediatrics
University of Toronto
Cardiologist
Department of Cardiology
The Hospital for Sick Children
Toronto, Ontario, Canada

Michele A. Frommelt, MD

Associate Professor
Department of Pediatrics
Medical College of Wisconsin
Staff Physician
Department of Pediatric Cardiology
Children's Hospital of Wisconsin
Milwaukee, Wisconsin

Michael A. Gatzoulis, MD, PhD, FACC, FESC

Professor of Cardiology
Congenital Heart Disease
Consultant Cardiologist
Royal Brompton Hospital
National Heart & Lung Institute
Imperial College
London, England, United Kingdom

Tal Geva, MD

Professor
Department of Pediatrics
Harvard Medical School
Chief, Division of Noninvasive
Imaging
Department of Cardiology
Children's Hospital Boston
Boston, Massachusetts

Michael Gewitz, MD

Physician-in-Chief
Chief, Pediatric Cardiology
Maria Fareri Children's Hospital at
Westchester Medical Center
Professor and Vice Chairman
Department of Pediatrics
New York Medical College
Valhalla, New York

Nancy S. Ghanayem, MD

Associate Professor
Department of Pediatrics, Division of
Critical Care
Medical College of Wisconsin
Clinical Director, Cardiac
Critical Care
Children's Hospital of Wisconsin
Milwaukee, Wisconsin

Therese M. Giglia, MD, FACC, FAAP, SCCM

Attending Cardiologist
Cardiac Center
Children's Hospital of Philadelphia
Philadelphia, Pennsylvania

Julie S. Glickstein, MD, FAAP, FAAC

Clinical Professor of Pediatrics
Department of Pediatrics
Columbia University College of
Physicians and Surgeons
Attending Physician
Department of Pediatrics,
Division of Pediatric Cardiology
Children's Hospital of New York
Presbyterian
New York, New York

Caren S. Goldberg, MD, MS

Associate Professor
Department of Pediatrics
University of Michigan Medical Center
Pediatric Cardiologist
Department of Pediatrics, Division of
Pediatric Cardiology
C.S. Mott Children's Hospital
Ann Arbor, Michigan

Elizabeth Goldmuntz, MD

Associate Professor of Pediatrics
Department of Pediatrics
University of Pennsylvania Perelman
School of Medicine
Associate Physician
Division of Cardiology, Department of
Pediatrics
The Children's Hospital of
Philadelphia
Philadelphia, Pennsylvania

Steven C. Greenway, MSc, MD, FRCPC

Clinical Fellow
Labatt Family Heart Centre
The Hospital for Sick Children
Toronto, Ontario, Canada

Donald J. Hagler, MD

Professor of Pediatrics and Medicine
Department of Pediatrics and Medicine
Pediatric Cardiology and Cardiovascu-
lar Diseases
Pediatric Cardiac Catheterization
Laboratory
Mayo Clinic College of Medicine
Rochester, Minnesota

Frank L. Hanley, MD

Co-Director and Professor of
Cardiothoracic Surgery
Children's Heart Center
Lucile Packard Children's Hospital at
Stanford
Stanford, California

George M. Hoffman, MD

Medical Director
Division of Anesthesiology
Children's Hospital of Wisconsin
Professor, Anesthesiology and Critical
Care
Medical Director and Chief, Pediatric
Anesthesiology
Associate Director, Pediatric Intensive
Care Unit
Medical College of Wisconsin
Milwaukee, Wisconsin

Timothy M. Hoffman, MD

Associate Professor
Department of Pediatrics
The Ohio State University College of
Medicine
Medical Director, Heart Transplant
and Heart Failure Program
The Heart Center
Nationwide Children's Hospital
Columbus, Ohio

Kirk R. Hutchinson, PhD, MS

Department of Physiology
The University of Arizona
Tucson, Arizona

Ralf J. Holzer, MD

Associate Professor of Pediatrics
The Ohio State University Medical
Center
Assistant Director
The Heart Center Cardiac
Catheterization and Interventional
Therapy
Nationwide Children's Hospital
Columbus, Ohio

John Lynn Jefferies, MD, MPH, FAAP, FACC

Associate Professor, Pediatric
Cardiology and Adult Cardiovascu-
lar Diseases
Director, Advanced Heart Failure,
Cardiomyopathy, and Ventricular
Assist Device Programs
Co-Director, Cardiovascular Genetics
Associate Director, Heart Institute
Research Core
The Heart Institute
Cincinnati Children's Hospital Medical
Center
Cincinnati, Ohio

Jonathan N. Johnson, MD

Assistant Professor
Department of Pediatrics
Mayo Clinic College of Medicine
Senior Associate Consultant
Department of Pediatrics, Division of
Pediatric Cardiology
Mayo Clinic
Rochester, Minnesota

Paul R. Julsrud, MD

Professor of Radiology
College of Medicine
Consultant
Department of Radiology
Mayo Clinic
Rochester, Minnesota

Gregory L. Kearns, PharmD, PhD

Professor
Department of Pediatrics and
Pharmacology
University of Missouri–Kansas City
Chairman
Medical Research
The Children's Mercy Hospital
Kansas City, Missouri

Thomas R. Kimball, MD

Professor
Department of Pediatrics
University of Cincinnati College of
Medicine
Medical Director
Heart Institute
Cincinnati Children's Hospital Medical
Center
Cincinnati, Ohio

Ganga Krishnamurthy, MBBS

Assistant Professor
Department of Pediatrics
Columbia University
Director, Neonatal Cardiac Care
Department of Pediatrics
Morgan Stanley Children's Hospital of
New York
New York, New York

John D. Kugler, MD

DB & Paula Varner Professor of
Pediatrics
Professor of Internal Medicine
Department of Pediatrics
University of Nebraska College of
Medicine
Clinical Professor, Creighton
University
School of Medicine
Department of Pediatrics
Creighton University School of
Medicine
Director of Patient Care Services,
Cardiology
Department of Cardiology
Children's Hospital & Medical Center
Omaha, Nebraska

Lary A. Latson, MD

Director, Pediatric International
Cardiology and Adult Congenital
Cardiology
Departments of Pediatric Cardiology
and Adult Cardiology
Joe DiMaggio Children's Hospital/
Memorial Health Care System
Hollywood, Florida

Peter C. Laussen, MBBS

Professor of Anesthesia
Harvard Medical School
Chief, Division of Cardiovascular
Critical Care
Department of Cardiology
Children's Hospital Boston
Boston, Massachusetts

Anthony Y. Lee, MD

Clinical Assistant Professor
Department of Pediatrics
The Ohio State University College of
Medicine
Attending Physician
Cardiothoracic Intensive Care Unit
Nationwide Children's Hospital
Columbus, Ohio

Mark B. Lewin, MD

Professor and Chief
Division of Pediatric Cardiology
Department of Pediatrics
University of Washington School of
Medicine
Heart Center Co-Director
Department of Cardiology
Seattle Children's Hospital
Seattle, Washington

D. Scott Lim, MD

Associate Professor
Department of Pediatrics and
Medicine
University of Virginia
Director of Cardiac Catheterization
Laboratory
Departments of Pediatrics and
Medicine
University of Virginia Health System
Charlottesville, Virginia

Angela E. Lin, MD

Associate Clinical Professor
Department of Pediatrics
Harvard Medical School
Staff Geneticist
Medical Genetics
MassGeneral Hospital for Children
Boston, Massachusetts

Frederick R. Long, MD

Clinical Professor
Department of Radiology
Ohio State University
Section Chief, Body MR and CT
Department of Radiology
Nationwide Children's Hospital,
Columbus, Ohio

Angela Lorts, MD

Assistant Professor
Division of Cardiology
Cincinnati Children's Hospital Medical
Center
Cincinnati, Ohio

Pamela A. Lucchesi, PhD

Professor
Department of Pediatrics
The Ohio State University
Director
Center for Cardiovascular and
Pulmonary Research
Nationwide Children's Hospital
Columbus, Ohio

Andrew S. Mackie, MD, SM, FRCP(C)

Assistant Professor
Department of Pediatrics and Public
Health Sciences
University of Alberta
Staff Cardiologist
Department of Pediatrics
Stollery Children's Hospital
Edmonton, Alberta, Canada

Katsuhide Maeda, MD, PhD

Clinical Assistant Professor of
Cardiothoracic Surgery
Division of Pediatric Cardiac
Surgery
Department of Cardiothoracic
Surgery
Stanford University School
of Medicine
Stanford, California

Joseph J. Maleszewski, MD

Assistant Professor of Pathology
Departments of Laboratory Medicine
and Pathology
Mayo Clinic
Rochester, Minnesota

Bradley S. Marino, MD, MPP, MSCE

Associate Professor
Department of Pediatrics
University of Cincinnati College of
Medicine
Staff Cardiac Intensivist
Cardiac Intensive Care Unit
Cincinnati Children's Hospital
Medical Center
Cincinnati, Ohio

Barry J. Maron, MD

Director, Hypertrophic
Cardiomyopathy Center
Minneapolis Heart Institute
Foundation
Minneapolis, Minnesota

Luciana Martins, BA, MSc, PhD

Senior Lecturer, Luso-Brazilian
Studies
Director, Centre for Iberian and Latin
American Visual Studies
Chair of Exams
External BA Programme Director
Birkbeck, University of London
London, England,
United Kingdom

Gerald R. Marx, MD

Associate Professor
Department of Pediatrics
Harvard Medical School
Senior Associate
Department of Cardiology
Boston Children's Hospital
Boston, Massachusetts

G. Paul Matherne, MD

Professor
Department of Pediatrics
University of Virginia
Pediatric Cardiology Division Head
Department of Pediatrics
University of Virginia Health System
Charlottesville, Virginia

Richard Eugene McClead, Jr., MD, MHA

Professor and Vice-chairman
Department of Pediatrics
The Ohio State University
Medical Director, Quality Improvement
Services
Department of Pediatrics
Nationwide Children's Hospital
Columbus, Ohio

Brian W. McCrindle, MD, MPH

Staff Cardiologist and Senior
Scientist
Department of Pediatrics
The Hospital for Sick Children
Toronto, Ontario, Canada

Jerry R. Mendell, MD

Professor of Pediatrics and
Neurology
Department of Pediatrics
Ohio State University
Director of Center for Gene Therapy
Department of Pediatrics
Nationwide Children's Hospital
Columbus, Ohio

Luc L. Mertens, MD, PhD

Associate Professor
Department of Pediatrics
University of Toronto
Section Head of Echocardiography
Department of Cardiology
Hospital for Sick Children
Toronto, Ontario, Canada

Erik C. Michelfelder, Sr., MD

Associate Professor
Department of Pediatrics
University of Cincinnati College of
Medicine
Co-Director, Cardiac Imaging
Services
Director, Fetal Heart Program
The Heart Institute
Cincinnati Children's Hospital Medical
Center
Cincinnati, Ohio

L. Luann Minich, MD

Professor of Pediatrics
Department of Pediatric
Cardiology
University of Utah/Primary Children's
Hospital
Salt Lake City, Utah

John W. Moore, MD, MPH

Professor of Pediatrics
Chief, Section of Cardiology
Department of Pediatrics
University of California, San Diego
School of Medicine
Director, Division of Cardiology
Children's Specialists of
San Diego
San Diego, California

Phillip Moore, MD, MBA

Professor of Clinical Pediatrics
Department of Pediatrics
University of California,
San Francisco
Director, Congenital Catheterization
Laboratory
Department of Pediatric Cardiology
University of California
San Francisco
San Francisco, California

Antoon F.M. Moorman, PhD

Professor in Embryology
Head of the Department of
Anatomy, Embryology, and
Physiology
Academic Medical Centre, University
of Amsterdam
Amsterdam, The Netherlands

Adrian M. Moran, MD

Associate Clinical Professor
Division Director, Department of
Pediatric Cardiology
Maine Medical Center
Pediatric Cardiology Associates
Portland, Maine

Kathleen A. Mussatto, PhD, RN

Nurse Scientist
Herma Heart Center
Children's Hospital of Wisconsin
Milwaukee, Wisconsin

Shobha Natarajan, MD

Assistant Professor
Department of Clinical Pediatrics
Perelman School of Medicine,
University of Pennsylvania
Attending Physician
Department of Cardiology/Cardiac
Center
The Children's Hospital of
Philadelphia
Philadelphia, Pennsylvania

Jane W. Newburger, MD, MPH

Commonwealth Professor of Pediatrics
Harvard Medical School
Department of Cardiology
Children's Hospital Boston
Boston, Massachusetts

David G. Nykanen, MD

Associate Professor
College of Medicine
University of Central Florida
Co-Director
The Heart Center
Arnold Palmer Hospital for Children
Orlando, Florida

Patrick W. O'Leary, MD, FASE, FACC

Professor of Pediatrics
Division of Pediatric Cardiology
Mayo Clinic
Rochester, Minnesota

Timothy M. Olson, MD

Professor
Department of Medicine and Pediatrics
College of Medicine, Mayo Clinic
Consultant, Division of Pediatric
Cardiology
Department of Medicine and Pediatrics
Mayo Clinic
Rochester, Minnesota

Stephen M. Paridon, MD

Professor of Pediatrics
Department of Pediatrics, Division of
Cardiology
Perelman School of Medicine
The University of Pennsylvania
Medical Director, Exercise Physiology
Laboratory
Department of Pediatrics, Division of
Cardiology
The Children's Hospital of Philadelphia
Philadelphia, Pennsylvania

Francesco Parisi, MD

Medical Director
Department of Pediatric Cardiology
and Cardiac Surgery
Bambino Gesù Pediatric Hospital and
Research Institute
Rome, Italy

Anjali Patwardhan, MD, MRCPI, MRCPCH, DCH, MBA, MSc

Assistant Professor
Department of Pediatric Rheumatology
University of Missouri Health Care
Columbia, Missouri

John Pepper, MA, MChir, FRCS, FESC

Professor of Cardiothoracic Surgery
Royal Brompton Hospital
National Heart & Lung Institute
Imperial College
London, England, United Kingdom

John R. Phillips, MD

Associate Professor
Department of Pediatrics
West Virginia University School of
Medicine
Pediatric Cardiologist
Department of Pediatrics
West Virginia University Children's
Hospital
Morgantown, West Virginia

Paolo T. Pianosi, MD

Associate Professor
Department of Pediatric and
Adolescent Medicine
Mayo Clinic
Rochester, Minnesota

Arthur S. Pickoff, MD

Professor and Chair
Departments of Pediatrics and
Community Health
Assistant Dean for Clinical Research
Wright State University Boonshoft
School of Medicine
The Children's Medical Center of
Dayton
Dayton, Ohio

Andrew J. Powell, MD

Associate Professor
Department of Pediatrics
Harvard Medical School
Director, Cardiac MRI
Department of Cardiology
Children's Hospital Boston
Boston, Massachusetts

Matina Prapa, MD

PhD Fellow
Royal Brompton Hospital
National Heart & Lung Institute
Imperial College
London, England, United Kingdom

Lourdes R. Prieto, MD

Associate Professor
Department of Pediatrics
Cleveland Clinic Lerner College of
Medicine of Case Western Reserve
University
Director, Catheterization Laboratory
Center for Pediatric and Congenital
Heart Disease
Cleveland Clinic Foundation
Cleveland, Ohio

Marlene Rabinovitch, MD

Professor of Pediatrics
Department of Pediatrics
Stanford University School of Medicine
Stanford, California

Andrew N. Redington, MD, FRCP

Professor of Pediatrics
University of Toronto
Head of Cardiology
Department of Pediatrics
Hospital for Sick Children
Toronto, Ontario, Canada

Sharon L. Roble, MD

Assistant Professor
Division of Cardiovascular Medicine
The Ohio State University
Nationwide Children's Hospital
Columbus, Ohio

S. Lucy Roche, MB ChB, MRCPCH (UK), MD

Assistant Professor
Department of Medicine—Cardiology
University of Toronto
Staff Cardiologist
Adult Congenital & Pediatric
Cardiology
Toronto General Hospital
Toronto, Ontario, Canada

Lindsay Rogers, MD

Pediatric Cardiology Fellow
The Children's Hospital of
Philadelphia
Philadelphia, Pennsylvania

Stephen J. Roth, MD, MPH

Associate Professor
Department of Pediatrics
Stanford University School of
Medicine
Medical Director
Cardiovascular Intensive Care Unit
Lucile Packard Children's Hospital
Palo Alto, California

Agustin E. Rubio, MD

Assistant Professor
Department of Pediatrics
University of Washington School of
Medicine
Cardiologist, Cardiac Catheterization
Services
Department of Cardiology
Seattle Children's Hospital
Seattle, Washington

Jennifer M. Rutledge, MD, FACC

Clinical Associate Professor
Department of Pediatrics
University of Alberta Hospital
Edmonton, Alberta, Canada

Ritu Sachdeva, MBBS, FACC, FAAP

Associate Professor
Department of Pediatrics, Division of
Pediatric Cardiology
University of Arkansas for Medical
Sciences
Medical Director, Heart Station
Division of Pediatric Cardiology
Arkansas Children's Hospital
Little Rock, Arkansas

Sameh M. Said, MD

Fellow
Cardiovascular Surgery
Mayo Clinic
Rochester, Minnesota

J. Philip Saul, MD

Professor of Pediatrics,
Chief, Pediatric Cardiology
Department of Pediatrics
Medical University of South
Carolina
Charleston, South Carolina

Douglas J. Schneider, MD

Associate Professor
Department of Pediatrics
University of Kentucky
Director, Cardiac Catheterization
Laboratory
Medical Director, Congenital Heart
Clinic
Kentucky Children's Hospital
Lexington, Kentucky

Robert E. Shaddy, MD

Professor of Pediatrics
Department of Pediatrics
University of Pennsylvania
Perelman School of Medicine
Chief, Division of Pediatric
Cardiology
Vice Chair, Department of
Pediatrics
Department of Pediatrics
The Children's Hospital of
Philadelphia
Philadelphia, Pennsylvania

Norman H. Silverman, MD

Academic Specialist
Department of Pediatrics
University of California, San Francisco
School of Medicine
San Francisco, California

Candice K. Silversides, MD

Head of Obstetric Medicine
Mount Sinai Hospital
Staff Cardiologist
Toronto Congenital Cardiac
Centre for Adults
Toronto General Hospital
Toronto, Ontario, Canada

Samuel C. Siu, MD, SM

Gunton Professor and Divisional Chair
of Cardiology
Department of Medicine
Schulich School of Medicine and
Dentistry
City Wide Chief of Cardiology
Medical Leader, Cardiac Program
Department of Medicine
London Health Sciences Centre and
St. Joseph's Health Care
London, Ontario, Canada

Aleksander Sizarov, MD

Researcher
Heart Failure Research Center,
Academic Medical Center
University of Amsterdam
Amsterdam, The Netherlands

Jeffrey F. Smallhorn, MBBS, FRACP, FRCP(C)

Professor of Pediatrics
Department of Pediatrics
University of Alberta
Pediatric Cardiologist
Department of Pediatrics
Stollery Children's Hospital
Edmonton, Alberta, Canada

Gary A. Smith, MD, DrPH

Professor
Department of Pediatrics,
Epidemiology, and Emergency
Medicine
The Ohio State University
Director
Center for Injury Research
and Policy
Nationwide Children's Hospital
Columbus, Ohio

Christopher S. Snyder, MD

Head of Pediatric Electrophysiology
Department of Pediatrics
Ochsner Clinic Foundation
New Orleans, Los Angeles

Charles H. Spencer, MD

Professor of Clinical Pediatrics
Department of Pediatrics
Ohio State University
Chief, Section of Rheumatology
Department of Pediatrics
Nationwide Children's Hospital
Columbus, Ohio

Deepak Srivastava, MD

The Younger Family Director
Professor
Departments of Pediatrics and
Biochemistry & Biophysics
Wilma and Adeline Pirag Distinguished
Professor
Pediatric Developmental
Cardiology
Gladstone Institute of Cardiovascular
Disease
University of California
San Francisco, California

Paul Stephens, Jr., MD

Clinical Associate Professor
of Medicine
Department of Pediatrics
University of Pennsylvania School of
Medicine
Staff Cardiologist
Department of Pediatrics
Children's Hospital of Philadelphia
Philadelphia, Pennsylvania

Thomas Taghon, DO

Assistant Clinical Professor of
Anesthesiology
Department of Anesthesiology
The Ohio State University College of
Medicine
Vice Chair, Quality Improvement
Department of Anesthesiology and
Pain Medicine
Nationwide Children's Hospital
Columbus, Ohio

Lloyd Y. Tani, MD

Professor of Pediatrics and Division
Chief, Pediatric Cardiology
Department of Pediatrics
University of Utah School
of Medicine
Chief, Pediatric Cardiology
Department of Cardiology
(Pediatrics)
Primary Children's Medical
Center
Salt Lake City, Utah

Kathryn A. Taubert, PhD

Chief Science Officer
World Heart Federation
Geneva, Switzerland
Adjunct Professor
University of Texas Southwestern
Medical Center
Dallas, Texas

David F. Teitel, MD

Professor of Pediatrics
Division Chief, Pediatric Cardiology
University of California,
San Francisco
Medical Director, Pediatric
Heart Center
UCSF Benioff Children's Hospital
San Francisco, California

Ravi R. Thiagarajan, MBBS, MPH

Associate Professor of Pediatrics
Department of Pediatrics
Harvard Medical School
Senior Associate in Cardiology
Department of Cardiology
Children's Hospital Boston
Boston, Massachusetts

Jeffrey A. Towbin, MD, FAAP, FACC, FAHA

Executive Co-Director
The Heart Institute
Cincinnati Children's Hospital Medical
Center
Chief, Pediatric Cardiology
Department of Pediatrics
University of Cincinnati
Cincinnati, Ohio

James S. Tweddell, MD

The S. Bert Litwin Chair
Department of Cardiothoracic
Surgery
Children's Hospital of Wisconsin
Professor of Surgery and Pediatrics
Chair, Division Cardiothoracic
Surgery
Medical College of Wisconsin
Milwaukee, Wisconsin

Nathaniel W. Taggart, MD

Assistant Professor
Department of Pediatric and
Adolescent Medicine
Mayo Clinic College of Medicine
Consultant
Division of Pediatric Cardiology
Mayo Clinic
Rochester, Minnesota

George F. Van Hare, MD

Director, Pediatric Cardiology
Department of Pediatrics
Washington University in St. Louis
Co-Director, St. Louis Children's
and Washington University
Heart Center
St. Louis Children's Hospital
St. Louis, Missouri

Jodie K. Votava-Smith, MD

Advanced Fellow in Fetal Cardiology
The Heart Institute
Cincinnati Children's Hospital Medical
Center
Cincinnati, Ohio

Paul M. Weinberg, MD

Professor of Pediatrics and Pediatric
Pathology and Laboratory
Medicine
Associate Professor of Radiology
Department of Pediatrics
Perelman School of Medicine at The
University of Pennsylvania
Senior Cardiologist, Consultant in
Pathology and Radiology (MRI)
Department of Pediatrics,
Division of Cardiology, Pathology,
Radiology
The Children's Hospital of
Philadelphia
Philadelphia, Pennsylvania

Stephen E. Welty, MD

Professor of Pediatrics-Neonatology
Head, Section of Neonatology
Department of Pediatrics
Baylor College of Medicine
Chief, Neonatology Service
Texas Children's Hospital
Houston, Texas

Gil Wernovsky, MD

Professor of Pediatrics
University of Pennsylvania School of
Medicine
Associate Chief
Division of Pediatric Cardiology
Children's Hospital of
Philadelphia
Philadelphia, Pennsylvania

Char Witmer, MD

Attending Physician
Hemostasis and Thrombosis
Center
The Children's Hospital of
Philadelphia
Philadelphia, Pennsylvania

Loren E. Wold, PhD, FAHA

Assistant Professor
Department of Pediatrics/Physiology
and Cell Biology
The Ohio State University
Principal Investigator
Center for Cardiovascular and
Pulmonary Research
The Research Institute at Nationwide
Children's Hospital
Columbus, Ohio

Gail E. Wright, MD

Clinical Associate Professor of Pediatrics
Division of Pediatric Cardiology
Lucile S. Packard Children's Hospital
at Stanford University
Palo Alto, California

Ali N. Zaidi, MD

Assistant Professor, Pediatrics and
Internal Medicine
Department of Pediatrics, Division of
Pediatric Cardiology
Department of Internal Medicine,
Division of Cardiovascular
Medicine
The Ohio State University College of
Medicine
Director, Research, Columbus Ohio
Adult Congenital Heart Disease
Program
Department of Pediatrics, Division of
Pediatric Cardiology
The Heart Center, Nationwide
Children's Hospital
Columbus, Ohio

PREFACE

With this eighth edition of *Moss and Adams' Heart Disease in Infants, Children, and Adolescents*, the editors have attempted to garner updated and useful information from authors who are presently leading their various areas of our discipline. The field of genetics is ever expanding, as are arenas of care, diagnosis, and long-term evaluation. The responses from the authors reflect a careful approach to each chapter, and for that we are grateful. We have added chapters on quality of life, quality and safety, pharmacology, and research design that should prove useful to all of the readership, especially cardiology fellows who are about to take the sub-Board examination. Again, we thank authors who previously contributed to earlier editions as well as those who have joined authorship in this edition. It is they who deserve the appreciation of the readership of this text.

With the availability of an electronic version of the text, we have been able to move various appendices, the chapter on *The Development of Pediatric Cardiology*, and movies to

the online portion, leaving room for more text in the printed volumes. Additionally, we have included sub-Board-like questions for the various chapters in the electronic version. Hopefully this will be useful for those taking and recertifying the certifying examinations. It is important to note that present members of the sub-Board of Pediatric Cardiology did not participate in this component of the book. An editor who has not been a sub-Board member for some time (HDA) prepared these questions. The questions are not part of the sub-Board examination and have not been "lifted" from the examination, as Dr. Allen is far enough removed so as not to recall or know any questions on the present examination.

Hugh D. Allen, MD, FACC, FAAP, FAHA
David J. Driscoll, MD
Robert E. Shaddy, MD
Timothy F. Feltes, MD

ACKNOWLEDGMENTS

The authors deserve any positive credit for usefulness of this text.

The staff of Wolters Kluwer/Lippincott Williams & Wilkins has been fantastic. The advice, patience, and courage of Fran DeStefano; the organization, persistence, and attention to detail of Leanne Vandetty; and the recent addition of Julie Goolsby are most appreciated.

George Emmanouilides, MD, remains a wonderful and respected counselor for this text. Forrest Adams, MD, is still active and was a driving force from the beginning. Many thanks to each of you from all of us in the discipline.

I (HDA) am most grateful to my administrative assistant, Jayne Henry, for her attention to detail in translating my edits of the chapters.

TRIBUTE TO MOSS, ADAMS, & EMMANOUILIDES



Arthur J. Moss, MD (1914–2004)

*Pediatrician, Pediatric Cardiologist, Educator
Professor of Pediatrics, Emeritus
University of California, Los Angeles
Chairman, Department of Pediatrics (1967–1977)
Chairman, Executive Committee, Section on Cardiology,
American Academy of Pediatrics (1967–1968)*



Forrest H. Adams, MD (1919. . .)

*Pediatrician, Pediatric Cardiologist, Investigator, Educator
Professor of Pediatrics, Emeritus
University of California, Los Angeles
Director, Division of Cardiology
Department of Pediatrics (1952–1978)
Chair, Sub-board of Pediatric Cardiology (1967–1969)
President, American College of Cardiology (1971–1972)*



George C. Emmanouilides, MD (1926. . .)

*Pediatrician, Pediatric Cardiologist, Educator, Advocate,
Neonatologist, Investigator
Professor of Pediatrics, Emeritus
University of California, Los Angeles
Chief, Division of Pediatric Cardiology
Department of Pediatrics
Harbor–UCLA Medical Center
Torrance, California (1963–1995)
Chair, Executive Committee of Section on Cardiology, American
Academy of Pediatrics (1978–1980)
Distinguished Physician Award—Hellenic Society of New York (1992)*

Structure and Function of the Cardiovascular System

Cardiac Anatomy and Examination of Cardiac Specimens

William D. Edwards ■ Joseph J. Maleszewski

A fundamental understanding of cardiac anatomy forms the cornerstone of diagnostic pediatric cardiology and is a prerequisite for the proper interpretation of clinical cardiovascular imaging. In this chapter, cardiac anatomy is presented segmentally, with an emphasis on comparisons between analogous right-sided and left-sided structures. Although standard and commonly accepted anatomic terminology is used, anglicized forms are also provided in parentheses—for example, *crista terminalis* (terminal crest).

MEDIASTINUM

General Features

In keeping with their embryonic origins as midline structures, the heart and great vessels occupy the midthorax within the mediastinum. The anatomic borders of the mediastinum are as follows:

1. Anteriorly, the sternum and its adjacent ribs
2. Posteriorly, the vertebral column and its adjacent ribs
3. Laterally, the medial aspects of the parietal pleurae (pleurae)
4. Superiorly, the plane of the first rib
5. Inferiorly, the diaphragm

The mediastinum, in turn, is divided into four regions (Fig. 1.1). The heart, aortic arch, and descending thoracic aorta are located in the middle, superior, and posterior regions, respectively. Also located within the mediastinum are the esophagus, trachea, right and left main bronchi, thymus, lymph nodes, autonomic nerves, thoracic duct, and small vessels (including bronchial, esophageal, azygos, and hemiazygos).

Cardiac Size

The size of the heart relative to the thoracic cage varies with age. Radiographically, on a posteroanterior (PA) film, the normal cardiothoracic ratio is 60% or less for newborns and 50% or less in children and adults (Fig. 1.2). However, these ratios are applicable only for full respiratory inspiration, a condition that may be difficult to attain in newborns and infants. Accurate assessment of the great vessels by chest radiography also may be hampered by the overlying thymus.

Cardiac size also is proportional to body size and correlates better with body surface area and weight than with height. In well-conditioned athletes, with physiologic cardiac hypertrophy, heart weights may approach or slightly exceed the upper limits of normal. Heart weight varies with gender as well and, for the same body size, is greater in girls than in boys during infancy and childhood. By the time a body weight of 25 kg is achieved, however, heart weights are similar between genders, and beyond 35 kg of body weight, heart weights in boys exceed those in girls by about 10% (1). This trend continues throughout adult life and increases with body size, from 15% at 70 kg, to 20% at 100 kg, to 25% at 150 kg (2).

In general, the normal human heart is roughly the size of one's fist. In this regard, it is important to emphasize that a patient's heart size should be similar in size to the patient's fist, not the examiner's. This obvious fact easily can be forgotten when one is viewing cardiac images and not taking into account the size of the patient.

Cardiac Position

Within the mediastinum, the cardiac apex normally is directed leftward, anteriorly, and inferiorly, and this constitutes

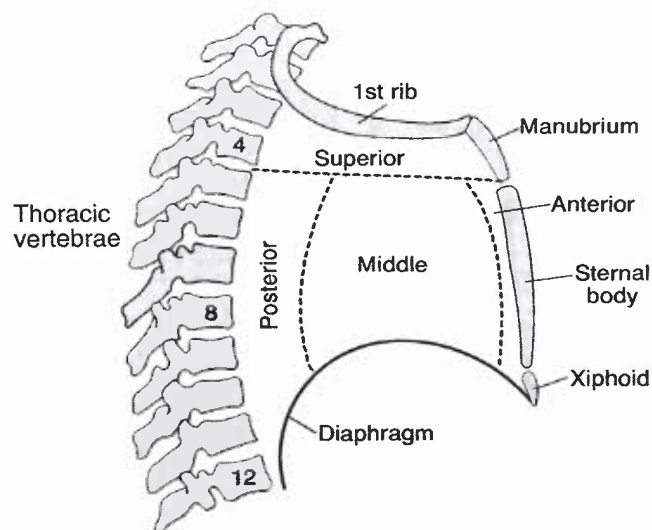


Figure 1.1. Mediastinum, shown schematically. Viewed from a right lateral perspective, the mediastinum has four divisions.

levocardia. In newborns, the apical direction is more horizontal than in children or adults.

However, once the heart is removed from the chest, whether literally at autopsy or technically by projecting an image onto a video monitor, the extracardiac reference points are lost, and

orientation becomes a matter of convenience. Traditionally, photographs of cardiac specimens have been oriented with the apex down, and echocardiographic four-chamber images of the heart often are projected similarly. As a result, confusion has arisen concerning the true anatomic positions of the cardiac chambers and valves.

PERICARDIUM

General Features

The pericardium both covers the heart, as the epicardium, and surrounds it, as the parietal pericardium, much like a fluid-filled balloon covers a fist that is pressed into it. Between the two layers, within the pericardial sac, serous pericardial fluid (≤ 25 mL in adults) serves to lubricate the heart and allow its relatively friction-free movement within the chest. In addition, the parietal pericardium limits the diastolic dimensions of the heart.

Parietal Pericardium

The parietal pericardium represents a tough, flask-shaped sac that surrounds the heart and attaches along the great vessels, such that the ascending aorta and main pulmonary artery are intrapericardial (Fig. 1.3A). Similarly, the terminal 2 to 4 cm of the superior vena cava also is located within the pericardial



Figure 1.2. Cardiothoracic ratio. In posteroanterior chest radiograms, the relative size of the cardiac silhouette changes with age. **A:** Two-day-old newborn. **B:** Three-year-old child. **C:** Thirty-one-year-old man.

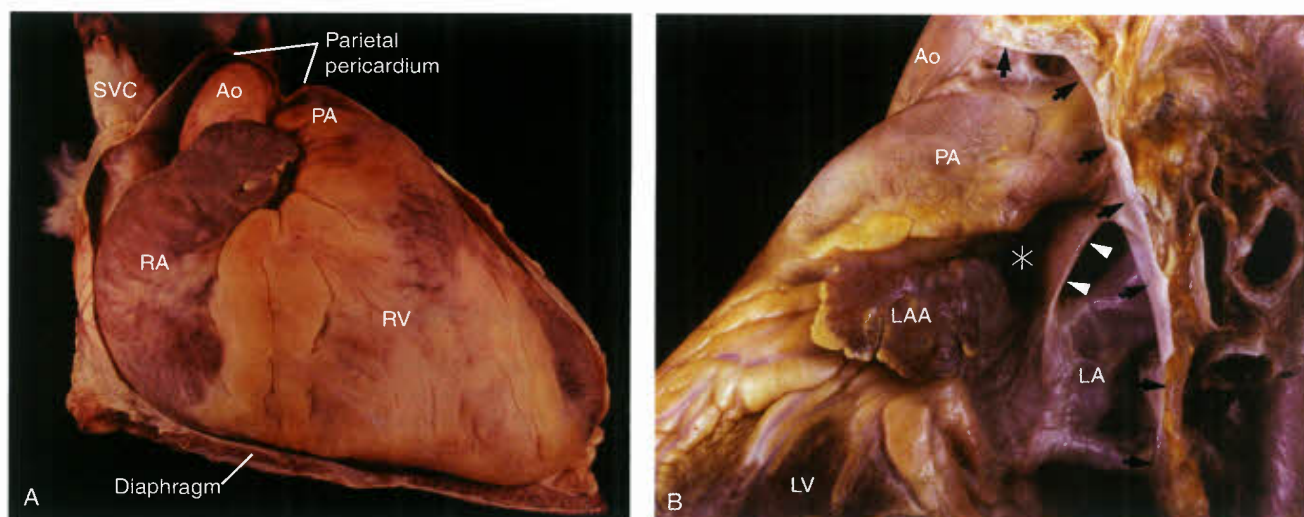


Figure 1.3. Parietal pericardium. A: With the anterior aspect of the parietal pericardium removed, the intrapericardial position of the great vessels is apparent. B: With most of the parietal pericardium excised, the pericardial reflection can be identified (arrows), as can the ligament of Marshall (arrowheads) and the transverse sinus (asterisk) (left lateral view). (See Appendix 1.1 at <http://solution.lww.com> for abbreviations.)

sac, as are shorter lengths of the pulmonary veins and the inferior vena cava.

For patients with total anomalous pulmonary venous connection, the confluence of pulmonary veins is located within the pericardial sac behind the heart. In contrast, the right and left pulmonary arteries and the ductus arteriosus are extrapericardial structures, and surgical procedures restricted to these vessels do not require a pericardial incision.

The parietal pericardium consists of an outer fibrous layer and an inner serous layer of mesothelial cells. The fibrous layer is densely collagenous and is ≤ 1 mm thick in adults. Its outer surface also normally contains variable amounts of adipose tissue, especially near the diaphragm, that can cause apparent thickening of the pericardium, as well as contribute to the cardiac silhouette radiographically.

Because the fibrous pericardium contains little elastic tissue, it cannot distend acutely. Consequently, the rapid accumulation of as little as 200 mL of pericardial fluid in adults generally produces hemodynamic features of cardiac tamponade. However, in the setting of chronic enlargement of the heart, as occurs with normal body growth or with cardiac dilation, stretching and growth of the parietal pericardium do take place to accommodate the increasing cardiac volume. Such growth is capable of accommodating >1 L of chronic pericardial effusion.

Visceral Pericardium (Epicardium)

The visceral pericardium, or epicardium, covers the heart and the intrapericardial portions of the great vessels. It consists of a delicate lining of mesothelial cells and the subjacent adipose tissue, coronary vessels, and nerves along the surface of the heart. Adipose tissue tends to accumulate within the atrioventricular (AV), interventricular, and interatrial grooves (sulci) and along the acute margin of the right ventricle and the coronary branches. Prominent tags of fat cover the origins of the coronary arteries, between the aorta and the atrial appendages. With increasing age, epicardial fat increases in amount and may infiltrate into the atrial septum, particularly within the limbus of the fossa ovalis.

Because the heart must be compliant enough to enlarge during ventricular diastole and to contract during systole, the

normal visceral pericardium has no dense fibrous component. Even so, it does have appreciable mechanical strength, as evidenced by the fact that, following coronary interventions complicated by arterial perforation, the overlying epicardium readily withstands coronary blood pressure and thereby deters rupture into the pericardial sac.

Pericardial Reflection

The junction between the parietal and visceral layers occurs along the great vessels and is known as the pericardial reflection. That portion involving the great veins forms the oblique sinus, a cul-de-sac (shaped like an inverted U) along the posterior aspect of the left atrium. Between the great arteries, anterosuperiorly, and the atrial walls, posteroinferiorly, is a tunnel-shaped structure, the transverse sinus (Fig. 1.3B). Nearby, the ligament of Marshall represents the embryonic remnant of a left superior vena cava.

Intraoperatively, in the setting of pulmonary atresia, if a remnant of the hypoplastic or atretic main pulmonary artery exists, it will be found along the ascending aorta, anterosuperior to the transverse sinus. Conversely, a persistent left superior vena cava will abut the left pulmonary artery, posterior to the transverse sinus.

Following operative procedures that include an anterior pericardiotomy, the development of fibrinous pericarditis is the rule and may be accompanied by a friction rub. As healing takes place, fibrin is replaced by fibrovascular granulation tissue, from which oozing of blood may occur as small vessels are eroded by repeated contact between the parietal and visceral layers with each heartbeat. For this reason, the pericardium generally is left open postoperatively so that accumulations of blood or fluid can be drained into one of the pleural cavities and removed through a chest tube.

Within a few days, however, the raw and inflamed surfaces generally begin to adhere to the overlying sternum, effectively closing the pericardium. When this occurs, oozing of blood from the pericardial surfaces can result in the insidious development of postoperative cardiac tamponade. Furthermore, in supine patients, localized accumulations of blood within the oblique sinus can produce isolated left

atrial tamponade, which can be readily detected by bedside echocardiography.

Over time, organization of fibrinous exudates often results in the development of diffuse fibrous adhesions between the parietal pericardium and the epicardial surface, although progression to constriction is rare. However, fibrous adhesions may increase the risk of subsequent cardiac operations by obscuring the locations of epicardial coronary arteries or, when dissected free, by causing appreciable intraoperative bleeding while the patient is heparinized.

EXTERNAL TOPOGRAPHY

General Features

The AV groove (sulcus) defines the plane of the base of the heart, which contains the four major cardiac valves. The anterior and inferior interventricular grooves indicate the plane of the underlying ventricular septum. Externally, the two ventricles are similar in size and the atria are appreciably smaller than the ventricles, even though all four internal chamber volumes are similar. Along the surface of the heart, the right and circumflex coronary arteries travel in the right and left AV grooves, respectively, and the left anterior and posterior descending coronary arteries course along the anterior and inferior interventricular grooves, respectively. Thus, by external inspection alone, surgeons and pathologists can assess the location of the coronary arteries and the presence of hypoplastic or dilated chambers.

Base–Apex Characteristics

The ventricles, being roughly conical, have a base (at the base of the heart) and an apex. The base–apex direction (or axis) for both ventricles is leftward, anterior, and inferior, and the two directions are roughly parallel. However, in crisscross hearts, the ventricular apical directions cross and are often perpendicular.

Because the left base–apex length normally is greater than that of the right, the left ventricular apex generally forms the

true apex of the heart. However, the right ventricle may form the cardiac apex when the left ventricle is hypoplastic or when the right ventricle is dilated. Rarely, the interventricular groove is quite deep apically and results in a heart with a bifid apex.

The cardiac apex normally is located along the left mid-clavicular line at the fourth or fifth intercostal space. Clinically, the point of maximal impulse usually corresponds to the anteroapical region of the left ventricle rather than to the true cardiac apex.

External Landmarks

The junction between the anterior and inferior free walls of the right ventricle forms a sharp angle known as the acute margin, the basal aspect of which delineates the right shoulder of the heart. Analogously, the rounded lateral wall of the left ventricle forms an ill-defined obtuse margin, and its basal aspect represents the left shoulder of the heart. Thus, coronary vessels supplying this region are known as obtuse marginal branches of the circumflex artery. Along the inferior (diaphragmatic) aspect of the heart, the AV, interventricular, and interatrial grooves form a cross-shaped intersection called the crux cordis (crux of the heart).

Chambers and Great Vessels

To properly interpret the various cardiac imaging modalities, one must understand not only the normal size and shape of the cardiac chambers and great vessels but also their relative positions three-dimensionally (Fig. 1.4). In this regard, only the right atrium is anatomically named correctly. It is truly a right lateral chamber, whereas the left atrium lies in the midline posteriorly and is not a left-sided structure. The right ventricle is a right anterior chamber, and the left ventricle is a left posterior structure. Although not striking, the atria are located slightly superiorly relative to the ventricles. Positionally, the aorta arises posteriorly, inferiorly, and to the right of the main pulmonary artery. In patients with congenitally malformed hearts, the relative sizes and positions of the cardiac chambers and great vessels may vary considerably from normal.

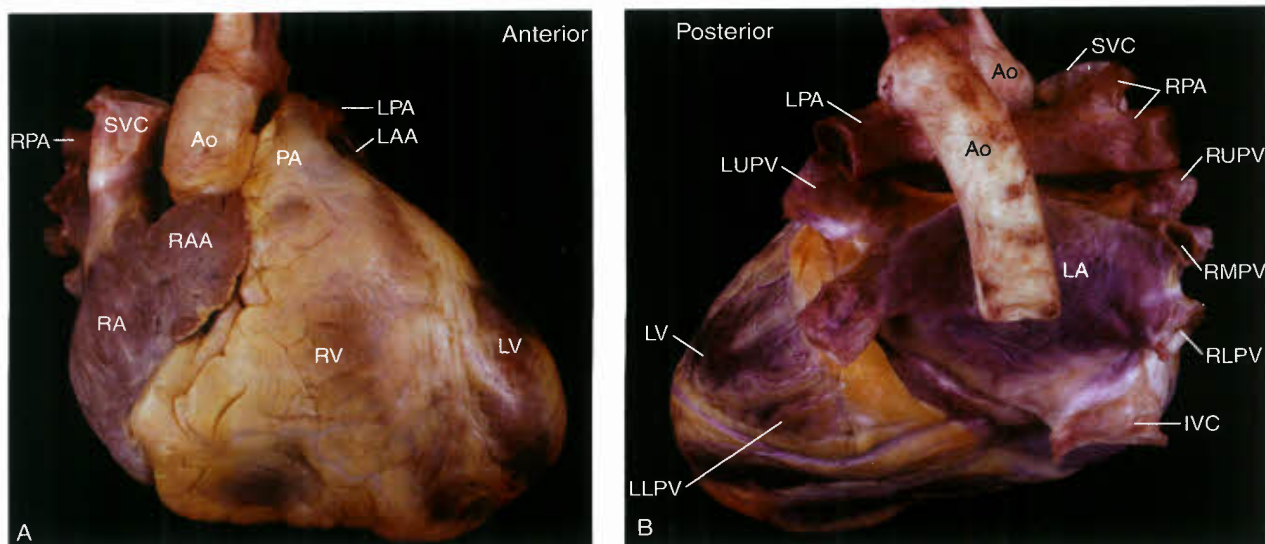


Figure 1.4. External cardiac anatomy. The heart and great vessels are shown from the anterior (A), posterior (B), right lateral.

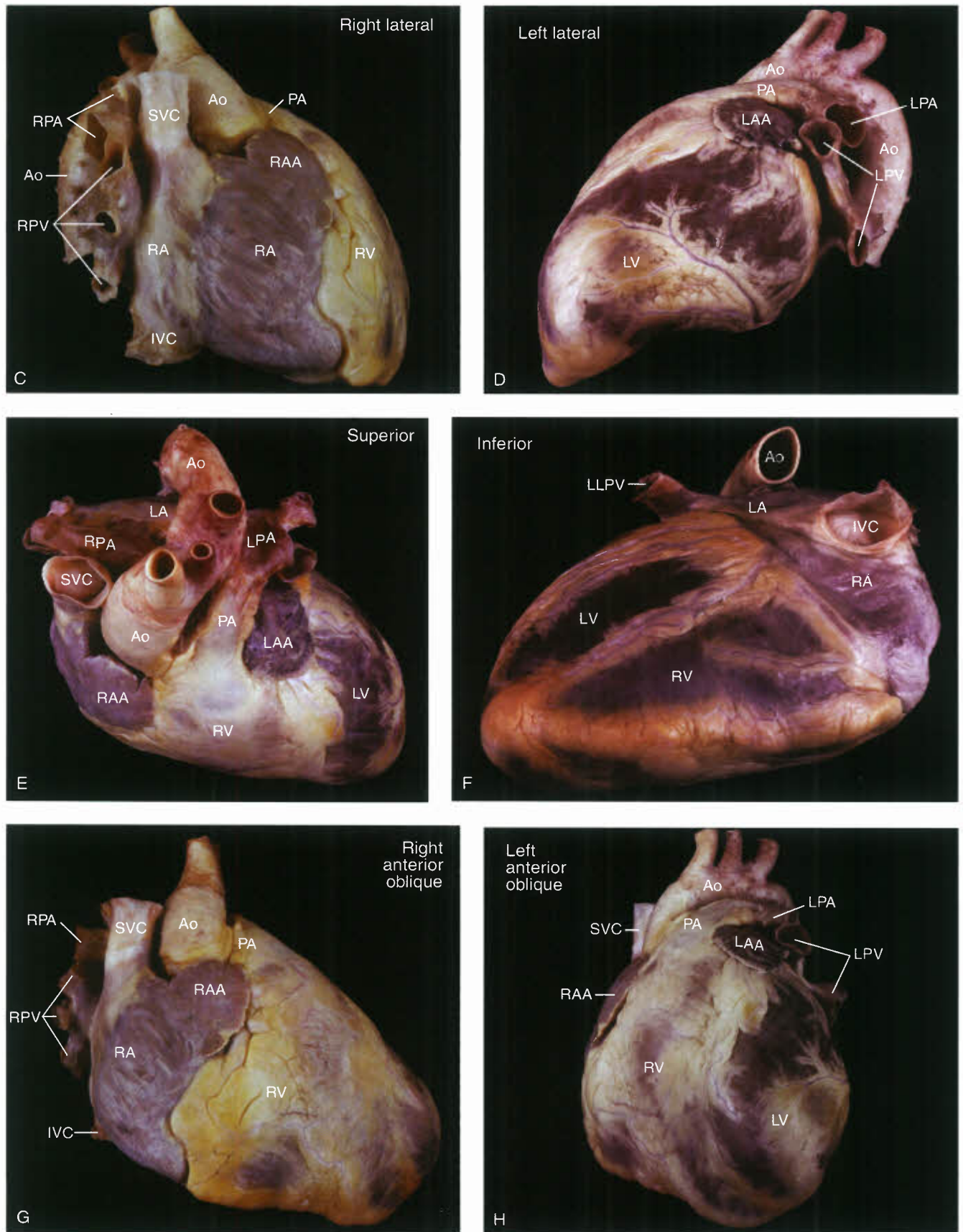


Figure 1.4. (Continued) (C), left lateral (D), superior (E), inferior (F), right anterior oblique (G), and left anterior oblique (H) anatomic perspectives, as indicated for each view. (See Appendix 1.1 at <http://solution.lww.com> for abbreviations.)

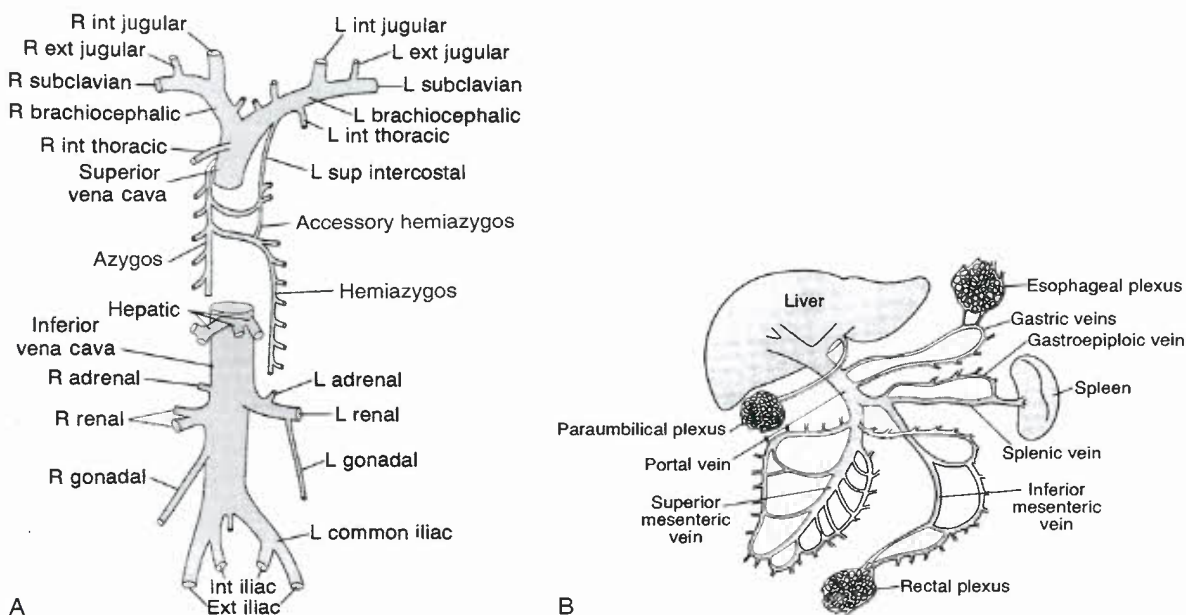


Figure 1.5. Systemic veins, shown schematically. **A:** The systemic veins include the superior and inferior venae cavae and their tributaries. **B:** The portal circulation drains the abdominal digestive system and the spleen. (See Appendix 1.1 at <http://solution.lww.com> for abbreviations.)

GREAT VEINS

Superior Vena Cava

The internal jugular and subclavian veins merge to form brachiocephalic (or innominate) veins bilaterally (Fig. 1.5). Their junctions usually are guarded by venous valves (3). The brachiocephalic veins enter the mediastinum at the level of the first rib, posterior to the sternoclavicular joint. The left brachiocephalic or innominate vein is two to three times the length of its right-sided counterpart and lies along the anterosuperior aspect of the aortic arch and its brachiocephalic branches.

Each innominate vein receives internal mammary (thoracic) and pericardiophrenic veins, and the left also receives the inferior thyroidal vein.

Both brachiocephalic veins merge to form the superior vena cava, which lies just anteriorly to the right pulmonary artery and against the posterolateral aspect of the ascending aorta. The azygos vein arches over the right bronchus and empties into the superior vena cava posteriorly. The superior vena cava, as a right lateral structure, contributes to the right superior border of the radiographic frontal cardiac silhouette (Fig. 1.6). Approximately one-third to one-half of its length is intrapericardial as it approaches the right atrium.

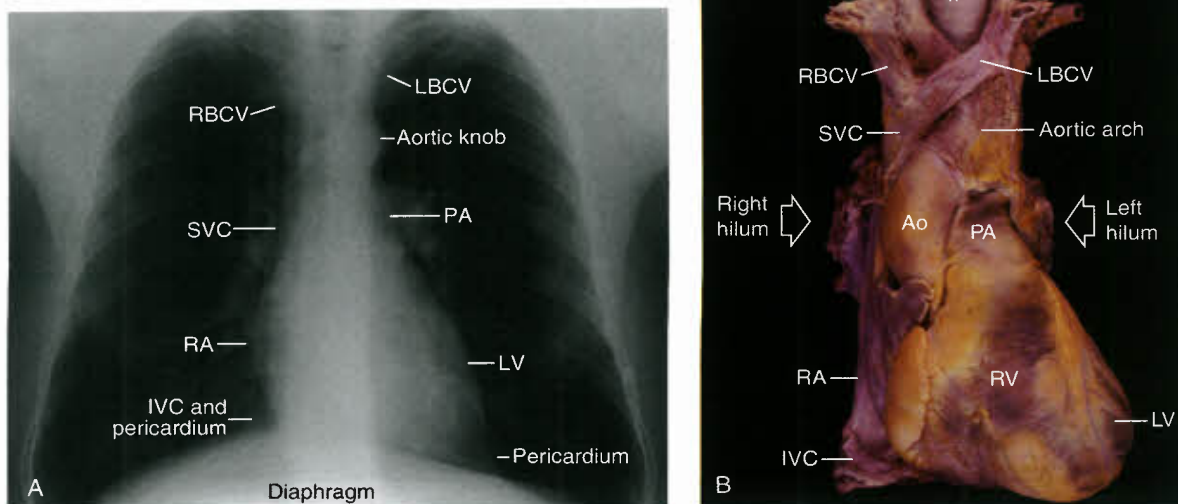


Figure 1.6. Heart and great vessels. **A:** The borders of the frontal cardiac silhouette are demonstrated on a chest radiogram. **B:** An anterior view of a cardiac specimen is shown, for comparison with A. (See Appendix 1.1 at <http://solution.lww.com> for abbreviations.)

The right internal jugular vein, right brachiocephalic vein, and superior vena cava provide a short and relatively straight intravascular route to the right atrium and tricuspid orifice that may be used for obtaining endomyocardial biopsy specimens from the right ventricle. Subclavian veins often are used for the placement of transvenous pacemaker leads, and both the subclavian and internal jugular veins are used for the insertion of pressure-monitoring catheters. Indwelling catheters and pacemaker leads can become coated with shallow thrombus, particularly at sites of contact with vascular walls, which may become sources of embolization or infection.

Inferior Vena Cava

The inferior vena cava receives systemic venous drainage from the legs, retroperitoneal viscera, and the portal circulation (Fig. 1.5). Because the veins from the abdominal digestive system drain through the liver, ingested substances are metabolized before they gain access to the remainder of the body. The suprahepatic portion of the inferior vena cava is only a few centimeters in length and, after traversing the diaphragm, joins the inferior surface of the right atrium.

The ostium of the inferior vena cava is guarded by a diminutive crescent-shaped flap of tissue, the eustachian valve. Although generally small, this valve of the inferior vena cava can become so large that it produces a double-chambered right atrium (cor triatriatum dexter) and can be so obstructive to the tricuspid valve inflow that underdevelopment of the right ventricle results.

Interestingly, the vertebral venous plexus does not directly join the inferior vena cava. Rather, it drains into the intracranial, intercostal, lumbar, and lateral sacral veins, as well as into the portal system via the rectal venous plexus. Accordingly, infections or metastases may spread to the vertebral bodies or central nervous system through this vascular network.

Coronary Sinus

The coronary sinus travels in the left AV groove and receives not only the great cardiac vein but also the posterior, middle, and small cardiac veins. It empties into the right atrium near the atrial septum and the orifice of the inferior vena cava. During electrophysiologic studies in patients with the Wolff-Parkinson-White preexcitation syndrome and left-sided bypass tracts, a multielectrode catheter can be positioned within the coronary sinus and great cardiac vein, adjacent to the mitral valve ring, to localize the aberrant conduction pathways. During cardiac operations, cardioplegic solution may be administered retrogradely into the coronary sinus.

The coronary sinus ostium is guarded by a crescent-shaped valve, the thebesian valve. A commissure exists between the valves of the coronary sinus and the inferior vena cava. From this commissure, a small cord, the tendon of Todaro, travels just beneath the endocardium and inserts into the membranous septum. Rarely, an unroofed coronary sinus drains directly into the left atrium, or the coronary sinus ostium is atretic.

The valves of the inferior vena cava and coronary sinus both are derived from the embryonic right venous valve. When either is enlarged and fenestrated, the term Chiari net (or network) may be applied.

Pulmonary Veins

Superior (upper) and inferior (lower) pulmonary veins from each lung join the posterolateral aspects of the left atrium. Owing to the midline nature of the left atrium, the right-sided

veins are similar in length to their left-sided counterparts. As a variation of normal, a middle lobe vein from the right lung may enter the left atrium separately rather than first joining the upper lobe vein. In other cases, the upper and lower pulmonary veins, particularly from the left lung, can merge and join the left atrium as a single vein.

The right and left lower pulmonary veins each travel along the inferior aspect of the corresponding main bronchus. In contrast, the two upper veins each course anteriorly to their respective bronchus and, at the pulmonary hilum, lie anteriorly to the right intermediate and left main pulmonary arteries. Thus, because the upper pulmonary veins travel anteriorly and the pulmonary arteries travel posteriorly (moving from the heart to the hilus), the veins are posterior to the arteries at the level of the left atrium but lie anteriorly to the arteries at the level of the pulmonary hilum.

Interestingly, the media of the pulmonary veins, within 1 to 3 cm of the left atrium, contain myocardial cells rather than smooth muscle cells. Consequently, these regions can function as sphincters during atrial systole and thereby minimize retrograde blood flow back into the lungs. These venous myocytes also can be the nidus for atrial fibrillation. Because the pulmonary veins normally are thin walled and distended under low pressure, they are prone to extrinsic compression either by a native structure, such as thrombus or neoplasm, or by synthetic materials, such as a conduit or surgical hemostatic packing material.

ATRIA

General Features

The right and left atria serve as receiving chambers for blood returning from the systemic and pulmonary venous systems, respectively. They also have an endocrine function, particularly the right atrium. In the setting of right atrial dilation or congestive heart failure, atrial natriuretic peptide is released from secretory granules within myocytes, as part of the cardiovascular system for sodium and body fluid homeostasis.

Right Atrium

The right atrium is a right lateral chamber that, along with the venae cavae, forms the right lateral border of the radiographic frontal cardiac silhouette (Fig. 1.6). It receives blood from the two venae cavae, coronary sinus, and numerous small thebesian veins, and it expels blood across the tricuspid valve and into the right ventricle. Structurally, the right atrium consists of free-wall and septal components.

Free Wall

Internally, the free wall has a smooth posterior region and a more muscular anterior region (Fig. 1.7). The posterior aspect receives the two venae cavae and has a vein-like appearance, in keeping with its embryologic origin from the sinus venosus. In contrast, the anterior aspect exhibits a muscular wall and a large pyramidal appendage. A prominent C-shaped ridge of muscle, the crista terminalis, serves to separate the two regions and forms one of the tracts for internodal conduction.

Numerous pectinate muscles arise from the terminal crest and travel as parallel ridges along the anterior aspect of the free wall. *Pectinatus* is Latin for comb, and the crista terminalis and pectinate muscles may be likened to the backbone and teeth of a comb, respectively. An irregular arrangement of pectinate muscles also is found within the atrial appendage, and, as a result, atrial pacemaker leads can be lodged readily in

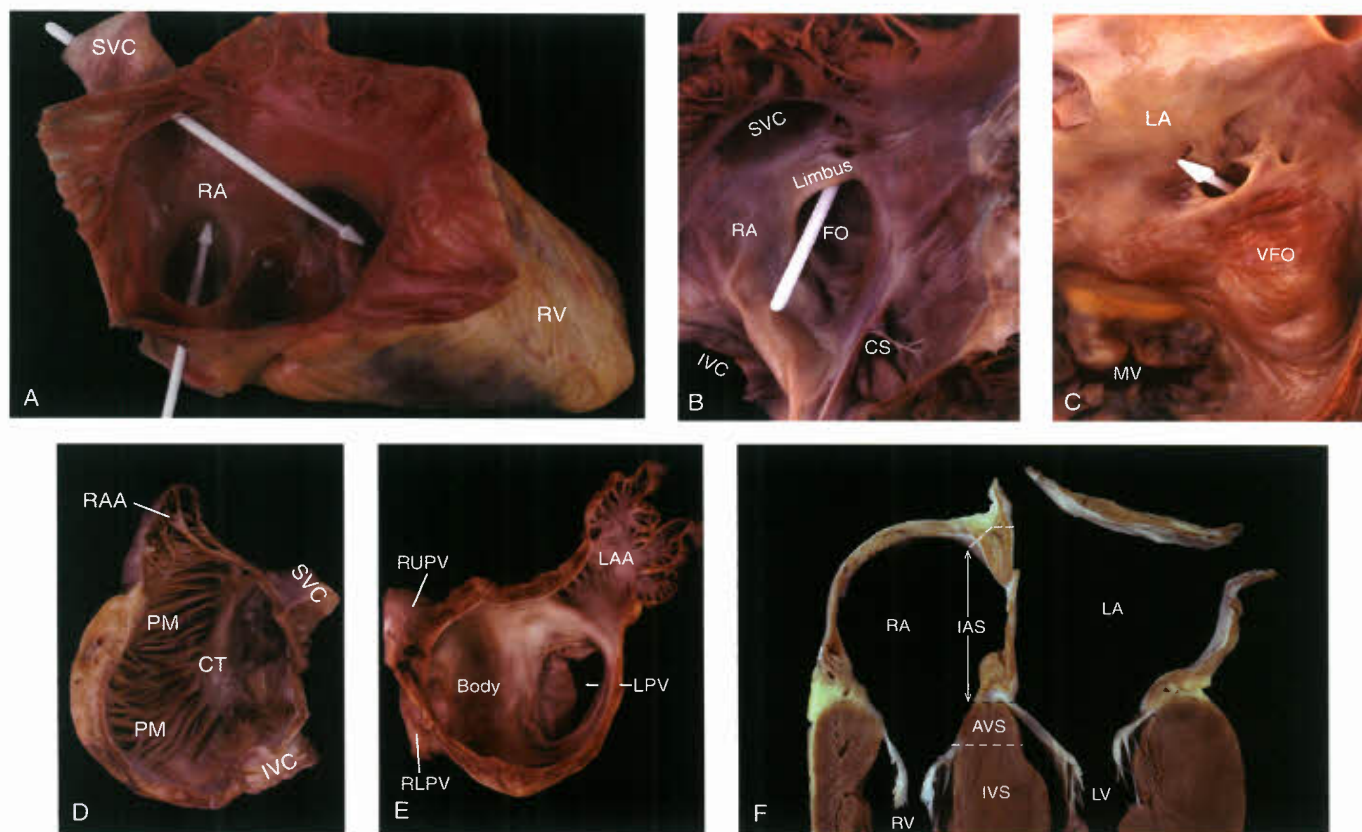


Figure 1.7. Comparison of right and left atria. **A:** Opened right atrium. Two arrow-shaped probes show that the superior vena cava is directed toward the tricuspid orifice and the inferior vena cava is directed toward the fossa ovalis. **B and C:** Atrial septum. A white probe in the patent foramen ovale passes between the limbus and valve of the fossa ovalis in the right atrium (**B**) and exits through the ostium secundum in the left atrium (**C**). **D and E:** Atrial free walls. The right atrial wall (**D**, viewed from a left lateral perspective) contains a crista terminalis and pectinate muscles, whereas the left atrial wall (**E**, viewed from an anterior perspective) contains neither of these structures. **F:** The interatrial and AV septa are demonstrated in a four-chamber slice of the heart. (See Appendix 1.1 at <http://solution.lww.com> for abbreviations.)

this area. The right atrial appendage rests against the ascending aorta and overlies the proximal right coronary artery.

When right atrial enlargement is associated with stasis to blood flow, thrombus may form between the pectinate muscles, particularly within the appendage. Transvenous pacemaker leads and intracardiac catheters often produce linear contact lesions at the cavoatrial junction, and these usually become lined by shallow mural thrombi.

It is important to note that the atrial wall between the ridges of pectinate muscles is generally <1 mm thick and can be perforated by catheters and pacemaker leads. Although the posterior half of the free wall (derived from the sinus venosus) is also only about 1 mm thick, it has a thicker endocardium and, therefore, is less prone to perforation. In adolescents and adults, the pectinate muscles are 2 to 4 mm thick, and the crista terminalis may achieve a thickness of 3 to 6 mm.

Septum

When viewed from the right, the septum has an interatrial component (between the right and left atria) and an AV component (between the right atrium and left ventricle). The interatrial portion is relatively small, and its most prominent feature is the fossa ovalis (4). This consists of a horseshoe-shaped muscular rim—the limbus, which forms a pathway

for internodal conduction—and a central sheet of thin fibrous tissue—the valve of the fossa ovalis (Fig. 1.7). In adolescents and adults, the limbus averages 4 to 8 mm in thickness, and the valve is about 1 mm thick. Embryologically, the valve of the fossa ovalis represents the first septum that develops (septum primum), and the limbus represents the second septum that forms (septum secundum).

During fetal and neonatal life, the valve of the fossa ovalis represents a paper-thin, delicate, translucent membrane. As such, it readily is torn (or stretched) during balloon atrial septostomy procedures. With increasing age, however, the progressive deposition of collagen and elastin produces a thicker, tougher, opaque valve (5). As a result, transseptal procedures may be more difficult in older children, adolescents, and adults.

In contrast to the fossa ovalis, the foramen ovale represents a potential passageway between the two atria. It courses between the anterosuperior aspect of the limbus and the valve of the fossa ovalis and then through a natural valvular perforation, the ostium secundum, and into the left atrium (Fig. 1.7). Although the foramen ovale is patent throughout fetal life, it functionally closes soon after birth, as left atrial pressure begins to exceed that in the right atrium, and the valve of the fossa ovalis becomes pressed against the limbus, thereby effectively closing the foramen.

In approximately two-thirds of individuals, the foramen ovale closes permanently during the first year of life, as fibrous tissue seals the valve to the limbus of the fossa ovalis. Thus, in about one-third of infants, children, and adolescents, this flap valve is not sealed (patent foramen ovale) and closes only when the pressure in the left atrium exceeds that in the right atrium. During the Valsalva maneuver, for example, a small right-to-left shunt can be detected echocardiographically in persons with a patent foramen ovale. In adolescents and adults, the foramen ovale ranges from 2 to 10 mm in maximal potential diameter, with a mean size of 5 to 6 mm (6).

In the setting of pronounced atrial dilation, the atrial septum can be stretched to such an extent that the limbus no longer covers the ostium secundum, resulting in a valvular-incompetent patent foramen ovale—an acquired atrial septal defect. In contrast, fenestrations of the valve are the most common cause of congenital atrial septal defects. Excessive valve tissue may undulate during the cardiac cycle and form an aneurysm of the fossa ovalis (see Chapter 28).

Because the tricuspid valve annulus attaches to the septum lower (more apically) than the mitral annulus, septal myocardium is interposed between the right atrium and the left ventricle. This constitutes the AV septum (Fig. 1.7). Although this is primarily a muscular septum, on average 10 mm thick in adults, it also contains a membranous portion that is only about 1 mm thick. The AV portion of the membranous septum is located at the anterosseptal tricuspid commissure (when viewed from the right side of the heart) and beneath the right posterior aortic commissure (as seen from the left side).

The AV septum corresponds to the triangle of Koch, an important anatomic surgical landmark because it contains the AV node and the proximal (penetrating) portion of the AV (His) bundle. Thus, during tricuspid annuloplasty procedures, care must be taken to avoid injury to the conduction system. When defects occur in the muscular AV septum, the mitral annulus usually drops to the same level as the tricuspid annulus, so that the defect becomes primarily interatrial, and the AV conduction tissues are displaced inferiorly.

Finally, a medial portion of the free wall lies against the right aortic sinus, which bulges somewhat into the atrial cavity as the torus aorticus (aortic bulge). This protuberance is bordered by the limbus of the fossa ovalis, the ostium of the appendage, the tricuspid annulus, and the AV septum. During transseptal procedures, care must be taken to stay within the confines of the valve of the fossa ovalis to avoid perforation along the aortic protuberance, which could result in trauma to the adjacent aortic root or coronary arteries. Rarely, atrial septal defect closure devices have eroded into the aortic root (see Chapter 13).

Because of hemodynamic streaming within the right atrium during intrauterine life, poorly oxygenated blood from the superior vena cava is directed toward the tricuspid orifice, whereas well-oxygenated placental blood within the inferior vena cava is directed by the eustachian valve toward the foramen ovale and into the left atrium. Consequently, the most oxygenated blood in the fetal circulation travels, via the left side of the heart, to the coronary arteries, upper extremities, and the rapidly developing central nervous system. Throughout postnatal life, this orientation of the venae cavae is maintained (Fig. 1.7). As a result, transseptal procedures are performed more easily via the inferior vena cava, in contrast to right ventricular biopsies, which are performed more readily by a superior vena caval approach.

Left Atrium

The left atrium is a midline posterior chamber that receives pulmonary venous blood and expels it across the mitral valve

and into the left ventricle. By virtue of its posterior location, the body of the left atrium does not contribute to the borders of the radiographic frontal cardiac silhouette. However, the left atrial appendage, when enlarged, may produce a bulge along the left cardiac border, between the left ventricle and the left pulmonary artery.

Interposed between the left atrium and the vertebral bodies are the esophagus, to the right, and the descending thoracic aorta, to the left. Furthermore, the bifurcated pulmonary artery and left bronchus travel along the superior aspect of the left atrium, and the left and posterior aortic sinuses may indent the atrial wall as the aortic protuberance (torus aorticus). During transesophageal echocardiography, the transducer is placed close to the left atrium and provides excellent visualization of the atria, AV valves, and great vessels.

In the setting of left atrial dilation, the left bronchus is pushed upward, as can be seen radiographically, and the esophagus is displaced rightward. When a left superior vena cava persists, the coronary sinus into which it drains generally is quite dilated, in some cases indenting the left atrial wall, and should not be mistaken echocardiographically for the descending thoracic aorta. As on the right side, the left atrium consists of a free wall and a septum.

Free Wall

The free wall includes a dome-shaped body, which receives the pulmonary veins, and a finger-like appendage. These two regions are separated externally by the left atrial coronary vein and ligament of Marshall and internally by the ostium of the appendage. The left atrial body, although 1 to 3 mm thick and infiltrated by cardiac myocytes, is derived embryologically from the common pulmonary vein and internally maintains a smooth vein-like appearance. The endocardium is opaque and gray-white, owing to the deposition of collagen and elastin, and is thicker and less compliant than that in the other three chambers.

The left atrial appendage rests along the left AV groove and covers the proximal circumflex coronary artery and, in some individuals, the left main coronary artery. The appendage contains numerous small pectinate muscles, has a variable number of lobes or blind-ended pouches, and is tortuous and may fold on itself. Outside the appendage, the body of the left atrium contains no pectinate muscles, and there is no crista terminalis.

As the left upper pulmonary vein joins the left atrium, an infolded ridge often forms where the ostium of the pulmonary vein is contiguous with that of the atrial appendage. This should not be mistaken as a partial form of cor triatriatum (triatrial heart).

Septum

When viewed from the left, the septum is entirely interatrial. Along its anterosuperior border, the valve of the fossa ovalis contains one or more fenestrations, representing the embryologic counterpart of the ostium secundum. If a probe passed through the fenestrations enters the right atrium, the foramen ovale is considered patent. Neither the limbus of the fossa ovalis nor the AV septum is visible from within the left atrium. Several small thebesian veins drain directly into the left atrial cavity, particularly along the septum.

Comparison of the Atria

With regard to the atrial septum, the limbus of the fossa ovalis is a feature of the right atrium, and the ostium secundum is characteristic of the left atrium (Fig. 1.7). The free wall of the right atrium contains the crista terminalis and pectinate muscles, whereas that of the left atrium does not (Table 1.1). Moreover, the right atrial appendage is large and pyramidal,

TABLE 1.1 Comparison of Right-Sided and Left-Sided Anatomic Fractures of Cardiac Segments

Right Atrium	Left Atrium
Limbus of fossa ovalis (limb of oval fossa)	Ostium secundum
Large pyramidal appendage	Small finger-like appendage
Crista terminalis (terminal crest)	No crista terminalis
Pectinate muscles	No pectinate muscles
Receives venae cavae and coronary sinus ^a	Receives pulmonary veins ^a
Tricuspid Valve	Mitral Valve
Low septal annular attachment	High septal annular attachment
Septal cordal attachments	No septal cordal attachments
Triangular orifice (midleaflet level)	Elliptical orifice (midleaflet level)
Three leaflets and commissures	Two leaflets and commissures
Three papillary muscles	Two large papillary muscles
Empties into right ventricle	Empties into left ventricle
Right Ventricle	Left Ventricle
Tricuspid–pulmonary discontinuity	Mitral–aortic continuity
Muscular outflow tract	Muscular–valvular outflow tract
Septal and parietal bands	No septal or parietal band
Large apical trabeculations	Small apical trabeculations
Coarse septal surface	Smooth upper septal surface
Crescentic in cross sections ^a	Circular in cross section ^a
Thin free wall (3–5 mm) ^a	Thick free wall (12–15 mm) ^a
Receives tricuspid valve	Receives mitral valve
Pulmonary Valve	Aortic Valve
Empties into main pulmonary artery	Empties into ascending aorta

^aVariable feature.

whereas the left atrial appendage is smaller and finger-like. Although the superior vena cava and the pulmonary veins can anomalously join the contralateral atrium, the inferior vena cava almost invariably joins the morphologic right atrium.

Thus, the distinguishing features of a morphologic right atrium are the limbus of the fossa ovalis, connection of the inferior vena cava, and a large pyramidal appendage. The limbus can be detected with four-chamber imaging, and the course of the inferior vena cava and the morphology of the atrial appendage can be assessed by either invasive or noninvasive imaging. Identification of the crista terminalis and pectinate muscles is possible by direct inspection at operation or autopsy but not consistently by imaging procedures.

ATRIOVENTRICULAR VALVES

General Features

The AV valves serve to maintain unidirectional blood flow and to electrically separate the atria and ventricles. Each valve has five components. The annulus, leaflets, and commissures form the valvular apparatus, and the chordae tendineae (tendinous cords) and papillary muscles form the tensor apparatus.

The annulus of each valve is somewhat saddle shaped rather than being truly planar and represents an ill-defined

ring of fibrous tissue from which the leaflets arise. Although the mitral annulus is a continuous ring of collagen, the tricuspid annulus is not and exhibits loose connective tissue at the points of annular discontinuity. Consequently, ventricular dilation leads more readily to annular dilation of the tricuspid valve than that of the mitral valve. During the first two decades of life, valvular growth correlates better with age than with body height, weight, or surface area (1).

Leaflets represent delicate flaps of connective tissue. Owing to direct cordal insertions along their leading edges, the free edges have a serrated appearance. Tendinous cords also insert along the ventricular aspect of each leaflet (the valve pocket or undersurface) and thereby support the leaflet during ventricular systole. On the atrial aspect, the closing edge represents an ill-defined junction between the thinner body (or clear zone) and the thicker contact region (or rough zone) of the leaflet. During valve closure, apposing leaflets contact one another along the surfaces between the free and closing edges (Fig. 1.8). In about 50% of fetuses and infants, blood cysts occur as small (<3 mm) purple nodules along the contact surfaces of the mitral and tricuspid valves and generally disappear within 1 year (7).

Microscopically, each leaflet exhibits two major layers. A fibrous layer (fibrosa) forms the strong structural backbone of the valve and is continuous from the annulus proximally to the sites of cordal insertion distally. In contrast, the spongy layer (spongiosa) acts as a shock absorber and becomes prominent along the contact regions of each leaflet. Because the leaflets are

thin and compliant and are attached only at the annulus and papillary muscles, rapid opening and closure of the valve is possible.

A commissure represents the site along a valve annulus where two leaflets meet. Commissures always have an underlying papillary muscle and a fan-like array of tendinous cords that attach to both leaflets, in contrast to congenital clefts, which have neither. Although each leaflet has two major commissures, it also may be divided further into several regions, or scallops, by minor commissures, each of which has a small underlying papillary muscle.

The tendinous cords act as strong fibrous guy wires to anchor and support the leaflets. Accordingly, they restrict excessive valvular excursion during ventricular systole and prevent valvular prolapse into the atrium. Because a cord generally branches several times, more than 150 cords normally insert into the free edge or ventricular aspect of each valve, which tends to distribute the systolic force of ventricular blood evenly along the undersurface of each leaflet (8,9). If the tendinous cords are malformed, weakened, or insufficient in number, a portion of the leaflet can begin to bulge and prolapse, leading to valvular regurgitation. This commonly occurs not only with myxomatous valves but also with common AV valves and at least one of the two AV valves in a double-inlet left ventricle (10).

Papillary muscles can be single, multiheaded, or a fused group. By being positioned directly beneath a commissure and by receiving tendinous cords from two adjacent leaflets, a papillary muscle tends to pull its two leaflets toward each other during ventricular systole, thereby facilitating valve closure. Ventricular contraction also contributes to valve closure by decreasing the annular dimension and shortening the base–apex length of the chamber. Thus, papillary muscle ischemia or ventricular dilation may produce valvular regurgitation, as can be seen with the tricuspid valve after severe birth asphyxia or in the setting of persistent pulmonary hypertension of the newborn.

Tricuspid Valve

Because of the normal rightward bowing of the ventricular septum, the tricuspid annulus is shaped like a reversed D when viewed from its ventricular aspect (Fig. 1.8). However, at midleaflet level, the orifice becomes triangular. Annular dimensions vary with the cardiac cycle, decreasing by about 20% in circumference and 33% in area during systole, owing to contraction of the right ventricular myocardium (11). The plane of the tricuspid annulus faces toward the right ventricular apex.

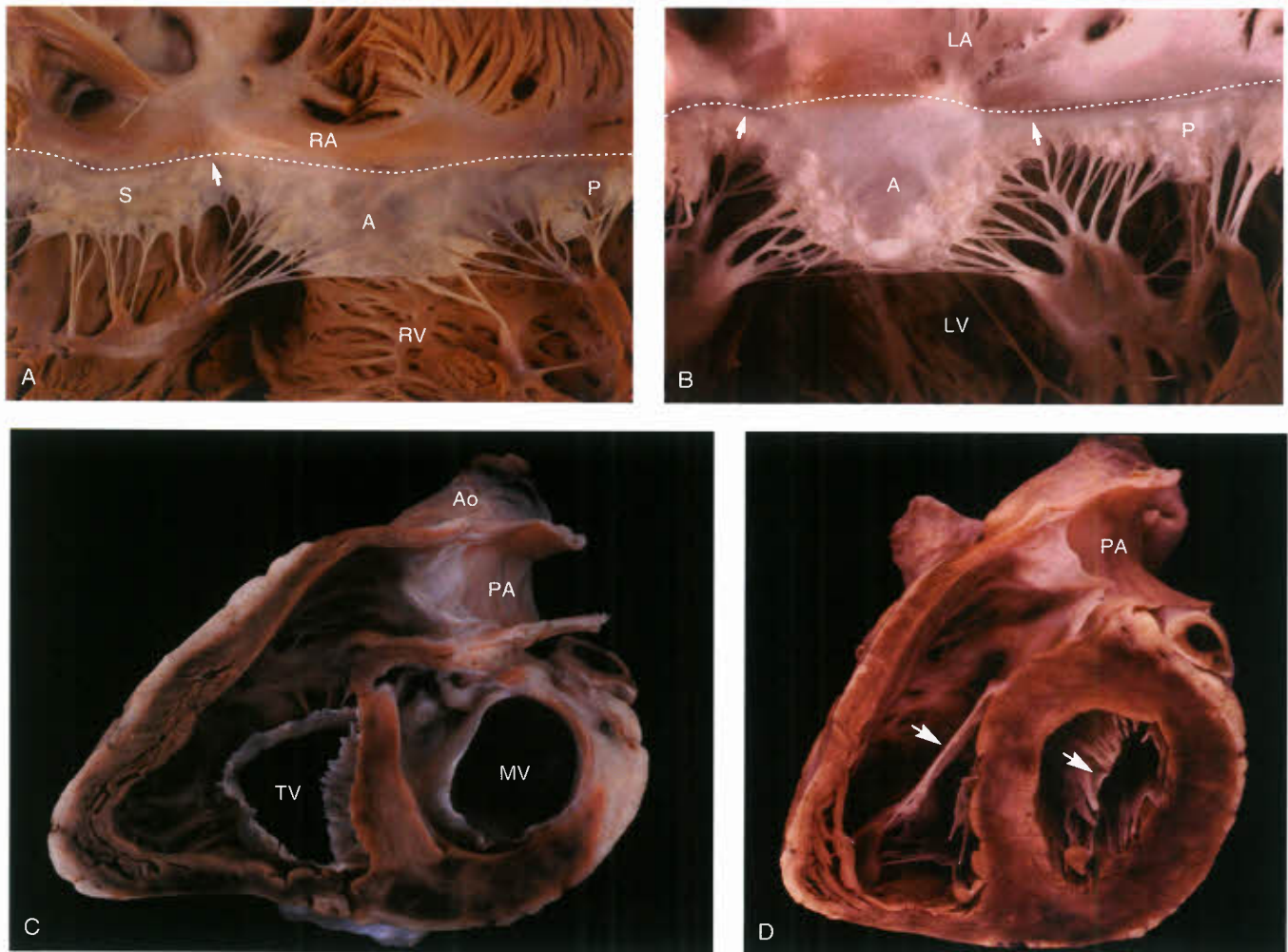


Figure 1.8. Comparison of right and left AV valves. **A:** The tricuspid valve normally has three leaflets. The membranous septum is located along its annulus (*dashed line*), at the anterosseptal commissure (*arrow*). **B:** The mitral valve has two leaflets, with papillary muscles beneath each commissure. **C and D:** In short-axis views, the tricuspid orifice is shaped like a reversed D at the annular level (**C**) and like a triangle at the midleaflet level (**D**). In contrast, the mitral orifice is elliptical at both levels. As shown in **D**, the anterior leaflet (*arrow*) of each valve is a midcavitary structure that divides its ventricle into inflow and outflow regions. (See Appendix 1.1 at <http://solution.lww.com> for abbreviations.)

Whereas the septal and posterior leaflets lie against the ventricular septum and inferior wall of the right ventricle, respectively, the anterior leaflet forms a prominent intracavitary curtain that partially separates the inflow and outflow tracts. The anterior leaflet is the most mobile of the three, and the septal leaflet, by virtue of its numerous direct cordal attachments along the ventricular septum, is the least mobile. The relative sizes of the three leaflets vary appreciably from person to person (9).

Among the three papillary muscles, the anterior muscle is the largest and most well formed. It originates from the acute margin of the right ventricle, may be single or bifid, and provides cordal insertions to the anterior and posterior leaflets. The posterior papillary muscle arises from the inferior wall near the septum, and the posterior and septal leaflets receive cords not only from this small muscle but also from accessory papillary muscles and trabeculations. The medial papillary muscle (also called the papillary muscle of the conus or the muscle of Lancisi) emanates along the superior aspect of the septal band, at the level of the membranous septum, and has cordal attachments to the septal and anterior leaflets. Although prominent in infants and children, it commonly merges with the septal band and becomes small or absent by adulthood.

Of the three commissures, the anteroseptal is the most variable. It traverses the midportion of the membranous septum, dividing it into AV and interventricular regions. Leaflet tissue is deficient at this commissure in about 10% of hearts, and the membranous septum fills the 1- to 7-mm gap between the anterior and septal leaflets (12). This commissure is also characteristically deficient in partial AV septal defects.

Mitral Valve

The mitral annulus changes shape during the cardiac cycle, from circular in diastole to elliptical during systole. However, at the midleaflet level, the diastolic orifice is elliptical or football shaped. The annular circumference and area also decrease by approximately 15% and 25%, respectively, during ventricular systole (13). Unlike the tricuspid annulus, the mitral annulus is directed more toward the midportion of the septum than toward the apex. Although the entire annular circumference connects to the overlying left atrium, only a C-shaped portion attaches to the underlying left ventricular free wall. The remaining 30% of the annulus is intracavitary, is attached to the anterior mitral leaflet, and is continuous with the aortic valve annulus.

Therefore, the anterior mitral leaflet, like the anterior tricuspid leaflet, forms an intracavitary curtain that partially separates the inflow and outflow tracts (Fig. 1.8). However, unlike its right-sided counterpart, it actually forms part of the outflow tract and may contribute to subaortic obstruction in such disorders as hypertrophic cardiomyopathy. Whereas the anterior leaflet is semicircular, the posterior leaflet is rectangular and usually is subdivided by minor commissures into three or more semicircular scallops. Only the mitral valve has just two leaflets; the other three valves each have three leaflets or cusps.

Interestingly, the surface areas of the anterior and posterior leaflets are almost identical and together provide nearly twice the area needed to close the systolic annular orifice (14). However, because some folding and puckering of leaflet tissue, as well as appreciable surface area for contact between leaflets, are needed to ensure a competent seal, the mitral leaflets are not as redundant as they might first appear.

The mitral valve has two major commissures, beneath which are located the two major papillary muscles, anterolateral and posteromedial. In addition to the usual tendinous cords, two thick and prominent strut cords, one from each papillary muscle, attach to the ventricular aspect of the

anterior leaflet and offer additional support (15). In about 50% of subjects, cordal structures known as left ventricular pseudotendons arise from a papillary muscle and insert onto either the septum or the opposite papillary muscle. In contrast, attachment of cords from a mitral leaflet to the ventricular septum is distinctly abnormal and is usually associated with AV septal defects or straddling mitral valves.

Both papillary muscles originate from the left ventricular free wall and can have thicknesses similar to those of the ventricular wall. They occupy the middle third of the left ventricular base–apex length, not only in normal hearts but also in hypertrophied and dilated hearts. In the setting of hypertrophic cardiomyopathy, the mitral papillary muscles may be particularly prominent and occupy a substantial portion of the potential volume of the left ventricular chamber.

The anterolateral papillary muscle commonly is single with a midline groove and usually has a dual blood supply from the left anterior descending and circumflex coronary arteries. In contrast, the posteromedial papillary muscle generally is multiple or else bifid or trifid, and it most commonly is nourished solely by the right coronary artery. The anterolateral muscle usually is larger and extends closer to the mitral annulus than the posteromedial muscle.

Comparison of Atrioventricular Valves

The tricuspid valve has three leaflets, commissures, and papillary muscles, whereas the mitral valve has only two of each. Other differences also exist that may be of clinical use (Fig. 1.8 and Table 1.1).

From a practical standpoint, identification of the lower septal insertion of the tricuspid annulus, as distinct from the mitral, can be assessed with four-chamber images (Fig. 1.7F) in both normal and malformed hearts. Exceptions include partial AV septal defects and double-inlet ventricles, in which the two valves achieve the same annular level. Along the septum, the distance between the mitral and tricuspid insertions is <0.8 cm/m² body surface area in normal hearts and is greater than this in the Ebstein malformation (16).

The insertion of numerous cords directly onto the septum is a reliable distinguishing feature of the tricuspid valve. Finally, the tricuspid valve virtually always connects to a morphologic right ventricle, whereas the mitral valve connects to a morphologic left ventricle. Differences also exist between the two valves with regard to annular size and orifice shape.

VENTRICLES

General Features

Normally, a ventricle receives blood through an AV valve from an atrium and pumps it across a semilunar valve into a great artery. Because all four major cardiac valves lie in the same plane, at the base of the heart, blood entering and exiting a ventricle follows a V-shaped course. During ventricular systole, both the base–apex length and the short-axis diameter decrease and not only expel blood from the chamber but also assist closure of the AV valve by decreasing its annular size.

Heart weight, which roughly corresponds to ventricular mass, is related to body surface area or weight for all age groups (1,2). During the first two decades of life, thicknesses of the right and left ventricular free walls and the ventricular septum correlate better with age than with body size. In normal hearts, the ratio between ventricular septal and left ventricular free-wall thicknesses is 1.1 (range 0.8 to 1.4), and the ratio between left and right ventricular thicknesses is 3

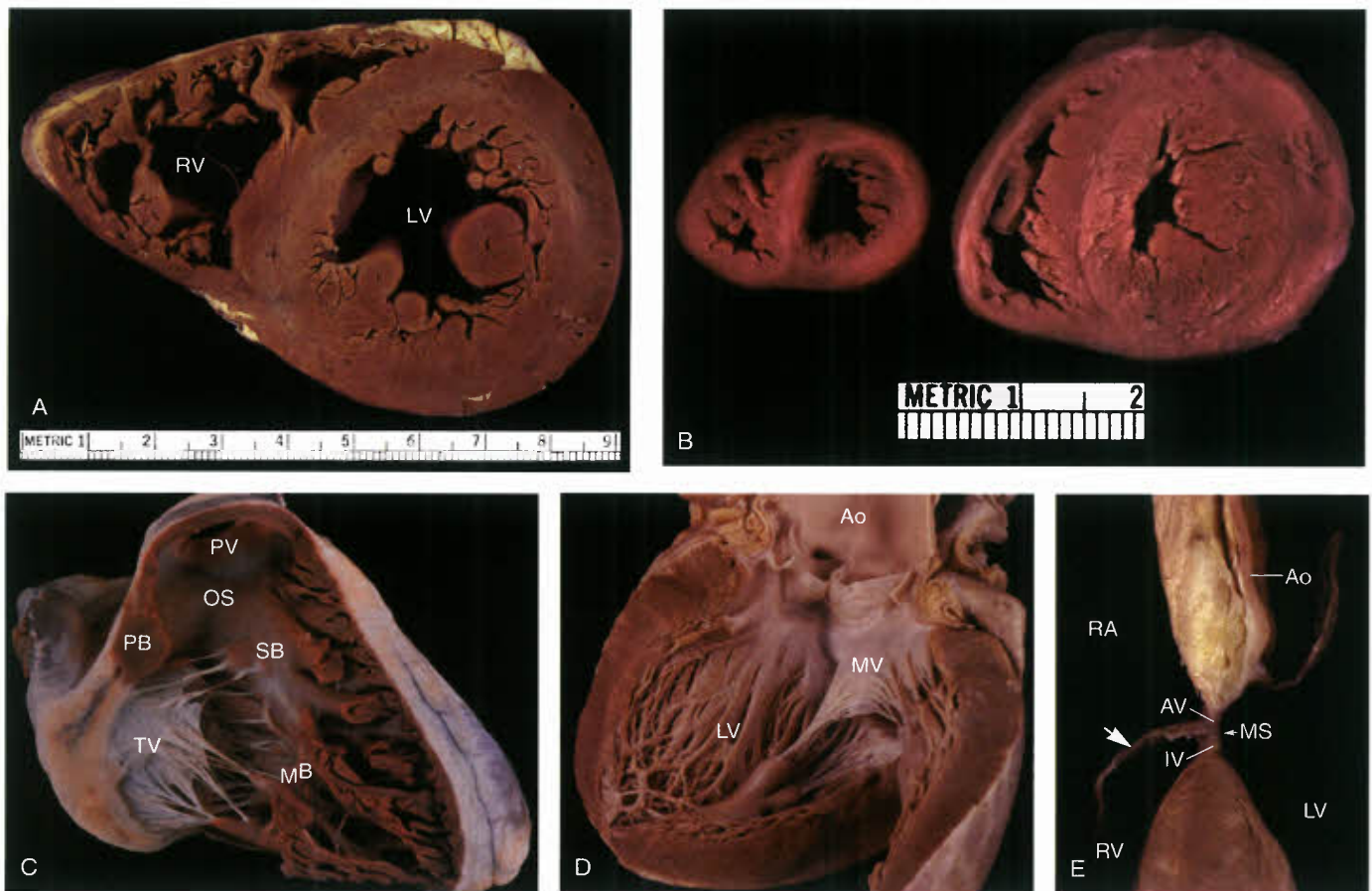


Figure 1.9. Comparison of right and left ventricles. **A:** In cross section, the right ventricle is crescent shaped, the left ventricle is circular, and the wall thickness of the left ventricle is three to four times that of the right ventricle. **B:** The fetal heart (*to the left*) exhibits prominent right ventricular hypertrophy, whereas by the age of 3 months, the infant's heart (*to the right*) shows regression of hypertrophy. **C:** The right ventricle receives a tricuspid valve, has prominent anteroapical trabeculations, and has a muscular outflow track that separates the tricuspid and pulmonary valves. The parietal and septal bands and the outlet septum form the crista supraventricularis (supraventricular crest). **D:** The left ventricle, in contrast, receives a mitral valve, has shallow apical trabeculations, and exhibits direct continuity between the mitral and aortic valves. **E:** The membranous septum is divided into AV and interventricular components by the septal tricuspid leaflet (*arrow*). (See Appendix 1.1 at <http://solution.lww.com> for abbreviations.)

(range 2 to 5). Autopsy measurements of wall thickness tend to correspond to end-systolic rather than end-diastolic dimensions (17).

It is important to note that the right ventricle in fetuses and neonates differs from that in older persons. During fetal life, the presence of a patent ductus arteriosus is associated with equalization of aortic and pulmonary artery pressures and a state of physiologic pulmonary hypertension. Thus, during fetal and neonatal life, right ventricular hypertrophy is evident and the thickness of the right ventricle is similar to that of the left (Fig. 1.9).

Right Ventricle

As a right anterior chamber, the right ventricle normally does not contribute to the radiographic frontal cardiac silhouette. The anterior and inferior surfaces of its free wall merge along the acute margin of the heart and form an angle of 45 to 75 degrees. This, along with rightward bowing of the ventricular septum, results in a crescent-shaped chamber in the short-axis view. Conditions such as pulmonary hypertension that impose a pressure or volume overload on the right ventricle and cause

its hypertrophy and dilation may be attended by straightening of the septum so that both ventricles become D-shaped on cross section. In extreme cases, such as an Ebstein anomaly or total anomalous pulmonary venous connection, leftward bowing of the septum can result not only in a reversal in ventricular short-axis shapes but also in possible obstruction of the left ventricular outflow tract.

Anatomically, the right ventricle can be divided into inlet, trabecular, and outlet regions. This concept of a tripartite chamber correlates well with the embryologic development of the right ventricle. The inlet portion is associated with the tricuspid valve, and its border is defined by the cordal insertions. Anteroapically, prominent muscle bundles traverse the chamber from septum to free wall and demarcate the trabecular region. It is in this region that biopsy tissue is obtained and transvenous pacemaker leads are lodged. The remainder of the ventricle is relatively smooth walled and forms the outlet region, which is a collar of myocardium known as the conus (meaning cone), infundibulum (meaning funnel), or right ventricular outflow tract.

Within the right ventricle, a nearly circular ring of muscle known as the crista supraventricularis forms an unobstructed opening into the outlet region. It consists of a parietal band, an

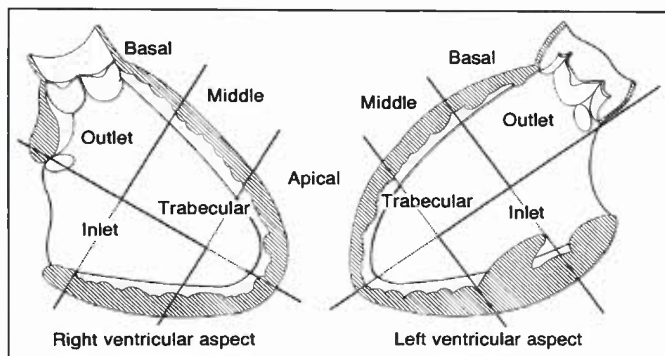


Figure 1.10. Ventricular septum, shown schematically. For each ventricle, the septum is roughly triangular-shaped. One side forms the anterior border, and one forms the inferior border. The third side is located at the cardiac base and is associated with AV and semilunar valves. (See text for further description.)

outlet septum, a septal band, and a moderator band (Fig. 1.9). The parietal band is a free-wall structure that separates the tricuspid and pulmonary valves. Lying beneath the right-left commissure of both semilunar valves, the outlet septum separates the two ventricular outflow tracts and tilts approximately 45 degrees relative to the remainder of the ventricular septum. The septal band is a Y-shaped structure with a long, broad stem and smaller inferior and anterior limbs. The two limbs, in turn, cradle the outlet septum and give rise to the medial tricuspid papillary muscle. Apically, the septal band merges with the apical trabeculations and gives rise to the moderator band, which inserts at the base of the anterior tricuspid papillary muscle. The right bundle branch travels along the septal and moderator bands.

When viewed from a right anterior oblique perspective, the ventricular septum is shaped like a triangle, the vertexes of which correspond to the apex, pulmonary annulus, and the most inferior aspect of the tricuspid annulus. Normally, the distance from the apex to the pulmonary valve annulus is about 25% greater than that from the apex to the tricuspid annulus. The membranous septum lies midway between the pulmonary valve annulus and the inferior aspect of the tricuspid annulus.

Using these landmarks, the surface of the ventricular septum can be divided into six regions that are useful for localizing the position of septal defects (Fig. 1.10) (18). A line drawn from the membranous septum to the apex divides the septum into anterior and inferior halves. By dividing the base–apex length into thirds (basal, middle, and apical), the six regions are obtained. The basal and middle regions inferiorly correspond to the inlet portion of the right ventricle, and the two apical regions plus the anterior middle region match the anterobasal trabecular area. The remaining anterobasal region corresponds to the outlet septum.

Left Ventricle

The left ventricle is a left posterior chamber that forms the left border of the radiographic frontal cardiac silhouette (Fig. 1.6). It consists of septal and free-wall components, and its entrance and exit are guarded by the mitral and aortic valves, respectively. The left ventricle is circular in short-axis cross section and is somewhat wedge shaped in the long-axis view. Three-dimensionally, it is shaped like a strawberry and is approximated mathematically as a truncated ellipsoid (Fig. 1.11). It is



Figure 1.11. Three-dimensional shape of the left ventricle. The left ventricle in humans is shaped like a strawberry, here shown whole and in long-axis. Rather than being facetious, this analogy serves to emphasize the complex shape of the chamber. Thus, mathematical formulas used for the determination of chamber volume or myocardial mass are accurate only insofar as they also accurately reflect the actual shape of the left ventricle. In disease states that are commonly attended by appreciable alterations in ventricular shape, the use of standard formulas may result in determinations that are considerably inaccurate.

of interest that, whereas a conical chamber (as in aortic stenosis) uses the least energy for systolic contraction and a spherical chamber (remodeling in dilated cardiomyopathy) requires the least expenditure of energy for diastolic filling, the normal elliptical left ventricular chamber expends the least total systolic and diastolic energy (19).

In the left ventricle, muscle bundles follow a spiral course from apex to base and also form several different layers that crisscross one another. As a result of this arrangement, systole is characterized by twisting or wrenching contractions that effectively wring blood out of the left ventricle, and diastole creates a vortex that literally sucks blood into the left ventricular chamber.

The free wall is thickest basally and then gradually tapers toward the apex. Interestingly, the tip of the apex, called the apical thin point, averages only 1 to 2 mm in thickness, even in hypertrophied hearts. In contrast, the muscular septum forms a rounded peak at its basal summit and becomes thickest at its midportion owing to the contribution of the right ventricular septal band. Then, after thinning a bit, the septum remains relatively constant in thickness and tapers only as it fuses with the apical portion of the free wall.

Direct fibrous continuity exists between the anterior mitral leaflet and the left and posterior aortic cusps, and this region is reinforced bilaterally by the right and left fibrous trigones (see “Base of the Heart” section later in this chapter). In some hearts, small bundles of myocytes are embedded in this fibrous tissue and afford a minor degree of muscular separation between the two valves. With persistence of the left parietal band (so-called double conus), this muscle bundle causes appreciable valvular separation as is often seen in a double-outlet right ventricle.

As in the right ventricle, the septal surface of the left ventricle is roughly triangular. However, in contrast, the distances from the apex to the mitral annulus and from the apex to the aortic annulus are similar. The inflow length is appreciably shorter than the outflow length only with AV septal defects. The membranous septum and the site of mitral–aortic valvular continuity lie at a level midway between the aortic valve annulus and the most inferior portion of the mitral annulus. Thus, in long-axis scans, a line drawn from the point of valvular continuity to the apex will divide the ventricle into an inferior inflow region and an anterosuperior outflow region and allow identification of the site of the membranous septum.

The ventricular apex is characterized by small, shallow trabeculations, and the apical one-half to two-thirds of the septal surface is also finely trabeculated. More basally, the septum is smooth walled, and subendocardially, the left bundle branch travels in this region. The membranous septum lies beneath the right posterior aortic commissure (Fig. 1.9). Because the septal tricuspid leaflet inserts along its midportion, the membranous septum consists of AV and interventricular components, and their relative sizes vary inversely, depending on the level of tricuspid insertion. Moreover, the entire membranous septum varies considerably in size among individuals and tends to be largest in patients with Down syndrome. Septal defects in this region generally are associated with focal elevation of the tricuspid annulus to the level of the mitral valve so that the communication is interventricular rather than atrioventricular.

The outflow tract of the left ventricle is formed by the upper septum, the anterobasal free wall, and the anterior mitral leaflet. Abnormalities in any of these structures may be associated with outflow tract obstruction. Examples include the discrete and tunnel forms of subaortic stenosis and hypertrophic cardiomyopathy. It is found along the anterior free wall, at the entrance to the outflow tract. The anterolateral muscle of the left ventricle is a prominent trabeculation that may cause outflow tract obstruction in association with certain anomalies (20,21). By cardiac imaging, such prominent trabeculations may be misinterpreted as mural thrombus.

Conditions such as aortic stenosis that impose a pressure overload on the left ventricle induce concentric hypertrophy without appreciable dilation (pressure hypertrophy). In contrast, disorders that produce a volume overload, such as chronic aortic regurgitation, are attended not only by concentric hypertrophy but also by chamber dilation (volume hypertrophy). Although pressure and volume hypertrophy each increase the ventricular mass, only pressure hypertrophy is consistently associated with an increased wall thickness. In volume hypertrophy, dilation masks the degree of hypertrophy, and wall thicknesses often are normal although muscle mass is increased (Fig. 1.12). Consequently, when the left ventricle is dilated, wall thickness cannot be used as a reliable indicator of hypertrophy.

As a general rule, only in myocarditis or hyperacute allograft rejection does the left ventricle become dilated without coexistent hypertrophy, owing to the acute nature of the disorder. It also is important to recognize that hypertrophy, with or without dilation, decreases myocardial compliance and may hinder diastolic filling. Many forms of congenital heart disease are associated with moderate to marked degrees

of ventricular hypertrophy, and, as a result, there may be difficulty in achieving adequate myocardial preservation during long operations. Moreover, marked hypertrophy does not always regress significantly following reparative procedures and may become a source for ischemic injury as the patient survives into adulthood.

Comparison of Ventricles

Because the AV valves travel with their corresponding ventricles, the identification of these valves (by noting their different annular insertion levels along the septum) provides an indirect but reliable clinical means of establishing ventricular morphology. The presence of continuity or discontinuity between the AV and semilunar valves is also useful and can be evaluated using various scanning techniques (Table 1.1). Coarse apical trabeculations, indicative of a right ventricle, are identified more readily by angiography than by echocardiography. Although differences in wall thickness and ventricular shapes are characteristic in normal hearts, they often do not apply in malformed hearts.

SEMILUNAR VALVES

General Features

The semilunar valves connect the ventricles to the great arteries and serve to maintain unidirectional blood flow. They consist of an annulus, cusps, and commissures. Because they have no tensor apparatus (tendinous cords and papillary muscles), the semilunar valves are simpler than the AV valves, and their opening and closure are primarily passive processes.

Behind each cusp is an outpouching of the great artery that imparts a tribulbous, or cloverleaf, shape to the arterial root. The junction between the sinus portion of a great artery and its distal tubular portion forms a prominent ridge, the sinotubular junction. From the right and left aortic sinuses, proximal to this junction, arise the right and left coronary arteries, respectively. These often are incorrectly called the right and left coronary sinuses; the coronary sinus, of course, is a venous structure that empties into the right atrium.

The annulus of each semilunar valve assumes the shape of a triradiate crown, the three points of which attain the level of the sinotubular junction and demarcate the commissures. A commissure, in turn, represents the site at which two

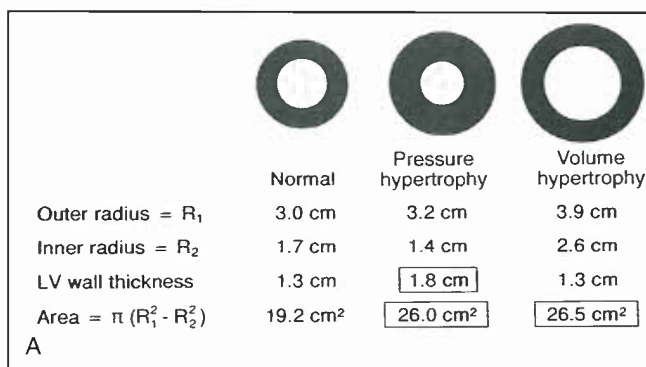


Figure 1.12. Geometry of left ventricular hypertrophy and dilation in short-axis views. **A:** As shown schematically, compared with the normal state, pressure hypertrophy produces an increase in both wall thickness and surface area, whereas volume hypertrophy (with chamber dilation) increases the surface area but not the wall thickness. **B:** Compared with a normal heart (center), the heart with pressure hypertrophy (left) has a thick left ventricular wall, but the one with volume hypertrophy (right) has a normal wall thickness.

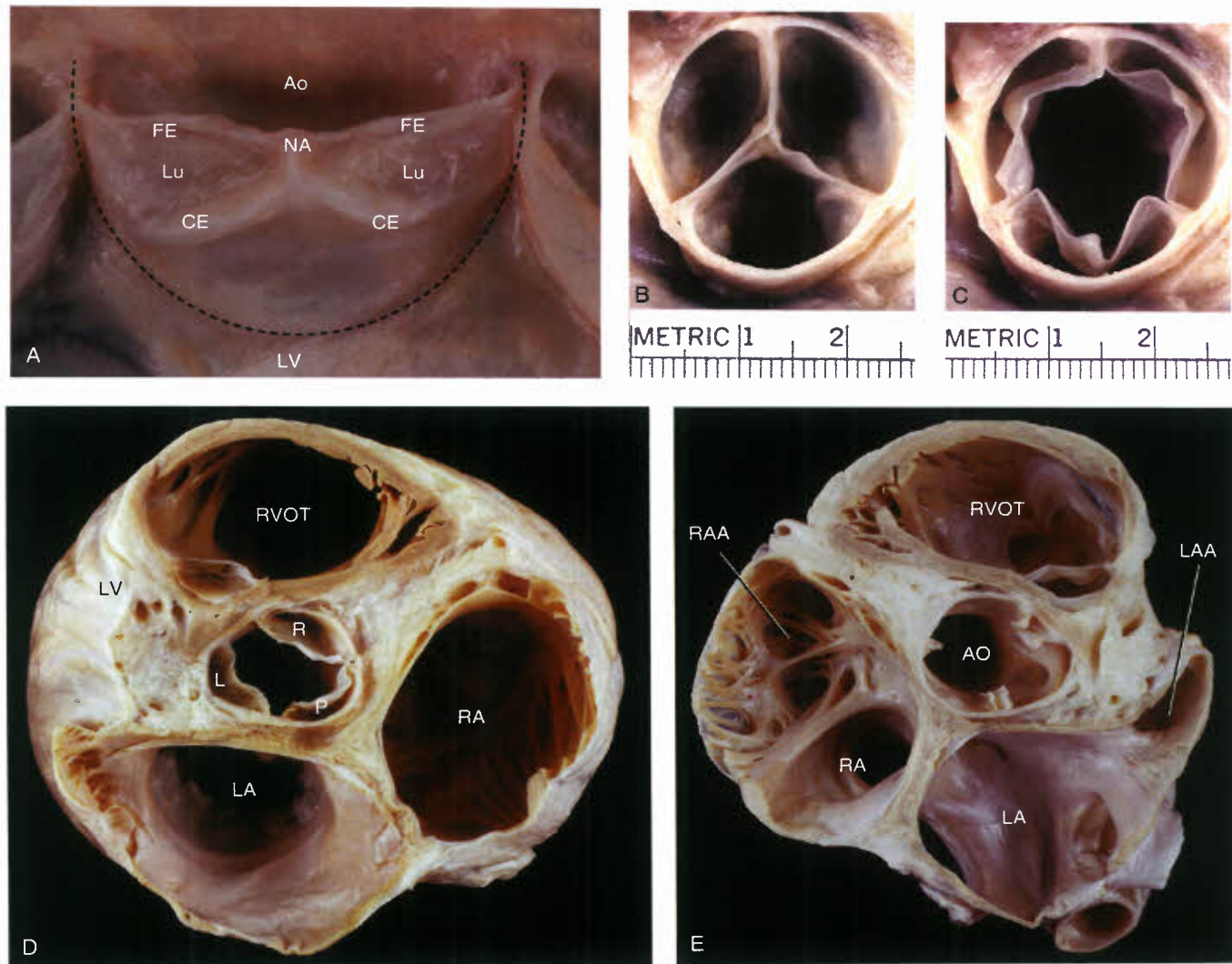


Figure 1.13. Semilunar valves. **A:** Each cusp is pocket shaped and has a free edge, a closing edge, a nodule of Arantius, and two contact regions (lunulae). The annulus (*dotted line*) for each cusp is U shaped. **B and C:** The aortic valve, viewed from above, is shown in simulated opened (**B**) and closed (**C**) positions. **D and E:** Tomographic sections at the level of the aortic valve show adjacent structures as viewed from above (**D**) and below (**E**). (See Appendix 1.1 at <http://solution.lww.com> for abbreviations.)

cusps meet along the annulus. Because the valvular orifice approximates the level of the sinotubular junction, autopsy measurements of the arterial diameter and circumference at this level correlate well with clinical measurements of orifice size (1). During the first two decades of life, normal valve size correlates better with age than with parameters of body size.

As half-moon-shaped (semilunar) structures, the cusps represent pocket-like flaps of delicate fibrous tissue. The leading edge of each cusp is its free edge, beneath which lies a shallow biscalloped ridge, the closing edge, along the ventricular surface of the cusp (Fig. 1.13). At the center of each cusp, along the free edge, is a small fibrous mound, the nodule of Arantius. To either side of this nodule, between the free and closing edges, are two crescent-shaped areas called lunulae that represent the contact surfaces between adjacent cusps during valve closure. The arterial surface of each cusp, in conjunction with its arterial sinus, forms the valve pocket.

Like the AV valves, the semilunar valves histologically consist of fibrous (fibrosa) and spongy (spongiosa) layers. Cusps contain little elastic tissue and therefore have little elastic recoil. As passively mobile structures, they have no memory of

shape and no tendency to assume either an opened or a closed position. During isovolumetric ventricular contraction, expansion of the arterial root may produce commissural separation and thereby initiate valvular opening. Each cusp moves in undulating fashion toward its arterial sinus during ventricular systole and then back toward the center of the arterial lumen during ventricular diastole as retrograde blood flow fills each valve pocket.

Pulmonary Valve

The pulmonary valve lies closest to the chest wall, near the upper left sternal border, and its orifice is directed toward the left shoulder. Because the right ventricular myocardium extends onto the pulmonary sinuses, the valve appears partially submerged within a crater of infundibular muscle. The anterosuperior limb of the septal band extends onto the left pulmonary sinus, and trabeculations parallel to the parietal band insert onto the right pulmonary sinus. Trabecular extensions onto the anterior sinus are less prominent. In the setting

of pulmonary atresia with an intact ventricular septum, failure to recognize these features has resulted in burrowing into the pericardial sac rather than into the pulmonary artery during closed operations (Brock procedure). Although the Brock procedure is no longer performed, it is important to remember this potential complication during cardiac catheter manipulations.

Aortic Valve

The annulus of the aortic valve is a midline structure, and its orifice is directed toward the right shoulder. Consequently, its systolic murmurs are best heard along the upper right sternal border and radiate toward the neck. Although the valve cusps are similar in size, in only about 10% of hearts are they truly equal in size. Thus, a minor degree of inequality is the rule, and in two-thirds of hearts, either the right or the posterior cusp is larger than the other two.

By virtue of its central position, the aortic valve and its sinuses contact all four cardiac chambers, an important consideration in evaluating aortic sinus aneurysms of congenital or infectious origin. The right aortic sinus abuts the basal ventricular septum and right ventricular parietal band and is covered in part by the right atrial appendage. In contrast, the left aortic sinus rests against the anterior left ventricular free wall and a portion of the anterior mitral leaflet, abuts the left atrial free wall, and is covered in part by the main pulmonary artery and left atrial appendage. Finally, the posterior aortic sinus overlies the basal ventricular septum and a part of the anterior mitral leaflet, forms part of the transverse sinus, abuts the atrial septum, and indents both atrial free walls as the torus aorticus (aortic bulge).

Comparison of Semilunar Valves

The semilunar valves are named according to the great artery into which they empty, not the ventricle from which they arise. During fetal development and infancy, the aortic and pulmonary valves are virtually identical. However, during childhood, the aortic cusps begin to thicken and become more opaque than the pulmonary cusps as a result of higher left-sided pressures, and this process continues throughout life. The annular dimensions of the aortic and pulmonary valves are similar

from birth through the first four decades of life, but beyond the age of 40 years, the rate of age-related annular dilation is greater for the aortic valve than for the pulmonary valve.

Base of the Heart

The cardiac base is defined by the plane of the AV groove (sulcus) and houses the four cardiac valves (Fig. 1.14). It also contains the fibrous cardiac skeleton, whose purpose is to weld together the valvular annuli, to fuse together but also electrically separate the atria and the ventricles, and to provide a firm foundation against which the ventricles can contract. The cardiac skeleton contains not only the four major valve annuli but also their intervalvular fibrous attachments (the right, left, and intervalvular fibrous trigones and the conus ligament).

The centrally located aortic valve forms the cornerstone of the cardiac skeleton, and its fibrous extensions anchor and support the other three valves. The intervalvular fibrous trigone is interposed between the left-posterior aortic commissure and the anterior mitral leaflet, and the left and right fibrous trigones project from each side and attach to the remainder of the anterior mitral leaflet. Thus, the left, intervalvular, and right fibrous trigones provide the anatomic substrate for direct mitral-aortic valvular continuity.

The membranous septum, in conjunction with the right fibrous trigone, fuses the right posterior aortic commissure to the anteroseptal tricuspid commissure. Therefore, the right fibrous trigone (also known as the central fibrous body) welds together the aortic, mitral, and tricuspid valves and forms the largest and strongest component of the cardiac skeleton. Even in the setting of a membranous ventricular septal defect, this connection is maintained, so that the region of mitral-tricuspid continuity forms the posterior wall of the defect. Near the right-left aortic commissure is a diminutive connection between the aortic and pulmonary valves, the conus ligament (or ligament of Krehl). Thus, each aortic valve commissure is fused to one of the other three valves: left-posterior commissure to mitral valve, right-posterior commissure to tricuspid valve, and right-left commissure to pulmonary valve.

Although schematic drawings of the cardiac base generally show the four valves in the same plane, they actually do not lie in the same plane or even in parallel planes. Because of the intertwining of the great arteries, the aortic and pulmonary

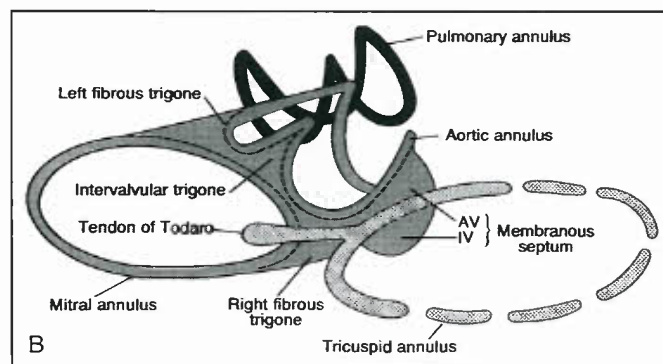
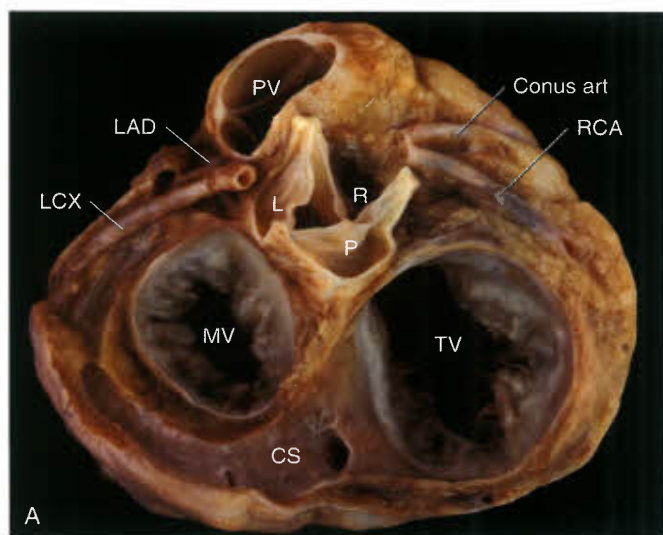


Figure 1.14. Base of the heart. A: The aortic valve is located centrally and abuts the other three cardiac valves. B: The cardiac skeleton, shown schematically, consists of four valvular annuli, three fibrous trigones, a membranous septum, and the tendon of Todaro. (See Appendix 1.1 at <http://solution.lww.com> for abbreviations.)

valves are skewed 60 to 90 degrees as the valvular orifices are directed toward opposite shoulders. Moreover, the tricuspid and mitral valves are skewed 10 to 15 degrees, such that their annuluses approach one another at the membranous septum and diverge along the inferior wall as the coronary sinus is interposed between them. These angles may vary somewhat during the course of the cardiac cycle.

GREAT ARTERIES

General Features

The great arteries include the aorta, pulmonary arteries, and ductus arteriosus. Although the aorta and pulmonary artery represent elastic vessels, the ductus arteriosus has a unique microscopic appearance that changes during fetal and neonatal life.

In the fetus and neonate, the aorta and pulmonary arteries are similar in thickness and in the number of elastic laminae within their medial layers. During the first several months of life, and consequent to the postnatal decrease in pulmonary artery pressure and resistance, the mediastinal pulmonary arteries attenuate and decrease in thickness, and their elastic fibers become irregular and fragmented. Beyond the first year of life, the thickness of the main pulmonary artery is normally less than half that of the adjacent ascending aorta, although the diameters of the two great arteries remain similar.

Interestingly, for patients with persistent pulmonary artery hypertension after birth (as with large unoperated ventricular septal defects), the medial thickness and elastic pattern in the pulmonary arteries remain similar to those in the aorta. In contrast, in patients who develop primary pulmonary hypertension later in life, their pulmonary arteries become thickened and the medial elastic layers retain the appearance of a pulmonary artery rather than that of an aorta.

Pulmonary Arteries

The main pulmonary artery emanates from the right ventricle and travels to the left of the ascending aorta in the general direction of the left shoulder. As it bifurcates, the left pulmonary

artery continues as a smooth arch and courses over the left bronchus, whereas the right pulmonary artery arises at a right angle and travels beneath the aortic arch and behind the superior vena cava. Creation of a Glenn anastomosis between the superior vena cava and right pulmonary artery takes advantage of the close proximity of these two vessels. The main and left pulmonary arteries contribute to the upper left border of the radiographic frontal cardiac silhouette (Fig. 1.6). Because the pulmonary arteries do not exhibit bilateral mirror-image symmetry, the spatial relationship of the main and lobar arteries to their adjacent bronchi differs between the right and left lungs and can be used to determine pulmonary morphology and sidedness (Fig. 1.15; also see Figs. 2.5 and 2.6).

During childhood, the tracheobronchial cartilage is pliable and may be compressed by hypertensive pulmonary arteries. Chronic compression of the left main and right middle lobe bronchi may contribute to the development of recurrent bronchopneumonia or atelectasis in the corresponding lobes. Furthermore, rightward displacement of the aortic arch by a dilated and hypertensive pulmonary trunk can produce tracheal indentation, which may be detected radiographically, and hoarseness owing to compression of the left recurrent laryngeal nerve.

The pulmonary circulation often is referred to as the central or lesser circulation. Within the human lung, pulmonary arteries travel with their corresponding airways and pulmonary veins course within the interlobular septa (*not* septae) (22). Because the pulmonary circulation represents a low-pressure and low-resistance system, its arteries and veins are normally thin walled. In general, pulmonary arteries >1 mm in diameter are elastic vessels, and those <1 mm represent muscular resistance arteries. Because pulmonary arterioles normally contain little medial muscle, the term arteriolar resistance is inaccurate.

During fetal life, a state of physiologic pulmonary hypertension exists owing to patency of the ductus arteriosus and equalization of aortic and pulmonary arterial pressures. As a result, the medial thickness of muscular pulmonary arteries resembles that of systemic arteries. After birth, as the ductus arteriosus closes and pulmonary arterial pressure decreases, attenuation of medial smooth muscle occurs, such that the ratio of medial thickness to external diameter decreases from 20% to 25% in fetuses to <10% in infants 3 to 6 months of age (Fig. 1.16).

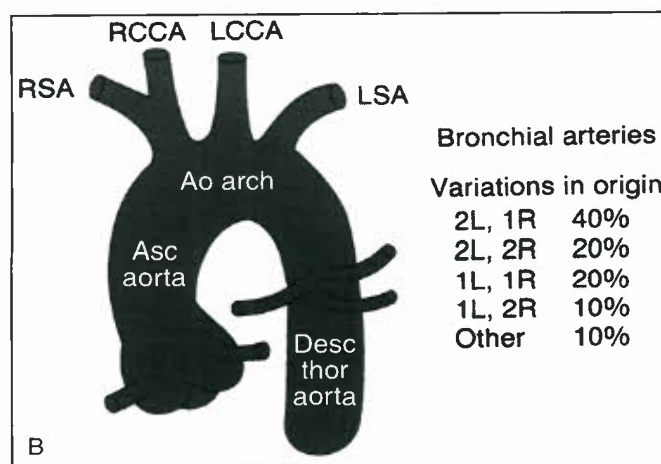
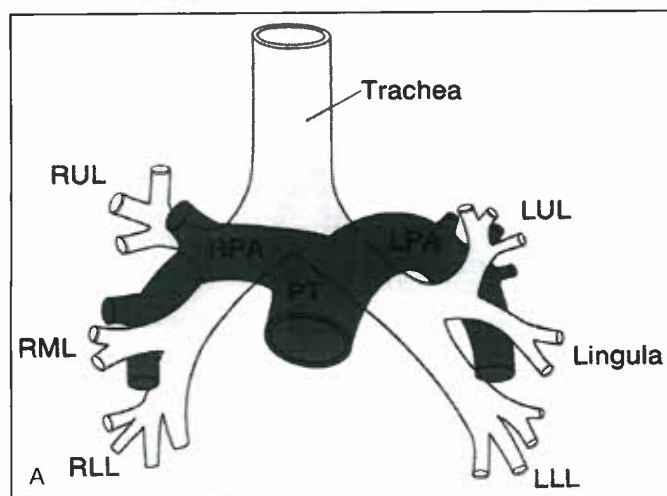


Figure 1.15. Pulmonary and bronchial arteries, shown schematically. A: The right and left pulmonary arteries are not mirror-image structures, and neither are the right and left bronchial trees. B: Bronchial arteries usually arise from the descending thoracic aorta at the level of the carina, but they vary in number. (See Appendix 1.1 at <http://solution.lww.com> for abbreviations.)

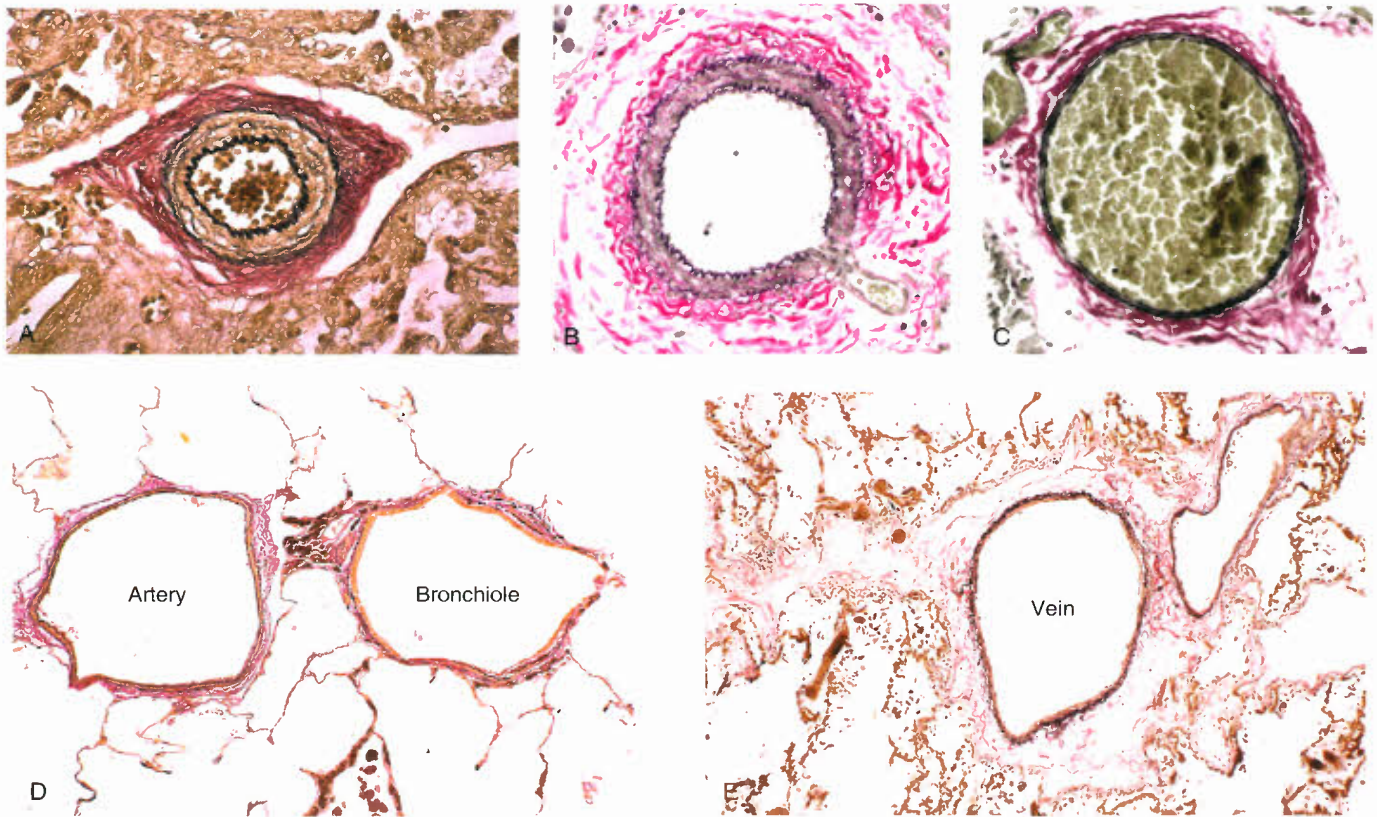


Figure 1.16. Microscopic appearance of the pulmonary circulation. A–C: The medial thickness of muscular pulmonary arteries changes after birth, as shown at birth (A), in a 5-month-old (B), and in a 7-month-old (C). D and E: Pulmonary arteries (D) travel with their airways, and pulmonary veins (E) travel within the interlobular septa. (Elastic van Gieson stain; A–C, high power; D and E, medium power.)

The pulmonary arteries serve to transport systemic venous blood to the lungs for oxygenation and for the release of carbon dioxide. In contrast, nutrition of the bronchial and pulmonary vascular walls is provided by bronchial arteries that arise from the descending thoracic aorta (Fig. 1.15).

Aorta

The aorta is the major elastic artery of the systemic circulation. It arises at the level of the aortic valve annulus and terminates at its bifurcation into the common iliac arteries, at the level of the umbilicus and the fourth lumbar vertebra. The aorta may be divided into four regions: ascending aorta, aortic arch, descending thoracic aorta, and abdominal aorta (Fig. 1.17). Of note, the ascending aorta and aortic arch are derived embryologically from the neural crest, while the descending thoracic aorta and abdominal aorta are derived from the primitive vascular mesenchyme. This fact may help to explain the different pathologic conditions observed in the different aortic regions.

The ascending aorta lies to the right of the main pulmonary artery and is located almost entirely within the pericardial sac. It consists of sinus and tubular portions, which are demarcated by the sinotubular junction, the site at which the discrete form of supravalvular aortic stenosis occurs. The right and left coronary arteries, as the only major branches from the ascending aorta, arise from the right and left aortic sinuses, respectively. During childhood and adolescence, the dimensions of the ascending aorta are related to age and body size.

The aortic arch normally travels over the left bronchus, defining a left aortic arch, and over the right pulmonary artery.

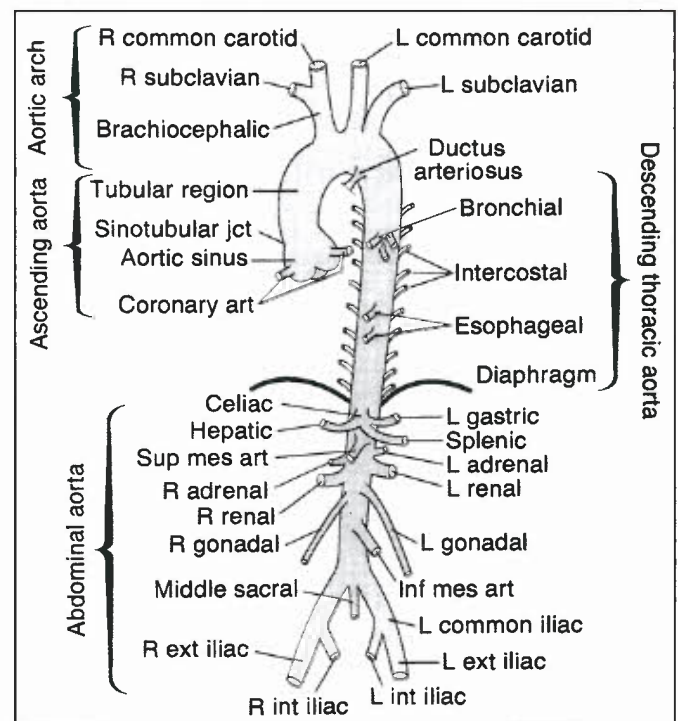


Figure 1.17. Systemic arteries, shown schematically. The aorta consists of ascending, arch, descending thoracic, and abdominal regions. (See Appendix 1.1 at <http://solution.lww.com> for abbreviations.)

From the top of the arch, the brachiocephalic (or innominate), left common carotid, and left subclavian arteries arise, in that order. In about 10% of individuals, the left common carotid artery originates from the brachiocephalic artery, and in 5%, the left vertebral artery arises from the aorta, between the left common carotid and left subclavian arteries. The aortic arch contributes to the left superior border of the radiographic frontal cardiac silhouette and forms the aortic knob.

When the aorta courses over the right bronchus, a right aortic arch exists, and the arch vessels show mirror-image branching. Aberrant retroesophageal subclavian arteries arise from the side of the arch rather than from its top. Most aortic coarctations occur opposite the ductus arteriosus, just distal to the left subclavian artery.

The descending thoracic aorta lies adjacent to the left atrium, esophagus, and vertebral column. Its posterolateral branches are the paired intercostal arteries, and its anterior branches include the bronchial, esophageal, mediastinal, pericardial, and superior phrenic arteries. The bronchial arteries also may arise from the intercostal or subclavian arteries or, rarely, from a coronary artery. Bronchial veins drain not only into the azygos and hemiazygos veins but also into the pulmonary veins (23).

The abdominal aorta lies to the left of midline, adjacent to the vertebral column. Its major lateral branches are retroperitoneal and include the renal, adrenal, lumbar, and inferior phrenic arteries. Although the gonadal arteries originate more anteriorly, they too are retroperitoneal. In contrast, all other branches that arise anteriorly represent intraperitoneal arteries that supply the digestive system, including the celiac artery (with its left gastric, splenic, and hepatic branches) and the superior and inferior mesenteric arteries. Distally, the aorta bifurcates into the common iliac arteries and also gives rise to the middle sacral artery.

Ductus Arteriosus

During fetal life, the ductus arteriosus provides an avenue for communication between the pulmonary and systemic circulations. It is interposed between the proximal portion of the left pulmonary artery and the undersurface of the aortic arch; during intrauterine life, its diameter is similar to that of the descending thoracic aorta and is larger than that of the right or left pulmonary artery. Most of the right ventricular output bypasses the lungs and enters the aorta via the ductus arteriosus. However, soon after birth and with expansion of the lungs, the ductus functionally closes, pulmonary vasodilation occurs, and the entire right cardiac output passes through the lungs (see Chapters 27 and 31).

Throughout gestation, structural changes take place that prepare the ductus arteriosus for rapid functional closure soon after birth (24). Initially, this vessel has the appearance of a muscular artery, in contrast to the elastic arteries to which it connects. During the third trimester, proliferative fibroelastic intimal cushions become prominent and medial thickening results from smooth muscle proliferation and the deposition of collagen, elastin, and glycoproteins. Ultrastructurally, medial smooth muscle cells change from the secretory to the contractile type. Blurring of intimal-medial junctions, coupled with haphazard arrangement of muscle bundles, produces an appearance similar to that of fibromuscular dysplasia. Adventitial elastic fibers become prominent, particularly at each end of the artery.

Constriction of the ductus arteriosus occurs within 24 to 48 hours of birth in term neonates and is mediated by a combination of rising systemic oxygen tension and decreasing circulating prostaglandin E₂ (PGE₂) and prostacyclin (PGI₂) levels. Ductal vasoconstriction, over the next several weeks,

is accompanied by focal medial necrosis, medial edema, disruption of the internal elastic lamina, and mural thrombosis. Subsequently, the deposition of elastin within the arterial wall becomes marked, and focal areas of calcification are the rule, resulting in complete and permanent closure of the ductus arteriosus, persisting from then on as the ligamentum arteriosum. Not surprisingly, ductal closure is hampered in both infants born at high altitude where oxygen tension is lower and in those born prematurely. Both genetic factors and prenatal infection may also play a role in patients with ductus arteriosus patency.

In general, closure of the ductus arteriosus begins near the pulmonary artery and progresses toward the aorta. If this process is incomplete, a small ductal diverticulum remains that characteristically emanates from the undersurface of the aortic arch. Rarely, ductal aneurysms, dissections, or ruptures occur and may be associated with underlying connective tissue disease, surgical manipulation, or active/healed arteritis.

CORONARY CIRCULATION

Coronary Arteries

The right and left coronary arteries arise from their corresponding aortic sinuses. Their ostia (ostiums) are circular to elliptical and originate midway between the aortic valve commissures and about two-thirds of the distance between the annulus and the sinotubular junction. The right coronary artery originates nearly perpendicularly from the right aortic sinus. In contrast, the left main coronary artery arises at an acute downward angle and travels parallel to its aortic sinus wall.

The major epicardial arteries include the left main, left anterior descending, circumflex, and right coronary arteries. Branches of the left anterior descending artery are called diagonals, whereas branches of the right and circumflex arteries are called marginals (Fig. 1.18). Septal perforators represent long intramural branches of the anterior and posterior descending arteries that supply the ventricular septum and, hence, are not epicardial branches.

Proximally, the right coronary artery travels between the main pulmonary artery and the right atrium and is covered by the right atrial appendage. Throughout its course within the right AV groove, the right coronary artery is embedded in epicardial adipose tissue. In about 60% of subjects, the first branch is the conus coronary artery, which supplies the right ventricular outflow tract; in the other 40%, this artery arises independently from the right aortic sinus (25). The descending septal artery nourishes the infundibular septum. Marginal branches include several small vessels and a prominent acute marginal artery.

Beyond the acute margin, along the inferior surface of the heart, the length of the right coronary artery varies inversely with that of the circumflex artery. In about 70% of human hearts, the right coronary artery gives rise not only to the posterior descending branch, as the dominant coronary artery, but also to posterolateral branches, thereby nourishing the right ventricular free wall, the inferoseptal wall of the left ventricle, the posteromedial mitral papillary muscle, and the AV nodal artery.

The left main coronary artery lies between the main pulmonary artery and the left atrium and is covered by the left atrial appendage. It bifurcates into left anterior descending and circumflex branches in most individuals but trifurcates in some, with an intermediate artery emanating between the other two vessels. A short (<8 mm) left main artery often is associated with left coronary dominance. The vast majority of left coronary artery blood flow takes place during ventricular diastole.

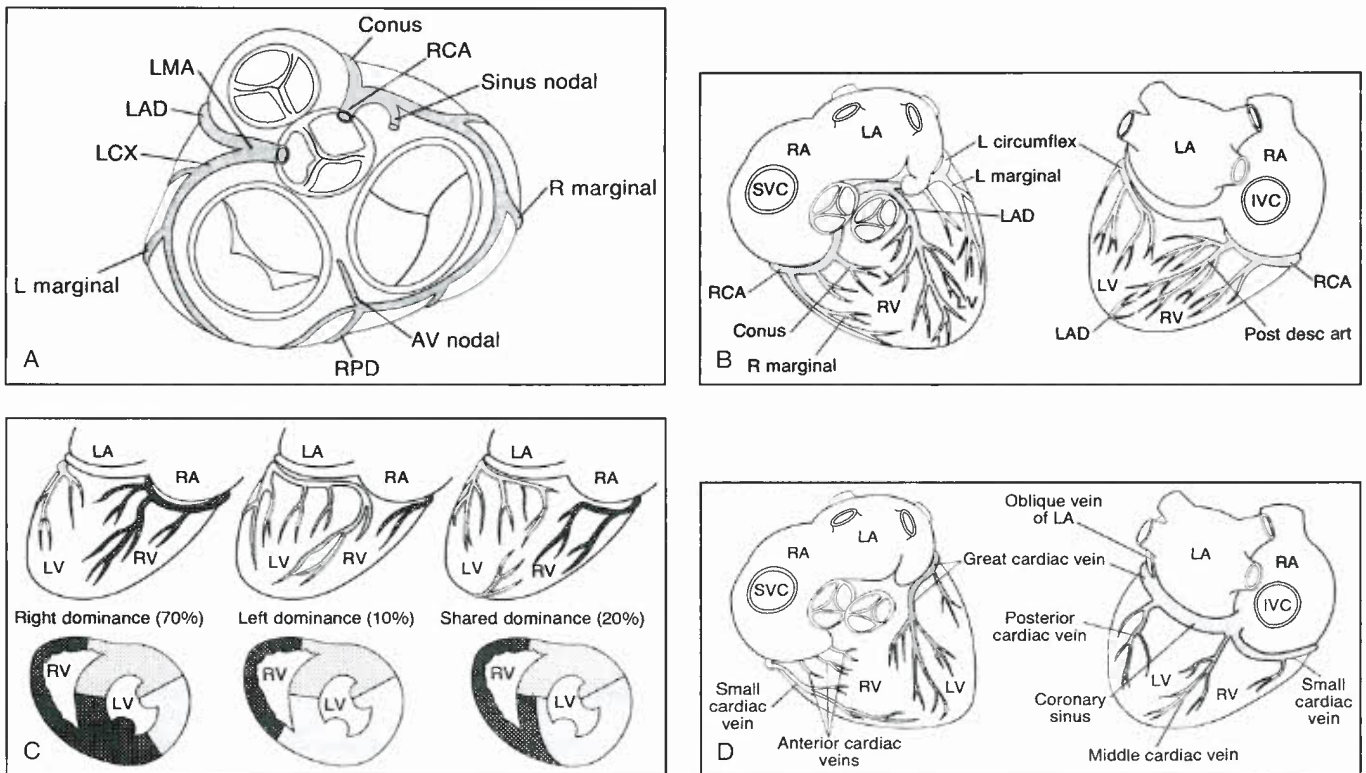


Figure 1.18. Coronary circulation, shown schematically. **A:** The right and circumflex arteries travel in the AV groove, near the tricuspid and mitral valves, respectively (cardiac base). **B:** The anterior and posterior descending arteries travel in the interventricular groove and demarcate the plane of the ventricular septum (superior and inferior views). **C:** Coronary dominance is determined by the origin of the posterior descending branch. **D:** The anterior cardiac veins empty directly into the right atrium, whereas the other major epicardial veins drain into the coronary sinus. (See Appendix 1.1 at <http://solution.lww.com> for abbreviations.)

Traveling within the anterior interventricular groove, the left anterior descending artery wraps around the apex and extends for a variable distance in the posterior interventricular groove. Including its diagonal and septal perforating branches, this vessel supplies the anteroseptal and anterolateral walls, part of the anterolateral mitral papillary muscle, and the entire apex of the left ventricle. Bridges of myocardium cover small lengths of the left anterior descending artery in about 10% of human hearts, but usually do not interfere with diastolic myocardial perfusion (26).

The circumflex coronary artery travels within adipose tissue in the left AV groove. It generally terminates just beyond its obtuse marginal branches and nourishes the lateral wall of the left ventricle and part of the anterolateral mitral papillary muscle. In about 10% of subjects, the circumflex artery also supplies the posterior descending branch, constituting left coronary dominance, and the inferoseptal wall of the left ventricle, posteromedial mitral papillary muscle, and AV nodal artery. About 20% of human hearts exhibit shared coronary dominance, such that both the right and circumflex arteries provide posterior descending branches.

The sinus nodal artery arises from the right coronary artery in about 60% of hearts and from the circumflex artery in 40%, but its artery of origin does not depend on patterns of coronary dominance. In contrast, the AV nodal artery arises from the dominant coronary artery and, therefore, originates from the right coronary artery in 90% of human hearts. The AV (His) bundle receives a dual blood supply from the AV nodal artery and the first septal perforator of the left anterior descending artery. Nourishment for the right and left bundle branches is provided by other septal perforator branches of the anterior and posterior descending arteries.

The right and circumflex coronary arteries travel in the AV groove and thereby define the plane of the cardiac base. Similarly, the anterior and posterior descending coronary arteries course within the interventricular grooves and indicate the plane of the ventricular septum. Consequently, for surgeons and pathologists, the epicardial coronary arteries are reliable external landmarks for determining relative chamber sizes and valve locations.

Coronary Veins

The coronary veins and cardiac lymphatics work in concert to remove excess fluid from the myocardial interstitium and the pericardial sac. The venous circulation of the heart consists of a coronary sinus system, an anterior cardiac venous system, and a thebesian venous system (Fig. 1.18). The great cardiac vein travels beside the left anterior descending and circumflex coronary arteries to merge with the coronary sinus. At this site is a bicuspid venous valve, known as Vieussens valve. The coronary sinus, in turn, receives the left-posterior, middle, and small cardiac veins, as well as several smaller tributaries, before joining the right atrium. Along the anterobasal aspect of the right ventricular free wall, three or four anterior cardiac veins either empty directly into the right atrium or first join a common collecting vein. Finally, numerous small thebesian veins drain directly into a cardiac chamber, particularly the right atrium or right ventricle.

As an aside, the human heart normally has eight valves. There are four major valves (aortic, mitral, tricuspid, and pulmonary). The right atrium contains three valves (of the fossa ovalis, inferior vena cava, and coronary sinus). The eighth is Vieussens valve, the ostial valve of the great cardiac vein.

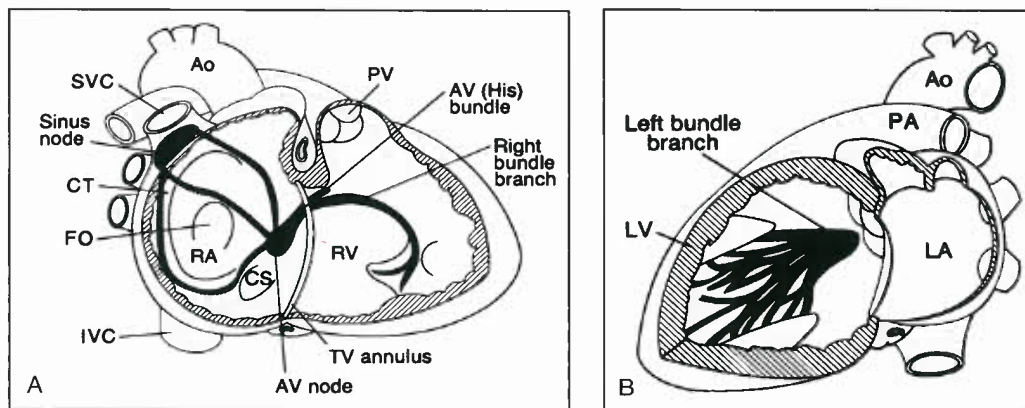


Figure 1.19. Cardiac conduction, shown schematically. **A:** Right heart. The sinus node and AV node are both right atrial structures, whereas the AV (His) bundle travels through the right fibrous trigone to reach the summit of the ventricular septum. The right bundle branch travels along the septal and moderator bands. **B:** Left heart. The left bundle branch forms a broad sheet of fibers along the septal surface. (See Appendix 1.1 at <http://solution.lww.com> for abbreviations.)

Cardiac Lymphatics

Within the ventricular myocardium is an interconnecting network of delicate lymphatic channels that drain toward the epicardial surface. Along the epicardial surface, the right and left lymphatic channels form and accompany their respective coronary arteries in retrograde fashion toward the aortic root. These are joined by lymphatic channels from the conduction system and a few sparse lymphatic vessels from the atria and the valves (27). As the right and left lymphatic channels coalesce, they travel along the ascending aorta to the undersurface of the aortic arch and drain into a pretracheal lymph node. Next, they course between the superior vena cava and the brachiocephalic artery to join a cardiac lymph node before emptying into the right lymphatic duct. Lymphatics from the parietal pericardium drain into either the right lymphatic duct or the thoracic duct.

CARDIAC CONDUCTION SYSTEM

General Features

The cardiac conduction system consists of the sinus node, internodal tracts, and AV conduction tissues (Fig. 1.19). Its function is influenced by sympathetic and parasympathetic innervation, circulating catecholamines, patency of its nutrient blood supply, regional acid-base or electrolyte disturbances, mechanical trauma (such as sutures, synthetic patches, or ablation procedures), and involvement by neoplasm or infection.

The sinus and AV nodes are both right atrial structures with similar microscopic features, conduction velocities, and action potentials (Table 1.2). Similarities also exist in the structure, conduction velocities, and action potentials of the AV (His) bundle, right and left bundle branches, and working cardiac

TABLE 1.2 Comparison of Components of the Cardiac Conduction System

Site	Location	Cell Types	Cell Diameter (mm)	Conduction Velocity (m/s)	Action Potential
Sinus node	Right atrial subepicardium	P cells	5–10	<0.05	
		Transitional cells	5–10		
Internodal tracts	Atrial septum and free walls	Atrial myocytes	10–15	0.3–0.4	
AV node	Right atrial subendocardium	P cells	5–10	0.1	
		Transitional cells	5–10		
		Purkinje cells	30–60		
AV (His) bundle	Tricuspid valve annulus and ventricular septal summit	Purkinje cells	30–60	2–3	
		Ventricular myocytes	10–20		
Bundle branches	Ventricular subendocardium	Purkinje cells	30–60	2–3	
		Ventricular myocytes	10–20		
Ventricular myocardium	Ventricular septum and walls	Ventricular myocytes	10–20	0.3–0.4	

myocytes. All components of the cardiac conduction system are specialized cardiac myocytes, not nerves, whose major function is conduction rather than contraction.

Sinus Node

As the primary pacemaker of the heart, the sinus node represents a right atrial structure that is located subepicardially, along the terminal groove near the superior cavoatrial junction (Fig. 1.20 and Table 1.2). Because it is found at the border between areas derived from the sinus venosus and the embryonic atrium, the pacemaker often is referred to as the sinoatrial node. It is shaped like a flattened ellipse, through which a prominent sinus nodal artery passes. Numerous autonomic nerves approach the sinus node at both its poles.

Microscopically, the node is characterized by a complex interwoven pattern of P cells and transitional cells, within a fibrous stroma, and an outer coat of working atrial myocytes

(28). Because these specialized cells primarily are concerned with conduction rather than contraction, they have fewer contractile elements and expend less energy than working myocytes. Although P cells are thought to be the source of impulse formation, changes in autonomic input may alter the actual pacing site within the node.

Among patients with the asplenia syndrome and right isomerism, bilateral sinus nodes may be encountered. In contrast, in the setting of polysplenia and left isomerism, the sinus node can be congenitally absent or malpositioned. During surgical operations such as the Mustard and Fontan procedures, the sinus node and its artery are susceptible to injury.

Internodal Tracts

Whether specialized conduction pathways exist between the sinus and AV nodes has been the subject of much controversy. Electrophysiologic studies support the concept

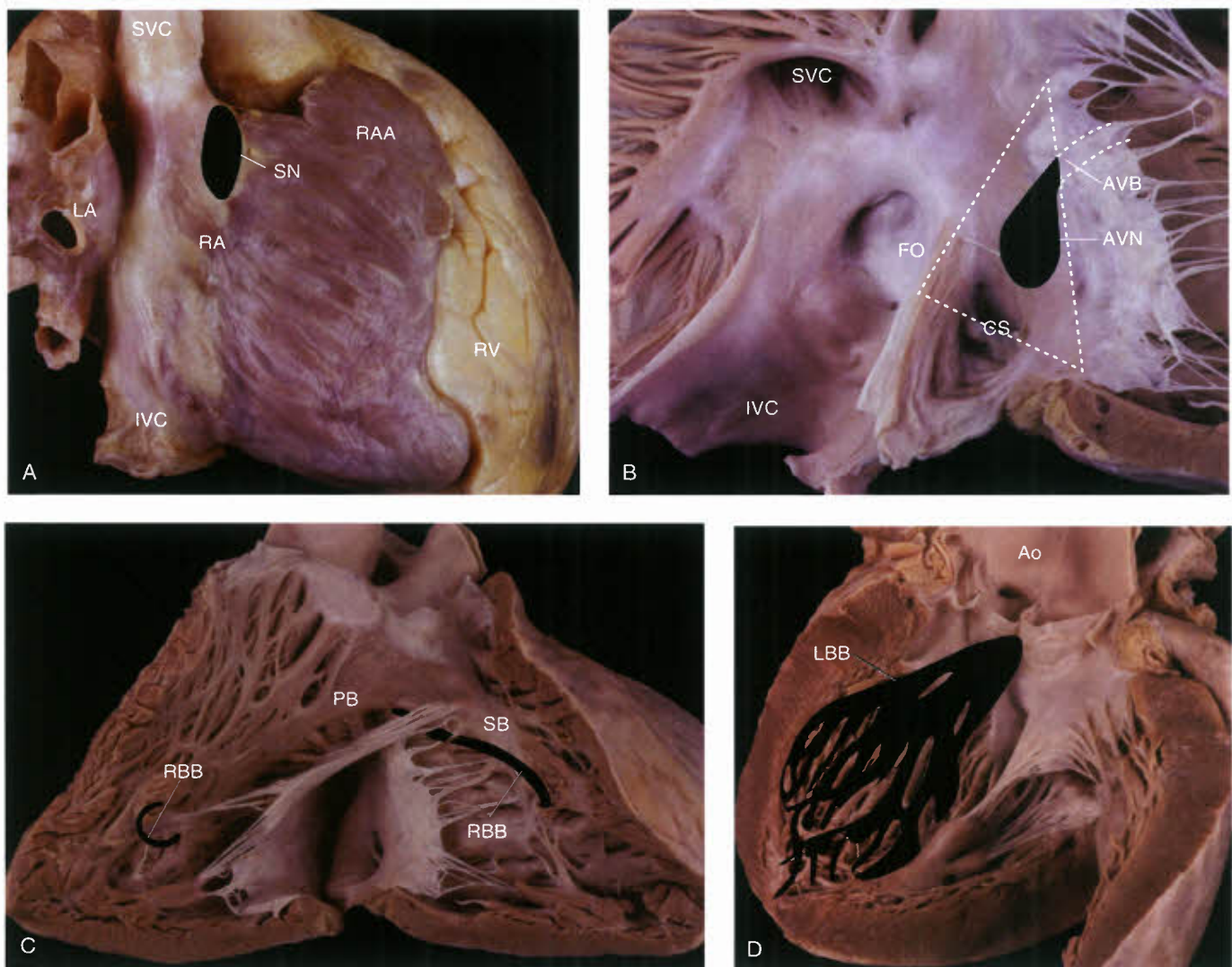


Figure 1.20. Location of the cardiac conduction system (indicated in *black ink*). **A:** The sinus node lies subepicardially in the terminal groove of the right atrium (right lateral view). **B:** The AV node represents a subendocardial right atrial structure that lies within the triangle of Koch (*dashed lines*), and the AV (His) bundle travels through the tricuspid annulus to rest along the summit of the ventricular septum. **C:** The right bundle branch is a small cordlike structure that courses along the septal and moderator bands (opened right ventricle). **D:** In contrast, the left bundle branch represents a broad sheet of fibers that travels subendocardially along the left side of the ventricular septum. (See Appendix 1.1 at <http://solution.lww.com> for abbreviations.)

of preferential pathways, but morphologic studies do not. Recent investigations suggest that both views may be correct. The three internodal tracts identified electrophysiologically correspond to those regions of the atrial septum and right atrial free wall, such as the crista terminalis, that contain the greatest concentration of myocytes. Thus, microscopically, these regions consist of working atrial myocytes rather than specialized P, transitional, or Purkinje cells.

Because the septal preferential pathways near the fossa ovalis travel anterosuperiorly in its limbus, internodal conduction disturbances would not be expected following a Rashkind balloon atrial septostomy, in which the valve of the fossa ovalis is torn, or a Blalock–Hanlon posterior atrial septectomy. However, for operations in which the atrial septum is resected, as in the Mustard and Fontan procedures, such disturbances can occur. Similarly, disruption of the crista terminalis may interfere with normal internodal conduction.

Atrioventricular Node

Like the sinus node, the AV node is a right atrial structure that is richly innervated by parasympathetic and sympathetic fibers. In contrast, it is located subendocardially, rather than subepicardially, within the triangle of Koch and adjacent to the right fibrous trigone (or central fibrous body). The triangle of Koch, in turn, corresponds to the AV septum and is bordered by the septal tricuspid annulus, coronary sinus ostium, and tendon of Todaro, a subendocardial fibrous cord that travels from the thebesian–eustachian valvular commissure to the membranous septum (Fig. 1.20). The AV nodal artery, or several of its branches, travel near the node but not necessarily through it, and venous and lymphatic channels are abundant in and around the node.

Microscopically, the AV node consists of a complex interwoven pattern of specialized cardiac muscle cells within a fibrous matrix, similar to the sinus node (28). Proximally, at its junction with the internodal tracts, the AV nodal tissues are loosely arranged and consist primarily of transitional cells and a few working atrial myocytes. Centrally, the node is more compact and is characterized by an interlacing arrangement of P cells. Distally, Purkinje cells begin to form parallel bundles as the node merges with the His bundle. Around its periphery, the AV node contains transitional cells and an outer insulating coat of collagen.

Because of its right atrial location near the tricuspid annulus, the AV node is susceptible to injury during annuloplasty procedures for tricuspid regurgitation and during plication procedures for the Ebstein malformation. In the setting of AV septal defects, involving the expected site of the AV node, the node and His bundle are displaced posteroinferiorly and are associated with relatively specific electrocardiographic alterations. Interestingly, in hearts affected by congenitally corrected transposition of the great arteries, both anterior and posterior AV nodes are observed, usually with a sling of His bundle tissue between the two.

Atrioventricular (His) Bundle

The AV (His) bundle arises from the distal portion of the AV node and travels through the central fibrous body (right fibrous trigone) to reside along the basal ventricular septum, adjacent to the membranous septum. It thereby represents the only normal avenue for electrical conduction between the atrial and ventricular myocardium. Within the central fibrous body, the AV bundle is related closely to the annuli of the aortic, mitral, and tricuspid valves, and its location is somewhat variable along the basal ventricular septum. Thus, during operative procedures involving these valves or a membranous

ventricular septal defect, care must be taken to avoid injury to the His bundle. In some cases of congenital AV block, discontinuity exists between the AV node and the AV bundle.

Microscopically, the AV bundle can be divided into two regions: the penetrating portion, which courses through the central fibrous body, and the branching portion, which gives rise to the right and left bundle branches. Both regions are characterized by numerous parallel bundles of Purkinje cells and working ventricular myocytes, separated by delicate fibrous tissue (28). During fetal and neonatal life, these conduction bundles often are dispersed or separated within the central fibrous body. The final destination of each bundle within the right or left ventricle is probably determined by its position proximally within the penetrating portion of the His bundle. Like an electrical wire, the entire AV bundle is insulated by a dense fibrous sheath.

In many individuals, additional connections exist between the AV conduction system and the atrial and ventricular myocardium. In some, atrial myocardium either joins the distal AV node via the atrionodal bypass tracts of James or connects to the AV bundle through the atriofascicular tracts of Brechenmacher. In others, nodoventricular and fasciculoventricular bypass fibers of Mahaim link the AV node and AV bundle, respectively, to the underlying ventricular septal myocardium. These accessory pathways are apparently nonfunctional in most individuals, although they may produce ventricular preexcitation in some.

However, ventricular preexcitation more often is associated with aberrant bypass tracts that span the annulus of the tricuspid or mitral valve, traveling either through the fibrous ring or within the adipose tissue in the AV groove. Such bypass tracts can be single or multiple and may be identified by electrophysiologic mapping. In contrast, nodules of specialized conduction tissue, representing the bundles of Kent, are located in the right lateral AV groove but usually do not provide a connection between atria and ventricles.

Bundle Branches

The right bundle branch emanates from the distal portion of the AV (His) bundle and forms a cord-like structure that travels along the septal and moderator bands toward the anterior tricuspid papillary muscle. In contrast, the left bundle branch represents a broad fenestrated sheet of subendocardial conduction fibers that spreads along the septal surface of the left ventricle. As it courses toward the ventricular apex and both mitral papillary muscles, the left bundle branch may separate into two or three indistinct fascicles. Left ventricular pseudotendons also may contain conduction tissue from the left bundle branch (29). Microscopically, the bundle branches consist of Purkinje cells and ventricular myocytes (28).

In the setting of a membranous ventricular septal defect, the AV conduction tissues travel along the posteroinferior rim of the defect. However, if AV discordance coexists, the conduction fibers course along the anterosuperior aspect of the defect. For the outlet, inlet, and muscular forms of ventricular septal defect, the AV conduction tissues generally are remote from the defect. Interestingly, following a right ventriculotomy for reconstruction of the right ventricular outflow tract, the electrocardiogram characteristically exhibits a pattern of right bundle branch block, even though the right bundle has not been disrupted.

Cardiac Innervation

Because the embryonic heart tube first forms in the future neck region, its autonomic innervation also originates from this level. From the cervical ganglia arise three pairs of cervical sympathetic cardiac nerves, which intertwine as they join the cardiac plexus between the great arteries and the tracheal bifurcation.

Several thoracic sympathetic cardiac nerves arise from the upper thoracic ganglia and also join the cardiac plexus. From the parasympathetic vagus nerves emanate the superior and inferior cervical vagal cardiac nerves and the thoracic vagal cardiac nerves, which also enter the cardiac plexus. These nerves then descend from the cardiac plexus onto the heart and innervate the coronary arteries, conduction system, and myocardium. In addition, afferent nerves concerned with pain and various reflexes ascend from the heart toward the cardiac plexus.

Transplanted hearts are completely denervated early after transplantation and can respond only to circulating substances, such as catecholamines, but usually not to autonomic impulses. Moreover, because afferent pathways are also lost, coronary obstruction owing to chronic transplant vasculopathy may be associated with undetected myocardial ischemia, because chest pain cannot develop.

EXAMINATION OF CARDIAC SPECIMENS

General Features

Evaluation of cardiopulmonary specimens from patients with congenital heart disease entails more than documentation of the underlying anomalies, although this is certainly important. The recognition of malformations in other organ systems is necessary for the identification of various syndromes, which can have implications for genetic counseling. In addition, the presence of secondary obstructive lesions in the pulmonary vasculature may be more significant in explaining the demise of a patient than the underlying cardiac anomalies. Other processes, such as infections or protein-losing enteropathy, also may be important.

In the 21st century, it is distinctly uncommon for subjects with congenital heart disease to have received no interventional therapy, either in the operating room or in the cardiac catheterization laboratory. Hence, the investigation of cardiopulmonary specimens also entails an evaluation of old and recent procedures, addressing not only their effectiveness but also their secondary effects on the heart and the pulmonary circulation. This includes recognition not only of the complications of therapy but also of the beneficial effects, such as the regression of obstructive pulmonary vascular disease.

Pathologists who evaluate treated forms of congenital heart disease often act in the capacity of a medical archeologist, searching for the telltale results of procedures performed at various times in the past. In complex cases, accurate conclusions can be reached only if accurate and complete historical information is available concerning clinical diagnoses and previous procedures. For example, in patients with multiple interventions, the results of reconstruction and takedown procedures may so alter the underlying morphology that identification of the original anomalies or even previous procedures becomes difficult or impossible.

To relay this information to one's clinical colleagues, a pathologist should not only provide a written report, often with schematic diagrams, but also be prepared to review the actual specimen with others. Such reviews may represent informal sessions, formal conferences, or publications, and therefore can involve the specimen itself or its photographs. In this regard, methods of dissection and photography should be chosen that display the lesions most clearly and accurately. Details of these various methods are discussed below. If one does not have the time, training, or interest to dissect operated hearts with congenital anomalies, referral to a pathologist who does represents a reasonable option.

In the past, for the dissection of congenitally malformed hearts, it was recommended that the heart and lungs be maintained as one intact specimen. Based on personal experience,

however, if the pulmonary arterial and venous connections are normal, then the lungs can be removed from the heart without compromising the accuracy of the evaluation. In fact, both the inspection and photography of the heart generally are easier if the lungs and tracheobronchial tree are removed (but not discarded). In contrast, the entire thoracic aorta with appreciable lengths of its brachiocephalic branches should remain attached to the cardiac specimen.

Inflow–Outflow Method

In the inflow–outflow method, the heart is opened according to the direction of blood flow (30). First, scissors are used to make an incision from the inferior vena cava to the right atrial appendage. The superior vena cava is left unopened so as not to disturb the region of the sinus node. Both the inflow and outflow cuts for the right ventricle are made about 0.5 cm from the ventricular septum, with either scissors or a knife, from the right atrium to the ventricular apex and then from the apex to the pulmonary artery. Contrary to older recommendations, there is no reason to avoid cutting through an abnormal valve when using this method of dissection.

The left atrium is best opened from a point between the right upper and lower pulmonary veins to the tip of the left atrial appendage. In contrast to the right ventricle, the left ventricular inflow tract is opened not along the septum but rather along the lateral wall, between the mitral papillary muscles, from the left atrium to the left ventricular apex. From the apex to the aortic valve, the outflow cut follows the junction with the ventricular septum, generally forming a gentle inverted S-shaped curve. Whereas the inflow cut is best made with a long knife, the outflow cut is best accomplished using a scalpel.

Once the aortic annulus is crossed, scissors can be used to continue cutting through the left aortic cusp. Because of the normal intertwining of the great arteries, further dissection into the ascending aorta requires transection of the main pulmonary artery. The aortic arch is then opened along its left lateral border and, as a continuous dissection, the descending thoracic aorta is opened posteriorly, between the paired intercostal arteries. Once the great arteries are opened, the origins of the coronary arteries and the patency of the ductus arteriosus can be evaluated.

The inflow–outflow method of cardiac dissection is easy to learn and quick to perform. Although it has withstood the test of time and is currently the most popular dissection method among pathologists, it is recommended primarily for normal hearts and perhaps for simple or unoperated forms of congenital heart disease (Fig. 1.21A,B).

Base-of-Heart Method

Removal of the atria and the great arteries just above their corresponding valves allows visualization and inspection of the cardiac base (Fig. 1.14). This method is useful for the evaluation of valvular anomalies or the effects of valvular surgery on nearby structures (Fig. 1.21C). For example, following tricuspid annular plication for an Ebstein anomaly, possible kinking of the right coronary artery may be investigated by this method.

Window Method

In selected cases, hearts prepared by perfusion fixation, paraffin infiltration, or plastination may be examined by cutting windows from the cardiac chambers or great vessels (Fig. 1.21D). In this manner, the interior of the heart or vessels can be viewed without greatly disturbing the internal structures. Although such specimens can be visually stunning, their preparation and photography can be difficult.

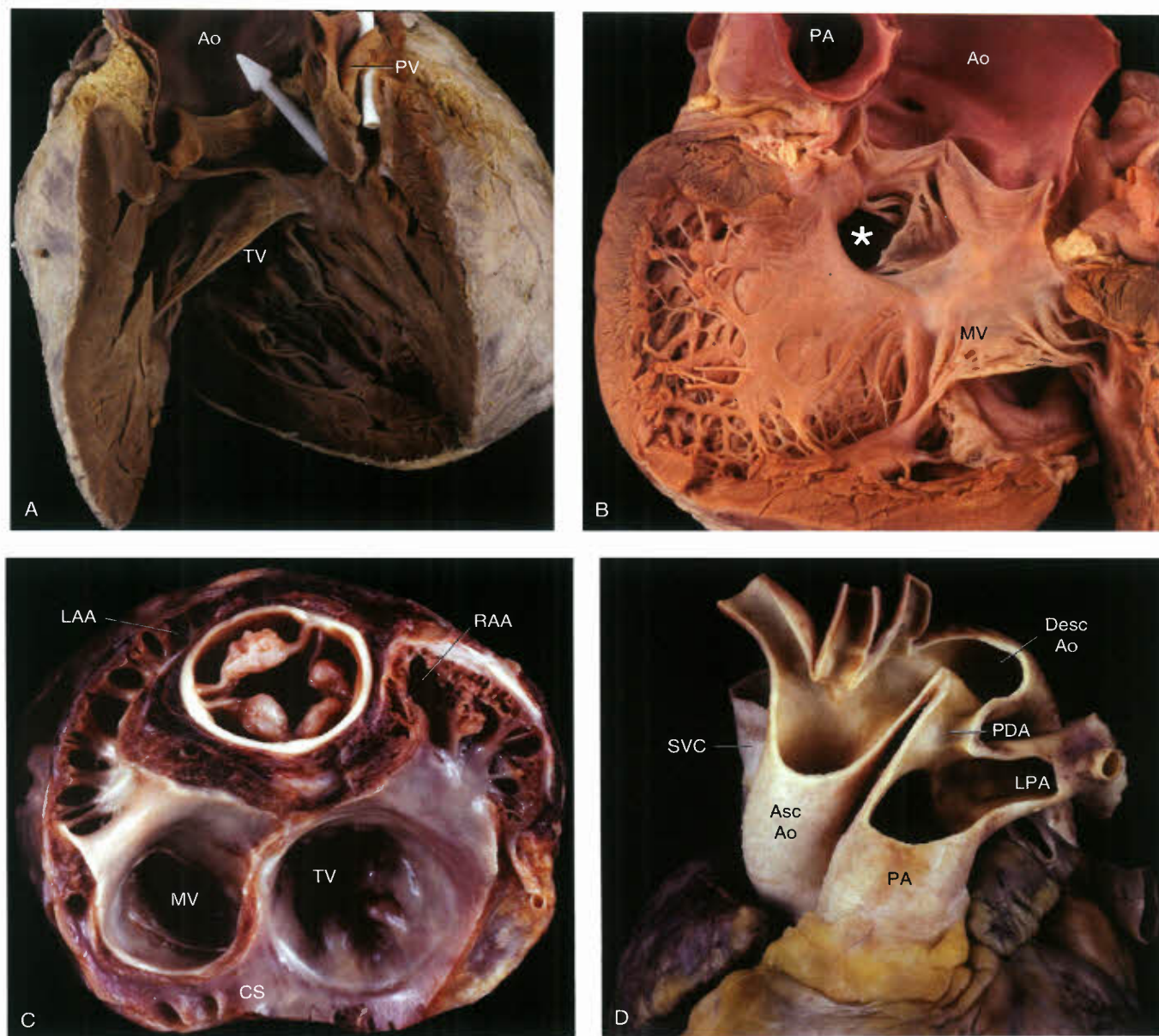


Figure 1.21. Nontomographic methods of dissection in malformed hearts. A and B: Inflow–outflow method. In (A), the right ventricle in a specimen with tetralogy of Fallot is opened to display the ventricular septal defect (with an arrow-shaped probe coming from the left ventricle), overriding aorta, and pulmonary stenosis (probe). In (B), an opened left ventricle demonstrates the position of a membranous ventricular septal defect (*). C: Base-of-heart method. The atria and great arteries have been removed to show the cardiac valves in a case of truncus arteriosus. D: Window method. The great arteries have been unroofed to demonstrate a patent ductus arteriosus. (See Appendix 1.1 at <http://solution.lww.com> for abbreviations.)

Tomographic Method

In the tomographic method, the heart is bisected (divided into two pieces) by one plane of section. With the bread-slice technique, multiple sections are made parallel to the AV groove, producing numerous ventricular slices. For the past several decades, this popular method has been used by pathologists for the evaluation of ischemic heart disease. It is identical to the short-axis method used in clinical imaging and represents the most common method of cardiac dissection used at our institution for the evaluation of acquired heart disease. It also may be performed concomitantly with the base-of-heart method.

In addition to the short-axis method, the long-axis and four-chamber planes represent other tomographic sections commonly obtained clinically and may be correlated with anatomic features in normal hearts. Other planes, parallel to the standard anatomic directions, also have been used clinically, not only for transesophageal echocardiography but also for magnetic resonance imaging (31). These include frontal (coronal), parasagittal (lateral), and horizontal (transverse) planes of section. In cardiac specimens, any of the aforementioned tomographic planes can be applied not only to normal hearts but also to acquired and congenital forms of heart disease (Figs. 1.22–1.25) (32).

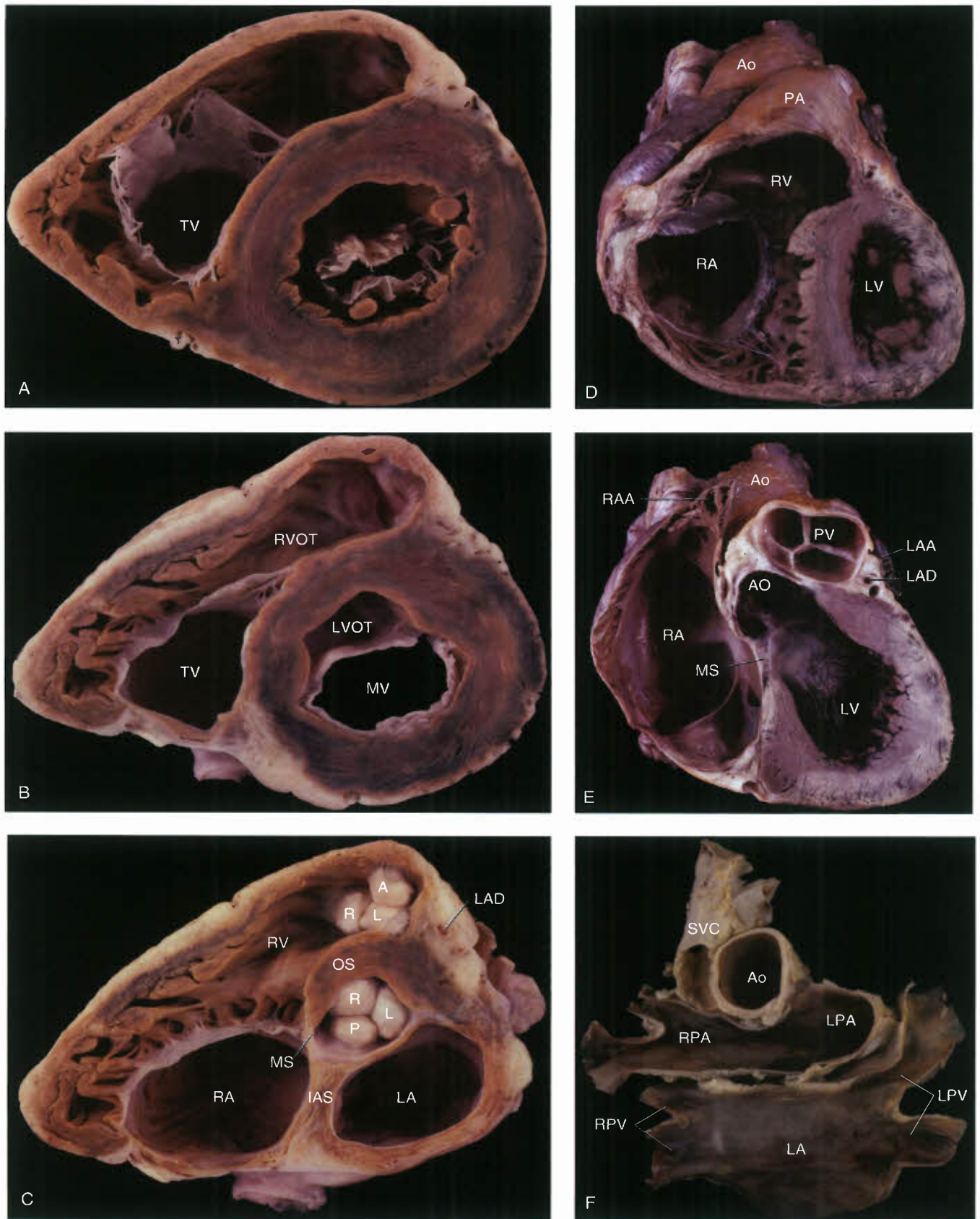


Figure 1.22. Tomographic methods of cardiac dissection (short-axis and frontal views), shown in normal hearts. A–C: Short-axis views, at the levels of the mitral valve orifice (A), left ventricular outflow tract (B), and aortic valve (C). D–F: Frontal (coronal) views, at the levels of the ventricular septum (D), membranous septum (E), and left atrium (F). (See Appendix 1.1 at <http://solution.lww.com> for abbreviations.)

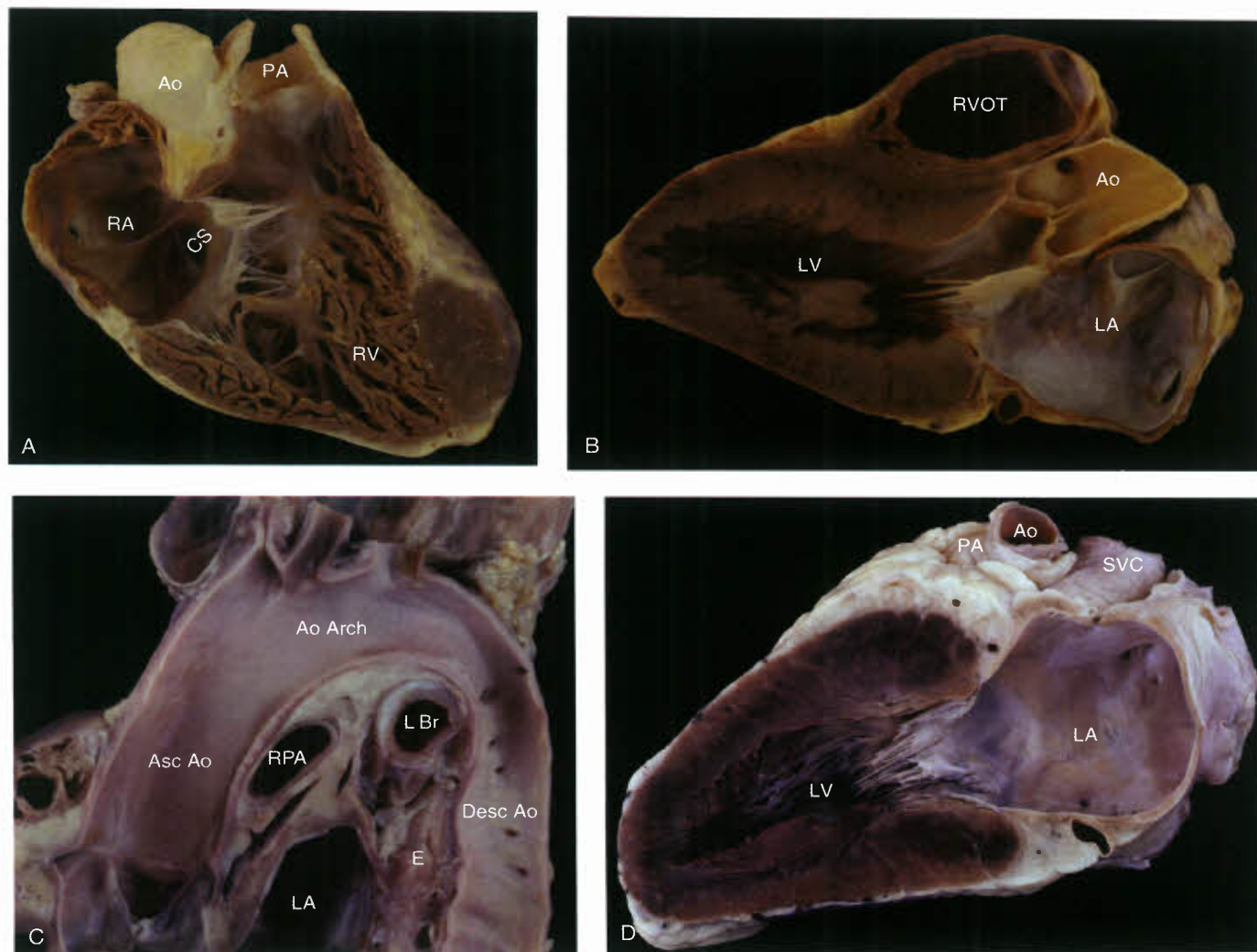


Figure 1.23. Tomographic methods of cardiac dissection (long-axis and two-chamber views), shown in normal hearts. A and B: Long-axis views show inflow and outflow tracts of right ventricle (A) and left ventricle (B). C: Long-axis view of thoracic aorta shows left bronchus and right pulmonary artery traveling beneath aortic arch. D: Two-chamber view demonstrates inflow tract of left ventricle. (See Appendix 1.1 at <http://solution.lww.com> for abbreviations.)

Although the tomographic method of cardiac dissection has been used by anatomists and pathologists for more than a century, it has not been accepted widely, probably because it is time-consuming and requires prior fixation (preferably perfusion fixation). Nonetheless, perhaps no other technique allows the assessment of intracardiac relationships as well as the cross-sectional method. For congenitally malformed hearts, tomographic sections are particularly well suited for demonstrating not only the primary anomalies and various interventions but also their secondary effects on the heart. Thus, photographs of specimens dissected tomographically provide clarity as teaching tools and correlate well with current clinical imaging modalities.

Technically, the best cardiac cross sections are generally achieved when a perfusion-fixed specimen is cut in one continuous cut with a very sharp knife. Sawing motions are to be avoided. Moreover, after one section has been made and documented photographically, the specimens can be glued back together and resectioned along another tomographic plane. For this purpose, any of the readily available cyanoacrylate glues (such as Krazy Glue or Super Glue) will suffice. The best results are attained with smooth dry surfaces; roughened sur-

faces (such as those produced by using scissors) may adhere poorly.

Photography of Cardiac Specimens

It is difficult to overestimate the role of photography in the teaching of congenital heart disease. Although schematic diagrams are helpful, the visualization of actual specimens often is necessary for an appreciation of three-dimensional features. In this regard, the well-planned dissection and photography of a classic lesion may be remembered far longer than written words (33). Having access to the most expensive photographic equipment, however, does not guarantee good results. Careful planning and attention to detail are more important.

The use of a high-resolution digital camera has essentially replaced film-based cameras in the field of specimen photography. However, certain basic rules of photography still apply. For example, to increase the depth of field of focus, the aperture should be as small as possible (achieved by setting the f-stop as large as possible, preferably 16 or greater). One of the simplest yet most important factors for attaining high-quality

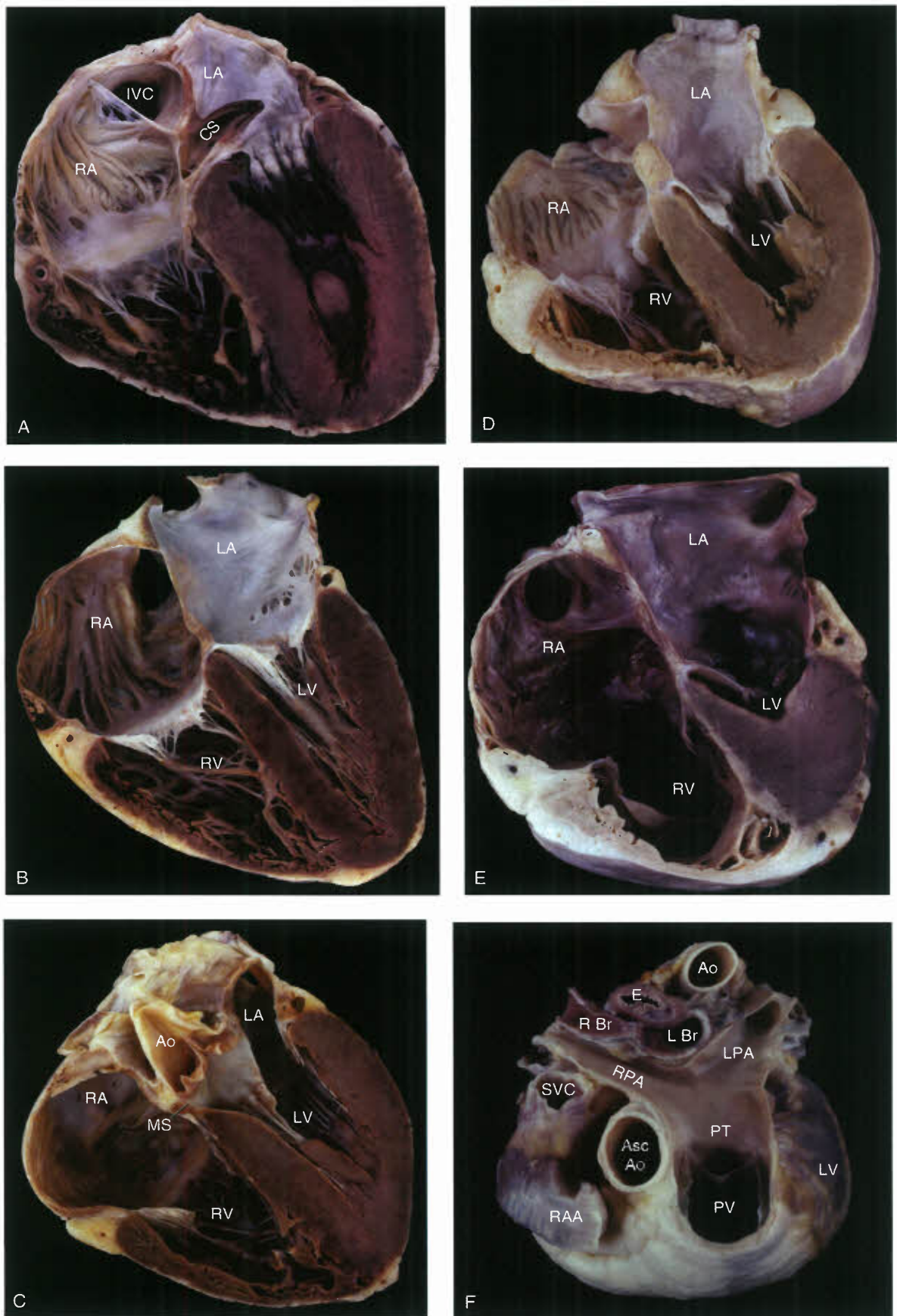


Figure 1.24. Tomographic methods of cardiac dissection (four-chamber and horizontal views) shown in normal hearts. A–C: Four-chamber views, at levels of coronary sinus (A), fossa ovalis (B), and aortic valve (C). D–F: Horizontal (transverse) views at levels of ventricular inflow (D) and outflow (E) tracts and pulmonary artery (F). (See Appendix 1.1 at <http://solution.lww.com> for abbreviations.)

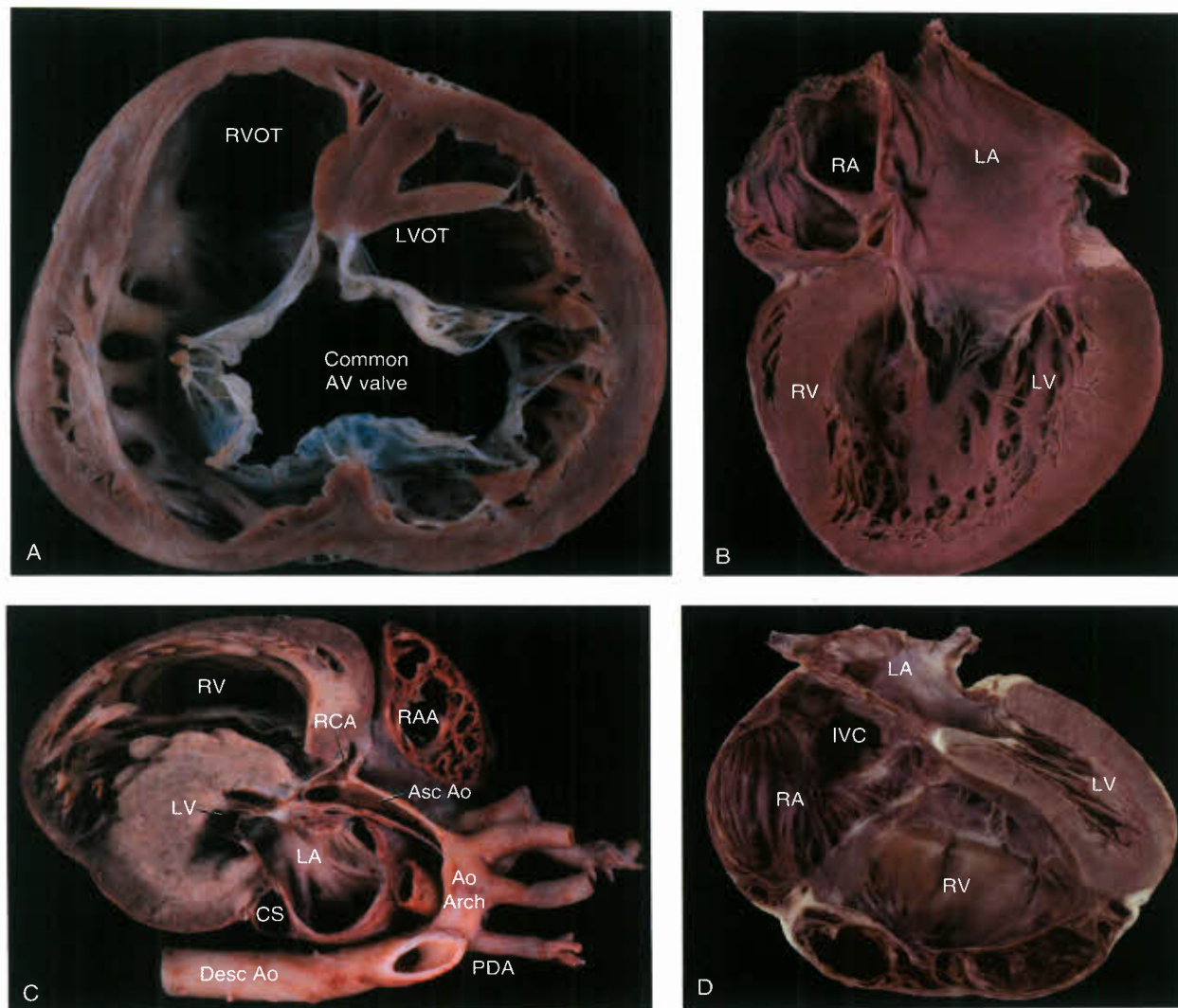


Figure 1.25. Tomographic methods of dissection in malformed hearts. **A:** Short-axis view of common AV valve in complete AV septal defect. **B:** Short-axis view of right anteriosuperior aorta in complete transposition of the great arteries. **C:** Long-axis view of hypoplastic left ventricle in aortic atresia. **D:** Four-chamber view of right-sided dilation in an Ebstein malformation. (See Appendix 1.1 at <http://solution.lww.com> for abbreviations.)

photographs is the initial focusing of the camera. Few things can ruin a photograph as quickly and irreversibly as failure to attend to sharp focusing.

The use of black or white backgrounds is favored over backlighting through translucent sheets of colored plastic. In this regard, it is important to note that standard black poster board, available from art supply stores, is generally made with water-soluble ink and will stain the specimens.

Because fresh specimens have shiny surfaces that produce extensive glare, tissues should be fixed before being photographed. Maintenance of lifelike colors can be achieved by fixation in formalin for only brief periods (5 to 15 minutes) or in nonformalin fixatives such as Kaiserling or Jores (32). For perfusion-fixed specimens that have been in formalin less than a week, colors may be partially restored by soaking the tissues in 80% ethanol for 15 to 30 minutes. Specimens are then thoroughly dried with paper towels to eliminate reflective glare.

In some cases, pins are necessary to hold thin or collapsible structures in position. From a technical perspective, a piece of black cardboard is placed on a piece of similarly sized corkboard, and the specimen is placed on the cardboard. Pins of

various sizes are then used to stabilize the specimen, and the heads of the pins are removed with cutting pliers so they will not be visible in the photograph (32). For example, 46 pins were used in Figure 1.7E to hold the atrial walls and valve leaflets upright. Probes, arrows, transillumination, and normal specimens (for comparison) also may be used to highlight specific morphologic features.

REFERENCES

1. Scholz DG, Kitzman DW, Hagen PT, et al. Age-related changes in normal human hearts during the first 10 decades of life. Part I (Growth): a quantitative anatomic study of 200 specimens from subjects from birth to 19 years old. *Mayo Clin Proc* 1988;63:126–136.
2. Kitzman DW, Scholz DG, Hagen PT, et al. Age-related changes in normal human hearts during the first 10 decades of life. Part II (Maturity): a quantitative anatomic study of 765 specimens from subjects 20 to 99 years old. *Mayo Clin Proc* 1988;63:137–146.
3. Harmon JV Jr, Edwards WD. Venous valves in subclavian and internal jugular veins: frequency, position, and structure in 100 autopsy cases. *Am J Cardiovasc Pathol* 1987;1:51–54.

4. Sweeney LJ, Rosenquist GC. The normal anatomy of the atrial septum in the human heart. *Am Heart J* 1979;98:194–199.
5. Hutchins GM, Moore GW, Jones JF, et al. Postnatal endocardial fibroelastosis of the valve of the foramen ovale. *Am J Cardiol* 1981;47:90–94.
6. Hagen PT, Scholz DG, Edwards WD. Incidence and size of patent foramen ovale during the first 10 decades of life: an autopsy study of 965 normal hearts. *Mayo Clin Proc* 1984;59:17–20.
7. Zimmerman KG, Paplanus SH, Dong S, et al. Congenital blood cysts of the heart valves. *Hum Pathol* 1983;14:699–703.
8. Seccombe JF, Cahill DR, Edwards WD. Quantitative morphology of normal human tricuspid valve: autopsy study of 24 cases. *Clin Anat* 1993;6:203–212.
9. Roberts WC. Morphologic features of the normal and abnormal mitral valve. *Am J Cardiol* 1983;51:1005–1028.
10. Becker AE, de Wit APM. Mitral valve apparatus: a spectrum of normality relevant to mitral valve prolapse. *Br Heart J* 1979;42:680–689.
11. Tei C, Pilgrim JP, Shah PM, et al. The tricuspid valve annulus: study of size and motion in normal subjects and in patients with tricuspid regurgitation. *Circulation* 1982;66:665–671.
12. Restivo A, Smith A, Wilkinson JL, et al. Normal variations in the relationship of the tricuspid valve to the membranous septum in the human heart. *Anat Rec* 1990;226:258–263.
13. Ormiston JA, Shah PM, Tei C, et al. Size and motion of the mitral valve annulus in man. I: a two-dimensional echocardiographic method and findings in normal subjects. *Circulation* 1981;64:113–120.
14. Ranganathan N, Lam JHC, Wigle ED, et al. Morphology of the human mitral valve. II: the valve leaflets. *Circulation* 1970;41:459–467.
15. Lam JHC, Ranganathan N, Wigle ED, et al. Morphology of the human mitral valve. I: chordae tendineae: a new classification. *Circulation* 1970;41:449–458.
16. Shiina A, Seward JB, Tajik AJ, et al. Two-dimensional echocardiographic-surgical correlation in Ebstein's anomaly: preoperative determination of patients requiring tricuspid valve plication vs replacement. *Circulation* 1983;68:534–544.
17. Prakash R, Umali SA. Comparison of echocardiographic and necropsy measurements of left ventricular wall thickness in patients with coronary artery disease. *Am J Cardiol* 1984;53:838–841.
18. Hagler DJ, Edwards WD, Seward JB, et al. Standardized nomenclature of the ventricular septum and ventricular septal defects, with applications for two-dimensional echocardiography. *Mayo Clin Proc* 1985;60:741–752.
19. Hutchins GM, Bulkley BH, Moore GW, et al. Shape of the human cardiac ventricles. *Am J Cardiol* 1978;41:646–654.
20. Wafae N, Warde M, Vieira MC. Morphologic study of one septal trabecula carnea of the left ventricle. *Bull Assoc Anat (Nancy)* 1990;74:33–36.
21. Draulens-Noe HA, Wenink AC. Anterolateral muscle bundle of the left ventricle in atrioventricular septal defect: left ventricular outflow tract and subaortic stenosis. *Pediatr Cardiol* 1991;12:183–188.
22. Edwards WD. Pathology of pulmonary hypertension. *Cardiovasc Clin* 1988;18:321–359.
23. Cudkowicz L. Bronchial arterial circulation in man: normal anatomy and responses to disease. *Lung Biol Health Dis* 1979;14:111–232.
24. Silver MM, Freedom RM, Silver MD, et al. The morphology of the human newborn ductus arteriosus: a reappraisal of its structure and closure with special reference to prostaglandin E1 therapy. *Hum Pathol* 1981;12:1123–1136.
25. Edwards BS, Edwards WD, Edwards JE. Aortic origin of conus coronary artery: evidence of postnatal coronary development. *Br Heart J* 1981;45:555–558.
26. Kramer JR, Kitazume H, Proudfit WL, et al. Clinical significance of isolated coronary bridges: benign and frequent condition involving the left anterior descending artery. *Am Heart J* 1982;103:283–288.
27. Miller AJ. *Lymphatics of the Heart*. New York, NY: Raven Press, 1982:107–180, 318–325.
28. Ferrans VJ, Rodriguez ER. Ultrastructure of the normal heart. In: Silver MD, ed. *Cardiovascular Pathology*. New York, NY: Churchill Livingstone, 1991:43–101.
29. Abdulla AK, Frustaci A, Martinez JE, et al. Echocardiography and pathology of left ventricular “false tendons.” *Chest* 1990;98:129–132.
30. Layman TE, Edwards JE. A method for dissection of the heart and major pulmonary vessels. *Arch Pathol* 1966;82:314–320.
31. Seward JB, Khandheria BK, Freeman WK, et al. Multiplane transesophageal echocardiography: image orientation, examination technique, anatomic correlations, and clinical applications. *Mayo Clin Proc* 1993;68:523–551.
32. Ackermann DM, Edwards WD. Anatomic basis for tomographic analysis of the pediatric heart at autopsy. *Perspect Pediatr Pathol* 1988;12:44–68.
33. Edwards WD. Photography of medical specimens: experiences from teaching cardiovascular pathology. *Mayo Clin Proc* 1988;63:42–57.

Classification and Terminology of Cardiovascular Anomalies

William D. Edwards ■ Joseph J. Maleszewski

PERSPECTIVES ON NOMENCLATURE

Through 5,000 years of recorded human history, only during the past 60 have treatments become available to substantially improve the quality of life and increase the longevity of children with cardiac anomalies. Within these 60 years, diagnostic and interventional procedures have been developed that have defined the frontiers of medical technology and creativity. During these exciting and innovative times, however, seeds were also sown, in the form of redundant and overlapping terminology, that have inadvertently led to difficulty and confusion for those interested in the subject of congenital heart disease.

Diversity of Terminology

Drawings and descriptions of malformed hearts date back to the 18th century, and in the mid-19th century, Peacock (1) published 18 cases in his classic series. However, it is the categorization of 1,000 malformed hearts by Dr. Maude E. Abbott at McGill University, published by the American Heart Association in 1936, that stands as a landmark in the classification of congenital heart disease (2). Since that time, others have examined large numbers of cases, both from autopsies and from living patients, and have proposed different systems of classification and nomenclature (3–13). Furthermore, numerous classifications have been adopted for individual anomalies, such as ventricular septal defects, and for groups of anomalies, such as hearts with univentricular atrioventricular connections.

Each new system, however, has reflected not only the state of knowledge at the time of its formulation but also the particular interests or biases of its creators. Thus, among the various classifications, some researchers have emphasized surgical anatomy, some embryogenesis, others spatial relationships such as atrial sidedness and the positions of ventricles and great arteries, and still others clinical features such as cyanosis and altered pulmonary blood flow. Not surprisingly, the introduction of new systems of classification has been attended by changes in terminology, primarily to clarify or simplify certain concepts. But as newer terms have been introduced, older terms have rarely been abandoned. As a result, the nomenclature for congenital heart disease has become a sea of synonyms, adding confusion rather than clarity to an already complex subject (Appendix 2.1, at <http://solution.lww.com>).

Unity from Diversity

Is the development of a unified system of nomenclature a realistic and worthwhile goal? If so, who should decide on the acceptable terminology? And what price will be paid to gain unity at the expense of diversity? Although such a system would limit the confusing number of synonyms that now exist, it also could limit our perspective as certain terms (such as

those with an embryologic basis) are purged from our rich and diverse heritage.

Nevertheless, a movement is already well under way to establish such a unified system. Uniform acceptance, however, will probably be achieved only following the publication of a consensus report from an international group that represents all disciplines dealing with congenital heart disease. To date, such attempts have met with only limited success (14). The system that is eventually chosen should be accurately descriptive, internally consistent, clinically usable, readily codable in a database, and applicable to all forms of congenital heart disease. New terms should be accepted only if they are necessary, brief, and specific (3).

Until such a consensus report is available, it is premature to endorse a specific system of nomenclature. However, at least at an institutional level, those dealing with patients having congenital heart disease should agree to speak the same clinical language and to prescribe to a single system of terminology. For this chapter, the approach and terminology suggested by Anderson et al. (4) are emphasized, with some modifications. Commonly used Latin terms and their anglicized counterparts are provided in Appendix 2.2 at <http://solution.lww.com>.

Although the notation system proposed by Van Praagh (3) is not emphasized in this chapter, it is favored at some institutions and warrants summarization. The situs (sidedness) is determined separately for the atria, ventricles, and great arteries. Atrial situs may be solitus (S), inversus (I), or ambiguous (A). Ventricular situs is solitus or D-loop (D), inversus or L-loop (L), or ambiguous (X). Great arterial situs is designated as solitus (S), inversus (I), D-transposition/malposition (D), L-transposition/malposition (L), or ambiguous or anterior transposition/malposition (A). Abbreviations are listed within the parentheses, with the ventriculoarterial arrangement included before the parentheses and any atrioventricular malalignments or other anomalies stated after the parentheses. Thus, TGA (S,D,D) would correspond to complete transposition of the great arteries.

SEQUENTIAL SEGMENTAL ANALYSIS

For evaluating patients with suspected congenital heart disease, it is helpful to consider the heart as a segmented structure represented by three regions—atria, ventricles, and great arteries (3–6). Each region, in turn, is partitioned into two components, usually right-sided and left-sided. Atrioventricular valves serve as connectors between atria and ventricles, and semilunar valves join the ventricles to the great arteries. There are only a limited number of possible connections between the three major regions, regardless of their spatial orientations. In practice, each region is evaluated independently, following the direction of blood flow: (a) systemic and pulmonary veins, (b) atria, (c) atrioventricular valves, (d) ventricles and

right ventricular outflow tract (infundibulum or conus), (e) semilunar valves, and (f) great arteries.

In a systematic manner, right-sided and left-sided structures at each level are evaluated according to their morphology, their relative positions, their connections to proximal and distal segments, and the presence and location of shunts, obstructions, and valvular regurgitation (7). This constitutes the sequential segmental method for investigation of congenital heart disease, and it represents a diagnostic cornerstone both for clinicians and for pathologists. Before applying this method, however, it is important to determine the cardiac position and the visceral situs (sidedness).

CARDIAC POSITION AND APICAL DIRECTION

With regard to the position of the heart in the chest, two questions arise that can be answered independently: Where is the heart located, and what is the direction of the cardiac apex? Unfortunately, the terms levocardia, dextrocardia, and mesocardia are commonly used to answer both questions, thus imparting an element of ambiguity (3,4). Although the approach described below is not universally accepted, it does provide clarity by defining the cardiac location and apical direction separately and by avoiding the ambiguous Latin terms.

Location in the Chest

Within the thorax, the heart can be described positionally as left-sided (normal), right-sided, or midline. This designation is particularly useful radiographically, before a patient has been evaluated by other imaging techniques.

The position of the heart in the mediastinum is affected not only by underlying cardiac malformations but also by abnormalities in adjacent structures. It can be displaced by conditions that distort the shape of the thorax, such as severe scoliosis or an elevated diaphragm, or that alter the size of thoracic structures, such as a hypoplastic lung or diaphragmatic hernia. Rightward displacement of the heart constitutes dextroposition, a leftward shift represents levoposition, and shifts toward the midline are called mesoposition.

In rare instances, sternal or diaphragmatic defects exist and are associated with an extrathoracic heart, or ectopia cordis (ectopic heart). This condition may be partial or complete and can be further categorized as cervical, thoracocervical, thoracic, thoracoabdominal, or abdominal.

Orientation in the Chest

The direction in which the ventricles are aligned defines the base–apex axis of the heart and may be leftward, rightward, or midline (Figs. 2.1 and 2.2). Leftward ventricles represent

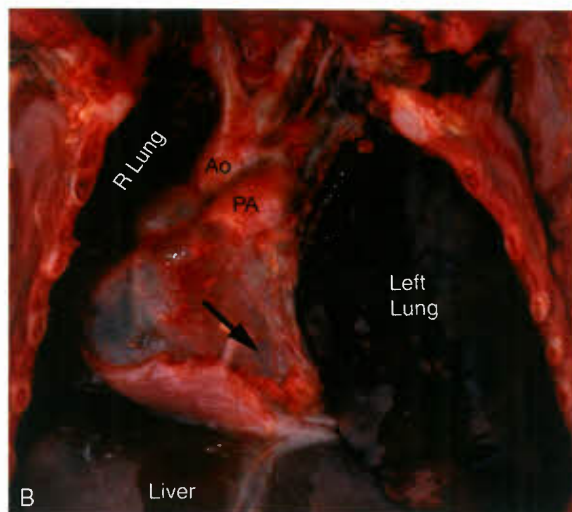
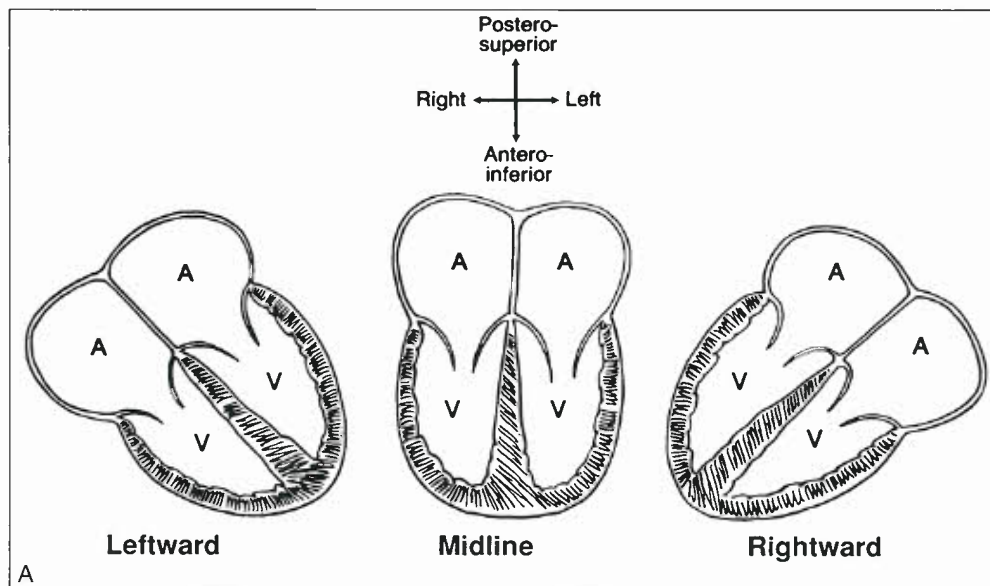


Figure 2.1. Cardiac base–apex axis.

A: The three types are shown schematically and are independent of cardiac position or situs. B: The ventricular apex is leftward (arrow), even though a hypoplastic right lung has caused dextroposition of the entire heart. (See Appendix 1.1 at <http://solution.lww.com> for abbreviations.)

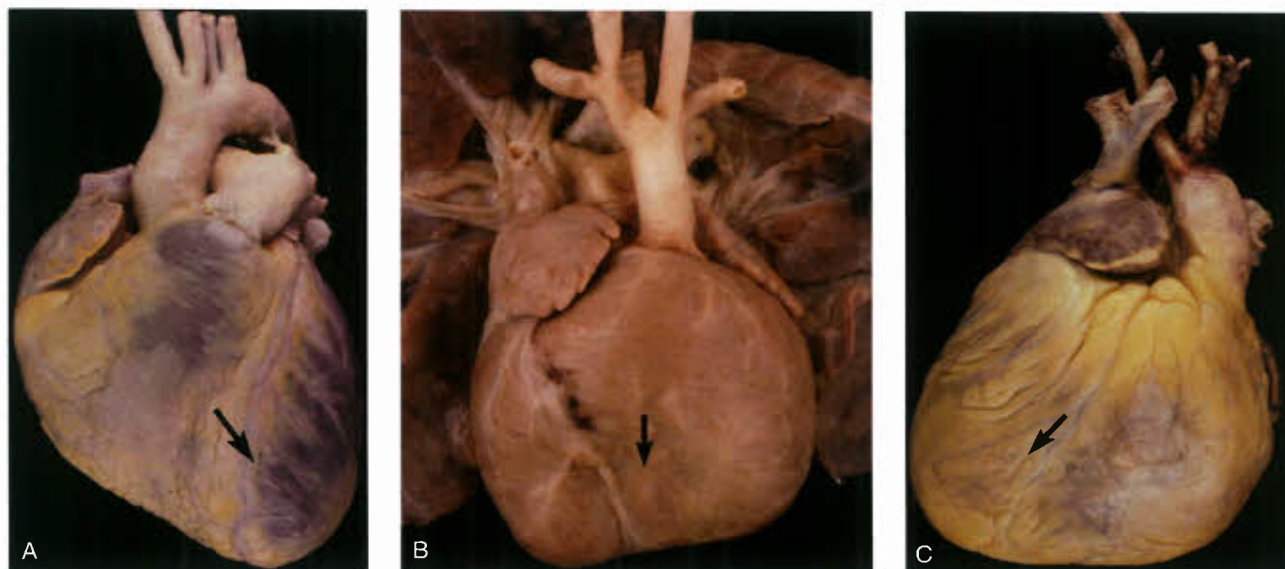


Figure 2.2. Cardiac base–apex axis (arrows) shown in three specimens, viewed anteriorly. **A:** Normal heart, with a leftward apex. **B and C:** Congenitally corrected transposition of the great arteries, showing a box-shaped midline apex (**B**) and a rightward apex (**C**).

the normal state and are characterized by an apex that is directed leftward, anteriorly, and somewhat inferiorly. The extent of these three directions is variable and is influenced by age, body build, and the level and functional state of the diaphragm. Ventricles with a rightward apex are directed to the right of midline. In contrast, midline ventricles are often box shaped and exhibit two apices that are directed anteriorly and inferiorly (7).

The base–apex axis is independent of cardiac location and displacements. For example, a patient with a hypoplastic right lung could have a right-sided heart, owing to dextroposition, and still exhibit a leftward apex (Fig. 2.1B).

The base–apex axis is also independent of cardiac sidedness. Thus, the presence of a leftward apex does not necessarily imply normal sidedness (*situs solitus*), and a right-sided apex does not always coincide with mirror-image sidedness (*situs inversus*). A midline apex, on the other hand, usually is associated with cardiac isomerism (*situs ambiguus*).

VISCERAL SIDEDNESS (SITUS)

All major organ systems begin their embryologic development as midline structures with bilateral mirror-image symmetry. However, three organ systems (cardiovascular, respiratory, and digestive) later acquire asymmetry and are thereby characterized by sidedness (*situs* or handedness), which is genetically determined. Sidedness may be normal, mirror-image, isomeric, or indeterminate. Right isomerism indicates bilateral right-sidedness, whereas left isomerism denotes bilateral left-sidedness.

Isomerism and Splenic Anomalies

The relationship between isomerism and splenic anomalies is intriguing (8). The splenic anlage, rather than originating as a midline structure, appears to be left-sided from its inception. Thus, when right isomerism exists, the spleen is usually absent (asplenia syndrome). Left isomerism, in contrast, is generally

associated with multiple spleens (polysplenia syndrome) that are confined to only one side of the vertebral column. Occasionally, subjects with asplenia or polysplenia have normal hearts, and, rarely, those with atrial isomerism have normal spleens.

Abnormalities may affect the entire body, as in total mirror-image sidedness (*situs inversus totalis*), or can involve individual organ systems. Moreover, sidedness may vary between systems, particularly in conditions associated with isomerism. Although the term *atriovisceral situs* enjoys common usage, it does not always allow an accurate description of sidedness in right isomerism and left isomerism. Consequently, it is recommended that the sidedness of cardiovascular, respiratory, and digestive systems be designated separately (7).

Cardiac Sidedness (Situs)

Cardiac sidedness is determined by the position of the morphologic right atrium (Fig. 2.3). It is not determined by the direction of the cardiac apex, the positions of the ventricles or great arteries, or the sidedness of noncardiac viscera. The morphologic right atrium is normally right-sided but is left-sided in *situs inversus* (mirror-image sidedness). Bilateral right atria define right cardiac isomerism, and bilateral left atria constitute left cardiac isomerism (Fig. 2.4) (14). In some cases of polysplenia, one chamber represents a left atrium, but the other has a hybrid appearance that is morphologically neither left nor right; this constitutes indeterminate cardiac sidedness. In practice, an accurate determination of cardiac sidedness depends on an accurate distinction between right and left atrial morphology, as discussed in this chapter and in Chapter 1. Although all investigators agree on the concept of normal and mirror-image cardiac sidedness, some have questioned the existence of atrial isomerism (9).

Pulmonary Sidedness (Situs)

Pulmonary sidedness is determined by the positions of the morphologic right and left lungs (Fig. 2.5). Pulmonary morphology,

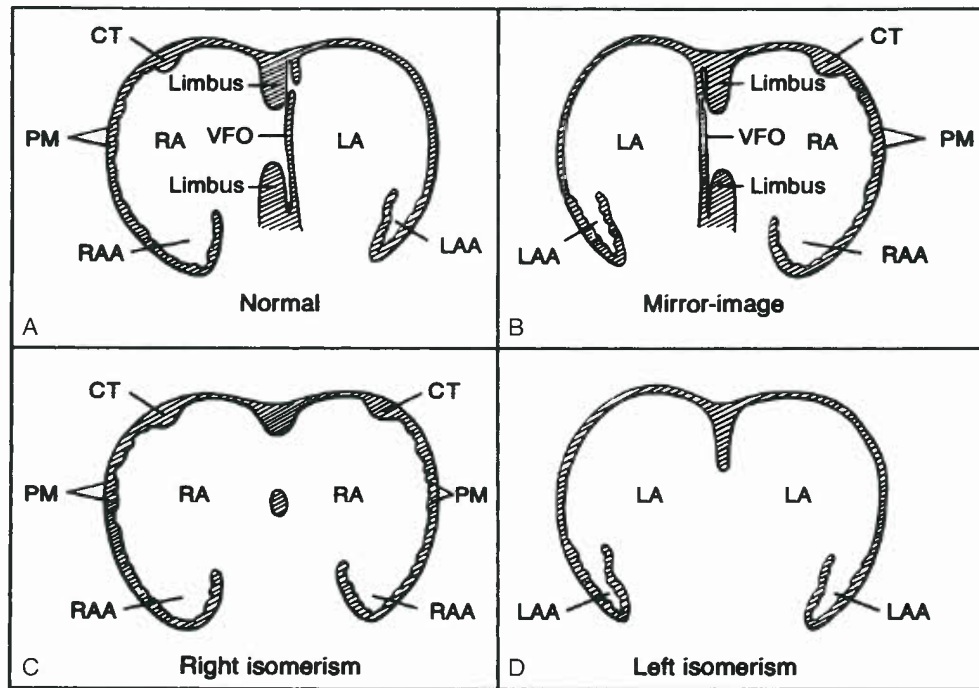


Figure 2.3. Cardiac situs (sidedness), shown schematically. A: Situs solitus, with right-sided morphologic right atrium. B: Situs inversus, with left-sided morphologic right atrium. C and D: Situs ambiguus, with bilateral morphologic right atria (right isomerism) (C) and bilateral morphologic left atria (left isomerism) (D). (See Appendix 1.1 at <http://solution.lww.com> for abbreviations.)

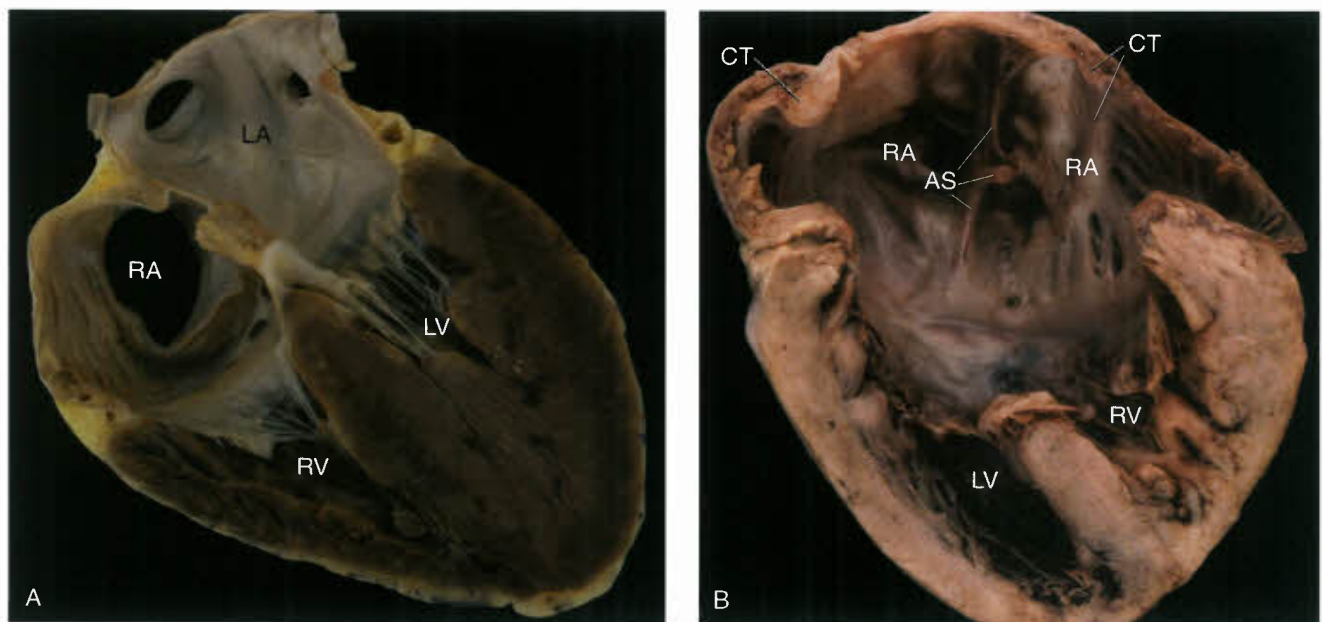


Figure 2.4. Cardiac situs in two specimens, displayed in the four-chamber format. A: Situs solitus. B: Situs ambiguus, with right isomerism. A crista terminalis is present bilaterally. Ventricular inversion is also present but plays no role in determining cardiac sidedness. (See Appendix 1.1 at <http://solution.lww.com> for abbreviations.)

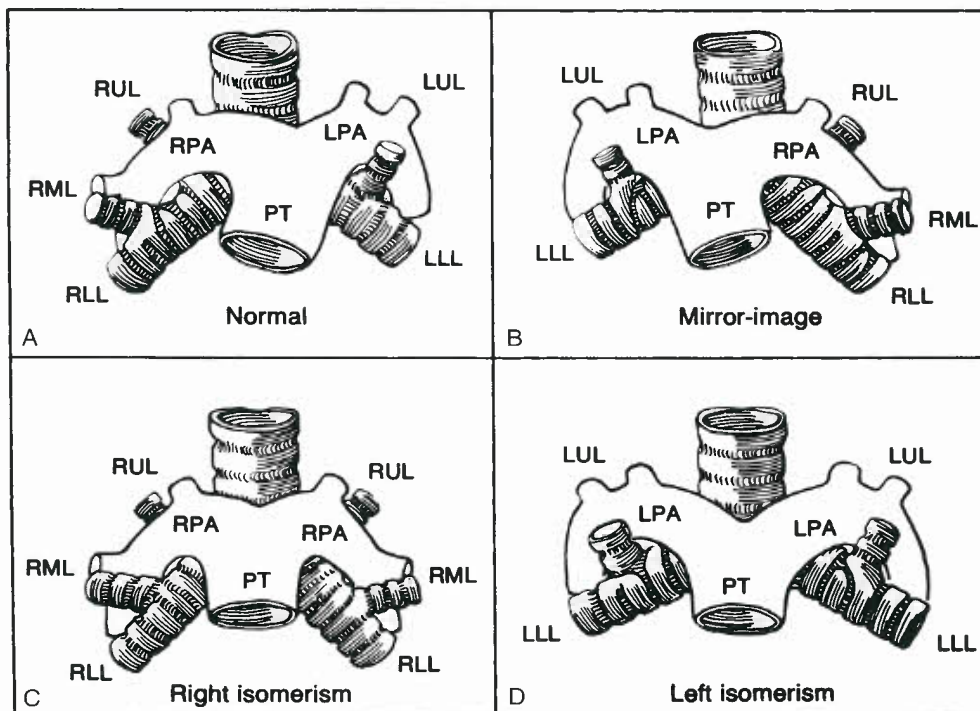


Figure 2.5. Pulmonary situs, shown schematically. A: Situs solitus, with right pulmonary anterior to its upper lobe bronchus and with left pulmonary artery posterior to its upper lobe bronchus. B: Situs inversus, with mirror-image morphology. C and D: Situs ambiguus, with bilateral morphologic right lungs (right isomerism) (C) and bilateral morphologic left lungs (left isomerism) (D). (See Appendix 1.1 at <http://solution.lww.com> for abbreviations.)

in turn, is defined by the relationship of the pulmonary arteries to their adjacent bronchi, and not by the number of lobes. The pulmonary artery of a morphologic right lung travels anterior to its upper and intermediate bronchi, whereas that of a morphologic left lung travels superior to its main bronchus and posterior to the upper lobe bronchus.

Clinically, pulmonary sidedness may be inferred by comparing the relative lengths of the two main bronchi, as measured on a chest radiograph that shows an air bronchogram. Normally, the distance from the carina to the origin of the upper lobe bronchus is 1.5 to 2.5 times greater for the morphologic left lung than for the right lung, and this ratio holds true regardless of the sidedness of the aortic arch (which is determined by the bronchus over which the aorta travels) (10). With pulmonary isomerism, this ratio approaches unity because the lengths of the two mirror-image bronchi are similar (Fig. 2.6).

Although most examples of bilateral trilobed lungs do correspond to cases of right isomerism or asplenia syndrome, bilateral bilobed lungs more often occur as a variation of normal morphology than as a manifestation of left isomerism or polysplenia.

Abdominal Sidedness (Situs)

Abdominal sidedness is determined by the location of the liver and stomach, with the spleen and pancreas generally on the same side of the vertebral column as the stomach (Fig. 2.7). The state of the spleen can be evaluated by clinical imaging, thus supplanting the less reliable method of identifying Howell-Jolly bodies in peripheral blood smears. At autopsy, splenic morphology should always be designated in patients with congenital heart disease.

In the asplenia syndrome, the liver is commonly midline with two mirror-image right lobes (right hepatic isomerism), and the biliary tree is patent and is usually associated with a single gallbladder (Fig. 2.8). The position of the stomach and pancreas can be left-sided, right-sided, or midline. Malrotation of the bowel is the rule, such that the cecum and appendix may be located in any of the abdominal quadrants. Finally, the aorta and inferior vena cava travel together on the same side of the vertebral column, a unique feature that can be demonstrated by abdominal imaging.

Interestingly, with the polysplenia syndrome, the sidedness of the abdominal viscera may be indeterminate (ambiguous), mirror-image (inversus), or even normal (solitus). Although the spleens are multiple, they are all located on the same side of the vertebral column as the stomach. The gallbladder is single, but biliary atresia may occur. As a rule, the inferior vena cava fails to join the heart directly and exhibits azygos continuation, with connection to the superior vena cava.

MORPHOLOGY OF CARDIAC SEGMENTS

Accurate identification of right-sided and left-sided structures is an essential feature of the sequential segmental approach to the diagnosis of congenital heart disease. For consistency and reproducibility of diagnoses, definitions of even the most commonly used terms are helpful.

In this regard, a distinction between the terms connection and drainage is necessary because the two are not synonymous. *Connection* is an anatomic term that implies a direct link between two structures. In contrast, *drainage* is a hemodynamic term that refers to the direction of blood flow.

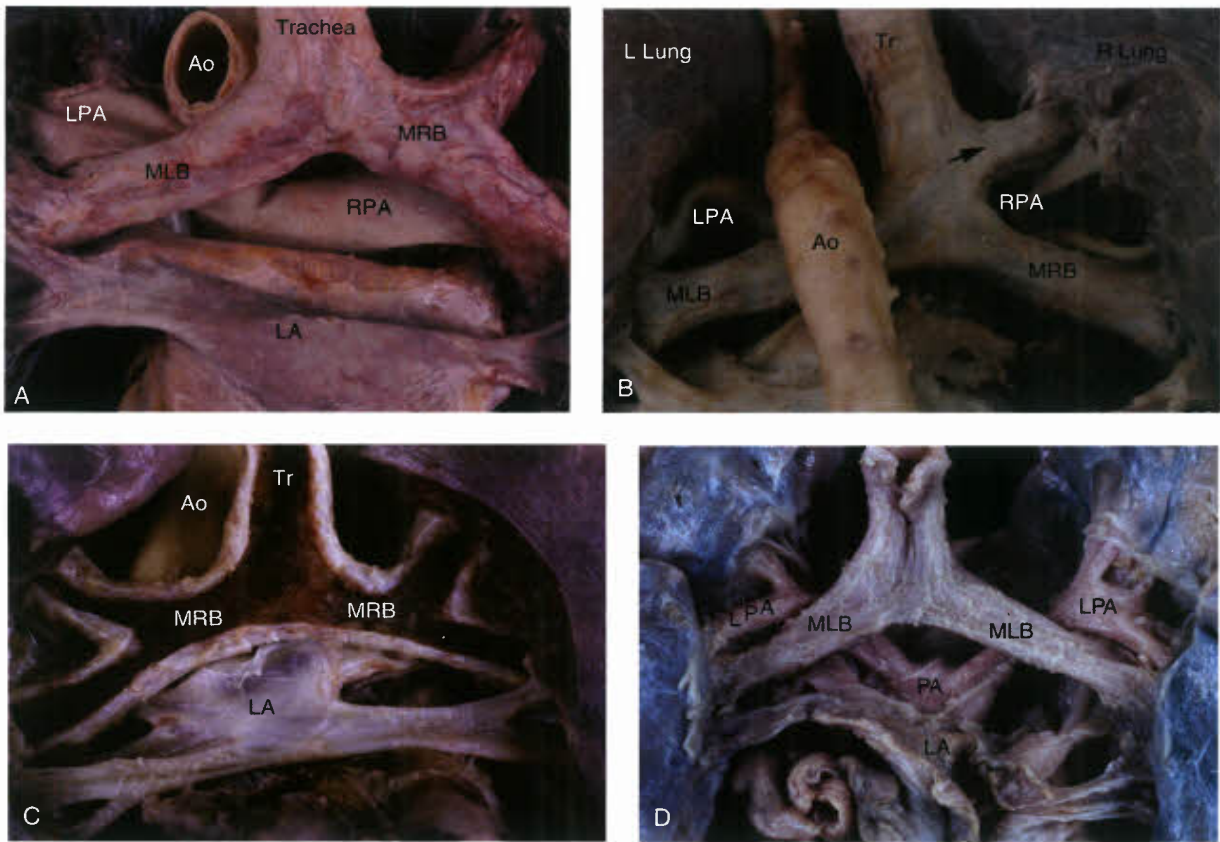


Figure 2.6. Pulmonary situs in four specimens, viewed posteriorly. A: Normal situs, with long left bronchus and short right bronchus. B: Normal situs, with tracheal origin of the right upper lobe bronchus (bronchus suis) (*arrow*). C: Right pulmonary isomerism, with short bronchi of similar length (the posterior wall of the airways has been removed). D: Left pulmonary isomerism, with long bronchi of similar length. (See Appendix 1.1 at <http://solution.lww.com> for abbreviations.)

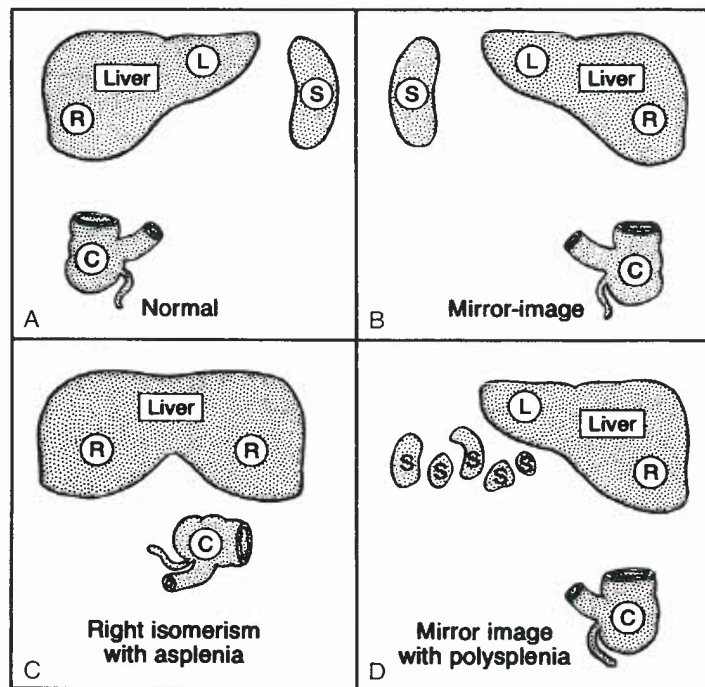


Figure 2.7. Abdominal situs, drawn schematically. A: Situs solitus, with right-sided liver, left-sided spleen (also stomach and pancreas, not shown), and cecum in right lower quadrant. B: Situs inversus, with mirror-image morphology. C: Situs ambiguus with right isomerism shows liver with two right lobes, malrotation of the bowel (indicated by the abnormal position of the cecum), and asplenia. D: Situs ambiguus with left isomerism shows polysplenia; other features are variable. (See Appendix 1.1 at <http://solution.lww.com> for abbreviations.)

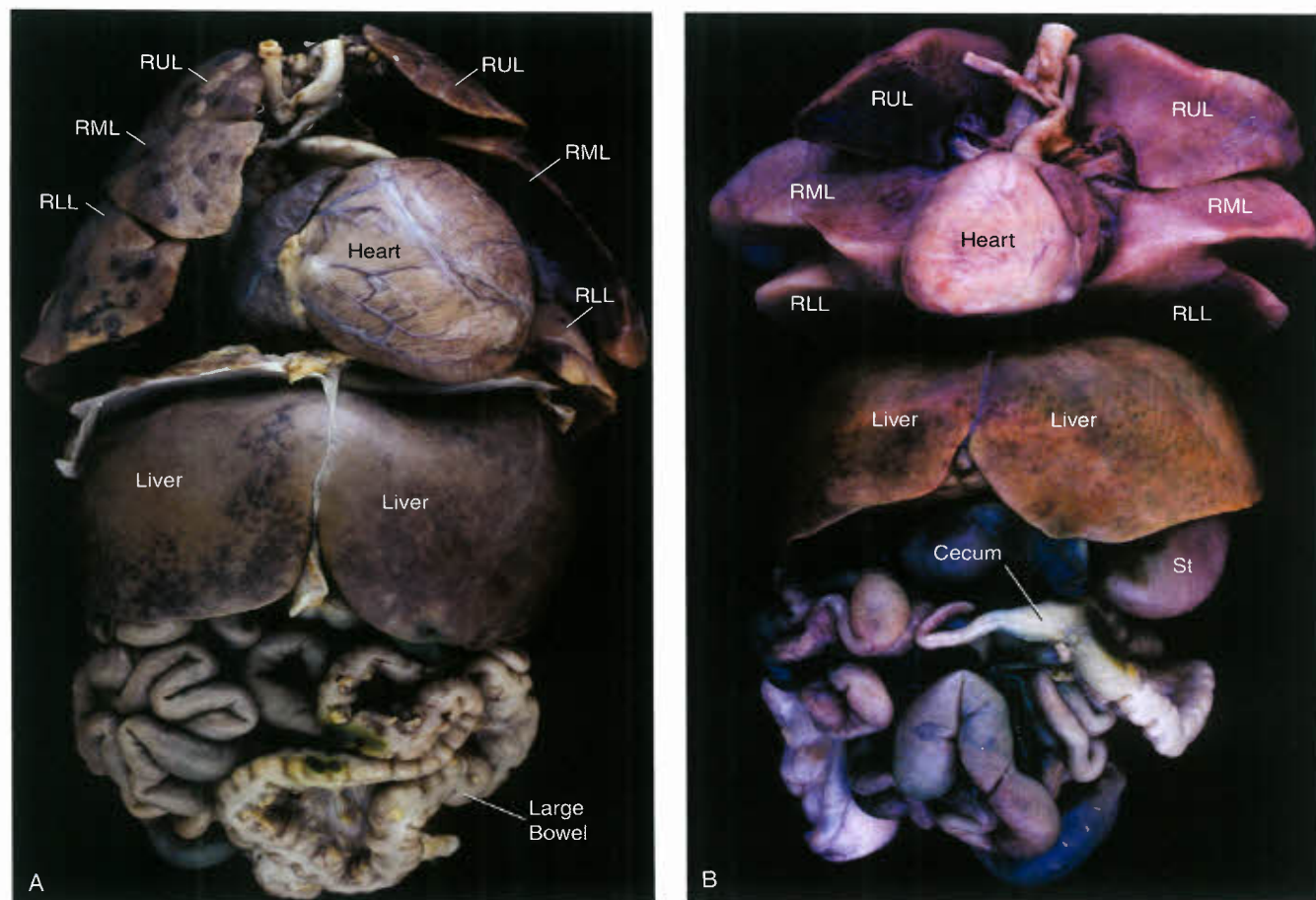


Figure 2.8. Abdominal situs in two patients, with thoracoabdominal organs viewed anteriorly. **A** and **B**: Both patients had the asplenia syndrome, with right isomerism of the heart, lungs, and abdominal organs. Both exhibit a midline symmetric liver and malrotation of the bowel (with the small bowel to the right and the large bowel to the left). (As an aside, cardiac situs is not affected by the cardiac base–apex axis, which is leftward in **A** and rightward in **B**.) (See Appendix 1.1 at <http://solution.lww.com> for abbreviations.)

A distinction also should be drawn between single and common, as applied to cardiac chambers and valves. *Single* implies that the corresponding contralateral structure is entirely absent. Tricuspid atresia with a single-inlet ventricle is one example. In contrast, the term *common* indicates bilateral components with absent septation. Examples are a common atrium, a common atrioventricular valve, and a common truncal artery (truncus arteriosus [TA]).

Superior Vena Cava

When the superior vena cava is single and right-sided, as normally occurs, no further designation is necessary. The term left superior vena cava is recommended for its left-sided counterpart, and distinction should be made between right-sided and left-sided structures in the setting of bilateral venae cavae. With bilateral veins, the presence or absence of a brachiocephalic (innominate) venous bridge between the two should also be described.

Inferior Vena Cava

The inferior vena cava, or at least its suprahepatic segment, almost invariably connects to the inferior aspect of the

morphologic right atrium. Rarely, and usually in patients with polysplenia, this connection is interrupted, and the vein empties into the superior vena cava through a direct connection with the azygos or hemiazygos vein, representing azygos continuation of the inferior vena cava. In such cases, the hepatic veins generally connect directly to one or both atria via the suprahepatic segment of the inferior vena cava (9).

Coronary Sinus

The coronary sinus normally joins the right atrium. Rarely, its ostium is atretic. Moreover, variable portions of the vein may be unroofed and produce a left atrial fistula. Complete unroofing is commonly referred to as absence of the coronary sinus and may be associated with asplenia syndrome and direct left atrial connection of a left superior vena cava, or may be an isolated anomaly with resultant creation of an atrial septal defect of coronary sinus type.

Pulmonary Veins

Normally, the four pulmonary veins join the body of the left atrium separately. As a variant of normal, the upper and lower

veins, most commonly from the left lung, merge and connect to the left atrium as a single vein. Another variant is independent connection of the right middle lobar vein directly to the left atrium.

In the setting of anomalous pulmonary venous connection or severe left-sided obstructive lesions, a vessel connecting the pulmonary veins to the left brachiocephalic, or innominate, vein has been referred to as a persistent superior vena cava, vertical vein, or a levoatrial cardinal vein. For these anomalies, perhaps the term collateral vein would suffice (analogous to collateral arteries in cases of pulmonary atresia with ventricular septal defect).

Atria

Definition

By definition, an atrium is a cardiac receiving chamber that usually is interposed between the great veins and an atrioventricular valve. Occasionally, it may exist either between the great veins and an adjacent atrium, as in tricuspid atresia or cor triatriatum (triatrial heart), or between an atrium and an atrioventricular valve, as in total anomalous pulmonary venous connection. Triatrial hearts can be described as having a subdivided left atrium, a double-chamber left atrium, or an accessory left atrial chamber. Rarely, the right atrium is subdivided by an enlarged valve of the inferior vena cava.

Right Atrium

The morphologic right atrium is characterized by connections from the venae cavae and coronary sinus and by connections to one or both atrioventricular valves, with drainage into one or both ventricles. Its septal surface is defined by an interatrial portion, with the limbus and valve of the fossa ovalis, and by an atrioventricular portion. The free wall harbors not only a large pyramidal appendage but also a crista terminalis and numerous pectinate muscles outside the appendage (11). The crista terminalis forms a boundary between the smooth-walled posterior aspect of the free wall, derived from the sinus venosus, and the muscular anterior aspect, derived from the embryologic right atrium.

Left Atrium

In contrast, the morphologic left atrium has neither a crista terminalis nor pectinate muscles other than in its appendage. This appendage is more finger shaped than pyramidal, with several small outpouchings or lobes. The main body of the left atrium is smooth walled, like the common pulmonary vein from which it is derived, and only the appendage remains as a remnant of the embryologic atrium. The body and main pulmonary veins become infiltrated by cardiac myocytes that can produce left atrial contraction. The left side of the atrial septum is entirely interatrial. Its smooth surface is interrupted only by a crescentic rim that forms the residual border of the ostium secundum.

Common Atrium

A common atrium is the result of absence, or near absence, of the atrial septum. It almost always is associated with an atrioventricular septal defect, with or without asplenia syndrome. In most cases, a characteristic band or bar of myocardium spans the midportion of the atrium as the only septal remnant. The two atrial free walls can be morphologically right and left, or they may be bilaterally right or bilaterally left.

Indeterminate Atrial Morphology

Occasionally, atrial morphology may be impossible to determine with certainty. This most often occurs in patients with right or left isomerism. With left isomerism in particular, one atrium often has a hybrid structure with some anatomic features of each atrium. In addition, previous surgical procedures with ligation of the atrial appendages or excision of the atrial septum may so distort the chambers that determination of atrial morphology is impossible.

Diagnostic Criteria

Cardiac sidedness is established by the location of the right and left atria (10) (Fig. 2.9). In this regard, anatomic landmarks in the atrial septum are useful for distinguishing between normal cardiac sidedness (*situs solitus*) and mirror-image cardiac sidedness (*situs inversus*). The limbus of the fossa ovalis always faces the morphologic right atrium. However, in the setting of atrial isomerism (*situs ambiguus*), most of the atrial septum is characteristically absent. As a result, anatomic landmarks in the atrial free walls must be used to determine cardiac sidedness. Only the parts of the free wall that are derived from the embryologic atrium are used for this purpose, not those derived from the sinus venosus or common pulmonary vein. With this in mind, the structural landmarks of a morphologic right atrium are a large pyramidal appendage, pectinate muscles, and a crista terminalis. In contrast, the hallmark of a morphologic left atrium includes only a tortuous appendage with side branches, but without pectinate muscles or a crista terminalis. Using these criteria, right and left isomerism can readily be established in most cases.

Atrioventricular Valves

Definition

Atrioventricular valves not only connect the atria to the ventricles but also serve to separate them electrically. Because these valves travel with their respective ventricles, a morphologic tricuspid valve connects to a morphologic right ventricle, and a morphologic mitral valve connects to a morphologic left ventricle. In normal hearts, viewed in a four-chamber format, the tricuspid valve ring attaches to the septum more apically than does the mitral annulus (Fig. 2.9). Identification of this arrangement by clinical imaging allows determination not only of atrioventricular valve morphology but also of ventricular morphology.

Tricuspid Valve

The normal tricuspid valve consists of three leaflets, three major commissures, and three papillary muscles. Although its annulus is elliptical (but saddle shaped), the shape of its orifice at the midleaflet (or midventricular) level is more triangular. The septal tricuspid leaflet has numerous direct cordal insertions along the ventricular septum, and the anterior leaflet forms an intraventricular curtain that separates the inflow and outflow tracts. Additionally, the tricuspid and pulmonary valves are separated by the muscular right ventricular outflow tract.

Mitral Valve

Like the tricuspid valve, the mitral valve has an elliptical (but saddle-shaped) annulus and an intraventricular anterior leaflet that separates the inflow and outflow tracts. However, the mitral valve has only two leaflets, two major commissures, and

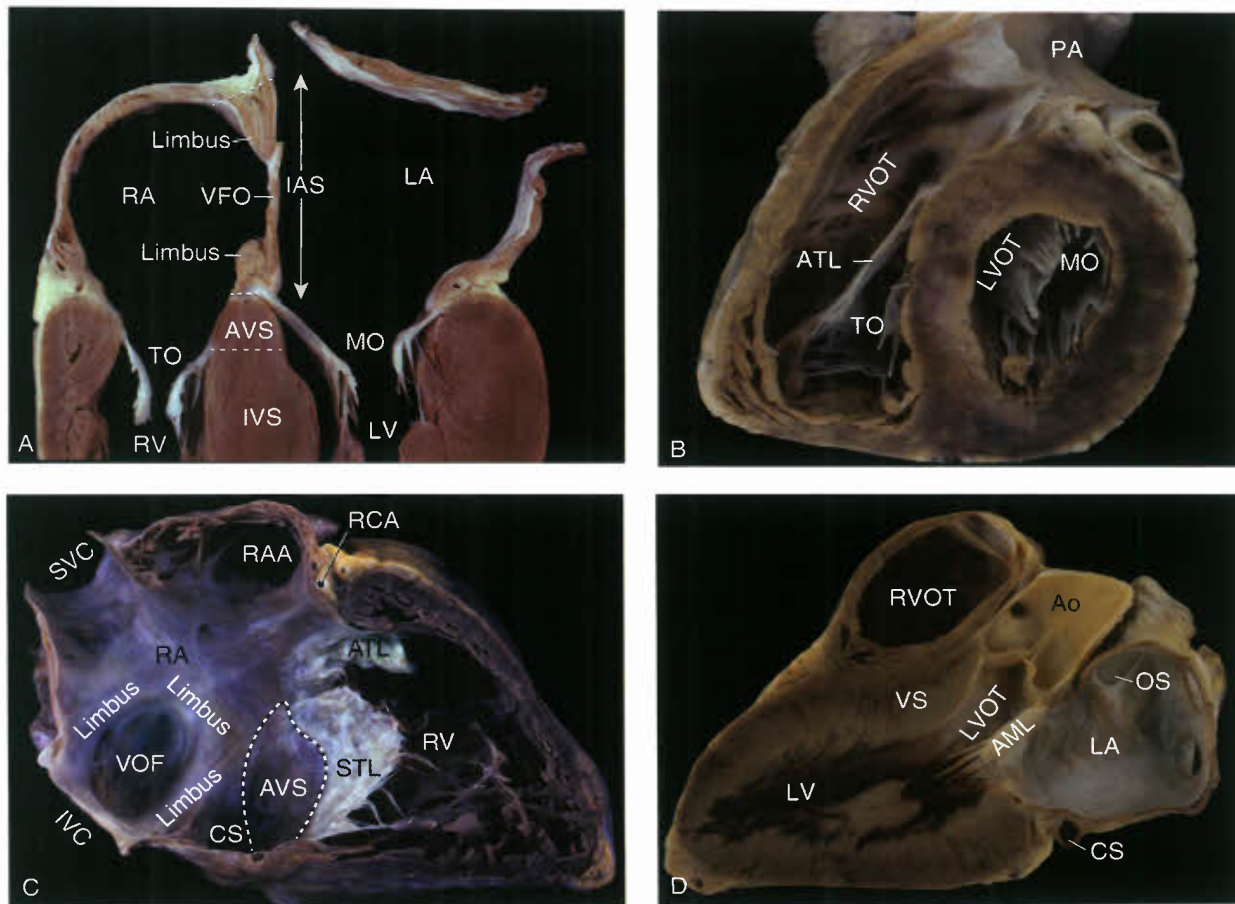


Figure 2.9. Characteristic anatomic features of atria, atrioventricular valves, and ventricles in four specimens of normal hearts. **A:** The atrioventricular septum and the more apical attachment of the tricuspid valve ring, compared with the mitral valve, are best evaluated in a four-chamber view. **B:** The triangular tricuspid orifice and elliptical mitral orifice, at midleaflet level, are shown in a short-axis view, as are the septal insertions of tendinous cords from the septal tricuspid leaflet. **C and D:** Right-sided and left-sided features can readily be compared between a two-chamber view of the right heart (**C**) and a long-axis view of the left heart (**D**). (See Appendix 1.1 at <http://solution.lww.com> for abbreviations.)

two papillary muscle groups rather than three, and because the papillary muscles attach to the left ventricular free wall, there are normally no septal insertions of tendinous cords. Moreover, in contrast to the muscular separation that exists between the tricuspid and pulmonary valves, the mitral annulus is in direct continuity with the aortic valve ring, such that the anterior mitral leaflet forms a part of the left ventricular outflow tract.

Common Atrioventricular Valve

With complete atrioventricular septal defects, the presence of a common valve, rather than distinct tricuspid and mitral valves, renders four-chamber imaging unsuitable for determining ventricular morphology. Similarly, in partial atrioventricular septal defects, the mitral valve ring generally attaches to the septum at the same level as the tricuspid annulus, producing an interatrial septal defect and interfering with the identification of ventricular morphology.

Right and Left Atrioventricular Valves

A double-inlet left ventricle is characterized by papillary muscle insertions from both atrioventricular valves into the

morphologic left ventricle. In many cases, the valves have mirror-image mitral morphology, or one of the valves (with right-ventricular straddling) has indeterminate, or hybrid, morphology with mitral and tricuspid features. Designation simply as right-sided or left-sided atrioventricular valves rather than as mitral, tricuspid, or hybrid minimizes the likelihood of confusion.

Diagnostic Criteria

The most reliable feature that allows distinction between tricuspid and mitral valves is the more apical septal attachment of the tricuspid valve when viewed in a four-chamber format (Fig. 2.9). For conditions in which this cannot be assessed, other features should be assessed, including septal cordal attachments, indicative of a tricuspid valve, and direct continuity with a semilunar valve, indicative of a mitral valve.

Ventricles

Definition

A ventricle represents an endocardial-lined chamber within the ventricular muscle mass. Other proposed definitions have been

a source of disagreement and controversy (12,13). Although normal ventricles are characterized by inlet, trabecular, and outlet regions, they are not defined by the presence of all three or by the presence of any one in particular. Hypoplastic ventricles, as described below, frequently consist of only one or two components. It is important to emphasize that, with only rare exceptions, virtually all human hearts contain two ventricular chambers. Hence, the terms single ventricle and univentricular heart are inaccurate.

Right Ventricle

A morphologic right ventricle is characterized by a heavily trabeculated anteroapical region (4). Other definitive features relate to the inlet region and the anatomic details of the tricuspid valve, as discussed earlier. The normal right ventricular outflow tract (infundibulum or conus) represents a collar of muscle that separates the tricuspid and pulmonary valves. Rarely, in the case of a double-outlet left ventricle, the infundibular region may originate entirely from the contralateral ventricle. To conceptualize this and other conotruncal anomalies, the heart may be considered as consisting of five chambers (two atria, two ventricles, and an infundibulum) in which the infundibulum can attach to one or both ventricles, in various orientations (15).

Left Ventricle

A morphologic left ventricle has fine apical trabeculations. However, in patients with a double-inlet left ventricle, the presence of four sets of papillary muscles produces a muscular apex that can be misinterpreted as a morphologic right ventricle, particularly by echocardiography.

Common Ventricle

A common ventricle is characterized by virtual absence of the ventricular septum and by a free wall that morphologically is part right ventricle and part left ventricle. This represents an exceedingly rare condition. Accordingly, other anomalies that resemble a common ventricle should be considered before rendering a diagnosis. Among patients with a common-inlet right ventricle, the hypoplastic left ventricle may be so diminutive that it is difficult to identify even at autopsy and may lead to a misdiagnosis of common ventricle.

Ventricular Morphology

If ventricular morphology cannot be determined with confidence, the term indeterminate may be applied. This designation is usually reserved for the rare condition in which only one ventricular chamber can be identified. Such a chamber has either ambiguous morphologic features or has right and left ventricular free walls with an absent ventricular septum (a common ventricle).

Hypoplastic Ventricle

Underdeveloped ventricles have an appreciably smaller chamber size than expected, although their muscular walls may either be normal in thickness or hypertrophied, depending on the pressures generated within the chamber. Structurally, either they exhibit inlet, trabecular, and outlet components or they are deficient and consist of only one or two of these regions.

In the setting of tricuspid or mitral atresia, for example, the inlet portion of the affected ventricle is either absent or very diminutive. Similarly, with pulmonary or aortic atresia, the outlet region is usually incompletely formed. For combined tricuspid and pulmonary atresia or combined mitral and aortic atresia, the interposed ventricle is severely hypoplastic and generally consists primarily of a trabecular component.

A hypoplastic ventricle that is positioned along the antero-superior surface of the heart and gives rise to a great artery is virtually always a morphologic right ventricle. Conversely, a small chamber that occupies the posteroinferior aspect of the heart and does not connect to a great artery is almost invariably a morphologic left ventricle. Thus, the use of terms such as outlet chamber, trabecular pouch, and rudimentary chamber is probably unnecessary.

Criteria

In practice, the most reliable features that allow distinction between morphologic right and left ventricles are the nature of the apical trabeculations, the morphology of the associated atrioventricular valve, and the state of continuity between the atrioventricular and semilunar valves (Fig. 2.9). Even in the setting of a hypoplastic ventricle, the other ventricle should be assessable at all three levels. Trabeculations and valvular discontinuity can be determined angiographically, and valvular morphology and discontinuity are readily evaluated echocardiographically.

In normal hearts, the short-axis shapes and wall thicknesses of the ventricles differ appreciably. The left ventricle has a thick wall and a circular chamber, whereas the right ventricle is thin walled and more crescent shaped. Neither of these features, though, is reliable for distinguishing ventricular morphology. Right ventricular hypertrophy or left ventricular atrophy is encountered relatively frequently and produces either ventricles of similar thickness or a thick right ventricle and thin left ventricle, respectively. Likewise, straightening or leftward bowing of the ventricular septum may occur and result in mirror-image D-shaped chambers or a crescentic left ventricle, respectively.

Semilunar Valves

A semilunar valve serves to connect a ventricle to a great artery and is named according to the artery into which it empties. It is not named according to the ventricle from which it emanates or according to its relative position in the chest. Semilunar valves include aortic, pulmonary, and truncal valves. Normal semilunar valves consist of three pocket-like cusps, three commissures, and a fibrous annulus shaped like a triradiate crown. When malformed, they can have an abnormal number of cusps, be hypoplastic or dysplastic, or exhibit a combination of these features.

Great Arteries

Definition

The great arteries include the aorta, main pulmonary artery, TA, and ductus arteriosus. Distinction between the aorta, pulmonary artery, and TA is based solely on their branching patterns (Fig. 2.10); there are no other distinguishing features. In contrast, the identification of a ductus arteriosus is based on its position and its lack of tortuosity or branching.

Aorta

The aortic arch is normally left-sided, traveling over the left bronchus. In contrast, a right aortic arch travels over the right bronchus and is almost always associated with mirror-image brachiocephalic arterial branching. A double aortic arch, although rare, travels over both bronchi. The sidedness of the aortic arch is not associated with appreciable lengthening of the subclavian bronchus and therefore does not interfere with the radiographic determination of pulmonary situs (10). Consequently, even with a right aortic arch, the length of the right bronchus will be substantially less than that of the left bronchus.

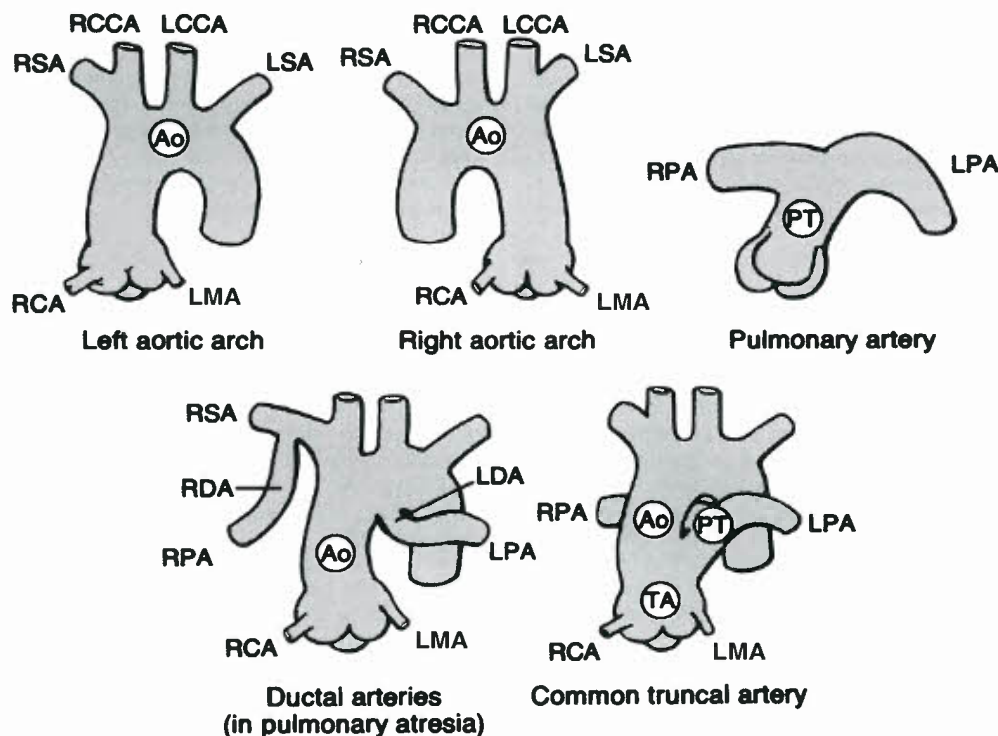


Figure 2.10. The different types of great arteries are illustrated schematically, as viewed anteriorly. A right aortic arch travels over the right main bronchus, and its brachiocephalic branching is the mirror-image of normal. (See Appendix 1.1 at <http://solution.lww.com> for abbreviations.)

Pulmonary Artery

The mediastinal pulmonary arteries maintain their characteristic Y shape when severely hypoplastic and occasionally even when atretic. They do not branch further before entering the lungs. In addition, each artery has a unique relationship to its adjacent bronchus (Fig. 1.15 and 2.5). Rarely, the right or left pulmonary artery anomalously arises from the ascending aorta. In contrast, the smaller bronchial arteries originate from the descending thoracic aorta, often form several branches, and course along the major bronchi to enter the lungs. Systemic collateral arteries usually have a similar origin and distribution.

Truncus Arteriosus

The TA represents a common vessel that has not divided into the ascending aorta and main pulmonary artery. Accordingly, it gives rise to the coronary, systemic, and pulmonary circulations. In patients with pulmonary atresia and a ventricular septal defect, in whom no remnant of the main pulmonary artery can be identified, the single artery that emanates from the heart is an aorta and not a common TA, because the right and left pulmonary arteries do not originate from it.

Ductus Arteriosus

Embryologically, the ductus arteriosus is bilateral. The left-sided structure is simply referred to as the ductus arteriosus. It travels between the most proximal portion of the left pulmonary artery and the undersurface of the aortic arch. In the setting of a left aortic arch, a right-sided ductus arteriosus, if present, will connect the proximal portion of the right subclavian artery to the right pulmonary artery. For a right aortic arch with mirror-image brachiocephalic branching, the opposite applies. A ductus arteriosus is not tortuous and does not form branches.

POSITIONS OF CARDIAC SEGMENTS

Once the cardiac segments are defined morphologically, their spatial orientations are next recorded. Three segments are evaluated: atria, ventricles, and great arteries. The positions of the atrioventricular and semilunar valves are addressed later when segmental connections are evaluated.

Atria

The spatial relationship between the atria is important because the position of the morphologic right atrium determines cardiac sidedness (Figs. 2.3 and 2.4). If the right atrium is right-sided, then the cardiac situs is normal, or solitus. On the other hand, if it is left-sided, then the situs is mirror-image, or inversus.

Ventricles

The location of the ventricles is determined by the position of the cardiac apex and the plane of the ventricular septum. In hearts with a leftward apex, the two ventricles occupy right-anterior and left-posterior positions. Conversely, with a rightward apex, they are usually right-posterior and left-anterior. A midline apex is generally characterized by a vertical midline septum with side-by-side ventricles.

For hearts with univentricular atrioventricular connections and a hypoplastic right ventricle, the ventricular septum is often tilted midway between vertical and horizontal. Rarely, the septum is horizontal, resulting in superoinferior ventricles (upstairs-downstairs), with the morphologic right ventricle on top. Finally, in crisscross hearts with twisted atrioventricular connections, the ventricular septum may also acquire a partial

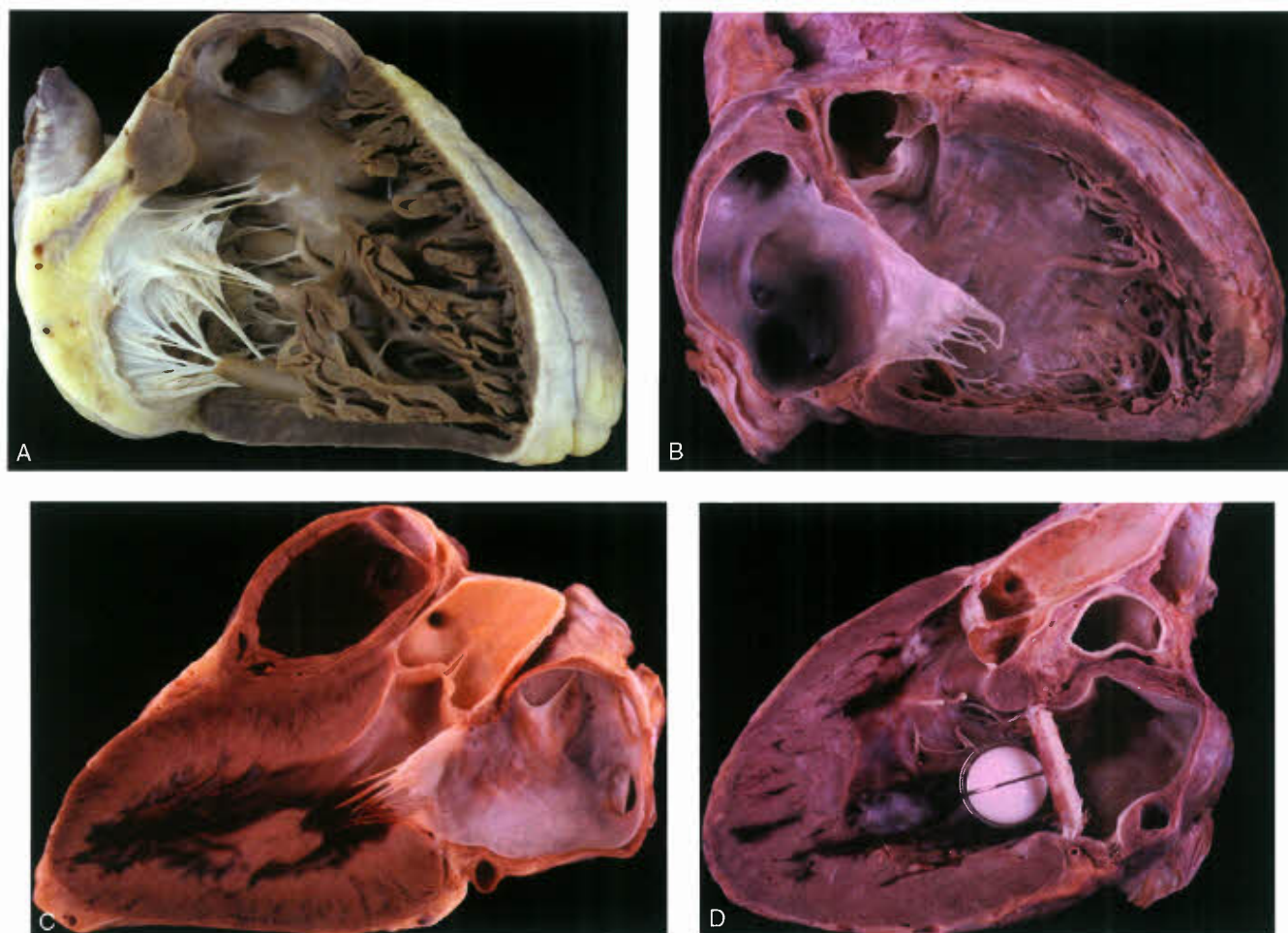


Figure 2.11. Ventricular sidedness. A, B: Right-sided ventricles. A normal right-sided morphologic right ventricle has been dissected by removal of its free wall (A). A mirror-image right-sided morphologic left ventricle is shown from a patient with atrioventricular discordance (B). C, D: Similar views are provided of a normal morphologic left ventricle (C), and a mirror-image left-sided morphologic right ventricle from a patient with atrioventricular discordance who underwent tricuspid valve replacement (D).

spiral twist, such that the relative positions of the ventricular chambers change as one travels from the cardiac base toward the apex.

In each of the aforementioned positions, the ventricles may be normal or mirror image in morphology. Mirror-image ventricles have also been referred to by various researchers as L-loop ventricles, ventricular situs inversus, or ventricular inversion (Fig. 2.11) (3).

Great Arteries

The position of the ascending aorta is generally described in relation to the main pulmonary artery (Fig. 2.12). Normal hearts are characterized by a right-posterior aorta. Abnormalities in aortic position are important to assess because each generally occurs in only a limited number of conditions. For the vast majority of malformed hearts, the aortic position is either normal or occupies a position that is dextroposed, right lateral, right anterior, or left anterior (Fig. 2.13). Only rarely are other positions encountered.

A slightly anterior shift of the aorta, to a position midway between right posterior and right lateral, is termed

dextroposition of the aorta (in contrast to dextroposition of the entire heart) and is commonly encountered in tetralogy of Fallot, double-outlet right ventricle, and atrioventricular septal defects. A right-anterior aorta is most frequently associated with complete transposition of the great arteries, and a left-anterior aorta most often occurs in patients with either congenitally corrected transposition of the great arteries or a double-inlet left ventricle.

CONNECTIONS OF CARDIAC SEGMENTS

Once the morphology and positions of the cardiac segments are determined, the manner in which they join to one another can be evaluated. Connections exist at three levels: venoatrial, atrioventricular, and ventriculoarterial. Abnormal venoatrial connections are related to malformations involving the sinus venosus, common pulmonary vein, and their derivatives.

In contrast, cardiac valves form the mortar that connects atria to ventricles and ventricles to great arteries. These connections, however, do not necessarily imply patency for blood flow. For example, in aortic atresia, identification of

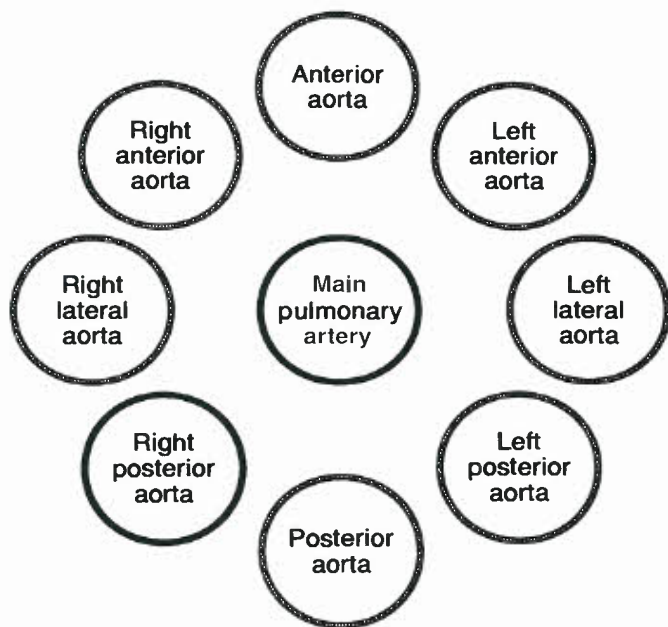


Figure 2.12. The possible positions of the ascending aorta relative to the main pulmonary artery are shown schematically, as viewed from below (from apex toward base).

an imperforate valve between the left ventricle and the ascending aorta is indicative of a concordant connection, despite the fact that blood does not flow between the two. The presence of overriding valves can interfere with the determination of atrioventricular and ventriculoarterial connections, as discussed below.

Venoatrial Connections

Normally, the superior and inferior venae cavae and the coronary sinus connect to the morphologic right atrium and the pulmonary veins join the morphologic left atrium. Anomalies may involve the systemic veins, pulmonary veins, or both, and they can involve all or only some of the veins. Consequently, the connection of each venous structure should be evaluated separately.

Atrioventricular Connections

Only four possible modes of atrioventricular connection exist: concordance, discordance, univentricular, and ambiguous (Figs. 2.4B, 2.14, and 2.15). The univentricular connections, in turn, include three subtypes: double inlet, single inlet, and common inlet.

If an atrioventricular valve is atretic, it is important to distinguish between the presence of an imperforate fibrous membrane, in which the connection can be determined, and absence of the atrioventricular connection on that side of the heart. Most cases of tricuspid atresia, for example, are characterized by an absent right atrioventricular connection rather than by an identifiable valvular plug. By clinical imaging, the membranous septum should not be misinterpreted as an imperforate tricuspid valve.

Concordance and Discordance

Concordance denotes the normal state and indicates that the morphologic right atrium is connected to the morphologic

right ventricle and that the left atrium is connected to the left ventricle. In contrast, connection of the right atrium to the left ventricle and of the left atrium to the right ventricle constitutes atrioventricular discordance, which corresponds to ventricular inversion or L-loop ventricles.

Univentricular Atrioventricular Connections

When both atria are joined to only one ventricle, the connection is univentricular, and three variants are recognized: double-inlet ventricle, in which two atrioventricular valves are present; single-inlet ventricle, in which only one valve is present and there is no grossly identifiable remnant of the other valve; and common-inlet ventricle, in which a common atrioventricular valve connects both atria to only one ventricle. Thus, it is the connection, and not the heart, that is univentricular.

Ambiguous Atrioventricular Connection

With either right or left cardiac isomerism, the atrioventricular connection, by definition, is ambiguous or mixed. In the setting of right isomerism, for example, the right-sided morphologic right atrium might be connected to a morphologic right ventricle (concordance), and the left-sided morphologic right atrium would then join a morphologic left ventricle (discordance). For complex cases such as this, a description of the atrioventricular connection is recommended.

Ventriculoarterial Connections

Like connections at the atrioventricular level, those at the ventriculoarterial level are limited in number. Possibilities include concordance, discordance, and double, single, and common outlets (Figs. 2.16 and 2.17). Occasionally, with an atretic pulmonary or aortic valve, the ventricle to which the corresponding great artery is connected cannot be distinguished with certainty, and the ventriculoarterial connection is considered indeterminate.

Concordance and Discordance

Concordance refers to the normal state, in which the morphologic right ventricle is connected to the pulmonary artery and the morphologic left ventricle is linked to the aorta. By comparison, discordance corresponds to right ventricular origin of the aorta and left ventricular origin of the pulmonary artery and is synonymous with transposition of the great arteries.

When the atrioventricular connection is concordant and the ventriculoarterial connection is discordant, the malformation is called complete transposition, which results in complete separation of the systemic and pulmonary circulations, except at the sites of shunts. In contrast, congenitally corrected transposition is characterized by ventriculoarterial discordance and atrioventricular discordance, which results in normal blood flow but a systemic workload on the morphologic right ventricle. Because the term great vessels refers to either the great arteries or the great veins, use of the term great arteries is favored for the transposition complexes.

Double, Single, and Common

When both great arteries emanate from only one ventricular chamber, the ventriculoarterial connection is considered double outlet. It is important to recognize that a double-outlet connection is not synonymous with the diagnostic entity known as double-outlet right ventricle. This form of connection includes not only double-outlet right ventricle but also double-outlet left ventricle and most cases of tetralogy of Fallot.

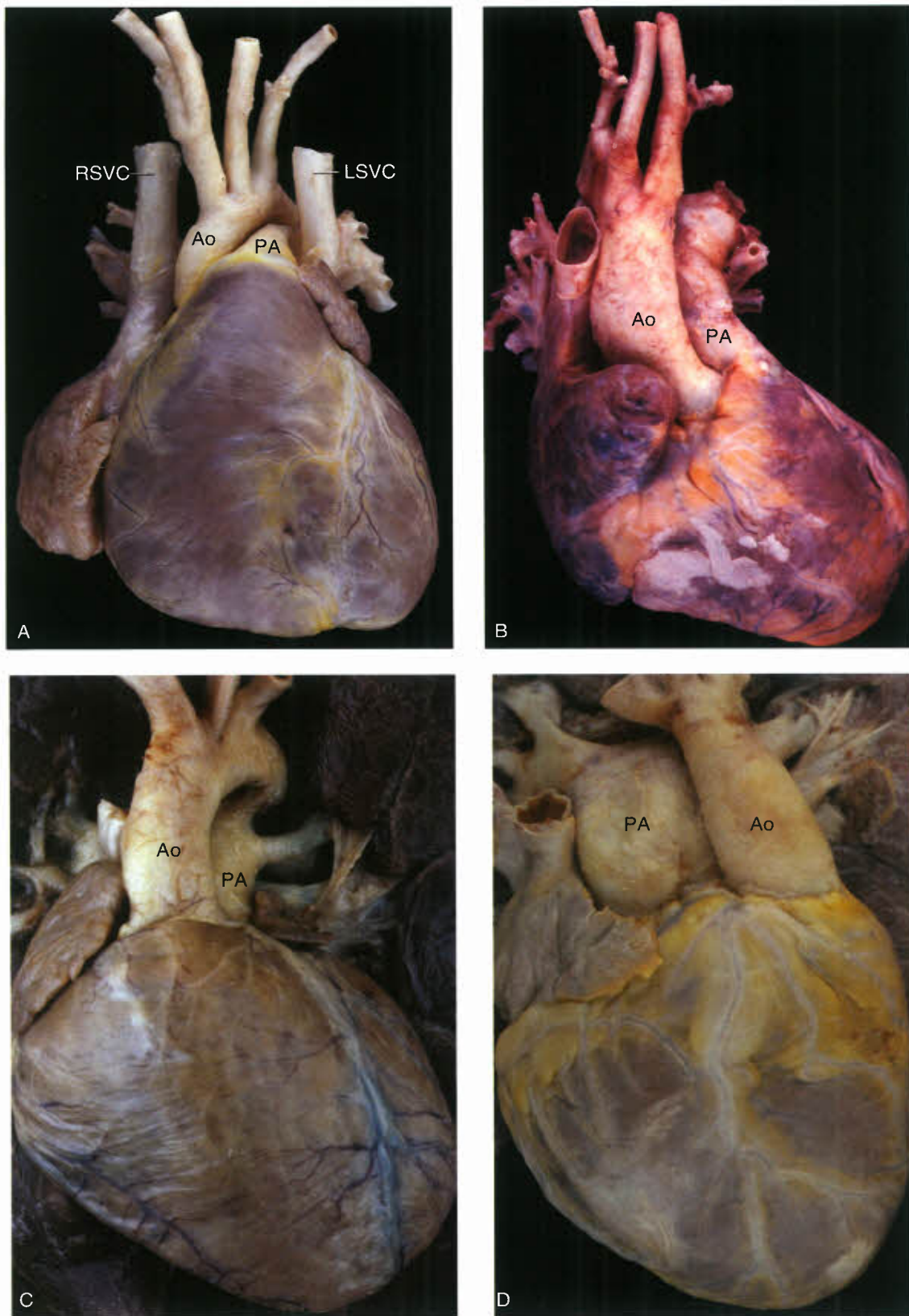


Figure 2.13. Aortic positions in four types of congenital heart disease. **A:** The aortic position is normal in this example of supra-ventricular aortic stenosis with bilateral superior venae cavae. **B:** A right lateral aorta is associated with tetralogy of Fallot and a right aortic arch with mirror-image brachiocephalic branching. **C:** The aorta is right-anterior in this case of complete transposition of the great arteries. **D:** The aortic position in this patient is left-anterior and is associated with a double-inlet left ventricle. (See Appendix 1.1 at <http://solution.lww.com> for abbreviations.)

Figure 2.14. The six possible atrioventricular connections are shown schematically. **Upper panel:** Concordance is synonymous with the normal state, and discordance is synonymous with ventricular inversion. For either right or left cardiac isomerism, the atrioventricular connection is always ambiguous. **Lower panel:** There are three possible univentricular atrioventricular connections: double inlet, single inlet, and common inlet. (See Appendix 1.1 at <http://solution.lww.com> for abbreviations.)

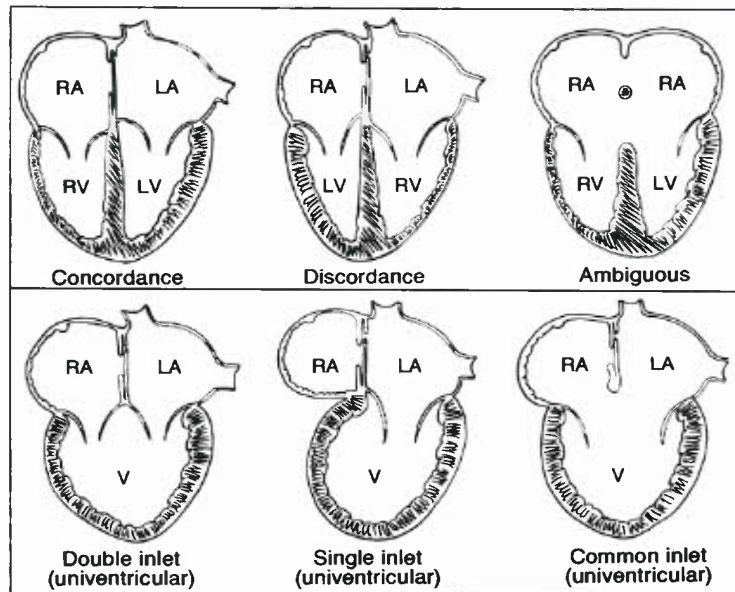
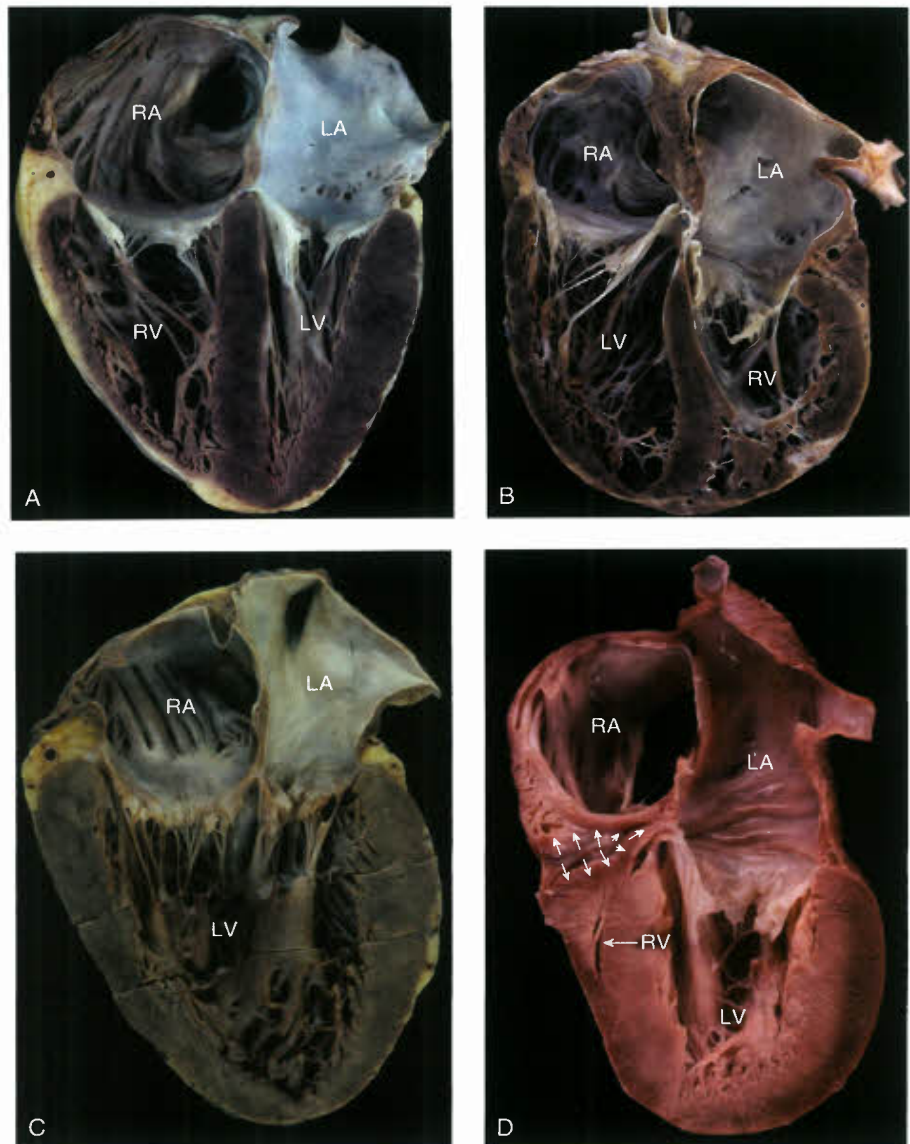


Figure 2.15. Four types of atrioventricular connection, shown in a four-chamber (or three-chamber) format. **A:** Concordance. **B:** Discordance. **C:** Double-inlet left ventricle. **D:** Tricuspid atresia with single-inlet left ventricle and absent right atrioventricular connection (arrows). (See Appendix 1.1 at <http://solution.lww.com> for abbreviations.)



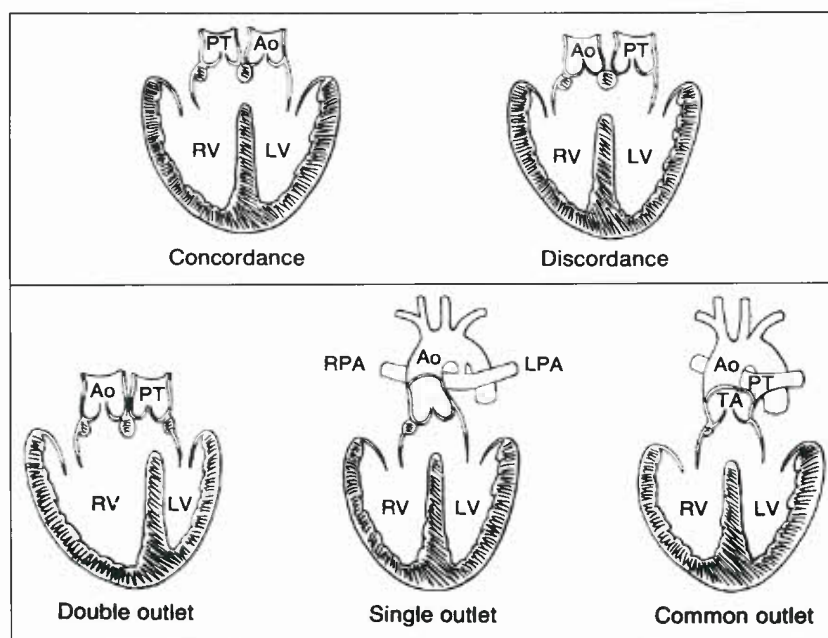


Figure 2.16. The five possible ventriculoarterial connections are shown schematically. **Upper panel:** Concordance indicates the normal state, and discordance is synonymous with transposition of the great arteries. **Lower panel:** There are three other possible connections: double outlet, which usually involves a right ventricle; single outlet, which includes pulmonary atresia with ventricular septal defect; and common outlet, which represents TA. (See Appendix 1.1 at <http://solution.lww.com> for abbreviations.)

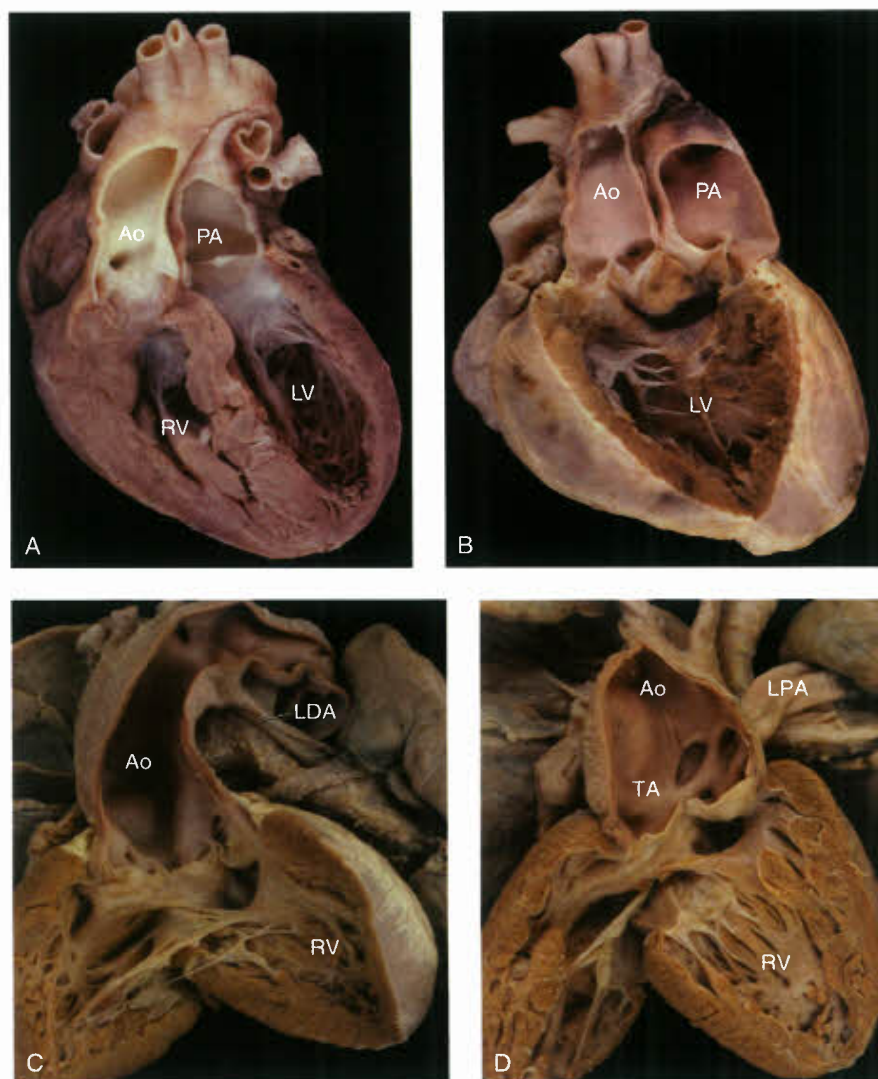


Figure 2.17. Four types of ventriculoarterial connection, viewed anteriorly. **A:** Discordance, in complete transposition of the great arteries. **B:** Double-outlet connection, in double-outlet right ventricle. **C:** Single-outlet connection, in pulmonary atresia with a ventricular septal defect and ductal origin of the pulmonary arteries. **D:** Common-outlet connection, in TA. (See Appendix 1.1 at <http://solution.lww.com> for abbreviations.)

Morphologic criteria exist to distinguish tetralogy of Fallot from cases of double-outlet right ventricle with subpulmonary stenosis and a subaortic ventricular septal defect. Interestingly, patients with tetralogy of Fallot and a complete atrioventricular septal defect usually have Down syndrome and a low surgical mortality rate, whereas those with double-outlet right ventricle and a complete atrioventricular septal defect characteristically have atrial isomerism and a high surgical mortality rate.

Among patients with pulmonary atresia and a ventricular septal defect, there exists a group in whom no remnant of the pulmonary valve or proximal portion of the pulmonary artery can be identified. As a result, only the aorta arises from the ventricles, constituting a single-outlet ventriculoarterial connection. In general, this situation does not pertain to aortic valve atresia because the ascending aorta, although hypoplastic, must remain patent to provide coronary blood flow, thus allowing its ventricular connection to be readily determined.

A common-outlet connection is characteristic of TA, in which this vessel represents the undivided aortic and pulmonary roots. Although hearts with single-outlet and common-outlet connections are quite similar, only in the setting of TA do the pulmonary arteries arise proximally from this vessel rather than from the ductus arteriosus or systemic collateral arteries.

Overriding and Straddling Valves

Definition of Overriding Valves

Overriding may be defined as biventricular emptying of an atrioventricular valve or biventricular origin of a semilunar valve.

It is a property of the valve annulus and is always associated with a malalignment ventricular septal defect. The presence of annular overriding may interfere with accurate determination of cardiac connections. As a further complication in living patients, the extent of overriding may vary throughout the cardiac cycle and may appear to vary with different angles of view.

Malalignment

For overriding atrioventricular valves, the atrial and ventricular septa are malaligned. This may represent a lateral shift, a rotational shift, or a combination of the two (Fig. 2.18). The ventricular septal defect tends to involve the basal portion of the inlet septum. For the assessment of atrioventricular connections, an atrium is considered to join the ventricle into which >50% of the valve orifice empties (Fig. 2.19). A common atrioventricular valve is usually associated with concordant or discordant connections, although a common-inlet arrangement applies if >75% of the valve orifice empties into only one of the two ventricles.

Overriding of the semilunar valves is associated with malalignment of the outlet septum relative to the remainder of the ventricular septum. Malalignment can be lateral, rotational, or a combination of these (Figs. 2.18 and 2.20). The ventricular septal defect is located beneath the overriding artery and is either membranous or outlet in location, or a combination of the two. As with the atrioventricular valves, the 50% rule also applies to the semilunar valves (Fig. 2.21).

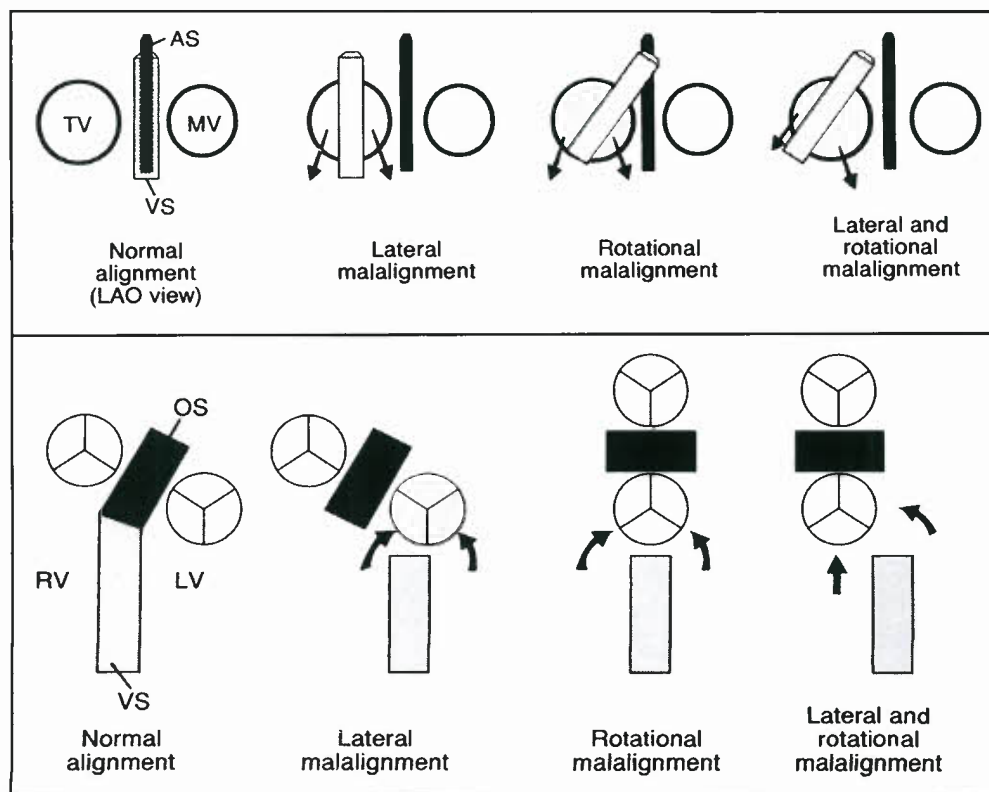


Figure 2.18. The types of annular overriding and septal malalignment are illustrated schematically. **Upper panel:** Atrioventricular valves are shown, with lateral and rotational malalignments between the atrial and ventricular septa. **Lower panel:** Semilunar valves are shown, with lateral and rotational malalignments between the ventricular and outlet septa. (See Appendix 1.1 at <http://solution.lww.com> for abbreviations.)

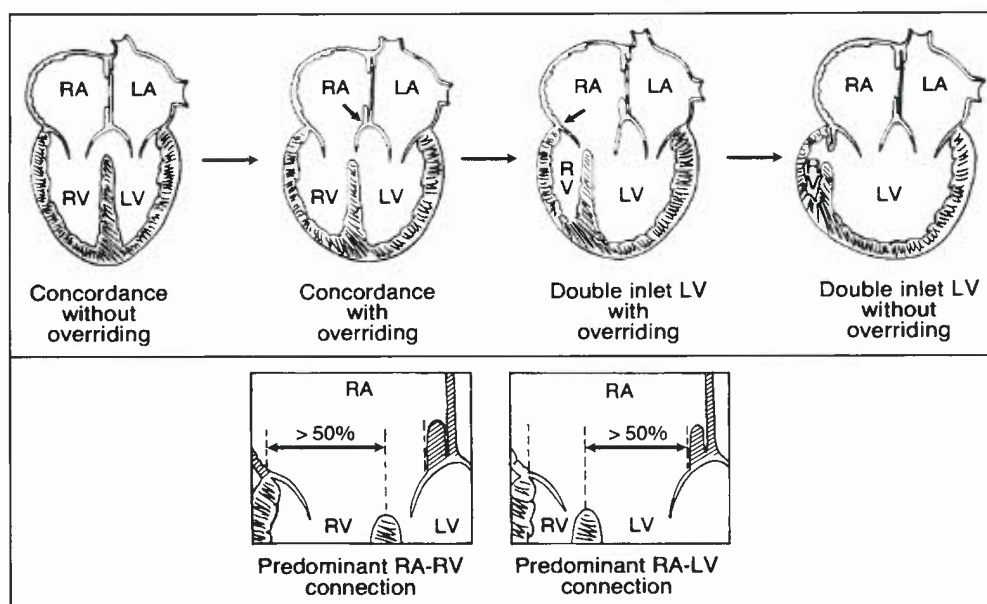


Figure 2.19. The effect of overriding atrioventricular valves on the determination of atrioventricular connections. **Upper panel:** With progressive leftward shifting of the atrial septum, the connections change from concordant to double-inlet left ventricle. **Lower panel:** The two insets illustrate the 50% rule. (See Appendix 1.1 at <http://solution.lww.com> for abbreviations.)

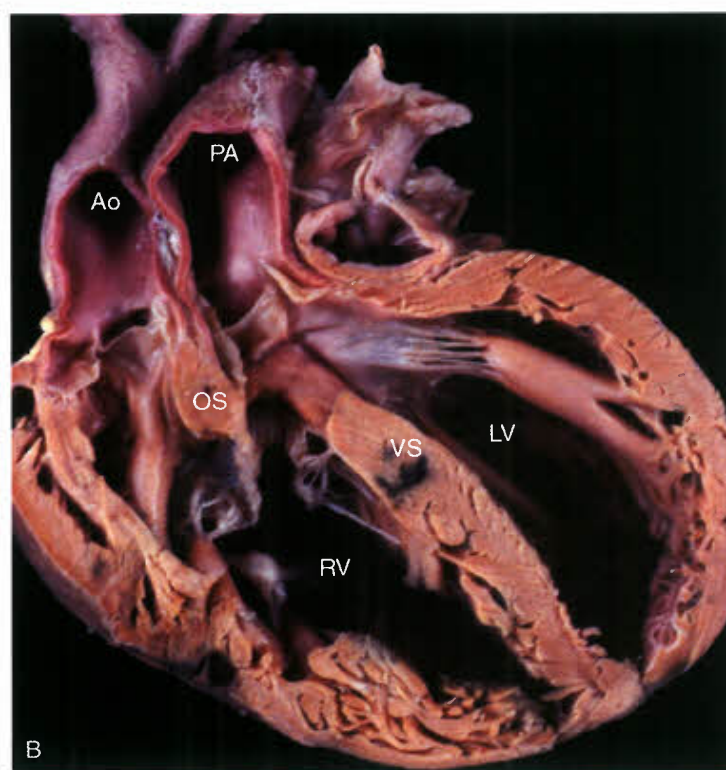
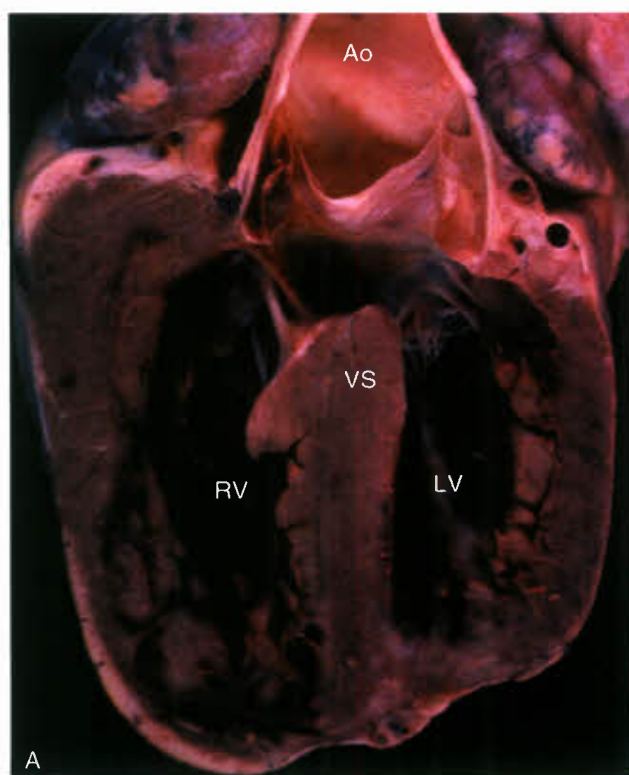
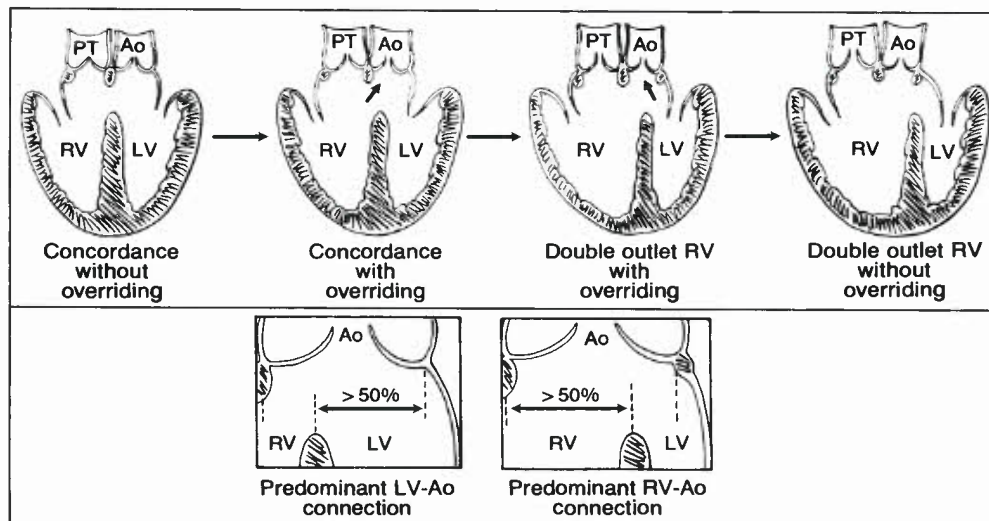


Figure 2.20. Overriding semilunar valves, in two cardiac specimens. **A:** An overriding aortic valve in tetralogy of Fallot. **B:** An overriding pulmonary valve in complete transposition of the great arteries. (See Appendix 1.1 at <http://solution.lww.com> for abbreviations.)

Figure 2.21. The effect of overriding semilunar valves on the determination of ventriculoarterial connections. **Upper panel:** With progressive rightward shifting of the outlet septum, the connection changes from concordant to double-outlet right ventricle. **Lower panel:** The two insets illustrate the 50% rule. (See Appendix 1.1 at <http://solution.lww.com> for abbreviations.)

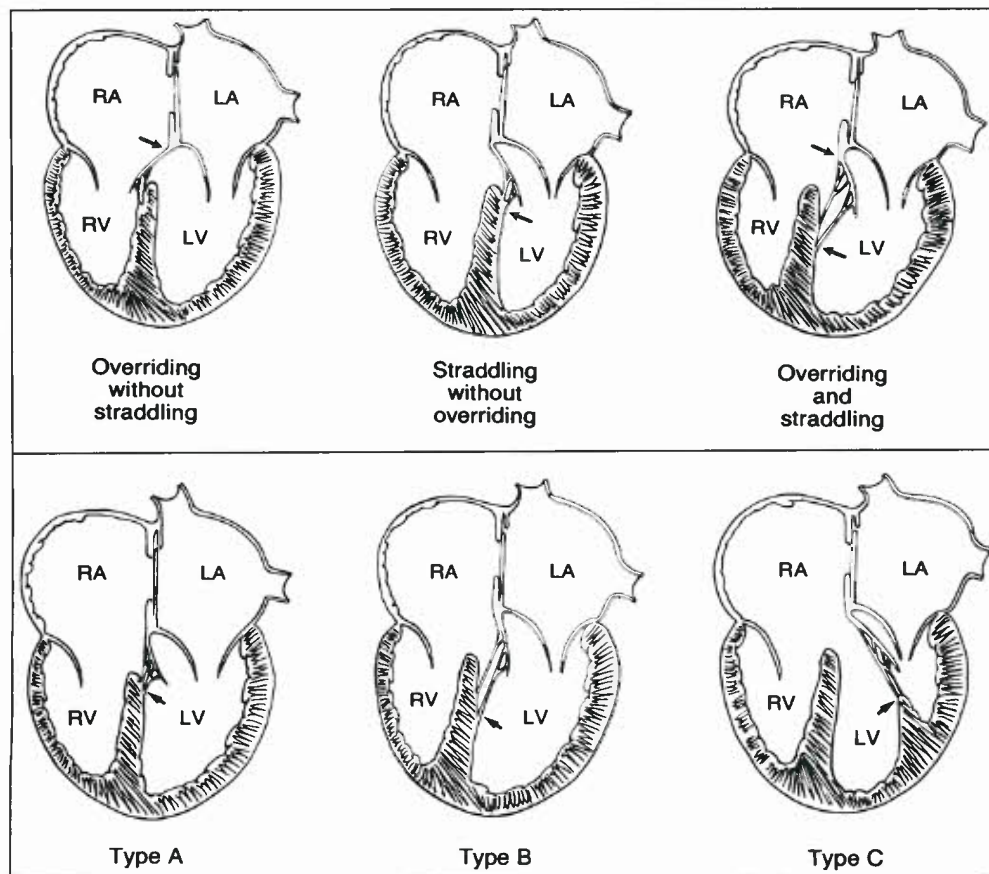


Definition of Straddling Valves

In contrast to annular overriding, *straddling* involves the anomalous insertions of chordae tendineae (tendinous cords) or papillary muscles into the contralateral ventricle (Figs. 2.22 and 2.23). Thus, straddling involves only the atrioventricular

valves and requires the presence of a ventricular septal defect. Although straddling does not affect the evaluation of atrioventricular connections, it is important that it be identified preoperatively because its presence may preclude certain types of surgical repair or may necessitate valve replacement. Cordal straddling may occur alone or in conjunction with annular overriding.

Figure 2.22. Overriding and straddling atrioventricular valves are shown schematically. **Upper panel:** Overriding and straddling are compared (see text for definitions). **Lower panel:** The three types of straddling are determined by the sites or cordal insertion into the contralateral ventricle along the crest (type A) or body (type B) of the ventricular septum, or onto the ventricular free wall (type C). (See Appendix 1.1 at <http://solution.lww.com> for abbreviations.)



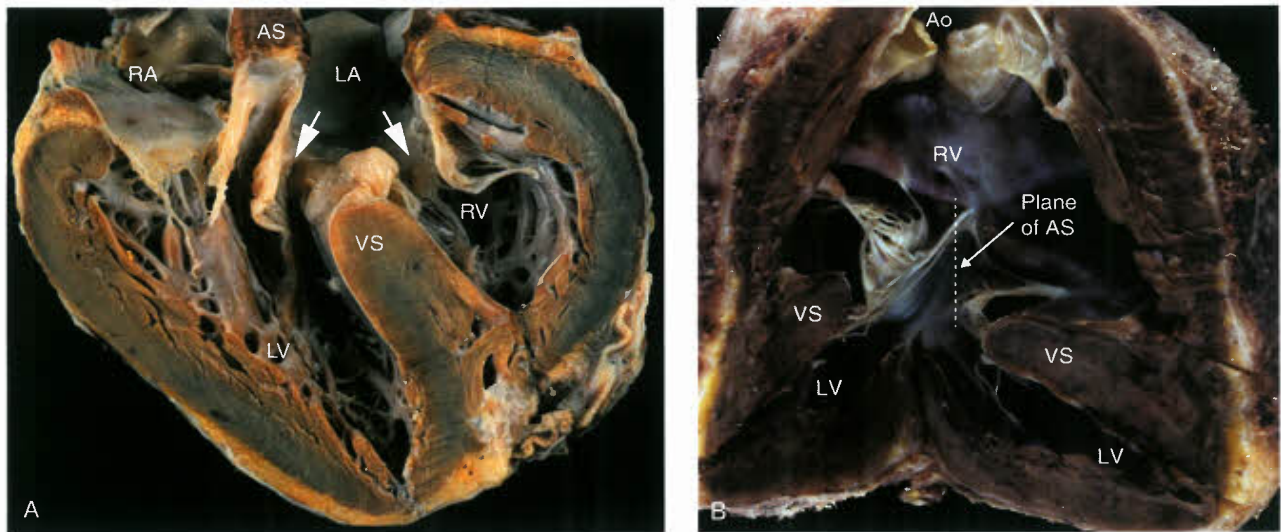


Figure 2.23. Overriding and straddling atrioventricular valves in two specimens. **A:** Straddling without overriding of the left-sided tricuspid valve (arrows) in a heart with atrioventricular discordance. **B:** Overriding and straddling of both atrioventricular valves is associated with rotational malalignment of the atrial and ventricular septa in a case of superoinferior ventricles with a horizontal ventricular septum. (See Appendix 1.1 at <http://solution.lww.com> for abbreviations.)

REFERENCES

1. Peacock TB. *On Malformations of the Human Heart*. London, UK: John Churchill, 1858.
2. Abbott ME. *Atlas of Congenital Cardiac Disease*. New York, NY: American Heart Association, 1936.
3. Van Praagh R. Diagnosis of complex congenital heart disease: morphologic-anatomic method and terminology. *Cardiovasc Intervent Radiol* 1984;7:115–120.
4. Anderson RH, Becker AE, Freedom RM, et al. Sequential segmental analysis of congenital heart disease. *Pediatr Cardiol* 1984;5:281–288.
5. Van Praagh R. The segmental approach to diagnosis in congenital heart disease. *Birth Defects* 1972;8:4–23.
6. de la Cruz MV, Nadal-Ginard B. Rules for the diagnosis of visceral situs, truncoconal morphologies and ventricular inversions. *Am Heart J* 1972;84:19–32.
7. Edwards WD. Congenital heart disease. In: Schoen FJ, ed. *Interventional and Surgical Cardiovascular Pathology: Clinical Correlations and Basic Principles*. Philadelphia, PA: WB Saunders, 1989:281–367.
8. Anderson C, Devine WA, Anderson RH, et al. Abnormalities of the spleen in relation to congenital malformations of the heart: a survey of necropsy findings in children. *Br Heart J* 1990;63:122–128.
9. Van Praagh R, Van Praagh S. Atrial isomerism in the heterotaxy syndromes with asplenia, or polysplenia, or normally formed spleen: an erroneous concept. *Am J Cardiol* 1991;66:1504–1506.
10. Macartney FJ, Partridge JB, Shinebourne EA, et al. Identification of atrial situs. In: Anderson RH, Shinebourne EA, eds. *Paediatric Cardiology* 1977. Edinburgh, UK: Churchill Livingstone, 1978:16–26.
11. Sharma S, Devine W, Anderson RH, et al. The determination of atrial arrangement by examination of appendage morphology in 1842 autopsied specimens. *Br Heart J* 1988;60:227–231.
12. Van Praagh R, David I, Van Praagh S. What is a ventricle? The single ventricle trap. *Pediatr Cardiol* 1982;2:79–84.
13. Anderson RH, Macartney FJ, Tynan M, et al. Univentricular atrioventricular connection: the single ventricle trap unsprung. *Pediatr Cardiol* 1983;4:273–280.
14. Van Mierop LHS. Diagnostic code for congenital heart disease. *Pediatr Cardiol* 1984;5:331–362.
15. Van Praagh R, Van Praagh S. Embryology and anatomy: keys to the understanding of complex and congenital heart disease. *Coeur* 1982;13:315–336.

Development of Myocardial Structure and Function

Pamela A. Lucchesi ■ Kirk R. Hutchinson ■ Luciana Martins ■ Loren E. Wold

The structure and function of the myocardium undergoes dynamic changes during fetal life and in postnatal maturation to adulthood. These processes are regulated by a number of hormones, neurotransmitters, growth factors, and mechanical forces. The development of the coronary circulation is tightly coordinated with myocardial growth to ensure an adequate supply of oxygen and metabolic substrates. A complete understanding of the physiologic processes that regulate myocardial structure and function is a necessary prerequisite to understand the pathogenesis of congenital and acquired heart disease. This chapter describes the developmental changes in cardiac structure and excitation–contraction (E–C) coupling along with cell–cell and cell–matrix interactions at the cellular and tissue levels. Postnatal changes in autonomic innervation are summarized. The effects of these changes on myocardial systolic and diastolic dysfunction are also discussed.

It is important to note that the majority of studies on developmental changes in myocardial structure and function have been performed in zebra fish, chick embryos, and rodents, with some additional data taken from higher mammals and humans. While the process of E–C coupling is very similar, there is significant spatiotemporal variability in structural development across mammalian species. Unless otherwise noted, the majority of the developmental changes described in this chapter focus on data from rodent models and humans. Second, most of our understanding of developmental changes in myocardial structure and function is limited to the left ventricle (LV), especially during the postnatal period. Finally, many important concepts and molecular mechanisms have been omitted because they are beyond the scope of this chapter.

MYOCARDIAL STRUCTURE

The heart is a complex organ composed of multiple cell types that can be grouped into conducting, supporting, and functional cells (Fig. 3.1). The cellular constituents of the heart include cardiac myocytes, cardiac fibroblasts, endothelial cells, and vascular smooth muscle cells. The conducting cells are mainly Purkinje fibers that propagate the action potential from the atrium to the ventricle. Purkinje fibers are responsible for rapid communication and propagation of the signal throughout the heart. While cardiac myocytes are responsible for the mechanical function of the heart, they comprise only approximately 30% of the total number of cells. Cardiac fibroblasts predominate in conferring structural integrity to the heart (1). Dynamic cross talk between cardiac myocytes and cardiac fibroblasts plays a crucial role in myocardial development and structural remodeling.

CARDIAC FIBROBLASTS AND THE EXTRACELLULAR MATRIX

The cardiac fibroblast is the most abundant noncardiac myocyte cell type present within the postnatal mature heart. Cardiac fibroblasts play an extensive role in cardiac development and remodeling. They are the main cell types responsible for the deposition of extracellular matrix (ECM) proteins and also dynamically remodel the ECM through the secretion of matrix metalloproteinases and their tissue inhibitors. Fibroblasts also act as a source of growth factors, mitogens, and cytokines that signal to neighboring myocytes. Cardiac fibroblasts are derived from different cell lineages at different developmental stages. During embryonic development, they are mesenchymal in origin and are derived from the proepicardial organ. Fibroblasts also arise from the differentiation of bone-marrow-derived circulating fibrocytes (2). In the neonatal and adult heart, cardiac fibroblasts arise from resident cells via epithelial–mesenchymal transformation and from bone-marrow-derived cells (3).

The ECM provides structural support to the heart, facilitates mechanical and chemical signaling during myocardial development, and helps to maintain normal homeostasis in the adult heart in response to physiologic stressors and injury. Components of the ECM include interstitial collagens, elastin, fibronectin, proteoglycans, glycoproteins, cytokines, growth factors, and proteases. The most abundant extracellular collagens are the fibrillar collagens, type I and III. Elastic fibers are present in close association to collagen and are responsible for maintaining normal elasticity of the cellular framework. Fibronectin influences cellular properties, including cellular growth. Proteoglycans and glycoproteins appear to play a role in signaling and ECM turnover and serve as a reservoir for latent growth factors (e.g., transforming growth factor (TGF)- β , epidermal growth factor).

The collagen network of the myocardium begins forming during fetal development (3). Cardiac fibroblasts become enmeshed in this network, which allows them to contract the endomysial collagen, exerting mechanical force on the myocytes (Fig. 3.2). In addition, this organization allows fibroblasts to maintain structural integrity of the heart through cell–cell and cell–ECM interactions, as well as through proliferation and ECM degradation and synthesis. In the adult myocardium, this network includes the epimysium that surrounds large groups of muscle fibers, the perimysium arising from the epimysium that surrounds smaller groups of muscle fibers, and the endomysium that tethers individual fibers to each other and the adjacent vasculature (4,5). In addition to acting as scaffolding for cells and vessels, the collagen network also coordinates the delivery of force generated by myocytes, serving as a viscoelastic medium facilitating compression and recoil properties of the tissue (6).

Cardiac fibroblasts are regulated by mechanical and molecular signals during cardiac development. Mechanical

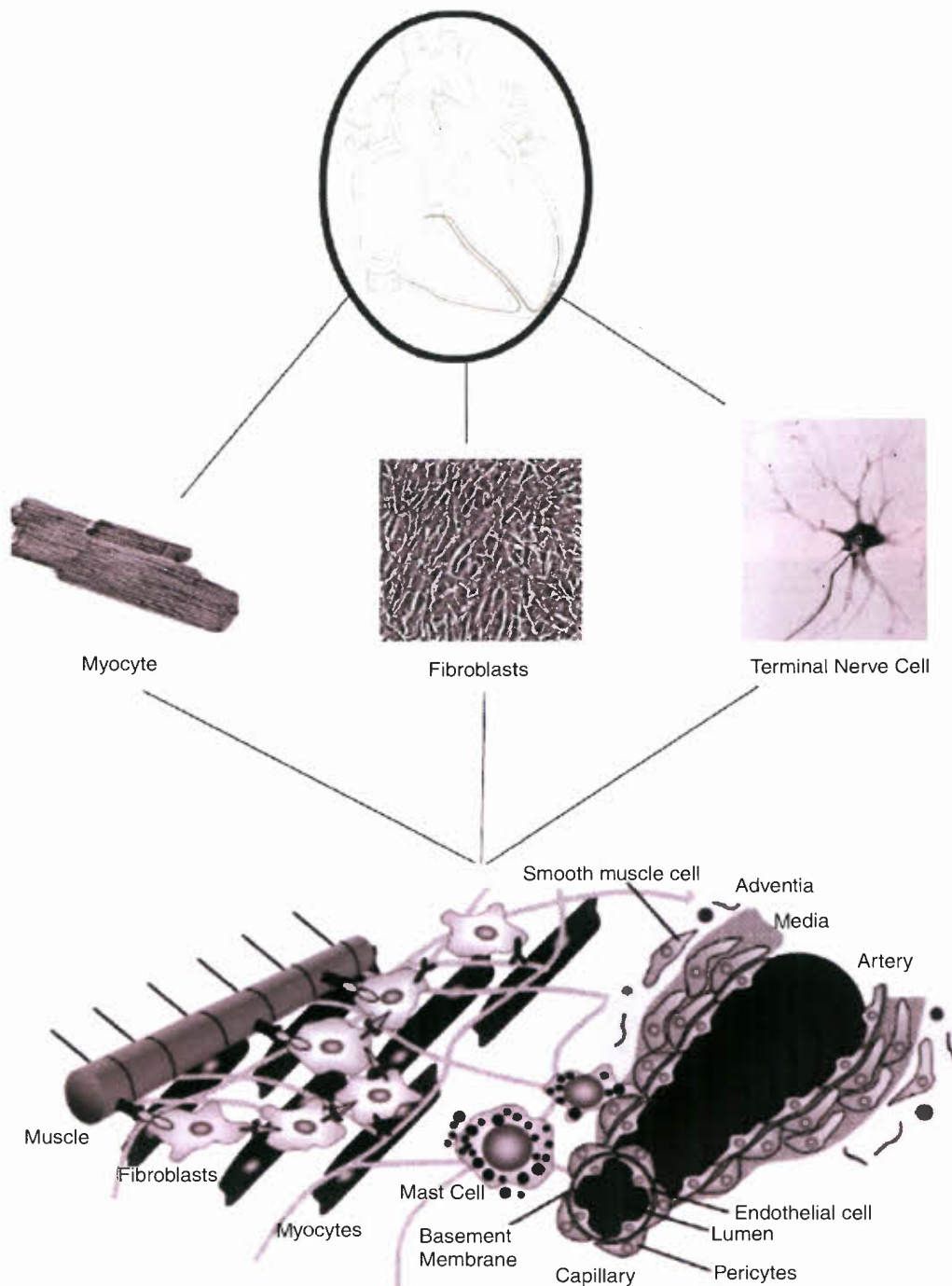


Figure 3.1. Schematic representation of the major cell types of the heart, including myocytes, fibroblasts, blood vessels, and nerve terminals. (Modified from Baudino T.A., et al. Cardiac fibroblasts: friend or foe? *Am J Physiol Heart Circ Physiol* 2006;291:H1015-H1026.)

stimulation of fibroblasts causes a marked increase in integrin receptors and secretion of ECM proteins, cytokines, and growth factors. Angiotensin, endothelin, and TGF- β also stimulate matrix deposition, while the inflammatory cytokines such as interleukin 1- β and tumor necrosis factor- α inhibit matrix deposition and promote matrix degradation by matrix metalloproteinases (7).

Basement Membrane

A specialized area of the matrix termed the basement membrane or basal lamina surrounds all cells in the myocardium except

cardiac fibroblasts. The primary components of the basal lamina are laminin, type IV collagen, and the proteoglycan perlecan. Type IV collagen assembles into a sheet-like mesh and provides tensile strength. Type IV collagen is coated by perlecan that binds to integrins and dystroglycans on the plasma membrane to stabilize the basement membrane structure against mechanical forces. Perlecan is expressed at high levels throughout embryogenesis in the heart where it is required to ensure mechanical stability until cell-cell contacts have formed and matured (8). Cardiac deletion of perlecan encoded by *HSPG2* in mice is lethal to the embryo due to basement membrane deterioration, blood leakage into the myocardium, and cardiac asystole (9).

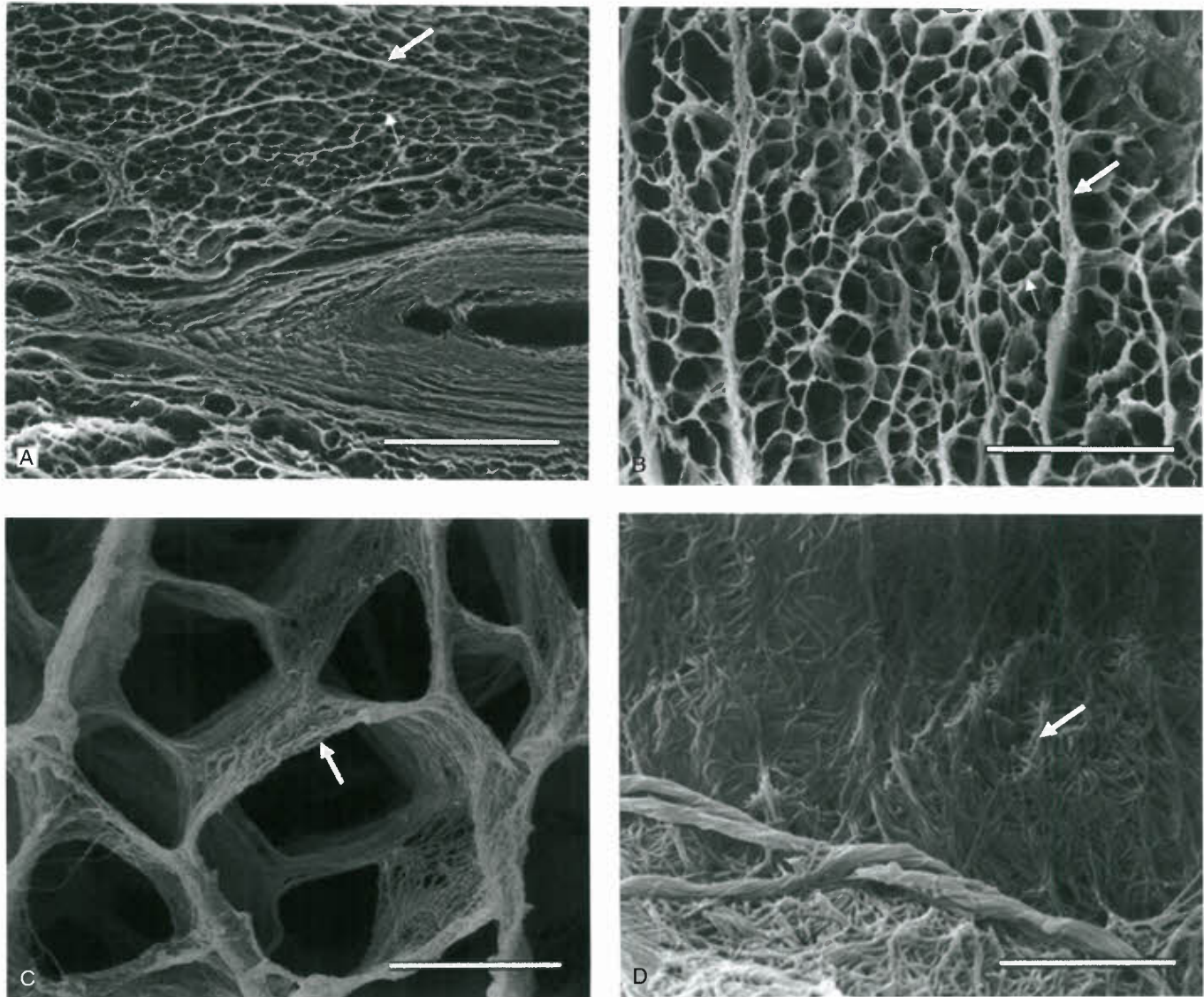


Figure 3.2. Connective tissues of the human heart (transverse section). **A:** The collagen network around cardiomyocytes and small vessels is clearly observed. *Thick arrow:* perimysium; *thin arrow:* endomysium). **B:** The interstitial connective tissue consisting of perimysial and endomysial components presents a honeycomb shape. The perimysium (*thick arrow*) surrounds groups of cardiomyocytes, and the endomysium (*thin arrow*) surrounds each cardiomyocyte. **C:** The endomysium supports and connects individual cardiomyocyte fascicles. **D:** At higher magnification, collagen fibers show interconnections on the surface of cardiomyocytes. Thin collagen strands are probably collagen III (*arrow*). Scale bar = 3 μm ; magnification $\times 10,000$. (From Kanzaki Y, Terasaki F, Okabe M, et al. Three-dimensional architecture of cardiomyocytes and connective tissue in human heart revealed by scanning electron microscopy. *Circulation* 2010;122:1973–1974, with permission.)

CARDIAC MYOCYTES

Cardiac myocytes have two major mechanistic functions: force generation by myofibrils in response to E–C coupling and force transmission across cell bundles mediated by the integration of electromechanical signals at the intercalated disc. Myocytes also communicate with the ECM and other cardiac cells through costameres.

Plasma Membrane

The plasma membrane (or sarcolemma) is the region of the cell that contains ion pumps, channels, and exchangers that contribute

to action potential propagation as well as maintenance of proper ionic and chemical gradients. The flow of ions controlled by these proteins is essential for proper myocyte function and directly regulates cellular contraction and relaxation. Numerous G-protein-coupled receptors and cytokine and growth factor receptors are located on the plasma membrane and are responsible for transducing changes in the local neurohormonal milieu into intracellular signals that regulate cell growth and function.

Na⁺- and K⁺-ATPases and Exchangers

The Na⁺/K⁺-ATPase maintains the ionic gradient across the sarcolemmal membrane by pumping Na⁺ out of the cell and

K⁺ into the cell against their respective concentration gradients. Since under physiologic conditions, three Na⁺ are removed from the cell but only two K⁺ are taken up per pump cycle, the ATPase generates a small outward current. Both the maintenance of the ionic gradient and the electrogenic property of Na⁺/K⁺-ATPase are required to maintain resting Ca²⁺ levels (10).

The Na⁺/K⁺-ATPase is composed of α - and β -subunits. The α -subunit contains the binding sites for ATP, Na⁺, K⁺, and cardiac glycosides, and is thus largely responsible for the catalytic, transport, and pharmacologic characteristics of the ATPase. The smaller β -subunit modulates the transport characteristics of the ATPase and plays an important role in its proper membrane insertion (10). There are three Na⁺/K⁺ pump α -subunits in the heart that display similar ion affinities and ATPase activity, but different affinities for cardiac glycosides and distinct subcellular localizations. In the rodent heart, the low-digitalis affinity α_1 isoform predominates through all phases of development, while there is a postnatal transition from the neonatal α_3 isoform to the adult α_2 isoform that occurs within the second week of postnatal life (11). However, in humans, the α_1 isoform has high affinity for cardiac glycosides. Three different isoforms of the Na⁺/K⁺-ATPase in the adult human heart, $\alpha_1\beta_1$, $\alpha_2\beta_1$, and $\alpha_3\beta_1$, are expressed with different affinities for various cardiac glycosides (12). To date, there have been no human studies characterizing developmental changes in Na⁺/K⁺-ATPase isoform expression.

Na⁺/K⁺-ATPase activity indirectly regulates other plasma membrane transporters that require an inward Na⁺ gradient. The cardiac Na⁺/Ca²⁺ exchanger (NCX1) is the major Ca²⁺ extrusion mechanism in cardiac myocytes. It functions by utilizing the Na⁺ electrochemical gradient to mediate the electrogenic countertransport of three Na⁺ ions for one Ca²⁺ ion across the sarcolemmal membrane (13). This exchanger is bidirectional and capable of moving Ca²⁺ in either direction across the sarcolemma.

The plasma membrane also contains a high-affinity, low-capacity Ca²⁺-ATPase that extrudes Ca²⁺ from the cell in an ATP-dependent process. This pump functions as a fine-tuner of cell Ca²⁺, lowering it to the submicromolar level (14), thereby maintaining low amounts of intracellular Ca²⁺ during basal conditions.

Na⁺ Channels, Ca²⁺ Channels, and K⁺ Channels: The Cardiac Action Potential

Under resting conditions, the membrane potential (V_m) is set by the intracellular and extracellular concentrations of Na⁺ and K⁺ and the conductance properties of ion channels on the plasma membrane (Fig. 3.3). This equilibrium potential (voltage at which there is no net flow) for a single ion is described by the Nernst equation. In ventricular myocytes, the resting V_m (~−86 mV) is close to that predicted by the Nernst equations for K⁺ (15). In order to elicit an action potential, any electrical stimulus must depolarize the membrane to a threshold value (~−65 mV) – the lowest membrane potential that causes activation of voltage-sensitive Na⁺ channels.

Phase 0: The rapid depolarization phase and action potential amplitude is due to Na⁺ entry through voltage-sensitive Na⁺ channels encoded by the SCN5A gene. Once open, these channels rapidly inactivate at higher V_m and undergo a refractory period in which the channels become unresponsive to any further stimulation. This voltage-dependent activation and inactivation of the channel are important clinically since changes in its expression or gating properties can change action potential amplitude and durations, leading to arrhythmias (15). For

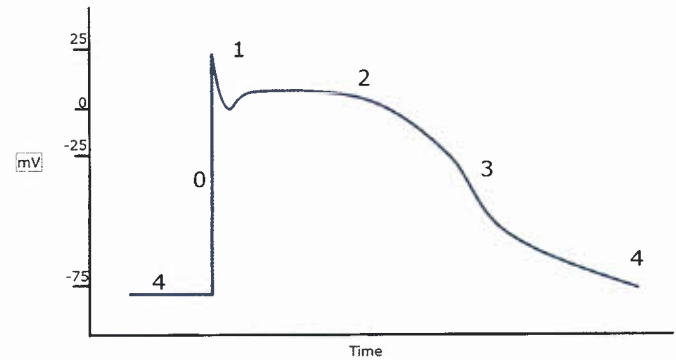


Figure 3.3. Schematic representation of the cardiac action potential.

example, gain-of-function mutants in SCN5A prolong the action potential duration and are one cause of long Q-T syndrome (16). Loss-of-function mutants decrease the inward Na⁺ current and are associated with Brugada syndrome, a disorder characterized by susceptibility to ventricular arrhythmias in structurally normal hearts that may cause syncope or sudden death (17).

Phase 1: Early repolarization. The brief repolarization phase results in the notch between the end of the upstroke and the beginning of the plateau phase. This transient outward current is largely due to activation of K⁺ channels. There are numerous K⁺ channels present in the sarcolemma that are characterized by their gating properties and substances that regulate their opening (e.g., K_{ACh} , K_{Ca}) and closing (e.g., K_{ATP}) (18). The K⁺ channels involved in this phase are outward rectifier K_v channels.

Phase 2: The plateau phase. Ca²⁺ enters the cell through voltage-gated L-type Ca²⁺ channels, which are composed of two subunits (α and α_1) that form the ion pore. These channels are regulated by membrane potential and the inward Ca²⁺ concentration gradient. In the adult heart, the majority of Ca²⁺ influx occurs through this channel, although fetal myocytes also express T-type Ca²⁺ channels that may contribute to E–C coupling. During this phase, delayed outward rectifier K⁺ channels begin to open and the positive V_m drives K⁺ efflux from the cell.

Phase 3: K⁺ efflux through outward rectifier K⁺ channels and Ca²⁺-activated K⁺ channels (K_{Ca} or BK channels) dominates this repolarization phase. Mutations in the KCNQ1 gene encoding a delayed rectifier K⁺ channel are also associated with long QT syndrome (19). On the other hand, activation of the K_{Ca} channel by Ca²⁺ explains why the QT interval is diminished by cardiac glycosides (15). Expression of these channels changes over the course of cardiac development, which likely influences changes in the action potential duration and repolarization (20,21).

Phase 4: Restoration of ionic concentrations: This phase is largely driven by K⁺ flux through inwardly rectifying K⁺ channels. The Na⁺/K⁺-ATPase also maintains the resting membrane potential.

Sarcoplasmic Reticulum

The sarcoplasmic reticulum (SR) is a network of tubular membranes that surround the myofibrils and are involved in the regulation of Ca²⁺ concentrations (Fig. 3.4). The SR is composed of two distinct regions that are involved in Ca²⁺ regulation: the junctional SR regulates Ca²⁺ storage

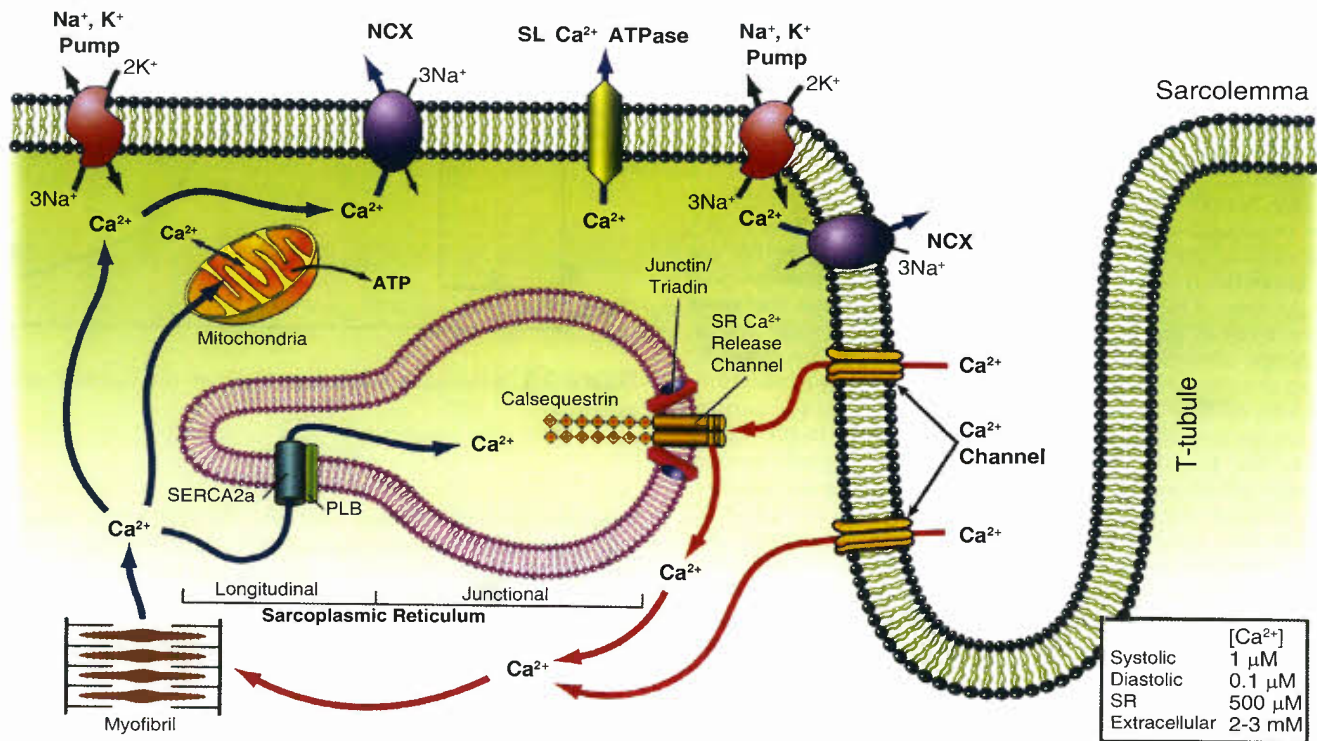


Figure 3.4. Pumps and channels regulate Ca²⁺ signaling, the key modulator of contraction and relaxation. Following depolarization, Ca²⁺ enters the cells through the sarcolemma and causes Ca²⁺-induced Ca²⁺ release from the SR, initiating contraction. Relaxation occurs when most of the Ca²⁺ is resequenced into the SR. SR, sarcoplasmic reticulum; SL, sarcolemma; PLB, phospholamban; NCX, Na–Ca exchanger.

and release, while the longitudinal SR regulates Ca²⁺ uptake. Release of SR Ca²⁺ is a tightly regulated process, and proper functioning of the SR is imperative for normal heart function. The SR contains ryanodine Ca²⁺ release channels that play a primary role in E–C coupling (22) (see below). The cardiac SR Ca²⁺-ATPase (SERCA2a) pumps Ca²⁺ into the SR against its concentration gradient. SERCA2a is the main player in restoring diastolic Ca²⁺ levels and terminating Ca²⁺-dependent force activation. The function of SERCA2a can be modulated by several indirect and direct factors. The most predominant indirect mechanism is inhibition by the phosphoprotein phospholamban. Phosphorylation of phospholamban via β -adrenergic stimulation and enhanced cAMP-dependent protein kinase A activity (PKA) relieves SERCA2a inhibition (23). SERCA2a is also under the direct control of Ca²⁺/calmodulin-dependent protein kinase II, which has been shown to phosphorylate SERCA2a and enhance its Ca²⁺ transport capacity (23). During development, the SR content of the heart changes wherein the immature heart SR content is dramatically less (24,25) than in the mature heart (26).

T-Tubules

The system of T-tubules extends transversely into the center of the myocyte and envelops the myofibril at the level of the Z-disk, forming couplings with the SR. This allows transmission of the action potential to the cellular interior, leading to rapid activation of the cell. In humans, T-tubules are noted at 30 weeks gestation (27). The development of T-tubule net-

works appears variable, with myocytes from animals that are well developed at birth having well-developed T-tubule systems and those from less well-developed neonates lacking mature T-tubule networks. These variations in T-tubule development may account for the variability in E–C coupling between mature and immature heart cells.

Sarcomere

The sarcomere (Fig. 3.5), or the functional unit of heart muscle, is defined as the region between two Z-lines and is composed of thick (myosin) and thin (actin) filaments. The regions of the sarcomere include the I-band, which contains thin filaments, troponin, and tropomyosin; the A-band, which is a region of overlapping thick and thin filaments; and the M-band (located in the center of the A-band) containing thick filaments linked to titin and myosin-binding protein.

Thin Filaments

The thin filaments are composed of two strands of actin monomers. There are two isoforms of actin, skeletal and cardiac α -actin, that differ by four amino acids. Early in human heart development, both α -actin isoforms are expressed (28). As development progresses, however, the content of skeletal α -actin is decreased, while the cardiac isoform is increased; however, the mechanisms of this isoform switch have not been delineated. The Tn complex is composed of three proteins: TnT, TnI, and TnC (29). TnT facilitates binding of the

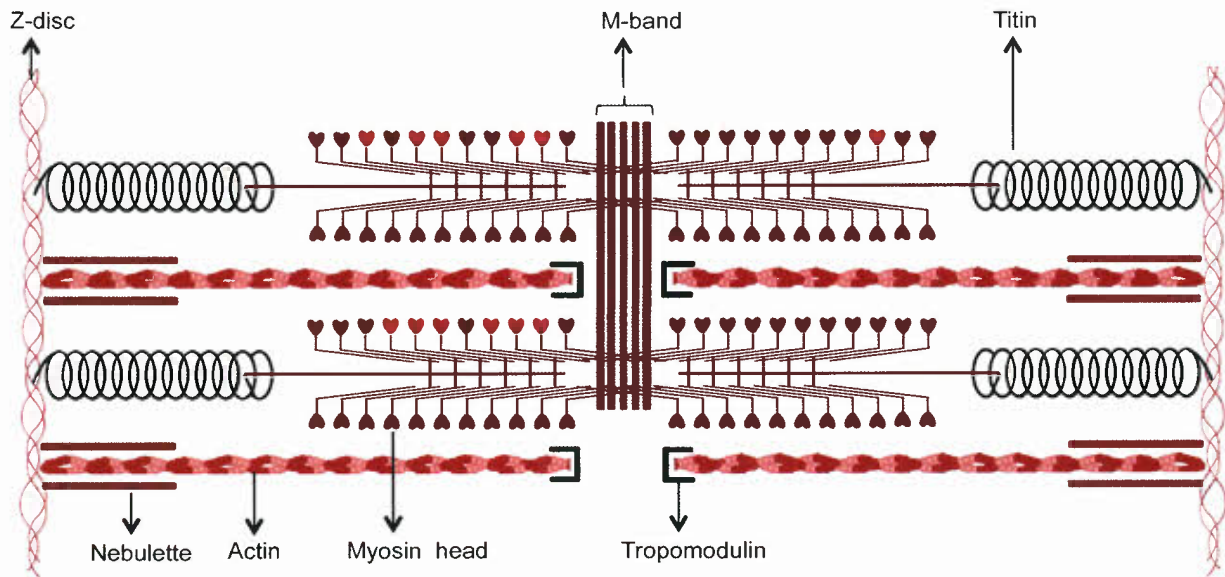


Figure 3.5. Protein composition of the sarcomere. Titin, extending from the Z band to the thick filament, connects to myosin by myosin-binding protein C. Several proteins support the thin filaments, including nebulin (connecting the thin filaments to the Z band) and tropomodulin (linked to the ends of thin filaments). (Redrawn from Katz AM. *Molecular and Cellular Basis of Contraction and Relaxation*. Figure 1-8. In: Colucci WS, ed. *Atlas of Heart Failure: Cardiac Function and Dysfunction*. 4th ed.)

troponin complex to tropomyosin. TnI is a strong inhibitor of actin–myosin interactions, binding to TnC during systole and actin during diastole (Fig. 3.6) (30). TnT is involved in binding the troponin complex to tropomyosin. Tropomyosin is evident in both α and β isoforms that wind together to form a coil. TnI is a strong inhibitor of actin–myosin interactions, whereby TnI binds to TnC during systole and actin during diastole. TnI also has skeletal and cardiac forms, and both are expressed in immature hearts (31). During development of the heart, the skeletal isoform is changed to the cardiac isoform,

Diastole

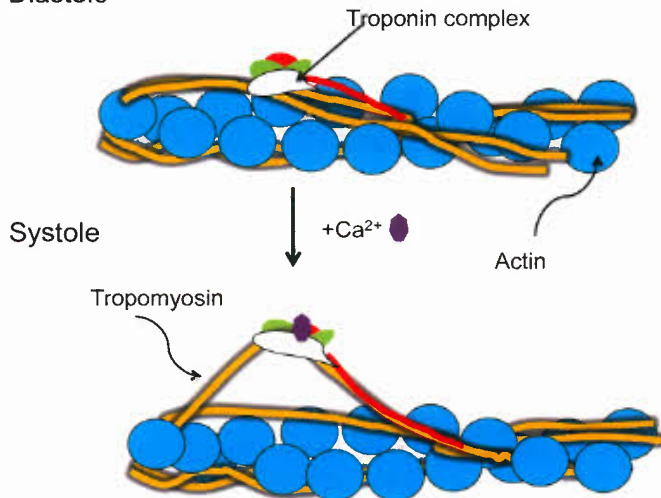


Figure 3.6. Interaction of the troponin–tropomyosin complex with an actin filament. During diastole, troponin I covers the adenosine triphosphate (ATP)-reactive site on the actin filament. When Ca^{2+} binds to troponin C during systole, a conformational change causes TnT to lift tropomyosin and TnI away from the ATP-reactive site to permit actin–myosin interaction. (Redrawn from McBride BF, White CM. *Levosimendan: Implications for Clinicians*. *J Clin Pharmacol* 2003;43:1071–1081, with permission.)

which could help to explain the changes in cardiac function during development (32,33). TnC binds Ca^{2+} and a conformational change causes TnT to lift tropomyosin and TnI away from the ATP-reactive site to permit actin–myosin interaction leading to contraction.

The distribution of thin filament subunits is altered during heart development and likely contributes to developmental changes in myocardial contraction. The regulation of TnI has been well studied in the heart and has two isoforms, cardiac TnI and slow skeletal TnI. Slow skeletal TnI is the major isoform during development, and a switch occurs at birth to cardiac TnI (34,35). This switch is postulated to account for the decrease in calcium sensitivity found in the adult heart as compared to the neonatal heart (33). TnT has multiple isoforms. Studies in the rat heart have demonstrated that TnT1 is a major isoform in the fetal heart with a switch to TnT2 in the neonate (36), but in human studies, TnT1 is a predominant isoform in both the fetus and adult, while TnT2 is only found in the fetal heart (30). Interestingly, TnC does not seem to change expression during development.

Changes in actin and tropomyosin also occur during development. In the fetus, the predominant actin isoform is α -skeletal actin and this is replaced by α -cardiac actin in the adult heart (37). Tropomyosin also has two major isoforms, α and β . In the adult heart, these two forms are present at approximately equal levels, but during development β -tropomyosin has lower expression levels. During late fetal development, expression of this β isoform increases to adult levels and this is postulated to be inversely correlated with heart rate (37).

Thick Filaments

Myosin is the most abundant protein in the myocyte, with two heavy chains and four light chains. The two heavy chains of myosin wind together to form the thick filament, with the myosin heads projecting up from the long axis of the thick filament to form cross-bridges. In the presence of Ca^{2+} , the myosin heads bind to actin to initiate contraction. In the first step, the myosin head, due to its intrinsic ATPase activity, becomes activated by ATP hydrolysis, allowing the head to attach to

actin and form a cross-bridge. The interaction elicits a conformational change in the myosin head that pulls the actin filament inward (“power stroke”). ADP is then released and a new molecule of ATP binds to the myosin head, causing it to release the actin filament. If intercellular Ca^{2+} remains elevated, myosin will undergo another cross-bridge cycle.

Myocytes contain two types of myosin heavy chain (MHC): α -MHC and β -MHC. Detailed expression studies in mouse embryos demonstrate that the predominant isoform in the developing ventricles is MHC- β , while MHC- α expression is localized to the developing atria. MHC- β is found as early as E7.5 in the mouse embryonic heart (38). In early postnatal life in the rodent, there is a switch from MHC- β to MHC- α in the ventricles. Recent studies demonstrate the role of the microRNA miR-208 in regulating this switch and that miR-208 mediates the effects of thyroid hormones (THs), which are known to affect MHC- α and MHC- β expression levels (39).

In human ventricles, β -MHC is the predominant form during all stages of life (40). Interestingly, α -MHC is found in only very small amounts in the human ventricle, but mutations in this protein are linked to both hypertrophic and dilated cardiomyopathy (41). Expression of the myosin light chain (MLC) does not appear restricted in the early to midfetal stages of development, but by late fetal life, MLC1A is restricted to the atria and MLC1V to the ventricles. This expression is maintained in adulthood.

Myosin-binding protein C is a protein associated with the thick-filament myosin that is found within the A band and functions as a tether to hold the thick filaments together. Mutations in myosin-binding protein C have been linked to hypertrophic cardiomyopathy (42,43) and may account for potential alterations in cardiac contractile function during development (44).

Z-disk

The Z-disks demarcate individual sarcomeres and directly interact with all myofilament proteins except myosin. α -Actinin is the primary protein that makes up the backbone of the Z-disk and cross-links the ends of actin to adjacent sarcomeres (45). Proteins in the Z-disk also bind the intermediate filament desmin to link the sarcomere to the intercalated disc and costameres at the plasma membrane (see following section). This unique structure allows the integration of signals from the cytoskeleton, ECM, and those induced by mechanical stress (45).

Titin

Titin is the largest protein known, spanning half of the sarcomere from Z-disk to M-band (Fig. 3.5). Titin's remarkable elasticity is due to its I-band domain that is composed of three sequence elements that develop passive tension as the sarcomere is stretched. These three elements are composed of distal and proximal Ig segments, a unique N2B segment, and the PEVK segment (named for its rich composition of proline [P], glutamate [E], valine [V], and lysine [K] residues). Tension generated by these elements is responsible for pressure generated during diastole and accounts for approximately 80% of passive pressure at physiologic sarcomere lengths (46). Titin's passive force is modulated during development and in response to pathologic changes in hemodynamic load. This occurs primarily by differential splicing primarily in the Ig and PEVK segments, which leads to three different isoform classes with variable compliance (47). The stiffer N2B isoform is the shortest of these and is approximately 3 MDa. The second class is the more compliant N2BA isoform, which is approximately 3.3 to 3.5 MDa, and contains additional PEVK segments and a varying number of additional Ig domains.

The relationship of titin to cardiac development and disease is complex. A dramatic isoform switch occurs during cardiac development in mammals, from fetal N2BA titin expressed before birth to a mix of smaller N2BA/N2B isoforms found postnatally. Adult rat hearts almost exclusively have N2B titin isoform (48,49). These changes in titin isoform composition during heart development affect myofibrillar extensibility, passive force generation, and alter cardiac stiffness (50). In humans, N2BA/N2B ratios vary with disease from an increased ratio in dilated cardiomyopathy (more compliant) (46,51–53) to decreased ratios in aortic stenosis (less compliant) (46,52–54).

MITOCHONDRIA AND METABOLISM

As the heart develops, it requires an abundant amount of energy to grow, differentiate, and mature. Cellular mitochondria are the key “powerhouses” of energy production, generating abundant amounts of ATP for use in cellular processes. Relative to other organs, the heart contains a high number of mitochondria to accommodate this energy need.

Mitochondria are rectangular-shaped with an inner membrane that folds into numerous compartments termed cristae. The cristae create a greatly expanded intracellular surface area to accommodate the membrane-bound enzymes of the electron transport chain responsible for generating ATP in the inner matrix. Myocytes contain two distinct types of mitochondria: subsarcolemmal mitochondria located beneath the plasma membrane and interfibrillar mitochondria located between myofibrils in parallel rows. The number, size, and volume of mitochondria increase during development (55–58), coupled with lengthening of the cristae.

The adult heart is primarily a postmitotic organ with minimal regenerative capacity. Proper functioning of cellular mitochondria is therefore critical for proper functioning of the heart. The electron transport chain is naturally somewhat “leaky,” and release of high-energy electrons from this chain generates reactive oxygen species that then react with macromolecular components of the cell (proteins, lipids, mitochondrial DNA, etc.). Though the mechanisms are not well understood, it is thought that increases in oxidative damage to cellular macromolecules due to this mitochondrial leakage play a significant role in the aging process.

Cellular metabolism and energetics undergo major shifts during the switch from fetal life to adulthood. The heart utilizes predominately glucose and lactate before birth. Following birth, there is a shift toward increased left ventricular workload. At this stage, the heart switches to fatty acids that supply reducing equivalents to the mitochondrial electron transport chain as its primary substrates for metabolism (59).

CELL–CELL AND CELL–EXTRACELLULAR MATRIX INTERACTIONS

Cell–Extracellular Matrix Interactions

Cardiac myocyte contraction causes cellular deformation and shortening (Fig. 3.7). During this process, the contractile machinery must remain connected to the surrounding ECM; otherwise, movement would be improperly transmitted, which would increase the risk of membrane damage (60). Cells maintain strong connection to the ECM through two specialized complexes, costameres and dystrophin glycoprotein complexes.

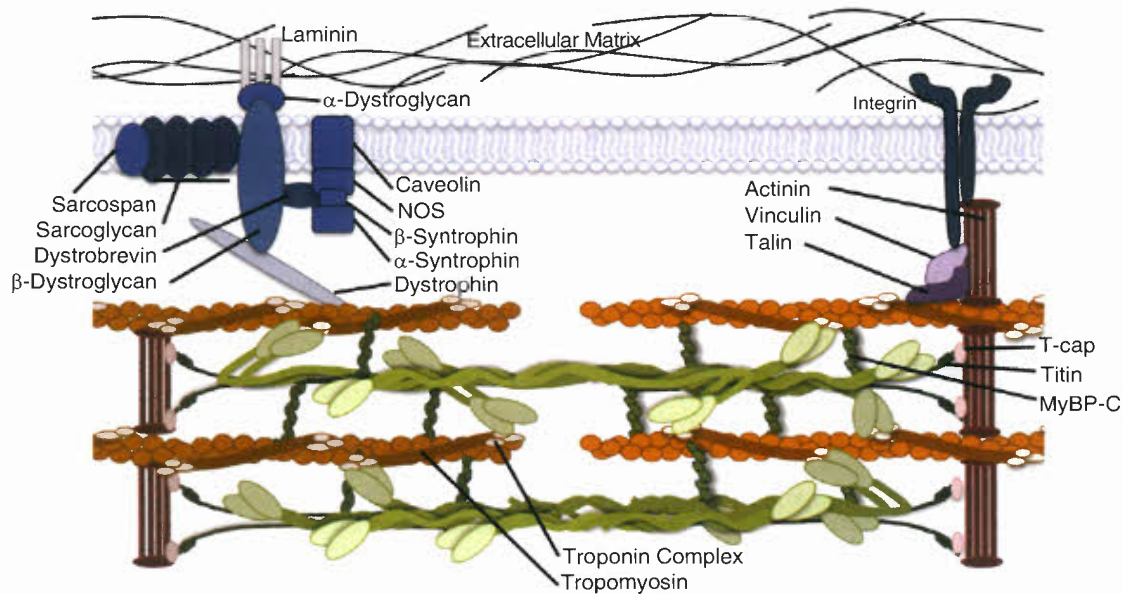


Figure 3.7. Extracellular matrix–cardiac myocyte interactions. Attachment to the ECM is mediated by costameres composed of the dystroglycan–glycoprotein complex and the integrin complex. Force transduction and intracellular signaling are coordinated through the costamere. The unique roles of each of these proteins are critical to appropriate structure and function of the heart. T-cap, titin cap; MyBP-C, myosin-binding protein C. (From Harvey PA, Leinwand LA. The cell biology of disease: cellular mechanisms of cardiomyopathy. *J Cell Biol* 2011;194:355–365.)

Costameres

Costameres are a complex protein structure that forms a physical connection between the ECM and underlying outer Z-disks of underlying sarcomeres. This complex acts to transmit the contractile forces generated by the myofilaments directly to the ECM. Members of the integrin family of transmembrane proteins are found in costameres. Integrins bind directly to specific peptide sequences in the basal lamina proteins collagen IV and laminin and to Type I and III collagens and fibronectin in the ECM. Integrins are heterodimeric proteins consisting of single α - and β -subunits. Cardiac myocytes express multiple α -subunits (α_1 -, α_3 -, α_5 -, α_6 -, α_9 -, and α_v -subunits), whereas the predominant β -subunit is β_1 and, to a lesser extent, β_{1D} (61). Different combinations of these subunits allow integrins to bind to specific ECM components. The α -subunit directly binds to the matrix proteins, while the cytoplasmic tail of β -integrin interacts with several cytoskeletal proteins (vinculin, talin, filamin) that directly link to α -actinin at the Z-disk and cytoskeletal actin. This spatial organization of integrin-associated costameres allows them to act as key mechanical sensors that transduce changes in mechanical forces to cellular signaling cascades that mediate sarcomere assembly, gene expression, cell migration, and survival. This type of “outside-in” signaling is the primary mechanism that regulates cardiac myocyte growth in response to changes in hemodynamic load (61).

Costameres play a key role in sarcomere assembly. Sustained changes in myocardial wall stress and strain result in myocyte growth or atrophy. For example, cells elongate in response to sustained diastolic strain by adding sarcomeres in series, while they thicken in response to increased systolic stress by adding sarcomeres in parallel (62). The precise mechanisms by which new sarcomeres are added to the myofilament are unknown. Russell and colleagues performed a series of gene overexpression or deletion studies in neonatal cardiac myocytes that suggest that integrins activate signaling cascades (e.g., protein kinase C- ϵ) that “loosen” the Z-disk, weakening

actin binding and stimulating actin capping and myofilament formation (62–64).

The molecular composition of integrins and the ECM changes throughout development, suggesting that these two factors may contribute to myocardial morphogenesis. One example is the coordinated regulation of fibronectin and β_1 -integrins. The levels of fibronectin and β_1 -integrin are elevated in the developing myocardium, which allow myocytes to spread and proliferate, but in adult cells that have lower levels of these proteins, myocytes only attach weakly to fibronectin. Both neonatal and adult cells bind strongly to laminin and collagen IV in the basal lamina (65).

Dystrophin-Associated Glycoprotein Complexes

The dystrophin-associated glycoprotein complex provides a strong mechanical link from the cardiac cytoskeleton to the ECM and appears to colocalize with costameres. Components of this complex include dystrophin, dystroglycan, sarcoglycans, and dystrobrevins. Mutations in these proteins result in plasma membrane damage in striated muscle as seen in muscular dystrophy-associated cardiomyopathies. Loss of normal dystrophin function in the heart produces four-chamber dilation, reduction in left ventricular function, and arrhythmias (66). Since dystrophin complex-related cardiomyopathies are covered in great detail in a later Chapter (58), this section is restricted to an overview of dystrophin complex organization and function, as well as functional classes of mutations.

Dystrophin is a rigid cytoplasmic protein that anchors dystroglycan to the cytoskeletal filamentous actin (67). Removal of dystrophin from the dystrophin glycoprotein complex makes this complex unstable and leads to its loss from the plasma membrane, rendering the cell susceptible to damage from contraction (68). Specifically, the loss of membrane integrity allows Ca^{2+} entry into the cell, which in turn activates

Ca^{2+} -sensitive proteases leading to cellular degradation and release of cardiac myocyte proteins such as creatine kinase into the bloodstream (69,70). In cardiac myocytes, mutations in dystrophin also affect the function of stretch-activated ion channels that normally open in response to stretch during ventricular filling (70).

Heterodimeric dystroglycan is a protein central to the dystrophin glycoprotein complex that spans the sarcolemma and binds to laminin in the surrounding basal lamina through its α -dystroglycan subunit and to dystrophin through the cytoplasmic, C-terminus of its β -dystroglycan subunit (71,72). Sarcoglycans are transmembrane glycoprotein complexes composed of six isoforms (α , β , δ , ϵ , γ , and ζ) that are thought to stabilize the interactions between α and β dystroglycans. Dystrobrevin binds to dystrophin and the sarcoglycan complexes and also plays an important role as a structural scaffold linking the dystrophin glycoprotein complex to intermediate filaments (73). The intermediate filaments, in turn, encircle the Z-lines of each myofibril. Mutations in dystrobrevin have been associated with left ventricular noncompaction, a recently defined cardiomyopathy characterized by a pattern of prominent trabecular meshwork and deep trabecular recesses (74).

Cell–Cell Interactions

Intercalated discs (Fig. 3.8) are highly organized and specialized components of the cardiac myocyte that maintain structural integrity and synchronized contraction of cardiac tissue. Intercalated discs are located at the longitudinal ends of the rod-shaped cardiac myocytes where contact and cell–cell communication occurs, and are composed of three different

types of connections: adherens junctions, desmosomes, and gap junctions. Adherens junctions and desmosomes provide mechanical coupling for force transmission and reinforce cardiac myocyte structure, whereas gap junctions are essential for rapid electrical transmission between cells.

Components of adherens junctions include the transmembrane cadherin (*N*-cadherin) responsible for cell–cell adhesion, the cytoplasmic catenins (α - β - γ [plakoglobin]) that bind to cadherin and regulate adhesion, and other catenin-related proteins including vinculin and α -actinin that link the intercalated discs to the cytoskeleton catenins (75). Adherens junctions hold cells tightly together as the heart expands and contracts and act as the anchor point where myofibrils are attached, enabling transmission of contractile forces from one cell to another (76). Because actin filaments also pull against cadherins, these junctions also mediate the bidirectional transmission of cytoskeletal tension between cells (65).

Desmosomes also consist of intercellular and intracellular components. The desmosomal cadherins, desmocollin, and desmoglein interact in a heterophilic manner in the extracellular space to connect with adjacent cells. The cytoplasmic component of desmosomes consists of the proteins plakoglobin (γ -catenin), plakophilin, and desmoplakin, the latter of which connects the desmosome to intermediate filaments such as desmin (76). Desmin also links the Z-disk to costameres. Thus, desmin is uniquely situated to integrate signals from both cell–cell and cell–matrix interactions to ensure cellular integrity, force transmission, and biochemical signaling (45). Given this crucial role, it is not surprising that mutations in desmin lead to cardiomyopathy (77).

The gap junctions maintain electrical coupling of individual myocytes to form an electrical syncytium. Gap junctions ensure

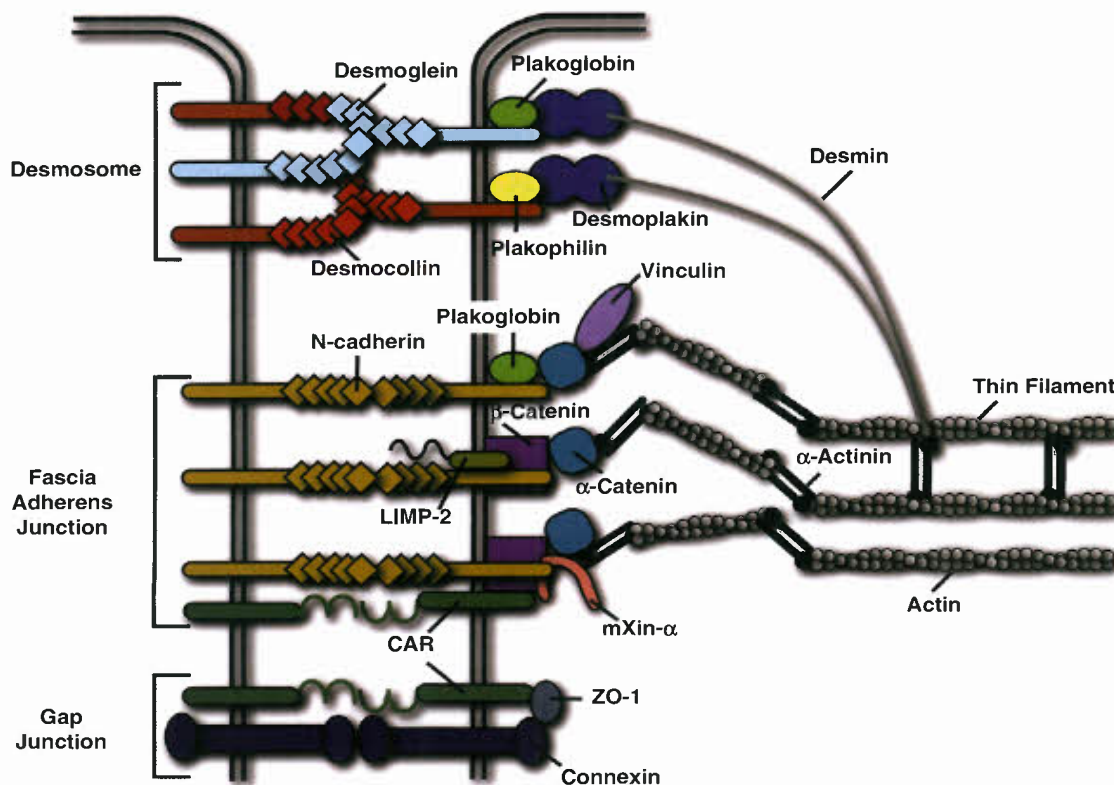


Figure 3.8. Schematic representation of the major cell–cell complexes of the cardiac intercalated disc. (Reprinted from Sheikh F, Ross RS, Chen J. Cell–cell communications. *Trends Cardiovasc Med* 2010;19:182–190, with permission from Elsevier.)

the proper propagation of the electrical impulse, which triggers sequential and coordinated contraction of the cardiac myocytes. One gap junction channel consists of heptamers of the core protein connexin, of which 20 members have been identified in human (78). The main connexins expressed in the heart are connexins-40, -43, -45, and -37. In ventricular myocytes, the embryonic isoforms are connexin-40 and -43, but connexin-40 expression gradually decreases during development (79). These isoforms also exhibit distinct regional, cell type-specific and chamber-specific expression, with different isoforms present in the conduction system as compared to the ventricular myocardium (80). Six connexins combine to form one connexon that extends from the plasma membrane of one cell to dock with a connexin of an adjacent cell, creating an intercellular gap (78).

Gap junctions regulate numerous functions; the most well-known action of gap junctions is the rapid transmission of action potentials throughout the myocardium. However, connexins also allow the diffusion of metabolites and second messengers, including glucose, ATP, Ca^{2+} , cyclic nucleotides (cAMP, cGMP), and inositol phosphates (78). Connexins may also be involved in gene transcription and cell growth control through interactions with a number of cytoplasmic proteins including zona-occludens-1 (ZO-1) and actin.

Gap junction channel assembly, membrane localization, gating, and degradation are regulated by a variety of stimuli including voltage, ionic concentrations, pH, phosphorylation, and local protein interactions. For example, increases in cAMP increase the trafficking and assembly of connexins at the intercalated disk, whereas protein kinase C decreases the unitary conductance of gap junction channels (80–82).

During cardiac myocyte development and maturation, large changes in the spatiotemporal distribution of gap junctions, desmosomes, and adherens junctions occur. In the mature myocardium, all three are clustered in a bipolar pattern (perpendicular to the long axis) on the ends of the myocyte. However, during embryological development, adherens junctions are also found on the lateral membranes where they seem to be able to sense mechanical forces along the transverse axis and are thought to play an important role in myofibrillogenesis (65,83). At the perinatal stage, the adherens junctions no longer surround the entire cell, but are restricted to intercalated discs between cells. Interestingly, this polarization coincides temporally with an increase in cardiac output at birth to support the needs of the newborn, suggesting that maturation of contractility provides mechanical inputs for cadherin movement to the longitudinal border (65).

Unlike adherens junctions, gap junctions exhibit a distinct pattern of localization and are not restricted to the intercalated disc until 4 weeks after birth (84). Indeed, there is some evidence that the adherens junction complex may “prime” gap junction formation either by bringing adjacent cell membranes in close apposition or through cadherin–catenin-mediated changes in gene expression (85).

Several cardiac disorders have recently been identified in which defective electromechanical coupling between cardiac myocytes leads to degenerative cardiomyopathies characterized by contractile impairment and electrical disorders. Mutations in the desmosomal complex result in arrhythmogenic right ventricular cardiomyopathy such as those observed in Naxos disease (76,86). Mutations in proteins in the adherens junctions are associated with heart failure and dilated cardiomyopathy (75).

CORONARY VASCULATURE

The functional and metabolic demands of the developing heart require a tightly coupled growth of the coronary vasculature. As the myocardium grows and the walls thicken, passive oxygen

and nutrient diffusion is replaced by the vascular plexus that remodels to form the mature coronary circulation (87). The initiation of blood flow requires several events including the formation of the initial vascular plexus, lumen formation, initiation of heart contraction, and the entry of erythrocytes into circulation. The coordinate development of myocardium with formation of the coronary vasculature depends upon complex molecular communication between the epicardium, the subepicardial mesenchyme, and the myocardium (88). Finally, mechanical (stretch), hemodynamic (flow), and metabolic (hypoxia) signals provide additional developmental cues.

Blood vessel formation in the heart occurs by a combination of vasculogenesis and angiogenesis. Vasculogenesis is the *de novo* formation of blind-ended, tubular structures that result from the migration and incorporation of endothelial precursor cells. The origin of the endothelial cells is still somewhat controversial. Originally thought to be derived from the neural crest (89), it is now generally accepted that these cells originate from the proepicardial organ. The proepicardial organ is a transient extracardiac cell population located on the septum transversum; cells from this region migrate to the surface of the developing heart to form the epicardium. A subpopulation of these epicardium-derived progenitor cells undergoes epithelial-to-mesenchymal transition (EMT) to generate a population of cells that migrate into the underlying myocardium to give rise to endothelial cells, vascular smooth muscle cells, pericytes, and cardiac fibroblasts (87,88). Vascular smooth muscle cells of the main coronary arteries also originate from the neural crest, while coronary vein smooth muscle is derived from atrial cardiac myocytes (90,91). More recent data suggest that new coronary vessels arise from angiogenic sprouts from the sinus venosus, the major vessel that returns circulating blood to the developing heart. In this scenario, sprouting venous endothelial cells dedifferentiate as they migrate through the myocardium to form the coronary plexus and then redifferentiate and remodel into capillaries, arteries, and veins (92).

The signals that regulate coronary development are derived from both the epicardium and cardiac myocytes. Both metabolic (hypoxia) and mechanical factors stimulate growth factors that promote angiogenesis (93). The epicardium initially acts as a signaling center by secreting a variety of growth factors such as basic fibroblast growth factor (FGF), retinoic acid, TGF- β , and erythropoietin to promote cardiac myocyte proliferation and prepare the epicardium for EMT (88). EMT is promoted by growth factors secreted by both the epicardium and myocytes. Platelet-derived growth factor, FGF family members, angiopoietins, and bone morphogenetic proteins promote EMT and endothelial tube formation. Vascular endothelial growth factor (VEGF) plays multiple roles in coronary vessel development including EMT, coronary endothelial cell proliferation, migration, and tube formation and also promotes connection of the coronary plexus to the aortic root (88,89). VEGF is also the molecular link between hypoxia and angiogenesis. As the growing myocardium increases its oxygen consumption, localized hypoxia triggers hypoxia-inducible factor 1 α , which in turn drives the expression of VEGF.

Physiologic feedback between the myocardium and coronary vessels also occurs via mechanical stimuli. Mechanical stretch of the myocardium potentially induces VEGF secretion. For example, experimentally induced increases in diastolic filling (e.g., bradycardia, volume overload) cause increased myocardial angiogenesis (94) through a VEGF-dependent pathway (93,95). This effect appears to be due to increased cyclic stretch of cardiac myocytes, since cultured cells secrete VEGF in response to mechanical stretch (96).

As the heart begins to contract, the network of blood vessels initially contains only plasma followed by erythrocytes as they dislodge from blood islands (97). As blood flows through

the developing vessels, endothelial cells become exposed to shear stress, which is a function of fluid flow velocity and viscosity. Endothelial cells are equipped with a variety of “mechanosensors” that respond to shear stress and stimulate the expression of a variety of genes required for endothelial function and differentiation of arteries and veins (98). The coronary vasculature continues to grow postnatally to keep pace with increasing mass of the myocardium. In humans, the number of arterioles and capillaries steadily increases during the first postnatal year (99). Blood flow continues to drive the remodeling of the large arteries, while FGF and VEGF signaling modulate arteriolar and capillary growth (87,100).

MYOCARDIAL GROWTH AND REMODELING

Cardiac myocytes display two developmentally regulated types of growth. During fetal and early neonatal life in rats, cardiac myocytes actively proliferate (101). In the neonatal mouse heart, the ability to regenerate after injury is lost by 7 days of age, a time point that coincides with the loss of cardiac myocyte proliferative capacity (102,103). After this time point, increased cardiac myocyte growth is largely limited to hypertrophy of existing myocytes (104). Numerous signaling pathways have been shown to regulate cardiac myocyte growth. One common target of these pathways are microRNAs (miRs), small noncoding RNAs that cause coordinated posttranscriptional repression of genes by binding to distinct sequences usually located within the 3′-untranslated region of target mRNAs. It is becoming increasingly evident that miRs are important regulators of cardiac growth and function (105). For example, pioneering work by Olson’s group has identified miR-15 family members as potent inhibitors of cardiac myocyte proliferation by repressing the expression of multiple cell cycle genes (102).

TH elicits pleiotropic actions on the cardiovascular system throughout development, postnatal maturation, and adult life. In rodent cardiac myocytes, triiodothyronine (T_3) is the biologically active TH as the heart lacks tissue deiodinases required for the conversion of T_3 to thyroxine (T_4) (106). The majority of TH effects are elicited through classical nuclear TH receptors (TH- α and TH- β) that are members of a superfamily of nuclear hormone receptors that regulate gene transcription (107). TH- α receptors have distinct actions depending upon their hormone-binding state. At early embryonic stages when hormone levels are low, unliganded TH- α receptors repress expression of TH-dependent genes (108). During later stages of development, TH levels trigger the conversion of TH- α to a ligand-bound state and induce myoblasts to differentiate and express a cardiac-specific phenotype. Studies in neonatal rat myocytes indicate that TH also promotes the postnatal myosin isoform switch from the fetal β -MHC isoform to the adult α -MHC form and similar isoform shifts in troponins, MLCs, and titin (48,106,109). Additional functions of TH in cardiac innervation are discussed below.

APOPTOSIS

Cells of the heart can die by either necrosis, apoptosis (programmed cell death), or autophagy (110). Apoptosis, or programmed cell death, is a key mechanism of cardiomyocyte loss in adult heart failure. Only recently, however, has apoptosis been recognized as a key regulator of normal cardiac development (111). Both intrinsic (controlled by mitochondrial activity) and extrinsic (receptor-mediated) apoptotic pathways regulate this process (112). Several proteins in the

mitochondrial pathway include caspases (3, 6, and 9) as well as proteins encoded by the mammalian *Bcl-2* family of antiapoptotic genes (110). The extrinsic pathway involves tumor necrosis factor- α or the Fas-ligand binding to their respective cell surface receptors (113).

During development, precursor cells are recruited to the heart where they proliferate and differentiate into cardiomyocytes, fibroblasts, smooth muscle cells, as well as endocardial and endothelial cells. Proper cardiovascular remodeling during development requires strict coordination between this proliferation/differentiation and temporal activation of apoptotic events.

Myocyte proliferation and apoptosis are highest during the early stages of cardiac development. Fiorina et al. (111) showed that the number of apoptotic myocyte nuclei decreases in the third trimester (as compared to the second trimester) in human fetal heart samples. They concluded that there is a delicate balance between myocyte proliferation and death, and that this is a key mechanism in maintaining a proper heart weight/body weight ratio. Indeed, myocyte apoptosis remains relatively high up to 6 months postnatal prior to declining into adulthood.

During development, the right ventricle and left ventricle are exposed to similar volume loads. After birth, however, as the foramen ovale and ductus arteriosus close, the LV is exposed to a greater peripheral resistance than the right ventricle. Myocyte apoptosis in the right ventricle is four times higher than in the LV24 hours postnatally, and this apoptosis decreases over time (114). Overall, it is clear that apoptosis plays a key role in the transition from fetal to postnatal life; thus, it may be a target for the design of pharmacologic agents to enhance fetal heart development.

MYOCARDIAL FUNCTION

Excitation–Contraction Coupling

E–C coupling refers to the process that couples an action potential (excitation) with an intracellular Ca^{2+} transient and subsequent cross-bridge cycling and contraction. Although much attention has been paid to the mechanisms that couple surface membrane depolarization to Ca^{2+} release from the SR (Ca^{2+} -induced Ca^{2+} release), it is important to remember that changes in thick- and thin-filament expression and Ca^{2+} sensitivity also modulate the contractile response to the Ca^{2+} transient. In this section, we first provide an overview of E–C coupling in the mature myocardium, and then discuss how this process changes during development.

The “excitation” component of E–C coupling depends upon the macromolecular complex termed the Ca^{2+} release unit. Structurally, this unit is located at the T-tubule–SR junction or “triad junction” composed of a single T-tubule flanked on either side by a terminal cisternae of the SR (115). Plasma membrane L-type Ca^{2+} channels act as the voltage sensor of the complex. In response to the action potential, Ca^{2+} enters the local microenvironment through these channels to elicit Ca^{2+} release from the SR through ryanodine receptors. Ryanodine receptors bind to numerous regulatory proteins that modulate its Ca^{2+} binding (calmodulin), gating properties (FKBP 12.6), and its Ca^{2+} release (triadin, junction) or proteins that buffer SR Ca^{2+} stores (calsequestrin) (116). In this way, the ryanodine receptor is able to respond to surface depolarization in a manner that depends on the Ca^{2+} load within the SR (117). This junctional arrangement also serves as the “local control” model that describes the summation of spontaneous Ca^{2+} release or Ca^{2+} sparks from the ryanodine receptor. Ca^{2+} sparks are the fundamental units of SR Ca^{2+} release at rest (where they occur as random, stochastic events) and during E–C coupling

(116,118). During E–C coupling, thousands of Ca^{2+} sparks are synchronized by the action potential, such that the local rises in $[\text{Ca}^{2+}]$, completely overlap in time and space, making the Ca^{2+} transient appear uniform (116).

As discussed in previous sections, the “contraction” portion of E–C coupling results from Ca^{2+} binding to TnC, the binding of TnC to TnI, and the resultant dissociation of TnI from actin that increases the number of cross-bridges for force generation. The amount of force developed depends on the amplitude and duration of the Ca^{2+} transients and the Ca^{2+} sensitivity of the myofilaments. While the Ca^{2+} -induced Ca^{2+} release mechanism largely dictates the Ca^{2+} transient amplitude (with a minor component from reverse mode NCX1 exchange), SR Ca^{2+} reuptake by SERCA2a (~70%) and Ca^{2+} extrusion via the NCX1 exchanger (~30%) are the major determinants of Ca^{2+} transient duration (116).

Myofilament Ca^{2+} sensitivity is largely determined by the type of troponin isoform present. For instance, the presence of slow skeletal TnI in embryonic and early postnatal hearts is associated with an increased Ca^{2+} affinity and a decreased rate of Ca^{2+} dissociation from TnC (119). In the mature myocardium, phosphorylation of TnI by PKA (in response to β -adrenergic stimulation) decreases the Ca^{2+} affinity of the troponin complex and increases the rate of Ca^{2+} dissociation. Myofilament Ca^{2+} sensitivity is reduced by acidosis (116) and increased in response to a new class of inotropic drugs including levosimendan (120).

Changes in E–C coupling occur throughout development. Embryonic myocytes have a poorly developed T-tubule system and SR, making the fetal heart more dependent upon L-type Ca^{2+} channels and Ca^{2+} influx across the plasma membrane (121). Ryanodine receptors are expressed in neonatal myocytes, but are not involved in Ca^{2+} -induced Ca^{2+} release until the T-tubule system matures 2 weeks following birth (122). Interestingly, fetal and neonatal myocytes from early stages of cardiac development display spontaneous Ca^{2+} oscillations that are independent of membrane depolarization or Ca^{2+} influx but seem to originate from inositol trisphosphate receptor-gated channels (123). These oscillations may lead to subsarcolemmal release of Ca^{2+} from ryanodine receptors to elicit spontaneous contractions (124).

REGULATION OF E–C COUPLING

As the heart continues to mature following birth, there are considerable changes in myocardial performance. The myocardium increases contractility, diastolic relaxation, volume, and cardiac output. These postnatal changes in cardiac function reflect the developmental regulation of ion channels, receptors for neurotransmitters, and alterations in cell signaling cascades. Multiple mechanisms underlie these phenotypic changes and are classified as intrinsic (e.g., mechanical load), extrinsic (autonomic innervation, TH status), or structural (125).

Intrinsic Regulation

Changes in heart rate increase myocardial contractile force according to the cardiac force–frequency relationship, initially described by Bowditch more than a century ago (126). The force–frequency relationship is an important intrinsic regulatory mechanism of cardiac contractility and describes the relationship between force and velocity, where shortening velocity increases in a hyperbolic manner as force is reduced (127). The underlying cellular mechanisms are related to rate-dependent changes in Ca^{2+} availability (13) and myofilament Ca^{2+} sensitivity (128).

The length-dependent Ca^{2+} activation of the thin filament plays a critical role in the steep force–length relationship of cardiac muscle (Frank–Starling relationship). Quite simply, this relationship describes the observation that when cardiac myocytes are stretched longitudinally, they develop proportionally more force at a given submaximal Ca^{2+} concentration than they do at shorter myofilament lengths (129). The molecular mechanisms that underlie this intrinsic regulatory mechanism are unclear, but have been proposed to involve myofilament lattice spacing (increase in the local concentration of myosin heads due to longitudinal stretch), titin (exertion of radial force at long sarcomere lengths to pull thick and thin filaments together), or increased Ca^{2+} sensitivity of the thin filament (130). This relationship underlies the Frank–Starling mechanism that is discussed in a subsequent section of this chapter.

Sympathetic Innervation

The development of the autonomic nervous system depends upon the secretion of local trophic growth factors. The most important are the neurotrophin family members of nerve growth factor (NGF) and neurotrophins 3 and 4. Cardiac myocytes secrete NGF to promote sympathetic nerve sprouting, survival, and maintenance (131,132). Interestingly, innervation is also modulated by “neurorepellants” such as semaphorin 3a (Sema 3a) that inhibit neuronal growth. In fact, Sema 3a may be partly responsible for patterning of sympathetic innervation in an epicardial to endocardial gradient since Sem3a-deficient mice exhibit disrupted spatial patterning (133,134). These results suggest that the overall balance between NGF and Sema 3a dictates sympathetic nerve development in the heart.

The main neurotransmitters of the sympathetic nervous system are norepinephrine in presynaptic nerves and acetylcholine in postsynaptic ganglia (132). Norepinephrine stimulates both α (α_1) and β (β_1 and β_2) adrenergic receptors (ARs) in cardiac tissue. Similar to humans, the rodent heart expresses predominantly β_1 -ARs with a small fraction (15%–25%) of β_2 -receptors (135). Following β_1 -adrenergic stimulation, the G_s -dependent activation of adenylate cyclase causes an increase in cAMP and activation of PKA. PKA phosphorylates a number of proteins involved in E–C coupling that increase the peak Ca^{2+} transient amplitude (L-type Ca^{2+} channels, ryanodine receptors) and contractility coupled with an increase in the kinetics of cell shortening (TnI, phospholamban). The cAMP–PKA system also alters gene expression and cardiac growth. β_2 -Receptors elicit similar effects but display developmentally regulated responses to catecholamines. For example, β_2 -receptors have higher affinity for epinephrine than norepinephrine and neonatal receptors are more sensitive to physiologic concentrations of these neurohormones compared to β_2 -receptors in adult hearts (134).

Sympathetic innervation appears to be delayed in the rat ventricle since sympathetic nerve terminals are not observed until the third week after birth and do not fully mature to the adult pattern until 5 weeks postnatally (135), and both chronic and inotropic responses to β -adrenergic agonists are significantly weaker in 2-week-old mice compared to adult mice (136). The onset of sympathetic innervation of the mammalian ventricle is associated with functional alterations in several ion channels, including the inward Na^+ current, the L-type Ca^{2+} channel, the inward rectifier K^+ current, and delayed rectifier K^+ currents (125). These changes are likely due to a combination of altered gene expression, membrane compartmentalization, and posttranslational modifications.

In humans, parasympathetic activity in the heart is controlled by superior, inferior, and thoracic branches of the vagal nerve (132,137). The parasympathetic nervous system

uses acetylcholine as its main neurotransmitter. Acetylcholine exerts its actions predominately through M_2 cholinergic receptors although a perinatal involvement of M_1 receptors has been reported (138,139). Parasympathetic innervation of the rat heart is first detected a few days before birth, although maturation of atrial innervation is not completed until 30 to 60 days after birth (135,140). The most significant effects of parasympathetic innervation occur in the atrium, where acetylcholine interacts with M_2 receptors in the sinoatrial node and conductive tissue to increase K^+ channel activation and inhibits the pacemaker current. Both of these effects contribute to the well-known negative chronotropic actions of vagal stimulation. Inotropic effects of the parasympathetic nerves in the ventricular myocardium are primarily through antagonism of β -adrenergic stimulation largely through M_2 receptor- G_i -mediated inhibition of adenylyl cyclase.

Overall, the functional interactions of the autonomic nervous system on the neonatal heart seem to favor a net excitatory state (135). Prior to the onset of sympathetic innervation, both the β_1 -AR and β_2 -AR are functionally active and contribute to the positive chronotropic and inotropic effects of circulating catecholamines in the neonate. The cardiac ARs are responsive to adrenal catecholamines. Since β_2 -ARs have higher affinity for epinephrine versus norepinephrine, the excitatory β_2 -adrenergic signaling cascade may be more responsive to circulating rather than neuronally derived catecholamines (134). With the onset of sympathetic innervation, the resultant changes in AR density, increases in G_s/G_i ratios, and changes in ion channel expression and activation allow the maturing heart to become more responsive to norepinephrine release from local nerve terminals.

Thyroid Hormone

It is well recognized that TH regulates the expression of ARs and levels of adenylyl cyclase in the developing and adult heart. This is crucial in the neonate to ensure the transition to extrauterine life and postnatal cardiac growth and to facilitate β -adrenergic signaling prior to the arrival of sympathetic nerve terminals (141). TH also regulates the expression of several proteins involved in E-C coupling including α -MHC, titin, SERCA2a, the Na^+/K^+ -ATPase, and the NCX1 exchanger (49,142) and promotes mitochondrial biogenesis and oxidative phosphorylation (143). The observed changes in heart rate, cardiac output, and systemic vascular resistance in animal models and in patients with altered thyroid status underscore the importance of TH in normal cardiovascular function. In general, hyperthyroidism is associated with tachycardia, increased cardiac output, and systemic vasodilation. Conversely, hypothyroidism correlates with bradycardia and mild hypertension (144). Of note, plasma TH levels drop as much as 60% in infants and children undergoing cardiac bypass surgery. Promising results have been obtained in several small-scale clinical studies using T_3 therapy in infants and children undergoing cardiopulmonary bypass, showing that this therapy improves postoperative cardiac function (145,146). Early results from a larger multicenter placebo-controlled randomized trial (T_3 supplementation in infants and children undergoing cardiopulmonary bypass, TRICC) suggest that T_3 supplementation improves cardiac function in patients younger than 5 months of age and decreases the need for inotropic support (147).

Structural Changes

At the level of the cytoskeleton, changes in the relative content, posttranslational modification, arrangement, and isoform expression of various proteins can alter diastolic performance

and lead to dysfunction. Multiple studies have examined the contribution of microtubules (tubulin) (121) and intermediate filaments (desmin) (148) to relaxation, where aberrant changes can lead to increased stiffness. Early work by Tagawa et al. (149) examined cardiomyocytes using a method of single-cell mechanical loading of myocytes. They found that cytoskeletal stiffness and viscosity increased significantly in cats exposed to pressure overload hypertrophy. This apparent stiffness and viscosity was reversed and cardiomyocyte function was restored upon the addition of the microtubule depolymerization drug colchicine.

The intermediate filament desmin reinforces myocyte sarcomeres and contributes to the overall diastolic tone. Dynamic increases in desmin have been noted in models of diastolic dysfunction including microembolization (leading to global ischemia) in sheep (150) and ventricular septal defects in pigs (151). In addition to changes in relative abundance, reports have suggested that posttranslational modification (nitration) of this protein is associated with oxidative stress-induced systolic and diastolic dysfunction (152).

Sarcomeric titin is attributed with providing much of the passive elastic properties of the cardiac muscle. Over the normal operating range of sarcomere lengths ($<2.2 \mu m$), titin contributes to sarcomeric stiffness more than the microfilaments and intermediate filaments that provide $<10\%$ of the elastic force (153). Shifts in the relative content of the larger more compliant N2BA isoform versus the smaller and stiffer N2B isoform are implicated in multiple forms of diastolic dysfunction, including aortic stenosis (154), hypothyroidism-induced LV dysfunction (53), and pacing-induced cardiac failure (155,156).

In summary, the combination of neurohormonal programming, autonomic innervation, and mechanical forces coordinate postnatal cardiac growth and E-C coupling in order to increase cardiac output to meet the metabolic demands of the rapidly growing organism.

LV CHAMBER FUNCTION

Systole

Cardiac output is tightly matched to meet the metabolic needs of the body via feedback mechanisms that prevent a mismatch between supply and demand. Systole refers to the process of force generation and shortening in the LV, where blood is ejected into the systemic circulation, a process that is initiated by the coordinated propagation of the action potential. Systolic ejection is regulated by three phenomena: end-diastolic fiber length (the Frank-Starling mechanism), afterload, and intrinsic myocardial contractility.

Pioneering work in the late 19th century by Otto Frank (157) and in the early 20th century by Ernest Starling and colleagues (158,159) determined that the cardiac ejection volume (stroke volume) of the heart increases in response to increased preload (diastolic filling of the heart). As described earlier, this response is mediated by an increased responsiveness of the myofilament apparatus to Ca^{2+} at longer sarcomere lengths (160). The Frank-Starling mechanism ensures that over a physiologic range, on average, the same amount of blood is pumped out of the left and right ventricles.

Afterload (also referred to as aortic resistance/impedance) is the work that the LV must overcome to eject a given volume of blood (stroke volume). Afterload has an inverse relationship with stroke volume. This relationship is most notably evident in cases of arterial hypertension, where the increased afterload results in a decreased stroke volume in the LV. To alleviate the effects of afterload, it is common to administer vasodilators in order to increase forward ejection fraction.

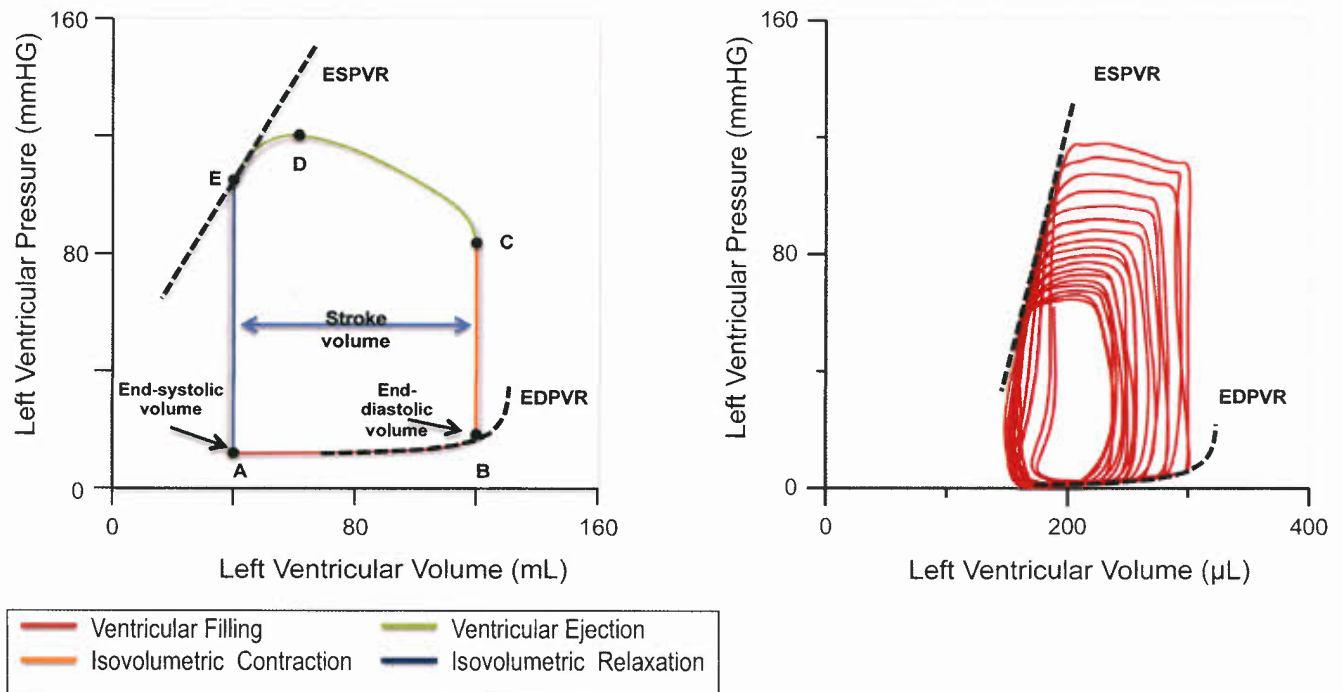


Figure 3.9. A: Schematic of a PV loop generated by a normal human LV. The loop is constrained by the end-diastolic pressure–volume relationship (EDPVR) and by the end-systolic pressure–volume relationship (ESPVR). See text for further details. B: A series of pressure–volume loops were obtained in a rat heart by occluding the inferior vena cava, in order to obtain load-independent measures of contractility (slope of ESPVR or E_{es}) and LV compliance (slope of EDPVR).

Diastolic Relaxation

Diastole occurs at the beginning of isovolumic relaxation (see Fig. 3.9) and ends with mitral valve closure. This allows ventricular filling and involves the interaction between active, energy-dependent processes (myocardial relaxation) that primarily influence early ventricular filling and passive processes, such as loading conditions and myocardial compliance. Active LV relaxation is dependent upon the rate of myocyte $SR\ Ca^{2+}$ reuptake by SERCA2a and by titin. The rate of global LV myocardial relaxation is reflected by the monoexponential course of LV pressure fall. Tau is a widely accepted invasive measure of the rate of LV relaxation.

The role of the ECM is also paramount in regulating diastolic function in the context of normal function and disease. As discussed in preceding sections, the ECM forms the scaffold that tethers and signals to the cardiac myocyte, and changes in the makeup or content of the ECM can be detrimental to diastolic filling. The ECM forms a scaffold that is composed primarily of collagen fibers, which allow for the transmission of mechanical force generated by cardiomyocytes. A multitude of evidence reveals that collagen can also regulate myocardial stiffness and diastolic and systolic function via contribution from changes in collagen volume fraction, collagen isoform composition (collagen I/III ratio), and collagen cross-linking contribution (161).

PRESSURE–VOLUME LOOP ANALYSES OF CONTRACTILE FUNCTION

Although currently limited in clinical use, pressure–volume (PV) analysis is potentially a powerful tool that could be applied for use in assessment of pediatric diseases. The procedure

requires the introduction of a catheter (commonly through the femoral artery) into the LV that reads simultaneous pressure and volume during the cardiac cycle. These values are then displayed by plotting instantaneous ventricular pressure versus volume. A typical trace is shown in Figure 3.9A. At point *a*, filling of the LV chamber begins during diastole after the mitral valve opens and continues to point *b*. The pressure does not change substantially due to progressive LV relaxation and passive compliance. The small increase in pressure just prior to point *b* reflects the contribution of atrial contraction to LV filling. With the onset of LV isovolumetric contraction (line *b–c*), the pressure rises steeply but volume does not change since both the mitral and aortic valves are closed. When the rise in ventricular pressure exceeds the diastolic pressure in the aorta (point *c*), the aortic valve opens, and during the first phase of ejection (rapid ejection, line *c–d*), the large reduction in volume is associated with increased LV pressure. This is followed by a period of reduced ejection and a decrease in LV pressure. This phase corresponds to the onset of cardiac myocyte relaxation. Once the pressure falls below systolic aortic pressure, the aortic valve closes (point *e*). As the ventricle continues to relax, the pressure decreases but volume remains constant since the mitral valve has not yet opened. This phase is referred to as isovolumetric relaxation. When the LV pressure falls below that in the left atrium, the mitral valve opens again and the cycle repeats.

This method can be used to determine load-dependent indices of systolic function, including, but not limited to, the following systolic parameters: ejection fraction, the first derivative ($+dp/dt$) of the rate of developed pressure, stroke work (area within the PV loop), and stroke volume. Load-dependent parameters used for analysis of diastolic function include end-diastolic pressure, tau, and $-dp/dt$. Furthermore, load-independent function can be evaluated using PV analysis, which is accomplished by occluding either the inferior vena cava or the descending thoracic aorta using a balloon

catheter (Fig. 3. 9B). This generates a series of PV curves that allow for the measurement of indices of load-independent contractility including end-systolic elastance (Ees; slope of the end-systolic PV relationship curve) and preload-recrutable stroke work. The relationship generated from the end-systolic elastance has been shown to have a high correlation with the Frank-Starling relationship of the heart, with steeper slopes indicating increased contractility. Although this systolic relationship is generally considered nonlinear, a line can be fit to this curve as long as the volume axis intercept is also examined. For instance, a shift in the Ees line to the left (such as that occurring following administration of a β -adrenergic agonist) accompanied by little change in slope would indicate an increase in contractility since there is increased end-systolic pressure generation at a common volume. Afterload can also be assessed using PV analysis by comparing the stroke volume of the ventricular contraction to the end-systolic pressure required to eject (higher end-systolic pressure with common stroke volumes would indicate a higher afterload).

Furthermore, left ventricular chamber stiffness can be assessed using this series of PV curves. This relationship, which is based on the points in the end-diastolic pressure-volume relationship (EDPVR), provides an accurate assessment of compliance, with shift to the right and down indicating increased compliance. Several extrinsic and intrinsic factors determine these end-diastolic properties. Extrinsic factors are pericardial restraint and ventricular interaction. Intrinsic factors include myocardial stiffness (cardiomyocytes and ECM), myocardial tone, chamber geometry, and wall thickness (162).

EMERGING CONCEPTS AND CONCLUSION

Research into the developing myocardium is still in its infancy, with numerous studies emerging within the last 5 years. Recently, the role of cardiac-resident stem cells in the prenatal and postnatal heart has become a popular area of study, with suggestions that the heart can regulate its own internal environment by recruitment of stem cells to areas within the heart for growth and maturation (163–166). Gene therapy is also increasingly popular in the developing heart, with studies suggesting that genes can be delivered to the myocardium to regulate expression and control growth (167–169). These areas of research will likely continue to increase our understanding of the developing heart and how it functions, and assist in developing novel therapeutic approaches for the treatment of pediatric cardiovascular diseases.

REFERENCES

- Ottaviano FG, Yee KO. Communication signals between cardiac fibroblasts and cardiac myocytes. *J Cardiovasc Pharmacol* 2011;57:513–521.
- Borg TK, Baudino TA. Dynamic interactions between the cellular components of the heart and the extracellular matrix. *Pflugers Arch* 2011;462:69–74.
- Souders CA, Bowers SL, Baudino TA. Cardiac fibroblast: the renaissance cell. *Circ Res* 2009;105:1164–1176.
- Weber KT. Cardiac interstitium in health and disease: the fibrillar collagen network. *J Am Coll Cardiol* 1989;13:1637–1652.
- Kanzaki Y, Terasaki F, Okabe M, et al. Three-dimensional architecture of cardiomyocytes and connective tissue in human heart revealed by scanning electron microscopy. *Circulation* 2010;122:1973–1974.
- Burlew BS, Weber KT. Connective tissue and the heart. Functional significance and regulatory mechanisms. *Cardiol Clin* 2000;18:435–442.
- Spinale FG. Myocardial matrix remodeling and the matrix metalloproteinases: influence on cardiac form and function. *Physiol Rev* 2007;87:1285–1342.
- Sasse P, Malan D, Fleischmann M, et al. Perlecan is critical for heart stability. *Cardiovasc Res* 2008;80:435–444.
- Costell M, Gustafsson E, Aszodi A, et al. Perlecan maintains the integrity of cartilage and some basement membranes. *J Cell Biol* 1999;147:1109–1122.
- Glitsch HG. Electrophysiology of the sodium-potassium-ATPase in cardiac cells. *Physiol Rev* 2001;81:1791–1826.
- Lucchesi PA, Sweadner KJ. Postnatal changes in Na,K-ATPase isoform expression in rat cardiac ventricle. Conservation of biphasic ouabain affinity. *J Biol Chem* 1991;266:9327–9331.
- Hauck C, Potter T, Bartz M, et al. Isoform specificity of cardiac glycosides binding to human Na⁺,K⁺-ATPase α 1 β 1, α 2 β 1 and α 3 β 1. *Eur J Pharmacol* 2009;622:7–14.
- Reuter H, Zobel C, Brixius K, et al. The force-frequency relationship is dependent on Ca(2⁺)-influx via L-type- and SR-Ca(2⁺)-channels in human heart. *Basic Res Cardiol* 1999;94:159–170.
- Guerini D, Coletto L, Carafoli E. Exporting calcium from cells. *Cell Calcium* 2005;38:281–289.
- Katz A. *Physiology of the Heart*. Philadelphia, PA: Lippincott Williams & Wilkins, 2006.
- Shah M, Akar FG, Tomaselli GF. Molecular basis of arrhythmias. *Circulation* 2005;112:2517–2529.
- Antzelevitch C, Brugada P, Borggreffe M, et al. Brugada syndrome: report of the second consensus conference: endorsed by the heart rhythm society and the European heart rhythm association. *Circulation* 2005;111:659–670.
- Snyders DJ. Structure and function of cardiac potassium channels. *Cardiovasc Res* 1999;42:377–390.
- Bokil NJ, Baisden JM, Radford DJ, et al. Molecular genetics of long QT syndrome. *Mol Genet Metab* 2010;101:1–8.
- Nakamura TY, Sturm E, Pountney DJ, et al. Developmental expression of NCS-1 (fresenius), a regulator of Kv4 K⁺ channels, in mouse heart. *Pediatr Res* 2003;53:554–557.
- Morrissey A, Parachuru L, Leung M, et al. Expression of ATP-sensitive K⁺ channel subunits during perinatal maturation in the mouse heart. *Pediatr Res* 2005;58:185–192.
- Bers DM. Macromolecular complexes regulating cardiac ryanodine receptor function. *J Mol Cell Cardiol* 2004;37:417–429.
- Frank KF, Bolck B, Erdmann E, et al. Sarcoplasmic reticulum Ca²⁺-ATPase modulates cardiac contraction and relaxation. *Cardiovasc Res* 2003;57:20–27.
- Maylie JG. Excitation-contraction coupling in neonatal and adult myocardium of cat. *Am J Physiol* 1982;242:H834–H843.
- Nassar R, Reedy MC, Anderson PA. Developmental changes in the ultrastructure and sarcomere shortening of the isolated rabbit ventricular myocyte. *Circ Res* 1987;61:465–483.
- Harrer JM, Haghighi K, Kim HW, et al. Coordinate regulation of SR Ca(2⁺)-ATPase and phospholamban expression in developing murine heart. *Am J Physiol* 1997;272:H57–H66.
- Kim HD, Kim DJ, Lee IJ, et al. Human fetal heart development after mid-term: morphometry and ultrastructural study. *J Mol Cell Cardiol* 1992;24:949–965.
- Boheler KR, Carrier L, de la Bastie D, et al. Skeletal actin mRNA increases in the human heart during ontogenic development and is the major isoform of control and failing adult hearts. *J Clin Invest* 1991;88:323–330.
- Parmacek MS, Solaro RJ. Biology of the troponin complex in cardiac myocytes. *Prog Cardiovasc Dis* 2004;47:159–176.
- Anderson PA, Malouf NN, Oakeley AE, et al. Troponin T isoform expression in humans. A comparison among normal and failing adult heart, fetal heart, and adult and fetal skeletal muscle. *Circ Res* 1991;69:1226–1233.
- Bodor GS, Oakeley AE, Allen PD, et al. Troponin I phosphorylation in the normal and failing adult human heart. *Circulation* 1997;96:1495–1500.
- Kobayashi T, Solaro RJ. Calcium, thin filaments, and the integrative biology of cardiac contractility. *Annu Rev Physiol* 2005;67:39–67.
- Siedner S, Kruger M, Schroeter M, et al. Developmental changes in contractility and sarcomeric proteins from the early embryonic to the adult stage in the mouse heart. *J Physiol* 2003;548:493–505.
- Saggin L, Gorza L, Ausoni S, et al. Troponin I switching in the developing heart. *J Biol Chem* 1989;264:16299–16302.
- Hunkeler NM, Kullman J, Murphy AM. Troponin I isoform expression in human heart. *Circ Res* 1991;69:1409–1414.
- Jin JP, Lin JJ. Rapid purification of mammalian cardiac troponin T and its isoform switching in rat hearts during development. *J Biol Chem* 1988;263:7309–7315.
- Katz AM. *Physiology of the Heart*. New York, NY: Raven Press, 1992.
- Lyons GE, Schiaffino S, Sassoon D, et al. Developmental regulation of myosin gene expression in mouse cardiac muscle. *J Cell Biol* 1990;111:2427–2436.
- van Rooij E, Sutherland LB, Qi X, et al. Control of stress-dependent cardiac growth and gene expression by a microRNA. *Science* 2007;316:575–579.
- Reiser PJ, Portman MA, Ning XH, et al. Human cardiac myosin heavy chain isoforms in fetal and failing adult atria and ventricles. *Am J Physiol Heart Circ Physiol* 2001;280:H1814–H1820.
- Carniel E, Taylor MR, Sinagra G, et al. Alpha-myosin heavy chain: a sarcomeric gene associated with dilated and hypertrophic phenotypes of cardiomyopathy. *Circulation* 2005;112:54–59.
- Schlossarek S, Mearini G, Carrier L. Cardiac myosin-binding protein C in hypertrophic cardiomyopathy: mechanisms and therapeutic opportunities. *J Mol Cell Cardiol* 2011;50:613–620.
- James J, Robbins J. Signaling and myosin-binding protein C. *J Biol Chem* 2011;286:9913–9919.

44. Vikstrom KL, Leinwand LA. Contractile protein mutations and heart disease. *Curr Opin Cell Biol* 1996;8:97-105.
45. Frank D, Frey N. Cardiac z-disc signaling network. *J Biol Chem* 2011;286:9897-9904.
46. Chung CS, Granzier HL. Contribution of titin and extracellular matrix to passive pressure and measurement of sarcomere length in the mouse left ventricle. *J Mol Cell Cardiol* 2011;50:731-739.
47. Lahmers S, Wu Y, Call DR, et al. Developmental control of titin isoform expression and passive stiffness in fetal and neonatal myocardium. *Circ Res* 2004;94:505-513.
48. Kruger M, Linke WA. The giant protein titin: a regulatory node that integrates myocyte signaling pathways. *J Biol Chem* 2011;286:9905-9912.
49. Kruger M, Sachse C, Zimmermann WH, et al. Thyroid hormone regulates developmental titin isoform transitions via the phosphatidylinositol-3-kinase/AKT pathway. *Circ Res* 2008;102:439-447.
50. Linke WA. Sense and stretchability: the role of titin and titin-associated proteins in myocardial stress-sensing and mechanical dysfunction. *Cardiovasc Res* 2008;77:637-648.
51. Lee EJ, Peng J, Radke M, et al. Calcium sensitivity and the frank-starling mechanism of the heart are increased in titin N2B region-deficient mice. *J Mol Cell Cardiol* 2010;49:449-458.
52. LeWinter MM, Granzier H. Cardiac titin: a multifunctional giant. *Circulation* 2010;121:2137-2145.
53. LeWinter MM, Wu Y, Labeit S, et al. Cardiac titin: structure, functions and role in disease. *Clin Chim Acta* 2007;375:1-9.
54. Granzier H, Labeit S. Cardiac titin: an adjustable multi-functional spring. *J Physiol* 2002;541:335-342.
55. Smolich JJ, Walker AM, Campbell GR, et al. Left and right ventricular myocardial morphometry in fetal, neonatal, and adult sheep. *Am J Physiol* 1989;257:H1-H9.
56. Rolph TP, Jones CT, Parry D. Ultrastructural and enzymatic development of fetal guinea pig heart. *Am J Physiol* 1982;243:H87-H93.
57. Barth E, Stammler G, Speiser B, et al. Ultrastructural quantitation of mitochondria and myofilaments in cardiac muscle from 10 different animal species including man. *J Mol Cell Cardiol* 1992;24:669-681.
58. Judge S, Leeuwenburgh C. Cardiac mitochondrial bioenergetics, oxidative stress, and aging. *Am J Physiol Cell Physiol* 2007;292:C1983-C1992.
59. Leone TC, Kelly DP. Transcriptional control of cardiac fuel metabolism and mitochondrial function. *Cold Spring Harb Symp Quant Biol* 2011;76:175-182.
60. Demonbreun AR, Lapidos KA, Heretis K, et al. Myoferlin regulation by NFAT in muscle injury, regeneration and repair. *J Cell Sci* 2010;123:2413-2422.
61. Samarel AM. Costameres, focal adhesions, and cardiomyocyte mechanotransduction. *Am J Physiol Heart Circ Physiol* 2005;289:H2291-H2301.
62. Russell B, Curtis MW, Koshman YE, et al. Mechanical stress-induced sarcomere assembly for cardiac muscle growth in length and width. *J Mol Cell Cardiol* 2010;48:817-823.
63. Heidkamp MC, Bayer AL, Scully BT, et al. Activation of focal adhesion kinase by protein kinase C epsilon in neonatal rat ventricular myocytes. *Am J Physiol Heart Circ Physiol* 2003;285:H1684-H1696.
64. Mansour H, de Tombe PP, Samarel AM, et al. Restoration of resting sarcomere length after uniaxial static strain is regulated by protein kinase C-epsilon and focal adhesion kinase. *Circ Res* 2004;94:642-649.
65. McCain ML, Parker KK. Mechanotransduction: the role of mechanical stress, myocyte shape, and cytoskeletal architecture on cardiac function. *Pflugers Arch* 2011;462:89-104.
66. Romfh A, McNally EM. Cardiac assessment in duchenne and becker muscular dystrophies. *Curr Heart Fail Rep* 2010;7:212-218.
67. Rybakova IN, Patel JR, Ervasti JM. The dystrophin complex forms a mechanically strong link between the sarcolemma and costameric actin. *J Cell Biol* 2000;150:1209-1214.
68. Lapidos KA, Kakkar R, McNally EM. The dystrophin glycoprotein complex: signaling strength and integrity for the sarcolemma. *Circ Res* 2004;94:1023-1031.
69. Constantin B, Sebillé S, Cognard C. New insights in the regulation of calcium transfers by muscle dystrophin-based cytoskeleton: implications in DMD. *J Musc Res Cell Motil* 2006;27:375-386.
70. Kaspar RW, Allen HD, Montanaro F. Current understanding and management of dilated cardiomyopathy in duchenne and becker muscular dystrophy. *J Am Acad Nurse Pract* 2009;21:241-249.
71. Ervasti JM, Campbell KP. A role for the dystrophin-glycoprotein complex as a transmembrane linker between laminin and actin. *J Cell Biol* 1993;122:809-823.
72. Gumerson JD, Michele DE. The dystrophin-glycoprotein complex in the prevention of muscle damage. *J Biomed Biotechnol* 2011;2011:210797.
73. Nakamori M, Takahashi MP. The role of alpha-dystrobrevin in striated muscle. *Int J Mol Sci* 2011;12:1660-1671.
74. Ichida F. Left ventricular noncompaction. *Circ J* 2009;73:19-26.
75. Sheikh F, Ross RS, Chen J. Cell-cell connection to cardiac disease. *Trends Cardiovasc Med* 2009;19:182-190.
76. Noorman M, van der Heyden MA, van Veen TA, et al. Cardiac cell-cell junctions in health and disease: electrical versus mechanical coupling. *J Mol Cell Cardiol* 2009;47:23-31.
77. Goldfarb LG, Dalakas MC. Tragedy in a heartbeat: malfunctioning desmin causes skeletal and cardiac muscle disease. *J Clin Invest* 2009;119:1806-1813.
78. Giepmans BN. Gap junctions and connexin-interacting proteins. *Cardiovasc Res* 2004;62:233-245.
79. Perriard JC, Hirschy A, Ehler E. Dilated cardiomyopathy: a disease of the intercalated disc? *Trends Cardiovasc Med* 2003;13:30-38.
80. Hesketh GG, Van Eyk JE, Tomaselli GF. Mechanisms of gap junction traffic in health and disease. *J Cardiovasc Pharmacol* 2009;54:263-272.
81. Lampe PD, TenBroek EM, Burt JM, et al. Phosphorylation of connexin43 on serine368 by protein kinase C regulates gap junctional communication. *J Cell Biol* 2000;149:1503-1512.
82. Solan JL, Lampe PD. Connexin phosphorylation as a regulatory event linked to gap junction channel assembly. *Biochim Biophys Acta* 2005;1711:154-163.
83. Imanaka-Yoshida K, Knudsen KA, Linask KK. N-cadherin is required for the differentiation and initial myofibrillogenesis of chick cardiomyocytes. *Cell Motil Cytoskeleton* 1998;39:52-62.
84. Angst BD, Khan LU, Severs NJ, et al. Dissociated spatial patterning of gap junctions and cell adhesion junctions during postnatal differentiation of ventricular myocardium. *Circ Res* 1997;80:88-94.
85. Fujimoto K, Nagafuchi A, Tsukita S, et al. Dynamics of connexins, E-cadherin and alpha-catenin on cell membranes during gap junction formation. *J Cell Sci* 1997;110:311-322.
86. Delmar M, McKenna WJ. The cardiac desmosome and arrhythmogenic cardiomyopathies: from gene to disease. *Circ Res* 2010;107:700-714.
87. Riley PR, Smart N. Vascularizing the heart. *Cardiovasc Res* 2011;91:260-268.
88. Olivey HE, Svensson EC. Epicardial-myocardial signaling directing coronary vasculogenesis. *Circ Res* 2010;106:818-832.
89. Tomanek RJ, Ishii Y, Holifield JS, et al. VEGF family members regulate myocardial tubulogenesis and coronary artery formation in the embryo. *Circ Res* 2006;98:947-953.
90. Gittenberger-de Groot AC, DeRuiter MC, Bergwerff M, et al. Smooth muscle cell origin and its relation to heterogeneity in development and disease. *Arterioscler Thromb Vasc Biol* 1999;19:1589-1594.
91. Vrancken Peeters MP, Gittenberger-de Groot AC, Mentink MM, et al. Smooth muscle cells and fibroblasts of the coronary arteries derive from epithelial-mesenchymal transformation of the epicardium. *Anat Embryol (Berl)* 1999;199:367-378.
92. Red-Horse K, Ueno H, Weissman IL, et al. Coronary arteries form by developmental reprogramming of venous cells. *Nature* 2010;464:549-553.
93. Tomanek RJ, Zheng W, Yue X. Growth factor activation in myocardial vascularization: therapeutic implications. *Mol Cell Biochem* 2004;264:3-11.
94. Chen Y, Torry RJ, Baumbach GL, et al. Proportional arteriolar growth accompanies cardiac hypertrophy induced by volume overload. *Am J Physiol* 1994;267:H2132-H2137.
95. Zheng W, Brown MD, Brock TA, et al. Bradycardia-induced coronary angiogenesis is dependent on vascular endothelial growth factor. *Circ Res* 1999;85:192-198.
96. Seko Y, Takahashi N, Shibuya M, et al. Pulsatile stretch stimulates vascular endothelial growth factor (VEGF) secretion by cultured rat cardiac myocytes. *Biochem Biophys Res Commun* 1999;254:462-465.
97. Jones E. The initiation of blood flow and flow induced events in early vascular development. *Semin Cell Dev Biol* 2011;22:1028-1035.
98. Jones EA, le Noble F, Eichmann A. What determines blood vessel structure? Genetic prespecification vs. hemodynamics. *Physiology (Bethesda)* 2006;21:388-395.
99. Kurosawa S, Kurosawa H, Becker AE. The coronary arterioles in newborns, infants and children. A morphometric study of normal hearts and hearts with aortic atresia and complete transposition. *Int J Cardiol* 1986;10:43-56.
100. Tomanek RJ, Sandra A, Zheng W, et al. Vascular endothelial growth factor and basic fibroblast growth factor differentially modulate early postnatal coronary angiogenesis. *Circ Res* 2001;88:1135-1141.
101. Wadhawan R, Tseng YT, Stabila J, et al. Regulation of cardiac beta 1-adrenergic receptor transcription during the developmental transition. *Am J Physiol Heart Circ Physiol* 2003;284:H2146-H2152.
102. Porrello ER, Johnson BA, Aurora AB, et al. Mir-15 family regulates postnatal mitotic arrest of cardiomyocytes. *Circ Res* 2011;109:670-679.
103. Porrello ER, Mahmoud AI, Simpson E, et al. Transient regenerative potential of the neonatal mouse heart. *Science* 2011;331:1078-1080.
104. Li F, Wang X, Capasso JM, et al. Rapid transition of cardiac myocytes from hyperplasia to hypertrophy during postnatal development. *J Mol Cell Cardiol* 1996;28:1737-1746.
105. Small EM, Olson EN. Pervasive roles of microRNAs in cardiovascular biology. *Nature* 2011;469:336-342.
106. Dillmann WH. Cellular action of thyroid hormone on the heart. *Thyroid* 2002;12:447-452.
107. White P, Burton KA, Fowden AL, et al. Developmental expression analysis of thyroid hormone receptor isoforms reveals new insights into their essential functions in cardiac and skeletal muscles. *FASEB J* 2001;15:1367-1376.
108. Sato Y, Buchholz DR, Paul BD, et al. A role of unliganded thyroid hormone receptor in postembryonic development in *Xenopus laevis*. *Meck Dev* 2007;124:476-488.
109. Dieckman LJ, Solaro RJ. Effect of thyroid status on thin-filament Ca²⁺ regulation and expression of troponin I in perinatal and adult rat hearts. *Circ Res* 1990;67:344-351.

110. Pierdominici M, Ortona E, Franconi F, et al. Gender specific aspects of cell death in the cardiovascular system. *Curr Pharm Des* 2011;17:1046–1055.
111. Fiorina P, Corradi D, Pinelli S, et al. Apoptotic/myogenic pathways during human heart development. *Int J Cardiol* 2004;96:409–417.
112. Madden SD, Donovan M, Cotter TG. Key apoptosis regulating proteins are down-regulated during postnatal tissue development. *Int J Dev Biol* 2007;51:415–423.
113. Berry NC, Sosnovik DE. Cardiomyocyte death: insights from molecular and microstructural magnetic resonance imaging. *Pediatr Cardiol* 2011;32:290–296.
114. Takeda K, Yu ZX, Nishikawa T, et al. Apoptosis and DNA fragmentation in the bulbus cordis of the developing rat heart. *J Mol Cell Cardiol* 1996;28:209–215.
115. Beard NA, Casarotto MG, Wei L, et al. Regulation of ryanodine receptors by calsequestrin: effect of high luminal Ca^{2+} and phosphorylation. *Biophys J* 2005;88:3444–3454.
116. Bers DM. Cardiac excitation-contraction coupling. *Nature* 2002;415:198–205.
117. Dulhunty AF. Excitation-contraction coupling from the 1950s into the new millennium. *Clin Exp Pharmacol Physiol* 2006;33:763–772.
118. Wier WG, ter Keurs HE, Marban E, et al. Ca^{2+} 'sparks' and waves in intact ventricular muscle resolved by confocal imaging. *Circ Res* 1997;81:462–469.
119. Davis JP, Tikunova SB. Ca^{2+} exchange with troponin C and cardiac muscle dynamics. *Cardiovasc Res* 2008;77:619–626.
120. Hoffman TM. Newer inotropes in pediatric heart failure. *J Cardiovasc Pharmacol* 2011;58:121–125.
121. Schroder EA, Tobita K, Tinney JP, et al. Microtubule involvement in the adaptation to altered mechanical load in developing chick myocardium. *Circ Res* 2002;91:353–359.
122. Ziman AP, Gomez-Viquez NL, Bloch RJ, et al. Excitation-contraction coupling changes during postnatal cardiac development. *J Mol Cell Cardiol* 2010;48:379–386.
123. Janowski E, Cleemann L, Sasse P, et al. Diversity of Ca^{2+} signaling in developing cardiac cells. *Ann New York Acad Sci* 2006;1080:154–164.
124. Janowski E, Berrios M, Cleemann L, et al. Developmental aspects of cardiac Ca^{2+} signaling: interplay between Ryr- and IP(3)R-gated Ca^{2+} stores. *Am J Physiol Heart Circ Physiol* 2010;298:H1939–H1950.
125. Qu J, Robinson RB. Cardiac ion channel expression and regulation: the role of innervation. *J Mol Cell Cardiol* 2004;37:439–448.
126. Bowditch HP. Über die eigenthümlichkeiten der reizbarkeit, welche die muskelfasern des herzens zeigen. *Arb Physiol Anstalt Leipzig* 1871;6:139–176.
127. McDonald KS. The interdependence of Ca^{2+} activation, sarcomere length, and power output in the heart. *Pflügers Arch* 2011;462:61–67.
128. Tong CW, Gaffin RD, Zawieja DC, et al. Roles of phosphorylation of myosin binding protein-C and troponin I in mouse cardiac muscle twitch dynamics. *J Physiol* 2004;558:927–941.
129. Holloway CJ, Cochlin LE, Emmanuel Y, et al. A high-fat diet impairs cardiac high-energy phosphate metabolism and cognitive function in healthy human subjects. *Am J Clin Nutr* 2011;93:748–755.
130. Campbell KS. Impact of myocyte strain on cardiac myofilament activation. *Pflügers Arch* 2011;462:3–14.
131. Ieda M, Kanazawa H, Ieda Y, et al. Nerve growth factor is critical for cardiac sensory innervation and rescues neuropathy in diabetic hearts. *Circulation* 2006;114:2351–2363.
132. Hildreth V, Anderson RH, Henderson DJ. Autonomic innervation of the developing heart: origins and function. *Clin Anat* 2009;22:36–46.
133. Ieda M, Fukuda K. New aspects for the treatment of cardiac diseases based on the diversity of functional controls on cardiac muscles: the regulatory mechanisms of cardiac innervation and their critical roles in cardiac performance. *J Pharmacol Sci* 2009;109:348–353.
134. Ieda M, Tsuchihashi T, Ivey KN, et al. Cardiac fibroblasts regulate myocardial proliferation through beta1 integrin signaling. *Dev Cell* 2009;16:233–244.
135. Robinson RB. Autonomic receptor-effector coupling during post-natal development. *Cardiovasc Res* 1996;31 [Spec No:E68–E76].
136. Xiao H, Zhang YY, Du XJ, et al. Developmental changes in the geometry, function and responsiveness of the mouse heart to beta-adrenergic stimulation as determined by high-resolution echocardiography. *Clin Exp Pharmacol Physiol* 2010;37:826–832.
137. Kawashima T. The autonomic nervous system of the human heart with special reference to its origin, course, and peripheral distribution. *Anat Embryol (Berl)* 2005;209:425–438.
138. Sun LS, Roberts LA, Rosen MR, et al. The positive chronotropic effect of acetylcholine has muscarinic and nicotinic components in the neonatal rat heart. *J Pharmacol Exp Ther* 1988;247:585–589.
139. Rosen MR, Steinberg SF, Danilo P Jr. Developmental changes in the muscarinic stimulation of canine purkinje fibers. *J Pharmacol Exp Ther* 1990;254:356–361.
140. Marvin WJ Jr, Hermsmeyer K, McDonald RI, et al. Ontogenesis of cholinergic innervation in the rat heart. *Circ Res* 1980;46:690–695.
141. Pracyk JB, Slotkin TA. Thyroid hormone regulates ontogeny of beta adrenergic receptors and adenylate cyclase in rat heart and kidney: effects of propylthiouracil-induced perinatal hypothyroidism. *J Pharmacol Exp Ther* 1992;261:951–958.
142. Klein I, Ojamaa K. Thyroid hormone and the cardiovascular system. *N Engl J Med* 2001;344:501–509.
143. Marin-Garcia J. Thyroid hormone and myocardial mitochondrial biogenesis. *Vascul Pharmacol* 2010;52:120–130.
144. Klein I. Thyroid and the heart: the intimacy is strained. *Thyroid* 2011;21:469–470.
145. Bettendorf M, Schmidt KG, Grulich-Henn J, et al. Tri-iodothyronine treatment in children after cardiac surgery: a double-blind, randomised, placebo-controlled study. *Lancet* 2000;356:529–534.
146. Mainwaring RD, Capparelli E, Schell K, et al. Pharmacokinetic evaluation of triiodothyronine supplementation in children after modified fontan procedure. *Circulation* 2000;101:1423–1429.
147. Portman MA, Slee A, Olson AK, et al. Triiodothyronine supplementation in infants and children undergoing cardiopulmonary bypass (TRICC): a multicenter placebo-controlled randomized trial: age analysis. *Circulation* 2010;122:S224–S233.
148. Maloyan A, Osinska H, Lammerding J, et al. Biochemical and mechanical dysfunction in a mouse model of desmin-related myopathy. *Circ Res* 2009;104:1021–1028.
149. Tagawa H, Wang N, Narishige T, et al. Cytoskeletal mechanics in pressure-overload cardiac hypertrophy. *Circ Res* 1997;80:281–289.
150. Monreal G, Nicholson LM, Han B, et al. Cytoskeletal remodeling of desmin is a more accurate measure of cardiac dysfunction than fibrosis or myocyte hypertrophy. *Life Sci* 2008;83:786–794.
151. Monreal G, Youtz DJ, Phillips AB, et al. Right ventricular remodeling in restrictive ventricular septal defect. *J Mol Cell Cardiol* 2010;49:699–706.
152. Lord KC, Shenouda SK, McIlwain E, et al. Oxidative stress contributes to methamphetamine-induced left ventricular dysfunction. *Cardiovasc Res* 2010;87:111–118.
153. Granzier HL, Irving TC. Passive tension in cardiac muscle: contribution of collagen, titin, microtubules, and intermediate filaments. *Biophys J* 1995;68:1027–1044.
154. Williams L, Howell N, Pagano D, et al. Titin isoform expression in aortic stenosis. *Clin Sci (Lond)* 2009;117:237–242.
155. Wu JC, Sung HC, Chung TH, et al. Role of N-cadherin- and integrin-based costameres in the development of rat cardiomyocytes. *J Cell Biochem* 2002;84:717–724.
156. Wu Y, Bell SP, Trombitas K, et al. Changes in titin isoform expression in pacing-induced cardiac failure give rise to increased passive muscle stiffness. *Circulation* 2002;106:1384–1389.
157. Frank O. Zur dynamik des herzmuskels. *Z Biol* 1895;32:370–437.
158. Patterson SW, Starling EH. On the mechanical factors which determine the output of the ventricles. *J Physiol* 1914;48:357–379.
159. Markwalder J, Starling EH. On the constancy of the systolic output under varying conditions. *J Physiol* 1914;48:348–356.
160. de Tombe PP, Mateja RD, Tachampa K, et al. Myofilament length dependent activation. *J Mol Cell Cardiol* 2010;48:851–858.
161. Hutchinson KR, Stewart JA Jr, Lucchesi PA. Extracellular matrix remodeling during the progression of volume overload-induced heart failure. *J Mol Cell Cardiol* 2010;48:564–569.
162. Leite-Moreira AF. Current perspectives in diastolic dysfunction and diastolic heart failure. *Heart* 2006;92:712–718.
163. Laflamme MA, Murry CE. Heart regeneration. *Nature* 2011;473:326–335.
164. Urbanek K, Cabral-da-Silva MC, Ide-Iwata N, et al. Inhibition of Notch1-dependent cardiomyogenesis leads to a dilated myopathy in the neonatal heart. *Circ Res* 2010;107:429–441.
165. Kaushal S, Jacobs JP, Gossett JG, et al. Innovation in basic science: stem cells and their role in the treatment of paediatric cardiac failure—opportunities and challenges. *Cardiol Young* 2009;19:74–84.
166. Mishra R, Vijayan K, Colletti EJ, et al. Characterization and functionality of cardiac progenitor cells in congenital heart patients. *Circulation* 2011;123:364–373.
167. Sayed D, Abdellatif M. MicroRNAs in development and disease. *Physiol Rev* 2011;91:827–887.
168. van Weerd JH, Koshiba-Takeuchi K, Kwon C, et al. Epigenetic factors and cardiac development. *Cardiovasc Res* 2011;91:203–211.
169. Rapti K, Chaanine AH, Hajjar RJ. Targeted gene therapy for the treatment of heart failure. *Can J Cardiol* 2011;27:265–283.

David F. Teitel ■ Steven C. Cassidy ■ Jeffrey R. Fineman

The circulation can be divided into its central components, consisting of the central arteries, veins, and, in the fetus, central shunts, and its peripheral components, consisting of the various regional vascular beds. Each component undergoes significant changes throughout fetal and postnatal development. General physiologic principles of blood flow will be presented first, followed by specific considerations pertaining to blood flow through the central and peripheral circulations, including developmental changes.

PHYSIOLOGY

General Physiology

Physical Determinants of Flow

Physical factors that regulate flow through a vascular bed exert their effects through the hydraulic equivalent of Ohm's law (resistance equation) and the Poiseuille-Hagen relationship. In vascular terms, Ohm's law states that resistance to flow between two points along a tube equals the pressure difference between the two points divided by flow. With vascular resistance R and blood flow Q , the mean pressure decrease that occurs from the artery (P_a) to the vein (P_v) can be derived from the formula

$$R = \frac{P_a - P_v}{Q}$$

To assess changes in arterial blood pressure in response to changes in flow and resistance, the formula can be rearranged as

$$P_a = Q \times R + P_v$$

Thus, elevation of arterial blood pressure may occur in response to an increase in either vascular resistance or blood flow. However, these factors are not independent; for example, arterial blood pressure may remain constant when blood flow increases if the increased flow causes vascular resistance to decrease. This can occur by the recruitment of partially or fully closed arterioles—if the product $Q \times R$ does not increase, arterial pressure does not.

Further factors that affect the resistance to flow can be approximated by the Poiseuille-Hagen relationship, which describes the relationship of pressure and flow of a Newtonian fluid flowing through a straight, round glass tube:

$$R = \frac{8l\eta}{\pi r^4}$$

where l is the length of the tube, r is its internal radius, and η is the fluid viscosity. Blood is not Newtonian. The walls of the small arteries are not smooth, and the arteries branch, curve, and taper. Blood flow is pulsatile, so that additional energy (and therefore a higher pressure) is needed to overcome inertia and to accelerate the blood at each ejection. Because of short distances between arterial branch points, laminar flow is unlikely in peripheral vascular beds, and viscous pressure losses are greater than in a classical physical model. Arteries are also distensible, and the continuously changing transvascular pressure alters their radii. Lastly, vascular beds are composed of many blood vessels in parallel. These vessels are not all open all the time, and they may differ in radii in different zones. For all of these reasons, pressure–flow relationships are not linear.

Despite these complicating factors, the general principles of changes in physical factors such as viscosity and radius apply. Vascular resistance is directly related to the viscosity of blood perfusing the vascular bed and inversely related to its cross-sectional area (r^4). Increasing viscosity or decreasing vessel radius therefore leads to an elevation of both arterial pressure and vascular resistance when blood flow remains constant (1).

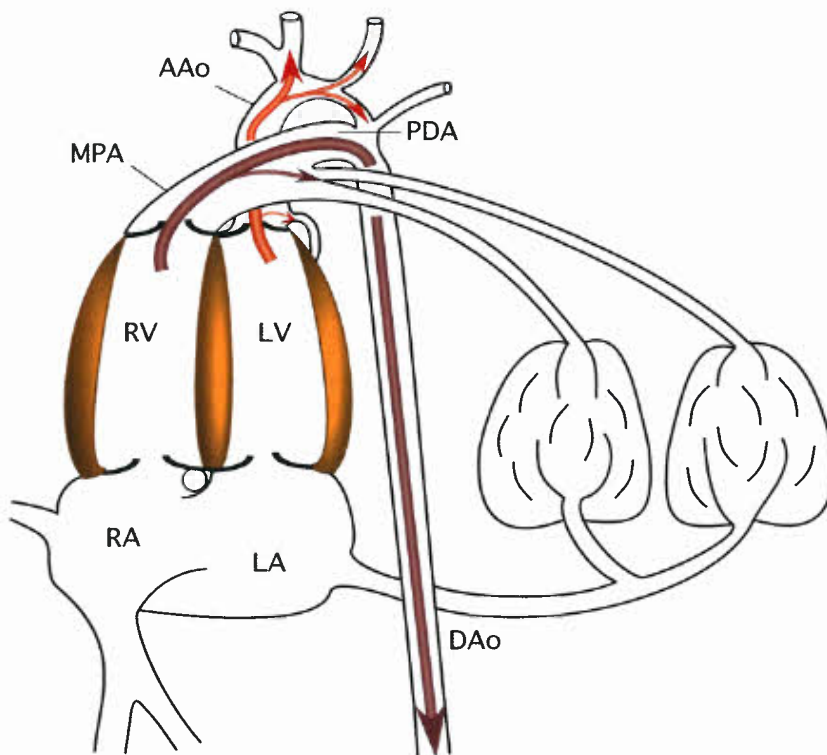
CENTRAL CIRCULATION

The central circulation is structured very differently in the fetus, primarily to accommodate the different site of oxygen uptake. In the postnatal state, oxygen uptake occurs in the pulmonary vascular bed, which is perfused independently by the right ventricle; the left ventricle separately supplies the regional systemic vascular beds with fully oxygenated blood. In the fetal state, oxygen uptake occurs in the placenta, which is perfused in parallel with the systemic vascular beds. To deliver relatively highly oxygenated blood to the metabolically active tissues (such as the heart and brain) and to deliver less oxygenated blood to the placenta for oxygen uptake, central shunts and preferential blood flow patterns exist. Shunts are present in the venous system (ductus venosus), the heart (foramen ovale), and the arterial system (ductus arteriosus) and are remarkably efficient at achieving this goal. At birth, these shunts are abolished over a very short period of time, and the mature postnatal central circulation is established within the first few days of life.

Fetal Circulation

The presence of central shunts allows the fetal circulation to be remarkably efficient at distributing oxygen and substrate. Figure 4.1 demonstrates that the fetal ventricles primarily perform their postnatal functions: The fetal right

Figure 4.1. Preferential pattern of ventricular output. The left ventricle (LV) directs most of its highly saturated blood (red arrow) via the ascending aorta (AAo) to the highly metabolic heart and upper body. The right ventricle (RV) primarily ejects less oxygenated blood (purple arrow) via the main pulmonary artery (MPA) primarily down the ductus arteriosus (PDA) and via the descending aorta (DAo) to the placenta for oxygen uptake. RA, right atrium; LA, left atrium.



ventricle supplies most of its blood via the ductus arteriosus and descending aorta to the placenta for oxygen uptake, and the left ventricle supplies most of its blood via the ascending aorta to the heart and brain for oxygen delivery. For the central venous circulation to facilitate the efficient performance of these tasks, the least saturated venous blood should be directed to the right ventricle and the most saturated should be directed to the left. To appreciate how this is achieved, it is best to consider the five components of the central venous circulation in turn. These components are the venous returns from the upper body, the myocardium, the lungs, the lower body, and the placenta.

The least saturated blood returns from the upper body, via the superior vena cava, and from the myocardium, via the coronary sinus. This blood is directed appropriately, through the tricuspid valve to the right ventricle. The leftward and superior course of the eustachian valve directs >95% of the blood flowing caudally from the superior vena cava away from the foramen ovale and toward the tricuspid valve. In addition, the location of the coronary sinus caudad to the foramen ovale causes venous blood from the myocardium to flow through the tricuspid valve to the right ventricle (Fig. 4.1). Blood returning from the lungs has an intermediate saturation, but by the nature of the normal drainage of the pulmonary veins to the left atrium, preferential flow to the right ventricle is not possible. However, pulmonary blood flow is a relatively small portion of combined venous return. It represents no more than 8% of combined ventricular output in the sheep fetus (2), and about twice that in the human, at most being 25% (3), so that it does not have a significant effect on oxygen delivery.

Inferior vena caval return comes from the remaining two sources, the lower body and the placenta. Most lower body flow, except that from the liver, ascends the distal inferior vena cava. This stream of relatively desaturated blood enters the lateral margin of the right atrium and is directed primarily through the tricuspid valve. Placental (umbilical venous) and liver venous return is more complicated (Fig. 4.2). Under

normal conditions in the fetal sheep, about 55% of the highly saturated umbilical venous return ascends via the ductus venosus to the inferior vena cava–right atrium junction, where it preferentially crosses the foramen ovale (2). Slightly less than half of the remaining umbilical venous return enters the left lobe of the liver, from which it reaches the left hepatic vein (4). The left hepatic vein joins the ductus venosus near the inferior vena cava, so that this highly saturated blood is also directed toward the foramen ovale. The limbus of the foramen ovale helps to direct this blood into the left atrium. The remainder of the umbilical venous blood, along with >95% of the poorly saturated portal venous blood, is directed to the right lobe of the liver. From the right lobe, this much less saturated blood enters the right hepatic vein and tends to stream with the blood of the distal inferior vena cava to the tricuspid valve. The hepatic artery, which carries blood that is moderately well saturated, constitutes <10% of hepatic blood flow in the fetus, so it does not significantly contribute to oxygen supply. Hepatic arterial blood is distributed to both lobes of the liver, with the right lobe receiving somewhat more (4).

Thus, preferential streaming patterns among the different sources of venous return allow most of the poorly saturated blood from the upper body, myocardium, and lower body to reach the right ventricle, and the more highly saturated umbilical venous return to reach the left ventricle. Although the separation of fetal venous return and ventricular output according to its level of blood oxygenation is not as efficient as the postnatal separation, it is quite remarkable in its ability to allow the right and left ventricles to perform their normal postnatal functions of delivery of blood for oxygen uptake and oxygen supply, respectively.

Postnatal Circulation

The changes in the central circulation at birth are primarily caused by external events rather than by primary changes in

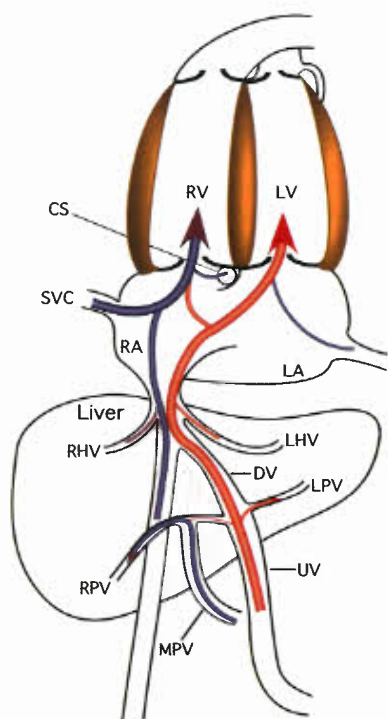


Figure 4.2. Preferential pattern of venous return to the right (RV) and left (LV) ventricles. More highly saturated blood (red arrow) from the umbilical vein (UV) passes via the ductus venosus (DV) and left hepatic vein (LHV) to the left atrium (LA) and LV. Less saturated blood (blue arrows) from the lower body via the inferior vena cava (IVC, not shown), from the main and right portal veins (MPV and RPV) via the right hepatic vein (RHV), from the coronary sinus (CS), and from the superior vena cava (SVC) passes to the right atrium (RA) and RV.

the circulation itself. Most important of these external events are the rapid and large decrease in pulmonary vascular resistance and the disruption of the umbilical-placental circulation. The various mechanisms responsible for the decrease in pulmonary vascular resistance are discussed later in this chapter. This decrease has profound effects on the central shunts in the systemic circulation. Abruptly at birth, the ductus arteriosus changes from a right-to-left conduit of blood to the descending aorta, to a left-to-right conduit of blood to the lungs, until it closes in the first hours or days of life. This shunt may be prolonged in the premature infant, causing a steal of blood from the regional systemic vascular beds of greatest resistance. The physiologic basis of normal closure of the ductus arteriosus and problems associated with delayed closure are discussed elsewhere (see Chapter 19).

As previously mentioned, the ductus venosus carries umbilical venous return primarily to the left heart. Although the amount of umbilical venous blood that enters the ductus venosus is variable and is greatly affected by stresses such as hypoxemia, changes in flow do not appear to be caused by active vasoconstriction of the ductus venosus, but rather, occur passively in accordance with changes in umbilical blood flow. At birth, the umbilical-placental circulation is abolished, causing a marked reduction in ductus venosus flow and in flow to the left lobe of the liver. However, portal venous flow through the ductus venosus increases from <5% to >50% by 1 hour of age so that, despite an increase in portal venous flow at birth, blood flow to the liver itself actually decreases substantially (5). This shunt of portal venous blood through the ductus

venosus is transient, generally lasting for 1 day to 2 weeks. The functional closure of the ductus venosus is probably a passive phenomenon, although it has been demonstrated that the isolated ductus venosus can respond to adrenergic stimulation and prostanoids. In the intact newborn lamb, it can dilate in response to prostaglandin E_1 (6). Thus, its closure may be partly induced by the same hormonal changes that are implicated in the closure of the ductus arteriosus.

Although vasoactive processes are involved in the closure of the ductus arteriosus, and may be involved in closure of the ductus venosus, closure of the foramen ovale at birth is entirely passive, secondary to alterations in the relative return of blood to the right and left atria. Prior to birth, direct left atrial return via the pulmonary veins is only modest, $\leq 25\%$ of combined venous return. Thus, the pressure gradient from the right atrium to the left maintains a large flow of blood through the foramen ovale, which appears as a wind sock bulging into the left atrium. With the onset of oxygen ventilation, the proportion of combined venous return that directly enters the left atrium via the pulmonary veins increases dramatically, to >50% (2). This is because of the marked increase in pulmonary blood flow, which includes a transient left-to-right shunt through the ductus arteriosus. Left atrial pressure thus exceeds right, and the redundant flap of tissue of the foramen ovale that previously bowed into the left atrium is now pressed against the septum. Small left-to-right shunts may be visualized in the newborn by color Doppler ultrasonography, but these shunts are not hemodynamically significant. Although patency of the foramen ovale may be present for several years, shunts of any significance occur only when the primum septum is deficient, thus forming a secundum atrial septal defect (see Chapter 28).

PULMONARY CIRCULATION

Although considerable information is available regarding the complex physiologic regulation of pulmonary vascular resistance, the exact mechanisms involved in intrinsic relaxation and constriction of the pulmonary vascular smooth muscle are not completely understood. The important functional role of the vascular endothelium and its interactions with smooth muscle are only now being brought to light. The pulmonary vessels not only produce many vasoactive substances, but also actively metabolize many. Changes in pulmonary vascular resistance can occur at different levels within the circulation, and vasoactive substances and their properties may change during passage through the pulmonary vascular bed. Accurate physiologic characterization of the pulmonary circulation varies with the gender, age, and species of the model used and the exact compartment of the pulmonary circulation evaluated. Whether all the principles that apply to systemic vascular smooth muscle also apply to the pulmonary circulation is not yet clear. However, the final common pathway by which vascular smooth muscle constricts is by Ca^{2+} -mediated stimulation of excitation-contraction coupling. Relaxation occurs mainly either through a cyclic guanosine monophosphate (cGMP)- or cyclic adenosine monophosphate (cAMP)-mediated mechanism. Many interacting factors are responsible for the physiologic and physical control of pulmonary vascular resistance in the fetus and for its normal decrease after birth.

MORPHOLOGIC DEVELOPMENT

The stage of morphologic development of the pulmonary circulation affects the vascular responses in the perinatal period.

In the fetus and newborn, all small pulmonary arteries have a thicker medial smooth muscle layer in relation to diameter than similar arteries in adults. This increased muscularity is partly responsible for the increased vasoreactivity and pulmonary vascular resistance in the fetus, particularly near term. In fetal lamb lungs, when perfusion is fixed at pressures equivalent to those *in utero*, the muscle is most prominent in the smallest resistance arteries (identified as fifth- and sixth-generation arteries; external diameter 20 to 50 μm), and over the latter half of gestation, the thickness remains constant in relation to diameter.

Similar observations using slightly different techniques have been made in human lungs. In these, the small pulmonary arteries are identified by their relationship to airways. Preacinar arteries course proximal to or along with terminal bronchioli; intra-acinar arteries course along with respiratory bronchioli or alveolar ducts, or within the alveolar walls. In arteries traced along the airways toward the alveoli, a point is reached at which the completely encircling medial smooth muscle coat gives way to a region of incomplete muscularization. In these partially muscularized arteries, the smooth muscle is arranged in a spiral or helix. The muscle then disappears from the arteries that are still larger than capillaries (nonmuscularized small pulmonary arteries). In these arteries, an incomplete pericyte layer is found within the endothelial basement membrane; in the nonmuscular portions of the partially muscular small pulmonary arteries are intermediate cells (i.e., cells intermediate in position and structure between pericytes and mature smooth muscle cells). These cells are precursor smooth muscle cells. Under certain conditions, such as hypoxia, they may rapidly differentiate into mature smooth muscle cells.

In the near-term fetus, only about half the precapillary arteries (those associated with respiratory bronchioli) are muscularized or partially muscularized, and the alveoli are free of muscular arteries. In the first 4 to 6 weeks after birth, there is progressive involution of the circumferential medial smooth muscle with overall reduction in medial muscular thickness of the walls of the small pulmonary arteries. In adults, circumferential muscularization extends peripherally along the intraacinar arteries so that most are completely muscularized, although with only a very thin layer of smooth muscle; this adult-like pattern is reached at about puberty.

During fetal growth, the number of small arteries increases greatly. In humans the main preacinar pulmonary arterial branches that accompany the larger airways are developed by 16 weeks' gestation. However, the intraacinar circulation follows alveolar development late in gestation and after birth, and arteries multiply as alveoli develop, a process generally complete by about 10 years of age (7,8).

There is an important new appreciation of the co-development and regulation of vascular and alveolar growth. These interactions likely have significant clinical implications particularly in conditions of lung hypoplasia, where vascular hypoplasia is emerging as an important clinical problem (9).

Fetal Circulation

In the fetus, gas exchange occurs in the placenta and pulmonary blood flow is low, supplying nutritional requirements for lung growth and allowing the lung to serve a metabolic or paraendocrine function. Pulmonary blood flow in near-term fetal lambs (term being 145 days of gestation) is about 100 mL/100 g wet lung weight (8% to 10% of combined ventricular output). Pulmonary blood flow is low despite the dominance of the right ventricle, which in the fetus ejects 55% to 60% of total cardiac output. Most of the right ventricular output is diverted away from the lungs through the widely patent

ductus arteriosus to the descending thoracic aorta and the placenta for oxygenation (Fig. 4.1). In young fetuses at about 0.5 gestation, 3% to 4% of total cardiac output perfuses the lungs; this increases to about 6% at 0.8 gestation, corresponding temporally with the onset of the release of surface active material into lung fluid. There is a further progressive slow increase thereafter to 8% to 10% near term. Fetal pulmonary arterial mean blood pressure increases progressively with gestation and at term is about 50 mm Hg, exceeding mean aortic blood pressure by 1 to 2 mm Hg. Total pulmonary vascular resistance early in gestation is extremely high relative to that in the infant or adult, probably owing to the small number of small arteries present. Total pulmonary vascular resistance decreases progressively over the last half of gestation, with growth of new arteries and an overall increase in cross section. However, when lung growth is accounted for, the pulmonary vascular resistance per unit of lung tends to increase over late gestation (10,11).

Transitional Circulation

At birth, with initiation of pulmonary ventilation, pulmonary vascular resistance decreases rapidly and is associated with an eightfold to tenfold increase in pulmonary blood flow. In normal full-term lambs, pulmonary arterial blood pressure decreases to near-adult levels within 2 to 3 hours. In humans this takes longer, and by 24 hours of age, mean pulmonary arterial blood pressure may be half systemic. After the initial rapid decrease in pulmonary vascular resistance and pulmonary arterial blood pressure, there is a slow, progressive decrease, with adult levels reached after 2 to 6 weeks (Fig. 4.3). This is due to vascular remodeling, muscular involution, and rheologic changes.

Physiologic Regulation of Pulmonary Vascular Resistance

As previously discussed, pulmonary vascular resistance in the fetal lung is initially high and decreases slightly throughout the final third of gestation. Many factors, including mechanical effects, state of oxygenation, and the production of vasoactive substances, regulate the tone of the fetal pulmonary circulation. The most prominent factor associated with high fetal pulmonary vascular resistance is the normally low blood and alveolar O_2 tension. In the fetal lamb, resistance is further increased by hypoxemia and lowered by increasing oxygen tension, a vasoactive response that becomes active in the latter third of gestation. The exact mechanism and site of hypoxic pulmonary vasoconstriction in the fetal pulmonary circulation remains unclear. In isolated fetal pulmonary arteries, oxygen modulates the production of both prostacyclin and endothelium-derived nitric oxide (EDNO): two potent vasoactive substances that may in part underlie the responses of the developing pulmonary circulation to changes in oxygenation. In addition to the low oxygen environment, many substances constrict the pulmonary circulation of the fetus, such as α agonists, thromboxane, and the leukotrienes. However, their role, if any, in the maintenance of the high fetal pulmonary vascular resistance does not appear prominent (12–14). In addition to the production of vasoconstrictors, the fetal pulmonary circulation actively and continuously produces vasodilating substances that modulate the degree of vasoconstriction under normal conditions and may play a more active role during periods of fetal stress. These substances are mainly endothelially derived and include EDNO and prostacyclin (PGI_2). EDNO is synthesized by the oxidation of the guanidino nitrogen moiety of L-arginine.

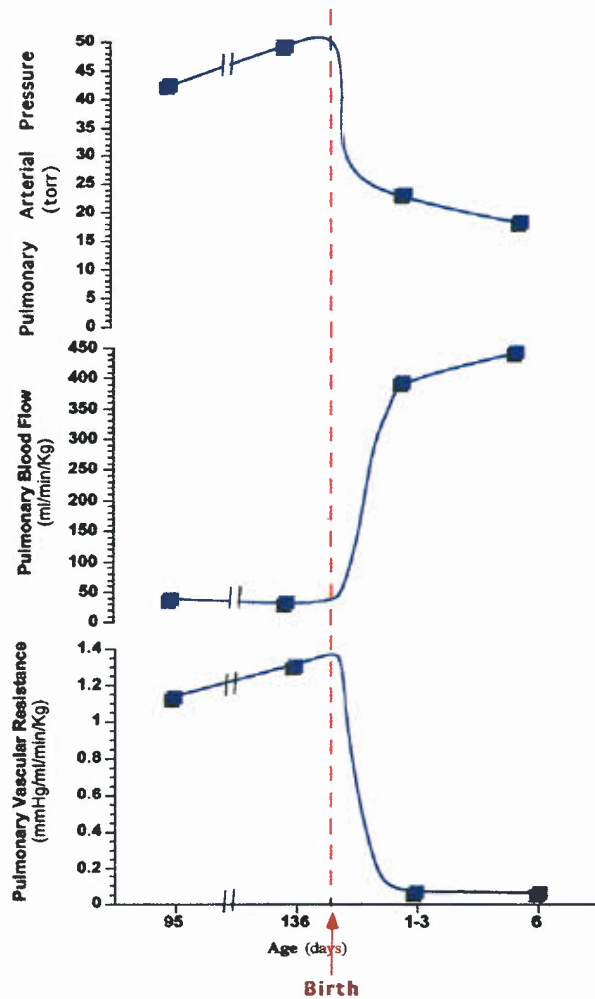


Figure 4.3. The changes in pulmonary arterial pressure, blood flow, and vascular resistance that occur around birth. (Data from Morin FC III, Egan E. Pulmonary hemodynamics in fetal lambs during development at normal and increased oxygen tension. *J Appl Physiol* 1992;73:213–218; and Soifer SJ, Morin FC III, Kaslow DC, et al. The developmental effects of prostaglandin D₂ on the pulmonary and systemic circulation in the newborn lamb. *J Dev Physiol* 1983;5:237–250.)

After certain stimuli, such as shear stress or the receptor binding of specific vasodilators (endothelium-dependent vasodilators), nitric oxide (NO) is synthesized by the activation of NO synthase, and NO is then released from the endothelial cells. Once released from endothelial cells, NO diffuses into vascular smooth muscle cells and activates soluble guanylate cyclase, the enzyme that catalyzes the production of guanosine-3'-5'-cyclic monophosphate (cGMP) from guanosine-5'-triphosphate. Activation of guanylate cyclase increases the concentrations of cGMP, thus initiating a cascade that results in smooth muscle relaxation (Fig. 4.4). Endothelial production of NO and cGMP has been demonstrated in the fetal, newborn, and adult pulmonary vasculature. In fetal lambs, inhibition of EDNO synthesis produces marked increases in resting fetal pulmonary vascular resistance and inhibits the oxygen-induced decrease in pulmonary vascular resistance. In addition, studies of intrapulmonary arteries and isolated lung preparations of the sheep show maturational increases in NO-mediated relaxation during the late fetal and early postnatal period. These data suggest that basal EDNO production is an important mediator of both normal fetal pulmonary vascular tone and the dramatic decrease in resistance that occurs with the onset of oxygen ventilation at birth (15–17). Prostacyclin is synthesized primarily in vascular endothelial cells and produces vasodilation by activating adenylate cyclase via receptor G protein-coupled mechanisms. Activation of adenylate cyclase results in increased adenosine 3',5'-cyclic monophosphate (cAMP) concentrations, thus initiating a cascade that results in smooth muscle relaxation. Although there is a maturational increase in PGI₂ production throughout gestation, basal PGI₂ activity does not appear to be an important mediator of resting fetal pulmonary vascular tone. Interestingly, endothelin-1 (ET-1) is another potent endothelially derived vasoactive factor with both vasodilating and vasoconstricting effects. The hemodynamic effects of ET-1 are mediated by at least two distinct receptor populations, ET_A and ET_B. ET_A receptors are located on vascular smooth muscle cells and are likely responsible for the vasoconstricting effects of ET-1, whereas most ET_B receptors are located on endothelial cells and are likely responsible for the vasodilating effects of ET-1. The predominant effect of exogenous ET-1 in the fetal and newborn pulmonary circulation is vasodilation, mediated via ET_B receptor activation and EDNO release. However, the predominant effect in the juvenile and adult pulmonary circulation is vasoconstriction, mediated via ET_A receptor activation. In fetal lambs, selective ET_A receptor blockade produces small

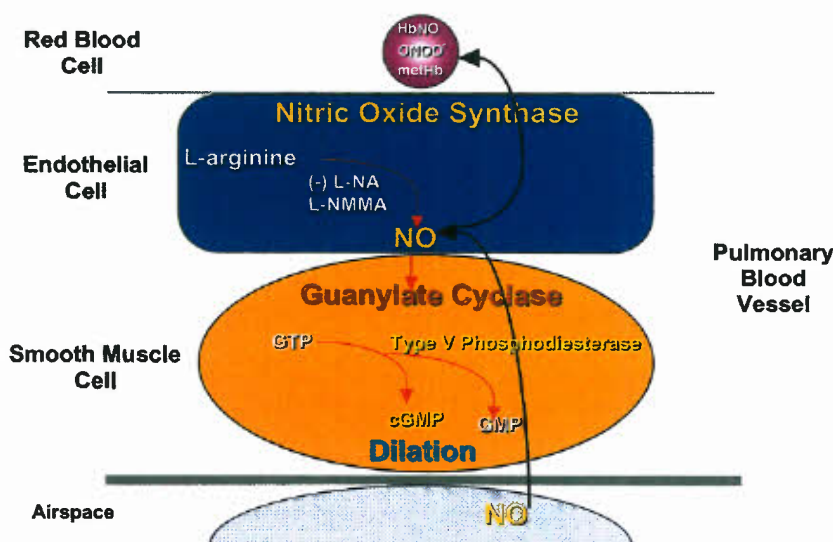


Figure 4.4. Schematic of the nitric oxide (NO)-cGMP pathway. Endogenous NO is produced from L-arginine within the pulmonary vascular endothelial cell. After diffusing into the smooth muscle cell, NO activates guanylate cyclase. The resulting increase in cGMP concentration induces relaxation. Exogenous NO (inhaled NO) diffuses from the airspace into the smooth muscle cell, where it activates guanylate cyclase. When it diffuses into the bloodstream, NO binds to hemoglobin to form methemoglobin and is inactivated.

decreases in resting fetal pulmonary resistance, suggesting a potential, minor role for basal ET-1-induced vasoconstriction in maintaining the high fetal pulmonary vascular resistance. Although plasma concentrations of ET-1 are increased at birth, animal data suggest that basal ET-1 activity does not play an important role in mediating the transitional or resting postnatal pulmonary circulation (18).

The decrease in pulmonary vascular resistance and increase in pulmonary blood flow with ventilation were, for a long time, thought mainly to be due to the increase in alveolar oxygen tension with a contribution from the physical expansion of the lung. The role of oxygen was supported by increased pulmonary flow with hyperbaric oxygenation without ventilation. Some pulmonary vasodilation occurs by inflating the lungs with a low oxygen-containing gas mixture that does not change arterial blood gas composition. Adding oxygen completes the vasodilator process. The exact mechanisms of oxygen-induced pulmonary vasodilation during the transitional circulation remain unclear. The increase in alveolar or arterial oxygen tension may decrease pulmonary vascular resistance either directly via potassium channel activation or indirectly by stimulating the production of vasodilator substances such as PGI₂, bradykinin, adenosine, adenosine-5'-triphosphate, or EDNO. Inflating the lung with a low-oxygen gas mixture may lower pulmonary vascular resistance by either physical or chemical mechanisms. One mechanism operates through changes in alveolar surface tension. Another more important mechanism is the production and release of prostaglandins (predominantly PGI₂), which occurs either with mechanical stimulation of the lung or with rhythmic lung expansion (19,20).

Exogenous prostaglandins, particularly PGI₂, lower pulmonary vascular resistance in the fetus. In addition, inhibiting prostaglandin production with indomethacin before fetal lung ventilation attenuates the subsequent decrease in pulmonary vascular resistance that occurs after the initial (~first 30 seconds) rapid decrease in resistance. However, exogenous PGE₂ and PGI₂ also produce systemic vasodilation in fetal animals, whereas systemic vascular resistance normally rises when ventilation begins. Therefore, other prostaglandins, such as PGD₂, could be involved in pulmonary vasodilation. In newborn animals, PGD₂ produces greater pulmonary than systemic vasodilation; this differential effect is lost by about 12 to 15 days of age, when PGD₂ produces pulmonary vasoconstriction. This is similar to the effects of histamine, a modest pulmonary vasodilator in the immediate perinatal period and later a pulmonary vasoconstrictor. Both PGD₂ and histamine are released from mast cells, which increase in number in the lungs over the last portion of gestation; after birth, they decrease markedly. Thus, the stimulus of lung expansion may cause mast cells to degranulate, release PGD₂ and histamine, and contribute to the initial postnatal pulmonary vasodilation.

Adenosine and adenosine triphosphate also produce potent pulmonary vasodilation in the fetus via purine receptor activation. Animal studies suggest that their release at birth has a significant role in oxygen-induced pulmonary vasodilation. Bradykinin, another vasoactive agent, also is a potent pulmonary vasodilator in the fetus. However, bradykinin receptor blockade does not attenuate the decrease in pulmonary vascular resistance at birth in the lamb, casting doubt over the importance of bradykinin in postnatal pulmonary vasodilation.

Endothelium-derived NO has been implicated as an important mediator of the decrease in pulmonary vascular resistance at birth associated with increased oxygenation. For example, inhibition of NO synthesis attenuates the increase in pulmonary blood flow owing to oxygenation of fetal lambs induced by either maternal hyperbaric oxygen exposure or *in utero* ventilation with oxygen. *In utero* ventilation

without changing fetal blood gases increases epithelial nitric oxide synthase (eNOS) gene expression in lung parenchyma of fetal lambs; this is further increased by ventilation with 100% oxygen. *In vitro* data reveal a maturational increase in EDNO production from late gestation to the early postnatal period that is modulated, in part, by oxygen. Moreover, both acute and chronic inhibition of NO synthesis prior to delivery significantly attenuate the normal increase in pulmonary blood flow at birth. These data suggest an important role for EDNO activity during the transitional circulation. However, the immediate decrease in pulmonary vascular resistance minutes after birth is not attenuated by NO inhibition. Therefore, there appear to be at least two components to the decrease in pulmonary vascular resistance with the initiation of ventilation and oxygenation. First, pulmonary vasodilation is caused by physical expansion of the lung and the production of prostaglandins (PGI₂ and PGD₂). This probably is independent of fetal oxygenation and results in an increase in pulmonary blood flow and decrease in pulmonary vascular resistance. Second, there is a further maximal pulmonary vasodilation associated with fetal oxygenation that is independent of prostaglandin production; it is most likely caused by the synthesis of EDNO, although the exact stimuli for EDNO production have not yet been defined. Both components are necessary for the successful transition to extrauterine life.

Control of the perinatal pulmonary circulation, therefore, probably reflects a balance between factors producing active pulmonary vasoconstriction (leukotrienes, low oxygen, and possibly even ET-1 acting through the ET_A receptor) and those leading to pulmonary vasodilation (EDNO, ET-1 acting through the ET_B receptor, bradykinin, and prostaglandins). The dramatic increase in pulmonary blood flow after birth most likely reflects a shift from active pulmonary vasoconstriction to active pulmonary vasodilation. It is possible that arachidonic acid metabolism shifts from lipoxygenase products in the fetus toward cyclo-oxygenase products owing either to mechanical stimulation with lung expansion or to the higher oxygen environment after birth.

After the immediate postnatal period, the more important factors affecting pulmonary vascular tone and resistance are oxygen concentration, pH, the basal production of EDNO, the effects of alveolar distention, and perhaps the production of other vasoactive agents such as histamine, 5-hydroxytryptamine, ET-1, prostanoids, thromboxanes, and the leukotrienes. The interaction of oxygen and pH is particularly important. Decreasing oxygen tension and decreases in pH elicit vasoconstriction of the resting pulmonary circulation. The mechanisms of acute hypoxic pulmonary vasoconstriction remain unclear and are the subject of several extensive reviews. Acidosis potentiates hypoxic pulmonary vasoconstriction, and alkalosis reduces it. The exact mechanism of pH-mediated pulmonary vasoactive responses also remains incompletely understood, but appears to be independent of pCO₂ (7,17). More recent data suggest that potassium channels play an important role in mediating these responses (21,22).

POSTNATAL PERIPHERAL CIRCULATION

The peripheral circulation is composed of a wide variety of regional vascular beds, each with its own characteristics. Several mechanisms regulate blood flow to these beds and affect each bed to a varying degree. These include central regulatory mechanisms such as neural activity and hormonal levels, and local mechanisms including local metabolic and pressure-flow (autoregulation) control. These mechanisms are first

presented, and then the individual vascular beds are discussed, according to their primary control mechanisms.

Controls Over the Peripheral Circulation

Neural Control

Neural control of the systemic circulation allows rapid regulation of the circulation and provides simultaneous control of different parts of the peripheral circulation. It is the primary mechanism responsible for the minute-to-minute control of blood pressure and regional blood flow distribution in the resting state and in response to acute stresses. Neural regulation consists of feedback information (afferent limb) provided by various mechanoreceptors and chemoreceptors, central integration of that information in the medulla oblongata, and effector mechanisms (efferent limb) within the autonomic nervous system, composed primarily of sympathetic nerves. Nearly all blood vessels in the body are innervated by the sympathetic vasoconstrictor nerves; some are also innervated by sympathetic and parasympathetic vasodilator nerves. The extent and type of innervation vary from one vascular bed to another.

The primary afferent limb of the neural control mechanisms consists of mechanoreceptors in the carotid sinuses and aortic arch, which respond to changes in pressure (baroreceptors). Two types of baroreceptors have been identified. Type 1 receptors control dynamic changes in blood pressure; type 2 receptors are responsible for control of resting blood pressure (23). These receptors respond to mechanical stretch of the arterial wall and send nerve impulses to the cardioinhibitory and vasomotor centers of the medulla oblongata. Stimulation of carotid sinus receptors results in slowing of heart rate, vasodilation, and a decrease in arterial blood pressure. Smooth muscle in the walls of these baroreceptor regions is innervated by vasoconstrictor efferent fibers, suggesting that sympathetic activity may modify baroreceptor responses.

Mechanoreceptors are also found in the walls of the atria and ventricles. These receptors are located in the walls of both atria at the venoatrial junctions (24), and are scattered throughout the left ventricle and interventricular septum. Two kinds of atrial receptors have been described. Type A receptors fire during atrial contraction and respond to changes in atrial pressure, and type B receptors fire during ventricular systole and respond to changes in atrial volume (25). Type A receptors stimulate and type B receptors inhibit sympathetic vasoconstrictor activity. These receptors provide feedback to the hypothalamus and inhibit secretion of antidiuretic hormone (vasopressin) (25). Atrial stretch causes secretion of atrial natriuretic peptide (ANP), which is discussed in more detail later. Atrial receptors also alter sympathetic stimulation of the renal circulation (23). By these mechanisms, atrial stretch receptors play an important role in regulation of intravascular volume. They are also responsible for the increase in heart rate caused by the Bainbridge reflex (24).

Two different types of mechanoreceptors are found in ventricular myocardium. The first fire in a pulsatile manner in time with cardiac rhythm and are small in number. The second respond to mechanical stimulation and to various drugs and chemicals through nonmyelinated afferent nerves known as C fibers (24). Stimulation of C fibers, primarily located in the left ventricle, causes hypotension and bradycardia by parasympathetic stimulation and sympathetic inhibition (24). There is evidence to suggest that carotid baroreceptors are more important for control of sympathetic regulation of muscle blood flow, whereas cardiac receptors are more important for control of sympathetic regulation of kidney blood flow.

Chemoreceptors also play a significant role in the central control of the circulation, particularly during acute stresses. Under normoxemic and normocapnic conditions, they exert little effect, but hypoxemia and hypercapnia increase sympathetic vasoconstrictor activity in addition to stimulating respiratory rate and effort. The primary locations of these chemoreceptors are in the carotid body, aortic arch, and brain (the latter is likely the mechanism of the Cushing reflex), but they also exist in coronary vessels, muscle, and lung.

Central integration of neural control of the circulation occurs primarily in the medullary cardiovascular centers, which also control respiration. Higher centers, such as the hypothalamus, modulate the medullary activity. The only afferent component that appears to have continuous input to the central control is the arterial baroreceptors.

Central mechanisms in the medulla control the efferent output of the sympathetic and parasympathetic neural systems, the efferent limb of neural control of the circulation. The primary efferent effectors are the sympathetic vasoconstrictor fibers. Their nerve endings contain the vasoconstrictor norepinephrine, which is released on nerve stimulation. They innervate the "resistance vessels," which are systemic arterioles that constrict upon this sympathetic stimulation. Other substances are present at the neurovascular junction, including monoamines, polypeptides, purines, and amino acids, all of which can influence the release and the effects of norepinephrine (23). Impulses carried through vasoconstrictor fibers contribute the normal vascular tone or baseline constriction that is present at rest in most vascular beds and thus are the main mechanism for regulating blood pressure in the unstressed state. These vasoconstrictor fibers are more prevalent in skeletal muscles, where intrinsic tone is fairly high under resting conditions. They are much less prevalent in the cerebral and coronary beds. Sympathetic vasoconstriction of larger arteries and of veins changes their volume and therefore changes the circulating volume; these vessels are known as capacitance vessels.

Sympathetic stimulation by vasodilator fibers increases blood flow to a vascular bed. These fibers are primarily found in the vascular beds of skeletal muscle. The transmitter in vasodilator fibers is thought to be acetylcholine, although in primates it may be epinephrine. These vasodilator fibers may cause a small anticipatory increase of blood flow to the skeletal muscle. However, once muscle exercise begins, local vasodilation probably plays a more important role.

The parasympathetic system primarily controls heart function and rate and has a very limited role in control of the peripheral circulation. The transmitter stored in nerve endings of the parasympathetic system is acetylcholine. Parasympathetic vasodilator fibers are found in the cerebral and myocardial circulations and in the bladder, rectum, and external genitalia. Their effects are important for local vasodilation in the latter group, but have very little role in vascular tone in the brain and the heart.

Hormonal Control

Hormonal control of the peripheral circulation can best be described as vascular constriction or dilation in response to circulating hormones. The vasculature in the peripheral circulation is responsive to various hormones, including catecholamines, angiotensin II, vasopressin, eicosanoids, NO, and peptide hormones.

Catecholamines are the hormones of the adrenergic system. Adrenergic receptors to catecholamines are present in the smooth muscle throughout the peripheral vascular system and can be categorized as α and β receptors. Stimulation of α receptors causes vascular smooth muscle to contract, causing vasoconstriction; stimulation of β receptors causes vascular smooth muscle to relax, causing vasodilation. These receptors

are responsive to both endogenous catecholamines and sympathomimetic drugs. Norepinephrine, an α -adrenergic agonist, is secreted by the adrenal medulla and is carried by the bloodstream to receptors in the peripheral vasculature. Preganglionic sympathetic fibers innervate the adrenal medulla and stimulate norepinephrine secretion. There is, therefore, central control of this hormonal regulation. Epinephrine is also secreted by the adrenal medulla, but it is a much weaker vascular stimulant and tends to exert a β -agonistic effect at physiologic concentrations.

Angiotensin II, a powerful vasoconstrictor, is produced by activation of the renin-angiotensin-aldosterone system. The juxtaglomerular apparatus in the kidney secretes renin in response to decreased renal arterial pressure or a decrease in extracellular fluid volume. Renin, in turn, cleaves angiotensinogen to angiotensin I, which is then converted to angiotensin II by a converting enzyme found in lung and vascular endothelium. Angiotensin II has direct vasoconstrictor properties, acts centrally to stimulate the vasoconstrictor centers of the brain, and stimulates the secretion of antidiuretic hormone (vasopressin). Antidiuretic hormone is synthesized in the hypothalamus and secreted by the posterior pituitary. It is a very potent vasoconstrictor but plays a minimal role in regulation of the circulation under resting conditions.

Prostaglandins and other eicosanoids play a small role in regulation of flow in the systemic circulation and have been discussed in detail above. Another group of hormones that participate in regulation of the systemic circulation are the natriuretic peptides. At the present time, the three main natriuretic peptides are ANP (atrial natriuretic peptide), BNP (brain natriuretic peptide), and CNP (C-type natriuretic peptide), although new members of this family are continually being discovered. ANP is released from atrial myocytes of both atria and in smaller amounts from the ventricular myocytes. Ventricular production of ANP decreases with maturation; large amounts of ANP are produced in fetal ventricular myocardium, and only small amounts are produced by adult ventricles (26). ANP is released in response to stretch of either atrium. Increased circulating levels of ANP are detected when left atrial pressure is elevated even when the right atrial pressure is normal. In the kidney, ANP decreases tubular reabsorption of sodium. In the circulatory system, ANP has vasodilator and cardioinhibitory effects (26). Circulating levels of ANP are increased in certain pathophysiologic conditions, such as congenital heart disease associated with elevated atrial pressures, congestive heart failure, valve disease, hypertension, coronary artery occlusion, and atrial arrhythmias (26). BNP is secreted from the ventricles, responding to volume expansion and pressure overload similarly to ANP. Its mechanism of action is also similar, binding to BNP receptors which subsequently causes an increase in intracellular cGMP levels. BNP is important because it has been found to be one of the most specific and sensitive biomarkers for heart failure. CNP is quite different than ANP and BNP. It is thought to be stored locally, in endothelial cells, particularly in the coronary and mesenteric circulations. It acts via G_i proteins to inhibit adenyl cyclase and activate phospholipase-C. It hyperpolarizes smooth muscle cells, leading to vasodilation, and is thought by some investigators to be the endothelium-derived hyperpolarizing factor (EDHF) discussed below (27).

Endothelial Function

The vascular endothelium plays an important role in regulating vascular tone, platelet adhesion, and inflammation. Receptors are present on the endothelial cell membrane for a number of locally produced and remotely secreted hormones and other substances, including peptides, kinins, amines, nucleotides, and eicosanoids. The endothelium responds to changes in

blood flow and stretch and generally promotes vasodilation (28). The endothelium produces vasoactive substances in response to different stimuli to mediate this effect.

Vasodilator substances produced by the endothelium include PGI_2 , EDNO, adenosine, and EDHF (28). PGI_2 and EDNO have been discussed above. The identity of EDHF has yet to be determined but many investigators think that it is CNP. It produces hyperpolarization of vascular smooth muscle cells (28) by activating K^+ channels, thereby inhibiting voltage-gated calcium channels, lowering cytosolic calcium, and promoting relaxation (29). Vasoconstrictor substances produced by the endothelium include ET-1, a locally acting peptide hormone also discussed earlier in this chapter. Angiotensin II is also produced in the endothelium by angiotensin-converting enzyme, found in vascular endothelial cells. Other vasoconstrictor factors are postulated to be produced by the endothelium, but are yet to be identified (28).

Local Metabolic Control

In addition to local endothelial release of vasoactive hormones described above, tissues have the ability to regulate their own blood flow in response to changes in metabolic demands by changes in their chemical milieu. The local chemical environment of arterioles can cause vasodilation or, to a lesser extent, vasoconstriction. For example, a decrease in pO_2 , an increase in pCO_2 , or an increase in H^+ or K^+ concentration each causes arteriolar vasodilation independent of endothelial function. Many cells other than endothelial cells will release adenosine, a potent vasodilator, in response to increased metabolism or decreased oxygen tension.

Red Blood Cell Control

Recently, red blood cells have been postulated to be a major factor in the regulation of local blood flow (30). It has been proposed that the sensor is deoxygenated hemoglobin. By a variety of mechanisms, deoxygenation may cause the release of vasodilatory compounds from the red blood cell, or may cause the red blood cell to release factors that stimulate endothelial release of vasodilatory compounds. Three possible mechanisms of this action have been proposed. First, red blood cells have been shown to be able to release ATP in a deoxygenation-dependent manner; this, in turn, is capable of promoting the endothelial production of NO and other local vasodilators. An important finding is that ATP can be propagated upstream, which is necessary if deoxygenated red blood cells in capillaries are to be capable of inducing arteriolar dilation. Second, there is evidence of direct red blood cell release of NO from S-nitrosohemoglobin on deoxygenation. NO is rapidly inactivated in red blood cells by interacting with oxygenated hemoglobin to form methemoglobin and nitrate, and it binds to deoxygenated hemoglobin to form nitrosylhemoglobin. It is thought that the latter compound contains some vasodilatory potential, carried in red blood cells in the S-nitrosohemoglobin form. Lastly, it has been proposed that small amounts of local nitrite produced by NO oxidation can react with deoxygenated hemoglobin, when taken up in the red blood cell, to produce NO, which then escapes from the cell.

Autoregulation

Blood flow to tissues remains relatively constant over a wide range of arterial blood pressure owing to autoregulation. The mechanisms of this phenomenon are largely unknown. Several hypothetical mechanisms exist, including local metabolic control, myogenic activity of vascular smooth muscle, tubuloglomerular feedback in the kidney, and tissue pressure. These mechanisms may act alone or in combination. The metabolic hypothesis suggests that blood flow is closely linked to tissue

metabolism. Reduction of inflow of blood would cause an accumulation of vasodilator substances such as those discussed above, which would in turn cause vasodilation and increased blood flow. In organs with high oxygen consumption, autoregulation of blood flow is dependent on tissue oxygenation. A second proposed mechanism of autoregulation is myogenic control (31). According to this theory, increased intravascular pressure stimulates vasoconstriction of vascular smooth muscle. A venous-arterial reflex has been described in which an increase in venous pressure causes arteriolar constriction, probably by a neurally mediated mechanism (31). A tubuloglomerular feedback mechanism may help to autoregulate renal blood flow. According to this hypothesis, increased renal blood pressure and flow increase the concentration of solutes in the tubular fluid; this increase is sensed in the macula densa, causing vasoconstriction by an unknown mechanism. Tissue pressure is another possible mechanism for autoregulation. By this proposed mechanism, increased tissue pressure in areas in encapsulated organs or in the brain leads to decreased blood flow to those areas. Autoregulation seems to play a more significant role in control of resting blood flow in vital organs such as the brain and heart and becomes significant in other areas during times of increased metabolic demand.

Specific Regional Vascular Beds

The different regional vascular beds in the fetus and child are controlled to varying extents by the different mechanisms discussed above. Generally, the highly metabolically active organs such as the brain and heart are primarily regulated by local mechanisms, whereas the less active beds are under central neural and hormonal controls. Specialized beds such as the renal and hepatic circulations, which receive blood for unique activities such as metabolic degradation and excretion, hematopoiesis, and blood pressure control, have unique combinations of control mechanisms. The myocardium is not discussed in this section because it is considered elsewhere (see Chapter 3).

Cerebral Circulation

The cerebral circulation of the fetus and neonate has been the most extensively studied and characterized. It is unique in four main respects. First, there is a blood-brain barrier created by a continuous lining of endothelial cells linked by tight junctions and by degradative enzymes; thus, changes in circulating concentrations of various constituents such as H^+ and catecholamines may have a limited effect. Second, the large arteries form a significant component of the resistance circuit, having been shown to respond in a similar fashion to the arterioles in response to stresses such as hypoxia (32). Third, the cerebral circulation is encased in a closed box, the skull, so that perfusion pressure is particularly important to blood flow characteristics. And fourth, there is great heterogeneity in blood flow patterns to the different regions of the brain. They have very different resting blood flows and are controlled to different extents by different mechanisms. For example, in the fetus, the greatest blood flow occurs in the oldest regions phylogenetically: The brain stem receives the most, then the cerebellum, and last, the cortex. In the newborn, the pattern is immediately reversed, with the cortex receiving the greatest blood flow, then the cerebellum, and last, the brain stem (33). These differences are thought to exist because of differences in sensitivity to hypoxia and hyperoxia.

Autoregulation is an essential component in the control of cerebral blood flow. To limit the risk of hemorrhage and inadequate blood supply to the brain in the face of acute increases and decreases in blood pressure, it is important that flow remains constant over a wide range of perfusion pressures in the range of 60 to 160 mm Hg. At higher blood pressure,

autoregulation is lost, and blood flow becomes dependent on mean arterial pressure. At pressures below the autoregulation range, cerebral blood flow falls resulting in ischemia (34).

In the brain, several mediators of autoregulation have been found. It appears that alterations in local adenosine concentrations mediate the autoregulatory response. Interstitial levels of adenosine increase during hypotension, an adenosine analogue increases blood flow in the autoregulatory range, and autoregulation is abolished by blocking the adenosine receptor (35). Prostanoids are another group of vasoactive substances that have been implicated in the control of autoregulation. Dilator prostanoids such as prostacyclin increase in response to hemorrhage, and cyclooxygenase inhibition decreases cerebral blood flow and the response to hypotension. There is evidence that neuronally derived NO participates in vasodilation during hypertension (36). Whether or not NO plays a role in autoregulation of cerebral blood flow is still controversial (37).

Autoregulation has been demonstrated in young fetal sheep as early as 93 days' gestation (~ 0.67 gestation) and exists over a wide range of mean cerebral arterial pressures (35). However, the lower limit of this range is close to the normal mean perfusion pressure, putting the fetus at relatively high risk for hypotension-associated problems. This is particularly important in the subependymal germinal matrix, which exists until about 36 weeks' gestation in the human fetus, and in the choroid plexus, which are the primary sites of intraventricular hemorrhage in the premature infant. In the sick preterm and term infant, autoregulation has been shown to be absent (38), a circumstance that may predispose these infants to brain injury such as intracranial hemorrhage. At birth, studies are conflicting as to whether the autoregulatory range increases significantly. However, the lower limit of the autoregulatory range is much further below the normal mean perfusion pressure than it is in the premature infant.

Another major regulating factor of cerebral blood flow is blood oxygen concentration. Because of the critical importance of oxygen delivery to the brain, this is not surprising. However, although it had been assumed that pCO_2 is a more important determinant of cerebral blood flow, studies have shown that the fetus and newborn are relatively insensitive to pCO_2 changes but can change blood flow twofold to threefold in response to changes in arterial pO_2 (35). In the immature brain, oxygen sensitivity follows the same hierarchy as flow patterns. The brain stem is most sensitive and the cortex is least sensitive to changes in pO_2 . This is perhaps a protective mechanism to permit the maintenance of basic autonomic function during profound hypoxia. The mechanisms behind oxygen sensitivity are not certain, although local factors produced by the endothelium probably play a considerable role. In addition to vasoactive substances, oxygen may have a direct effect on various ATP-mediated reactions (32).

Carbon dioxide also has a significant effect on cerebral blood flow, although less than in the mature brain, and, like oxygen, has its greatest effects on the brain stem (33). Moreover, this effect has been demonstrated in all regions of the brain as early as 0.4 gestation in the fetal sheep (39). Because of the blood-brain barrier, this effect is specific to a change in pCO_2 ; cerebral blood flow does not change in the face of metabolic acidosis or alkalosis. The effect of pCO_2 appears to be exerted by changing extracellular brain H^+ , but how this change in H^+ then affects the production or release of endothelium-derived vasoactive substances is not known. It is apparent, however, that prostanoids are significantly involved in this response (40). Recent evidence has demonstrated that hypoxia disrupts cerebral autoregulation, but hypocapnia augments the cerebral autoregulation response (41).

Other factors also can modulate cerebral blood flow, including sympathetic innervation, circulating hormones such

as vasopressin and catecholamines, and blood hematocrit level, but it is clear that this highly metabolically active organ is under exquisite control from very early in gestation by a host of local regulatory mechanisms.

Peripheral Tissues

In contrast to the cerebral circulation, the peripheral circulation (skin, muscle, and bone) is primarily under central control. The vasoactivity of each component of the peripheral tissues is controlled somewhat differently. For example, the skin is predominantly under α -adrenergic tone with no significant autoregulation, whereas the muscle has a higher proportion of β -adrenergic control and has intact autoregulation. This group of vascular beds is presented together because the primary control of vascular tone of these beds and the responses to major stresses such as hypotension and hypoxemia are similar and are predominantly mediated by the autonomic nervous system and circulating hormones. Because peripheral blood flow is needed primarily for growth and thermoregulation in the developing organism and essential oxygen demands are small, central controls that limit flow during stress can be invoked with few sequelae. Thus, from early fetal life, a large variety of vascular receptors develop, including α_2 -adrenergic, β_1 - and β_2 -adrenergic, dopaminergic A1 and A2, vasopressinergic V1, Endothelin A and B, muscarinic, etc. They transduce alterations in levels of circulating and synaptic compounds via various intracellular second messengers, into alterations of peripheral vascular smooth muscle tone.

Early in gestation, the peripheral circulation is predominantly under α -adrenergic influences, with little cholinergic tone. Changes in basal tone can be demonstrated with the administration of α -adrenergic agonists and not by β -agonists or cholinergic agents. Similarly, blocking of α -adrenergic activity invokes a large decrease in peripheral vascular resistance, whereas the dominant effect of β -adrenergic blockade is to slow heart rate. Although parasympathetic tone is limited in early gestation, receptors are present and can be stimulated. Late in gestation, resting activity increases rapidly toward the high levels normally seen after birth. Very early in fetal life, response of autonomic receptors requires that circulating catecholamines be secreted by the adrenal medulla and nonadrenal chromaffin tissue; innervation is a significantly later event than receptor development. As innervation proceeds rapidly in early fetal life, neural mechanisms can be invoked to alter peripheral blood flow. The primary neural mechanisms invoked are the central vasomotor controls, which are primarily medullary, peripheral baroreceptors located in the carotid sinus and peripheral chemoreceptors located in the carotid and aortic bodies. Activity of both the baroreceptor and chemoreceptor mechanisms has been documented early in gestation, and although the manifestations may be blunted by the existence of central shunts and the umbilical-placental circulation, peripheral vasoconstriction is evident. The critical importance of baroreceptor control of the peripheral circulation is demonstrated by the marked fluctuations in arterial blood pressure induced by sinoaortic denervation in immature fetal sheep (42).

In addition to circulating catecholamines and the autonomic nervous system, other circulating hormones exert significant effects on the peripheral circulation throughout fetal and postnatal life. The renin-angiotensin system probably plays a major role in controlling peripheral vascular tone even in the young fetus; infusion of angiotensin II significantly increases peripheral vascular resistance (43). Plasma vasopressin increases during hypotension in the fetus and the newborn (44). Although ANP has been demonstrated as early as 21 weeks in the human fetus and does appear to have a small effect on blood volume, there is no evidence of a peripheral vascular effect (45).

NO plays a role in vasodilation of the skin and muscle, but its role is limited. In response to whole-body heating, NO contributes about 30% of the vasodilation of the skin (46). In contrast, with local heating, NO is primarily responsible for vasodilation. During exercise, NO also plays a modest role in increasing peripheral blood flow for local homeostasis. There is a balance achieved between local vasodilation, sympathetic vasoconstriction, and whole-body blood pressure control (46) to allow maintenance of local homeostasis and central blood pressure. NO plays no significant role in blood pressure control during exercise.

Last, circulating hormones can affect the peripheral circulation indirectly via their effects on the central nervous system as well as in peripheral autonomic ganglia and the adrenal medulla. The roles of vasopressin and angiotensin II in the central control of the peripheral circulation are not clear, but these agents, along with various neurotransmitters, apparently exert significant controls via stimulation and inhibition of various central regions. Endogenous opioids are intimately involved in the cardiovascular response to shock by exerting both central and adrenal medullary effects in the adult. Endogenous opioids at concentrations higher than those seen in the mother have been demonstrated throughout gestation, and fetal plasma β -endorphin levels have been shown to increase in response to maternal hypoxemia (47).

Renal Circulation

Aspects unique to the renal circulation are its exceptionally high blood flow because of the requirements of glomerular ultrafiltration, the presence of two distinct capillary beds to allow filtration and reabsorption, and the delayed maturational processes in regional blood flow and its controls as compared with other systemic vascular beds.

Blood flow to the adult kidney represents up to 25% of cardiac output. Most of this flow courses via the afferent arterioles in the renal cortex to the glomerular capillary bed. This capillary bed is under relatively high pressure to allow for a large production of ultrafiltrate into the renal collecting system. Distal to an efferent arteriolar system that significantly decreases hydrostatic pressure, significantly less blood passes to the medullary capillary bed. This low pressure in addition to osmotic forces favors the reuptake of the filtrate. Within the two regions, the cortex and medulla, there is preferential distribution of blood as well. The outer cortex receives a relatively small proportion of cortical blood and is composed of small glomeruli with low single-nephron glomerular filtration. The inner or juxtaglomerular cortex receives far more blood flow per weight and is composed of very large glomeruli with high filtration rates. The medulla is composed of the outer medulla (the descending and thick ascending limbs of the loops of Henle and collecting duct segments) and the inner medulla (thin segments of the loops of Henle and the terminal portions of the collecting system). The inner medulla is perfused by the vasa recta and receives the least blood per weight and at very slow transit times. This is critical to the reuptake of ultrafiltrate and thus concentration of urine: There is an inverse relationship between inner medullary blood flow and urine osmolality.

Under normal conditions, the primary mechanism for control of renal cortical blood flow is autoregulation, which matures quite late. Autoregulation in the kidney consists of two mechanisms, tubuloglomerular feedback and renal myogenic response (48). Tubuloglomerular feedback involves sensing flow in the region of the macula densa that results in alteration in vascular tone in adjacent arterioles, likely involving adenosine or ATP. Myogenic response refers to vasoconstriction of afferent renal arterioles in response to increased transmural pressure. Both mechanisms participate in regulation of renal flow and protection from renal injury from hypertension (48).

Autoregulation is present in the newborn of most species but is of reduced efficiency. Because the immature kidney excretes far more prostanoids than the mature kidney, it is possible that impaired autoregulation is caused not so much by an immaturity of the mechanisms controlling autoregulation as by an overabundance of prostanoid production. In normal conditions, however, there is no evidence that prostanoids play a role in the control of renal blood flow. A mechanism unique to the kidney that contributes to autoregulatory control of renal blood flow is tubuloglomerular feedback. This mechanism is a single-nephron phenomenon and is initiated by alterations in filtrate and solute flow from the proximal to distal tubule. An alteration in either distal tubule reabsorption or fluid delivery alters the blood flow and glomerular filtration, probably by constriction or dilation of the afferent arteriole. The renin-angiotensin system mediates afferent arteriolar vasoconstriction so that glomerulotubular feedback depends on an intact and mature juxtaglomerular apparatus and renin-angiotensin system. The immature kidney does not show tubuloglomerular feedback until after birth, probably because of an immature renin-angiotensin system. In addition to the elevated renal prostanoids already discussed, basal levels of angiotensin II are elevated so that the ability of the juxtaglomerular apparatus to further activate the system is greatly limited; moreover, the immature renal vasculature is relatively insensitive to the constrictor effects of angiotensin II. Thus, unlike in the cerebral circulation, fine control of renal blood flow in resting conditions is significantly impaired in the fetus and newborn.

During stress, however, autonomic rather than autoregulatory mechanisms predominate and act primarily to limit renal blood flow. Both α_1 - and α_2 -adrenergic receptors are present in the kidney throughout fetal and postnatal life, and stimulation of both by neural discharge or circulating catecholamines causes renal vasoconstriction, redistributing blood away from the kidney as blood is distributed away from the peripheral circulation. Dopaminergic and β -adrenergic receptors are also present across development, although dopamine-2 receptor density decreases with age (49). Stimulation of both causes vasodilation but their physiologic significance is uncertain in the immature kidney. There is no evidence of resting β -adrenergic tone, and β -adrenergic blockade does not enhance α -adrenergically mediated vasoconstriction in the fetal sheep. However, the adult is more sensitive to stimulation of both β -adrenergic and dopaminergic receptors, developing significantly more vasodilation.

The role of other circulating factors in the control of cortical blood flow in the young is less significant and often less clear. The renin-angiotensin system has been discussed in regard to autoregulation. Although it is very important to the autoregulatory ability of the adult kidney, the renin-angiotensin system has significantly limited effects on autoregulation in the very young. Although captopril increases renal blood flow in the newborn lamb (50), this may be caused by its inhibition of kininase II in the kallikrein-kinin system, rather than by inhibition of angiotensin-converting enzyme. Similar to angiotensin, vasopressin is not known to have effects on resting renal blood flow in the young (51), despite the presence of V1 receptors.

Control over medullary flow in the adult kidney is primarily by vasopressin, with no evidence of autoregulation. As medullary flow decreases in response to release of vasopressin, the osmotic gradient increases and uptake of the resorbate increases. As mentioned, the medulla consists of two distinct zones with complex vasculature to allow the countercurrent multiplication and exchange critical to the reuptake of the vast majority of the ultrafiltrate. It is in the inner medulla that the extreme concentration of the urine occurs and the greatest sensitivity to vasopressin exists.

In addition to regional and developmental differences in the control of cortical and medullary blood flow, there are significant developmental differences in intrarenal regional blood flows and flow distribution, as suggested above. Up to 25% of cardiac output is distributed to the kidney in the adult, with about 90% of that flow being cortical. Most of that cortical flow is distributed to the larger juxtamedullary nephrons, yielding a very high glomerular filtration rate. Conversely, the immature kidney receives far less blood, and the distribution of that blood is less specific. The very low cortical flow is associated with a markedly reduced glomerular filtration rate in the fetus and newborn, and the relatively high medullary flow with limited vasopressin sensitivity is associated with poor concentrating ability. The lesser renal blood flow is caused only in small part by fewer nephrons. Glomerulogenesis is complete in the human by 36 weeks' gestation, yet the kidneys still account for only about 5% of cardiac output at birth. Over the first weeks of life, both renal blood flow and glomerular filtration rate double as afferent arteriolar resistance decreases. The ultimate increase in renal blood flow and ultrafiltration is related to further alterations in the renal vasculature, particularly in conjunction with the large increase in the size of glomeruli, which is not complete until late adolescence.

In summary, the renal vascular and glomerular beds are very immature at birth, so that renal function and control over renal blood flow and its distribution are limited. Throughout much of childhood, maturation proceeds, although most is accomplished in the first few months of life. The control mechanisms of renal flow are centered on three requirements: maintenance of adequate ultrafiltration in the cortex, maintenance of filtrate concentration in the medulla, and redistribution of blood away from the kidney in periods of stress. The three functions are primarily controlled by different mechanisms that mature at different rates.

Splanchnic Circulation

The splanchnic circulation consists of the vascular beds of the spleen, gastrointestinal tract, and liver. Similar to the renal circulation, the splanchnic circulation receives about 25% of cardiac output in the adult, but it is also a large reservoir of blood, containing about 20% to 25% of total blood volume. Thus, response to stresses such as hemorrhage leads not only to redistribution of blood flow away from the splanchnic circulation but also to mobilization of blood volume from that vascular bed to the central vessels and other organs. Control over the splanchnic bed in response to stress is primarily central rather than local, with neurohumoral catecholamine stimulation being the major mechanism controlling vasoconstriction. Stimulation of both carotid and aortic baroreceptors causes sympathetic neural stimulation of splanchnic resistance and capacitance vessels and large decreases in splanchnic blood flow and volume. Also, secondary to the active vasoconstriction of the resistance (arterial) component of the splanchnic circulation are decreases in the venous capacitance size. It appears that approximately half the decrease in splanchnic blood volume is secondary to active vasoconstriction of the capacitance (venous) system and half secondary to its passive decrease in volume. Specific to the splanchnic bed is the property that exercise and thermal stresses also induce large decreases in flow and volume with redistribution to the skeletal muscle and skin, respectively. The afferent limbs of these responses are uncertain because, unlike with hemorrhage, stimulation of baroreceptors does not occur. Responses specific to the individual components of the splanchnic vascular bed are discussed next.

The spleen has significant sympathetic adrenergic innervation and responds to stimulation with vasoconstriction. Although there are β -adrenergic receptors as well as

α -adrenergic receptors, the former are less active. In addition to sensitivity to adrenergic stimulation, human splenic arterioles respond to vasopressin and angiotensin with vasoconstriction. There is no evidence of autoregulatory or other local controls over splenic blood flow. Thus, in response to stress, central mechanisms direct blood flow away from the spleen. Unlike other mammals, humans do not show significant reduction in splenic venous capacitance with stimulation, so it does not contribute significantly to the blood reservoir when mobilized with stress. It is the other components of the splanchnic circulation that contribute to increasing blood volume during hypovolemic stresses.

The gastrointestinal tract has a more complex vascular bed, controlled by a greater variety of mechanisms. Like the splenic vessels, the mesenteric vessels are richly innervated with sympathetic nerves, which respond to stimulation with vasoconstriction, although there are some vasodilatory β -adrenergic receptors as well. Constriction of the venous effluent vessels in addition to the passive decrease in venous capacitance causes mobilization of blood volume from this large reservoir. The intestinal circulation also responds similarly to the splenic circulation during hemorrhage, with marked vasoconstriction in response to increases in angiotensin II and vasopressin. However, unlike the splenic circulation, the intestinal circulation escapes from vasoconstriction as vascular resistance decreases and flow increases secondary to autoregulatory escape. This escape phenomenon is not well defined, but it is probably secondary to sensitivity of the arteriolar bed to vasodilator metabolites such as adenosine, in much the same way that adenosine is involved in local regulation of other vascular beds, such as the cerebral and myocardial circulations. This metabolic mechanism may explain why the fed adult dog, which has a greater oxygen extraction under normal pressure, exhibits better autoregulation than the fasted dog. This greater local regulatory response during conditions of greater oxygen extraction is also evident in the young (35 days) pig during hypoxic and ischemic stresses (52). However, similar to but not as pronounced as the case in the renal vascular bed, autoregulatory mechanisms are immature in the newborn, both at rest and in hypoxic and ischemic conditions.

The response of the intestinal circulation to feeding is also of interest. In anticipation of food, the response is central in origin and largely sympathetic, causing vasoconstriction. Once food has been ingested, there are major local vascular responses related to the type of food, the products of digestion in different parts of the intestine, and the secondary effects of various gastrointestinal hormones. The hydrolytic products of carbohydrates and fat are particularly potent local vasodilators and appear to act on a metabolic basis similar to that of autoregulation by increasing local oxygen consumption. Local hormones that may play a role in vasodilation include cholecystokinin, secretin, gastrin, glucagon, and vasoactive intestinal polypeptide. The overall response to feeding yields increases in local blood flow of $\leq 300\%$ within 60 to 90 minutes (53). Because of the large increase in oxygen consumption, however, these increases are not enough to meet the increased metabolic demand, so that oxygen extraction also increases.

The hepatic circulation is even more complex, receiving both highly oxygenated blood from the hepatic arteries and blood of lesser saturation but greater substrate concentrations from the portal vein. The incorporation of umbilical venous blood in the fetal circulation was discussed earlier. A review by Lauth and Greenway (54) clearly describes the hepatic circulation and its control. The portal vein terminates in the hepatic sinusoids, and the hepatic arterioles split into a complex capillary network that also drains into the sinusoids. These vessels, along with the biliary ductules and lymph vessels and nerves,

occupy the portal triad. In these sinusoids, which allow free contact with the hepatic cells, the blood passes radially away from the center of the hepatic glomus to the periphery, where it passes into the hepatic venules on its way to the hepatic veins and inferior vena cava. As the blood passes from the center (zone 1) to the periphery (zone 3), near the hepatic venules, different metabolic activities predominate.

As with the kidney, blood flow to the liver is large (about 25% of cardiac output in the adult) and far exceeds its metabolic demand for oxygen. As with the intestinal circulation, hepatic blood volume is large (about 10% of total blood volume) and is mobilized during periods of stress. Conversely, as hepatic venous pressure increases, hepatic blood volume increases greatly because of the large compliance of these capacitance vessels. There are also sphincters described in the hepatic venules that may regulate hepatic blood volume by varying sinusoidal volume and portal resistance. These sphincters respond to norepinephrine and angiotensin.

Portal venous blood contributes about 75% of hepatic blood flow, and this flow is determined primarily by mechanisms that regulate splenic and intestinal flow, although presinusoidal sphincters exist as well. Alterations in hepatic venous pressure affect neither portal flow nor its intrahepatic distribution. The hepatic arterial circulation is innervated in a similar fashion as the mesenteric arterial circulation and responds prominently to α -adrenergic stimulation during stress, as well as to other stress hormones such as angiotensin II and vasopressin. Similarly, there are vasodilatory β_2 -adrenergic receptors and there is some responsiveness to vasodilatory gastrointestinal hormones such as glucagon, secretin, and pentagastrin. An additional regulatory mechanism of hepatic arterial flow exists that is somewhat analogous to intestinal autoregulation. Although there is no autoregulation within the arterial circulation, as portal venous flow decreases, there is a reciprocal increase in hepatic arterial flow. The mechanism is thought to be adenosine regulated. Adenosine is released into the central sinusoids and comes in contact with the hepatic arterioles; as portal flow decreases, the washout of adenosine from this region is decreased, and thus more is present to dilate the hepatic arterioles (53).

Perhaps the largest changes in regional blood flow in the perinatal period occur in the liver, but this is not because of maturation of the hepatic circulation but rather because of loss of the umbilical-placental circulation. Prior to birth, the primary source of hepatic blood flow is the umbilical vein, which joins the portal venous blood in the portal sinus. About 45% of umbilical venous return passes to the liver, with the right lobe receiving somewhat more than the left (4). Portal venous blood is distributed much more unequally, with almost all of it passing to the right lobe, which therefore is perfused with blood of much lower hemoglobin oxygen saturation compared with the left. Hepatic arterial blood flow is very limited in the fetus and is distributed approximately equally to the two lobes. At birth, the loss of the umbilical-placental circulation is not associated with immediate closure of the ductus venosus, which can remain patent for several days (25). Some portal venous blood is shunted away from the liver to the inferior vena cava via the ductus venosus. This, along with the absence of an immediate increase in hepatic arterial flow causes a marked reduction in hepatic blood flow at birth and a halving of oxygen consumption (2). By 1 week of age, hepatic blood flow increases and oxygen consumption returns to fetal levels, although hepatic arterial blood flow remains at the very low fetal levels, contributing only 5% of total hepatic blood flow. The mechanisms that underlie the increase in hepatic flow and oxygen consumption in early postnatal life and the subsequent increase in hepatic arterial flow are uncertain, as are the implications of these changes on liver function and maturation.

REFERENCES

1. Roos A. Poiseuille's law and its limitations in vascular systems. *Med Thorac* 1962;19:224-238.
2. Teitel DF, Iwamoto HS, Rudolph AM. Effects of birth-related events on central blood flow patterns. *Pediatr Res* 1987;22:557-566.
3. Rasanen J, Wood DC, Weiner S, et al. Role of the pulmonary circulation in the distribution of human fetal cardiac output during the second half of pregnancy. *Circulation* 1996;94:1068-1073.
4. Edelstone DI, Rudolph AM, Heymann MA. Liver and ductus venosus blood flows in fetal lambs in utero. *Circ Res* 1978;42:426-433.
5. Townsend SF, Rudolph CD, Rudolph AM. Changes in ovine hepatic circulation and oxygen consumption at birth. *Pediatr Res* 1989;25:300-304.
6. Adeagbo AS, Coceani F, Olley PM. The response of the lamb ductus venosus to prostaglandins and inhibitors of prostaglandin and thromboxane synthesis. *Circ Res* 1982;51:580-586.
7. Levin DL, Rudolph AM, Heymann MA, et al. Morphological development of the pulmonary vascular bed in fetal lambs. *Circulation* 1976;53:144-151.
8. Reid L. The pulmonary circulation: remodeling in growth and disease. *Am Rev Respir Dis* 1979;119:531-546.
9. Thebaud B, Abman SH. Bronchopulmonary dysplasia: where have all the vessels gone? Roles of angiogenic growth factors in chronic lung disease. *Am J Respir Crit Care Med* 2007;175:978-985.
10. Rudolph AM, Heymann MA. Circulatory changes during growth in the fetal lamb. *Circ Res* 1970;26:289-299.
11. Lewis AB, Heymann MA, Rudolph AM. Gestational changes in pulmonary vascular responses in fetal lambs in utero. *Circ Res* 1976;39:536-541.
12. Rudolph AM, Yuan S. Response of the pulmonary vasculature to hypoxia and H⁺ ion concentration changes. *J Clin Invest* 1966;45:399-411.
13. Cassin S. Role of prostaglandins and thromboxanes in the control of the pulmonary circulation in the fetus and newborn. *Semin Perinatol* 1980;4:101-107.
14. Fineman JR, Soifer SJ, Heymann MA. Regulation of pulmonary vascular tone in the perinatal period. *Annu Rev Physiol* 1995;57:115-134.
15. Furchgott RF. Role of endothelium in responses of vascular smooth muscle. *Circ Res* 1983;53:557-573.
16. Ignarro LJ. Biological actions and properties of endothelium-derived nitric oxide formed and released from artery and vein. *Circ Res* 1989;65:1-21.
17. Shaul PW. Nitric oxide in the developing lung. *Adv Pediatr* 1995;42:367-414.
18. Yanagisawa M, Kurihara H, Kimura S, et al. A novel potent vasoconstrictor peptide produced by vascular endothelial cells. *Nature* 1988;332:411-415.
19. Leffler CW, Hessler JR, Green RS. The onset of breathing at birth stimulates pulmonary vascular prostacyclin synthesis. *Pediatr Res* 1984;18:938-942.
20. Soifer SJ, Fineman JR, Heymann MA. The pulmonary circulation. In: Gluckman PA, Heymann MA, eds. *Pediatrics and Perinatology. The Scientific Basis*. Kent, England: Edward Arnold, 1996:749-755.
21. Cornfield DN, Resnik ER, Herron JM, et al. Pulmonary vascular K⁺ channel expression and vasoreactivity in a model of congenital heart disease. *Am J Physiol Lung Cell Mol Physiol* 2002;283:L1210-L1219.
22. Vander Heyden MA, Halla TR, Madden JA, et al. Multiple Ca²⁺-dependent modulators mediate alkalosis-induced vasodilation in newborn piglet lungs. *Am J Physiol Lung Cell Mol Physiol* 2001;280:L519-L526.
23. Ebert TJ, Stowe DF. Neural and endothelial control of the peripheral circulation—implications for anesthesia: Part I, Neural control of the peripheral vasculature. *J Cardiothorac Vasc Anesth* 1996;10:147-158.
24. Linden RJ. Function of cardiac receptors. *Circulation* 1973;48:463-480.
25. Little RC, Little WC. The output of the heart and its control. In: *Physiology of the Heart and Circulation*. Chicago, IL: Year Book Medical, 1989:165-198.
26. Athanassopoulos G, Cokkinos DV. Atrial natriuretic factor. *Prog Cardiovasc Dis* 1991;33:313-328.
27. Rose RA, Giles WR. Natriuretic peptide C receptor signalling in the heart and vasculature. *J Physiol* 2008;586:353-366.
28. Stowe DF, Ebert TJ. Neural and endothelial control of the peripheral circulation—implications for anesthesia: Part II, Endothelium-mediated effects in the normal and diseased circulation. *J Cardiothorac Vasc Anesth* 1996;10:159-171.
29. Archer SL, Gragasin FS, Wu X, et al. Endothelium-derived hyperpolarizing factor in human internal mammary artery is 11,12-epoxyeicosatrienoic acid and causes relaxation by activating smooth muscle BK(Ca) channels. *Circulation* 2003;107:769-776.
30. Jensen FB. The dual roles of red blood cells in tissue oxygen delivery: oxygen carriers and regulators of local blood flow. *J Exp Biol* 2009;212:3387-3393.
31. Johnson PC. Autoregulation of blood flow. *Circ Res* 1986;59:483-495.
32. Longo LD, Pearce WJ. Fetal and newborn cerebral vascular responses and adaptations to hypoxia. *Semin Perinatol* 1991;15:49-57.
33. Szymonowicz W, Walker AM, Cussen L, et al. Developmental changes in regional cerebral blood flow in fetal and newborn lambs. *Am J Physiol* 1988;254:H52-H58.
34. Cipolla MJ. The cerebral circulation. In: Granger DN, Granger J, eds. *Integrated Systems Physiology: From Molecule to Function*. San Rafael, CA: Morgan and Claypool Life Sciences, 2010.
35. Laudignon N, Beharry K, Farri E, et al. The role of adenosine in the vascular adaptation of neonatal cerebral blood flow during hypotension. *J Cereb Blood Flow Metab* 1991;11:424-431.
36. Talman WT, Nitschke Dragon D. Neuronal nitric oxide mediates cerebral vasodilation during acute hypertension. *Brain Res* 2007;1139:126-132.
37. Toda N, Ayajiki K, Okamura T. Cerebral blood flow regulation by nitric oxide: recent advances. *Pharmacol Rev* 2009;61:62-97.
38. Boylan GB, Young K, Panerai RB, et al. Dynamic cerebral autoregulation in sick newborn infants. *Pediatr Res* 2000;48:12-17.
39. Habgood MD, Jones SE, Maroni JM, et al. Cerebral blood flow in the anaesthetized immature sheep fetus and the response to hypercapnia. *Exp Physiol* 1991;76:495-505.
40. Wagerle LC, Mishra OP. Mechanism of CO₂ response in cerebral arteries of the newborn pig: role of phospholipase, cyclooxygenase, and lipoxygenase pathways. *Circ Res* 1988;62:1019-1026.
41. Ogoh S, Nakahara H, Ainslie PN, et al. The effects of oxygen on dynamic cerebral autoregulation: crucial role of hypocapnia. *J Appl Physiol* 2009;108:538-543.
42. Itskovitz J, LaGamma EF, Rudolph AM. Baroreflex control of the circulation in chronically instrumented fetal lambs. *Circ Res* 1983;52:589-596.
43. Iwamoto HS, Rudolph AM. Effects of angiotensin II on the blood flow and its distribution in fetal lambs. *Circ Res* 1981;48:183-189.
44. Zubrow AB, Daniel SS, Stark RI, et al. Plasma vasopressin, renin and catecholamines during nitroprusside-induced hypotension in the newborn lamb. *J Perinat Med* 1989;17:271-277.
45. Hargrave BY, Iwamoto HS, Rudolph AM. Renal and cardiovascular effects of atrial natriuretic peptide in fetal sheep. *Pediatr Res* 1989;26:1-5.
46. Joyner MJ, Casey DP. The catecholamines strike back. What NO does not do. *Circ J* 2009;73:1783-1792.
47. Wardlaw SL, Stark RI, Daniel S, et al. Effects of hypoxia on beta-endorphin and beta-lipotropin release in fetal, newborn, and maternal sheep. *Endocrinology* 1981;108:1710-1715.
48. Loutzenhiser R, Griffin K, Williamson G, et al. Renal autoregulation: new perspectives regarding the protective and regulatory roles of the underlying mechanisms. *Am J Physiol Regul Integr Comp Physiol* 2006;290:R1153-R1167.
49. Felder RA, Nakamura KT, Robillard JE, et al. Dopamine receptors in the developing sheep kidney. *Pediatr Nephrol* 1988;2:156-162.
50. Robillard JE, Nakamura KT. Neurohormonal regulation of renal function during development. *Am J Physiol* 1988;254:F771-F779.
51. Robillard JE, Weitzman RE. Developmental aspects of the fetal renal response to exogenous arginine vasopressin. *Am J Physiol* 1980;238:F407-F414.
52. Nowicki PT, Miller CE, Edwards RC. Effects of hypoxia and ischemia on autoregulation in postnatal intestine. *Am J Physiol* 1991;261:G152-G157.
53. Vatner SF, Franklin D, Van CR. Mesenteric vasoactivity associated with eating and digestion in the conscious dog. *Am J Physiol* 1970;219:170-174.
54. Lauth WW, Greenway CV. Conceptual review of the hepatic vascular bed. *Hepatology* 1987;7:952-963.

Diagnostic and Therapeutic Methods

History and Physical Examination

Steven C. Cassidy ■ Hugh D. Allen ■ John R. Phillips

Despite the availability of advanced imaging technologies, a thorough history and physical examination is the core of evaluating children with suspected heart disease. Although the basics of obtaining a history and physical examination are similar in all patients, this chapter emphasizes specific issues when evaluating a child with possible cardiac pathology.

HISTORY

To obtain an accurate history, it is important to establish rapport with the patient and parents. Meetings are often short and first impressions are lasting, so the first encounter is critical. The examiner should sit and carefully listen to the details provided by the patient and parents. The history is the predominant vehicle that defines the first encounter. *Many aspects of the history are age specific. Therefore, historical information should be elicited from the patient, as age and maturity allow, and from the parents as observers*

Parents often research their child's illnesses on the Internet or through the media and may come to a visit with preconceived notions and, perhaps, opinionated or anecdotal information. The examiner must be prepared for this and discuss the patient's condition in a nonconfrontational and open manner. In that way, an honest and positive patient-physician relationship will be established.

Newborns and Infants

Congenital heart disease often presents in early infancy because of observed abnormalities in the appearance or behavior of the infant. Because an infant's primary physical exertion is eating, a thorough feeding history should be obtained. If the mother has had previous children, she may offer insight into differences in feeding habits between the patient and her other children. The feeding history should be as quantitative as possible. Frequency of feeding, volume of milk or formula (and type of formula,

especially regarding kcal/oz information) consumed, and the length of time to finish a feeding should be obtained for both bottle- and breast-fed infants. Most newborns feed 2 to 3 oz every 2 to 3 hours. It is common for children with congestive heart failure to take breaks during a feeding because of rapid breathing or to fall asleep during feeding only to awaken after a few minutes and feed a small amount again. Generally, normal infants should be able to complete their feeding in <30 minutes. A longer time to finish each feeding, low volume consumed, excessive diaphoresis, and increased work of breathing during feeding are signs of heart failure or poor cardiac output. As pulmonary vascular resistance declines over the first 4 to 6 weeks of life, irritability and fussiness with feeding may indicate angina and ischemia in a child with an anomalous left coronary artery from the pulmonary artery. This is often confused with colic or reflux.

The presence of cyanosis should be determined. Cyanosis may be central or peripheral. Central cyanosis, which reflects true arterial desaturation, is characterized by blueness of the tongue and oral mucosa. Central cyanosis is most likely related to cardiac or respiratory disease. Children in shock also may appear cyanotic owing to venous stasis, right-to-left intrapulmonary shunting, or increased peripheral oxygen extraction. Acrocyanosis, or blueness of the hands and feet related to skin temperature, is normal. Similarly, blueness of the skin around the mouth or other parts of the face can often be attributed to alterations in skin blood flow or vasomotor instability, and should be considered to be a normal variant. Cyanosis may be more difficult to recognize in the anemic patient, because with decreased hemoglobin, similar levels of desaturation may not produce sufficient quantities of reduced hemoglobin (>5 g/%) to be clinically apparent.

If there has been observed cyanosis, it is important to distinguish between constant cyanosis and episodic cyanosis. In most forms of cyanotic congenital heart disease, cyanosis is constant. Constant cyanosis should suggest the presence of congenital heart disease with hypoxemia related to transposition physiology, inadequate pulmonary blood flow, or intracardiac mixing. Episodic cyanosis may be due to hypoxemia

related to hypercyanotic episodes from tetralogy of Fallot physiology (see Chapter 43). This can occur in tetralogy of Fallot, in some patients with double-outlet right ventricle, or in patients who have subpulmonic stenosis associated with a univentricular circulation.

Differential cyanosis of the upper and lower body in a newborn, although much less common, can also be an important finding. Lower body cyanosis with a pink upper body suggests right-to-left shunting at the level of the ductus arteriosus, seen in patients with persistent pulmonary hypertension of the newborn. Upper body cyanosis with pink lower extremities may indicate transposition of the great arteries with an aortic arch obstruction. In this circumstance, the lower body is perfused by the reversing ductus arteriosus that carries pulmonary venous blood via the left ventricle to the pulmonary artery.

The parent or caregiver's observation of the infant's breathing patterns should be documented. Unlabored ("happy") tachypnea often accompanies cyanotic heart disease, whereas increased work of breathing and sometimes grunting are associated with left-sided obstructive lesions or respiratory illness. Grunting with closure of the glottis provides positive end-expiratory pressure and is seen in infants who have pulmonary edema. Parents may also observe intercostal or subcostal retractions when the child is undressed. If the infant has been symptomatic from birth, some first-time parents may not recognize mild respiratory symptoms such as tachypnea.

Finally, newborns and infants who have heart diseases may have diaphoresis. This can occur during feedings or during sleep. Diaphoresis in this circumstance generally indicates activation of the sympathetic nervous system in patients who have low cardiac output.

The time at which signs and symptoms of heart disease begin may be a clue to the type of cardiac lesion. Commonly, murmurs detected early in the neonatal period originate from atrioventricular valve regurgitation or semilunar valve stenosis. Most newborns with acyanotic congenital heart disease are asymptomatic at birth. As the transition from fetal to postnatal circulation is completed, symptoms specific to the physiology of the defect become evident. For example, ductal-dependent left-sided obstructive lesions usually present in the first week of life as the ductus arteriosus closes, resulting in markedly decreased cardiac output and signs of shock. On the other hand, children with significant left-to-right shunt lesions typically are asymptomatic until 4 weeks of age or later, when pulmonary vascular resistance decreases to near adult levels and pulmonary overcirculation ensues. This may also be the first time a murmur is heard.

Toddlers and Preschoolers

Toddlers and preschoolers, like infants, are generally unable to give the examiner a true subjective history, so again, history in this age group is largely observational. Symptoms may be somewhat nonspecific. Again, feeding and breathing symptoms should be sought. As children become more physically active, parents may observe inability of children in this age group to sustain physical activity. Parents can be questioned regarding comparisons of these patients to siblings and age-mates about sustaining play or physical activity. Growth and developmental history is also important at this age. As they approach school age, children can sometimes voice subjective complaints, but often this is simplified to what the parent concludes is chest discomfort.

Older Children and Adolescents

As childhood progresses through school age and adolescence, the primary historian should be the patient. The parents should be asked additional pertinent historical and observational

information. Adolescents should have the right to speak privately, especially about drug use, sexual behavior, and other personal matters. A clinician should not betray their confidentiality and should not divulge to others the information revealed in confidence.

Older children and adolescents can be questioned much like adults regarding cardiovascular symptoms. Recognize that children with congenital heart disease may be symptomatic from birth and therefore may not experience a change in symptoms, as would a previously healthy adult with acquired heart disease. Older children and adolescents should be specifically questioned about their ability to tolerate exercise and physical activity. This may include the ability to participate in recreational activity and sports, but should also include activities of daily living such as walking or stair climbing. Shortness of breath with activity should be noted. Cyanosis with physical activity may indicate persistence or new appearance of a cardiac right-to-left shunt.

In older patients, a sleep history should be sought. Older patients may have paroxysmal nocturnal dyspnea or orthopnea with congestive heart failure. One should inquire about the patient's comfort when lying supine in bed, and if they require sleeping with elevation of the head by more than one pillow. Nocturnal awakening and shortness of breath can occur in heart failure with postural redistribution of edema fluid, particularly if there is pulmonary vein or mitral stenosis.

Palpitations are a common complaint in older children, and it is most helpful to have the subjective description of the events by the patient. The patient may describe transient or sustained sensation of an abnormal heartbeat, ranging from the sensations of the heart "skipping a beat" to the sensation of the heart beating hard or fast. The details of the symptoms should be carefully teased out to determine the circumstances in which they occur (e.g., rest vs. exercise), the frequency and duration of the complaint, and any associated symptoms such as fatigue, shortness of breath, or chest pain. It is often helpful to ask the parent about the appearance of the patient during these symptoms, specifically asking about pallor, breathing, and diaphoresis.

Chest pain at rest is a common complaint in adolescents and is generally noncardiac in nature. Again, in this circumstance, a subjective history is most helpful. The examiner should inquire about the nature of the pain, as well as its location, and duration. The examiner should ask the patient whether the pain is affected by breathing movements, cough, or arm and shoulder movements. Any other exacerbating or alleviating maneuvers should be sought. Chest pain with exercise should be questioned. Although chest pain with exercise is commonly associated with adult coronary disease, it is uncommonly associated with congenital heart disease. Exercise-induced chest pain may be found in patients with diseases resulting in significant left ventricular hypertrophy, congenital coronary artery abnormalities, or coronary abnormalities associated with Kawasaki syndrome, or can be due to noncardiac conditions such as exercise-induced bronchospasm.

Syncope is another symptom that is a frequent reason for Cardiology referral and may be due to a cardiac cause. When a patient presents with syncope as a complaint, the circumstances of the event and presyncopal symptoms are of greatest importance. Patients should be asked to describe where they were, what they were doing, and how they felt at the time of the event. Most postural syncope will occur when the patient is upright, generally standing. Often it occurs in a warm environment after a period of prolonged standing, but may also occur in some upon standing quickly from a sitting or supine position or while standing after a period of intense exercise. Dizziness or light-headedness, visual changes, feeling hot, or nausea often precede postural syncope. The examiner should inquire about presence of these presyncopal symptoms at other times when the patient has not lost consciousness. Additional

information that may be helpful includes the patient's daily intake of fluids and caffeine. Syncope without prodrome should be considered more significant for the possibility of a sudden severe arrhythmia.

Some patients may complain about edema, or swelling, although it is less commonly related to congenital heart disease in children and adolescents. The location of this edema is dependent upon the predominant posture of the individual. Patients who are upright much of the time may complain of swelling of their feet and ankles or of shoes that are tight at the end of the day. Younger patients who are supine much of the time may have sacral edema or puffiness of the face and eyelids.

Past Medical and Surgical History

The past medical history should include documentation of significant illnesses, previous hospitalization, previous operations, immunization status, and symptoms of poor growth as an infant. A detailed catalogue of previous cardiac and cardiothoracic procedures should be documented, including catheterizations, catheter interventions, and cardiac surgeries. The examiner should ask about the presence of other congenital anomalies and syndromes that may be associated with heart disease. Other illnesses and chronic conditions, immunization history, and allergies should be queried and documented.

Prenatal and Birth History

When evaluating a newborn for the first time, it is important to obtain details about the pregnancy. Details of the maternal health during pregnancy should be obtained, including maternal illnesses, medications, toxic exposures, and pregnancy-related complications. The infant of a mother with gestational diabetes, for example, has an increased risk of cardiac defects. Similarly, the relationship between maternal lupus and congenital heart block is well recognized. Maternal exposure to teratogens associated with cardiac defects (Table 5.1) should be part of the prenatal history (see Chapters 25 and 27). Smoking during pregnancy has been linked to small-for-gestational-age newborns but not specific cardiac defects. Congenital infections may lead to specific types of cardiac diseases. One example is rubella, which has been associated with patent ductus arteriosus and pathologic peripheral pulmonary stenosis. The use of illicit drugs may indicate an increased risk for human immunodeficiency virus infection, which has been associated with infantile cardiomyopathy. The age of the mother is important to determine her risk for offspring with chromosomal abnormalities such as trisomy 21. Complications such as toxemia, birth asphyxia, fetal distress, and low birth weight

may result in perinatal insult to the myocardium, leading to a generalized cardiomyopathy. The gestational age and birth history, including perinatal monitoring, method of delivery, and infant's Apgar scores, should be noted, and cyanosis, color, and perfusion status should be assessed.

Family History

A family history of relatives, especially siblings, born with heart defects indicates a higher than normal risk of congenital heart defects. For a couple that has already had a child with a left-sided obstructive lesion (i.e., hypoplastic left heart syndrome), the risk of congenital heart defects in subsequent children is increased. In most centers, a history of siblings with significant congenital heart lesions would prompt a referral to a pediatric cardiologist for a detailed fetal echocardiogram. A complete family history also should include the presence or absence of syndromes associated with congenital heart disease such as Marfan syndrome, Holt-Oram syndrome, long QT syndrome, and idiopathic sudden death. A positive family history for these diseases may warrant screening of other family members.

In the family history, one should identify the presence of premature myocardial infarction and hypercholesterolemia that may prompt cholesterol screening. The presence of congenital heart diseases in family members, and valve abnormalities such as bicuspid aortic valve should be determined. Heritable conditions such as hypertrophic cardiomyopathy should be specifically questioned. As in the infant, a family history of idiopathic sudden death in a close relative should prompt careful evaluation of the patient's QTc interval on a surface electrocardiogram.

Review of Systems, Social History

A review of systems and social history should include specific information regarding the patient's eating and exercise habits. School performance and sports participation should be assessed. A careful respiratory review of systems should be obtained. The clinician should make a private interview available to the adolescent. A history of tobacco and illicit drug use can then be determined. A discussion of personal habits gives the examiner an opportunity to advise about risk factors for coronary artery disease. This information is pertinent to the cardiac evaluation and aids in building the patient-physician relationship.

PHYSICAL EXAMINATION

Preparation and Strategy

We will now discuss the parts of the cardiac physical examination, including assessment of vital signs, inspection, palpation, percussion, and auscultation. Before the clinician proceeds with the examination, the patient should undress. The child may be covered with a blanket or wear a medical examination gown. The privacy and modesty of older children and adolescents must be respected. A staff member chaperone should be present during the examination of a patient of the opposite sex. Every child is different, so each examination must be individualized to be successful. The examiner must wash his or her hands or use sanitizing hand gel while being observed by the patient and parents doing so.

For the physician to perform a successful examination, the patient must be quiet and cooperative. This requires tact, patience, and innovation on the part of the examiner. If the infant is happiest in the mother's lap, then he or she should

TABLE 5.1 Common Teratogens and Their Associated Cardiac Defects

Teratogen	Cardiac Defect
Alcohol	ASD, VSD
Lithium	Ebstein's anomaly
Retinoic acid	Conotruncal abnormalities
Valproic acid	ASD, VSD, AS, PA/IVS, CoA

AS, aortic valve stenosis; ASD, atrial septal defect; CoA, coarctation of the aorta; PA/IVS, pulmonary atresia with intact ventricular septum; VSD, ventricular septal defect.

be allowed to stay there. The mother should feed or play with the child during inspection or palpation. The order of the examination can be adjusted based on cooperation to obtain the most information. For example, if the child is asleep, auscultation should be performed before palpation. In anxious toddlers and infants, often it is useful to auscultate before palpating, and any supine examination should be left for last. Toddlers can be examined through a combination of distraction and play. Older children can be approached in a more traditional “head-to-toe” approach used in adult patients.

The clinician should develop a routine (and stay with it) for listening to heart sounds so that each portion of the cardiac cycle is examined at several locations. At each location, it is important to focus on one sound or one interval at a time, in a systematic and consistent way. Most examiners start at the apex and work to the left lower and left upper sternal borders, then right upper sternal border. The clinician should be sure to auscultate the left subclavicular area, both axillae, the liver, the head, and the back. At each location, one must listen to the first heart sound, throughout systole, the second heart sound, and throughout diastole.

Equipment

There are several choices in stethoscope design, and choice of the best stethoscope is personal. Some advocate single tubing, whereas others prefer double-tubed devices. Some of the newer digital stethoscopes are quite useful, but may not accurately reproduce heart sounds as heard with an unamplified stethoscope. Whichever the instrument, the tubing must be intact, relatively short, and of sufficient bore. The earpieces must fit comfortably into the examiner's ears, and should be chosen to completely seal in the examiner's ears to reduce interference from ambient noise. Chest pieces vary in size. Larger diaphragms on adult stethoscopes may make localization of heart sounds more difficult, but is it possible to use a larger diaphragm by placing only a portion of the diaphragm on the chest wall. Chest pieces with a diaphragm and bell are essential to evaluate both high- and low-frequency sounds, respectively. In infants and small children, it is possible to hear high-frequency sounds by pressing on the bell, thereby creating a diaphragm with the skin. The examiner should become accustomed to his or her personal stethoscope and how it transmits heart and lung sounds.

Different types of manometers have been developed for blood pressure measurement. Although many hospitals are phasing out mercury manometers, they have been the most accurate tools for blood pressure measurement. Aneroid sphygmomanometers are the next most reliable, and are more commonly available. Although automated instrument (such as Dinamap) pressures are easy to obtain, these measurements are reliable only in quiet cooperative patients, and diastolic pressures are often unreliable. It is best to develop the skill of obtaining manual blood pressure for greatest reliability. A range of blood pressure cuffs of different sizes should be available so that infants through adults can be assessed.

A pulse oximeter has become a standard piece of equipment for noninvasive screening of a patient's oxygen saturation using photoplethysmography. There are several varieties of these devices from larger units to portable devices that clip on a fingertip. These devices should be kept in a well-maintained state and calibrated per manufacturer's recommendations.

Vital Sign Assessment

Heart rate, respiratory rate, and blood pressure are vital to a complete cardiac examination. They should be assessed at each visit.

Heart Rate and Respiratory Rate

The importance of changes in heart rate and respiratory rate are noted throughout this chapter. Often, changes in heart rate and respiratory rate are the first harbingers of myocardial dysfunction, pulmonary congestion, or arrhythmia, even before changes in blood pressure occur. Respiratory rate should be counted with the patient unaware that it is being done, and preferably while sleeping in infants. Postural changes in heart rate and blood pressure should be determined in patients with postural dizziness or syncope.

Blood Pressure Measurement

On the initial visit, blood pressures should be measured in both upper extremities and at least one lower extremity. The standard technique for measuring blood pressure should be used. First, the length of the bladder of the cuff should be 80% of the circumference of the limb, and the width of the cuff should cover at least two-thirds of the length of the extremity. If only the arm pressure is to be measured, the patient should be sitting. Finally, to obtain an accurate measurement, the cuff should be deflated slowly. Care should be taken to not compress the artery with the head of the stethoscope. Listening to the brachial or popliteal arteries yields the Korotkoff sounds that are used; first and fifth are now the standard. For comparison between upper and lower extremities, it is best to obtain both while the patient is supine. If the sounds cannot be heard, systolic pressure can be obtained by palpating the first pulsation of an artery distal to the cuff or by using a handheld Doppler probe over the distal artery as the cuff is deflated. Another alternative, especially helpful in uncooperative infants, is using the flush technique. This is done by manually blanching the hand or foot, inflating the blood pressure cuff, releasing the hand or foot, and slowly deflating the cuff until intense redness is seen in the previously pale extremity, estimating mean arterial pressure. Serial upper and lower body blood pressure measurements are important for following patients with coarctation of the aorta and other aortic arch anomalies.

Pulse Oximetry Screening

Pulse oximeter saturation measurement has become commonplace and has often become considered to be a fifth vital sign. It has been suggested that in newborn infants, early mild desaturation detected by screening pulse oximetry may allow earlier detection of congenital heart diseases (1), potentially leading to earlier treatment and decreased morbidity and mortality from significant congenital heart disease. It has been suggested that spot check of pulse oximeter saturation be performed in every newborn after 24 hours of life prior to hospital discharge, with 95% accepted as lower limit of normal. If a newborn fails to maintain oxygen saturation >95%, further screening would be planned. Currently, insufficient data are available to determine if this is cost-effective or if it should become standard of care in newborns. Despite the lack of such evidence, at least one state has passed legislation mandating newborn screening by pulse oximetry at the time of this writing, and several other states are considering mandating this screening. There has been a recent statement by the American Heart Association and American Academy of Pediatrics calling for future studies about screening by pulse oximeter saturation (1). Pulse oximetry is also used as a tool to follow the degree of cyanosis in patients known to have cyanotic heart diseases, and is followed serially at visits. Serial measurement of oxygen saturation in patients with acyanotic heart diseases is not necessary.

Growth Parameters

Height, weight, and head circumference should be measured in all patients, and serially tracked and plotted on growth charts at subsequent visits. Patients who have heart disease may have difficulty with weight gain or linear growth. Generally, head circumference is spared in all but the sickest patients. Newborns and young infants should establish which percentile curve that their growth parameters will follow. Falling consistently through percentiles or a plateau in growth of any of the parameters should be considered significant. After repair of a hemodynamically significant heart problem, infants often have a reassuring period of “catch-up” growth.

General Appearance

The physical examination actually starts at first contact, as soon as the room is entered. The examiner should take advantage of the time while interviewing the parent to observe the child. Each patient should be inspected for general appearance, nutritional status, dysmorphic features, color, and comfort. A thorough inspection often will clue the examiner to the cause and severity of an illness. The child's general appearance and comfort should be noted. Is the child fussy or playful? Is he or she well nourished? Are dysmorphic features or chromosomal abnormalities present? As discussed elsewhere in the text, specific cardiac lesions will accompany specific syndromes. The child's breathing pattern should be observed. Patients with severe heart failure, pulmonary edema, or pericardial restriction (tamponade, constrictive pericarditis) are more comfortable sitting up. Forcing such a patient into the supine position may result in respiratory failure. Patients should be allowed to determine the position in which they are most comfortable. The child's activity level, including feeding in infants, may be observed. In the infant, feeding constitutes exercise, which may elicit increased work of breathing, tachypnea, or diaphoresis.

Cyanosis and Clubbing

The child's color (i.e., pink, cyanotic, pale) should be noted. True cyanosis requires desaturation of 5 g% of hemoglobin and is difficult to detect unless the arterial saturation is $\leq 85\%$ in a child with normal hemoglobin levels. The best indicator of arterial desaturation is central cyanosis of the gums and tongue. The oral mucosa has a rich vascular supply and is free of pigmentation. Acrocyanosis that occurs in a cold environment or after bathing nearly always is a normal finding and is not true cyanosis. In the older child, long-standing cyanosis is usually accompanied by digital clubbing. The loss of the angle between the nail and the cuticle area is consistent and is often the earliest finding of clubbing. Cyanosis also results from respiratory disease or central nervous system disorders. During initial screening of infants, or if cyanosis is suspected, pulse oximetry should be obtained. In newborns with severe desaturation on oximetry, obtaining arterial blood gas analysis provides additional information about the degree of hypoxemia and if there is evidence of hypercarbia or acidemia.

Breathing Pattern

Resting breathing patterns can offer information regarding the patient's hemodynamic state. If the infant has central cyanosis, it is usually accompanied by a nonlabored tachypnea that results from hypoxic respiratory drive. Grunting is a physiologic means of producing positive end-expiratory pressure and often accompanies pulmonary edema. Nasal flaring and intercostal and subcostal retractions may be present.

If the infant is severely distressed, the head will bob with respiratory effort.

Neck Veins

Neck vein distention suggests impaired right ventricular filling. It may not be apparent in infants and toddlers because of their relatively short neck and relatively increased subcutaneous tissue. Neck vein distension is best observed with the patient positioned 30 degrees upright. Measurement of the height of neck vein distension above the manubrium can be used to quantify central venous pressure. Cannon A waves may be seen in patients with atrial contraction against a closed tricuspid valve. Regular cannon A waves can be found in patients with supraventricular tachycardia or atrial flutter. Irregular cannon A waves can indicate complete heart block.

Bobbing of the head may be seen in patients with significant aortic regurgitation. This is caused by increased carotid arterial pulsations striking the angles of the mandibles. The patient appears to be nodding “yes.” Patients with significant tricuspid regurgitation will exhibit lateral head movement. This occurs when regurgitant blood in the superior vena cava strikes the right mandibular angle. The patient appears to be nodding “no.”

Respiratory Examination

A careful respiratory system examination is important in assessing the cardiovascular system, as many heart diseases cause abnormalities in lung findings. This should include observation, percussion of the lung fields over the back while upright, and auscultation. Observation should include the presence of retractions, use of accessory muscles of respiration, and symmetry of chest wall motion with breathing, as discussed above. Patients who have asymmetric chest wall motion in the postoperative period should be evaluated for diaphragmatic paralysis from phrenic nerve injury. Percussion is a sensitive method for detecting pleural effusions postoperatively or in patients with heart failure. Auscultation of the breath sounds may reveal rales or crackles, wheezing, or rhonchi. Wheezing is of particular interest, as it is the most common pulmonary auscultatory finding in infants and toddlers with congestive heart failure due to either overcirculation or cardiomyopathy. In patients who present with a first episode of wheezing, heart disease should be considered as a potential cause. Stridor may be present in patients who have vascular rings or slings causing airway compression, or in patients who have absent pulmonary valve with associated severe pulmonary artery dilation.

Unexpected changes in the respiratory examination after surgery may be of significant importance. Most infants with appropriate palliation or surgical treatment of their heart disease will have fewer symptoms and findings on a respiratory examination. Raspy breathing or stridor in a postoperative patient should trigger investigation of the vocal cords that may be injured from direct trauma from endotracheal intubation, or paralyzed from injury to the recurrent pharyngeal nerve. Asymmetric chest wall movement again may indicate diaphragmatic hemiparesis due to phrenic nerve injury.

Cardiovascular Examination

There are three parts to a complete cardiovascular system examination. These include observation/inspection, palpation, and auscultation. Percussion is of little value for assessment of heart size and is not commonly performed to evaluate the heart.

OBSERVATION/INSPECTION

In addition to the general inspection described above, there can be observed findings that are specific to the cardiovascular system. Inspection of the chest wall may reveal chest wall surgical scars that suggest particular lesions. A right thoracotomy is used for placement of a right Blalock-Thomas-Taussig shunt, atrial septal defect repair, or mitral valve surgery. A midline sternotomy is used for most heart operations, especially if cardiopulmonary bypass is used. A left thoracotomy is used for patent ductus ligation, coarctation repair, or placement of a left Blalock-Thomas-Taussig shunt.

The clinician should inspect the chest for asymmetry or pulsatility. The transverse aorta sits under the suprasternal notch. Pulsations of the suprasternal notch may be visible in the presence of significant aortic runoff lesions such as aortic regurgitation. A left parasternal precordial bulge often is noted in patients with right ventricular volume overload (i.e., atrial septal defect). Examining a patient for a precordial bulge is best done with the patient supine, shoulders square on the examination table, with the examiner bending and looking tangentially across the chest. Because the dilated right ventricle is below the left precordium, the developing cartilaginous rib cage will expand to accommodate the structure. As the ribs ossify, the left precordial bulge remains. With the patient supine and the examiner at the feet of the patient, the point of maximal impulse can sometimes be observed. It is usually located in the left fourth intercostal space in the midclavicular line. In dextrocardia, it is on the right. It is displaced downward and laterally with left ventricular volume overload. Left ventricular hypertrophy does not usually alter the location of the point of maximal impulse.

PALPATION

Palpation of peripheral pulses, the chest, the abdomen, and the back should be included in each cardiac examination. Palpation of the extremities (peripheral) to assess pulses and perfusion and of the precordium (central) to assess activity and thrills should be performed.

Peripheral Palpation, Pulses

Pulses should be assessed, noting regularity and quality of the pulsations. Pulse rate changes with the age of the patient. A fast pulse rate for age may indicate arrhythmia or congestive heart failure. A slow pulse rate usually reflects athletic conditioning; however, atrioventricular block or drug effect should be considered. Irregularity of pulse rate may indicate an arrhythmia. However, a change in pulse rate with respiration is normal (sinus arrhythmia).

It is important to palpate pulses simultaneously in the upper and lower extremities, specifically right brachial or radial and right femoral pulses. Bilateral brachial pulses should be palpated simultaneously as well. If there is a delay between the upper and lower extremity pulses or absence of femoral pulsations, coarctation of the aorta should be considered. Diminished pulses are ominous in children and may suggest cardiac failure or shock. Absent or weak pulses in the left arm may result from previous subclavian flap repair of a coarctation of the aorta or in the right arm from systemic-to-pulmonary artery shunts (i.e., classic Blalock-Thomas-Taussig shunt). Bounding pulses reflect aortic runoff as in aortic regurgitation, patent ductus arteriosus, or arteriovenous malformations.

Assessment of tissue perfusion includes determining the quality of the peripheral pulses, as well as skin temperature

and capillary refill. Peripheral pulses should be full and easily palpable, not thready. Skin temperature should be determined, as should transition of central to peripheral cutaneous temperature. Temperature is best assessed using the dorsal aspect of the fingers. Change in temperature from central to peripheral can be determined by running the backs of the fingers from proximal to distal on the upper or lower extremities. Patients who have cool peripheral extremities who are warm centrally may be volume depleted or have low cardiac output. Capillary refill time is the time required for blanching to disappear after manually pressing on an extremity, and should be 3 seconds or less. While testing capillary refill, the clinician should examine the extremities for abnormalities associated with congenital heart disease, such as clubbing, finger-like thumbs (Holt-Oram syndrome), webbing of the digits, or polydactyly.

Central Palpation, Chest Wall

The chest should be palpated for the point of maximal impulse, precordial activity, and thrills. The location of the point of maximal impulse suggests the ventricular dominance. The chest should be palpated with a fingertip to confirm its location. With left ventricular dominance, the point of maximal impulse is palpated at the left midclavicular line or apex. A point of maximal impulse located at the lower left sternal border or xiphoid process suggests right ventricular dominance. Patients with dextrocardia will have a point of maximal impulse on the right side of the chest. Occasionally, an impulse will have a double contour or heave in the presence of volume overload (i.e., mitral regurgitation). In the face of pressure overload, a well-localized, sharp rising impulse or tap may be detected.

Precordial activity should be assessed. A hyperactive precordium suggests heart disease with volume overload. Volume overload may result from a large left-to-right shunt (i.e., a large ventricular septal defect or patent ductus arteriosus) or severe valve regurgitation (i.e., aortic and mitral insufficiency). In addition, left precordial bulging often is noted in patients with significant right ventricular volume overload.

Thrills are vibrations detected distal to jet lesions that are transmitted to the chest wall. Left precordial thrills are best felt with the metacarpal heads of the hand while the examiner is positioned to the right of the supine patient. Gently placing a fingertip in the suprasternal notch in supine patients will allow detection of aortic pulsations and thrills in patients with aortic valve disease. A thrill also may be palpable over the carotid arteries. Thrills located over the right upper sternal border are aortic in origin and are felt in patients with aortic valve stenosis. Left upper sternal border thrills are pulmonic in origin and generally indicate pulmonary valve stenosis, or occasionally, patent ductus arteriosus. A thrill may be felt over the left lower sternal border due to the jet of a restrictive ventricular septal defect as it strikes the endocardial surface of the right ventricle and transmits to the chest wall. Stenotic right ventricle-to-pulmonary artery conduits may produce a thrill. These are usually felt along the left sternal border.

In patients with pulmonary hypertension and elevated pulmonary arterial diastolic pressure, the pulmonic valve closure (P2) is often palpable at the left upper sternal border.

Palpation of the chest wall is also an important assessment in patients who present with the complaint of chest pain. Palpation of the costal-chondral joints should be performed to elicit tenderness. The pectoralis muscles should be palpated to determine if they are tender from injury. Placing the hands on the sides and performing gentle pressure with the palms will flex the costal-chondral joints to determine if there is pain with movement. It may be of additional benefit to have the patient perform some pectoralis muscle exercise to try to

reproduce chest pain. This could include “bench press” of the examiner’s hands, or having the patient try to bring elbows together in front of the chest against resistance to try to reproduce the patient’s symptoms.

AUSCULTATION

“Sound is the organized movement of molecules caused by a vibrating body in some medium” (2). In the case of heart sounds and murmurs, the medium is blood. Vibrations are produced by the cessation or propulsion of blood within the heart that, in turn, create sound that then radiates through the thorax, across the skin, and ultimately to the examiner through a stethoscope. The ability to identify heart sounds and murmurs and relate them to other clinical findings is an essential step in the evaluation of heart disease.

Classical teaching of cardiac auscultation suggests listening to the four valve areas and left sternal border (3). However, many of the cardiac sounds associated with congenital heart disease are heard in places other than the classic valve areas or left precordium. Listening between the valve areas will yield findings of subtle cardiac abnormalities that may not be even audible in the classic auscultation areas. For example, murmurs from some small muscular ventricular septal defects can be very localized, and are often heard midway between the tricuspid and pulmonary areas, at the mid left sternal border. Murmurs caused by coronary fistulae may be best heard at the lower right sternal border. And in patients who have dextrocardia, the cardiac sounds may best be auscultated entirely over the right precordium. A careful survey of where sounds are best heard is prudent. In patients with normal cardiac position, the pattern of auscultation might best be a large figure of eight, with the lower portion at the cardiac apex, and the upper portion being at the right sternal border, encompassing all of the left sternal border and much of the right sternal border.

Heart Sounds

Vibration of the valve apparatus, myocardium, pericardium, blood, or chest wall have all been implicated in the production of heart sounds (4–7). The timing of the first heart sound corresponds to the closure of the tricuspid and mitral valves. The second heart sound corresponds to the closure of the aortic and pulmonary valves. It has been shown that these sounds are not produced by coaptation of the valve leaflets, but rather the sudden deceleration of blood flow following closure of the valves. In turn, deceleration and cessation of blood flow cause surrounding cardiac structures and tissue to vibrate, producing audible sound (8,9).

The first heart sound (S1) occurs with closure of the mitral and tricuspid valves. There are four components to the first heart sound, but only the second and third are audible to the human ear. The first heart sound is typically a discrete, single low-frequency sound heard best at the left lower sternal border. The first heart sound is usually single in infancy. With aging, splitting of the first heart sound often becomes apparent. As with the second sound, splitting of the first heart sound varies with respiration. The timing of a split first heart sound can be confused with an early systolic ejection click. Typically, heart sounds are low in frequency, and clicks higher in frequency, but occasionally the distinction is difficult.

The second heart sound (S2) has two components that coincide with aortic and pulmonary valve closure. The aortic component (A2) precedes the pulmonary component (P2) because left ventricular contraction ends slightly before right ventricular contraction. Ordinarily, P2 is softer than A2.

Elevated pulmonary arterial diastolic pressure, as seen with pulmonary vascular obstructive disease, will cause the pulmonic valve to close crisply and accentuate P2.

The second heart sound is best heard at the mid and upper left sternal border. In the immediate newborn period, the second sound may sound single. Beyond the first 1 to 2 days of life, splitting of the second heart sound with respiration is expected, with splitting during inspiration and superimposition of the aortic and pulmonary closure sounds during expiration.

Abnormal splitting of S2 is an important finding when diagnosing heart disease. The interval of the split can increase in circumstances that prolong right ventricular ejection, such as atrial septal defects, total anomalous pulmonary venous connection, pulmonary valve stenosis, and right bundle branch block. Narrow splitting of S2 occurs with early closure of the pulmonary valve (i.e., pulmonary hypertension) or delayed aortic valve closure (i.e., severe aortic valve stenosis). Paradoxical splitting can occur in severe aortic valve stenosis, where left ventricular ejection is prolonged. A single second heart sound is not normal, and may represent atresia of an arterial valve, transposition, or pulmonary hypertension. Any heart disease that shifts the pulmonary valve away from the chest wall, such as D-transposition of the great arteries, will cause the second heart sound to be single. When the pulmonary artery is not adjacent to the chest wall, the softer pulmonary closure often becomes inaudible to the stethoscope. The second heart sound often becomes single and loud during pulmonary hypertension, as the timing of pulmonary closure becomes earlier.

The third heart sound (S3) may be heard early in diastole with rapid filling. It is a low-frequency sound, best appreciated with the bell of the stethoscope at the apex or left lower sternal border. Early in diastole, rapid ventricular filling causes vibration of the cardiac structures, producing a third heart sound. Many older children will have a normal soft third heart sound heard as a dull, low-frequency, middiastolic thud at the apex. An apical S3 is frequently heard in normal children and competitive athletes. Third heart sounds in older children should be considered to be normal. If a third heart sound is heard in the context of tachycardia, it is more likely to be a pathologic gallop than a normal sound. Later in diastole, atrial contraction augments ventricular filling.

If the ventricle is resistant to further distention, as in cardiomyopathy, the poorly compliant myocardium will vibrate, producing a fourth heart sound. Audible fourth heart sounds (S4) are almost always pathologic and are often found in patients with congestive heart failure. It is a low-frequency sound heard at the end of diastole just before S1. It is associated with rapid filling of the ventricle during atrial contraction and is heard in congestive heart failure and conditions of decreased ventricular compliance (i.e., cardiomyopathy). Its presence, often in the context of tachycardia, may sound like a gallop. When a gallop rhythm is heard, it is often difficult to distinguish whether a third or fourth heart sound is present. This is often called a “summation gallop” as it may represent one or both of these sounds, S3 and S4.

Clicks

Ejection clicks occur soon after S1 and are associated with semilunar valve stenosis (i.e., aortic or pulmonary valve stenosis) or with dilated great arteries. Aortic valve clicks are heard at the apex or right upper sternal border, and do not vary with respiration. Pulmonary valve clicks are heard along the left sternal border and are louder with expiration. Clicks associated with dilation of the aorta or pulmonary arteries are best heard over the vessel, at the right and left upper sternal borders, respectively.

A midsystolic, apical click is heard in the diagnostic finding of mitral valve prolapse. A midsystolic click may be accompanied by a late systolic murmur. Standing after squatting may accentuate a mitral valve click or regurgitant murmur in patients with mitral valve prolapse.

Friction Rubs

Friction rubs are pericardial sounds caused by movement of pericardial surfaces against one another. Friction rubs sound like the sound made by squeezing a paper bag or plastic wrap, occur in sync with heart rate, and are most often heard over the cardiac apex. Friction rubs are frequently heard in the 24 to 48 hours after cardiac surgery, especially when indwelling mediastinal chest tubes are in place. Pericarditis or other pericardial disease can cause a friction rub, although with large pericardial effusions, friction rubs can disappear.

Other Heart Sounds

Bruits are murmur-like sounds that can be heard in places other than the precordium as the case with arteriovenous malformations. Arteriovenous malformations may be responsible for unexplained cardiomegaly. In those instances, the clinician should listen for a bruit over the fontanelle or liver. In severe aortic regurgitation, one should listen over the femoral arteries for “pistol shot” sounds. The lungs should be examined for wheezing, rales, or abnormal breath sounds.

Heart Murmurs

Heart murmurs are thought to be the auditory representations of turbulent flow within the heart or blood vessels that is transmitted through the vessels, mediastinum, and the chest wall to the skin. Turbulence is described as highly disturbed flow that produces random fluctuations of velocity and pressure within the blood and vibration of the surrounding tissue. Turbulence can be described by the physical characteristic of Reynolds number. “The Reynolds number is a dimensionless quantity often used to describe the characteristics of steady flow through straight tubes at which transition from laminar to turbulent flow would occur” (10). The Reynolds number is defined as

$$Re = [(density\ of\ fluid)(velocity) / (tube\ diameter)] / viscosity\ of\ fluid$$

Although the cardiovascular system varies from the steady state conditions noted above, the transition to turbulent blood flow is thought to typically occur at a Reynolds number >2,000. There is debate whether murmurs are a direct result of turbulence or a consequence of turbulence.

Turbulent blood flow produces vibrations of the surrounding vessel in several ways. Direct impact of a jet against cardiac structures is the easiest to comprehend. However, several other mechanisms of creating vibration have been suggested (10). Eddy currents, for example, are produced adjacent to high-velocity jets. Like ripples in a pond, they produce vibrations as they strike the vessel wall. Second, pressure is lower in a moving fluid compared with stationary fluid. Therefore, the higher pressure outside of the moving fluid pushes the vessel wall toward the lower pressure fluid. This is called the Bernoulli effect. Fluctuations in the intensity of the Bernoulli effect may cause vibration of the vessel wall. Last, high turbulent flow can cause cavitation or the forming of bubbles of vapor in a liquid. Theoretically, these bubbles cause vibrations as they strike the vessel wall.

Heart murmurs should be evaluated in terms of intensity, timing, location, transmission, and quality (i.e., harsh, vibratory, etc.).

Intensity

The intensity of a murmur is relatively easy to determine, but is somewhat subjective. The intensity of a murmur is graded from I to VI where

- Grade I. Barely audible and may require several cycles to detect
- Grade II. Soft, but easily audible
- Grade III. Moderately loud murmur without a thrill
- Grade IV. Loud murmur with a thrill
- Grade V. Loud murmur heard with the stethoscope barely off the chest
- Grade VI. Loud murmur heard without the stethoscope touching the chest

The intensity of a murmur may reflect the pressure difference between the heart chambers or vessels where the abnormality exists causing the murmur. For example, as the severity of the aortic or pulmonary valve stenosis progresses, the associated murmur may increase in intensity reflecting a larger valve gradient. As ventricular septal defects become more restrictive, the associated murmur may become louder, reflecting a greater pressure difference between the ventricles. Murmur intensity when grade III or less does not help to distinguish innocent from pathologic murmurs. Any murmur that is grade IV or louder should be considered to be abnormal.

Timing

Heart murmurs should be described based on their timing during the cardiac cycle (Fig. 5.1). The timing of heart murmurs can be broken down into systolic murmurs (ejection and S1 coincident), diastolic murmurs (early diastolic, middiastolic, and late diastolic/presystolic), and continuous murmurs.

SYSTOLIC MURMURS

Systolic murmurs can be classified further as ejection or S1 coincident, based on the onset of the murmur relative to S1.

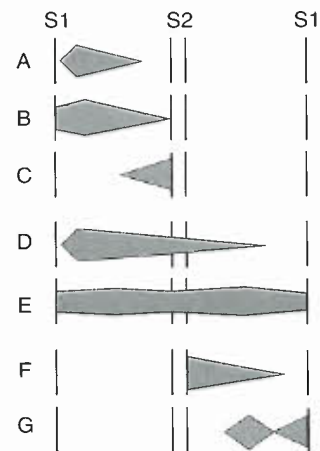


Figure 5.1. Diagram outlining timing of heart murmurs. This figure demonstrates the classification of heart murmurs based on their timing during the cardiac cycle. (A) represents the timing of systolic ejection murmurs, (B) S1 coincident murmurs, (C) late systolic murmurs, (D) continuous murmurs of vascular origin, (E) continuous venous hum, (F) early diastolic murmurs, and (G) mid and late diastolic murmurs.

Ejection Murmurs

The onset of systolic ejection murmurs occurs a short time after S1. Murmurs of this timing are separated from S1 by the period of isovolumic contraction and occur during the ejection phase of systole, while the aortic and pulmonary valves are open (Fig. 5.1A). They may be long or short and usually have a crescendo-decrescendo quality. They should end prior to S2. Ejection murmurs are the result of either obstructed blood flow through a stenotic semilunar valve or excessive volume through a normal semilunar valve. They are heard best over the site of altered flow (i.e., aortic, right upper sternal border; pulmonary, left upper sternal border) and radiate in the direction of flow.

Ejection murmurs associated with obstructed blood flow are heard with semilunar valve stenosis, subvalvular or supravulvular aortic or pulmonary stenosis, branch pulmonary artery stenosis, and hypertrophic obstructive cardiomyopathy. Ejection murmurs caused by excessive volume through the pulmonary valve are heard in atrial septal defects, pulmonary valve regurgitation, and anomalous pulmonary venous drainage. Commonly, an ejection murmur through the pulmonary valve is detected during pregnancy because of increased circulating volume. Ejection murmurs caused by excessive volume through the aortic valve are heard with aortic regurgitation, patent ductus arteriosus, and systemic arteriovenous malformations. Ejection murmurs are also heard when viscosity is decreased, such as with anemia.

S1-Coincident Murmurs

S1-coincident murmurs start with S1, and often obscure S1 as a separate sound (Fig. 5.1B). They may last through much of systole and are sometimes referred to as holosystolic or pansystolic murmurs (Figs. 5.1B and 5.2). S1-coincident murmurs occur when blood flows from a high-pressure chamber to a low-pressure chamber during what should be an isovolumic period in early systole. They are associated with ventricular septal defect and mitral or tricuspid valve regurgitation. When associated with valve regurgitation, their location corresponds with the tricuspid (left lower sternal border) and mitral (apex) valves. In the case of a ventricular septal defect, an S1-coincident murmur is heard along the left sternal border and may radiate to the right. The frequency or pitch of a ventricular septal defect murmur is directly proportional to the pressure drop through the defect; the higher the frequency, the smaller the ventricular septal defect (11). Mitral and tricuspid regurgitation murmurs are typically higher frequency and “blowing” in quality, being best heard in their respective valve areas.

Late Systolic Murmurs

Murmurs from mitral valve regurgitation due to mitral valve prolapse can occur in late systole (Fig. 5.1C). Often these murmurs are preceded by a midsystolic click. Typically, these murmurs are heard at the cardiac apex in the mitral valve area and are blowing in quality.

DIASTOLIC MURMURS

Diastolic murmurs are differentiated based on the timing of their onset during diastole: early diastolic, middiastolic, and late systolic/presystolic.

Early Diastolic Murmurs

Early diastolic murmurs begin immediately after S2 and are decrescendo in intensity as the pressure difference between artery and ventricle decreases during diastole (Fig. 5.1F). They are the result of early diastolic backflow from the great artery into the heart through an incompetent semilunar valve.

Aortic regurgitation murmurs arise from the higher diastolic pressure in the aorta and are therefore high pitched. They are heard best with the diaphragm of the stethoscope at the left mid-sternal border and radiate toward the apex. As the diastolic pressure gradient decreases, the murmur decreases in intensity. Listening while the patient leans forward and exhales accentuates the aortic regurgitation murmur.

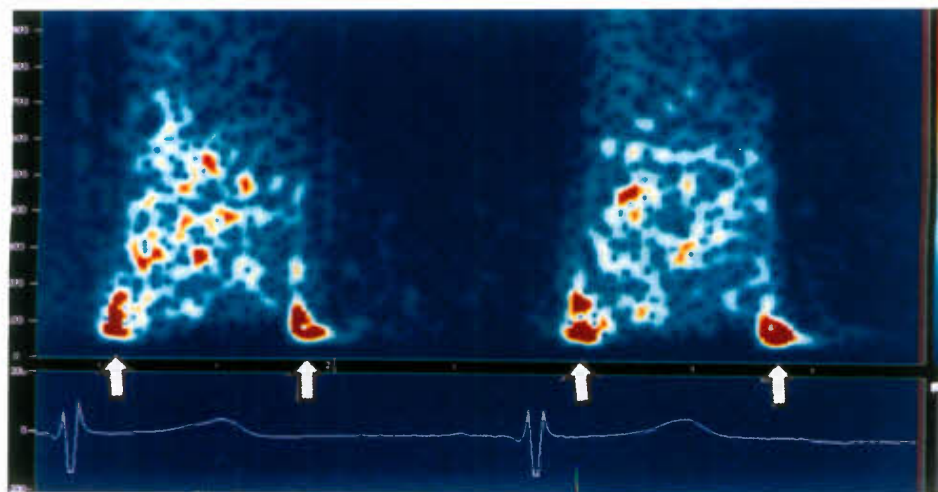
Pulmonary regurgitation murmurs are also heard in early diastole. They are medium-low pitched murmurs unless there is diastolic pulmonary hypertension, in which case they are higher pitched. They are heard from the left upper to midsternal border and radiate down the left sternal border.

Middiastolic Murmurs

Middiastolic murmurs occur during the rapid filling phase of diastole when blood crosses the atrioventricular valves (Fig. 5.1G). They are low-pitched, often rumbling noises and best heard with the bell of the stethoscope. Pathologic narrowing or thickening of the mitral or tricuspid valves (i.e., mitral and tricuspid stenosis) causes a middiastolic murmur. Excessive flow through a normal-sized atrioventricular valve is heard as a middiastolic rumble and is erroneously referred to as “relative stenosis.” If the valve is held partially closed by an aortic regurgitation jet, a middiastolic murmur results, called the Austin-Flint murmur.

Mitral valve stenosis, ventricular septal defect, patent ductus arteriosus, and mitral regurgitation cause mitral valve middiastolic murmurs that are heard at the apex. Tricuspid

Figure 5.2. Digital phonocardiographic image demonstrating the S1-coincident murmur of a ventricular septal defect. The scale on the left denotes frequency of sound. The color scale on the right depicts intensity of sound. The corresponding electrocardiogram is plotted below. Arrows correspond to S1 and S2. The color display between S1 and S2 represents the various frequencies and intensities of the murmur. (From Balster DA, Chan DP, Rowland DG, et al. Digital acoustic analysis of precordial innocent versus ventricular septal defect murmurs in children. *Am J Cardiol* 1997;79:1552–1555, with permission from Elsevier.)



valve stenosis, atrial septal defect, and anomalous pulmonary venous return cause tricuspid valve middiastolic murmurs that are heard along the left lower sternal border.

Late Diastolic Murmurs

Presystolic murmurs also are caused by flow through narrowed atrioventricular valves (Fig. 5.1G). They occur late in diastole as a result of atrial contraction pushing blood through the narrowed valve into the ventricle. The murmur will accentuate with atrial contraction and will be absent if the patient is in atrial fibrillation. They are low-frequency murmurs heard in true mitral and tricuspid valve stenosis. They are rare in children, due to the low prevalence of children with true atrioventricular valve stenosis.

CONTINUOUS MURMURS

Continuous murmurs begin in systole and continue into, and often, through diastole (Fig. 5.1D,E). These murmurs almost always are vascular in origin. They are caused by aortopulmonary (dependent) (i.e., patent ductus arteriosus, surgical aortopulmonary) shunts or arteriovenous (obligate) connections (atrioventricular fistula, coronary–cameral fistula), turbulent flow in arteries (coarctation, severe branch pulmonary artery stenosis), or turbulent flow through veins (venous hum).

The most common pathologic aortopulmonary continuous murmur is heard in patent ductus arteriosus. It is loudest in systole and softest during diastole, giving it a “machinery” characteristic. It is continuous because of the constant pressure gradient between the aorta and pulmonary arteries and increases during systole because of a larger pressure gradient. In patients with levocardia, it is best heard at the left infraclavicular area. A surgically placed aortopulmonary shunt murmur sounds similar to that of the patent ductus arteriosus.

Other continuous murmurs arising from arterial malformations include coronary artery fistulae, pulmonary arteriovenous fistulae, bronchial collateral vessels, and pulmonary vessels arising from a truncus arteriosus. Coronary artery fistulas may empty into the right atrium, right ventricle, left ventricle, or pulmonary artery. These continuous murmurs may be louder in diastole. The location of the murmur will differ with each abnormality; however, it will usually be located on the lower pressure side of the abnormal connection.

Continuous murmurs occasionally are heard in patients with peripheral pulmonary arterial stenosis in whom flow into distal vessels varies and in patients with coarctation of the aorta who have large collateral vessels. Patients who are surgically palliated with bilateral pulmonary artery bands often have continuous murmurs. Murmurs due to peripheral pulmonary arterial stenosis of any cause will radiate over the lung fields, and be heard in the axillae and over the back.

Venous murmurs can be benign, as in the venous hum. They usually are heard over the left or right upper chest and disappear with changes in head position or compression of the jugular vein, and are truly continuous (Fig. 5.1E). They are typically low in frequency, vary with respiration, and are best heard with the patient upright.

In obstructed forms of total anomalous pulmonary venous return, a soft, high-pitched continuous murmur may be heard over the site of obstruction. The site of the murmur is determined by the locus of drainage, for example, over the liver.

Dynamic Auscultation

Patients should be examined in several positions to assess positional changes in murmurs and other findings. At a minimum, patients who are able to sit independently should be examined while sitting and supine. Older children should also

be examined while standing, and sometimes while squatting. Adolescents, patients being screened for sports participation, and patients with collagen vascular disorders should be examined supine and upright, including squatting to standing (dynamic auscultation) to detect the click and murmur of mitral valve prolapse or the ejection murmur of hypertrophic cardiomyopathy. This maneuver first places increased afterload on the heart, enlarging the left ventricle. Then, with standing, the ventricle is relatively unloaded, allowing mitral valve prolapse or dynamic outflow obstruction to be more manifest to the examiner. The change in position from supine to sitting often makes an innocent Still murmur softer. Reclining a patient from sitting to supine should make an innocent venous hum disappear completely.

Abdominal Examination

The abdominal examination is important and often fraught with difficulty, especially in the infant. To conduct a thorough examination, it may be best to palpate the abdomen last. The clinician should remember to warm his or her hands before starting. Bending his or her knees so that the abdominal muscles relax may relax a child who is tense or ticklish. It is generally possible to palpate the deeper aspects of the abdomen and maintain pressure during inspiration. The size and texture of the liver and spleen should be assessed, palpating above the pelvic brim and working slowly upward until the liver edge or spleen tip is felt. With increased venous pressure, the liver will be enlarged and its capsule may be tender. Percussion is also important to determine the location of the upper margin of the liver to determine liver span. This is particularly useful if the lungs are hyperinflated. Hyperinflation pushes the liver below the costal margin, giving a false impression of liver enlargement. In this case, percussion is a more accurate method for assessing liver size. Percussion over the lower left ribs for displacement or absence of the stomach air bubble can help to define splenomegaly.

Back Examination

Patients with congenital heart disease, especially those with chronically enlarged hearts and connective tissue disorders, have a high incidence of scoliosis. Other diseases that have cardiac manifestations such as Marfan syndrome can be associated with scoliosis. Therefore, examination of the spine for the presence of scoliosis should be part of the cardiac physical.

INNOCENT MURMURS

Innocent murmurs are the sound of noisy blood flow coursing through a structurally normal heart. They are heard in 50% or more of children at some time or another, particularly at around 3 or 4 years of age. They are accentuated by increased cardiac output, as when a child is excited, anemic, or febrile. Auscultation with the ability to differentiate pathologic murmurs from benign murmurs is the method of choice for diagnosing innocent murmurs. In general, innocent murmurs are low in intensity, and low in frequency. They are generally not harsh in quality. Most innocent murmurs, with the exception of the venous hum, are systolic ejection in timing. Innocent murmurs are not associated with abnormalities in the palpation exam (displaced point of maximal impulse or pulse abnormalities) and are associated with normal heart sounds. The presence of a click should be a clue that an associated murmur is not innocent.

Still Murmur

The most common innocent systolic murmur of childhood is Still murmur. It has many descriptions, including innocent, vibratory, functional, normal, and physiologic murmur. It is a systolic ejection murmur heard loudest somewhere between the left lower sternal border and the apex. Described as having a vibratory, musical, or twanging string quality, its usual intensity is grade I to III/VI. It is a low-frequency murmur in the range of 150 Hz (12). The murmur is heard best with the patient supine. This murmur also varies significantly with respiration, becoming softer and less vibratory during inspiration. As with all innocent murmurs, the electrocardiogram and chest radiograph are normal. The exact cause of this innocent murmur has not been determined. Suggestions include relatively smaller aortic size resulting in increased velocity of blood through the aorta during ejection, left ventricular false tendons, exaggerated vibrations with ventricular contraction, and increased cardiac output (13–15). Whatever the cause, the heart is normal, and a detailed imaging evaluation is unnecessary for diagnosis.

Pulmonary Flow Murmur of Childhood

A second innocent systolic ejection murmur is the pulmonary flow murmur. Commonly detected in thin-chested adolescents between 8 and 14 years of age, it is heard maximally over the pulmonary area. Although it resembles the ejection murmur of pulmonary stenosis, it is not particularly harsh in quality, and not accompanied by a click or thrill. Its intensity is 1 to 3/6, and the second heart sound should have normal splitting with the P2 component sounding normal. This murmur is frequently heard in patients who have increased cardiac output from fever, anemia, or pregnancy. If this murmur is heard in the presence of fever, and is not present when afebrile, it may not require any further evaluation. If the murmur of pulmonary flow is present in a patient who is not in an increased output state, lesions of increased pulmonary flow, such as atrial septal defects, should be considered.

Pulmonary Flow Murmur of Infancy

Also referred to as a peripheral pulmonary flow (peripheral pulmonary stenosis) murmur, this murmur is commonly heard during the newborn period and early infancy, particularly in premature infants. It is an ejection murmur that radiates from the left upper sternal border over the lung fields to both axillae and the back. Theories of its origin include the relatively small size of the branch pulmonary arteries immediately after birth, as well as their angle of the takeoff from the main pulmonary artery during the newborn period (16,17). Whatever the cause, it usually disappears by 6 months of age. If the murmur persists past 6 months of age, structural abnormalities of

the pulmonary artery tree, or lesions that increase pulmonary blood flow such as atrial septal defect should be considered.

Venous Hum

The venous hum murmur, as discussed above, is the only innocent murmur that is not systolic ejection in its timing. This murmur is low frequency and truly incessant when the patient is upright. Typically, this is a low-frequency noise that sounds more like a motor running in the background. Generally, some variation in pitch and intensity occur with respiratory and cardiac cycles. This murmur will cease with maneuvers that occlude the neck veins, either by direct compression using a thumb, or by turning the patient's head to look over the contralateral shoulder. Gravity driven, this murmur should also completely disappear with the patient flat in a supine position.

REFERENCES

1. Mahle WT, Newburger JW, Matherne GP, et al. Role of pulse oximetry in examining newborns for congenital heart disease: a scientific statement from the American Heart Association and American Academy of Pediatrics. *Circulation* 2009;120:447–458.
2. Stevens SS, Warshofsky F. *Sound and Hearing*. Alexandria, VA: Time-Life Science Library, 1980.
3. Bickley LS, Szilagyi PG. *Bates' Guide to Physical Examination and History Taking*. Philadelphia, PA: Lippincott Williams & Wilkins, 2007:313.
4. Dock W, Grandell F, Taubman F. The physiologic third sound, its mechanism and relation to protodiastolic gallop. *Am Heart J* 1955;50:449–464.
5. Ozawa Y, Smith D. Origin of the third heart sound: 1. studies in dogs. *Circulation* 1983;67:393–398.
6. Dunn FL, Dickerson WJ. Third heart sound: possible role of pericardium in its production. *Circ Res* 1955;3:51–55.
7. Reddy PS, Meno F, Cutiss EI, et al. The genesis of gallop sounds: investigation by quantitative phono- and apex cardiography. *Circulation* 1981;63:922–933.
8. Leatham A. *Auscultation of the Heart and Phonocardiography*. London, UK: J & A Churchill, 1970.
9. Shaver JA, Leonard JJ, Leon DF. *Examination of the Heart. Part 4: Auscultation of the Heart*. Dallas, TX: American Heart Association, 1990.
10. Nichols WW, O'Rourke MF. *McDonald's Blood Flow in Arteries*. Philadelphia, PA: Lea & Febiger, 1990.
11. Balster DA, O'Connell D, McCreary M, et al. Frequency analysis of heart murmurs correlates to severity of ventricular septal defect. Paper presented at the American Academy of Pediatrics. San Francisco, CA, October, 2004.
12. Balster DA, Chan DP, Rowland DG, et al. Digital acoustic analysis of precordial innocent versus ventricular septal defect murmurs in children. *Am J Cardiol* 1997;79:1552–1555.
13. Klewer SE, Donnerstein RL, Goldberg SJ. Still's-like innocent murmur can be produced by increasing aortic velocity to a threshold value. *Am J Cardiol* 1991;68:810–812.
14. Stein P, Sabbah H. Aortic origin of innocent murmurs. *Am J Cardiol* 1977;39:665–671.
15. Stein P, Sabbah H, Lakier J. Origin and clinical relevance of musical murmurs. *Int J Cardiol* 1983;4:103–112.
16. Danilowicz DA, Rudolph AM, Hoffman JIE, et al. Physiologic pressure differences between main and branch pulmonary arteries in infants. *Circulation* 1972;45:410–419.
17. Miyake T, Yokoyama T. Evaluation of transient heart murmur resembling pulmonary artery stenosis in term infants by Doppler and M-mode echocardiography. *Jpn Circ J* 1993;57:77–83.

Exercise Screening and Sports Participation

Julie A. Brothers ■ Paul Stephens, Jr. ■ Stephen M. Paridon

Over the last 30 years, there has been a significant increase in the rates of overweight and obesity in children in developed countries. Concurrently, there has been a decline in physical activity in children and adolescents. The reasons for these trends are multiple and include a shift to a high-fructose diet, increased fat and processed food consumption, and increased sedentary activity such as watching television and video gaming. The result is a young population at risk for an epidemic of hypertension, type II diabetes, and early atherosclerotic coronary disease (1,2). Recent data on obesity trends in children with congenital heart disease (CHD) indicate their incidence of obesity is similar to that of the general pediatric population. The risks for complications of obesity appear to be at least as great in this population as in the general population (3,4). Given these trends, there is an essential need to promote routine vigorous physical activity in both the general pediatric population and, in particular, the CHD population.

Balanced with the need to promote physical activity as an essential part of a healthy lifestyle is the need to keep children and adolescents safe from the risk of sudden cardiac death (SCD) during physical activity. Although SCD is very rare in the pediatric and young adult population, congenital cardiac defects, either myopathies or structural abnormalities, are the major causes of these events (5,6). SCD occurs very rarely in patients with known congenital cardiac disease. Much more commonly, it happens to those athletes not previously suspected of having cardiac abnormalities. There are few evidence-based recommendations for the screening of athletes for risks of SCD. Much controversy surrounds this topic. There are even fewer evidence-based data regarding the screening and participation for athletic activities for children and adolescents with known CHD. What information is available is restricted to adolescents and young adults, and, importantly, current recommendations are restricted to competitive sports. There is essentially no information on the safety or screening of preadolescents with CHD for physical activity. As well, there are almost no evidence-based guidelines for children and adolescents with CHD wanting to participate in leisure or recreational activities. Likewise, guidelines for activities of daily living especially for young adults with CHD are very limited.

The goal of this chapter is to discuss the current state of knowledge for athletic screening and participation in children with CHD. It broadly discusses the current recommendations regarding physical activity promotion in the pediatric, adolescent, and young adult populations. It also discusses the differences and various types of physical activity such as those of daily living, leisure sports, and organized competitive athletics. As well, differences in physiologic requirements of various athletic activities and their associated risks are discussed. The current methods and recommendations for screening for SCD during physical activity are reviewed. Controversies regarding the type and timing of screening are addressed. Finally, what is known about the ability to participate in and the risks of athletic activities for the individual groups of congenital cardiac

defects is discussed with emphasis on what is known about preathletic screening and recommendations for activities of daily living, leisure and recreational athletics, and participation in competitive sports.

PHYSICAL ACTIVITY AND EXERCISE

Physical performance during exercise depends on the individual's strength, endurance, and skill in performing a given athletic activity. These in turn may be influenced by a number of factors such as age, sex, height, weight, and especially cardiovascular conditioning. The ability to successfully and safely undertake a given athletic activity depends on the combination of these factors and the requirements of the activity.

All athletic activities can be roughly broken down into their "static" and "dynamic" components (7). The static component is the amount of maximal voluntary contraction (MVC) of the exercising muscles required to perform the activity. This is what is traditionally considered isometric activity or the muscles working against resistance. Examples of activities requiring high static forces are weight lifting and wrestling. The cardiovascular effects of isometric activity depend on the intensity of the activity (e.g., the percentage of MVC required) and the size and number of the muscle groups involved in the activity. Contraction of muscles during isometric activity results in an increase in peripheral vascular resistance (PVR) with a consequent rise in systolic, diastolic, and mean blood pressures. The degree of increase in these values depends on the size of the muscle group and the percentage of MVC achieved but may result in systolic blood pressures in excess of 300 mm Hg with heavy weight lifting. On the other hand, cardiac output and total body minute oxygen consumption (VO_2) are relatively unchanged by brief severe static activity (8–10).

The dynamic component of exercise can be thought of as the activity that results in muscle contraction and body movement. These activities are usually repetitive and against low resistance (7,9). This is what is thought of as isotonic activity. An example of a highly isotonic activity is long-distance running. The cardiovascular effects of high dynamic activity are quite different from static activity. The metabolic demands of the exercising muscle are much greater. The VO_2 may rise 10-fold or more from resting values with highly dynamic activity. To meet this oxygen demand, cardiac output may rise fivefold or more in well-conditioned athletes. Although systolic blood pressure rises as the cardiac output increases, vasodilation of the vascular bed of the exercising muscles results in a significant drop in PVR with highly dynamic exercise. Thus, dynamic exercise results primarily in a volume load being placed on the heart as opposed to the pressure load that results from highly static activity.

In truth, there are no pure "static" or "dynamic" activities, and all athletic activities are to some degree a combination of

Increasing Static Component ↑	III. High (>50% MVC)	Bobsledding/Luge*, Field events (throwing), Gymnastics*, Martial arts*, Sailing, Sport climbing, Water skiing*, Weight lifting*, Windsurfing*	Body building*, Downhill skiing*, Skateboarding*, Snowboarding*, Wrestling*	Boxing*, Canoeing/Kayaking Rowing Speed skating*, Triathlon Cycling*, Decathlon
	II. Moderate (20–50% MVC)	Archery, Auto racing*, Diving*, Equestrian*, Motorcycling	Football*, Field events (jumping), Figure skating*, Rodeoing*, Rugby*, Running (sprint) Surfing*, Synchronized swimming	Basketball*, Ice Hockey*, Cross-Country Skiing (skating technique), Lacrosse*, Running (middle distance), Swimming, Team handball
	I. Low (<20% MVC)	Billiards, Bowling, Cricket, Curling, Golf, Riflery	Baseball/Softball*, Fencing, Table tennis, Volleyball	Badminton, Cross- country Skiing (classic technique), Tennis, Race walking, Running (long distance), Field Hockey*, Soccer*, Racquetball, Squash, Orienteering
		A. Low (<40% Max O ₂)	B. Moderate (40–70% Max O ₂)	C. High (>70% Max O ₂)
		Increasing Dynamic Component →		

Figure 6.1. Classification of sports. This classification is based on peak static and dynamic components achieved during competition. It should be noted that higher values may be reached in training. The increasing dynamic component is defined in terms of the estimated percent of maximal oxygen consumption (Max VO₂) achieved and results in an increasing cardiac output. The increasing static component is related to the estimated percent of MVC reached and results in an increasing blood pressure load. The lowest total cardiovascular demands (cardiac output and blood pressure) are shown in green and the highest in red. Blue, yellow, and orange depict low moderate, moderate, and high moderate total cardiovascular demands, respectively. *denotes collision risk. (From Mitchell JH, Haskell W, Snell P. Task Force 8: classification of Sports. *J Am Coll Cardiol* 2005;45:1364–1367, with permission from Elsevier.)

both types. Figure 6.1 shows the relative amounts of static and dynamic forces required for various types of competitive sports that was published as part of the 36th Bethesda Conference on Competitive Sports Participation in Athletes with Heart Disease (7). Increasing dynamic activity requires a higher VO₂ while increasing static activity requires a higher percentage of MVC. There are sports such as rowing and cycling that require both high static and high dynamic components.

This figure has been widely published and used by clinicians to help to make recommendations for activities for their patients with heart disease. It is important to remember that the values for this table refer only to competitive sports in adolescents and adults. The contents of this table have little or no relevance to competitive sports participation in the preadolescent population. Much of preadolescent competitive sport training focuses on learning basic skills and coordination. Strength and endurance training have very little or no place in competitive sports at this age. Any parent will tell you that soccer played by a group of 7-year-olds bears almost no relationship to soccer being played by a group of 17-year-olds. Understanding these differences is crucial since it impacts directly on the ability of athletes with CHD in these age groups to successfully and safely participate in the athletic activity.

Types of Physical Activity

Physical activities can be divided into three broad types of activities: (a) activities of daily living, (b) leisure and recreational sports, and (c) competitive sports. All patients with CHD

participate in the first type of activity. Many also participate in the one or both of the latter two types. Understanding the differences between these types of activities is important to being able to assess the capabilities and safety of individuals with CHD to perform these activities.

Activities of Daily Living

“Activities of daily living” is an inclusive term that encompasses all the physical activities required by an individual as part of his or her routine daily tasks. These requirements will vary greatly depending on the age of the individual as well as many other unique circumstances. There have been attempts to quantify the amount of physical activity that occurs during typical activities of daily living among different ages of children, adolescents, and young adults both with and without CHD. These studies used various types of motion detectors as well as recall questionnaires. The results of these studies were mixed, but generally indicated that children and adolescents with CHD perform significantly less physical activity as part of their daily routine (11–13). This difference was most pronounced in boys with CHD compared to their healthy peers (12,13). It is also worth noting that most children tend to overestimate the amount of physical activity they perform (14,15).

The reasons for this difference in physical activity associated with daily living among children with CHD are not clear. There is at least some evidence that this is due to activity restrictions that have been imposed by physicians, parents, and in some cases by the children themselves (16). This has been seen even in children with relatively trivial cardiac conditions. The consequence of these restrictions may well be quite significant. Recent studies of obesity trends in children with CHD are alarming. Obesity in this population mirrors that of the general pediatric population and occurs even in populations with otherwise excellent cardiac repair and normal or near-normal exercise capacities (3,4,17). There is at least some evidence that the amount of obesity is related to daily amounts of physical activity.

Assessment of activities of daily living is even more important in the case of young adults with CHD. These activities will usually include those required for employment. The intensity of physical activity can obviously vary greatly from individual to individual depending on the nature of their employment. Although this may seem obvious, the little research available would suggest that this aspect of patient care is largely ignored by the patients and their physicians. Of concern is the finding that the most common reason patients do not seek information about appropriate level of physical activities is a mistaken belief that all activities are safe to perform (18).

Leisure and Recreational Sports

Leisure and recreational sports are physical activities that are engaged in without pressure to participate and are performed at the individual's desire and comfort level. In short, they are activities that are undertaken without formal coaching. This definition encompasses a broad category of activities. Although there may be no formal coaching, some of these activities have significant organization and structure. Intramural sports at the high school or college level may often fall into this category. Less structured activities such as playground “pick-up” games as well as physical activities that may be undertaken by an individual such as cycling or jogging would also fall under this category of leisure or recreational sports. A careful history of these activities is an important part of the assessment of a patient with CHD. Clearly, the intensity with which these leisure activities are performed may vary widely with the age and circumstances in which they are undertaken. This also highlights the importance of understanding the difference and

intensity of sports at a recreational as opposed to a competitive level. Intramural flag football has little in common with competitive high school football. For this reason, it does not make sense to use the information in Figure 6.1 on the intensity of this sport to determine if it is safe for a patient with CHD to play at an intramural level.

Competitive Sports

Competitive sports are those that are generally organized, coached, and played at high skill levels. They often, but not always, require high-intensity physical activity (see Fig. 6.1). The intensity with which an individual participates in competitive sports is influenced by their personal motivation as well as the outside influences of the coach, other team members, parents and other family members, and spectators. The end result is the potential for the individuals to push themselves to participate beyond the level they might otherwise choose to or which might be considered safe by their physician.

It is also important to remember that training is a significant part of competitive sports. The training for competitive sports may in many cases be of higher intensity than participation in the actual sport. For example, weight training and physical conditioning undertaken by high school athletes playing baseball may easily exceed the intensity of the activity they achieve in the actual game. When considering the safety of participation of an individual with CHD in a particular sport, the requirements of training must be considered equally with the sporting activity itself.

It is also important to remember, as stated earlier, that “competitive” does not necessarily mean the same thing for all ages. None of the factors that influence high levels of performance in adolescents and adults, such as coaching and spectators, are likely to have much of an effect on young children. Especially at early ages, children are very unlikely to perform beyond a level that they would otherwise choose to self-limit. As such, these “competitive” sports should be thought of more as activities to teach basic physical skills rather than true competitive athletics (19).

Promoting Physical Activities and Exercise in Patients with Congenital Heart Disease

Given the concerns of growing obesity and sedentary lifestyles in the population with CHD, what should the recommendations be for physical activity in this population? Regardless of age, in the vast majority of the population, the recommended level of 60 minutes of moderate to vigorous physical activities per day is probably appropriate. This level of activity corresponds to approximately 50% to 60% of maximal VO_2 or 70% of maximal heart rate (20). As will be discussed later in this chapter, this is a level of physical activity that is often achieved in recreational activity or in many cases through competitive sports and is both safe and desirable for many individuals with simple congenital heart defects. Often with minor CHD, minimal formal testing may be required prior to individuals undertaking this level of activity. In more complex defects and usually following an operative repair, more formal studies including electrocardiogram (ECG), echocardiogram, and exercise testing may be indicated. The need and the rationalization for these tests will be discussed for the individual defects.

In individuals with complex defects and residual cardiac dysfunction, studies from the adult heart failure literature suggest that they would still benefit from routine regular physical activity. However, these patients may need physical activity programs that are more specifically designed for their degree of cardiac fitness (21–23). In these circumstances,

formal exercise testing with assessment of VO_2 , work rate, and heart rate is very useful in generating an exercise prescription. This can be used to instruct the patient in the types and intensity of activities that are both safe and beneficial. These prescriptions are usually based on what is referred to as **FITT**-factors. **FITT** is an acronym for Frequency, Intensity, Time and Type. All four factors should be included when generating an exercise prescription and address both activities with primarily dynamic and static components to assure optimal physical conditioning (24). This type of activity classification is used throughout this chapter in making recommendations for activities in individual congenital cardiac defects.

PREPARTICIPATION SCREENING FOR UNDIAGNOSED CARDIAC CONDITIONS

Incidence of Sudden Cardiac Death

SCD in individuals younger than 35 years of age during or just after exercise is almost always attributable to structural or functional cardiac disease (25). In the United States, the most common cardiac causes of SCD are hypertrophic cardiomyopathy (HCM), commotio cordis, coronary artery anomalies, other cardiomyopathies, electrical abnormalities (e.g., long QT syndrome, catecholaminergic polymorphic ventricular tachycardia, Brugada syndrome), myocarditis, Marfan syndrome, aortic valve disease, atherosclerotic coronary artery disease (CAD), and others (25–28). Because there is no mandatory reporting system in the United States, the exact frequency of SCD is unknown. Published reports have relied on public media, catastrophic insurance claims, and electronic databases. From these, estimates of SCD range from 1:160,000 to 1:300,000 for competitive athletes aged 12 to 35 years (25,27,28). These may underestimate the true incidence of SCD since without mandatory reporting, it is likely that some cases are missed. Indeed, there are other studies that have reported a higher incidence of SCD in the United States, ranging from 1:9,000 in United States military recruits (29) to 1:67,000 in a retrospective survey of college athletes aged from 18 to 23 years (30–34). In the Veneto region of Italy, prior to implementing a national screening program, the incidence of SCD was 1:28,000 for competitive athletes aged from 12 to 35 years. This is based on a mandatory registry of SCD in the region (35).

Risk of SCD appears to differ based on gender, race, and activity. SCD occurs more often in males than females (26,27,36), which may be explained by the greater participation rates in males compared to females in competitive athletics. In the United States, African Americans are at greater risk than Caucasians for SCD (36). Participation in soccer and basketball carries the highest risk of SCD, but this may be explained by the popularity and higher participation rates in these sports compared to other activities (26).

Although debatable, most agree that regular training for athletic competition is associated with an increased risk of SCD in those athletes who have underlying occult cardiovascular disease compared to sedentary young individuals. In 2003, Corrado et al. reported the incidence of sudden death in the athletic and nonathletic young population (12 to 35 years) in the Veneto region of Italy. These authors demonstrated that participating in competitive sports increased the risk of sudden death in adolescents and young adults by 250%. They reported an incidence of sudden death of 2.3 (2.62 in the males and 1.07 in females) per 100,000 athletes per year from all causes and of 2.1 per 100,000 athletes per year from cardiovascular disease (5).

Purpose of Preparticipation Screening

Why do we perform preparticipation screening? Is the purpose to prevent SCD or is it to identify those children with cardiovascular abnormalities that may place them at increased risk for SCD? The answer appears to be the latter. The American Heart Association (AHA) states that preparticipation screening is the “systematic practice of medically evaluating large, general populations of athletes before participation in sports for the purpose of identifying (or raising suspicion of) abnormalities that could provoke disease progression or sudden death” (37) (Fig. 6.2). Similarly, according to the 36th Bethesda Conference Guidelines “the ultimate objective of pre-participation screening carried out in general populations of trained athletes is the recognition of “silent” cardiovascular abnormalities that can progress or cause sudden cardiac death” (38). The American Academy of Pediatrics recently published guidelines for preparticipation screening, with the goal to “uncover conditions that might require further investigation or treatment” that would hinder the health and safety of the athlete (39). Thus, it appears that the main goal of screening is to discover underlying cardiovascular disease that has the potential for SCD. Based on estimates from several studies using noninvasive testing, approximately 1 in 500 young athletes may have an underlying cardiac condition that places them at increased risk of SCD (35,37,40–43). Many cardiovascular conditions, once identified, can be treated to help reduce the risk of SCD. Treatment may include activity restriction, pharmacotherapy, electrophysiology studies and procedures, implantable cardioversion defibrillator placement, and in some cases, surgical repair.

Current Preparticipation Screening Recommendations

Both the AHA and the European Society of Cardiology (ESC) agree that preparticipation screening of young athletes is warranted; however, controversy exists between the U.S. and European recommendations on the inclusion of a 12-lead ECG as part of routine screening (37,44). The first consensus statement on preparticipation screening in the United States

was published by the AHA in 1996 and was reaffirmed in 2007 (37,45). This statement recommended a detailed personal and family history and physical examination (Fig. 6.2). A 12-lead ECG was not included. One of the major issues with this approach is that many athletes with a predisposition to SCD are asymptomatic, with normal histories and physical examinations. Often, the first sign of an underlying cardiovascular condition is SCD in up to 60% to 80% of these athletes (26,46,47). The limited value of history and physical examination alone was noted in a retrospective analysis of 115 high school and collegiate athletes who died suddenly. The authors found that cardiovascular abnormalities were suspected by standard history and physical examination screening in only 3% of the examined athletes and screening led to the accurate diagnosis in only one athlete (26). In the United Kingdom, prospective studies using history and physical examination were not efficacious in identifying those with underlying cardiovascular conditions associated with SCD (48).

The current recommendations from the ESC, endorsed by the International Olympic Committee (IOC) and several professional sports organizations, include a 12-lead ECG in addition to the screening history and physical examination (44,49). For over 25 years, Italy has evaluated several million athletes annually, under a state-subsidized screening program (44). The evaluation is performed by specially trained physicians who work in centers dedicated to preparticipation screening of athletes and is performed starting at age 12 to 14 years and repeated at least every 2 years (44). The protocol also incorporates guidelines for further investigations if any cardiovascular abnormality is found or suspected.

Benefits of Mandatory Preparticipation Electrocardiogram Screening

In the United States, the inclusion of additional noninvasive tests, such as the 12-lead ECG, to preparticipation screening of young athletes is highly debated (50–53). The European recommendations are based on several studies demonstrating increased sensitivity using ECG to detect occult cardiovascular pathology compared with history and physical examination alone (35,40–43).

Figure 6.2. The American Heart Association Pre-participation Screening of Competitive Athletes Recommendations (12-Elements) (Adapted from Maron BJ, Thompson PD, Puffer JC, et al. Cardiovascular pre-participation screening of competitive athletes. A statement for health professionals from the Sudden Death Committee (clinical cardiology) and Congenital Cardiac Defects Committee (cardiovascular disease in the young), American Heart Association. *Circulation* 1996;94:850–856.).

^aIn middle and high school athletes, parental verification of medical history is recommended.

^bNot vasovagal (neurocardiogenic); particularly concerning if related to exercise.

^cAuscultation should be done both while supine and standing, or with Valsalva maneuver, in order to identify murmurs of dynamic left ventricular outflow tract obstruction.

Medical History^a

- Chest pain on exertion
- Chest pain with exercise
- Syncope/near syncope that is unexplained^b
- Unexplained or excessive dyspnea/fatigue with exertion
- Prior heart murmur
- Elevated systemic blood pressure

Family History

- Premature death < 50 years from heart disease, sudden or otherwise, ≥ 1 relative
- Disability from heart disease in a close relative < 50 years of age
- Knowledge of certain cardiac conditions in relatives: hypertrophic or dilated cardiomyopathy, long QT syndrome or other ion channelopathies, Marfan syndrome, or clinically significant arrhythmias

Physical Examination

- Heart murmur^c
- Evaluation of femoral pulses, to exclude aortic coarctation
- Physical characteristics of Marfan syndrome
- Brachial artery blood pressure (sitting, in both arms)

Genetic cardiomyopathies are the most common cause of SCD in young athletes. In the United States, HCM is most common while in Italy, arrhythmogenic right ventricular cardiomyopathy (ARVC) predominates (25,35). While cardiomyopathy is definitively diagnosed with cardiac imaging, ECG screening can detect approximately 95% of those with HCM and 80% with ARVC (54,55). Corrado et al. (56) reported on a 17-year experience of preparticipation screening that included ECG in the Veneto region of Italy. During 1979 to 1996, a consecutive series of 33,735 young athletes was evaluated. Of these athletes, 1,058 were disqualified for medical reasons and 621 (1.8%) because of the recognition of clinically relevant cardiovascular abnormalities. Among the athletes screened, 22 (0.07%) showed both clinical and echocardiographic evidence of HCM, which accounted for 3.5% of the cardiovascular causes for disqualification. The authors showed that, when compared to history and physical examination alone, ECG had 77% greater power to identify HCM. Similarly, a population-based study of 4,111 young adult athletes in the United States using ECG found a diagnosis of HCM in 7 (0.17%) by echocardiography, 5 of whom had an abnormal ECG (71%) (57). The Italian ECG-based preparticipation screening model has also been shown to have a high negative predictive value (99.98%) in excluding HCM in those young athletes who have normal ECG (58). This model was found to be effective in reducing rates of SCD from ARVC with a significant decline (84%) in incidence rates from the prescreening to the postimplementation of screening era (35).

In 2006, Corrado et al. reported on a prospective observational analysis of 42,386 young athletes, evaluating the rate of SCD in those undergoing screening to those nonathletes who did not have preparticipation screening over more than 25 years. Results were compared for the era prior to use of ECG for preparticipation screening to the 25-year era with ECG screening. There was a 90% reduction in mortality in young athletes since the beginning of the screening period. The rate of SCD in nonathletes remained constant over the same period. The reduction appeared to be due to fewer cases of SCD from cardiomyopathies (mainly ARVC) and to increased identification of cardiomyopathies at time of screening (35). Recently, Wilson et al. evaluated 1,074 junior athletes (ages 10 to 27) and 1,646 physically active schoolchildren (age 14 to 20) in the United Kingdom using personal and family history, physical examination, and resting ECG. Nine athletes (0.3%) were found to have cardiovascular abnormalities predisposing them to SCD. All were detected by ECG alone as none had symptoms or family history of SCD (59).

Concerns about Mandatory Preparticipation Electrocardiogram Screening

In the United States, obstacles exist to implementation of an obligatory national screening of competitive athletes using ECG. Some of these obstacles include the large population of athletes to be screened (10 to 12 million), diverse ethnic and racial population in the United States, and the recognition that it is impossible to absolutely eliminate the risks associated with competitive sports (5).

Another main concern regarding the use of ECG during preparticipation screening relates to the high false-positive rate. In the study by Corrado et al. (35), a 7% false-positive rate with 2% of athletes being disqualified was reported; only 0.2% of athletes were ultimately disqualified for potentially fatal cardiac conditions. This raises concerns regarding unnecessary further investigations and/or false disqualification of an athlete who is not actually at increased risk for SCD (60). Several recent studies have been published utilizing strict ECG criteria when screening athletes to take into account

the physiologic adaptation to heart structure and function in athletes ("athlete's heart") affecting the interpretation of ECGs. In the study by Wilson et al., the authors reported a false-positive rate of 3.7% using history, physical examination, and ECG with 1.9% false positives due to ECG alone (59). Hevia et al. (61) evaluated 1,220 amateur athletes in Spain using history, physical examination, and 12-lead ECG and found 6.14% of ECGs were abnormal with 2 cases of HCM diagnosed by ECG. There were 15 cases with positive criteria on history or physical examination, but none were found to have cardiac disease by echocardiography (1.2% false-positive rate). In 2007, Pelliccia et al. (62) described ECG abnormalities on 32,652 amateur athletes (median age 17 years) undergoing preparticipation screening in Italy and found 12% had abnormalities but only 40% of those abnormalities (4.8% of the population) required further diagnostic testing.

Two recent studies have further called into question the usefulness of 12-lead ECG as part of preparticipation screening of athletes. Maron et al. (63) compared sudden death rates in Minnesota, where ECG is not part of routine screening, to that of the Veneto region of Italy, where ECG screening is mandatory. Over a 23-year period, the SCD rate of high school athletes in Minnesota was 1.06 per 100,000 person-years and 1.87 per 100,000 person-years in Italy. These data demonstrated that the SCD rate was low in both locations and does not support a reduced mortality rate due to use of ECG in preparticipation screening. As well, Steinvil et al. (64) reported on the sudden death rate prior to and after mandatory preparticipation screening program in Israel. This screening consisted of medical history, physical examination, ECG, and exercise stress testing. The authors found no significant difference between the average yearly incidences of SCD (2.54 per 100,000 person-years) in the decade prior to mandatory screening compared to the decade after (2.66 events per 100,000 person-years). The authors also called into question the findings from Italy (35) from which the ESC based their current guidelines (44), noting that the Italian study only looked at the 2-year period preceding the enforcement of ECG screening and compared this to mortality rates 25 years later. Instead, it may be that there were abnormally high mortality rates in Italy in 1980 and 1981 (mandatory screening was enforced in 1982) but if they had looked prior to those dates, they may have found great variability in the SCD rates, as was found in Israel (35,64).

As well, as with any screening tool, ECG does not detect all conditions that predispose an athlete to SCD. In particular, congenital coronary anomalies and premature atherosclerotic CAD cannot be identified by ECG alone. These cause up to 20% of SCD in young athletes in the United States (26). There are also a small percentage of people with HCM who have normal ECG; however, it is believed that these may represent a milder phenotype and may have a lower risk for cardiac-related sudden death (65).

Electrocardiogram Analysis

The evaluation of studies looking at false-positive and false-negative rates for ECG screening may be strongly affected by what is defined as normal and abnormal in an individual study. There are physiologic changes in structure and function that are considered benign in athletes but are atypical in a sedentary individual. These ECG changes that were once thought of as abnormal are now understood to be training-related changes. To clarify physiologic ECG changes in athletes from pathologic ones, the ESC recently published a statement with recommendations on ECG interpretations (66). These are summarized in Table 6.1. The main change from previous guidelines is the elimination of isolated QRS voltage criteria

TABLE 6.1 Classification of Abnormalities of the Athlete's ECG

Common and Training-Related ECG Changes	Uncommon and Training-Unrelated ECG Changes
Sinus bradycardia	T-wave inversion
First-degree AV block	ST-segment depression
Incomplete RBBB	Pathologic Q waves
Early repolarization	Left atrial enlargement
Isolated QRS voltage criteria for LVH	Left-axis deviation/left anterior hemiblock
	Right-axis deviation/left posterior hemiblock
	Right ventricular hypertrophy
	Ventricular preexcitation
	Complete LBBB or RBBB
	Long- or short-QT interval
	Brugada-like early repolarization

Common or training changes generally require no additional investigation. Uncommon changes should be further evaluated prior to sports participation.

Modified from Corrado D, Pelliccia A, Heidbuchel H, et al. Recommendations for interpretation of the 12-lead electrocardiogram in the athlete. *Eur Heart J* 2010;31(2):243–259.

for left ventricular hypertrophy (LVH) as abnormal. Several studies have demonstrated a high incidence (up to 80%) of ECGs from trained athletes that meet ECG LVH criteria (S wave in V1 + R wave in V5 >35 mm) (66).

Further, since most normative data for ECGs are based on Caucasian males, they may not extrapolate well to other populations. For instance, female adolescent athletes often have T-wave inversions in the right precordial leads, which may be mistaken for ARVC (67). Research has also shown that ethnicity impacts physiologic responses to exercise and, as such, may manifest with ECG patterns that are classified as abnormal. This is especially true of athletes of African and Afro-Caribbean descent. In a study by Magalski et al. (68) evaluating ECG patterns in 1,959 elite male football players in the United States, the authors found marked repolarization abnormalities, often limited to the right precordial leads (V₁–V₄), in 30% of African American athletes compared with 13% of Caucasian athletes. Another study from the United Kingdom suggested that certain electrocardiographic abnormalities found in black athletes may be variants of normal and not evidence of pathology. This study demonstrated that black athletes with ECG abnormalities limited to the right precordial leads did not have evidence of cardiomyopathy by echocardiography and, when followed long-term, these athletes had no increased cardiovascular morbidity or mortality (69).

Economic Consequence of Preparticipation Screening

When examining the cost-benefit ratio of preparticipation screening, one has to examine the cost of the ECG added to the cost of history and physical examination alone. There is high variability in reports of cost-effectiveness estimates based on different statistics used for rates of SCD, false-positive rates of ECG, and costs of ECG and additional screening (70). For example, since there are >10 million athletes in the United States, if an ECG costs \$50, it would cost \$500 million for electrocardiographic screening of all athletes. Based on the Italian

experience, we would estimate that 890,000 ECGs would be positive in the United States. This will result in ordering an echocardiogram at an approximate cost of \$1,500 per test. Thus, the total cost of an Italian/European-based screening program in the United States would be \$1.84 billion. This is coupled with the above data and is probably underestimating EKG and echo costs.

Fuller et al. (71) assessed the cost-effectiveness of using history and physical examination alone with the addition of a 12-lead ECG and found that adding an ECG was more cost-effective, costing \$44,000 per life-year saved if ECG screening was used on high school athletes in the United States compared with \$84,000 per life-year saved by history and examination alone. Recently, Wheeler et al. (72) evaluated the cost-effectiveness of preparticipation screening of U.S. athletes from ages 14 to 22 using cardiac-focused history and physical examination alone or with the addition of ECG. The authors found that the addition of 12-lead ECG saves 2.1 life-years per 1,000 athletes screened (\$89 per athlete) with a cost-effectiveness ratio of \$42,900 per life-year saved compared with history and physical examination alone.

Start-up costs of a preparticipation screening program in countries such as the United States, where there is not an established program in place, would be significant. There are not only costs in developing the necessary infrastructure for both the evaluation as well as the treatment of athletes but also the costs for physicians who would need to undergo more formalized training. There are also the costs and resources needed for those who have ECG abnormalities, since they almost always necessitate further evaluation, including visits with a cardiovascular specialist and noninvasive imaging, such as echocardiography. In those for whom the ECG is a false positive, the costs of additional testing are not only financial, but physical and psychological too. The athlete may experience anxiety awaiting further evaluation, will likely be restricted from exercise, and may be disqualified from the sport. This highlights the need for a program in which quick evaluation and results are provided to those who have abnormalities found at the initial screening process (37,73).

SPECIFIC CONGENITAL CARDIAC LESIONS

Shunt Lesion

Atrial Septal Defect, Ventricular Septal Defect, Atrioventricular Septal Defect and Patent Ductus Arteriosus

When exercise capacity is measured by formal exercise testing in patients with either small or repaired shunt lesions, many patients are found to have a low aerobic capacity (74,75). While residual cardiac disease or, more rarely, a persistent degree of pulmonary hypertension (PHT) with exercise may be the cause of this finding in a few cases (75), the cause in the majority of patients with these shunt lesions is a sedentary lifestyle with physical inactivity. Regular exercise participation, exercise training, and in many cases competitive sports participation may be beneficial for the majority of these patients.

Atrial Septal Defect

In patients with atrial septal defect (ASD), blood flows left to right across the atrial defect during diastole as a consequence of the greater right ventricular compliance. The total amount of blood across the shunt is negligible in small defects, and patients should have a normal exercise capacity. However, in larger defects the greater shunt size leads to right ventricular volume overload that could potentially cause PHT during exercise (75). In addition, this shunt flow may limit preload to the left ventricle at higher heart rates. If this occurs, this may lead to a mildly reduced exercise capacity. After ASD closure, nearly all patients resume full exercise capacity. In the current surgical and interventional era, repair outside of early childhood is rare. Residual PHT or atrial arrhythmias are very rare during childhood or at any age following early childhood repair. The guidelines from the 36th Bethesda Conference do not limit competitive activity in children who have their defects closed. The only patients in whom exercise should be restricted are those with a large ASD and mild pulmonary artery hypertension. Low-intensity competitive sports (IA) are recommended until the defect is closed (76). In Europe the guidelines from the task force of the ESC on sports for children with CHD and a left-to-right shunt (ASD) are for no limitations on physical exercise or sports activities (77). This also holds true for leisure sports and other physical activities.

After interventional device closure of the ASD, the patient may resume light sport activities approximately 10 to 14 days after intervention (i.e., when the puncture site at the groin has healed completely). To minimize risk of dislodgement, contact sports should be avoided for 6 months at which time the device should be completely covered by the endocardium. After surgical patch closure, there are no restrictions after the thoracotomy has healed.

Ventricular Septal Defect

In those patients with highly restrictive ventricular septal defects (VSD) with a pulmonary-to-systemic flow ratio (Qp/Qs) of $<1.5/1$, there will only be a small shunt from the left to right ventricle (RV). During exercise, the shunt will remain relatively small. In those with moderate-size defects (Qp/Qs 1.5–2), there is usually low pulmonary artery pressure and resistance and only mild left ventricular volume overload. In these patients, dynamic exercise is usually well tolerated. Because isometric exercise increases systemic afterload much more than pulmonary afterload, this form of exercise can result in an increase in both pulmonary flow and Qp/Qs , making isometric exercise somewhat less well tolerated. Those patients with large VSD ($Qp/Qs > 2$) with normal pulmonary pressures

and resistances have similar exercise hemodynamics compared to those with moderate-size defects. However, if there is PHT, neither dynamic nor isometric exercise is well tolerated. In the presence of significantly elevated PVR, the pulmonary vascular bed is unable to handle the increased blood flow associated with the exercise and right-to-left shunting may occur.

In two studies of children during submaximal exercise testing, reduced values for ventilatory anaerobic threshold were found in about half of 43 patients with native VSD (mean $86 \pm 12\%$ of normal) and with surgically closed VSD (mean $86 \pm 12\%$ of normal) (74,75). The only variable that correlated with a lower level of exercise performance was greater physical inactivity during daily life. Children with a VSD (repaired or unrepaired) should be encouraged to be physically active and to adopt a healthy lifestyle. If low levels of exercise performance are found, increasing physical activity should be encouraged. Previous studies in small groups of children with congenital heart defects, including those with VSD, have shown improvement in maximal work rate on the bicycle ergometer, without a change in maximal VO_2 after a 6-week home-based conditioning program (78).

Atrioventricular Septal Defects

Patients with an atrioventricular septal defect (AVSD) who do not have Down syndrome should follow the same recommendations as for VSD. The only exception is those individuals who have significant mitral regurgitation. Those with moderate to severe mitral regurgitation should be restricted from exercise if they have either severe volume overload of the left atrium and/or left ventricle or evidence of PHT. For those patients with Down syndrome, discussion with the primary physician and cardiologist should occur before undertaking any exercise program. While physical activity is important and encouraged in this population, they may need to be restricted from contact sports and other activities that may jar the neck due to the high rate of atlantoaxial instability in people with Down syndrome (79).

Patent Ductus Arteriosus

For patients with a patent ductus arteriosus (PDA), the hemodynamics are similar to those found in patients with VSD. When in isolation, PDA closure is nearly always performed percutaneously. The same recommendations for activity apply as after percutaneous ASD closure.

Evaluation Prior to Exercise and Sports Participation

Most patients with well-repaired or hemodynamically insignificant residual shunt defects need little evaluation beyond routine outpatient care prior to participating in either recreational or competitive athletics. This will generally include a physical examination, ECG, chest x-ray, and echocardiogram. In cases where there is additional concern of significant residual abnormalities or pulmonary disease, additional testing including exercise testing may be needed (76).

Leisure Activities and Activities of Daily Living

In patients with well repaired or hemodynamically insignificant ASD, VSD, PDA, and AVSD, no limitation exists for leisure activities or activities of daily living. These children can and should participate normally in physical exercise without restrictions. It is recommended that they perform 60 minutes of moderate to vigorous physical activity on 5 days per week or more (20) (see Table 6.2).

Competitive Sports

According to the Bethesda guidelines, since most children have ASDs closed before they are active in competitive sports,

exercise usually is not restricted. The only patients in whom exercise should be restricted are those with a large ASD (unrepaired) and mild pulmonary artery hypertension. Low-intensity competitive sports (IA) are recommended until the defect is closed (see Fig. 6.1). For those athletes with surgical or device closure of an ASD, if there is no evidence of PHT or ventricular or atrial ectopy, they can participate in all sports 3 to 6 months after the operation or device closure (76). For those with VSDs, athletes with small to moderate defects and normal pulmonary artery pressure can participate in all sports while those with large defects and normal pulmonary artery pressure can participate after VSD closure. Those with large unrepaired defects and elevated pulmonary vascular resistance cannot participate in competitive sports (76). For those who want to participate in competitive athletics after surgical or device closure of a VSD, if there is no evidence of PHT or ventricular or atrial ectopy, the patient can participate in all sports 3 to 6 months after successful intervention (76). Limitations for competitive sports are only in patients with pulmonary arterial hypertension (PAH) (77). Information on exercise recommendations for the patients with PHT can be found in the section on PHT later in this chapter.

Left-Sided Obstructive Lesions

Aortic Stenosis

Congenital aortic stenosis occurs in three major subtypes: subvalvar, valvar, and supravalvar. Subvalvar disease is a result of a subaortic muscular ridge, a fibromuscular ridge and/or tunnel, or a discrete subaortic membrane. Subaortic obstruction is also associated with a distorted aortic valve leaflet resulting in regurgitation. Congenitally stenotic aortic valves can be isolated, as is seen in the unicommissural or bicommissural lesions, or they can be found in association with posterior malalignment type VSD, abnormalities of the mitral valve, hypoplasia of the aortic arch, and aortic coarctation. Supravalvar aortic stenosis at the sinotubular junction is typically seen in patients with Williams syndrome, in familial supraaortic stenosis and rarely with familial dyslipidemias (80, 81), or as spontaneous mutations in otherwise normal individuals. Except in severe cases or in the presence of other significant defects, exercise performance is usually normal or near normal.

Evaluation Prior to Exercise and Sports Participation

It is important to distinguish symptomatic from asymptomatic patients who have aortic stenosis. A previous history of exercise-induced syncope or lightheadedness, dyspnea with exercise without an ostensible pulmonary etiology, or angina may indicate that these patients are at higher risk of SCD compared

to asymptomatic patients. These patients therefore should be evaluated for possible surgery or catheter-based interventions. Guidelines grading the degree of stenosis have been previously reported and have been used to make recommendations regarding sports participation in competitive athletes. However, these guidelines are admittedly conservative and based upon scant literature (76). Most of the previously reported patients with aortic stenosis who died suddenly had a high incidence of ECG abnormalities. LVH and/or strain should be assessed when making recommendations for competitive sports. Graded exercise testing may be helpful in unmasking important findings, such as blunted blood pressure response or ventricular ectopy, in asymptomatic patients.

Leisure Activities and Activities of Daily Living

As stated above, most patients with aortic stenosis are asymptomatic and have normal exercise tolerance. Patients with mild disease need no restrictions and should follow the recommendations in Table 6.2. Patients with moderate stenosis should follow the recommendations for bicuspid aortic valve syndrome (see Table 6.3). It is unknown if regular physical training slows the progression of stenosis or insufficiency in this disorder. It is believed that repetitive, maximally strenuous isometric exercise may hasten valve deterioration; therefore, these activities should be minimized or avoided completely. Physical training, however, is helpful in hastening recovery in patients with CHD who have had surgical intervention (82–84).

Competitive Sports

Patients with valvar aortic stenosis are at risk for SCD during exercise (26,85). However, the true risk is unknown. In adults, syncope, dizziness, angina pectoris, or dyspnea with exercise are associated with SCD. Recent data suggest that the risk of SCD during exercise in patients who had balloon valvuloplasty as infants may not be as high as previously believed (86). Until more data are available, the guidelines from the 36th Bethesda Conference are probably reasonable. Athletes with mild aortic stenosis, a normal resting ECG, and no history of exercise-related symptoms can participate in all forms of competitive sports. Patients with mild stenosis should be reevaluated periodically to continue with competitive sports. Athletes with moderate aortic stenosis who have mild or no LVH, normal response to treadmill exercise testing, and no exercise-induced symptoms can participate in low static/low-to-moderate dynamic and moderate static/low-to-moderate dynamic exercise (classes IA, IB, and IIA) (see Fig. 6.1). Individualized exercise prescriptions in borderline cases are reasonable in light of the finding of the lower risk of sudden death than was previously believed (86).

TABLE 6.2

Recommendations Following the F.I.T.T. Principle for Recreational Activities and Exercise Training in Children and Adolescents with ASD/VSD/AVSD/PDA and No Hemodynamically Significant Residual Disease

F.I.T.T.	Cardiovascular (dynamic) Training	Muscle (static) Training
Frequency	Moderate: daily Vigorous: 3–5×/wk	3–5×/wk
Intensity	Moderate: 55%–60% of max $\dot{V}O_2$ to Heavy: below 80% of max $\dot{V}O_2$	Moderate to High: 20%–50% MVC to >70% MVC
Time	Most of daily 60 min activity	As part of daily 60 min activity
Type	Predominantly dynamic activity: e.g., running, jumping, cycling, swimming, inline skating, skateboarding, soccer	Predominantly static activity: e.g., gymnastics, climbing, push-ups, martial arts, ball sports practice

$\dot{V}O_2$, minute oxygen consumption; MVC, maximum voluntary contraction.

TABLE 6.3

Recommendations Following the F.I.T.T. Principle for Recreational Activities and Exercise Training in Children and Adolescents with Bicuspid Aortic Valve Syndrome^a

F.I.T.T.	Cardiovascular (dynamic) Training	Muscle (static) Training
Frequency	3–4×/wk	1–2×/wk
Intensity	Constant load training at low to moderate intensity: 40%–60% of max $\dot{V}O_2$	Low intensity: (i.e., 1–5 lb Dumbbells), 10–15 repetitions for separate small muscle group
Time	60 min per session	Include up to 30 min strength training in total time.
Type	Low static sports, like cycling, walking, swimming	Dumbbell exercises, light gymnastics.

$\dot{V}O_2$, minute oxygen consumption.

^aPatients with no aortic root dilation and no significant stenosis or regurgitation may follow recommendations in Table 6.2.

Subvalvar and supra-avalvar aortic stenosis probably warrant similar exercise recommendations as valvar aortic stenosis, even in light of slightly different pathophysiologies.

Bicuspid Aortic Valves

Bicuspid or bicommissural aortic valves are the most common type of congenital heart malformation, estimated to occur in 0.5% of the population. Males are affected three times more often than females (87,88). Many providers investigate for Turner syndrome when a female is found to have a bicuspid aortic valve. In females with bicuspid aortic valve in association with coarctation, Turner syndrome or Turner mosaicism should be strongly considered. The typical bicuspid aortic valve has two recognizable lines of cusp apposition. Fusion of the right and left or right and noncoronary cusps results in valves that are prone to either regurgitation or stenosis or both. Abnormalities of the aortic root, sinotubular junction, and ascending aorta occur as part of this lesion (89–91). Dilation of the root and ascending aorta is common, even in patients who do not have stenosis or regurgitation. The risk of spontaneous rupture may occur in these patients but with much less frequency compared to Marfan syndrome patients. There is a tendency to dilate the aortic root in patients with fusion of the right and left coronary cusps, while dilation of the ascending aorta appears to be more common in patients with fusion of the right and noncoronary cusps (92,93).

Evaluation Prior to Exercise and Sports Participation

Bicuspid aortic valves should be considered when there is a family history of aortic valve problems in first-degree relatives (siblings or parents) given the reported vertical transmission rate as high as 33% with this defect. The physical finding of an aortic ejection click is frequently found with this anomaly, and a stenotic or regurgitant murmur may be present. Four extremity blood pressure assessments will help rule out coexisting aortic coarctation. ECG screening is uniformly performed but is typically not helpful when no significant murmurs are present on the physical examination. ECG is essential in determining the diagnosis and assessing the hemodynamic significance of the lesion or lesions. Exercise stress testing is not usually helpful, unless important stenosis and/or regurgitation is found echocardiographically or if coarctation of the aorta is also identified. Magnetic resonance imaging (MRI) may be helpful in assessing the caliber of the ascending aorta in patients who have difficult ECG windows. Cardiac catheterization may rarely be needed to confirm the gradient in patients who appear to have moderate-to-severe stenosis and may be helpful for risk stratification.

Leisure Activities and Activities of Daily Living

These patients should follow the guidelines listed above for aortic stenosis. Minimizing the exposure to significant static activities should be emphasized in those patients with evidence of aortic root dilation. These recommendations are summarized in Table 6.3.

Competitive sport

Patients with isolated bicuspid aortic valve without stenosis, regurgitation, or aortic dilation may participate in all competitive sports. Although there is information to suggest that regular athletic training may increase aortic dimensions, the actual risk associated with this progression is unknown (94). There is evidence that endurance training may improve the elastic properties of the aorta (95–99). Close follow-up is warranted, and annual ECG may be helpful (100) but should be individualized to the patient. Intense, repetitive isometric activities may enhance aortic stiffness (101) and dilation (102); however, in the absence of aortic root dilation, isometric activities are currently acceptable (103).

Exercise restrictions are implemented for regurgitant and/or stenotic aortic valves, and the degree of restriction is commensurate with the degree of the hemodynamic abnormality (103). Mild aortic dilation does not typically indicate exercise restrictions; however, frequent (annual) assessment is required in athletes, with attention to both the absolute dimension and rate of change. Current recommendations are summarized below. In younger preadolescent ages, the aortic root size should be indexed to the appropriate body mass Z-score.

1. Patients with isolated bicuspid aortic valve without important stenosis or regurgitation and no more than mild aortic dilation (<40 mm) may participate in all competitive sports.
2. Patients with moderate (<45 mm) aortic dilation that is stable (not rapidly progressive) may participate in low static/low-to-moderate dynamic competitive sports without risk of bodily collision.
3. Patients with progressive (>5 mm per year) or severe aortic dilation (>45 mm) are permitted to engage in low static/low dynamic exercise only.

Coarctation of the Aorta

Aortic coarctation is narrowing of the aortic isthmus, defined as the segment of the aorta between the origin of the subclavian artery and ductal ampulla/ligament. It is commonly associated with abnormalities of the aortic valve, VSD, mitral valve abnormalities, hypoplasia of the transverse aortic arch, and hypoplastic left heart syndrome. Histologic abnormalities

involving the elastic media at the site of the coarctation are integral to this lesion. Older unoperated patients are also at risk for the development of and rupture of intracranial aneurysms. This risk exists even in operated patients. The cardiovascular risk of CAD, stroke, heart failure, aortic and cerebral aneurysmal rupture, and SCD occur even after successful early repair (104). Exercise capacity is reduced in these patients despite the adequacy of the repair (105,106). Chronically elevated systolic blood pressure may play a role in cardiovascular morbidity and mortality. Endothelial dysfunction, reduced vessel elasticity, and enhanced baroreceptors may all play a role in the development of chronic systolic hypertension and the commonly found systolic hypertensive rise to graded dynamic or isometric exercise (107–109).

Evaluation Prior to Exercise and Sports Participation

Medical and surgical history, including the presence and/or repair of associated lesions, four extremity blood pressures, and a resting ECG are essential in the initial evaluation of patients with coarctation of the aorta. Previous information regarding cardiac catheterizations is also important, particularly in patients who have had balloon dilation of native coarctation or dilation of recurrent/residual coarctation. The presence of an upper-to-lower extremity blood pressure gradient should alert the physician to the presence of a possible residual coarctation.

Laboratory studies include the baseline resting ECG to assess for the presence of LVH. Echocardiography is very useful in the detection of residual gradients, associated lesions, and the site of the residual obstruction, if present, as well as LVH. MRI with three-dimensional reconstruction offers exquisite detail of aortic anatomy and may be useful in determining the site of residual obstruction or aneurysm. Maximal exercise testing can be useful to assess the blood pressure response to exercise in these patients. This response may be abnormal even in the absence of a residual coarctation. This may be related to residual abnormal vascular reactivity that may be seen in these patients as stated above.

Leisure Activities and Activities of Daily Living

There are significant numbers of studies examining exercise performance in patients with repaired coarctation of the aorta but longitudinal data regarding the risk of intense exercise participation and training are sparse. Those patients with good repairs (e.g., resting gradient of <20 mm Hg, no juxtaductal aneurysm), normal resting and exercise blood pressures, and no other associated cardiac abnormalities should engage in regular moderate to vigorous recreational activities as outlined in Table 6.2. Those patients with hypertension in the absence of residual coarctation should follow the recommendations listed later in this chapter for systemic hypertension. Patients with a bicuspid aortic valve should follow the recommendations for bicuspid valves in Table 6.3.

Competitive Sports

Patients with isolated coarctation of mild degree (<20 mm Hg systolic blood pressure gradient) may participate in all sports; however, activities that have a maximally strenuous isometric component should probably be discouraged. Patients with residual obstruction should be referred for either catheter-based or surgical intervention prior to participating in competitive sports (76). Resting or exercise-induced hypertension in the absence of a residual gradient should be treated as discussed in the section on systemic hypertension. As with recreational activities, competitive sports in patients with repaired coarctation and bicuspid aortic valve should defer to the section on bicuspid aortic valve.

Right-Sided Obstructive Lesions

Pulmonary Stenosis

Valvar pulmonary stenosis (PS) is the most common type of right ventricular outflow obstruction and is caused by fused leaflets in most cases. The degree of obstruction is variable, but is typically mild and may regress spontaneously. More advanced obstruction results in right ventricular hypertrophy and/or strain, and if left untreated, can result in exercise intolerance (110), and/or atrial arrhythmias secondary to right atrial dilation. Most patients with advanced obstruction benefit from intervention, typically balloon valvuloplasty. Freedom from reintervention and exercise capacity have been reported to be quite favorable; however, the long-term impact of chronic pulmonary regurgitation as a result of the intervention remains to be seen (111,112). Mild PS (peak gradient <30 mm Hg) does not appear to significantly impact exercise performance. However, moderate (30 to 50 mm Hg peak gradient) or severe (>50 mm Hg) stenosis impairs performance, but typically improves after intervention.

Evaluation Prior to Exercise and Sports Participation

Prior to participation in routine physical activity, patients with PS should have a complete cardiovascular physical examination. A resting ECG should be obtained. Further studies will depend on the severity of the stenosis and the extent of any associated additional cardiac abnormalities. An echocardiogram, Holter monitor, and exercise testing should be considered in any patient with more than mild PS. Additional imaging studies such as cardiac MRI or computed tomography (CT) scan may be needed in select patients with significant right ventricular dilation or dysfunction.

Leisure Activities and Activities of Daily Living

Patients with mild PS not associated with a pressure overloaded RV, no ECG abnormalities, and normal exercise tolerance are encouraged to pursue normal activities (see Table 6.2) (76,113,114). Patients with treated PS and no significant hemodynamic abnormalities (mild stenosis, no more than moderate regurgitation) and a normal ECG should also be encouraged to participate in recreational activities without restrictions. Similar recommendations apply for patients with moderate stenosis and no more than moderate regurgitation.

For patients with residual regurgitation associated with a dilated RV with normal RV systolic wall motion (see Table 6.4). If RV dysfunction is present, recreational activities and daily living activities may be limited. These patients may benefit from a formal exercise prescription to help optimize both their dynamic and static exercise performance (see Table 6.5). Patients with severe stenosis should be restricted from exercise until they can undergo repair.

Competitive Sports

Patients with mild PS, normal RV size and function and no more than mild regurgitation, normal ECG, and no RV hypertrophy, may participate in all sports (76,115). Patients with moderate stenosis, no more than mild regurgitation, normal RV size and function, normal ECG, and no more than mild RV hypertrophy can participate in no more than moderate dynamic and mild isometric sports (see Fig. 6.1) (76,115). Patients with no or mild stenosis but with significant regurgitation associated with RV dilation but normal RV function and are asymptomatic, can participate in low-intensity aerobic activities (see Fig. 6.1). Patients with severe stenosis should not engage in competitive sports but they can resume sports 3 to 6 months after successful intervention. Types of activities depend upon residual hemodynamic findings (see above) (76,115).

TABLE 6.4 Recommendations Following the F.I.T.T. Principle for Recreational Activities and Exercise Training in Children and Adolescents with PS and ToF and Moderate Residual Lesions and No Right Ventricular Dysfunction

F.I.T.T.	Cardiovascular (dynamic) Training	Muscle (static) Training
Frequency	3–5×/wk to daily	3–5×/wk
Intensity	Moderate: 40%–60% of max VO_2	Low to moderate: 20%–50% MVC
Time	Most of daily 60 min activity	As part of daily 60 min activity
Type	Moderate dynamic activities including swimming, table tennis, walking	Static activities including gymnastics, ball sports, light weights

VO_2 , minute oxygen consumption; MVC, maximum voluntary contraction.

Tetralogy of Fallot

Exercise performance in Tetralogy of Fallot (TOF) has probably been studied more than in any other congenital cardiac abnormality. Valvotomy and outflow tract patches typically result in pulmonary regurgitation and dilation of the RV. Significant ventricular dilation can lead to arrhythmias as can scarring associated with ventriculotomies. Residual stenosis, regurgitation, and branch pulmonary artery stenosis have all been independently associated with diminished exercise performance, and inefficient ventilation during exercise. The latter is manifested as high ventilatory equivalents for carbon dioxide (minute ventilation is high when compared to carbon dioxide excretion) as well as a steep rise in the slope of minute ventilation relative to carbon dioxide production (116–119). Exercise capacity varies widely in this population. It may range from severely depressed to, in some cases, well above normal. This heterogeneity in exercise performance reflects both the heterogeneity of the defect itself as well as the broad spectrum of residual disease seen following operative repair. Those patients with significant pulmonary regurgitation accompanied by biventricular systolic dysfunction appear to have the lowest exercise capacity (117). These are often young adults with long-standing residual right-sided abnormalities. Patients with restrictive right ventricular mechanics may not develop significant right ventricular dilation despite severe pulmonary regurgitation and often appear to have more preserved exercise capacity at long-term follow-up (120,121). QRS prolongation is associated with

dilated RVs, and the absolute measurement (>180 ms) as well as the rate of change of the QRS duration may be important prognosticators for the risk of SCD during exercise. Other factors associated with ventricular arrhythmias and possibly with SCD include older age at repair, residual right ventricular outflow tract obstruction with increased right ventricular systolic pressure, RV dilation and dysfunction, and left ventricular systolic dysfunction (122–125). Premature atrial and ventricular ectopy is commonly observed on exercise testing and can be seen in as many as 50% of patients. However, fast atrial or ventricular couplets or runs of arrhythmias are not common during exercise testing and are likely a cause for concern.

Recent studies in young adults have shown a significant predictive value of exercise testing for identifying patients at risk for either SCD or death from heart failure as well as the need for hospitalization for heart failure. Several studies assessing the role of exercise training in a controlled environment have also demonstrated improvement in exercise performance in this population despite the presence of important residual lesions (pulmonary regurgitation, RV dysfunction). Of note is that in one such study, patients with documented ventricular arrhythmias were excluded from participation (126).

Evaluation Prior to Exercise and Sports Participation

Evaluation prior to participation in regular physical activity should be similar to that for PS with residual cardiac abnormalities. All patients should have regular Holter monitoring

TABLE 6.5 Recommendations Following the F.I.T.T. Principle for Recreational Activities and Exercise Training in Children and Adolescents with PS and ToF and Residual Lesions with Right Ventricular Dysfunction^a

F.I.T.T.	Cardiovascular (dynamic) Training	Muscle (static) Training
Frequency	3–5×/wk to daily	3–5×/wk
Intensity	Low to moderate: 30%–60% of max VO_2	Low to moderate: 20%–50% MVC
Time	Most of daily 60 min activity	As part of daily 60 min activity
Type	Low to moderate dynamic activities including walking, swimming	static activities including light gymnastics, ball sports, light weights

VO_2 , minute oxygen consumption; MVC, maximum voluntary contraction.

^aConsider formal exercise prescription in patients with significant cardiac dysfunction or deconditioning.

and exercise testing to evaluate arrhythmias and assess cardiopulmonary capacity during exercise. Exercise testing combined with imaging studies, such as MRI, may be helpful in identifying patients who could benefit from pulmonary valve replacement. This may be especially useful in the late adolescent and young adult age group.

Leisure Activities and Activities of Daily Living

Because of the heterogeneity of this population, recommendations for activities and sports participation will vary widely depending on the state of the individual patient. Asymptomatic patients with normal or only mild RV dilation, normal right ventricular pressure, and systolic function who have no documented arrhythmias at rest and during exercise should be encouraged to pursue regular physical activities without restrictions (see Table 6.2).

Asymptomatic patients with significant pulmonary regurgitation who have at least moderate right ventricular dilation, but with preserved right ventricular function and no arrhythmias at rest or during exercise should follow recommendations as delineated in Table 6.4.

Asymptomatic patients with significant regurgitation, significant right ventricular dilation, and abnormal function may engage in mild dynamic exercise assuming no arrhythmias at rest or during exercise. These patients as well as the symptomatic patients described in the following paragraph may benefit from a formal exercise prescription to better assess their individual limitations and to assure that they are performing activities that are safe and appropriate for their individual capacities. Depending on the patient, this may be based on recommendations in Tables 6.4 or 6.5.

Symptomatic patients with residual right ventricular lesions and/or left ventricular dysfunction, patients with right ventricular to systemic systolic pressures ratios of two-thirds or more, patients with important residual intracardiac shunts, and patients with documented sustained atrial or ventricular arrhythmias that are refractory to treatment should engage in only low dynamic, low static activities (see Table 6.5).

Competitive Sports

Repaired patients with normal or near-normal RV pressure, with no more than mild RV volume overload, no important residual shunt, and no arrhythmias at rest or during exercise may engage in all competitive sports without restriction, except in Europe (76,115). The recent extraordinary performance of an American freestyle snow boarder is testament of the safety of the pursuit of athletic competition at very high level in repaired patients who do not have significant residual lesions. Patients with pulmonary regurgitation with dilated RVs, elevated RV pressures to one-half or more of the systemic systolic pressure, or with atrial or ventricular arrhythmias should only engage in low static, low dynamic sports (see Fig. 6.1) (76).

Ebstein Anomaly

There is scant literature regarding exercise performance and the risk associated with exercise in patients with Ebstein anomaly. Heterogeneity in this patient population is great and will vary with the severity of the valvular abnormalities as well as with the presence and degree of atrial right to left shunting. Oxygen consumption is reduced compared to normal. However, patients have improved exercise performance after tricuspid valvuloplasty and ASD closures (127). Patients repaired at a younger age who have lower cardiothoracic ratios on chest x-ray at the time of intervention appear to have the best outcomes. Preoperative patients frequently have cyanosis at rest that worsens with exercise. Even after surgical intervention,

most patients have fairly limited exercise capacity with an average maximal VO_2 of 50% of predicted. Chronotropic impairment may be present. Reduced right ventricular and left ventricular stroke volumes may limit cardiac output and therefore exercise performance, even in adult patients who are fully saturated (128). Similar to patients with TOF and single ventricles, ventilatory inefficiency during exercise can be significant as a result of pulmonary abnormalities as well as right-to-left intra-arterial shunting if an ASD is present.

Evaluation Prior to Exercise and Sports Participation

Evaluation prior to participation in regular physical activity should be similar to that outlined for patients with TOF. Exercise testing and Holter monitoring are useful to assess exercise-induced arrhythmias and evidence of preexcitation. Exercise testing is also useful to evaluate the presence and degree of desaturation with exercise.

Leisure Activities and Activities of Daily Living

Asymptomatic, acyanotic patients with no more than mild tricuspid regurgitation, normal left ventricular systolic function, and no resting or exercise-induced arrhythmias may engage in all activities (Table 6.2). Asymptomatic patients with moderate tricuspid regurgitation and normal arterial saturation with supraventricular arrhythmias that are controlled may participate in low-level dynamic and no more than moderately isometric physical activities (see Table 6.5). Symptomatic patients at rest or during exercise, those with important right atrial or right ventricular dilation, severe regurgitation, left ventricular dysfunction, or chronic atrial or ventricular arrhythmias, should not engage in physical exercise.

Competitive Sports

Asymptomatic, acyanotic patients with no more than mild tricuspid regurgitation, normal left ventricular systolic function, and no resting or exercise-induced arrhythmias may engage in all competitive sports (76). Asymptomatic patients with no more than moderate tricuspid regurgitation, normal arterial saturation, and no resting or exercise-induced arrhythmias may participate in low dynamic and low static competitive sports (76) (see Fig. 6.1).

Patients with severe Ebstein anomaly characterized as severe regurgitation and evidence of right ventricular dysfunction (desaturation, exercise-induced arrhythmias, or symptoms during exercise or rest) should not engage in competitive sports. Patients who have had surgical intervention may participate in selected competitive sports 3 months after surgery if they are asymptomatic, have no or mild tricuspid valve regurgitation, and have no resting or exercise-induced arrhythmias.

D-Transposition of the Great Arteries

Prior to approximately 25 years ago, D-transposition of the great arteries (D-TGA) was repaired using the atrial switch operation, either the Mustard or Senning. Therefore, almost all patients with this type of procedure are in at least their third or fourth decade of life. Exercise performance in this population is usually moderately compromised with maximal VO_2 in the range of 60% to 70% of predicted. Many patients may be more severely limited even in performing activities of daily living to varying degrees. The reasons for poor exercise performance are multiple and may include poor systemic right ventricular function, chronotropic impairment, tricuspid valve regurgitation, and ridged atrial baffles that limit augmentation of ventricular preload (129–133).

Because of the long-term problems with the atrial switch operations, the current approach has been to perform an

arterial switch operation whenever possible. Most patients after the arterial switch operation have near-normal exercise performance (on average, 87% of predicted maximal VO_2) (134–140). However, as this population has moved into adolescent and young adult ages, there is evidence to suggest that their exercise performance has somewhat declined (137–139). The reasons for this decline are unclear but may be related at least in part to lack of physical activity and rising rates of obesity (3,4). Symptomatic and asymptomatic occlusion of coronary vessels, myocardial perfusion imaging defects, wall-motion abnormalities on stress echocardiography and diminished coronary reserve have been noted in approximately 10% to 12% of patients following the arterial switch operation (134,136,137,140–142). These findings raise concerns regarding the risk of highly competitive sports in these patients as well as the potential risks of acquired atherosclerotic coronary disease and subsequent activity-related myocardial ischemia as this population ages. Additionally, dilation of the aortic root is seen with increasing frequency as this population ages. Despite these concerns, sudden death after this operation is uncommon. To date, the need for surgical intervention has been quite low, and indications for reoperation are not clear. The risk for aortic rupture or dissection during activity in this population is not known but given the presence of scar tissue surrounding the aortic root and the presence of a suture line, it is probably much less than with aortic root dilation from connective tissue diseases. The effects of aortic root dilation on the coronary arteries are also unknown (143–145).

Evaluation Prior to Exercise and Sports Participation

Patients with the atrial switch operation will be almost exclusively adults, and most will have some degree of significant cardiac dysfunction. A thorough evaluation such as what was outlined above for patients with TOF with significant residual defects is warranted. Routine exercise testing is useful to assess for the presence of arrhythmias and chronotropic response. In addition, this testing is useful in judging exercise capacity and potential limitations. This information will be useful in helping to counsel patients about jobs and daily living activities as well as recreational sports and the need for physical rehabilitation, when necessary.

Following the arterial switch operation, a complete history and physical examination are also needed. An echocardiogram to assess for function, aortic root dilation, and pulmonary artery stenosis should be included. An exercise test may help to unveil hidden residual hemodynamic abnormalities or arrhythmias as well as to evaluate presence of ECG changes suggestive of myocardial ischemia. Myocardial perfusion imaging during exercise stress testing, stress echocardiography, and MRI may also be considered if abnormalities are suspected, especially in cases where resting conduction abnormalities on the ECG limit the interpretation of ST segment changes. Some authorities believe that ECG, echocardiography, and stress testing should be repeated every 2 years. However, there are no reliable data to suggest that this approach to screening frequency is superior to individual provider judgment.

Leisure Activities and Activities of Daily Living

The rare patients with atrial switch physiology who are asymptomatic and without residual abnormalities (ventricular dysfunction and no resting or exercise-induced arrhythmias) are encouraged to engage in a variety of recreational sports without restrictions (115,146). Because most of these patients will have some degree of cardiac, pulmonary, and/or musculoskeletal abnormalities, following the guidelines in Tables 6.4 and 6.5 is generally appropriate. Individual exercise prescriptions

based on exercise testing may frequently be useful to help with assessing the feasibility and safety of occupational as well as recreational activities.

Asymptomatic patients following repair using the arterial switch operation with no and/or minor residual lesions (small VSD, mild neopulmonary or neo-aortic stenosis or insufficiency), extra systoles without fast couplets or arrhythmias, and no exercise-induced arrhythmias are encouraged to engage in recreational sports without restrictions (see Table 6.2). Asymptomatic patients with hemodynamically significant residual lesions (ventricular dysfunction, hypertrophy, or dilation; neopulmonary stenosis >30 mm Hg; moderate or more neo-aortic regurgitation or arrhythmias at rest or during exercise) should be evaluated on an individual basis by their cardiologist. These patients generally should be able to exercise to their own tolerance level, avoid intravascular volume depletion, and be allowed to rest when fatigued. Maximally strenuous isometric activities, even for brief time periods, should probably be avoided. This makes sense as well for those patients with significant aortic root dilation. They may benefit from following the guidelines for patients with a bicuspid aortic valve and root dilation (see Table 6.3). However, as stated above, the risks of physical activities in this group of patients are unknown.

Competitive Sports

Almost without exception, patients repaired by the atrial switch operation are beyond the age when they would be likely to engage in organized competitive athletics. For the very rare patient with exceptionally good function who desires to participate in a recreational sport at a high level, comprehensive individual evaluation by their cardiologist should be undertaken prior to participation.

Asymptomatic patients repaired by the arterial switch operation with only minor residual lesions who have no significant arrhythmias at rest or during exercise and no evidence of exercise-induced myocardial ischemia may participate in competitive sports without restrictions. Sports with a combined high dynamic and high isometric component are not contraindicated, but are discouraged (see Fig. 6.1) (7,115). Patients with either symptoms possibly attributable to residual lesions or those with hemodynamically significant residual lesions are advised not to participate in competitive sports. Their cardiologist may prescribe sports with low dynamic and low isometric components depending upon the residual lesions and the needs of the patient.

Congenitally Corrected Transposition of the Great Arteries

Congenitally corrected transposition of the great arteries (ccTGA) is a relatively rare defect. Although ccTGA can occasionally occur with no other associated abnormalities, more than 90% of patients will have some additional defect or dysfunction. These additional defects may include VSD, tricuspid valve abnormalities, and left ventricular outflow obstruction. It is often these additional defects that are responsible for the decreased exercise performance in ccTGA. Abnormalities of the conduction system resulting in heart block are also common and adversely affect exercise performance.

Until recently, most patients with ccTGA were palliated with operations that resulted in the RV remaining the systemic pumping chamber. Therefore, studies of exercise performance in ccTGA are essentially restricted to these types of palliation. There are no significant data on the exercise performance after the so-called “double switch” operation.

Most exercise data are from studies in young adult populations with ccTGA comparing them to patients with D-TGA with atrial switch physiology. On average, the two groups are similar with maximal VO_2 of approximately 60% of predicted

for age and sex (147,148). The reasons for decreased exercise tolerance are similar to D-TGA: poor systemic RV function, tricuspid insufficiency, and chronotropic impairment. Interestingly, patients with ccTGA appear to be able to increase their stroke volume with exercise to a greater degree than those with D-TGA. This is a consequence of the lack of an atrial baffle in ccTGA allowing for better maintenance of right ventricular preload with exercise (132).

Evaluation Prior to Exercise and Sports Participation

Patients with ccTGA should have, in addition to a physical exam, a resting echocardiogram to assess right ventricular and left ventricular function, tricuspid valve function, and the presence and degree of ventricular outflow obstruction. A Holter monitor is useful to assess presence of conduction abnormalities. A maximal graded exercise test is useful to measure physical working capacity, aerobic capacity, chronotropic response, and presence of arrhythmias.

Leisure Activities and Activities of Daily Living

In most cases, activity recommendations for patients with ccTGA are similar to those with D-TGA repaired with an atrial switch operation. Regular recreational activities of light to moderate aerobic intensities should be encouraged on a daily level. Static activity should be at a low level especially in the presence of significant tricuspid insufficiency. In certain cases where there are little or no other associated abnormalities, higher levels of activity may be encouraged. This decision should be based on preparticipation evaluations and exercise testing.

Competitive Sports

As with leisure activity, recommendations for competitive sports are similar to those with D-TGA repaired with the atrial switch operation. These recommendations are to restrict to low dynamic and low static activities. Also, as with leisure activities, exceptions may be indicated in the rare patient with no significant associated abnormalities and normal ventricular and atrioventricular valve function. Frequent assessment of such patients is needed to assure safe participation in more vigorous activities.

Single Ventricle Physiology

Although patients with Fontan physiology have improved exercise tolerance compared to unoperated patients with single ventricles, their aerobic performance remains, in most cases, well below that of their age-matched peers and is also lower than that of most patients with other types of congenital heart defects. Most Fontan patients have a maximal VO_2 which approximates 65% to 70% of predicted, and have chronotropic impairment, reduced stroke volume, and impaired ventilatory inefficiency (149,150). Diminished muscle bulk and function may also contribute to reduced exercise tolerance (151). Submaximal aerobic capacity appears to be somewhat better preserved in this population. This finding may reflect the limited ability of this physiology to maintain ventricular preload at higher heart rates (149). Energy loss through the Fontan circuitry due to turbulence may limit the ability to augment cardiac output with exercise (152). Heart block and the loss of sequential atrioventricular conduction and sinus node dysfunction may also affect performance. There are increasing data showing that aerobic capacity and exercise tolerance declines in this population as they progress through their second and third decade of life. A significant decline in aerobic performance has been associated with onset of symptomatic heart failure and cardiac death or need for heart transplantation (23).

Evaluation Prior to Exercise and Sports Participation

Prior to undertaking a regular physical activity or conditioning program, patients with stable Fontan physiology should have a thorough baseline evaluation. Baseline testing should include an ECG, echocardiography to rule out hemodynamic derangements that may negatively impact the Fontan circuit, and a Holter monitor to assess for occult arrhythmias. A graded exercise test is extremely useful to measure aerobic and physical working capacities. Systemic oxygen saturation should be assessed throughout the test. Evaluating pulmonary function at rest and exercise may be quite useful in unmasking associated pulmonary abnormalities that may impact on exercise performance.

Leisure Activities and Activities of Daily Living

Patients with stable Fontan physiology are typically able to engage in normal daily activities without impairment. Patients should be encouraged to perform moderate to vigorous activities daily. Although exercise performance is quite limited in this group of patients, the variation in performance is great. On formal exercise testing, up to 25% to 30% of patients with Fontan physiology will have aerobic capacities within the range of normal for healthy age-matched peers. Not surprisingly, these patients tend to cluster in the preadolescent age range. These patients can and often do keep up with their peers with all levels of recreational activity.

At the other extreme, a significant portion of patients with Fontan physiology have quite limited exercise performance. These patients are often adolescents and young adults. These patients may have difficulty even with routine activities of daily living. Exercise training in accordance with the FITT principle, Table 6.6, has been shown to improve exercise capacity in Fontan patients (151,153–157). Patients should be allowed to rest when fatigued, maintain adequate hydration, and avoid bodily collision if taking antithrombotic medication.

Competitive Sports

The issue of participation in competitive sports in this population is complex. For reasons stated above, most adolescents and young adults with Fontan physiology are unlikely to be able to successfully compete in sports with moderate or greater dynamic and static requirements (Fig. 6.1). Therefore, the recommendations of the Bethesda Conference restricting them from those activities are a reasonable default position (76). Because there are exceptional patients in this age range with normal exercise capacity, a case-by-case evaluation should be made for these patients who may wish to compete at higher levels of intensity. The risks should be carefully evaluated and discussed with the patient and family.

As previously mentioned, preadolescent patients with Fontan physiology may often have normal or near normal exercise capacity. Also, as discussed earlier in this chapter, the nature of competitive sports in this population is significantly different from that of adolescent and adult level sports. There are no compelling data to support restricting this population from participation on the basis of their physiology alone. Rather, restrictions should be based on the patient's ability and assessment of their risks as outlined above.

In all patients with Fontan physiology, certain concerns should be addressed. Patients should not participate in competitive sports in which a risk of bodily collision could result in significant injury for those patients on antithrombotic medication, who are pacemaker-dependent or have implantable cardioverters/defibrillators. Patients must be allowed to rest when fatigued and maintain adequate hydration to minimize spontaneous clot formation, particularly those patients with atrial fenestrations.

TABLE 6.6 Recommendations Following the F.I.T.T. Principle for Recreational Activities and Exercise Training in Children and Adolescents with Fontan Procedure^a

F.I.T.T.	Cardiovascular (dynamic) Training	Muscle (static) Training
Frequency	3–5×/wk to daily	3–5×/wk
Intensity	Low to Moderate: 30%–60% of max $\dot{V}O_2$	Low: 20%–30% MVC
Time	30 min	15–30 min
Type	Walking, swimming, stationary cycle	light weights

$\dot{V}O_2$, minute oxygen consumption; MVC, maximum voluntary contraction.

^aConsider formal exercise prescription in patients with significant cardiac dysfunction or deconditioning.

Pulmonary Hypertension and Eisenmenger Syndrome

The classification of PHT was recently updated at the 4th World Symposium on Pulmonary Hypertension in 2008. In the pediatric population, the vast majority of patients who will be evaluated by a cardiologist will be in the PAH group. This includes patients with idiopathic, heritable, and PHT from CHD. This latter group also contains those patients with Eisenmenger physiology (158).

Functional classification for PHT is divided into four classes by the World Health Organization (see Table 6.7) (159). Class 1 patients are asymptomatic at rest and exercise. Class 2 patients are symptomatic with leisure activities and some activities of daily living. Classes 3 and 4 are significantly symptomatic even with activities that are generally less than those required for daily living. Even those patients who are Class 1 and 2 may be at significant risk with physical activity. SCD is a common cause of death in this population and occurs frequently during some type of physical activity. Of note, patients with Eisenmenger syndrome often have a more severe functional classification and yet are at lower risk for SCD with activities. The presence of a large cardiac shunt permits systemic cardiac output and coronary perfusion to be maintained in the face of a sudden increase in pulmonary

resistance or a drop in systemic resistance. Patients with PAH and a structurally normal heart may be unable to maintain cardiac output and system blood pressure with exercise in the face of significantly elevated pulmonary vascular resistance (160).

Evaluation Prior to Exercise and Sports Participation

This population is at high risk for adverse events with exercise even if they are completely asymptomatic. Evaluation and risk stratification of patients with PHT is complex and requires extensive testing that often includes noninvasive imaging studies and, frequently, cardiac catheterization to assess pulmonary vascular reactivity. This evaluation should be undertaken by a practitioner who is experienced in the diagnosis and treatment of PHT (160).

Evaluation of exercise performance is very useful in both initial risk stratification and subsequent monitoring of disease progression and therapeutic interventions. In mild cases, formal metabolic exercise testing can be used to monitor patients. In more severe cases, a 6-minute walk test has been shown to be useful both to monitor disease progression and to assess the efficacy of intervention. This type of testing may be needed as frequently as every 3 to 6 months (160).

TABLE 6.7 Functional Classification for Pulmonary Hypertension According to the World Health Organization

Class	Description
Class I	Patients with PHT but without resulting limitation of physical activity. Ordinary physical activity does not cause undue dyspnea or fatigue, chest pain, or near syncope.
Class II	Patients with PHT resulting in slight limitation of physical activity. They are asymptomatic at rest. Ordinary daily physical activities result in excessive dyspnea or fatigue.
Class III	Patients with PHT resulting in marked limitation of physical activity. They are asymptomatic at rest. Less than ordinary daily activities result in excessive dyspnea, fatigue, chest pain, or near syncope.
Class IV	Patients with PHT with inability to carry out any physical activity without symptoms. These patients demonstrate signs and symptoms of right heart failure. Dyspnea and fatigue may be present at rest. Symptoms are increased by any physical activity.

Modified from Galie N, Hoeper HM, Humbert M, et al. Guidelines for the diagnosis and treatment of pulmonary hypertension. *Eur Heart J* 2009;30:2493–2537.

Leisure Activities and Activities of Daily Living

Because of the broad range of symptoms and the unpredictable risk of sudden death in many of these patients, it is very difficult to make any generalized recommendations regarding physical activity in this population. With rare exceptions, activity should be of low intensity and have both a low dynamic and static requirement (see Table 6.8). In more symptomatic patients, a formal exercise prescription may be useful (161). These patients may be quite deconditioned and their quality of life may be significantly improved by simple activities designed to improve their musculoskeletal conditioning. This may initially need to be in a structured and monitored location rather than a home-based program. Regardless of the level of activity, frequent reassessment is necessary in all patients. Exercise recommendations may be liberalized or restricted based on the patient's clinical course (160). There has been a very significant improvement in the clinical course of patients with PHT over the last decade as a result of treatment with several new classes of therapeutic agents. Many patients will have a marked improvement in the symptoms with onset of therapy. For this reason, the need to frequently reassess exercise capacity and recommendations in this population cannot be overemphasized (160).

Most of the recommendations of PAH also apply for patients PHT from Eisenmenger Syndrome. Exercise capacity is often limited by both cardiac and peripheral factors (160,162). However, as stated above, these patients are at less risk for sudden drops in systemic cardiac output and blood pressure. Exercise-related SCD appears to be significantly less common compared to patients with PAH. This would suggest that if these patients can tolerate somewhat more vigorous physical activity, it may be undertaken with less risk. Careful and frequent monitoring of exercise symptoms and capacity are still essential (160).

Competitive Sports

Given the high-risk nature of this population, restriction from any competitive sport is probably warranted. Special circumstances may occur when participation in low static and dynamic sports may be considered on an individual basis for Class 1 patients. There are, however, no significant data that would allow accurate assessment of risk for an individual patient.

Heart Transplantation

Exercise capacity as measured by both aerobic capacity and musculoskeletal strength is significantly decreased in the pediatric population following heart transplantation. The causes of these limitations are multifactorial. The few reports of exercise

testing in pediatric heart transplant patients have reported aerobic capacities, as measured by maximal VO_2 , of 50% to 60% of healthy age and sex matched peers (163–165). These values are not significantly different from those reported in the adult population. The reasons for this finding appear to be due to both central and peripheral factors combining to impair aerobic capacity. Especially in early posttransplant periods, stroke volume is limited. This may be due to systolic impairment but more importantly to diastolic dysfunction with high cardiac filling pressures. Abnormalities of autonomic innervation and function also impact on cardiac output during exercise. At least initially there is a loss of autonomic innervation to the heart. This significantly decreases chronotropic reserve and blunts the time course of the chronotropic response. There is some evidence for reinnervation and improved chronotropy late after transplant in some patients or as a response to cardiac training (discussed below). In addition to the cardiac effects, autonomic tone is abnormal in the peripheral vasculature. Brachial reactivity is impaired and systemic vascular resistance is increased (166–169).

Limitations of the peripheral exercising musculature are most likely at least as important as central mechanisms in limiting aerobic capacity. Following heart transplant, skeletal muscle mass is often reduced by 20% of normal. Capillary density is also significantly decreased. This may reflect the marked deconditioning in these patients that occurs prior to transplantation but may also be the result of immunosuppressant therapy. These changes result in an impaired ability of the exercising muscle to extract oxygen. Muscle strength is significantly impaired, especially in the early transplant period. Bone demineralization is a frequent finding. This may result in stress and compression fractures. Use of ongoing immunosuppressant medications may continue to exacerbate the problem of demineralization.

Serial studies of exercise performance following pediatric heart transplants are limited. Recent studies of Davis et al. (163) and Dipchand et al. (165) are conflicting. Both show early improvement in aerobic capacity and working capacity. Davis saw a decline of improvement after about 3 years while Dipchand's population remained steady with some patients showing a decrease associated with the onset of graft vasculopathy. The reason for these findings are unclear but are probably the combined improvement of systolic and especially diastolic function in the immediate posttransplant period as well as the longer term improvement in musculoskeletal conditioning, even in the absence of formal rehabilitation. In addition, improved chronotropy suggests at least some patients benefit from autonomic reinnervation of the donor heart.

TABLE 6.8

Recommendations Following the F.I.T.T. Principle for Recreational Activities and Exercise Training in Children and Adolescents with Pulmonary Hypertension^a

F.I.T.T.	Cardiovascular (dynamic) Training	Muscle (static) Training
Frequency	3–5×/wk	3–5×/wk
Intensity	Low intensity: 20%–40% of max VO_2	Low: 20% of MVC
Time	60 min per session	Included in cardiovascular training session
Type	Predominantly dynamic activity: e.g., walking either on a treadmill or an open course.	Major muscle groups, upper, and lower limbs and torso. Exercise aims at correct technique and breathing pattern to avoid the Valsalva maneuver.

VO_2 , minute oxygen consumption; MVC, maximum voluntary contraction.

^aIf the patient is WHO Class II or greater, formal exercise testing and prescription should be considered to assign intensity and types of activities.

Evaluation Prior to Exercise and Sports Participation

Like patients with PHT, those who have undergone heart transplantation represent a unique population. They should be evaluated for physical activity by physicians and health care providers who have specialized knowledge in this area. Assessment of systolic and diastolic function by echocardiography and cardiac catheterization is routine in this population and should be a part of any preparticipation evaluation. As the period of time from transplantation lengthens, the risk for development of graft dysfunction and, most importantly, coronary graft vasculopathy increases. Routine exercise testing, myocardial perfusion imaging, and even selective coronary angiography are essential parts of screening to assure safe participation in physical activity.

Unlike many congenital cardiac conditions, following heart transplantation, noncardiac medical issues may be just as important as cardiac functioning in determining the ability to perform certain activities. Muscle mass loss and deconditioning, bone mineral loss, and other end-organ dysfunction are all potentially important factors to assess especially in the early posttransplant period. These children usually benefit from exercise testing and a thorough physical therapy evaluation. Often a structured rehabilitation program that transitions to a home activity program is desirable for newly transplanted patients.

Leisure Activities and Activities of Daily Living

There are no evidence-based studies assessing the types, safety, or benefit of sports and exercise participation in children following heart transplantation. In a very small interview study of mixed solid organ transplant patients, Olausson et al. (170) reported that most expressed the opinion that they lived normal lives. Ross et al. (171) reported on the long-term survival of a cohort of pediatric heart transplantation patients at 10 and 20 years after transplant. They state that “physical rehabilitation and return to normal lifestyle has been nearly 100%.” They cite two anecdotal cases of patients participating in vigorous competitive sports. In an editorial, Fricker (172) listed a series of recommendations for pediatric heart transplantation patients:

1. Exercise should be encouraged, not discouraged.
2. All patients should be in a monitored rehabilitation program within 3 months following transplantation.
3. Return to age-appropriate activities including physical education class within 6 months after transplantation.
4. Endurance activities will be better tolerated than intermittent high-intensity activity.
5. Participation in competitive sports should be individualized with detailed yearly reevaluation of participation.

Absent any studies on leisure activity in this population, this appears to be a reasonable approach. Patients with no evidence of graft vasculopathy, other musculoskeletal problems, or end-organ dysfunction should be encouraged to engage in vigorous recreational activity (see Table 6.9).

Competitive Sports

There is an equal lack of data in the adult and pediatric populations regarding competitive sports participation following heart transplantation. A number of case reports and small studies show that heart transplant recipients can train and compete often quite successfully in vigorous athletic activity. However, the numbers in these studies are too small to allow generalization to the entire transplant population regarding the safety and benefits of such training. Given these limitations, the recommendations from the 36th Bethesda Conference on Eligibility Recommendations for Competitive Athletes with Cardiovascular Abnormalities are probably appropriate (173):

1. Because of special issues involved with transplant patient management, decisions as to the feasibility of athletic competition for cardiac transplant recipients should be made in conjunction with the patient's transplant cardiologist.
2. Athletes with no coronary luminal narrowing, no exercise-induced ischemia, and normal exercise capacity for age can generally participate in all competitive sports as appropriate for their exercise capacity.
3. Athletes with coronary luminal narrowing should be risk stratified as outlined in the recommendations by Thompson et al. (173).

In the absence of any better data, these recommendations are probably a good basis, at least, for the evaluation of the adolescent population as well.

DEFECTS THAT ARE ASSOCIATED WITH SUDDEN CARDIAC DEATH IN ATHLETES

Congenital Coronary Artery Abnormalities

The congenital coronary anomalies in which there is often an increased risk of myocardial ischemia and SCD are those in which the anomalous vessel arises from the inappropriate

TABLE 6.9

Recommendations Following the F.I.T.T. Principle for Recreational Activities and Exercise Training in Children After Heart Transplantation without Coronary Artery Disease

F.I.T.T.	Cardiovascular (dynamic) Training	Muscle (static) Training
Frequency	3–5×/wk	3–5×/wk
Intensity	Moderate to Heavy: near VAT (55%–65% of max $\dot{V}O_2$).	Moderate: 20%–50% of MVC
Time	60 min per session	Included in cardiovascular training session
Type	Predominantly dynamic activity: e.g., walking, jogging, running, cycling, running games	Major muscle groups, upper, and lower limbs and torso. Exercise aims at correct technique and breathing pattern to avoid the Valsalva maneuver.

$\dot{V}O_2$, minute oxygen consumption; MVC, maximum voluntary contraction; VAT, ventilatory anaerobic threshold.

Modified after McBride MG, Binder TJ, Paridon SM. Safety and feasibility of inpatient exercise training in pediatric heart failure: a preliminary report. *J Cardiopulm Rehabil Prev* 2007;27(4):219–222.

sinus of Valsalva and courses intramurally between the aorta and pulmonary artery, with the anomalous left coronary artery from the right sinus carrying the greatest risk of SCD. Indeed, these anomalies are the second leading cardiovascular cause of SCD in young athletes in the United States (25). Identification of coronary anomalies is challenging because many individuals do not experience warning symptoms. The first symptom may be SCD. A screening ECG is almost always normal in these patients. In those who complain of *exertional* chest pain, palpitations, dizziness, presyncope, or syncope, the presence of an anomalous coronary artery must be considered. Transthoracic echocardiography with color Doppler should be performed to demonstrate coronary anatomy. When an anomalous coronary artery is suspected, confirmatory imaging such as cardiac MRI, ultrafast CT, and occasionally coronary angiography are almost always utilized. In those for whom the left main coronary arises aberrantly, surgery is usually indicated. The management of asymptomatic patients with anomalous right coronary artery has not been defined, with some opting for surgery and others opting for medical management, including exercise restriction. The relative risks and benefits of surgical versus nonsurgical management of these defects are far from clear.

Evaluation Prior to Exercise and Sports Participation

Children with congenital coronary anomalies should have a baseline physical examination and ECG, and a resting echocardiogram to delineate coronary anatomy, evaluate heart function, assess atrioventricular and aortic valve regurgitation, and assess resting wall-motion abnormalities. A maximal graded exercise stress test, usually with nuclear myocardial perfusion and/or stress echocardiography should be performed. Besides measuring aerobic and physical working capacities, the stress test will help assess for evidence of ischemia, exercise-induced symptoms, and exercise-induced arrhythmias. A Holter monitor is useful to evaluate for arrhythmias.

Leisure Activities and Activities of Daily Living

If maximal graded exercise testing and other provocative testing are normal, most practitioners would encourage asymptomatic children and young adults with anomalous right

coronary artery from the left sinus of Valsalva to participate in leisure sports and daily physical activities (174). Regular recreational activities of at least moderate aerobic intensities should be encouraged (see Table 6.10). Static training should be at a moderate level as well. Those who have exertional symptoms, evidence of ischemia on provocative testing, and those with anomalous left coronary artery from the right sinus of Valsalva should refrain from recreational activities until further treatment, likely surgery.

Competitive Sports

The current guidelines in the United States recommend exclusion from competitive sports once the diagnosis of anomalous coronary artery has been confirmed (76). If the patient undergoes surgery, the Bethesda guidelines allow for full participation in competitive sports 3 months after a successful operation, as long as there is no evidence of ischemia, ventricular tachycardia, or ventricular dysfunction during a maximal graded exercise stress test (76). An imaging study during exercise, such as nuclear myocardial perfusion and/or stress echocardiography may be helpful in evaluating postoperative ischemia in addition to the exercise stress test. There are no long-term data addressing the effectiveness of surgery in reducing risk of SCD in this population.

Acquired Coronary Disease

Kawasaki Disease

Kawasaki disease is the most common cause of acquired heart disease in children in the United States (175). Ischemic heart disease that can lead to myocardial infarction and SCD can occur due to coronary aneurysms, together with progressive coronary artery stenosis (176). The risk of SCD due to extent of CAD appears to change over time. For the first 20 years after the onset of Kawasaki disease, patients without evidence of coronary aneurysm or with initial transient dilation on echocardiography appear to have no greater risk for ventricular tachyarrhythmias and SCD than that of the general population (176). Those with aneurysms that regress to normal lumen diameter may have persisting structural and functional coronary abnormalities (176). Suda and colleagues recently reported the long-term prognosis (median 19 year follow-up)

TABLE 6.10

Recommendations Following the F.I.T.T. Principle for Recreational Activities and Exercise Training in Children and Adolescents with Coronary Anomalies and Acquired Coronary Disease

F.I.T.T.	Cardiovascular (dynamic) Training	Muscle (static) Training
Frequency	Moderate: daily Vigorous: $\geq 3\times/\text{wk}$	$\geq 3\times/\text{wk}$
Intensity	Moderate: 55%–60% of max VO_2 to heavy (below 80% of max VO_2)	Moderate: 20%–50% MVC
Time	Most of daily ≥ 60 min activity	As part of daily ≥ 60 min activity
Type	Predominantly dynamic activity: e.g., running, jumping, cycling, swimming, inline skating, skateboarding, soccer	Predominantly static activity: e.g., gymnastics, climbing, push-ups, martial arts, ball sports practice

VO_2 , minute oxygen consumption, MVC: maximum voluntary contraction.

These recommendations apply to those patients with no evidence by history or testing of exercise-induced myocardial ischemia and no coronary artery stenosis* Patients with anomalous left coronary artery, even if asymptomatic, should refrain from physical activity until after surgical repair.

of patients with giant coronary aneurysms that did not regress and, instead, remodeled over time, leading to intimal thickening and risk of ischemic heart disease. Of the 76 patients initially followed, 7 died and 1 underwent heart transplantation. In addition, there were numerous catheter and surgical coronary interventions with cumulative coronary intervention rates of 28%, 43%, and 59% at 5, 15, and 25 years after disease onset, respectively (177). Certainly, in patients with Kawasaki disease, risk associated with physical activity and exercise depends on the degree of coronary involvement. Paridon et al. (178) reported on 46 children and adolescents with a history of Kawasaki disease and showed that maximal oxygen consumption was within normal limits without a difference based on coronary artery status (i.e., none, regressed, or current aneurysms). Another study focusing on children with persistent coronary aneurysms also showed normal peak oxygen consumption, workload, and anaerobic threshold when compared to control subjects (179).

Evaluation Prior to Exercise and Sports Participation

Children with Kawasaki disease should have, in addition to a physical examination and ECG, a resting echocardiogram to evaluate heart function and presence and size of coronary aneurysms. A maximal graded exercise test in conjunction with nuclear myocardial imaging and/or stress echocardiography can be helpful in assessing evidence of ischemia, wall-motion abnormalities, and presence of exercise-induced arrhythmias.

Leisure Activities and Activities of Daily Living

Because of the overall cardiovascular benefits associated with physical activity and exercise, it is recommended that all patients with Kawasaki disease remain physically active and avoid a sedentary lifestyle (76). Regular recreational activities of at least moderate level should be encouraged daily. Static training should be at least at a moderate level as well (see Table 6.10).

Competitive Sports

For competitive athletics, the risk is dependent on coronary artery status. The following recommendations are from the 36th Bethesda Conference guidelines for competitive athletes (76). Those patients without coronary artery abnormalities or transient coronary artery ectasia may participate in all sports after 6 to 8 weeks from disease onset. Similarly, those with regressed aneurysms can participate in all competitive sports as long as there is no evidence of exercise-induced ischemia using exercise stress testing with myocardial perfusion imaging. For those patients with isolated small- to medium-sized aneurysms in one or more coronary arteries without exercise-induced ischemia or arrhythmia and with normal left ventricular function are thought to be at low risk for ischemia. They may participate in low to moderate static and dynamic competitive sports (class IA, IB, IIA, and IIB) (see Fig. 6.1). Ischemia evaluations using exercise stress testing with myocardial perfusion imaging should be repeated at 1- to 2-year intervals.

Patients with at least one large coronary aneurysm, multiple (segmented), or complex aneurysms with or without obstruction to coronary artery blood flow may participate in class IA and IIA sports in the absence of reversible ischemia and exercise-induced arrhythmias on exercise stress testing and normal left ventricular function. Annual exercise stress testing with myocardial perfusion imaging should be performed to monitor the development of ischemia.

Patients with recent myocardial infarction or revascularization should not participate in competitive sports until their recovery is complete, which is usually 6 to 8 weeks. After their recovery, those with normal left ventricular function and exercise tolerance and absence of reversible ischemia on myocardial perfusion testing, and exercise-induced arrhythmias may participate in class IA and IB sports. Those with left ventricular ejection fraction <40%, exercise intolerance, or exercise-induced ventricular tachyarrhythmias should not be allowed to participate in competitive sports. As well, patients who are taking anticoagulants and/or antiplatelet drugs (aspirin, clopidogrel) should not participate in sports that pose danger of high-speed collision.

Atherosclerotic Coronary Artery Disease

Atherosclerotic CAD is the primary cause of exercise-induced SCD in adults older than 35 years, with those who are habitually sedentary at highest risk (115). In younger athletes (i.e., <35 years old), acute exercise-related ischemia is rarely caused by CAD, except in those with dyslipidemias that place them at high risk for premature atherosclerosis. The most common dyslipidemias in children and young adults are: heterozygous familial hypercholesterolemia, familial defective apoB100, polygenic hypercholesterolemia, familial combined hyperlipidemia, and familial hypertriglyceridemia. Patients with these dyslipidemias seldom have manifest CAD in childhood or young adulthood. As well, those with obesity-related dyslipidemia almost never develop atherosclerotic CAD during childhood and young adulthood. For those patients with extremely rare genetic dyslipidemias (i.e., homozygous familial hypercholesterolemia or sitosterolemia), risk of premature CAD is significantly increased during childhood and young adulthood.

The diagnosis of atherosclerotic CAD is made by having any of the following: history of myocardial infarction, history suggestive of angina pectoris in conjunction with evidence of inducible ischemia, and/or coronary atherosclerosis demonstrated using coronary imaging (173). In general, for people at risk for developing CAD, a sedentary lifestyle increases risk, whereas physical training reduces the risk of SCD during exercise (115).

Evaluation Prior to Exercise and Sports Participation

Most patients with the common genetic dyslipidemias and those with lifestyle-related hypercholesterolemia need little evaluation beyond routine care, including a physical examination, by the primary care pediatrician. These children do not manifest CAD at a young age and should not need further imaging studies performed. Patients with the rare genetic dyslipidemias, such as homozygous familial hypercholesterolemia, should have in addition to a physical examination and ECG, an annual resting echocardiogram to evaluate heart function and for aortic valve disease. Maximal graded exercise stress testing should be considered in adolescence, especially those with aortic valve regurgitation on echocardiography. If there are abnormalities noted on the exercise stress test, coronary angiography should be performed especially if there is high suspicion of atherosclerotic disease based on echocardiographic findings and worrisome family history (180). Electron beam computerized tomography may be useful in evaluating atherosclerosis, but this technology has not been adequately studied in children.

Leisure Activities and Activities of Daily Living

In the absence of evidence for exercise-related myocardial ischemia or laboratory evidence of more than mild coronary artery stenosis, regular recreational activities of vigorous to moderate levels should be encouraged daily. Static training

should be at a moderate level as well (see Table 6.10). Indeed, regular physical activity and recreational sports should be encouraged in patients at risk for and with CAD as this helps improve overall cardiovascular health (173). Those who have had a recent myocardial infarction or myocardial revascularization should not participate in physical activity until recovery is complete. These patients would likely benefit from cardiac rehabilitation as part of their recovery (173).

Competitive Sports

There is a lack of data on the presence and severity of CAD in competitive athletes. For this reason, the Bethesda conference guidelines are based on adult data from nonathletes with CAD, with two levels of risk assigned based on testing (173). It is likely that the risk of an exercise-related event increases with both the intensity of the competitive sport as well as the severity of disease in the athlete himself. Those with mildly increased risk are defined as: preserved left ventricular systolic function at rest (i.e., ejection fraction > 50%), normal exercise tolerance for age, absence of exercise-induced ischemia or complex ventricular arrhythmias, absence of hemodynamically significant stenosis (>50% luminal diameter narrowing) by coronary angiography, and/or successful myocardial revascularization. Those considered at substantially increased risk exhibit any of the following: impaired left ventricular systolic function at rest (i.e., ejection fraction < 50%), exercise-induced myocardial ischemia or complex ventricular tachyarrhythmias, or hemodynamically significant coronary arterial stenosis by coronary angiography. Based on these definitions, the recommendations are for those in the mildly increased risk group to participate in low dynamic and low/moderate static competitive sports (classes IA and IIA) but not in highly competitive activity. However, in those with very low exercise risk, select athletes may be allowed to compete in higher intensity sports. Also, these recommendations are not for children with dyslipidemias and no evidence of CAD (e.g., the vast majority of children with lipid abnormalities). This group should be treated as other healthy children and not be restricted from competitive athletics. Athletes in the substantially increased risk group should be restricted to low-intensity competitive sports (class IA).

Once CAD is established, it is necessary to stress that even in those athletes for whom risk is only mildly increased, competitive exercise may transiently increase the risk of an exercise-related adverse event.

Hypertrophic Cardiomyopathy

HCM is the leading cause of SCD in U.S. athletes and can have variable phenotypes. Four major phenotypes have been described and it is important to recognize that SCD can occur in all. Most patients have inherited cardiomyopathy due to mutations in sarcomeric protein genes, and gene tests to identify these mutations are readily available but expensive. Some patients who are genotype positive but phenotype negative may have myocardial disarray and disorder prior the development of clinically detectable hypertrophy (181-183). Patients who are genotype positive without clinically detectable hypertrophy can be of any age but are usually younger than 14 years (184,185). The risk of SCD in genotype positive but phenotype negative patients appears to be lower compared to phenotype positive individuals. Numerous screening programs to detect HCM have been attempted. The high cost of testing, the low prevalence rate (1 in 500 in adults, likely lower in children) and subsequent low detection rate, and the possibility of inappropriate disqualification of competitors with athlete's heart makes universal screening problematic.

Evaluation Prior to Exercise and Sports Participation

All athlete candidates require a careful medical history with particular attention to a history of syncope or dizziness during athletic competition, dyspnea with exertion, angina, and palpitations. Family history may include sudden death in members <40 years, a finding that should prompt the examiner to consider inherited types of cardiac disease. Systolic murmurs that are louder in the standing position after squatting may alert the examiner to dynamic outflow tract obstruction. ECGs are abnormal in approximately 90% of affected individuals. Echocardiography typically identifies affected individuals, but mild hypertrophy may mimic athlete's heart. Diastolic dysfunction due to myocardial disarray can be detected utilizing Doppler tissue imaging and may predate significant hypertrophy. Gene testing can identify young family members who have no ostensible expression of the disease. In the absence of gene testing, family members of affected individuals should have ECG and echocardiographic screening every few years until adolescence at which time annual screening is suggested.

Leisure Activities and Activities of Daily Living

Asymptomatic patients should pursue a healthy lifestyle, be allowed to regulate their own activities, rest when fatigued, and maintain hydration. Intravascular volume depletion worsens dynamic outflow tract obstruction and should be avoided. Electrolyte disturbances that may result from dehydration likely increase the risk of malignant arrhythmias. Isometric activities should be kept to a minimum.

Competitive Sports

Athletes with a probable or definitive diagnosis of HCM should be excluded from all but low-intensity sports, irrespective of age and gender and cardiac phenotype. Asymptomatic athletes with phenotype negative, genotype positive cardiomyopathy without a family history of SCD may participate in all competitive sports. At the time of this writing, there are no convincing data that these patients are at risk of a sudden catastrophic event as a result of vigorous exercise. Until such data exist, there appears to be no compelling evidence that would preclude these individuals from athletic competition.

Asymptomatic patients with implantable cardioverter-defibrillators should not engage in athletic competition, with the exception of low-intensity sports. Sports with danger of bodily collision in this setting should also be avoided. The availability of external cardioverter-defibrillators does not change the above recommendations at the time of this writing. However, it is expected that present day studies may alter recommendations for patients with HCM who have external or internal cardioverter-defibrillator availability.

Other Cardiomyopathies

Less common cardiomyopathies include dilated, restrictive, or mixed physiology. These cardiomyopathies arise from a variety of etiologies, such as genetic, chemical or toxic, and postinfectious. Exercise performance in this population may vary from severely limited to normal depending on the degree of ventricular dysfunction. Because of the heterogeneity of these diseases it is not possible to make generalized recommendations regarding physical activities and sports participation.

Limited data on exercise ability are available in some of these groups. Patients who have received anthracycline therapy as part of a chemotherapeutic treatment may develop a slowly progressive, dose-dependent, dilated cardiomyopathy as children or young adults. Exercise performance may be normal in patients who are only mildly affected and this may remain stable for many years (186,187). However, symptoms

will frequently occur in patients with significant, progressive decline in cardiac function. The presence of a restrictive physiologic component especially in the presence of PHT may greatly increase the risk in these postanthracycline population.

Noncompaction cardiomyopathy is a relatively newly recognized entity (188,189). The incidence of this type of cardiomyopathy is unknown. Patients may present with severe heart failure but are often completely asymptomatic and identified by an echocardiogram performed for an unrelated cause. For this reason, the risk for exercise in this population is largely unknown.

Evaluation Prior to Exercise and Sports Participation

Because of the heterogeneity of this group, each patient should be evaluated by a clinician familiar with the type of cardiomyopathy. ECGs and Holter monitors are useful to assess for the presence of arrhythmias. Echocardiograms are useful to assess systolic and diastolic function, as well as the presence of noncompaction, and monitor the development of PHT. More specific assessment of the myocardium and its function may be needed using testing such as MRI in certain cases. Exercise testing should be performed to assess aerobic and physical working capacity, evaluate incidence of arrhythmias, and symptoms suggestive of an inability to maintain cardiac output with increasing exercise intensity.

Leisure Activities and Activities of Daily Living

As stated above, the high degree of heterogeneity in this population precludes any meaningful generalized statements concerning leisure physical activity. However, almost all of the patients will benefit from routine physical activity of some type. Quality of life and physical working capacity have been shown to be improved in adults by routine exercise programs even in patients with advance heart failure (21). There are much less data for children but these also suggest that physical conditioning can be improved in severely symptomatic patients (190). Highly structured rehabilitation is not needed in most mild cases, although a formal exercise prescription is often useful to help guide the patient's activities. Often, little or no restrictions on leisure or daily living activities are needed in most mildly affected cases.

Competitive Sports

There are no data on risk stratification for competitive sports in the pediatric cardiomyopathy population. As a consequence, restriction from all but low static and dynamic activities appears to be a reasonable default approach. Individual exceptions to this approach may be warranted in rare very mild cases where testing would suggest that the risk for sudden death is low, and normal or high physical working capacity and aerobic capacity are preserved.

Arrhythmias and Cardiac Channelopathies

Approximately one-third of all SCDs occurring during athletic activities in the pediatric and young adult age range are not associated with any evidence of structural heart disease or cardiomyopathy (25). These deaths are most likely due to arrhythmias. Defects in the cardiac sodium and potassium channels are those most associated with SCD during athletics. These include long QTc syndrome and Brugada Syndrome. The evaluation of these defects and their risk of SCD are discussed in a separate chapter (see Chapter 16).

Systemic Hypertension

Systemic hypertension is the most common cardiovascular problem diagnosed in adolescent and young adult athletes. As

was stated at the beginning of this chapter, there is an epidemic of obesity in the pediatric and adolescent population. This is translating into a growing number of cases of essential hypertension in the pediatric age range (191,192). Fortunately, this is one of the few cardiovascular abnormalities where exercise and competitive sports are not only often safe but may be beneficial in its control. Certainly, data from young adults suggest that vigorous dynamic and resistance exercise results in prolonged lowering of blood pressure and reduction in the likelihood of developing essential hypertension.

Evaluation Prior to Exercise and Sports Participation

Evaluation for hypertension should conform to the guidelines of the National High Blood Pressure Education Program Working Group on High Blood Pressure in Children and Adolescents (193). Especially in preadolescent patients, secondary causes of hypertension that may impact on eligibility to compete should be carefully evaluated.

Leisure Activity and Activities of Daily Living

All patients with systemic hypertension should be encouraged to participate in regular vigorous recreational activities as part of treatment for their hypertension. Patients with Stage 1 hypertension and no end-organ damage (including increased left ventricular mass) should be encouraged to engage in routine moderate to high dynamic and static activities similar to those patients with well-repaired CHD and no exercise restrictions (Table 6.2). Care may be needed if these patients have metabolic syndrome and significant obesity. An exercise evaluation and prescription may be needed in these cases to avoid the risk of orthopedic injuries when undertaking a vigorous new unsupervised activity program.

Patients with more severe hypertension, Stage 2, and certainly patients with evidence of increased left ventricular mass, should have appropriate control of their hypertension. Once the hypertension is controlled, these patients should also be encouraged to engage in regular recreational activity as part of their hypertension management.

Competitive Sports

Patients with Stage 1 hypertension and no cardiac or other end-organ abnormalities can and should be encouraged to participate in competitive sports. Blood pressure should be monitored routinely after beginning competition. Patients with Stage 2 hypertension should not participate in competitive sports until the hypertension is controlled and there is no evidence of cardiac or other end-organ damage.

REFERENCES

1. Williams CL, Hayman LL, Daniels SR, et al. Cardiovascular health in childhood: a statement for health professionals from the Committee on Atherosclerosis, Hypertension, and Obesity in the Young (AHOY) of the Council on Cardiovascular Disease in the Young, American Heart Association. *Circulation* 2002;106:143–160.
2. Hayman LL, Williams CL, Daniels SR, et al. A Statement for Health and Education Professionals and Child Health Advocates from the Committee on Atherosclerosis, Hypertension, and Obesity in Youth (AHOY) of the Council on Cardiovascular Disease in the Young, American Heart Association. *Circulation* 2004;110:2266–2275.
3. Pasquali SK, Marino BS, Pudusseri A, et al. Risk factors associated with obesity after congenital heart surgery. *Congenit Heart Dis* 2008;3:376–394.
4. Pasquali SK, Marino BS, Pudusseri A, et al. Risk factors and comorbidities associated with obesity in children and adolescents following the arterial switch operation and Ross procedure. *Am Heart J* 2009;158:473–479.
5. Corrado D, Basso C, Rizzoli G, et al. Does sports activity enhance the risk of sudden death in adolescents and young adults? *J Am Coll Cardiol* 2003;42:1959–1963.

6. Maron BJ. Sudden death in young athletes. *N Engl J Med* 2003;349:1064-1075.
7. Mitchell JH, Haskell W, Snell P, et al. Task Force 8: classification of Sports. *J Am Coll Cardiol* 2005;45:1364-1367.
8. Lock JE, Einzig S, Moller JH. Hemodynamic responses to exercise in normal children. *Am J Cardiol* 1978;41:1278-1284.
9. Asmussen E. Similarities and dissimilarities between static and dynamic exercise. *Circulation Res* 1981;48:3-10.
10. MacDougall JD, Tuxen D, Sale DG, et al. Arterial blood pressure response to heavy resistance exercise. *J Appl Physiol* 1985;85:785-790.
11. Arvidsson D, Slinde F, Hulthen L, et al. Physical activity, sports participation and aerobic fitness in children who have undergone surgery for congenital heart defects. *Acta Paediatr* 2009;98:1475-1482.
12. Fredriksen PM, Ingjer E, Thaulow E. Physical activity in children and adolescents with congenital heart disease. Aspects of measurements with an activity monitor. *Cardiol Young* 2000;10:98-106.
13. Kao CC, Chang PC, Chiu CW, et al. Physical activity levels of school-age children with congenital heart disease in Taiwan. *Appl Nurs Res* 2009;22:191-197.
14. Barber G, Heise CT. Subjective estimates of exercise ability: comparison to objective measurements. *Pediatr Exerc Sci* 1991;3:327-332.
15. Rogers R, Reybrouck T, Weymans M, et al. Reliability of subjective estimates of exercise capacity after total repair of Tetralogy of Fallot. *Acta Paediatr* 1994;83:866-869.
16. Bergman AB, Stamm SJ. The morbidity of cardiac nondisease in schoolchildren. *N Engl J Med* 1967;276:1008-1013.
17. Stefan MA, Hopman WM, Smythe JF. Effect of activity restriction owing to heart disease on obesity. *Arch Pediatr Adolesc Med* 2005;159:477-481.
18. Swan L, Hillis WS. Exercise prescription in adults with congenital heart disease: a long way to go. *Heart* 2000;83:685-687.
19. Bernhardt DT, Gomez J, Johnson MD, et al. Strength training by children and adolescents. *Pediatrics* 2001;107:1470-1472.
20. Strong WB, Malina RM, Blimkie CJR, et al. Evidence based physical activity for school-age youth. *J Pediatr* 2005;146:732-737.
21. Carvalho VO, Mezzani A. Aerobic exercise training intensity in patients with chronic heart failure: principles of assessment and prescription. *Eur J Cardiovasc Prev Rehabil* 2010;DOI:10.1097/HJR.0b013e32833a9c63.
22. Giardini A, Hager A, Lammers AE, et al. Ventilatory efficiency and aerobic capacity predict event-free survival in adults with atrial repair for complete transposition of the great arteries. *J Am Coll Cardiol* 2009;53:1548-1555.
23. Diller GP, Giardini A, Dimopoulos K, et al. Predictors of morbidity and mortality in contemporary Fontan patients: results from a multicenter study including Cardiopulmonary Exercise Testing in 321 patients. *Eur Heart J* 2010;24:3073-3083.
24. Pollock ML, Gaesser GA, Butcher JD, et al. ACSM position stand: the recommended quantity and quality of exercise for developing and maintaining cardiorespiratory and muscular fitness, and flexibility in healthy adults. *Med Sci Sports Exerc* 1998;30:975-991.
25. Maron BJ, Doerer JJ, Haas TS, et al. Sudden deaths in young competitive athletes: analysis of 1866 deaths in the United States, 1980-2006. *Circulation* 2009;119:1085-1092.
26. Maron BJ, Shirani J, Poliac LC, et al. Sudden death in young competitive athletes. Clinical, demographic, and pathological profiles. *JAMA* 1996;276:199-204.
27. Maron BJ, Gohman TE, Aeppli D. Prevalence of sudden cardiac death during competitive sports activities in Minnesota high school athletes. *J Am Coll Cardiol* 1998;32:1881-1884.
28. Van Camp SP, Bloor CM, Mueller FO, et al. Nontraumatic sports death in high school and college athletes. *Med Sci Sports Exerc* 1995;27:641-647.
29. Eckart RE, Scoville SL, Campbell CL, et al. Sudden death in young adults: a 25-year review of autopsies in military recruits. *Ann Intern Med* 2004;141:829-834.
30. Drezner JA, Rogers KJ, Zimmer RR, et al. Use of automated external defibrillators at NCAA Division I universities. *Med Sci Sports Exerc* 2005;37:1487-1492.
31. Berger S, Utech L, Fran HM. Sudden death in children and adolescents. *Pediatr Clin North Am* 2004;51:1653-1677,ix-x.
32. Asif I, Harmon K, Drezner J, et al. Incidence and etiology of sudden death in NCAA athletes. *Clin J Sport Med* 2010;20:136.
33. Drezner JA, Rao AL, Heistand J, et al. Effectiveness of emergency response planning for sudden cardiac arrest in United States high schools with automated external defibrillators. *Circulation* 2009;120:518-525.
34. Chugh SS, Reinier K, Balaji S, et al. Population-based analysis of sudden death in children: the Oregon Sudden Unexpected Death Study. *Heart Rhythm* 2009;6:1618-1622.
35. Corrado D, Basso C, Pavei A, et al. Trends in sudden cardiovascular death in young competitive athletes after implementation of a preparticipation screening program. *JAMA* 2006;296:1593-1601.
36. Maron BJ, Carney KP, Lever HM, et al. Relationship of race to sudden cardiac death in competitive athletes with hypertrophic cardiomyopathy. *Am Coll Cardiol* 2003;41:974-980.
37. Maron BJ, Thompson PD, Ackerman MJ, et al. Recommendations and considerations related to preparticipation screening for cardiovascular abnormalities in competitive athletes: 2007 update: a scientific statement from the American Heart Association Council on Nutrition, Physical Activity, and Metabolism: endorsed by the American College of Cardiology Foundation. *Circulation* 2007;115:1643-1655.
38. Maron BJ, Douglas PS, Graham TP, et al. Task force 1: preparticipation screening and diagnosis of cardiovascular disease in athletes. *J Am Coll Cardiol* 2005;45:1322-1326.
39. American Academy of Family Physicians, American Academy of Pediatrics, American College of Sports Medicine, et al. *PPE PreParticipation Physical Evaluation*. 4th ed. Elk Grove Village, IL: American Academy of Pediatrics, 2010.
40. Fuller CM, McNulty CM, Spring DA, et al. Prospective screening of 5,615 high school athletes for risk of sudden cardiac death. *Med Sci Sports Exerc* 1997;29:1131-1138.
41. Wilson MG, Basavarajah S, Whyte GP, et al. Efficacy of personal symptom and family history questionnaires when screening for inherited cardiac pathologies: the role of electrocardiography. *Br J Sports Med* 2008;42:207-211.
42. Bessem B, Groot FP, Nieuwland W. The Lausanne recommendations: a Dutch experience. *Br J Sports Med* 2009;43:708-715.
43. Baggish AL, Hutter AM Jr, Wang F, et al. Cardiovascular screening in college athletes with and without electrocardiography: a cross-sectional study. *Ann Intern Med* 2010;152:269-275.
44. Corrado D, Pelliccia A, Bjornstad H, et al. Study Group of Sport Cardiology of the Working Group of Cardiac Rehabilitation and Exercise Physiology and the Working Group of Myocardial and Pericardial Diseases of the European Society of Cardiology. Cardiovascular pre-participation screening of young competitive athletes for prevention of sudden death: proposal for a common European protocol. Consensus Statement of the Study Group of Sport Cardiology of the Working Group of Cardiac Rehabilitation and Exercise Physiology and the Working Group of Myocardial and Pericardial Diseases of the European Society of Cardiology. *Eur Heart J* 2005;26:S16-S24.
45. Maron BJ, Thompson PD, Puffer JC, et al. Cardiovascular pre-participation screening of competitive athletes. A statement for health professionals from the Sudden Death Committee (clinical cardiology) and Congenital Cardiac Defects Committee (cardiovascular disease in the young), American Heart Association. *Circulation* 1996;94:850-856.
46. De Noronha SV, Sharma S, Papadakis M, et al. Aetiology of sudden cardiac death in athletes in the United Kingdom: a pathological study. *Heart* 2009;95:1409-1414.
47. Basso C, Maron BJ, Corrado D, et al. Clinical profile of congenital coronary artery anomalies with origin from the wrong aortic sinus leading to sudden death in young competitive athletes. *J Am Coll Cardiol* 2000;35:1493-1501.
48. Wilson MG, Basavarajah S, Whyte GP, et al. Efficacy of personal symptom and family history questionnaires when screening for inherited cardiac pathologies: the role of electrocardiography. *Br J Sports Med* 2008;42:207-211.
49. Ljungqvist A, Jenouire PJ, Engebretsen L, et al. The international Olympic committee (IOC) consensus statement on periodic health evaluation of elite athletes, March 2009. *Clin J Sport Med* 2009;19:347-365.
50. Chaitman BR. An electrocardiogram should not be included in routine preparticipation screening of young athletes. *Circulation* 2007;116:2610-2614.
51. Myerburg RJ, Vetter VL. Electrocardiograms should be included in preparticipation screening of athletes. *Circulation* 2007;116:2616-2626.
52. Drezner J, Berger S, Campbell R. Current controversies in the cardiovascular screening of athletes. *Curr Sports Med Rep* 2010;9:86-92.
53. Steinvil A, Chundadze T, Zeltser D, et al. Mandatory electrocardiographic screening of athletes to reduce their risk for sudden death: proven fact or wishful thinking? *J Am Coll Cardiol* 2011;57:1291-1296.
54. Maron BJ. Distinguishing hypertrophic cardiomyopathy from athlete's heart physiological remodeling: clinical significance, diagnostic strategies and implications for preparticipation screening. *Br J Sports Med* 2009;43:649-656.
55. Corrado D, Basso C, Fontaine G. Clinical profile of young competitive athletes who dies suddenly of arrhythmic right ventricular cardiomyopathy/dysplasia: a multicenter study. *Pacing Clin Electrophysiol* 2002;25:544.
56. Corrado D, Basso C, Schiavon M, et al. Screening for hypertrophic cardiomyopathy in young athletes. *N Engl J Med* 1998;339:364-369.
57. Maron BJ, Gardin JM, Flack JM, et al. Prevalence of hypertrophic cardiomyopathy in a general population of young adults: echocardiographic analysis of 4111 subjects in CARDIA study. *Circulation* 1995;92:785-789.
58. Pelliccia A, Di Paolo FM, Corrado D, et al. Evidence for efficacy of the Italian national pre-participation screening programme for identification of hypertrophic cardiomyopathy in competitive athletes. *Eur Heart J* 2006;27:2196-2200.
59. Wilson MG, Basavarajah S, Whyte GP, et al. Efficacy of personal symptom and family history questionnaires when screening for inherited cardiac pathologies: the role of electrocardiography. *Br J Sports Med* 2008;42:207-211.
60. Thompson PD, Levine BD. Protecting athletes from sudden cardiac death. *JAMA* 2006;296:1648-1650.
61. Hevia AC, Fernandez MM, Palacio JM, et al. ECG as a part of the preparticipation screening programme: an old and still present international dilemma. [published online ahead of print April 15, 2011] *Br J Sports Med* doi:10.1136/bjsm.2009.063958.
62. Pelliccia A, Culasso F, Di Paolo FM, et al. Prevalence of abnormal electrocardiograms in a large, unselected population undergoing pre-participation cardiovascular screening. *Eur Heart J* 2007;28:2006-2010.
63. Maron BJ, Haas TS, Doerer JJ, et al. Comparison of U.S. and Italian experiences with sudden cardiac deaths in young competitive athletes

- and implications for preparticipation screening strategies. *Am J Cardiol* 2009;104:276–280.
64. Steinvil A, Chundadze T, Zeltser D, et al. Mandatory electrocardiographic screening of athletes to reduce their risk for sudden death: proven fact or wishful thinking? *J Am Coll Cardiol* 2011;57:1291–1296.
 65. McLeod CJ, Ackerman MJ, Nishimura RA, et al. Outcome of patients with hypertrophic cardiomyopathy and a normal electrocardiogram. *J Am Coll Cardiol* 2009;54:229–233.
 66. Corrado D, Pelliccia A, Heidbuchel H, et al. Recommendations for interpretation of the 12-lead electrocardiogram in the athlete. *Eur Heart J* 2010;31:243–259.
 67. Papadakis M, Basavarajaiah S, Rawlins J, et al. Prevalence and significance of T-wave inversions in predominantly Caucasian adolescent athletes. *Eur Heart J* 2009;30:1728–1735.
 68. Magalski A, Maron BJ, Main ML, et al. Relation of race to electrocardiographic patterns in elite American football players. *J Am Coll Cardiol* 2008;51:2250–2255.
 69. Basavarajaiah S, Boraita A, Whyte G, et al. Ethnic differences in left ventricular remodeling in highly trained athletes relevance to differentiating physiologic left ventricular hypertrophy from hypertrophic cardiomyopathy. *J Am Coll Cardiol* 2008;51:2256–2262.
 70. Drener J, Corrado D. Is there evidence for recommending electrocardiogram as part of the pre-participation examination? *Clin J Sport Med* 2011;21:18–24.
 71. Fuller CM. Cost effectiveness analysis of screening of high school athletes for risk of sudden cardiac death. *Med Sci Sports Exerc* 2000;32:887–890.
 72. Wheeler MT, Heidenreich PA, Froelicher VF, et al. Cost-effectiveness of preparticipation screening for prevention of sudden cardiac death in young athletes. *Ann Intern Med* 2010;152:276–286.
 73. Chandra N, Papadakis M, Sharma S. Preparticipation screening of young competitive athletes for cardiovascular disorders. *Phys Sports Med* 2010;38:54–63.
 74. Reybrouck T, Weymans M, Stijns H, et al. Ventilatory anaerobic threshold for evaluating exercise performance in children with congenital left-to-right intracardiac shunt. *Pediatr Cardiol* 1986;7:19–24.
 75. Reybrouck T, Rogers R, Weymans M, et al. Serial cardiorespiratory exercise testing in patients with congenital heart disease. *Eur J Pediatr* 1995;154:801–806.
 76. Graham J, Thomas P, Driscoll DJ, et al. 36th Bethesda Conference: Recommendations for Determining Eligibility for Competition in Athletes with Cardiovascular Abnormalities. Task Force 2: Congenital Heart Disease. *J Am Coll Cardiol* 2005;45:1326–1333.
 77. Hirth A, Reybrouck T, Bjarnason-Wehrens B, et al. Recommendations for participation in competitive and leisure sports in patients with congenital heart disease: a consensus document. *Eur J Cardiovasc Prev Rehabil* 2006;13:293–299.
 78. Goldberg B, Frapp RR, Lister G, et al. Effect of physical training on exercise performance of children following surgical repair of congenital heart disease. *Pediatrics* 1981;68:691–699.
 79. Pueschel SM, Scola FH. Atlantoaxial instability in individuals with Down syndrome: epidemiologic, radiographic, and clinical studies. *Pediatrics* 1987;80:555–560.
 80. Kolansky DM, Cuchel M, Clark BJ. Longitudinal evaluation and assessment of cardiovascular disease in patients with homozygous familial hypercholesterolemia. *Am J Cardiol* 2008;102:1438–1443.
 81. Aboulhoss J, Child JS. Left ventricular outflow obstruction: subaortic stenosis, bicuspid aortic valve, supravalvular aortic stenosis, and coarctation of the aorta. *Circulation* 2006;114:2412–2422.
 82. Ruttenberg HD, Adams TD, Orsmond GS, et al. Effects of exercise training on aerobic fitness in children after open heart surgery. *Pediatr Cardiol* 1983;4:19–24.
 83. Longmuir PE, Tremblay MS, Goode RC. Postoperative exercise training develops normal levels of physical activity in a group of children following cardiac surgery. *Pediatr Cardiol* 1990;11:126–130.
 84. Dua JS, Cooper AR, Fox KR, et al. Exercise training in adults with congenital heart disease: feasibility and benefits. *Int J Cardiol* 2010;138:196–205.
 85. Basso C, Corrado D, Thiene G. Cardiovascular causes of sudden death in young individuals including athletes. *Cardiol Rev* 1999;7:127–135.
 86. Brown DW, Dipilato AE, Chong EC, et al. Sudden unexpected death after balloon valvuloplasty for congenital aortic stenosis. *J Am Coll Cardiol* 2010;56:1939–1946.
 87. Basso C, Boschello M, Perrone C, et al. An echocardiographic survey of primary school children for bicuspid aortic valve. *Am J Cardiol* 2004;93:661–663.
 88. Nistri S, Basso C, Marzari C, et al. Frequency of bicuspid aortic valve in young male conscripts by echocardiogram. *Am J Cardiol* 2005;96:718–721.
 89. Russo CF, Cannata A, Lanfranconi M, et al. Is aortic wall degeneration related to bicuspid aortic valve anatomy in patients with valvular disease? *J Thorac Cardiovasc Surg* 2008;136:937–942.
 90. Silberbach M. Bicuspid aortic valve and thoracic aortic aneurysm: toward a unified theory. *J Am Coll Cardiol* 2009;53:2296–2297.
 91. Tadros TM, Klein MD, Shapira OM. Ascending aortic dilatation associated with bicuspid aortic valve: pathophysiology, molecular biology, and clinical implications. *Circulation* 2009;119:880–890.
 92. Schaefer BM, Lewin MB, Stout KK, et al. The bicuspid aortic valve: an integrated phenotypic classification of leaflet morphology and aortic root shape. *Heart* 2008;94:1634–1638.
 93. Schaefer BM, Lewin MB, Stout KK, et al. Usefulness of bicuspid aortic valve phenotype to predict elastic properties of the ascending aorta. *Am J Cardiol* 2007;99:686–690.
 94. Galanti G, Stefani L, Toncelli L, et al. Effects of sports activity in athletes with bicuspid aortic valve and mild aortic regurgitation. *Br J Sports Med* 2010;44:275–279.
 95. Cameron JD, Dart AM. Exercise training increases total systemic arterial compliance in humans. *Am J Physiol* 1994;266:H693–H701.
 96. Kakiyama T, Sugawara J, Murakami H, et al. Effects of short-term endurance training on aortic distensibility in young males. *Med Sci Sports Exerc* 2005;37:267–271.
 97. Kakiyama T, Matsuda M, Koseki S. Effect of physical activity on the distensibility of the aortic wall in healthy males. *Angiology* 1998;49:749–757.
 98. Sugawara J, Otsuki T, Tanabe T, et al. The effects of low-intensity single-leg exercise on regional arterial stiffness. *Jpn J Physiol* 2003;53:239–241.
 99. Sugawara J, Otsuki T, Tanabe T, et al. Physical activity duration, intensity, and arterial stiffening in postmenopausal women. *Am J Hypertens* 2006;19:1032–1036.
 100. Michelena HI, Desjardins VA, Avierinos JF, et al. Natural history of asymptomatic patients with normally functioning or minimally dysfunctional bicuspid aortic valve in the community. *Circulation* 2008;117:2776–2784.
 101. Bertovic DA, Waddell TK, Gatzka CD, et al. Muscular strength training is associated with low arterial compliance and high pulse pressure. *Hypertension* 1999;33:1385–1391.
 102. BabaeeBigi MA, Aslani A. Aortic root size and prevalence of aortic regurgitation in elite strength trained athletes. *Am J Cardiol* 2007;100:528–530.
 103. Bonow RO, Carabello B, De Leon AC, et al. ACC/AHA guidelines for the management of patients with valvular heart disease: a report of the American College of Cardiology/American Heart Association Task Force on Practice Guidelines (Committee on Management of Patients with Valvular Heart Disease). *J Am Coll Cardiol* 1998;32:1486–1582.
 104. Toro-Salazar OH, Steinberger J, Thomas W, et al. Long-term follow-up of patients after coarctation of the aorta repair. *Am J Cardiol* 2002;89:541–547.
 105. Diller GP, Dimopoulos K, Okonko D, et al. Exercise intolerance in adult congenital heart disease: comparative severity, correlates, and prognostic implication. *Circulation* 2005;112:828–835.
 106. Gratz A, Hess J, Hager A. Self-estimated physical functioning poorly predicts actual exercise capacity in adolescents and adults with congenital heart disease. *Eur Heart J* 2009;30:497–504.
 107. de Divitiis M, Pilla C, Kattenhorn M, et al. Vascular dysfunction after repair of coarctation of the aorta: impact of early surgery. *Circulation* 2001;104:I-165–I-170.
 108. Hanson E, Eriksson BO, Sivertsson R. Baroreceptor reflexes after coarctectomy. *Clin Physiol* 1981;1:503–509.
 109. Beekman RH, Katz BP, Moorehead-Steffens C, et al. Altered baroreceptor function in children with systolic hypertension after coarctation repair. *Am J Cardiol* 1983;52:112–117.
 110. Nishimura RA, Pieroni DR, Bierman FZ, et al. Second natural history study of congenital heart defects. Pulmonary stenosis: echocardiography. *Circulation* 1993;87:173–179.
 111. Chen CR, Cheng TO, Huang T, et al. Percutaneous balloon valvuloplasty for pulmonic stenosis in adolescents and adults. *N Engl J Med* 1996;335:21–25.
 112. Roos-Hesselink JW, Meijboom FJ, Spitaels SE, et al. Long-term outcome after surgery for pulmonary stenosis (a longitudinal study of 22–33 years). *Eur Heart J* 2006;27:482–488.
 113. Kavey RE, Daniels SR, Lauer RM, et al. American Heart Association Guidelines for Primary Prevention of Atherosclerotic Cardiovascular Disease Beginning in Childhood. *Circulation* 2003;107:1562–1566.
 114. Marcus BH, Williams DM, Dubbert PM, et al. Physical activity intervention studies: what we know and what we need to know: a scientific statement from the American Heart Association Council on Nutrition, Physical Activity, and Metabolism (Subcommittee on Physical Activity); Council on Cardiovascular Disease in the Young; and the Interdisciplinary Working Group on Quality of Care and Outcomes Research. *Circulation* 2006;114:2739–2752.
 115. Pelliccia A, Fagard R, Bjornstad HH, et al. Recommendations for competitive sports participation in athletes with cardiovascular disease: a consensus document from the Study Group of Sports Cardiology of the Working Group of Cardiac Rehabilitation and Exercise Physiology and the Working Group of Myocardial and Pericardial Diseases of the European Society of Cardiology. *Eur Heart J* 2005;26:1422–1445.
 116. Giardini A, Specchia S, Coutosombas G, et al. Impact of pulmonary regurgitation and right ventricular dysfunction on oxygen uptake recovery kinetics in repaired tetralogy of Fallot. *Eur J Heart Fail* 2006;8:736–743.
 117. Giardini A, Specchia S, Tacy TA, et al. Usefulness of cardiopulmonary exercise to predict long-term prognosis in adults with repaired tetralogy of Fallot. *Am J Cardiol* 2007;99:1462–1467.

118. Frigiola A, Tsang V, Bull C, et al. Biventricular response after pulmonary valve replacement for right ventricular outflow tract dysfunction: is age a predictor of outcome? *Circulation* 2008;118:S182-S190.
119. Sutton NJ, Peng L, Lock JE, et al. Effect of pulmonary artery angioplasty on exercise function after repair of tetralogy of Fallot. *Am Heart J* 2008;155:182-186.
120. Gatzoulis MA, Clark AL, Cullen S, et al. Right ventricular diastolic function 15 to 35 years after repair of tetralogy of Fallot. Restrictive physiology predicts superior exercise performance. *Circulation* 1995;91:1775-1781.
121. Gatzoulis MA, Elliott JT, Guru V, et al. Right and left ventricular systolic function late after repair of tetralogy of Fallot. *Am J Cardiol* 2000;86:1352-1357.
122. Gatzoulis MA, Balaji S, Webber SA, et al. Risk factors for arrhythmia and sudden cardiac death late after repair of tetralogy of Fallot: a multicentre study. *Lancet* 2000;356:975-981.
123. Steeds RP, Oakley D. Predicting late sudden death from ventricular arrhythmia in adults following surgical repair of tetralogy of Fallot. *QJM* 2004;97:7-13.
124. Ghai A, Silversides C, Harris L, et al. Left ventricular dysfunction is a risk factor for sudden cardiac death in adults late after repair of tetralogy of Fallot. *J Am Coll Cardiol* 2002;40:1675-1680.
125. Knauth AL, Gauvreau K, Powell AJ, et al. Ventricular size and function assessed by cardiac MRI predict major adverse clinical outcomes late after tetralogy of Fallot repair. *Heart* 2008;94:211-216.
126. Therrien J, Fredriksen P, Walker M, et al. A pilot study of exercise training in adult patients with repaired tetralogy of Fallot. *Can J Cardiol* 2003;19:685-689.
127. MacLellan-Tobert SG, Driscoll DJ, Mottram CD, et al. Exercise tolerance in patients with Ebstein's anomaly. *J Am Coll Cardiol* 1997;29:1615-1622.
128. Trojnarowska O, Szyszka A, Gwizdala A, et al. Adults with Ebstein's anomaly—cardiopulmonary exercise testing and BNP levels exercise capacity and BNP in adults with Ebstein's anomaly. *Int J Cardiol* 2006;111:92-97.
129. Roos-Hesselink JW, Meijboom FJ, Spitaels SE, et al. Decline in ventricular function and clinical condition after Mustard repair for transposition of the great arteries (a prospective study of 22-29 years). *Eur Heart J* 2004;25:1264-1270.
130. Norozi K, Buchhorn R, Alpers V, et al. Relation of systemic ventricular function quantified by myocardial performance index (Tei) to cardiopulmonary exercise capacity in adults after Mustard procedure for transposition of the great arteries. *Am J Cardiol* 2005;96:1721-1725.
131. Moons P, De Bleser L, Budts W, et al. Health status, functional abilities, and quality of life after the Mustard or Senning operation. *Ann Thorac Surg* 2004;77:1359-1365; discussion 1365.
132. Derrick GP, Narang I, White PA, et al. Failure of stroke volume augmentation during exercise and dobutamine stress is unrelated to load-independent indexes of right ventricular performance after the Mustard operation. *Circulation* 2000;102:III154-III159.
133. Paridon SM, Humes RA, Pinsky WW. The role of chronotropic impairment during exercise after the Mustard operation. *J Am Coll Cardiol* 1991;17:729-732.
134. Hovels-Gürich HH, Krämer NA, Schulze A, et al. The cardiologic status of youngsters and young adults after neonatal arterial switch operation with a simple transposition of big vessels. *Clin Res Cardiol* 2008;97:671.
135. Reybrouck T, Eyskens B, Mertens L, et al. Cardiorespiratory exercise function after the arterial switch operation for transposition of the great arteries. *Eur Heart J* 2001;22:1052-1059.
136. Mahle WT, McBride MG, Paridon SM. Exercise performance after the arterial switch operation for D-transposition of the great arteries. *Am J Cardiol* 2001;87:753-758.
137. Pasquali SK, Marino BS, McBride MG, et al. Coronary pattern and age impact exercise performance late after the arterial switch operation. *J Thorac Cardiovasc Surg* 2007;134:1207-1212.
138. de Koning WB, van Osch-Gevers M, Ten Harkel AD, et al. Follow-up outcomes 10 years after arterial switch operation for transposition of the great arteries: comparison of cardiologic health status and health-related quality of life to those of the a normal reference population. *Eur J Pediatr* 2008;167:995-1004.
139. Fredriksen PM, Pettersen E, Thaulow E. Declining aerobic capacity of patients with arterial and atrial switch procedures. *Pediatr Cardiol* 2009;30:166-171.
140. Giardini A, Khambadkone S, Rizzo N, et al. Determinants of exercise capacity after arterial switch operation for transposition of the great arteries. *Am J Cardiol* 2009;104:1007-1012.
141. Hauser M, Bengel FM, Kuhn A, et al. Myocardial blood flow and flow reserve after coronary reimplantation in patients after arterial switch and Ross operation. *Circulation* 2001;103:1875-1880.
142. Oskarsson G, Pesonen E, Munkhammar P, et al. Normal coronary flow reserve after arterial switch operation for transposition of the great arteries: an intracoronary Doppler guidewire study. *Circulation* 2002;106:1696-1702.
143. Cohen MS, Marino BS, McElhinney DB, et al. Neo-aortic root dilation and valve regurgitation up to 21 years after staged reconstruction for hypoplastic left heart syndrome. *J Am Coll Cardiol* 2003;42:533-540.
144. Murakami T, Takei K, Ueno M, et al. Aortic reservoir function after arterial switch operation in elementary school-aged children. *Circ J* 2008;72:1291-1295.
145. Bove T, De Meulder F, Vandenplas G, et al. Midterm assessment of the reconstructed arteries after the arterial switch operation. *Ann Thorac Surg* 2008;85:823-830.
146. Hirth A, Reybrouck T, Bjarnason-Wehrens B, et al. Recommendations for participation in competitive and leisure sports in patients with congenital heart disease: a consensus document. *Eur J Cardiovasc Prev Rehabil* 2006;13:293-299.
147. Ohuchi H, Hiraumi Y, Tasato H, et al. Comparison of the right and left ventricle as a systemic ventricle during exercise in patients with congenital heart disease. *Am Heart J* 1999;137:1185-1194.
148. Fredriksen PM, Chen A, Veldtman G, et al. Exercise capacity in adult patients with congenitally corrected transposition of the great arteries. *Heart* 2001;85:191-195.
149. Paridon SM, Mitchell PD, Blaufox A, et al. A cross-sectional study of exercise performance during the first two decades of life following the Fontan procedure. *J Am Coll Cardiol* 2008;52:99-107.
150. Anderson PA, Sleeper LA, Mahony L, et al. Contemporary outcomes after the Fontan procedure: a pediatric heart network multicenter study. *J Am Coll Cardiol* 2008;52:85-98.
151. Brassard P, Bedard E, Jobin L, et al. Exercise capacity and impact of exercise training in patients after a Fontan procedure: a review. *Can J Cardiol* 2006;22:489-495.
152. Whitehead K, Pekkan K, Kitajima H, et al. Non-linear power loss during exercise in single ventricle patients after the Fontan: insights from computational fluid dynamics. *Circulation* 2007;116:1-165-1-17.
153. McCall R, Humphrey R. Exercise training in a young adult late after a Fontan procedure to repair single ventricle physiology. *J Cardiopulm Rehabil* 2001;21:227-230.
154. Minamisawa S, Nakazawa M, Momma K, et al. Effect of aerobic training on exercise performance in patients after the Fontan operation. *Am J Cardiol* 2001;88:695-698.
155. Opocher F, Varnier M, Sanders SP, et al. Effects of aerobic exercise training in children after the Fontan operation. *Am J Cardiol* 2005;95:150-152.
156. Rhodes J, Curran TJ, Camil L, et al. Impact of cardiac rehabilitation on the exercise function of children with serious congenital heart disease. *Pediatrics* 2005;116:1339-1345.
157. Moalla W, Gauthier R, Maingourd Y, et al. Six-minute walking test to assess exercise tolerance and cardiorespiratory responses during training program in children with congenital heart disease. *Int J Sports Med* 2005;26:756-762.
158. Simonneau G, Robbins I, Beghetti M, et al. Updated clinical classification of pulmonary hypertension. *J Am Coll Cardiol* 2009;54:S43-S54.
159. Barst RJ, McGoon M, Torbicki A, et al. Diagnosis and differential assessment of pulmonary arterial hypertension. *J Am Coll Cardiol* 2004;43:S40-S47.
160. Galie N, Hoeper MM, Humbert M, et al. Guidelines for the diagnosis and treatment of pulmonary hypertension: The Task Force for the Diagnosis and Treatment of Pulmonary Hypertension of the European Society of Cardiology (ESC) and the European Respiratory Society (ERS), endorsed by the International Society of Heart and Lung Transplantation (ISHLT). *Eur Heart J* 2009;30:2493-2537.
161. Mereles D, Ehlken N, Kreuscher S, et al. Exercise and respiratory training improve exercise capacity and quality of life in patients with severe chronic pulmonary hypertension. *Circulation* 2006;114:1482-1489.
162. Martinez-Quintana E, Miranda-Calderin G, Ugarte-Lopetegui A, et al. Rehabilitation program in adult congenital heart disease patients with pulmonary hypertension. *Congenit Heart Dis* 2010;5:44-50.
163. Davis JA, McBride MG, Chrisant MR, et al. Longitudinal assessment of cardiovascular exercise performance after pediatric heart transplantation. *J Heart Lung Transplant* 2006;25:626-633.
164. Patel JN, Kavey RE, Pophal SG, et al. Improved exercise performance in pediatric heart transplant recipients after home exercise training. *Pediatr Transplant* 2008;12:336-340.
165. Dipchand AI, Manlhiot C, Russell JL, et al. Exercise capacity improves with time in pediatric heart transplant recipients. *J Heart Lung Transplant* 2009;28:S85-S90.
166. Haykowsky M, Eves N, Figgures L, et al. Effect of exercise training on VO₂peak and left ventricular systolic function in recent cardiac transplant recipients. *Am J Cardiol* 2005;95:1002-1004.
167. Richard R, Verdier JC, Duvallet A, et al. Chronotropic competence in endurance trained heart transplant recipients: heart rate is not a limiting factor for exercise capacity. *J Am Coll Cardiol* 1999;33:192-197.
168. Singh TP, Curran TJ, Rhodes J. Cardiac rehabilitation improves heart rate recovery following peak exercise in children with repaired congenital heart disease. *Pediatr Cardiol* 2007;28:276-279.
169. Braith RW, Schofield RS, Hill JA, et al. Exercise training attenuates progressive decline in brachial artery reactivity in heart transplant recipients. *J Heart Lung Transplant* 2008;27:S2-S9.
170. Olausson B, Urbult Y, Hansson S, et al. Transplanted children's experiences of daily living: children's narratives about their lives following transplantation. *Pediatr Transplant* 2006;10:S75-S85.
171. Ross M, Kouretas P, Gamberg P, et al. Ten- and 20-year survivors of pediatric orthotopic heart transplantation. *J Heart Lung Transplant* 2006;25:261-270.

172. Fricker FJ. Should physical activity and/or competitive sports be curtailed in pediatric heart transplant recipients? *Pediatr Transplant* 2002;6:267–269.
173. Thompson PD, Balady GJ, Chaitman BR, et al. Task force 6: coronary artery disease. *J Am Coll Cardiol* 2005;45:1348–1353.
174. Brothers J, Gaynor JW, Paridon S, et al. Anomalous aortic origin of a coronary artery with an interarterial course: understanding current management strategies in children and young adults. *Pediatr Cardiol* 2009;30:911–921.
175. Newberger JW, Takahashi M, Gerber MA. Diagnosis, treatment, and long-term management of Kawasaki disease: a statement for health professionals from the Committee on Rheumatic Fever, Endocarditis and Kawasaki Disease, Council on Cardiovascular Disease in the Young. *Circulation* 2004;110:2747–2771.
176. Kato H, Sugimura T, Akagi T. Long-term consequences of Kawasaki disease: a 10 to 21 year follow-up study of 594 patients. *Circulation* 1996;94:1379–1385.
177. Suda K, Iemura M, Nishiono H, et al. Long-term prognosis of patients with Kawasaki disease complicated by giant coronary aneurysms: a single-institution experience. *Circulation*, 2011;123:1836–1842.
178. Paridon SM, Galioto FM, Vincent JA, et al. Exercise capacity and incidence of myocardial perfusion defects after Kawasaki disease in children and adolescents. *J Am Coll Cardiol* 1995;25:1420–1424.
179. Rhodes J, Hijazi ZM, Marx GR, Fulton DR. Aerobic exercise function with persistent coronary artery aneurysms secondary to Kawasaki disease. *J Pediatr Cardiol* 1996;17:226–230.
180. Kolansky DM, Cuchel M, Clark BJ, et al. Longitudinal evaluation and assessment of cardiovascular disease in patients with homozygous familial hypercholesterolemia. *Am J Cardiol* 2008;102:1438–1443.
181. Rosenzweig A, Watkins H, Hwang DS, et al. Preclinical diagnosis of familial hypertrophic cardiomyopathy by genetic analysis of blood lymphocytes. *N Engl J Med* 1991;325:1753–1760.
182. Panza JA, Maron BJ. Relation of electrocardiographic abnormalities to evolving left ventricular hypertrophy in hypertrophic cardiomyopathy. *Am J Cardiol* 1989;63:1258–1265.
183. Ho CY, Sweitzer NK, McDonough B, et al. Assessment of diastolic function with Doppler tissue imaging to predict genotype in preclinical hypertrophic cardiomyopathy. *Circulation* 2002;105:2992–2997.
184. Maron BJ, McKenna WJ, Danielson GK, et al. American College of Cardiology/European Society of Cardiology clinical expert consensus document on hypertrophic cardiomyopathy: a report of the American College of Cardiology Foundation Task Force on Clinical Expert Consensus Documents and the European Society of Cardiology Committee for Practice Guidelines. *J Am Coll Cardiol* 2003;42:1687–1713.
185. Maron BJ. Hypertrophic cardiomyopathy: a systematic review. *JAMA* 2002;287:1308–1320.
186. Silber JH, Cnaan A, Clark BJ, et al. Enalapril to prevent cardiac function decline in long-term survivors of pediatric cancer exposed to anthracyclines. *J Clin Oncol* 2004;22:820–828.
187. Hogarty AN, Leahey A, Zhao H, et al. Longitudinal evaluation of cardiopulmonary performance during exercise after bone marrow transplantation in children. *J Pediatr* 2000;136:311–317.
188. Chin TK, Perloff JK, Williams RG, et al. Isolated noncompaction of left ventricular myocardium: a study of eight cases. *Circulation* 1990;82:507–513.
189. Ichida F, Hamamichi Y, Miyawaki T, et al. Clinical features of isolated noncompaction of the ventricular myocardium: long-term clinical course, hemodynamic properties, and genetic background. *J Am Coll Cardiol* 1999;34:233–240.
190. McBride MG, Binder TJ, Paridon SM. Safety and feasibility of inpatient exercise training in pediatric heart failure: a preliminary report. *J Cardipulm Rehabil Prev* 2007;27:219–222.
191. Ostchega Y, et al. Trends of elevated blood pressure among children and adolescents: data from the National Health and Nutrition Examination Survey 1988–2006. *Am J Hypertens* 2009;22:56–59.
192. McCrindle BW. Assessment and management of hypertension in children and adolescents. *Nat Rev Cardiol* 2010;7:155–163.
193. The National High Blood Pressure Education Program Working Group on High Blood Pressure in Children and Adolescents. The fourth report on the diagnosis, evaluation, and treatment of high blood pressure in children and adolescents. *Pediatrics* 2004;114:555–576.

The ability to perform work or to exercise is a basic function of life, and many disease states affect this ability. Children are, or ought to be, by nature, physically active whether in spontaneous school yard play or in any number of organized activities. Accurate and reproducible measurement of work performance or exercise capacity provides a means to quantify a dimension of disease severity and assess one aspect of quality of life; to assess the effects of treatment and training; and, in some instances, to identify previously unrecognized disease. Despite a proliferation of noninvasive measurement techniques, much of our knowledge of exercise physiology still comes from studies in adults. Thus, the field of pediatric work physiology has had to draw many conclusions by extrapolation from these studies, an inherently flawed approach that readers must bear in mind.

BASIC EXERCISE PHYSIOLOGY

Work, Energy, and Power

Exercise involves utilization of energy and its transformation into mechanical work. Because work equals force multiplied by distance, the unit for work is the newton-meter, or joule (J). There is a constant relationship between energy and work as described by the relationship one kilocalorie (kcal) being equal to 4.1868 joules (J). Power is work performed per unit time, expressed as joules/second, but commonly referred to as watt (W) ($1 \text{ W} = 1 \text{ J/s}$). Older nomenclature used the kilopond-meter (kpm), where one kilopond is the force acting on a 1 kg mass at the normal *G*-force (on earth), such that $1 \text{ W} = 6.12 \text{ kpm/min}$.

From the mechanical perspective, there are two types of exercise: isotonic (dynamic) and isometric (static). Isotonic exercise implies alternate rhythmic contraction and relaxation of muscles against resistance. Isometric exercise involves muscular contraction against a fixed resistance with little (if any) muscle shortening. Clinical exercise testing can be done using either isotonic or isometric exercise. Usually, however, clinical exercise testing is done using isotonic forms of exercise, such as cycling, walking, and running. From the energetics perspective, the chemical energy required to perform work can arise from aerobic or anaerobic sources. Use of oxygen is a major contributor to ATP synthesis in light to moderate exercise regardless of duration: so-called aerobic exercise. In contrast, short sprints, or heavy isotonic and isometric exercise, can be accomplished without oxygen, at least for brief periods. In anaerobic exercise, muscle energy is supported by the phosphocreatine (PCr)-ATP system followed by glycolysis, not through mitochondrial oxidative phosphorylation that requires oxygen consumption. However, in real life it is exceedingly unlikely that such a dichotomy exists when a child plays in fits, starts, and stops, which typically characterize

daily play. During incremental exercise, one can observe—and many have investigated—a level of work or intensity of exercise below which one allegedly accomplishes aerobically and above which one continues anaerobically, or at least anaerobic energy sources predominate. Many of these conclusions have been reached by gas-exchange analysis or measurement of blood lactate levels. More recent results employing near-infrared spectroscopy (NIRS) paint a different picture—one demonstrating an early, continuous, but complementary role of anaerobic metabolism to the primacy of aerobic metabolism during exercise. Because energy is necessary to perform work and requires combustion of oxygen, there is a predictable relationship between aerobic work and oxygen consumption or uptake ($\dot{V}\text{O}_2$) as shown in Figure 7.1. This approximates 10 mL O_2 per minute per watt in normal, healthy adults (1,2) but oxygen cost of work (mechanical efficiency) tends to be higher in children and is somewhat age dependent (3).

If one excludes so-called tests of anaerobic capacity such as Wingate, exercise testing strategies have evolved over the past century from classical steady-state procedures, incremental or otherwise, to non-steady-state procedures. The latter have largely supplanted the former, and increments can be discrete (e.g., 1 to 2 minutes each) or continuous, also known as ramp protocols. The difference between steady-state and non-steady-state exercise can best be understood by considering energy utilization at onset of exercise. If one were to immediately change from walking to running on a treadmill, or unloaded pedaling to 50 W on a cycle ergometer, work rises in an instant but $\dot{V}\text{O}_2$ does not rise nearly so quickly. This step-up in power requires adjustments to ventilation and cardiac output in order to meet the energy requirement to perform the additional work. Until the cardiopulmonary system adapts to this increment, the exercising muscles utilize anaerobic energy sources such as ATP and PCr replenished by rate-limiting glycolytic pathways. In doing so, the exercising muscles incur an O_2 debt, which is simply the area under the curve shown in Figure 7.2. Once the cardiopulmonary system has made the necessary transition in terms of ventilation and cardiac output, such that energy required to perform the additional work can be provided aerobically, exercise is considered steady state. The time course of the rise to steady state is described by a time constant (τ), and mathematically it can be shown that steady state is achieved over a time equal to approximately five to six time constants. The term exercise “kinetics” has been coined to describe this transition process. Time constants for heart rate (HR) and $\dot{V}\text{O}_2$, but not for cardiac output, have been reported in children and, in general, are shorter (smaller) compared to those in adults (4,5). The distinction becomes an important consideration should one attempt to apply certain physiologic principles, such as solving the Fick equation, to non-steady-state exercise measurements. In general, measurements such as cardiac output that employ solving the Fick equation, or measurement of physiologic dead space by the Bohr equation, should be based on measurements done

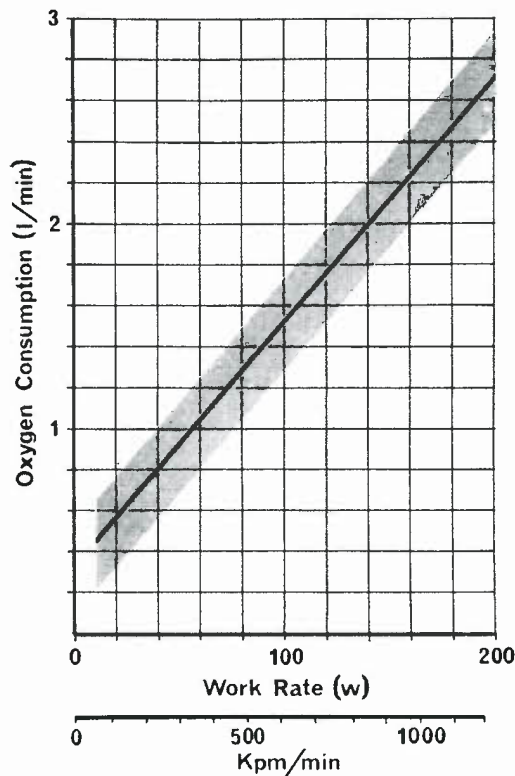


Figure 7.1. Diagrammatic illustration of the relationship between oxygen consumption and workload. (From Godfrey S. *Exercise Testing in Children*. London, UK: WB Saunders Co. Ltd., 1974, with permission).

during steady-state exercise. That does not necessarily mean that non-steady-state measures of such parameters are invalid but simply that they should be interpreted with caution. It has been amply demonstrated that many measurements made during non-steady-state, progressive exercise provide results or values very similar to those made during conventional, steady-state, tests. This is one reason, other than practicality,

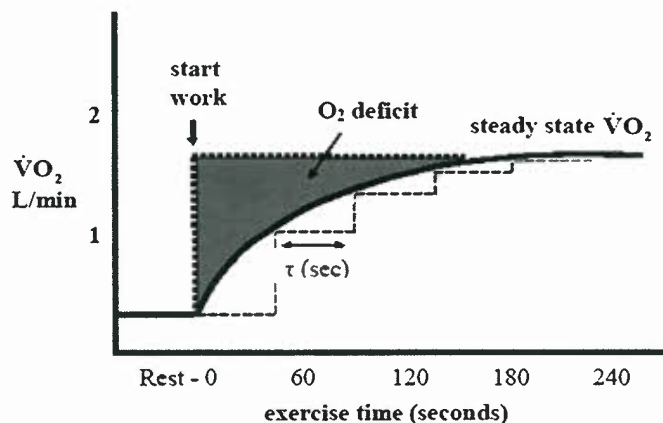


Figure 7.2. Schematic plot showing rest-work transition, plotting oxygen uptake versus time, in order to illustrate two concepts: (i) oxygen deficit, that is, $\dot{V}O_2$, which would be required if all metabolic requirement to perform work were met instantaneously by aerobic mechanisms, and (ii) time constant (τ , seconds), which is the time required to reach 50% of the plateau value. As a rule, the plateau is reached in the equivalent time of five to six time constants.

that non-steady state, incremental, or ramp exercise protocols largely have replaced the classical steady-state methods.

Exercise requires a complex and intricate interaction of multiple organ systems, and abnormalities in any of these organ systems will affect and potentially limit performance. The four principal systems involved in transferring oxygen from the atmosphere to the myocyte mitochondria—lungs, heart, blood, and muscle—are intimately linked in series and overall transport and utilization of oxygen depends on all components functioning optimally and in concert. When any one of these organ systems reaches maximal functional capacity, further exercise will be limited. An exercise test has the potential to reveal the limiting organ system by applying the engineering principle of stress testing, rather than providing a specific diagnosis in a patient presenting with exercise intolerance. A more fundamental approach is to ask whether oxygen supply (pulmonary/cardiovascular/blood transport), oxygen utilization (substrate availability, enzyme function) independent of oxygen supply, or converting chemical into mechanical energy (muscle efficiency) imposes the limiting factor for maximum work capacity. In health, the scale tips toward oxygen supply as the limiting step; thus, the circulatory system and specifically total oxygen transport capacity—product of cardiac output and O_2 carrying capacity ($\dot{Q}O_2$)—become the factor limiting performance. In a maximal exercise test to voluntary exhaustion, most healthy subjects cease exercise because of leg discomfort or fatigue, though some will complain of dyspnea, as the reason(s) for being unable to continue. This presumably reflects leg muscle fatigue, where O_2 demand exceeds O_2 supply to (or utilization by) muscle mitochondria.

Maximal-Aerobic Power

Many different indices can be used to describe fitness or maximal exercise capacity. The amount of work a person can perform could be used to define exercise capacity but maximum aerobic power or maximum oxygen uptake ($\dot{V}O_{2\max}$) achieved during exercise is probably the best index. $\dot{V}O_{2\max}$ is defined by a plateau in $\dot{V}O_2$ that occurs despite continued exercise, proof that work can be performed using anaerobic energy production, but the amount that can be performed anaerobically is limited. This concept evolved using discontinuous, quasi-steady-state, exercise protocols nearly a century ago. A plot of $\dot{V}O_2$ versus work will reach an asymptotic $\dot{V}O_2$ if and only if the subject is able and willing to continue exercise, making it crucial to ensure that a subject's effort is maximal in order to properly determine $\dot{V}O_{2\max}$. It is difficult to motivate untrained subjects and most children to exercise to that asymptotic $\dot{V}O_2$, as continuing becomes intolerable such that a plateau is seldom observed in children. Thus, the concept of $\dot{V}O_{2\max}$ has given way to the more practical " $\dot{V}O_{2\text{peak}}$ ". The terms $\dot{V}O_{2\text{peak}}$ or peak work capacity have been coined to refer to a symptom- or discomfort-limited clinical exercise test, also known as voluntary exhaustion. In practice, there is little or no difference between $\dot{V}O_{2\text{peak}}$ and $\dot{V}O_{2\max}$ (6,7).

Maximum cardiac output is closely correlated with maximum oxygen uptake, although this concept continues to be the subject of debate among exercise physiologists (8). Oxygen supply to the exercising muscle is determined by oxygen carrying capacity (a function of hemoglobin) and rate of transport from the cardiopulmonary source to its destination, that is, cardiac output. This can be expressed mathematically as the product of cardiac output and oxygen content of the blood, or $\dot{Q}O_2$. It follows that reductions in cardiac output (and hemoglobin level) will reduce $\dot{V}O_{2\max}$; conversely, experimentally increasing $\dot{Q}O_2$ will raise $\dot{V}O_{2\max}$ (9,10). Exercising larger (as opposed to smaller) muscle groups or more (vs. fewer) muscle

groups will result in higher $\dot{V}O_{2\max}$. Higher $\dot{V}O_{2\max}$ can be best achieved by treadmill exercise than by cycle exercise because more muscle groups are working when one performs treadmill exercise. The larger exercising muscle mass is an important determinant of many exercise parameters; for example, greater muscle mass involved in exercise also dictates the relative contribution of stroke volume (SV) and HR in determining cardiac output during exercise. Indeed, some measure of lean leg volume or muscle cross-sectional area is perhaps the single best predictor of $\dot{V}O_{2\max}$. There is some evidence that as children grow into adults, their leg volume increases in greater proportion to their body mass. Because body mass—or better still, lean leg mass—increases considerably during the period of growth and maturation, $\dot{V}O_{2\max}$ rises considerably when expressed in absolute terms (L/min), particularly in postpubertal males (Fig. 7.3A). If $\dot{V}O_{2\max}$ were related to lean body mass, there ought to be no difference between boys and girls in achievable values of $\dot{V}O_{2\max}$, at least not before puberty. On the other hand, $\dot{V}O_{2\max}$ normalized for weight ($mL/kg/min$) remains relatively constant in boys between ages 6 and 18 years, whereas in girls $\dot{V}O_{2\max}$ remains relatively constant between the ages of 6 and 13 years, but levels off or even declines slightly after puberty in girls (Fig. 7.3B).

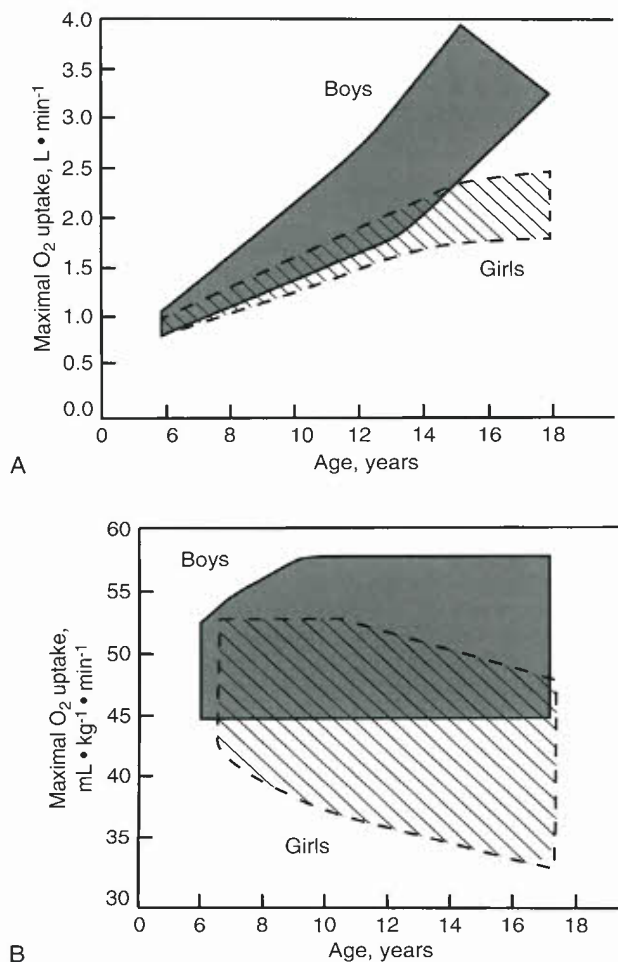


Figure 7.3. Part A illustrates a composite graph of $\dot{V}O_{2\max}$ in absolute terms versus age in children, whereas part B depicts the relationship with $\dot{V}O_{2\max}$ normalized for body mass. (From Bar-Or O, Rowland TW. *Pediatric Exercise Medicine—From Physiologic Principles to Health Care Application*. Champaign, IL: Human Kinetics, 2004, with permission).

This decline in girls probably represents the effect of increased body fat (or decreased lean body mass) coupled with the recently demonstrated trend in decreasing levels of daily physical activity in adolescent girls. Thus, in adolescence, it is fair to say that boys have a higher $\dot{V}O_{2\max}$ than girls, whether expressed in absolute or relative terms, but apart from this generalization the picture remains unclear. Prior to that age, $\dot{V}O_{2\max}$ of boys and girls differs little although even this conclusion depends on the center, exercise protocol, and methods.

There are two important caveats to any conclusion or statement about $\dot{V}O_{2\max}$ in pediatrics: one pertains to longitudinal versus cross-sectional study data, and the other concerns the method of scaling or normalization of the data (as noted above). Investigators have searched for the best method of indexing $\dot{V}O_2$ and considerable controversy persists as to the best method, if one indeed exists. Based on the dimensionality theory, an exponent of body length was proposed using an exponent from 1.5 to 3.21, and Astrand and Rodahl (11) suggested using length to the 2.9 power. Body weight (mass) expressed simply in kilograms has been criticized as a method for explaining growth-related changes because it led to spurious correlations, misinterpretation of data, and erroneous conclusions. Exponents for body mass or weight ranging from 0.7 to 1.0 have been reported (12,13). This is particularly relevant given our current obesity epidemic. In the final analysis, the most commonly accepted and simplest method of indexing $\dot{V}O_2$ in clinical exercise testing is to use body weight (kilograms), but with recognition of the limitations of this approach. Said limitations become particularly relevant to compilation of normal reference standards that are inevitably derived from large cross-sectional sampling of a pediatric population, usually without regard to stage of physical development and pubertal maturation. Longitudinal studies have clearly shown that there are differences in the change of $\dot{V}O_{2\max}$ over the age span 8 to 16 years. There are different individual trajectories for $\dot{V}O_{2\max}$ during these growth years, which depend not only on age, sex, height, and weight but also on training (14,15). In essence, the so-called normal range is merely a composite of individual single time-point data. Thus, if one studies the same individual repeatedly over his/her growth years, which is probably more meaningful in the clinical arena, one must bear in mind the pitfalls of applying normal population reference standards to an individual patient.

There appear to be minor racial differences in $\dot{V}O_{2\max}$, at least in North American studies. Several small studies have shown lower $\dot{V}O_{2\max}$ in African American children compared with Caucasian children. African American children have slightly smaller lung volumes than Caucasian children of similar standing height, and this alters ventilatory strategy during exercise slightly, but ventilation is not thought to limit exercise in health. One study concluded that slightly lower hemoglobin values and levels of habitual activity in African American children accounted for part of the lower $\dot{V}O_{2\max}$ observed (16).

Considerable attention has focused on the so-called anaerobic threshold as a surrogate measure of maximal aerobic power. Theoretically, it might allow assessment of exercise capacity using a submaximal exercise study, a potential advantage in children who have difficulty achieving a true $\dot{V}O_{2\max}$. The term anaerobic threshold has given way to the term ventilatory threshold (VT) in recent years, in recognition of the fact that this time point during incremental exercise does not reflect the "onset" of anaerobic metabolism as was once hypothesized (17). The ventilatory (anaerobic) threshold (VT or VAT) is defined as $\dot{V}O_2$ at which there is a disproportionate increase in minute ventilation (\dot{V}_E) relative to oxygen uptake. A rise in mixed expired O_2 concentration is observed at this point. There frequently is a disproportionate rise in lactate production at this point as well, hence

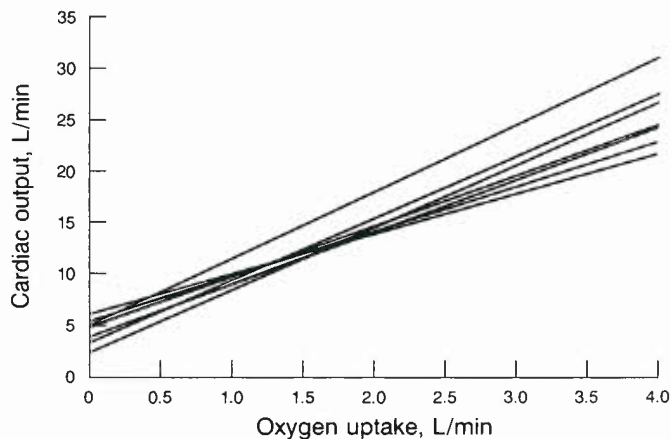


Figure 7.4. The relationship of cardiac output to oxygen uptake for normal persons. The various lines represent measurements from different laboratories using a variety of techniques for measuring cardiac output.

the term anaerobic threshold, but an increased lactate is not necessary for the disproportionate rise in \dot{V}_E to occur (18). Breath-by-breath measurement of ventilatory indices and brief incremental workloads are preferable for determining the anaerobic threshold. There are several methods of identifying this point, but the V-slope method is the most common and likely the most reliable in pediatrics (19). This point must also be distinguished from the second inflection or respiratory compensation point. At this juncture during incremental exercise, \dot{V}_E increases out of proportion to $\dot{V}CO_2$, such that $\dot{V}_E/\dot{V}CO_2$ also begins to rise, and end-tidal CO_2 partial pressure begins to fall. This change is attributed to the H^+ -mediated drive to breathe created by blood lactic acid accumulation that has outstripped buffering capacity. Reybrouck et al. (20) reported an inability to detect a VAT in 10% of children. In normal boys, they found a gradual decrease in VAT between ages 8 and 16 years. VAT was lower for girls than for boys. When expressed as a percentage of $\dot{V}O_{2max}$, VAT declined from approximately 65% in 8-year-old boys to approximately 55% in 16-year-old boys. It decreased from 62% in 8-year-old girls to approximately 55% in 16-year-old girls, similar to adult values. Apropos the earlier discussion pertaining to the concept of a “threshold” during an incremental exercise test, more recent studies indeed demonstrated (i) strong correlation between lactate (ventilatory) threshold during incremental cycle exercise and exaggerated reduction in muscle oxygenation measured by NIRS and (ii) muscle deoxygenation trends recorded during short-duration, high-intensity exercise indicate that substantial aerobic metabolism persists during such exercise (21).

CARDIAC RESPONSES TO EXERCISE

The importance of cardiac output and $\dot{Q}O_2$ as a determinant of exercise capacity has already been stated. Cardiac output (\dot{Q}) rises linearly with increasing $\dot{V}O_2$ (Fig. 7.4), the relationship described by

$$\dot{Q} = k\dot{V}O_2 + 4$$

where k averages somewhere between 5 and 7 (22). The intercept, 4, is obviously somewhat dependent on the size of the subject but is a good approximation for children within the

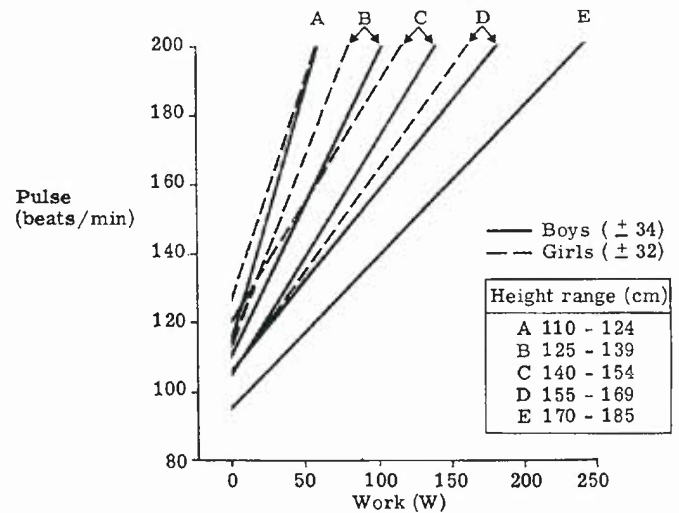


Figure 7.5. Heart rate versus work in children, illustrating sex and size (height) differences. (From Godfrey S. *Exercise Testing in Children*. London, UK: WB Saunders Co. Ltd., 1974, with permission).

“testable” age range (23). These relationships were obtained from steady-state exercise studies, but more recent work done during non-steady-state, progressive tests employing ramp or short-duration (e.g., 2 minute) step increments suggest this linearity may not be maintained. Stringer et al. (24) demonstrated a noticeable leveling or plateau in the $\dot{Q} - \dot{V}O_2$ relationship in four out of five subjects using invasive methods to measure \dot{Q} during ramp exercise to voluntary exhaustion Beck et al. (25) showed that 38% of 72 healthy adults demonstrated nonlinearity in their $\dot{Q} - \dot{V}O_2$ relationship during progressive exercise and that subjects with higher $\dot{V}O_{2max}$ tended to exhibit a leveling off \dot{Q} when plotted versus $\dot{V}O_2$. Rowland (26) recently demonstrated slight nonlinearity in the $\dot{Q} - \dot{V}O_2$ relationship in preadolescent boys during progressive, maximal exercise with 3-minute increments, but the departure was so slight that one could still parsimoniously estimate a linear trajectory. The discrepancy between steady-state and non-steady-state behavior of the $\dot{Q} - \dot{V}O_2$ function is likely the result of different time constants for \dot{Q} versus $\dot{V}O_2$. In other words, if one of these variables reaches steady state more quickly than the other, there will be increasing divergence from the steady-state relationship (5 to 7 L/min per L/min $\dot{V}O_2$), eventually creating a curved function when one is plotted against the other. Since time constants for HR and $\dot{V}O_2$ are faster in children than in adults, this non-linearity may not be so evident in children. However, the dearth of data on kinetics of \dot{Q} in children (and paucity of such data in adults) prevents one from drawing firm conclusions, and underscores deficits in our understanding the dynamics of non-steady-state exercise in children.

Cardiac output is the product of HR \times SV. Stroke volume is dependent on preload, afterload, and myocardial contractility. Clinically useful proxy measures for these could be end-diastolic volume (EDV), blood pressure, and shortening fraction or preferably ejection fraction (EF), respectively. End-systolic volume (ESV) is the difference between EDV and SV, and since $EF = 100(SV/EDV)$, the basic determinants of \dot{Q} are HR, EDV, and EF.

Heart Rate

For normal persons, increased HR during exercise is the major determinant of increased cardiac output. There is a more or less linear relationship between HR and work. The “more or less”

qualification is warranted because some children will show a lesser increment in HR with step changes in work at near-maximal exercise. Indeed, Godfrey et al. (23) have shown that a plot of HR versus logarithm $\dot{V}O_2$ yield a linear plot. It can be seen from Figure 7.5 that, in general, smaller children will have higher HR than larger children at any given work, and girls will have slightly higher HR than boys—particularly after puberty. Maximum heart rate (HR_{max}) that can be achieved is an important determinant of $\dot{V}O_{2max}$. For subjects between 5 and 20 years of age, HR_{max} is about 190 to 205 beats per minute (bpm). The HR_{max} for children younger than 5 years of age probably is similar, but it is difficult to motivate these young children to perform a truly maximal test. For subjects older than 20 years, HR_{max} is equal to $210 - 0.65 \times \text{age}$. The reasons for the decline of HR_{max} with age are unclear but may be related to fibrosis and scarring of the sinoatrial node. Maximum heart rate will vary slightly depending on the exercise protocol used and the type of exercise performed. For example, a slightly higher HR_{max} is obtained for treadmill than for cycle exercise.

Four typical HR patterns during progressive or incremental exercise are illustrated in Figure 7.6. The “normal” graph represents the HR response of a normal subject with an HR_{max} of 200 bpm and $\dot{V}O_{2max}$ of 2.5 L/min. While achieving predicted HR_{max} could be considered indicative of a maximum effort, very fit individuals can continue exercising while HR remains at its maximum value for 1 to 2 minutes. Obviously, this can occur only at the expense of extreme anaerobic energy production. The curve labeled “conditioned” illustrates the HR response if the subject improves his or her physical fitness. With improved fitness, resting HR declines, the so-called training bradycardia. Maximum heart rate does not increase, but it occurs at a higher $\dot{V}O_{2max}$. The curve labeled “deconditioned” illustrates the effect on HR response of deconditioning. Resting HR is higher than control, and HR_{max} occurs at a lower $\dot{V}O_{2max}$. The curve labeled “submaximal” could represent simply inadequate effort, but this curve also is typical of patients with chronotropic insufficiency, that is, low HR_{max} , which occurs in many patients with heart disease with or without prior cardiac surgery.

Stroke Volume

In contrast to the relative ease with which HR is measured, SV measurement has been a daunting challenge because of the invasive nature of methods available in the past. Therefore, our

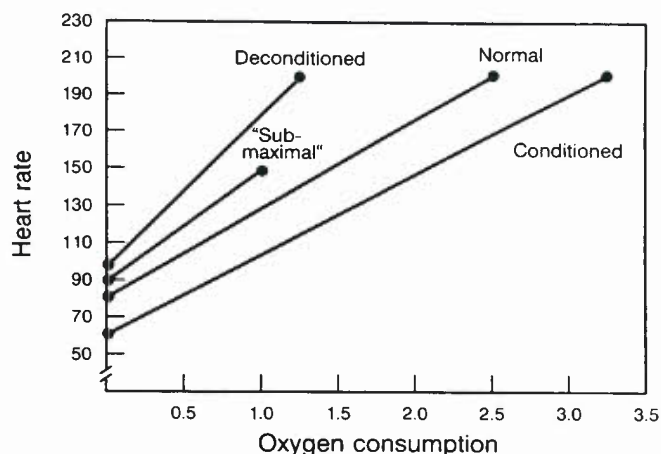
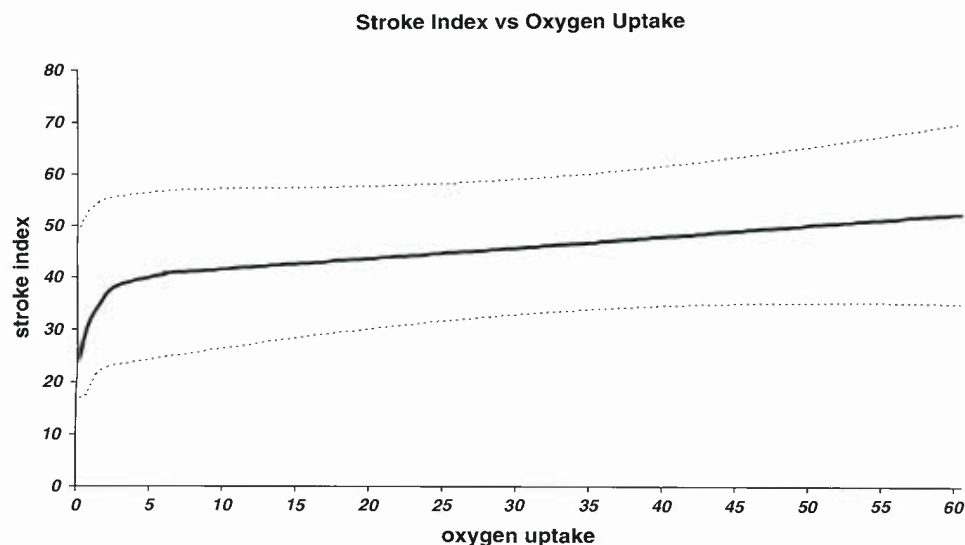


Figure 7.6. Diagrammatic representation of the relationship between heart rate response to exercise and oxygen consumption. Four different conditions are depicted.

understanding of the behavior of SV during exercise in children has largely been by extrapolation of work done in adults, or based on a limited number of small pediatric studies. Changes in SV during exercise depend to some extent on the position in which exercise is performed. SV approaches its maximum in the supine position, such that when exercise is performed supine there is limited rise in SV. The change in SV that occurs with upright exercise in children is illustrated in Figure 7.7. SV increases primarily early in exercise and increases little thereafter. Thus, the change in cardiac output effected by change in SV occurs early in exercise, and additional changes of cardiac output depend predominantly on the HR.

Parsing the circulatory adaptations to cardiac performance during exercise, one can see that EDV and EF must increase as well in order to explain the rise in SV and fall in ESV. The limits of SV augmentation will be reached when the rapidly increasing HR limits ventricular filling during diastole. Since most ventricular filling occurs in early diastole, left ventricular relaxation and compliance become important variables in the EDV response to exercise. As mentioned in the section above, some children will show a lesser increment in HR with step changes in work at near-maximal exercise. Unless one achieves a plateau for $\dot{V}O_2$, it follows that cardiac output is still rising,

Figure 7.7. Normal range of SV in healthy children plotted against oxygen uptake, with 95% confidence interval. (From Pianosi PT, unpublished data).



which implies that SV must continually increase even near maximal exercise. As simple as this logic appears, demonstrating this has been a challenge, and was the topic of a recent debate in the physiology literature (27). In adults, conventional wisdom states that on average, SV levels off beyond 30% to 40% of $\dot{V}O_2$ max, and most studies (nearly all done in adults) indicate that SV falls at or near maximal exercise except in highly trained individuals in whom it may still rise slightly. Rowland et al. (28) reached similar conclusions in boys. In contrast, Eriksson et al. (29), in one of the few invasive studies of upright cardiac output in children, noted that six of eight subjects achieved their largest SV at maximal exercise. There is a decline in ventricular diastolic compliance with age that is not evident in childhood, but over several decades the ventricles become less compliant and active relaxation becomes impaired. It should therefore come as no surprise that healthy children ought to, in fact, be able to continuously increase SV during progressive exercise, presumably because the younger myocardium has better relaxation kinetics and compliance. Although this supposition remains to be proven, recent work suggests a steady but gradual rise in SV in children during progressive exercise (30).

Another approach to this question is to examine a surrogate measure for SV that can be determined from simple, noninvasive measurements. Rearranging the Fick equation:

$$SV \cdot HR = \frac{\dot{V}O_2}{C_aO_2 - C_vO_2}$$

one obtains:

$$SV \cdot (C_aO_2 - C_vO_2) = \frac{\dot{V}O_2}{HR}$$

The right side of the equation is termed the oxygen pulse, and gives some idea of SV if one assumes a value for arteriovenous O_2 content difference. There is good evidence from adult studies that $C_aO_2 - C_vO_2$ rises linearly with increasing work (24,31). HR and $\dot{V}O_2$ obviously can be measured fairly easily during exercise with modern metabolic carts, and the quotient $\dot{V}O_2/HR$ is known as the oxygen-pulse (mL/beat). While this approach may have some validity in healthy adults, including those with heart failure, there are too many underlying assumptions that render it unwise to extrapolate this approach to pediatric subjects. Moreover, there is a similar dearth of published normal values for oxygen pulse in children (32), an area ripe for future research.

Blood Pressure

During isotonic exercise, systolic blood pressure increases whereas diastolic blood pressure changes little, though, on average, may vary within 10 mm Hg from resting level. Larger children have a higher blood pressure at submaximal and maximal exercise than smaller children (Fig. 7.8). Among similar-sized children, boys have higher peak systolic blood pressure than girls. African American children have a greater blood

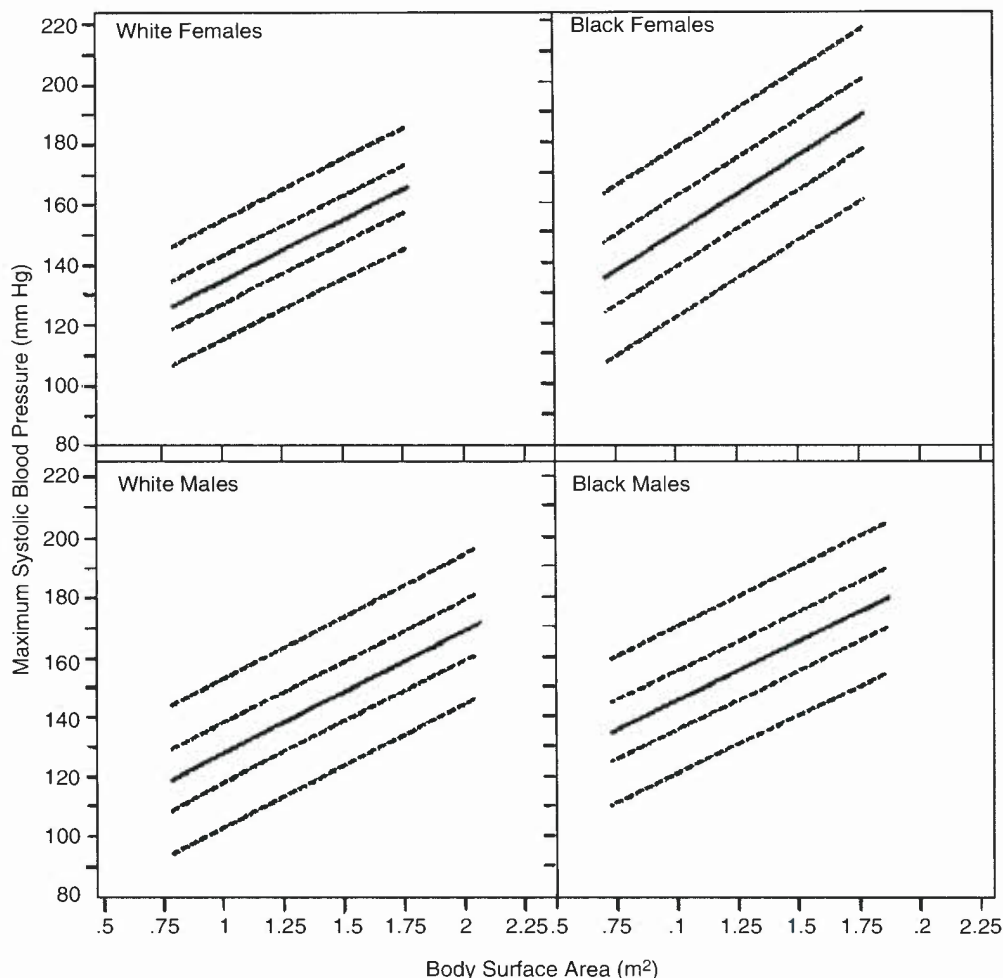


Figure 7.8. Nomograms for systolic blood pressure at peak exercise in children according to race and sex. Solid lines represent 50th percentiles, and dashed lines represent (top to bottom) 95th, 75th, 25th, and 5th, percentiles, respectively. (From Alpert BS, Flood NL, Strong WB, et al. Responses to ergometer exercise in a healthy biracial population of children. *J Pediatr* 1982;101:538–545. Copyright Mosby-Year Book, Inc. Reprinted with permission.)

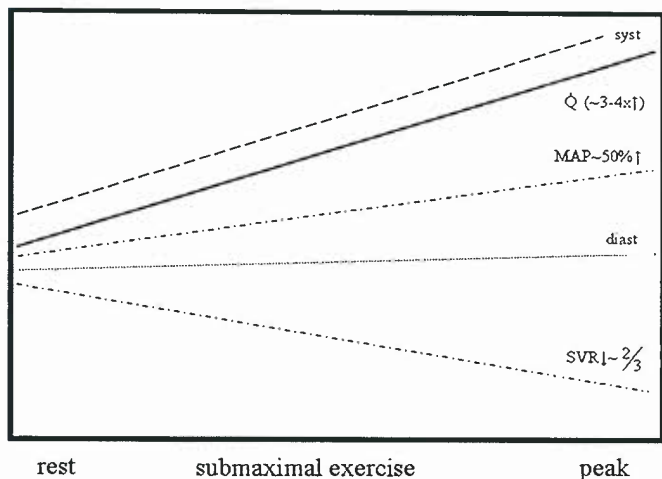


Figure 7.9. Composite Schematic illustration of changes in cardiovascular parameters (systolic and diastolic BP, cardiac output [\dot{Q}], mean arterial pressure and systemic vascular resistance) during exercise in children. Magnitude of each relative change shown gathered and derived from different published sources of normative pediatric exercise data.

pressure response to exercise than white children (33). Mean arterial pressure (MAP) increases during isotonic exercise are due to increased cardiac output and higher systolic pressure, despite a rather marked reduction in total systemic resistance ($SVR = MAP/\dot{Q}$) as shown in Figure 7.9. In contradistinction to this pattern, blood pressure response to isometric exercise is quite different from that during isotonic exercise. With isometric exercise, both systolic and diastolic pressure will increase. Indeed, with power weight lifting, systolic blood pressure may reach 400 mm Hg.

Regulation of Circulation during Exercise

It is important to appreciate the dynamics of this process, that is, the mechanisms leading to the rise in HR, SV, and BP, with exercise as this provides insights into the regulation of circulation. Many physiologic systems involving bulk flow (blood, air) have models in basic physics such as electrical analogues, for example, voltage = current \times resistance. An electrical circuit is characterized by a capacitance or an inductance, and inductance can be in phase or out of phase. Inductance is defined as the property of a circuit to oppose any change in current, and when a circuit has an inductive component, current lags voltage. Capacitance is the property of a circuit to oppose any change in voltage, and current leads voltage in a capacitance circuit. The circulatory equivalents are obviously pressure (voltage) and flow (current). Conceptualizing the cardiovascular system as a capacitance circuit is a useful paradigm. During exercise, the heart must pump more per beat, into a systemic circulation under higher pressure, and in turn receives more blood return from the exercising limbs via the muscle pump phenomenon. Blood pressure rises in response to this increased flow through the circuit but there are concomitant changes in distribution of this increased cardiac output to other vascular beds geared to maintain central blood volume and perfusion through exercising muscles. In order for this process to accommodate the requirements of dynamic exercise of increasing intensity, total peripheral vascular resistance must fall significantly. Whether pressure leads flow or lags flow in the cardiovascular system is a subject of intense interest to physiologists because it cuts to the heart of control of circulation during exercise.

An interesting model to study this paradigm is postural orthostatic tachycardia syndrome (POTS) or adolescent autonomic dysfunction as it is called in pediatric circles (35). POTS comprises a constellation of symptoms and affected individuals represent a heterogeneous population who share certain abnormalities in the regulation of circulation. One hypothesis argues that after some initiating event, deconditioning plays a major pathophysiologic role (35). Functionally, a conceptual model with three groups: “low-flow,” “normal-flow,” and “high-flow” patients with POTS has been developed (36), and our experience at Mayo clinic lends some early support to this concept (37). Patients with low-flow POTS demonstrate low blood flow and high arterial resistance, attributed to abnormalities in local blood-flow regulation and mild hypovolemia. In contrast, normal-flow POTS patients exhibit normal flow and systemic resistance in supine position, and manifest increased peripheral resistance after standing. This is thought to result from splanchnic pooling and distributive hypovolemia. High-flow POTS patients display low arterial resistance and high blood flow with increased cardiac output, possibly attributable to a hyperadrenergic state or long-tract autonomic neuropathy. One of the most consistent findings in patients with POTS is the presence of relative low blood volume, which can result in decreased venous return (preload). In response to this, normal physiologic responses generate tachycardia, to provide a compensatory increase in cardiac output. The symptoms and pathology of POTS are consistent with relative central hypovolemia, in which systemic volume may be normal but a state of intrathoracic hypovolemia exists (38). Many of these signs and symptoms can result from prolonged bed rest or following spaceflight—conditions that cause deconditioning. A recent study found that many of these pathophysiologic changes improved after a period of aerobic training (39).

The electrical analogue described above may prove useful in understanding the pathophysiology of this syndrome, that is, whether the cardiovascular system behaves as a capacitance or inductance circuit. Examination of Figure 7.9 gives one some idea of how alterations in one parameter, for example, hyperdynamic circulation with changes in cardiac output exceeding those predicted from the normal $\dot{Q} - \dot{V}O_2$ relationship, might compensate for low MAP in a patient with POTS whose systolic pressure barely nudges above resting levels. In this scenario, the circulatory system acts like a capacitance circuit in as much as current (cardiac output) leads voltage (pressure). In contrast, the circulatory system of low- and normal-flow POTS patients appears to behave more like an inductance circuit, where current (flow) lags voltage (pressure). Nonessential (from the point of view of meeting exercise needs) circulatory beds such as the gut act as large inductance coils, sapping the current (blood flow) during upright exercise. Such modeling may answer the “how” but not necessarily the “why” POTS patients respond to exercise as they do.

Fitness

Improved fitness occurs with repetitive exercise—the “training effect”. From a strict physiologic standpoint, improved fitness implies an increase in $\dot{V}O_{2\max}$. Many studies in adults have demonstrated increases in $\dot{V}O_{2\max}$ as a result of a conditioning or fitness program. In children, it has been more difficult to demonstrate this effect, probably because “normal” children simply are more fit than “normal” adults to begin with; hence, it is more difficult to demonstrate a change in fitness in normal children. However, a recent longitudinal study in athletic children demonstrated that the type of physical activity did indeed affect the change in $\dot{V}O_{2\max}$ during childhood (14). The importance of this observation may become more relevant in

TABLE 7.1

Physiologic Changes Associated with Trained or Conditioned State

Cardiovascular		Ventilatory		Cellular (Muscle)	
Heart volume	↑	Maximal minute volume	↑	Glycogen stores	↑
LV dimension	↑	Ventilatory equivalents	N or ↓	Oxidative enzymes succinyl dehydrogenase, cytochrome C oxidase, acyl CoA synthetase	↑
		Submaximal or maximal			
LV thickness	↑			Mitochondria—number ^a	↑
Ventricular filling	↑			Mitochondria—volume ^a	↑
Stroke volume	↑			Myoglobin content ^a	↑
Submaximal HR	↓				
Maximal HR	↓				

^aDemonstrated only in adults, not in children.

N = No Change.

Adapted from Bar-Or O, Rowland TW. *Pediatric Exercise Medicine*. Champaign, IL: Human Kinetics, 2004.

this era of increasing childhood obesity and decreasing fitness levels in today's youth.

As demonstrated in Figure 7.6, resting HR decreases with improved fitness, and HR_{max} occurs at a higher $\dot{V}O_{2max}$. It is apparent from this figure that submaximal HR is lower at any $\dot{V}O_2$ in the fit person compared with that in the unfit person. These adjustments of HR occur because of the increase in SV that occurs with conditioning. Also, changes in the parasympathetic and sympathetic regulation of HR probably play an important role, with a relatively greater parasympathetic (vagal) influence on HR in the fit person. Changes in fitness or conditioning are not limited to changes in function of the cardiovascular system. The ventilatory changes listed are not the result of changes in resting lung function but are due to improved oxygen delivery and utilization, which thereby reduce ventilatory requirements in heavy exercise. Important changes also occur in subcellular changes in muscle and indeed, it is these changes that can contribute more to improved fitness with training. These are listed in the Table 7.1. Fitness can be improved with regular episodes of sustained exercise. Conversely, deconditioning occurs if regular exercise is not done. Because children with heart disease may be sedentary, some component of reduced aerobic capacity in these patients may result from deconditioning.

VENTILATORY RESPONSE TO EXERCISE

Ventilation increases because of increases in both tidal volume (V_T) and breathing frequency (Fig. 7.10). Similar to HR, submaximal respiratory rates (RR) are higher in younger children at any given work rate. As children grow, the respiratory rate at peak exercise declines, particularly above age 12 to 13 years. Younger children will typically achieve a peak RR of 60 breaths per minute, whereas older children will generally achieve RR of 50 breaths per minute in early adolescence to 40 breaths per minute in late adolescence, at maximal exercise. In part this is due to the obligate dead space ventilation, but is largely due to the relatively larger increase in

vital capacity with growth allowing more room for V_T recruitment. Tidal volume, in general, does not level off with increasing exercise intensity, though some individuals with marked hyperventilation at maximal exercise actually will sacrifice V_T for higher breathing frequency. V_T increases commensurate

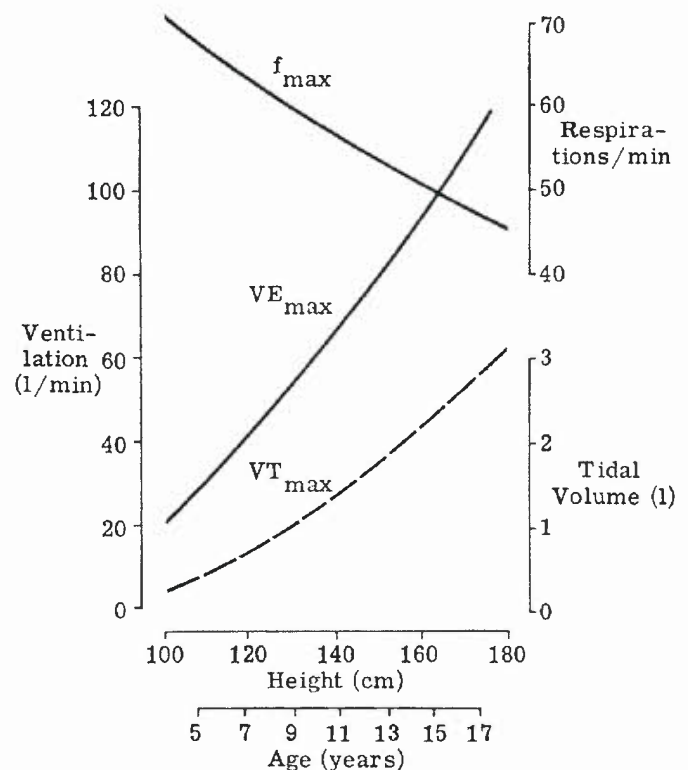


Figure 7.10. Relationships between ventilatory variables at maximum exercise in healthy children of varying age and height. (From Godfrey S. *Exercise Testing in Children*. London, UK: WB Saunders Co. Ltd., 1974, with permission).

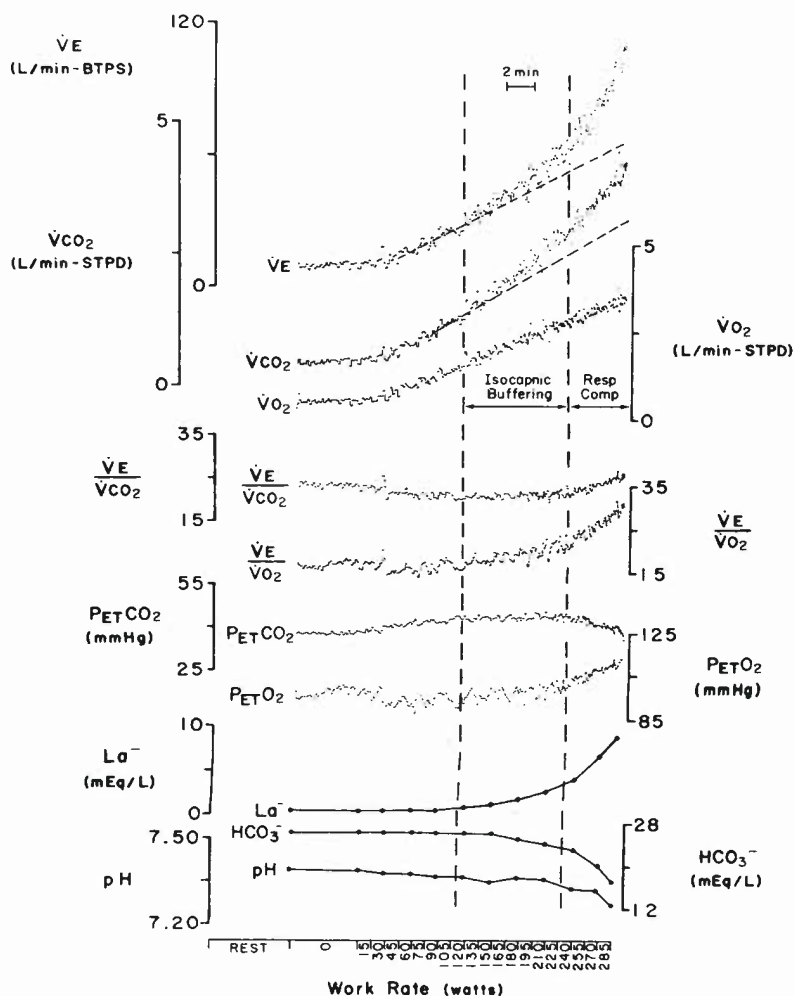
with growth of vital capacity during childhood and adolescence but at maximal exercise V_T reaches a level at least 40% and as much as 60% of vital capacity regardless of age. This is accomplished by encroaching somewhat on the expiratory reserve volume but predominantly by tapping into the larger inspiratory reserve volume. This strategy has important implications in determining the cause(s) of exertional dyspnea.

The relationship between ventilation and work is linear until (VAT) is attained. Ventilation most closely tracks carbon dioxide output ($\dot{V}CO_2$) during exercise and the ventilatory response to progressive exercise can be characterized as $\Delta\dot{V}_E/\Delta\dot{V}CO_2$. This slope falls slightly with age and growth during childhood (40). The ventilatory equivalent for CO_2 ($\dot{V}_E/\dot{V}CO_2$) dictates the volume of air breathed relative to the volume of CO_2 produced. By analogy, the ventilatory equivalent for O_2 ($\dot{V}_E/\dot{V}O_2$) describes the volume of air breathed relative to the volume of O_2 consumed. These parameters traditionally have been measured during steady-state exercise. $\dot{V}_E/\dot{V}O_2$ declines early in exercise as a result of better ventilation and blood flow matching in the lungs as pulmonary blood flow increases and flow redistributes to the apices of the lungs. The point during exercise when $\dot{V}_E/\dot{V}O_2$ begins to increase describes the VAT. The gas exchange ratio (R value) is the quotient $\dot{V}CO_2/\dot{V}O_2$. Normally it is measured during steady-state conditions and reflects the mixture of energy sources consumed at rest or exercise; as such, it becomes a measure of the cellular respiratory quotient (RQ). Children consuming a ketogenic (high fat) diet will have an R near 0.7, but the typical resting value is usually

approximately 0.8, again reflecting the carbohydrate and fat mix of a child's average daily food consumption. During incremental exercise both $\dot{V}O_2$ and $\dot{V}CO_2$ creep upward with increasing work, but $\dot{V}CO_2$ does so at a slightly faster rate than $\dot{V}O_2$. This gradual rise in $\dot{V}CO_2$ relative to $\dot{V}O_2$ means that R value approaches unity as power rises. Beyond this point $\dot{V}CO_2$ then rises disproportionately to $\dot{V}O_2$ as exercise continues above the VAT. Exercise hyperpnea that was linearly related to $\dot{V}CO_2$ maintains its tight coupling for a variable period even after the point when $\dot{V}_E/\dot{V}O_2$ begins to increase (VAT) (Fig. 7.11). In other words, at VAT the slope of $\dot{V}_E/\dot{V}O_2$ increases, but the slope of $\dot{V}_E/\dot{V}CO_2$ does not, until increasing work results in acidosis. At this point \dot{V}_E increases disproportionately to $\dot{V}CO_2$, resulting in a rise in $\dot{V}_E/\dot{V}CO_2$. As power inches further toward maximum and \dot{V}_E outpaces metabolic requirement ($\dot{V}CO_2$), an inflection point in $\dot{V}_E/\dot{V}CO_2$ occurs. This constitutes the respiratory compensation point, and is characterized by hyperventilation with reduction of arterial PCO_2 , generally reaching the low thirties (mm Hg)—lower in younger children compared with adolescents (41).

When exercise ceases at the point of voluntary exhaustion, \dot{V}_E is typically 60% to 70% of maximum voluntary ventilation (MVV), leaving a "ventilatory reserve" of roughly 30% to 40%. Persons with pulmonary disease who encroach on this breathing reserve achieve maximal \dot{V}_E exceeding 70%, and sometimes 100%, of MVV. How is this possible? Caution must be used in assessing the relationship between \dot{V}_E during exercise and MVV measured at rest because obtaining a

Figure 7.11. Changes in ventilatory indices, serum lactate, bicarbonate, and pH with increasing work. The vertical lines represent the onset of the VAT (left line) and the threshold for decompensated acidosis (right line). (From Wasserman K, Hansen J, Sue D, et al. *Principles of Exercise Testing and Interpretation*. Philadelphia, PA: Lea & Febiger, 1987.)



true measure of rest MVV depends greatly on subject effort. If the subject does not make a good effort, a factitiously low MVV will be recorded, and the relationship with \dot{V}_E during exercise will be misleading. A true MVV should approximate 1-second forced expiratory volume (FEV_1) \times 35 or 40. This long-held index has other limitations, principally because the operating lung volume of the resting MVV maneuver differs from the actual operating lung volume during exercise. A better way to determine whether exercise is limited by ventilation is by measurement of tidal flow-volume loops during exercise (42), which may have the added advantage of detecting vocal cord dysfunction, an increasingly recognized cause of exertional dyspnea. This is depicted in Figure 7.12, and has recently been studied in normal children (43,44). In a manner analogous to SV, V_T normally increases both by breathing at a lower end-expiratory lung volume (equivalent to LV-ESV) and attaining a higher end-inspiratory lung volume (higher LV-EDV). A small contribution comes from the expiratory reserve volume whereas the lion's share of V_T recruitment occurs by tapping into inspiratory reserve volume.

Diffusion limitation is seldom, if ever, a problem during routine clinical exercise testing. It may become a factor at extremes of exercise in high-performance athletes, as transit

time through the pulmonary capillaries may be short enough (very high levels of cardiac output) to preclude equilibration of alveolar and end-capillary PO_2 . Such an individual might even experience arterial desaturation if she/he had an intrinsically low hypoxic ventilatory response (45). Normal, healthy children should not exhibit desaturation even at maximal exercise but this area has not been studied specifically in children with the exception of one report (46). These authors concluded (with a few caveats) that exertional desaturation can occur in 25% to 33% of physically active children with normal (vs. supranormal) $\dot{V}O_{2\max}$ values. Given the technical difficulties in precise determination of oxygen saturation by pulse oximetry during exercise, healthy skepticism seems warranted.

METHODOLOGY OF EXERCISE TESTING

Types of Exercise and Ergometers

Treadmill and stationary cycles are the two most frequently used ergometers for clinical exercise testing. Neither is inherently superior to the other; each has advantages and disadvantages. Most people can walk reasonably efficiently, but not everyone can cycle efficiently. Children younger than 4 or 5 years of age may have more difficulty using a cycle ergometer than a treadmill. On the other hand, a treadmill may be more dangerous than a cycle because the subject can fall from the treadmill. Also, it is more difficult to hear the Korotkoff sounds when the subject is running or jogging on a treadmill than when he or she is cycling. If the subject is connected to numerous monitoring devices, cycling may be preferable because it involves less movement of the trunk and extremities. In general, it is easier to calibrate a treadmill than a cycle ergometer.

The two general types of cycle ergometers are the mechanically braked and electronically braked. With a mechanically braked cycle ergometer, power changes with changes of pedaling frequency. With an electronically braked cycle ergometer, moderate changes in pedaling frequency do not affect power substantially. Thus, for untrained subjects, who may have difficulty maintaining a steady pedaling frequency, electronically braked cycles are preferable. Other, less frequently used ergometers are handgrip ergometers and arm crank ergometers. The arm-crank ergometer is useful for subjects who are unable to walk or cycle or for whom physiologic measurement of upper extremity function is of interest.

Exercise Protocols

There is no "best" exercise protocol. Examiners should select or create a protocol that best allows measurement of the responses to exercise that are of particular interest. One may use a protocol that has been standardized in another laboratory. Ideally, protocols should be standardized and data obtained for a "normal" population in the laboratory in which the clinical exercise testing is done. Power increments should not be excessive; otherwise, some subjects may stop exercise before a maximum cardiorespiratory effort has been achieved. Power increments too small result in unnecessarily long tests, which can be a challenge in a child with short attention span. In general, exercise protocols should be designed such that the duration of the exercise test is 8 to 12 minutes, since children become disinterested with longer tests and effort wanes. The Three well-standardized protocols for treadmill exercise are detailed in Tables 7.2 to 7.4.

The Bruce protocol is arguably the most commonly employed in children. For children and subjects incapable of much exercise, a modified Bruce protocol can be used in

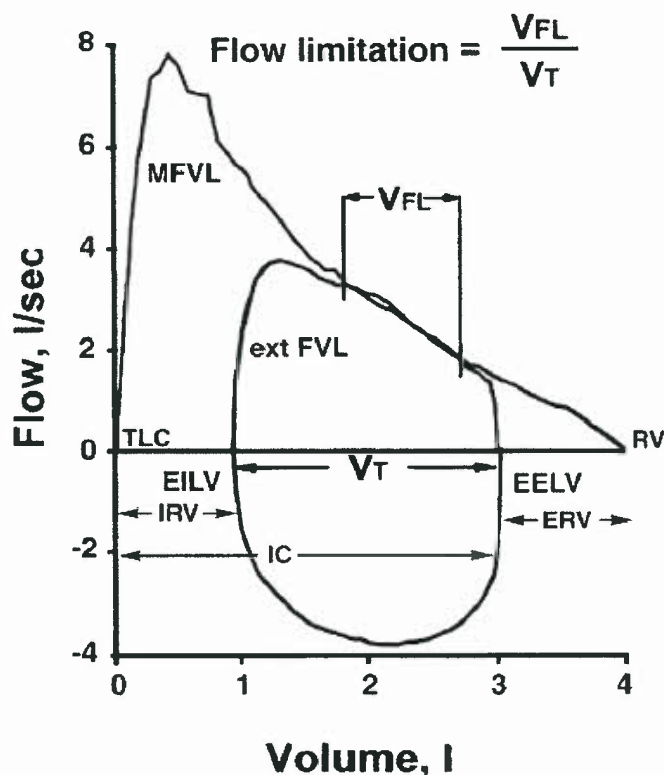


Figure 7.12. New method to assess ventilatory limitation to exercise. Exercise tidal flow volume loops (ext FVL) are superimposed within the maximal flow volume loop (MFVL) determined at rest, and any overlap is considered evidence of flow limitation (V_{FL}). EELV and EILV are end-expiratory and end-inspiratory lung volumes, respectively; while IRV and ERV are inspiratory and expiratory reserve volumes, respectively. Lung volume is plotted on the abscissa with total lung capacity (TLC) at the origin, while flow is on the ordinate, with expiration above the volume axis and inspiration below. (From Johnson BD, Weisman IM, Zeballos RJ, et al. Emerging concepts in the evaluation of ventilatory limitation during exercise: the exercise tidal flow-volume loop. *Chest* 1999;116:488–503. Reprinted with permission from the American College of Chest Physicians.)

TABLE 7.2 Bruce Treadmill Protocol

Stage ^a	Belt Speed (mph)	Incline (%Grade)	METs ^b
(Modified Bruce)	1.7	0	2.3
(Modified Bruce)	1.7	5	3.5
1	1.7	10	4.5
2	2.5	12	7.0
3	3.4	14	10.0
4	4.2	16	12.9
5	5.0	18	15.0
6	5.5	20	16.9
7	6.0	22	19.1

^a3-minute stages.^bMETs are multiples of resting O₂ uptake. One MET equals an O₂ uptake of 3.5 mL/kg/min.From Bruce R. Exercise testing in coronary artery disease. *Ann Clin Res* 1971;3:323–332, with permission.

which the initial two steps use a belt speed of 1.7 mph and an incline of 0% and 5%, respectively (47). For cycle testing, the James (48) protocol is useful because the 3-minute duration of each work increment make it very likely that steady state is achieved at each load. On the other hand, the large jump in power (50 W for child with body surface area (BSA) more than 1.2 m²) results in some smaller children being unable to persevere despite not having achieved their true maximum work capacity or aerobic power. Ramp protocols may come to be used more and more frequently as investigators acquire the equipment to perform this type of study. The ramp protocol uses a constantly increasing workload where the increment, regardless of magnitude, occurs as a gradual and continuous procedure instead of a step each minute. Obviously, this protocol is not suited for assessing physiologic functions that require steady-state exercise. A good compromise is the standard

TABLE 7.3 Balke Treadmill Protocol

Stage ^a	Belt Speed (mph)	Incline (%Grade)
1	3.3	0
2	3.3	2
3	3.3	3
4	3.3	4
5	3.3	5
6	3.3	6
7	3.3	7
Etc.	Etc.	Etc.

^a1-minute stages.From Balke J, Ware R. An experimental study of "physical fitness" of Air Force personnel. *U.S. Armed Forces Med J* 1959;10:675–688.**TABLE 7.4 James Cycle Protocol**

Stage ^a	kpm/min		
	<1 m ² BSA	1–1.19 m ² BSA	>1.2 m ² BSA
1	200	200	200
2	300	400	500
3	500	600	800
4	600	700	1000
5	700	800	1200
6	800	900	1400
7	900	1000	1600
8	1000	1100	1800

^a3-minute stages.

BSA body surface area.

From James FW, Kaplan S, Glueck CJ, et al. Responses of normal children and young adults to controlled bicycle exercise. *Circulation* 1980;61:902–12, with permission.

incremental cycle ergometer protocol with increments in work every 1 or 2 minutes, with the size of the increments tailored to the anticipated maximum capacity for each subject, such that test duration is 8 to 12 minutes. This will also provide enough data points to plot and analyze physiologic parameters with confidence.

TECHNIQUES OF SPECIFIC MEASUREMENTS

Heart Rate and Electrocardiogram

HR, one of the basic indices of cardiac response to exercise, is measured from the electrocardiogram (ECG), which can be done manually by averaging several R-R intervals. Alternatively, the ECG signal can be processed through a tachometer, and a direct recording of HR based on one or more R-R intervals can be obtained. At least three leads of the standard surface ECG should be displayed or recorded continuously during, and for 5 to 10 minutes after completion of, an exercise test. The examiner should have the option of viewing various combinations of leads so that inferior, right, and left precordial cardiac events can be assessed. A complete ECG should be recorded at rest, at least once during each workload, and for several intervals after exercise. Ideally, the ECG should have several recording speeds. Obtaining an ECG at a speed of 50 mm/sec facilitates assessment of ST segment changes. Continuous recording of the ECG at 5 mm per second paper speed facilitates detection of arrhythmias.

Appropriate application of the ECG electrodes and leads and electric shielding of the cable connecting the leads to the electrocardiograph are important for obtaining high-quality, artifact-free recordings. The subject's skin should be cleansed with alcohol and abraded lightly to reduce electric skin resistance. Most commercially available electrodes are prepackaged with electrode paste; occasionally, however, no paste is present, and these electrodes must be discarded or paste applied before using them. Note that pregelled electrodes have a limited shelf life due to chemical changes in the conducting paste,

and should be discarded if they are old and signal quality visibly deteriorates. The wire leads connecting the individual electrodes to the ECG cable should be secured to the subject's torso to minimize artifact from movement of these electrodes during exercise. This can be accomplished by loosely wrapping the torso with an elastic bandage or by using a commercially available knit shirt. The presence of artifact on the ECG usually indicates a loose lead-electrode interface, a poorly applied electrode, or inadequate electrode paste.

Blood Pressure

Blood pressure is an essential measurement in evaluating the cardiovascular response to exercise. Blood pressure can be measured directly with an indwelling arterial catheter or, more commonly, indirectly with a cuff, a sphygmomanometer, and a stethoscope. Numerous commercially available electronic units are available to measure blood pressure indirectly during exercise. The accuracy and precision of these "black boxes," however, must be a concern. Devices designed to inflate and deflate the cuff automatically coupled to a microphone that can be secured over the brachial artery are useful. It is critical to use an appropriate-size cuff. The bladder of the cuff should encircle the arm completely, and the width of the cuff should be at least two-thirds the length of the upper arm. An oversized cuff should be available to measure leg blood pressure when indicated. It should be remembered that accurate measurement of diastolic blood pressure during exercise is extremely difficult, particularly during treadmill exercise, because the pounding feet and the noise of the treadmill make it difficult to hear Korotkoff sounds. Direct (intra-arterial) blood pressure measurement allows nearly instantaneous beat-to-beat monitoring of blood pressure with a high level of precision. Because of peripheral amplification, however, measurement of blood pressure in the distal vascular system (radial or brachial artery) overestimates central aortic blood pressure (Fig. 7.13). In addition, this technique is invasive and potentially painful, which limits its usefulness in children.

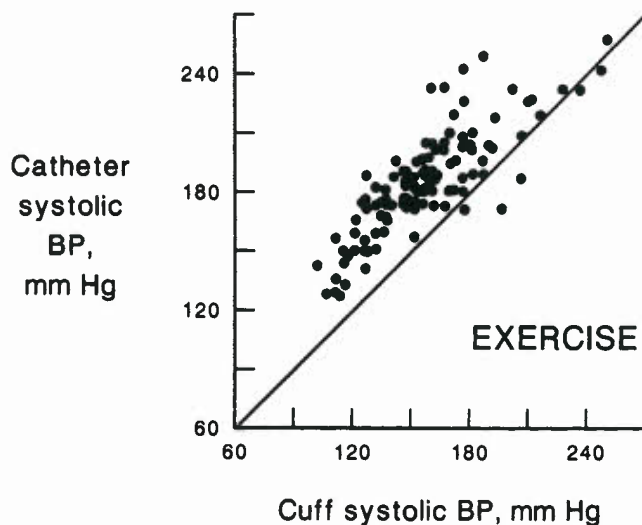


Figure 7.13. The relationship between systolic blood pressure measured using an indwelling radial artery cannula and arm blood pressure measured with a sphygmomanometer. Note that the blood pressures measured using a radial artery catheter are greater than those using a sphygmomanometer. (Reproduced from Rassmussen P, Staats B, Driscoll D, et al. Direct and indirect blood pressure during exercise. *Chest* 1985;87:743–748, with permission.)

Cardiac Output and Stroke Volume

The two techniques used most frequently to measure cardiac output (\dot{Q}) relatively noninvasively and without the need for radioactive material are the CO_2 and the acetylene-helium ($\text{C}_2\text{H}_2\text{-He}$) rebreathing techniques, although third, similar technique—nitrous oxide (N_2O)—has recently been reevaluated. The renewed interest in inert gas (N_2O and acetylene) has occurred with the advent of newer, less finicky, gas analyzers.

The CO_2 rebreathing technique (Fig. 7.14) is based on the Fick principle for CO_2 :

$$\dot{Q} = \frac{\dot{V}\text{CO}_2}{C_v\text{CO}_2 - C_a\text{CO}_2}$$

where $\dot{V}\text{CO}_2$ is the volume of carbon dioxide produced, $C_v\text{CO}_2$ is mixed venous blood CO_2 content, and $C_a\text{CO}_2$ is the systemic arterial blood CO_2 content. $\dot{V}\text{CO}_2$ is measured directly, arterial CO_2 content is calculated from the measurement of systemic arterial blood PCO_2 , and mixed venous CO_2 content is calculated from the measurement of end-tidal (alveolar) PCO_2 , assuming equilibrium with mixed venous PCO_2 and alveolar PCO_2 during the rebreathing maneuver. The latter maneuver can be done by the classical equilibrium or the exponential technique (49,50). The latter is simpler during incremental exercise and better tolerated because it utilizes lower CO_2 concentration in the rebreathing mixture. Inhaled CO_2 can create an unpleasant taste and transient headache in high concentrations. The need to measure systemic arterial PCO_2 is a disadvantage of this technique because it is invasive. Systemic arterial PCO_2 can be estimated from end-tidal PCO_2 , or by assuming a normal anatomic dead space in a subject with normal pulmonary function and solving for PaCO_2 using the Bohr equation, since all parameters in this equation are directly measured except for PaCO_2 . Note that one must account for instrument dead space (mouthpiece, face mask). Ultimately however, such approximations introduce additional potential error into the technique. Furthermore the concentration of CO_2 in the rebreathing mixture as well as the volume of the rebreathing mixture must be adjusted to the patient's size and exercise intensity. The future of this method is uncertain because of two recently described methodologic issues: the accuracy of measuring PCO_2 in a high O_2 mixture (51) and the solution to the equation relating CO_2 partial pressures to contents (52). The former problem, known as the collision-broadening effect, effectively limits the CO_2 rebreathing technique to laboratories employing a mass spectrometer to measure exhaled gas concentrations, while the latter underscores the need to know (rather than assume) blood pH and PCO_2 . Until these issues are clarified, healthy critical evaluation of papers using the indirect Fick (CO_2) technique would seem justified.

The $\text{C}_2\text{H}_2\text{-He}$ rebreathing technique to measure cardiac output is based on the principle that acetylene diffuses from the alveolus to the pulmonary capillary (53). The concentration of the acetylene in the rebreathing system declines relative to the volume of effective pulmonary blood flow (Fig. 7.15). This technique actually measures effective pulmonary blood flow rather than systemic blood flow, but in the absence of significant right-to-left or left-to-right intracardiac or intrapulmonary shunt, it is a reliable approximation of cardiac output. The other caveat is that the technique is heavily dependent on even distribution of the inspired gas and will thus be less accurate in patients with lung disease characterized by mismatching of ventilation and perfusion. It is necessary to include a gas that does not diffuse out of the alveolus (e.g., helium) to determine the volume of the entire

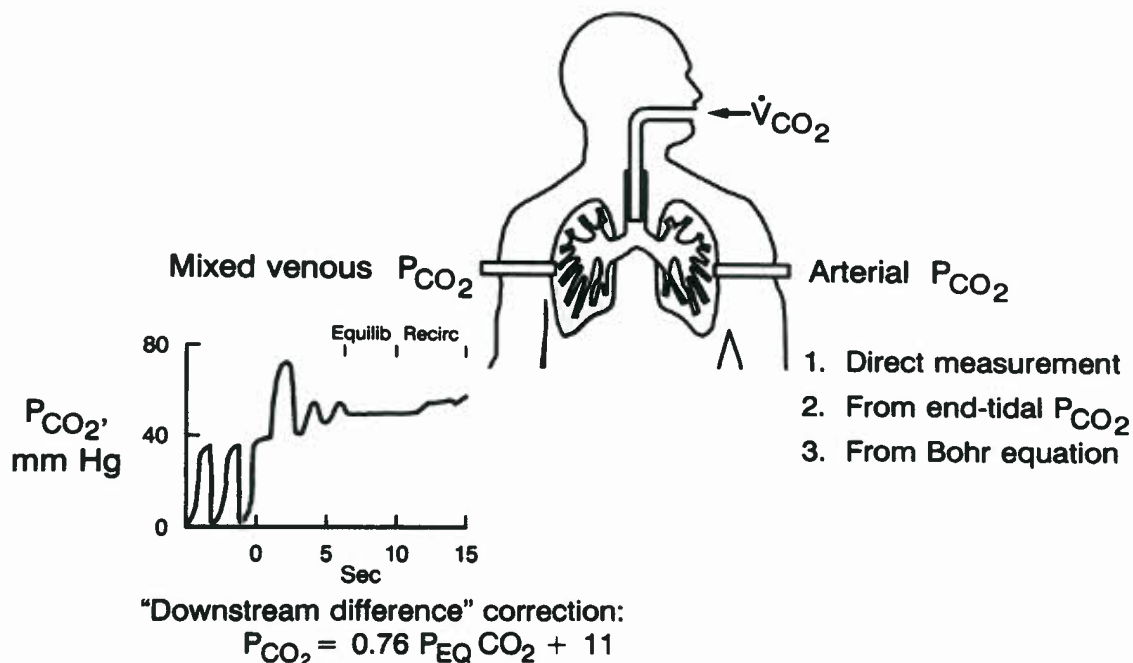
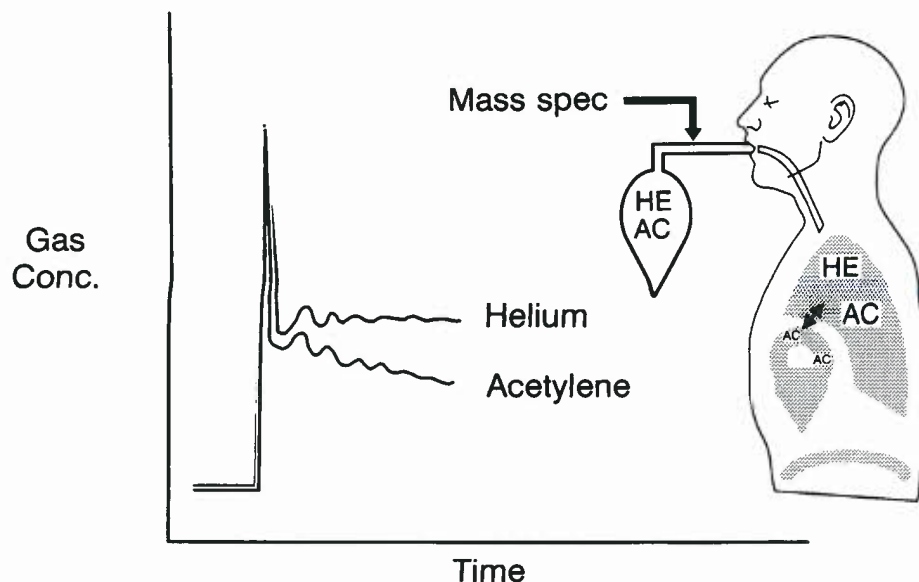


Figure 7.14. Diagrammatic representation of the CO_2 rebreathing method of assessing cardiac output. See text for determination of $PaCO_2$.

respiratory system and rebreath apparatus. This technique is completely noninvasive and tolerated well by children. Technically, it is simpler to perform the C_2H_2 -He than the CO_2 rebreath maneuver because the concentration of acetylene, helium, oxygen, and nitrogen used as the rebreath mixture is constant, only the volume of the mixture needs to be altered, depending on the subject's tidal volume. Subjects find the C_2H_2 -He rebreathing technique more comfortable, with less feeling of dyspnea during the procedure than with CO_2 rebreathing. One pediatric study compared C_2H_2 -He versus a somewhat modified CO_2 rebreath maneuvers, and found that only half the CO_2 rebreath maneuvers provided data that could be analyzed (54).

N_2O is highly soluble in blood and rebreathing N_2O was first described as another inert gas technique to measure cardiac output nearly 50 years ago, but has recently undergone reexamination. Like C_2H_2 -He rebreathing, N_2O rebreathing measures effective pulmonary blood flow, and suffers from the same limitations as acetylene method. An insoluble tracer gas is required, and recent studies used SF_6 for this purpose since it is highly insoluble and achieves equilibrium within the bag-lung rebreathing system. When this method was in its infancy, two studies in children (using helium or argon tracers) were published, one of which found the method compared very well with CO_2 rebreathing measurements of cardiac output (55). More recent studies in adults with (56) and without heart

Figure 7.15. Diagram of the acetylene-helium rebreathing technique for measuring effective pulmonary blood flow. Note that with rebreathing there is a constant decay in the concentration of acetylene in the rebreathing system. This occurs because acetylene passes across the alveolar membrane and is taken up by the pulmonary blood flow.



failure have compared N₂O rebreathing with (57) invasive and (58) noninvasive (CO₂) methods of measuring cardiac output. The study by Jarvis et al. (57) was very comprehensive and compared direct Fick, thermodilution, N₂O and C₂H₂ rebreathing methods (plus a 1-step CO₂ rebreathing technique). There are many ways to compare results of different methods of measurement. One is to report bias, that is, how closely one method approximates the gold standard, and precision, that is, how reproducible is the method, or alternatively, what is the variance of repeated trials. These authors concluded that inert gas methods were precise, but tended to underestimate the results obtained by the gold standard method(s) during exercise.

No similar study has been reported in children, nor is one likely. The fact is that these inert gas methods offer promise for using the lungs to measure cardiac output noninvasively in children. Whereas the CO₂ nontechnique can give accurate results in children with lung disease characterized by significant ventilation-perfusion mismatch, provided one *measures* rather than estimates PaCO₂, the same *cannot* be said for inert gas methods. They are predicated on adequate mixing of inspired gas, such that gas contents in the bag mix quickly with alveolar gas. Only once that occurs can these methods accurately measure pulmonary blood flow, which equals cardiac output for all intents and purposes.

The past decade has witnessed several publications on echocardiographic measurement of cardiac output during exercise. With this method, SV is estimated by standard Doppler echocardiographic techniques (59). The cross-sectional area of the ascending aorta is first calculated at rest with subjects in the sitting position from the maximal diameter of the aorta measured by two-dimensional echocardiography (long-axis view) at the sinotubular junction (inner edge to inner edge) assuming the aorta to be circular. Velocity of ascending aorta blood flow is determined with a continuous-wave transducer positioned in the suprasternal notch. The velocity-time integral (VTI) for each beat is calculated off-line by tracing the velocity curve contour over time. The termination of each contour was marked by aortic valve closure. Five to eight curves with the highest values and most distinct spectral envelopes should be averaged for each workload. SV is estimated as the product of the mean VTI and the cross-sectional area of the ascending aorta. The method is reasonably accurate, provided enough beats are averaged to compute stroke volume, since SV is affected by phase of breathing (60), and one risks overestimation of SV and hence cardiac output if one chooses the “best-looking” VTI. The technique also is critically dependent on accurate measurement of aortic valve area. Moreover, obtaining a satisfactory window at the suprasternal notch during heavy exercise can be a challenge both to the person holding the transducer and to the hyperpneic subject. Thus, echocardiographic measurement of cardiac output is very operator dependent, but despite these limitations the method is a choice among the noninvasive options. It has been extensively used by Rowland and coworkers (28,61,62) to study cardiac responses to exercise during the growth period of childhood.

Before concluding this section, one should be aware of the potential for impedance cardiography as a useful clinical and research tool in the pediatric exercise laboratory. It has never gained widespread acceptance because of uncertainty over its theoretical foundations, and because of equivocal findings of previous reports comparing this method with more accepted methods of measuring cardiac output. Recent work may change this thinking (30, 63–67), so a brief description is worthwhile. The theory behind the method models the thorax as a cylinder or truncated cone whose electrical impedance changes in proportion to the electrical conductivity of the blood within, simultaneously with mechanical systole. A tiny, biologically inactive AC current is discharged by one set of electrodes, while another set measures the impedance of the

thoracic contents to this current. SV is computed from thoracic impedance measurements using one of a number of published equations, which contain all or some the following terms:

$$SV = r \cdot (L^2/Z_0^2) \cdot VET \cdot (dZ/dt_{\min})$$

where r is the blood resistivity, a function of packed cell volume; L is the distance between electrodes; Z_0 is the baseline thoracic impedance; VET is the ventricular ejection time; and dZ/dt_{\min} is the maximum rate of fall in impedance. Most devices compute ventricular ejection time from the ECG tracing, though one (30) uses a microphone on the chest to detect the second heart sound. This unique impedance cardiograph required measurement of Z_0 and interelectrode distance (30), whereas others did not (63–67). The most recent iteration of this technology measures the relative phase shift ($\Delta\Phi$) of a radiofrequency signal passing through the thorax (instead of amplitude changes in impedance to an AC microcurrent) between paired electrodes during aortic ejection, which are tightly correlated to blood flow rate (65). This parameter allegedly has a higher signal to noise ratio and simplified the SV equation to:

$$SV = C \cdot VET \cdot (d\Phi/dt_{\max})$$

where C was termed a constant of proportionality, and $d\Phi/dt_{\max}$ is the rate of change in relative phase shift of the impedance signal. Despite claims, it significantly underestimated (bias) cardiac output during exercise in healthy adults compared with an inert gas rebreathing method, and the authors commented that subjects were required to maintain a relatively stable upper body position to reduce signal artifact (66). The precision of impedance cardiography was very good in children, with realistic results reported, though since no comparator measure was employed, one cannot comment on its bias (67). Future studies will determine its role, but it offers a simple, unobtrusive method for measuring cardiac output during exercise in children that yields results comparable to other methods.

Ventilation Measurements

The following indices of ventilation are measured: respiratory rate (RR), tidal volume (V_T), minute ventilation (\dot{V}_E or \dot{V}_I , depending on whether one measures inspired or expired ventilation), oxygen uptake ($\dot{V}O_2$), carbon dioxide production ($\dot{V}CO_2$), end-tidal CO₂, O₂, and mixed-expired CO₂ and O₂. From these measurements, the ventilatory equivalents for oxygen ($\dot{V}_E/\dot{V}O_2$) and CO₂ ($\dot{V}_E/\dot{V}CO_2$) and gas exchange ratio (RER) can be measured. Noninvasive (ear or finger oximetry) measurement of blood oxygen saturation is useful to document the presence or absence, and degree, of hypoxemia. There is very good correlation between blood oxygen saturation measured by pulse oximetry and that measured by direct blood gas analysis at least for oxygen saturations above 75%.

Several technical advances have been made in the measurement of ventilation and gas exchange during exercise, particularly with gas analyzers. This technology has improved in as much as large, cantankerous, mass spectrometers have also been replaced by smaller and more user-friendly gas analyzers permitting determination of concentrations of several gases at one time. Because of smaller size, newer portable metabolic carts containing all the essential tools are now readily available. Some of the old standards such as fuel cell or zirconium oxide O₂ analyzers and infrared CO₂ analyzers remain the workhorses of many such systems, though infrared CO₂

analysis may no longer be considered accurate if employed to analyze CO_2 concentration in high O_2 mixtures. In addition, hardware and software are available to measure indices of ventilation in a breath-by-breath fashion. There are several essential requirements of an ideal system: low sampling volume, rapid sampling rate with ultrafast response times. Software algorithms must account for these delays in computing breath-by-breath $\dot{V}\text{O}_2$ and $\dot{V}\text{CO}_2$, since the actual concentration of the gas at any instant must be matched with the exhaled volume at that same time point, in order to calculate the concentration–time integral.

It no longer is necessary to use timed gas collection into cumbersome Douglas bags and Tissot spirometers. Some commercially available systems still employ a mixing chamber, much smaller than devices used for timed collections, from which mixed expired gases (O_2 and CO_2) are sampled in real time. This requires not only that gas in the chamber is well mixed before expulsion, but also that these concentrations must then be matched with minute volume measured at approximately the same time. By and large, these methods have given way to accurate and reliable respiratory mass flow sensors, Pitot tubes, pneumotachographs, and turbine flowmeters. Measurement of ventilatory indices requires the use of a mouthpiece and a nose clip or a tightly fitting mask, and the latter can be oronasal or partition oral and nasal flow. Most children will tolerate a mouthpiece and nose clip. It is important to have different-sized mouthpieces and three-way respiratory valves available so that the dead space of the system can be minimized for small children. Valve or mask dead spaces volumes typically should be approximately 50 to 70 mL. It is equally important that such exercise systems recognize and subtract valve or mask dead space volume from the total \dot{V}_E before calculating $\dot{V}_E/\dot{V}\text{O}_2$ and $\dot{V}_E/\dot{V}\text{CO}_2$ ratios or slopes. Failure to do so, particularly in children, can result in large error given the smaller tidal volumes of younger children.

REFERENCES

- Hansen JE, Sue DY, Wasserman K. Predicted values for clinical exercise testing. *Am Rev Respir Dis* 1975;112:S49–S55.
- Wasserman K, Whipp BJ. Exercise physiology in health and disease. *Am Rev Respir Dis* 1975;112:219–249.
- Bar-Or O, Rowland TW. *Pediatric Exercise Medicine—From Physiological Principles to Health Care Application*. Champaign, IL: Human Kinetics, 2004:7–11.
- Williams CA, Carter H, Jones AM, et al. Oxygen uptake kinetics during treadmill running in boys and men. *J Appl Physiol* 2001;90:1700–1706.
- Zanconato S, Cooper DM, Armon Y. Oxygen cost and oxygen uptake dynamics and recovery with 1 min of exercise in children and adults. *J Appl Physiol* 1991;71:993–998.
- Howley ET. $\dot{V}\text{O}_2$ max and the plateau—needed or not? *Med Sci Sports Exerc* 2007;39:101–102.
- Rossiter HB, Kowalchuk JM, Whipp BJ. A test to establish maximum O_2 uptake despite no plateau in the O_2 uptake response to ramp incremental exercise. *J Appl Physiol* 2006;100:764–770.
- Saltin B, Calbet JAL, Wagner PD. Point:counterpoint in health and normoxic environment, $\dot{V}\text{O}_2$ max is limited primarily by cardiac output and locomotor muscle blood flow. *J Appl Physiol* 2006;100:744–748.
- Wagner PD. Determinants of maximal transport and utilization. *Annu Rev Physiol* 1996;58:21–50.
- di Prampero PE. Factors limiting maximal performance in humans. *Eur J Appl Physiol* 2003;90:420–429.
- Astrand P-O, Rodahl K. *Textbook of Work Physiology: Physiological Basis of Exercise*. New York, NY: McGraw-Hill, 1977:450.
- Welsman JR, Armstrong N, Nevill AM, et al. Scaling $\dot{V}\text{O}_2$ max for differences in body size. *Med Sci Sports Exerc* 1996;28:259–265.
- Cooper Dan M, Weiler-Ravell D, Whipp BJ, et al. Aerobic parameters of exercise as a function of body size during growth in children. *J Appl Physiol* 1984;56:628–634.
- Baxter-Jones A, Goldstein H, Helms P. The development of aerobic power in young athletes. *J Appl Physiol* 1993;75:1160–1167.
- Armstrong N, Welsman JR, Nevill AM, et al. Modeling growth and maturation changes in peak oxygen uptake in 11–13 year olds. *J Appl Physiol* 1999;87:2230–2236.
- Andreacci JL, Robertson RJ, Dube JJ, et al. Comparison of maximal oxygen consumption between black and white prepubertal and pubertal children. *Pediatr Res* 2004;56:706–713.
- Washington RL. Cardiorespiratory testing: anaerobic threshold/respiratory threshold. *Pediatr Cardiol* 1999;20:12–15.
- Hagberg JM, Coyle EF, Carroll JF, et al. Exercise hyperventilation in patients with McArdle's disease. *J Appl Physiol* 1982;52:991–994.
- Hebestreit H, Staschen B, Hebestreit A. Ventilatory threshold: a useful method to determine aerobic fitness in children? *Med Sci Sports Exerc* 2000;32:1964–1969.
- Reybrouck T, Weymans M, Stijns H, et al. Ventilatory anaerobic threshold in healthy children: age and sex differences. *Eur J Appl Physiol* 1985;54:278–284.
- Bhambhani YN. Muscle oxygenation trends during dynamic exercise measured by near infrared spectroscopy. *Can J Appl Physiol* 2004;29:504–523.
- Rowell LB. Circulatory adjustments to dynamic exercise. In: Rowell LB, ed. *Human Circulation Regulation During Physical Stress*. New York, NY: Oxford University Press, 1986:213–256.
- Godfrey S, Davies CTM, Wozniak E, et al. Cardio-respiratory response to exercise in normal children. *Clin Sci* 1971;40:419–431.
- Stringer WW, Whipp BJ, Wasserman K, et al. Non-linear cardiac output dynamics during ramp-incremental cycle ergometry. *Eur J Appl Physiol* 2005;93:634–639.
- Beck KC, Randolph LN, Bailey KR, et al. Relationship between cardiac output and oxygen consumption during upright cycle exercise in healthy humans. *J Appl Physiol* 2006;101:1474–1480.
- Rowland T. Circulatory “efficacy” during progressive aerobic exercise in children: insights from the $\dot{Q} - \dot{V}\text{O}_2$ relationship. *Eur J Appl Physiol* 2007;101:61–66.
- Gonzalez-Alonzo J, Warburton DER, Gledhill N. Point:counterpoint. stroke volume does/does not decline during exercise at maximal effort in healthy individuals. *J Appl Physiol* 2008;104:275–280.
- Rowland T, Popowski B, Ferrone L. Cardiac responses to maximal upright cycle exercise in healthy boys and men. *Med Sci Sports Exerc* 1997;29:1146–1151.
- Eriksson BO, Grimby G, Saltin B. Cardiac output and arterial blood gases during exercise in pubertal boys. *J Appl Physiol* 1971;31:348–352.
- Pianosi P. Measurement of exercise cardiac output by thoracic impedance in healthy children. *Eur J Appl Physiol* 2004;92:425–430.
- Stringer WW, Hansen JE, Wasserman K. Cardiac output estimated non-invasively from oxygen uptake during exercise. *J Appl Physiol* 1997;83:908–912.
- Washington RL, van Gundy JC, Cohen C, et al. Normal aerobic and anaerobic exercise data for North American school-age children. *J Pediatr* 1988;112:223–233.
- Strong W, Miller M, Striplin M, et al. Blood pressure response to isometric and dynamic exercise in healthy black children. *Am J Dis Child* 1978;132:587–591.
- Johnson JN, Mack KJ, Kuntz NL, et al. Postural orthostatic tachycardia syndrome: a clinical review. *Pediatr Neurol* 2010;42:77–85.
- Joyner MJ, Masuki S. POTS versus deconditioning: the same or different? *Clin Auton Res* 2008;18:300–307.
- Meadow MS, Stewart JM. The postural tachycardia syndrome. *Cardiol Rev* 2007;15:67–75.
- Burkhardt BEU, Fischer PR, Brands CK, et al. Exercise performance in adolescents with autonomic dysfunction. *J Pediatr* 2010;158:15–19.e1.
- Stewart JM. Chronic orthostatic intolerance and the postural tachycardia syndrome (POTS). *J Pediatr* 2004;145:725–730.
- Fu QI, vanGundy TB, Galbreath MM, et al. Cardiac origins of postural orthostatic tachycardia syndrome. *J Am Coll Cardiol* 2010;55:2858–2868.
- Cooper DM, Kaplan MR, Baumgarten L, et al. Coupling of ventilation and CO_2 production during exercise in children. *Pediatr Res* 1987;21:568–572.
- Ohuchi H, Kato Y, Tasato H, et al. Ventilatory response and arterial blood gases during exercise in children. *Pediatr Res* 1999;45:389–396.
- Johnson BD, Weisman IM, Zeballos RJ, et al. Emerging concepts in the evaluation of ventilatory limitation during exercise: the exercise tidal flow-volume loop. *Chest* 1999;116:488–503.
- Nourry C, Deruelle F, Fabre C, et al. Exercise flow-volume loops in prepubescent aerobically trained children. *J Appl Physiol* 2005;99:1912–1921.
- Swain KE, Rosenkranz SK, Beckman B, et al. Expiratory flow limitation during exercise in prepubescent boys and girls: prevalence and limitations. *J Appl Physiol* 2010;108:1267–1274.
- Dempsey JA, Wagner PD. Exercise-induced arterial hypoxemia. *J Appl Physiol* 1999;87:1997–2006.
- Nourry C, Fabre C, Bart F, et al. Evidence of exercise-induced arterial hypoxemia in prepubescent trained children. *Pediatr Res* 2004;55:674–681.
- Cumming GR, Everatt D, Hastman L. Bruce treadmill in children: normal values in a clinic population. *Am J Cardiol* 1978;41:69–75.
- James F, Kaplan S, Glueck C, et al. Responses of normal children and young adults to controlled bicycle exercise. *Circulation* 1980;61:902–912.
- Godfrey S. *Exercise Testing in Children*. London, UK: WB Saunders, 1974:45–50.
- Jones NL. *Clinical Exercise Testing*. Toronto, ON: WB Saunders, 1988:187–195.
- Hornby L, Coates AL, Lands LC. Effect of analyzer on determination of mixed venous Pco_2 and cardiac output during exercise. *J Appl Physiol* 1995;79:1032–1038.

52. Sun, Xing-Guo, Hansen JE, et al. Carbon dioxide pressure-concentration relationship in arterial and mixed venous blood during exercise. *J Appl Physiol* 2001;90:1798–1810.
53. Triebwasser J, Johnson R, Burpo R, et al. Noninvasive determination of cardiac output by a modified acetylene re-breathing procedure utilizing mass spectrometer measurements. *Aviat Space Environ Med* 1977;48:203–209.
54. Rosenthal M, Bush A. The simultaneous comparison of acetylene or carbon dioxide flux as a measure of effective pulmonary blood flow in children. *Eur Respir J* 1997;10:2586–2590.
55. Zeidifard E, Godfrey S, Davies EE. Estimation of cardiac output by an N₂O rebreathing method in adults and children. *J Appl Physiol* 1976;41:433–438.
56. Agostoni P, Cattadori G, Apostolo A, et al. Non-invasive measurement of cardiac output during exercise by inert gas rebreathing technique: a new tool for heart failure evaluation. *J Am Coll Cardiol* 2005;46:1779–1781.
57. Jarvis SS, Levine BD, Prisk GK, et al. Simultaneous determination of the accuracy and precision of closed-circuit cardiac output rebreathing techniques. *J Appl Physiol* 2007;103:867–874.
58. Jalovljjevic DG, Nunan D, Donovan G, et al. Comparison of cardiac output determined by different rebreathing methods at rest and peak exercise. *Eur J Appl Physiol* 2008;102:593–599.
59. Calafiore P, Stewart WJ. Doppler echocardiographic quantitation of volumetric flow rate. *Cardiol Clin* 1990;8:191–202.
60. Du Quesnay MC, Stoute GJ, Hughson RL. Cardiac output in exercise by impedance cardiography during breath holding and normal breathing. *J Appl Physiol* 1987;62:101–107.
61. Rowland TW, Goff D, Martel L, et al. Influence of cardiac functional capacity on gender differences in maximal oxygen uptake in children. *Chest* 2000;117:629–635.
62. Rowland TW, Obert P. L. Doppler echocardiography for the estimation of cardiac output with exercise. *Sports Med* 2002;32:973–986.
63. Tordi N, Mourot L, Matusheski B, et al. Measurements of cardiac output during constant exercise: comparison of two non-invasive techniques. *Int J Sports Med* 2004;25:145–149.
64. Ruddy R, Lonsdorfer-Wolf E, Charloux A, et al. Non-invasive cardiac output evaluation during a maximal progressive exercise test, using a new impedance cardiograph device. *Eur J Appl Physiol* 2001;85:202–207.
65. Keren H, Burkhoff D, Squara P. Evaluation of a noninvasive continuous cardiac output monitoring system. *Am J Physiol Heart Circ Physiol* 2007;293:H583–H589.
66. Elliot A, Hull JH, Nunan D, et al. Application of bioreactance for cardiac output assessment during exercise in healthy individuals. *Eur J Appl Physiol* 2010;109:945–951.
67. Welsman J, Bywater K, Farr C, et al. Reliability of peak $\dot{V}O_2$ and maximal cardiac output assessed using thoracic impedance in children. *Eur J Appl Physiol* 2005;94:228–234.

Echocardiography: Basic Principles and Imaging

Thomas R. Kimball ■ Erik C. Michelfelder

Although utilization of imaging modalities other than echocardiography (e.g., computed tomography and magnetic resonance imaging) has increased in the evaluation of congenital heart disease (1,2), echocardiography remains the principal diagnostic modality in the field of pediatric cardiology (3). The echocardiography laboratory is often the patient's last "diagnostic stop" before surgical or catheter intervention, which necessitates the most complete anatomic and physiologic description of the cardiovascular system possible and requires unprecedented detail in the echocardiographic evaluation. In addition, pediatric echocardiographers find themselves with two important challenges today: (a) to define, with the help of other imaging specialists, the roles of not only echocardiography but other emerging imaging technologies in the evaluation of complex anatomy in children and adults with congenital heart disease (4) and (b) to oversee the expanding utilization of echocardiography among not only our cardiology colleagues but also other noncardiology health care providers—utilization precipitated in part by poorer auscultatory skills of personnel and increased miniaturization and decreased cost of cardiac ultrasound technology (5,6).

HISTORY

In 1877, Pierre Curie, then only 18 years old, and his older brother, Jacques, found the basis for the field that would later be known as ultrasound by discovering the piezoelectric effect in which mechanical distortion of crystals produces an electric potential and vice versa. Although this was a landmark discovery, it was not until many years later, in fact not until after the 1912 sinking of the Titanic (which catalyzed efforts to create systems aiding ships in earlier detection of icebergs), that the field of ultrasound began to develop (7). Eventually, in World War II, ultrasound waves formed the basis of Sound Navigation and Ranging (SONAR) (8).

The successful use of ultrasound as a diagnostic medical technique was simultaneously pioneered in the 1940s and 1950s by four groups: (a) the Massachusetts Institute of Technology (MIT; Bolt, Ballantine, Ludwig, and Heuter), (b) the University of Illinois (Fry, Fry, and Kelly), (c) the University of Colorado (Howry and Holmes), and (d) the University of Minnesota (Wild and Reid). The MIT group developed A (amplitude)-mode ultrasound, a method of displaying the intensity of reflected waves as spikes of various heights on an oscilloscope. The Illinois group is renowned for using ultrasound to detect breast cancer. The Colorado group developed B (brightness)-mode imaging, a method of displaying the intensity of the reflected ultrasound waves as dots of various brightness along a single scan line, the progenitor to two-dimensional (2-D) ultrasound. They expanded this concept by creating the B-29 gun turret water-bath scanner in which both patient and transducer were immersed. The Minnesota group

perfected pulsed ultrasound techniques that permit a single transducer to act as both a transmitter and a receiver in real time and, by incorporating a water interface in the transducer head, created the first hand-held scanner, thus eliminating the need for patient immersion (7,8).

Applying ultrasound for cardiac diagnosis was first performed at the University of Lund, Sweden (Edler and Hertz) in 1953. A B-mode detector with continuous moving film to obtain real-time images of the heart in waveform provided the first M(motion)-mode echocardiogram (7,8). Twenty years later, M-mode echocardiography was applied to congenital heart disease by Goldberg, Allen, Sahn, Meyer and others (9,10). In the late 1970s and early 1980s, the application of 2-D echocardiography to congenital heart disease allowing complete, accurate, and detailed diagnoses was successfully completed by pioneers such as Sahn, Snider, Silverman, Williams, Stevenson, and others (11–20). Each stressed a thoughtful, considered approach that coupled the evolving field of echocardiography to the established fields of cardiac morphology, pathology, and embryology, eventually forging the way for children, infants, and neonates to receive medical and surgical treatment after an assessment that was completely noninvasive. In the 1990s and early 2000s, ultrasound technology became increasingly miniaturized so that echocardiography began to enjoy broader use including as a bedside adjunct to the physical examination in more unique settings such as the emergency room and the intensive care unit. Such applications have created special challenges for the pediatric echocardiography community which must respond to the training and quality assurance issues associated with a wider user base without being exclusionary. With other imaging modalities such as cardiac MRI becoming more established, echocardiographers will need to work with other imaging specialists to define the role of each of these cardiac imaging tools in the diagnostic workup in all the disease states and patient population which we manage.

PHYSICS OF TWO-DIMENSIONAL ECHOCARDIOGRAPHY

The piezoelectric effect occurs when an electric potential applied to a crystal results in mechanical distortion because of alignment of the crystal's molecular dipoles. This, in turn, causes the crystal to resonate producing ultrasonic waves. A sound wave requires a deformable medium for its propagation because it is mechanical in nature, consisting of a series of compressions and expansions (rarefaction) of the molecules in the medium. The velocity of sound depends on the type of tissue through which it is traveling (1,540 m/s in soft tissue, 330 m/s in air). The wave has characteristics that define its existence (Fig. 8.1).

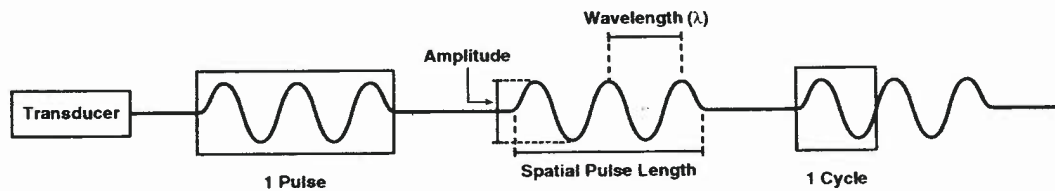


Figure 8.1. The anatomy of a wave. Sound travels with a velocity (c) dependent on the medium through which it propagates (for soft tissue, $c = 1540$ m/s). The wavelength (λ) is the distance between two consecutive and equivalent parts. The frequency (ν) is the number of compressions per unit of time expressed in Hertz. The frequency and wavelength are inversely proportional to each other through the velocity of sound ($\nu\lambda = c$). The amplitude is the pressure difference between nadir and peak. In echocardiography, waves are emitted as pulses consisting of wave cycles. Therefore, the spatial pulse length is the distance from the beginning of a single pulse train to its end.

The echocardiographic transducer does not emit ultrasound continuously but rather emits pulses rapidly ($\sim 1,000$ pulses/s) and quickly ($\sim 1 \mu\text{s}$ for every pulse). Therefore, the transducer is operating as a transmitter for an extremely short time (0.1% of the time). During a 30-minute examination, the transducer has transmitted pulses for <2 seconds. When the transducer is not emitting sound waves, it is in its receiver mode awaiting the return of reflected ultrasound.

Eight Equations that Form the Basis of Two-Dimensional and Doppler Echocardiography

Equation 1: The Basis of Image Generation

$$\%R = \{(Z_2 - Z_1) / (Z_2 + Z_1)\}^2 \times 100 \quad [1]$$

where

$\%R$ = percent reflection of ultrasound signal

Z_n = impedance in medium_n = $\rho_n c_n$

ρ_n = density of medium_n

c_n = speed of sound in medium_n

As an ultrasound beam travels through the body, some of its energy will be reflected back to the transducer and some of its energy will continue to be transmitted forward. In considering the amount of reflected energy, it is helpful to consider the concept of momentum, which is the product of mass (m) of an object and its velocity (v) (momentum = mv). A speeding semitractor trailer (high velocity, huge mass) has much greater momentum than a pedaling bicyclist (slow velocity, small mass). Consider the well-known novelty of a set of metallic balls suspended adjacent to each other as a pendulum (Fig. 8.2). An outside ball is drawn away from the stationary balls and is released, striking the stationary balls, resulting in the outside ball on the opposite side to move away from the stationary balls. If the first outside ball were the size of a pea, it would strike the stationary balls and merely bounce away from them. It does not have sufficient momentum (because of relatively small mass) to cause any perturbation in the stationary balls. It is therefore merely reflected backward.

Acoustic impedance is the ultrasound equivalent to momentum; density replaces mass, and speed of sound replaces velocity (21). If the acoustic impedance is the same between two media (the equivalent of a large metallic ball in the example above), ultrasound will be readily transmitted through the media interface; however, a mismatch in the impedance between the two media (the equivalent of a pea-sized ball in the example above) will result in reflection of ultrasound.

Equation 2: The Basis of Image Resolution (Part I)

$$\text{SPL} = n(\lambda) = n(c/\nu) \quad [2]$$

where

SPL = spatial pulse length

λ = wavelength

n = number of cycles in a pulse of ultrasound

c = speed of sound

ν = transmission frequency

Axial resolution (resolution along the axis of the ultrasound beam) of a nonpulsed wave is approximately equivalent to its wavelength. A bat feeding at twilight emits ultrasound waves at a frequency of 100 kHz, which provides excellent resolution for catching insects in air ($\lambda = c/\nu = 330 \text{ m/s} \div 100,000 \text{ cycles/s} = 3.3 \text{ mm}$) but provides an unacceptable resolution if an eccentric bat were to try fatuously to echo-locate cardiac anatomy through soft tissue ($1,540 \text{ m/s} \div 100,000 \text{ cycles/s} = 15.4 \text{ mm}$). With pulsed ultrasound, the axial resolution is dependent on

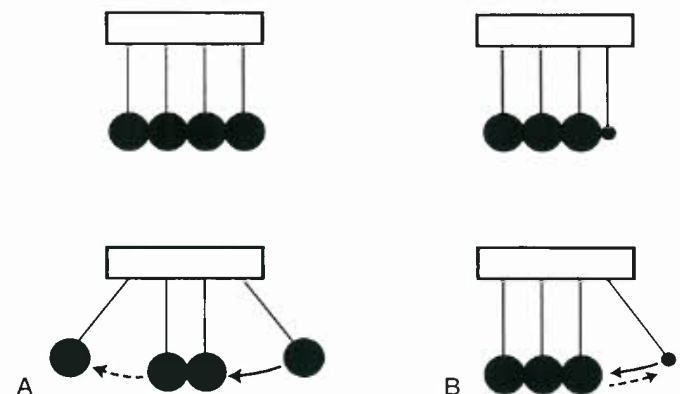


Figure 8.2. In mechanics, energy transfer is dependent on momentum. A: After an outside ball of equivalent size to the stationary balls is released, it strikes the stationary balls, resulting in movement of the outside ball on the opposite side. The ball has sufficient momentum to cause effective energy transfer to the stationary balls. B: After an outside ball of smaller size is released, it strikes the stationary balls and is reflected off of them. This ball has insufficient momentum to result in energy transfer. Acoustic impedance is the ultrasound equivalent to momentum. In ultrasound, energy transfer is dependent on impedance. If the impedances between two media are similar, ultrasound will be readily transmitted. If there is a mismatch in impedance, ultrasound will be reflected.

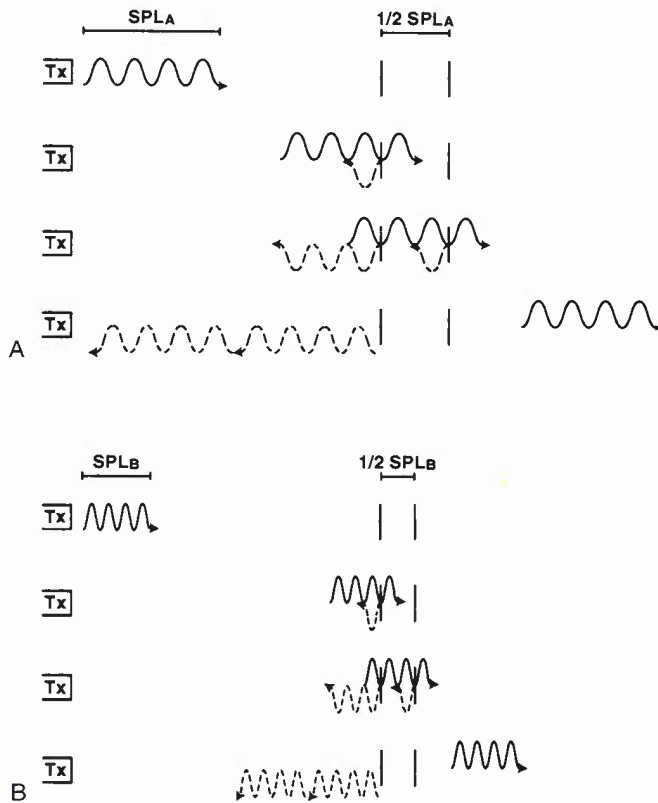


Figure 8.3. The axial resolution (resolution along the axis of the ultrasound beam) is dependent on the spatial pulse length (SPL). The shorter the SPL, the better the resolution. Resolution can be no better than $1/2$ of the SPL. **A:** The transducer emits pulses of sound waves (solid line) with a relatively long SPL of SPL_A . This train of pulses can distinguish two objects that are separated by a distance of $1/2 SPL_A$ but not closer because the transducer would not have finished receiving the reflected wave from the proximal object before arrival of the reflected wave from the distal object. **B:** The transducer emits pulses of sound with a shorter SPL of SPL_B . These train of pulses can distinguish two objects that are closer together but still not closer than $1/2 SPL_B$ (reflected waves shown as dashed lines).

having a short spatial-pulse length. This can be achieved by either decreasing the number of wave cycles in an ultrasound pulse or decreasing the wavelength (i.e., increasing the transmission frequency). The best possible axial-point separation resolution is equal to $1/2$ of the spatial-pulse length (Fig. 8.3). Using Equation 2, a 10-MHz transducer emitting a train of three pulsed ultrasonic waves will yield a point separation resolution of approximately 0.46 mm ($3 \times 154,000 \text{ cm/s} \div 10,000,000 \text{ cycles/s}$). A 2.5-MHz transducer will have an approximate resolution of 1.8 mm. The poorer axial resolution of a transducer of this frequency therefore limits its usefulness in evaluating anatomy of smaller magnitude, for example, the luminal diameter of a coronary artery or the diameter of a small septal defect.

Equation 3: The Basis of Image Resolution (Part II)

$$D = (d^2 v) / (4c) \quad [3]$$

where

D = depth of near field
 d = diameter of transducer
 v = transmission frequency of transducer
 c = speed of sound

Lateral resolution is the ability to resolve objects that are perpendicular to the beam axis and is dependent not only on transducer frequency but also on the beam width. For a nonfocused transducer, the ultrasonic beam consists of a near field with narrow beam width and good lateral resolution (the Fresnel zone) and a far field where the beam width diverges rapidly limiting resolution (the Fraunhofer zone) (21). The depth of the near field is extended by increasing the frequency or the footprint diameter of the transducer (Equation 3 and Fig. 8.4).

An example is afforded by imaging a newborn. For the parasternal and apical views, a small-diameter, high-frequency probe is advantageous because the cardiac structures are not at a deep depth and the small footprint can be placed between the acoustically unfriendly ribs. For subcostal imaging, a larger-diameter transducer provides great advantage by extending the near field to the level of the cardiac structures improving their resolution.

Lateral resolution can be improved by focusing, which causes the beam width to narrow more distally where it would otherwise begin to diverge. Focusing can be accomplished by external devices (such as mirrors or lenses) or by electronic means;

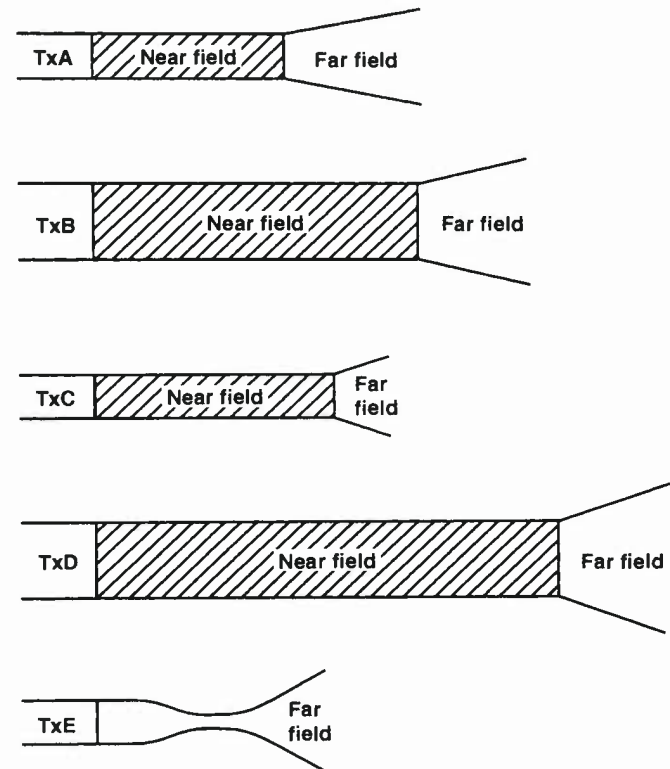


Figure 8.4. The lateral resolution (resolution perpendicular to the axis of the ultrasound beam) is dependent not only on transmission frequency but also on the beam width of the transducer. The beam is relatively narrow in the near field of the transducer. In the far field, the ultrasound beam begins to diverge and lateral resolution deteriorates. Transducer A has a relatively small diameter and, therefore, a relatively shallow near field. The diameter of transducer B is larger, thereby extending the near field. Near-field depth can be increased even when using a smaller-diameter transducer if transducer frequency is increased (transducer C). Near-field depth is optimized with transducers having relatively large diameters and emitting ultrasound of high frequency (transducer D). Lateral resolution can also be improved by focusing the transducer crystal; however, focusing has the disadvantage of the beam diverging rapidly beyond the focal zone (transducer E).

however, focusing results in two important disadvantages: (a) the focal zone is closer to the transducer face than the nonfocused near-field zone and (b) the far-field divergence of a focused beam is greater than the divergence of a nonfocused beam.

Equation 4: The Yin–Yang Relationship between Resolution and Penetration

$$L = \mu v z \quad [4]$$

where

L = intensity attenuation loss (in decibels)

μ = intensity attenuation coefficient approximately 0.8 dB/cm/MHz for soft tissue

v = transducer frequency (in MHz)

z = distance traveled in the medium by ultrasound wave (in cm)

The energy of the ultrasound wave is decreased by tissue interactions. Attenuation describes the loss of intensity resulting from scattering (reflection at small interfaces) and absorption (energy transformation) (21). Equation 4 demonstrates that intensity loss is greatest (or penetration is poorest) not only at deeper tissue depths but also when using a transducer with a higher frequency, precisely the frequency needed to enhance resolution (Equations 2 and 3). Thus, echocardiography requires a constant balancing act between optimizing resolution without sacrificing penetration and vice versa.

Equation 5: The Basis of Temporal Resolution

$$F = (c) / (2DNn) \quad [5]$$

where

F = frame rate

c = speed of sound

D = sampling depth

N = number of sampling lines per frame

n = number of focal zones used to produce one image

Motion during 2-D echocardiography is portrayed by rapid presentation of successive single image frames, similar to viewing a motion picture film. A single image frame is generated by successive electronic stimulation of each element in the transducer to initiate an ultrasound pulse, which propagates down (and is received up) successive scan lines (one scan

line typically extends through 1 to 3 degrees of the sector). In addition, the superimposition of a color Doppler sector on the image increases the time for a pulse to propagate down and up a scan line. The time required for the pulse to travel down one scan line to the depth of interest and back to the transducer imposes a restriction on how quickly the next element is stimulated, how rapidly a frame is acquired, and how soon the next frame can be produced. The frame rate (expressed in Hz) quantitates the speed of this process (21).

Temporal resolution can be optimized by narrowing the sector size (of both the image and the color Doppler region), thereby decreasing the number of scan lines, or by decreasing the depth range (Equation 5 and Fig. 8.5). A practical, easy-to-remember rule of thumb to optimize frame rate is to ensure that the subject of interest fills the sector wedge completely, eliminating imaging of superfluous tissue at the lateral and inferior aspects of the sector. Since M-mode and Doppler echocardiography have better temporal resolution, these modalities may be more useful when measuring events which are occurring quickly.

Equation 6: The Doppler Equation

$$v_d = [2v_0(V)(\cos \theta)] \div c \quad [6]$$

where

v_d = the observed Doppler frequency shift

v_0 = the transmitted frequency of sound

V = blood flow velocity

θ = the intercept angle between the ultrasound beam and the direction of blood flow

c = the velocity of sound in human tissue

The Doppler principle states that the frequency of a transmitted wave is altered when the source of the wave is in motion (e.g., the siren on an ambulance racing by a pedestrian). The principle is also applicable when the source of the wave is stationary and the “receiver” of the wave is in motion. The observed change in frequency under these circumstances is termed the Doppler shift, after Christian Johann Doppler, who described this phenomenon in 1842 when studying the light waves emitted with the motion of binary stars. The phenomenon is apparent (in the ambulance example reference above) when the ambulance’s wailing siren is perceived as having an increased pitch as it approaches and decreased pitch as it races away.

A stationary surfer waiting to catch a wave encounters the same number of wave crests per minute as emitted by the source.

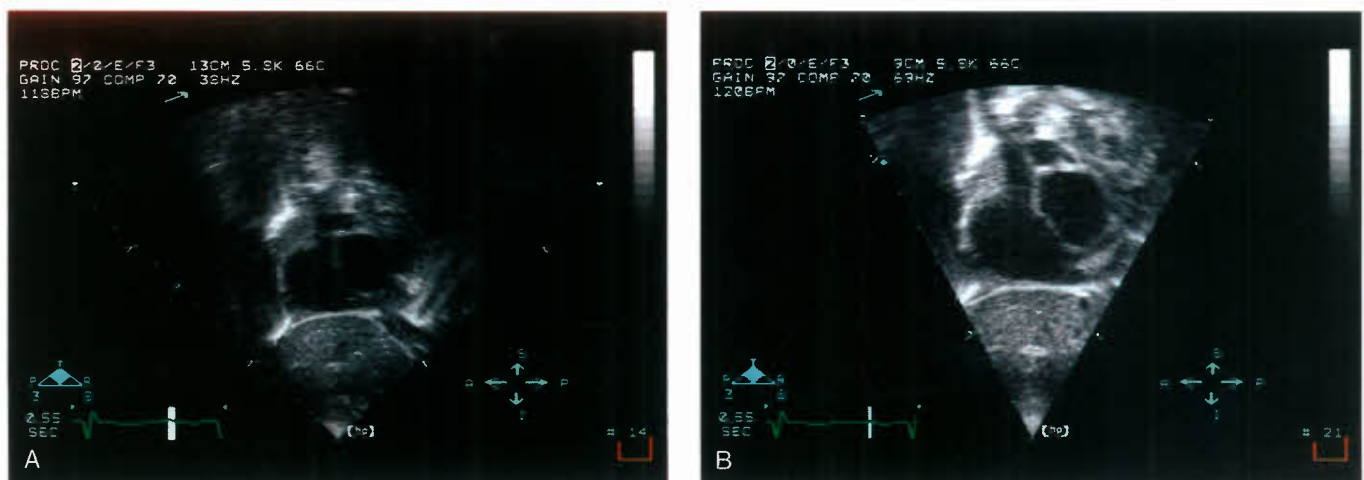


Figure 8.5. Two subcostal sagittal images demonstrating the factors that impact temporal resolution (arrows). **A:** The sampling depth is 13 cm, and the sector size is wide, yielding a frame rate of 38 Hz. **B:** The sampling depth has been decreased to 9 cm and the sector scan narrowed so that the image fills the entire sector and the frame rate has increased to 69 Hz.

If the surfer paddles away from the beach toward the ocean, he perceives an increase in the wave frequency because he is swimming toward the wave source. If he reverses his direction and heads to the beach (away from the source), he encounters fewer wave crests. If he moves faster in either direction, the difference between the actual and observed frequency of wave crests (the frequency shift) increases. The only instance in which the actual and observed frequencies coincide is when the surfer is stationary.

In medical ultrasound and echocardiography, the Doppler principle is applied using transmitted sound waves to strike moving red blood cells. Sound waves are transmitted by a stationary transducer, strike red blood cells in motion, and the returning “backscattered” sound pulses are Doppler shifted in frequency in relation to the velocity and direction in which the blood cells are moving. Doppler principles are also applied to evaluate tissue motion by Doppler tissue imaging. In these instances, since tissue moves at a much slower speed than blood, a low pass filter is applied to the returning ultrasound signal to allow the low velocity tissue reflections to pass and the high velocity blood signals to be filtered out.

Doppler ultrasound is used primarily to assess velocity of moving structures, whether it be the velocity of blood flow through the heart and vasculature or the velocity of the ventricular myocardium. It is therefore appropriate to rearrange the Doppler equation to solve for velocity:

$$V = [c (v_d)] \div [2 v_o \cos \theta]$$

As the speed of sound (c) and the transmitted frequency (v_o) are constant, and the frequency shift (v_d) can be very accurately measured, it becomes apparent that the main source of potential error in Doppler estimation of velocity arises from the intercept angle, θ , between the sound beam and the direction of blood/tissue motion. Consider the surfer analogy above. If the surfer were moving toward the ocean (toward the wave source) at an oblique angle, then the “frequency shift” (i.e., the difference between the actual and observed frequency of wave crests) would be less than if he were heading directly into the wave source. The observed velocity is the velocity vector parallel to the insonation beam. The true velocity of his movement would not be known unless we were to account for his oblique travel pattern relative to the wave source. This can be determined by dividing the frequency shift by the cosine of θ (the intercept angle between the wave source and his direction of travel). If the true velocity vector is aligned with the ultrasound beam (i.e., $\theta = 0$), then $\cos \theta$ is one and the observed velocity is the true velocity. However, if the true velocity vector and insonation beam are not aligned, the observed velocity will be smaller than the true velocity, unless angle correction is performed. For intercept angles < 20 degrees, $\cos \theta$ is small, and is not felt to result in significant underestimation of the flow velocity. At greater intercept angles, correction for $\cos \theta$ is needed (Fig. 8.6). In clinical application, Doppler evaluation is generally avoided at higher intercept angles to avoid inaccuracy and the need for angle correction.

Equation 7: The Basis of Aliasing

$$V_{\max} = (c^2) \div [8 v_o D \cos \theta] \quad [7]$$

where

V_{\max} = the maximum measurable velocity of blood

c = the velocity of sound in tissue

v_o = the transmitted frequency of sound

D = depth of interest

θ = the intercept angle between the ultrasound beam and the direction of blood flow

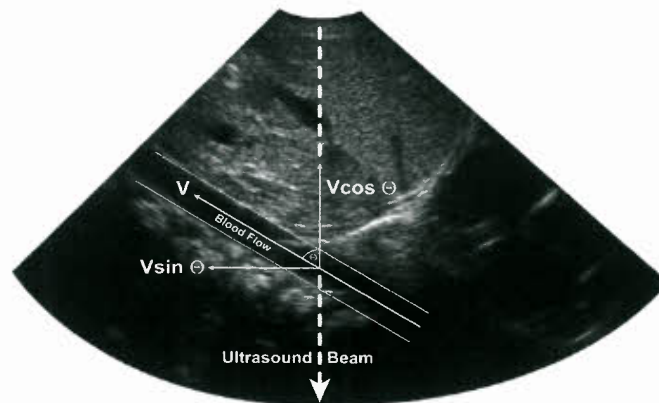


Figure 8.6. Angle correction for Doppler velocity assessment. The measured Doppler velocity is the velocity vector parallel to the line of insonation (dotted line). The velocity of interest, in this case the velocity of red blood cells coursing through the abdominal aorta or the true velocity, is related to the measured velocity by the cosine of the angle, θ , between the direction of flow and the line of insonation. For $\theta > 20$ degrees, the cosine function becomes significantly less than 1, and will result in significant underestimation of the true velocity, V . The Doppler equation allows calculation of the true velocity even when the angle between the insonation beam and the vector of the true velocity is significant by dividing the frequency shift by $\cos \theta$.

If the Doppler sampling rate is not adequate, the frequency of the reflected wave is sampled only intermittently, data must be inferred, and the wave is misinterpreted as having a lower frequency—a phenomenon called aliasing. The phenomenon is apparent in older Western movies when the wheel of a stagecoach is perceived as rotating backwards while the stagecoach is obviously moving forward. The movie consists of a series of stop-action photographs, which when shown one after the other, give the appearance of motion. If the stagecoach moves very fast, the wheel turns very fast and turns too great a revolutionary arc between successive photographs. The problem is solved by decreasing the time between successive photographs so the wheel turns a smaller arc between photographs (Fig. 8.7). Equation 7 demonstrates that the maximum measurable velocity of blood can be increased by decreasing the transducer frequency and/or sampling at a shallower depth. Since the latter is usually not alterable, increasing the aliasing (or Nyquist limit) is achieved by exchanging to a lower frequency transducer.

The phenomenon of aliasing and the value of using lower frequency transducers for sampling higher blood velocities are also understood by contemplating the concept of pulse repetition frequency (PRF) in the context of Equation 6. Since it requires a minimum of two pulses per wave cycle to define frequency unambiguously, the minimum PRF to sample a reflected wave's frequency is twice the Doppler shift. Therefore a more reasonable PRF is achieved by minimizing the Doppler shift. It is clear from Equation 6 that at any given blood velocity and Doppler angle, a lower Doppler shift (i.e., low v_d) is only achieved by reducing transducer frequency (i.e., low v_o).

Equation 8: The Bernoulli Equation

$$\Delta P = \frac{1}{2} \rho (V_2^2 - V_1^2) + \rho \int dV / dt(ds) + R(V) \quad [8]$$

where

ΔP = the pressure difference across an obstructive orifice

V_1 = the flow velocity proximal to the obstruction

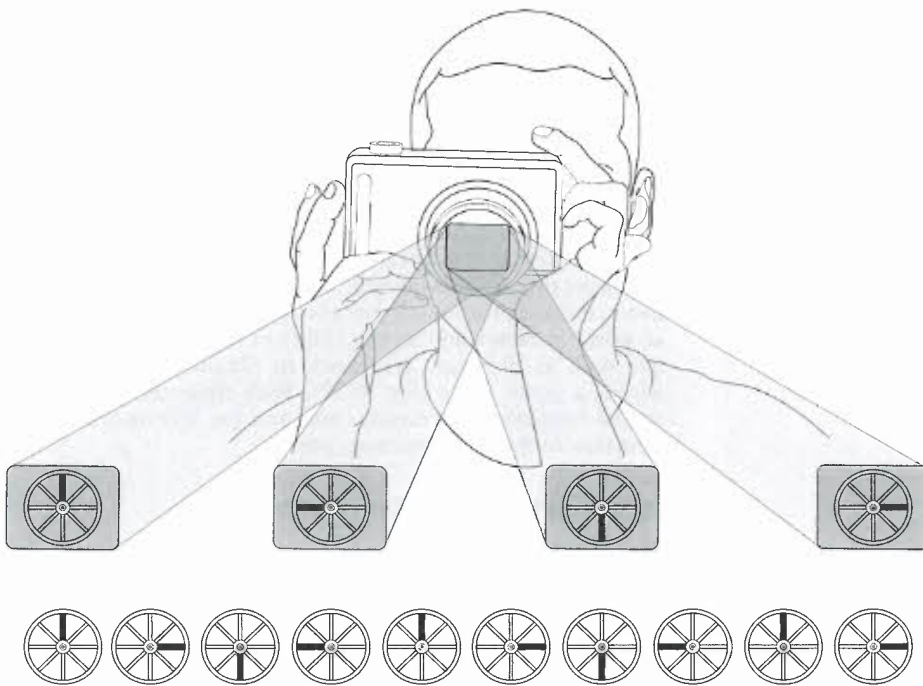


Figure 8.7. The principle of aliasing is similar to the phenomenon in old Western movies of a wheel of a stagecoach appearing to rotate backward when the stagecoach is obviously moving forward. The movie consists of a series of stop-action photographs which when placed in sequential order give the appearance of motion. If the series of photographs are captured at too low a frequency (top row) any spoke on the wheel (e.g., the highlighted, bold spike), will appear to be rotating backward (in this case, appearing to rotate 90 degrees counterclockwise each time an image is captured). It is only when the frequency of snapping photographs is high enough (bottom row), that the true forward rotation of the wheel is appreciated (in this case, rotating 90 degrees clockwise each time an image is snapped).

V_2 = the flow velocity distal to the obstruction
 ρ = the mass density of blood = 1,060 kg/m³
 dV = change in velocity over time (dt)
 ds = distance over which change in pressure occurs
 R = viscous resistance in blood vessel
 V = velocity of blood flow

The first term, $\frac{1}{2} \rho (V_2^2 - V_1^2)$, represents convective acceleration through the flow orifice. This portion of the equation becomes $4 (V_2^2 - V_1^2)$ when substituting the blood density of 1,060 kg/m³ into the equation, multiplying by $\frac{1}{2}$ and, multiplying by the conversion factor of 0.0075 which converts kg/m/s² (a pascal) to mm Hg. In addition, in most clinical conditions, the proximal flow velocity is < 1 m/s, and is considered negligible. Thus, the first term can be simplified as $4V_2^2$. The second term $(\rho dV/dt (ds))$ describes energy expended to accelerate fluid at the onset of flow; clinical measurements are usually made at peak flow, thus, this term can be assumed to be zero. The third term $R (V)$ describes energy lost overcoming viscous friction along the walls of the vessel, and is felt to be of little impact in most clinical circumstances. Therefore, the Bernoulli equation can be simplified, acknowledging the assumptions above:

$$\Delta P = 4V_2^2 \quad [9]$$

It is important to understand that when the assumptions used to simplify the Bernoulli equation may not apply, the approach to estimating pressure gradients may need to be modified. A common example of such an instance is in estimation of pressure drops where the proximal velocity (V_1) is greater than 1 m/s such as across an aortic coarctation, stenotic and regurgitant semilunar valves (where the regurgitant volume may result in an increase in V_1), multiple obstructions in series, and in the setting of high cardiac output. Viscous resistance may not be negligible in other circumstances where the obstruction is long and narrow (22) such as across Blalock-Taussig shunts, or across tunnel-type obstructions, for example, tubular obstruction of the left ventricular outflow tract.

THE EXAMINATION

General Considerations

Echocardiographic Windows

There are four major echocardiographic windows to the heart (Fig. 8.8): (a) parasternal, (b) apical, (c) subcostal, and (d) suprasternal notch. (A fifth window, the right parasternal window, obtained with the patient in a right lateral decubitus position, is used for obtaining an accurate Doppler gradient in patients with aortic valve stenosis.) The examination usually is performed in this same order, beginning with the least noxious (parasternal) window and finishing with the potentially most noxious (suprasternal notch) window. In complex cases associated with abnormal situs or cardiac position, the examination may alternatively begin with the apical or subcostal windows so that the echocardiographer can become oriented for the other views.

Parasternal and apical imaging is performed with the patient in a left lateral decubitus position. A dropout mattress is essential for obtaining the apical view. During subcostal imaging, the patient lies supine, sometimes flexing the knees, thereby relaxing the abdominal muscles. Suprasternal imaging is performed with a roll under the shoulders to extend the neck. When using the right parasternal view for Doppler interrogation of valvar aortic stenosis, the patient should be positioned in a right lateral decubitus position.

Planes of the Heart and Technique of Sweeping: Thinking in Three Dimensions

Three-dimensional (3-D) imaging is enjoying more routine use for clinical purposes. However, the challenge and essence of pediatric echocardiography continue to be acquiring all the necessary 2-D images, mentally synthesizing them into a 3-D model, and conveying this 3-D representation to others by narrative or visual tools.

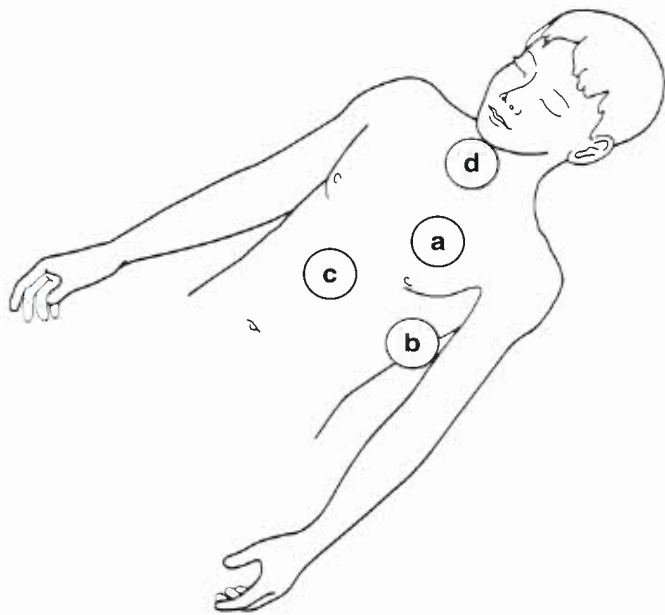


Figure 8.8. There are four main echocardiographic windows: (a) parasternal, (b) apical, (c) subcostal, and (d) suprasternal notch. The parasternal and apical windows are obtained with the patient in a left lateral decubitus position using a drop-out mattress. Subcostal images are obtained with the patient supine and sometimes with the knees flexed. Suprasternal notch images are obtained with a roll under the shoulders so that the neck is hyperextended. Additional windows include the right parasternal with the patient in a right lateral decubitus position useful for the Doppler interrogation of valvar aortic stenosis and the right apical view along the right anterior axillary line used when imaging patients with dextrocardia.

The spatial location of any part of an object is defined and understood by considering it in relation to the three planes (transverse (axial), sagittal, and coronal) in which the object exists (Fig. 8.9). Each of the four standard echocardiographic windows affords the opportunity to image the heart from one or more of these three planes. From the parasternal window, the long (sagittal) and short (axial) planes are shown. From the apical and subcostal windows, the four-chamber (coronal) and two-chamber (sagittal) planes are demonstrated. Finally, from the suprasternal notch window, the sagittal and axial axes of the upper thoracic vasculature are imaged. Sweeping the transducer through the nearly parallel planes within each of the acoustic windows mimics the ability of other imaging modalities such as magnetic resonance to obtain parallel “slices” within a given plane (Fig. 8.10). With these techniques, the spatial relationships become clear, and the 3-D mental reconstruction of the heart becomes possible.

Optimizing the Doppler Examination

The robustness of Doppler echocardiography as a tool for evaluating cardiac physiology is only manifest when its practitioners exhibit precise and diligent technique. Doppler spectral envelopes must be sharp and free of feathering. A sharp envelope is first achieved by aligning the ultrasound beam as parallel to the flow as possible. Traditionally, color Doppler is used before application of pulsed or continuous wave Doppler to determine the precise location and direction of a jet. The transducer position on the chest is then moved accordingly so that the flow is directed either exactly toward or opposite to it. The best transducer position for the Doppler examination may therefore be offset from the most ideal position for 2-D imaging. Not only the spectral display but also the audio component from the Doppler signal is often helpful in determining if one is localized in the vena contracta and parallel to flow. Second, the practitioner must be careful to avoid overgaining the

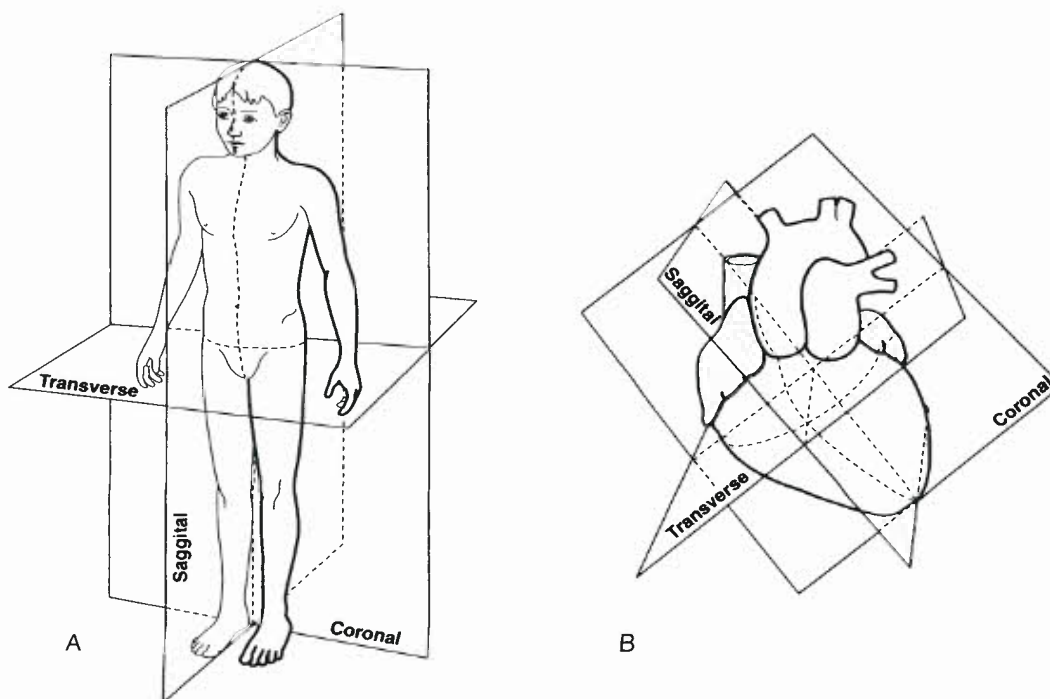


Figure 8.9. A: There are three imaging planes of the body: sagittal, coronal, and transverse. B: There are also three imaging planes of the heart. The cardiac imaging planes are rotated leftward and anterior because the heart's axes are rotated leftward and anterior relative to the body's.

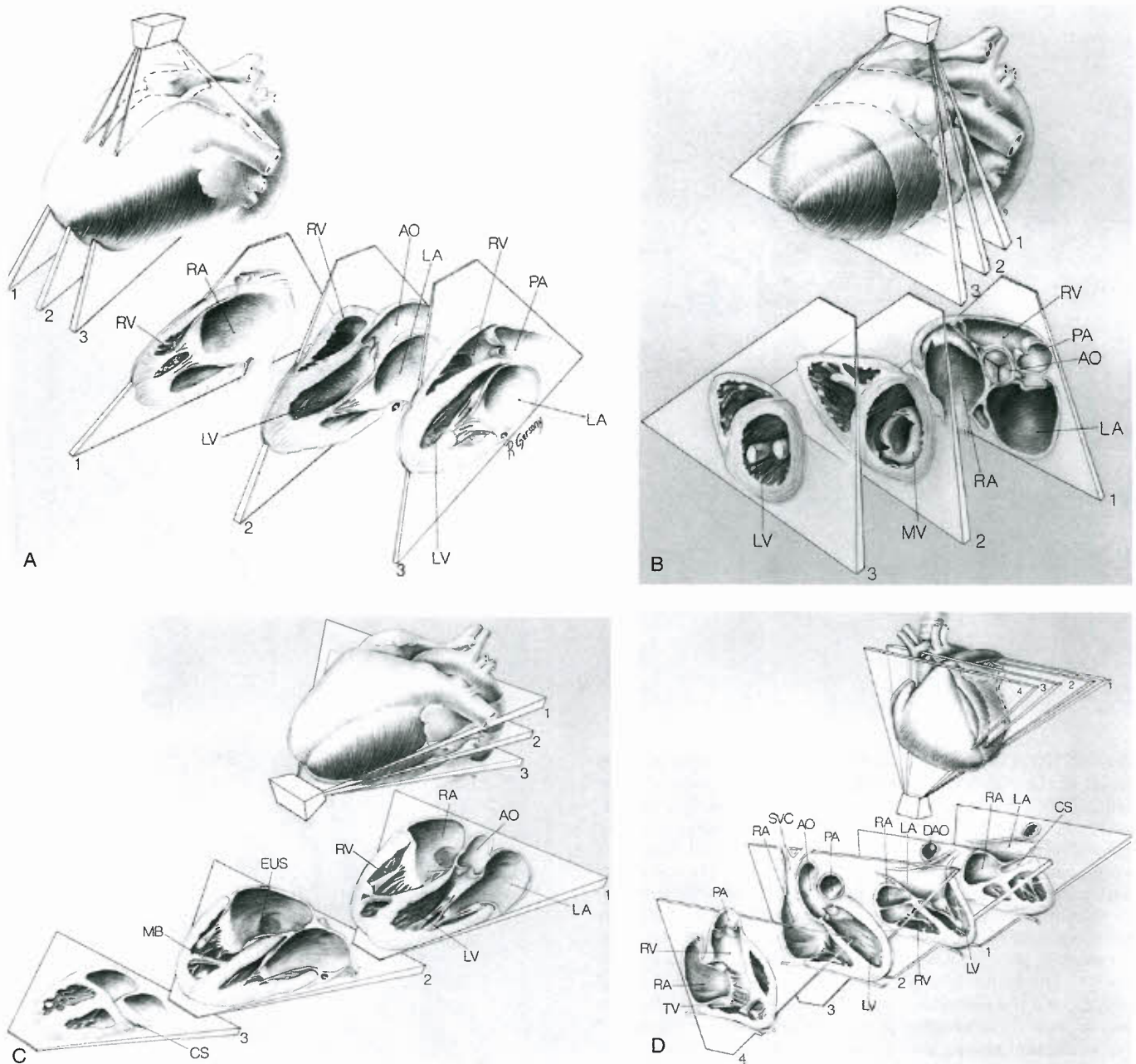


Figure 8.10. The family of sweeps for each of the imaging planes of the heart. **A:** The parasternal long-axis sweeps consist of the rightward tricuspid valve view (1), the standard long-axis plane (2), and the leftward pulmonary valve view (3). **B:** The parasternal short-axis sweeps consist of the superior basal view (1), the standard plane at the level of the mitral valve (2), and the inferior papillary muscle view (3). **C:** The apical sweeps consist of the anterior five-chamber view (1), the standard apical four-chamber view (2), and the posterior coronary sinus view (3). **D:** The subcostal coronal sweeps consist of the posterior coronary sinus view (1), the standard four-chamber view (2), the anterior left ventricular outflow tract view (3), and the extremely anterior right ventricular outflow tract view (4). (*Continued*)

spectral display which can cause indistinct envelopes. Third, the spectral display of interest should fill as much of the screen as possible by shifting the baseline up or down and decreasing the Doppler scale. In this way, the envelope is made as large as possible minimizing the effect of imprecise Doppler envelope planimetry (Fig. 8.11). Fourth, tracing the Doppler envelope must be careful, precise, and steady. The operator must know if a trace of modal velocity (for continuity equation) or of peak (or mean) velocity (for pressure gradients) is most appropriate (Fig. 8.12).

Color Flow Doppler

With its development in the 1980s, color flow Doppler revolutionized echocardiography by providing an efficient overview of flow across a relatively vast region of interest making it extremely valuable in screening for normal and abnormal flows across valves, vessels, and septa. The color Doppler modality interrogates flow with multiple pulsed Doppler sample volumes placed successively along multiple scan lines. For each sampling gate, the baseline frequency is compared to the

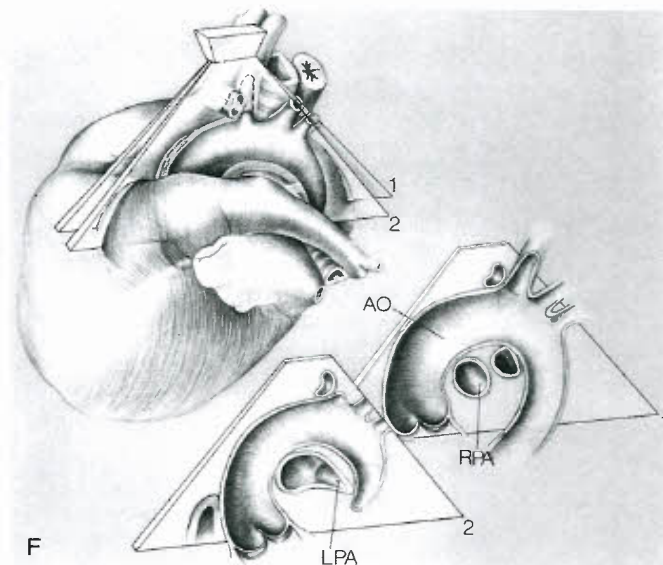
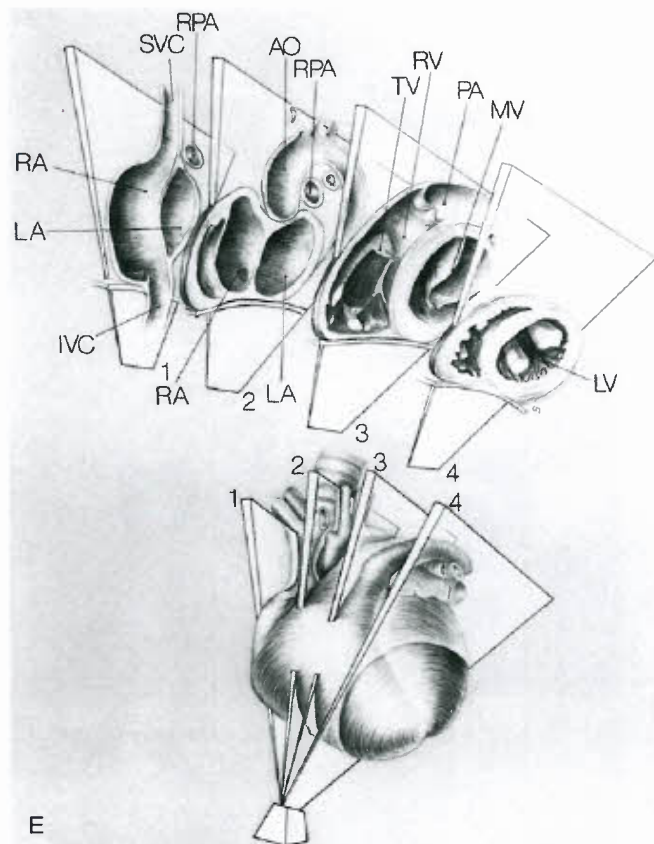
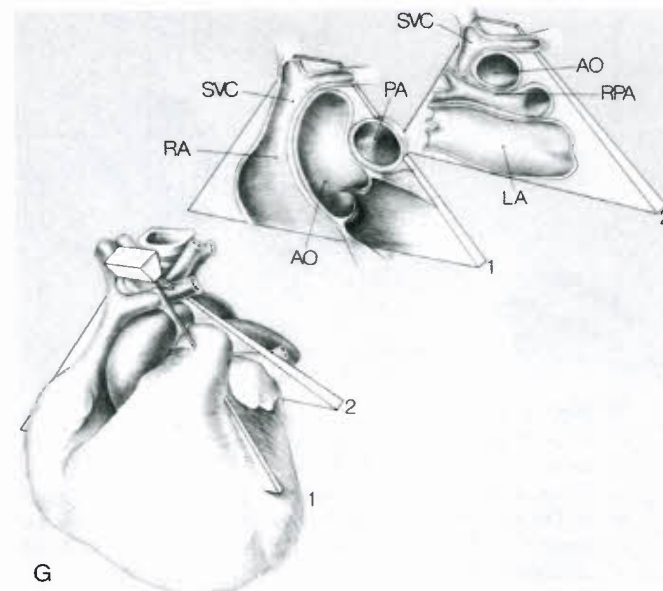


Figure 8.10. (Continued). E: The subcostal sagittal sweeps consist of the rightward systemic venous return view (1), the slightly leftward left ventricular outflow tract view (2), the leftward right ventricular outflow tract view (3), and the extremely leftward ventricular view (4). F: The suprasternal long-axis sweeps consist of the standard aortic arch view (1), the rightward superior vena caval view (not shown), and the leftward left pulmonary artery view (2). G: The suprasternal short-axis sweeps consist of the very anterosuperior strap vessels view (not shown), the anterosuperior vena cava and innominate vein view (1), the standard right pulmonary artery and left atrial view (2), and the posterior descending aorta view (not shown). Even though these imaging planes are defined and illustrated here as discrete planes, the technique of sweeping is a process that allows acquisition of dozens of imaging planes tangential to these. The technique of sweeping through these imaging planes in orthogonal views is critical to understanding the 3-D anatomy. AO, aorta; CS, coronary sinus; DAO, descending aorta; EUS, Eustachian valve; IVC, inferior vena cava; LA, left atrium; LPA, left pulmonary artery; LV, left ventricle; MB, moderator band; MV, mitral valve; PA, pulmonary artery; RA, right atrium; RPA, right pulmonary artery; RV, right ventricle; SVC, superior vena cava; TV, tricuspid valve. (Reprinted from Snider AR, Serwer GA, Ritter SB, eds. *Echocardiography in Pediatric Heart Disease*. 2nd ed. St. Louis, MO: Mosby-Year Book, 1997:27–52, with permission from Elsevier.)



received frequency. Pixels in the image are arbitrarily assigned a color (red for flow toward the transducer and blue for flow away from the transducer) and the color intensity is based on the magnitude of the mean velocity. The color Doppler scale should be actively manipulated throughout the examination—using low velocity scales when interrogating venous velocities (e.g., those across/in antegrade atrioventricular valves, atrial

septum, cavopulmonary shunt, and systemic and pulmonary venous velocities) or velocities generated from lower pressure gradients (e.g., in the coronary arteries, across a large VSD or patent ductus arteriosus [PDA]) and high velocity scales when interrogating arterial flows or flows generated from high pressure gradients (e.g., atrioventricular valve regurgitation, restrictive VSD or PDA). The examiner must actively think

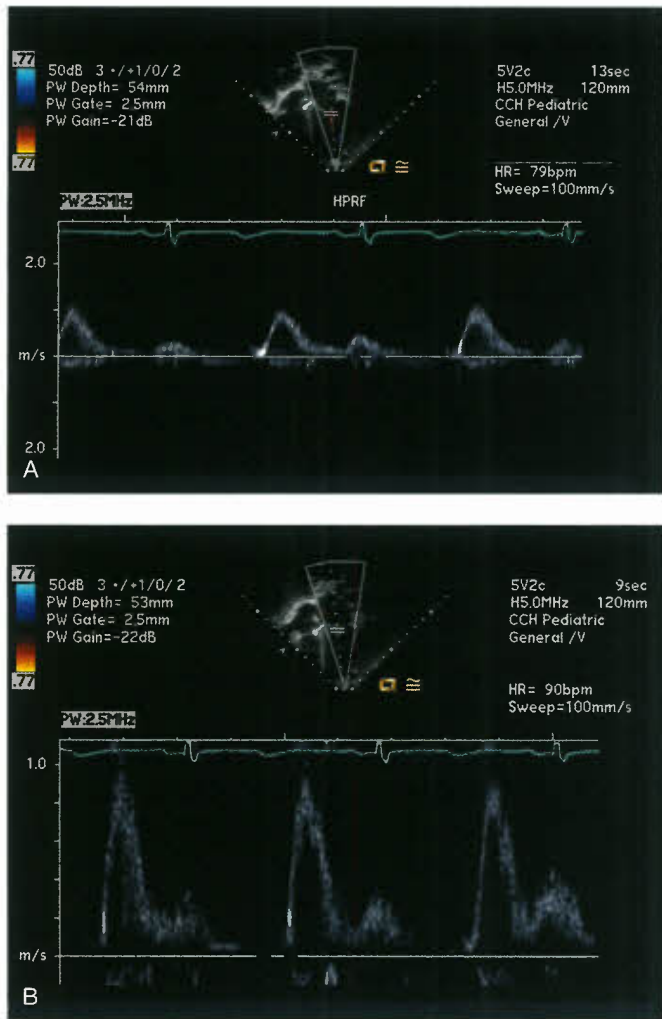


Figure 8.11. Mitral valve Doppler spectral profile recorded with (A) inappropriate and (B) appropriate scale and baseline shift. It is important to fill as much of the Doppler display area, thereby enlarging the Doppler spectral profile as much as possible thus minimizing error in measurement (B).

about and anticipate expected physiology during the study so that the color scale is appropriately adjusted (Fig. 8.13). For example, in a toddler being evaluated for a suspected ventricular septal defect (VSD), interrogation of the septum with a high color Doppler scale is appropriate. However, using such a high color scale in the investigation for a VSD in a newborn would likely miss the low velocity shunt flow since the shunt is driven by a very low pressure gradient due to the normally elevated pulmonary vascular resistance in the newborn period. The examiner would need to interrogate the ventricular septum with a low velocity color Doppler scale in this instance. These flows then need to be more carefully and precisely interrogated and quantitated with either pulsed or continuous wave Doppler. Because of the massive amount of data, a color Doppler sector should be kept as narrow as acceptable to improve accuracy and/or temporal resolution (see Section Equation 5: The Basis of Temporal Resolution)

Pulsed Wave Doppler

Pulsed wave Doppler, along with continuous wave Doppler, is the principal echocardiographic tool for evaluating cardiovascular physiology. Pulsed Doppler causes the transducer to

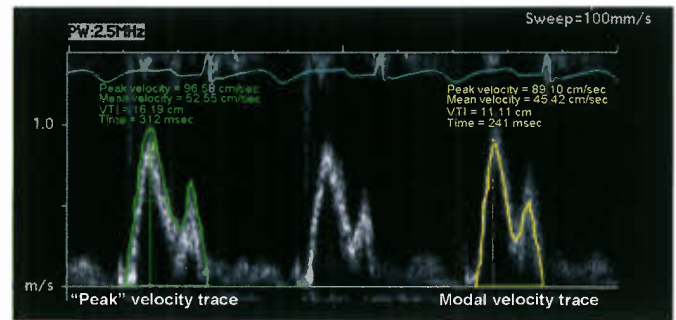


Figure 8.12. Mitral valve Doppler spectral profile demonstrating the difference between a “peak” velocity trace (green on the left waveform) and modal velocity trace (yellow on the right waveform). The “peak” velocity trace follows the outside edge of the Doppler spectral contour while the modal velocity trace follows the midline of the contour. “Peak” velocity traces are used to obtain peak and mean pressure gradients across valves and orifices. Modal velocity traces are used in the continuity equation and in calculation of cardiac output. Note that there can be a potentially large difference in the values obtained from a “peak” and modal velocity trace. (e.g., 31% difference in the two velocity time integrals (VTI) in this case)

alternately transmit and receive short ultrasound bursts. The time between transmission and reception allows calculation of the depth of the signal or “range-gating” which provides the operator with the Doppler frequency shift at a specific location. A disadvantage with the technique is that the maximal detectable frequency shift is limited—the Nyquist limit (see Section Equation 7: The Basis of Aliasing). However, the Nyquist limit can be extended by shifting the baseline of the spectral display, exchanging to a lower frequency transducer, or moving to a different imaging plane so that the structure of interest is at a shallower depth if possible. High-PRF is a technique in which volleys of pulses of ultrasound are sent before reception of prior pulses. This technique increases the Nyquist limit but causes some range ambiguity.

Continuous Wave Doppler

With the continuous wave Doppler modality, the transducer is continuously transmitting and receiving ultrasound signals. The disadvantage of this process is the absence of range gating, but a major advantage is that the sampling rate is infinite so there is no longer a limit to the maximal frequency shift. The spectral display consists of a composite of signals with the maximal velocity representing the peak velocity at any depth in the plane of the ultrasound beam. Lower velocities are often visible within the spectral envelope allowing calculation of “corrected gradients” in which the lower proximal velocity (V1) is subtracted from the higher distal velocity (V2) as is performed for the evaluation of a gradient across an aortic coarctation.

Approach to the Pediatric Patient

A cheerful environment is important in relieving anxiety. Bright-colored rooms filled with toys and stuffed animals capturing the environment of the patient’s own bedroom can make the child feel more comfortable. Rooms should be equipped with television and DVD players so that patients can be entertained during the examination. Warm ultrasound gel also helps in reducing stress. For infants, light dimmers and an infant warmer will facilitate a comfortable environment. Formula should be available for further comforting of infants.

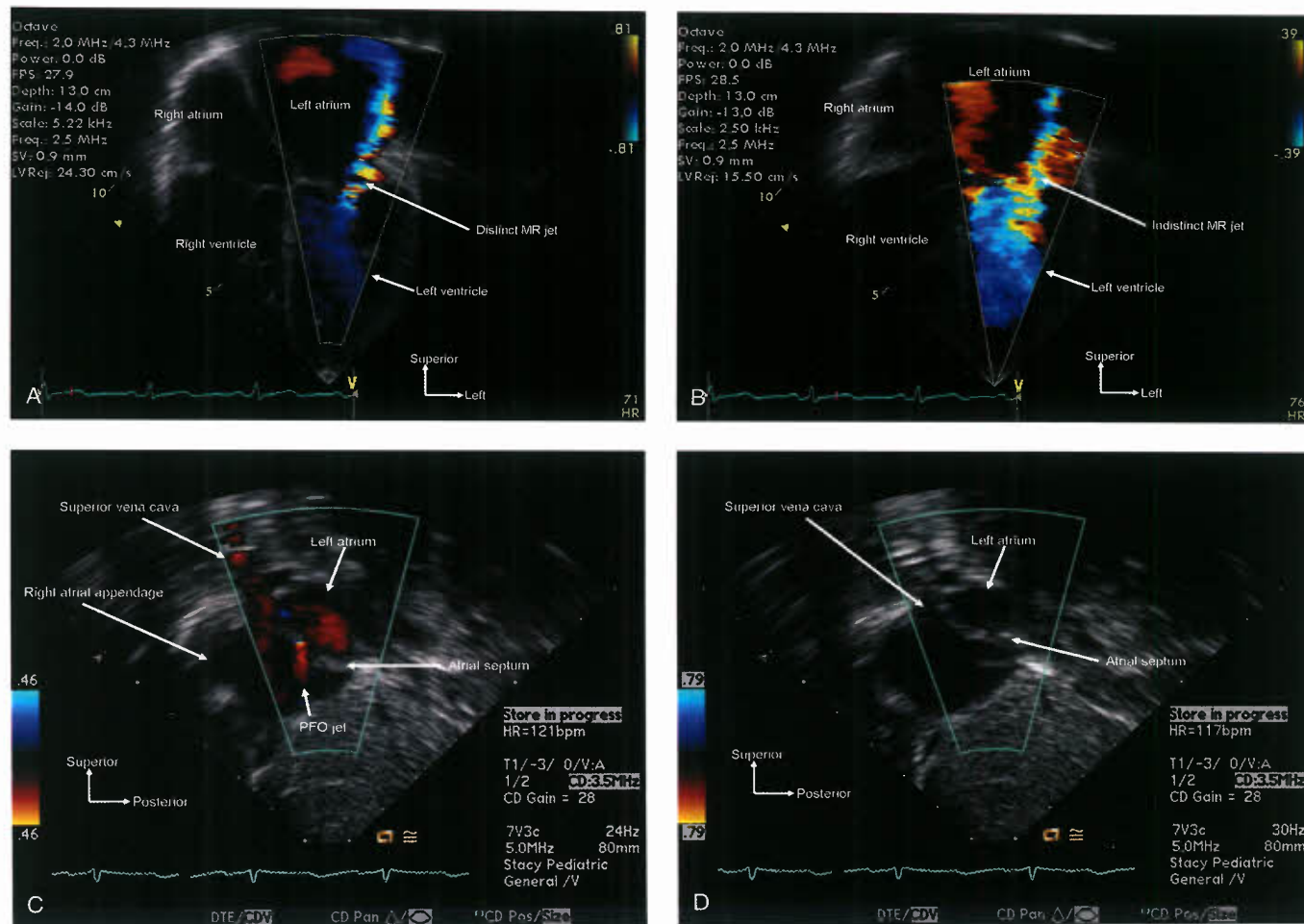


Figure 8.13. Series of four images demonstrating inappropriate and appropriate color aliasing limits during the echocardiographic examination. Throughout an echocardiographic examination the echocardiographer must actively decrease and increase the color aliasing limit depending on the expected velocity of the color jet being interrogated. For example, in evaluating high-velocity jets such as mitral insufficiency, color aliasing limits should be high as in this apical four-chamber view shown in (A) where the velocity limit is 81 cm/s. This provides a clean, crisp, and interpretable display of the mitral insufficiency flow. Inappropriate low color aliasing limit as in (B) (39 cm/s) produces an indistinct display of the mitral insufficiency jet. On the other hand, when evaluating a low-velocity color jet such as a patent foramen ovale (PFO) the color aliasing velocity should be lower to enhance recognition and display as in the subcostal image (C) where the aliasing velocity is 46 cm/s. If the aliasing velocity is set too high (79 cm/s in this example), detection of the low-velocity PFO jet may be impossible (D).

Even in a nonthreatening environment, patients over 6 months and under 3 years of age often require sedation. Presedation guidelines delineating the fasting requirements and describing the sedation procedure need to be sent to parents before the echocardiography visit. Chloral hydrate (75 to 100 mg/kg administered orally) or pentobarbital (5 mg/kg orally) are commonly used agents for sedation. In order to remain compliant with increasingly strict regulations from the Centers for Medicare and Medicaid Services, many pediatric laboratories are electing to employ anesthesiologist and/or nurse anesthetists for the administration and monitoring of conscious sedation. Monitoring and resuscitation equipment should be available in each room in the event of an adverse reaction or complication.

Echocardiography: Robust Phenotyping Tool

Echocardiography represents a “physiologic microscope” which singularly provides phenotypic observations on an

“experimental preparation” (the pediatric cardiovascular system) with minimal interference from external noxious influences. Therefore, unique opportunities to evaluate both cardiovascular anatomy and physiology are afforded that are not available with other imaging modalities, for example, during magnetic resonance imaging when the patient may have to endure an examination of prolonged duration or during catheterization when the heart is probed with catheters.

Defining Anatomy: Segmental Approach

The echocardiographic examination is performed, and the interpretation is presented using a segmental approach (23–27) which requires complete definition of eight features of cardiac anatomy (Table 8.1). This is a two-step process. The first is the proper identification of a structure which requires the abilities of imaging and recognizing the specific features of

TABLE

8.1

Segmental Approach to Defining Cardiac Anatomy by Echocardiography

Anatomic Feature	Diagnostic Possibilities
Thoracoabdominal situs	Solitus Inversus Ambiguous
Cardiac position	Levocardia Mesocardia Dextrocardia
Atria	Solitus (S) Inversus (I) Ambiguous (A)—bilateral right- and left-sidedness
<i>Atrioventricular connection</i>	Concordant Discordant Atresia Double inlet Common Straddling Criss-cross
Ventricles	d-looped (D) l-looped (L) x-indeterminate
Conus	Subpulmonic Subaortic Bilateral Absent or very deficient
<i>Ventriculoarterial connection</i>	Concordant Discordant Double outlet Single outlet
Great vessels	Solitus (S) Inversus (I) Transposed (D, L, A) Side-by-side

A complete segmental description of the heart by echocardiography begins by defining these eight features which include the three segments of the heart (shown in bold) and the two junctional segments (shown in italics). The letters in parentheses following the diagnostic possibilities for the three cardiac segments are frequently used as abbreviated three-letter descriptors of these segments: the first initial describing atrial situs, the second describing ventricular topology, and the third describing the great vessel relationship. For example, (S, D, S) describes a normal heart, while (I, L, I) describes mirror image dextrocardia. Following description of the morphology, intrinsic (e.g., pulmonary stenosis), myocardial (e.g., hypertrophic cardiomyopathy), septal (e.g., tetralogy or Fallot), orientation (e.g., criss-cross heart), defect (e.g., ventricular septal defect or aortopulmonary window) pathology is described.

each cardiac structure. The second is determining the spatial and physiologic relationships of a properly identified structure to the other structures (both cardiac and noncardiac) in the thoracoabdominal cavity. Accurate morphology can be accomplished definitively only by imaging chamber septal structures. Next, other malformations (e.g., cardiac shunts, valve function) and physiology (biventricular function, chamber sizes, pressure estimates) are described. To ensure that no anatomy or physiology is left undescribed, it is helpful during both the

performance and interpretation of the examination to imagine the course of a red blood cell traveling through the heart, beginning in the systemic veins and terminating in the systemic arteries.

Abdominal Situs and Cardiac Position

Abdominal situs is best determined from a transverse view of the abdomen below the diaphragm (Fig. 8.14). In this view the positions of the liver and the gastric bubble can be ascertained. In patients with abdominal situs solitus, the stomach is on the left and the liver is on the right. In patients with abdominal situs inversus, the opposite is true.

The position of the heart in the thoracic cavity is identified most easily from an apical four-chamber or subcostal coronal view. The position of the transducer on the chest from where a standard apical four-chamber view is obtained defines the position of the cardiac apex. From the subcostal coronal view, the side of the cardiac apex is determined (Fig. 8.15). The normal position of the heart in the left chest is termed levocardia. The mesocardic term refers to a cardiac position over the patient's midline.

Dextrocardia indicates that the heart lies in the right side of the chest. There are three main categories of dextrocardia. The first is termed dextroposition and refers to a condition in which the heart is pushed into the right chest by either a mass in the left chest (e.g., diaphragmatic hernia) or deficiencies in right-sided chest structures. The apex remains pointed to the left, atrial situs, ventricular topology, and great vessel relationships are normal, and cardiac pathology, if any, is not complex. In the other two types of dextrocardia, termed dextroversion and mirror-image dextrocardia, the apex is pointed to the patient's right. Dextroversion refers to a condition in which there is atrial situs solitus with a rightward-pointing apex. Ventricular inversion (atrioventricular discordance) and associated pathology similar to that seen in congenitally corrected transposition of the great vessels is frequently associated. Mirror-image dextrocardia is a condition with atrial situs inversus and a rightward-pointing apex. These patients' anatomy is "mirror image" to that of a patient with levocardia and atrial situs solitus and their anatomy is best appreciated by imagining a mirror placed on a patient with levocardia and situs solitus at the patient's midline in a sagittal position. In this way, one appreciates that structures that are normally far left (e.g., left ventricle) are in a far right position in a patient with mirror image dextrocardia. Structures that are closer to the midline (e.g., the superior vena cava [SVC]) are in a midline position in a patient with mirror image dextrocardia. There may be major and complex pathology associated with mirror image dextrocardia. However, in situs inversus totalis (a condition in which all body organs are on the contralateral side of the body from which they usually reside), the heart may be completely normal.

When evaluating a patient with any of these three types of dextrocardia, the echocardiographer must maintain left/right conventions rather than attempting to make the image look familiar. Specifically, the echocardiographer must remain true to the established echocardiographic convention that the **right** side of the screen/monitor in the parasternal short-axis, apical four-chamber, and subcostal coronal view is always the **left** side of the patient. This convention is maintained by the echocardiographer rotating the transducer so that the "orientation mark" on the transducer is pointing to the patient's left in these imaging planes. There will be a tendency (which must be resisted) for the echocardiographer to rotate the transducer to an unusual or atypical position to attempt to make the image look "normal." In some instances, this is problematic because it could reverse the left/right echocardiographic conventions.

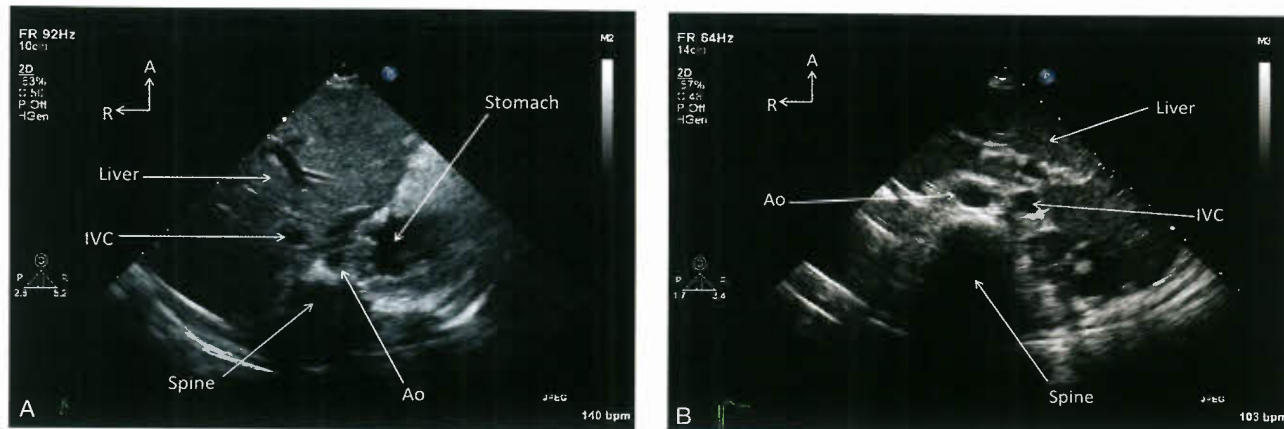


Figure 8.14. Subcostal transverse abdominal views in a patient with abdominal situs solitus (A) and in a patient with abdominal situs inversus (B). With abdominal situs solitus, the liver is on the patient's right and the stomach is on the left. In abdominal situs inversus, the liver is on the left and the stomach is on the right. A, anterior; Ao, descending abdominal aorta; IVC, inferior vena cava; R, right.

Venous Return and Atria

Situs

The fact that an atrial chamber is on the patient's right or left or that it receives a particular venous structure does not allow a conclusion regarding atrial morphology. Atrial situs can be deduced only by evaluation of the atrial appendages and the septal structures.

The atrial appendages are consistently committed to their respective atria and are distinctly morphologically different. The right atrial appendage is short, fat, and broad-based and best seen in the subcostal sagittal view, as well as the parasternal long-axis view (Fig. 8.16A). The left atrial appendage is long, thin, and narrow-based and best seen in the parasternal short-axis and apical four-chamber views (Fig. 8.16B). The atrial appendages have pectinate muscles (raised parallel ridges resembling the teeth of a comb) which also help make them distinct. These muscles of the right atrial appendage extend into the right atrium (RA) whereas the pectinate muscles of the left atrial appendage are confined to the appendage and do not extend into the atrium (28,29).

The unique septal structures of the RA are the embryonic valves—Eustachian and Thebesian—seen in the subcostal coronal and sagittal views. The unique left atrial septal structure is the flap valve seen in the apical and subcostal coronal and sagittal views (Fig. 8.17). In heterotaxy syndrome with bilateral right- or left-sidedness and common atrium, the atrial septal structures will not be obvious and atrial situs will be indeterminate or ambiguous.

SYSTEMIC VEINS AND RIGHT ATRIUM

The innominate veins are identified in the suprasternal short-axis view. Both innominate veins are identified and traced downstream as they join to form the right superior vena cava (RSVC) which, in turn, is followed to its entrance into the heart (Fig. 8.18). The left innominate vein is traced upstream to identify a possible left superior vena cava (LSVC) (Fig. 8.19). Alternatively, a suprasternal notch long-axis view can be swept leftward from the aortic arch to demonstrate a LSVC in its long axis (Fig. 8.20). These maneuvers are particularly important in (a) any patient undergoing surgical repair

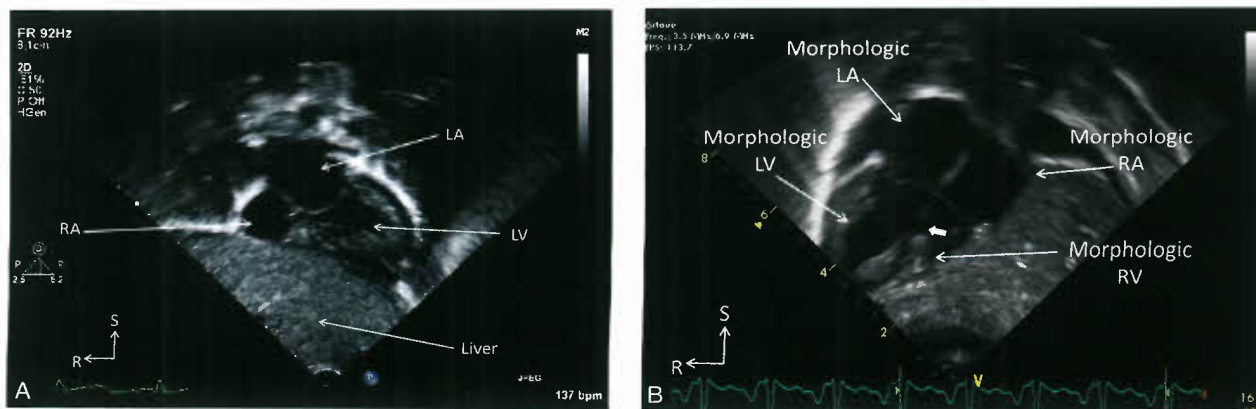


Figure 8.15. Subcostal coronal views of a patient with levocardia (A) and a second patient with dextrocardia (B). In the patient with dextrocardia, the apex of the heart is pointing to the patient's right. The patient has mirror image dextrocardia so that the morphologic left atrium (LA) and left ventricle are on the patient's right and the morphologic right atrium (RA) and right ventricle (RV) are on the patient's left. The patient also has a small midmuscular ventricular septal defect (block arrow). R, right; S, superior.

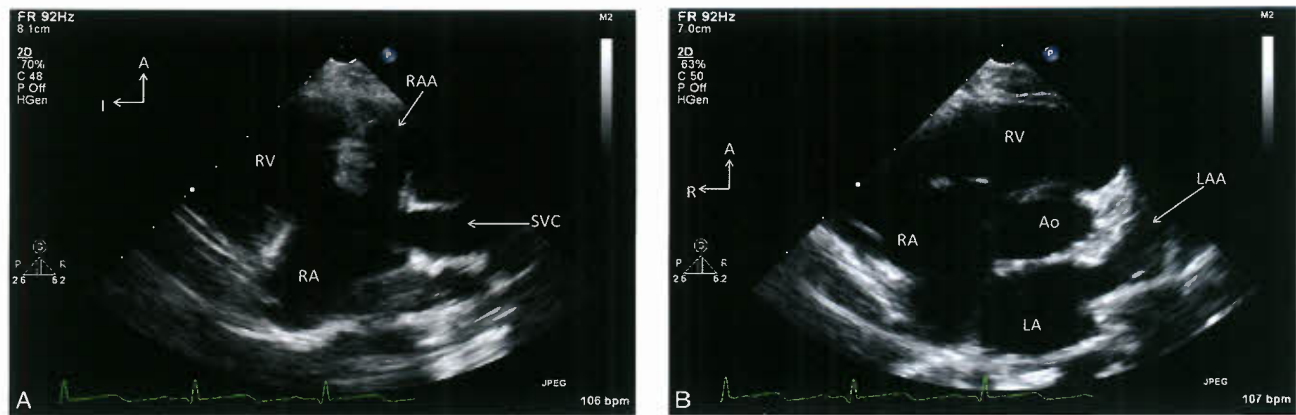


Figure 8.16. Echocardiographic imaging of the atrial appendages. **A:** The right atrial appendage (RAA) is broad based and is best seen in the subcostal plane and, as shown here, in the parasternal long view swept rightward. **B:** The left atrial appendage (LAA) is long and thin and is best seen in the parasternal short-axis view (**B**). A, anterior; Ao, aorta; I, inferior; LA, left atrium; RA, right atrium; RV, right ventricle; SVC, superior vena cava.

using cardiopulmonary bypass since a surgeon may have to cannulate both SVCs (when present) in the absence of a left innominate vein and (b) the newborn with single-ventricle physiology, who will undergo eventual bilateral bidirectional cavopulmonary anastomoses in the presence of bilateral SVC without an innominate vein. In patients with unexplained cyanosis or systemic emboli or with absent innominate vein without dilated coronary sinus, the presence of a LSVC draining directly into the left atrium (LA) should be investigated. This may require using agitated saline contrast (see Section Contrast Echocardiography).

The inferior vena cava (IVC) is identified in the subcostal transverse abdominal and subcostal coronal and sagittal views (Fig. 8.14). Anyone performing cardiac catheterization needs to be alerted for interruption of the IVC. This is apparent in the transverse abdominal view where a large venous vessel immediately posterior to the aorta (the azygous or hemiazygous vein) is seen and there is notable absence of an IVC candidate anterior to the aorta (Fig. 8.21).

The entrance of the coronary sinus into the RA can be seen in the subcostal coronal and the apical four-chamber views. The size and possible unroofing of the coronary sinus can be

assessed in a posterior sweep from the standard apical four-chamber and parasternal long-axis views.

ATRIAL SEPTUM

The atrial septum is examined in the subcostal coronal and sagittal views. With the increasing responsibility of echocardiographers to define atrial septal rims for device closure of atrial septal defect (ASD), the complexity of the atrial septum is gaining a new appreciation. The size of an ASD, as well as the degree of remaining atrial septal rim tissue for anchoring of possible ASD closure device and total atrial septal length for maximum possible diameter for said device, are best evaluated by using both these views to give information from two mutually orthogonal planes. In addition, the rim between aorta and defect can be assessed in the parasternal short-axis view.

Superior and inferior vena caval sinus venosus defects are best seen in the subcostal sagittal view. The transducer should be swept gradually and deliberately posterior and rightward to investigate for possible associated partial anomalous pulmonary venous return. Secundum ASDs are best seen in the same imaging planes. The ostium primum defect

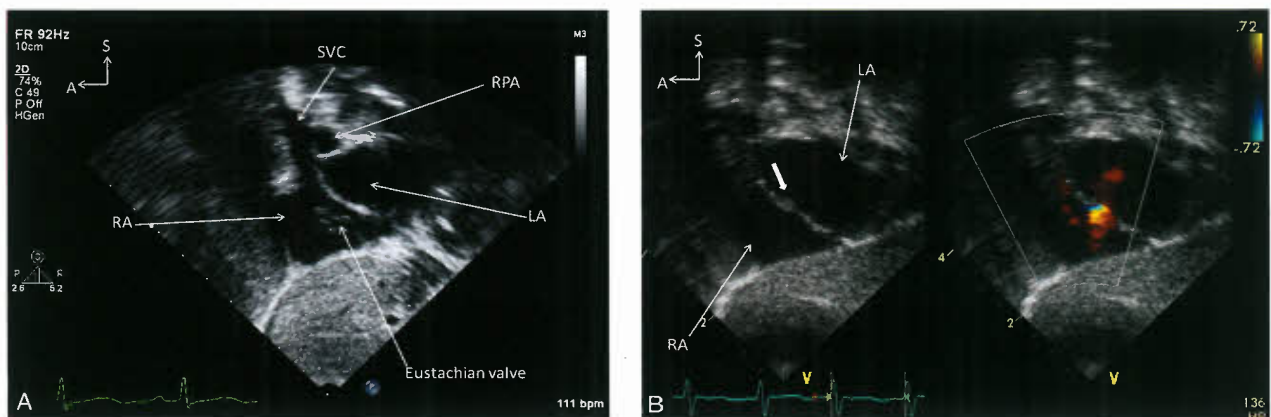


Figure 8.17. Subcostal sagittal views demonstrating Eustachian valve (**A**) and flap valve (block arrow in **B**). These unique septal structures are the most reliable method for defining the morphologic right and left atrium (RA and LA), respectively. The color panel of Figure B demonstrates a small left-to-right shunt from the LA to the RA through the patent foramen ovale caused by the flap valve. A, anterior; I, inferior; IVC, inferior vena cava; P, posterior; RPA, right pulmonary artery; S, superior; SVC, superior vena cava.

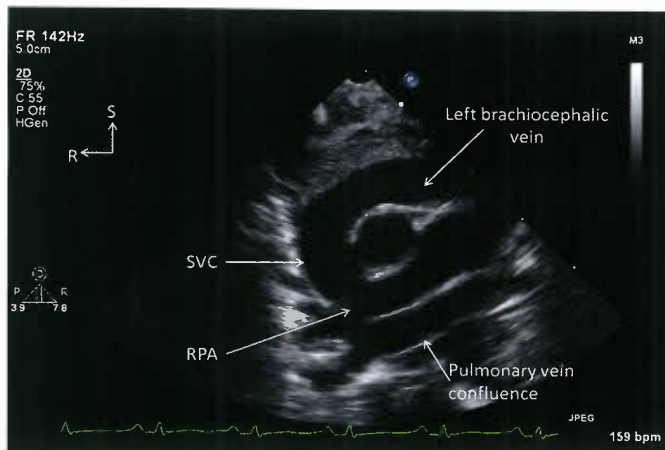


Figure 8.18. Suprasternal notch short-axis view demonstrating the left brachiocephalic vein draining into the right superior vena cava (SVC) in a patient with total anomalous pulmonary venous return of the supracardiac type. The pulmonary veins drained to a pulmonary vein confluence immediately superior to the roof of the LA. Pulmonary venous flow then continued through a vertical vein, the left brachiocephalic vein and the SVC resulting in dilatation of the latter two structures. R, right; RPA, right pulmonary artery; S, superior; SVC, superior vena cava.

is related to the crux of the heart and is therefore best seen in the apical view. The coronary sinus defect is visualized by sweeping the transducer posterior from the standard apical four-chamber view.

PULMONARY VEINS AND LEFT ATRIUM

The pulmonary veins are identified most easily from the suprasternal short-axis plane (Fig. 8.22). Alternatively, the pulmonary veins can be visualized from the parasternal short-axis and apical four-chamber views. An extreme rightward sweep (tilt right from the SVC, RA, IVC views) in the subcostal sagittal plane consistently reveals the right upper pulmonary vein. Parasagittal imaging from the bicaval view can show the right

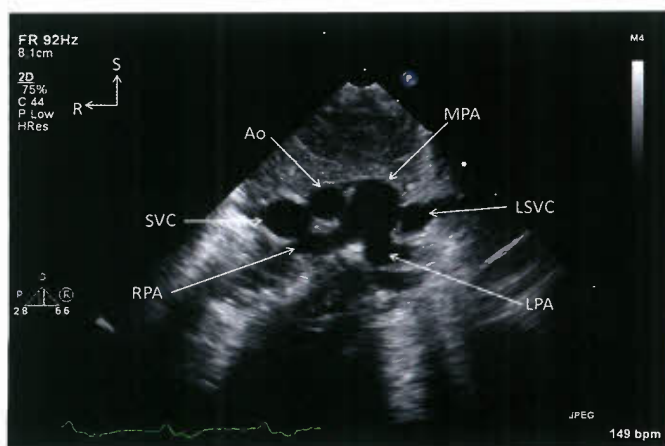


Figure 8.19. High suprasternal notch short-axis view demonstrating not only the normal anatomy and relationships of the right superior vena cava (SVC), ascending aorta (Ao), and main pulmonary artery (MPA), but also the additional finding of a left superior vena cava (LSVC) in cross section just leftward of the MPA. LPA, left pulmonary artery; R, right; RPA, right pulmonary artery; S, superior.

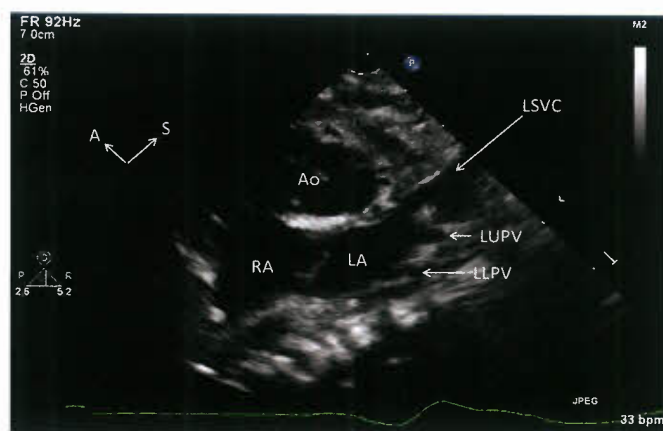


Figure 8.20. Hybrid suprasternal notch oblique axis view of left superior vena cava (LSVC), which in this patient is draining directly into the roof of the left atrium (LA) due to complete unroofing of the coronary sinus. A, anterior; LLPV, left lower pulmonary vein; LUPV, left upper pulmonary vein; RA, right atrium; S, superior.

pulmonary veins (with a rightward sweep) and the left pulmonary veins (with a leftward sweep) in cross section as they course into the LA. Color Doppler with a low velocity aliasing limit can aid in visualizing the individual pulmonary veins (30). Anomalous pulmonary venous pathways, the confluences from which they emanate, and the entrances of the pulmonary veins into the confluences should be investigated from the suprasternal short axis view (supracardiac drainage), parasternal and apical views (cardiac drainage), and subcostal coronal and sagittal views (infracardiac drainage). Unlike systemic venous anomalies, in which color Doppler demonstrates flow coursing toward the heart, these anomalous pulmonary venous pathways will have color Doppler flow coursing away from the heart, often the first sign that makes an echocardiographer aware of this condition.

The LA is best evaluated in the apical four-chamber and the subcostal coronal and sagittal views. Membranes (e.g., supra-valvar stenosing mitral ring and cor triatriatum) are identified in the apical four-chamber view. The diagnostic relationship of these membranes relative to the left atrial appendage (i.e., membrane of cor triatriatum upstream from the LA appendage

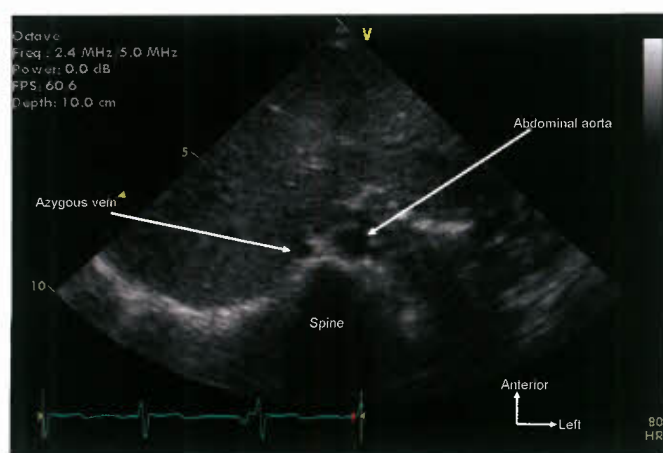


Figure 8.21. Subcostal transverse abdominal view demonstrating the features of interrupted inferior vena cava (IVC). There is no venous structure identified anterior to the aorta. Instead, there is a venous structure which is adjacent and slightly posterior to the aorta. The structure is also rightward of the aorta indicating that it is an azygous continuation of interrupted IVC.

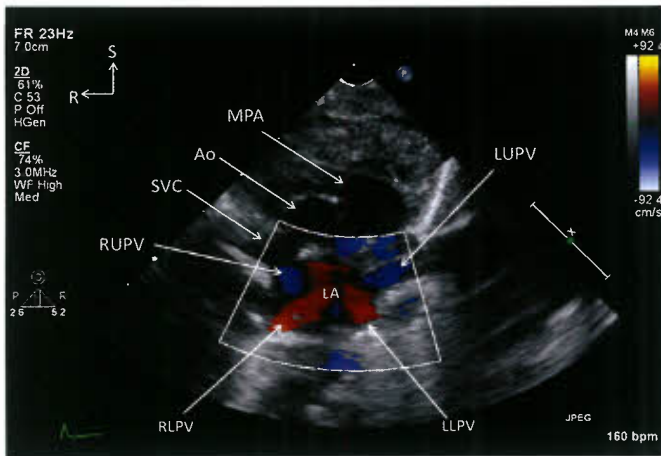


Figure 8.22. Suprasternal notch short-axis view with color Doppler demonstrating the four pulmonary veins draining normally into the left atrium. Ao, ascending aorta; LA, left atrium; LLPV, left lower pulmonary vein; LUPV, left upper pulmonary vein; MPA, main pulmonary artery; RLPV, right lower pulmonary vein; RUPV, right upper pulmonary vein; R, right; S, superior; SVC, superior vena cava.

orifice and membrane of supravalvar stenosing mitral ring downstream in the mitral valve funnel itself) is visualized from the apical four-chamber view.

Atrioventricular Connection

TYPE

The septal structures of the atrioventricular valves serve as the only consistent feature allowing morphologic diagnosis. The tricuspid valve has an intimate relationship with the ventricular septum (i.e., septophilic), with multiple chordal attachments emanating from its septal leaflet, seen best in the apical four-chamber view. On the other hand, the mitral valve has no chordal attachments with the ventricular septum (septophobic), and all of its attachments course to the left ventricular free wall (Fig. 8.23). In addition, the hinge point of the septal leaflet of the tricuspid valve is inferior to the hinge point of the anterior leaflet of the mitral valve. Because each atrioventricular valve is associated with its appropriate ventricle (i.e., tricuspid valve with right ventricle, mitral valve with left ventricle), the atrioventricular connection can be determined as concordant (RA to right ventricle and LA to left ventricle) or discordant (RA to left ventricle and LA to right ventricle). Atrietic atrioventricular connections are easily identified in the apical and subcostal views. The relationship of the atrioventricular valves to each other in double-inlet connections are explored in the parasternal views. The five leaflets of the common atrioventricular valve (superior/anterior bridging, right superior, right mural, inferior/posterior bridging, and left mural) are best seen in a right anterior oblique subcostal view (midway between the coronal and sagittal views). In this view, the presence or absence of a tongue of tissue connecting the two bridging leaflets should be identified first to allow the establishment of a complete (absent connecting tissue) or partial (present connecting tissue) atrioventricular septal defect. Then the degree of bridging of the superior leaflet and its attachments are identified, allowing for Rastelli classification (Fig. 8.24). Straddling and criss-cross connections are seen in the apical four-chamber and subcostal views. A straddling atrioventricular valve (valve attachments to contralateral ventricle) must be distinguished from mere overriding (valve annulus partially displaced over the ventricle) in these views. Criss-cross atrioventricular relationships necessitate deliberate and slow sweeping of the transducer anteriorly and posteriorly in the

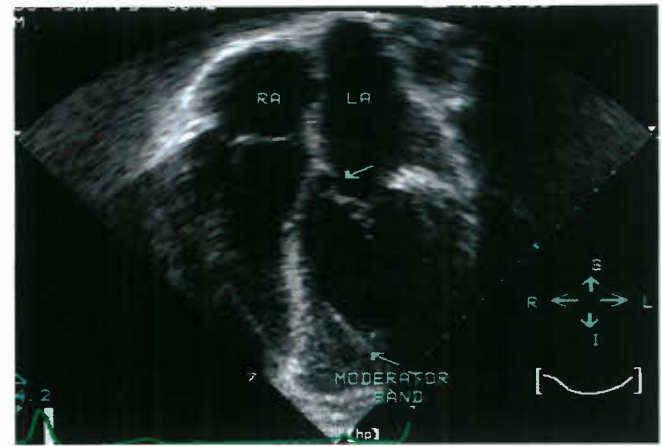


Figure 8.23. Apical four-chamber view in a patient with ventricular inversion with congenitally corrected transposition of the great vessels {S, L, L}. The left-sided atrioventricular valve has attachments to the ventricular septum, whereas the right-sided valve does not, allowing diagnosis of a left-sided tricuspid valve and a right-sided mitral valve. In addition, the septal hinge point of the tricuspid valve is inferior to that of the mitral valve, which is another distinguishing feature of a tricuspid valve. There is a moderator band near the apex of the left-sided ventricle, further defining this ventricle as a morphologic right ventricle. I, inferior; LA, left atrium; RA, right atrium; S, superior.

subcostal coronal or superiorly and inferiorly in the parasternal short-axis views with careful, simultaneous observation of each valve's upstream atrium and downstream ventricle.

TRICUSPID VALVE

The tricuspid valve is examined in the parasternal long-axis plane (sweeping right from the standard plane), the apical four-chamber view, and the subcostal coronal and sagittal views. The septal leaflet and its attachments to the interventricular

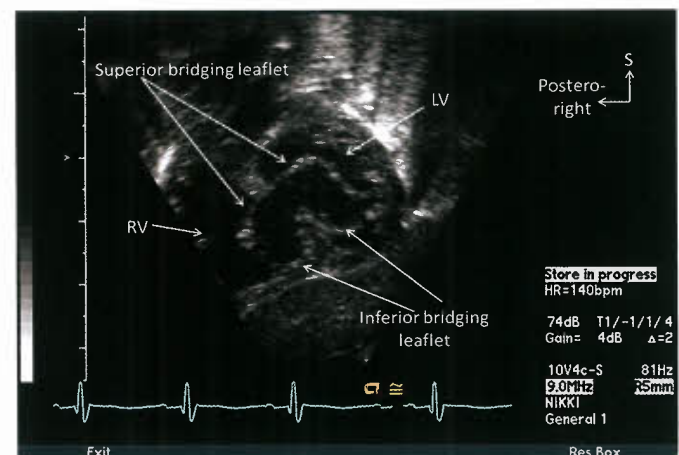


Figure 8.24. The subcostal oblique view (a hybrid between coronal and sagittal views) of a common atrioventricular valve. The five leaflets of the common atrioventricular valve are shown including the superior and inferior bridging leaflets. The commissure of the superior bridging leaflet attaches to the inferior portion of the outlet septum identifying this as a Rastelli type A atrioventricular septal defect. There is a well-defined left mural leaflet between the papillary muscles which are well spaced. Right accessory and right mural leaflets can be seen in the right ventricular portion of the common valve. LV, left ventricle; RV, right ventricle; S, superior.

septum are best seen in the apical four-chamber view. Also, in this view, the posterior leaflet (with a slight posterior sweep) or the anterior leaflet (with a slight anterior sweep) is seen on the lateral portion of the right ventricular wall. The anterior leaflet and its attachments to the conal papillary muscle (Lancisi) are best visualized in the subcostal coronal view sweeping anteriorly.

In the evaluation of Ebstein anomaly, the degree of atrialization of the right ventricle is assessed from the apical four-chamber view. From here, the septal attachments of the septal leaflet are appreciated. The posterior mural leaflet is seen with a slight posterior sweep from the apical four-chamber view. A portion of the anterior mural leaflet can be seen with an anterior sweep from the apical four-chamber view but the subcostal coronal view is required to visualize the displacement of the anterior leaflet into the right ventricular outflow tract and the degree to which it obstructs it. The tricuspid valve annulus size, which is important to assess in conditions of right ventricular hypoplasia (e.g., pulmonary atresia with intact ventricular septum) and conditions of right ventricular volume overload (e.g., postoperative tetralogy of Fallot with pulmonary regurgitation or hypoplastic left heart syndrome after Norwood), should be evaluated in the apical four-chamber view.

MITRAL VALVE

The mitral valve is visualized in the parasternal, apical four-chamber, subcostal coronal, and sagittal views. The size of the mitral annulus, which is important in determining suitability for biventricular repair in cases of relative left-sided hypoplasia, should be performed in the orthogonal planes of the parasternal long-axis and apical four-chamber views. The papillary muscles, important to assess for repair of complete atrioventricular septal defect and for diagnosing parachute mitral valve, are best visualized in the parasternal short-axis and subcostal sagittal sweeps. Mitral stenosis is assessed in the parasternal long-axis and the apical four-chamber views, where the degree of leaflet excursion can be seen clearly. Mitral valve prolapse is best identified in the parasternal long-axis and apical four-chamber views. Clefting of the mitral valve and double orifice mitral valve are usually seen in the parasternal short-axis sweep.

Ventricles

VENTRICULAR MORPHOLOGY

During embryologic development, the heart begins as a straight tube anchored cephalad by the truncus arteriosus and caudad by the sinus venosus. The tube undergoes differential and rapid growth in its midsection which, because of the anchoring, forces it to bend to the right or the left. Bend to the right results in the right ventricle developing to the right and the left ventricle to the left (D-looping). Bend to the left results in the opposite situation (L-looping). Definition of the embryologic type of ventricular looping first requires clear identification of ventricular morphology. The septal structures once again provide the definitive criteria for this evaluation. The first criterion is the type of atrioventricular valve entering the ventricle (see preceding section on Atrioventricular Connection, Type). The right ventricle also can be identified by its coarse, large, and extensive trabeculations along the septum and free wall. One of these trabeculations, the moderator band, is particularly prominent running transversely from free wall to septum in the inferior third of the right ventricular cavity in the apical view (Fig. 8.23). Once ventricular morphology has been established, the ventricular looping is determined. This is performed by imagining one is standing in the right ventricle facing the right ventricular face of the interventricular septum. The palm of one hand is placed against the septum. The looping is determined by which of the two hands allow the thumb to point into the atrioventricular valve and the fingers to point into the outflow tract. If the right hand meets these criteria, the ventricles are D-looped. If the left hand meets these criteria, the ventricles are L-looped.

RIGHT VENTRICLE

The size of the right ventricle and its relative contribution to the ventricular apex in conditions such as complete atrioventricular septal defect and pulmonary atresia with intact ventricular septum are best assessed from the apical four-chamber view. Because the three portions of the right ventricle (inlet, trabecular, and conus) do not lie in a single plane, visualization of the entire right ventricular cavity requires sweeping of the transducer through multiple planes in the subcostal coronal and sagittal views.

VENTRICULAR SEPTUM

The ventricular septum is composed of two components: (a) the membranous septum, which is an extremely small (5 mm in diameter in the adult heart) and superior portion wedged between the tricuspid and aortic valves; and (b) the large muscular septum. The membranous septum consists of two portions separated by the septal leaflet of the tricuspid valve: the pars atrioventricularis, where left ventricular to RA shunts occur, and the pars interventricularis, where VSDs are located. The muscular septum consists of three portions: the inlet portion, which is inferior to the membranous septum and is between the atrioventricular valves; the trabecular portion, which extends from the membranous septum to the apex; and the conal (or outlet or infundibular) septum, immediately below the pulmonary valve.

Many VSDs typically occur along embryologic fusion lines (e.g., a perimembranous outlet VSD is along the fusion line between the membranous and conal septa). VSDs within the membranous septum can be assessed in the parasternal long and short-axes, apical five-chamber, and subcostal views. In the basal short-axis view where the subpulmonary and subaortic regions can be imaged simultaneously, it can be determined whether an outlet VSD is below the crista supraventricularis (infracristal outlet VSD) or above the crista (supracristal outlet VSD, also known as subpulmonic or doubly committed VSDs). The membranous septum is seen well in the parasternal long-axis sweep from the standard view toward the tricuspid valve. In the apical view, the transducer should be swept anteriorly so that the left ventricular outflow tract and aorta are visualized. VSDs within the conal septum are assessed in the parasternal long axis sweeping left toward the pulmonary valve, in the basal short-axis, and in the subcostal coronal and sagittal views. The trabecular septum is so large that defects within it need to be localized preferably describing their position in two orthogonal planes and in relation to nearby landmarks. One classification system assigns the VSD as anterior, midmuscular, apical, or posterior. Anterior trabecular VSDs can be missed if the echocardiographer is not interrogating consciously for them. Perhaps the best view is the parasternal long-axis view sweeping to the left. The midmuscular VSDs can be seen in the standard parasternal long and short-axes views and apical four-chamber views. VSDs in the posterior trabecular septum are visualized best in the parasternal short-axis view or in the apical view swept posteriorly. Apical trabecular defects are best seen in the apical four-chamber view inferior to the moderator band. Inlet VSDs are best visualized in the short axis sweeping inferiorly toward the atrioventricular valves and in the standard apical four-chamber view at the level of the atrioventricular valves. These are distinguished from atrioventricular septal defects by close echocardiographic inspection of the hinge points of the atrioventricular valve annuli, which remain normal (i.e., mitral hinge point slightly superior to that of the tricuspid valve) with an inlet VSD and at identical heights with an atrioventricular septal defect.

LEFT VENTRICLE

The size of the left ventricle, which is particularly important in evaluating atrioventricular septal defects and variants of hypoplastic left heart with relative left-sided hypoplasia, is

investigated in the apical four-chamber view. The left ventricular outflow tract, which is important to visualize for membranous and subvalvar stenosis, is seen by a slight anterior tilt of the transducer. Equally valuable for the visualization of the subaortic region is the parasternal long-axis view in which the left ventricular outflow tract is at a slightly shallower depth, improving imaging, or the subcostal coronal view. Trabeculations, the diagnostic feature of left ventricular noncompaction, are best seen at the cardiac apex or lateral wall from a true apical four-chamber view with the apex clearly visible in the sector and with careful, deliberate sweeps in the parasternal short axis from the mitral valve annulus inferiorly to the cardiac apex. It is from this and the parasternal short-axis view that the echocardiographer can assess whether trabeculations are deep and/or extensive enough to meet diagnostic criteria for left ventricular noncompaction (31,32). Others have suggested that a diagnostic ratio for left ventricular noncompaction has little if any pathoanatomical basis. These authors suggest that the mere presence of trabeculations indicate noncompaction (33,34).

Conal Morphology

The conus (or infundibulum) is the cavitory space formed by the muscular segment of the heart that connects the ventricles with the great arteries and separates the atrioventricular and semilunar valves. Abnormalities in conal development consist of variations in the presence, length, and diameters of the subpulmonary and subaortic conus. These variations can lead to (or be associated with) complex malformations, such as tetralogy of Fallot, interrupted aortic arch, transposition of the great vessels, and double-outlet right ventricle.

SUBPULMONIC

In the normal heart, the conus is the nearly vertical tubular outflow portion of the right ventricle, which is separated from the nearly horizontal right ventricular inflow portion by distinct muscle bands. These muscle bands form a near-circular rim formed by the parietal band anteriorly, the crista supraventricularis posteriorly, and the septal band medially and prohibit pulmonary valve to atrioventricular valve continuity. The subpulmonary conus is best identified in the subcostal views. Leftward anterior deviation of the conal septum leading to a narrowed conus and subvalvar pulmonary stenosis in tetralogy of Fallot is evident in these views. Posterior deviation of the conal septum with VSD results in left ventricular outflow tract obstruction and is associated with interrupted aortic arch. The conal septum in this lesion is best assessed from the parasternal long-axis view.

SUBAORTIC

Persistence of the subaortic conus and involution of the subpulmonic conus is the usual conal relationship in D- (or L-) transposition of the great vessels (35). The subaortic conus is evident on the subcostal coronal and sagittal views. Persistence of subaortic conus prohibits continuity of the aortic valve to either atrioventricular valve. Involution of the subpulmonary conus allows continuity between the pulmonary valve and both atrioventricular valves in transposition of the great vessels. An extremely unusual variant of conal morphology is a subpulmonic conus in the setting of D-transposition of the great vessels.

BILATERAL

Bilateral persistence of the subarterial conus usually results in double-outlet right ventricle. Because the main goal of surgical correction of double outlet right ventricle is to connect the aorta with the morphologic left ventricle through the VSD, it is important to determine the conal relationships with each other and with the great vessels. In double-outlet right ventricle, the relationship of the great arteries with each other is

an inaccurate method by which to determine the infundibular relationships. Particularly important is to determine which conus has the interventricular septum as one of its walls, to localize the VSD with respect to the conus, and to determine the connection of the conus to the aorta.

When two conuses are present, their relationship may be classified as either (a) anterior/posterior or (b) side-by-side (36). With anterior/posterior conal relationship, the VSD is usually subaortic; with the side-by-side relationship, the defect is usually subpulmonic. The conal relationship can be determined by subcostal coronal and sagittal imaging with anterior/posterior and left/right sweeping, respectively. With an anterior/posterior conal relationship, the outlet septum inserts anteriorly separating the anterior conus from most of the interventricular septum and, thus, the VSD. With a side-by-side conal relationship, the outlet septum inserts near the crux of the heart separating the lateral conus from the interventricular septum and VSD.

Bilateral conus also can be associated with D-transposition of the great vessels with VSD, a more anterior and superior location of the pulmonary root than in patients with a subaortic conus only, and discontinuity between the pulmonary and mitral valves (as well as between the aortic and tricuspid valves). L-Transposition of the great vessels also can be associated, although rarely, with bilateral conus evident in the subcostal views.

ABSENT

A rare type of D-transposition can exist in the context of bilaterally deficient subarterial conus (37). This results in an unusual heart in which D-transposition of the great vessels exists with a doubly committed VSD and a posterior aorta. These relationships can be identified by parasternal and subcostal coronal and sagittal imaging (Fig. 8.25).

Ventriculoarterial Connection

TYPE

If the aorta arises from the left ventricle and the pulmonary artery arises from the right ventricle, the relationship is concordant. When the aorta arises from the right ventricle and the pulmonary artery from the left ventricle, the relationship is discordant. The third type of ventriculoarterial connection is double outlet, almost always from the right ventricle. The ventricular origins of aorta and pulmonary artery are evident on the parasternal long-axis view, sweeping the transducer inferiorly from the basal short-axis view, the apical five-chamber view, and the subcostal coronal and sagittal views. A great vessel should be related to a ventricle by at least 50% of its dimension to be considered committed to it. Determining the extent of commitment of a great vessel to the right ventricle is best performed in the parasternal long- and short-axis view sweeps, the apical five-chamber view, and the subcostal coronal and sagittal views. The final type of ventriculoarterial connection is single outlet (truncus arteriosus). This entity can be diagnosed in the parasternal long axis, where a single trunk with pulmonary arteries arising from it can be seen. The basal short-axis view is notable for absence of a pulmonary valve; the pulmonary artery branches arising from the trunk also can be seen in this view. The subcostal coronal and sagittal views are usually diagnostic for this entity.

Great Vessels

RELATIONSHIP

The aorta courses superiorly toward the thoracic inlet before coursing posteriorly, gives rise to strap vessels as it courses posteriorly, and has coronary arteries arising from its root. The pulmonary artery courses posteriorly almost immediately after it arises from the heart and bifurcates shortly after its origin. The most helpful views for identifying the great vessels

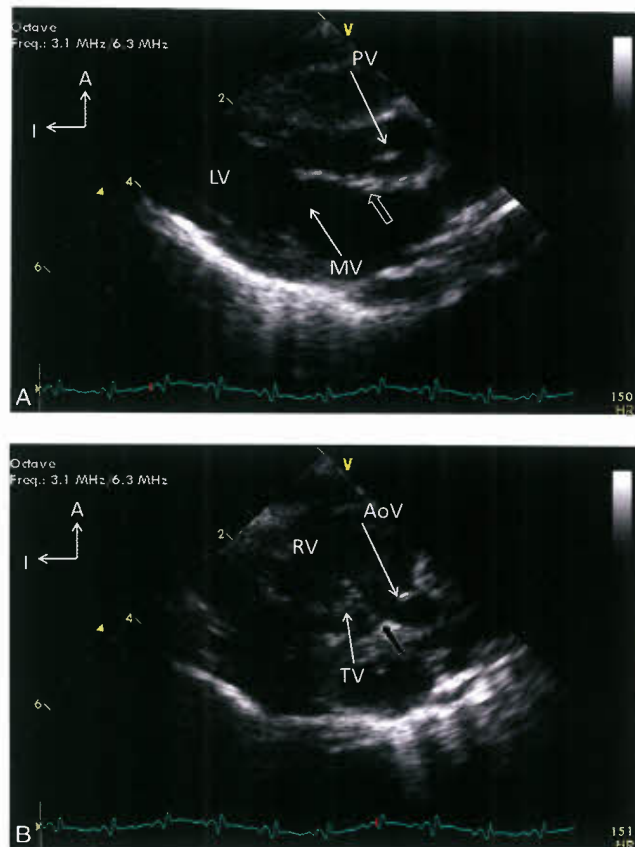


Figure 8.25. Parasternal long-axis images of a patient with bilaterally absent conus resulting in transposition of the great vessels (i.e., ventriculoarterial discordance) with not only mitral-pulmonic continuity (arrowhead in standard parasternal long-axis view (A) but also tricuspid-aortic continuity (arrowhead in parasternal long-axis view swept right and inferiorly (B)). A, anterior; AoV, aortic valve; I, inferior; LV, left ventricle; MV, mitral valve; PV, pulmonary valve; RV, right ventricle; TV, tricuspid valve.

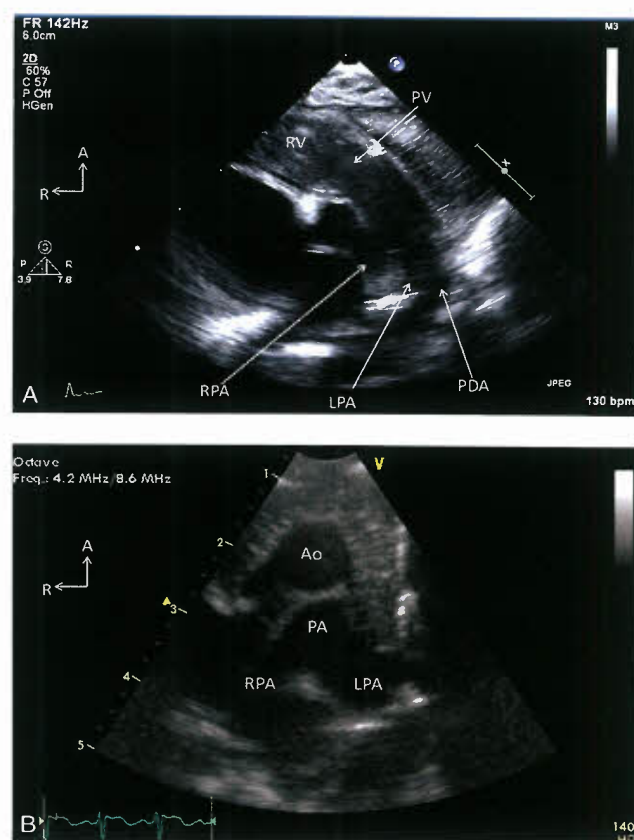


Figure 8.26. Parasternal short-axis images demonstrating different relationships between the great vessels. **A:** An echocardiogram from an infant demonstrates the identifying features of a pulmonary artery with its bifurcation into right and left pulmonary arteries (RPA, LPA). This view is called the “3 finger view” as it also demonstrates the PDA. The great vessels are normally related with the pulmonary valve (PV) lying anterior and left of the aorta. **B:** In a patient with D-transposition of the great vessels, both semilunar valves are in cross section in the parasternal short-axis view. The aorta (Ao) is identified as the anterior and slightly rightward vessel. The main pulmonary artery (PA) lies posterior to the Ao and bifurcates into RPA and LPA. A, anterior; R, right; RV, right ventricle.

are the parasternal short-axis view at the base and even more superiorly, the suprasternal notch long- and short-axis views, and the subcostal coronal and sagittal views (Fig. 8.26).

Situs solitus of the great vessels describes the normal relative position of the aortic annulus located rightward and posterior to the pulmonary annulus. This relationship is best seen in the parasternal short-axis view, but it is also obvious in the parasternal long-axis sweeps and the subcostal coronal and sagittal views.

Situs inversus of the great vessels describes the relative position of the aortic annulus located leftward and posterior to the pulmonary valve annulus in mirror image dextrocardia. Note that the term “inversus” in this context does not signify transposition. It is merely the designation given to normally related great vessels in a mirror-image relationship (i.e., the aorta continues to arise from the left ventricle and the pulmonary artery from the right ventricle). This relationship is evident in a right parasternal short-axis view and in the subcostal coronal and sagittal sweeps.

Transposition of the great vessels is diagnosed when there is a discordant ventriculoarterial relationship. By definition, then, it is impossible to diagnose double-outlet right ventricle with transposition. Instead, this is referred to as double-outlet right ventricle with **malposition** of the great vessels. Transposition of the great vessels can exist with the aorta right and

anterior (D), left and anterior (L), and directly anterior (A) to the pulmonary artery. In addition, the aorta may exist side-by-side or even posterior to the pulmonary artery. These relationships are best diagnosed in the basal short-axis and subcostal coronal and sagittal views.

MAIN AND BRANCH PULMONARY ARTERIES

The main and branch pulmonary arteries are best seen in the basal (and more superior) short-axis and subcostal coronal and sagittal views. In addition, the right pulmonary artery is best seen in the suprasternal short-axis view. The left pulmonary artery usually can be seen when sweeping the standard suprasternal long-axis view to the left.

Pulmonary valve stenosis is evident in the parasternal basal short-axis view. Frequently, continued clockwise rotation of the transducer can yield an *en face* view of the pulmonary valve. Supravalvar pulmonary stenosis is best visualized in this view. Aortopulmonary window is usually evident on the parasternal short-axis view and careful, deliberate sweeps between the aorta and main pulmonary artery in the subcostal coronal and sagittal views.

AORTA AND BRANCH VESSELS

The aorta, which lies more posterior in the center of the heart, can be visualized in many different views, including the parasternal long- and short-axis views, the apical five-chamber view, the subcostal views, and the suprasternal notch views. The aortic arch is best seen in the subcostal oblique view and the suprasternal notch views.

Valve morphology in aortic stenosis can be understood by examining the parasternal views. The short-axis views allow determination of dysplasia and number of leaflets. Supravalvar stenosis, root dilation, and sinotubular effacement are best measured in the parasternal long-axis view.

The side of the aortic arch (important in tetralogy of Fallot, truncus arteriosus, hypoplastic left heart, vascular rings, and before tracheoesophageal fistula repair) is diagnosed by sweeping the transducer in the suprasternal long-axis view and noting the relationship of the arch to the trachea, the rings of which resemble a stack of coins. Equally important is sweeping the transducer in the suprasternal notch short-axis view from the origin of the aorta superiorly toward the arch and branch vessels and then back inferiorly and posteriorly following the descending aorta. Using this view, the transducer should also be swept superiorly to follow the course of each branch vessel arising from the arch. In a normal, left-sided aortic arch, the first branch vessel is a right brachiocephalic artery that can be shown to bifurcate into right subclavian and carotid arteries (Fig. 8.27). In a right-sided aortic arch, the first branch vessel is usually a left brachiocephalic artery, which usually bifurcates into a left subclavian and carotid arteries. In either case, the first branch vessel should be followed to its bifurcation. If no bifurcation is present, anomalous origin of the ipsilateral subclavian artery should be suspected. Likewise, superior sweeping from the origin of each of the other strap vessels upstream should be performed deliberately to completely delineate the strap vessel anatomy.

Arch hypoplasia, coarctation, and interruption are best diagnosed from the suprasternal long- and short-axis views. The proximal (the segment between brachiocephalic and common carotid artery origins) and distal (the segment between common carotid artery and subclavian artery origins) transverse arch should be imaged and measured.

Aortopulmonary collateral vessels (important in tetralogy of Fallot and single ventricle/Fontan physiology) are best seen in the suprasternal notch long- and short-axis views. The subcostal oblique view of the descending aorta also allows identification of these vessels.

Coronary Arteries

The coronary arteries are best seen in the parasternal short-axis views. The coronary arteries can also be seen in the apical four-chamber view as they course in the atrioventricular grooves. The midportion of the right coronary artery is seen in the subcostal coronal view. Frequently, the origin of the left coronary artery and the left anterior descending coronary artery are seen in the subcostal coronal view or a leftward sweep from the standard parasternal long-axis view. The posterior descending coronary artery is more difficult to visualize but investigators have had success in imaging it adjacent to the cross section of the coronary sinus from an apical two-chamber view (38).

Anomalous coronary artery origins and courses are important to delineate in transposition of the great vessels, tetralogy of Fallot, anomalous origin of the left (or more rarely, the right) coronary artery from the pulmonary artery, dilated cardiomyopathy, and exertional syncope and are seen in the parasternal short axis. If 2-D imaging in the short-axis view shows isolated dilation of a proximal coronary artery, a coronary artery fistula or anomalous origin of a coronary artery should

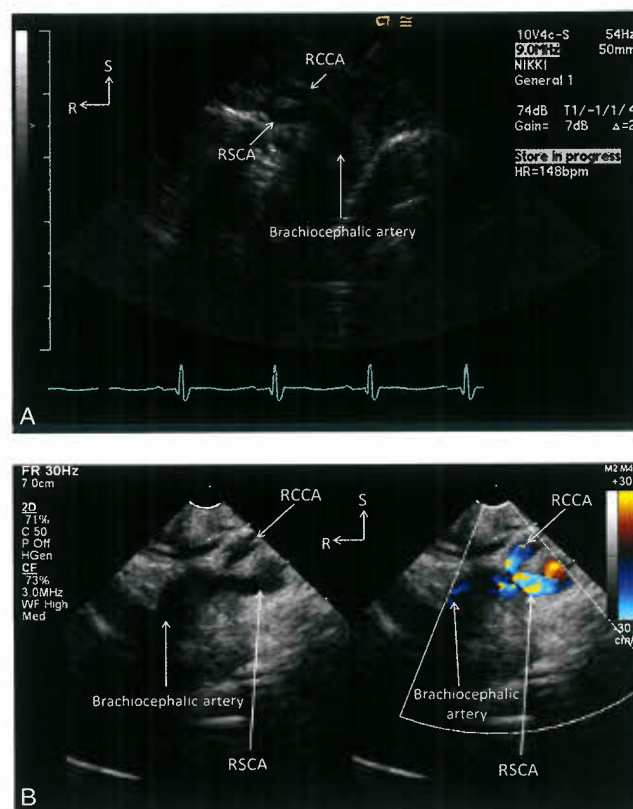


Figure 8.27. Suprasternal notch short-axis views in a patient with left aortic arch (A) and a second patient with right aortic arch (B). In each view, the transducer is swept superiorly to demonstrate the bifurcation of the brachiocephalic artery. In the patient with a left aortic arch, the first strap vessel arising from the aortic arch is the brachiocephalic artery which bifurcates toward the right into right subclavian (RSCA) and right common carotid arteries (RCCA), indicating a left aortic arch. In the second patient with a right aortic arch (B), the first strap vessel is a left brachiocephalic artery, and it bifurcates to the left into the left subclavian (LSCA) and left common carotid (LCCA) arteries, indicating a right aortic arch. Color Doppler can be helpful in tracking these arteries distally to determine their branching patterns as shown by the color Doppler panel in B. R, right; S, superior.

be suspected. The entire extent of the coronary artery must be interrogated for fistulous communications from all imaging planes. The main and branch pulmonary arteries should be carefully imaged for an anomalously arising coronary artery. Simultaneous use of color Doppler is extremely helpful when investigating for coronary artery fistulae or anomalous origin of a coronary artery. Coronary cameral sinusoids, seen within high pressure ventricles such as the right ventricle in pulmonary atresia with intact ventricular septum, are best visualized in the apical four-chamber view with simultaneous use of color Doppler. Evaluation of the coronary arteries during and following Kawasaki disease for aneurysms and stenoses should be performed in all the aforementioned imaging planes so that almost the entire extent of the coronary artery is interrogated.

TRANSESOPHAGEAL ECHOCARDIOGRAPHY

In 1991, Ritter (39) reported initial experience of biplane transesophageal echocardiography (TEE) to evaluate congenital heart disease in patients as small as 2.4 kg without complications,

and it later became clear that intraoperative echocardiography allowed immediate revision of initial repair and improved patient outcome (40). In addition, TEE has become standard for guidance of defect-closure devices during interventional catheterization procedures (41), guidance of balloon atrial septostomy, and evaluation for thrombi (42).

Approach

The probe should be inspected carefully for any defects before it is inserted into the oropharynx. Probe size should be chosen on the basis of the patient's weight. Generally, current pediatric size TEE probes can be safely used in patients as small as 3.5 kg; recently, use of newer "micro-TEE" probes have been reported in infants as small as 1.7 kg (43). Esophageal intubation can be enhanced with the neck slightly flexed and the patient in a slight left lateral decubitus position. Under no circumstances should the probe be forced into the posterior pharynx; sometimes direct visualization with a laryngoscope for difficult intubations is necessary.

Probe manipulation consists of the transesophageal equivalents of transthoracic sweeps: withdrawing or advancing the transducer superiorly and inferiorly within the esophagus, rotating the transducer left and right, ante- or retroflexing the transducer, or flexing left or right (Fig. 8.28). In addition, the imaging plane can be mechanically adjusted from 0 to 180 degrees in the case of multiplane TEE probes (Fig. 8.29), or from horizontal to vertical imaging planes in the case of biplane imaging (Fig. 8.30). Currently, multiplanar TEE probes are available widely in pediatric sizes, so increasingly, multiplane (rather than biplane) imaging is performed.

The examination should proceed in a segmental manner with identification of the systemic venous return moving the transducer superiorly and inferiorly in the esophagus in the longitudinal and transverse views. The atrial septum should be examined in these same views. The tricuspid valve is best visualized in the transverse four-chamber view and the longitudinal plane with rightward rotation. The interventricular septum is visualized in the transverse four-chamber view, sweeping the longitudinal view from left to right and in the transgastric views. The right ventricular outflow tract and pulmonary valve are seen in a superior transverse view, in the longitudinal view swept leftward from the aorta, and in the longitudinal gastric view. On multiplane imaging, the tricuspid valve, right ventricular outflow tract, pulmonary valve, and membranous/outlet interventricular septum can also be imaged in a 60- to 70-degree plane (Fig. 8.31). Pulmonary veins are best seen in the transverse plane by sweeping right and left. The mitral valve is investigated from the transverse four-chamber view and the longitudinal plane with a far leftward sweep. The left ventricular outflow tract and the aorta are evaluated in a slightly superior sweep from the transverse four-chamber view and in the longitudinal view between the SVC and the pulmonary artery. On multiplane imaging, the left ventricular outflow tract, aorta, and outlet interventricular septum are also imaged well at an imaging angle of approximately 120 degrees (Fig. 8.32).

Complications from TEE are rare; however, there are reports of upper-airway obstruction secondary to esophageal hematoma (44), compression of an aberrant right subclavian artery (45), accidental endotracheal tube extubation, and esophageal burns and tears resulting from defective or improperly maintained probes. In a large review of 1,650 transesophageal studies in the pediatric population (46), Stevenson reported an approximately 3% incidence of complications, most of which were related to airway complications (e.g., airway occlusion or displacement of the endotracheal tube) in small infants.

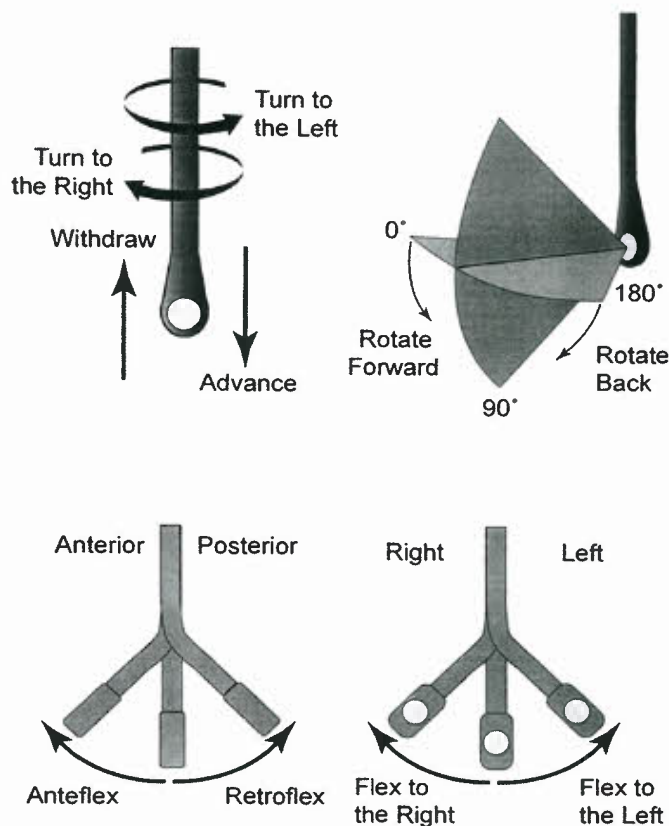


Figure 8.28. Terminology used to describe the various transesophageal probe manipulations that can be employed during imaging studies. (Reprinted from Shanewise JS, et al. ASE/SCA Guidelines for Performing a Comprehensive Intraoperative Multiplane Transesophageal Echocardiography Examination: Recommendations of the American Society of Echocardiography and the Society of Cardiovascular Anesthesiologists Task Force for Certification in Perioperative Transesophageal Echocardiography. *J Am Soc Echocardiogr* 1999;12:884-900, with permission from Elsevier.)

Intraoperative Transesophageal Echocardiography

The value of intraoperative TEE is in evaluating residual problems relating to ventricular outflow tract obstruction, semilunar valve insufficiency, septal defects, atrioventricular valve insufficiency and stenosis, and ventricular function and wall-motion abnormalities. Stevenson et al. (47) reported that reoperation occurred in 7.5% of cases as a result of residual findings on intraoperative TEE. Ungerleider et al. (40) showed a similarly low rate of reoperation, but also demonstrated a significant impact on length of stay and hospital costs for patients undergoing immediate reoperation because of intraoperative echocardiographic findings. In addition, the knowledge that a repair is satisfactory helps guide bypass weaning and immediate postoperative care. Although intraoperative imaging can confirm adequate surgical repair/palliation, findings can evolve postoperatively due to changing hemodynamics, loading conditions, or other factors, which may make repeat imaging necessary or advisable. For example, the degree of valvar regurgitation seen on pre-discharge echocardiography is often different than on intraoperative transesophageal study in patients following repair of atrioventricular septal defects (48,49) and atrioventricular valve regurgitation (50).

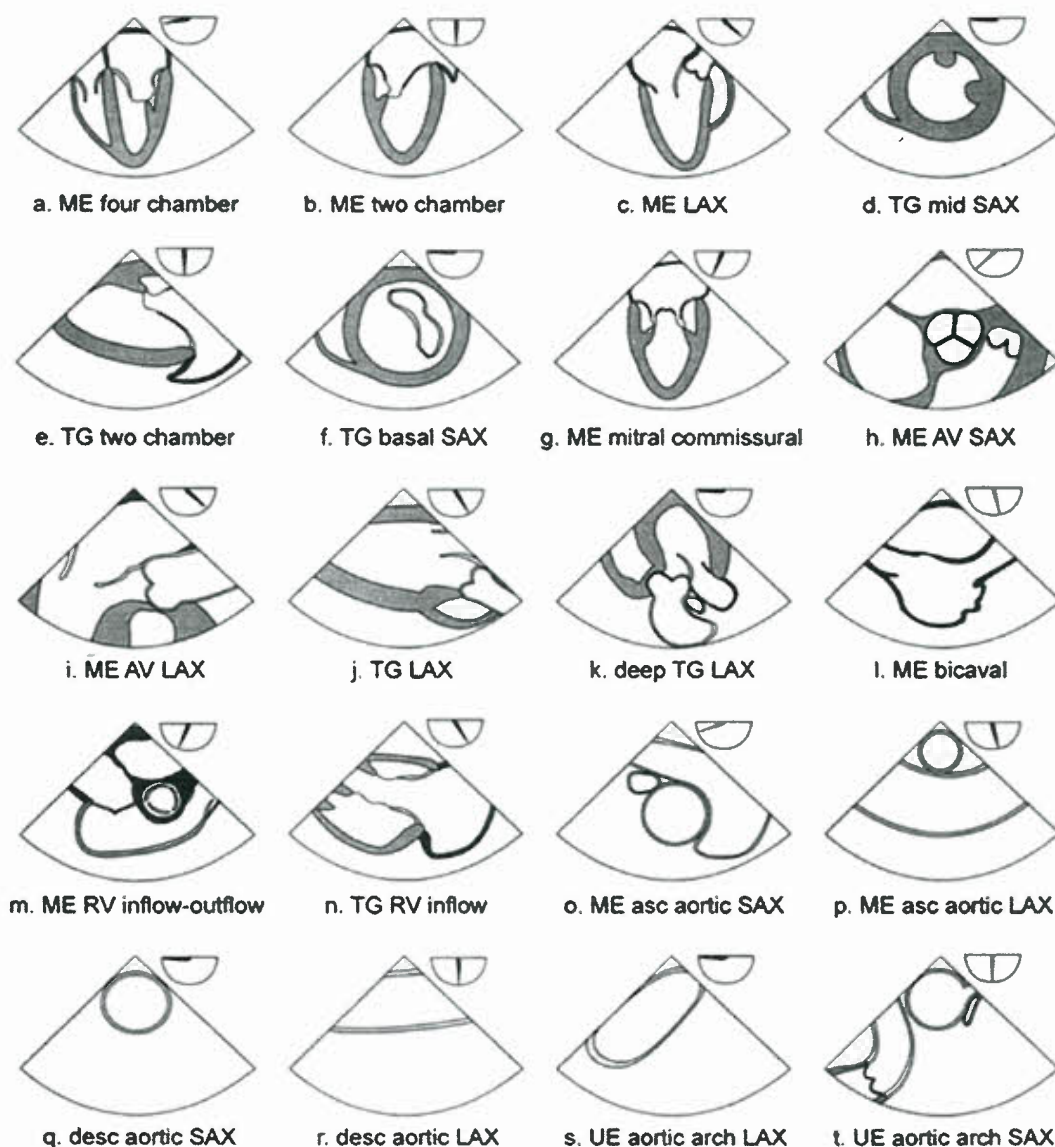


Figure 8.29. There are multiple imaging planes available during multiplane TEE based on level of the transducer and rotational angle. AV, aortic valve; LAX, long axis; ME, midesophagus; RV, right ventricle; SAX, shortaxis; TG, transgastric; UE, upper esophagus. (Reprinted from Shanewise JS, et al. ASE/SCA Guidelines for Performing a Comprehensive Intraoperative Multiplane Transesophageal Echocardiography Examination: Recommendations of the American Society of Echocardiography and the Society of Cardiovascular Anesthesiologists Task Force for Certification in Perioperative Transesophageal Echocardiography. *J Am Soc Echocardiogr* 1999;12:884–900, with permission from Elsevier.)

Guidance of Transcatheter Device Closure

TEE has proven value in guiding interventional catheterization procedures; this is discussed in detail in Chapter 13.

Evaluation for Thrombi and Complications of Endocarditis

Consideration of performing TEE should be given when there is suspicion of thrombi (i.e., because of neurologic changes, dysrhythmias, spontaneous contrast on the transthoracic echocardiogram). Patients with the Fontan procedure, particularly those with an atriopulmonary anastomosis, are at high risk for developing thrombi in the RA, IVC, or pulmonary artery (51) (Fig. 8.33).

TEE may have utility in the evaluation of suspected infective endocarditis in children, but may not be necessary when transthoracic imaging is adequate (52,53). Although TEE has been shown to be significantly more sensitive than transthoracic echo in diagnosing valvular vegetations and abscesses in adults with suspected endocarditis (54–56), higher quality acoustic windows in the pediatric population in general may negate the improvements in diagnostic sensitivity seen with use of TEE in adults (52,53). Moreover, the use of TEE in children is generally performed under conditions of endotracheal intubation and deep sedation/anesthesia, making the performance of TEE more invasive in this population. Therefore, TEE should be performed in any patient with suspected endocarditis, in whom the transthoracic study is negative or inconclusive due to technical inadequacies. Alternatively, in the patient with confirmed endocarditis, TEE may be useful in

more fully delineating the cardiac sequelae, such as perivalvar abscess and extent of vegetations (52).

STRESS ECHOCARDIOGRAPHY

Stress echocardiography is a valuable adjunct to the standard examination in two general instances. First, if there is a

concern in a patient with coronary artery disease (e.g., due to Kawasaki Disease, cardiac transplant vasculopathy, arterial switch operation, et al.), stress echocardiography may be helpful. In these circumstances, stress echocardiography is used to determine the physiologic significance of the anatomic abnormalities. A stressor is administered (e.g., exercise or pharmacologic) with the intention of increasing myocardial oxygen demand. In normal coronary arteries, blood flow increases to

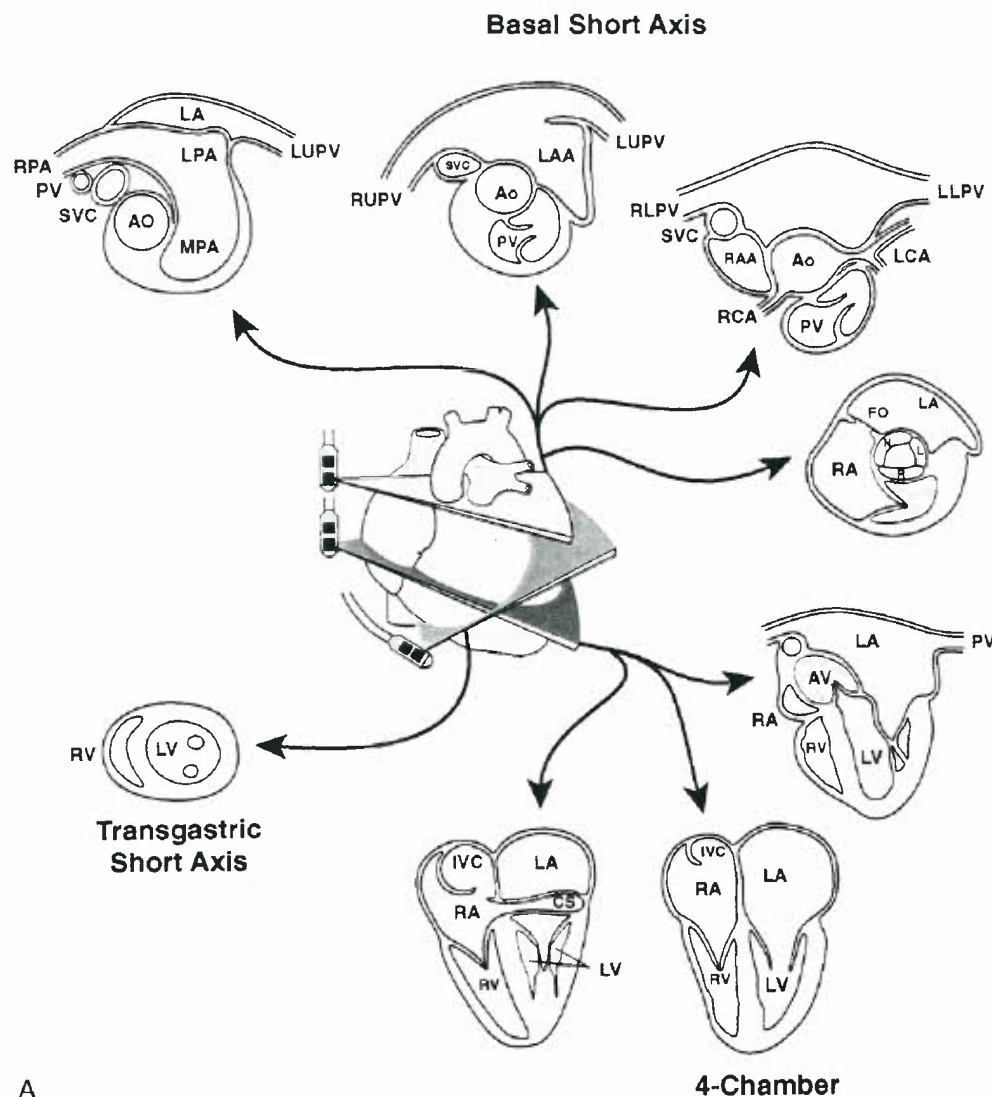


Figure 8.30. There are two basic imaging planes used in pediatric TEE: the horizontal imaging plane (A) and the vertical imaging plane (B). Omniplane probes can image at planes intermediate between these two. Imaging can be performed in three basic esophageal positions: the midesophagus, the upper esophagus at the base of the heart, and transgastrically. Horizontal-plane imaging in the midesophagus provides the four-chamber view, coronary sinus view, and pulmonary vein view. Horizontal imaging in the higher esophagus provides views of the base of the heart, including the aorta, coronary arteries, pulmonary valve, branch pulmonary arteries, pulmonary veins, and superior vena cava (SVC). Horizontal imaging in the transgastric view yields a short-axis view of the ventricles. Vertical imaging in the midesophagus provides views of the left ventricular outflow tract and the mitral valve. Vertical imaging in the higher esophagus provides views of the right ventricular outflow tract, main pulmonary artery, branch pulmonary arteries, left ventricular outflow tract, aorta, SVC, and atrial septum. Transgastric vertical plane imaging provides images of the left ventricular and right ventricular outflow tracts. A, aorta; AO, aorta; AV, aortic valve; CS, coronary sinus; FO, foramen ovale; IVC, inferior vena cava; LA, left atrium; LAA, left atrial appendage; LCA, left carotid artery; LLPV, left lower pulmonary valve; LPA, left pulmonary artery; LPV, left pulmonary valve; LUPV, left upper pulmonary valve; LV, left ventricle; MPA, main pulmonary artery; PV, pulmonary valve; RA, right atrium; RAA, right atrial appendage; RCA, right coronary artery; RPA, right pulmonary artery; RUPV, right upper pulmonary valve; RV, right ventricle; SVC, superior vena cava.

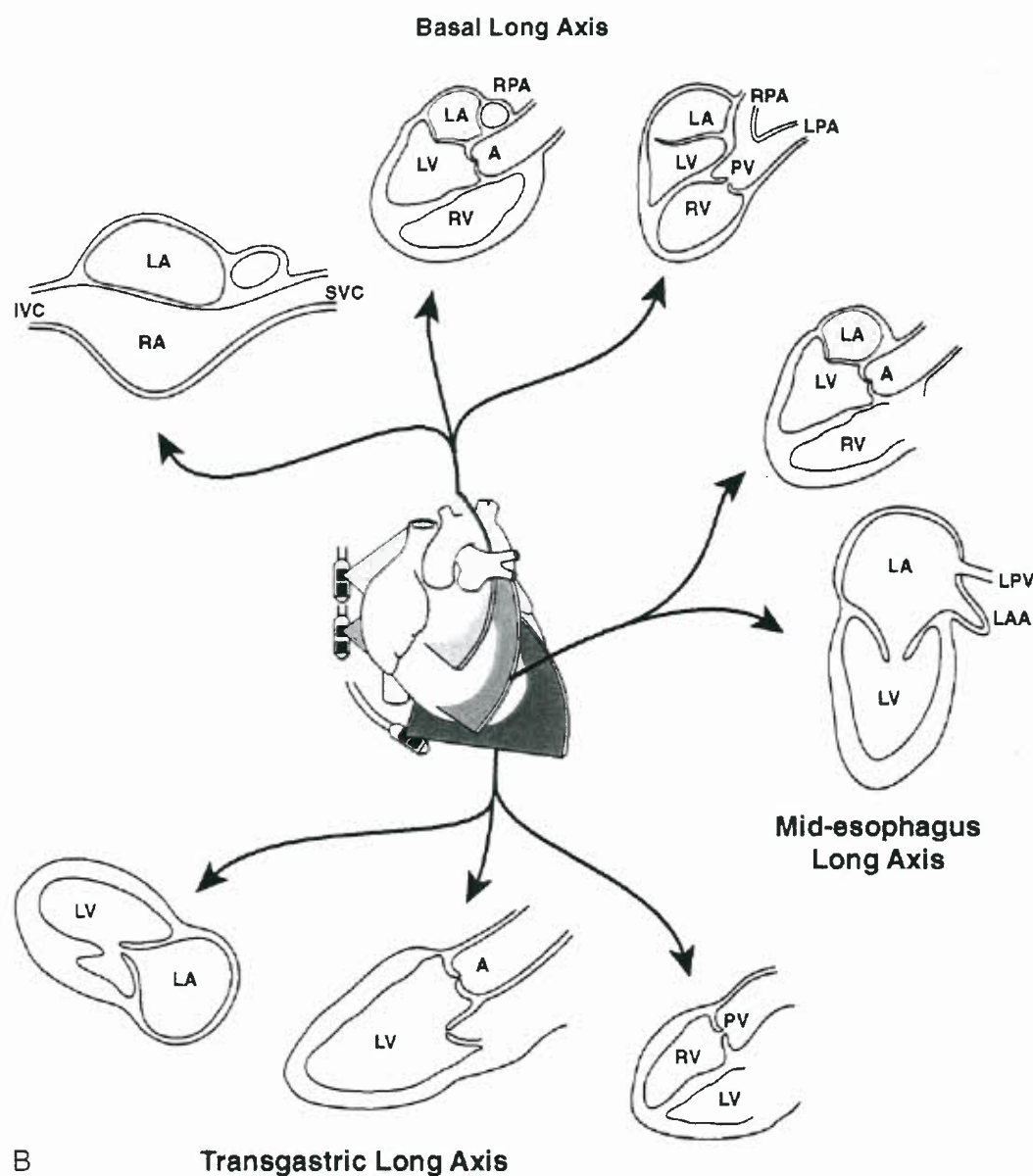


Figure 8.30. (Continued)

meet this demand. However, if in a diseased coronary artery, flow is compromised; ischemia is induced to the myocardial segment supplied by that coronary artery which is manifest on the echocardiogram by altered wall motion of that segment.

The second general use of stress echocardiography is evaluating a patient's hemodynamics in a setting other than the resting state. Children are rarely sedentary. Yet, echocardiographic examinations are largely performed when the child is in a resting, supine state—a condition that the child is actually experiencing for only brief moments during the day. These resting examinations shed little light on the child's typically more active physiology which, ironically, becomes apparent only after the patient leaves the laboratory. An echocardiographic assessment with the addition of a stressing agent provides greater insight into the hemodynamics present during the active state typical of children. One simple approach is the force-frequency relationship—increasing frequency of contraction induced by cardiac pacing (57) results in increased contractile force generation (as measured by ejection phase indices or by wall stress relations) with a maximal force (F_{\max}) at a

stimulus frequency of approximately 175 beats/min (Treppe phenomenon). Thereafter, the response becomes inverted (increased frequency results in decreased force). In the chronically failing heart due, for example, to dilated cardiomyopathy, mitral insufficiency, or diabetic cardiomyopathy, F_{\max} is depressed due to decreased activity of the calcium adenosine triphosphatase in the sarcoplasmic reticulum (SERCA-2) (58). Another, similar approach is the assessment of contractile reserve. In chronic heart failure, a rise in circulating catecholamines is accompanied by decreased beta receptor density and downregulation of receptors leading to a poor response to inotropic agents (59). Poor contractile response to exogenous catecholamines, therefore, has prognostic value in identifying the marginal ventricle more likely to require chronic medications, assist devices, and possibly transplant (60) and is associated with overexpression of apoptosis-related proteins (61–63). The magnitude of augmentation of cardiac performance during cardiovascular stress is termed contractile reserve and can be assessed noninvasively using exercise or pharmacologic stress (64–66).

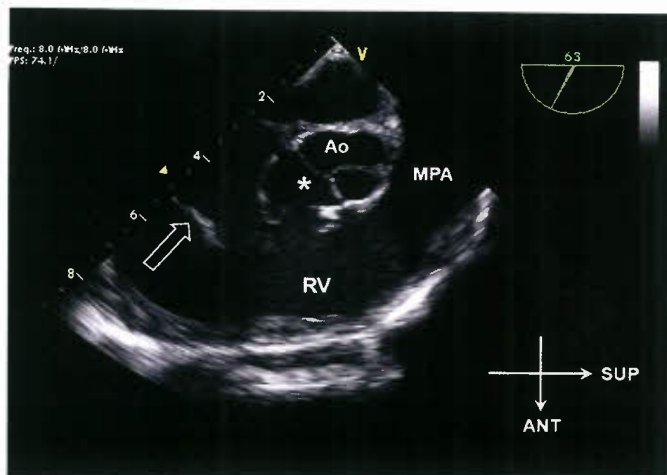


Figure 8.31. Multiplane TEE at midesophagus with imaging angle at approximately 60 degrees. This imaging plane allows demonstration of the aortic valve (Ao) in short axis, as well as the right ventricular (RV) body and outflow tract. The proximal main pulmonary artery (MPA) can also be imaged, as well as the pulmonary valve (open arrow). The tricuspid valve (open arrow) can also be noted. Note the perimembranous ventricular septal defect (asterisk) in this image. ANT, anterior; SUP, superior.

Technical Aspects

In pediatrics, the usual stressors are exercise and dobutamine (67,68). Exercise is the reference standard, and most of the other stressing agents are employed to mimic it. However, exercise has the disadvantages of (a) patient movement and respiration, which impair echocardiographic imaging; and (b) lack of threshold dosing (the entire stress dose is given without the option for early termination). Since imaging is so poor during exercise, echocardiography must be performed

immediately after exercise, necessitating a hurried process to acquire images before the exercise dose dissipates (usually <60 seconds). Dobutamine infusion offers a controlled environment in which dosing can be gradually increased or terminated on the basis of immediate echocardiographic feedback. Imaging is usually excellent because there is no patient movement or deep respirations. The main disadvantage of dobutamine is that it does not duplicate exercise exactly.

For an exercise echocardiogram, imaging is performed in four echocardiographic planes (parasternal long- and short-axis, apical two- and four-chamber views) with the patient in a left lateral decubitus position before, immediately after, and 20 minutes after exercise. For a dobutamine stress echocardiogram, imaging is performed in the same four planes at rest, at each dobutamine dose, at peak heart rate, and 20 to 30 minutes after termination of dobutamine. Dobutamine is given in consecutive doses of 10, 20, 30, 40, and 50 mcg/kg/min. Atropine (0.01 mg/kg) is administered to augment the heart rate, if necessary. The test is terminated if (a) target heart rate (85% of age-related maximal heart rate) is achieved, (b) adverse reactions occur, (c) the electrocardiogram shows abnormalities (e.g., significant ST segment depression or significant dysrhythmia), (d) the patient's rating of perceived exertion is excessive (exercise), or (e) the maximum dose has been given (dobutamine).

Wall Motion Abnormalities

Wall motion abnormalities are the diagnostic feature of a myocardial perfusion deficit during a stress echocardiogram. Detection of a wall motion abnormality is the most difficult part of a stress echocardiogram. It is essential that pediatric cardiologists contemplating the introduction of stress echocardiography into their laboratories receive and maintain adequate training in the interpretation of wall motion from adult cardiologists. In evaluating wall motion, it frequently helps to first examine the overall end-systolic cavity size. If there is little or no change at peak heart rate versus rest, abnormal wall motion is diagnosed and each segment examined in detail to detect specific regional wall motion abnormalities. In addition, an abnormality seen in one view should be verified by examination of the same or adjacent segment in another view.

Diagnosis of pathology based on myocardial wall motion during stress is based on four basic response patterns: normal motion at rest and normal motion during stress indicates normal myocardium; normal motion at rest and abnormal motion during stress indicates ischemic myocardium; abnormal motion at rest and abnormal motion during stress indicates necrotic myocardium; and abnormal motion at rest and normal or biphasic response during stress indicates viable myocardium (hibernating myocardium) (69).

Wall motion scoring systems have been defined by segmenting the left ventricle into 16 or 17 segments and assigning a score of "1" to a segment with normal motion, "2" to a segment that is hypokinetic, "3" to a segment that is akinetic, and "4" to a segment that is dyskinetic. The sum of segment scores divided by the number of visualized segments is the wall motion score index (70).

Wall motion scoring systems are based on subjective assessment. Strain imaging and 3-D echocardiography have also been used to enhance detection of, and to quantify, wall motion abnormalities during stress echocardiography in adults but experience is lacking in children (71,72).

Whereas stress echocardiography administered to unmask occult coronary artery disease requires a large stressing dose to maximize myocardial oxygen consumption, administration of stress for assessment of contractile reserve requires far less but nevertheless still substantial dosing (dobutamine

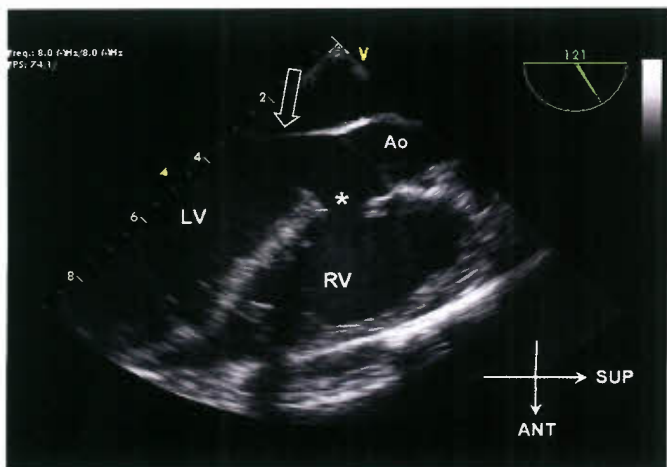


Figure 8.32. Multiplane TEE at midesophagus with imaging angle at approximately 120 degrees. The mitral valve anterior leaflet (open arrow), left ventricle (LV), outflow tract, and aortic valve (Ao) can be demonstrated in this plane. Portions of the right ventricular (RV) outflow tract, and an outlet ventricular septal defect (asterisk) are also noted. ANT, anterior; SUP, superior.

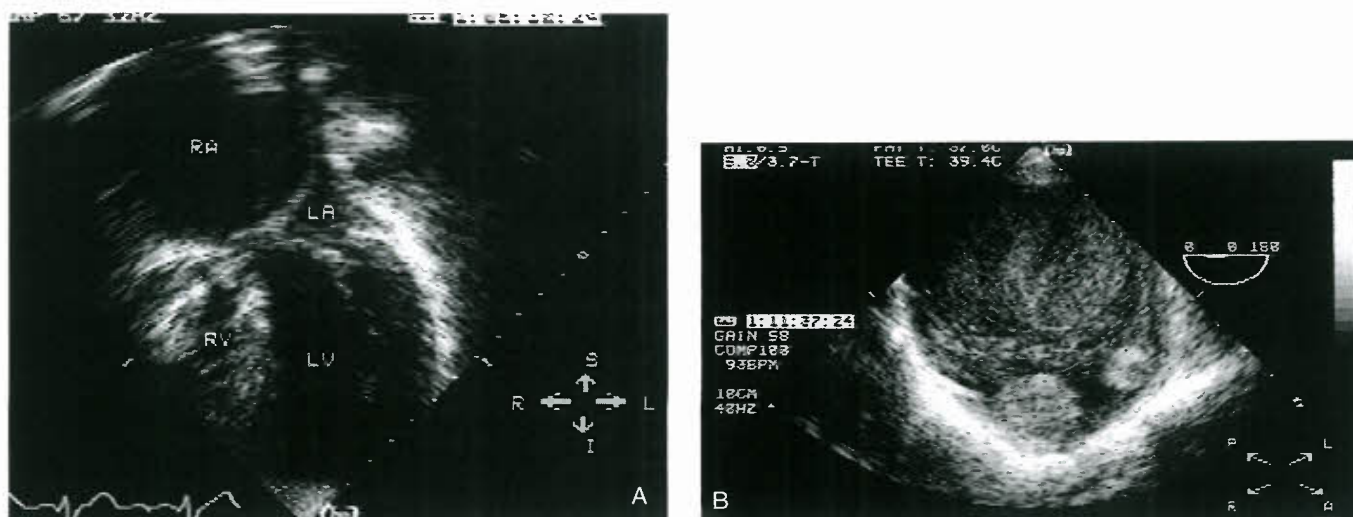


Figure 8.33. A: Transthoracic apical four-chamber view in an adolescent patient with pulmonary atresia and intact ventricular septum who had previously undergone a classic Fontan procedure with the right atrium (RA) directly anastomosed to the pulmonary artery. The electrocardiogram shows atrial fibrillation/flutter. The patient was being evaluated for the possibility of thrombi before DC cardioversion. This echocardiogram revealed no obvious thrombi. In particular, the RA appeared free of thrombus. B: Transesophageal echocardiogram of the RA in the horizontal plane. There is marked spontaneous contrast indicative of a thrombogenic milieu. In addition, there are two large thrombi on the RA free wall. Further imaging revealed thrombi in the midcavity of the RA and at the inferior vena cava orifice. Transthoracic echocardiography may lead to false-negative results, and TEE is often necessary to evaluate for thrombi, particularly in patients with classic Fontan operation. A, anterior; I, inferior; LA, left atrium; LV, left ventricle; P, posterior; RV, right ventricle.

at ~ 20 mcg/kg/min) (73). Normal responses of left ventricular performance (shortening fraction) and contractility (VCF_d difference) to exercise and dobutamine stress have been established (73,74) (Fig. 8.34). Stress echocardiography can also be used to assess the changing behavior of various cardiac lesions during altered activity levels (Fig. 8.35). For example, the gradients in hypertrophic cardiomyopathy, coarctation, pulmonary or aortic valvar stenoses (75), and the pulmonary artery pressure in patients with suspected pulmonary hypertension can all be evaluated with echocardiography during stress.

THREE-DIMENSIONAL ECHOCARDIOGRAPHY

The goal of the echocardiographic examination is to create and convey a 3-D reconstruction of the heart. Historically, 3-D reconstruction has been a mental process dependent on the ability of the viewer to spatially “render” a 3-D image of the heart using 2-D images. This can clearly be improved on by an actual visual 3-D reconstruction. Three-dimensional images can be produced with any medical imaging technique, but echocardiography is uniquely qualified because images are tomographic, are acquired at a relatively high rate, can be triggered to an appropriate phase of the electrocardiogram, and can be acquired from any angle.

Evolution of current 3-D ultrasound systems progressed from static to dynamic, and ultimately, to real-time 3-D imaging. Static 3-D images were initially obtained from a single volume of “voxels”—a volume of pixels—by sweeping the ultrasound transducer through the area of interest. Although this can be achieved by sweeping the ultrasound probe through the area of interest by linear, fan-like or rotational sweeps, this technique was ultimately supplanted by rotational acquisition (76,77). Dynamic 3-D imaging is also possible, but portrayal of the heart in motion was dependent on reconstruction

algorithms that were in turn dependent on 2-D image quality, and were often deemed impractical due to the long and tedious nature of data acquisition and data analysis. The current state-of-the-art in 3-D imaging is represented by real-time 3-D imaging. Several recently developed ultrasound systems (78) feature matrix array transducers, which allow acquisition of high-quality, pyramidal image volumes (Fig. 8.36). Advances in 3-D ultrasound processing and faster computing times has currently made “real-time” 3-D imaging possible (79), which is likely to lead to increasing use in the future. Recently, development of higher frequency, matrix array TEE probes has resulted in excellent 3-D image quality in real time (80). Currently, 3-D echocardiography has the potential to add to what 2-D imaging can offer in pediatric heart disease in several areas: (a) anatomic imaging in the setting of structural heart disease, (b) quantitative evaluation of chamber volumes and function, and (c) guidance during cardiac interventional procedures.

Anatomic Imaging in Structural Heart Disease

Three-dimensional echocardiographic reconstruction has the potential to provide unique information regarding cardiac anatomy. Recent reports have demonstrated that 3-D imaging of the atrioventricular valves may augment clinicians’ understanding of the mechanisms of atrioventricular valve regurgitation during valve repair in atrioventricular septal defects (81–83) (Fig. 8.37), and in a variety of congenital heart lesions, including the tricuspid valve in hypoplastic left heart syndrome (83) and in Ebstein anomaly (84). Three-dimensional assessment of aortic valve area in the setting of valvar aortic stenosis has also been described (85,86). Assessment of both native and prosthetic mitral valve abnormalities has been shown to be both feasible and accurate using 3-D techniques (80,87).

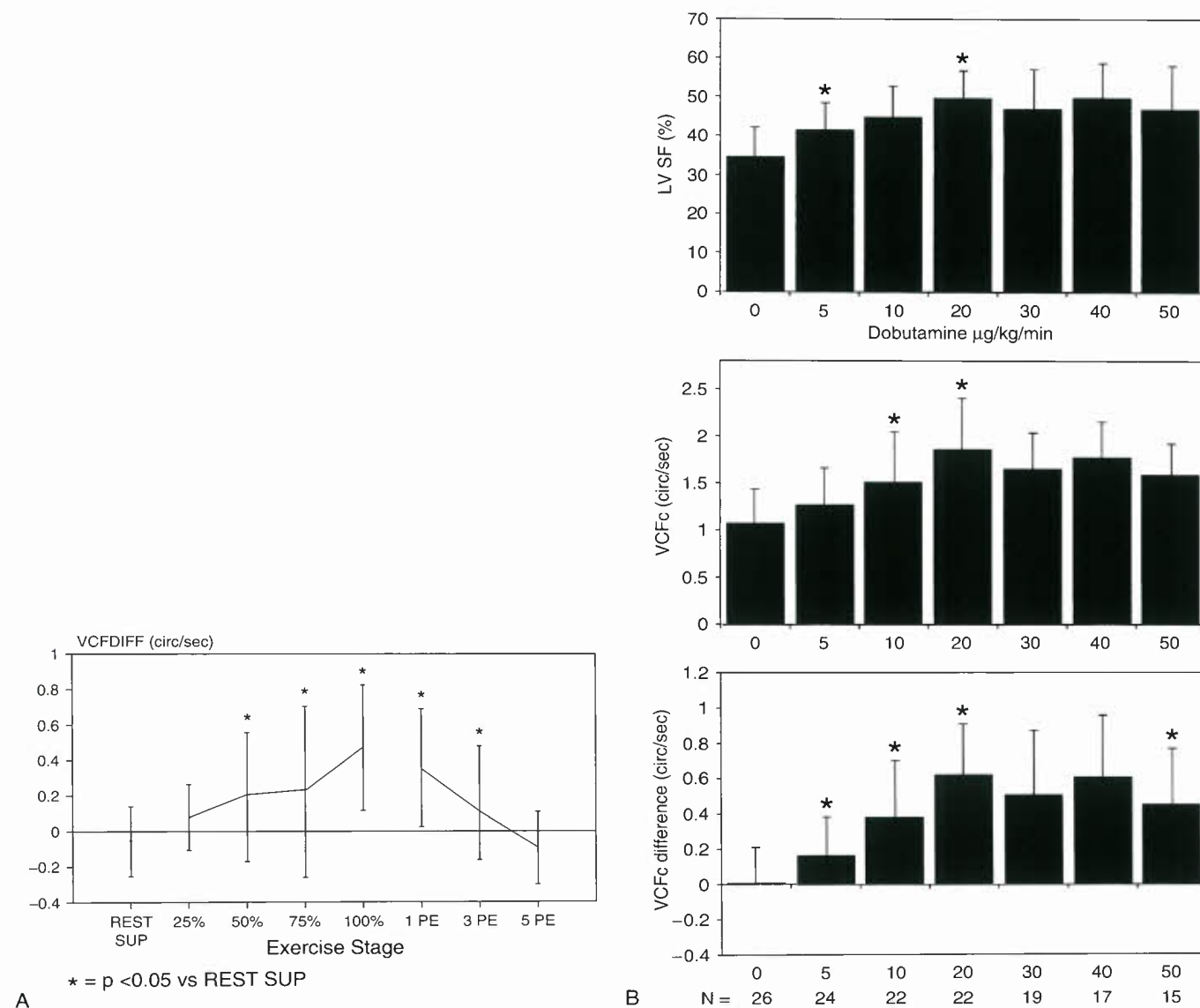


Figure 8.34. Normal responses to VCF difference, a quantitative measure of left ventricular contractility, in children during exercise (A) and during dobutamine stress (B). (Reprinted from Kimball TR, Mays WA, Khoury PR, et al. Echocardiography determination of left ventricular preload, afterload, and contractility during and after exercise. *J Pediatr* 1993;122:S92-S93, with permission from Elsevier. Reprinted from Michelfelder EC, Witt SA, Khoury P, et al. Moderate-dose dobutamine maximizes left ventricular contractile response during dobutamine stress echocardiography in children. *J Am Soc Echocardiogr* 2003;16:144, with permission from Elsevier.)

Three-dimensional echocardiography can also add incremental imaging data in the setting of both ASD and VSD (88,89). With 3-D echocardiography, anatomy can be viewed from unique perspectives, for example, that of the surgeon (90) (Fig. 8.38). In addition, particularly complex anatomy may be better visualized (91). This may be specifically useful, for example, in determining the relation of the VSD to the great vessels in double-outlet right ventricle.

Quantitation of Cardiac Chamber Volumes and Function

From the quantitative standpoint, it is now possible to evaluate cardiac volumes by real-time 3-D echocardiography. Reliable quantitation of both left atrial (92,93) and

left ventricular volumes and left ventricular ejection fraction (94) is possible, and is comparable to values obtained utilizing cardiac magnetic resonance imaging techniques. Research also indicates that right ventricular volumes can be measured accurately in the pediatric population with a variety of congenital heart lesions (95,96). This information may be helpful in evaluating right ventricular size in patients with relative right ventricular hypoplasia (e.g., in pulmonary atresia with intact ventricular septum) and evaluating right ventricular function in the setting of postoperative tetralogy of Fallot or in systemic right ventricles (e.g., hypoplastic left heart syndrome or transposition of the great arteries following atrial switch procedure). Altmann et al. (97) have also demonstrated that 3-D echocardiographic measurements of single ventricular volume and mass are also accurate and suggest this technique for assessing cardiovascular status in this

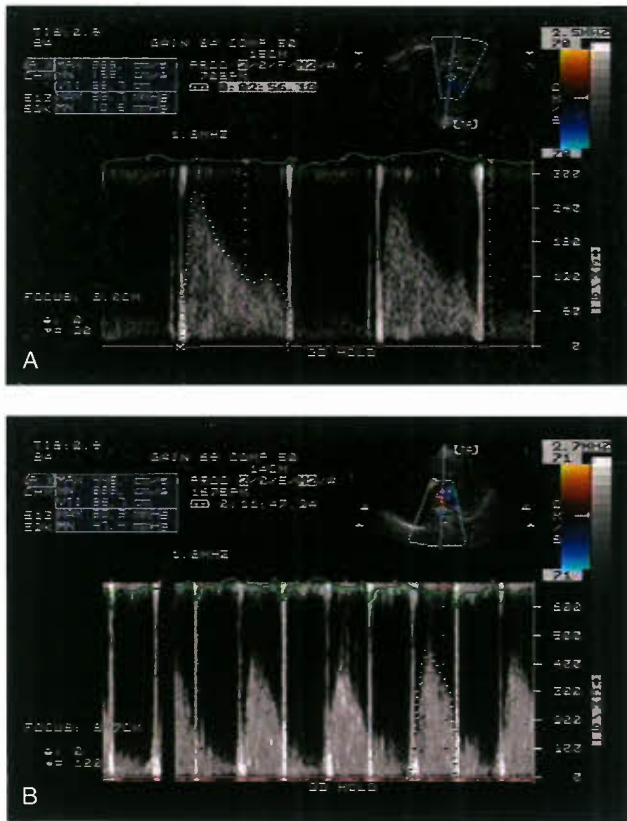


Figure 8.35. Mitral valve Doppler tracings from an apical four-chamber view in a 16-year-old male with a prosthetic mitral valve at baseline (A) and at peak exercise (B). The mean mitral valve gradient at baseline is 10.5 mm Hg. With exercise, the mean gradient increases to 47 mm Hg.

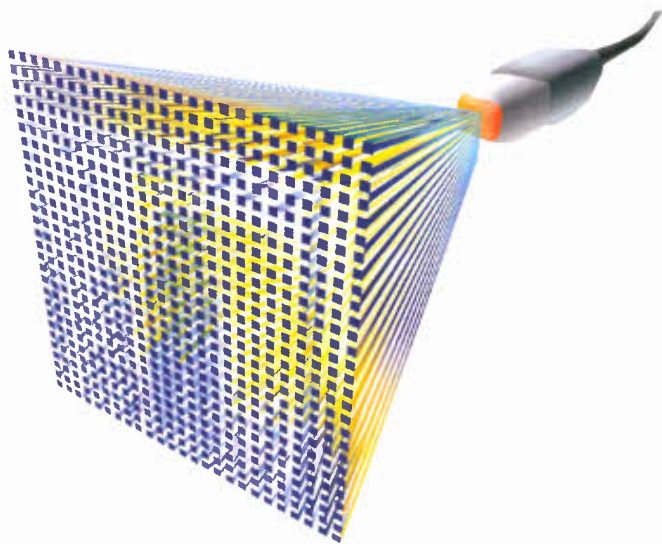


Figure 8.36. With a matrix array transducer, “full volume” 3-D images can be obtained. Thousands of imaging elements in the transducer head allows acquisition of “voxels” in either real time at a smaller (30 to 50 degrees) sector angle, or by electrocardiographically gated acquisition of smaller volume sectors that are integrated into a volume with a larger (90 degrees) sector angle.

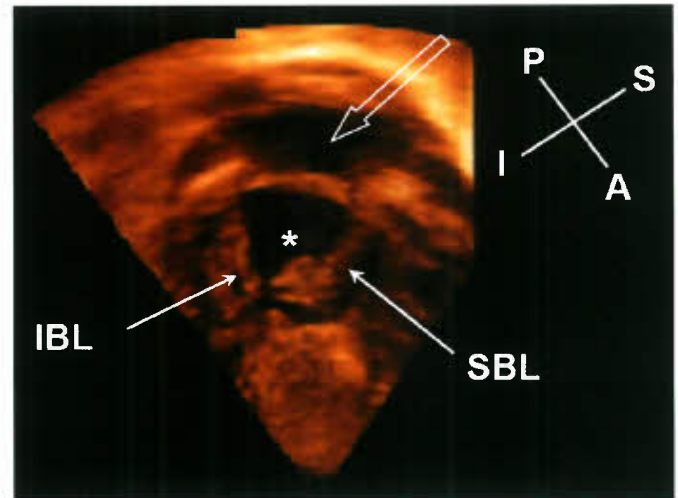


Figure 8.37. Three-dimensional imaging of an atrioventricular septal defect. Three-dimensional image processing of this apical view has removed the right atrial and right ventricular free walls and allows visualization of the right atrial and right ventricular septal surface, including imaging of the primum atrial septal defect (*open arrow*) and inlet ventricular septal defect (*asterisk*). The superior (SBL) and inferior (IBL) bridging leaflets of the common atrioventricular valve can also be seen. A, anterior; I, inferior; P, posterior; S, superior. (Image courtesy of Dr. Girish Shirali, Medical University of South Carolina.)

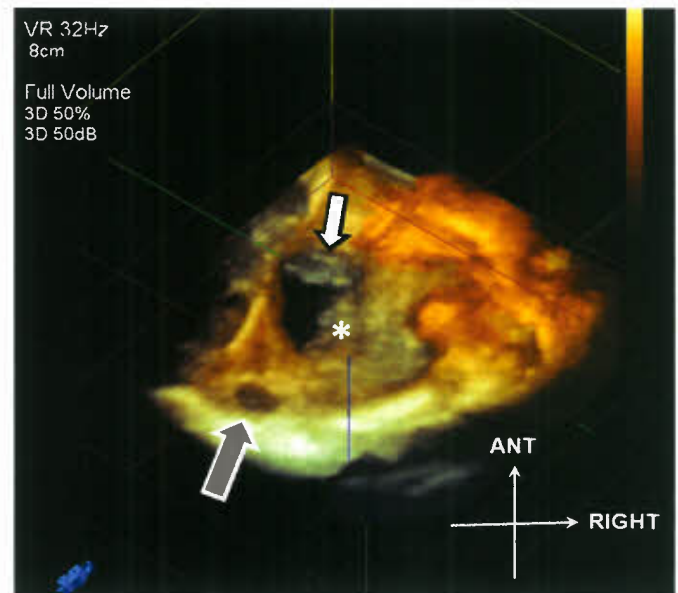


Figure 8.38. Three-dimensional, “surgeon’s view” of the tricuspid valve. The anterior (*white arrow*) and posterior (*asterisk*) tricuspid valve leaflets can be identified; the septal leaflet is open but oriented into the plane of the image. The floor of the RA and coronary sinus ostium (*grey arrow*) is also demonstrated. ANT, anterior.

high-risk population. Other emerging quantitative modalities in 3-D echocardiography include 3-D assessment of intra-ventricular regional function and dyssynchrony (98–100), although these techniques are not yet widely used, particularly in the pediatric population.

3-D Guidance of Cardiac Interventional Procedures

Three-dimensional echocardiography is gaining increasing use in both the intraoperative setting and during catheter-based interventional procedures.

ECHOCARDIOGRAPHIC EVALUATION OF INTERVENTIONAL PROCEDURES

As the field of transcatheter cardiac intervention has expanded the availability of devices and interventions, echocardiographic techniques to evaluate and monitor these procedures have also necessarily expanded. In this section, we review common techniques in echocardiographic evaluation of device deployment in the catheterization laboratory. Following an early experience in transcatheter intervention using only angiography, TEE quickly became established as a vital imaging tool during these procedures (101), particularly during device closure of atrial and ventricular septal (41) defects. As new septal occluder devices continued to be developed, TEE continued to demonstrate its utility in guiding device deployment and assessing outcomes for both atrial (102–104) and ventricular septal (105,106) occluder devices.

Subsequently, intracardiac echocardiography (ICE) was reported. ICE employs a small (10 F, 3.2 mm) catheter with a high frequency ultrasound transducer in its tip. These transducers could image in a longitudinal plane with a sector angle of 90 degrees, and a depth of penetration to 12 cm. ICE was also reported to be useful and effective in demonstrating pertinent anatomy and monitoring device deployment, particularly during device occlusion of ASDs and patent foramina ovale (107–110). A potential advantage of ICE imaging is that it does not require general anesthesia or intubation, as is often necessary in children undergoing TEE (107).

Three-dimensional echocardiography has also been described as a potentially useful modality in the pre- and postprocedure evaluation of the atrial septum before and after device occlusion of ASD (111). More recently, real-time 3-D TEE has proven useful for determining atrial septal anatomy, defect size, rim dimensions, and device position (Fig. 8.39) in the interventional catheterization laboratory (112,113), and may actually reduce fluoroscopy time during these procedures (112).

Regardless of the echocardiographic modality being employed, the goals of echocardiographic evaluation before, during, and after device deployment include: (a) pre-procedure assessment of pertinent anatomy; (b) monitoring during intervention and device deployment; and (c) anatomic assessment after device deployment.

Atrial Septal Defect

In general, only secundum ASDs or patent foramen ovale are amenable to device occlusion. Care should be taken to inspect the defect for size and location. Measurement of the defect size on 2-D imaging should be performed. Assessment of tissue rims around the defect is important in determining the ability of the device to anchor around the defect margins (Fig. 8.40A). The position of the ASD relative to other important cardiac structures, for example, right pulmonary veins, mitral valve, aorta,

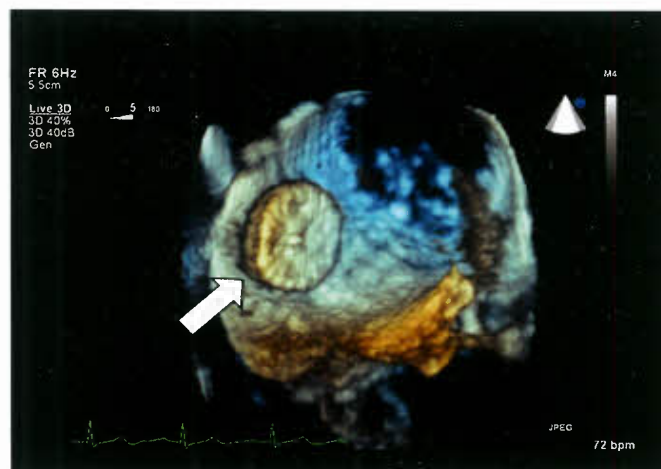


Figure 8.39. Real-time, three-dimensional transesophageal echocardiogram after deployment of an atrial septal defect occluder device. The left atrial disc of the device can be seen centrally along the left atrial aspect of the interventricular septum (arrow). (Image courtesy of Phillips Medical Co., Bothell, WA.)

and coronary sinus should be noted. During the procedure, the position of sheaths and guidewires should be documented and communicated to the interventionalist. As most ASD occluder devices now consist of a dual “disk” design, deployment of the left atrial disk in the LA should be confirmed, then proper seating of the disc upon the atrial septum is noted. Full deployment of the right atrial disc and assessment of the entire device relative to its position on the atrial septum, presence/absence of residual shunting, and potential impingement on adjacent structures should be evaluated prior to release of the device. Findings should be reevaluated following release of the device from its guidewire (Fig. 8.40B). It is important that unique characteristics of each device be known and understood during the imaging evaluation (102,103,114–116).

Ventricular Septal Defect

Specific devices for closure of perimembranous (105,117) and muscular (106,118) VSDs have been reported. Care should be taken to inspect the defect for size and location. Measurement of the defect size on 2-D imaging should be performed. Assessment of tissue rims around the defect are important in determining the ability of the device to anchor around the defect margins, and to assess the potential of the device to impinge on other important cardiac structures, for example, atrioventricular valve and chordal apparatus. During the procedure, the position of sheaths and guidewires should be documented and communicated to the interventionalist. Deployment of the device into the left ventricle should be confirmed (Fig. 8.41A), and then proper seating of the disc upon the ventricular septum noted (Fig. 8.41B). Full deployment of the device and assessment of the entire device relative to presence/absence of residual shunting, and potential impingement on adjacent structures should be evaluated prior to release of the device. Findings should be reevaluated following release of the device from its guidewire to rule out device embolization (Fig. 8.41C).

Patent Ductus Arteriosus

Transcatheter therapy for PDA most commonly consists of either coil occlusion with Gianturco coils (119,120)

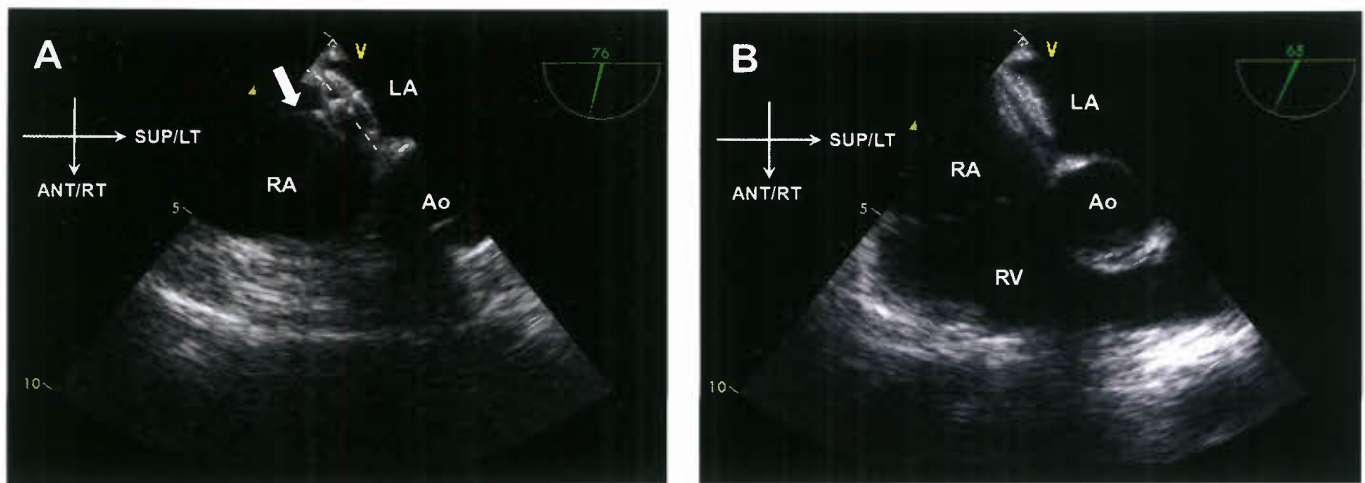


Figure 8.40. Transesophageal imaging during device occlusion of a secundum atrial septal defect (ASD). In panel A, the ASD device is seen straddling the ASD. Rim tissue (*dotted lines*) can be seen between both left atrial (LA) and right atrial (RA) discs. The device has not been released from the guidewire (*white arrow*). In panel B, the device has been fully deployed, and now sits flush against the atrial septum. ANT, anterior; Ao, aorta; LT, left; RT, right; RV, right ventricle; SUP, superior.

or device occlusion, for example, the Amplatzer ductal occluder (119,121,122). Most frequently echocardiography is utilized to assess preprocedure ductal size and morphology, and to evaluate residual shunting postdevice placement.

In addition to assessing residual ductal level shunting, it is important to screen for evidence of device impingement on adjacent vessels, particularly the proximal left pulmonary artery (121).

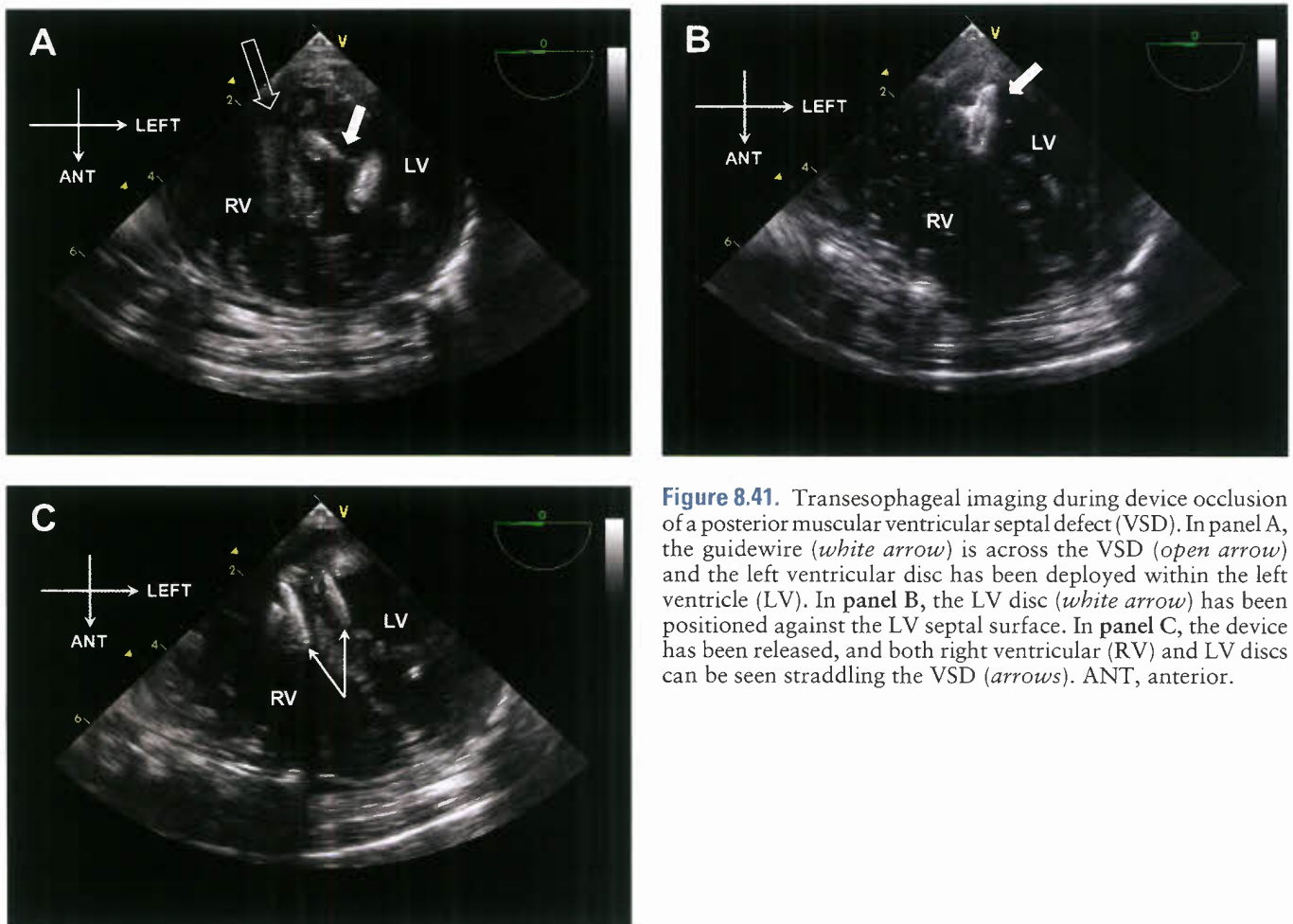


Figure 8.41. Transesophageal imaging during device occlusion of a posterior muscular ventricular septal defect (VSD). In panel A, the guidewire (*white arrow*) is across the VSD (*open arrow*) and the left ventricular disc has been deployed within the left ventricle (LV). In panel B, the LV disc (*white arrow*) has been positioned against the LV septal surface. In panel C, the device has been released, and both right ventricular (RV) and LV discs can be seen straddling the VSD (*arrows*). ANT, anterior.

CONTRAST ECHOCARDIOGRAPHY

Contrast echocardiography involves administration of one of two distinct contrast agents—agitated saline or commercially available transpulmonary contrast. Although both are administered through an intravenous line, each has a distinct purpose and use.

Agitated Saline Contrast Echocardiography

Principle

Agitation of saline produces microbubbles of gas (10 to 100 μ in diameter) which pass through the circulation until they are filtered and absorbed by transit into a capillary bed. With a systemic intravenous injection, therefore, the microbubble “cloud” will follow the downstream flow of blood, pass into the large systemic veins, and enter the right-sided cardiac structures. In the absence of right-to-left shunts, the microbubbles should not be present in the left side of the heart because of filtering and absorption in the pulmonary capillary bed. The presence of contrast in the left side of the heart after an intravenous injection of agitated saline, therefore, is a very sensitive marker for the existence of a right-to-left intrapulmonary or intracardiac shunt (123). Likewise, the presence of contrast in the right side of the heart after a left heart injection (e.g., in the operating room or cardiac intensive care unit through a left atrial line) is indicative of an intracardiac left-to-right shunt.

Technique

First, the injection site should be considered. For example, a right antecubital injection is sufficient if one needs to opacify the right heart for investigation of an intracardiac right-to-left shunt. However, if one is suspecting drainage of a LSVC into a coronary sinus or the LA directly, the injection site should be through the left antecubital vein to ensure that “contrast” enters the LSVC. In this instance, a right antecubital vein injection would not ensure opacification of a LSVC since the “contrast” would pass through the right innominate vein and preferentially enter the RSVC bypassing a communicating vein (which may not even be present) and the LSVC. In the case of unusual Glenn and Fontan connections it may be necessary to inject into a lower extremity vein to preferentially fill the left pulmonary artery. Sometimes agitated saline contrast should be administered through central catheters during cardiac catheterization, for example, to pinpoint the exact location of a Fontan leak.

Two syringes (one empty, the other filled with saline [~3 mL for newborn, ~20 mL for adult]) are connected to a stopcock. The stopcock is connected to the intravenous line close to its entry into the body. Addition of a small amount (0.25 to 0.5 mL) of the patient’s blood will enhance contrast opacification (124). Agitation is achieved by turning the stopcock off to the patient and forcefully pushing the saline (or saline/blood mixture) alternately between the two syringes for approximately 30 seconds. The sonographer should obtain a view (usually the apical four-chamber view) in which both right and left heart structures are imaged simultaneously so that the contrast can be visualized passing (a) through the right heart to verify that the contrast injection was indeed adequate and (b) through the left heart to verify if a right-to-left shunt is indeed present. The stopcock is then turned on to the patient and the contrast is pushed rapidly into the vein. In older patients, a Valsalva maneuver may be performed to enhance the ability to detect a right-to-left shunt.

Indications

Agitated saline contrast is helpful whenever a right-to-left intrapulmonary or intracardiac shunt is suspected but cannot be detected or definitively diagnosed by standard echocardiographic modalities. These scenarios include the patient with a suspected thromboembolic stroke, unexplained cyanosis,

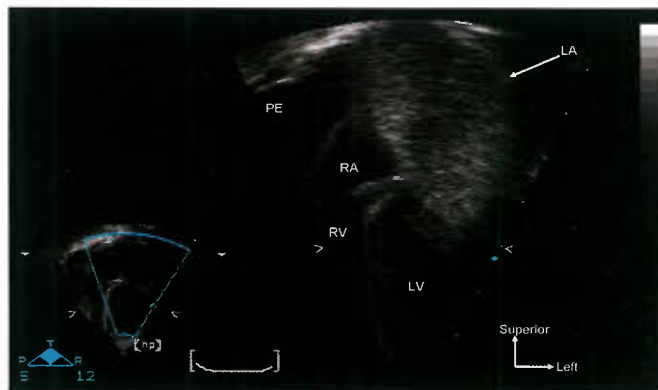


Figure 8.42. Apical four-chamber view during administration of agitated saline contrast in the left antecubital vein demonstrates dense opacification of the left atrium (LA) supportive of the suspected diagnosis of a left superior vena cava draining directly into the roof of the LA. (This patient also has a moderate pericardial effusion [PE].) LV, left ventricle; RA, right atrium; RV, right ventricle.

suggestion of an intracardiac shunt on an echocardiogram with suboptimal windows, poor oxygen saturations following Glenn or Fontan operation (125), suspected baffle leak following atrial switch procedure for transposition, suspected unroofed coronary sinus, and liver disease with suspected hepatopulmonary syndrome (126,127) (Fig. 8.42).

With intrapulmonary shunts, as seen in pulmonary arteriovenous malformations occurring in cavopulmonary connections and in the hepatopulmonary syndrome, microbubbles in the left heart usually appear three to four cardiac cycles after the contrast cloud appears in the right heart. With intracardiac shunts such as atrial or VSDs, unroofed coronary sinus, or atrial baffle leak, microbubbles appear in the left heart almost immediately upon appearance in the right heart. The exact site of initial left heart microbubble appearance should also be carefully noted since the location of the right-to-left shunt can be pinpointed to either that level or upstream to it.

Diagnosis of the hepatopulmonary syndrome is one of the leading indications for agitated saline contrast. This syndrome is a well-defined cause of hypoxemia in patients with liver disease and carries an incidence as high as 29% (126). It is due to abnormal intrapulmonary vascular dilation resulting in excess perfusion (of deoxygenated blood) for the given state of ventilation. This pathophysiology is in distinction from that occurring in the other well-recognized cardiopulmonary complication, portopulmonary hypertension, which is characterized by abnormal pulmonary vasoconstriction and obliterative vascular remodeling. Alteration in the hepatic synthesis or metabolism of vasoactive pulmonary substances, nitric oxide and possibly endothelin-1, are believed to be integral to the development of intrapulmonary vascular dilation in the hepatopulmonary syndrome (126,128). A particularly interesting congenital etiology of the hepatopulmonary syndrome is the Abernethy Malformation because its initial presentation is one of dyspnea and cyanosis rather than of frank liver disease (127). The malformation is due to congenital absence of the portal vein, which results in a diversion of portal blood away from the liver and directly into the vena cava.

Transpulmonary Contrast Echocardiography

PRINCIPLE

Unlike agitated saline, commercially available transpulmonary contrast agents consist of a suspension of microspheres designed to pass through the pulmonary capillary bed and densely opacify the left heart structures (129). These microspheres are 10-fold smaller than the microbubbles created with saline agitation

(1 to 10 μ vs. 10 to 100 μ) (129). The microspheres consist of an internal gas (air or fluorocarbon) encapsulated by an external shell (aggregated albumin, galactose, or lipid). After an intravenous injection, the microspheres will follow the downstream course of the blood into the right heart and pulmonary vasculature. The microspheres are sufficiently small and the diffusion of the gas is sufficiently limited by its low partition coefficient that the microspheres pass through the capillary bed into the left heart. Because the acoustic impedance of the microspheres is much lower than that of the blood, the ultrasound waves are scattered and reflected at the microsphere-blood interface.

TECHNIQUE

All contrast agents are activated by suspending the microspheres through agitation of the vial, sometimes with a commercially supplied mechanical agitator. The contrast agent can then be administered intravenously by infusion or bolus. Although pediatric dosages have not been established, 50% of the adult dose produces excellent left heart opacification without side effects (130) (Fig. 8.43). Contrast effect persists for approximately 3 to 5 minutes. The ultrasound system should be set to low power or mechanical index so that bubble destruction is minimized. With this setting, the myocardium will appear black and the contrast-filled cavity will be white. Adverse reactions have not been reported in children. In adults, adverse reactions are extremely rare and when present consist of allergic reaction, headache, flushing, and nausea. In the presence of an intracardiac shunt, the microspheres can bypass filtering by the lung and enter the arterial circulation directly. It is believed that the larger (up to 32 μ) microspheres which constitute a very small percentage of the total suspension and which are normally filtered by the lungs can pass into the left heart and produce arterial occlusions in this setting. Therefore, no transpulmonary contrast agent should ever be administered to a patient with a known or suspected intracardiac shunt.

INDICATIONS

Currently, contrast agents are approved for the use of heart opacification and endocardial visualization only. Therefore, they are indicated when traditional echocardiographic modalities yield suboptimal myocardial and endocardial visualization. Most often this is necessary during stress echocardiography when visualization of all myocardial segments is required to adequately assess integrity or compromise of coronary perfusion (130,131).

Additionally, contrast agents may be beneficial in the evaluation of right ventricular function since the right ventricular endocardium and myocardium can be very difficult to visualize.

DIGITAL ARCHIVING AND TELE-/WEB-BASED ECHOCARDIOGRAPHY

The laboratory of our past collected nondiscrete, analog wave-form signals of varying voltages that were stored to videotape, conforming to the National Television Standards set in the 1940s. Now, the digital laboratory of our present uses technology enabling gray scale storage of each pixel in the echocardiographic image by conversion into a series of binary digits. The depth of binary storage dictates the resolution. For example, an 8-bit depth binary system stores the image as series of eight digits (e.g., 00000000, 00000001, and so on) providing $2^8 = 256$ shades of gray. This level is more than sufficient when one considers that the human eye can distinguish only 50 shades of gray. The digital image has almost complete fidelity to the true real-time image.

Digital imaging comes with a considerable storage burden. Typically, a freeze-frame ultrasound image has 512 lines of information with 512 samples per line, resulting in approximately 262,000 pixels per frame. Each pixel is described by an 8-bit binary system, resulting in approximately 2 million bits of data to describe a single frame. At ultrasound frame rates of 45 frames/s, it therefore requires 283 MB of storage to save a single 3-second (~ 5 beat) sweep. A typical study of 60 to 80 clips and a few still frames approaches 20 to 25 GB of data! Guidelines for the management of this massive amount of digital echocardiographic data have been developed by the American Society of Echocardiography (132).

Compression of digital data aids in practical storage and transmission. There are two types of compression: lossless and lossy. Lossless compression ensures that no data are lost but provides only a modest 3:1 reduction in data storage. Lossy compression (e.g., Joint Photography Expert Group method, or JPEG) reduces data storage by 20:1 allowing transmission of video through computer networks and without loss of image quality compared with super Video Home System (VHS) video (133). The Motion Picture Expert Group (MPEG) method is a second compression process that uses a motion picture prediction algorithm exploiting redundancy between preceding

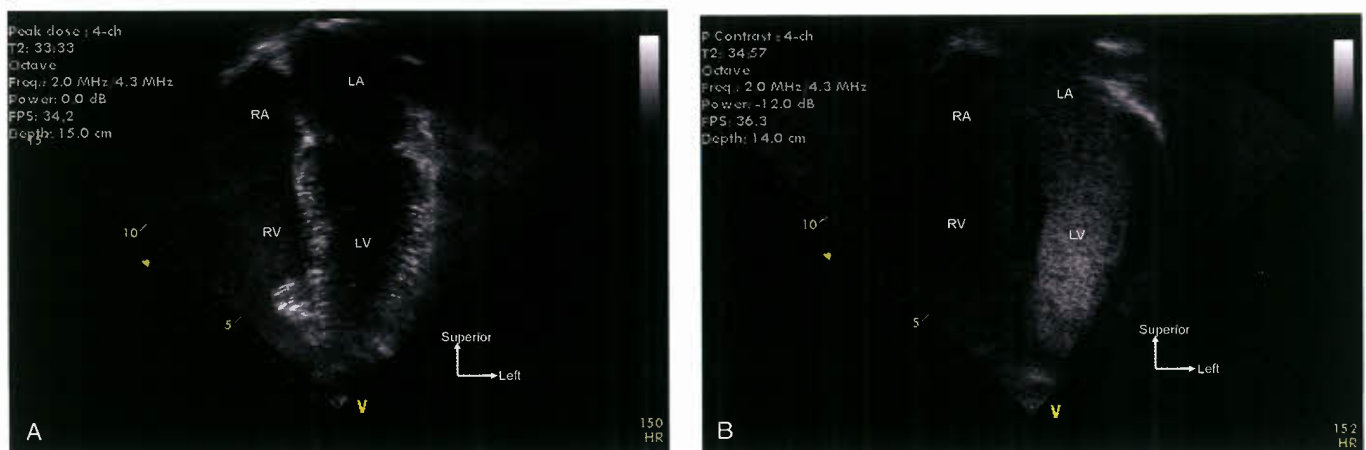
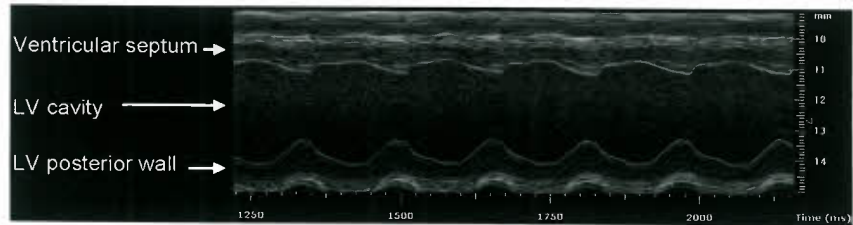


Figure 8.43. Apical four-chamber views at peak heart rate during dobutamine stress echocardiogram without (A) and with (B) transpulmonary contrast agent. Although the noncontrast image (A) is reasonably clear and most wall segments can be identified, the contrast image (B) makes identification of all wall segments (particularly those at the apex) easy.

Figure 8.44. An M-mode echocardiogram of the left ventricle of a mouse using a high-frequency (40 MHz) transducer demonstrates excellent resolution of the ventricular septum, left ventricular cavity, and left ventricular posterior wall.



and subsequent images, thereby offering better motion-image quality, higher compression ratios (e.g., 1,500:1), and easier integration into a computer network. Disadvantages to MPEG compression are that it is not yet validated for echocardiography, is not standardized within DICOM (the Digital Imaging and Communications in Medicine Standard), and has inferior still-frame image quality (134,135).

Despite the large amount of data created with digital echocardiographic image acquisition, image management has been relatively facile and has indeed improved efficiency in the pediatric echocardiography laboratory (136). Computer technology has continued to improve so that images have been routinely attached to web-based journal articles (137). Importantly, images can be transferred easily through web-based networks and onto personal digital devices allowing for reading of echocardiograms from and in remote sites as long as web access is available (138). Acquiring and reading echocardiograms in this manner has been shown to be diagnostically accurate (139).

Further, this technology has had profound impact on (a) more timely diagnosis of critically ill patients, (b) better determination of need for cardiology consult, and (c) preventing unnecessary transfers for the purpose of merely obtaining an echocardiogram (140–142).

RESEARCH ECHOCARDIOGRAPHY

Because of its ease of use, portability, low cost, absence of side effects, and high diagnostic accuracy; echocardiography is a robust research tool. The American Society of Echocardiography has established guidelines for the appropriate use of echocardiography in clinical trials (143). Echocardiography has been used successfully to provide mechanistic insights into disease processes and therapeutic outcomes, to provide both cross-sectional and longitudinal data in large epidemiologic studies, and to measure functional and structural changes now considered to be end points. The Framingham Heart Study was the first epidemiologic study to use echocardiographic measurements (144). The single largest application of echocardiography in epidemiologic studies has been the measurement of left ventricular mass and its change with antihypertensive therapy (145–149). Recently, the use of echocardiography has been expanded to clinical trials investigating cardiac resynchronization therapy for congestive heart failure. Echocardiography has been instrumental to demonstrate that remodeling due to resynchronization therapy is associated with less risk of subsequent ventricular tachyarrhythmia (150). In addition, echocardiography is the major tool for providing detailed phenotypes for large human genetic studies (151).

The use of echocardiography for any research purpose necessitates establishing methods to limit measurement variability. Intra- and interobserver variability should be measured and repeated periodically. Protocols for training qualification need to be developed. A minimum number of sonographers and readers should be used to limit the effects of interobserver variability. Only contemporary equipment should be used. Digital archiving should be established to provide a bioinformatic data bank of echocardiographic images. These practices

are best established by the creation of a core research laboratory which can guarantee adequate training of peripheral sites and accurate, reproducible data analysis (143,152,153).

Echocardiography has also been instrumental in animal research, most notably in the phenotyping of transgenic mice (154–159). Previous phenotyping methods (Langendorf preparation, histologic examination) necessitated sacrifice of the animal. This prohibited not only acquisition of longitudinal data and also further breeding. Mouse echocardiography is performed using high-frequency transducers (at least 15 MHz) while the animal is anesthetized with 2% inhaled isoflurane and kept warm on a heated examination table. Parasternal and apical images are obtained and quantitative data include left ventricular dimensions, function, mass, and aortic and mitral valve Doppler velocities (Fig. 8.44). If the animal has undergone microcatheterization of the left ventricle or a systemic artery, pressure data can be coupled with simultaneous echocardiographic left ventricular dimensional data to create pressure-dimension loops or end-systolic wall stress data, powerful indices of ventricular function (see above) (Fig. 8.45) (159).

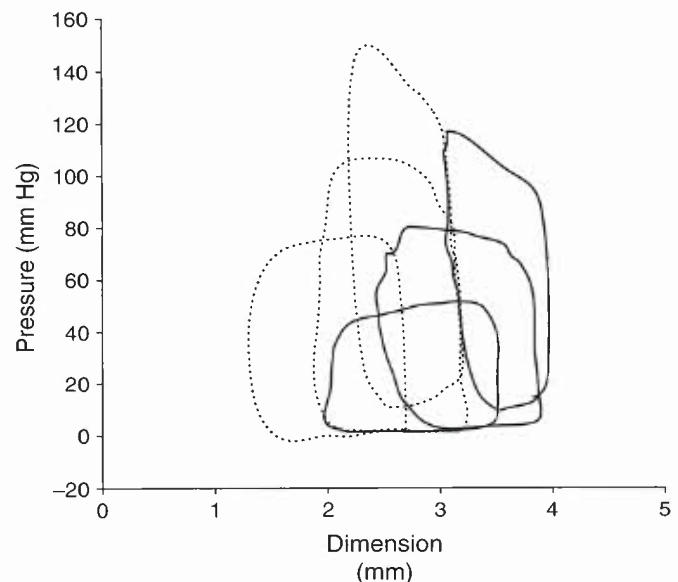


Figure 8.45. Left ventricular pressure-dimension loops in control mice (*thin lines*) and hypothyroid mice (*thick lines*) derived from simultaneous M-mode echocardiography and catheterization of the left ventricle. Afterload was manipulated with phenylephrine and nitroprusside infusion to create a family of pressure-dimension loops from which end-systolic relations can be measured. At any given end-systolic dimension, the end-systolic pressure is less in the hypothyroid mice versus the control mice indicating depressed contractility in the hypothyroid mice. (From Williams RV, Lorenz JN, Witt SA, et al. End-systolic stress-velocity and pressure-dimension relationships by transthoracic echocardiography in mice. *Am J Physiol* 1998;274(Heart Circ Physiol 43):H1828–H1835).

Recently, the development of high-frequency ultrasound transducers (30 to 70 MHz) has allowed imaging of hearts in mouse pups or even mouse embryos (160–166). This echocardiographic technique, more appropriately called ultrasound biomicroscopy, involves mounting the anesthetized pup or pregnant ewe on a microscope stage embedded with heating elements to keep the animal warm and which can be moved spatially in x , y , and z planes using three micromanipulator knobs similar to using a microscope. Embryonic mice imaging is extremely valuable since many transgenic mice models are embryonic lethal. Doppler signals are apparent as early as the eighth embryonic day, essentially the heart tube stage (gestational age of mouse = 18.5 days). Four chambers can be identified with echocardiography at embryonic day 11.5 and septation is evident by ultrasound at embryonic day 13.5. Resolution has improved significantly with these higher frequency transducers such that it will now be possible to phenotype transgenic mice models targeted for maldevelopment of the cardiac valves. Using such equipment, investigators have studied the origins of adult cardiovascular disease. Specifically, it has been shown in transgenic studies, for example, that prenatal diet has profound influences on adult cardiovascular mechanics as assessed by echocardiography (167).

THE FUTURE

For years, echocardiography enjoyed a status to itself as the premier diagnostic modality for pediatric cardiovascular disease. This is no longer true. Now, echocardiography shares the stage of noninvasive cardiac imaging with a variety of other modalities, including cardiac magnetic resonance imaging, positron emission tomography, metabolic imaging, and perfusion imaging. Echocardiographers and other pediatric cardiologists need to understand that these modalities complement, rather than replace, echocardiography. For example, cardiac magnetic resonance imaging excels in imaging both extracardiac anatomy and also the spatial relationships of cardiovascular anatomy in relation to other structures in the thoracic cavity. The former has been difficult and the latter impossible for the pediatric echocardiographer. Because of these complementary niches of the various imaging modalities, patient care has improved to unprecedented levels. Nevertheless, the myriad of diagnostic tests provides echocardiographers with at least two challenges.

First, pediatric echocardiographers must resist complacency. There may be a tendency to become less rigorous during the echocardiographic exam knowing that other imaging modalities may later be employed. If difficult anatomy can be diagnosed accurately with echocardiography, the expense, the inconvenience, and potential risk of other imaging modalities will be avoided. We need to remain compulsive and true to our specialty and continue to bring the same rigor and compulsiveness to the exam that we have employed in the past. This will involve not only efforts at the bedside and in the echocardiography laboratory but also efforts at a more communal level such as the continued development of guidelines and standards for the performance of quality echocardiographic examinations (168,169).

The second challenge is one of “imaging responsibility” to our patients and our health care system. We must realize that we are responsible for recognizing and resisting the lure of employing all of the diagnostic armamentarium available to us. The challenge is to partner with our colleagues managing these other imaging modalities to develop pathways in the diagnostic approach for our patients. Such an approach will necessarily be diagnosis- and age- specific and, indeed, in some instances may not utilize echocardiography. In all cases,

however, imagers must join together to develop strategies that bring the greatest value to the patient...an approach that is most accurate with the least cost.

Because of continued miniaturization of computer and ultrasound equipment, hand-carried ultrasound devices have been used for medical diagnostics. Most of these devices now have the capabilities of even the most technologically advanced ultrasound systems but are the size of a small laptop computer or even a mobile phone. Using such devices, echocardiographers can provide point-of-service care more effectively. More importantly, these devices expand the community that can now receive and benefit from the diagnostic power of echocardiography. In addition, the devices improve diagnostic accuracy by complementing the cardiac physical examination in even tertiary care centers.

Although auscultation has been the traditional foundation of the cardiac physical examination, many primary care physicians and even some cardiologists have imperfect auscultatory skills. For example, diagnostic accuracy of current resident physicians using auscultation alone is notoriously poor (170–172). It is likely that these skills will continue to decline as resident physicians cope with the competing forces of having to learn vast amounts of newer medical information within the time constraints imposed by resident work hour regulations. Hand-carried ultrasound devices extend the diagnostic accuracy of echocardiography from the ultrasound laboratory to the time and place of the physical examination. By complementing stethoscope use with a hand-held system, an examiner can not only hear the heart but see it as well, thereby improving diagnostic accuracy (173). Implementation of a hand-carried ultrasound device program into the medical school curriculum significantly increases the diagnostic accuracy of the physical examination performed by medical students (174). Even the accuracy of the cardiovascular examination performed by board-certified cardiologists is enhanced by their use of a hand-carried device (175,176). In pediatrics, hand-held ultrasound has been shown to have similar diagnostic accuracy as traditional ultrasound systems and its use is speculated to only increase (177).

The increased availability of echocardiography made possible by hand-carried devices has tempted other noncardiac specialists to practice cardiac ultrasound (178,179). While this has the potential benefit of enhancing overall patient care by improving diagnostic accuracy, it also emphasizes the need for responsible practice of ultrasound. It is the duty of the echocardiography community to develop standards for the practice of hand-carried ultrasound and ensure that they are met (180).

The situation is similar to stethoscope use. Most physicians who use a stethoscope are not cardiologists; the diagnostic accuracy of the stethoscope varies according to its user, and cardiologists have greater expertise in its use. Likewise, hand-carried ultrasound devices are currently being used by a variety of health care providers, for example, emergency room physicians, neonatologists, and even robots (181–184).

However, as with the stethoscope, it would be expected and need to be indoctrinated as standard of care, that when a noncardiologist identified a patient with suspected pathology using a hand-held device, the patient would be referred to a cardiologist for further evaluation.

The development and expansion of hand-held ultrasound devices speaks to us as physicians, specifically to the reasons as to why many of us chose medicine as our career. We have a powerful, robust tool in echocardiography; a tool with which we can do much good by providing very advanced medical care to an even vaster population. There is great value in the fact that hand-held devices allow us to provide increased availability to our tertiary care populations at surrounding satellite clinics improving medical care by obviating the need for lengthy, stressful and time-consuming journeys to the central facility. But there is perhaps greater value and meaning in

the fact that hand-held devices allow us to spread echocardiographic technology to those patients who would otherwise never benefit from it — the patients utilizing the underserved urban and rural health clinics and the patients in developing countries (185–187). As investigators from the Cedars Sinai Medical Center state, it is this use of echocardiography that truly makes “an impossible mission possible” (186).

REFERENCES

- Samyn MM. A review of the complementary information available with cardiac magnetic resonance imaging and multi-slice computed tomography (CT) during the study of congenital heart disease. *Int J Cardiovasc Imag* 2004;20:569–578.
- Ellis AR, et al. Utility of computed tomographic angiography in the preoperative planning for initial and repeat congenital cardiovascular surgery. *Cardiol Young* 2010;20:262–268.
- Minich LL, Tani LY, Paul JJ. Technological advances to extend the echocardiographic imaging of pediatric patients. *Pediatr Cardiol* 2002;23:257–265.
- Broberg C, Meadows AK. Advances in imaging: the impact on the care of the adult with congenital heart disease. *Prog Cardiovasc Dis* 2011;53:293–304.
- Ageliki KA, et al. Accuracy of cardiac auscultation in asymptomatic neonates with heart murmurs: comparison between pediatric trainees and neonatologists. *Pediatr Cardiol* 2011;32:473–477.
- Azhar AS, Habib HS. Accuracy of the initial evaluation of heart murmurs in neonates: do we need an echocardiogram? *Pediatr Cardiol* 2006;27:234–237.
- Kelves BH. Looking through women: the development of ultrasound and mammography. In: *Naked to the Bone: Medical Imaging in the Twentieth Century*. Reading, MA: Addison-Wesley, 1997:228–250.
- Goldberg BB, Kimmelman BA. *Medical Diagnostic Ultrasound: A Retrospective on its 40th Anniversary*. Rochester, NY: Eastman Kodak Company, 1988:2–19.
- Goldberg SJ, Allen HD, Sahn DJ. *Pediatric and Adolescent Echocardiography: A Handbook*. Chicago, IL: Year Book Medical Publishers, 1975.
- Baylen B, et al. Left ventricular performance in the critically ill premature infant with patent ductus arteriosus and pulmonary disease. *Circulation* 1977;55:182–188.
- Snider AR, et al. Congenital left ventricular inflow obstruction evaluated by two-dimensional echocardiography. *Circulation* 1980;61:848–855.
- Clyman RJ, et al. Prenatal administration of betamethasone for prevention of patent ductus arteriosus. *J Pediatr* 1981;98:123–126.
- Snider AR, et al. Doppler evaluation of left ventricular diastolic filling in children with systemic hypertension. *Am J Cardiol* 1985;56:921–926.
- Snider AR. Two-dimensional and Doppler echocardiographic evaluation of heart disease in the neonate and fetus. *Clin Perinatol* 1988;15:523–565.
- Bierman FZ, Williams RG. Subxiphoid two-dimensional imaging of the interatrial septum in infants and neonates with congenital heart disease. *Circulation* 1979;60:80–90.
- Bierman FZ, Williams RG. Prospective diagnosis of d-transposition of the great arteries in neonates by subxiphoid, two-dimensional echocardiography. *Circulation* 1979;60:1496–1502.
- Bierman FZ, Fellows K, Williams RG. Prospective identification of ventricular septal defects in infancy using subxiphoid two-dimensional echocardiography. *Circulation* 1980;62:807–817.
- van Doesburg NH, Bierman FZ, Williams RG. Left ventricular geometry in infants with d-transposition of the great arteries and intact interventricular septum. *Circulation* 1983;68:733–739.
- Stevenson JG, Kawabori I, Guntheroth WG. Noninvasive detection of pulmonary hypertension in patent ductus arteriosus by pulsed Doppler echocardiography. *Circulation* 1979;60:355–359.
- Stevenson JG, et al. Pulsed Doppler echocardiographic evaluation of ventricular septal defect patches. *Circulation* 1984;70:138–146.
- Hedrick WR, Hykes DL, Starchman DE. *Ultrasound Physics and Instrumentation*. St. Louis, MO: Mosby-Year Book, 1995:1–90.
- Yoganathan AP, et al. Review of hydrodynamic principles for the cardiologist: applications to the study of blood flow and jets by imaging techniques. *J Am Coll Cardiol* 1988;12:1344–1353.
- Anderson RH, et al. Sequential segmental analysis of congenital heart disease. *Pediatr Cardiol* 1984;5:281–287.
- Jacobs JP, et al. The nomenclature, definition and classification of cardiac structures in the setting of heterotaxy. *Cardiol Young* 2007;17:1–28.
- Hagler DJ. Echocardiographic segmental approach to complex congenital heart disease in the neonate. *Echocardiography* 1991;8:467–475.
- Van Praagh R. Diagnosis of complex congenital heart disease: morphologic-anatomic method and terminology. *Cardiovasc Intervent Radiol* 1984;7:115–120.
- Van Praagh R. The importance of segmental situs in the diagnosis of congenital heart disease. *Semin Roentgenol* 1985;20:254–271.
- Ho SY, Anderson RH, Sanchez-Quintana D. Gross structure of the atriums: more than an anatomic curiosity? *Pacing Clin Electrophysiol* 2002;25:342–350.
- Zhang YQ, et al. Echocardiographic assessment of juxtaposition of the right atrial appendage in children with congenital heart disease. *Echocardiography* 2010;27:878–884.
- Kimball TR, et al. Color flow mapping to document normal pulmonary venous return in neonates with persistent pulmonary hypertension being considered for extracorporeal membrane oxygenation. *J Pediatr* 1989;114:433–437.
- Jenni R, Rojas J, Oechslin E. Isolated noncompaction of the myocardium. *N Engl J Med* 1999;340:966–967.
- Chin TK, et al. Isolated noncompaction of left ventricular myocardium. A study of eight cases. *Circulation* 1990;82:507–513.
- Finsterer J, Stollberger C. No rationale for a diagnostic ratio in left ventricular hypertrabeculation/noncompaction. *Int J Cardiol* 2011;146:91–92.
- Stollberger C, Finsterer J. Left ventricular hypertrabeculation/noncompaction. *J Am Soc Echocardiogr* 2004;17:91–100.
- Van Praagh R, et al. Transposition of the great arteries with posterior aorta, anterior pulmonary artery, subpulmonary conus and fibrous continuity between aortic and atrioventricular valves. *Am J Cardiol* 1971;28:621–631.
- de la Cruz MV, et al. The infundibular interrelationships and the ventriculoarterial connection in double outlet right ventricle. Clinical and surgical implications. *Int J Cardiol* 1992;35:153–164.
- Pasquini L, et al. Conal anatomy in 119 patients with d-loop transposition of the great arteries and ventricular septal defect: an echocardiographic and pathologic study. *J Am Coll Cardiol* 1993;21:1712–1721.
- Margossian R, et al. Predictors of Coronary Artery Visualization in Kawasaki Disease. *J Am Soc Echocardiogr* 2011;24:53–59.
- Ritter SB. Transesophageal real-time echocardiography in infants and children with congenital heart disease. *J Am Coll Cardiol* 1991;18:569–580.
- Ungerleider RM, et al. Intraoperative echocardiography during congenital heart operations: experience from 1,000 cases. *Ann Thorac Surg* 1995;60:S539–S542.
- van der Velde ME, et al. Transesophageal echocardiographic guidance of transcatheter ventricular septal defect closure. *J Am Coll Cardiol* 1994;23:1660–1665.
- Fyfe DA, et al. Transesophageal echocardiography detects thrombus formation not identified by transthoracic echocardiography after the Fontan operation. *J Am Coll Cardiol* 1991;18:1733–1737.
- Zyblewski SC, et al. Initial experience with a miniaturized multiplane transesophageal probe in small infants undergoing cardiac operations. *Ann Thorac Surg* 2010;89:1990–1994.
- Saphir JR, et al. Upper airway obstruction after transesophageal echocardiography. *J Am Soc Echocardiogr* 1997;10:977–978.
- Bensky AS, O'Brien JJ, Hammon JW. Transesophageal echo probe compression of an aberrant right subclavian artery. *J Am Soc Echocardiogr* 1995;8:964–966.
- Stevenson JG. Incidence of complications in pediatric transesophageal echocardiography: experience in 1650 cases. *J Am Soc Echocardiogr* 1999;12:527–532.
- Stevenson JG, et al. Transesophageal echocardiography during repair of congenital cardiac defects: identification of residual problems necessitating reoperation. *J Am Soc Echocardiogr* 1993;6:356–365.
- Kim HK, et al. Predictive value of intraoperative transesophageal echocardiography in complete atrioventricular septal defect. *Ann Thorac Surg* 2005;80:56–59.
- Lee HR, et al. Usefulness of intraoperative transesophageal echocardiography in predicting the degree of mitral regurgitation secondary to atrioventricular defect in children. *Am J Cardiol* 1999;83:750–753.
- Honjo O, et al. Discrepancy between intraoperative transesophageal echocardiography and postoperative transthoracic echocardiography in assessing congenital valve surgery. *Ann Thorac Surg* 2006;82:2240–2246.
- Fyfe DA, et al. The utility of transesophageal echocardiography during and after Fontan operations in small children. *Am Heart J* 1991;122:1403–1415.
- Ayres NA, et al. Indications and guidelines for performance of transesophageal echocardiography in the patient with pediatric acquired or congenital heart disease: report from the task force of the Pediatric Council of the American Society of Echocardiography. *J Am Soc Echocardiogr* 2005;18:91–98.
- Humpl T, McCrindle BW, Smallhorn JE. The relative roles of transthoracic compared with transesophageal echocardiography in children with suspected infective endocarditis. *J Am Coll Cardiol* 2003;41:2068–2071.
- Lowry RW, et al. Clinical impact of transesophageal echocardiography in the diagnosis and management of infective endocarditis. *Am J Cardiol* 1994;73:1089–1091.
- Pedersen WR, et al. Value of transesophageal echocardiography as an adjunct to transthoracic echocardiography in evaluation of native and prosthetic valve endocarditis. *Chest* 1991;100:351–356.
- Shively BK, et al. Diagnostic value of transesophageal compared with transthoracic echocardiography in infective endocarditis. *J Am Coll Cardiol* 1991;18:391–397.
- Khoury SF, et al. Effects of thyroid hormone on left ventricular performance and regulation of contractile and Ca²⁺-cycling proteins in the baboon.

- Implications for the force-frequency and relaxation-frequency relationships. *Circ Res* 1996;79:727-735.
58. Mulieri LA, et al. Altered myocardial force-frequency relation in human heart failure. *Circulation* 1992;85:1743-1750.
 59. Fowler MB, et al. Assessment of the beta-adrenergic receptor pathway in the intact failing human heart: progressive receptor down-regulation and subsensitivity to agonist response. *Circulation* 1986;74:1290-1302.
 60. Pratali L, et al. Prognostic significance of the dobutamine echocardiography test in idiopathic dilated cardiomyopathy. *Am J Cardiol* 2001;88:1374-1378.
 61. Ho YL, et al. The correlation between expression of apoptosis-related proteins and myocardial functional reserve evaluated by dobutamine stress echocardiography in patients with dilated cardiomyopathy. *J Am Soc Echocardiogr* 2003;16:931-936.
 62. Paraskevaidis IA, Adamopoulos S, Kremastinos DT. Dobutamine echocardiographic study in patients with nonischemic dilated cardiomyopathy and prognostically borderline values of peak exercise oxygen consumption: 18-month follow-up study. *J Am Coll Cardiol* 2001;37:1685-1691.
 63. Naqvi TZ, et al. Myocardial contractile reserve on dobutamine echocardiography predicts late spontaneous improvement in cardiac function in patients with recent onset idiopathic dilated cardiomyopathy. *J Am Coll Cardiol* 1999;34:1537-1544.
 64. Klewer SE, et al. Dobutamine stress echocardiography: a sensitive indicator of diminished myocardial function in asymptomatic doxorubicin-treated long-term survivors of childhood cancer. *J Am Coll Cardiol* 1992;19:394-401.
 65. De Wolf D, et al. Dobutamine stress echocardiography in the evaluation of late anthracycline cardiotoxicity in childhood cancer survivors. *Pediatr Res* 1996;39:504-512.
 66. Suarez WA, et al. Preclinical cardiac dysfunction in transfusion-dependent children and young adults detected with low-dose dobutamine stress echocardiography. *J Am Soc Echocardiogr* 1998;11:948-956.
 67. Pahl E, et al. Feasibility of exercise stress echocardiography for the follow-up of children with coronary involvement secondary to Kawasaki disease. *Circulation* 1995;91:122-128.
 68. Kimball TR, Witt SA, Daniels SR. Dobutamine stress echocardiography in the assessment of suspected myocardial ischemia in children and young adults. *Am J Cardiol* 1997;79:380-384.
 69. Sicari R, et al. Stress Echocardiography Expert Consensus Statement—Executive Summary: European Association of Echocardiography (EAE) (a registered branch of the ESC). *Eur Heart J* 2009;30:278-289.
 70. Bourdillon PD, et al. Regional wall motion index for infarct and noninfarct regions after reperfusion in acute myocardial infarction: comparison with global wall motion index. *J Am Soc Echocardiogr* 1989;2:398-407.
 71. Aggeli C, et al. Real-time three-dimensional dobutamine stress echocardiography for coronary artery disease diagnosis: validation with coronary angiography. *Heart* 2007;93:672-675.
 72. Hanekom L, et al. Incremental value of strain rate analysis as an adjunct to wall-motion scoring for assessment of myocardial viability by dobutamine echocardiography: a follow-up study after revascularization. *Circulation* 2005;112:3892-3900.
 73. Michelfelder EC, et al. Moderate-dose dobutamine maximizes left ventricular contractile response during dobutamine stress echocardiography in children. *J Am Soc Echocardiogr* 2003;16:140-146.
 74. Kimball TR, et al. Echocardiographic determination of left ventricular preload, afterload, and contractility during and after exercise. *J Pediatr* 1993;122:S89-S94.
 75. Cyran SE, et al. Aortic "recoarctation" at rest versus at exercise in children as evaluated by stress Doppler echocardiography after a "good" operative result. *Am J Cardiol* 1993;71:963-970.
 76. Ludomirsky A, et al. Transthoracic real-time three-dimensional echocardiography using the rotational scanning approach for data acquisition. *Echocardiography* 1994;11:599-606.
 77. Roelandt J, et al. Precordial three-dimensional echocardiography with a rotational imaging probe: methods and initial clinical experience. *Echocardiography* 1995;12:243-252.
 78. Wang XF, et al. Live three-dimensional echocardiography: imaging principles and clinical application. *Echocardiography* 2003;20:593-604.
 79. Bu L, et al. Rapid full volume data acquisition by real-time 3-dimensional echocardiography for assessment of left ventricular indexes in children: a validation study compared with magnetic resonance imaging. *J Am Soc Echocardiogr* 2005;18:299-305.
 80. Sugeng L, et al. Live 3-dimensional transesophageal echocardiography initial experience using the fully-sampled matrix array probe. *J Am Coll Cardiol* 2008;52:446-449.
 81. Hlavacek AM, et al. Real-time three-dimensional echocardiography is useful in the evaluation of patients with atrioventricular septal defects. *Echocardiography* 2006;23:225-231.
 82. Barrea C, et al. Three-dimensional echocardiography improves the understanding of left atrioventricular valve morphology and function in atrioventricular septal defects undergoing patch augmentation. *J Thorac Cardiovasc Surg* 2005;129:746-753.
 83. Takahashi K, et al. Two-dimensional versus transthoracic real-time three-dimensional echocardiography in the evaluation of the mechanisms and sites of atrioventricular valve regurgitation in a congenital heart disease population. *J Am Soc Echocardiogr* 2010;23:726-734.
 84. Vertukattil JJ, Bharucha T, Anderson RH. Defining Ebstein's malformation using three-dimensional echocardiography. *Interact Cardiovasc Thorac Surg* 2007;6:685-690.
 85. Otani K, et al. Assessment of the aortic root using real-time 3D transesophageal echocardiography. *Circ J* 2010;74:2649-2657.
 86. Suradi H, et al. Feasibility of using real time "Live 3D" echocardiography to visualize the stenotic aortic valve. *Echocardiography* 2010;27:1011-1020.
 87. Sugeng L, et al. Real-time three-dimensional transesophageal echocardiography in valve disease: comparison with surgical findings and evaluation of prosthetic valves. *J Am Soc Echocardiogr* 2008;21:1347-1354.
 88. Tantengco MV, et al. Dynamic three-dimensional echocardiographic reconstruction of congenital cardiac septation defects. *Pediatr Cardiol* 1997;18:184-190.
 89. van den Bosch AE, et al. Characterization of atrial septal defect assessed by real-time 3-dimensional echocardiography. *J Am Soc Echocardiogr* 2006;19:815-821.
 90. Vogel M, et al. Three-dimensional echocardiography can simulate intraoperative visualization of congenitally malformed hearts. *Ann Thorac Surg* 1995;60:1282-1288.
 91. Salustri A, et al. Transthoracic three-dimensional echocardiography in adult patients with congenital heart disease. *J Am Coll Cardiol* 1995;26:759-767.
 92. Anwar AM, et al. Assessment of left atrial volume and function by real-time three-dimensional echocardiography. *Int J Cardiol* 2008;123:155-161.
 93. Khankirawatana B, et al. Left atrial volume determination by three-dimensional echocardiography reconstruction: validation and application of a simplified technique. *J Am Soc Echocardiogr* 2002;15:1051-1056.
 94. Soliman OI, et al. Accuracy and reproducibility of quantitation of left ventricular function by real-time three-dimensional echocardiography versus cardiac magnetic resonance. *Am J Cardiol* 2008;102:778-783.
 95. Grison A, et al. Three-dimensional echocardiographic evaluation of right ventricular volume and function in pediatric patients: validation of the technique. *J Am Soc Echocardiogr* 2007;20:921-929.
 96. van der Zwaan HB, et al. Clinical value of real-time three-dimensional echocardiography for right ventricular quantification in congenital heart disease: validation with cardiac magnetic resonance imaging. *J Am Soc Echocardiogr* 2010;23:134-140.
 97. Altmann K, et al. Comparison of three-dimensional echocardiographic assessment of volume, mass, and function in children with functionally single left ventricles with two-dimensional echocardiography and magnetic resonance imaging. *Am J Cardiol* 1997;80:1060-1065.
 98. Baker GH, et al. Left ventricular dysfunction is associated with intraventricular dyssynchrony by 3-dimensional echocardiography in children. *J Am Soc Echocardiogr* 2008;21:230-233.
 99. Horstman JA, Monaghan MJ, Gill EA. Intraventricular dyssynchrony assessment by real-time three-dimensional echocardiography. *Cardiol Clin* 2007;25:253-260.
 100. Krenning BJ, et al. Guiding and optimization of resynchronization therapy with dynamic three-dimensional echocardiography and segmental volume—time curves: a feasibility study. *Eur J Heart Fail* 2004;6:619-625.
 101. van der Velde ME, Perry SB, Sanders SP. Transesophageal echocardiography with color Doppler during interventional catheterization. *Echocardiography* 1991;8:721-730.
 102. Hijazi ZM, et al. Transesophageal echocardiographic results of catheter closure of atrial septal defect in children and adults using the Amplatzer device. *Am J Cardiol* 2000;85:1387-1390.
 103. Salameh KJ, et al. Unique echocardiographic features associated with deployment of the Amplatzer atrial septal defect device. *J Am Soc Echocardiogr* 2001;14:128-137.
 104. Thanopoulos BD, et al. Closure of atrial septal defects with the Amplatzer occlusion device: preliminary results. *J Am Coll Cardiol* 1998;31:1110-1116.
 105. Thanopoulos BD, et al. Transcatheter closure of perimembranous ventricular septal defects with the Amplatzer asymmetric ventricular septal defect occluder: preliminary experience in children. *Heart* 2003;89:918-922.
 106. Thanopoulos BD, et al. Transcatheter closure of muscular ventricular septal defects with the amplatzer ventricular septal defect occluder: initial clinical applications in children. *J Am Coll Cardiol* 1999;33:1395-1399.
 107. Bartel T, et al. Intracardiac echocardiography is superior to conventional monitoring for guiding device closure of interatrial communications. *Circulation* 2003;107:795-797.
 108. Bartel T, et al. Intracardiac echocardiography: an ideal guiding tool for device closure of interatrial communications. *Eur J Echocardiogr* 2005;6:92-96.
 109. Koenig P, et al. Role of intracardiac echocardiographic guidance in transcatheter closure of atrial septal defects and patent foramen ovale using the Amplatzer device. *J Interv Cardiol* 2003;16:51-62.
 110. Mullen MJ, et al. Intracardiac echocardiography guided device closure of atrial septal defects. *J Am Coll Cardiol* 2003;41:285-292.
 111. Maeno YV, Benson LN, Boutin C. Impact of dynamic 3D transesophageal echocardiography in the assessment of atrial septal defects and occlusion by the double-umbrella device (CardioSEAL). *Cardiol Young* 1998;8:368-378.
 112. Balzer J, et al. Feasibility, safety, and efficacy of real-time three-dimensional transesophageal echocardiography for guiding device closure of interatrial communications: initial clinical experience and impact on radiation exposure. *Eur J Echocardiogr* 2010;11:1-8.
 113. Roberson DA, et al. Three-dimensional transesophageal echocardiography of atrial septal defect: a qualitative and quantitative anatomic study. *J Am Soc Echocardiogr* 2011;24:600-610.

114. Magni G, et al. Two- and three-dimensional transesophageal echocardiography in patient selection and assessment of atrial septal defect closure by the new DAS-Angel Wings device: initial clinical experience. *Circulation* 1997;96:1722-1728.
115. Butera G, et al. CardioSEAL/STARflex versus Amplatzer devices for percutaneous closure of small to moderate (up to 18 mm) atrial septal defects. *Am Heart J* 2004;148:507-510.
116. Law MA, et al. Long-term follow-up of the STARFlex device for closure of secundum atrial septal defect. *Catheter Cardiovasc Interv* 2009;73:190-195.
117. Fu YC. Transcatheter device closure of muscular ventricular septal defect. *Pediatr Neonatol* 2011;52:3-4.
118. Thanopoulos BD, Rigby ML. Outcome of transcatheter closure of muscular ventricular septal defects with the Amplatzer ventricular septal defect occluder. *Heart* 2005;91:513-516.
119. Gudauskas TM, et al. Comparison of two transcatheter device strategies for occlusion of the patent ductus arteriosus. *Catheter Cardiovasc Interv* 2008;72:675-680.
120. Liang CD, Ko SF, Huang SC. Echocardiographic guidance for transcatheter coil occlusion of patent ductus arteriosus in the catheterization laboratory. *J Am Soc Echocardiogr* 2003;16:476-479.
121. Thanopoulos BV, et al. Further experience with catheter closure of patent ductus arteriosus using the new Amplatzer duct occluder in children. *Am J Cardiol* 2010;105:1005-1009.
122. Wang JK, et al. Transcatheter closure of moderate to large patent ductus arteriosus with the Amplatzer duct occluder. *Catheter Cardiovasc Interv* 2007;69:572-578.
123. Thanigaraj S, et al. Comparison of transthoracic versus transesophageal echocardiography for detection of right-to-left atrial shunting using agitated saline contrast. *Am J Cardiol* 2005;96:1007-1010.
124. Fan S, et al. Superiority of the combination of blood and agitated saline for routine contrast enhancement. *J Am Soc Echocardiogr* 1999;12:94-98.
125. Chang RK, et al. Bubble contrast echocardiography in detecting pulmonary arteriovenous shunting in children with univentricular heart after cavopulmonary anastomosis. *J Am Coll Cardiol* 1999;33:2052-2058.
126. Hoeper MM, Krowka MJ, Strassburg CP. Portopulmonary hypertension and hepatopulmonary syndrome. *Lancet* 2004;363:1461-1468.
127. Alvarez AE, et al. Abernethy malformation: one of the etiologies of hepatopulmonary syndrome. *Pediatr Pulmonol* 2002;34:391-394.
128. Ashrafian H, Swan L. The mechanism of formation of pulmonary arteriovenous malformations associated with the classic Glenn shunt (superior cavopulmonary anastomosis). *Heart* 2002;88:639.
129. Christiansen C, et al. Physical and biochemical characterization of Albunex, a new ultrasound contrast agent consisting of air-filled albumin microspheres suspended in a solution of human albumin. *Biotechnol Appl Biochem* 1994;19:307-320.
130. Zilberman MV, Witt SA, Kimball TR. Is there a role for intravenous transpulmonary contrast imaging in pediatric stress echocardiography? *J Am Soc Echocardiogr* 2003;16:9-14.
131. Jung PH, et al. Effect of contrast application on interpretability and diagnostic value of dobutamine stress echocardiography in patients with intermediate coronary lesions: comparison with myocardial fractional flow reserve. *Eur Heart J* 2008;29:2536-2543.
132. Thomas JD, et al. Guidelines and recommendations for digital echocardiography. *J Am Soc Echocardiogr* 2005;18:287-297.
133. Karson TH, et al. Digital storage of echocardiograms offers superior image quality to analog storage, even with 20:1 digital compression: results of the Digital Echo Record Access Study. *J Am Soc Echocardiogr* 1996;9:769-778.
134. Thomas JD. Digital storage and retrieval: the future in echocardiography. *Heart* 1997;78:19-22.
135. Thomas JD, Main ML. Digital echocardiographic laboratory: where do we stand? *J Am Soc Echocardiogr* 1998;11:978-983.
136. Mathewson JW, et al. Conversion to digital technology improves efficiency in the pediatric echocardiography laboratory. *J Am Soc Echocardiogr* 2002;15:1515-1522.
137. Feigenbaum H. Journal of the American society of echocardiography case reports with digital images. *J Am Soc Echocardiogr* 2005;18:619.
138. Sable C. Telemedicine applications in pediatric cardiology. *Minerva Pediatr* 2003;55:1-13.
139. Grant B, et al. Remote diagnosis of congenital heart disease: the impact of telemedicine. *Arch Dis Child* 2010;95:276-280.
140. Sable CA, et al. Impact of telemedicine on the practice of pediatric cardiology in community hospitals. *Pediatrics* 2002;109:E3.
141. Mulholland HC, et al. Application of a low cost telemedicine link to the diagnosis of neonatal congenital heart defects by remote consultation. *Heart* 1999;82:217-221.
142. Gomes R, et al. Pediatric cardiology and telemedicine: seven years' experience of cooperation with remote hospitals. *Rev Port Cardiol* 2010;29:181-191.
143. Gottdiener JS, et al. American Society of Echocardiography recommendations for use of echocardiography in clinical trials. *J Am Soc Echocardiogr* 2004;17:1086-1119.
144. Savage DD, et al. The spectrum of left ventricular hypertrophy in a general population sample: the Framingham Study. *Circulation* 1987;75:126-133.
145. Gardin JM, et al. Relation of echocardiographic left ventricular mass, geometry and wall stress, and left atrial dimension to coronary calcium in young adults (the CARDIA study). *Am J Cardiol* 2005;95:626-629.
146. Lonn E, et al. Effects of ramipril on left ventricular mass and function in cardiovascular patients with controlled blood pressure and with preserved left ventricular ejection fraction: a substudy of the Heart Outcomes Prevention Evaluation (HOPE) Trial. *J Am Coll Cardiol* 2004;43:2200-2206.
147. Devereux RB, et al. Prognostic significance of left ventricular mass change during treatment of hypertension. *JAMA* 2004;292:2350-2356.
148. Daniels SR, et al. Left atrial size in children with hypertension: the influence of obesity, blood pressure, and left ventricular mass. *J Pediatr* 2002;141:186-190.
149. Daniels SR, et al. Effect of lean body mass, fat mass, blood pressure, and sexual maturation on left ventricular mass in children and adolescents. Statistical, biological, and clinical significance. *Circulation* 1995;92:3249-3254.
150. Barshesht A, et al. Reverse Remodeling and the Risk of Ventricular Tachyarrhythmias in the MADIT-CRT (Multicenter Automatic Defibrillator Implantation Trial-Cardiac Resynchronization Therapy). *J Am Coll Cardiol* 2011;57:2416-2423.
151. Cripe L, et al. Bicuspid aortic valve is heritable. *J Am Coll Cardiol* 2004;44:138-143.
152. Hole T, et al. Differences between echocardiographic measurements of left ventricular dimensions and function by local investigators and a core laboratory in a 2-year follow-up study of patients with an acute myocardial infarction. *Eur J Echocardiogr* 2002;3:263-270.
153. Galderisi M, et al. Recommendations of the European Association of Echocardiography: how to use echo-Doppler in clinical trials: different modalities for different purposes. *Eur J Echocardiogr* 2011;12:339-353.
154. Wilkins BJ, et al. Calcineurin/NFAT coupling participates in pathological, but not physiological, cardiac hypertrophy. *Circ Res* 2004;94:110-118.
155. Schultz Jel J, et al. Accelerated onset of heart failure in mice during pressure overload with chronically decreased SERCA2 calcium pump activity. *Am J Physiol Heart Circ Physiol* 2004;286:H1146-H1153.
156. Bueno OF, et al. Calcineurin Abeta gene targeting predisposes the myocardium to acute ischemia-induced apoptosis and dysfunction. *Circ Res* 2004;94:91-99.
157. Schultz Jel J, et al. TGF-beta1 mediates the hypertrophic cardiomyocyte growth induced by angiotensin II. *J Clin Invest* 2002;109:787-796.
158. Sussman MA, et al. Hypertrophic defect unmasked by calcineurin expression in asymptomatic tropomodulin overexpressing transgenic mice. *Cardiovasc Res* 2000;46:90-101.
159. Williams RV, et al. End-systolic stress-velocity and pressure-dimension relationships by transthoracic echocardiography in mice. *Am J Physiol* 1998;274:H1828-H1835.
160. Phoon CK, et al. Embryonic heart failure in NFATc1-/- mice: novel mechanistic insights from in utero ultrasound biomicroscopy. *Circ Res* 2004;95:92-99.
161. Phoon CK, Turnbull DH. Ultrasound biomicroscopy-Doppler in mouse cardiovascular development. *Physiol Genomics* 2003;14:3-15.
162. Ji RP, et al. Onset of cardiac function during early mouse embryogenesis coincides with entry of primitive erythroblasts into the embryo proper. *Circ Res* 2003;92:133-135.
163. Phoon CK, Aristizabal O, Turnbull DH. Spatial velocity profile in mouse embryonic aorta and Doppler-derived volumetric flow: a preliminary model. *Am J Physiol Heart Circ Physiol* 2002;283:H908-H916.
164. Zhou YQ, et al. Abnormal cardiac inflow patterns during postnatal development in a mouse model of Holt-Oram syndrome. *Am J Physiol Heart Circ Physiol* 2005;289:H992-H1001.
165. Zhou YQ, et al. Comprehensive transthoracic cardiac imaging in mice using ultrasound biomicroscopy with anatomic confirmation by magnetic resonance imaging. *Physiol Genomics* 2004;18:232-244.
166. Zhou YQ, et al. Applications for multifrequency ultrasound biomicroscopy in mice from implantation to adulthood. *Physiol Genomics* 2002;10:113-126.
167. Knight BS, et al. Developmental regulation of cardiovascular function is dependent on both genotype and environment. *Am J Physiol Heart Circ Physiol* 2009;297:H2234-H2241.
168. Lai WW, et al. Guidelines and standards for performance of a pediatric echocardiogram: a report from the Task Force of the Pediatric Council of the American Society of Echocardiography. *J Am Soc Echocardiogr* 2006;19:1413-1430.
169. Picard MH, et al. American Society of Echocardiography recommendations for quality echocardiography laboratory operations. *J Am Soc Echocardiogr* 2011;24:1-10.
170. Mangione S, Nieman LZ. Cardiac auscultatory skills of internal medicine and family practice trainees. A comparison of diagnostic proficiency. *JAMA* 1997;278:717-722.
171. Mangione S. Cardiac auscultatory skills of physicians-in-training: a comparison of three English-speaking countries. *Am J Med* 2001;110:210-216.
172. Gaskin PR, et al. Clinical auscultation skills in pediatric residents. *Pediatrics* 2000;105:1184-1187.
173. Kobal SL, Atar S, Siegel RJ. Hand-carried ultrasound improves the bedside cardiovascular examination. *Chest* 2004;126:693-701.
174. Decara JM, et al. Use of hand-carried ultrasound devices to augment the accuracy of medical student bedside cardiac diagnoses. *J Am Soc Echocardiogr* 2005;18:257-263.
175. Spencer KT, et al. Physician-performed point-of-care echocardiography using a laptop platform compared with physical examination in the cardiovascular patient. *J Am Coll Cardiol* 2001;37:2013-2018.

176. Kobal SL, et al. Usefulness of a hand-carried cardiac ultrasound device to detect clinically significant valvular regurgitation in hospitalized patients. *Am J Cardiol* 2004;93:1069–1072.
177. Li X, et al. Will a handheld ultrasound scanner be applicable for screening for heart abnormalities in newborns and children? *J Am Soc Echocardiogr* 2003;16:1007–1014.
178. Spurney CF, et al. Use of a hand-carried ultrasound device by critical care physicians for the diagnosis of pericardial effusions, decreased cardiac function, and left ventricular enlargement in pediatric patients. *J Am Soc Echocardiogr* 2005;18:313–319.
179. Kirkpatrick JN, et al. Effectiveness of echocardiographic imaging by nurses to identify left ventricular systolic dysfunction in high-risk patients. *Am J Cardiol* 2005;95:1271–1272.
180. Labovitz AJ, et al. Focused cardiac ultrasound in the emergent setting: a consensus statement of the American Society of Echocardiography and American College of Emergency Physicians. *J Am Soc Echocardiogr* 2010;23:1225–1230.
181. El-Khuffash AF, McNamara PJ. Neonatologist-performed functional echocardiography in the neonatal intensive care unit. *Semin Fetal Neonatal Med* 2011;16:50–60.
182. Sehgal A, McNamara PJ. Does point-of-care functional echocardiography enhance cardiovascular care in the NICU? *J Perinatol* 2008;28:729–735.
183. Delgorte C, et al. A tele-operated mobile ultrasound scanner using a lightweight robot. *IEEE Trans Inf Technol Biomed* 2005;9:50–58.
184. Takeuchi R, et al. Field testing of a remote controlled robotic tele-echo system in an ambulance using broadband mobile communication technology. *J Med Syst* 2008;32:235–242.
185. Kobal SL, et al. Hand-carried cardiac ultrasound enhances healthcare delivery in developing countries. *Am J Cardiol* 2004;94:539–541.
186. Kobal SL, et al. Making an impossible mission possible. *Chest* 2004;125:293–296.
187. Kirkpatrick JN, et al. Hand-carried cardiac ultrasound as a tool to screen for important cardiovascular disease in an underserved minority health care clinic. *J Am Soc Echocardiogr* 2004;17:399–403.

Echocardiographic Assessment of Cardiac Dimensions, Cardiac Function, and Valve Function

Luc L. Mertens ■ Mark K. Friedberg

QUANTIFICATION OF CHAMBER DIMENSIONS AND CARDIAC STRUCTURES

Accurate measurements of valves, chambers, and vessels are essential to the diagnosis and management of patients with congenital and pediatric heart disease. The American Society of Echocardiography published recommendations for quantification of chamber sizes and function in adults (1,2) and for quantification of cardiac structures in the pediatric population (3). One of the important differences between measurements in adult and pediatric patients is the effect of growth or body size on measurements. As dimensions of cardiovascular structures correlate best with body surface area (BSA), indexing the size of cardiovascular structures for BSA has become a commonly used practice. The Haycock formula ($BSA [m^2] = 0.024265 \times \text{weight [kg]}^{0.5378} \times \text{height [cm]}^{0.3964}$) has been recommended for BSA calculation. Correction for BSA is based on the assumption that there is a linear relationship between the cardiac measurement and the BSA. This has been shown to be a simplification as the linear relationship does not hold for the entire spectrum and there is increased variance in the measurements with increasing BSA related to confounding factors like blood pressure, obesity, and physical activity (4). To overcome this limitation, the use of z-scores has been proposed as a practical alternative (4). Z-scores are based on measurements of cardiovascular structures in a normal population encompassing a wide range of BSA. The z-score represents the number of standard deviations a measurement lies from the mean value at a specific BSA. For instance, z-score of -3.5 for an aortic valve annulus diameter indicates that the value is 3.5 standard deviations below the mean value for that particular BSA. Z-scores for different cardiovascular structures have been published (5,6), but the effect of gender and race on cardiovascular measurements may necessitate establishing normal values based on population mix seen in a specific laboratory.

Detailing the measurement of each individual cardiovascular structure is beyond the scope of this chapter. The reader is referred to recently published guidelines for this purpose (3). In this chapter, the evaluation of cardiac function and chamber quantification are discussed in more detail. In congenital heart disease, chamber quantification can be challenging due to the variable shapes of the ventricles including the right ventricle (RV) and the univentricular heart.

The authors acknowledge the contributions of Drs. Kimball and Michelfelder to this chapter in the previous edition.

QUANTIFICATION OF THE LEFT VENTRICLE

The importance of accurately measuring left ventricle (LV) size cannot be overstated. Measurement of LV chamber dimensions at end systole and end diastole (linear dimensions, areas, or volumetric measurements) are used to assess LV remodeling (degree of LV dilation) and function. Measurements of LV wall thickness and mass are important to identify LV hypertrophy.

Linear measurements of LV chamber size and wall thickness have been traditionally obtained using M-mode measurements from the parasternal short- or long-axis views just below the tips of the mitral valve leaflets (Fig. 9.1). M-mode measurements have a very high temporal resolution albeit at the expense of low spatial resolution. It can be difficult to obtain a perpendicular M-mode through the LV resulting in oblique planes that overestimate LV dimensions and increase measurement variability. If not well standardized, M-mode measurements can be highly variable. This was shown by Lipshultz et al. (7) who compared the M-mode measurements made in local echocardiography laboratories and in a core laboratory. This study showed poor agreement between the core laboratory and local laboratory measurements with relatively wide limits of agreement. To overcome these problems, the recent American Society of Echocardiography recommendations suggested using measurements obtained from two-dimensional (2-D) imaging in place of M-mode for LV chamber quantification. Two-dimensional short-axis imaging just distal to the mitral valve leaflets is recommended (Fig. 9.2) for measuring the internal LV diameter and the inferolateral and septal wall thickness at end diastole and end systole. However, there are inadequate data to determine if 2-D linear measurements are indeed more reproducible than those obtained by M-mode. Another limitation is that currently all published normal z-score data are based on M-mode measurements and not on 2-D imaging. Following these recommendations, new normal data sets of cardiac dimensions will hopefully be obtained.

2-D and 3-D Techniques

Beyond linear measurements of LV dimensions, it is also possible to calculate LV volumes using either 2-D or 3-D techniques. Two 2-D techniques (the area-length method and the biplane Simpson's method) are currently recommended. The area-length method requires measuring the LV major-axis length from a subcostal or apical four-chamber view combined with an area calculation from a subcostal or parasternal short-axis view. The volume is calculated using the formula $LV \text{ volume} = 5/6 \times CSA \times LV \text{ length}$. As a geometrical formula, this requires a normal LV shape. The biplane Simpson's method is based on summation of disks and requires delineating the endocardial borders in the apical four-chamber and

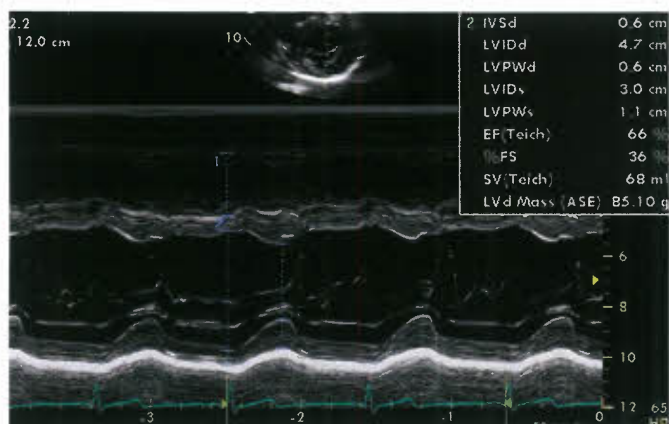


Figure 9.1. M-mode measurements. M-mode measurement is obtained from a parasternal short-axis view of the left ventricle just inferior to the mitral valve leaflets. End-diastolic (at the QRS complex) and end-systolic (at point of minimal diameter) measurements are obtained and fractional shortening and ejection fraction are calculated. EF, ejection fraction; IVSd, inter-ventricular septum at end diastole; LVPWd, left ventricular posterior wall thickness at end diastole; LVIDs, left ventricular end-systolic dimensions; %FS, percent fractional shortening; SV, stroke volume; LVD Mass, left ventricular mass.

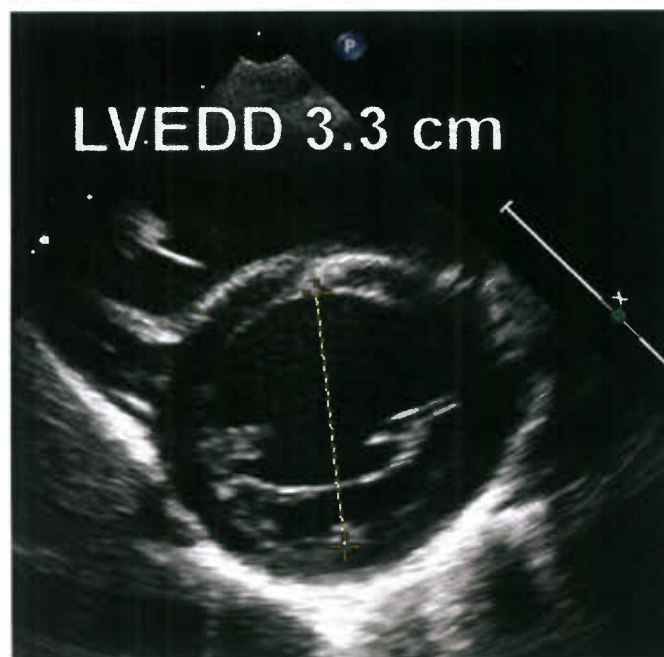


Figure 9.2. Two-dimensional measurement of LV dimensions. The left ventricular end-diastolic dimension (LVEDD) is measured from a parasternal short-axis view just inferior to the mitral valve leaflets.

two-chamber views (Fig. 9.3). Therefore, images should be optimized to allow delineation of the endocardium and LV length as suboptimal border detection and foreshortening of the LV are major problems that result in underestimation of the LV volumes. There have been only a few studies that have investigated the reproducibility of these volumetric methods in the pediatric population. Their accuracy was studied in an adult population where the biplane Simpson's method for calculating LV volumes was compared to cardiac magnetic resonance imaging (MRI) in patients after acute myocardial infarction (8). This study showed a relatively weak correlation ($r = 0.61$, $p < 0.01$) between the echocardiographic and

MRI measurements suggesting that the biplane Simpson's method is not very accurate and the agreement between measurements is not very strong. The accuracy and reproducibility of these measurements is crucial as LV volumes are used for therapeutic decisions (for instance, LV end-systolic volume in aortic regurgitation). These measurements are also used for calculating ejection fraction (EF) as discussed below. The smaller the LV, the larger is the effect of the measurement error. This is especially important in the borderline LV in patients with aortic stenosis where LV volume calculations may determine a biventricular versus a univentricular treatment approach.

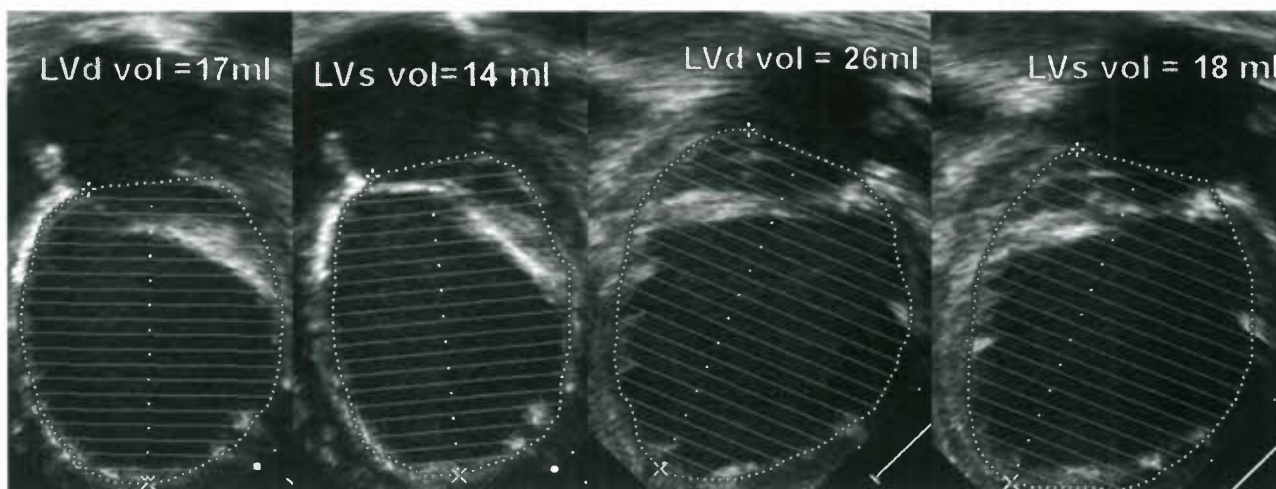


Figure 9.3. Use of biplane Simpson's rule in calculating left ventricular (LV) volume in patients with severe LV dysfunction. The first two images from the left show the apical four-chamber view in end diastole and end systole, respectively. The next two images are obtained from the apical two-chamber view also in end diastole and end systole, respectively. LV volumes in end diastole and end systole can be calculated. Based on the biplane measurements, the LV ejection fraction in this example is 22%.

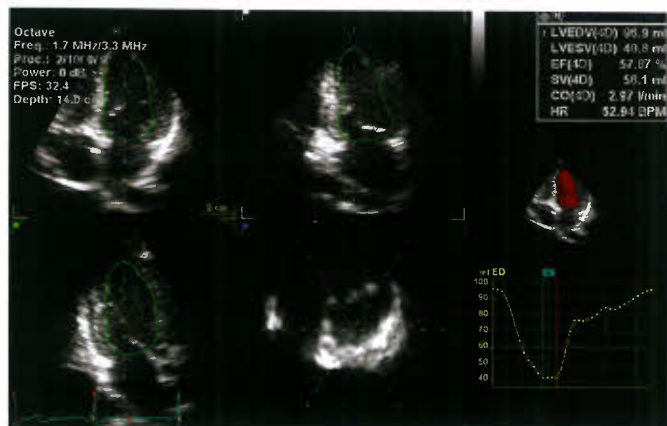


Figure 9.4. Three-dimensional (3-D) echocardiography to assess LV volumes. Three-dimensional echocardiography and (semi-) automated analysis of 3-D volumes is used to measure LV volumetric changes throughout the cardiac cycle. The images represent an apical four-chamber (left upper), an apical two-chamber (right upper), and an apical three-chamber (left lower) cut through the LV volume. The planes through the volumes are illustrated in the right lower panel. On the right of the images, the result of volumetric analysis is shown. LVEDV, left ventricular end-diastolic volume; LVESV, left ventricular end-systolic volume; EF, ejection fraction; SV, stroke volume; CO, cardiac output; HR, heart rate. The lower panel shows the volume–time curve.

Calculating volumes based on 2-D images will always be influenced by assumptions of LV shape and geometry. Three-dimensional echocardiography overcomes this problem as full 3-D volumetric data sets can be obtained using newer generation matrix probes. Most ultrasound systems calculate LV volumes using (semi-) automated analysis algorithms (Fig. 9.4). This results in improved reproducibility as it eliminates observer bias in determining endocardial borders. Hence, the intra- and interobserver variability of 3-D methods are much lower compared to 2-D-based volumetric calculations. Moreover, 3-D echocardiography is more accurate for determination of LV volumes than 2-D when compared to cardiac MRI (9–11). In a pediatric population, 3-D echocardiography has been shown to be the most reliable method for quantification of LV volumes (12). Therefore, it is likely to replace other methods in the foreseeable future. It is important to recognize, however, that the feasibility of the 3-D methods is limited as it is not always possible to obtain good quality 3-D data sets in every patient.

Left Ventricular Mass

Calculation of LV mass can also be useful in pediatric patients. In patients with arterial hypertension, LV mass indexed for BSA or height has been shown to correlate well with disease severity and has diagnostic and therapeutic implications (13). LV mass is usually calculated using the Devereux formula ($\text{LV mass} = 0.8 \times \{1.04[(\text{LVIDd} + \text{PWTd} + \text{SWTd})^3 - (\text{LVIDd})^3]\} + 0.6 \text{ g}$, where LVIDd is the left ventricular end-diastolic dimension, PWTd is the diastolic posterior wall thickness, and SWTd is the diastolic septal wall thickness) from M-mode or 2-D echocardiography. As LV mass is strongly related to body size, various methods have been proposed to correct LV mass for body size. The best correction in the adult population seems to be to index LV mass in grams by height in meters to the 2.7th power (1). Khoury et al. (14) showed that this correction works well for

children >9 years of age but that below that age, there is a significant variation for this index in normal controls. Foster et al. (13) have recently shown that in a pediatric population LV mass-for-height centile curves (and z-scores) are the better method for normalizing LV mass.

The 2-D-based method only works for concentric hypertrophy as it assumes that the LV walls are homogeneously thickened. This assumption is often inaccurate as even in arterial hypertension the basal LV septum is often thicker than the rest of the LV walls, resulting in overestimation of overall LV mass by the Devereux formula. The formula cannot be used in patients with asymmetric hypertrophic cardiomyopathy. Three-dimensional methods can also be used to quantify LV mass and have been shown to correlate better with MRI measurements of LV mass as they are less dependent on geometrical assumptions (15).

QUANTIFICATION OF THE RIGHT VENTRICLE

Assessment of RV dimensions and volumes is even more challenging compared to the LV due to its more complex geometrical shape (difficult to describe by a simple geometrical formula) and anterior position into the chest (anterior wall in the near field of the ultrasound beam reducing spatial resolution) (16). The American Society of Echocardiography has published recent guidelines for assessment of the right heart in adults (2). The American Society of Echocardiography pediatric guidelines also contain updated recommendations for measuring RV dimensions and functions (3). Linear measurements have been used to assess RV size. In the pediatric recommendations, various measurements obtained from the apical four-chamber view have been proposed (Fig. 9.5). These include measuring RV end-diastolic diameters at the basal and midcavity levels, RV end-diastolic length, and also end-diastolic and end-systolic RV areas. A problem with these measurements is the lack of normal data precluding calculation of z-scores. Another problem is that measurements from the apical four-chamber view include only the inlet and the apical portions of the RV and do not account for the RV outlet. Therefore, measurements of the RV outflow tract from either a parasternal short-axis or long-axis view should be made. Z-scores are available for RV outflow end-diastolic dimensions from M-mode, but these mainly reflect RVOT dilation and do not portray remodeling of the remainder of the RV cavity. All 2-D-based methods have been shown to underestimate RV volumes when compared to cardiac MRI volumetric calculations. This is mainly due to foreshortening in the 2-D images (it can be difficult to image the true RV apex by echo) and difficulties in defining the endocardial borders. The RV wall is relatively thin (compacted myocardial thickness of around 3 to 5 mm in the adult heart) and has coarse trabeculations causing variability in endocardial border definition. Also for the RV, 3-D echocardiography is a promising tool for assessing RV volumes. Specific analysis software has become available for quantifying RV volumes from 3-D data sets. Full volumetric acquisition can be difficult, especially when the RV is very large, which limits the feasibility of the 3-D methods. Studies have shown that good quality 3-D data sets can only be obtained in 55% to 75% of patients (17–19). A second problem is that 3-D methods tend to underestimate RV volumes compared to cardiac MRI in patients with congenital heart disease (17–19). Studies have suggested that the larger the ventricle, the more important the underestimation. This is probably related to difficult visualization of the endocardial borders as well as the anatomical landmarks like the pulmonary valve.

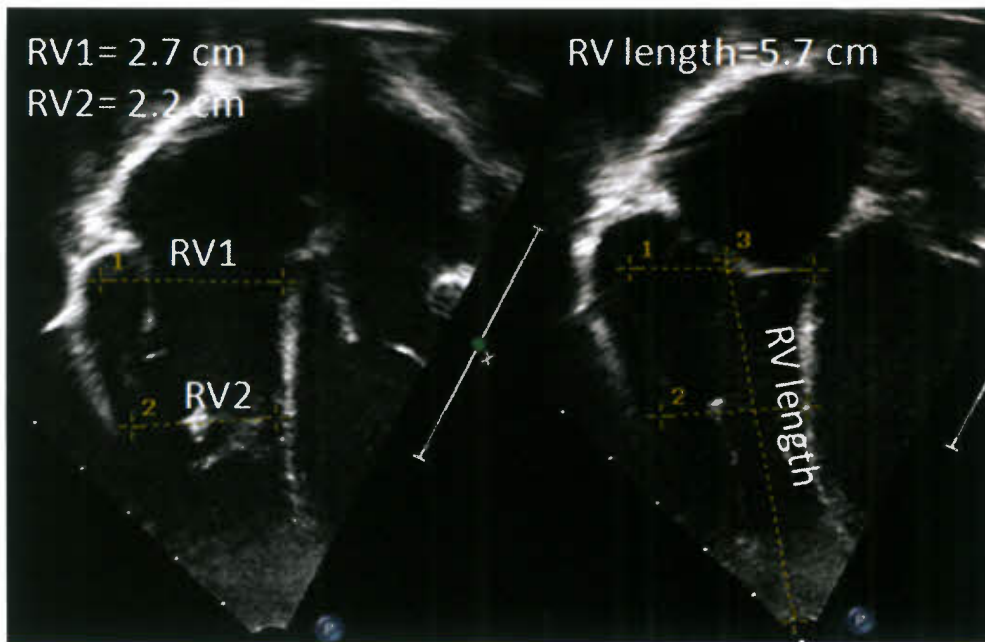


Figure 9.5. Measurement of right ventricular (RV) 2-D dimensions. From the apical four-chamber view, RV width is measured just below the tricuspid valve (RV1) and in the mid part of the RV (RV2). RV length is also measured just after tricuspid valve closure from the mid of the tricuspid valve to the apex of the RV.

QUANTIFICATION OF THE UNIVENTRICULAR HEART

Assessing chamber dimensions of the univentricular heart can be challenging due to the variable morphology. First, it is important to know whether the morphology of the dominant ventricle is that of a left, right, or indeterminate morphology. The methods used for measuring the right and left ventricles can be applied to the univentricular heart, but “normal” values for the univentricular heart of either LV or RV morphology are unavailable. Moreover, the size of the ventricle will be influenced by the type of palliation and associated volume loading. A shunted single ventricle will be larger compared to the same ventricle after total cavopulmonary anastomosis. Three-dimensional volumes can also be calculated based on full volumetric data sets. It should be noted, however, that the software used for (semi-) automated calculation of LV and RV volumes assumes a specific geometric shape and has not been validated for single ventricles. Soriano et al. used the method of disk summation to measure the volumes of single ventricles (20). The echocardiographic results were accurate when compared to the MRI results but the method requires extensive off-line manual tracing and processing, limiting its application in clinical practice.

EVALUATION OF SYSTOLIC VENTRICULAR FUNCTION

When evaluating systolic function, it is important to consider the different levels evaluated by the various functional indices. Overall cardiovascular function can be defined as the delivery of blood to the tissues at a rate commensurate with oxygen consumption. This integrates cardiac and vascular function. To describe cardiac function, a distinction between ventricular and myocardial function can be made. Ventricular function is the pump activity generating an adequate cardiac output at low filling pressures. Myocardial function is the phasic shortening and force generation at the fiber or segmental level, followed

by lengthening and force decay. Cardiac function can thus be studied at the level of fiber mechanics, regional or segmental myocardial function, and global pump function (Fig. 9.6). At each level (fiber, segment, or ventricle), there is a component of force development and resulting deformational changes. *Fiber mechanics* describes the relationship between active myocardial fiber force development (contractility) and fiber shortening. The degree of shortening is influenced by the precontraction muscle length (preload) and by the force opposing shortening after the onset of contraction (afterload). The frequency of stimulation will also influence fiber shortening as increased frequency results in increased contractile force development (force-frequency relationship). Echocardiography cannot directly study fiber mechanics. At the level of *regional or segmental* function, regional force development within a segment will result in regional myocardial deformation. At the segmental level, myocardial force is better described as regional wall stress that is influenced by active contractile force development, pressure, wall geometry (wall thickness, regional wall curvature), and segmental interaction. Current echocardiographic techniques allow quantification of regional myocardial deformation as segment shortening, thickening, and rotation (also called regional myocardial strain or deformation). This allows study of regional ventricular wall mechanics. Global pump function is the product of interaction between the different contractile segments resulting in ventricular pressure generation and, when the outlet valve opens, in ejection of blood from the ventricle. On the pump level, ventricular performance is determined by myocardial function (influenced by preload, afterload, and heart rate) and efficient segment interaction (synchronicity of contraction). When interpreting an echocardiographic index of global function, such as EF, it is important to understand that it is influenced by myocardial function and its determinants, synchronicity of contraction, and global ventricular geometry. An EF of 45%, for example, has a completely different implication in a ventricle with severe mitral regurgitation, LV dilation, and left bundle branch block compared to the same EF in a patient with severe aortic stenosis and normal conduction. For interpretation of measurements, it is important to know which physiologic parameters influence the echocardiographic parameters. All too often, measurements are determined to

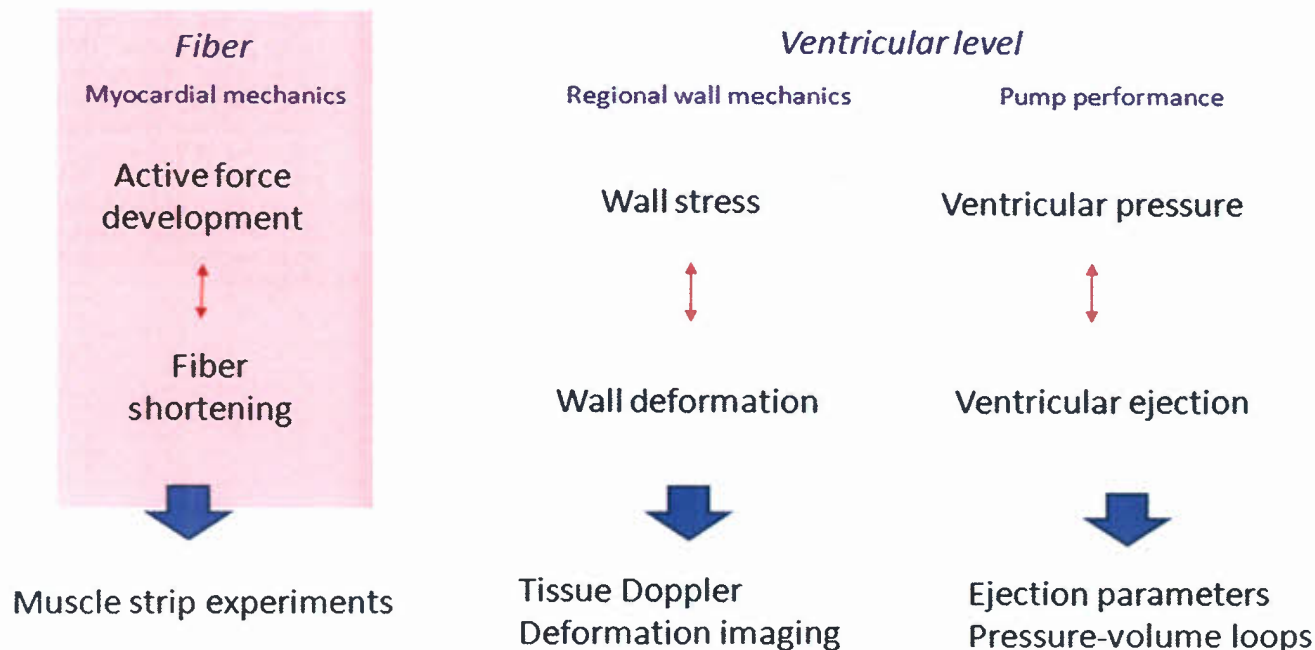


Figure 9.6. Assessment of ventricular function from fiber to pump level. At the fiber level, active force development results in fiber shortening. This relationship can be studied in muscle strip experiments. On the segmental level, regional wall stress is the composite of regional force development and loading on the regional segment. Force development in a segment will result in segmental deformation. Echocardiographically, regional wall motion and deformation can be studied by tissue Doppler and myocardial-deformation imaging. On the pump level, generation of ventricular pressure results in ejection of blood. This can be assessed using ejection parameters like ejection fraction by echocardiography. Invasively this can be studied by pressure-volume loops.

be indices of “contractility,” while there are very few, if any, that are not influenced by loading conditions. Knowledge on the reliability, reproducibility, and accuracy of the methods to assess ventricular function will also influence interpretation of the results. This is especially important for serial evaluation of patients over time. A program of continuous quality improvement for an echocardiographic laboratory should include regular evaluations of the reliability of the measurements in the individual laboratory (21).

A wide variety of different echocardiographic parameters and indices have been developed for assessing ventricular function. This in itself indicates that no single parameter adequately provides all the necessary information. The echocardiographer needs to integrate information from different parameters to comprehensively describe systolic function. In this chapter, the most commonly used indices will be discussed with a description of their measurement, reproducibility, accuracy, availability of normal values, and the influence of loading conditions.

The most commonly used parameter for assessing LV function, probably is percent shortening fraction (%SF) defined as the percentage change in LV dimension from end diastole to end systole. Percent shortening fraction was traditionally measured using M-mode echocardiography from either the parasternal long-axis or short-axis view just below the level of the mitral valve leaflets. The recent recommendations for quantification advise measuring %SF based on 2-D short-axis cuts (either parasternal or subcostal) through the LV. The disadvantage of using 2-D instead of M-mode is the lower temporal resolution. This can be an important problem at higher heart rates, especially in neonates. It can also be difficult to identify end diastole and end systole on 2-D short-axis views. Percent shortening fraction is defined as

$$(\text{LVEDD} - \text{LVESD}) / \text{LVEDD} \times 100$$

where LVEDD is the left ventricular end-diastolic dimension and LVESD is the left ventricular end-systolic dimension. The normal value ranges between 28% and 38%. Values <28% suggest reduced systolic function, while values >38% indicate hyperdynamic function. In most patients, %SF is relatively easy to measure yielding high feasibility. After adequate standardization of acquisition and analysis, variability should be between 10% and 15%. Percent SF has important limitations that should be taken into account when used for clinical decision making. First, %SF measures the apposition of two opposing walls (basal septum and inferolateral wall) as a measure of global systolic function. This assumes that there are no regional differences in wall motion while, in reality, different conditions are associated with regional wall motion abnormalities. In congenital heart disease, hypokinesia and dyskinesia of the interventricular septum occur in the presence of RV volume loading (e.g., large atrial septal defect). This can cause paradoxical septal motion with the septum moving away from the inferolateral wall during systole (Fig. 9.7). Paradoxical septal motion can also be present in the immediate postoperative (post bypass) period and in the presence of left bundle branch block where maximal systolic motion of the inferolateral wall and septum do not occur simultaneously. All these conditions affect measurement of %SF. In cases of regional myocardial dysfunction, such as after myocardial infarction where the inferolateral and basal septum are not involved, measurement of %SF can overestimate global function. Percent SF is also influenced by preload and afterload and does not directly reflect intrinsic myocardial function. Volume loading will generally increase %SF. An example is the increased %SF in patients with mitral and aortic regurgitation. Pressure loading generally decreases %SF, especially when acute changes occur. A typical example would be an acute increase in arterial blood pressure resulting in an

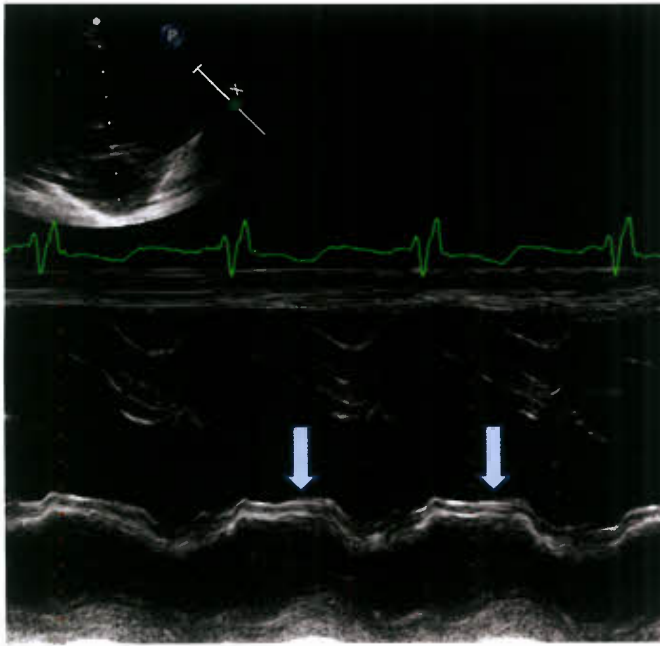


Figure 9.7. Paradoxical motion of the interventricular septum in a patient with a large atrial septal defect. M-mode obtained from a parasternal short-axis view through the dilated RV and smaller LV. The arrows show the motion of the interventricular septum in the direction of the RV in systole. This paradoxical systolic motion makes it impossible to use shortening fraction as a measure for LV systolic function in this setting.

immediate decrease in %SF. This does not reflect an acute decrease in myocardial contractility but rather the increased loading on the heart. A final important limitation is the dependency of the calculation on LV geometry. When hypertrophy of the wall occurs, as happens in the context of chronic arterial hypertension or hypertrophic cardiomyopathy, endocardial changes and dimension changes are influenced by the thickened wall resulting in an overestimation of systolic function.

Ejection fraction is a volumetric measurement reflecting the percentage change in LV volume from end diastole to end systole. It is defined as

$$EF = (LVEDV - LVESV) / LVEDV \times 100$$

where LVEDV is the LV volume at end diastole and LVESV is the LV volume at end systole. LV volumes can be calculated using M-mode echocardiography, 2-D echocardiography, and 3-D echocardiography. As previously mentioned, the recommended 2-D-based methods are the area-length method and the biplane Simpson's method to quantify EF. Three-dimensional echocardiography has been introduced more recently and has been shown to be more reproducible compared to the biplane Simpson's method. Normal values for EF range between 54% and 75%. EF is a good parameter for global pump function and takes into account regional wall motion abnormalities. Like %SF, the method is load dependent with increased volume loading resulting in higher EF and increased pressure loading decreasing EF.

VCF–End-Systolic Wall Stress Relationship

To overcome the load dependency of the SF and EF measurements, alternative methods have been developed that attempt

to correct for the effect of afterload or wall stress. The velocity of circumferential fiber shortening (VCF) measures the velocity of dimensional changes during ejection. Fiber shortening only occurs during ejection and therefore the mean VCF shortening can be calculated as

$$VCF = \%SF / \text{ejection time}$$

ET can be calculated from an M-mode of the aortic valve with very high temporal resolution. VCF_c should be corrected for heart rate as fiber shortening is influenced by heart rate. The heart rate corrected value can be calculated as

$$VCF_c (\text{circ} / \text{s}) = [(\%SF) \times (RR)^{0.5}] / (ET)$$

where SF is shortening fraction, RR is R to R interval, and ET is ejection time. The corrected VCF_c is relatively insensitive to preload changes but highly sensitive to changes in contractility and afterload. When corrected for afterload, the measurement thus becomes a good parameter for contractility. The problem is how to clinically define afterload. As “fiber shortening” is calculated by measuring ventricular dimensional changes, the same assumptions can be made to calculate “wall stress.” This is based on the Laplace formula where wall stress in a passive tube is related to ventricular pressure and cavity size and inversely related to wall thickness ($\sigma = (Pr)/2h$). Higher ventricular pressure and larger ventricular size increase wall stress while a thicker wall reduces wall stress. Assumptions for both meridional and circumferential wall stress can be derived from M-mode measurements, pressure measurements, and initially, carotid pulse tracing was used to estimate end-systolic wall stress. While peak stress determines the degree of hypertrophy, end-systolic stress is the most important parameter determining systolic shortening (22). The formula that is used to calculate meridional (longitudinal) end-systolic wall stress is

$$ESWS (g / \text{cm}^2) = [1.35(Pes)(LVES)] \div [(4)(hes)(1 + hes / LVES)],$$

where 1.35 is the conversion factor from mm Hg to g/cm^2 , Pes is the end-systolic pressure derived from linear interpolation of the dicrotic notch on the pulse trace assigning the systolic blood trace to its peak and the diastolic pressure to its nadir, LVES is the left ventricular end-systolic dimension, and hes is the left ventricular end-systolic wall thickness. Circumferential end-systolic wall stress can also be calculated with the addition of the LV long-axis end-systolic length from the mitral annulus to the LV apex in the apical four-chamber view (L). Thus, circumferential $ESWS (g/\text{cm}^2) = [(1.35)(Pes)(LVES/2hes)] \times [1 - (LVES)/2(L)]$. Both parameters can be obtained from an M-mode echocardiogram of the LV with simultaneous indirect carotid artery pulse trace and blood pressure determination. This makes the method quite cumbersome. Simplified versions include using mean or peak systolic pressures instead of end-systolic estimated pressures (23). Colan et al. (24) found a direct negative correlation between VCF_c and end-systolic meridional wall stress. This seems logical as higher afterload can be expected to reduce the velocity of fiber shortening for the same myocardial contractility. The relationship between VCF_c and end-systolic wall stress within the normal range has been published (24,25).

Abnormal LV contractility is defined as values for wall stress versus VCF_c falling below the normal expected range. In younger children, the linearity of the relationship was questioned and it was shown that wall stress as calculated in the formula misrepresents afterload in children and young adults

with abnormal left geometry (26). The relationship between VCF_c and wall stress only holds with a normal wall thickness-to-chamber ratio. When this ratio is increased (e.g., hypertrophic cardiomyopathy), meridional wall stress underestimates fiber stress; when the ratio is decreased (e.g., dilated cardiomyopathy), meridional wall stress overestimates fiber stress. The method has been applied in a number of different clinical conditions, especially for the evaluation of cardiac contractility in pediatric patients exposed to anthracyclines. Lipshultz et al. (27) demonstrated that the velocity of fiber shortening versus wall stress is a useful index for following patients after exposure to anthracyclines. Before the wall stress- VCF_c relationship (or contractility) becomes abnormal, an increase in wall stress is measured in some postchemotherapy patients, mainly related to a change in wall thickness-chamber dimension ratio (28). Overall, the added benefit of measuring and calculating the VCF_c relationship is still uncertain. More advanced calculations have been proposed to calculate midwall shortening and even fiber stress, but, apart from use in research, the clinical applicability and the use of these methods in clinical decision making are currently limited, and clinical decision making is still mainly based on calculation of EF.

Doppler Indices of Ventricular Function

Measurement of EF and %SF provides information on global pump function based on dimensional changes. Derived parameters such as VCF_c and wall stress were developed in an attempt to yield information on myocardial and even fiber function. As all these parameters are based on calculations involving geometrical dimensions, their use in congenital heart disease is limited. As an alternative to measuring geometrical changes, Doppler data have been used to quantify ventricular systolic function. Initially, blood pool velocity measurements were made, and more recently tissue Doppler was introduced to measure the velocity of myocardial motion. The advantage of these methods is that they can be obtained independently of ventricular geometry.

One of the proposed blood pool measurements is *maximal* dP/dt based on a CW Doppler signal obtained through an AV-valve regurgitant jet. From invasive pressure measurements, the maximal rate of rise in LV pressure during the isovolumic contraction period (dP/dt_{max}) has been used as an invasive index for LV function. As Doppler velocity measurements represent pressure gradients, the slope of the CW regurgitant jet represents the speed of pressure rise within the ventricle. Practically, dt is calculated between 1 m/s and 3 m/s; dP between those two time points calculated by the Bernoulli equation is 32 mm Hg. dP/dt can then be calculated by the following formula: $dP/dt = 32 \text{ mm Hg/time interval in seconds}$. In the normal LV, dP/dt is 1,200 mm Hg/s or more. The same calculation can be applied to the RV or the univentricular heart. As dP/dt is measured before aortic valve opening, it is independent from changes in afterload but its measurement is influenced by preload changes. As the time interval measured on the Doppler trace is very short and the settings used to obtain the spectral Doppler tracings can be variable, the reliability and accuracy of the method are limited. This confines its use in daily clinical practice. Assessment of cardiac function by measuring blood flow velocity during ventricular ejection is another logical approach. Doppler signals across the aortic and pulmonary valves can provide timing intervals that are used to assess ventricular function. The time period between the onset of the QRS-complex and the onset of outflow is called the pre-ejection period. This period shortens when the function improves. When the pre-ejection period is corrected for ET, the PEP/ET ratio is a parameter for systolic function. One of the problems is that ET is very sensitive to afterload changes and is heart rate dependent. Moreover, the PEP time interval is short and

its measurement influenced by the spectral Doppler settings. A logical next step is to combine inflow and outflow Doppler measurements in the assessment of ventricular function. The myocardial performance index (MPI) was introduced as a nongeometrical index that incorporates both systolic and diastolic time intervals in expressing global ventricular function (29). MPI is defined as

$$(ICT + IRT) / ET$$

where ICT is the isovolumetric contraction time, IRT is the isovolumetric relaxation time, and ET is the ejection time (Fig. 9.8). When systolic dysfunction is present, ICT will prolong and ET shortens resulting in a prolongation of MPI. When diastolic dysfunction is present, the effect of IRT is dependent on the type of diastolic dysfunction. A relaxation abnormality will increase ICT but elevated filling pressures will have the opposite effect as an increase in left atrial (LA) pressure will shorten IRT. Thus, IRT is strongly dependent on preload and filling pressures while ET is influenced by afterload. Normal MPI values for the LV are 0.35 ± 0.03 and for the RV are 0.28 ± 0.04 . MPI has been proposed as an index for global ventricular performance as it incorporates systolic and diastolic function and will also be influenced by loading conditions. MPI has been shown to be a sensitive but not very specific marker of cardiac performance. Nevertheless, in certain diseases like pulmonary hypertension, amyloid heart disease, and pulmonary hypertension, it has strong predictive value (30,31).

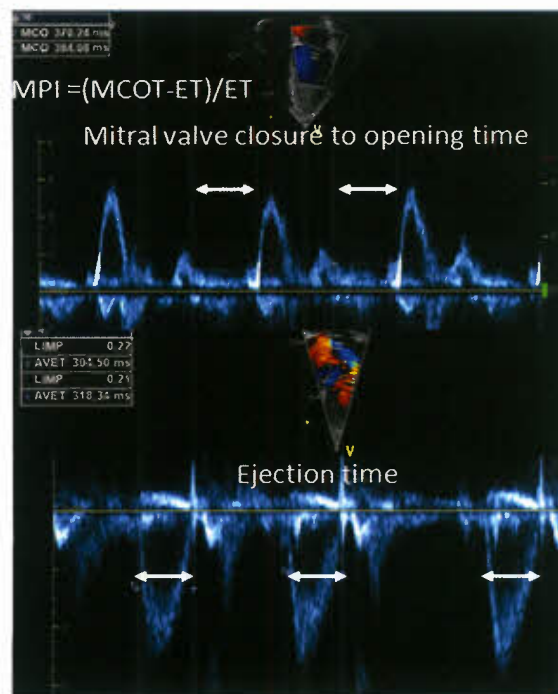


Figure 9.8. Myocardial performance index (MPI). The sum of isovolumetric relaxation and contraction time is calculated by measuring mitral valve closure to opening time (MCO) and subtracting the LV ejection time (ET). The difference between these two intervals is the isovolumic time. The total isovolumic time divided by the ET gives the MPI. The MCO is measured on the mitral inflow pattern as shown in the upper part of the picture. The LVET is measured on the aortic outflow as illustrated in the lower part of the figure.

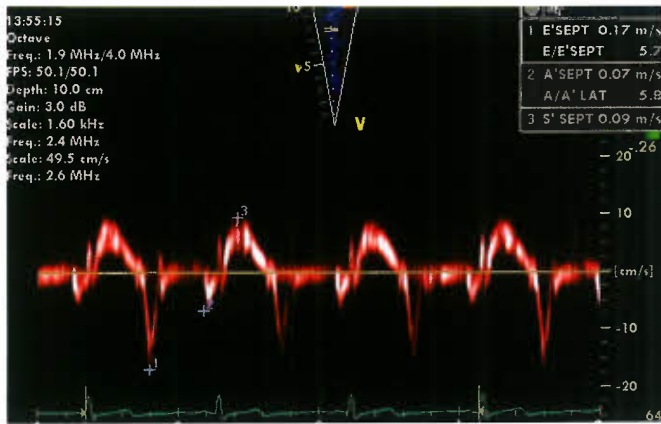


Figure 9.9. Typical longitudinal tissue Doppler tracing obtained in the basal part of the interventricular septum from an apical four-chamber view. Alignment with longitudinal LV motion is extremely important to obtain reliable measurements. Peak systolic velocity (S') (3), peak early diastolic velocity (E') (1), and peak late diastolic velocity (A') (2) are measured.

Apart from measuring flow velocities, Doppler has also been used for measuring myocardial velocities or tissue Doppler velocities. Tissue velocities are lower than most blood pool velocities but have higher amplitudes. Thus by adjusting Doppler filter settings, tissue Doppler velocities can be selectively measured (Fig. 9.9). Pulsed-wave tissue Doppler was developed first, followed by color tissue Doppler. Pulsed Doppler typically measures velocities in a single segment while color tissue Doppler measures velocities in an entire wall or chamber. While pulsed Doppler measures peak velocities, color tissue Doppler measures mean velocities. Therefore, color tissue Doppler velocities are approximately 15% to 20% lower than pulsed Doppler velocities. Color Doppler has the advantage of measuring velocities in different myocardial segments simultaneously while pulsed Doppler samples a single segment in a given time. Typically, pulsed tissue Doppler tracings are obtained at the mitral and tricuspid annulus or basal lateral wall and interventricular septal segments to study longitudinal motion in systole and diastole. A typical pattern of myocardial motion comprises an isovolumic spike followed by a systolic velocity wave. The systolic wave can be biphasic, especially in the lateral wall segments. In diastole, early and late

(during atrial contraction) diastolic velocities can be measured. Experimental studies have confirmed that, for normal myocardium, changes in segmental systolic velocities are closely linked to changes in contractility but are also influenced by loading conditions. Cardiac translational motion and tethering between segments (a noncontractile segment passively pulled by a normally contracting segment) also influences tissue Doppler velocities. As a Doppler technique, it is, by definition, angle dependent and influenced by machine settings and technical optimization. When the methods are well-standardized, tissue Doppler velocities can be measured with reasonable intra- and interobserver variability. Differences between different machines from different vendors have been described, especially for color Doppler measurements (32). At present, the use of systolic velocities is limited mainly to the assessment of ventricular dyssynchrony as will be discussed later in this chapter. Diastolic velocities, on the other hand, have become a key component in diastolic function assessment (see below). In the assessment of systolic function, the spike that occurs during the isovolumetric contraction period has been shown to be potentially useful (33). The mean acceleration of this spike, also called myocardial isovolumic acceleration (IVA), can be measured (Fig. 9.10) and has been described to be a relatively load-independent parameter for contractile function. As isovolumic contraction is a short-lived event (30 to 40 ms), calculation of IVA requires obtaining images at high temporal resolution (>200 frames/s) and the reproducibility of the measurements can be difficult if the method is not well-standardized. An interesting physiologic characteristic of IVA is its heart-rate dependency. Contractility increases with heart rate as described by the force–frequency relationship and IVA has been shown to be able to study this relationship in normal children and in disease (34). This indeed may be its main application as, due to its heart rate dependency, baseline values of IVA are highly variable. The measurement thus requires heart rate manipulation with ventricular pacing or exercise testing.

Ventricular Strain and Strain Rate

To overcome the problem of cardiac motion and translation as well as to neutralize the effect of intersegmental tethering, myocardial strain imaging was developed. Strain is defined as the deformation of a myocardial segment and is a dimensionless unit. Strain rate is the speed at which the deformation occurs and is expressed as strain/second. Initially, strain calculations were based on myocardial tissue Doppler velocities by measuring velocity gradients within the myocardium. In the radial direction, for instance, the endocardium moves faster

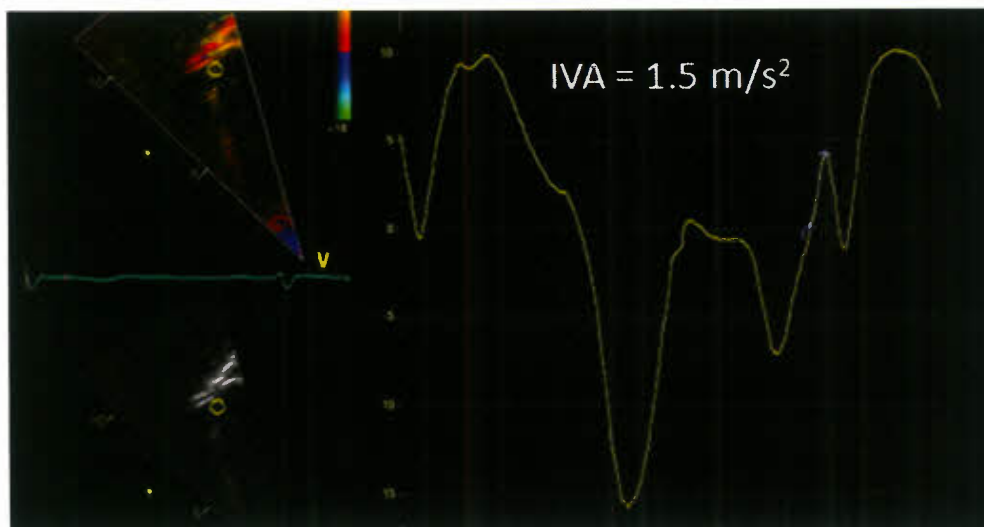


Figure 9.10. Isovolumetric acceleration measured in the RV lateral annulus from an apical four-chamber view. The measurement is performed using color tissue Doppler traced at high frame rates (>180 frames/s). The acceleration of the isovolumetric spike is measured from the baseline to the peak.

than the epicardium and the gradient between epi- and endocardial velocities correspond to radial strain rate. Temporal integration of the strain rate curve results in the measurement of strain. Tissue Doppler-derived strain measurements are quite cumbersome and require extensive off-line processing with large intra- and interobserver variability if not well standardized. Moreover, tissue Doppler velocities are angle dependent, limiting the measurement of myocardial deformation in certain directions (mainly longitudinal and radial). More recently, it has become possible to measure the strain and strain rate based on speckle tracking imaging. “Speckles” are gray-scale reflectors within the myocardium and their motion can be tracked in two or three dimensions (Fig. 9.11). The change in distance between the speckles throughout the cardiac cycle can be measured and strain and strain rate derived. The advantage is that this technique is angle independent and most vendors have developed a relatively user-friendly software interface that allows calculation of myocardial strain in different directions (longitudinal, radial, and circumferential). If well standardized, the reproducibility is reasonable but there are considerable differences between strain packages from different vendors, especially for radial strain measurements (35). Speckle tracking techniques perform reasonably well for longitudinal strain, but less well for circumferential and especially radial strain. Technical improvements are likely to occur. The first and probably most important application of strain imaging is quantification of regional myocardial function. This is especially useful when regional wall motion abnormalities are present due to regional myocardial perfusion problems or electromechanical dyssynchrony (Fig. 9.12). Other applications mainly relate to the early detection of myocardial

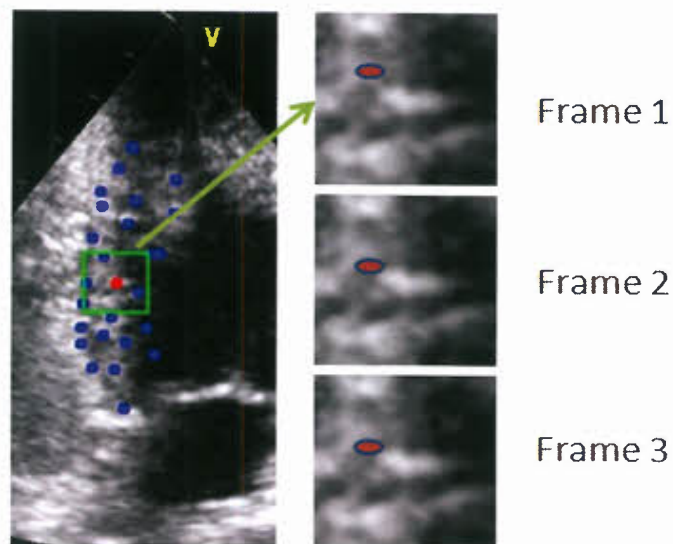


Figure 9.11. Speckle tracking. Speckles are reflectors within the myocardium. They can be tracked throughout the cardiac cycle frame by frame. The motion of the speckles in 2-D or even 3-D space can be used to calculate myocardial deformation. This image is taken from an apical two-chamber view, and speckles within the inferior wall are magnified. The way these speckles move can be traced in 2-D on a frame-by-frame basis as illustrated in the right panels.

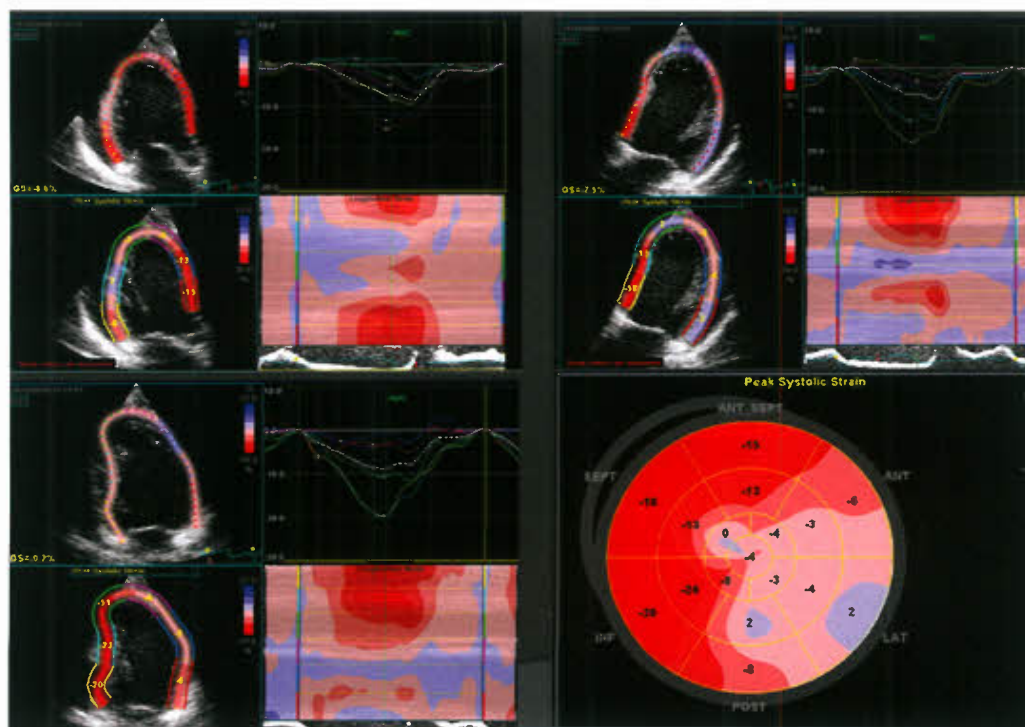


Figure 9.12. Longitudinal LV strain in a 13-year-old girl who developed a myocardial infarction based on abnormal origin of the left coronary artery from the right cusp with posterior looping and intramural course. The **left upper panel** represents the strain curves obtained from the apical three-chamber view, the **left lower panel** represents the strain curves obtained from the apical two-chamber view, and the **right upper panel** represents the strain curves from the apical four-chamber view. Longitudinal strain measurements are significantly reduced in the inferolateral wall segments (*light pink and blue areas*). The figure on the **lower right** demonstrates the recommended method for displaying strain data with all 17 cardiac segments portrayed in a bull's-eye type format. This allows an objective quantification of regional myocardial function. In this patient, the *light pink and blue areas* in the inferolateral wall segments represent the extent of the myocardial infarction on regional myocardial function.

dysfunction, where in certain diseases like Duchenne muscular dystrophy and patients exposed to anthracyclines, changes in systolic strain can be observed prior to changes in other cardiac parameters. Using strain imaging, a detailed study of myocardial wall mechanics is possible. When interpreting strain data, it should be remembered that strain measurements are influenced by ventricular size and loading conditions. The clinical usefulness of all deformation measurements still needs to be proven.

Assessment of Right Ventricular Function

The echocardiographic methods to assess ventricular systolic function were mainly developed to assess LV function. The more complex geometry of the RV, its anterior position within the chest, its coarse trabeculations, and its different physiology, make it more difficult to apply these echocardiographic methods for the assessment of RV systolic function (16). Cardiac MRI is considered the current clinical reference standard for measuring RV volumes and EF. By echocardiography, RV function is often assessed by subjective “eyeballing.” A reasonable echocardiographic surrogate for EF is the measurement of percent fractional area change (%FAC) from an apical four-chamber view. The RV end-diastolic area (RVEDA) and RV end-systolic area (RVESA) are measured and %FAC is calculated as $(RVEDA - RVESA)/RVEDA$ (Fig. 9.13). The %FAC has been shown to have a reasonable correlation with MRI EF, but as delineation of the RV lateral wall can be difficult, it can have significant interobserver variability. The %FAC is not very reliable when the RV outflow tract is dysfunctional as this part of the RV is not imaged from the apical four-chamber view and not included in the measurement.

As the RV fibers are more longitudinally oriented, longitudinal deformation in the RV is more important than radial and circumferential deformation, at least in the nonhypertrophied RV. Thus, the study of longitudinal RV function seems more important compared to the study of LV longitudinal

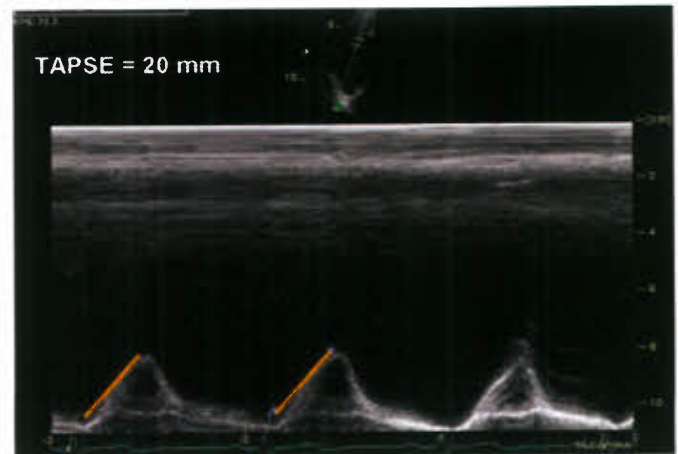


Figure 9.14. Tricuspid annular planar systolic excursion (TAPSE). An M-mode cursor is placed through the tricuspid valve annulus at the RV free wall and longitudinal displacement of the annulus is measured on the M-mode tracing (*lines* on figure). In this case, TAPSE is 2.7 cm, which is within the normal range (>1.7 cm).

function. The easiest method for assessing longitudinal function is by measuring the tricuspid annulus systolic planar excursion (TAPSE) by M-mode (Fig. 9.14). In adults, the normal excursion is >17 mm. For children, TAPSE is dependent on ventricular size and normal values for children have been published (36). TAPSE is easy to measure and correlates relatively well with EF measurements if there is no significant regional RV dysfunction or tricuspid regurgitation. TAPSE is a potentially useful method for serial follow-up of patients.

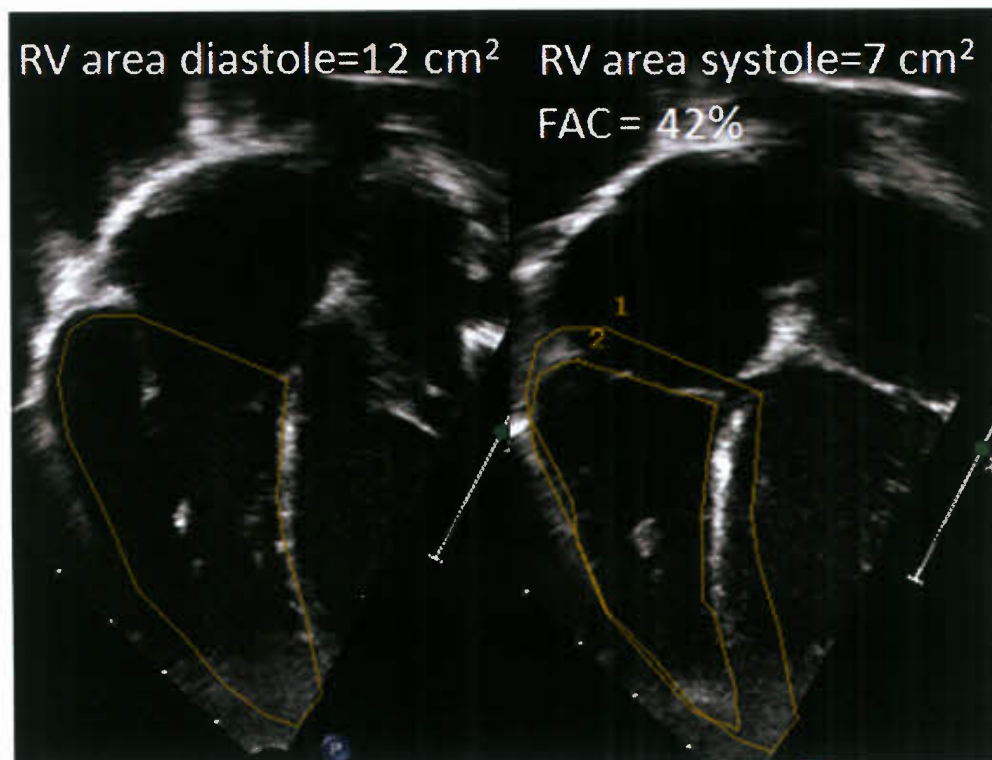


Figure 9.13. Right ventricular fractional area change (FAC). From the apical four-chamber view, the RV is imaged so that the endocardial borders can be tracked as well as possible. The RV area is measured at end diastole and at end systole and FAC is calculated as a percentage.

Systolic tissue Doppler velocities at the tricuspid annulus can also be measured with the same limitations as for the LV. IVA has been used in the RV but requires heart rate manipulation if the force–frequency response is to be studied. RV longitudinal strain measurements have also been proposed and have been shown to correlate well with global EF in systemic RVs but less well in patients after tetralogy of Fallot (TOF) repair. This is probably related to the influence of more radial and circumferential strain in patients with more hypertrophied RVs (37).

RV volumes and EFs can also be measured by 3-D echocardiography or by 2-D-based 3-D reconstruction methods. Software for analysis of RV volumes is available and the volumes obtained using these methods have been shown to correlate well with MRI-derived volumes (Fig. 9.15). However, feasibility is a problem as it can be very difficult to acquire the entire RV volume in a single volumetric data set. Another problem is endocardial border detection that can be challenging in the low-resolution 3-D data sets. Finally, it has been shown that 3-D echo tends to underestimate RV volumes compared to MRI, especially in dilated RVs.

Systolic Function of the Univentricular Heart

With advances in surgical palliation of univentricular congenital heart disease, patients now survive longer and the univentricular heart must support both the systemic and pulmonary circulations over many years. Functional evaluation of these ventricles is largely based on subjective assessment. Three-dimensional echocardiography using a method of disks analysis has been shown to correlate well with MRI-based volumetric calculations but requires extensive tracing of the myocardium and is cumbersome. Moreover, the feasibility of this method is limited by the difficulty of capturing the entire volume of the dominant ventricle into a single data set. More work is needed to develop a method to assess volumes in single RVs. Tissue Doppler and strain imaging are promising methods to assess myocardial function in single ventricles but one of their major limitations is that abnormal geometry, ventricular size, and loading conditions affect strain and strain rate values. Therefore, at present, there is no adequate quantitative method to assess the univentricular heart.

Ventricular/ventricular Interaction

In congenital heart, the ventricular–ventricular interactions are important for both systolic and diastolic function assessment. The interventricular septum is an important interface between both ventricles: in RV volume overload, the diastolic flattening of the interventricular septum interferes with LV filling and can influence LV output. In case of pulmonary regurgitation after TOF repair, RV dilation has been shown to influence LV filling and pulmonary valve replacement results in better LV filling and improvement in cardiac output (38). Systolic flattening of the interventricular septum is an important phenomenon in RV hypertension that influences LV systolic and also diastolic function (39,40). Description of the septal position in systole and diastole should therefore be part of the assessment of cardiac function. Apart from the influence of the interventricular septum, the epicardial fibers, which are shared between the RV and LV, also influence interventricular cross-talk. In experimental electrically isolated hearts, it has been demonstrated that up to 20% to 40% of the RV systolic pressure and volume output is generated by LV contraction (41,42). How this is important for patients with congenital heart disease needs further exploration. The electrical interreaction between both ventricles is also very important as discussed further in the section on dyssynchrony evaluation.

ASSESSMENT OF VALVE FUNCTION

Semilunar Valves and Great Vessels

Quantitative Morphometric Evaluation

Quantitative anatomic assessment of the proximal great vessels and their branches is important in a number of circumstances. It is routine to perform a quantitative evaluation of the aortic structures from the level of the valve annulus through the distal aortic arch. Evaluation of the aortic root itself consists of 2-D assessment of the aortic annular dimension, dimension of the aorta at the level of the sinuses of Valsalva, and dimension of the sinotubular junction, ascending

Figure 9.15. Three-dimensional echocardiography to calculate RV volumes. This is based on obtaining a full volumetric data set of the RV and using a semiautomated tracking method to measure RV volume. The **left panel** represents the reconstructed RV volume with the tricuspid valve on the right and the pulmonary valve level on the left of the volume. The **right panels** represent the cuts through the volumetric data sets that are traced to reconstruct the RV volume. The **right upper** is the coronal plane, the **middle** the transverse plane, and the **lower** the sagittal plane.



aorta, proximal and distal transverse aortic arch, and aortic isthmus. In general, 2-D axial resolution is superior to lateral resolution. Therefore, aortic root dimensions are best assessed in the parasternal long axis with the proximal ascending aorta and aortic root perpendicular to the ultrasound beam. Different techniques for measuring the aortic root have been proposed and when using normal data, it is important to know which technique was used to establish the reference values. Measurements can be obtained during early to midsystole as suggested by the pediatric guidelines (3), but most of the normal reference papers have used diastolic measurements of the aortic root. Roman et al. (43) and the more recent paper by Gautier et al. (44) both measured the aortic root at end diastole and also used a leading edge to leading edge technique, which means that they included the anterior wall of the aorta in the measurement but not the posterior wall. The alternative technique is to measure the aortic root between the anterior and posterior inner edges. This is the method used in other imaging modalities like cardiac MRI and cardiac CT and the increased image resolution of echocardiography should allow use of the inner-edge technique.

The aortic valve is magnified in the parasternal long-axis view and the annulus measured from the inner edge of the proximal valve insertion hinge point within the arterial root to the inner edge of the opposite hinge point (Fig. 9.16). The sinus of Valsalva and sinotubular junction are also measured from the parasternal long-axis view. To visualize the aortic root and ascending aorta, it may be necessary to move the transducer one or two intercostal spaces higher (high left parasternal view). The ascending aorta is measured at the level where it crosses the right pulmonary artery. Imaging of the transverse arch and isthmus is usually done in long-axis images of the aortic arch from the suprasternal notch window. Measurements should be performed at the level of the proximal transverse arch (between the innominate and left carotid arteries), the distal transverse arch (between the left carotid and left subclavian arteries), and the aortic isthmus (the narrowest segment distal to the left subclavian artery).

The pulmonary valve is best measured from the parasternal long-axis outflow view, although it can also be measured from the parasternal short-axis view (lower resolution) (Fig. 9.17).

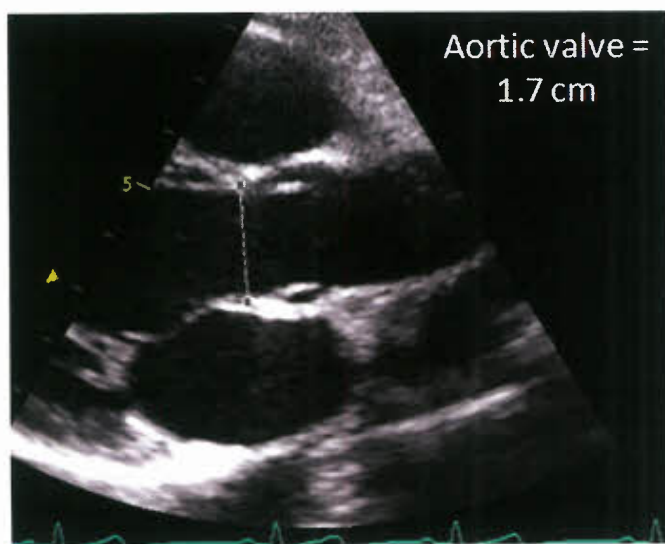


Figure 9.16. Measurement of the aortic valve annulus. A zoomed parasternal long-axis view of the aortic valve is used. The measurement is performed in early systole. The measurement is made at the aortic valve hinge points.

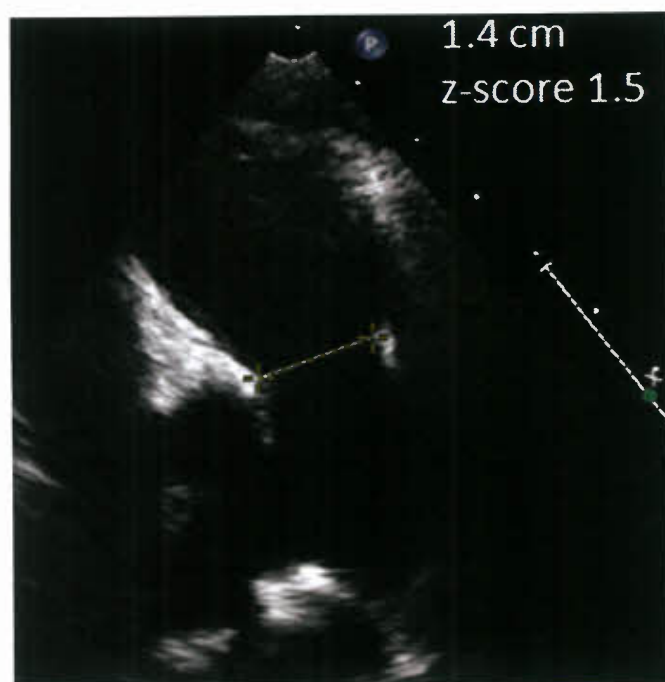


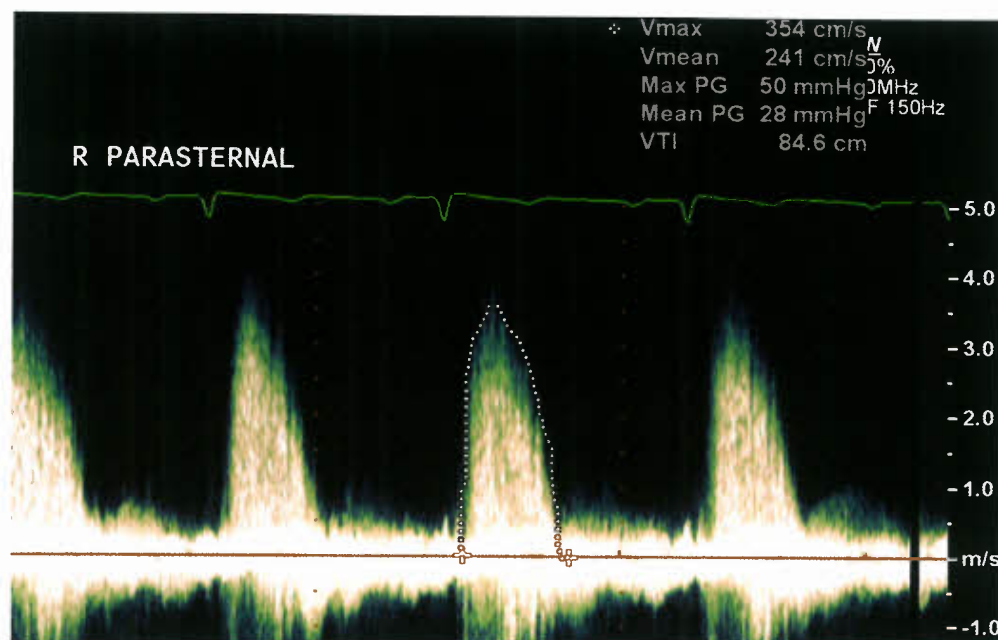
Figure 9.17. Pulmonary valve measurement. In this parasternal short-axis view, the pulmonary valve annulus is measured at the hinge point of the valve leaflets in early systole.

The main pulmonary artery can be measured between the sinotubular junction and the bifurcation. The proximal right pulmonary artery is best measured from the suprasternal view where it crosses behind the aorta. The left pulmonary artery is best measured from the suprasternal or ductal view.

Semilunar Valve Stenosis

Prior to measuring gradients, the level of obstruction needs to be determined by 2-D and color Doppler imaging. Subvalvar and supra-valvar stenosis should be excluded. The severity of aortic and pulmonary valve stenosis in pediatric heart disease is based on Doppler measurement of the peak and mean transvalvular gradient. As with all Doppler assessments, interrogation of transvalvular flow jets should be performed with an angle of insonation as parallel to the direction of flow as possible to minimize underestimation of the valve gradient. As such, aortic valve gradients are most accurately assessed from either the apical window or from a high right parasternal window, with the ultrasound plane angled inferiorly toward the ascending aorta (Fig. 9.18). Suprasternal windows can also be helpful. For the pulmonary valve, the parasternal short- and long-axis views can be used and in infants and smaller children, subcostal imaging can be useful. The peak instantaneous Doppler velocity is measured and the gradient calculated using the Bernoulli equation. This is different from the peak-to-peak gradient measured in the cardiac catheterization laboratory by pullback of the catheter across the valve. The peak instantaneous pressure gradient is calculated from the peak instantaneous flow velocity that occurs across the semilunar valve at a single time point in systole. When peak-to-peak gradients are measured by pullback of the catheter in the cardiac catheterization laboratory, the gradient is expressed as the difference between the peak pressure upstream of the valve (or point of obstruction) and peak pressure proximal to the valve, which does not occur simultaneously in the cardiac cycle. The peak-to-peak gradient measured by echocardiography will often be higher compared to the peak-to-peak gradient measured by catheterization. The mean aortic

Figure 9.18. Continuous wave Doppler tracing obtained in patient with aortic stenosis from the right parasternal window with the patient in a right lateral decubitus position. This position and view frequently affords the best Doppler alignment with the aortic stenosis jet. Peak gradient as well as mean gradient are measured on the tracing.



gradient can be obtained by tracing the flow profile. Mean gradients correlate better with peak-to-peak gradients obtained in the catheterization laboratory. For the pulmonary valve, the peak instantaneous gradient correlates better with the peak-to-peak gradient on pullback—and this explains why for assessing severity of pulmonary valve stenosis, the peak instantaneous gradient is used—while for the aortic valve, the mean gradient is considered to better correlate with the peak-to-peak gradient.

When interpreting gradients, it is important to consider the ventricular function. A low gradient across the aortic valve with poor LV systolic function can result in underestimation of the severity of stenosis. Any factor causing increased flow in the LV outflow such as hyperdynamic ventricular function, anemia, and associated aortic insufficiency will result in higher gradients. As cardiac catheterization is often performed under general anesthesia, it is not unusual to find significant differences in the gradient before and after induction of general anesthesia. Another factor influencing the assessment of Doppler gradients in children is the pressure recovery phenomenon. Potential energy is converted into kinetic energy when blood accelerates across the vena contracta. Some of this energy dissipates into heat related to turbulence and viscous losses. Some of the kinetic energy reconverts to potential energy, resulting in pressure increase distal to the stenosis. This phenomenon is more important when the aorta is smaller and results in overestimation of pressure gradients. Other formulas have been proposed that allow better prediction of the catheter peak-to-peak gradient, but have not been extensively validated.

If there is uncertainty regarding the importance of a semilunar valve stenosis, it can also be useful to try to estimate right or LV pressure, using atrioventricular (AV) valve regurgitation. RV systolic pressure can be assessed by measuring the peak velocity of the tricuspid regurgitant jet. The RV systolic pressure = $4 (\text{TR peak velocity})^2 + \text{estimated right atrial (RA) pressure}$. In general, RA pressure is estimated to be around 5 mm Hg unless there is clinical evidence of elevated RA pressure. LV systolic pressure can be estimated based on the mitral regurgitant jet using the same formula. It can, however, be more difficult to estimate LA pressure.

Calculation of Valve Areas

Because of the aforementioned factors influencing calculation of pressure gradients, estimation of aorta valve area is

recommended in the adult patient with aortic stenosis (45). The recommended method to measure aortic valve area is the continuity equation. This equation, based on the principle of conservation of mass, states that with no net loss of fluid from the system, the volumetric flow at area *A* must be equal to the volumetric flow at area *B*. The equation is therefore stated as

$$A_1 V_1 = A_2 V_2,$$

where *A* is the cross-sectional area of either position 1 or 2, and *V* is the mean velocity of the modal spectral profile at either position 1 or 2.

As the mean flow velocity, *V*, equals the velocity–time integral of flow divided by the ET, and as the ETs across both areas 1 and 2 are essentially the same, the continuity equation is further simplified as follows:

$$A_1 (\text{VTI}_1) = A_2 (\text{VTI}_2),$$

where VTI is the velocity–time integral of flow across either area 1 or 2.

The continuity equation is most frequently used in clinical studies to estimate the effective aortic valve area in the setting of aortic stenosis. By rearranging the continuity equation, the effective valve area of a stenotic aortic valve can be solved for as follows:

$$A_{\text{AOV}} = (A_{\text{LVOT}} \times \text{VTI}_{\text{LVOT}}) / \text{VTI}_{\text{AOV}},$$

where A_{AOV} is the cross-sectional area of the effective aortic valve orifice, A_{LVOT} is the cross-sectional area of the LV outflow tract (LVOT), solved by measuring the diameter of the LVOT in the parasternal long-axis view, VTI_{LVOT} is the velocity–time integral of flow across the LVOT, and VTI_{AOV} is the velocity–time integral across the stenotic aortic valve.

Using the continuity equation, it has been demonstrated that the aortic valve areas calculated in children by Doppler correlate well to aortic valve areas calculated by the Gorlin equation on cardiac catheterization, although Doppler methods tend to underestimate catheter areas slightly (46). In normal children and adolescents,

it has been shown that aortic valve area indexed to BSA is approximately $1.33 \text{ cm}^2/\text{m}^2$ (47), which is very close to values obtained in normal adults (48). Due to the potential inaccuracies in measurement of the LV outflow tract and the larger error associated with the assumption that the outflow tract is circular, the calculation of the valve area is not widely applied in pediatric echocardiography. Direct planimetry by 2-D and 3-D methods have been proposed but due to doming, funnel-type opening of the valve leaflets, the actual orifice is difficult to identify and true *en-face* views of the valves are difficult to obtain. Three-dimensional methods could potentially help to resolve this problem but have not been validated in pediatric cardiology.

Aortic Valve Insufficiency

Isolated aortic regurgitation in the pediatric population is relatively uncommon, but it can be seen, particularly in children with bicuspid aortic valves. More often, aortic regurgitation is seen in conjunction with an abnormal aortic valve that features both aortic stenosis and insufficiency. Evaluation of neo-aortic insufficiency, however, can be important following aortic valve replacement by pulmonary autograft (Ross procedure), in hypoplastic left heart syndrome following a Norwood reconstruction or following an arterial switch operation in transposition of the great arteries. In general, methods for assessing aortic regurgitation can be divided into (a) assessment of LV end-diastolic and end-systolic dimensions and volumes (see section above) and (b) assessment of the aortic regurgitation severity using Doppler methods.

Hemodynamically significant aortic regurgitation results in enlargement of the LV with an increase in LV end-diastolic dimensions and volume. In case of preserved LV function, hyperdynamic LV function is often associated with LV dilatation (Frank-Starling relationship) causing the LV end-systolic dimension to remain low. With progressive aortic regurgitation and associated LV dysfunction, the end-systolic dimensions (and volume) will increase. In adult patients, it has been proposed that aortic valve replacement or repair be undertaken for end-systolic dimensions $>55 \text{ mm}$ to protect against irreversible myocardial damage and risk of sudden death (49). In children, a z-score of >4.0 has been suggested but this is not based on good prospective data. Due to the effect of loading conditions on most echocardiographic functional parameters, it is uncertain which parameter best detects early ventricular dysfunction.

Apart from assessing the effect of chronic regurgitation on the LV size and function, the severity of aortic regurgitation needs to be assessed. Different methods should be combined for a com-

prehensive assessment. Pulsed-wave Doppler flow patterns in the distal aortic arch and descending aorta can be used to assess severity of aortic regurgitation. Significant aortic regurgitation results in holodiastolic flow reversal in the distal aortic arch up to the descending aorta at the level of the diaphragm (Fig. 9.19). Color Doppler interrogation of the aortic insufficiency jet itself can also be performed and various measurements made on the color Doppler images: (a) *Jet width or cross-sectional area*. This is measured immediately below the aortic valve, within 1 cm of the valve (for adults). In the long-axis view, jet width relative to the LV outflow tract dimension can be measured. From the parasternal short-axis view, the cross-sectional area relative to the LV outflow tract area can be measured. The criteria to define severe AR are ratios of $>65\%$ for jet width and $>60\%$ for jet area. This has not been well validated in pediatric aortic regurgitation. (b) *Measurement of the vena contracta*. The vena contracta is defined as the smallest diameter of flow at the level of the aortic valve, immediately below the region of flow convergence. It is different from the jet width that is measured in the LVOT. A vena contracta $>0.6 \text{ cm}$ in adults is associated with severe AI but no data are available for children. (c) *CW Doppler of the regurgitant jet*. The best signals are usually obtained from the apical windows. The most commonly used parameter is the pressure half-time of the aortic insufficiency velocity profile (the time required for the initial peak gradient between aorta and LV to decrease by half). A pressure half-time $>500 \text{ ms}$ usually indicates mild AR, whereas a value $<200 \text{ ms}$ is consistent with severe AR. The problem with this measurement is that it is influenced by LV end-diastolic pressure and the presence of diastolic dysfunction. Increased end-diastolic pressure will shorten the duration of regurgitant flow.

Regurgitant volume, regurgitant fraction, and effective regurgitant orifice area can all be directly estimated by a combination of Doppler and 2-D echocardiography. Estimation of regurgitant volume and EROA can also be done using color flow Doppler imaging of the regurgitant jet and the proximal isovelocity surface area (PISA). These methods are rarely applied in pediatric echocardiography laboratories due to high variability and inadequate validation.

Pulmonary Valve Regurgitation

In theory, all the techniques described for aortic valve regurgitation could be used to assess severity of pulmonary valve regurgitation. In practice, pulmonary valve regurgitation is most commonly graded using color Doppler flow. Flow reversal in the pulmonary artery is assessed and, in general, the presence

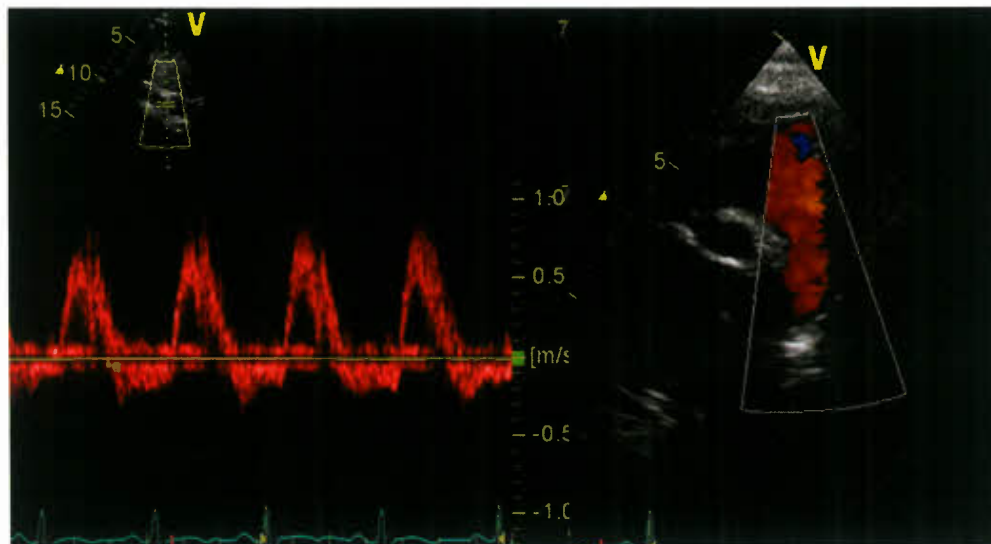


Figure 9.19. Patient with severe aortic regurgitation. Holodiastolic backflow in the abdominal aorta is shown on the pulsed Doppler tracing in the abdominal aorta. Color Doppler also shows the diastolic retrograde flow in the descending thoracic aorta.

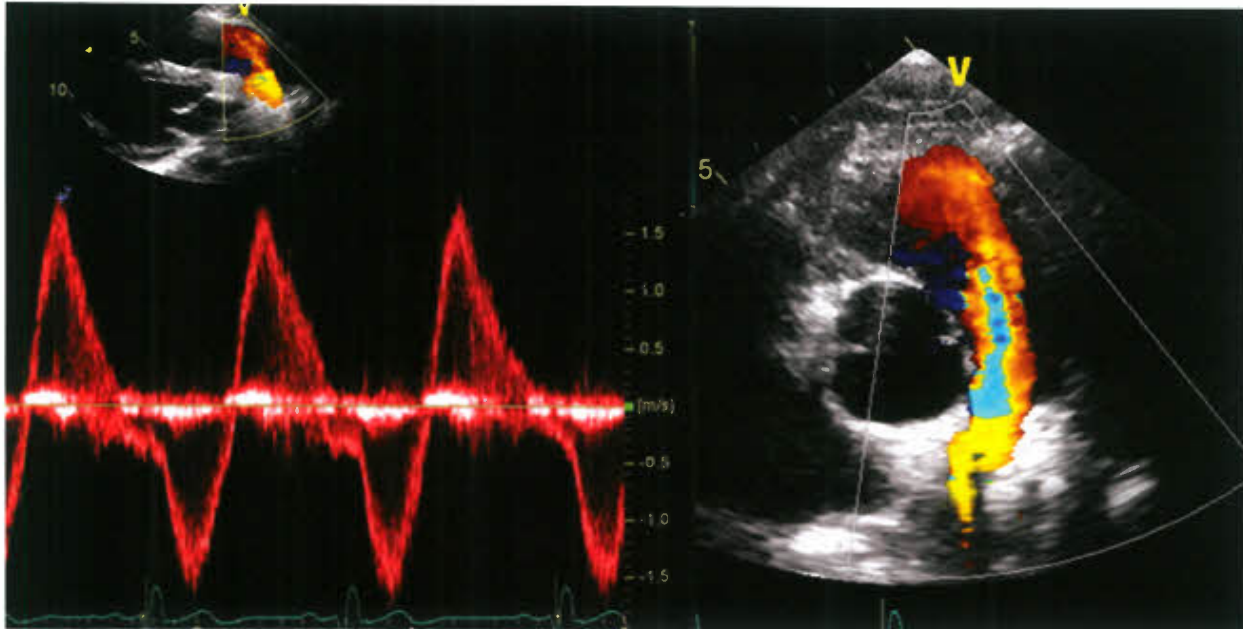


Figure 9.20. Severe pulmonary regurgitation after TOF repair. A wide regurgitant jet can be seen in the main pulmonary artery originating distally from the right pulmonary artery. The Doppler pattern shows the protodiastolic duration of the jet with its termination late in diastole.

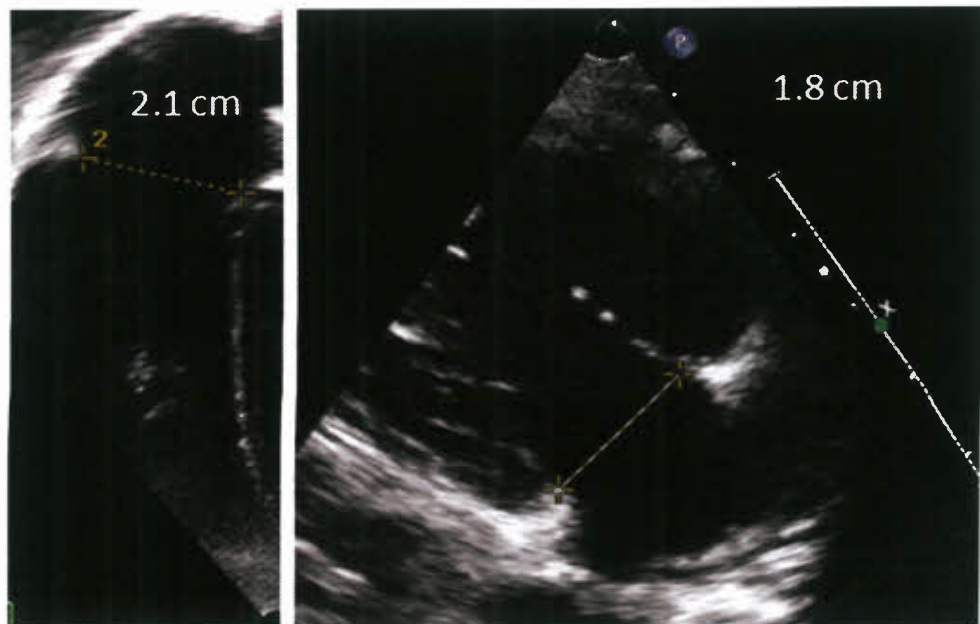
of flow reversal in the distal branch pulmonary arteries is seen in severe pulmonary regurgitation (Fig. 9.20). Jet width relative to the RV OFT dimension can be measured. Finally pressure half-time and duration of the pulmonary regurgitant flow relative to the total time of diastole can be used to quantify severity of pulmonary regurgitation. These, however, are influenced by RV end-diastolic pressure. The impact of pulmonary regurgitation on RV dimensions and function can be assessed as discussed in the section on RV volume and function. Based on cardiac MRI data, a RV end-diastolic volume between 150 and 170 mL/m² has been proposed as an indication for pulmonary valve replacement.

ATRIOVENTRICULAR VALVE SIZE AND FUNCTION

Quantitative Morphometric Evaluation

The annuli of the tricuspid and mitral valves have an elliptical and saddle-like shape and are best measured from the apical four-chamber view and parasternal long-axis view (Figs. 9.21 and 9.22). The diameters of the valves should be measured in early diastole at the frame after maximal excursion of the leaflets from inner edge to inner edge at the hinge points of the leaflets. The values should be expressed as z-scores. The area of valves can be calculated using the formula of an ellipse. Planimetry based on

Figure 9.21. Measurement of the tricuspid valve in two planes. **Left panel** shows the apical four-chamber view and **right panel** the parasternal long-axis inflow view. The valve is measured in diastole with the leaflets open.



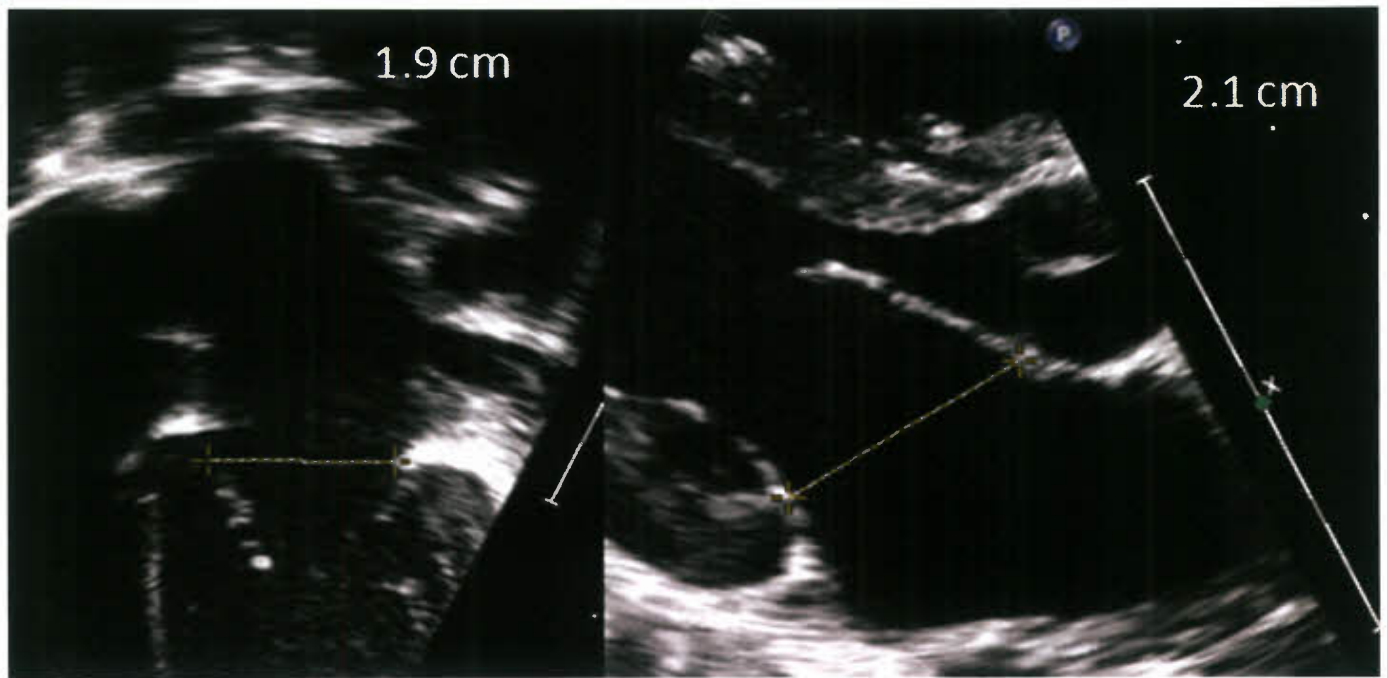


Figure 9.22. Measurement of the mitral valve in two planes. **Left panel** shows the apical four-chamber view and **right panel** the parasternal long-axis view. The valve is measured in diastole with the leaflets open.

2-D or 3-D images can also be used to measure AV valve size. Tricuspid and mitral valves annular sizes are important in valve disease as well as in the assessment of ventricular size.

Mitral or Tricuspid Stenosis

Mitral and especially tricuspid valve stenosis are rare congenital lesions. Echocardiography is used to define the mechanisms contributing to valvar narrowing and requires a detailed description of the supralvalvar region (supralvalvular ring), leaflets (thickened, reduced mobility), chordae

(short chordae in case of arcade mitral valve), and papillary muscles (parachute mitral valve). In patients with AV valve stenosis, the Doppler flow will usually be turbulent and its velocity elevated. The early peak velocity can be increased in cases of elevated filling pressures associated with LV diastolic dysfunction, which should be distinguished from mitral valve stenosis. The best method to assess AV-valve stenosis severity is by calculation of mean gradients using the mitral or tricuspid inflow signal (Fig. 9.23). For the tricuspid valve, there can be considerable influence of respiration on the inflow gradient with an increasing gradient during inspiration and decreasing gradient during expiration. Therefore, the gradient should be

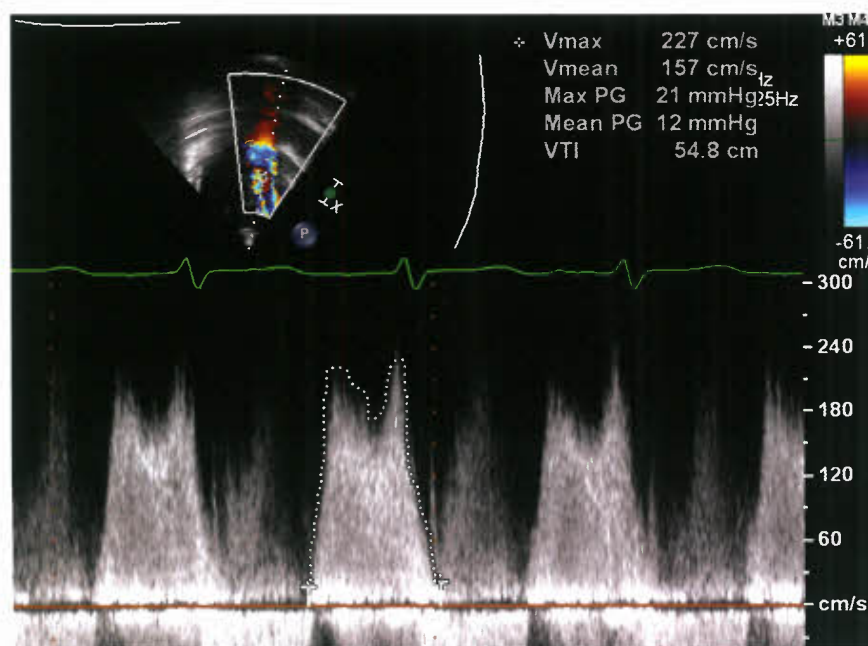


Figure 9.23. Mitral stenosis. Continuous wave Doppler signal through the inflow in the LV. The mean gradient across the valve is calculated.

averaged over at least three to five cardiac cycles. Heart rate and associated AV-valve regurgitation will also influence the calculated mean gradient. The severity of mitral valve stenosis can also be assessed by calculating the pressure half-time (the time needed for the peak early diastolic pressure to decline by 50%). A pressure half-time <60 ms is normal. A pressure half-time ($T_{1/2}$) >100 ms is indicative of significant mitral stenosis. Based on mitral valve pressure half-time, mitral valve area can be measured based on the formula ($220/T_{1/2}$). However, this calculation is not usually applicable in children due to higher heart rates influencing $T_{1/2}$. Effective orifice size can also be measured by the continuity equation, although again, this is more problematic in children. Direct planimetry based on 2-D or 3-D short-axis views of the mitral valve has been proposed but has not been well validated. Therefore, in practice, the most commonly used method is calculation of the mean gradient across the valve. The presence of an atrial septal defect/patent foramen ovale can lead to atrial decompression and lowering of atrial pressures resulting in a reduction of the gradient across the mitral valve. Therefore, in addition to the heart rate, the presence of an atrial communication should also be noted.

Atrioventricular Valve Insufficiency

In pediatric heart disease, assessment of AV insufficiency continues to be largely semiquantitative based on color Doppler. In adult echocardiography, more quantitative methods have been proposed including measurement of the vena contracta, regurgitant jet area, calculation of the regurgitant volume, regurgitant fraction, and effective regurgitant orifice area from the continuity equation and from the PISA. However, the utility of these indices in children is limited, and none of these have been adequately validated.

DIASTOLIC VENTRICULAR FUNCTION

Diastolic function describes the ability of the ventricles to fill with blood from the atria and pulmonary or systemic veins under low pressure. Echocardiographic assessment of diastolic function is based on Doppler assessment of AV inflow and the pulmonary (or systemic) veins with supplemental assessment by tissue Doppler, color-M-mode, and deformation imaging. Despite the multitude of available indices and techniques, echo assessment of diastolic function remains a challenging area in pediatric cardiology. At the same time, as our understanding of the importance of diastolic function in both acquired and congenital pediatric heart disease evolves, there is a need to correctly assess diastolic function in children.

Diastolic Physiology

Ventricular diastole can be defined as the time between semilunar valve closure and AV valve closure. This period is further divided into isovolumic relaxation, rapid early filling, diastasis, and filling during atrial systole (Fig. 9.24). Although useful, this definition is simplistic in that relaxation begins in some ventricular segments while other segments are still contracting. Moreover, diastolic function is intimately connected to the preceding systole through recoil, restoring forces, and ventricular suction effects that are linked to energy built up in systole and also connected to ventricular contractile synchrony. Likewise, a prolonged systole due to ventricular dysfunction will compromise diastolic duration (50). Thus, systolic and diastolic functions are intimately linked (50,52).

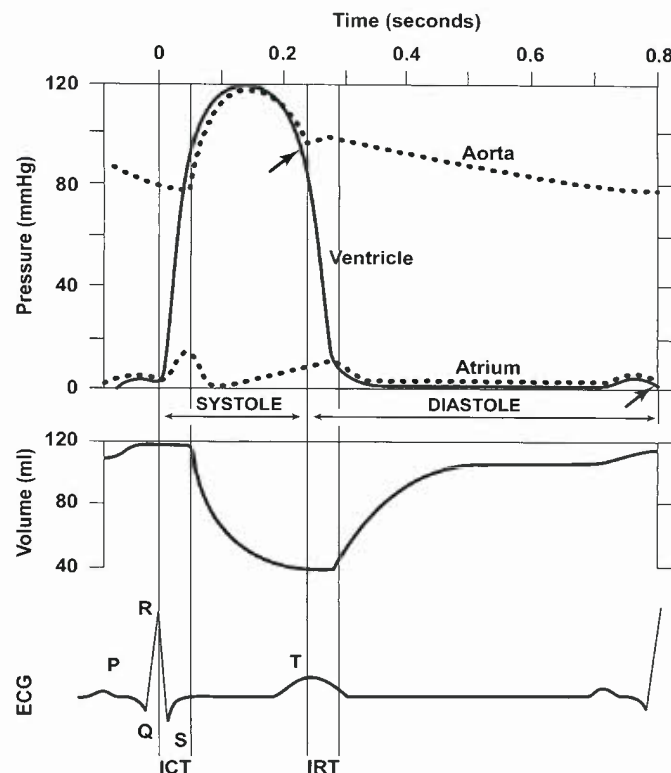


Figure 9.24. Physiologic tracing of left ventricular (solid line), left atrial (dotted line), and aortic (dash-dot line) pressure during the cardiac cycle. Diastole is defined as the time between aortic valve closure (arrow, top left) and mitral valve closure (arrow, bottom right). Isovolumic relaxation (IVRT) occurs between aortic valve closure and mitral valve opening. ECG, electrocardiogram; ICT, isovolumic contraction time.

Diastole is a complex process with both active and passive components. Ventricular relaxation is characterized by a decrease in ventricular pressure for a given ventricular volume. Initially, the pressure decrease is rapid and as the pressure in the ventricle falls below the pressure in the great vessels, the semilunar valves close. Mechanically, this initial decrease in ventricular pressure can be considered the onset of diastole. As the ventricular pressure declines further, it falls below the atrial pressure and the AV valves are swept open by blood rushing from the atria into the rapidly relaxing ventricles. Thus, a period exists between semilunar valve closure and AV valve opening characterized by a sharp fall in ventricular pressure without change in ventricular volume. In fact, most ventricular relaxation occurs in this isovolumic period. As the AV valves open, there is rapid filling in early diastole, which ceases temporarily when ventricular and atrial pressures equilibrate during diastasis. Further filling of the ventricle subsequently occurs during atrial contraction. Thus, early diastole is dependent primarily on ventricular relaxation, while filling in late diastole is determined to a large degree by ventricular compliance, defined as the change in pressure for a given change in volume. Overall, through their effect on the trans-mitral pressure gradient, ventricular relaxation and ventricular compliance are the two major determinants of diastolic function.

The timing and rate of ventricular relaxation are dependent on preload, afterload, myocardial relaxation, and mechanical synchrony. Myocardial relaxation is an active process involving rapid removal of intracellular Ca^{2+} controlled

predominantly by the sarcoendoplasmic Ca^{2+} -ATPase. Development of the sarcoplasmic reticulum and calcium handling in the myocyte is an age-dependent process that is relatively immature in the fetus and neonate. Age will therefore impact the rate of ventricular relaxation and the observed Doppler variables describing this phenomenon (53). The rate of relaxation will also be influenced by the degree of systolic shortening in the preceding cardiac cycle as well as by elastic recoil in early diastole from forces created in systole. In addition, the myocardium has viscous properties that require greater force to induce rapid expansion than more gradual expansion. These properties are likely most important when rapid filling occurs in early diastole and during atrial systole. Passive filling is impacted by atrial pressure, heart rate, and the elastic properties of the ventricle. The degree of ventricular filling during atrial systole is further modified by ventricular compliance and atrial function. The interplay of factors impacting diastolic function and affecting the transmitral gradient is portrayed in Figure 9.25. In turn, ventricular filling pressures are influenced not only by ventricular or myocardial properties, but by a variety of additional factors. This complicates isolated assessment of ventricular and myocardial diastolic properties by echo. Likewise, heart rate has a profound impact on diastolic duration (54,55). Therefore, growth and its associated change in heart rate will influence diastole and its assessment by echo. At high heart rates, there is exponential shortening of the diastolic duration with elimination of diastasis and fusion of early and late AV inflow and tissue Doppler waves into a single summation wave. Fusion between early and late diastolic waves of AV inflow or tissue velocities limits echo assessment of diastolic function in children with high heart rates.

History of Doppler Diastolic Assessment

Our understanding of the progression of LV diastolic dysfunction became clearer in 1992, when Appleton and Hatle (56) described the natural history of diastolic dysfunction. Using Doppler echocardiography, they demonstrated that diastolic dysfunction occurred in progressive sequence that could be characterized by Doppler echocardiography analysis of transmitral and pulmonary venous flow profiles. Subsequent work in additional techniques such as Tissue Doppler Imaging (TDI) (57–59) further refined assessment of diastolic ventricular function.

In adults, ventricular diastolic dysfunction has been classically described as progressing along a spectrum of increasing severity, divided into three main stages. In mild (stage I)

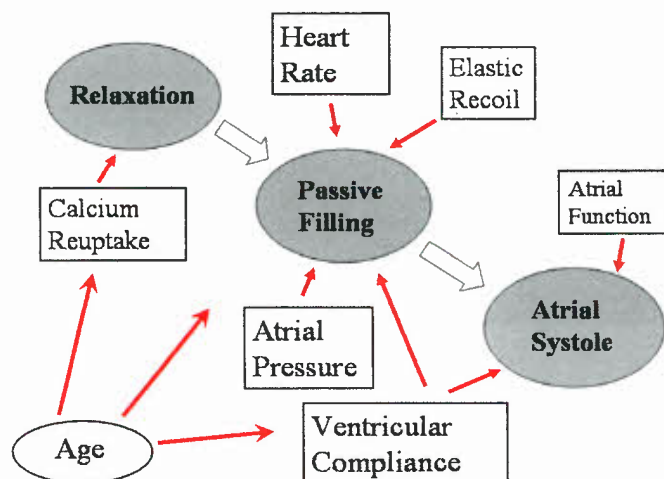


Figure 9.25. Factors influencing diastolic function.

diastolic dysfunction, the predominant abnormality is impaired ventricular relaxation. In moderate (stage II) diastolic dysfunction, pseudonormal function—described below—is noted. In the most severe (stage III) diastolic dysfunction, restrictive physiology is present. A fourth stage of irreversible restrictive physiology is also considered and portrays worse prognosis. Whether this paradigm of progressive diastolic worsening through these defined stages holds true for children is still under investigation. Our impression is that it is less common to see isolated stage 1 diastolic dysfunction in children, except in specific circumstances such as some children with ventricular hypertrophy secondary to hypertrophic cardiomyopathy or systemic hypertension (60). Rather, we often note concomitant abnormalities of relaxation and compliance, with predominance of decreased compliance. Nonetheless, the adult paradigm of staged progression currently provides the best working framework to assess and report diastolic dysfunction and its severity (61).

Echocardiographic Evaluation of Diastolic Function

Regardless of the stage of diastolic dysfunction, a standard protocol for evaluating LV diastolic function in children should be used (3). As no single echo index adequately describes diastolic dysfunction, a comprehensive examination is needed incorporating multiple parameters with interpretation and integration of the information by the echocardiographer. Echocardiographic assessment of diastolic function is usually centered on (a) transmitral Doppler flow, (b) pulmonary venous flow patterns, and (c) TDI of the lateral and medial mitral annulus. Color M-mode and deformation imaging are adjunct modalities.

Transmitral Doppler Flow Evaluation

Transmitral flow is obtained using a 1 to 2 mm pulsed Doppler sample placed between the tips of the mitral leaflets. A normal transmitral Doppler flow pattern (Fig. 9.26) features an early triangular diastolic E wave, with rapid acceleration and deceleration. The E wave includes the flow profile of early ventricular filling, while the E-wave deceleration phase reflects equalization between ventricular and atrial pressures. Therefore, an increase or decrease in filling pressures will shorten or lengthen the E-wave deceleration time, respectively. E-wave deceleration occurs after most early filling has occurred and is largely influenced by ventricular compliance. After cessation of the E wave, there is a period of diastasis (“separation” in ancient Greek), where little or no flow is seen. The quiescence of diastasis ends with the onset of the transmitral “A” wave, which begins after electrical activation of the atria (onset of the ECG P wave) and includes flow occurring during atrial systole. In addition, by enlarging the pulsed-wave Doppler sample volume and positioning it more medially so that it straddles the LV inflow and outflow, a simultaneous display of both mitral inflow and LV outflow can be obtained. The isovolumic relaxation time (IVRT) can then be measured as the interval between cessation of systolic flow and onset of mitral inflow. For a comprehensive diastolic function evaluation, the peak E- and A-wave velocities, E-wave deceleration time, A-wave duration, and IVRT should be measured. The peak E-wave/peak A-wave velocity ratio is also calculated (3). Although not commonly assessed, some authors advocate for measurement of the mitral flow velocity at the onset of atrial contraction. This “E at A” velocity affects the peak velocity and duration of the mitral A wave and hence important parameters such as the E/A ratio, the duration of pulmonary A-wave reversal relative to mitral A-wave duration.

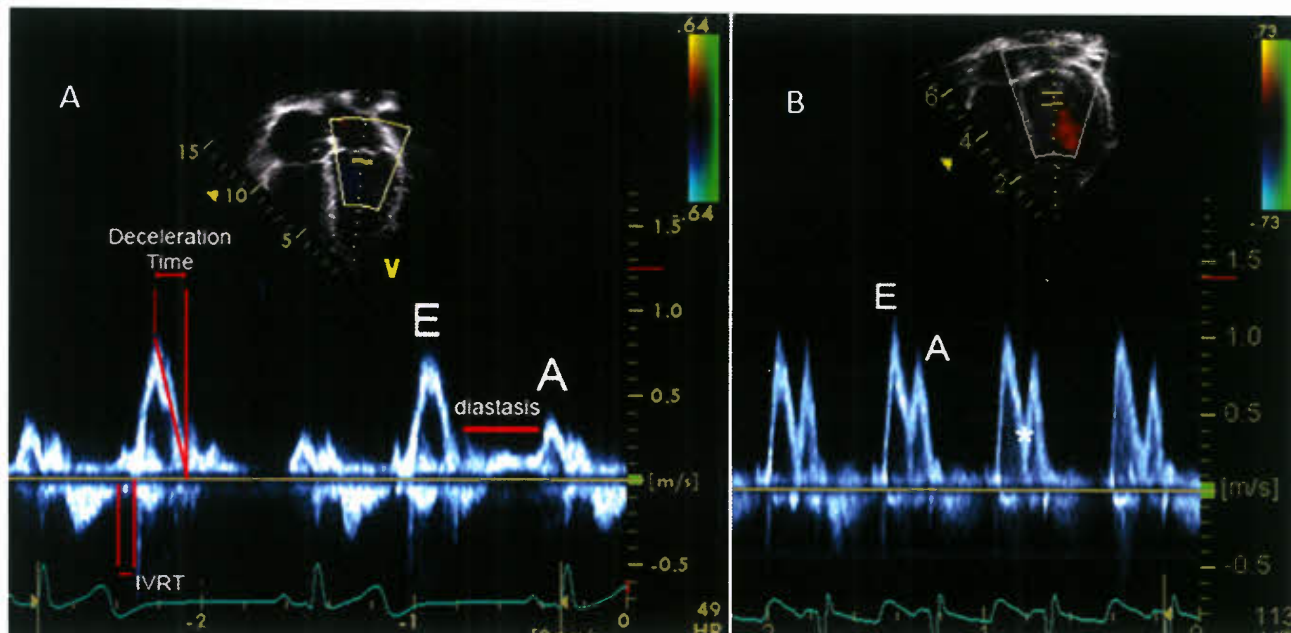


Figure 9.26. Mitral inflow at slow heart rate (panel A): Pulsed Doppler of the mitral inflow. The cursor is positioned at the tips of the mitral leaflets. Early (E) and late (A) diastolic waves are seen. Minimal flow is seen in diastasis—the period between the E and A waves. The isovolumic relaxation time (IVRT), measured from cessation of LV outflow to onset of mitral inflow and E-wave deceleration time (DT) are depicted. Mitral inflow at fast heart rate (panel B). Doppler of mitral inflow. Due to the fast heart rate, there is no diastasis and the E and A waves begin to overlap. At higher heart rates, these will merge into a single inflow wave. The asterisks depicts the “E at A” point. This is the point where the E and A waves merge when the E wave does not reach the baseline.

Pulmonary Venous Doppler Flow Analysis

Pulmonary venous flow is usually assessed from the apical four-chamber view by placing a 5-mm pulsed Doppler sample volume in the right pulmonary vein. The pulmonary venous flow features a low velocity phasic flow pattern consisting of

a systolic S wave, an early diastolic D wave, and a late diastolic reversal during atrial systole (A-wave reversal). During a comprehensive diastolic function assessment, the peak S- and D-wave velocities and the duration and peak velocity of the pulmonary venous A wave are measured, and the S-wave/D-wave velocity ratio is calculated (Fig. 9.27). Of these, the

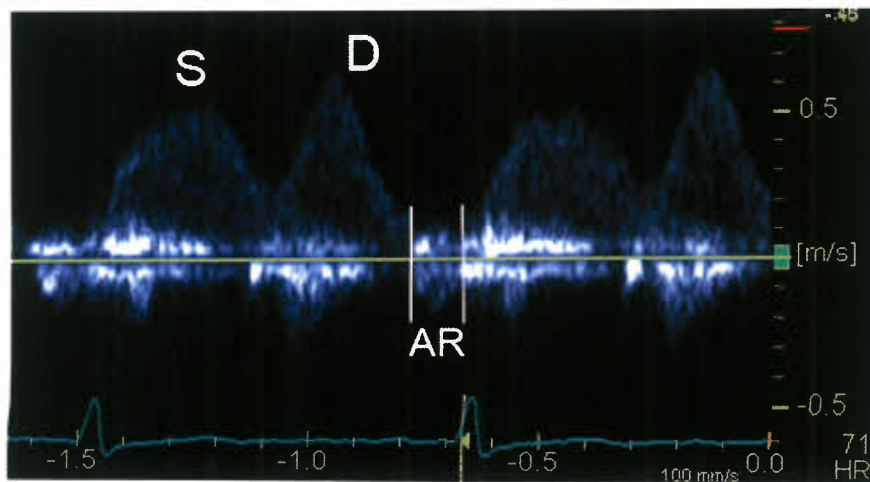


Figure 9.27. Pulmonary vein Doppler: Pulsed Doppler of a right pulmonary vein obtained from the apical view in a normal child. A systolic (S) and diastolic (D) wave are seen. In adults, a reduced S wave compared to the D wave would be abnormal and suggestive of delayed relaxation. However, this is commonly seen in normal children. The S wave often comprises an early and late component (S1, S2). This can be subtly discerned in the second cardiac cycle. Following the electrocardiographic P wave and atrial contraction, there is a small amount of flow reversal back into the pulmonary vein (AR). The duration and peak velocity of this flow reversal are measured as indirect indicators of ventricular compliance.

duration of the A-wave reversal relative to the mitral inflow A-wave duration is considered most useful as an indicator of ventricular compliance and reflects filling pressures in adults and in children (62). Of note, in the largest study of pediatric echo Doppler diastolic values to date, a small, but important, number of normal children were found to have increased duration of pulmonary vein A-wave reversal (62). Data in healthy infants and young children are limited to a small number of children (63).

Doppler Myocardial Velocity Assessment

TDI is a Doppler modality in which myocardial motion can be displayed both by color Doppler velocity maps and by pulsed Doppler spectral display. Tissue motion features low velocity and high amplitude signals; therefore, TDI presets optimize low-pass filters and lower-gain amplification to allow display of tissue velocities. This is in contrast to blood flow velocities, for which high-velocity and low-amplitude signals require different Doppler settings (Fig. 9.28).

Color tissue Doppler is derived from mean velocities and values are approximately 20% lower than the peak values depicted by pulsed tissue Doppler. Both color and pulsed TDI are easy to acquire and can be readily incorporated into the routine clinical exam. Color TDI is more convenient to interrogate large areas of myocardium in a single acquisition with subsequent off-line analysis of regions of interest anywhere in the data set. However, to date, the largest pediatric data sets in normal children report pulsed TDI values (64–68).

In addition, most literature investigating usefulness of TDI in relation to hemodynamics and in relation to clinical outcomes has used pulsed TDI. Therefore, for clinical assessment of LV diastolic function, it is conventional to use pulsed-wave Doppler assessment of the lateral and medial mitral valve annulus and to obtain the spectral display necessary for diastolic function evaluation (Fig. 9.28). TDI yields an early and late diastolic wave, mirroring AV inflow, but in the opposite direction (from the apical window, diastolic tissue velocities are below the baseline—moving away from the transducer). Typically, the peak tissue E-wave ($E_a[E']$) and A-wave ($A_a[A']$) velocities are measured. While the peak E'/A' -wave velocity ratio can be calculated, most research has focused on the utility of the early diastolic velocity (E'). This early diastolic tissue motion reflects diastolic relaxation and peak E' values correlate with the time constant of pressure decay in the LV (τ) (69). Tissue velocities are influenced by afterload, and although they

are also influenced by preload, they are less so than mitral inflow velocities. As abnormal loading is a hallmark of many types of congenital heart disease, thereby complicating interpretation of diastolic function through mitral inflow patterns alone, tissue Doppler velocities may play a useful adjunctive role. However, it should be noted that tissue Doppler velocities are less influenced by loading when ventricular relaxation is impaired. In the presence of normal relaxation, loading will have a greater influence on diastolic tissue velocities. In adults, out of all the various echo indices, E' is one of the best discriminators between normal and abnormal. Therefore, in the American Society of Echocardiography guidelines, grading of diastolic dysfunction begins with the E' velocity as well as LA volume (61). Whether or not this technique is applicable in children remains to be shown. It should also be remembered that the E' is sampled at a specific location, but is used to reflect on “global” ventricular properties, which may not hold true in all individuals. Importantly, the E' velocity or the related E'/E' ratio has also been shown to have prognostic value in a variety of adult and pediatric conditions including ischemic heart disease, valvular disease, dilated cardiomyopathy, hypertrophic cardiomyopathy, LV noncompaction, transplant rejection, and diabetes (70–75). A major practical advantage of TDI is that it is easy to obtain and yields robust signals, even when imaging windows are poor. High temporal resolution ensures that peak velocities are captured even when heart rates are high. An important pitfall of TDI is that tissue velocities may arise from passive myocardial motion due to translational motion of the entire heart in the chest or tethering of the interrogated passive segment to adjacent actively contracting or relaxing segments. Measurement of longitudinal velocities partly overcomes tethering effects as longitudinal motion is less affected by tethering. Tissue velocities change rapidly over the first year of life and are highly correlated to LV end-diastolic dimensions and mass (65). These characteristics should be taken into account when interpreting E' peak values in children. In addition, the IVRT derived from tissue Doppler imaging (TDI) may be useful as a parameter of LV relaxation (76) and normal data are available in children (77). Likewise, the $IVRT'/IVRT$ has been shown to correlate with LV filling pressures (76).

Estimation of Left Atrial Volume

In the absence of mitral stenosis or mitral regurgitation, estimation of LA volume is one of the most important parameters to assess chronic elevation of LV filling pressures (78).

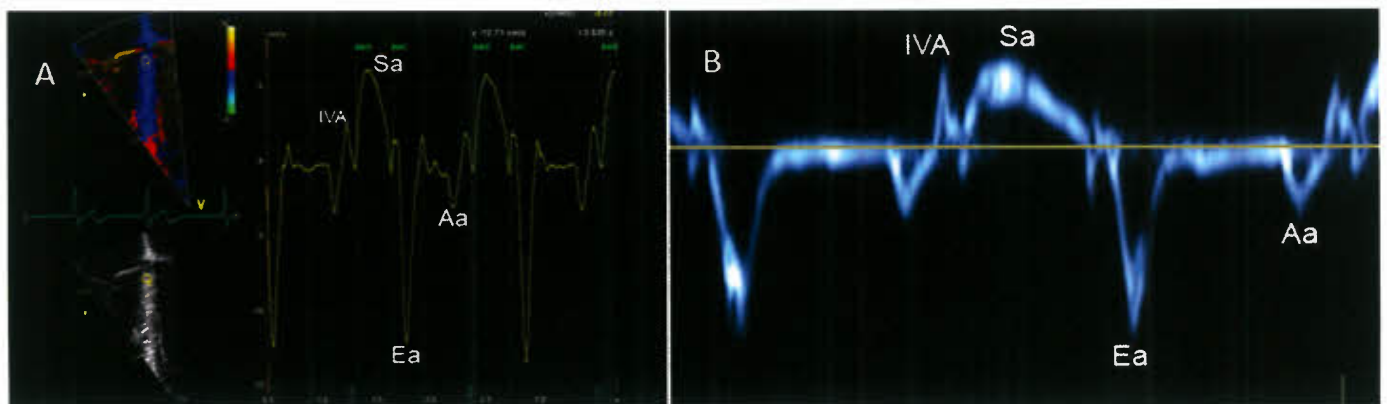


Figure 9.28. Color and pulsed Doppler in the assessment of diastolic function. Color (panel A) and pulsed (panel B) tissue Doppler sampled at the basal interventricular septum. In the color TDI image, aortic valve opening (AVO) and closure (AVC) are depicted (green lines). Systolic (Sa), early diastolic (E'), and late diastolic (A') waves are seen. Note that tissue velocity directions are a mirror image of atrioventricular valve inflow.

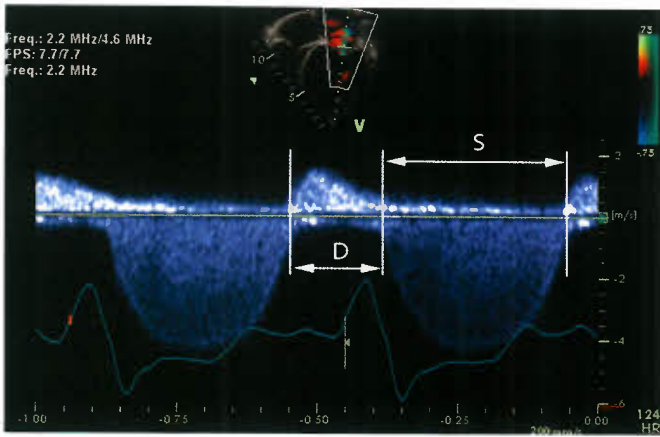


Figure 9.29. Continuous wave Doppler of mitral regurgitation in a child with dilated cardiomyopathy. The duration of mitral regurgitation represents the systolic duration (S). The remainder of the cardiac cycle represents diastolic duration (D). In ventricular dysfunction, systolic duration is prolonged compromising diastolic duration. This problem is aggravated by the relatively fast heart rate of 124 beats per minute in this patient where systolic duration is twice that of diastolic duration.

Normal values have been published in children (79) (Fig. 9.29). As filling pressures are related in part to LV compliance, increased LA volume has been associated with increasing severity of LV diastolic function (80) in a variety of conditions including in hypertrophic cardiomyopathy (79,81,82) and in both adult (81) and pediatric hypertension (83). Because increased filling pressures are related to clinical symptoms and outcomes, LA volume has been correlated to mortality in various types of heart disease in adults as well as in hypertrophic cardiomyopathy (84). LA volume can be measured using the biplane methods of discs (85), imaging the left atrium orthogonally in the apical two- and four-chamber views (Fig. 9.30), by the area length method or by 3-D echocardiography (3,86). Echocardiographic estimates of LA volume correlate well with estimates by cineangiography (87) and computed tomography (88), and can be compared to published normal values (87,89).

Color M-mode

Normal ventricular relaxation propagates from apex to base and, as will be subsequently discussed, is enhanced by recoil and untwisting of the LV. These mechanics produce a suction effect that allows rapid filling of the ventricle at low filling pressures via creation of intraventricular pressure gradients from base to apex. These pressure gradients can be calculated from Doppler by solving for the Euler equation, a derivative of the Bernoulli equation (90). The same phenomenon can be simply imaged by color M-mode as the flow propagation into the LV. This is done most practically by placing a color Doppler map between base and apex and placing an M-mode cursor through the mitral inflow. The color scale is lowered and the slope of the first aliasing velocity line is measured as the propagation velocity (V_p) (Fig. 9.31). The V_p is a measure of LV relaxation and has been found to correlate with tau in children with congenital heart disease (60). As the V_p is related to relaxation, the E/V_p ratio can be used to estimate mean LA pressures much in the same way as the E/E' ratio. Some adult laboratories have proposed using a qualitative assessment of this measure (91), but in children, it has been our experience that qualitative assessment is difficult. In adults, normal values are >50 cm/s. Although one pediatric paper found that age did not significantly impact V_p , as for many diastolic parameters, a large range of values were found in normal children (92). As the mitral leaflets are opened by blood flowing into the ventricle, measuring the slope of mitral excursion in early diastole by M-mode may be a simple surrogate for V_p (93).

Deformation Imaging

The rate of diastolic tissue relaxation can be assessed during the isovolumic relaxation period using speckle tracking to measure the global diastolic strain rate during IVRT (Fig. 9.32). This more direct assessment of LV myocardial relaxation will be less influenced by localized abnormalities at the mitral annulus or basal septum, where the E' tissue velocities are measured (91), but is limited by use of relatively low frame rates in relation to a very rapid event. Likewise, the degree of myocardial expansion (relaxation) at certain time points in diastole can be used as indicators of myocardial relaxation. Accordingly, the percentage of strain in early

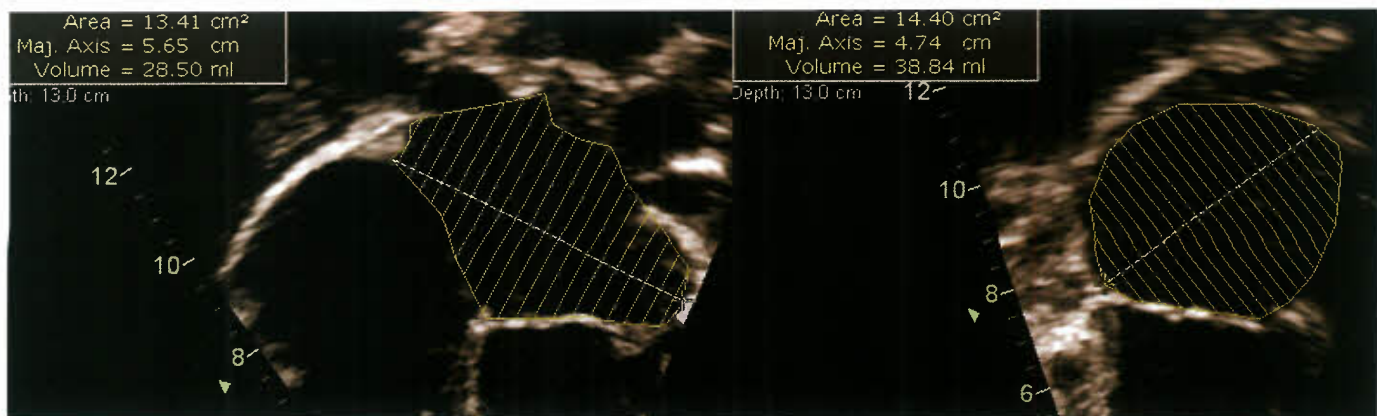


Figure 9.30. LA volume by Simpson's method. Left atrial volumes are calculated by Simpson's method of discs. The left atrium is planimetered in two orthogonal planes (four-chamber view, left panel and two-chamber view, right panel) to obtain both area and length. Volume is then calculated as $0.85 A_1 A_2/L$. LA volume > 32 mL/m² are abnormal.

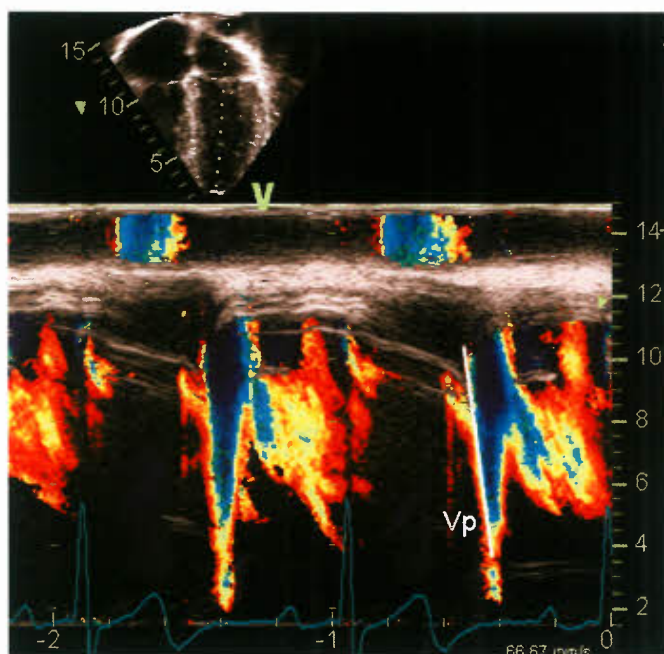


Figure 9.31. The velocity of flow propagation (V_p) into the left ventricle (LV), an index of LV relaxation, is obtained by color M-mode. An M-mode scan line is placed from the LV apex through the mitral valve with simultaneous color Doppler flow. The color scale (Nyquist limit) is lowered until aliasing is obtained. The slope between the first and second aliasing velocity is measured as the V_p . A more shallow slope indicates impaired relaxation. Normal data for pediatric V_p are not available.

diastole has been proposed as an index of relaxation (94). However, in children, diastolic strain and especially strain rate measurements are hampered by poor reliability (35). This is likely related in part to inadequate capture of the very rapid early relaxation, especially in young children, using relatively low frame rates currently accepted for 2-D speckle tracking echocardiography. Strain and strain rate are not currently recommended for routine clinical assessment of diastolic function according to the guidelines of the American Society of Echocardiography (95).

The LV contracts with a twisting motion, and the subsequent rapid untwisting motion in early diastole contributes to LV filling. Twisting in systole and untwisting in diastole is calculated as the net difference in rotation between base and apex. Normal basal systolic rotation is clockwise (when viewed from the apex), whereas the apex rotates in the counterclockwise direction. In diastole, directions are reversed. Ventricular untwisting can be measured by color TDI techniques (96), but is more easily imaged using speckle tracking echocardiography (97) from rotation measured at the base and at the apex in short-axis images. The rate of untwisting may be an even more informative parameter and correlates with tau (98). In normal young children, one study has found especially vigorous untwisting and recoiling of the apex during isovolumic relaxation and early diastole (99). This contrasts a previous study that found slower untwisting during isovolumic relaxation in infants, with subsequent increase over age (100). Decreased rotation mechanics have been demonstrated in various diseases of myocardial dysfunction including hypertension, hypertrophic cardiomyopathy, and nonischemic and ischemic heart disease in adults (101,102), and dilated cardiomyopathy in children (103). However, as untwisting is

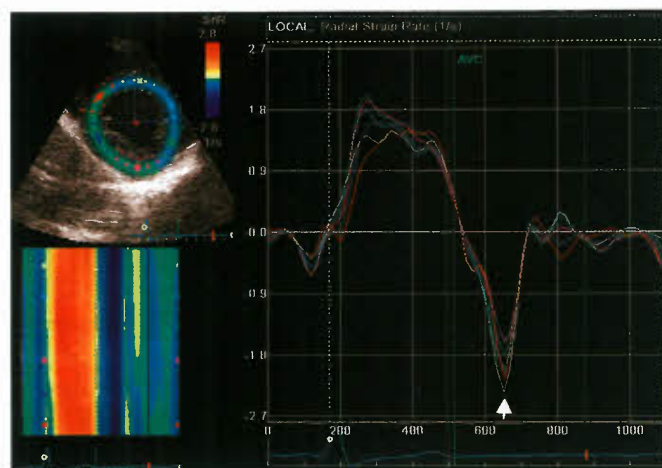


Figure 9.32. Left ventricular early diastolic radial strain rate obtained from 2-D speckle-tracking echocardiography in a parasternal short-axis plane at the papillary muscle level. Peak early diastolic strain rate is marked by the arrow. The top left panel is the reference image. The lower left panel depicts strain rate in color M-mode format. The x-axis is time. The y-axis is the various myocardial segments with the top portion indicating the anterospetum and continuing clockwise (around the transverse plane of the LV from top to bottom in the figure). The blue color depicts the diastolic strain rate and gives the same information shown in the curves. Although, this measurement reflects early diastolic relaxation, we do not advocate for its use as a routine clinical parameter as frame rates are low compared to the rapid sequence of the event.

strongly related to systolic twisting and end-systolic volume, it is not a “pure” indicator of diastolic relaxation (97). While rotation mechanics values have now been published in normal children (99), validation studies and demonstration of the usefulness of this index in clinical practice are still lacking.

Normal Echocardiographic Diastolic Function

In the normal LV, ventricular relaxation leads to a rapid fall in LV pressure during isovolumic relaxation creating a pressure gradient in early systole between the left atrium and LV. Early diastolic flow into the LV is driven by this pressure gradient, producing the mitral valve E wave. During diastasis, there is minimal pressure gradient between left atrium and LV with cessation of flow and lack of Doppler signal. During atrial systole, a LA–LV pressure gradient recurs to produce late diastolic filling—the mitral valve A wave.

The normal E-wave/A-wave velocity ratio in children between 3 years of age and adulthood is approximately 2.3 ± 0.6 , with mitral valve A-wave duration of approximately 140 \pm 21 ms (62). The normal pattern of mitral inflow is portrayed in Figure 9.26. It is optimal to interpret the E/A ratio when the mitral inflow velocity at onset of atrial contraction is <20 cm/s. However, this is dependent on heart rate and it is not feasible to lower heart rates in children for the purposes of this examination. Likewise, both IVRT and mitral E-wave deceleration time are heart rate dependent. Nomograms for deceleration time versus heart rate have been published (62). It has been proposed that correcting the IVRT for heart rate by dividing by the square root of the cardiac cycle length identifies a normal heart rate corrected IVRT of 63 ± 7 ms in children from several months

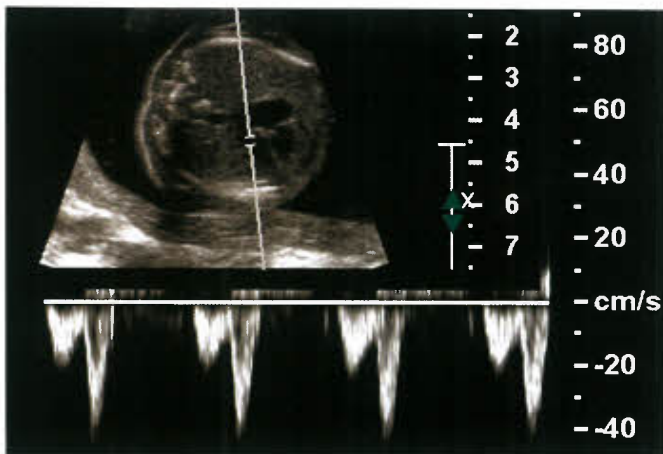


Figure 9.33. Fetal inflow pattern. A typical mitral inflow pattern on a fetal exam obtained from an apical four-chamber view with $E < A$ and prolonged IRTs.

to 20 years of age (104). In infants <2 months of age and in the fetus, myocardial immaturity produces a pattern of impaired relaxation with reversed E and A waves and TDI E' and A' waves. Thus, in the fetus and neonate, E-wave/A-wave ratios <1 and prolonged IVRTs are noted (Fig. 9.33); the degree to which these indices differ from normal children and adolescents is a function of myocardial maturity. Thus these changes are seen more dramatically in the fetus than in the newborn and in the newborn more than in the 2- to 3-month-old infant. The maturation from fetal to childhood patterns generally occurs by 3 months of age (105).

Normal pulmonary venous flow (Fig. 9.27) has typical S and D waves and usually a small atrial systolic A wave. The S wave may have two components: S1 and S2. In younger children, the S-to-D velocity ratio is typically <1, a finding that differs from the older adolescent and adult population for which the S/D-wave velocity ratio in normal subjects is typically >1. The normal pulmonary venous S-wave/D-wave ratio in children 3 to 17 years of age is 0.8 ± 0.2 . In children, a small atrial systolic flow reversal of short duration is often present (62,106). The pulmonary venous A-wave velocity is 21 ± 5 cm/s with duration of approximately 130 ± 20 ms (102).

TDI assessment of mitral annular velocities (Fig. 9.28) in the normal LV shows an E'-wave/A'-wave velocity ratio >1. Relaxation of the ventricle produces movement of the mitral valve annulus away from the transducer in the apical four-chamber view; atrial systole produces a mitral annular A' wave, reflecting the motion of the mitral annulus away from the transducer with late systolic ventricular filling. Normal values for both mitral and tricuspid annular velocities in children have been published (65,68,107).

ABNORMALITIES OF LEFT VENTRICULAR DIASTOLIC FUNCTION

Stage I Diastolic Dysfunction: Impaired Relaxation

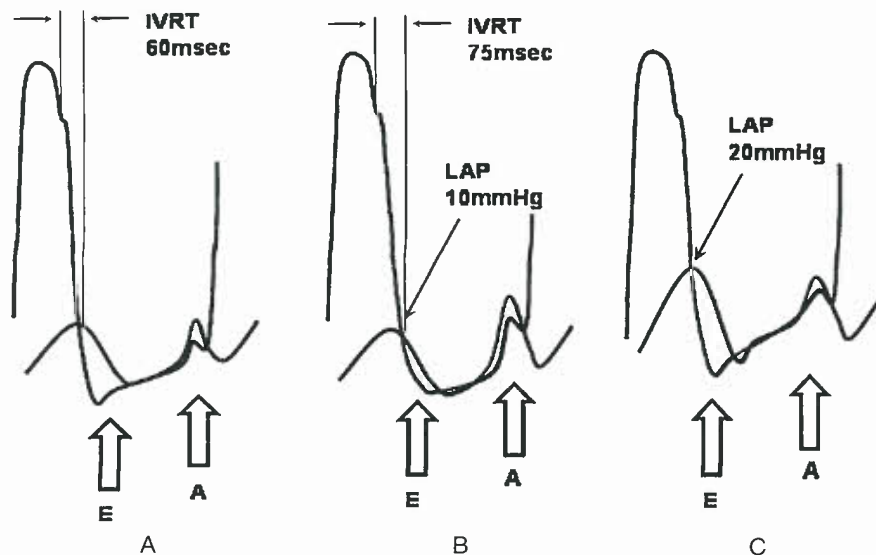
In the earliest stages of diastolic dysfunction, the rate of ventricular relaxation is impaired. Delayed LV relaxation results in a slower decline in LV pressure resulting in a diminished gradient between the left atrium and LV in early diastole and a diminished mitral E-wave velocity. The slow relaxation also results in a lengthening of the IVRT and E-wave deceleration time. As a result, there is a compensatory increase in late filling during atrial systole, producing an augmented mitral A wave. These changes occur when ventricular compliance and LA and LV end-diastolic pressures are at near normal levels.

In the pulmonary veins, delayed relaxation results in reduced early diastolic flow, resulting in an augmented systolic S wave and a diminished D wave. This results in an increased S/D-wave velocity ratio. This index should be interpreted with caution in children as many normal children have higher S than D waves in the pulmonary veins. As atrial pressures are near normal at this stage of dysfunction, atrial systolic flow reversal remains absent or small (Fig. 9.34). TDI of the lateral mitral annular velocities will demonstrate a decrease in the peak E' velocity, corresponding to decrease in early diastolic ventricular relaxation. The E'/A' velocity ratio will therefore be <1 in this setting (Fig. 9.35).

Stage II: Pseudonormal Diastolic Dysfunction

Diastolic function indices in stage II dysfunction are summarized in Figure 9.35. As diastolic dysfunction advances,

Figure 9.34. Physiologic left ventricle (LV)/left atrial pressure relation with normal diastolic function and two stages of diastolic dysfunction. A: Normal ventricular relation produces a normal rise in the pressure gradient between the left atrium and LV at the conclusion of isovolumic relaxation. This results in a normal mitral E wave. Normal atrial contraction at end-diastole produces a normal mitral A wave. B: Impaired relaxation prolongs the IVRT and results in a diminished pressure gradient between the left atrium and LV in early diastole. This results in a diminished mitral E wave, with a compensatory increase in the mitral A wave during atrial systole. C: Rising left atrial pressure restores the early diastolic gradient between the left atrium and LV, resulting in a pseudonormal E-wave velocity. LAP, left atrial pressure.



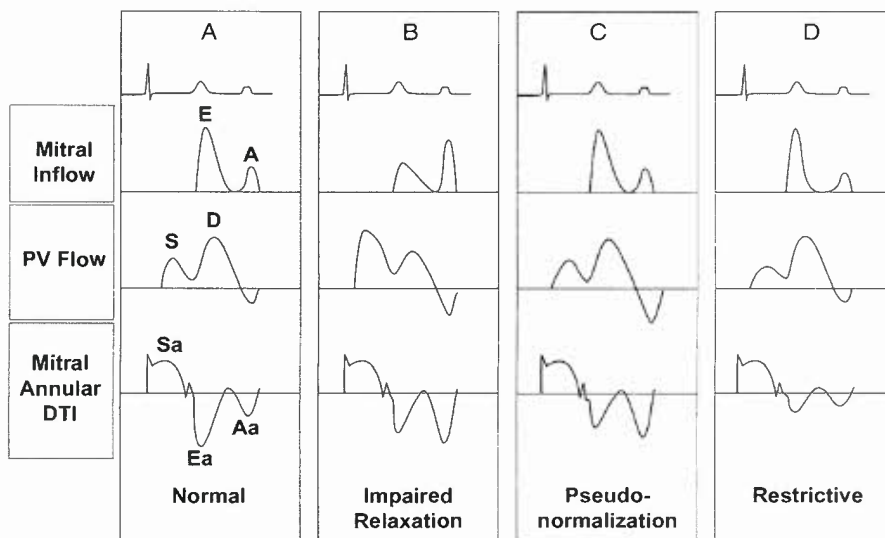


Figure 9.35. Progression from normal diastolic function (A) to early (B,C) and advanced (D) phases of diastolic dysfunction with demonstration of the associated changes in the mitral inflow, pulmonary venous flow, and mitral annular Doppler tissue imaging indices. TDI, Tissue Doppler Imaging; PV, pulmonary venous.

ventricular compliance progressively diminishes along with continued abnormalities in ventricular relaxation. Ventricular filling becomes dependent on a compensatory increase in LA pressure. The increase in LA pressure has several effects: an increase in the left atrium to LV pressure gradient in early diastole produces an increase in the mitral E-wave velocity and a shortening of the IVRT by producing early mitral valve opening. Progressive decreases in ventricular compliance result in shortening of the E-wave deceleration time. These changes lead to so-called pseudonormalization of the mitral inflow Doppler pattern. Although tissue Doppler, deformation imaging, and color M-mode help differentiate pseudonormal from normal, inspection of the M-mode, 2-D echo, and mitral inflow Doppler themselves can be useful to differentiate normal from pseudonormal. A heart with vigorous left and right ventricular contraction, normal wall thickness, and normal left and right ventricular and atrial sizes is most likely normal. A normal-sized but “hypercontractile” appearing left atrium, with increased annular excursion toward the pulmonary veins suggests reduced early diastolic LV filling and impaired ventricular relaxation. Likewise, in pseudonormalization, although the E/A ratio appears normal, the E wave is often higher than normal (due to the elevated atrial pressure), and higher than the LV outflow velocity. Finally, the Valsalva maneuver that impairs LA filling, thereby reducing the E wave velocity, can be used to unmask delayed relaxation when a pseudonormal pattern is present.

The pulmonary venous flow profile features a decrement in the magnitude of the S wave and an increase in the D wave, resulting in a diminished S-/D-wave velocity ratio. The pulmonary venous A-wave velocity and duration will increase as ventricular compliance worsens. In adult studies, pulmonary venous A-wave velocities of >35 cm/s or pulmonary venous A-wave durations that exceed the mitral A-wave duration by ≥ 30 ms have been reported to distinguish normal mitral inflow profiles from pseudonormal mitral inflow profiles (61,108). In the pediatric population, the difference between pulmonary venous A-wave duration and mitral A-wave duration can identify children with elevated LV filling pressures. However, these methods are adequately predictive only when the LV end-diastolic pressures are >18 mm Hg (62).

The pattern of mitral annular velocities remains largely unchanged in the setting of pseudonormal dysfunction. Abnormal relaxation will again result in a diminished E'

velocity and an E'/A' velocity ratio of <1 . Thus, TDI can be useful to distinguish normal from pseudonormal mitral valve inflow profiles (69,109). This is particularly true when obtaining technically adequate pulmonary venous A-wave profiles on transthoracic echocardiography proves difficult, or when LA pressure is modestly elevated. An additional index of diastolic function that has been correlated to elevations in ventricular filling pressures is the ratio of transmitral E wave to lateral mitral annular velocity (or the average of the lateral and septal velocities)—the E/E' ratio. This ratio was found to correlate with pulmonary capillary wedge pressures in the presence of delayed relaxation (110,111). However, in one study, the E/E' ratio did not successfully predict elevated pulmonary capillary wedge pressures in adults with decompensated advanced heart failure (112). In light of these findings, further validation is required in children to assess the usefulness of the E/E' ratio in specific conditions. The relation between the onset of mitral filling to the onset of mitral annular tissue motion can also be used to assess LA pressures and differentiate pseudonormal from normal. In the normal heart, there is vigorous relaxation with suction of blood early in diastole. Therefore, the E' wave will appear slightly earlier or simultaneously with the mitral E inflow. In the presence of impaired ventricular relaxation and with increased atrial pressure driving filling, the E wave will precede the tissue E' wave.

Stage III Diastolic Dysfunction: Restrictive Physiology

As diastolic dysfunction worsens, a restrictive pattern emerges. The changes on Doppler parameters are summarized in Figure 9.35. LA pressure and LV stiffness are very high. The increase in LA pressure results in rapid inflow of blood into the LV during early diastole, producing a tall E wave. However, low LV compliance causes premature termination of early ventricular filling with narrowing of the E wave and further shortening of the E-wave deceleration. Likewise, due to the low compliance, filling in late diastole is reduced resulting in a small A wave. Transmitral Doppler findings therefore feature an increased E-/A-wave ratio, typically >2 , and further shortening of the E-wave deceleration time, which is typically <150 ms in adult studies (108) and shorter still in children. Of note, severe restrictive physiology results in a rapid rise in intraventricular pressures during diastolic filling, which will occasionally produce diastolic mitral regurgitation, especially

when the AV conduction delay is prolonged. These findings can be appreciated on color flow-Doppler imaging (113,114).

In the pulmonary veins, there is further worsening of the trend seen in pseudonormal dysfunction, with further decreases in the fraction of systolic pulmonary venous flow and further increases in the diastolic fraction, resulting in further reduction in the S-/D-wave velocity ratio. The magnitude and duration of the atrial systolic reversal frequently becomes quite pronounced.

TDI in restrictive physiology will demonstrate decreased E' velocities (58,109). Overall, the magnitude of annular velocities—both E' and A' waves—is low, given the combined effects of severely decreased relaxation and compliance. The E/E' ratio will be higher than in preceding stages of dysfunction.

A further, more severe stage of restrictive physiology is proposed in the adult literature (stage 4). This stage is characterized by similar or worse parameters than stage 3, but a negative response to the Valsalva maneuver, indicating irreversible disease.

Difficulties in Distinguishing Normal from Abnormal Diastolic Function in Children

Throughout this section we have discussed differences between adults and children and difficulties, especially in children, in interpreting diastolic function. Patterns and values considered abnormal in adults are often found in normal children. In addition, parameters are affected by age, heart size, heart rate, variable loading conditions, the heterogeneity of congenital heart disease, and whether the disease process is acute or chronic, compensated, or decompensated. Although normal pediatric reference data are available, there is a wide range of normal values reported in the literature. This pertains both to Doppler-flow parameters, TDI parameters, and deformation parameters (62,64). Furthermore, large areas of overlap in many indices have been found between normal children and those with increased filling pressures (62). Lack of validation of adult paradigms and correlation of abnormal echo-diastolic parameters compared with invasive reference methods in various diseases are additional limitations.

Constrictive Pericarditis

Constrictive pericarditis, although uncommon in children, can manifest very similar diastolic findings to restrictive physiology. The transmitral flow pattern can be very similar and feature an increased E-/A-wave ratio and a shortened E-wave deceleration time. Several findings can help distinguish constrictive pericarditis from restrictive cardiomyopathy. In constrictive pericarditis, simultaneous respirometry will reveal increased variation in the mitral valve E-wave velocities (>25%) and augmentation of pulmonary venous flows during respiration, that are not seen with restrictive physiology (115). In addition, Doppler assessment of the hepatic venous flow will show increased atrial systolic flow reversal during expiration with constriction and during inspiration with restrictive physiology (116). TDI in constrictive pericarditis will show a normal E' velocity in constriction, where the myocardium is relatively normal, compared with a low E' velocity in the diseased muscle of restrictive physiology (109). It is important to remember that in constrictive pericarditis, there may be a normal E/E' ratio despite elevated filling pressures due to the normal E' velocity (117). It should also be noted that the aforementioned findings have not been validated in pediatric studies of constrictive and restrictive physiology.

Assessment of Diastolic Function During Exercise

The ability of the heart to increase its relaxation and suction effect in response to the increased cardiac output during exercise, at a time when diastole is significantly shortened, is

a key component of cardiac physiology. Therefore, assessment of diastolic function and diastolic reserve during the provocative physiology of exercise may be valuable (118). In response to exercise, untwisting of the heart is augmented allowing rapid filling in a shorter time period (96). This augmentation is closely linked to increased systolic twisting demonstrated by speckle tracking (97,119). Although multiple diastolic parameters can be assessed, the E/E' ratio is commonly used. Abnormal hearts will demonstrate relative worsening of relaxation with decreased E' velocities and an increased E/E' ratio. Studies in children are limited.

Doppler Assessment of Right Ventricular Diastolic Function

Diastolic dysfunction of the RV (either in a systemic or pulmonary position or as a single ventricle) can also be assessed by Doppler techniques. However, it is less clear what specific findings are representative of normal baseline ventricular diastolic function in these instances. There has been work describing diastolic dysfunction, for example, in the single ventricle (100,111), but it is likely that diastolic dysfunction will need to be stratified for severity within a specific diagnosis. Moreover, variations of flow patterns with respiration are prevalent on the right side of the heart; therefore, diastolic findings will need interpretation in view of their phase of respiration.

Diastolic function of the RV can be assessed by assessment of transtricuspid Doppler flow patterns, TDI of the lateral tricuspid annulus, and assessment of the systemic venous inflow. Unlike the LV, however, in which echocardiographic diastolic indices have been validated in large adult populations, assessment of RV diastolic dysfunction in children has historically been confined to assessment in several fairly heterogeneous circumstances such as, postoperative TOF (120–122), systemic RVs, and single RV physiology (123,124). As such, normal diastolic function is difficult to define in these circumstances, and diastolic findings are often compared within a specific population against other clinical parameters. In addition, the Doppler profile of tricuspid inflow is often less sharp than that of mitral inflow, making precise and reproducible measurements more difficult. Nonetheless, published normal values for both tricuspid inflow Doppler flow profiles (65,125,126) and tricuspid annular velocities (65,127) exist for the pediatric population, and can be used to evaluate RV diastolic function in the same way as one would assess diastolic function of the LV. Both systemic venous and transtricuspid flow can vary significantly during respiration (125); diastolic assessments of the RV and systemic venous inflow should therefore be standardized for phase of respiration using simultaneous respirometry. Respirometry can be particularly helpful in assessing systemic venous flow patterns, as these can often be important in distinguishing restrictive diastolic physiology from a more constrictive pattern as described above. Pulsed-wave Doppler assessment of flow in the proximal pulmonary artery is also useful when RV diastolic dysfunction is suspected, as antegrade flow in the main pulmonary artery during atrial systole that occurs in both inspiration and expiration, has been associated with restrictive RV physiology in postoperative TOF (Fig. 9.36) (121,127). RA dilation in the absence of tricuspid regurgitation could be considered as an important parameter for RV diastolic dysfunction but in contrast to the left atrium, no good normal values are present for the pediatric age range and no good method has been developed for measuring RA volumes. RA area can be measured. Flow in the hepatic veins should also be recorded. Significant flow reversal in the hepatic veins during atrial contraction is a sign of elevated RV end-diastolic pressure but no specific cutoff values have been provided (Fig. 9.37).

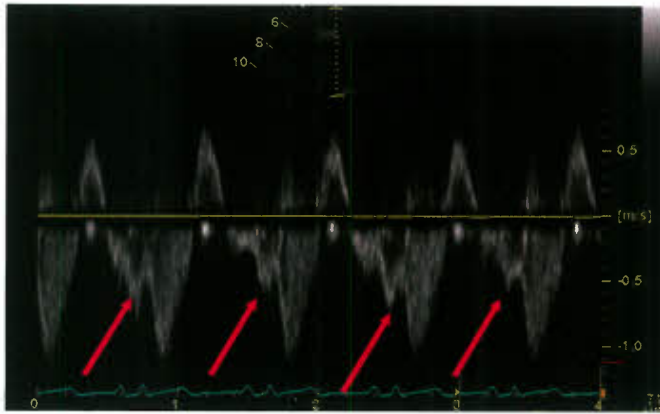


Figure 9.36. Restrictive RV physiology in a patient after tetralogy of Fallot repair. Pulsed-wave Doppler tracing obtained at the level of the pulmonary valve. This patient had severe pulmonary regurgitation as indicated by the short pressure half-time and only early diastolic flow reversal. During atrial contraction antegrade flow across the pulmonary valve can be recorded (arrows). This suggests that RV end-diastolic pressure during atrial contraction exceeds pulmonary diastolic pressure, which is consistent with restrictive RV physiology.

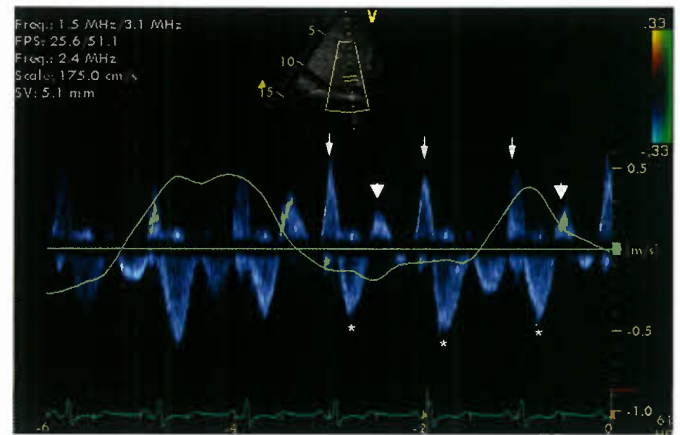


Figure 9.37. Pulsed Doppler sampled in the hepatic vein of a patient with hypertrophic cardiomyopathy. Respirometry is seen in green. Findings are consistent with restrictive features with systolic antegrade flow (asterisks), retrograde flow in early diastole (arrowheads), and marked flow reversal after atrial contraction (arrows). In this patient these abnormalities are present during inspiration and expiration.

EVALUATION OF VENTRICULAR SYNCHRONY

Normal cardiac activation and contraction is rapid and homogeneous with coordinated contraction of the atria to fill the ventricles at end-diastole, homogenous contraction between the different segments of the systemic ventricle, and the activation of the left and RVs within 50 to 80 ms (129). Dyssynchrony refers to the incoordinate or heterogeneous activation and contraction of the cardiac chambers, especially the ventricles. Electrical dyssynchrony refers to slow and inhomogeneous activation of the ventricles and is most commonly measured using the QRS duration from the surface electrocardiogram. Mechanical dyssynchrony refers to the heterogeneous contraction of the cardiac chambers and is most commonly and easily measured using echocardiography. With the increasing evidence and recognition that ventricular dyssynchrony is a risk factor for ventricular dysfunction and increased morbidity and mortality in patients with heart failure (130,131), and with the advent of cardiac resynchronization therapy (CRT) using biventricular or multisite pacing to treat ventricular dyssynchrony (132,133), it has become important to diagnose dyssynchrony, identify likely responders to CRT, and to optimize pacemaker settings after implantation (134,135). Some studies have suggested that echo may be useful to guide the optimal site of lead placement during pacemaker implantation for CRT (136,137). Three levels of dyssynchrony are generally identified: (a) atrioventricular dyssynchrony—the timing between atrial systole and ventricular diastole, (b) interventricular dyssynchrony—incoordinate contraction between the left and RVs, and (c) intraventricular dyssynchrony—incoordinate contraction between different segments of the LV or RV.

QRS duration is the most widely accepted criteria to diagnose ventricular dyssynchrony for the purposes of predicting response to CRT (138,139). However, approximately one-third of adult patients do not respond to CRT based on standard criteria using QRS duration (140). One assumption was that these patients may not have mechanical dyssynchrony and therefore did not respond to CRT or conversely that ECG might not be sensitive enough to detect the presence of regional abnormalities arising from distal conduction disease not reflected in the QRS duration. Therefore, echo criteria to determine mechanical dyssynchrony, especially LV intraventricular dyssynchrony,

have been investigated in the hope of better identifying patients who may respond to CRT. Early trials based on single-center experiences and largely based on TDI of mechanical dyssynchrony showed that echo could identify patients likely to respond to CRT better than QRS duration alone (141–145). Unfortunately, this experience was not confirmed in a large prospective randomized multicenter trial (PROSPECT) using either clinical improvement or a decrease in ventricular volumes (reverse remodeling) as outcomes (146). Likewise, echo criteria of mechanical dyssynchrony failed to predict response to CRT in heart failure patients with a narrow QRS duration using an increase in peak oxygen consumption during exercise as the outcome (147). These trials have left the field with much uncertainty as to the role of echo in assessment of dyssynchrony and in choosing candidates for CRT. Currently, echo criteria are not recommended to implement or withhold CRT from a patient (148). Nonetheless, many authors believe that mechanical dyssynchrony is an important component of ventricular dysfunction, that CRT addresses this phenomenon, and that echo holds the greatest potential to measure mechanical dyssynchrony given its high spatial and temporal resolution, its availability, and the ability for serial measurements, especially in patients with an implanted pacemaker, which is currently a relative contraindication to MRI (135,149,150). Some authors have advocated for using a more broad-based echocardiographic approach, assessing atrioventricular, intraventricular, and interventricular dyssynchrony as possible discrete mechanisms that may be present in different patients, thereby tailoring CRT to the underlying type of dyssynchrony (151). The question remains what is the best way to evaluate abnormal electromechanical coupling, measure mechanical dyssynchrony, and what is the ability of any given method to predict response to CRT? Currently there is no simple or single answer to these questions. The field continues to evolve, and multiple echo indices to measure mechanical dyssynchrony have been published. In children, answers are far more vague with limited data and there are no published values to predict response to CRT.

In the following section, we will summarize the main echo indices and modalities currently used to measure mechanical dyssynchrony. Many other dyssynchrony indices have been investigated but are beyond the scope of this text.

ECHOCARDIOGRAPHIC ASSESSMENT OF THE ATRIOVENTRICULAR DELAY

Assessment of the AV delay is most commonly assessed after CRT implantation when optimizing device settings. This assessment is not necessary in every patient (148). Although several methods are available, AV dyssynchrony is most easily measured using pulsed Doppler of the mitral inflow by the iterative method (visual assessment). Optimal filling occurs when the systemic inflow E and A waves are clearly identified and separated from one another. The end of the A wave should be aligned with the QRS complex and/or mitral valve click (148).

ASSESSMENT OF INTERVENTRICULAR DYSSYNCHRONY

The interventricular delay is measured as the delay between the onset of LV and RV ejection (Fig. 9.38). This is most easily measured from the onset of ECG Q wave to the onset of pulsed Doppler flow in the LV and RV outflow tracts or proximal aorta and pulmonary artery (148). Although this index

has not traditionally been used to predict response to CRT, it is one of the most reliably measured indices, may identify adults with increased response to CRT, and may be important in children with congenital heart disease (152,153).

ASSESSMENT OF INTRAVENTRICULAR DYSSYNCHRONY

To date, echo assessment of mechanical dyssynchrony has largely focused on assessment of intraventricular dyssynchrony as this parameter is thought to be most predictive of CRT in adults.

M-mode

The most common M-mode dyssynchrony index is the septal-posterior wall delay measured from peak excursion of the septum to peak excursion of the posterior wall. A delay of more than 130 ms is considered abnormal in adults (154). Assessment of a very limited segment of the heart, difficulties in identifying the peak excursion when wall motion is flat as is commonly seen in ventricular dysfunction, and motion arising from tethering of the interrogated segment to adjacent segments limits the utility of this index. In the presence of left bundle branch block, a sharp thinning-thickening (or lengthening-shortening) motion of the septum in the preejection period (termed the “septal flash”), which can be demonstrated by M-mode or by tissue-Doppler imaging, has been found by one group to have a high specificity for response to CRT in adults as judged by reverse LV remodeling (151).

Tissue Doppler Imaging

To date, TDI, usually by color TDI with off-line analysis, has been the most common method to assess mechanical intraventricular dyssynchrony. TDI indices can be measured at any point of the ventricular myocardium to give information on regional wall motion. Because of this feature, TDI indices are not only useful in the assessment of ventricular function, but may be valuable in assessing ventricular dyssynchrony and response to CRT (155). Multiple TDI dyssynchrony indices based on TDI have been published. These generally measure the time to onset or peak systolic motion in a varying number of LV segments using the QRS complex as a reference. One of the most commonly used indices calculates the time-to-peak systolic motion (during ejection) in 12 LV basal and mid segments, assessed from the apical four-, three-, and two-chamber views, and expresses the heterogeneity of longitudinal motion as a standard deviation (Fig. 9.39) (156,157). Other indices measure the difference in time-to-peak systolic longitudinal motion between 2, 4, or 12 LV segments (143,148). However, indices based on the measurement of a single-tissue velocity point, which is often variable and difficult to identify, tend to have poor intra- and interobserver reliability (146). A promising approach integrates multiple points along the LV velocity curve essentially analyzing the motion of the wall throughout the systole. The relative delay between the two segments of interest (the shift in curves) can then be calculated using cross-correlation computation (158). This computation is not yet routinely available on common commercial ultrasound analysis platforms. The major advantage of TDI for mechanical dyssynchrony analysis is the ability to easily and quickly obtain data from multiple segments simultaneously (in the same cardiac cycle) at high frame rates. Major disadvantages include difficulties in identifying peak systolic motion when multiple

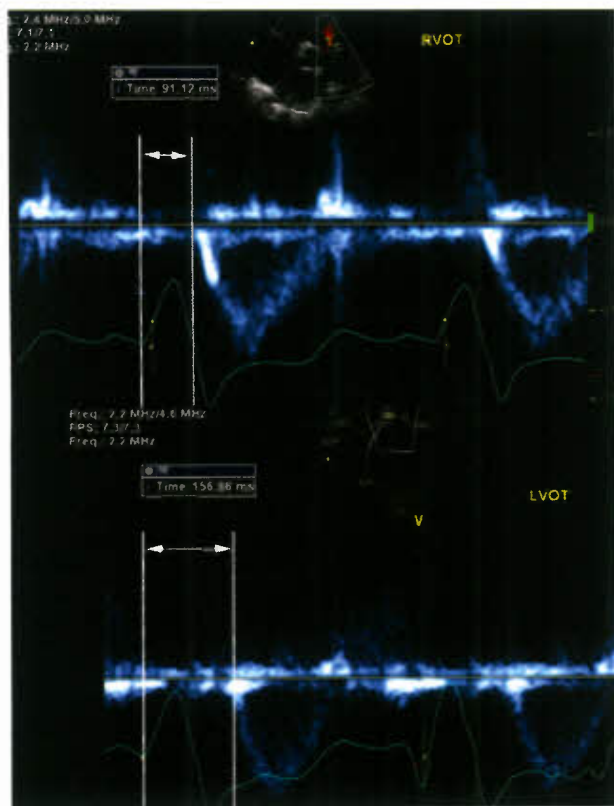


Figure 9.38. The interventricular delay represents the delay in ejection between the left ventricle (LV) and the right ventricle (RV). This is calculated as the time difference between the onset on QRS complex as the reference (*first white line*) and the onset of pulmonary (RVOT, *top panel*) and aortic (LVOT, *bottom panel*) ejection, respectively. In this example there is a 66 msec delay between onset of ejection of the RV and subsequently the LV (*second white line*), which is prolonged. It is important to acquire the samples at the same heart rate. In this example there is a small difference in heart rate between the two images (<10%). The measurement cannot be used when heart rate is significantly different at time of sampling.

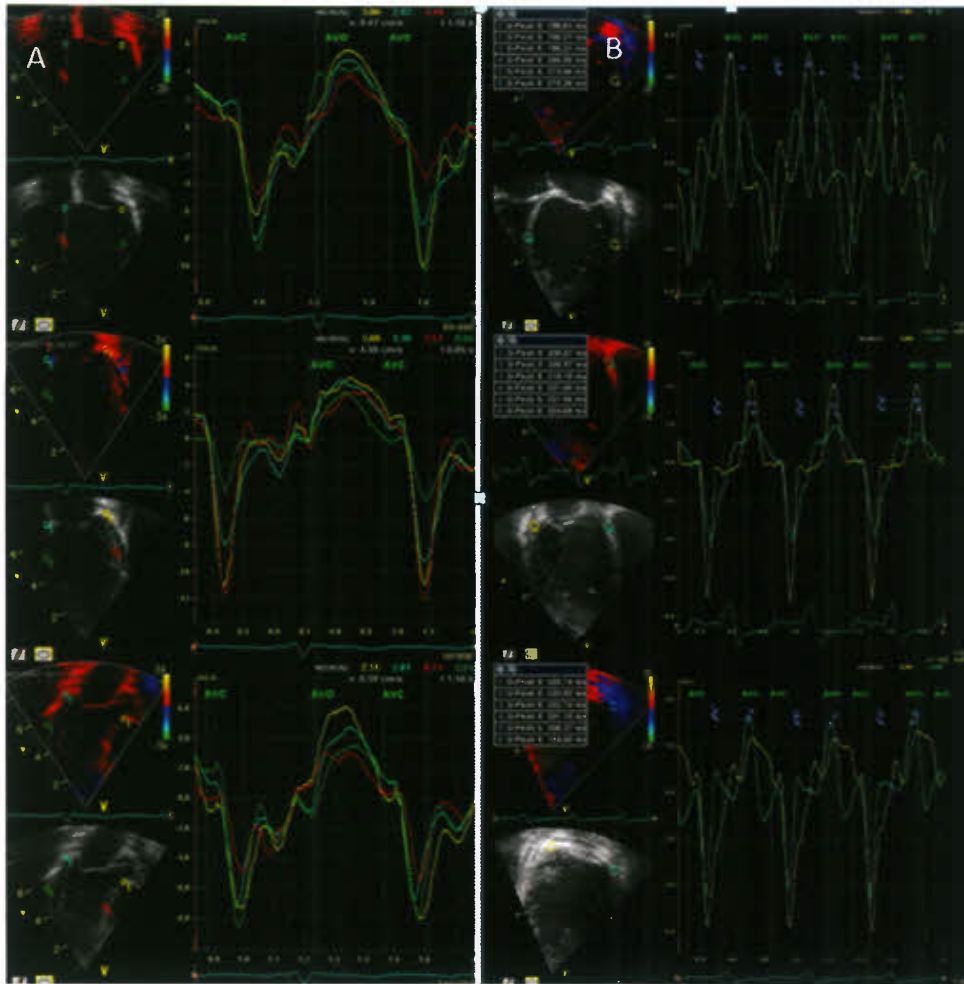


Figure 9.39. Assessment of left ventricular (LV) intraventricular dyssynchrony using tissue Doppler to measure the left ventricular dyssynchrony (Yu) index. Aortic valve opening and closing are marked by the *green lines* to delineate ventricular ejection. In **panel A** 12 tissue Doppler curves are obtained from the basal and mid regions from apical 4 (top), 2 (middle), and 3 (bottom) chamber views. The time to peak velocity is measured using the onset of the QRS complex as a reference point. The standard deviation of the time to peak velocity during ejection is measured as the dyssynchrony index. In this normal example, tissue velocities reach their peak nearly simultaneously so that the standard deviation of time to peak velocity curves is low. In contrast, **panel B** shows curves from a patient with dilated cardiomyopathy where different segments reach peak velocity at different times. This would increase the standard deviation of time to peak velocity and indicate LV intraventricular dyssynchrony. For the sake of clarity, only 6 of the 12 segments sampled are shown.

peaks are present or when a clear peak is not visible. Wall motion profiles may differ between segments complicating analysis. These factors lead to poor reproducibility. Moreover, motion of the interrogated segment may be passive due to translation of the entire heart or due to tethering of a noncontractile segment to adjacent segments. The importance of tethering in children, who generally do not have discrete regions of infarcted myocardium except in very specific circumstances, is unknown.

Deformation Imaging

Because of the poor results predicting response to CRT using tissue Doppler techniques and because of its high intra- and interobserver reliability, echo measurement of dyssynchrony using deformation imaging is increasing (159,160). One method measures the delay between time-to-peak radial strain between the septum and posterior wall (similar to the M-mode technique) at mid-ventricular level with a 130 ms cutoff quoted in the adult literature (Fig. 9.40) (161). Adding the radial septal to posterior wall delay to longitudinal assessment by TDI may increase the ability of echo to predict response to CRT (162). Other authors have used the delay between time-to-peak longitudinal strain in the septum and lateral wall. By measuring active contraction, strain imaging overcomes the problem of passive translational motion and tethering. However, the utility of deformation imaging to predict the response to CRT in large populations and in multicenter setting needs validation. Other disadvantages include a lower frame rate

than tissue Doppler (for speckle tracking), lack of standardization for which segments to measure and as for TDI measurements, how large the region of interest should be (163), and relatively poor reproducibility. Despite the theoretical benefits of deformation imaging, our practical experience has been that it is difficult to obtain reliable strain curves for dyssynchrony measurements in a substantial proportion of children with ventricular dysfunction.

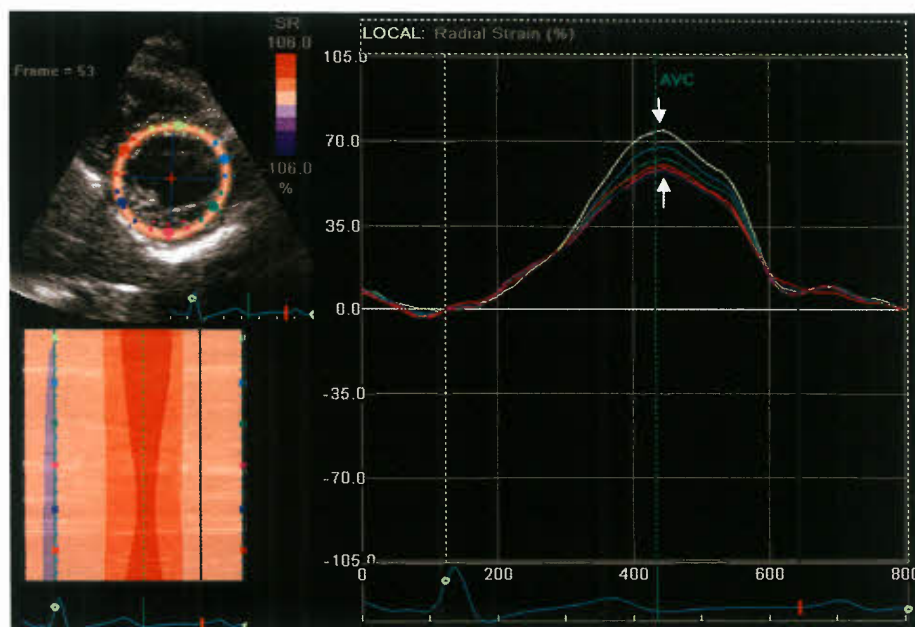
Three-Dimensional Echocardiography

LV dyssynchrony can be readily measured by 3-D echo in adults and children (164,165). The full LV 3-D volume is segmented by postprocessing software into subvolumes around the LV central meridional axis. The standard deviation of time to minimal volume between 12 and 16 subvolumes is then used as a dyssynchrony index (Fig. 9.41). To account for different heart rates, the dyssynchrony index can be expressed as a percentage of the cardiac cycle length. Disadvantages of 3-D echo are the low frame rates and the indirect assessment of wall motion through assessment of volume change.

Assessment of Mechanical Dyssynchrony in Children

Dyssynchrony has been shown to be important in children and adolescents in a number of acquired and congenital conditions. Data on RV and LV dyssynchrony by various modalities

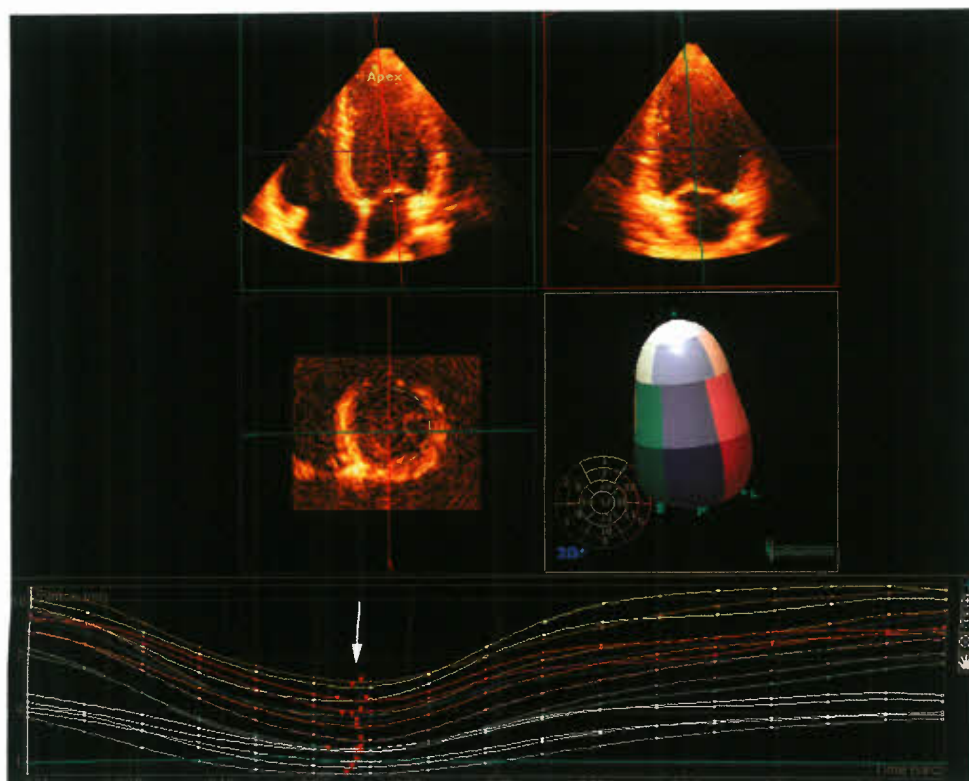
Figure 9.40. Radial strain curves obtained in six segments from a mid parasternal short-axis cut. Note that peak systolic strain occurs nearly simultaneously in the six measured segments.



derived from normal populations are emerging but are still limited (166–168). More importantly, to date, there are no data pertaining to mechanical dyssynchrony cut-points that may predict response to CRT in children. Likewise, the largest published CRT experience in children has not described mechanical dyssynchrony (169–171). Most studies have largely been restricted to investigating the prevalence of dyssynchrony in various conditions and investigating its impact on cardiac function, exercise capacity, and clinical outcomes. In children with dilated cardiomyopathy, and in normal controls, the degree of radial deformation (which is related to contractility) was found

to be related to the time it took to develop peak deformation, thereby providing a direct link between timing of contraction and regional function (172). Indeed, systolic dyssynchrony measured by TDI and by strain is prevalent in children with dilated cardiomyopathy, even when the QRS duration is narrow (173,174). Mechanical dyssynchrony was not significantly linked to death or transplant in a relatively small study using TDI assessment (175), although by 3-D assessment, it has been linked to LV EF (165). Diastolic dyssynchrony has also been found to be prevalent in this population and is possibly linked to increased risk for death or transplant (176).

Figure 9.41. Three-dimensional synchrony. Three-dimensional left ventricular (LV) full volume. After tracing the endocardial borders, a LV volume is generated and tracked over the cardiac cycle. The post-processing software generates 17 subvolumes around the meridional axis. The change in each subvolume over the cardiac cycle is represented in the curves at the bottom of the figure. In this example, all subvolumes reach minimal volume at approximately the same time (*arrow*) depicting synchronous LV contraction.



Dyssynchrony, demonstrated by echo, is also important in children with congenital heart disease. RV wall motion abnormalities are commonly found after repair of TOF and in the systemic RV after atrial switch procedures where pulsed tissue-Doppler has demonstrated opposing longitudinal motion in the RV free wall (177,178). These abnormalities were related to electrical activation (QRS duration) and risk for arrhythmia. Indeed, after surgical repair of TOF, where right bundle branch block is common, electromechanical interactions seem to be important, especially when involving the infundibulum as shown by pulsed tissue Doppler, M-mode, and deformation imaging (179,180). These wall abnormalities may also impact TOF patients' responses to exercise. During exercise, even asymptomatic TOF patients develop both RV and LV dyssynchrony as shown by TDI (181). Likewise an increased interventricular delay has been linked with decreased exercise capacity and increased risk for ventricular arrhythmias during exercise (153). Wall motion abnormalities impacting ventricular function have also been found in the LV in TOF patients, where an increased delay between time-to-peak deformation between the lateral wall and septum has been associated with decreased global LV function (178). LV dyssynchrony and dysfunction in congenital disease affecting the RV may stem from adverse ventricular-ventricular interactions (182–185) as LV dyssynchrony was more prevalent in the presence of abnormal septal motion, more pulmonary regurgitation, larger RV volumes, and right bundle branch block (182,185). RV mechanical dyssynchrony has been demonstrated using vector velocity imaging, a form of deformation imaging, in children with hypoplastic left heart syndrome (186). The amount of dyssynchrony differed between different stages of palliation. Whether this dyssynchrony constitutes a marker for later development of ventricular dysfunction in this population, is unknown. However, in the failing systemic RV, mechanical dyssynchrony may be an important component of the response to CRT (187). Acutely after surgery, biventricular pacing is likely superior to single-site pacing in terms of wall motion and hemodynamics, as assessed by TDI (155). Indeed, increased mechanical dyssynchrony by tissue Doppler and strain imaging may be associated with decreased cardiac output after congenital heart disease surgery, and this may respond to biventricular pacing.

CORONARY ARTERY PHYSIOLOGY

Coronary artery physiology and pathology play an important role in congenital conditions, and assessment of coronary artery physiology is gaining an increasingly important role for the pediatric and congenital echocardiographer. In children, coronary artery abnormalities are predominantly related to (a) an abnormal origin or course (e.g., left coronary artery arising from the right facing sinus), (b) inflammatory diseases (e.g., Kawasaki disease), (c) problems related to surgical reimplantation (e.g., repair of anomalous left coronary artery from the pulmonary artery, arterial switch procedure, pulmonary autograft (Ross) procedure), (d) early atherosclerosis, (e) reduced flow related to high end-diastolic pressure (e.g., LV outflow tract obstruction, cardiomyopathy), and (f) compression of the coronary arteries (e.g., myocardial bridging in hypertrophic cardiomyopathy). The specific etiology in question will influence the type and extent of imaging performed. Two-dimensional and color flow echocardiography are useful for imaging coronary artery origins, course, aneurysms, and dilatation, but are less useful for detecting coronary artery stenosis, aside from perhaps coronary ostial stenosis.

Coronary echocardiography or ultrasound can be divided into the following broad categories:

1. Direct imaging of the coronary arteries
2. Assessment of regional myocardial function at rest and during stress that may indicate perfusion abnormalities in specific myocardial territories
3. Vascular imaging to detect early atherosclerosis

In this section, we refer to general imaging of coronary artery physiology. Specific abnormalities are covered in the respective chapters.

Coronary physiology can be assessed by studying peripheral arterial structure and function or by direct interrogation of the coronary arteries themselves.

The peripheral arteries serve as surrogate windows for the study of coronary artery physiology. Carotid intima-medial thickness is a precursor of atherosclerosis (188,189) and can be measured by high-frequency ultrasound (15 MHz).

Peripheral arterial endothelial function is assessed by brachial artery flow-mediated dilation. This technique involves inflating a sphygmomanometer cuff placed on the forearm or upper arm to a pressure of 100 to 150 mm Hg above the systolic pressure for 4 to 5 minutes. The brachial artery diameter immediately after cuff deflation is compared with the baseline diameter before inflation. The technique produces very subtle changes and must be performed in a highly controlled environment free of extraneous influences. Both carotid intima-medial thickness and brachial artery flow-mediated dilation have been used successfully to show impairment of vascular function, and therefore, presumably coronary arterial function in children with insulin-dependent diabetes mellitus (190,191). Vascular function can also be assessed by applanation tonometry, a nonultrasound technique that necessitates noninvasive capture of a large artery waveform using high-fidelity transducers and from which cardiovascular risk can be assessed (192).

Direct Assessment of the Coronary Arteries

Two-dimensional and color-flow imaging of the coronary arteries can show anomalous origins, abnormal branching patterns and courses of the coronary arteries, coronary aneurysms and/ or dilation, and coronary fistulae. Direct assessment of the coronary arteries is still limited and a coronary abnormality should be considered when other signs of myocardial ischemia or infarction are present, such as global or regional ventricular dysfunction, ventricular and atrial enlargement, the presence of mitral regurgitation, echogenic papillary muscles or myocardium, and flow reversal in the left anterior descending artery by color flow Doppler in anomalous origin of the left coronary artery from the pulmonary artery.

Direct functional assessment of the coronary arteries largely rests on Doppler assessment of coronary flow although it is not routinely performed in most pediatric clinical institutions. Nonetheless, Doppler flow velocities have been found to correlate well with invasive measurements by Doppler guide wire in adults and in pediatric studies, albeit in a small number of subjects (193–195). Normal values for Doppler flow velocities at rest in the left coronary artery have been published in a cohort of over 300 children (196), and have been studied in the branch coronary arteries (197). Velocities, which ranged up to 60 cm/s in young children, decreased with age and increased with heart rate.

Coronary flow reserve reflects the increase in coronary flow in response to stimuli such as pharmacologic agents

(e.g., adenosine triphosphate, and dipyridamole) and exercise. It is calculated as the ratio of the peak (or mean) diastolic velocity after hyperemic stimulation to the baseline peak (or mean) diastolic velocity and reflects the resistance of the coronary bed, its ability to maintain constant flow when myocardial perfusion pressure changes (autoregulation), and the ability to augment blood flow in response to stress (198). Coronary flow reserve is affected not only by stenosis or compression of the proximal coronary arteries, such as in Kawasaki disease (195,199) or hypertrophic cardiomyopathy (200), but also by abnormalities in the distal coronary microvasculature such as in dilated cardiomyopathy, where decreased coronary flow reserve by Doppler echo has been linked to worse outcome (201,202). More reassuringly, normal coronary flow reserve has been found in a small study of children after arterial switch operation for transposition of the great arteries, although a number of children with variant left coronary anomaly demonstrated abnormal coronary flow reserve by cardiac positron emission tomographic imaging in response to adenosine (203). These normal findings in most children after the arterial switch operation mirror an invasive study using a Doppler guidewire and (204) may predict lower risk for atherosclerosis in the following decade (205). On the other hand, past publications have found that while coronary artery anatomy is not a determinant of outcome after the arterial switch operation, a portion of children may have silent ischemia without echocardiographic abnormalities at rest (206). Whether these children will demonstrate abnormal coronary flow reserve is unknown. Echo Doppler assessment of coronary flow reserve in the right coronary artery has also been shown to be feasible in an adult population, using a coronary Doppler flow wire as a reference (203).

Given the important limitations of echocardiography in detecting coronary anomalies, especially those related to coronary stenosis and perfusion abnormalities, there should be a low threshold to proceed to other imaging modalities when there is a clinical suspicion of coronary stenosis or a perfusion abnormality. Alternative imaging modalities for this indication include computerized tomography, cardiac MRI, nuclear imaging, and especially coronary angiography, which remains the reference standard.

Coronary Perfusion

One of the major uses of stress echocardiography is in the assessment of coronary perfusion (204). Myocardial ischemia develops when myocardial oxygen demand exceeds supply. Ischemia can manifest by angina (a relatively late manifestation evident by patient history), a metabolic abnormality (a relatively early manifestation evident by positron emission tomography), or several intermediate manifestations such as ST-segment depression on the electrocardiogram or poor radioisotope perfusion on a thallium scan. On the echocardiogram, ischemia is manifested by a new or worsening regional wall motion abnormality. In children, stress echocardiography for coronary assessment can be useful for a variety of indications including Kawasaki disease, detection of coronary artery vasculopathy in the transplanted heart (205,206), and after the arterial switch operation. In children, although an abnormal DSE correlates relatively well with angiographic abnormalities in the coronary vessels (206), one of the main problems is the low pretest probability of an abnormality resulting in a low positive predictive value of the exam. It is currently our institutional practice to limit routine dobutamine stress echocardiography for detection of transplant vasculopathy to patients who are more than 3 years after transplant and who have risk factors for rejection or previous rejection.

REFERENCES

- Lang R, Bierig M, Devereux R, et al. Recommendations for chamber quantification. *Eur J Echocardiogr* 2006;7:79–108.
- Rudski LG, Lai WW, Afilalo J, et al. Guidelines for the echocardiographic assessment of the right heart in adults: a report from the American Society of Echocardiography endorsed by the European Association of Echocardiography, a registered branch of the European Society of Cardiology, and the Canadian Society of Echocardiography. *J Am Soc Echocardiogr* 2010;23:685–713; quiz 786–688.
- Lopez L, Colan SD, Frommelt PC, et al. Recommendations for quantification methods during the performance of a pediatric echocardiogram: a report from the Pediatric Measurements Writing Group of the American Society of Echocardiography Pediatric and Congenital Heart Disease Council. *J Am Soc Echocardiogr* 2010;23:465–495; quiz 576–577.
- Sluysmans T, Colan SD. Theoretical and empirical derivation of cardiovascular allometric relationships in children. *J Appl Physiol* 2005;99:445–457.
- Petersen MD, Du W, Skeens ME, et al. Regression equations for calculation of z scores of cardiac structures in a large cohort of healthy infants, children, and adolescents: an echocardiographic study. *J Am Soc Echocardiogr* 2008;21:922–934.
- Daubeney PE, Blackstone EH, Weintraub RG, et al. Relationship of the dimension of cardiac structures to body size: an echocardiographic study in normal infants and children. *Cardiol Young* 1999;9:402–410.
- Lipshultz SE, Easley KA, Orav EJ, et al. Reliability of multicenter pediatric echocardiographic measurements of left ventricular structure and function: the prospective P(2)C(2) HIV study. *Circulation* 2001;104:310–316.
- Jenkins C, Brinknell K, Chan J, et al. Comparison of two- and three-dimensional echocardiography with sequential magnetic resonance imaging for evaluating left ventricular volume and ejection fraction over time in patients with healed myocardial infarction. *Am J Cardiol* 2007;99:300–306.
- Jacobs LD, Salgo IS, Goonewardena S, et al. Rapid online quantification of left ventricular volume from real-time three-dimensional echocardiographic data. *Europ Heart J* 2006;27:460–468.
- Mor-Avi V, Lang RM. Three-dimensional echocardiographic evaluation of the heart chambers: size, function, and mass. *Cardiol Clin* 2007;25:241–251.
- Muraru D, Badano LP, Piccoli G, et al. Validation of a novel automated border-detection algorithm for rapid and accurate quantitation of left ventricular volumes based on three-dimensional echocardiography. *Eur J Echocardiogr* 2010;11:359–368.
- Lu X, Xie M, Tomberlin D, et al. How accurately, reproducibly, and efficiently can we measure left ventricular indices using M-mode, 2-dimensional, and 3-dimensional echocardiography in children? *Am Heart J* 2008;155:946–953.
- Foster BJ, Mackie AS, Mitsnefes M, et al. A novel method of expressing left ventricular mass relative to body size in children. *Circulation* 2008;117:2769–2775.
- Khoury PR, Mitsnefes M, Daniels SR, et al. Age-specific reference intervals for indexed left ventricular mass in children. *J Am Soc Echocardiogr* 2009;22:709–714.
- Caiani EG, Corsi C, Sugeng L, et al. Improved quantification of left ventricular mass based on endocardial and epicardial surface detection with real time three dimensional echocardiography. *Heart* 2006;92:213–219.
- Mertens LL, Friedberg MK. Imaging the right ventricle-current state of the art. *Nat Rev Cardiol* 2010;7:551–563.
- Grewal J, Majdalany D, Syed I, et al. Three-dimensional echocardiographic assessment of right ventricular volume and function in adult patients with congenital heart disease: comparison with magnetic resonance imaging. *J Am Soc Echocardiogr* 2010;23:127–133.
- Khoo NS, Young A, Occhleshaw C, et al. Assessments of right ventricular volume and function using three-dimensional echocardiography in older children and adults with congenital heart disease: comparison with cardiac magnetic resonance imaging. *J Am Soc Echocardiogr* 2009;22:1279–1288.
- van der Zwaan HB, Helbing WA, McGhie JS, et al. Clinical value of real-time three-dimensional echocardiography for right ventricular quantification in congenital heart disease: validation with cardiac magnetic resonance imaging. *J Am Soc Echocardiogr* 2010;23:134–140.
- Soriano BD, Hoch M, Ithuralde A, et al. Matrix-array 3-dimensional echocardiographic assessment of volumes, mass, and ejection fraction in young pediatric patients with a functional single ventricle: a comparison study with cardiac magnetic resonance. *Circulation* 2008;117:1842–1848.
- Picard MH, Adams D, Bierig SM, et al. American Society of Echocardiography recommendations for quality echocardiography laboratory operations. *J Am Soc Echocardiogr* 2010;24:1–10.
- Colan SD, Parness IA, Spevak PJ, et al. Developmental modulation of myocardial mechanics: age- and growth-related alterations in afterload and contractility. *J Am Coll Cardiol* 1992;19:619–629.
- Rowland DG, Gutgesell HP. Noninvasive assessment of myocardial contractility, preload, and afterload in healthy newborn infants. *Am J Cardiol* 1995;75:818–821.

24. Colan SD, Borow KM, Neumann A. Left ventricular end-systolic wall stress-velocity of fiber shortening relation: a load-independent index of myocardial contractility. *J Am Coll Cardiol* 1984;4:715-724.
25. Kimball TR, Daniels SR, Khoury P, et al. Age-related variation in contractility estimate in patients less than or equal to 20 years of age. *Am J Cardiol* 1991;68:1383-1387.
26. Gentles TL, Colan SD. Wall stress misrepresents afterload in children and young adults with abnormal left ventricular geometry. *J Appl Physiol* 2002;92:1053-1057.
27. Lipshultz SE, Colan SD, Gelber RD, et al. Late cardiac effects of doxorubicin therapy for acute lymphoblastic leukemia in childhood. *N Engl J Med* 1991;324:808-815.
28. Lipshultz SE, Lipsitz SR, Sallan SE, et al. Chronic progressive cardiac dysfunction years after doxorubicin therapy for childhood acute lymphoblastic leukemia. *J Clin Oncol* 2005;23:2629-2636.
29. Tei C, Dujardin KS, Hodge DO, et al. Doppler echocardiographic index for assessment of global right ventricular function. *J Am Soc Echocardiogr* 1996;9:838-847.
30. Dujardin KS, Tei C, Yeo TC, et al. Prognostic value of a Doppler index combining systolic and diastolic performance in idiopathic dilated cardiomyopathy. *Am J Cardiol* 1998;82:1071-1076.
31. Tei C, Dujardin KS, Hodge DO, et al. Doppler index combining systolic and diastolic myocardial performance: clinical value in cardiac amyloidosis. *J Am Coll Cardiol* 1996;28:658-664.
32. Koopman LP, Slorach C, Manhiot C, et al. Myocardial tissue doppler velocity imaging in children: comparative study between two ultrasound systems. *J Am Soc Echocardiogr* 2010;23:929-937.
33. Vogel M, Cheung MM, Li J, et al. Noninvasive assessment of left ventricular force-frequency relationships using tissue Doppler-derived isovolumic acceleration: validation in an animal model. *Circulation* 2003;107:1647-1652.
34. Roche SL, Vogel M, Pitkanen O, et al. Isovolumic acceleration at rest and during exercise in children normal values for the left ventricle and first non-invasive demonstration of exercise-induced force-frequency relationships. *J Am Coll Cardiol* 2011;57:1100-1107.
35. Koopman LP, Slorach C, Hui W, et al. Comparison between different speckle tracking and color tissue Doppler techniques to measure global and regional myocardial deformation in children. *J Am Soc Echocardiogr* 2010;23:919-928.
36. Koestenberger M, Ravekes W, Everett AD, et al. Right ventricular function in infants, children and adolescents: reference values of the tricuspid annular plane systolic excursion (TAPSE) in 640 healthy patients and calculation of z score values. *J Am Soc Echocardiogr* 2009;22:715-719.
37. Pettersen E, Helle-Valle T, Edvardsen T, et al. Contraction pattern of the systemic right ventricle shift from longitudinal to circumferential shortening and absent global ventricular torsion. *J Am Coll Cardiol* 2007;49:2450-2456.
38. Coats L, Khambadkone S, Derrick G, et al. Physiological consequences of percutaneous pulmonary valve implantation: the different behaviour of volume- and pressure-overloaded ventricles. *Eur Heart J* 2007;28:1886-1893.
39. Ama R, Leather HA, Segers P, et al. Acute pulmonary hypertension causes depression of left ventricular contractility and relaxation. *Eur J Anaesthesiol* 2006;23:824-831.
40. Rex S, Missant C, Claus P, et al. Effects of inhaled iloprost on right ventricular contractility, right ventriculo-vascular coupling and ventricular interdependence: a randomized placebo-controlled trial in an experimental model of acute pulmonary hypertension. *Crit Care* 2008;12:R113.
41. Santamore WP, Dell'Italia LJ. Ventricular interdependence: significant left ventricular contributions to right ventricular systolic function. *Prog Cardiovasc Dis* 1998;40:289-308.
42. Santamore WP, Gray L Jr. Significant left ventricular contributions to right ventricular systolic function. Mechanism and clinical implications. *Chest* 1995;107:1134-1145.
43. Roman MJ, Devereux RB, Kramer-Fox R, et al. Two-dimensional echocardiographic aortic root dimensions in normal children and adults. *Am J Cardiol* 1989;64:507-512.
44. Gautier M, Detaint D, Fermanian C, et al. Nomograms for aortic root diameters in children using two-dimensional echocardiography. *Am J Cardiol* 2010;105:888-894.
45. Baumgartner H, Hung J, Bermejo J, et al. Echocardiographic assessment of valve stenosis: EAE/ASE recommendations for clinical practice. *J Am Soc Echocardiogr* 2009;22:1-23; quiz 101-102.
46. Friedberg MK, Silverman NH. Cardiac ventricular diastolic and systolic duration in children with heart failure secondary to idiopathic dilated cardiomyopathy. *Am J Cardiol* 2006;97:101-105.
47. Mohammed A, Mertens L, Friedberg MK. Relations between systolic and diastolic function in children with dilated and hypertrophic cardiomyopathy as assessed by tissue Doppler imaging. *J Am Soc Echocardiogr* 2009;22:145-151.
48. Yip GW, Zhang Y, Tan PY, et al. Left ventricular long-axis changes in early diastole and systole: impact of systolic function on diastole. *Clin Sci (Lond)* 2002;102:515-522.
49. Ichihashi K, Sato A, Shiraishi H, et al. Tissue Doppler combined with pulsed-wave Doppler echocardiography for evaluating ventricular diastolic function in normal children. *Echocardiography* 2011;28:93-96.
50. Spitaels S, Arbogast R, Fouron JC, et al. The influence of heart rate and age on the systolic and diastolic time intervals in children. *Circulation* 1974;49:1107-1115.
51. Sarnari R, Kamal RY, Friedberg MK, et al. Doppler assessment of the ratio of the systolic to diastolic duration in normal children: relation to heart rate, age and body surface area. *J Am Soc Echocardiogr* 2009;22:928-932.
52. Appleton CP, Hatle LK. The natural history of left ventricular filling abnormalities: assessment by two-dimensional and Doppler echocardiography. *Echocardiography* 1992;9:438-457.
53. Garcia MJ, Ares MA, Asher C, et al. An index of early left ventricular filling that combined with pulsed Doppler peak E velocity may estimate capillary wedge pressure. *J Am Coll Cardiol* 1997;29:448-454.
54. Garcia MJ, Thomas JD, Klein AL. New Doppler echocardiographic applications for the study of diastolic function. *J Am Coll Cardiol* 1998;32:865-875.
55. Swaminathan S, Ferrer PL, Wolff GS, et al. Usefulness of tissue Doppler echocardiography for evaluating ventricular function in children without heart disease. *Am J Cardiol* 2003;91:570-574.
56. Border WL, Kimball TR, Witt SA, et al. Diastolic filling abnormalities in children with essential hypertension. *J Pediatr* 2007;150:503-509.
57. Nagueh SF, Appleton CP, Gillebert TC, et al. Recommendations for the evaluation of left ventricular diastolic function by echocardiography. *J Am Soc Echocardiogr* 2009;22:107-133.
58. O'Leary PW, Durongpisitkul K, Cordes TM, et al. Diastolic ventricular function in children: a Doppler echocardiographic study establishing normal values and predictors of increased ventricular end-diastolic pressure. *Mayo Clin Proc* 1998;73:616-628.
59. Ayabakan C, Ozkutlu S. Normal patterns of flow in the superior caval, hepatic and pulmonary veins as measured using Doppler echocardiography during childhood. *Cardiol Young* 2003;13:143-151.
60. Roberson DA, Cui W, Chen Z, et al. Annular and septal Doppler tissue imaging in children: normal z-score tables and effects of age, heart rate, and body surface area. *J Am Soc Echocardiogr* 2007;20:1276-1284.
61. Eidem BW, McMahon CJ, Cohen RR, et al. Impact of cardiac growth on Doppler tissue imaging velocities: a study in healthy children. *J Am Soc Echocardiogr* 2004;17:212-221.
62. Ayabakan C, Ozkutlu S. Left ventricular myocardial velocities in healthy children: quantitative assessment by tissue Doppler echocardiography and relation to the characteristics of filling of the left ventricle. *Cardiol Young* 2004;14:156-163.
63. Kapusta L, Thijsen JM, Cuypers MH, et al. Assessment of myocardial velocities in healthy children using tissue Doppler imaging. *Ultrasound Med Biol* 2000;26:229-237.
64. Mori K, Hayabuchi Y, Kuroda Y, et al. Left ventricular wall motion velocities in healthy children measured by pulsed wave Doppler tissue echocardiography: normal values and relation to age and heart rate. *J Am Soc Echocardiogr* 2000;13:1002-1011.
65. Sohn DW, Chai IH, Lee DJ, et al. Assessment of mitral annulus velocity by Doppler tissue imaging in the evaluation of left ventricular diastolic function. *J Am Coll Cardiol* 1997;30:474-480.
66. McMahon CJ, Pignatelli RH, Nagueh SF, et al. Left ventricular non-compaction cardiomyopathy in children: characterisation of clinical status using tissue Doppler-derived indices of left ventricular diastolic relaxation. *Heart* 2007;93:676-681.
67. McMahon CJ, Nagueh SF, Eapen RS, et al. Echocardiographic predictors of adverse clinical events in children with dilated cardiomyopathy: a prospective clinical study. *Heart* 2004;90:908-915.
68. McMahon CJ, Nagueh SF, Pignatelli RH, et al. Characterization of left ventricular diastolic function by tissue Doppler imaging and clinical status in children with hypertrophic cardiomyopathy. *Circulation* 2004;109:1756-1762.
69. Wang M, Yip GW, Wang AY, et al. Peak early diastolic mitral annulus velocity by tissue Doppler imaging adds independent and incremental prognostic value. *J Am Coll Cardiol* 2003;41:820-826.
70. Troughton RW, Prior DL, Frampton CM, et al. Usefulness of tissue doppler and color M-mode indexes of left ventricular diastolic function in predicting outcomes in systolic left ventricular heart failure (from the ADEPT study). *Am J Cardiol* 2005;96:257-262.
71. Fyfe DA, Ketchum D, Lewis R, et al. Tissue Doppler imaging detects severely abnormal myocardial velocities that identify children with pre-terminal cardiac graft failure after heart transplantation. *J Heart Lung Transplant* 2006;25:510-517.
72. Rudko R, Przewlocki T, Pasowicz M, et al. IVRT/IVRT index is a useful tool for detection of elevated left ventricular filling pressure in patients with preserved ejection fraction. *Echocardiography* 2008;25:473-481.
73. Cui W, Roberson DA, Chen Z, et al. Systolic and diastolic time intervals measured from Doppler tissue imaging: normal values and Z-score tables, and effects of age, heart rate, and body surface area. *J Am Soc Echocardiogr* 2008;21:361-370.
74. Geske JB, Sorajja P, Nishimura RA, et al. The relationship of left atrial volume and left atrial pressure in patients with hypertrophic cardiomyopathy: an echocardiographic and cardiac catheterization study. *J Am Soc Echocardiogr* 2009;22:961-966.
75. Taggart NW, Cetra F, O'Leary PW, et al. Left atrial volume in children without heart disease and in those with ventricular septal defect or patent ductus arteriosus or hypertrophic cardiomyopathy. *Am J Cardiol* 2010;106:1500-1504.

76. Pritchett AM, Mahoney DW, Jacobsen SJ, et al. Diastolic dysfunction and left atrial volume: a population-based study. *J Am Coll Cardiol* 2005;45:87-92.
77. Mattioli AV, Zennaro M, Bonatti S, et al. Regression of left ventricular hypertrophy and improvement of diastolic function in hypertensive patients treated with telmisartan. *Int J Cardiol* 2004;97:383-388.
78. Menon SC, Ackerman MJ, Cetta F, et al. Significance of left atrial volume in patients < 20 years of age with hypertrophic cardiomyopathy. *Am J Cardiol* 2008;102:1390-1393.
79. Daniels SR, Witt SA, Glascock B, et al. Left atrial size in children with hypertension: the influence of obesity, blood pressure, and left ventricular mass. *J Pediatr* 2002;141:186-190.
80. Yang H, Woo A, Monakier D, et al. Enlarged left atrial volume in hypertrophic cardiomyopathy: a marker for disease severity. *J Am Soc Echocardiogr* 2005;18:1074-1082.
81. Sauter HJ, Dodge HT, Johnston RR, et al. The Relationship of Left Atrial Pressure and Volume in Patients with Heart Disease. *Am Heart J* 1964;67:635-642.
82. Poutanen T, Jokinen E, Sairanen H, et al. Left atrial and left ventricular function in healthy children and young adults assessed by three dimensional echocardiography. *Heart* 2003;89:544-549.
83. Hofstetter R, Bartz-Bazzanella P, Kentrup H, et al. Determination of left atrial area and volume by cross-sectional echocardiography in healthy infants and children. *Am J Cardiol* 1991;68:1073-1078.
84. Kircher B, Abbott JA, Pau S, et al. Left atrial volume determination by biplane two-dimensional echocardiography: validation by cine computed tomography. *Am Heart J* 1991;121:864-871.
85. Hiraishi S, DiSessa TG, Jarmakani JM, et al. Two-dimensional echocardiographic assessment of left atrial size in children. *Am J Cardiol* 1983;52:1249-1257.
86. Greenberg NL, Vandervoort PM, Thomas JD. Instantaneous diastolic transmitral pressure differences from color Doppler M mode echocardiography. *Am J Physiol* 1996;271:H1267-1276.
87. Lester SJ, Tajik AJ, Nishimura RA, et al. Unlocking the mysteries of diastolic function: deciphering the Rosetta Stone 10 years later. *J Am Coll Cardiol* 2008;51:679-689.
88. Hashimoto I, Uese K, Watanabe S, et al. Assessment of variables affecting flow propagation velocity of the left ventricle in healthy children. *Pediatr Int* 2007;49:305-309.
89. Friedberg MK, Silverman NH. Mitral valve leaflet excursion velocity in the pediatric population: a comparable diastolic index to the color M-mode propagation velocity. *J Am Soc Echocardiogr* 2005;18:142-147.
90. Pena JL, da Silva MG, Faria SC, et al. Quantification of regional left and right ventricular deformation indices in healthy neonates by using strain rate and strain imaging. *J Am Soc Echocardiogr* 2009;22:369-375.
91. Mor-Avi V, Lang RM, Badano LP, et al. Current and Evolving Echocardiographic Techniques for the Quantitative Evaluation of Cardiac Mechanics: ASE/EAE Consensus Statement on Methodology and Indications Endorsed by the Japanese Society of Echocardiography. *J Am Soc Echocardiogr* 2011;24:277-313.
92. Notomi Y, Martin-Miklovic MG, Oryszak SJ, et al. Enhanced ventricular untwisting during exercise: a mechanistic manifestation of elastic recoil described by Doppler tissue imaging. *Circulation* 2006;113:2524-2533.
93. Wang J, Khoury DS, Yue Y, et al. Left ventricular untwisting rate by speckle tracking echocardiography. *Circulation* 2007;116:2580-2586.
94. Notomi Y, Popovic ZB, Yamada H, et al. Ventricular untwisting: a temporal link between left ventricular relaxation and suction. *Am J Physiol Heart Circ Physiol* 2008;294:H505-513.
95. Takahashi K, Al Naami G, Thompson R, et al. Normal rotational, torsion and untwisting data in children, adolescents and young adults. *J Am Soc Echocardiogr* 2010;23:286-293.
96. Notomi Y, Srinath G, Shiota T, et al. Maturation and adaptive modulation of left ventricular torsional biomechanics: Doppler tissue imaging observation from infancy to adulthood. *Circulation* 2006;113:2534-2541.
97. Takeuchi M, Borden WB, Nakai H, et al. Reduced and delayed untwisting of the left ventricle in patients with hypertension and left ventricular hypertrophy: a study using two-dimensional speckle tracking imaging. *Eur Heart J* 2007;28:2756-2762.
98. Bertini M, Nucifora G, Marsan NA, et al. Left ventricular rotational mechanics in acute myocardial infarction and in chronic (ischemic and nonischemic) heart failure patients. *Am J Cardiol* 2009;103:1506-1512.
99. Jin SM, Noh CI, Bae EJ, et al. Decreased left ventricular torsion and untwisting in children with dilated cardiomyopathy. *J Korean Med Sci* 2007;22:633-640.
100. Schmitz L, Schneider MB, Lange PE. Isovolumic relaxation time corrected for heart rate has a constant value from infancy to adolescence. *J Am Soc Echocardiogr* 2003;16:221-222.
101. Schmitz L, Xanthopoulos A, Koch H, et al. Doppler flow parameters of left ventricular filling in infants: how long does it take for the maturation of the diastolic function in a normal left ventricle to occur? *Pediatr Cardiol* 2004;25:482-491.
102. de Marchi SF, Bodenmuller M, Lai DL, et al. Pulmonary venous flow velocity patterns in 404 individuals without cardiovascular disease. *Heart* 2001;85:23-29.
103. Rychik J, Tian ZY. Quantitative assessment of myocardial tissue velocities in normal children with Doppler tissue imaging. *Am J Cardiol* 1996;77:1254-1257.
104. Rakowski H, Appleton C, Chan KL, et al. Canadian consensus recommendations for the measurement and reporting of diastolic dysfunction by echocardiography: from the Investigators of Consensus on Diastolic Dysfunction by Echocardiography. *J Am Soc Echocardiogr* 1996;9:736-760.
105. Rajagopalan N, Garcia MJ, Rodriguez L, et al. Comparison of new Doppler echocardiographic methods to differentiate constrictive pericardial heart disease and restrictive cardiomyopathy. *Am J Cardiol* 2001;87:86-94.
106. Nagueh SF, Mikati I, Kopelen HA, et al. Doppler estimation of left ventricular filling pressure in sinus tachycardia. A new application of tissue Doppler imaging. *Circulation* 1998;98:1644-1650.
107. Sundereswaran L, Nagueh SF, Vardan S, et al. Estimation of left and right ventricular filling pressures after heart transplantation by tissue Doppler imaging. *Am J Cardiol* 1998;82:352-357.
108. Mullens W, Borowski AG, Curtin RJ, et al. Tissue Doppler imaging in the estimation of intracardiac filling pressure in decompensated patients with advanced systolic heart failure. *Circulation* 2009;119:62-70.
109. Appleton CP, Hatle LK, Popp RL. Demonstration of restrictive ventricular physiology by Doppler echocardiography. *J Am Coll Cardiol* 1988;11:757-768.
110. Appleton CP, Hatle LK, Popp RL. Relation of transmitral flow velocity patterns to left ventricular diastolic function: new insights from a combined hemodynamic and Doppler echocardiographic study. *J Am Coll Cardiol* 1988;12:426-440.
111. Klein AL, Cohen GI, Pietrolungo JF, et al. Differentiation of constrictive pericarditis from restrictive cardiomyopathy by Doppler transthoracic echocardiographic measurements of respiratory variations in pulmonary venous flow. *J Am Coll Cardiol* 1993;22:1935-1943.
112. Oh JK, Hatle LK, Seward JB, et al. Diagnostic role of Doppler echocardiography in constrictive pericarditis. *J Am Coll Cardiol* 1994;23:154-162.
113. Ha JW, Oh JK, Ling LH, et al. Annulus paradoxus: transmitral flow velocity to mitral annular velocity ratio is inversely proportional to pulmonary capillary wedge pressure in patients with constrictive pericarditis. *Circulation* 2001;104:976-978.
114. Ha JW, Oh JK, Pelikka PA, et al. Diastolic stress echocardiography: a novel noninvasive diagnostic test for diastolic dysfunction using supine bicycle exercise Doppler echocardiography. *J Am Soc Echocardiogr* 2005;18:63-68.
115. Doucende G, Schuster I, Rupp T, et al. Kinetics of left ventricular strains and torsion during incremental exercise in healthy subjects: the key role of torsional mechanics for systolic-diastolic coupling. *Circ Cardiovasc Imaging* 2010;3:586-594.
116. Brill S, Alexopoulos N, Latsios G, et al. Tissue Doppler imaging and brain natriuretic peptide levels in adults with repaired tetralogy of Fallot. *J Am Soc Echocardiogr* 2005;18:1149-1154.
117. Gatzoulis MA, Clark AL, Cullen S, et al. Right ventricular diastolic function 15 to 35 years after repair of tetralogy of Fallot. Restrictive physiology predicts superior exercise performance. *Circulation* 1995;91:1775-1781.
118. Gatzoulis MA, Norgard G, Redington AN. Biventricular long axis function after repair of tetralogy of Fallot. *Pediatr Cardiol* 1998;19:128-132.
119. Border WL, Michelfelder EC, Glascock BJ, et al. Color M-mode and Doppler tissue evaluation of diastolic function in children: simultaneous correlation with invasive indices. *J Am Soc Echocardiogr* 2003;16:988-994.
120. Olivier M, O'Leary P W, Pankratz VS, et al. Serial Doppler assessment of diastolic function before and after the Fontan operation. *J Am Soc Echocardiogr* 2003;16:1136-1143.
121. Riggs TW, Snider AR. Respiratory influence on right and left ventricular diastolic function in normal children. *Am J Cardiol* 1989;63:858-861.
122. Zoghbi WA, Habib GB, Quinones MA. Doppler assessment of right ventricular filling in a normal population. Comparison with left ventricular filling dynamics. *Circulation* 1990;82:1316-1324.
123. Frommelt PC, Ballweg JA, Whitstone BN, et al. Usefulness of Doppler tissue imaging analysis of tricuspid annular motion for determination of right ventricular function in normal infants and children. *Am J Cardiol* 2002;89:610-613.
124. Cullen S, Shore D, Redington A. Characterization of right ventricular diastolic performance after complete repair of tetralogy of Fallot. Restrictive physiology predicts slow postoperative recovery. *Circulation* 1995;91:1782-1789.
125. Durrer D, van Dam RT, Freud GE, et al. Total excitation of the isolated human heart. *Circulation* 1970;41:899-912.
126. Bader H, Garrigue S, Lafitte S, et al. Intra-left ventricular electromechanical asynchrony. A new independent predictor of severe cardiac events in heart failure patients. *J Am Coll Cardiol* 2004;43:248-256.
127. Lamia B, Tanabe M, Kim HK, et al. Quantifying the role of regional dyssynchrony on global left ventricular performance. *JACC Cardiovasc Imaging* 2009;2:1350-1356.
128. Cazeau S, Leclercq C, Lavergne T, et al. Effects of multisite biventricular pacing in patients with heart failure and intraventricular conduction delay. *N Engl J Med* 2001;344:873-880.
129. Bristow MR, Saxon LA, Boehmer J, et al. Cardiac-resynchronization therapy with or without an implantable defibrillator in advanced chronic heart failure. *N Engl J Med* 2004;350:2140-2150.

130. Bax JJ, Abraham T, Barold SS, et al. Cardiac resynchronization therapy: Part 2—issues during and after device implantation and unresolved questions. *J Am Coll Cardiol* 2005;46:2168–2182.
131. Gorcsan J III, Oyenuga O, Habib PJ, et al. Relationship of echocardiographic dyssynchrony to long-term survival after cardiac resynchronization therapy. *Circulation* 2010;122:1910–1918.
132. Dohi K, Suffoletto M, Ganz L, et al. Utility of echocardiographic tissue synchronization imaging to redirect left ventricular lead placement for improved cardiac resynchronization therapy. *Pacing Clin Electrophysiol* 2005;28:461–465.
133. Becker M, Franke A, Breithardt OA, et al. Impact of left ventricular lead position on the efficacy of cardiac resynchronization therapy: a two-dimensional strain echocardiography study. *Heart* 2007;93:1197–1203.
134. Epstein AE, DiMarco JP, Ellenbogen KA, et al. ACC/AHA/HRS 2008 Guidelines for Device-Based Therapy of Cardiac Rhythm Abnormalities: a report of the American College of Cardiology/American Heart Association Task Force on Practice Guidelines (Writing Committee to Revise the ACC/AHA/NASPE 2002 Guideline Update for Implantation of Cardiac Pacemakers and Antiarrhythmia Devices) developed in collaboration with the American Association for Thoracic Surgery and Society of Thoracic Surgeons. *J Am Coll Cardiol* 2008;51:e1–62.
135. Vardas PE, Auricchio A, Blanc JJ, et al. Guidelines for cardiac pacing and cardiac resynchronization therapy: The Task Force for Cardiac Pacing and Cardiac Resynchronization Therapy of the European Society of Cardiology. Developed in collaboration with the European Heart Rhythm Association. *Eur Heart J* 2007;28:2256–2295.
136. Birnie DH, Tang AS. The problem of non-response to cardiac resynchronization therapy. *Curr Opin Cardiol* 2006;21:20–26.
137. Yu CM, Fung JW, Zhang Q, et al. Tissue Doppler imaging is superior to strain rate imaging and postsystolic shortening on the prediction of reverse remodeling in both ischemic and nonischemic heart failure after cardiac resynchronization therapy. *Circulation* 2004;110:66–73.
138. Yu CM, Gorcsan J III, Bleeker GB, et al. Usefulness of tissue Doppler velocity and strain dyssynchrony for predicting left ventricular reverse remodeling response after cardiac resynchronization therapy. *Am J Cardiol* 2007;100:1263–1270.
139. Bax JJ, Bleeker GB, Marwick TH, et al. Left ventricular dyssynchrony predicts response and prognosis after cardiac resynchronization therapy. *J Am Coll Cardiol* 2004;44:1834–1840.
140. Yu CM, Bleeker GB, Fung JW, et al. Left ventricular reverse remodeling but not clinical improvement predicts long-term survival after cardiac resynchronization therapy. *Circulation* 2005;112:1580–1586.
141. Zhang Q, van Bommel RJ, Fung JW, et al. Tissue Doppler velocity is superior to strain imaging in predicting long-term cardiovascular events after cardiac resynchronization therapy. *Heart* 2009;95:1085–1090.
142. Chung ES, Leon AR, Tavazzi L, et al. Results of the Predictors of Response to CRT (PROSPECT) trial. *Circulation* 2008;117:2608–2616.
143. Beshai JE, Grimm RA, Nagueh SF, et al. Cardiac-resynchronization therapy in heart failure with narrow QRS complexes. *N Engl J Med* 2007;357:2461–2471.
144. Gorcsan J III, Abraham T, Agler DA, et al. Echocardiography for cardiac resynchronization therapy: recommendations for performance and reporting—a report from the American Society of Echocardiography Dyssynchrony Writing Group endorsed by the Heart Rhythm Society. *J Am Soc Echocardiogr* 2008;21:191–213.
145. Yu CM, Sanderson JE, Gorcsan J III. Echocardiography, dyssynchrony, and the response to cardiac resynchronization therapy. *Eur Heart J* 2010;31:2326–2337.
146. Bleeker GB, Mollema SA, Holman ER, et al. Left ventricular resynchronization is mandatory for response to cardiac resynchronization therapy: analysis in patients with echocardiographic evidence of left ventricular dyssynchrony at baseline. *Circulation* 2007;116:1440–1448.
147. Parsai C, Bijnens B, Sutherland GR, et al. Toward understanding response to cardiac resynchronization therapy: left ventricular dyssynchrony is only one of multiple mechanisms. *Eur Heart J* 2009;30:940–949.
148. van Bommel RJ, Bax JJ, Abraham WT, et al. Characteristics of heart failure patients associated with good and poor response to cardiac resynchronization therapy: a PROSPECT (Predictors of Response to CRT) sub-analysis. *Eur Heart J* 2009;30:2470–2477.
149. D'Andrea A, Caso P, Sarubbi B, et al. Right ventricular myocardial activation delay in adult patients with right bundle branch block late after repair of Tetralogy of Fallot. *Eur J Echocardiogr* 2004;5:123–131.
150. Pitzalis MV, Iacoviello M, Romito R, et al. Cardiac resynchronization therapy tailored by echocardiographic evaluation of ventricular asynchrony. *J Am Coll Cardiol* 2002;40:1615–1622.
151. Pham PP, Balaji S, Shen I, et al. Impact of conventional versus biventricular pacing on hemodynamics and tissue Doppler imaging indexes of resynchronization postoperatively in children with congenital heart disease. *J Am Coll Cardiol* 2005;46:2284–2289.
152. Yu CM, Chau E, Sanderson JE, et al. Tissue Doppler echocardiographic evidence of reverse remodeling and improved synchronicity by simultaneously delaying regional contraction after biventricular pacing therapy in heart failure. *Circulation* 2002;105:438–445.
153. Yu CM, Fung WH, Lin H, et al. Predictors of left ventricular reverse remodeling after cardiac resynchronization therapy for heart failure secondary to idiopathic dilated or ischemic cardiomyopathy. *Am J Cardiol* 2003;91:684–688.
154. Fornwalt BK, Arita T, Bhasin M, et al. Cross-correlation quantification of dyssynchrony: a new method for quantifying the synchrony of contraction and relaxation in the heart. *J Am Soc Echocardiogr* 2007;20:1330–1337 e1331.
155. Delgado V, Ypenburg C, van Bommel RJ, et al. Assessment of left ventricular dyssynchrony by speckle tracking strain imaging comparison between longitudinal, circumferential, and radial strain in cardiac resynchronization therapy. *J Am Coll Cardiol* 2008;51:1944–1952.
156. Tanaka H, Hara H, Saba S, et al. Prediction of response to cardiac resynchronization therapy by speckle tracking echocardiography using different software approaches. *J Am Soc Echocardiogr* 2009;22:677–684.
157. Dohi K, Onishi K, Gorcsan J III, et al. Role of radial strain and displacement imaging to quantify wall motion dyssynchrony in patients with left ventricular mechanical dyssynchrony and chronic right ventricular pressure overload. *Am J Cardiol* 2008;101:1206–1212.
158. Gorcsan J III, Tanabe M, Bleeker GB, et al. Combined longitudinal and radial dyssynchrony predicts ventricular response after resynchronization therapy. *J Am Coll Cardiol* 2007;50:1476–1483.
159. Fornwalt BK, Thomas JA, Bhasin M, et al. Effects of region of interest tracking on the diagnosis of left ventricular dyssynchrony from Doppler tissue images. *J Am Soc Echocardiogr* 2008;21:234–240.
160. Kapetanakis S, Kearney MT, Siva A, et al. Real-time three-dimensional echocardiography: a novel technique to quantify global left ventricular mechanical dyssynchrony. *Circulation* 2005;112:992–1000.
161. Baker GH, Hlavacek AM, Chessa KS, Fleming DM, Shirali GS. Left ventricular dysfunction is associated with intraventricular dyssynchrony by 3-dimensional echocardiography in children. *J Am Soc Echocardiogr* 2008;21:230–233.
162. Hui W, Slorach C, Bradley TJ, et al. Measurement of right ventricular mechanical synchrony in children using tissue Doppler velocity and two-dimensional strain imaging. *J Am Soc Echocardiogr* 2010;23:1289–1296.
163. Cui W, Gambetta K, Zimmerman F, et al. Real-time three-dimensional echocardiographic assessment of left ventricular systolic dyssynchrony in healthy children. *J Am Soc Echocardiogr* 2010;23:1153–1159.
164. Ten Harkel AD, Van Osch-Gevers M, Helbing WA. Real-time transthoracic three dimensional echocardiography: normal reference data for left ventricular dyssynchrony in adolescents. *J Am Soc Echocardiogr* 2009;22:933–938.
165. Dubin AM, Janousek J, Rhee E, et al. Resynchronization therapy in pediatric and congenital heart disease patients: an international multicenter study. *J Am Coll Cardiol* 2005;46:2277–2283.
166. Janousek J, Gebauer RA, Abdul-Khaliq H, et al. Cardiac resynchronization therapy in paediatric and congenital heart disease: differential effects in various anatomical and functional substrates. *Heart* 2009;95:1165–1171.
167. Cecchin F, Frangini PA, Brown DW, et al. Cardiac resynchronization therapy (and multisite pacing) in pediatrics and congenital heart disease: five years experience in a single institution. *J Cardiovasc Electrophysiol* 2009;20:58–65.
168. Friedberg MK, Slorach C. Relation between left ventricular regional radial function and radial wall motion abnormalities using two-dimensional speckle tracking in children with idiopathic dilated cardiomyopathy. *Am J Cardiol* 2008;102:335–339.
169. Chen CA, Hsiao CH, Wang JK, et al. Implication of QRS prolongation and its relation to mechanical dyssynchrony in idiopathic dilated cardiomyopathy in childhood. *Am J Cardiol* 2009;103:103–109.
170. Friedberg MK, Silverman NH, Dubin AM, et al. Mechanical dyssynchrony in children with systolic dysfunction secondary to cardiomyopathy: a Doppler tissue and vector velocity imaging study. *J Am Soc Echocardiogr* 2007;20:756–763.
171. Friedberg MK, Roche SL, Balasingam M, et al. Evaluation of mechanical dyssynchrony in children with idiopathic dilated cardiomyopathy and associated clinical outcomes. *Am J Cardiol* 2008;101:1191–1195.
172. Friedberg MK, Roche SL, Mohammed AF, et al. Left ventricular diastolic mechanical dyssynchrony and associated clinical outcomes in children with dilated cardiomyopathy. *Circ Cardiovasc Imaging* 2008;1:50–57.
173. Vogel M, Sponring J, Cullen S, et al. Regional wall motion and abnormalities of electrical depolarization and repolarization in patients after surgical repair of tetralogy of Fallot. *Circulation* 2001;103:1669–1673.
174. Vogel M, Derrick G, White PA, et al. Systemic ventricular function in patients with transposition of the great arteries after atrial repair: a tissue Doppler and conductance catheter study. *J Am Coll Cardiol* 2004;43:100–106.
175. Uebing A, Gibson DG, Babu-Narayan SV, et al. Right ventricular mechanics and QRS duration in patients with repaired tetralogy of Fallot: implications of infundibular disease. *Circulation* 2007;116:1532–1539.
176. van der Hulst AE, Roest AA, Delgado V, et al. Relationship between temporal sequence of right ventricular deformation and right ventricular performance in patients with corrected tetralogy of Fallot. *Heart* 2011;97:231–236.
177. Roche SL, Grosse-Wortmann L, Redington AN, et al. Exercise induces biventricular mechanical dyssynchrony in children with repaired tetralogy of Fallot. *Heart* 2010;96:2010–2015.
178. Abd El Rahman MY, Hui W, Yigitbasi M, et al. Detection of left ventricular asynchrony in patients with right bundle branch block after repair of tetralogy of Fallot using tissue-Doppler imaging-derived strain. *J Am Coll Cardiol* 2005;45:915–921.

179. Tzemos N, Harris L, Carasso S, et al. Adverse left ventricular mechanics in adults with repaired tetralogy of Fallot. *Am J Cardiol* 2009;103:420–425.
180. Veeram Reddy SR, Du W, Zilberman MV. Left ventricular mechanical synchrony and global systolic function in pediatric patients late after ventricular septal defect patch closure: a three-dimensional echocardiographic study. *Congenit Heart Dis* 2009;4:454–458.
181. Liang XC, Cheung EW, Wong SJ, et al. Impact of right ventricular volume overload on three-dimensional global left ventricular mechanical dyssynchrony after surgical repair of tetralogy of Fallot. *Am J Cardiol* 2008;102:1731–1736.
182. Friedberg MK, Silverman NH, Dubin AM, et al. Right ventricular mechanical dyssynchrony in children with hypoplastic left heart syndrome. *J Am Soc Echocardiogr* 2007;20:1073–1079.
183. Janousek J, Tomek V, Chaloupecky VA, et al. Cardiac resynchronization therapy: a novel adjunct to the treatment and prevention of systemic right ventricular failure. *J Am Coll Cardiol* 2004;44:1927–1931.
184. Davis PH, Dawson JD, Mahoney LT, et al. Increased carotid intimal-medial thickness and coronary calcification are related in young and middle-aged adults. The Muscatine study. *Circulation* 1999;100:838–842.
185. Davis PH, Dawson JD, Riley WA, et al. Carotid intimal-medial thickness is related to cardiovascular risk factors measured from childhood through middle age: The Muscatine Study. *Circulation* 2001;104:2815–2819.
186. Trigona B, Aggoun Y, Maggio A, et al. Preclinical noninvasive markers of atherosclerosis in children and adolescents with type 1 diabetes are influenced by physical activity. *J Pediatr* 2010;157:533–539.
187. Singh TP, Groehn H, Kazmers A. Vascular function and carotid intimal-medial thickness in children with insulin-dependent diabetes mellitus. *J Am Coll Cardiol* 2003;41:661–665.
188. Nurnberger J, Keflioglu-Scheiber A, Opazo Saez AM, et al. Augmentation index is associated with cardiovascular risk. *J Hypertens* 2002;20:2407–2414.
189. Hozumi T, Yoshida K, Akasaka T, et al. Noninvasive assessment of coronary flow velocity and coronary flow velocity reserve in the left anterior descending coronary artery by Doppler echocardiography: comparison with invasive technique. *J Am Coll Cardiol* 1998;32:1251–1259.
190. Harada K, Yasuoka K, Tamura M, et al. Coronary flow reserve assessment by Doppler echocardiography in children with and without congenital heart defect: comparison with invasive technique. *J Am Soc Echocardiogr* 2002;15:1121–1126.
191. Noto N, Karasawa K, Kanamaru H, et al. Non-invasive measurement of coronary flow reserve in children with Kawasaki disease. *Heart* 2002;87:559–565.
192. Aoki M, Harada K, Takada G. Normal values for left anterior descending coronary artery flow velocity assessed by transthoracic Doppler echocardiography in healthy children. *Tohoku J Exp Med* 2003;199:211–217.
193. Aoki M, Harada K, Takada G. Noninvasive visualization and measurement of posterior descending coronary artery flow velocity by transthoracic Doppler echocardiography in normal children. *Am J Cardiol* 2003;91:376–379.
194. Hoffman JI. Maximal coronary flow and the concept of coronary vascular reserve. *Circulation* 1984;70:153–159.
195. Hiraishi S, Hirota H, Horiguchi Y, et al. Transthoracic Doppler assessment of coronary flow velocity reserve in children with Kawasaki disease: comparison with coronary angiography and thallium-201 imaging. *J Am Coll Cardiol* 2002;40:1816–1824.
196. Cortigiani L, Rigo F, Gherardi S, et al. Prognostic implications of coronary flow reserve on left anterior descending coronary artery in hypertrophic cardiomyopathy. *Am J Cardiol* 2008;102:1718–1723.
197. Rigo F, Gherardi S, Galderisi M, et al. The prognostic impact of coronary flow-reserve assessed by Doppler echocardiography in non-ischaemic dilated cardiomyopathy. *Eur Heart J* 2006;27:1319–1323.
198. Rigo F, Ciampi Q, Ossena G, et al. Prognostic value of left and right coronary flow reserve assessment in nonischemic dilated cardiomyopathy by transthoracic Doppler echocardiography. *J Card Fail* 2011;17:39–46.
199. Turner DR, Muzik O, Forbes TJ, et al. Coronary diameter and vasodilator function in children following arterial switch operation for complete transposition of the great arteries. *Am J Cardiol* 2010;106:421–425.
200. Oskarsson G, Pesonen E, Munkhammar P, et al. Normal coronary flow reserve after arterial switch operation for transposition of the great arteries: an intracoronary Doppler guidewire study. *Circulation* 2002;106:1696–1702.
201. Britten MB, Zeiher AM, Schachinger V. Microvascular dysfunction in angiographically normal or mildly diseased coronary arteries predicts adverse cardiovascular long-term outcome. *Coron Artery Dis* 2004;15:259–264.
202. Hutter PA, Bennink GB, Ay L, et al. Influence of coronary anatomy and reimplantation on the long-term outcome of the arterial switch. *Eur J Cardiothorac Surg* 2000;18:207–213.
203. Lethen H, P Tries H, Kersting S, et al. Validation of noninvasive assessment of coronary flow velocity reserve in the right coronary artery. A comparison of transthoracic echocardiographic results with intracoronary Doppler flow wire measurements. *Eur Heart J* 2003;24:1567–1575.
204. Sicari R, Nihoyannopoulos P, Evangelista A, et al. Stress echocardiography expert consensus statement: European Association of Echocardiography (EAE) (a registered branch of the ESC). *Eur J Echocardiogr* 2008;9:415–437.
205. Dipchand AI, McCrindle BW, Lee K, et al. Dobutamine/atropine stress echocardiography: feasibility, safety and early results in paediatric heart transplant recipients. *J Heart Lung Transplant* 2001;20:232.
206. Dipchand AI, Bharat W, Manlhiot C, et al. A prospective study of dobutamine stress echocardiography for the assessment of cardiac allograft vasculopathy in pediatric heart transplant recipients. *Pediatr Transplant* 2008;12:570–576.

Since publication of the previous edition of this textbook, the field of cardiovascular magnetic resonance imaging (CMR) has continued to experience rapid evolution in technology and clinical applications. During the past decade, developments in hardware design, computer sciences, and imaging sequences have led to a marked expansion of the clinical utility of CMR in patients with congenital and acquired pediatric heart disease. CMR is rarely used as the first or the sole diagnostic imaging test. It complements echocardiography, provides a noninvasive alternative to x-ray angiography, and overcomes many of the limitations of these modalities. For example, in contrast to echocardiography, acoustic windows and body size do not limit CMR, and, unlike cardiac catheterization, CMR does not use ionizing radiation. In today's clinical practice, CMR is increasingly used in concert with other imaging modalities (most commonly echocardiography) for assessment of cardiac anatomy and function, measurements of blood flow, tissue characterization, and, more recently, evaluation of myocardial perfusion and viability. This chapter reviews common CMR techniques and discusses the clinical applications of CMR in patients with congenital and acquired pediatric heart disease.

INDICATION FOR MAGNETIC RESONANCE IMAGING EVALUATION OF CONGENITAL HEART DISEASE

The indications for CMR in patients with congenital heart disease (CHD) continue to expand. Given that CMR has been shown to provide helpful diagnostic information in most types of CHD, it is not practical to list individual anomalies in which the test is indicated. In general, the clinical reasons for a CMR examination fall into one or more of the following categories:

1. When transthoracic echocardiography cannot provide the required diagnostic information
2. When clinical assessment and other diagnostic tests are inconsistent
3. As an alternative to diagnostic cardiac catheterization with its associated risks and higher cost
4. To obtain diagnostic information for which CMR offers unique advantages

In clinical practice, CMR is typically ordered after other imaging studies have been performed and additional diagnostic information is required. Table 10.1 summarizes the primary referral diagnoses in 1,334 consecutive CMR examinations performed in 1,183 patients at Children's Hospital Boston in 2003 to 2004 (1), illustrating the wide range of cardiovascular anomalies evaluated.

It is worth noting that the role of CMR in infants and toddlers is more limited than that in older patients.

Because poor acoustic windows are less common in infants, echocardiography can provide the necessary diagnostic information in most patients, and CMR under sedation or anesthesia is reserved for those in whom additional information is necessary. A review of 99 consecutive CMR examinations in patients younger than 1 year of age during a 4-year period (January 1999 through December 2002) at Children's Hospital Boston found that delineation of the thoracic vasculature was the most common indication (55%), followed by assessment of airways compression (25%) and evaluation of cardiac tumors (6%) (272). In the future, CMR will likely assume a greater role in this age group, primarily as an alternative to diagnostic cardiac catheterization. Examples of such scenarios include delineation of sources of pulmonary blood supply in tetralogy of Fallot (TOF) with pulmonary atresia and preoperative assessment of candidates for a bidirectional Glenn shunt.

MAGNETIC RESONANCE IMAGING TECHNIQUES

Background

In magnetic resonance imaging (MRI), magnetic fields and radiofrequency (RF) energy are used to stimulate nuclei in selected regions of the body to emit radio waves that are then processed to construct images. The primary source of signals used to construct MR images is derived from hydrogen protons (^1H). The ^1H protons can be thought of as tiny bar magnets that, when placed in a strong magnetic field, will align and precess (rotate) around the axis of the magnetic field. The highest concentrations of ^1H protons are in water and fat. Through the use of a strong static magnetic field, much weaker but rapidly varying magnetic field gradients, and short pulses of RF energy, the ^1H protons (also referred to as *spins*) in selected regions of the body are stimulated to emit RF waves. These RF waves are then used to construct MR images (Fig. 10.1). The strength of the static magnetic field in most clinical scanners used for CMR is either 1.5 or 3.0 Tesla (T) (1 Tesla = 10,000 gauss [G]; the strength of earth's magnetic field at its surface is ~0.5 G).

As with any other diagnostic modality, an in-depth knowledge of underlying MRI physics is essential for maximizing its utility and understanding its pitfalls and limitations. This, in turn, enhances the quality of the interpretation of the imaging data. A detailed discussion of MRI physics is beyond the scope of this chapter and can be found in other sources (2,3). Selected imaging sequences commonly used in CMR are described together with their clinical applications later in this chapter.

Cardiac and Respiratory Gating

Because most CMR techniques acquire data over multiple heartbeats, cardiac and respiratory motions during image acquisition

TABLE 10.1

Primary Referral Diagnoses in 1,334 CMR Examinations at Children's Hospital Boston

Referral Diagnosis	Number of Studies	Percent
Tetralogy of Fallot	270	20.2
Aorta	198	14.8
Coarctation	116	
Other	82	
Complex 2 Ventricle	187	14.0
TGA	78	
S/p arterial switch	35	
S/p atrial switch	43	
Single ventricle	134	10.0
Septal defects	72	5.4
ASD	39	
VSD	33	
Anomalies of the pulmonary veins	46	3.4
Arrhythmogenic right ventricular cardiomyopathy	41	3.1
Pulmonary atresia with intact ventricular septum	29	2.2
Vascular anomalies (other than aorta)	25	1.9
Kawasaki disease	24	1.8
Congenital coronary anomaly	22	1.6
Cardiac tumor/mass	22	1.6
Vascular ring	21	1.6
Other	243	18.2

ASD, atrial septal defect; TGA, transposition of the great arteries; VSD, ventricular septal defect.

result in image blurring. Several techniques have been developed to overcome this problem. The most common approach to compensate for cardiac motion is to synchronize or “gate” image acquisition with the cardiac cycle. The cardiac cycle is tracked using either the electrocardiogram (ECG) or an optical pulse sensor placed on an extremity (called “peripheral gating”) (Fig. 10.2). Electrocardiographic gating can be accomplished with a high-quality standard ECG trace or with a vectorcardiogram (VCG) signal (4). More recently, a new technique called “self-gating,” which relies on cardiac motion and avoids the use of ECG triggering altogether, has been described (5). Blurring due to respiratory motion can be avoided either by having the patient hold his breath for periods of 5 to 10 seconds during data acquisition or by synchronizing image data acquisition to the respiratory as well as to the cardiac cycle. Another approach that reduces blurring from respiratory motion is to repeat the image acquisition several times and average the data. Respiratory motion can be tracked by either a bellows device placed around the abdomen or by MR navigator pulse that concurrently tracks the position of the diaphragm or cardiac border (Fig. 10.3) (6).

A more desirable approach to avoid motion-induced image blurring is to acquire the MR data fast enough so that cardiac and respiratory motions are adequately resolved. Advances in gradient coil performance, parallel acquisition techniques, and image reconstruction methods have allowed real-time CMR at 20 to 24 frames per second, albeit at the expense of spatial and temporal resolutions (7–10). Real-time imaging may be particularly useful when a patient has an irregular rhythm and to evaluate respiratory-related variations in blood flow and septal position (11). This technology, which is now commercially available on some clinical scanners, may obviate the need for ECG and respiratory triggering.

SEDATION AND MONITORING

Patients undergoing CMR examinations must remain still in the scanner bore for up to 60 minutes to minimize motion artifact during image acquisition and allow planning of successive imaging sequences. Accordingly, the need for performing the examination under sedation or anesthesia and an assessment of the risk–benefit ratio for proceeding under these circumstances should be determined well before the examination date. Multiple factors are taken into account when deciding whether a patient should have an examination with sedation, including the length of the anticipated examination protocol, the child's developmental age and maturity, the child's experience with prior procedures, and the parents' opinion of their child's capability to cooperate with the examination. True claustrophobia in the pediatric age group is rare. In general, most children 7 years of age and older can cooperate sufficiently for a good-quality CMR study. Parents should be provided with a detailed description of the examination and asked to discuss it with their child in an age-appropriate manner in advance to increase the likelihood of a successful study. After proper screening, parents can be allowed into the scanner room to help their child complete the examination. Allowing patients to listen to music or watch movies through a specialized MRI-compatible audiovisual system may reduce anxiety and improve patient cooperation (12).

Strategies for sedation and anesthesia in CMR vary and often depend on institutional preference and resources such as availability of qualified pediatric anesthesiologists. Although it is possible to wait for young children to fall into a natural sleep using a “feed and swaddle” approach, this method may be time-consuming and complicated by early awakening. Sedation can be achieved with a variety of medications (e.g., pentobarbital, propofol, fentanyl, midazolam, chloral hydrate) and is a reasonable approach (13–19). Its principal drawbacks are an unprotected airway and reliance on spontaneous respiratory effort with the associated risks of aspiration, airway obstruction, and hypoventilation. In addition, because images are often acquired over several seconds, respiratory motion will degrade image quality. This motion artifact can be reduced by synchronizing image data acquisition to the respiratory cycle tracked either by a bellows device around the abdomen or by navigator echoes that concurrently image the position of the diaphragm or heart. An alternative strategy to reduce respiratory motion artifacts is to acquire multiple images at the same location and average them, thereby minimizing variations from respiration. The principal limitations of both these strategies are prolonged scan times and incomplete elimination of respiratory motion that can lead to reduced image quality.

Because of these safety and image quality concerns, we and others frequently prefer to perform CMR examinations

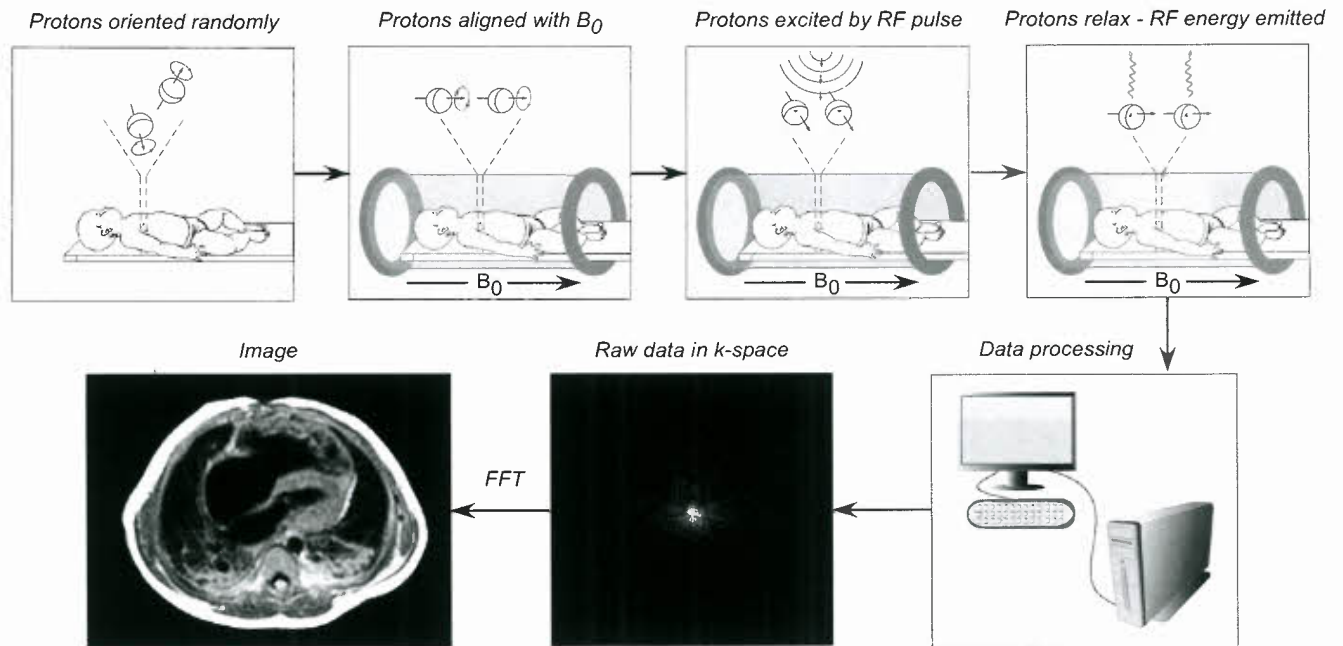


Figure 10.1. From signal to image. Top panel: Outside the scanner's magnetic field, the orientation of the spinning (precessing) protons is random. Once inside the scanner, the protons are aligned with the direction of the static magnetic field (B_0). Excitation by a brief pulse of RF energy perturbs the protons into a state of higher energy. Once the RF pulse ceases, the protons return to their original state of energy (relaxation) and emit RF energy. Lower panel: The emitted RF energy is captured by receiver coils (antennas) and undergoes through a series of electronic filters. The raw MR signal is stored as an array of numbers called " k -space." By applying fast Fourier transformation (FFT), the raw MR data stored in k -space is translated into an image.

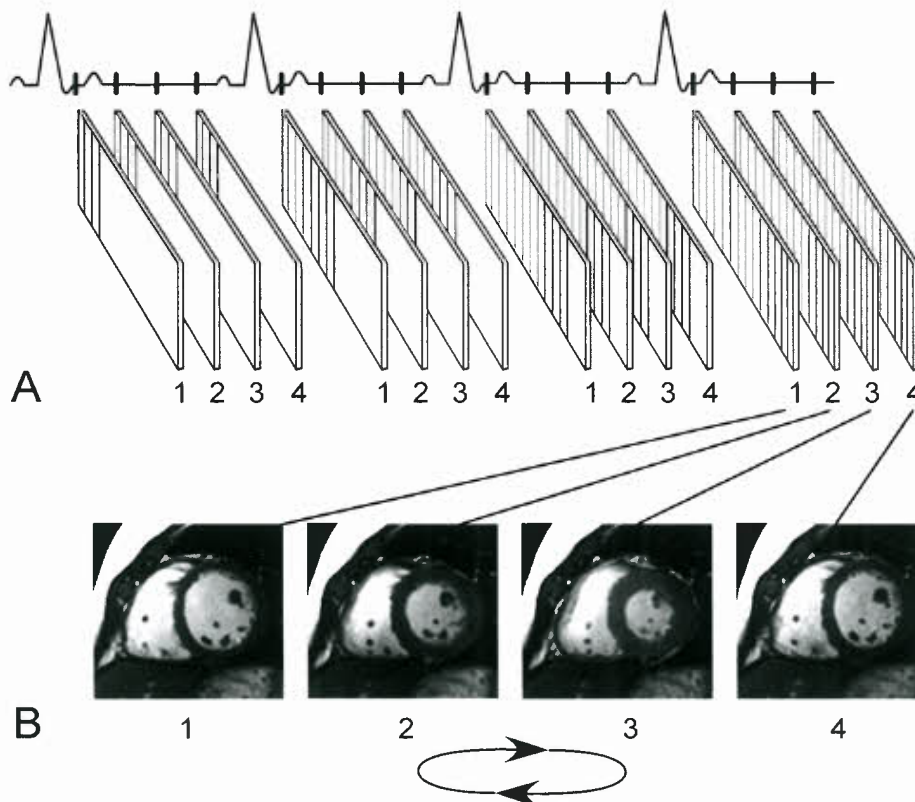


Figure 10.2. Cine MRI. A: Schematic representation of image data acquisition. Using the ECG signal, the cardiac cycle is divided into multiple, equally spaced acquisition windows. Several lines of k -space are acquired during each acquisition window (a technique called *segmented k -space*). Over several heartbeats, a series of images spanning the cardiac cycle is reconstructed and viewed in cine loop mode (B).

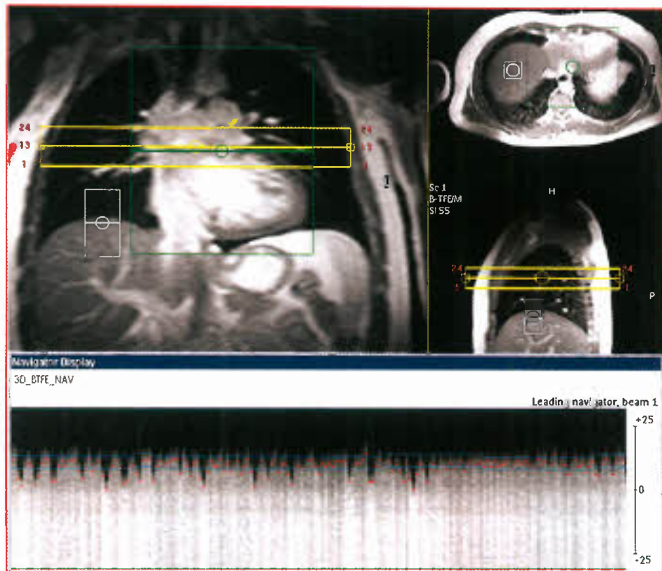


Figure 10.3. Respiratory navigator. The navigator beam is positioned over the right hemidiaphragm and includes lung and liver tissues (top). The motion of the right hemidiaphragm is continuously displayed (bottom) along with the acceptance window (horizontal lines). Only data acquired when the position of the right hemidiaphragm is registered within the acceptance window are used for image reconstruction.

under general anesthesia in children who cannot undergo an awake examination (20,21). This approach, described in detail elsewhere (2,22), is safe, consistently achieves adequate sedation, protects the airway, and offers control of ventilation. Respiratory motion artifact can be completely eliminated by suspending ventilation in conjunction with neuromuscular blockade. Breath-hold periods of 30 to 60 seconds are typically well tolerated, and allow multiple locations to be scanned efficiently.

When utilizing either sedation or anesthesia, it is important that both the nurses and physicians have sufficient experience with these procedures in children with cardiovascular disorders. Continuous monitoring of the ECG, pulse oximetry, end-tidal carbon dioxide, anesthetic gases, blood pressure, and temperature with an MRI-compatible physiologic monitoring system is required (Fig. 10.4). MRI-compatible anesthesia machines are available that can be located in the scanner room and connected to the patient's endotracheal tube by an extended breathing circuit. To maximize patient safety and examination quality, it is recommended that different health care providers be responsible for supervising the imaging and sedation/anesthesia aspects of the study and that both communicate closely with each other.

PATIENT PREPARATION

Prior to bringing the patient into the scanner room, the physician and technologists should review the patient's history, safety screening form, and the most recent chest radiograph to identify implanted devices that may be hazardous in the MRI environment or produce image artifact. A detailed discussion on MRI safety can be found at the end of this chapter and elsewhere (23–25).

Following safety screening, physiologic monitoring devices and hearing protection (for both awake and anesthetized



Figure 10.4. MRI suite equipped with (1) MR-compatible anesthesia machine, (2) physiologic monitoring equipment, and (3) ceiling-mounted in-room scan controls and monitors.

patients) are put in place. A high-quality ECG signal is essential for optimum image quality in cardiac-gated sequences. The signal should be checked both when the patient is outside and then inside the scanner bore. In patients with dextrocardia, ECG leads are best placed on the right chest. Because young children dissipate body heat faster than adults, the scanner room temperature should be adjusted and prewarmed blankets applied to minimize heat loss.

The imaging coil should be chosen to maximize the signal-to-noise ratio over the entire body region to be examined. Because CHD often involves abnormalities of the thoracic vasculature, the coil will usually need to be large enough to cover the entire thorax rather than just the heart. Adult head or knee coils are often appropriate for infants weighing <10 kg, and adult cardiac coil for medium-sized children weighing between 10 and 40 kg. More recently, multichannel coils designed specifically for cardiovascular imaging in infants and young children have become commercially available (Fig. 10.5). Adequate coil coverage and placement should be confirmed early in the examination by reviewing the localizing images.

SAFETY

Standard clinical imaging scanners present no known hazards to biologic materials. Guidelines set by the Food and Drug Administration (FDA) keep the strength of the magnetic fields and the deposition of RF energy well below levels that could cause significant biologic effects. Animal studies evaluating the influence of static magnetic fields have not demonstrated significant biologic effects for fields of up to 2 T (26). Millions of patients have undergone MRI studies without any noticeable immediate or long-term sequelae. The incidence of complications related to CMR examination in patients with CHD is low (1.6%), most of which are minor and transient (1). Not surprisingly, infants with severe cardiorespiratory compromise referred to CMR from the cardiac intensive care unit are more susceptible to adverse events such as transient hypotension and hypoxemia.

Investigations on pregnant human subjects exposed to MR imaging or the MR environment have not demonstrated any adverse outcomes. Current guidelines state that pregnant patients can be accepted to undergo MR scans



Figure 10.5. Multichannel RF coils used in CMR imaging in infants, children, and adults. **A:** 8-channel knee coil used in infants weighing 4 kg or less; **B:** 8-channel pediatric coil used in patients weighing between 4 kg and 10 kg; **C:** 5-channel cardiac coil used in patients weighing between 10 kg and 30 kg; and **D:** 32-channel cardiac coil used in patients weighing 30 kg or more. These body weights are approximates and other considerations are taken into account when selecting a coil for an individual patient.

at any stage of pregnancy if the risk–benefit ratio to the patient warrants that the study be performed (27). Thus, when maternal and fetal health considerations necessitate diagnostic studies, MRI is preferable to methods that use x-rays, such as computed tomography (CT) or standard angiography.

Gadolinium contrast is commonly used in CMR examinations in patients of all ages for angiography and for assessment of myocardial viability, first-pass perfusion, and diffuse fibrosis (28–30). It is important to note that the FDA has not approved the use of contrast agents in CMR; hence its use is off-label. The incidence of adverse events related to gadolinium contrast is very low. In patients with CHD, Dorfman et al. (1) reported an event rate of 0.84%—all were minor and transient events such as nausea, vomiting, or sensation of warmth. Anaphylactic reaction to gadolinium contrast is

exceptionally rare (31). Nephrogenic systemic fibrosis (NSF), previously known as nephrogenic fibrosing dermopathy, is a well recognized but incompletely understood systemic disease characterized by progressive multiple-organ fibrosis. An association between NSF and gadolinium administration was recognized in 2006 (32). Subsequent investigations found that patients with renal failure were at risk for developing this rare but severe complication (33,34). Consequently, most institutions have adopted a policy to avoid using gadolinium contrast in patients with impaired renal function (35). A recent study has shown no new cases of NSF since the institution of a policy of avoiding use of gadolinium contrast in patients with glomerular filtration rate lower than 60 mL/min/m² (36).

Implanted metallic objects are of particular concern in the MR environment since they could potentially undergo undesirable movements if the magnetic field were sufficiently

TABLE 10.2

Safety Considerations and Image Artifacts due to Implanted Devices used in Patients with CHD

Device	Safety ^a	Image Artifact ^b	Comment
Pacemaker	RC	2	The assertion that presence of a pacemaker/defibrillator is an absolute contraindication to MRI has been challenged (23) Careful assessment of risks and benefits, informed consent, and proper precautions are required.
AICD	CI	2	
Permanent pacemaker lead—no generator	RC	1	Experiments in animal models found heating of permanent pacemaker leads (306)
Temporary pacemaker lead—no generator	OK	1	
Sternal wire	OK	2	
Hemostatic vascular clips	OK	1–2	
Stent	*		
Stainless steel	OK	3	
Non- or minimally ferromagnetic	OK	1	
Vascular occluding coil	*		
Stainless steel	OK	3	
Nonferromagnetic (e.g., platinum, nickel-titanium, other composites)	OK	1	
Occluding devices	*		
Rashkind occluder	OK	3	
Clamshell	OK	3	
CardioSEAL	OK	2	
StarFLEX	OK	2	
Amplatzer	OK	2	
Prosthetic heart valves	OK	2	

CI, contraindication; RC, relative contraindication; OK, no known adverse events related to clinical MRI.

^aSafety grade in a 1.5T scanner with commercially available imaging sequences:

^bExtent of image artifact: 1) none or trivial; 2) small on standard gradient echo sequences (GRE) and minimal on spin echo (SE) sequences; 3) large (several centimeters) on GRE and remains substantial on SE sequences.

* Some centers advocate avoiding MRI for an arbitrarily period of time after implantation (usually for several weeks), but such practice is not supported by conclusive published data. A decision to perform MRI examination shortly after cardiac surgery or implantation of a biomedical device must weigh the risk–benefit ratio for the individual patient. (From Shellock FG. Metallic surgical instruments for interventional MRI procedures: evaluation of MR safety. *J Magn Reson Imaging* 2001;13:152–157, with permission from John Wiley and Sons.)

strong and if they contained sufficient ferromagnetic material (Table 10.2). Fortunately, surgical clips and sternotomy wires implanted in the chest and abdomen are typically only weakly ferromagnetic. Furthermore, these devices quickly become immobilized by surrounding fibrous tissue, and MRI can safely be used to study patients with these implants. The wires and clips, however, may cause localized image artifact. Similarly, MRI can be used to image patients with implanted intravascular coils, stents, and occluding devices once the implants are believed to be immobile. Many centers choose to avoid exposing these patients to MRI for an arbitrarily chosen period of time after implantation (usually for several weeks), but such practice is not supported by conclusive published data. A decision to perform MRI examination shortly after cardiac surgery or implantation of a biomedical device must weigh the risk–benefit ratio for the individual patient (37).

Several devices are considered either a relative or absolute contraindication to MRI (37–39). Presence of an intracranial, intraocular, and intracochlear metallic object is considered a contraindication to MRI. The presence of a cardiac pacemaker is also considered a contraindication to MRI (40) although

some reports have suggested that scanning patients who have modern pacemakers may be possible (23,41–44). In 2011, the FDA gave conditional approval to a pacemaker designed specifically to be MRI compatible (45).

Because MRI scanners attract ferromagnetic objects, extreme caution should be used in approaching magnets with objects containing iron or other ferromagnetic materials. Only specially designed MRI-compatible physiologic monitoring equipment should be used in conjunction with MRI studies. There have been several reported cases of patient burns resulting from the use of MRI-incompatible pulse oximeters and ECG monitoring devices.

SUPERVISION AND INTERPRETATION OF MRI EXAMINATION

Detailed pre-examination planning is crucial, given the wide array of imaging sequences available and the often-complex nature of the clinical, anatomic, and functional issues in

patients with CHD. The importance of a careful review of the patient's medical history, including details of all cardiovascular surgical procedures, interventional catheterizations, findings of previous diagnostic tests, and current clinical status, cannot be overemphasized. As with echocardiography and cardiac catheterization, CMR examination of CHD is an interactive diagnostic procedure that requires online review and interpretation of the data by the supervising physician. The unpredictable nature of the anatomy and hemodynamics often require adjustment of the examination protocol, modification of imaging planes, changing sequences, and adjustment of imaging parameters. Reliance on standardized protocols and postexamination review alone in these patients may result in incomplete or even erroneous interpretation.

CLINICAL APPLICATIONS

CMR Examination Techniques

The building blocks of any MRI examination are called “pulse sequences” (Fig. 10.6). An MRI pulse sequence describes the way the magnetic field gradients and RF pulses are applied to produce images with particular characteristics. During the course of a CMR examination, the examiner selects the pulse sequences and prescribes imaging locations and planes to acquire the image data to address specific clinical questions. Some of the pulse sequences used in CMR practice are described below together with their clinical applications.

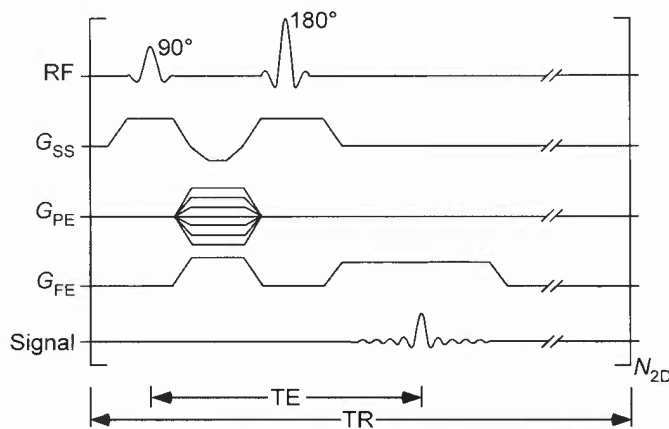


Figure 10.6. Timing diagram of a SE pulse sequence. The x-axis represents time. The first step is the simultaneous application of a 90-degree RF pulse and a slice-selective gradient (G_{SS}) pulse. The next step is the application of a slice-selective 180-degree RF pulse to refocus the transverse magnetization that lost phase coherence due to inhomogeneities in the magnetic field. To locate the MR signal in space (spatial localization), multiple frequency encoding (G_{PE}) and single-phase encoding (G_{FE}) gradients are applied. The time at which the MR signal (echo) is recorded is called *echo time*, or TE. This sequence results in the acquisition of one line of k -space data. The sequence is repeated N_{2D} times, each with a different phase-encoding value, until all lines of k -space are collected and a 2-D image is reconstructed. The time from onset of one sequence to the next is called *repetition time*, or TR.

Assessment of Cardiovascular Anatomy

Evaluation of cardiovascular anatomy and function in patients with CHD is often inseparable. Several MRI sequences can be used for anatomic delineation; each has particular advantages and provides specific information. In practice, the anatomy in question is often assessed by more than one imaging sequence, yielding overlapping information that increases diagnostic confidence.

Spin Echo MRI

With spin echo (SE) imaging, the MR signal is produced by applying a brief RF pulse that tips the magnetization vector of the hydrogen atoms (spins) 90 degrees relative to the axis of the main magnetic field, followed by a 180-degree refocusing RF pulse (Fig. 10.6). Because of the relatively long time interval between tissue excitation and data sampling, flowing blood will leave the image plane by the time the signal is sampled. The result is an image in which flowing blood appears black, whereas more stationary tissues produce MR signals displayed in varying shades of gray or white (“black blood” imaging) (Fig. 10.7A). Other features of SE pulse sequences include a single image per cardiac cycle (static imaging), high tissue contrast, and, compared with gradient echo pulse sequences, relative insensitivity to inhomogeneities in the magnetic field. In clinical practice, such inhomogeneities are mostly owing to ferromagnetic implants such as sternal wires, prosthetic heart valves, stents, coils, or other implants. SE sequences can also be modified to alter tissue contrast and characterize the composition of structures (e.g., T1 and T2 weighting) (Fig. 10.7B). Standard SE requires several minutes (usually 2 to 4 minutes, depending on heart rate and imaging parameters) to acquire an image dataset. Fast or turbo spin echo (FSE or TSE) requires a much shorter image acquisition time because instead of acquiring a single-phase encoding line for each 90 degrees RF pulse, multiple-phase encoding lines are acquired in rapid succession (called “echo train”). As a result, image acquisition can be completed during 10 to 15 seconds of breath holding. In the TSE sequence, the blood signal is nulled by an inversion pulse (called *double inversion recovery*) rather than relying on blood flow alone.

Standard SE was the workhorse of CMR during the 1980s. In today's clinical practice, standard SE has been largely replaced by FSE or TSE with double inversion recovery (2). Examples of clinical applications include assessment of tissue characteristics (e.g., cardiac tumors), vessel wall imaging (e.g., aortic dissection), evaluation of the pericardium, and anatomic imaging in patients with metallic implants such as stents and prosthetic valves.

Gradient Echo Cine MRI

Gradient echo MR is a class of pulse sequences that produce bright blood images. The fundamental difference between SE and gradient echo sequences is that in the latter the initial RF pulse tips the spins at an angle (called *flip angle*) <90 degrees. Gradient echo sequences are generally faster than SE sequences because the time between spin excitation and signal detection (called “echo time” or TE) is much shorter. The signal from stationary or relatively slow-moving tissues (such as the myocardium) is gray because the spins within the selected slice have reduced signal intensity (i.e., partially saturated) by the rapid repetition of the RF pulse. This is because the spins do not have sufficient time to return to their original unexcited state during the short interval between RF pulses, which result in

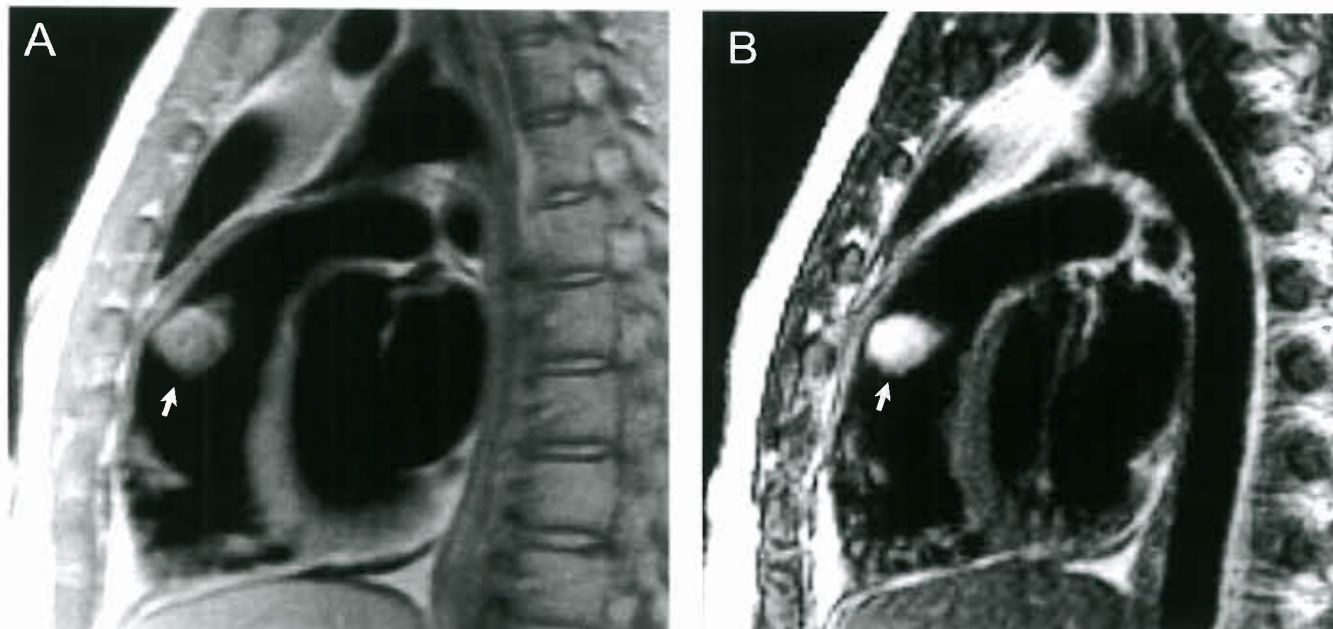


Figure 10.7. Short-axis FSE image in a patient with hemangioma of the RVOT. **A:** T1-weighted image showing a slightly hyperintense globular tumor (arrow); **B:** T2-weighted image showing the tumor is markedly hyperintense, consistent with a vascular tumor.

a relatively weak signal. On the other hand, blood that flows into the slice contains unsaturated spins that produce relatively strong signals, hence the term “bright blood” imaging (Fig. 10.8). An important feature of gradient echo sequences is high imaging speed, which allows reconstruction of multiple images during the cardiac cycle that can be displayed in cine loop format. Compared with SE techniques, gradient echo sequences have a relatively low tissue contrast and are more susceptible to inhomogeneities within the magnetic field.

ECG- or VCG-triggered steady-state free precession (SSFP) is the most commonly used cine MRI technique for assessment of cardiovascular anatomy and ventricular function. The brightness of a given tissue in this case is determined primarily by the ratio of T2 to T1 relaxation times, which results in high contrast between the blood pool ($T2/T1 = 360 \text{ ms}/1200 \text{ ms} = 0.3$) and the myocardium ($T2/T1 = 75 \text{ ms}/880 \text{ ms} = 0.085$) and clearly depicts the boundaries of cardiovascular structures (Fig. 10.8) (46). This sequence is known by several proprietary names, including true fast imaging with steady precession, balanced fast field echo (bFFE), and fast imaging employing steady state acquisition (FIESTA). The acquisition time of SSFP cine MRI is short, typically requiring 4 to 10 seconds for each location depending on heart rate, spatial resolution, and other acquisition parameters. The SSFP sequence, however, is highly sensitive to inhomogeneities in the magnetic field such as those induced by implanted metallic devices.

A segmented *k*-space fast (also termed “turbo”) gradient recalled echo (fast GRE) sequence was used extensively during the 1990s, and its accuracy and reproducibility in measuring ventricular dimensions and function have been validated (47,48). Compared with SSFP, the distinction between blood and myocardium on fast GRE images is less sharp, the contrast-to-noise ratio and the temporal resolution are lower, image acquisition time is longer, and images are more susceptible to blood flow effects. On the other hand, fast GRE is less susceptible to inhomogeneities in the magnetic field than SSFP.

In clinical practice, an ECG-gated gradient echo cine MRI sequence is prescribed across the anatomy of interest to yield a stack of contiguous cross-sectional slices that can be displayed on a computer workstation in a multilocation, multiphase (cine loop) format. ECG-gated segmented *k*-space SSFP cine MRI is the sequence of choice for evaluation of cardiac anatomy and function because of its excellent blood–myocardium contrast, high spatial and temporal resolutions, and short acquisition time. Use of a parallel imaging technique (e.g., sensitivity encoding or SENSE) further shortens acquisition

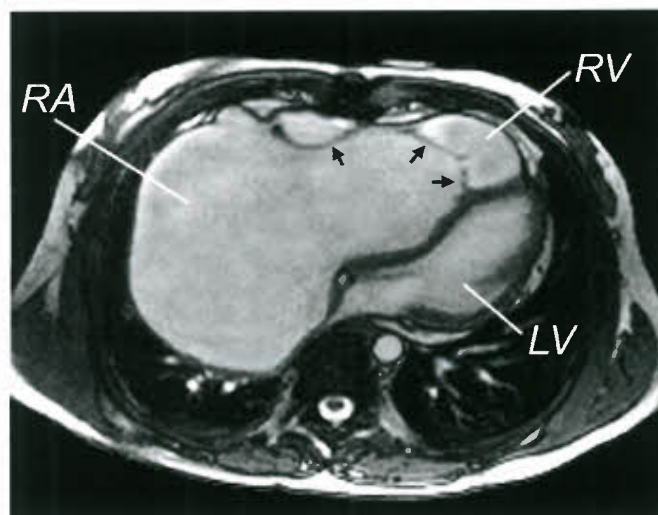


Figure 10.8. ECG-triggered SSFP image in the axial plane in a patient with severe Ebstein anomaly. Note the apical displacement of the tricuspid valve (black arrows), “atrialization” of the right ventricular inflow, markedly dilated right atrium (RA), and the compressed LV.

time (49). The SSFP sequence allows detailed imaging of the cardiac chambers, the atrioventricular and semilunar valves, the papillary muscles and chordae tendineae, the membranous septum, septum primum, and blood vessels (Fig. 10.8). The SSFP sequence, however, is relatively less sensitive to flow disturbances due to stenotic or regurgitant jets compared to fast GRE. Alternatively, a velocity-encoded cine (VEC) MRI sequence can be prescribed when further delineation of abnormal flow jets is desirable.

Three-Dimensional Steady State Free Precession MRI

This cardiac-triggered SSFP technique acquires a 3-D image volume over a period of 4 to 7 minutes of free breathing (50,51). The motion of the diaphragm is tracked with a navigator pulse and image data is accepted only when the position of the diaphragm lies within a narrow window defined by the operator (Fig. 10.3), thus avoiding artifacts from respiratory motion. The volume elements (voxels) of the image dataset are typically isotropic, which allows off-line reformatting of the image volume in any arbitrary plane. This imaging technique does not require administration of contrast agents and provides high-resolution static imaging of both intracardiac and extracardiac anatomy (Fig. 10.9).

Coronary Artery Imaging

The origin and course of the epicardial coronary arteries can be evaluated by several MRI techniques. Most of the published experience with MRI evaluation of the coronary arteries is based on a cardiac-triggered, navigator-gated, free-breathing 3-D magnetic resonance angiography (MRA) sequence (52). This technique has been used successfully in patients with various congenital anomalies of the coronary arteries (Fig. 10.10) and in Kawasaki disease (53–57).

Contrast-Enhanced Three-Dimensional MRA

Gadolinium (Gd)-enhanced 3-D MRA is ideally suited for imaging of extracardiac vascular anatomy. Examples of common clinical applications include imaging of the aorta and its branches, pulmonary arteries, pulmonary veins, systemic veins, aortopulmonary and venous–venous collateral vessels, systemic-to-pulmonary artery shunts, conduits, and vascular grafts (14,58). Although this technique is mostly used for imaging of extracardiac anatomy, we have also found it useful in the evaluation of intra-atrial systemic and pulmonary baffles (e.g., Mustard or Senning operations and Fontan palliation), as well as for imaging of the outflow tracts (e.g., repaired TOF and the arterial switch operation [ASO]). In addition, Gd-enhanced 3-D MRA clearly delineates the spatial relationships between vascular structures, the tracheo-bronchial tree, chest wall, spine, and other landmarks that may be useful for planning interventional catheterization or surgical procedures (Fig. 10.11). More recently, imaging acceleration techniques have been applied to shorten the acquisition time to 2 to 5 seconds, thereby permitting multiple 3-D volume sets to be acquired as the contrast passes through the circulation, producing a “time-resolved” 3-D MRA (59). However, given the trade-offs between spatial and temporal resolutions, the clinical utility of this imaging technique awaits further study.

In practice, the contrast (e.g., gadopentetate dimeglumine 0.2 mmol/kg) is infused through a peripheral intravenous cannula either by hand or by a power injector. The patient is

instructed to hold his/her breath and imaging acquisition is initiated. The time delay between start of contrast injection and data acquisition is determined either by a magnetic resonance (MR) fluoroscopic method that allows real time visualization of the arrival of the contrast bolus to the heart or by a bolus tracking technique. Two or more sequential 3-D MRA data acquisitions are usually obtained 10 to 15 seconds apart during suspended respiration.

Ventricular Function

Technique. ECG- or VCG-triggered SSFP is the preferred cine MRI technique for assessment of ventricular function. In patients in whom image artifacts from metallic implants obscure the ventricles, a fast (turbo) GRE sequence can be used because it is less susceptible to inhomogeneities in the magnetic field (60). ECG-triggered SSFP cine MRI is acquired during short periods of breath holding. Depending on heart rate and image acquisition parameters (matrix size, number of k -space lines per segment, and the scanner's gradient system capabilities), high-resolution acquisition may last 7 to 10 seconds per slice. A modest decrease in spatial and temporal resolutions will lower the acquisition time to 4 to 5 seconds while producing diagnostically acceptable images. The use of SENSE technology allows shorter acquisitions time by a factor of 2 to 4 seconds (at the expense of reduced signal-to-noise ratio), an increase in spatial or temporal resolutions while maintaining the same acquisition time, or a combination of the two. Patients are instructed to hold their breath at end expiration to minimize variations in the position of the diaphragm and, consequently, the heart. In patients who are incapable of holding their breath, images are acquired during free breathing either with multiple signal averages, with respiratory triggering, or with real-time MR fluoroscopy (61,62).

Quantitative evaluation of ventricular function is achieved by obtaining a series of contiguous SSFP cine MRI slices that cover the ventricles in short-axis (Fig. 10.12). This involves the following steps:

- Two-chamber plane (also known as vertical long-axis plane):* A slice is prescribed parallel to the plane of the interventricular septum based on previously obtained scout images in the axial (transverse) plane (Fig. 10.12A). In patients with a biventricular heart and a systemic left ventricle (LV), the slice extends from the center of the mitral valve to the LV apex. In patients with a systemic right ventricle (RV) (e.g., atrial switch operation for transposition of the great arteries [TGA]), it is advantageous to place the slice between the center of the tricuspid valve and the RV apex. In patients with a single ventricle, the slice is placed between the center of the atrioventricular (AV) valve(s) and the ventricular apex. This acquisition accounts for the orientation of the ventricles in the transverse plane of the chest.
- Four-chamber plane (also known as horizontal long-axis plane):* A stack of slices (usually four) is prescribed from an end-diastolic image of a slice acquired perpendicular to the previous two-chamber cine sequence (Fig. 10.12B). This acquisition accounts for the superior–inferior orientation of the ventricles in the chest.
- Short-axis plane:* Multiple equidistant slices are prescribed from an end-diastolic image of the previous four-chamber cine sequence covering the ventricles from the plane of the AV valve(s) to the cardiac apex (Fig. 10.12C). The first slice is placed at the level of the AV annuli by connecting the right coronary artery (seen in cross section in the right AV groove) with the left circumflex coronary artery (seen in the left AV groove). Subsequent slices

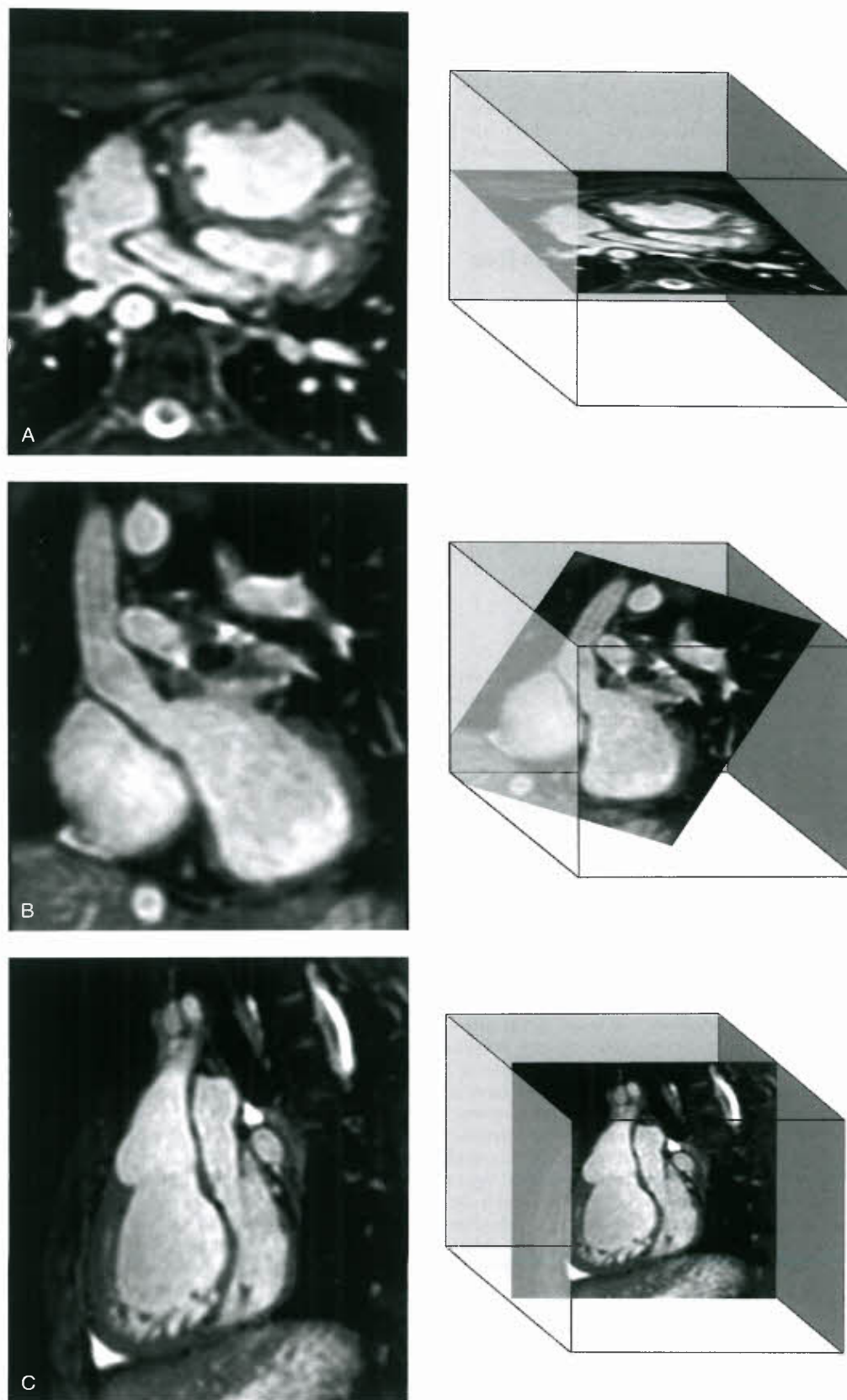


Figure 10.9. Free-breathing (navigator-gated), ECG-triggered, isotropic, 3-D SSFP imaging in a patient with Mustard palliation of TGA. The 3-D data volume is reformatted off-line in multiple user-defined planes. **A:** Transverse view of the pulmonary venous pathway. **B:** Oblique view depicting the superior vena cava pathway. **C:** Oblique sagittal view of the left and right ventricular outflow tracts.



Figure 10.10. Free-breathing (navigator-gated), ECG-triggered, 3-D coronary magnetic resonance angiogram (MRA) showing anomalous origin of the right coronary artery from the left aortic sinus of Valsalva.

are positioned in equidistance through the cardiac apex (Fig. 10.12D). In most patients, 12 slices will cover the ventricles from base to apex with adjustment of slice thickness between 4 and 8 mm and the interslice spacing from 0 to 2 mm. Using these guidelines, the range

of ventricular lengths covered is 4.8 to 12 cm. In some infants, the number of slices can be reduced, whereas in older patients with markedly dilated ventricles, or in those with abnormally shaped ventricles (e.g., basal RV “shoulder” protruding past the plane of the tricuspid valve), the number of slices may need to be increased. We prefer not to increase the slice thickness >8 mm and interslice spacing >2 mm to avoid partial volume effect and to minimize extrapolation of interslice data.

Image Analysis. Accurate determination of ventricular volume requires clear depiction of the blood–myocardium boundary. Adjustment of the image brightness and contrast on the computer screen can facilitate visualization of that boundary. By tracing the blood–endocardium boundary, the slice’s blood pool volume is calculated as the product of its cross-sectional area and thickness (which is prescribed by the operator). The left ventricular papillary muscles and the major trabeculations of the RV (e.g., septal and moderator bands) are excluded from the blood pool and are considered part of the myocardium (63,64). Ventricular volume is then determined by summation of the volumes of all slices. The process can be repeated for each frame in the cardiac cycle to obtain a continuous time–volume loop or it may be performed only on end-diastolic (maximal area) and end-systolic (minimal area) frames to calculate diastolic and systolic volumes. From these data one can calculate left and right ventricular ejection fractions and stroke volumes. Since the patient’s heart rate at the time of image acquisition is known, one can calculate left and right ventricular outputs as the product of stroke volume and heart rate. Ventricular mass is calculated by tracing the epicardial borders and calculating the epicardial volume, subtracting the endocardial volume, and multiplying the resultant muscle volume by the specific gravity of the myocardium (1.05 g/mL).



Figure 10.11. Gadolinium-enhanced 3-D MRA of scimitar syndrome. A: Subvolume maximal intensity projection; B: 3-D volume rendering (*posterior view*). L, left; R, right.

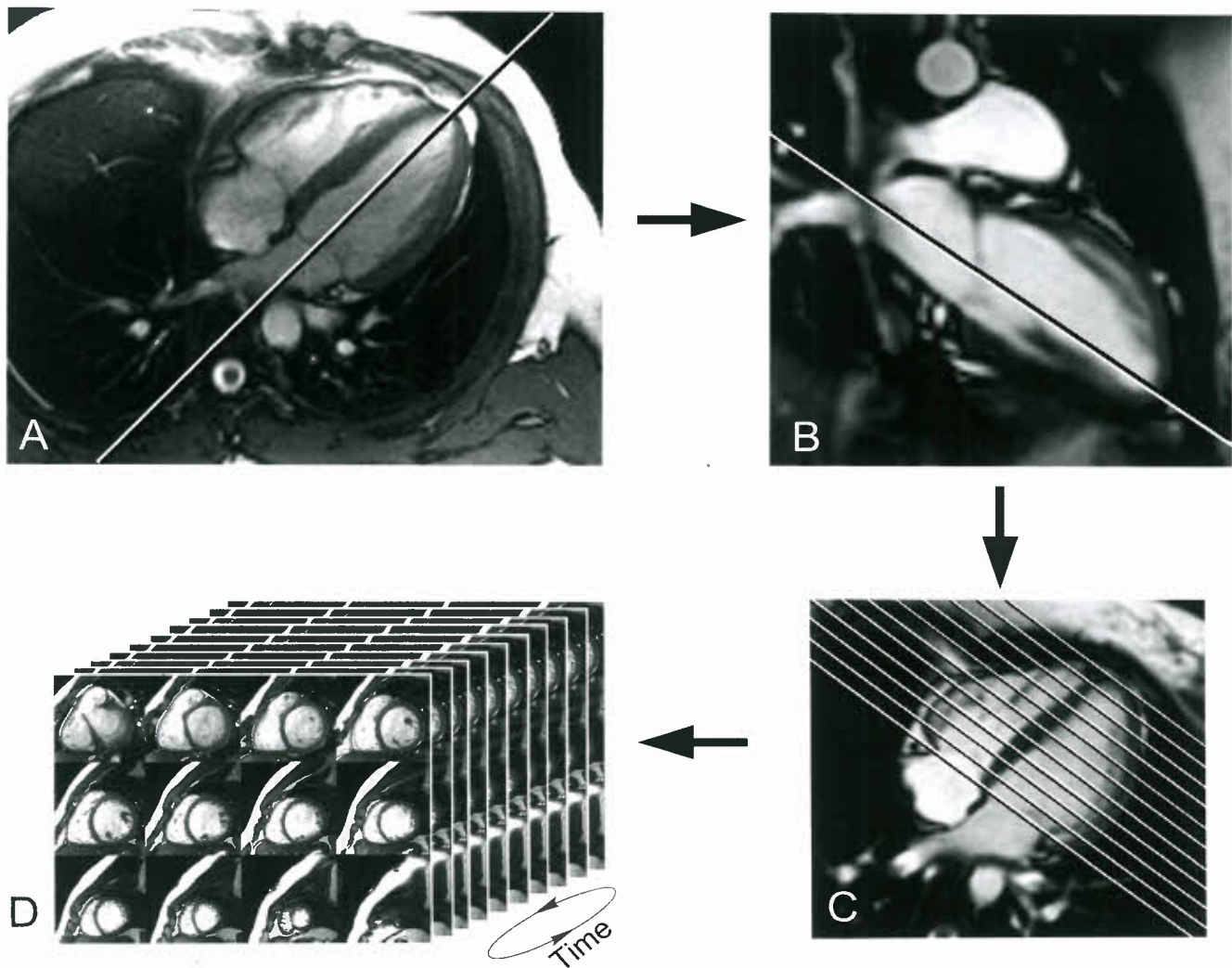


Figure 10.12. Evaluation of ventricular volumes and mass. **A:** Using a localizing image obtained in the axial (transverse) plane, a two-chamber (also known as vertical long-axis) plane is prescribed as shown; **B:** Prescription of the four-chamber plane from an end-diastolic image of the previous two-chamber cine sequence; **C:** Prescription of the short-axis plane from an end-diastolic image of the previous four-chamber cine sequence extending from the plane of the AV valves through the cardiac apex; **D:** The short-axis stack is viewed in cine mode.

Several approaches to measurements of biventricular size and function have been reported. In general, these can be divided into two broad categories: (a) methods that rely on summation of discs (Simpson principle) (65); and (b) methods that rely on modeling the chamber or extrapolation of sparse data (66–68). In the first category, each of the slices covering the ventricles is contoured at least once at end diastole (largest volume) and at end systole (smallest volume). Some groups have advocated the use of images obtained in axial or oblique long-axis planes (69,70). The major advantage of this approach, as compared with analysis based on short-axis images, is the ease of determining the planes of the AV and semilunar valves. This advantage is likely responsible for the slightly higher reproducibility of measurements using older software (70). However, this approach limits evaluation of ventricular mass because the epicardial and endocardial borders of the diaphragmatic wall of the heart are not clearly defined. Recent development of techniques that incorporate cross-references between long-axis and short-axis images has greatly reduced the difficulty in determining valve plane on short-axis images (Fig. 10.12) (71). Moreover,

most reports on normal values as well as the majority of the literature on ventricular size and function in CHD and acquired heart disease are based on analysis of short-axis images (63,72,73).

In the second category, either a formula based on a geometrical model or extrapolation from sparse data is used to generate ventricular volumes (66–68). The major advantage of this approach is shorter analysis time but it is disadvantaged by reduced accuracy.

In our center, ventricular volumes and mass are measured from short-axis cine SSFP images (64). Cross-referencing the short-axis images with left and right ventricular two-chamber (vertical long-axis) and four-chamber (horizontal long-axis) cine SSFP facilitates accurate determination of the AV and semilunar valves planes during systole and diastole (71). To optimize interstudy reproducibility in patients followed longitudinally, contours should be compared side-by-side with those from previous studies. Saving the contour files along with previous studies facilitates this comparison. On average, total analysis time is approximately 25 minutes and decreases with operator experience (71).

Manufacturers of MRI scanners and several third-party companies offer software packages that automatically perform the above calculations. Development of algorithms for automatic border detection has facilitated the application of these techniques, but further refinements are required to improve its accuracy (74–77).

Potential Sources of Errors in Determining Ventricular Volumes by MRI. Translational motion of the ventricles in the base-to-apex direction is most prominent at the base of the heart. Given that the prescribed short-axis slices are fixed in space, there is significant through-plane motion in the basal slices during the cardiac cycle. As a result, the first (and sometimes also the second) most basal slices may contain atrial blood pool during part of the cardiac cycle because the AV junction has moved out of the imaging plane during systole. To avoid erroneous inclusion of the atrial blood pool in the calculation of ventricular volume, the image dataset is examined to distinguish between ventricular and atrial structures. In general, when a slice contains a ventricular chamber throughout the cardiac cycle, the chamber's cross-sectional area decreases in systole and its wall thickness increases. In contrast, in a slice containing ventricular myocardium in diastole and atrial blood pool in systole, the chamber's cross-sectional area increases and wall thickness decreases. Recent development of techniques that incorporate cross-references between long-axis and short-axis images has greatly reduced the difficulty in determining valve plane on short-axis images (71).

Another potential source of error in measurements of ventricular volumes is when the left ventricular papillary muscles and the right ventricular trabeculations are traced in an inconsistent fashion during systole and diastole. For example, exclusion of the papillary muscles from the blood pool in diastole, but not in systole, will lead to underestimation of end-systolic volume, stroke volume, and ejection fraction.

Inconsistent position of the diaphragm during breath holding can lead to spatial variations in the location of the ventricles during acquisition of the short-axis images. This source of error in volume calculation can be minimized by instructing the patient to hold breath at end expiration (78,79).

Accuracy, Reproducibility, and Reference Values of Ventricular Volumes and Function by CMR. The combination of a 3-D dataset, clear distinction between the blood pool and the myocardium, and high spatial and temporal resolutions allow for accurate measurements of any cardiac chamber regardless of its morphology and without geometric assumptions. Much research was performed in the late 1980s and early 1990s on in vitro phantoms, animal models, and in human subjects to validate the accuracy of CMR measurements of ventricular volumes and mass (80–86). More recently, attention has focused on investigating the test characteristics of CMR assessment of chamber dimensions and function, and on comparison of its accuracy and reproducibility with those of echocardiography and radionuclide techniques (87–90). Germain et al. (91) in a study of 20 patients with “good echocardiographic windows,” found that the mean (\pm SD) interstudy variability of CMR measurement of left ventricular mass was $6.75 \pm 3.8\%$ compared with $11 \pm 6.4\%$ for M-mode echocardiography. Bellenger et al. (92) calculated that the sample size required to detect changes in left ventricular volumes, ejection fraction, and mass by CMR in patients with heart failure were substantially smaller compared with published values for 2-D echocardiography. For example, to detect a 10-mL change in end-diastolic volume (with 90% power and $p < 0.05$), 12 subjects must be studied by CMR versus 121 patients examined by 2-D echocardiography; a 3% change in ejection fraction requires 15 CMR versus 102

echocardiograms; and a 10-g change in mass requires 9 CMR versus 273 echocardiograms. Ioannidis et al. (93) compared the accuracy of single-photon emission computed tomography (SPECT) for assessment of left ventricular volumes and ejection fraction with that of CMR. Although the two modalities correlated well, compared with CMR, there was a substantial variation in individual measurements by SPECT. Half of the SPECT ejection fraction determinations deviated by at least 5% from CMR-obtained values and one in four deviated by at least 10%. In patients with CHD, Mooij et al. (71) demonstrated low interobserver coefficient of variations in 60 children, most with abnormalities affecting the right heart. The coefficient of variations for RV volumes and mass ranged from 6.4% to 11.3% and for LV volumes and mass from 3.6% to 10.5%.

Because CMR techniques continue to evolve, different imaging sequences may yield different measurements of ventricular dimensions and function. Several studies have compared the normal range of left and right ventricular mass, volume, and ejection fraction measured by cine SSFP with values obtained by the fast (turbo) GRE cine technique (94). In general, compared with fast GRE, measurements based on cine SSFP resulted in larger ventricular volumes, lower mass, and similar ejection fraction. Importantly, both intraobserver and interobserver variations were lower with SSFP measurements. The range of SSFP-based left and right ventricular volumes, mass, and ejection fraction in 60 healthy subjects ranging in age from 20 to 65 years was published by Alfakih et al. (63). Other groups have published similar data in healthy adults (72,95). Several reports on SSFP-based normal values of ventricular dimensions in children have been published (73,96,97), but data in infants and young children are still lacking.

Assessment of Myocardial Function

Although ejection fraction and other ejection phase indices such as shortening fraction and velocity of circumferential fiber shortening are useful markers of ventricular function and provide valuable prognostic information, they are influenced by preload, afterload, heart rate, and the contractile state of the myocardium. Moreover, load-dependent ejection phase indices such as ejection fraction can be normal despite depressed contractility and, conversely, can be depressed despite having normal contractility. Therefore, assessment of ventricular function by load-independent indexes provides useful information on the contractile state of the myocardium. A detailed discussion of ventricular mechanics is beyond the scope of this chapter and can be found elsewhere (98,99).

Assessment of the contractile state of the myocardium by CMR has been investigated by Setser et al. (100) using normalized maximal ventricular power. An alternative approach is to adjust ejection phase variables such as ejection fraction, velocity of fiber shortening, or wall strain to end-systolic stress. With knowledge of left ventricular end-systolic volume, mass, and pressure (estimated based on mean arterial blood pressure measured by sphygmomanometry), end-systolic stress can be estimated as follows (99):

$$P = (2/3)\sigma_p(\ln V_0 - \ln V_c)$$

where

V_c is cavity volume

V_0 is chamber volume (cavity volume + myocardial volume)

σ_p is average of orthogonal fiber stresses $(\sigma_{p\phi} + \sigma_{p\theta})/2$.

It should be noted that experience with this method in CMR is lacking.

Analysis of Regional Wall Motion

A simple qualitative approach is to visually evaluate segmental ventricular wall motion and thickening imaged from long- and short-axis cine SSFP sequences. The LV is divided into 17 segments, as recommended by the American Heart Association (Fig. 10.13) (101) and the RV is divided into nine segments as described by Klein et al. (102) (Fig. 10.14). Ventricular wall motion is classified as normal (appropriate systolic wall motion normal to the local wall segment accompanied by myocardial thickening indicative of fiber shortening), hypokinesis (reduced systolic motion and wall

thickening), akinesis (no appreciable systolic wall motion and no change in wall thickness), or dyskinesis (outward systolic wall motion without myocardial thickening). A more objective approach is to define the endocardial and epicardial boundaries of the ventricles throughout the cardiac cycle, and, using commercially available software, quantitatively analyze wall motion and myocardial thickening (103). The main drawback of this approach is that it is time-consuming, which hinders its acceptance into routine clinical practice. However, improvements in automatic border detection can shorten the process and may lead to increased use of this technique.

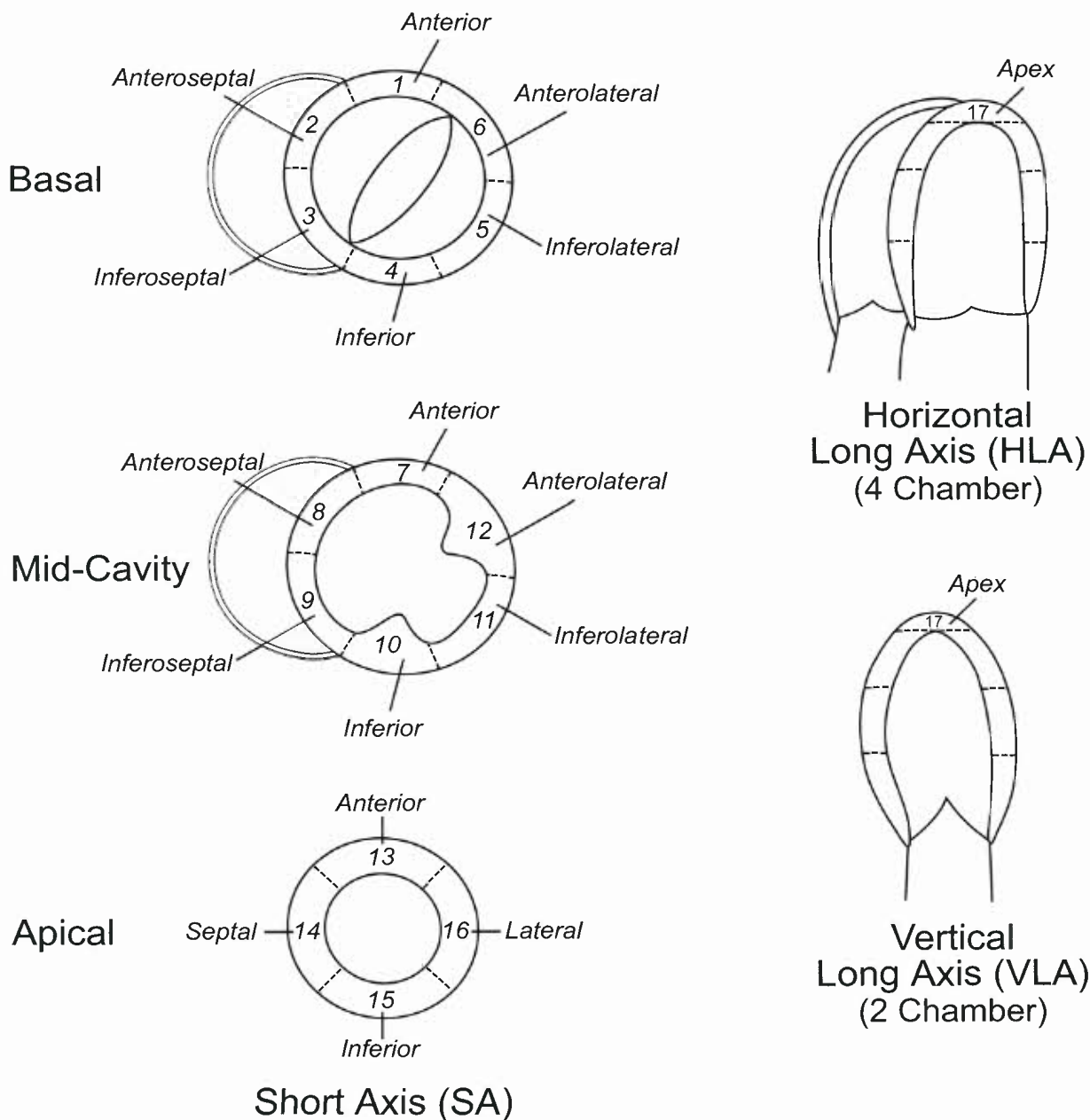


Figure 10.13. Left ventricular wall segments. Ant, anterior; Inf, inferior; Lat, lateral; LV, left ventricle; MV, mitral valve; PM, papillary muscles; Post, posterior; RV, right ventricle; SAX, short-axis; Sept, septal. (Adapted and modified from Cerqueira MD, Weissman NJ, Dilsizian V, et al. Standardized myocardial segmentation and nomenclature for tomographic imaging of the heart: a statement for health care professionals from the Cardiac Imaging Committee of the Council on Clinical Cardiology of the American Heart Association. *Circulation* 2002;105:539–542 with permission.)

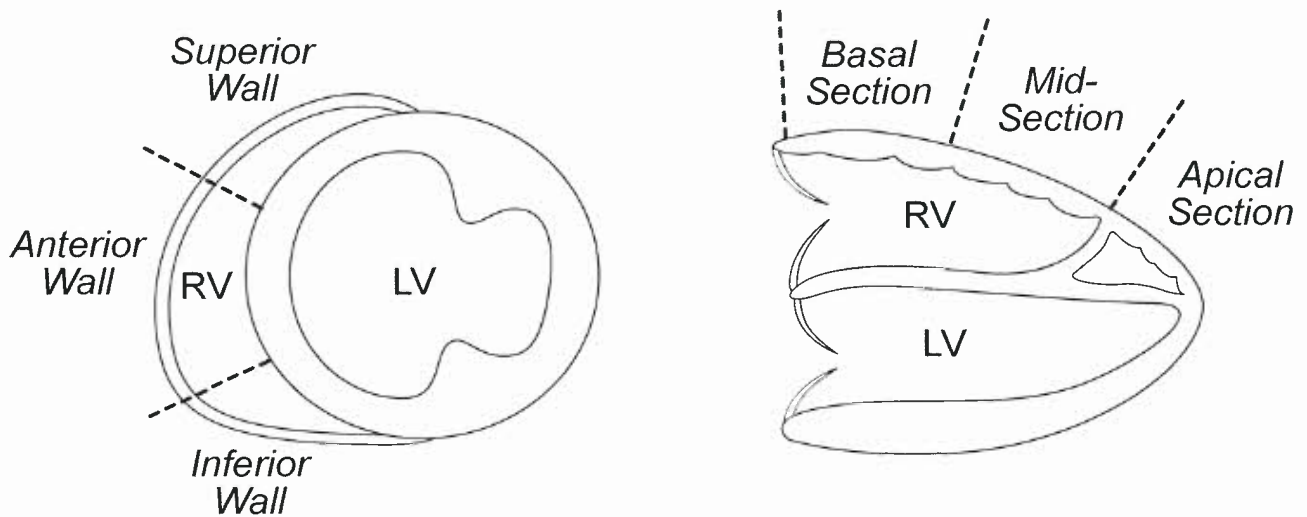


Figure 10.14. Right ventricular wall segments. (Adapted and modified from Klein SS, Graham TP Jr, Lorenz CH. Noninvasive delineation of normal right ventricular contractile motion with magnetic resonance imaging myocardial tagging. *Ann Biomed Eng* 1998;26:756–763.)

Analysis of Myocardial Strain and Stress

Analysis of myocardial strain provides information on regional myocardial function. Although myocardial strain can be calculated from velocity information obtained by phase-velocity cine MRI technique (similar to tissue Doppler imaging), most investigators favor a technique called *myocardial tagging* using spatial modulation of magnetization (SPAMM) (104). This technique is a modification of cine gradient echo MRI that allows tracking of myocardial motion in two or three spatial dimensions over time. Using a preparatory RF pulse, saturation bands or “tags” that appear as dark lines or stripes are applied across the image at end diastole (Fig. 10.15). On subsequent images, the stripes (tags) will remain unchanged on stationary tissue such as the chest wall and spine but will change their position on moving tissues such as ventricular myocardium. As the myocardium moves during the cardiac cycle, the tags follow it and their rotation, translation, and deformation can be tracked allowing for calculation of myocardial strain and strain rate (105). This analysis can be done during systole or diastole and in two or three dimensions (106). Early studies with myocardial tagging were mostly done by manual tracking of the tags, a time-consuming process that hindered the clinical use of this technique. A modified technique for the analysis of myocardial tagging data, harmonic phase imaging (HARP), greatly shortens analysis time because it does not require manual tracing of the tags (107). This technique relies on automatic analysis of the raw MRI data for changes in phase between images. With recent advances in automatic analysis of the tag data and fast image acquisition and display techniques, it is now possible to evaluate myocardial strain in real time (10).

Myocardial tagging has been shown to be an important research tool in the study of normal left (108–110) and right (102,111) ventricular mechanics in healthy volunteers. In the clinical arena, analysis of wall strain by myocardial tagging has provided useful information in patients with ischemic and valvular heart disease (112–115). In a study of 211 patients with chest pain, Kuijpers et al. (116) demonstrated that myocardial tagging detects more segments with regional wall motion abnormalities by dobutamine stress CMR (DSMR) than visual assessment alone. Evaluating patients with CHD, Fogel et al. (117–119) used myocardial tagging to characterize patterns of wall motion and strain in patients with functionally

single ventricles. As new fast MRI techniques coupled with automatic analysis of myocardial tagging become more widely available, the clinical application of ventricular strain analysis will likely expand. Further research is required to determine the clinical implications of the strain data and how it can be used to assess prognosis and guide patient management.

Tissue tracking, which is a relatively new method to assess myocardial motion and deformation by echocardiography (120), has recently been successfully applied to CMR (Fig. 10.16) (121). By comparing differences in signal intensities (speckles) from one frame to the next, specialized software tracks the motion of the myocardium and calculates displacement, strain, and strain rate in user-defined regions of the ventricles. Advantages of this technique include the ability to perform the analysis on existing cine CMR images and no requirement for additional sequences such as myocardial tagging. Using this technique, Ortega et al. (122) recently demonstrated in patients with repaired TOF that indexes of left ventricular dyssynchrony were associated with death and sustained ventricular tachycardia.

Stress CMR

There is a growing body of literature on the use of DSMR in the evaluation of myocardial ischemia in adults with coronary artery disease (see discussion in the section on myocardial ischemia below). Several studies have evaluated the use of stress CMR in patients with CHD. In a study of 32 children with congenital and acquired pediatric heart disease, Strigl et al. (123) demonstrated the feasibility of dobutamine CMR for evaluation of stress-induced wall motion abnormalities. Using a protocol that included dobutamine doses up to 40 $\mu\text{g/kg/min}$ and atropine to attain a target heart rate ($0.85 \times [220 - \text{age}]$), the authors demonstrated excellent interobserver agreement (100%) for test positivity and good agreement (92%) for segmental wall motion score. Tulevski et al. (124,125) used a low-dose (15 $\mu\text{g/kg/min}$) dobutamine to evaluate the functional reserve of the LV and RV in asymptomatic and minimally symptomatic patients with repaired TGA, physiologically corrected TGA, and pulmonary outflow obstruction. Compared with controls, patients with systemic RV had decreased functional reserve. In another study from the same group, Dodge-Khatami et al. (126) showed that the functional reserve of the systemic ventricle is comparable in healthy adults and in patients with unoperated, physiologically

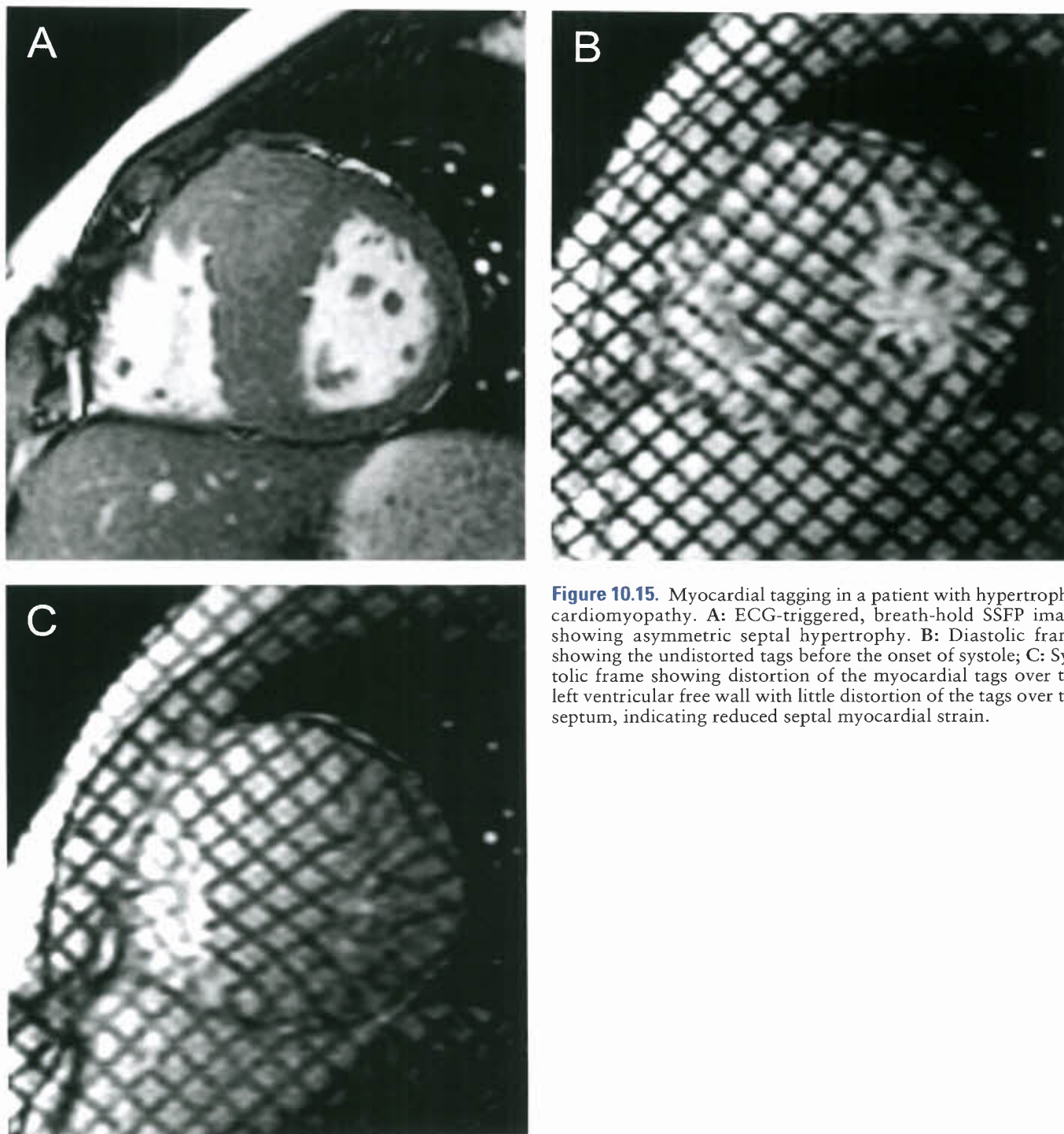


Figure 10.15. Myocardial tagging in a patient with hypertrophic cardiomyopathy. **A:** ECG-triggered, breath-hold SSFP image showing asymmetric septal hypertrophy. **B:** Diastolic frame showing the undistorted tags before the onset of systole; **C:** Systolic frame showing distortion of the myocardial tags over the left ventricular free wall with little distortion of the tags over the septum, indicating reduced septal myocardial strain.

corrected TGA. Roest et al. (127) demonstrated the feasibility of assessing biventricular dimensions and function by CMR during supine exercise, a method that provides an alternative to pharmacologic stress.

Diastolic Function

Diastole is a complex process during which the force of the myofibers is restored (128). A detailed discussion of diastolic ventricular mechanics is beyond the scope of this chapter and can be found elsewhere in this text. Researchers have utilized

various modalities and a wide array of parameters to assess diastolic function, such as changes in pressure and chamber dimensions, wall thinning, myocardial velocities and strain, and a wide range of flow-derived variables obtained by Doppler interrogation of the AV valves and pulmonary veins. With the exception of direct pressure measurements, MRI can also evaluate all of the above variables (129–134). For example, Helbing et al. (129) used CMR to measure blood flow through the tricuspid and pulmonary valves as well as changes in right ventricular dimensions to assess diastolic function after TOF repair. Although the data derived from analysis of blood flow

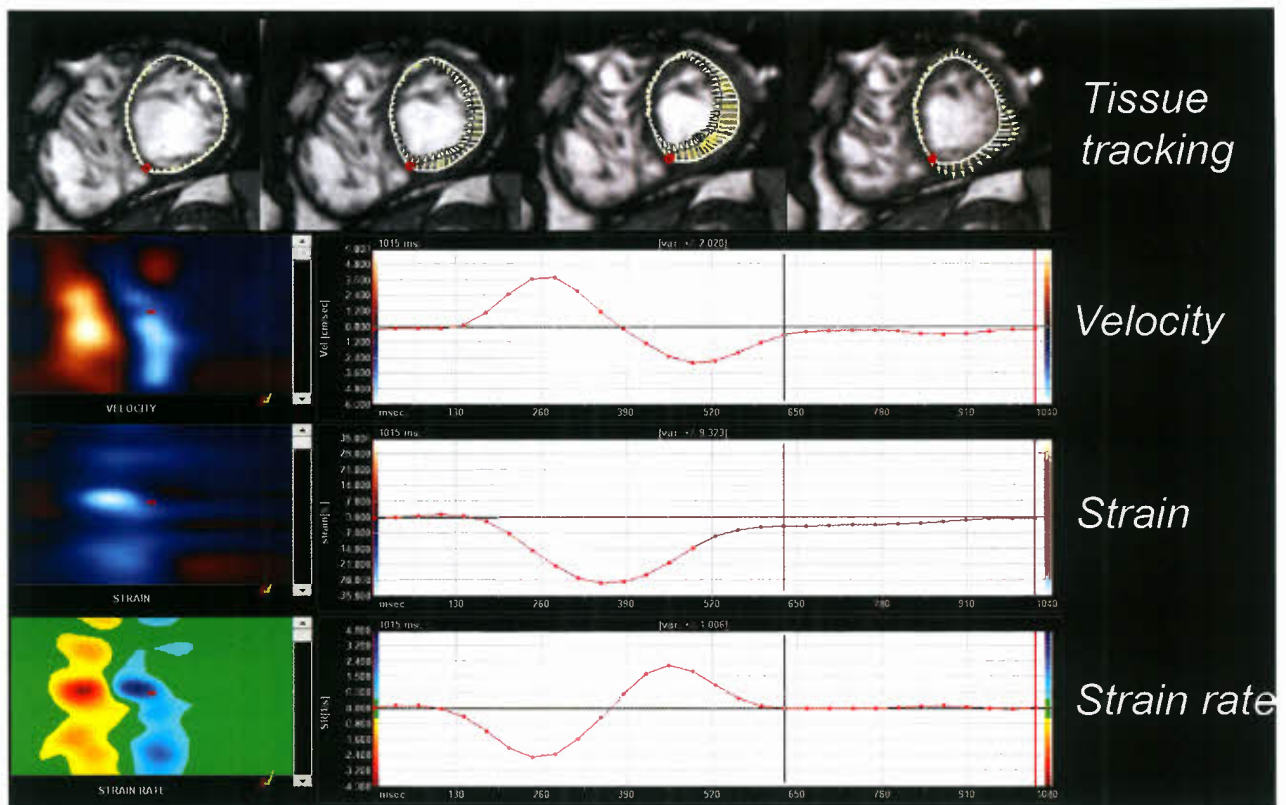


Figure 10.16. Tissue tracking CMR. The software tracks the motion of the left ventricular myocardium throughout the cardiac cycle on short-axis cine SSFP images (top panel), analogous to speckle tracking echocardiography. The tissue velocity, strain, and strain rate versus time are calculated (lower three panels).

and chamber dimensions by MRI are not fundamentally different from similar data obtained by other techniques, MRI offers an advantage in terms of its ability to track tissue motion and deformation during the cardiac cycle using tissue tagging techniques (131,133,135). Fogel et al. (131) used myocardial tagging to study left ventricular diastolic strain in 11 infants with structurally normal heart. They demonstrated inhomogeneities in both circumferential lengthening (E_2) and radial thinning (E_1). Another investigation has demonstrated in a canine model that measurements of the velocity of myocardial untwisting and recoil rate assessed by MRI using tissue tagging correlate closely with the time constant of relaxation or tau (τ) ($r = -0.86$), was unaffected by left atrial pressure, and that τ but not loading conditions was an independent predictor of the recoil rate (133). Thus, the rate of recoil of torsion derived by tissue tagging may provide a noninvasive preload independent isovolumic phase measure of ventricular relaxation.

Flow Analysis

Quantitative and qualitative assessment of blood flow is frequently used in functional MR evaluation of congenital and acquired pediatric heart disease (136). Qualitative evaluation of abnormal flow patterns is used to visualize turbulent flow jets related to stenotic or regurgitant valves or abnormal communications between cardiac chambers or blood vessels (e.g., septal defects, patent ductus arteriosus (PDA), systemic-to-pulmonary shunts, etc.). Site-specific quantification of flow rate, flow velocity, stroke volume, and minute flow can, in principal, be measured across any blood vessel within the central cardiovascular system.

Technique. An ECG-gated VEC MRI sequence, a type of gradient echo sequence, can be used to measure blood flow velocity and quantify blood flow rate (136,137). The VEC MRI technique is based on the principle that the signal from hydrogen nuclei (such as those in blood) flowing through specially designed magnetic field gradients accumulates a predictable phase shift that is proportional to its velocity. Multiple phase images are constructed across the cardiac cycle in which the signal amplitude (intensity) of each voxel is proportional to mean flow velocity within that voxel. Using specialized software, regions of interest around a vessel are defined, and the flow rate is automatically calculated as the product of the mean velocity and the cross-sectional area (Fig. 10.17).

In practice, an imaging plane is prescribed perpendicular to the vessel of interest and two sets of multiphase images are reconstructed following a VEC MRI acquisition: a set of *magnitude images* that provide anatomic information and a set of *phase images* in which the velocity information is encoded. For each acquisition, the operator prescribes the field of view, matrix size, and slice thickness, which, in turn, determine spatial resolution. Greil et al. (138), in an in vitro study using a pulsatile flow model, found that spatial resolution is important for accurate measurements of flow rate by VEC MRI with an optimal number of pixels within the cross section of the vessel of interest ≥ 16 . Other variables such as the angle between the prescribed imaging plane and flow direction, velocity encoding range, flip angle, and slice thickness must also be considered. Other known caveats of quantitative assessment of blood flow by VEC MRI include flow aliasing and dephasing secondary to turbulent flow. Aliasing can be avoided by prescribing a velocity encoding range higher than the maximal velocity within the target vessel. Avoiding dephasing secondary to turbulent

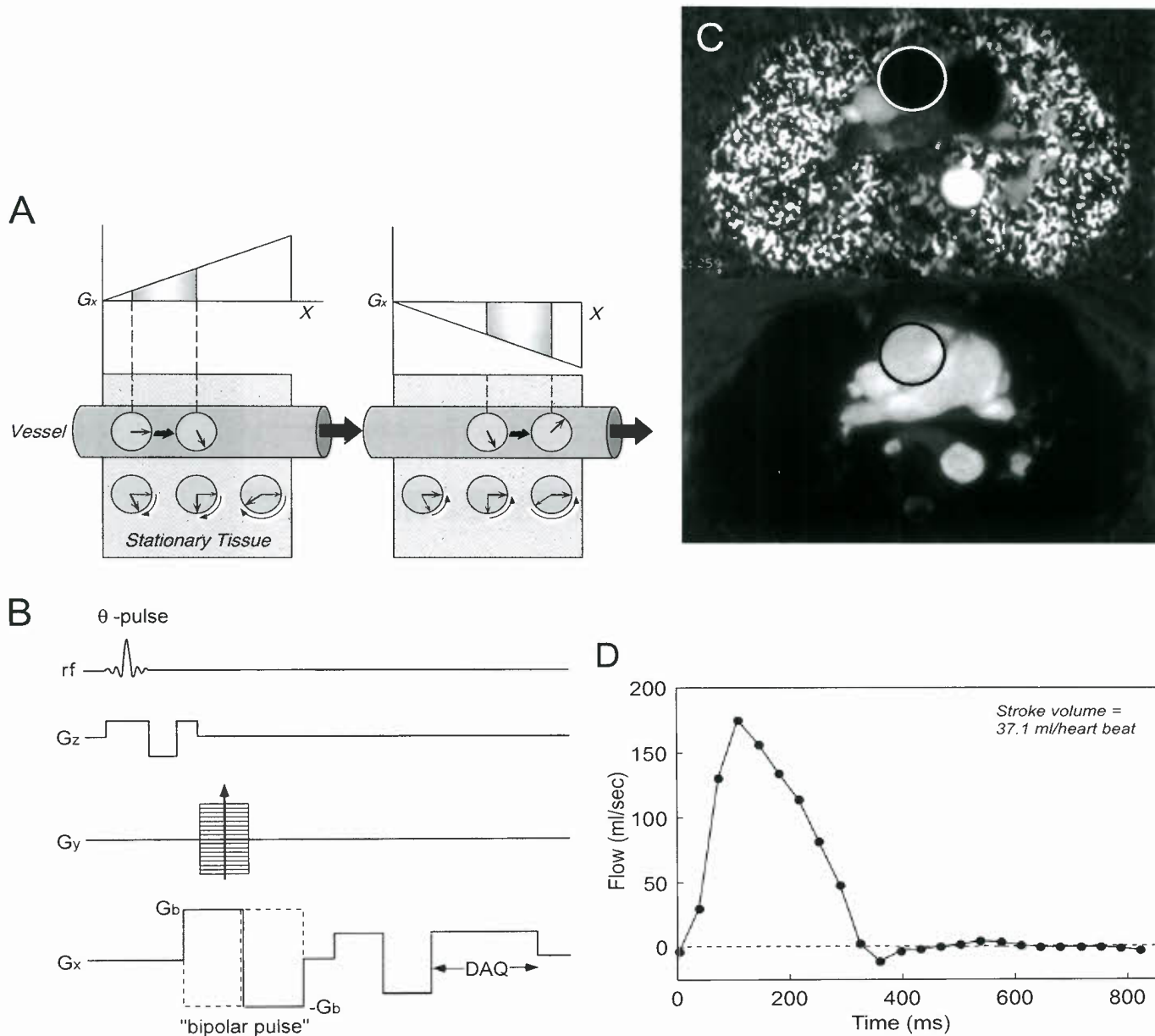


Figure 10.17. Flow velocity cine MRI. **A:** Schematic representation of phase velocity encoding. **Left panel:** A magnetic field gradient (G_x) is briefly applied in the velocity encoding direction (x) causing phase variations to develop. **Right panel:** The gradient is then reversed so that it has equal magnitude and duration but opposite polarity. In stationary tissue, there is no net phase shift because the reversal of the gradient field cancels the effect of the initial gradient application. In contrast, flowing blood in the vessel is now in a different location and is therefore exposed to a different gradient strength (shaded region). Consequently, a net phase shift will result that is proportional to flow velocity. **B:** A typical phase-velocity cine MRI pulse sequence diagram (rf, radiofrequency; G_z , slice select gradient; G_y , frequency select gradient; G_x , phase encoding gradient; DAQ, data acquisition window). **C:** Transverse (axial) view of phase-velocity cine MRI perpendicular to the ascending aorta. **Top panel:** Phase-sensitive image. The signal intensity in this image is linearly proportional to flow velocity. Flow direction is encoded in black (inferior-to-superior) or white (superior-to-inferior). **Bottom panel:** Magnitude image reconstructed based on the amplitude of the tissue signal intensity. To measure the flow in the ascending aorta, a region of interest (*circle*) is placed using off-line computer software. **D:** Flow-time curve. Instantaneous flow rates are calculated multiple times during the cardiac cycle by integrating the flow velocities across the vessel cross-sectional area. The area under the curve represents the stroke volume. Minute flow is calculated by multiplying the stroke volume by the heart rate.

blood flow can be achieved by shortening the echo time, prescribing a thinner slice thickness, or repositioning the imaging slice proximal or distal to the turbulent jet.

Accuracy of Blood Flow Measurements by MRI. VEC MRI flow calculations have been shown by in vitro and in vivo studies to be accurate and reproducible (138–143). In vitro studies have demonstrated that measurements of continuous flow are accurate within 5% of reference standard (144,145). Greil et al. (138) demonstrated that the accuracy and reproducibility of in vitro pulsatile flow measurements by VEC MRI is $0.8 \pm 1.5\%$. Evans et al. (143) found a strong correlation ($r^2 = 0.99$) with a 95% confidence interval of ± 0.07 L/min over a range of flow rates 0.125 to 1.9 L/min. Powell et al. (140), in a phantom model that mimics flow condition in the aorta of a child (flow rates 1.25 to 3.5 L/min), found a similarly strong correlation, a close agreement (bias = -0.045 L/min), and 95% limits of agreement of -0.19 to 0.1 L/min.

The accuracy of in vivo VEC MRI measurements of blood flow has been demonstrated by numerous studies. Investigators have used ventricular stroke volume, thermodilution, Fick principle, indicator dilution, and flow probe measurements as reference standards, showing strong correlations with VEC MRI (140,146–152). Hundley et al. (151) found that ascending aorta flow in 23 adults was within 4% of flow measurements by the Fick method and within 5% measured by thermodilution. Evans et al. (143), in a study of 10 adult subjects, demonstrated an average difference between pulmonary (Q_p) and systemic (Q_s) flow ratio of 5%. Powell et al. (140), in a study of 20 healthy volunteers, found that Q_p/Q_s closely approximated unity (mean \pm SD = 0.99 ± 0.1 , range 0.85 to 1.19). Beerbaum et al. (139), in a study of 50 children

with atrial or ventricular septal defects (VSDs) who underwent concomitant cardiac catheterization, reported a mean difference between VEC MRI and oximetry of 2% (2SD = -20% to $+26\%$). Powell et al. (153), in a study of 20 patients with atrial septal defect (ASD), found a mean difference between VEC MRI and oximetry of 2.3% with a reproducibility of repeat VEC MRI flow measurements of $1.1 \pm 4.2\%$ in the main pulmonary artery and $0.7 \pm 5.4\%$ in the ascending aorta (Fig. 10.18).

Clinical Applications. Measurements of blood flow are an integral element of functional assessment by MRI in a wide range of clinical scenarios. Examples include measurement of cardiac output (151,154), pulmonary-to-systemic flow ratio in patients with intra- and extracardiac shunts (139–141,153,155,156), regional flow to selected organs or vascular beds (e.g., patients with vascular malformations) (157–159), valvular regurgitation in patients with native and postoperative lesions (e.g., pulmonary regurgitation after TOF repair) (160–170), differential lung perfusion (e.g., branch pulmonary artery stenosis) (171–173), quantification of aortopulmonary collateral flow (174,175), AV valve inflow (129), estimation of pressure gradient (170,176,177), and a variety of other clinical scenarios.

Keeping in mind the known limitations of VEC MRI (136,138,178), site-specific quantification of flow rate, flow velocity, stroke volume, and minute flow can provide useful hemodynamic information in a wide range of clinical scenarios. Pharmacologic stress can be used to provide additional information on functional reserve (179). For example, using either dipyridamole or adenosine for vasodilation of the coronary vascular bed, coronary flow reserve can be assessed (180). An inherent strength of functional assessment by MRI

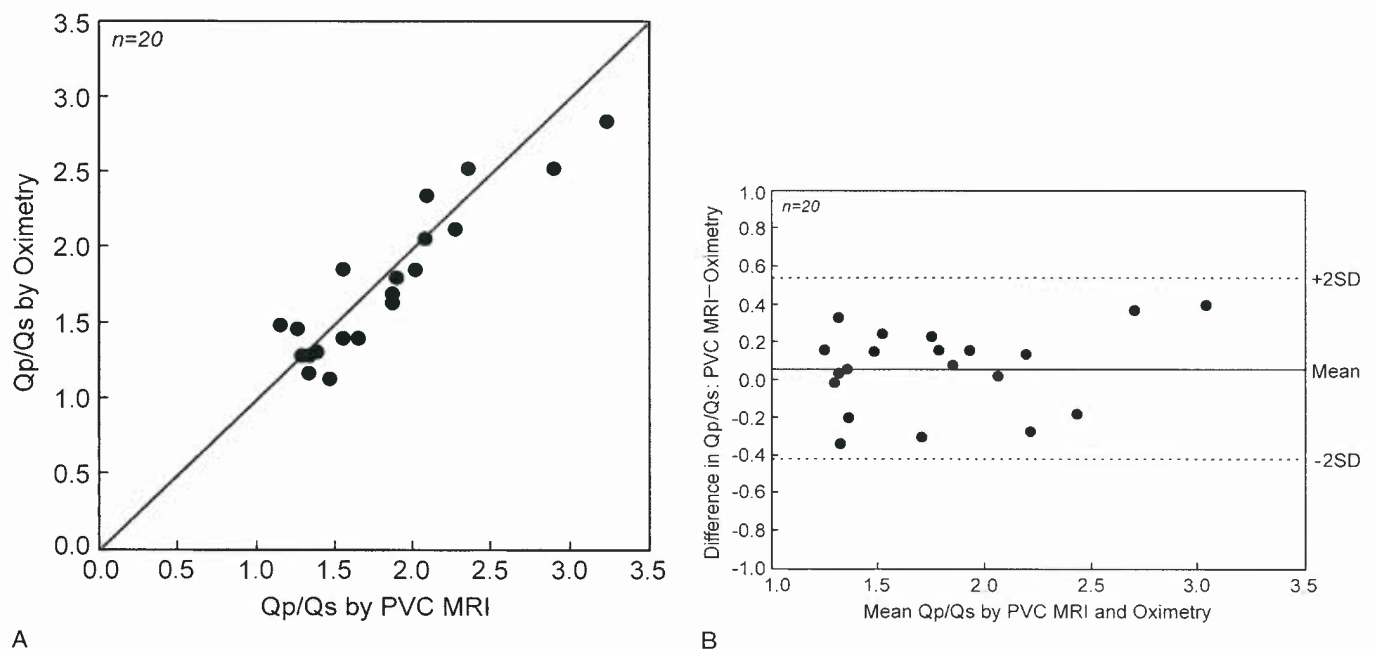


Figure 10.18. Accuracy of phase velocity cine (PVC) MRI measurements of blood flow in 20 patients with interatrial shunt (From Hundley WG, Meshack BM, Willett DL, et al. Comparison of quantitation of left ventricular volume, ejection fraction, and cardiac output in patients with atrial fibrillation by cine magnetic resonance imaging versus invasive measurements. *Am J Cardiol* 1996;78:1119–1123, with permission). A: Mean pulmonary-to-systemic (Q_p/Q_s) flow ratio by oximetry versus mean Q_p/Q_s by PVC MRI. B: The difference in Q_p/Q_s versus mean Q_p/Q_s by PVC MRI and oximetry. The mean difference was 0.06 L/min (solid line) and ± 2 standard deviations from the mean (95% limits of agreement) were -0.42 and 0.54 L/min (dashed lines). (Reprinted from Powell et al. Comparison between phase-velocity cine magnetic resonance imaging and invasive oximetry for quantification of atrial shunts. *Am J Cardiol* 2003;91:1523–1525, with permission from Elsevier.)

is the ability to measure the same variable by different methods, thus allowing for internal validation of the functional data. For example, in a patient with an ASD, the pulmonary-to-systemic flow ratio can be assessed based on (a) flow measurements in the main pulmonary artery and ascending aorta; (b) flow measurements through the tricuspid and mitral valves (typically obtained in a single acquisition perpendicular to plane of the AV valves); and (c) LV and RV stroke volumes obtained by short-axis cine MR. Although standard VEC MRI techniques require 2 to 4 minutes of data acquisition in each site, developments of faster imaging strategies (e.g., segmented k space acquisition and parallel processing) have greatly shortened the acquisition time (156,181–184). Although these techniques allow for data acquisition during a short period of breath holding (10 to 14 seconds), the physiologic effects of suspended respiration may alter intrathoracic pressure and affect flow measurements. Sakuma et al. (185) demonstrated that flow measurements during large lung volume breath holding significantly underestimated cardiac output (4.47 ± 0.63 vs. 6.09 ± 0.49 L/min), whereas cardiac output measurements during small lung volume breath-holding was similar to that obtained during free breathing. Development of real-time velocity-encoded techniques has a potential utility analogous to color Doppler in echocardiography (169). This technique has recently proved valuable in providing unique physiologic information in patients with Fontan circulation (186).

The preceding discussion focused on through-plane flow measurements. When velocity information is measured in the three orthogonal planes (anterior–posterior, superior–inferior, and through plane), multidimensional flow imaging and shear stress calculation can be accomplished (187–190). 3-D flow vector mapping is a useful adjunct to cine flow imaging because it provides dynamic 3-D flow maps that can readily detect abnormal flow patterns (Fig. 10.19).

Myocardial Perfusion and Viability

Compared with the adult population, myocardial ischemia related to coronary artery disease is uncommon in infants and children. In the pediatric population, ischemia may be associated with congenital coronary abnormalities such as

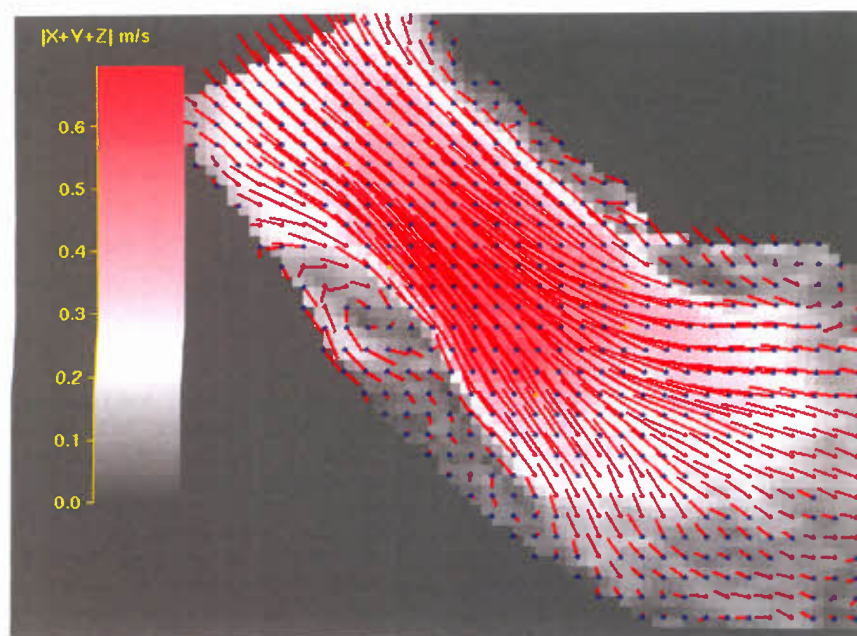
anomalous origin of a coronary artery from the pulmonary artery or from the opposite sinus of Valsalva, or acquired conditions, most notably Kawasaki disease. Alternatively, the coronary circulation may be compromised in postoperative patients, especially those whose procedure involved relocation of the coronary arteries (e.g., ASO). Patients who have undergone heart transplantation are also at risk for the development of accelerated coronary artery disease and abnormalities of the coronary microvasculature.

In comparison with nuclear techniques, cardiac MRI is a relatively young tool for detection of myocardial ischemia and viability. As a result, one should remember during the subsequent discussion that the available data on its clinical utility and applicability are considerably smaller than for the more established techniques. This limitation is perhaps offset by the fact that data specific to children and young adults are scarce for all of the non-invasive techniques. The feasibility of assessing myocardial perfusion and viability by CMR in children and patients with CHD has been demonstrated with encouraging results (191–195).

Myocardial Ischemia. Currently, the two most widely used CMR techniques to detect ischemia are DSMR and first-pass myocardial perfusion (196–198). DSMR is performed using a protocol similar to dobutamine stress echocardiography (DSE) with increasing doses of dobutamine up to 40 to 50 $\mu\text{g/kg/min}$ and the addition of atropine if necessary to reach the target heart rate. The goal of the test is to detect ventricular myocardium supplied by a stenotic coronary artery. At rest, the myocardial blood supply/demand ratio may be sufficient to allow normal wall motion and thickening. However, with increasing metabolic demand under pharmacologic stress, ischemia may be induced and wall motion is impaired. Imaging is usually performed with breath-hold cine SSFP MRI, thereby providing high-quality images of left ventricular wall motion and thickening. Nagel et al. (199) compared the sensitivity and specificity of DSMR with that of DSE in 208 patients for the detection of >50% coronary artery stenosis determined by coronary angiography. Compared with DSE, DSMR was more sensitive (86.2% vs. 74.3%), had a higher specificity (85.7% vs. 69.8%), and better accuracy (86% vs. 72.7%) ($p < 0.05$ for all). CMR has a particular advantage over echocardiography in patients who have poor acoustic windows (up to 15% of studies in adults).

First-pass myocardial perfusion CMR can also be used to diagnose myocardial ischemia. After intravenous injection of a

Figure 10.19. 3-D flow vector mapping in the aortic root and proximal ascending aorta in a patient with Marfan syndrome. The origin of the flow is depicted as a *blue dot* and the *red line* represents the direction and velocity of the flow.



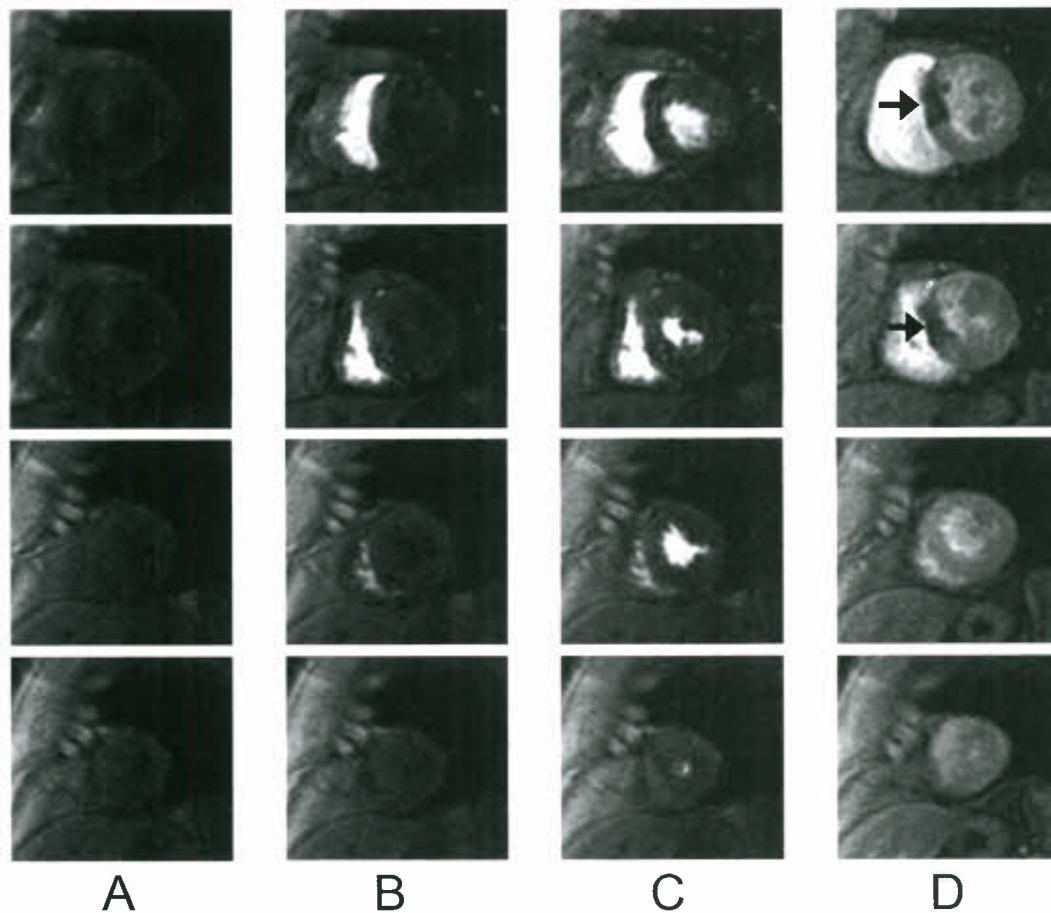


Figure 10.20. First-pass myocardial perfusion in a patient with anterior septal myocardial infarction. **A:** Four short-axis slices (top frame, basal slice; bottom frame, apical slice) before arrival of the contrast; **B:** The contrast enters the RV; **C:** The contrast enters the LV but not the coronary arteries (note the bright signal from the blood pool but not from the myocardium); **D:** Segments with well-perfused myocardium show bright signal whereas the hypoperfused anterior septal segment remains dark (arrows).

gadolinium-based contrast agent, the enhancement pattern of the myocardium is evaluated during the first transit of the bolus through the heart. The appearance of contrast will be attenuated, both in amplitude and rate, in regions of compromised coronary blood flow (Fig. 10.20). In practice, the contrast (e.g., gadopentetate dimeglumine 0.05 to 0.1 mmol/kg) is infused through a large bore cannula using a power injector at a rate of 3 to 5 mL/s. With the patient holding his or her breath, the heart is rapidly imaged in multiple planes for approximately 30 seconds using a cardiac-triggered fast gradient hybrid echo-planar or cine SSFP pulse sequences. An inversion preparation pulse is also used which minimizes the signal from myocardium and thus enhances the relative increase in signal intensity produced by the T1-shortening effects of the contrast agent. Because exercise stress cannot be readily done in the MRI scanner, most perfusion studies are performed with vasodilators such as adenosine or dipyridamole. Both qualitative and quantitative analysis have been reported; the latter is done typically by constructing time-intensity curves of myocardial regions and calculating a perfusion reserve index (200,201).

Myocardial Viability. In addition to detection of ischemia, CMR can also be used to differentiate viable from nonviable myocardium. Myocardial delayed enhancement (MDE) imaging, also known as late gadolinium enhancement (LGE) imaging, has become the dominant MRI technique to assess viability (202). It is based on the observation that in necrotic myocardium and in areas where the myocardium is replaced

by collagen (e.g., scar tissue) the washout kinetics of gadolinium-based MRI contrast agents is delayed and its volume of distribution is increased. Consequently, nonviable myocardium appears bright or hyperenhanced compared with viable myocardium when imaged with a segmented inversion recovery fast gradient echo sequence after contrast injection (Fig. 10.21). In practice, MDE imaging is performed 10 to 20 minutes after administration of 0.1 to 0.2 mmol/kg of gadolinium-based contrast. The optimal inversion time is selected using inversion-recovery fast multishot echo-planar imaging, such as a Look-Locker sequence (203). Using this inversion time, MDE is then performed in ventricular short- and long-axis planes.

Several studies in both animals and humans have shown that this technique is effective at identifying the presence, location, and size of acute and chronic myocardial infarction (204–213). Klein, et al. (214) found close agreement between MDE imaging and positron emission tomography (PET) scar size measurements in 31 patients with ischemic heart failure. Because of its superior spatial resolution, MDE is more sensitive than SPECT in patients with small or subendocardial infarctions (215). Most importantly, the transmural extent of MDE can be used to predict improvement in contractile function after revascularization in patients with acute and chronic coronary artery disease (216–219). Another promising clinical application of MDE imaging is detection of myocardial fibrosis in patients with hypertrophic cardiomyopathy (220). Kim et al. (221) demonstrated that the extent of myocardial fibrosis assessed by MDE can be used to stratify risk in these

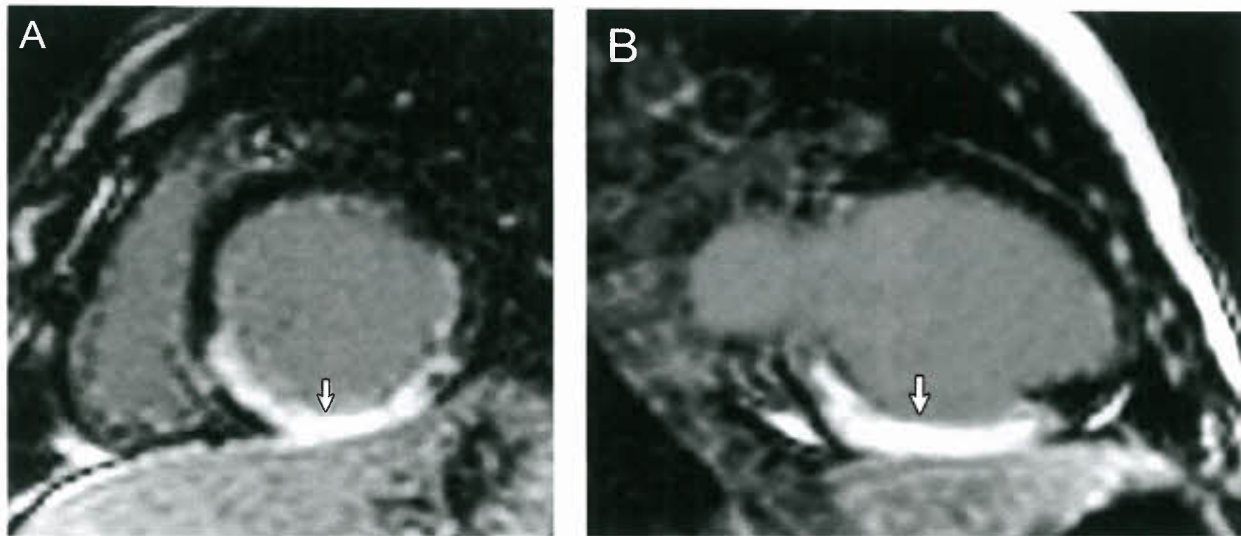


Figure 10.21. MDE imaging in a 4-year-old patient with Kawasaki disease complicated by coronary artery aneurysms and occlusion of the left circumflex coronary artery. **A:** Short-axis view showing enhancement of the inferior wall (arrow), consistent with transmural myocardial infarction; **B:** Long-axis view showing the base-to-apex extent of the infarct.

patients. Other groups have recently found similar results (222–225). In pediatric and CHD patients, Prakash et al. (191) studied 30 patients with a median age of 13 years (range 0.3 to 40 years) whose diagnoses included repaired CHD in 15, cardiomyopathy in 6, cardiac tumor in 3, dysplastic LV in 2, congenital coronary anomaly in 2, and coronary artery aneurysm following Kawasaki disease in 2. They found good agreement between MRI evaluation of myocardial perfusion and viability and analysis of segmental wall motion, as well as coronary angiography ($n = 10$) and SPECT ($n = 6$). More recently, studies have demonstrated the usefulness of MDE imaging to evaluate endomyocardial scar tissue in patients with systemic RV (193), repaired TOF (192,226,227), endocardial fibroelastosis in hypoplastic left heart syndrome (228), and late after Fontan operation (194).

Diffuse Myocardial Fibrosis. Although contrast-enhanced MDE imaging has been shown to accurately evaluate myocardial necrosis and scar tissue in ischemic and nonischemic heart disease, the technique cannot evaluate diffuse interstitial fibrosis. Several groups have recently developed CMR techniques to measure diffuse myocardial fibrosis based on postgadolinium T1 mapping (29,229–231). Myocardium with more fibrosis will have a higher concentration of gadolinium contrast and thus a shorter T1. Azevedo et al. (232), in a study of 54 adult patients with aortic valve stenosis, demonstrated good agreement between CMR and histologic measurements of diffuse left ventricular fibrosis. Given that this technique holds promise as a noninvasive means to measure diffuse myocardial fibrosis, further studies addressing its accuracy, reproducibility, and clinical usefulness in patients with acquired and CHD are warranted (229).

Tissue Characteristics

Assessment of the myocardium, pericardium, blood vessels wall, and extracardiac tissue for pathologic changes can be valuable in a variety of clinical circumstances. MRI offers a distinct advantage over other modalities for the evaluation of soft tissues because of its ability to discern even minor changes in tissue composition. By manipulations of T1 and T2 weightings and by applying a variety of prepulses or suppression of signals from specific tissue elements such as fat or water, tissue composition can be evaluated. Clinical applications include assessment of myocardial architecture

(e.g., myocardial noncompaction (233,234) and ventricular aneurysm (235,236), evaluation of cardiac and pericardial tumors (Fig. 10.22) (237,238), vessel wall imaging (e.g., aortic dissection (240,241), assessment of the myocardium for fatty infiltration or other pathologic changes (e.g., arrhythmogenic right ventricular cardiomyopathy (242,243), evaluation of the pericardium (e.g., constrictive pericardium (244,245), and assessment of myocardial iron load (245).

In practice, MRI assessment of tissue characteristics is based on the use of several imaging sequences. FSE sequence is used for morphologic imaging of the myocardium, pericardium, blood vessel walls, and extracardiac structures. Manipulations of image contrast (T1, T2, or proton density weighting) and the addition of prepulses (e.g., triple inversion recovery, T2

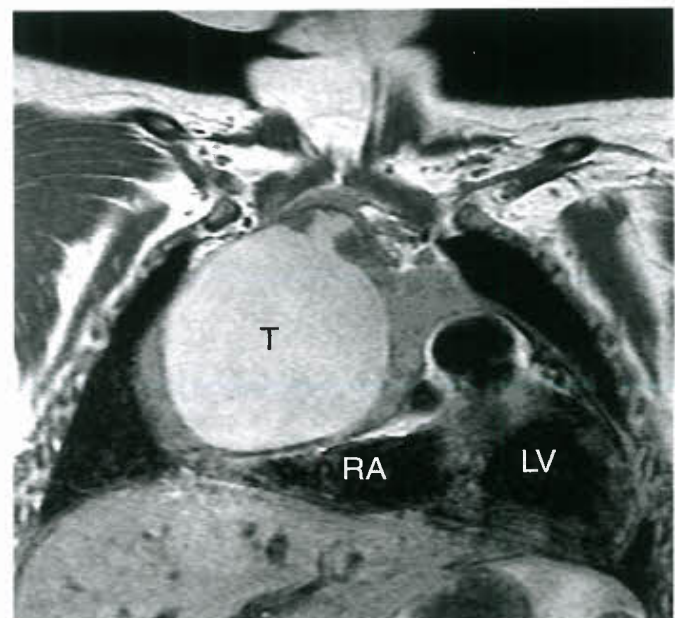


Figure 10.22. Coronal plane T1-weighted FSE image in a patient with pericardial teratoma (T). Note the compressed RA. LV, left ventricle.

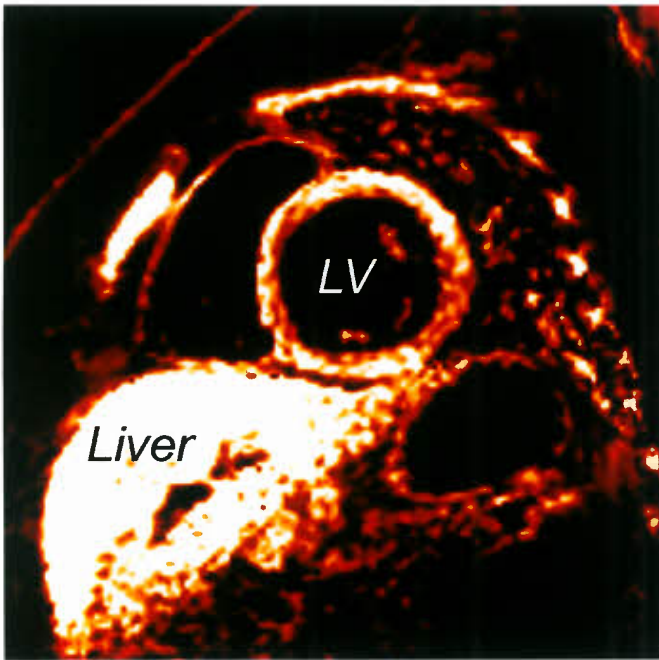


Figure 10.23. MRI assessment of myocardial and liver iron using T2* mapping in a patient with thalassemia major. Note the high signal intensity in the liver and in the left ventricular myocardium, corresponding to high iron concentrations in these organs.

preparation, and fat or water saturation) result in highlighting or suppression of specific tissue characteristics. T2* mapping is used to evaluate myocardial and liver iron concentrations (Fig. 10.23) (246–248). Gradient echo sequences provide information on signal intensity and, more important, on motion of the tissue in question. First-pass myocardial perfusion, early and late enhancement after intravenous administration of gadolinium-based contrast, and myocardial tagging can provide additional diagnostic information about tissue characteristics.

EXAMPLES OF CLINICAL APPLICATIONS OF CMR

Shunt Lesions

Atrial Septal Defect

CMR can be helpful in selected patients with a known or suspected ASD, usually adolescents and adults with inconclusive clinical and echocardiographic findings. For example, CMR provides a noninvasive alternative to transesophageal echocardiography and to diagnostic catheterization in patients with right ventricular volume overload, in whom transthoracic echocardiography cannot demonstrate the source of the left-to-right shunt (249–253). CMR can visualize different types of atrial-level defects, including secundum, primum, sinus venosus, and coronary sinus septal defects. In patients with sinus venosus defect, CMR can provide all the necessary information required for surgical planning. The goals of the CMR examination include delineation of the location and size of the ASD, its relations to key neighboring structures, its size, suitability for transcatheter versus surgical closure, and functional assessment of the hemodynamic burden, including pulmonary-to-systemic flow ratio, and RV size and function.

Although SE sequences have been used to diagnose ASDs, thin structures such as septum primum may not be clearly demonstrated, leading to an overestimation of the defect's

size or to a false positive diagnosis. Cine MRI using SSFP is capable of providing high-quality imaging of the atrial septum and the adjacent anatomic structures, including the vena cavae, pulmonary veins, and the AV valves. The atrial septum is imaged in at least two planes by obtaining a stack of ECG-triggered multiphase SSFP images, a stack in the axial or four-chamber planes, and a stack in an oblique sagittal plane (Fig. 10.24). Additional cine SSFP imaging is performed in the short-axis plane across the ventricles to quantify LV and RV volumes and function. This stack also allows qualitative assessment of RV systolic pressure based on the configuration of the interventricular septum. The septal geometry is concave toward the RV when the RV/LV pressure ratio is low and assumes a flat configuration, or even a concave shape toward the LV, as the RV/LV pressure ratio increases. Interpretation of the hemodynamic significance of septal configuration may be confounded by factors such as inhomogeneous contraction of the RV, intraventricular conduction delay (e.g., right or left bundle branch block, preexcitation), and a high LV pressure.

Measurement of the pulmonary-to-systemic flow ratio (Q_p/Q_s) is clinically helpful in patients with ASD. Several studies have shown that flow measurements in the main pulmonary artery (Q_p) and ascending aorta (Q_s) using VEC MRI agree closely with catheterization-based oximetry (139,153,254,255). In the absence of AV valve regurgitation or an additional shunt, Q_p/Q_s can also be measured by VEC MRI in the ventricular short-axis plane perpendicular to the mitral (Q_s) and tricuspid valve (Q_p) inflows. A third option is to compare the RV and LV stroke volumes obtained by the short-axis cine SSFP. In clinical practice, it is recommended to measure the Q_p/Q_s ratio by more than one method in order to evaluate the data for internal consistency. Flow velocity mapping across the ASD using VEC MRI can be used to further delineate the defect. Color-coded in-plane flow velocity mapping (Fig. 10.24B) or 4-D flow velocity mapping can characterize the flow across the defect (256).

Non-ECG triggered Gd-enhanced 3-D MRA sequence is not ideally suited for evaluation of secundum ASDs due to blurring of thin intracardiac structures. However, this sequence is helpful in the evaluation of sinus venosus septal defects, especially since these defects invariably involve the pulmonary veins (Fig. 10.25).

Ventricular Septal Defect

CMR is rarely used primarily for the evaluation of a VSD. In our experience, only 7 of 1,119 CMR examinations (0.6%) were requested for evaluation of an isolated VSD, primarily for assessment of ventricular dimensions and function and Q_p/Q_s measurement in patients with inadequate or inconsistent echocardiographic data. Many other CMR studies, however, were performed for other indications in patients in whom a VSD was present.

VSDs can be imaged by gradient echo (preferably SSFP) or SE sequences obtained in any combination of planes (Fig. 10.26). The four-chamber plane provides a base-to-apex view of the septum, whereas the short-axis plane images the interventricular septum from anterior–superior to posterior–inferior. Additional imaging in other planes should be performed if the location of the defect and its relation to neighboring key structures (e.g., AV or semilunar valves) is not demonstrated by imaging in standard planes. Measurement of ventricular dimensions and function is a key element of the CMR evaluation in a patient with VSD. Quantification of Q_p/Q_s provides additional hemodynamic information and can be achieved either by VEC MRI flow measurements in the ascending aorta and main pulmonary artery, across the mitral and tricuspid valves, or by comparison of the LV and RV stroke volumes. In the presence of additional shunts (e.g., ASD or PDA) or valve regurgitation, calculation of Q_p/Q_s must be adjusted to account for the effect of the additional flow.

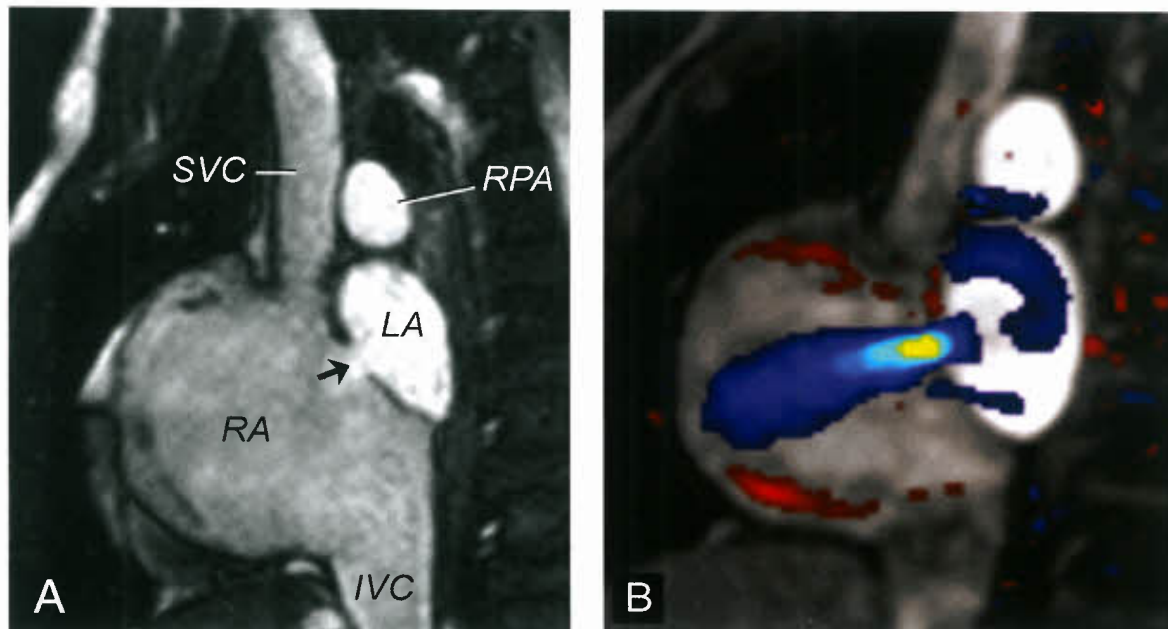


Figure 10.24. Secundum ASD. A: Oblique sagittal SSFP image showing a centrally located defect (arrow); B: Color-coded phase-velocity cine MRI showing flow from the left atrium (LA) to the RA through the defect. LA, left atrium; IVC, inferior vena cava; RA, right atrium; RPA, right pulmonary artery; SVC, superior vena cava.

Patent Ductus Arteriosus

CMR is seldom requested primarily for assessment of an isolated PDA. In several types of complex CHD, evaluation of the ductus arteriosus is an important element of the examination. For example, in patients with TOF and pulmonary atresia, the

ductus arteriosus can be an important source of pulmonary blood supply (257,258). Gd-enhanced 3-D MRA is a particularly helpful imaging technique in these patients because it allows accurate delineation of all sources of pulmonary blood supply, including a PDA, aortopulmonary collateral vessels, and the central pulmonary arteries (259). Another clinical circumstance in which MRI evaluation of a PDA may be requested is the adult with CHD in whom limited acoustic windows can hamper echocardiographic evaluation. Imaging of a PDA can be accomplished by several MRI sequences (Fig. 10.27). If a PDA is detected, it is vital to also evaluate the direction of flow across the duct by VEC MRI, to assess the hemodynamic burden by measurements of ventricular volumes and function, to measure the Q_p/Q_s , and to assess RV pressure by septal position in the short-axis plane.

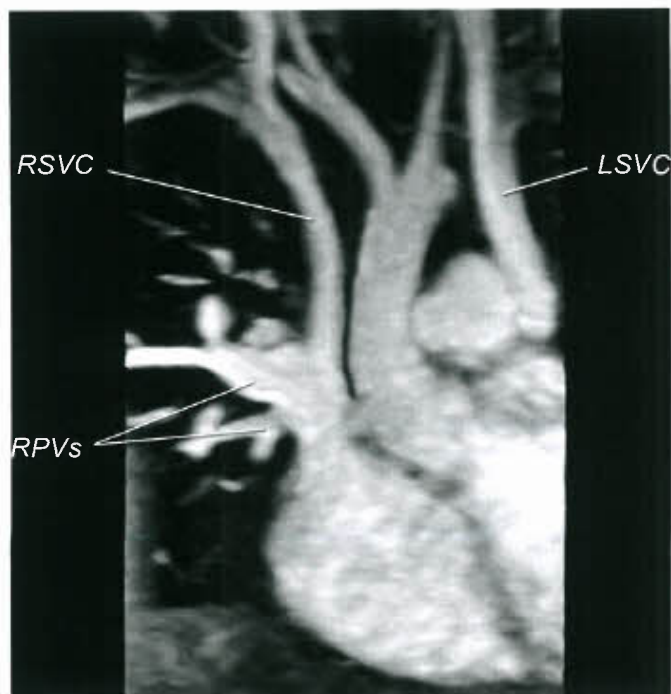


Figure 10.25. Maximal intensity projection Gd-enhanced 3-D MRA showing drainage of right pulmonary veins (RPVs) to the cardiac end of the right superior vena cava (RSVC) in a patient with sinus venosus defect and bilateral superior vena cavae. LSVC, left superior vena cava.

Anomalies of the Aorta

Coarctation of the Aorta

The use of MRI to image anomalies of the aortic arch dates back to the early 1980s (260). While those studies provided mostly static anatomical information, the advent of new imaging sequences has greatly expanded the diagnostic capabilities of CMR to include comprehensive anatomic and functional evaluation. In adults with CHD, Therrien et al. (261) have shown that the combination of clinical assessment and MRI provides a better “cost-effective” yield compared with a combination that relies on echocardiography as the primary imaging modality. Others have shown the utility of CMR in infants and children with coarctation and other anomalies of the aortic arch (176,262,263).

The objectives of the CMR evaluation of suspected or repaired aortic coarctation include (a) detailed imaging of the aorta including the proximal brachiocephalic arteries and the descending aorta to the level of the renal arteries; (b) imaging of blood flow throughout the thoracic aorta to detect high-velocity flow jets suggestive of stenosis; (c) detection of collateral vessels that bypass the coarctation site; (d) assessment of

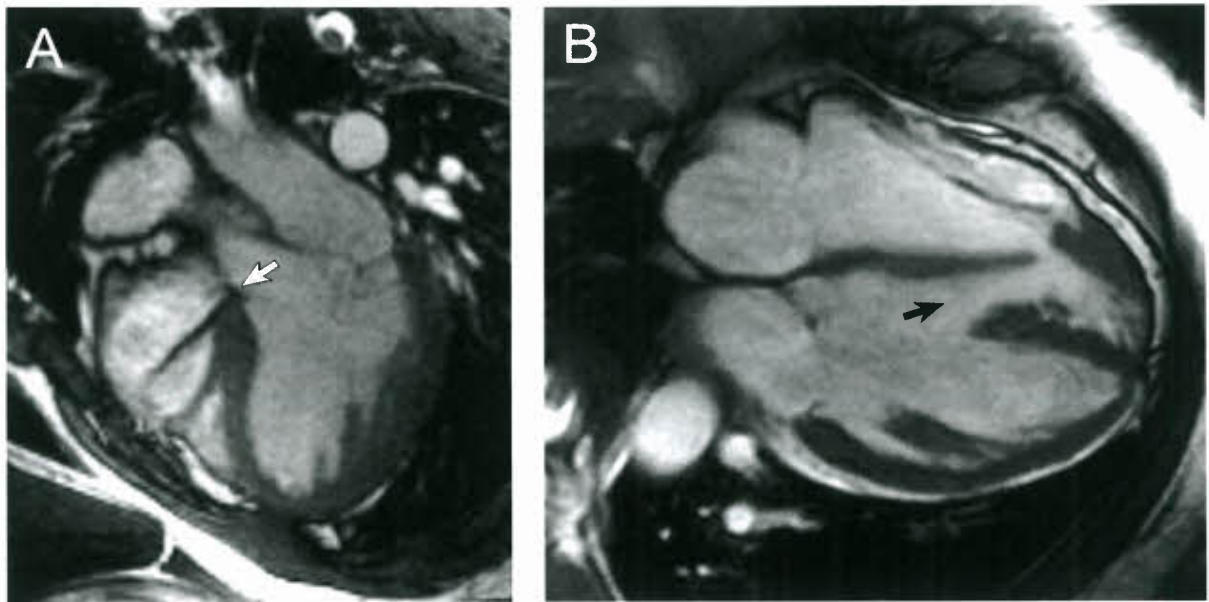


Figure 10.26. ECG-triggered, breath-hold, cine SSFP imaging of VSD. A: Small membranous VSD (arrow); B: Large muscular VSD (arrow).

left ventricular mass, volumes, and function; and (e) detection of any associated lesions.

Much of the anatomic information is gleaned from the Gd-enhanced 3-D MRA, including the anatomy of the aorta, imaging of collateral vessels, and cross-sectional measurements of the aorta in various locations (Fig. 10.28). A 3-D SSFP sequence provides an alternative to contrast MRA when an intravenous cannula cannot be placed or if there is a contraindication to the use of Gd. A SE sequence with double inversion recovery provides high-resolution imaging of the

aortic wall. This may be particularly important in cases with discrete coarctation comprised of a thin “shelf” that protrudes into the aortic lumen and in patients with atypical location of the coarctation such as in the abdomen (Fig. 10.29). Gradient echo sequences are helpful for detection of signal void due to high-velocity turbulent jets.

Evaluation of the hemodynamic significance of coarctation is an important element of the CMR examination. Several investigations compared the anatomic features and the extent of collateral blood flow with coarctation diameter measured

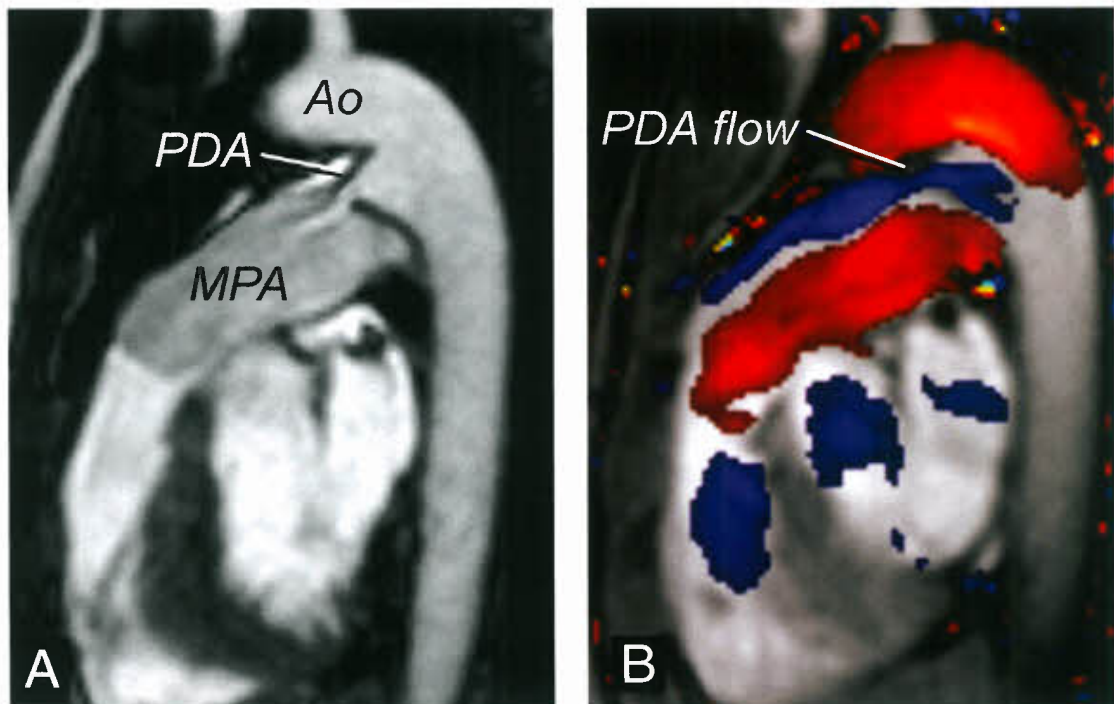


Figure 10.27. MRI evaluation of PDA. A: Cine SSFP in an oblique sagittal plane showing small PDA; B: Color-coded cine phase velocity MRI showing flow from the aortic isthmus (Ao) to the main pulmonary artery (MPA).

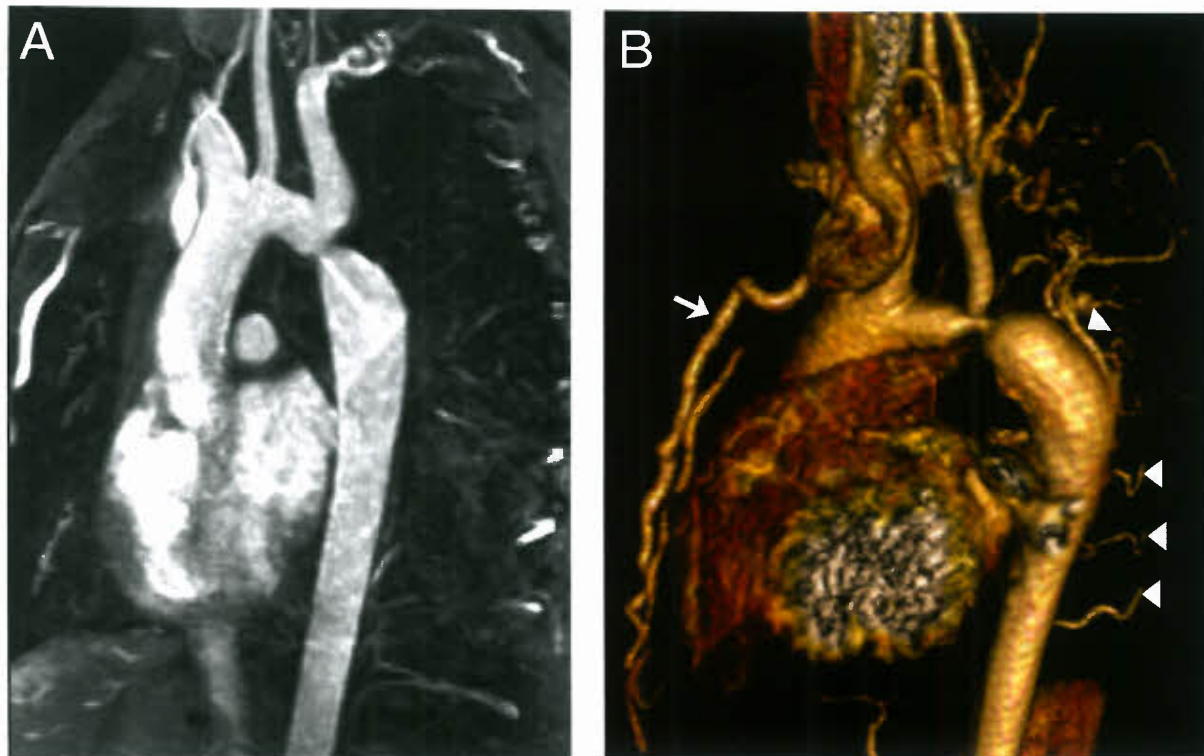


Figure 10.28. Gadolinium-enhanced 3-D MRA in patients with severe aortic coarctation. **A:** Maximal intensity projection; **B:** 3-D volume rendering showing prominent internal mammary arteries (*arrow*) and collateral vessels to the descending aorta (*arrowheads*).

by x-ray angiography (262,263), blood pressure measurements by sphygmomanometry (264), and Doppler assessment of flow velocity (265). Riquelme et al. (266) showed a correlation coefficient of 0.99 between gradient echo cine MRI measurement of coarctation diameter and angiography. Simpson et al. (262) and Mendelsohn et al. (263) reported correlation coefficients of 0.9 and 0.91, respectively. Other groups have focused on the percent increase in descending aorta flow from collateral vessels to assess CoA severity. Steffens et al. (267) reported that the percent increase in flow correlated with the

diameter of the CoA segment ($r = 0.94$), with arm-to-leg blood pressure difference ($r = 0.84$), and with Doppler gradient ($r = 0.76$). More recently, Araoz et al. (264) demonstrated that the percent increase in descending aorta flow in 19 patients with repaired coarctation more accurately reflected the degree of narrowing than arm-to-leg blood pressure measurements. We have developed a CMR-based model to predict the probability of hemodynamically significant coarctation defined as a pressure gradient ≥ 20 mm Hg measured by catheterization (268). The combination of the smallest cross-sectional area of the

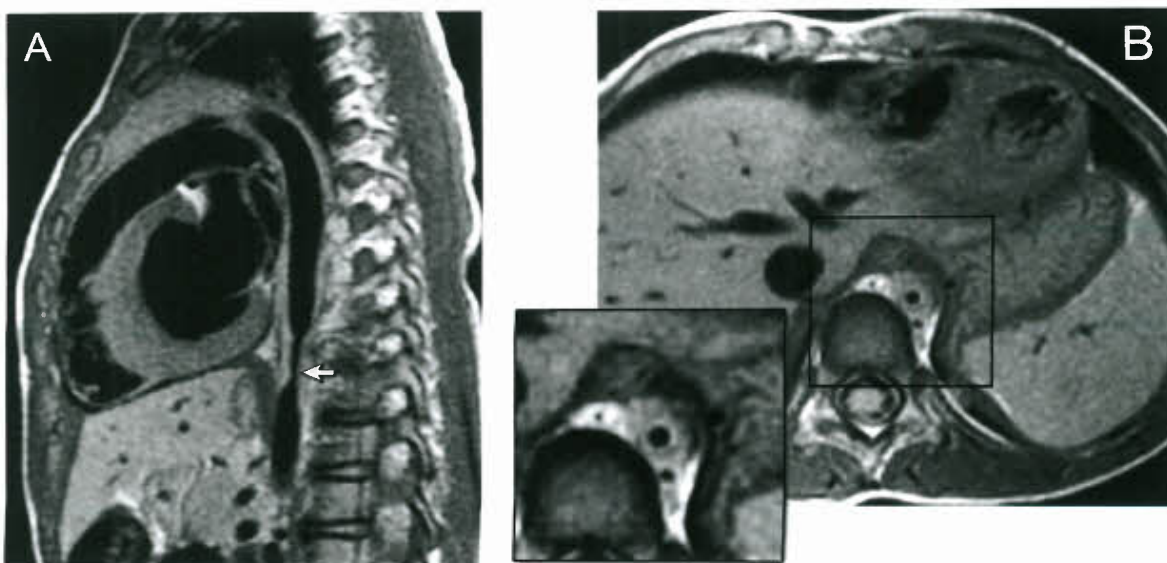


Figure 10.29. FSE imaging showing severe long-segment abdominal coarctation in a 5-year-old patient with Takayasu arteritis. **A:** Sagittal view; **B:** Axial (transverse) view showing marked thickening of the aortic wall.

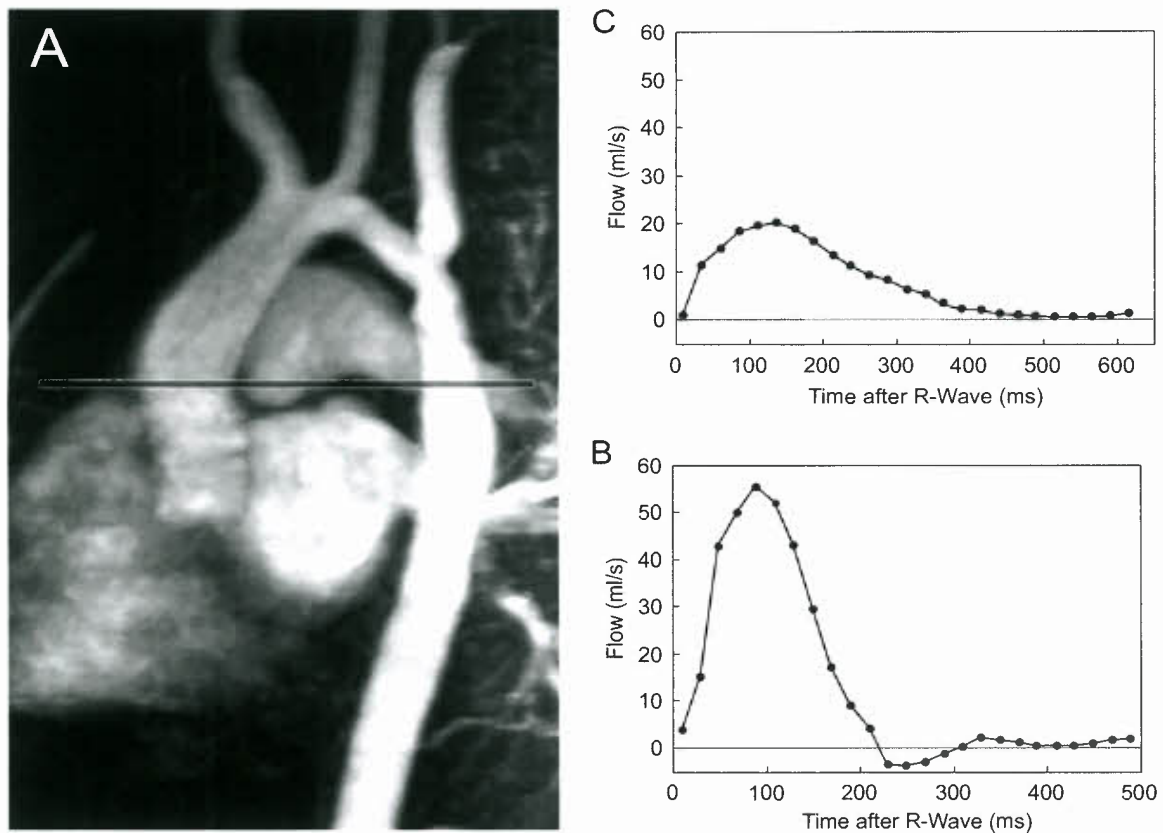


Figure 10.30. Evaluation of coarctation severity based on flow pattern in the descending aorta and the smallest cross-sectional area of the coarctation segment (268). **A:** Imaging plane for flow measurements in the ascending and descending aorta; **B:** Descending aorta flow pattern in a patient with repaired coarctation and no residual obstruction. Note the sharp upstroke and short deceleration phase; **C:** Descending aorta flow pattern in a patient with severe coarctation. Note the shallow upstroke and prolonged deceleration.

aorta (measured from the Gd-enhanced 3-D MRA) and the heart rate-adjusted mean deceleration of flow in the descending aorta (measured by VEC MRI distal to the CoA) (Fig. 10.30) predicted coarctation severity group with 95% sensitivity, 82% specificity, 90% positive and negative predictive values, and an area under the receiver-operator characteristics curve of 0.94. Muzzarelli et al. (269) recently demonstrated that the optimal location for assessing the flow profile in the descending aorta is at the level of the diaphragm.

Aortic Aneurysm and/or Dissection

Severe dilation, aneurysm formation, and dissection can complicate the course of some congenital cardiac defects such as bicommissural aortic valve and TOF, and are common in patients with Marfan syndrome and other connective tissue disorders. CMR is an ideal modality for longitudinal noninvasive assessment of the aorta, especially in adolescents and adults in whom the echocardiographic windows are often limited. In contrast to CT, CMR does not expose the patients to the risks of ionizing radiation and can also provide functional information such as measuring aortic regurgitation fraction and left ventricular dimensions and function. In patients with suspected acute dissection who may require emergent intervention, CT angiography might be more readily available.

The imaging strategy for assessment of aortic aneurysm is modified from the protocol used for aortic coarctation. Both spin and gradient echo sequences are acquired in planes perpendicular and parallel to the long-axis of the aorta (Fig. 10.31A). The branch vessels of the aorta are also examined

to determine for extension of an aneurysm, dissection, or obstruction. A stack of thin-sliced ECG-triggered SSFP cine is acquired perpendicular to the aortic root and ascending aorta. This sequence allows accurate measurements of orthogonal dimensions of the dilated aortic segment during systole. In addition, the aortic wall is examined in detail for evidence of dissection and VEC MRI is used to evaluate aortic valve function. This technique can also be used to distinguish between flow in the true and false lumen of aortic dissection. Gd-enhanced MRA is particularly helpful for evaluation of tortuous aortic segments and branch vessels (Fig. 10.31B).

Vascular Rings and Pulmonary Artery Sling

Vascular rings constitute an uncommon form of congenital vascular anomaly in which the trachea and esophagus are encircled completely by vascular structures. Rings are formed by abnormal persistence and/or regression of components of the aortic arch complex. MRI is ideally suited for evaluation of vascular rings and LPA sling because it provides good visualization of the airways and the vasculature, imaging can be performed in any plane, and there is no exposure to ionizing radiation (270,271). The main drawback of MRI is the need for sedation given that most patients with vascular rings are too young to cooperate. Although vascular rings account for fewer than 1% of patients with CHD, they account for 10% of all CMR examinations in our laboratory in patients younger than 1 year of age (272). Although multirow detector CT with contrast can provide excellent imaging of the airways and vasculature, this technique is associated with a significant exposure to ionizing radiation.

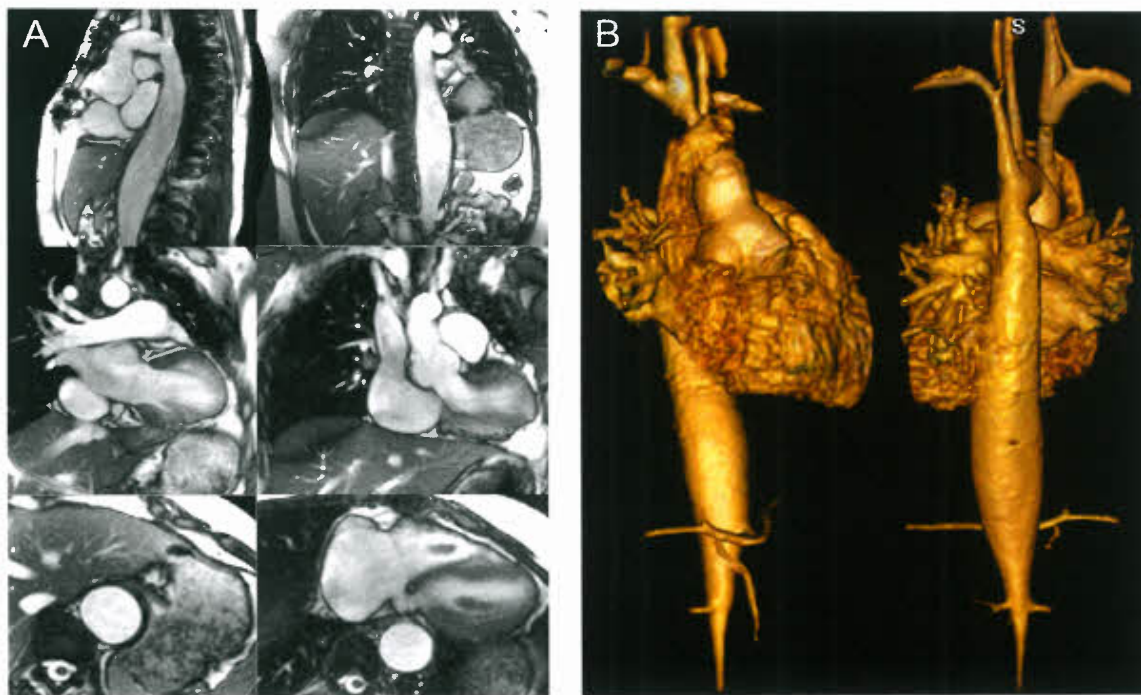


Figure 10.31. Large aneurysm of the descending aorta in a patient with connective tissue disorder who underwent replacement of the ascending aorta and transverse arch. **A:** SSFP cine MRI in multiple planes; **B:** Volume rendered reconstruction of Gd-enhanced 3-D MRA. The left panel shows an anterior view and the right panel shows a posterior view.

On the other hand, the potential ability of CT to obtain good quality images without general anesthesia and endotracheal intubation is advantageous (see Chapter 11).

MRI evaluation of vascular rings and left pulmonary artery sling can be accomplished by a combination of SE, free-breathing isotropic 3-D SSFP, and Gd-enhanced 3-D MRA (Fig. 10.32A). Thin (2 to 3 mm) contiguous FSE with double inversion recovery slices provide excellent visualization of the

trachea, main stem bronchi, and the vasculature. In addition to the axial plane, imaging of the trachea in oblique coronal and sagittal planes parallel to its long axis can be helpful. Occasionally, FSE imaging may not be able to distinguish stenotic from atretic aortic segments with confidence. Gd-enhanced 3-D MRA can be used to determine if any segment of the vascular ring does not have luminal continuity and is ideally suited for 3-D reconstruction (Fig. 10.32B).

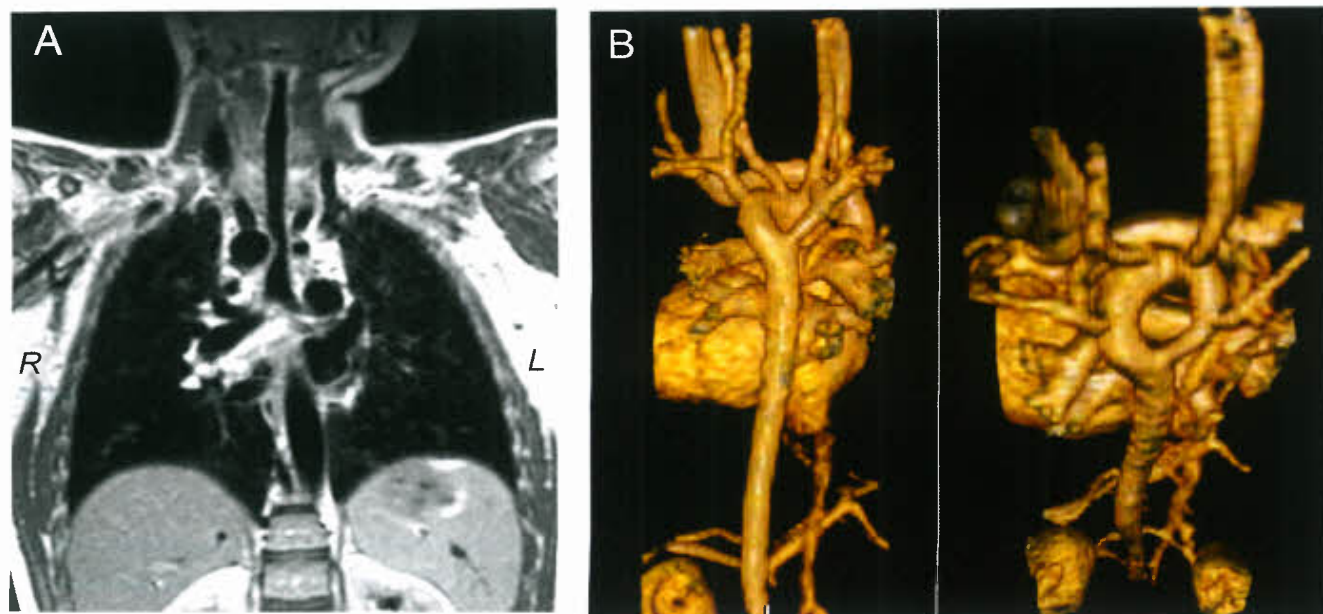


Figure 10.32. Vascular ring consisting of a double aortic arch. **A:** FSE with double inversion recovery sequence in the coronal plane showing tracheal compression and cross-sections of the larger right and the smaller left arches; **B:** Volume rendered reconstruction of Gd-enhanced 3-D MRA. The left panel shows a posterior view and the right panel shows a superior view.

Pulmonary Artery Anomalies

Most anomalies of the pulmonary arteries occur in association with other CHD. For example, stenosis, hypoplasia, and/or discontinuity of the branch pulmonary arteries are commonly associated with TOF. Congenitally absent branch pulmonary artery without additional CHD is a rare anomaly. It is characterized by absence of the mediastinal pulmonary artery on the opposite side of the aortic arch in most cases (Fig. 10.33) (273). A ligamentum arteriosum can usually be found between the base of the subclavian artery and peripheral pulmonary arteries at the hilum of the ipsilateral lung. Early diagnosis and establishment of vascular continuity between the main pulmonary artery and the peripheral branches on the affected side may promote growth of the pulmonary vascular bed and reduce the likelihood of complications. Another condition where a branch pulmonary artery is absent is agenesis of the corresponding lung. In contrast to congenitally absent branch pulmonary artery without associated anomalies, in agenesis of a lung, the ipsilateral pulmonary veins are absent as well.

Other rare anomalies of the branch pulmonary arteries include origin from the ascending aorta (so-called hemitruncus) and crossed pulmonary arteries.

Spin and gradient echo cine sequences can be used to assess the central pulmonary arteries but these techniques may have a limited ability to depict very small and tortuous vessels, especially in infants (see discussion on MRI evaluation of pre-operative TOF). Gd-enhanced 3-D MRA provides excellent depiction of the pulmonary arterial tree, including the second- and third-generation branches. This sequence has been shown to image pulmonary arterial branches as small as 1 mm even in the absence of antegrade blood flow, as is the case in congenitally absent branch pulmonary artery without associated anomalies (Fig. 10.29) (259).

Systemic and Pulmonary Venous Anomalies

Although referral to CMR primarily for evaluation of the pulmonary veins accounts for only 3.4% of cases in our hospital, evaluation of the systemic and pulmonary veins is integral

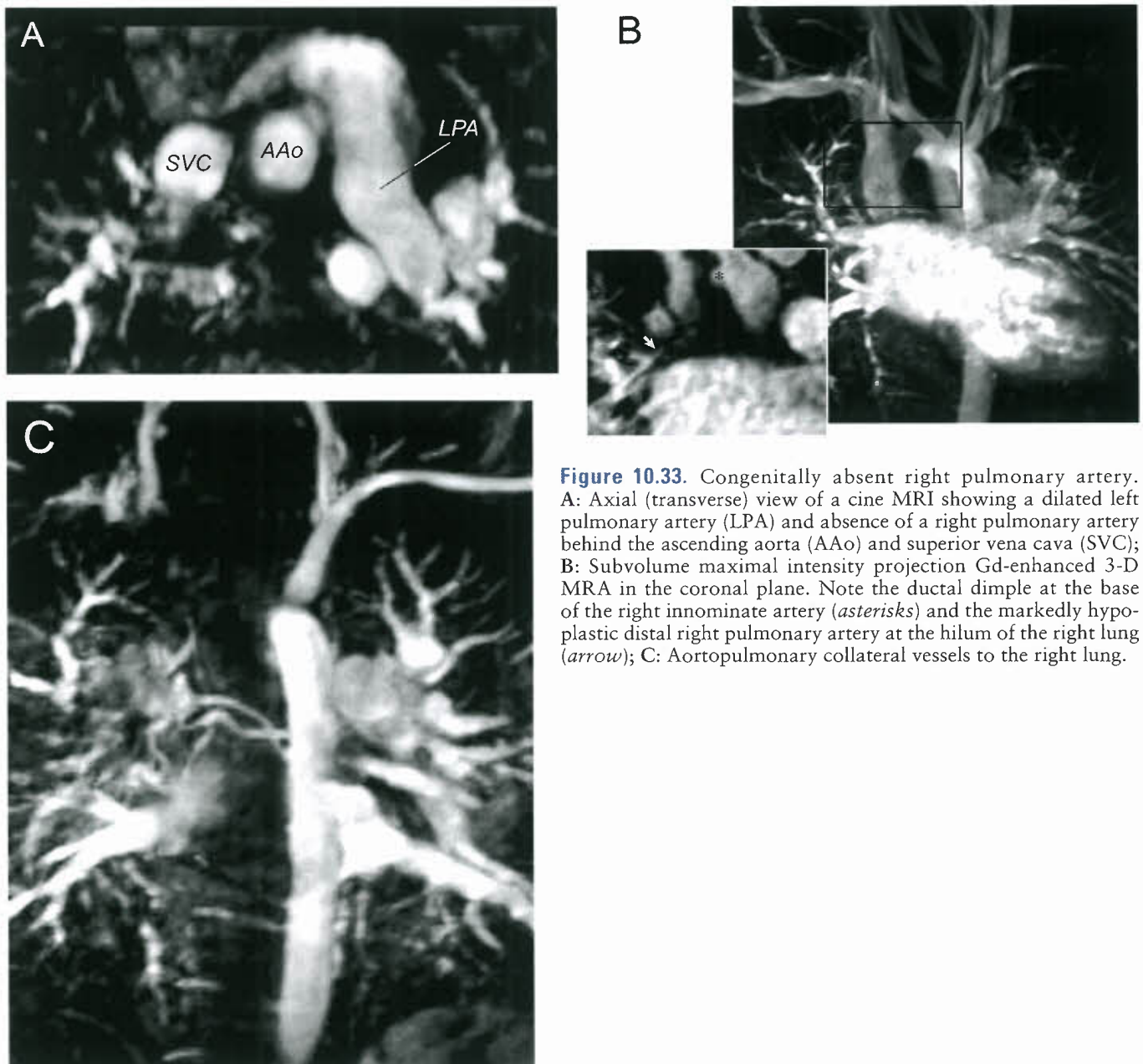


Figure 10.33. Congenitally absent right pulmonary artery. A: Axial (transverse) view of a cine MRI showing a dilated left pulmonary artery (LPA) and absence of a right pulmonary artery behind the ascending aorta (AAo) and superior vena cava (SVC); B: Subvolume maximal intensity projection Gd-enhanced 3-D MRA in the coronal plane. Note the ductal dimple at the base of the right innominate artery (*asterisks*) and the markedly hypoplastic distal right pulmonary artery at the hilum of the right lung (*arrow*); C: Aortopulmonary collateral vessels to the right lung.



Figure 10.34. Volume rendered reconstruction of Gd-enhanced 3-D MRA in a patient with partially anomalous pulmonary venous connection of the left upper pulmonary vein (arrow) to the left innominate vein.

to a comprehensive CMR evaluation in patients with CHD. Venous anomalies are often associated with other CHD and unsuspected, but clinically important, abnormalities can be detected on examinations performed for other indications. Gd-enhanced 3-D MRA is particularly helpful for anatomic evaluation of systemic and pulmonary venous anomalies (Fig. 10.34) (58,274). Gradient echo sequences can be used to depict an abnormal blood flow pattern such as a turbulent jet. A FSE sequence can be used to provide high-resolution imaging of vessel wall, such as in patients with pulmonary veins stenosis. VEC MRI is used to measure blood flow in selected vessels to assess regional blood flow (274). Applications include measurement of Q_p/Q_s , the fractional flow to each lung in patients with pulmonary veins stenosis, and the direction of flow in the azygous vein in a patient with narrowing of the superior vena cava.

Tetralogy of Fallot

TOF is the most frequent diagnosis among patients referred for CMR evaluation at Children's Hospital Boston (Table 10.1). Unlike infants in whom echocardiography generally provides all the necessary diagnostic information for surgical repair (258,275), MRI assumes an increasing role in adolescents and adults with TOF in whom the acoustic windows are frequently limited (160). CMR is useful in both preoperative and postoperative assessment of TOF, but the focus of the examination is different.

Preoperative MRI

In most patients with unrepaired TOF, the central question for the CMR examination is to delineate all sources of pulmonary blood flow—pulmonary arteries, aortopulmonary collateral

vessels, and the ductus arteriosus. Several studies have shown that SE and 2-D gradient echo cine MRI techniques provide excellent imaging of the central pulmonary arteries and major aortopulmonary collaterals (257,276). However, these MRI techniques require relatively long scan times for complete anatomical coverage, and small vessels (<2 mm) may not be detected. Furthermore, these 2-D techniques are not optimal for imaging long and tortuous blood vessels. Gd-enhanced 3-D MRA is ideally suited to image these vessels (Fig. 10.35). Compared with conventional x-ray angiography, MRA has been shown to be highly accurate in depicting all sources of pulmonary blood supply in patients with complex pulmonary stenosis or atresia, including infants with multiple small aortopulmonary collaterals (259).

Cine SSFP is used to assess ventricular dimensions and function, the right ventricular outflow tract (RVOT) as well as dynamic flow imaging of valve function. When the origins and proximal course of the left and right coronary arteries are not known from other imaging studies, they should be imaged either by a coronary MRA sequence or by a FSE sequence in the axial or aortic root short-axis planes. Particular attention is paid to the exclusion of a major coronary artery crossing the RVOT.

Postoperative MRI

CMR has been used extensively for assessment of postoperative TOF patients of all ages, but its greatest clinical utility is in adolescents and adults (168,277,278). Many studies have shown that the degree of pulmonary regurgitation measured by VEC MRI is closely associated with the degree of RV dilation (149,279–281). Another factor that affects RV function is the presence and extent of an aneurysm in the RVOT (226,282). Quantitative assessment of RV and LV dimensions and function is a key element of CMR evaluation in patients with repaired TOF (Fig. 10.36) (64). The degree of RV dysfunction is an important determinant of clinical status late after TOF and is also closely associated with LV function, likely through ventricular–ventricular interaction (283,284). Taken together with clinical assessment and electrophysiologic data, information derived from CMR on pulmonary regurgitation fraction, RV and LV dimensions and function, presence and extent of a RVOT aneurysm, and presence of branch pulmonary artery stenosis is used to direct clinical care in patients with repaired TOF (192,278,285–287).

The goals of the CMR examination, therefore, include quantitative assessment of left and right ventricular volumes, mass, stroke volumes, and ejection fraction; imaging the anatomy of the RVOT, pulmonary arteries, aorta, and aortopulmonary collaterals; and quantification of pulmonary regurgitation, tricuspid regurgitation, pulmonary-to-systemic flow ratio, and detection of scar tissue, especially in the RVOT. CMR examination protocols for evaluation of repaired TOF have been published (277,278).

Transposition of the Great Arteries

CMR is seldom requested for preoperative assessment of infants with D-loop TGA because echocardiography usually provides all necessary diagnostic information (288). In postoperative TGA, CMR assumes an increasing role due to its ability to noninvasively evaluate most clinically relevant issues (124,193,289–291).

Postoperative Atrial Switch (Senning or Mustard Operation)

The goals of CMR evaluation of postoperative atrial switch include (a) quantitative evaluation of the size and function of the systemic RV (Fig. 10.36A) (292); (b) imaging of

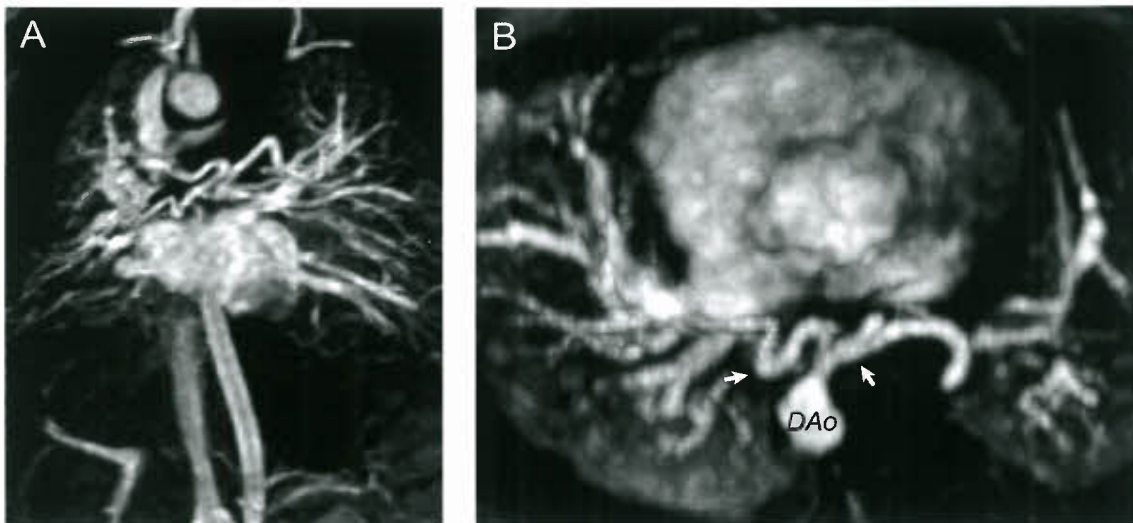


Figure 10.35. Subvolume maximal intensity projection Gd-enhanced 3-D MRA showing aortopulmonary collateral vessels (*arrows*) in a newborn with TOF and pulmonary atresia. **A:** Coronal plane; **B:** Axial (transverse) plane.

the systemic and pulmonary venous pathways for obstruction and/or baffle leak(s) (Fig. 10.36B); (c) assessment of tricuspid valve regurgitation; (d) evaluation of the left and right ventricular outflow tracts for obstruction; (e) detection of aortopulmonary collateral vessels and other associated anomalies; (f) evaluation of the coronary arteries (293); and (g) detection of myocardial fibrosis and/or scar tissue (193,293). The response of the systemic RV to pharmacologic stress (dobutamine) or to exercise can be tested by CMR, but the clinical utility of this information awaits further study (125,289).

Postoperative Arterial Switch

The long-term concerns in patients after the ASO relate primarily to the technical challenges of the operation—transfer of the coronary arteries from the native aortic root to the neo-aortic root (native pulmonary root) and the transfer of the pulmonary arteries anterior to the neoascending aorta. Consequently, the goals of CMR evaluation of postoperative arterial switch include (a) evaluation of global and regional LV and RV size and function; (b) evaluation of the left and right ventricular outflow tracts for obstruction; (c) qualitative estimation of RV systolic pressure based on the configuration

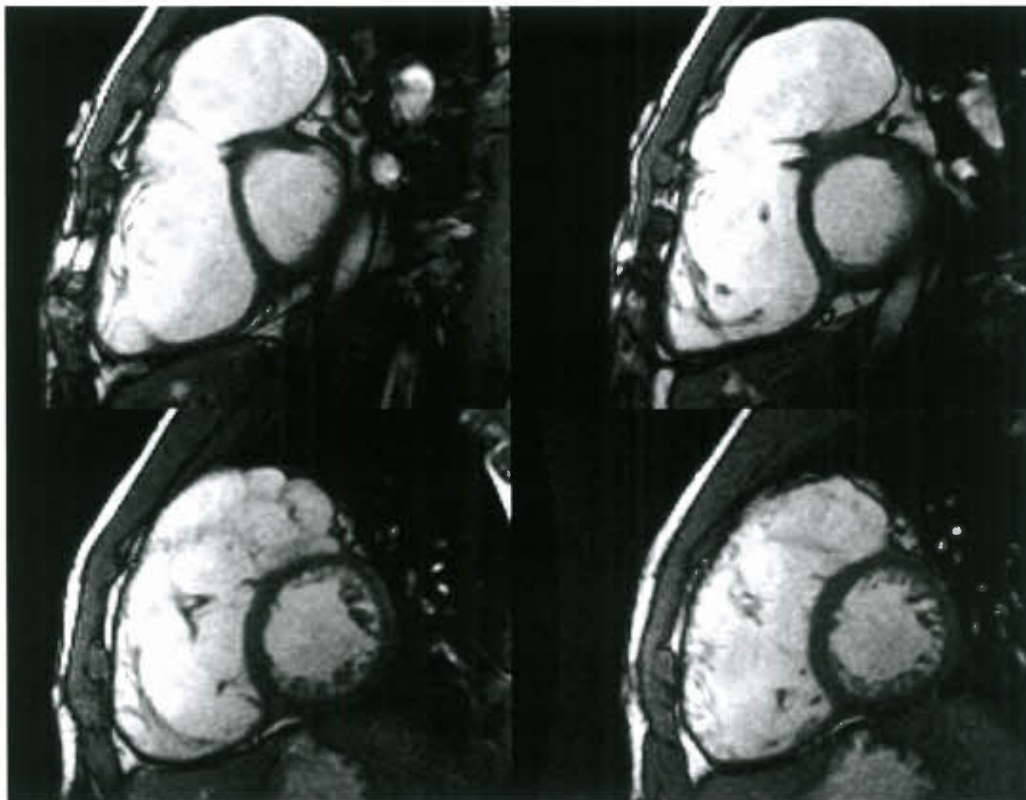


Figure 10.36. Short-axis, ECG-triggered, breath-hold, cine SSFP imaging in a patient with TOF, severe pulmonary regurgitation, and markedly dilated RV.

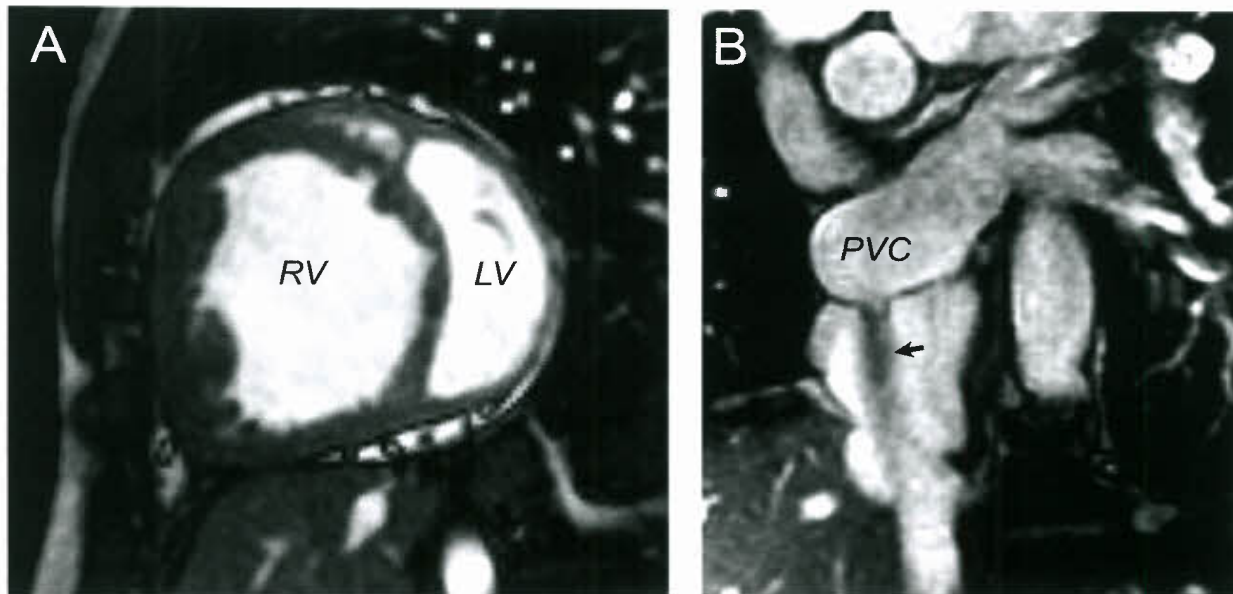


Figure 10.37. ECG-triggered, breath-hold, cine SSFP imaging in a patient with Mustard palliation of D-loop TGA. A: Short-axis view showing the dilated and hypertrophied RV, which compresses the thin-walled LV; B: Baffle leak (arrow) with flow from the pulmonary venous chamber (PVC) to the systemic venous chamber.

of the interventricular septum; (d) imaging of the great vessels with emphasis on evaluation of the pulmonary arteries for stenosis and the aortic root for dilation (Fig. 10.38); (e) detection of aortopulmonary collateral vessels and other associated anomalies; (f) evaluation of the origins and proximal course

of the coronary arteries (51,294); and (g) detection of myocardial ischemia, fibrosis, and/or scar tissue (290). The role of myocardial perfusion and viability imaging in this population deserves further study, especially with regard to the sensitivity, specificity, and predictive values of these techniques for detection of myocardial ischemia and the prognostic implications of myocardial fibrosis and/or scar tissue detected by delayed myocardial enhancement.



Figure 10.38. Volume rendered reconstruction of Gd-enhanced 3-D MRA in a patient with ASO for D-loop TGA. Note the relationship between the pulmonary arteries and the ascending aorta resulting from the Lecompte maneuver.

Single Ventricle and Fontan

Before Stage I Palliation

CMR has an important role in the diagnostic evaluation and follow-up of patients with anatomic and functional single ventricle. Echocardiography is the primary imaging tool during the initial evaluation since most patients present in the newborn period or early infancy and their acoustic windows are typically adequate. CMR is used before the first palliative procedure only in selected cases, usually to evaluate incompletely diagnosed extracardiac anatomy such as anomalies of the aortic arch, pulmonary arteries, and venous anomalies.

Before Stage II Palliation

The role of CMR increases after the first palliative surgical procedure. CMR may be requested to assess potential complications or sequelae of the first operation such as residual or recurrent aortic arch obstruction, stenosis or compression of branch pulmonary arteries or pulmonary veins, aortopulmonary or ventriculopulmonary shunts, airway compression, and others. In patients who are candidates for a bidirectional Glenn shunt or a hemi-Fontan procedure (second-stage palliation), CMR can substitute routine diagnostic catheterization in selected patients (295). Evidence from two retrospective studies suggests that in a substantial number of patients who are candidates for a second-stage palliation cardiac catheterization data do not change the surgical plan (296,297). Although some of these patients undergo a concomitant transcatheter intervention (e.g.,

balloon dilation of coarctation or coil occlusion of aortopulmonary collaterals), the indications for and the clinical benefits from such procedures are not clearly defined. Whereas echocardiography can provide much of the anatomic and functional information in these patients, there are circumstances in which parts of the anatomy may not be fully defined and additional quantitative functional data may be desired. CMR can potentially fulfill these goals (Fig. 10.39). Brown et al. (298) in a prospective randomized clinical trial

of CMR versus routine catheterization showed that CMR is a safe, effective, and less costly alternative to routine catheterization in the evaluation of selected patients before bidirectional Glenn operation. Another retrospective analysis showed that a noninvasive diagnostic algorithm effectively screened for patients who are unsuitable for a Fontan operation and that omission of routine preoperative hemodynamic assessment at catheterization did not impair prediction of adverse postoperative outcomes (299).

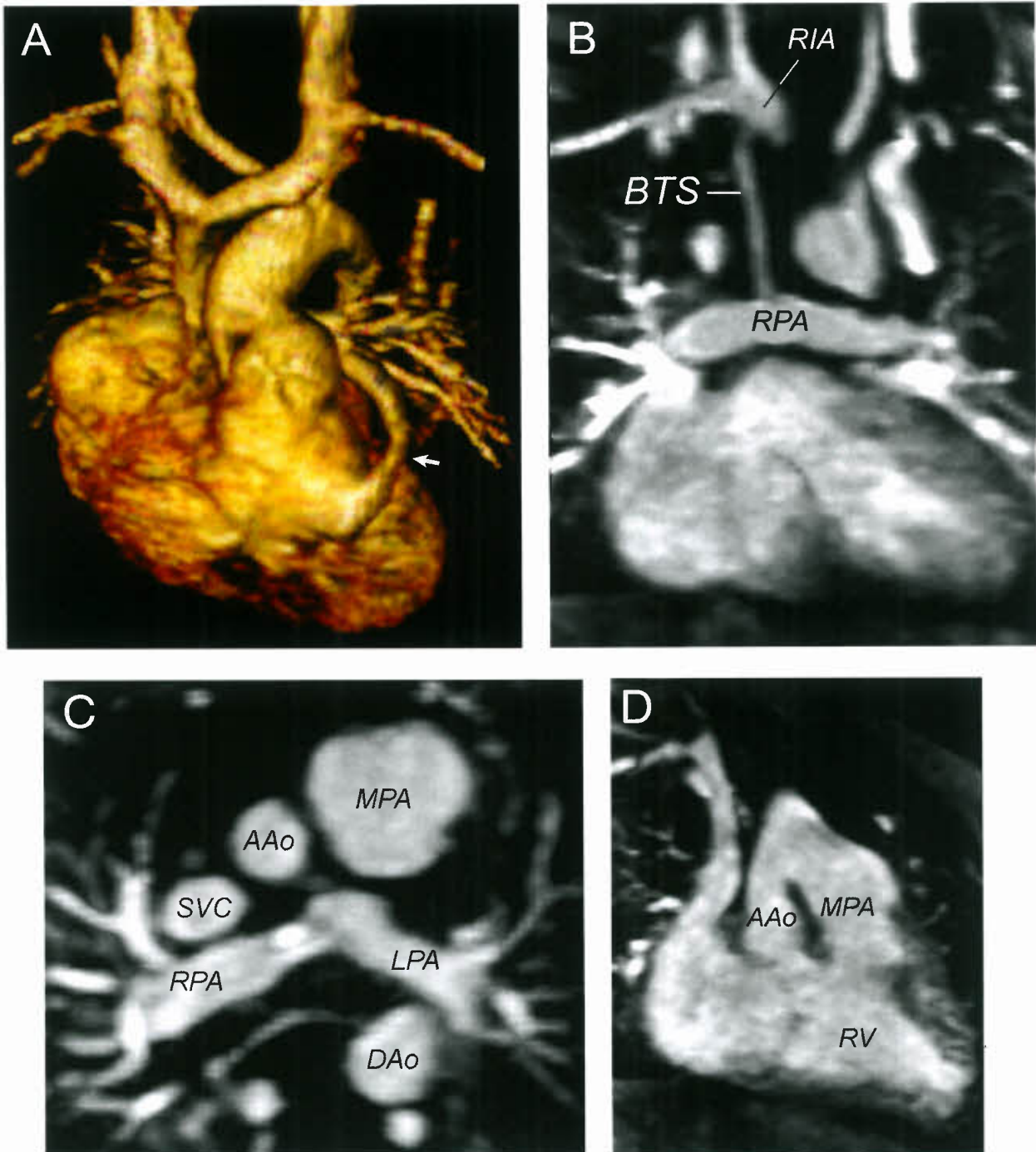


Figure 10.39. MRI evaluation of hypoplastic left heart syndrome after stage I palliation. **A:** Volume rendered reconstruction of Gd-enhanced 3-D MRA showing the RV-to-pulmonary artery conduit (*arrow*) and the arterial anastomoses; **B:** maximal intensity projection of a modified right Blalock-Taussig shunt (BTS); **C:** maximal intensity projection image in the axial (transverse) plane showing the branch pulmonary arteries; **D:** maximal intensity projection image showing the anastomosis between the main pulmonary artery and the native ascending aorta; (*Continued*)

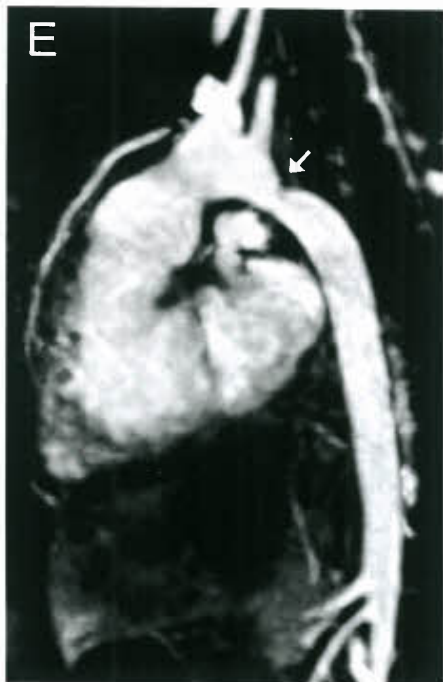


Figure 10.39. (Continued) E: maximal intensity projection image of the reconstructed aorta showing mild coarctation (arrow). AAo, ascending aorta; DAo, descending aorta; LPA, left pulmonary artery; MPA, main pulmonary artery; RIA, right innominate artery; RPA, right pulmonary artery.

The goals of the CMR examination in patients who are candidates for a second-stage palliation include the following: (a) anatomy of the systemic and pulmonary veins; (b) anatomy of the branch pulmonary arteries; (c) anatomy of the thoracic aorta with an emphasis on exclusion of arch obstruction; (d) presence and distribution of aortopulmonary and venous collaterals, including quantification of collateral flow (174,175); (e) quantitative assessment of systemic ventricular function; (f) quantitative assessment of valve regurgitation; (g) evaluation of the atrial septum for restriction; and (h) detection of myocardial fibrosis or scar tissue (228).

Before and after Fontan Palliation

The role of CMR in the evaluation of patients before and after the Fontan operation is growing (300). Several investigators explored the use of clinical criteria and noninvasive imaging to supplant routine cardiac catheterization in low-risk patients before a Fontan operation (299,301,302). These studies noted that a substantial proportion of patients can undergo surgery without a preceding catheterization and emphasized the role of CMR. After Fontan, CMR is increasingly used for surveillance of late complications (198,303). Several reports have used CMR as an investigational tool to study blood flow dynamics within the Fontan pathways and to delineate the distribution of inferior and superior caval flow to each lung (171,172,186,187,303,304). Myocardial tagging has proved an important investigational tool in the evaluation of myocardial mechanics in patients with functional single ventricle and Fontan circulation, demonstrating asynchrony and impaired regional wall motion (117). Cine SSFP is the preferred method for assessment of ventricular

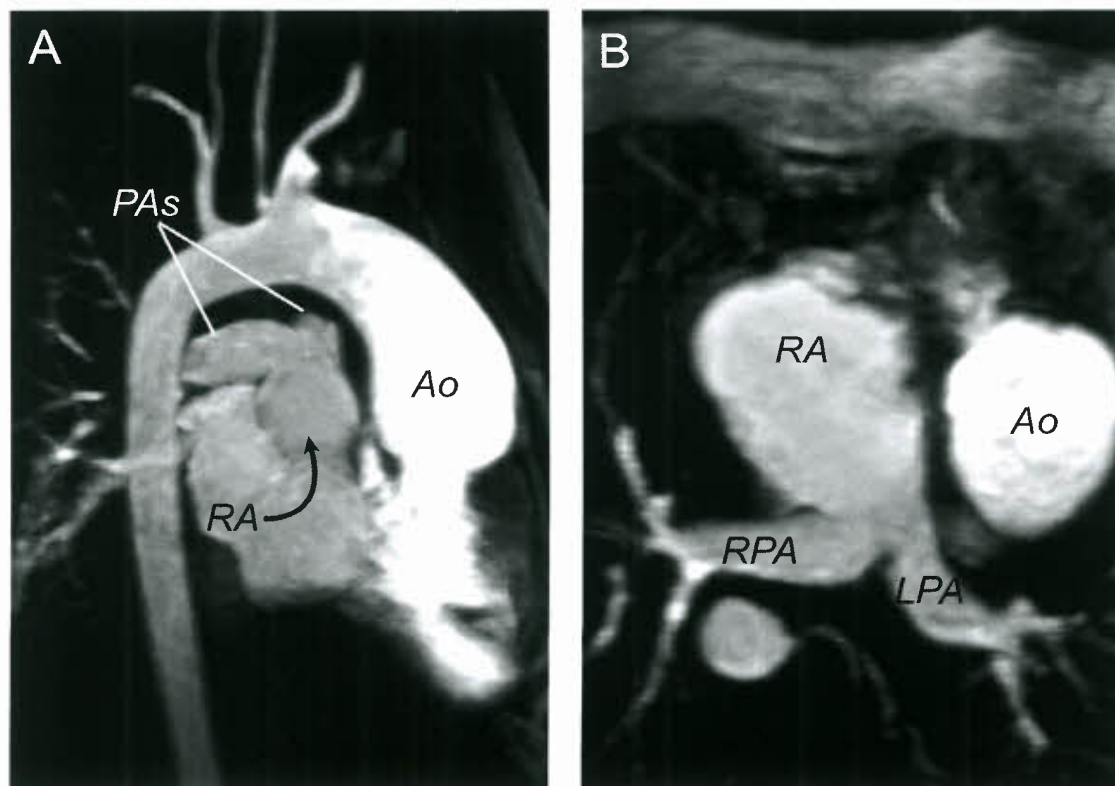


Figure 10.40. Subvolume maximal intensity projection image of Fontan pathway in a patient with atriopulmonary anastomosis. A: Oblique sagittal view showing the atriopulmonary anastomosis (curved arrow); B: Oblique transverse view showing the atriopulmonary anastomosis and branch pulmonary arteries. Ao, aorta; LPA, left pulmonary artery; PAs, pulmonary arteries; RPA, right pulmonary artery.

size and function (305) and LGE imaging is used for assessment of myocardial scar (194).

The goals of the CMR examination in patients with the Fontan circulation include (a) assessment of the pathways from the systemic veins to the pulmonary arteries for obstruction and a thrombus (Fig. 10.40); (b) detection of Fontan baffle fenestration or leaks; (c) evaluation of the pulmonary veins for compression; (d) measurements of systemic ventricular volumes, mass, and function; (e) detection of myocardial fibrosis; (f) imaging of the systemic ventricular outflow tract for obstruction; (g) quantitative assessment of the AV and semilunar valve(s) for regurgitation; (h) imaging the aorta for obstruction or an aneurysm; (i) measurement of aortopulmonary collateral flow; and (j) detection of systemic venous or systemic-to-pulmonary venous collateral vessels.

An important limitation of CMR in patients with Fontan circulation is the frequent presence of metallic implants (e.g., stainless steel coils, stents, occluding devices) that produce image artifacts. Garg et al. (60) reviewed the CMR studies of 120 consecutive CMR examinations from 1996 to 2003 and found that artifacts from metallic implants were present in 54% of the studies. Major artifacts (mostly caused by stainless steel coils) were present in 36% of patients, and in 20% the artifact precluded complete volumetric assessment of the systemic ventricle. More recently, however, use of nonferromagnetic coils has greatly reduced the frequency imaging artifacts in patients with Fontan circulation. CT can be used as an alternative to CMR in patients with large image artifacts as well as in those with relative contraindications to CMR (e.g., pacemaker).

REFERENCES

- Dorfman AL, Odegard KC, Powell AJ, et al. Risk factors for adverse events during cardiovascular magnetic resonance in congenital heart disease. *J Cardiovasc Magn Reson* 2007;9:793-798.
- Mulkern RV, Chung T. From signal to image: magnetic resonance imaging physics for cardiac magnetic resonance. *Pediatr Cardiol* 2000;21:5-17.
- Axel L. Physics and technology of cardiovascular MR imaging. *Cardiol Clin* 1998;16:125-133.
- Chia JM, Fischer SE, Wickline SA, et al. Performance of QRS detection for cardiac magnetic resonance imaging with a novel vectorcardiographic triggering method. *J Magn Reson Imaging* 2000;12:678-688.
- Larson AC, White RD, Laub G, et al. Self-gated cardiac cine MRI. *Magn Reson Med* 2004;51:93-102.
- Spuentrup E, Buecker A, Stuber M, et al. Navigator-gated coronary magnetic resonance angiography using steady-state-free-precession: comparison to standard T2-prepared gradient-echo and spiral imaging. *Invest Radiol* 2003;38:263-268.
- Wetzel SG, Lee VS, Tan AG, et al. Real-time interactive duplex MR measurements: application in neurovascular imaging. *AJR Am J Roentgenol* 2001;177:703-707.
- Buecker A, Adam GB, Neuerburg JM, et al. Simultaneous real-time visualization of the catheter tip and vascular anatomy for MR-guided PTA of iliac arteries in an animal model. *J Magn Reson Imaging* 2002;16:201-208.
- Plein S, Smith WH, Ridgway JP, et al. Measurements of left ventricular dimensions using real-time acquisition in cardiac magnetic resonance imaging: comparison with conventional gradient echo imaging. *MAGMA* 2001;13:101-108.
- Sampath S, Derbyshire JA, Atalar E, et al. Real-time imaging of two-dimensional cardiac strain using a harmonic phase magnetic resonance imaging (HARP-MRI) pulse sequence. *Magn Reson Med* 2003;50:154-163.
- Korperich H, Gieseke J, Barth P, et al. Flow volume and shunt quantification in pediatric congenital heart disease by real-time magnetic resonance velocity mapping: a validation study. *Circulation* 2004;109:1987-1993.
- Lemaire C, Moran GR, Swan H. Impact of audio/visual systems on pediatric sedation in magnetic resonance imaging. *J Magn Reson Imaging* 2009;30:649-655.
- Gutierrez FR. Magnetic resonance imaging of congenital heart disease. *Top Magn Reson Imaging* 1995;7:246-257.
- Masui T, Katayama M, Kobayashi S, et al. Gadolinium-enhanced MR angiography in the evaluation of congenital cardiovascular disease pre- and postoperative states in infants and children. *J Magn Reson Imaging* 2000;12:1034-1042.
- Schlesinger AE, Hernandez RJ. Magnetic resonance imaging in congenital heart disease in children. *Tex Heart Inst J* 1996;23:128-143.
- Fogel MA, Donofrio MT, Ramaciotti C, et al. Magnetic resonance and echocardiographic imaging of pulmonary artery size throughout stages of Fontan reconstruction. *Circulation* 1994;90:2927-2936.
- Beekman RP, Hoorntje TM, Beek FJ, et al. Sedation for children undergoing magnetic resonance imaging: efficacy and safety of rectal thiopental. *Eur J Pediatr* 1996;155:820-822.
- Didier D, Ratib O, Beghetti M, et al. Morphologic and functional evaluation of congenital heart disease by magnetic resonance imaging. *J Magn Reson Imaging* 1999;10:639-655.
- Fogel MA, Weinberg PM, Parave E, et al. Deep sedation for cardiac magnetic resonance imaging: a comparison with cardiac anesthesia. *J Pediatr* 2008;152:534-539, 539 e1.
- Baker E. What's new in magnetic resonance imaging? *Cardiol Young* 2001;11:445-452.
- Holmqvist C, Larsson EM, Stahlberg F, et al. Contrast-enhanced thoracic 3D-MR angiography in infants and children. *Acta Radiol* 2001;42:50-58.
- Odegard KC, DiNardo JA, Tsai-Goodman B, et al. Anaesthesia considerations for cardiac MRI in infants and small children. *Paediatr Anaesth* 2004;14:471-476.
- Martin ET, Coman JA, Shellock FG, et al. Magnetic resonance imaging and cardiac pacemaker safety at 1.5-Tesla. *J Am Coll Cardiol* 2004;43:1315-1324.
- Shellock FG. Prosthetic heart valves and annuloplasty rings: assessment of magnetic field interactions, heating, and artifacts at 1.5 Tesla. *J Cardiovasc Magn Reson* 2001;3:317-324.
- Ahmed S, Shellock FG. Magnetic resonance imaging safety: implications for cardiovascular patients. *J Cardiovasc Magn Reson* 2001;3:171-182.
- Wolff S, James TL, Young GB, et al. Magnetic resonance imaging: absence of in vitro cytogenetic damage. *Radiology* 1985;155:163-165.
- Kanal E, Barkovich AJ, Bell C et al. ACR guidance document for safe MR practices: 2007. *AJR Am J Roentgenol* 2007;188:1447-1474.
- Moriarty JM, Finn JP, Fonseca CG. Contrast agents used in cardiovascular magnetic resonance imaging: current issues and future directions. *Am J Cardiovasc Drugs* 2010;10:227-237.
- Osorio J. New CMR approach to measure diffuse myocardial fibrosis. *Nat Rev Cardiol* 2010;7:542.
- Prakash A, Powell AJ, Geva T. Multimodality noninvasive imaging for assessment of congenital heart disease. *Circ Cardiovasc Imaging* 2010;3:112-125.
- Shepherd M, Lata S, Mani S, et al. Anaphylaxis to gadolinium radiocontrast: a case report and review of the literature. *J La State Med Soc* 2009;161:282-284.
- Grobner T. Gadolinium—a specific trigger for the development of nephrogenic fibrosing dermopathy and nephrogenic systemic fibrosis? *Nephrol Dial Transplant* 2006;21:1104-1108.
- Runge VM. Gadolinium and nephrogenic systemic fibrosis. *AJR Am J Roentgenol* 2009;192:W195-W196; discussion W197.
- Perazella MA. Advanced kidney disease, gadolinium and nephrogenic systemic fibrosis: the perfect storm. *Curr Opin Nephrol Hypertens* 2009;18:519-525.
- Altun E, Martin DR, Wertman R, et al. Nephrogenic systemic fibrosis: change in incidence following a switch in gadolinium agents and adoption of a gadolinium policy—report from two U.S. universities. *Radiology* 2009;253:689-696.
- Wang Y, Alkasab TK, Narin O, et al. Incidence of Nephrogenic Systemic Fibrosis after Adoption of Restrictive Gadolinium-based Contrast Agent Guidelines. *Radiology* 2011;260:105-111.
- Shellock FG. Metallic surgical instruments for interventional MRI procedures: evaluation of MR safety. *J Magn Reson Imaging* 2001;13:152-157.
- Sawyer-Glover AM, Shellock FG. Pre-MRI procedure screening: recommendations and safety considerations for biomedical implants and devices. *J Magn Reson Imaging* 2000;12:92-106.
- Rutledge JM, Vick GW III, Mullins CE, et al. Safety of magnetic resonance imaging immediately following Palmaz stent implant: a report of three cases. *Catheter Cardiovasc Interv* 2001;53:519-523.
- Shellock FG, Spinazzi A. MRI safety update 2008: part 2, screening patients for MRI. *AJR Am J Roentgenol* 2008;191:1140-1149.
- Hofman MB, de Cock CC, van der Linden JC, et al. Transesophageal cardiac pacing during magnetic resonance imaging: feasibility and safety considerations. *Magn Reson Med* 1996;35:413-422.
- Gimbel JR, Johnson D, Levine PA, et al. Safe performance of magnetic resonance imaging on five patients with permanent cardiac pacemakers. *Pacing Clin Electrophysiol* 1996;19:913-919.
- Sorrentino RA. A novel MRI-safe dual-chamber pacemaker system: its time has come. *Heart Rhythm* 2011;8:74-75.
- Pulver AF, Puchalski MD, Bradley DJ, et al. Safety and imaging quality of MRI in pediatric and adult congenital heart disease patients with pacemakers. *Pacing Clin Electrophysiol* 2009;32:450-456.
- Mitka M. First MRI-safe pacemaker receives conditional approval from FDA. *JAMA* 2011;305:985-986.
- Carr JC, Simonetti O, Bundy J, et al. Cine MR angiography of the heart with segmented true fast imaging with steady-state precession. *Radiology* 2001;219:828-834.

47. Bax JJ, Lamb H, Dibbets P, et al. Comparison of gated single-photon emission computed tomography with magnetic resonance imaging for evaluation of left ventricular function in ischemic cardiomyopathy. *Am J Cardiol* 2000;86:1299–1305.
48. Bellenger NG, Burgess MI, Ray SG, et al. Comparison of left ventricular ejection fraction and volumes in heart failure by echocardiography, radionuclide ventriculography and cardiovascular magnetic resonance; are they interchangeable? *Eur Heart J* 2000;21:1387–1396.
49. Tso J, Kozerke S, Boesiger P, et al. Optimizing spatiotemporal sampling for k-t BLAST and k-t SENSE: application to high-resolution real-time cardiac steady-state free precession. *Magn Reson Med* 2005;53:1372–1382.
50. Sorensen TS, Korperich H, Greil GF, et al. Operator-independent isotropic three-dimensional magnetic resonance imaging for morphology in congenital heart disease: a validation study. *Circulation* 2004;110:163–169.
51. Beerbaum P, Sarikouch S, Laser KT, et al. Coronary anomalies assessed by whole-heart isotropic 3D magnetic resonance imaging for cardiac morphology in congenital heart disease. *J Magn Reson Imaging* 2009;29:320–327.
52. Manning WJ, Stuber M, Danias PG, et al. Coronary magnetic resonance imaging: Current status. *Curr Probl Cardiol* 2002;27:275–333.
53. Greil GF, Stuber M, Botnar RM, et al. Coronary magnetic resonance angiography in adolescents and young adults with kawasaki disease. *Circulation* 2002;105:908–911.
54. Taylor AM, Thorne SA, Rubens MB, et al. Coronary artery imaging in grown up congenital heart disease: complementary role of magnetic resonance and x-ray coronary angiography. *Circulation* 2000;101:1670–1678.
55. Aydogan U, Onursal E, Cantez T, et al. Giant congenital coronary artery fistula to left superior vena cava and right atrium with compression of left pulmonary vein simulating cor triatriatum—diagnostic value of magnetic resonance imaging. *Eur J Cardiothorac Surg* 1994;8:97–99.
56. Danias PG, Stuber M, McConnell MV, et al. The diagnosis of congenital coronary anomalies with magnetic resonance imaging. *Coron Artery Dis* 2001;12:621–626.
57. Boxer RA, LaCorte MA, Singh S, et al. Noninvasive diagnosis of congenital left coronary artery to right ventricle fistula by nuclear magnetic resonance imaging. *Pediatr Cardiol* 1989;10:45–47.
58. Greil GF, Powell AJ, Gildein HP, et al. Gadolinium-enhanced three-dimensional magnetic resonance angiography of pulmonary and systemic venous anomalies. *J Am Coll Cardiol* 2002;39:335–341.
59. Mohrs OK, Petersen SE, Voigtlaender T, et al. Time-resolved contrast-enhanced MR angiography of the thorax in adults with congenital heart disease. *AJR Am J Roentgenol* 2006;187:1107–1114.
60. Garg R, Powell AJ, Sena L, et al. Effects of metallic implants on magnetic resonance imaging evaluation of Fontan palliation. *Am J Cardiol* 2005;95:688–691.
61. Kaji S, Yang PC, Kerr AB, et al. Rapid evaluation of left ventricular volume and mass without breath-holding using real-time interactive cardiac magnetic resonance imaging system. *J Am Coll Cardiol* 2001;38:527–533.
62. Schalla S, Nagel E, Lehmkuhl H, et al. Comparison of magnetic resonance real-time imaging of left ventricular function with conventional magnetic resonance imaging and echocardiography. *Am J Cardiol* 2001;87:95–99.
63. Alfakih K, Plein S, Thiele H, et al. Normal human left and right ventricular dimensions for MRI as assessed by turbo gradient echo and steady-state free precession imaging sequences. *J Magn Reson Imaging* 2003;17:323–329.
64. Samyn MM, Powell AJ, Garg R, et al. Range of ventricular dimensions and function by steady-state free precession cine MRI in repaired tetralogy of Fallot: right ventricular outflow tract patch vs. conduit repair. *J Magn Reson Imaging* 2007;26:934–940.
65. Alfakih K, Thiele H, Plein S, et al. Comparison of right ventricular volume measurement between segmented k-space gradient-echo and steady-state free precession magnetic resonance imaging. *J Magn Reson Imaging* 2002;16:253–258.
66. Hergan K, Schuster A, Fruhwald J, et al. Comparison of left and right ventricular volume measurement using the Simpson's method and the area length method. *Eur J Radiol* 2008;65:270–278.
67. Sheehan FH, Kilner PJ, Sahn DJ, et al. Accuracy of knowledge-based reconstruction for measurement of right ventricular volume and function in patients with tetralogy of Fallot. *Am J Cardiol* 2010;105:993–999.
68. Moroseos T, Mitsumori L, Kerwin WS, et al. Comparison of Simpson's method and three-dimensional reconstruction for measurement of right ventricular volume in patients with complete or corrected transposition of the great arteries. *Am J Cardiol* 2010;105:1603–1609.
69. Strugnell WE, Slaughter RE, Riley RA, et al. Modified RV short axis series—a new method for cardiac MRI measurement of right ventricular volumes. *J Cardiovasc Magn Reson* 2005;7:769–774.
70. Alfakih K, Plein S, Bloomer T, et al. Comparison of right ventricular volume measurements between axial and short axis orientation using steady-state free precession magnetic resonance imaging. *J Magn Reson Imaging* 2003;18:25–32.
71. Mooij CF, de Wit CJ, Graham DA, et al. Reproducibility of MRI measurements of right ventricular size and function in patients with normal and dilated ventricles. *J Magn Reson Imaging* 2008;28:67–73.
72. Hudsmith LE, Petersen SE, Francis JM, et al. Normal human left and right ventricular and left atrial dimensions using steady state free precession magnetic resonance imaging. *J Cardiovasc Magn Reson* 2005;7:775–782.
73. Buechel EV, Kaiser T, Jackson C, et al. Normal right- and left ventricular volumes and myocardial mass in children measured by steady state free precession cardiovascular magnetic resonance. *J Cardiovasc Magn Reson* 2009;11:19.
74. Fu JC, Chai JW, Wong ST. Wavelet-based enhancement for detection of left ventricular myocardial boundaries in magnetic resonance images. *Magn Reson Imaging* 2000;18:1135–1141.
75. Makowski P, Sorensen TS, Therkildsen SV, et al. Two-phase active contour method for semiautomatic segmentation of the heart and blood vessels from MRI images for 3D visualization. *Comput Med Imaging Graph* 2002;26:9–17.
76. Zimmer Y, Akselrod S. An automatic contour extraction algorithm for short-axis cardiac magnetic resonance images. *Med Phys* 1996;23:1371–1379.
77. Yezzi A, Jr., Kichenassamy S, Kumar A, et al. A geometric snake model for segmentation of medical imagery. *IEEE Trans Med Imaging* 1997;16:199–209.
78. Holland AE, Goldfarb JW, Edelman RR. Diaphragmatic and cardiac motion during suspended breathing: preliminary experience and implications for breath-hold MR imaging. *Radiology* 1998;209:483–489.
79. Raichura N, Entwistle J, Leverment J, et al. Breath-hold MRI in evaluating patients with pectus excavatum. *Br J Radiol* 2001;74:701–708.
80. Ostrzega E, Maddahi J, Honma H, et al. Quantification of left ventricular myocardial mass in humans by nuclear magnetic resonance imaging. *Am Heart J* 1989;117:444–452.
81. Maddahi J, Cruces J, Berman DS, et al. Noninvasive quantification of left ventricular myocardial mass by gated proton nuclear magnetic resonance imaging. *J Am Coll Cardiol* 1987;10:682–692.
82. Keller AM, Peshock RM, Malloy CR, et al. In vivo measurement of myocardial mass using nuclear magnetic resonance imaging. *J Am Coll Cardiol* 1986;8:113–117.
83. Katz J, Milliken MC, Stray-Gundersen J, et al. Estimation of human myocardial mass with MR imaging. *Radiology* 1988;169:495–498.
84. Florentine MS, Grosskreutz CL, Chang W, et al. Measurement of left ventricular mass in vivo using gated nuclear magnetic resonance imaging. *J Am Coll Cardiol* 1986;8:107–112.
85. Caputo GR, Tscholakoff D, Sechtem U, et al. Measurement of canine left ventricular mass by using MR imaging. *AJR Am J Roentgenol* 1987;148:33–38.
86. Koch JA, Poll LW, Godehardt E, et al. In vitro determination of cardiac ventricular volumes using MRI at 1.0 T in a porcine heart model. *Int J Cardiovasc Imaging* 2001;17:237–242.
87. Semelka RC, Tomei E, Wagner S, et al. Interstudy reproducibility of dimensional and functional measurements between cine magnetic resonance studies in the morphologically abnormal left ventricle. *Am Heart J* 1990;119:1367–1373.
88. Semelka RC, Tomei E, Wagner S, et al. Normal left ventricular dimensions and function: interstudy reproducibility of measurements with cine MR imaging. *Radiology* 1990;174:763–768.
89. Doherty NE III, Fujita N, Caputo GR, et al. Measurement of right ventricular mass in normal and dilated cardiomyopathic ventricles using cine magnetic resonance imaging. *Am J Cardiol* 1992;69:1223–1228.
90. Doherty NE III, Seelos KC, Suzuki J, et al. Application of cine nuclear magnetic resonance imaging for sequential evaluation of response to angiotensin-converting enzyme inhibitor therapy in dilated cardiomyopathy. *J Am Coll Cardiol* 1992;19:1294–1302.
91. Germain P, Roul G, Kastler B, et al. Inter-study variability in left ventricular mass measurement: comparison between M-mode echography and MRI. *Eur Heart J* 1992;13:1011–1019.
92. Bellenger NG, Davies LC, Francis JM, et al. Reduction in sample size for studies of remodeling in heart failure by the use of cardiovascular magnetic resonance. *J Cardiovasc Magn Reson* 2000;2:271–278.
93. Ioannidis JP, Trikalinos TA, Danias PG. Electrocardiogram-gated single-photon emission computed tomography versus cardiac magnetic resonance imaging for the assessment of left ventricular volumes and ejection fraction: a meta-analysis. *J Am Coll Cardiol* 2002;39:2059–2068.
94. Plein S, Bloomer TN, Ridgway JP, et al. Steady-state free precession magnetic resonance imaging of the heart: comparison with segmented k-space gradient-echo imaging. *J Magn Reson Imaging* 2001;14:230–236.
95. Maceira AM, Prasad SK, Khan M, et al. Reference right ventricular systolic and diastolic function normalized to age, gender and body surface area from steady-state free precession cardiovascular magnetic resonance. *Eur Heart J* 2006;27:2879–2888.
96. Robbers-Visser D, Boersma E, Helbing WA. Normal biventricular function, volumes, and mass in children aged 8 to 17 years. *J Magn Reson Imaging* 2009;29:552–559.
97. Sarikouch S, Peters B, Gutberlet M, et al. Sex-specific pediatric percentiles for ventricular size and mass as reference values for cardiac MRI: assessment by steady-state free-precession and phase-contrast MRI flow. *Circ Cardiovasc imaging* 2010;3:65–76.
98. Colan SD. Assessment of ventricular and myocardial performance. In: Fyler DC, ed. *Nadas' Pediatric Cardiology*. Philadelphia, PA: Hanley & Belfus, 1992:225–248.
99. Regan DM. Calculation of left ventricular wall stress. *Circ Res* 1990;67:245–252.
100. Setser RM, Sayre K, Flacke S, et al. Assessment of ventricular contractility during cardiac magnetic resonance imaging examinations using normalized maximal ventricular power. *Ann Biomed Eng* 2001;29:974–982.

101. Cerqueira MD, Weissman NJ, Dilsizian V, et al. Standardized myocardial segmentation and nomenclature for tomographic imaging of the heart: a statement for healthcare professionals from the Cardiac Imaging Committee of the Council on Clinical Cardiology of the American Heart Association. *Circulation* 2002;105:539–542.
102. Klein SS, Graham TP Jr, Lorenz CH. Noninvasive delineation of normal right ventricular contractile motion with magnetic resonance imaging myocardial tagging. *Ann Biomed Eng* 1998;26:756–763.
103. Lamb HJ, Singleton RR, van der Geest RJ, et al. MR imaging of regional cardiac function: low-pass filtering of wall thickness curves. *Magn Reson Med* 1995;34:498–502.
104. Reichek N. MRI myocardial tagging. *J Magn Reson Imaging* 1999;10:609–616.
105. Fogel MA. Assessment of cardiac function by magnetic resonance imaging. *Pediatr Cardiol* 2000;21:59–69.
106. Haber I, Metaxas DN, Axel L. Three-dimensional motion reconstruction and analysis of the right ventricle using tagged MRI. *Med Image Anal* 2000;4:335–355.
107. Garot J, Bluemke DA, Osman NF, et al. Fast determination of regional myocardial strain fields from tagged cardiac images using harmonic phase MRI. *Circulation* 2000;101:981–988.
108. Fonseca CG, Oxenham HC, Cowan BR, et al. Aging alters patterns of regional nonuniformity in LV strain relaxation: a 3-D MR tissue tagging study. *Am J Physiol Heart Circ Physiol* 2003;285:H621–H630.
109. Tustison NJ, Davila-Roman VG, Amini AA. Myocardial kinematics from tagged MRI based on a 4-D B-spline model. *IEEE Trans Biomed Eng* 2003;50:1038–1040.
110. O'Dell WG, McCulloch AD. Imaging three-dimensional cardiac function. *Annu Rev Biomed Eng* 2000;2:431–456.
111. Haber I, Metaxas DN, Geva T, et al. Three-dimensional systolic kinematics of the right ventricle. *Am J Physiol Heart Circ Physiol* 2005;289:H1826–H1833.
112. Chin BB, Esposito G, Kraitchman DL. Myocardial contractile reserve and perfusion defect severity with rest and stress dobutamine (99 m)Tc-sestamibi SPECT in canine stunning and subendocardial infarction. *J Nucl Med* 2002;43:540–550.
113. Saito I, Watanabe S, Masuda Y. Detection of viable myocardium by dobutamine stress tagging magnetic resonance imaging with three-dimensional analysis by automatic trace method. *Jpn Circ J* 2000;64:487–494.
114. Mankad R, McCreery CJ, Rogers WJ Jr, et al. Regional myocardial strain before and after mitral valve repair for severe mitral regurgitation. *J Cardiovasc Magn Reson* 2001;3:257–266.
115. Setser RM, White RD, Sturm B, et al. Noninvasive assessment of cardiac mechanics and clinical outcome after partial left ventriculectomy. *Ann Thorac Surg* 2003;76:1576–1585; discussion 1585–1586.
116. Kuijpers D, Ho KY, van Dijkman PR, et al. Dobutamine cardiovascular magnetic resonance for the detection of myocardial ischemia with the use of myocardial tagging. *Circulation* 2003;107:1592–1597.
117. Fogel MA, Gupta KB, Weinberg PM, et al. Regional wall motion and strain analysis across stages of Fontan reconstruction by magnetic resonance tagging. *Am J Physiol* 1995;269:H1132–H1152.
118. Fogel MA, Weinberg PM, Chin AJ, et al. Late ventricular geometry and performance changes of functional single ventricle throughout staged Fontan reconstruction assessed by magnetic resonance imaging. *J Am Coll Cardiol* 1996;28:212–221.
119. Fogel MA, Weinberg PM, Gupta KB, et al. Mechanics of the single left ventricle: a study in ventricular-ventricular interaction II. *Circulation* 1998;98:330–338.
120. Amundsen BH, Crosby J, Steen PA, et al. Regional myocardial long-axis strain and strain rate measured by different tissue Doppler and speckle tracking echocardiography methods: a comparison with tagged magnetic resonance imaging. *European journal of echocardiography: the journal of the Working Group on Echocardiography of the European Society of Cardiology* 2009;10:229–237.
121. Hor KN, Gottliebson WM, Carson C, et al. Comparison of magnetic resonance feature tracking for strain calculation with harmonic phase imaging analysis. *JACC Cardiovasc Imaging* 2010;3:144–151.
122. Ortega M, Triedman JK, Geva T, et al. Relation of left ventricular dyssynchrony measured by cardiac magnetic resonance tissue tracking in repaired tetralogy of Fallot to ventricular tachycardia and death. *Am J Cardiol* 2011;107:1535–1540.
123. Strigl S, Beroukhim R, Valente AM, et al. Feasibility of dobutamine stress cardiovascular magnetic resonance imaging in children. *J Magn Reson Imaging* 2009;29:313–319.
124. Tulevski II, van der Wall EE, Groenink M, et al. Usefulness of magnetic resonance imaging dobutamine stress in asymptomatic and minimally symptomatic patients with decreased cardiac reserve from congenital heart disease (complete and corrected transposition of the great arteries and subpulmonic obstruction). *Am J Cardiol* 2002;89:1077–1081.
125. Tulevski II, Lee PL, Groenink M, et al. Dobutamine-induced increase of right ventricular contractility without increased stroke volume in adolescent patients with transposition of the great arteries: evaluation with magnetic resonance imaging. *Int J Card Imaging* 2000;16:471–478.
126. Dodge-Khatami A, Tulevski II, Bennis GB, et al. Comparable systemic ventricular function in healthy adults and patients with unoperated congenitally corrected transposition using MRI dobutamine stress testing. *Ann Thorac Surg* 2002;73:1759–1764.
127. Roest AA, Kunz P, Lamb HJ, et al. Biventricular response to supine physical exercise in young adults assessed with ultrafast magnetic resonance imaging. *Am J Cardiol* 2001;87:601–605.
128. Grossman W. Diastolic function and heart failure: an overview. *Eur Heart J* 1990;11:2–7.
129. Helbing WA, Niezen RA, Le Cessie S, et al. Right ventricular diastolic function in children with pulmonary regurgitation after repair of tetralogy of Fallot: volumetric evaluation by magnetic resonance velocity mapping. *J Am Coll Cardiol* 1996;28:1827–1835.
130. Eroglu AG, Sarioglu A, Sarioglu T. Right ventricular diastolic function after repair of tetralogy of Fallot: its relationship to the insertion of a 'transannular' patch. *Cardiol Young* 1999;9:384–391.
131. Fogel MA, Weinberg PM, Hubbard A, et al. Diastolic biomechanics in normal infants utilizing MRI tissue tagging. *Circulation* 2000;102:218–224.
132. Kroft LJ, Simons P, van Laar JM, et al. Patients with pulmonary fibrosis: cardiac function assessed with MR imaging. *Radiology* 2000;216:464–471.
133. Dong SJ, Hees PS, Siu CO, et al. MRI assessment of LV relaxation by untwisting rate: a new isovolumic phase measure of tau. *Am J Physiol Heart Circ Physiol* 2001;281:H2002–H2009.
134. Paelinck BP, Lamb HJ, Bax JJ, et al. Assessment of diastolic function by cardiovascular magnetic resonance. *Am Heart J* 2002;144:198–205.
135. Young AA, Cowan BR, Occleshaw CJ, et al. Temporal evolution of left ventricular strain late after repair of coarctation of the aorta using 3D MR tissue tagging. *J Cardiovasc Magn Reson* 2002;4:233–243.
136. Powell AJ, Geva T. Blood flow measurement by magnetic resonance imaging in congenital heart disease. *Pediatr Cardiol* 2000;21:47–58.
137. Pelc NJ, Herfkens RJ, Shimakawa A, et al. Phase contrast cine magnetic resonance imaging. *Magn Reson Q* 1991;7:229–254.
138. Greil G, Geva T, Maier SE, et al. Effect of acquisition parameters on the accuracy of velocity encoded cine magnetic resonance imaging blood flow measurements. *J Magn Reson Imaging* 2002;15:47–54.
139. Beerbaum P, Korperich H, Barth P, et al. Noninvasive quantification of left-to-right shunt in pediatric patients: phase-contrast cine magnetic resonance imaging compared with invasive oximetry. *Circulation* 2001;103:2476–2482.
140. Powell AJ, Maier SE, Chung T, et al. Phase-velocity cine magnetic resonance imaging measurement of pulsatile blood flow in children and young adults: in vitro and in vivo validation. *Pediatr Cardiol* 2000;21:104–110.
141. Hundley WG, Li HF, Lange RA, et al. Assessment of left-to-right intracardiac shunting by velocity-encoded, phase-difference magnetic resonance imaging: a comparison with oximetric and indicator dilution techniques. *Circulation* 1995;91:2955–2960.
142. Robertson MB, Kohler U, Hoskins PR, et al. Quantitative analysis of PC MRI velocity maps: pulsatile flow in cylindrical vessels. *Magn Reson Imaging* 2001;19:685–695.
143. Evans AJ, Iwai F, Grist TA, et al. Magnetic resonance imaging of blood flow with a phase subtraction technique: in vitro and in vivo validation. *Invest Radiol* 1993;28:109–115.
144. Firmin DN, Nayler GL, Kilner PJ, et al. The application of phase shifts in NMR for flow measurement. *Magn Reson Med* 1990;14:230–241.
145. Ku DN, Biancheri CL, Pettigrew RI, et al. Evaluation of magnetic resonance velocimetry for steady flow. *J Biomech Eng* 1990;112:464–472.
146. Sondergaard L, Thomsen C, Stahlberg F, et al. Mitral and aortic valvular flow: quantification with MR phase mapping. *J Magn Reson Imaging* 1992;2:295–302.
147. Firmin DN, Nayler GL, Klipstein RH, et al. In vivo validation of MR velocity imaging. *J Comput Assist Tomogr* 1987;11:751–756.
148. Kondo C, Caputo GR, Semelka R, et al. Right and left ventricular stroke volume measurements with velocity-encoded cine MR imaging: in vitro and in vivo validation. *AJR Am J Roentgenol* 1991;157:9–16.
149. Rebergen SA, Chin JG, Ottenkamp J, et al. Pulmonary regurgitation in the late postoperative follow-up of tetralogy of Fallot: volumetric quantitation by nuclear magnetic resonance velocity mapping. *Circulation* 1993;88:2257–2266.
150. Rebergen SA, Ottenkamp J, Doornbos J, et al. Postoperative pulmonary flow dynamics after Fontan surgery: assessment with nuclear magnetic resonance velocity mapping. *J Am Coll Cardiol* 1993;21:123–131.
151. Hundley WG, Li HF, Hillis LD, et al. Quantitation of cardiac output with velocity-encoded, phase-difference magnetic resonance imaging. *Am J Cardiol* 1995;75:1250–1255.
152. Matsumura K, Nakase E, Haiyama T, et al. Determination of cardiac ejection fraction and left ventricular volume: contrast-enhanced ultrafast cine MR imaging vs IV digital subtraction ventriculography. *AJR Am J Roentgenol* 1993;160:979–985.
153. Powell AJ, Tsai-Goodman B, Prakash A, et al. Comparison between phase-velocity cine magnetic resonance imaging and invasive oximetry for quantification of atrial shunts. *Am J Cardiol* 2003;91:1523–1525.
154. Hundley WG, Meshack BM, Willett DL, et al. Comparison of quantitation of left ventricular volume, ejection fraction, and cardiac output in patients with atrial fibrillation by cine magnetic resonance imaging versus invasive measurements. *Am J Cardiol* 1996;78:1119–1123.
155. Brenner LD, Caputo GR, Mostbeck G, et al. Quantification of left to right atrial shunts with velocity-encoded cine nuclear magnetic resonance imaging. *J Am Coll Cardiol* 1992;20:1246–1250.

156. Beerbaum P, Korperich H, Gieseke J, et al. Rapid left-to-right shunt quantification in children by phase-contrast magnetic resonance imaging combined with sensitivity encoding (SENSE). *Circulation* 2003;108:1355-1361.
157. Buonocore MH. Estimation of total coronary artery flow using measurements of flow in the ascending aorta. *Magn Reson Med* 1994;32:602-611.
158. Kolbitsch C, Lorenz IH, Hormann C et al. The impact of increased mean airway pressure on contrast-enhanced MRI measurement of regional cerebral blood flow (rCBF), regional cerebral blood volume (rCBV), regional mean transit time (rMTT), and regional cerebrovascular resistance (rCVR) in human volunteers. *Hum Brain Mapp* 2000;11:214-222.
159. Sommer G, Noorbehesht B, Pelc N, et al. Normal renal blood flow measurement using phase-contrast cine magnetic resonance imaging. *Invest Radiol* 1992;27:465-470.
160. Geva T, Sahn, DJ, Powell AJ. Magnetic resonance imaging of congenital heart disease in adults. *Prog Pediatr Cardiol* 2003;17:21-39.
161. Holmqvist C, Oskarsson G, Stahlberg F, et al. Functional evaluation of extracardiac ventriculopulmonary conduits and of the right ventricle with magnetic resonance imaging and velocity mapping. *Am J Cardiol* 1999;83:926-932.
162. Walker PG, Houliand K, Djurhuus C, et al. Motion correction for the quantification of mitral regurgitation using the control volume method. *Magn Reson Med* 2000;43:726-733.
163. Walker PG, Oyre S, Pedersen EM, et al. A new control volume method for calculating valvular regurgitation. *Circulation* 1995;92:579-586.
164. Globits S, Higgins CB. Assessment of valvular heart disease by magnetic resonance imaging. *Am Heart J* 1995;129:369-381.
165. Reid SA, Walker PG, Fisher J, et al. The quantification of pulmonary valve haemodynamics using MRI. *Int J Cardiovasc Imaging* 2002;18:217-225.
166. Dohmen PM, Hotz H, Lembcke A, et al. Magnetic resonance imaging of stentless xenografts for reconstruction of right ventricular outflow tract. *Semin Thorac Cardiovasc Surg* 2001;13:24-27.
167. Kuehne T, Saeed M, Reddy G, et al. Sequential magnetic resonance monitoring of pulmonary flow with endovascular stents placed across the pulmonary valve in growing Swine. *Circulation* 2001;104:2363-2368.
168. Helbing WA, de Roos A. Clinical applications of cardiac magnetic resonance imaging after repair of tetralogy of Fallot. *Pediatr Cardiol* 2000;21:70-79.
169. Nayak KS, Pauly JM, Kerr AB, et al. Real-time color flow MRI. *Magn Reson Med* 2000;43:251-258.
170. Mitchell L, Jenkins JP, Watson Y, et al. Diagnosis and assessment of mitral and aortic valve disease by cine-flow magnetic resonance imaging. *Magn Reson Med* 1989;12:181-197.
171. Fogel MA, Weinberg PM, Rychik J, et al. Caval contribution to flow in the branch pulmonary arteries of Fontan patients with a novel application of magnetic resonance presaturation pulse. *Circulation* 1999;99:1215-1221.
172. Fratz S, Hess J, Schwaiger M, et al. More accurate quantification of pulmonary blood flow by magnetic resonance imaging than by lung perfusion scintigraphy in patients with fontan circulation. *Circulation* 2002;106:1510-1513.
173. Henk CB, Schlechta B, Grampp S, et al. Pulmonary and aortic blood flow measurements in normal subjects and patients after single lung transplantation at 0.5 T using velocity encoded cine MRI. *Chest* 1998;114:771-779.
174. Whitehead KK, Gillespie MJ, Harris MA, et al. Noninvasive quantification of systemic-to-pulmonary collateral flow: a major source of inefficiency in patients with superior cavopulmonary connections. *Circ Cardiovasc Imaging* 2009;2:405-411.
175. Grosse-Wortmann L, Al-Otay A, Yoo SJ. Aortopulmonary collaterals after bidirectional cavopulmonary connection or Fontan completion: quantification with MRI. *Circ Cardiovasc Imaging* 2009;2:219-225.
176. Rupprecht T, Nitz W, Wagner M, et al. Determination of the pressure gradient in children with coarctation of the aorta by low-field magnetic resonance imaging. *Pediatr Cardiol* 2002;23:127-131.
177. Ebberts T, Wigstrom L, Bolger AF, et al. Estimation of relative cardiovascular pressures using time-resolved three-dimensional phase contrast MRI. *Magn Reson Med* 2001;45:872-879.
178. van der Geest RJ, Reiber JH. Quantification in cardiac MRI. *J Magn Reson Imaging* 1999;10:602-608.
179. Pennell DJ, Firmin DN, Burger P, et al. Assessment of magnetic resonance velocity mapping of global ventricular function during dobutamine infusion in coronary artery disease. *Br Heart J* 1995;74:163-170.
180. Schwitter J, DeMarco T, Kneifel S, et al. Magnetic resonance-based assessment of global coronary flow and flow reserve and its relation to left ventricular functional parameters: a comparison with positron emission tomography. *Circulation* 2000;101:2696-2702.
181. Shibata M, Sakuma H, Isaka N, et al. Assessment of coronary flow reserve with fast cine phase contrast magnetic resonance imaging: comparison with measurement by Doppler guide wire. *J Magn Reson Imaging* 1999;10:563-568.
182. Rodriguez-Gonzalez AO. Arterial flow determined with half Fourier echo-planar imaging. *Arch Med Res* 2000;31:470-485.
183. Thompson RB, McVeigh ER. Fast measurement of intracardiac pressure differences with 2D breath-hold phase-contrast MRI. *Magn Reson Med* 2003;49:1056-1066.
184. Prakash A, Garg R, Marcus EN, et al. Faster flow quantification using sensitivity encoding for velocity-encoded cine magnetic resonance imaging: in vitro and in vivo validation. *J Magn Reson Imaging* 2006;24:676-682.
185. Sakuma H, Kawada N, Kubo H, et al. Effect of breath holding on blood flow measurement using fast velocity encoded cine MRI. *Magn Reson Med* 2001;45:346-348.
186. Hjortdal VE, Emmertsen K, Stenbog E, et al. Effects of exercise and respiration on blood flow in total cavopulmonary connection: a real-time magnetic resonance flow study. *Circulation* 2003;108:1227-1231.
187. Be'eri E, Maier SE, Landzberg MJ, et al. In vivo evaluation of Fontan pathway flow dynamics by multidimensional phase-velocity magnetic resonance imaging. *Circulation* 1998;98:2873-2882.
188. Kohler U, Marshall I, Robertson MB, et al. MRI measurement of wall shear stress vectors in bifurcation models and comparison with CFD predictions. *J Magn Reson Imaging* 2001;14:563-573.
189. Oyre S, Ringgaard S, Kozerke S, et al. Accurate noninvasive quantitation of blood flow, cross-sectional lumen vessel area and wall shear stress by three-dimensional paraboloid modeling of magnetic resonance imaging velocity data. *J Am Coll Cardiol* 1998;32:128-134.
190. Morgan VL, Roselli RJ, Lorenz CH. Normal three-dimensional pulmonary artery flow determined by phase contrast magnetic resonance imaging. *Ann Biomed Eng* 1998;26:557-566.
191. Prakash A, Powell AJ, Krishnamurthy R, et al. Magnetic resonance imaging evaluation of myocardial perfusion and viability in congenital and acquired pediatric heart disease. *Am J Cardiol* 2004;93:657-661.
192. Babu-Narayan SV, Kilner PJ, Li W, et al. Ventricular fibrosis suggested by cardiovascular magnetic resonance in adults with repaired tetralogy of Fallot and its relationship to adverse markers of clinical outcome. *Circulation* 2006;113:405-413.
193. Babu-Narayan SV, Goktekin O, Moon JC, et al. Late gadolinium enhancement cardiovascular magnetic resonance of the systemic right ventricle in adults with previous atrial redirection surgery for transposition of the great arteries. *Circulation* 2005;111:2091-2098.
194. Rathod RH, Prakash A, Powell AJ, et al. Myocardial fibrosis identified by cardiac magnetic resonance late gadolinium enhancement is associated with adverse ventricular mechanics and ventricular tachycardia late after Fontan operation. *J Am Coll Cardiol* 2010;55:1721-1728.
195. Whitham JK, Hasan BS, Schamberger MS, et al. Use of cardiac magnetic resonance imaging to determine myocardial viability in an infant with in utero septal myocardial infarction and ventricular noncompaction. *Pediatr Cardiol* 2008;29:950-953.
196. Chotenimitkhun R, Hundley WG. Identification of left ventricular myocardial ischemia and cardiac prognosis with cardiovascular magnetic resonance: updates from 2008 to 2010. *Curr Cardiol Rep* 2011;13:77-85.
197. Bettencourt N, Chiribiri A, Schuster A, et al. Assessment of myocardial ischemia and viability using cardiac magnetic resonance. *Curr Heart Fail Rep* 2009;6:142-153.
198. Strzelczyk J, Attali A. Cardiac magnetic resonance evaluation of myocardial viability and ischemia. *Semin Roentgenol* 2008;43:193-203.
199. Nagel E, Lehmkühl HB, Bocksch W, et al. Noninvasive diagnosis of ischemia-induced wall motion abnormalities with the use of high-dose dobutamine stress MRI: comparison with dobutamine stress echocardiography. *Circulation* 1999;99:763-770.
200. Nagel E, Klein C, Paetsch I, et al. Magnetic resonance perfusion measurements for the noninvasive detection of coronary artery disease. *Circulation* 2003;108:432-437.
201. Schwitter J, Nanz D, Kneifel S, et al. Assessment of myocardial perfusion in coronary artery disease by magnetic resonance: a comparison with positron emission tomography and coronary angiography. *Circulation* 2001;103:2230-2235.
202. Kwong RY, Korlakunta H. Diagnostic and prognostic value of cardiac magnetic resonance imaging in assessing myocardial viability. *Top Magn Reson Imaging* 2008;19:15-24.
203. Nkongchu K, Santyr G. Phase-encoding strategies for optimal spatial resolution and T1 accuracy in 3D Look-Locker imaging. *Magn Reson Imaging* 2007;25:1203-1214.
204. Dendale P, Franken PR, Block P, et al. Contrast enhanced and functional magnetic resonance imaging for the detection of viable myocardium after infarction. *Am Heart J* 1998;135:875-880.
205. Kim RJ, Fieno DS, Parrish TB, et al. Relationship of MRI delayed contrast enhancement to irreversible injury, infarct age, and contractile function. *Circulation* 1999;100:1992-2002.
206. Gerber BL, Garot J, Bluemke DA, et al. Accuracy of contrast-enhanced magnetic resonance imaging in predicting improvement of regional myocardial function in patients after acute myocardial infarction. *Circulation* 2002;106:1083-1089.
207. Perin EC, Silva GV, Sarmiento-Leite R, et al. Assessing myocardial viability and infarct transmural extent with left ventricular electromechanical mapping in patients with stable coronary artery disease: validation by delayed-enhancement magnetic resonance imaging. *Circulation* 2002;106:957-961.
208. Motoyama S, Kondo T, Anno H, et al. Relationship between thrombolytic therapy and perfusion defect detected by Gd-DTPA-enhanced fast magnetic resonance imaging in acute myocardial infarction. *J Cardiovasc Magn Reson* 2001;3:237-245.

209. Sandstede JJ, Lipke C, Beer M, et al. Analysis of first-pass and delayed contrast-enhancement patterns of dysfunctional myocardium on MR imaging: use in the prediction of myocardial viability. *AJR Am J Roentgenol* 2000;174:1737-1740.
210. Lauerma K, Niemi P, Hanninen H, et al. Multimodality MR imaging assessment of myocardial viability: combination of first-pass and late contrast enhancement to wall motion dynamics and comparison with FDG PET-initial experience. *Radiology* 2000;217:729-736.
211. Kim RJ, Hillenbrand HB, Judd RM. Evaluation of myocardial viability by MRI. *Herz* 2000;25:417-430.
212. Bax JJ, de Roos A, van Der Wall EE. Assessment of myocardial viability by MRI. *J Magn Reson Imaging* 1999;10:418-422.
213. Kim RJ, Chen EL, Lima JA, et al. Myocardial Gd-DTPA kinetics determine MRI contrast enhancement and reflect the extent and severity of myocardial injury after acute reperfused infarction. *Circulation* 1996;94:3318-3326.
214. Klein C, Nekolla SG, Bengel FM, et al. Assessment of myocardial viability with contrast-enhanced magnetic resonance imaging: comparison with positron emission tomography. *Circulation* 2002;105:162-167.
215. Wagner A, Mahrholdt H, Holly TA, et al. Contrast-enhanced MRI and routine single photon emission computed tomography (SPECT) perfusion imaging for detection of subendocardial myocardial infarcts: an imaging study. *Lancet* 2003;361:374-379.
216. Kim RJ, Wu E, Rafael A, et al. The use of contrast-enhanced magnetic resonance imaging to identify reversible myocardial dysfunction. *N Engl J Med* 2000;343:1445-1453.
217. Choi KM, Kim RJ, Gubernikoff G, et al. Transmural extent of acute myocardial infarction predicts long-term improvement in contractile function. *Circulation* 2001;104:1101-1107.
218. Knuesel PR, Nanz D, Wyss C, et al. Characterization of dysfunctional myocardium by positron emission tomography and magnetic resonance: relation to functional outcome after revascularization. *Circulation* 2003;108:1095-1100.
219. Beek AM, Kuhl HP, Bondarenko O, et al. Delayed contrast-enhanced magnetic resonance imaging for the prediction of regional functional improvement after acute myocardial infarction. *J Am Coll Cardiol* 2003;42:895-901.
220. Wilson JM, Villareal RP, Hariharan R, et al. Magnetic resonance imaging of myocardial fibrosis in hypertrophic cardiomyopathy. *Tex Heart Inst J* 2002;29:176-180.
221. Kim RJ, Judd RM. Gadolinium-enhanced magnetic resonance imaging in hypertrophic cardiomyopathy: in vivo imaging of the pathologic substrate for premature cardiac death? *J Am Coll Cardiol* 2003;41:1568-1572.
222. Leonardi S, Raineri C, De Ferrari GM, et al. Usefulness of cardiac magnetic resonance in assessing the risk of ventricular arrhythmias and sudden death in patients with hypertrophic cardiomyopathy. *Eur Heart J* 2009;30:2003-2010.
223. Gosling OE, Bellenger N, Spurrell P. Risk assessment with cardiac magnetic resonance imaging in hypertrophic cardiomyopathy. *Heart* 2009;95:1843.
224. Efthimiadis GK, Pagourelas ED. Delayed hyperenhancement magnetic resonance imaging for sudden cardiac death risk stratification in hypertrophic cardiomyopathy. *J Am Coll Cardiol* 2009;55:77.
225. Nazarian S, Lima JA. Cardiovascular magnetic resonance for risk stratification of arrhythmia in hypertrophic cardiomyopathy. *J Am Coll Cardiol* 2008;51:1375-1376.
226. Wald RM, Haber I, Wald R, et al. Effects of regional dysfunction and late gadolinium enhancement on global right ventricular function and exercise capacity in patients with repaired tetralogy of Fallot. *Circulation* 2009;119:1370-1377.
227. Oosterhof T, Mulder BJ, Vliegen HW, et al. Corrected tetralogy of fallot: delayed enhancement in right ventricular outflow tract. *Radiology* 2005;237:868-871.
228. Tworetzky W, del Nido PJ, Powell AJ, et al. Usefulness of magnetic resonance imaging of left ventricular endocardial fibroelastosis in infants after fetal intervention for aortic valve stenosis. *Am J Cardiol* 2005;96:1568-1570.
229. Broberg CS, Chugh SS, Conklin C, et al. Quantification of diffuse myocardial fibrosis and its association with myocardial dysfunction in congenital heart disease. *Circ Cardiovasc Imaging* 2010;3:727-734.
230. Sparrow P, Messroghli DR, Reid S. Myocardial T1 mapping for detection of left ventricular myocardial fibrosis in chronic aortic regurgitation: pilot study. *AJR Am J Roentgenol* 2006;187:W630-W635.
231. Flett AS, Hayward MP, Ashworth MT, et al. Equilibrium contrast cardiovascular magnetic resonance for the measurement of diffuse myocardial fibrosis: preliminary validation in humans. *Circulation* 2010;122:138-144.
232. Azevedo CF, Nigri M, Higuchi ML, et al. Prognostic significance of myocardial fibrosis quantification by histopathology and magnetic resonance imaging in patients with severe aortic valve disease. *J Am Coll Cardiol* 2010;56:278-287.
233. Bax JJ, Atsma DE, Lamb HJ, et al. Noninvasive and invasive evaluation of noncompaction cardiomyopathy. *J Cardiovasc Magn Reson* 2002;4:353-357.
234. Hamamichi Y, Ichida F, Hashimoto I, et al. Isolated noncompaction of the ventricular myocardium: ultrafast computed tomography and magnetic resonance imaging. *Int J Cardiovasc Imaging* 2001;17:305-314.
235. Frances CD, Shlipak MG, Grady D. Left ventricular pseudoaneurysm: diagnosis by cine magnetic resonance imaging. *Cardiology* 1999;92:217-219.
236. McMahon CJ, Moniotte S, Powell AJ, et al. Usefulness of magnetic resonance imaging evaluation of congenital left ventricular aneurysms. *Am J Cardiol* 2007;100:310-315.
237. Kiaffas MG, Powell AJ, Geva T. Magnetic resonance imaging evaluation of cardiac tumor characteristics in infants and children. *Am J Cardiol* 2002;89:1229-1233.
238. Mackie AS, Kozakewich HP, Geva T, et al. Vascular tumors of the heart in infants and children: case series and review of the literature. *Pediatr Cardiol* 2005;26:344-349.
239. Sakuma H, Bourne MW, O'Sullivan M, et al. Evaluation of thoracic aortic dissection using breath-holding cine MRI. *J Comput Assist Tomogr* 1996;20:45-50.
240. Moore NR, Parry AJ, Trotman-Dickenson B, et al. Fate of the native aorta after repair of acute type A dissection: a magnetic resonance imaging study. *Heart* 1996;75:62-66.
241. van der Wall EE, Kayser HW, Bootsma MM, et al. Arrhythmogenic right ventricular dysplasia: MRI findings. *Herz* 2000;25:356-364.
242. Midiri M, Finazzo M. MR imaging of arrhythmogenic right ventricular dysplasia. *Int J Cardiovasc Imaging* 2001;17:297-304.
243. Breen JF. Imaging of the pericardium. *J Thorac Imaging* 2001;16:47-54.
244. White CS. MR evaluation of the pericardium. *Top Magn Reson Imaging* 1995;7:258-266.
245. Mollet NR, Dymarkowski S, Volders W, et al. Visualization of ventricular thrombi with contrast-enhanced magnetic resonance imaging in patients with ischemic heart disease. *Circulation* 2002;106:2873-2876.
246. Deborah Chirnomas S, Geukes-Foppen M, Barry K, et al. Practical implications of liver and heart iron load assessment by T2*-MRI in children and adults with transfusion-dependent anemias. *Am J Hematol* 2008;83:781-783.
247. Taher AT, Musallam KM, Wood JC, et al. Magnetic resonance evaluation of hepatic and myocardial iron deposition in transfusion-independent thalassemia intermedia compared to regularly transfused thalassemia major patients. *Am J Hematol* 2010;85:288-290.
248. Wood JC, Tyszkla JM, Carson S, et al. Myocardial iron loading in transfusion-dependent thalassemia and sickle cell disease. *Blood* 2004;103:1934-1936.
249. Baur LH, Vliegen HW, van der Wall EE, et al. Imaging of an aneurysm of the sinus of Valsalva with transthoracic echocardiography, contrast angiography and MRI. *Int J Card Imaging* 2000;16:35-41.
250. Taylor AM, Stables RH, Poole-Wilson PA, et al. Definitive clinical assessment of atrial septal defect by magnetic resonance imaging. *J Cardiovasc Magn Reson* 1999;1:43-47.
251. Holmvang G. A magnetic resonance imaging method for evaluating atrial septal defects. *J Cardiovasc Magn Reson* 1999;1:59-64.
252. Dinsmore RE, Wismer GL, Guyer D, et al. Magnetic resonance imaging of the interatrial septum and atrial septal defects. *AJR Am J Roentgenol* 1985;145:697-703.
253. Holmvang G, Palacios IF, Vlahakes GJ, et al. Imaging and sizing of atrial septal defects by magnetic resonance. *Circulation* 1995;92:3473-3480.
254. Sieverding L, Jung WI, Klose U, et al. Noninvasive blood flow measurement and quantification of shunt volume by cine magnetic resonance in congenital heart disease: preliminary results. *Pediatr Radiol* 1992;22:48-54.
255. Rebergen SA, van der Wall EE, Helbing WA, et al. Quantification of pulmonary and systemic blood flow by magnetic resonance velocity mapping in the assessment of atrial-level shunts. *Int J Card Imaging* 1996;12:143-152.
256. Valverde I, Simpson J, Schaeffter T, et al. 4D phase-contrast flow cardiovascular magnetic resonance: comprehensive quantification and visualization of flow dynamics in atrial septal defect and partial anomalous pulmonary venous return. *Pediatr Cardiol* 2010;31:1244-1248.
257. Powell AJ, Chung T, Landzberg MJ, et al. Accuracy of MRI evaluation of pulmonary blood supply in patients with complex pulmonary stenosis or atresia. *Int J Card Imaging* 2000;16:169-174.
258. Mackie AS, Gauvreau K, Perry SB, et al. Echocardiographic predictors of aortopulmonary collaterals in infants with tetralogy of Fallot and pulmonary atresia. *J Am Coll Cardiol* 2003;41:852-857.
259. Geva T, Greil GF, Marshall AC, et al. Gadolinium-enhanced 3-dimensional magnetic resonance angiography of pulmonary blood supply in patients with complex pulmonary stenosis or atresia: comparison with x-ray angiography. *Circulation* 2002;106:473-478.
260. Amparo EG, Higgins CB, Shafton EP. Demonstration of coarctation of the aorta by magnetic resonance imaging. *AJR Am J Roentgenol* 1984;143:1192-1194.
261. Therrien J, Thorne SA, Wright A, et al. Repaired coarctation: a "cost-effective" approach to identify complications in adults. *J Am Coll Cardiol* 2000;35:997-1002.
262. Simpson IA, Chung KJ, Glass RF, et al. Cine magnetic resonance imaging for evaluation of anatomy and flow relations in infants and children with coarctation of the aorta. *Circulation* 1988;78:142-148.
263. Mendelsohn AM, Banerjee A, Donnelly LF, et al. Is echocardiography or magnetic resonance imaging superior for precoarctation angioplasty evaluation? *Cathet Cardiovasc Diagn* 1997;42:26-30.
264. Araoz PA, Reddy GP, Tarnoff H, et al. MR findings of collateral circulation are more accurate measures of hemodynamic significance than arm-

- leg blood pressure gradient after repair of coarctation of the aorta. *J Magn Reson Imaging* 2003;17:177-183.
265. Mohiaddin RH, Kilner PJ, Rees S, et al. Magnetic resonance volume flow and jet velocity mapping in aortic coarctation. *J Am Coll Cardiol* 1993;22:1515-1521.
 266. Riquelme C, Laissy JP, Menegazzo D, et al. MR imaging of coarctation of the aorta and its postoperative complications in adults: assessment with spin-echo and cine-MR imaging. *Magn Reson Imaging* 1999;17:37-46.
 267. Steffens JC, Bourne MW, Sakuma H, et al. Quantification of collateral blood flow in coarctation of the aorta by velocity encoded cine magnetic resonance imaging. *Circulation* 1994;90:937-943.
 268. Nielsen JC, Powell AJ, Gauvreau K, et al. Magnetic resonance imaging predictors of coarctation severity. *Circulation* 2005;111:622-628.
 269. Muzzarelli S, Ordoñez KG, Hope MD, et al. Diagnostic value of the flow profile in the distal descending aorta by phase-contrast magnetic resonance for predicting severe coarctation of the aorta. *J Magn Reson Imaging* 2011;33:1440-1446.
 270. Donato R, Lentini S, Di Bella G. Magnetic resonance angiography for diagnosis of right aortic arch with vascular ring. *Arch Cardiovasc Dis* 2010;103:631-633.
 271. Banka P, Geva T, Powell AJ, et al. Images in cardiovascular medicine: right aortic arch with aberrant left innominate artery: a rare vascular ring. *Circulation* 2009;120:264-265.
 272. Tsai-Goodman B, Geva T, Odegard KC, et al. Clinical role, accuracy, and technical aspects of cardiovascular magnetic resonance imaging in infants. *Am J Cardiol* 2004;94:69-74.
 273. Ten Harkel AD, Blom NA, Ottenkamp J. Isolated unilateral absence of a pulmonary artery: a case report and review of the literature. *Chest* 2002;122:1471-1477.
 274. Grosse-Wortmann L, Al-Otay A, Goo HW, et al. Anatomical and functional evaluation of pulmonary veins in children by magnetic resonance imaging. *J Am Coll Cardiol* 2007;49:993-1002.
 275. Need LR, Powell AJ, del Nido P, et al. Coronary echocardiography in tetralogy of Fallot: diagnostic accuracy, resource utilization and surgical implications over 13 years. *J Am Coll Cardiol* 2000;36:1371-1377.
 276. Holmqvist C, Hochbergs P, Björkhem G, et al. Pre-operative evaluation with MR in tetralogy of Fallot and pulmonary atresia with ventricular septal defect. *Acta Radiol* 2001;42:63-69.
 277. Kilner PJ, Geva T, Kaemmerer H, et al. Recommendations for cardiovascular magnetic resonance in adults with congenital heart disease from the respective working groups of the European Society of Cardiology. *Eur Heart J* 2010;31:794-805.
 278. Geva T. Repaired tetralogy of Fallot: the roles of cardiovascular magnetic resonance in evaluating pathophysiology and for pulmonary valve replacement decision support. *J Cardiovasc Magn Reson* 2011;13:9.
 279. Roest AA, Helbing WA, Kunz P, et al. Exercise MR imaging in the assessment of pulmonary regurgitation and biventricular function in patients after tetralogy of Fallot repair. *Radiology* 2002;223:204-211.
 280. Niezen RA, Helbing WA, van der Wall EE, et al. Left ventricular function in adults with mild pulmonary insufficiency late after Fallot repair. *Heart* 1999;82:697-703.
 281. Niezen RA, Helbing WA, van der Wall EE, et al. Biventricular systolic function and mass studied with MR imaging in children with pulmonary regurgitation after repair for tetralogy of Fallot. *Radiology* 1996;201:135-140.
 282. Davlouros PA, Kilner PJ, Hornung TS, et al. right ventricular function in adults with repaired tetralogy of Fallot assessed with cardiovascular magnetic resonance imaging: detrimental role of right ventricular outflow aneurysms or akinesia and adverse right-to-left ventricular interaction. *J Am Coll Cardiol* 2002;40:2044-2052.
 283. Geva T, Sandweiss BM, Gauvreau K, et al. Factors associated with impaired clinical status in long-term survivors of tetralogy of Fallot repair evaluated by magnetic resonance imaging. *J Am Coll Cardiol* 2004;43:1068-1074.
 284. Tobler D, Crean AM, Redington AN, et al. The left heart after pulmonary valve replacement in adults late after tetralogy of Fallot repair. *Int J Cardiol* 2011.
 285. Oosterhof T, van Straten A, Vliegen HW, et al. Preoperative thresholds for pulmonary valve replacement in patients with corrected tetralogy of Fallot using cardiovascular magnetic resonance. *Circulation* 2007;116:545-551.
 286. Buechel ER, Dave HH, Kellenberger CJ, et al. Remodelling of the right ventricle after early pulmonary valve replacement in children with repaired tetralogy of Fallot: assessment by cardiovascular magnetic resonance. *Eur Heart J* 2005;26:2721-2727.
 287. Knauth AL, Gauvreau K, Powell AJ, et al. Ventricular size and function assessed by cardiac MRI predict major adverse clinical outcomes late after tetralogy of Fallot repair. *Heart* 2008;94:211-216.
 288. Blume ED, Altmann K, Mayer JE, et al. Evolution of risk factors influencing early mortality of the arterial switch operation. *J Am Coll Cardiol* 1999;33:1702-1709.
 289. Roest AA, Lamb HJ, van der Wall EE, et al. Cardiovascular response to physical exercise in adult patients after atrial correction for transposition of the great arteries assessed with magnetic resonance imaging. *Heart* 2004;90:678-684.
 290. Manso B, Castellote A, Dos L, et al. Myocardial perfusion magnetic resonance imaging for detecting coronary function anomalies in asymptomatic paediatric patients with a previous arterial switch operation for the transposition of great arteries. *Cardiol Young* 2010;20:410-417.
 291. Johansson B, Babu-Narayan SV, Kilner PJ, et al. 3-dimensional time-resolved contrast-enhanced magnetic resonance angiography for evaluation late after the mustard operation for transposition. *Cardiol Young* 2010;20:1-7.
 292. Lorenz CH, Walker ES, Graham TP Jr, et al. Right ventricular performance and mass by use of cine MRI late after atrial repair of transposition of the great arteries. *Circulation* 1995;92:II233-II239.
 293. Taylor AM, Dymarkowski S, Hamaekers P, et al. MR coronary angiography and late-enhancement myocardial MR in children who underwent arterial switch surgery for transposition of great arteries. *Radiology* 2005;234:542-547.
 294. Rajiah P, Setser RM, Desai MY, et al. Utility of free-breathing, whole-heart, three-dimensional magnetic resonance imaging in the assessment of coronary anatomy for congenital heart disease. *Pediatr Cardiol* 2011;32:418-425.
 295. Muthurangu V, Taylor AM, Hegde SR, et al. Cardiac magnetic resonance imaging after stage I Norwood operation for hypoplastic left heart syndrome. *Circulation* 2005;112:3256-3263.
 296. Brown DW, Gauvreau K, Moran AM, et al. Clinical outcomes and utility of cardiac catheterization prior to superior cavopulmonary anastomosis. *J Thorac Cardiovasc Surg* 2003;126:272-281.
 297. McMahon CJ, Eidem BW, Bezold LJ, et al. Is cardiac catheterization a prerequisite in all patients undergoing bidirectional cavopulmonary anastomosis? *J Am Soc Echocardiogr* 2003;16:1068-1072.
 298. Brown DW, Gauvreau K, Powell AJ, et al. Cardiac magnetic resonance versus routine cardiac catheterization before bidirectional Glenn anastomosis in infants with functional single ventricle: a prospective randomized trial. *Circulation* 2007;116:2718-2725.
 299. Prakash A, Khan MA, Hardy R, et al. A new diagnostic algorithm for assessment of patients with single ventricle before a Fontan operation. *J Thorac Cardiovasc Surg* 2009;138:917-923.
 300. Fogel MA. Is routine cardiac catheterization necessary in the management of patients with single ventricles across staged Fontan reconstruction? *Neonatology* 2005;26:154-158.
 301. Ro PS, Rychik J, Cohen MS, et al. Diagnostic assessment before Fontan operation in patients with bidirectional cavopulmonary anastomosis: are noninvasive methods sufficient? *J Am Coll Cardiol* 2004;44:184-187.
 302. Banka P, McElhinney DB, Bacha EA, et al. What is the clinical utility of routine cardiac catheterization before a Fontan operation? *Pediatr Cardiol* 2010;31:977-985.
 303. Whitehead KK, Sundareswaran KS, Parks WJ, et al. Blood flow distribution in a large series of patients having the Fontan operation: a cardiac magnetic resonance velocity mapping study. *J Thorac Cardiovasc Surg* 2009;138:96-102.
 304. Dasi LP, Whitehead K, Pekkan K, et al. Pulmonary hepatic flow distribution in total cavopulmonary connections: extracardiac versus intracardiac. *J Thorac Cardiovasc Surg* 2011;141:207-214.
 305. Prakash A, Travison TG, Fogel MA, et al. Relation of size of secondary ventricles to exercise performance in children after fontan operation. *Am J Cardiol* 2010;106:1652-1656.
 306. Luechinger R, Zeijlemaker VA, Pedersen EM, et al. In vivo heating of pacemaker leads during magnetic resonance imaging. *Eur Heart J* 2005;26:376-383; discussion 325-327.

Cardiac Computed Tomography in Children with Congenital Heart Disease

Frederick R. Long ■ Joachim G. Eichhorn

INTRODUCTION

Computed tomography (CT) and magnetic resonance imaging (MRI) are advanced imaging techniques that can provide 3-D representations of cardiovascular anatomy and functional hemodynamic information that is not limited by field of view or acoustic window as can occur with echocardiography, the primary modality for imaging children with congenital heart disease (CHD). Thus, CT and MRI are supplementary examinations to echocardiography that may substitute the need for more invasive catheter angiography (1–4). The most common clinical indications for CT are to evaluate the extracardiac vascular anatomy (thoracic, coronary, and pulmonary artery and vein connections). In addition, CT and MRI can provide quantitative hemodynamic information that is more accurate and reproducible than echocardiography in following disease progression and timing intervention in children with CHD (5,6).

Assuming equal expertise and access to state-of-the-art hardware, the choice of whether to perform a CT or MRI exam depends upon the unique advantages or disadvantages of CT versus MRI for each individual patient (Table 11.1). Due to the theoretical risk of ionizing radiation in causing cancer, which is greater in infants and children than in adults, MRI is the preferred exam when all other considerations are equal (7). The chief advantages of CT over MRI are much shorter examination times, 2 to 15 seconds versus 30 to 45 minutes, and greater spatial resolution, $0.4 \times 0.4 \times 0.4$ mm versus $0.9 \times 1.1 \times 1.2$ to 2.4 mm (8,9).

The short examination time may preclude the need for sedation. Thus, CT may be preferred in critically ill infants who may not tolerate a longer MRI procedure or who can be examined without sedation or in emergent situations such as in the evaluation of suspected aortic dissection (10). Because of the better spatial resolution, CT may be preferred to image small structures such as the coronary arteries or the small vascular structures in newborns and infants (Figs. 11.1 and 11.2). CT is the modality of choice for imaging the lung parenchyma and airways, to evaluate peripheral pulmonary artery and vein stenosis, and pulmonary emboli (6). Of course, CT should replace MRI in patients with metallic clips, coils, and stents that are not proven safe for MRI or result in unacceptable degradation of MR image quality due to magnetic susceptibility artifacts. MRI is specifically contraindicated in patients with pacemakers or defibrillators. MRI is the modality of choice for quantifying ventricular volumes and function, blood flow, and myocardial perfusion and viability (6).

METHODS AND TECHNIQUE

CT Angiography (CTA) Protocol

Both CT and MRI can be considered advanced imaging techniques not only because of the highly detailed 3-D diagnostic information that they provide but also because their successful

performance requires special expertise and careful technique. The CTA protocol includes a number of factors: patient preparation and positioning, whether ECG-gating or sedation is used; the amount, rate, and timing of intravenous contrast injection; and other parameters such as pitch, slice thickness, and radiation exposure settings. All of these factors are highly dependent on the type of scanner used and the size of the patient (11). In general, a 0.5- to 1.2-mm collimation or slice thickness with a pitch of 1 to 1.5 is used with 8–320 detector scanners to maximize spatial resolution (11). Other major factors are described in detail below.

Sedation and Controlling Respirations

Motion of any kind creates artifacts and blurring that degrade images. In infants and young children, the inability to hold still and to breath hold may significantly degrade image quality. A child may suddenly move, start crying, or just suddenly take in a big breath, particularly during contrast injection. Fast scan speeds cannot compensate for such gross movements.

In infants and young children who are free-breathing and who do not make sudden movements, the fast scan speeds using 8- to 16-slice or greater multidetector scanners can usually compensate for respiratory motion. Adequate chest CTA studies have been reported in free-breathing infants using only oral or rectal sedation or without any sedation. Some institutions report acquiring successful CT exams in neonates without sedation by feeding the infant and wrapping him/her in a blanket (12). The possibility to perform the exam without sedation represents a major potential advantage of CT over MRI.

In general, we sedate our pediatric patients with CHD with the assistance of general anesthesia. This level of support optimizes the safety of our patients who tend to be high-risk infants with complex CHD and who may be hemodynamically unstable. At the same time, image quality is optimized by ensuring that the patient will remain still.

Other advantages of anesthesia assistance include the ability to acquire the CT examination at optimized inspiratory and expiratory lung volumes, depending on the indication. In general, the vascular anatomy is better displayed during an inspiratory breath hold. Exams done during an expiratory breath hold are used to evaluate for tracheomalacia, bronchomalacia, and air trapping. In addition, anesthesia assistance can make intravenous access nontraumatic to the child. IV access is often difficult in infants with CHD as in other sick children. With anesthesia assistance, the IV can be placed after inhalation induction that has the benefit of having a vasodilatory effect (13).

Anesthesiologists also have access to very short-acting sedative drugs (sevoflurane, propofol, and remifentanyl) that are better suited for the short duration of a CT scan (13). In addition, by using short-acting drugs, endotracheal intubation can

TABLE 11.1 Choice of method**MRI ...**

Spatial resolution ≥ 1 mm: more likely for older children, great vessels, follow-up

Functional evaluation

CT ...

Spatial resolution 0.5 mm: primary diagnostics

Lung diagnostics, associated complications

Stents, pacemaker, small and critically ill children

Always, when a rapid cardiac evaluation is necessary!

be avoided by providing facemask ventilation. Breath holding can be achieved while performing facemask ventilation using controlled ventilation technique (14,15). Controlled ventilation involves positive-pressure face mask hyperventilation to induce a transient respiratory pause. During an induced breath hold, we apply positive airway pressure of 15 to 25 cm water pressure to inflate the lungs. By titrating short-acting agents so that spontaneous respirations are not completely suppressed, atelectasis, or partial/complete collapse of the lung, can be minimized. Endotracheal intubation with complete

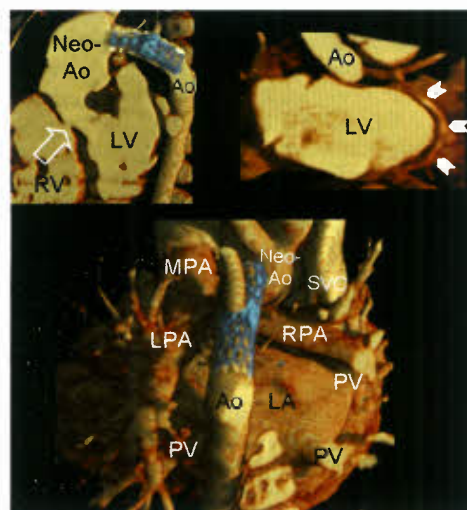


Figure 11.1. An 8-month-old boy with type B interrupted aortic arch after Damus-Kaye-Stansel anastomosis, aortic arch repair, pulmonary homograft, and aortic stent placement (two “overlapping” stents in blue). Three-dimensional volume-rendered images shown were acquired during controlled ventilation with deep conscious sedation on an eight-slice MDCT following 25 mL contrast by hand injection. The 6-second scan demonstrates in a single shot the following relevant information (in order from *top to bottom, left to right*): correct position of the stent, mild left subclavian artery stenosis, left ventricle (LV) outflow tract to the native aorta, LV outflow tract to the neo-aorta (Neo-Ao) (appreciate the small ventricular septal defect marked by the *arrow*) and coronary arteries (*small arrows*). Ao, aorta; LA, left atrium; LPA, left pulmonary artery; MPA, main pulmonary artery; PV, pulmonary vein; RPA, right pulmonary artery; RV, right ventricle; SVC, superior vena cava.

suppression of spontaneous respirations often results in large areas of dependent atelectasis that may obscure vascular anatomy, especially the assessment of the pulmonary veins.

Intravenous Contrast Injection

The usual dose of intravenous iodinated contrast media is 2 mL/kg with an iodine concentration of 240 to 370 mg/mL. The greater the iodine concentration, the better the vascular enhancement, but this also increases the contrast viscosity. Nonionic contrast media is used exclusively to decrease the risk of anaphylaxis, contrast-induced nephropathy, gastrointestinal upset, and complications from potential contrast extravasation into the soft tissues (11,16,17).

CTA image quality is critically dependent on the level of aortic enhancement that requires adequate delivery and timing of the intravenously administered bolus of iodinated contrast media. In general, the more rapid the rate of contrast injection, the greater will be the level of vascular enhancement. The degree of enhancement is inversely related to body weight (17), which is an advantage when imaging small infants.

Contrast injection rate is limited by the size and location of the peripheral intravenous line. The antecubital location is the preferred location due to larger vein size. If this site is not feasible, a forearm/hand vein and foot vein are alternatives. When possible, the right upper extremity should be used to limit streak artifact across the aortic arch (11).

The optimal injection rate for CTA is 1 to 5 mL/s depending on the age of the patient and indication. For example, injection rates of 1 mL/s are sufficient for studies in infants and can be obtained by hand injection through a 24-gauge angiocatheter (12). Rates of ≥ 2 mL/s, which are optimal for older infants and young children, require the use of a power injector and at least a 22-gauge peripheral angiocatheter (Fig. 11.3). Rates of 3 to 5 mL/s require a 20-gauge catheter (18,19). Rates of approximately ≥ 5 mL/s are usually used for coronary artery evaluation or to detect pulmonary emboli in adult-sized patients (20).

The use of indwelling central venous and percutaneously inserted central catheter (PICC) lines for contrast injection is in general avoided because the lines limit contrast injection rates to ≤ 1 mL/s as per manufacturing guidelines (21). Power PICC lines that are designed to be power injected are exceptions to this rule. Umbilical venous catheters (UVC) have been used when peripheral venous access is not possible. A potential problem could arise if the UVC line terminates in an occluded ductus venosus (12). Diagnostic CTA exams can be performed, although with difficulty, while a patient is treated with extracorporeal membrane oxygenation (22).

Timing of the Contrast Bolus

The objective is to synchronize imaging with the delivery of the bolus of intravenous contrast when the region of interest is at its peak of enhancement. Various methods of timing have been used and include automated bolus tracking, the use of a precontrast test bolus, and empiric methods (17). In older children and adults, almost any method will work well, but in infants, it is much more difficult due to the greater potential differences in cardiac output and the small size of the contrast bolus. For example, in infants, the test bolus may be the size of the study bolus, and bolus tracking may be limited by the post trigger delay in scan initiation. When injecting a small amount of contrast for infants weighing <10 kg, the delay from the start of injection to start of scanning can be empirically estimated by the circulation time of 12 to 15 seconds. When injecting a large amount of contrast in an adult-sized patient, empirically starting the scan at the end of contrast injection should capture near peak aortic enhancement (17).

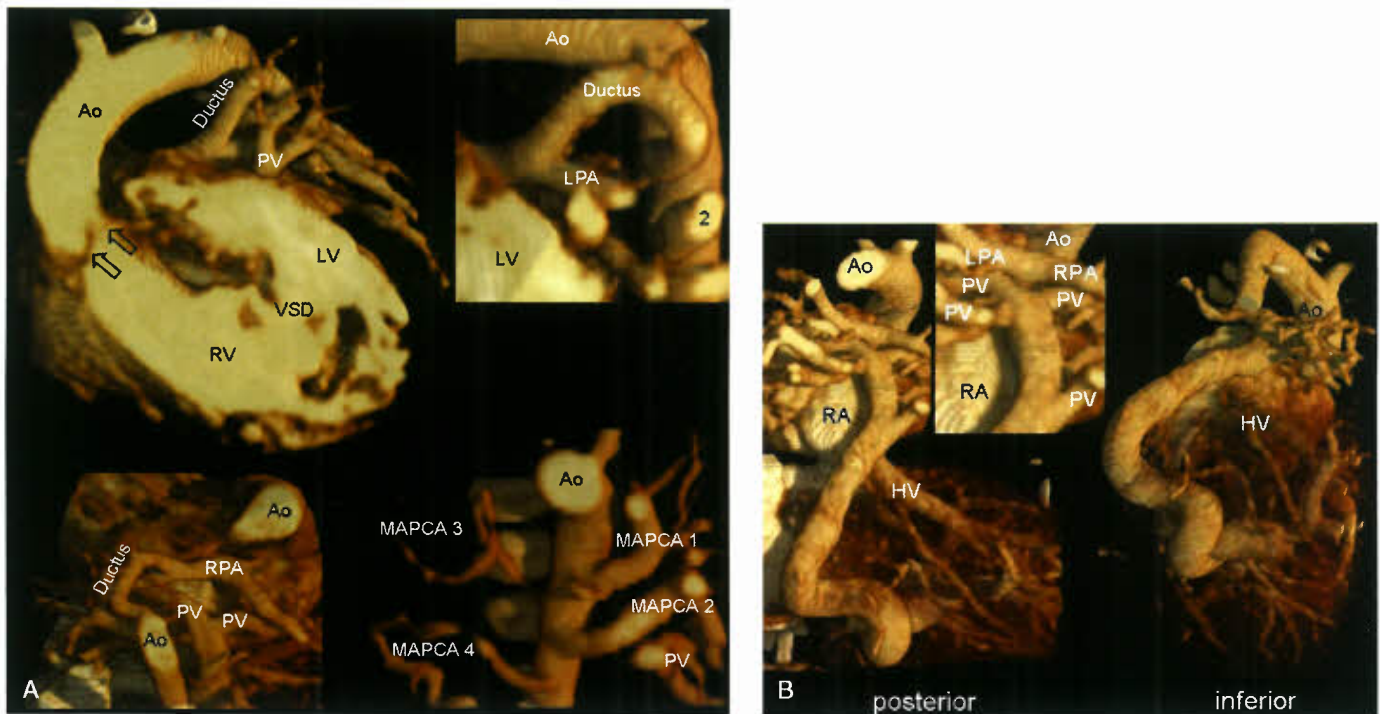


Figure 11.2. A 3-kg newborn with heterotaxia and total anomalous pulmonary venous drainage to the portal vein. Three-dimensional volume-rendered images obtained on a 64-slice MDCT scanner following hand injection of 6 mL of contrast in the UVC. **A:** Images (right to left and top to bottom) show the aortic valve (arrows) and ventricular septal defect (VSD) as well as a ductus and MAPCAs arising from the aorta to supply the lung and the pulmonary arteries. **B:** Image shows the confluence of the pulmonary veins (PV) draining across the diaphragm to the liver. Appreciate the size of <1 mm of the PV. Ao, Aorta; HV, hepatic veins; RA, right atrium; LV and RV, left and right ventricle.



Figure 11.3. A 5-month-old boy with pulmonary stenosis (arrow). Coronal reformatted MIP image obtained using a 22-gauge IV in left hand at 2 mL/s by power injector (20 mL Optiray 320) using a 64-slice MDCT. Contrast enhancement exceeded 600 HU.

A method that utilizes the contrast-covering time concept makes use of the advantages of bolus tracking but compensates for the trigger delay by adjusting the injected flow rate of contrast. This requires a dual power injector (9).

In patients who have undergone a Fontan procedure, the lack of proper contrast mixing in the right atrium due to the sluggish, slow blood flow through the Fontan circuit often results in suboptimal contrast enhancement of the pulmonary arteries and may mimic a thrombosis. By employing simultaneous injections of contrast in both upper- and lower-extremity veins and by monitoring enhancement of the pulmonary arteries by using bolus tracking, this problem can be minimized (23). One may need to be ready to perform a delayed second-phase CT scan if the dual injection method is unsuccessful. Because intravascular contrast enhancement persists longer when using gadolinium and MRI, evaluation of Fontan anatomy is easier with MRI (24).

Radiation Protection

In part because of the success and proliferation of CT for medical imaging, safety concerns regarding the potential hazards of ionizing radiation from frequent and indiscriminate use of diagnostic CT examinations have in recent years come to the forefront. Because of the uncertainty of what risks, if any, can be attributed to repeated exposures of low levels of ionizing radiation used for medical imaging, a conservative approach has been adopted by health professionals to limit radiation exposure as low as reasonably achievable (ALARA) (7,25).

Dose Reduction – a multifactorial issue

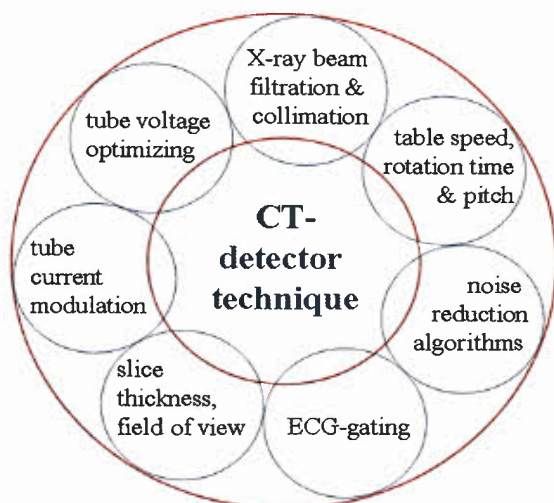


Figure 11.4. Dose reduction—a multifactorial issue.

The radiation exposure from a given exam is influenced by many factors (Fig. 11.4): the type of scanner, for example, dual source, electron beam etc.; the vendor of the scanner; the use of shielding; the use of dose modulation software; the kilovolt potential (kVp); tube current or milliamperes (mA); collimation; rotation speed and pitch; and whether ECG or other type of gating is used (26). There are a number of suggested ALARA protocols in the literature (9,11,12).

The radiation dose received is proportional to the square root of the kilovolt potential (kVp) and is directly related to tube current or milliamperes (mA) times the duration of exposure (seconds). Because of the reduced x-ray attenuation secondary to lower body mass in children, the exposure settings can be reduced without loss in image quality (Figs. 11.5 and 11.6). When intravenous contrast is used, a lower kVp is advantageous in that it accentuates the beam absorption properties of the high atomic weight of iodine (16). Reducing the kVp to 80 in infants and small children thus allows reduction in dose while at the same time enhancing vascular contrast. The ALARA principle dictates that the milliamperes used should be adjusted according to patient weight (27).

The estimated effective doses of CTA using pediatric ALARA protocols in infants ranges from 1.1 to 1.7 mSv using nongated and 2.2 to 3.4 mSv for gated multidetector computed tomography (MDCT) (9). With a dual-source scanner, effective doses for gated and nongated CT are <1 mSv. To put these radiation dose exposures in perspective, the average natural background dose for living 1 year in Ohio is estimated to be 3 mSv and in Germany 2.3 mSv.

Electrocardiograph Gating

A non-ECG-gated acquisition is optimal for most CT exams in CHD, which are obtained to evaluate the extracardiac vasculature. Not only is there no radiation dose penalty but also nongated exams are faster and extracardiac structures are more susceptible to respiratory motion than cardiac pulsation artifact.

With the fast temporal resolution of 165 ms using 64-slice MDCT, electrocardiographic (ECG) gating is possible. Retrospective ECG gating is necessary for a comprehensive evaluation of the coronary arteries and allows reconstruction of the



Figure 11.5. A 6-month-old boy with history of pulmonary atresia and small right pulmonary artery (RPA). A 1.25 mm axial image obtained during controlled ventilation with deep conscious sedation on an eight-slice MDCT following 15 mL contrast by hand injection at 120 kVp and 40 mAs (effective dose estimate of 150 mrem).

CT data so as to be able to perform functional analyses such as ventricular wall motion and ventricular volume and ejection fraction calculations, typically the domain of MRI. Few studies have compared MRI and CT in functional assessment. One such study found no difference between MRI and CT in assessing right ventricle function in adults with tetralogy of Fallot (28,29).

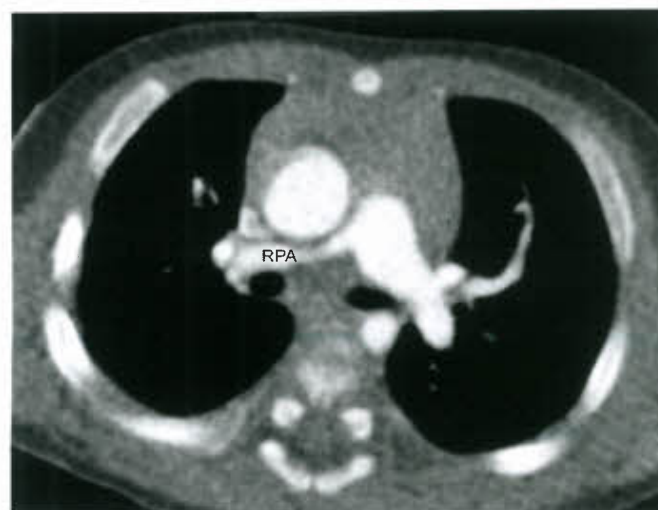


Figure 11.6. A 3-month-old boy with hypoplastic right heart syndrome and small right pulmonary artery (RPA). A 1.25 mm axial image obtained during controlled ventilation with deep conscious sedation on an eight-slice MDCT following 10 mL contrast by hand injection at 80 kVp and 20 mAs (effective dose estimate 28 mrem). The radiation dose was decreased 80% compared with example shown in Figure 11.5 without loss of diagnostic quality.



Figure 11.7. Three-dimensional volume-rendered image of the coronaries in a 3-month-old boy with heart rate of 111 acquired in 3 seconds using ECG gating without sedation on a 64-slice MDCT scanner (GE Volume CT). Ao, aorta. (Images courtesy of Dr. Hauschild, San Diego Children's Hospital.)

In retrospective gating, the tube current is on during the whole cardiac cycle, for approximately five heart beats using a 64-MDCT system, so that data can be reconstructed during the most motion-free phases. This boosts the radiation dose three to four times compared to a nongated exam. The dose can be lessened by approximately 25% by using tube current modulation that reduces the beam strength during nonoptimal phases, near end-diastole and end-systole (20). There are limitations in successfully retrospective gating if the heart rate is too fast, which depends on the particular scanner used, with an upper limit of approximately 110 beats per minute on a 64-slice scanner (Fig. 11.7).

In prospective ECG gating, there is no dose penalty, but one cannot perform functional analysis, and the heart rates permissible are limited to <65 to 80 beats per minute. The x-ray beam is on only during a predetermined phase of the cardiac cycle with significant radiation dose savings (77 to 87%) (30,31). In adults, prospective gating resulted in images of similar quality to retrospectively gated coronary artery exams (30). The improved temporal resolution of dual-source scanners of <100 ms allows prospective gating in the systolic phase to image coronary arteries in babies who have high heart rates. Dual-source prospective gating mode may allow the entire thorax of a baby to be scanned in 1.3 seconds at a low radiation exposure of 0.5 mSv (32).

CT Scanners

Electron beam CT scanners are rarely used in CHD evaluation due to their poorer spatial resolution (3 mm). MDCT scanners are the current mainstay for cardiac imaging. Sixty-four channel scanners have the necessary spatial and temporal resolution for coronary imaging. The use of two simultaneous x-ray sources (dual source) coupled with two corresponding detectors allows a temporal resolution of <100 μ s because each of two arrays travels only 90 degrees to acquire sufficient data. The latest generation MDCT scanners utilizing 128 to

320 detectors have the potential to image the heart of an adult-sized patient almost instantaneously but the gantry is too wide to be of practical use for a small infant's heart.

Postprocessing CT Data Set

MDCT acquires a large volumetric isotropic data set of high spatial resolution, submillimeter in all three planes. Thus, MDCT excels at 3-D modeling. Interactively reviewing this data set at an independent workstation adds considerable diagnostic value, particularly in the setting of complex CHD in small children. The important relationships gleaned from this analysis can be saved as multiplanar two-dimensional (2-D) or 3-D reconstructions, which are ideal for discussions in case conferences and in therapeutic planning. A combination of 2-D multiplanar and 3-D maximum-intensity projection and volume-rendered images is most commonly used in the evaluation of CHD (4). A clear understanding of how the various reconstruction algorithms work and their pitfalls is necessary in order to avoid misrepresentation of the data due to partial volume averaging or artifacts (33).

INDICATIONS FOR CARDIAC CT

Problems in defining intracardiac morphology by echocardiography are usually handled with MRI even in infants because of the added functional information provided. The most common indications for CT are to evaluate the extracardiac vasculature in newborns and infants.

Pulmonary Arteries

The creation and maintenance of good pulmonary blood flow is a central theme in the management of CHD and is the goal of several common surgical procedures used to treat CHD: modified Blalock-Thomas-Taussig shunt, Glenn shunt, and Fontan procedure. Problems with the pulmonary arteries often occur postoperatively, such as with the arterial switch procedure, or are prevalent in certain conditions, such as tetralogy of Fallot. In children with pulmonary atresia/severe tetralogy, CT is helpful in identifying the source of pulmonary blood flow by determining the confluence and location of the mediastinal pulmonary arteries (5,34,35), the presence and size of a patent ductus arteriosus, and the presence and location of major aortopulmonary collaterals (MAPCAs) (36) and to identify pulmonary artery stenosis prior to surgery or as a postsurgical complication (Figs. 11.8–11.10).

Systemic and Pulmonary Veins

Left superior vena cava is more common in patients with CHD (37,38). In children with total or partial anomalous pulmonary venous return, CT is helpful in delineating the course and connections of the pulmonary veins and site of insertion of the draining vein and can identify postoperative vein obstruction (39–42). Total anomalous pulmonary venous return (TAPVR) is associated with heterotaxy syndrome (Figs. 11.11 and 11.12).

Aorta and Vascular Rings

Aortic coarctation may be difficult to differentiate from hypoplasia or interrupted aortic arch by echocardiography, particularly in the setting of a large patent ductus arteriosus. Echocardiography may also have difficulty

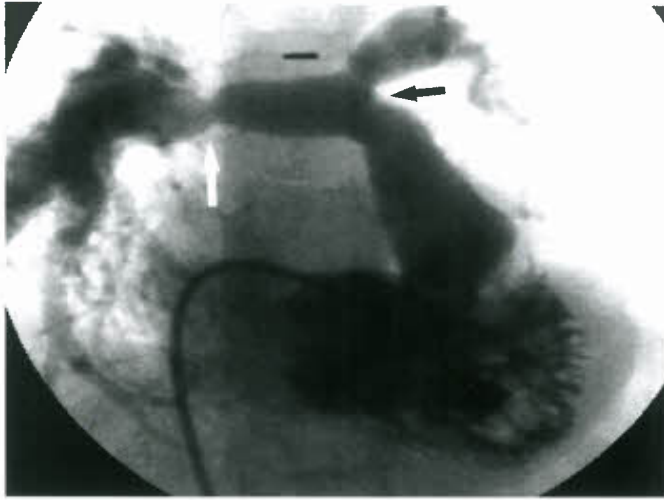


Figure 11.8. A 2-year-old boy with history of tetralogy of Fallot status after complete repair. Digital angiography spot film following injection of the right ventricle shows bilateral pulmonary artery stenoses (*white arrow*, right pulmonary artery; *black arrow*, left pulmonary artery).

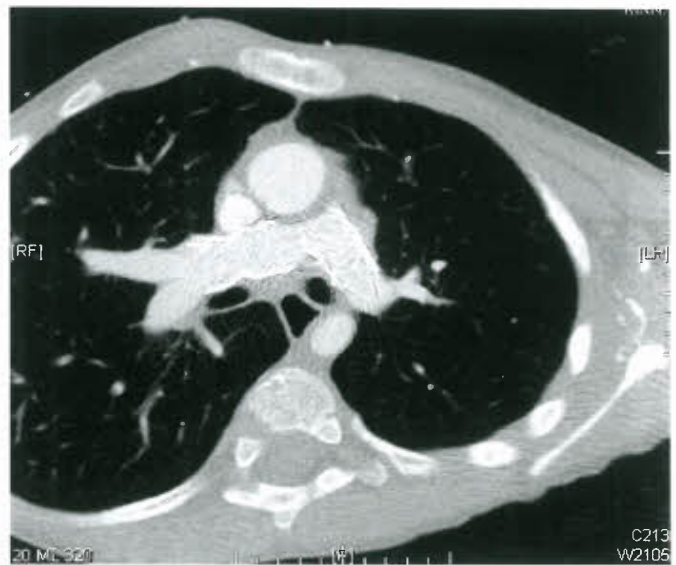


Figure 11.10. Same child as in Figure 11.8. A 1.25 mm axial image obtained during controlled ventilation with deep conscious sedation on an eight-slice MDCT scanner following angioplasty and placement of bilateral pulmonary artery stents. Note lack of major stent artifacts.

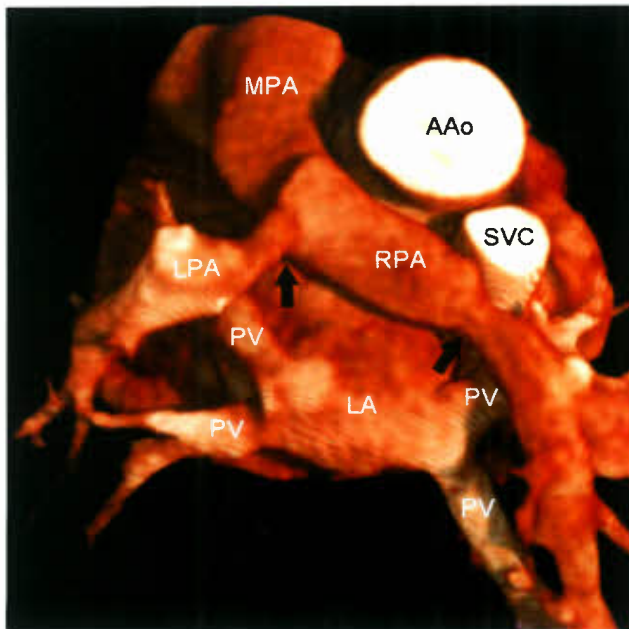


Figure 11.9. Same child as in Figure 11.8. The 3-D volume-rendered image of heart (posterior view) obtained during controlled ventilation with deep conscious sedation on an eight-slice MDCT depicts the nature and extent of bilateral pulmonary artery stenoses (*arrows*) more clearly. MPA, main pulmonary artery; RPA, right pulmonary artery; LPA, left pulmonary artery; PV, pulmonary vein; LA, left atrium; AAO, ascending aorta; SVC, superior vena cava.

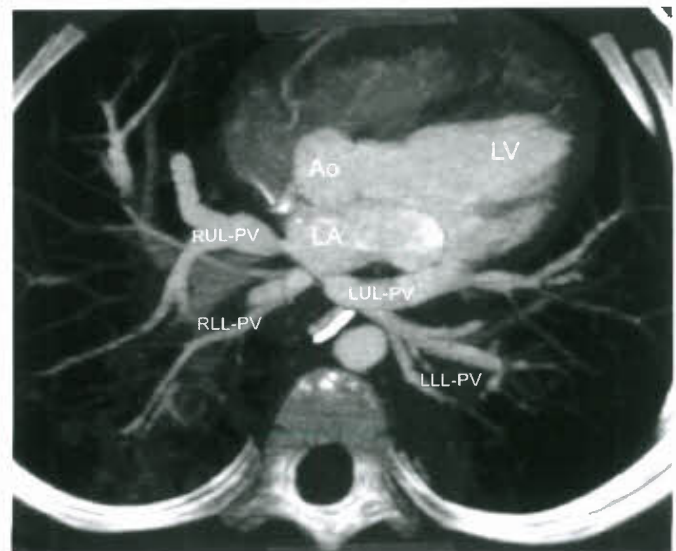


Figure 11.11. A 2-year-old boy who presented with right-sided heart failure. A 1.25-mm axial image obtained during controlled ventilation with deep conscious sedation on an eight-slice MDCT scanner at 100 kVp and 40 mAs shows stenoses of the pulmonary veins at their insertions into LA. Ao, aorta; LA, left atrium; LLL-PV and RLL-PV, left and right lower lung-pulmonary vein; LUL-PV and RUL-PV, left and right upper lung-PV; LV, left ventricle.



Figure 11.12. Three-dimensional volume-rendered posterior coronal image of the same child as in Figure 11.11. MPA, main pulmonary artery; RPA, right pulmonary artery; LPA, left pulmonary artery; PV, pulmonary vein; LA, left atrium; AAo, ascending aorta; SVC, superior vena cava; IVC, inferior vena cava.

assessing the branching pattern of the great vessels in these disorders. Some vascular rings may have subtle findings (Fig. 11.13). There may be critical aortic aneurysmal dilatation in infantile Marfan syndrome, critical aortic stenosis (supra valvular and diffuse) in Williams syndrome, or small pseudoaneurysms as a complication of surgical or intravascular treatment.

Airway Abnormalities

Airway stenosis or malacia may occur secondary to prolonged intubation or to a vascular ring (Fig. 11.14) or extrinsic compression by dilated pulmonary arteries or therapeutic stents. CT may also identify a tracheal bronchus (43) or a bridging bronchus (44), which are associated with CHD (Fig. 11.15). A bridging bronchus is a lobar or segmental bronchus that arises from the contralateral bronchus.

Coronary Arteries

In infants and children, there is often no need for a comprehensive evaluation of coronary artery anatomy as in adults with atherosclerotic disease with the exception of aneurysms as a complication of Kawasaki disease (Fig. 11.16). Rather, it is important to delineate the origin and course of the proximal coronary arteries to identify anomalies that may interfere with a safe surgical correction or that may result in sudden death as in a young athlete. Potential anomalies of significance include anomalous origin from the contralateral aortic sinus (Fig. 11.17), single coronary artery, interarterial course of a coronary artery, pulmonary artery origin, high takeoff, and multiple ostia of the coronary arteries (45,46).

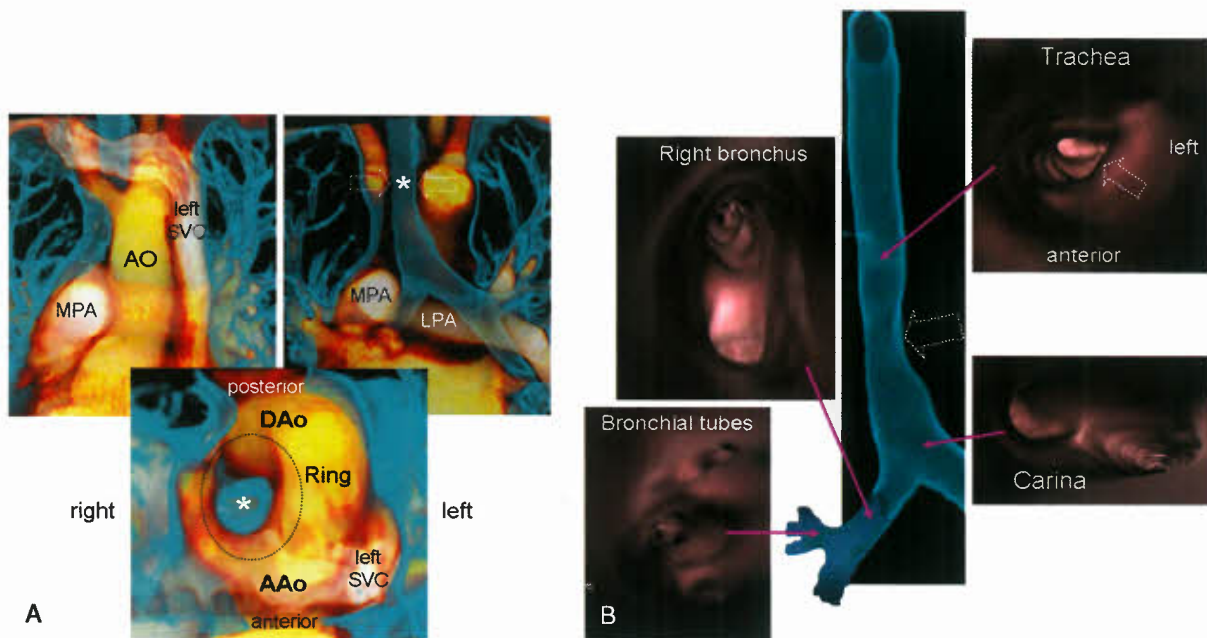
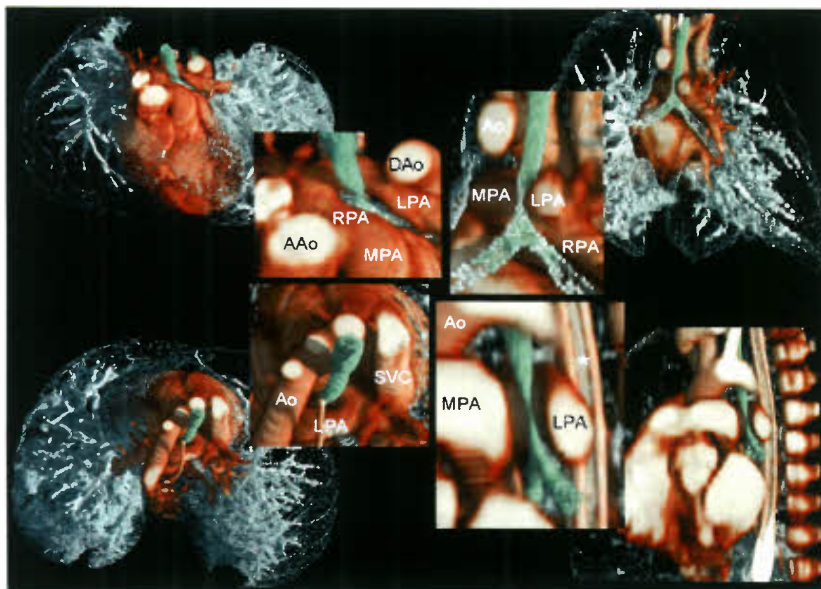


Figure 11.13. A 2-year-old with situs inversus and dextrocardia had acute respiratory distress and suspected vascular ring. Left side (A) shows a volume rendering of the vascular anatomy depicting a double aortic arch with a dominant left-sided and a hypoplastic right-sided arch. The ring encloses the trachea marked by an asterisk. B: Virtual tracheobronchoscopic views and fly-through of the trachea upon rerendering the same CT dataset. The arrows show the place and direction of the tracheal impression due to the pulsations of the ring. The pink arrows mark the position of the corresponding view. AAo and DAo, ascending and descending aorta, SVC, superior vena cava; MPA, main pulmonary artery.

Figure 11.14. A 3.5-month-old boy with pulmonary artery sling. Multiple volume-rendered images show compression of trachea (*green*) by the anomalous course of the left pulmonary artery (LPA). Note virtual bronchograms of lungs (*turquoise*) highlighting the capability of CT to simultaneously assess both heart and lungs. Left in anteroposterior and right in a left lateral view. MPA, main pulmonary artery; LPA, left pulmonary artery and RPA, AAO and DAAO, ascending and descending aorta.



The ability to visualize the proximal coronary arteries is inconsistent on nongated MDCT but better the older the child especially if they are capable of a breath hold (45,47). Gated MRI exams, particularly with good navigator sequences, are often successful in this regard in older children. In neonates, infants, and young children, gated CT exams are necessary to reliably assess the proximal coronary arteries (48). This requires fast temporal

resolution such as a 64 or greater MDCT or dual-source scanner (49). Breath holding may not be necessary in neonates (48).

There is an increased incidence of coronary artery anomalies in CHD. Presurgical identification is particularly important in patients with transposition of the great vessels, tetralogy of Fallot, truncus arteriosus, and pulmonary atresia with intact ventricular septum (45).

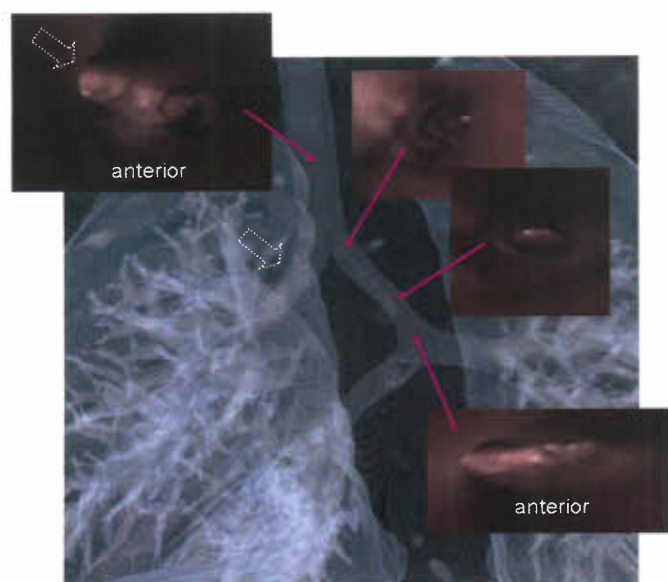


Figure 11.15. A 1.5-year-old child with bridging bronchus. Virtual tracheobronchoscopic views. The *pink arrows* mark the position of the corresponding view into and down the tracheo-bronchial system. After the "first" bifurcation (or the origin of a so-called bronchus suis or pig bronchus [arrow]), stenosis and cartilaginous tracheal rings could be appreciated (funnel trachea). The bronchial tree is getting wider with the origin of the "bridging bronchus" (the "real" right main bronchus).

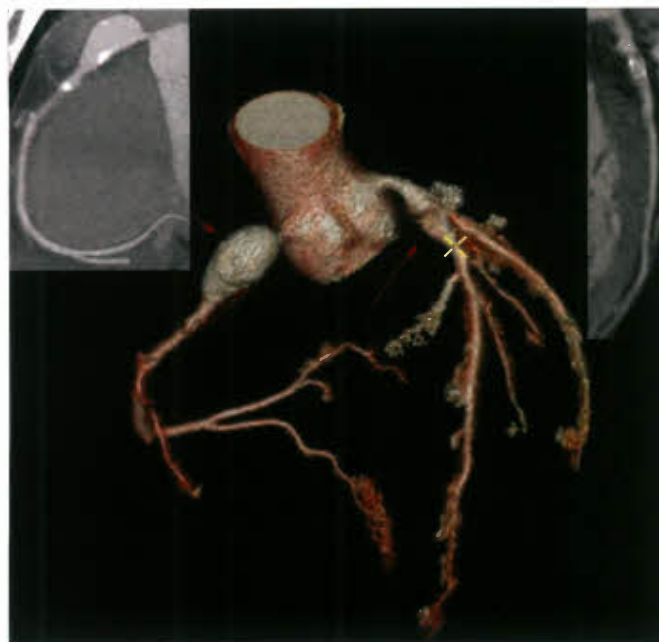


Figure 11.16. Three-dimensional volume-rendered image of the coronaries of a young adult patient 15 years after Kawasaki disease: giant aneurysm of the right coronary artery and fusiform aneurysm of the left coronary artery including its bifurcation. The small images show curved MPR (multiplanar reconstruction) of the both arteries. Calcifications could be appreciated as wide spots in the vessel wall.

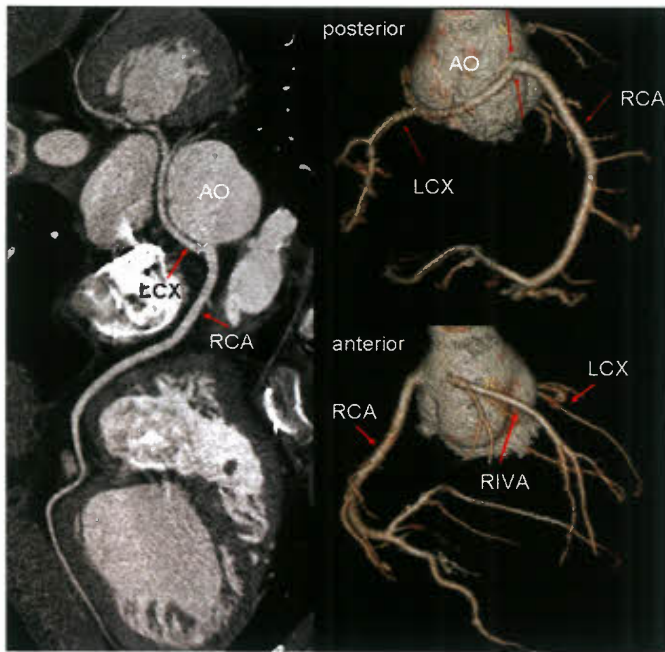


Figure 11.17. A 12-year-old boy was assessed with a 256-slice MDCT in a 3-second scan with prospective ECG gating (heart rate of 75 beats per minute). CTA shows an unknown anomaly of the coronary arteries. Left side; in a curved MP reformatted image, the left circumflex artery (LCX) arises from the right coronary artery (RCA) and follows a retroaortic pathway. On the right side, volume-rendered image shows the origins of all the coronary arteries. RIVA, ramus interventricularis anterior. (Courtesy of Dr. G. Gitsioudis, Heidelberg.)

Stents

Transcatheter placement of endovascular metallic stents is a common nonoperative way to treat stenoses of the pulmonary and systemic arteries and veins in children with CHD (50). A frequent complication of stents is the development of in-stent luminal narrowing due to intimal hyperplasia, stent

fracture (Fig. 11.18), and stent-related vascular narrowing or aneurysms (51,52). Conventional digital angiography is the gold standard for identifying in-stent restenosis, but it is not practical for long-term follow-up due to the fact that it is invasive and results in radiation exposure. In contrast to sonography and MRI, MDCT is surprisingly free of artifacts from the metallic component of stents (Fig. 11.19). (52). CT has been shown to accurately identify in-stent restenosis, even in small coronary arteries (53–55), but it is limited in detecting very mild intimal proliferation due to volume averaging from the metallic struts (56–58).

The ability of MRI to evaluate stents is dependent on the magnetic susceptibility of the material used as well as on the geometry and orientation of the struts and on the orientation of the stent in the main magnetic field (58,59). Stent artifacts are due not only to the induced magnetic field inhomogeneity but also are caused by radiofrequency shielding. For example, an MR black-blood imaging sequence, which is resistant to field inhomogeneity, still results in poor images due to shielding. MR seems to be able to provide diagnostic information on stent patency in stents made out of nitinol and tantalum and when high flip angle magnetic resonance angiography sequences are used (60,61).

CONCLUSION

CT technology continues to evolve new hardware and software modifications that result in faster scan times to reduce the need for sedation and to image better the coronary arteries while at the same time significantly lowering the radiation dose. With current ALARA protocols and MDCT scanners, CT provides a 3-D submillimeter evaluation of the heart and great vessels in a matter of seconds with little motion artifacts, potentially without the need for general anesthesia, and with much less radiation exposure than commonly thought. This powerful diagnostic tool plays an important role in infants and young children and the most critically ill children with CHD as a supplement to ultrasound evaluation and thereby decreases the number of diagnostic cardiac catheterizations needed and the radiation dose and sedation times utilized in the interventional cardiac lab.

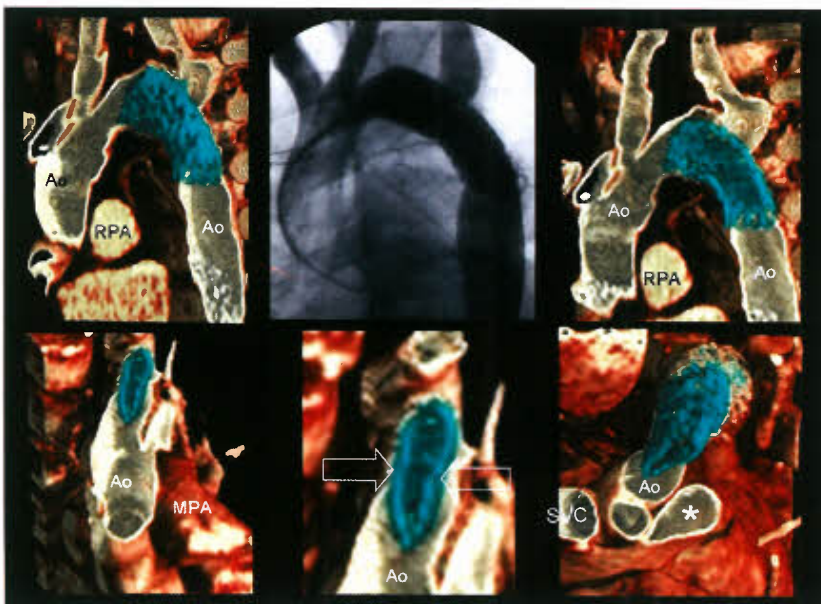


Figure 11.18. A 7-year-old girl with history of aortic coarctation postangioplasty and aortic stent placement (green). Multiple volume-rendered images from an eight-slice MDCT obtained during a voluntary breath hold of the aortic arch show inward collapse of lumen of stent (arrows) on coronal projection not seen on sagittal views or on digital angiogram (top middle). MPA, main pulmonary artery; RPA, right pulmonary artery; Ao, aorta.

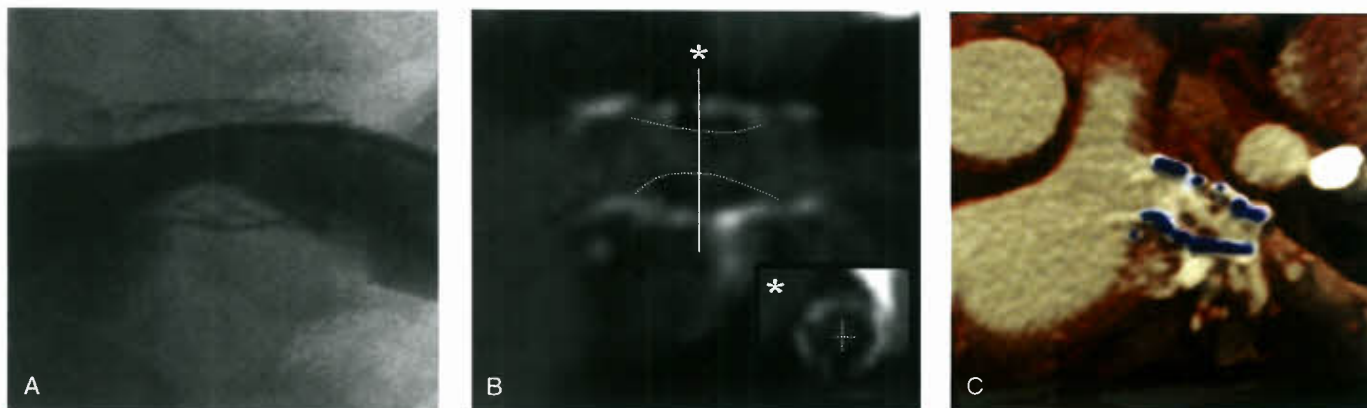


Figure 11.19. A 4-year-old child with an LPA stent. **A:** Digital angiogram shows narrowing or a moderate in stent restenosis which is greatest at its mid-portion. **B:** CTA 2-D multiplanar reconstruction of stent. **C:** Three-dimensional volume rendering shows stent (blue dashes).

REFERENCES

- Lee T, Tsai IC, Fu YC, et al. Using multidetector-row CT in neonates with complex congenital heart disease to replace diagnostic cardiac catheterization for anatomical investigation: initial experiences in technical and clinical feasibility. *Pediatr Radiol* 2006;36:1273–1282.
- Beier UH, Jelnin V, Jain S, et al. Cardiac computed tomography compared to transthoracic echocardiography in the management of congenital heart disease. *Catheter Cardiovasc Interv* 2006;68:441–449.
- Haramati LB, Glickstein JS, Issenberg HJ, et al. MR imaging and CT of vascular anomalies and connections in patients with congenital heart disease: significance in surgical planning. *Radiographics* 2002;22:337–347; discussion 48–49.
- Dillman JR, Hernandez RJ. Role of CT in the evaluation of congenital cardiovascular disease in children. *AJR Am J Roentgenol* 2009;192:1219–1231.
- Matsui H, Yasukochi S, Haseyama K, et al. Quantification of right and left ventricular volumes in children with congenital heart disease by multidetector-row computed tomography. *Pediatr Cardiol* 2007;28:267–271.
- Chan FP. MR and CT imaging of the pediatric patient with structural heart disease. *Semin Thorac Cardiovasc Surg* 2008;20:393–399.
- Brenner D, Elliston C, Hall E, et al. Estimated risks of radiation-induced fatal cancer from pediatric CT. *AJR Am J Roentgenol* 2001;176:289–296.
- Hlavacek AM. Imaging of congenital cardiovascular disease: the case for computed tomography. *J Thorac Imaging* 2010;25:247–255.
- Tsai IC, Chen MC, Jan SL, et al. Neonatal cardiac multidetector row CT: why and how we do it. *Pediatr Radiol* 2008;38:438–451.
- Kawano T, Ishii M, Takagi J, et al. Three-dimensional helical computed tomographic angiography in neonates and infants with complex congenital heart disease. *Am Heart J* 2000;139:654–660.
- Hellinger JC, Pena A, Poon M, et al. Pediatric computed tomographic angiography: imaging the cardiovascular system gently. *Radiol Clin North Am* 2010;48:439–467, x.
- Krishnamurthy R. Neonatal cardiac imaging. *Pediatr Radiol* 2010;40:518–527.
- Schmid E, Johr M. Current discussions in pediatric anesthesia. Pediatric Anesthesia Symposium in Zurich, September 17–18, 2004. *Anaesthesist* 2005;54:163–165.
- Long FR, Castile RG, Brody AS, et al. Lungs in infants and young children: improved thin-section CT with a noninvasive controlled-ventilation technique-initial experience. *Radiology* 1999;212:588–593.
- Long FR, Castile RG. Technique and clinical applications of full-inflation and end-exhalation controlled-ventilation chest CT in infants and young children. *Pediatr Radiol* 2001;31:413–422.
- Siegel MJ. Multiplanar and three-dimensional multi-detector row CT of thoracic vessels and airways in the pediatric population. *Radiology* 2003;229:641–650.
- Bae KT. Intravenous contrast medium administration and scan timing at CT: considerations and approaches. *Radiology* 2010;256:32–61.
- Behrendt FF, Bruners P, Keil S, et al. Impact of different vein catheter sizes for mechanical power injection in CT: in vitro evaluation with use of a circulation phantom. *Cardiovasc Intervent Radiol* 2009;32:25–31.
- Schwab SA, Uder M, Anders K, et al. Peripheral intravenous power injection of iodinated contrast media through 22G and 20G cannulas: can high flow rates be achieved safely? A clinical feasibility study. *Rofo* 2009;181:355–361.
- Taylor CM, Blum A, Abbara S. Patient preparation and scanning techniques. *Radiol Clin North Am* 2010;48:675–686.
- Rigsby CK, Gasber E, Seshadri R, et al. Safety and efficacy of pressure-limited power injection of iodinated contrast medium through central lines in children. *AJR Am J Roentgenol* 2007;188:726–732.
- Friedman BA, Schoepf UJ, Bastarrica GA, et al. Computed tomographic angiography of infants with congenital heart disease receiving extracorporeal membrane oxygenation. *Pediatr Cardiol* 2009;30:1154–1156.
- Prabhu SP, Mahmood S, Sena L, et al. MDCT evaluation of pulmonary embolism in children and young adults following a lateral tunnel Fontan procedure: optimizing contrast-enhancement techniques. *Pediatr Radiol* 2009;39:938–944.
- Takawira F, Ayer JG, Onikul E, et al. Evaluation of the extracardiac conduit modification of the Fontan operation for thrombus formation using magnetic resonance imaging. *Heart Lung Circ* 2008;17:407–410.
- Brody AS, Frush DP, Huda W, et al. Radiation risk to children from computed tomography. *Pediatrics* 2007;120:677–682.
- Paul JF, Abada HT. Strategies for reduction of radiation dose in cardiac multislice CT. *Eur Radiol* 2007;17:2028–2037.
- Herzog C, Mulvihill DM, Nguyen SA, et al. Pediatric cardiovascular CT angiography: radiation dose reduction using automatic anatomic tube current modulation. *AJR Am J Roentgenol* 2008;190:1232–1240.
- Raman SV, Cook SC, McCarthy B, et al. Usefulness of multidetector row computed tomography to quantify right ventricular size and function in adults with either tetralogy of Fallot or transposition of the great arteries. *Am J Cardiol* 2005;95:683–686.
- Nicol ED, Stirrup J, Roughton M, et al. 64-Channel cardiac computed tomography: intraobserver and interobserver variability, part 2: global and regional ventricular function, mass, and first pass perfusion. *J Comput Assist Tomogr* 2009;33:169–174.
- Shuman WP, Branch KR, May JM, et al. Prospective versus retrospective ECG gating for 64-detector CT of the coronary arteries: comparison of image quality and patient radiation dose. *Radiology* 2008;248:431–437.
- Blankstein R, Shah A, Pale R, et al. Radiation dose and image quality of prospective triggering with dual-source cardiac computed tomography. *Am J Cardiol* 2009;103:1168–1173.
- Paul JF, Rohnean A, Sigal-Cinqualbre A. Multidetector CT for congenital heart patients: what a paediatric radiologist should know. *Pediatr Radiol* 2010;40:869–875.
- Johnson PT, Fishman EK. Postprocessing techniques for cardiac computed tomographic angiography. *Radiol Clin North Am* 2010;48:687–700.
- Khatri S, Varma SK, Khatri P, et al. 64-slice multidetector-row computed tomographic angiography for evaluating congenital heart disease. *Pediatr Cardiol* 2008;29:755–762.
- Hayabuchi Y, Mori K, Kitagawa T, et al. Accurate quantification of pulmonary artery diameter in patients with cyanotic congenital heart disease using multidetector-row computed tomography. *Am Heart J* 2007;154:783–788.
- Hayabuchi Y, Inoue M, Watanabe N, et al. Assessment of systemic-pulmonary collateral arteries in children with cyanotic congenital heart disease using multidetector-row computed tomography: comparison with conventional angiography. *Int J Cardiol* 2010;138:266–271.
- Rigatelli G. Congenitally persistent left superior vena cava: a possible unpleasant problem during invasive procedures. *J Cardiovasc Med (Hagerstown)* 2007;8:483–487.
- Demos TC, Posniak HV, Pierce KL, et al. Venous anomalies of the thorax. *AJR Am J Roentgenol* 2004;182:1139–1150.
- Moral S, Ortuno P, Aboal J. Multislice CT in congenital heart disease: partial anomalous pulmonary venous connection. *Pediatr Cardiol* 2008;29:1120–1121.
- Lakshminrusimha S, Wynn RJ, Youssfi M, et al. Use of CT angiography in the diagnosis of total anomalous venous return. *J Perinatol* 2009;29:458–461.

41. Ho ML, Bhalla S, Bierhals A, et al. MDCT of partial anomalous pulmonary venous return (PAPVR) in adults. *J Thorac Imaging* 2009;24:89–95.
42. Hirsch R, Gottliebson W, Crotty E, et al. Computed tomography angiography with three-dimensional reconstruction for pulmonary venous definition in high-risk infants with congenital heart disease. *Congenit Heart Dis* 2006;1:104–110.
43. Ming Z, Lin Z. Evaluation of tracheal bronchus in Chinese children using multidetector CT. *Pediatr Radiol* 2007;37:1230–1234.
44. Baden W, Schaefer J, Kumpf M, et al. Comparison of imaging techniques in the diagnosis of bridging bronchus. *Eur Respir J* 2008;31:1125–1131.
45. Goo HW, Seo DM, Yun TJ, et al. Coronary artery anomalies and clinically important anatomy in patients with congenital heart disease: multislice CT findings. *Pediatr Radiol* 2009;39:265–273.
46. Sundaram B, Kreml R, Patel S. Imaging of coronary artery anomalies. *Radiol Clin North Am* 2010;48:711–727.
47. Goo HW, Park IS, Ko JK, et al. Visibility of the origin and proximal course of coronary arteries on non-ECG-gated heart CT in patients with congenital heart disease. *Pediatr Radiol* 2005;35:792–798.
48. Tsai IC, Lee T, Chen MC, et al. Visualization of neonatal coronary arteries on multidetector row CT: ECG-gated versus non-ECG-gated technique. *Pediatr Radiol* 2007;37:818–825.
49. Ben Saad M, Rohnan A, Sigal-Cinqualbre A, et al. Evaluation of image quality and radiation dose of thoracic and coronary dual-source CT in 110 infants with congenital heart disease. *Pediatr Radiol* 2009;39:668–676.
50. Peters B, Ewert P, Berger F. The role of stents in the treatment of congenital heart disease: current status and future perspectives. *Ann Pediatr Cardiol* 2009;2:3–23. PMID:2840765.
51. Hamzeh RK, El-Said HG, Moore JW. Left main coronary artery compression from right pulmonary artery stenting. *Catheter Cardiovasc Interv* 2009;73:197–202.
52. Eichhorn JG, Jourdan C, Hill SL, et al. CT of pediatric vascular stents used to treat congenital heart disease. *AJR Am J Roentgenol* 2008;190:1241–1246.
53. Das KM, El-Menyar AA, et al. Contrast-enhanced 64-section coronary multidetector CT angiography versus conventional coronary angiography for stent assessment. *Radiology* 2007;245:424–432.
54. Pugliese F, Cademartiri F, van Mieghem C, et al. Multidetector CT for visualization of coronary stents. *Radiographics* 2006;26:887–904.
55. Suzuki S, Furui S, Kuwahara S, et al. Detection of in-stent restenosis of coronary stents using 40-detector row computed tomography in vitro. *J Comput Assist Tomogr* 2008;32:252–258.
56. Eichhorn JG, Long FR, Hill SL, et al. Assessment of in-stent stenosis in small children with congenital heart disease using multi-detector computed tomography: a validation study. *Catheter Cardiovasc Interv* 2006;68:11–20.
57. Blum MB, Schmook M, Scherthaner R, et al. Quantification and detectability of in-stent stenosis with CT angiography and MR angiography in arterial stents in vitro. *AJR Am J Roentgenol* 2007;189:1238–1242.
58. Eichhorn JG, Long FR, Jourdan C, et al. Usefulness of multidetector CT imaging to assess vascular stents in children with congenital heart disease: an in vivo and in vitro study. *Catheter Cardiovasc Interv* 2008;72:544–551.
59. Bartels LW, Smits HF, Bakker CJ. MR imaging of vascular stents: effects of susceptibility, flow, and radiofrequency eddy currents. *J Vasc Interv Radiol* 2001;12:365–371.
60. Hamer OW, Finkenzeller T, Borisch I, et al. In vivo evaluation of patency and in-stent stenoses after implantation of nitinol stents in iliac arteries using MR angiography. *AJR Am J Roentgenol* 2005;185:1282–1288.
61. Nordmeyer J, Gaudin R, Tann OR, et al. MRI may be sufficient for noninvasive assessment of great vessel stents: an in vitro comparison of MRI, CT, and conventional angiography. *AJR Am J Roentgenol* 2010;195:865–871.

Nathaniel W. Taggart ■ Allison K. Cabalka

Cardiac catheterization has a long and illustrious history, beginning in 1929 when Werner Forssmann (1), a surgical resident and future urologist, performed the first cardiac catheterization from an arm vein—on himself. He was subsequently awarded the Nobel Prize for his discovery. In the 1950s, the catheterization laboratory was used to understand the physiology of congenital heart defects. By the 1960s to 1970s, advances in cardiac surgery required more detailed anatomic information, which was addressed using axial angiography (2,3). In the 1980s, 2-D echocardiography made it possible for many patients to be diagnosed and treated without cardiac catheterization. In the 1990s, transesophageal echocardiography, computerized tomography, and magnetic resonance imaging were used to produce detailed cardiac images, further decreasing the need for diagnostic cardiac catheterization. However, as more complex cardiac conditions are treated, more detailed physiologic data are necessary for the evaluation and treatment of children with congenital or acquired heart defects. This chapter discusses the acquisition of hemodynamic data and angiographic images. Interventional techniques are discussed separately in Chapter 13.

DIAGNOSTIC CARDIAC CATHETERIZATION AND ANGIOGRAPHY

Indications

A thorough diagnostic cardiac catheterization provides complete physiologic and anatomic data. With the appropriate team, the risk of cardiac catheterization is low—usually less than the risk associated with clinical decisions based on inadequate information. The three major indications for performing a diagnostic cardiac catheterization are as follows:

1. A complete anatomic diagnosis or necessary hemodynamic information cannot be obtained by noninvasive methods.
2. Clinical signs and symptoms are not consistent with a patient's diagnosis.
3. A patient's clinical course is not progressing as expected.

Indications for catheterization in specific lesions are covered subsequently in the relevant chapters pertaining to each lesion.

Techniques

Planning the Study

In order to acquire complete and accurate information from cardiac catheterization, the cardiologist must have a clear understanding of the specific question(s) to be answered. Necessary preparation before cardiac catheterization includes a

thorough review of the patient's complete history and physical examination, including all previous pertinent noninvasive studies, cardiac catheterizations, and reviewing operative notes from all prior surgeries. Additional laboratory studies should be obtained as indicated by the clinical findings including electrolytes in patients taking diuretics, blood urea nitrogen and creatinine if there is concern for renal insufficiency, and blood typing for any patient in whom the complication risk is significant or in whom intervention potentially may be needed. Patients referred for cardiac catheterization may be severely ill or have various comorbidities. Recognition of these coexisting conditions and appropriate anticipation of potential complications is vitally important. Precatheterization planning should incorporate discussion of the case with the anesthesiologist. Airway management and the use of conscious sedation versus general anesthesia should be discussed and planned in advance of the catheterization procedure.

If a patient is anemic, transfusion prior to cardiac catheterization can optimize the baseline hemodynamic condition. Cyanotic patients who have significantly elevated hemoglobin levels are at increased risk of stroke during cardiac catheterization, due to polycythemia. Partial exchange transfusion may be considered prior to catheterization, but currently is rarely performed.

Premedication, Sedation, and Anesthesia

Physicians and institutions vary in their approaches to premedication, sedation, and anesthesia. Management is influenced by the diversity of cardiac defects and the expertise of the cardiologist and anesthesiology team. The goals of premedication and sedation or anesthesia are to decrease anxiety, facilitate parental separation, ensure comfort, promote amnesia, and facilitate the safe and efficient performance of the procedure. At the same time, sedation and mechanical ventilation may affect intracardiac hemodynamic measurements and can influence the applicability of the data acquired during the catheterization. The level of sedation during the catheterization and the use of supplemental oxygen should be discussed explicitly with the anesthesiologist before the beginning of the procedure. It is now standard to assign a person other than the primary cath physician to be responsible for sedation and airway monitoring. In most cases, this should be a cardiac anesthesiologist, particularly for patients with complex congenital heart disease, elevated pulmonary vascular resistance, or depressed myocardial function.

Prior to the catheterization, in general, pediatric patients should not have solid food for 8 hours, but may have milk or infant formula up to 6 hours prior, breast milk up to 4 hours before, with clear liquids up to 2 hours before the procedure. Certain patients should have an intravenous (IV) line placed in (preferably in an upper extremity) before arriving in the cath lab; this facilitates administering IV fluid (to ensure hydration) and sedation, especially in cyanotic or polycythemic patients.

Premedications can be administered orally or intravenously. Some children are best treated with mask induction first, prior to IV placement. The periprocedure management should be individualized for each patient based upon his or her age, level of anxiety, and specific cardiac defect/physiology.

Local anesthesia is administered prior to starting percutaneous access. Lidocaine is the usual anesthetic, which is painful when initially injected. Premedication diminishes the discomfort to lidocaine infiltration, as does buffering the lidocaine with sodium bicarbonate, pretreatment with a topical anesthetic cream (lidocaine 2.5% and prilocaine 2.5%), use of a small needle (25 gauge) to infiltrate the skin prior to infiltrating deeper tissues, and a slow rate of lidocaine infiltration. The dose of lidocaine should not exceed 6 mg/kg, as an excessive dose or accidental IV administration can cause seizures. Care should also be taken to assure that lidocaine is not injected intravascularly.

Effective sedation and analgesia can be maintained during the procedure using various IV medications, including fentanyl, midazolam, ketamine, and propofol. Cardiac depressant agents (e.g., propofol) must be used cautiously or avoided in patients with depressed cardiac function. Vasodilator agents should typically be avoided in patients with tetralogy of Fallot or similar physiology due to severe pulmonary outflow obstruction where systemic vasodilation may produce increasing right-to-left shunt. Conversely, ketamine can increase the systemic vascular resistance and may be useful in certain clinical settings. When administering sedative medications, it is important to observe any changes in heart rate, blood pressure, and pulse oximetry and to have appropriate airway support immediately available. In the current era, the majority of congenital cardiac catheterization procedures in pediatric patients are performed with general anesthesia, so the involvement of a cardiac anesthesiologist is paramount to assure a safe procedure.

Vascular Access

Establishing reliable vascular access is a vital early step to conducting a safe and efficient cardiac catheterization. Particularly in young children and neonates, hurried attempts at vascular access can result in significant bleeding or vessel damage, which in turn makes access more difficult.

Vascular access is most commonly obtained in the femoral system, with the catheterization procedure described as antegrade from the venous system or retrograde from the arterial system. Right heart catheterization is performed in an antegrade fashion through the great veins. Left heart catheterization is often performed in a retrograde fashion, but can also be accomplished antegrade across an atrial septal defect, patent foramen ovale (PFO), or via transseptal puncture. The type and location of vascular access necessary to perform the study are dictated both by the patient's particular anatomy and the objectives of the catheterization. For example, patients with a bidirectional cavopulmonary superior vena cava (SVC) to pulmonary artery anastomosis require internal jugular (IJ) or subclavian vein access to enter the pulmonary arterial tree.

Patients with congenital heart disease who have undergone multiple prior catheterizations and surgical operations may have obstruction of the systemic veins or femoral arteries, complicating vascular access. Previous catheterization reports can provide insight into difficulty with vascular access and whether complete vessel occlusion has been documented. Certainly, it is helpful to future operators if this is documented in the medical record, if not also with a digital record of the hand injection of contrast in the femoral venous system for confirmation. In such cases, alternative sites of vascular access should be explored. Occasionally, vascular ultrasound with color flow Doppler or other imaging modalities may be necessary prior to catheterization to identify available sites. The most common sites of venous access for cardiac catheterization are femoral,

IJ, and subclavian. Percutaneous arterial access is almost exclusively achieved via the femoral artery. Other modes of venous access include use of the umbilical vein or artery in the newborn or transhepatic route in patients who have multiple obstructed systemic veins.

Femoral Approach

Atraumatic percutaneous entry of the femoral vessels should be possible in nearly all pediatric patients. This requires knowledge of the anatomy, attention to detail, excellent technique, and patience. The most common approach, using a plain beveled needle with Seldinger technique, is described here (4).

The patient is positioned on the catheterization table with the hips elevated slightly, and the legs restrained in a straight or slightly inward rotation. Conversely, some physicians prefer to have the legs rotated outward in a more "frog-legged" position; this displaces the femoral vessels to a more lateral position. The anatomic landmarks are identified both before and after draping the patient. Consistent landmarks for determining the site of vessel entry are the anterior superior iliac spine, the symphysis pubis, the inguinal ligament, and the femoral pulse. In small patients, the inguinal ligament is palpable. The femoral vessels should be entered 1 to 2 cm below the inguinal ligament to ensure reliable hemostasis at the completion of the procedure. Vessel entry above the inguinal ligament is likely to result in a labial or scrotal hematoma or the more significant complication of retroperitoneal bleeding.

After the skin has been cleansed and a sterile field established, bony and soft tissue landmarks are again palpated to locate the femoral neurovascular bundle. This bundle courses vertically in the upper thigh and passes below the inguinal ligament approximately midway between the symphysis pubis and the anterior superior iliac spine. The femoral artery lies lateral to the vein and medial to the femoral nerve. Palpating the femoral pulse provides a reliable landmark for infiltration of anesthetic and, ultimately, needle puncture of the vein or artery. Ideally, the right femoral vein is accessed, as it provides a straight course to the right atrium (except in patients with situs inversus). Ultrasound with color flow Doppler can help determine vessel patency prior to attempted needle puncture. In the event that vessel patency cannot be documented by ultrasound, attention should be turned to the left-sided femoral vessels, which should also be evaluated by ultrasound. Due to the risk of complications, the use of ultrasound guidance for femoral access is becoming more commonplace (5) except in very young infants in whom the ultrasound probe may compress the vessels.

Once the vessel and surrounding landmarks have been identified, the overlying skin is infiltrated with a small amount of lidocaine, administered gradually to minimize the pain associated with administration. Too large a volume of lidocaine, particularly in small children, can distort the underlying vessels and make access more difficult. Once the skin is appropriately numbed, a hollow-bore needle, preferably with a short bevel, is introduced at a 30- to 45-degree to the skin, 1 to 2 cm below the inguinal ligament. The needle should be inserted using an "advance and wait" technique, observing for backflow of blood between 1- and 2-mm advances. If no backflow of blood occurs, once the needle is advanced to the bone, it should be withdrawn slowly and blood return monitored. It is also possible to advance the needle slowly with application of gentle aspiration using a syringe at this point if one is not used initially. Once consistent blood return is obtained, the needle is stabilized, and the soft end of the guide wire is advanced through the needle into the vessel lumen. The wire should advance freely; any resistance should be investigated. When accessing the femoral vein, the wire position can be confirmed with brief fluoroscopic imaging,

typically advancing the wire into the distal IVC. When accessing the femoral artery, it should be advanced to the lower abdominal aorta. Once the wire position has been confirmed, the needle is removed and an appropriate-sized hemostatic sheath is placed over the wire and advanced until the sheath hub is at the skin. The sheath is cleared of air by drawing back on a syringe attached to the sheath. Prompt blood return again confirms the position of the sheath within the vessel space, and connection to the monitoring pressure transducer confirms venous or arterial pressure.

When advancing the introducer wire through the needle, if the wire meets resistance immediately upon leaving the needle tip, it is most likely in the extravascular space and should be removed. If there is resistance to removing the wire, then the entire system should be removed to be sure that the wire is not sheared off beyond the end of the needle bevel. However, if the wire extends well beyond the tip of the needle before meeting resistance, the vessel may be obstructed. Obstruction can be confirmed by a small injection of contrast through the needle, using a slip-tip syringe, and imaged under fluoroscopy. This image of the obstructed vessel should be recorded and documented in the catheterization report for future reference.

Internal Jugular Approach

The IJ vein is the most common approach used when femoral veins are obstructed. It is the preferred approach for right ventricular endomyocardial biopsies (except in very young patients). The IJ vein is entered outside the thorax, so there is a low risk of pneumothorax. For appropriate positioning, the patient's head must remain turned to one side; thus in a sedated patient (particularly an infant), the airway may be compromised. Therefore, general anesthesia with endotracheal intubation is commonly used for IJ access. The right IJ vein is preferred (to the left) because it offers a more direct course into the right atrium, and the apex of the lung is lower on the right side. The patient is positioned with a soft towel roll under the neck to slightly hyperextend it with the head turned to the left. Landmarks to be identified before and after draping the patient are the carotid pulse and the two divisions of the sternocleidomastoid muscle. The right IJ vein lies below the sternocleidomastoid muscle, anterior and lateral to the carotid artery. Ultrasound guidance is mandatory for IJ access, and the IJ vein is visualized just lateral to the carotid artery. This spatial relationship is not universal, however. A growing body of evidence mandates that ultrasound guidance be used during puncture of the IJ vein to improve access success and decrease vascular complications (6–9). The IJ vein is distinguished from the carotid artery as gentle pressure with the transducer compresses the vein, and the artery has obvious pulsations with the heart rate. The skin is infiltrated with a small amount of lidocaine. With simultaneous ultrasound guidance, the access needle is advanced with constant gentle aspiration on the syringe until a free flow of blood return is obtained. Using fluoroscopic guidance, a guide wire is passed through the needle, into the vein, and is then advanced into the right atrium (or pulmonary artery in a cavopulmonary anastomosis).

Subclavian Approach

The subclavian vein is posterior to the clavicle, superficial and inferior to the subclavian artery, lying partly on the pleura. As a result, complications of subclavian vein access include pneumothorax, hemothorax, and intravascular air. Complications are more likely to occur when there is pulmonary parenchymal disease, pulmonary hypertension, or anatomic thoracic abnormalities (including previous surgery).

The patient is positioned with a small roll under the shoulders. Airway adequacy is verified before proceeding. Prior to draping the patient and again before vessel entry, one should

identify important landmarks, specifically the suprasternal notch and the depression at the lateral third of the clavicle. With the usual anatomy of a right SVC and left innominate vein, left subclavian vein access is preferred. In the region of clavicular depression, the skin, subcutaneous tissues, and clavicular periosteum are infiltrated with lidocaine. The needle, with attached syringe, is advanced gently through the skin until it contacts the clavicle, then it is “walked” under the clavicle. The needle must be oriented anteriorly to avoid entering the subclavian artery or the apex of the lung. Once under the clavicle, the needle is advanced slowly with constant gentle aspiration until a steady venous blood return is obtained. Using fluoroscopic guidance, the soft end of a wire is advanced through the vein into the right atrium (or the pulmonary artery in a cavopulmonary anastomosis). Due to negative intrathoracic pressure, air will be sucked into the vein if the needle is left open to air or if there is a mismatch between the size of the needle lumen and the wire diameter, especially if the patient is breathing spontaneously. Because of the risk of intravascular air, a sheath with a bleedback valve is always used.

Umbilical Approach

Umbilical venous access is generally possible until the third day of life. The umbilical artery may be cannulated up to 1 week of age. It is best to avoid maneuvering a wire directly through the umbilical vessels. Often, infants arrive in the cath lab with umbilical lines in place. An indwelling umbilical vein catheter with its tip in the right atrium can be exchanged over a 0.018- to 0.021-in guide wire for a sheath and dilator; the sheath should be long enough to cross the ductus venosus and just enter the right atrium, but not so long as to puncture the right atrium. An indwelling umbilical arterial line may be exchanged over a wire; however, the circuitous course of this vessel makes catheter exchanges difficult. The use of a sheath in the umbilical artery is optional.

Catheter manipulation is difficult from the umbilical vessels. An umbilical venous catheter is directed toward the roof of the left atrium, across the PFO. Directing it to any other location will usually require the use of a deflecting wire. With an umbilical arterial catheter, the initial inferior loop that the umbilical artery takes before joining the internal iliac artery limits the ability to manipulate the catheter. It is important to use very gentle technique during cardiac catheterization in the newborn heart, as the cardiac walls are very thin—especially in the atria and left ventricular apex—and the chambers are small. Since small sheaths and catheters (3 and 4 Fr) can be placed in the femoral vessels, the benefits of improved catheter manipulation make a femoral approach preferable in most cases, even when the umbilical vessels are available.

Hepatic Approach

In the mid to late 1990s, transhepatic venous access was first described as an alternative to traditional venous access sites in limited clinical situations (10,11). When femoral, jugular, or subclavian venous access to the right atrium is not possible, a hemostatic sheath can be placed within a hepatic vein. This is particularly useful for device closure of an atrial septal defect when the IVC is interrupted or thrombosed. Overall, however, transhepatic venous access is infrequently used.

After the appropriate sterile preparation and local anesthesia (including infiltration of into the hepatic parenchyma), the skin is punctured along the mid to anterior axillary line at the subcostal margin using a long 21 or 22 gauge needle with or without an obturator. The needle is directed posteriorly, superiorly, and medially, toward the left shoulder. Historically, the needle is advanced under fluoroscopic guidance, but some have advocated for ultrasound guided access (12). When the tip of the needle is approximately 1 cm from midline, the obturator

is removed. Blood return with or without gentle aspiration suggests that the needle is in the vascular space. Positioning is then confirmed with a contrast injection; if contrast flows to the heart, the needle is in an appropriate hepatic vein, whereas if contrast flows into the liver parenchyma, the needle is in a portal vein and should be repositioned. Once the needle is found to be within an adequately sized hepatic vein, a 0.018-in wire is passed through the needle into the right atrium or SVC. With the needle removed, a stiff introducer is advanced over the wire, which is then exchanged for a larger 0.035- or 0.038-in wire. The introducer is then exchanged for the necessary hemostatic sheath with the tip of the sheath positioned in the low right atrium.

Catheter manipulation through hepatic venous access may be more troublesome than traditional femoral venous access. Directing catheters into the right ventricle and pulmonary arteries frequently requires creative use of preshaped catheters and deflecting wires.

Hepatic venous access also carries the risk of some unique complications, including intraperitoneal bleeding, hemobilia, gall bladder perforation, portal vein thrombosis, and liver abscess or peritonitis. Closure of the hepatic tract following sheath removal may depend on the need for ongoing anticoagulation, size of sheath used, and hemodynamic status; often hemostasis may be obtained with pressure (13).

Catheters and Wires

Functioning competently in the congenital cardiac catheterization lab requires an understanding of the various equipment and tools available to the cardiologist. Specifically, the cardiologist needs a practical familiarity with the different catheters and wires available in the cath lab.

For the most part, catheters are hollow, allowing for transmission of pressure measurements, sampling of blood, and infusion of medications or contrast. In general, catheters can be classified as end-hole or side-hole. For the most part, end-hole catheters are used for hemodynamic measurements, blood gas sampling, and contrast injection into smaller vessels by hand. Angiographic injections are primarily performed using side-hole catheters. Catheters may be straight or shaped. Figure 12.1 illustrates some examples of different catheter shapes.

Right heart catheterization is typically performed using soft, balloon-tipped catheters. An end-hole balloon wedge catheter

is used for hemodynamic pressure measurement and blood gas sampling. When the balloon is inflated with a small volume of CO₂ and with small amount of manual torque, the catheter will follow the flow of venous blood into right atrium, across the tricuspid valve into the right ventricle and from the right ventricle into the pulmonary arteries. With the balloon-tipped end-hole catheter positioned in a distal branch pulmonary artery, gentle balloon inflation of the balloon allows for measurement of pulmonary artery wedge pressure. Angiography of the right heart is usually performed using a balloon-tipped angiographic catheter, which has side holes proximal to the balloon.

Left heart catheterization is typically performed using smaller caliber, thin-walled, but more rigid, catheter. A pigtail catheter is advanced to the descending aorta over a wire. With the wire removed, the catheter end is curled, allowing it to be advanced and withdrawn in the aorta without engaging smaller branch arteries. However, in order to advance the pigtail catheter into the left ventricle, a soft, typically tight-J-tipped wire is used to cross the aortic valve to prevent leaflet damage. Pressure measurements, blood sampling, and angiography can all be performed using the pigtail catheter.

Wires can be used to direct or stabilize catheters. Like catheters, wires come in many different diameters. Most wires have a soft distal end, which comes in various contours, including straight, J-tipped, and angled. Wires advanced through hollow catheters are used to probe and enter vessels that may be otherwise difficult to access with the catheter alone, such as stenotic branch pulmonary arteries or tortuous collateral vessels. Wires can also be used to cross a PFO for access to the left atrium and pulmonary veins. Stiff wires are used to stabilize catheters for angioplasty and valvuloplasty. Stiff, extra-long wires are valuable for maintaining position while exchanging one catheter for another.

Many other catheters and wires of various sizes, lengths, and contours are available for use depending upon the specific clinical scenario, but an expansive discussion is beyond the scope of this chapter.

Catheter Manipulation

A detailed discussion of catheter manipulation is beyond the scope of this chapter, but several points deserve mention. In the neonate and infant, cardiac tissue is thin. Perforation can occur easily, especially in the atrial appendages, right ventricular

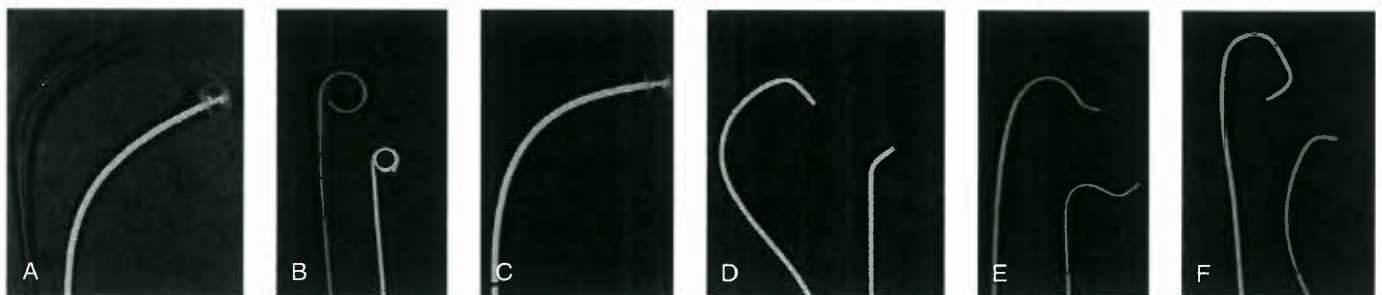


Figure 12.1. A: Angiographic catheters, the NIH catheter (USCI, Billerica, MA), and the Berman angiographic catheter (arrow, Reading, PA) have side holes but no end hole. The NIH catheter is a relatively stiff catheter, and with the angled tip, it responds well to torque maneuvering. The Berman catheter is soft and balloon tipped; it can be flow directed but it is more difficult to effectively torque. B: Pigtail catheters (Medi-Tech, Watertown, MA; and UMI, Ballston Spa, NY). These are thin-walled catheters that have both end and side holes, designed to deliver a large volume of contrast quickly for ventriculography. They may be angled and may have radio-opaque markers to facilitate making measurements. Note the smaller diameter curve on the right catheter, which is better for neonates and infants. C: Balloon wedge pressure catheter (arrow). This is an end-hole, balloon-tipped catheter that is not used for angiographic purposes; however, it may be used for hand injections (with or without balloon-occlusion). D: End-hole catheters. There are many preformed end-hole catheters designed for selective entry of noncoronary vessels. The catheters may be used for selective angiography by hand injection. Pictured are Cobra and Berenstein (Medi-Tech) catheters. E,F: Coronary artery catheters. These catheters are designed for selective hand injection of normally originating right and left coronary arteries. Pictured are the Amplatz left and right (E) and the Judkins left and right (F) (Cook, Bloomington, IN) coronary catheters.

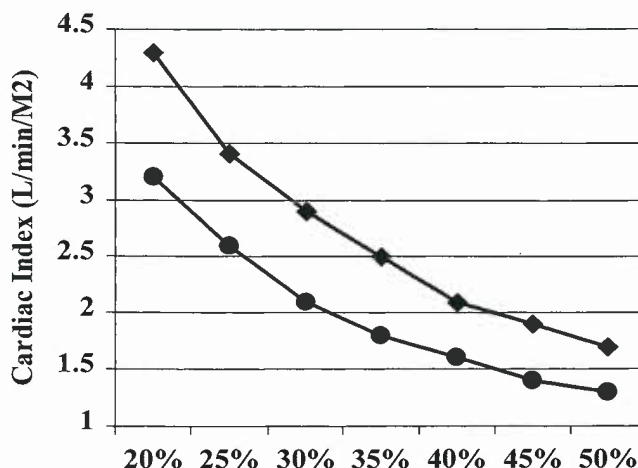
outflow tract, left ventricular apex, and aortic valve cusps. The risk of perforation can be decreased by gentle catheter manipulation, using small movements, the use of balloon catheters, and a thorough understanding of the cardiac anatomy and the desired catheter route and destination. The importance of reviewing *all* previous imaging studies *before* the catheterization cannot be overemphasized. If a catheter is too straight to manipulate to the desired location (e.g., across the tricuspid valve), it may be safely curved outside the body, in a hepatic vein, or using a tip-deflecting or shaped wire, rather than within the heart. The small catheters used in infants and children can be damaged by vigorous manipulation. Thin-walled catheters, such as pigtails, should be advanced over a wire. Large catheter loops in the atrium or right ventricular outflow tract can cause hemodynamic instability owing to reflex bradycardia or tricuspid valve insufficiency; therefore, one needs to pay attention to all parts of the catheter, not just the tip.

Collection of Hemodynamic Data

The purpose of a diagnostic heart catheterization is to collect data that will be used to define the patient's condition and make management decisions. The calculations made using data obtained during catheterization assume that blood samples and pressure measurements were obtained at a steady physiologic state. Changes in oxygenation, ventilation, heart rate, and blood pressure will directly affect these calculations and may produce inaccurate data that, in turn, can result in suboptimal patient management. Because a true "steady state" is rarely encountered in the cath lab, it is important to recognize any changes in heart rate, blood pressure, and oxygen saturation and how these changes will affect the accuracy of the data. The patient's condition, oxygen saturation (or blood gas) samples, and hemodynamic data must be continually assessed for validity. The operator should be constantly aware of the patient's hemodynamic state, and inconsistencies in the data must be clarified before the catheters are removed. Initial interpretation of all data obtained should be performed before leaving the cath lab to be certain that the information deemed necessary has been obtained. Although separated for purposes of discussion, the collection of hemodynamic/pressure data and oxygen sampling occurs simultaneously during the initial phases of the catheterization procedure.

Diagnostic heart catheterization typically begins with assessment of the initial arterial blood pressure, venous filling pressures, and measurements of oxygen saturations in the SVC and femoral artery. These data provide immediate information about the patient's initial hemodynamic status, which is a crucial aspect of the procedure. One needs to assess initial blood pressure to be sure that the hemodynamic data recorded will be valid. Detection of shunts and quantifying resistance depends on the measurement of various flow indices, and for the purposes of this discussion, oxygen content (saturation) will be used as the primary indicator with respect to these calculations (see further discussion below). Children with an SVC saturation <60% or arterial saturation <70% have limited cardiac reserve. All factors influencing their conditions (i.e., body temperature, ventilatory status, acid-base balance, and volume status) should be assessed at the start of the procedure and maintained at an optimal steady state during the procedure. Since variation in any of these factors can affect the data obtained during catheterization, all procedures should be completed as expeditiously as possible.

Any abnormal data must be verified promptly in the cath lab. Abnormal pressure tracings should be compared to those expected or to baseline, and transducers recalibrated frequently to be sure they are properly zeroed. When sampling saturations, for instance, elevated pulmonary artery saturation should prompt the operator to identify whether the catheter was partially wedged or whether there is a left-to-right shunt. In addition, a significant "step-up" in saturation between



Difference in arterial-venous oxygen saturation

Figure 12.2. Graph displaying the relationship between cardiac index and varying arteriovenous oxygen saturations using an assumed oxygen consumption = 140 mL/min/m². Note the greater cardiac index with a hemoglobin of 12 g/dL (diamonds) compared with 16 g/dL (circles).

consecutive cardiac chambers suggests the presence of a left-to-right shunt.

After collecting all saturations and pressures, and before proceeding to angiography, it is important to assess the pulmonary and systemic flows, resistances, and flow ratios. Systemic flow index can be estimated by recognizing that an arterial-venous (A-V) oxygen (O₂) saturation difference of 20% to 25% corresponds to a "normal" cardiac index of approximately 3.5 L/min/m². A larger A-V O₂ difference correlates with a lower cardiac index. In addition, for a given A-V O₂ difference, the higher the hemoglobin level, the lower the flow index (Fig. 12.2). A simple formula to estimate pulmonary flow index (Q_p) compared to systemic flow index (Q_s) is the ratio of pulmonary A-V O₂ divided by systemic A-V O₂. Details of calculations for flow indices and resistance are discussed later in this chapter.

Measurement of Hemodynamic Variables

The primary goals of any detailed hemodynamic catheterization are to measure pressures in all of the pertinent cardiac structures/chambers and to obtain oxygen samples in these structures, in order to calculate systemic and pulmonary flow indices and vascular resistance.

Pressure Measurements

In the cath lab, pressures are most often measured using fluid-filled catheters connected to pressure-sensitive transducers. The change in pressure (force/unit area) in the cardiac chamber or vessel is transmitted along a column of incompressible fluid (saline or blood) contained within a nonexpansile tube (catheter) to a transducer. The transducer contains a diaphragm that moves a small distance (in a linear fashion) in response to change in pressure. The movement of the diaphragm is transmitted to an electronic strain gauge. The strain gauge converts pressure changes into voltage changes. These voltage changes are then converted into an electric signal, which is displayed as a waveform over time on a computer monitor. Systolic and diastolic pressures are measured instantaneously as the peak and trough, respectively, of the waveform. A mean pressure is obtained by electronic damping of the signal over several cardiac cycles. The system is calibrated to a zero point at level of the center of the heart. It is

important to understand potential sources of error and artifact in the pressure tracings obtained. Two important concepts are frequency response (the ratio of output amplitude to input amplitude over the range of frequencies of the input pressure wave) and damping (the dissipation of the energy of oscillation of a pressure measurement system). Inaccurate pressure waveforms frequently are related to deterioration of the frequency response or to overdamping or underdamping. Other references contain a more complete discussion of these principles (14). Eight potential sources of pressure tracing artifact and recommendations for identifying the source of artifact and error are listed below:

1. Loose connections in the system: These usually result in an overdamped tracing. Backup of blood into the transducer tubing is an indication of a loose connection.
2. Air in the system: This is probably the most common cause of measurement error. Air may be introduced into the system at any of the connections, or dissolved air may come out of the saline used to flush the system. Air is compressible and its presence in the system lowers the frequency response. As a result, information inherent in the applied pressure wave is lost, producing what is commonly referred to as a damped tracing. Another indication of air in the system is the amplification of high-frequency input, producing overshoot or "fling" in the tracing. The appearance of a small amount of blood with obvious pulsatility in the transducer tubing is an indication that there is air in the system.
3. Inaccurate calibration or baseline drift: Even if the transducers are properly calibrated or "zeroed" at the beginning of the procedure, movement of either the patient or the transducers, or electric drift of the baseline, may result in inaccurate pressure recordings. Although small errors in calibration may be inconsequential in arterial recordings, they can have a significant impact in the measurement of venous pressures and pulmonary vascular resistance.
4. Partial catheter obstruction: This is usually the result of the catheter clotting or kinking. This usually occurs when small or thin-walled catheters are used. If blood is allowed to remain in the catheter lumen for any length of time, deposition of fibrin or platelets will reduce the lumen size, decreasing the frequency response.
5. Catheter "fling": The appearance of fling (a tall, narrow spike) on a pressure recording has many causes. Overshoot, produced by air in the system, has been discussed. Rapid movement of the catheter tip, which may occur if the tip lies in a turbulent jet, can result in superimposition of high-frequency oscillations on the pressure recording. If the catheter is contacted by a cardiac structure (such as the mitral valve), the superimposed oscillation can alter the waveform dramatically. At times, these conditions are unavoidable. To minimize this error, use the mean systolic pressure rather than the peak systolic pressure, or inject a small amount of blood or contrast media in the tubing to intentionally damp the system.
6. End-hole artifact: When a column of blood stops suddenly against an end-hole catheter, kinetic energy is transformed into pressure energy, and the recorded pressure is falsely elevated. Similarly, when a column of blood is moving away from an end-hole catheter, the pressure recorded will be less than the true intravascular pressure, in proportion to the velocity of flow. This explains why the pressure in a stenotic proximal pulmonary artery has a lower peak systolic pressure than the distal larger vessel.
7. Peripheral pulse wave amplification: Both the peak systolic pressure and the pulse pressure are amplified with increasing distance from the aortic valve. The mean pressure, however, remains the same. This phenomenon is demonstrated by recording the pressure tracing during a pullback around the aortic arch, where the systolic pressure increases from the ascending to the descending aorta. While peripheral

pulse wave amplification is a physiologic phenomenon and not an artifact, per se, it may lead one to incorrectly interpret pressure data. When comparing the ascending aorta systolic pressure with the femoral or radial artery systolic pressure, failure to take into account pulse wave amplification will result in underestimation of a pressure gradient across an aortic valve or coarctation of the aorta.

8. Catheter entrapment: An end-hole catheter placed in a small or heavily trabeculated ventricle can trap a small volume of fluid, resulting in an exaggerated pressure elevation during systole. This error can be eliminated by slightly withdrawing the catheter or deflating the balloon (if a balloon-tipped catheter is used). If these maneuvers are not possible, the pressure should be recorded using a side-hole catheter, provided that all of the side holes are within the chamber or vessel of interest.

Transducer-tipped wire catheters, such as the Radi wire, allow direct pressure measurement without relying on the propagation of fluid waves through a fluid-filled catheter (15). Such wire catheters consist of a floppy wire end distal to the transducer, which prevents the manometer from being damaged or puncturing the vessel or chamber wall. The pressure wire is connected to an analyzer system that displays numeric pressures and waveforms on a monitor. The pressure wire is introduced through an end-hole catheter. When the manometer reaches the end of the catheter, the wire and catheter pressures are calibrated on the monitoring system. The pressure wire is then advanced from the catheter into the vessel or chamber in question. Pressure wire manometry allows simultaneous pressure measurements in two contiguous locations, such as simultaneous ascending and descending aorta pressures in a patient with coarctation of the aorta. This technique may also be used to carefully record the pressure differential across a mechanical valve, with very gentle manipulation of the wire across the prosthetic valve opening. In the case of an aortic prosthesis, the retrograde catheter remains in the ascending aorta, whereas the pressure wire is advanced retrograde across the valve into the left ventricle. The thin pressure wire is also useful for obtaining pressure measurements distal to narrow communications that may be difficult to access with a catheter alone, such as the pulmonary artery pressure in child whose sole source of pulmonary blood flow is via a modified Blalock-Thomas-Taussig shunt (16).

Right Heart Catheterization

Characteristic right heart waveforms are shown in Figure 12.3 and normal hemodynamic pressure values for children are shown in Table 12.1. There are three characteristic waves in the right atrial tracing; a, c, and v waves. The a wave represents atrial systole and occurs just after the P wave on the electrocardiogram. The c wave is due to either right ventricular contraction or tricuspid valve closure, whereas the v wave results from filling of the right atrium against a closed tricuspid valve. The decrease in pressure after the a wave is the x descent, which is due to atrial relaxation. The decrease in pressure after the v wave is the y descent, which represents the opening of the tricuspid valve in early diastole.

Normally, the right atrial a wave exceeds the v wave by 2 to 3 mm Hg, neither wave exceeds 8 mm Hg, and both waves are within 5 mm Hg of the mean right atrial pressure. An elevated a wave is seen in the context of restricted right ventricular filling, such as tricuspid stenosis or a noncompliant right ventricle (e.g., pulmonic stenosis, pulmonary atresia, or pulmonary hypertension). So-called cannon a waves may be seen with certain arrhythmias, when atrial contraction occurs after right ventricular contraction has closed the tricuspid valve. Elevated v waves are seen with tricuspid regurgitation,

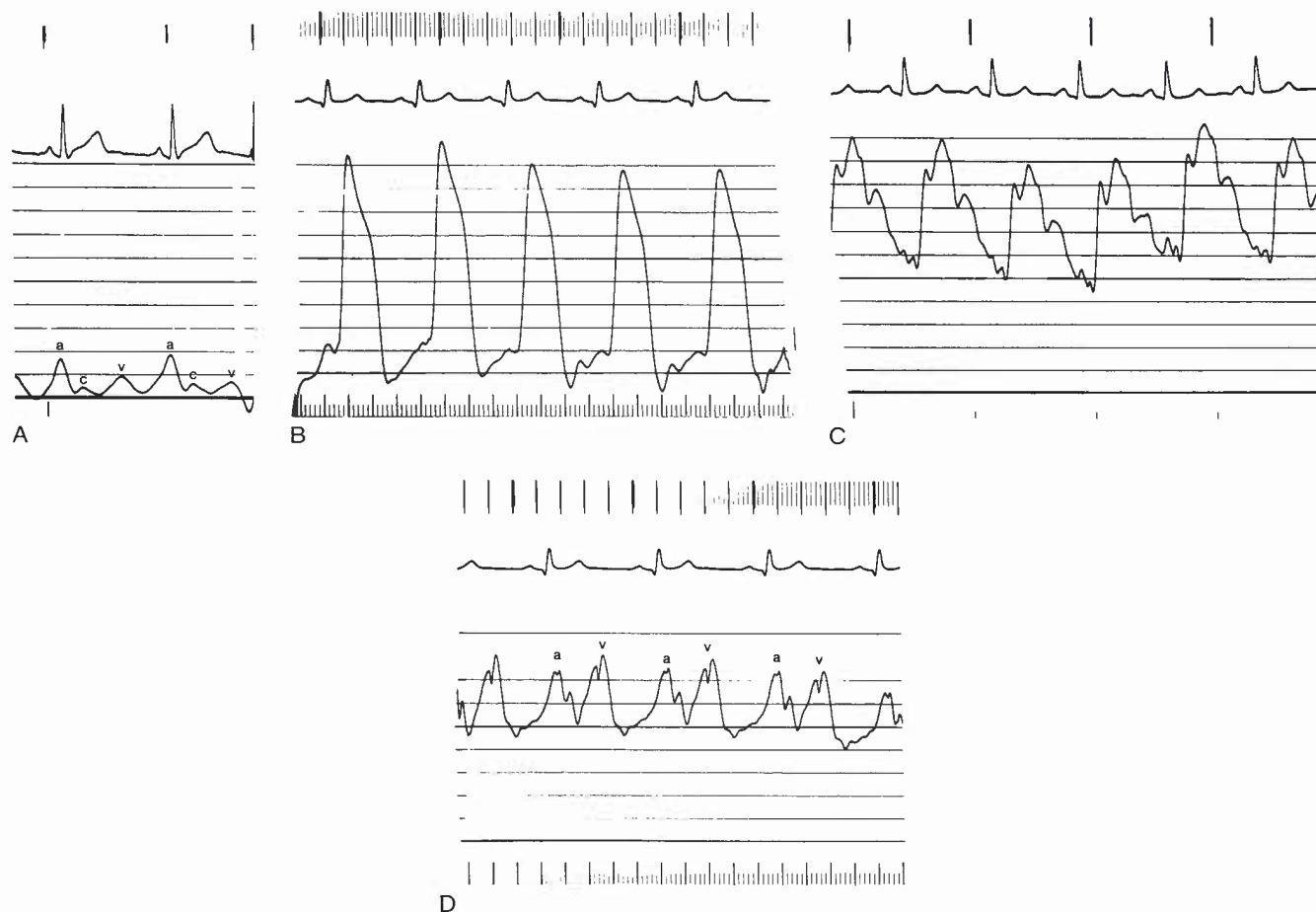


Figure 12.3. Right heart pressures (each horizontal line = 2 mm Hg). A: Right atrium: a wave = 3, c wave = 1, v wave = 2. B: Right ventricle: 20/0.2. C: Pulmonary artery: 20/10. D: Pulmonary capillary wedge: a wave = 14, v wave = 16.

Ebstein anomaly, or a left ventricular-to-right atrial shunt. The right atrium and venae cavae are compliant structures that can accept a large volume of blood with minimal change in pressure; thus, the v wave may not necessarily be elevated in the aforementioned conditions. Elevation of the mean pressure is seen with any condition that elevates the a wave or v wave, or in the context of myocardial failure. Low right atrial pressure (<1 to 2 mm Hg) suggests hypovolemia. Marked variability of the a wave and mean pressure may be seen with atri-

oventricular dissociation or with obstructive airway disease. A patient who is breathing spontaneously but has significant airway obstruction may have negative intrathoracic pressure and subatmospheric right atrial pressure, which may result in the introduction of air into the system if the catheter is not properly connected or the hub is maintained below the level of the chamber.

The right ventricular pressure tracing has a rapid upstroke during isovolumic contraction, a plateau during systolic ejection, a decline to near zero during isovolumic relaxation, and a slow rise to the end-diastolic pressure during diastolic filling. Normally, the peak systolic pressure is <30 mm Hg, and the end-diastolic pressure is <8 mm Hg. Except in the context of tricuspid valve stenosis, the end-diastolic pressure corresponds to (and should be equal to) the right atrial a wave. Right ventricular systolic pressure is elevated in the presence of a large ventricular septal defect, right ventricular outflow tract obstruction, and pulmonary hypertension. Recordings should be obtained in the apex and in the outflow tract to confirm the absence of any intracavitary gradient.

The normal pulmonary artery systolic pressure is equal to the right ventricular systolic pressure (<30 mm Hg), and the mean pressure is <20 mm Hg. Pulmonary artery diastolic pressure begins with the dicrotic notch caused by valve closure, and the end-diastolic pressure is typically 2 to 3 mm Hg higher than the wedge pressure. Increased pulmonary artery pressure occurs with distal obstruction to flow, such as with peripheral pulmonary stenosis, pulmonary arteriolar obstruction, pul-

TABLE 12.1

Normal Hemodynamic Pressure Measurements in Children

Chamber/Vessel	Systolic	Diastolic	Mean
Right atrium			3 ± 1
Right ventricle	25 ± 5	4 ± 2	
Pulmonary artery	22 ± 4	10 ± 3	13 ± 3
PA wedge			8 ± 2
Left ventricle	110 ± 12	9 ± 2	

Values are compiled from data published in references. All pressures are in mm Hg. PA, pulmonary artery.

monary thromboembolism, pulmonary venous obstruction, or left atrial hypertension (due to other causes such as cor triatriatum, mitral stenosis, or left ventricular diastolic dysfunction). Pulmonary artery pressure is also elevated in the presence of aorta-pulmonary artery communications (such as patent ductus arteriosus or aortopulmonary window) or a significant ventricular septal defect (if there is no pulmonic stenosis). In the presence of pulmonary hypertension, a pulse pressure of <40% of the peak systolic pressure suggests a fixed resistance, whereas a wide pulse pressure (>60% of the peak systolic pressure) suggests high flow and low resistance.

Systolic pressure gradients between right ventricle and pulmonary artery are due to right ventricular outflow tract obstruction, although gradients of 5 mm Hg may be normal. Gradients ≤ 10 mm Hg may be seen with structurally normal pulmonary valves and increased blood flow, as with a large atrial septal defect. In the setting of very severe branch stenosis or a very tight pulmonary artery band, the catheter may produce enough obstruction of the vessel as it crosses the stenosis that the pressure distally resembles the wedge pressure tracing.

Pulmonary artery wedge pressure is usually a good reflection of the left atrial and left ventricular end-diastolic pressures because of the absence of valves in the pulmonary circulation. When an end-hole catheter is appropriately wedged in a pulmonary artery branch, the distal pulmonary venous pressure is transmitted retrograde through the capillary bed and arterioles to the catheter tip. When using a balloon-tipped wedge catheter (end-hole), the catheter is advanced as far as it can into the distal pulmonary artery and the balloon is partially inflated while monitoring the tracing for its characteristic appearance. The wedge tracing should have the characteristic a and v wave appearance of an atrial tracing (Fig. 12.3). The wedged catheter position is confirmed by observation of the characteristic left atrial waveform or by withdrawal of fully saturated blood. When small catheters are used, it may not be possible to withdraw a blood sample from the wedged position. Interpretation of the wedge pressure must be guided by an understanding of the anatomy. The pulmonary artery wedge pressure does not reflect the left ventricular end-diastolic pressure when there is pulmonary vein stenosis, cor triatriatum, mitral stenosis, or anomalous pulmonary venous return. When the wedge pressure is elevated, these lesions must be confirmed or ruled out by direct measurement of the left atrial or left ventricular end-diastolic pressure.

Left Heart Catheterization

Characteristic left heart waveforms are shown in Figure 12.4 and normal pressure values for are shown in Table 12.1. The

normal left atrial mean pressure is 6 to 10 mm Hg (depending on age), which is several mm Hg higher than the right atrial mean pressure. In contrast to the right atrium, the left atrial v wave is usually higher than the a wave, and neither is >5 mm Hg above the mean pressure. An elevated a wave is seen with defects resulting in left atrial outflow obstruction (mitral stenosis, supravalle mitral membrane) or with diseases that impair left ventricular compliance (aortic stenosis, coarctation of the aorta). The a wave may be dominant with an atrial septal defect, as a large atrial septal defect allows transmission of pressure across the septum, or with diseases that elevate the right atrial a wave. Elevated v waves typically occur with mitral regurgitation. Elevation of the left atrial mean pressure (and both the a and v waves) may be encountered with large left-to-right shunts at the ventricular or great vessel level or as a sign of left ventricular failure. If the end-diastolic pressures in the left atrium and left ventricle are not equal, some form of mitral valve obstruction is present. Higher gradients (>8 to 10 mm Hg) suggest structural mitral stenosis, whereas lower gradients suggest physiologic stenosis due to increased blood flow across the valve, such as from a large ventricular septal defect. When transseptal technique is used to enter the left atrium, one can use a smaller diameter catheter to advance into the left ventricle and simultaneously measure left atrial and left ventricular pressure.

The peak systolic pressure in the left ventricle should be equal to or up to 5 mm Hg greater than the peak systolic pressure in the ascending aorta. A gradient between the left ventricle and the aorta is present in dynamic left ventricular obstruction (as in hypertrophic cardiomyopathy), subaortic stenosis, or aortic valve stenosis. The normal aortic pressure is a reflection of left ventricular stroke volume and systemic vascular resistance. Near the aortic valve, the arterial waveform displays a relatively slow upstroke, a broad peak, and a near-linear drop to end-diastole. In the distal arteries, the peak becomes sharper, the dicrotic notch (representing the decrease in pressure with closure of the aortic valve) becomes more obvious, and pulse wave amplification occurs.

The pulse pressure in the ascending aorta is usually 25 to 50 mm Hg, or <50% of the peak systolic aortic pressure. Increased pulse pressure and low diastolic pressure may be seen with aortic insufficiency, a ruptured sinus of Valsalva, or conditions in which there is a low-resistance diastolic runoff such as patent ductus arteriosus, aortopulmonary collaterals, aortopulmonary window, truncus arteriosus, and systemic AV fistula. A narrow pulse pressure may be encountered in pericardial tamponade or low cardiac output states. A gradient between the ascending and descending aorta suggests coarctation of the aorta.



Figure 12.4. Left heart pressures. A: Left atrium (each horizontal line = 2 mm Hg): a wave = 13, v wave = 16. B: Left ventricle (each horizontal line = 10 mm Hg): 98/0.6. C: Aorta (each horizontal line = 10 mm Hg): 98/50.

Derived Hemodynamic Variables

Measurement of cardiac output, in terms of pulmonary and systemic blood flow, is a necessary first step to quantifying shunt volume and vascular resistance. Because cardiac output cannot be measured directly, it can be estimated using the indicator dilution technique described by Fick (17). The indicators most commonly used are oxygen or cold saline (thermodilution) (18). Various analogies have been used to explain the concept of the Fick principle. In one analogy, a coal-bearing train, representing blood, passes through a coal-loading station (capillary bed) at a constant but unknown rate (cardiac output). The train consists of a series of cars (hemoglobin), each of which have a known load of coal (oxygen content). By knowing the rate of delivery of the coal (oxygen uptake) and the amount of coal in the cars before and after the station, one can easily calculate the rate at which the train is moving through the station. In quantitative terms, cardiac output can be calculated as follows:

- Blood flows at an unknown rate.
- An indicator is present in the blood in a measurable concentration.
- The indicator is added or removed at a known rate.
- Measurement of the change in concentration of the indicator allows one to calculate flow as follows:

$$\text{Flow} = \frac{\text{Rate of addition or removal}}{\text{Change in concentration}}$$

Oxygen in the Blood

Oxygen is the most common indicator that is used for purposes of calculating flow and resistance in the congenital cardiac patient. Because the quantity of oxygen in the blood that is being sampled directly affects the calculation of cardiac flow rates, it is important to be able to accurately measure or estimate the oxygen content of a blood sample.

Oxygen is carried in the blood in two forms: either attached to hemoglobin or dissolved in plasma. The amount of oxygen bound to hemoglobin is influenced by many factors including the partial pressure of oxygen (pO_2). In addition, the affinity of hemoglobin for oxygen is inversely affected by hydrogen ion concentration, partial pressure of carbon dioxide, level of 2,3-diphosphoglycerate (DPG), and temperature. Affinity for oxygen is also affected by the type of hemoglobin. For example, hemoglobin F (fetal hemoglobin) has a higher affinity for oxygen than the more common hemoglobin A.

The term oxygen capacity refers to the amount of oxygen that can be bound by hemoglobin in blood; maximum oxygen capacity is 1.36 mL O_2 per 1 g of hemoglobin. Thus, oxygen capacity (mL O_2 /dL) can be calculated as

$$\text{Oxygen capacity (mL } O_2 / \text{dL)} = \text{Hemoglobin (g / dL)} \times (1.36 \text{ mL } O_2 / \text{g of hemoglobin})$$

The actual amount of oxygen bound to hemoglobin in a given sample of blood is calculated as the oxygen capacity multiplied by the oxygen saturation of hemoglobin. Oxygen saturations in the blood samples are measured spectrophotometrically. Oxidized hemoglobin and reduced hemoglobin have different spectral absorptions at 650 nm but similar ones at 805 nm. Oximeters measure the absorption at 650 nm to represent the amount of oxidized hemoglobin and the absorption at 805 nm to represent total hemoglobin; the ratio of these two numbers is the oxygen saturation. The method is most accurate at oxygen saturations between 60% and 95%, as long as there are no other substances in the blood that affect the spectral absorption (e.g., carboxyhemoglobin).

It is important to remember that oxygen saturation values report only the amount of oxygen that is *bound* to hemoglobin and does not account for *dissolved* O_2 . In room air, the vast majority of oxygen in the blood is bound to hemoglobin, whereas the amount of dissolved oxygen is very small, so dissolved O_2 is typically ignored in calculations made in room air at baseline. In contrast, if the patient is inhaling 100% oxygen, with pO_2 values that may reach 500 mm Hg, dissolved oxygen becomes very important relative to the amount bound to hemoglobin, and this must be accounted for in the calculations.

Dissolved oxygen in plasma is determined by the solubility coefficient of oxygen, temperature, and the pO_2 . At 37°C (body temperature), the amount of oxygen dissolved in blood is 0.003 mL/mm Hg/dL. As mentioned, the amount of oxygen dissolved in plasma is usually not significant enough to include in the calculations for the patient breathing room air, but accounting for dissolved oxygen becomes very important when the patient is breathing 100% oxygen or has low hemoglobin. To put this in perspective, in arterial blood with a pO_2 of 100 mm Hg (typical for an oxygen saturation of 100% in room air), there is only 3 mL of dissolved oxygen *per liter*. This amount of oxygen is small relative to the amount of oxygen bound to hemoglobin. However, if the patient is receiving supplemental oxygen, with the $pO_2 > 100$ mm Hg, dissolved oxygen contributes more significantly to the total oxygen content and must be considered in hemodynamic calculations. In this situation, for example, if the arterial pO_2 is 500, there will be 15 mL of dissolved oxygen per liter, a much greater percentage that must be accounted for in assuring accurate calculations. Dissolved oxygen should also be considered in the setting of low hemoglobin, as the carrying capacity of the blood is lower; therefore, the relative percentage accounted for by dissolved oxygen is higher.

The *total* oxygen content in a sample of blood is the sum of dissolved oxygen in the blood and the oxygen that is bound to hemoglobin:

Oxygen content

$$(\text{mL } O_2 / \text{L}) = \left[\frac{(\text{Oxygen capacity} \times \text{Sp}O_2) + }{(pO_2 \times 0.003 \text{ mL/mm Hg/dL})} \right] \times 10 \text{ dL/L}$$

In room air, one typically uses only the oxygen content of *hemoglobin* for calculations instead of the total oxygen content of the *blood*, due to the fact that dissolved oxygen contributes very little. The use of the expanded formula for oxygen content in calculations is mandatory in the patient with (or without) a left-to-right shunt in whom the hemodynamic study is repeated in 100% oxygen in order to determine pulmonary vasoreactivity. If dissolved oxygen is not accounted for in flow calculations, the amount of flow/shunt may be overestimated. Conversely, the resistance estimated based on these flow calculations will be *underestimated*, a very important issue for decisions that are made based on the data obtained.

For example, if the hemoglobin is 11.5 g/dL, the femoral artery oxygen saturation is 99%, and the PaO_2 is 106 mm Hg, the oxygen content is calculated as follows:

$$\begin{aligned} \text{Oxygen capacity} &= 11.5 \text{ g / dL} \times 1.36 \text{ mL / g} \\ &= 15.6 \text{ mL } O_2 / \text{dL blood} \end{aligned}$$

$$\begin{aligned} \text{Dissolved oxygen} &= 106 \text{ mm Hg} \times 0.003 \text{ mL / mm Hg / dL} \\ &= 0.32 \text{ mL } O_2 / \text{dL blood} \end{aligned}$$

$$\begin{aligned} \text{Oxygen content} &= [(15.6 \text{ mL / dL} \times 0.99) + 0.32 \text{ mL / dL}] \\ &\quad \times 10 \text{ dL / L} = 154 + 3.2 \\ &= 157 \text{ mL } O_2 / \text{L blood} \end{aligned}$$

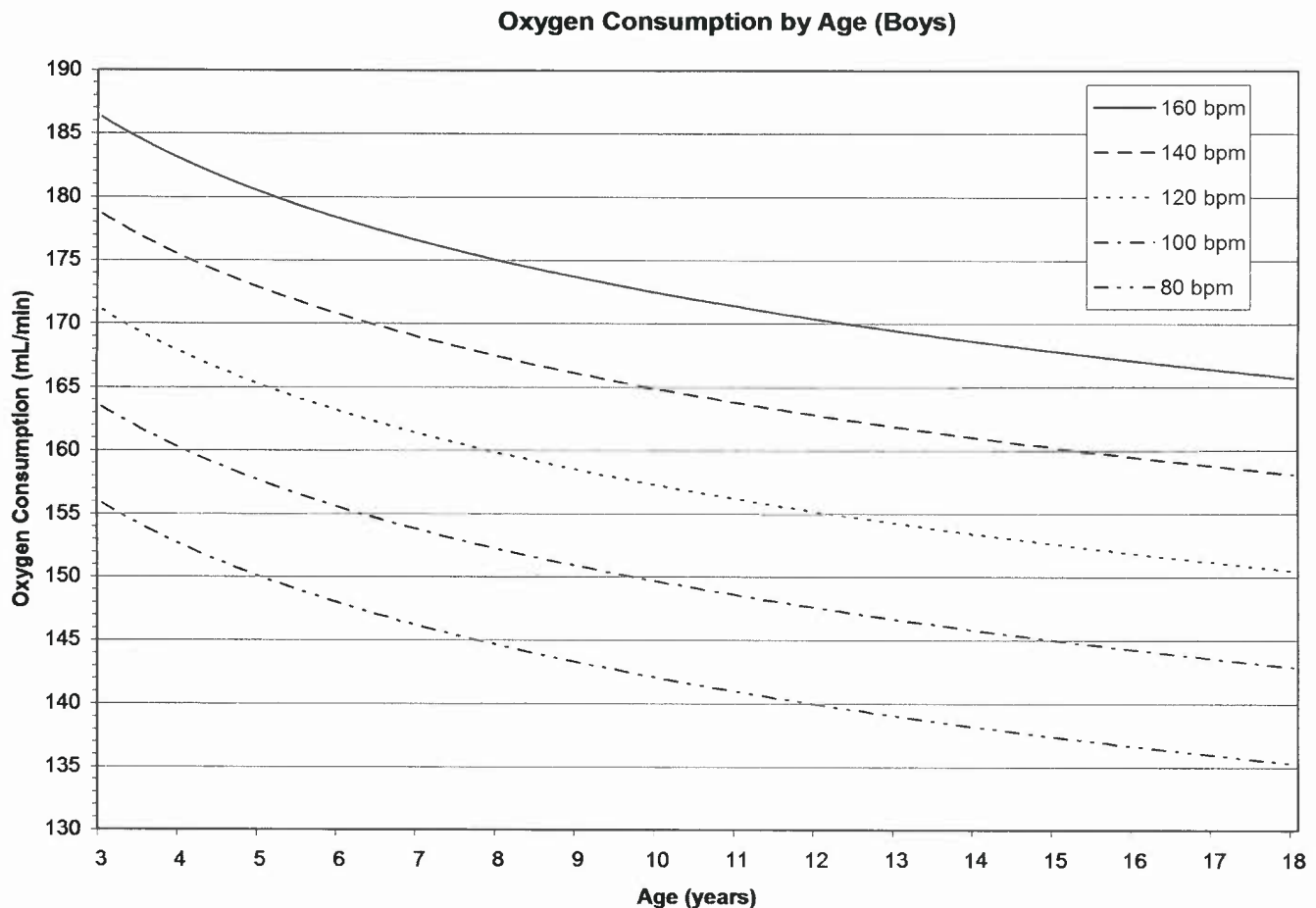


Figure 12.5. Oxygen consumption curves (boys, in mL/min).

If the femoral artery PaO_2 is 566 and the oxygen saturation is 100%, the oxygen content is calculated as follows:

$$\begin{aligned}\text{Oxygen capacity} &= 11.5 \text{ g/dL} \times 1.36 \text{ mL/g} \\ &= 15.6 \text{ mL O}_2 / \text{dL blood}\end{aligned}$$

$$\begin{aligned}\text{Dissolved oxygen} &= 566 \text{ mm Hg} \times 0.003 \text{ mL/mm Hg/dL} \\ &= 1.70 \text{ mL O}_2 / \text{dL blood}\end{aligned}$$

$$\begin{aligned}\text{Oxygen content} &= [(15.6 \text{ mL/dL} \times 1.0) + 1.70 \text{ mL/dL}] \\ &\quad \times 10 \text{ dL/L} = 156 + 17 \\ &= 173 \text{ mL O}_2 / \text{L blood}\end{aligned}$$

Oxygen Method for Calculation of Cardiac Output

When cardiac output is calculated using the Fick method, the indicator is oxygen. The rate of change of the indicator is the oxygen consumption (VO_2). It is assumed that measurements are taken at a steady-state condition; thus VO_2 by tissues equals oxygen uptake by the lungs. VO_2 may be measured or assumed. In the current era, it is most common to use the assumed values for purposes of calculations because the actual measurement of VO_2 is quite cumbersome. It is often difficult to maintain a steady state in the pediatric patient in order to measure a reliable VO_2 . Furthermore, measurement of VO_2 requires spontaneous respirations, and since procedures are often performed under

general anesthesia, this measurement would have to be performed at a different time than when the oxygen saturation samples are being obtained. Assumed values that are most often used for calculations are based on the formulas of Lafarge and Meittinen (19) and are derived from measurements made in 879 patients using the Douglas bag method. Values for patients 3 to 18 years of age and at various heart rates are listed in Figures 12.5 and 12.6.

There are specific equations for applying the Fick principle to the calculation of the systemic and pulmonary flow (Table 12.2). Possible sources of error include inaccuracy of the value used for oxygen consumption, inaccurate sample for the mixed venous saturation, and absence of a steady-state condition.

The systemic flow (Q_s) is equal to the VO_2 divided by the change in oxygen content across the body (oxygen content of the aorta minus the SVC).

$$Q_s = \text{VO}_2 / (\text{oxygen content of aorta} - \text{oxygen content of SVC})$$

If the patient is breathing room air, the amount of dissolved oxygen can be ignored, simplifying the equation to:

$$\begin{aligned}Q_s &= \text{VO}_2 / [\text{hemoglobin} \times 1.36 \times 10 \\ &\quad \times (\text{aorta sat} - \text{SVC sat})]\end{aligned}$$

Similarly, the pulmonary flow (Q_p) is equal to the VO_2 divided by the change in oxygen content across the lungs (oxygen content of the pulmonary vein minus oxygen content of the pulmonary artery).

Oxygen Consumption by Age (Girls)

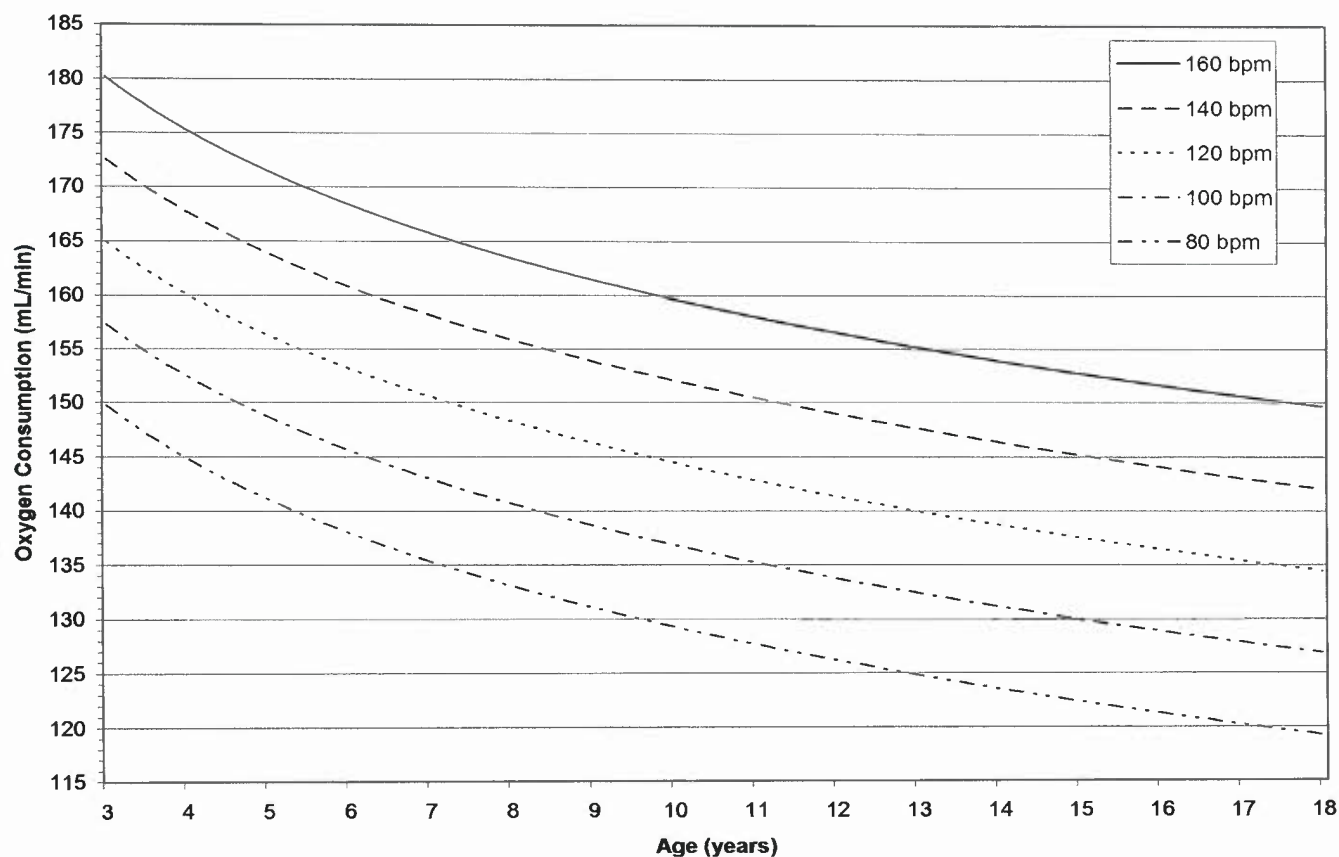


Figure 12.6. Oxygen consumption curves (girls, in mL/min).

$$Q_p = \frac{VO_2}{(\text{pulm vein oxygen content} - \text{pulm art oxygen content})}$$

And if ignoring dissolved oxygen:

$$Q_p = \frac{VO_2}{[\text{hemoglobin} \times 1.36 \times 10 \times (\text{pulm vein sat} - \text{pulm art sat})]}$$

It is important to remember the units assigned to each factor in these equations. The unit for cardiac output is L/min. The unit for VO_2 is mL O_2 /min. Oxygen content is measured as mL O_2 /L of blood. Though not illustrated in the above equations, final flow index in children is normally reported as cardiac index, which is obtained by dividing the output by the patient's body surface area (BSA) given in m^2 . Since flows are indexed to BSA, inaccurate measurement of patient length, especially in infants, may be another source of error. Note: if the final VO_2 value that is used in this formula is not indexed to BSA, the final cardiac output calculation is divided by the BSA to index the value accordingly. This correction does not need to be done if the VO_2 is already indexed! The factor of 10 in the denominator converts the value from g/dL to g/L in order to report the cardiac index value in L/min/ m^2 .

Thermodilution Method

With the thermodilution method, the indicator is temperature. A double-lumen thermodilution (Swan-Ganz) catheter is used. A bolus of cold saline of a known temperature (room

temperature, $\sim 21^\circ\text{C}$) is injected through the proximal port (positioned in the right atrium). A thermistor for measuring temperature is located near the catheter tip (positioned in the pulmonary artery). Saline cools the blood as they mix together; the degree of cooling of the blood is inversely proportional to the magnitude of flow and directly proportional to several factors: the volume of saline injected, the temperature difference between the injectate and the blood, and the specific heats of the injectate and the blood. The thermodilution cardiac output measurement is an automated system (including the injector) and the calculations are performed by a computer. To minimize error, three to five sequential injections of cold saline are performed over 1 to 2 minutes. The technique is simple, precise, and easily allows serial measurements to compare interventions in the cath lab or intensive care unit. The thermodilution method (as with any indicator dilution method) requires complete mixing; thus, it is most accurate when there is a mixing chamber proximal to the thermistor (i.e., the right ventricle). The thermodilution method is used in patients who do not have intracardiac or great vessel level shunts or significant tricuspid/pulmonary valve insufficiency. Possible sources of error include inconsistent volume of injectate, variable temperature of the blood or injectate, apposition of the thermistor to a vessel wall, and inadequate mixing. Thorough mixing is particularly problematic in venous systems with low flow (e.g., bidirectional cavopulmonary anastomosis, Fontan circulation). This method of determining cardiac output is less frequently used in the congenital cardiac patient because of all of these factors.

TABLE 12.2 Commonly Used Equations for Calculating Flow, Resistant, and Shunt

Oxygen capacity

$$\text{O}_2 \text{ Capacity (mL O}_2\text{/dL)} = \text{Hemoglobin (g/dL)} \times 1.36$$

Dissolved oxygen

$$\text{Dissolved O}_2 \text{ (mL O}_2\text{/dL)} = 0.003 \times \text{pO}_2 \text{ (mm Hg)}$$

Oxygen content

$$\text{O}_2 \text{ content (mL O}_2\text{/L)} = [(\text{O}_2 \text{ Capacity} \times \text{SpO}_2) + \text{Dissolved O}_2] \times 10$$

Systemic blood flow

$$Q_s = \frac{\text{VO}_2}{\text{SAO}_2 \text{ Content} - \text{MVO}_2 \text{ Content}}$$

Pulmonary blood flow

$$Q_p = \frac{\text{VO}_2}{\text{PVO}_2 \text{ Content} - \text{PAO}_2 \text{ Content}}$$

Q_p/Q_s estimation

$$Q_p/Q_s = \frac{\text{Aosat} - \text{SVC sat}}{\text{PV sat} - \text{PA sat}}$$

Effective systemic/pulmonary blood flow

$$Q_{ES} = Q_{EP} = \frac{\text{VO}_2}{\text{PVO}_2 \text{ Content} - \text{MVO}_2 \text{ Content}}$$

Shunt volume

$$Q_{L-R} = Q_p - Q_{EP} \quad Q_{L-R} = Q_p - Q_{EP}$$

Shunt percentage

$$\text{Shunt}_{L-R} = \frac{Q_p - Q_{EP}}{Q_p} = 1 - \frac{\text{PV sat} - \text{PA sat}}{\text{PV sat} - \text{MV sat}}$$

$$\text{Shunt}_{R-L} = \frac{Q_s - Q_{ES}}{Q_s} = 1 - \frac{\text{Aosat} - \text{MV sat}}{\text{PV sat} - \text{MV sat}}$$

Systemic vascular resistance

$$R_s = \frac{\text{pAo}_{\text{mean}} - \text{pRA}_{\text{mean}}}{Q_s}$$

Pulmonary vascular resistance

$$R_p = \frac{\text{pPA}_{\text{mean}} - \text{pLA}_{\text{mean}}}{Q_p}$$

pO₂, partial pressure of oxygen; VO₂, oxygen consumption (mL O₂/min); Q_s, systemic blood flow in (L/min); SA, systemic arterial; MV, mixed venous; Q_p, pulmonary blood flow (L/min); PV, pulmonary vein; PA, pulmonary artery; Q_{ES}, effective systemic blood flow; Q_{EP}, effective pulmonary blood flow; Q_{L-R}, left-to-right shunt volume (L/min); Q_{R-L}, right-to-left shunt volume (L/min); Shunt_{L-R}, left-to-right shunt percentage; Shunt_{R-L}, right-to-left shunt percentage; R_s, systemic vascular resistance (Wood units); pAo_{mean}, mean aortic pressure; pRA_{mean}, mean right atrial pressure; R_p, pulmonary vascular resistance (Wood units); pPA_{mean}, mean pulmonary artery pressure; pLA_{mean}, mean left atrial pressure.

Intracardiac Shunts

For practical purposes, it is assumed that with normal cardiovascular connections, the oxygen saturation in all right heart structures (i.e., SVC, right atrium, right ventricle, and pulmonary artery) would be equal. Similarly, the oxygen saturation in the left heart structures (pulmonary veins, left atrium, left ventricle, and aorta and its branches) would be equal.

In reality, oxygen saturation varies between the SVC and coronary sinus, and complete mixing does not occur until systemic venous return reaches the pulmonary artery. An increase in oxygen saturation between different sites of the right heart would give precise information on the location and magnitude of left-to-right shunts, whereas a decrease in saturation between successive chambers of the left heart would define a right-to-left shunt.

To evaluate possible intracardiac shunts in the cath lab, it is necessary to understand four assumptions inherent in these calculations and to be certain they are applicable. The first assumption is that the patient is at steady state. While this may be true if the patient is asleep or resting quietly, as conditions change during the measurements, errors may be introduced. Therefore, it is best to obtain all samples as rapidly and safely possible to minimize perturbations in patient steady state. The second assumption is that an oxygen saturation sample is an accurate representation of the chamber or vessel. This is often the case, but oxygenation sampling is fraught with difficulty; scattered areas of pulmonary parenchymal disease or atelectasis may lead to inhomogeneous oxygenation of pulmonary artery flow. Similarly, the right atrium is a difficult site for obtaining a representative sample because of streaming from the highly saturated renal vein, the less saturated hepatic vein, and the very low saturated coronary sinus. Inferior vena cava saturation is usually higher at rest than the SVC saturation, but during general anesthesia, the SVC saturation may be higher. The third assumption is that all blood entering a chamber does so in an antegrade fashion, and, therefore, the sample is not “contaminated” by blood from a distal chamber. Certainly, this is not the case when there is atrioventricular or semilunar valve regurgitation. For example, a right ventricle saturation may be falsely elevated when there is pulmonary regurgitation and a patent ductus arteriosus. The fourth assumption is that the patient’s hemodynamic state in the cath lab represents the baseline hemodynamic state. This is probably the most difficult assumption to support; at one end of the spectrum, inadequate sedation results in a terrified or combative child, while at the other end of the spectrum is general anesthesia. Neither condition represents a normal physiologic state. The best an operator can do is to establish the conditions of the cardiac catheterization, then maintain these same conditions in a “steady state” until a complete set of measurements has been obtained.

Quantitative Assessment of Shunts

Use of the Fick principle to calculate pulmonary flow (Q_p) and systemic flow (Q_s) has been discussed. Calculation of left-to-right and right-to-left shunts requires understanding the concept of *effective* pulmonary flow (Q_{ep}) and *effective* systemic flow (Q_{es}). The formulas discussed subsequently are also presented in Table 12.2. The Q_{ep} is the volume of systemic venous return (i.e., “blue” blood) that flows to the lungs to be oxygenated. Q_{ep} is calculated by using the oxygen saturation of the “red” blood flowing out of the lungs (pulmonary vein) minus the saturation of the “blue” blood flowing into the lungs (SVC) using the following equation:

$$Q_{ep} = \text{VO}_2 / [\text{hemoglobin} \times 1.36 \times 10 \times (\text{pulm vein sat} - \text{SVC sat})]$$

Therefore, if the patient has no left-to-right shunt, the mixed venous saturation and pulmonary artery saturation are the same, and all of the pulmonary blood flow is “effective,” that is Q_p = Q_{ep}.

The Q_{es} is the volume of pulmonary venous return (i.e., “red” blood) that flows to the body. For all patients in a steady hemodynamic state:

$$Q_{ep} = Q_{es}$$

Simply stated, the amount of “blue” blood that flows to the lungs is equal to the amount of “red” blood that flows to the body.

When there is a left-to-right shunt, some oxygenated blood recirculates through the lungs, thus $Q_p > Q_{ep}$. The volume of a left-to-right shunt is the difference between the total pulmonary flow (Q_p) and the effective pulmonary flow (Q_{ep}):

$$Q_{L-R} = Q_p - Q_{ep}$$

Similarly, when there is a right-to-left shunt, some of the deoxygenated “blue” blood bypasses the lungs and recirculates through the body, thus $Q_s > Q_{es}$. The volume of a right-to-left shunt is the difference between the total systemic flow (Q_s) and the effective systemic flow (Q_{es}):

$$Q_{R-L} = Q_s - Q_{es}$$

Since $Q_{ep} = Q_{es}$, then:

$$Q_{R-L} = Q_s - Q_{ep}$$

Mathematically, the ratio of pulmonary flow to systemic flow is Q_p/Q_s . Calculating the Q_p/Q_s is simple and can be done immediately once the appropriate saturation samples are obtained when assessing shunt lesions. Since the oxygen consumption is in the numerator of both the Q_p and Q_s equations, it cancels out, leaving the following equation:

$$Q_p / Q_s = \frac{\text{systemic A - V oxygen difference}}{\text{pulmonary A - V oxygen difference}}$$

If the patient is breathing room air, dissolved oxygen is negligible, and the calculation of Q_p/Q_s can be stated in terms of oxygen saturation samples as follows:

$$Q_p / Q_s = \frac{(\text{Aorta sat} - \text{SVC sat})}{(\text{pulm vein sat} - \text{pulm art sat})}$$

When the pulmonary blood flow is markedly increased (e.g., pulmonary artery saturation 89%), the difference in pulmonary vein and pulmonary artery saturation is small (e.g., 99% to 89%), so the normal error of 2% to 3% that may occur with each measurement becomes significant. Thus, when there is a large left-to-right shunt, the Q_p/Q_s is simply reported as “greater than 3:1.”

Qualitative Assessment of Shunts

During right heart catheterization, some degree of variability in oxygen saturation from one chamber to the next is expected, typically between 1% and 2% from sample to sample. In a seminal study from 1979, Freed et al. investigated the normal variation between oxygen samples throughout the right heart in over 1,000 catheterizations in children with aortic or pulmonic stenosis who had no intracardiac shunts (confirmed by dye curves or angiography) (20). The mean oxygen saturations were similar in the SVC, right atrium, right ventricle, and pulmonary artery. The oxygen saturation sample in the proximal chambers was subtracted from the pulmonary artery sample to determine the variability in the absence of a left-to-right shunt. The standard deviation of the pulmonary artery and SVC difference was 2.9%, that of the pulmonary artery and right atrium difference was 1.8%, and that of the pulmonary artery–right ventricle difference was 1.8%. Thus, in the absence of a shunt, a step-up of >6% at the atrial level, 4% at the ventricular level, and 4% at the great vessel level will occur <5% of the time (i.e., twice the standard deviation).

Increases of >9%, 6%, and 6%, respectively (i.e., three times the standard deviation), would be expected no more than 1% of the time, thus would be highly unlikely in the absence of intracardiac shunting. Qualitatively, if there is a step-up in oxygen saturations in the right heart, there is a left-to-right shunt. Conversely, there is a right-to-left shunt if there is a step-down in oxygen saturations in the left heart. Quantitative methods are discussed later in the chapter, and must be used if one wants to define the caliber of the shunt.

The sample in the true SVC is taken in the mid-portion, superior to the entrance of the azygous vein and inferior to the innominate vein (both of which may have a higher saturation than the mid-SVC). Sampling too high in the SVC, near the IJ vein, will provide a “falsely” low value for mixed venous saturation use in calculations because of cerebral extraction. However, general anesthesia can also result in a higher than normal SVC saturation. High mid-SVC saturation also may be seen in the presence of a high-output state, partial or total anomalous pulmonary venous return to the SVC or innominate vein, or an arteriovenous fistula. A low mid-SVC saturation may be present when the systemic arterial saturation is low (pulmonary venous desaturation, right-to-left shunt) or with a low cardiac output state (high tissue extraction).

The right atrial sample should be obtained at the lateral midatrial wall to avoid the low saturation stream from the coronary sinus and to facilitate mixing from the inferior and superior venae cavae streams. A step-up of >9% is highly suggestive of a left-to-right shunt from an atrial septal defect, anomalous pulmonary venous connection, a left ventricle-to-right atrium shunt, a ventricular septal defect with tricuspid insufficiency, or a shunt from the aorta (ruptured sinus of Valsalva aneurysm, coronary artery fistula). However, the absence of a significant step-up in the right atrium does not completely rule out a left-to-right shunt.

The right ventricular saturation should be approximately equal to that in the right atrium; a step-up of >6% suggests a left-to-right shunt. A step-up at the ventricular level may be seen with a low atrial septal defect (where the oxygenated blood preferentially streams into the right ventricle), a ventricular septal defect, a ruptured sinus of Valsalva aneurysm, a coronary AV fistula draining into the right ventricle, or a left-to-right shunt at the great vessel level with significant pulmonary valve insufficiency.

A step-up of >6% at the pulmonary artery level is seen with a high outlet ventricular septal defect, patent ductus arteriosus, aortopulmonary window, coronary artery fistula into the pulmonary artery, anomalous origin of the coronary artery from the pulmonary artery also with fistula, or a surgical aortopulmonary communication.

Similar data for the qualitative detection of right-to-left shunts are not available. If the aortic saturation is <92% (sea level, normal ventilation) or if there is >3% decrease in oxygen saturation on the left side of the heart, a right-to-left shunt is likely present. Pulmonary vein desaturation results most commonly from hypoventilation (sedation), pulmonary parenchymal disease, or pulmonary edema. Administering 100% oxygen will increase the pulmonary vein saturation and the systemic artery saturation, allowing one to distinguish between pulmonary parenchymal disease and a right-to-left shunt. Pulmonary vein desaturation that does not resolve with administration of 100% oxygen suggests an intrapulmonary shunt, such as from a pulmonary arteriovenous malformation. Left atrial desaturation, with normal pulmonary vein saturation, usually results from a right-to-left shunt through an atrial septal defect or PFO. This is a necessary shunt with tricuspid atresia and is seen frequently with tricuspid stenosis, Ebstein anomaly of the tricuspid valve, pulmonary atresia or severe pulmonic stenosis, or severe pulmonary vascular disease. Right-to-left atrial shunt may be seen with any disease

that markedly decreases right ventricular compliance or leads to right ventricular failure. Occasionally, right-to-left atrial shunting can occur even in the presence of normal right-sided pressures and resistances. This condition, called platypnea-orthodeoxia syndrome, produces cyanosis and dyspnea, which is due to cyanosis from right-to-left shunting across a PFO as one changes position from supine to sitting. A rare congenital defect, a persistent left SVC to the left atrium, also can cause left atrial desaturation.

Left ventricular desaturation may occur with any lesion that produces desaturation in the pulmonary veins or left atrium. Right-to-left shunting at the ventricular level occurs when the right ventricular systolic pressure is equal to or greater than left ventricular systolic pressure (e.g., a ventricular septal defect and elevated pulmonary vascular resistance or right ventricular outflow tract obstruction). Right-to-left shunting can occur during diastole if the right ventricular diastolic pressure exceeds that of the left ventricle, even if the right ventricular systolic pressure is less than that of the left ventricle. Occasionally, the streaming effect of a right-to-left shunt through a ventricular septal defect is such that the desaturation is not detected at the ventricular level but is detected in the ascending aorta (e.g., tetralogy of Fallot).

A decrease in oxygen saturation between the left ventricle and aorta requires both a communication between the aorta and the pulmonary artery and increased pulmonary vascular resistance. Typically, this is a patent ductus arteriosus or aortopulmonary window, combined with either pulmonary vascular obstructive disease or peripheral pulmonary stenosis. A decrease in saturation from the ascending to the descending aorta occurs with the combination of a patent ductus arteriosus and coarctation of the aorta; this right-to-left shunt from the pulmonary artery to the descending aorta causes differential cyanosis—saturated, pink upper extremities and desaturated, blue lower extremities.

Equal oxygen saturations in the aorta and pulmonary artery occur with lesions that cause complete mixing at any level. Occasionally, even when complete mixing is expected, different saturations may be found in the pulmonary artery and aorta due to intracardiac streaming patterns. For example, most patients with truncus arteriosus have preferential streaming, resulting in lower saturation in the pulmonary artery and higher saturation in the aorta.

In children who have transposition of the great arteries with intact ventricular septum, the pulmonary artery saturation is always higher than the aortic saturation, defining “transposition physiology.” With transposition of the great arteries and a large ventricular septal defect, there may be complete mixing, thus equal saturations in the pulmonary artery and aorta, but in some patients, streaming may still produce less favorable mixing, thereby increasing the importance of atrial level mixing in these patients to improve aortic saturations. If the saturation in the descending aorta is higher than that in the ascending aorta, the child has transposition of the great arteries with a patent ductus arteriosus and coarctation of the aorta (or interrupted aortic arch), causing reversed differential cyanosis—desaturated, blue upper extremities and saturated, pink lower extremities.

Vascular Resistance

Cardiac catheterization may be needed in children to assess pulmonary vascular resistance in order to determine operability or to plan therapy (e.g., in the setting of primary pulmonary hypertension). It is crucial that the data used for this calculation are collected meticulously, calculations are performed correctly, and the limitations of the resultant value are appreciated. The basic formula for vascular resistance shows us that resistance is related to the pressure drop across the vascular

bed divided by the flow across the vascular bed. Mathematical assessment of vascular resistance is based on laws of Poiseuille and Ohm (which describes electrical resistance). Poiseuille's law states that the resistance to flow across a vascular bed is related to the difference in mean pressure at inflow to outflow divided by the amount of flow. Neither concept perfectly describes a biologic system for several reasons. Blood flow is pulsatile (i.e., not constant) and not laminar, vascular walls are distensible (not rigid), and blood is not a homogeneous fluid. In addition, vascular resistance is not a fixed entity; it is a dynamic set of blood vessels changing in response to numerous mechanical and neurohormonal factors. Adapting these equations and applying them to the vascular bed results in the currently used simplified equation for calculation of vascular resistance (R):

$$R = \Delta P / Q$$

where

ΔP = change in pressure across the vascular bed

Q = flow in the vascular bed

Specific formulas for vascular resistance are found in Table 12.2. One can see from this formula, if rearranged as $R \times Q = \Delta P$, that increases in pressure difference (ΔP) across a vascular bed may be due either to resistance (R) or flow (Q) or both. Normal values for vascular resistance have been developed, and it is against these values that any one patient's hemodynamic situation is compared.

For example, if a sedated patient in the cath lab is hypoventilated, hypercarbia and acidosis develop; both factors cause an elevation of pulmonary vascular resistance. Another important factor affecting pulmonary resistance is pulmonary capillary recruitment that requires a minimal distending pressure. When there is decreased pulmonary flow or pressure (e.g., tetralogy of Fallot, restrictive aortopulmonary shunt, cavopulmonary anastomosis), there is derecruitment of capillaries in the pulmonary vasculature, resulting in an elevated resistance (21). There is no method to predict if (and how much) the pulmonary resistance will decrease with increased flow or pressure. Nevertheless, the concept of vascular resistance is very important in managing patients with congenital heart defects.

The pulmonary vascular resistance (R_p) equation is

$$R_p = \Delta \text{ Pulmonary pressure} / \text{Pulmonary blood flow}$$

where Δ pulmonary pressure is the change in pressure across the pulmonary vascular bed (i.e., pulmonary artery mean pressure – left atrial mean pressure), often called the transpulmonary gradient.

Similarly, the equation for systemic vascular resistance is

$$R_s = \Delta \text{ Systemic pressure} / \text{Systemic blood flow}$$

where Δ systemic pressure is the change in pressure across the systemic vascular bed (i.e., systemic arterial mean pressure – right atrial mean pressure).

When assessing the pulmonary vascular reactivity to various medications, a drop in pulmonary pressure may be related to the medicine decreasing the systemic resistance. In such situations, calculating the relative resistances of the pulmonary and systemic vasculature may provide useful information:

$$R_p / R_s = \text{Pulmonary vascular resistance} / \text{Systemic vascular resistance}$$

This “hybrid” vascular resistance unit, the Wood unit, is defined in mm Hg/L/min; it is used for pediatric hemodynamic calculations. Because of the considerable size range of pediatric patients, Wood units are indexed to BSA by *multiplying* by the BSA and are reported as “Wood units·m²” (mm Hg/L/min·m²). Indexing these units allows for comparison between patients

of different sizes (22). The normal range for indexed pulmonary resistance is 1 to 3 Wood units·m². The normal range for indexed systemic resistance is 20 to 28 Wood units·m².

When calculating the pulmonary vascular resistance in patients with normal pulmonary artery pressures, the numerator (i.e., Δ pressure) is a small number (4 to 10 mm Hg), similar in magnitude to the denominator (i.e., the pulmonary blood flow, 2 to 8 L/min). Thus, a 1- to 2-mm Hg error in pressure measurement can result in a large error in the calculated R_p . Thus, it is crucial to make sure the pulmonary artery and left atrial pressures are measured accurately. If there is concern for measurement error, recalibrate or change transducers to verify the pressures obtained.

Oxygen and Nitric Oxide Inhalation Studies

For patients with pulmonary hypertension, it is not only important to calculate pulmonary vascular resistance but also to identify whether elevated pulmonary vascular resistance is fixed or reactive to certain pharmacologic interventions. To answer this question in the cardiac cath lab, patients who have elevated pulmonary vascular resistance are given 100% inhaled oxygen or nitric oxide (usually 20 to 80 ppm). These drugs have pulmonary vasodilatory effects as is discussed in Chapter 20. Hemodynamic measurements (and baseline calculations) are performed first in room air and then repeated after giving oxygen and/or nitric oxide for several minutes. Patients with elevated pulmonary vascular resistance that is fixed may not exhibit a significant increase in left-to-right shunt (if present) or significant decrease in resistance after receiving oxygen or nitric oxide. On the other hand, patients with reactive pulmonary hypertension will show a significant decrease in pulmonary vascular resistance index and R_p/R_s (23).

Valve Area and Pressure Gradient

The pressure gradient across a valve is a function of both the flow across the valve and the orifice size. At normal flow rates, cardiac valves offer little resistance to flow. As the flow increases, a small pressure gradient may develop across a normal valve (e.g., a large left-to-right shunt through a ventricular septal defect resulting in a flow gradient across a normal pulmonary valve). Conversely, at low flow rates (e.g., shock), there may be little pressure gradient across a severely obstructed valve (e.g., neonatal critical aortic stenosis). Adult cardiologists describe valve stenosis in terms of the valve area, rather than the pressure gradient, as the valve area calculation takes into consideration flow rate. In general, the orifice area for most valves is 2.5 cm². However, most pediatric cardiologists describe valve gradients in terms of the peak pressure gradient across the valve. These pressure gradients are meaningful only when considered in conjunction with the transvalvar flow or cardiac output.

Valve area is calculated using the Gorlin formula (Table 12.3) that incorporates cardiac output, heart rate, and pressure curves on either side of the stenotic lesion (incorporating time lines, in order to calculate systolic ejection or diastolic filling time, and calibrated for pressure) (24). Flow across a valve is not continuous throughout the cardiac cycle. Flow occurs across the aortic and pulmonary valves, in systole, and across the mitral and tricuspid valves in diastole. The systolic ejection time is the period during which the aortic valve is open and blood is flowing across the valve and it is determined from simultaneous pressure tracings of the left ventricle and ascending aorta. The two points at which the ventricular tracing crosses the aortic tracing represent the opening and closing of the aortic valve. The time between these points is the systolic ejection time. The diastolic filling period is the time during which the mitral valve is open and blood is flowing across the valve. It is determined from simultaneous pressure tracings of the left atrium and left ventricle. The two points at which the left ventricular tracing

TABLE 12.3 Calculation of Valve Areas Using the Gorlin Formula

Calculation of the aortic valve area:

Determine cardiac output (in mL), systolic ejection time (in s/beat), and R-R interval (in seconds).

Calculate systolic flow:

$$\text{Systolic flow} = \frac{\text{cardiac output} \times \text{R-R interval}}{60 \times \text{systolic ejection time}}$$

Determine mean aortic valve gradient (mm Hg, by planimetry):

$$\text{Aortic valve area (cm}^2\text{)} = \frac{\text{systolic flow}}{44.5 \times \sqrt{\text{mean systolic gradient}}}$$

Calculation of mitral valve area:

Determine cardiac output (in mL), diastolic filling time (in s/beat), and R-R interval (in seconds).

Calculate diastolic flow:

$$\text{Diastolic flow} = \frac{\text{cardiac output} \times \text{R-R interval}}{60 \times \text{diastolic filling time}}$$

Determine mean mitral valve gradient (mm Hg, by planimetry):

$$\text{Mitral valve area} = \frac{\text{Diastolic flow}}{37.8 \times \sqrt{\text{mean diastolic gradient}}}$$

crosses the left atrial tracing represent the opening and closing of the mitral valve. The time between these points is the diastolic filling period. Because the left atrium is rarely directly entered except in the presence of an atrial septal defect or PFO, it is more common to utilize simultaneous pressure tracings of the left ventricle and the pulmonary artery capillary wedge. These tracings must be realigned to compensate for the time delay of the pulmonary wedge tracing. In adult patients (who have slower heart rates), the wedge tracing is delayed by 50 to 70 ms; in pediatric patients (who have faster heart rates), the wedge tracing is moved to the left so that the v wave is bisected by or just precedes the downstroke of the left ventricular tracing. Once the appropriate ejection or filling period is determined, flow across the valve is calculated from the Gorlin equation according to the formulas provided in Table 12.3.

The mean aortic valve gradient is most accurately determined by planimetry of the area between the left ventricular and aortic tracings during the systolic ejection time. The mean mitral valve gradient is most accurately determined by planimetry of the area between the left ventricular and the left atrial (or pulmonary capillary wedge) tracings during the diastolic filling period. Previously, planimetry was done by manual tracing or averaging multiple parallel lines; now computer programs easily perform planimetry.

In patients with congenital heart defects, particularly intracardiac or extracardiac shunts, determining the valve area is challenging, as the flow may be different across each valve. For example, with a ventricular septal defect, flow across the mitral valve is greater than flow across the aortic valve as a portion of left ventricular preload is ejected across the defect rather than the aortic valve. When the flow across a valve cannot be accurately determined, the valve area cannot be calculated. However, most of this information can be obtained from noninvasive means such as detailed 2-D and Doppler echocardiography.

ANGIOGRAPHY

Basic Concepts

In this era of highly developed noninvasive imaging techniques, the role of cardiac and vascular angiography is complementary and remains essential for the evaluation and management of selected conditions. The goals of angiography should be defined prior to the procedure, as determined by the information that is available from noninvasive studies, such as echocardiography, magnetic resonance imaging, and computer tomographic imaging, and further delineated during the procedure based on the hemodynamic and oximetric data obtained.

This section covers basic angiography issues, including contrast agents, radiation exposure, catheters, and camera angles. Angiographic imaging of selected defects is discussed.

Contrast Media

Contrast media are radiopaque due to the iodine content and classified as either ionic (high osmolality) or nonionic (low osmolality) compounds. Both types yield excellent image quality but have widely different side effect profiles. The main hemodynamic and cardiovascular effects of contrast agents are directly related to osmolality, sodium content, and the agent's effect on serum calcium. For this reason, it is important to measure the most important portion of the hemodynamic data prior to use of a significant amount of contrast.

The relative advantages and disadvantages of ionic versus nonionic contrast media have been discussed extensively in the literature (25). Ionic media are generally not recommended for use in the pediatric patient due to their more significant adverse physiologic and hemodynamic effects. The effects of using ionic media include: a rapid shift of interstitial and intracellular fluid into the vascular space, binding of serum calcium, an increase in pulmonary artery and left atrial pressures, reflex tachycardia, a sensation of intense heat or pain, coughing (pulmonary artery injection), and the potential for exacerbation of pulmonary hypertension. Nonionic media are routinely used for the pediatric or complex congenital patient, as these agents are safer, well tolerated, but more expensive. The older published guidelines for maximum contrast dosage typically state a maximum of 4 mL/kg as a limit for routine angiography during a procedure; however, studies using the newer contrast agents (with lower side effect profile) have not been conducted (26). It is prudent to assure that each patient receives adequate hydration during and after the catheterization procedure.

Allergic reactions to contrast agents are unusual without prior exposure. If a patient has had a known allergic reaction to contrast, a premedication regimen that includes administration of a corticosteroid and antihistamine should be utilized. Careful observation for any allergic reaction in such patients following injection of a very small dose of contrast should be performed before administering a bolus of contrast for angiography. Repeat dosing of these medications may be necessary depending on the length of the procedure. Allergy to shellfish may portend sensitivity to iodine, which is usually present in contrast media.

Radiation Dose and Exposure

Compared with other diagnostic procedures performed in pediatric patients, cardiac catheterization produces a relatively large dose of radiation. In adults, the cardiac catheterization radiation dose is about 600 times the dose of a chest x-ray view (27). Pediatric patients undergoing complex diagnostic

evaluation or therapeutic cardiac catheterization are typically exposed to longer fluoroscopy times, thus a higher radiation dose. Thus, it is imperative that the catheterization goals be defined as well as possible ahead of time to minimize the exposure to radiation. For certain complex conditions (e.g., pulmonary atresia, complex functional single ventricle physiology), an increasingly aggressive treatment approach may result in an increased number of catheterizations at an earlier age, particularly in those patients who need intervention. Although it is difficult to quantitate the risk from radiation exposure in the cath lab, the probability of a fatal cancer per fluoroscopically guided procedure has been reported at approximately 0.07% (28).

Factors that affect the radiation dose include the duration of exposure, the BSA exposed, and the current (mA) and voltage (kV) used to generate the image. Although the patient's risk associated with the radiation exposure should be less than that associated with untreated congenital heart defects or incomplete diagnosis, the cardiologist must be aware of issues that affect both the patient and staff exposure to radiation, doing everything possible to minimize this exposure. As technology has advanced, technical modifications that have reduced radiation exposure during cardiac catheterization include the transition to digital-only systems, high-power x-ray tubes that allow copper filtration (inserted to reduce skin dose), last image storage, and improved detector efficiency (28,29).

Patient Dose

Cineangiography is associated with a markedly higher radiation dose per unit time than fluoroscopy, typically about 15 times higher (29,30). Thus, in a simple diagnostic catheterization, cineangiography accounts for most of the radiation exposure. However, in lengthy interventional cases, fluoroscopy time contributes significantly to the total radiation dose. Simultaneous biplane imaging (either with fluoroscopy or cineangiography) doubles the radiation dose compared with single-plane imaging. Similarly, the radiation dose increases with frame rate; pulsed fluoroscopy at 30 frames per second is twice the dose of pulsed fluoroscopy at 15 frames per second. For basic catheter manipulation, the fluoroscopic frame rate can be set lower, if extensive procedure time is anticipated; however, this will detract from image quality. By selecting the lowest frame rate necessary (fluoroscopy and cineangiography) and judiciously minimizing the use of biplane fluoroscopic imaging, the cardiologist can significantly reduce the radiation dose to the patient and cath lab personnel. One must always balance radiation dose with image quality (29).

Recent improvements in cath lab equipment also have reduced the radiation dosage. In particular, the use of digital flat panel imaging systems has decreased the radiation dosage from 25% to 50% when compared to prior use of conventional film systems (28). Collimation of the x-ray beam is another important factor in reducing radiation exposure. When the beam is collimated to the smallest area needed to view the pertinent structures, there is not only reduction in the volume of patient tissue exposed and radiation scatter to personnel, but there is improvement in image quality. Current modern systems allow for virtual collimation based on the last image stored, so that additional exposure is not needed to set these fields (28). Wedge filters should be positioned in the corners of the radiographic field to further improve image quality, but should not be considered a major strategy for reduction of radiation exposure. One must remember that electronic magnification modes will increase patient radiation dosage, so it is recommended that the lowest level of magnification that provides good image quality be used (29).

Cath Lab Personnel Exposure

The previous discussion of radiation exposure is not only relevant to the patient but to the staff in the cath lab. The following considerations also apply to the protection of personnel.

Scatter of the x-ray beam is the major source of personnel exposure in the cath lab, although as a general rule the intensity of scatter to the operator is 1/1,000 of the patient skin dose. It is approximately 10 times greater with cineangiography than with fluoroscopy. Increasing patient size, field size, and angled views will all increase scatter. Lead shielding and increased distance from the patient provide the best protection against exposure from x-ray scatter; the radiation dose decreases rapidly as one moves away from the patient ($1/r^2$) (27). Distance from the patient is more easily maximized during angiography when using an automatic injector system, thereby reducing exposure. The operators' hands should not be seen in the x-ray field (29).

All staff working in the cardiac cath lab must wear "lead" aprons. New aprons, which are not made of lead, can be as much as 50% lighter than a lead apron, making them more comfortable to wear and producing less fatigue. They are made from several layers of very light fabric; each layer absorbs a different wavelength of radiation but covers the same radiation spectrum as a lead apron. Those personnel likely to have their backs to the patient during the procedure (e.g., staff obtaining equipment, performing transesophageal echocardiography) should wear lead aprons that completely wrap around them. A thyroid collar reduces the exposure risk to the thyroid by approximately one half. Wraparound leaded eyeglasses reduce ocular exposure by approximately one-fifth. Regular eyeglasses with glass lenses provide some protection; eyeglasses with plastic lenses provide virtually no protection.

Additional measures that are helpful to reduce the overall amount of radiation exposure to both the patient and the staff include

1. Intermittent use of the fluoroscopy with reduction in fluoroscopic frame rate to the minimum needed for visualization of pertinent catheter course and cardiac structures
2. Careful attention to catheter pressure tracings by the operator in order to correlate with catheter course on fluoroscopy
3. Use of biplane fluoroscopy only when necessary
4. Cineangiography for recording essential information, with the use of either cineangiography at a lower frame rate or a "store fluoroscopy" capability for less important functions, such as recording balloon inflations.
5. The field of interest should be centered in the detector, with appropriate filters, collimators in use, and the detector as close to the patient as possible.
6. Liberal use of lead shields for positioning between the operator's hands and the x-ray beam and for shielding of other cath lab personnel, such as anesthesia at the head of the cath lab table.

Angiography

The importance of good technique when performing angiography cannot be overemphasized. It is critical to assess the status of the patient prior to and during angiography, making sure that the patient is properly positioned on the table and will not move significantly during the injection of contrast. It is preferable to deliver the bolus of contrast within one cardiac cycle, where feasible, in order to provide the opacification needed for detailed angiography. Catheters used for angiography are thin walled and have multiple side

holes to allow rapid delivery of contrast media at relatively high pressures without catheter recoil (Fig. 12.1). If catheter recoil is anticipated, then the rate of contrast injection can be slowed or the rise time to maximum pressure can be increased. Catheter tips should be free within the cardiac chambers or vessels (to prevent staining or injection into tissue), the body or shaft of the catheter should be positioned to support the catheter during injection to prevent excessive recoil, and the catheter should be positioned in or just proximal to the area of interest. When positioned in a ventricle, a balloon-tipped angiographic catheter may cause less ectopy than other catheters.

It is common during interventional procedures to make calibrated measurements of structures that are defined angiographically. During diagnostic studies, vessel size and ventricular function also can be quantitated in order to provide a thorough assessment of anatomy and function. A given catheter's French size (1 Fr = 0.33 mm) may be used as a reference for calibration to determine the x-ray magnification, allowing absolute measurements to be made from the angiogram; however, small errors in measurement may contribute to larger calibration errors since many structures being measured in the congenital patient are larger than the catheter itself. More accurate measurements may be obtained using a marker catheter, which has radio-opaque bands placed 1 or 2 cm apart (compared with a catheter that may be only 1 to 3 mm in diameter), but the x-ray beam must be perpendicular to the catheter to avoid foreshortening, which causes a calibration error. The most accurate method of calibration is that which is built into the imaging system itself, with the patient positioned at isocenter on the table, whereby automated calibration references allow for measurement of structures or vessels from stored fluoroscopic or angiographic images.

Imaging of the Biventricular Heart

Position of the Camera, Image Intensifier/Detector, and Radiographic Source

Camera angles refer specifically to the angles of the flat panel detectors with respect to the table or patient's chest. As viewed from the flat panel detector, the image plane is perpendicular to a line drawn between the x-ray tube and the detector. For example, in a straight frontal view, the frontal plane detector is positioned at 0 degree and the lateral detector is positioned at 90 degrees for the corresponding orthogonal view. These systems allow independent positioning of the tubes; however, a 90-degree relationship between the two detectors is most often maintained so as to provide corresponding orthogonal views of complex congenital structures.

The importance of angled views for imaging congenital heart lesions was first described by Taussig in the 1940s (31). Subsequently, several manuscripts have described the use of angled views (axial angiography) in the cardiac cath lab (28). While increasingly complicated surgical and transcatheter interventional techniques require more sophisticated angled views and camera adjustment, certain standard angles may be used for common lesions and traditional structural orientation. Again, familiarity with the anatomy and structures that need to be defined during angiographic assessment is required, so that adjustments in camera angles can be made to optimize structural definition. Understanding the views needed and planning ahead may reduce overall radiation exposure (29). An exhaustive discussion of the use of angled views in congenital heart disease is beyond the scope of this chapter; however, basic imaging of the biventricular heart and of several other common defects is discussed below.

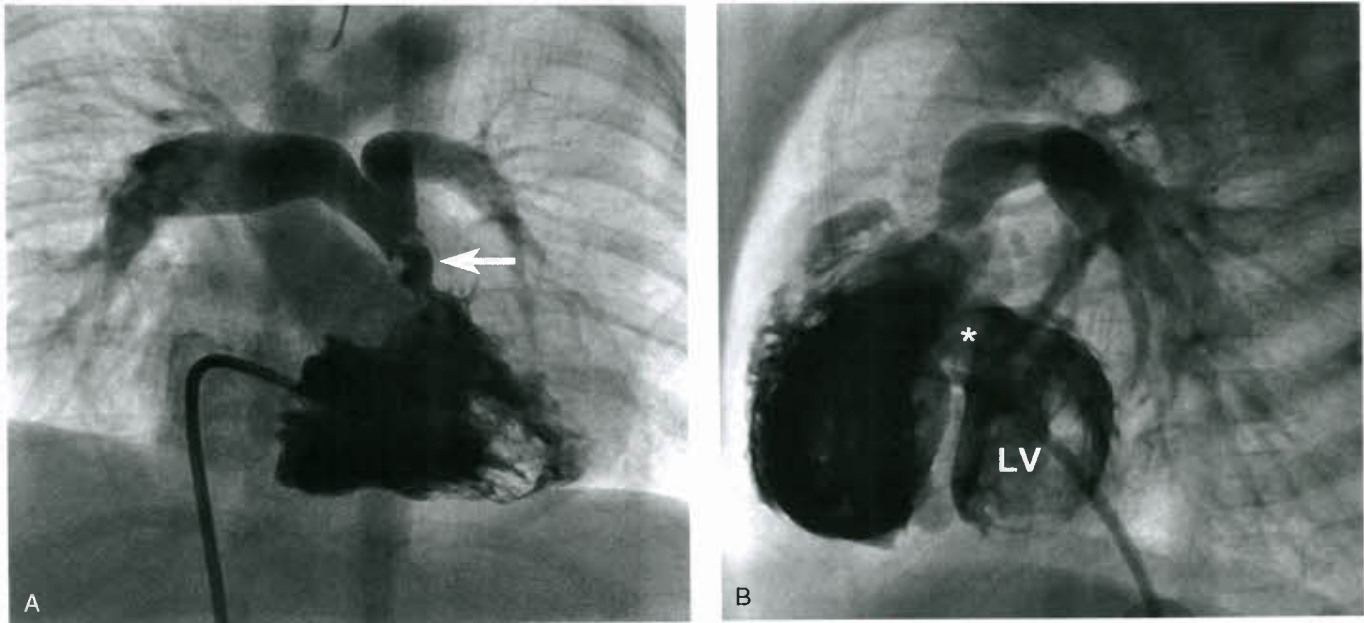


Figure 12.7. Infant with tetralogy of Fallot. **A:** Straight AP frontal plane view of right ventricular injection shows the infundibular stenosis and thickened pulmonary valve leaflets (*arrow*), in addition to the pulmonary artery bifurcation. **B:** 90-degree straight lateral projection again shows right ventricle well in addition to the right-to-left shunt through the VSD (*) with filling of the left ventricle (LV).

Right Ventricle and Pulmonary Arteries. The right ventricle is most often imaged in the frontal and straight lateral views (Fig. 12.7). Occasionally, 0 to 25 degrees of cranial angulation is added to the frontal plane detector to provide better definition of the outflow tract. Note the following:

1. Neither view displays the interventricular septum well as the normal right ventricle wraps around the left ventricle. The interventricular septum should be imaged from a left ventricular injection (unless there is simple transposition of the great arteries).
2. The right ventricular outflow tract and main pulmonary artery (MPA) take a posterior course from the heart. Without cranial angulation, there may be overlay of structures (Fig. 12.8); this is most accentuated when the MPA is dilated. The straight 90-degree lateral view displays the infundibulum (Fig. 12.8) and the pulmonary valve well in almost all patients.
3. The right pulmonary artery (RPA) courses posterior to the ascending aorta and travels laterally into the right chest, alongside of and anterior to the right bronchus. It is well seen in the frontal view and almost completely foreshortened in the lateral view. For example, maintaining the detectors at a 90-degree relationship, if the catheter in the RPA is fully foreshortened in the lateral view (adjusted LAO so one is looking “down the barrel” of the catheter), then one can be assured that the frontal plane view (simultaneously adjusted with right anterior oblique [RAO] angulation) will fully display the length of the vessel for accurate measurement.
4. The left pulmonary artery (LPA) courses posteriorly in the chest, anterior to the descending aorta, over and behind the left bronchus. Its most proximal portion may not be well seen in the frontal plane but is better visualized in the lateral view, sometimes with LAO angulation to prevent foreshortening (similar, but “opposite,” to the technique to visualize the RPA). The distal portion of the LPA can be

seen well in a straight lateral view but is foreshortened in the frontal view.

Left Ventricle and Aorta. The left ventricle is imaged using RAO and left anterior oblique (LAO) with cranial angulation (Fig. 12.9A). For an RAO view, the frontal image intensifier has 20 to 30 degrees of straight rightward angulation, whereas the lateral image intensifier has 60 to 70 degrees of leftward angulation with 20 to 30 degrees of cranial angulation. Images created with these projections are shown in Figure 12.9B–F. Note the following:

1. The RAO view displays the anterior portion of the interventricular septum (between the arrowheads in Fig. 12.9B). An anterior muscular ventricular septal defect or a defect arising from conal septal hypoplasia would be displayed in this view as a jet of contrast coursing superiorly into the right ventricular outflow tract. The mitral valve is visualized, and mitral insufficiency (if present) would be noted.
2. The LAO/cranial view displays the membranous, midmuscular, and apical portions of the ventricular septum (Fig. 12.9D). A qualitative assessment of left ventricular function can be performed in this view, and when calibrated systems are in place, the ventricle can be measured in diastole and systole to provide ejection fraction and volumes.
3. Neither view optimally profiles the inlet portion of the ventricular septum.
4. The right coronary artery can be seen in both the RAO and LAO/cranial views, outlining the position of the tricuspid valve. The left main coronary artery is seen in the LAO/cranial view coursing posteriorly from the aortic root, bifurcating into the left anterior descending branch anteriorly and the circumflex branch posteriorly.
5. The aortic valve is imaged well from a left ventricular injection, and the leaflets should be thin and barely visible when normal (Fig. 12.9E,F).

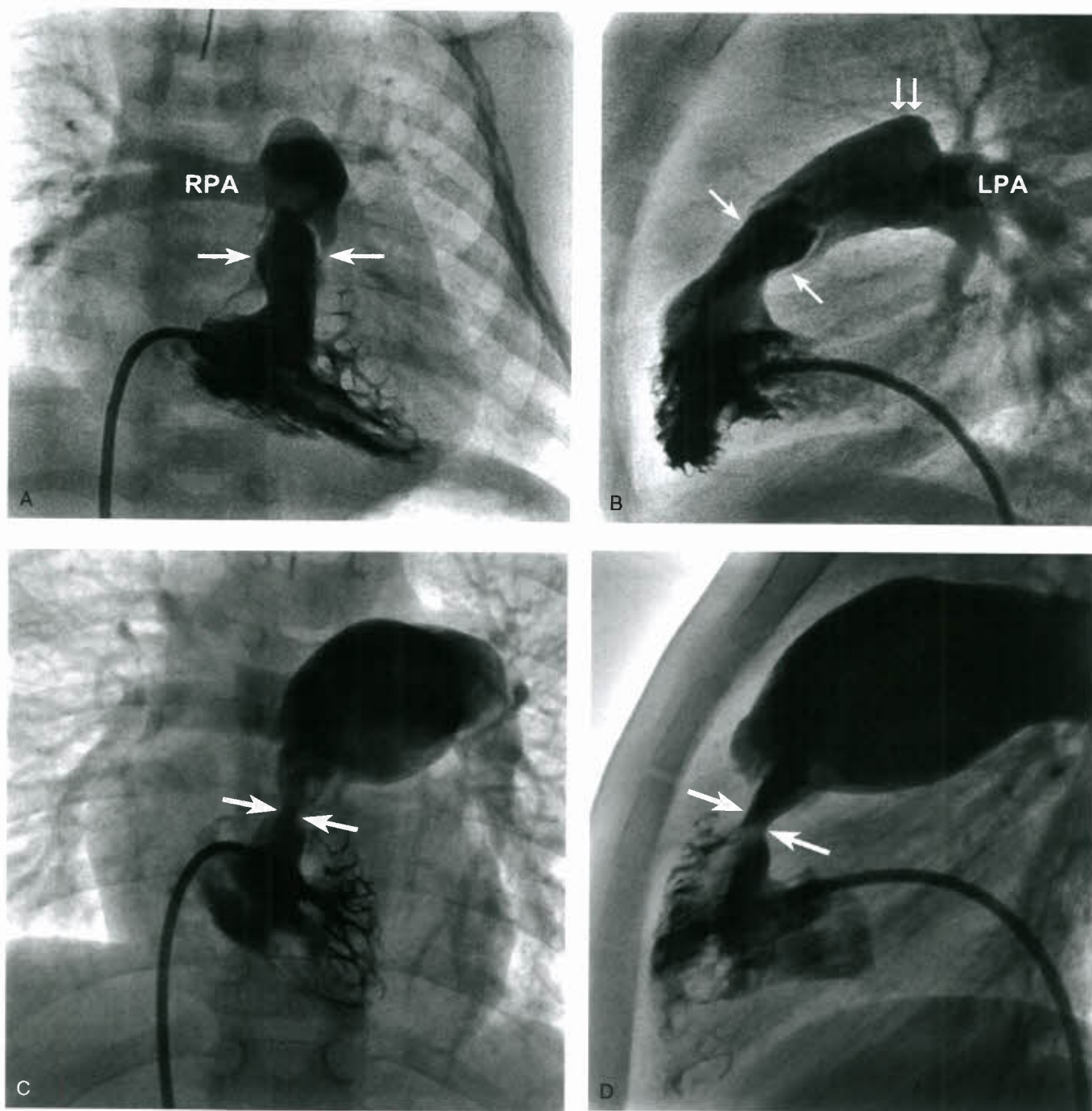


Figure 12.8. Right ventricular (RV) angiogram in an infant with severe pulmonary valve stenosis. In the frontal projection (A), the right pulmonary artery (RPA) is seen well, but the left, which courses posteriorly, is foreshortened. Note the hinge points (*arrows*) of the thickened pulmonary valve that domes in systole and the narrow jet of contrast passing through the valve. The lateral projection (B) displays the thickened, doming pulmonary valve (*arrows*). Most of the left pulmonary artery (LPA) is seen well in this view, but the right pulmonary artery is more foreshortened. There is a prominent ductus diverticulum (*double arrow*). C,D: RV angiogram in an older child with long-standing pulmonary stenosis following balloon valvuloplasty. Frontal plane view (C) shows very dynamic infundibular stenosis (*arrows*) with hyperdynamic RV function and prominent trabeculations. Lateral view demonstrates the dynamic infundibular narrowing well (*arrows*). In both views, there is significant poststenotic dilation of the main pulmonary artery.

For atrioventricular septal defects (which are not commonly seen in the cath lab for purposes of diagnostic angiography but for determination of pulmonary resistance in the older patient) and posterior muscular ventricular septal defects, visualization of the inlet portion of the ventricular septum is required. This requires

more cranial and more vertical angulation than the usual LAO/cranial view and is best displayed in the hepatoclavicular view (Fig. 12.10). For this, the lateral detector is moved to 40 degrees of leftward angulation and 40 degrees of cranial angulation, whereas the frontal camera has 30 degrees of rightward angulation.

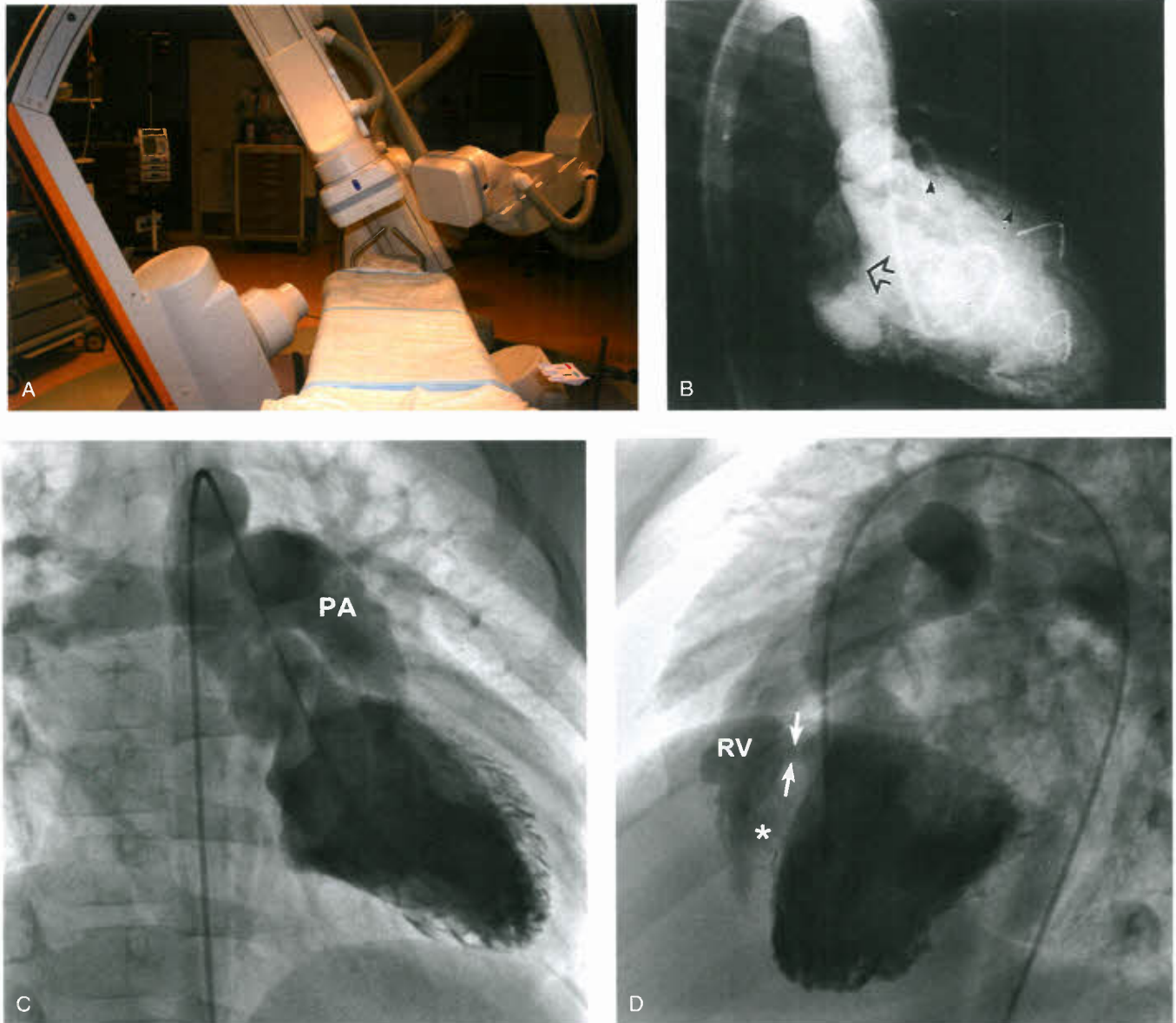


Figure 12.9. A: Biplane cardiac cath lab with the c-arms positioned for right anterior oblique (RAO) and long axial oblique projections. The frontal flat panel detector has 20 degrees of rightward angulation, while the lateral flat panel detector has 70 degrees of leftward and 25 degrees of cranial angulation. B: Retrograde left ventriculogram, RAO projection. The anterior muscular septum is indicated by the two *arrowheads*; a ventricular septal defect in this region would appear as a superiorly directed contrast jet. The mitral valve is indicated by the *open arrow*, and mitral insufficiency (if present) would be seen in this view. C,D: Retrograde left ventriculogram in a child with tricuspid atresia, normally related great arteries and a restrictive muscular ventricular septal defect (VSD). Frontal plane (C) with 27 degrees RAO angulation shows contrast appearing in the pulmonary artery (PA), but the ventricular septum is not profiled well from this angle. The corresponding LAO view (D; 61 degrees LAO, 19 degrees cranial) profiles the ventricular septum well and shows both the midmuscular VSD (*arrows*) and the tiny apical trabecular VSDs (*) in addition to the hypoplastic right ventricular chamber (RV).

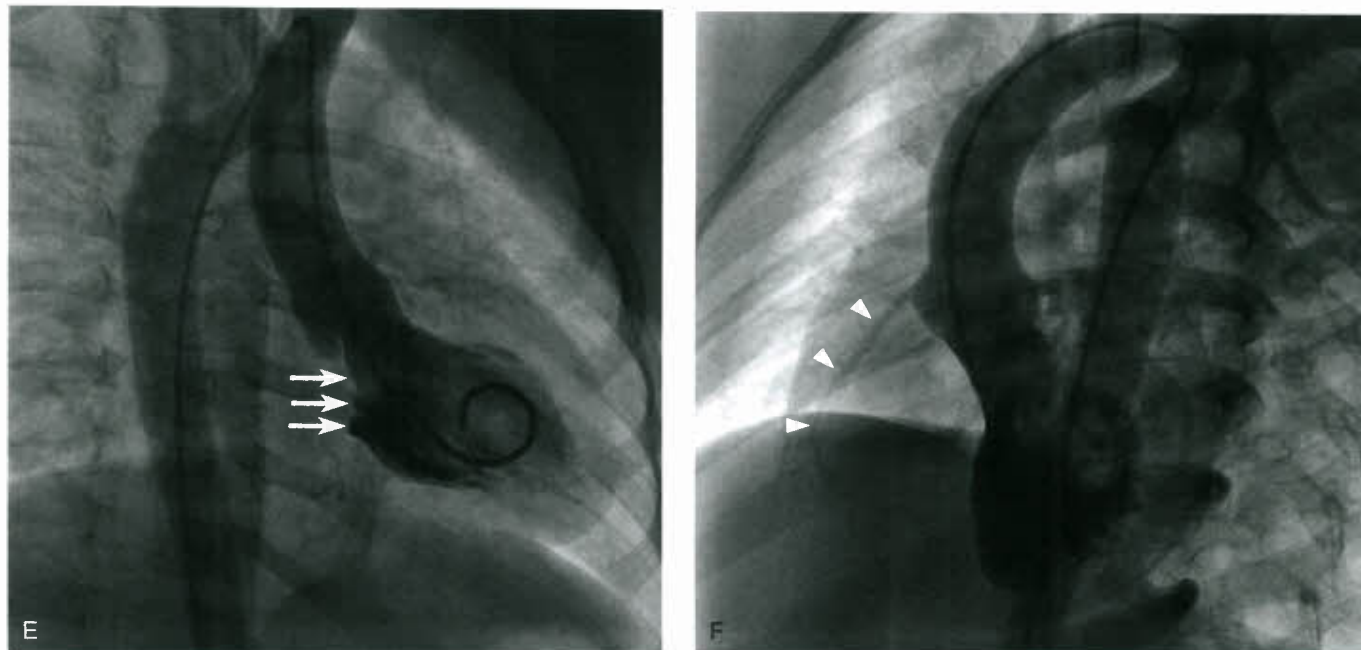


Figure 12.9. (Continued) E,F: Retrograde LV injection in an infant with a complex vascular ring shows thin aortic valve leaflet in the RAO projection (E) with competent mitral valve (*three arrows*). LAO projection (F) shows the intact ventricular septum very well; the right coronary (*arrowheads*) courses anterior to the right ventricle (which is not opacified in this patient with intact septum).

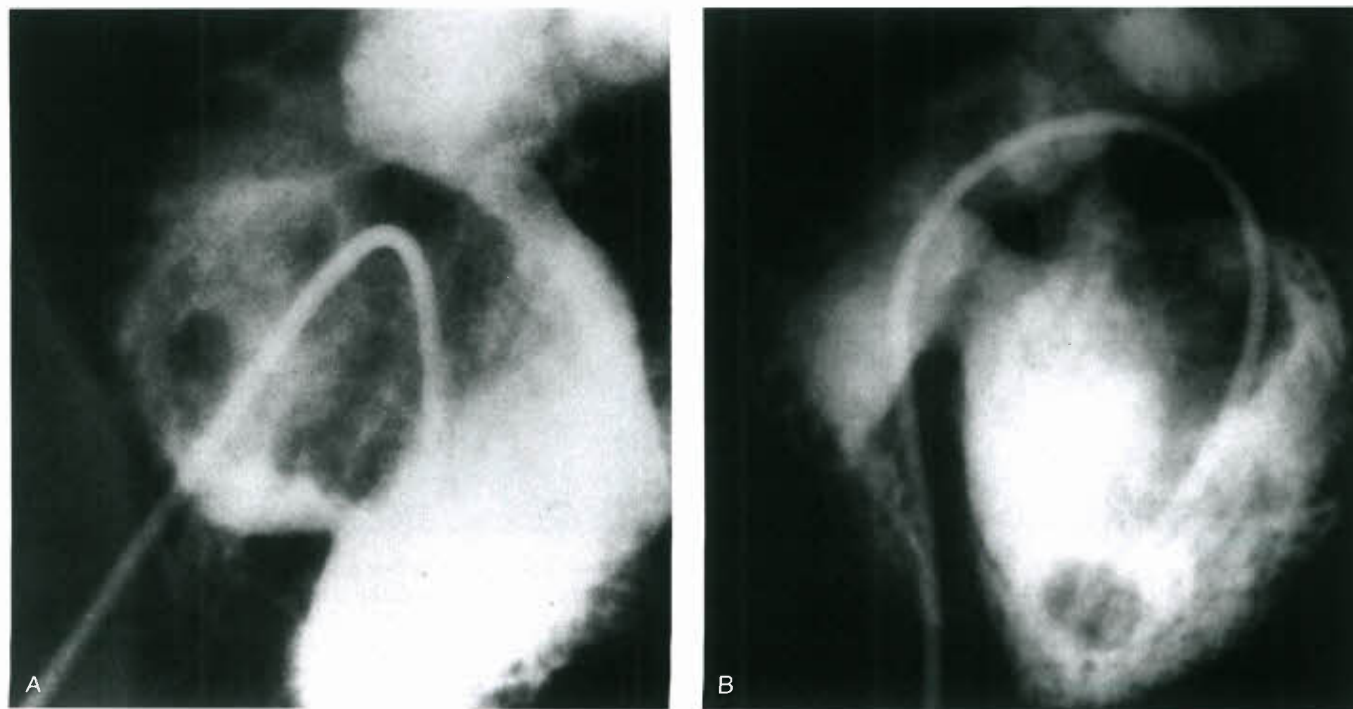


Figure 12.10. Hepatoclavicular view. A: Left ventriculogram in a child with a complete atrioventricular septal defect. The left ventricle is densely opacified, and contrast has crossed a large ventricular septal defect to outline the common atrioventricular valve (as negative contrast or dark appearance). The right ventricle is not yet fully opacified in this frame. B: Left ventriculogram in a child with tricuspid atresia. The large ventricular septal defect and moderately hypoplastic right ventricle are well seen.

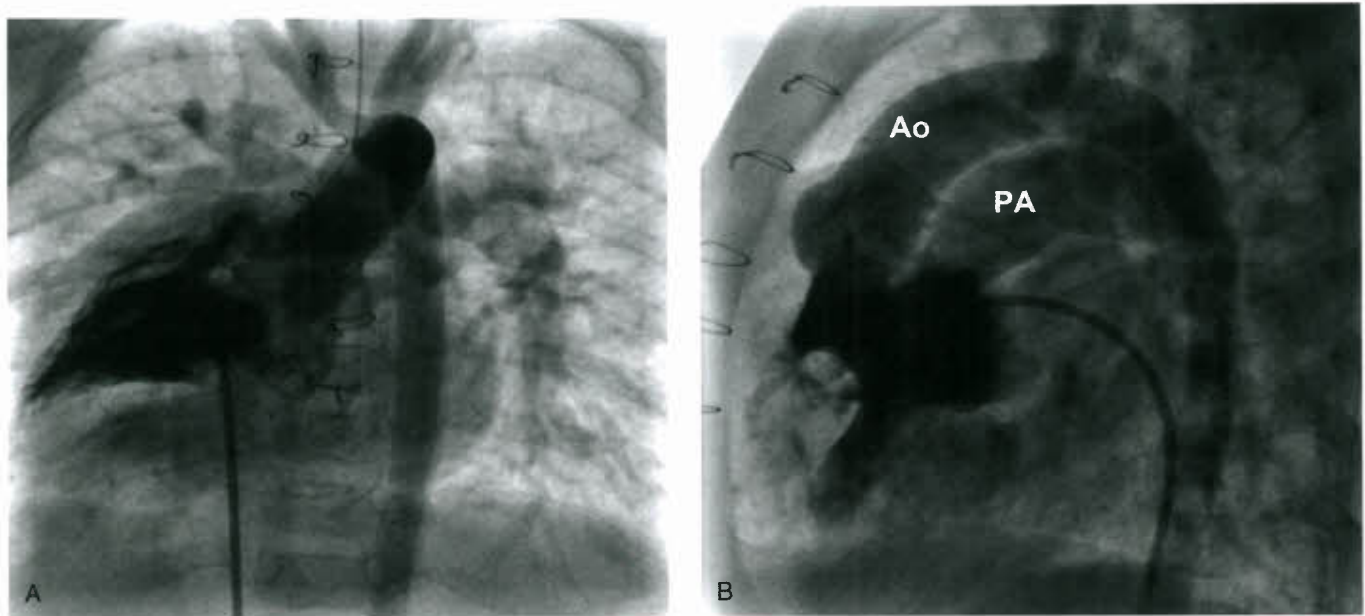


Figure 12.11. Straight AP (A) and lateral (B) views of a right ventricular injection in a patient with d-transposition of the great arteries, ventricular septal defect, and complex upstairs–downstairs ventricular arrangement. Both great arteries fill from the RV injection, although the aorta is more densely opacified and appears directly in front of the pulmonary artery in the frontal plane (A). In the straight lateral plane (B), it is now possible to appreciate the direct anterior (aorta, Ao)/posterior (pulmonary artery, PA) relationship of the great vessels more easily than in a complex angled view. Using such views will aid surgical planning when reoperation is necessary, so that the surgeon may appreciate the relationship of the great vessels to the sternum.

Specific Techniques

Aorta and Pulmonary Arteries

In more complex arrangements of the great vessels, it is often preferred to perform angiography in straight PA and lateral planes in order to define the left–right relationship of the vessels as defined in the frontal plane and, correspondingly, the anterior–posterior relationship in the lateral plane (Fig. 12.11).

Central Pulmonary Arteries

In some patients, particularly those who have tetralogy of Fallot, it is not possible to obtain sufficient cranial angulation to display the pulmonary artery bifurcation in the frontal plane view. Although routine catheterization of infants with tetralogy of Fallot is uncommon, postoperative angiography may be performed if pulmonary branch stenosis is suspected and warrants intervention. The catheter must be positioned beyond the right ventricular outflow tract, as contrast in the right ventricle will obscure the pulmonary arteries. Preferably, RAO and LAO projections, both with cranial angulation, may display the proximal right and left branch pulmonary arteries, respectively. In other cases, where this does not provide adequate visualization of the individual branches, extreme caudal angulation may display the central pulmonary artery bifurcation. Selective pulmonary artery injection will usually be necessary before intervention is undertaken so that detailed anatomy and calibrated measurements can be accurately obtained (Fig. 12.12A,B). In the case of very severe branch stenosis, balloon occlusion angiography with the catheter positioned in the contralateral PA may be used to fill the stenotic vessel (Fig. 12.12C,D).

Left SVC or Venous Collateral Vessels. Definition of the venous drainage of the upper body is necessary prior to a cavopulmonary anastomosis. An angiogram in the left innominate vein will display a left SVC or venous collateral vessels, if they are present. The angiogram may be performed using either a side-hole angiographic catheter positioned at the junction of the left IJ and subclavian veins or with an end-hole catheter using a balloon-occlusion technique. The balloon catheter is positioned in the innominate vein just medial to the left jugular vein, the balloon is inflated (occluding the innominate vein), 2 to 5 mL of contrast is hand injected, and then the balloon is deflated, allowing the contrast to drain via the right SVC into the heart (Fig. 12.13).

Pulmonary Angiography through a Sano, Modified Blalock-Thomas-Taussig Shunt, or Cavopulmonary Anastomosis

Current Norwood stage I palliation for hypoplastic left heart syndrome is carried out with either a Sano modification or a modified Blalock-Thomas-Taussig shunt as a source for pulmonary blood flow. In patients with the Sano modification, a right ventricular injection may show the pulmonary arteries fairly well but the Sano shunt is better visualized in the lateral projection due to overlap of the structures in the frontal plane projection (Fig. 12.14). A modified Blalock-Thomas-Taussig shunt can be easily accessed with a soft-tipped catheter in order to perform an angiogram in the shunt; this provides definition of the shunt caliber and pulmonary artery branch anatomy. With retrograde access, an angled-tip, 0.025 in, hydrophilic wire and a 4 Fr end-hole catheter (such as an internal mammary artery catheter or Judkins right) facilitates this procedure and minimizes negative hemodynamic effects. It is possible to directly measure pulmonary artery pressure if the catheter can be advanced through the shunt without hemodynamic

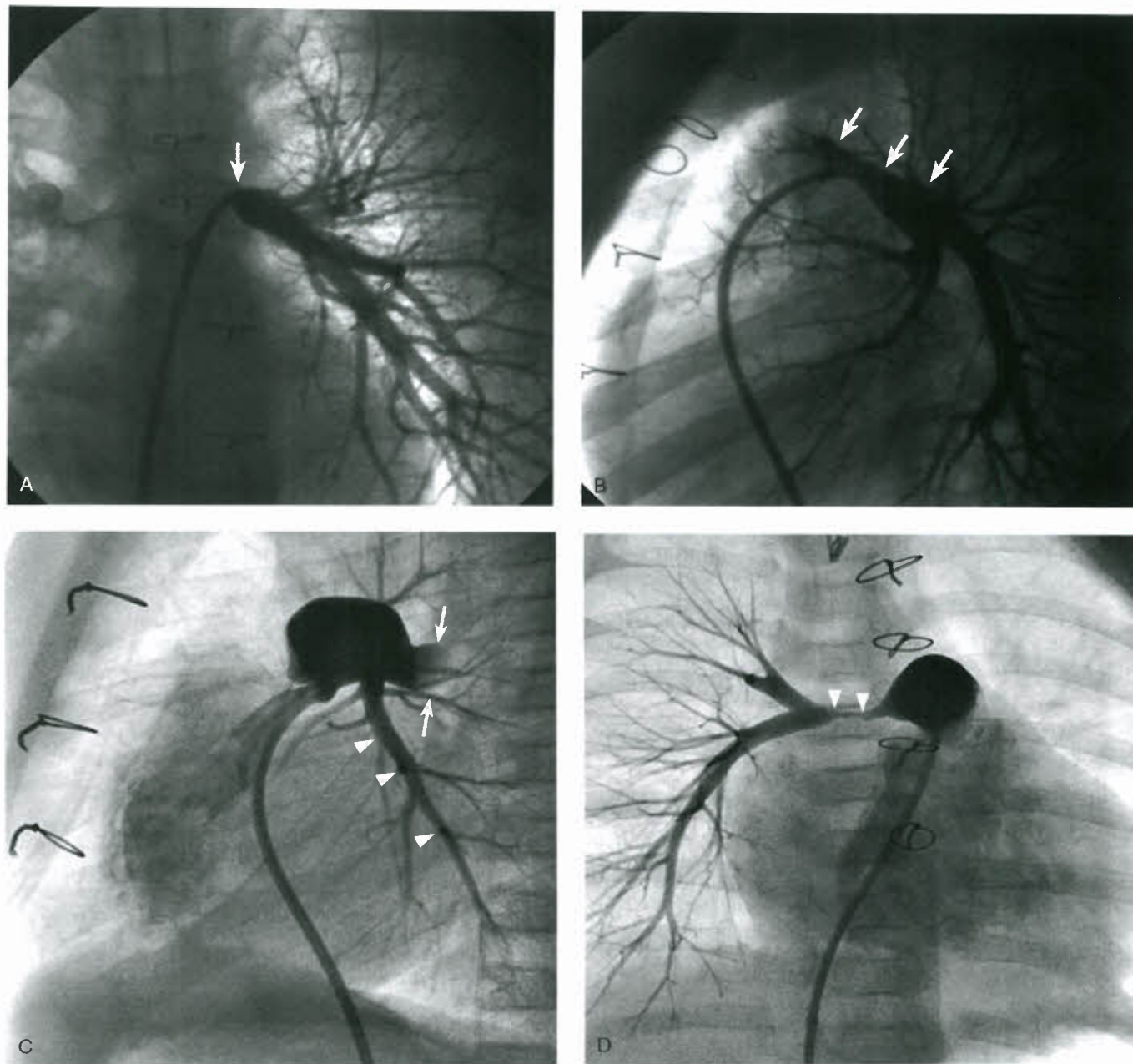


Figure 12.12. Examples of pulmonary artery branch stenosis. **A, B:** Selective left pulmonary artery (LPA) injection in a patient with proximal LPA stenosis. With the frontal plane detector angled at 16 degrees cranial/6 RAO, the proximal LPA stenosis (*arrow*) is completely foreshortened (**A**). This assures the operator that the orthogonal view (**B**) fully depicts the stenosis (*arrows*) and that measurement of this segment will be accurate. **C, D:** Severe right pulmonary artery (RPA) stenosis in a patient who had repair of anomalous left coronary originating from the mid-RPA. Balloon occlusion is performed with the angiographic catheter in the proximal LPA to occlude flow distally (**C**, *open arrows*), forcing contrast into the tightly stenotic RPA (*arrowheads*). Note the reduced perfusion of the RPA branches, which appear fully distributed (**D**), and is better seen on the corresponding AP view).

embarrassment, and the tip is free without pressure dampening. A selective pulmonary artery injection can also be performed by hand. Additional hand injections can be performed in the shunt with this catheter in order to demonstrate the anatomy more specifically (Fig. 12.14D). In some cases, the pulmonary arteries may be imaged without crossing the shunt, particularly if the patient has low saturations (unless intervention

is anticipated). A balloon-tipped angiographic catheter can be advanced antegrade through the heart into the subclavian artery, distal to the origin of the shunt. The balloon is inflated, occluding the distal subclavian artery, while a power injection of 0.5 to 1 mL/kg of contrast is performed. Positioning the side holes directly over the shunt origin prevents dense filling of the aorta, which would obscure the pulmonary arteries.

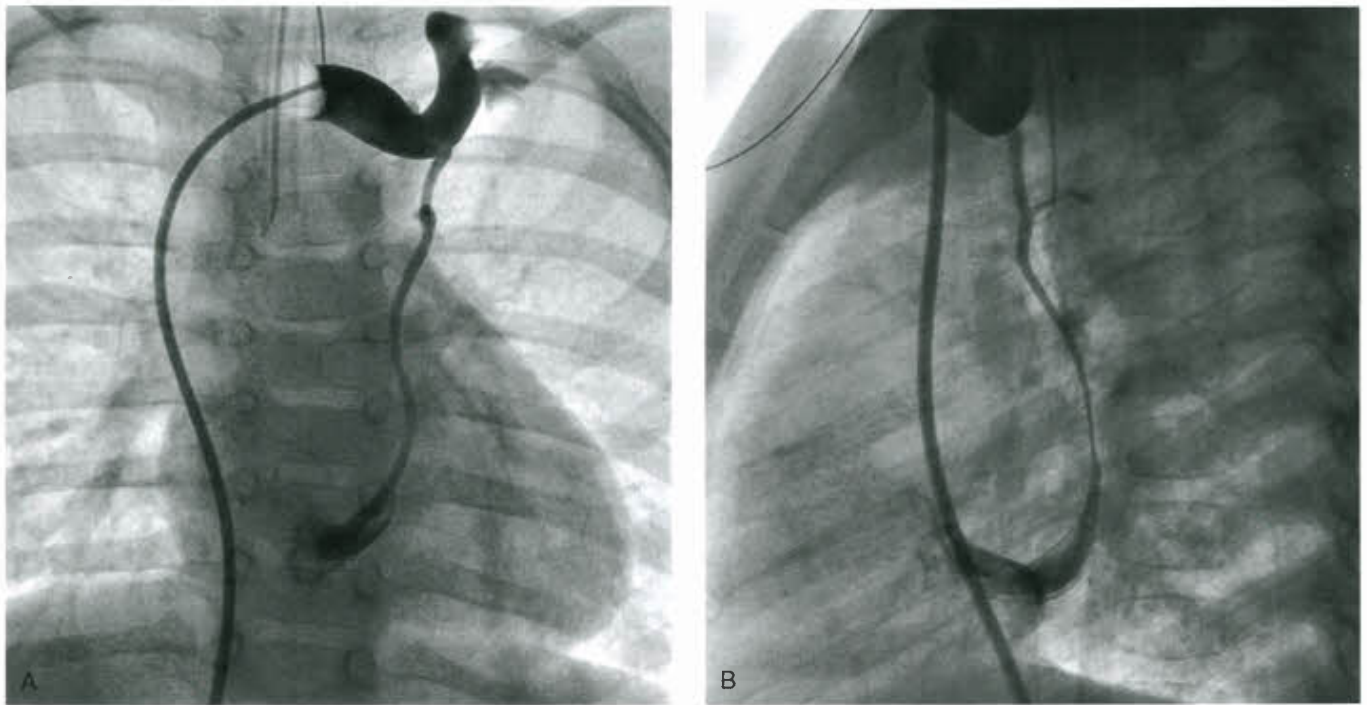


Figure 12.13. A,B: Balloon occlusion hand injection of contrast in the innominate vein fills a diminutive left superior vena cava (SVC) that drains to the coronary sinus. Lateral view (B) demonstrates posterior course of the left SVC to coronary sinus.

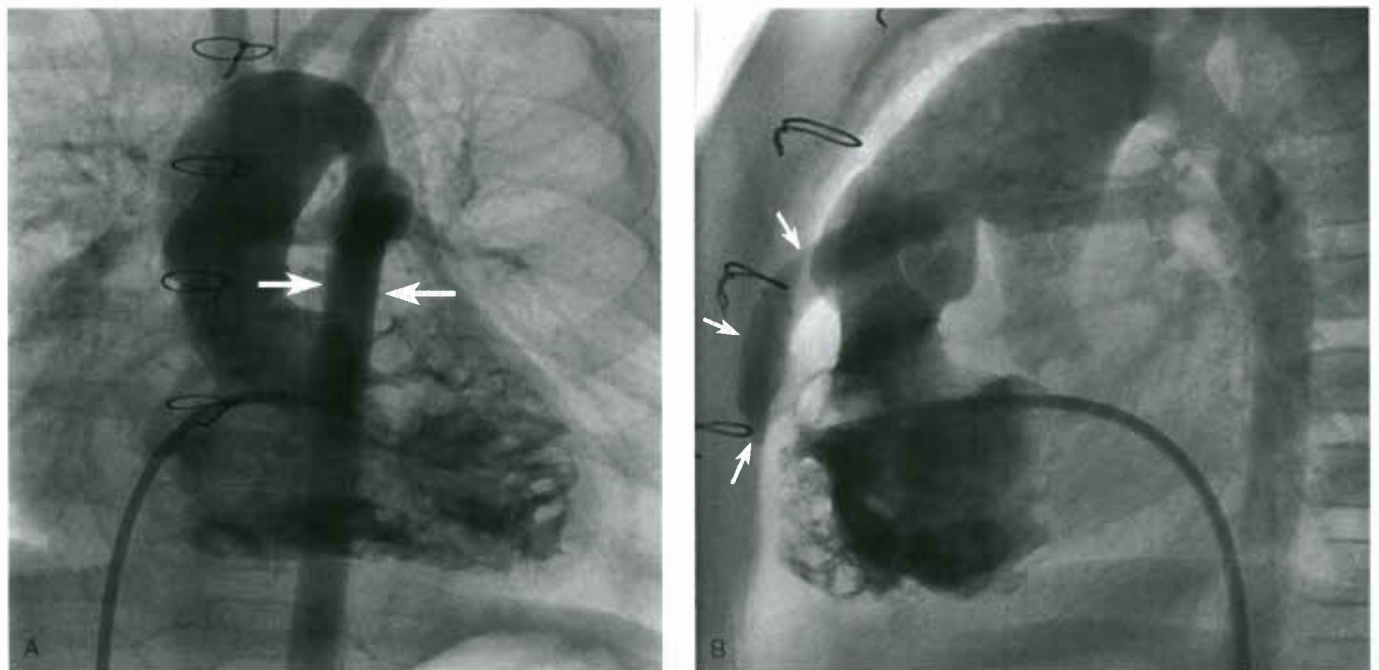


Figure 12.14. A,B: Right ventricular angiography in an infant with hypoplastic left heart syndrome, following Norwood Stage I with Sano modification (right ventricle to pulmonary artery conduit). A: In the straight frontal plane view, the Sano shunt (*arrows*) lies directly in front of the descending aorta, making it very difficult to see if there is stenosis in the Sano shunt. B: Lateral view nicely demonstrates the position of the Sano shunt (*arrows*) without evidence of stenosis in the Sano conduit itself (prominent right ventricular muscle bundles are present at origin). This view also shows the entire neo-aortic arch very well.

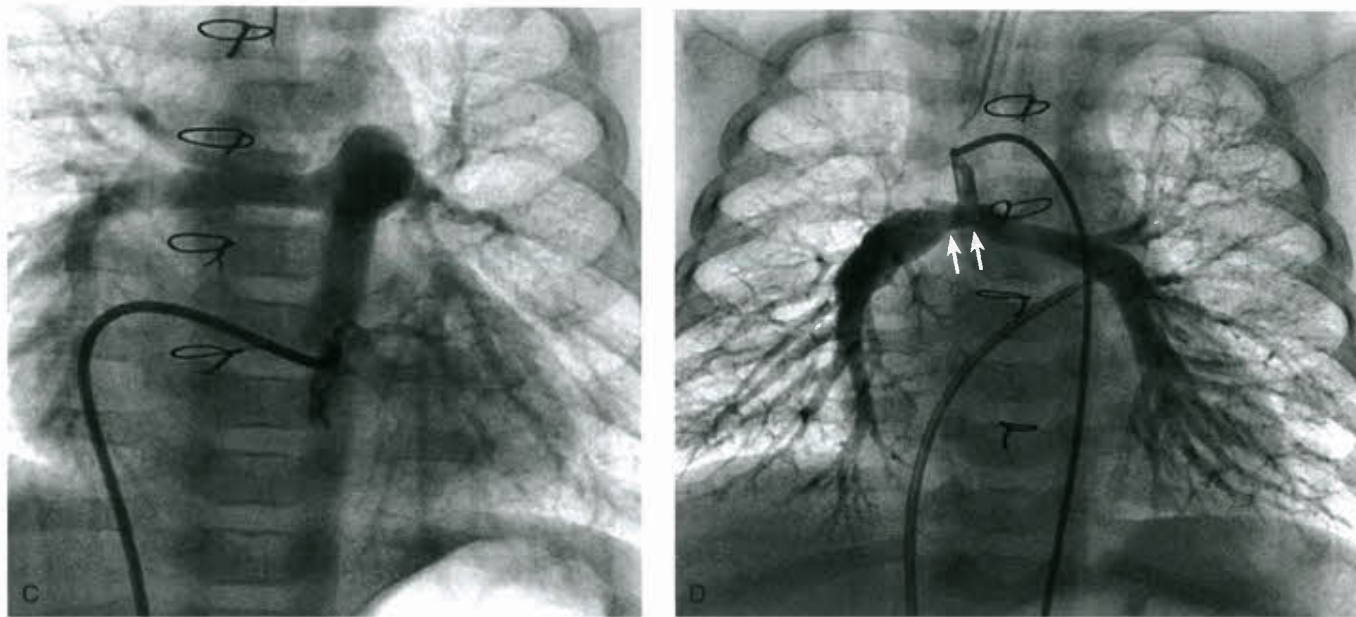


Figure 12.14. (Continued) C: More selective catheter injection in the proximal Sano shunt fills the pulmonary arteries well. D: Retrograde end-hole catheter injection by hand into the mid-portion of a Modified Blalock-Taussig shunt shows typical stenosis (*double arrow*) in the right pulmonary artery immediately adjacent to the shunt insertion; pulmonary arteries are well distributed.

For patients who have advanced through stage II palliation, usually a conversion to bidirectional cavopulmonary anastomosis, IJ access is needed and the pulmonary angiogram is performed with the angiographic catheter positioned in the distal SVC (Fig 12.15).

Pulmonary Vein Wedge Angiography

When the pulmonary arteries cannot be imaged by direct injection or by injection of an aortopulmonary shunt or aortopulmonary collateral, pulmonary vein wedge angiography

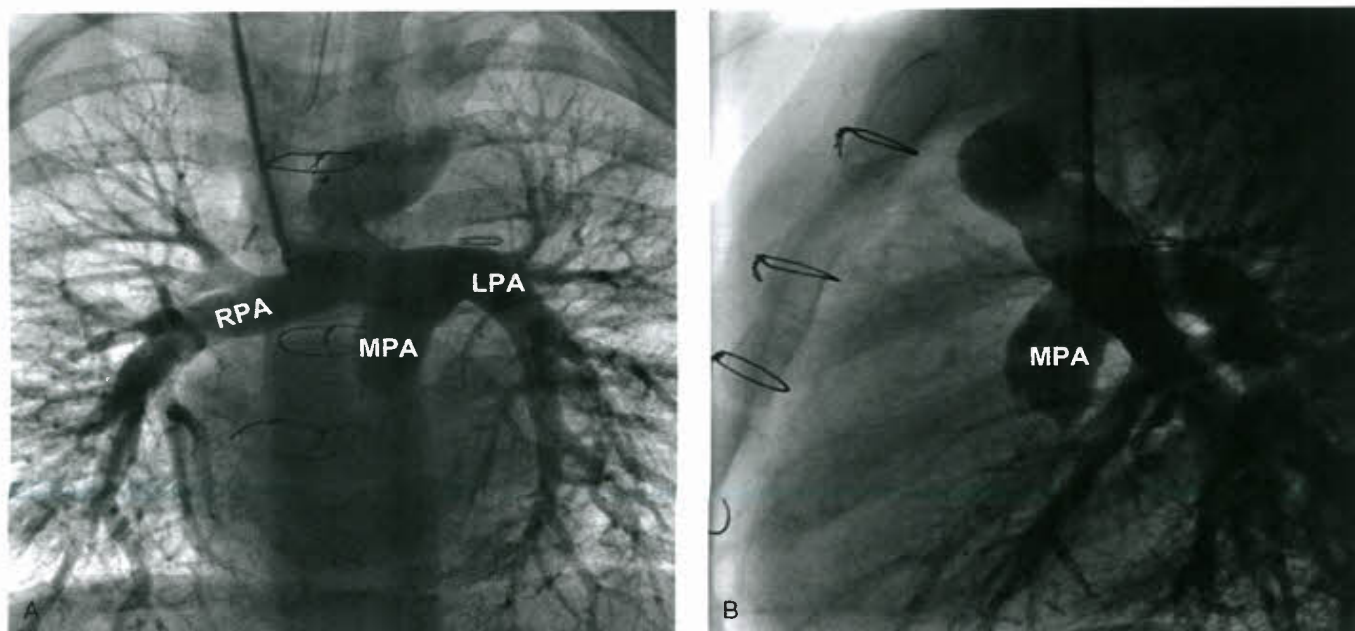


Figure 12.15. A,B: Injection via the angiographic catheter positioned in the distal superior vena cava to pulmonary artery anastomosis shows normal-size and normally distributed pulmonary arteries. MPA, main pulmonary artery; RPA, right pulmonary artery; LPA, left pulmonary artery.

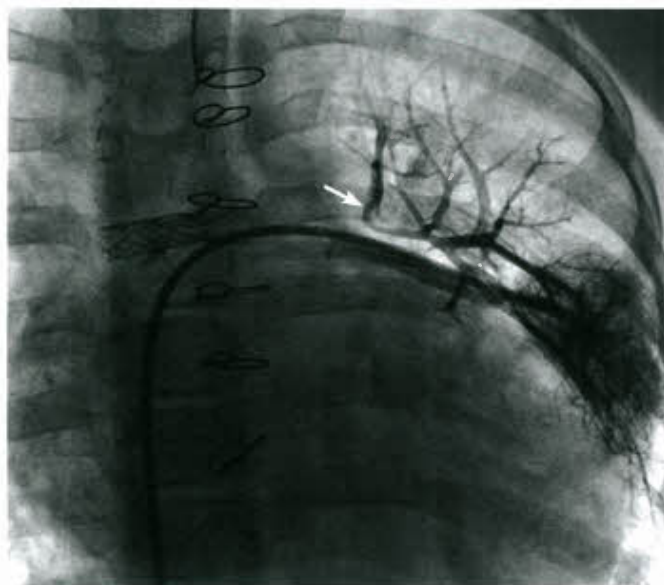


Figure 12.16. Pulmonary vein wedge injection with the capillary bed filling retrograde into a very diminutive left upper lobe artery (*arrow*) in a patient with complex pulmonary atresia/ventricular septal defect.

may be necessary (32). An end-hole catheter is advanced antegrade into the pulmonary vein, typically through the patent foramen or atrial septal defect. With free flow of blood upon drawing back on the syringe, a 5- to 12-mL syringe containing 1 to 4 mL of contrast (0.3 mL/kg, maximum 4 mL) is held in vertical position and a small amount of blood is drawn into the syringe. The contrast forms a separate layer in the syringe below the blood and the pulmonary vein is occluded by advancing the catheter. The contrast and saline are slowly hand injected to backfill the pulmonary capillary bed and pulmonary artery (Fig. 12.16), continuously watching the

appearance of the vascular bed on the monitor. If the contrast is injected too rapidly, the capillaries may rupture into the airways, causing coughing and respiratory distress. On the other hand, if there is significant flow to that pulmonary artery from an aortopulmonary collateral vessel, visualization by a hand injection may be difficult and it may be necessary to balloon-occlude the collateral vessel during the vein wedge injection.

Selective Coronary Arteriography

In some pediatric patients, adequate imaging of the coronary arteries is achieved with an aortic root injection, or even a left ventriculogram. Indications for selective coronary angiography include a coronary artery fistula (including pulmonary atresia with intact ventricular septum), Kawasaki disease, heart transplant, and coronary ischemia (Fig. 12.17). Coronary catheter size refers to the diameter of curvature of its preformed distal end: a Judkins Left or JL-2 catheter is preformed to access the left coronary artery with a 2-cm diameter of curvature of the distal tip. The proper size catheter is a function of the aortic root diameter. Some pediatric patients who require selective coronary angiography (e.g., previous arterial switch procedure, heart transplant) have atypical locations of the coronary artery origins. Successful cannulation of the coronary arteries requires an understanding of the anatomy and choosing the appropriate catheter for this anatomy; often an aortic root injection will provide a good road map if there is difficulty with selective cannulation. When the aorta arises from the right ventricle (transposition of the great arteries), antegrade selective coronary angiography can be performed, but the retrograde approach is still preferred.

Definition of Aortopulmonary Collateral Vessels

In patients with obstructed pulmonary flow (tetralogy of Fallot, pulmonary atresia, complex single ventricle), accurate definition of the collateral supply to the pulmonary arteries is crucial prior to surgical or transcatheter intervention. Initially, an aortogram is performed to display all aortopulmonary collateral vessels. In an infant, this may be accomplished

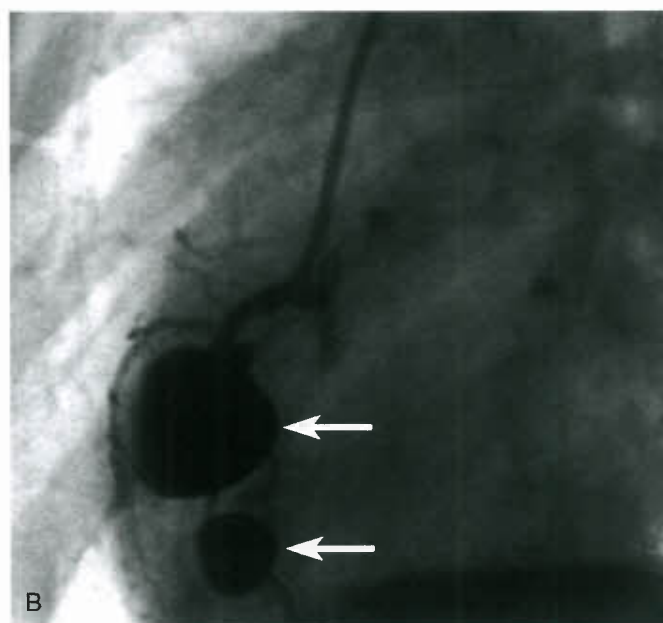
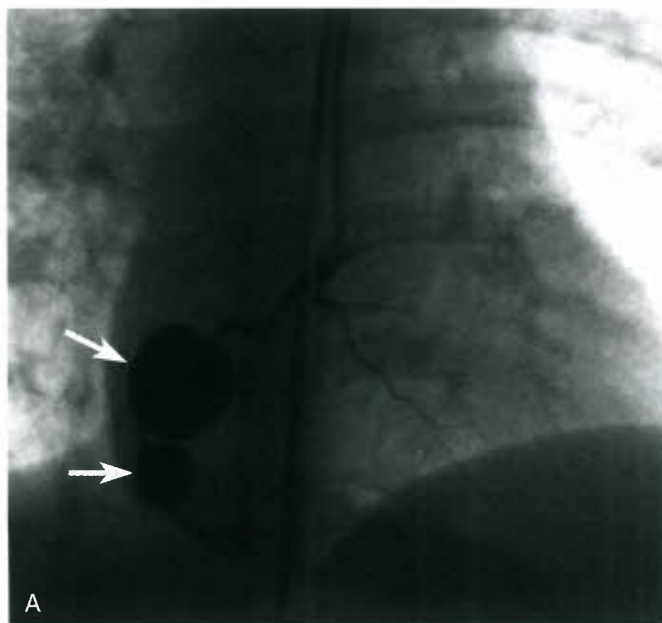


Figure 12.17. Selective coronary artery angiography in a patient with history of infantile Kawasaki disease and giant coronary aneurysms seen on echocardiography. A,B: Right coronary injection shows two large aneurysms (*arrow*).

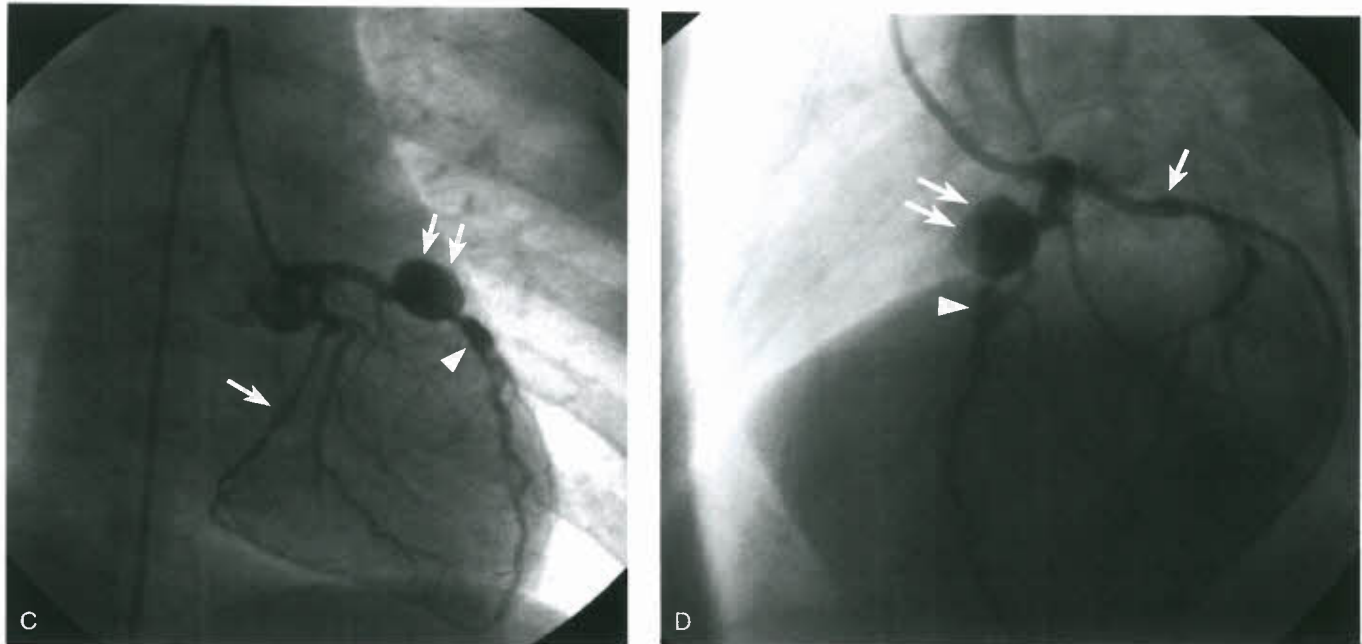


Figure 12.17. (Continued) C,D: Left coronary injection shows large proximal aneurysm in the left anterior descending branch (double arrow) with more distal smaller aneurysm (arrowhead); there is a small saccular aneurysm in the circumflex artery (arrow).

by an antegrade angiography (Fig. 12.18A), balloon-occlusion injection in the descending aorta (Fig. 12.18B), or with a retrograde aortic angiogram (Fig. 12.18C). Once the collateral vessels are identified, individual selective hand injections are typically performed in each of the collaterals, defining the

pulmonary segments supplied by the collateral and whether there is communication with the “true” pulmonary arteries (Fig. 12.18D). Aortopulmonary collateral or dilated bronchial vessels can occur in patients with transposition of the great arteries, although in most cases, they are of no physiologic

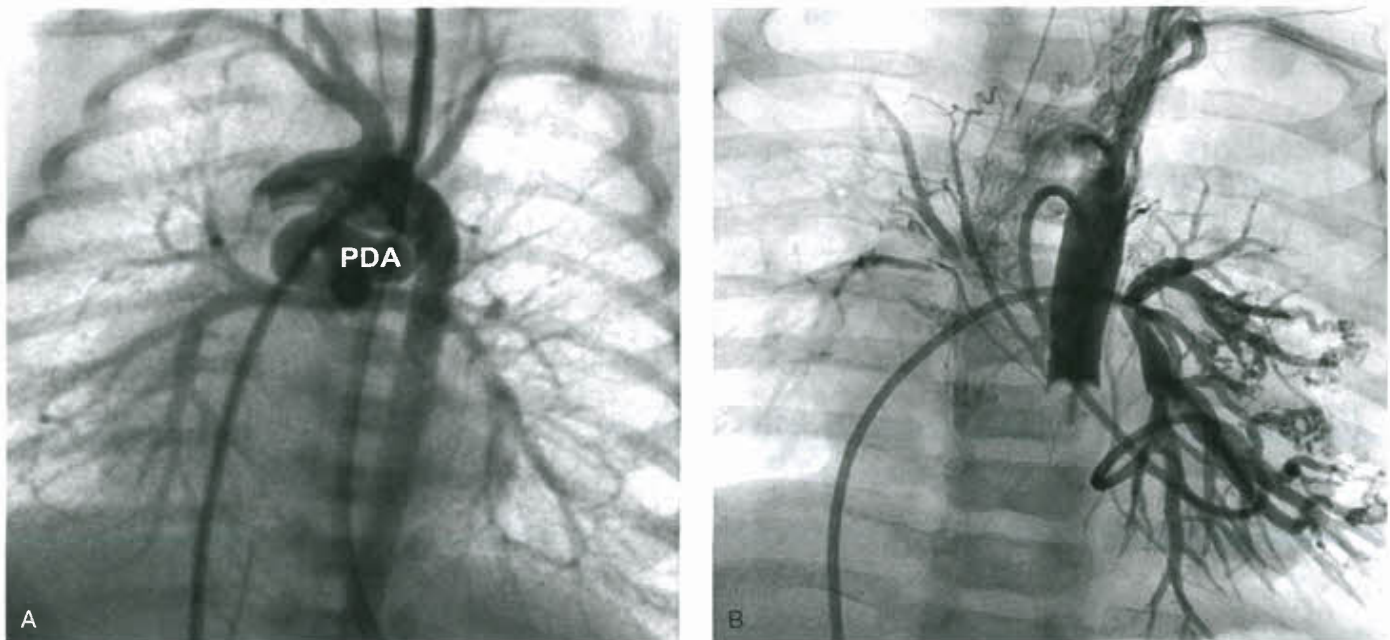


Figure 12.18. A: Antegrade angiography with catheter advanced from right ventricle into ascending aorta in an infant with tetralogy of Fallot/pulmonary atresia and a large tortuous patent ductus arteriosus supplying diminutive but confluent pulmonary arteries (subsequent angios, not shown, did not demonstrate collaterals). B: Balloon occlusion aortogram in an infant with very complex pulmonary atresia/intact ventricular septum/Alagille syndrome. Injection is performed with the catheter-advanced antegrade through the atrial septal defect, left ventricle, and aortic valve, with the catheter positioned just above the diaphragm. The balloon is inflated so that contrast fills the proximal descending aorta outlining the very complex collateral supply.

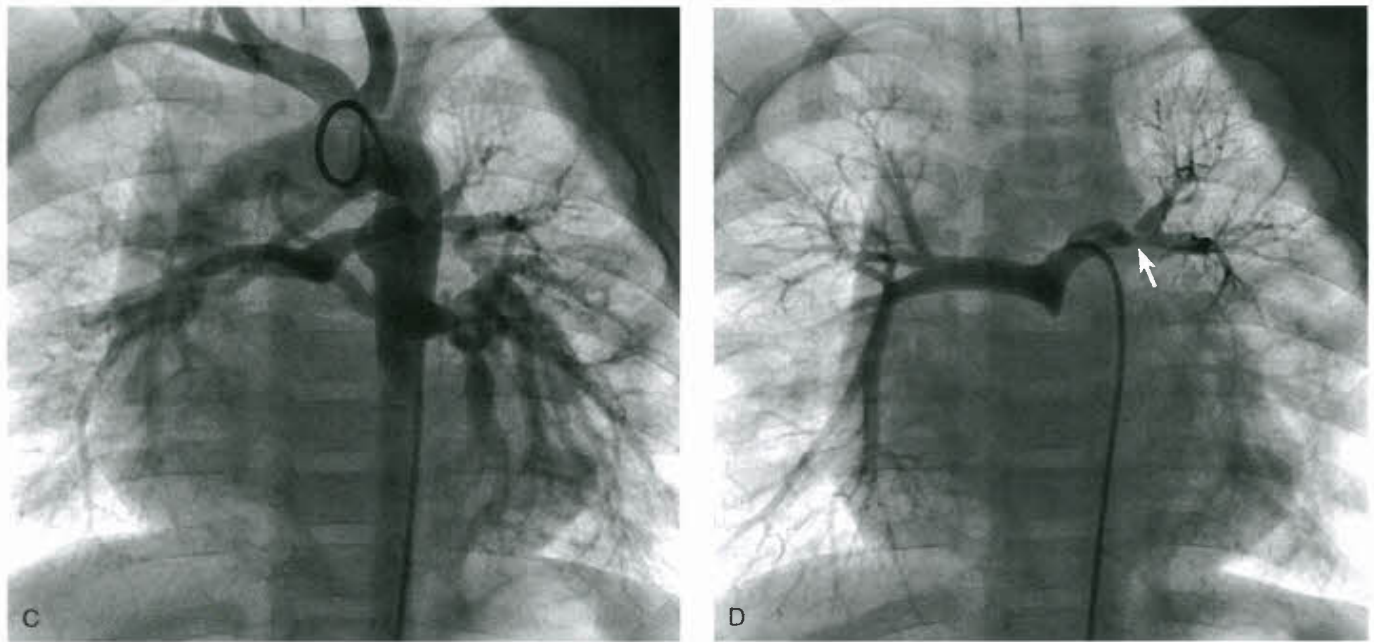


Figure 12.18. (Continued) C: Retrograde aortogram in complex pulmonary atresia/VSD provides a “road map” of the collateral vessels before selective angiography is undertaken. D: Selective hand injection with an end-hole catheter fills the true pulmonary artery confluence in this same patient (as in panel C).

significance; a descending aortogram should identify these vessels, which can then be selectively injected and potentially coiled if hemodynamically important (33).

Complications

Although patients referred for cardiac catheterization are now smaller and have more complex cardiac abnormalities, the procedure has become safer. Complication rates are higher for interventional procedures than diagnostic procedures and are more frequent in neonates and infants than older patients. The most common complication is related to vascular access (34). Mortality rates, currently reported at approximately 0.25% to 0.29%, are usually related to the severity of illness in this population (34,35).

Arrhythmias

Arrhythmias during cardiac catheterization are common and are usually related to catheter contact with the atrial wall or ventricular myocardium. Such benign arrhythmias resolve with catheter repositioning. Careful catheter manipulation and, in some lesions, using tip-deflector wires or balloon-tipped catheters to diminish irritation of the myocardium are helpful in avoiding arrhythmias. Catheter-induced atrioventricular block can easily occur in children with atrioventricular discordance (S, L, L), but can also occur in children with D-transposition of the great arteries (S, D, D) and tetralogy of Fallot, particularly during passage of a catheter from the right ventricle to the aorta. Atrioventricular block generally resolves spontaneously, but if prolonged or associated with hemodynamic compromise, temporary transvenous pacing may be necessary (34).

Hypoventilation

The combination of pharmacologic sedation and physical immobilization during cardiac catheterization may foster hypoventilation. In the current era, approximately

three-fourths of congenital cardiac catheterizations will be performed with general anesthesia, which minimizes these risks (35). Continuous pulse oximetry saturation monitoring, end-tidal CO₂ monitoring (in intubated patients), and arterial blood gas sampling all aid in assuring maintenance of stable airway status during the procedure. The position of the endotracheal tube should be checked during initial fluoroscopy. Regardless of whether conscious sedation or general anesthesia is utilized, careful attention to airway management is required in all cases.

Embolism

Although pulmonary or systemic emboli are rare during cardiac catheterization in children, the potential for an embolic event is real, and the results can be devastating. Air, thrombus, broken wires, or catheters all can embolize. Conditions that increase the risk of an embolic event include the use of large sheath size (particularly when placed in the left heart or with a right-to-left shunt), cyanosis with erythrocytosis or anemia, and prolonged catheter manipulation in the ascending aorta or transverse arch. Precautions that decrease the risk of an embolism include systemic heparinization (50 to 100 U/kg as an initial bolus dose with appropriate monitoring of the activated clotting time according to locally available assays), frequent aspiration and flushing of catheters, use of carbon dioxide to inflate balloon catheters, and positioning the arterial catheter distal to the brachiocephalic vessels.

Cardiac Perforation

Improved catheter technology and better noninvasive definition of the cardiac anatomy have resulted in fewer complications, including cardiac perforation. The most common sites of cardiac perforation are the atrial appendages (especially if the heart is viewed in only one plane), the right ventricular outflow tract of small infants, the right ventricle during endomyocardial biopsy (particularly in smaller children with myocarditis), the left ventricular apex, and the aortic valve cusps.

Pushing a wire or Brockenbrough needle through the wall of the heart usually does not cause a problem as the puncture site is very small; however, passage of anything larger (e.g., dilator, catheter, sheath) through the atrial wall is likely to require surgical repair. Perforations in the ventricle are more likely to seal over without needing surgery.

When hypotension occurs during or shortly after cardiac catheterization, cardiac perforation resulting in tamponade must be considered. An echocardiogram should be obtained immediately. Fluoroscopically, there are two clues to alert the staff about a pericardial effusion: an enlarged cardiac silhouette with absent movement of the cardiac silhouette. Therefore, it is important to know the cardiac size, shape, and motion prior to starting the catheterization. When cardiac perforation occurs, initial treatment includes removal of the catheter and observation. Any coagulopathy should be corrected. If clinically indicated, pericardiocentesis is performed and a pericardial drain (pigtail catheter) is placed. By connecting a stopcock and sterile IV tubing to the pericardial drain, the blood can be reinfused into a venous catheter to aid in maintaining hemodynamic stability while monitoring the rate of persistent bleeding closely. If there is continued accumulation of pericardial blood, surgical repair should be immediately arranged.

Hypercyanotic Episode

Despite appropriate precautions (hydration, sedation, careful catheter manipulation), infants and children with tetralogy of Fallot and some forms of double-outlet single ventricle with infundibular pulmonary stenosis are at risk for a hypercyanotic episode ("tet spell") during or shortly after cardiac catheterization. This complication occurs more frequently in small, cyanotic infants. Often, thorough echocardiographic assessment will have determined much of the anatomy, leaving one or more specific remaining questions to be expeditiously answered during catheterization (e.g., coronary artery anatomy, distal pulmonary artery anatomy, additional ventricular septal defects, and collateral vessels). If possible, avoiding deliberate catheter manipulation across the tightly stenotic pulmonary outflow tract may lessen catheter-induced hypoxemia. Increasing cyanosis, fluctuating arterial oxygen saturations, metabolic acidosis, all can be indications of an impending hypercyanotic episode. Appropriate treatment includes administration of volume (saline, or red blood cells if very anemic), IV phenylephrine or other peripheral vasoconstrictors, sodium bicarbonate (for acidosis), and intubation (if not already performed). General anesthesia can be helpful but may not "break" a hypercyanotic episode in a patient who was consciously sedated for the procedure.

Patient with Pulmonary Vascular Disease

It has been long documented that there is an increased risk associated with cardiac catheterization in patients with markedly elevated pulmonary vascular resistance (36). The periprocedural mortality has been reduced significantly by advances in airway management, sedation, and pharmacologic management of pulmonary hypertension, in addition to a safe procedure carried out by a team of experienced pediatric cardiologists and cardiac anesthesiologists. Indications for catheterization include baseline hemodynamic evaluation, assessment of pulmonary reactivity using pharmacologic agents, and uncommonly, potential for intervention to create an atrial septal defect. In most cases, pulmonary artery angiography should be avoided, as it could precipitate acute, sometimes fatal, pulmonary artery vasoconstriction.

Peripheral Vascular Injury

Vascular complications are among the most common complications following congenital cardiac catheterization (34). Factors contributing to peripheral vascular injury include small vessel size (in infants), large catheter or sheath size, multiple previous entries into the vessel, multiple catheter exchanges, and improper technique for achieving vascular access or hemostasis. Measures that reduce the incidence and severity of peripheral vascular injury should include attention to the following: skilled percutaneous access, use of ultrasound to visualize the vascular structures, use of finely tapered sheaths and dilators over appropriate-sized wires, systemic heparinization, and efficient execution of the procedure minimizing the time catheters are in the vessel (37). At the end of the procedure, the catheters and sheaths should be aspirated to remove any thrombus and then removed, allowing the vessel to bleed back briefly. Hemostasis is achieved by applying pressure with one or two fingers cephalad to the site of percutaneous entry, which should be at the site of entry into the vessel. Routine use of sandbags or mechanical devices to apply pressure to percutaneous sites is contraindicated in pediatric catheterization procedures.

After a diagnostic catheterization, pulse loss is rare. Even in small infants, the use of a 3 Fr pigtail catheter tapered to a 0.021-in wire should allow a safe retrograde arterial catheterization (although the catheter flow rate is low). When loss of a pulse occurs, heparin is continuously infused until the pulse returns or for 12 to 24 hours. There is likely a component of arterial spasm, and heparin may prevent thrombus formation at the site of spasm. If the pulse does not return, treatment with a thrombolytic agent may be instituted unless contraindications are present (38,39).

Latex Allergy

Latex allergy can result in a wide range of symptoms, from contact urticaria to life-threatening anaphylaxis. Overwhelming anaphylaxis generally occurs during surgery and results from patient exposure to surgical latex gloves. This problem has occurred in patients who previously had minor symptoms caused by contact with latex (38). However, there have been no reports of anaphylaxis from the use of intravascular latex catheter balloons. For any patient with any history of latex allergy undergoing cardiac catheterization, standard institutional protocols for latex precautions should be observed.

ACKNOWLEDGMENT

The authors wish to acknowledge previous authors of this chapter, Drs. Ronald G. Grifka, Nancy D. Bridges, Michael P. Freed, Martin P. O'Laughlin, and Charles E. Mullins. Many of their initial contributions remain as core information in this chapter.

Textbook References That Exclusively Discuss Cardiac Catheterization, Angiography, and Intervention

1. Mullins CE. *Cardiac Catheterization in Congenital Heart Disease: Pediatric and Adult*. Malden, MA: Blackwell Publishing, 2006.
2. Lock JE, Keane JF, Perry SB. *Diagnostic and Interventional Catheterization in Congenital Heart Disease*. 2nd ed. New York: Springer Publishing, 2000.
3. Freedom RM, Mawson JB, Yoo SJ, et al. *Congenital Heart Disease: Textbook of Angiocardiography*. Malden, MA: Blackwell Publishing, 1997.
4. Baim D. *Grossman's Cardiac Catheterization, Angiography, and Intervention*. 7th ed. Philadelphia, PA: Lippincott Williams & Wilkins, 2005.

REFERENCES

- Forssmann W. Die sondierung des rechten herzen. *Klin Wochenschr* 1929;8:2085–2087.
- Barger LM Jr, Elliott LP, Soto B, et al. Axial cineangiography in congenital heart disease. Section I. Concept, technical and anatomic considerations. *Circulation* 1977;56:1075–1083.
- Elliott LP, Barger LM Jr, Bream PR, et al. Axial cineangiography in congenital heart disease. Section II. Specific lesions. *Circulation* 1977;56:1048–1093.
- Lock JE, Keane JF, Fellows KE. *Diagnostic and Interventional Catheterization in Congenital Heart Disease*. Boston, MA: Martinus Nijhoff, 1987.
- Iwashima S, Ishikawa T, Ohzeki T. Ultrasound-guided versus landmark-guided femoral vein access in pediatric cardiac catheterization. *Pediatr Cardiol* 2008;29:339–342.
- Chuan WX, Wei W, Yu L. A randomized-controlled study of ultrasound prelocation vs anatomical landmark-guided cannulation of the internal jugular vein in infants and children. *Paediatr Anaesth* 2005;15:733–738.
- Hosokawa K, Shime N, Kato Y, et al. A randomized trial of ultrasound image-based skin surface marking versus real-time ultrasound-guided internal jugular vein catheterization in infants. *Anesthesiology* 2007;107:720–724.
- Roth B, Marciniak B, Engelhardt T, et al. Anatomic relationship between the internal jugular vein and the carotid artery in preschool children—an ultrasonographic study. *Paediatr Anaesth* 2008;18:752–756.
- Wigmore TJ, Smythe JF, Hacking MB, et al. Effect of the implementation of NICE guidelines for ultrasound guidance on the complication rates associated with central venous catheter placement in patients presenting for routine surgery in a tertiary referral centre. *Br J Anaesth* 2007;99:662–665.
- Shim D, Lloyd TR, Cho KJ, et al. Transhepatic cardiac catheterization in children. Evaluation of efficacy and safety. *Circulation* 1995;92:1526–1530.
- Shim D, Lloyd TR, Beekman RH III. Transhepatic therapeutic cardiac catheterization: a new option for the pediatric interventionalist. *Cathet Cardiovasc Interv* 1999;47:41–45.
- Johnston TA, Donnelly LF, Frush DP, et al. Transhepatic catheterization using ultrasound-guided access. *Pediatr Cardiol* 2003;24:393–396.
- Ebeid MR. Transhepatic vascular access for diagnostic and interventional procedures: techniques, outcome, and complications. *Cathet Cardiovasc Interv* 2007;69:594–606.
- Yang SS, Bentivoglio LG, Maranhao V, et al. *From Cardiac Catheterization Data to Hemodynamic Parameters*. 2nd ed. Philadelphia, PA: FA Davis Co., 1978.
- Gorge G, Erbel R, Niessing S, et al. Miniaturized pressure-guide-wire: evaluation in vitro and in isolated hearts. *Cathet Cardiovasc Diagn* 1993;30:341–347.
- Everett AD, Matherne GP. Feasibility of pulmonary artery pressure measurements in infants through aorto-pulmonary shunts using a micromanometer pressure wire. *Pediatr Cardiol* 2003;24:336–337.
- Fick A. Über die messung des blutquantums in den herzventrikeln. *Sitz der Physik-Med Ges Wurtzberg* 1870:16.
- Ganz W, Donoso R, Marcus HS, et al. A new technique for measurement of cardiac output by thermodilution in man. *Am J Cardiol* 1971;27:392–396.
- LaFarge CG, Miettinen OS. The estimation of oxygen consumption. *Cardiovasc Res* 1970;4:23–30.
- Freed MD, Miettinen OS, Nadas AS. Oximetric detection of intracardiac left-to-right shunts. *Br Heart J* 1979;42:690–694.
- Wagner WW Jr. Capillary recruitment in the pulmonary microcirculation. *Chest* 1988;93:855–885.
- Vargo TA. Cardiac catheterization: hemodynamic measurements. In: Garson A, et al., ed. *The Science and Practice of Pediatric Cardiology*. 2nd ed. Baltimore, MD: Williams & Wilkins, 1998:961–993.
- Hill KD, Lim DS, Everett AD, et al. Assessment of pulmonary hypertension in the pediatric catheterization laboratory: current insights from the Magic registry. *Cathet Cardiovasc Interv* 2010;76:865–873.
- Gorlin R, Gorlin SG. Hydraulic formula for calculation of the area of the stenotic mitral valve, other cardiac valves, and central circulatory shunts. I. *Am Heart J* 1951;41:1–29.
- Bettmann MA. Radiographic contrast agents—a perspective. *New Engl J Med* 1987;317:891–893.
- Mullins CE. *Cardiac Catheterization in Congenital Heart Disease: Pediatric and Adult*. Malden, MA: Blackwell, 2006.
- Moore R. *Imaging Principles of Cardiac Angiography*. Queenstown, MD: Aspen, 1990.
- Onnasch DG, Schroder FK, Fischer G, et al. Diagnostic reference levels and effective dose in paediatric cardiac catheterization. *Br J Radiol* 2007;80:177–185.
- Justino H. The ALARA concept in pediatric cardiac catheterization: techniques and tactics for managing radiation dose. *Pediatr Radiol* 2006;36:146–153.
- Hirshfeld JW Jr, Balter S, Brinker JA, et al. ACCF/AHA/HRS/SCAI clinical competence statement on physician knowledge to optimize patient safety and image quality in fluoroscopically guided invasive cardiovascular procedures. A report of the American College of Cardiology Foundation/American Heart Association/American College of Physicians Task Force on Clinical Competence and Training. *J Am Coll Cardiol* 2004;44:2259–2282.
- Taussig H. *Congenital Malformations of the Heart*. New York: The Commonwealth Fund, 1947.
- Nihill MR, Mullins CE, McNamara DG. Visualization of the pulmonary arteries in pseudotruncus by pulmonary vein wedge angiography. *Circulation* 1978;58:140–147.
- Wernovsky G, Bridges ND, Mandell VS, et al. Enlarged bronchial arteries after early repair of transposition of the great arteries. *J Am Coll Cardiol* 1993;21:465–470.
- Mehta R, Lee KJ, Chaturvedi R, et al. Complications of pediatric cardiac catheterization: a review in the current era. *Cathet Cardiovasc Interv* 2008;72:278–285.
- Bergersen L, Marshall A, Gauvreau K, et al. Adverse event rates in congenital cardiac catheterization—a multi-center experience. *Cathet Cardiovasc Interv* 2010;75:389–400.
- Keane JF, Fyler DC, Nadas AS. Hazards of cardiac catheterization in children with primary pulmonary vascular obstruction. *Am Heart J* 1978;96:556–558.
- Freed MD, Keane JF, Rosenthal A. The use of heparinization to prevent arterial thrombosis after percutaneous cardiac catheterization in children. *Circulation* 1974;50:565–569.
- Sussman GL, Tarlo S, Dolovich J. The spectrum of IgE-mediated responses to latex. *JAMA* 1991;265:2844–2847.
- Wessel DL, Keane JF, Fellows KE, et al. Fibrinolytic therapy for femoral arterial thrombosis after cardiac catheterization in infants and children. *Am J Cardiol* 1986;58:347–351.

Ralf J. Holzer ■ John P. Cheatham

Catheter-based techniques, whether palliative or corrective, are now the accepted therapy for many congenital cardiac defects. Interventional or, better termed, therapeutic catheterizations were initiated by Dotter and Judkins (1), who first reported the treatment of peripheral vascular lesions during a catheterization in 1964, when they dilated a stenotic peripheral vessel through a cut-down on the vessel. The next major innovative accomplishment and the first intracardiac therapeutic catheterization procedure for pediatric congenital heart disease (CHD) was the balloon atrial septostomy (BAS) done by Rashkind and Miller (2) in 1966. This procedure really “set the stage” for all therapeutic catheterization procedures used today. In 1968, Porstmann et al. (3) reported the first non-surgical corrective procedure in the catheterization laboratory with their description of a technique for closure of a patent ductus. Vascular occlusion coils were introduced by Gianturco et al. (4) in 1975, and in 1976, King et al. (5) were the first to describe the closure of atrial septal defects (ASDs) in the catheterization laboratory. Even though their device has not found widespread use, it set the stage for future development of transcatheter devices. One of the largest contributions to interventional cardiology has probably been made by Gruentzig, a Swiss native who in 1976 reported on dilation of peripheral vessels with noncompliant balloons. This initiated a rapid innovative spurt within the congenital cardiac community during which narrowed lesions at various locations were treated with balloon angioplasty, frequently initially in a noncontrolled fashion. In 1982, Dr. Jean Kan (6) reported the first successful transcatheter static balloon pulmonary valvuloplasty (BPV) and Dr. James Lock et al. (7) in 1988 used the clamshell device to occlude a ventricular septal defect (VSD) using a percutaneous approach. Dr. Charles Mullins introduced endovascular stents into the management of patients with congenital cardiac lesions (8), and the long list of innovations reached another milestone when Dr. Phillip Bonhoeffer et al. (9), a German cardiologist working in France in 2000, performed the first transcatheter pulmonary valve replacement in a human. Transcatheter valve therapies and other interventional therapies to treat patients with structural heart disease have rapidly increased over the past few years. Another milestone was reached when the Melody valve (Medtronic, Minneapolis, MN) gained Food and drug administration (FDA) Humanitarian device exemption (HDE) approval in January 2010. These therapies are not limited anymore to patients with CHD. In fact, transcatheter aortic valve implantations in adults have overtaken transcatheter valve therapies in the congenital population, with several thousands of implantations of the CoreValve (Medtronic, Minneapolis, MN) in adults having been performed thus far.

In this section, the most important therapeutic catheterization procedures performed as of this writing are discussed. This chapter is not intended as a complete and exhaustive textbook of interventional techniques, but instead should give the reader a general overview of therapeutic catheterization.

It should be emphasized that not every pediatric cardiologist, or, for that matter, every center, should offer every therapeutic catheterization procedure. For any procedures to be performed at any particular institution, minimal specific skills are required, special techniques must be mastered and maintained, and a large inventory of specialized and expensive catheters and devices must be stocked to offer the patient an optimal procedure. Absence of appropriate qualifications and equipment can result in unnecessary risk to the patient without a reasonable chance of the therapeutic catheterization procedure being successfully accomplished. In fact, even if the patient is not acutely harmed by the attempt, it is important to be aware of the fact that the next procedure in a more appropriate setting might be compromised by a previously unsuccessful attempt.

We have used and expanded upon this chapter published in other editions of this textbook and therefore acknowledge the previous contributions made by Drs. Nancy Bridges, Martin O’Laughlin, Charles Mullins, and Michael Freed.

ADVERSE EVENTS AND QUALITY IMPROVEMENT

For many years, reporting of procedure-related adverse events was limited mostly to single-center retrospective experiences, often without any clearly and consistently applied criteria of what would be considered an adverse event, and how its severity should be defined (10–12). Over the years, several multi-center registries have captured procedural outcomes including efficacy and occurrence of adverse events, which included the Valvuloplasty and Angioplasty of Congenital Anomalies (VACA) registry, Mid-Atlantic Group of Interventional cardiology (MAGIC), and Congenital Cardiovascular Interventional Study Consortium (CCISC) (13–15). The data derived from these registries often provided the only prospective multicenter outcome data for many types of procedures.

A more systematic capture of procedure-related adverse events was accomplished recently through the Congenital Cardiac Catheterization Project on Outcomes (C3PO) multi-institutional registry (16), using definitions for event severity and preventability as defined in the International Pediatric Congenital Cardiology Code nomenclature (17). This registry documented not insignificant rates of adverse events, 10% for diagnostic cases and 20% for interventional procedures. Higher severity (level 3 to 5) adverse events occurred in 9% of interventional cases and 5% of diagnostic cases.

However, to accurately compare adverse event rates and outcome between institutions and operators, an adjustment for case mix and hemodynamic vulnerability is required. Using consensus-based and empirical methods and methods derived from the C3PO dataset, Bergersen et al. (18) recently reported on

procedure-type risk groups, separating different types of diagnostic and interventional procedures into four different risk groups, ranging from diagnostic procedures performed in patients over 1 year of age (Risk Group 1) to balloon angioplasty of four or more pulmonary artery branches (Risk Group 4).

Following the definition of procedure-type risk groups, Bergersen et al. reported on hemodynamic variables associated with vulnerability for AE, which were determined based on an empirical analysis of the C3PO data set. The combination of variables that were identified to offer the best predictive performance for high severity adverse events included systolic main PA pressure ≥ 45 mm Hg (two-ventricle) or mean PA pressure ≥ 17 mm Hg (single-ventricle), systemic ventricular end-diastolic pressure ≥ 18 mm Hg, mixed venous saturations $< 60\%$ (two-ventricle) or mixed venous saturation $< 50\%$ (single-ventricle), and systemic saturations $< 95\%$ (two-ventricle) or $< 78\%$ (single-ventricle) (19,20).

However, incidence of adverse events and efficacy of an interventional procedure do not exclusively depend on patient-specific characteristics and procedure type. In fact, Holzer et al. (20,21) found that operator experience of < 10 years was an important independent risk factor for procedure-related higher severity adverse events for both pulmonary artery rehabilitation and BPV.

These various quality improvement efforts have culminated in the development of Improving Pediatric and Adult Congenital Treatment Registry and National Cardiovascular Data Registry, which were designed to capture all catheterization procedures performed nationwide within the United States in pediatric and adult patients with CHD. While the registry is only in its first year of data collection, hopefully it will eventually allow operators and institutions to compare performance objectively on a national level (22).

THE INTERVENTIONAL ARMAMENTARIUM

General Considerations

The spectrum of transcatheter procedures available for the treatment of children and adults with CHD has rapidly increased over the last three decades. While the technical skills of the operator combined with a sound anatomic and hemodynamic understanding of a patient's condition remain without a doubt the most important ingredients for the successful outcome of an interventional catheter procedure, the choice of the appropriate equipment is almost equally important for a successful outcome. With rapid progress that is being made in the development of new and more refined equipment, the operator has an inherent responsibility to keep up-to-date with these development efforts and to avoid procedural failures in situations where the use of a different type of equipment may lead to a very different outcome. Even though most interventional meetings center on new device developments, the choice of appropriate balloons, catheters, sheaths, and wires is in many situations even more important for a successful outcome. It is beyond the scope of this discussion to describe all available balloon catheters, but operators have to make a well-informed decision on which balloon to use based on profile, rated maximum pressure, available lengths, and degree of compliance and adjust their choices to suit specifically the therapeutic intervention that is intended. For example, balloon-in-balloon (BIB) catheters (NuMED, Hopkinton, MA) are specifically suited for stent deployment, but the family of high-pressure Mullins balloons (NuMED, Hopkinton, MA) or ultrahigh-pressure Atlas balloons (Bard Peripheral Vascular, Inc., Tempe, AZ) aid exquisitely when high-pressure balloon angioplasty or stent re-expansion to a larger diameter is required.

Even though transcatheter devices have long been available for the management of congenital cardiac lesions, the greatest progress has been made through introduction of a large variety of newer devices that were specifically developed for individual congenital cardiac lesions over the past 10 years. This progress has enabled many procedures to be safely performed in a much wider range of clinical centers. In this chapter, a variety of device-specific sections have been taken with permission from an article on this topic that was published in "Expert Review of Medical Devices" (23).

The following discussion is centered on transcatheter devices that are presently approved or investigated within the United States and includes a discussion of devices available for occlusion of septal defects as well as occlusion of vascular structures. The spectrum of devices that is discussed below is not intended to be complete, but rather represents subjective choices of the authors.

Devices for Occlusion of Septal Defects

The development of transcatheter devices for the occlusion of septal defects has been progressing at a rapidly accelerating pace, ever since King et al. (5) first described a percutaneous technique to close ASDs. Various devices are presently approved by the FDA, either for regular use or under a HDE, while others are presently being evaluated in phase I and II clinical trials. Even though devices are usually developed to address a specific type of septal defect, it is not uncommon that they are also used for occlusion of other types of defects on an "off-label" basis, once regular premarket approval (PMA) has been obtained.

The AMPLATZER Septal Occluder (ASO) gained FDA approval in December 2001 for occlusion of secundum ASDs as well as fenestrations after surgical completion of a Fontan-type circulation. It is presently the most frequently used transcatheter device for occlusion of septal defects within the United States and worldwide. Modifications of the principle device design have since been developed to accommodate the specific requirements of patent foramen ovale (PFO) (AMPLATZER PFO Occluder), multifenestrated ASD (AMPLATZER Cribiform Septal Occluder), muscular VSD (AMPLATZER Muscular VSD Occluder), perimembranous VSD (AMPLATZER Membranous VSD Occluder), and postmyocardial infarction VSD (AMPLATZER Muscular VSD (Postmyocardial Infarction) Occluder), most of which are presently undergoing or have just completed phase I or phase II FDA-sponsored clinical trials. The AMPLATZER Muscular VSD Occluder is approved for use in "high-risk" muscular VSDs. Figure 13.1 shows the family of AMPLATZER devices. (All of these devices are manufactured by AGA Medical Corporation, Golden Valley, MN.)

The CardioSEAL ASD occlusion device (Nitinol Medical Technologies, Boston, MA) was developed as a successor to the Clamshell device. At the same time as the ASO was approved, the CardioSEAL device gained regular use approval by the FDA for occlusion of "high-risk" muscular VSDs, under a registry requirement. Furthermore, it gained HDE approval for occlusion of PFO in patients with associated recurrent stroke who were taking therapeutic Warfarin. A self-centering modification of the CardioSEAL device, the STARFlex Occluder had been evaluated for the treatment of PFO and stroke (CLOSURE I) but is no longer marketed (24,25).

Another device that has recently acquired FDA PMA for the occlusion of ASD is the HELEX Septal Occluder (W.L. Gore & Associates, Flagstaff, AZ) (26). A variety of other devices have been used outside the United States but have not gained FDA approval (27–30).

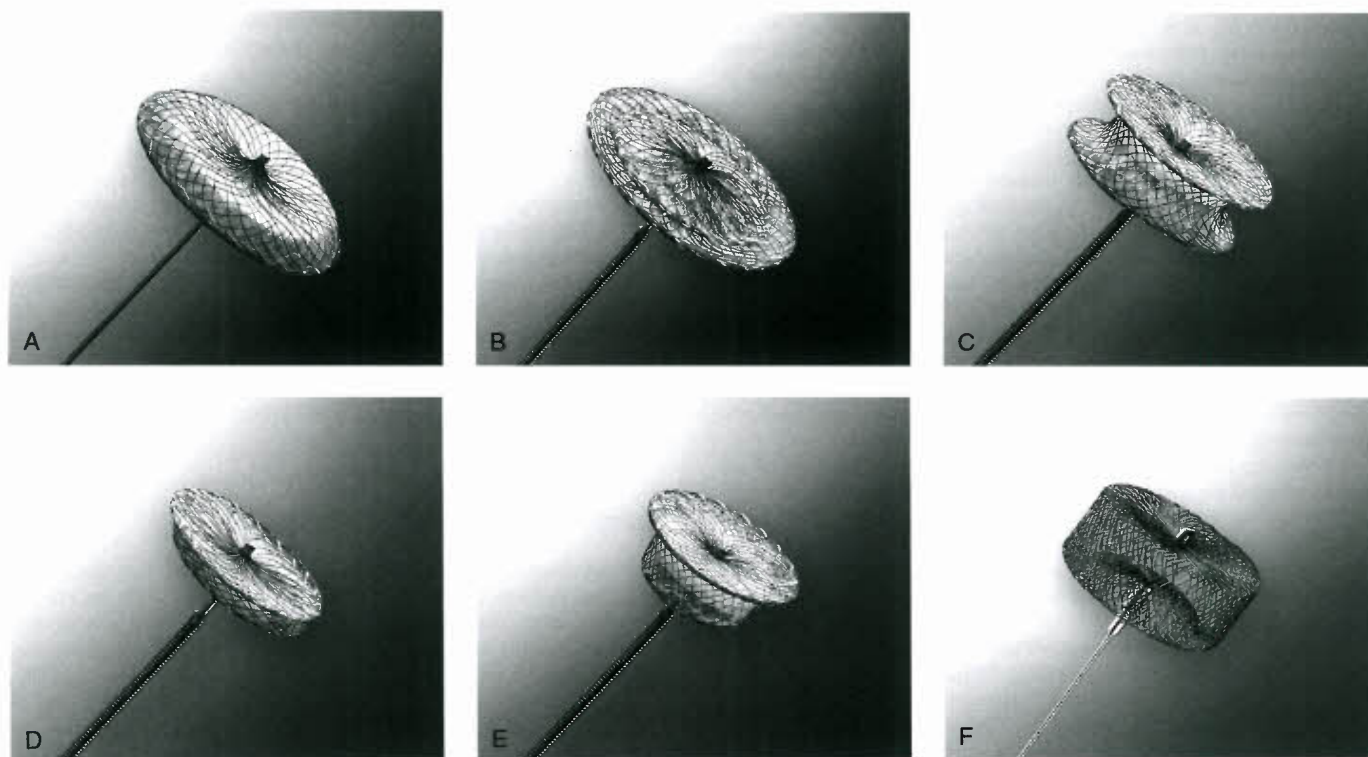


Figure 13.1. AMPLATZER Devices. (A) AMPLATZER Septal Occluder, (B) AMPLATZER PFO Occluder, (C) AMPLATZER Muscular VSD Occluder, (D) AMPLATZER Membranous VSD Occluder, (E) AMPLATZER Duct Occluder, and (F) AMPLATZER Vascular Plug. The images were provided by AGA Medical Corporation, Golden Valley, MN.

AMPLATZER Septal Occluder

The ASO, first described in 1997, is a double-disc device formed of 0.005-inch Nitinol mesh (31,32). It consists of two discs that are linked to each other through a central connecting waist. Dacron fabric is incorporated into each disc as well as the connecting waist to enhance thrombosis. The device size is defined by the diameter of the connecting waist and is available in sizes from 4 to 38 mm. A 40-mm device is available outside the United States. The connecting waist has a length between 3 and 4 mm with the diameter of the left atrial disc exceeding the connecting waist by 12 to 16 mm, while the diameter of the right atrial disc exceeds the connecting waist by 8 to 10 mm.

AMPLATZER Cribriform Septal Occluder

A device that is less frequently used, the AMPLATZER Cribriform Septal Occluder, has very specific characteristics that make it an excellent choice for closing multifenestrated ASDs. The device was introduced in 2003 and has recently gained FDA PMA after completing phase II clinical US trials (33). Its design resembles the AMPLATZER PFO Occluder, with the notable exception of both discs being equally sized. It is available in sizes of 18, 25, and 35 mm diameter. The thin central connecting waist allows a much larger area of the device to be available to cover the atrial septum when compared to the ASO, while at the same time avoiding any septal distortion through the central connecting waist. This not only makes it an excellent choice for multifenestrated ASDs but it also allows stabilization of an associated aneurysmal atrial septum. However, placement of the device through the most central defect is important and therefore high-quality transesophageal

echocardiography (TEE) or intracardiac echocardiography (ICE) guidance is imperative to achieve the desired result.

AMPLATZER PFO Occluder

The design of the AMPLATZER PFO Occluder, albeit similar to the ASO, accommodates very specific morphological characteristics of the PFO. Similar to the ASO, the PFO Occluder is a double-disc device formed of 0.005-inch (18- and 25-mm device) or 0.006-inch (35-mm device) Nitinol wire mesh. However, it is non-self-centering and consists of two discs that are linked to each other through a central connecting waist, with Dacron fabric being incorporated into each disc. The connecting waist is thin with a length of 3 mm, thereby accommodating the tunnel-type morphology of a PFO without distorting the atrial septal anatomy. In contrast to the ASO, the right atrial disc is equal or larger in size than the left atrial disc. The device is available in three size configurations of right and left atrial disc: 18/18 mm (18-mm device) (34), 25/18 mm (25-mm device), and 35/25 mm (35-mm device). The relatively large size of the discs in relation to the connecting waist makes this device particularly useful to flatten any coexisting atrial septal aneurysm. Its clinical use was first described in 2000 by Waight et al. (35). The device has investigational device exemption approval and is being evaluated in the RESPECT trial.

AMPLATZER Muscular VSD Occluder

The AMPLATZER Muscular VSD Occluder was added to the interventional armamentarium in 1999 (36,37). Similar to most AMPLATZER devices, it is a double-disc device made of 0.0005-inch Nitinol mesh wire. Both discs are equal in size and exceed the diameter of the central connecting waist by

8 mm. Dacron fabric is incorporated into both discs as well as the central connecting waist, which has a length of 7 mm to accommodate the increased septal thickness of muscular VSD. This determines the size of the device, which is available from 4 to 18 mm.

AMPLATZER Muscular VSD (Postmyocardial Infarction) Occluder

The AMPLATZER Muscular VSD (Postmyocardial Infarction) Occluder was first described in 2003 in a small series by Goldstein et al. (38). It was developed as a modification of the AMPLATZER Muscular VSD Occluder to take account of the increased septal thickness in adults. It is a double-disc device made of 0.0005-inch Nitinol mesh wire. The discs are symmetrical and slightly larger than those of the muscular VSD device and exceed the connecting waist by 10 mm. The length of the central connecting waist is 10 mm, which is longer than the waist of the muscular VSD Occluder. The device is available in sizes from 16 to 24 mm. Similar to the muscular VSD device, Dacron fabric is incorporated into both discs and the central connecting waist.

AMPLATZER Membranous VSD Occluder

The inherent morphological and anatomical characteristics of perimembranous VSD in the past have resulted in suboptimal outcomes of attempts at percutaneous device closure (39). The AMPLATZER Membranous VSD Occluder is the first device that has been specifically designed for occlusion of these defects. It was first described in a natural swine model in 2000 with Hijazi et al. (41) reporting the first clinical experience in 2002 (40).

In contrast to other AMPLATZER devices, the Membranous VSD Occluder is an asymmetrical double-disc device made of 0.004-inch Nitinol wire mesh. The asymmetrical left-ventricular disc exceeds the central connecting waist at the superior, aortic end by just 0.5 mm and at the inferior, apical end by about 5.5 mm. A platinum marker is incorporated into the apical end of the left ventricular (LV) disc to aid device positioning. In contrast, the right ventricular (RV) disc is symmetrical in relation to the connecting waist and exceeds its diameter by a total of 4 mm. The connecting waist has a length of just 1.5 mm and the device is available with the diameter of the connecting waist ranging from 4 to 18 mm.

HELEX Septal Occluder

The HELEX Septal Occluder was first described by Zahn et al. (26) in 2001. Its frame is made of a long Nitinol wire, with a strip of polytetrafluoroethylene (PTFE) fabric attached alongside. Three “eyelets” are embedded along the device to facilitate accurate positioning, one at each end and one in central position between both discs. In its deployed status, the device forms two circular discs that are composed by the spiraling Nitinol wire with its attached PTFE membrane. The device is available in sizes from 15 to 35 mm (diameter of discs) in 5-mm increments with a device to defect ratio of 1.7 to 2:1 being recommended. When compared to the ASO, this device has a lower profile and a more atraumatic contour. It is delivered through a 9 Fr catheter, rather than relying on a long sheath. Its also creates less distortion of the atrial septum prior to its release.

Devices for Occlusion of Vascular Structures

Porstmann et al. (3) introduced a technique of transcatheter closure of the ductus arteriosus in 1968. The procedure was complicated and required a large arterial cannulation and as a result, this technique never found widespread use.

Rashkind and Cuaso, while still working on the septostomy balloon, also developed a device for closure of the patent ductus. This device was a small umbrella that attached to the ductus by tiny hooks at the ends of the umbrella arms. The first successful use of this early device was reported in 1979 (42). It was modified into a double umbrella that is fixed in the ductus by a spring mechanism of the arms expanding against the vessel walls. Even though the device had undergone extensive trials, resulting in more than 700 prospectively monitored patent ductus arteriosus (PDA) occlusion procedures performed in the United States, it never quite made it to regular use approval (43,44). However, the extensive experience gained in this process formed the basis upon which virtually all subsequent devices have been developed.

A large variety of devices have been developed to facilitate occlusion of vascular structures. Embolization coils have been used by general interventional radiologists for almost three decades (4). However, it was not until the 1980s that these were introduced into the interventional armamentarium of the pediatric cardiologist, initially for occlusion of abnormal collateral vessels (45) and subsequently in 1992 for the occlusion of patent arterial ducts in children (46). Gianturco coils are available in a variety of sizes but the lack of a controlled release mechanism ultimately stimulated the development of Jackson coils, which are presently only available outside the United States (47), and its US counterpart, the Flipper coil (Cook, Bloomington, IN). An MRI compatible modification of the Gianturco and Flipper coil, the MRye coil (Cook, Bloomington, IN) was introduced in 2006 and has since evolved as the most commonly used coil to date, mainly due to the notably lower incidence of MRI artifact (48).

Even though coils were and still are used “off-label” for the occlusion of the patent arterial duct, it was not until 2003 that a custom-made device designed specifically for the occlusion of the PDA gained FDA PMA (49). The AMPLATZER Duct Occluder (ADO) (AGA Medical Corporation, Golden Valley, MN), which was first introduced into clinical use in 1997, has since remained the only device approved specifically for this indication (49). However, a modification of the device, the ADO II (AGA Medical Corporation, Golden Valley, MN) is presently undergoing phase II clinical trials in the United States (50–52). In addition, the Nit-Occlud PDA occlusion device (pfm AG, Cologne, Germany), a modification of the Duct-Occlud device, has undergone phase II clinical trials with promising results (53,54). An additional “coil modification,” the Gianturco-Grifka Vascular Occlusion Device (GGVOD) (Cook, Bloomington, IN) has gained FDA approval, even though its cumbersome delivery technique has prevented its widespread use. A large variety of additional coils is available for regular use, such as Target coils (Target therapeutics, Fremont, CA), Tornado coils (Cook, Bloomington, IN), and Nester coils (Cook, Bloomington, IN). However, these are less frequently used in congenital cardiac interventions and therefore are not discussed further in this chapter.

Further additions to the interventional armamentarium include the AMPLATZER Vascular Plug, which was first described in 2003. It has since acquired regular use approval for peripheral arterial and venous embolizations (55). A modification, the AMPLATZER Vascular Plug II (AGA Medical Corporation, Golden Valley, MN) has since gained PMA approval. Other devices are available internationally, but not approved in the United States.

AMPLATZER Duct Occluder and Duct Occluder II

The ADO was first introduced into clinical use in 1997 (49). It is, at present, the most commonly used device to close medium- or larger-sized PDA. The device is mushroom-shaped and made of 0.005-inch Nitinol wire mesh. The central skirt of the device is cone-shaped with the pulmonary end being

about 1 to 2 mm smaller than the aortic end. A microscrew for attachment of the delivery cable is recessed into the pulmonary end of the device. The device is further expanded at the aortic end through a symmetrical retention disc, in which the diameter exceeds the size of the aortic end of the skirt by about 4 to 6 mm. Dacron fabric is incorporated into the retention disc and the skirt. The size of the device, defined by a combination of the diameters at aortic and pulmonary end of the skirt, is available from 5/4 to 16/14 mm. The total length of the device ranges from 5 to 8 mm.

The ADO II was first described in 2009, and is presently undergoing phase II clinical trials within the United States (50–52). In contrast to the standard Duct Occluder, the ADO II is a double-disc device with a central connecting waist. The connecting waist has a length of either 4 or 6 mm and a diameter between 3 and 6 mm. The two discs exceed the diameter of the connecting waist by 6 mm. The device is made from triple layered mesh of braided 144 Nitinol wire and does not incorporate any polyester fabric. Due to its symmetric shape, it can be delivered antegrade as well as retrograde, using 4 or 5 Fr delivery catheters.

AMPLATZER Vascular Plug and Vascular Plug II

The use of the AMPLATZER Vascular Plug in transcatheter therapy of congenital cardiac lesions was first reported in 2003 (55). The device is cylindrical in shape and formed of 0.0015- to 0.003-inch 144 Nitinol wire mesh. It is available in diameters from 4 to 16 mm in 2-mm increments, with a device length of 7 to 8 mm. In contrast to other AMPLATZER devices, Dacron fabric is not incorporated into the device.

The AMPLATZER Vascular Plug II is a modification of the standard vascular plug, consisting of three segments instead of just one. It is made of a triple layered mesh of braided 144 Nitinol wire and is available in diameters from 3 to 22 mm. The device can be delivered through 5 to 9 Fr Guide catheters. The Plug II has shown excellent occlusive properties, even for higher flow arterial structures that could not be occluded with the standard vascular plug (56,57).

Embolization Coils

Stainless steel coils for embolization of vascular structures have been introduced in the early 1970s (4) and have since undergone few modifications. At present, “Gianturco” embolization coils (Cook, Bloomington, IN) are made of stainless steel spring wire (0.004 to 0.008 inch) with synthetic Dacron fibers being added for increased thrombogenicity. Each extended spring coil has a stiffening “core” wire that facilitates the forming of a coil of variable length and diameter, once the extending forces are removed. The coils are delivered in their extended length, requiring delivery catheters of 0.025, 0.035, 0.038, or 0.052 inch, depending on the size of the spring coil. The coils are available in diameters between 2 and 15 mm and a length that allows formation between 1.1 to 5.3 loops. Even though the 0.035- and 0.038-inch varieties are most frequently used, 0.025- and 0.052-inch coils have maintained their usefulness for very specific occasions. The detachable Flipper coil (Cook, Bloomington, IN) is a variation of the standard 0.035-inch Gianturco coil and includes a controlled release mechanism. It became available in the United States in 2001. However, early versions of this coil lacked thrombogenic Dacron fibers, and the 0.035 coil remains less robust than the 0.038 inch standard Gianturco coil (58). Modifications of the standard Gianturco and the Flipper coils were first described in 2008 (48). These coils include the MRye coil and the MRye Flipper coil (Cook Medical, Bloomington, IN), which are made of MRye super alloy with a very similar design to the standard coils. However, the MRye coil is only available in the 0.035- and 0.038-inch varieties.

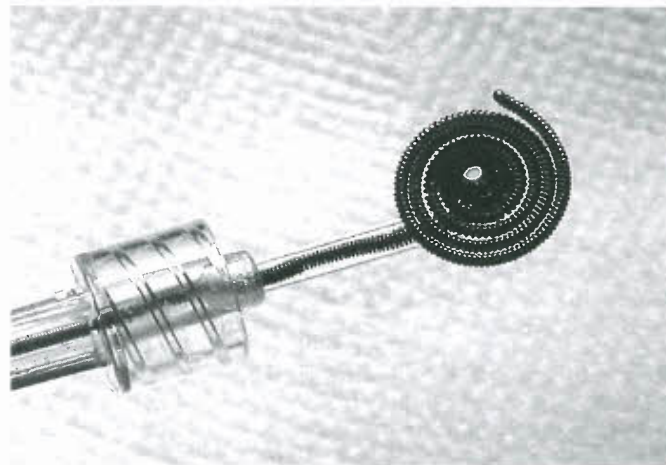


Figure 13.2. Nit-Occlud PDA occlusion system. The image shows the aortic spiral disc with the device still attached to the delivery system.

Nit-Occlud

The Nit-Occlud PDA occlusion system, developed as a successor to the Duct-Occlud device, was introduced in 2001. The device is made up of wound 0.01 inch Nitinol wire, which forms a secondary helix-type loop, thereby conforming to a “double opposing cone” shape (Fig. 13.2) (53,54,58). The device has reinforced distal windings at the aortic end that prevent it from pulling through the PDA, while tighter and softer central windings allow the device to conform to the narrow portions of the PDA at the pulmonary end, thereby allowing more efficient occlusion of the duct. No fabric is attached to the device, with occlusion being facilitated through the metal windings alone. The device is available in three principal versions, the Nit-Occlud Flex, the Nit-Occlud Medium, and the Nit-Occlud Stiff, which differ from each other through an increasing stiffness. The devices are available in various dimensions, with the distal (aortic) diameter ranging from 4 to 14 mm, while the proximal pulmonary winding diameter ranges from 4 to 6 mm. A phase II clinical trial evaluating the Nit-Occlud has been completed in the United States and results are expected soon.

Other Devices and Device Modifications

In 1995, Grifka et al. (59) reported on the evaluation of a new vascular occlusion device in a canine model. The “Gianturco-Grifka Vascular Occlusion Device” is essentially an oblong nylon bag that is filled with a long, stainless steel spring guide-wire. The length of the wire determines the size of the device, which is available in diameters of 3, 5, 7, and 9 mm. A radio-opaque marker is attached to the proximal end of the bag. The GGVOVOD has been used to occlude a variety of tubular structures, including shunts and pulmonary AVMs, but its design and cumbersome delivery technique make it less suitable for occlusion of the standard type A PDA (58,60,61).

In addition to the aforementioned, a wide variety of devices has been used “off-label” to occlude the patent arterial duct and other vascular communications, including the AMPLATZER Muscular VSD Occluder (62), the AMPLATZER Septal Occluder (63), the buttoned device (64), and the AMPLATZER Vascular Plug (55).

Endovascular Stents

Charles E. Mullins, MD pioneered the introduction of endovascular stents into the armamentarium of the congenital

cardiac interventionalist in the late 1980s and early 1990s (8,65). The most common indications for stent placement include rehabilitation of branch pulmonary artery stenosis as well as treatment of primary and recurrent coarctation of the aorta or aortic arch obstructions. However, stents are also used to rehabilitate stenotic lesions in systemic and pulmonary veins and to maintain patency of structures that would otherwise close, such as the arterial duct or a foramen ovale. Endovascular stents are particularly helpful in locations that are either inaccessible to surgical techniques or where the scarring resulting from surgical intervention is unlikely to achieve an improvement of the lesion, which applies to thin-walled vessels such as distal pulmonary arteries or pulmonary veins.

Virtually all approved stents that are used in the US in transcatheter therapy of congenital cardiovascular lesions have not been designed specifically for these indications and are therefore used on an “off-label” basis. The choice of which stent to use for a particular lesion depends not only on age and size of the patient but also on expected adult dimensions of the vascular structure that is being treated, the morphology of the specific lesion, the presence of side branches that need to be crossed, expected future surgical procedures as well as previous surgical, and transcatheter procedures and their outcome.

An ideal stent would combine a variety of characteristics that are often exclusive to each other and may require opposing design goals:

- Low profile that allows introduction through small delivery sheaths.
- Easy crimpability or availability as premounted stents.
- Possibility for re-expansion with maximum achievable diameter being sufficient to accommodate the growth of a vessel to adult size.
- High degree of flexibility for placement around curved structures.
- Allow rehabilitation of vessels that are overlapped by the placed stent through the stent meshwork/cells (e.g., open cell design).
- High radial force to accommodate very tight and scarred lesions.
- Rounded atraumatic edges that avoid damage to the vessel and the balloon upon which it is mounted.
- Nonexisting or low degree of stent-shortening during expansion.
- Stent material that is MRI compliant, noncorrosive, and does not lead to increased blood levels of metal.
- Low risk of neointimal proliferation, possibly through internal coating.
- Possibility of biodegradable material with a platform to sustain drug coating to minimize tissue reaction.

Unfortunately, the ideal stent does not exist; therefore, a careful decision has to be made on which to use. Dr. Charles Mullins always emphasized that the interventional cardiologist should not create a later surgical stenosis by failure of the stent to be able to be dilated to the adult-sized diameter of the vessel. However, it is important to note that the use of premounted and smaller diameter stents as a “palliative” procedure to relieve critical vascular narrowing in small infants and children, who will have later surgery as a “staged repair” or conduit change, is now a very important treatment option. When judging the suitability of stent implantation, one always has to remember that suboptimal balloon angioplasty may result in impaired interval growth of the pulmonary arterial tree. Furthermore, recent studies have shown that small diameter stents can be intentionally fractured when necessary with the use of high-pressure balloons (66). In addition, surgeons are well equipped to excise or patch a stent when necessary (67).

Table 13.1 summarizes the most important characteristics of those larger diameter stents that are presently most frequently used in treatment of CHD in the United States. The Cheatham-Platinum (CP) stent (NuMED, Hopkinton, NY), as well as its covered variety, is available in the United States for compassionate and investigational use (COAST II trial) only, but is approved outside the United States as the only stent specifically approved for the treatment of CHD,

TABLE 13.1 Stents

Name (Manufacturer)	Material	Max Diameter (mm)	Available Length (mm)	Profile	Radial Force	Flex	Short	Nontraumatic Edges	Crimp	Cells
Genesis XD (Cordis)	Stainless steel	18	19, 25, 29, 39, 59	+	+	0	–	0	++	Closed
Palmaz XL (Cordis)	Stainless steel	25+	31, 40, 50	–	++	–	–	–	+	Closed
IntraStent DoubleStrut LD (EV3)	Stainless steel	18	16, 26, 36, 56, 76	+	–	++	++	+	0	Open
Mega LD (EV3)	Stainless steel	18	16, 26, 36	0	+	++	++	+	0	Open
Max LD (EV3)	Stainless steel	25	16, 26, 36	–	++	+	++	+	–	Open
Cheatham Platinum 8z (NuMED)	Platinum/ Iridium + Gold	25	22–45	–	++	0	–	++	+	Closed

Characteristics of the most commonly used endovascular stents in CHD (United States). Manufacturers listed are Cordis (Cordis, Warren, NJ), EV3 (EV3, Plymouth, MN), and NuMED (NuMED, Hopkinton, NY). The table describes various stent characteristics, ranging from “–” (poor stent characteristic) to “++” (excellent stent characteristic). Max, Maximum; Flex, Flexibility; Short, Stent shortening; Crimp, Crimpability; Cells, Open or closed cell design.

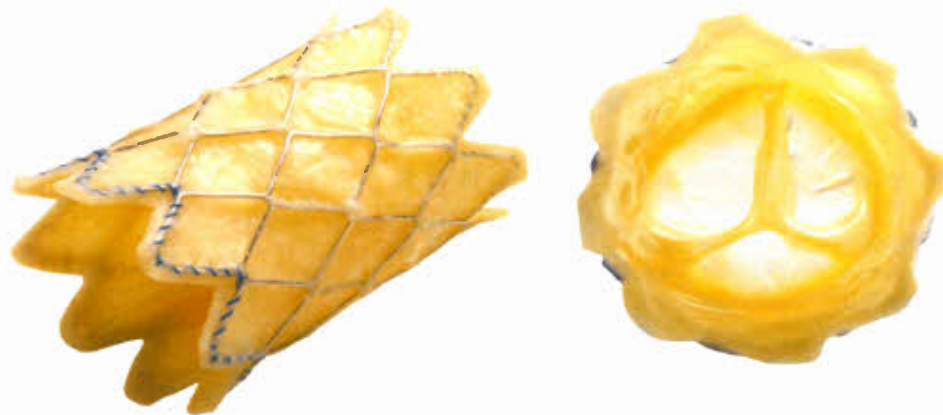
and has favorable design characteristics for the use in native and recurrent coarctation. Covered stents are especially useful for the treatment of ruptured vessels, including aortic aneurysms. Even though the early versions of the Palmaz stent (P108, P188, and P308) (Johnson & Johnson, Warren, NJ) as well as the “ITI Double Strut” and “Double Strut LD” stent (Intra Therapeutics, Inc., St Paul, NM) are still available, they have largely been replaced by the Genesis XD stents (Cordis, Warren, NJ) as well as the EV3 Mega LD and Max LD stents (EV3, Plymouth, MN), and are therefore not listed in this summary. Smaller diameter stents that are used in the congenital pediatric population include self-expandable Nitinol stents, the premounted Palmaz Blue stents (Cordis, Warren, NJ), the premounted Cook Formula 418 stents (Cook, Bloomington, IN), and various coronary stents.

The use of intravascular stents has provided a definitive solution to the problem of overdilation that is frequently required when performing standard balloon angioplasty. There has been extensive favorable experience and up to 15 years’ follow-up in patients with pulmonary artery branch stenosis and systemic vein stenosis. In the single-center series of Mullins and associates at Texas Children’s Hospital, more than 655 stents were implanted in 340 patients with pulmonary artery and systemic vein stenoses. The largest group of patients in this series had lesions involving the central pulmonary arteries in postoperative patients and postoperative central systemic vein or systemic venous baffle stenosis. Many of these stenotic veins had a totally occluded initial lumen; some of the venous channels were intentionally perforated with a wire or long needle. The mean vessel diameter increased from 5 to 12 mm, and there was lasting success, with <0.5% showing restenosis during the follow-up period. The number of complications from the procedure or the stents themselves was minimal.

Melody Valve

Since Dr. Phillip Bonhoeffer et al. (9) performed the first transcatheter pulmonary valve replacement in a human in 2000, more than a thousand of these procedures have been performed worldwide. In January 2010, the Melody valve (Medtronic, Minneapolis, MN) gained FDA HDE approval in the United States (68,69). Its use is indicated for dysfunctional right ventricular outflow tract (RVOT) conduits larger than 16 mm, even though the valve has also been used for other indications (70,71). The Melody transcatheter pulmonary valve is a bovine jugular venous valve that is sutured within an 8-zig, 28-mm Covered CP stent (Fig. 13.3). The valve is mounted on a 18-, 20-, or 22-mm BiB balloon, which is a part of the specifically designed Ensemble delivery system (Fig. 13.3).

Figure 13.3. Melody valve. Transcatheter pulmonary valve implantation. **Left:** Side view of the transcatheter bovine jugular venous valve mounted on a CP stent. **Right:** *En face* view of a bovine jugular venous valve mounted on a CP stent.



HOW TO CREATE, ENLARGE, AND MAINTAIN INTRA-ATRIAL COMMUNICATIONS

Balloon Atrial Septostomy

BAS, introduced by Rashkind and Miller (2) in 1966, is a life-saving procedure and one of the few remaining indications for an emergency catheterization in infants. BAS should be available in every institution that cares for infants with CHD. Because of septal thickening with age, BAS is consistently effective only in infants younger than 1 month of age. The BAS procedure is indicated in all infants with simple transposition of the great arteries (TGA) who are younger than 1 month of age with a restrictive intra-atrial communication, and not otherwise scheduled for immediate surgical correction. Emergency BAS is imperative in any infant with simple TGA who exhibits evidence of acidosis as a result of an inadequate intra-atrial communication. This procedure also may be indicated for palliation in other congenital heart lesions in equally young infants, in whom all systemic, pulmonary, or mixed venous blood must traverse through a restrictive intra-atrial communication to return to the active circulation. These lesions include complex single-ventricle defects associated with hypoplastic right or left ventricles and some instances of total anomalous pulmonary venous connection. BAS is rarely indicated in cases of pulmonary valve atresia and intact ventricular septum (IVS). It can be extremely hazardous in left-sided heart hypoplasia if the left atrium is diminutive, as there is a heightened risk of perforation or avulsion of atrial appendage or pulmonary vein. In such cases, static balloon dilation of the atrial septum may be preferable (72).

The preferable approach for performing a BAS is percutaneously through the femoral vein. In addition, BAS can be accomplished successfully using an umbilical venous approach. For acute, temporary palliation, many of these procedures can be performed under echocardiographic guidance in the neonatal intensive care unit, but whenever possible, the availability of fluoroscopy in the cardiac catheterization laboratory adds an additional safety margin to the procedure. BAS catheters are available from variety of manufacturers and in different designs. The classical Miller-Edwards balloon septostomy catheter (Edwards Lifescience, Irvine, CA) is a single lumen catheter with a fairly compliant latex balloon at the end, that is rated up to 4 mL capacity but can be inflated with larger quantities if required. It requires the use of a 7 Fr sheath and is still in widespread use, even though newer catheter varieties offer more favorable balloon characteristics. Because of the single lumen, it cannot be tracked over a wire and the fairly high compliance often requires large balloon inflations to successfully perform a septostomy, which is a considerable disadvantage especially in smaller infants under 3 kg. Other

catheter varieties include the USCI Rashkind balloon catheter (USCI, Glens Falls, NY), which have a 6 Fr shaft, and the newer NuMED Z5 atrioseptostomy catheters (NuMED, Hopkinton, NY) that are available on a 4 or 5 Fr shaft and can be passed through a 5 or 6 Fr introducer. These balloons have the advantage of being noncompliant at inflation volumes of 1 or 2 mL, which is very important when attempting to tear, rather than stretch the atrial septum. The balloons also have the additional benefit of being able to be passed over a wire.

Once the deflated balloon catheter is introduced into the venous system and while it is observed on fluoroscopy or by echocardiography, it is advanced through the right atrium and through the foramen ovale or small ASD into the left atrium. While continually observed on fluoroscopy and/or 2-D echocardiography, the balloon is inflated with dilute contrast to the maximum diameter of the balloon or, in the smaller atrium, to the maximum diameter tolerated within the particular left atrium. It is essential to determine that the balloon is completely free within the left atrium before initiating the “jerk” across the septum. Failure to do so can result in laceration or even separation of the left atrium from the pulmonary veins. The balloon is pulled rapidly or, better stated, “jerked” across the atrial septum into the right atrium using as forceful and rapid, but at the same time, as short and controlled a pull as possible. Especially when using the fairly noncompliant NuMED atrioseptostomy catheters, it is important to avoid pulling the balloons into the inferior vena cava (IVC), as the rapid “jerk” can easily create a laceration or disruption of the IVC–RA junction. The entire procedure should be performed one to four times or until no resistance to withdrawal of the fully inflated balloon is encountered or until enlargement of the defect and looseness or “flipping” of the septum primum tissue are documented by echocardiography. Following a successful septostomy, there should be an immediate equalization or near equalization of pressures across the atrial septum. Performed carefully with precise attention to details, the procedure carries only a small risk; yet it has the potential for a dramatic improvement in the infant's hemodynamic and symptomatic status.

Blade Atrial Septostomy and Balloon Atrial Septoplasty

In infants over 1 month of age, and certainly for older children who might require an atrial septostomy for palliation of their cardiac defect, the atrial septum usually is frequently too tough or thick for a simple BAS to tear the septum. In 1975, Park et al. introduced the Park Blade Septostomy Catheter (Cook, Inc., Bloomington, IN) and the blade atrial septostomy procedure to obviate this difficulty. A collaborative study from 1978 to 1982 (73) demonstrated the safety and effectiveness of the blade procedure. The indications for blade atrial septostomy are the same as considered for a balloon septostomy or for surgical atrial septostomy that otherwise would be needed in the older infant.

Blade catheters are available with three different blade lengths: 1.0, 1.34, and 2.0 cm. The two smaller blades (the PBS 100 and 200) are available on a 6 Fr catheter, and the 2.0-cm blade (the PBS 300) is on an 8 Fr catheter. Both blade catheter sizes require a sheath one size larger than the catheter shaft for smooth introduction.

The most consistent method of delivering the blade into the left atrium is to pass a long Mullins sheath over a catheter or dilator from the femoral vein through the right atrium, through the septum, (either through the PFO or through a transseptal puncture) into the left atrium. The blade catheter is advanced through this sheath, and the sheath is withdrawn well into the IVC. The blade is opened carefully in the left atrium while it is continuously observed on fluoroscopy. Transesophageal echocardiographic guidance can add an additional safety margin to this procedure.

The tip is directed anteriorly and to either the patient's right or left side. In contrast to the balloon septostomy, the blade catheter is withdrawn slowly in a controlled but at the same time, forceful maneuver until the blade snaps through the septum. The “blading” is repeated four to eight times while changing the angle of extension of the blade as necessary and changing the blade direction from side to side until there is no further resistance to the withdrawal of the fully opened blade catheter.

The blade septostomy is followed by a balloon septostomy. In most patients, this can be accomplished using the Rashkind balloon technique; however, in larger or older patients, when the septum is tough or resistant to tearing, the blade incision can be extended by the use of static dilation balloons placed in the defect and inflated. Alternatively, balloon dilation alone after transseptal placement of a guidewire can be effective in creating or enlarging an ASD. The resultant defect will be somewhat smaller than the balloon or balloons used for dilation, so the balloon catheters must be oversized relative to the final defect diameter desired. As a result of the combined blade and ballooning, equalization of pressures between the two atria as well as a measurable increase in the mixing of the systemic and pulmonary venous blood should occur. In most cases, an adequate and permanent ASD is created, palliating the patient indefinitely or until a more permanent correction is possible. Stenting of the atrial septum has been performed in a few cases to ensure a lasting opening. The blade atrial septostomy can be accomplished in patients of any age or any size. Prior to the introduction of the transhepatic approach, congenital absence or acquired blockage of the IVC had been the only absolute prohibition to a blade atrial septostomy.

With the availability of larger cutting balloons of up to 8 mm in diameter (Boston Scientific, Boston, MA), the combination of static cutting balloon septoplasty, followed by the use of larger diameter static balloons or standard BAS, has become an important alternative to blade atrial septostomy in patients with a thickened atrial septum. The smaller the pre-existing septal defect, the higher the likelihood that the use of cutting balloon will achieve an adequate result (Fig. 13.4). This is especially important if the patient size is rather small making it prohibitive to use even a small PBS 100 blade catheter. If the existing intra-atrial communication is stretched, cutting balloon septoplasty may be unfeasible, and it may be more beneficial to perform a transseptal puncture to start with a “fresh” diminutive opening to facilitate a better result of cutting balloon atrial septoplasty. More technical details are provided in the section on Hybrid Palliation of Hypoplastic Left Heart Syndrome (HLHS), where atrial septal interventions are particularly important and challenging (72).

Transseptal Puncture

Access to left heart structures is required at times to obtain accurate left atrial pressure recordings or to facilitate interventional procedures such as the creation or closure of an intra-atrial communication or balloon mitral valvuloplasty (BMVP). In addition, access to left heart structures from a venous approach avoids the use of larger sheaths in the femoral artery, which can be especially beneficial in small children and infants. Most catheterization laboratories use the standard Brockenbrough transseptal needle, while the use of radiofrequency (RF) energy has added a more controlled technique specifically for infants with small left atria (74).

The Brockenbrough needle is available in sizes of 62 and 72 cm of usable length, and is usually used in conjunction with a transseptal Mullins introducer set (Cook, Bloomington, IN). A fairly stiff exchange length wire is placed in SVC or preferably innominate vein, and the Mullins sheath and dilator are advanced to a position within the SVC. The wire is withdrawn and the transseptal needle is advanced through the sheath to a

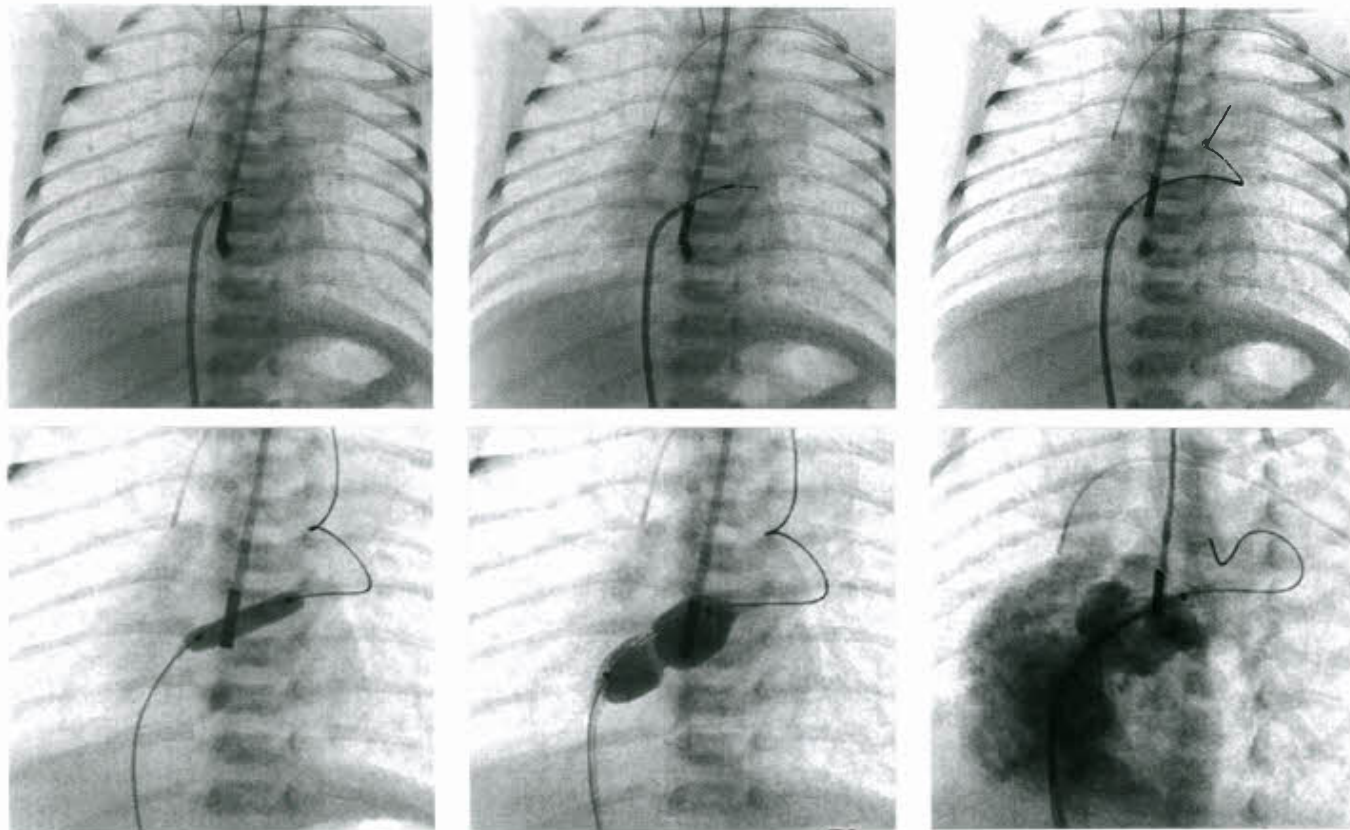


Figure 13.4. Septoplasty. RF perforation of the atrial septum followed by cutting and standard atrial balloon septoplasty in a 7-day-old infant with hypoplastic left heart syndrome, intact atrial septum, and a restrictive decompressing vein. Images (from left to right and top to bottom) demonstrate the RF wire across the atrial septum, the coaxial catheter advanced over the RF wire into the LA, and wire position through the coaxial catheter into the decompressing vein. Cutting balloon septoplasty is followed by standard balloon atrial septoplasty and final left atrial angiography demonstrating the newly created intra-atrial communication. An intracardiac echocardiographic probe is utilized in TEE position.

position just 1 to 2 mm below the tip of the dilator. On occasions, difficulty can be encountered when introducing the transseptal needle through the hub or dilator and sheath, at which point the two components should be separated temporarily by 1 to 2 cm to allow passage of the needle through the hub. Once the needle has been positioned appropriately, the whole system is flushed and the needle is connected to a pressure monitoring system. There is usually a 1- to 2-cm separation between the needle and the hub of the dilator and care must be taken to maintain this distance throughout the procedure. Needle, sheath, and dilator are then removed carefully as one unit with the system being gently pointed towards the patient's left scapula (and posterior) when withdrawing from the SVC and sliding along the atrial septum. Any harsh movement or torque should be avoided at this stage as it can create injury to adjacent vessel or chamber walls. Once the unit has passed about two-thirds of the atrial septal length inferiorly, one often notices the tip of the dilator suddenly moving slightly to the left while advancing into the fossa ovalis. At this stage, sheath dilator and needle are withdrawn inferiorly for a further few millimeters just below the limbus of the ovale fossa. The sheath and dilator are then fixed, while the needle is advanced slightly out of the tip of the dilator until it fully engages the dilator. At this point, the whole unit is advanced while carefully observing the recorded pressure tracing and maintaining a left and posterior direction. The operator usually feels a slight "pop" when the needle traverses the atrial septum and this should be

followed by the emergence of left atrial pressure tracing. If any untoward resistance or inappropriate pressure tracings appear, the operator should stop any advances of needle, sheath, and dilator. If a position is unclear, a small amount of contrast can be instilled through the needle.

If a left atrial pressure tracing is obtained, the entire system is advanced slightly further towards the patient's left to allow at least the proximal portion of the dilator to pass through the atrial septum. This is performed in very diminutive steps while maintaining careful observation for left atrial pressure tracings. At this point, the needle is withdrawn just inside the dilator to add additional stiffness to the system and the Mullins sheath is advanced over the dilator and needle across the atrial septum into the left atrium. If at any stage during the procedure, doubt about the accurate position occurs, the system is withdrawn in very small steps until either appropriate pressure recording reoccurs or a small amount of contrast confirms the sheath's location.

An alternative to the use of the classical Brockenbrough needle is the use of RF energy. At the present time, two techniques of RF perforation of the atrial septum are available, depending on patient's size and left atrial size. In larger patients, the Toronto transseptal catheter can be used in combination with the 8 Fr Torflex transseptal sheath and dilator (Both: Baylis Medical Corporation, Montreal, Quebec, Canada). The Toronto transseptal catheter is curved at the end by about 210 degrees to avoid continued perforation of adjacent structures once

the atrial septum is traversed. It also has a slightly increased stiffness when compared to the Nykanen RF perforation wire (Baylis Medical Corporation, Montreal, Quebec, Canada) that is specifically suited to allow tracking of the transseptal sheath across the perforated atrial septum. Initial positioning of the transseptal sheath is very similar to the Brockenbrough transseptal technique. However, instead of using a stiff and forceful needle to traverse the atrial septum, low-power and high-intensity electrical current is used to allow the transseptal catheter to advance through the atrial septum, usually with minimal force and a much lower risk of injuring adjacent structures.

In small infants, especially in neonates with a small left atrium, the curve of the Toronto transseptal catheter is too large to fit snugly into the small left atrium. Therefore, in these patients, a 5 Fr JR catheter is used to obtain an appropriate position along the atrial septum to facilitate RF puncture (Fig. 13.4). A 180-cm 0.035-inch outer diameter coaxial injectable catheter (Baylis Medical Corporation, Montreal, Quebec, Canada) is loaded over a 260-cm 0.024-inch Nykanen RF perforation wire and the RF wire is advanced to the tip of the positioned JR catheter. The use of TEE-guided perforation of the atrial septum has greatly improved the safety and success of this challenging procedure. In infants <3 kg, placing the 8 Fr ICE catheter (Acuson-Siemens Co., Mountain View, CA) transesophageally has been suggested by Hill et al. (75) as an additional form of guidance for the transseptal puncture. Once an accurate position is confirmed with hand injections of contrast through the side-port of a Touhy Borst adapter, RF energy is applied, while also exerting a gentle push on the RF wire. Once perforation has occurred, an orienting injection of contrast can be performed through the Touhy Borst adapter, before advancing the coaxial catheter over the RF wire across the perforated lesion. The RF wire is then exchanged to an appropriate exchange-length wire that can be preshaped according to the size of the left atrium. This positioned wire then facilitates cutting balloon septoplasty, possibly followed by BAS or standard septoplasty using larger balloon diameters, depending on the size of the intra-atrial communication that is required.

BALLOON AORTIC VALVULOPLASTY

The possibility of creating significant aortic regurgitation has always been the main concern when considering balloon dilation of congenitally stenotic aortic valves, especially in infants and small children. In 1984, Lababidi et al. reported for the first time on a series of 23 patients with congenital aortic valve stenosis, in whom the procedure was documented to be safe and effective (31). Despite this report, general acceptance of the technique was relatively slow. One of the fundamental problems of the procedure to this day remains the risk of creating significant aortic insufficiency, which then may accelerate the need for any surgical aortic valve procedure. While this is less of a concern in the adolescent, where all other treatment options are available in such a situation, problems are more significant in the infant who has a moderate degree of aortic valve stenosis, where severe aortic regurgitation may force a surgical procedure to be performed at an age where one would have otherwise preferably waited for the patient to grow.

Several other centers have demonstrated that the results of balloon aortic valve dilation approximated the results of surgical valvotomy but with less risk and less morbidity. However, the disease has very wide morphological variations, ranging from the critically ill neonate with borderline LV and left ventricular outflow tract size and a very dysplastic aortic valve to the young adult with isolated valvar stenosis and well-formed aortic valve.

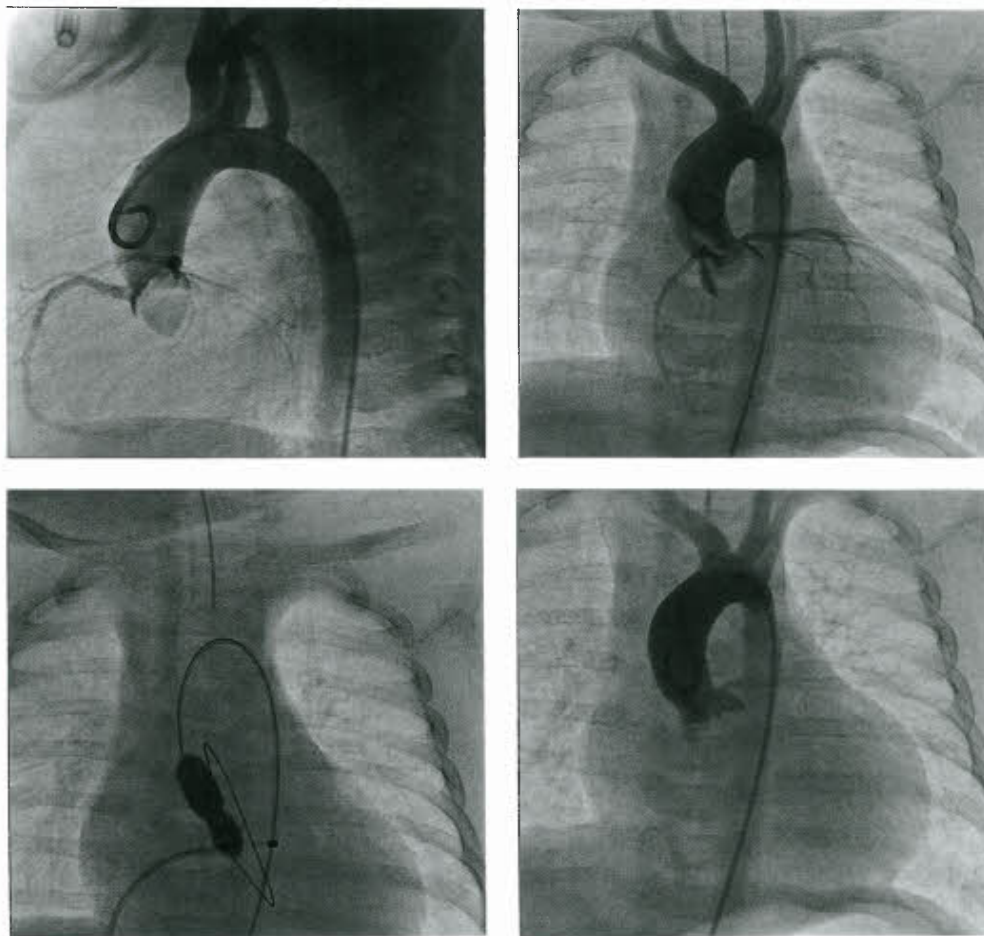
The decision when to take a patient with congenital aortic valve stenosis to the catheterization laboratory is not always straightforward. Many factors have to be considered including peak and mean Doppler gradients, age and gender, electrocardiogram (EKG) findings, LV function and degree of Left ventricular hypertrophy, symptoms, exercise tolerance, and desire to exercise competitively, valve morphology and preexisting aortic insufficiency, as well as associated lesions such as coarctation or mitral valve (MV) disease. Guidelines for the treatment of congenital aortic valve stenosis in children are derived from the adult population (76), where a peak-to-peak gradient in excess of 60 mm Hg in asymptomatic patients is considered an indication for transcatheter intervention. However, in symptomatic patients, or with the presence of ischemic or repolarization changes on EKG, a gradient of 50 mm Hg should be used. However, peak systolic gradients are only meaningful if LV function is normal. Documented aortic valve stenosis in the critically ill neonate with a dilated left ventricle and poor LV function is an indication for transcatheter intervention irrespective of any obtained transvalvar gradient.

Balloon aortic valvuloplasty is now considered a standard technique performed in virtually any center that offers interventional treatment for congenital cardiac lesions (Fig. 13.5). In contrast to BPV, where the vast majority of patients can be expected not to require any further transcatheter or surgical intervention, aortic valvuloplasty is usually palliative in nature, and not infrequently aimed at delaying an inevitable surgical procedure, be it valve replacement or Ross procedure, until a time when the child has reached close-to-adult size. A surgical series reporting the results of surgical aortic valvuloplasty documented freedom from aortic valve replacement (AVR) of 72% at 10 years and 60% at 18 years (77). This is very similar to the results of transcatheter aortic valvuloplasty where freedom from AVR of 79% at 10 years and 53% at 20 years has been reported (78).

In general, aortic valve dilation is performed retrograde with a catheter introduced into the femoral artery. While an antegrade approach with transseptal puncture offers a slight advantage in maintaining a centered balloon position across the aortic valve during balloon inflation, the technique is more cumbersome and is associated with risk of injuring the MV apparatus with resulting mitral insufficiency, and is therefore not routinely employed. An end-hole catheter is passed from the femoral artery across the aortic valve to a stable position in the left ventricle. A double-balloon technique with the introduction procedure repeated from both femoral arteries may offer advantages for the aortic valve dilation in selected older patients, even though today, the spectrum of available balloons usually allows a successful employment of a single-balloon technique.

The catheter/wire passage retrograde across the stenotic aortic orifice is the most difficult maneuver in the entire procedure, and therefore should ideally be performed only once during the procedure. Before crossing the aortic valve, an aortogram with 25 degrees left anterior oblique (LAO)/cranial angulation of the anteroposterior (AP) and straight lateral projection should initially be performed to exactly delineate the size of the aortic valve annulus, while at the same time demonstrating any angiographic evidence of preexisting aortic valve insufficiency. The exact technique for passing the wire or catheter into the left ventricle varies from operator to operator. A Judkins right coronary catheter curve or multipurpose catheter is used by some operators with success in crossing the aortic valve from this approach. However, the Judkins left coronary catheter may offer advantages in many patients, as the curvature is automatically directed to the leftward and posterior opening of the congenitally stenotic aortic valve. Once the valve is crossed, an end-hole catheter (not Judkins left) is advanced over the wire into the left ventricle, and the wire

Figure 13.5. Aortic valvuloplasty. Balloon aortic valvuloplasty in a 3-month-old infant with congenital aortic stenosis (Gradient: Pre: 92 mm Hg, Post: 25 mm Hg). **Top left and right:** Aortogram in lateral and AP projection profiling the doming aortic valve annulus. **Bottom left:** Balloon inflation centered across the aortic valve with concomitant rapid RV pacing for cardiac output control. **Bottom right:** Aortogram after balloon valvuloplasty documenting absence of aortic insufficiency.



replaced with an extra stiff exchange-length wire with a long floppy tip, which is looped within the ventricle to protect the ventricular apex from perforation by the catheter tip and to minimize ventricular ectopy. A LV angiogram is optional. If an atrial communication is present, hemodynamic evaluation can be performed by advancing a catheter antegrade into the left ventricle with simultaneous pressure recording in the ascending aorta. The same approach is then also used for LV angiography. In neonates and infants, a floppy-tipped coronary wire with a relatively stiff body may be advanced across the valve and allowed to loop in the left ventricle. Care has to be taken to prevent the wire from being ejected from the left ventricle and therefore, once positioned, wire control should be maintained throughout the procedure. By using a floppy-tipped, high-torque guidewire, the wire does not need to be changed, and the first catheter to cross the valve can be the dilation balloon (thus minimizing the period of potential low output). The use of stiffer exchange wires and longer dilation balloons may aid in maintaining an exact position of the balloons across the valve during inflation and, in turn, eliminate the "shear" trauma to the valve from balloon movement during inflation. With the wire secured within the left ventricle, the deflated balloon is manipulated through arterial sheaths and passed retrograde over the wire. We do not believe that direct introduction of the balloon through the skin should have any role to play, as the balloon profile of balloons has considerably decreased, thereby allowing the appropriately sized balloon to be introduced through fairly small sheaths. In addition, it is quite conceivable that the pulling of a deflated balloon directly through the femoral and iliac arteries may cause more harm

to the vessel than using the appropriately sized sheath. Once the balloon is positioned across the stenotic valve, the balloon is rapidly inflated to the recommended maximal pressure and then rapidly deflated.

One difficulty of the procedure is to keep the balloon positioned across the aortic valve during inflation. Once it is inflated, the balloon tends naturally to move towards the ascending aorta because of the ejecting forces created by the left ventricle. It is generally difficult to push against these forces (unless using an antegrade approach), but a longer balloon length aids this process. Adenosine has been used to achieve a temporary cardiac standstill, but its timing in relation to balloon inflation is often difficult to predict. A more controllable method of reducing the cardiac output is through rapid RV pacing (79). The rate of pacing can be adjusted prior to balloon inflation to achieve a drop in blood pressure by at least 50% and these settings are then available to be used during the inflation process. An inflation device that can be operated using a single hand is preferential, as this allows the operator to use the other hand to maintain control of the balloon catheter, making very fine adjustments while the balloon is inflated. The balloon is then immediately and rapidly deflated, with the entire process taking no more than 5 to 10 seconds. Arterial pressures should be monitored throughout the procedure. To limit the potential damage to the aortic valve, only one inflation should be performed provided that the operator is assured that (a) the balloon remained properly positioned in the valve; (b) the balloon was of adequate size; and (c) the waist disappeared. Regardless of the technique, a marked drop in systemic pressure, a rise in LV pressure, and resultant bradycardia may

transiently result. The double-balloon technique using two balloons placed side by side across the valve may minimize this problem, but more importantly one has to avoid prolonged inflations with any technique when performing aortic balloon dilations. With successful valve dilation, after the balloon is deflated, both the blood pressure and heart rate should return spontaneously to normal.

For a single-balloon technique, the initial balloon is chosen with a diameter of about 80% to 90% of the measured aortic annulus diameter. After each set of inflations, the hemodynamic result and the degree of aortic insufficiency are evaluated. If no or only a mild change in the degree of aortic insufficiency has been observed with still a significant residual gradient (>35 mm Hg), repeat dilation valvuloplasty is done with a balloon sized just 1 to 2 mm above the one previously used. Brown et al. (78) recently demonstrated that freedom from AVR was improved when comparing patients with a residual gradient of <30 mm Hg to those with a gradient in between 30 and 39 mm Hg. Even more importantly, freedom from AVR was better in patient with a gradient of <35 mm Hg and having moderate to severe aortic regurgitation. This compared to those with more than 35 mm Hg gradient but only mild aortic regurgitation suggests that the residual gradient may be more important when compared to aortic insufficiency than previously thought.

When using the double-balloon technique, the combined diameters of the two balloons should approximate 1.2 times the measured diameter of the aortic annulus. Because of the extensive manipulation in the left side of the heart and arteries, all these patients are systemically anticoagulated with heparin at the beginning of the procedure.

In the past, the most common complication of aortic balloon dilation was damage to the femoral arteries by the large balloon dilation catheters. This problem has been minimized by newer lower-profile balloon designs, use of the double-balloon technique where required, and diligent monitoring of ACT levels throughout the procedure. When arterial damage does occur, it usually can be managed medically or, rarely, surgically. In small infants, because of the increased risk of femoral artery injury from the introduction of the dilating balloon catheters into the vessels, several other approaches to aortic valve dilation have been described. The prograde approach, first passing a catheter, then a wire, and finally the balloon from the femoral vein to the right atrium, foramen ovale, left atrium, left ventricle, and prograde across the aortic valve is chosen by some. Although frequently successful, this approach has a high incidence of failure in delivering the balloons and, even more disturbing, a significant incidence of damage to the MV apparatus.

Another approach is through a controlled cutdown on the carotid artery. As a result of extensive experience with extracorporeal membrane oxygenation (ECMO) and the safe introduction of cannulae into the carotid arteries, several centers, with the help of pediatric or vascular surgeons, dilate aortic valves in infants from this approach. The approach is direct to the aortic valve, requires less catheter manipulation and less overall time, and has resulted in no reported complications related to the technique. The ideal procedure for the small infant is still to be determined.

With a conservative dilation of the aortic valve, the gradient should be reduced to a gradient ≤ 35 mm of Hg. This usually can be accomplished without inducing significant aortic insufficiency, no more than that seen after surgical valvotomy. Furthermore, as highlighted above, recent data by Brown et al. (78) suggest that the residual gradient may be more important when compared to aortic insufficiency than previously thought, and reducing the gradient to <35 mm Hg may be more important, even if it were achieved at the expense of moderate aortic insufficiency. However, the treatment approach has to

be tailored to the individual patient, and specifically in infants, gradient reductions to <40 mm Hg may be sufficient to delay the need for early aortic valve surgery. The long-term results, like those for surgical valvotomy, will be palliative; however, the catheter balloon dilation procedure is accomplished without a sternotomy or cardiopulmonary bypass with their inherent risks and morbidity. Balloon dilation of congenital aortic valve stenosis in pediatric patients and young adults is now the standard initial procedure for this lesion in most centers.

BALLOON PULMONARY VALVULOPLASTY

With the development of the special, larger-dilation balloons, a transcatheter technique for balloon pulmonary valve dilation was first introduced by Kan et al. (6) in 1982. The technique performed acutely was successful and, at the same time, carried little risk over and above the basic risk of a catheterization. By December 1986, 28 centers, voluntarily reporting to a collaborative registry (VACA), demonstrated the successful and safe application of the technique in more than 680 cases of pulmonary valve stenosis (80). With these data and many subsequent reports of successful use (81,82), balloon dilation has been accepted as the standard therapeutic procedure for pulmonary valvar stenosis. It is applicable to patients of all ages from the newborn period throughout adult life. With its excellent results and low rate of procedure-related complications, maximum instantaneous systolic Doppler gradients of as little as 35 mm Hg, when combined with evidence of RV hypertrophy, should be considered an indication for BPV (83).

The degree of pulmonary valve stenosis is documented by accurate hemodynamic measurements in the catheterization laboratory. However, if the pulmonary valve is not easily crossed, RV angiography should be obtained prior to further attempts at crossing the valve.

The valve anatomy, size, and exact location are visualized angiographically, with standard AP (with some cranial angulation) and lateral being the most appropriate projections. Accurate determination of the valve annulus diameter is obtained using appropriate calibration techniques. With this information available, a long exchange guidewire is passed through an end-hole catheter into a distal pulmonary artery. The left pulmonary artery (LPA) is preferable for this position because of the straighter course from the valve and main pulmonary artery (MPA) to the left. However, in neonates with a patent arterial duct, the wire may be passed through the duct into the descending aorta (DAO). The chosen wire should be fairly stiff to allow the balloon to track over the wire and across the stenosed pulmonary valve. In infants and smaller children, a stiff 0.018 wire with a floppy tip is frequently appropriate for this purpose. However, infants with critical pulmonary stenosis and a closed arterial duct may poorly tolerate placement of a wire or catheter across the valve; therefore, the valve should only be crossed when all equipment have been prepared to immediately proceed with BPV.

McCrindle (84) documented that the optimum balloon diameter should be between 1.2 and 1.3 times the size of the pulmonary valve annulus for a "single-balloon" dilation. Lower balloon to valve annulus ratios are associated with an increased risk of recurrent or residual pulmonary valve stenosis, while ratios in excess of 1.4 are associated with an increased risk of clinically significant pulmonary insufficiency (84).

The choice of balloon catheters that can be used for this procedure is wide and depends to a degree on the individual valve morphology. In general, inflation pressures of more than six atmospheres are rarely necessary in patients with typical valve morphology, and therefore low pressure balloons such as Tyshak II (NuMED, Hopkinton, NY) with a lower profile are

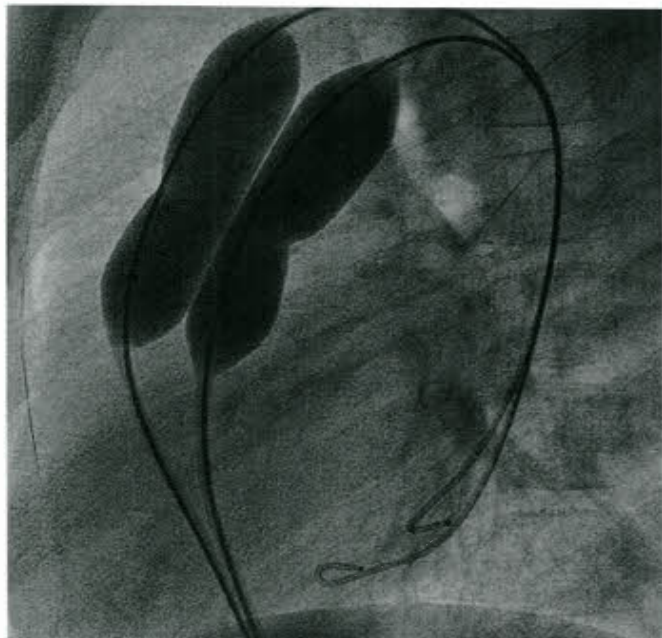


Figure 13.6. Pulmonary valvuloplasty. BPV in a 5-year-old boy with valvar and supra-valvar pulmonary stenosis, using the double-balloon technique to facilitate the use of higher inflation pressures.

the preferred initial balloon types to be utilized. However, the maximum rated inflation pressures decline sharply when using the larger varieties of these balloons. Therefore, high-pressure balloons, such as ZMed II (NuMED, Hopkinton, NY), or the double-balloon technique should be considered in these situations as the primary approach to balloon valvuloplasty (Fig. 13.6). High-pressure balloons may also be more beneficial when dealing with very dysplastic thickened pulmonary valves in the older patient or if there is associated supra-valvar narrowing. In neonates with critical pulmonary valve stenosis and a closed arterial duct, a low profile balloon with fairly rapid deflation characteristics such as the Tyshak II balloon should be used. Very low profile balloons, such as the mini Tyshak balloons (NuMED, Hopkinton, NY), may cross the valve more readily, but their very slow deflation characteristics make these balloons an inappropriate choice in patients who have critical pulmonary stenosis without a patent arterial duct. If the valve cannot be crossed with the appropriate sized balloon, smaller coronary balloons can facilitate predilating the valve to allow the larger balloon to be subsequently passed.

With the wire fixed in place in the distal pulmonary artery, the end-hole catheter is removed and the catheter with its deflated balloon is passed over this wire until the center of the balloon length is positioned exactly at the area of the stenotic valve. The balloon is then rapidly inflated to the pressure recommended by the manufacturer and is observed for the appearance of a circumferential indentation or "waist" in the balloon. Full inflation results in disappearance of the waist. An inflation device that can be operated using a single hand is preferential, as this allows the operator to use the other hand to maintain control of the balloon catheter, making very fine adjustments as the balloon is inflated. The balloon is then immediately and rapidly deflated, with the entire process taking no more than 5 to 10 seconds. Arterial pressures should be monitored throughout the procedure. In contrast to balloon aortic valvuloplasty, more than one inflation is usually performed to assure the operator that (a) the balloon

remained properly positioned in the valve; (b) the balloon was of adequate size; and (c) the waist disappeared early and at low pressures during subsequent inflations. When a single balloon is used, there is a significant drop in both systemic blood pressure and heart rate during inflation. With successful valve dilation, after the balloon is deflated, both the blood pressure and heart rate should return spontaneously to normal.

To avoid the marked drop in systemic blood pressure and to reduce the trauma to the peripheral introductory veins, a double-balloon technique was introduced (85). This technique also allows the use of higher inflation pressures in patients with a large pulmonary valve annulus, where a single balloon would provide an inadequate rated burst pressure. The double-balloon technique uses two separate balloon catheters, each on a smaller shaft and with a smaller balloon "profile." Each is introduced into a separate vein. With this technique, a second exchange wire is introduced from the opposite femoral vein and positioned across the pulmonary valve into a distal pulmonary artery, possibly next to the first wire. Two smaller-diameter balloon dilation catheters are advanced over the separate wires and centered in the valve orifice, and the two balloons are simultaneously inflated. Various formulae have been used to estimate the equivalence of double-balloon to single-balloon technique (83), ultimately resulting in comparison charts that allow choice of sizes of the two smaller balloons, depending on the size that would have been chosen if a single-balloon technique would have been used. However, a combined diameter of 150% to 160% of the pulmonary valve annulus can be used as a guide to choose the appropriate balloon sizes.

Reported success criteria for BPV have been variable. The VACA registry, dating back as much as 15 years, defined a gradient on follow-up of equal to or above 35 mm Hg as procedural failure (86). Holzer et al. (21) defined procedural success as either a reduction of the peak systolic RV/MPA gradient to <25 mm Hg, or a reduction of the valvar gradient by at least 50%, or a reduction of the RV/systemic pressure ratio by at least 50%. However, with pure valve stenosis and a closed PDA, regardless of the initial gradient, one should expect to reduce the pressure gradient across the nondysplastic pulmonary valve to <10 mm Hg by balloon valvuloplasty in most patients, with an equivalent reduction in the RV to systemic pressure ratio.

If the initial results are suboptimal, the balloon size should be increased up to 130% to 140% of the pulmonary valve annulus, and high pressure balloons should be used, after obtaining an intermittent angiographic evaluation, using, for example, a multitrack catheter that is positioned over the *in situ* guidewire in the RVOT. However, it is important to recognize that relief of the valvar stenosis may unmask a dynamic infundibular obstruction in some cases, resulting in a persistent residual RV outflow gradient (Fig. 13.7). This secondary area of obstruction can be documented by pressure recording during careful catheter withdrawal from the pulmonary artery to the RVOT or with simultaneous pressure recordings from a double-lumen catheter or from separate catheters in each of the two areas. Experience has shown that the infundibular obstruction is dynamic and that it will regress with time. This is particularly notable in adult patients undergoing BPV. Fawzy et al. (87,88) reported an incidence of infundibular gradients in excess of 30 mm Hg in 46% of 93 adult patients undergoing BPV. All these patients were recatheterized within 6 to 24 months, documenting a decrease in the mean infundibular gradient from 43 to 25 mm Hg. In <10% of patients, a dysplastic pulmonary valve is encountered, with thickened, redundant leaflets resembling a "cauliflower"; frequently supra-valve stenosis may coexist. This condition is more common in some genetic conditions, such as Noonan's syndrome. A higher-pressure balloon is usually required with a gradient reduction frequently less than what would be

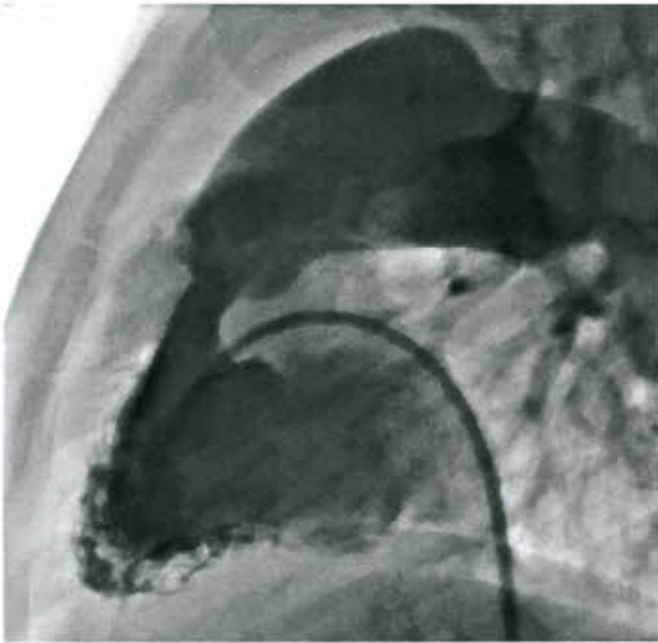


Figure 13.7. Subpulmonary stenosis after BPV. Dynamic subpulmonary stenosis seen on angiography in a 3-year-old child after undergoing BPV. Hemodynamic evaluation after BPV documented no residual valvar gradient, but a 10 to 15 mm Hg subvalvar gradient.

expected with nondysplastic valves. Within the recent multicenter experience from the C3PO registry reported by Holzer et al. (21), acute procedural success was 77%, with independent risk factors for procedural failure being the presence of a genetic syndrome, complex two-ventricle anatomy, presence of supravalue pulmonary stenosis, a hemodynamic vulnerability score of two or more, and the need for balloon inflation above 8 atmospheres.

Procedure-related serious adverse events are rare. In a multicenter registry (C3PO) including 290 patients, Holzer et al. (21) recently reported an incidence of moderate adverse events in 3% of patients and major adverse events in <1%. There was no incidence of procedure-related death, and independent predictors of higher level adverse events included among others, age below 1 month, complex two-ventricle anatomy, two or more parameters of hemodynamic vulnerability, and operator experience of <10 years.

The long-term effects of the procedure have not yet been determined. However, studies so far have documented rates of restenosis between 5% to 11% within 10 years after the procedure (81,82). The risk of recurrence or restenosis may be greater in patients who present in infancy or with very dysplastic pulmonary valves as well as those in whom an undersized balloon was used in the initial procedure. Holzer et al. (21) recently reported an incidence of early reinterventions of 12% in neonates that underwent BPV. So far, reports have not provided evidence to suggest an increased risk of patients requiring pulmonary valve replacement because of pulmonary insufficiency, secondary to BPV. Dr. Charles Mullins pointed out that in the presence of otherwise normal heart and lungs, the regurgitant fraction is usually small and at low diastolic pressure, due to 80% to 85% of the ejection fraction having “diffused completely into the distal pulmonary capillary bed by the end of systole.” However, we have also learned that progressive RV dilation secondary to pulmonary insufficiency should be considered a potential indication for pulmonary valve replacement.

PERFORATION OF THE ATRETIC PULMONARY VALVE

The diagnosis of PA/IVS is usually made within the neonatal period. Pulmonary blood flow after birth is maintained through a patent arterial duct until a more definitive source of pulmonary blood supply can be established. An intra-atrial communication allows the systemic venous return to pass into the systemic circulation. The long-term prognosis of patients with PA/IVS can be extremely poor, especially when a diminutive right ventricle is combined with an RV-dependent coronary circulation with multiple coronary abnormalities. In this situation, patients may require cardiac transplantation early in life. However, while patients with the diagnosis of PA/IVS and a single-ventricle pathway usually have a very poor long-term outcome, the outlook for those patients with a biventricular or a “one-and-a-half ventricle” circulation is much better.

Perforation of the atretic pulmonary valve plate has an important role to play within the available treatment modalities for these patients (74). Achieving antegrade pulmonary flow not only acutely decompresses the right ventricle but more importantly serves as an incentive to facilitate further growth of an initially hypoplastic right ventricle. While a variety of sharp instruments as well as laser-guided techniques have been used to perforate the atretic pulmonary valve, these techniques are often poorly controlled and associated with a variably high risk of creating inadvertent injury to surrounding structures, often with disastrous results. Consequently, the use of RF energy was introduced into therapeutic cardiac catheterization in the early 1990s as an alternative to laser-guided perforation of the pulmonary valve plate (89).

The equipment presently most frequently used to achieve perforation of the atretic pulmonary valve with RF energy is the Nykanen RF perforation wire and the Baylis RF puncture generator (both from Baylis Medical Corporation, Montreal, Quebec, Canada). Suitability for transcatheter RF perforation of the pulmonary valve plate is ascertained by 2-D echocardiography with minimal criteria in most cases being the presence of a tripartite right ventricle as well as a membranous atretic pulmonary valve with a well-formed infundibulum (90). Vascular access is routinely obtained via right femoral venous cannulation. A femoral arterial pressure monitoring line is placed. Initial hemodynamic evaluation includes measurement of RV and systemic arterial pressures, followed by RV angiography with 20-degree cranial angulation of the frontal tubes and standard lateral projection. This allows measurement of the pulmonary valve plate diameter and exclusion of RV-dependent coronary circulation. Further angiography is obtained in the left ventricle in the same projection. The combination of these two ventriculograms allows documentation of the relationship between the blind-ending RV infundibulum and MPA. A 5 Fr Judkins 2.5 right coronary artery catheter is placed below the pulmonary valve plate within the RVOT using a Touhy Borst adapter to allow passage of the RF wire and simultaneous contrast injections. Once the RF wire and coaxial catheter are loaded and accurate positioning is confirmed, RF energy is applied while maintaining a gentle push on the RF wire towards the valve membrane. In most patients, a power setting of 5 W per second for 2 seconds should be sufficient to perforate the pulmonary valve plate. It is important for the operator to be particularly suspicious of creating a false track if high-power settings are required. RF energy is discontinued once the wire has advanced through the valve plate. Appropriate position is confirmed using contrast injection through the Touhy Borst adapter. The coaxial catheter is then advanced over the RF wire into the MPA and the RF wire is exchanged to a 0.014- or 0.018-inch coronary wire, which can be directed either to a position in a distal branch

pulmonary artery or preferably through the PDA into DAO. Even though a wire position in the distal pulmonary arteries or preferably across the PDA must be established, this should not be attempted with the Nykanen RF wire, as it can easily cause perforation of the MPA (74). The use of a coaxial catheter is a significant advantage when comparing the Baylis to the Osyka RF system that is still in widespread use elsewhere. A low-profile balloon valvuloplasty catheter, such as the Mini-Tyshak (NuMED, Hopkinton, NY), with a diameter of about 130% of the valve plate annulus is then advanced over the coronary wire and balloon dilation performed (Fig. 13.8). In cases where the balloon catheter cannot be advanced across the valve, sequential dilation can be performed starting with a lower profile 2.5-mm coronary balloon. Trackability can also be improved through arterial fixation or snaring of the coronary wire (91). Balloon valvuloplasty is followed by assessment of

the pressure gradient across the pulmonary valve as well as the RV-to-systemic pressure ratio, and a final RV angiogram is performed to document the result of the procedure.

Many studies have reported on the outcome of RF perforation of the pulmonary valve and results have been summarized by Benson et al. (92–97). Most series are very small and include less than five patients. The overall procedural mortality is about 8% with incidence of procedural complications being about 15%.

It has been advocated that the combination of ductal stenting with RF perforation in one single procedure may reduce the number of transcatheter interventions and prevent prolonged postprocedural care. Approximately 50% of all neonates undergoing successful perforation and balloon valvuloplasty require additional pulmonary blood flow (98), even though it remains difficult to predict this for each individual

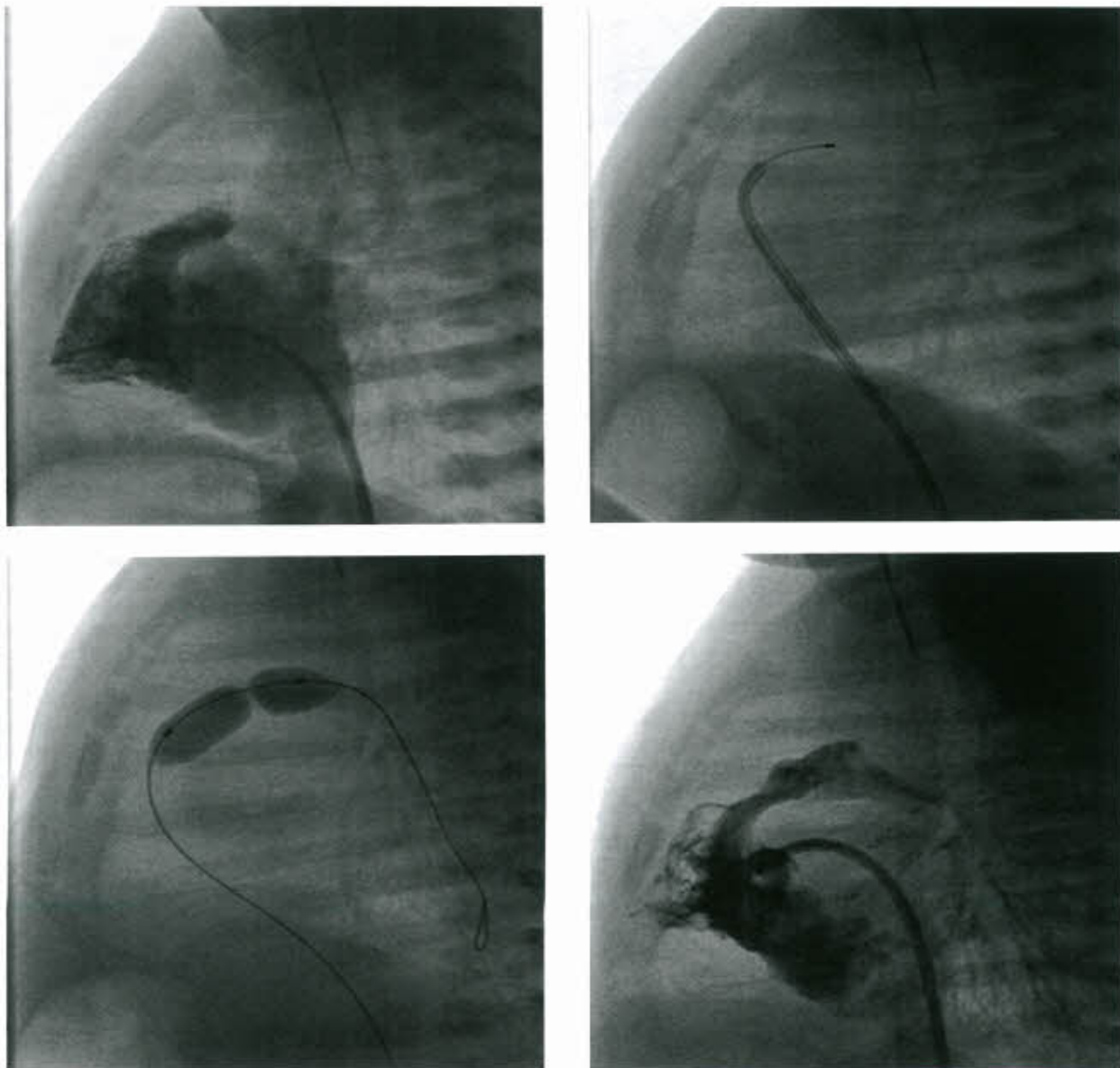


Figure 13.8. RF perforation in pulmonary atresia (PA)/IVS. RF perforation of the pulmonary valve plate in a neonate with PA and IVS. **Top left:** RV angiogram delineating the RVOT. **Top right:** RF wire across the pulmonary valve plate. **Bottom left:** Balloon valvuloplasty with a wire positioned in distal RPA. **Bottom right:** RV angiogram demonstrating the newly created continuity between right ventricle and MPA.

patient. Some authors have suggested to use the tricuspid valve z-score (95), but this has not consistently been identified of being predictive of the need for pulmonary blood flow augmentation. Regardless, after failing to wean from prostaglandin E infusion after 5 to 7 days, one should proceed with either PDA stenting or surgical aortopulmonary shunt placement. If performed appropriately, this technique allows up to 75% of suitable patients to ultimately sustain a biventricular or one-and-a-half ventricle circulation (74).

TRANSCATHETER TREATMENT OF STENOTIC AV VALVES

Mitral Valve Dilation

When discussing balloon dilation of stenotic atrioventricular (AV) valves, it is very important to distinguish between congenitally stenotic AV valves and acquired AV valve stenosis as a result of rheumatic fever. In many countries outside the United States, rheumatic MV stenosis is still a common lesion in children. These acquired valve lesions with commissural fusion lend themselves naturally to a dilation procedure, which has been demonstrated to be effective in children. In contrast, the anatomy of congenital mitral stenosis (MS) is quite variable and is generally less favorable for balloon dilation, although the procedure has occasionally been effective for this lesion. The decision to proceed with balloon valvuloplasty of congenital MS should be based on a complete echocardiographic assessment of MV anatomy.

The MV is approached from the femoral vein using a transseptal approach into the left heart. A variety of techniques has been described that include predilating the atrial septum to allow passing a single large mitral dilation balloon, the passing of two balloons through two large transseptal sheaths, the passing of two balloons over separate guidewires without long sheaths and without the need for specific dilation of the septum, as well as a double-balloon technique using a multi-track system over a single guidewire (NuMED, Hopkinton, NY) (99). The Inoue balloon (Toray Industries, Houston, TX) is a custom-made hourglass-shaped balloon that is available as a complete set, including sheath, guidewire and mandrill. It specifically facilitates balloon valvuloplasty using a single-balloon technique without the use of a guidewire in the left ventricle (Fig. 13.9). The Inoue balloon is available in three sizes, allowing balloon dilation diameters between 22 and 30 mm. Its use has demonstrated success in treating rheumatic MV stenosis (100).

When using a double-balloon technique, the left atrium is entered and one or two separate transseptal punctures are made. Exchange wires are manipulated from the right atrium through previously positioned catheters or long sheaths across the septum, across the MV, and into the left ventricle with the “transition” and floppy portions of the wires looped in the ventricle. It is important to remember that if a guidewire is to be used for balloon dilation, a balloon-tipped end-hole catheter should be initially directed from the left atrium across the MV to lessen the chance of crossing between chordal attachments. Once the wires are in place, either the two long sheath/dilator sets or the two separate “uncovered” balloons are passed over the wires into the left atrium. The balloons are advanced and positioned across the MV. The sheaths are withdrawn off the balloons and the balloons are simultaneously inflated. Again, longer balloons (5 to 6 cm in older children and adolescents) help to stabilize during inflation. The sum of the two balloon diameters equals the measured or estimated maximal normal MV diameter for a patient of that particular body size. The two balloons allow an adequate total balloon diameter for the

much larger mitral annulus without coincident destruction of the entry veins or the atrial septum during balloon passage. As with any interventional catheterization, these patients should be anticoagulated with heparin.

The initial success of transcatheter balloon dilation of congenital MV stenosis appears equal to that of surgical commissurotomy, depending on the MV apparatus. However, the total experience is limited, and the duration of the relief of the obstruction is unpredictable. McElhinney et al. (101) recently described a series of 108 patients with congenital MS who underwent BMVP or surgical intervention at a median age of 18 months. BMVP was effective in creating a reduction of the mean gradient by 38%, while significant mitral regurgitation was identified as a result in 28% of procedures. Overall 5-year survival was 69%, while patients at the later stages of the institutional experience had a 5-year survival of 87%. The early mortality was similar for balloon valvuloplasty and surgical mitral valvuloplasty, while the need for initial MV replacement was a significant predictor of worse acute and long-term outcomes. The 5-year survival free from failure of biventricular repair after balloon valvuloplasty was 75%. While the authors suggested that the initial procedure for congenital MS in patients with either typical congenital MS or double orifice MV should be balloon valvuloplasty, they conceded that the surgical approach is more appropriate in patients with supravalle mitral ring and parachute MV.

While in general a parachute MV is not a contraindication to balloon valvuloplasty, the procedure is probably less likely to be effective when there is a single papillary muscle or severe shortening or virtual absence of the chordal apparatus (the “arcade-type” MV). Ultimately, it is difficult to predict which intervention is the more appropriate for congenital MS and most series report institutional preferences. As such, comparisons between surgical and percutaneous approach are biased at best.

Tricuspid Valve Dilation

Congenital tricuspid stenosis, as well as rheumatic, carcinoid, and rare other types of acquired tricuspid valve stenosis, occur less frequently than MS, but, as with MS, may be amenable to balloon valve dilation. Congenital forms of tricuspid valve stenosis are usually associated with other cardiac lesions and, similar to MV stenosis, are less amenable to balloon valvuloplasty than rheumatic tricuspid valve stenosis. The diagnosis of tricuspid stenosis is confirmed hemodynamically. As much information as possible about the valve anatomy and the exact location of the obstruction is obtained by echocardiography and angiography. The tricuspid valve is approached by passing one or two guidewires across the valve, either into the pulmonary artery or to the RV apex. With the use of the calculated or estimated maximum tricuspid valve annulus diameter according to the patient's body surface area, the balloon diameter or combined balloon diameters are chosen to equal this measurement (except in cases of annular hypoplasia). The dilation balloons are introduced through standard venous sheaths and over the wires. When the balloons are positioned across the stenotic valve, they are inflated simultaneously. Disappearance of the indentations or waists in the balloons at maximal inflation is sought. As with MV dilation, the use of the longer balloons facilitates appropriate positioning and maintaining positioning across the valve during dilation. A successful dilation should eliminate any transvalvar gradient. Experience with tricuspid valve dilation is limited, but, on the basis of even limited experience and minimal risk, this procedure is offered to the appropriate patients before considering surgery for tricuspid stenosis.

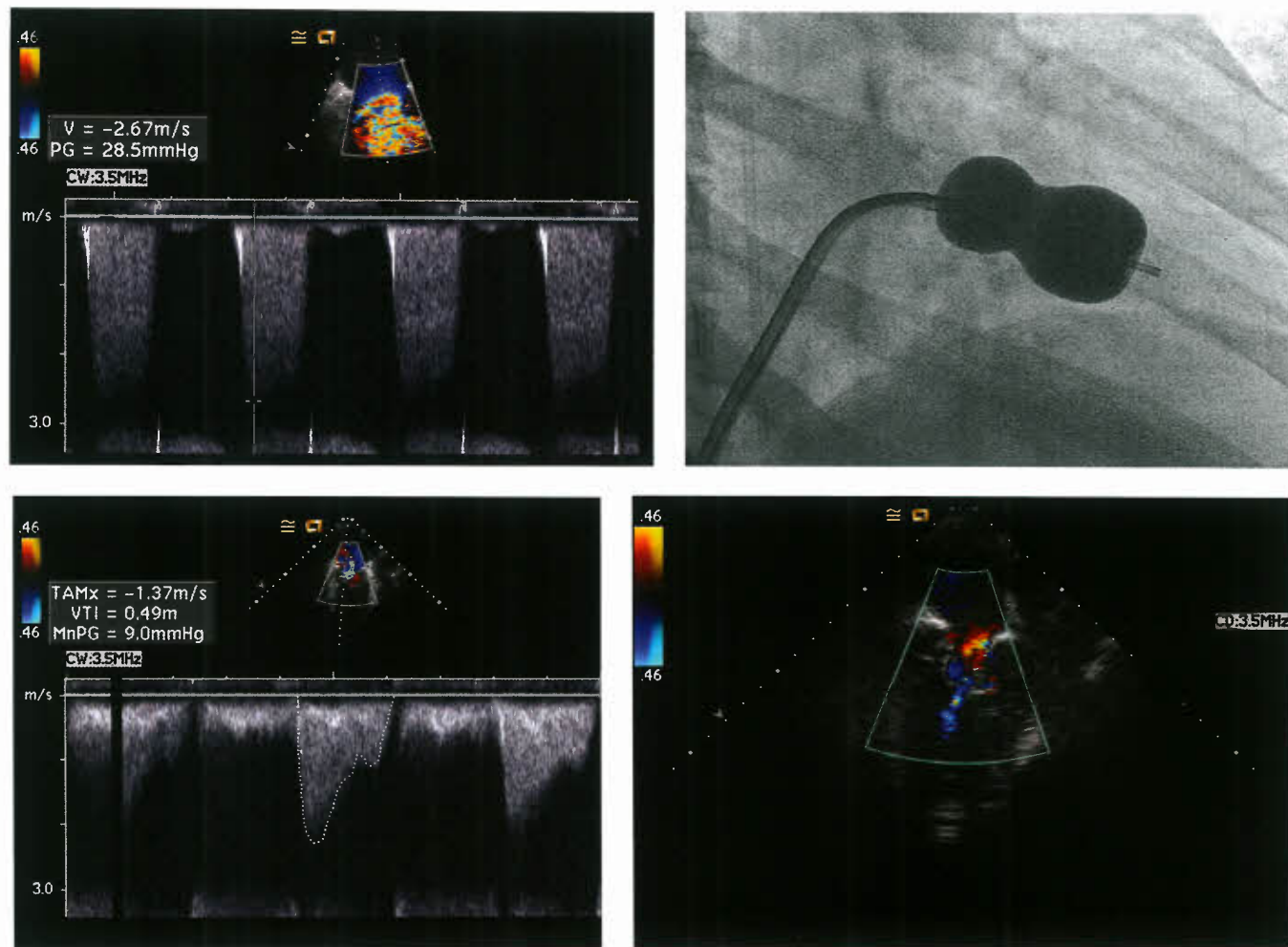


Figure 13.9. Mitral “Inoue” balloon valvuloplasty. A 38-year-old woman with rheumatic MV stenosis. Inoue BMVP reduced the mean gradient from 28 to 9 mm Hg with mitral regurgitation increasing from trivial to mild. **Top left:** 28 mm Hg mean Doppler gradient across MV prior to balloon valvuloplasty. **Bottom left:** 9 mm Hg mean Doppler gradient across MV postballoon valvuloplasty. **Top right:** Inoue balloon inflated across MV. **Bottom right:** Mild mitral insufficiency by color Doppler after balloon valvuloplasty.

TRANSCATHETER MANAGEMENT OF COARCTATION, RECOARCTATION, AND AORTIC ARCH OBSTRUCTIONS

Dilation of peripheral arteries was the first therapeutic catheterization procedure and represents yet another area in which the vascular radiologist introduced the techniques. Dotter and Judkins (1) reported on the dilation of atherosclerotic peripheral arteries at the same time that Rashkind and colleagues were working on the atrial septostomy catheter.

The technique for dilation of vessel stenosis uses small, cylindrical, fixed maximal diameter dilating balloons passed over a spring guidewire, positioned across the area of stenosis, and inflated with relatively high pressures. This stretches or tears the area of stenosis up to the predetermined diameter of the balloon. This balloon technique is not only used to treat recurrent or native coarctation of the aorta (Fig. 13.10), but similarly is used for branch pulmonary artery stenoses as well as central and peripheral venous stenoses. As many vessel dilation procedures are associated with immediate recoil and subsequent restenosis, the addition of balloon-expandable

stents has further improved upon the available therapeutic interventional armamentarium and is frequently the treatment of choice in adult patients.

In 1979, Sos et al. (102) first experimented with balloon angioplasty of native coarctation in postmortem specimens and this was followed by some fundamental work by Dr. James Lock in the early 1980s. He performed balloon angioplasty on excised human coarctation segments as well as experimentally induced coarctation in lambs (103,104). He showed that balloon angioplasty achieved its therapeutic result by creating micro- or macroscopic intimal and medial tears over a variable distance in the vessel. These intimal injuries appeared to have healed completely on late pathologic examination, leaving the ballooned segment with a normal looking intima. The studies also documented that a balloon diameter of less than twice the size of the coarctation segment was unlikely to achieve a successful dilation, while diameters greater than three times appeared to carry a higher risk of deep and extensive tears.

Dr. Ronald Grifka et al. (105) and Dr. Charles E. Mullins' group from Texas Children's Hospital set the stage for early evaluation of endovascular stent therapy to treat coarctation (Fig. 13.11). In animal experiments, they implanted Palmaz

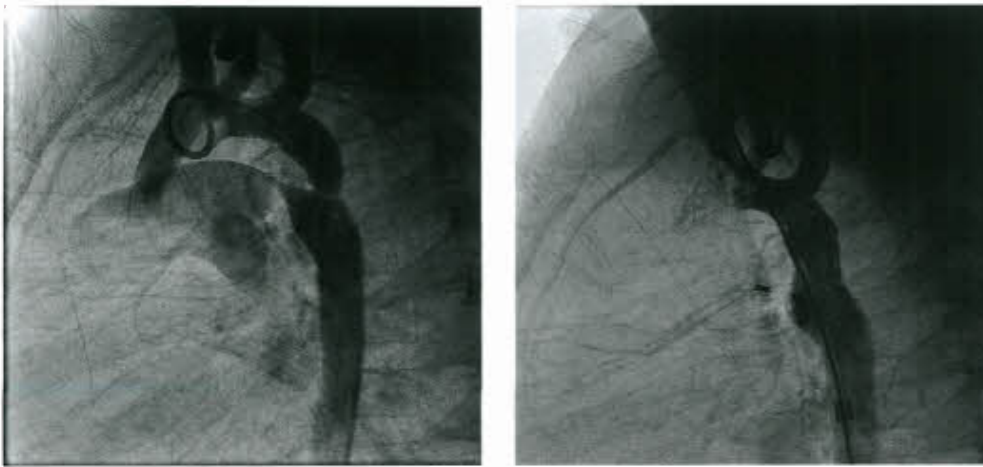


Figure 13.10. Coarctation and PDA. A 14-month-old child was referred for elective PDA closure. Coarctation with 30 mm Hg peak systolic gradient was incidentally found during procedure. PDA was closed with 6/4-mm ADO, followed by placement of a 19-mm Genesis XD in DAO, completely abolishing the gradient. **Left:** PDA and coarctation prior to intervention. **Right:** Postintervention.

P308, P188, and P108 stents in the abdominal aorta and documented that stents can be safely redilated after initial stent implantation. Dr. Andrew Redington et al. (106) added to this in 1993 by implanting a self-expandable stent into a 10-week-old girl who had previously had palliative surgery for hypoplastic left heart syndrome. While one should generally avoid endovascular stent therapy in small infants, in some very rare circumstances, the implantation of a low profile stent in very sick infants may be justifiable, even though one has to accept that these low-profile stents are not expandable to adult size and therefore will eventually require surgical removal. In 1995, Suarez de Lezo et al. (107) reported the first large series of stent implantation to treat native and recurrent coarctation in humans using the Palmaz stent and in 1999 Cheatham (108) first reported on a new stent design, the CP stent, which is also available in a PTFe-covered variety. Holzer et al. (109) at Nationwide Children's Hospital recently reported a larger experience of stent therapy for complex aortic arch lesions, which further expanded the indications for transcatheter stent therapy with excellent results (Fig. 13.11).

One of the major difficulties when comparing the various treatment modalities for native or recurrent coarctation of the aorta, such as surgery, balloon angioplasty, and endovascular stenting, is the fundamental lack of prospective, evidence-based data (110). As such, one has to rely on institutional series (110), the results of which are necessarily influenced by not only the skill of the individual interventional cardiologist and cardiac surgeon in the respective institution but also by the common institutional policy and experience in treating these lesions.

Similar to the comparison of surgical and interventional approaches to coarctation, the decision between balloon

angioplasty and primary stenting is often dependent on the individual institutional policy, rather than being guided by evidence-based data. While both balloon angioplasty and endovascular stenting have an important role to play in the primary management of aortic coarctation, there are a number of valid reasons that make primary stenting the more suitable treatment modality, if the size of the patient permits this procedure. First, the results of balloon angioplasty are limited due to elastic recoil of the coarcted segment and the rigidity of an endovascular stent obviously overcomes this problem. Second, the degree of trauma to the aortic vessel wall plays an important factor in the potential development of complications such as aneurysm formation. While balloon angioplasty often requires a degree of overexpansion of the coarctation and adjacent vessel wall to achieve a maintainable result, endovascular stenting allows having a successful result while dilating the vessel wall only to the desired diameter—overexpansion is not required. Finally, a subgroup of longer-segment coarctation or arch hypoplasia typically has a poorer outcome after balloon angioplasty alone.

Even though primary endovascular stenting offers significant benefits, it is usually avoided in small children and infants, because of the potential for injury to the arterial vessels and access sites as well as the higher likelihood of developing in-stent stenosis when stents are only expanded to fairly small diameters. As with any other aspect of interventional therapy, the catheterization laboratory has to be equipped to allow the operator to deal with potential complications that are specific to the procedure performed (Fig. 13.12).

The goal of the procedure is to achieve reduction in the gradient to <10 mm Hg or a 90% or greater relief of the

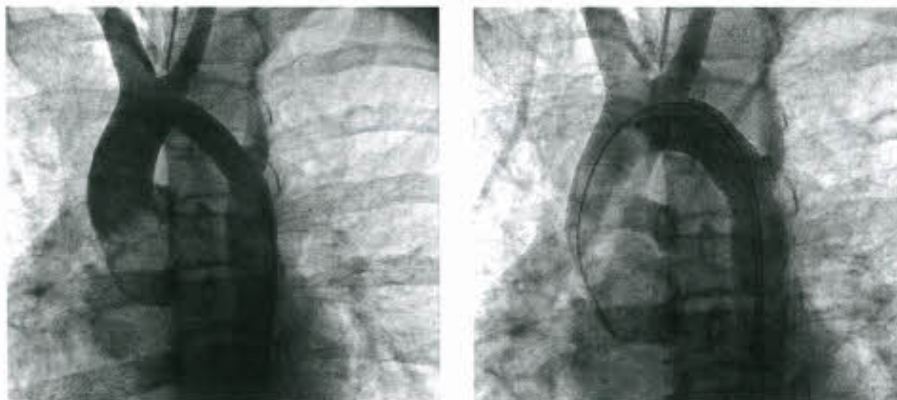
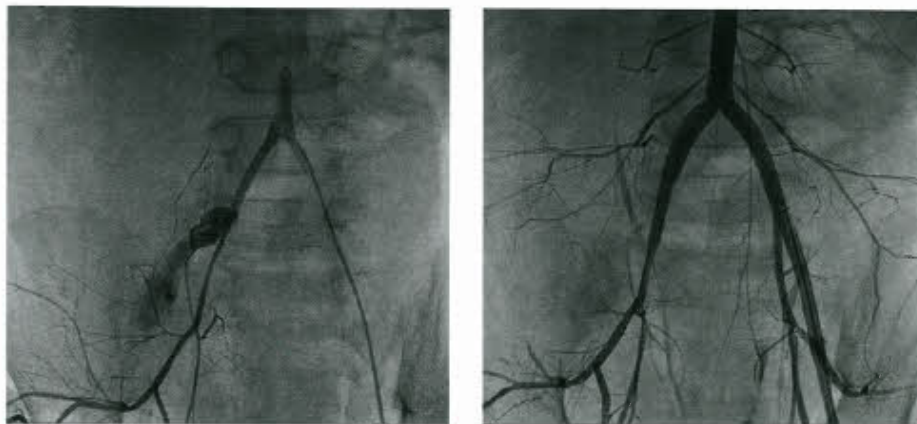


Figure 13.11. Complex arch stenting. A 15-year-old child with coarctation repair (end-to-end) during infancy had Shone's complex with transverse arch hypoplasia. Placement of a 36-mm Max LD stent in the transverse arch led to a gradient reduction from 22 mm Hg peak systolic to 2 mm Hg peak systolic. **Left:** Aortogram before stent placement. **Right:** Aortogram after stent placement.

Figure 13.12. Iliac rupture. A 9-year-old boy with localized coarctation undergoing placement of a Max LD stent with complete abolishment of the gradient. Upon sheath removal injury to right iliac artery occurred that was treated through implantation of a covered Atrium Cast stent. **Left:** Injured iliac artery with significant extravasation of contrast, **Right:** Same vessel after placement of the covered stent.



obstruction angiographically. In an observational study, Zabal et al. (111) analyzed a cohort of 54 consecutive adult patients who underwent transcatheter treatment for coarctation with the primary endpoint being a composite index of failure, made up of heart-related death, a gradient on follow-up of more than 20 mm Hg, the need for reintervention, or complications such as aneurysm formation. They identified that a residual gradient of more than 10 mm Hg was associated with a significantly higher failure index. While this is not a prospective or randomized study, it does fit with the results of other observational series and appears to be a good guideline when delivering interventional therapy to these patients.

With the present techniques and equipment, dilation and/or stent implantation for native or recurrent coarctation appears to be successful in achieving immediate relief of the obstruction in more than 90% of cases. Holzer et al. (112) recently reported the results of the CCISC registry on stent implantation for aortic coarctation, documenting acute composite procedural success of 96%. However, the cumulative composite procedural success decreased to 86% at intermediate follow-up (3 to 18 months) and 77% at long-term follow-up (>18 months).

Balloon angioplasty alone for native coarctation in smaller children and infants has lower long-term success rates and the results are frequently not well maintained, with up to 66% recoarctation rate. An additional concern when discussing transcatheter interventions for native coarctation is the potentially greater incidence of aortic aneurysm formation in the area of the coarctation dilation. Aneurysms have occurred both immediately and late after the coarctation dilation. Catastrophic events as a direct result of these aneurysms are rare. However, the follow-up data are limited, and the long-term outcome is uncertain, at best. Data from the CCISC registry suggest that the incidence of aortic wall complications after stent implantation for native coarctation on medium-term follow-up is less with stent implantation than with balloon angioplasty or surgery (13% vs. 44% vs. 25%)(113). From several surgically removed segments and from intravascular ultrasound (IVUS) of the area, it appears that both the aortic intima and media are often disrupted, with only the adventitial layer constraining the aortic pressure. Another concern with these aneurysms, particularly following an otherwise successful dilation, is that if subsequent surgery is necessary, it could be more hazardous because of the disappearance of collaterals following a hemodynamically successful dilation. As more follow-up information is gathered regarding dilation of native coarctation, this technique appears more reasonable for discrete lesions in patients over 7 to 12 months of age (114). Continued long-term follow-up is still recommended. In the

larger child, primary stent therapy for native coarctation is a suitable treatment alternative to balloon angioplasty, even though aneurysms can occur with these stent implants. It has been suggested that gradual conservative expansion of these stents be performed over two or three procedures, especially in tight lesions, to reduce the incidence of dissection or aneurysm formation.

The technique itself is relatively straightforward. The coarctation and adjacent aorta are visualized by quantitative angiography, usually using lateral as well as LAO projections. IVUS can further assist the preinterventional assessment of coarctation, and may be specifically useful in the postoperative group of patients (115–117). If balloon angioplasty alone is performed, a balloon of the same diameter as the narrowest aortic diameter adjacent to the coarctation is prepared. A “J” or curved-tip stiff guidewire is positioned retrograde through the coarctation, around the aortic arch, and into the aortic root or occasionally into the right innominate artery. The dilation balloon catheter is passed over the wire and across the area of coarctation. When the balloon is centered in the coarctation, it is inflated to the manufacturer’s listed maximum pressure. The inflation may be repeated several times until the waist in the balloon or the gradient disappears. In smaller children and infants, cutting balloon angioplasty frequently adds an additional treatment alternative in patients where endovascular stent placement should be avoided.

In the slightly larger patient, when the results of the dilation are not satisfactory and where larger sheaths can be introduced into the arteries, intravascular stents can be used to support the dilated segment of aorta. When stents are used, it is imperative that only stents that eventually can be dilated to the full diameter of the adult DAO are used. In smaller patients with an expected diameter below average adult size, the Genesis XD or the Mega LD stents with a maximum expandable diameter of up to 18 mm would be perfectly appropriate. If larger maximum diameters are required, the Max LD, the CP, or older Palmaz XL (Cordis, Warren, NJ) stents with maximum expandable diameters beyond 25 mm are available, even though the (covered) NuMED CP stent is approved in the United States under an investigational protocol only (COAST/COAST II). If aortic arch vessels must be crossed, the Mega or Max LD stents offer additional advantages because of their open-cell design, which can be expanded to avoid having the side branches of the aortic arch covered by the cells of the stent wire mesh (Fig. 13.13). In contrast, the ePTFE-covered variety of the CP stent is specifically useful for very tight coarctation where an increased risk of injury to the aortic wall is expected as well as in the adult population where catastrophic aortic rupture



Figure 13.13. Three-dimensional (3-D) rotational angiography of open cell stent extending over arch vessels. 3-D reconstruction of a rotational angiogram taken in a 3-year-old child with complex CHD who underwent stent placement of the transverse arch using a 26-mm Mega LD stent (no residual gradient), completely opening the cells to the single side branch using a 10-mm balloon.

has been reported (118–120). Stents implanted in children can gradually be expanded to adult size in subsequent transcatheter procedures to accommodate a child's growth. It is hoped that the prospective enrollment of patients undergoing balloon angioplasty, stent therapy, or surgical treatment in the CCISC, organized by Dr. Thomas Forbes in Detroit with participating centers worldwide, will help shed light on this subject.

Transcatheter management of coarctation in the adult has some important differences when compared to its management in the younger child. For example, limiting factors in younger children when considering endovascular stent therapy, include the potential for injury to the arterial vessels and access sites due to the need for larger sized hemostatic sheaths as well as the higher likelihood of developing in-stent stenosis when stents are only expanded to fairly small diameters. These problems are of a much lesser concern when dealing with an adult. The goal of the interventional procedure in adults is similar to children: To achieve reduction in the gradient to <10 mm Hg or a 90% or greater relief of the obstruction angiographically.

It has been advocated that the risk of catastrophic aortic injury during or after balloon angioplasty and/or stent placement in the adult (118–120) is higher than what would be expected in the younger child, especially when treating primary coarctation. In the adult, coarctation or recoarctation do not always have the morphological correlate of a “high grade” and “tight” stenosis. Many adult patients with systemic and exercise induced hypertension may present with “just” a 20 to 30 mm Hg upper-to-lower limb blood pressure gradient with an angiographic discrepancy between coarcted segment and the aorta at the diaphragm of not more than 30% to 50%. To achieve an adequate result with balloon angioplasty alone, one would ideally have to expand the area to at least twice the size of the coarctation segment (103,104). However, using this as a guide would lead to significant overdilation of not only the coarcted segment but also the adjacent “healthy” aorta. Primary stent therapy is therefore the treatment of choice in adults with primary or recurrent coarctation, as it not only avoids the need for overexpansion but also has a lower risk of recurrence when compared to balloon angioplasty.

While the risk of catastrophic aortic injury cannot be eliminated, it can be minimized through the diligent use of diagnostic techniques such as IVUS (115,117). IVUS allows to evaluate the integrity and structure of the aortic wall above, below, and within the coarcted segment. This not only identifies areas with medial and intimal disruption as could relate from a previous attempt at balloon angioplasty but it also allows clear definition of the extension of the abnormal vessel wall, thereby allowing choice of a stent that is of sufficient length to cover the full length of the abnormal vasculature.

Some institutions advocate preexpansion of the coarcted segment as a means of testing aortic wall compliance prior

to stent implantation. However, this has the disadvantage of potentially extending a intimal-medial tear into healthy vasculature that subsequently may not be covered during stent placement, therefore potentially acting as a “nidus” for aneurysm formation, especially at the areas immediately adjacent to the placed stent. In adults with very “tight” coarctation, it may be beneficial to expand the aorta not to the full intended diameter in a single procedure but instead adopting a staged approach where the stent is dilated over two or three sessions up to its desired final diameter, thereby allowing the aorta to heal between interventional procedures, with a reduced risk of catastrophic aortic wall injury. However, even with a very careful and considerate approach, the risks of treating adult coarctation cannot be fully eliminated and therefore whenever possible, the availability of an approved covered stent variety as a primary or rescue intervention could potentially enhance the safety of these procedures (Fig. 13.14). Covered stents have also been successfully used to exclude aortic aneurysms at the site of (re)coarctation (Fig. 13.15).

It is important to minimize the potential risk of aneurysm formation and other vascular complications after transcatheter therapy of (re)coarctation. The freshly injured vessel wall should be protected from any hypertensive strain and as such, at least temporary placement of the patient on antihypertensive medications such as beta-receptor blockers (even in the normotensive patient), may potentially reduce the incidence of early vascular complications after transcatheter therapy. During follow-up, it is important to investigate the potential development of aneurysms at the site of interventional therapy, which can occur even after stent therapy. A multislice CT scan or MRI should be performed within 6 to 12 months after the interventional procedure.

REHABILITATION OF (BRANCH) PULMONARY ARTERY STENOSIS

Transcatheter therapy of all varieties of branch pulmonary artery stenoses is a widely accepted standard procedure, in large part because most of these lesions are not amenable to surgical repair. However, rehabilitation of branch pulmonary artery stenoses can be one of the most challenging tasks in congenital pediatric patients. Transcatheter therapy has to strive to achieve the optimum possible outcome that sometimes requires repeated and staged procedures to achieve some improvement for an individual complex patient. The treatment modalities available include the use of cutting balloons, standard balloon angioplasty, or the placement of endovascular stents.

The individual success of treating these lesions is sometimes difficult to assess, but in patients with a biventricular

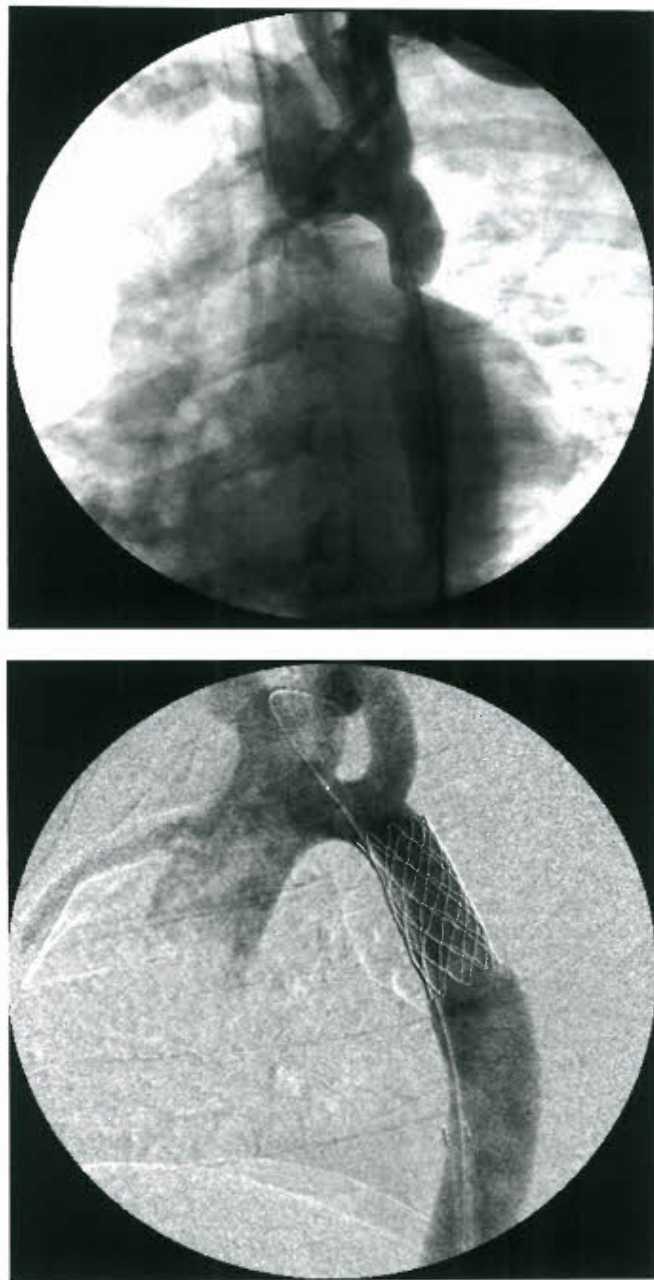


Figure 13.14. Coarctation in pregnancy. A 34-year-old pregnant woman was hospitalized during her 24th week gestation with severe systemic hypertension. Evaluation demonstrated severe coarctation of the aorta. Significant concern for fetus and mother lead to transcatheter placement of a covered NuMED CP stent, with complete abolishment of the gradient. Fluoroscopy time was minimized and appropriate radiation protection measures were taken. **Top:** Aortogram demonstrating near interruption before stent placement. **Bottom:** Aortogram after stent placement.

circulation, a reduction in the RV to systemic pressure ratio is a good indicator for a successful outcome. Individual pressure gradients to branch pulmonary arteries may be less meaningful, and in fact angiographically significant branch pulmonary artery stenoses can be associated with surprisingly low-pressure gradients, especially for isolated lesions and in the presence of significant pulmonary insufficiency. However,

when assessing these gradients across individual stenoses, it is important to avoid a catheter-induced damping and therefore the use of pressure wires such as the RADI pressure wire (Radi Medical Systems, Wilmington, MA) may aid in accurately assessing the hemodynamic data. The angiographic appearance of the vessel before and after transcatheter intervention is equally important, and while one should strive to aim to achieve a “normal” vessel diameter, frequently the percentage of improvement in the anatomic measured stenosis is a good outcome parameter. Rotational angiography with 3-D reconstruction is a new tool that is in particular suited for patients that require complex pulmonary artery rehabilitation. The 3D reconstructions allow to visualize the complete pulmonary artery tree and the best angulations can be chosen to profile individual lesions (Fig. 13.16). This not only provides better imaging of individual lesions but may also lead to a reduction in the overall amount of contrast needed, especially in patients who require multilevel pulmonary artery rehabilitation. The amount of contrast for individual rotational angiograms can be further reduced by using rapid RV pacing during the rotational acquisition.

While standard balloon angioplasty can be performed using a normal balloon-over-the-wire technique, it is frequently helpful to place long sheaths towards the area of intended interventional therapy to facilitate simultaneous therapies of adjacent lesions, balloon exchanges, and subsequent placement of stents if required (Fig. 13.17). In many patients, especially in adults, placements of long sheaths from a femoral venous approach may be difficult. Therefore, alternative approaches should be considered. Internal jugular venous or transhepatic approaches offer the advantages of eliminating some of the double-S-curves that have to be traversed from a femoral venous approach, while also using a shorter sheath length and allowing improved “pushability” of the catheter.

Standard balloon angioplasty alone rarely achieves a sustainable long-term improvement to an individual stenosis and as such is usually only performed in situations where other forms of transcatheter treatment are not available or where the size of the patient or vessel prevents the use of endovascular stents that can be expanded to adult size. No absolute rules exist for determining the correct balloon size; it appears that the balloon should preferably be larger than two times the diameter of the stenotic segment while avoiding exceeding a diameter of three times the actual narrowing. However, when using standard balloon angioplasty, “overdilation” of a vessel is frequently required to achieve an adequate outcome. In very resistant stenoses, the use of high-pressure balloons should be employed, rather than exceeding the size of the dilation balloons. Cutting balloon angioplasty is available for maximum diameters of up to 8 mm and is a suitable alternative to endovascular stenting especially in small distal pulmonary arteries (121,122). It is frequently beneficial to “score” very tight stenoses that can be followed either by standard balloon angioplasty or by endovascular stent placement if required.

Standard balloon angioplasty of pulmonary branch stenosis has not been highly successful at correcting the lesions and many of the vessels that initially are dilated satisfactorily reconstrict immediately (recoil) with the deflation of the balloon or, if not immediately, a short time later. Few of these dilated vessels are maintained at a normal diameter. The true success rate at achieving a vessel of normal diameter with no gradient is <20%; at the same time, there is a definite morbidity and even mortality with the procedure. It is not possible to determine in advance which case will be successful, so the procedure is often performed as a therapeutic trial. Frequently, pulmonary artery rehabilitation is a staged procedure, where reinterventions are not necessarily a sign of procedural failure, but more importantly reflect a consciously chosen staged therapeutic strategy with frequent early reinterventions to

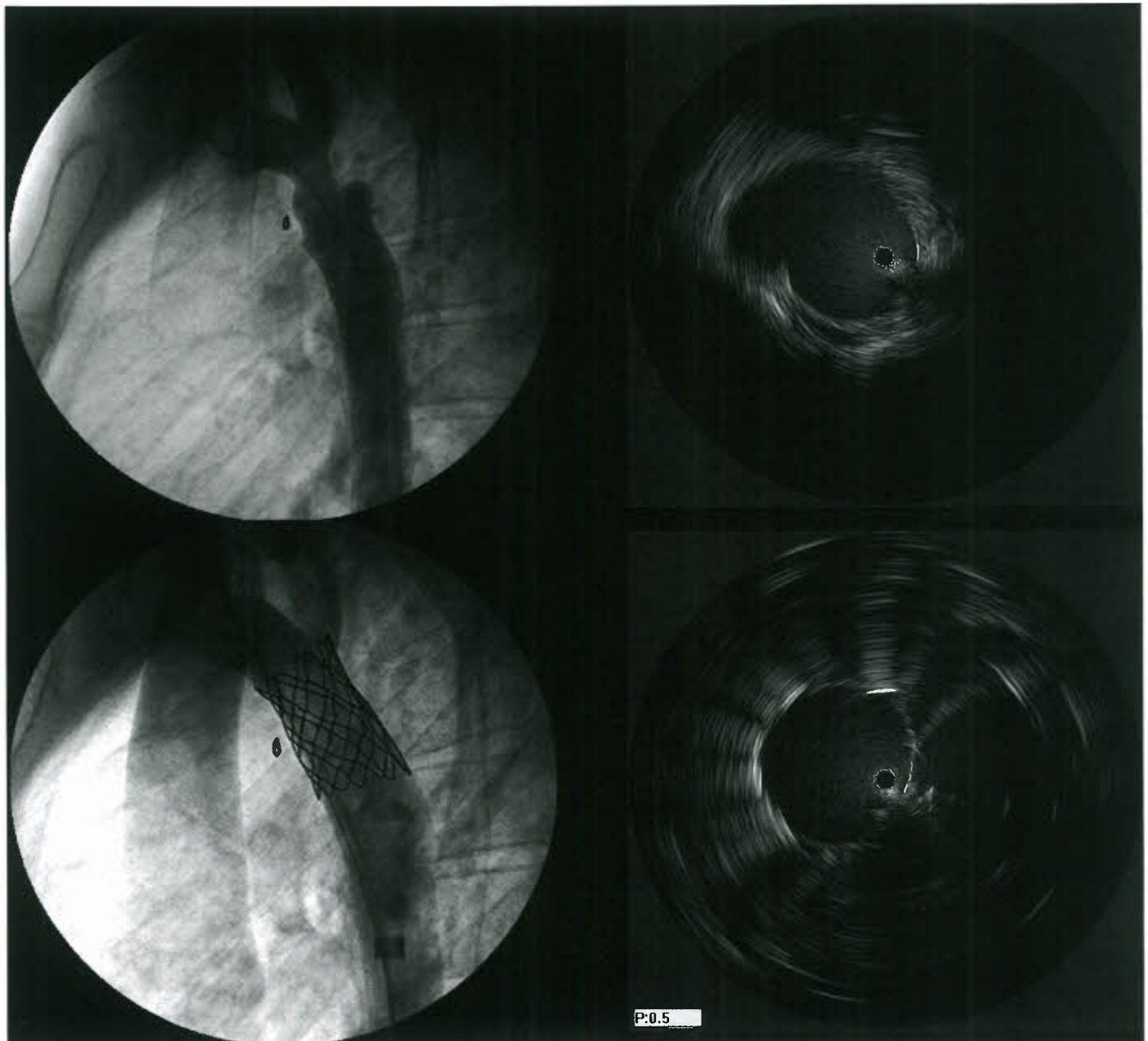


Figure 13.15. Adult coarctation with aneurysm. A 23-year-old man who underwent GoreTex patch augmentation earlier in life and subsequently developed recoarctation with a 22 mm Hg peak systolic gradient and associated posterior aneurysm. Placement of a cove red CP stent completely abolished the residual gradient and excluded the posterior aneurysm. **Top left:** Aortogram before stent placement. **Bottom left:** Aortogram after stent placement. **Top right:** IVUS before stent placement demonstrating the aortic aneurysm. **Bottom right:** IVUS after stent placement with complete exclusion of the aneurysm.

achieve optimum pulmonary growth. This was highlighted in the results from the C3PO registry where 22% of patients required early reinterventions within the first 3 years of the procedure (20).

The clinical use of intravascular stents in patients with congenital heart lesions was introduced in 1989 by Mullins and colleagues with the use of large Johnson and Johnson Interventional System (JJIS; Sommerville, NJ) iliac stents in branch pulmonary artery and central systemic vein stenoses. The experience with stents in these lesions has significantly changed the approach to branch pulmonary stenosis. Results in eliminating any gradients and opening the vessels to their normal diameters have been excellent (8). The implant dilation does not require overdilation of the vessel to achieve a normal

end diameter. The initial results are often sustained over years. In addition, it has been demonstrated that if the appropriate stents are implanted initially, these stents can be dilated further in the future up to the adult diameter of the vessel. In the 25 years since their introduction for this use, intravascular stents have become the primary mode of therapy for branch pulmonary artery stenoses in most large institutions that provide care for congenital heart patients.

Implanting stents that may not be expandable to adult size (such as premounted stents) may be indicated in certain infants and small children undergoing a “palliative” procedure. Holzer et al. (123) recently presented a series of pulmonary arterial stent implantation in children weighing <15 kg and documented that stent implantation may prevent or defer

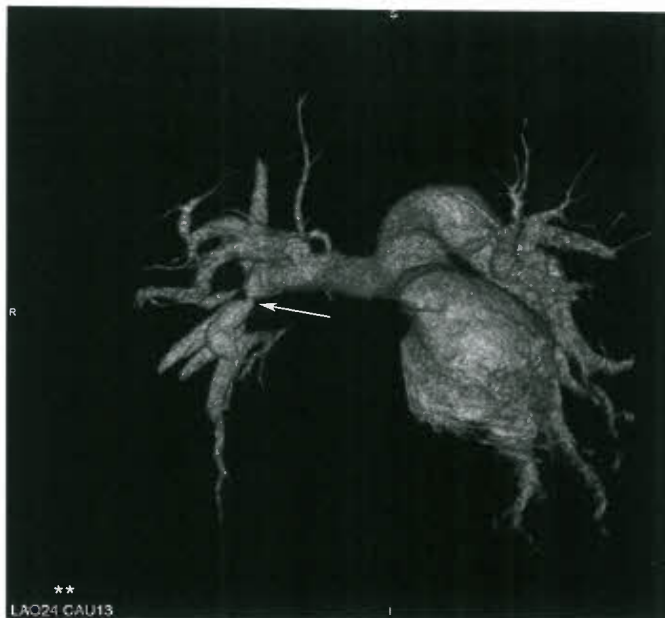


Figure 13.16. Three-dimensional (3-D) reconstruction of rotational angiography of pulmonary arteries. A 5-year-old girl with TOF-PA-MAPCAs who underwent unifocalization without VSD closure at 6 months of age, followed by two surgical reinterventions and subsequent interventional catheterization within the following 12 months. 3-D rotational angiography facilitates better delineation of an RLL branch PA stenosis (arrows). The image can be rotated until the lesion is best profiled and the allowable angles are displayed (asterisks) that then allows the operator to choose the same angulations for 2-D acquisitions.

the need for subsequent surgical intervention to a time when this can be performed with a lower risk. Similar results were documented in a larger series by Stanfill et al. (67). Furthermore, *in situ* stents may not necessarily present a major difficulty for the surgeons and can be excised or patched where required (67,123). While this may be challenging, it may present the preferred treatment alternative for selected patients. Furthermore, the meshwork of small diameter stents can be potentially fractured using ultra-high-pressure balloons, as recently shown by Maglione et al. (66). This would then allow implantation of stents that can be expanded to adult diameter to accommodate growth of a child and vessel.

The delivery and implantation of intravascular stents in the branch pulmonary arteries are performed through the use of long sheaths and these procedures are usually a fairly complex undertaking. An end-hole catheter is advanced well beyond the lesion to be treated and is replaced with a stiff exchange wire. Appropriate and diligent guidewire positioning is a key to successful stent therapy. A long sheath/dilator large enough in diameter to accommodate the stent mounted on the appropriate delivery balloon is passed over the wire beyond the area of stenosis. This is usually one of the most challenging parts of the procedure and may require changing the approach from femoral venous to internal jugular or transhepatic in selected patients. The chosen long sheath should be kink-resistant and reinforced if possible, such as the Super ArrowFlex sheath (Arrow, Reading, PA), but these suitable sheaths are presently not available in all sizes that would accommodate larger sized balloon-stent combinations, as required in many adult patients. The dilator is then removed over the wire, leaving the sheath and wire in place. The balloon with the mounted stent

is advanced over the wire and through the long sheath to the area of stenosis. The sheath is withdrawn off the balloon/stent; when the stent is verified to be in the exact position, the balloon is inflated, expanding the stent into the lesion and with deflation of the balloon, fixes the vessel at the dilated diameter (Fig. 13.18). During stent positioning, angiography can either be obtained through the sidearm of the long hemostatic sheath or by using an additional angiographic catheter advanced from a separate venous entry site. In order to achieve precise delivery and positioning of the stent, specialized balloon delivery catheters are often helpful. The BIB balloon catheter allows adjustment of the partially deployed stent after inflation of the inner balloon alone, before full deployment using the outer balloon. When expanding the stent to a diameter ≥ 12 mm, the BIB catheter is chosen. The addition of rapid RV pacing also reduces systolic stent movement during deployment.

Pulmonary artery rehabilitation requires a high amount of technical expertise and is not without risks. The results from the C3PO registry documented an incidence of high severity adverse events of 10% in 1,315 procedures (20). Independent risk factors for high severity adverse events were age below 1 month, two or more indicators of hemodynamic vulnerability, use of cutting balloons, and operator experience of <10 years. The use of cutting balloons likely reflected the severity of the underlying lesions, rather than cutting balloons themselves being a risk factor for adverse events. The study also found that technical complications such as stent migration were more common for proximal pulmonary artery lesions, while, for example, reperfusion injuries (Fig. 13.19) as manifested through bleeding from the endotracheal tube were more common for lobar or mixed lesions. Acute changes in distal PA pressures of more than 150% and a mean distal PA pressure of more than 20 mm Hg have been found to be risk factors for reperfusion injury (124). In patients with multiple pulmonary artery stenosis, it is therefore often important to treat as many lesions as possible, allowing a decrease of the pulmonary artery pressures rather than treating only individual lesions that then may lead more readily to a reperfusion injury in the treated segment.

TRANSCATHETER MANAGEMENT OF PULMONARY VEIN STENOSES

Surgical as well as transcatheter interventions for pulmonary vein stenoses have a uniformly bad long-term outcome (125,126). Pulmonary vein stenoses are frequently not isolated. Transcatheter interventions, whether (cutting) balloon angioplasty or endovascular stenting, are often performed as a “last resort” in patients in whom no other treatment alternatives are available before considering heart-lung transplantation. These procedures are technically challenging and have a higher than average associated procedural risk. The procedures are often acutely successful but restenosis is observed in the majority of cases. Attempted dilation of these lesions may be recommended in an infant or child who is severely symptomatic. The experience with intravascular stents in pulmonary vein stenosis to date has had no better medium- or long-term results than (cutting) balloon angioplasty alone, but has been associated with a high percentage of complications including systemic stent embolization. However, in selected patients, short-term results of endovascular stenting may be superior to cutting balloon angioplasty and as such may serve as a temporizing measure in critically ill children (Fig. 13.20). Stents have been surgically placed into pulmonary veins under direct vision as well as during brief ECMO support as “hybrid” procedures. The ultimate prognosis of these lesions remains poor. Where transseptal access is required and patients are of

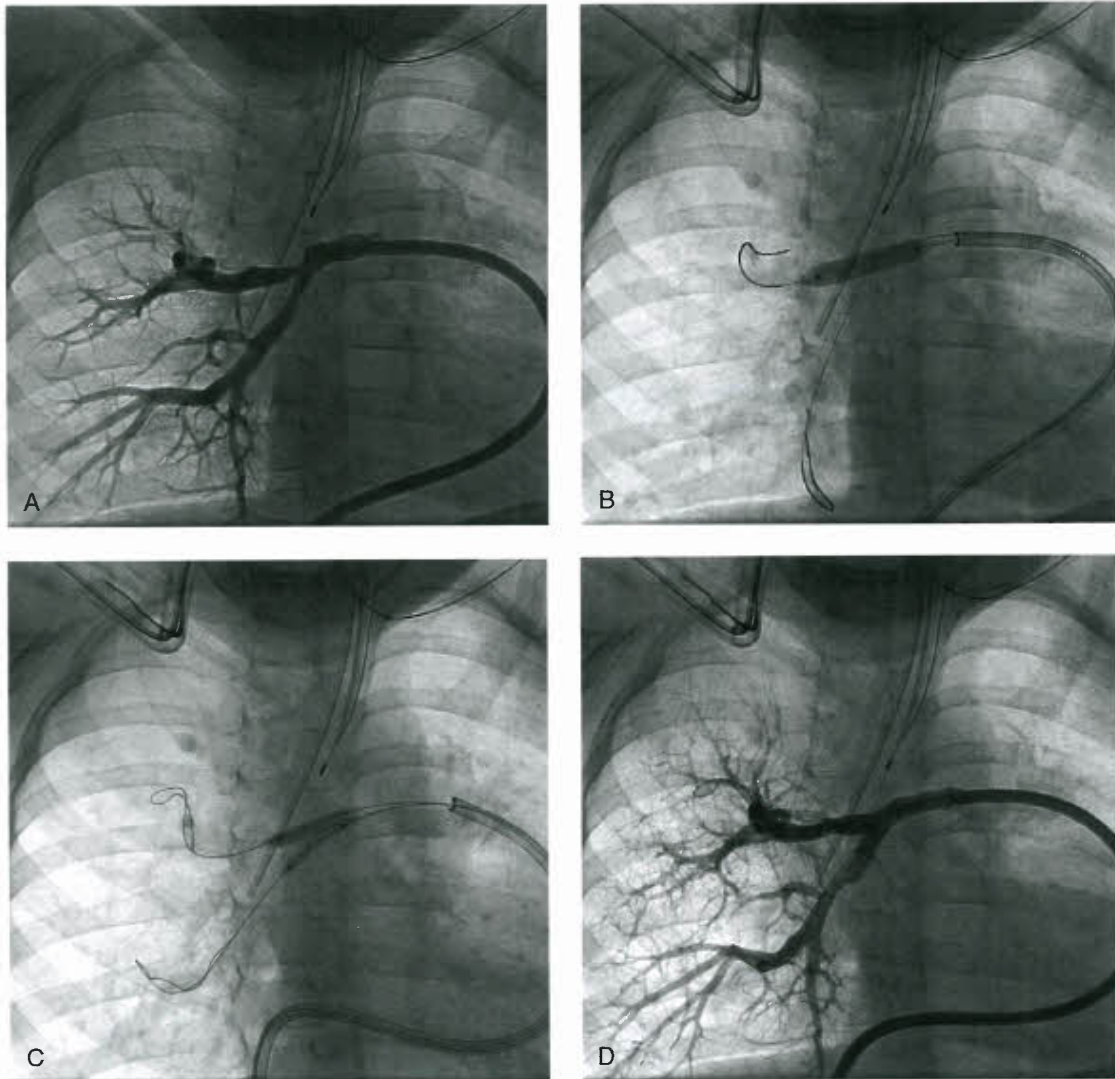


Figure 13.17. Pulmonary atresia with ventricular septal defect (PAVSD). Major aortopulmonary collateral arteries (MAPCAS)—PA rehab of multiple lesions. A 2-year-old girl with PAVSD and MAPCAS, RLL and Right middle lobe (RML) stenosis (A). A long braided sheath is placed in the proximal RPA with wires positioned in both RML and RLL branches to allow PA rehabilitation in quick succession. Initially cutting balloon angioplasty is performed of RML (B), then cutting balloon angioplasty of RLL, followed by simultaneous standard BA of both RML and RLL (C), with good angiographic result (D, trivial LLL aneurysm).

appropriate size, the use of steerable transseptal sheaths can significantly improve access especially to the right pulmonary veins.

TRANSCATHETER MANAGEMENT OF SYSTEMIC VEIN STENOSES

Dilation of stenosed systemic veins, particularly those narrowed after surgical or other interventions, often is acutely successful and carries little risk. Zahn et al. (127) recently demonstrated the feasibility of transcatheter interventions even in freshly operated lesions. The surgical alternative for these lesions is poor to nonexistent. Like pulmonary branch stenosis, the results are not uniform or predictable. As with balloon dilation of other vessels, there is immediate hemodynamic, anatomic, and symptomatic improvement. However, stenosis recurs in many cases. The technique for dilation of

systemic veins, as with the other vascular balloon dilation procedures, involves crossing the stenosed lesion with a catheter and exchanging the catheter for a wire over which the dilation balloon (or balloons) can be advanced across the lesion. The balloon size varies between two and three times the diameter of the stenosed segment. The balloons are inflated in the lesion to the pressure recommended for the particular balloons. Balloon angioplasty is frequently the preferred intervention when fairly fresh thrombotic material is responsible for the stenosis, as placement of endovascular stents often does not offer additional advantages due to protrusion of thrombotic material through the struts of the placed stent (unless covered stents are used). However, if a vascular stenosis is the cause of an acute vascular thrombosis, stent implantation is usually preferable to balloon angioplasty alone (128).

Similar to results seen in pulmonary artery branch stenoses, the incidence of restenosis is high. Therefore, primary therapy for the more long-standing venous lesions has become the implantation of intravascular stents. In many patients, the

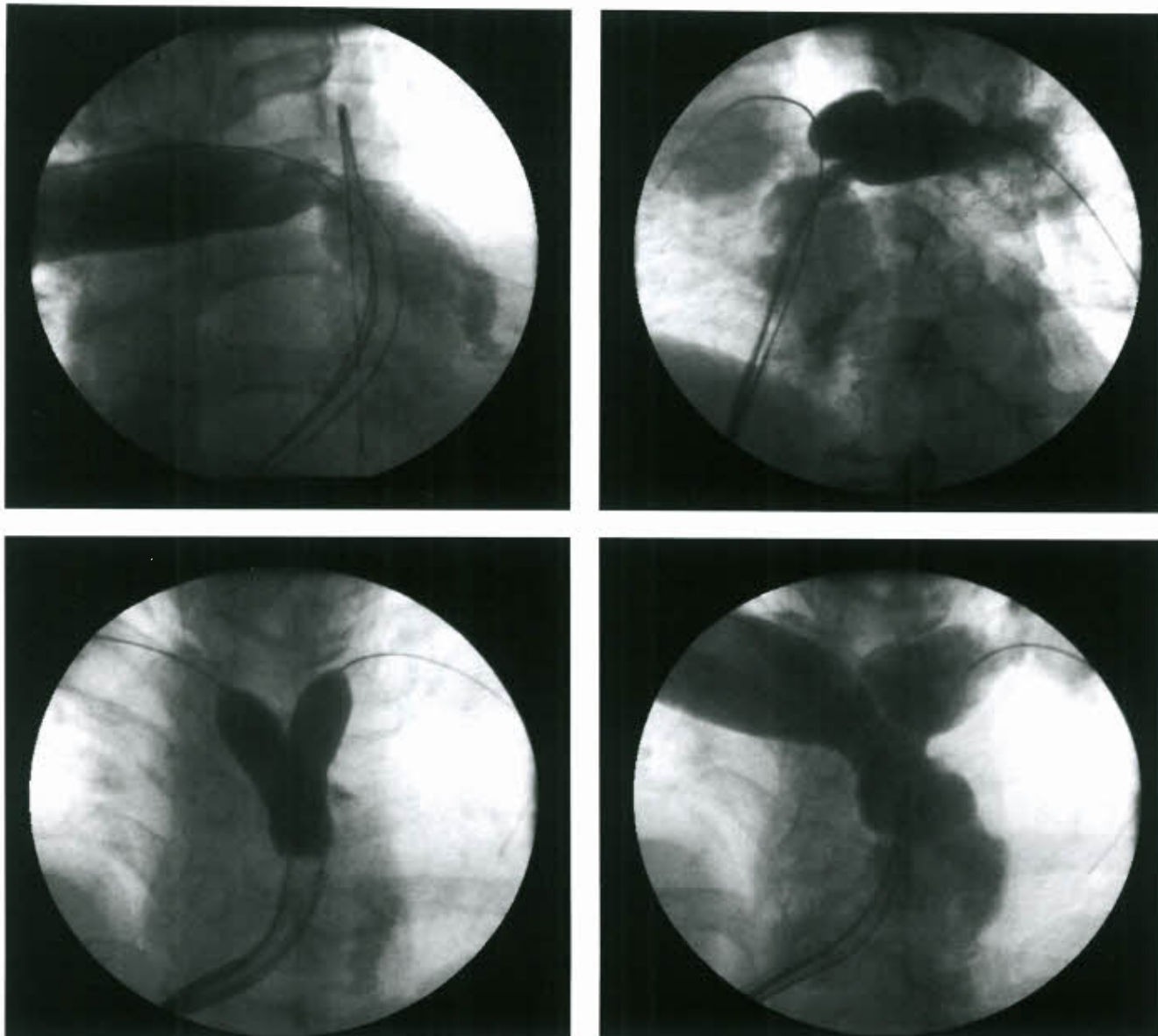


Figure 13.18. “Kissing” stents for bilateral branch PS. Bilateral branch pulmonary artery stenosis after repair of tetralogy of Fallot. Implantation of “kissing” stents to the PAs abolished 25 mm Hg gradients to the branch PAs and reduced the RV/systemic pressure ratio from 60% to 35%. **Top left:** RPA origin stenosis. **Top right:** LPA origin stenosis. **Bottom left:** Simultaneous expansion of “kissing” stents (Genesis XD and Max LD). **Bottom right:** Angiographic result after stent deployment.

use of RF energy combined with the subsequent placement of covered stents may allow the recanalization of even completely obstructed venous structures (Fig. 13.21) (74). As with any other lesion, stents are chosen to be expandable to adult size, and therefore usually include the Genesis XD or the Max/Mega LD stents, or the covered CP stent, if available. The venous stent delivery procedure is similar to other intravascular stent deliveries in congenital heart lesions with the stents delivered over a stiff wire and through a long sheath. For stent delivery, a single balloon of a diameter similar to that of the adjacent nearest normal vein is used. Results of central venous stent implantations have been excellent. No adverse reactions or long-term complications of the stents have occurred. Some venous restenoses have occurred when stents were dilated to a diameter significantly larger than the adjacent vessel at the time of implant.

In these instances, the lumen within the stent “remodels” with neointima to the size of the normal adjacent vessel.

TRANSCATHETER THERAPY AFTER “ATRIAL SWITCH”

Prior to the establishment of the “arterial switch procedure” as the primary technique to treat patients with TGA, a large number of patients have been palliated using a modified Mustard or Senning procedure. These patients have continued to survive into adulthood, often with very minimal early limitations in their overall cardiopulmonary exercise capacity. However, it has gradually become very clear that the “atrial

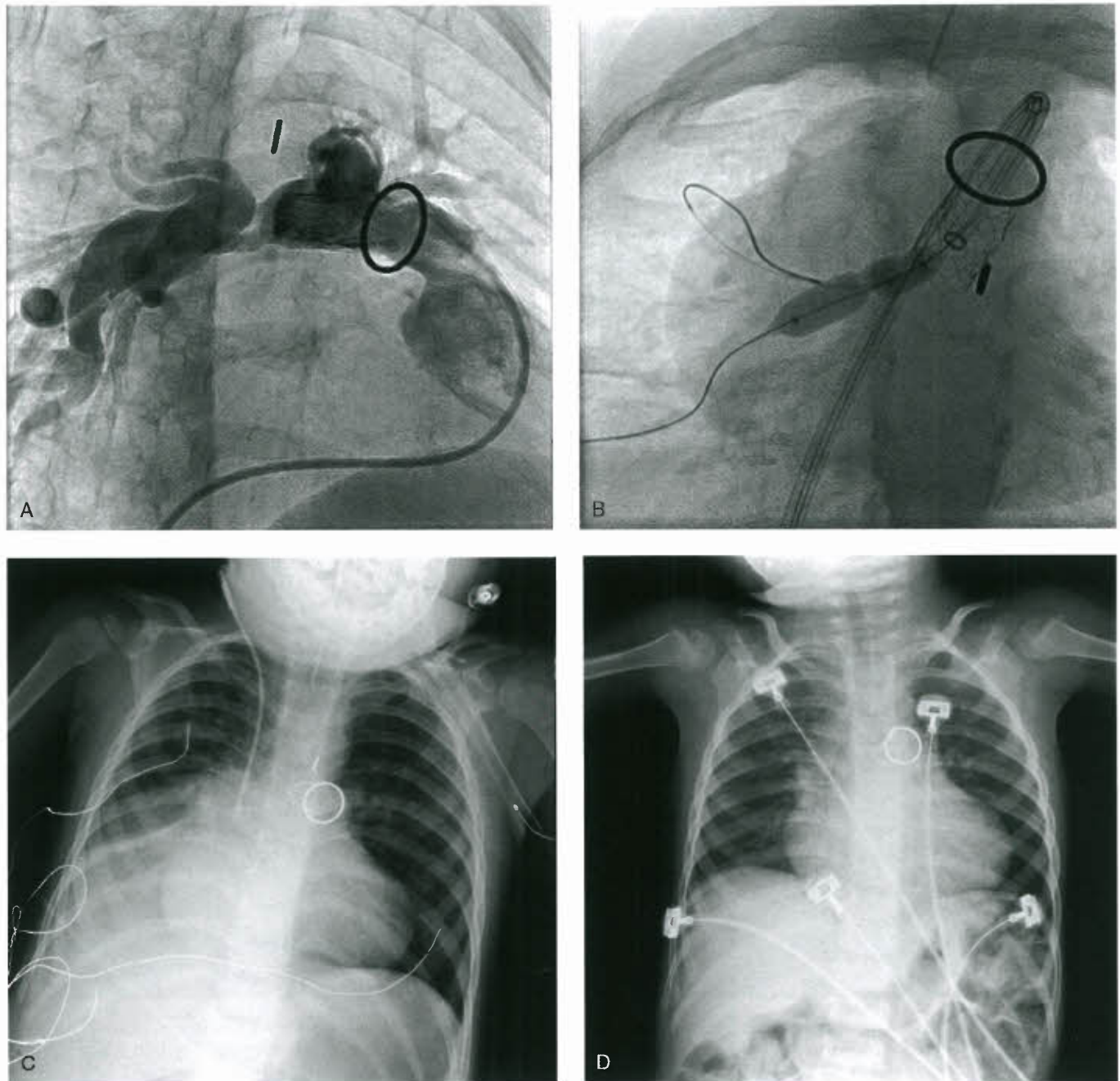


Figure 13.19. Reperfusion injury after PA rehab. A 2-year-old boy with TOF-PA-MAPCAs and DiGeorge syndrome who underwent a surgical shunt at 2.5 months of age and unifocalization with RVPA conduit at 1 year of age. **A:** MPA angiography showing significant distal RPA stenoses. **B:** Serial balloon dilation of distal RPA and lobar branches. **C:** Chest X-ray demonstrating associated reperfusion injury primarily to the right lower lobe (RLL). **D:** Follow-up chest x-ray demonstrating the radiographic appearance of this segment having returned to baseline.

switch” procedures have not “corrected” these patients, but instead have created a long-term palliation with very favorable early results. As a result of their often fairly normal overall cardiovascular status, many patients have been “lost to follow up” or have only been followed up in large intervals without very detailed diagnostic studies being performed on a regular basis. However, as these patients have survived into adulthood, more patients have become symptomatic from problems that are related to the early palliation and are frequently amenable to transcatheter and/or electrophysiological therapy. These problems include systemic and pulmonary venous baffle

limb obstructions, baffle leaks, left ventricular outflow tract obstruction, atrial and ventricular arrhythmias, conduction anomalies, and sudden death. In addition, RV function is frequently found to be reduced, often manifesting itself with an increasing amount of tricuspid regurgitation.

The workup prior to any transcatheter intervention should include an exercise study with documentation for potential arrhythmias or desaturations on exercise, a transthoracic or preferably transesophageal echocardiographic evaluation with documentation of any potential baffle leak or baffle obstruction, and Holter recording. An MRI will enhance the

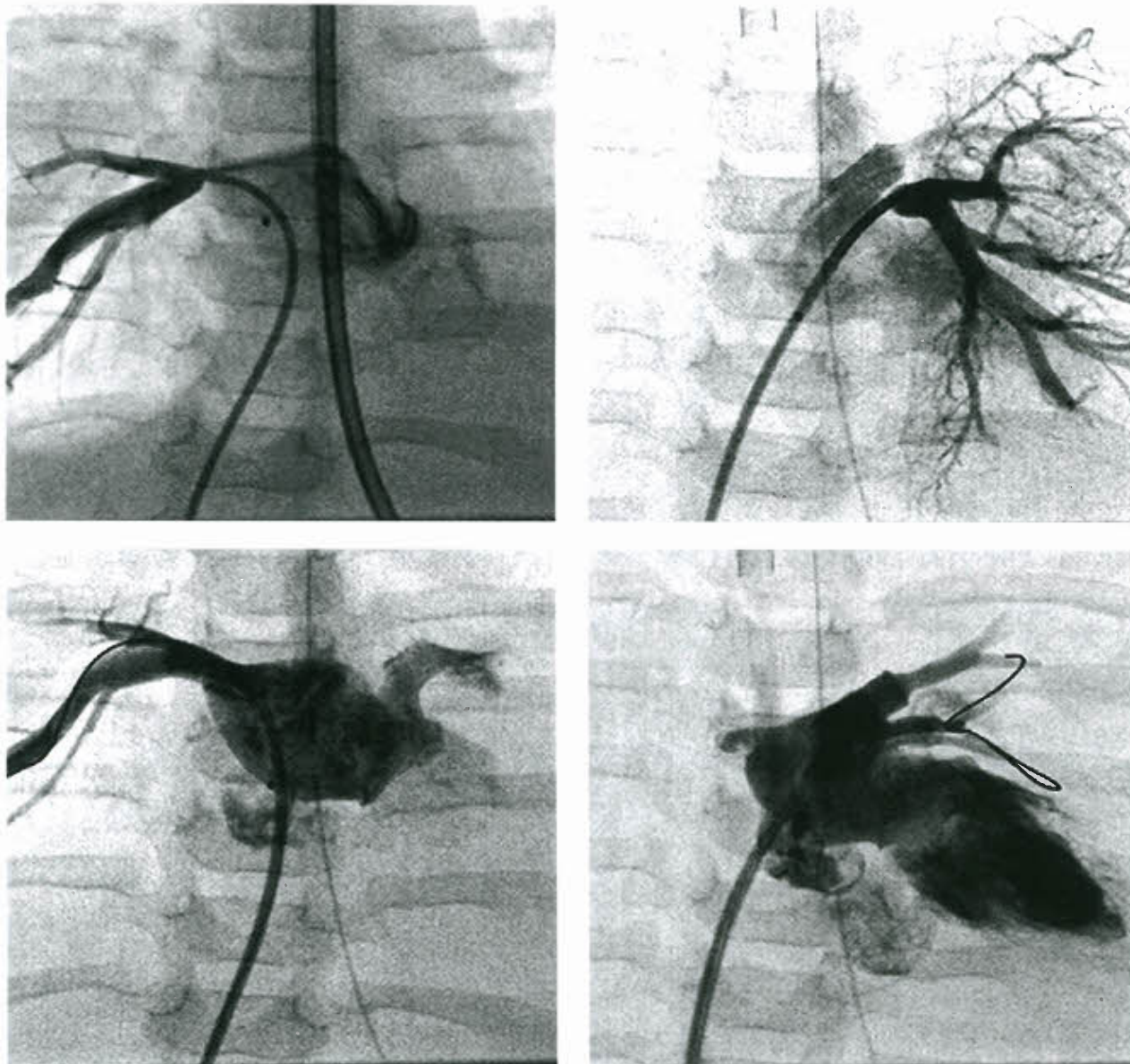


Figure 13.20. Stenting of pulmonary vein stenosis. A 13-month-old infant with Adams-Oliver Syndrome, primary pulmonary hypertension and pulmonary vein stenoses (procedure performed on ECMO support). **Top left:** Right lower pulmonary vein stenosis. **Bottom left:** Right lower pulmonary vein after stent implantation. **Top right:** Left lower pulmonary vein stenosis with drainage partially via stented left upper pulmonary vein. **Bottom right:** Left pulmonary veins after stent placement in upper and lower pulmonary vein.

sensitivity in detecting baffle leaks and baffle obstructions, while also providing RV functional parameters. The electrophysiology team has to be closely involved in preparing these procedures, deciding upon the best physical location (adult or pediatric hospital) and the order in which each individual part of the procedure is performed. This may not only include the pediatric, but in some patients also the adult electrophysiology team who may have greater expertise in, for example, complex pacing lead extractions. For example, a patient with a permanent pacemaker and a lead fracture may benefit from lead extraction at an adult center. The same patient could then be transferred with a temporary pacing lead to the specialized congenital interventional center, where stent therapy of a coexisting SVC baffle limb stenosis is performed, which then allows the pediatric electrophysiologist

to place new transvenous pacing leads through the newly “opened up” SVC.

In general, most patients will usually undergo a combined procedure, during which the interventional cardiologist initially performs a full left- and right-heart hemodynamic evaluation (ideally obtaining jugular venous as well as femoral venous access), which will give some idea of potential pulmonary or systemic baffle limb stenoses. Angiograms of SVC, IVC, right atrium, as well as pulmonary arteries further delineate any areas of stenosis, while also documenting the presence of any baffle leaks. TEE evaluation should be performed during the procedure to better delineate the baffle leaks and specifically their distance to AV valves as well as documenting the location of any pulmonary venous baffle limb stenosis. If multiple abnormalities are identified, it is very important to

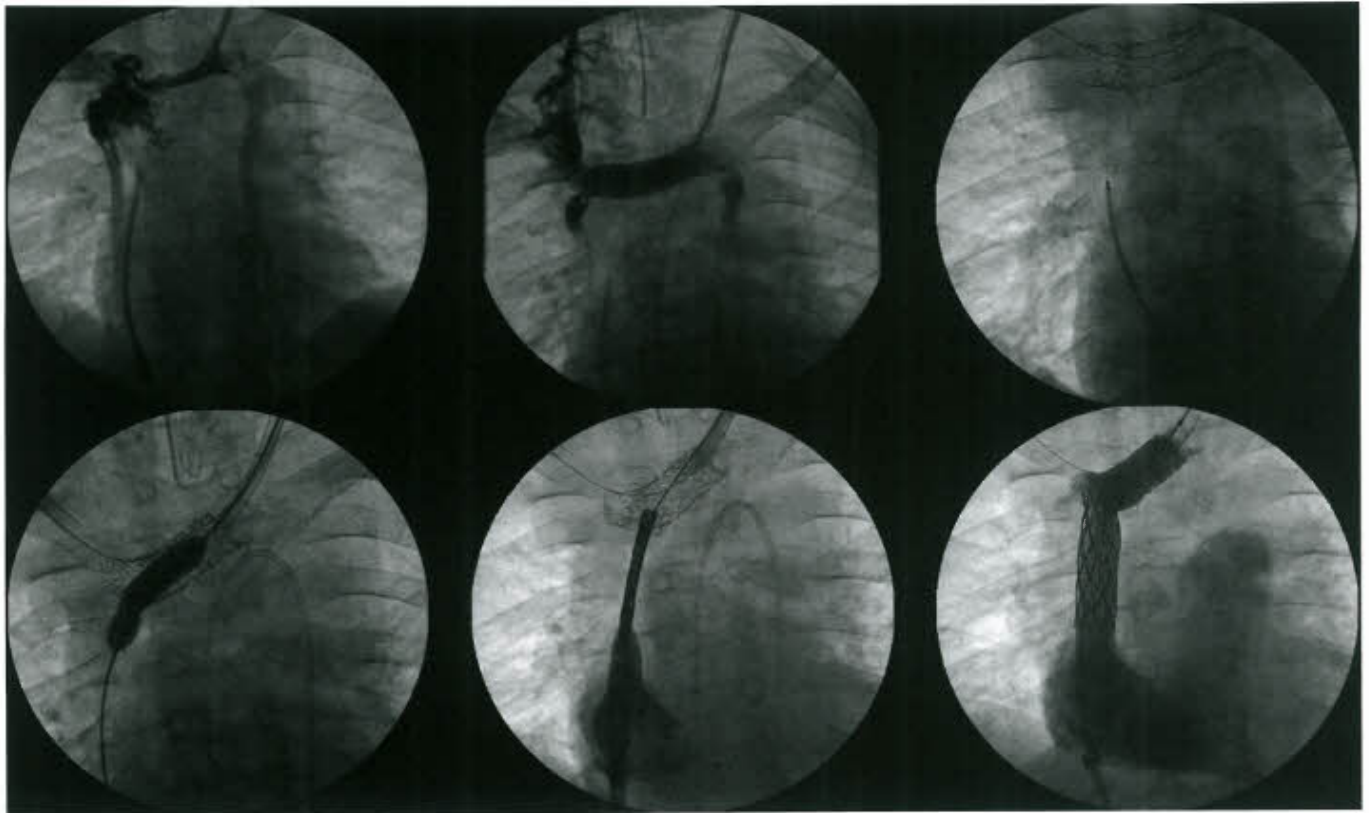


Figure 13.21. Recanalization of SVC obstruction. Recanalization of an obstructed SVC and stenotic innominate vein in a 16-year-old boy. **Top left:** Occluded SVC and stenotic innominate vein with collateral formation. **Top middle:** Innominate vein appearance after placement of a Mega LD stent. **Top right:** RF wire positioning from right atrium to innominate vein. **Bottom left:** Balloon angioplasty of the open cell Mega LD stent (over wire loop). **Bottom middle:** Final positioning of a covered NuMED CP stent in SVC. **Bottom right:** Final result with significantly improved drainage from innominate vein via SVC to right atrium.

involve the cardiac surgical team during the procedure. That allows determining which lesions may require surgical revision, while deciding at the same time whether other lesions could/should be addressed during the transcatheter procedure. The pediatric electrophysiologist usually follows the interventional cardiologist with an evaluation of AV conduction as well as an electrophysiology study to detect atrial and ventricular arrhythmias. This is then followed by either implantable cardioverter defibrillator (ICD) or pacemaker implantation if required, frequently through the newly stented SVC.

Many cardiologists have in the past adopted a “wait and see” approach when faced with baffle limb obstructions or baffle leaks. However, even though an obstructed SVC baffle limb with a well-formed collateral circulation in an asymptomatic patient may not necessarily cause any immediate problems, rebuilding this vessel not only prepares these patients for the potential of ICD or pacing leads placed later in life but also prevents the baffle stenosis to become completely obstructed, which would pose a higher challenge for any transcatheter management needed in the future. Symptomatic SVC obstructions do benefit from transcatheter management in any patient, while any IVC baffle limb stenoses, if left untreated, have the potential of impairment of hepatic flow characteristics with secondary hepatomegaly and ascites. Pulmonary venous baffle limb stenoses may lead to pulmonary congestion as well as elevated pulmonary arterial pressures and should therefore be treated with the same degree of aggressiveness as MS in a patient with an otherwise normal intracardiac anatomy. Finally, baffle leaks are potential causes for right-to-left

shunting and paradoxical embolism, which can be a particular problem in patients with pacing or ICD leads and/or frequent atrial arrhythmias. Baffle leaks can also lead to desaturation during exercise or even at rest, thereby may contribute to a reduced exercise tolerance, while moderate shunts add unwanted volume loading to the already reduced RV function. At this institution, we have therefore adopted an approach that attempts to eliminate any residual anatomic or morphological abnormalities as much as possible through transcatheter therapy, which has been documented to be an excellent form of therapy for these lesions with very favorable results (129).

SVC baffle limb rehabilitation is best preformed using an internal jugular venous approach, placing a stiff wire with a floppy tip within the left ventricle. Some SVC baffle limb stenoses may require high pressures during balloon expansion and frequently the placed stents must be further expanded using high-pressure Mullins balloons (NuMED, Hopkinton, MA). Stents that are expandable to diameters in excess of 18 mm, such as the Max LD stent (EV3, Plymouth, MN) or the (covered) CP stent (NuMED, Hopkinton, MA), are most suitable to treat these baffle limb obstructions. Stents should only be placed across a baffle leak after the leak itself has been occluded using a transcatheter device (Fig. 13.22). Where approved and available, a combination of baffle leak and obstruction can be more readily treated using covered stents. Pulmonary venous baffle limb stenoses can be addressed either by a transeptal approach or by using a retrograde aortic approach through right ventricle and tricuspid valve. The short length of these lesions usually makes them less amenable to intravascular

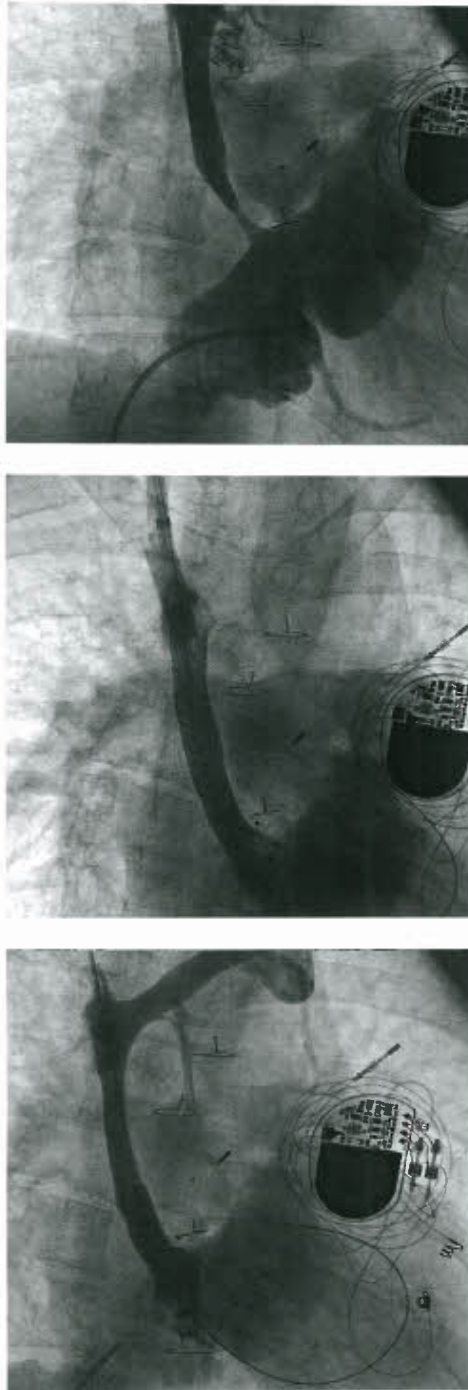


Figure 13.22. Mustard baffle leak and stenosis. A 25-year-old patient with a history of Mustard atrial switch procedure for TGA. Hemodynamic evaluation demonstrated a SVC baffle limb stenosis with near-interruption and a 10 mm Hg mean gradient as well as a stenotic SVC. Additionally, a baffle leak was identified at the inferior end of the SVC baffle. **Top:** SVC angiogram delineates the severe SVC baffle limb stenosis and the baffle leak to the right of the stenotic area. **Middle:** SVC angiogram after occlusion of the baffle leak using an 8-mm ASDO and placement of a 36-mm Max LD within the SVC baffle limb, demonstrating no residual angiographic shunt and significantly improved SVC baffle limb. **Bottom:** Angiogram in SVC after placement of two additional Max LD stents in SVC, thereby rehabilitating the hypoplastic SVC from innominate vein insertion to baffle limb (mean residual gradient 1 mm Hg).

stent therapy, but some improvement can be achieved using high-pressure balloon angioplasty.

The experience of managing these patients at our institution using a combined team approach was presented by Holzer et al. (130) in 2006 (Fig. 13.23). Between December 2002 and April 2006, 81% of all patients who were followed after atrial switch procedure underwent transcatheter evaluation. Electrophysiologic or pacing procedures were performed in the same setting in 15 patients. SVC baffle limb stenosis was found in 75% of patients, while IVC baffle limb stenosis was seen in about 11%. Seven percent of patients had a pulmonary venous baffle limb stenosis, while 57% of patients had baffle leaks. Only three patients had none of the aforementioned abnormalities. Stent therapy was performed for 19 SVC baffle limb obstructions and 2 IVC baffle limb obstructions. Devices for baffle leaks were implanted in 11 patients, while 5 patients received a covered stent for a combination of baffle limb stenosis and leak. One patient underwent balloon angioplasty of a pulmonary venous baffle limb stenosis and three patients had RF perforation of a completely obstructed SVC baffle limb. Most patients with pulmonary venous baffle limb stenosis underwent surgical revision—the same applied for three patients with large baffle leaks and insufficient distance to the AV valves. After stent implantation, the gradient across the baffle limb was reduced significantly from a mean of 3 mm Hg to a mean of 1 mm Hg, while the mean diameter improved significantly from 8.3 to 18 mm. Transcatheter baffle leak occlusion was performed or attempted in 17 patients, while three patients had unsuitable locations of the baffle leak, requiring surgical revision. Complete closure of the baffle leaks was achieved in about 82% of patients. Trivial residual leaks were seen in two patients, usually around small right atrial trabeculations. Complications were rare and only encountered in two patients, including atrial tachycardia requiring medical management in one and temporary complete heart block (CHB) in another. Over a follow-up period of up to 3.7 years, one patient underwent a repeated intervention for closure of a residual baffle leak after surgical baffle revision, while three patients underwent surgical correction for large baffle leaks or pulmonary venous baffle limb stenoses.

These data demonstrate clearly that patients after atrial switch have significant pathology that can be treated in the catheterization laboratory. Patients after “atrial switch” procedure require a team approach to identify and treat any residual anatomic lesions. Transcatheter and electrophysiologic therapy have important roles within the multidisciplinary management of these patients.

DEVICE CLOSURE OF SEPTAL DEFECTS

Transcatheter Closure of Atrial Septal Defects

At the present time, the AMPLATZER Septal Occluder is the most commonly used device to close intra-atrial communications worldwide as well as in the United States, ranking superior with regards to closure rates, rates of complications, and ease of use. However, prospective clinical trials that compare this device with other available devices in a controlled and randomized fashion have not been conducted.

Preparation for Transcatheter ASD Closure

Transcatheter closure of ASDs is usually performed under general anesthesia using TEE as guidance for device deployment and delivery. However, studies have documented that ICE is equally suitable for echocardiographic guidance, thereby allowing these procedures to be performed under conscious or deep sedation in older children and adults (131,132).

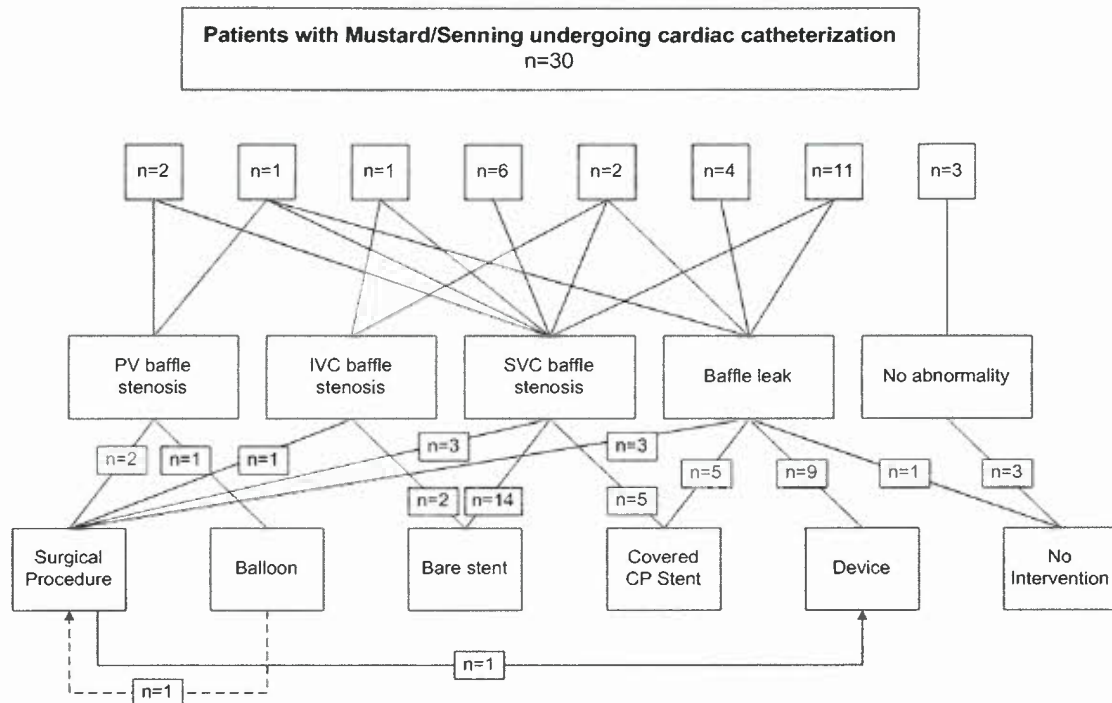


Figure 13.23. “Atrial Switch” catheterizations at Nationwide Children’s Hospital. Findings and procedures performed in 30 patients who underwent cardiac catheterization at Nationwide Children’s Hospital. All young adult patients had previously undergone a surgical “atrial switch” procedure for TGA.

Every study requires a full echocardiographic evaluation of the ASD. This should include assessment of the defect size in different planes (four-chamber view, short axis view, and SVC view), confirmation of normal pulmonary venous drainage, and evaluation of the AV valves for the presence of preexisting AV valve regurgitation. It is extremely important to evaluate all septal rims, including the superior rim with distance to pulmonary vein insertion and SVC, the inferior rim towards the AV valves, the anterior retroaortic rim, and the posterior-inferior rim that is in continuity with the IVC. It can at times be difficult to achieve a clear definition of the posterior-inferior rim toward the IVC with TEE, in which case ICE has a clear advantage. Although studies have documented that closure of ASDs even with multiple septal rim deficiency is feasible, this clearly increases demands of the operator’s technical skills (133,134).

Vascular access is usually obtained via the right femoral vein, placing an additional arterial monitoring cannula in the right femoral artery. Additional venous access from the right or left femoral veins may be necessary for ICE. In patients with bilateral occluded femoral veins, device deployment and delivery should usually be performed using transhepatic access, which may even provide better alignment of the device to the atrial septum (135). Internal jugular venous access is the least preferable access route and is unsuitable for device delivery in most patients. Heparin at a dose of 100 IU/kg is administered to maintain an activated clotting time of >200 seconds. A standard hemodynamic left and right heart catheter evaluation should be performed prior to device closure. This should include evaluation of pulmonary artery pressures, pulmonary vascular resistance, and estimation of the atrial level shunt. Angiographic evaluation of the ASD through an injection in the right upper pulmonary vein is not uniformly required but may aid as a roadmap for device orientation especially when

larger defects are being closed in smaller children. Angiography is usually performed using 35 degree LAO and cranial angulation. However, as the ASD’s position varies between patients, so does the best view to *en-face* profile the atrial septum. Therefore, tube angulations should be adjusted after initial angiography to achieve a better profile of the atrial septum. This view is then used throughout the device delivery and deployment process. In general, biplane views are not necessary to aid ASD device closure and, in fact, may hinder accessibility to the patient for the echocardiographer.

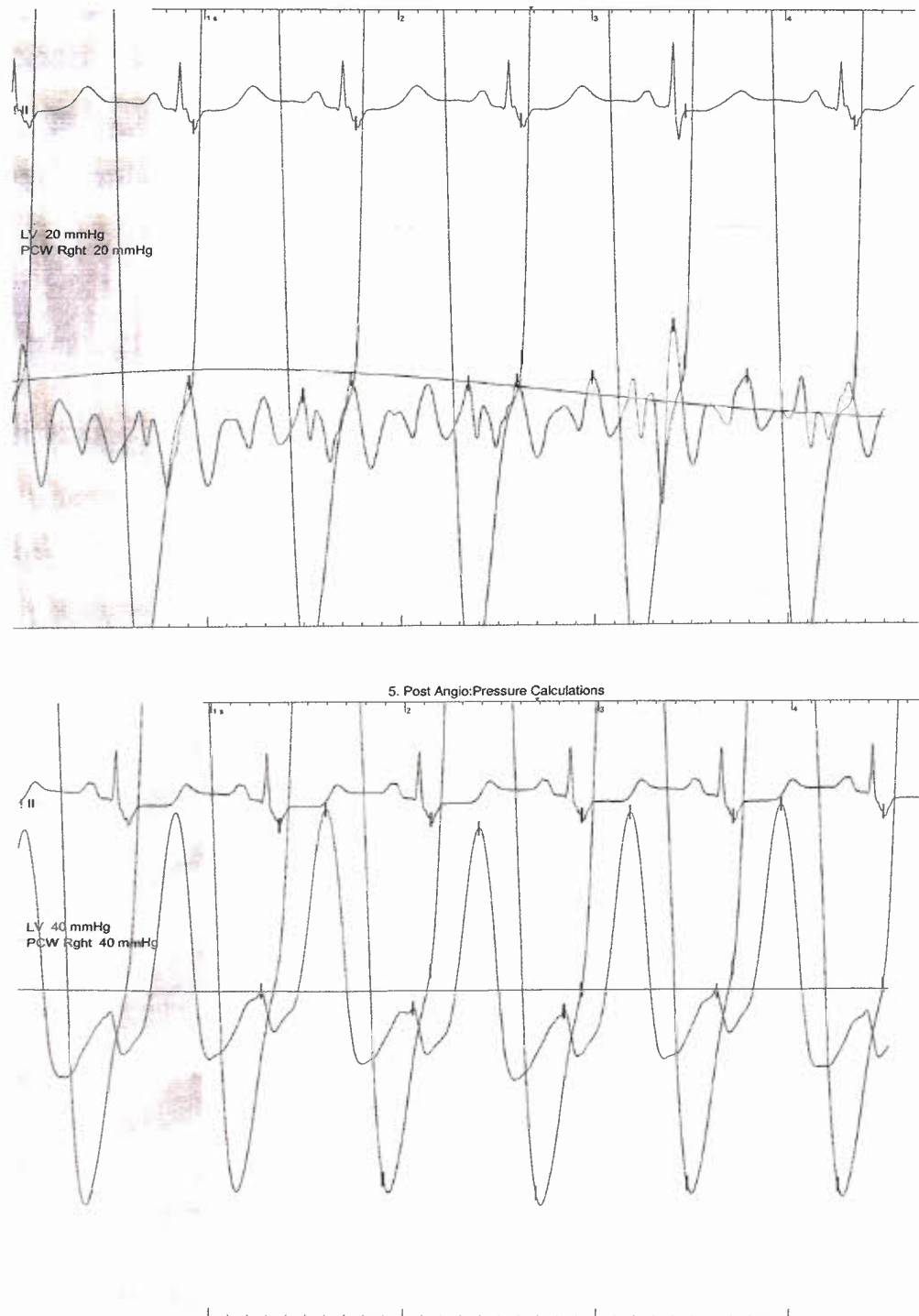
Even though the technical aspects of the treatment of adults with ASDs are not dissimilar to the treatment of smaller children (Fig. 13.27), the physiological effects of closing the intra-atrial communication have to be considered and evaluated very carefully, especially in older patients who have evidence of LV diastolic dysfunction. Closure of large intra-atrial communications in “unprepared” patients with LV diastolic dysfunction can lead to a significant increase in left atrial pressure due to the loss of “pop-off” via the atrial septum, with resulting pulmonary edema and ventilator dependency (136). The left atrial/wedge pressure should be evaluated at baseline as well as after test occlusion of the defect. In many patients, placing the device across the defect without release and then recording pulmonary artery wedge pressure via a second catheter eliminate the potential of the balloon size interfering with the obtained pressure tracing. While a small increase (<5 mm Hg) in left atrial pressures may be acceptable and reasonably well tolerated, an increase of left atrial pressure by a mean of 10 mm Hg or more is clearly prohibitive to occlusion of the septal defect (Fig. 13.24). Preferably, the treatment of any patient in whom these physiologic changes are expected, such as in older patients with a large ASD and systemic hypertension and/or LV dysfunction, should be optimized prior to engaging in any transcatheter procedure. This should include aggressive

diuretic therapy as well as afterload reducing agents. If a patient, despite appropriate pretreatment, still develops significant left atrial hypertension after test-occlusion, the placement of a fenestrated device may be necessary. Fenestrations within the device have been described, such as creating a communication through the ASO (AGA Medical Corporation, Golden Valley, MN), which can be created by direct puncture through the central connecting waist of the device using a larger sized dilator (137). Alternatively, if these fenestrations need to be maintained for a longer period of time, placement of a short endovascular stent through the device may be beneficial (138).

Technique of ASD Closure Using the AMPLATZER Septal Occluder

The left upper pulmonary vein is entered using either a wedge, multipurpose, or Judkins right coronary catheter and a pre-shaped, exchange length, extra stiff, j-tipped wire is advanced. Most operators would at this stage perform static “Doppler stop-flow” balloon sizing under echocardiographic guidance, using either an 18-, 24-, or 34-mm AGA sizing balloon (AGA Medical Corporation, Golden Valley, MN) or a NuMED sizing balloon (NuMED, Hopkinton, NY). It is extremely

Figure 13.24. Wedge pressure and ASD closure. Pulmonary arterial wedge pressure in a 70-year-old woman who was considered for transcatheter ASD closure. Top LV and wedge tracing before closure documenting a mean wedge pressure of 9 mm Hg. Bottom LV and wedge tracing after ASD occlusion with a 34-mm ASO deployed but not released, documenting an increased mean wedge pressure of 32 mm Hg and an increase in Left ventricular end-diastolic pressure (LVEDP). The device was subsequently recaptured and the ASD was left open.



important to expand the balloon until the atrial level shunt is just abolished. The dimensions are then recorded on echocardiography as well as on cine recording. However, unless a mild waist is visible, cine recordings can be misleading at times, as the angle of the atrial septum in relation to the sizing balloon may vary. One should clearly avoid any oversizing in an attempt to achieve a clear waist on the balloon, as oversizing of the device has been linked to the rare but serious complication of device erosion into the aortic root that has been described after ASD closure using the ASO (139). Many centers now completely avoid balloon sizing, especially in small children, and instead use an averaged maximum diameter taken from the three standard views to determine the appropriate device size. One would then add 25% to this diameter to determine the appropriate device size, which is often very similar to the ASD size determined when using color flow mapping. In patients with a deficient retroaortic rim where the two discs are expected to hug the aortic root on either side, the device size may have to be increased further. By subtracting 12 to 14 mm (depending on the device size), one can then estimate the maximum LA disc size that is suitable to close the defect without exceeding the septal length. Where balloon sizing is performed, the AGA sizing balloon may be advanced directly through the skin without the use of a hemostatic sheath, while the NuMED sizing balloon (NuMED, Hopkinton, MA) can pass through an 8 Fr sheath.

Once the device size has been determined, the appropriate delivery sheath is placed over the guidewire into the mouth of the left upper pulmonary vein. In addition to the standard AGA 45 degree delivery sheath, other long hemostatic sheaths can be used. The dilator and wire are gently removed and extreme care must be taken to avoid any inadvertent air entry into the sheath and left atrium at this stage. The device is then prepared for delivery, attaching either a Touhy-Borst adapter or the standard bleed-back valve that is supplied with the AGA delivery system to the loader. The delivery cable is passed through the assembly and the device, after being carefully inspected, is screwed onto the cable avoiding any force on the screwing mechanism. The device is then loaded under water seal and the whole assembly flushed with hand-warm saline. Once the loader is screwed onto the delivery sheath, the device is pushed forward under fluoroscopic guidance until the tip of the sheath is reached. The deployment is conducted under simultaneous echocardiographic and fluoroscopic guidance. The whole assembly is then pulled back until the tip of the delivery sheath exits the mouth of the pulmonary vein, at which stage the delivery sheath is pulled back while fixing the delivery cable to deploy the left atrial disc. Once the LA disc has been deployed, the position and orientation of the device are further evaluated on echocardiography, and while gently pulling towards the atrial septum, the alignment of device and septum are evaluated. At this stage, gentle rotation of the sheath may aid a better alignment. Once alignment appears suitable, the central connecting waist is deployed allowing "self-centering" and the whole assembly is pulled back against the atrial septum. In quick succession, this is followed by deployment of the right atrial disc once the connecting waist stents the defect itself. If the device pulls through the septum, the device is recaptured, the delivery sheath repositioned, and the deployment process started again. Various techniques have been used to achieve better alignment of the device, such as the use of specialized s-curved delivery sheaths (Hausdorf sheath, Cook, Bloomington, IN), deployment of the left atrial disc into the left or right upper pulmonary vein, use of a dilator advanced through additional venous access to prevent the device from pulling through the defect, and use of Judkins right coronary guide catheters for smaller devices (134,140,141). Before release, the device must be carefully evaluated by echocardiography. This should include assess-

ment for residual shunts around the device, obstruction of adjacent structures, as well as possible interference with the AV valves. The tension of the delivery cable will frequently distort device orientation and allow a moderate shunt between the separated discs. A careful push/pull action of the delivery cable should clearly demonstrate that the two discs are separate in all echocardiographic views as well as on fluoroscopy and the device should not easily be displaced through this very gentle push/pull maneuver. On occasions, right atrial angiography through the delivery sheath may be helpful to unmask inappropriate device position. Once the operator and the echocardiographer are satisfied with the device position, the device is released through counterclockwise rotation of the delivery cable using the supplied pin vice. The device usually reorients itself into a more appropriate position and therefore a final echocardiographic assessment is performed after release of the device (Fig. 13.25).

More challenging defects that require additional operator expertise are those with multifenestrated atrial septum, multiple larger ASDs, or those in very small children. Figure 13.26 demonstrates closure of multiple ASD using two ASO, while Figure 13.27 demonstrates closure of a multifenestrated atrial septum using the AMPLATZER Cribriform Septal Occluder. ASD closure in small children is particularly challenging, due to the small left atrial size and the relationship between device size and limited septal length in these patients (Fig. 13.28). In small children, especially when the weight is below 3 kg, the ICE catheter can be used as echocardiographic guidance in TEE position. Because of the reduced left atrial size, it is often necessary to pull up the TEE probe prior to device deployment, to avoid the device being tilted into an unfavorable position due to impingement of the TEE probe posteriorly (which frequently would let a device pull through the anterior retroaortic rim).

Results of ASD Closure Using the AMPLATZER Septal Occluder

Procedure or device-related complications after ASD device closure are extremely rare. Even though the risk of device embolization is low at about 0.5%, it can occur, especially when attempting to close very large defect with deficient rims in adults (142). Therefore, it is mandatory that any physician attempting to close ASDs be sufficiently trained and skilled in device retrieval, using, for example, a Gooseneck snare (Microvena Corporation, White Bear Lake, MN). The AMPLATZER Septal Occluder can usually be snared and recaptured into a sheath that is 2 Fr size larger than recommended by the manufacturer for that specific device, but attempts at snaring should only be performed within the atria, aorta, or pulmonary arteries. If a device has embolized into a ventricle, frequently manifesting itself with new and persisting ventricular arrhythmias, then surgical retrieval is usually indicated in order to avoid tricuspid or MV chordal injury. When a device is snared, one has to carefully manipulate the retrieval sheath to allow the screw of the device to readily advance into the sheath; otherwise capture of the device would not be possible (Fig. 13.29).

Early electrophysiological abnormalities are common within the first 24 hours after ASD device closure (143), but most of these resolve quickly and persistent rhythm or conduction disturbances 1 year after device closure are extremely rare (144). A release of nickel from the device with a peak at 1-month postimplantation has been described (145). However, its clinical significance is questionable and reports of clinically significant allergic reactions to nickel after device implantation are rare (146,147).

One of the most serious complications after ASD closure is erosion of the device into the aortic root, observed at an incidence of 0.1% (139). Even though the exact cause and risk factors for device erosion into the aortic root have not been

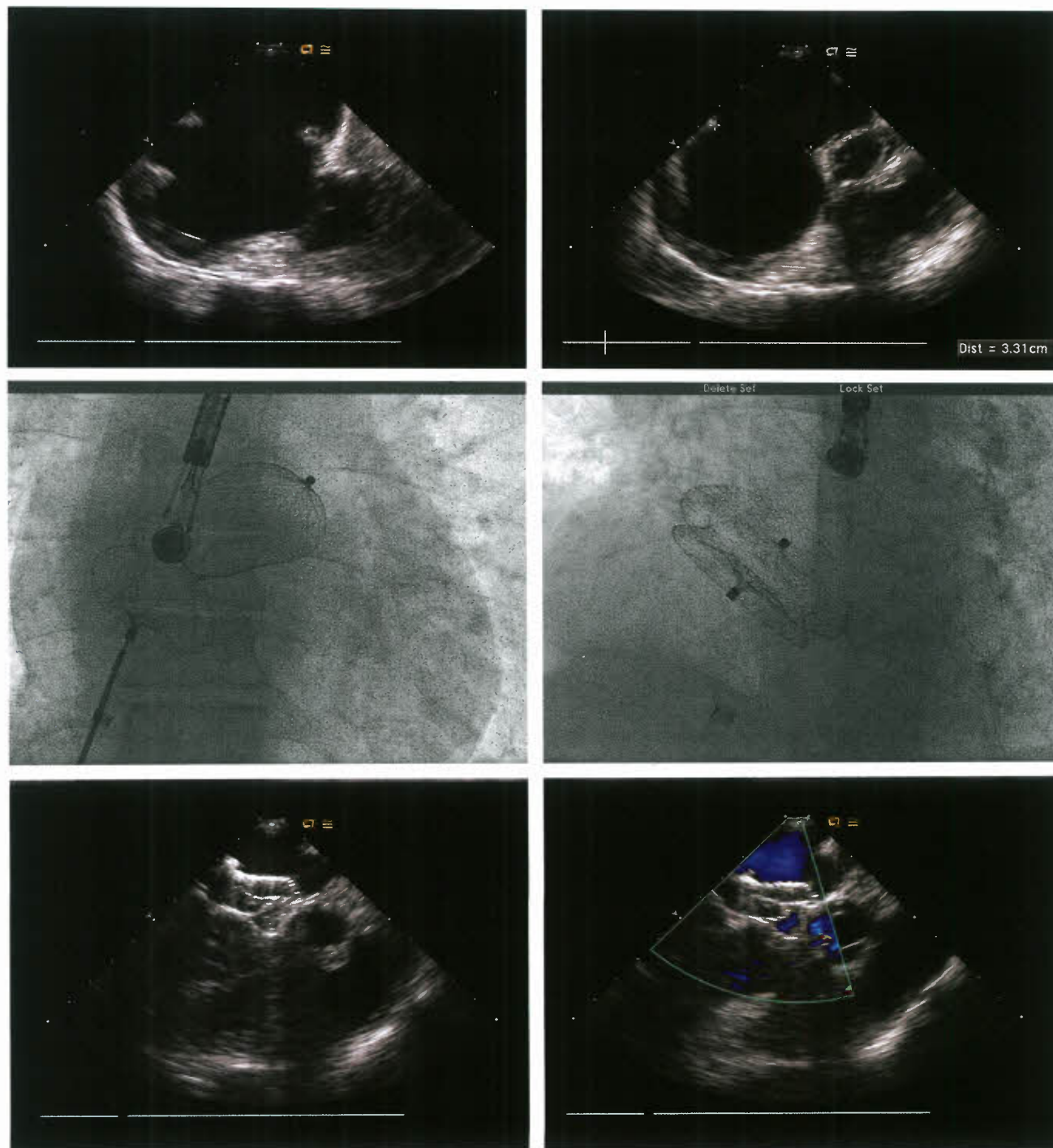


Figure 13.25. Closure of large secundum ASD. Closure of a large 32- to 34-mm secundum ASD using a 36-mm ASO. The device was deployed using a LUPV technique to achieve appropriate alignment with the atrial septum. **Top left:** Modified four-chamber view documenting larger ASD. **Top right:** Short axis view documenting large ASD with deficient retroaortic rim. **Middle left:** LUPV deployment technique. **Middle right:** Device postrelease. **Bottom left and right:** Short axis view without and with color flow mapping after release, documenting excellent device position and no significant residual shunt.

identified, oversizing has been a concern in these patients (139). Most cases of erosion (Fig. 13.30) present in adults within a few days of the procedure with symptoms of chest pain and echocardiographic evidence of a pericardial effusion. However, device erosion can occur with more subtle symptoms several months after the procedure and may only be diagnosed after

fatal erosion into the aortic root has occurred. While there is no valid tool available that identifies device erosion at an early stage, symptoms of chest pain or the presence of a pericardial effusion should alert the cardiologist to this potentially fatal complication. A multislice volume-rendered CT scan with 3D reconstruction allows evaluation of the device from all

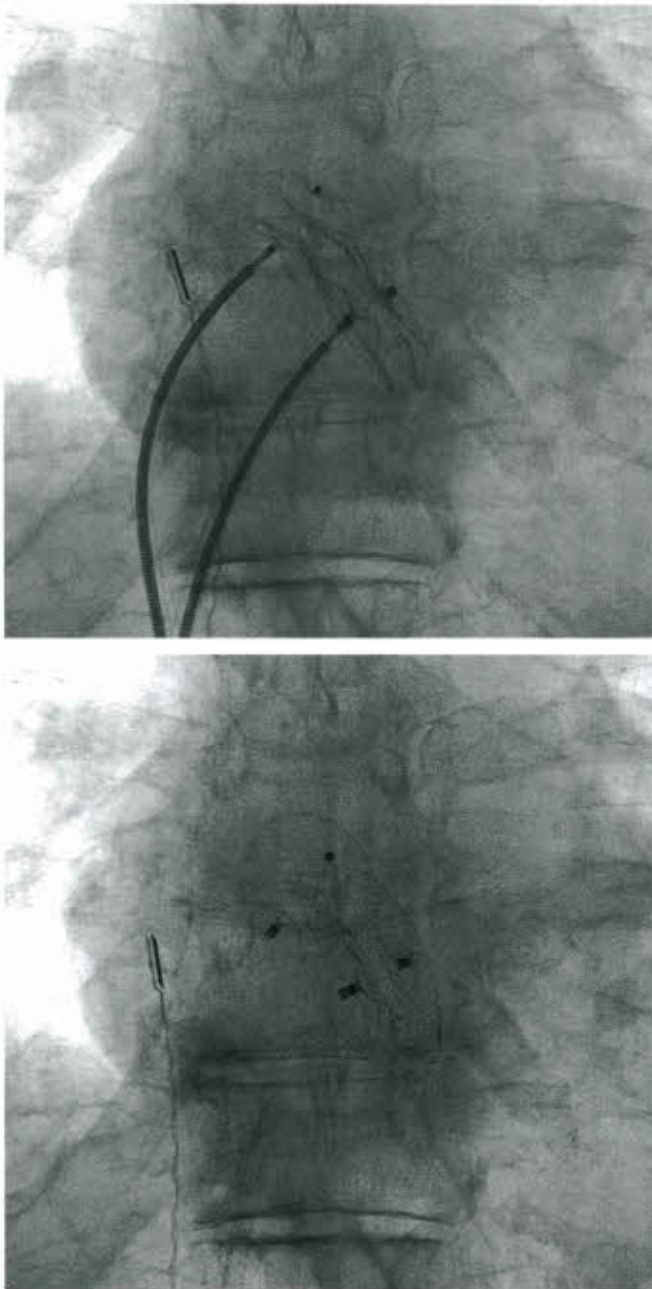


Figure 13.26. Closure of multiple ASDs. Closure of two secundum ASDs in a 59-year-old-man using 20- and 13-mm ASO. **Top:** Two devices deployed but not released with the larger device being “sandwiched” within the smaller device. **Bottom:** Both devices after release.

views and as such can potentially demonstrate the relationship between device, atrial wall, and aortic root (Fig. 13.31).

Closure rates are excellent with residual shunts being <5% at 1-year follow-up (32,134,148,149). The RV diastolic diameter tends to decrease after ASD closure suggesting some degree of remodeling when the exposure to volume loading is eliminated (150).

While technically challenging, ASD closure in small children can be successfully performed. Holzer and colleagues reported on 26 patients with a weight below 10 kg (2.4 to 10 kg) in whom ASD closure was attempted. Rim deficiencies were present in 31% of patients and the overall procedural

success was 95%, with one unsuccessful procedure being related to a deficiency of the inferior rim.

ASD Closure Using the Helex Septal Occluder

Delivery of the Helex Septal Occluder is slightly more challenging than the ASO. The deployment technique has been previously described in various articles (151–154). Jones et al. (154) reported on the results of 135 patients who were enrolled in an FDA phase II multicenter trial. Device delivery was successful in 119/135 (88%) patients. The incidence of device embolization requiring catheter retrieval was 1.7%. At 12-month follow-up, 73% of defects were completely occluded, 25% had a clinically insignificant residual shunt, while 2% had a clinically significant residual shunt. The HELEX Septal Occluder appears to be more suitable for smaller defects, rather than large ones. In contrast to the ASO, balloon sizing is essential and a device at least twice the size of the stretched diameter (stop-flow) should be used. Serious complications such as erosions into the aortic root that have been described with the AMPLATZER devices have not been observed with the HELEX Septal Occluder thus far, which is an important advantage when considering the use of the HELEX Septal Occluder for smaller ASD and PFO.

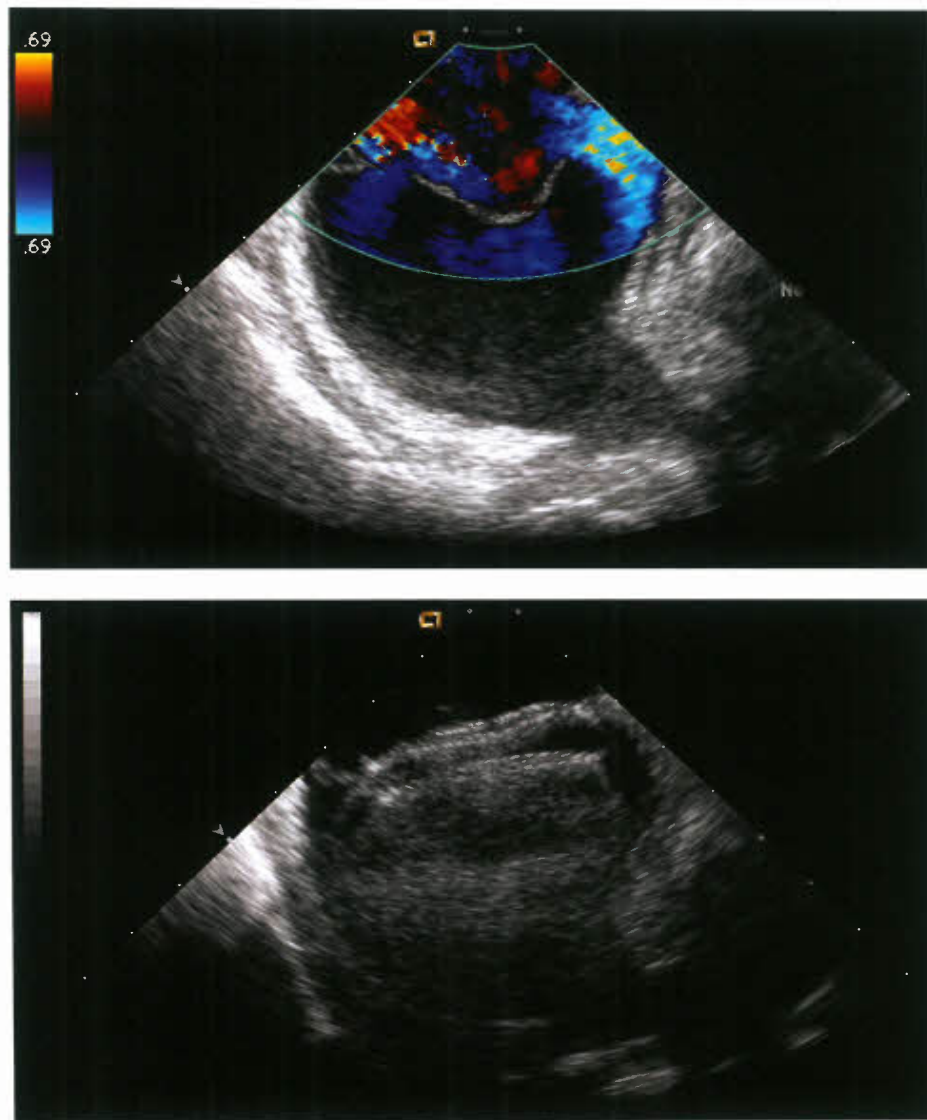
ASD Closure Using the CardioSEAL and STARFlex Devices

Technical details of ASD closure using these devices have been described elsewhere (25). In 2000, Carminati et al. (155) reported on the European multicenter experience of using the CardioSEAL and STARFlex double umbrella devices to close intra-atrial communications in 334 patients with a mean age of 12 years. Implantation was achieved in 97% of patients, with early device embolization being seen in 4% of procedures, most of which required surgical removal of the device. Residual shunting has been observed more frequently when compared to the ASO. Immediately after the procedure, 41% of patients had a detectable residual shunt that decreased gradually to 21% at 12-month follow-up. However, when excluding trivial leaks, the rate of complete closure was as high as 93% at 1-year follow-up. Two patients required late explantation of the device, one due to malposition and one due to late embolization. Fractures of the device arms were seen in 6% of patients, not associated with clinically significant adverse events. Device erosions into adjacent structures were not observed and no patient died as a result of the device implantation. Unfortunately, only defects ≤20 mm can be reliably closed using these devices, a significant limitation for patients with larger defects.

Some Comments on PFO Closure

Device closure of PFO using the ASO is very similar to ASD closure and technically fairly straightforward in most patients. Balloon sizing may avoid choosing a device that is too large for the individual patient, even though most ASO will fall in the range from 12 to 18 mm. The not-yet approved AMPLATZER PFO Occluder (AGA Medical Corporation, Golden Valley, MN) is specifically helpful for the longer tunnel-like PFO and also aids in the stabilization of an associated septal aneurysm. It is currently investigated in a Randomized Evaluation of Recurrent Stroke Comparing PFO Closure to Established Current Standard of Care Treatment (RESPECT). The presence of an atrial level right-to-left shunt should be evaluated before and after PFO closure using either bubble contrast echocardiography or transcranial Doppler. The recently approved AMPLATZER Cribriform Septal Occluder (AGA Medical Corporation, Golden Valley, MN) may have some use in transcatheter closure of PFO.

Figure 13.27. Closure of multifenestrated ASD. Multifenestrated atrial septum with at least three separate shunts on echo color flow mapping. **Top:** Multifenestrated septum before device placement associated with atrial septal aneurysm. **Bottom:** Atrial septum after device placement—note the flat appearance of the device and septum without a significant central waist.



The HELEX Septal Occluder has also been used frequently in Europe to occlude PFO. Sievert et al. (156) reported their experience of 33 patients and identified residual shunts at 6-month follow-up in 5.5% of patients, without any procedure or device-related complications. No recurrent neurological event was observed in these patients during a mean follow-up of 12 months (156). Within the US, the use of the HELEX Septal Occluder to close PFO in patients with cryptogenic stroke as compared to standard therapy with Aspirin, is presently being evaluated in the REDUCE trial. Similar to the ASO and the HELEX Septal Occluder, the (no longer available) STARFlex Occluder was evaluated for the treatment of PFO and stroke (CLOSURE I trial) (24,25).

Transcatheter Closure of Fontan Fenestrations

Transcatheter closure of fenestrations created surgically during the completion of a Fontan is usually considered in patients who have transcutaneous oxygen saturations equal to or below 90% after completion of Fontan. While the CardioSEAL ASD occlusion device had standard use approval under the FDA for occlusion of these defects, many other approved

devices have been used on an off-label basis and the most commonly used devices for this indication are presently the smaller varieties of the ASO (Fig. 13.32) (157,158). While in general, these defects are closed in a similar fashion to secundum ASDs, there are a few important considerations. Balloon test occlusion of the fenestration should be undertaken for 10 to 15 minutes, allowing for careful evaluation of right atrial pressures, systemic pressure, oxygen, and cardiac index. If test occlusion is well tolerated, the defect can be closed using a variety of approaches. Even though the jugular venous approach is unsuitable for occlusion of ASDs, small surgically created fenestrations are usually more amenable to this approach, as the small size of the defect allows a much harder pulling force to be exerted that overcomes the disadvantages otherwise encountered through inappropriate alignment. The location of surgical fenestrations may be close to the tricuspid valve and therefore careful echocardiographic assessment is necessary to avoid the device dropping into the tricuspid apparatus. Ideally, the left atrial disc should be deployed close to the fenestration. In many cases, the smallest device size of an ASO (4 mm) is sufficient for occlusion. In patients with extracardiac Fontan circulation and a short tubular connection to the atrial mass, the ADO may be more suitable to close this fenestration (159).

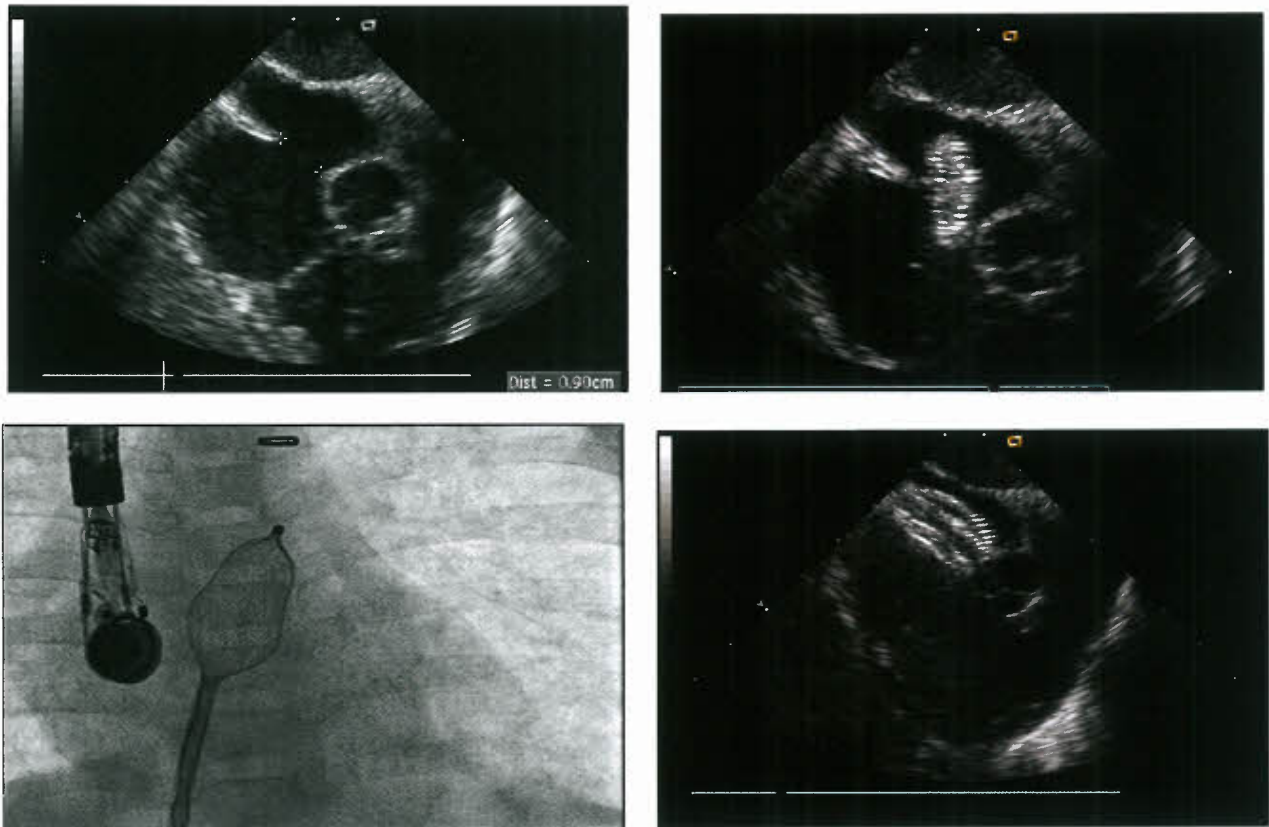


Figure 13.28. ASD closure in infancy. An 8 months (6.5 kg) ex-premature ventilator-dependent infant with bronchopulmonary dysplasia and a moderate (9 mm, unstretched) secundum ASD with deficient retroaortic rim (**Top left**). **Top right**: Standard deployment technique was unsuccessful in aligning the device with the atrial septum, **Bottom left**: Left upper pulmonary venous deployment technique. **Bottom right**: Device alignment and position after release (11-mm ASO). Patient was subsequently weaned off the ventilator.

Transcatheter Closure of Ventricular Septal Defects

Background and History

Transcatheter closure of muscular VSDs was first attempted on a compassionate basis using the larger Rashkind PDA occluding device (7). In 1988, Lock et al. (7) reported on a series of six patients in whom muscular VSDs—including postinfarct VSDs—were closed using the Rashkind device. Although the device and technique were successful in some cases, the device frequently was too small and resulted in significant residual leaks or actual embolization of the device. Some shortcomings of the Rashkind device were overcome by the design and larger sizes of the Clamshell device, making this a useful technique for some otherwise difficult to treat VSDs (160). Its successor, the Cardio-SEAL, had been used to close a variety of muscular VSDs (161). However, the most commonly used approved device for closure of muscular VSD is the AMPLATZER Muscular VSD Occluder.

Other devices have been used “off-label” to close muscular as well as perimembranous (39) VSDs, including the buttoned device (162), detachable coils (163–165), and the ASO (166). However, these devices as well as the approved Cardio-SEAL device were designed for different indications and as such are not generally adapted to suit the very different anatomical and morphological parameters (such as septal thickness) that are encountered with muscular VSDs.

It was not until 1999 when Thanopoulos first reported on the use of a custom-made device for closure of muscular VSDs (37). Results of the AMPLATZER Muscular VSD Occluder have been encouraging (167–170). In contrast to muscular

VSDs, perimembranous defects pose much higher demands on device design due to their proximity to the aortic valve, and early trials with “off-label” use of the Rashkind double umbrella were quickly abandoned (39). In 2002, Hijazi et al. (41) first reported on the use of a custom-designed device to close perimembranous VSDs and phase I trials investigating the AMPLATZER Membranous VSD Occluder were conducted in the United States (171) (Fig. 13.33). However, a serious and worrisome complication after implantation of the AMPLATZER Membranous VSD Occluder is the development of CHB. Its incidence in reported studies ranged from 2% to 3% (171,172). More recent reports of even higher incidence of CHB have appeared in several international registries, up to 4% to 5%. Even though heart block may develop during the procedure itself (173), it has been reported to occur at any time from within a few days to within a few months after an otherwise uncomplicated procedure (172,174). So far, no specific factors have been identified that allow prediction of these serious events. Because of the high reported incidence of AV block at present, the device is presently not approved for closure of perimembranous VSDs (and therefore the technique is not described in this section). Device modifications that may allow a reduction in external forces exposed onto the conduction system are presently being evaluated.

Technique of Muscular VSD Closure Using the AMPLATZER Muscular VSD Occluder

The principle technique for device closure of muscular as well as perimembranous VSDs is similar, with the device usually being deployed from an antegrade approach. For apical

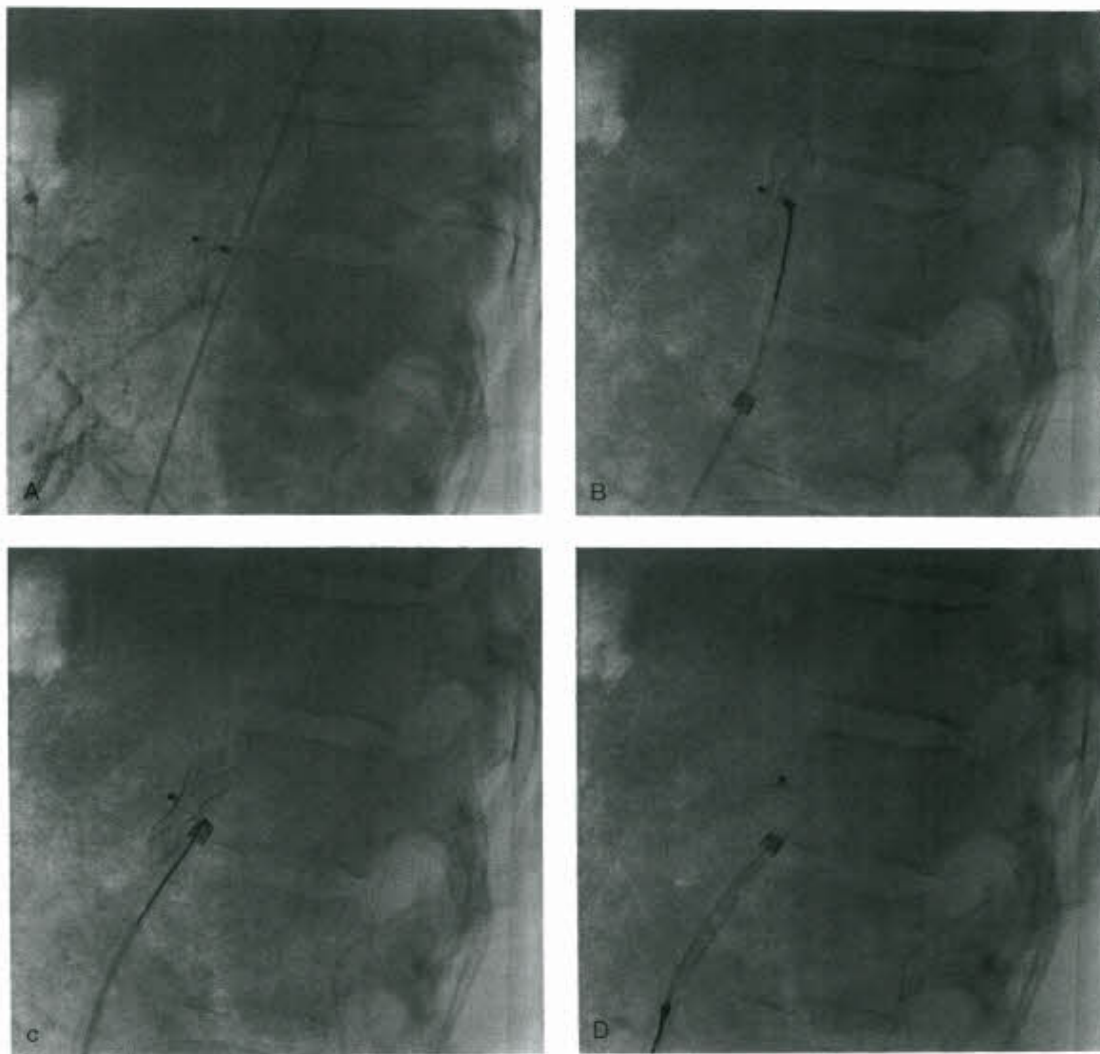


Figure 13.29. ASO device retrieval. A 29-year-old man who underwent ASD closure using a 20-mm ASO. The following day the device was found to have embolized to the DAO (A). The device was snared using a Gooseneck snare (B) and subsequently the screw aligned with the retrieval sheath (C). The device was recaptured into the sheath (D).

and mid muscular locations of the defects, the device delivery usually is from the superior vena cava (SVC); defects in the anterior muscular septum generally are approached from the IVC. This combination of circumstances results in a complex delivery technique requiring an arterial-venous guidewire “rail” passing from the arterial approach to the left ventricle, through the defect into the right ventricle, and ultimately being exteriorized either via femoral or internal jugular vein.

The procedure is performed using continuous TEE. After an initial hemodynamic evaluation and LV angiography, the VSD is usually crossed from the LV using a Judkins right coronary catheter and a 0.035-inch exchange length angled glide wire. The wire is snared using an Amplatz Gooseneck snare (Microvena Corporation, White Bear Lake, MN) either in SVC or in pulmonary arteries and exteriorized via femoral vein or internal jugular vein, thereby establishing a “rail” that can then be used to advance the appropriate diameter long delivery sheath through the defect and into the left ventricle. Device delivery is similar to that of the ASO for ASD closure. However, especially the closure of posterior-inferior defects is frequently complicated by delivery sheath kinking. Because of the complexity of the procedure, transcatheter muscular VSD closure should be limited to a few centers that have the

necessary interventional expertise. A perventricular approach described later in this chapter is preferred over a percutaneous approach for small infants, due to the higher incidence of adverse events associated with percutaneous device delivery in that population (175).

Results of Transcatheter Closure of Muscular VSDs

An early multicenter US experience of 75 patients was reported by Holzer et al. (170) in 2004. Procedure and device-related complications occurred in up to 39% of patients, almost a quarter of which were classified as major. The mortality in this early multicenter trial was 2.6%. Weight below 10 kg has been identified as a significant risk factor for adverse events. Closure rates were 40% immediately after device deployment, and increased further to 92% at 12-month follow-up (170). In 2005, Thanopoulos and Rigby (169) reported one case of subsequent development of CHB 1 year after device implantation in a series of 30 patients with a median follow-up of 2.2 years. Closure rates as high as 93% were described. Reports suggest that the relatively high rate of procedure-related complications in infants might be reduced through a perventricular approach through the beating heart without

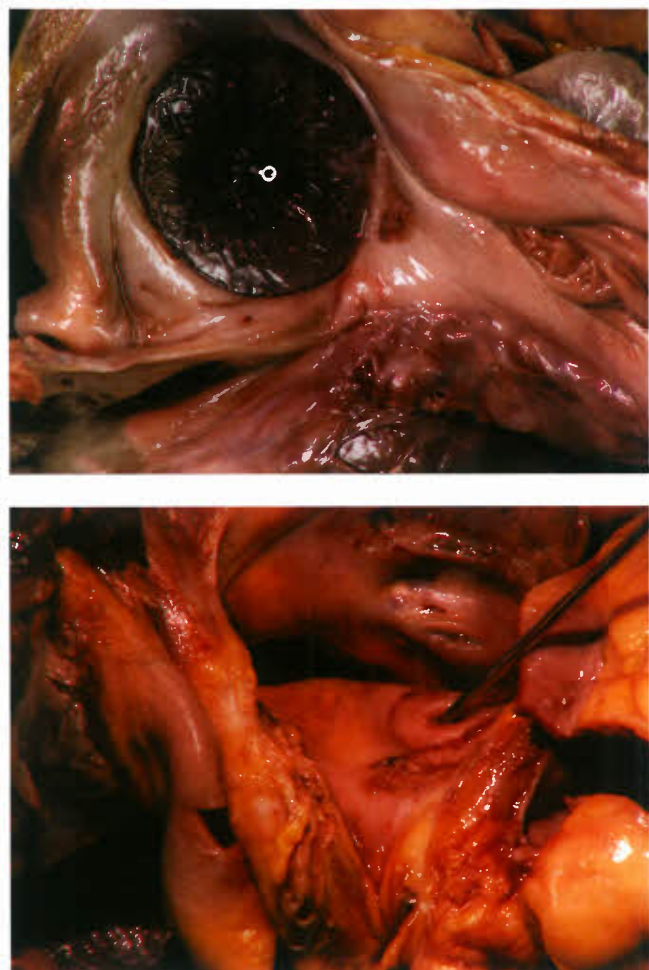


Figure 13.30. ASO erosion. Pathology specimen after erosion of the AMPLATZER Septal Occluder through the left atrial wall into the aorta is shown here. The ASO is seen “endothelialized” with the edge of the device against the LA free wall (top). A probe is placed through the aortic erosion adjacent to the erosion seen in the roof of the LA (bottom).

need for cardiopulmonary bypass (168,176). It has been suggested that when the advantages and disadvantages of the surgical approach to muscular ventricular defects are weighed against the risks and difficulties of the catheterization technique, the transcatheter route may be an effective alternative in selected patients with a decreased morbidity.

Postinfarction muscular VSDs require very specific considerations. In 2004, Holzer et al. (177) reported on 18 patients in whom occlusion of a postinfarct VSD was attempted using the AMPLATZER Muscular VSD (postmyocardial infarction) Occluder. A device was successfully placed in 89% of procedures, with early 30-day mortality being about 28%. On follow-up, two patients underwent recatheterization to close a residual VSD. At a median follow-up of 332 days, 20% of patients had complete closure, 60% had a small residual shunt, and a further 20% had a moderate residual shunt (177). Even though results of device closure of postmyocardial infarction VSD are poor, they have to be interpreted in context with the background of early surgical mortality being as high as 27% to 46%, with the mortality in untreated patients exceeding 90% (178–180). Unfortunately, so far, the device design for postinfarction VSD remains suboptimal, both in sizes available and device configuration. Residual shunts are not uncommon.

It is possible that the addition of further Dacron fabric to the device may help. From our own experience, we have found that the maximum available device size of 24 mm is frequently insufficient to occlude larger postinfarct VSDs. Whether a per-ventricular approach may aid in reducing the perioperative mortality has not been evaluated.

TRANSCATHETER OCCLUSION OF PATENT DUCTUS ARTERIOSUS

At present, the most commonly used device to close medium or larger sized arterial ducts in the United States is the ADO which was introduced in 1997 (49). It presently is the only device that has been FDA approved specifically for closure of the patent arterial duct. However, many small PDAs are still being occluded using a variety of coils. The Nit-Occlud device is awaiting FDA approval, while the ADO II is presently undergoing phase II clinical trials in the United States.

Coil occlusion of the arterial duct can be performed using either an antegrade or retrograde approach. For very small PDA, a retrograde arterial approach is usually sufficient. Before crossing the patent arterial duct, an aortogram is performed just at the origin of the PDA using standard lateral projection as well as 30-degree right anterior oblique projection of the AP tube. Measurements of the pulmonary arterial end, the aortic end, and the total length of the arterial duct and its midportion are made. According to a classification by Krichenko et al. (181), the arterial duct can be described angiographically as classically cone-shaped (type A), short with a narrow aortic end (type B), tubular (type C), having multiple constrictions (type D), or elongated conical with a distant constriction (type E). Hemodynamic evaluation is performed prior to angiography, including assessment for any pressure gradient across the aortic arch as well as a full right heart catheterization in cases where an antegrade ductal closure is anticipated. Care should be taken to avoid inadvertently entering the duct before angiographic evaluation can be completed, as that may trigger ductal spasm that may make it impossible to obtain accurate measurements and could in the worst-case lead to the patient having to be rescheduled for a repeat procedure (Fig. 13.34). The antegrade approach has the advantage of allowing angiographic evaluation before the coil is completely deployed but both techniques are equally used and suitable.

A coil usually twice the size of the pulmonary end of the duct is chosen and coils are deployed in a way to allow placement of about one loop being distal to the pulmonary arterial end, while the remainders of the loops are placed in the ductal ampulla. The length of the coil is usually three to five loops and depends on the length of the aortic ampulla. Delivery of Flipper or Jackson coils (or the newer MRye Flipper coils) is technically fairly easy and the controlled release mechanism allows an extra safety margin to prevent inadvertent coil embolization. If the coil position appears suboptimal, the coil can be recaptured and redeployed into a more appropriate position. However, Flipper coils with their reduced amount of filament are not always suitable to close especially medium sized PDAs. Therefore, techniques have been developed that allow delivery of the standard Gianturco coils in a more controlled fashion, such as the use of a snare (182) or biptome (183) to hold onto the coil, the use of a tightened catheter tip (184), or the use of a balloon (185) to tamp the coil within the ductus during deployment. Even without these aids, closure of many arterial ducts is feasible using just the standard Gianturco coils, as has been demonstrated through many successful procedures, performed before any other devices became available. If a residual shunt is present after placement of a coil, attempts should be made to place an additional coil. Residual



Figure 13.31. ASO relation to aortic root. Multislice volume rendered CT scan demonstrating the relation of the ASO to the aortic root in a patient who developed chest pain after transcatheter ASD closure. Arrowheads point to the device. **Left:** On-face view of the ASO in relation to the aorta. **Right:** Profile view of the ASO in relation to the aorta (Images provided by Stephen Cook, MD).

shunts not only fail to abolish the risk of bacterial endocarditis, but in addition are associated with an increased risk of intravascular hemolysis (186). Sufficient time (10 to 15 minutes) should be given to allow clotting to occur before attempting to place an additional coil, which is usually placed using a retrograde approach. The duct is carefully crossed using, for example, a 0.018 V18 wire or a 0.035 angled glide wire. A soft 4 Fr catheter, such as a glide catheter, should then be tracked over the wire and advanced carefully across the PDA before placing an additional coil that is usually of smaller diameter than the one that was originally placed. Before introduction of the ADO, many moderate- to large-sized PDAs were occluded using multiple coils in this fashion (187).

The technique of closing the arterial duct using the ADO has been described in detail by Masura et al. (49). After hemodynamic and angiographic evaluation, the PDA is crossed antegrade and a 0.035-inch exchange length wire is advanced into the DAO. An appropriate delivery sheath is advanced over the wire with the tip positioned in the lower DAO. The wire is then removed and the device is loaded in a way similar to the ASO. The device size is chosen so that the pulmonary end of the skirt is about 2 mm larger than the size of the narrowest PA portion of the arterial duct. In a typical type A PDA with a 3- to 4-mm pulmonary arterial end, one would therefore choose an 8/6-mm ADO. However, in very small patients, the device size is chosen to be frequently on the smaller side, while very large PDA may require a device notably larger than just 2 mm above the narrowest PDA segment. The device is advanced until it reaches the tip of the delivery sheath. At this point, the whole assembly is gradually withdrawn in small increments. One should begin to deploy the retention disc when a position just in mid-portion of the DAO opposite to the PDA insertion is reached. It is important to use the angiographic recordings as a roadmap when deploying the device, with specifically the anterior end of the trachea and its relation to the PDA as a reference point. Once the retention disc is deployed, the whole assembly is withdrawn into the mouth of the aortic ductal ampulla, at which point the skirt is deployed while fixing the delivery cable and retracting the sheath. In type E PDA, tubular type C PDA, or elongated arterial ducts with a typical cone

shape, it may be necessary to withdraw (or begin to deploy) the retention disc inside the PDA. Once the device is deployed, a Pigtail catheter is advanced and positioned opposite the PDA in the DAO. Aortography is then performed, carefully evaluating for the presence of any residual shunt around the device. One can repeat the aortogram after 10 to 15 minutes to allow clotting to occur if required. Without any residual shunt, the device can be released and its position should again be evaluated through a final angiogram (Fig. 13.35). Pressure recordings in the ascending and DAO, as well as LPA and MPA should be obtained before and after device deployment. Even though the device is only recommended for use in infants above 5 kg, it is our experience that the ease with which the device can be recaptured if the position is not satisfactory should allow an attempt at PDA occlusion in any duct beyond the neonatal period, even if the patient's weight is below 5 kg (Fig. 13.36). The key to successful deployment in small patients is not necessarily the size of the PDA, but more so its length.

As an alternative to deployment of the ADO, the ADO II can be deployed using either an antegrade or a retrograde approach due to the symmetric shape of the device. The deployment technique is otherwise very similar to the ADO, with one disc being deployed at the aortic ampulla, the central portion within the PDA, and the more proximal disc deployed at pulmonary arterial opening of the duct (antegrade approach, Fig. 13.37). For some type C, type D, and type E PDAs, the AMPLATZER Vascular Plug II can be used successfully, again using usually an antegrade approach (Fig. 13.38) (56).

Results of PDA Closure

In 1999, Patel et al. (188) reported their experience of PDA coil occlusion in 149 patients. Out of 146 patients who had coils implanted, the rate of immediate complete closure was 97%. In three of four patients with a residual shunt, complete occlusion was achieved during a second transcatheter procedure, while the residual shunt spontaneously resolved in another. The study documented zero mortality and very low morbidity. Coil migration during the procedure was seen in six patients (4%); four were successfully retrieved. Recanalization

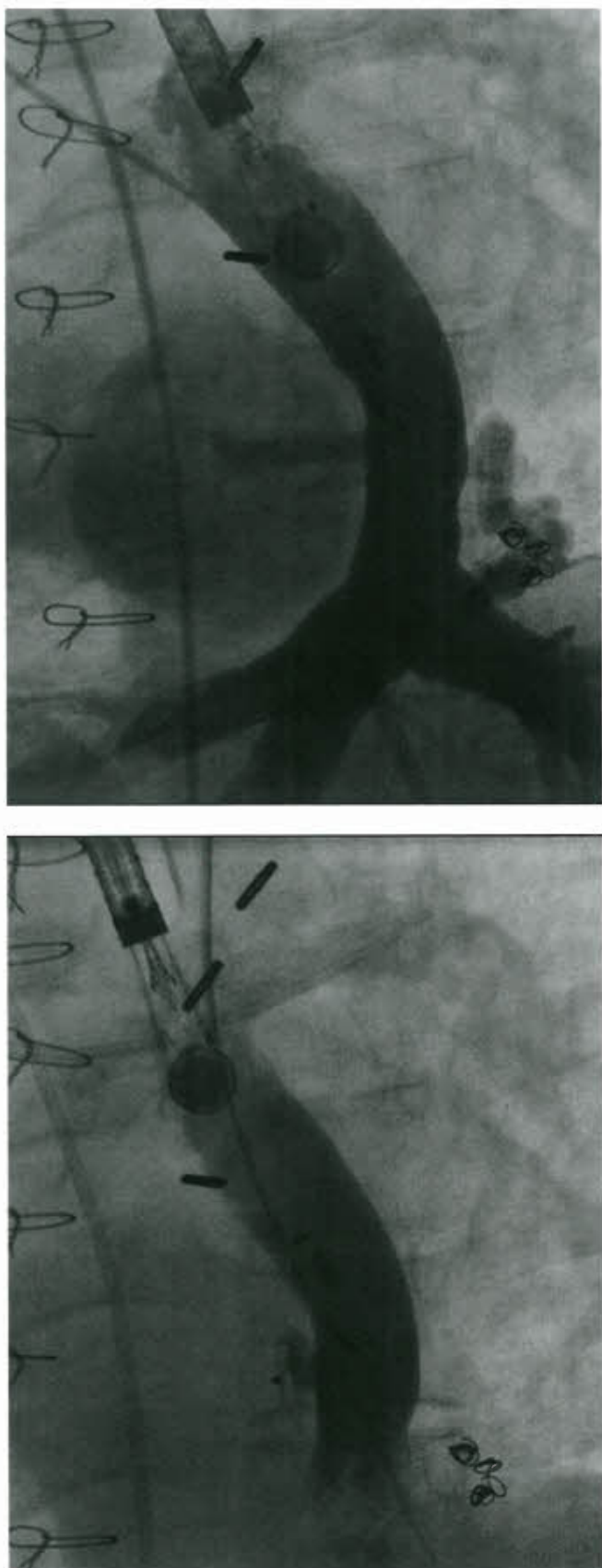


Figure 13.32. Closure of Fontan Fenestration. An 18-year-old girl with heterotaxy and an extracardiac Fontan (hepatic confluence to LPA). Fenestration occluded using 5-mm ASO. Top: Before occlusion. Bottom: After occlusion.

or delayed coil migration was not observed during a median follow-up period of 3 years. The risk of inadvertent coil embolization when attempting to close large PDA with a PA diameter in excess of 4 mm, has been documented to be as high as 16% (187). However, most published data about PDA coil occlusion preceded the introduction of the controlled release Flipper coil as well as the introduction of the ADO, which is now available for moderate- or large-sized PDA. As such, the rate of inadvertent embolization can today be expected to be <1%, if full use is made of all available devices and techniques.

Pass et al. (189) reported the results of a multicenter US trial evaluating the ADO, which enrolled 484 patients with a median age of 1.8 years between 1999 and 2002. The ADO was successfully implanted in 99% of suitable patients. Occlusion rates increased from 76% immediately at the end of the procedure to 89% at day one postprocedure and further to 99.7% at 1-year follow-up. For the ADO II, Saliba et al. (190) reported closure rates 94% at 24 hours.

Major complications were reported in 2.3% of patients while the incidence of minor adverse events was about 4.8%. Partial occlusion of the LPA was seen in two patients. However, no case of significant aortic obstruction was identified. Device embolization occurred in two patients, necessitating surgical retrieval in one. Vascular complications or blood loss requiring transfusion were reported in 18 patients and one patient died of overwhelming sepsis 5 months after the procedure. Embolized ADOs are more difficult to retrieve compared to other AMPLATZER devices, because of the recess of the microscrew into the device. Therefore, devices are usually retrieved using at least a 4 Fr larger delivery sheath allowing collapse of a device that has been snared circumferentially. Ducts of atypical (non-type A) morphology are technically more challenging and may require variations in the type and positioning of devices used.

Even though the AMPLATZER Vascular Plug has been used to occlude persistent arterial ducts (55,191), caution has to be applied for this indication, because the lack of Dacron fabric in these devices may prevent complete occlusion in moderate-sized high-flow PDA, as was demonstrated in a patient with a type C PDA (192,193). However, this does not appear to be a problem when using the AMPLATZER Vascular Plug II, with its triple-layered Nitinol mesh and improved occlusive properties (56).

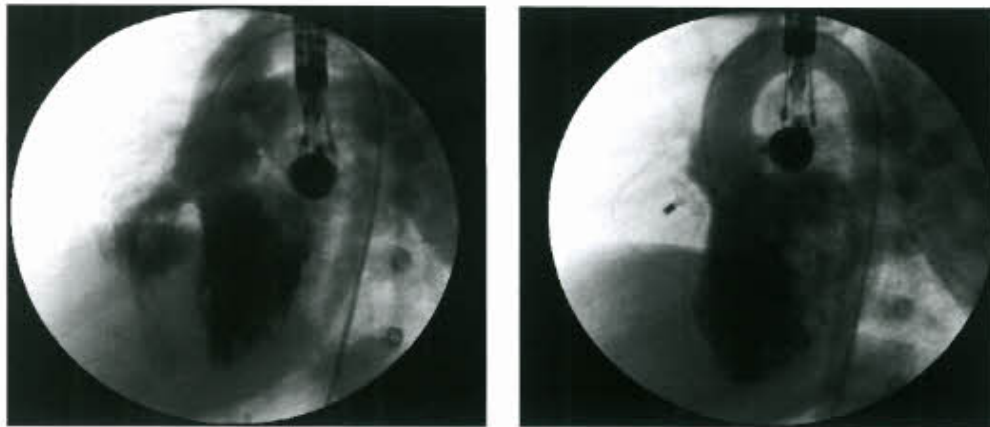
In 2003, Chisolm and colleagues reported on 19 patients in whom a Nit-Occlud was implanted as part of the phase II US clinical trial. Devices used were either Nit-Occlud Flex or Nit-Occlud Medium of various sizes. At 24 hours, 17/19 (89%) had no residual flow, while there was trivial residual flow in one and a small degree of residual flow in another patient. Procedural complications or device embolizations were not observed (53). In 2005, Celiker et al. (54) reported a closure rate up of 93% after 6 months.

CLOSURE OF OTHER PERSISTENT OR ABNORMAL VASCULAR COMMUNICATIONS

Techniques for embolization of abnormal or persistent arterial or arteriovenous vascular structures have been available for more than 30 years. Embolization techniques were developed and perfected primarily by vascular radiologists working in the abdominal viscera, gastrointestinal areas, and central nervous system, particularly in “end artery” vessels. Many materials and devices, including the patient’s own clotted blood, Gelfoam, colloidal plugs, “glues,” detachable balloons, and coil occlusion devices have been used for these peripheral occlusions.

Gianturco (Cook, Inc.) coils, and their MRI compatible successor the MRye coils, are the most commonly used occlusion

Figure 13.33. Closure of Perimembranous VSD. Closure of a perimembranous VSD. **Left:** Before closure. **Right:** After closure.



devices for patients with congenital cardiac defects. These coils are made of spring wire with polyester fibers enmeshed in the coils. They are available in several sizes and multiple diameters and lengths. The coil is introduced into the delivery catheter through a straight metal “loader” as a straight wire. When it is delivered by extrusion out of distal end of the catheter, it coils

like a small “pigtail.” Once delivery with this particular coil has been started, there is no way of withdrawing the coil back into the catheter. The Gianturco coil occludes the vessel by creation of a mass of fabric and wire where a thrombus forms. The coil occlusion device usually is delivered into a vessel with a discrete distal narrowing, where it will fix in place and not migrate further through the vessel. Often, several coils are placed in a single vessel to achieve complete occlusion. In the absence of a distal narrowing or some other type of device for fixation, coils are generally only usable in tubular structures with a distended diameter up to 7 to 8 mm. For larger vessels or vessels without an area of discrete stenosis, coils can be used in conjunction with other intravascular occlusion devices to complete the occlusion of the vessel. Other devices that are available to occlude slightly larger vascular structures include the AMPLATZER Vascular Plug (Fig. 13.36), The AMPLATZER Plug II (Fig. 13.37), the ADO, and the GGVOD.

Many abnormal collateral vessels or persistent surgically created systemic to pulmonary artery shunts are associated with more complex lesions. These vessels should be occluded when systemic flow competes with normal pulmonary flow, particularly after the major defect is corrected. These communications were traditionally delivered during the corrective surgical procedure or as a separate procedure. Other lesions in which these devices may be useful are AV fistulae, including systemic, coronary–cameral, and peripheral as well as pulmonary AV fistulae. In these lesions, it is critical to identify the stenotic or “end” vessel into which the device can be fixed in order to reduce the dangers of migration to a vital structure. A variety of other persistent and abnormal vascular communications can be occluded with the available devices, including a left SVC to the left atrium, systemic to pulmonary artery shunts in postoperative tetralogy of Fallot or PA patients, persistent systemic venous to atrial connections after the Fontan or Glenn procedures (Fig. 13.39), and others.

As early as 1989, Perry et al. (45) reported on their experience of occluding 77 vessels in 54 patients using Gianturco coils. The rates of total or subtotal occlusion immediately during the procedure were as high as 95%. Complications included six cases of inadvertent embolization into the pulmonary or systemic circulation, half of which were retrieved using transcatheter techniques and half of which were left without symptoms. This study, however, represents early results. Current practice is to continue to place multiple coils until complete or near complete occlusion of a vessel is confirmed angiographically, and detachable Flipper coils are usually preferred for any attempted occlusion that may be associated with a slightly higher risk of inadvertent coil embolization.

Hill et al. (192) reported a multicenter experience of 52 patients in whom 84 vessels were occluded using 89 AMPLATZER Vascular Plugs. The most commonly occluded



Figure 13.34. Ductal Spasm. PDA in spasm after catheter manipulation (A) and after waiting for 30 minutes for spasm to resolve (B).

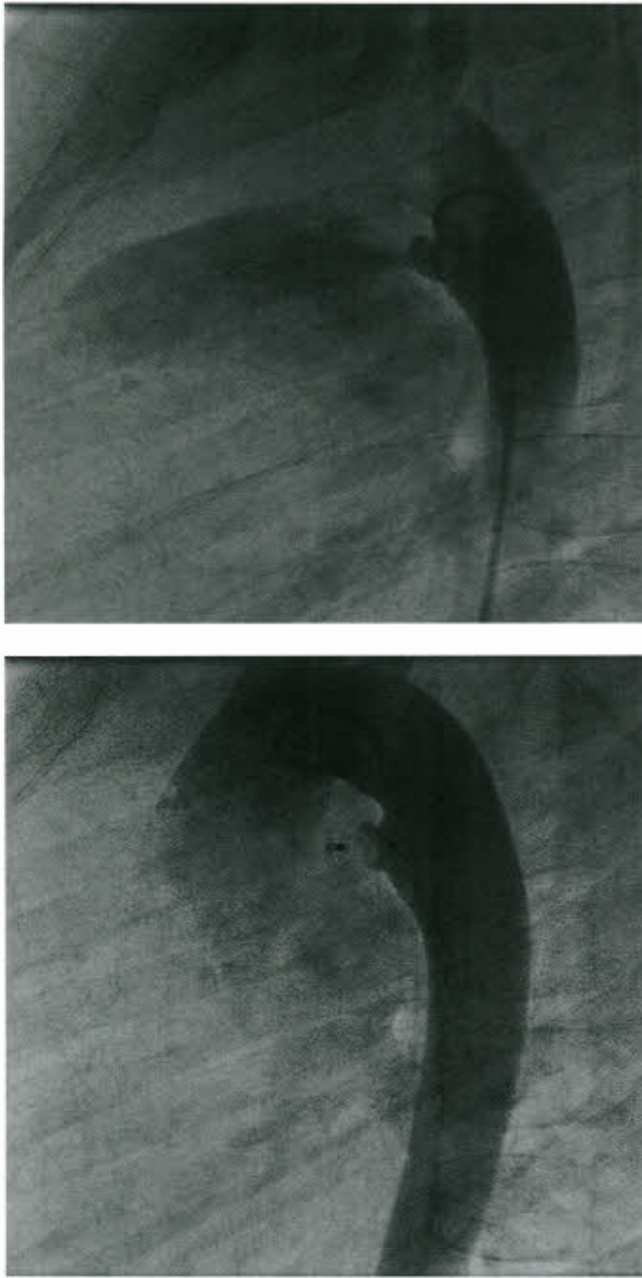


Figure 13.35. PDA closure with ADO. A 9-year-old girl with a medium sized PDA who underwent PDA occlusion using an AMPLATZER Duct Occluder. **Top:** Before closure. **Bottom:** After closure.

vessels included 45 aortopulmonary or venovenous collaterals, 28 pulmonary AVMs, 7 transhepatic tracts, and 4 shunts. Complete occlusion of the vascular structure was accomplished within 10 minutes in 94% of implanted devices. More than one vascular plug was required for five vascular structures. Two vascular plugs were electively removed due to residual shunts.

RETRIEVAL OF FOREIGN BODIES

With the proliferation of various types of chronic parenteral therapy, central line monitoring, chronic indwelling intravenous chemotherapeutic devices, and now the catheter-delivered therapeutic devices, the nonsurgical removal of embolized for-



Figure 13.36. PDA closure in a formerly premature neonate. A 3 months ex-premature infant with BPD who remained CPAP dependent. Catheterization documented a moderate tubular type C PDA, measuring approximately 2 to 2.5 mm throughout its length (**top**) with a $Q_p:Q_s$ of 2.5:1. PDA was successfully closed with a 4-mm Vascular Plug II. **Middle:** Aortogram with device still attached to delivery cable. **Bottom:** Aortogram after release of the device.

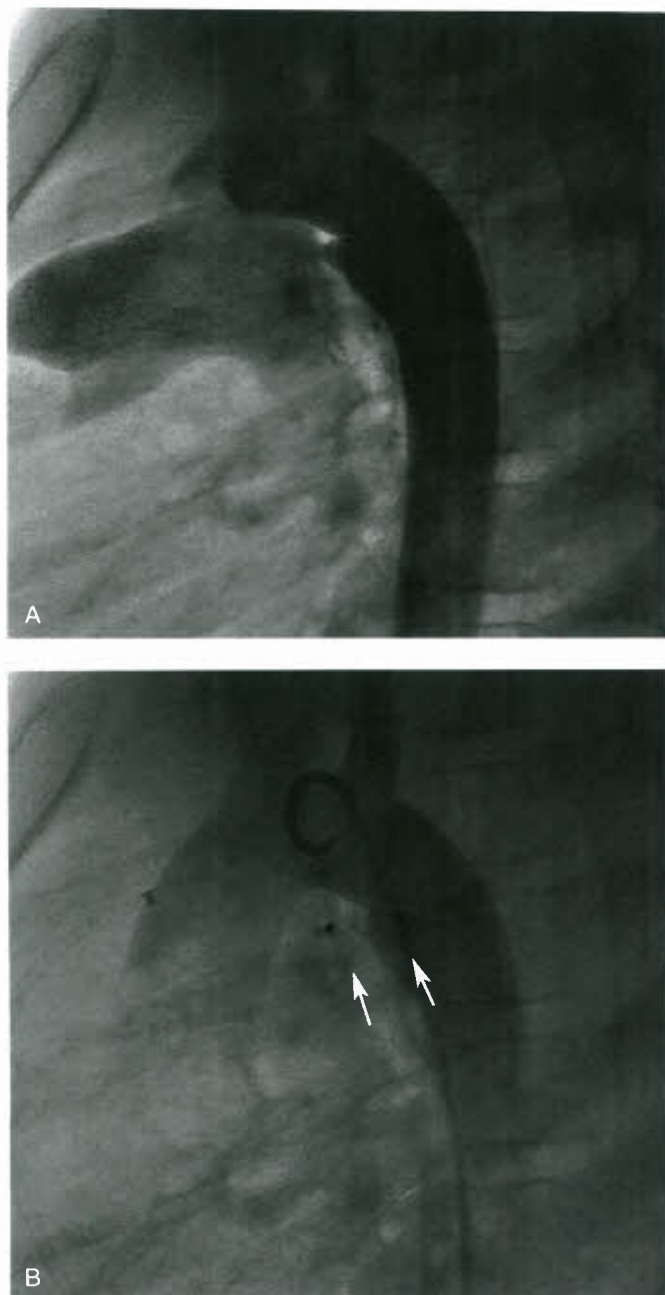


Figure 13.37. PDA closure with ADO II. A Male with a moderate type A PDA (A). Image (B) is an aortogram after occlusion with a 5° -- 4 mm ADO II (arrows point to the two symmetrical discs).

eign bodies from the heart or great vessels has become a more frequent challenge for the interventional cardiologist. The pediatric interventional cardiologist, who is more familiar with complex intracardiac anatomy and with the routine use of biplane fluoroscopy, is generally best qualified to perform these procedures, regardless of the patient's age. Fortunately, and thanks mostly to urologists, a variety of catheter devices is available for the grabbing, snaring, looping, or lassoing of any type of debris that work its way into the vascular system and must be available in any interventional catheterization laboratory.

Most of embolized materials end up in the pulmonary artery branches. Retrieval involves the delivery of a large sheath (8 to 15 Fr, depending on size and shape of the foreign body

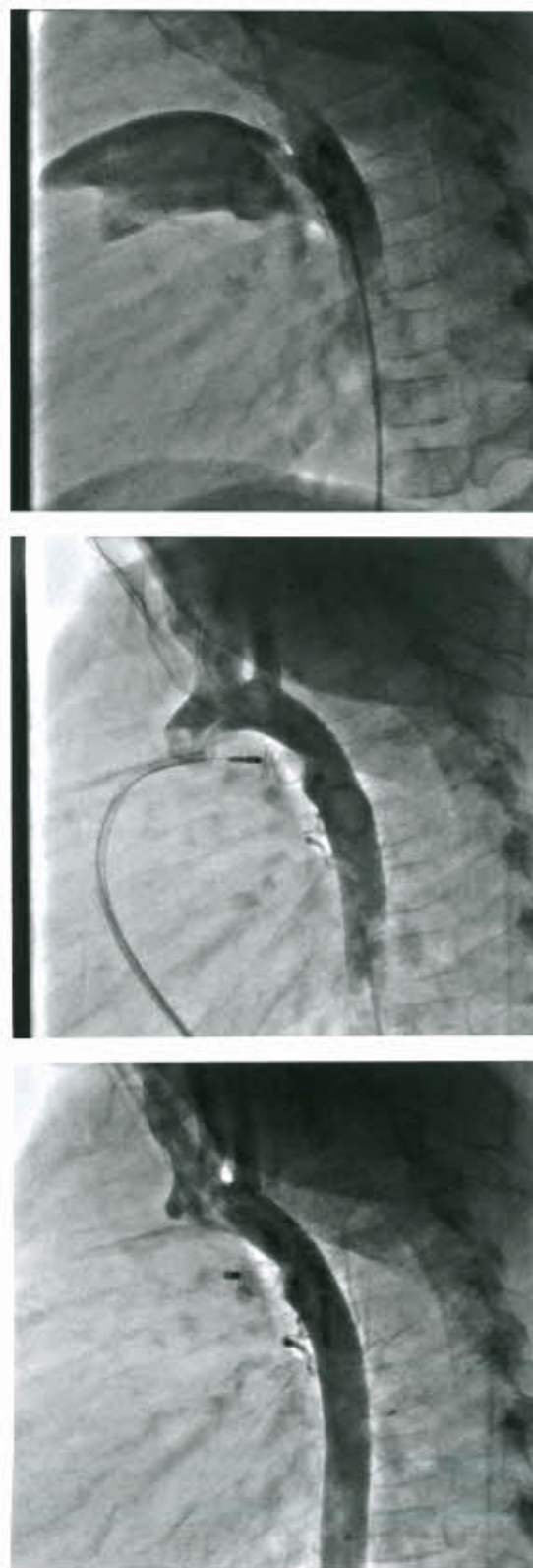


Figure 13.38. PDA closure with plug II. A 16-month-old male infant with a moderate tubular (type C) PDA (top) and a $Q_p:Q_s$ of 2.5:1 (Middle); aortogram showing a 6-mm vascular plug II deployed and (bottom); aortogram after release of the device.

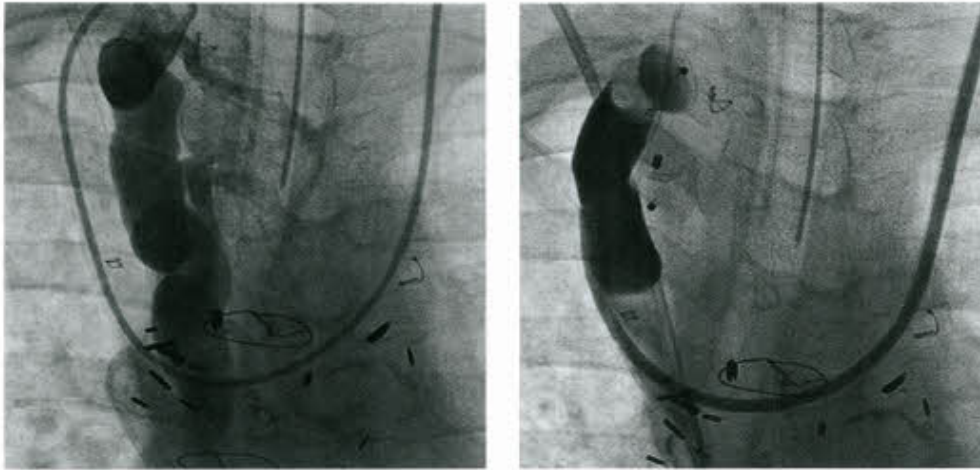


Figure 13.39. Closure of venovenous collaterals. A 10-year-old girl with HLHS, status post-Norwood procedure and bidirectional Glenn shunt, with low transcutaneous saturations. A large venovenous collateral was occluded using two 16-mm AMPLATZER Vascular Plugs. **Left:** Collateral before occlusion. **Right:** Collateral after occlusion.

that is to be retrieved) into the specific branch pulmonary artery just proximal to the foreign body. The specific type of retrieval catheter used is determined by the size of the patient, the type of foreign body, and exactly how and where the foreign body is situated within the vascular system. Then, either directly through the sheath or through a catheter delivered through the sheath, the particular retrieval device is advanced to the foreign body and manipulated to grasp it. Once firmly grasped, the foreign material is withdrawn into the large sheath and out of the body through the sheath. With the use of the large, long sheaths with these retrieval devices, it is usually no longer necessary to perform a venous cutdown even for the final removal of the foreign body from the vessel or skin entry site.

One of the most common iatrogenic foreign bodies retrieved by the congenital interventional cardiologist is an embolized ASO, which is described above (Fig. 13.29).

MANAGEMENT OF PERIPROSTHETIC LEAKS

Periprosthetic leaks are notoriously difficult to treat. A variety of devices has been used successfully in selected patients, by either an antegrade or a retrograde approach (194–201). However, the crescent-shaped form of many of these defects combined with the biophysical characteristics of the adjacent prosthetic valves does not lend themselves for the use of any of the currently available transcatheter devices, and complications such as impairment of the prosthetic valve or wire entrapment have been documented (202,203). Development efforts are presently underway to design a custom-made device specifically designed for the closure of periprosthetic leaks, which will hopefully improve upon the currently available devices that have been used for these indications.

TRANSCATHETER PULMONARY VALVE REPLACEMENT

The groundbreaking work by Dr. Phillip Bonhoeffer has initiated one of the most exciting developments in transcatheter therapy of recent years. Patients with significant conduit dysfunction have so far required surgical (re)placement of a valved conduit between the right ventricle and pulmonary arteries. The longevity of these conduits has been limited, necessitating further conduit replacements every 5 to 15 years for recurrent

conduit stenosis or new or recurrent valve insufficiency. The prospect of frequent open-heart procedures is very undesirable in this group of patients, who usually already have undergone a series of cardiac surgical procedures, each adding further potential insults to global left and RV function. In addition, because of scarring, these operations are potentially very difficult to perform. As such, a less-invasive procedure that would further extend the need for surgical conduit replacement was most desirable.

In 2000, Bonhoeffer et al. (9) reported on the first human implantation of a stent-mounted valve into an RV-PA conduit in a 12-year-old boy. The technique has been modified since and until now more than 1,000 patients have received a transcatheter-stented valve in the pulmonary position (204). The Melody valve utilizes a bovine jugular venous valve that is preserved in glutaraldehyde and mounted within a 28-mm-long CP stent. The valve is ideally implanted into a preexisting RV-PA conduit, preferably with a degree of associated stenosis, and expanded up to a diameter of 18, 20, or 22 mm. At the present time, in the United States, the valve is not approved for use in patients with a native pulmonary valve, a patched RVOT, or positions outside the RVOT such as the tricuspid valve.

Implantation of the Melody valve requires careful pre-procedural planning and patient selection, closely involving the adult congenital team. Patients with significant conduit stenosis pose different procedural challenges than those with predominant valve insufficiency. Once a patient has been identified to require pulmonary valve or conduit replacement, he/she should be reviewed by the interventional team to assess whether he/she would be a suitable candidate for the Melody valve. Patients with very large nonstenotic conduits with diameters of 25 mm or more are generally questionable candidates. Using the 22-mm Ensemble delivery system, the outer diameter of the Melody valve is approximately 24 mm, and therefore any inner diameter of a conduit larger than this would be insufficient to securely anchor the Melody valve. While the valve could theoretically be mounted on a 24-mm BiB balloon, this technique is more challenging and is not the standard technique approved in the United States. When deciding about the size of a conduit, one has to bear in mind that conduits that house a bioprosthetic valve, such as the Hancock conduit, usually have an inner diameter at the valve ring of about 2 mm less than the nominal size of the conduit. Once a patient has been found to be a suitable candidate, a careful diagnostic and hemodynamic evaluation is performed within the catheterization laboratory. Particular attention has to be paid to the location of the coronary arteries in relation to the desired implantation site of

the Melody valve (Fig. 13.40). For this purpose, a balloon of similar size as the intended Melody valve is advanced over a stiff guidewire into pulmonary position and inflated, while a simultaneous aortogram is obtained. To allow visualization of the coronary arteries through the balloon, very diluted contrast (20%) is used. If any doubt exists about the coronary arteries, selective coronary angiograms can be performed. In addition to lateral projection, caudal and LAO projection usually profile the left coronary artery very well in relation to the balloon position. In addition to evaluating the coronary anatomy, pretreatment of a stenotic right ventricle to pulmonary artery (RVPA) conduit may be required. As stent fracture is one of the most common complications seen after Melody valve implantation, operators may want to eliminate the majority of conduit narrowing prior to implantation of the Melody valve, in order to reduce the radial force on the valve. For this purpose, balloon sizing is undertaken. If, at low pressure, the waist seen in the balloon is 80% or less than that of the desired diameter, a smaller balloon is used. This gradual approach may limit

the injury that is being caused to the conduit through balloon angioplasty. Prestenting the RVPA conduit has been favored by many operators, implanting sometimes as many as four to five stents to give the conduit enough radial strength to reduce the risk of subsequent stress fractures of the implanted Melody valve (Figs. 13.41 and 13.42). Furthermore, if a Melody valve is implanted without eliminating the stenosis sufficiently through prestenting, very little can be done subsequently if the Melody valve shows some recoil as a response to external radial forces. Once the “landing zone” for the Melody valve has been prepared in such a fashion, a Lunderquist extra stiff wire (Cook, Bloomington, IN) is placed in the most appropriately sized branch pulmonary artery, which then facilitates advancement of the Ensemble delivery system and eventually deployment of the Melody valve. The crimping process, predilation of the entry site, and advancement of the Melody valve have been described elsewhere and are therefore not described in detail in this section (Fig. 13.43). ICE is a useful tool to evaluate valve function after implantation (Fig. 13.44).

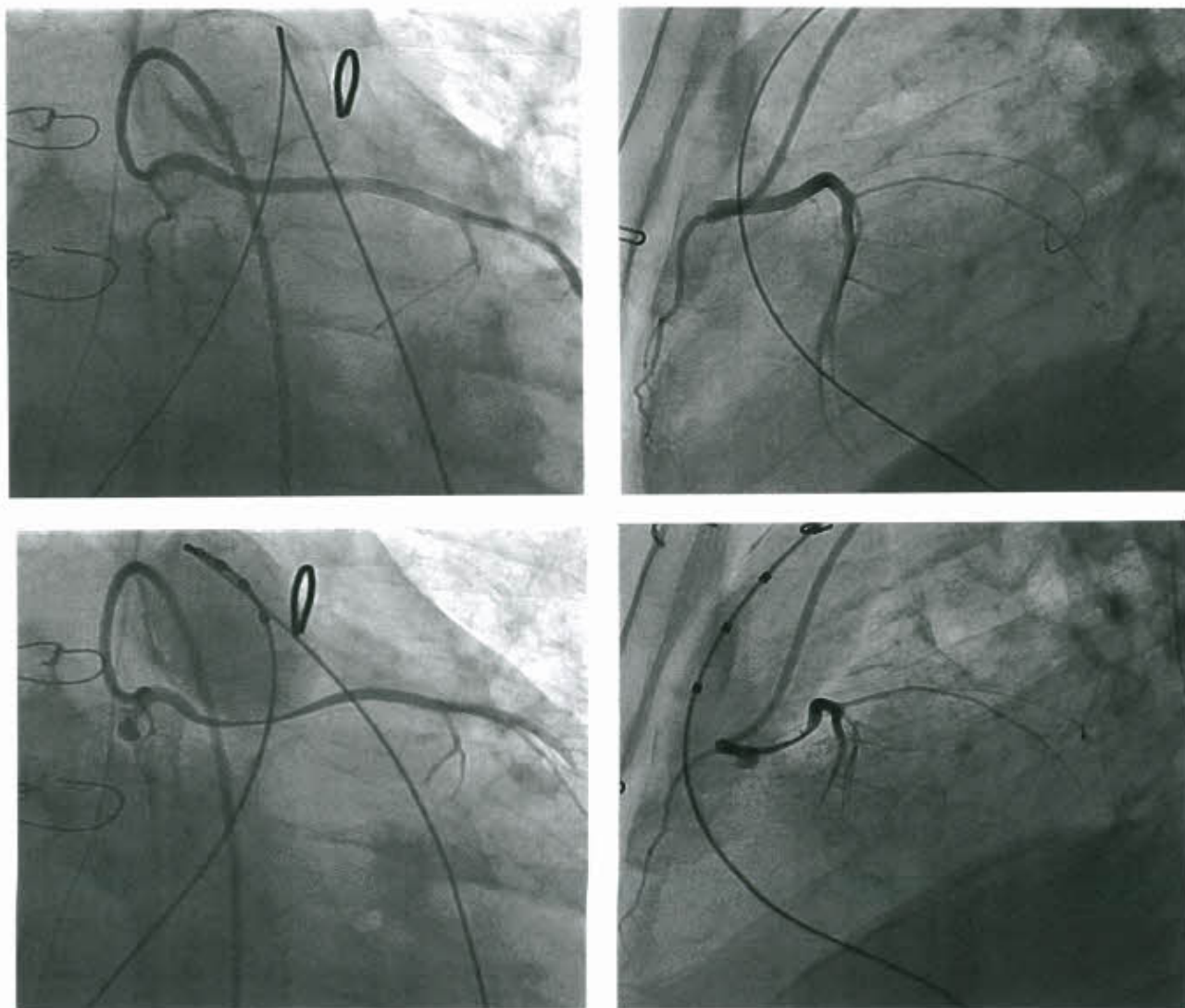


Figure 13.40. Melody valve and coronary compression. A patient with tetralogy of Fallot and the LAD coronary artery arising from the RCA is evaluated for Melody TPV implant. A selective LAD injection in steep caudal angulation and a lateral view (**top**) is shown. A guidewire has been placed through the RVOT into the LPA. There is no observed obstruction to coronary flow. However, with inflation of the balloon in the RV-PA homograft, there is clear compression of the LAD branch (**bottom**). Implant of any bare metal stent or the Melody TPV would result in coronary ischemia. Therefore, this patient was referred for surgical pulmonary valve replacement.

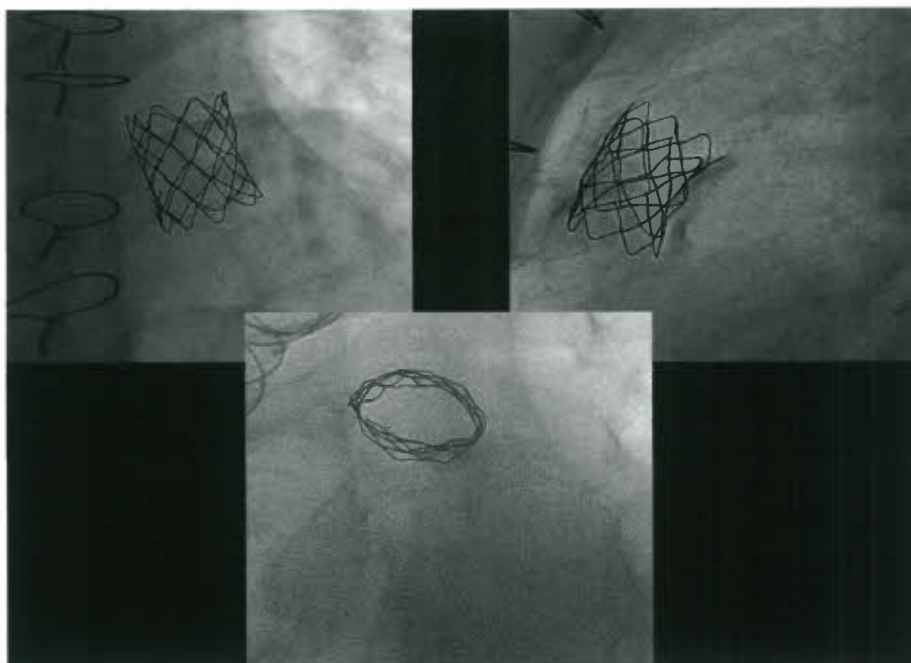


Figure 13.41. Melody valve stent fracture. A patient underwent implantation of the transcatheter Melody valve within a homograft. After balloon compliance testing, the Melody TPV is implanted in a homograft. After 1 year, the patient's systolic gradient increased and fluoroscopic examination of the valve demonstrated multiple fractures and loss of stent integrity (**bottom**). The patient was successfully treated with a new valve after two bare metal stents were placed to reinforce the original valve.

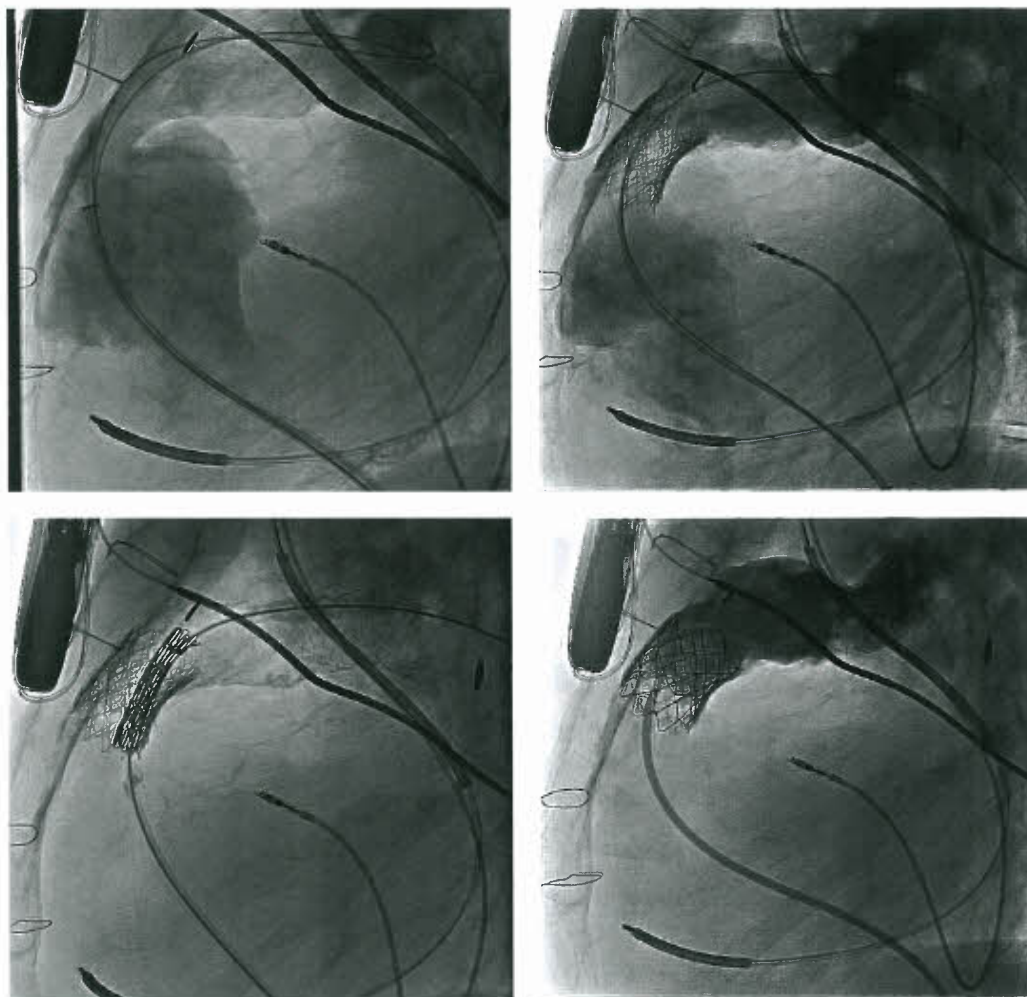
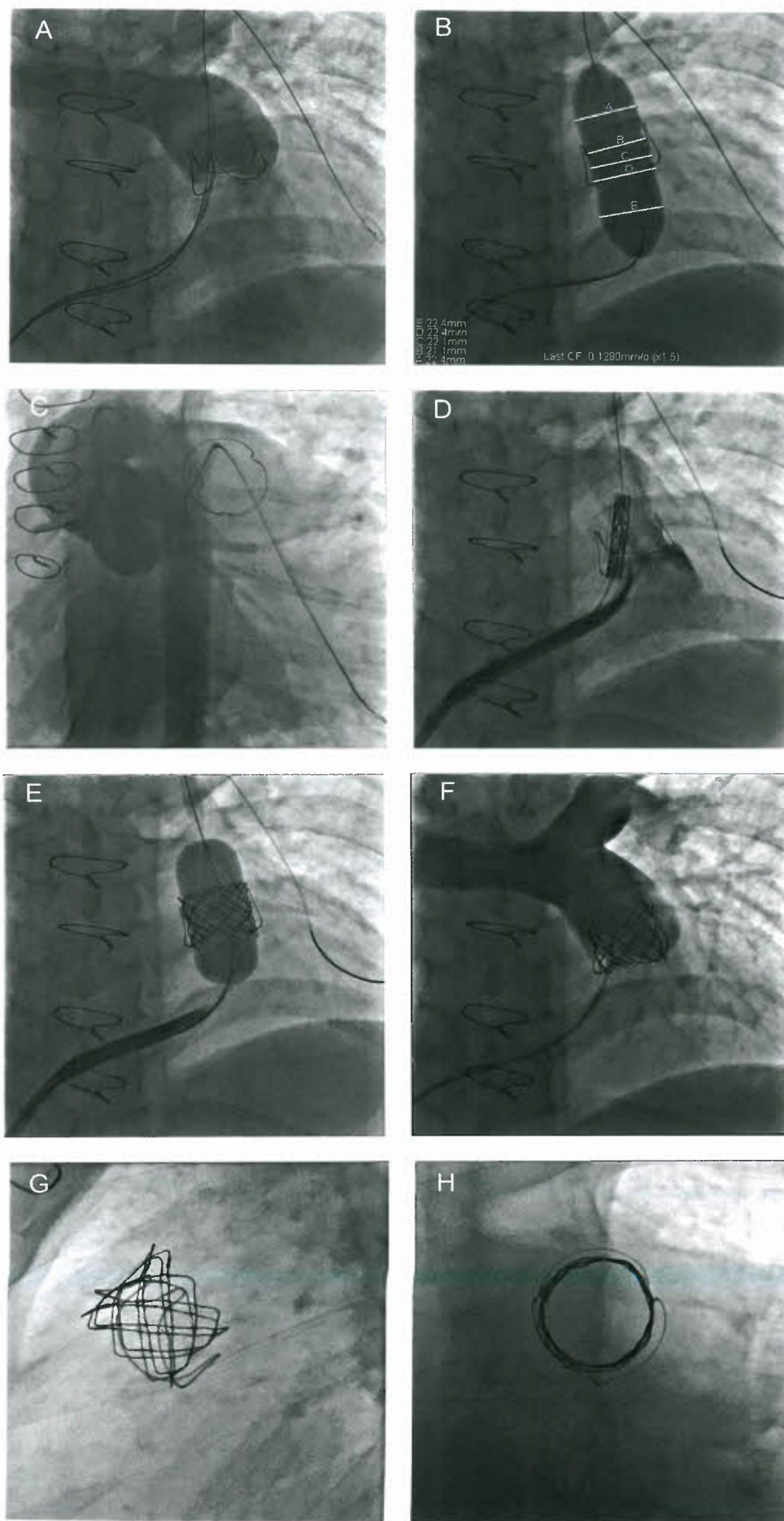


Figure 13.42. Melody valve and pretesting. There is increasing evidence that pretesting conduits using bare metal stents where a noncompliant surrounding environment exists may reduce the incidence of Melody TPV fatigue fractures and prolong the life span of the valve. In this very complicated patient who had multiple surgeries as well as an ICD, an RV angiogram demonstrates the narrowed conduit (**top left**). Four Palmaz XL stents were implanted until recoil of the stent was not observed and the PA angiogram demonstrated wide open PR (**top right**). The Melody TPV was then implanted within the bare metal stents (**bottom left**) and a repeat PA angiogram showed no residual stenosis or regurgitation (**bottom right**).

Figure 13.43. Procedural stages of Melody valve implant. The following images demonstrate the procedural steps for Melody TPV implant in a patient with a degenerating bioprosthetic pulmonary valve. A PA angiogram shows combined pulmonary valve stenosis and regurgitation (A). Balloon compliance testing is next performed to assess the suitability for valve implant (B). This is followed by testing for coronary artery compression (C). During delivery of the Melody valve, the outer sheath of the Ensemble BDS is withdrawn and a small angiogram is performed to confirm the appropriate position for implant (D). Next the inner balloon (E) of the BIB catheter are expanded, fully deploying the Melody valve. A repeat PA angiogram demonstrates no residual stenosis or regurgitation (F). Fluoroscopy at the end of the procedure nicely demonstrates the Melody TPV inside the metal struts of the bioprosthetic valve in the AP, Lateral, and Down-The-Barrel view (G,H).



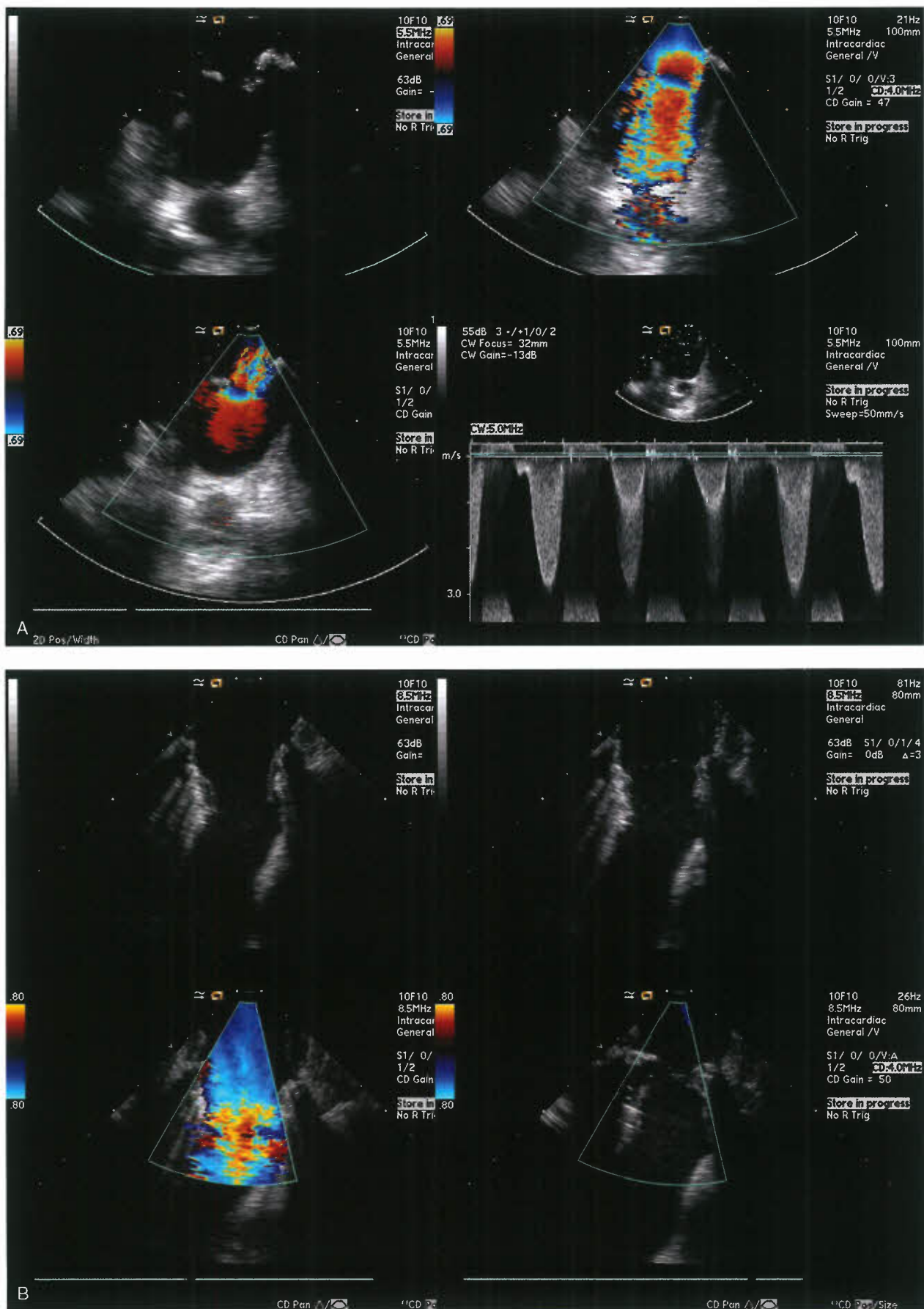


Figure 13.44. ICE evaluating Melody valve function. ICE has become a very important tool to evaluate the degenerating conduit valve as well as the newly implanted Melody TPV. The catheter is placed in the RVOT directly beneath the valve. Severely thickened and immobile valve leaflets are seen with systolic velocities over 3 m/sec and a wide diastolic color jet indicating significant PR (A). After the Melody TPV implant, nice thin leaflets are seen in systole and diastole with no significant residual stenosis or regurgitation (B).

The results of the expanded US Multicenter trial have recently been published by McElhinney et al. (68). Melody valve implantation was attempted in 124 patients, excluding, among others, 6 patients in whom valve implantation was not attempted due to coronary compression. Procedure-related serious adverse events occurred in 6% of patients including one death from intracranial hemorrhage after coronary artery dissection and one valve explantation after conduit rupture. Importantly, freedom from Melody valve dysfunction or reintervention was 94% at 1 year, and functional improvement in NYHA class was seen in most patients, even though long-term results after Melody valve implantation have yet to be confirmed. As an alternative to the Melody valve, the Carpentier-Edwards valve is presently undergoing trials within the US and may be suitable for larger RV-PA conduits (205,206).

HYBRID PROCEDURES

For many years, the relationship between the cardiothoracic surgeon and cardiac interventionalist was marked by competition and occasional “turf wars” between both groups, especially when dealing with acquired heart disease in adults. However, one of the most valuable lessons learned over the past decade is the need to embrace a collaborative approach between the congenital interventionalist and cardiac surgeon. Today, it should be commonplace to find a cardiac surgeon giving advice in the cardiac catheterization laboratory, while an interventionalist may aid his/her surgical colleague in the operating room by providing specific interventional techniques in selected patients. It should be routine and standard to involve the surgical team in any patient who is expected to undergo further surgical procedures prior to engaging in any transcatheter intervention. These discussions must be open and directed towards the specific patient who is being considered for interventional and/or surgical treatment. For example, in a patient undergoing transcatheter evaluation in preparation for conduit replacement, it may well be justified to place a stent for a more distal pulmonary artery stenosis, while proximal branch stenosis is not addressed because it is felt that this lesion could easily be treated during subsequent conduit replacement. Knowledge of the combined treatment capabilities allows the development of new and complex treatment strategies. One of the most notable examples of this cooperation has been in the “fenestrated Fontan” patients, in whom the immediate surgical morbidity is dramatically reduced by a purposeful “conduit” fenestration, which can subsequently be closed in the catheterization laboratory once the patient has recovered from the initial procedure. Another dramatic example of this type of collaboration is in patients with pulmonary valve atresia and VSD, in whom the surgical creation of a right ventricle to pulmonary artery connection early in the course of management provides the cardiologist access to the pulmonary vessels for dilation and intrapulmonary stenting in preparation for eventual definitive repair. This type of cooperation with inclusion of the adjunct procedures of the cardiologist in the staging of the surgery will contribute to better outcomes for many patients with extremely complex lesions.

In addition to the aforementioned collaboration between cardiac surgeons and cardiac interventionalists, a selection of new therapeutic hybrid catheterization and surgical procedures has been added to the spectrum of therapeutic interventions in complex CHD. These include the staged “hybrid approach” to the management of hypoplastic left heart syndrome (207–209), periventricular closure of VSDs (168,176), and intraoperative stent placements (210). Results of the multi-institutional C3PO registry documented a significant increase in the number of hybrid procedures performed over

a 2-year study period, with PDA stent placement, periventricular VSD closure, and intraoperative stent placement being the most commonly performed hybrid interventions (211).

Hypoplastic Left Heart Syndrome

Hypoplastic left heart syndrome carries a grave short- and long-term prognosis despite improvements that have been made in the traditional staged surgical approach. Even though surgical management has evolved over time, the basic concept has remained the same and as such, any possible improvements are capped by the limitations of this basic surgical approach. Using the conventional palliative surgical approach, the 5-year survival has been documented in multicenter experiences to be as low as 54% (212). The stage I Norwood- or Sano-type palliation in the neonate appears to carry the greatest risk contributing to the high morbidity and mortality in these patients. This is not surprising, given the many physiological changes that occur in the neonatal period that significantly influence the overall balance of this very fragile circulation. Combining this with an additional insult of a major open-heart procedure results in quite variable outcomes among institutions with mortality ranging from just under 10% to in excess of 50%. This has led to the development of alternative treatment strategies that are based upon smaller off-pump interventions in the early neonatal period that can be performed with minimal morbidity and mortality, thereby deferring the need for major cardiac surgical procedures, allowing the necessary time for improved growth and development of the patient and cardiac structures. This sets the stage for a subsequent comprehensive surgical procedure that combines the classical bidirectional Glenn shunt with a Norwood-type palliation as well as potential setup for subsequent transcatheter completion of the Fontan-type circulation. This staged approach requires a close collaboration between the cardiac surgeon, interventional cardiologist, and Heart Center staff. As is the case with many new innovative techniques, modifications have evolved over time as a result of the associated learning curve.

In 2002, Akintuerk et al. (213) reported on their experience with 11 patients who underwent transcatheter stenting of the arterial duct using balloon-expandable Jo stents, followed by bilateral pulmonary arterial banding 1 to 3 days after the transcatheter procedure. Balloon atrial septoplasty or BAS was performed on an as-needed basis. This early palliation was followed by a bidirectional Glenn procedure as well as a Damus-Kaye-Stanzel procedure and arch reconstruction between the age of 3.5 and 6 months. Two deaths were encountered in this series.



Figure 13.45. Hybrid Stage I for HLHS—Setup. Team approach during a Hybrid Stage I palliation in the specifically designed Hybrid Catheterization Suites.



Figure 13.46. Hybrid Catheterization Suite. Hybrid cardiac catheterization suite at Nationwide Children's Hospital.

In 2003, Michel-Behnke et al. (207) of the same group published an updated experience of 20 patients with very similar results.

The technique has further been modified by Galantowicz and Cheatham (208). Initial attempts at a sole transcatheter

technique with implantation of the AMPLATZER PA Flow Restrictor (AGA Medical, Golden Valley, MN) and PDA stents had a suboptimal outcome with significant hemodynamic compromise due to the combination of the stiffness of delivery cable as well as the need for placing a long sheath through tricuspid and pulmonary valves into the branch PAs, resulting in significant regurgitation. The approach was thus modified to a true hybrid technique, in which the cardiac surgeon initially performs bilateral pulmonary arterial banding, followed by transpulmonary placement of a stent to maintain patency of the arterial duct during the same procedure. This technique is performed preferably in a specially designed hybrid cardiac catheterization or operative suite that facilitates the specific needs of the cardiac surgeon as well as the interventional cardiologist (Fig. 13.45). The first suite dedicated to "hybrid" therapies in complex CHD opened in June 2004 at Nationwide Children's Hospital in Columbus (Fig. 13.46).

After LPA and right pulmonary artery (RPA) bands are placed using a 3.5- or 3.0-mm GoreTex tube that are cut into 1- to 2-mm-wide strips, the PDA stent is delivered through a short delivery sheath placed transpulmonary directly through a purse-string secured by snares. The initial choice of stents included balloon expandable premounted Genesis (Cordis, Warren, NJ) or Formula 418 stents (Cook, Bloomington, IN) but more recently self-expandable Protégé (EV3, Plymouth, MN) stents have been implanted and are felt to be more

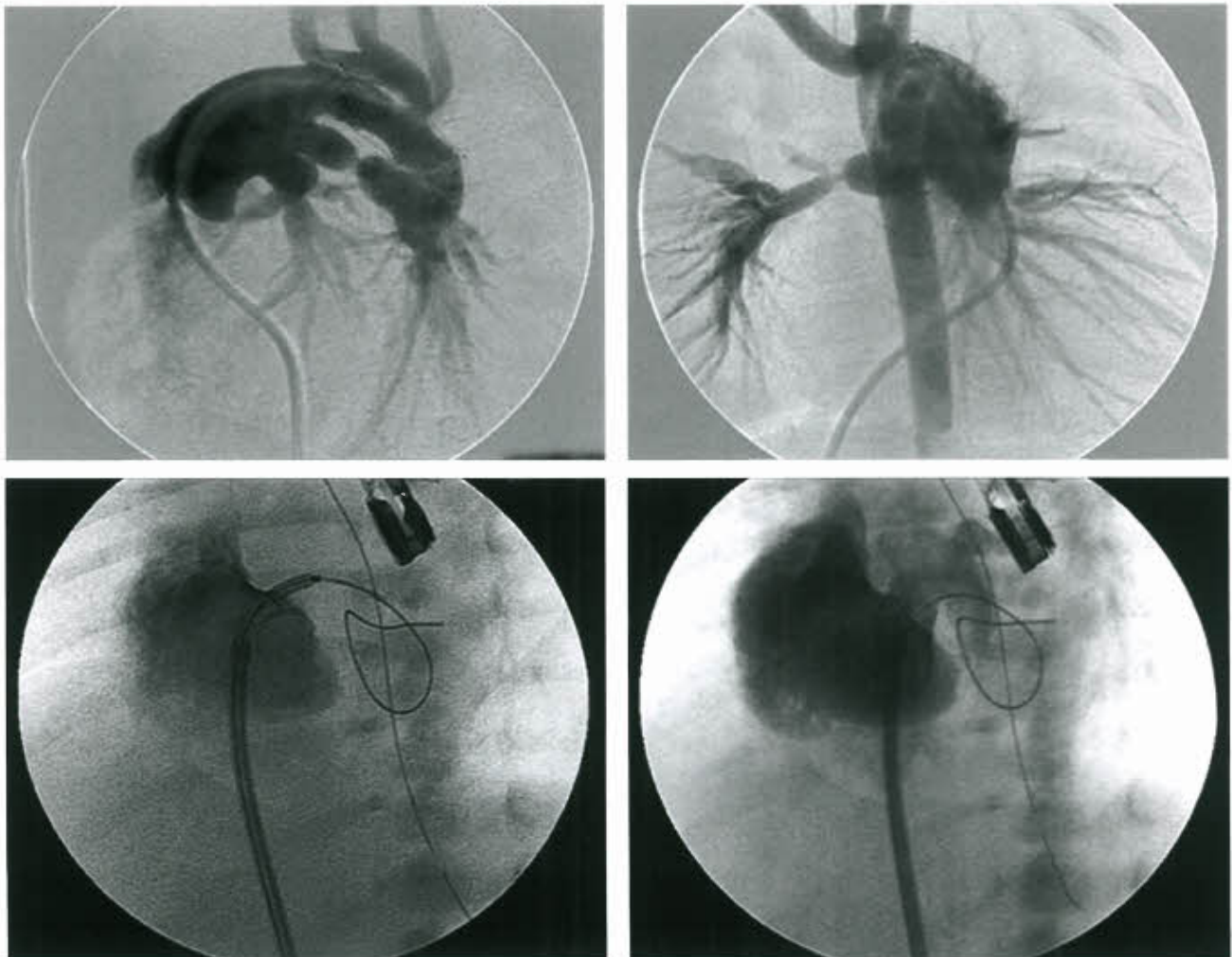


Figure 13.47. Hybrid Stage I for HLHS—Procedure. A 2-day-old infant with hypoplastic left heart syndrome undergoing stage I palliation. **Top left and right:** MPA angiogram after placement of bilateral PA bands and a PDA stent. **Bottom left:** Placement of a stent across a restrictive intra-atrial communication. **Bottom right:** Angiogram after placement of a stent across the restrictive intra-atrial communication.

beneficial due to the increased flexibility when compared to the balloon expandable varieties. Additionally, the feasibility of allowing to “drag” the partially deployed stent backwards if required during the delivery process is useful. The use of these stents has become even more appropriate since the length of the delivery sheath has been decreased from 135 to 80 cm.

The hybrid stage I procedure is feasible for the majority of patients with hypoplastic left heart syndrome (Fig. 13.47), an exception being those patients with stenosis of the retrograde aortic arch with accelerated flow noted on screening Doppler echocardiography. In these patients, a classical Norwood-type procedure remains the preferred treatment choice. Size has not been an issue with hybrid stage I palliation being successfully performed in preterm neonates as small as 1.1 kg. After the hybrid stage I procedure, patients are usually evaluated prior to discharge for the presence of any significant atrial-level restriction and BAS or atrial septoplasty is performed in virtually all patients, unless a very large ASD is present. In patients with hypoplastic left heart syndrome, this procedure can be extremely challenging and may require a wide variety of techniques, such as RF perforation of the atrial septum, use of (cutting) balloon septoplasty, atrial septal stent placement, or BAS with a smaller 1-mL balloon catheters. Frequently, a combination of these techniques is used to achieve successful

relief of any atrial level restriction (72). Patients are closely monitored during the follow-up period not only for the development of recurrent atrial-level restriction but also for the presence of any obstruction at the level of the retrograde aortic arch or the PDA stent, as well as assessing the flow to both branch PAs. Ideally, a single catheterization procedure is performed prior to the comprehensive stage II procedure. This includes assessment of the distal pulmonary artery pressures using a pressure wire such as the Radi pressure wire (Radi Medical Systems, Uppsala, Sweden), and an assessment for any residual or recurrent stenosis across the PDA stent or retrograde arch (Fig. 13.48). A septostomy at this stage usually allows the use of a larger septostomy balloon and is performed if any significant atrial-level restriction is identified.

The comprehensive stage II procedure is mostly a surgical undertaking, often combined with completion angiography. It combines a bidirectional Glenn shunt with debanding of the pulmonary arteries and patch pulmonary artery augmentation, if required. A Damus-Kaye-Stanzel anastomosis is performed with arch reconstruction. The PDA stent is removed and atrial septectomy is performed. If a transcatheter Fontan completion is considered, radio-opaque bands can be placed across the IVC and a blind-ending pouch of SVC below the pulmonary arteries is created. Another radiopaque marker facilitates subsequent

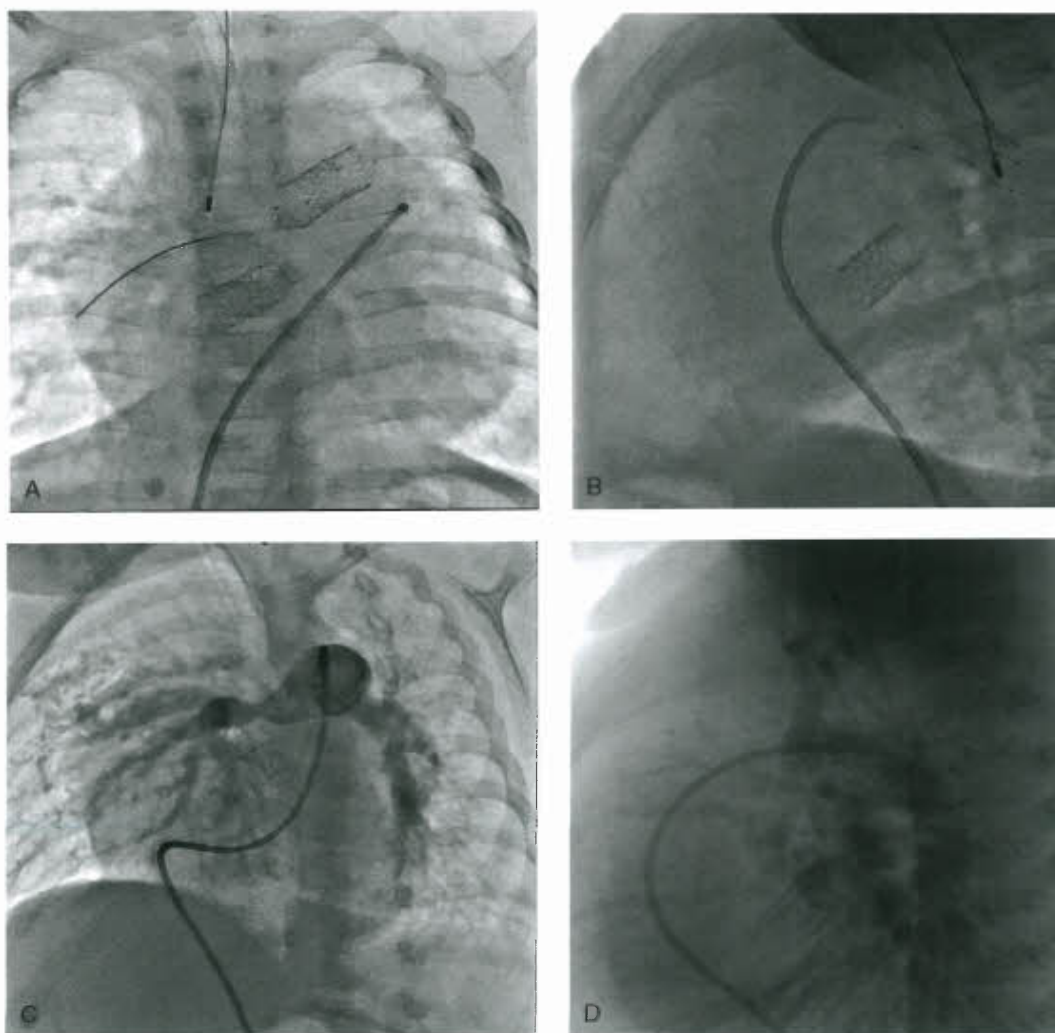


Figure 13.48. Transcatheter evaluation after Hybrid Stage I palliation. A 5-month-old infant with a h/o Hybrid stage I palliation and ASD stent placement. Catheterization prior to comprehensive stage II includes pressure recording with pressure wires in RPA (A), LPA, retrograde arch (B), Dao through stent, and ASD. Angiograms in MPA and PDA stent show the RPA band (C), LPA band, PDA stent and retrograde arch (D).

transcatheter completion of a Fontan-type circulation. The transcatheter completion of the Fontan-type circulation requires the availability of a covered balloon expandable stent, which can be implanted between IVC and SVC-pouch. A catheter-based approach was first described by Hausdorf et al. (214) but it was only recently that this approach had been modified by Galantowicz and Cheatham (209). However, its practical use has been limited in the United States due to the lack of FDA approval of the covered stent. Outside the US, the covered varieties of the NuMED CP stent are more widely available and this has resulted in further development of this technique pursued by larger Canadian centers (215).

The hybrid approach has been documented to achieve acceptable short- and mid-term outcome in patients with hypoplastic left heart syndrome. Galantowicz et al. (216) reported a 97% hospital survival after Hybrid Stage I palliation, with a combined survival up to and including comprehensive stage II palliation of more than 80% in standard patients with HLHS. This compares very well to other purely surgical series. One of the main problems after Hybrid stage I palliation is the development of in-stent stenosis within the stented arterial duct, which not only leads to obstruction for the right ventricle but even more importantly can create or worsen obstruction of flow to the retrograde arch. Egan et al. (217) recently reported histological results taken from stented PDA segments

that documented that neointimal proliferation after PDA stent placement were the “result of inflammation, extracellular matrix deposition, and smooth muscle-cell proliferation in the peristut region.” Identifying those patients who are at risk of developing retrograde arch obstruction after PDA stent placement has been a particular challenge. Egan et al. (218) reported that patients with smaller aortic roots, higher baseline retrograde arch velocities, and a larger angle between retrograde arch and PDA on angiography may be at higher risk of developing retrograde arch obstruction.

This technique is still evolving and with refinements in patient selection, further improved morbidity and mortality should be realized. Special efforts are being made to evaluate the neurodevelopmental outcome in these patients, which ultimately may be the most important factor in comparing the surgical and the hybrid approach for palliation of HLHS.

Perventricular Closure of Ventricular Septal Defects

Device closure of muscular VSDs using the AMPLATZER Muscular VSD Occluder has been shown to be safe and effective. However, even though the transcatheter approach can be safely and effectively performed in most patients, patient weight below 10 kg has been associated with a significantly

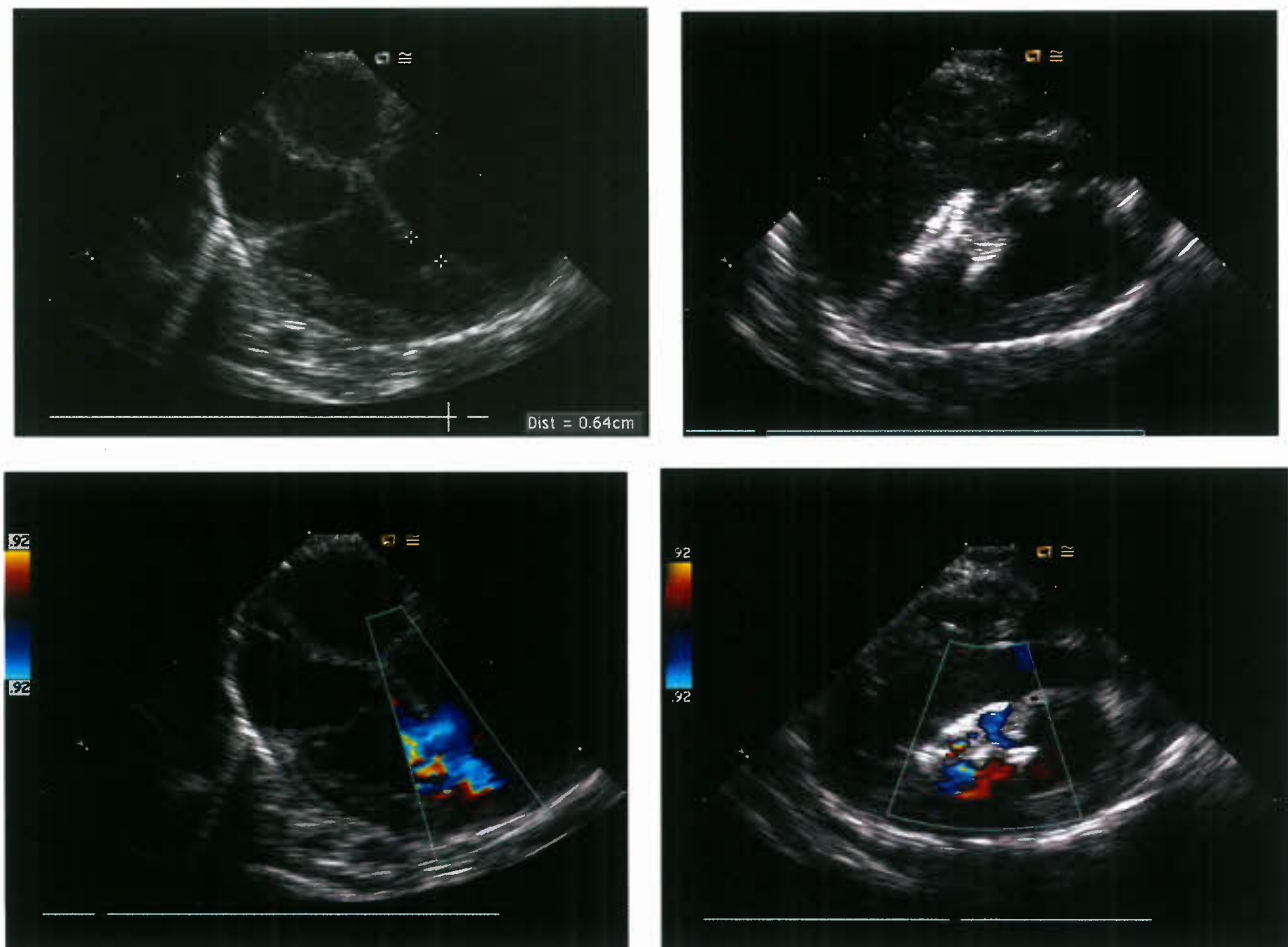


Figure 13.49. Perventricular VSD closure. Closure of a moderate-sized muscular VSD in a 3-month-old infant using a perventricular “Hybrid” approach. **Top left:** Four-chamber view demonstrates large VSD. **Bottom left:** Four-chamber view with color flow mapping demonstrates VSD. **Top right:** Long-axis view documents excellent device position after VSD closure. **Bottom right:** Long-axis view with color flow mapping demonstrates only minimal foaming through the device after release.

higher risk of procedure- or device-related complications and a higher risk of procedural failure (170,219). This is mainly related to the need of establishing an arteriovenous wire loop and the use of a long and relatively stiff delivery system, which in infants, frequently not only stents open the tricuspid and aortic valves but also creates a significant amount of tension that may result in bradycardia and/or temporary heart block. As a result, a periventricular approach has been adopted that combines the safety of the hybrid surgical approach, avoidance of cardiopulmonary bypass, and relatively short procedure time. In this approach, the heart is exposed through a midline sternotomy off cardiopulmonary bypass. Under TEE and/or epicardial echo guidance, the appropriate entry site in relation to the VSD is identified and secured by placing a purse-string around its location at the RV free wall. Subsequently, a direct puncture is performed with the needle directed towards the VSD. A 0.035-inch angled glide wire is used to cross the VSD. An appropriately sized short hemostatic sheath can then be advanced across the VSD under echo guidance, keeping an appropriate distance from the LV free wall and the MV apparatus. The correctly sized AMPLATZER Muscular VSD Occluder is then loaded and advanced across the sheath and deployed under echo guidance, again, being specifically careful to establish some distance to the MV apparatus before deploying the LV disc. Once deployed across the VSD, device position is evaluated for any evidence of residual shunts or interference with adjacent structures that could create, for example, mitral or tricuspid regurgitation. Once a satisfactory device position has been confirmed, the device is released followed by a final echo evaluation (Fig. 13.49). The earliest experience describing this technique was reported by Bacha et al. (176) in 2003. In 2005, a multicenter experience documented successful application of this technique in 12/13 patients without mortality (168). At follow-up, residual shunts were present in two patients, without evidence of volume overload, congestive heart failure, or pulmonary hypertension. Modifications of this periventricular approach to facilitate closure of perimembranous VSDs have been evaluated in animal experiments by Amin (220).

Intraoperative Stent Placement and Other Hybrid Procedures

The cooperation between cardiac surgeon and interventional cardiologist is not limited to the management of infants with HLHS or periventricular VSD closure. The “hybrid approach” can and has been adopted to a variety of lesions and indications, including the stent placement in a variety of locations (Fig. 13.50) on and off cardiopulmonary bypass, vascular access in preterm Neonates requiring interventional therapy (such as carotid cutdown or direct puncture via sternotomy), and intraoperative balloon occlusion of aortopulmonary collaterals or shunts (Fig. 13.51). The ability of the surgeon to provide safe access to a vascular structure not amenable to conventional transcatheter therapy and the ability of the interventionalist to use less-invasive techniques and materials creates a unique “marriage” benefiting patients with complex CHD. The essential ingredients to achieve a successful outcome of these procedures are the close cooperation between the surgeon and interventionalist as well as their flexibility to adopt nonstandard approaches that are specifically tailored towards each individual patient.

Intraoperative stent placement is aided by the direct visualization in the operative field and can be further enhanced through the use of endoscopic equipment that facilitates a more detailed view of the stenosed or compressed area. The decision about intraoperative stent placement often is made in the catheterization laboratory, especially when evaluating

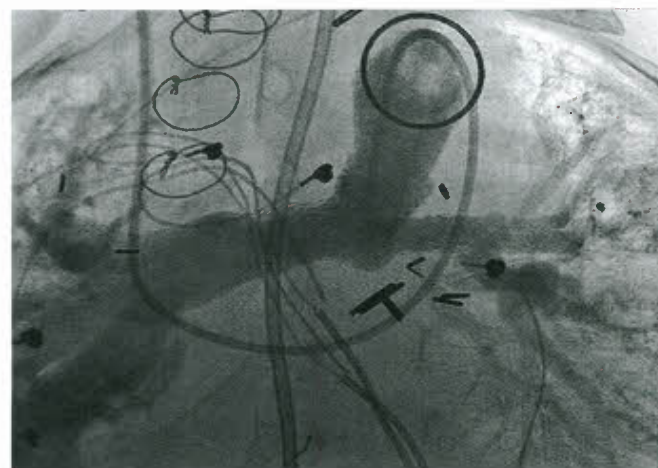
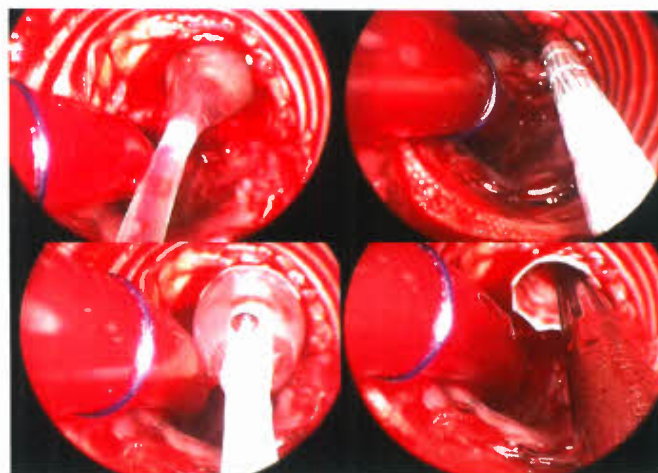
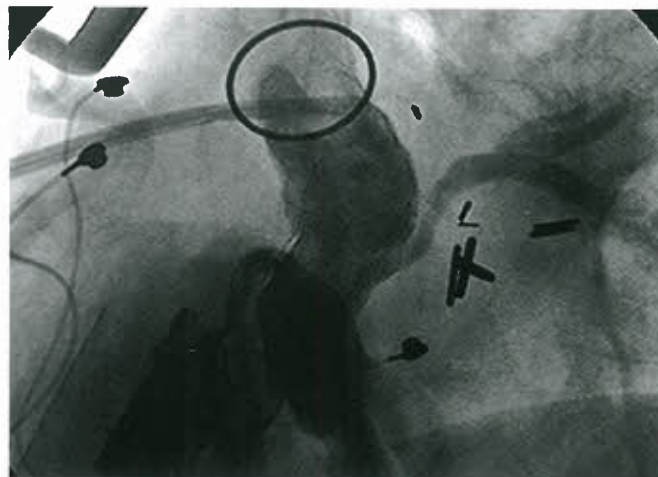


Figure 13.50. Intraoperative PA stenting. A 7-year-old girl with complex CHD who underwent intraoperative LPA stent placement during a Mustard procedure. **Top:** PA angiogram demonstrates a severely hypoplastic LPA. **Middle:** Intraoperative PA rehabilitation monitored endoscopically, from left to right and top to bottom, cutting balloon angioplasty, (covered) stent positioning followed by expansion, stent appearance after expansion. **Bottom:** PA angiogram demonstrates significantly improved LPA appearance.

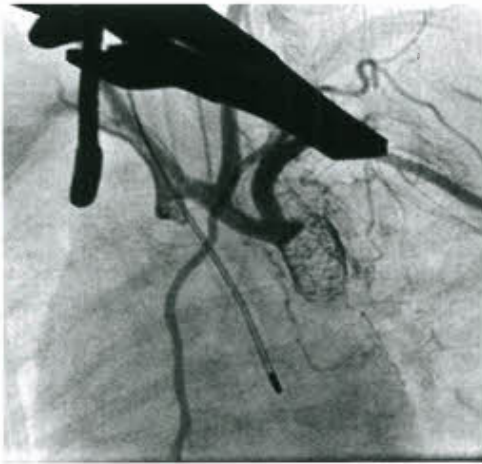


Figure 13.51. Stent placement via carotid cutdown. A 2-month-old boy premature infant (2.1 kg), who initially underwent Hybrid stage 1 palliation for complex CHD developed a significant recoarctation distal to the left subclavian artery (LSA) and therefore underwent “Hybrid” placement of a premounted stent using a surgical carotid cutdown. **Left:** Almost complete interruption distal to LSA before stent placement. **Right:** Aortogram after stent placement demonstrates significantly improved flow through the DAO.

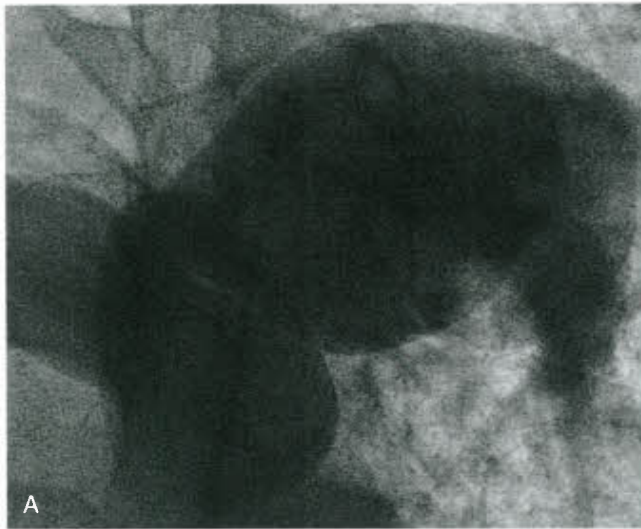


Figure 13.52. Intraoperative stent placement in proximal PA in adult using endoscopic guidance. A 42-year-old patient with history of Tetralogy of Fallot repair and free pulmonary insufficiency. Presurgical catheterization documented an LPA kink (A,B). Intraoperative endoscopic evaluation documented a ridge/fold at the proximal LPA (C), which was successfully treated by intraoperative stent placement (D).

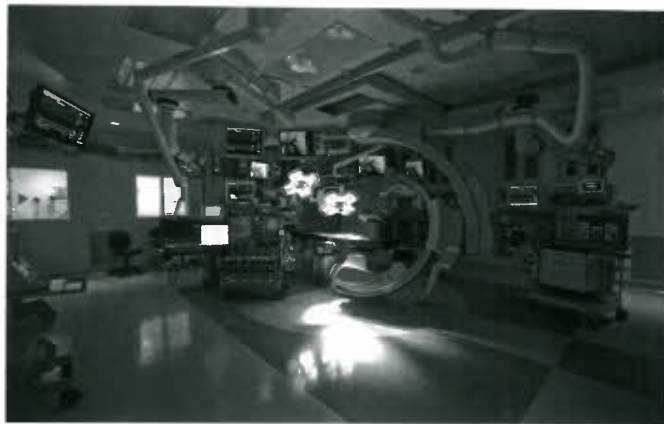


Figure 13.53. Hybrid operating suite. “Hybrid” operating suite at Nationwide Children’s Hospital in Columbus, Ohio, with large amount of floor space and various adjustable monitors combined with strategically placed booms. Equipment includes among others a ceiling-mounted cardiac flat-panel detector (Toshiba America Medical systems, Tustin, CA).

adult patients who are expected to undergo surgical conduit or pulmonary valve replacement. While proximal branch PA stenoses may be easily addressed during the surgical intervention, a more distal stenosis should usually be treated in the cardiac catheterization laboratory. Any residual branch PA stenosis after surgical pulmonary valve replacement burdens extra strain on the already reduced RV function, and therefore appropriate rehabilitation of these lesions is extremely important in achieving a quick postoperative recovery of RV function. However, a very proximal branch PA stenosis may not necessarily always indicate the need for surgical angioplasty. In fact, a nonobstructed RVOT may not always be treated with placement of a pulmonary valve, rather than placing an RV-PA conduit and as such a proximal branch PA stenosis may be better treated by placing an endovascular stent rather than performing patch

angioplasty with its fairly high recurrence risk (Fig. 13.52). In many instances, the ultimate decision whether to stent or to surgically treat the stenosis will be made intraoperatively. Intraoperative stent placement is a valid treatment option for these patients, with recent studies having documented very good results (221).

In addition, it is essential to have a high-resolution, digital, mobile C-arm readily available to obtain intraoperative angiograms whenever necessary. Hybrid Cardiothoracic Operative Suites with integrated permanent imaging equipment (Fig. 13.53) allow even more complex CHD to be treated using innovative management strategies. However, appropriate radiation protection is essential during these procedures, especially to surgeon and other operating room staff who are not accustomed to working with fluoroscopic equipment. While the need for radiation protection for staff and patients in the catheterization laboratory is frequently emphasized (222), the radiation protection used is usually impractical for surgeons in the operating room. As a result, Sawdy et al. (223) recently reported the use of lightweight radiation protection drapes that can be used during these hybrid procedures.

Holzer et al. (224) recently published the results of completion angiography performed after 32 cardiac surgical procedures, identifying unexpected pathology in 56% of procedures, leading to therapeutic changes or interventions in 28% of patients (Fig. 13.54). Other examples of important pathology identified through intraoperative C-arm angiography have been reported by Shuhaiber et al. (225). These reports emphasize that completion angiography after cardiac surgical repair may be an underutilized diagnostic modality, with potentially as important an impact on outcome as has been established with routine intraoperative TEE.

SUMMARY

The therapeutic cardiac catheterization procedures discussed in this chapter represent significant advances in the care of patients with CHD. The procedures are ordinarily performed

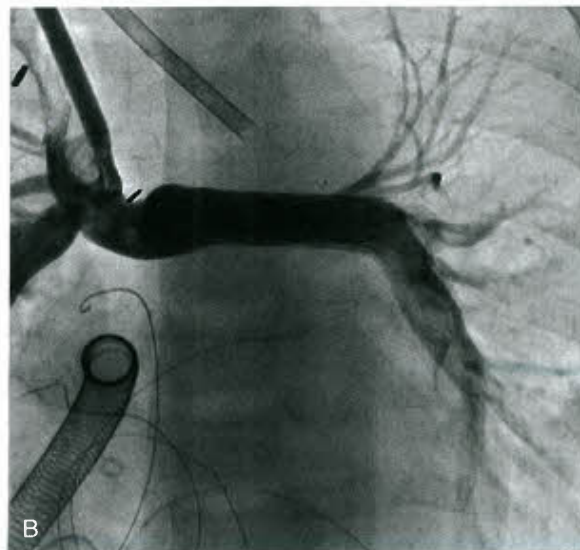
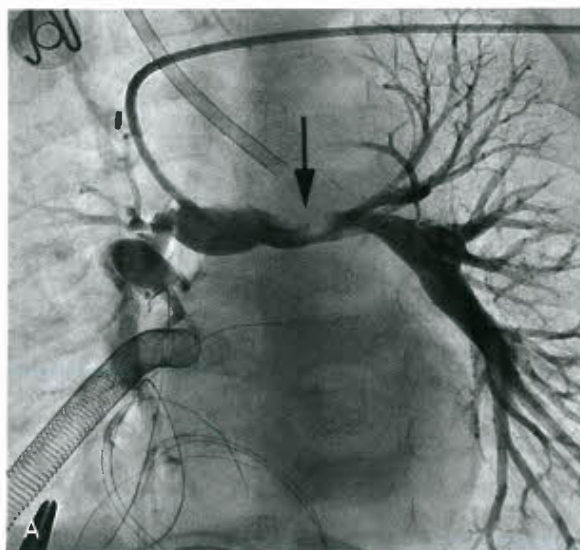


Figure 13.54. Exit angio after comprehensive stage II with inraop LPA stent. A 6-month-old boy infant with HLHS and previous Hybrid Stage I palliation. Exit angiography after comprehensive Stage II palliation documented a significant stenosis (patch-folding) of the mid-portion of the LPA (A). A 25-mm Genesis XD stent was implanted and expanded to 7 mm with very good angiographic result (B).

without an incision, cardiopulmonary bypass, or chest tubes. Some of the therapeutic procedures are possible only in the catheterization laboratory, and the subsequent surgery is possible only after preparation in the catheterization laboratory.

Even with the additional expense of the specialized catheters and devices and the added cost of the more extensive catheterization procedures, the direct costs of the therapeutic procedure in the catheterization laboratory are significantly lower than those for the comparable surgical procedure. The indirect savings for a patient or the patient's family may be even greater. The patient and family are away from home and work for only 1 or 2 days for the entire hospital stay. Following the catheterization procedure, the patient can return home and immediately return to full activity of either school or work. These advantages of therapeutic catheterization procedures have led to their wide acceptance.

However, therapeutic catheterization has advanced beyond the confines of the cardiac catheterization laboratory. Many "cutting-edge" procedures can only be facilitated through the unique cooperation between cardiac surgeon and interventional cardiologist and as such, patient care is advanced through this combined expertise. With further developments and improvements in catheter and surgical techniques, it is to be expected that additional nonsurgical or "hybrid" corrections will become standard within the next several years (226–229).

REFERENCES

- Dotter CT, Judkins MP. Transluminal treatment of arteriosclerotic obstruction. Description of a new technic and a preliminary report of its application. *Circulation* 1964;30:654–670.
- Rashkind WJ, Miller WW. Creation of an atrial septal defect without thoracotomy. A palliative approach to complete transposition of the great arteries. *JAMA* 1966;196:991–992.
- Porstmann W, Wierny L, Warnke H. Closure of ductus arteriosus persists without thoracotomy. 2. *Fortschr Geb Rontgenstr Nuklearmed* 1968;109:133–148.
- Wallace S, Gianturco C, Anderson JH, et al. Therapeutic vascular occlusion utilizing steel coil technique: clinical applications. *AJR Am J Roentgenol* 1976;127:381–387.
- King TD, Thompson SL, Steiner C, et al. Secundum atrial septal defect. Nonoperative closure during cardiac catheterization. *JAMA* 1976;235:2506–2509.
- Kan JS, White RI Jr, Mitchell SE, et al. Percutaneous balloon valvuloplasty: a new method for treating congenital pulmonary-valve stenosis. *N Eng J Med* 1982;307:540–542.
- Lock JE, Block PC, McKay RG, et al. Transcatheter closure of ventricular septal defects. *Circulation* 1988;78:361–368.
- O'Laughlin MP, Perry SB, Lock JE, et al. Use of endovascular stents in congenital heart disease. *Circulation* 1991;83:1923–1939.
- Bonhoeffer P, Boudjemline Y, Saliba Z, et al. Percutaneous replacement of pulmonary valve in a right-ventricle to pulmonary-artery prosthetic conduit with valve dysfunction. *Lancet* 2000;356:1403–1405.
- Vitiello R, McCrindle BW, Nykanen D, et al. Complications associated with pediatric cardiac catheterization. *J Am Coll Cardiol* 1998;32:1433–1440.
- Tavli V, Kayhan B, Okur FF, et al. Complications of pediatric cardiac catheterization: 18-month study. *Turk J Pediatr* 2000;42:294–297.
- Cassidy SC, Schmidt KG, Van Hare GF, et al. Complications of pediatric cardiac catheterization: a 3-year study. *J Am Coll Cardiol* 1992;19:1285–1293.
- Everett AD, Ringel R, Rhodes JF, et al. Development of the MAGIC congenital heart disease catheterization database for interventional outcome studies. *J Interv Cardiol* 2006;19:173–177.
- Forbes TJ, Garekar S, Amin Z, et al. Procedural results and acute complications in stenting native and recurrent coarctation of the aorta in patients over 4 years of age: a multi-institutional study. *Catheter Cardiovasc Interv* 2007;70:276–285.
- Allen HD, Mullins CE. Results of the Valvuloplasty and Angioplasty of Congenital Anomalies Registry. *Am J Cardiol* 1990;65:772–774.
- Bergersen L, Marshall A, Gauvreau K, et al. Adverse event rates in congenital cardiac catheterization—a multi-center experience. *Catheter Cardiovasc Interv* 2010;75:389–400.
- Franklin RC, Jacobs JP, Tchervenkov CI, et al. Bidirectional crossmap of the Short Lists of the European Paediatric Cardiac Code and the International Congenital Heart Surgery Nomenclature and Database Project. *Cardiol Young* 2002;12:431–435.
- Bergersen L, Gauvreau K, Marshall A, et al. Procedure-type risk categories for pediatric and congenital cardiac catheterization. *Circ Cardiovasc Interv* 2011;45:188–194.
- Bergersen L, Gauvreau K, Foerster SR, et al. Catheterization for Congenital Heart Disease Adjustment for Risk Method (CHARM). *JACC Cardiovasc Interv* 2011;4:1037–1046.
- Holzer RJ, Gauvreau K, Kreutzer J, et al. Balloon angioplasty and stenting of branch pulmonary arteries: Adverse events and procedural characteristics—results of a multi-institutional registry. *Circ Cardiovasc Interv* 2011;4:287–296.
- Holzer RJ, Gauvreau K, Kreutzer J, et al. Safety and efficacy of balloon pulmonary valvuloplasty: A multicenter experience. *J Am Coll Cardiol* 2012 Mar 15. doi: 10.1002/ccd.23473. [Epub ahead of print]
- Martin GR, Beekman RH, Ing FF, et al. The IMPACT registry: IMproving Pediatric and Adult Congenital Treatments. *Semin Thorac Cardiovasc Surg Pediatr Card Surg Annu* 2010;13:20–25.
- Holzer R, Chisolm J, Hill SL, et al. Transcatheter devices used in the management of patients with congenital heart disease. *Expert Rev Med Devices* 2006;2:603–615.
- Furlan AJ, Reisman M, Massaro J, et al. Study design of the CLOSURE I Trial: a prospective, multicenter, randomized, controlled trial to evaluate the safety and efficacy of the STARFlex septal closure system versus best medical therapy in patients with stroke or transient ischemic attack due to presumed paradoxical embolism through a patent foramen ovale. *Stroke* 2010;41:2872–2883.
- Hausdorf G, Kaulitz R, Paul T, et al. Transcatheter closure of atrial septal defect with a new flexible, self-centering device (the STARFlex Occluder). *Am J Cardiol* 1999;84:1113–1116, A10.
- Zahn EM, Wilson N, Cutright W, et al. Development and testing of the Helix septal occluder, a new expanded polytetrafluoroethylene atrial septal defect occlusion system. *Circulation* 2001;104:711–716.
- Sideris EB, Sideris SE, Thanopoulos BD, et al. Transvenous atrial septal defect occlusion by the buttoned device. *Am J Cardiol* 1990;66:1524–1526.
- Rao PS, Berger F, Rey C, et al. Results of transvenous occlusion of secundum atrial septal defects with the fourth generation buttoned device: comparison with first, second and third generation devices. International Buttoned Device Trial Group. *J Am Coll Cardiol* 2000;36:583–592.
- O'Laughlin MP. Microvena atrial septal defect occlusion device—update 2000. *J Interv Cardiol* 2001;14:77–80.
- Hausdorf G, Schneider M, Franzbach B, et al. Transcatheter closure of secundum atrial septal defects with the atrial septal defect occlusion system (ASDOS): initial experience in children. *Heart* 1996;75:83–88.
- Lababidi Z, Wu JR, Walls TJ. Percutaneous balloon aortic valvuloplasty: results in 23 patients. *Am J Cardiol* 1984;53:194–197.
- Masura J, Gavora P, Formanek A, et al. Transcatheter closure of secundum atrial septal defects using the new self-centering amplatzer septal occluder: initial human experience [see comment]. *Catheter Cardiovasc Diagn* 1997;42:388–393.
- Cheatham JP, Hill SL, Chisolm JL. Initial results using the new cribriform Amplatzer septal occluder for transcatheter closure of multifenestrated atrial septal defects with septal aneurysm. *Catheter Cardiovasc Interv* 2003;60:126.
- Ewert P, Kretschmar O, Peters B, et al. Preliminary experience with a new 18 mm Amplatzer PFO occluder for small persistent foramen ovale. *Catheter Cardiovasc Interv* 2003;59:518–521.
- Waight DJ, Cao QL, Hijazi ZM. Closure of patent foramen ovale in patients with orthodeoxia-platypnea using the amplatzer devices [see comment]. *Catheter Cardiovasc Interv* 2000;50:195–198.
- Amin Z, Gu X, Berry JM, et al. New device for closure of muscular ventricular septal defects in a canine model. *Circulation* 1999;100:320–328.
- Thanopoulos BD, Tsaousis GS, Konstadopoulou GN, et al. Transcatheter closure of muscular ventricular septal defects with the amplatzer ventricular septal defect occluder: initial clinical applications in children. *J Am Coll Cardiol* 1999;33:1395–1399.
- Goldstein JA, Casserly IP, Balzer DT, et al. Transcatheter closure of recurrent postmyocardial infarction ventricular septal defects utilizing the Amplatzer postinfarction VSD device: a case series [Review] [12 refs]. *Catheter Cardiovasc Interv* 2003;59:238–243.
- Rigby ML, Redington AN. Primary transcatheter umbrella closure of perimembranous ventricular septal defect. *Br Heart J* 1994;72:368–371.
- Gu X, Han YM, Titus JL, et al. Transcatheter closure of membranous ventricular septal defects with a new nitinol prosthesis in a natural swine model. *Catheter Cardiovasc Interv* 2000;50:502–509.
- Hijazi ZM, Hakim F, Haweleh AA, et al. Catheter closure of perimembranous ventricular septal defects using the new Amplatzer membranous VSD occluder: initial clinical experience. *Catheter Cardiovasc Interv* 2002;56:508–515.
- Rashkind WJ, Cuaso CC. Transcatheter closure of patent ductus arteriosus; successful use in a 3.5 kilogram infant. *Pediatr Cardiol* 1979;1:3–7.
- Rashkind WJ, Mullins CE, Hellenbrand WE, et al. Nonsurgical closure of patent ductus arteriosus: clinical application of the Rashkind PDA Occluder System. *Circulation* 1987;75:583–592.
- Rashkind WJ. Therapeutic interventional procedures in congenital heart disease. *Radiol Diagn* 1987;28:449–460.

45. Perry SB, Radtke W, Fellows KE, et al. Coil embolization to occlude aortopulmonary collateral vessels and shunts in patients with congenital heart disease. *J Am Coll Cardiol* 1989;13:100-108.
46. Cambier PA, Kirby WC, Wortham DC, et al. Percutaneous closure of the small (less than 2.5 mm) patent ductus arteriosus using coil embolization. *Am J Cardiol* 1992;69:815-816.
47. Uzun O, Hancock S, Parsons JM, et al. Transcatheter occlusion of the arterial duct with Cook detachable coils: early experience. *Heart* 1996;76:269-273.
48. Grifka RG, Fenrich AL, Tapio JB. Transcatheter closure of patent ductus arteriosus and aorto-pulmonary vessels using non-ferromagnetic Inconel MREye embolization coils. *Catheter Cardiovasc Interv* 2008;72:691-695.
49. Masura J, Walsh KP, Thanopoulos B, et al. Catheter closure of moderate- to large-sized patent ductus arteriosus using the new Amplatzer duct occluder: immediate and short-term results. *J Am Coll Cardiol* 1998;31:878-882.
50. Forsey J, Kenny D, Morgan G, et al. Early clinical experience with the new Amplatzer Ductal Occluder II for closure of the persistent arterial duct. *Catheter Cardiovasc Interv* 2009;74:615-623.
51. Morgan G, Tometzki AJ, Martin RP. Transcatheter closure of long tubular patent arterial ducts: the Amplatzer Duct Occluder II-A new and valuable tool. *Catheter Cardiovasc Interv* 2009;73:576-580.
52. Bhole V, Miller P, Mehta C, et al. Clinical evaluation of the new Amplatzer duct occluder II for patent arterial duct occlusion. *Catheter Cardiovasc Interv* 2009;74:762-769.
53. Chisolm JL, Hill SL, Hardin J, et al. Initial experience with the nit-occlud PDA occlusion system for closure of patent ductus arteriosus. *Catheter Cardiovasc Interv* 2003;60:123.
54. Celiker A, Aypar E, Karagoz T, et al. Transcatheter closure of patent ductus arteriosus with Nit-Occlud coils. *Catheter Cardiovasc Interv* 2005;65:569-576.
55. Holzer R, Cao QL, Sandhu S, et al. The Amplatzer vascular plug—an addition to our interventional armamentarium. *Pediatr Cardiol* 2004;26:6-8.
56. Ng B, Schneider DJ, Hokanson JS. Closure of tubular patent ductus arteriosus in infants and small children with the Amplatzer Vascular Plug II. *Congenit Heart Dis* 2011;6:64-69.
57. Mordasini P, Gralla J, Brekenfeld C, et al. Preliminary experimental evaluation of the immediate angiographic occlusion time with use of the AMPLATZER vascular plug II for carotid artery occlusion. *J Vasc Interv Radiol* 2010;21:1873-1877.
58. Mullins CE. *Cardiac catheterization in congenital heart disease*. Vol. 1. Malden, MA: Blackwell, 2006.
59. Grifka RG, Mullins CE, Gianturco C, et al. New Gianturco-Grifka vascular occlusion device. Initial studies in a canine model. *Circulation* 1995;91:1840-1846.
60. Hoyer MH, Leon RA, Fricker FJ. Transcatheter closure of modified Blalock-Taussig shunt with Gianturco-Grifka Vascular Occlusion Device [see comment]. *Catheter Cardiovasc Interv* 1999;48:365-367.
61. Ebeid MR, Gaymes CH, Smith JC, et al. Gianturco-Grifka vascular occlusion device for closure of patent ductus arteriosus. *Am J Cardiol* 2001;87:657-660.
62. Demkow M, Ruzyllo W, Siudalska H, et al. Transcatheter closure of a 16 mm hypertensive patent ductus arteriosus with the Amplatzer muscular VSD occluder. *Catheter Cardiovasc Interv* 2001;52:359-362.
63. Pedra CA, Sanches SA, Fontes VF. Percutaneous occlusion of the patent ductus arteriosus with the amplatzer device for atrial septal defects. *J Invasive Cardiol* 2003;15:413-417.
64. Rao PS, Sideris EB, Haddad J, et al. Transcatheter occlusion of patent ductus arteriosus with adjustable buttoned device. Initial clinical experience. *Circulation* 1993;88:1119-1126.
65. Mullins CE, O'Laughlin MP, Vick GW, III, et al. Implantation of balloon-expandable intravascular grafts by catheterization in pulmonary arteries and systemic veins. *Circulation* 1988;77:188-199.
66. Maglione J, Bergersen L, Lock JE, et al. Ultra-high-pressure balloon angioplasty for treatment of resistant stenoses within or adjacent to previously implanted pulmonary arterial stents. *Circ Cardiovasc Interv* 2009;2:52-58.
67. Stanfill R, Nykanen DG, Osorio S, et al. Stent implantation is effective treatment of vascular stenosis in young infants with congenital heart disease: acute implantation and long-term follow-up results. *Catheter Cardiovasc Interv* 2008;71:831-841.
68. McElhinney DB, Hellenbrand WE, Zahn EM, et al. Short- and medium-term outcomes after transcatheter pulmonary valve placement in the expanded multicenter US melody valve trial. *Circulation* 2010;122:507-516.
69. Zahn EM, Hellenbrand WE, Lock JE, et al. Implantation of the melody transcatheter pulmonary valve in patients with a dysfunctional right ventricular outflow tract conduit early results from the U.S. Clinical trial. *J Am Coll Cardiol* 2009;54:1722-1729.
70. Robb JD, Harris MA, Minakawa M, et al. Melody valve implantation into the branch pulmonary arteries for treatment of pulmonary insufficiency in an ovine model of right ventricular outflow tract dysfunction following tetralogy of fallot repair. *Circ Cardiovasc Interv* 2011;4:80-87.
71. Eicken A, Fratz S, Hager A, et al. Transcatheter Melody valve implantation in "tricuspid position" after a Fontan Bjork (RA-RV homograft) operation results in biventricular circulation. *Int J Cardiol* 2010;142:e45-e47.
72. Holzer RJ, Wood A, Chisolm JL, et al. Atrial septal interventions in patients with hypoplastic left heart syndrome. *Catheter Cardiovasc Interv* 2008;72:696-704.
73. Park SC, Neches WH, Mullins CE, et al. Blade atrial septostomy: collaborative study. *Circulation* 1982;66:258-266.
74. Holzer RJ, Hardin J, Hill SL, et al. Radiofrequency Energy—A Multifaceted Tool for the Congenital Interventionist. *Congenital Cardiol Today* 2006;4:1-8.
75. Hill SL, Mizelle KM, Vellucci SM, et al. Radiofrequency perforation and cutting balloon septoplasty of intact atrial septum in a newborn with hypoplastic left heart syndrome using transesophageal ICE probe guidance. *Catheter Cardiovasc Interv* 2005;64:214-217.
76. Bonow RO, Carabello BA, Chatterjee K, et al. ACC/AHA 2006 guidelines for the management of patients with valvular heart disease: a report of the American College of Cardiology/American Heart Association Task Force on Practice Guidelines (writing Committee to Revise the 1998 guidelines for the management of patients with valvular heart disease) developed in collaboration with the Society of Cardiovascular Anesthesiologists endorsed by the Society for Cardiovascular Angiography and Interventions and the Society of Thoracic Surgeons. *J Am Coll Cardiol* 2006;48:e1-e148.
77. Polimenakos AC, Sathanandam S, Elzein C, et al. Aortic cusp extension valvuloplasty with or without tricuspidization in children and adolescents: long-term results and freedom from aortic valve replacement. *J Thorac Cardiovasc Surg* 2010;139:933-941; discussion 941.
78. Brown DW, Dipilato AE, Chong EC, et al. Aortic valve reinterventions after balloon aortic valvuloplasty for congenital aortic stenosis intermediate and late follow-up. *J Am Coll Cardiol* 2010;56:1740-1749.
79. Daehnert I, Rotzsch C, Wiener M, et al. Rapid right ventricular pacing is an alternative to adenosine in catheter interventional procedures for congenital heart disease. *Heart* 2004;90:1047-1050.
80. Stanger P, Cassidy SC, Girod DA, et al. Balloon pulmonary valvuloplasty: results of the Valvuloplasty and Angioplasty of Congenital Anomalies Registry. *Am J Cardiol* 1990;65:775-783.
81. Jarrar M, Betbout F, Farhat MB, et al. Long-term invasive and noninvasive results of percutaneous balloon pulmonary valvuloplasty in children, adolescents, and adults. *Am Heart J* 1999;138:950-954.
82. Rao PS, Galal O, Patnana M, et al. Results of three to 10 year follow up of balloon dilatation of the pulmonary valve. *Heart* 1998;80:591-595.
83. Mullins CE. Pulmonary valve balloon dilation. In: Mullins CE, ed. *Cardiac catheterization in congenital heart disease*. Vol. 1. Malden, MA: Blackwell, 2006:430-440.
84. McCrindle BW. Independent predictors of long-term results after balloon pulmonary valvuloplasty. Valvuloplasty and Angioplasty of Congenital Anomalies (VACA) Registry Investigators. *Circulation* 1994;89:1751-1759.
85. Mullins CE, Nihill MR, Vick GW, III, et al. Double balloon technique for dilation of valvular or vessel stenosis in congenital and acquired heart disease. *J Am Coll Cardiol* 1987;10:107-114.
86. McCrindle BW. Independent predictors of long-term results after balloon pulmonary valvuloplasty. Valvuloplasty and Angioplasty of Congenital Anomalies (VACA) Registry Investigators. *Circulation* 1994;89:1751-1759.
87. Fawzy ME, Hassan W, Fadel BM, et al. Long-term results (up to 17 years) of pulmonary balloon valvuloplasty in adults and its effects on concomitant severe infundibular stenosis and tricuspid regurgitation. *Am Heart J* 2007;153:433-438.
88. Fawzy ME, Galal O, Dunn B, et al. Regression of infundibular pulmonary stenosis after successful balloon pulmonary valvuloplasty in adults. *Catheter Cardiovasc Diagn* 1990;21:77-81.
89. Redington AN, Cullen S, Rigby ML. Laser or radiofrequency pulmonary valvotomy in neonates with pulmonary atresia and intact ventricular septum—description of a new method avoiding arterial catheterization. *Cardiol Young* 1992;2:387-390.
90. Cheatham JP. To perforate or not to perforate—that's the question...or is it? just ask Richard & excl. *Catheter Cardiovasc Diagn* 1997;42:403-404.
91. Latson L, Cheatham J, Froemming S, et al. Transductal guidewire "rail" for balloon valvuloplasty in neonates with isolated critical pulmonary valve stenosis or atresia. *Am J Cardiol* 1994;73:713-714.
92. Benson LN, Nykanen D, Collison A. Radiofrequency perforation in the treatment of congenital heart disease [68 refs]. *Catheter Cardiovasc Interv* 2002;56:72-82.
93. Gournay V, Piechaud JF, Delogu A, et al. Balloon valvotomy for critical stenosis or atresia of pulmonary valve in newborns. *J Am Coll Cardiol* 1995;26:1725-1731.
94. Walsh KP, Abdulhamed JM, Tometzki JP. Importance of right ventricular outflow tract angiography in distinguishing critical pulmonary stenosis from pulmonary atresia. *Heart* 1997;77:456-460.
95. Alwi M, Kandavello G, Choo KK, et al. Risk factors for augmentation of the flow of blood to the lungs in pulmonary atresia with intact ventricular septum after radiofrequency valvotomy. *Cardiol Young* 2005;15:141-147.
96. Wang JK, Wu MH, Chang CI, et al. Outcomes of transcatheter valvotomy in patients with pulmonary atresia and intact ventricular septum. *Am J Cardiol* 1999;84:1055-1060.
97. Justo RN, Nykanen DG, Williams WG, et al. Transcatheter perforation of the right ventricular outflow tract as initial therapy for pulmonary valve atresia and intact ventricular septum in the newborn [see comment]. *Catheter Cardiovasc Diagn* 1997;40:408-413.
98. Cheatham JP. The transcatheter management of the neonate and infant with pulmonary atresia and intact ventricular septum. *J Interv Cardiol* 1998;11:363-387.

99. Bonhoeffer P, Piechaud JF, Sidi D, et al. Mitral dilatation with the Multi-Track system: an alternative approach. *Cathet Cardiovasc Diagn* 1995;36:189–193.
100. Inoue K, Owaki T, Nakamura T, et al. Clinical application of transvenous mitral commissurotomy by a new balloon catheter. *J Thorac Cardiovasc Surg* 1984;87:394–402.
101. McElhinney DB, Sherwood MC, Keane JF, et al. Current management of severe congenital mitral stenosis: outcomes of transcatheter and surgical therapy in 108 infants and children. *Circulation* 2005;112:707–714.
102. Sos T, Sniderman KW, Rettke-Sos B, et al. Percutaneous transluminal dilatation of coarctation of thoracic aorta post mortem. *Lancet* 1979;2:970–971.
103. Lock JE, Castaneda-Zuniga WR, Bass JL, et al. Balloon dilatation of excised aortic coarctations. *Radiology* 1982;143:689–691.
104. Lock JE, Niemi T, Burke BA, et al. Transcutaneous angioplasty of experimental aortic coarctation. *Circulation* 1982;66:1280–1286.
105. Grifka RG, Vick GW III, O'Laughlin MP, et al. Balloon expandable intravascular stents: aortic implantation and late further dilation in growing minipigs. *Am Heart J* 1993;126:979–984.
106. Redington AN, Hayes AM, Ho SY. Transcatheter stent implantation to treat aortic coarctation in infancy. *Br Heart J* 1993;69:80–82.
107. Suarez dL, Pan M, Romero M, et al. Percutaneous interventions on severe coarctation of the aorta: a 21-year experience. *Pediatr Cardiol* 2005;26:176–189.
108. Cheatham JP. Stenting of coarctation of the aorta. *Catheter Cardiovasc Interv* 2001;54:112–125.
109. Holzer RJ, Chisolm JL, Hill SL, et al. Stenting complex aortic arch obstructions. *Catheter Cardiovasc Interv* 2008;71:375–382.
110. Egan M, Holzer RJ. Comparing balloon angioplasty, stenting and surgery in the treatment of aortic coarctation. *Expert Rev Cardiovasc Ther* 2009;7:1401–1412.
111. Zabala C, Attie F, Rosas M, et al. The adult patient with native coarctation of the aorta: balloon angioplasty or primary stenting? [see comment]. *Heart* 2003;89:77–83.
112. Holzer R, Qureshi S, Ghasemi A, et al. Stenting of aortic coarctation: acute, intermediate, and long-term results of a prospective multi-institutional registry—Congenital Cardiovascular Interventional Study Consortium (CCISC). *Catheter Cardiovasc Interv* 2010;76:553–563.
113. Forbes TJ, Kim DW, Du W, et al. Comparison of surgical, stent and balloon angioplasty treatment of native coarctation of the aorta. *JACC* 2011;58(25):2664–2674.
114. Fletcher SE, Nihill MR, Grifka RG, et al. Balloon angioplasty of native coarctation of the aorta: midterm follow-up and prognostic factors. *J Am Coll Cardiol* 1995;25:730–734.
115. DeGroff CG, Rice MJ, Reller MD, et al. Intravascular ultrasound can assist angiographic assessment of coarctation of the aorta. *Am Heart J* 1994;128:836–839.
116. Tong AD, Rothman A, Atkinson RL, et al. Intravascular ultrasound imaging of coarctation of the aorta: animal and human studies. *Am J Card Imaging* 1995;9:250–256.
117. Xu J, Shiota T, Omoto R, et al. Intravascular ultrasound assessment of regional aortic wall stiffness, distensibility, and compliance in patients with coarctation of the aorta. *Am Heart J* 1997;134:93–98.
118. Tan JL, Mullen M. Emergency stent graft deployment for acute aortic rupture following primary stenting for aortic coarctation. *Catheter Cardiovasc Interv* 2005;65:306–309.
119. Hijazi ZM. Catheter intervention for adult aortic coarctation: be very careful! [comment]. *Catheter Cardiovasc Interv* 2003;59:536–537.
120. Varma C, Benson LN, Butany J, et al. Aortic dissection after stent dilatation for coarctation of the aorta: a case report and literature review. *Catheter Cardiovasc Interv* 2003;59:528–535.
121. Bergersen L, Jenkins KJ, Gauvreau K, et al. Follow-up results of Cutting Balloon angioplasty used to relieve stenoses in small pulmonary arteries. *Cardiol Young* 2005;15:605–610.
122. Bergersen LJ, Perry SB, Lock JE. Effect of cutting balloon angioplasty on resistant pulmonary artery stenosis. *Am J Cardiol* 2003;91:185–189.
123. Holzer RJ, Chisolm JL, Hill S, et al. PA rehabilitation using endovascular stents in children with a weight below 15 kg: Stents are for kids too. *Catheter Cardiovasc Interv* 2006;67:836.
124. Arnold LW, Keane JF, Kan JS, et al. Transient unilateral pulmonary edema after successful balloon dilatation of peripheral pulmonary artery stenosis. *Am J Cardiol* 1988;62:327–330.
125. Seale AN, Daubeney PE, Magee AG, et al. Pulmonary vein stenosis: initial experience with cutting balloon angioplasty. *Heart* 2006;92:815–820.
126. Devaney EJ, Chang AC, Ohye RG, et al. Management of congenital and acquired pulmonary vein stenosis. *Ann Thorac Surg* 2006;81:992–995; discussion 995–996.
127. Zahn EM, Dobrolet NC, Nykanen DG, et al. Interventional catheterization performed in the early postoperative period after congenital heart surgery in children. *J Am Coll Cardiol* 2004;43:1264–1269.
128. Thrush PT, Mackman CA, Lawrence P, et al. Interventional strategies for complete vascular occlusions. *Pediatr Cardiol* 2011;32(6):713–723.
129. Daehnert I, Hennig B, Wiener M, et al. Interventions in leaks and obstructions of the interatrial baffle late after Mustard and Senning correction for transposition of the great arteries. *Catheter Cardiovasc Interv* 2005;66:400–407.
130. Holzer RJ, Hill SL, Chisolm JL, et al. Transcatheter Management of Patients after “atrial switch”—State of the Art. *Catheter Cardiovasc Interv* 2006;68:475.
131. Koenig P, Cao QL, Heitschmidt M, et al. Role of intracardiac echocardiographic guidance in transcatheter closure of atrial septal defects and patent foramen ovale using the Amplatzer device. *J Interv Cardiol* 2003;16:51–62.
132. Zanchetta M, Rigatelli G, Pedon L, et al. Transcatheter atrial septal defect closure assisted by intracardiac echocardiography: 3-year follow-up. *J Interv Cardiol* 2004;17:95–98.
133. Du ZD, Koenig P, Cao QL, et al. Comparison of transcatheter closure of secundum atrial septal defect using the Amplatzer septal occluder associated with deficient versus sufficient rims. *Am J Cardiol* 2002;90:865–869.
134. Varma C, Benson LN, Silversides C, et al. Outcomes and alternative techniques for device closure of the large secundum atrial septal defect. *Catheter Cardiovasc Interv* 2004;61:131–139.
135. Holzer RJ, Chisolm J, Hill S, et al. Transhepatic cardiac catheterization in complex congenital heart disease: where there is a will there is a way. *Congenital Cardiol Today* 2005;3:1–7.
136. Ewert P, Berger F, Nagdyman N, et al. Masked left ventricular restriction in elderly patients with atrial septal defects: a contraindication for closure? *Catheter Cardiovasc Interv* 2001;52:177–180.
137. Holzer R, Cao QL, Hijazi ZM. Closure of a moderately large atrial septal defect with a self-fabricated fenestrated Amplatzer septal occluder in an 85-year-old patient with reduced diastolic elasticity of the left ventricle. *Catheter Cardiovasc Interv* 2005;64:513–518.
138. Cheatham JP. Now we are making a hole in a device meant to close a hole: Why? How? Is there a better answer? *Catheter Cardiovasc Interv* 2005;64:519–521.
139. Amin Z, Hijazi ZM, Bass JL, et al. Erosion of Amplatzer septal occluder device after closure of secundum atrial septal defects: review of registry of complications and recommendations to minimize future risk. *Catheter Cardiovasc Interv* 2004;63:496–502.
140. Wahab HA, Bairam AR, Cao QL, et al. Novel technique to prevent prolapse of the Amplatzer septal occluder through large atrial septal defect. *Catheter Cardiovasc Interv* 2003;60:543–545.
141. Berger F, Ewert P, Abdul-Khalik H, et al. Percutaneous closure of large atrial septal defects with the Amplatzer Septal Occluder: technical overkill or recommendable alternative treatment? *J Interv Cardiol* 2001;14:63–67.
142. Levi DS, Moore JW. Embolization and retrieval of the Amplatzer septal occluder. *Catheter Cardiovasc Interv* 2004;61:543–547.
143. Hill SL, Berul CI, Patel HT, et al. Early ECG abnormalities associated with transcatheter closure of atrial septal defects using the Amplatzer septal occluder. *J Interv Card Electrophysiol* 2000;4:469–474.
144. Hessling G, Hycs S, Brockmeier K, et al. Cardiac dysrhythmias in pediatric patients before and 1 year after transcatheter closure of atrial septal defects using the amplatzer septal occluder. *Pediatr Cardiol* 2003;24:259–262.
145. Ries MW, Kampmann C, Rupprecht HJ, et al. Nickel release after implantation of the Amplatzer occluder. *Am Heart J* 2003;145:737–741.
146. Gordon BM, Moore JW. Nickel for your thoughts: survey of the Congenital Cardiovascular Interventional Study Consortium (CCISC) for nickel allergy. *J Invasive Cardiol* 2009;21:326–329.
147. Lai DW, Saver JL, Araujo JA, et al. Pericarditis associated with nickel hypersensitivity to the Amplatzer occluder device: a case report. *Catheter Cardiovasc Interv* 2005;66:424–426.
148. Masura J, Gavora P, Podnar T. Long-term outcome of transcatheter secundum-type atrial septal defect closure using Amplatzer septal occluders. *J Am Coll Cardiol* 2005;45:505–507.
149. Fischer G, Stieh J, Uebing A, et al. Experience with transcatheter closure of secundum atrial septal defects using the Amplatzer septal occluder: a single centre study in 236 consecutive patients. *Heart* 2003;89:199–204.
150. Veldtman GR, Razack V, Siu S, et al. Right ventricular form and function after percutaneous atrial septal defect device closure. *J Am Coll Cardiol* 2001;37:2108–2113.
151. Latson LA, Zahn EM, Wilson N. Halex septal occluder for closure of atrial septal defects. *Curr Interv Cardiol Rep* 2000;2:268–273.
152. Delaney JW, Chan KC, Rhodes JF, Jr. The design and deployment of the HELEX septal occluder. *Congenit Heart Dis* 2006;1:202–209.
153. Javois AJ, Van Bergen AH, Husayni TS. Technical considerations for closing secundum atrial septal defect in the small child with the HELEX Septal Occluder via transhepatic access. *Catheter Cardiovasc Interv* 2006;67:127–131.
154. Jones TK, Latson LA, Zahn E, et al. Results of the U.S. multicenter pivotal study of the HELEX septal occluder for percutaneous closure of secundum atrial septal defects. *J Am Coll Cardiol* 2007;49:2215–2221.
155. Carminati M, Giusti S, Hausdorf G, et al. A European multicentric experience using the CardioSEAL and Starflex double umbrella devices to close interatrial communications holes within the oval fossa. *Cardiol Young* 2000;10:519–526.
156. Sievert H, Horvath K, Zadan E, et al. Patent foramen ovale closure in patients with transient ischemia attack/stroke. *J Interv Cardiol* 2001;14:261–266.
157. Tofeig M, Walsh KP, Chan C, et al. Occlusion of Fontan fenestrations using the Amplatzer septal occluder. *Heart* 1998;79:368–370.
158. Cowley CG, Badran S, Gaffney D, et al. Transcatheter closure of fontan fenestrations using the Amplatzer septal occluder: initial experience and follow-up [see comment]. *Catheter Cardiovasc Interv* 2000;51:301–304.

159. Rueda F, Squitieri C, Ballerini L. Closure of the fenestration in the extra-cardiac Fontan with the Amplatzer duct occluder device [see comment]. *Catheter Cardiovasc Interv* 2001;54:88-92.
160. Bridges ND, Perry SB, Keane JF, et al. Preoperative transcatheter closure of congenital muscular ventricular septal defects. *N Eng J Med* 1991;324:1312-1317.
161. Pienvichit P, Piemonte TC. Percutaneous closure of postmyocardial infarction ventricular septal defect with the CardioSEAL septal occluder implant [see comment]. *Catheter Cardiovasc Interv* 2001;54:490-494.
162. Sideris EB, Walsh KP, Haddad JL, et al. Occlusion of congenital ventricular septal defects by the buttoned device. "Buttoned device" Clinical Trials International Register. *Heart* 1997;77:276-279.
163. Chaudhari M, Chessa M, Stumper O, et al. Transcatheter coil closure of muscular ventricular septal defects. *J Interv Cardiol* 2001;14:165-168.
164. Kalra GS, Verma PK, Singh S, et al. Transcatheter closure of ventricular septal defect using detachable steel coil. *Heart* 1999;82:395-396.
165. Latiff HA, Alwi M, Kandhavel G, et al. Transcatheter closure of multiple muscular ventricular septal defects using Gianturco coils. *Ann Thorac Surg* 1999;68:1400-1401.
166. Lee EM, Roberts DH, Walsh KP. Transcatheter closure of a residual post-myocardial infarction ventricular septal defect with the Amplatzer septal occluder. *Heart* 1998;80:522-524.
167. Margiocco ML, Bulmer BJ, Sisson DD. Percutaneous occlusion of a muscular ventricular septal defect with an Amplatzer muscular VSD occluder. *J Vet Cardiol* 2008;10:61-66.
168. Bacha EA, Cao QL, Galantowicz ME, et al. Multicenter experience with periventricular device closure of muscular ventricular septal defects. *Pediatr Cardiol* 2005;26:169-175.
169. Thanopoulos BD, Rigby ML. Outcome of transcatheter closure of muscular ventricular septal defects with the Amplatzer ventricular septal defect occluder. *Heart* 2005;91:513-516.
170. Holzer R, Balzer D, Cao QL, et al. Amplatzer Muscular Ventricular Septal Defect I. Device closure of muscular ventricular septal defects using the Amplatzer muscular ventricular septal defect occluder: immediate and mid-term results of a U.S. registry. *J Am Coll Cardiol* 2004;43:1257-1263.
171. Fu YC, Bass J, Amin Z, et al. Transcatheter closure of perimembranous ventricular septal defects using the new Amplatzer membranous VSD occluder: results of the U.S. phase I trial. *J Am Coll Cardiol* 2006;47:319-325.
172. Holzer R, de Giovanni J, Walsh KP, et al. Transcatheter closure of perimembranous ventricular septal defects using the amplatzer membranous VSD occluder: immediate and mid-term results of an international registry. *Catheter Cardiovasc Interv* 2006;68:620-628.
173. Masura J, Gao W, Gavora P, et al. Percutaneous closure of perimembranous ventricular septal defects with the eccentric Amplatzer device: multicenter follow-up study. *Pediatr Cardiol* 2005;26:216-219.
174. Yip WC, Zimmerman F, Hijazi ZM. Heart block and empirical therapy after transcatheter closure of perimembranous ventricular septal defect. *Catheter Cardiovasc Interv* 2005;66:436-441.
175. Holzer R, Balzer D, Cao QL, et al. Device closure of muscular ventricular septal defects using the Amplatzer muscular ventricular septal defect occluder: immediate and mid-term results of a U.S. registry. *J Am Coll Cardiol* 2004;43:1257-1263.
176. Bacha EA, Cao QL, Starr JP, et al. Periventricular device closure of muscular ventricular septal defects on the beating heart: technique and results. *J Thorac Cardiovasc Surg* 2003;126:1718-1723.
177. Holzer R, Balzer D, Amin Z, et al. Transcatheter closure of postinfarction ventricular septal defects using the new Amplatzer muscular VSD occluder: results of a U.S. registry. *Catheter Cardiovasc Interv* 2004;61:196-201.
178. Crenshaw BS, Granger CB, Birnbaum Y, et al. Risk factors, angiographic patterns, and outcomes in patients with ventricular septal defect complicating acute myocardial infarction. GUSTO-I (Global Utilization of Streptokinase and TPA for Occluded Coronary Arteries) trial investigators. *Circulation* 2000;101:27-32.
179. Cooley DA. Postinfarction ventricular septal rupture. *Semin Thorac Cardiovasc Surg* 1998;10:100-104.
180. Dalrymple-Hay MJ, Monro JL, Livesey SA, et al. Postinfarction ventricular septal rupture: the Wessex experience. *Semin Thorac Cardiovasc Surg* 1998;10:111-116.
181. Krichenko A, Benson LN, Burrows P, et al. Angiographic classification of the isolated, persistently patent ductus arteriosus and implications for percutaneous catheter occlusion. *Am J Cardiol* 1989;63:877-880.
182. Sommer RJ, Gutierrez A, Lai WW, et al. Use of preformed nitinol snare to improve transcatheter coil delivery in occlusion of patent ductus arteriosus. *Am J Cardiol* 1994;74:836-839.
183. Hays MD, Hoyer MH, Glasow PF. New forceps delivery technique for coil occlusion of patent ductus arteriosus. *Am J Cardiol* 1996;77:209-211.
184. Kuhn MA, Latson LA. Transcatheter embolization coil closure of patent ductus arteriosus—modified delivery for enhanced control during coil positioning. *Catheter Cardiovasc Diagn* 1995;36:288-290.
185. Dalvi B, Goyal V, Narula D, et al. New technique using temporary balloon occlusion for transcatheter closure of patent ductus arteriosus with Gianturco coils. *Catheter Cardiovasc Diagn* 1997;41:62-70.
186. Henry G, Danilowicz D, Verma R. Severe hemolysis following partial coil occlusion of patent ductus arteriosus [see comment] [8 refs]. *Catheter Cardiovasc Diagn* 1996;39:410-412.
187. Hijazi ZM, Geggel RL. Transcatheter closure of large patent ductus arteriosus (≥ 4 mm) with multiple Gianturco coils: immediate and mid-term results. *Heart* 1996;76:536-540.
188. Patel HT, Cao QL, Rhodes J, et al. Long-term outcome of transcatheter coil closure of small to large patent ductus arteriosus. *Catheter Cardiovasc Interv* 1999;47:457-461.
189. Pass RH, Hijazi Z, Hsu DT, et al. Multicenter USA Amplatzer patent ductus arteriosus occlusion device trial: initial and one-year results. *J Am Coll Cardiol* 2004;44:513-519.
190. Saliba Z, El-Rassi I, Abi-Warde MT, et al. The Amplatzer Duct Occluder II: a new device for percutaneous ductus arteriosus closure. *J Interv Cardiol* 2009;22:496-502.
191. Hoyer MH. Novel use of the Amplatzer plug for closure of a patent ductus arteriosus [see comment]. *Catheter Cardiovasc Interv* 2005;65:577-580.
192. Hill SL, Hijazi ZM, Hellenbrand WE, et al. Evaluation of the AMPLATZER vascular plug for embolization of peripheral vascular malformations associated with congenital heart disease. *Catheter Cardiovasc Interv* 2006;67:113-119.
193. Cheatham JP. Not so fast with that Novel use: does AVP = PDA? [comment]. *Catheter Cardiovasc Interv* 2005;65:581-583.
194. Martinez CA, Cohen H, Ruiz CE. Simultaneous aortic and mitral metallic paravalvular leaks repaired through one delivery sheath. *J Invasive Cardiol* 2011;23:E19-E21.
195. Larman M, Lasa G, Sanmartin JC, et al. Transapical technique as an alternative approach to paravalvular leak closure. *Rev Esp Cardiol* 2011;64:80-82.
196. Kursaklioglu H, Barcin C, Ilysoy A, et al. Percutaneous closure of mitral paravalvular leak via retrograde approach: with use of the Amplatzer duct occluder II and without a wire loop. *Tex Heart Inst J* 2010;37:461-464.
197. Chiam PT, Ding ZP, Sin YK, et al. How should I treat a percutaneous transcatheter mitral paravalvular leak closure? *EuroIntervention* 2010;6:653-659.
198. Hourihan M, Perry SB, Mandell VS, et al. Transcatheter umbrella closure of valvular and paravalvular leaks. *J Am Coll Cardiol* 1920:1371-1377.
199. Moore JD, Lashus AG, Prieto LR, et al. Transcatheter coil occlusion of perivalvular mitral leaks associated with severe hemolysis. *Catheter Cardiovasc Interv* 2000;49:64-67.
200. Boudjemline Y, Abdel-Massih T, Bonhoeffer P, et al. [Percutaneous closure of a paravalvular mitral regurgitation with Amplatzer and coil prostheses] [French]. *Arch Mal Coeur Vaiss* 2002;95:483-486.
201. Piechaud JF. Percutaneous closure of mitral paravalvular leak. *J Interv Cardiol* 2003;16:153-155.
202. Mandegar MH, Roshanali F. Prosthetic valve malfunction after Amplatzer closure of paravalvular leak. *Ann Thorac Surg* 2011;91:614.
203. Martinez CA, Cohen H, Ruiz CE. Wire entrapment through an aortic paravalvular leak. *J Invasive Cardiol* 2010;22:E119-E121.
204. Khambadkone S, Coats L, Taylor A, et al. Percutaneous pulmonary valve implantation in humans: results in 59 consecutive patients. *Circulation* 2005;112:1189-1197.
205. Boone RH, Webb JG, Horlick E, et al. Transcatheter pulmonary valve implantation using the Edwards SAPIEN transcatheter heart valve. *Catheter Cardiovasc Interv* 2010;75:286-294.
206. Garay F, Webb J, Hijazi ZM. Percutaneous replacement of pulmonary valve using the Edwards-Cribier percutaneous heart valve: first report in a human patient. *Catheter Cardiovasc Interv* 2006;67:659-662.
207. Michel-Behnke I, Akintuerk H, Marquardt I, et al. Stenting of the ductus arteriosus and banding of the pulmonary arteries: basis for various surgical strategies in newborns with multiple left heart obstructive lesions. *Heart* 2003;89:645-650.
208. Galantowicz M, Cheatham JP. Lessons learned from the development of a new hybrid strategy for the management of hypoplastic left heart syndrome. *Pediatr Cardiol* 2005;26:190-199.
209. Galantowicz M, Cheatham JP. Fontan completion without surgery. *Semin Thorac Cardiovasc Surg Pediatr Card Surg Annu* 2004;7:48-55.
210. Hjortdal VE, Redington AN, de Leval MR, et al. Hybrid approaches to complex congenital cardiac surgery. *Eur J Cardiothorac Surg* 2002;22:885-890.
211. Holzer R, Marshall A, Kreutzer J, et al. Hybrid procedures: adverse events and procedural characteristics—results of a multi-institutional registry. *Congenit Heart Dis* 2010;5:233-242.
212. Ashburn DA, McCrindle BW, Tchervenkov CI, et al. Outcomes after the Norwood operation in neonates with critical aortic stenosis or aortic valve atresia. *J Thorac Cardiovasc Surg* 2003;125:1070-1082.
213. Akintuerk H, Michel-Behnke I, Valeske K, et al. Stenting of the arterial duct and banding of the pulmonary arteries: basis for combined Norwood stage I and II repair in hypoplastic left heart. *Circulation* 2002;105:1099-1103.
214. Hausdorf G, Schneider M, Konertz W. Surgical preconditioning and completion of total cavopulmonary connection by interventional cardiac catheterisation: a new concept. *Heart* 1996;75:403-409.
215. Crystal M, Yoo S, Van Arsdell GS, et al. Catheter-based completion of the Fontan: a non-surgical approach. *Catheter Cardiovasc Interv* 2006;68:460.
216. Galantowicz M, Cheatham JP, Phillips A, et al. Hybrid approach for hypoplastic left heart syndrome: intermediate results after the learning curve. *Ann Thorac Surg* 2008;85:2063-2070; discussion 2070-2071.
217. Egan MJ, Trask AJ, Baker PB, et al. Histopathologic evaluation of patent ductus arteriosus stents after hybrid stage I palliation. *Pediatr Cardiol* 2011;32:413-417.

218. Egan MJ, Hill SL, Boettner BL, et al. Predictors of retrograde aortic arch obstruction after hybrid palliation of hypoplastic left heart syndrome. *Pediatr Cardiol* 2011;32:67–75.
219. Holzer R, De Giovanni JV, Walsh KP, et al. Transcatheter closure of perimembranous ventricular septal defects using the amplatzer membranous VSD occluder: immediate and mid term results of an international registry. *Catheter Cardiovasc Interv* 2006;68:620–628.
220. Amin Z, Danford DA, Lof J, et al. Intraoperative device closure of perimembranous ventricular septal defects without cardiopulmonary bypass: preliminary results with the perventricular technique. *J Thorac Cardiovasc Surg* 2004;127:234–241.
221. Holzer RJ, Chisolm JL, Hill SL, et al. “Hybrid” stent delivery in the pulmonary circulation. *J Invasive Cardiol* 2008;20:592–598.
222. Chambers CE, Fetterly KA, Holzer R, et al. Radiation safety program for the cardiac catheterization laboratory. *Catheter Cardiovasc Interv* 2011;77:546–556.
223. Sawdy JM, Gocha MD, Olshove V, et al. Radiation protection during hybrid procedures: innovation creates new challenges. *J Invasive Cardiol* 2009;21:437–440.
224. Holzer RJ, Sisk M, Chisolm JL, et al. Completion angiography after cardiac surgery for congenital heart disease: complementing the intraoperative imaging modalities. *Pediatr Cardiol* 2009;30:1075–1082.
225. Shuhaiber JH, Bergersen L, Pigula F, et al. Intraoperative assessment after pediatric cardiac surgical repair: initial experience with C-arm angiography. *J Thorac Cardiovasc Surg* 2010;140:e1–e3.
226. Lock JE, Rome JJ, Davis R, et al. Transcatheter closure of atrial septal defects. Experimental studies. *Circulation* 1989;79:1091–1099.
227. Latson LA, Benson LN, Hellenbrand WF, et al. Transcatheter closure of ASD—early results of multi-center trial of the Bard clamshell septal occluder. *Circulation* 1991;84:544–544.
228. Schlesinger AE, Folz SJ, Beckman RH. Transcatheter atrial septal defect occlusion devices: normal radiographic appearances and complications. *J Vasc Interv Radiol* 1992;3:527–533.
229. Latson LA. The CardioSEAL device: History, techniques, results. *J Interv Cardiol* 1998;11:501–505.

Development and Functional Maturation of the Cardiac Conduction System

Aleksander Sizarov ■ Antoon F.M. Moorman ■ Arthur S. Pickoff

In this chapter, current concepts regarding the formation of the cardiac conduction system, along with developmental aspects of cardiac electrophysiology, are summarized. Genetic regulation of the early specification of the conduction system and the electrophysiologic characteristics of the maturing heart are discussed in conjunction with morphologic considerations.

RECOGNITION OF THE CONDUCTION TISSUES IN THE POSTNATAL HEART

All cardiac muscle possesses the capacity to conduct, making the term “conduction system” a bit ambiguous. A small subset of cardiomyocytes, nonetheless, has specific electrophysiologic properties, accompanied by a distinct cellular morphology and pattern of gene expression. These cardiomyocytes make up the so-called specialized conduction system of the heart. The conduction system consists of the sinus node, the atrioventricular (AV) node, the AV bundle (known better in the clinical setting as the bundle of His), its branches, and the ventricular network of Purkinje fibers (Fig. 14.1A). Each time the heart beats, contraction is triggered by a wave of electrical activity spontaneously generated in the sinus node. The depolarizing impulse propagates rapidly through the atrial chamber myocardium, to be collected and delayed in the AV node, and again spreads very rapidly to the ventricular muscular mass through the bundle of His, its branches, and the ramifications of the Purkinje fibers. Comprehensive histologic descriptions of the cardiac nodes and the fast-conducting tracts were published over a century ago (1–4) and have served as the “gold standard” for the identification of the specialized conduction tissues.

The characteristic aggregation of the cardiomyocytes at specific locations, either as nodes or as tracts, makes it possible to recognize them as anatomic components of the conduction system by routine histology (Fig. 14.1B). In the human heart, the sinus node (SN) occupies a subepicardial position at the lateral aspect of the junction of the superior caval vein (SCV) and right

atrium (RA) (5). The node characteristically is horseshoe shaped in the fetus, and usually assumes a more spindle-like shape with development. By light microscopy, the cells of the SN morphologically are distinct from the surrounding atrial myocardium; they are smaller, more compact, and contained within a fibrous matrix (6). A tail of nodal cells extends inferiorly from the SN along the terminal crest of the atrium. The AV node is located within the right atrial wall at the apex of the triangle of Koch, which is bordered by the septal leaflet of the tricuspid valve, the tendon of Todaro, and the mouth of the coronary sinus (7). Histologically, the AV node consists of a zone of loosely arranged “transitional” atrial cells that blend and extend into the surrounding atrial myocardium and, adjacent to the central fibrous body, a compact zone of closely grouped small cells (8). Two inferior extensions from the compact zone have been described that extend toward the hinges of the mitral and tricuspid valves (9,10). The compact zone of the AV node continues to penetrate the central fibrous body, at which point it contacts the bundle of His. Subsequent to penetrating the central fibrous body, and at the crest of the muscular portion of the ventricular septum and beneath the membranous septum, the bundle of His becomes the branching bundle, which gives rise to the right and left bundle branches (1,8,11). These then course along the surface of the ventricular septum toward the apex of the heart as muscular tracts insulated from the rest of the ventricular myocardium by fibrous tissue. The left bundle branch divides further into three fascicles. Under light microscopical inspection, the cells of the bundle branches appear slightly larger than the surrounding myocardial cells. The terminations of the bundle branches continue as a widespread network of Purkinje fibers, which in the human heart are little different from the adjacent working cardiomyocytes. They are subendocardially localized, and branch into small transmural ramifications (12). The so-called AV ring bundles (13), and septal and retroaortic (RAo) root branches (14,15), generally are not considered as components of the definitive AV conduction system in the normal adult heart. They still can be traced, however, in neonatal human hearts (Fig. 14.2), and can persist as histologically recognizable structures. In rare circumstances, these remnants may provide the substrate for

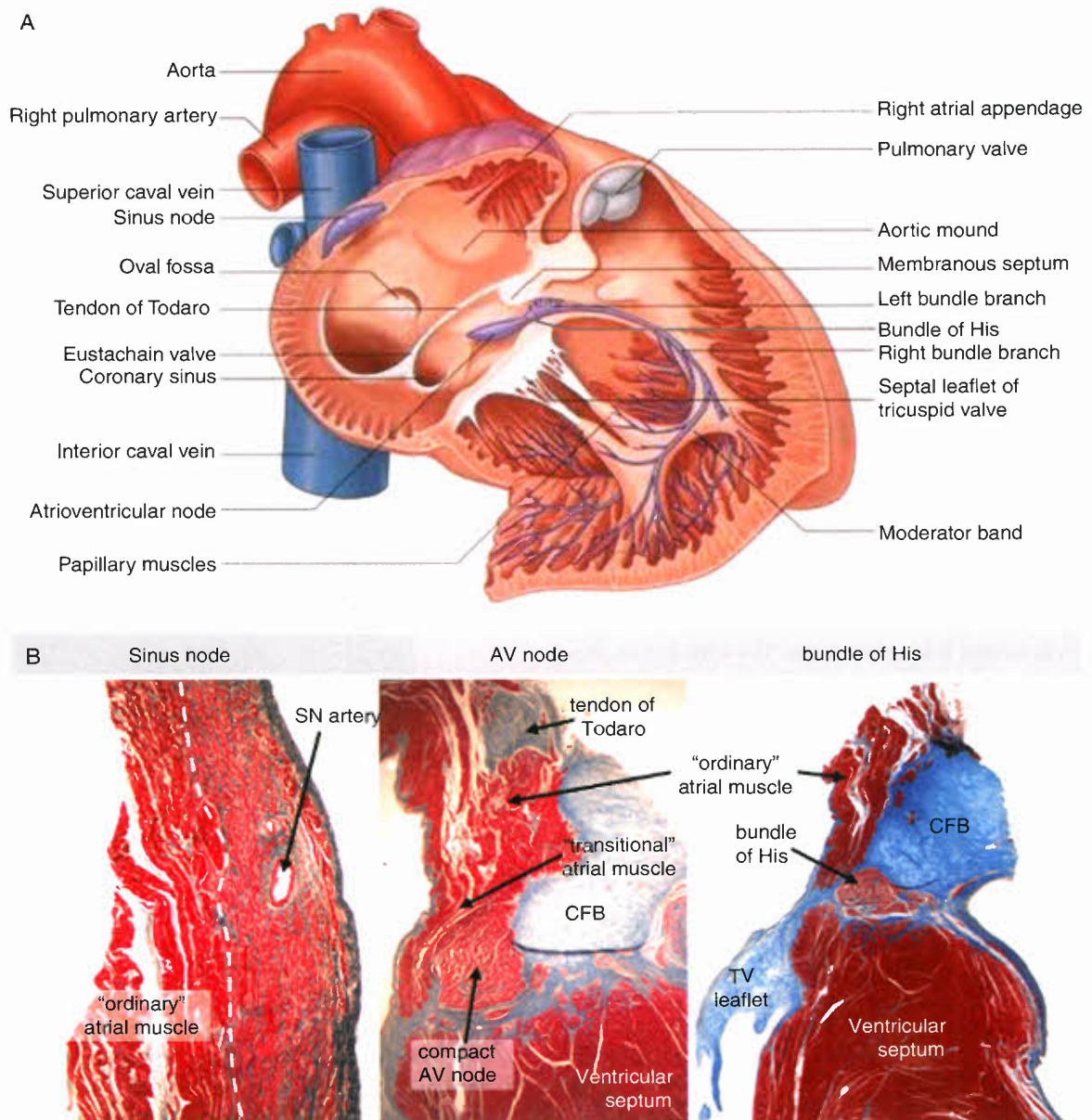


Figure 14.1. Anatomy and histology of the cardiac conduction system in the postnatal heart. **Panel A** shows schematic representation of the location of the conduction system components in relation to the external and internal cardiac anatomy (Modified from Heart and Great Vessels. In: Standring S (Ed.). *Gray's Anatomy: The Anatomical Basis of Clinical Practice*. 40th ed. Churchill Livingstone, 2008; pp 959–987.) The lateral wall of the RA and RV was removed to expose the conduction tissues (depicted in blue). **Panel B** shows histological sections through the sinus node, AV node and penetrating portion of the bundle of His in the heart of a 7-month-old child. Sections were stained using Masson's trichrome technique, which stains muscle tissue in red and collagen fibers in blue. Note the differential staining within the cardiac nodes and the bundle of His, the latter being additionally surrounded by connective tissue. The AV node comprises the compact part and more loosely arranged fibers of the so-called transitional atrial cells. AV, atrioventricular; CFB, central fibrous body; SN, sinus node; TV, tricuspid valve.

some forms of ventricular preexcitation in otherwise normally structured hearts (16). Additionally, in the setting of complex congenital malformations, these remnants may constitute the AV conduction axis at aberrant locations (see below).

The sporadic appearance of individual cardiomyocytes resembling so-called Purkinje cells in the atrial musculature between the cardiac nodes, and in the pulmonary venous sleeves, caused some authors to conclude that these cells constitute specialized conduction tissue at these ectopic locations (17,18). In the postnatal heart, however, the preferential con-

duction that exists within the atrial musculature is explained by the orientation of the cardiomyocytes, rather than the existence of specialized tracts (19). As discussed later, the maintenance of the primary myocardium phenotype, or insufficient maturation of the working myocardium of the terminal crest, the sleeves around the pulmonary veins, and the ventricular outflow tracts (OFTs) during cardiac development could provide the substrates for abnormal automaticity in the postnatal heart. In terms of gross histology, however, these areas are indistinguishable from the remainder of the working myocardium (20–22).

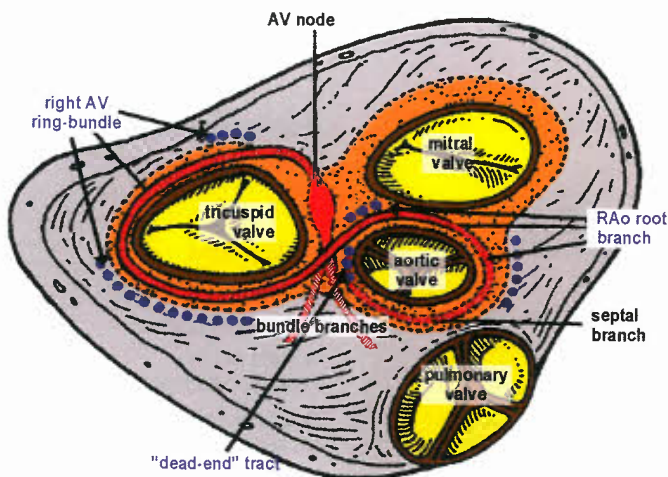


Figure 14.2. Definitive and “residual” components of the AV conduction system. The derivatives of the “primary ring” (depicted in red) from which the AV conduction system is derived are projected on the superior view of the aortic-mitral fibrous unit (orange) of the postnatal heart. Blue dots indicate the areas of remnants of the “residual” derivatives of the “primary ring,” which can be found in neonatal human hearts. AV, atrioventricular; RAo, retroaortic. (Modified from Wesels A, Mijnders TA, de Gier-de Vries C, et al. Expression of myosin heavy chain in neonatal human hearts. *Cardiol Young* 1992;2:318–334.)

THE BASIC BUILDING PLAN OF THE MAMMALIAN HEART

A fundamental question in cardiac development relates to the establishment of the correct disposition of the chambers and the conduction system. In the early developing heart, it is not possible to identify, histologically, components of the conduction system as one can in the postnatal heart. Subsequent to formation of its chambers, nonetheless, the embryonic heart produces coordinated contractions and relaxations of the atria and ventricles, which is reflected in the nearly “adult-like” electrocardiogram (23) (Fig. 14.3). The developing heart consists of several building blocks with distinct conduction and contraction properties, which allow for efficient pumping function of the heart despite the absence of a definitive conduction system and valves (24).

Early cardiac development starts around 20 days of human embryonic life (see Table 14.1). The first step is the formation of a primary heart tube from the cardiogenic mesoderm, the latter known as the cardiac crescent. The primary heart tube in vertebrate embryos is little more than a myocardialized part of the splanchnic mesodermal layer folded and protruding into the coelomic cavity. It encompasses a narrow lumen lined by a single layer of endothelial cells, with a thick acellular layer of cardiac jelly separating the endothelium from the outer myocardial layer (25,26). This simple myocardial tube produces unidirectional peristaltic waves of contractions, which propel the blood from the inflow to the outflow part of the heart tube. Not all mesodermal cells fated to become cardiomyocytes do so immediately. At the venous and arterial poles, along with the dorsal mesocardium, which are the sites of attachment of the primary heart tube to the dorsal part of the embryo, differentiating cells from the pool of cardiac progenitors, the so-called second heart field, are added to the heart (27–29). This permits the slowly proliferating primary heart tube to significantly elongate during a relatively short period of time (30,31). Concomitantly, the primary heart

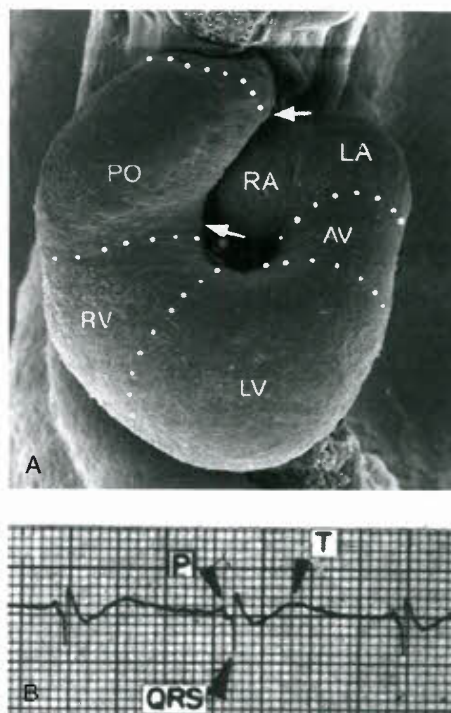


Figure 14.3. Configuration and electrocardiogram of the early chamber-forming heart in the chicken embryo. **Panel A** shows a scanning electron microscopic image of a stage 17 chicken looping heart, where ballooning of the atrial and ventricular chambers has just been initiated at the outer curvature of the heart tube. Arrows point to the angles at the caudal and cranial borders of the proximal outflow (PO) tract. (From Männer J. The anatomy of cardiac looping. *Clin Anat* 2009;22:21–35, with permission.) **Panel B** shows an electrocardiogram derived from a chicken embryonic heart at a comparable stage of development. Note the almost “adult-like” ECG, including the isoelectric interval between the P wave and QRS complex. AV, atrioventricular canal; LA/RA, left/right atrium; LV/RV, left/right ventricle. (From Paff GH, Boucek RJ, Harrell TC. Observations on the development of the electrocardiogram. *Anat Rec* 1968;160:575–582, with permission.)

tube loops ventrally and rightward, so that it becomes possible to recognize its outer and inner curvatures (Fig. 14.4). At localized areas of the outer curvature, the primary cardiomyocytes start to proliferate, at the same time initiating a genetic program governing their differentiation toward the working myocardium phenotype characterized by expression of fast-conducting gap-junctional proteins and atrial natriuretic factor (ANF) (31–33) (Fig. 14.5). The myocardium of the ballooning atrial and ventricular chambers remains flanked by the primary myocardium of the AV canal, the inner curvature, and the OFT. These flanking segments retain the primitive phenotype characterized by long-lasting contractions and slow conduction (24). After initiation of chamber formation, a new myocardial structure, the systemic venous sinus, or sinus venosus, is formed at the inflow region of the heart (34). Similar to the myocardium of the primary heart tube, the myocardium of the venous sinus initially escapes further differentiation, does not express fast-conducting connexins, and is characterized by high intrinsic automaticity, ensuring dominant pacemaker activity at the inflow of the heart (35–38). At this stage, the basic cardiac building plan, consisting of fast-conducting chambers flanked by slow-conducting myocardium of the

TABLE 14.1 Comparison of the Developmental Stages in the Human, Mouse, and Chicken Embryos

Human Carnegie Stages*	Human Embryonic Days	Mouse (Embryonic Days)	Chicken (HH Stages)
10	22–23	8.0	9–10
12	26–28	9.5	13–14
14	31–35	10.5	18–20
16	38–41	12.0	24–24
18	45–48	14.5	28–29
20	51–53	15.5	31–32
23	56–58	17.5	34–35

HH, Hamburger-Hamilton (see Hamburger V, Hamilton HL. A series of normal stages in the development of the chick embryo. *J Morph* 1951;88:49–92).

*O’Rahilly R, Müller F. *Developmental Stages in Human Embryos. Including a Revision of Streeter’s “Horizons” and a Survey of the Carnegie Collection*. Washington, DC: Carnegie Institution, 1987; publication 647.

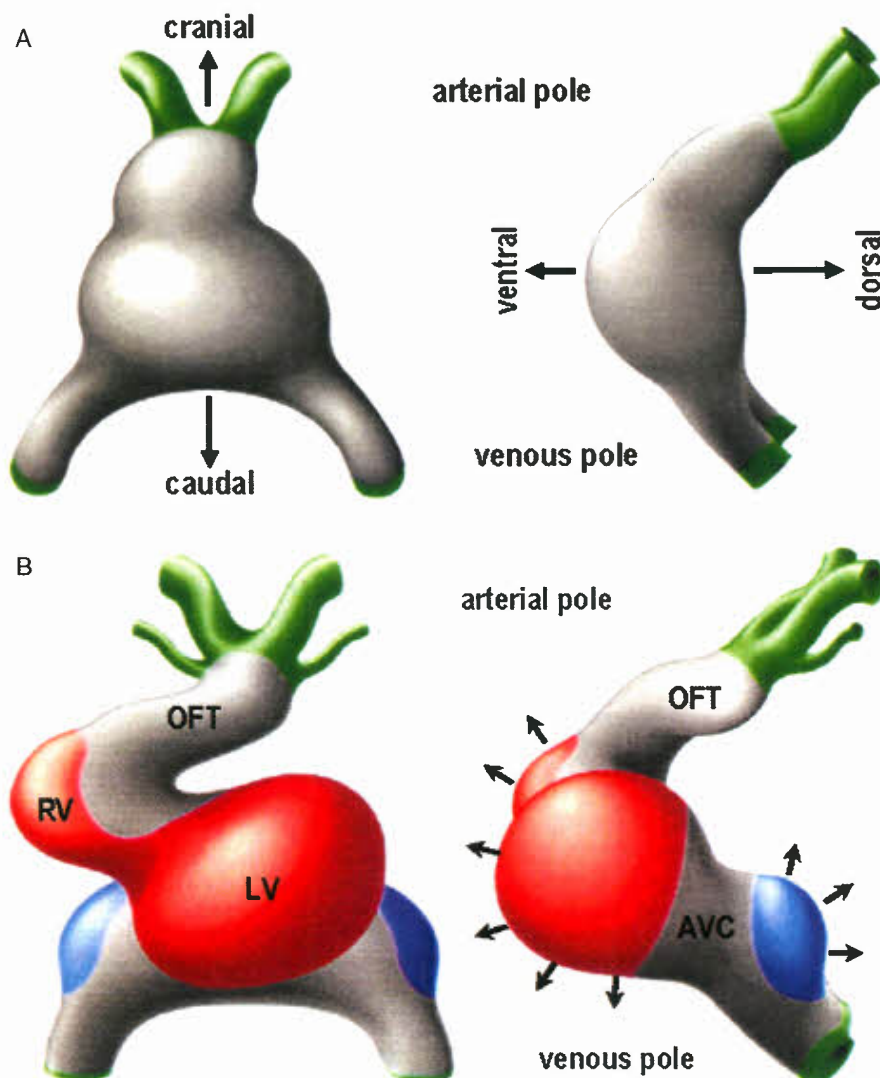


Figure 14.4. Morphogenesis of the early heart tube in mammals. **Panel A** depicts the prototypic linear heart tube as seen in ventral (left) and right lateral (right) views, while **panel B** shows the prototypic looping and chamber-forming heart tube in similar views. The primary myocardium is indicated in gray, the secondary myocardium of the atrial chambers ballooning at the dorsal aspect of the heart tube (arrows) is indicated in blue, and the myocardium of the ventricular chambers growing ventrally along the outer curvature of the heart tube (arrows) is indicated in red. At the linear tube stage no secondary myocardium is present. In the human embryonic heart, the chamber myocardium is first seen locally at the stage of looping and does not involve the entire circumference of the tube. Note that the primary myocardium of the venous pole, the atrioventricular canal (AVC), and the outflow tract (OFT) is contiguous, with no signs of separate rings of so-called specialized tissue. AVC, atrioventricular canal; LV/RV, left/right ventricle; OFT, outflow tract. (Modified from Moorman AFM, Christoffels VM. Cardiac chamber formation: development, genes, and evolution. *Physiol Rev* 2003;83:1223–1267.)

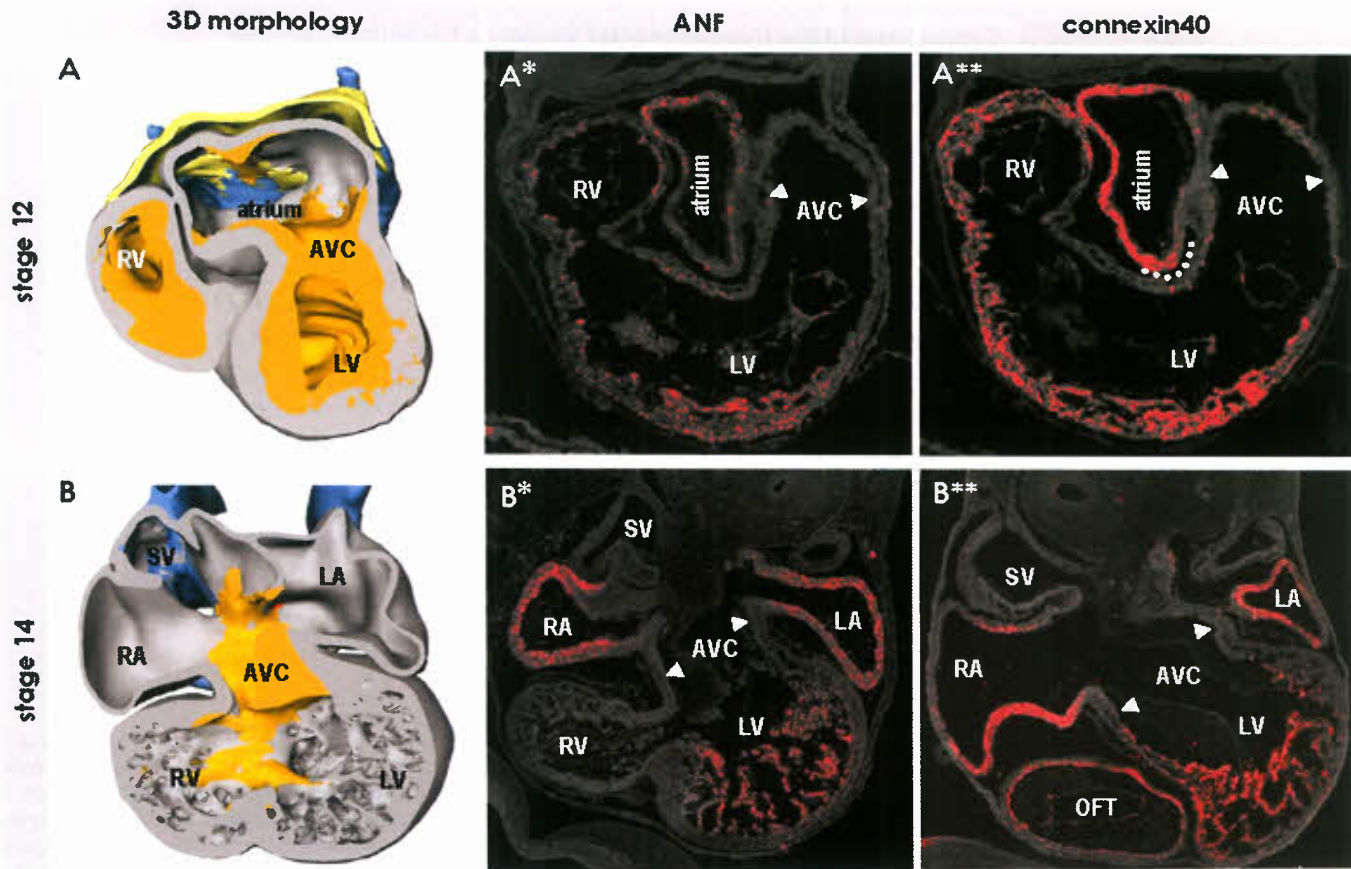


Figure 14.5. Three-dimensional and molecular analysis of chamber formation in the human embryonic heart. Two different stages are shown. Panels A,A*,A** show a 3-D model and immunohistochemical stainings for chamber markers in the stage 12 embryonic heart, when the chamber formation is initiated. Note, that the walls of the atrioventricular canal (AVC) and inner curvature (*dotted line* in A**) do not express atrial natriuretic factor (ANF) and connexin40, while the walls of the atrial and ventricular chambers are positive for these markers. Panels B,B*,B** show a 3-D model and stainings in the stage 14 heart, when septation between the atrial and ventricular chambers is initiated. Now clearly two separate atria are formed and the ventricular chambers possess an extensive meshwork of trabeculations. Note, that the walls of the venous sinus (SV) and AVC (*arrowheads*) are still negative for chamber markers. AVC, atrioventricular canal; LA/RA, left/right atrium; LV/RV, left/right ventricle; OFT, outflow tract; SV, sinus venosus. (Modified from Sizarov A, Ya J, de Boer BA, et al. Formation of the building plan of the human heart: morphogenesis, growth, and differentiation. *Circulation* 2011;123:1125–1135.)

venous sinus, atrioventricular canal (AVC), and OFT serves as a blueprint for the formation, at appropriate positions, of the specialized pacemaking and conduction system (39).

THE SINUS NODE

Initiation of the Heart Beat

Subsequent to its formation, the primitive heart tube immediately commences regular waves of peristaltic contractions. At the beginning, the initiation of contraction is observed in the middle of the straight heart tube (40), where excitation–contraction coupling of the cardiomyocytes has progressed sufficiently to produce active shortening of the myofibrils. Studies in chicken embryos using voltage-sensitive dyes detecting spontaneous electrical depolarization have demonstrated that pacemaker activity can be identified along the whole primary heart tube prior to any contractile activity (41)

(Fig. 14.6A). However, the earliest spontaneous pacemaking activity always is located at the inflow of the primary heart tube (38) (Fig. 14.6B). During further development, the pacemaking activity in already differentiated myocardium is suppressed, while newly added myocardium at the venous pole assures this site remains the dominant pacemaker site (38,42), ensuring efficient unidirectional pumping of the blood. The pacemaking mechanism in the adult SN is very complex, and involves multiple currents through different ion channels (43). It is still incompletely characterized in the embryonic heart. Very early in embryonic life, prior to the development of true pacemaker ion current(s), shuttling of calcium in and out of the sarcoplasmic reticulum through an inositol triphosphate-dependent mechanism may be responsible for pacemaker activity (44). Mouse embryos that are deficient for the hyperpolarization-activated cyclic nucleotide-gated cation channel 4 (HCN4), the major isoform producing the I_f (“funny” current), have extremely low heart rates and die in utero (45), suggesting an important role of I_f in the pacemaking mechanism of the embryonic heart.

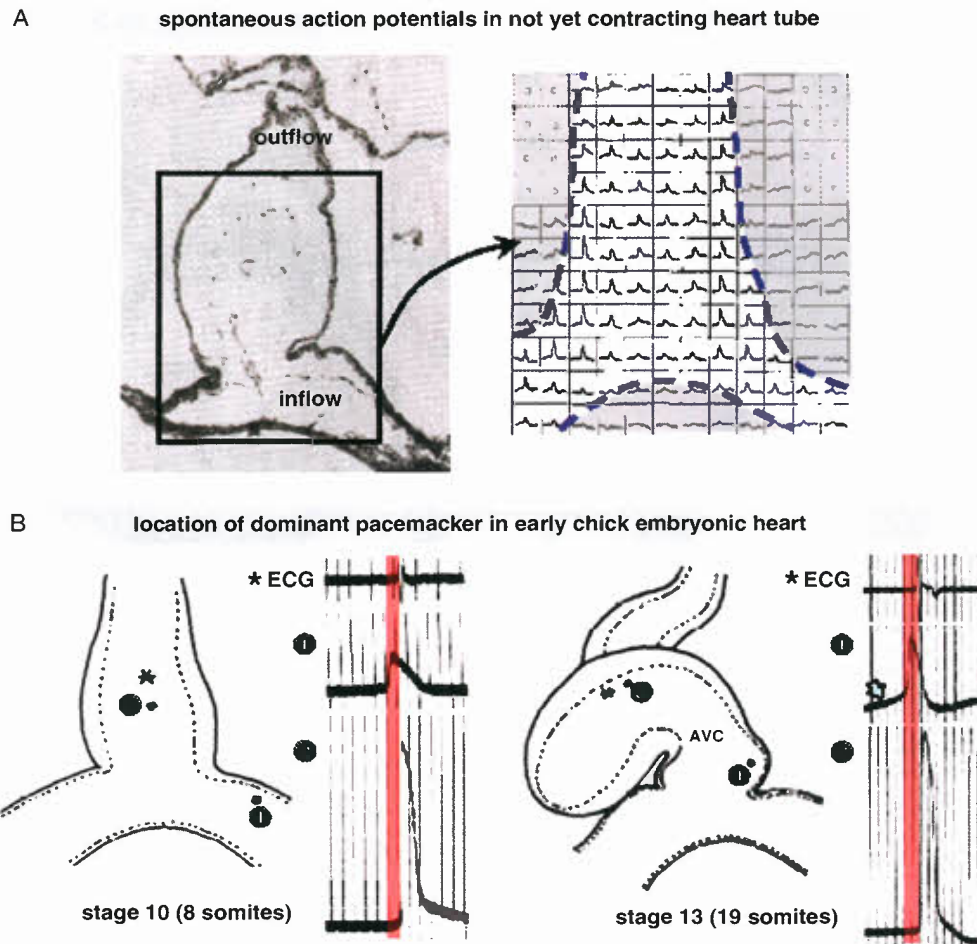


Figure 14.6. Initiation of the heart beat. **Panel A** shows that in the very early chicken embryonic heart (about stage 9), which is not yet contracting, action potentials of spontaneous depolarization can be detected over the entire heart tube. **Panel B** shows that the earliest action potentials always are registered at the most caudal end of the heart. Note, that the interval between the upstroke of the action potentials measured at proximal (1) and distal (2) sites of the heart tube remains remarkably similar at stage 13 as compared to very young stage 9 (*red bars* in **panel B**). The initial phase of the caudal action potential, however, already resembles at stage 13 the slow depolarization period of the definitive pacemaker action potential (*arrow* in **panel B**). AVC, atrioventricular canal; E, site of ECG registration. (Modified from Kamino K, Komuro H, Sakai T, et al. Functional pacemaking area in the early embryonic chick heart assessed by simultaneous multiple-site optical recording of spontaneous action potentials. *J Gen Physiol* 1988;91:573–591; and Van Mierop LHS. Localization of pacemaker in chick embryo heart at the time of initiation of heartbeat. *Am J Physiol* 1967;212:407–415.)

Development of the Sinus Node

The primary heart tube, although consisting of cardiomyocytes, which all possess pacemaker activity (40,46), does not contain the precursors of the cells destined to form the definitive sinus node, as at this stage the cardiomyocytes forming the systemic venous sinus have not yet been added to the heart (34). Early investigations of the developing cardiac conduction tissues in mammalian and human embryos were, of necessity, limited to search for clusters of histologically “specialized” cardiomyocytes at the locations they occupy in the postnatal heart. There are numerous comprehensive descriptions of the morphologic changes during development of the SN in the human embryonic and fetal heart (47–51). Although these studies were based on comparable histologic stainings, they led to very different hypotheses about its development. Thus, in the human, the SN had been hypothesized to develop from a so-called sinatrial ring (49,50). This concept depended on the presence of “specialized” rings of myocardium between segments of the pri-

mary heart tube, which, in turn, were believed to develop into the distinct parts of the definitive conduction system. Numerous molecular studies in experimental animals, and now in human hearts, have revealed that this is not the case.

From analyses of various transgenic mouse models, it is known that correct expression of several transcription factors is needed for the formation of the SN at its normal location (52) (Fig. 14.7). Until embryonic day 9 to 9.5 in mouse, and approximately 26 to 28 days in humans, the homeobox transcription factor *Nkx2.5* is expressed in all myocardium, but not in the mesenchymal cells at the caudal ventral side of the inflow tract (34,36). These cells express the T-box transcription factor *Tbx18* in a strictly complementary pattern, and differentiate into cardiomyocytes forming sinus muscle, and ultimately the sinus node. Genetic lineage analyses have provided strong evidence for the origin of the entire venous sinus from these cardiac progenitor cells. Taking into account that these cells are the precursors of the sinus node, this finding is consistent with the previous observation that the elongating heart tube shows

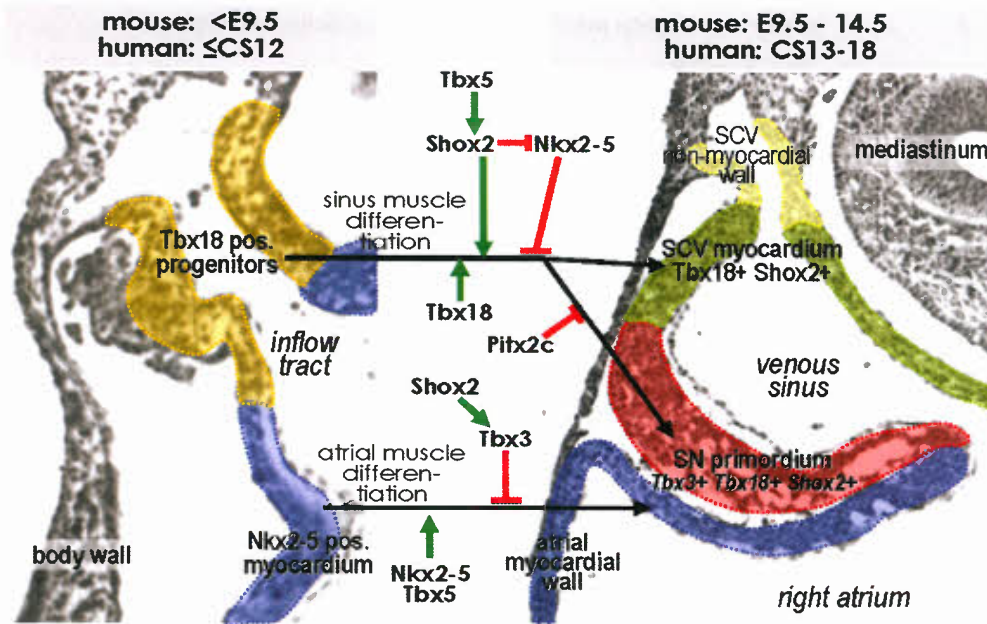


Figure 14.7. Molecular pathways regulating sinus node (SN) development. The SN develops from the sinus myocardium, which in turn differentiates from the Tbx18-positive and Nkx2-5-negative mesenchyme at the inflow region of the early chamber-forming heart. Depicted transcription factors regulate the formation of the boundaries and zones of expression and differentiation of atrium, SN and the myocardial sleeve of superior caval vein (SCV). Green arrows indicate positive regulation and red lines suppression of the sinus muscle and atrial muscle differentiation. For more details, see text. CS, Carnegie stage; E, embryonic day; pos, positive; SCV, superior caval vein; SN, sinus node. (Modified from Christoffels VM, Smits GJ, Kispert A, et al. Development of the pacemaker tissues of the heart. *Circ Res* 2010;106:240–254.)

an increase in beat rate (53). Furthermore, Tbx18-deficient mice fail to form the large head component of the sinus node, demonstrating that Tbx18 is crucial for the recruitment of inflow region mesenchyme into the myocardial lineage, which is essential for the formation of the SN (54). In the human embryonic heart, the systemic venous sinus is first discernable at 28th day of human development as a small hollow structure upstream from the common atrial chamber. It initially has nonmyocardial walls expressing Tbx18 and HCN4, and is no more than the confluence of the systemic venous channels entering the heart. During the next stages, the venous sinus shifts to the right, and its walls become muscular and thickened, particularly its right lateral part (36,55,56) (Figs. 14.8 and 14.9). This thickened structure, which may be considered as the sinus nodal primordium, is traceable at its specific location along the right side of the sinuatrial junction till the end of the embryonic period, when it already begins to resemble the SN of the postnatal heart (50). Early specification of the sinus nodal primordium in the mouse embryonic heart is regulated by another T-box transcription factor Tbx3 (57), which is expressed in the human embryonic heart in an almost identical pattern. Tbx3 represses the expression of the fast-conducting connexins 40 and 43, thus allowing newly added sinus myocardium to escape from further differentiation toward working myocardium (Fig. 14.9). Forced expression of Tbx3 in the atrial myocardium of the postnatal mouse heart leads to the development of ectopic functional pacemaker tissue, thus identifying Tbx3 as a key regulator of the sinus nodal phenotype (57). The suppression of the formation of the SN at the left side of the sinuatrial junction in the mouse heart is regulated by the transcription factor Pitx2c (42), which, in vertebrates, plays a crucial role in the establishment of the left/right asymmetry of the inner organs, including the heart (58). Accordingly, dual

sinus nodes are present in Pitx2c-deficient mice and in humans with right isomerism of atrial appendages (59).

During the mid-stages of human and mouse gestation, the expression of HCN4 and pacemaker activity becomes confined to the SN itself by an as yet undiscovered mechanism. The myocardium derived from the sinus muscle, with the exception of the SN itself, matures to produce a phenotype comparable to that of the atrial working myocardium, including upregulated expression of connexins 40 and 43, and downregulated expression of HCN4 (42). The failure of complete “atrialization” of this myocardium in some individuals could explain the presence of ectopic automaticity, and the initiation of ectopic atrial tachycardias.

THE AV CONDUCTION AXIS

The Development of the AV Conduction System

The myocardium of the primary heart tube is characterized by slow transmission of the electrical impulse. With ongoing development, the primary myocardium at specific locations along the outer curvature of the looping heart tube begins to further differentiate and expand to form the atrial and ventricular chambers, which are characterized by fast conduction of the depolarizing electrical impulse, and matching synchronous contractions (32,60). The ballooning chambers remain flanked by the primary myocardium of the venous sinus, inner curvature, AVC and OFT, which escapes further differentiation, and retains the more primitive phenotype displaying high automaticity, slow conduction, and long-lasting contractions (24). The different components of the definitive AV conduction system are formed

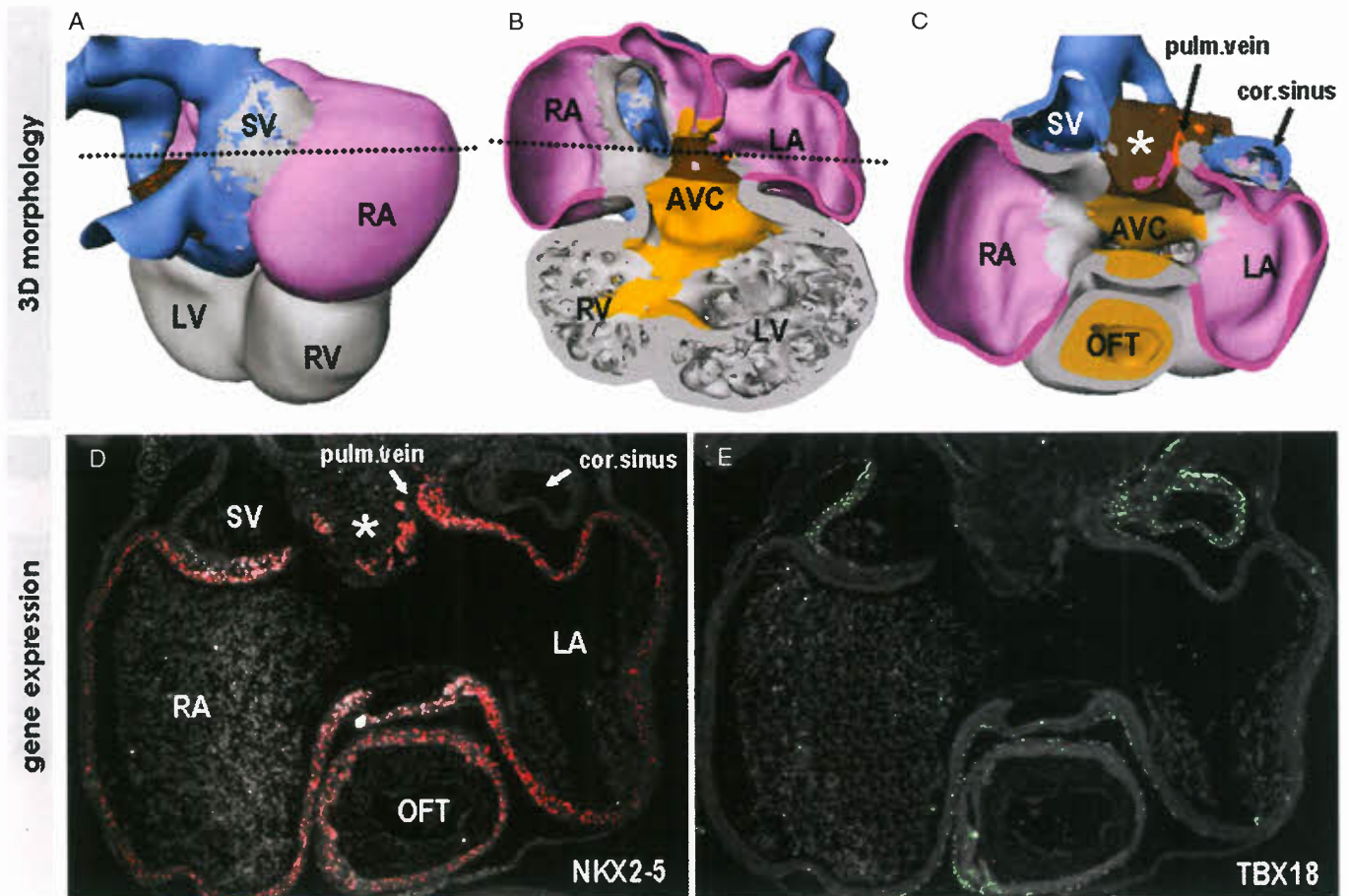


Figure 14.8. Three-dimensional and molecular analysis of the venous pole of the embryonic human heart. Panels A through C show different views of the 3-D model of a stage 14 human embryonic heart, on which the expression domain of fast-conducting gap-junctional protein connexin40 was projected (depicted in pink). Note that the myocardial wall of the venous sinus (asterisk) is negative for connexin40. Lines in (A) and (B) refer to the level of the transverse cut shown in panel C and histological sections shown in panels D and E. Serial sections through the venous sinus were stained for the transcription factor NKX2-5, which is not expressed in the walls of systemic venous tributaries (venous sinus, coronary sinus), and TBX18, which is expressed specifically in the walls of the venous sinus and coronary sinus and not in the rest of the cardiac muscle. Asterisk points to the vestibular spine. AVC, atrioventricular canal; cor, coronary; LA/RA, left/right atrium; LV/RV, left/right ventricle; OFT, outflow tract; pulm, pulmonary; SV, sinus venosus. (Modified from Sizarov A, Anderson RH, Christoffels VM, et al. Three-dimensional and molecular analysis of the venous pole of the developing human heart. *Circulation* 2010;122:798–807.)

in situ from this primary myocardium (61). The hypothesis that the conduction system may have contributions from the cardiac neural crest cells (62–64) has not been supported by overt evidence. In chicken embryos, retrovirus-labeled neural crest cells were not traced in the conduction system components (65), demonstrating that the entire conduction system has a myogenic origin. The cells derived from the neural crest differentiate in part into the autonomic nerves, which, in turn, influence the conduction properties through the AV conduction axis (66).

Although in the embryonic heart it is not possible to recognize the components of the AV conduction axis as seen in the postnatal heart, and the common atrium is in muscular continuity with the developing ventricles through the AVC musculature (67), the chamber-forming heart already displays coordinated atrial and ventricular contractions and a proper AV delay. As with the sinus node, standard histology does not permit the unambiguous identification of different tissue types. Nonetheless, investigators at the beginning of the previous century attempted to identify the precursors of the AV conduction

system in the human embryonic heart (47–49,68–73), but their conclusions were far from comparable. The AV node was claimed to represent a part of the original AVC, and it was suggested that the bundle of His arose from the nodal tissue by a process of active growth (47). Others hypothesized that the development of the AV node occurred through further specialization of the earlier appearing bundle of His (48). Still others postulated that the formation of the AV conduction system occurred through fusion of different parts of the “specialized” myocardial rings (49). More accurate insights into the development of the AV conduction system were gained from studies on the changes in expression of neural tissue antigen GIN2 during human cardiac development (74,75). Initially, in the early chamber-forming heart, GIN2 expression marks the so-called primary foramen, which is bordered by the right-sided aspect of the AVC and the crest of the ventricular septum. With ongoing development, the AVC expands and shifts rightward, establishing a direct connection between the RA and the right ventricle (RV), marked by the expression of GIN2.

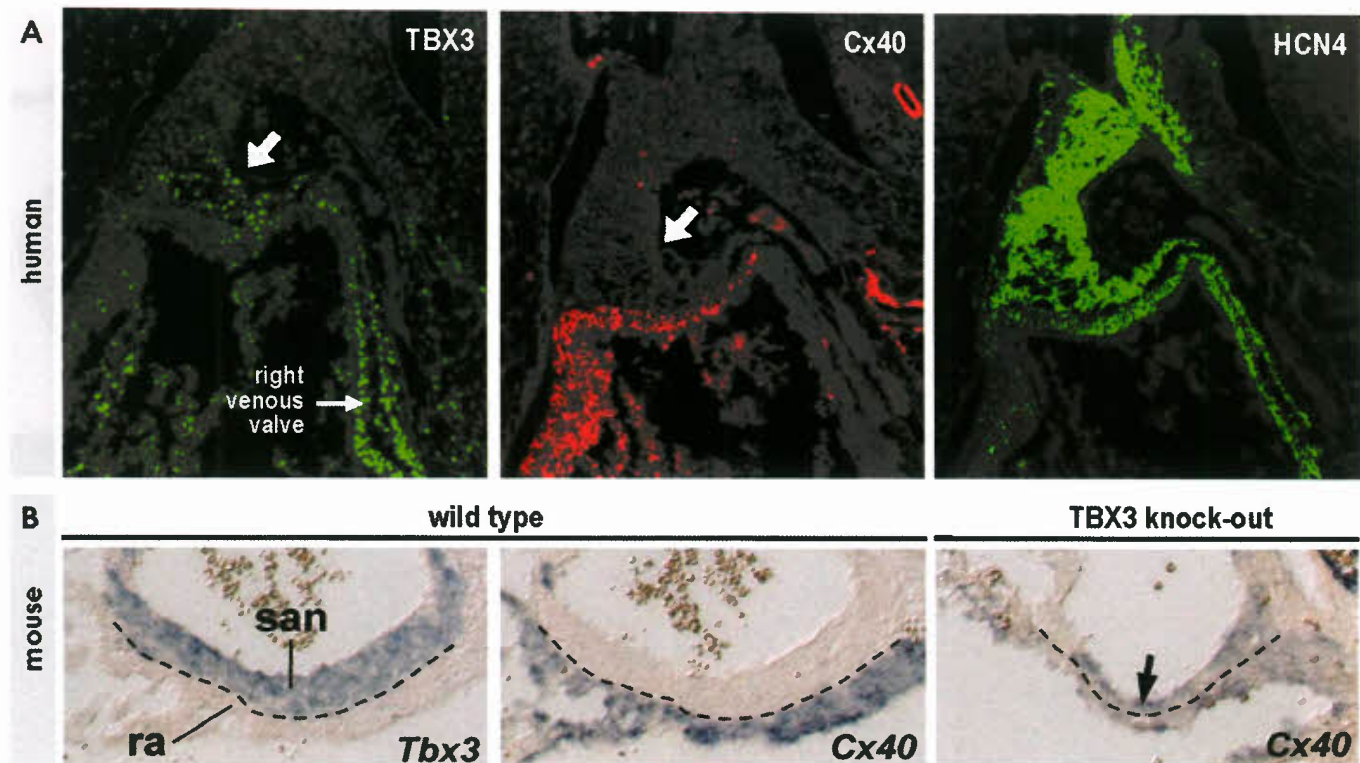


Figure 14.9. Gene expression in the SN primordium. **Panel A** shows serial sections taken through the SN primordium (arrow) of a stage 16 human embryonic heart and stained immunohistochemically for the transcription factor TBX3 (left), gap-junctional protein connexin40 (Cx40, middle) and pacemaker ion-channel HCN4 (right). Note that TBX3 only is expressed in a part of the thickened wall of the venous sinus, which at this stage of development is in its entirety positive for HCN4 and negative for connexin40. **Panel B** shows the sinoatrial boundary in the mouse. In the hearts of wild-type mouse the expression of *Tbx3* and connexin40 are strictly complementary, while in the mouse heart, in which *Tbx3* was knocked-out, expression of connexin40 is extended into the sinus node. ra, right atrium; san, sinoatrial node. (From Hoogaars WMH, Engel A, Brons JF, et al. *Tbx3* controls the sinoatrial node gene program and imposes pacemaker function on the atria. *Genes Dev* 2007;21:1098–1112, with permission.)

A leftward extension of the anterior aspect of the GIN2-positive ring becomes evident at later stages, when the subaortic OFT becomes positioned above the left ventricle. In addition to the GIN2 expression on the crest of ventricular septum, at late stages, GIN2 positivity is also present along the surface of the ventricular septum, resembling the branches of the bundle of His (74) (Fig. 14.10). Although the functional significance of the expression of the neural tissue antigen GIN2 in the developing heart is still unknown, this marker has helped in the understanding of the development of the correct AV and ventriculo-arterial arrangements (76,77), and demonstrated that the entirety of the AV conduction axis developed from the primary ring myocardium.

Our insight into the molecular mechanisms regulating the further development of the AVC has increased over the last decade (Fig. 14.11). One of the earliest events is the activation of the bone morphogenetic protein (Bmp) signaling pathway, with *Bmp2* as one of the main players (78,79). This small signaling molecule activates the expression of another T-box transcriptional factor, *Tbx2*, which along with the transcription factors *Tbx3* and *Msx2* prevents expression of the chamber myocardium-specific genes, thus protecting the AVC muscle from further differentiation (80–83). Another T-box transcription factor, *Tbx20*, directly interferes with Bmp/Smad signaling to suppress *Tbx2* expression in the chambers, thereby confining *Tbx2* expression to the prospective AVC region (84). The combined action of the widely expressed transcription factors

Nkx2-5, *Tbx5*, and *Id2* (inhibitor of DNA binding), having more limited domain of expression, is now known to be crucial for the development of the AV conduction system in the mouse heart (85). In addition, recent lineage analyses in the mouse has provided evidence that structures, such as the coronary sinus, epicardium, vestibular spine, and ventricular septal myocardium, do not contribute to the formation of the AV node (86), as had been suggested previously (87,88) (Fig. 14.12). Current studies support the view that the embryonic AVC, although proliferating very slowly, grows sufficiently to provide the precursor cells for the AV node, AV ring bundles, and lower atrial rims. The same lineage studies also showed that the so-called lower nodal cells of the mouse heart and the ventricular parts of the AV conduction system, including the bundle of His, bundle branches, and the septal branch are not derived from the AVC, but have a ventricular origin (86). A cross-comparison of the genome-wide expression profiles of the cardiomyocytes from the AVC at E10.5 and the AV node at E17.5 in mouse revealed that the majority of differentially expressed transcripts at the E10.5 AVC had maintained this expression profile at the E17.5 AV node. Moreover, the AV nodal cells showed an extensive neurogenic gene expression profile, which is significantly different from that of the AVC, demonstrating that the AV node substantially specializes during development (89).

The myocytes making up the bundle of His and its branches are distinct from the myocytes of the AV node in terms of gene expression, as well as in their electrophysiological properties.

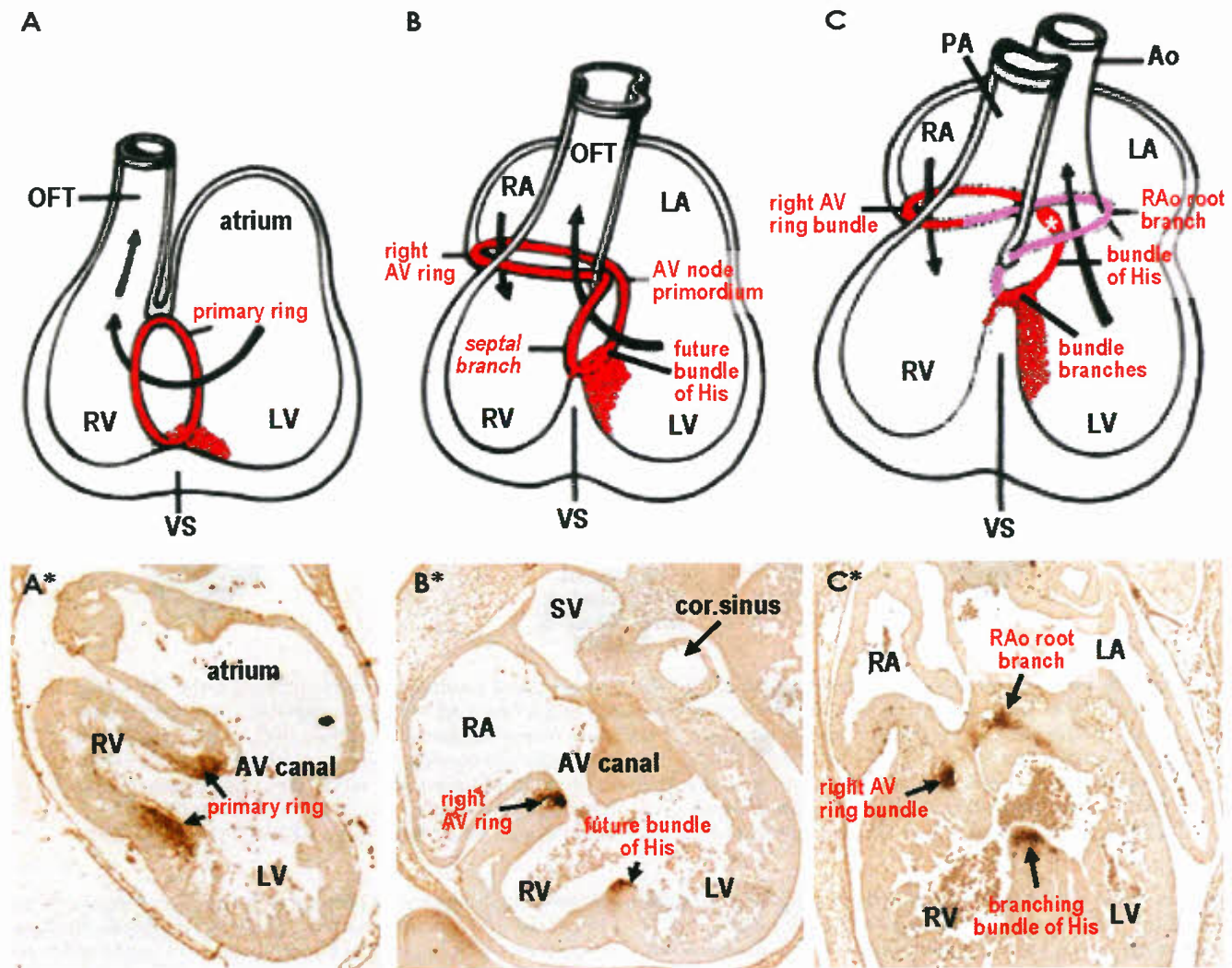


Figure 14.10. Development of the AV junction in the human embryonic heart based on the expression of neural tissue antigen GIN2. In the stage 13 to 14 heart (panels A,A*) a single ring of GIN2-staining tissue is identified, which marks the myocardium of the crest of the ventricular septum and right-sided part of AV canal surrounding the primary foramen connecting the cavities of the left and right ventricular chambers. In the stage 15 to 16 heart (panels B,B*) the GIN2 staining marks the rightward expansion of the AV canal, which establishes a direct connection between the RA and RV. In the stage 18 to 23 heart (panels C,C*) the leftward extension of the ventral part of GIN2-positive ring occurs as the subaortic OFT becomes positioned over the left ventricle. These drawings illustrate the development of the AV conduction system as a derivative of the GIN2-positive myocardium encircling the “primary” foramen in the earliest stages. The drawings show that the so-called septal branch and retroaortic (RAo) root branch can be recognized as transient structures in the developing human heart, which lose their GIN2 expression during late stages of development. AV, atrioventricular; cor, coronary; LA/RA, left/right atrium; LC/RV, left/right ventricle; VS, ventricular septum. (Modified from Wessels A, Vermeulen JL, Verbeek FJ, et al. An immunohistochemical analysis of the distribution of the neural tissue antigen GIN2 in the embryonic human heart. *Anat Rec* 1992;232:97–111.)

A variety of origins of the bundle of His have been proposed (90), but it is generally agreed that the bundle forms in situ by differentiation of the cardiomyocytes on the crest of the developing ventricular septum (61). Once more, *Tbx3* plays an important role in this process (91). From the outset, the crest of the ventricular septum is in direct continuity with the myocardium of the AVC dorsally and ventrally (92). Despite their distinct developmental origins, both the atrial and ventricular parts of the developing AV conduction axis express similar sets of molecular markers, including *Tbx3* and *HCN4*, and both initially are negative for fast-conducting connexins 40 and 43 (61) (Fig. 14.13). Although specified precursors of the bundle of His and its branches are present from the outset

of ventricular septation, they are not initially functionally able to rapidly propagate the electrical impulse (93).

Formation of the AV Plane of Fibrous Insulation

In the normal human adult heart, there are no other muscular connections between the atria and ventricles than the AV conduction axis, which is responsible for the delay of impulse propagation from the atria to the ventricles, this occurring in the AV node, and the uniform and rapid distribution of the impulse to the ventricular chambers through the bundle of His and its branches. As we already have emphasized, in the

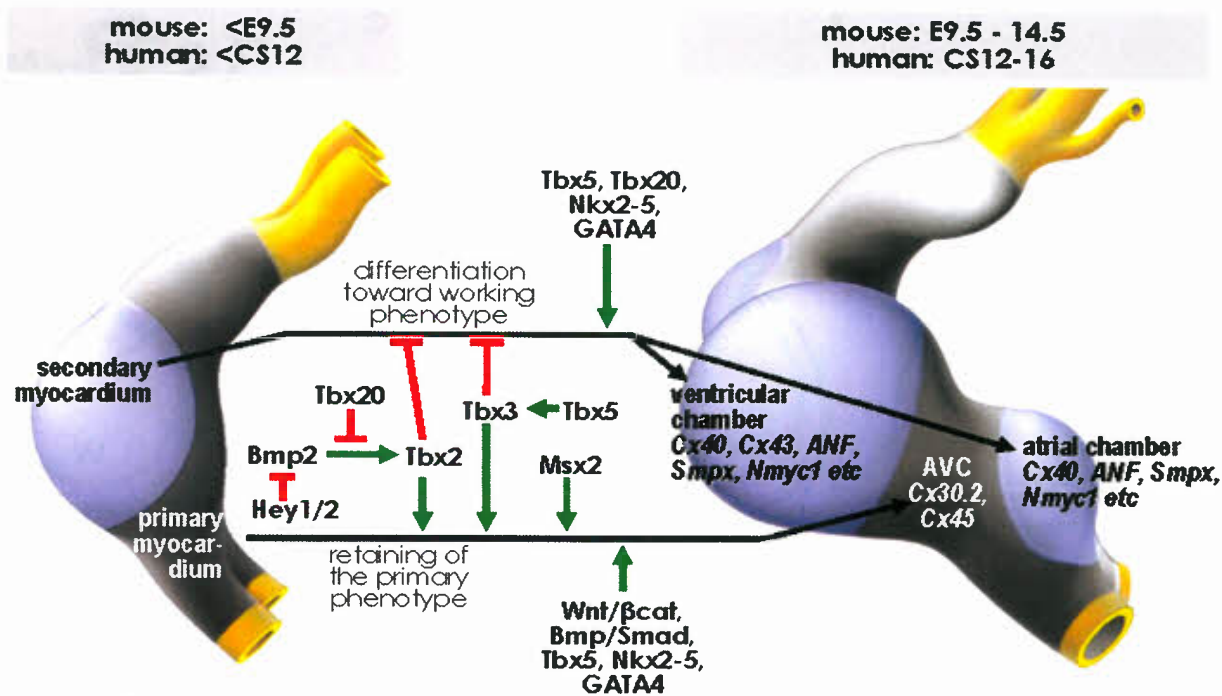


Figure 14.11. Molecular pathways regulating the development and boundary establishment of the AV canal and chamber myocardium. *Green arrows* indicate positive regulation and *red lines* suppression for differentiation towards the working phenotype or retention of the more primitive phenotype. Note that broadly expressed transcription factors Tbx5, GATA5, and NKX2-5 play role in both processes, pointing to the importance of the cooperative action of several factors in regulating the fate of the cardiomyocyte. ANF, atrial natriuretic factor; AVC, atrioventricular canal; CS, Carnegie stage; E, embryonic day. (Modified from Christoffels VM, Smits GJ, Kispert A, et al. Development of the pacemaker tissues of the heart. *Circ Res* 2010;106:240–254.)

embryonic heart, the atrial myocardium is contiguous with the myocardium of the ventricles throughout the AV junction (67). At these stages, the physical insulation by fibrous tissue is not essential because of the intrinsic property of slow propagation of the cardiac impulse by the AVC myocardium (24,87). In the septating heart, the AVC myocardium is sandwiched between the epicardially derived tissues of the AV groove at the epicardial side, and the endocardially derived AV cushion at the endocardial side (94). Due to the growth of the ventricular and atrial chambers, the significant thickening of the free walls of the ventricles, particularly at their bases, and the relatively slow proliferation of the AVC myocardium, the connective tissue of the AV grooves becomes invaginated between the atrial and ventricular myocardial masses, creating the mesenchymal insulation plane (Fig. 14.14). The molecular mechanisms driving the fusion of the epicardially derived tissue with the AV cushions, which finalizes the AV insulation, are not fully understood, but an essential role of epicardially derived cells in this process is well established (95).

With exception of the muscular connection through the bundle of His, the AV myocardial continuity is essentially interrupted at approximately 12 weeks of human development (67). In the fetal and early neonatal human heart, however, multiple tiny myocardial strands have been observed crossing the otherwise fully formed plane of AV insulation (15,96). Persistence of these remnants of the AVC musculature was suggested to be the substrate for electrical preexcitation of the ventricles, which may result in the Wolff-Parkinson-White syndrome, the most prevalent type of supraventricular tachyarrhythmias in children (97). An important characteristic of these bundles is their high conductivity due to the expression of fast-conducting connexin 43 (98), which can lead in specific circumstances to life-threatening arrhythmias. The myocardial

strands found in normal neonatal hearts, however, are derived from the AVC, and our own studies, as yet unpublished, suggest they retain the AVC phenotype and are negative for connexins 40 and -43, making it unlikely that the mere failure of their disappearance is sufficient to explain the phenomenon of ventricular preexcitation with rapid AV conduction.

The Bmp-receptor 1a, also known as *Alk3*, and the transcription factor *Tbx2* have been shown to play an important role in the correct formation of the plane of insulation on the left side of the mouse heart (79,99). In the absence of myocardial *Alk3* or *Tbx2* expression, not only does connective tissue fail to form between the atrial and ventricular chambers, but also the persisting myocardial strands become fast conducting, and are thus capable of causing preexcitation. The formation of accessory pathways with fast conduction properties, therefore, involves both abnormalities in the development of the fibrous insulation *and* the differentiation of the originally slow-conducting AVC myocardium into fast-conducting working myocardial phenotype.

The bundle of His, which remains the only muscular connection between the atrial and ventricular chambers after completion of the formation of the insulation plane, becomes gradually isolated from the myocardium of the ventricular septum by a connective tissue sheath originating, most probably, from the epicardially derived tissues of the AV grooves. In fetal hearts, the cardiomyocytes of the AV node and bundle of His remain in contact with the myocardium of the ventricular septum (Fig. 14.15). Persistence of these connections between the AV node (or bundle of His) and the ventricular myocardium during further maturation in the fetal period may constitute the slow-conducting substrate of one of the variants of so-called Mahaim-type reentry tachycardia, although similar slow-conducting AV connections can be demonstrated along the entire right AV ring, likely representing persisting remnants of the AV ring tissues (16).

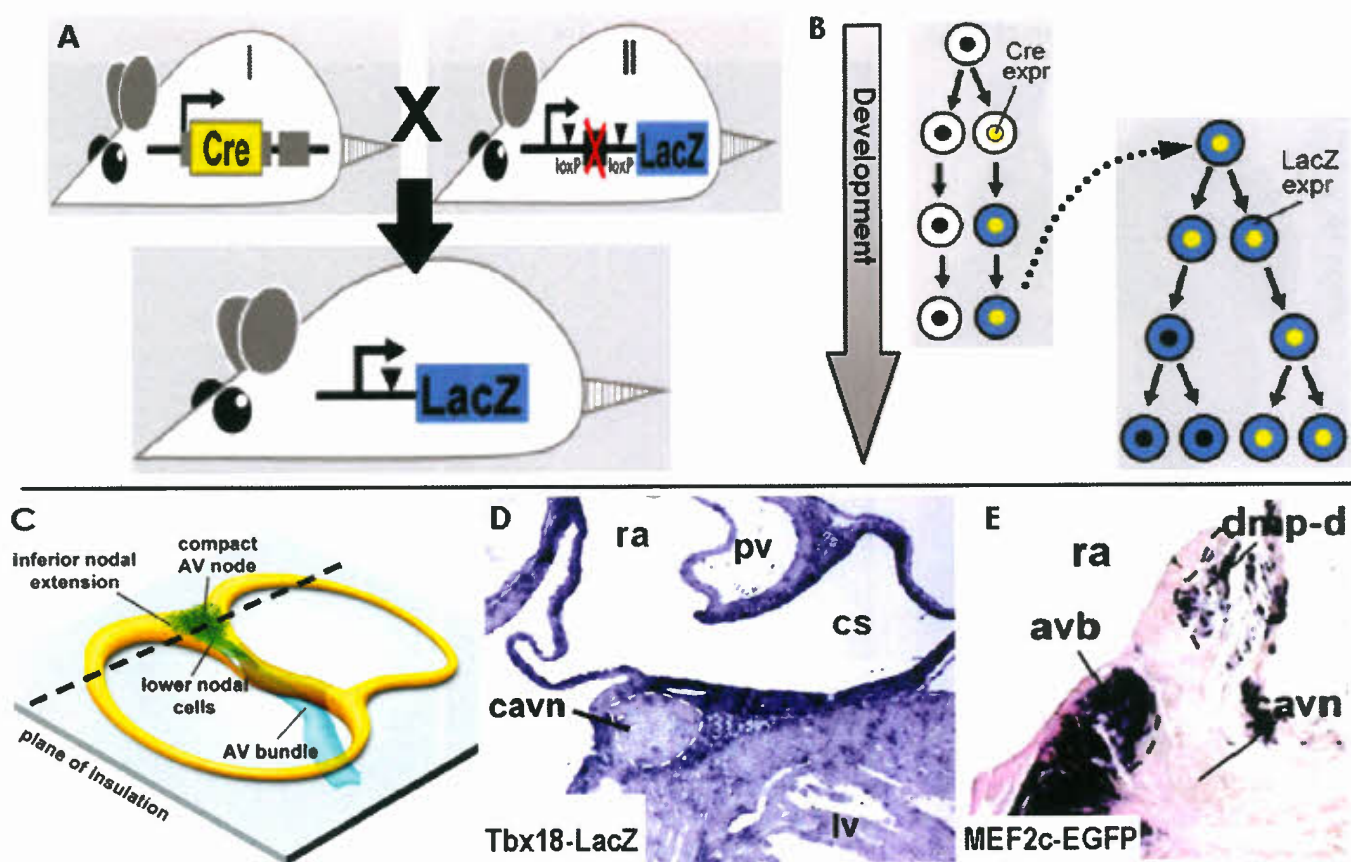


Figure 14.12. Lineage analysis of the developing atrioventricular (AV) node in the mouse heart. **Panel A** and **B** schematically demonstrate the methodology utilized to follow the fate of cells in vivo. In mouse line I the transgene *Cre* (Causes a recombination event) is introduced under the direction of a tissue-specific promoter. Another transgenic mouse line (II) holds a construct consisting of a promoter, which is active in all body cells, and the reporter gene (here the bacterial gene *LacZ*, but it can also be *EGFP*), expression of which is prevented by the STOP sequence (depicted by) upstream of the reporter gene. This STOP sequence is flanked by so-called *loxP* sites, which are recognized by the enzyme *Cre*. When both mice are crossed, the STOP sequence is irreversibly removed in all cells where *Cre* is expressed, by which the reporter gene is then activated in the original cells and their offspring. Subsequently these cells can be labeled by staining for the reporter gene (blue cells in **panel B**), even when the endogenous gene driving *Cre* expression is no longer active. This technique makes it possible to study the origin of the cells of the different components of the mature mammalian four-chambered heart. (Modified from Horsthuis T et al. Can recent insights into cardiac development improve our understanding of congenitally malformed hearts? *Clin Anat* 2009;22:4–20.) Such a study was performed to assess the developmental origin of the AV node, where several tissues have been suggested to contribute, including the myocardial wall of the coronary sinus and the dorsal mesenchymal protrusion, or vestibular spine. **Panel C** shows the AV plane of insulation with the AV rings, the AV node and AV bundle. The dashed line shows the plane of sectioning through the AV node of the postnatal mouse heart shown in **(D)** and **(E)**. The compact atrioventricular node (cavn) is not stained and remains free of recombination, when the *Tbx18* (**panel D**) or *MEF2c* (**panel E**) promoter is used to drive *Cre* expression. This implies that neither the sinus muscle, which is marked by the expression of *Tbx18*, nor the myocardium derived from the dorsal mesenchymal protrusion (dmp-d), which expresses the *MEF2c* enhancer contributes to the AV node, lending no support to the hypothesis that coronary sinus or dorsal mesenchymal protrusion-derived myocardium contribute to the formation of the AV node. Instead the entire AV bundle, along with the so-called lower nodal cells, is derived from ventricular myocardium. avb, atrioventricular bundle; cs, coronary sinus; EGFP, enhanced green fluorescent protein; expr, expression; lv, left ventricle; pv, pulmonary vein; ra, right atrium. (Modified from Aanhaanen WT, Mommersteeg MT, Norden J, et al. Developmental origin, growth, and three-dimensional architecture of the atrioventricular conduction axis of the mouse heart. *Circ Res* 2010;107:728–736.)

DEVELOPMENT OF THE VENTRICULAR CONDUCTION NETWORK

In the postnatal heart, the electrical impulse, after being delayed in the AV node, is transmitted via the ventricular conduction network consisting of the bundle branches and Purkinje fibers.

The main function of the ventricular conduction network is the rapid propagation and uniform distribution of the impulse to the ventricular muscle mass. The fast-conducting properties of the ventricular conduction system (VCS) are due to the high expression of connexins 40 and 43— proteins, which form gap junctions with high conductance properties (100). As with the ventricular working myocardium, the cardiomyocytes

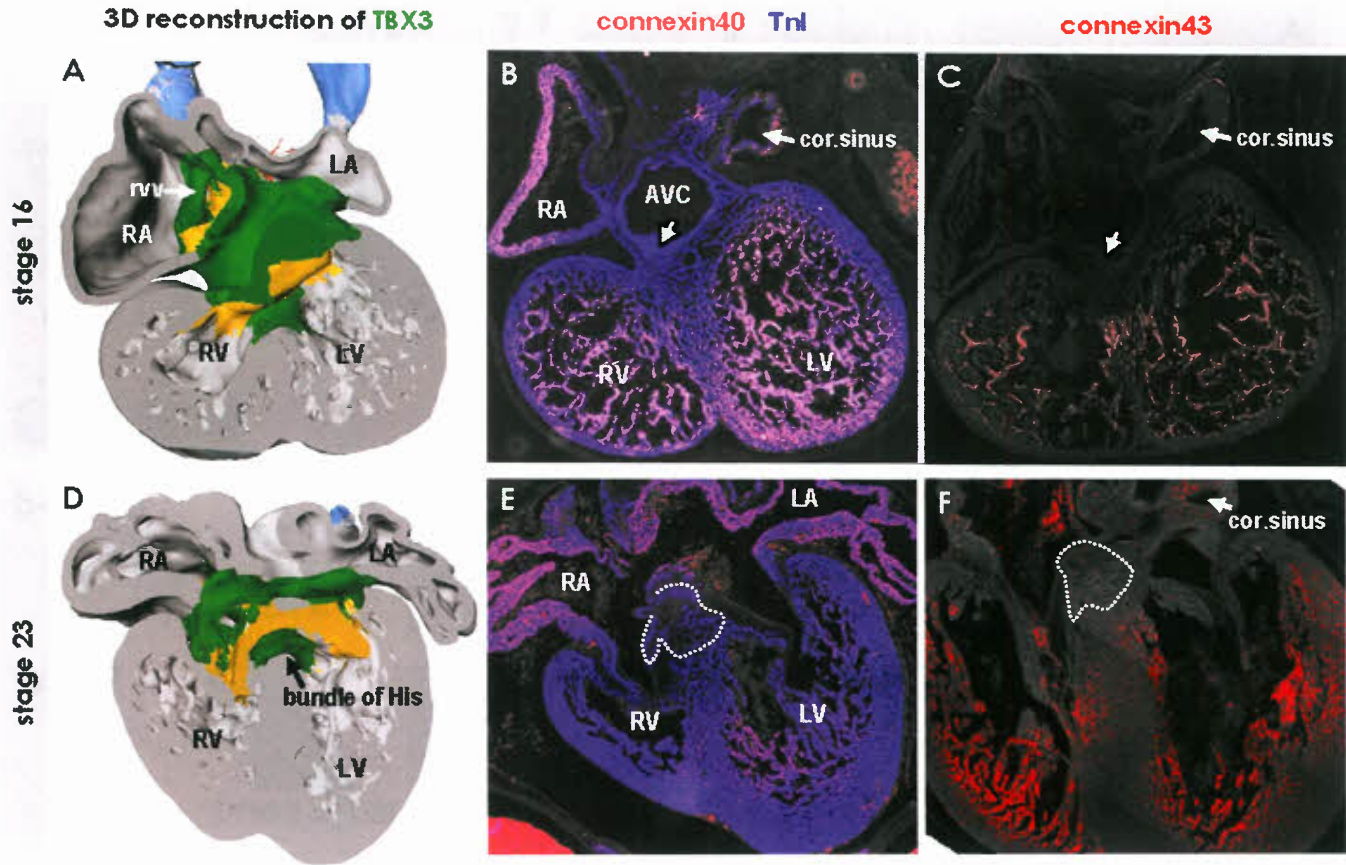


Figure 14.13. Three-dimensional and molecular analysis of the developing AV conduction system in the developing human heart. Panels A and D show a four-chamber cut through the 3-D models of the human embryonic heart with incomplete (stage 16) and complete (stage 23) septation, upon which the expression of the conduction system marker TBX3 was projected (shown in green). TBX3, which represses myocardial differentiation, marks the tissues that will retain their primitive phenotype and will develop in part into the conduction system of the heart. Histological sections taken through the dorsal part of the AV canal were stained for the fast-conducting gap-junctional proteins connexin40 and -43 (panels B and C). The TBX3-positive myocardium of the developing AV node lacks expression of these connexins (arrow). At later stages the domains of TBX3 expression already resemble the postnatal configuration of the AV system. The AV node primordium (outlined by the dashed line in panels E and F) does not express connexins 40 and 43, being a slow conducting structure. 3-D, three-dimensional; AVC, atrioventricular canal; cor, coronary; LA/RA, left/right atrium; LV/RV, left/right ventricle; rrv, right venous valve. (Modified from Sizarov A, Devalla DH, Anderson RH, et al. Molecular analysis of patterning of conduction tissues in the developing human heart. *Circ Arrhythm Electrophysiol*, 2011;4:532–542.)

of the postnatal VCS are specialized in fast conduction. Unlike the working myocytes, however, they have a poorly developed contractile apparatus, and even display some degree of automaticity, resembling the embryonic primitive phenotype (61). In embryonic hearts that do not have discernable bundle branches or a Purkinje fiber network, fast conduction within the developing ventricles already is present at stages when the trabeculations just have appeared. It has been established that the development of the mature pattern of ventricular activation and formation of the Purkinje fiber network are closely related to the development of the ventricular trabeculations (65). The cavities of the ventricles in the early embryonic heart contain an extensive meshwork of trabeculations attaching to the thin outer ventricular wall, which, similar to the trabeculations, expresses the fast-conducting connexins 40 and -43 (31,80,101). Thus, there is a molecular substrate for the preferential rapid conduction of the electrical impulse through the ventricular trabeculations to the ventricular musculature in the embryonic heart without a fully differentiated true ventricular conduction network.

During normal heart development, proliferation ceases in the trabeculations soon after their formation, while the outer ventricular wall becomes highly proliferative to form the compact myocardial layer (31,102), thus meeting the increasing demand to produce more powerful contractions. The newly formed compact layer of the ventricular wall, unlike the trabecular myocardium, does not express connexin 40. The extent of the trabeculations within the ventricular chambers does not change significantly during development compared to the enormous growth of the compact layer (Fig. 14.16). This suggests that failure of proper formation of the compact ventricular wall and abnormal continuing growth of the trabecular layer are responsible for the so-called noncompaction cardiomyopathy, where the extensive trabecular network coexists with a compact layer of decreased thickness (103).

The observation that so-called Purkinje myocytes along with myocardial markers also express markers reminiscent of neuronal cells has resulted in much debate about the origin of the ventricular conduction system. Most of the data

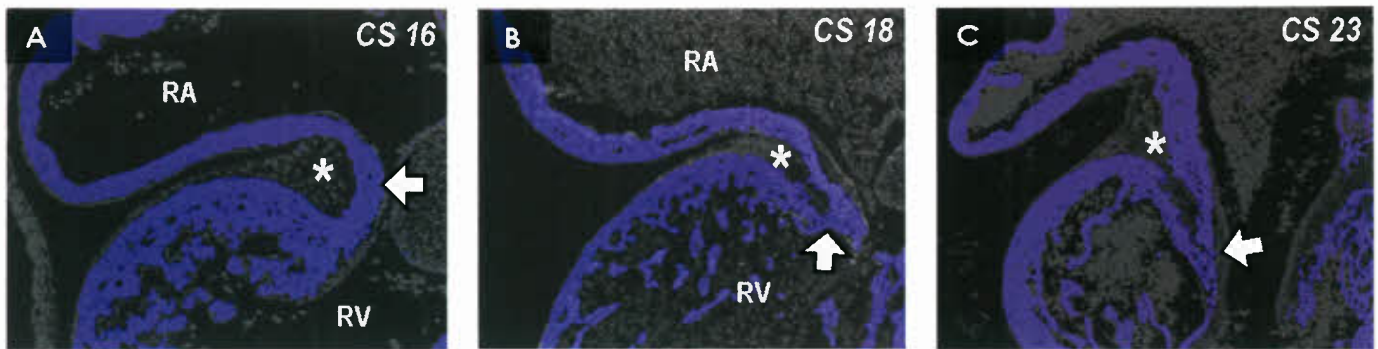


Figure 14.14. Early stages of the formation of the AV plane of insulation in the human heart. These photomicrographs show the right part of the AV canal in a stage 16 heart and the right AV junction in later stages. Sections were immunohistochemically stained for the myocardial marker troponin I (shown in blue). The asterisk points to the subepicardial mesenchymal tissue accumulated in the AV groove. At stage 16, atrial and ventricular myocardium are contiguous through the AV canal musculature (arrow in panel A). This continuity is markedly reduced already two stages later (arrow in panel B). Note, that at the latest embryonic stage there are still myocardial fibers connecting the atrial myocardial with the ventricular wall (arrow in panel C). CS, Carnegie stage; RA, right atrium; RV, right ventricle.

regarding the induction of the VCS have come from studies in chicken embryos, where fate-mapping experiments have unequivocally demonstrated that the entire conduction system has a myocardial origin (65). Individual ventricular myocyte precursor cells give rise to a series of progeny that migrate preferentially vertically to form the meshwork of trabeculations (104, our unpublished observations). From mouse studies, it is known that neuregulin-1 and Notch signaling are necessary and sufficient, to form the ventricular trabeculations through regulating the relative proportion of the embryonic ventricular cardiomyocytes that form the trabecular and compact myocardium (105,106). Another signaling molecule, endothelin-1, secreted by endocardial cells

covering the ventricular trabecular myocardium, probably in response to increasing biomechanical forces such as shear stress and pressure in the walls of the ventricular chambers, has been shown to play an important role in the induction of the Purkinje fiber network in the chicken embryonic heart (107,108). Current models of the development of the ventricular conduction network involve neuregulin signaling-mediated induction and formation of ventricular trabecular myocardium and endothelin signaling-mediated differentiation of subendocardial myocytes into Purkinje myocytes (61,65,109) (Fig. 14.17), with recent lineage studies in the mouse supporting a biphasic mode of formation of the VCS (110).

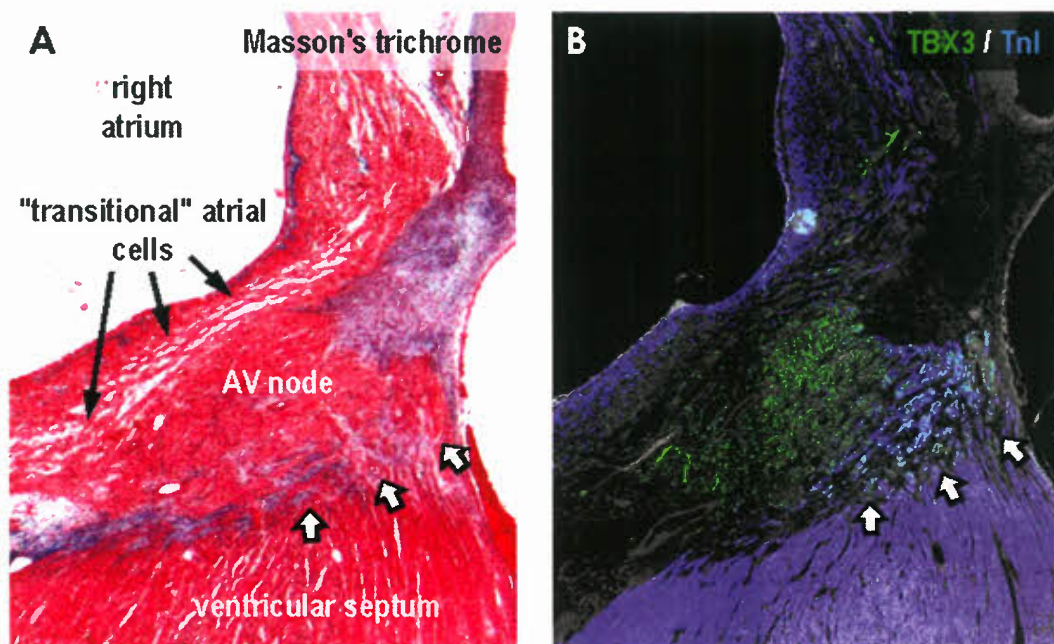


Figure 14.15. Histological and molecular analysis of the AV node in the early human fetus. Serial sections of a 13 week fetal heart were stained using Masson's trichrome (panel A) and immunohistochemistry for TBX3 and the myocardial marker troponin I. Note the tiny myocardial tracts still crossing the forming plane of insulation (arrows). These myocytes are positive for the conduction system marker TBX3 and are, thus, the remnants of the embryonic conduction tissues. AV, atrioventricular; TnI, troponin I.

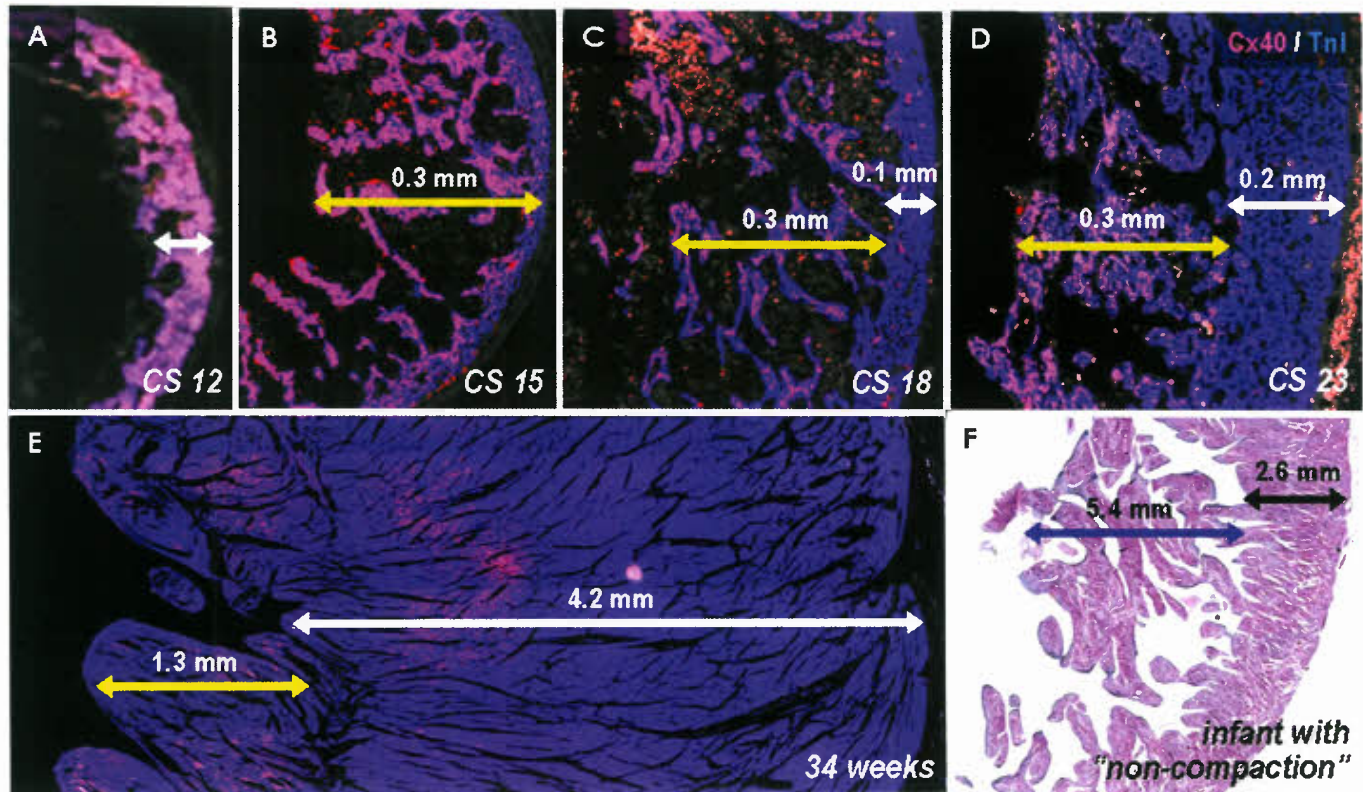


Figure 14.16. Development of the compact ventricular myocardial wall and the Purkinje system in the human heart. Histological sections through the left ventricular free wall were double stained for troponin I (shown in blue) and connexin40 (shown in pink). In the ventricles at Carnegie stages (CS) 12 through 15 connexin40 is expressed transmurally and no overt compact layer is present. After stage 15 the connexin40-negative compact layer of the ventricular wall forms and expands at the epicardial side. Note that the thickness of the trabecular component of the ventricular wall remains the same between stages 15 and 23 (yellow arrows). At the end of the embryonic period connexin40 becomes confined to the trabecular myocardium only, whereas the compact layer in the late normal fetal heart expands considerably (panel E). Note, that in the infant heart with left ventricular “noncompaction” (panel F) the compact layer of the ventricular wall is underdeveloped, while trabecular layer is abnormally expanded. (Modified from Freedom RM, Yoo SJ, Perrin D, et al. The morphological spectrum of ventricular noncompaction. *Cardiol Young* 2005;15:345–364.)

DEVELOPMENTAL ASPECTS OF CARDIAC ELECTROPHYSIOLOGY

A great variety of ion channels, connexins, and calcium-handling molecules determines the different properties of the action potential in the various types of myocytes in the heart (111). The action potential and the rapid changes in voltage differences across the cell membrane are determined by shifts in intra- and extracellular concentrations of several ions, including sodium, potassium, and calcium. Such shifts in ionic concentrations are achieved through active and passive flows of the ions through the different channels, ion pumps, and gap junctions, together constituting the ion currents. Action potentials have a number of characteristics, such as the upstroke velocity, which is the speed of membrane depolarization; the duration, this being the time from the initiation of depolarization to complete repolarization of the cell membrane; the amplitude, in other words the extent of decrease of the negative membrane charge; and the so-called plateau phase, which is the period of relative stability during the membrane depolarized state. The different types of cardiomyocytes display distinct action potential characteristics (Fig. 14.18). During development and maturation of the heart, dramatic changes occur in these characteristics (112,113), affecting myocardial conduction and

refractoriness properties, which, in turn, influence the physiologic function of the maturing heart.

Pacemaking in the Maturing Heart

In the early embryonic heart, all cardiomyocytes are capable of generating the electrical impulse, albeit with gradients of pacemaking dominance, decreasing from the venous to the arterial pole (38,46). In chicken embryos, the earliest activation has been recorded in the systemic venous sinus and both atria (114). Later in development, the origin of the electrical impulse becomes confined to the region of the sinus node. In the immature postnatal heart, nonetheless, there are considerable shifts of the primary pacemaking site over a much wider area than that occupied by the morphologically recognizable sinus nodal cells (115). Down- and upregulation of several ion currents in the adult sinus nodal and atrial working myocardial cells are required to allow a small SN to drive the depolarization of a large mass of atrial chamber myocardium (116). The high expression of HCN4, the ion channel responsible for the pacemaker “funny” current, and Cav3.1, the T-type voltage-gated calcium channel, are essential in the spontaneous depolarization process. Equally important is the

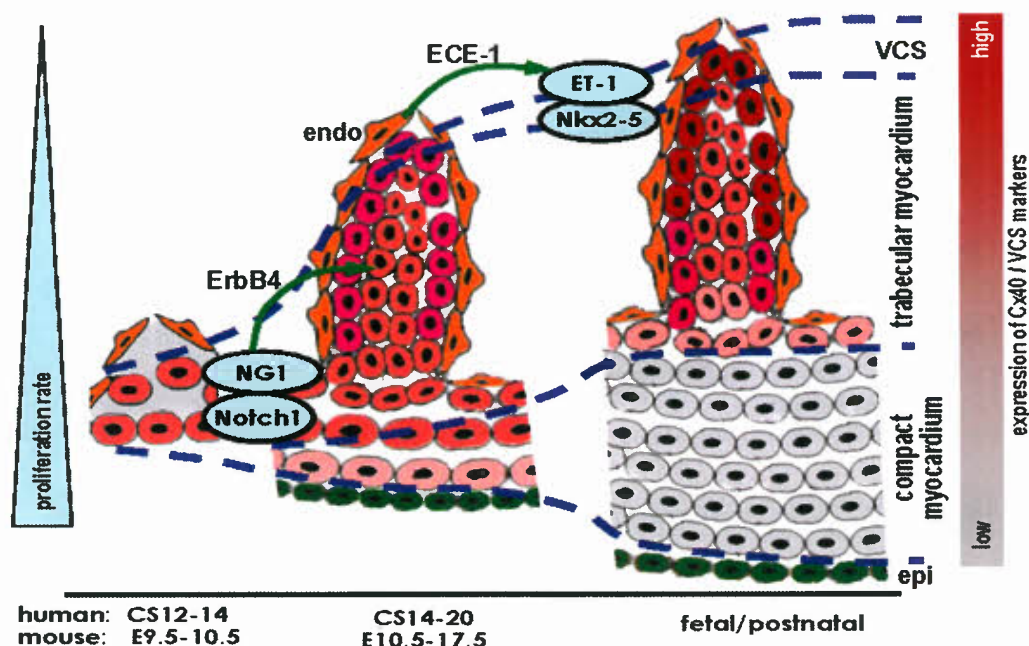


Figure 14.17. Schematic model for the development of the ventricular trabeculations and Purkinje fiber network. At early stage of chamber formation the ventricular wall is 3 to 4 cell thick and only tiny trabeculations are present. Neuregulin-1 (NG1) and Notch1 play important roles in the induction of the formation of extensive meshwork of trabeculae in the consecutive stages. The endothelial cells (endo) then signal, via endothelin-1 (ET-1) and endothelin converting enzyme (ECE-1), to initiate the induction and maturation of the ventricular conduction system (VCS), where transcription factor Nkx2-5 also plays an important role. Expression of connexin40 and other VCS markers is depicted in a gradient from red (high) to gray (no expression). Epi indicates epicardium. Cx40, connexin40; CS, Carnegie stage; ECE-1, endothelin converting enzyme 1; E, embryonic day; endo, endocardium; epi, epicardium; ET-1, endothelin-1; NG1, neuregulin-1; VCS, ventricular conduction system. (Modified from Christoffels VM, Moorman AF. Development of the cardiac conduction system: why are some regions of the heart more arrhythmogenic than others? *Circ Arrhythm Electrophysiol* 2009;2:195–207; Mikawa T, Hurtado R. Development of the cardiac conduction system. *Semin Cell Dev Biol* 2007;18:90–100; and Wagner M, Siddiqui MA. Signal transduction in early heart development (II): ventricular chamber specification, trabeculation, and heart valve formation. *Exp Biol Med (Maywood)* 2007;232:866–880.)

low expression, or virtual absence, of the fast-conducting connexins 40 and 43, of the inward-rectifying potassium channel Kir2.1, and of the sodium-channel Nav1.5. These latter currents are responsible, respectively, for the stabilization of the membrane resting potential and its rapid upstroke in the cardiomyocytes of the atrial and ventricular chambers (43,115). The establishment of sharper borders between the domains of expression of these functional proteins likely is responsible for the progressive confinement of the site of pacemaking to the sinus nodal region of the heart. The timing of changes in the expression of these ion channels in the human maturing heart is not yet characterized. Our preliminary results from studies in late embryonic and early fetal human hearts indicate that there is a gradual decrease of HCN4 expression in the myocardium of the atrium, the pulmonary and systemic venous sleeves, and the AV junction, with subsequent confinement and strong expression of HCN4 to the developing SN (Fig. 14.19). Failure of downregulation of the expression of HCN4 in these structures during later stages of development may provide a substrate for arrhythmogenic ectopic foci in the postnatal heart.

Propagation of the Electrical Impulse in the Atrial Myocardium

After generation of the impulse and breakthrough from the sinus node, the electrical impulse spreads rapidly and uniformly over both right and left atrial chambers as a broad wave front (117),

which is reflected in the P wave of the surface electrocardiogram (118). Conflicting interpretations of studies from the beginning of the previous century on the conduction of the heart beat from the SN toward the AV node (119) stimulated extensive research aimed at discovering “specialized” internodal pathways for the preferential conduction of the impulse between the two cardiac nodes (120,121). Histologic studies failed to identify the presence of distinct insulated myocardial tracts within the atrial musculature (20), while functional studies have provided evidence that anisotropy, or unidirectional orientation of the atrial muscle fibers, is responsible for the slightly faster conduction within some areas of the atrial musculature (19,122). In the embryonic heart, nonetheless, it is possible to recognize molecularly distinct pathways within the developing RA that extend from the sinus nodal primordium toward the developing AV node (Fig. 14.20). The cardiomyocytes making up these “tracts” express the transcription factor Tbx3 and neural tissue antigen HNK-1, both considered to represent markers of the conduction system (123,124) (though expression of HNK-1 was found also outside the developing conduction system) (124,125). It is likely that remnants of the Tbx3- and HNK1-positive areas of the primary myocardium in the postnatal heart are the substrates for abnormal automaticity that result in ectopic atrial tachycardias seen in children. Paroxysmal atrial fibrillation, originating from the myocardial sleeves of the pulmonary veins, is more prevalent in adults, and developmentally unrelated.

Age-related changes in the functional and cellular electrophysiologic properties of the atrium are well recognized. In rat and dog atrial myocardium, action potentials recorded in

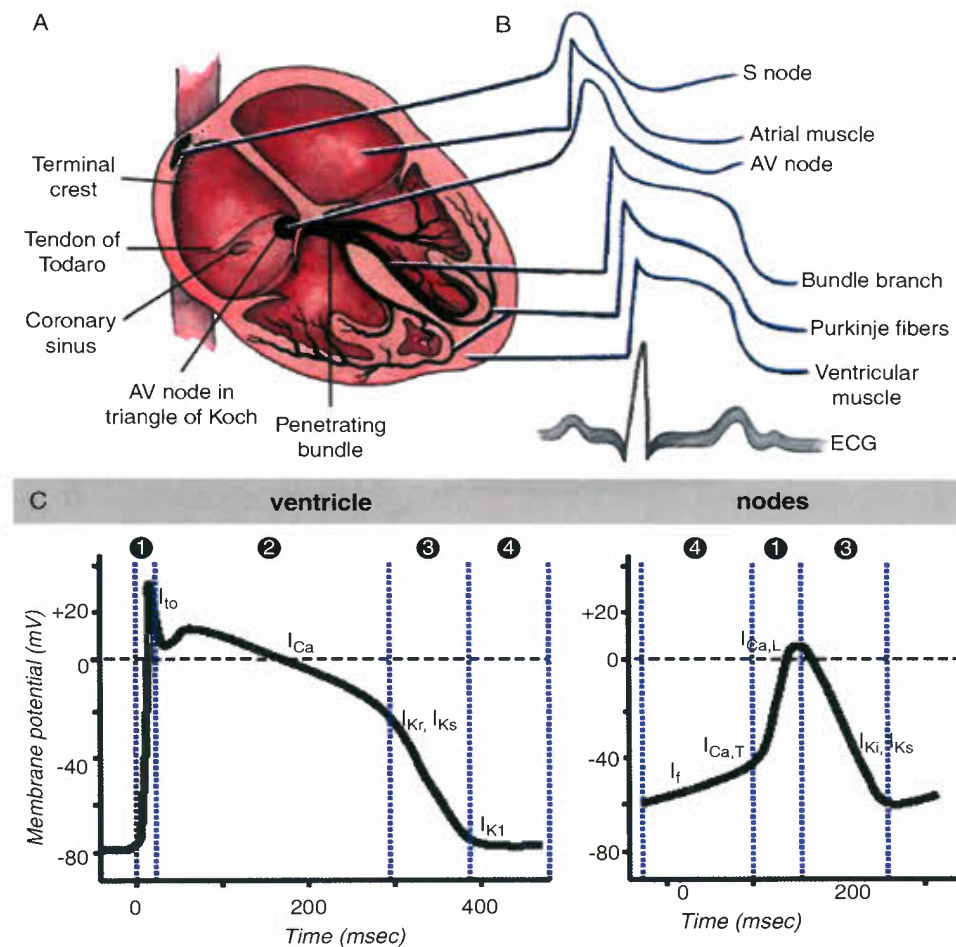


Figure 14.18. Cellular electrophysiology of the cardiac conduction system of the adult human heart. **Panel A** shows schematically the location of the components of the human pacemaking and conduction system, while **panel B** shows the schematic representation of the action potentials in the different cardiomyocytes. Note, that the slowly conducting sinus (S) and atrioventricular (AV) nodes have a distinct morphology of the action potential as compared to the action potentials from the rapidly conducting chamber myocardium, bundle branch and Purkinje fibers. The nodal action potential is characterized by a slow upstroke velocity (phase 1 in the right-sided **panel C**), relatively high (i.e., less negative) resting membrane potentials of about -60 mV, the absence of the plateau phase, and spontaneous depolarization during phase 4. The action potential of the atrial and ventricular chambers, bundle branches and Purkinje fibers (left-sided **panel C**) is, in turn, characterized by the low and stable resting membrane potential of about -90 mV, very rapid upstroke velocity, and presence of the plateau phase (2) during relatively stable depolarized state of the cardiomyocyte membrane. Both types of action potentials have the phase of rapid repolarization (phase 3), during which the potential of the membrane returns to its resting value. The action potential is longest in the Purkinje fibers and shortest in the atrial cardiomyocytes. **Panel C** depicts also the ionic currents (designated as I), which are responsible for the depolarization or repolarization phases of the action potential: $I_{Ca-L/T}$, L- and T-type calcium current; I_f , “funny” current; I_{K1} , inward-rectifier potassium current; $I_{Kr/Ks}$, rapid- and slow components of delayed-rectifier potassium current; I_{Na} , sodium current; I_{to} , transient outward potassium current. AV, atrioventricular; ECG, electrocardiogram; S node, sinus node.

newborn animals are characterized by a shorter plateau phase and duration than in older animals (126). Very limited data exist concerning the maturation of these electrophysiologic characteristics in the developing human heart. In the early human fetus, from 12 to 16 weeks of gestation, action potentials recorded from atrial and ventricular myocardium are comparable with those in the adult, and by mid-gestation conduction velocities are only slightly slower than those in the adult heart (93,127,128). Increasing action potential plateau and duration as a function of age have also been observed in atrial myocardium of the human postnatal heart (129). Shorter atrial refractory periods due to the shorter action potential durations (APDs) in the immature atrium may facilitate the conduction of very closely coupled

impulses, and could render the newborn atrium more susceptible to intraatrial reentry (130,131) (Fig. 14.21). This partly may explain the occurrence of atrial arrhythmias such as atrial flutter in the otherwise healthy fetus or newborn infant (132).

Physiology of the Maturing AV Conduction System

As we have emphasized, a delay in conduction between the atrium and ventricle can be observed already in the early chamber-forming chicken heart. Action potentials recorded from the AVC myocardium of such young embryonic hearts exhibit a characteristic low upstroke velocity and long duration (24,87),

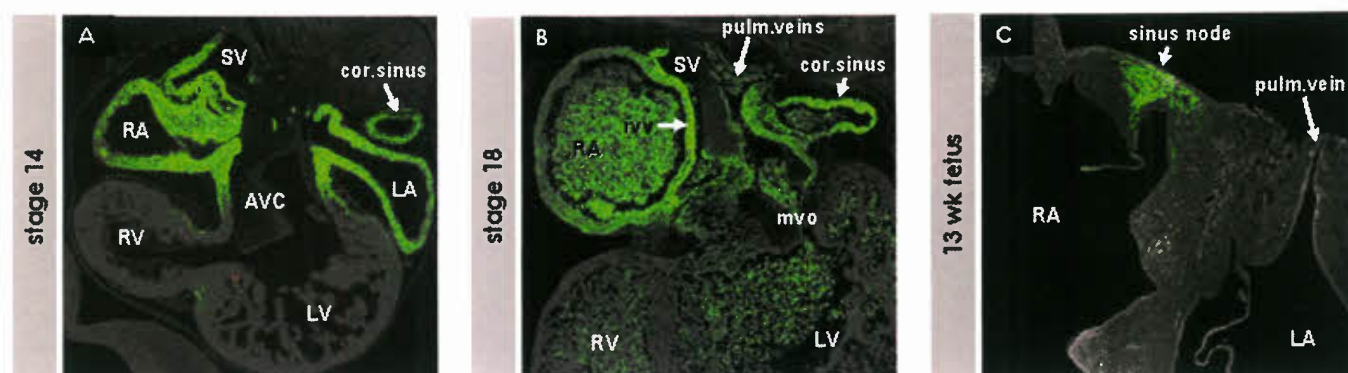


Figure 14.19. Expression of the pacemaker channel HCN4 reflects the progressive maturation of the differentiating myocardium in the human heart. Histological sections of human embryonic and fetal hearts were immunohistochemically stained to show the expression of the pacemaker ion channel HCN4 (depicted in green), which is responsible for the spontaneous depolarization of the nodal cells. In the relatively early embryonic heart (panel A) HCN4 is broadly expressed, in the systemic venous tributaries, atrial chambers and AV canal, but not in the ventricular chambers. In the late embryonic heart (panel B), HCN4 expression declines in the atrial walls, but remains high in the venous and coronary sinus, and AV junctions. Note, the weak expression of HCN4 in the walls of the pulmonary veins. In the early fetal heart (panel C) HCN4 expression at the venous pole is present only in the sinus node, not in the atrial walls or pulmonary vein myocardial sleeves. AVC, atrioventricular canal; cor, coronary; LA/RA, left/right atrium; LV/RV, left/right ventricle; mvo, mitral valve orifice; pulm, pulmonary; SV, sinus venosus.

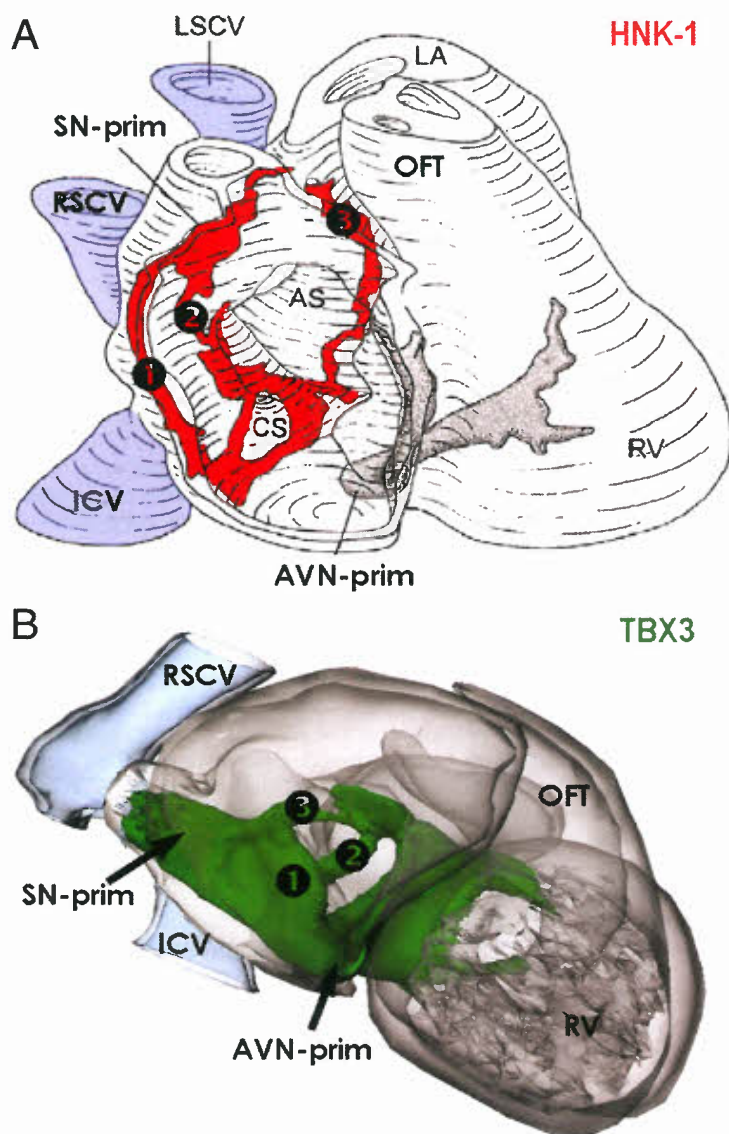


Figure 14.20. Presence of the internodal “tracts” in the human embryonic heart. Panel A shows a 3-D reconstruction of the expression of neural tissue antigen HNK-1 shown in red for the atrial part and in gray for the AV part of its expression domain in a stage 18 human embryonic heart. The view is from the right after removing the lateral part of the RA. Three HNK-1-positive “tracts” are present running from the SN primordium (SN-prim) toward the AV node primordium (AVN-prim), but not connecting with the developing AV node. These three HNK-1-positive “tracts” run in the right venous valve (1), in the left venous valve (2), and in the spurious septum and ventral wall of the RA (3). The last “tract” converges with the so-called retroaortic node region dorsal to the OFT. (From Blom NA, Gittenberger-de Groot AC, DeRuiter MC, et al. Development of the cardiac conduction tissue in human embryos using HNK-1 antigen expression: possible relevance for understanding of abnormal atrial automaticity. *Circulation* 1999;99:800–806, with permission.) Panel B shows a 3-D reconstruction of the expression of the transcription factor TBX3 (shown in green) in a stage 16 human embryonic heart. The view is from the right with the myocardium (gray) made transparent. There are also three “tracts” of TBX3-positive myocardium identifiable, running in the right venous valve (1), in the leading edge of the atrial septum (2) and in the spurious septum and ventral wall of the RA (3). The TBX3-positive “tracts” are, unlike the HNK-1-positive tissues, in direct continuity with the developing AV node region. AS, atrial septum; AVN-prim, atrioventricular nodal primordium; CS, coronary sinus; ICV, inferior caval vein; LSCV/RSCV, left/right superior caval vein; LV/RV, left/right ventricle; OFT, outflow tract; SN-prim, sinus nodal primordium.

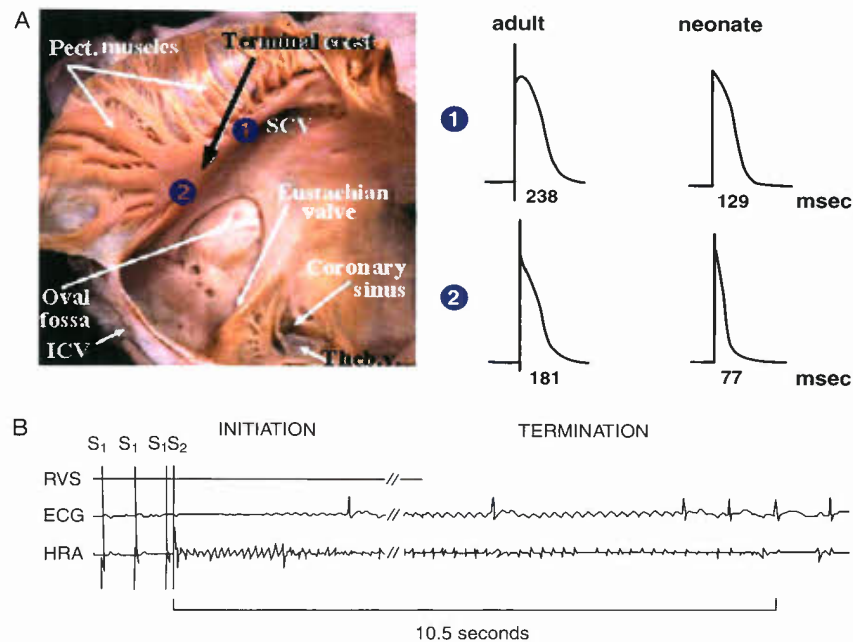


Figure 14.21. Developmental aspects of the conduction through the atrial myocardium. **Panel A** shows action potentials recorded from morphologically similar sites along the terminal crest (depicted by 1 and 2 in the left-sided photo of the opened right atrium) in adult and newborn dogs. In contrast to the adult, neonatal atrial potentials have little or no plateau phase and are significantly shorter in duration. (Modified from Anderson RH, Cook AC. The structure and components of the atrial chambers. *Europace* 2007;9:vi3-vi9; and Spach MS et al. Multiple regional differences in cellular properties that regulate repolarization and contraction in the right atrium of adult and newborn dogs. *Circ Res* 1989;65:1594-1611.) **Panel B** shows how the introduction of a premature extrastimulus (S₂) to the RA of a newborn dog (during gentle vagal stimulation, RVS) results in the induction of a long train of atrial fibrillation/flutter. Similar but shorter runs of atrial fibrillation/flutter can be induced in the absence of vagal stimulation. Such repetitive responses become less common at older ages. HRA, high right atrium; RVS, right vagal stimulation train; ECG, electrocardiogram lead II; ICV, inferior caval vein; Pect, pectinated; S₁, S₂, paced stimuli; SCV, superior caval vein; Theb.v, Thebesian valve. (Modified from Pickoff AS, Stolfi A. Modulation of electrophysiological properties of canine heart by tonic parasympathetic stimulation. *Am J Physiol* 1990;258:H38-H44.)

which are the electrophysiologic characteristics reflecting slowing of conduction. AV delay, including Wenckebach's periodicity, also has been described in the embryonic rat heart prior to formation of the AV conduction system (133). In the embryonic rat heart, acetyl cholinesterase can be detected in the myocardium adjacent to the endocardial cushions, but not in the free walls of the atria and ventricles (134). This may indicate that a cholinergic mechanism is already in some manner linked to the AV delay observed at these early developmental stages, when the heart is not yet innervated.

Individual cardiomyocytes have different types of contact with each other. One type of contact consists of the so-called gap junctions. Gap junctions are highly specialized protein channels that connect adjacent myocytes and allow the passive passage of electrical current, or the flow of charged ions, via a low-resistance pathway from one cell to the next (135). The connexons making up the gap junction may consist of different types of connexins, which vary in their conductivity. Expression of different connexin isoforms results in gap junctions with differing conduction properties. In the early fetal human heart, both the AV node and bundle of His, as well as the lower rims of the atrial chambers, do not express the fast-conducting connexins 40 and 43, which is reflected in their slow conduction (our unpublished observations). This explains the AV delay and absence of ventricular pre-excitation in the setting of incomplete formation of the fibrous annulus and the fibrous sheath of the bundle of His (93). The refractory period of the AV junction in the human fetal heart, moreover, is significantly longer than that of the ventricular

myocardium, thus protecting the ventricles from being excited by supraventricular impulses in its vulnerable period (93). During later fetal stages, concomitant with the fibrous insulation of the bundle of His from the myocardium of the ventricular septum cardiomyocytes making up the bundle upregulate the expression of connexin40, changing it to a rapidly conducting structure. In human hearts, however, this does not affect the PR interval of the fetal magnetocardiogram, which remains unchanged between the 20th and 42nd gestational weeks (136).

In the postnatal heart, important differences in electrophysiology and morphology of the AV junction have been reported between children and adults. Routine histology has shown that the inferior extension of the AV node is much smaller in neonatal and infant hearts when compared to the adult (137). In human and canine young hearts, the antegrade AV refractory periods (the time when no transmission of the electrical impulse is possible) are typically shorter, and intact retrograde, or ventriculoatrial, conduction is more common (138,139). In contrast, cellular electrophysiologic studies of the AV node in neonatal and adult rabbits have shown no significant differences in action potential characteristics, resting AV nodal conduction times, or Wenckebach intervals between the two age groups (140). It also has been reported that, in calf, goat, and pig newborn hearts, the AV node lacks the ability to function as an effective filter of very rapid or premature beats, resulting in very fast conduction and ventricular fibrillation (141-143). Species differences, therefore, may exist in the degree of postnatal maturation of AV nodal function.

In young children, there is a much lower incidence of the so-called dual AV nodal physiology and AV nodal reentry tachycardia as compared to adults (144,145). Dual physiology of the AV node involves two functionally distinct myocardial pathways through the node, the so-called fast and slow pathways, which are currently thought to be the main substrates for AV nodal reentry tachycardia (146).

Developmental Aspects of the VCS and Working Myocardium

The conduction velocity in the synchronously contracting ventricular chambers of the septating heart has been estimated to be more than ten times faster than in the primary myocardium of the looping heart tube (24,87,133). It has been shown that the “mature” apex-to-base activation pattern of the ventricles is present in the embryonic rabbit heart prior to the completion of ventricular septation (147). As we have already discussed, there is preferential conduction through the ventricular trabecular myocardium due to the high expression of the fast-conducting connexins. The morphology and gene expression patterns of the developing ventricular chambers are very similar in the rabbit, mouse, chicken,

and human, suggesting conservation of the electrical activation pattern between these species. The critical role of expression of connexins during development for normal conduction is demonstrated by the abnormal, often lethal, disturbances of cardiac conduction observed in transgenic mice with deficiencies of these specific connexin isoforms (148,149). In the developing chicken and rat heart, cellular electrophysiologic changes in myocyte action potential characteristics of working myocardium promote an increase in conduction velocity with maturation. Increases in the upstroke velocity and amplitude of the action potential in the ventricular cardiomyocytes, and therefore ventricular conduction velocities, have been noted in both species during embryonic development (150,151). These changes may be the result of the switch from slow to fast sodium ion channels, responsible for the rapid upstroke phase (152), and the increase of the resting membrane potential, which also contributes to a higher action potential upstroke velocity. The developmental aspects of the maturing Purkinje fiber network mainly have been described in fetal and young postnatal canine hearts. Age-dependent increases in action potential upstroke velocity, amplitude, resting membrane potential, and duration have been described. In addition, changes in the ultrastructure of the developing canine Purkinje myocytes, including changes in cell shape, increases in cross-sectional area, and the development of intercalated discs and desmosomes undoubtedly contribute to the increase in conduction velocity noted with maturation (153–155). There are no data on the functional maturation of the Purkinje network in the human beside morphologic analyses in the mid-gestation fetal hearts (156).

Protection against rapid ventricular rates also depends in part on electrophysiologic properties of the conduction system at sites distal to the AV node. In the adult dog, APDs increase along the length of the Purkinje system, with the longest duration occurring just proximal to the site of subendocardial insertion, which functions as a physiologic gate that offers protection against closely coupled impulses. This electrophysiologic gate is not functional in the newborn heart, since nearly uniform APDs are recorded along the entire length of the Purkinje system (157) (Fig. 14.22). This could render the neonatal ventricular myocardium vulnerable to closely coupled impulses that might arise distal to the AV node.

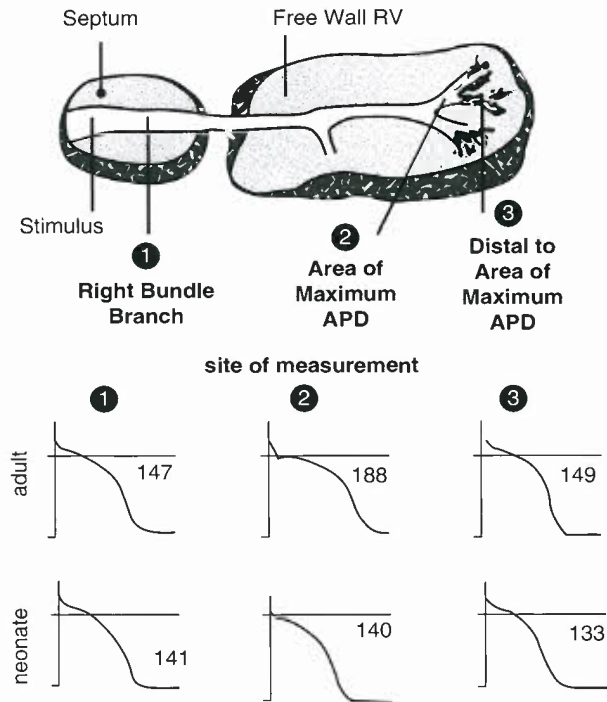


Figure 14.22. Developmental aspects of the conduction through the Purkinje fiber network. Action potentials were recorded at three separate sites along the VCS of the newborn and adult dog. Site 1 corresponds to the proximal right bundle branch, site 2 just proximal to the distal ramifications of the ventricular conduction system, and site 3 within the distal ramifications within right ventricle (RV). Note, that in the adult dog, the longest action potential duration (APD) is recorded at site 2. This abrupt increase in APD at site 2 functions as a physiologic gate, capable of blocking the conduction of closely coupled impulses to the ventricles. This abrupt increase in APD is not observed in the newborn canine heart (i.e., the physiologic gate is absent). (Modified from Myerburg RJ et al. Electrophysiological properties of the canine peripheral A-V conducting system. *Circ Res* 1970;26:361–378; and Unterreker WJ, Danilo P Jr, Rosen MR. Developmental changes in action potential duration, refractoriness, and conduction in the canine ventricular conducting system. *Pediatr Res* 1984;18:53–58.)

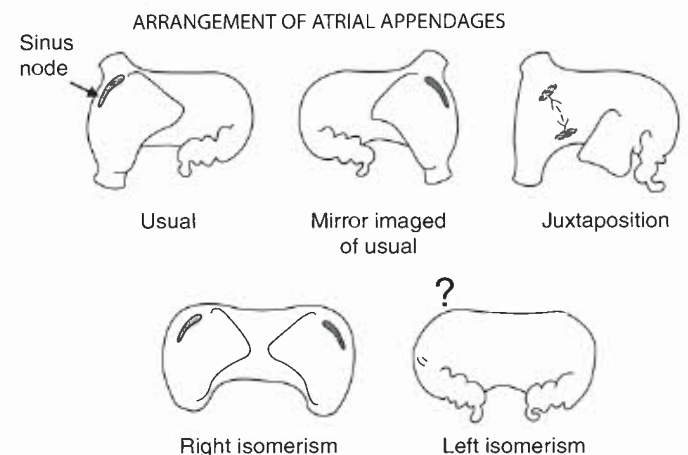


Figure 14.23. Localization of the SN in variations of arrangement of the atrial appendages. In the usual arrangement (atrial situs solitus), the SN is located at the junction of the superior vena cava and RA. The reverse occurs in atrial situs inversus (*mirror imaged*). In juxtaposition of the atrial appendages, the SN becomes displaced along the right atrial anterior wall. In right isomerism there are bilateral sinus nodes. In left atrial isomerism the SN is highly variable, being absent, displaced, and/or hypoplastic. (From Ho SY. Clinical pathology of the cardiac conduction system. *Novartis Found Symp* 2003;250:210–221, with permission.)

THE CONDUCTION SYSTEM IN CONGENITALLY MALFORMED HEARTS

While the majority of malformed hearts have more-or-less normal arrangements of the conduction system, there can be significant deviations from the norm (158,159). During late embryonic development of the heart, the spatial distribution of the conduction system markers *Tbx3* (123) and *GLN2/HNK1* (74,124) is reminiscent of the location of the definitive and “residual” components, the latter being the largely regressing components of the developing conduction system still seen in the postnatal heart.

Malposition of the SN may occur in left juxtaposition of the atrial appendages, where anterior displacement of the SN is observed; in right isomerism, where bilateral sinus nodes are formed; and in left isomerism, where a SN may not be identifiable (Fig. 14.23). In the setting of some congenital cardiac

malformations, there is considerable aberration in the course of the AV conduction axis (159), which can be explained well on the basis of knowledge of the developing conduction system. Incomplete formation of the RV, as seen in tricuspid atresia, double-inlet left ventricle, and straddling tricuspid valve represents incomplete rightward transfer of the right side of the AV canal. In these defects, the AV conduction system always is located at the junction of the inferocaudal aspect of the ventricular septum carrying the bundle of His, and the AV junction where the AV node forms. The position of the AV node and bundle of His is thus determined by the relative positions of the right and left ventricles, and the degree of underdevelopment of the right AV ring. In transposition of the great arteries with AV discordance, the AV node and bundle of His are located anteriorly (160). A similar analysis applies to the formation of the conduction system in the setting of AV septal defect with common AV junction (161) and other malformations (Fig. 14.24).

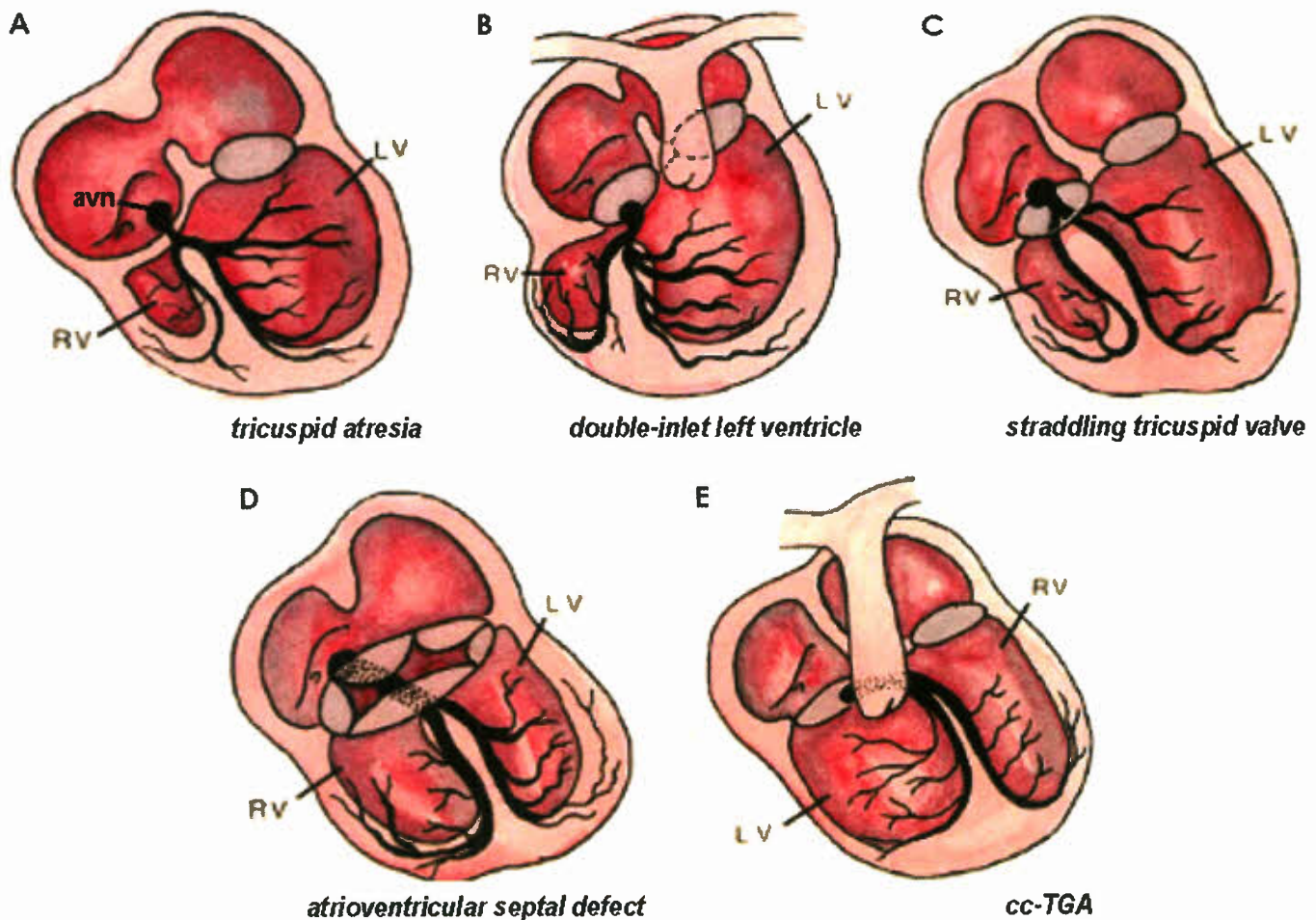


Figure 14.24. Disposition of the AV conduction system components in congenitally malformed hearts. In the setting of tricuspid atresia (panel A), the atrioventricular node (avn) is positioned on the floor of the blindly ended right atrium. The conduction system extends onto the crest of the muscular ventricular septum, coursing inferoposterior to the rim of the ventricular septal defect (VSD). In double-inlet left ventricle (panel B), the AV node and the bundle of His are positioned anteriorly, at the site where the right AV ring is in contact with the crest of the muscular ventricular septum, which separates the left ventricle from the outlet chamber (the incomplete right ventricle). In hearts with straddling tricuspid valve (panel C), the AV node and the bundle of His are positioned at the postero-inferior site along the right AV ring and its contact with the muscular ventricular septum. In AV septal defect with common AV junction (panel D), the AV node is positioned posteriorly and inferiorly outside the triangle of Koch, as the central fibrous body is absent. The relatively long bundle of His runs along the inferior rim of the muscular ventricular septum. In congenitally corrected transposition of the great arteries (cc-TGA, panel E), the AV node is positioned anteriorly near the atrial septum. The long bundle of His is related to the pulmonary OFT and runs in anterocephalad direction, passing anteriorly to the rim of the VSD, if present. LV/RV, left/right ventricle.

REFERENCES

1. Tawara S. *Reizleitungssystem des Säugetierherzens: Eine anatomisch-Histologische Studie Über das Atrioventrikulärbündel und die Purkinje'schen Fäden*. Jena: Verlag von Gustav Fischer, 1906.
2. Keith A, Flack M. The form and nature of the muscular connections between the primary divisions of the vertebrate heart. *J Anat Physiol* 1907;41:172–189.
3. Aschoff L. Referat über die Herzstörungen in ihren Beziehungen zu den Spezifischen Muskelsystem des Herzens. *Verh Dtsch Pathol Ges* 1910;14:3–35.
4. Mönckeberg JG. Beiträge zur normalen und pathologischen Anatomie des Herzens. *Verh Dtsch Pathol Ges* 1910;14:64–71.
5. Sánchez-Quintana D, Cabrera JA, Farré J, et al. Sinus node revisited in the era of electroanatomical mapping and catheter ablation. *Heart* 2005;91:189–194.
6. James TN. Anatomy of the human sinus node. *Anat Rec* 1961;141:109–139.
7. Koch W. Weiter mitteilungen über den Sinusknoten des Herzens. *Verh Dtsch Ges Pathol* 1909;13:85–92.
8. Anderson RH, Becker AE, Brechenmacher C, et al. The human atrioventricular junctional area: a morphological study of the AV node and bundle. *Eur J Cardiol* 1975;3:11–25.
9. Becker AE, Anderson RH. Morphology of the atrioventricular junctional area. In: Wellens HJJ, Lie KI, Janse MJ, eds. *The Conduction System of the Heart: Structure, Function and Clinical Implications*. Leiden: Stenford Kroese BV, 1976;263–286.
10. Inoue S, Becker AE. Posterior extensions of the human compact atrioventricular node: a neglected anatomic feature of potential clinical significance. *Circulation* 1998;97:188–193.
11. Masing GK, James TN. Anatomical configuration of the His bundle and bundle branches in the human heart. *Circulation* 1975;53:609–621.
12. Oosthoek PW, Virág S, Lamers WH, et al. Immunohistochemical delineation of the conduction system. II: the atrioventricular node and Purkinje fibers. *Circ Res* 1993;73:482–491.
13. Anderson RH, Davies MJ, Becker AE. Atrioventricular ring specialized tissue in the human heart. *Eur J Cardiol* 1974;2:219–230.
14. Kurosawa H, Becker AE. Dead-end tract of the conduction axis. *Int J Cardiol* 1985;7:13–20.
15. Wessels A, Mijnders TA, de Gier-de Vries C, et al. Expression of myosin heavy chain in neonatal human hearts. *Cardiol Young* 1992;2:318–334.
16. Anderson RH, Ho SY, Gillette PG, et al. Mahaim, Kent and abnormal atrioventricular conduction. *Cardiovasc Res* 1996;31:480–491.
17. Sherf L, James TN. Fine structure of cells and their histologic organization within internodal pathways of the heart: clinical and electrocardiographic implications. *Am J Cardiol* 1979;44:345–369.
18. Perez-Lugones A, McMahon JT, Ratliff NB, et al. Evidence of specialized conduction cells in human pulmonary veins of patients with atrial fibrillation. *J Cardiovasc Electrophysiol* 2003;14:803–809.
19. Spach MS, Kootsey JM. The nature of electrical propagation in cardiac muscle. *Am J Physiol* 1983;244:H3–H22.
20. Anderson RH, Ho SY, Smith A, et al. The internodal atrial myocardium. *Anat Rec* 1981;201:75–82.
21. Ho SY, Cabrera JA, Tran VH, et al. Architecture of the pulmonary veins: relevance to radiofrequency ablation. *Heart* 2001;86:265–270.
22. Boukens BJ, Christoffels VM, Coronel R, et al. Developmental basis for electrophysiological heterogeneity in the ventricular and outflow tract myocardium as a substrate for life-threatening ventricular arrhythmias. *Circ Res* 2009;104:19–31.
23. Paff GH, Boucek RJ, Harrell TC. Observations on the development of the electrocardiogram. *Anat Rec* 1968;160:575–582.
24. de Jong F, Op't Hof T, Wilde AA, et al. Persisting zones of slow impulse conduction in developing chicken hearts. *Circ Res* 1992;71:240–250.
25. Arguello C, de la Cruz MV, Gómez CS. Experimental study of the formation of the heart tube in the chick embryo. *J Embryol Exp Morphol* 1975;33:1–11.
26. Stalsberg H, DeHaan RL. The precardiac areas and formation of the tubular heart in the chick embryo. *Dev Biol* 1969;19:128–159.
27. de la Cruz VM, Sanchez Gomez C, et al. Experimental study of the development of the truncus and the conus in the chick embryo. *J Anat* 1977;123:661–686.
28. Cai CL, Liang X, Shi Y, et al. Isl1 identifies a cardiac progenitor population that proliferates prior to differentiation and contributes a majority of cells to the heart. *Dev Cell* 2003;5:877–889.
29. Buckingham M, Meilham S, Zaffran S. Building the mammalian heart from two sources of myocardial cells. *Nat Rev Genet* 2005;6:826–837.
30. van den Berg G, Abu-Issa R, de Boer BA, et al. A caudal proliferating growth center contributes to both poles of the forming heart tube. *Circ Res* 2009;104:179–188.
31. Sizarov A, Ya J, de Boer BA, et al. Formation of the building plan of the human heart: morphogenesis, growth, and differentiation. *Circulation* 2011;123:1125–1135.
32. Christoffels VM, Habets PE, Franco D, et al. Chamber formation and morphogenesis in the developing mammalian heart. *Dev Biol* 2000;223:266–278.
33. Moorman AFM, Christoffels VM. Cardiac chamber formation: development, genes, and evolution. *Physiol Rev* 2003;83:1223–1267.
34. Christoffels VM, Mommersteeg MT, Trowe MO, et al. Formation of the venous pole of the heart from an Nkx2-5-negative precursor population requires Tbx18. *Circ Res* 2006;98:1555–1563.
35. Soufan AT, van den Hoff MJ, Ruijter JM, et al. Reconstruction of the patterns of gene expression in the developing mouse heart reveals an architectural arrangement that facilitates the understanding of atrial malformations and arrhythmias. *Circ Res* 2004;95:1207–1215.
36. Sizarov A, Anderson RH, Christoffels VM, et al. Three-dimensional and molecular analysis of the venous pole of the developing human heart. *Circulation* 2010;122:798–807.
37. Lieberman M, Paes de Carvalho A. The electrophysiological organization of the embryonic chick heart. *J Gen Physiol* 1965;49:351–363.
38. van Mierop LHS. Localization of pacemaker in chick embryo heart at the time of initiation of heartbeat. *Am J Physiol* 1967;212:407–415.
39. Moorman AF, Soufan AT, Hagoort J, et al. Development of the building plan of the heart. *Ann NY Acad Sci* 2004;1015:171–181.
40. Patten BM, Kramer TC. The initiation of contraction in the embryonic chicken heart. *Am J Anat* 1933;53:349–375.
41. Kamino K, Komuro H, Sakai T, et al. Functional pacemaking area in the early embryonic chick heart assessed by simultaneous multiple-site optical recording of spontaneous action potentials. *J Gen Physiol* 1988;91:573–591.
42. Mommersteeg MTM, Hoogaars WMH, Prall OWJ, et al. Molecular pathway for the localized formation of the sinoatrial node. *Circ Res* 2007;100:354–362.
43. Mangoni ME, Nargeot J. Genesis and regulation of the heart automaticity. *Physiol Rev* 2008;88:919–982.
44. Mery A, Aimond F, Menard C, et al. Initiation of embryonic cardiac pacemaker activity by inositol 1,4,5-triphosphate-dependent calcium signaling. *Mol Biol Cell* 2005;16:2414–2423.
45. Stieber J, Herrmann S, Feil S, et al. The hyperpolarization-activated channel HCN4 is required for the generation of pacemaker action potentials in the embryonic heart. *Proc Natl Acad Sci USA* 2003;100:15235–15240.
46. Patten BM. Initiation and early changes in the character of the heart beat in vertebrate embryos. *Physiol Rev* 1949;29:31–47.
47. Walls EW. The development of the specialized conducting tissue of the human heart. *J Anat* 1947;81:93–110.
48. Navaratnam V. The development of the specialized musculature of the human heart. *Ceylon J Med Sci* 1965;14:68–80.
49. Wenink ACG. Development of the human cardiac conduction system. *J Anat* 1976;121:617–631.
50. Anderson RH, Ho SY, Becker AE, et al. The development of the sinoatrial node. In: Bonke FIM ed. *The Sinus Node: Structure, Function and Clinical Relevance*. Leiden: Martinus Nijhoff Medical Division, 1978;166–182.
51. Lichnovský V, Obrucnik M, Málek V, et al. Development of the conduction system of the human embryonic and foetal heart. Differentiation of the sinoatrial node. *Folia Morphol (Praha)* 1979;27:31–35.
52. Christoffels VM, Smits GJ, Kispert A, et al. Development of the pacemaker tissues of the heart. *Circ Res* 2010;106:240–254.
53. DeHaan RL. Development of pacemaker tissue in the embryonic heart. *Ann NY Acad Sci* 1965;127:7–18.
54. Wiese C, Grieskamp T, Airik R, et al. Formation of the sinus node head and differentiation of sinus node myocardium are independently regulated by Tbx18 and Tbx3. *Circ Res* 2009;104:388–397.
55. Los JA. Die Entwicklung des Septum sinus venosi cordis. Die Herzentwicklung des Menschen, von einer vergessenen Struktur aus untersucht. *Z Anat Entwicklung* 1960;122:173–196.
56. Steding G, Xu JW, Seidl W, et al. Developmental aspects of the sinus valves and the sinus venosus septum of the right atrium in human embryos. *Anat Embryol (Berl)* 1990;181:469–475.
57. Hoogaars WMH, Engel A, Brons JF, et al. Tbx3 controls the sinoatrial node gene program and imposes pacemaker function on the atria. *Genes Dev* 2007;21:1098–1112.
58. Levin M. Left-right asymmetry in embryonic development: a comprehensive review. *Mech Dev* 2005;122:3–25.
59. Ho SY, Seo JW, Brown NA, et al. Morphology of the sinus node in human and mouse hearts with isomerism of the atrial appendages. *Br Heart J* 1995;74:437–442.
60. Moorman AF, Schumacher CA, de Boer PA, et al. Presence of functional sarcoplasmic reticulum in the developing heart and its confinement to chamber myocardium. *Dev Biol* 2000;223:279–290.
61. Christoffels VM, Moorman AF. Development of the cardiac conduction system: why are some regions of the heart more arrhythmogenic than others? *Circ Arrhythm Electrophysiol* 2009;2:195–207.
62. Gorza L, Schiaffino S, Vitadello M. Heart conduction system: a neural crest derivative? *Brain Res* 1988;457:360–366.
63. Poelmann RE, Jongbloed MR, Molin DG, et al. The neural crest is contiguous with the cardiac conduction system in the mouse embryo: a role in induction? *Anat Embryol (Berl)* 2004;208:389–393.
64. Nakamura T, Colbert MC, Robbins J. Neural crest cells retain multipotential characteristics in the developing valves and label the cardiac conduction system. *Circ Res* 2006;98:1547–1554.
65. Mikawa T, Hurtado R. Development of the cardiac conduction system. *Semin Cell Dev Biol* 2007;18:90–100.

66. Hildreth V, Webb S, Bradshaw L, et al. Cells migrating from the neural crest contribute to the innervation of the venous pole of the heart. *J Anat* 2008;212:1–11.
67. Wessels A, Markman MW, Vermeulen JL, et al. The development of the atrioventricular junction in the human heart. *Circ Res* 1996;78:110–117.
68. Mall FP. On the development of the human heart. *Am J Anat* 1912;13:249–298.
69. Sanabria T. Recherches sur la différenciation du tissu nodal et connecteur du cœur des mammifères. *Arch Biol* 1936;47:2–70.
70. Anderson RH, Taylor IM. Development of atrioventricular specialized tissue in human heart. *Br Heart J* 1972;34:1205–1214.
71. Truex RC, Marino TA, Marino DR. Observations on the development of the human atrioventricular node and bundle. *Anat Rec* 1978;192:337–350.
72. Obrucnik M, Lichnovský V. Development of the conduction system of the human heart. *Folia Morphol (Praha)* 1980;28:278–281.
73. Doménech-Mateu JM, Arbó-Palau A, Martínez-Pozo A. Study of the development of the atrioventricular conduction system. *Anat Rec* 1991;230:73–85.
74. Wessels A, Vermeulen JL, Verbeek FJ, et al. An immunohistochemical analysis of the distribution of the neural tissue antigen GIN2 in the embryonic human heart. *Anat Rec* 1992;232:97–111.
75. Moorman AF, Christoffels VM. Development of the cardiac conduction system: a matter of chamber development. *Novartis Found Symp* 2003;250:25–34.
76. Lamers WH, Wessels A, Verbeek FJ, et al. New findings concerning ventricular septation in the human heart. Implications for maldevelopment. *Circulation* 1992;86:1194–1205.
77. Lamers WH, Moorman AF. Cardiac septation: a late contribution of the embryonic primary myocardium to heart morphogenesis. *Circ Res* 2002;91:93–103.
78. Ma L, Lu MF, Schwartz RJ, et al. Bmp2 is essential for cardiac cushion epithelial-mesenchymal transition and myocardial patterning. *Development* 2005;132:5601–5611.
79. Gaussin V, Morley GE, Cox L, et al. Alk3/Bmpr1a receptor is required for development of the atrioventricular canal into valves and annulus fibrosus. *Circ Res* 2005;97:219–226.
80. Christoffels VM, Hoogaars WMH, Tessari A, et al. T-box transcription factor Tbx2 represses differentiation and formation of the cardiac chambers. *Dev Dyn* 2004;229:763–770.
81. Harrelson Z, Kelly RG, Goldin SN, et al. Tbx2 is essential for patterning the atrioventricular canal and for morphogenesis of the outflow tract during heart development. *Development* 2004;131:5041–5052.
82. Chen YH, Ishii M, Sucov HM, et al. Msx1 and Msx2 are required for endothelial-mesenchymal transformation of the atrioventricular cushions and patterning of the atrioventricular myocardium. *BMC Dev Biol* 2008;8:75.
83. Boogerd KJ, Wong LY, Christoffels VM, et al. Msx1 and Msx2 are functional interacting partners of T-box factors in the regulation of connexin 43. *Cardiovasc Res* 2008;78:485–493.
84. Singh R, Horsthuis T, Farin HF, et al. Tbx20 interacts with smads to confine Tbx2 expression to the atrioventricular canal. *Circ Res* 2009;105:442–452.
85. Moskowitz IP, Kim JB, Moore ML, et al. A molecular pathway including Id2, Tbx5, and Nkx2-5 required for cardiac conduction system development. *Cell* 2007;129:1365–1376.
86. Aanhaanen WT, Mommersteeg MT, Norden J, et al. Developmental origin, growth, and three-dimensional architecture of the atrioventricular conduction axis of the mouse heart. *Circ Res* 2010;107:728–736.
87. Arguello C, Alanis J, Pantoja O, et al. Electrophysiological and ultrastructural study of the atrioventricular canal during the development of the chick embryo. *J Mol Cell Cardiol* 1986;18:499–510.
88. Patten BM. The development of the sinoventricular conduction system. *Univ Mich Med Bull* 1956;22:1–21.
89. Horsthuis T, Buermans HP, Brons JF, et al. Gene expression profiling of the forming atrioventricular node using a novel tbx3-based node-specific transgenic reporter. *Circ Res* 2009;105:61–69.
90. Virág Sz, Challice CE. The development of the conduction system in the mouse embryo heart. IV. Differentiation of the atrioventricular conduction system. *Dev Biol* 1982;89:25–40.
91. Bakker ML, Boukens BJ, Mommersteeg MT, et al. Transcription factor Tbx3 is required for the specification of the atrioventricular conduction system. *Circ Res* 2008;102:1340–1349.
92. Virág Sz, Challice CE. The development of the conduction system in the mouse embryo heart. II. Histogenesis of the atrioventricular node and bundle. *Dev Biol* 1977;56:397–411.
93. Janse MK, Anderson RH, van Capelle FJ, et al. A combined electrophysiological and anatomical study of the human fetal heart. *Am Heart J* 1976;91:556–562.
94. de Lange FJ, Moorman AF, Anderson RH, et al. Lineage and morphogenetic analysis of the cardiac valves. *Circ Res* 2004;95:645–654.
95. Kolditz DP, Wijffels MC, Blom NA, et al. Epicardium-derived cells in development of annulus fibrosus and persistence of accessory pathways. *Circulation* 2008;117:1508–1517.
96. Hahuri ND, Gittenberger-De Groot AC, Kolditz DP, et al. Accessory atrioventricular myocardial connections in the developing human heart. *Circulation* 2008;117:2850–2858.
97. Ko JK, Deal BJ, Strasburger JF, et al. Supraventricular tachycardia mechanisms and their age distribution in pediatric patients. *Am J Cardiol* 1992;69:1028–1032.
98. Peters NS, Rowland E, Bennett JG, et al. The Wolff-Parkinson-White syndrome: the cellular substrate for conduction in the accessory atrioventricular pathway. *Eur Heart J* 1994;15:981–987.
99. Aanhaanen WT, Boukens BJ, Sizarov A, et al. Defective Tbx2-dependent patterning of the atrioventricular canal myocardium causes accessory pathway formation in mice. *J Clin Invest* 2011;121:534–544.
100. Jansen JA, van Veen TA, de Bakker JM, et al. Cardiac connexins and impulse propagation. *J Mol Cell Cardiol* 2010;48:76–82.
101. Delorme B, Dahl E, Jarry-Guichard T, et al. Expression pattern of connexin gene products at the early developmental stages of the mouse cardiovascular system. *Circ Res* 1997;81:423–437.
102. Sedmera D, Reckova M, DeAlmeida A, et al. Spatiotemporal pattern of commitment to slowed proliferation in the embryonic mouse heart indicates progressive differentiation of the cardiac conduction system. *Anat Rec* 2003;274A:773–777.
103. Freedom RM, Yoo SJ, Perrin D, et al. The morphological spectrum of ventricular noncompaction. *Cardiol Young* 2005;15:345–364.
104. Mikawa T, Fischman DA. The polyclonal origin of myocyte lineages. *Annu Rev Physiol* 1996;58:509–521.
105. Grego-Bessa J, Luna-Zurita L, del Monte G, et al. Notch signaling is essential for ventricular chamber development. *Dev Cell* 2007;12:415–429.
106. Hertig CM, Kubalak SW, Wang Y, et al. Synergistic roles of neuregulin-1 and insulin-like growth factor-I in activation of the phosphatidylinositol 3-kinase pathway and cardiac chamber morphogenesis. *J Biol Chem* 1999;274:37362–37369.
107. Hall CE, Hurtado R, Hewett KW, et al. Hemodynamic-dependent patterning of endothelin converting enzyme 1 expression and differentiation of impulse-conducting Purkinje fibers in the embryonic heart. *Development* 2004;131:581–592.
108. Reckova M, Rosengarten C, DeAlmeida A, et al. Hemodynamics is a key epigenetic factor in development of the cardiac conduction system. *Circ Res* 2003;93:77–85.
109. Wagner M, Siddiqui MA. Signal transduction in early heart development (II): ventricular chamber specification, trabeculation, and heart valve formation. *Exp Biol Med (Maywood)* 2007;232:866–880.
110. Miquerol L, Moreno-Rascon N, Beyer S, et al. Biphasic development of the mammalian ventricular conduction system. *Circ Res* 2010;107:153–161.
111. Schram G, Pourrier M, Malnyk P, et al. Differential distribution of cardiac ion channel expression as a basis for regional specialization in electrical function. *Circ Res* 2002;90:939–950.
112. Davies MP, An RH, Doevendans P, et al. Developmental changes in ionic channel activity in the embryonic murine heart. *Circ Res* 1996;78:15–25.
113. Yokoshiki H, Tohse N. Developmental changes of ion channels. In: Sperelakis N, Kurachi Y, Terzic A, Cohen MV eds. *Heart Physiology and Pathophysiology*. 4th ed. San Diego, CA: Academic Press, 2000;719–735.
114. Sedmera D, Wessels A, Trusk TC, et al. Changes in activation sequence of embryonic chick atria correlate with developing myocardial architecture. *Am J Physiol* 2006;291:H1646–H1652.
115. Boyett MR, Honjo H, Kodama I. The sinoatrial node: a heterogeneous pacemaker structure. *Cardiovasc Res* 2000;47:658–687.
116. Joyner RW, van Capelle FJ. Propagation through electrically coupled cells. How a small SA node drives a large atrium. *Biophys J* 1986;50:1157–1164.
117. Lewis T, Meakins J, White PD. The excitatory process in the dog's heart. Part I. The auricles. *Phil Trans R Soc London* 1914;205:375.
118. Katz LN. The genesis of the electrocardiogram. *Physiol Rev* 1947;27:398–435.
119. Eyster JAE, Meek WJ. Experiments on the origin and conduction of the cardiac impulse. VI. Conduction of the excitation from the sinoauricular node to the right auricle and auriculoventricular node. *Arch Intern Med* 1916;18:775.
120. Liebman J. Are there internodal tracts? Yes. *Int J Cardiol* 1985;7:174–185.
121. James TN. The internodal pathways of the human heart. *Prog Cardiovasc Dis* 2001;43:495–535.
122. Spach MS, Lieberman M, Scott JG, et al. Excitation sequences of the atrial septum and the AV node in isolated hearts of the dog and rabbit. *Circ Res* 1971;29:156–172.
123. Hoogaars WM, Tessari A, Moorman AF, et al. The transcriptional repressor Tbx3 delineates the developing central conduction system of the heart. *Cardiovasc Res* 2004;62:489–499.
124. Blom NA, Gittenberger-de Groot AC, DeRuiter MC, et al. Development of the cardiac conduction tissue in human embryos using HNK-1 antigen expression: possible relevance for understanding of abnormal atrial automaticity. *Circulation* 1999;99:800–806.
125. Blom NA, Gittenberger-de Groot AC, Jongeneel TH, et al. Normal development of the pulmonary veins in human embryos and formulation of a morphogenetic concept for sinus venous defects. *Am J Cardiol* 2001;87:305–309.
126. Cavoto FV, Kellier GJ, Roberts J. Electrophysiological changes in the rat atrium with age. *Am J Physiol* 1974;226:1293–1297.
127. Gennser G, Nilsson E. Excitation and impulse conduction in the human fetal heart. *Acta Physiol Scand* 1970;79:305–320.
128. Tuganowski W, Cekanski A. Electrical activity of a single fibre of the human embryonic heart. *Pflügers Arch* 1971;323:21–26.

129. Escande D, Loisanse D, Planche C, et al. Age-related changes of action potential plateau shape in isolated human atrial fibers. *Am J Physiol* 1985;249:H843-H850.
130. DuBrow IW, Fisher EA, Amat-y-Leon F, et al. Comparison of cardiac refractory periods in children and adults. *Circulation* 1975;51:485-491.
131. Pickoff AS, Singh S, Flinn CJ, et al. Atrial vulnerability in the immature canine heart. *Am J Cardiol* 1985;55:1402-1406.
132. Strasburger JF, Cheulkar B, Wichman HJ. Perinatal arrhythmias: diagnosis and management. *Clin Perinatol* 2007;34:627-652.
133. Lloyd TR, Baldwin HS. Emulation of conduction system functions in the hearts of early mammalian embryos. *Pediatr Res* 1990;28:425-428.
134. Lamers WH, te Kortschot A, Los JA, et al. Acetylcholinesterase in prenatal rat heart: a marker for the early development of the cardiac conductive tissue? *Anat Rec* 1987;217:361-370.
135. van Veen TA, van Rijen HVM, Op't Hof T. Cardiac gap junction channels: modulation of expression and channel properties. *Cardiovasc Res* 2001;51:217-229.
136. Kahler C, Schleussner E, Grimm B, et al. Fetal magnetocardiography: development of the fetal cardiac time intervals. *Prenat Diagn* 2002;22:408-414.
137. Waki K, Kim JS, Becker AE. Morphology of the human atrioventricular node is age dependent: a feature of potential clinical significance. *J Cardiovasc Electrophysiol* 2000;11:1144-1151.
138. Pickoff AS, Singh S, Flinn CJ, et al. Maturation changes in ventriculo-atrial conduction in the intact canine heart. *J Am Coll Cardiol* 1984;3:162-168.
139. McCormack J, Gelband H, Xu H, et al. Atrioventricular nodal function in the immature canine heart. *Pediatr Res* 1988;23:99-103.
140. Hewett KW, Gaymes CH, Noh C-I, et al. Cellular electrophysiology of neonatal and adult rabbit atrioventricular node. *Am J Physiol* 1991;260:H1674-H1684.
141. Preston JB, McFadden S, Moe GK. Atrioventricular transmission in young mammals. *Am J Physiol* 1959;197:236-240.
142. Moore EN. Atrioventricular transmission in newborn calves. *Ann NY Acad Sci* 1965;127:113-126.
143. Gough WB, Moore EN. The differences in atrioventricular conduction of premature beats in young and adult goats. *Circ Res* 1975;37:48-58.
144. Cohen MI, Wieand TS, Rhodes LA, et al. Electrophysiologic properties of the atrioventricular node in pediatric patients. *J Am Coll Cardiol* 1997;29:403-407.
145. van Hare GF. Developmental aspects of atrioventricular node reentry tachycardia. *J Electrocardiol* 2008;41:480-482.
146. Katritsis DG, Camm AJ. Atrioventricular nodal reentrant tachycardia. *Circulation* 2010;122:831-840.
147. Rothenberg F, Nikolski VP, Watanabe M, et al. Electrophysiology and anatomy of embryonic rabbit hearts before and after septation. *Am J Physiol* 2005;288:H344-H351.
148. Kirchhoff S, Kim JS, Hangendorff A, et al. Abnormal cardiac conduction and morphogenesis in connexin 40 and connexin 43 double deficient mice. *Circ Res* 2000;87:399-405.
149. Gutstein DE, Morley GE, Tamaddon H, et al. Conduction slowing and sudden arrhythmic death in mice with cardiac-restricted inactivation of connexin 43. *Circ Res* 2001;88:333-339.
150. Couch JR, West TC, Hoff HE. Development of the action potential of the prenatal rat heart. *Circ Res* 1969;24:19-31.
151. Sperelakis N, Shigenobu K. Changes in membrane properties of chick embryonic hearts during development. *J Gen Physiol* 1972;60:430-453.
152. Shigenobu K, Sperelakis N. Development of sensitivity to tetrodotoxin of chick embryonic hearts with age. *J Mol Cell Cardiol* 1971;3:271-286.
153. Rosen MR, Legato MJ, Weiss RM. Developmental changes in impulse conduction in the canine heart. *Am J Physiol* 1981;240:H546-H554.
154. Danilo P, Reder RF, Binah O, et al. Fetal canine cardiac Purkinje fibers: electrophysiology and ultrastructure. *Am J Physiol* 1984;246:H250-H260.
155. Legato MJ, Weintraub M, McCord GM, et al. The morphology of the developing canine conducting system: bundle branch and Purkinje cell architecture from birth to week 12 of life. *J Mol Cell Cardiol* 1991;23:1063-1076.
156. Forsgren S, Carlsson E, Strehler E, et al. Ultrastructural identification of human fetal Purkinje fibres: a comparative immunocytochemical and electron microscopic study of composition and structure of myofibrillar M-regions. *J Mol Cell Cardiol* 1982;14:437-449.
157. Untereker WJ, Danilo P Jr, Rosen MR. Developmental changes in action potential duration, refractoriness, and conduction in the canine ventricular conducting system. *Pediatr Res* 1984;18:53-58.
158. Ho SY. Clinical pathology of the cardiac conduction system. *Novartis Found Symp* 2003;250:210-221.
159. Kurosawa H, Becker AE. *Atrioventricular Conduction in Congenital Heart Disease: Surgical Anatomy*. Berlin, Germany: Springer-Verlag, 1987.
160. Anderson RH, Becker AE, Arnold R, et al. The conducting tissues in congenitally corrected transposition. *Circulation* 1974;50:911-923.
161. Thiene G, Wenink AC, Frescura C, et al. Surgical anatomy and pathology of the conduction tissues in atrioventricular defects. *J Thorac Cardiovasc Surg* 1981;82:928-937.

George F. Van Hare ■ Anne M. Dubin

In this era of easily available high-resolution imaging techniques, does electrocardiography (ECG) still have a place in the diagnosis and management of children with congenital heart disease? Certainly, for the noninvasive diagnosis of arrhythmias and cardiac conduction disorders, there is no substitute for careful analysis of the ECG. In addition to the assessment of arrhythmias, the ECG is important in the diagnosis and management of heart disease in children. Although rarely diagnostic of the type of congenital heart disease, the ECG should be thought of in the same way as the physical examination. It provides clues to the likely diagnosis, provides information about the severity of the condition, and may be indicative of other associated problems. Additionally, review of the ECG may identify important discrepancies as compared with the patient's presumed diagnosis, prompting further testing or a more careful review of the existing data. Most experienced pediatric cardiologists consider a cardiology consultation incomplete without a review of the ECG.

THE HISTORY OF ELECTROCARDIOGRAPHY

Although Augustus Waller was the first to record an ECG in a human (1), Willem Einthoven of The Netherlands is considered the father of electrocardiography. In 1901, Einthoven published a description of the string galvanometer, a device ideally suited for recording the rapidly changing and weak currents of cardiac electrical activity present on the body surface (2). During subsequent work, Einthoven identified the major waveforms of the ECG, and initially named them A, B, C, and D. He subsequently changed the naming system to P, Q, R, S, and T waves (Fig. 15.1), leaving room at either end of the alphabet for naming of new, as yet undiscovered, waves (as later came to pass when the U wave was described). The string galvanometer proved useful for the study of the ECG. The investigations of Einthoven and Sir Thomas Lewis dominated the early years of ECG studies, and they are credited with bringing the ECG to the bedside (3). This was not anticipated by Waller: "I certainly had no idea that the electrical signs of the heart's action could ever be utilized for clinical investigation" (1). Recordings in children followed, and Ziegler (4) reviewed the early reports on the use of the ECG in children. In 1913, Hecht published a "comprehensive" study, evaluating all three standard bipolar leads (I, II, III) in ECG tracings from hundreds of premature infants, term infants, and children with normal and abnormal hearts. By the late 1930s, the distinctive developmental changes that occur in the ECGs of normal infants and children had been described (4).

PRINCIPLES AND TECHNICAL CONSIDERATIONS IN RECORDING THE ELECTROCARDIOGRAM

The Scalar Electrocardiogram

The heart is an electrically active organ, and the current flows that result in cardiac contraction can be recorded from the body surface. How these electrical events are transmitted to the body surface is a complex topic and involves characteristics both of the heart as a current source as well as of the chest, which acts as a conductor (5,6). These characteristics change in the presence of congenital defects and other forms of cardiac disease as well as with normal growth and development.

The basic principle of the ECG is that electrical potentials generated by the heart can be accounted for by considering these electrical events to be equivalent to those generated by a dipole source in a homogeneous volume conductor (the equivalent dipole model). This concept has the limitation of seriously oversimplifying these events, especially in the assumption of homogeneity of conduction through the chest. The scalar ECG can be thought of as the record of voltage variation of this dipole with respect to time, in the particular orientation of the lead recorded. Cardiac electrical activity, of course, generates potentials in three dimensions, so any particular lead provides a very small amount of the potentially available information that can be recorded. For this reason, the conventional ECG includes 12 or 15 leads, arranged to give recordings along a variety of lead orientations to better represent the cardiac activity in three dimensions. The choice of these leads evolved as studies of the ECG progressed and, in retrospect, may not represent the best of all possible lead systems. However, these particular leads are deeply entrenched in modern cardiology practice.

Electrocardiographic interpretation begins with artifact-free ECG recordings. In addition to accurate electrode placement, cleaning of the skin with alcohol or acetone is essential to lower the skin resistance. ECG recordings in active infants and toddlers can be a technical challenge.

The standard ECG record consists of 12 leads recorded from nine body surface locations with the patient in the supine position (7). The ideal recorder should have the capability of displaying 3 to 12 leads simultaneously. The standard configuration usually is modified in children and adults with congenital heart disease, to record additional right (V3R, V4R) and left (V7) chest leads. Interpretation of rhythm disturbances ideally is accomplished by viewing a rhythm strip with 12 simultaneously recorded leads so that transient events, such as premature beats, can be assessed in all leads simultaneously.

Electrocardiograms can be recorded at various "paper speeds" and at various voltage standardizations (although

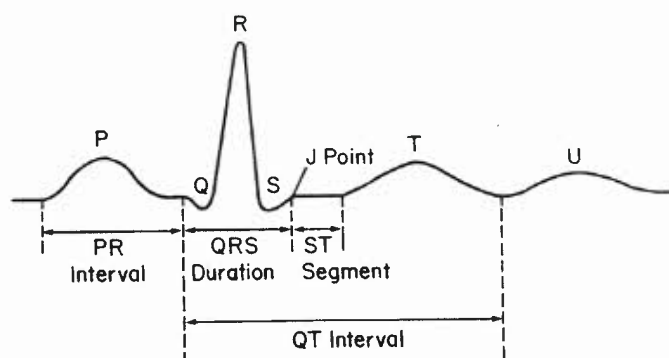


Figure 15.1. Scalar ECG showing P, Q, R, S, T, and U waves. The J point is shown, as well as the standard intervals (PR interval, QRS duration, ST segment, and QT interval).

modern systems acquire the tracings digitally and may be interpreted online without ever being printed on paper). Paper speeds of 12.5, 25, and 50 mm/s have been used, but 25 mm/s is standard. Standard ECG recording paper has major time divisions at 5-mm intervals and minor time divisions at 1-mm intervals. Therefore, at a paper speed of 25 mm/s, each large block corresponds to 0.20 seconds (200 ms), and 1 second is represented by five large blocks. Each small block represents 0.04 seconds (40 ms). In terms of voltage, full standardization refers to 1.0 mV/10 mm in vertical deflection on the recording, whereas half standardization refers to 0.5 mV/10 mm. It is important that the ECG reader always checks standardization prior to interpreting the ECG because the use of half standardization is common when large voltages cause overlap between leads. The choice of paper speed and gain may have an impact on the reproducibility of interval measurements (8). With the exception of the signal-averaged ECG, it is uncommon to discuss or report ECG voltages in terms of millivolts. It is much more common to discuss them in terms of millimeters of amplitude at full standardization. Therefore, for the remainder of this chapter, millimeters at full standardization is used rather than millivolts.

Vectorcardiography

Vectorcardiography was developed to correct some basic limitations of the conventional lead system and to display the data obtained by the ECG in a potentially more useful format. The dipole varies in magnitude and direction with time. The scalar ECG allows the presentation of the magnitude only, as it varies with time, and one needs to infer the direction of forces from the lead chosen. Each instant, the heart generates a force that has both magnitude and direction. This vector force changes with time and traces a loop during the duration of the QRS complex, which occupies all three dimensions. The vectorcardiography lead system allows a reasonably faithful representation of this three-dimensional loop as two-dimensional frontal, sagittal, and horizontal planes (Fig. 15.2). Several lead systems have been used. They each have their advantages and disadvantages. The Frank (9) system has been the most widely used, but the McFee system also has been used. The QRS vectorcardiogram, then, consists of a loop that starts at the beginning of the QRS, ends with the end of the QRS, and is displayed on paper in three planes.

Because of the need for special equipment, technical expertise, and the inconvenience of multiple leads, vectorcardiograms rarely are obtained in modern pediatric cardiology practice. Also, because of high-quality echocardiography,

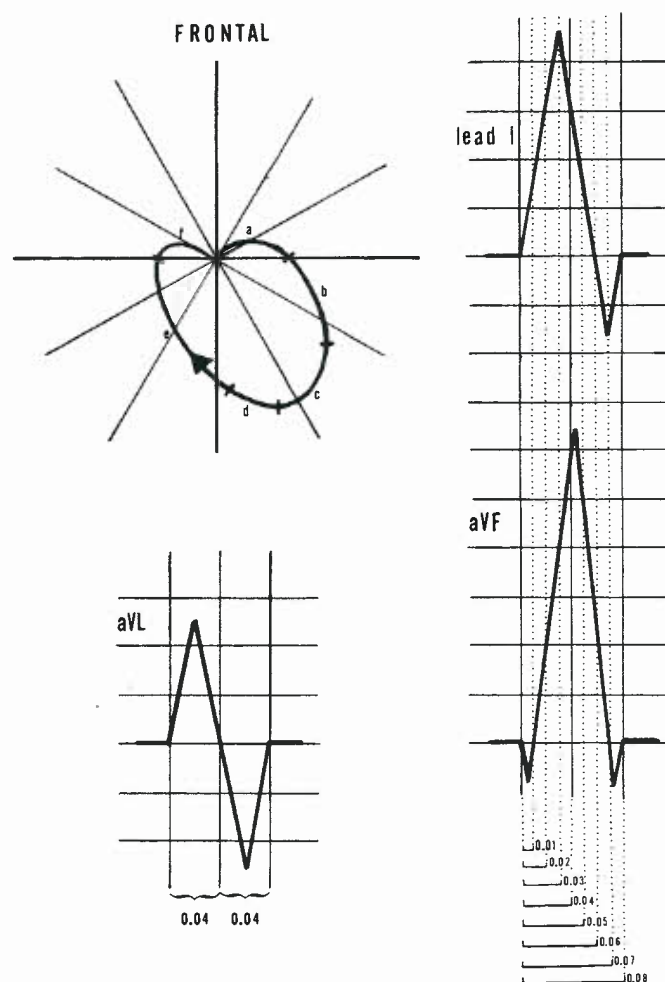


Figure 15.2. Diagrammatic representation of a typical normal frontal plane vector loop (top left) with corresponding scalar ECG leads I, aVL, and aVF. The loop is clockwise in the frontal plane and lasts for 0.08 seconds. Each lettered segment corresponds to a portion of the QRS interval: a, 0 to 0.01 seconds; b, 0.01 to 0.03 seconds; c, 0.03 to 0.04 seconds; d, 0.04 to 0.055 seconds; e, 0.055 to 0.07 seconds; f, 0.07 to 0.08 seconds.

vectorcardiography has limited utility. Still, the best electrocardiographers think in terms of vectors even when interpreting the scalar ECG. Rather than memorizing patterns of QRS morphology and axis, they view the standard scalar ECG as a representation of the vector forces that vary with time, and perhaps understand the ECG better than those who simply “pattern read.”

Body Surface Mapping

A natural extension of the technique of ECG and vectorcardiography is the use of body surface mapping. To obtain the spatial-temporal representation of cardiac electrical potentials on the body surface, simultaneous measurement of potentials are needed at a number of sites (from 24 to 200) on the anterior and posterior torso. Several excellent reviews have addressed the specific details, including number and location of electrodes (10), electrode type (11), sample rate (12), digital collection and processing of ECG signals (13,14), and construction of maps (13). These techniques

are investigational and require specialized equipment and a high level of computerization. Recent developments in solving the "inverse problem" in electrocardiology have allowed for so-called electrocardiographic imaging in which epicardial potentials are computed from information available on the body surface. This approach has shown promise in the noninvasive evaluation of cardiac conduction abnormalities such as Wolff-Parkinson-White (WPW) syndrome and other electrical abnormalities of the heart (15).

Esophageal Electrocardiography

Because the esophagus normally is behind the left atrium and is in close proximity to the heart, an electrode placed in the esophagus will record atrial activity more locally than the standard ECG leads (16). This is especially useful in evaluating cardiac rhythm disturbances, particularly in situations where the P wave is difficult to find on the surface ECG (3). For example, when there is atrial flutter with 2:1 atrioventricular (AV) conduction, flutter waves may not be obvious on the surface ECG. Even if one observes atrial activity on the surface ECG, it may not be apparent that there are twice as many atrial deflections as ventricular deflections. The esophageal ECG solves this problem by recording atrial electrograms that are as large as or larger than the simultaneously recorded ventricular electrograms.

To obtain artifact-free esophageal ECGs, a soft bipolar electrode that has widely spaced large electrodes is used. Several are commercially available from 7 to 10 F in size. The catheter is positioned at the proper site and the signal filtered, usually employing band-pass filtering at 10 to 1,000 Hz, to eliminate the low-frequency respiratory artifact (16). Electrode placement is similar to nasogastric tube placement. The insertion depth for recording the maximum atrial deflection can be estimated from the patient's height (17,18). The ideal position is the site at which the atrial electrogram is about equal to the ventricular electrogram amplitude, and both are as large as possible. Positioning too distally will yield a large ventricular electrogram and a small atrial electrogram, and positioning too proximally will yield low amplitudes of both electrograms.

Signal-Averaged Electrocardiography

Under normal circumstances, the amplitude of P waves and ST segments is <2.5 mm, and T waves do not exceed 10 mm in the precordial leads. On the other hand, precordial R and S waves may have amplitudes of 30 to 40 mm. Interest in low-level potentials has led to the development of the signal-averaged ECG as a way of eliminating noise, which may exceed 0.03 mV peak to peak, and improving the signal-to-noise ratio.

The principal interest in the signal-averaged ECG has been to identify small high-frequency potentials either during the PR interval or during late QRS and ST segment (19). High-frequency potentials during the ST segment may result from areas of slow conduction that have been observed in myocardial infarction and associated ventricular arrhythmias (20). Interest in high-frequency potentials during the PR interval has focused on detecting depolarization within the His-Purkinje system.

The basic principle is that averaging a periodic, repetitive signal will reduce random noise to <0.001 mV, thereby enhancing the detection of low-amplitude signals. The signals are recorded at very high gain and are band-pass filtered. Waveforms usually are averaged over several minutes. Sensitivity and specificity of the technique for predicting adult patients at risk for ventricular arrhythmias have been reported. Reports of this technique for pediatric patients have been limited (21),

but it has been used to identify patients with arrhythmogenic right ventricular dysplasia (22).

24-Hour Ambulatory Electrocardiography

Named after Dr. N. J. Holter (23), the 24-hour ambulatory ECG, or Holter ECG, is an important tool in the diagnostic armamentarium of the pediatric cardiologist. It is used for various indications and is, perhaps, the most effective method to diagnose transient events such as AV block and other conduction disorders.

Modern Holter equipment records two or three channels of the ECG for 24 hours, either onto a cassette tape or digitally into a flash memory card in the recorder (24). The digital recording system has the advantage of being smaller and lighter and avoids the mechanical problems of cassette tape drag and damaged tapes. The ECG leads chosen for recording generally are modified chest leads and most closely resemble leads V1 and V5. The ECG is obtained using chest leads that are applied after adequate skin preparation, and the chest is often wrapped in an elastic bandage. The recorder can be worn on the belt, placed in a backpack, or suspended from a strap. The recorders have a digital clock for linking events with actual times, as well as a patient-activated event marker that allows the patient to annotate episodes of cardiac symptoms.

The recording is scanned using a computerized analysis system that provides both a full disclosure of the entire recording, as well as summary data regarding average, maximum, and minimum heart rates. Computerized algorithms allow the identification, characterization, and enumeration of premature atrial and ventricular contractions, as well as higher grades of ectopy and episodes of abnormal tachycardia. The patient keeps a diary of events while wearing the Holter recorder, and any such episodes of interest can be printed out and evaluated as part of the scanning process. The algorithms for arrhythmia diagnosis are limited in their applicability to pediatric patients, and the technician who scans and prints the report must be experienced in pediatric Holter scanning and supervised by a pediatric cardiologist (25–27).

Transtelephonic Event Recording

One limitation of Holter monitoring is that to record a transient symptomatic event, the event must occur spontaneously during the period that the patient is wearing the recorder. Thus, Holter monitoring often fails to record such events when they do not occur many times per day. Accordingly, to capture a symptomatic event, transtelephonic event recording allows longer periods of monitoring in a cost-effective manner (28,29). Several types of recorders are available. The simplest is a small device that records a single ECG channel for 30 to 60 seconds into the memory of the device when a button is pushed. It may have electrodes built into the device that contact the chest, or can be attached to the patient by several ECG electrodes or by wrist electrodes. These recorders have the disadvantage that the episode must be long enough for the recorder to be applied. This problem can be minimized by using a recorder that resembles a wristwatch, does not require additional electrodes, and can be worn continuously. An alternative to this simple type of recorder is the so-called memory-loop recorder. This recorder resembles a small Holter recorder, is attached to the patient by means of chest electrodes, and is worn continuously. Rather than recording and storing all the ECG data while worn, the device temporarily stores about 60 seconds of ECG data. When the patient experiences a symptom, he or she presses a button on the unit, causing it to store the 30 seconds of data that occurred prior

to pressing the button as well as a short amount of data following the episode.

The recorder stores the episode as an oscillatory audio signal. After an episode is captured by the recorder, the patient or a parent can transmit the ECG by playing back the stored audio signal over the telephone to the monitoring center, where the ECG is converted back to an ECG waveform and printed out for interpretation.

Also available are implantable loop recorders (ILR), which are implanted in the subcutaneous tissue on the chest wall and are active for up to 3 years. The device incorporates a continuous loop recording of the heart rhythm that is stored when the device is activated by the patient or parent. There is also an autoactivation component that allows the device to automatically record rhythms that are out of a preset range. Remote monitoring is available so that patients can transmit recorded data over phone lines using equipment at home (30). This device is useful for pediatric patients with syncope and/or palpitations (31). These are ideal when noninvasive methods have failed to document the rhythm particularly in cases of very infrequent events.

HOW TO READ A PEDIATRIC ELECTROCARDIOGRAM

An organized approach to evaluating the ECG is important to avoid failure to consider each characteristic of the ECG. Many advise that these characteristics be evaluated in a particular order, for example, by assessing the P wave first, the QRS second, and so on. The order, of course, is less important than a careful review of all the aspects of the recording (Table 15.1). Often pediatric ECGs are interpreted in light of extensive knowledge of the patient's condition. Clearly, the more information the reader has about the patient's condition, the more relevant the ECG interpretation will be. However, one often reads ECGs with no clinical information except the patient's age. For this reason, the ECG is considered a laboratory test. ECG attributes (e.g., intervals, voltages) are distributed within

a population. Thus, the prevalence of an abnormality depends on the normal cutoff points one picks. Just as the presence of a murmur does not necessarily mean that a patient has valvular stenosis, an "abnormal" ECG does not necessarily mean that the patient has heart disease. An example of this pitfall is the presence of a chest deformity (e.g., pectus excavatum or scoliosis) about which the ECG reader may not have information and needs to interpret the ECG. Even if the reader knows about the deformity, he or she may not know what constitutes normal for such a situation.

Pediatric ECG features are age dependent (Table 15.2). The PR interval, ST segment, and T wave are heart rate dependent as well. The most comprehensive tabulation of age- and heart rate-dependent ECG measures was provided by Davignon et al. (32,33).

The zero-voltage baseline, which is the reference level for ECG voltage measurements, is based on the fact that no potential differences exist on the body surface at that instant. At slow heart rates, the T-P or U-P interval is a good approximation of the voltage baseline. At faster heart rates, the P wave may be superimposed on the previous T-U wave. In this situation, the PR segment is the best alternative. When measuring a large deflection, choice of baseline selection is relatively unimportant. However, when measuring a low-level potential (e.g., ST segment), or attempting to determine onset of a waveform (e.g., QRS), choice of the baseline is critical—maybe as important as the measurement of interest.

Detailed descriptions of arrhythmia diagnosis are found elsewhere in this text. Likewise, the ECG patterns characterizing various forms of complex congenital heart disease are addressed in the chapters dealing with those diseases.

Rate and Rhythm

Ventricular Rate

Heart rate is determined by measuring the R-R interval. It often is more useful to think of cycle length than heart rate, because on the standard ECG there seldom is an entire minute's worth of heartbeats to count. Cycle length and heart rate have a reciprocal relationship. Cycle length (in milliseconds) is measured directly as the R-R interval. Heart rate is calculated by dividing the measured cycle length by 60,000 ms/min. Heart rate is highly dependent on age, body temperature, autonomic tone, and physical activity. For example, in a 14-year-old, a resting heart rate (cycle length) of 150 beats per minute (400 ms) would be abnormally high. However, it might be a perfectly normal rate for an apprehensive toddler during ECG recording. Similarly, a resting heart rate of 50 beats per minute (1,200 ms) in a healthy adolescent would be normal, whereas the same heart rate in an infant would signify bradycardia.

Origin of the Pacemaker

On most ECGs, there will be normal AV conduction with P waves preceding each QRS complex. It is important to determine if the P wave originates from the sinus node or elsewhere. The vector of a sinus P wave is from top to bottom and right to left (positive in leads I, II, and aVF). The P wave in sinus rhythm is biphasic in lead V1, initially being upright followed by a brief downward deflection. If the P wave does not have these characteristics, it does not originate from the sinus node and has an "ectopic" location. One must ascertain its origin, for example, a rhythm in which the P wave is inverted in leads I and aVL is termed a left atrial rhythm, whereas a P wave that is inverted in leads II, III, and aVF is termed a low right atrial rhythm (also known as a coronary sinus rhythm).

The rhythm may be regular, irregular, or regular with intermittent but predictable phases of irregularity. The last would

TABLE 15.1 Characteristics for Evaluation of the Electrocardiogram

Rate and rhythm
Ventricular rate
Origin of the pacemaker
AV conduction
Atrial enlargement/hypertrophy
Ventricular depolarization
QRS axis deviation
Bundle branch blocks
Pre-excitation
Hypertrophy
Initial forces
Ventricular repolarization
QT interval
ST segment, T wave, and U waves

TABLE 15.2 Normal ECG Standards for Children by Age

	0–1 d	1–3 d	3–7 d	7–30 d	1–3 mo	3–6 mo	6–12 mo	1–3 y	3–5 y	5–8 y	8–12 y	12–16 y
Heart rate per minute	94–155 (122)	91–158 (122)	90–166 (128)	86–182 (149)	120–179 (149)	105–185 (141)	108–169 (131)	89–152 (119)	73–137 (109)	65–133 (100)	62–130 (91)	60–120 (80)
Frontal plane QRS axis (degrees)	59–189 (135)	64–197 (134)	76–191 (133)	0–160 (109)	30–115 (75)	7–105 (60)	6–98 (55)	7–102 (55)	6–104 (56)	10–139 (65)	6–116 (60)	9–128 (59)
PR lead II (s)	0.08–0.16 (0.107)	0.08–0.14 (0.108)	0.07–0.15 (0.102)	0.07–0.14 (0.100)	0.07–0.13 (0.098)	0.07–0.15 (0.105)	0.07–0.16 (0.106)	0.08–0.15 (0.113)	0.08–0.16 (0.119)	0.09–0.16 (0.123)	0.09–0.17 (0.128)	0.09–0.18 (0.135)
QRS duration, V5 (s)	0.02–0.07 (0.05)	0.02–0.07 (0.05)	0.02–0.07 (0.05)	0.02–0.08 (0.05)	0.02–0.08 (0.05)	0.02–0.08 (0.05)	0.03–0.08 (0.05)	0.03–0.08 (0.06)	0.03–0.07 (0.06)	0.03–0.08 (0.06)	0.04–0.09 (0.06)	0.04–0.09 (0.07)
P-wave amplitude, lead II	0.5–2.8 (1.6)	0.3–2.8 (1.6)	0.7–2.9 (1.7)	0.7–3.0 (1.9)	0.7–2.6 (1.5)	0.4–2.7 (1.6)	0.6–2.5 (1.6)	0.7–2.5 (1.5)	0.3–2.5 (1.4)	0.4–2.5 (1.4)	0.3–2.5 (1.4)	0.3–2.5 (1.4)
Q-wave amplitude, aVF	0.1–3.4 (1.0)	0.1–3.3 (1.0)	0.1–3.5 (1.1)	0.1–3.5 (1.2)	0.1–3.4 (0.9)	0–3.2 (0.9)	0–3.3 (1.0)	0–3.2 (0.9)	0–2.9 (0.6)	0–2.5 (0.6)	0–2.7 (0.5)	0–2.4 (0.4)
Q-wave amplitude, V6	0–1.7 (0.1)	0–2.2 (0.1)	0–2.8 (0.1)	0–2.8 (0.4)	0–2.6 (0.3)	0–2.6 (0.3)	0–3.0 (0.4)	0–2.8 (0.6)	0.1–3.3 (0.8)	0.1–4.6 (0.8)	0.1–2.8 (0.6)	0–2.9 (0.4)
R amplitude, V1	5–26 (13)	5–27 (15)	3–25	3–12 (12)	3–19 (10)	3–20 (10)	2–20 (9) (10)	2–18	1–18 (8) (8)	1–14 (7)	1–12 (5)	1–10 (4)
S amplitude, V1	1–23 (8)	1–20 (9)	1–17 (7)	0–11 (4)	0–13 (5)	0–17 (6)	1–18 (7)	1–21 (8)	2–22 (10)	3–23 (12)	3–25 (12)	3–22 (11)
R amplitude, V6	0–12 (4)	0–12 (5)	1–12 (5)	3–16 (8)	5–21 (12)	6–22 (13)	6–23 (13)	6–23 (13)	8–25 (15)	8–26 (16)	9–25 (16)	7–23 (14)
S amplitude, V6	0–10 (4)	0–9 (3)	0–10 (4)	0–10 (3)	0–7 (3)	0–10 (3)	0–8 (2)	0–7 (2)	0–6 (2)	0–4 (1)	0–4 (1)	0–4 (1)
R/S ratio, V1	0.1–9.9 (2.2)	0.1–6 (2.0)	0.1–9.8 (2.8)	1.0–7.0 (2.9)	0.3–7.4 (2.2)	0.1–6.0 (2.3)	0.1–4.0 (1.8)	0.1–4.3 (1.4)	0.03–2.7 (0.9)	0.02–2.0 (0.8)	0.02–1.9 (0.6)	0.02–1.8 (0.5)
R/S ratio, V6	0.1–9 (2)	0.1–12 (3)	0.1–10 (2)	0.1–12 (4)	0.2–14 (5)	0.2–18 (7)	0.2–22 (8)	0.3–27 (10)	0.6–30 (11)	0.9–30 (12)	1.5–33 (14)	1.4–39 (15)

All values are 2nd percentile to 98th percentile (mean). All amplitudes of waves are given in millimeters at full standardization, that is, 1 mm = 10 mV.
 Derived from percentile charts in Davignon A, Rautaharju P, Boisselle E, et al. Normal ECG standards for infants and children. *Pediatr Cardiol* 1979;1:123–152.

be a description of phasic sinus arrhythmia, which results from normal autonomic effects influences that mediate accelerations and decelerations of the sinus node in response to respiration. One also may observe tachyarrhythmias such as atrial tachycardia or AV reciprocating tachycardia rather than sinus rhythm.

Atrioventricular Conduction

One assesses conduction both by measurement of the PR interval and the relationship of P waves to QRS complexes. The PR interval is age, activity, and heart rate dependent. Impaired AV conduction is described as first-, second-, or third-degree AV block. Abbreviated conduction, manifested by a short PR interval, occurs in WPW syndrome, glycogen storage disease, and the presence of a low atrial pacemaker located closer to the AV node.

Atrial Enlargement and Hypertrophy

The right atrium is to the right, superior, and anterior to the left atrium. During normal sinus rhythm, the right atrium begins to depolarize before the left atrium, so that the first 0.04 to 0.06 seconds of the P wave are due mostly to right atrial activation. Thus, effects of atrial enlargement may be manifested early, to the left and inferior (right atrial) or late and posterior (left atrial) portion of the P wave. If sinus rhythm is not present, for example, with an ectopic atrial rhythm or an electronic atrial pacemaker, these criteria are not applicable. The ECG criterion for right atrial enlargement is the presence of a peaked, tall P wave in lead II (Fig. 15.3). The upper limit of normal for the P wave amplitude is 2.5 mm over the age of 6 months, and 3.0 mm from 0 to 6 months (Table 15.2). This can be accompanied by a biphasic or tall P wave in lead V1. The criteria for left atrial enlargement include a broad notched P wave in lead II (P-wave duration >0.10 to 0.12 seconds) and/or a deep, slurred biphasic P wave in V1, particularly when the terminal negative component is broad and deep. Biatrial enlargement is considered to be present when signs of both right and left atrial enlargement are present.

Ventricular Depolarization

Normally, ventricular depolarization occurs virtually simultaneously at many sites, resulting in a QRS of brief duration. QRS duration is age dependent (Table 15.2). It is <80 ms from infancy through age 8 years, and <90 ms throughout childhood and early adolescence. QRS duration is an objective measure that can be determined reliably using computerized ECG recording systems. QRS duration may be prolonged by right or left bundle branch block (LBBB), ventricular preexcitation, or a ventricular pacemaker. The term *intraventricular conduction delay* is reserved for those situations when QRS is prolonged but does not fit any of the above categories.

Axis Deviation

Axis is an ECG measurement derived from the equivalent dipole model. The electrical axis is the direction of the predominant vector of a wavefront in the frontal plane. It is a physiologic abstraction and an oversimplification because it does not take into account the time-dependent changes in vector forces that occur during atrial and ventricular depolarization. Still, it has been a popular ECG measure, and some prefer to call the axis the mean frontal plane vector. The simplest way to present the concept is to represent leads I and aVF on a Cartesian system (Fig. 15.4), designating lead I as 0 (left) to 180 degrees (right) and lead aVF as 90 (inferior) to 270 degrees (superior), with the other limb leads corresponding to other angles in the frontal plane. The axis can be calculated for all three waves of the ECG. For example, using the system shown in Figure 15.4, one first determines a quadrant by looking at leads I and aVF. Once the quadrant is established, the frontal lead, which is most isoelectric, is identified. The mean QRS axis is perpendicular to this lead.

QRS and P axes are measured reliably by automated ECG interpretation systems, and normal values have been tabulated (4,32,33). However, the same concepts can be applied to the ST segment, initial part of the QRS complex, and so on.

Frontal plane QRS axis deviation is age dependent. Right axis deviation is present when the QRS axis is more positive

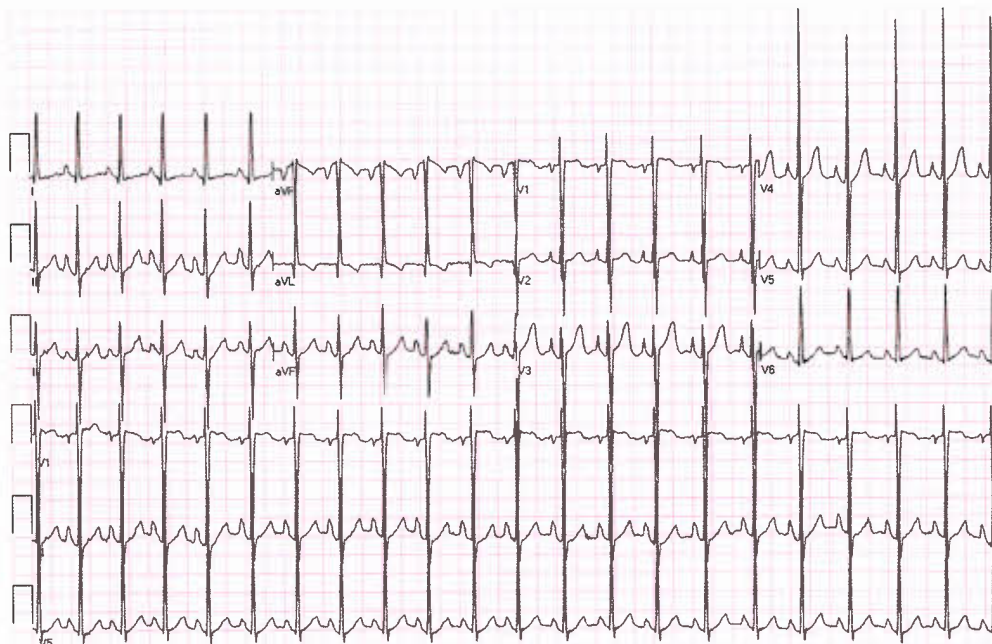


Figure 15.3. A 6-month-old with tricuspid atresia and normally related great vessels. The ECG shows right atrial enlargement and left axis deviation.

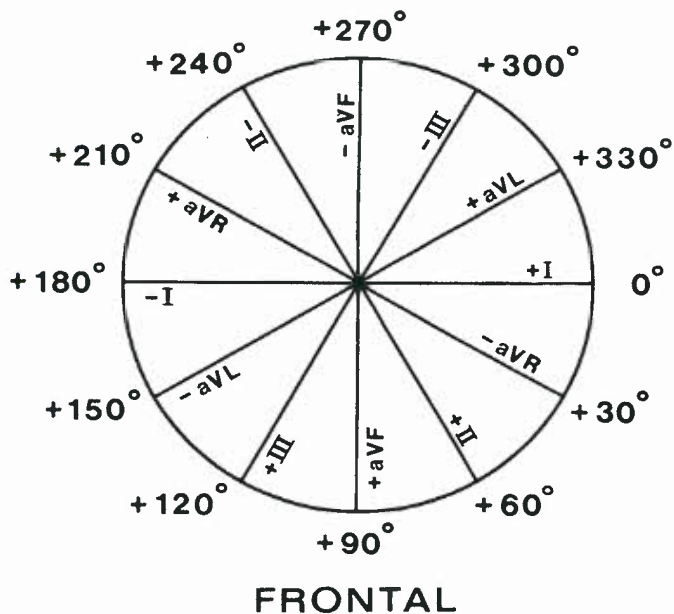


Figure 15.4. Reference frame for the frontal plane according to Einthoven's equilateral triangle. The lines are drawn through the center to the negative terminus of each lead. Thus, the 360 degrees are divided into multiple 30-degree sections.

than normal, and left axis deviation is present when the QRS axis is less than normal. Right axis deviation is a criterion for right ventricular hypertrophy (RVH), albeit a very poor one. In pediatric patients, left axis deviation is not a criterion for left ventricular hypertrophy (LVH). The QRS axis is *superior* when it is between -60 and -100 degrees. The axis is *indeterminate* (neither left nor right or northwest) when it is between -100 degrees and $+210$ degrees.

The most important pattern in pediatric patients is the so-called abnormally superior vector or abnormally superior axis. This occurs in patients with AV septal (canal) defects. The main QRS axis is superior, but the initial forces are inferior,

so that leads II, III, and aVF inscribe a small r wave followed by a large S wave. This pattern of initial forces separates the abnormally superior vector from other causes of axis deviation (Fig. 15.5).

Bundle Branch Block

Bundle branch block exists when there is prolongation of the QRS. Because the distal conduction system is divided into left and right bundle branches, which depolarize the left and right ventricles respectively, block in one of the bundle branches will lead to delayed activation of the corresponding ventricle. Thus, the diagnosis is based on knowledge of anatomy and analysis of the terminal vector forces of the QRS complex. For example, because the right ventricle is to the right, anterior and superior in relation to the left ventricle, right bundle branch block (RBBB) will give rise to terminal forces that are rightward, anterior, and superior. Furthermore, the left bundle normally divides into two fan-like sheets of specialized conduction tissue: The anterior and posterior fascicles. Delay or block in either fascicle will result in a characteristic ECG pattern.

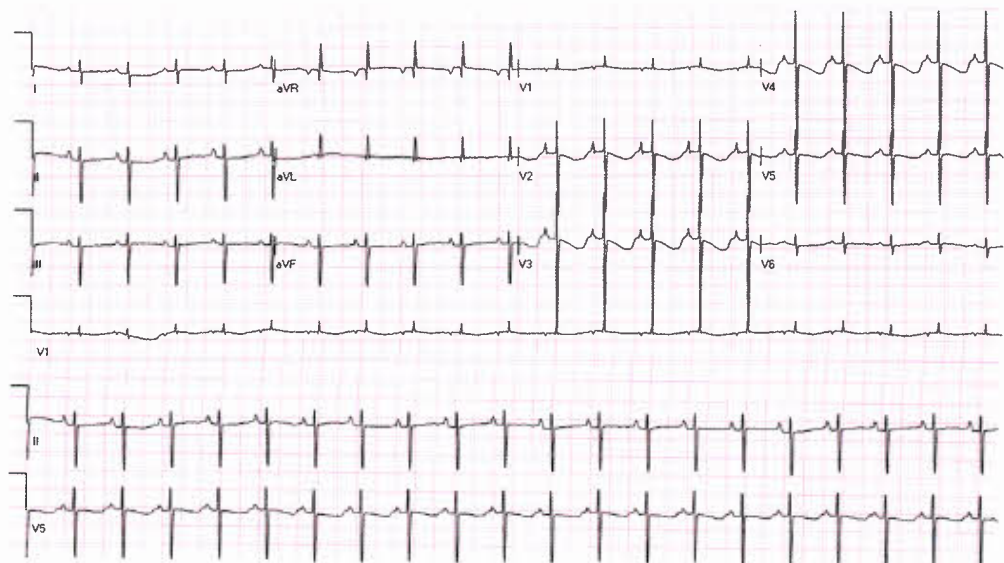
In practice, it is not always possible to differentiate bundle branch block from severe ventricular hypertrophy. This is because severe hypertrophy can result in a prolonged QRS that mimics bundle branch block. In the hypertrophied heart, endocardial activation is presumed to be on time, but epicardial activation is delayed owing to prolonged conduction time through the hypertrophied ventricular wall.

Right Bundle Branch Block

In RBBB, the QRS complex is wide and has a characteristic morphology of a rapid initial deflection followed by a slurred slower portion of the QRS. This reflects the rapid depolarization of the left ventricle followed by the slower depolarization of the right ventricle through ventricular muscle. The criteria for complete right bundle branch block includes a QRS above the upper limit for age in combination with normal initial forces and terminal conduction delay that is directed anteriorly, to the right and superior (wide and slurred S in leads I, V5, and V6; slurred R waves in leads aVR, V1, and V2; and wide and slurred S in leads II, III, and aVF) (Fig. 15.6).

The most common cause of RBBB is surgical closure of ventricular septal defects, especially in tetralogy of Fallot. When

Figure 15.5. Newborn with a complete AV septal (canal) defect. Note typical abnormally superior axis (northwest axis) along with right atrial enlargement.



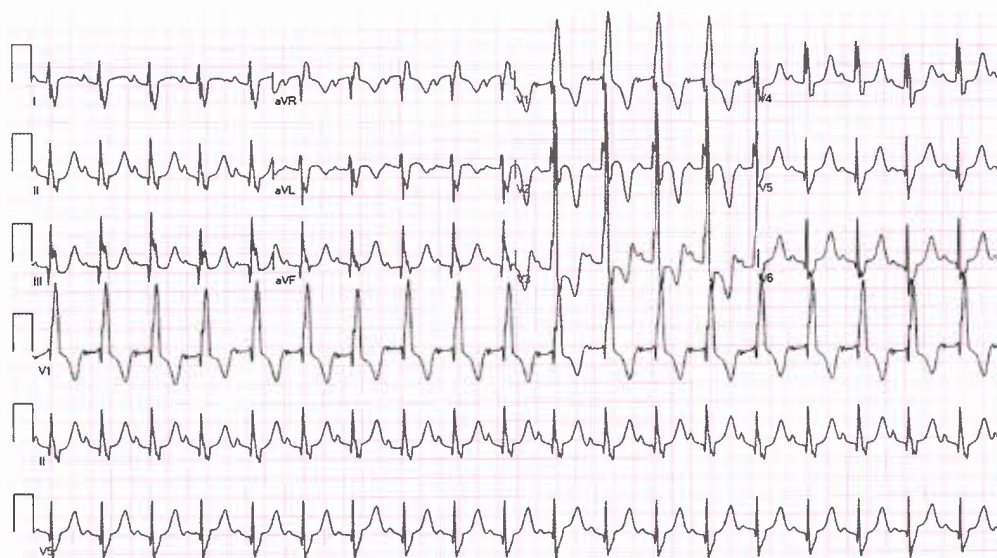


Figure 15.6. A 3-year-old following repair of tetralogy of Fallot. Note Q waves in inferior leads, documenting normal left anterior fascicular conduction.

the ECG demonstrates RBBB, it is not possible to diagnose RVH. The usual markers of ischemia also are lost because of associated ST- and T-wave abnormalities.

"Incomplete" Right Bundle Branch Block

An RSR prime pattern in lead V1 with a normal or slightly prolonged QRS duration has been termed incomplete RBBB. However, this pattern of ventricular conduction occurs in normal children. Further complicating matters, this pattern commonly occurs with right ventricular overload and frequently is present in patients with secundum atrial septal defects. Because of the prevalence of this pattern in normal children, it is perhaps better to refer to this as minor right ventricular conduction delay and not necessarily abnormal.

Left Bundle Branch Block

Just as delay or block in the right bundle branch results in RBBB, delay or block in the main left bundle branch results in late activation of the left bundle and LBBB. The QRS is prolonged, slurred, and directed leftward, posteriorly, and

inferiorly. The criteria for LBBB include an abnormally prolonged QRS duration, absent normal initial forces (no Q waves in leads aVL and V6), and notched slurred QRS complexes that are directed leftward and posteriorly (QS or rS in lead V1 and a tall notched R wave in lead V6).

LBBB is uncommon in children. It is usually the result of surgery on the left ventricular outflow tract. It also occurs with hypertrophic cardiomyopathy, myocarditis, or dilated cardiomyopathy (Fig. 15.7). As with RBBB, it is difficult, if not impossible, to assess hypertrophy and ischemic changes when LBBB is present.

Left Anterior Hemiblock

Normally, the left anterior fascicle is responsible for activation of the anterior and superior portion of the left ventricle, which occurs just ahead of activation of the posterior-inferior region by way of the left posterior fascicle. Block in the left anterior fascicle results in sequential activation of the left ventricle. The posterior-inferior region of the left ventricle is activated prior to the anterior-superior region. This results in abnormal QRS

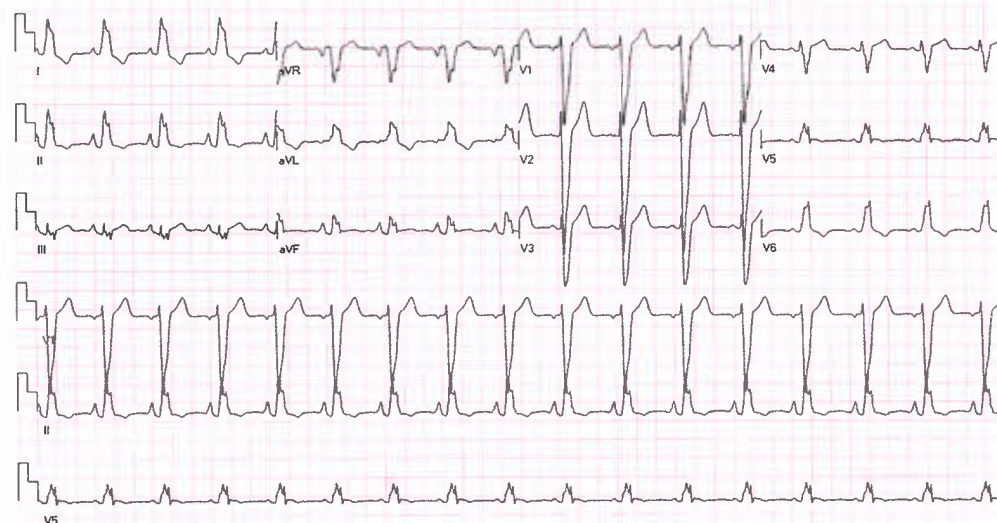


Figure 15.7. Left bundle branch block in a 15-year-old patient following resection of a subaortic membrane.

activation, with two sequential vectors: The initial forces are directed inferiorly and then spread in an anterior and superior fashion. This produces marked left axis deviation (<-30 degrees) with an rS in the inferior limb leads (II, III, and aVF). The QRS is normal or only minimally prolonged.

This conduction abnormality is relatively rare in children without congenital heart disease. It can occur with myocarditis, ischemia, or after cardiac surgery on the left ventricular outflow tract or ventricular septal defect closure. Tricuspid atresia and AV septal defects have ECG findings consistent with left anterior hemiblock (abnormally superior vector or axis) (34,35). However, these conditions do not have a true conduction defect, but rather, are related to the abnormal development of the conduction system.

Left Posterior Hemiblock

The activation sequence in left posterior hemiblock is the opposite of that seen with anterior hemiblock. The left ventricle depolarizes first in the anterior and superior region and then in the posterior and inferior portion. This produces an axis that is oriented rightward and inferiorly (120 degrees) with a normal QRS duration. Initial forces are directed superiorly (Q waves in leads II, III, and aVF). Left posterior hemiblock can be difficult to diagnose because most infants will have a rightward axis; this diagnosis should be reserved for a sudden change in axis between serial ECGs. It can result from surgical trauma and myocarditis.

Bifascicular Block

RBBB in combination with left anterior hemiblock occurs most commonly following repair of tetralogy of Fallot (10% of such patients). The ECG reflects the combination of these two conduction abnormalities. The initial forces, which in RBBB reflect only the left ventricle, initially are directed inferiorly and subsequently superiorly owing to left anterior hemiblock. The rest of the QRS complex reflects the characteristic terminal rightward and superior slurring of RBBB (Fig. 15.8).

RBBB and left posterior hemiblock is rare and difficult to diagnose by ECG. It is characterized by RBBB with initial rightward forces. Because most children who develop RBBB following surgery have preexisting RVH, it is difficult to distinguish RBBB with left posterior hemiblock from preexisting RVH.

Preexcitation

Preexcitation describes an abnormal depolarization of the ventricle prior to normal conduction through the His-Purkinje system. This takes place because of activation via an accessory connection between the two chambers.

Wolff-Parkinson-White Pattern

Wolff-Parkinson-White syndrome results from the presence of an accessory pathway that connects the atria directly to ventricular muscle. Conduction occurs both across the normal conduction system (AV node and His-Purkinje system) and across the accessory pathway. The ECG has a characteristic appearance of a short PR interval and a wide QRS complex (see Chapters 17 and 18). A delta wave or slurred upstroke of the QRS, indicating conduction from atrial to ventricular muscle, is characteristic of the syndrome. The terminal part of the complex may be wide or narrow, depending on the degree of conduction via the AV node. Children who have this finding are subject to episodes of reciprocating AV tachycardia. To diagnose WPW syndrome, a patient must have both the characteristic pattern of preexcitation as well as episodes of supraventricular tachycardia or atrial fibrillation. Therefore, the electrocardiographer should read the ECG as showing a "WPW pattern" or "ventricular pre-excitation."

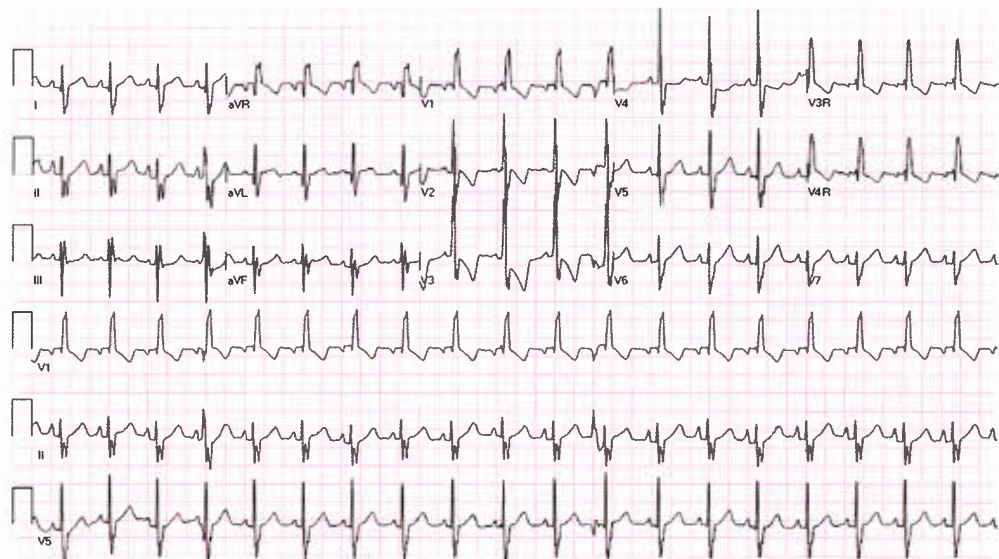
Mahaim Pathway

The Mahaim pathway is a particular type of accessory pathway that inserts into the right bundle branch or right ventricle and incorporates AV node-like tissue. There are several types. The most common is the atriofascicular pathway, with nodofascicular and fasciculoventricular pathways being less common (36). A Mahaim pattern of pre-excitation is one in which there is a widened QRS with an appearance similar to that in WPW, but in which there is a normal PR interval.

Lown-Ganong-Levine Syndrome

This entity exists when there is a short PR interval without a QRS abnormality in association with episodes of abnormal tachycardia. With the advent of invasive electrophysiologic testing, this entity has essentially disappeared from the literature, most likely owing to the fact that there does not seem to be a clear electrophysiologic correlate to the

Figure 15.8. Right bundle branch block with left anterior hemiblock following complete repair in an 11-month-old with tetralogy of Fallot and AV septal (canal) defect. Note lack of initial Q waves in leads II, III, and aVF.



so-called Lown-Ganong-Levine (LGL) syndrome. Most of these patients, in fact, were adults who had atrial fibrillation with fast AV node conduction. When there is a short PR interval with a normal QRS morphology and duration, one should simply read the ECG as showing a short PR interval rather than the LGL pattern.

Hypertrophy

Criteria for ECG determination of ventricular hypertrophy rely largely on whether QRS voltages in specific leads exceed normal values. The criteria were derived empirically, based on studies of normal infants or on comparison of ECG measurements with findings at cardiac catheterization, surgery, or autopsy. Interpretation of criteria for hypertrophy depends on the assumption that cardiac-torso geometry is normal or near normal and the ventricular depolarization sequence is normal (i.e., no bundle branch block). Because of the proximity effect, the closer the heart is to a particular precordial lead, the greater the observed voltage, regardless of the underlying cardiac pathology. Limb leads give rise to little or no proximity effect (6). This effect is particularly important in infants who have relatively thin chests. Consequently, some leads are better for determining certain types of hypertrophy. Still, if one approaches the problem of ventricular hypertrophy by thinking in terms of the vector forces involved, combined with the knowledge of cardiac anatomy and the relative positions of the right and left ventricle in the chest, the criteria for RVH and LVH will not seem entirely arbitrary. That is, the right ventricle is to the right, anterior, and superior, so that increased forces to the right, anterior, and superior suggest RVH. Likewise, the left ventricle is to the left, inferior, and posterior, and increased forces directed to the left, inferior, and posterior suggest LVH. Leads V5 and V6 may be used to judge left-right forces, leads V1 and V2 can be used for judging anterior-posterior forces, and aVF is the best lead for judging inferior-superior forces.

Left Ventricular Hypertrophy

In general, criteria for LVH are based on QRS voltage criteria and repolarization criteria. The voltage criteria involve voltage increase, and the repolarization criteria refer to the shift of the T-wave axis in the direction opposite to the QRS. Voltage criteria involve R and S waves in leads V1, V6, and aVF

and Q wave amplitude in lead V6. These measurements are compared with known normal standards that vary with age. The repolarization criteria refer to T-wave negativity in the lateral precordial leads and the angle (>100 degrees) between the frontal plane QRS and T axis.

R-wave amplitude greater than the 98th percentile for age in lead V6 and S-wave amplitude greater than the 98th percentile in lead V1 have been used to predict LVH. Unfortunately, hypertrophy may be present with normal left-sided forces, and normal children can have R waves in lead V6 that are above the 98th percentile. The large S wave in lead V1 owing to increased posterior forces is a much better criterion for LVH (Fig 15.9).

Patients with LVH usually have increased inferior forces manifesting a tall R wave in aVF, but this also may occur in RVH. In the absence of RVH, this criterion is helpful in supporting a diagnosis of LVH, particularly in a patient with prominent mid-precordial voltages because the limb leads are not prone to proximity effect.

In newborns, if an adult pattern of R-wave progression is evident, rather than the neonatal pattern, LVH is likely. That is, when a newborn manifests small R waves and deep S waves over the right precordium progressing to tall R waves and small S waves in the left lateral precordium, it suggests that there is left ventricular dominance. This corresponds to the vectorcardiographic finding of a wide-open counterclockwise loop in the horizontal plane.

T-wave abnormalities are the most reliable indication of LVH. A so-called strain pattern consists of inverted T waves in the inferior leads (II, III, and aVF) and left precordial leads (V5 and V6). One can compare the frontal plane T-wave axis with the QRS axis, and the difference between these is the QRS-T angle. Normally it is very small, and a wide QRS-T angle of >100 degrees is supportive of the diagnosis of LVH but is not specific (Fig. 15.9). T-wave abnormalities in LVH sometimes can be associated with depression of the ST segment. T-wave inversion also may be a sign of ischemia or myocardial inflammation; thus, these causes must be excluded prior to the diagnosis of LVH being made.

Left axis deviation is supportive of the diagnosis of LVH, especially in infancy. Left anterior hemiblock also may cause left axis deviation.

Abnormally prominent Q waves in the left lateral precordium (leads V5 and V6) may result from hypertrophy of the



Figure 15.9. An 8-month-old male with left ventricular hypertrophy. Note that the ECG is half-standard, and there is a T wave abnormality.

left ventricular portion of the interventricular septum, or perhaps from abnormal position of the left relative to the right ventricle owing to hypertrophy. A dilated volume-loaded left ventricle, which occurs with aortic valve insufficiency or patent ductus arteriosus, tends to produce deep Q wave in the lateral leads. On the other hand, with severe LVH, as might be seen with severe pressure loading, small or absent Q waves occur.

Right Ventricular Hypertrophy

Criteria for RVH are more specific than for LVH and include voltage and repolarization criteria. Because of normal right ventricular predominance in the neonate and the rapid changes in T-wave vectors in the first 2 weeks of life, the ECG interpretation of RVH in infants may be difficult.

R-wave amplitude in lead V1 that is greater than the 98th percentile for age is a very specific finding for RVH beyond the neonatal period. It has been used to estimate right ventricular pressure in isolated pulmonary stenosis using the following formula: Peak systolic right ventricular pressure = R-wave height, in mm \times 5 (34). An R wave in V1 that is >20 mm correlates with a right ventricular pressure that is at least systemic (37).

An abnormally deep S wave in V6 (>98 th percentile) is a very sensitive indicator of RVH. It often occurs in patients with increased right ventricular pressure secondary to chronic lung disease. When this pattern occurs with right atrial enlargement, it is characteristic of cor pulmonale. This criterion is less specific than the R wave in lead V1 because of the possibility of posterobasal LVH, in which large terminal superior and rightward forces result from hypertrophy of this late-activating portion of the left ventricle.

The R/S ratio is well established for various ages. If it is abnormally increased in lead V1, or abnormally decreased in lead V6, RVH is likely. However, it is rare for an abnormal R/S ratio to occur as an isolated finding, and this criterion should, therefore, be applied in conjunction with other findings of RVH.

T-wave orientation changes with age. Normally, it is upright until 4 to 7 days of age. Between 1 week of age and adolescence it is negative, and reverts to upright again in many individuals in adolescence and adulthood. An upright T wave after 7 days of age but before adolescence is a sensitive indicator of increased right ventricular pressure. The sensitivity

of this measure increases when R-wave amplitude also is considered. Mild RVH is manifested by normal R-wave amplitude but an upright T wave. Moderate RVH is manifested by increased R-wave amplitude and an upright T wave, whereas severe RVH is manifested by an increased R-wave amplitude and inversion of the T wave (Fig. 15.10).

A qR pattern also can be indicative of RVH, especially in conjunction with a tall R wave [typically >10 mm (Fig. 15.11)]. It also occurs with l-looping of the ventricles (abnormal septal depolarization), anterior myocardial infarction, and WPW syndrome.

An RSR prime pattern can be associated with right ventricular volume overload, as seen with atrial septal defects, but also may be a normal finding. It should be used to diagnose RVH only when the R prime amplitude is large.

Right axis deviation alone is not a criterion for RVH, but can be used to support other findings suggestive of RVH. Another cause of right axis deviation is left posterior hemiblock.

As in LVH, the R-wave progression across the precordial leads may be helpful. The neonatal pattern, consisting of tall R waves and small S waves in the right precordium, progressing to small R waves and deep S waves in the left lateral precordium, suggests right ventricular dominance (Fig. 15.12). When this pattern occurs in older children, rather than the normal adult-type R-wave progression, it suggests severe RVH. This corresponds to a completely clockwise loop in the horizontal plane.

Biventricular Hypertrophy

The diagnosis of biventricular hypertrophy (BVH) is made most easily when there are clear criteria present for both RVH and LVH. This often is manifest by normal R-wave progression across the precordium, but with increased voltages, so that there are both large R and S waves in leads V1 and V6. Proximity effect may produce prominent voltages in normal children in the mid-precordial leads (V3 to V5) without increases in leads V1 or V6 or any of the limb leads. In this situation, one should not diagnose hypertrophy, but should instead note the presence of prominent mid-precordial voltage. However, if the total voltage (R plus S) in lead V4 is >60 mm, BVH is likely (the Katz-Wachtel criterion).

Some electrocardiographers diagnose BVH when there are clear criteria for hypertrophy of one chamber and normal

Figure 15.10. A 4-month-old with hypoplastic left heart syndrome. Note that the tracing is recorded at half-standard.



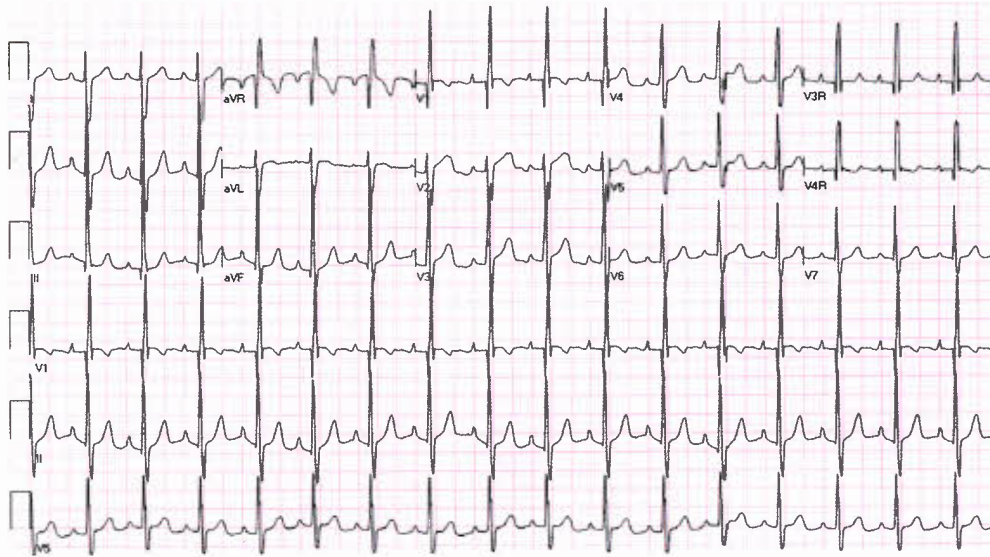


Figure 15.11 A 3-year-old following repair of truncus arteriosus with significant conduit obstruction. Note the qR in the right precordial leads, as well as the terminal rightward conduction delay, in this case due to hypertrophy.

voltages arising from the other chamber (e.g., >98th percentile R in V6 with greater than mean S in V6). They reason that the predominance of one chamber cancels or masks voltage from the other chamber, and therefore normal voltages could reflect hypertrophy. Although this approach makes some sense, in practice it seems to be dependent on the magnitude of the hypertrophy involved (i.e., it is more likely to be true if one chamber is severely hypertrophied). This criterion also suffers from the oversimplified viewpoint that R and S waves arise from one chamber only. For example, it would be incorrect to believe that for patients with LVH, the S wave in V6 and the S wave in lead aVF reflect only right ventricular forces, because the posterobasal portion of the left ventricle depolarizes later than the rest of the left ventricle. LVH also may include the posterobasal portion of the left ventricle, with normal to increased S waves in leads V6 or aVF without BVH.

Low QRS Voltage

Reduced QRS voltage is a nonspecific finding that may occur with various conditions, including myocarditis, pericardial

effusion, and generalized edema. Low voltage is present when the QRS amplitude is <5 mm in all limb leads and <10 mm in all precordial leads. While not always present, when associated with ST-segment change, it is characteristic of myocarditis.

Initial Forces

The Q wave occurs at the beginning of the QRS complex. One normally finds a small (<4 mm) Q wave in leads V5 and V6, and aVF. This is because normal initial depolarization, made up of several different areas of endocardial activation including the septum, is rightward, superior, and anterior. There are only a few specific situations when the presence or absence of certain types of Q waves may be of clinical significance. If the QRS duration is prolonged, no specific significance can be attached to Q waves. For the diagnosis of myocardial infarction, Q-wave duration should be ≥ 40 ms (38). Q-wave amplitude is lead dependent but in all cases should exceed 4 mm. A qR pattern in lead V1 signifies RVH, and deep Q waves in leads II, III, aVF, V5, and V6 are indicative of left septal hypertrophy, usually as part of LVH. Finally, in patients with

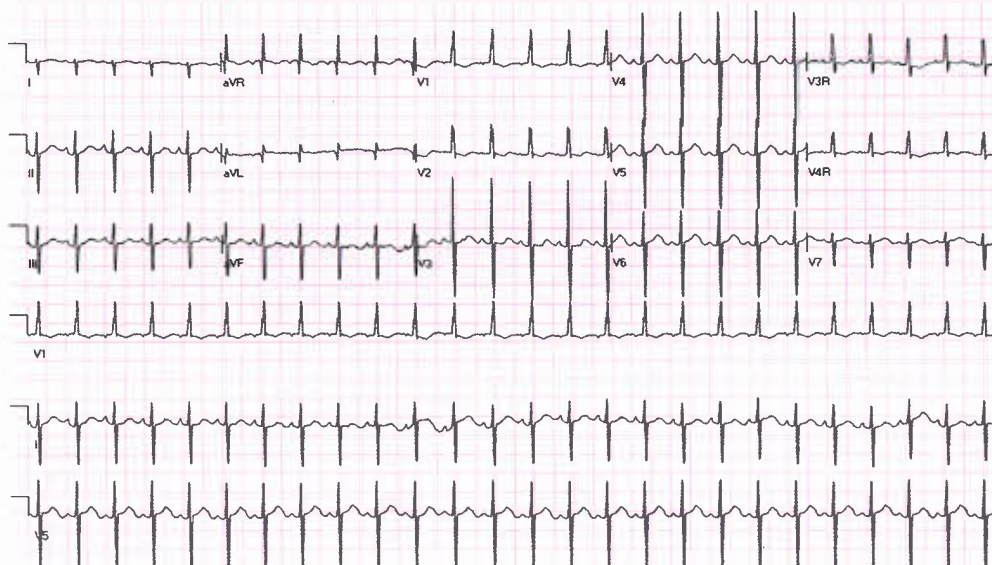


Figure 15.12 A 3-day-old male infant with critical coarctation. The ECG shows RVH. Note that all leads are half-standard.

congenitally corrected transposition of the great arteries and ventricular inversion, initial forces are posterior and to the left, producing a small Q wave in V1 or a qS complex, with absence of the normal Q wave in leads V5 and V6.

Ventricular Repolarization

Considered from the standpoint of a single cardiac cell action potential, repolarization is simply defined and begins immediately following depolarization. However, viewed from the perspective of the whole heart, repolarization is more difficult to characterize (39). In the normal heart, the subendocardium depolarizes before the subepicardium, but the subepicardium repolarizes before the subendocardium. This figures prominently in ECG features during the ST segment and T wave. There is an age-dependent overlap between the end of depolarization and the onset of repolarization. In childhood, repolarization potentials appear on an average of 10 ms before the end of ventricular depolarization (J point) (40).

QT Interval

There has been considerable debate regarding the best way to measure the rest and exercise QT interval. In supine patients at rest, the technical difficulty is determination of the end of the T wave, which may be fused with the U wave as it gradually blends with the baseline (40,41). Furthermore, Davignon et al. (32) demonstrated that the QT interval is both age and heart rate dependent. Attempts to correct for heart rate usually involve Bazett's formula ($QT_c = QT \text{ interval divided by the square root of the preceding R-R interval}$, where QT_c is the corrected QT interval). However, this may be inaccurate at low heart rates, often seen in adolescents. A number of alternative proposals have been made for correcting the QT (42). Technical problems are compounded during exercise because of the difficulty in identifying the ECG baseline. They also are complicated by variations in the RR interval that occur in children due to sinus arrhythmia. The choice of RR interval to be measured is critical in calculating the corrected QT interval. Garson (43) has suggested measuring the shortest RR interval. Calculating the QT_c from that interval, he found that a cutoff of 460 ms for QT_c identifies 98.4% of known long QT syndrome patients but only 3.8% of normal control subjects. In patients with QRS abnormality, and especially QRS prolongation due to bundle branch block, measurement of the QT_c is less useful, as it tends to be quite long in otherwise normal patients. The corrected JT interval has been proposed as a potential solution to this conundrum, and although normal standards for this measurement exists, it is not yet clear that this method reliably separates patients with prolonged QT syndrome and RBBB from other patients with RBBB (44).

The QT interval may be prolonged on a congenital basis (45,46) or as the result of antiarrhythmic drugs or electrolyte imbalance (47). The significance of a prolonged QT interval in an asymptomatic child is hard to determine. There seems to be little disagreement that a QT of 400 ms is normal and a QT of 480 ms is abnormal. However, there is disagreement as to the significance of intermediate values, especially in asymptomatic patients. Family history is, of course, important. Even in patients with pathologic prolongation of the QT interval, no ECG feature has been identified (not even the QT interval) that predicts which patients will develop symptoms or torsades de pointes (48).

ST Segment, T Waves, and U Waves

ST Segment

Identifying the true baseline is extremely important when analyzing the ST segment. This is an important practical problem

when the heart rate is increased as during exercise or with fever. ST segments >1 mm are said to be elevated and ST segments <-0.5 mm are considered depressed. However, in an analysis of average (0 to 50 ms) ST-segment potentials, the maximum and minimum potentials were age dependent. Maximum potentials (1.1 to 3.7 mm) occurred during adolescence. Minimum ST-segment potentials (0.4 to 1.2 mm) occurred during childhood (40,41). Interpretation of apparent ST-segment abnormalities requires careful attention to the clinical situation and important age-dependent and technical limitations.

T Waves

The sequence of ventricular depolarization, as characterized by the time difference between the earliest and latest area to depolarize, is an important determinant of the T wave (i.e., asynchronous depolarization influences the ECG patterns). Abnormalities of depolarization have a direct effect on repolarization. Therefore, T-wave abnormalities may be entirely owing to QRS abnormalities. Such abnormalities are termed secondary T-wave abnormalities as opposed to primary T-wave abnormalities, which reflect actual abnormalities of repolarization not simply caused by changes in the QRS (49).

U Waves

Little is known about the source or significance of U waves. They are quite common in young people, but Spach et al. (40,41) did not find them in children <8 years of age. U waves usually are apparent in the mid-precordial leads (V2 to V5), and they often overlap the T wave, resulting in TU fusion. The latter feature may complicate measurement of the QT interval. The amplitude of U waves is about 10% that of T waves (range 4% to 28%). The U-wave amplitude is heart rate sensitive. When U waves are large and difficult to separate from the T wave, they may indicate prolonged QT syndrome. On the other hand, long QT syndrome often is misdiagnosed in the presence of prominent mid-precordial U waves (50).

Specific Abnormalities Affecting the ST Segment, T Wave, and U Wave

Early Repolarization

Early repolarization usually occurs in adolescents and is associated with ST-segment elevation. This is seen best in the anterior and mid-precordial leads (V2 to V4) (Fig. 15.13). Because repolarization normally begins before depolarization ends, this term is a misnomer. Elevation of the ST segment may be explained by the normal age-dependent changes of ST-segment potentials. It can mimic changes associated with pericarditis and may be confusing in the evaluation of adolescents with chest pain. With early repolarization, J-point elevation often disappears with exercise. Serial ECGs may be helpful in separating early repolarization from the typical evolution of ST- and T-wave abnormality in pericarditis. Recent attention to this pattern of "early repolarization" in adults has identified it as a significant risk factor for sudden death, but clear criteria for separating at-risk patients from the large population of normals are, so far, lacking (51).

Pericarditis and Pericardial Effusions

Pericarditis is the most common cause of ST-segment elevation in children. There are a series of changes that occur as pericarditis evolves. Initially the ST segment is elevated with a normal T wave, thought to be secondary to subepicardial myocarditis. The ST segment then returns to normal, but the

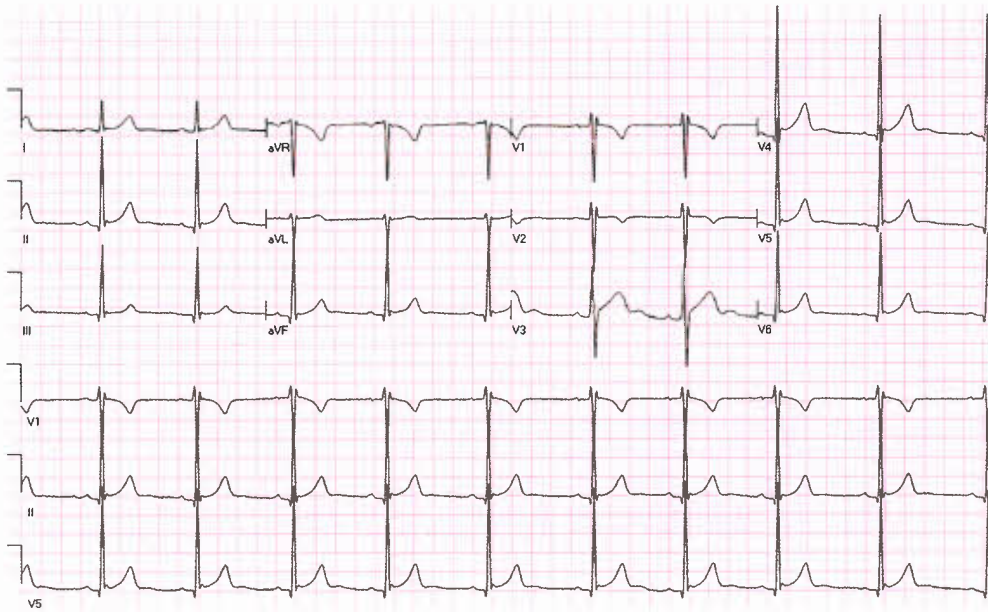


Figure 15.13. Early repolarization in a 16-year-old seen on a 12-lead ECG at full standardization. Note the 2 mm ST-segment elevation in leads V3–V6.

T wave becomes flat and then inverted. Characteristically, these findings differ from ischemic changes in that they involve all leads (46). Pericardial effusions can result in diminished QRS voltages and, rarely, electrical alternans (alternating QRS amplitude).

Myocarditis

Myocarditis usually results in flattened or inverted T waves and low-voltage QRS patterns. The QT interval may be prolonged. AV block and intraventricular conduction delay also can occur.

Ischemia

Myocardial ischemia is rare in children, but there are certain situations in which it must be considered. These include Kawasaki disease and congenital coronary artery abnormalities. Myocardial ischemia initially presents as distortion of the T wave, which becomes tall and peaked in the leads near the affected myocardial segment. The ST segment may be affected. If ischemia is reversed promptly, these changes will resolve. If ischemia persists, however, the myocardium will progress to the injury stage. The ECG may show deviation in the ST segments. The ST segments may become elevated or depressed depending on whether the injury is endocardial or epicardial. Reversal of ischemia may reverse these changes. Further injury will result in infarction, which appears on the ECG as a decrease in R-wave voltage and appearance of abnormal Q waves facing the infarcted segment (38).

Myocardial ischemia in an infant is caused by congenital coronary abnormalities, the most common being anomalous origin of the left coronary from the pulmonary artery. These infants usually present with ischemia or infarction of the anterior and septal areas (distribution of the left anterior descending coronary artery). They have deep Q waves in leads I, aVL, and V3 to V6. There also is loss of the mid-precordial R wave with a normal R wave in V1 and V6.

Kawasaki disease is an acquired cause of myocardial infarction in children. The ECG is characterized initially by low QRS voltages and nonspecific T-wave changes typical of myocarditis. These may progress to a myocardial infarction pattern.

Potassium Imbalance

Hyperkalemia produces tall peaked T waves. However, this finding is nonspecific and insensitive because normal children may have peaked T waves, and those with hyperkalemia may not have peaked T waves. As the potassium level increases, the T waves become more peaked and an intraventricular conduction delay results in a widened QRS along with PR prolongation (Fig. 15.14). The resultant ECG may resemble a sine wave or wide ventricular tachycardia. At concentrations of 9 mEq/L atrial standstill, AV block and ventricular fibrillation can occur.

Hypokalemia is associated with decreased T-wave amplitude. As potassium levels decrease, a U wave becomes apparent and the ST segment becomes depressed. Hypokalemia will enhance the arrhythmogenic effects of digoxin.

Calcium and Magnesium Imbalance

Hypercalcemia shortens the QT interval by shortening the ST segment. It also produces sinus rate slowing and sinoatrial block. Hypocalcemia lengthens the QT interval by prolonging the ST segment. A low magnesium level may enhance the effects of a low calcium level. In some infants the ECG will normalize only after both calcium and magnesium are corrected.

THE NORMAL ELECTROCARDIOGRAM

Developmental Changes

The hallmark of the ECG changes in the normal infant and child are the age-related transitions of QRS morphology, QRS duration, and the pattern of the ST segment and T wave (32,53–55). During normal development, there is a gradual decrease in heart rate and an increase in P-wave duration, PR interval, and QRS duration. Compared with those at older ages, the QRS voltages are low during the first several months of life. The mean QRS axis in the frontal plane moves in a direction from right to left. Although one might hypothesize that the observed increase in PR interval and QRS duration

Figure 15.14. A 14-year-old patient with renal failure and a potassium level of 7.7 mmol/L. The ECG shows the characteristic findings of hyperkalemia.



are related to changes in the size of the heart or the AV node, this hypothesis has not been borne out in studies in large animals.

The right ventricular dominance of the infant was one of the first age-dependent ECG changes to be recognized. The changes in depolarization of the ventricles during the first year of life occur in an orderly progression. In the newborn, the principal QRS potentials result from the right ventricle. The transition of the ECG from right ventricular dominance at birth to the pattern of left ventricular dominance lags behind hemodynamic changes. Loss of right ventricular dominance starts at about 1 month of age, and left ventricular dominance is well established by 1 year. These changes are appreciated best by the R-wave progression in the precordial leads during the first year of life. At birth and for the first several weeks of life there are tall R waves and small S waves in the right and anterior precordium (V3R, V4R, and V1), and deep S waves and small R waves in the left precordium (V6 and V7). This corresponds to a clockwise vector loop in the horizontal plane. With the establishment of left ventricular dominance, the precordial leads progress to a more adult pattern by 2 months of age, with deeper S waves in the right and anterior precordium and taller S waves in the left precordium, corresponding to a counterclockwise vector loop in the horizontal plane. At this age, however, there is still a prominent R wave in V1. By 1 year of age, the precordial R-wave progression is similar to that in the adult, with small R waves and deep S waves in the right and anterior precordium.

T waves change in a characteristic way, but the age-related patterns of repolarization are more difficult to interpret than the depolarization changes. The changes in right ventricular pressure that occur rapidly in the first days of life in normal infants have very little effect on the P wave or the QRS complex but have a great effect on the T wave. In the first minutes after birth, the T-wave vector is anterior and to the left (upright in V1 and V6). The T-wave vector may swing rightward in the next several hours, producing flattening or inversion of the T wave in the left lateral leads. Over the next 7 days, the T-wave vector moves posterior and leftward, producing an inverted T wave in V1 and an upright T wave in V6. Finally, the T wave becomes upright again in V1 after 7 or 8 years of age, but may remain inverted throughout adolescence (so-called juvenile T-wave pattern).

Preterm Infant

Compared with the ECG of term infants, the initial ECG of the premature infant is notable for its shorter QRS duration. The PR interval and QT interval also are shorter. The ECG of the premature infant is characterized by less right ventricular dominance at birth than the ECG of the full-term infant (56,57). At 1 year of age, the heart rate of the premature infant exceeds that of the term infant. Furthermore, precordial voltages are lower in the 1-year-old infant who was premature (57). The reduced precordial voltages may occur in the absence of bronchopulmonary dysplasia. Whether these differences are related to intrinsic myocardial differences of the premature versus term infant or to altered cardiac-torso geometry is unknown.

The Athlete

Athletes can have unusual ECG findings. For example, Oakley and Oakley (58) evaluated ten athletes with ECGs with voltage criteria for LVH (seven patients), nonspecific ST-segment and T-wave changes (three patients), and Q-wave changes suggestive of anterior myocardial infarction. No cardiac abnormalities were found after extensive evaluation. Balady et al. (59) reported QRS duration ≥ 100 ms in 60% of athletes, and 13% had ST-segment and T-wave changes that mimicked acute ischemia. Atrial enlargement was rare. Bjornstad et al. (60) reported athletes with sinus bradycardia and prolonged PR and QT intervals. They suggested that different criteria for ventricular hypertrophy were warranted for athletes.

Gender and Racial Differences

There are gender and racial ECG differences (61–63). The racial differences usually are not apparent until the preteen (ages 6 to 10) years. By 11 to 14 years of age, both sex and race differences are noted. It is important to know that the widely used normal standards published by Davignon (32) were based on 2,141 white children. In general, voltages in both limb and precordial leads are increased in males when compared with females and in blacks as compared with whites. Differences are not noted between black and white

females. There are differences in left ventricular posterior wall thickness among males (62). Similar findings occur in children with hypertension. It may be that the larger voltages on the ECG represent an early sign of increased left ventricular mass (64).

GUIDELINES AND INDICATIONS

In children, the primary uses of ECG include initial evaluation of patients with suspected cardiovascular disease and serial evaluation of the patient with known cardiovascular disease. The ECG is indispensable for evaluation of the patient with known or suspected disorders of rhythm and conduction, including patients with palpitations and syncope. ECGs also are indicated for determining the response to antiarrhythmic drugs or drugs with potential cardiac effects (e.g., tricyclic antidepressants). Although there is great interest in the possibility of widespread population-based screening for unrecognized cardiac disease using the ECG, there appears to be little rationale for routine ECG screening of asymptomatic, ostensibly normal young patients who are \leq age 40 years. The principal weakness of the ECG is its high rate of false positive findings, which when applied to a population with a very low prior probability, will lead to massive numbers of inappropriately identified individuals who require further testing. This argument applies to routine well-child examination as well as to pre-participation screening for athletes (65). Similarly, controversy exists regarding the need for ECG evaluation prior to the initiation of stimulant medication. While the American Heart Association has listed this as a class 2 indication (reasonable but not mandatory) (66) the American Academy of Pediatrics does not recommend such testing (67).

REFERENCES

- Burchell HB. A centennial note on Waller and the first human electrocardiogram. *Am J Cardiol* 1987;59:979-983.
- Fournier M. Willem Einthoven—the electrophysiology of the heart. *Medicamundi* 1976;21:65-70.
- Fisch C. Evolution of the clinical electrocardiogram. *J Am Coll Cardiol* 1989;14:1127-1138.
- Ziegler RF. *Electrocardiographic Studies in Normal Infants and Children*. Springfield, IL: Charles C Thomas Publisher, 1951:3-9.
- Barr RC. The electrocardiogram and its relationship to excitation of the heart. In: Sperelakis N, ed. *Physiology and Pathophysiology of the Heart*. Boston, MA: Kluwer Academic Publishers, 1989:175-194.
- Plonsey R. The biophysical basis for electrocardiography. In: Liebman J, Plonsey R, Gillette PC, eds. *Pediatric Electrocardiography*. Baltimore, MD: Williams & Wilkins, 1982:1-14.
- Bailey JJ, Berson AS, Garson A Jr, et al. Recommendations for standardization of leads and of specifications for instruments in electrocardiography and vector cardiography: report of the Committee on Electrocardiography and Cardiac Electrophysiology of the Council on Clinical Cardiology, American Heart Association. *Circulation* 1990;81:730-739.
- Murray A, McLaughlin NB, Bourke JP, et al. Errors in manual measurement of qt intervals. *Br Heart J* 1994;71:386-390.
- Frank E. An accurate, clinically practical system for spatial vector cardiography. *Circulation* 1956;13:737-749.
- Barr RC, Spach MS, Herman-Giddings GS. Selection of the number and positions of measuring locations for electrocardiography. *IEEE Trans Biomed Eng* 1971;18:125-138.
- Kavuru MS, Vesselle H, Thomas CW. Advances in body surface potential mapping (BSPM) instrumentation. In: Liebman J, Plonsey R, Rudy Y, eds. *Pediatric and Fundamental Electrocardiography*. Boston, MA: Martinus Nijhoff, 1987:315-326.
- Barr RC, Spach MS. Sampling rates required for digital recording of intracellular and extracellular cardiac potentials. *Circ Res* 1977;55:40-48.
- Thomas CW, Lee D. Methodology in constructing body surface potential maps. In: Liebman J, Plonsey R, Rudy Y, eds. *Pediatric and Fundamental Electrocardiography*. Boston, MA: Martinus Nijhoff, 1987:329-346.
- Barr RC, Spach MS. Construction and interpretation of body surface maps. *Prog Cardiovasc Dis* 1983;26:33-42.
- Ghosh S, Rhee EK, Avari JN, et al. Cardiac memory in patients with Wolff-Parkinson-White syndrome: noninvasive imaging of activation and repolarization before and after catheter ablation. *Circulation* 2008;118:907-915.
- Barold SS. Filtered bipolar esophageal electrocardiography. *Am Heart J* 1972;83:431.
- Benson DW Jr, Sanford M, Dunnigan A, et al. Transesophageal atrial pacing threshold: role of interelectrode spacing, pulse width and catheter insertion depth. *Am J Cardiol* 1984;53:63-67.
- Benson DW Jr. Transesophageal electrocardiography and cardiac pacing: state of the art. *Circulation* 1987;75:III86-III92.
- Simson MB. Use of signals in the terminal QRS complex to identify patients with ventricular tachycardia after myocardial infarction. *Circulation* 1981;64:235-242.
- Boineau JP, Cox JL. Slow ventricular activation in acute myocardial infarction: a source of re-entrant ventricular contractions. *Circulation* 1978;45:702-713.
- Zimmermann M, Friedli B, Adamec R, et al. Frequency of ventricular late potentials and fractionated right ventricular electrograms after operative repair of tetralogy of Fallot. *Am J Cardiol* 1987;13:737-749.
- Blomstrom-Lundqvist C, Hirsch I, Olsson SB, et al. Quantitative analysis of the signal-averaged QRS in patients with arrhythmogenic right ventricular dysplasia. *Eur Heart J* 1988;9:301-312.
- Holter J. Radioelectrocardiography: a new technique for cardiovascular studies. *Ann N Y Acad Sci* 1957;65:913-923.
- Knoebel SB, Crawford MH, Dunn MI, et al. Guidelines for ambulatory electrocardiography: report of ACC/AHA task force on assessment of diagnostic and therapeutic cardiovascular procedures. *Circulation* 1989;79:206-215.
- Southall DP, Johnston F, Shinebourne EA, et al. A 24-hour ECG study of heart rate and rhythm patterns in a population of healthy children. *Br Heart J* 1981;45:281-291.
- Dickinson DE, Scott O. Ambulatory electrocardiographic monitoring in 100 healthy teenage boys. *Br Heart J* 1984;51:179-183.
- Southall DP, Richards JM, Mitchell P, et al. Study of cardiac rhythm in healthy newborn infants. *Br Heart J* 1980;43:14-20.
- Dick M, McFadden D, Crowley D, et al. Diagnosis and management of cardiac rhythm disorders by transtelephonic electrocardiography in infants and children. *J Pediatr* 1979;94:612-615.
- Goldstein MA, Hesslein P, Dunnigan A. Efficacy of transtelephonic electrocardiographic monitoring in pediatric patients. *Am J Dis Child* 1990;144:178-182.
- Furukawa T, Maggi R, Bertolone C, et al. Effectiveness of remote monitoring in the management of syncope and palpitations. *Europace* 2011;13:431-437.
- Rossano J, Bloemers B, Sreeram N, et al. Efficacy of implantable loop recorders in establishing symptom-rhythm correlation in young patients with syncope and palpitations. *Pediatrics* 2003;112:e228-e233.
- Davignon A, Rautaharju P, Barselle E, et al. Normal ECG standards for infants and children. *Pediatr Cardiol* 1979;80;1:123-134.
- Liebman J. Tables of normal standard. In: Liebman J, Plonsey R, Gillette PC, eds. *Pediatric Electrocardiography*. Baltimore, MD: Williams & Wilkins, 1982:82-133.
- Dick M, Fyler DC, Nadas AS. Tricuspid atresia: the clinical course in 101 patients. *Am J Cardiol* 1975;36:327-337.
- Campbell RM, Dick M II, Hees P, et al. Epicardial and endocardial activation in patients with endocardial cushion defects. *Am J Cardiol* 1983;51:277-281.
- Sallee D, Van Hare GF. Preexcitation secondary to fasciculoventricular pathways in children: a report of three cases. *J Cardiovasc Electrophysiol* 1999;10:36-42.
- Cayler GG, Onley P, Nadas AS. Relation of systolic pressure in the right ventricle to the electrocardiogram. *N Engl J Med* 1958;258:979-982.
- Towbin JA, Bricker JT, Garson A Jr. Electrocardiographic criteria for diagnosis of acute myocardial infarction in childhood. *Am J Cardiol* 1992;69:1545-1548.
- Spach MS, Barr RC. Origin of epicardial ST-T wave potentials in the intact dog. *Circ Res* 1976;39:475-487.
- Spach MS, Barr RC, Benson DW Jr, et al. Body surface low-level potentials during ventricular repolarization with analysis of the ST segment. *Circulation* 1979;59:822-836.
- Spach MS, Barr RC, Warren RB, et al. Isopotential body surface mapping in subjects of all ages: emphasis on low-level potentials with analysis of the method. *Circulation* 1979;59:805-821.
- Rautaharju PM, Warren JW. Estimation of QT prolongation: a persistent, avoidable error in computer electrocardiography. *J Electrocardiol* 1990;23:111-117.
- Garson A Jr. How to measure the QT interval—what is normal? *Am J Cardiol* 1993;72:14B-16B.
- Berul CI, Sweeten TL, Dubin AM, et al. Use of the rate-corrected JT interval for prediction of repolarization abnormalities in children. *Am J Cardiol* 1994;74:1254-1257.
- Moss AL, Schwartz PJ, Crampton RS, et al. The long QT syndrome: prospective longitudinal study of 328 families. *Circulation* 1991;84:1135-1144.
- Keating M. Linkage analysis and long QT syndrome. *Circulation* 1992;85:1973-1986.

47. Singh BN. When is QT prolongation antiarrhythmic and when is it proarrhythmic? *Am J Cardiol* 1989;63:867–869.
48. Benhorin J, Merri M, Alberti M, et al. Long QT syndrome: new electrocardiographic characteristics. *Circulation* 1990;82:521–527.
49. Surawicz B. The pathogenesis and clinical significance of primary T wave abnormalities. In: Schlant RC, Hurst JW, eds. *Advances in Electrocardiography*. New York, NY: Grune & Stratton, 1972:377–421.
50. Taggart NW, Haglund CM, Tester DJ, et al. Diagnostic miscues in congenital long-QT syndrome. *Circulation* 2007;115:2613–2620.
51. Haissaguerre M, Derval N, Sacher F, et al. Sudden cardiac arrest associated with early repolarization. *N Engl J Med* 2008;358:2016–2023.
52. Spodick DH. Electrocardiogram in acute pericarditis. *Am J Cardiol* 1974;33:470–474.
53. Liebman J. The normal electrocardiogram. In: Liebman J, Plonsey R, Gillette PC, eds. *Pediatric Electrocardiography*. Baltimore, MD: Williams & Wilkins, 1982:144–171.
54. Walsh Z. The electrogram during the first week of life. *Br Heart J* 1963;25:784–794.
55. Hait G, Gasul BM. The evolution and significance of T wave changes in the normal newborn during the first seven days of life. *Am J Cardiol* 1963;12:494–504.
56. Sreenivasan V, Fisher BJ, Liebman J, et al. Longitudinal study of the standard electrocardiogram in the healthy premature infant during the first year of life. *Am J Cardiol* 1973;31:57–63.
57. Walsh EP, Long P, Ellison RC, et al. Electrocardiograms of the premature infant at 1 year of age. *Pediatrics* 1986;77:353–356.
58. Oakley DM, Oakley CM. Significance of abnormal electrocardiograms in highly trained athletes. *Am J Cardiol* 1982;50:985–989.
59. Balady GJ, Cadigan JB, Ryan TJ. Electrocardiogram of the athlete: an analysis of 289 professional football players. *Am J Cardiol* 1984;53:1339–1343.
60. Bjornstad H, Storstein L, Meen HD, et al. Electrocardiographic findings in athletic students and sedentary controls. *J Cardiol* 1991;79:290–305.
61. Rao PS. Racial differences in electrocardiograms and vectorcardiograms between black and white adolescents. *J Electrocardiol* 1985;18:309–313.
62. Hashida E, Nishi T. Constitutional and echocardiographic variability of the normal electrocardiogram in children. *J Electrocardiol* 1988;21:231–237.
63. Rao PS, Thapar MK, Harp RJ. Racial variations in electrograms and vectorcardiograms between black and white children and their genesis. *J Electrocardiol* 1984;17:239–252.
64. Aristimuno GG, Foster TA, Berenson GS, et al. Subtle electrocardiographic changes in children with high levels of blood pressure. *Am J Cardiol* 1984;54:1272–1276.
65. Steinvil A, Chundadze T, Zeltser D, et al. Mandatory electrocardiographic screening of athletes to reduce their risk for sudden death proven fact or wishful thinking? *J Am Coll Cardiol* 2011;57:1291–1296.
66. Vetter VL, Elia J, Erickson C, et al. Cardiovascular monitoring of children and adolescents with heart disease receiving medications for attention deficit/hyperactivity disorder [corrected]: a scientific statement from the American Heart Association Council on cardiovascular Disease in the Young Congenital Cardiac Defects Committee and the Council on Cardiovascular Nursing. *Circulation* 2008;117:2407–2423.
67. Perrin JM, Friedman RA, Knilans TK. Cardiovascular monitoring and stimulant drugs for attention-deficit/hyperactivity disorder. *Pediatrics* 2008;122:451–453.

Cardiac Channelopathies, Syncope, and Sudden Death

Michael J. Ackerman

In the United States, an estimated 300,000 to 400,000 individuals die suddenly each year with the vast majority secondary to coronary artery disease in the elderly (1). Fewer than 10,000 of these deaths involve people <35 years of age. Sudden cardiac death (SCD) in children, adolescents, and young adults is infrequent with an incidence between 1.3 and 8.5 per 100,000 patient-years (2). Sudden death under the age of 1 year can be attributed to infection, cardiovascular anomalies, child abuse/negligence, accidents, homicide, or metabolic/genetic disorders. However, 70% to 80% of these infantile deaths have no identifiable cause and are labeled as sudden infant death syndrome (SIDS) (3,4). SIDS remains the leading cause of postneonatal infant death and the third leading cause of infant mortality overall in the United States with an estimated incidence of 0.57 per 1,000 live births (5,6).

Beyond the first year of life, the cause and manner of death can be established from a comprehensive medicolegal investigation that includes an autopsy (7,8). For nearly half of young victims from 1 to 35 years of age, there are no apparent warning signs and sudden death often occurs as the sentinel event. The postmortem investigation is critical to determine the cause and manner of death (2). A postmortem examination may detect a noncardiac cause of the death such as asthma, epilepsy, or pulmonary embolism. However, SCD is the prevailing cause of sudden death in the young, with structural cardiovascular abnormalities often evident at autopsy, including hypertrophic cardiomyopathy (HCM) (Chapter 54), arrhythmogenic right ventricular cardiomyopathy (ARVC) (Chapters 18 and 39), congenital coronary artery anomalies (Chapter 32), and myocarditis (Chapter 56) (8,9).

In contrast, approximately one-third of sudden deaths involving previously healthy children, adolescents, and young adults have no identifiable abnormalities at autopsy, and the death is classified as autopsy-negative sudden unexplained death (SUD) (7,8,10–12). The exact prevalence of SUD, particularly in children, is unclear. Potentially lethal and heritable channelopathies such as congenital long QT syndrome (LQTS), catecholaminergic polymorphic ventricular tachycardia (CPVT), and Brugada syndrome (BrS) leave no clues at autopsy. The absence of any material evidence should prompt coroners, medical examiners, and forensic pathologists to consider that a fatal arrhythmia might have caused SUD (7,13–16). Accordingly, a cardiac channel molecular autopsy, potentially, can elucidate the pathogenic mechanism and establish probable cause and manner of SUD (17–21). Most often, the arrhythmias associated with these cardiac channelopathies spontaneously return to normal sinus rhythm resulting in an episode of “just” syncope. As such, it is paramount to distinguish the ordinary benign faint from a sudden death warning sign.

In this chapter, we summarize some recent population-based investigations of sudden death in the young to better understand its frequency and causes. Next, the pathologic bases, clinical

evaluation and diagnosis, and therapeutic management of the cardiac channelopathies are detailed. Finally, we will examine the features of fainting spells that may allow discrimination between common but benign vasovagal/neurocardiogenic syncope and much rarer but, potentially lethal, cardiac channelopathy-precipitated (arrhythmic) syncope.

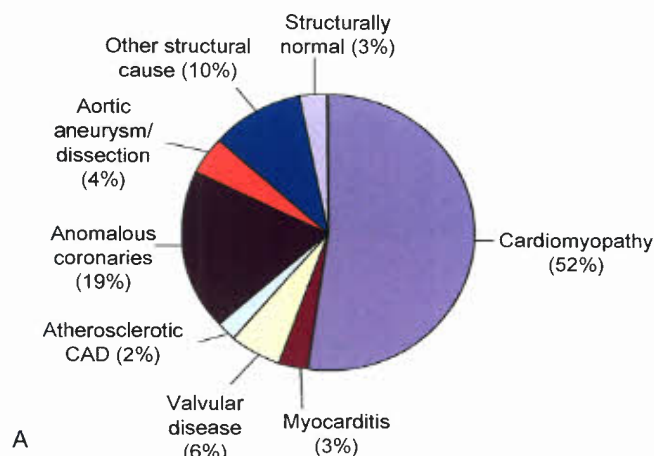
THE PREVALENCE AND CAUSES OF SUDDEN DEATH IN THE YOUNG

Maron et al. (8) demonstrated that HCM was the most frequent cause of SCD involving young competitive athletes. In this setting, over one-third of SCDs were attributed to HCM, and an additional 10% had an unexplained increase in cardiac mass, representing “possible HCM” (Fig. 16.1A). Autopsy-negative SUD accounted for only 3% of cases. The preponderance of athletes were male (90%) and collapsed during or instantaneously following a daytime training session (90%). Accordingly, HCM represents the most common cause of SCD on the athletic field in the United States.

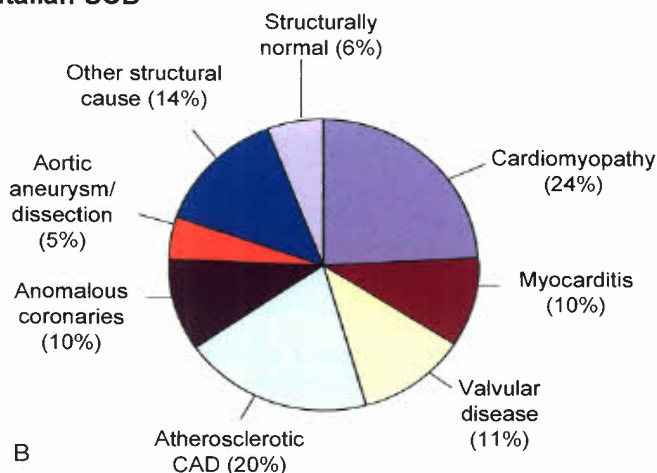
In 2001, Corrado et al. (9) noted that ARVC overshadowed HCM as the most frequent cardiomyopathy associated with SCD in young Italians (Fig. 16.1B). In this autopsy review of 273 cases of Italian SCD, atherosclerotic coronary artery disease prevailed at 20% followed by ARVC (13%) and HCM (7%). Hearts were identified as structurally normal (SUD) in 6% of cases of SUD. In 2005, Puranik et al. (12) reviewed the autopsy reports from 427 young victims of unexpected sudden death (ages 5 to 35 years) over a 10-year period in eastern Sydney, Australia (Fig. 16.1C). This population-based cohort included ≥90% of all sudden deaths that occurred in this urban population during the study period. Excluded were traumatic, accidental, selected drownings, and death from drug intoxications. SCD was determined for more than half of these SUDs. Cardiomyopathies accounted for only 16% of their SCDs and only 6% of deaths were attributed to HCM. Instead, autopsy-negative SUD (29%) was the leading cause of SCD (Fig. 16.1C) with nearly 10% of the decedents with structurally normal hearts deemed to have LQTS.

Further, a 25-year review of autopsies performed on American military recruits by Eckart et al. (22) showed a non-traumatic sudden death rate of 13 per 100,000 recruit years among a monitored 6.3 million men and women aged 18 to 35 years (Fig. 16.1D). Of the 126 sudden deaths, 108 (86%) were related to exercise. Half of the sudden deaths were attributed to an identifiable cardiac abnormality after a postmortem investigation. However, 35% of the sudden deaths were classified as autopsy-negative SUD (22). Several cases were identified as having a family history of sudden premature death suggesting a heritable predisposition for a malignant arrhythmia (22).

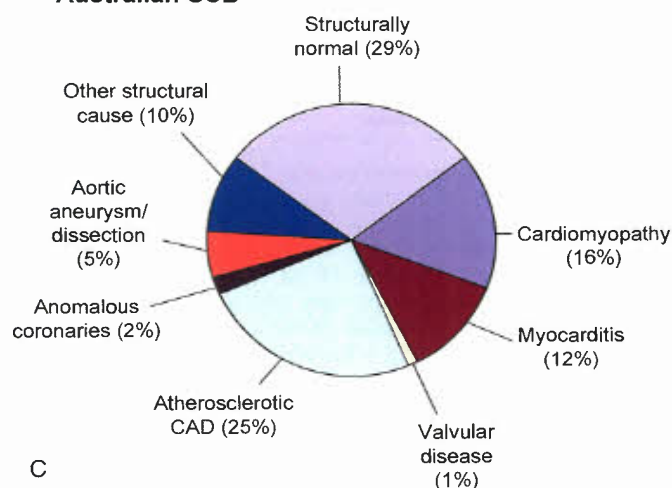
Athletic Field SCD



Italian SCD



Australian SCD



American Military Recruits SCD

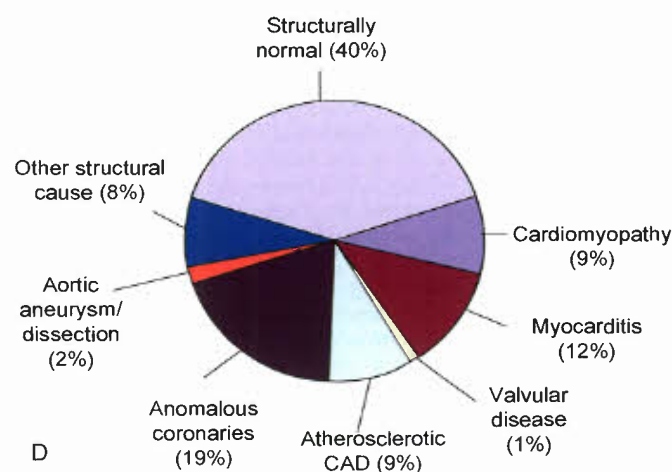


Figure 16.1. Epidemiology of sudden death in the young. A comparison of data from four cohorts. A: $N = 134$; mean age: 17 years. Frequency of cardiomyopathy subtypes: hypertrophic cardiomyopathy (HCM) 36%, dilated cardiomyopathy (DCM) 3%, arrhythmogenic right ventricular dysplasia (ARVD) 3%, and unexplained increase in cardiac mass ("possible HCM") 10%. (Maron BJ, Shirani J, Poliac LC, et al. Sudden death in young competitive athletes. Clinical, demographic, and pathological profiles. [see comment]. *JAMA* 1996;276:199–204.) B: $N = 273$; mean age: 24 years. Frequency of cardiomyopathy subtypes: HCM 7%, DCM 4%, and ARVD 13%. A significant fraction of those included in "Other structural causes" (24/38) had histological evidence of conduction system abnormalities. (Corrado D, Basso C, Thiene G. Sudden cardiac death in young people with apparently normal heart. *Cardiovasc Res* 2001;50:399–408) C: $N = 241$; mean age: 27 years. Frequency of cardiomyopathy subtypes: HCM 6%, DCM 5%, ARVD 2%, and idiopathic left ventricular hypertrophy (LVH) 3%. (Puranik R, Chow CK, Duflo JA, et al. Sudden death in the young. *Heart Rhythm* 2005;2:1277–1282.) D: $N = 108$; mean age: 19 years. Frequency of cardiomyopathy subtypes: HCM 8%, DCM 1%, and ARVD 1%. "Structurally normal" includes the diagnosis of arrhythmia disorders, such as LQTS, as well as all sudden unexplained deaths. In some instances, minimal structural abnormalities were noted at autopsy, but these were felt to be insufficient to cause sudden death. †"Cardiomyopathy" includes those with HCM, DCM, ARVD, and those with unexplained increase in cardiac mass not meeting strict criteria for HCM (i.e., "possible HCM"). CAD, coronary artery disease. (Eckart RE, Scoville SL, Campbell CL, et al. Sudden death in young adults: a 25-year review of autopsies in military recruits. *Ann Intern Med* 2004;141:829–834, Ref. 22; From Tester DJ, Ackerman MJ. The role of molecular autopsy in unexplained sudden cardiac death. *Curr Opin Cardiol* 2006;21:166–172, with permission, Ref. 23.)

Morentin et al. (11) scrutinized all sudden nonviolent deaths in persons 1 to 35 years of age occurring in Spain from 1991 to 1998. Among the 107 cases of sudden death, 18% were considered SUD. Thirteen died following sudden collapse, and six were discovered dead in bed. In one-fifth of these SUDs, death occurred in relation to physical exertion (including swimming) or extreme emotion. Antecedent

symptoms compatible with cardiac arrhythmia were evident in >25% of the SUD cases.

These population-based studies suggest that while the majority of SCD stem from identifiable morphologic abnormalities found at autopsy, nearly one-third of sudden deaths involving previously healthy children, adolescents, and young adults are autopsy-negative SUD.

AUTOPSY-NEGATIVE SUDDEN UNEXPLAINED DEATH

Assessment of Family Members

In cases of autopsy-negative SUD, a cardiac and genetic evaluation of first- and second-degree relatives and/or a molecular autopsy may elucidate the underlying mechanism of the sudden death. Although arrhythmias can be isolated events, some may represent manifestations of inherited arrhythmia syndromes with increase risk for syncope, cardiac arrest, or SCD in relatives when there is a family history of sudden death. Thus, first-degree relatives of the decedent should have a comprehensive cardiovascular evaluation including an extensive personal and family history, physical examination, 12-lead electrocardiogram, treadmill stress test, 24-hour Holter monitoring, and an echocardiogram.

In 2003, Behr et al. (10) performed a detailed cardiovascular evaluation of 109 first-degree relatives of 32 cases of SUD and showed that 22% of these families had evidence of inherited cardiac disease with the majority having features suggestive of LQTS. Similarly, in 2005, Tan et al. (24) found that 28% of families had an identifiable cardiac channelopathy including CPVT and LQTS following a clinical assessment of first-degree relatives of young SUD victims. In a 2008 follow-up study by Behr et al., a diagnosis of inheritable heart disease was made in 53% of first-degree relatives of SUD victims following a comprehensive clinical evaluation; 70% being diagnosed with either LQTS (53%) or BrS (17%). Strikingly, 30% of the families evaluated reported a family history of additional unexplained premature sudden deaths under the age of 45 years, and nearly 20% of the decedents had a prior history of syncope.

In 2010, van der Werf et al. identified a certain or probable diagnosis in 47 (33%) of 140 families of SUD victims (aged 1 to 50 years) following a clinical cardiac assessment. Around 96% of these 47 families were diagnosed with an inherited cardiac disease (21% LQTS, 17% CPVT, 15% BrS, and 15% ARVC). The diagnostic yield among families depended upon the age of the decedent ranging from a high of 70% when the decedent was between ages of 1 and 10 years to a low of 21% when the decedent was between 41 and 49 years of age. Many of these sudden death victims had antecedent warning signs prior to their own death, including syncope in 15% and a family history of young sudden death in 29%. However, there was no prior clinical diagnosis of an inherited cardiac disease for either the decedent or any other family member.

Incomplete penetrance and variable expression are hallmarks of the various cardiac channelopathies that lead to “concealed” forms of these disorders (25). Therefore, clinical assessment of surviving family members of SUD victims may be insufficient to detect LQTS, CPVT, or BrS in unsuspected individuals. A molecular autopsy involving postmortem cardiac channel genetic testing is a tool for the forensic pathologist/medical examiner/coroner to provide the answer to unexplained deaths in the young and subsequently benefit other family members.

Molecular Autopsy Investigations of SUD

In 2004, Chugh et al. (21) identified 12 cases of SUD following a comprehensive postmortem analysis of a consecutive series of 270 adult (age ≥ 20 years) cases of SCD occurring over a 13-year period. Postmortem genetic analysis of the LQTS-susceptibility genes revealed an identical *KCNH2* mutation in 2 of these 12 (17%) cases of autopsy-negative SUD. Similarly, Di Paolo et al. (26) performed LQTS molecular autopsies on

10 cases of juvenile (ages 13 to 29 years) SUD and identified *KCNQ1* mutations in 2 individuals.

In 2007, Tester and Ackerman completed the largest molecular autopsy series of SUD to date (27,28). Comprehensive mutational analysis of all 60 translated exons in the LQTS-associated genes (*KCNQ1*, *KCNH2*, *SCN5A*, *KCNE1*, and *KCNE2*) along with targeted analysis of the CPVT1-susceptibility gene (*RYR2*) was conducted on a series of 49 medical examiner referred cases of SUD. Over one-third of these SUD cases had a presumably pathogenic cardiac channel mutation with mutations in *RYR2*, alone, accounting for nearly 15% of the cases (27,29). In this series, sudden death was the sentinel event in all but four mutation-positive SUD cases. However, many had a positive family history of cardiac events, yet no family members had been diagnosed with either LQTS or CPVT. Overall, approximately half of the 17 decedents with a cardiac channel mutation detected by postmortem genetic testing exhibited potential warning signs, either personally or in the family. The repeated observations of unheeded warning signs of syncope and/or family history of sudden death in nearly 15% to 30% of young SUD victims emphasize the importance of heeding potential warning signs.

Population-based studies involving the evaluation of relatives and molecular autopsy investigations of the decedent show that identifiable and potentially treatable cardiac channelopathies (including LQTS, CPVT, and BrS) account for approximately one-third of autopsy-negative SUD in the young. In addition, approximately 10% to 15% of SIDS may be due to these cardiac channelopathies (19,30–36).

THE CARDIAC CHANNELOPATHIES

The discipline of *Cardiac Channelopathies* unofficially commenced in 1995 with the discovery of mutations in genes encoding critical ion channels of the heart as the pathogenic basis for congenital LQTS (37,38). Besides classical autosomal dominant (Romano-Ward) LQTS and autosomal recessive (Jervell and Lange-Nielsen) LQTS, the cardiac channelopathies now include Andersen-Tawil syndrome (ATS), Timothy syndrome (TS), drug-induced *torsades de pointes* (DI-TdP), short QT syndrome (SQTS), CPVT, BrS, idiopathic ventricular fibrillation, early repolarization syndrome, progressive cardiac conduction disease or familial atrioventricular conduction block or Lev-Lenegre disease, and familial atrial fibrillation. Even primary cardiomyopathies like dilated cardiomyopathy (DCM) can be due to genetically mediated perturbations in ion channels, specifically the *SCN5A*-encoded cardiac sodium channel (37–39).

Overall, cardiac channelopathies may affect as many as 1 in 1,000 persons, may lie dormant for decades or present with SIDS, and may or may not manifest signature electrocardiographic features (Fig. 16.2). Collectively, these cardiac channelopathies represent treatable conditions when recognized. In general, the cardinal events of the cardiac channelopathies comprise *syncope*, *seizures*, and *SCD*. Unfortunately, SCD can be the sentinel event.

Autosomal Dominant Long QT Syndrome (Romano-Ward)

Congenital LQTS is the prototypic cardiac channelopathy with an estimated prevalence of 1 in 2,000 to 2,500 persons. Clinically, LQTS is characterized by abnormal cardiac repolarization resulting in QT interval prolongation (Fig. 16.2A) that predisposes patients to TdP (Fig. 16.2B). Palpitations seldom represent the sole indicator of an episode of TdP. The

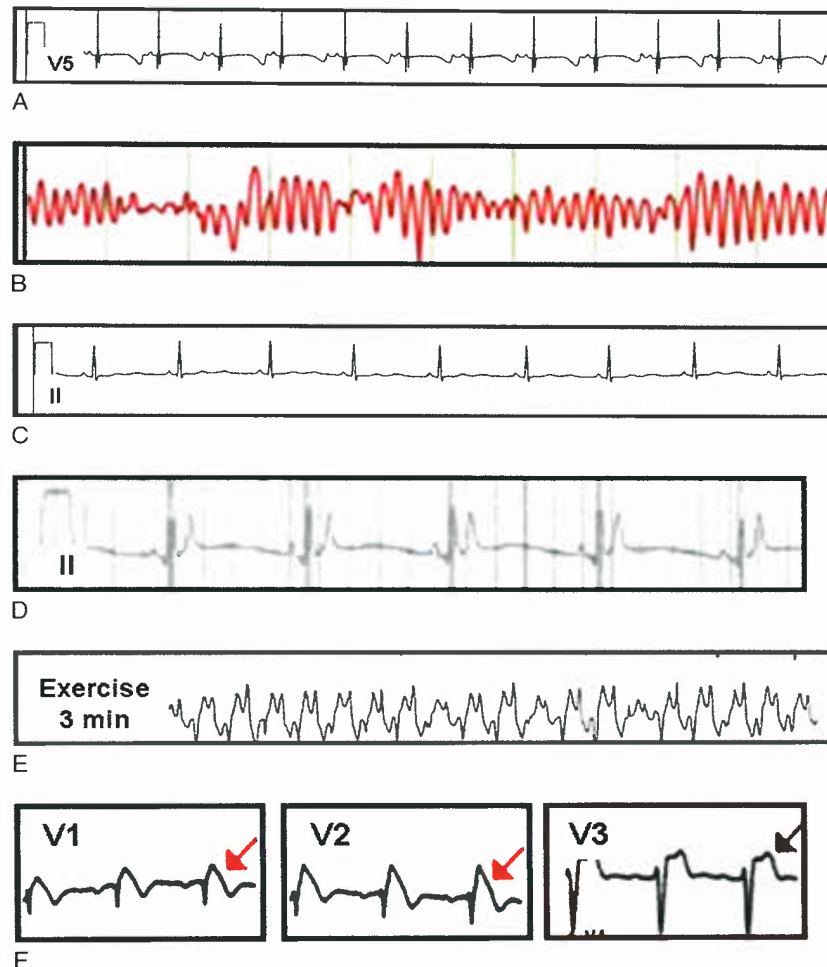


Figure 16.2. Signature electrocardiographic features of various channelopathies. A: QT prolongation—an example of a patient with extreme QT prolongation ($QT_c > 650$ ms). Note, the ST segment and T-wave morphology would predict LQT3, but this patient is among the 25% who are genotype negative. Also, the computer-calculated QT_c was 362 ms underscoring the mandate to independently compute the QT_c . B: *Torsade de pointes* (“twisting of the points”)—hallmark arrhythmia of LQTS. C: Abnormal U wave in ATS—although subtle, this lead II recording is quite abnormal characterized by normal QT interval, long isoelectric segment between the end of the T wave on the start of the U wave and long-duration U wave in this female with an ATS1-associated mutation in *KCNJ2*. D: Short QT interval— QT_c of approximately 250 ms. E: Exercise-induced bidirectional VT seen in CPVT. F: Coved ST segment elevation in BrS (type I Brugada ECG pattern) in precordial leads V1 and V2 and a saddle back profile (type II Brugada ECG pattern) in V3. (From Ackerman MJ. Heritable cardiac channelopathies. In: Wyszynski DF, Correa-Villasenor A, Graham TP, eds. *Congenital Heart Defects: From Origin to Treatment*. New York, NY: Oxford University Press, 2010:131–140, with permission, Ref. 40).

most common form of LQTS is autosomal dominant LQTS, previously known as Romano-Ward syndrome (41,42).

Hundreds of mutations in 13 distinct LQTS-susceptibility genes have been identified and generally involve either loss-of-function potassium channel mutations or gain-of-function sodium channel mutations. Except for four rare subtypes that stem from perturbations in key cardiac channel interacting proteins or structural membrane-scaffolding proteins (ankyrin B-, caveolin 3-, yotiao-, and syntrophin α -LQTS) (43–46), LQTS is a pure “channelopathy” resulting from mutations in cardiac channel α - and β -subunits. The majority of LQTS is due to mutations in either the *KCNQ1*-encoded I_{Ks} potassium channel (LQT1, 30% to 35%), the *KCNH2*-encoded I_{Kr} potassium channel (LQT2, 25% to 30%), or the *SCN5A*-encoded I_{Na} sodium channel (LQT3, 5% to 10%) (47,48).

The past decade of LQTS research has provided numerous genotype–phenotype relationships (Fig. 16.3). Genotype–ECG

relationships include broad-based T waves in LQT1, low-amplitude or notched T waves in LQT2, and long ST isoelectric segment with normal T-wave morphology in LQT3 (51,52). Gene-specific arrhythmia triggers have been observed including: exertion in LQT1 (particularly swimming), auditory triggers and the postpartum period in LQT2, and events during sleep in LQT3 (49,53–56). Importantly, the response to β -blockers is strongly influenced by the underlying genotype with which patients with LQT1 realize superior protection than patients with either LQT2 or LQT3 (57).

In the presence of a clinical diagnosis of LQTS, the yield of LQTS genetic testing is about 75% (58). Generally accepted indications for LQTS genetic testing are summarized in Table 16.1. However, genetic tests for LQTS and the other cardiac channelopathies must be scrutinized and interpreted with great caution and must not be viewed as binary tests (50,59). These genetic tests are probabilistic tests. Some mutations will

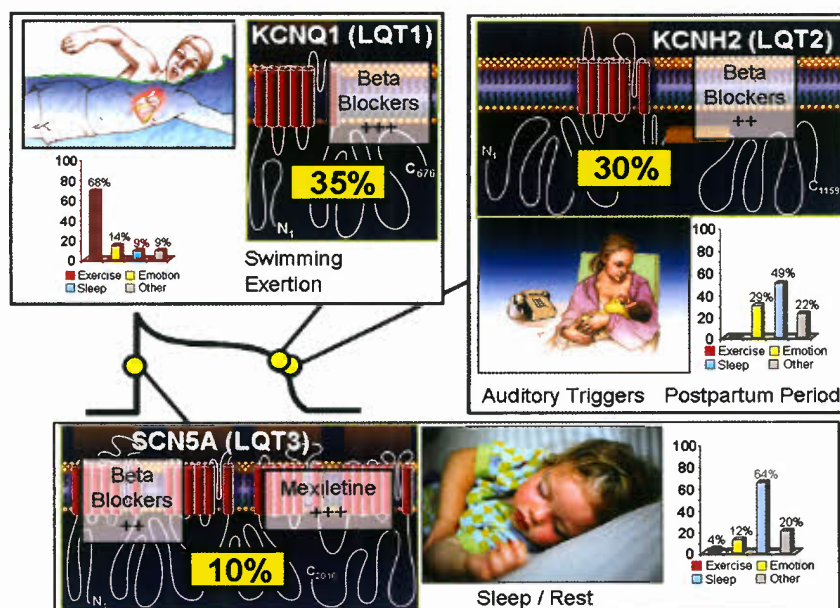


Figure 16.3. Genotype–phenotype correlations in LQTS. Seventy-five percent of clinically strong LQTS is due to mutations in three genes (35% *KCNQ1*, 30% *KCNH2*, and 10% in *SCN5A*) encoding for ion channels that are critically responsible for the orchestration of the cardiac action potential. Genotype–phenotype correlations have been observed, including swimming/exertion and LQT1, auditory triggers/postpartum period and LQT2, and sleep/rest and LQT3. The bar graphs represent genotype–phenotype data from Ref. 49. Also illustrated is the relative gene-specific effectiveness in β -blocker therapy where β -blockers are extremely protective in LQT1 patients and moderately protective in LQT2 and LQT3. Direct late sodium current blockers like mexiletine, flecainide, and ranolazine may be protective in LQT3. (From Tester DJ, Ackerman MJ. Genetic testing for potentially lethal, highly treatable inherited cardiomyopathies/channelopathies in clinical practice. *Circulation* 2011;123:1021–1037, with permission, Ref. 50.)

be definite disease-causative mutations, whereas other genetic variants may not be pathogenic (50).

Individuals with LQTS may or may not display the hallmark repolarization abnormality of QT interval prolongation (Fig. 16.2A). In fact, approximately 40% to 50% of patients with genotype-positive LQTS have a normal resting QTc (25). This observation reinforces the critical role of genetic testing. In general, a heart rate-corrected QT interval (QTc) > 480 ms in *postpubertal* females or > 470 ms in *postpubertal* males should prompt a thorough investigation for LQTS. These values represent the 99th percentile in the distribution of QTc values. Previously, a QTc > 440 ms (males) or > 450 ms (females) has been considered “borderline” QT prolongation. In fact, the 2009 AHA/ACC/HRS (American College of Cardiology/American Heart Association/Heart Rhythm Society) guidelines denote that a QTc \geq 450 ms in adult males

and \geq 460 ms in adult females must be considered “prolonged QTc.” Although 50% of patients with genetically proven LQTS have a QTc < 460 ms, these cutoff values would result in an unacceptably high rate of false positives if used as part of a screening program. Using these cutoff values, an estimated 15% to 20% of the entire population would have “borderline QT prolongation” and 5% to 10% of adults would satisfy the guidelines definition of “prolonged QTc” (Fig. 16.4). In addition, these QTc values are based upon an accurate measurement of the QTc (62). It is absolutely critical to measure the QTc manually. Relying on the computer-derived QTc is unacceptable. Calculation of an average QTc from either lead II or V5 is recommended. Simply using the beat yielding the maximum QTc yields too many false positives. Furthermore, these QT distributions do not apply to 24-hour ambulatory ECG recordings.

TABLE 16.1 Generally Accepted Indications for LQTS Genetic Testing

1. Persons with unequivocal and unexplained QT prolongation (i.e., QTc \geq 500 ms).
2. Persons with clinically suspected LQTS regardless of (a) baseline QTc or (b) history of prior negative genetic testing in research laboratories or with commercially available targeted exon testing. (Rationale: Mutation detection methods over the past decade have changed significantly and false negatives have been demonstrated.)
3. All first-degree relatives of a genotype positive index case (genetic testing extended to other degrees of relatedness by “following the genetic trail” down the appropriate path of concentric first-degree relatives). For example, confirmatory genetic testing demonstrates the index case’s LQT1-associated mutation in the father. Accordingly, the father’s parents and siblings (second-degree relatives to the index case) should be offered testing. Next, if, say, the paternal aunt (to the index case) tests positive, now all of her children (cousins or third-degree relatives to the index case) should be tested and so forth.

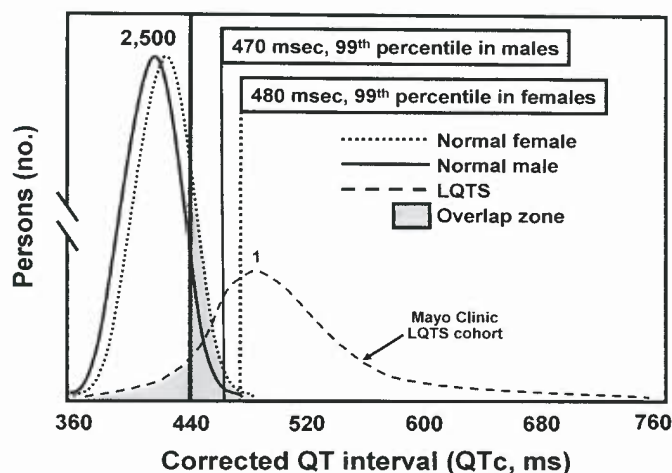


Figure 16.4. Distribution of QTc in health and LQTS. Shown is the distribution of QTc values derived from healthy postpubertal males and females (Mason JW, Ramseth DJ, Chanter DO, et al. Electrocardiographic reference ranges derived from 79,743 ambulatory subjects. *J Electrocardiol* 2007;40:228–234, Ref. 60). The QTc distribution for LQTS is derived from analysis of the ECGs of all patients with mutation-proven LQTS who have been evaluated in Mayo Clinic's LQTS Clinic. (Adapted from Taggart NW, Haglund CM, Tester DJ, et al. Long QT syndrome. *Circulation* 2007;115:2613–2620; Johnson JN, Ackerman MJ. Long QT syndrome. In: Yan G, Kowey PR, eds. *Management of Cardiac Arrhythmias*. New York, NY: Humana Press, 2011:419–440, with permission, Ref. 61.)

Efforts to unmask concealed LQTS (genotype-positive/resting ECG negative) include exercise stress testing and epinephrine QT stress testing (63–67). With exercise stress testing, failure to shorten the QT interval appropriately suggests LQTS. However, this failure to shorten during exercise is principally an LQT1-specific response. Thus, the presence of normal QT interval shortening during exercise does *not* exclude LQTS. Similarly, during infusion of low-dose epinephrine (≤ 0.1 mcg/kg/min), the presence of paradoxical lengthening (>30 ms) of the absolute QT interval is suggestive (75% positive predictive value) of concealed LQT1 (68).

The features present in the composite clinical diagnostic scorecard known as the “Moss, Comptom, and Schwartz LQTS score” should be used to gauge the clinical probability of the presence of LQTS in an index case (Table 16.2) (69). This score includes ECG parameters (QTc, TdP, T-wave alternans, and notched T-waves) and the personal and family history. Importantly, this score does not apply to family members. In addition, the metrics utilized are more sensitive than specific. For example, an asymptomatic 17-year-old girl with no family history but a QTc of 481 ms is awarded 3 points and a qualitative label of “intermediate probability” LQTS. Although statistically more likely to have LQTS than a woman with the same story but a QTc of only 420 ms, this “intermediate probability” LQTS-labeled female still has *only* a 4% chance of actually having LQTS. One must avoid not only missing LQTS when it is there but also overdiagnosing it when it is not there. In our center, approximately 40% of the patients who have sought a second opinion following a diagnosis of LQTS were dismissed as otherwise healthy (70). Common and recurring miscues included miscalculation of the QTc and overinterpretation of the significance of a borderline QTc value in the context of nonarrhythmic syncope.

Overall, the annual mortality associated with LQTS is around 1% per year with the highest risk subset around 5% to

TABLE

16.2

Clinical Probability Scores for Index Case Evaluation for SQTS and LQTS

SQTS	Diagnostic Criteria	LQTS
ECG parameters—must be included in the diagnosis		
QTc (Bazett formula)		
	≥ 480 ms	3
	460–470 ms	2
	450–459 ms (males only)	1
0	371–459 ms (“normal” QTc for female patient)	0
0	371–450 ms (“normal” QTc for male patient)	0
1	351–370 ms	
2	331–350 ms	
3	<330 ms	
	Torsade de pointes ^a	2
	T-wave alternans	1
	≥ 3 leads with notched T-waves	1
	Bradycardia (<2 nd percentile for age)	0.5
1	Jpoint–Tpeak interval < 120 ms	
Clinical history		
2	History of sudden cardiac arrest	
2	Documented polymorphic VT or VF ^a	
1	History of syncope ^a	
	Without stress	1
	With stress	2
1	Atrial fibrillation	
	Congenital deafness	0.5
Family history		
	Family history of LQTS ^b	1
2	Family history of SQTS ^b	
1	Unexplained sudden death: first-degree family member $< \text{age } 30^b$	0.5
1	Sudden infant death syndrome (SIDS) ^b	
Genotype		
2	Genotype positive	
1	Variant of uncertain significance (VUS) in a culprit gene	

Low probability: ≤ 2 points (SQTS), ≤ 1 point (LQTS); intermediate probability: 3 points (SQTS), 2–3 points (LQTS); and high probability: ≥ 4 points (SQTS and LQTS). Electrocardiogram must be recorded in the absence of modifiers known to shorten or lengthen the QT interval. Jpoint–Tpeak must be measured in the precordial lead with the greatest amplitude T wave. A minimum of 1 point must be obtained in the ECG section in order to obtain additional points.

^aSyncope and torsade de pointes are mutually exclusive.

^bCannot count the same family member twice. VF, ventricular fibrillation; VT, ventricular tachycardia. SQTS criterion adapted from Gollob MH, Redpath CJ, Roberts JD. The short QT syndrome: proposed diagnostic criteria. *J Am Coll Cardiol* 2011;57:802–812; LQTS criterion adapted from Schwartz PJ, Moss AJ, Vincent GM, et al. Diagnostic criteria for the long QT syndrome. An update. *Circulation* 1993;88:782–784.

8% per year. Indicators of increased risk for SCD include a QTc > 500 ms (71,72), a history of TdP-mediated syncope (72,73), prepubertal males and postpubertal females (74), and events occurring during the first year of life (75). Genetic risk factors include multiple mutations, LQT2 or LQT3 genotype (71), and the presence of higher risk mutations based on molecular location and cellular function (76–81). Both symptomatic and asymptomatic patients with LQTS must avoid medications that prolong the QT interval (www.qtdrugs.org). In addition, patients should maintain adequate hydration/electrolyte replenishment in the setting of vomiting and diarrhea that could cause hypokalemia. Asymptomatic patients >40 years of age, especially those with nondiagnostic QTc values at rest, may not require active intervention but this must be individualized.

In general, all symptomatic patients and all asymptomatic patients <40 years of age should receive medical, surgical, and/or device-related therapy. β -Blockers, preferably nadolol or propranolol, should be considered standard therapy for all patients with either LQT1 or LQT2 (57,82). In contrast, the protective role of β -blockers for patients with LQT3 is controversial and confusing. Initial clinical reports failed to demonstrate clear efficacy (57). Subsequently, *in vitro* cellular studies raised the concern of a possible proarrhythmic effect of β -blockers for LQT3 (83). These observations likely catalyzed the overuse of internal cardioverter defibrillators (ICDs) in the management of patients with LQT3 (84,85). β -Blocking drugs, particularly propranolol, are reemerging as initial treatment of choice for LQT3 (unpublished data). Additionally, genotype-targeted therapy with late sodium current blockers such as mexiletine, flecainide, or ranolazine may be considered as stand-alone or concomitant therapy with propranolol (57,86,87).

Despite a class IIb guideline recommendations for an ICD in any patient diagnosed with LQTS (88), more appropriate indications for an ICD include (a) aborted cardiac arrest (regardless of genotype) as secondary prevention, (b) breakthrough cardiac event despite adequate medical therapy, (c) intolerance of primary pharmacotherapy, and (d) prior LQTS-triggered cardiac events plus QTc > 550 ms (particularly in LQT2 women) (84,85,89). In general, a single lead ICD system is preferred unless pacing is required. Conversely, there is probably little role for pacemaker-only therapy except possibly in LQT2 when a pause-dependent premature ventricular contraction triggering mechanism is suspected or documented. Usually however, if a pacemaker is contemplated for therapy, a dual-chamber PM/ICD should be utilized instead.

A unilateral left cardiac sympathetic denervation (LCSD) involving surgical ablation of the lower half of the left stellate ganglion along with the left-sided thoracic ganglia T2 through T4 is indicated either for patients receiving recurrent ventricular fibrillation (VF)-terminating ICD shocks or patients who do not tolerate adequate doses of appropriate drugs (90,91). LCSD also could be considered for patients with a pharmacotherapeutic breakthrough events. Also, LCSD may be useful as a “bridge to ICD” for those patients at high risk for an LQTS-triggered cardiac event but who are high risk for ICD-related complications such as infants and children. According to the 2005 Bethesda Conference no. 36 guidelines, competitive sports are restricted (except class IA activities of golf, cricket, bowling, billiards, and riflery) in all patients with symptomatic LQTS (except possibly LQT3) (92). However, these guidelines/expert opinion-based recommendations are not accepted uniformly within the community of both pediatric and adult heart rhythm specialists especially for the athlete with LQTS and an ICD (www.icdsportsregistry.com) (93,94). Currently, there is guidelines-based support for relaxing these competitive sports restrictions for patients with concealed LQTS defined as genotype positive but asymptomatic with QTc < 480 ms in females and <470 ms in males.

Autosomal Recessive LQTS (Jervell and Lange-Nielsen)

In contrast to Romano-Ward LQTS, autosomal recessive LQTS (Jervell and Lange-Nielsen syndrome, JLNS) is extremely rare affecting one per million persons. The cardiac phenotype generally is more severe and, in fact, primary prevention with a β -blocker plus ICD therapy or β -blocker plus LCSD therapy is indicated for JLNS. JLNS involves homozygous or compound heterozygous (“double hit”) mutations in the I_{Ks} potassium channel. Type 1 JLNS (JLN1) arises from such double mutations in *KCNQ1* (i.e., double LQT1), whereas type 2 JLNS (JLN2) stems from double mutations in *KCNE1* (double LQT5). These genes encode, respectively, the Kv7.1's α - and β -subunits of the critical phase 3 repolarizing potassium current, I_{Ks} . By definition, both parents of a child with JLNS are obligate affected individuals with either LQT1 or LQT5. That is, the cardiac phenotype in JLNS is a dominant trait although the parents generally have an asymptomatic course and minimal, if any, manifest QT prolongation. In contrast, the deafness is a recessive trait. This same I_{Ks} potassium channel is critical for potassium homeostasis of the endolymph in inner ear.

Multisystem or Complex LQTS

ATS is a multisystem disorder that includes skeletal and facial features, periodic paralysis, and abnormal cardiac repolarization. Loss-of-function mutations involving the *KCNJ2*-encoded inwardly rectifying potassium channel (Kir2.1) is implicated in the pathogenesis of approximately 50% to 60% of ATS (95). Unlike the classical forms of LQTS, however, the abnormal repolarization in ATS1 is better characterized as normal QT interval, prolonged QU intervals, with prolonged/abnormal U waves (Fig. 16.2C) (96). The incidence of sudden death is less in ATS than the major subtypes of LQTS.

TS is a rare multisystem disorder that includes abnormal cardiac repolarization, syncope and sudden death, syndactyly, and significant learning disability. Mutations in the α subunit of the L-type calcium channel ($Ca_v1.2$) encoded by *CACNA1C* (particularly a specific missense mutation G406R) have been identified (97). The mutation results in near complete loss of voltage-dependent channel *inactivation* of $Ca_v1.2$ producing QT prolongation secondary to increased calcium influx (i.e., gain-of-function phenotype). Although extremely rare, TS is associated with a very severe phenotype, and primary prevention ICD therapy probably is indicated. Like LQTS, genetic testing for both ATS and TS is available.

Short QT Syndrome

There are three genetic subtypes of SQTS, each representing the antithesis of loss-of-function, potassium channel-mediated LQTS, and ATS (98–101). The three SQTS subtypes stem from gain-of-function mutations in *KCNH2*, *KCNQ1*, and *KCNJ2*. These mutant potassium channels accelerate cardiac repolarization. Electrocardiographically, the characteristic ECG finding is a short QT interval (QTc \leq 330 ms), with tall, symmetrical, peaked T-waves (Fig. 16.2D).

Recently, diagnostic criteria for SQTS have been proposed. The SQTS score awards points not only for the QT interval but also for the personal and family history (Table 16.2) (102). These patients present with sudden death, syncope, palpitations, and, sometimes, paroxysmal atrial fibrillation. The age at which sudden death occurs varies from 3 months to 70 years. Most patients have a family history of sudden death. The degree of incomplete penetrance, variable expressivity, and overall prevalence of SQTS are poorly understood. However, SQTS is thought

to be much less common than LQTS. Examples of family members who are genotype positive for a SQTs-associated mutation but a normal resting QT interval have been reported.

Most patients have easily inducible VF during electrophysiologic studies and have short atrial and ventricular refractory periods. The therapy of choice is an ICD. However, these patients are at increased risk of inappropriate shocks from T-wave oversensing. ICD detection algorithms may decrease the risk of inappropriate shocks. Adjunctive pharmacotherapy with drugs like propafenone, quinidine, dofetilide, or sotalol may help prolong the QT interval and decrease the potential for VF.

Catecholaminergic Polymorphic Ventricular Tachycardia

CPVT is characterized by exercise/stress-induced syncope and/or sudden death in the setting of a structurally normal heart with a normal QT interval (103). CPVT clinically mimics concealed type 1 LQTS but is far more malignant than concealed (normal QT interval) LQTS. In fact, 3% to 4% of patients referred for LQTS genetic testing actually have CPVT-associated mutations (104). Initially, CPVT was described in children, but more recent studies suggest that the age at presentation can vary from infancy to 40 years. In one-third of patients with CPVT, there is a family history positive for juvenile sudden death (105). The hallmark electrocardiographic feature of CPVT is exercise or isoproterenol-induced ventricular arrhythmias, particularly bidirectional VT (Fig. 16.2E). However, the vast majority of mutation-proven CPVT patients in our clinic never have exhibited CPVT's trademark arrhythmia during stress testing. Also, bidirectional VT during exercise has been reported in ATS and LQTS. Importantly, a patient with a history of exertional syncope, normal QT interval at rest, and exercise-induced ventricular ectopy is far more likely to have CPVT than LQTS. Moreover, a history of exercise-induced seizures should prompt investigation for the possibility of either LQTS or CPVT before concluding that it is epileptogenic in origin (106–108).

The pathogenic substrates for CPVT involve key components of intracellular calcium-induced calcium release from the sarcoplasmic reticulum. Type 1 CPVT (CPVT1) stems from mutations in the *RYR2*-encoded cardiac ryanodine receptor or calcium release channel and accounts for approximately 60% of CPVT (109,110). Mutations in *RYR2* confer a *gain-of-function* phenotype to the calcium release channel resulting in increased calcium leak during sympathetic stimulation, particularly in diastole. In contrast to the autosomal dominant/sporadic CPVT1, CPVT2 is autosomal recessive, very rare, and is due to mutations in *CASQ2*-encoded calsequestrin (111,112). Mutations in *KCNJ2*, the same gene for both ATS and SQTs, also may contribute to CPVT (113).

β -Blockers are first-line therapy for patients with symptomatic CPVT. However, because CPVT is more aggressive than LQTS and because β -blockers appear less protective in CPVT compared to LQT1 (105), concomitant therapy with either calcium channel blocking agents (verapamil), flecainide, and/or LCSD should be considered strongly (114–117). An ICD never should be implanted as stand-alone therapy because of the potential for a refractory ICD storm in a CPVT patient whereby the first VF-terminating shock only transiently restores normal sinus rhythm before VF recurs with ultimate failure of the device to restore order.

Brugada Syndrome

The BrS is characterized by typical ECG findings of cove-type ST elevation (type 1 BrS ECG, Fig. 16.2F) in the right precordial leads (V1 to V3) with or without incomplete or complete right bundle branch block, and an increased risk of sudden

death (118). The prevalence of a spontaneous Brugada ECG pattern in the general population is estimated to range from 0.05% to 0.6%. The characterization of a cove-type ST elevation (type I Brugada ECG pattern) or saddle back ST segment elevation (type II Brugada ECG pattern) reflects distinct differences in the risk of sudden death. Overall, the saddle-back-type ST elevation is more common in the general population and far less specific for BrS.

The majority of patients with symptomatic BrS both in Europe and Japan have a cove-type ST elevation (119). The type I Brugada ECG pattern may be present at rest or when unmasked with class I sodium channel blockers including ajmaline, flecainide, or procainamide. Provocative testing with class I agents is used strictly for diagnosis and is of no prognostic value. Superior performance of ajmaline during provocative testing has been demonstrated but this medication is not available in the United States. Increased sensitivity with the resting ECG is achieved by placing the right precordial leads of V1 and V2 in the second intercostal space (Fig. 16.5) (120,121).

Patients more often are male, and often present with SCD due to VF or with syncope due to polymorphic VT. The age of diagnosis ranges from 2 months to 77 years, with a mean of approximately 40 years. Up to 20% of patients diagnosed with idiopathic VF initially may have BrS. An estimated 10% to 20% of patients with BrS also have atrial fibrillation.

In contrast to LQT3 that is due to *gain-of-function* mutations involving the *SCN5A*-encoded cardiac sodium channel $Na_v1.5$, 20% to 30% of BrS is due to *loss-of-function* mutations in *SCN5A* (BrS1) (122,123). To date, over 300 BrS1-causing mutations have been identified in *SCN5A* (124). Over the past 2 years, 10 additional BrS-susceptibility genes: *GPD1L*, *CACNA1C*, *CACNB2*, *CACNA2D1*, *SCN1B*, *SCN3B*, *KCNE3*, *HCN4*, *KCNJ8*, and *KCND3* have been identified (125–134). *GPD1L*-, *SCN1B*-, *SCN3B*-, *KCNE3*-, *HCN4*-, *KCNJ8*-, and *KCND3*-BrS appear to be extremely uncommon (<1% frequency for each) and thus no meaningful genotype–phenotype relationships exist at this point. BrS secondary to dysregulation of the L-type calcium channel complex may be more common (~10%) (126,129). For the most part, there is no apparent difference in clinical outcome for patients with BrS1 versus the majority of patients with *SCN5A*-negative BrS. Patients with BrS1 tend to have longer HV intervals. Patients with BrS1 and a nonsense or frameshift mutation resulting in premature truncations of $Na_v1.5$ exhibit a more severe phenotype (often with concomitant evidence of conduction disease), than patients with a missense mutations (135). Genetic testing is available commercially for BrS1. The *a priori* yield is approximately 25% (50) (www.brugadadrugs.org).

The outcome of patients with BrS depends strongly on the presence of symptoms and the spontaneous presence of a type 1 BrS ECG pattern. In patients who present with aborted sudden death, nearly 66% had documented VF or sudden death in a 4.5-year follow-up period (136). In comparison, only 19% of patients who presented with syncope had VF or sudden death (136). This percentage decreased further to 8% in asymptomatic patients. Therefore, an ICD is indicated for all symptomatic patients (either aborted cardiac arrest or arrhythmic syncope) with BrS (119).

The role of programmed electrical stimulation (PES) for risk stratification of asymptomatic individuals remains unclear (137–140). Proponents of PES–(electrophysiologic study) EPS would advise ICD therapy as primary prevention for asymptomatic patients with inducible VF. Opponents suggest that there is no role for an EPS in the evaluation of BrS. Because BrS-associated events are infrequent in children and adolescents, there is essentially *no* role for an EPS in the *asymptomatic* pediatric patient with only a spontaneous or provoked type I Brugada ECG pattern. Besides ICD therapy for secondary

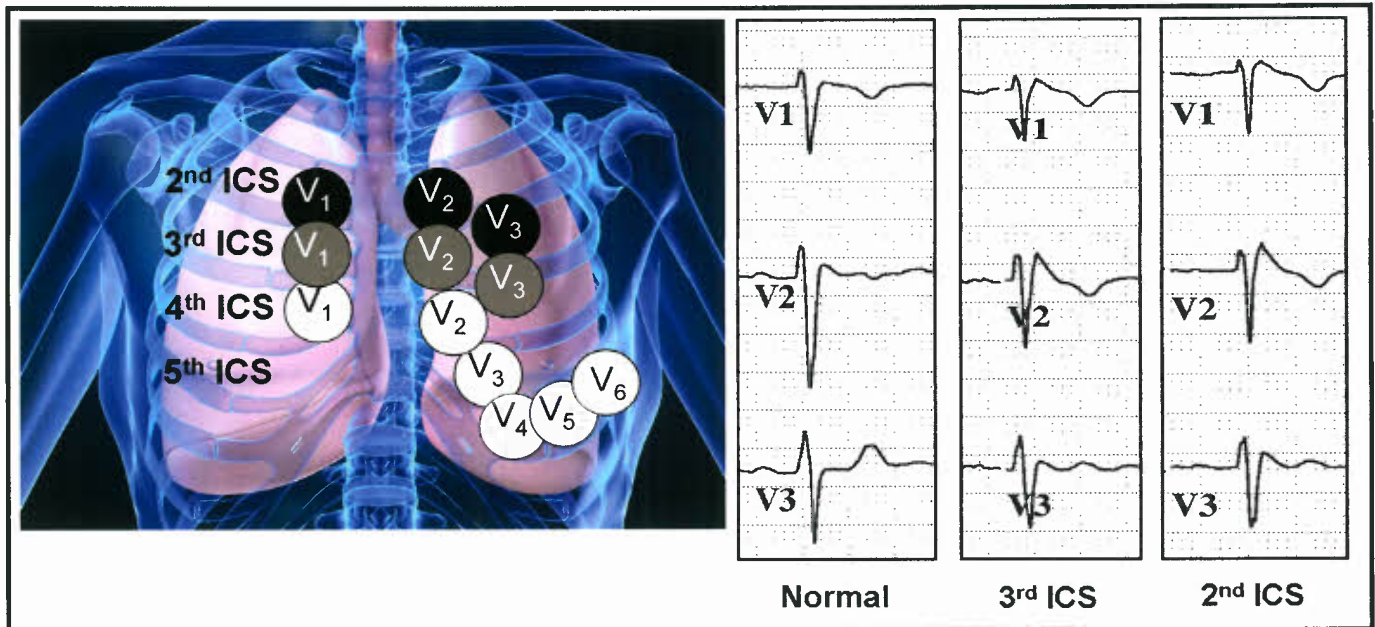


Figure 16.5. High-lead ECG protocol to unmask a type I Brugada ECG pattern. The type I (coved-type), type II (saddle-back), and type III Brugada ECG patterns are shown in the **upper left panel** with the type I Brugada ECG pattern being most sensitive/specific for the presence of BrS. The high-lead ECG protocol (**bottom left panel**) is used to unmask a type I Brugada ECG pattern shown in **bottom right panel**. After obtaining a standard 12-lead ECG (**left panel**), the right precordial leads V1–V3 are moved up one intercostal space and the ECG is repeated (**middle panel**), and then the V1–V3 leads are moved up another intercostal space and the ECG is repeated (**right panel**). As shown, conversion into a positive type I Brugada ECG pattern is equivalent to a positive drug challenge with agents like ajmaline, procainamide, or flecainide. This simple noninvasive maneuver may be as sensitive as a procainamide challenge although not equal to an ajmaline challenge. Ajmaline is a superior provocative agent but is not available in the United States.

prevention, there may be a role for quinidine in patients with recurrent VF-terminating ICD shocks (141). Aggressive management of febrile illnesses is warranted as fever appears to be an arrhythmic trigger for patients with BrS (142,143).

DISTINGUISHING FEATURES OF “COMMON YET BENIGN” SYNCOPE FROM “SUDDEN DEATH WARNING SIGN” SYNCOPE

It is estimated that approximately half of patients with channelopathies may be asymptomatic and long lived, while the other half will have at least one arrhythmia-mediated cardiac event. For most, that first cardiac event will be arrhythmic syncope with spontaneous resolution (i.e., self-terminating TdP/VF). In contrast to these channelopathies with a combined prevalence of 1 per 1,000, syncope while in normal sinus rhythm (i.e., vasovagal or neurocardiogenic syncope) is extremely common in the general population. Unless there is documentation of the rhythm at the time of the faint, distinguishing the common faint from a potential sudden death warning depends on the circumstances during and surrounding the faint.

Greater than 95% of all syncopal episodes involving otherwise healthy adolescents and young adults are innocuous. Approximately 15% of children and 25% of military recruits (age 17 to 26) have had one syncopal episode (144,145). Syncope will affect up to 20% of males and up to 50% of females by the age of 20, and results in approximately 1 of every 1,200 visits to a pediatric emergency department (144,146,147). However, important cardiac pathology is found in fewer than 5% of children and adolescents with syncope

(148). One of the first population-based studies involving syncope in children and adolescents showed that the incidence of syncope coming to medical attention was between 71.9 and 125.8 per 100,000 population. There was a greater incidence for girls than for boys and the peak incidence was between 15 and 19 years of age (149). In this study, syncope was associated with an acute illness (25%), a noxious stimulus (21%), prescription medication (18%), emotion (12%), bodily function (11%), and/or shower/bath/standing in church (9%). Exertion accounted only for 4% of the syncopal episodes. The vast majority of subjects had a diagnosis of benign vasovagal/neurocardiogenic syncope. Notably, the small subset with a potentially lethal cardiac condition was found among the subjects who fainted during exercise. More recently, investigators from a study involving nearly 500 subjects who fainted concluded that 95% had a noncardiac cause of their syncope, while 3% had LQTS, 1% had another arrhythmia, and 0.4% had a cardiomyopathy (150). An abrupt-onset faint with negligible prodrome that occurred *during* exercise (*not at the conclusion of a SK race*) or during an acute auditory trigger helped to separate those with a sudden death predisposing cardiac condition from the large group of patients with benign syncope.

Although there is only a 3% to 5% chance of important heart disease (i.e., cardiac channelopathy or cardiomyopathy) among all youthful fainters, the pretest probability increases to approximately 35% for a young person with an *exercise-triggered faint*. With an odds ratio > 10 stemming from knowing the patient's history, it is critical that a faint during exercise be viewed as potentially serious. However, it is even more critical to be sure that the faint indeed was exercise-triggered. Here, many *faux pas* have been committed. The history must be gathered carefully. What may initially be described as exercise-associated syncope may, in fact, have occurred after exercise or while the

subject was watching others exercise. An accurate history is extremely important when evaluating a patient who has fainted.

For the patient who truly had a sudden death warning faint, a thorough review of the patient's clinical history and family history is vital. The family history should seek to (a) identify any relatives with similar episodes of unexplained, abrupt onset syncope, (b) identify any relatives diagnosed previously with any form of heart disease, (c) identify any relatives who died suddenly and unexpectedly before the age of 50 years, and (d) identify any relatives who drowned or were involved in single motor vehicle accidents. This should be followed by careful scrutiny of the patient's 12-lead ECG, 24-hour ambulatory ECG, treadmill stress test, and echocardiogram.

Exercise-induced fainting is associated with a 35% chance, not a 100% chance, of an important heart condition. In other words, such a faint does *not* mandate that a diagnosis of a cardiac condition be made. This must be kept in clear view as many of these syndromes have been overdiagnosed seemingly compelled by an obligation to find something wrong with the person who faints during exercise. Benign vasovagal/neurocardiogenic syncope, indeed, can occur "during exercise" but this conclusion must be arrived at only *after* intense investigation.

Even though the vast majority of pediatric patients have a benign mechanism for their syncope, the clinical evaluation of syncope often results in extensive costly testing and possible referral to a pediatric cardiologist for further evaluation (151). In any case of emergency department referral for syncope, especially when cardiac disease is suspected, an ECG is the diagnostic test of choice. If there was a low index of suspicion before the ECG, a normal ECG should probably prompt dismissal from further cardiac evaluation. One must exercise caution when assessing the QTc in the emergency department following a faint that occurred earlier that day. In this setting, the prevalence of borderline QTc values may be even greater because cardiac repolarization may be reacting to the faint rather than suggesting the presence of a substrate responsible for the faint. Previously, we noted that 38% of fainters and 31% of controls had a QTc between 420 and 470 ms that often prompted premature considerations of "borderline" LQTS (152). More recently, a large review of nearly 1,600 patient ECGs obtained in an adult emergency department demonstrated that 35% of patients had a QTc > 450 (males) or > 460 ms (females) (153). The QTc distribution curves shown for otherwise healthy individuals in Figure 16.4 are right shifted among patients seeking medical attention.

Managing the patient who fainted after a prodrome and in the setting of overheating/dehydration, venipuncture/sight of blood, prolonged standing, or during micturition can be vexing. Although not life threatening, these faints are a nuisance for the patient and the family. Although not really a cardiac condition, it often is the pediatric cardiologist who is asked to evaluate these patients. Diagnostic tests should be kept to a minimum. Aggressive hydration (60 to 80 oz of noncaffeinated beverage or until urine is clear) and liberal salt intake often are all that is necessary. Increasing aerobic fitness can help decrease these spells. Drug therapy is entirely trial-and-error, and polypharmacy should be discouraged. Medications tried include β -blockers, vasoconstrictors like midodrine, salt-retaining drugs like Florinef, and selective serotonin reuptake inhibitors.

REFERENCES

- Virmani R, Burke AP, Farb A. Sudden cardiac death. *Cardiovasc Pathol* 2001;10:275–282.
- Liberthson RR. Sudden death from cardiac causes in children and young adults. *New Engl J Med* 1996;334:1039–1044.
- Cote A, Russo P, Michaud J. Sudden unexpected deaths in infancy: what are the causes? *J Pediatr* 1999;135:437–443.
- Arnestad M, Vege A, Rognum TO. Evaluation of diagnostic tools applied in the examination of sudden unexpected deaths in infancy and early childhood. *Forensic Sci Int* 2002;125:262–268.
- Dwyer T, Ponsonby AL, Blizzard L, et al. The contribution of changes in the prevalence of prone sleeping position to the decline in sudden infant death syndrome in Tasmania. *JAMA* 1995;273:783–789.
- Kinney HC, Thach BT. The sudden infant death syndrome. *New Engl J Med* 2009;361:795–805.
- Chugh SS, Kelly KL, Titus JL. Sudden cardiac death with apparently normal heart. *Circulation* 2000;102:649–654.
- Maron BJ, Shirani J, Poliac LC, et al. Sudden death in young competitive athletes. Clinical, demographic, and pathological profiles.[see comment]. *JAMA* 1996;276:199–204.
- Corrado D, Basso C, Thiene G. Sudden cardiac death in young people with apparently normal heart. *Cardiovasc Res* 2001;50:399–408.
- Behr E, Wood DA, Wright M, et al. Cardiological assessment of first-degree relatives in sudden arrhythmic death syndrome. *Lancet* 2003;362:1457.
- Morentin B, Suarez-Mier MP, Aguilera B. Sudden unexplained death among persons 1–35 years old. *Forensic Sci Int* 2003;135:213–217.
- Puranik R, Chow CK, Dufloy JA, et al. Sudden death in the young. *Heart Rhythm* 2005;2:1277–1282.
- Wever EF, Robles de Medina EO. Sudden death in patients without structural heart disease. *J Am Coll Cardiol* 2004;43:1137–1144.
- Ackerman MJ. Cardiac channelopathies: it's in the genes. *Nat Med* 2004;10:463–464.
- Ackerman MJ. Cardiac causes of sudden unexpected death in children and their relationship to seizures and syncope: genetic testing for cardiac electrophathies. *Semin Pediatr Neurol* 2005;12:52–58.
- Goldenberg I, Moss AJ, Zareba W. Sudden cardiac death without structural heart disease: update on the long QT and Brugada syndromes. *Curr Cardiol Rep* 2005;7:349–356.
- Ackerman MJ, Tester DJ, Porter CJ, et al. Molecular diagnosis of the inherited long-QT syndrome in a woman who died after near-drowning. *New Engl J Med* 1999;341:1121–1125.
- Priori SG, Napolitano C, Giordano U, et al. Brugada syndrome and sudden cardiac death in children. *Lancet* 2000;355:808–809.
- Ackerman MJ, Siu BL, Sturner WQ, et al. Postmortem molecular analysis of SCN5A defects in sudden infant death syndrome. *JAMA* 2001;286:2264–2269.
- Ackerman MJ, Tester DJ, Driscoll DJ. Molecular autopsy of sudden unexplained death in the young. *Am J Forensic Med Pathol* 2001;22:105–111.
- Chugh SS, Senashova O, Watts A, et al. Postmortem molecular screening in unexplained sudden death. *J Am Coll Cardiol* 2004;43:1625–1629.
- Eckart RE, Scoville SL, Campbell CL, et al. Sudden death in young adults: a 25-year review of autopsies in military recruits. *Ann Intern Med* 2004;141:829–834.
- Tan HL, Hofman N, van Langen IM, et al. Sudden unexplained death: heritability and diagnostic yield of cardiological and genetic examination in surviving relatives. *Circulation* 2005;112:207–213.
- Priori SG, Napolitano C, Schwartz PJ. Low penetrance in the long-QT syndrome: clinical impact. *Circulation* 1999;99:529–533.
- Di Paolo M, Luchini D, Bloise R, et al. Postmortem molecular analysis in victims of sudden unexplained death. *Am J Forensic Med Pathol* 2004;25:182–184.
- Tester DJ, Ackerman MJ. Postmortem long QT syndrome genetic testing for sudden unexplained death in the young. [see comment]. *J Am Coll Cardiol* 2007;49:240–246.
- Tester DJ, Spoon DB, Valdivia HH, et al. Targeted mutational analysis of the RyR2-encoded cardiac ryanodine receptor in sudden unexplained death: a molecular autopsy of 49 medical examiner/coroner's cases. *Mayo Clin Proc* 2004;79:1380–1384.
- Tester DJ, McCormack J, Ackerman MJ. Prenatal molecular genetic diagnosis of congenital long QT syndrome by strategic genotyping. *Am J Cardiol* 2004;93:788–791.
- Tester DJ, Ackerman MJ. Sudden infant death syndrome: how significant are the cardiac channelopathies? *Cardiovasc Res* 2005;67:388–396.
- Tester DJ, Dura M, Carturan E, et al. A mechanism for sudden infant death syndrome (SIDS): stress-induced leak via ryanodine receptors. *Heart Rhythm* 2007;4:733–739.
- Van Norstrand DW, Ackerman MJ. Sudden infant death syndrome: do ion channels play a role? *Heart Rhythm* 2009;6:272–278.
- Arnestad M, Crotti L, Rognum TO, et al. Prevalence of long-QT syndrome gene variants in sudden infant death syndrome. [see comment]. *Circulation* 2007;115:361–367.
- Wang DW, Desai RR, Crotti L, et al. Cardiac sodium channel dysfunction in sudden infant death syndrome. *Circulation* 2007;115:368–376.
- Van Norstrand DW, Valdivia CR, Tester DJ, et al. Molecular and functional characterization of novel glycerol-3-phosphate dehydrogenase 1 like gene (GPD1-L) mutations in sudden infant death syndrome. *Circulation* 2007;116:2253–2259.
- Van Norstrand DW, Pundi KN, Tester DJ, et al. Identification of cardiac sodium channel beta subunit mutations in sudden infant death syndrome. *Heart Rhythm* 2008;5:S94.
- Curran ME, Splawski I, Timothy KW, et al. A molecular basis for cardiac arrhythmia: HERG mutations cause long QT syndrome. *Cell* 1995;80:795–803.
- Wang Q, Shen J, Li Z, et al. Cardiac sodium channel mutations in patients with long QT syndrome, an inherited cardiac arrhythmia. *Hum Mol Genet* 1995;4:1603–1607.

38. Olson TM, Michels VV, Ballew JD, et al. Sodium channel mutations and susceptibility to heart failure and atrial fibrillation. [see comment]. *JAMA* 2005;293:447-454.
39. Romano C, Gemme G, Pongiglione R. [Rare Cardiac Arrhythmias of the Pediatric Age. I. Repetitive Paroxysmal Tachycardia]. *Minerva Pediatr* 1963;15:1155-1164.
40. Ward O. A new familial cardiac syndrome in children. *J Ir Med Assoc* 1964;54:103-106.
41. Mohler PJ, Schott JJ, Gramolini AO, et al. Ankyrin-B mutation causes type 4 long-QT cardiac arrhythmia and sudden cardiac death. *Nature* 2003;421:634-639.
42. Vatta M, Ackerman MJ, Ye B, et al. Mutant caveolin-3 induces persistent late sodium current and is associated with long-QT syndrome. *Circulation* 2006;114:2104-2112.
43. Chen L, Marquardt ML, Tester DJ, et al. Mutation of an A-kinase-anchoring protein causes long-QT syndrome. *Proc Natl Acad Sci* 2007;104:20990-20995.
44. Ueda K, Valdivia C, Medeiros-Domingo A, et al. Syntrophin mutation associated with long QT syndrome through activation of the nNOS-SCN5A macromolecular complex. *Proc Natl Acad Sci USA* 2008;105:9355-9360.
45. Splawski I, Shen J, Timothy KW, et al. Spectrum of mutations in long-QT syndrome genes. KVLQT1, HERG, SCN5A, KCNE1, and KCNE2. *Circulation* 2000;102:1178-1185.
46. Tester DJ, Will ML, Haglund CM, et al. Compendium of cardiac channel mutations in 541 consecutive unrelated patients referred for long QT syndrome genetic testing. *Heart Rhythm* 2005;2:507-517.
47. Zhang L, Timothy KW, Vincent GM, et al. Spectrum of ST-T-wave patterns and repolarization parameters in congenital long-QT syndrome: ECG findings identify genotypes. *Circulation* 2000;102:2849-2855.
48. Moss AJ, Zareba W, Benhorin J, et al. ECG T-wave patterns in genetically distinct forms of the hereditary long QT syndrome. *Circulation* 1995;92:2929-2934.
49. Ackerman MJ, Tester DJ, Porter CJ. Swimming, a gene-specific arrhythmogenic trigger for inherited long QT syndrome. *Mayo Clin Proc* 1999;74:1088-1094.
50. Wilde AA, Jongbloed RJ, Doevendans PA, et al. Auditory stimuli as a trigger for arrhythmic events differentiate HERG-related (LQTS2) patients from KVLQT1-related patients (LQTS1). *J Am Coll Cardiol* 1999;33:327-332.
51. Moss AJ, Robinson JL, Gessman L, et al. Comparison of clinical and genetic variables of cardiac events associated with loud noise versus swimming among subjects with the long QT syndrome. *Am J Cardiol* 1999;84:876-879.
52. Schwartz PJ, Priori SG, Spazzolini C, et al. Genotype-phenotype correlation in the long-QT syndrome: gene-specific triggers for life-threatening arrhythmias. *Circulation* 2001;103:89-95.
53. Khositseth A, Tester DJ, Will ML, et al. Identification of a common genetic substrate underlying postpartum cardiac events in congenital long QT syndrome. *Heart Rhythm* 2004;1:60-64.
54. Moss AJ, Zareba W, Hall WJ, et al. Effectiveness and limitations of beta-blocker therapy in congenital long-QT syndrome. *Circulation* 2000;101:616-623.
55. Tester DJ, Will ML, Haglund CM, et al. Effect of clinical phenotype on yield of long QT syndrome genetic testing. *J Am Coll Cardiol* 2006;47:764-768.
56. Kapa S, Tester DJ, Salisbury BA, et al. Genetic testing for long-QT syndrome: distinguishing pathogenic mutations from benign variants. *Circulation* 2009;120:1752-1760.
57. Tester DJ, Ackerman MJ. Genetic testing for potentially lethal, highly treatable inherited cardiomyopathies/channelopathies in clinical practice. *Circulation* 2011;123:1021-1037.
58. Viskin S, Rosovski U, Sands AJ, et al. Inaccurate electrocardiographic interpretation of long QT: the majority of physicians cannot recognize a long QT when they see one. [see comment]. *Heart Rhythm* 2005;2:569-574.
59. Vincent GM, Jaiswal D, Timothy KW. Effects of exercise on heart rate, QT, QTc and QT/QTc in the Romano-Ward inherited long QT syndrome. *Am J Cardiol* 1991;68:498-503.
60. Ackerman MJ, Khositseth A, Tester DJ, et al. Epinephrine-induced QT interval prolongation: a gene-specific paradoxical response in congenital long QT syndrome. *Mayo Clin Proc* 2002;77:413-421.
61. Shimizu W, Noda T, Takaki H, et al. Epinephrine unmasks latent mutation carriers with LQT1 form of congenital long-QT syndrome. *J Am Coll Cardiol* 2003;41:633-642.
62. Wong JA, Gula LJ, Klein GJ, et al. Utility of treadmill testing in identification and genotype prediction in long-QT syndrome. *Circ Arrhythm Electrophysiol* 2010;3:120-125.
63. Viskin S, Postema PG, Bhuiyan ZA, et al. The response of the QT interval to the brief tachycardia provoked by standing: a bedside test for diagnosing long QT syndrome. *J Am Coll Cardiol* 2010;55:1955-1961.
64. Vyas H, Hejlik J, Ackerman MJ. Epinephrine QT stress testing in the evaluation of congenital long-QT syndrome: diagnostic accuracy of the paradoxical QT response. *Circulation* 2006;113:1385-1392.
65. Schwartz PJ, Moss AJ, Vincent GM, et al. Diagnostic criteria for the long QT syndrome. An update. *Circulation* 1993;88:782-784.
66. Taggart NW, Haglund CM, Tester DJ, et al. Diagnostic miscues in congenital long-QT syndrome. [see comment]. *Circulation* 2007;115:2613-2620.
67. Priori SG, Schwartz PJ, Napolitano C, et al. Risk stratification in the long-QT syndrome. *New Engl J Med* 2003;348:1866-1874.
68. Liu JF, Jons C, Moss AJ, et al. Risk factors for recurrent syncope and subsequent fatal or near-fatal events in children and adolescents with long QT syndrome. *J Am Coll Cardiol* 2011;57:941-950.
69. Hobbs JB, Peterson DR, Moss AJ, et al. Risk of aborted cardiac arrest or sudden cardiac death during adolescence in the long-QT syndrome. *JAMA* 2006;296:1249-1254.
70. Locati EH, Zareba W, Moss AJ, et al. Age- and sex-related differences in clinical manifestations in patients with congenital long-QT syndrome: findings from the International LQTS Registry. *Circulation* 1998;97:2237-2244.
71. Spazzolini C, Mullally J, Moss AJ, et al. Clinical implications for patients with long QT syndrome who experience a cardiac event during infancy. [see comment]. *J Am Coll Cardiol* 2009;54:832-837.
72. Moss AJ, Zareba W, Kaufman ES, et al. Increased risk of arrhythmic events in long-QT syndrome with mutations in the pore region of the human ether-a-go-go-related gene potassium channel. *Circulation* 2002;105:794-799.
73. Moss AJ, Shimizu W, Wilde AA, et al. Clinical aspects of type-1 long-QT syndrome by location, coding type, and biophysical function of mutations involving the KCNQ1 gene. *Circulation* 2007;115:2481-2489.
74. Jons C, Moss AJ, Lopes CM, et al. Mutations in conserved amino acids in the KCNQ1 channel and risk of cardiac events in type-1 long-QT syndrome. *J Cardiovasc Electrophysiol* 2009;20:859-865.
75. Shimizu W, Moss AJ, Wilde AA, et al. Genotype-phenotype aspects of type 2 long QT syndrome. *J Am Coll Cardiol* 2009;54:2052-2062.
76. Shimizu W, Horie M, Ohno S, et al. Mutation site-specific differences in arrhythmic risk and sensitivity to sympathetic stimulation in the LQT1 form of congenital long QT syndrome. *J Am Coll Cardiol* 2004;44:117-125.
77. Nagaoka I, Shimizu W, Itoh H, et al. Mutation site dependent variability of cardiac events in Japanese LQT2 form of congenital long-QT syndrome. *Circ J* 2008;72:694-699.
78. Villain E, Denjoy I, Lupoglazoff JM, et al. Low incidence of cardiac events with B-blocking therapy in children with long QT syndrome. *Eur Heart J* 2004;25:1405-1411.
79. Shimizu W, Antzelevitch C. Differential effects of beta-adrenergic agonists and antagonists in LQT1, LQT2 and LQT3 models of the long QT syndrome. *J Am Coll Cardiol* 2000;35:778-786.
80. Schwartz PJ, Spazzolini C, Priori SG, et al. Who are the long-QT syndrome patients who receive an implantable cardioverter-defibrillator and what happens to them?: Data from the European long-QT syndrome implantable cardioverter-defibrillator (LQTS ICD) registry. *Circulation* 2010;122:1272-1282.
81. Horner JM, Kinoshita M, Webster TL, et al. Implantable cardioverter defibrillator therapy for congenital long QT syndrome: a single-center experience. *Heart Rhythm* 2010;7:1616-1622.
82. Schwartz PJ, Priori SG, Locati EH, et al. Long QT syndrome patients with mutations of the SCN5A and HERG genes have differential responses to Na⁺ channel blockade and to increases in heart rate. Implications for gene-specific therapy. *Circulation* 1995;92:3381-3386.
83. Moss AJ, Windle JR, Hall WJ, et al. Safety and efficacy of flecainide in subjects with long QT-3 syndrome (DeltaKPQ mutation): a randomized, double-blind, placebo-controlled clinical trial. *Ann Noninvasive Electrocardiol* 2005;10:59-66.
84. Epstein AE, DiMarco JP, Ellenbogen KA, et al. ACC/AHA/HRS 2008 guidelines for device-based therapy of cardiac rhythm abnormalities: executive summary: a report of the American College of Cardiology/American Heart Association Task Force on Practice Guidelines (Writing Committee to Revise the ACC/AHA/NASPE 2002 Guideline Update for Implantation of Cardiac Pacemakers and Antiarrhythmia Devices) developed in collaboration with the American association for thoracic surgery and society of thoracic surgeons. *J Am Coll Cardiol* 2008;51:2085-2105.
85. Zareba W, Moss AJ, Daubert JP, et al. Implantable cardioverter defibrillator in high-risk long QT syndrome patients. *J Cardiovasc Electrophysiol* 2003;14:337-341.
86. Moss AJ, McDonald J. Unilateral cervicothoracic sympathetic ganglionectomy for the treatment of long QT interval syndrome. *New Engl J Med* 1971;285:903-904.
87. Schwartz PJ, Priori SG, Cerrone M, et al. Left cardiac sympathetic denervation in the management of high-risk patients affected by the long-QT syndrome. *Circulation* 2004;109:1826-1833.
88. Zipes DP, Ackerman MJ, Estes NA III, et al. Task force 7: arrhythmias. *J Am Coll Cardiol* 2005;45:1354-1363.
89. Lampert R, Cannom D. Sports participation for athletes with implantable cardioverter-defibrillators should be an individualized risk-benefit decision. *Heart Rhythm* 2008;5:861-863.
90. Lampert R, Cannom D, Olshansky B. Safety of sports participation in patients with implantable cardioverter defibrillators: a survey of heart rhythm society members. *J Cardiovasc Electrophysiol* 2006;17:11-15.
91. Plaster NM, Tawil R, Tristani-Firouzi M, et al. Mutations in Kir2.1 cause the developmental and episodic electrical phenotypes of Andersen's syndrome. *Cell* 2001;105:511-519.
92. Zhang L, Benson DW, Tristani-Firouzi M, et al. Electrocardiographic features in Andersen-Tawil syndrome patients with KCNJ2 mutations: characteristic T-U-wave patterns predict the KCNJ2 genotype. *Circulation* 2005;111:2720-2726.
93. Splawski I, Timothy KW, Sharpe LM, et al. Cav1.2 calcium channel dysfunction causes a multisystem disorder including arrhythmia and autism. *Cell* 2004;119:19-31.
94. Gussak I, Brugada P, Brugada J, et al. Idiopathic short QT interval: a new clinical syndrome? *Cardiology* 2000;94:99-102.
95. Brugada R, Hong K, Dumaine R, et al. Sudden death associated with short-QT syndrome linked mutations in HERG. *Circulation* 2004;109:30-35.

96. Bellocq C, van Ginneken AC, Bezzina CR, et al. Mutation in the KCNQ1 gene leading to the short QT-interval syndrome. *Circulation* 2004;109:2394-2397.
97. Priori SG, Pandit SV, Rivolta I, et al. A novel form of short QT syndrome (SQT3) is caused by a mutation in the KCNJ2 gene. [see comment]. *Circ Res* 2005;96:800-807.
98. Gollob MH, Redpath CJ, Roberts JD. The short QT syndrome: proposed diagnostic criteria. *J Am Coll Cardiol* 2011;57:802-812.
99. Leenhardt A, Lucet V, Denjoy I, et al. Catecholaminergic polymorphic ventricular tachycardia in children: a 7-year follow-up of 21 patients. *Circulation* 1995;91:1512-1519.
100. Tester DJ, Kopplin LJ, Will ML, et al. Spectrum and prevalence of cardiac ryanodine receptor (RyR2) mutations in a cohort of unrelated patients referred explicitly for long QT syndrome genetic testing. *Heart Rhythm* 2005;2:1099-1105.
101. Priori SG, Napolitano C, Memmi M, et al. Clinical and molecular characterization of patients with catecholaminergic polymorphic ventricular tachycardia. *Circulation* 2002;106:69-74.
102. Johnson JN, Tester DJ, Bass NE, et al. Cardiac channel molecular autopsy for sudden unexpected death in epilepsy. *J Child Neurol* 2010;25:916-921.
103. Johnson JN, Hofman N, Haglund CM, et al. Identification of a possible pathogenic link between congenital long QT syndrome and epilepsy. *Neurology* 2009;72:224-231.
104. McCormick JM, McAlister H, Crawford J, et al. Misdiagnosis of long QT syndrome as epilepsy at first presentation. *Ann Emerg Med* 2009;54:26-32.
105. Laitinen PJ, Brown KM, Plippo K, et al. Mutations of the cardiac ryanodine receptor (RyR2) gene in familial polymorphic ventricular tachycardia. *Circulation* 2001;103:485-490.
106. Priori SG, Napolitano C, Tiso N, et al. Mutations in the cardiac ryanodine receptor gene (hRyR2) underlie catecholaminergic polymorphic ventricular tachycardia. *Circulation* 2001;103:196-200.
107. Lahat H, Eldar M, Levy-Nissenbaum E, et al. Autosomal recessive catecholamine- or exercise-induced polymorphic ventricular tachycardia: clinical features and assignment of the disease gene to chromosome 1p13-21. *Circulation* 2001;103:2822-2827.
108. Postma AV, Denjoy I, Hoorntje TM, et al. Absence of calsequestrin 2 causes severe forms of catecholaminergic polymorphic ventricular tachycardia. *Circ Res* 2002;91:E21-E26.
109. Tester DJ, Arya P, Will M, et al. Genotypic heterogeneity and phenotypic mimicry among unrelated patients referred for catecholaminergic polymorphic ventricular tachycardia genetic testing. *Heart Rhythm* 2006;3:800-805.
110. Wilde AAM, Bhuiyan ZA, Crotti L, et al. Left cardiac sympathetic denervation for catecholaminergic polymorphic ventricular tachycardia. *New Engl J Med* 2008;358:2024-2029.
111. Collura CA, Johnson JN, Moir C, et al. Left cardiac sympathetic denervation for the treatment of long QT syndrome and catecholaminergic polymorphic ventricular tachycardia using video-assisted thoracic surgery. *Heart Rhythm* 2009;6:752-759.
112. Rosso R, Kalman JM, Rogowski O, et al. Calcium channel blockers and beta-blockers versus beta-blockers alone for preventing exercise-induced arrhythmias in catecholaminergic polymorphic ventricular tachycardia. *Heart Rhythm* 2007;4:1149-1154.
113. Watanabe H, Chopra N, Laver D, et al. Flecainide prevents catecholaminergic polymorphic ventricular tachycardia in mice and humans. *Nat Med* 2009;15:380-383.
114. Brugada P, Brugada J. Right bundle branch block, persistent ST segment elevation and sudden cardiac death: a distinct clinical and electrocardiographic syndrome. A multicenter report. *J Am Coll Cardiol* 1992;20:1391-1396.
115. Antzelevitch C, Brugada P, Borggreffe M, et al. Brugada syndrome: report of the Second Consensus Conference. *Heart Rhythm* 2005;2:429-440.
116. Shimizu W, Matsuo K, Takagi M, et al. Body surface distribution and response to drugs of ST segment elevation in Brugada syndrome: clinical implication of eighty-seven-lead body surface potential mapping and its application to twelve-lead electrocardiograms. *J Cardiovasc Electrophysiol* 2000;11:396-404.
117. Sangwatanaroj S, Prechawat S, Sunsaneewitayakul B, et al. New electrocardiographic leads and the procainamide test for the detection of the Brugada sign in sudden unexplained death syndrome survivors and their relatives. *Eur Heart J* 2001;22:2290-2296.
118. Chen Q, Kirsch GE, Zhang D, et al. Genetic basis and molecular mechanism for idiopathic ventricular fibrillation. *Nature* 1998;392:293-296.
119. Vatta M, Dumaine R, Antzelevitch C, et al. Novel mutations in domain I of SCN5A cause Brugada syndrome. *Mol Genet Metab* 2002;75:317-324.
120. Kapplinger J, Tester D, Alders M, et al. An international compendium of mutations in the SCN5A-encoded cardiac sodium channel in patients referred for Brugada syndrome genetic testing. *Heart Rhythm* 2010;7:33-46.
121. London B, Michalec M, Mehdi H, et al. Mutation in glycerol-3-phosphate dehydrogenase 1 like gene (GPD1-L) decreases cardiac Na⁺ current and causes inherited arrhythmias. *Circulation* 2007;116:2260-2268.
122. Antzelevitch C, Pollevick GD, Cordeiro JM, et al. Loss-of-function mutations in the cardiac calcium channel underlie a new clinical entity characterized by ST-segment elevation, short QT intervals, and sudden cardiac death. *Circulation* 2007;115:442-449.
123. Watanabe H, Koopmann TT, Le Scouarnec S, et al. Sodium channel β 1 subunit mutations associated with Brugada syndrome and cardiac conduction disease in humans. *J Clin Invest* 2008;118:2260-2268.
124. Delpón E, Cordeiro JM, Nunez L, et al. Functional effects of KCNE3 mutation and its role in the development of Brugada syndrome. *Circ Arrhythm Electrophysiol* 2008;1:209-218.
125. Burashnikov E, Pfeiffer R, Barajas-Martinez H, et al. Mutations in the cardiac L-type calcium channel associated with inherited J-wave syndromes and sudden cardiac death. *Heart Rhythm* 2010;7:1872-1882.
126. Hu D, Barajas-Martinez H, Burashnikov E, et al. A mutation in the beta3 subunit of the cardiac sodium channel associated with Brugada ECG phenotype. *Circ Cardiovasc Genet* 2009;2:270-278.
127. Ueda K, Hirano Y, Higashiesato Y, et al. Role of HCN4 channel in preventing ventricular arrhythmia. *J Hum Genet* 2009;54:115-121.
128. Haissaguerre M, Chatelet S, Sacher F, et al. Ventricular fibrillation with prominent early repolarization associated with a rare variant of KCNJ8/KATP channel. *J Cardiovasc Electrophysiol* 2009;20:93-98.
129. Medeiros-Domingo A, Tan B-H, Crotti L, et al. Gain-of-function mutation S422L in the KCNJ8-encoded cardiac KATP channel Kir6.1 as a pathogenic substrate for J-wave syndromes. *Heart Rhythm* 2010;7:1466-1471.
130. Giudicessi JR, Ye D, Tester DJ, et al. Transient outward current (Ito) gain-of-function mutations in the KCND3-encoded Kv4.3 potassium channel and Brugada syndrome. *Heart Rhythm* 2011;8:7.
131. Merregalli PG, Tan HL, Probst V, et al. Type of SCN5A mutation determines clinical severity and degree of conduction slowing in loss-of-function sodium channelopathies. *Heart Rhythm* 2009;6:341-348.
132. Brugada J, Brugada R, Antzelevitch C, et al. Long-term follow-up of individuals with the electrocardiographic pattern of right bundle-branch block and ST-segment elevation in precordial leads V1 to V3. *Circulation* 2002;105:73-78.
133. Priori SG, Napolitano C, Gasparini M, et al. Natural history of Brugada syndrome: insights for risk stratification and management. *Circulation* 2002;105:1342-1347.
134. Brugada J, Brugada R, Brugada P. Determinants of sudden cardiac death in individuals with the electrocardiographic pattern of Brugada syndrome and no previous cardiac arrest. *Circulation* 2003;108:3092-3096.
135. Eckardt L, Probst V, Smits JPP, et al. Long-term prognosis of individuals with right precordial ST-segment-elevation Brugada syndrome. *Circulation* 2005;111:257-263.
136. Probst V, Veltmann C, Eckardt L, et al. Long-term prognosis of patients diagnosed with Brugada syndrome: results from the FINGER Brugada syndrome registry. *Circulation* 2010;121:635-643.
137. Belhassen B, Glick A, Viskin S. Efficacy of quinidine in high-risk patients with Brugada syndrome. *Circulation* 2004;110:1731-1737.
138. Saura D, Garcia-Alberola A, Carrillo P, et al. Brugada-like electrocardiographic pattern induced by fever. *Pacing Clin Electrophysiol* 2002;25:856-859.
139. Antzelevitch C, Brugada R. Fever and Brugada syndrome. *Pacing Clin Electrophysiol* 2002;25:1537-1539.
140. Lewis DA, Dhala A. Syncope in the pediatric patient. The cardiologist's perspective. *Pediatr Clin North Am* 1999;46:205-219.
141. Murdoch BD. Loss of consciousness in healthy South African men: incidence, causes and relationship to EEG abnormality. *South Afr Med J* 1980;57:771-774.
142. Pratt JL, Fleisher GR. Syncope in children and adolescents. *Pediatr Emerg Care* 1989;5:80-82.
143. Wieling W, Ganzeboom KS, Saul JP. Reflex syncope in children and adolescents. *Heart* 2004;90:1094-1100.
144. Driscoll DJ, Edwards WD. Sudden unexpected death in children and adolescents. *J Am Coll Cardiol* 1985;5:118B-121B.
145. Driscoll DJ, Jacobsen SJ, Porter CJ, et al. Syncope in children and adolescents. *J Am Coll Cardiol* 1997;29:1039-1045.
146. Ritter S, Tani LY, Etheridge SP, et al. What is the yield of screening echocardiography in pediatric syncope? *Pediatrics* 2000;105:E58.
147. Steinberg LA, Knillans TK. Syncope in children: diagnostic tests have a high cost and low yield. *J Pediatr* 2005;146:355-358.
148. Khositseth A, Martinez MW, Driscoll DJ, et al. Syncope in children and adolescents and the congenital long QT syndrome. *Am J Cardiol* 2003;92:746-749.
149. Seftchick MW, Adler PH, Hsieh M, et al. The prevalence and factors associated with QTc prolongation among emergency department patients. *Ann Emerg Med* 2009;54:763-768.
150. Tester DJ, Ackerman MJ. The role of molecular autopsy in unexplained sudden cardiac death. *Curr Opin Cardiol* 2006;21:166-172.
151. Ackerman MJ. Heritable cardiac channelopathies. In: Wyszynski DF, Correa-Villasenor A, Graham TP, eds. *Congenital Heart Defects: From Origin to Treatment*. New York, NY: Oxford University Press, 2010:131-140.
152. Mason JW, Ramseth DJ, Chanter DO, et al. Electrocardiographic reference ranges derived from 79,743 ambulatory subjects. *J Electrocardiol* 2007;40:228-234.
153. Johnson JN, Ackerman MJ. Long QT syndrome. In: Yan G, Kowey PR, eds. *Management of Cardiac Arrhythmias*. New York, NY: Humana Press, 2011:419-440.

Electrophysiology Studies and Electrophysiologic Therapeutic Catheterization

J. Philip Saul ■ John D. Kugler

This chapter begins by describing the indications, objectives, and techniques for performing electrophysiologic studies, intracardiac and esophageal, in the pediatric patient without congenital heart disease and pediatric and adult patients with congenital heart disease. These groups are hereafter referred to as *pediatric and adult congenital* when appropriate, where pediatric refers to neonates, infants, children, and adolescents. Following the technical aspects of performing such studies, the use of catheter techniques for arrhythmia therapy in the same group is covered in detail.

ELECTROPHYSIOLOGIC STUDIES—DIAGNOSTIC

Several aspects of electrophysiologic studies in pediatric and adult congenital patients have changed over the past two decades. This chapter emphasizes these changes while reviewing the established age-related and disease-related principles (1–4). The expanding therapeutic use of catheter ablation has had a major impact on various aspects of intracardiac electrophysiologic study, including not only the objectives and techniques during the study but also indications for the study. In addition to the influence of ablation, indications for electrophysiologic studies have changed because of the data from large multicenter studies involving specific arrhythmias and underlying disease processes. Although specific indications for electrophysiologic studies relative to the underlying disease, symptom, or arrhythmia are discussed primarily in other chapters, the objectives are discussed, with emphasis on comparing intracardiac and transesophageal techniques. The advantages and limitations of each technique, as viewed in the context of age, risk/benefit, therapy, and addressing the relevant clinical questions are also addressed.

PLANNING THE STUDY

The clinical questions addressed by the electrophysiologic study should be asked in advance, and the procedure should be planned and guided in this manner. The planning should include choice of intracardiac and/or transesophageal technique, needed preprocedure studies (e.g., electrocardiography [ECG], Holter monitoring, exercise testing, imaging studies); preparation or education of the patient and family; choice of sedation or general anesthesia; preparation of the patient in the procedure room or catheterization laboratory; types of equipment (catheters, sheaths); planned recording, pacing, or ablation protocols (with strategies for each); and administration of provocative or antiarrhythmic drugs. All of these issues are addressed.

INTRACARDIAC TECHNIQUE

Educational and Emotional Preparation of Patient and Family

The importance of patient and family preparation cannot be overemphasized. The potentially long duration of the study, the use of multiple catheters and protocols, and particularly the inclusion of an ablation necessitate relieving patient and family anxiety, which, in turn, enhances patient cooperation. Age-related patient and family preparation begins with the pediatric electrophysiologist and is continued by pediatric cardiac/congenital heart disease electrophysiology nurses. Educational materials can be helpful at all levels.

Sedation and Anesthesia

Sedation is required for virtually all pediatric patients, and most laboratories have transitioned to using general anesthesia or *deep* sedation delivered by an anesthesiologist for all electrophysiologic and nonelectrophysiologic catheter procedures. *Moderate* sedation, in which the patient can still respond when addressed, is generally reserved for older less anxious patients undergoing just a diagnostic or transesophageal electrophysiology study. There has been a shift toward anesthesia over sedation for any electrophysiologic study as dedicated pediatric anesthesia services have become more available.

The pain and discomfort of an ablation procedure does not appear to be very much higher than that for a typical diagnostic catheterization, even accounting for some patients feeling pain during the application of radiofrequency (RF) energy. Thus, general anesthesia is by no means necessary. However, many pediatric electrophysiologists began using general or near general anesthesia for most patients early in the ablation experience for two reasons. First and foremost, uncontrolled patient movement that dislodges the catheter may inadvertently occur at a critical point in the procedure, particularly if the RF application produces pain. One of the authors of this chapter (Saul), in fact experienced an isolated case of complete heart block early in his ablation experience that occurred in part from untimely movement of an uncooperative patient during ablation of a midseptal accessory pathway (AP) (5), leading the Children's Hospital in Boston to replace heavy, often disorienting sedation with general anesthesia for most patients. Second, most centers have found that even older cooperative children and young adults find a long procedure much more tolerable under anesthesia and are more willing to return for follow-up procedures, when needed. Currently, virtually all pediatric electrophysiologists use general anesthesia for ablation procedures.

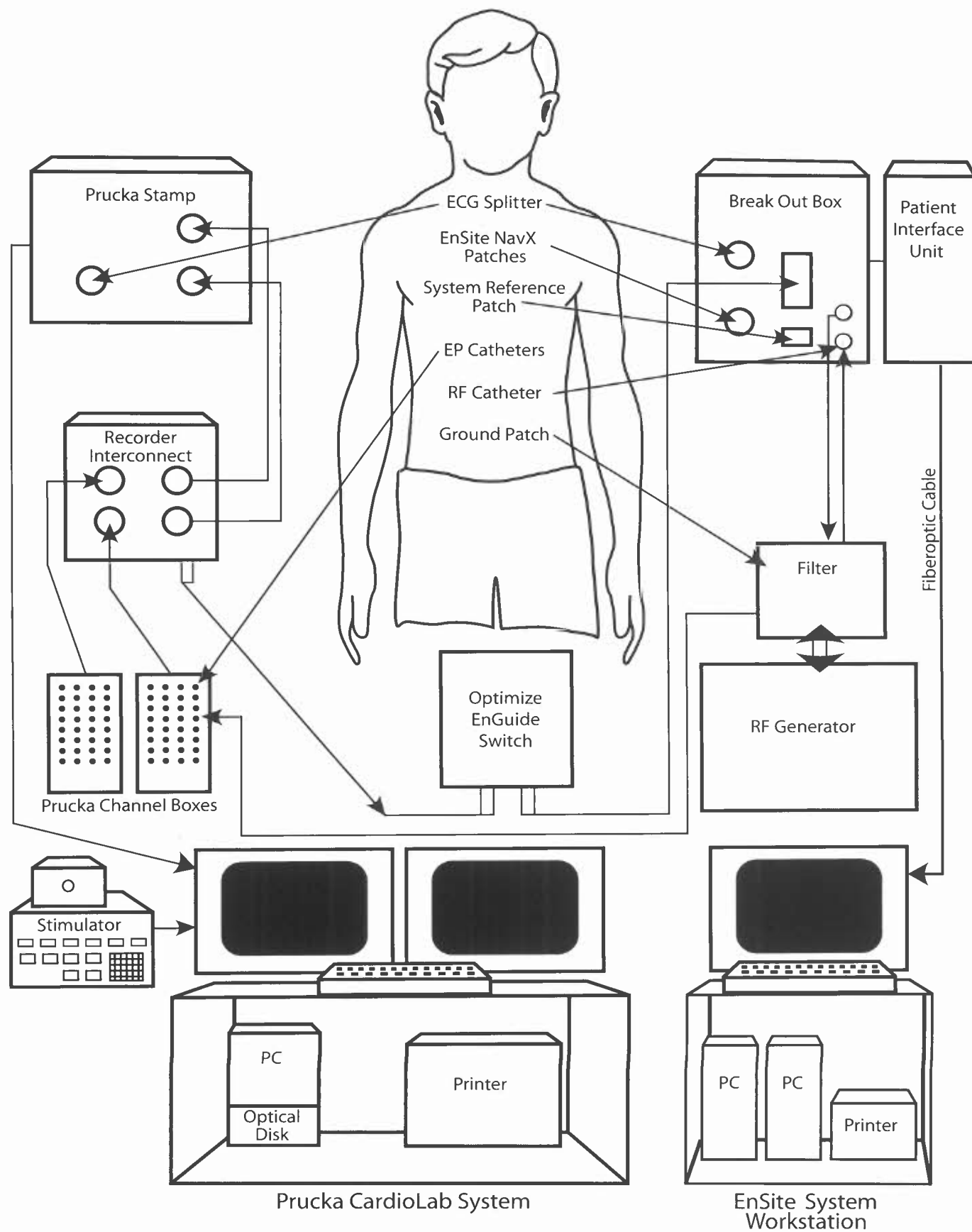


Figure 17.1. Diagram showing the major components of an electrophysiology (EP) cardiac laboratory (lab). An EP lab can be configured using equipment from several companies. In this illustration, the Prucka CardioLab System (General Electric Healthcare, UK) is interfaced with the electronic stimulator. Together, they provide the system by which conventional electrogram recordings are displayed and pacing protocols are performed and recorded. A 3-D mapping system can interface with the conventional system to enhance mapping (see text) and minimize use of fluoroscopy. In this example, the EnSite NavX (St. Jude Medical, St. Paul, MN) provides the ability to view nonfluoroscopic images (see Fig. 17.5) of the catheter positions at the EnSite Workstation also with simultaneous conventional electrogram recordings. As is shown in Figure 17.5, much greater detailed 3-D mapping images can be generated using the intracardiac balloon/electrode array EnSite system. Integration of preprocedure cardiac magnetic resonance images or computed tomographic images can be downloaded and interfaced into the 3-D recording system.

Sedation and anesthesia agents generally are not standardized in electrophysiology laboratories, with multiple appropriate regimens used; however, there are a few common themes. In general, anticholinergic agents should be avoided because of their electrophysiologic effects. These include agents like chlorpromazine and the drying agents atropine and glycopyrrolate. Most sedative regimens include a narcotic (e.g., meperidine, morphine, or fentanyl) for pain and benzodiazepines for sedative amnesia (e.g., diazepam or midazolam). Midazolam may be a better choice than diazepam because of its demonstrated lack of electrophysiologic effect (6,7). Antiemetics like phenergan or droperidol are acceptable, if necessary, but preferably avoided. Continuous intravenous propofol has gained increased acceptance as a deep sedative at lower doses and as a general anesthetic at a higher dose (8). With propofol's low incidence of postprocedure nausea and vomiting, patients recover faster with less lingering sedation, and because of the decreased vomiting, Valsalva-related catheter site bleeding is minimized. The electrophysiologic effects of propofol in children appear to be minimal and similar to isoflurane-based anesthetics (9).

Preparation of the Patient in the Catheterization Laboratory

Initial patient preparation involves positioning and then comforting the patient on the table. When a long procedure is planned, securing the arms above the shoulders may promote the undesired complication of brachial plexus injury. Although positioning the arms inferiorly along the thorax interferes with the straight lateral fluoroscopy view, rotating slightly to 10 to 20 degrees right anterior oblique (RAO) with the anterior-posterior tubes and 80 to 70 degrees left anterior oblique (LAO) with the lateral tubes alleviates this problem while still providing acceptable views for catheter introduction. All limb and chest surface ECG leads are placed initially, allowing for a choice of displayed leads. Selection of a displayed lead is based on the underlying arrhythmia or conduction disturbance. When a contemporary digital recording system is used, a full 12-lead ECG is available at any time regardless of the fewer displayed leads.

Many pediatric electrophysiologists now use 3-D mapping systems. Depending on the system used, the initial room setup and preparation of the patient involves steps that are required for proper functioning of the system (e.g., pads placed/positioned, connections, and interfacing as illustrated in Fig. 17.1). Routine use of the disposable (and translucent) defibrillation pad and lead system has improved cardioversion and emergency defibrillation efficiency and probably has improved the safety of the intracardiac study.

Sheath and Catheter Placement

In patients undergoing electrophysiologic study, special care is needed when infiltrating skin and subcutaneous areas with lidocaine (1–4). Studies have shown that therapeutic and, therefore, antiarrhythmic serum concentrations have been achieved with routine use of 2% lidocaine (10). One percent or, ideally, 0.5% concentration given in sufficient amounts to achieve local anesthesia, but not in increased volume, is recommended to avoid therapeutic lidocaine serum concentration.

The number, size, and location of the sheaths relates to the age and size of the patient, the underlying arrhythmia, and objectives of the study. In most studies, the number of sheaths varies between one and five, with the maximum number consisting of three in the femoral veins, up to two in the internal jugular vein, and one in the femoral artery. Sheath sizes usually correlate directly with the size of the patient and vary between 4 and 8 French (Fr). The 7 or 8 Fr sheaths are helpful when intravenous drug administration is required because a side-arm sheath larger than the catheter permits free, unobstructed flow of fluid into the vein. In addition, some ablation catheters have larger tips and require an 8 Fr sheath for introduction.

The ultimate number and location of the sheaths also depend on the success of catheter manipulation and preference of the operator. For example, the coronary sinus (CS) catheter can be advanced from the inferior or superior vena cava. From the inferior caval approach, a catheter can be manipulated into the CS from the femoral vein/inferior vena cava (IVC) by looping the catheter in the right atrium or by directly advancing it from the right atrium (2,3). If this is either not successful or not desirable, a sheath or catheter can be advanced from the superior vena caval approach. This is accomplished from the arm (the median basilic vein in the left arm is preferred), neck (either internal jugular, but right is preferred), or subclavian vein (either right or left) approach (2,3). A limitation to the arm approach is that the arm is extended throughout the procedure, which can be uncomfortable to the patient and can interfere with the lateral fluoroscopy tube positioning. An advantage to the internal jugular vein is that its larger size can more easily accommodate a second sheath if needed (e.g., in a patient such as the one shown in Figure 17.2, in whom a mapping or ablation catheter is manipulated from above to reach a location along the tricuspid annulus not accessible from the femoral approach).

Although not mandated, to enhance safety a femoral artery cannula allows access to monitor arterial blood pressure continuously throughout the procedure. When a sheath is placed in the femoral artery for retrograde access to the left ventricle, a side-arm sheath one size larger than the catheter permits accurate pressure recordings. Otherwise, a small plastic cannula/dilator is used.

The use of anticoagulation to minimize thromboembolic complications varies among laboratories and is difficult

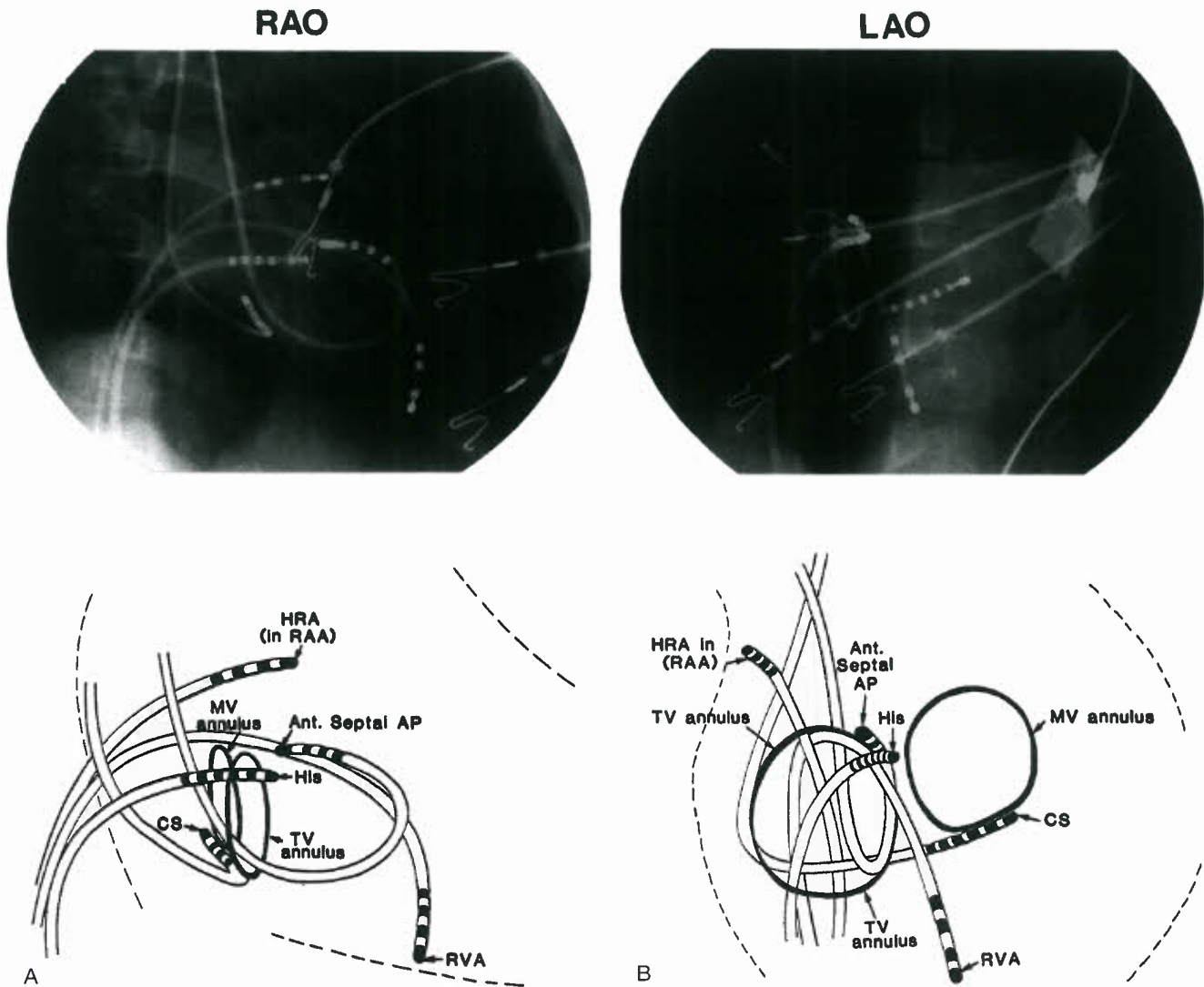


Figure 17.2. Right anterior oblique (RAO) and left anterior oblique (LAO) single-frame radiographs (top) from biplane cine with accompanying diagrammatic illustrations (bottom) showing multiple-electrode catheter positions during an intracardiac electrophysiologic study in a 6-year-old boy with WPW syndrome (right anterior septal accessory AV pathway). **A:** The RAO view (anterior–posterior tubes rotated 45 degrees) provides the operator with a direct anterior–posterior view (right to left, respectively, as viewed in the radiograph and illustration), with the AV valves nearly perpendicular to the operation. **B:** The corresponding LAO biplane view (lateral tubes rotated 45 degrees) provides the operator with a direct left–right view (tricuspid valve annulus on left and mitral valve annulus on right, with septal area between). Note that three 6 Fr catheters were advanced from the femoral veins and positioned in the high right atrium (HRA), right atrial appendage (RAA), right ventricular apex (RVA), and His position. Two 6 Fr catheters were advanced from the right internal jugular vein and positioned in the coronary sinus (CS) posterior to the mitral valve (MV) annulus and under the tricuspid valve (TV) leaflet anterior (ant. septal) to the His catheter where the accessory AV pathway (AP) was located. The tricuspid valve annulus and the mitral valve annulus are depicted in positions predicted by the catheter positions to demonstrate approximate locations. The surface electrocardiographic leads and skin electrodes, as well as RF and defibrillation skin pads, are not labeled. (See Fig. 17.8 for recordings from these electrode catheters in this patient.)

to analyze because it is difficult to separate the diagnostic procedure from the various interventional procedures (catheter ablation and the techniques used for ablation). Zhou et al. (11) reviewed the literature to show that heparin use does not eliminate the risk of thromboembolic complications during RF catheter ablation. Anfinssen et al. (12) in a randomized study in adults showed that heparin administration immediately after sheath placement significantly decreased hemostatic activation. In a separate study, these investigators also showed that the procedure duration prior to heparin administration determined

hemostatic activation and fibrinolysis independent of RF ablation (RFA) (13). Tse et al. (14) found both platelet and coagulation activation during RFA, but platelet activation was not found during cryoablation. The heparin dose varies among laboratories, but the initial dose is usually 70 to 100 U/kg, to a maximum of 5,000 U. Ongoing heparin anticoagulation can be provided by a continuous intravenous infusion (e.g., 15 to 20 U/kg/h) or by boluses. To follow the degree of optimal anticoagulation during long procedures, the activated clotting time (ACT) is measured one to three times per hour to achieve a desired

value of 200 to 300 seconds, except when a 3-D balloon array mapping system is used within the left atrium or ventricle and an ACT of >300 seconds is desirable. For typical studies, most laboratories administer 100 U/kg of heparin after all the sheaths are in, monitor the ACT every 30 to 60 minutes, and give additional boluses of heparin to keep the ACT >200 seconds.

Electrode Catheters

The catheter sizes vary from 2 to 7 Fr. Traditionally, 4 Fr catheters were used virtually only for infants, whereas 5 Fr catheters most often were used in young children, and 6 and 7 Fr catheters were used for adolescents and adult-sized patients. Smaller (2 to 3 Fr) catheters can be used for intracardiac recordings as well as for epicardial mapping (by advancing the catheters from the CS into the very small branches throughout the epicardial surface) (15). These small catheters may be used in small children to record intracardiac electrograms throughout the conduction system. Although these small catheters may be difficult to manipulate, up to three catheters can be used in the same sheath. Also, 2 Fr active fixation catheters (e.g., Medtronic, Inc.) can be used in patients such as those with preexcitation/Wolff-Parkinson-White (WPW) syndrome who undergo a single-catheter short-duration study to assess risk of rapid A-V conduction of atrial fibrillation. These small catheters can be used in any size patients with the advantage of minimizing the venous puncture site—and therefore skin, muscle, and vein trauma—allowing quick recovery with low groin morbidity.

Catheter electrodes vary in number and interval distance. Traditionally, catheters used for recording and pacing were in a quadripolar configuration, whereas catheters used primarily for recording and mapping contain between 6 and 12 electrodes. However, currently, catheters with 6 to 10 electrodes often are used for multiple purposes, such as recording/mapping in the CS and atrial pacing. Similarly, some catheters are designed to record atrial and His potentials from proximal electrodes, while distal electrodes are used to pace the ventricle. Specially formed catheters also are available for the His location with an “S” shaped tip providing stable seating between the anterior and septal tricuspid leaflets. These catheters tend to work best in larger pediatric patients. Short (1 to 2 mm) interelectrode distances for the bipoles, separated by 5 to 10 mm spacing allow high quality electrograms and precise mapping, while spanning a larger region of the heart.

The number of catheters used during a study depends not only on the size of the patient and the underlying problem but also on whether the electrophysiologist prefers the minimum or maximum possible amount of catheter manipulation during the study. If the least amount of catheter manipulation is desired, more catheters are positioned initially, and these are left in place for the duration of the procedure. Electrophysiologists who use more catheters prefer the advantage of simultaneous recording from the multiple catheters to optimize data collection. If multiple changes in catheter positions are deemed acceptable, fewer catheters initially are placed. Use of fewer catheters requires moving the catheter from one area to another and perhaps back to the original position during the study. However, it may not be possible without using mapping systems (described later, e.g., the NavX system, St. Jude Medical, Minneapolis, MN, and shown in Fig. 17.3) to return the catheter to the precise original location, and electrogram consistency may be compromised or the arrhythmia affected by the catheter movement (e.g., arrhythmia may not be inducible thereafter, so optimal gathering and recording of information is lost). Also, with each catheter position change, the otherwise satisfactorily sedated patient may become disturbed, in the absence of anesthesia.

Manipulation and placement of electrode catheters involves several factors, including patient size and age, underlying

arrhythmia, objectives of the individual study, size and type of catheters (e.g., steerable), and underlying cardiac and blood vessel anatomy.

Catheter access to the left atrium or ventricle is desirable for several reasons, usually for the purpose of recording and stimulation of the left atrium and ventricle for evaluation and mapping of supraventricular tachyarrhythmias. With increasing use of catheter ablation, left-sided APs or ectopic arrhythmia foci require catheter access to the left side. The location of the CS provides precise mapping of APs along the mitral valve annulus. For left-sided atrial and ventricular ectopic foci and for ablation catheter manipulation, a lone catheter within the CS is insufficient. This has prompted use of the retrograde arterial approach or the transseptal approach via a patent foramen ovale or a transseptal needle and sheath (Brockenbrough) technique. Limitations are associated with each technique (2,16).

Biplane (rather than single-plane) fluoroscopy is not essential but becomes more critical as the procedure becomes more complicated. It helps minimize the risk of perforation and enhances procedural efficiency, while maximizing the precision of catheter manipulation during mapping. For mapping, especially when it involves the tricuspid annulus, mitral annulus, and posterior septal area, the positioning of the fluoroscopy x-ray tubes in a perpendicular alignment to the long and short cardiac axes optimizes recognition of anatomic relationships (Fig. 17.2). This involves rotation of the anterior-posterior tubes to approximately 30 degrees RAO position and the lateral tube perpendicular at about 60 degrees LAO position. In addition, 10 to 15 degrees of caudal angulation of the LAO tube provides a view directly orthogonal to the mitral annulus, facilitating mapping of left-sided APs (Fig. 17.4).

Recording and Stimulation Technique

The display and recording of the intracardiac electrograms are undertaken after catheter placement. Most electrograms are displayed and recorded in a bipolar fashion, although unipolar electrograms are obtainable easily and can be helpful for mapping arrhythmia foci (17). Various recordings and stimulation systems are commercially available, and some laboratories customize systems. Most laboratories use a digital computer-based system that maximizes recording and stimulation efficiency by eliminating manual switching of catheter connections, eliminating paper recordings, providing a database/reporting system, and providing online measurements with freeze-scope capability (Fig. 17.1). The 3-D mapping systems, used primarily when ablation is planned, incorporate the temporal and spatial (anatomic) details and therefore provide much more precise diagnostic data (see Interventional section for more details) (18). Also, many 3-D systems have the capacity to capture continuous rhythm for analysis when sustained tachyarrhythmias are not inducible or when the arrhythmia is associated with intolerable hemodynamics. The 3-D mapping systems have added an important diagnostic component to electrophysiologic studies and also have provided increased safety by decreasing radiation exposure because catheter manipulation can be performed without, or by minimizing, fluoroscopy (19,20). Regardless of the specific 3-D system used, Packer (18) summarizes the minimal general requirements as follows: (i) accurately replicate the cardiac anatomy underlying the arrhythmia, (ii) provide a plausible representation of activation of that chamber, as linked to the specific anatomic site of data acquisition, (iii) readily capture and intelligibly display other details of physiology, and (iv) catalogue the site of interventions. These features are illustrated in Figures 17.5 to 17.7.

A standard method or order of electrogram display and recording on the optical disk monitor does not exist, but typical

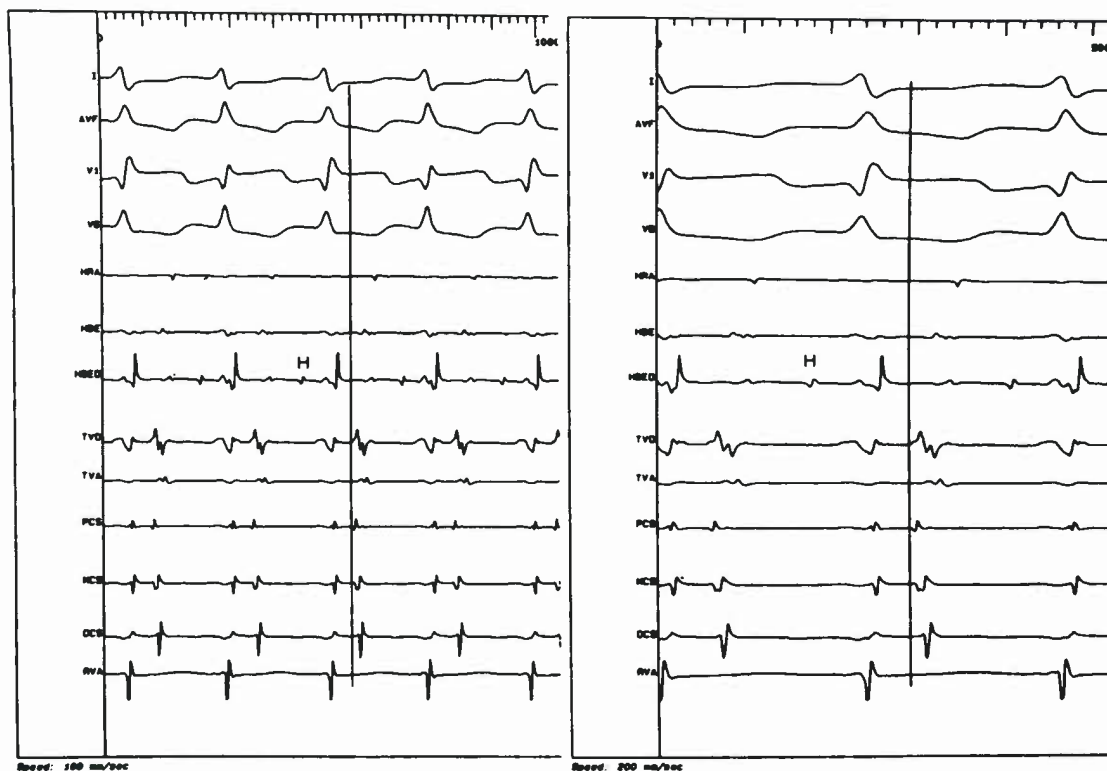


Figure 17.3. Two recordings in a 3-year-old boy with incessant, fast (220-ms cycle length; rate 272 beats per minute), orthodromic reciprocating AV reentrant SVT that demonstrate the advantage of fast recording speed. **Left:** Using a recording speed of 100 mm/s, the earliest retrograde (conduction via posterior septal accessory AV pathway) atrial activation was difficult to determine. The atrial activation closest to the vertical line appeared to be either from the distal pair of electrodes on the tricuspid valve annulus mapping catheter (TVD) located at the posterior septal area or from the proximal pair of electrodes on the coronary sinus (PCS) catheter, located approximately 0.5 cm into the CS from the os. **Right:** By doubling the recording speed to 200 mm/s, the earliest electrogram not only appeared to be more easily detected by the TVD electrodes but also the low-amplitude earliest electrogram appeared to be from the accessory AV pathway (see also Fig. 17.3). (Other abbreviations are as described in Fig. 17.8).

examples are illustrated in Figure 17.8. It is advantageous to record at least three or four simultaneous surface ECGs, including two perpendicular limb leads to elicit P or QRS frontal plane axis changes and one or two chest leads to maximize detection of bundle branch changes. A major effort should be undertaken to record a His bundle electrogram (HBE). Virtually all mechanisms of arrhythmias and conduction system disturbances are definitive only when an HBE is recorded. When the usual catheter position (superior or septal tricuspid valve annulus) fails to elicit an HBE, advancing a catheter retrogradely to

the noncoronary aortic sinus can allow successful recording. With catheters used for both recording and stimulation, the distal pair of electrodes is best suited for pacing consistency, and all proximal pairs are then used for recording. Because of fast tachycardia rates in children, fast recording capability (200 mm/s or higher) is essential to differentiate electrograms recorded by the various electrode catheters (Fig. 17.3).

The pacing and recording protocols used are variable, and emphasis should be on flexibility and patient-specific diagnosis and findings. The specific protocols chosen should be adapted to

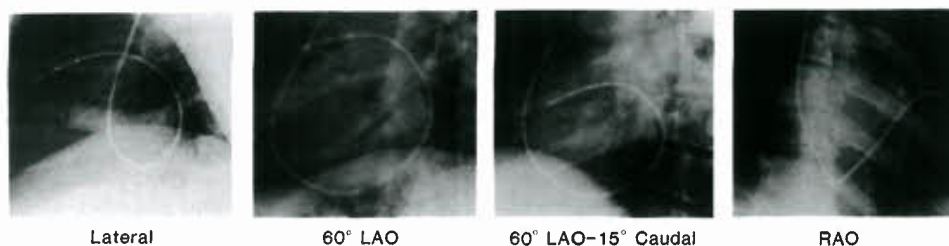


Figure 17.4. Catheter projections for ablation procedures. Note how left anterior oblique (LAO) view plus caudal angulation maximally elongates the mitral annulus. (From Saul JP, Hulse JE, DeW, et al. Catheter ablation of accessory atrioventricular pathways in young patients: use of long vascular sheaths, the transseptal approach and a retrograde left posterior parallel approach. *J Am Coll Cardiol* 1993;21:571-583, with permission.)

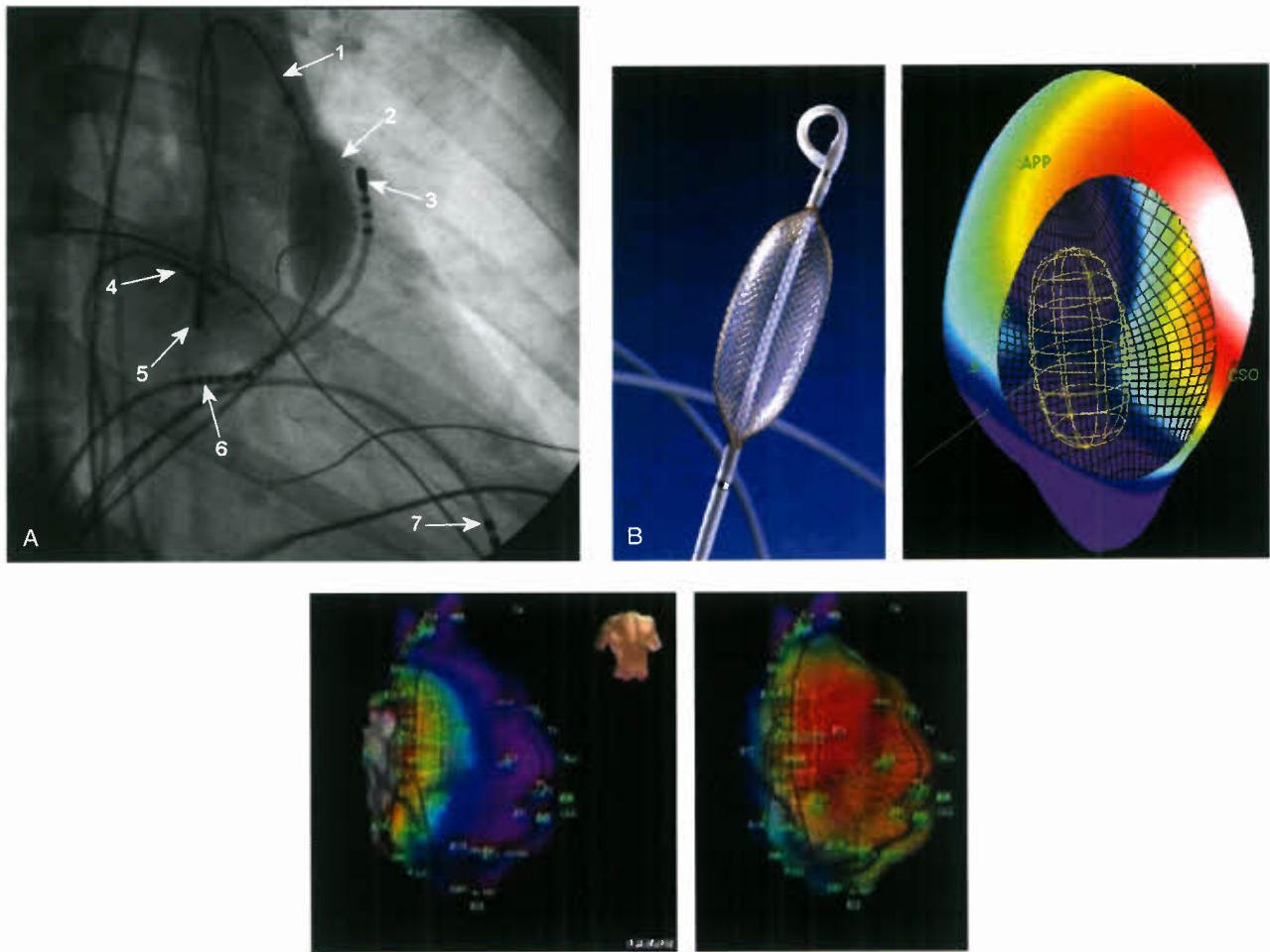


Figure 17.5. This figure shows the use of the EnSite 3-D intracavitary balloon noncontact mapping system (St. Jude Medical, St. Paul, MN). (A, top left) Fluoroscopic RAO image is shown: (1) wire in main pulmonary artery placed to enable advancing the balloon/mesh catheter, (2) 64-electrode mesh inflated balloon in the right ventricular outflow tract (RVOT), (3) mapping/ablation catheter in RVOT, (4) high right atrial catheter, (5) retrograde mapping/ablation catheter in aortic root/sinus, (6) His catheter, and (7) RV apex catheter. (B, top middle) Picture of mapping balloon shows a grid of wires criss-crossing the surface of the balloon, creating 64 individual electrodes. (top right) A computer reconstruction of the right atrium (CSO, coronary sinus os; APP, appendage) showing the endocavitary location of the balloon and voltages on the endocardial surface at a single point in time. Activation is currently septal, shown by the white color above the CSO. (Bottom Panels) Right atrium during intra-atrial reentry tachycardia (IART) in a 14-year-old boy after an atriopulmonary Fontan operation. The torso shows these are slight RAO projections. The atrium is large and bulbous. Although a little fuzzy, an area of presumed block secondary to a right lateral atrial scar is shown by a dark line along the anterolateral RA. When played as a movie the tachycardia proceeded around the scar inferior to superior on the anterior surface and superior to anterior on the posterolateral. The two images show posterior activation on the left and lateral activation on the right. The image of the balloon can be seen within the chamber.

the patient as they relate to the preprocedure diagnosis, but they also should remain flexible during the study, dependent on ongoing elicited findings. It is beyond the scope of this chapter to provide examples of protocols for each specific type of arrhythmias and conduction disturbances. Most can be found either elsewhere in this chapter or in the literature (2–4,16,21–23). However, in Table 17.1, a list of pacing protocols provides examples of options used during intracardiac studies. Also, with the advent of catheter ablation and with the advances in 3-D mapping technology, the techniques and objectives of mapping have assumed a major new role and are emphasized in the interventional section of this chapter. The important general mapping concepts include the fluoroscopic image, catheter manipulation techniques, various modes of pacing, nuances of electrogram recordings, and 3-D mapping (Figs. 17.1–17.4,17.8,17.9, Figs. 17.5–17.7).

Administration of Drugs

Intravenous drug administration during an intracardiac study encompasses three general categories: anesthetic drugs, provocative arrhythmic drugs, and antiarrhythmic drugs. Of the three, anesthetic drugs are the most commonly administered and were discussed earlier in this chapter. The most commonly used provocative arrhythmic drug is isoproterenol. Other less frequently used provocative drugs include epinephrine, atropine, aminophylline, phenylephrine, procainamide, or flecainide (for Brugada syndrome) (2,3,24–28). Because of sleep- or sedative-induced vagotonia, one of these provocative drugs may be necessary to induce or sustain tachycardia, which is essential to determine arrhythmia mechanisms and the site of arrhythmia foci or pathways. Also, some arrhythmias can be observed only

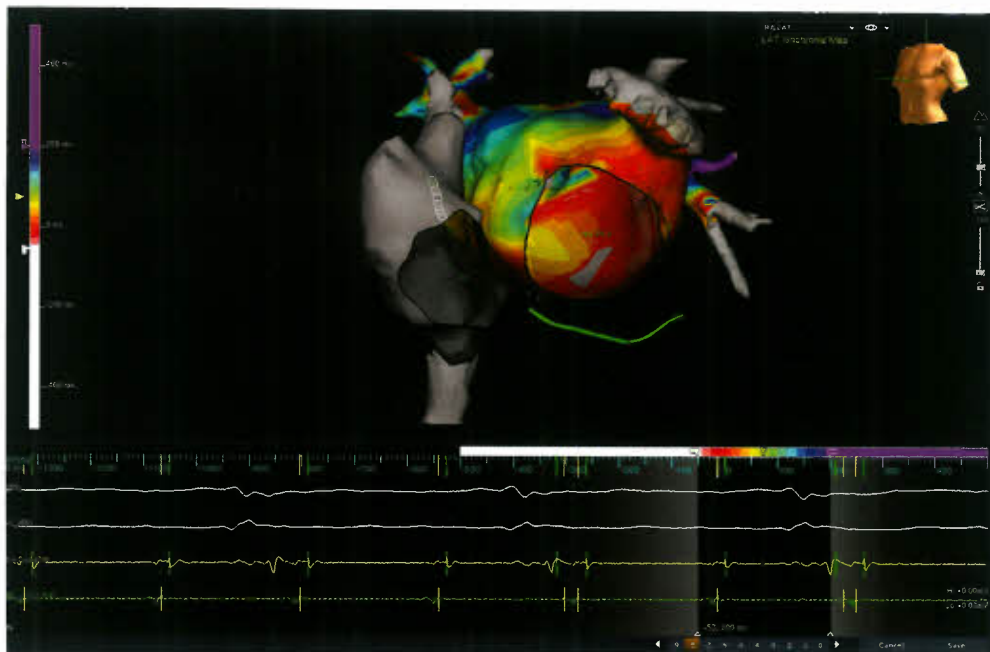
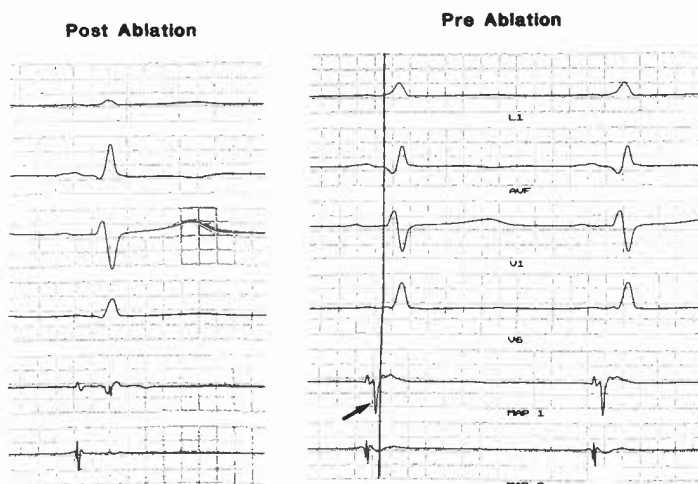


Figure 17.6. When imaging of multiple-catheter location is desired with or without the need for anatomic imaging detail, a mapping system such as NavX (St. Jude Medical, St. Paul, MN) or the latest fast mapping version of Biosense CARTO can be used. As shown in this image of the left and right atria, all the catheter locations can be seen. The CS catheter is under left atrium in *green*, and an ablation catheter can be seen in the right middle pulmonary vein through the right atrium. The torso shown in this is an LAO view. The system provides the ability to reflect real-time motion of catheter position, minimizing use of fluoroscopy and radiation exposure (see text). In addition, the catheters can be used to derive “geometry” by sequential positioning of any of the catheter electrodes at multiple sites along the endocardial chamber. With the new Velocity system shown here the geometry can be made out of multiple segments to create a realistic 3-D model of cardiac structures. This image is also improved by merging the catheter-acquired data with a CT image. Once the geometry is made, modifications like “cutting out” the tricuspid and mitral valves can be added, as shown here. Then signals can be acquired from any catheter electrodes and timing points derived to make a timing map. The timing map shown here is in the left atrium with early activation in *pink red* in the low lateral left atrium, probably near the left lower pulmonary vein. Activation proceeds anteriorly and superiorly to *yellow* and *blue* colors. The ECG and electrograms at the bottom include a window (*right lower*) that demonstrates where in the cardiac cycle the colors in the image correspond to. Although not shown in this patient, the location of ablation lesions or other points of interest can be easily added. (With permission from St. Jude Medical, St. Paul, MN.)

when the heart rate is lower or are observed better in the presence of second-degree AV block (e.g., atrial reentry tachycardia), situations where enhanced vagotonia is helpful and can be induced by an infusion of phenylephrine titrated to moderately

raise arterial pressure. The doses of isoproterenol and epinephrine continuous-drip infusions are similar and range from 0.01 to 0.1 $\mu\text{g/kg/min}$. Atropine (0.01 to 0.04 mg/kg) is used infrequently because it cannot be administered as a continuous drip

Figure 17.7. AP potentials. The first four signals are surface ECG leads. The second two come from the mapping/ablation catheter. Note that there is minimal preexcitation in the surface leads pre-ablation; however, a very large potential is seen in the distal electrode pair of the mapping catheter (*arrow*) preceding the surface QRS. This probable AP potential is no longer present after the ablation. (From Saul JP, Hulse JE, De W, et al. Catheter ablation of accessory AV pathways in young patients: use of long vascular sheaths, the transseptal approach and a retrograde left posterior parallel approach. *J Am Coll Cardiol* 1993;21: 571–583, with permission.)



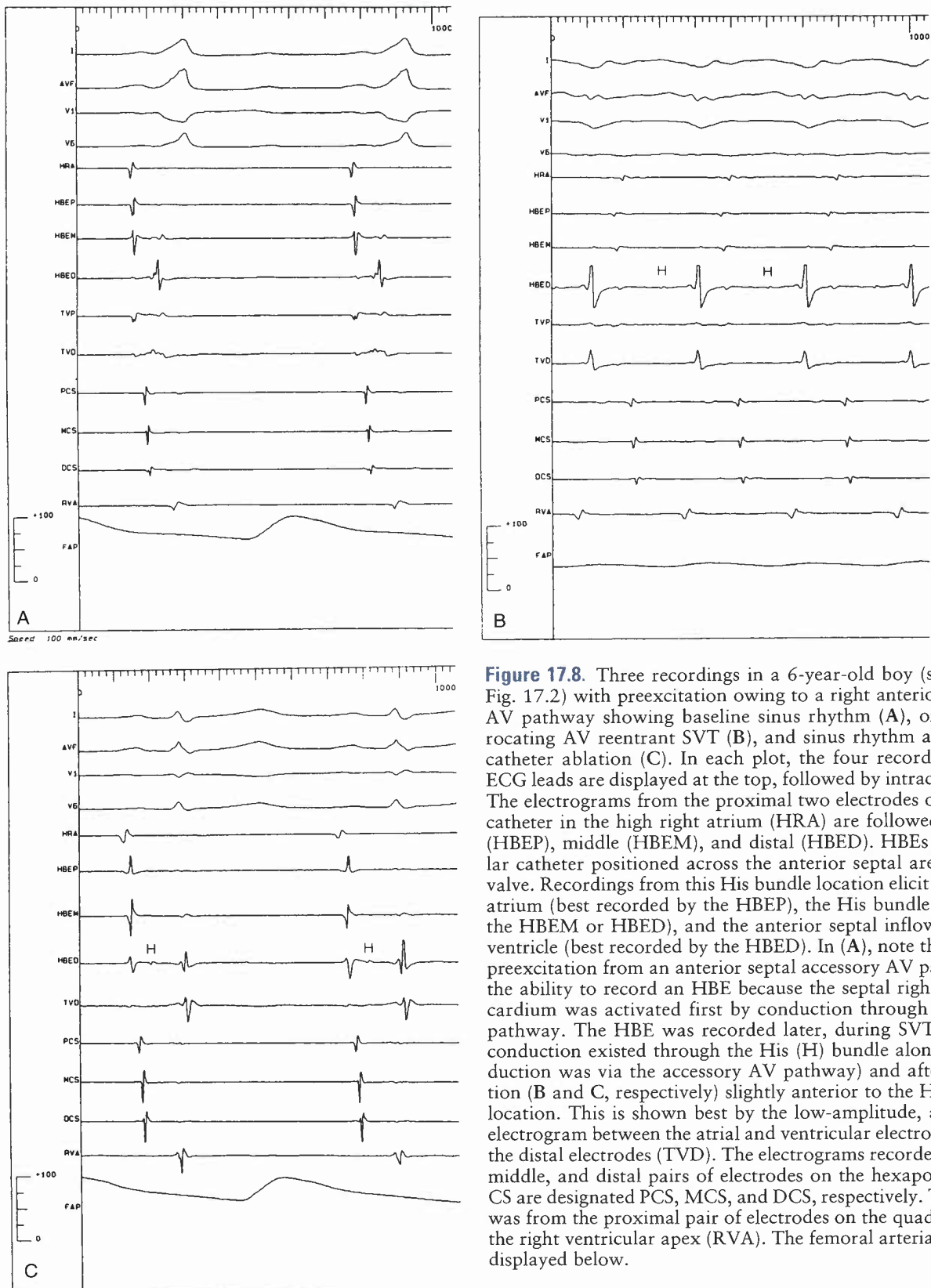


Figure 17.8. Three recordings in a 6-year-old boy (same patient as in Fig. 17.2) with preexcitation owing to a right anterior septal accessory AV pathway showing baseline sinus rhythm (A), orthodromic reciprocating AV reentrant SVT (B), and sinus rhythm after successful RF catheter ablation (C). In each plot, the four recordings from surface ECG leads are displayed at the top, followed by intracardiac recordings. The electrograms from the proximal two electrodes on the quadripolar catheter in the high right atrium (HRA) are followed by the proximal (HBEP), middle (HBEM), and distal (HBED). HBEs from the hexapolar catheter positioned across the anterior septal area of the tricuspid valve. Recordings from this His bundle location elicit activity in the low atrium (best recorded by the HBEP), the His bundle (best recorded by the HBEM or HBED), and the anterior septal inflow area of the right ventricle (best recorded by the HBED). In (A), note that the presence of preexcitation from an anterior septal accessory AV pathway eliminated the ability to record an HBE because the septal right ventricular myocardium was activated first by conduction through the accessory AV pathway. The HBE was recorded later, during SVT, when antegrade conduction existed through the His (H) bundle alone (retrograde conduction was via the accessory AV pathway) and after successful ablation (B and C, respectively) slightly anterior to the His bundle catheter location. This is shown best by the low-amplitude, almost continuous electrogram between the atrial and ventricular electrograms recorded by the distal electrodes (TVD). The electrograms recorded by the proximal, middle, and distal pairs of electrodes on the hexapolar catheter in the CS are designated PCS, MCS, and DCS, respectively. The next recording was from the proximal pair of electrodes on the quadripolar catheter in the right ventricular apex (RVA). The femoral arterial pressure (FAP) is displayed below.

and because of its longer-lasting effects. Phenylephrine can be given as a bolus of 0.50 to 1.0 $\mu\text{g}/\text{kg}$ and titrated as an infusion to the desired blood pressure.

Before the ablation era, antiarrhythmic drug administration during intracardiac electrophysiologic study commonly was used to assess drug safety and efficiency of planned chronic therapy

(29). Although chronic medical therapy still exists as a treatment option (especially for patients with ventricular arrhythmias), its use is declining because of the increased application of ablation treatment and cardioverter-defibrillator device options.

Antiarrhythmic drug administration also is used commonly to achieve acute effects. This is indicated most often in an

TABLE 17.1 Pacing Protocols for Intracardiac Electrophysiologic Study

1. Sinus node function
 - a. Sinus node recovery time
 - b. Sinoatrial conduction time
2. AV conduction
 - a. Continuous atrial decremental pacing
 - b. Premature atrial extrastimulus technique (during sinus and/or eight-beat drives of a-paced rhythm)
3. VA conduction
 - a. Continuous ventricular decremental pacing
 - b. Premature ventricular extrastimulus technique (during sinus and/or eight-beat drives of v-paced rhythm)
4. Atrial muscle conduction and refractory period
 - a. Premature atrial extrastimulus technique (during sinus and/or eight-beat drives of a-paced rhythm)
5. Ventricular muscle conduction and refractory period
 - a. Premature ventricular extrastimulus technique (during eight-beat drives of v-paced rhythm)
6. Induction of SVT
 - a. One or more of the following: Continuous atrial decremental pacing (or short bursts), premature atrial extrastimulus technique (using one or more drive cycle lengths, one to three extrastimuli, and one or more pacing sites such as HRA, LRA, CS), continuous ventricular decremental pacing, premature ventricular extrastimulus technique (during sinus and/or eight-beat drives of v-paced rhythm)
 - b. If unsuccessful, add provocative drug and repeat step 6a
7. Determine SVT mechanism, map location
 - a. Results of steps 6a, b
 - b. One or more of the following during underlying SVT rhythm with use of recording electrodes in several locations pertinent to type of tachycardia: Premature atrial extrastimulus technique (from one or more pacing sites such as HRA, LRA, CS), premature ventricular extrastimulus technique (from one or more pacing sites such as RV, LV)
8. Risk stratification in asymptomatic or symptomatic WPW
 - a. Premature atrial extrastimulus technique (using one or more drive cycle lengths, one or more pacing sites such as HRA, LRA, CS) to determine the antegrade effective refractory of the AP
 - b. Continuous atrial decremental pacing (or short bursts) to determine minimum cycle length for 1:1 conduction in the AP
 - c. Attempted induction of SVT as in steps 6a,b, and determine mechanism as in step 7
 - d. Premature right ventricular extrastimulus technique (using one or more drive cycle lengths) to determine the presence of retrograde conduction and the effective refractory of the AP.
 - e. Attempted induction of atrial fibrillation to determine the minimum preexcited RR interval during atrial fibrillation.
9. Induction of ventricular tachyarrhythmia
 - a. One or more of the following: Continuous ventricular decremental pacing (or short bursts), premature ventricular extrastimulus technique (using one or more drive cycle lengths, one to four extrastimuli, and one or more pacing sites such as RVA, RVOT, LV), continuous atrial decremental pacing, premature atrial extrastimulus technique (during sinus and/or eight-beat drives of v-paced rhythm)
 - b. If unsuccessful, add provocative drug and repeat step 8a
10. Determine VT mechanism, map location
 - a. Results of steps 8a, b

AV, atrioventricular; VA, ventriculoatrial; HRA, high right atrium; LRA, lower right atrium; CS, coronary sinus; SVT, supraventricular tachycardia; RV, right ventricle; LV, left ventricle; RVA, right ventricular apex; RVOT, RV outflow tract; VT, ventricular tachycardia.

attempt to block atrioventricular (AV) nodal conduction. The AV nodal blocking effects of verapamil, esmolol, propranolol, adenosine, or phenylephrine (as discussed above) are helpful to elucidate arrhythmia mechanisms and to distinguish the type of AV and ventriculoatrial (VA) conduction, if present (30–32).

Complications

Complications have been reported and analyzed for nonelectrophysiologic cardiac catheterizations in children (33–38). Only the 1998 report by Vitiello et al. (37) and the summary in a previous edition of this book by Kugler (16) have separate analyses of electrophysiologic studies. Vitiello et al. (37)

conducted an extensive statistical analysis (stepwise multiple logistic regression followed by categorical variable testing of models, which was further tested by Hosmer-Lemeshow's goodness of fit) of 4,952 consecutive cases (3,149 diagnostic, 1,371 interventional, 383 electrophysiologic, 41 ablation). Electrophysiologic procedures had the lowest rate of major complications at 0.7%, similar to the 0.8% of diagnostic procedures, and both were less than the interventional (ablations included in interventional) rate of 2.0%. An electrophysiologic study was not an independent risk factor for a complication. However, because ablation was included as an interventional procedure, it was an independent risk factor for complication during electrophysiologic study. It appears that addition of an ablation procedure increases the risk of

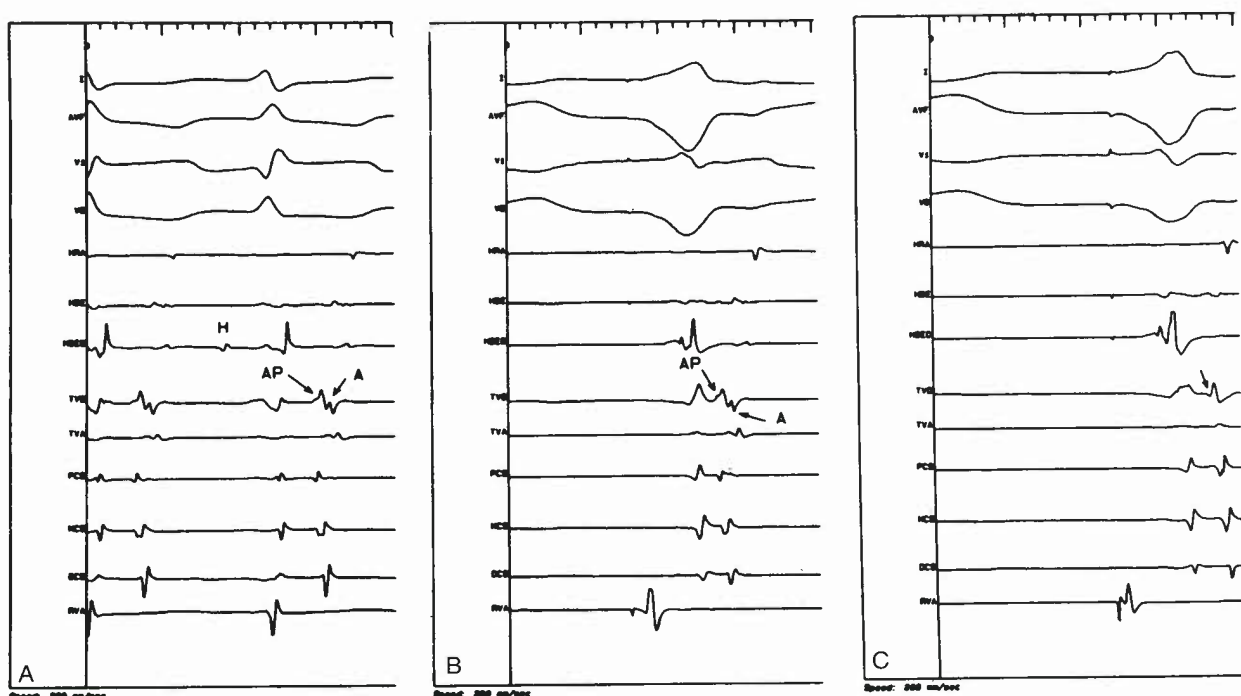


FIGURE 17.9. Three recordings from the same patient as in Fig. 17.10 demonstrating the recording of an electrogram from an accessory atrioventricular (AV) pathway (AP). **A:** During orthodromic reciprocating AV reentrant SVT (220-ms cycle length, same recording as in Fig. 17.3), an early, low-amplitude electrogram (arrow, AP) was recorded before a biphasic electrogram that appeared to be either a fusion with the following atrial (A) electrogram or a biphasic atrial electrogram. H, His bundle. **B:** During ventricular pacing (500-ms cycle length), a virtually identical electrogram was recorded (arrow, AP). **C:** During ventricular pacing at the same cycle length after successful RF catheter ablation, the AP electrogram was eliminated (arrow). Also, after the ablation, normal retrograde conduction was verified by several other pacing protocols (not shown). (Other abbreviations are as described in Fig. 17.8.)

the procedure to a level similar to that of other interventional catheter procedures (16). For the Pediatric Electrophysiology Society's catheter ablation registry, Schaffer et al. (39) studied the mortality rate and found a mortality rate of 0.12% for all procedures and a correlation of mortality with underlying heart disease (increased to 0.89%), greater number of energy applications, left-sided procedures, and lower body weight. The latter risk factor also was found in the single-center report of Rhodes et al. (38) for patients ≤ 5 kg, but they included only nonelectrophysiology catheterization procedures.

TRANSESOPHAGEAL TECHNIQUE

This section covers both the *isolated* transesophageal study, as well as one performed as a preliminary study for supraventricular tachycardia (SVT) inducibility or WPW syndrome risk stratification prior to a possible catheter ablation procedure. The primary difference is that sedation might be replaced by general anesthesia if an ablation is being considered to immediately follow the transesophageal procedure.

Educational and Emotional Preparation of Patient and Family

The preparation of the patient and family for a transesophageal study centers on explaining the technique and addressing expectations and concerns related to placement of the catheter followed by pacing and stimulation. Educational materials

backed by an honest but positive and confident approach during the explanation session are important in successfully achieving the goals of a transesophageal study in an older child or adolescent. In infants and small children, the same approach is modified and directed toward the parents.

Sedation

If general anesthesia is not being used as described above, mild to moderate sedation usually is sufficient to maximize patient cooperation while relieving discomfort and anxiety. For infants, children, and adolescents, intravenous midazolam (0.05 to 0.1 mg/kg) with morphine (0.05 to 0.1 mg/kg) or fentanyl (1 to 2 μ g/kg), is an effective analgesic/amnestic sedative combination. Before a peripheral intravenous line is established, oral diazepam (0.2 to 0.4 mg/kg) or intranasal midazolam (0.2 to 0.3 mg/kg) can also be used to control anxiety and thereby allow the patient to be more cooperative (40).

Preparation of Patient in the Procedure Room

Whether in an inpatient or outpatient setting, the transesophageal technique easily is adaptable to virtually any type of room or location where the patient can be comfortably supine and where sufficient space exists for equipment and monitoring. After peripheral intravenous access is established, the surface ECG leads are placed and connected. A direct current (DC) defibrillation and cardioversion system should be available, or chest pads can be placed routinely, as with most intracardiac studies. Sedation is administered as needed with appropriate

vital sign (heart rate, respiratory rate, and blood pressure) and oximetry monitoring protocols established. In most infants and children, comfortable extremity restraints are necessary to prevent withdrawal of the catheter by the patient. The success of a transesophageal study depends highly on a positive, encouraging approach during the procedure by the pediatric electrophysiologist, pediatric cardiology nurse, and associated personnel. A soothing, comforting manner is necessary for successful passage of the catheter, as well as for successful recording and stimulation because of the potential mild discomfort encountered during each of these steps.

Catheter Placement

Similar to passage of a nasogastric tube, initial placement of the catheter involves lubrication (KY type jelly usually is sufficient, but local lidocaine gel can be beneficial). Entry through the nares is followed by firm but gentle advancement through the posterior pharynx into the esophagus. Encouragement of repeated swallowing by the awake patient facilitates the catheter placement. The distance of catheter advancement required to reach the predicted area best suited for recording and pacing directly correlates with patient height (41) (Fig. 17.10). However, this predicted depth may not actually be the ideal location and minor adjustments may be necessary. The optimal catheter electrode position for pacing correlates with the largest atrial electrogram amplitude. Short distances (a few millimeters) of catheter withdrawal and advancement are performed until the maximum atrial electrogram amplitude is found. The catheter is then secured by taping it to the patient's face or nose.

Equipment and Recording/Stimulation Technique

The three major equipment components are the electrode catheter, the recording apparatus (monitor, strip-chart recorder), and the stimulator (Fig. 14.8). Successful transesophageal

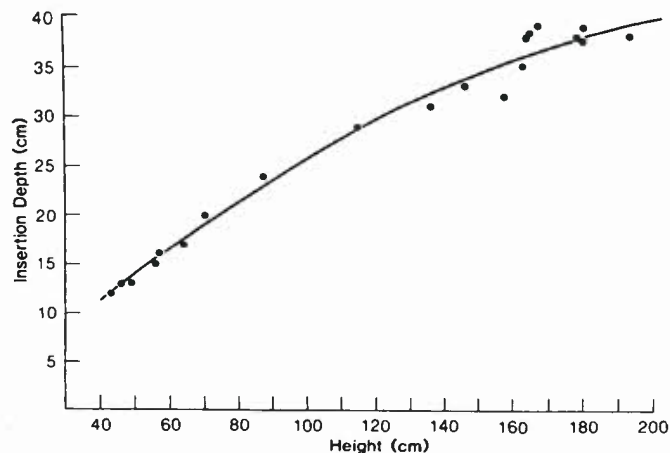


Figure 17.10. Graph of depth of transesophageal electrode catheter insertion (measured from distal electrode on catheter) from the nares in pediatric patients of various heights. By plotting the patient's height, in centimeters, the correlating distal electrode depth can be determined. After the distal electrode has been positioned at the predicted depth, small adjustments may be necessary for optimal recording and pacing. (From Benson DW Jr, Sanford M, Dunnigan A, et al. Transesophageal atrial pacing threshold: Role of interelectrode spacing, pulse width and catheter insertion depth. *Am J Cardiol* 1984;53:1102-1106, with permission.)

recording and stimulation in infants, children, and adolescents have been reported with various types of electrode catheters. Transesophageal electrode catheters differ in size (4 to 10 Fr), interelectrode distance (2 to 30 mm), and number of electrodes (bipolar, quadripolar, hexapolar). Although the adult "pill" electrode can be used in the older child and adolescent, the electrode catheter is better suited for the pediatric patient. Moreover, some transesophageal catheter manufacturers have been receptive to customized catheter design regarding electrode number and interelectrode distance. Benson et al. (41) found that the interelectrode distances (12, 22, and 28 mm) had no significant effect on pacing thresholds regardless of age or size of the patient. Essentially no data are available that compare catheter sizes in pediatric patients; however, intuitively, if electrode contact with the esophageal wall is an important goal, the largest possible catheter size should be used. In normal-sized newborn infants, the nares easily accommodate catheters in the 5 to 7 Fr range; however, a 10 Fr catheter can be placed through the mouth if there is difficulty with the smaller catheter in the nares. In older children and adult-sized adolescents, 10 Fr catheters are used most often. Bipolar electrode configuration limits the technique to either recording or pacing, so quadripolar electrode catheters have been designed to permit simultaneous pacing and recording, with the recording interelectrode distance shorter (2 mm) than the pacing interelectrode distance (12 to 30 mm). Most catheters used today are bipolar.

The recording equipment consists minimally of a strip-chart recorder with an ECG monitor. Without a monitor, the strip-chart recorder can run continuously and, therefore, also functions as the monitor. The recording system can be set up in a unipolar or bipolar fashion (Fig. 17.11). When possible, performing the procedure in the intracardiac EP laboratory allows use of the same digital recording system used for more complex studies, with all its inherent advantages and standard signal filtering capabilities.

A unipolar recording system is the simplest and involves the lowest investment in equipment because a preamplifier is not required. A three-channel ECG machine can function as both a strip-chart recorder and monitor (Fig. 17.11). A three-channel simultaneous-recording ECG machine uses one channel for a unipolar esophageal lead and the other two channels for two surface ECG leads. For example, the V1 chest lead is connected to one of the electrodes on the transesophageal catheter. The recordings from the V2 and V3 chest leads are then displayed or recorded simultaneously to permit comparison of the QRS and P waves on the surface leads with the electrograms from the unipolar esophageal lead (Figs. 17.11A and 17.12). Alternatively, two simultaneous unipolar esophageal electrograms, each from a separate esophageal electrode, can be displayed or recorded with the recording from one surface ECG lead. Recording during pacing is carried out either without the simultaneous transesophageal electrogram, by reconnecting the V1 chest lead to the V1 skin lead as illustrated in Figure 17.13, or with the simultaneous recording from a transesophageal lead (Figs. 17.11B and 17.14).

A bipolar system has the advantages of more reproducible and reliable atrial electrograms. The baseline wanders less, and the atrial electrograms are more distinct and the ventricular electrograms less prominent, which makes the recordings more distinguishable (Fig. 17.15). However, standard ECG filters are 0.05 to 50 Hz, which are still not ideal for high-quality bipolar electrograms. The simplest solution is to perform the study in the intracardiac electrophysiology laboratory where the recording system includes variable filtering as needed and the pacing systems can provide the necessary output. When using a standard 12-lead ECG machine, a bipolar recording can be achieved by connecting two esophageal electrodes to

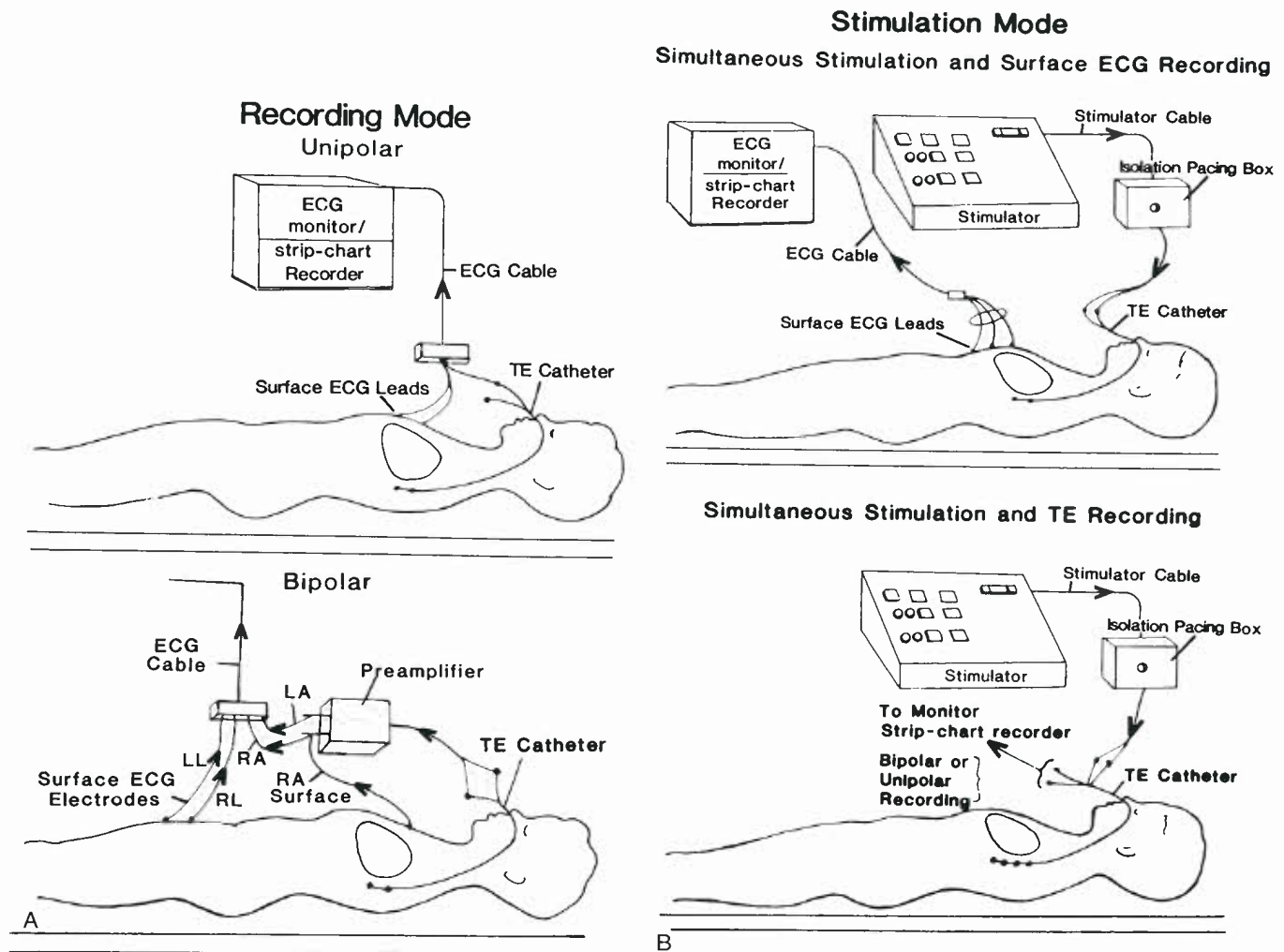


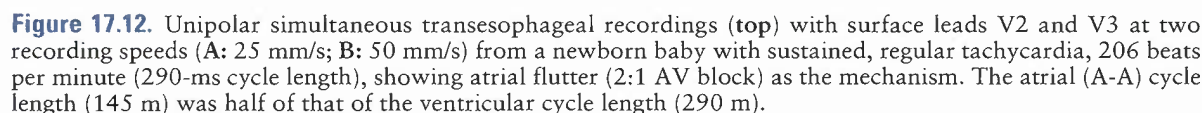
Figure 17.11. Diagrammatic illustration showing the recording and stimulation components of the transesophageal (TE) electrophysiologic technique. The recording mode (A) can be set up in a simple unipolar system (top) by connecting one esophageal electrode terminal to a surface ECG lead (e.g., V1) while recording one or two other simultaneous surface ECG leads (e.g., V2, V3). (See Figs. 17.12 and 17.15A for examples of unipolar recordings.) A bipolar recording system (bottom) can be used by adding a preamplifier. (See Fig. 17.15B for an example of a bipolar recording.) The stimulation mode (B) can be set up using either a bipolar or a quadripolar transesophageal electrode catheter. The bipolar electrode catheter permits only recording or stimulation, but not both simultaneously. An example of bipolar pacing using a bipolar electrode catheter is shown (top) with recording of the surface ECG during pacing. (See Fig. 17.13 for an example of ECG recording during pacing.) Simultaneous esophageal recording during pacing (bottom) can be accomplished in a unipolar or bipolar recording mode. (See Fig. 17.14 for an example of unipolar recording during pacing.) LA, left arm; LL, left leg; RA, right arm; RL, right leg.

the bipole of an ECG limb lead (e.g., right arm and left leg for lead II). Signal quality can be enhanced by the addition of a preamplifier between the catheter and the monitor/strip-chart recorder (Fig. 17.11A), but if it is not available, most studies can be performed adequately by adjusting the ECG high-pass filters to 0.5 or 1.0 Hz. A bipolar system is better than a unipolar system with regard to pacing-induced artifact, but the latter is not eliminated by a bipolar system because the high amplitudes and long pulse widths of bipolar transesophageal pacing present a problem in ECG recording and, therefore, measuring intervals. Benson et al. (42) have reported success using a prototype stimulus artifact suppressor that allowed for much-improved ECG recordings, but such a device rarely is used today.

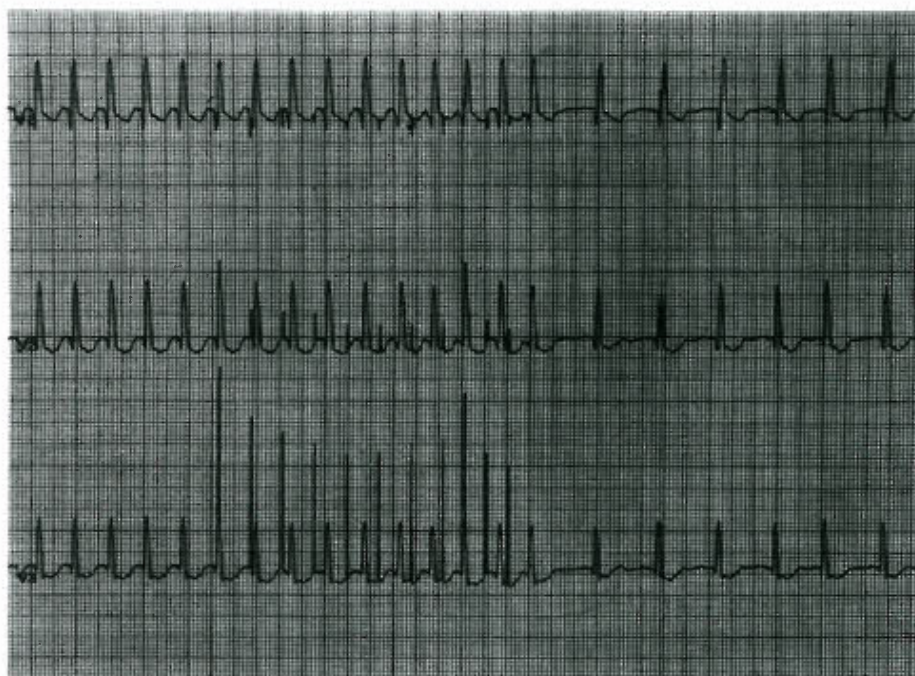
The stimulator system requires capability for a long pulse width (≥ 10 m) and high current (10 to 25 mA) (42,43).

Several investigators have shown that pulse widths greater than the standard 2 m for intracardiac pacing are necessary to overcome high impedance and to penetrate the esophagus to reach the atrial (paraseptal) myocardium, particularly in non-infants. Although reports of pulse width duration for successful transesophageal atrial pacing have included low values of ≤ 2 m, atrial pacing is most consistent and reproducible at 6 to 10 m and current of 10 to 15 mA (28,29). Delivery of stimulus current >15 mA (at a constant pulse width of 10 m) is associated with patient discomfort (41,43). Moreover, lower stimulus current is needed at higher pulse width settings (e.g., 15 or 22 m). Therefore, for patients with high thresholds, discomfort can be minimized by increasing the pulse width, limiting the current threshold with a goal of <15 mA.

Transesophageal atrial pacing is most successful and best tolerated when performed at stimulator outputs $\geq 20\%$ above



Ventricular transesophageal pacing has been accomplished in adults by stimulating at high outputs currents ranging from 20 to 30 mA with a pulse width of 40 m and by using a specially designed flexible lead passed into the stomach (45,46). In a case report of ventricular transesophageal pacing in a 2,400-g premature infant with congenital AV block, high output also was required: 10-ms pulse width with 45-V amplitude (current was not specified) (47). Overall success rates of



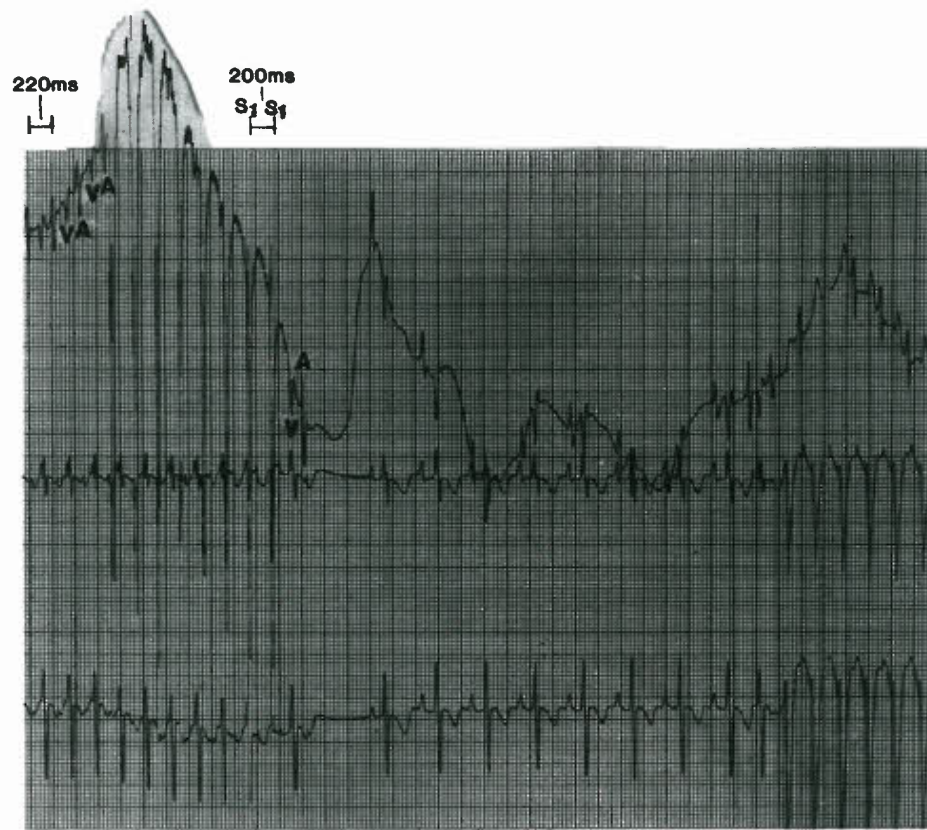


Figure 17.14. Unipolar transesophageal simultaneous recordings (top) with surface leads V2 and V3 from a 3-year-old boy with incessant normal and wide QRS SVT (220-ms cycle length) showing simultaneous transesophageal pacing (interelectrode distance 24 mm) and recording (interelectrode distance 2 mm). Using a quadripolar electrode catheter, the esophageal recording (V, ventricular; A, atrial) during tachycardia was interrupted by 8 beats of atrial pacing (200-ms cycle length), which converted the tachycardia to several beats of sinus before wide QRS reciprocating AV reentrant SVT recurred. Note the wandering baseline of the unipolar esophageal recording before, during, and after pacing.

stable transesophageal ventricular pacing have ranged from 50% to 75% in adult patients. Data are not available from a pediatric series.

The pacing protocols for transesophageal pacing are limited, on a practical basis, to atrial pacing. As with the intracardiac pacing protocols, the specific protocols should be suited to the patient and the preprocedure diagnosis. In Table 17.2, a list of pacing protocols provides examples of several options used during transesophageal electrophysiologic studies.

Administration of Drugs

Sedative, provocative arrhythmic, and antiarrhythmic drugs are administered intravenously as individually indicated, similar to the intracardiac studies discussed earlier. The major differences relate to the practical application to primarily supraventricular arrhythmias in transesophageal studies, contrasted with both supraventricular and ventricular arrhythmias in intracardiac studies. The one caveat

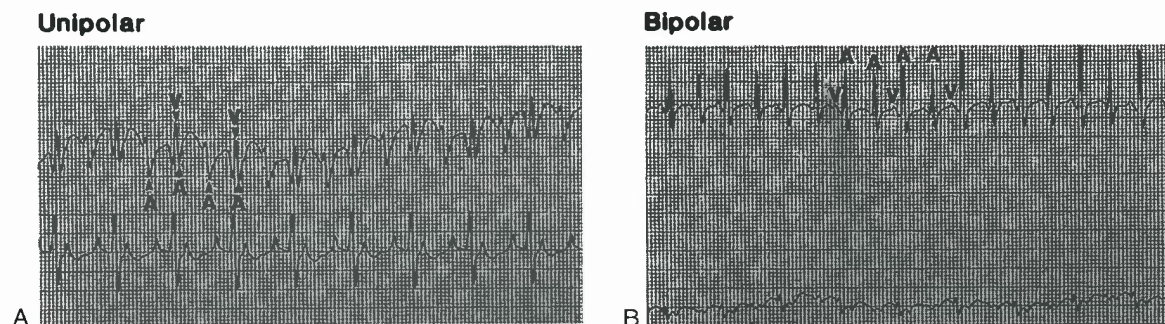


Figure 17.15. Two transesophageal recordings (50 mm/s) in a 2,250-g newborn with atrial flutter (150-ms atrial cycle length) and 2:1 AV block showing a comparison of unipolar (A) and bipolar (B) recordings. Note that the prominent ventricular electrogram and the wandering baseline in the unipolar recording are eliminated in the bipolar recording. Therefore, the atrial electrogram is better delineated in the bipolar recording.

TABLE 17.2

Pacing Protocols for Transesophageal Electrophysiologic Study

1. Sinus node function
 - a. Sinus node recovery time
2. AV conduction
 - a. Continuous atrial decremental pacing
 - b. Premature atrial extrastimulation technique (during sinus and/or eight-beat drive of a-paced rhythm)
3. Atrial muscle refractory period
 - a. Premature atrial extrastimulation technique (during sinus and/or eight-beat drive of a-paced rhythm)
4. Induction of SVT
 - a. One or more of the following: Short bursts of a-pacing, continuous atrial decremental a-pacing, premature atrial extrastimulation technique (using one or more drive cycle lengths and one to three extrastimuli)
 - b. If unsuccessful, add provocative drug and repeat 4a
5. Determine SVT mechanism
 - a. Results of 4a, b
 - b. Record transesophageal electrogram, determine intervals
6. Determine drug efficacy/safety
 - a. Administer drug
 - b. For efficacy, repeat provocative a-pacing modes that induced pacing before drug
 - c. For safety, repeat steps 1–3
7. Terminate tachycardia
 - a. One or more of the following: Short bursts of a-pacing, continuous atrial decremental pacing, premature atrial extrastimulation technique (using one or more drive cycle lengths and one to three extrastimuli)
8. Risk stratification in asymptomatic or symptomatic WPW
 - a. Premature atrial extrastimulus technique to determine the antegrade effective refractory of the AP
 - b. Continuous atrial decremental pacing (or short bursts) to determine minimum cycle length for 1:1 conduction in the AP
 - c. Attempted induction of SVT as in steps 4a,b, and determine mechanism as in steps 5
 - d. Attempted induction of atrial fibrillation to determine the minimum preexcited RR interval during atrial fibrillation.

AV, atrioventricular; SVT, supraventricular tachycardia.

is ventricular tachycardias (VTs) that are reproducibly induced and terminated with atrial pacing like “Belhassen” tachycardia (48,49), where diagnostic and follow-up efficacy studies can be performed with transesophageal techniques.

Complications

Complications of transesophageal studies are infrequent and predominantly inconsequential (41,50,51). Mechanical or anatomic problems such as undetected obstructions or mucosal trauma or placement in a bronchus can arise during passage of the catheter through the nares and pharynx. These usually are recognized and are transient. Using lower stimulation outputs, no esophageal mucosal damage has been documented even after hours of continuous pacing if outputs are reasonably low. However, with

excessively high outputs esophageal damage can occur. Although technically not a true complication, transesophageal pacing in rare cases causes intolerable discomfort that is sufficient to disrupt completion of the study. Ventricular arrhythmias may be induced from inadvertent ventricular pacing or from rapidly conducting atrial-paced beats (51–53). This rare but serious problem of induced ventricular arrhythmias requires readily accessible DC cardioversion/defibrillation and resuscitative equipment.

OBJECTIVES OF DIAGNOSTIC ELECTROPHYSIOLOGIC STUDIES AND COMPARISON OF INTRACARDIAC AND TRANSESOPHAGEAL TECHNIQUES

One or more of the objectives listed in Table 17.3 are pertinent during electrophysiologic studies. The specific objectives performed relate to several factors, including arrhythmia diagnosis, underlying cardiac diagnoses, planned therapy, and which electrophysiologic technique (intracardiac or transesophageal) is used. The following discussion outlines the advantages and limitations of the two techniques relative to the objectives of the electrophysiologic study.

Ample studies of electrophysiologic results for both intracardiac and transesophageal techniques involving the objectives listed in Table 17.3 have been reported. The ability of the two techniques to accomplish the objectives of an electrophysiologic study encompasses multiple factors. It is important to realize the advantages and limitations of the two techniques. In this manner, when presented with an individual patient with a specific diagnostic or therapeutic problem, either the intracardiac or transesophageal technique (or both) can be chosen. Although the intracardiac technique may be superior in accomplishing virtually all of the clinical objectives, limitations in terms of cost, higher risk, and application in small infants may dominate in specific situations, making the transesophageal technique the best choice for the individual patient.

In Table 17.3, a comparison of the two techniques is graded (by opinion only) on a scale ranging from 0 (–), indicating no ability to accomplish the objective, to 4 (+ + + +), indicating an approximately perfect (or universal) ability to accomplish the objective. The inability to routinely pace the ventricle is the major limitation to the transesophageal technique. Therefore, when the objectives that involve ventricular pacing are analyzed, the transesophageal technique is inferior. Another major limitation of the transesophageal technique involves the fixed site of recording and stimulation, which limits the ability to effectively evaluate mechanisms of supraventricular arrhythmias, sinus node function (increased distance to sinus node), AV conduction, and site of AV block (inability to record HBE). The inability to reach the effective refractory period of the atrium is occasionally overcome by increasing the energy output. This is a potential limitation to the transesophageal technique, especially when attempting to fully evaluate patients with preexcitation when the AP refractory period is limited by reaching the atrial refractory period first.

Although the major advantages of the intracardiac technique involve its superiority in accomplishing specific objectives, the transesophageal technique is far superior in terms of cost, time commitment, and risk. Therefore, in many situations, limitations of the transesophageal technique are outweighed by its advantages. Also, it may be better to use one technique for a patient with a specific arrhythmia, but in another patient with an identical arrhythmia it may be better to use the other technique. In some patients, particularly in unique situations in which catheter access is a problem, the transesophageal technique is used during an intracardiac electrophysiologic procedure to provide additional and/or optional atrial recording/pacing site.

TABLE 17.3

Comparison of Intracardiac and Transesophageal Techniques to Accomplish Objectives of the Electrophysiologic Study

Objective	Intracardiac	Transesophageal
1. Determine cause of unexplained symptoms suggesting arrhythmia	+++	++
2. Terminate AV reentrant SVT, AV nodal SVT, or intra-atrial reentry/atrial flutter	++++	+++
3. Determine mechanism of ECG-documented SVT to define treatment options	+++	++
4. Assess efficacy/safety of antiarrhythmic drug therapy for SVT	++	++
5. Assess efficacy/safety of antiarrhythmic therapy for ventricular arrhythmia	++	—
6. Assess sinus node function	++	+
7. Assess AV conduction	+++	+
8. Assess site of AV block	+++	—
9. Evaluate potential risk in patient with:		
a. Preexcitation	+++	++
b. Ventricular tachycardia	+++	—
10. Determine optimal mode of chronic pacemaker therapy for bradycardia pacing	++	+
11. Determine efficacy/safety and optimal mode of antitachycardia pacemaker therapy	++	+
12. Perform catheter ablation at same setting	+++	—
13. Assess efficacy/safety after catheter ablation	+++	+ ^a

AV, atrioventricular; SVT, supraventricular tachycardia.

^aSVT only.

Finally, as noted above, the transesophageal study may be used before a catheter ablation procedure in the same setting to test arrhythmia inducibility in a patient with undiagnosed palpitations or for risk stratification in a patient with asymptomatic WPW. By understanding the limitations and advantages of the two techniques the cardiologist can optimally recommend the appropriate technique for the individual patient.

ELECTROPHYSIOLOGIC STUDIES—THERAPEUTIC CATHETERIZATION

In 1932, based on surface electrocardiographic data alone, Wolferth and Wood (54) correctly hypothesized that the structural abnormality underlying WPW syndrome (55) was an accessory AV connection or AP. However, it was not until Sealy et al. (56) surgically cured a patient with WPW syndrome and a right-sided AP that the anatomic basis of the disease proposed so long before was confirmed. This milestone also heralded the beginning of a prolonged debate concerning the optimal management of symptomatic and asymptomatic WPW syndrome: medical, surgical, or none. That debate has now changed from “which” to “when,” as ablation procedures have progressed from application of uncontrolled miniexplosions generated by high-energy defibrillator shocks delivered through the tip of a catheter, to precise localization of the atrial or ventricular AP insertion sites followed by temperature-controlled heating or freezing of a small volume of myocardium with RF (57) or cryoenergy (58). However, despite these changes, several questions regarding the early and late implications of catheter therapy in small children whose myocardial development is still underway remain unanswered (59,60).

This introduction to interventional electrophysiologic catheterization uses the treatment of AP-mediated tachyarrhythmias as a focal point for discussion. However, catheter-based therapy now has been applied to the cure or modification of most pediatric

arrhythmias, including AV node reentry tachycardia (61), ectopic atrial tachycardia (EAT), atrial reentry/flutter, congenital junctional ectopic tachycardia (JET), and some forms of VT (62).

THE DECISION TO ABLATE: SAFETY VERSUS EFFICACY

One overriding theme in the management of arrhythmias in children compared to adults is an emphasis on *safety* over *efficacy*. Although there are few cases at any age where safety is not an important concern, the relatively benign course of many arrhythmias in childhood, the potential disruption even therapies such as permanent pacing cause for a child, and the fact that parents are usually the decision making surrogate for the child, often lead to a different decision tree for children than in adults. Furthermore, for some situations and technologies, there are important differences (e.g., - the potential for coronary damage with RF energy application at the AV groove, the size of the patient and the heart).

Ablation in patients with WPW syndrome is an excellent example of how decision making may be age dependent (63). In this chapter, the term WPW is used to describe the condition of preexcitation on the surface ECG, with or without coexisting tachycardia. Due to a variety of concerns, even the most symptomatic infant with WPW and paroxysmal SVT only rarely is a candidate for ablation (64–66). Myocardial (60) and potentially severe coronary injury (67–70) are more likely with ablation in this age-group than in older patients. Furthermore, about 40% of APs in infants spontaneously stop functioning in the first year of life (71,72), and an additional third of patients are unlikely to have symptoms between infancy and early childhood (73). In children over the age of 4 years with symptomatic arrhythmias, the balance between risks and benefits clearly shifts toward ablation therapy, but

generally only if the ablation can be performed safely (63). In contrast to the situation in infants, even asymptomatic patients with WPW between the ages of about 8 and 18 years can be managed more aggressively than adults. Unlike asymptomatic adults over the age of 28 years, who are unlikely to ever have symptoms (74,75), the older child with a high-risk AP is exactly the type of patient who may present with sudden arrhythmic death as their initial symptom. This leads to the recommendation that such patients undergo risk stratification and those who are *high risk* be offered catheter ablation as a therapeutic option (76). Furthermore, the guidelines for sports participation in patients with WPW recommend risk stratification prior to approval for this age-group (77). Other age-dependent differences in management decisions are addressed when discussing individual arrhythmias below.

ENERGY SOURCES

Various energy sources have been used for ablation of myocardial tissue. Although many of the techniques rely on the generation of heat to destroy tissue, alternate mechanisms include chemically induced cell death, application of high current densities to disrupt intracellular membranes, and cooling to burst them.

Direct Current

In 1979, Vedel et al. (78) reported the first use of a DC shock through a catheter to produce complete AV block (inadvertently, in that case). His findings soon led to the use of DC catheter ablation for intentional production of complete heart block in a limited number of patients with drug-refractory supraventricular arrhythmias (79). Although the method was moderately successful in producing clinically effective AV block (~90% of 127 patients in one large series), complications were sometimes severe, including production of new arrhythmias, cardiac tamponade, and sudden death (80). With the possible exception of one series (81), similar results were obtained when DC ablation techniques were applied for the elimination of accessory AV connections or VT; moderate success was attained with infrequent but serious complications (82). Based on the results in adults, appropriate skepticism concerning the use of DC ablation in small hearts led to limited use of the technique in pediatric patients. Although success

was possible, a high incidence of complications has resulted in there being no current circumstances in which DC ablation is recommended for the treatment of arrhythmias in children (83,84). The so-called low-energy DC ablation technique (2 to 40 J) introduced in 1986 (85) was significantly safer than standard DC ablation, even within the CS, but its introduction was nearly simultaneous with the much more controllable RF techniques described below.

Radiofrequency

The theoretical advantages of controlled lesion formation using RF current to heat tissue combined with an existing neurosurgical experience using RF current (86) led Huang et al. (87) to attempt closed-chest ablation of the AV node with catheter-delivered RF energy. Their use of relatively low power (<50 W) appeared to provide adequate tissue heating to induce permanent AV block without significant complications, such as perforation or proarrhythmia, and with a lesion that was histologically well demarcated. The appeal of this technique was noted immediately by several investigators, such that by 1987, reports of the use of this technique in humans for both AV node and AP ablation were beginning to appear (88).

Since 1987, a number of studies, both in vitro and in vivo, in adult animals have confirmed that the cause of myocardial cell death with RFA is tissue heating to a temperature greater than approximately 50°C (57). Tissue heating to >90°C to 100°C is associated with tissue boiling, coagulum formation on the tip of the catheter, an increase in impedance, and a decrease in delivered current (89). Cell death appears to occur almost immediately at temperatures above 52°C, suggesting that cell death is the result of both protein denaturation and dehydration. The histologic changes have been described as coagulation necrosis (87). Haines and Watson (57) demonstrated that the lesion size grows exponentially with time, with a half-time of about 18 seconds. The temperature decreases hyperbolically with distance away from the electrode tip (inversely proportional to the radial distance) so that the lesion dimensions are directly proportional to the temperature measured at the tip-tissue interface. We have demonstrated similar findings for RF lesions made in immature myocardium (Fig. 17.16) (60). Thus, theoretically it is possible to accurately control lesion size by controlling the RF power output such that a particular preset temperature is achieved at the tip-tissue interface.

Current commercial systems supply RF energy at 500 KHz using a generator that can either supply unmodulated voltage/

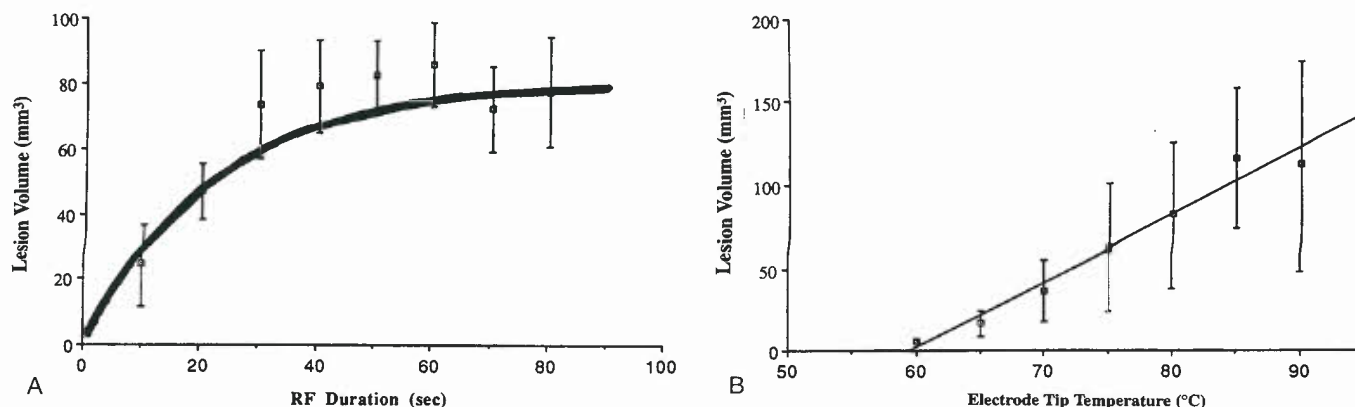
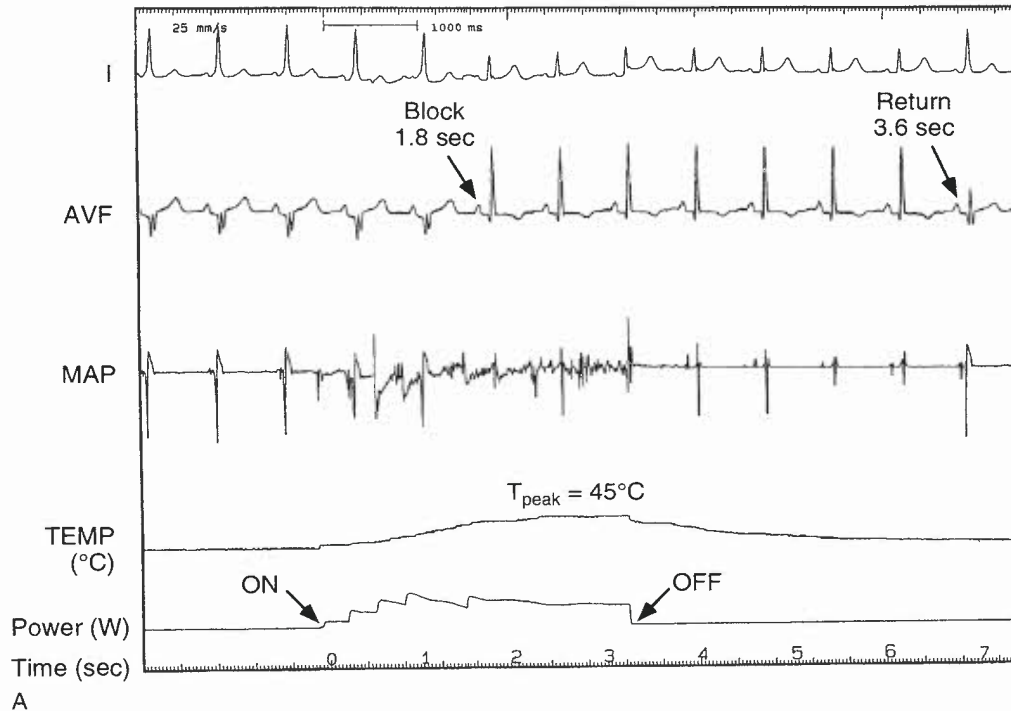


Figure 17.16. Lesion volume as a function of the duration of RF application (A) and the electrode tip temperature (B). Volume increases exponentially as a function of lesion duration. For (A), the tip temperature was held constant at 80°C. The time constant (time required to reach 63% of the ultimate asymptotic lesion size of 79 mm³) was 22 seconds. Ninety percent of the maximum lesion was reached by 45 seconds. Lesion volume appeared to grow linearly as a function of electrode tip temperature. Previous data in adult animals had shown linear increase in width and depth with tip temperature.

power or control the temperature of the catheter tip through power modulation between 0 and 50, 60, or 100 W, depending on the manufacturer and catheter used (90). Energy is delivered in a unipolar fashion from the catheter tip to one or two large skin reference electrodes, positioned either on the patient's chest,

buttocks, or leg. During each RF application, voltage, power, current, impedance, and temperature are available and can be monitored continuously. Appropriate filters are available in most recording systems so that intracardiac electrograms and surface ECG leads can be monitored during RF delivery (Fig. 17.17).

50° C Test



70°C Application

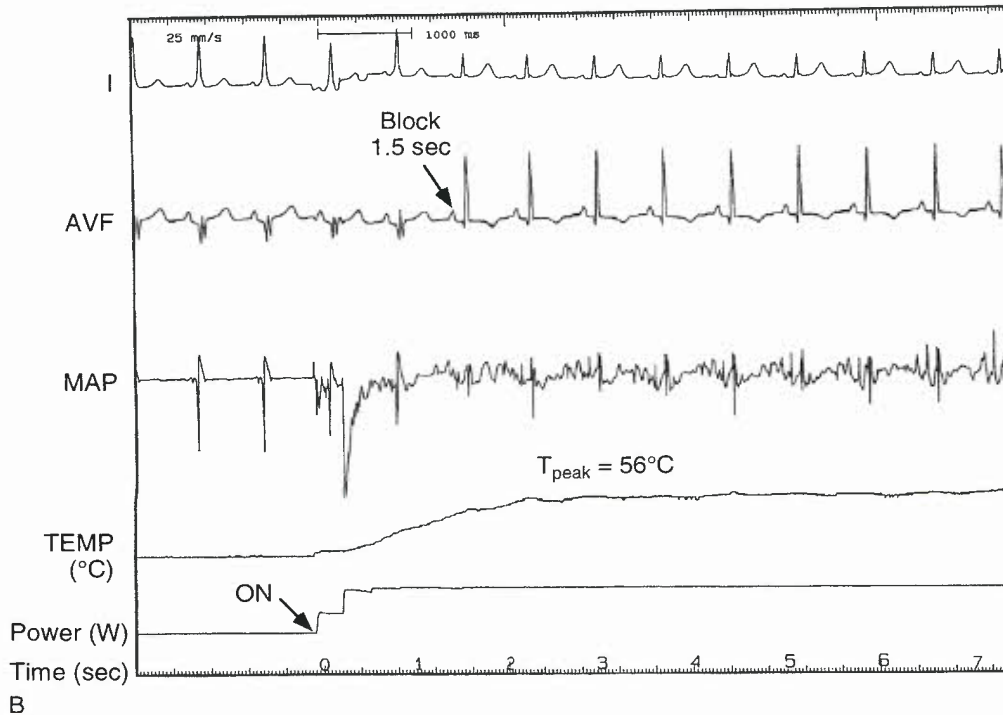


Figure 17.17. A: Test application with radiofrequency (RF) generator set to 50°C. Maximum temperature achieved is 45°C. AP block occurs after 1.8 seconds and power is turned off after 3.1 seconds. AP conduction returns 3.6 seconds after turning off the power. B: After return of AP conduction, a full application is delivered with the RF generator set to 70°C. Peak temperature achieved is 56°C, and AP conduction block occurs at 1.5 seconds.

Control of catheter tip temperature during power application has not necessarily improved the success rate of ablation procedures, but has (a) almost completely eliminated overheating, impedance increase, and coagulum formation, (b) helped determine whether inadequate heating rather than incorrect catheter location is responsible for lack of success at a particular site, and (c) allowed low temperature heat mapping by intentionally producing low-temperature (45°C to 50°C) applications, which cause reversible electrical changes in the tissue (Fig. 17.17) (91).

As noted above, chronic lesions in adult dogs appear to be well demarcated histologically and are approximately the same size as the acute lesions (87). However, in 1994, we reported that chronic atrial and ventricular lesions produced in immature (~1-month-old) sheep may increase in size during the subsequent 6 to 8 months of normal development (60). This finding may have important implications for the use of RFA in very small children.

Cooled-Tip Radiofrequency

As noted, one of the limitations in creating larger RF lesions is that high temperatures at the tip-tissue interface lead to boiling, coagulum formation, and impedance increase, preventing further delivery of RF energy to the tissue. Over the past few years, it has become apparent that tip cooling can decrease the tip-tissue interface temperature, allowing the delivery of more RF power, pushing the peak temperature further into the tissue, and increasing lesion size by as much as a factor of two (92). Tip cooling can be accomplished passively with a more thermally massive tip (e.g., 8 to 10 mm in length, gold, etc.) (93) or by actively using a variety of methodologies (e.g., shower head, internal flow, porous metal, sheath flow) (92,94), achieving lesion widths and depths of 10 to 15 mm. Although this technique already has been critically useful for treatment of a number of arrhythmias, there are two important caveats. First, lesions can be too large, creating unintentional damage to structures, such as coronary arteries and second, cooling will reduce lesion size when maximum power is already being delivered with a noncooled ablation tip.

Microwave

In contrast to RF heating, which primarily is resistive, microwaves heat with a propagating magnetic field that have the potential to heat tissue at a distance from the origin of the field. In vitro studies with microwave antennas have shown that the volume of heating is probably somewhat larger than that seen with RF, but is more dependent than RF on antenna construction characteristics, electromagnetic frequency, and geometry of the antenna in relation to the tissue (95). Although there are no commercial microwave systems available now, microwave ablation some day still may have a bearing on the treatment of VT or atrial flutter, where larger lesions may be necessary, than for common forms of SVT, where RF and cryo techniques have been adequate.

Cryotherapy

Catheter-based cryotherapy was introduced into the clinical arena around the year 2000 for ablation of a variety of cardiac arrhythmias (96–101), but there are limited reports of its use in children (98,102,103). Cryoablation has several potential advantages over RFA, including (a) reversible cryomapping prior to the production of a permanent lesion (100,104,105), (b) adherence of the catheter tip to the endocardium upon freezing, (c) a well-defined edge of the cryolesion (104), (d) minimal effects on adjacent coronary arteries (106,107), and (e) a lower incidence of thrombus (108,109). The first four of these issues

are particularly relevant to small children because of the close proximity of a variety of critical cardiac structures to the ablation target. The most common reported major complication during RFA in pediatric patients is AV block (66,110,111), and there appears to be a higher potential for coronary artery injury in this patient group (68–70,112,113), even during slow pathway modification (70). Both of these effects appear to be much less likely or absent with cryoablation (114). However, despite previous belief that cryoenergy did not have the same potential for RF lesion growth in immature myocardium as reported for RF energy (60), a recent report from Khairy et al. (109) demonstrated that, in fact, cryoenergy produces nearly identical late lesion characteristics to RF energy in immature swine.

Cryotherapy is performed with a system that cools the tip of a catheter by expanding a liquid gas within the tip and removing heat from the surrounding blood and tissue. Systems allow for both ice *mapping* at a tip temperature of –25 to –40°C where the catheter adheres and nearby tissue loses electrical activity but few cells are killed and *ablation* at a tip temperature of < –65°C where a lesion will be formed. Once cells freeze, they expand and burst. After 4 minutes at the ablation temperature, a typical lesion size is 3 to 6 mm in diameter, smaller than those seen for RF. One of the contrasting features of cryoablation compared to RF is that there is a much larger zone of reversibility as the lesion expands because tissue cooling above the freezing point will lead to loss of electrical activation well prior to the loss of viability. This feature has dramatically enhanced the safety profile in clinical trials to date. In fact, despite frequent use of the technology for septal tachycardia substrates, there are no reports of AV block with cryoablation (96,98–101), even in children as small as 20 kg, in the presence of a His potential (Fig. 17.28)(103).

The primary disadvantage of cryoablation is that inherent in its high level of safety is a smaller lesion size than for RFA. For ablation of septal tachycardia substrates (AV node modification, anterior and posterior septal pathways), cryoablation success rates have been statistically similar to those for RF techniques (96,98–101). However, recurrence rates have sometimes been higher (115). Most operators are less aggressive with RF in septal areas and have had to be highly aggressive with cryotherapy to achieve success. Furthermore, with one exception in which 97% success was reported in a series of 24 pediatric patients with left-sided APs (116), even aggressive application of cryoenergy has not yielded similar success rates to RF for ablation of nonseptal APs. Although the data are limited in very small children and infants, anecdotal evidence suggests that cryoablation may be effective for all AP locations in these unique patient groups. Because of its acute safety profile, the use of cryoablation is most important for septal substrates, small children, and patients with abnormal anatomy where the precise location of the AV conduction system is not known.

Other

Any energy source that creates tissue heat has the potential to ablate myocardium in a similar manner to RF and microwave energy. Laser energy has been used to successfully ablate ventricular myocardium in both normal animals and humans with VT (117–119). The use of high-power ultrasound delivered through a catheter also has been reported as a means of heat ablation. One potential advantage might be the simultaneous use of diagnostic ultrasound to monitor lesion production (120). Finally, chemical ablation achieved by delivering a toxic agent such as alcohol into the coronary artery or vein supplying the myocardium responsible for an arrhythmia has been used in both animals and humans. However, technical problems with selective delivery will probably prevent this technique from ever reaching widespread use.

Summary—Energy Sources

Several energy types are available currently for use in catheter ablation procedures. However, currently, for procedures in children, cryotherapy and RF energy with or without tip cooling appear to have the best safety and efficacy profile. Both energy sources can reproducibly control lesion characteristics through assessment of tip temperature and application time. In general, RFA is more effective, but for the reasons discussed above, cryoablation is safer. At this time, the balance between which source is used for which procedure depends on the arrhythmia substrate, the location of the target, including the proximity of the AV node and coronary arteries, and the preference of the center and operator.

PROCEDURE—GENERAL

Preablation

Prior to the ablation procedure, standard electrophysiologic techniques should be used to identify the tachycardia mechanism, and, if appropriate, the location of the arrhythmia substrate. Differences from the standard study are related primarily to the actual mapping and ablation. Although not absolutely necessary, biplane fluoroscopy is very useful for precise 2-D localization of catheter tip positions. For most APs and AV node modifications, cameras are placed in the 30-degree RAO and 60-degree LAO positions, with 10- to 15-degree caudal projections (Fig. 17.4). In addition to camera angles, the development of deflectable tipped catheters with closely spaced electrode configurations, which are now available from a number of manufacturers, has greatly facilitated accurate mapping and ablation in all parts of the heart.

Three-Dimensional Electroanatomic Mapping

Over the past 10 years, a few novel methods have been introduced to simultaneously present 3-D, detailed electrical and anatomic information, facilitating mapping and reducing fluoroscopy exposure. One, termed “nonfluoroscopic,” uses a technology similar to a global positioning system to identify the precise catheter tip position and orientation (Fig. 17.18) (CARTO, Biosense—Webster, Baldwin Park, CA). Another, termed “noncontact,” uses the electrical signals in the blood pool of a cardiac chamber to derive an inverse solution for the signals on the endocardial surface (Fig. 17.5) (EnSite—St. Jude Medical, St. Paul, MN). Other systems provide simpler 3-D localizations of the catheter electrodes, using either impedance (NavX—St. Jude Medical, St. Paul, MN Fig. 17.6, and Loca-Lisa, Medtronic, Minneapolis, MN) or ultrasound localization (RPM, Cardiac Pathways), and can catalog catheter locations and timing signals during either mapping or ablation. Although location identification with impedance-based systems like NavX can be less accurate than the magnetic-based CARTO system, impedance-based systems do allow for location and timing data from any catheter, consequently providing faster collection of both geometry and timing data. Consequently, most available systems now have a feature for impedance-based catheter location. The location tracking and cataloging feature is an important component of all 3-D systems, enabling the operator to be aware of where critical cardiac structures are, where applications have been made and their outcome. Although all of these systems have their limitations, including high cost for the CARTO catheter and EnSite balloon catheter, it is clear that they contribute significantly to our understanding of arrhythmias and their mechanisms, and probably enhance success for complex cases (121–126),

reduce radiation exposure (20), and make completely non-fluoroscopic procedures possible.

PROCEDURE—SUBSTRATE SPECIFIC

Accessory Pathways

Mapping

Jackman et al. (127) and others have described important electrogram characteristics that help identify the precise location of antegradely and retrogradely conducting APs. Electrograms should be examined for the presence of probable AP potentials (Fig. 17.7) as well as the shortest AV time in preexcited sinus rhythm or atrial-paced rhythm and the shortest VA time during orthodromic reciprocating tachycardia or ventricular-paced rhythm (127). To help localize left freewall and left posteroseptal APs, a multielectrode catheter may be used in the CS (Figs. 17.2, 17.4, 17.19, and 17.20), but is probably not always necessary because it is the electrogram from the tip of the ablation catheter that ultimately determines the final ablation site. Typically, a deflectable tipped mapping/ablation catheter is used to localize right-sided APs on the tricuspid annulus either from the right femoral vein or the left subclavian vein. These techniques have been well described elsewhere (5,127). Some of the 3-D mapping techniques described above may be particularly useful for septal APs, to better understand the local anatomy, identify the location of critical structures, and identify prior ablation locations.

Ablation Catheter Manipulation—General

After initial localization, additional mapping and RFA are performed with introduction of a large-tipped (4 to 10 mm) steerable electrode catheter. These catheters are now available from a number of manufacturers in multiple sizes (5, 6, 7, and 8 Fr tips) and with a variety of deflecting curve options. For technical reasons, cryoablation catheters are not available in <7 Fr. The following standard approaches to AP ablation have been reported (5,127).

Left Freewall Pathways

Left freewall APs can be approached using a deflectable-tipped catheter advanced retrograde from the aorta into the left ventricle (5,127) or transseptal (5). For the retrograde approach, an attempt is made to place the catheter tip under and perpendicular to the mitral leaflet (Ao-LV) (Fig. 17.7) or through the mitral valve and above the mitral leaflet (LV-LV) (Fig. 17.19).

For the transseptal approach, the area of the foramen ovale is first probed with the mapping/ablation catheter for patency. If not patent, a standard transseptal puncture is performed using any of a variety of techniques and sheaths (see below). The mapping/ablation catheter then is placed through the transseptal sheath into the left atrium. Generally, the tip of the ablation catheter is maneuvered so that fluoroscopically it appears to be near the AV groove, confirming such location by the electrical recording from the distal pair of electrodes. Then the catheter tip is manipulated through deflection, rotation, and longitudinal movement to map the left AV groove. In many cases, catheter stabilization for mapping and ablation can be enhanced by deflecting the catheter and pulling it back into the sheath until only the four electrodes protrude, giving the appearance of a hockey stick (Fig. 17.20). Then the sheath and catheter are moved along their long axis as a single unit from septum to lateral freewall and the catheter torqued either clockwise (posterior groove) or counterclockwise (anterior groove) within the sheath. Access to left lateral pathways in larger patients sometimes requires exchange

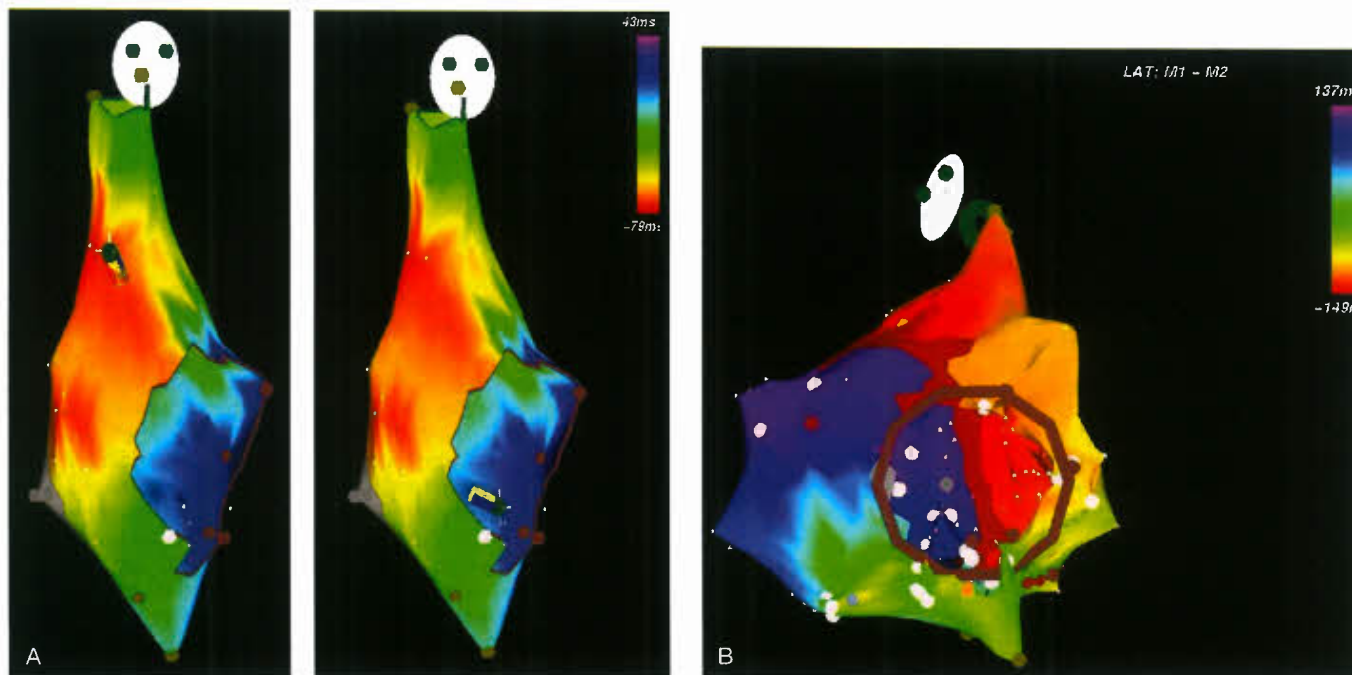
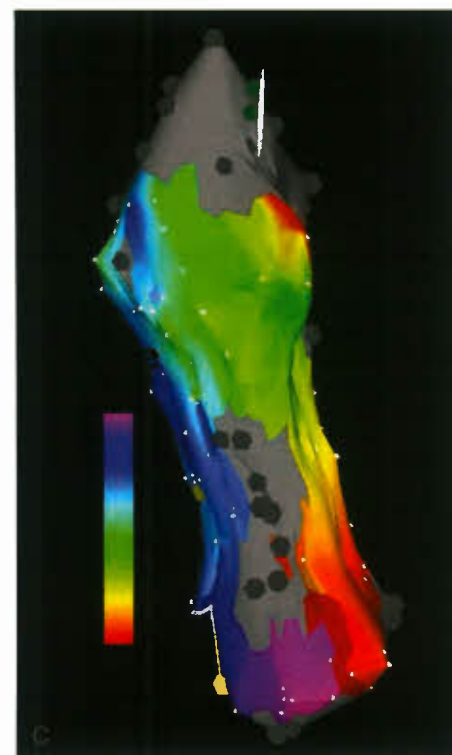


Figure 17.18. Three-dimensional mapping using the CARTO, Biosense nonfluoroscopic system. Color scales go from red–orange being the earliest activation to blue–purple being the latest (see scale bar in images). Gray represents an area of low voltage determined to be scar tissue. Each white dot represents one point where the catheter was placed and activation times determined. The “face” at the top of each image shows the direction of the image (A) sinus rhythm—RAO projection (see face) of the right atrium (RA) in an adult patient with prior repair of a VSD as a child. As expected with sinus rhythm, activation spreads from the antero-lateral RA down toward the tricuspid valve. Activation lasts 122 m, from 79 m before to 43 m after the fiducial point (bar at upper left). The two images show the mapping catheter tip in two different locations acquiring mapping data—high lateral RA on the left and low septal RA just behind the tricuspid valve on the right. **A:** Tricuspid valve is now seen *en face*. Activation now proceeds from high anterior (red) down the septum, under the tricuspid valve and up the lateral RA wall. Activation now lasts 286 m from 149 m before to 137 milliseconds after the fiducial point (bar at left), encompassing the entire cardiac cycle. This could be considered “typical” atrial flutter circling the tricuspid valve, but in a clockwise direction. **B:** Atrial reentry/flutter—LAO caudal image (see face) of the RA. **C:** Atypical intra-atrial reentry tachycardia (IART). Straight left lateral view of the septal surface of the RA (see edge of face with eyes forward). This 27-year-old patient with tricuspid atresia began to have IART soon after an atrioventricular Fontan. After failing multiple medications and catheter ablation procedures, he underwent a right atriotomy and conversion to a lateral tunnel, but continued to have IART. After many subsequent years of failed medical therapy, he underwent mapping with the CARTO system demonstrating extensive atrial scarring, and a single IART circuit was identified encircling a large septal scar or ASD patch. Note counterclockwise procession from red to yellow to green to blue to purple in this left septal view. Ablation was successful with an actively cooled-tip system to block conduction in the inferior segment of the circuit (around the purple color). The patient has been asymptomatic since.



of the typical Mullins-type transseptal sheath for one of a variety of specialized sheaths that are now available (see below).

Most operators today prefer the transseptal approach for left freewall pathways in both adults and children, because it generally is more consistent, cannot damage the aortic valve or the left or right coronary artery orifices, and theoretically is less likely to damage ventricular myocardium. However, the overall results and complications from the transseptal and retrograde techniques are similar.

Right Freewall Pathways

Right posterior and right posterior paraseptal pathways almost always can be approached from the right femoral vein with a deflectable-tipped catheter placed above the tricuspid valve (IVC-RA). Right lateral and right anterior pathways can be approached either from the right femoral vein and IVC or from the right internal jugular vein and superior vena cava (SVC). For right lateral pathways, most operators find the

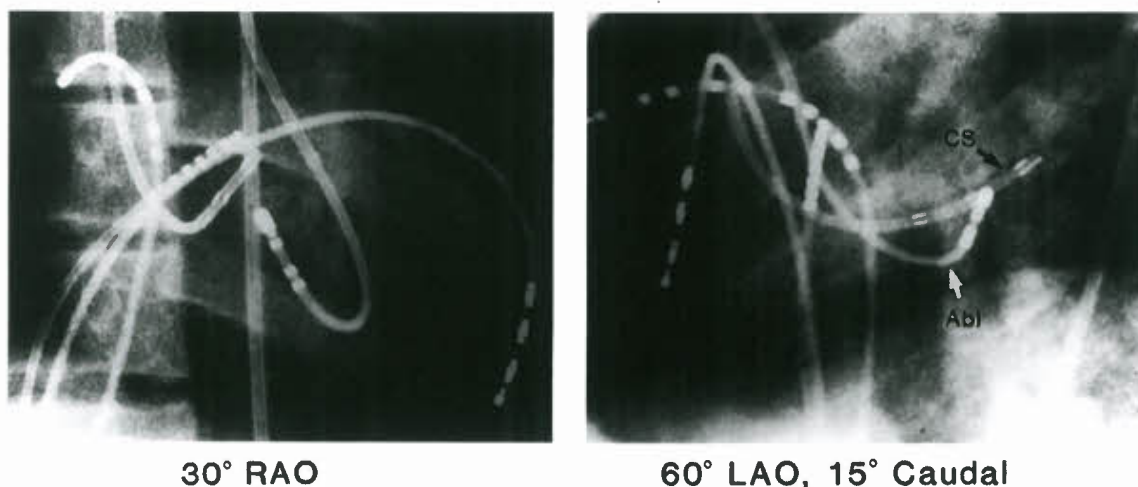


Figure 17.19. “Standard” retrograde approach from the aorta. The point of successful ablation is along the posterior AV groove at the sight of the large catheter tip. Note: overlapping of CS catheter in the LAO view, but catheter position well below the CS catheter in RAO view, indicating that the tip of the catheter is in the left ventricle.

use of a long vascular sheath (see below) very important to enhance catheter stability and improve access. Right anterior pathways also can be ablated on the ventricular side of the tricuspid leaflet (SVC-RV), using an approach from the SVC and placing the catheter tip through the tricuspid valve orifice (Fig. 17.2), as previously described (5).

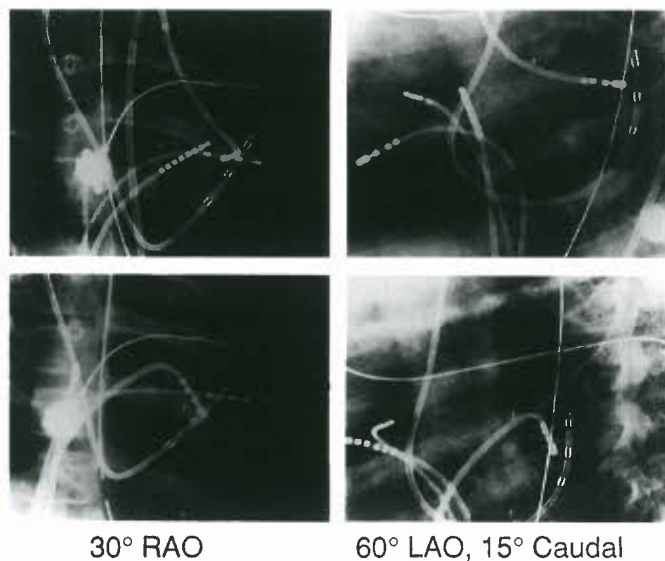


Figure 17.20. Transseptal approach. The top two cine frames show a failed attempt to place the catheter retrograde through the mitral valve on top of the mitral annulus. The transseptal approach (bottom two frames) was successful with the catheter in position very close to, but slightly different from, the retrograde mitral approach. Note the hockey-stick appearance of the catheter tip (arrow) using the transseptal approach. A “Jackman” orthogonal catheter is in the CS, an octapolar catheter is at the HIS bundle, and a quadripolar catheter is at the right ventricular apex. The deflectable ablation catheter has a large tip. (From Saul JP, Hulse JE, De W, et al. Catheter ablation of accessory atrioventricular pathways in young patients: use of long vascular sheaths, the transseptal approach and a retrograde left posterior parallel approach. *J Am Coll Cardiol* 1993;21:571–583, with permission.)

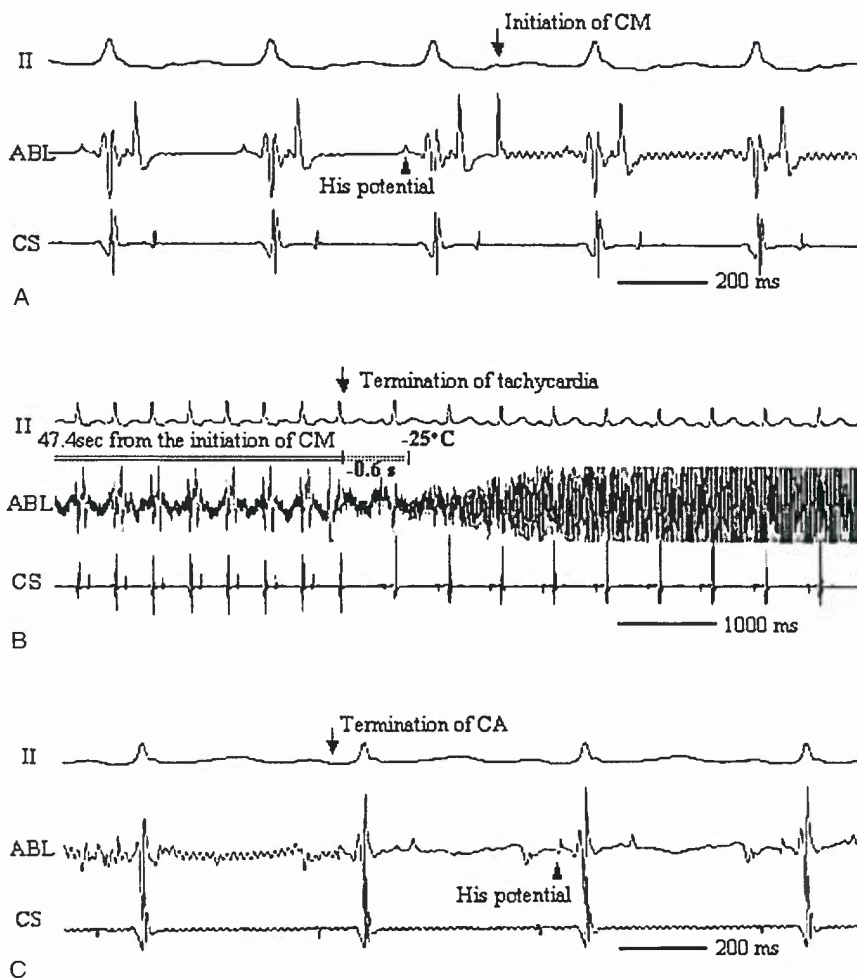
Posterior Septal Pathways

For left-sided septal pathways, the retrograde aortic technique can be used with an attempt to deflect the catheter tip under the mitral valve near the aortic annulus. Alternatively, a transseptal approach can be used by extending the catheter all the way around the mitral annulus to the area of the septum. However, many of these pathways are intimately related to the CS (128–137) and only can be ablated within or around the CS (5,5). The CS and the region around the os can be approached from the right atrium, using the right femoral vein/IVC or the subclavian vein/SVC. (IVC-CS and SVC-CS). Regardless of approach, one must be aware of the small size and close proximity of the coronary arteries in this region. In fact, over the last few years there has been a realization that the coronary arteries in the posterior septal region may be at a higher than previously realized risk for collateral damage during application of RF energy in this region (69,70,112,113,138). Consequently, many operators now perform preablation coronary angiograms for any pathway near the posterior septum to evaluate the proximity of the ablation site to a small coronary artery. Pathway locations “near” a small coronary artery are either not ablated or are ablated using cryotherapy, for the reasons stated above in the description of cryotherapy, and below in the discussion of safety. This issue is particularly important for small children and infants, who have smaller coronary arteries and shorter distances from the ablation sites to the coronary artery.

Right Anterior Septal Pathways

These pathways are perhaps the most difficult to ablate safely, because of the close proximity to the AV conduction system. As with other anterior right-sided pathways, they can be approached from below via the IVC or above via the SVC. It is not uncommon that the best location for AP ablation also has a relatively large His potential on the ablation catheter, raising concern about unintended damage to the normal AV conduction system (Fig. 17.21). In fact, permanent complete AV block has been reported during RFA in as many as 10% of patients with right anterior septal pathways (111,139,140). Although rapid junctional acceleration during application of RF energy in such locations may predict impending permanent AV conduction system damage, AV block can be quite sudden in onset and permanent. A number of techniques can be used

Figure 17.21. Successful cryoablation of a right anterior septal AP. **A:** ECG at the initiation of cryomapping during tachycardia. His potential can be seen on the ablation catheter. **B:** Termination of tachycardia during cryomapping. SVT terminates with VA block just 0.6 seconds before reaching -25°C and 47.4 seconds from the initiation of cryomapping. **C:** ECG at the termination of cryoablation shows sinus rhythm and a His potential still on the ablation catheter. CS, coronary sinus.



to help avoid AV block. We have found that approaching the AV groove from above via the SVC allows for somewhat easier separation of the ablation location from the bundle by deflecting the catheter superiorly away from the His bundle. If the ablation catheter is seen lateral to the His catheter in the LAO caudal view, theoretically the His bundle should be at least a few millimeters from the ablation location. However, the most important advance we have found for these pathways is the use of cryoablation (97,103,141–144). Cryo systems allow for (a) observation of the effects without junctional acceleration when close to the normal AV conduction system, (b) reversibility during mapping at higher temperatures around -30°C , (c) catheter adhesion, and (d) the ability to electrically test AV conduction continuously during ablation (Fig. 17.21). Furthermore, even if cryoablation is unsuccessful due to early recurrence (119), often it is possible to identify a safe location for the application of RF energy to permanently ablate the pathway. As with coronary injury for posterior septal pathways, AV conduction system damage may be an even more important issue in children than in adults because of the close proximity of all cardiac structures in the smaller heart, and the larger impact of needing permanent AV pacing in a child. Thus, despite a higher recurrence rate than with RF, cryoablation is probably the therapy of first choice for septal pathways in the pediatric patient.

Use of Long Vascular Sheaths

The approach to left and right freewall pathways in particular can often be improved by use of one of a variety of long

sheaths, including 6, 7, and 8 Fr straight and specially designed sheaths. The presence of the sheath provides catheter stability, markedly improves torque transmission from the catheter handle to the tip of the catheter, and allows for coaxial steering of the catheter tip (5). These characteristics may be critical for the atrial approach on either the right or left side, even when a patent foramen ovale is present. The set of sheaths that has gained the widest appeal is designed to facilitate an approach to the left and right AV groove in which the catheter tip ends up parallel to the plane of the groove (Swartz Left SL1–4 and Right SR0–4, St. Jude Medical, St. Paul, MN). However, any sheath that helps deliver the catheter to the correct location will facilitate stability and enhance efficacy. These sheaths seem to be most helpful for right freewall pathways, but are designed for use in every right and left-sided location.

Ablation

Ablation can be performed in either sinus rhythm or orthodromic reciprocating tachycardia. However, if performed in tachycardia, the catheter is likely to move when the AP blocks and the tachycardia terminates. Thus, catheter stability during ablation of retrograde conduction can be improved by performing the ablation during right ventricular pacing and observing for loss of retrograde VA conduction during the ablation (Fig. 17.22).

When RF energy is being used and permanent ablation is desired, the initial catheter tip set point is usually 70°C . However, as noted above, a particular site can be tested for success by setting the desired temperature to 50°C and stopping RF application

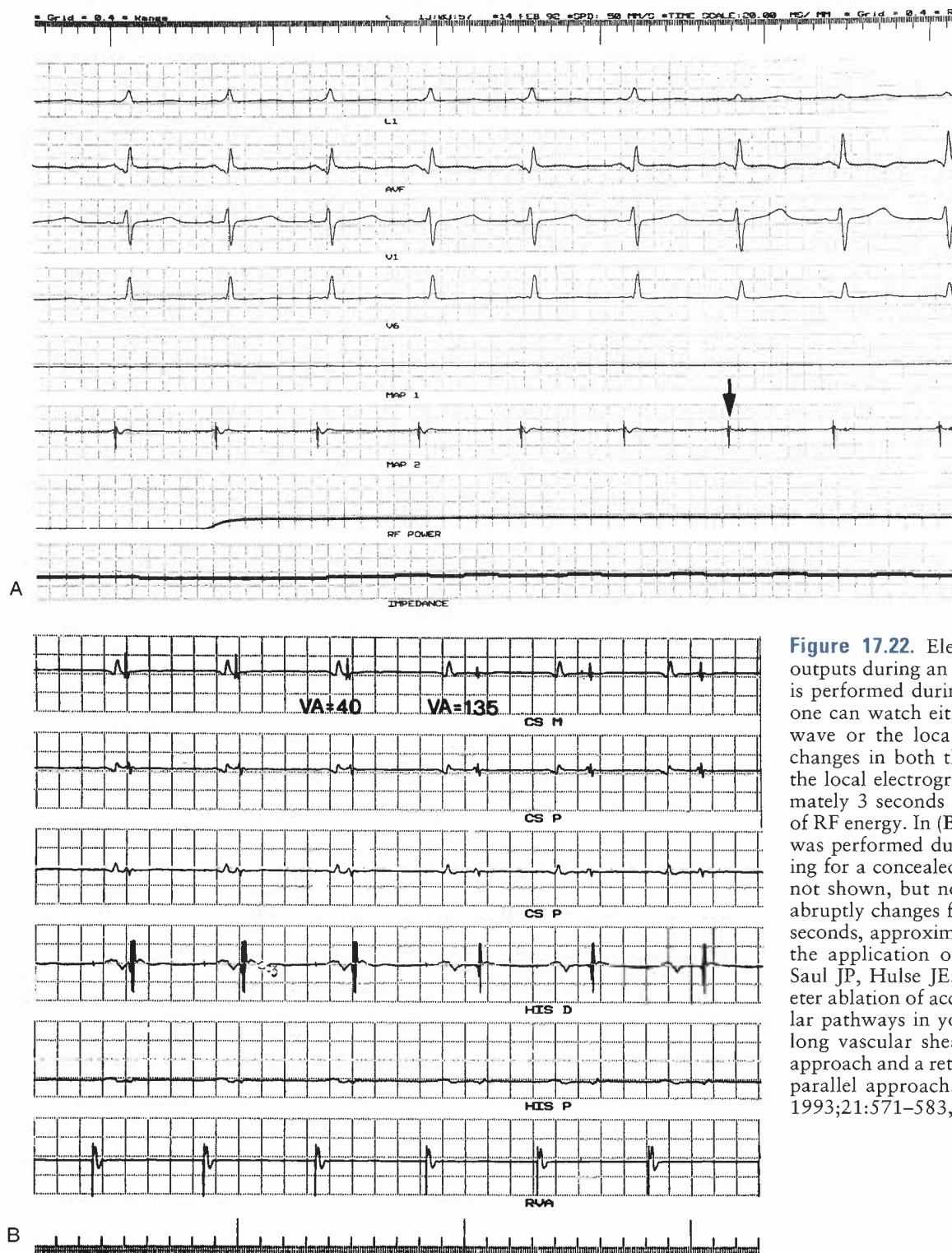


Figure 17.22. Electrograms and RF outputs during an ablation. When RFA is performed during sinus rhythm (A), one can watch either the surface delta wave or the local AV interval. Note changes in both the surface ECG and the local electrogram (arrow) approximately 3 seconds after the application of RF energy. In (B), the RF application was performed during ventricular pacing for a concealed AP. RF outputs are not shown, but note how AV interval abruptly changes from 40 to 135 milliseconds, approximately 6 seconds after the application of RF energy. (From Saul JP, Hulse JE, De W, et al. Catheter ablation of accessory atrioventricular pathways in young patients: use of long vascular sheaths, the transeptal approach and a retrograde left posterior parallel approach. *J Am Coll Cardiol* 1993;21:571–583, with permission.)

at 5 to 10 seconds if success is not achieved, reducing myocardial damage to an absolute minimum (Fig. 17.17) (91). Based on the observation that permanent success is associated with early disappearance of AP conduction (127,145), lesions should be made for only 5 to 10 seconds unless the delta wave disappears, tachycardia terminates, or there is a noted change in VA conduction. If any of these three conditions are met, the temperature should be set at 70°C and the RF application continued for 30 to 60 seconds. Without temperature monitoring, the delivered power is likely to be too high or too low. Thus, with temperature monitoring,

the delivered power varies dramatically in an individual patient between individual applications, depending on catheter tip location and stability, both of which are affected by respiratory activity. Consequently, when general anesthesia is used, asking the anesthesiologist to hold respiration in either expiration or inspiration can markedly reduce catheter movement, improving the accuracy and effectiveness of the ablation application while reducing the possibility for catheter dislodgement.

When cryoablation is used, the system may be used in either the mapping or ablation mode, as described above. In either

case, as with RF energy, the earlier the effect the more likely the conduction block will be permanent. AP block prior to 15 seconds after a tip temperature of -25°C is reached is desirable. Once AP block is observed, cryoablation is performed at the lowest possible temperature (-70°C to -80°C) for 4 minutes. There is evidence that repeating the application for 4 minutes in the same location (so-called freeze-thaw-freeze) will significantly increase the lesion size and reduce the risk of recurrence, which may be higher with cryoablation than RFA (97,103,141). However, as experience has been gained with cryotherapy, initial and long-term results have improved (97,100,114,146–148).

Following creation of a successful lesion, patients usually are observed in the electrophysiology laboratory for 30 to 60 minutes, after which repeat electrophysiologic testing is performed, sometimes with and sometimes without an infusion of isoproterenol. A bolus of adenosine also may be used to unmask residual AP function by briefly reducing or eliminating AV node function and enhancing AP conduction (149). Most patients can be discharged on the day of the procedure or the morning after.

Results

Regardless of pathway location, the presence of multiple pathways, catheter approach, or patient age, initial success rates for elimination of APs can be as high as 98% (5,62,150,151), and typically range between 85% and 95% (5,62,90,150,151,152). The most reliable outcome data in children probably come from the Prospective Assessment after Pediatric Catheter Ablation (PAPCA)(151,153,154) in which 2,761 ablation patients from a wide variety of US centers were enrolled prospectively and 481 of them followed for a period of 2 years. Overall initial success rates for AP ablation were about 94%, with results varying significantly by locations (left freewall 98%, right freewall 90%, left septal 88%, right septal 89%). Fluoroscopy times can be long compared to other pediatric catheter procedures, but have generally come down over time (155,156). High variance in the difficulty of individual procedures, combined with the variability between investigators, probably attests to a large number of poorly defined factors that affect each procedure. However, the overall high success rates, sometimes requiring a second procedure, also indicate that these factors can be overcome.

From the 481 PAPCA patients followed prospectively, 12.3% of the 361 with an AP substrate had a recurrence within 12 months of the procedure (153). As with initial success, recurrence also varied by pathway location, varying from 4.8% for left freewall pathways to 24.6% for right septal pathways. Left septal had the lowest rate at 4.8% and right freewall were intermediate at 15.8%. Although these rates may be higher than in other reports from single centers or uncontrolled registries, they are the only data from a prospectively controlled trial in children and the subjects have the broadest center representation of any prospective ablation trial. Thus, these recurrence rates may be the most accurate representation of what can be expected in the average pediatric ablation center.

Permanent Form of Junctional Reciprocating Tachycardia

The permanent form of junctional reciprocating tachycardia (PJRT) is not strictly a pediatric disease. However, it occurs primarily in young patients, causing a nearly incessant tachycardia that frequently is refractory to medical therapy, and often leads to ventricular dysfunction (157). Despite the name, PJRT is caused by a concealed (retrograde only) AP with decremental conduction properties that classically has been

described to have a posterior septal location (157). The results of RFA studies that can confirm a precise AP location have demonstrated that (a) the majority ($>95\%$) of these pathways can be ablated and (b) their location may be in almost any position around the AV groove (Fig. 17.23) (158). The high safety and efficacy of RFA for PJRT, combined with the fact that pharmacologic therapy often is ineffective, suggest that catheter ablation probably is appropriate as first-line therapy for this syndrome, particularly if ventricular dysfunction is present (159).

As with any other AP, the method of ablation of PJRT pathways is dependent on location. Because many of the pathways are posteroseptal, ablation within the mouth or veins of the CS often is necessary. For such cases, coronary angiography should be performed prior to ablation. If a small coronary artery is within 2 to 3 mm of the expected ablation site, cryoablation should be strongly considered in place of RF energy. If cryotherapy is either unavailable or ineffective, RF energy application should be minimized by reducing catheter size, temperature setpoint, and maximum power and/or duration. High-energy RF application with active or passive cooled-tip technology should be avoided if possible within the CS or used with extreme caution.

Mapping virtually always should be performed during tachycardia. The VA interval during tachycardia generally is long with a long isoelectric segment between the ventricular and atrial signals, and an AP potential may be present in as many as 75% of cases (160). Recurrence rates are higher than for typical APs, and some patients may require more than one procedure for initial success (150,153,158,160–163). Of note, despite the proximity to the AV node, AV block has not been reported in the larger series of patients with PJRT who have undergone RFA (158,160–162).

Atrioventricular Node Modification

Dual AV nodal physiology is the substrate for AV node reentry tachycardia. Regardless of whether this physiology is the result of anatomic or functional dissociation of AV nodal conduction, it now seems clear that either the fast or slow AV nodal pathways can be modified to eliminate AV node reentry. Most early reports using either DC or RF energy to modify the AV node concentrated on eliminating conduction over the fast AV nodal pathway by delivering energy to an area just proximal to the His bundle, where a relatively large atrial and relatively small or absent His potential were recorded (164,165). When successful (80% to 95% of cases), this so-called fast pathway ablation usually results in significant prolongation of the AH and PR intervals, and, unfortunately, regardless of the energy form used, most investigators have inadvertently produced complete AV block in 2% to 10% of patients (164). Although these characteristics make the technique undesirable for most children and adolescents, a small number of successful fast pathway ablations was reported in pediatric patients without significant complications (61,62). However, since around 1994, almost all AV node modifications have been directed at the “slow pathway” by positioning the catheter inferior and posterior to the AV node (166).

The advantages of the slow pathway technique are that normal AV node function can be preserved in the fast pathway and the risk of complete AV block is lower than with a fast pathway ablation (62,150,166). Importantly, even this small risk of AV block virtually has been eliminated by the use of cryoenergy in place of RF energy for slow pathway ablation. In fact, no cases of unintended permanent AV block have been reported using cryoablation for the treatment of AV node reentry (97,100,102,103,141,167). It should be

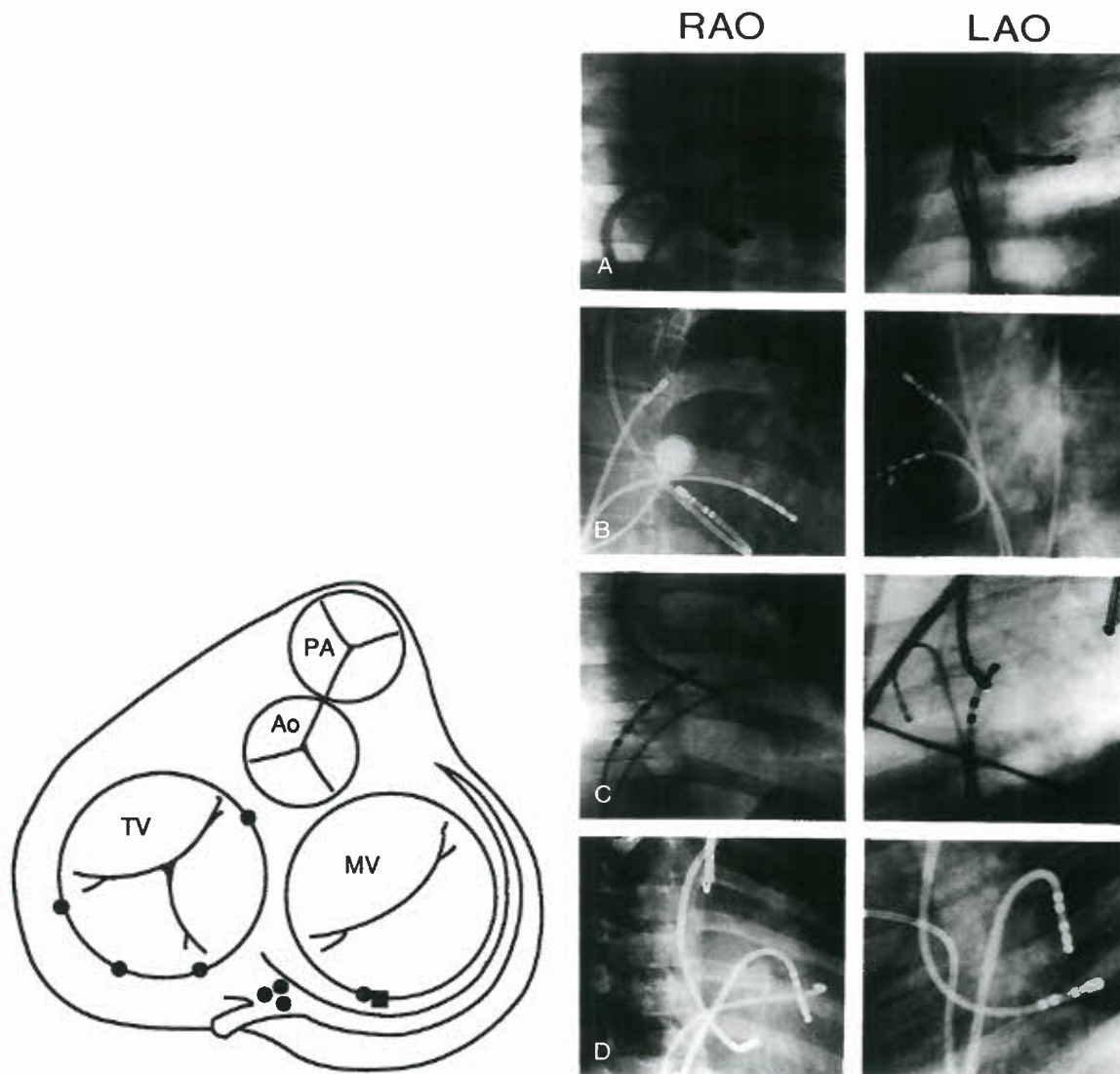


Figure 17.23. Location of APs leading to PJRT. The schematic diagram reveals pathway locations as identified by successful RFA site. Circles represent pathways causing PJRT while the square represents a typical concealed pathway found as a second pathway in one patient. Note that four pathways were located outside of the typical posteroseptal location. (A–D) show representative angiograms of catheter-electrode positions in four locations. In **panel A**, the large tipped ablation catheter approaches from the IVC. Its final position is in the mouth of the CS, near the ostium of the middle coronary vein (posteroseptal pathway). In **panel B**, the ablation catheter approaches from the SVC and loops upon itself in the RAO view; together with the LAO view, the findings demonstrate a right lateral position. In **panel C**, the ablation tip is positioned via the SVC and overlies the distal HIS electrode, indicating a right anterior pathway. In **panel D**, the large tip catheter positioned in the CS was used for mapping only. A deflectable tipped catheter with a “dumb-bell” shaped electrode was used for ablation, and was positioned using a transseptal approach from the IVC to the posterior mitral annulus (left posterior pathway). (From Ticho BS, Saul JP, Hulse JE, et al. Variable location of accessory pathways associated with the permanent form of junctional reciprocating tachycardia and confirmation with radiofrequency ablation. *Am J Cardiol* 1992;70:1559–1564, with permission.)

noted that AV block is possible with cryoablation and there is at least one anecdotal case the author JPS has been told about, but none has been demonstrated in a publication. Initial recurrence rates in the early reports were somewhat higher with cryoablation than RFA of the slow pathway (97,100,102,103,141,167). However, more recent reports have found recurrence rates under 5%, similar to those with RF Energy (148,147,168).

When mapping the slow pathway, some investigators have found that the presence of a small electrical potential

from a presumably discrete slow pathway potential is a highly sensitive indicator of an appropriate catheter position (166), while others have found this slow pathway potential to have very poor specificity (169). Thus, many ablation techniques have been developed, including a purely anatomic approach to the inferior aspects of the AV node (169) and the use of slow junctional acceleration as an indicator of slow pathway node proximity. This latter observation is not useful for cryoablation because cooling of the slow pathway does not lead to junctional acceleration as

does heating. Consequently, the technique with cryoablation focuses more on elimination of slow pathway conduction with only transient changes to fast pathway conduction as procedural endpoints (102,103).

Using RF energy to modify the slow AV nodal pathway, the PAPCA study investigators reported that between 97% and 99% of AV node reentry tachycardia can be eliminated in children <17 years of age, but with a 2.1% incidence of AV block (151). Similar success rates can be obtained with cryoablation, but as noted above, most if not all of the AV block can be avoided (97,100,102,141). Cryoablation may be particularly important in smaller children, in whom the close proximity of both the fast and slow pathways to each other and the bundle of His provides a much higher theoretical risk of inadvertent AV conduction system damage. This potential for AV block with the subsequent need for long-term electronic pacing has led to a formal guideline recommendation that RFA for well-controlled SVT be delayed until age 5 years (63). However, this recommendation occurred before the availability of cryotherapy, a likely modifying factor when the guidelines are updated.

In addition to the risk of AV block, we reported coronary damage in a child undergoing slow pathway modification with RF energy for AV node reentry resistant to drug therapy (70). After transient ST changes were observed, selective coronary angiography showed a dominant right coronary artery giving off a posterior left ventricular branch artery that had an 80% stenosis (Fig. 17.24). The vessel course was within 2 to 3 mm of where the catheter tip was placed during the last RF application. Acute management was conservative, and after 2 days, repeat angiography demonstrated some improvement with an approximately 50% stenosis. Repeat selective right coronary angiography 2 months later revealed complete resolution of the narrowing (Fig. 17.24). Although this is the first case of coronary injury reported for AV node modification, coronary damage has been reported in many other posterior locations during AP ablation in humans and experiments in animals (67–69,139,170–172). Furthermore, this case highlights several important issues regarding the potential for coronary artery injury during RFA in children.

First, coronary artery injury may occur with slow pathway ablation for atrioventricular nodal reentry tachycardia (AVNRT). Second, acute coronary artery injury has the potential to be missed and is likely an underreported phenomenon. Third, infants and young children may be at particular risk. The inflammatory component of tissue injury caused

by RF energy has been shown to invade layers of the right coronary artery, leading to acute narrowing when RF energy is applied to the atrial side of the lateral tricuspid annulus in pigs (67). Furthermore, maturation of this injury can result in significant late coronary stenosis (112). Thus, with RF energy application, coronary stenosis may occur acutely or be delayed. Our patient's injury was nearly missed because ST segment changes did not occur until 100 seconds after the last RF application and resolved spontaneously within minutes despite a significant persistent stenosis of the involved artery. Other instances of coronary artery injury following RFA also have been nearly missed because of this delay (69,172,173). Alternatively, cryoenergy has been shown to have minimal to no effects on coronary arteries in animals (114,174).

To absolutely minimize the chance of coronary injury in children, the following should be considered for patients under 20 kg undergoing slow pathway modification for AVNRT: (a) cryotherapy is the preferred ablation methodology, (b) in all patients where RF energy is used, selective coronary angiography of the artery supplying the posterior septum should be performed prior to ablation, (c) if a small coronary artery is within 2 to 3 mm of the expected ablation location, RF energy should not be delivered, and (d) if any RF energy is delivered, acute follow-up angiography should be performed post ablation (173).

Ectopic Atrial Tachycardia

EAT is an uncommon form of chronic SVT primarily occurring in pediatric patients that often leads to cardiomyopathy and can be difficult to control medically (175). EAT in children typically is due to automaticity in a single non-sinus focus, which may occur almost anywhere in the left or right atria but tends to occur more frequently in the locations shown in Fig. 17.25. Left-sided foci near the pulmonary veins are more common in children (176–178), as opposed to right atrial foci in adults (179). Although EAT has been reported to resolve spontaneously in a few cases, the sometimes devastating effects of the arrhythmia on cardiac function, combined with the hypothesis that the arrhythmia arises from a single non-sinus atrial focus, and some reports of successful surgical excision of the focus (175) led to relatively early attempts at eliminating EAT with DC catheter ablation techniques (180). These attempts were promising, but the technique never gained wide acceptance because of

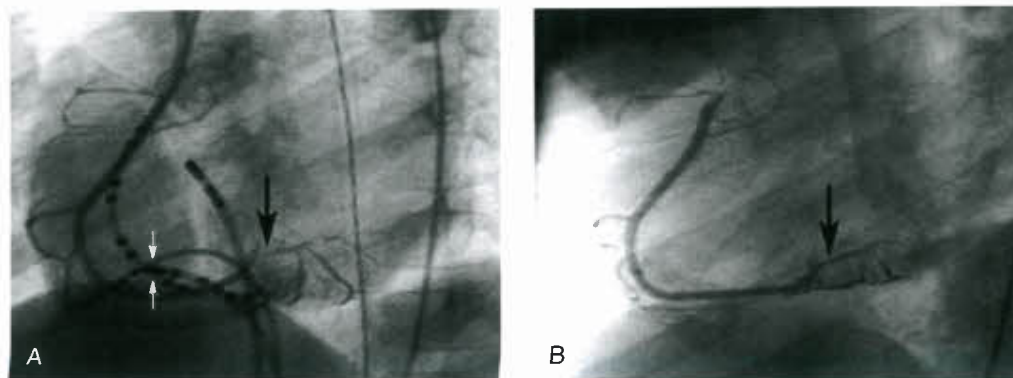


Figure 17.24. A: LAO projection of right coronary angiogram a few minutes after the ST segment changes in Figure 17.2 had spontaneously normalized. An approximately 80% stenosis (arrow) is seen in a posterior left ventricular branch off a dominant right coronary. The ablation catheter was moved away from the septum at the time of angiogram, but had been immediately adjacent to the stenosis during the RF application. B: Similar LAO projection of right coronary angiogram 2 months following ablation. Arrow marks area of prior stenosis, which is now resolved.

EAT Focus Location

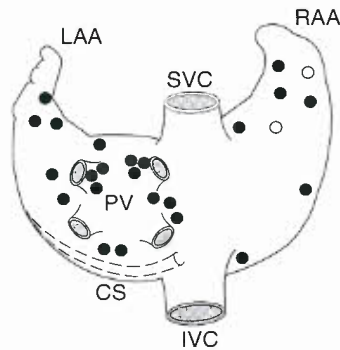


Figure 17.25. Location of EAT foci in the first 25 patients ablated at Children's Hospital in whom detailed mapping was possible. Closed circles ($n = 23$) indicate sites of successful ablation, and open circles ($n = 2$) indicate foci that could not be eliminated, in one case because of a broad area of fibrous dysplasia that was resected at surgery, and another patient because of multiple atrial foci of which this was only one. LAA, left atrial appendage; RAA, right atrial appendage; PV, pulmonary vein; SVC, superior vena cava; IVC, inferior vena cava.

the risks of acute damage and the fears of chronic myocardial damage associated with the DC technique. In addition, there was considerable speculation that elimination of one EAT focus was inadequate due to the later appearance of others, particularly for right-sided foci (175).

Impressively, the use of RF catheter ablation for EAT has revolutionized its treatment. The first reported experience in a group of 12 patients who all presented with cardiomyopathy and drug-resistant EAT demonstrated that in all but one patient with diffuse atrial dysplasia, RF catheter ablation could successfully and safely eliminate the arrhythmia without long-term recurrence up to a median of approximately 2 years (176,178). Furthermore, the data demonstrated that the arrhythmia focus is anatomically very small, because tachycardia termination took place in a median of 2.0 seconds after application of RF energy (Fig. 17.26). These results now have been confirmed in larger series in which up to 96% of EAT foci in children have been successfully eliminated with RFA (62,146,151). Because of these high success rates using ablation and the morbidity of drug therapy, the question of drug therapy generally has been reduced to one of whether it should be attempted at all in patients with ventricular dysfunction, and if so, how long should one wait for reversion to sinus rhythm before proceeding to ablation.

Initial procedure failure and late recurrence tend to be associated with the presence of multiple foci or intermittent EAT during the procedure. Multiple foci portend poorly for long-term success (175), both because there is increased difficulty in differentiating the foci during mapping and more than one focus seems to be indicative of other foci emerging after the ablation procedure. Fortunately, in the pediatric population, most EAT is due to a single non-sinus focus.

Overall, EAT ablation seems to be extremely low risk. Pulmonary vein stenosis is the only unique complication and can occur when the EAT focus is near or within a pulmonary vein (Fig. 17.25). Clinically significant stenosis has not been reported for a pediatric case, but it was previously quite common in adults undergoing focal or narrow circumferential atrial fibrillation ablation procedures in similar locations (181–183). There is also a potential for damage to the sinus node or the right phrenic nerve for foci that occurs along the crista terminalis, but injury is less likely in a patient who has

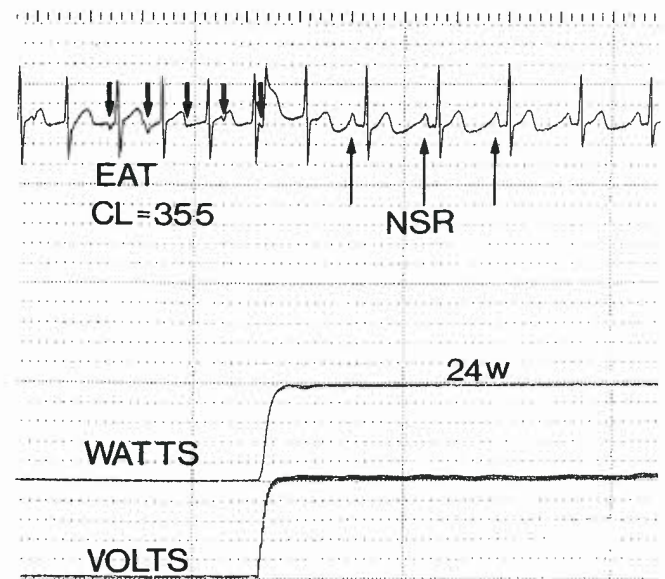


Figure 17.26. Ectopic atrial tachycardia ablation. Note how ectopic P waves terminate immediately at the onset of application of RF energy. (From Walsh EP, Saul JP, Hulse JE, et al. Transcatheter ablation of ectopic atrial tachycardia in young patients using radiofrequency current. *Circulation* 1992;86:1138–3346, with permission.)

never had heart surgery because the phrenic nerve continuously slides over the epicardial surface of the heart. Most other EAT foci are not near vital structures, such as the AV node or a coronary artery (Fig. 17.25).

Atrial Flutter or Fibrillation in the Absence of Other Heart Disease

In the pediatric patient, atrial reentry tachycardias are relatively rare in the absence of either structural or functional heart disease. The term *lone atrial flutter* or *fibrillation* has been applied here, referring to the isolated nature of the arrhythmia findings. However, both of these tachyarrhythmias occasionally are observed in pediatric patients. There are two age ranges for presentation. Perhaps the most common is during third trimester fetal life when atrial flutter accounts for up to a third of fetal tachycardias (184), often lasting through delivery and leading to ventricular dysfunction. Neonatal atrial flutter almost universally resolves without recurrence if the baby can be managed successfully during fetal and early neonatal life (185). Consequently, ablation therapy for such infants should not be necessary and has never been reported.

A second presentation peak occurs during adolescence when both atrial flutter and fibrillation may present in the absence of any identifiable structural, hormonal, or chemical cause. Although initial management should be conservative, in contrast to the infants, the arrhythmia typically recurs multiple times in this age group despite medical therapy, creating a need for ablation therapy similar to the scenario in adults. The use of catheter ablation has been reported for both flutter and fibrillation in young patients. Success rates have been over 90% for the flutter subgroup in a relatively large series of patients in the Pediatric Ablation Registry (110). Interestingly, acute success has also been reported in seven of eight pediatric patients with paroxysmal atrial fibrillation who underwent ablation of either a single ectopic atrial focus or pulmonary vein electrical isolation (186). Furthermore, one of the cases

we included in a series of EAT ablations in 1992 (176) was a 12-year-old boy who presented with recurrent atrial fibrillation that was eliminated permanently after ablation of a single left pulmonary vein ectopic focus.

Specific technical details for ablation of either atrial flutter or fibrillation in the larger child are not particularly different from those in adults (187–189), so they are not reviewed here. However, the decision of when to ablate can be quite different, particularly for fibrillation. After conversion from a first episode of one of these arrhythmias, either no therapy or a drug to block the AV node response is adequate. After recurrences, the threshold for ablation of atrial flutter can be similar to that in adults. The use of ablation therapy for the rare cases of atrial fibrillation in pediatric patients also is appealing, but the high emphasis on safety over efficacy noted above for all children necessitates that a decision to use RFA in this age group be considered only after failure of multiple antiarrhythmic agents. Furthermore, the technique chosen should be the most conservative in terms of safety, since complications such as pulmonary vein stenosis and stroke may be devastating to a child.

Intraatrial Reentry Tachycardia in the Presence of Congenital Heart Disease

Commonly known as atrial flutter, intraatrial reentry tachycardia (IART) is uncommon in children with structurally and functionally normal hearts, but quite common after surgery for congenital heart disease. Although the prevalence is highest after either an atrial repair of transposition of the great arteries (Mustard or Senning technique) (190) or after the Fontan repair (191), IART may occur after any repair that includes an atrial scar (atrial septal defect, tetralogy of Fallot, etc.) (192). IART generally is easy to convert to sinus rhythm with DC cardioversion or atrial pacing via an esophageal lead, an intracardiac lead, or an implantable antitachycardia device (193). However, prevention is critically important in some patients because IART can be life-threatening (190,193) and increases the likelihood of atrial thrombus formation. Unfortunately, prevention of IART is much more difficult than cardioversion, with drugs of all classes being generally ineffective and, even worse, often unsafe (194). Consequently, RF catheter ablation to either prevent IART (195,196) or to eliminate AV conduction and institute ventricular rate-responsive pacing recently has gained prominence as a therapeutic option. IART in postoperative congenital heart patients may have multiple circuits in the same patient and be much more complex to ablate than “typical” atrial flutter, which generally is treated easily by electrically dividing the tricuspid annulus–IVC isthmus (195) (Fig. 17.27). Despite these complexities and a relatively high recurrence rate (125,197), acute success rates were initially reported at about 75%. However, since 2002, we and others have approached a rate of 95% (121,125,195,197,198). The use of 3-D mapping techniques probably is most important in this patient group (Figs. 17.5, 17.6, 17.18). Recurrence remains a problem, probably secondary to inadequate lesion formation, but technologies that produce larger lesions, such as the tip cooling techniques described above, will appear to improve even late outcome (121,125,126).

Junctional Ectopic Tachycardia

In the pediatric population, unlike in adults, JET occurs in two relatively distinct settings: postoperative and congenital (199,200). The electrophysiologic characteristics of both varieties are similar to those of EAT (200), suggesting they also are due to abnormal automaticity, in this case arising from either low in the AV node or high in the His-Purkinje system. However, direct intracellular recordings have not been obtained.

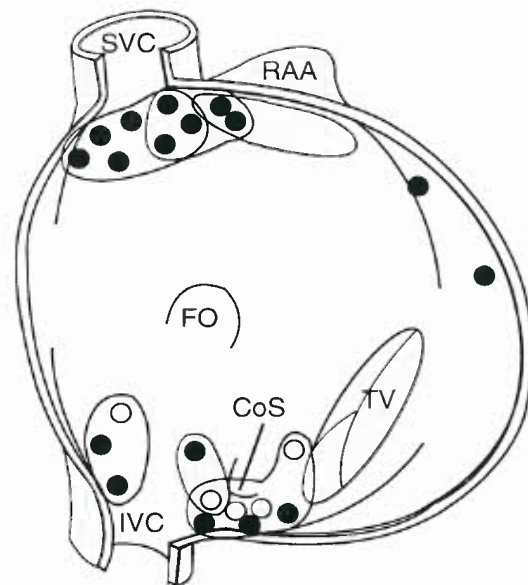


Figure 17.27. Sites of mapped exit points from zones of slow conduction at which ablation was attempted. In this schematic cartoon of the right atrium, *filled circles* represent 17 sites of successful termination of atrial reentry and *open circles* represent the presumed exit point of the circuit from the zone of slow conduction for five circuits not successfully ablated. A right atriotomy would normally be performed along the lateral reflected wall of the atrium in this view and may extend across the reflected opening to the base of the right atrial appendage; it is not possible to define with precision the sites of right atriotomy in individual cases. The crista terminalis would be expected to run along the line in which the right atrium has been opened in this view. SVC, superior vena cava; RAA, right atrial appendage; FO, fossa ovalis; CS, coronary sinus; TV, tricuspid valve; IVC, inferior vena cava. (Reprinted from Triedman JK, Saul JP, Weindling SN, et al. Radiofrequency ablation of intra-atrial reentrant tachycardia after surgical palliation of congenital heart disease American heart association. *Circulation* 1995;91:707–714, with permission.)

The postoperative and congenital forms of JET differ primarily in their duration and response to therapy (201–204). Postoperative JET typically is transient after ventricular septal defect repair, either alone or at the time of repair of more complex anomalies (205). It responds to cooling and a variety of antiarrhythmic agents (202–204). In contrast, congenital JET typically is chronic and incessant, but may resolve spontaneously over a period of years (200). Both JET types may result in severe hemodynamic compromise and appear to be exacerbated by both endogenous and exogenous adrenergic stimulation (200,204), and both arrhythmias seem to respond well to amiodarone (206).

The propensity for JET eventually to resolve spontaneously and the high theoretical risk of AV block from either catheter (83) or surgical (200) ablation of the JET focus in the AV junction suggest that JET initially may be best treated medically by minimizing adrenergic stimulation and beginning either intravenous or oral amiodarone (200,206,207), particularly in infants. However, anecdotal data from a few reports (207–213) and more recently a large series from a multicenter study (214) have demonstrated that with ablation, it is possible to eliminate JET while preserving AV conduction. The multicenter study from Collins et al. (214) reported ablation success in 83% of 17 patients undergoing RFA and 85% of

27 patients undergoing cryoablation, but few technical details were available in that report. Cryoablation was the preferred technology in recent years. Thus, when JET is resistant to medical therapy, persistent after a prolonged period of control, or producing intractable hemodynamic compromise, cryoablation probably should be attempted.

The specific details from the small number of reported cases of successful JET ablation provide few overarching recommendations to use when approaching these patients. Although in most cases, the region of interest has ended up in the anterior septum near the bundle of His, successful ablation in at least one case was reported in the posteroseptal region below the CS os, with the site identified using retrograde atrial activation as a guide (209). This region corresponds to the site used for slow pathway modification, and should be associated with a low incidence of permanent AV block. However, the data presented may be most consistent with frequent paroxysms of AV node reentry tachycardia triggered by junctional escape beats, and other investigators have not found mapping of earliest retrograde activation to be useful (211–213,215). Nonetheless, because this area generally is “safe,” initial attempts at ablation may be applied in the posterior septal region. If unsuccessful, mapping should focus on identifying the site of the earliest His potential during JET. Prior to ablation, the catheter should be moved very slightly posterior to that site, attempting to increase the atrial electrogram size and minimize the His activation from the distal ablation tip, similar to the methodology used in the past for fast pathway ablation. Most early reports of successful elimination of JET without causing AV block used this technique with brief, lower power applications of RF energy. However, there is probably a high risk of AV block in children using RF techniques, leading to the non-evidenced-based but probably appropriate switch to cryoenergy for ablation of JET. Figure 17.28 demonstrates the use of cryotherapy for ablation of JET in a 10-year-old with intermittently incessant tachycardia. Earliest His activation during tachycardia actually was found with retrograde mapping just under the aortic valve (Fig. 17.28). The intermittent nature of the JET in this case allowed for ablation during sinus rhythm. The high degree of safety of this methodology around the AV conduction system makes it ideal for both cryomapping and cryoablation, with successful elimination of the JET and preservation of the AV node, despite a catheter signal and location suggesting very close proximity to the His bundle. The outcome of cases like this (214) combined with the demonstrated reversibility of cryomapping applications suggests that cryotherapy should be the treatment of first choice for ablation of JET.

Ventricular Tachycardia

High success rates for both DC and RFA have been reported for two forms of VT in pediatric patients. In 1990, Morady et al. (215) first reported successful elimination of idiopathic

right-sided VT in 10 relatively young patients without structural heart disease using catheter-delivered DC energy. Other reports soon followed. In all of these series, pace mapping, as well as the site of earliest endocardial activation, were used as guides to the appropriate ablation site, but neither method was clearly superior. The youngest patient in any of these series was 18 years old, but a number of younger patients have since been reported (62,150,151,216–218). Both DC and RF energy also have been used to eliminate bundle branch reentry VT and idiopathic left VT by ablation of the right bundle branch or a left posterior Purkinje fiber (218,219). An entrainment technique that can identify sites most likely to ablate reentrant VT after myocardial infarction (220) has been used to successfully ablate reentrant VT in patients with tetralogy of Fallot and its variants (218,221–225).

COMPLICATIONS AND FOLLOW-UP

In children, acute major complications appear to occur in 1% to 2% of cases, and include complete AV block when ablating septal pathways (62,111,127,150,151), inadvertent coronary damage or coronary vein perforation (68–70,127,138), and vascular and embolic injury (61). Other minor complications have included Doppler-detectable increases in valvular regurgitation, minor vascular injury, and minor skin burns at the reference electrode skin site (5,62).

Follow-up studies have shown no evidence of new coronary abnormalities by traditional angiography at 1 to 6 months post ablation (5,127), and no significant increase in ventricular arrhythmias as late as 2 to 3 years. Importantly, however, acute coronary injury may not resolve (173), and animal studies have revealed coronary intimal thickening in arteries near the ablation site (69,112). Currently no data exist to assess the long-term effects of RF lesions on coronary function or arrhythmogenicity in developing infants and children.

The PAPCA study did not report any deaths in its 2,761 patients; however, in prior reports, death has been a rare complication of RFA procedures in children. Kugler et al. (62) reported a total of four procedure-related deaths in 4,135 children (0.097%) from 1991 to 1996, and Schaffer et al. (39) reported an incidence of 0.12% for patients with structurally normal hearts. The incidence was higher (0.89%) for patients with structural heart disease undergoing ablation.

SPECIAL CONSIDERATIONS FOR PEDIATRICS

Age (Infants)

There are three special considerations in infants that make their management different from the older patient when considering

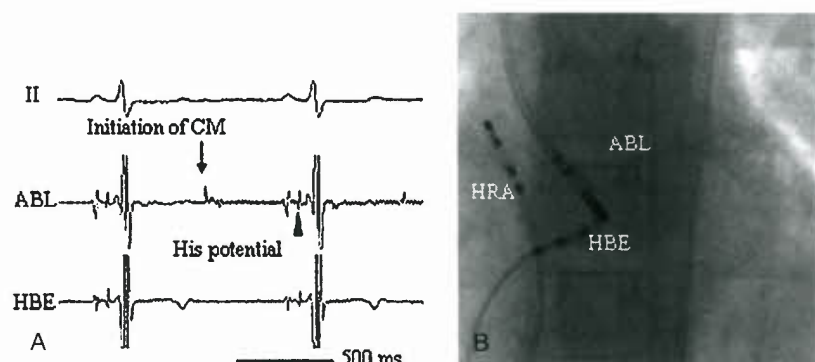


Figure 17.28. Successful cryoablation at location with His potential in a patient with JET. (A) Identical His potentials are clearly seen from the ablation catheter (retrograde approach through the aortic valve) and from the His catheter (in a usual position) just prior to initiation of cryomapping. (B) Fluoroscopic images in the anteroposterior (AP) view shows the cryoablation catheter overlapping the image of the His position catheter. ABL, ablation; HBE, His bundle electrogram.

catheter ablation. First, the risk of a sustained reentrant primary atrial tachycardia, such as atrial fibrillation, is very close to zero in the small structurally normal heart, making the risk of sudden death in infants with WPW very low (71,226). Second, in approximately 40% of infants, AP function will spontaneously disappear by 1 year of age (71,72). Finally, the known risks of any catheterization, combined with the specific risks of catheter ablation in this age group (59,66,227–229), suggest that pharmacologic control should be aggressively pursued prior to ablation. This last issue deserves further discussion.

In humans, myocardial cell division probably occurs through approximately 6 months of age (230). Although this finding could potentially protect the myocardium from long-term complications secondary to early injury, the observation has been made that ventriculotomy scars produced in newborn puppies (231) and RFA lesions in immature lambs (60) appear to increase in size during subsequent development. Furthermore, as noted above, in neonatal swine, both RF and cryo lesions have been noted to increase in size with age (109). In addition, in contrast to mature ablation scars from adult animals, late lesions from the neonatal lambs and swine often were invasive and poorly demarcated histologically from the surrounding tissue (60,109). The potential clinical importance of these results is underscored by a reported sudden death 2 weeks after an AP ablation in a 5-week-old, 3.2 kg infant (5,59). An echocardiogram from the infant at the time of a brief resuscitation, and autopsy findings, revealed relatively large lesions extending into the left ventricle from the intended mitral groove ablation site. Another heightened risk in infants is coronary artery damage due to the potentially close proximity of the coronaries to the ablation catheter and the reduced capacity for protective cooling during RF application in any small coronary artery. Although most reports of coronary damage have been limited to the posterior septum or a non-dominant right coronary (67,69,70), complete occlusion of the left circumflex artery has been reported in a 5-week-old, 5.0 kg infant undergoing RFA of a left lateral AP (68), as well as in older patients (172,232).

Despite these disturbing cases, nonpharmacologic therapy will be necessary in a small subset of the infants with AP-mediated tachycardia (228,233). Until accurate methods are available to assess lesion size in real time, alternative methodologies should be used in all infants. Data on the effects of cryotherapy suggest that this form of energy may be much less harmful to coronary arteries, even when in very close contact (114,174,234), due to the differing effects of cold and heat on connective tissue and the vascular inflammatory response. Coronary artery flow also protects the vessel through local warming during cryotherapy, similar to how flow protects through local cooling during RF energy application. If technical or other considerations require the use of RF energy, considerable caution should be used. RF lesion size is related to catheter tip size, RF power, tip temperature, and lesion duration (235,236). Thus, the following technical modifications should be adopted: (a) deliver energy in as atrial a location as possible, (b) use a 5 Fr catheter tip, (d) use *low temperature mapping* (50°C to 55°C) to identify the correct location prior to higher-temperature RF application (91), (d) use a lower-temperature set point of 60°C for the ablation lesion, and (e) use shorter duration lesions (7 to 10 times the time to effect, with a maximum of 30 to 40 seconds). The future development of real-time ultrasonographic or other modality monitoring of lesion size may also help reduce the procedural risks (237).

Size

Patient size by itself does not appear to affect the success rate of catheter ablation, but has distinctly influenced the catheter

approach. Some have advocated using the standard retrograde approach to left-sided APs, but with two modifications: (a) a smaller catheter (5 or 6 Fr), and (b) fewer catheters, one for the ablation and one additional diagnostic catheter, both modifications designed to avoid vascular complications. Other researchers, including our own group (5), have worried about producing inadvertent ventricular lesions and have found that manipulation of the ablation catheter inside small ventricles is more difficult, leading to the use of the transeptal approach to all left-sided pathways, as described above. In fact, using the atrial approach, smaller patient size may actually make catheter manipulation easier, as discussed below.

Preexcitation Syndromes in Patients with Structural Congenital Heart Disease

Though not only a pediatric issue, the combination of structural heart disease and arrhythmias will clearly be encountered often by the pediatric electrophysiologist. In agreement with previous studies (238,239), a review of this issue in all database patients with congenital heart disease at the Children's Hospital in Boston found that preexcitation syndromes are statistically increased in patients with Ebstein malformation, congenitally corrected transposition of the great arteries (ccTGV), and hypertrophic myopathy (196). Of course, pre-excitation also occurs in other patients with congenital heart disease, but with an incidence not statistically higher than the general population.

Ebstein Malformation

The association of WPW with Ebstein disease and with the left-sided tricuspid valve in ccTGV probably has its basis in the embryology of tricuspid valve formation (240–242). The leaflets of the AV valves normally develop through a process of undermining, or delamination of the interior surface of the embryonic ventricular myocardium. Separation of the atrium from the ventricle occurs through completion of this process and encroachment of fibrous tissue from the AV sulcus. The mitral valve and the anterior leaflet of the tricuspid valve are fully delaminated early in development; however, the posterior and septal leaflets of the tricuspid valve are not even fully formed by 3 months gestation (242). Ebstein disease appears to occur when there is arrested development of tricuspid valve formation sometime between delamination of the anterior and the posterior leaflets. The high prevalence of preexcitation combined with anatomic findings of accessory connections in a number of selected cases of Ebstein malformation (241,243) suggests that the arrested valve development results in remnants of muscular or specialized tissue connections that cross the AV groove. In fact, multiple pathways are common in these patients, often with a combination of a posteroseptal pathway and one or more additional freewall pathways.

The electrophysiology of the APs in patients with congenital heart disease is not particularly unique. Bidirectional, antegrade only and retrograde only pathways have been reported. Furthermore, these patients have the same range of tachyarrhythmias found in patients with structurally normal hearts: orthodromic and antidromic AV reciprocating tachycardia and other SVTs (AVNRT, atrial flutter/fib, and so on) with bystander participation of an antegradely conducting AP. However, the physiologic and clinical implications of the tachycardia may be markedly different in patients with congenital heart disease.

Abnormal hemodynamics, increased incidence of isolated atrial and ventricular ectopy, sometimes poor tolerance of antiarrhythmic therapy, and the need for surgical repair that

accompanies congenital heart disease all contribute to an increased need for aggressive arrhythmia management in this patient population. However, abnormal anatomy and atypical conduction systems may also enhance the difficulty and risks of either surgical or catheter ablation. Though difficult, RF catheter ablation results have been good enough to recommend the procedure in: (a) all patients requiring subsequent surgical repair to avoid postoperative arrhythmias as a complication and (b) most symptomatic patients over 1 year of age with significant structural lesions. A review of the reported cases of RFA in patients with congenital heart disease shows that most of the patients have Ebstein malformation (127,152,244–246). However, a significant portion has more complex anatomy with AV valve discordance and, often, heterotaxy. Multiple pathways are extremely common in this group, occurring between 30% and 80% of patients (127,243–245,247), compared to 5% to 10% in patients without congenital heart disease (127,152,248–250). It is interesting to note that similar to the patients with Ebstein malformation, patients with AV discordance had all of their APs associated with the tricuspid valve regardless of atrial situs, AV relationship, or valve function. This finding is in contrast to the more random location of APs reported for patients without congenital heart disease (127,152,248–253). Hypertrophic cardiomyopathy is the exception where pathways are more likely to be on the normal left-sided mitral valve.

Some aspects of the procedure in patients with Ebstein malformation are of special note. First, differentiation of atrial and ventricular signals and precise localization of the AV groove can be difficult, leading to a lack of specificity for what appear to be excellent signals in predicting a successful ablation site. In fact, very early ventricular activations, which might be termed “pseudo” AP potentials can often be seen near the AV groove (Fig. 17.29). This issue is particularly important for older patients who have large hearts with poorly defined AV grooves. The true AV groove is best identified by the right coronary artery. Use of a right coronary electrode wire can be considered (248,254), but may be difficult due to a diminutive right coronary artery, and may need to be in place for long periods when multiple pathways are present. A safer recommended alternative is continual display of the relevant coronary angiogram using a real-time biplane image storage and display system. As with any AP, searching for balanced atrial and ventricular electrograms during mapping is important. Despite these maneuvers, it may still be very difficult to define the AV groove in these patients, requiring more test applications of the ablation modality to identify the correct location. Catheter stabilization for freewall pathways in the largest hearts is difficult and is not sufficiently improved through the use of a long sheath or a variety of approaches (5) (see prior section). One observation that is difficult to prove statistically is that the smaller chamber size in smaller patients with structural heart disease is a technical asset in catheter ablation. In one series (244), a total of seven procedures lasting an average of 4.1 hours were required to ablate seven of nine accessory connections in six patients under 40 kg, whereas seven procedures lasting an average of 6.5 hours were used to ablate only three of seven connections in four patients who weighed over 40 kg.

As expected, it appears to be impossible to approach the ventricular side of the tricuspid valve in patients with Ebstein malformation. No specific reports have noted the use of *nonstandard* ablation technologies for the patient with Ebstein malformation, but a few observations can be made. Coronary damage has been reported on multiple occasions in patients with Ebstein anomaly (69), probably due to the thin RV wall and often diminutive right coronary artery. Consequently, despite the tendency to use higher-power active or passive cooling ablation systems for difficult cases, such technologies

should only be employed when an adequate distance between the catheter tip and the artery has been documented. The definition of “adequate” depends on the size of the nearby coronary artery—the larger the size, the safer the ablation. Furthermore, strong consideration should be given to the use of cryotherapy, at least as a mapping tool. Safety will be enhanced and the adhesion of the catheter may be particularly useful in the larger patients.

When multiple pathways are present, persistence may be the electrophysiologist’s best weapon for successful ablation. In general, 80% to 90% of patients can be rendered arrhythmia free by the procedure, with relatively infrequent major complications, such as permanent AV block (127,150,244,245). However, recurrence rates have been reported as high as 40%, particularly when multiple pathways are present (127,150,244,245).

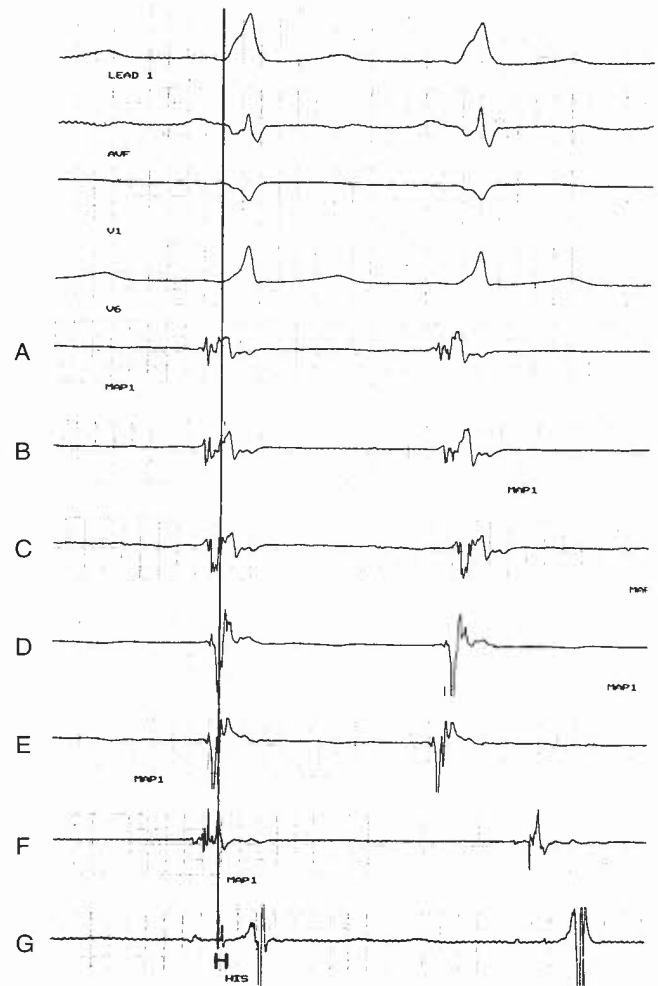


FIGURE 17.29. Electrograms near the AP with Ebstein malformation. Electrograms A through F were recorded with the distal pair of an ablating catheter very near the point of successful ablation shown in F. Note early ventricular activation in parts A through D, despite lack of success. Electrograms in parts D and E were not significantly different, but part E had transient success. F, the point of permanent success, probably has the earliest activation; however, the differences are much clearer in retrospect. The dark vertical line marks the point of earliest surface QRS activation for all electrograms. G shows the position of the atrial and HIS electrograms. Pathway location was posterior septal.

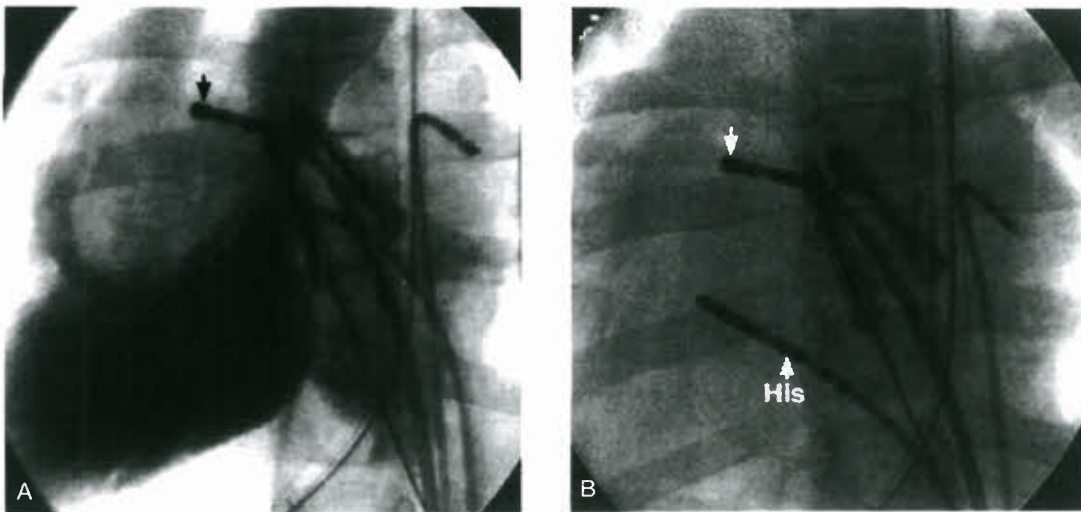
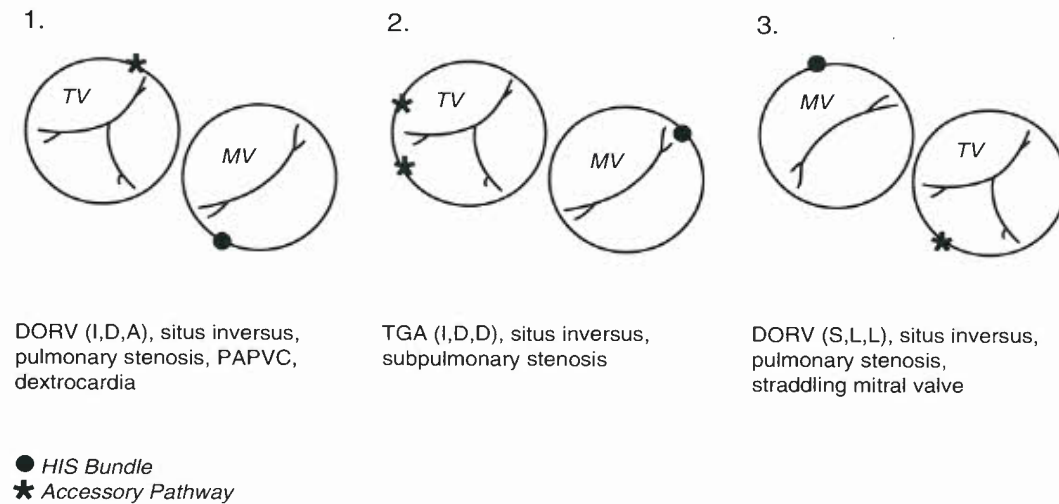


Figure 17.30. A: A cartoon demonstrating the locations of the mitral valve (MV), tricuspid valve (TV), the His bundle, and APs in three patients with preexcitation syndromes and atrioventricular discordance. Patient 1 corresponds with parts (A) and (B). The angiogram in the anteroposterior projection (B) illustrates the importance of defining the anatomy of the AV valves. The decapolar catheter (bottom white arrow in B) was advanced from the left-sided IVC across the mitral valve and positioned with the second pair of electrodes at the His bundle. The mapping catheter (black arrow in A, upper white arrow in B) was advanced from the IVC across the atrial septum to the right-sided (anatomic) left atrium and positioned at the location of the AP, which in this case was at the superior and anterior portion of the left-sided tricuspid valve. The unmarked catheter is an atrial pacing catheter in the left-sided right atrium. DORV, double outlet right ventricle; PAPVC, partial anomalous pulmonary venous connection; TGA, transposition of the great arteries.

Corrected Transposition

Ablation procedures in patients with AV discordance (S,L,L or I,D,D) require special considerations. First, detailed echocardiography and angiography are instrumental in defining the complex anatomy of the atria, the AV ring, and the CS, so that the cameras and catheters can be positioned appropriately (Fig. 17.30). Second, careful attention must be given to locating the normal conduction system. Virtually, all patients with AV discordance have had their AP associated with the tricuspid valve, while the His bundle has been associated more closely with the mitral valve. As predicted by Ho and Anderson (255), the normal conduction axis often is located at an anterior position along the AV groove. Once the “normal” and abnormal conduction fibers are located, electrophysiologic study and RFA of the APs can proceed with less risk

of damage to the normal conduction system. Mapping and ablation requires a detailed knowledge of the anatomy and often innovative approaches. For instance, for cases of atrial inversion (*right atrium* on the left, and vice versa) with AV discordance (I,D,D), an atrial approach to the right-sided tricuspid valve may require a *reverse* transeptal procedure from the left-sided IVC and right atrium to the right-sided left atrium. If present, the CS in such cases will also be reversed. AVNRT may also be present in these patients, requiring identification of the slow pathway of an AV node that is typically along the anterior mitral annulus. Clearly, the need for a detailed understanding of the anatomy in these cases cannot be overemphasized. Ablation technologies similar to those recommended above for Ebstein patients, including cryoablation as the preferred energy source, are applicable to AV discordance patients as well.

Double Atrioventricular Nodes

In hearts with discordant AV connections, the AV node typically is situated superior and anterior in the atrial wall near the antero-lateral quadrant of the mitral valve (240,255). A second AV node that often is present more inferiorly in the normal area of the triangle of Koch can also link to the ventricular conduction fibers posteriorly, usually inferior to a ventricular septal defect. If the posterior and anterior ventricular bundle branches link together, a conduction sling, sometimes referred to as a “Monckeberg sling,” is formed (Fig. 17.31) (240,256,257). These anatomic findings provide the substrate for a host of different modes of ventricular excitation or preexcitation and AV reciprocating tachycardias. However, prior to our reports, there had been no electrophysiologic documentation of this phenomenon (258,259).

In 2001, we reported seven such cases, all of whom had AV discordance (2-S,L,L and 1-I,D,D) and characteristics consistent with the diagnosis of two separate AV nodes (twin or double) (258). Five of the seven also had malaligned AV septal defects. The electrophysiologic findings included: (a) the existence of two discrete nonpreexcited QRS morphologies, each with an associated His-bundle electrogram and normal HV interval; (b) decremental as well as adenosine-sensitive anterograde and retrograde conduction; and (c) inducible AV reciprocating tachycardia with anterograde conduction over one AV node and retrograde conduction over the alternate AV node. Ventricular premature beats placed into tachycardia when the His was refractory could preexcite the atrium, indicating that the tachycardia involved two AV connections. In all cases, applications of RF energy at the site of the bidirectional pathway resulted in transient *junctional* acceleration with an identical QRS morphology to that generated by anterograde conduction over the targeted AV node and modified or eliminated antegrade and retrograde conduction at that site. Although there is a possibility that one or the other of these pathways was a *Mahaim-type* AV fiber, their locations and the presence of near-normal HV intervals, retrograde conduction, *orthodromic* tachycardia, and *junctional-type* acceleration during RFA all favor a second AV node. The precise etiology may make little difference for the management of such patients, but the phenomenon is important to be aware of to avoid damage to the more robust of the two conduction systems during ablation procedures performed prior to surgery in these patients with complex anatomy.

Clearly, an extensive understanding of the anatomy and electrophysiology should be obtained in such patients before proceeding to mapping and ablation. Furthermore, the lack of clarity in defining the anatomy of AV conduction in these patients suggests that ablation should first be undertaken using cryotherapy, proceeding to RF energy only if unsuccessful or after a recurrence. The one caveat to this recommendation is that low-power RF application may be helpful in identifying the location of the anterior and posterior AV nodes through their acceleration response when heated.

Preexcitation and Congenital Heart Disease: Summary

A few recommendations concerning catheter ablation in patients with congenital defects can be made: (a) an attempt should be made to carefully identify the location of the normal AV conducting system, particularly in patients with AV discordance, (b) the anatomic tricuspid valve is the most likely location for accessory connections, (c) smaller patient size may be an asset, (d) an atrial approach probably should be attempted first for connections around the tricuspid annulus (right or left sided), (e) the true AV groove should be well identified, using atrial and ventricular electrogram balance, a coronary angiogram, or if feasible and available, a coronary

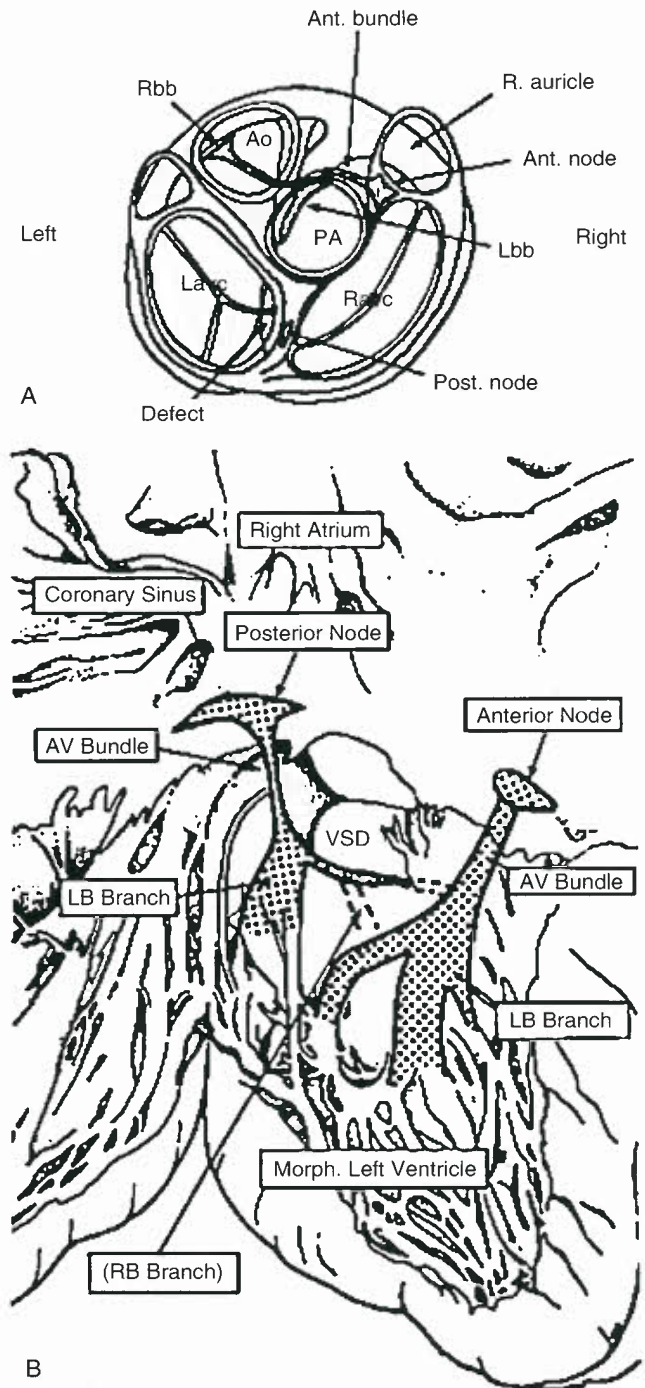


Figure 17.31. A: Diagram of the base of the heart and the AV conduction system in congenitally corrected transposition of the great arteries (corrected) as seen from above. Note the bicommissural mitral valve on the right and the tricommissural tricuspid valve on the left. The AV node may either lie posteriorly (Post. Node) in the septum in a somewhat normal location, anteriorly on the right-sided mitral valve (Ant. Bundle) or in both places (Anderson RH, Arnold R, Wilkinson JL. The conducting system in congenitally corrected transposition. *Lancet* 1973;1:1286–1288, with permission, Ref. 260). B: Diagram of the conduction system from a patient with corrected transposition in a criss-cross heart, with AV valve anatomy similar to that shown in (A). Note the dual conduction system with both the posterior and anterior AV nodes penetrating into the ventricles and near connection of the conduction systems within the ventricle.

mapping wire in larger patients, and (f) whenever possible, cryoenergy should be considered as the ablation technology to minimize the risk to the AV conduction system and adjacent small coronary arteries. With these caveats in mind, it appears that despite the difficulties of unusual anatomical landmarks and abnormally positioned conduction systems, most APs in patients with structural congenital heart disease can be ablated safely and effectively.

SUMMARY

Children are usually smaller than adults, but in general ablation techniques used in adults should not simply be miniaturized to fit the size of the pediatric patient. Multiple factors, including the distribution of arrhythmia mechanisms, ongoing myocardial development, potentially increased risk of vascular injury and AV node damage, as well as the effects of smaller cardiac size should all influence the ablation technique. An overriding theme in the child should be that safety takes precedence over efficacy. Thus, variations of technique should include the decision to ablate, the energy source and its delivery, the catheter approach to the heart and the AV ring, and the follow-up. For instance, because of its strong safety profile and despite lower efficacy, the use of cryotherapy may be even better suited to ablation in children than in adults. Attention to these factors probably is most important in infants. In addition, the pediatric patient is more likely to have the simultaneous presence of structural congenital heart disease, which in itself has a variety of implications for the decision to ablate and the procedure technique. Alternatively, there are numerous similarities between adult and pediatric patients. Specifically, regardless of age, it seems clear that a variety of techniques and approaches is necessary to successfully ablate APs in all locations around the AV groove.

REFERENCES

- Gillette PC, Blair HL. Intracardiac electrophysiology studies. In: Gillette PC, Garson AJ, eds. *Clinical Pediatric Arrhythmias*. Philadelphia, PA: WB Saunders, 1999:36–47.
- Kugler JD. Evaluation of pediatric patients with preexcitation syndromes. In: Benditt DG, Benson DW, Jr, eds. *Cardiac Preexcitation Syndromes, Origins, Evaluation and Treatment*. Leiden, Netherlands: Martinus Nijhoff, 1986:316–411.
- Kugler JD. Electrophysiologic studies. In: Allen HD, Gutgesell HP, Clark EB, et al, eds. *Moss and Adams' Heart Disease in Infants, Children, and Adolescents*. Baltimore, MD: Williams & Wilkins, 2001:452–467.
- Pass RH. Intracardiac electrophysiologic testing in pediatric patients. In: Walsh EP, Saul JP, Friedman JK, eds. *Cardiac Arrhythmias in Children and Young Adults with Congenital Heart Disease*. Philadelphia, PA: Lippincott Williams & Wilkins, 2001:57–94.
- Saul JP, Hulse JE, De W, et al. Catheter ablation of accessory atrioventricular pathways in young patients: use of long vascular sheaths, the transseptal approach and a retrograde left posterior parallel approach. *J Am Coll Cardiol* 1993;21:571–583.
- Yip AS, McGuire MA, Davis L, et al. Lack of effect of midazolam on inducibility of arrhythmias at electrophysiologic study. *Am J Cardiol* 1992;70:593–597.
- Kumagai K, Yamanouchi Y, Matsuo K, et al. Antiarrhythmic and proarrhythmic properties of diazepam demonstrated by electrophysiological study in humans. *Clin Cardiol* 1991;14:397–401.
- Lavoie J, Walsh EP, Burrows FA, et al. Effects of propofol or isoflurane anesthesia on cardiac conduction in children undergoing radiofrequency catheter ablation for tachydysrhythmias. *Anesthesiology* 1995;82:884–887.
- Erb TO, Hall JM, Ing RJ, et al. Postoperative nausea and vomiting in children and adolescents undergoing radiofrequency catheter ablation: a randomized comparison of propofol- and isoflurane-based anesthetics. *Anesth Analg* 2002;95:1577–1581.
- Erb TO, Kanter RJ, Hall JM, et al. Comparison of electrophysiologic effects of propofol and isoflurane-based anesthetics in children undergoing radiofrequency catheter ablation for supraventricular tachycardia. *Anesthesiology* 2002;96:1386–1394.
- Zhou L, Keane D, Reed G, et al. Thromboembolic complications of cardiac radiofrequency catheter ablation: a review of the reported incidence, pathogenesis and current research directions. [Review] [48 refs]. *J Cardiovasc Electrophysiol* 1999;10:611–620.
- Anfinson OG, Gjesdal K, Aass H, et al. When should heparin preferably be administered during radiofrequency catheter ablation? *Pacing Clin Electrophysiol* 2001;24:5–12.
- Anfinson OG, Gjesdal K, Brosstad F, et al. The activation of platelet function, coagulation, and fibrinolysis during radiofrequency catheter ablation in heparinized patients. *J Cardiovasc Electrophysiol* 1999;10:503–512.
- Tse HF, Kwong YL, Lau CP. Transvenous cryoablation reduces platelet activation during pulmonary vein ablation compared with radiofrequency energy in patients with atrial fibrillation. *J Cardiovasc Electrophysiol* 2005;16:1064–1070.
- Stabile G, De SA, Turco P, et al. Feasibility and safety of two French electrode catheters in the performance of electrophysiological studies. *Pacing Clin Electrophysiol* 1998;21:2506–2509.
- Kugler JD. Electrophysiologic studies. In: Emmanouilides GC, Riemen-schneider TA, Allen HD, et al, eds. *Moss and Adams' Heart Disease in Infants, Children, and Adolescents, Including the Fetus and Young Adult*. Baltimore, MD: Williams & Wilkins, 1995:347–366.
- Stevenson WG, Soejima K. Recording techniques for clinical electrophysiology. *J Cardiovasc Electrophysiol* 2005;16:1017–1022.
- Packer DL. Three-dimensional mapping in interventional electrophysiology: techniques and technology. *J Cardiovasc Electrophysiol* 2005;16:1110–1116.
- Clark J, Bockoven JR, Lane J, et al. Use of three-dimensional catheter guidance and trans-esophageal echocardiography to eliminate fluoroscopy in catheter ablation of left-sided accessory pathways. *Pacing Clin Electrophysiol* 2008;31:283–289.
- Miyake CY, Mah DY, Atallah J, et al. Nonfluoroscopic imaging systems reduce radiation exposure in children undergoing ablation of supraventricular tachycardia. *Heart Rhythm* 2011;8:519–525.
- Gillette PC, Garson AJ. *Clinical Pediatric Arrhythmias*. Philadelphia, PA: WB Saunders, 1999.
- Deal BJ, Wolff GS, Gelband H, eds. *Current Concepts in Diagnosis and Management of Arrhythmias in Infants and Children*. Armonk, NY: Futura Publishing, 1998.
- Yabek SM, Gillette PC, Kugler JD, eds. *The Sinus Node in Pediatrics*. New York: Churchill Livingstone, 1984.
- Przybylski J, Chiale PA, Halpern MS, et al. Unmasking of ventricular pre-excitation by vagal stimulation or isoproterenol administration. *Circulation* 1980;61:1030–1037.
- Toda I, Kawahara T, Murakawa Y, et al. Electrophysiological study of young patients with exercise related paroxysms of palpitation: role of atropine and isoprenaline for initiation of supraventricular tachycardia. *Br Heart J* 1989;61:268–273.
- Huycke EC, Lai WT, Nguyen NX, et al. Role of intravenous isoproterenol in the electrophysiologic induction of atrioventricular node reentrant tachycardia in patients with dual atrioventricular node pathways. *Am J Cardiol* 1989;64:1131–1137.
- Freedman RA, Swerdlow CD, Echt DS, et al. Facilitation of ventricular tachyarrhythmia induction by isoproterenol. *Am J Cardiol* 1984;54:765–770.
- Antzelevitch C, Brugada P, Borggreffe M, et al. Brugada syndrome: report of the second consensus conference. *Heart Rhythm* 2005;2:429–440.
- Kugler JD, Bansal AM, Cheatham JP, et al. Drug-electrophysiology studies in infants, children, and adolescents. *Am Heart J* 1985;110:144–154.
- Milstein S, Dunnigan A, Buetikofer J, et al. Usefulness of combined propranolol and verapamil for evaluation of surgical ablation of accessory atrioventricular connections in patients without structural heart disease. *Am J Cardiol* 1990;66:1216–1221.
- Dorostkar PC, Dick M II, Serwer GA. Effect of adenosine on atrioventricular conduction in children and young patients with supraventricular tachycardia. *Cardiol Young* 1996;6:308–314.
- Belhassen B. Adenosine triphosphate in cardiac arrhythmias: from therapeutic to diagnostic use. *Pacing Clin Electrophysiol* 2002;25:98–102.
- Stanger P, Heymann MA, Tarnoff H, et al. Complications of cardiac catheterization of neonates, infants, and children. A three-year study. *Circulation* 1974;50:595–608.
- Cohn HE, Freed MD, Hellenbrand WF, et al. Complications and mortality associated with cardiac catheterization in infants under one year: a prospective study. *Pediatr Cardiol* 1985;6:123–131.
- Mullins CE, Latson LA, Neches WH, et al. Balloon dilation of miscellaneous lesions: results of valvuloplasty and angioplasty of congenital anomalies registry. *Am J Cardiol* 1990;65:802–803.
- Cassidy SC, Schmidt KG, VanHare GF, et al. Complications of pediatric cardiac catheterization: a 3-year study. *J Am Coll Cardiol* 1992;19:1285–1293.
- Vitiello R, McCrindle BW, Nykanen D, et al. Complications associated with pediatric cardiac catheterization. *J Am Coll Cardiol* 1998;32:1433–1440.
- Rhodes JF, Asnes JD, Blafox AD, et al. Impact of low body weight on frequency of pediatric cardiac catheterization complications. *Am J Cardiol* 2000;86:1275–1278, A9.
- Schaffer MS, Gow RM, Moak JP, et al. Mortality following radiofrequency catheter ablation (from the Pediatric Radiofrequency Ablation Registry). Participating members of the Pediatric Electrophysiology Society. *Am J Cardiol* 2000;86:639–643.
- Latson LA, Cheatham JP, Gumbiner CH, et al. Midazolam nose drops for outpatient echocardiography sedation in infants. *Am Heart J* 1991;121:209–210.

41. Benson DW Jr, Sanford M, Dunnigan A, et al. Transesophageal atrial pacing threshold: role of interelectrode spacing, pulse width and catheter insertion depth. *Am J Cardiol* 1984;53:63-67.
42. Benson DW Jr, Javdar H, Strasburger JF. Utility of a stimulus artifact suppressor for transesophageal pacing. *Am J Cardiol* 1990;65:393-394.
43. Dick MJ, Campbell RM, Jenkins JM. Thresholds for transesophageal atrial pacing. *Cathet Cardiovasc Diagn* 1984;10:507-513.
44. Drago F, Turchetta A, Calzolari A, et al. Detection of atrial vulnerability by transesophageal atrial pacing and the relation of symptoms in children with Wolff-Parkinson-White syndrome and in a symptomatic control group. *Am J Cardiol* 1994;74:400-401.
45. McEneaney DJ, Cochrane DJ, Anderson JA, et al. A gastroesophageal electrode for atrial and ventricular pacing. *PACE* 1997;20:1815-1825.
46. McEneaney DJ, Escalona O, Anderson JA, et al. A gastroesophageal electrode for electrophysiological studies. *PACE* 1999;22:487-499.
47. Serwer GA, Eckerd JM, Kelly EE, et al. Emergency ventricular pacing from the esophagus in infancy. *Am J Cardiol* 1986;58:1105-1106.
48. German LD, Packer DL, Bardy GH, et al. Ventricular tachycardia induced by atrial stimulation in patients without symptomatic cardiac disease. *Am J Cardiol* 1983;52:1207.
49. Belhassen B, Shapira I, Pelleg A, et al. Idiopathic recurrent sustained ventricular tachycardia responsive to verapamil: an ECG-electrophysiologic entity. *Am Heart J* 1984;108:1034-1037.
50. Benson DW Jr, Dunnigan A, Benditt DG, et al. Transesophageal cardiac pacing: history, application, technique. *Clin Prog Pacing Electrophysiol* 1984;2:360-372.
51. Benson DW Jr. Transesophageal electrocardiography and cardiac pacing: state of the art. *Circulation* 1987;75:III86-III92.
52. Kugler JD, Danford DA, Gumbiner CH. Ventricular fibrillation during transesophageal atrial pacing in an infant with Wolff-Parkinson-White syndrome. *Pediatr Cardiol* 1991;12:36-38.
53. Sanatani S, Saul JP, Walsh EP, et al. Spontaneously terminating apparent ventricular fibrillation during transesophageal electrophysiological testing in infants with Wolff-Parkinson-White syndrome. *Pacing Clin Electrophysiol* 2001;24:1816-1818.
54. Wolferth CC, Wood FC. The mechanism of production of short PR intervals and prolonged QRS complexes in patients with presumably undamaged hearts: Hypothesis of an accessory pathway of auriculoventricular conduction (bunde of Kent). *Am Heart J* 1932;8:297-311.
55. Wolff L, Parkinson J, White PD. Bundle branch block with short P-R interval in healthy young people prone to paroxysmal tachycardia. *Am Heart J* 1930;5:685.
56. Sealy WC, Hattler BG, Blumenschein SD, et al. Surgical treatment of Wolff-Parkinson-White syndrome. *Ann Thorac Surg* 1969;8:1.
57. Haines DE, Watson DD. Tissue heating during radiofrequency catheter ablation: a thermodynamic model and observation in isolated perfused and superfused canine right ventricular free wall. *PACE* 1989;12:962-976.
58. Dubuc M, Talajic M, Roy D, et al. Feasibility of cardiac cryoablation using a transvenous steerable electrode catheter. *J Interv Card Electrophysiol* 1998;2:285-292.
59. Erickson CC, Walsh EP, Friedman JK, et al. Efficacy and safety of radiofrequency ablation in infants and young children <18 months of age. *Am J Cardiol* 1994;74:944-947.
60. Saul JP, Hulse JE, Papagiannis J, et al. Late enlargement of radiofrequency lesions in infant lambs. Implications for ablation procedures in small children. *Circulation* 1994;90:492-499.
61. Van Hare GF, Lesh MD, Scheinman M, et al. Percutaneous radiofrequency catheter ablation for supraventricular arrhythmias in children. *J Am Coll Cardiol* 1991;17:1613-1620.
62. Kugler JD, Danford DA, Deal BJ, et al. Radiofrequency catheter ablation for tachyarrhythmias in children and adolescents. The Pediatric Electrophysiology Society. *N Engl J Med* 1994;330:1481-1487.
63. Friedman RA, Walsh EP, Silka MJ, et al. NASPE Expert Consensus Conference: Radiofrequency catheter ablation in children with and without congenital heart disease. Report of the writing committee. North American Society of Pacing and Electrophysiology. [Review] [127 refs]. *Pacing Clin Electrophysiol* 2002;25:1000-1017.
64. Blafox AD, Denslow S, Felix GL, et al. Participating Members of the Pediatric Electrophysiology Society. Radiofrequency catheter ablation in Registry infants: when is it done and how do they fare? *Circulation* 2000;102(18):II-698.
65. Blafox AD, Paul T, Saul JP. Radiofrequency catheter ablation in small children: relationship of complications to application dose. *Pacing Clin Electrophysiol* 2004;27:224-229.
66. Blafox AD, Felix GL, Saul JP, et al. Radiofrequency catheter ablation in infants ≤18 months old: when is it done and how do they fare?: short-term data from the pediatric ablation registry. *Circulation* 2001;104:2803-2808.
67. Paul T, Bokenkamp R, Mahnet B, et al. Coronary artery involvement early and late after radiofrequency current application in young pigs. *Am Heart J* 1997;133:436-440.
68. Paul T, Kakavand B, Blafox AD, et al. Complete occlusion of the left circumflex coronary artery after radiofrequency catheter ablation in an infant. *J Cardiovasc Electrophysiol* 2003;14:1004-1006.
69. Bertram H, Bokenkamp R, Peuster M, et al. Coronary artery stenosis after radiofrequency catheter ablation of accessory atrioventricular pathways in children with Ebstein's malformation. *Circulation* 2001;103:538-543.
70. Blafox AD, Saul JP. Acute coronary artery stenosis during slow pathway ablation for atrioventricular nodal reentrant tachycardia in a child. *J Cardiovasc Electrophysiol* 2004;15:97-100.
71. Deal BJ, Keane JF, Gillette PC, et al. Wolff-Parkinson-White syndrome and supraventricular tachycardia during infancy: management and follow-up. *J Am Coll Cardiol* 1985;5:130-135.
72. Benson DW Jr, Dunnigan A, Benditt DG. Follow-up evaluation of infant paroxysmal atrial tachycardia: transesophageal study. *Circulation* 1987;75:542-549.
73. Perry JC, Garson A, Jr. Supraventricular tachycardia due to Wolff-Parkinson-White syndrome in children: early disappearance and late recurrence [see comments]. *J Am Coll Cardiol* 1990;16:1215-1220.
74. Klein GJ, Yee R, Sharma AD. Longitudinal electrophysiologic assessment of asymptomatic patients with the Wolff-Parkinson-White electrocardiographic pattern. [see comment]. *New Engl J Med* 1989;320:1229-1233.
75. Zardini M, Yee R, Thakur RK, et al. Risk of sudden arrhythmic death in the Wolff-Parkinson-White syndrome: current perspectives. *PACE* 1994;17:966-975.
76. Bromberg BI, Lindsay BD, Cain ME, et al. Impact of clinical history and electrophysiologic characterization of accessory pathways on management strategies to reduce sudden death among children with Wolff-Parkinson-White syndrome. *J Am Coll Cardiol* 1996;27:690-695.
77. Zipes DP, Garson A, Jr. 26th Bethesda conference: recommendations for determining eligibility for competition in athletes with cardiovascular abnormalities. Task Force 6: arrhythmias. [Review] [35 refs]. *Med Sci Sports Exerc* 1994;26:S276-S283.
78. Vedel J, Frank R, Fontaine G, et al. Bloc auriculo-ventriculaire intra-Hisien définitif induit au cours d'une exploration endoventriculaire droite. *Arch Mal Coeur* 1979;72:107-112.
79. Scheinman MM, Morady F, Hess DS, et al. Catheter-induced ablation of the atrioventricular junction to control refractory supraventricular arrhythmias. *JAMA* 1982;248:851-855.
80. Scheinman MM, Evans-Bell T. Catheter ablation of the atrioventricular junction: a report of the percutaneous mapping and ablation registry. *Circulation* 1984;70:1024-1029.
81. Warin JF, Haissaguerre M, D'Ilvernois C, et al. Catheter ablation of accessory pathways: technique and results in 248 patients. *PACE* 1990;13:1609-1614.
82. Sebag C, Laverge T, Millat B. Rupture of the stomach and the esophagus after attempted transcatheter ablation of an accessory pathway by direct current shock. *Am J Cardiol* 1989;63:890-891.
83. Gillette PC, Garson A Jr, Porter JC, et al. Junctional automatic ectopic tachycardia: new proposed treatment by transcatheter His bundle ablation. *Am Heart J* 1983;106:619-623.
84. Smith RT Jr, Gillette PC, Massumi A, et al. Transcatheter ablative techniques for treatment of the permanent form of junctional reciprocating tachycardia in young patients. *J Am Coll Cardiol* 1986;8:385-390.
85. Cunningham D, Rowland E, Rickards AF. A new low energy power source for catheter ablation. *PACE* 1986;9:1384-1390.
86. Cosman ER, Nashold BS, Ovelman-Levitt J. Theoretical aspects of radiofrequency lesions in the dorsal root entry zone. *Neurosurgery* 1984;15:945-950.
87. Huang SK, Bharati S, Graham AR, et al. Closed chest catheter desiccation of the atrioventricular junction using radiofrequency energy—a new method of catheter ablation. *J Am Coll Cardiol* 1987;9:349-358.
88. Borggreffe M, Budde T, Podczek A, et al. High frequency alternating current ablation of an accessory pathway in humans. *J Am Coll Cardiol* 1987;10:576-582.
89. Haines DE, Verow AF. Observations on electrode-tissue interface temperature and effects on electrical impedance during radiofrequency ablation of ventricular myocardium. *Circulation* 1990;82:1034-1038.
90. Calkins H, Prystowsky E, Carlson M, et al. Temperature monitoring during radiofrequency catheter ablation procedures using closed loop control. Atakr Multicenter Investigators Group. *Circulation* 1994;90:1279-1286.
91. Cote JM, Epstein MR, Friedman JK, et al. Low-temperature mapping predicts site of successful ablation while minimizing myocardial damage. *Circulation* 1996;94:253-257.
92. Nakagawa H, Yamanashi WS, Pitha JV, et al. Comparison of in vivo tissue temperature profile and lesion geometry for radiofrequency ablation with a saline-irrigated electrode versus temperature control in a canine thigh muscle preparation. *Circulation* 1995;91:2264-2273.
93. Langberg JJ, Gallagher M, Strickberger SA, et al. temperature-guided radiofrequency catheter ablation with very large distal electrodes. *Circulation* 1993;88:245-249.
94. Bergau D, Brucker GG, Saul JP. Porous metal tipped catheter produces larger radiofrequency lesions through tip cooling. *Circulation* 1993;88:1-164.
95. Whyne JG, Nath S, Haines DE. Microwave catheter ablation of myocardium in vitro. Assessment of the characteristics of tissue heating and injury. *Circulation* 1994;89:2390-2395.
96. Agnoletti G, Borghi A, Vignati G, et al. Fontan conversion to total cavopulmonary connection and arrhythmia ablation: clinical and functional results. *Heart* 2003;89:193-198.
97. Gaita F, Haissaguerre M, Giustetto C, et al. Safety and efficacy of cryoablation of accessory pathways adjacent to the normal conduction system. *J Cardiovasc Electrophysiol* 2003;14:825-829.

98. Gaita F, Antonio M, Riccardi R, et al. Cryoenergy catheter ablation: a new technique for treatment of permanent junctional reciprocating tachycardia in children. *J Cardiovasc Electrophysiol* 2004;15:263–268.
99. Lowe MD, Meara M, Mason J, et al. Catheter cryoablation of supraventricular arrhythmias: a painless alternative to radiofrequency energy. *Pacing Clin Electrophysiol* 2003;26:500–503.
100. Skanes AC, Yee R, Krahn AD, et al. Cryoablation of atrial arrhythmias. [Review] [26 refs]. *Cardiac Electrophysiol Rev* 2002;6:383–388.
101. Skanes AC, Dubuc M, Klein GJ, et al. Cryothermal ablation of the slow pathway for the elimination of atrioventricular nodal reentrant tachycardia. *Circulation* 2000;102:2856–2860.
102. Miyazaki A, Blafox AD, Fairbrother DL, et al. Prolongation of the fast pathway effective refractory period during cryoablation in children: a marker of slow pathway modification. *Heart Rhythm* 2005;2:1179–1185.
103. Miyazaki A, Blafox AD, Fairbrother DL, et al. Cryoablation for septal tachycardia substrates in pediatric patients: mid-term results. *J Am Coll Cardiol* 2005;45:581–588.
104. Rodriguez LM, Leunissen J, Hoekstra A, et al. Transvenous cold mapping and cryoablation of the AV node in dogs: observations of chronic lesions and comparison to those obtained using radiofrequency ablation. *J Cardiovasc Electrophysiol* 1998;9:1055–1061.
105. Dubuc M, Roy D, Thibault B, et al. Transvenous catheter ice mapping and cryoablation of the atrioventricular node in dogs. *Pacing Clin Electrophysiol* 1999;22:1488–1498.
106. Lustgarten DL, Bell S, Hardin N, et al. Safety and efficacy of epicardial cryoablation in a canine model. *Heart Rhythm* 2005;2:82–90.
107. Skanes AC, Jones DL, Teefy P, et al. Safety and feasibility of cryothermal ablation within the mid- and distal coronary sinus. *J Cardiovasc Electrophysiol* 2004;15:1319–1323.
108. Khairy P, Chauvet P, Lehmann J, et al. Lower incidence of thrombus formation with cryoenergy versus radiofrequency catheter ablation. *Circulation* 2003;107:2045–2050.
109. Khairy P, Guerra PG, Rivard L, et al. Enlargement of catheter ablation lesions in infant hearts with cryothermal versus radiofrequency energy: an animal study. *Circ Arrhythm Electrophysiol* 2011;4:211–217.
110. Kugler JD, Danford DA, Houston K, et al. Radiofrequency catheter ablation for paroxysmal supraventricular tachycardia in children and adolescents without structural heart disease. Pediatric EP Society, Radiofrequency Catheter Ablation Registry. *Am J Cardiol* 1997;80:1438–1443.
111. Schaffer MS, Silka MJ, Ross BA, et al. Inadvertent atrioventricular block during radiofrequency catheter ablation. Results of the Pediatric Radiofrequency Ablation Registry. Pediatric Electrophysiology Society. *Circulation* 1996;94:3214–3220.
112. Bokenkamp R, Wibbelt G, Sturm M, et al. Effects of intracardiac radiofrequency current application on coronary artery vessels in young pigs. *J Cardiovasc Electrophysiol* 2000;11:565–571.
113. Nakagawa H, Chandrasekaran K, Pitha J, et al. Early detection of coronary artery injury produced by radiofrequency ablation within the coronary sinus using intravascular ultrasound imaging. *Circulation* 1995;92:I–610.
114. Schneider HE, Kriebel T, Stahl M, et al. Double cryoenergy application (freeze-thaw-freeze) at growing myocardium: results of intracoronary artery angiography studies early after energy application. *Heart Rhythm* 2010;7:S1.
115. Bar-Cohen Y, Cecchin F, Alexander ME, et al. Cryoablation for accessory pathways located near normal conduction tissues or within the coronary venous system in children and young adults. *Heart Rhythm* 2006;3:253–258.
116. Gist KM, Bockoven JR, Lane J, et al. Acute success of cryoablation of left-sided accessory pathways: a single institution study. *J Cardiovasc Electrophysiol* 2009;20:637–642.
117. Haines DE. Thermal ablation of perfused porcine left ventricle in vitro with the neodymium-YAG laser hot tip catheter system. *Pacing Clin Electrophysiol* 1992;15:979–985.
118. Svenson RH, Littmann L, Colavita PG, et al. Laser photoablation of ventricular tachycardia: correlation of diastolic activation times and photoablation effects on cycle length and termination—observations supporting a macroreentrant mechanism. *J Am Coll Cardiol* 1992;19:607–613.
119. Wu G, Svenson RH, Littmann L, et al. Laser photoablation of experimental post-infarction ventricular tachycardia guided by three dimensional activation mapping. *Lasers Surg Med* 1997;20:119–130.
120. Lesh MD, Diederich C, Guerra PG, et al. An anatomic approach to prevention of atrial fibrillation: pulmonary vein isolation with through-the-balloon ultrasound ablation (TTB-USA). [Review] [20 refs]. *Thorac Cardiovasc Surg* 1999;47:347–351.
121. Blafox AD, Numan MT, Laohakunakorn P, et al. Catheter tip cooling during radiofrequency ablation of intra-atrial reentry: effects on power, temperature, and impedance. *J Cardiovasc Electrophysiol* 2002;13:783–787.
122. Love BA, Collins KK, Alexander ME, et al. Early results of radiofrequency ablation for intraatrial reentry tachycardia in congenital heart disease using electroanatomic mapping. *Circulation* 2000;102:II-698.
123. Love BA, Collins KK, Walsh EP, et al. Electroanatomic characterization of conduction barriers in sinus/atrially paced rhythm and association with intra-atrial reentrant tachycardia circuits following congenital heart disease surgery. *J Cardiovasc Electrophysiol* 2001;12:17–25.
124. Triedman JK. Arrhythmias in adults with congenital heart disease. *Heart* 2002;87:383–389.
125. Triedman JK, Alexander ME, Love BA, et al. Influence of patient factors and ablative technologies on outcomes of radiofrequency ablation of intra-atrial re-entrant tachycardia in patients with congenital heart disease. *J Am Coll Cardiol* 2002;39:1827–1835.
126. Triedman JK, DeLuca JM, Alexander ME, et al. Prospective trial of electroanatomically guided, irrigated catheter ablation of atrial tachycardia in patients with congenital heart disease. *Heart Rhythm* 2005;2:700–705.
127. Jackman WM, Wang XZ, Friday KJ, et al. Catheter ablation of accessory atrioventricular pathways (Wolff-Parkinson-White syndrome) by radiofrequency current [see comments]. *N Engl J Med* 1991;324:1605–1611.
128. Beukema WP, Van Dessel PF, van Hemel NM, et al. Radiofrequency catheter ablation of accessory pathways associated with a coronary sinus diverticulum. *Eur Heart J* 1994;15:1415–1418.
129. Chiang CE, Chen SA, Yang CR, et al. Major coronary sinus abnormalities: identification of occurrence and significance in radiofrequency ablation of supraventricular tachycardia. *Am Heart J* 1994;127:1279–1289.
130. Chiang CE, Chen SA, Yang CR, et al. Radiofrequency ablation of posteroseptal accessory pathways in patients with abnormal coronary sinus. *Am Heart J* 1993;126:1213–1216.
131. Giorgberide I, Saksena S, Krol RB, et al. Efficacy and safety of radiofrequency catheter ablation of left-sided accessory pathways through the coronary sinus. *Am J Cardiol* 1995;76:359–365.
132. Huang SK, Graham AR, Bharati S, et al. Short and long-term effects of transcatheter ablation of the coronary sinus by radiofrequency energy. *Circulation* 1988;78:416–427.
133. Langberg JJ, Griffin JC, Herre JM, et al. Catheter ablation of accessory pathways using radiofrequency energy in the canine coronary sinus. *J Am Coll Cardiol* 1989;13:491–496.
134. Lesh MD, van Hare G, Kao AK, et al. Radiofrequency catheter ablation for Wolff-Parkinson-White syndrome associated with a coronary sinus diverticulum. *PACE* 1991;14:1479–1484.
135. Sanchez-Quintana D, Ho SY, Cabrera JA, et al. Topographic anatomy of the inferior pyramidal space: relevance to radiofrequency catheter ablation. *J Cardiovasc Electrophysiol* 2001;12:210–217.
136. Shinbane JS, Lesh MD, Stevenson WG, et al. Anatomic and electrophysiologic relation between the coronary sinus and mitral annulus: implications for ablation of left-sided accessory pathways. *Am Heart J* 1998;135:93–98.
137. Tebbenjohanns J, Pfeiffer D, Jung W, et al. Radiofrequency catheter ablation of a posteroseptal accessory pathway within a coronary sinus diverticulum. *Am Heart J* 1993;126:1216–1219.
138. Khanal S, Ribeiro PA, Platt M, et al. Right coronary artery occlusion as a complication of accessory pathway ablation in a 12-year-old treated with stenting. *Catheter Cardiovasc Interv* 1999;46:59–61.
139. Kuck K, Schluter M, Guroy S. Preservation of atrioventricular nodal conduction during radiofrequency current catheter ablation of midseptal accessory pathways. *Circulation* 1992;86:1743–1752.
140. Schluter M, Siebels J, Duckeck W, et al. Catheter approaches to radiofrequency current ablation of posteroseptal accessory pathways. *J Am Coll Cardiol* 1992;19:27A.
141. Atrienza F, Arenal A, Torrecilla EG, et al. Acute and long-term outcome of transvenous cryoablation of midseptal and parahissian accessory pathways in patients at high risk of atrioventricular block during radiofrequency ablation. *Am J Cardiol* 2004;93:1302–1305.
142. Lanzotti ME, De PR, Tritto M, et al. Successful treatment of anteroseptal accessory pathways by transvenous cryomapping and cryoablation. *Ital Heart J* 2002;3:128–132.
143. Lee AW, Crawford FA Jr, Gillette PC, et al. Cryoablation of septal pathways in patients with supraventricular tachyarrhythmias. *Ann Thorac Surg* 1989;47:566–568.
144. Stobie P, Green MS. Cryoablation for septal accessory pathways: has the next ice age arrived? *J Cardiovasc Electrophysiol* 2003;14:830–831.
145. Laohaprasitiporn D, Walsh EP, Saul JP, et al. Predictors of permanence of successful radiofrequency lesions created with controlled catheter tip temperature. *Pacing Clin Electrophysiol* 1997;20:1283–1291.
146. Avari JN, Jay KS, Rhee EK. Experience and results during transition from radiofrequency ablation to cryoablation for treatment of pediatric atrioventricular nodal reentrant tachycardia. *Pacing Clin Electrophysiol* 2008;31:454–460.
147. Chan NY, Mok NS, Lau CL, et al. Treatment of atrioventricular nodal re-entrant tachycardia by cryoablation with a 6 mm-tip catheter vs. radiofrequency ablation. *Europace* 2009;11:1065–1070.
148. LaPage MJ, Saul JP, Reed JH. Long-term outcomes for cryoablation of pediatric patients with atrioventricular nodal reentrant tachycardia. *Am J Cardiol* 2010;105:1118–1121.
149. Tint D, Kun C, Beke I, et al. Adenosine-dependent concealed accessory pathway. *Pacing Clin Electrophysiol* 2011;1–3.
150. Tanel RE, Walsh EP, Triedman JK, et al. Five-year experience with radiofrequency catheter ablation: implications for management of arrhythmias in pediatric and young adult patients. *J Pediatr* 1997;131:878–887.
151. Van Hare GF, Javitz H, Carmelli D, et al. Prospective assessment after pediatric cardiac ablation: demographics, medical profiles, and initial outcomes. *J Cardiovasc Electrophysiol* 2004;15:759–770.
152. Calkins H, Langberg J, Sousa J, et al. Radiofrequency catheter ablation of accessory atrioventricular connections in 250 patients. Abbreviated

- therapeutic approach to Wolff-Parkinson-White syndrome. *Circulation* 1992;85:1337-1346.
153. Van Hare GF, Javitz H, Carmelli D, et al. Prospective assessment after pediatric cardiac ablation: recurrence at 1 year after initially successful ablation of supraventricular tachycardia. *Heart Rhythm* 2004;1:188-196.
 154. Van Hare GF, Carmelli D, Smith WM, et al. Prospective assessment after pediatric cardiac ablation: design and implementation of the multicenter study. *Pacing Clin Electrophysiol* 2002;25:332-341.
 155. Danford DA, Kugler JD, Deal B, et al. The learning curve for radiofrequency ablation of tachyarrhythmias in pediatric patients. *Am J Cardiol* 1995;75:587-590.
 156. Kugler JD, Danford DA, Houston KA, et al. Pediatric radiofrequency catheter ablation registry success, fluoroscopy time, and complication rate for supraventricular tachycardia: comparison of early and recent eras. *J Cardiovasc Electrophysiol* 2002;13:336-341.
 157. Critelli G, Gallagher JJ, Thiene G. The permanent form of junctional reciprocating tachycardia. In: Benditt DG, Benson DW, eds. *Cardiac Pre-excitation Syndromes, Origins, Evaluation and Treatment*. Boston, MA: Martinus Nijhoff, 1986:233-254.
 158. Ticho BS, Saul JP, Hulse JE, et al. Variable location of accessory pathways associated with the permanent form of junctional reciprocating tachycardia and confirmation with radiofrequency ablation. *Am J Cardiol* 1992;70:1559-1564.
 159. Fishberger SB, Colan SD, Saul JP, et al. Myocardial mechanics before and after ablation of chronic tachycardia. *Pacing Clin Electrophysiol* 1996;19:42-49.
 160. Haissaguerre M, Montserrat P, Warin JF, et al. Catheter ablation of left posteroseptal accessory pathways and of long RP' tachycardias with a right endocardial approach. *Eur Heart J* 1991;12:845-859.
 161. Ticho BS, Walsh EP, Saul JP. Ablation of permanent junctional reciprocating tachycardia. In: Huang SK, ed. *Radiofrequency Catheter Ablation of Cardiac Arrhythmias: Basic Concepts and Clinical Applications*. Mt. Kisco, NY: Futura Publishing, 1994:397-409.
 162. Gaita F, Haissaguerre M, Giustetto C, et al. Catheter ablation of permanent junctional reciprocating tachycardia with radiofrequency current. *J Am Coll Cardiol* 1995;25:648-654.
 163. Morady F, Scheinman MM, Kou WH, et al. Long-term results of catheter ablation of a posteroseptal accessory atrioventricular connection in 48 patients. *Circulation* 1989;79:1160-1170.
 164. Haissaguerre M, Warin JF, Lemetayer P, et al. Closed-chest ablation of retrograde conduction in patients with atrioventricular nodal reentrant tachycardia. *N Engl J Med* 1989;320:426-433.
 165. Huang SK, Bharati S, Graham AR, et al. Chronic incomplete atrioventricular block induced by radiofrequency catheter ablation. *Circulation* 1989;80:951-961.
 166. Jackman WM, Beckman KJ, McClelland JH, et al. Treatment of supraventricular tachycardia due to atrioventricular nodal reentry by radiofrequency catheter ablation of slow-pathway conduction. *N Engl J Med* 1992;327:313-318.
 167. Wong T, Segal OR, Markides V, et al. Cryoablation of focal atrial tachycardia originating close to the atrioventricular node. *J Cardiovasc Electrophysiol* 2004;15:838.
 168. Gaita F, Montefusco A, Riccardi R, et al. Acute and long-term outcome of transvenous cryothermal catheter ablation of supraventricular arrhythmias involving the perinodal region. *J Cardiovasc Med* 2006;7:785-792.
 169. Wathen M, Natale A, Wolfe K, et al. An anatomically guided approach to atrioventricular node slow pathway ablation. *Am J Cardiol* 1992;70:886-889.
 170. Benito F, Sanchez C. Radiofrequency catheter ablation of accessory pathways in infants. *Heart* 1997;78:160-162.
 171. Solomon AJ, Tracy CM, Swartz JF, et al. Effect on coronary artery anatomy of radiofrequency catheter ablation of atrial insertion sites of accessory pathways. *J Am Coll Cardiol* 1993;21:1440-1444.
 172. Chatelain P, Zimmermann M, Weber R, et al. Acute coronary occlusion secondary to radiofrequency catheter ablation of a left lateral accessory pathway. *Eur Heart J* 1995;16:859-861.
 173. Schneider HE, Kriebel T, Gravenhorst VD, et al. Incidence of coronary artery injury immediately after catheter ablation for supraventricular tachycardias in infants and children. *Heart Rhythm* 2009;6:461-467.
 174. Kriebel T, Hermann HP, Schneider H, et al. Cryoablation at growing myocardium: no evidence of coronary artery obstruction or intimal plaque formation early and late after energy application. *PACE* 2009;32:1197-1202.
 175. Garson A Jr, Smith RT, Moak JP, et al. Atrial automatic ectopic tachycardia in children. In: Touboul P, Waldo AL, eds. *Atrial Arrhythmias: Current Concepts and Management*. St. Louis, MO: Mosby Year Book, 1990:282-287.
 176. Walsh EP, Saul JP, Hulse JE, et al. Transcatheter ablation of ectopic atrial tachycardia in young patients using radiofrequency current [see comments]. *Circulation* 1992;86:1138-1146.
 177. Walsh EP. Ablation of ectopic atrial tachycardia in children. In: Huang SK, ed. *Radiofrequency Catheter Ablation of Cardiac Arrhythmias: Basic Concepts and Clinical Applications*. Mt. Kisco, NY: Futura Publishing, 1994:421-443.
 178. Walsh EP, Saul JP, Triedman JK, et al. Natural and unnatural history of ectopic atrial tachycardia: one institution's experience. *PACE* 1994;17:746.
 179. Tracy CM, Swartz JF, Fletcher RD, et al. Radiofrequency catheter ablation of ectopic atrial tachycardia using paced activation sequence mapping [see comments]. *J Am Coll Cardiol* 1993;21:910-917.
 180. Silka MJ, Gillette PC, Garson A Jr, et al. Transvenous catheter ablation of a right atrial automatic ectopic tachycardia. *J Am Coll Cardiol* 1985;5:999-1001.
 181. Haissaguerre M, Hocini M, Sanders P, et al. Catheter ablation of long-lasting persistent atrial fibrillation: clinical outcome and mechanisms of subsequent arrhythmias. *J Cardiovasc Electrophysiol* 2005;16:1138-1147.
 182. Haissaguerre M, Sanders P, Hocini M, et al. Pulmonary veins in the substrate for atrial fibrillation: the "venous wave" hypothesis. *J Am Coll Cardiol* 2004;43:2290-2292.
 183. Hsu LF, Jais P, Hocini M, et al. Incidence and prevention of cardiac tamponade complicating ablation for atrial fibrillation. *Pacing Clin Electrophysiol* 2005;28:S106-S109.
 184. Ko JK, Deal BJ, Strasburger JF, et al. Supraventricular tachycardia mechanisms and their age distribution in pediatric patients. *Am J Cardiol* 1992;69:1028-1032.
 185. Dunnigan A, Benson DW, Benditt DG. Atrial flutter in infancy: diagnosis, clinical features, and treatment. *Pediatrics* 1985;75:725-729.
 186. Nanthakumar K, Lau YR, Plumb VJ, et al. Electrophysiological findings in adolescents with atrial fibrillation who have structurally normal hearts. *Circulation* 2004;110:117-123.
 187. Cosio FG, Arribas F, Lopez-Gil M, et al. Atrial flutter mapping and ablation II. Radiofrequency ablation of atrial flutter circuits. [Review] [32 refs]. *Pacing Clin Electrophysiol* 1996;19:965-975.
 188. Kalman JM, Olgin JE, Saxon LA, et al. Electrocardiographic and electrophysiologic characterization of atypical atrial flutter in man: use of activation and entrainment mapping and implications for catheter ablation. *J Cardiovasc Electrophysiol* 1997;8:121-144.
 189. Manolis AS, Vassilikos V, Maounis TN, et al. Radiofrequency ablation in pediatric and adult patients: comparative results. *J Interv Cardiac Electrophysiol* 2001;5:443-453.
 190. Garson A Jr, Bink-Boelkens M, Hesslein PS, et al. Atrial flutter in the young: a collaborative study of 380 cases. *J Am Coll Cardiol* 1985;6:871-878.
 191. Fishberger SB, Wernovsky G, Gentles TL, et al. Factors that influence the development of atrial flutter after the fontan operation. *J Thorac Cardiovasc Surg* 1997;113:80-86.
 192. Bink-Boelkens MT, Meuzelaar KJ, et al. Arrhythmias after repair of secundum atrial septal defect: the influence of surgical modification. *Am Heart J* 1988;115:629-633.
 193. Rhodes LA, Walsh EP, Gamble WJ, et al. Benefits and potential risks of atrial antitachycardia pacing after repair of congenital heart disease. *Pacing Clin Electrophysiol* 1995;18:1005-1016.
 194. Weindling SN, Saul JP, Walsh EP. Efficacy and risks of medical therapy for supraventricular tachycardia in neonates and infants. *Am Heart J* 1996;131:66-72.
 195. Saul JP, Triedman JK. Radiofrequency ablation of intraatrial reentrant tachycardia after surgery for congenital heart disease. [Review] [35 refs]. *Pacing Clin Electrophysiol* 1997;20:2112-2117.
 196. Saul JP, Walsh EP, Triedman JK. Mechanisms and therapy of complex arrhythmias in pediatric patients. *J Cardiovasc Electrophysiol* 1995;6:1129-1148.
 197. Triedman JK, Bergau DM, Saul JP, et al. Efficacy of radiofrequency ablation for control of intraatrial reentrant tachycardia in patients with congenital heart disease. *J Am Coll Cardiol* 1997;30:1032-1038.
 198. Collins KK, Love BA, Walsh EP, et al. Location of acutely successful radiofrequency catheter ablation of intraatrial reentrant tachycardia in patients with congenital heart disease. *Am J Cardiol* 2000;86:969-974.
 199. Gillette PC. Diagnosis and management of postoperative junctional ectopic tachycardia. *Am Heart J* 1989;118:192-194.
 200. Villain E, Vetter VL, Garcia JM, et al. Evolving concepts in the management of congenital junctional ectopic tachycardia. A multicenter study [see comments]. [Review]. *Circulation* 1990;81:1544-1549.
 201. Sholler GF, Walsh EP, Saul JP, et al. Evaluation of a staged treatment protocol for postoperative rapid junctional ectopic tachycardia. *Circulation* 1988;78:II-597.
 202. Balaji S, Sullivan I, Deanfield J, et al. Moderate hypothermia in the management of resistant automatic tachycardias in children. *Br Heart J* 1991;66:221-224.
 203. Bash SE, Shah JJ, Albers WH. Hypothermia for the treatment of post-surgically accelerated junctional ectopic tachycardia. *J Am Coll Cardiol* 1987;10:1095-1099.
 204. Till JA, Rowland E. Atrial pacing as an adjunct to the management of post-surgical His bundle tachycardia. *Br Heart J* 1991;66:225-229.
 205. Walsh EP, Saul JP, Sholler GF, et al. Evaluation of a staged treatment protocol for rapid automatic junctional tachycardia after operation for congenital heart disease. *J Am Coll Cardiol* 1997;29:1046-1053.
 206. Perry JC, Fenrich AL, Hulse JE, et al. Pediatric use of intravenous amiodarone: efficacy and safety in critically ill patients from a multicenter protocol. *J Am Coll Cardiol* 1996;27:1246-1250.
 207. Figa FH, Gow RM, Hamilton RM, et al. Clinical efficacy and safety of intravenous Amiodarone in infants and children. *Am J Cardiol* 1994;74:573-577.

208. Balaji S, Gillette PC, Case CL. Successful radiofrequency ablation of permanent junctional reciprocating tachycardia in an 18-month-old child. *Am Heart J* 1994;127:1420-1421.
209. Ehler FA, Goldberger JJ, Deal BJ, et al. Successful radiofrequency energy ablation of automatic junctional tachycardia preserving normal atrioventricular nodal conduction. *Pacing Clinic Electrophysiology* 1993;16:54-61.
210. Rychik J, Marchlinski FE, Sweeten TL, et al. Transcatheter radiofrequency ablation for congenital junctional ectopic tachycardia in infancy. *Pediatr Cardiol* 1997;18:447-450.
211. Van Hare GF, Velvis H, Langberg JJ. Successful transcatheter ablation of congenital junctional ectopic tachycardia in a ten-month-old infant using radiofrequency energy. *PACE* 1990;13:730-735.
212. Young ML, Mehta MB, Martinez RM, et al. Combined alpha-adrenergic blockade and radiofrequency ablation to treat junctional ectopic tachycardia successfully without atrioventricular block. *Am J Cardiol* 1993;71:883-885.
213. Fishberger SB, Rossi AF, Messina JJ, et al. Successful radiofrequency catheter ablation of congenital junctional ectopic tachycardia with preservation of atrioventricular conduction in a 9-month-old infant. *Pacing Clinic Electrophysiol* 1998;21:2132-2135.
214. Collins KK, Van Hare GF, Kertesz NJ, et al. Pediatric nonpost-operative junctional ectopic tachycardia medical management and interventional therapies. *J Am Coll Cardiol* 2009;53:690-697.
215. Morady F, Kadish AH, DiCarlo L, et al. Long-term results of catheter ablation of idiopathic right ventricular tachycardia. *Circulation* 1990;82:2093-2099.
216. Paul T, Blaufox AT, Saul JP. Non-contact mapping and ablation of tachycardia originating in the right ventricular outflow tract. *Cardiol Young* 2002;12:294-297.
217. Gonzalez MB, Will JC, Tuzcu V, et al. Idiopathic monomorphic ventricular tachycardia originating from the left aortic sinus cusp in children: endocardial mapping and radiofrequency catheter ablation. [erratum appears in *Z Kardiol* 2003;92:970 Note: Tuzcu V [corrected to Tuzcu V]]. *Zeitschrift für Kardiologie* 2003;92:155-163.
218. Laohakunakorn P, Paul T, Knick B, et al. Ventricular tachycardia in non-postoperative pediatric patients: role of radiofrequency catheter ablation. *Pediatr Cardiol* 2003;24:154-160.
219. Langberg JJ, Desai J, Duller N, et al. Treatment of macroreentrant ventricular tachycardia with radiofrequency ablation of the right bundle branch. *Am J Cardiol* 1989;63:1010.
220. Stevenson WG, Khan H, Sager P, et al. Identification of reentry circuit sites during catheter mapping and radiofrequency ablation of ventricular tachycardia late after myocardial infarction. *Circulation* 1993;88:1647-1670.
221. Biblo LA, Carlson MD. Transcatheter radiofrequency ablation of ventricular tachycardia following surgical correction of tetralogy of Fallot. *Pacing Clinic Electrophysiol* 1994;17:1556-1560.
222. Burton ME, Leon AR. Radiofrequency catheter ablation of right ventricular outflow tract tachycardia late after complete repair of tetralogy of Fallot using the pace mapping technique. *Pacing Clinic Electrophysiol* 1993;16:2319-2325.
223. Chinushi M, Aizawa Y, Kitazawa H, et al. Successful radiofrequency catheter ablation for macroreentrant ventricular tachycardias in a patient with tetralogy of Fallot after corrective surgery. *Pacing Clinic Electrophysiol* 1995;18:1713-1716.
224. Goldner BG, Cooper R, Blau W, et al. Radiofrequency catheter ablation as a primary therapy for treatment of ventricular tachycardia in a patient after repair of tetralogy of Fallot. *Pacing Clinic Electrophysiol* 1994;17:1441-1446.
225. Moak JP. Radiofrequency ablation of arrhythmias in the pediatric patient. [Review] [47 refs]. *Curr Opin Cardiol* 1996;11:81-92.
226. Mantakas ME, McCue CM, Miller WW. Natural history of Wolff-Parkinson-White syndrome in infants and children: a review and a report of 28 cases. *Am J Cardiol* 1978;41:1097-1103.
227. Kugler JD. Radiofrequency catheter ablation for supraventricular tachycardia. Should it be used in infants and small children? [editorial; comment]. *Circulation* 1994;90:639-641.
228. Case CL, Gillette PC, Oslizlok PC, et al. Radiofrequency catheter ablation of incessant, medically resistant supraventricular tachycardia in infants and small children. *J Am Coll Cardiol* 1992;20:1405-1410.
229. Case CL, Gillette PC. Indications for catheter ablation in infants and small children with reentrant supraventricular tachycardia [letter]. *J Am Coll Cardiol* 1996;27:1551-1552.
230. Zak R. Development and proliferative capacity of cardiac muscle cells. *Circ Res* 1974;35:17-26.
231. Denfield SW, Kearney DL, Michael L, et al. Developmental differences in canine cardiac surgical scars. *Am Heart J* 1993;126:382-389.
232. Hope EJ, Haigney MC, Calkins H, et al. Left main coronary thrombosis after radiofrequency ablation: successful treatment with percutaneous transluminal angioplasty. *Am Heart J* 1995;129:1217-1219.
233. Erickson CC, Carr D, Greer GS, et al. Emergent radiofrequency ablation of the AV node in a neonate with unstable, refractory supraventricular tachycardia. *Pacing Clinic Electrophysiol* 1995;18:1959-1962.
234. Finelli A, Rewcastle JC, Jewett MA. Cryotherapy and radiofrequency ablation: pathophysiologic basis and laboratory studies. [Review] [48 refs]. *Curr Opin Urol* 2003;13:187-191.
235. Haines DE. The biophysics of radiofrequency catheter ablation in the heart: the importance of temperature monitoring. *PACE* 1993;16:586-591.
236. Haines DE, Watson DD, Verow AF. Electrode radius predicts lesion radius during radiofrequency energy heating. Validation of a proposed thermodynamic model. *Circ Res* 1990;67:124-129.
237. Chu E, Fitzpatrick AP, Chin MC, et al. Radiofrequency catheter ablation guided by intracardiac echocardiography. *Circulation* 1994;89:1301-1305.
238. Schiebeler GL, Adams P Jr, Anderson RC. The Wolff-Parkinson-White syndrome in infants and children: a review and a report of 28 cases. *Pediatrics* 1959;24:585-603.
239. Schiebeler GL, Adams P Jr, Anderson RC, et al. Clinical study of twenty-three cases of Ebstein's anomaly of the tricuspid valve. *Circulation* 1959;19:187.
240. Anderson RH, Becker AE, Arnold R, et al. The conducting tissues in congenitally corrected transposition. *Circulation* 1974;50:911-923.
241. Symons JC, Shinebourne EA, Joseph MC, et al. Criss-cross heart with congenitally corrected transposition: report of a case with d-transposed aorta and ventricular preexcitation. *Eur J Cardiol* 1977;5:493.
242. Van Mierop LHS, Kutsche LM, Victoria BF. Ebstein's anomaly. In: Adams FH, Emmanouilides GC, Riemenschneider TA, eds. *Heart Disease in Infants, Children and Adolescents*. Baltimore, MD: Williams & Wilkins, 1989:361-363.
243. Lev M, Gibson S, Miller RA. Ebstein's disease with Wolff-Parkinson-White syndrome: report of a case with a histopathologic study of possible conduction pathways. *Am J Cardiol* 1955;49:724-741.
244. Levine JC, Walsh EP, Saul JP. Radiofrequency ablation of accessory pathways associated with congenital heart disease including heterotaxy syndrome. *Am J Cardiol* 1993;72:689-693.
245. Van Hare GF, Lesh MD, Stanger P. Radiofrequency catheter ablation of supraventricular arrhythmias in patients with congenital heart disease: results and technical considerations. *J Am Coll Cardiol* 1993;22:883-890.
246. Kuck KH, Schluter M, Geiger M, et al. Radiofrequency current catheter ablation of accessory atrioventricular pathways. *Lancet* 1991;337:1557-1561.
247. Smith WM, Gallagher JJ, Kerr CR, et al. The electrophysiologic basis and management of symptomatic recurrent tachycardia in patients with Ebstein's anomaly of the tricuspid valve. *Am J Cardiol* 1982;49:1223-1234.
248. Lesh MD, Van Hare GF, Schamp DJ, et al. Curative percutaneous catheter ablation using radiofrequency energy for accessory pathways in all locations: results in 100 consecutive patients. *J Am Coll Cardiol* 1992;19:1303-1309.
249. Twidale N, Wang X, Beckman KJ, et al. Factors associated with recurrence of accessory pathway conduction after radiofrequency catheter ablation. *PACE* 1991;14:2042-2048.
250. Gallagher JJ, Pritchett ELC, Sealy WC, et al. The preexcitation syndromes. *Prog Cardiovasc Dis* 1978;20:285-327.
251. Cox JL, Gallagher JJ, Cain ME. Experience with 118 consecutive patients undergoing operation for the Wolff-Parkinson-White syndrome. *J Thorac Cardiovasc Surg* 1985;90:490-501.
252. Gillette PC, Garson A Jr, Kugler JD, et al. Surgical treatment of supraventricular tachycardia in infants and children. *Am J Cardiol* 1980;46:281-284.
253. Ott DA, Gillette PC, Garson A Jr, et al. Surgical management of refractory supraventricular tachycardia in infants and children. *J Am Coll Cardiol* 1985;5:124-129.
254. Weston LT, Hull RW, Laird JR. A prototype coronary electrode catheter for intracoronary electrogram recording. *Am J Cardiol* 1992;70:1492-1493.
255. Ho SY, Anderson RH. Embryology and anatomy of the normal and abnormal conduction system. In: Gillette PC, Garson A Jr, eds. *Pediatric Arrhythmias: Electrophysiology and Pacing*. Philadelphia, PA: Saunders, 1990:2-27.
256. Wenink ACG. Congenitally complete heart block with an interrupted Monckeberg sling. *Eur J Cardiol* 1979;9:89-99.
257. Bharati S, Rosen K, Steinfield L, et al. The anatomic substrate for preexcitation in corrected transposition. *Circulation* 1980;62:831-842.
258. Epstein MR, Saul JP, Weindling SN, et al. Atrioventricular reciprocating tachycardia involving twin atrioventricular nodes in patients with complex congenital heart disease. *J Cardiovasc Electrophysiol* 2001;12:671-679.
259. Walsh EP, Saul JP, Triedman JK, et al. Ablation of the "second conducting system": mahaim fibers and "double AV nodes" in congenital heart disease. *Circulation* 1994;90:1-100.
260. Anderson RH, Arnold R, Wilkinson JL. The conducting system in congenitally corrected transposition. *Lancet* 1973;1:1286-1288.

Disorders of Cardiac Rhythm and Conduction

Bryan C. Cannon ■ Christopher S. Snyder

Arrhythmias are common in the general pediatric population and frequently are an important clinical problem in patients with structural congenital heart disease. Arrhythmias have a broad spectrum of clinical presentations, ranging from no symptoms to sudden death. There is a wide variety of causes of arrhythmias and an even broader range of treatments. On the most basic level, arrhythmias can be divided into bradyarrhythmias and tachyarrhythmias.

SINUS NODE

The sinoatrial node is an extensive, subepicardial structure located on the crista terminalis of the right atrium between the inferior and superior vena cavae (1). The blood supply to the sinus node has three major variants, with the right coronary artery supplying it 60% of the time, left circumflex coronary artery 36%, and the remainder by both coronary arteries (2). The main function of the sinus node is electrical; therefore, it is dependent on ion channels. These cells have unique properties and exhibit a slow, spontaneous phase 4 depolarization known as the pacemaker potential that is affected by circulating catecholamines (3). The sinus node also has a very strong sympathetic and parasympathetic innervation through cardiac ganglionic plexi that directly affect the rate of depolarization. Increased sympathetic tone increases depolarization, while increased parasympathetic tone reduces depolarization. Disorders in any of these areas can result in abnormal sinus function resulting in bradyarrhythmias or tachyarrhythmias.

ANATOMY OF THE ATRIOVENTRICULAR NODE

The atrioventricular (AV) node is the electrical structure that connects the atrium to the ventricles. It is a complex structure made up of different structures that are based on variable cellular morphology and function. It generally is located at the base of the interatrial septum within the triangle of Koch. As with the sinus node, it has a very rich autonomic innervation with both sympathetic and parasympathetic neurons (4). Its main function is to allow delayed impulse transmission from the atrium to the ventricle. This delay ensures that the atria have a chance to contract before the ventricles are stimulated. When the sinus node fails, the AV node has automaticity and can function as an escape pacemaker.

The AV junction consists of transitional cells, specialized nodal cells (AV node), and the penetrating AV bundle (bundle of His) (Fig 18.1). The first part of the AV node is the transitional cells. These cells tend to be laid into tracts (i.e., the fast and slow pathways) that lead directly from the atrial myocardium into AV node proper (5). As the cells exit the compact

bundle, they begin to organize into larger individual bundles separated by fibrous tissue. As the lower cells progress even more distally, they form the penetrating AV bundle. The penetrating bundle is engulfed by the central fibrous body (CFB) and also is referred to as the bundle of His. Conduction exits the bundle of His into the ventricles via the left and right bundle branch and the Purkinje fibers. Abnormalities affecting this complex series of fibers at any level can result in AV block or tachyarrhythmias.

TACHYCARDIA

An abnormal mechanism of tachycardia, or tachyarrhythmia, results from an area other than the sinus node elevating the heart rate above the sinus rate or alternatively from an intrinsically abnormal sinus node. Tachyarrhythmias arise as a result of abnormal impulse initiation or conduction and may be classified in several different ways. One way to classify tachyarrhythmias is based on their mechanism of initiation and propagation. There are three basic mechanisms by which tachyarrhythmias start: reentry, abnormal automaticity, and triggered activity. It is important to understand these mechanisms because the clinical presentation and features of the tachycardia depend on their underlying mechanism.

Reentry is the most common form of tachyarrhythmia and is responsible for most supraventricular and many ventricular tachycardias (VTs). For reentry to occur, two distinct conducting pathways must be linked around an area of nonconducting tissue. One limb of the circuit must display slow conduction while the other limb has a long refractory period (Fig. 18.2). This type of arrhythmia can be terminated if one or both limbs of the tachycardia are disrupted. They usually have a rapid onset and offset (usually in a single beat) and may present with rates above 300 beats per minute. Examples of reentrant tachycardias are AV node reentry tachycardia, accessory pathway-mediated tachycardia, and atrial flutter.

Automaticity is the ability of a cell to depolarize spontaneously. With abnormal automaticity, there is either abnormally fast activation of cells that exhibit automatic function or development of spontaneous depolarization in cells that typically do not possess automaticity. Abnormal automaticity often has a metabolic cause (electrolyte disturbances, thyrotoxicosis, hypoxia, ischemia, fever, etc.). It can occur in otherwise normal children but also frequently is seen in acutely ill children and often exacerbated by intravenous sympathomimetics. The arrhythmias caused by abnormal automaticity show behavior similar to sinus rhythm in that they speed up and slow down according to metabolic changes and are generally refractory to direct current cardioversion. Examples of enhanced automaticity include atrial ectopic tachycardia (AET), junctional ectopic tachycardia (JET), and some forms of VT.

Figure 18.1. AV node anatomy. This diagram illustrates the location of the AV node within the triangle of Koch. One can follow the propagation of a sinus beat down the fast and slow pathways, through the compact AV node, located within the CFB, to its exit into the His bundle. CS, coronary sinus; IAS, intra-atrial septum; FO, foramen ovale; IVC, inferior vena cava; TrV, tricuspid valve; CFB, central fibrous body.

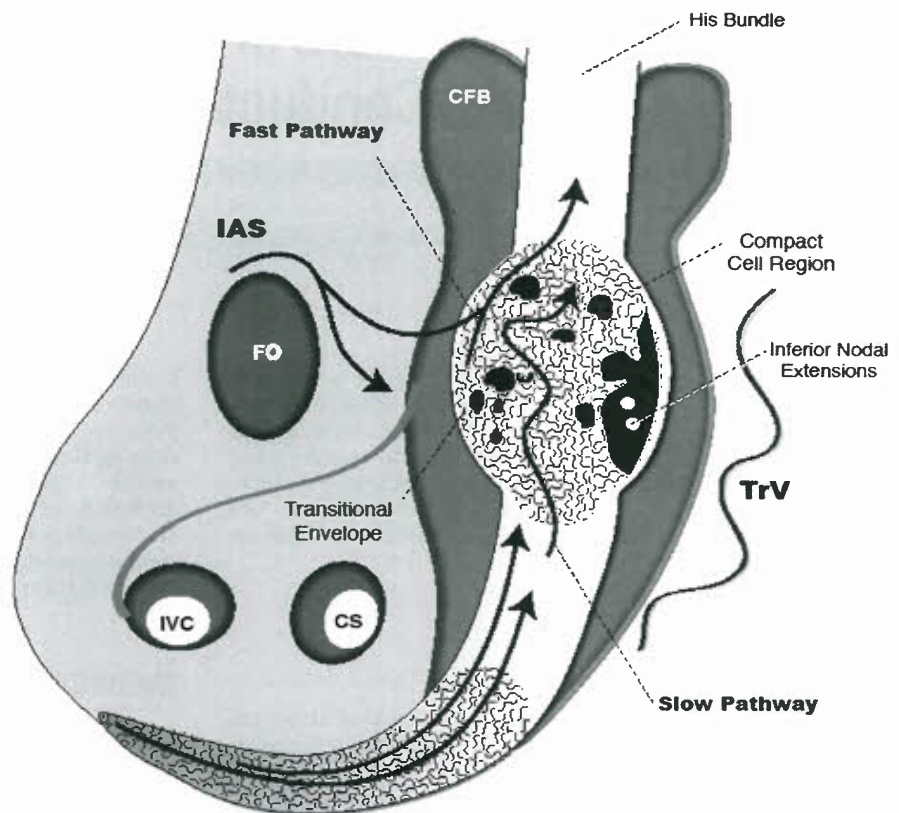


Figure 18.2. Mechanism of reentry.

A: Reentry involves two interconnected limbs of tissue that conduct electrical impulses with an area between the two with no electrical conduction. One limb has fast conduction with a long refractory period. The other limb has slower conduction but a shorter refractory period. **B:** If a premature impulse occurs, it may block in the rapidly conducting limb and conduct down the slow limb only. **C:** When the impulse reaches the connection between the two limbs, the faster conducting limb is no longer refractory and able to conduct a retrograde impulse. **D:** This retrograde impulse then activates the slowly conducting tissue setting up the reentrant circuit.

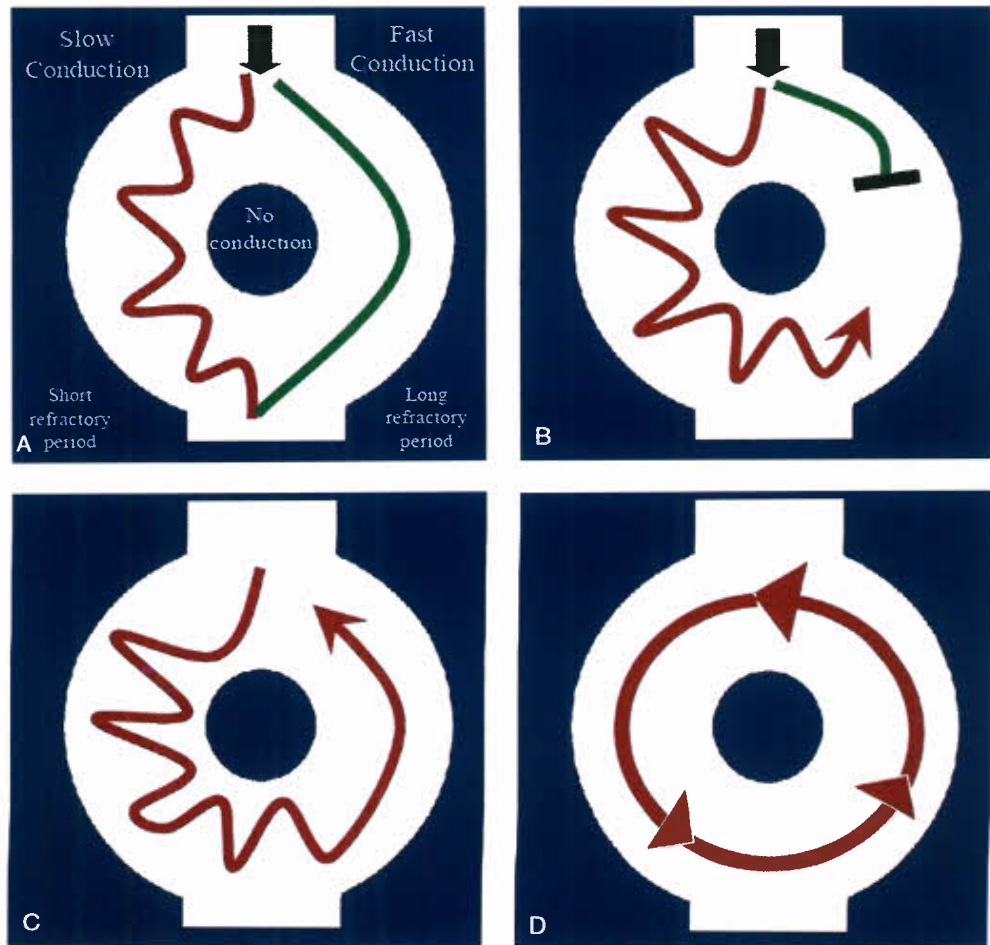


TABLE 18.1

Approximate Normal Resting Heart Rates in the Pediatric Population by Age

Age	Resting Heart Rate (bpm)
Birth-1 wk	90–160
1 wk–1 yr	100–170
1–2 y	80–150
3–7 y	70–135
7–10 y	65–130
11–15 y	60–120

The third and most rare mechanism of arrhythmogenesis is triggered activity, which has features of both automaticity and reentry. This is the result of an after-depolarization, which is an abrupt change in the membrane potential during the action potential (early after-depolarization) or following full repolarization (delayed after-depolarization). This may serve as a stimulus for an ensuing action potential, leading to a sustained arrhythmia. These after-depolarizations are a feature of many drug-induced arrhythmias (such as digitalis toxicity), and triggered activity is associated with the initiation of ventricular arrhythmias in long QT syndrome (6).

Clinical Presentation

Normal heart rates in pediatric patients are age dependent (Table 18.1). One must realize that these are normal *resting* heart rates. The challenge is actually obtaining an accurate resting heart rate. Palpation of a child's pulse or obtaining an ECG can lead to fear and/or anxiety, thereby increasing heart rate through significant sympathetic input. The maximum sinus heart rate that one can achieve is typically 220 beats per minute minus the patient's age. Although heart rates above 220 beats per minute rarely can be sinus in origin, heart rates in this range should warrant evaluation for an abnormal mechanism of tachycardia. Initiation and termination of tachycardia with a single beat also should raise suspicion for an abnormal mechanism of tachycardia. Syncope is a relatively uncommon presentation of tachycardia in the absence of other symptoms suggesting an arrhythmia or underlying channelopathy.

Evaluation

The most important aspect for diagnosis of tachyarrhythmias is the electrocardiogram (ECG). Documentation of the electrocardiographic rhythm during times of symptoms or tachycardia is the cornerstone for differentiation between sinus tachycardia and abnormal mechanisms of tachycardia. Ideally, this is performed as a 12-lead rhythm strip but may be done in any manner capable of recording and documenting the ECG. As arrhythmias may stop suddenly without warning, immediate documentation should be one of the first steps in managing a patient with a tachyarrhythmia following assessment for hemodynamic stability. The most helpful ECG for a specific diagnosis of a tachyarrhythmia is during times of "wobble": when a tachycardia, starts, stops, or changes. Therefore, a continuous ECG strip should be performed *during* the time of any intervention to terminate tachycardia, not just before and after.

At times, it can be difficult to diagnose the exact nature of a tachycardia based on an ECG or rhythm strip alone. In these cases, it may be necessary to use other diagnostic tools to characterize the tachycardia. Vagal maneuvers such as Valsalva or the dive reflex may be used to alter the tachycardia or in some instances terminate it. The dive reflex is initiated by placing a bag of ice over the entire face (including the nose and mouth) for a period of 10 to 15 seconds or submersing the entire face in an ice water mixture. Although this is a strong vagal stimulus, it may be alarming to parents, and care should be taken in small patients to avoid superficial damage to the skin from the ice. Other vagal maneuvers such as ocular stimulation, carotid massage, gagging, and rectal stimulation are best avoided in the pediatric setting.

Postoperatively, atrial temporary pacing wires can be used to obtain a pure atrial signal when it is difficult to determine the relationship of the P wave to the QRS during tachycardia. The two atrial pacing wires are connected to the white (right arm) and black (left arm) leads. This gives a distinct deflection representing atrial activity in lead I (see Fig. 18.3). Alternatively, a soft electrophysiology (EP) catheter (either a small transvenous catheter or a specialized catheter made for transesophageal pacing and recording) can be placed in the esophagus and connected to the ECG machine in a similar manner to obtain a recording of the left atrial signal.

A thorough history is also very important. Unfortunately, palpitations are a common complaint in children, especially among teenagers. Differentiation between tachyarrhythmias and sinus tachycardia due to other causes can be challenging. The onset and termination of tachycardia are important historic features. The onset of tachycardia frequently is described as sudden in both sinus tachycardia as well as tachyarrhythmias. The termination of tachycardia typically is gradual in sinus tachycardia. In a tachyarrhythmia, the termination may occur in a single beat. Dizziness can occur with both tachyarrhythmias and sinus tachycardia. If palpitations *precede* dizziness, this is more consistent with a tachyarrhythmia. If dizziness is the first symptom, a tachyarrhythmia is unlikely

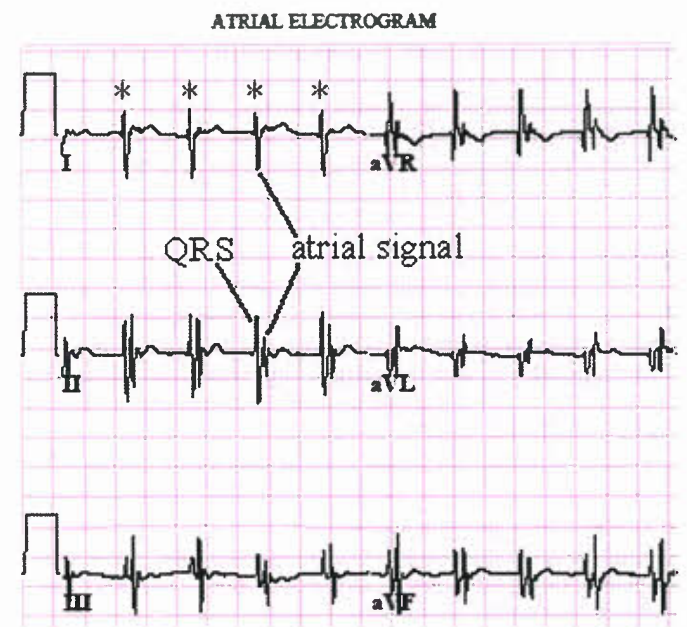


Figure 18.3. ECG tracing obtained using atrial temporary pacing wires. The two atrial pacing wires are connected to the right arm (*white*) and left arm (*black*) leads giving a pure atrial signal in lead I (marked by *asterisk*). Using this tracing, it is possible to delineate the atrial signal from the QRS complex

to be the source of symptoms. Quantification of the heart rate also can be challenging to obtain from a history because it is infrequent that an actual pulse is taken during an episode. Asking the child or parent to tap with his or her hand to approximate the symptoms may be a beneficial tool to estimate heart rate. Heart rates that are faster than one is able to count should prompt evaluation for a tachyarrhythmia.

Many tachyarrhythmias only occur with exercise as the increased catecholamine state may enhance conduction in the AV node, making reentrant tachycardias more likely or enhancing automaticity. In these particular circumstances, performing an exercise treadmill test may be indicated to elicit an abnormal tachycardia. Several different protocols can be used depending on the particular type of exercise that causes the tachycardia. The typical continuous escalating protocol (Bruce protocol) may be used or modified to replicate the type of activity that triggers the tachyarrhythmia.

As many patients who have tachyarrhythmias have a normal resting ECG when not in tachycardia, a 24-hour cardioscan or Holter monitor that records all ECG activity continuously for a 24-hour period rarely is helpful in diagnosing tachyarrhythmias unless symptoms happen daily. The monitor may be worn for 48 hours or even longer, but once again it is only helpful if symptoms occur while the monitor is being worn.

If symptoms happen only occasionally, one of two types of event monitors may be prescribed. The first is a small recording device containing electrodes that has the capability of recording an ECG only when activated. When a patient feels symptoms, he or she places the device on the chest and activates it, which then creates a recording of the rhythm at that time. The recordings then can be transmitted electronically to obtain an ECG during the symptoms. A second type of event monitor is a looping recorder. This device is connected by ECG monitoring electrodes to the patient and continuously records the rhythm. When the recording switch is activated, it has the capability to go back and record ECG tracings several minutes prior to the activation as well as following the activation. It also can be programmed to automatically record the rhythm if the heart rate exceeds or drops below a certain set rate. The external loop recorder may have issues with compliance because the ECG electrodes often are irritating to the skin and must be changed on a regular basis. A different type of loop recorder actually may be implanted under the skin to continuously record the cardiac rhythm, thus avoiding the problem of constantly having ECG leads attached. It functions similar to an external loop recorder. The loop recorder can then be downloaded to obtain the rhythm tracings. This can be done with the same programmer used to interrogate a pacemaker or can be done via a unit placed in the patient's home. An implantable loop recorder can be useful in pediatric patients for determining the presence or absence of an arrhythmia during symptoms of syncope, near syncope, and palpitations when conventional diagnostic testing such as ECG, Holter monitoring, and/or external loop recording is inconclusive (7). The drawback is the necessity for a minor surgery to implant the device with the need to remove the monitor when it is no longer needed or when the battery life ends (typically around 3 years after implantation). Fortunately, implantable loop recorders are rarely indicated in pediatric patients and should be reserved for cases when it is critical to document the presence and/or characteristics of an arrhythmia. After documentation of the tachycardia, it is then possible to characterize further the arrhythmia and plan a strategy for therapy.

Characterization of Tachycardias

One method for categorizing tachyarrhythmias is to examine the width of the QRS complex and divide the tachyarrhythmias

into narrow complex and wide complex. In making this distinction, one must take into account the duration of the QRS, which depends on the patient's age and history of cardiovascular surgery. In general, neonates have shorter QRS durations than other age groups. In a child <1 year old, a QRS duration of more than 80 milliseconds (two boxes on a standard ECG) should be considered wide. It is always important to measure the QRS duration as a QRS duration of 100 milliseconds may look narrow to the naked eye on an electronic monitor tracing present at the bedside. In general, narrow complex tachycardia originates from an area above the ventricles. The differential diagnosis of wide complex tachycardia, including VT, is discussed later in this chapter.

Sinus Arrhythmia

Although named as an arrhythmia, this phenomenon is related to increasing amounts of vagal tone and is entirely normal. In sinus arrhythmia, the P wave axis remains normal, but the heart rate increases with inspiration and decreases with expiration. It may be more prominent in younger patients with faster heart rates and is present at some point during 24-hour monitoring in almost all children (8). This variation in rate rarely exceeds 100% (e.g., from a rate of 60 to 120 beats per minute); if it does, it may signify an abnormality.

Narrow Complex Tachycardias

Supraventricular tachycardia (SVT) is the most common sustained arrhythmia in children, with an estimated incidence from 1 in 25,000 to as high as 1 in 250 children (9). The most common age at presentation in childhood is within the first 2 months of life (10).

SVT is defined as an abnormally rapid rhythm that originates proximal to the bifurcation of the bundle of His, is caused by an abnormal mechanism (specifically excluding sinus tachycardia), and does not have flutter waves on the surface ECG. Although most patients with SVT have a structurally normal heart, 20% of patients have structural heart disease (11).

One method for subdividing narrow complex tachycardias is to examine the relationship between the QRS complex and the P wave on the ECG. To do this, a line is drawn halfway between two successive QRS complexes. If the P wave is buried in the QRS complex or is visualized prior to the line between the two consecutive QRS complexes, the tachycardia is considered to be a short RP tachycardia. If the P wave is visualized after this line, it is considered to be a long RP tachycardia. The description of specific types of long RP versus short RP tachycardias is listed in Table 18.2.

Accessory Pathway–Mediated Tachycardia

In the normal heart, the atria and ventricles are isolated electrically from each other by the fibrous annulus of the tricuspid and mitral valves. The only way for electrical impulses to pass from the atria to the ventricles is through the AV node, which penetrates through the central fibrous body to conduct electrical impulses. An accessory pathway is an additional electrical conduction pathway from the atria to the ventricles. This pathway results from a defect in the fibrous annulus as the embryonic atria and ventricles become electrically isolated. This process occurs in all fetuses during cardiac development but regresses in most cases. Persistence of one of these connections creates an accessory pathway. Accessory pathways are derived from either normal ventricular myocardium or specialized conduction tissue. Accessory pathways can conduct antegrade only (Mahaim fibers), both antegrade and

TABLE 18.2 Characteristics of Narrow Complex Tachycardia

SVT Type	Incessant/ Paroxysmal	P Wave Axis	RP Relationship	Adenosine Response	Reentrant or Automatic
AVN (typical)	P	LSRA	Short	Terminate	Reentrant
AVN (atypical)	I	LSRA	Long	Terminate	Reentrant
WPW	P/I	Not HRA	Short	Terminate	Reentrant
URAP	P/I	Not HRA	Short	Terminate	Reentrant
PJRT	I	LSRA	Long	Terminate	Reentrant
Mahaim	P	LSRA	Short	Terminate	Reentrant/auto
AET	P/I	Not HRA	Long (may Wenckebach)	None or term	Automatic
NFAT	P	Not HRA	Long (may Wenckebach)	Terminate	Reentrant
JET	I	HRA	AV dissociated	None or slow	Automatic
Atrial Flutter	P/I	Not HRA	Long (may Wenckebach)	AV block	Reentrant

AVNRT, AV node reentry tachycardia; WPW, Wolff-Parkinson-White; URAP, unidirectional retrograde accessory pathway; PJRT, permanent form of junctional reciprocating tachycardia; AET, atrial ectopic tachycardia; NFAT, nonautomatic focal atrial tachycardia; JET, junctional ectopic tachycardia; HRA, high right atrium; LSRA, low septal right atrium.

retrograde (Wolff-Parkinson-White [WPW]), or retrograde only (unidirectional retrograde accessory pathway [URAP]).

There are two different mechanisms by which accessory pathways can cause SVT. In an *orthodromic* tachycardia, the conduction is antegrade through the AV node to the ventricle and then retrograde through the accessory pathway to the atrium (see Fig. 18.4A). This is the usual form of accessory

pathway-mediated tachycardia and results in a rapid rate with a narrow QRS complex. The other mechanism is termed *antidromic* tachycardia (see Fig. 18.4B). In this form of tachycardia, conduction is antegrade through the accessory pathway to the ventricle then retrograde through the AV node to the atrium and can only occur in accessory pathways with antegrade conduction. Because the activation of the ventricle is

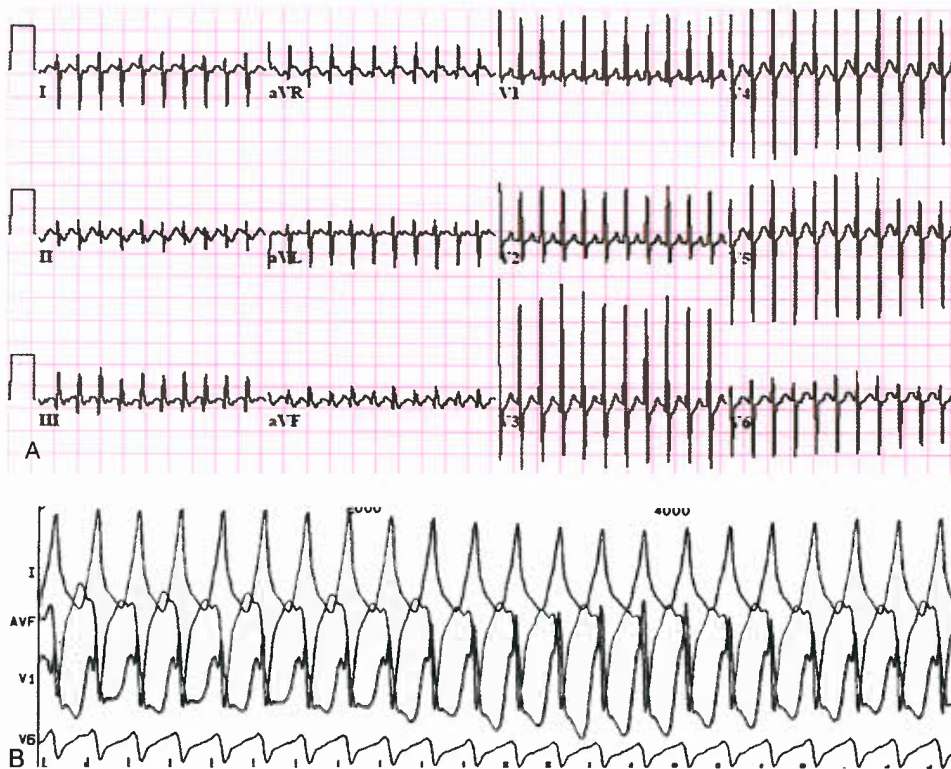


Figure 18.4. A: Orthodromic SVT using an accessory pathway. The rate is around 320 beats per minute and the QRS morphology is narrow as the antegrade activation is through the AV node and the retrograde activation is through the accessory pathway. B: Antidromic SVT induced during an EP study. The QRS morphology is wide and has the same activation pattern as the manifest preexcitation on the ECG in sinus rhythm as the antegrade limb is through the accessory pathway.

through the accessory pathway and not the AV node, this type of tachycardia is always a wide complex tachycardia. The activation of the ventricle will have the same pattern as the pattern of preexcitation seen on the surface ECG in sinus rhythm. Of note, in both types of tachycardia all four components (ventricle, accessory pathway, atrium, and AV node) are critical for maintaining the reentrant tachycardia circuit, and the tachycardia may be terminated in any one of these four limbs.

Wolff-Parkinson-White

In 1930, Drs Wolff, Parkinson, and White described an ECG syndrome consisting of a functional bundle branch block and a short PR interval in healthy people with paroxysms of tachycardia (12). This syndrome now bears their names. WPW syndrome or ventricular preexcitation involves the combination of three findings: a PR interval shorter than normal for the patient's age, a slurred upstroke of the QRS complex (i.e., a delta wave), and a QRS complex of longer duration than normal for age (see Fig. 18.5). There also frequently are changes in the ST or T waves. These findings may not be found in all leads, and the midprecordial leads (V2–V4) may be the most sensitive. Other clues to the presence of WPW are left axis deviation, the absence of Q waves in lead V6, abnormally wide Q waves in the limb leads (a pseudoinfarction pattern), junctional escape beat seen with a different QRS morphology, and accentuation or loss of preexcitation with a premature atrial contraction (PAC). The EP definition of preexcitation, or WPW, is a His to ventricle (HV) interval of <35 milliseconds.

Its incidence is 0.1% to 0.3% among the general population and is more prevalent in men than women (13–15). However, the true incidence of WPW may be much higher because many patients are asymptomatic. Although asymptomatic patients do not technically meet the definition for WPW “syndrome” (because they do not have tachycardia), these patients are still labeled as having WPW, although a more correct description would be ventricular preexcitation.

WPW has a known association with congenital heart disease, ranging from 9% to 32% of patients, so an echocardiogram generally is indicated (10,16–18). The structural cardiac diseases known to be associated with WPW include Ebstein anomaly of the tricuspid valve, corrected transposition of the great arteries, and hypertrophic cardiomyopathy; noncardiac associations include glycogen storage disease and tuberous

sclerosis. The majority of WPW cases tend to be sporadic in nature, but in a small minority of these patients (3%), there is an identifiable affected first-degree relative, and familial cases have been reported (7p3 chromosomal association) (19). In addition, approximately 9% of WPW patients have more than one accessory pathway (20). The incidence of multiple pathways may be as high as 20% of patients who have underlying congenital heart disease (21).

WPW may participate in arrhythmic substrates in two different ways. The first is as one of the limbs in a reentrant SVT. The second is conduction to the ventricle during atrial fibrillation. Many patients will present with symptomatic SVT, but some will have WPW discovered on an ECG done for other reasons. However, a significant percentage of incidentally discovered patients with WPW will develop an arrhythmia—15% after a mean follow-up of 37.7 months in a large Italian study (22). In higher-risk groups (patients with rapidly conducting accessory pathways or multiple pathways), this figure may be as high as 44% (23). In a large study of military personnel followed over 20 years, 23% with constant preexcitation developed reentrant SVT compared to 8.3% who only exhibited intermittent preexcitation (24).

Episodes of SVT decrease in frequency over the first year of life in >90% of patients. However, tachycardia recurs in approximately 30% of them at an average age of 7 to 8 years (18). Furthermore, there is evidence that in the first year of life the accessory pathway loses anterograde conduction in as many as 40% of patients and SVT becomes noninducible in a similar percentage, suggesting loss of retrograde conduction as well (25). However, if a WPW pattern persists on ECG, there is up to a 29-fold increased chance of SVT recurrence, requiring additional antiarrhythmic therapy to control SVT (26). If SVT presents after an age of 1 year, >90% of patients will have a recurrence (27).

Patients with WPW rarely present with symptoms of heart failure from the hemodynamic effects of preexcitation alone. This is presumed to be because of dyssynchronous ventricular contraction associated with an extremely preexcited rhythm (28). In addition, there is an improvement in ejection fraction after ablation of septal accessory pathways in pediatric patients (29) as well as rapid normalization of ventricular function and reverse left ventricular remodeling after elimination of ventricular preexcitation in adult patients (30).

Patients with WPW are at risk of developing atrial fibrillation. There are two likely mechanisms of paroxysmal atrial

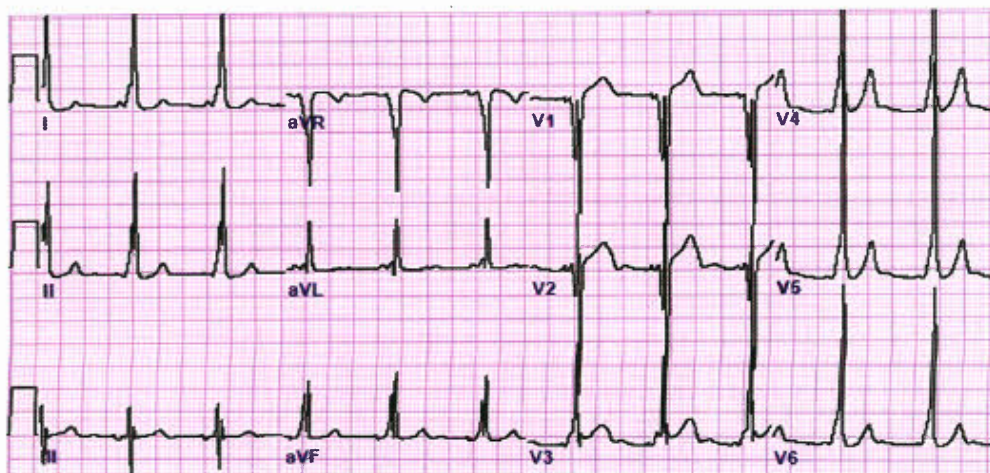


Figure 18.5. WPW with a shortened PR interval, widened QRS, and slurring of the upstroke of the QRS (Delta wave). Note the deep, wide Q wave in lead aVR (pseudoinfarction pattern) and the unusual appearance of the ST segments due to the preexcitation.

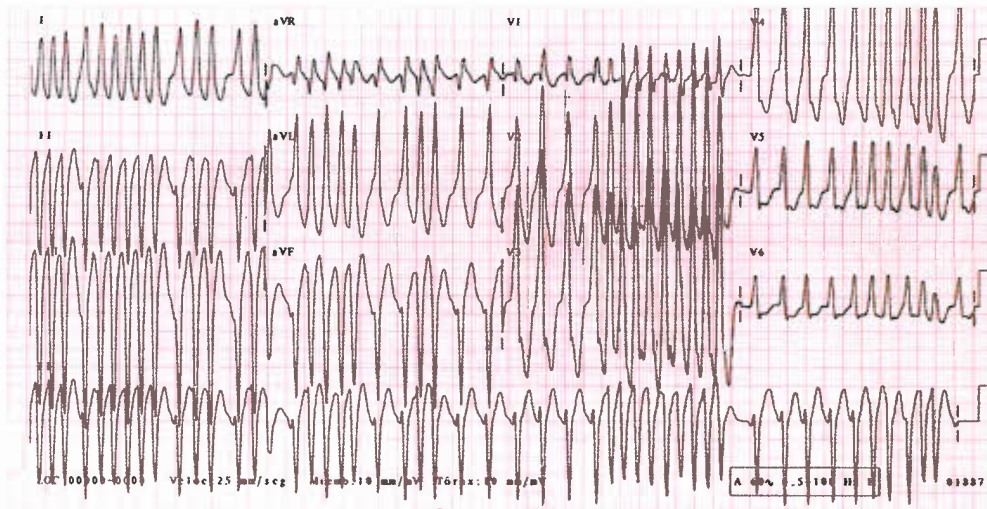


Figure 18.6. Atrial fibrillation in a patient with WPW. This creates an irregularly irregular wide complex tachycardia characteristic of this arrhythmia.

fibrillation in patients with WPW syndrome: one mechanism is reversible and directly related to the accessory pathway, while the other is intrinsic and accessory pathway-independent atrial vulnerability (31). Just as patients with multiple accessory pathways may be at a higher risk of SVT, they are also at a higher risk of atrial fibrillation (32). Atrial fibrillation as a presenting symptom occurs rarely, with an incidence of 6% in one study (33). Atrial fibrillation in WPW presents as a characteristic irregular wide complex tachycardia (see Fig. 18.6). This feature separates this arrhythmia from most VTs, which have a relatively constant cycle length. Rapid conduction through the accessory pathway may lead to VT or fibrillation with resultant hemodynamic collapse (34). Adenosine, digoxin, and calcium channel blockers typically are contraindicated in WPW patients in atrial fibrillation because they promote conduction through the accessory pathway rather than the AV node, precipitating ventricular arrhythmias. Direct current cardioversion is the preferred therapy, especially in the presence of rapid conduction down the accessory pathway.

The incidence of both malignant WPW syndrome resulting in cardiac arrest and WPW causing SVT is higher in patients with syncope than in patients who are otherwise asymptomatic (35). Therefore, syncope in a patient with WPW should prompt rapid referral for further diagnostic testing.

Risk Stratification

Risk stratification may be beneficial, even in asymptomatic individuals, because sudden cardiac death may be the first presentation of WPW syndrome in up to 1.4% of patients, according to an Italian study (22). However, other studies from the United States indicate that the overall sudden cardiac death rate is low (on the order of 0.0015 per patient-year) and that sudden cardiac death is extremely rare in patients who are asymptomatic at diagnosis (36). Rapid antegrade conduction through an accessory pathway is the primary risk factor for sudden cardiac death. Tachyarrhythmia inducibility and multiple accessory pathways also are risk factors for potentially life-threatening arrhythmic events (34). The risk of sudden cardiac death in patients younger than 8 years old is very small and is minimal in patients younger than 5. As invasive and noninvasive testing in this young age group may present challenges, it is acceptable to wait until ages 5 to 8 years to perform risk stratification. In a study by Bromberg et al. (37), cardiac arrest was the only distinguishing clinical

feature between high and low-risk groups and the first manifestation in 80% of the children of an accessory pathway that can precipitate a life-threatening arrhythmia. As patient history is not helpful in distinguishing high-risk groups in WPW, other methods of risk stratification need to be performed.

One method of stratifying patients with WPW by risk is to perform an exercise treadmill test. If there is loss of preexcitation, this suggests a low-risk accessory pathway (38,39) (see Fig. 18.7). The loss of preexcitation should occur in a single beat, rather than gradually, in order to classify the pathway as low risk based on the treadmill test (40). Although, intermittent preexcitation seen either on an ECG or 24-hour cardio monitor is a predictor of poor anterograde conduction through the accessory pathway, it has been observed in some patients with cardiac arrest (41).

The test that has held up as the best predictor for patients at risk for sudden death is the measurement of the shortest pre-excited RR interval (SPERRI) during atrial fibrillation, which can be performed if a patient presents in atrial fibrillation. Atrial fibrillation also can be induced by rapid atrial pacing from a transesophageal pacing probe (42) or by using a single transvenous pacing catheter placed in the atrium. During atrial fibrillation, two QRS complexes that show preexcitation are located and the *shortest* interval between two consecutive beats is measured in milliseconds. A SPERRI of 220 to 250 milliseconds and especially <220 milliseconds is more commonly seen in patients with WPW who have experienced cardiac arrest (37,43). These patients are candidates for ablation, or medical therapy to alter the conduction properties of the accessory pathway if ablation is not possible. However, an EP study is more useful to identify those at low risk of sudden death because the overall risk of sudden death in WPW is low. As many accessory pathways, particularly septal pathways, may

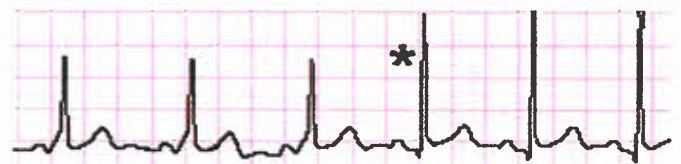


Figure 18.7. Loss of preexcitation in a single beat during an exercise treadmill test indicating a low-risk accessory pathway. The asterisk indicates the beat with loss of preexcitation.

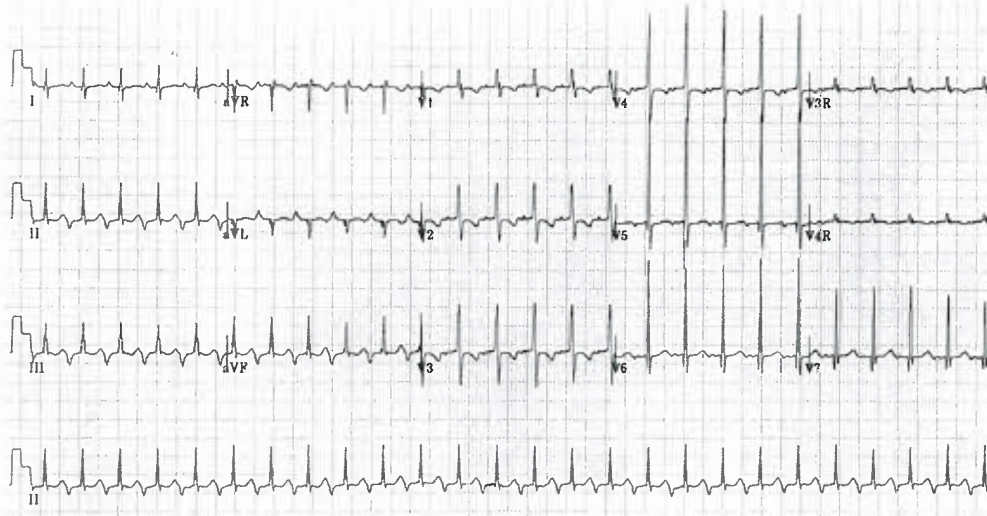


Figure 18.8. PJRT with deeply negative P waves in leads II, III, and aVF.

augment their conduction in the presence of catecholamines, it may be beneficial to perform the risk assessment while using an isoproterenol infusion (44). It is controversial whether the risks of performing an ablation of an accessory pathway (particularly one located in a high-risk location) outweigh the true risk of an arrhythmic sudden death, but eliminating conduction via catheter-based technology should be strongly considered in rapidly conducting pathways.

Unidirectional Retrograde Accessory Pathway

An accessory pathway may be present even when the surface ECG shows no overt manifestation. These pathways may conduct retrograde only (URAP) and, therefore, can be the cause of a reentrant SVT. The therapy and management of these accessory pathways are similar to those for WPW, but because there is no antegrade conduction, these patients are not at the same risk for sudden death from rapid conduction in atrial fibrillation.

Treatment of Supraventricular Arrhythmias

Treatment of supraventricular arrhythmias depends on patient age, severity of symptoms, spontaneous termination, length of symptoms, presence of other cardiac defects, and number of episodes. Medical treatment typically is effective, but does not address the underlying cause. Catheter ablation, particularly in patients older than 5 years of age should be considered. Ablation indications are discussed in another chapter in this book (see Chapter 17).

Permanent Junctional Reciprocating Tachycardia

A unique type of accessory pathway-mediated tachycardia is the permanent form of junctional reciprocating tachycardia. Initially, this tachycardia was thought to arise from the AV junction and thus was named a junctional reciprocating tachycardia. Later investigation actually showed this to be a slowly conducting accessory pathway, but the name permanent junctional reciprocating tachycardia (PJRT) has persisted. A PJRT fiber typically is located in the posterior septum on the right side of the heart, although fibers may be located in the midseptum or even on the left side of the heart. Because these fibers conduct slowly, the tachycardia presents as a long RP

where the P wave is visible easily on the surface ECG. The ECG in tachycardia has a classic morphology with deeply negative P waves in the inferior leads, II, III, and aVF (see Fig. 18.8). This type of tachycardia frequently is present immediately after birth but because of its relatively slow rate (150 beats per minute) may not be appreciated on routine examinations in newborns and infants. PJRT also tends to be an incessant tachycardia and may lead to a tachycardia-induced cardiomyopathy if left untreated (45).

Mahaim Fibers

Mahaim fibers are special types of accessory pathways connecting the atria to the ventricles bypassing at least part of the AV node. Descriptions of these fibers identify them as connecting either the atria to the fascicles (atriofascicular fibers), the bundle of His to the ventricles, the fascicles to the ventricles, or the atria to the bundle of His. These fibers generally are located on the right ventricular side of the heart but occur rarely on the left ventricular side. Because of their right-sided location, during tachycardia the patient's ECG has a left bundle branch block pattern. These pathways have unique properties similar to those of the AV node in that they often possess decremental conduction (conduct slower at a faster rate) and are typically catecholamine sensitive. Unlike most other accessory pathways, some of these fibers may have automaticity and are capable of depolarizing spontaneously (46). Tachycardia may result from this spontaneous depolarization or from reentrant tachycardia using the Mahaim fiber as the antegrade limb and the AV node as the retrograde limb. On the surface ECG in normal sinus rhythm, they often present as a normal PR interval with a slurred upstroke of the QRS (pseudo-preexcitation) resulting from ventricular depolarization through the Mahaim fiber (47). These fibers often times have only intermittent conduction, and although Mahaim fibers conduct antegrade, their risk for rapid ventricular conduction during atrial fibrillation likely is not present and therefore does not present a risk for sudden cardiac death.

Automatic Focus (Atrial Ectopic Tachycardia)

Atrial ectopic tachycardia (also known as ectopic atrial tachycardia) results when an abnormal focus of cells distinct from the sinus node in the atrium spontaneously depolarizes faster



Figure 18.9. These two irregular rhythms from different patients have a similar rate, but the underlying mechanism is different. The **top strip** represents an atrial tachycardia as there is a clear change in the P-wave axis from the normal sinus beats. The **bottom strip** represents a sinus arrhythmia which is a normal finding particularly in pediatrics with acceleration during inspiration and slowing during expiration with no change in the P wave axis or morphology.

than the underlying sinus node. AET can be incessant, and its rate may increase or decrease based on sympathetic tone and catecholamine state. Distinct P waves typically are visible, although the P waves may have an abnormal morphology or be notched (see Fig. 18.9). First-degree AV block or even Mobitz type I second-degree AV block (Wenckebach) may be present and provide clues about the presence of an abnormal tachycardia (48). The P waves at the onset of tachycardia are similar to the morphology of subsequent P waves in the tachycardia. Often times, the focus of the AET is in the right atrium along the crista terminalis or in the right atrial appendage (49). The P-wave axis in tachycardia frequently is abnormal on the surface ECG, unless its origin is near the sinus node or right upper pulmonary vein. When the focus is near the sinus node it shows as an upright P wave in lead I and aVF (similar to normal sinus rhythm), but the P wave frequently is negative (rather than biphasic) in lead VI, thus providing a clue to the presence of an ectopic atrial focus. In up to one-third of cases, multiple atrial foci may be the source of the tachycardia (50). Automatic focus atrial tachycardias account for 4% to 6% of SVT and are often incessant; these too can be associated with significant cardiac dysfunction (51).

The atrial rate in AET frequently displays periods of warming up and cooling down rather than a paroxysmal onset and termination. Often, this tachycardia appears initially as a wide QRS tachycardia. This occurs because of the refractory periods of the bundle branches that usually accommodate the faster rate and normalize. Adenosine can be useful in diagnosing this arrhythmia because it blocks the AV node without affecting the ectopic focus, and the arrhythmia generally does not terminate. However, some foci are adenosine sensitive, particularly those originating around the AV node (52). Cardioversion and overdrive pacing may temporarily suppress AET only to have it quickly resume its initial rate at least in part because of its catecholamine sensitivity.

Spontaneous resolution of AET is unlikely in children older than 3 years (53). For this reason, cardiac catheterization with ablation techniques generally is recognized as first-line therapy. However, in children younger than 6 months, there is a high incidence of spontaneous resolution of tachycardia with a low long-term incidence of recurrence. It is advisable to attempt medical control in these patients until the tachycardia resolves if the tachycardia is sustained or very rapid. Slower atrial tachycardias (<220 beats per minute) that are not incessant may not require therapy if the ventricular function is normal, although these patients require close follow-up.

Some arrhythmias that are difficult to control with medical therapy are caused by hamartomas within the myocardium. If reasonable control of the arrhythmia can be obtained with medication, they frequently will regress (54). In rare cases, when control cannot be achieved with maximal medication, the patient may require surgical excision of the tumor (55). These tumors frequently are visible to the naked eye as pale colored areas of the myocardium and can be excised.

Nonautomatic Focal Atrial Tachycardia

Nonautomatic focal atrial tachycardia (NAFAT) results from a small reentrant circuit within the atrium (i.e., micro-reentrant tachycardia) (56). This type of tachycardia, like other reentrant tachycardias, can be reproducibly induced with programmed atrial stimulation and can be terminated with adenosine. It commonly is located in the right atrium in patients with either normal or structurally diseased hearts (57). Although distinct from AET, its management is similar and is very amenable to ablation.

Chaotic Atrial Tachycardia

Chaotic atrial tachycardia or multifocal atrial tachycardia is a type of atrial tachycardia with multiple foci, which results in three or more P wave morphologies on the ECG. It has been described in children with otherwise normal hearts as well as in patients with acute viral bronchiolitis or advanced pulmonary disease. Because of the rapid chaotic nature of the tachycardia, it may be difficult to distinguish from atrial fibrillation. This type of tachycardia is difficult to treat and can be refractory to pace termination, DC cardioversion, and adenosine. This type of tachycardia is not amenable to ablation and typically is treated with medical therapy using Vaughn Williams class IA, IC, or III agents (see Table 18.3).

Junctional Ectopic Tachycardia

JET is an automatic focus tachycardia arising within or immediately adjacent to the AV junction. This tachycardia has a relatively high familial incidence. This tachycardia is, by definition, generally a narrow complex tachycardia with a QRS morphology identical to the QRS morphology in sinus rhythm (see Fig. 18.10). The classic description of this tachycardia is that there is no association between the P waves and the QRS complexes on the ECG. In reality, this tachycardia has all Junctional–Atrial (J–A) relationships from 1 to 1, to J–A Wenckebach, to no relationship. Retrograde P waves often are visualized in the terminal portion of the QRS. With adenosine, there may be loss of the retrograde conduction, resulting in dissociation of the P wave and the QRS. JET has two different forms: idiopathic JET, which is observed in a structurally normal heart, and postoperative JET.

Postoperative JET occurs in up to 6% of patients undergoing cardiac surgery and is seen more frequently with use of inotropic agents such as dopamine (58). Congenital JET is one of the rarest forms of SVT in infants and also one of the most difficult to treat. Congenital JET is presumed to be present from birth but may not be identified until months or years later. Patients with congenital JET have a wide range of clinical presentations. Patients with JET presenting at or younger than 6 months of age are more likely to have incessant JET

TABLE 18.3 Vaughan-Williams Classification**Class I**

- Block sodium channels
- Decrease speed of depolarization
- Slow conduction velocity
- Subdivided into Ia, Ib, and Ic

Class II

- Beta-blocking drugs
- Block adrenergic receptors
- Decrease sympathetic tone

Class III

- Block potassium channels
- Increase action potential duration

Class IV

- Calcium channel blockers
- Affect mainly SA and AV nodes
- Direct membrane effect

Class V

- Digitalis agents
- Affect mainly SA and AV nodes
- Act indirectly by increasing vagal tone

and to have faster JET rates, and the mortality rate in this population is approximately 4% (59). With current medical, ablative, and device therapies, the majority of patients have a good outcome.

Atrial Flutter

Atrial flutter is an uncommon arrhythmia in the pediatric population. It typically occurs in newborn infants and postoperatively in congenital heart disease patients. Newborn infants present within the first 2 days of life with tachycardia and frequently have signs of congestive heart failure (60). The ECG for these patients has the typical saw-toothed flutter waves (see Fig. 18.11) with atrial rates between 300 and 600 beats per minute and variable conduction to the ventricles. If the flutter waves cannot be distinguished easily on the ECG, adenosine can be given to reveal the flutter waves. Treatment is direct current-synchronized cardioversion with 0.5 to 1 J/kg. Atrial overdrive pacing also can be used if the atrial rate is slow, but this is more difficult to perform. Newborns with atrial flutter typically have no structural heart disease and have no further problems after successful cardioversion. A 24-hour cardioscan should be placed after cardioversion to rule out the rare reentrant tachycardias or atrial tachycardias that initiated the atrial flutter. Generally, the atrial flutter will not recur, and if no evidence of other arrhythmias is present, these infants do not require antiarrhythmic therapy and follow-up is not necessary (61).

Atrial Fibrillation

Atrial fibrillation is an uncommon arrhythmia in the pediatric population but is important to recognize. Atrial fibrillation presents as an irregularly irregular rhythm with the same QRS morphology as in sinus rhythm (see Fig. 18.12). Although P waves frequently are not visible in atrial fibrillation, they may be seen in patients with coarse atrial fibrillation. Atrial fibrillation can occur in the context of WPW or following extensive surgery involving the atrium such as a total cavopulmonary connection or atrial switch operation (Mustard or Senning). Patients who present with atrial fibrillation without evidence of structural heart disease warrant evaluation for other arrhythmias, such as reentrant SVT, that degenerate

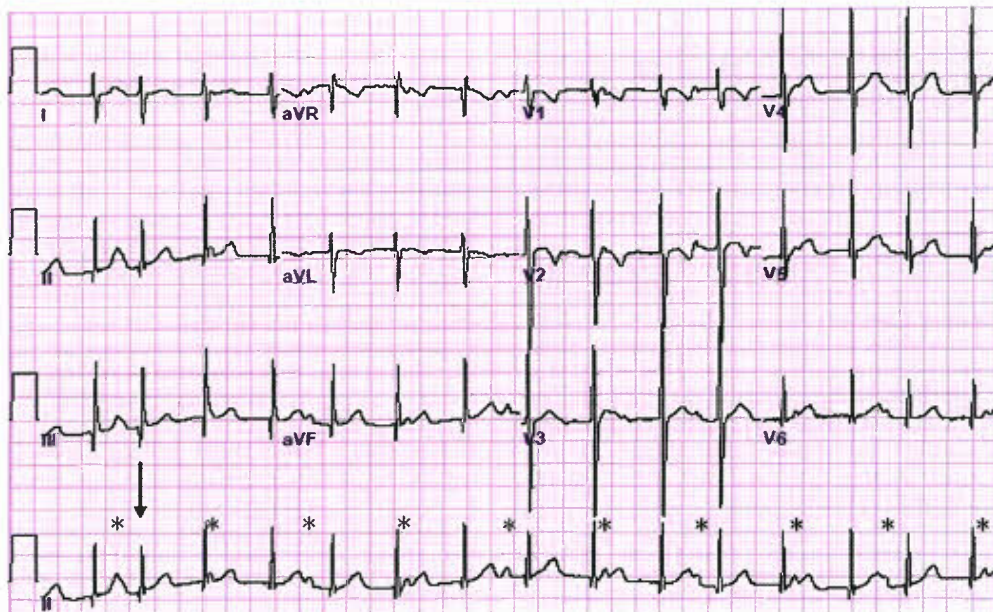


Figure 18.10. Slow JET. Note the narrow QRS morphology similar to sinus rhythm. The asterisks denote the underlying sinus rhythm P waves. There is no relationship between the P waves and the QRS, except for a single P wave that falls in a period where the AV node is not refractory from the ectopic junctional rhythm and is therefore able to conduct to the ventricle (sinus capture beat) denoted by the arrow. These sinus capture beats likely indicate that the underlying conduction in the AV node is intact.

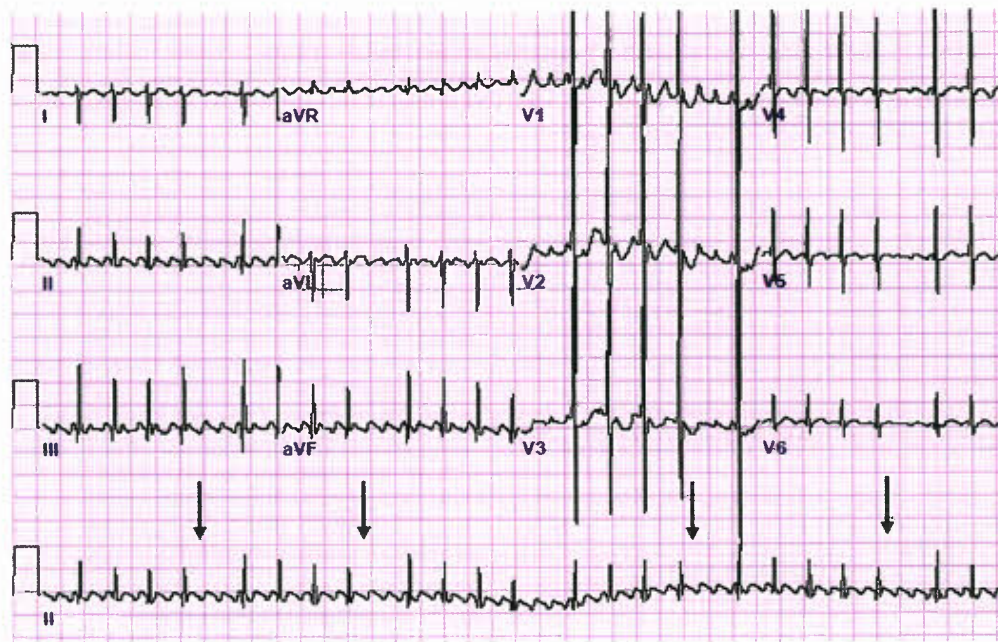


Figure 18.11. Neonatal atrial flutter with a saw-toothed pattern and an atrial rate of around 375 beats per minute. There is variable conduction through the AV node to the ventricles with predominantly 2:1 block, but also 3:1 block noted by the arrows.

into atrial fibrillation or an underlying channelopathy. If none are found, the problem could simply be primary or lone atrial fibrillation, which has been described in the late teenage years (62). Occasionally, atrial fibrillation may be the initial presentation of hyperthyroidism, myocarditis, or digoxin toxicity.

One of the initial therapies for chronic atrial fibrillation was ablation of the AV node with implantation of a permanent pacemaker. Because of the permanent loss of AV synchrony combined with the long-term need and dependence on a pacemaker as well as chronic anticoagulation, this therapy should be reserved only

for the most refractory and symptomatic cases of atrial fibrillation that have failed to respond to multiple medical therapies.

Intraatrial Reentrant Tachycardia

Intraatrial reentrant tachycardia (IART) occurs in patients who have undergone previous cardiac surgery either on or through their atria and are left with extensive scarring. This unique form of arrhythmia is similar to atrial flutter. It tends to have slower

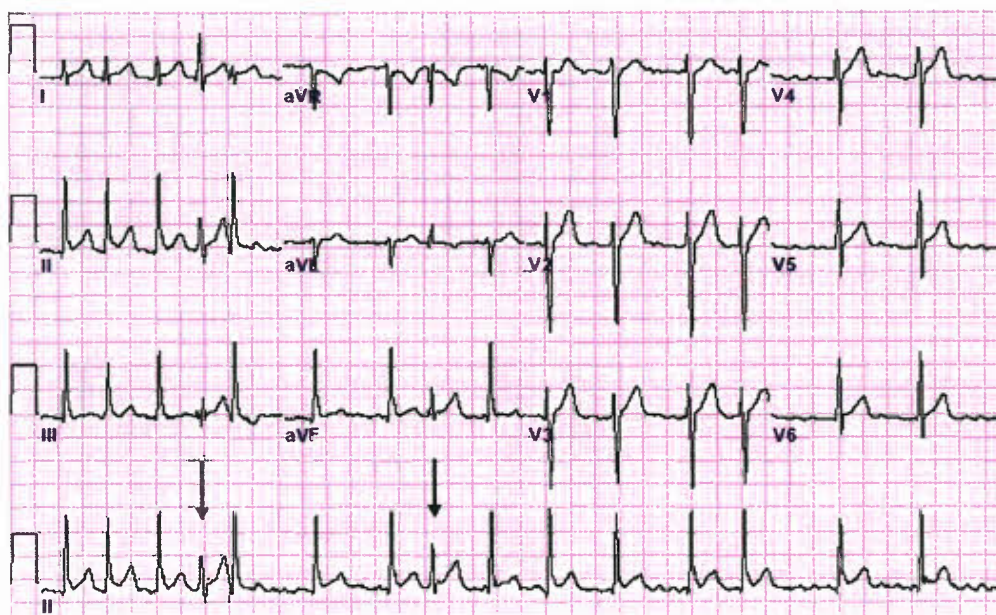


Figure 18.12. Atrial fibrillation with an irregularly irregular rhythm. This is coarse atrial fibrillation with visible atrial activity that is disorganized and chaotic. Some of the beats (noted by arrows) are conducted aberrantly through the AV node causing the QRS morphology to change.



Figure 18.13. Intra-atrial reentry tachycardia. The P waves of the tachycardia are frequently buried in the T waves or the QRS when the tachycardia has 2:1 conduction, especially in the presence of a bundle branch block. Note the flat isoelectric baseline between the P waves and the relatively small amplitude compared to atrial flutter.

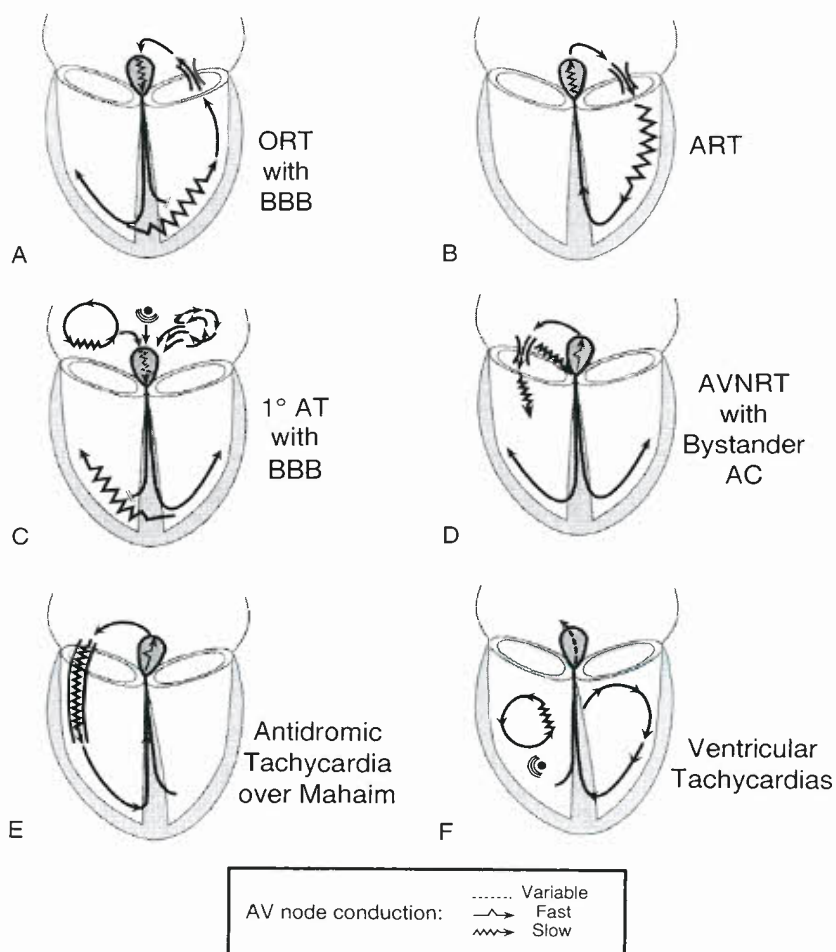
rates than atrial flutter, with atrial rates in the 140 to 200 beat per minute range. The ECG is different because there tends to be an isoelectric baseline between two consecutive P waves, unlike atrial flutter, where constant atrial activity creates the sawtoothed pattern (see Fig. 18.13). The P waves in IART may be

very small and are often missed, particularly if they are buried within the QRS complex or the T wave. Adenosine can be used to unmask this type of tachycardia. Because this type of tachycardia often occurs in patients with underlying sinus node dysfunction (SND), patients presenting with an unusually fast heart rate (>100 beats per minute) should be carefully examined for the presence of this arrhythmia. There is utility in placing epicardial ablation lesions in strategic positions (the so-called maze or maze-Cox III procedure) to prevent IART, and atrial fibrillation in pediatric patients and adults with congenital heart disease. This is particularly useful in patients who have had extensive atrial operations such as the Fontan procedure. Long linear probes can quickly form deep uniform lesions without the need to arrest the heart or place the patient on cardiopulmonary bypass. These lesions appear to have a relatively good long-term success even in the most complicated patients. For patients with atrial arrhythmias having a Fontan revision, there is up to a 76% recurrence without the placement of intraoperative ablation lesions (63). Physicians at most large centers routinely place ablation lesions (maze procedure) when doing a Fontan conversion. The late recurrence of atrial arrhythmias is only 13% to 22% (64,65).

Wide Complex Tachycardias

Wide complex tachycardias should be assumed to be VT until proven otherwise. However, there are several situations when a wide complex tachycardia may be supraventricular in origin (see Fig. 18.14). The most common scenario involves the presence of a SVT with aberrancy. With rapid onset of a tachycardia, either the left or right bundle branch may be

Figure 18.14. Diagrammatic representation of tachycardias with prolonged (wide) QRS. Such tachycardias may be due to (A) orthodromic reciprocating tachycardia (ORT) with bundle branch block (BBB), (B) antidromic tachycardia using an accessory AV connection (ART), (C) primary atrial tachycardia with BBB, (D) atrio-ventricular nodal reentry tachycardia (AVNRT) with a bystander accessory connection (AC), (E) tachycardia using a Mahaim fiber, or (F) ventricular tachycardia. Despite the diversity of mechanisms, ventricular tachycardia should be assumed until or unless additional data to the contrary are available.



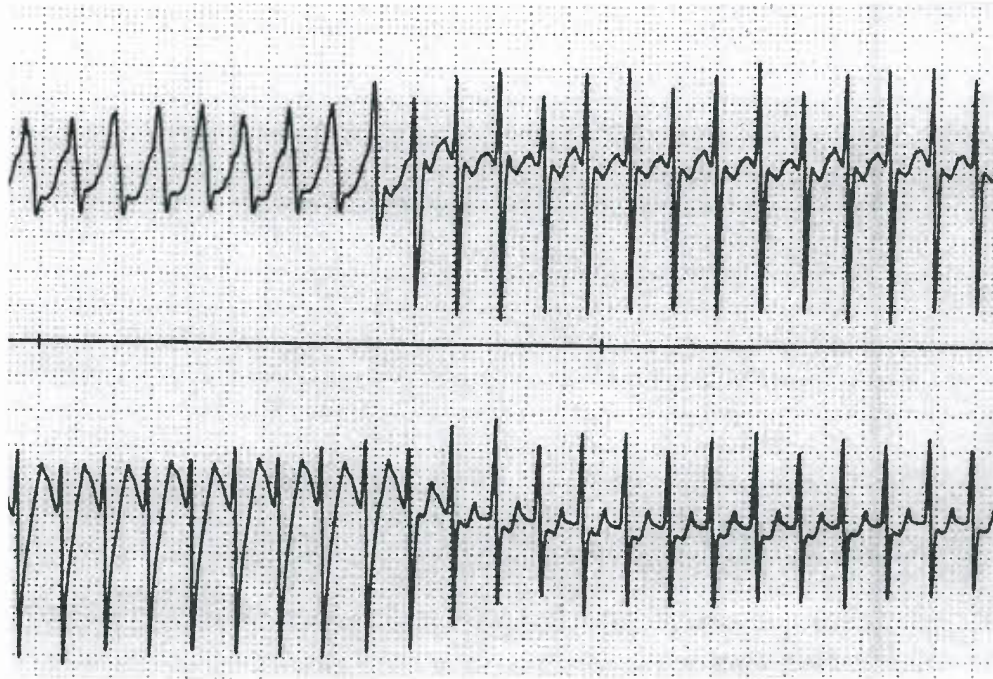


Figure 18.15. The initial portion of the tracing shows a wide complex tachycardia that subsequently changes to a narrow complex tachycardia at exactly the same rate. This is all SVT and not two different arrhythmias. The initial portion is aberrantly conducted. As the AV node and bundle branches accommodate to the faster rate, the SVT becomes narrow.

refractory and not able to conduct impulses. This results in a wide complex tachycardia on the ECG. A left bundle branch block pattern of aberrancy is much more common in neonates, while a right bundle branch block pattern is more common in children and adolescents. Frequently, the bundle will accommodate the tachycardia, and the QRS complex will become narrow (see Fig. 18.15). A second common scenario occurs when a SVT presents with a wide complex in the presence of an underlying bundle branch block on a baseline ECG or in the presence of preexcitation from WPW.

Most wide complex tachycardias except for ventricular fibrillation are relatively regular tachycardias. When an

irregular wide complex tachycardia is present, the possibility that this is atrial in origin should be raised.

Ventricular Tachycardia

VT is defined as three or more premature ventricular contractions (PVCs) in a row at a rate faster than 120 beats per minute. Slower rates, within around 10% to 20% of the underlying sinus rate, are referred to as accelerated ventricular rhythms and typically have a benign prognosis and treatment typically is not necessary (66) (see Fig. 18.16). A hallmark

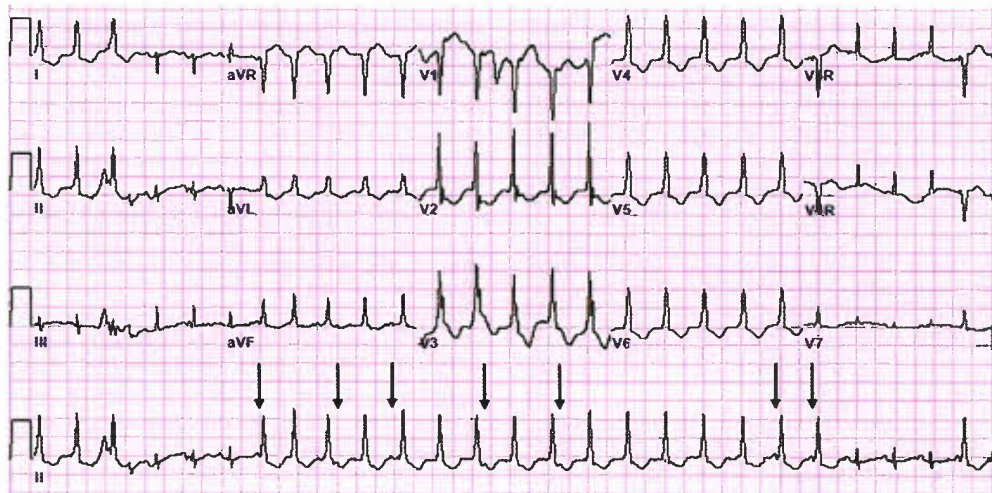


Figure 18.16. Accelerated ventricular rhythm. There is a wide complex rhythm that is within 20% of the underlying sinus rate and gradually overtakes the underlying sinus rhythm. There is no relationship between the ventricles and the atria (so-called VA dissociation) which distinguishes this as a ventricular arrhythmia (the arrows designate P waves that have no relationship to the tachycardia). This variant has a benign prognosis.

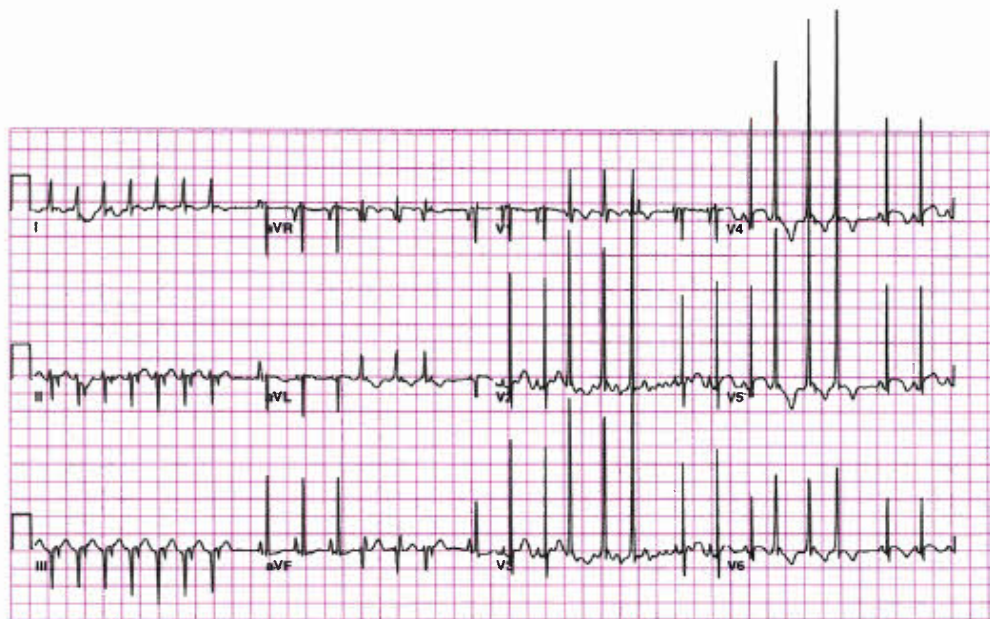


Figure 18.17. Ventricular tachycardia in a neonate. Note the relatively narrow complexes that are different from sinus beats and retrograde P waves in the initial portion of the tracing.

of VT is that the QRS complex is different than that of the sinus QRS complex but does not have to be wide. In infants younger than 2 years old, the QRS duration in VT can be as short as 0.06 seconds, and the rate can be as fast as 500 beats per minute (see Fig. 18.17). VT rarely can present as a narrow complex tachycardia in older patients as well. This occurs when the focus of the tachycardia is in close proximity to or contained within the normal conduction system. Most VTs, particularly in patients with structural heart disease, are reentrant in nature, although automatic foci occur in patients with structurally normal hearts.

In the normal pediatric population, spontaneous VT has an approximate incidence of 1/100,000 in the childhood years and may present any time between infancy and young adulthood (67). However, short episodes of VT can occur in up to 3% of otherwise healthy teenagers on routine Holter monitoring (68). In comparison to patients with structural heart disease or cardiomyopathy, patients with normal cardiac anatomy and function generally have a benign course. The presence of underlying heart disease, presence of symptoms, rapid rate of VT, and exacerbation of VT with exercise are risk factors for adverse events in nonischemic VT in children. Control of arrhythmias by ablation or antiarrhythmic medications may be indicated in this population (69). The chance of resolution is higher when the onset occurs during the first year of life (resolution in about 90% of patients) compared with onset beyond the first year of life to 15 years of age (resolution in about 50%). The clinical profile is more favorable for patients with right-sided VT (resolution in 76% and symptoms in 25%) compared with patients with left-sided VT (resolution in only 37% and symptoms in 67%) (70).

Two forms of VT are thought to be benign variants—right ventricular outflow tract tachycardia (left bundle branch block, inferior QRS axis on ECG) and idiopathic left VT (right bundle branch block, superior QRS axis on ECG). These tachycardias tend to be responsive to verapamil. The benign variant of VT originates from the right ventricular outflow tract in around 50% of patients (71). It is important to recognize underlying precipitating causes of VT—such as long QT syndrome,

arrhythmogenic right ventricular cardiomyopathy (ARVC), anomalous coronary arteries, and hypertrophic cardiomyopathy—because these patients may be at higher risk for sudden death. An echocardiogram is indicated in all patients with VT, and further imaging, including magnetic resonance imaging or cardiac catheterization, may be indicated in cases with a higher index of suspicion for underlying pathology.

More than 50% of pediatric patients with symptomatic or sustained VT have underlying structural heart disease, and another 25% may have at least subtle evidence of myopathy (72). Ventricular tachyarrhythmias in young infants may be associated with myocarditis, prolonged QT syndrome, severe electrolyte disturbances, or small hamartomas within the ventricular myocardium. In older children, VT may be associated with myocarditis, prolonged QT syndrome, medication overdose or toxicity, various forms of cardiomyopathy, arrhythmogenic right ventricular dysplasia, coronary artery abnormalities, and congenital heart disease both before and after surgery.

Patients with sustained or hemodynamically unstable ventricular arrhythmias or resuscitated sudden death episodes generally require placement of an implantable cardioverter defibrillator (ICD).

Torsades de pointes (also known as torsades) is an uncommon form of polymorphic VT with a characteristic twisting of the QRS complex around the isoelectric baseline (see Fig. 18.18). It commonly occurs in the presence of a channelopathy, such as *Brugada syndrome* or *long QT syndrome* (congenital or drug related), but may be associated with electrolyte abnormalities (particularly hypokalemia or hypomagnesemia), acid-base disturbances, endocrine disorders such as hypothyroidism, hyperparathyroidism or pheochromocytoma, myocardial ischemia, and myocarditis. Episodes typically are short lived and paradoxical and terminate spontaneously. However, longer episodes may progress to ventricular fibrillation and result in rapid hemodynamic compromise and sudden cardiac death (73). This tachycardia is unique in that it may respond to treatment with either isoproterenol or magnesium.



Figure 18.18. Torsades de pointes with its rapid polymorphic nature, and shifting of the QRS axis rapidly around an isoelectric baseline.

Tachycardia-Induced Cardiomyopathy

Although arrhythmias frequently occur in the context of depressed ventricular function, occasionally the *primary* cause of ventricular dysfunction is an arrhythmia. The ventricular dysfunction may be so severe that these patients may be listed for heart transplantation. One study showed that an incessant atrial tachycardia was present in 17% of patients listed for cardiac transplantation and accounted for 37% of patients initially diagnosed with idiopathic cardiomyopathy (74). The specific mechanisms of ventricular dysfunction secondary to tachyarrhythmias are poorly understood, but the arrhythmia typically is incessant. The minimum duration or heart rate necessary to develop dysfunction is unknown. Most studies suggest that patients who develop tachycardia-induced cardiomyopathy have heart rates >140 beats per minute (75). The origin of the tachycardia may be atrial or ventricular and may have an automatic focus or reentrant mechanism. SVTs are the most common cause of tachycardia-induced cardiomyopathy (76), although incessant ventricular arrhythmias may also result in cardiomyopathy. Ventricular rhythms causing cardiomyopathy are usually of automatic focus and frequently originate from the right or left ventricular outflow tract (77). Once an arrhythmia-causing tachycardia-induced cardiomyopathy is under control by either medication or catheter ablation, ventricular function typically normalizes. Many patients show a marked improvement as soon as 3 weeks after normalization of heart rate, although it may take up to 21 months to see a full recovery (78).

Premature Atrial Contractions

A PAC or supraventricular premature beat is a depolarization of atrial tissue that is distinct from sinus node tissue and manifests on ECG as a premature P wave. In most instances, it has a different morphology and axis from those of the sinus P waves. Most PACs are conducted to the ventricles with a normal QRS. Because the premature P wave occurs earlier and earlier, conduction to the ventricles may occur with a different QRS morphology than sinus rhythm (i.e., aberrantly conducted PAC). This occurrence may simulate a PVC. For any early QRS that has morphology different than that of the sinus beats, the preceding T wave should be examined carefully for a hidden

P wave. Occasionally, a premature P wave may occur so early that it results in no conduction to the ventricles. This situation may simulate sinus bradycardia because the premature P wave may conduct into the sinus node, delaying the next expected sinus impulse. In situations of paroxysmal bradycardia, especially those in which conducted PACs are on the same tracing, the T wave should also be searched carefully for the presence of hidden P waves. This phenomenon is especially common in newborn infants. Many tracings similar to the one in Figure 18.19 are interpreted as multiform PVCs with PACs and sinus bradycardia, when in fact most of these patients have only PACs, some of which conduct aberrantly and some of which block. PACs are common in the pediatric population. More than half of children have at least one PAC in a 24-hour monitoring period, and PACs occur more often in patients as they progress through their teenage years (8). Isolated PACs are benign and require further evaluation. If frequent PACs are noted on an

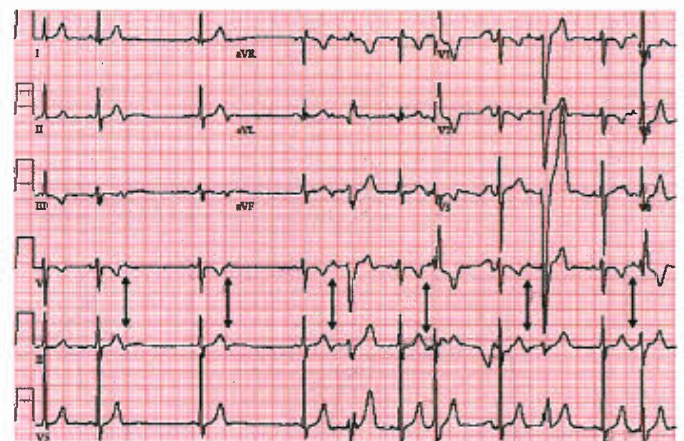


Figure 18.19. Premature atrial complexes are noted by the arrows. The first two PACs do not conduct to the ventricle (block). The next four complexes conduct to the ventricle but do not have a normal-appearing QRS (aberrantly conducted). The appearance of the aberrancy varies having both a left and a right bundle branch block morphology.

ECG or on monitoring strips, a 24-hour cardioscan monitor should be placed to exclude episodes of atrial tachycardia.

Premature Ventricular Contractions

A PVC is a premature QRS complex that does not have the same morphology as the sinus complex and is not preceded by a P wave. Especially in infants, PVCs may not have a broad QRS complex, but they have a morphology different than that of the sinus QRS. If all PVCs have similar morphology, they are referred to as uniform; if they have more than one morphology, they are called multiform. A ventricular couplet is defined as two PVCs in a row. Bigeminy is an alternating rhythm in which every other beat is a PVC, and trigeminy is when every third beat is a PVC.

Most children with PVCs have structurally normal hearts, and 40% of otherwise normal children may have PVCs seen on Holter monitoring (79). PVCs are multiform in up to 25% of patients, but there is no difference in prognosis from uniform PVCs (69). If the heart is completely normal, the prognosis for most children with uniform PVCs is good, and the condition is entirely benign. Although less well studied, the prognosis for uniform ventricular couplets is probably the same as for isolated PVCs. PVCs may spontaneously disappear, and PVCs with a right bundle branch block morphology may have a higher chance of resolution than PVCs with a left bundle branch block morphology (80). Rare cases of ventricular dysfunction occur as a direct result of PVCs in adults; with a PVC burden of >24%, this phenomenon is very rare in pediatrics (81).

Other factors that may be related to tachycardia-induced ventricular dysfunction are male gender, persistence of PVCs throughout the day, and the presence of repetitive monomorphic VT (82). If the history, physical examination, ECG (other than the rhythm), and echocardiogram are normal and the 24-hour cardioscan monitor shows only uniform PVCs and/or couplets, there is no need for medical therapy in these patients. It is prudent to repeat the cardioscan once after the initial evaluation to ensure that the ectopy has not changed or progressed. If a patient wishes to participate in competitive sports, an exercise treadmill test may be useful to determine the response of the ectopy to exercise.

Occasionally, PVCs are associated with long QT syndrome, myocarditis, hypertrophic cardiomyopathy, and congenital heart disease before or after surgery. Often in these patients, the resting ECG is abnormal, the ectopy is frequent (>1,000 PVCs an hour), or the PVCs are multiform. Closer surveillance is required in these patients, and they may require further evaluation.

Postoperative Arrhythmias

Hemodynamically significant postoperative arrhythmias are a frequent complication of pediatric cardiac surgery, occurring in about 15% of patients, with younger age and longer bypass

and cross-clamp times being risk factors for arrhythmia (83). JET and SVT are the most common postoperative arrhythmias (84). These arrhythmias may be transient and directly related to the cardiac surgery but also may be related to the underlying cardiac condition. Arrhythmias occurring more than 3 to 4 days following cardiac surgery may be an issue in the long-term care of these patients.

TREATMENT

All arrhythmias are mediated through the cardiac action potential. Antiarrhythmic medications affect the shape of the intracardiac action potential. They work by altering ion channels or blocking receptors. The Vaughan-Williams classification system was developed to help categorize antiarrhythmic drugs (85). This system organizes drugs based on their major mechanism of action—where they affect the cardiac cell membrane and subsequently the cardiac action potential (see Table 18.3). Changes in the action potential may change the conduction velocity, refractoriness, or automaticity (see Table 18.4).

Class I

Class I agents affect the sodium channels. They are divided into three categories: Ia, Ib, and Ic based on the effect they have on the action potential (see Fig. 18.20).

Class Ia agents slow the upstroke of the action potential, therefore prolonging its duration. This effect decreases conductivity and increases refractoriness.

Procainamide is a class Ia agent that suppresses normal and abnormal automaticity and slows conduction in accessory pathways in addition to being mildly vagolytic. Procainamide alters the ECG by increasing PR interval, QRS duration, and QT interval. It is metabolized approximately 35% by the liver, producing *N*-acetylprocainamide (NAPA), which prolongs the QT interval. The production of NAPA varies and is determined genetically. The other 65% is excreted by the kidneys. The therapeutic range is 4 to 12 mg/mL. NAPA levels have been measured in the past but have minimal therapeutic significance. Amiodarone and ranitidine increase procainamide levels. The intravenous dosage is a bolus of 10 to 15 mg/kg with close blood pressure monitoring. A continuous infusion of 30 to 80 micrograms (mcg)/kg/min can be employed. High doses have a negative inotropic effect, and caution should be exercised in patients with a prolonged QT interval, Brugada syndrome, left ventricular dysfunction, or sinus dysfunction. Because of this, procainamide generally is not a first-line agent. It can be used to treat supraventricular as well as VT if the tachycardia does not break with adenosine or immediately recurs after conversion. It also can be used in atrial fibrillation and atrial flutter. It is safe to use in neonates, but doses may need to be reduced in premature infants and those with renal dysfunction (86).

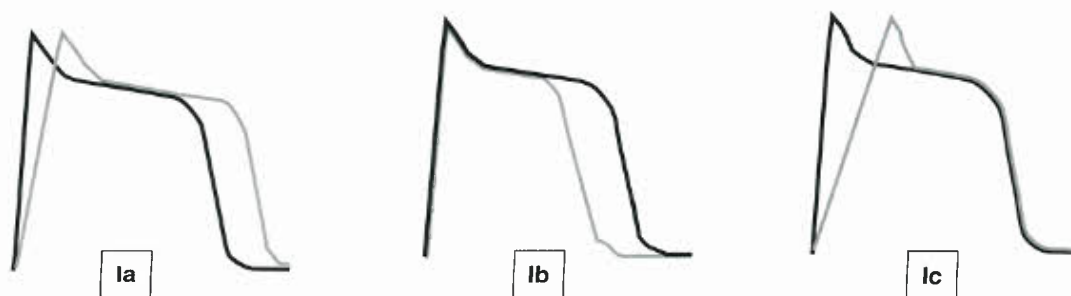


Figure 18.20. Changes in the action potential seen with Vaughan-Williams class I medications.

Class Ib agents have minimal effect on the upstroke of the action potential but do shorten its duration, which decreases refractoriness. Lidocaine is a Ib agent that inhibits fast inward sodium current, which primarily affects the ventricular myocardium. It shortens the action potential with no effect on QRS duration in sinus rhythm. It is highly selective for depressed myocardial tissue. The half-life is 5 to 10 minutes, and hypokalemia can decrease its effect. The typical loading dose of 1 mg/kg and infusion rate of 20 to 50 mg/kg/min can be titrated to achieve a therapeutic range of 1.5 to 5 mg/mL. Although not included in the 2010 Pediatric Advanced Life Support (PALS) guidelines, it may be useful in VT. Side effects include vertigo, tremor, seizures, obtundation, and bradycardia (in patients with SND). The hemodynamic effect is minimal at standard doses.

Unlike lidocaine, mexiletine is available in oral form. Outside of treatment for long QT syndrome, mexiletine is used only for frequent PVCs that cause symptoms or in patients with triggered VT (87). It rarely suppresses sustained VT and has prominent central nervous system side effects.

Class Ic drugs cause a marked slowing of upstroke of the action potential with minimal effect on the action potential duration. This results in a marked decrease in conductivity with little effect on refractoriness. The most commonly used agents are flecainide and propafenone.

Flecainide is a Ic agent that shortens conduction velocity with little effect on the sinus node but may exacerbate bradycardia in patients with SND. It is a pronounced negative inotropic agent. ECG effects include prolonging the PR and QRS intervals with minimal effect on the QT interval. The half-life changes with age: 12 hours in children <1 year old and >12 years old and 8 hours in children 1 to 12 years of age. Dairy products interfere with absorption, and patients may become toxic if dairy products are removed from their diet. Flecainide is 75% metabolized by the liver and 25% excreted by the kidneys. A therapeutic level is 0.2 to 1 mg/mL. QRS widening is infrequently seen at a therapeutic concentration and if present should warrant immediate evaluation for a high flecainide level. It is used in PJRT, AET, and SVT. Side effects include blurry vision (the most common side effect), dizziness, headache, fatigue, tremor, nausea, vomiting, and anorexia. It should be used with caution in patients with structural heart disease or primary cardiomyopathies. Severe proarrhythmia occurs in 1% to 3% of patients with abnormal hearts, and inpatient telemetry monitoring should be considered when initiating flecainide.

Class II

Beta-blockers have evolved over the years with the advent of newer and more selective agents. The first-generation beta-blockers are nonselective for beta-1 (predominantly located in the heart) and beta-2 (predominantly located in bronchial smooth cells) receptors and include propranolol and nadolol. Second-generation beta-blockers have relative selectivity for beta-1 receptors and include metoprolol, atenolol, and esmolol. Third-generation beta-blockers are selective or nonselective with potentially important ancillary properties and include carvedilol, which has the additional property of being an alpha-blocker that causes vasodilation.

Propranolol is a nonselective beta-blocker. In addition to its beta-blocking effects, it may have some direct effect on cell membrane stabilization. It is used in SVT, in ventricular arrhythmias (especially those that are catecholamine induced), and in atrial flutter or fibrillation to slow the ventricular response. More data exist regarding use in infancy, and there is a commercially available liquid preparation. Because of its rapid metabolism, it should be given 3 to 4 times a day or in a long-acting formulation.

Side effects include exacerbation of bronchospasm, hypoglycemia, depression, insomnia, fatigue, personality changes including aggression, and nightmares.

Nadolol is another nonselective beta-blocker that is similar in action to propranolol, but it has a preference for beta-1 receptors. It has a half-life of almost 24 hours, so it needs to be taken only once a day. It has been shown to be effective in the treatment of channelopathies such as long QT syndrome or catecholaminergic polymorphic VT (88,89).

Atenolol is a selective beta-1 antagonist. Because of its metabolism, it should be given 2 times per day in the pediatric population. It has been used in SVT, primary atrial tachycardias, and VTs, especially those exacerbated by catecholamines or exercise.

Although carvedilol is used more frequently in patients with heart failure, it has antiarrhythmic effects, particularly at high doses. It decreases ventricular ectopy in patients with dilated cardiomyopathy (90). Carvedilol likely has antiarrhythmic effects in addition to its beta-blocking properties—including alpha-adrenergic blocking effects and KCNH2 (HERG)-related potassium channel-blocking effects (shown in *in vitro* studies)—and has additional minimal blocking effects on sodium and calcium channels (91).

Esmolol, a short-acting selective beta-1 antagonist, is an excellent antiarrhythmic medication that can be delivered rapidly to the patient because its only form is intravenous. It has rapid clearance by erythrocyte esterases and has a half-life of 9 minutes in adults and 2 to 4 minutes in younger patients. The typical dose is 500 micrograms (mcg)/kg taken intravenously over 1 minute followed by a constant infusion at 25 mcg/kg/min. The infusion may be titrated upward until the desired effect is achieved, with a maximum of 200 mcg/kg/min. Side effects include decreased heart rate, decreased blood pressure, and, subsequently, a decreased cardiac index. Cardiac function typically recovers within 10 to 15 minutes of discontinuing the infusion.

Caution must be exercised when using beta-blockers in patients with reactive airway disease. In addition, mood changes including depression or aggression, constipation, fatigue as well as hypoglycemia can occur in children receiving beta-blockers.

Class III

Class III drugs inhibit potassium channels, which delays repolarization and prolongs the action potential.

Amiodarone is an antiarrhythmic agent with a complex array of actions, including sodium-channel inhibition, beta blockade, alpha-receptor blockade, and calcium channel-blocking activity. ECG changes can include prolongation of the PR interval, prolongation of the QT interval, a decrease in T wave amplitude, widening of the T wave, and a decrease in heart rate. It is one of the most potent antiarrhythmics, but also has the one of the most extensive side effect profiles. Amiodarone is poorly absorbed orally, with only 30% to 50% absorbed from the gastrointestinal tract, which may cause erratic bioavailability. It is highly lipophilic and distributes into many tissues. It may have a large volume of distribution (as high as 500 L), which can result in delayed onset of antiarrhythmic actions and delayed onset of side effects. The half-life ranges from 8 to 107 days. There is a poor correlation between plasma levels and efficacy, so measuring levels generally is not recommended. It is cleared by excretion in tears, sweat, and bile.

Toxicities are the primary limitation of using amiodarone and occur in up to 30% of pediatric patients (92). Many adverse reactions are related to the total cumulative dose. Photosensitivity is one of the most common side effects and is significant in up to 20% of patients. This sensitivity ranges

from susceptibility to sunburn to blue-gray discoloration of sun-exposed skin. Thyroid dysfunction is also a prominent adverse event in children. Amiodarone reduces peripheral conversion of T4 to T3, resulting in hypothyroidism (up to 10%) or hyperthyroidism. Other side effects include elevation of hepatic enzymes, weakness, peripheral neuropathy, corneal microdeposits resulting in decreased night vision, and esophageal reflux from paralysis of the lower esophageal sphincter. The most serious adverse reaction is pulmonary fibrosis, which is the only side effect that is not greatly improved or resolved by termination of amiodarone therapy (93). Fortunately, pulmonary fibrosis is extremely rare in children. Nausea is common with initiation but usually resolves with time. Amiodarone also can be given intravenously, but hypotension can occur with rapid intravenous loading, possibly because of the calcium-channel effects. Amiodarone typically does not have a significant effect on ventricular function, including in pediatric patients who have undergone recent cardiac surgery (94). It may be particularly useful in postoperative JET, which often is refractory to therapy (94). Loading should be initiated in the hospital to monitor for proarrhythmia and side effects.

In general, thyroid function tests and liver function tests should be performed at the start of therapy as a baseline and every 6 months while on amiodarone. Yearly ophthalmology examinations and pulmonary function tests (in patients able to comply, with particular attention paid to the carbon monoxide diffusing capacity) should be done to monitor for toxicity. Careful monitoring of digoxin, warfarin, and phenytoin levels should be performed because amiodarone increases levels of all these medications. Amiodarone-associated thyroid dysfunction is common in adults with congenital heart disease, with women and those with complex cyanotic lesions being at particular risk (95). In addition, amiodarone plus a beta-blocker may be effective for preventing shocks after an ICD implant (96).

Sotalol, another class III agent, initially was developed as a beta-blocker but also has the effect of prolonging the action potential as well as prolonging refractoriness. This results in prolongation of the QT interval. The drug's primary use is in SVT, but it is effective in VTs. It is well absorbed orally and is renally excreted with a half-life of 7 to 18 hours. Sotalol dosing is based on a nomogram and typically is dosed based on body surface area (60 to 200 mg/m²/day). The side effects are predominantly due to beta-blocking effects and include fatigue, dizziness, depression, headache, exacerbation of bronchospasm, bradycardia, AV block, and depression of cardiac function. Proarrhythmia can occur, with torsades de pointes being the most common, resulting from prolongation of the QT interval. The QT interval must be followed closely while patients are taking the drug because a corrected QTc <500 milliseconds has <2% risk of torsades, while a corrected QTc >550 milliseconds has a risk of torsades as high as 11%. Sotalol should be avoided in patients with hypokalemia or hypomagnesemia. Because of the incidence of symptomatic sinus bradycardia, AV block, and ventricular arrhythmias sotalol typically is initiated in the hospital with constant ECG monitoring (97).

Newer antiarrhythmic agents such as dofetilide and dronedarone may have utility in the treatment of arrhythmias in congenital heart disease patients, but there is limited experience with their use in children. Dofetilide, a class III antiarrhythmic agent, selectively inhibits the rapid component of the delayed rectifier potassium current, thus prolonging refractory periods (98). Dofetilide has been shown to be effective at controlling atrial arrhythmias in adult patients with congenital heart disease, but has a 15% incidence of excessive QT prolongation or torsades. Several patients in one study discontinued therapy because of waning effectiveness,

manifest by recurrence of their arrhythmias (99). Dronedarone is similar to amiodarone, although less potent, but has a better safety profile, lacking the thyroid, pulmonary, dermatologic, and neurologic toxicity (100). The efficacy and safety of dronedarone in patients with congenital heart disease remain to be determined. It may cause a rise in creatinine as well as liver dysfunction. An adult trial in advanced congestive heart failure patients was terminated prematurely because of excess mortality (101).

Class IV

Calcium channel blockers are Class IV agents in the Vaughn-Williams classification. Calcium channel blockers may be useful in AV node reentry tachycardia, idiopathic left VT, or right ventricular outflow tract tachycardia and to slow the ventricular response in atrial flutter or fibrillation. These drugs are relatively contraindicated in children younger than 1 year of age because of their greater sensitivity to negative inotropic effects, which may result in cardiovascular collapse and sudden death. They also are contraindicated in patients with WPW, as they may preferentially direct conduction down the accessory pathway, making ventricular fibrillation more likely.

Class V

Digoxin is classified as a Class V agent. It binds to Na-K-ATPase transport enzyme, which increases intracellular calcium via the Na-Ca exchange system. This results in an increase in vagal tone, which mediates EP effects, for instance, slowing AV node conduction and prolonging refractoriness. Applications for digoxin include controlling ventricular rate in primary atrial tachycardias and SVTs, particularly in fetal arrhythmias. Its effectiveness during exercise is limited because of low vagal tone; digoxin does not appear to blunt the heart rate during exercise. Caution should be used when giving digoxin to patients with WPW because it decreases the effective refractory period of the accessory pathway and may facilitate rapid conduction during atrial fibrillation. The half-life is age dependent: premature neonates, 60 hours; term neonates, 35 hours; infants, 18 hours; children, 37 hours; and adults, 35 to 48 hours. Adverse effects include nausea, vomiting, anorexia, headache, lethargy, confusion, and visual changes. Cardiac adverse effects include sinus bradycardia, AV block, supraventricular ectopy, ventricular ectopy, VT, and ventricular fibrillation. Digoxin may increase the risk of refractory ventricular arrhythmias or bradyarrhythmias after DC cardioversion. It is excreted primarily by the kidneys and must be used with extreme caution in patients with renal failure or the potential to develop renal dysfunction. Predisposing factors to toxicity also include increased myocardial sensitivity due to hypokalemia, hypomagnesemia, hypocalcemia, myocardial ischemia, myocarditis, and hypoxemia or taking drugs that decrease digoxin clearance, such as amiodarone, verapamil, spironolactone, or erythromycin.

Digitalis toxicity may present as a prolonged PR interval, ST segment changes, AV block, or ectopic junctional, atrial, or ventricular arrhythmias. Toxicity treatment may include atropine for bradycardia and AV block and lidocaine and/or phenytoin (class Ib antiarrhythmic) for tachycardias. High levels may require digoxin-immune Fab antibody therapy.

Adenosine

Adenosine works on specific receptors that are linked to potassium-channel stimulation located in the sinus and AV nodes.

TABLE 18.4 Pharmacologic Treatment of Arrhythmias

Treatment of Automaticity (AET)
Decrease phase 4 and 0 depolarization
β -Blocker (propranolol)
Sodium channel blocker (flecainide)
Alter surrounding tissue
Slow conduction ($\downarrow V_{max}$)
Na ⁺ channel blocker (flecainide)
Prolong refractoriness (TERP)
Class III agent (sotalol, amiodarone)
Treatment of reentry
Decrease conductivity of one limb
Na ⁺ -channel blockers (procainamide, flecainide)
β -Blockers (propranolol, atenolol)
Prolong refractoriness of one limb
Class Ia Agents (procainamide)
Class III Agents (sotalol, amiodarone)
Frequently, AVN is one limb of circuit
Calcium channel blockers (except in WPW)
β -Blockers
Treatment of triggered activity
Shorten action potential duration
Class Ib (mexiletine)
Suppress Afterdepolarizations
β -blockers (propranolol, atenolol, nadolol)

Activation of these receptors shortens the action potential duration. The EP effects include decreased rate of sinus node firing, slowing or block of AV nodal conduction, and shortening of atrial action potential. There is a biphasic response in the sinus node with an initial bradycardia that is a direct effect of activation of adenosine receptors followed by a subsequent sinus tachycardia that is an indirect effect from an autonomic reflex from carotid body chemoreceptors. Adenosine is metabolized rapidly by erythrocytes and endothelial tissue with a very short half-life of 1 to 5 seconds. The dose is usually 100 to 200 $\mu\text{g}/\text{kg}$, with a maximum dose of 12 mg, but doses of up to 400 $\mu\text{g}/\text{kg}$ may be given in refractory cases. Adenosine can be used in both the acute management of SVT to terminate reentrant arrhythmias and to establish the diagnosis in atrial arrhythmias. If the tachycardia is dependent on the AV node (AV node reentry tachycardia or accessory pathway-mediated tachycardia), it typically will terminate with adenosine. Atrial flutter or IART typically will not be affected by adenosine, but blocking the AV node and thus the ventricular response may reveal tachycardia that is masked by the QRS complex or T wave. Generally, automatic focus tachycardias (atrial or ventricular) are not affected but occasionally will terminate with adenosine administration. For this reason, an ECG recording during adenosine administration is very important. Adverse effects include chest discomfort, flushing, acute bronchospasm, and hypotension. The delayed chemoreceptor reflex may accelerate AV nodal conduction of atrial arrhythmias or precipitate atrial fibrillation. The initial bradycardia may precipitate torsades in patients with congenital or drug-induced prolonged QT. Patients who have had heart transplantation may be particularly sensitive to adenosine, resulting in long periods of ventricular asystole. A dose

of one-quarter to one-half the typical dose should be used in these patients.

In cases where adenosine is unsuccessful, it is important to determine the specific circumstances. If the adenosine is not given fast enough, there may be no response whatsoever. Other tachycardias (like sinus tachycardia) may temporarily slow down, but then immediately resume when the adenosine has been metabolized. Reentrant tachycardias using an accessory pathway may terminate, but then be reinitiated by a premature beat immediately after termination. Junctional or VTs may show temporary ventriculoatrial (VA) block with resultant VA dissociation without affecting the underlying tachycardia. As there are multiple reasons why adenosine “didn’t work,” it is important to obtain an ECG or rhythm strip during adenosine administration to determine the true response.

Magnesium

Magnesium also can be used as an antiarrhythmic agent, but its mechanism of action is not well established. Magnesium slows conduction in the AV node and suppresses after depolarizations. It should be considered as a first-line agent in patients with torsades de pointes, particularly those caused by congenital or drug-acquired long QT syndrome, and may have use in digitalis toxicity (102,103).

OTHER THERAPIES

In the case of reentrant tachycardias, pacing faster than the tachycardia cycle length can disrupt the circuit and terminate the tachycardia. This is particularly useful in the postoperative setting, where atrial and ventricular temporary pacing wires provide a means to pace the heart, or in the presence of implantable pacemakers or defibrillators. Alternatively, catheters can be placed transesophageally (for atrial flutter or reentrant SVT) or transvenously to pace terminate tachycardias. For patients presenting with intractable arrhythmias associated with poor ventricular function or myocarditis, mechanical support is an option until the tachycardia can be eliminated or controlled (104).

Defibrillation/Cardioversion

Defibrillation is the electrical conversion of a disorganized ventricular fibrillation into a normal rhythm. Cardioversion is the conversion of an organized tachycardia. For an organized tachycardia with a pulse, the energy should be delivered using a shock synchronized to the QRS complex. For ventricular fibrillation or torsades, an unsynchronized shock should be used. If the defibrillator is not able to sense QRS complexes, it will NOT discharge in the “synchronized” mode.

Defibrillation may be performed using either standard paddles or adhesive patches. Patches have the advantage of not requiring an operator to hold the paddles in position. For ventricular conversion, patches may be placed in the standard position of one patch to the right of the sternum and the other at the ventricular apex in the mid axillary line. For atrial tachycardias, it is beneficial to place the patches directly on the front and back of the chest. For unsuccessful cardioversions, it is important to differentiate from an unsuccessful defibrillation due to inadequate energy dose or improper paddle placement from termination with immediate reinitiation of the arrhythmia.

It is critically important to begin cardiopulmonary resuscitation (CPR) as soon as an arrest starts and defibrillate the heart as quickly as possible after an arrest. Even if there is an organized electrical activity on the ECG, one should always check a pulse to ensure that the electrical activity is creating a mechanical contraction. If no pulse is palpable, CPR should be resumed. It also is important to give sedation to awake patients as the energy delivered is a painful stimulus.

Antiarrhythmic medications may have an effect on defibrillation threshold from external defibrillators as well as ICDs. An increase in defibrillation thresholds is seen with flecainide, propafenone, amiodarone, and lidocaine, while sotalol and beta-blockers decrease defibrillation thresholds (105).

BRADYCARDIA

Bradycardias are defined as a heart rate less than normal for age. The most important distinction in bradycardias is differentiation of transient, functional slowing of the heart rate from that caused by an underlying disease of the conduction system.

Sinus Bradycardia

A hallmark feature of the sinus node is its adaptability to change. The majority of these changes are physiologic resulting from physical activity, fever, sleep, or illness. The autonomic nervous system plays a vital role in regulating the depolarizations and, therefore, the rate of sinoatrial nodal cell discharges. While the normal sinus rate for an adult is between 50 and 90 beats per minute, these rates vary in pediatrics based on age (see Table 18.1).

The definition of sinus bradycardia is a rhythm that originates in the sinoatrial node and is less than the lower rate acceptable for age (see Fig. 18.21). In addition, the axis of the P wave should be between 0 and 90 degrees (an upright P wave in leads I and aVF on the ECG), with each P resulting in normal AV activation. As previously stated, the sinus node may extend inferiorly to near the orifice of the inferior vena cava, therefore occasionally resulting in a slight shift in this P wave axis with a focus in the low right atrium resulting in a negative P wave in lead aVF on the ECG, but this is only seen at slower heart rates and typically reverts to the normal location at higher rates. Absolute limits for sinus bradycardia with a pediatric population have not been established firmly

because most of the studies performed in this area have not evaluated “normal” children (i.e., those without an indication for either an ECG or Holter monitor).

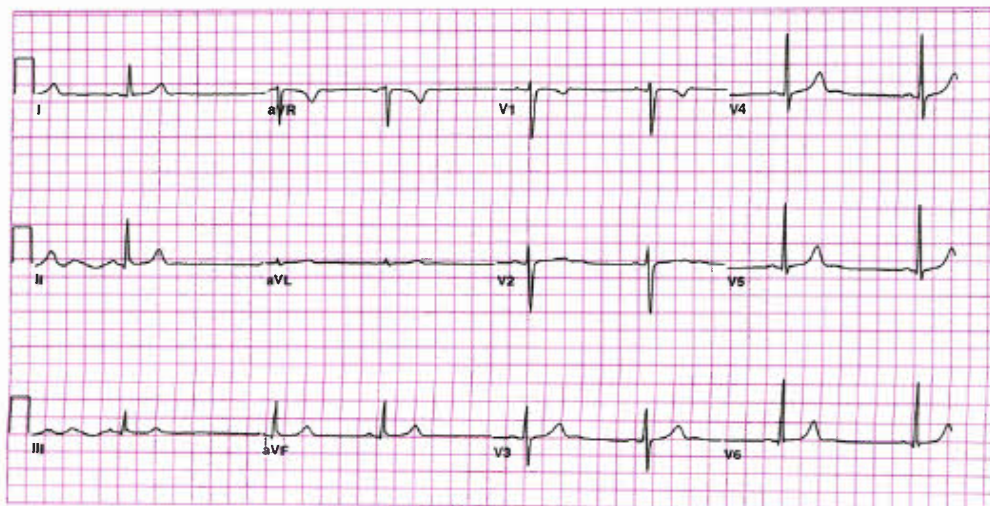
Sinus bradycardia is, in general, a benign entity that often occurs in athletes or during rest/sleep. Each person has his or her own set heart rate, and rates below “normal” values may be seen but may be completely normal and physiologically appropriate for an otherwise asymptomatic individual. Because of the general lack of symptoms, the true incidence of sinus bradycardia in the pediatric population is unknown. In a study performed on highly trained junior athletes, many subjects were found to have marked sinus bradycardia (106). Although the majority of patients with sinus bradycardia are asymptomatic, some may have symptoms of fatigue, syncope, exercise intolerance, sleepiness, and/or nightmares (107).

Common causes of sinus bradycardia include physical conditioning, anorexia, medications, or acute infections. Periods of abrupt sinus bradycardia and/or sinus arrest can occur in breath-holding spells or vasovagal/autonomic-mediated syncope. After a diagnosis of sinus bradycardia, a thorough history and review of symptoms is warranted to attempt to rule out a pathologic cause. Reversible causes of sinus bradycardia include such disorders as Cushing’s triad (acute increase in intracranial pressure, hypertension, and irregular respiration), hyperkalemia, hypercalcemia, hypoxia, hypothyroidism, hypothermia, and ingestions of such substances as beta-blockers, lithium, and digitalis (108). Rarely, cases of sinus bradycardia also may signify another disease such as myocarditis, diphtheria, or rheumatic fever (109).

The initial evaluation for a patient with bradycardia involves a complete history, physical examination, and an ECG. Having the patient do mild exercise (jumping jacks) in the office and then repeating an ECG may be sufficient evidence of normal sinus node functioning. If additional testing is necessary to confirm sinus bradycardia, other noninvasive tests such as a Holter monitor, an event monitor, or a 30-day loop recorder may be indicated. These tests have the advantage over the ECG in that the patient’s symptoms can be logged and directly correlated with symptoms. If these tests are not helpful or worry persists, the exercise stress test is another noninvasive test that can help rule out a pathologic sinus bradycardia. Invasive testing of the sinus node (sinus node recovery times or SNRTs) essentially has been abandoned in pediatrics because of its lack of sensitivity and specificity along with the ease of Holter monitoring and exercise stress testing.

The exercise stress test can be performed on children as young as 4 to 5 years old. This test is designed to give precise

Figure 18.21. Sinus bradycardia in a newborn. Note the slow rate with a normal P wave axis in an otherwise normal ECG. The pauses between two beats may be representative of underlying SND.



measurements of heart rate in response to an increasing load. The goal of exercise testing in a child with sinus bradycardia is to determine their maximal heart rate response. The diagnosis of SND—defined as any disturbance, impairment, or abnormality in the function of the sinus node—depends on the patient's effort, as the normal peak heart rate achievable during exercise stress testing is dependent on patient age and effort. The vast majority of patients who have an exercise test as an evaluation for sinus bradycardia achieves normal peak heart rates and therefore needs no further workup. Those patients who achieve a normal peak heart rate that is significantly lower than expected (typically <135 beats per minute) or have an exaggerated, rapid decline in heart rate during recovery may have SND rather than simple sinus bradycardia.

Treatment

The only reason to treat patients with sinus bradycardia is when symptoms of fatigue or syncope are temporally correlated with the presence of a slow heart rate on multiple occasions. Routine sinus bradycardia in the absence of any underlying cause or symptoms does not require treatment. Severe cases of autonomic dysfunction or breath-holding spells with frequent sinus pauses resulting in syncope may benefit from pacemaker placement, but this almost never is necessary, particularly in young children for whom the symptoms frequently will resolve by age 4 to 6. In addition, there is frequently a blood pressure drop in older patients that may result in continued symptoms and syncope despite an adequate heart rate.

Sinus Node Dysfunction

SND generally occurs in the setting of sinus bradycardia with slow escape rhythms and can be associated with tachyarrhythmias such as atrial fibrillation or flutter. This disorder is somewhat uncommon in the pediatric age group but becomes more prevalent in adults who had congenital heart surgery at earlier ages. There are two main groups of SND in the pediatric age group. In the first, disease is caused by a primary disorder associated with ion channels in the sinus node (a channelopathy). This is discussed in another chapter (see Chapter 16). Disease in the second group has causes such as vagal tone, congenital heart disease, postsurgical state, or a reversible cause including hypothyroidism or medications.

Most patients with SND, like those with sinus bradycardia, are asymptomatic. Multiple factors may be directly attributed to the fact that these patients, in spite of slow or absent sinus rhythm, are asymptomatic. First and foremost is that the presence of symptoms depends on the function of the remaining cardiac conduction system (atrium, AV node, and ventricles). If the patient has an appropriate atrial or junctional escape rhythm, they may be completely asymptomatic. Their clinical presentation also depends, in large part, upon age, with older patients tending to be asymptomatic, in part because they tend to self-limit and therefore symptoms such as exercise intolerance and fatigue go unnoticed. Infants with SND tend to present with poor feeding, lethargy, and failure to thrive while older children and adults are relatively asymptomatic. In studies performed on children with SND, almost 75% were asymptomatic (107,110). Those who experience symptoms may have only subtle signs of fatigue, inability to keep up with their peers, shortness of breath, syncope, or more marked symptoms of congestive heart failure or IART. Sudden death also has been reported in rare patients with SND, but these cases tend to involve primary SND and, contrary to popular belief, not secondary SND (111–113).

Etiology of sinus node dysfunction

There is a myriad of causes of SND in the pediatric age group, including ion channelopathies, malignancies, inflammatory disorders, cardiomyopathies, structural heart disease, and surgical damage. In addition, readily reversible causes include hypothyroidism, increased vagal tone, hypothermia, and medications. For this section, the focus is on the surgical and untreatable causes.

SND may result from cardiac surgery and disruption of the sinus node artery during the repair or during placement of the superior vena cava cannula for cardiopulmonary bypass (114a,114b,115). For a complete list of nonreversible, nongenetic causes of SND, please refer to Table 18.5.

The evaluation of SND is the same as for patients with sinus bradycardia. One clue that may help differentiate SND from sinus bradycardia is the complete absence of sinus node activity with slow escape rates or atrial flutter or fibrillation following a sinus pause as these are not typically seen in patients with a normal sinus node. If clinically indicated, laboratory evaluation including a drug screen, thyroid function tests and evaluation for rheumatic disorders, infections, or metabolic causes may be performed.

Treatment

When a reversible cause of SND has been excluded and symptomatic SND is present, the treatment is implantation of a permanent pacemaker. This includes patients with chronotropic incompetence as a result of required drug therapy.

Disorders of Atrioventricular Conduction

The term AV block describes an abnormality in the conduction of atrial impulses through the AV node to the ventricles.

TABLE 18.5

Nonreversible, Nongenetic Causes of SND

Congenital Heart Disease

Atrial septal defects, primum, secundum, and sinus venosus

Pulmonary stenosis

Ventricular septal defects

Transposition of the great arteries

Single ventricle

Patent ductus arteriosus

Coarctation of aorta

WPW syndrome

Cardiomyopathies

Idiopathic, hypertrophic, and infiltrative

Inflammatory

Muscular dystrophy, of all types, especially Emery-Dreifuss

Friedreich ataxia

Kawasaki disease

Other

Tumor

Guillain-Barré

Kearns-Sayre syndrome

This abnormality can range from a simple delay in impulse transmission, as in first-degree AV block, to a complete interruption of signal transmission, classified as complete, or third-degree, AV block. Each form of AV block has a distinct anatomic or physiologic cause for the electrical abnormality and can be either transient or permanent in nature. The cause of this arrhythmia may be structural cardiac disease, trauma, myocardial infarction or inflammation, or abnormal impulse propagation from an underlying cardiac channelopathy. In pediatric patients, the majority of block occurs in the AV node proper (116). The block can result from enhanced vagal tone, congenital heart disease, surgery, or infections such as Lyme disease (117).

First-Degree Atrioventricular Block

First-degree AV block is defined as prolonged conduction through the AV node that is greater than accepted for age (see Fig. 18.22). Although called “AV block,” it is not truly a block and a more correct terminology may be “prolonged PR interval.” The upper limit for the PR interval, like other ECG findings in pediatrics, varies with age, ranging from 70 milliseconds in infants to 200 milliseconds in adolescents. It manifests as prolongation of the PR interval with every P wave followed by a QRS complex. It can be caused by delay within the atrium, AV node, or His-Purkinje system. Generally, the finding is normal, with a prevalence of up to 8% of normal children (118). This ECG finding also has been described in patients with a patent ductus arteriosus (119). Other causes of first-degree AV block include increased vagal tone, acute rheumatic fever, Ebstein’s anomaly, medications (digoxin, calcium channel blockers, sotalol, amiodarone, and procainamide), and electrolyte disturbances (hyper- and hypokalemia and -calcemia as well as hypomagnesemia). Despite the severity of disorders and medications, this ECG finding has little clinical significance and generally requires no treatment. In some children, there is no underlying cause, and it may be considered normal for that individual.

Second-Degree Atrioventricular Block

Second-degree AV block is defined as the failure of at least one nonpremature atrial impulse to conduct to the ventricles. A number of different forms of second-degree AV block exist (see Fig. 18.23). These include Mobitz type I, Mobitz type II, 2:1 AV block, and high-grade second-degree AV

block (presence of some AV conduction, but more than two consecutive P waves fail to conduct).

Mobitz type I, or Wenckebach, is the most common type of second-degree AV block. Typical Wenckebach is characterized by the following four criteria (120):

1. Progressive prolongation of the PR intervals
2. PR interval prolongation at progressively decreasing increments
3. Progressive shortening of the RR interval
4. Eventual failure to conduct an atrial beat to the ventricle

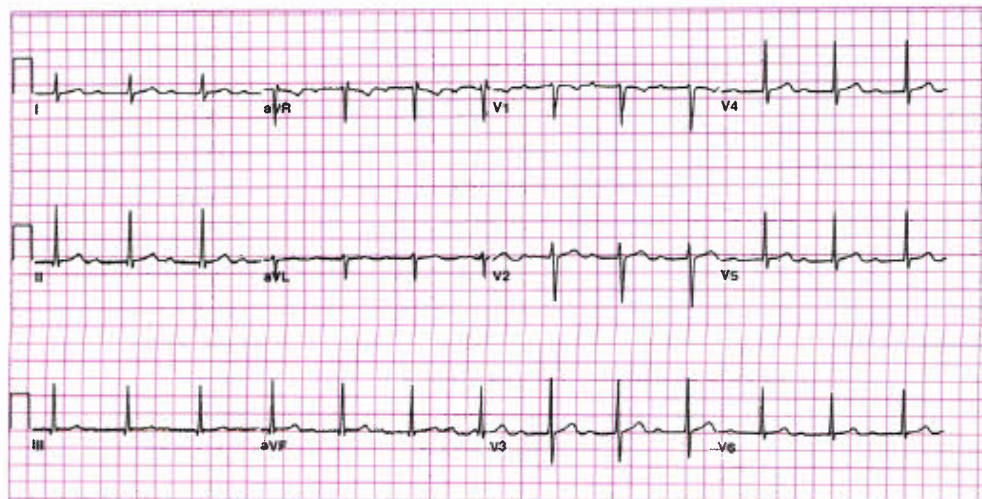
When Wenckebach occurs with a normal QRS duration, the location of the delay is in the AV node, proximal to the bundle of His (120). When the QRS duration is prolonged and Wenckebach occurs, the block may be in the AV node or within and/or below the His bundle.

This conduction abnormality most commonly is transient in nature and caused by vagal influence. The majority of episodes of Wenckebach occurs in healthy, asymptomatic patients during sleep or other times of high resting vagal tone. A small percentage of patients may have underlying AV node disease or a progressive conduction system disturbance. Wenckebach typically does not occur while awake except rarely in highly trained professional athletes. Wenckebach during exercise or at times of increased catecholamine state is pathologic and should be thoroughly evaluated for the presence of conduction system disease. If the Wenckebach is thought to be physiologic (particularly during sleep), no therapy is required and follow-up is unnecessary.

The pathologic form of second-degree AV block, or Mobitz type II, is characterized by a constant P-P interval without lengthening of the PR interval prior to the nonconducted P. This rare conduction abnormality generally but not always represents a conduction defect below the bundle of His (121). The most common reason for this problem in the pediatric population is myocarditis and/or postsurgical complications. Another potentially lethal cause has been described in patients who develop rejection after cardiac transplant (122,123) or who have posttransplant coronary artery disease (124). If a reversible cause for this form of AV block cannot be found, the recommendation is for implantation of a permanent pacemaker.

Another form of AV block that rarely occurs in pediatric patients is 2:1 AV block. This arrhythmia generally occurs in a patient during times of high vagal tone such as sleep but also may be seen in patients with long QT syndrome. It is impossible to classify 2:1 AV block as either type I or II because there

Figure 18.22. First-degree AV block. Note the prolonged PR interval with otherwise normal conduction in a 1:1 manner from the atrium to the ventricle. This finding is typically benign and related to an increased vagal tone or resting state. At faster heart rates, it may be a marker of atrial tachycardia or AV nodal conduction disease.



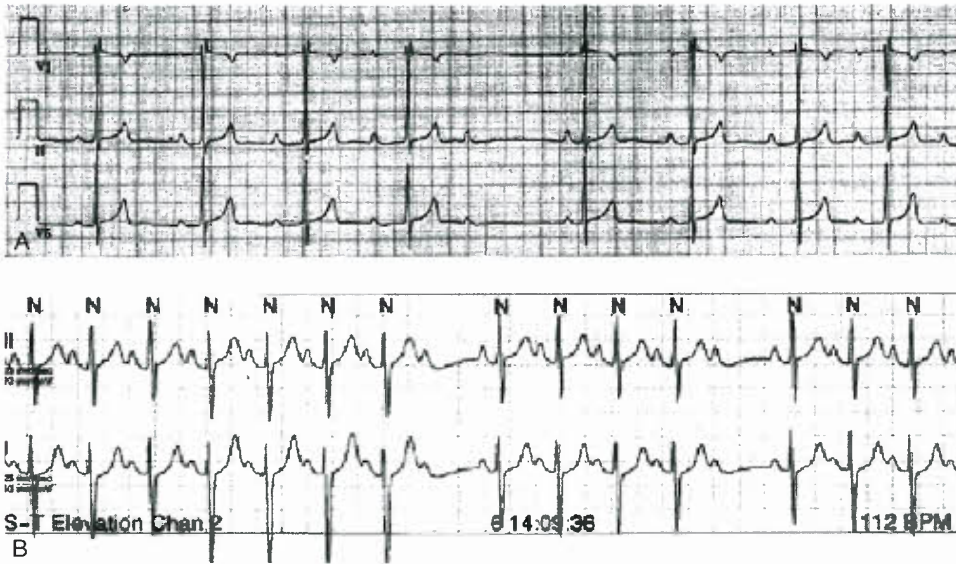


Figure 18.23. Second-degree AV block. A: Mobitz type I or Wenckebach with progressive prolongation of the PR interval followed by a dropped beat. This finding may be normal, particularly during sleep. B: Mobitz type II with no prolongation of the PR interval prior to a dropped beat. This type of block is always pathologic.

is no stable PR interval with successively conducted beats. The presence of Mobitz type I or Mobitz type II block on a long rhythm strip or 24-hour monitor may help to distinguish these two types. Differentiation also can be performed using an intracardiac tracing by looking for the presence of a bundle of His recording following the atrial depolarization. If the His is present, block occurs below the AV node. In addition, most patients who have Mobitz type II block have an underlying bundle branch block, although patients with Mobitz type I may as well. The treatment for 2:1 AV block is no different from that already outlined for type I and II AV block. The QT interval should be carefully measured in patients with 2:1 AV block as long QT syndrome can result in this finding.

High-grade or advanced second-degree AV block occurs when there are two or more successive sinoatrial impulses that are not propagated through the AV node. This form of AV block may have a reversible cause, such as acute myocarditis and rheumatic fever, an irreversible cause such as lupus or congenital cardiac disorders, or as a direct result of cardiac surgery (125–128). Patients with this conduction disorder need to be evaluated at regular intervals. The majority of these patients, regardless of symptoms, will require pacemaker implantation. In the asymptomatic patient with an unknown

cause of advanced second-degree AV block and a structurally normal heart, management would be similar to that of complete AV block (CAVB).

Complete Atrioventricular Block

CAVB, or third-degree AV block, is the complete failure of sinus atrial impulse conduction to the ventricles (Fig. 18.24). In addition, the atrial rate must be faster than the ventricular rate to assure that the AV dissociation is not caused by a junctional or ventricular rhythm (e.g., sinus bradycardia with junctional escape or an accelerated junctional or ventricular rhythm). This rhythm disturbance generally is diagnosed using an ECG and confirmed by a 24-hour Holter monitor. There is currently no indication for EP testing in patients with CAVB.

The incidence of congenital CAVB (CCAVB) in live-born infants is 1 in 20,000 (129). The majority of affected pediatric patients come from three distinct groups: those with structural cardiac disease, maternal connective tissue disorders, or cardiovascular surgery complications (130–132). In addition, other causes of CAVB have been described including infections, myopathies, and genetic disorders (133–135).

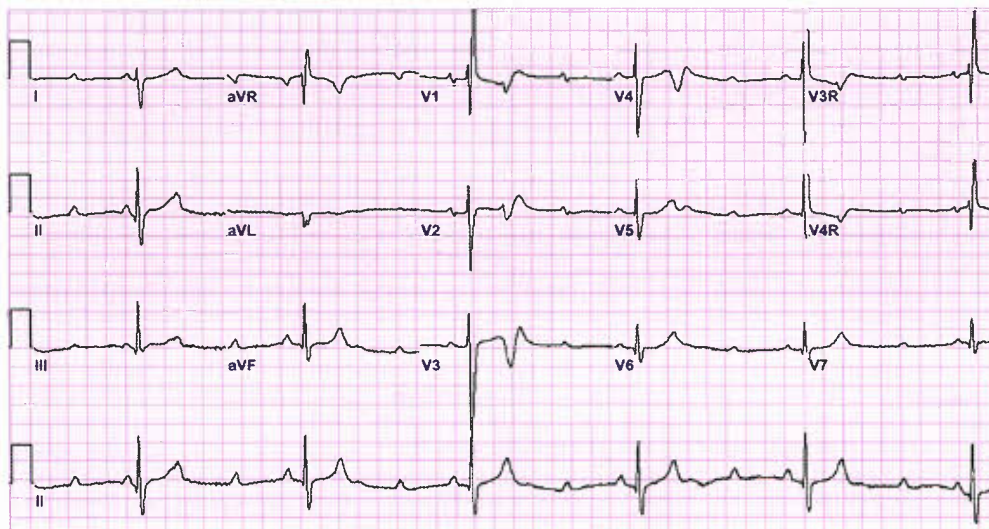


Figure 18.24. Complete AV block. The atrial rate is faster than the ventricular rate, there is no relationship between the P waves and the QRS complexes, and there are P waves that should conduct but do not.

The first major cause of CAVB is associated with structural cardiac disorders. The etiology of nonimmune CAVB has been postulated by Lev (136) to occur as the result of a developmental abnormality of the AV node. This can be caused by a complete absence of the AV node, lack of union between the AV node and distal conduction system, or the presence of an aberrant, nonfunctioning, or poorly functioning system. The most common structural cardiac abnormalities associated with CAVB are AV septal defects, both with and without associated left atrial isomerism and AV discordance with ventriculoarterial discordance (congenitally corrected transposition of the great arteries) (130,132). Additional cardiovascular malformations (tetralogy of Fallot, atrial septal defects, transposition of the great vessels, and tricuspid atresia) have been described, without any apparent association between the structural abnormality and the conduction defect (130,132).

A second major cause of CAVB can be attributed to maternal autoimmune disorders (137,138). It occurs in fetuses of mothers with systemic lupus erythematosus (SLE), Sjogren syndrome, rheumatoid arthritis, scleroderma, and undifferentiated connective tissue disorders (139–141). Specifically, it has been associated strongly with maternal autoantibodies designated as anti-SS-A/Ro, anti-SS-B/La, or both (142). Many women who deliver babies with CAVB do not have symptoms of any connective tissue disorder at the time, with half demonstrating only serologic evidence of their disease (143). In addition, the vast majority of mothers with SLE will not have offspring with CAVB. Their risk of conceiving an infant with CAVB is only 1 in 60 (144). If maternal autoantibodies to SSA/Ro are present, that risk, 1 in 20, increases dramatically (145). The risk of recurrence of CAVB in subsequent pregnancies is between 10% and 16% (142).

The mechanism of damage to the conduction system occurs when maternal antibodies cross the placenta and react with their corresponding antigens expressed on the surface of cells of the fetal cardiac conduction system, resulting in immunoglobulin deposition on the cells of the fetal conduction system and on the cardiac myocytes. This local inflammatory reaction leads to permanent damage to the fetal cardiac conduction system because of localized cellular apoptosis (146–150). Patients with antinuclear antibodies may have a higher incidence of long-term development of heart failure and death compared to those who are antibody negative (151).

The third major cause of CAVB is as a direct result of a surgical or catheter intervention that results in damage to the His bundle or AV node. In a number of surgical repairs, damage to the AV node is a known complication because of the close proximity between the defect and the conduction system. These defects include perimembranous ventricular septal defects, AV canal repairs, and congenitally corrected transposition of the great arteries with ventricular septal defect. In other repairs, such as aortic and mitral valve replacements, the prosthetic valve tissue often impinges on the normal AV conduction system, which also results in block.

AV block remains a relatively rare complication of cardiovascular surgery, affecting overall fewer than 3% of patients. A number of preoperative and intraoperative risks have been identified in these patients, including younger age, lower weights, and longer aortic cross clamp or cardiopulmonary bypass (84). Often this type of block is temporary and does not require long-term treatment although patients can be at an increased long-term risk for developing AV block. In this era of cardiovascular surgery, the majority of surgeons place temporary pacing wires at the time of repair that can be removed 2 to 3 days following surgery if no signs of conduction block have occurred (152). If any conduction block is noted, the heart can be paced until it is determined that normal conduction has returned or the patient requires a more permanent system.

Since the advent of catheter interventions for the treatment of arrhythmias or to occlude septal defects, an additional cause of AV block has emerged. EP procedures and a number of percutaneous catheter interventions also pose a risk of developing AV block either as an acute or late complication. The risk of AV block in these patients is thought to be as a direct result of impingement of the device (septal occluder or aortic or pulmonary valve) on the AV node (153–156). In the majority of patients, the AV block is noted acutely and can be rectified by device removal. However, some patients develop this as a late complication. These tend to be permanent.

In addition to these well-known causes, a small group of patients has been identified with a genetic mutation that results in CAVB. A mutation in the cardiac transcription factor NKX2.5 can result in familial atrial septal defects or hypoplastic left heart syndrome in an autosomal dominant inheritance pattern (157). AV node conduction abnormalities also occur in Holt-Oram syndrome and atrial septal defects. Patients with structurally normal hearts and a mutation in SCN5A, a sodium ion channel responsible for long QT and Brugada syndrome, can have a range of AV conduction abnormalities, including complete block (158). In addition, infections may produce AV block including acute rheumatic fever, Chagas disease, diphtheria, and Rocky Mountain spotted fever. Lyme disease also can present with high-grade AV block, which may be the only manifestation of this infection.

Symptoms and Treatment

Fetal Congenital Complete Atrioventricular Block

A wide range of symptoms has been identified in patients with CAVB. The symptoms that patients present with tend to depend, at least in part, on the patient's age at presentation. CCAVB, when identified in a fetus, can vary from asymptomatic to hydrops fetalis. Recent studies have documented exceptionally high mortality rates for these patients, ranging from 7% to 33% in infants and fetuses with structurally normal hearts and as high as 86% in those with structural cardiac lesions (130–132,143,159). Poor outcomes are associated with the presence of structural cardiac disease, hydrops, ventricular rates <55 beats per minute, AV valve regurgitation, dilated cardiomyopathy, prolonged corrected QT interval, or delivery at or before 32 weeks' gestation (130–132,143,159).

The goal of managing a fetus with CAVB is the birth of a healthy infant. This outcome can best be accomplished by early intervention at the first sign of the problems listed in the prior paragraph. Also, identification of fetuses at risk for developing CAVB is important, allowing the initiation of therapies to prevent the onset or progression of the conduction abnormality. These goals can be accomplished by increasing the fetal heart rate and/or contractility or by removing the inflammatory agents or modulating it through immune suppression.

The maternal or direct fetal administration of sympathomimetic agents such as ritodrine, terbutaline, isoproterenol, and salbutamol may improve both fetal heart rates and contractility (130,160–162). These medications are not given routinely as there frequently is no improvement because AV conduction has not been restored. However, it has been proposed that a trial of sympathomimetics should be considered in fetuses with CAVB with signs of deterioration (160). The reduction of the maternal antibody titer through plasmapheresis also has been performed but with variable results. Also, the use of intravenous gamma globulin has resulted in a complete reduction of the maternal anti-Ro antibody titer (163). Only a limited number of patients has had these therapies during pregnancy and they are not used in most centers.

The use of fluorinated steroids, dexamethasone and betamethasone for the treatment and prevention of CAVB also has been reported (130,131,142,164–166). In one study comparing the use of fluorinated steroids to an untreated control group, the use of steroids in fetuses that already had developed CAVB failed to restore any AV conduction but somewhat improved hydrops and other symptoms (167). Steroids administered soon after the onset of second-degree AV block may result in the permanent reversal of advanced AV conduction disorders in some fetuses, and fluorinated steroids should be considered in fetuses with early forms of AV block and/or hydrops.

In summary, fetal CAVB is a relatively rare condition with evolving management. It is recommended that all mothers with anti Ro and La antibodies (SSA and SSB) have an early fetal echocardiogram. In the fetus of a mother with a connective tissue disorder, early detection of advanced AV conduction abnormalities and/or hydrops should prompt the consideration to use fluorinated steroids with the goal of preventing the progression of the inflammatory process. In addition, referral to a center with expertise in high-risk obstetrics, fetal cardiology, and pediatric and neonatal pacemaker implantation and management should be considered strongly near the time of delivery.

CAVB in Infants, Children, and Young Adults

A wide array of symptoms occurs in infants, children, and young adults with structurally normal hearts and CAVB. These symptoms range from nothing to Stokes-Adams attacks (sudden transient episode of syncope) and sudden cardiac death. The underlying reason for symptoms or lack of symptoms is the patient's underlying escape rate and rhythm. Those patients with a reasonable junctional escape that is chronotropically competent tend to be relatively asymptomatic. Those with very slow resting heart rates that do not significantly increase with exercise tend to have symptoms of fatigue, syncope, nightmares, or even congestive heart failure.

After documentation of CCAVB in asymptomatic patients with an ECG, their evaluation includes a number of tests to determine whether they meet criteria for implantation of a pacing system. In patients newly diagnosed with CCAVB, an echocardiogram routinely is performed to evaluate for structural cardiac disease or myocarditis. If a congenital cardiac anomaly is a hemodynamically significant defect, then a pacing system is recommended if there are symptoms or if the heart rate is <70 regardless of symptoms. This recommendation stems from an increased incidence of death (29% vs. 8%) in patients with structural heart disease when compared to normal patients (168).

In asymptomatic patients with structurally normal hearts, the first test is a 24-hour Holter monitor to detect episodes of abrupt pauses >2 to 3 times the underlying cycle length, average heart rate <50 beats per minute, complex ventricular ectopy, wide QRS escape rhythm, VT, or symptoms associated with slow heart rates, all of which are indications for pacing. After the Holter monitor, the next test (in patients old enough to participate) is an exercise stress test. During the test, careful attention is paid to the patient's maximal heart rate at peak exercise and symptoms. If the patient has symptoms, an increase in ventricular ectopy or an episode of VT, pacing may be indicated. The final test, usually performed on an annual basis, is an echocardiogram to evaluate the size and function of the left ventricle.

CCAVB patients compensate for their reduced heart rate by increasing their left ventricular end diastolic volume and therefore their stroke volume. It is common to see ventricular dilation in these patients on echocardiography, but the function typically is normal or hyperdynamic. A decrease in function or extreme dilation is concerning and may require pacemaker implantation. In those patients with CCAVB who do not meet requirements for pacemaker implantation by their late teen

years, prophylactic pacemaker implantation may be considered. This is based on a large prospective study of adults with isolated congenital heart disease, in which the authors found that 50% of previously asymptomatic adult patients develop symptoms and 10% will die prematurely (169).

When surgical AV block is identified, these patients must be paced temporarily in the immediate postoperative phase. The underlying junctional escape rhythm in these patients is not reliable and may result in episodes of asystole. In addition, pacing allows a more appropriate ventricular rate and a restoration of AV synchrony that can be important to the patients' hemodynamic status. Paced patients with surgical AV block should be evaluated daily for return of native AV conduction. Atrial and ventricular lead capture thresholds should be adjusted to at least twice the safety margin (lowest output that reliably captures the myocardium). The patient should have implantation of a permanent pacing system if the AV block is not expected to resolve or persists at least 7 days following surgery. Without implantation of a pacing system in postoperative AV block, the mortality rate has been reported to be as high as 60% within the first year alone (170).

If temporary pacing for hemodynamically significant AV block is needed, there are several options. The first is transcutaneous pacing that can be performed through many external defibrillators. This may provide a temporary method for pacing the heart, but is not a good long-term solution and usually is not tolerable in an alert patient. Temporary pacing catheters also can be placed through the femoral or internal jugular veins to stimulate the heart. Pacing typically is performed in the ventricle regardless of the source of bradycardia to ensure an adequate ventricular rate to provide blood flow to the body. There are three types of catheters. The first uses a balloon to guide the catheter into position. This is helpful, unless there is ventricular asystole with no forward flow to guide the balloon into the ventricle. The second is a fixed curve or deflectable catheter used for EP studies that can be placed into the ventricle. In general, this requires fluoroscopic guidance in the cath lab to properly position. The final type is a temporary pacing catheter that has a small electrode tip that is actually screwed into the myocardium under fluoroscopic guidance. This technique has the advantage of having a stable position with little chance for dislodgement with subsequent loss of pacing capture, but is more difficult to place and remove. All of these are temporary solutions and require assessment for the need for a permanent pacing system after being in place for 1 to 2 days.

Bundle Branch Block

Synchronous depolarization of the left and right ventricles occurs through specialized conduction tissue and results in a narrow complex QRS on the ECG. This conduction tissue divides into a left and right bundle branch after the bundle of His. The right bundle continues into the right ventricular apex and then turns anteriorly and is contiguous with the moderator band. Typically, the left bundle branch quickly subdivides into a left anterior and left posterior fascicle resulting in activation of the left ventricle prior to the right ventricle.

When activation in one of these bundles is delayed, it results in a prolonged QRS duration for age. A right bundle branch block typically has a conduction delay in lead V1 with an initial positive deflection followed by a deflection below the baseline followed by another positive deflection (RSR' pattern). A left bundle branch will typically have this pattern in lead V6 (see Fig. 18.25).

This conduction delay may be congenital or acquired. Congenital autosomal dominant right bundle branch block is a hereditary condition that typically is associated with normal cardiac function and no long-term consequences. Congenital

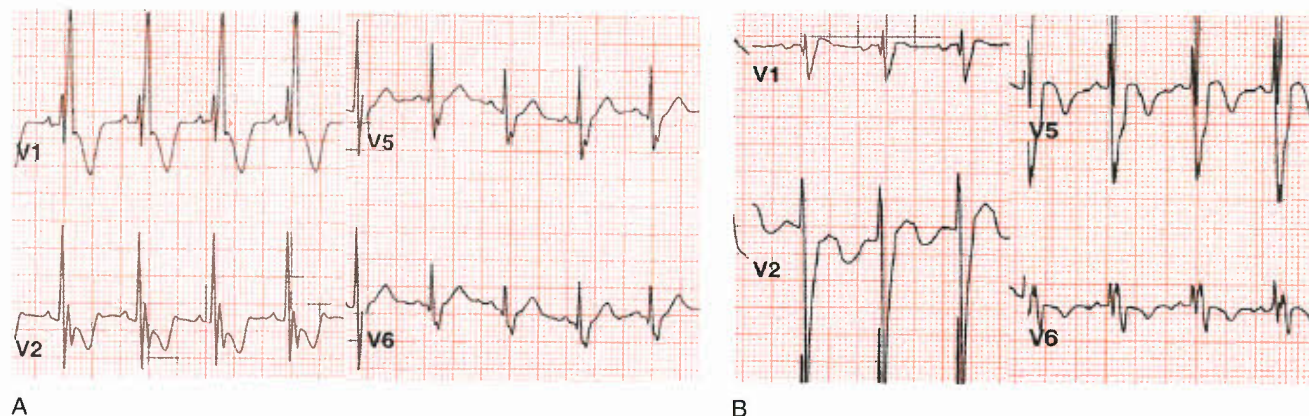


Figure 18.25. Bundle branch block. **A:** Right bundle branch block with an RSR' pattern in V1 and slurred S wave in V6. **B:** Left bundle branch block with an RSR' pattern in V6 and slurred S wave in V1.

right bundle branch block also occurs frequently with Ebstein anomaly of the tricuspid valve. Right bundle branch block also can occur in ARVC, myocarditis, following orthotopic heart transplantation or in Brugada syndrome (typically right bundle branch only in lead V1 and/or V2). More commonly right bundle branch block is acquired following cardiac surgery particularly following ventricular septal defect or AV canal repair. Left bundle branch block is rare in the pediatric population. Kearns-Sayre syndrome and myotonic dystrophy can present with first or second-degree AV block that may progress to higher levels of AV block and may therefore require early pacemaker implantation.

PACEMAKERS AND IMPLANTABLE CARDIOVERTER DEFIBRILLATORS

The original description of pediatric pacemaker implantations occurred in the 1960s and involved patients who had surgical CAVB (171). Since that time, the indication for pediatric devices has expanded and the technology has advanced. Only basic concepts are discussed as there is a large number of textbooks dedicated completely to a more in-depth examination of pacing and defibrillation indications, technology, and

implantation techniques. These devices consist of a generator that contains the battery, circuitry and computer, and a lead that connects the generator to the myocardium. Leads can be placed through the venous system and placed on the endocardial surface of the heart (transvenous leads) or affixed directly on the outer surface of the heart by a surgeon (epicardial leads). Newer lead technology allows the lead to be placed on the myocardium and communicate wirelessly to the generator.

Pacemakers perform four basic functions:

- Stimulate cardiac depolarization
- Sense intrinsic cardiac function
- Respond to increased metabolic demand by providing rate-responsive pacing
- Provide diagnostic information stored by the pacemaker

An ICD performs all of the above functions but is able to detect VT and deliver antitachycardia pacing or a shock through the device to attempt to cardiovert or defibrillate the patient. The North American Society of Pacing and Electrophysiology/British Pacing and Electrophysiology Group Generic (NBG) code was created as a standard method of describing the mode of pacing, the mode of sensing, and how the pacemaker will respond to the presence or absence of intrinsic beats.(172) (see Table 18.6).

TABLE 18.6 Revised NASPE/BPEG Generic Code

Position	1	2	3	4	5
Category	Chamber(s) paced	Chamber(s) Sensed	Response to sensing	Rate modulation	Multisite pacing
Letters used	0 = none A = atrial V = ventricle D = dual (A + V)	0 = none A = atrial V = ventricle D = dual (A + V)	0 = none T = triggered I = inhibit D = dual (T + I)	0 = none R = Rate modulation	0 = none A = atrial V = ventricle D = dual (A + V)

A triggered response is an active pacing response to a sensed event. This is used in dual-chamber pacemakers so that the underlying sinus rate can be "tracked" resulting in a 1:1 relationship between the atria and ventricles. An inhibit response results in the pacemaker not firing so that pacing does not occur when an intrinsic event is present. Rate modulation involves sensors in the device that increase the heart rate in response to motion to simulate the increase in heart rate seen with physical activity. Multisite pacing involves more than one pacing lead in a particular chamber to create a more synchronous contraction. (Adapted from Bernstein, et al. The revised NASPE/BPEG generic code for antibradycardia, adaptive-rate, and multisite pacing. North American Society of Pacing and Electrophysiology/British Pacing and Electrophysiology Group. *Pacing Clin Electrophysiol* 2002;25:260–264.)

The indications for pacing and defibrillation for children are relatively similar to those for adult patients, but due to patient size, activity level, longevity, and venous access, a number of unique considerations make the decision to implant a device not as straightforward. What type of device (single, dual, or multichamber) and how the device is implanted (transvenous versus epicardial) are the first decisions one must make after the decision to pace has been reached. These decisions are influenced by the patient's size, the presence of unrepaired structural cardiac disease or residual shunting, the inability to access the heart through the existing venous anatomy, and the necessity of device implantation.

The overall goal of any device is to improve the patient's underlying conduction abnormality while not limiting future decisions to upgrade the system. An example might be a

7-year-old patient with SND and intact AV node function: This patient's subclavian vein may be too small for implantation of a dual-chamber pacing system, but implanting a single-chamber system capable of pacing the atrium and allowing conduction down the intact AV node is a wise compromise. These decisions also may affect the ability to pace/defibrillate the patient through transvenous systems long term. The clinician's goal is to pace the patient in a manner that will allow for continued pacing throughout the patient's lifespan.

The 2008 guidelines for device-based therapy of cardiac rhythm abnormalities are categorized into different classes and different levels within each class. The indications for the implantation of a permanent pacing system in a pediatric patient are listed in Table 18.7 (173).

TABLE 18.7 Indications for Pacing in the Pediatric Population

Class I (Recommended)

1. Advanced second- or third-degree AV block associated with symptomatic bradycardia, ventricular dysfunction, or low cardiac output
2. SND with correlation of symptoms during age-inappropriate bradycardia
3. Postoperative advanced second- or third-degree AV block that is not expected to resolve or that persists at least 7 days after cardiac surgery
4. Congenital third-degree AV block with a wide QRS escape rhythm, complex ventricular ectopy, or ventricular dysfunction
5. Congenital third-degree AV block in the infant with a ventricular rate <55 bpm or with congenital heart disease and a ventricular rate <70 bpm

Class IIa (Is Reasonable)

1. Patients with congenital heart disease and sinus bradycardia (intrinsic or antiarrhythmic induced) for the prevention of recurrent episodes of intra-atrial reentrant tachycardia
2. Congenital third-degree AV block beyond the 1st year of life with an average heart rate <50 bpm, abrupt pauses in ventricular rate that are two or three times the basic cycle length, or associated with symptoms due to chronotropic incompetence
3. Sinus bradycardia with complex congenital heart disease with a resting heart rate <40 bpm or pauses in ventricular rate longer than 3 s
4. Patients with congenital heart disease and impaired hemodynamics due to sinus bradycardia or loss of AV synchrony.
5. Unexplained syncope in the patient with prior congenital heart surgery complicated by transient complete heart block with residual fascicular block after a careful evaluation to exclude other causes of syncope.

Class IIb (May Be Considered)

1. Transient postoperative third-degree AV block that reverts to sinus rhythm with residual bifascicular block because of the long-term risk for development of AV block
2. Congenital third-degree AV block in asymptomatic children or adolescents with an acceptable rate, a narrow QRS complex, and normal ventricular function
3. Asymptomatic sinus bradycardia after biventricular repair of congenital heart disease with a resting heart rate <40 bpm or pauses in ventricular rate longer than 3 s

Class III (Not Recommended)

1. Transient postoperative AV block with return of normal AV conduction in the otherwise asymptomatic patient
2. Asymptomatic bifascicular block with or without first-degree AV block after surgery for congenital heart disease in the absence of prior transient CAVB.
3. Asymptomatic type I second-degree AV block.
4. Asymptomatic sinus bradycardia with the longest relative risk interval <3 seconds and a minimum heart rate more than 40 bpm

Adapted from Epstein A, DiMarco J, Ellenbogen K, et al. ACC/AHA/HRS 2008 guidelines for device-based therapy of cardiac rhythm abnormalities. *J Am Coll Cardiol* 2008;5:E1–E62.

TABLE 18.8 Indications for Implantable Cardioverter-Defibrillator (ICD) Placement in Pediatric Patients**Class I (Recommended)**

1. ICD implantation is indicated in the survivor of cardiac arrest after evaluation to define the cause of the event and to exclude any reversible causes
2. ICD implantation is indicated for patients with symptomatic sustained VT in association with congenital heart disease who have undergone hemodynamic and electrophysiologic evaluation. Catheter ablation or surgical repair may offer possible alternatives in carefully selected patients

Class IIa (Is Reasonable)

1. ICD implantation is reasonable for patients with congenital heart disease with recurrent syncope of undetermined origin in the presence of either ventricular dysfunction or inducible ventricular arrhythmias at electrophysiologic study

Class IIb (May Be Considered)

1. ICD implantation may be considered for patients with recurrent syncope associated with complex congenital heart disease and advanced systemic ventricular dysfunction when thorough invasive and noninvasive investigations have failed to define a cause

Class III (Not Recommended)

1. ICD therapy is not indicated for patients who do not have a reasonable expectation of survival with an acceptable functional status for at least 1 year, even if they meet specific ICD implantation criteria
2. ICD therapy is not indicated for patients with incessant VT or ventricular fibrillation
3. ICD therapy is not indicated in patients with significant psychiatric illnesses that may be aggravated by device implantation or that may preclude systematic follow-up
4. ICD therapy is not indicated for NYHA Class IV patients with drug-refractory congestive heart failure who are not candidates for cardiac transplantation or implantation of a biventricular pacing device that incorporates both pacing and defibrillation capabilities.
5. ICD therapy is not indicated for syncope of undetermined cause in a patient without inducible ventricular tachyarrhythmias and without structural heart disease
6. ICD therapy is not indicated when ventricular fibrillation or VT is amenable to surgical or catheter ablation (e.g., atrial arrhythmias associated with WPW syndrome, right ventricular or LV outflow tract VT, idiopathic VT, or fascicular VT in the absence of structural heart disease)
7. ICD therapy is not indicated for patients with ventricular tachyarrhythmias due to a completely reversible disorder in the absence of structural heart disease (e.g., electrolyte imbalance, drugs, or trauma)

Adapted from Epstein A, DiMarco J, Ellenbogen K, et al. ACC/AHA/HRS 2008 Guidelines for device-based therapy of cardiac rhythm abnormalities. *J Am Coll Cardiol* 2008;51:E1–E62.

ICD therapy is the standard of care for prevention of sudden cardiac death in all age groups. The implantation of an ICD provides additional treatment in patients who experience life-threatening arrhythmias. The efficacy of ICDs to terminate ventricular arrhythmias has been proven in pediatric patients (174). The current indications for ICD implantation in pediatric patients and adults with congenital heart disease are based on data derived from adult studies and are located in Table 18.8. The main reason for ICD implantation has evolved over the years from secondary prevention of sudden cardiac death to their current use for primary prevention in patients with an increased risk for sudden death.

Biventricular Pacing

Cardiac resynchronization therapy (CRT) uses two separate pacing leads in the right and left ventricle to restore electrical and mechanical synchrony in patients with an intraventricular conduction delay. Despite varying causes of dyssynchrony, CRT has been successfully performed with good results. Although criteria for resynchronization have yet to be determined, research is currently being performed to guide clinicians as to which patients can benefit from this new technology. However,

several case series have indicated that CRT produces excellent results in children with a response rate around 85% to 90%, not only serving as a viable bridge to transplantation but also allowing many to be removed from transplantation lists because of improvement in symptoms and function (175–177). However, there is a relatively high complication rate for the procedure (including procedural deaths) and patients may require a surgical approach to place one or both pacing leads.

Follow-Up

After the implantation of a rhythm management device, they require close follow-up to ensure they are working appropriately. After initial implantation, the patient may be reevaluated relatively soon after implantation to ensure that the device is not infected and the incision is healing well. After this brief initial follow-up, patients then generally are evaluated in the office at 1 to 3 months after implantation and then at least once a year for the life of the device. During these visits, the device is interrogated to make sure the programming parameters are appropriate for the patient's age and lifestyle and the settings are optimized to maximize battery longevity. In addition to device interrogation, patients may have an ECG, Holter

monitor, chest x-ray (particularly during times of rapid linear growth), and exercise stress test to evaluate rate responsiveness and pacemaker function. Between visits, patient may perform device checks remotely through a telephone or wireless connection. These “transtelephonic checks” can give important information about battery status or problems with the device or lead. In addition, actual tracings of arrhythmias may be transmitted in patients with defibrillators who have had an ICD shock.

SUMMARY

Tachyarrhythmias and bradyarrhythmias are not uncommon in the pediatric age group. They have a wide variety of presentations and treatments. As our knowledge about these conditions continues to progress, specific therapies can be directed to diagnosing, curing, or preventing these conditions.

REFERENCES

- Dobrzynski H, Boyett MR, Anderson RH. New insights into pacemaker activity: promoting understanding of sick sinus syndrome. *Circulation* 2007;115:1921–1932.
- Nerantzis C, Anninos H, Koutsafitis P. Variation in the blood supply of the sinus node. *Surg Radiol Anat* 2010;32:983–984.
- Barbuti A, Baruscotti M, DiFrancesco D. The pacemaker current: from basic to the clinics. *J Cardiovasc Electrophysiol* 2007;18:342–347.
- Tawara S. Das Reizleitungssystem des Säugetierherzens: Eine Anatomisch-Histologische Studie Über Das Atrioventrikulärbündel Und Die Purkinjeschen Fäden. Jena, Germany, Verlag von Gustav Fischer, 1906.
- De Felice J, Challice CE. Anatomical and ultrastructural study of the atrioventricular region of the rabbit heart. *Circ Res* 1969;24:457–472.
- Priori SG, Napolitano C, Schwartz PJ. Electrophysiologic mechanisms involved in the development of torsades de pointes. *Cardiovasc Drugs Ther* 1991;5:203–212.
- Rossano J, Bloemers B, Sreeram N, et al. Efficacy of implantable loop recorders in establishing symptom-rhythm correlation in young patients with syncope and palpitations. *Pediatrics* 2003;112:e228–e233.
- Nagashima M, Matsushima M, Ogawa A, et al. Cardiac arrhythmias in healthy children revealed by 24-hour ambulatory ECG monitoring. *Pediatr Cardiol* 1987;8:103–108.
- Garson A, Gillette PC. Electrophysiologic studies of supraventricular tachycardia in children. II. Prediction of specific mechanism by noninvasive features. *Am Heart J* 1981;102:383–388.
- Perry JC, Garson A. Supraventricular tachycardia due to Wolff-Parkinson-White syndrome in children: early disappearance and late recurrence. *J Am Coll Cardiol* 1990;16:1215–1220.
- Snyder CS, Fenrich AL, Friedman RA, et al. Usefulness of echocardiography in infants with supraventricular tachycardia. *Am J Cardiol* 2003;91:1277–1279.
- Wolff L, Parkinson J, White PD. Bundle-branch block with short PR interval in healthy young people to paroxysmal tachycardia. *Am Heart J* 1930;6:685–704.
- De Bacquer D, De Backer G, Kornitzer M. Prevalences of ECG findings in large population based samples of men and women. *Heart* 2000;84:625–633.
- Sorbo MD, Buja GF, Miorelli M, et al. The prevalence of the Wolff-Parkinson-White syndrome in a population of 116,542 young males. *G Ital Cardiol* 1995;25:681–687.
- Sears GA, Manning GW. The Wolff-Parkinson-White pattern in routine electrocardiography. *Can Med Assoc J* 1962;87:1213–1217.
- Ko K, Deal BJ, Strasburger JF et al. Supraventricular tachycardia mechanisms and their age distribution in pediatric patients. *Am J Cardiol* 1992;69:1028–1032.
- Giardina AC, Ehlers KH, Engle MA. Wolff-Parkinson-White syndrome in infants and children: a long-term follow-up study. *Br Heart J* 1972;34:839–846.
- Deal BJ, Keane JF, Gillette PC, et al. Wolff-Parkinson-White syndrome and supraventricular tachycardia during infancy: management and follow-up. *J Am Coll Cardiol* 1985;5:130–135.
- Freed D II, Gillette PC. Familial WPW syndrome. *J Electrocardiol* 1983;16:111–112.
- Weng KP, Wolff GS, Young ML. Multiple accessory pathways in pediatric patients with Wolff-Parkinson-White syndrome. *Am J Cardiol* 2003;91:1178–1183.
- Chetaille P, Walsh EP, Triedman JK. Outcomes of radiofrequency catheter ablation of atrioventricular reciprocating tachycardia in patients with congenital heart disease. *Heart Rhythm* 2004;1:168–173.
- Pappone C, Santinelli V, Rosanio S, et al. Usefulness of invasive electrophysiologic testing to stratify the risk of arrhythmic events in asymptomatic patients with Wolff-Parkinson-White pattern: results from a large prospective long-term follow-up study. *J Am Coll Cardiol* 2003;41:239–244.
- Pappone C, Manguso F, Santinelli R, et al. Radiofrequency ablation in children with asymptomatic Wolff-Parkinson-White syndrome. *N Engl J Med* 2004;351:1197–1205.
- Fitzsimmons PJ, McWhirter PD, Peterson DW, et al. The natural history of Wolff-Parkinson-White syndrome in 228 military aviators: a long-term follow-up of 22 years. *Am Heart J* 2001;142:530–536.
- Benson DW Jr, Dunnigan A, Benditt DG. Follow-up evaluation of infant paroxysmal atrial tachycardia: transesophageal study. *Circulation* 1987;75:542–549.
- Tortorello TA, Snyder CS, Smith EO, et al. Frequency of recurrence among infants with supraventricular tachycardia and comparison of recurrence rates among those with and without preexcitation and among those with and without response to digoxin and/or propranolol therapy. *Am J Cardiol* 2003;92:1045–1049.
- Riggs TW, Byrd JA, Weinhouse E. Recurrence risk of supraventricular tachycardia in pediatric patients. *Cardiology* 1999;91:25–30.
- Emmel M, Balaji S, Sreeram N. Ventricular preexcitation associated with dilated cardiomyopathy: a causal relationship? *Cardiol Young* 2004;14:594–599.
- Tomaske M, Janousek J, Razeq V, et al. Adverse effects of Wolff-Parkinson-White syndrome with right septal or posteroseptal accessory pathways on cardiac function. *Europace* 2008;10:181–189.
- Udink ten Cate FE, Kruessell MA, Wagner K, et al. Dilated cardiomyopathy in children with ventricular preexcitation: the location of the accessory pathway is predictive of this association. *J Electrocardiol* 2010;43:146–154.
- Hamada T, Hiraki T, Ikeda H, et al. Mechanisms for atrial fibrillation in patients with Wolff-Parkinson-White syndrome. *J Cardiovasc Electrophysiol* 2002;13:223–229.
- Iesaka Y, Yamane T, Takahashi A, et al. Retrograde multiple and multifiber accessory pathway conduction in the Wolff-Parkinson-White syndrome: potential precipitating factor of atrial fibrillation. *J Cardiovasc Electrophysiol* 1998;9:141–151.
- Brembilla-Perrot B, Popescu I, Huttin O, et al. Risk of atrial fibrillation according to the initial presentation of a preexcitation syndrome. *Int J Cardiol* 2011.
- Klein GJ, Bashore TM, Sellers TD, et al. Ventricular fibrillation in the Wolff-Parkinson-White syndrome. *N Engl J Med* 1979;301:1080–1085.
- Brembilla-Perrot B, Chometon F, Groben L, et al. Are the results of electrophysiological study different in patients with a pre-excitation syndrome, with and without syncope? *Europace* 2008;10:175–180.
- Munger TM, Packer DL, Hammill SC, et al. A population study of the natural history of Wolff-Parkinson-White syndrome in Olmsted County, Minnesota, 1953–1989. *Circulation* 1993;87:866–873.
- Bromberg BI, Lindsay BD, Cain ME, et al. Impact of clinical history and electrophysiologic characterization of accessory pathways on management strategies to reduce sudden death among children with Wolff-Parkinson-White syndrome. *J Am Coll Cardiol* 1996;27:690–695.
- Sharma AD, Yee R, Guiraudon G, et al. Sensitivity and specificity of invasive and noninvasive testing for risk of sudden death in Wolff-Parkinson-White syndrome. *J Am Coll Cardiol* 1987;10:373–381.
- Bricker JT, Porter CJ, Garson A Jr, et al. Exercise testing in children with Wolff-Parkinson-White syndrome. *Am J Cardiol* 1985;55:1001–1004.
- Daubert C, Ollitrault J, Descaves C, et al. Failure of the exercise test to predict the anterograde refractory period of the accessory pathway in Wolff-Parkinson-White syndrome. *Pacing Clin Electrophysiol* 1988;11:1130–1138.
- Pietersen AH, Andersen ED, Sandoe E. Atrial fibrillation in the Wolff-Parkinson-White syndrome. *Am J Cardiol* 1992;70:38A–43A.
- Fenici R, Ruggieri MP, di Lillo M, et al. Reproducibility of transesophageal pacing in patients with Wolff-Parkinson-White syndrome. *Pacing Clin Electrophysiol* 1996;19:1951–1957.
- Santinelli V, Radinovic A, Manguso F, et al. The natural history of asymptomatic ventricular pre-excitation a long-term prospective follow-up study of 184 asymptomatic children. *J Am Coll Cardiol* 2009;53:275–280.
- Wellens HJJ, Brugada P, Roy D, et al. Effect of isoproterenol on the anterograde refractory period of the accessory pathway in patients with Wolff-Parkinson-White syndrome. *Am J Cardiol* 1982;50:180–184.
- Noë P, Van Driel V, Wittkamp F, et al. Rapid recovery of cardiac function after catheter ablation of persistent junctional reciprocating tachycardia in children. *Pacing Clin Electrophysiol* 2002;25:191–194.
- Haisaguerre M, Cauchemez B, Marcus F, et al. Characteristics of the ventricular insertion sites of accessory pathways with anterograde decremental conduction properties. *Circulation* 1995;91:1077–1085.
- Aliot E, de Chillou C, Revault d'Allones G, et al. Mahaim tachycardias. *Eur Heart J* 1998;19:E25–E31, E52–E53.
- Goldreyer BN, Gallagher JJ, Damato AN. The electrophysiological demonstration of atrial ectopic tachycardia in man. *Am Heart J* 1973;85:205–215.
- Tracy CM, Swartz JF, Fletcher RD, et al. Radiofrequency catheter ablation of ectopic atrial tachycardia using paced activation sequence mapping. *J Am Coll Cardiol* 1993;21:910–917.

50. Koike K, Hesslein PS, Finlay CD, et al. Atrial automatic tachycardia in children. *Am J Cardiol* 1988;61:1127-1130.
51. Naheed ZJ, Strasburger JF, Benson DW Jr, et al. Natural history and management strategies of automatic atrial tachycardia in children. *Am J Cardiol* 1995;75:405-407.
52. Iwai S, Badhwar N, Markowitz SM, et al. Electrophysiologic properties of para-Hisian atrial tachycardia. *Heart Rhythm* 2011;8:1245-1253.
53. Salerno JC, Kertesz NJ, Friedman RA, et al. Clinical course of atrial ectopic tachycardia is age-dependent: results and treatment in children <3 or ≥3 years of age. *J Am Coll Cardiol* 2004;43:438-444.
54. Abushaban L, Denham B, Duff D. 10 year review of cardiac tumours in childhood. *Br Heart J* 1993;70:166-169.
55. Gharagozloo F, Porter CJ, Tazelaar HD, et al. Multiple myocardial hamartomas causing ventricular tachycardia in young children: combined surgical modification and medical treatment. *Mayo Clin Proc* 1994;69:262-267.
56. Moltedo JM, Cannon BC, Fenrich AL, et al. Radiofrequency ablation of nonautomatic focal atrial tachycardia in children with structurally normal hearts. *J Interv Card Electrophysiol* 2009;26:225-229.
57. Sessler SP, Alexander ME, Berul CI, et al. Ablation of nonautomatic focal atrial tachycardia in children and adults with congenital heart disease. *J Cardiovasc Electrophysiol* 2006;17:359-365.
58. Hoffman TM, Bush DM, Wernovsky G, et al. Postoperative junctional ectopic tachycardia in children: incidence, risk factors, and treatment. *Ann Thorac Surg* 2002;74:1607-1611.
59. Collins KK, Van Hare GF, Kertesz NJ, et al. Pediatric nonpost-operative junctional ectopic tachycardia medical management and interventional therapies. *J Am Coll Cardiol* 2009;53:690-697.
60. Casey FA, McCrindle BW, Hamilton RM, et al. Neonatal atrial flutter: significant early morbidity and excellent long-term prognosis. *Am Heart J* 1997;133:302-306.
61. Texter KM, Kertesz NJ, Friedman RA, et al. Atrial flutter in infants. *J Am Coll Cardiol* 2006;48:1040-1046.
62. Kozłowski D, Budrejko S, Lip GY, et al. Lone atrial fibrillation: what do we know? *Heart* 2010;96:498-503.
63. Backer CL, Deal BJ, Mavroudis C, et al. Conversion of the failed Fontan circulation. *Cardiol Young* 2006;16:85-91.
64. Morales DL, Dibardino DJ, Braud BE, et al. Salvaging the failing Fontan: lateral tunnel versus extracardiac conduit. *Ann Thorac Surg* 2005;80:1445-1451.
65. Mavroudis C, Stewart RD, Backer CL, et al. Atrioventricular valve procedures with repeat fontan operations: influence of valve pathology, ventricular function, and arrhythmias on outcome. *Ann Thorac Surg* 2005;80:29-36.
66. MacLellan-Tobert SG, Porter CJ. Accelerated idioventricular rhythm: a benign arrhythmia in childhood. *Pediatrics* 1995;96:122-125.
67. Roggen A, Pavlovic M, Pfammatter JP. Frequency of spontaneous ventricular tachycardia in a pediatric population. *Am J Cardiol* 2008;101:852-854.
68. Dickinson DF, Scott O. Ambulatory electrocardiographic monitoring in 100 healthy teenage boys. *Br Heart J* 1984;51:179-183.
69. Rocchini AP, Chun PO, Dick M. Ventricular tachycardia in children. *Am J Cardiol* 1981;47:1091-1097.
70. Pfammatter JP, Paul T. Idiopathic ventricular tachycardia in infancy and childhood: a multicenter study on clinical profile and outcome. Working Group on Arrhythmias and Electrophysiology of the Association for European Pediatric Cardiology. *J Am Coll Cardiol* 1999;33:2067-2072.
71. Lemery R, Brugada P, Bella PD, et al. Nonischemic ventricular tachycardia. Clinical course and long-term follow-up in patients without clinically overt heart disease. *Circulation* 1989;79:990-999.
72. Davis AM, Gow RM, McCrindle BW, et al. Clinical spectrum, therapeutic management, and follow-up of ventricular tachycardia in infants and young children. *Am Heart J* 1996;131:186-191.
73. Roden DM. A practical approach to torsade de pointes. *Clin Cardiol* 1997;20:285-290.
74. Zimmerman FJ, Pahl E, Rocchini AP, et al. High incidence of incessant supraventricular tachycardia in pediatric patients referred for cardiac transplantation. *Pacing and Clin Electrophysiol* 1996;19:663.
75. Gelb BD, Garson A Jr. Noninvasive discrimination of right atrial ectopic tachycardia from sinus tachycardia in "dilated cardiomyopathy". *Am Heart J* 1990;120:886-891.
76. Gillette PC, Smith RT, Garson A Jr, et al. Chronic supraventricular tachycardia. A curable cause of congestive cardiomyopathy. *JAMA* 1985;253:391-392.
77. Umana E, Solares CA, Alpert MA. Tachycardia-induced cardiomyopathy. *Am J Med* 2003;114:51-55.
78. Packer DL, Bardy GH, Worley SJ, et al. Tachycardia-induced cardiomyopathy: a reversible form of left ventricular dysfunction. *Am J Cardiol* 1986;57:563-570.
79. Massin MM, Bourguignon A, Gérard P. Study of cardiac rate and rhythm patterns in ambulatory and hospitalized children. *Cardiology* 2005;103:174-179.
80. Beaufort-Krol GC, Dijkstra SS, Bink-Boelkens MT. Natural history of ventricular premature contractions in children with a structurally normal heart: does origin matter? *Europace* 2008;10:998-1003.
81. Baman TS, Lange DC, Ilg KJ, et al. Relationship between burden of premature ventricular complexes and left ventricular function. *Heart Rhythm* 2010;7:865-869.
82. Hasdemir C, Uluhan C, Yavuzgil O, et al. Tachycardia-induced cardiomyopathy in patients with idiopathic ventricular arrhythmias: the incidence, clinical and electrophysiologic characteristics, and the predictors. *J Cardiovasc Electrophysiol* 2011;22:663-668.
83. Delaney JW, Moltedo JM, Dziura JD, et al. Early postoperative arrhythmias after pediatric cardiac surgery. *J Thorac Cardiovasc Surg* 2006;131:1296-1300.
84. Rekawek J, Kansy A, Miszczak-Knecht M, et al. Risk factors for cardiac arrhythmias in children with congenital heart disease after surgical intervention in the early postoperative period. *J Thorac Cardiovasc Surg* 2007;133:900-904.
85. Vaughan Williams EM. Classification of antidysrhythmic drugs. *Pharmacol Ther* 1975;1:115-138.
86. Moffett BS, Cannon BC, Friedman RA, et al. Therapeutic levels of intravenous procainamide in neonates: a retrospective assessment. *Pharmacotherapy* 2006;26:1687-1693.
87. Moak JP, Smith RT, Garson A Jr. Mexiletine: an effective antiarrhythmic drug for treatment of ventricular arrhythmias in congenital heart disease. *J Am Coll Cardiol* 1987;10:824-829.
88. Fagundes A, DE Magalhães LP, Russo M, et al. Pharmacological treatment of electrical storm in catecholaminergic polymorphic ventricular tachycardia. *Pacing Clin Electrophysiol* 2010;33:e27-e31.
89. Schwartz PJ. Pharmacological and non-pharmacological management of the congenital long QT syndrome: the rationale. *Pharmacol Ther* 2011;131:171-177.
90. Cice G, Tagliamonte E, Ferrara L, et al. Efficacy of carvedilol on complex ventricular arrhythmias in dilated cardiomyopathy: double-blind, randomized, placebo-controlled study. *Eur Heart J* 2000;21:1259-1264.
91. Naccarelli GV, Lukas MA. Carvedilol's antiarrhythmic properties: therapeutic implications in patients with left ventricular dysfunction. *Clin Cardiol* 2005;28:165-173.
92. Guccione P, Paul T, Garson A Jr. Long-term follow-up of amiodarone therapy in the young: continued efficacy, unimpaired growth, moderate side effects. *J Am Coll Cardiol* 1990;15:1118-1124.
93. Garson A Jr, Gillette PC, McVey P, et al. Amiodarone treatment of critical arrhythmias in children and young adults. *J Am Coll Cardiol* 1984;4:749-755.
94. Haas NA, Camphausen CK. Acute hemodynamic effects of intravenous amiodarone treatment in pediatric patients with cardiac surgery. *Clin Res Cardiol* 2008;97:801-810.
95. Thorne SA, Barnes I, Cullinan P, et al. Amiodarone-associated thyroid dysfunction: risk factors in adults with congenital heart disease. *Circulation* 1999;100:149-154.
96. Connolly SJ, Dorian P, Roberts RS, et al. Optimal Pharmacological Therapy in Cardioverter Defibrillator Patients (OPTIC) Investigators. Comparison of beta-blockers, amiodarone plus beta-blockers, or sotalol for prevention of shocks from implantable cardioverter defibrillators: the OPTIC Study: a randomized trial. *JAMA* 2006;295:165-171.
97. Pfammatter JP, Paul T, Lehmann C, et al. Efficacy and proarrhythmia of oral sotalol in pediatric patients. *J Am Coll Cardiol* 1995;26:1002-1007.
98. Gwilt M, Arrowsmith JE, Blackburn KJ, et al. UK-68,798: a novel, potent and highly selective class III antiarrhythmic agent which blocks potassium channels in cardiac cells. *J Pharmacol Exp Ther* 1991;256:318-324.
99. Wells R, Khairy P, Harris L, et al. Dofetilide for atrial arrhythmias in congenital heart disease: a multicenter study. *Pacing Clin Electrophysiol* 2009;32:1313-1318.
100. Tamargo J, López-Farré A, Caballero R, et al. *Drugs Today (Barc)* 2011;47:109-133.
101. Kober L, Torp-Pedersen C, McMurray JJ, et al. Increased mortality after dronedarone therapy for severe heart failure. *N Engl J Med* 2008;358:2678-2687.
102. Gupta A, Lawrence AT, Krishnan K, et al. Current concepts in the mechanisms and management of drug-induced QT prolongation and torsade de pointes. *Am Heart J* 2007;153:891-899.
103. Tzivoni D, Banai S, Schuger C, et al. Treatment of torsade de pointes with magnesium sulfate. *Circulation* 1988;77:392-397.
104. Cooper DS, Jacobs JP, Moore L, et al. Cardiac extracorporeal life support: state of the art in 2007. *Cardiol Young* 2007;17:104-115.
105. Dopp AL, Miller JM, Tisdale JE. Effect of drugs on defibrillation capacity. *Drugs* 2008;68:607-630.
106. Sharma S, Whyte G, Elliott P, et al. Electrocardiographic changes in 1,000 highly trained junior elite athletes. *Br J Sports Med* 1999;33:319-324.
107. Yabek SM, Jarmakani JM. Sinus node dysfunction in children, adolescents, and young adults. *Pediatrics* 1978;61:593-598.
108. Moltedo JM, Porter GA, State MW, et al. Sinus node dysfunction associated with lithium therapy in a child. *Tex Heart Inst J* 2002;29:200-202.
109. Reidermann MI. Cardiac complications in adult diphtheria: analysis of 212 cases. *Praxis (Bern 1994)* 1996;85:1647-1651.

110. Yabek SM, Swenson R, Jamakani J. Electrocardiographic recognition of sinus node dysfunction in children and young adults. *Circulation* 1977;56:235-239.
111. Bricker J, Garson A Jr, Gillette P. A family history of seizures associated with sudden cardiac deaths. *Am J Dis Child* 1984;138:866-868.
112. Tomaske M, Keller D, Bauersfeld U. Sudden cardiac death: clinical evaluation of paediatric family members. *Europace* 2011;13:421-426.
113. Dos L, Teruel L, Ferreira I, et al. Late outcome of Senning and Mustard procedures for correction of transposition of the great arteries. *Heart* 2005;91:652-656.
- 114a. Smith P, Buhrman W, Levett J, et al. Supraventricular conduction abnormalities following cardiac operations. *J Thorac Cardiovasc Surg* 1983;85:105-115.
- 114b. El-Said G, Gillette P, Cooley D, et al. Protection of the sinus node in Mustard's operation. *Circulation* 1976;53:788-791.
115. Bink-Boelkens M, Velvis H, Homan van der Heide J, et al. Arrhythmias after atrial surgery in children. *Am Heart J* 1983;106:125-130.
116. Gillette P, Reitman M, Gursesell H, et al. Intracardiac electrophysiology in children and young adults. *Am Heart J* 1975;89:36-44.
117. Costello J, Alexanser M, Greco K, et al. Lyme carditis in children: presentation, predictive factors, and clinical course. *Pediatrics* 2009;123:835-841.
118. Scott O, Williams G, Fiddler G. Results of 24 hour ambulatory monitoring of electrocardiograms in 131 healthy boys age 10 to 13 years. *Br Heart J* 1980;44:304-308.
119. Mirowski M, Arevalo F, Medrano G, et al. Conduction disturbances in patients with patent ductus arteriosus: a study of 200 cases before and after surgery with determination of the PR interval. *Circulation* 1962;25:807-813.
120. Denes P, Levy L, Pick A, et al. The incidence of typical and atypical A-V Wenckebach periodicity. *Am Heart J* 1975;89:26-31.
121. Rosen K, Gunnar R, Rahimtoola S. Site and type of second degree AV block. *Chest* 1972;61:99-100.
122. Foerster A. The conduction system in human cardiac allografts. A histological and immunopathological study. *Pathol Res Pract* 1992;18:783-790.
123. Chan JB, Levi DS, Lai CK, et al. Cellular rejection of the conduction system after orthotopic heart transplantation for congenital atrioventricular block. *J Heart Lung Transplant* 2006;25:1371-1375.
124. Cannon BC, Denfield SW, Friedman RA, et al. Late pacemaker requirement after pediatric orthotopic heart transplantation may predict the presence of transplant coronary artery disease. *J Heart Lung Transplant* 2004;23:67-71.
125. Yu T, Gup G, Yang C. Reversible infra-Hisian atrioventricular block in acute myocarditis. *Chang Gung Med J* 2001;21:651-656.
126. Reddy D, Chun L, Yamamoto L. Acute rheumatic fever with advanced degree AV block. *Clin Pediatr* 1989;28:326-328.
127. Arkolaki EG, Simantirakis EN, Chrysostomakis SI, et al. Appropriate management of syncope in a patient with hypertrophic cardiomyopathy: rationale behind long-term cardiac rhythm monitoring. *Hellenic J Cardiol* 2009;50:144-146.
128. Limongelli G, Ducceschi V, D'Andrea A, et al. Risk factors for pacemaker implantation following aortic valve replacement: a single centre experience. *Heart* 2003;89:901-904.
129. Michaelsson M, Engle M. Congenital complete heart block: an international study of the natural history. *Cardiovasc Clin* 1972;4:85-101.
130. Schmidt K, Ulmer H, Silverman N, et al. Perinatal outcome of fetal complete atrioventricular block: a multicenter experience. *JACC* 1991;17:1360-1366.
131. Eronen M, Siren M, Ekblad H, et al. Short-and long-term outcome of children with congenital complete heart block diagnoses in utero or as a newborn. *Pediatrics* 2000;106:86-91.
132. Machado M, Tynan M, Curry P, et al. Fetal complete heart block. *Br Heart J* 1988;60:512-515.
133. Mulder T, Niyazov D, Kattash M, et al. A newborn with congenital complete atrioventricular block, lissencephaly and skeletal abnormalities: a case of suspected cytomegalovirus infection. *Congenit Heart Dis* 2010;5:486-490.
134. Hikita T, Wakita S, Mori Y, et al. Severe infantile myotubular myopathy with complete atrioventricular block. *Pediatr Int* 2008;50:698-700.
135. Pabst S, Wollnik B, Rohmann E, et al. A novel stop mutation truncating critical regions of the cardiac transcription factor NKX2-5 in a large family with autosomal-dominant inherited congenital heart disease. *Clin Res Cardiol* 2008;97:39-42.
136. Lev M. Pathogenesis of congenital atrioventricular block. *Prog Cardiovasc Dis* 1972;15:146.
137. McCue C, Mantakas M, Tingelstad J, et al. Congenital heart block in newborns of mothers with connective tissue disease. *Circulation* 1977;56:82-90.
138. Taylor P, Scott J, Gerlis L, et al. Maternal antibodies against fetal cardiac antigens in congenital complete heart block. *N Engl J Med* 1986;315:667-672.
139. Tan E. Antinuclear antibodies: diagnostic markers for autoimmune diseases and probes for cell biology. *Adv Immunol* 1989;44:93-152.
140. Meilof J, Smeenk R. Autoantibodies and their target antigens in Sjogren's Syndrome. *Neth J Med* 1992;40:140-147.
141. Waltuck J, Buyon J. Autoantibody-associated congenital heart block: outcome in mothers and children. *Ann Intern Med* 1994;120:544-551.
142. Buyon J, Heibert R, Copel J, et al. Autoimmune-associated congenital heart block: demographics, mortality, morbidity and recurrence rates obtained from a National Neonatal Lupus Registry. *JACC* 1998;31:1658-1666.
143. Michaelsson M, Riesenfeld T, Jonzon A. Natural history of congenital complete atrioventricular block. *Pacing Clin* 1997;20:2098-2101.
144. Goble M, Dick M, McCune J, et al. Atrioventricular conduction in children of women with systemic lupus erythematosus. *Am J Cardiol* 1993;71:94-98.
145. Ramsey-Goldman R, Hom D, Deng J, et al. Antia-SS-A antibodies and fetal outcome in maternal systemic lupus erythematosus. *Arthritis Rheum* 1986;29:1269-1273.
146. Watson R, Lane A, Barnett N, et al. Neonatal Lupus erythematosus. A clinical, serological and immunogenetic study with review of the literature. *Medicine* 1984;63:362-378.
147. Garcia S, Nascimento J, Bonfa E, et al. Cellular mechanism of the conduction abnormalities induced by serum from anti-Ro/SSA-positive patients in rabbit hearts. *J Clin Invest* 1994;93:718-724.
148. Horsfall A, Venables P, Taylor P, et al. Ro and La antigens and maternal anti-La idiotype on the surface of myocardial fibres in congenital heart block. *J Autoimmunity* 1991;4:165.
149. Thomas J, Edwards M, Park W, et al. Apoptosis as a possible cause of gradual development of complete heart block and fatal arrhythmias associated with absence of the AV node, sinus node and internodal pathways. *Circulation* 1996;93:1424-1438.
150. Tran H, Ohlsson M, Beroukas D, et al. Subcellular redistribution of la/SSb autoantigen during physiologic apoptosis in the fetal mouse heart and conduction system: a clue to the pathogenesis of congenital heart block. *Arthritis Rheum* 2002;46:202-208.
151. Sagar S, Shen WK, Asirvatham SJ, et al. Effect of long-term right ventricular pacing in young adults with structurally normal heart. *Circulation* 2010;121:1698-1705.
152. Moltedo JM, Rosenthal GL, Delaney J, et al. The utility and safety of temporary pacing wires in postoperative patients with congenital heart disease. *J Thorac Cardiovasc Surg* 2007;134:515-516.
153. Celiker A, Kafali G, Karagöz T, et al. The results of electrophysiological study and radio-frequency catheter ablation in pediatric patients with tachyarrhythmia. *Turk J Pediatr* 2003;45:209-216.
154. Nehgme RA, Huddleston AR, Cheatham JP. Progression to late complete atrioventricular block following amplatzer device closure of atrial septal defect in a child. *Pediatr Cardiol* 2009;30:367-370.
155. Butera G, Carminati M, Chessa M, et al. Transcatheter closure of perimembranous ventricular septal defects: early and long-term results. *J Am Coll Cardiol* 2007;50:1189-1195.
156. Walsh MA, Bialkowski J, Szkutnicki M, et al. Atrioventricular block after transcatheter closure of perimembranous ventricular septal defects. *Heart* 2006;92:1295-1297.
157. Elliott DA, Kirk EP, Yeoh T, et al. Cardiac homeobox gene NKX2-5 mutations and congenital heart disease: associations with atrial septal defect and hypoplastic left heart syndrome. *J Am Coll Cardiol* 2003;41:2072-2076.
158. Probst V, Hoorntje T, Hulsbeek M, et al. Cardiac conduction defect associated with mutation in SCN5A. *Nature Genet* 1999;23:20-21.
159. Groves A, Allan L, Rosenthal E. Outcome of isolated congenital complete heart block diagnosed in utero. *Heart* 1996;75:190-194.
160. Lopez L, Cha S, Leone C, et al. Use of sympathomimetic agents in fetal atrioventricular block. *Arg Bras Cardiol* 1994;63:297-298.
161. Bunyon J, Waltuck J, Kleinmaan C, et al. In utero identification and therapy of congenital heart block. *Lupus* 1995;4:116-121.
162. Yoshida H, Iwamoto M, Sakakibara H, et al. Treatment of fetal congenital complete heart block with maternal administration of beta-sympathomimetics. *Gynecol Obstet Invest* 2001;52:142-144.
163. Kaaja R, Julkunen H, Ammala P, et al. Congenital heart block: successful prophylactic treatment with intravenous gamma globulin and corticosteroid therapy. *Am J Obstet Gynecol* 1993;82:11-16.
164. Copel JA, Buyon JP, Kleinman CS. Successful in utero therapy of fetal heart block. *Am J Obstet Gynecol* 1995;173:1384-1390.
165. Bierman F, Baxi L, Jaffe I, et al. Fetal hydrops and congenital complete heart block: response to maternal steroid therapy. *J Pediatr* 1988;112:646-648.
166. Yamada H, Kato E, Ebina Y, et al. Fetal treatment of congenital heart block ascribed to anti-SSA antibody: case reports with observation of cardiohemodynamics and review of the literature. *Am J Reprod Immunol* 1999;42:226-232.
167. Saleeb S, Copel J, Friedman D, et al. Comparison of treatment with fluorinated glucocorticoids to the natural history of autoantibody-associated congenital heart block: retrospective review of the research registry for neonatal lupus. *Arthritis Rheum* 1999;42:2335-2345.
168. Michaelsson M, Engle MA. Congenital complete heart block: an international study of the natural history. *Cardiovasc Clin*. 1972;4(3):85-101.
169. Michaelsson M, Jonzon A, Riesenfeld T. Isolated congenital complete atrioventricular block in adult life. A prospective study. *Circulation* 1995;92:442-449.

170. Lillihei C, et al. Chronic post-surgical complete heart block. *J Cardiovasc Surg* 1973;46:436–456.
171. Elmqvist R, Landegren J, Petterson S, et al. Artificial pacemaker for treatment of Adams-Stokes syndrome and slow heart rate. *Am heart J* 1963;65:731–748.
172. Bernstein AD, Daubert JC, Fletcher RD, et al. The revised NASPE/BPEG generic code for antibradycardia, adaptive-rate, and multisite pacing. North American Society of Pacing and Electrophysiology/British Pacing and Electrophysiology Group. *Pacing Clin Electrophysiol* 2002;25:260–264.
173. Epstein A, DiMarco J, Ellenbogen K, et al. ACC/AHA/HRS 2008 guidelines for device-based therapy of cardiac rhythm abnormalities. *J Am Coll Cardiol* 2008;5:E1–E62.
174. Silka MJ, Bar-Cohen Y. Pacemakers and implantable cardioverter defibrillator in pediatric patients. *Heart Rhythm* 2006;3:1360–1366.
175. Janousek J, Gebauer RA. Cardiac resynchronization therapy in pediatric and congenital heart disease. *Pacing Clin Electrophysiol* 2008;31:S21–S23.
176. Karpawich PP. Pediatric cardiac resynchronization pacing therapy. *Curr Opin Cardiol* 2007;22:72–76.
177. Constans MM, Asirvatham SJ. An approach to overcoming specific difficulties with cardiac resynchronization therapy in children. *Indian Pacing Electrophysiol J* 2008;8:S105–S121.

Pediatric Cardiac Intensive Care

Physiology of the Preterm and Term Infant

Timothy M. Hoffman ■ Stephen E. Welty

INTRODUCTION

Approach to the care of the neonate with congenital heart disease is multidisciplinary. Regardless of where the patient is cared for (neonatal intensive care unit, cardiac intensive care unit) a firm understanding of neonatal physiology and development by the managing medical team is imperative to provide state-of-the-art interdisciplinary care. This chapter provides a unique perspective of the neonate from a multi-organ system approach. Cardiac lesion-specific data are outlined throughout the textbook; therefore this chapter does not include a discussion of these conditions. Instead, this chapter focuses on the complex interactions of multiple organ systems in neonates who also have congenital heart disease. In addition, an overview of lung development and the management of a patent ductus arteriosus in premature infants is presented.

TRANSITIONAL CIRCULATION

With the onset of spontaneous respiration at the time of birth, the low-resistance placenta is removed from the circulation, thus increasing systemic vascular resistance. Expansion of the lungs elicits an immediate decrease in the pulmonary vascular resistance as a result of physical recruitment of pulmonary vasculature and vasodilation of the pulmonary arteriolar bed in response to an elevated oxygen content. In turn, the shift of the systemic and pulmonary vascular resistances causes a reversal of flow of the ductus arteriosus from right to left to predominantly left to right. In theory, this change from fetal circulation causes an increase in pulmonary blood flow and a decrease in systemic venous return due to the lack of umbilical venous flow. Left atrial pressure increases and eventually exceeds the pressure in the right atrium leading to closure of the foramen ovale flap against the crista dividens, eliminating shunting at the atrial level. All of these alterations may be influenced by disease processes that affect the systemic and pulmonary vascular resistances, inhibiting the usual transition

to adult circulation (1,2). Additionally, after the initial precipitous fall in pulmonary vascular resistance, it continues to fall gradually in the first 48 hours of life and takes several weeks to fall to adult levels. In a normal neonate, the ductus generally closes functionally within several days of life.

PATENT DUCTUS ARTERIOSUS

Classic studies by Gittenburger-De Groot have described the sequence of events that occur in the infants that lead to functional and anatomic closure of the ductus arteriosus (3). The molecular events explaining closure and the predisposition of the ductus to remain patent in premature infants have been described (4–8). Ductal closure is dependent upon an initial ductal constriction which results from the development of hypoxia within the ductal media. Hypoxia mediates a series of molecular events that then lead to disruption of the internal elastic lamina and endothelial cell. Smooth muscle cells proliferate forming intimal mounds that impinge on the ductal lumen, ultimately leading to its anatomic closure. In premature infants, ductal constriction is essential for anatomical closure of the ductus arteriosus. But this alone may not be sufficient for ductal closure. Hypoxia in the muscular media may not occur and the post-constriction sequence fails to follow. Thus, premature infants may present with a symptomatic patent ductus arteriosus (PDA), especially those who are <30 weeks of gestation.

The incidence of PDA in premature infants is inversely related to gestational age. In a recent multicenter trial of indomethacin prophylaxis in premature infants weighing <1,000 g, the incidence of PDA in the placebo group was 50% (9). Premature infants with a PDA may present with classic findings of a left-to-right shunting lesion. In this case, infants typically have a systolic murmur, increased left precordial activity, sometimes with an associated thrill, bounding pulses, and a wide pulse pressure that also may be evident on umbilical arterial waveform tracings. Unfortunately, many infants with

a physiologically significant PDA may not have these findings. Thus there should be a high index of suspicion for a PDA even without classic physical findings in a premature infant who has lung disease. Doppler-echocardiography is the gold standard for diagnosing a PDA, and should be performed before treatment decisions are made.

Physiology of the PDA is secondary to overperfusion of the lung and possibly underperfusion of the systemic circulation. Infants' lungs are fully recruited at rest so that any increase in flow from left-to-right shunts predictably increases fluid filtration in the lung (10). Increased fluid filtration will lead to pulmonary edema if it exceeds the ability of the lymphatics to remove fluid, and pulmonary edema is frequently associated with pulmonary overcirculation from a PDA. The PDA may also steal from the systemic circulation. Animal studies have shown that even small shunts underperfuse systemic organs (10). Studies in extremely premature infants with a hemodynamically significant PDA observed that although total left ventricular output was increased, flow was decreased in the abdominal aorta, celiac, mesenteric, and renal arteries, while there were no differences in the anterior cerebral artery flow (11). While the changes in acute physiology are concerning, the effect of a PDA on the outcome of premature infants and the management of a PDA is controversial (12,13).

The management of the PDA in premature infants has changed dramatically over the last decade. The uniform findings from animal studies are that a PDA is associated with underperfusion of the systemic circulation and overcirculation of the pulmonary bed with the development of pulmonary edema (10,11). If these findings can be extrapolated to premature infants who weigh <1,000 g and approaches to preventing or treating the PDA lacked significant toxicity, it would support taking aggressive steps to prevent the development of a significant PDA, or at the very least, for treatment of these infants with a clinically significant PDA. Furthermore, epidemiologic data indicate that premature infants who develop a clinically significant PDA have higher rates of mortality and morbidity than do comparably sized infants who do not develop a significant PDA (14,15).

Treatment approaches include surgical ligation, pharmacologic treatment with cyclooxygenase inhibitors, or supportive medical management with fluid restriction, cardiovascular support, and therapy with diuretics. As recently as 1996, an analysis of strategies including prophylaxis, early treatment, and late treatment after overt symptoms indicated that the most reasonable approach to the PDA in premature infants is using indomethacin either prophylactically in high-risk populations or within the first few days of life when the PDA became evident prior to the development of overt symptoms (16). However, there have been marked improvements in perinatal care including an increased emphasis on the treatment of mothers who are at risk for delivering a premature infant with antenatal steroids (17,18). Likewise a more aggressive approach to noninvasive respiratory support strategies allows even premature infants born <1,000 g to be frequently not supported with pressors or mechanical ventilation in the first 24 hours of life. In this changing clinical context, aggressive treatment of the PDA in an infant with minimal lung disease and support has come into question. A recently published meta-analysis has concluded that prophylactic treatment of premature infants with cyclooxygenase inhibitors, while reducing the need for surgical ligation of the ductus and lowering the incidence of intraventricular hemorrhage, elicited no differences in survival or neurodevelopmental outcomes (19). Thus, a reasonable interpretation of the present clinical evidence supports the conclusion that the beneficial effect in closing the ductus in a population of infants who would have developed a symptomatic PDA may be offset by the deleterious effects of treating some infants

who would not have developed a PDA with a potent class of drugs with a significant frequency of side effects. Thus, treatment of a hemodynamically significant PDA appears to be the most prudent approach in extremely low birth weight infants. A recent meta-analysis comparing indomethacin with ibuprofen demonstrated no difference in efficacy in patients treated with ibuprofen, yet yielded a significantly lower incidence of side effects (20). This meta-analysis may lead to the conclusion that, at present, ibuprofen is the best treatment option for those with a symptomatic PDA. However, a recent analysis combining data from American and European studies found that ibuprofen therapy was associated with a greater risk of the development of bronchopulmonary dysplasia (BPD) than indomethacin therapy (21). Thus, the optimal choice of cyclooxygenase inhibitors remains unanswered.

Treatment of a PDA has taken a risk-based approach. If a premature infant with echocardiographic evidence of a PDA in the first week of life requires mechanical ventilation for support of lung disease that cannot be attributed to respiratory distress syndrome (RDS), treatment is warranted and a course of ibuprofen is probably the preferred choice. Furthermore, independent of the amount of cardiopulmonary support required, if a premature infant has clinical evidence of a PDA, such as wide pulse pressures, an active precordium, or a loud murmur and an echocardiogram demonstrates a ductus with evidence of left atrial or left ventricular enlargement, treatment is also warranted.

The role of surgical ligation in infants has become even less clear than the pharmacologic approach to treatment of a PDA. There is no evidence that early aggressive treatment with PDA ligation improves clinical outcomes (22), and recent evidence suggests that late ligation of a significant ductus arteriosus is associated with concerning long-term neurodevelopmental outcomes (23). These data do not exclude the need for surgical ligation, but rather may highlight the point that extremely premature infants who have a PDA evident after the first week of life define a population of infants at extremely high risk for long-term morbidity. However, based on the concerns about surgery, many clinicians choose to treat infants failing a course of cyclooxygenase inhibitors with fluid restriction and diuretics and defer ligation for the most symptomatic infants.

Lung Development

Lung development from the embryonic phase to the alveolar phase has been studied in humans and in many mammals (24–27). Furthermore, the molecular basis for lung development continues to be elucidated and a discussion of the mechanisms for lung development is beyond the scope of this chapter. However, since lung development proceeds through postnatal life for several years, understanding the effects on lung development of congenital heart disease, its treatment, and supportive medical care for lung disease is important. Overall lung development can be optimized in infants with respiratory disease and heart disease whether they are born prematurely or not.

Infants born as early as 23 weeks of gestation can survive. At 23 weeks of gestation, infants are still in the cannicular phase of lung development, which continues through 26 weeks of gestation. Despite the relatively immature lung architecture, including no identifiable alveoli and a thickened alveolar interstitium with a double capillary network, the lung can subserve enough air exchange function for the infant to survive. The sacular phase of lung development extends from 27 to 36 weeks of gestation and the alveolar phase starts at 37 weeks and proceeds through approximately 3 years of postnatal age. In infants born prematurely without heart disease, supportive care with mechanical ventilation and supplemental oxygen frequently

injures the lung and predisposes the infant to the development of chronic BPD (28). Furthermore, perinatal inflammation of the lung is frequently observed in premature infants, which also can injure the lung profoundly (29). The injury caused by lung support and/or inflammation leads to an arrest of lung development, and the lung function abnormalities can persist for years (30,31). Thus in infants, especially premature infants, who have heart disease and require supportive care delivered to the respiratory system, therapies should be pursued that limit lung injury and thereby limit aberrations in lung development, similar to treatment strategies being explored in infants born prematurely who do not have heart disease.

The most important intervention to improve the outcomes of premature infants is the administration of antenatal steroids to mothers who are at risk of delivering a premature infant. The landmark study by Liggins and Howie demonstrated a beneficial effect of antenatal steroids given to mothers who delivered infants at <34 weeks of gestation (32). These results have been verified by many other randomized, double-blinded, placebo control trials. While the initial studies focused on decreasing the incidence of respiratory distress, there was also evidence that antenatal corticosteroid (ACS) administration decreased mortality and other morbidities in premature infants (33–35). ACS administration enhanced lung and circulatory development. So much so that an NIH consensus statement stated strongly that ACS should be given to mothers with threatened premature delivery between 24 and 34 weeks of gestation (17). Details for ACS administration can be found in the NIH consensus statement. There is no present evidence that supports repeat ACS administration to those mothers who do not deliver within 1 week of steroid administration (18).

Surfactant administration has been shown to improve outcomes in premature infants. Exogenous surfactant has been given in prophylactic and rescue modes. In the prophylaxis studies of premature infants who were at high risk of having RDS, surfactant administration was given within 15 to 20 minutes of birth. This led to lower mortality rates and less morbidity than was seen in infants who were given surfactant after the diagnosis of RDS was established (selective) (36). These differences are less relevant in more mature infants. Thus, infants born after 30 weeks of gestation can be assessed for development of RDS and if RDS is present, surfactant should be delivered in the rescue mode (37).

In the last decade, as the antenatal steroid administration to mothers has increased and the expertise of noninvasive respiratory support has been enhanced, many infants, even extremely premature infants, are delivered with minimal lung disease so that a trial of noninvasive respiratory support with nasal continuous positive airway pressure (CPAP) may be reasonable. In 2008, the COIN (continuous positive airway pressure on intubation at birth) trial was published in which 610 infants between 25 and 28 weeks were randomized to either CPAP or intubation with surfactant at birth (38). While there were some differences favoring the CPAP group at 28 days of life, the outcomes at 36 weeks postmenstrual age for morbidity and mortality were not different. Another study by the SUPPORT study group (surfactant positive pressure and pulse oximetry randomized trial) enrolled 1,310 infants between 24 and 27 weeks of gestation which randomized similarly to the COIN study. The study results showed no statistically significant differences in the composite outcome of death or BPD at 36 weeks postmenstrual age (39). The combination of these findings suggest that infants born at 24 weeks of gestation up to 28 weeks of gestation who were exposed to maternal ACS and are vigorous at birth may be supported with CPAP without prophylactic surfactant. However, if the infants' oxygen requirement rises to >40%, administration of surfactant should then be considered.

Other therapeutic measures in premature infants that help to prevent development of BPD include: (a) monitoring to

prevent hyperoxemia and minimize exposure to supplemental oxygen and mechanical ventilation, (b) fluid restriction in the first few days of life (40), and (c) the institution of aggressive and early parenteral and enteral nutrition. The combination of therapies just discussed is supported in premature infants without congenital heart disease. However, there are no reports regarding the impact of congenital heart disease on lung development in premature infants, or on postnatal lung development in term infants. Acute management of premature infants with congenital heart disease is thus extrapolated from what has been observed in premature infants without heart disease.

PULMONARY HYPERTENSION

Abnormalities of smooth muscle development frequently influence acute cardiopulmonary physiology in newborn infants. Pulmonary hypertension is frequently present when there is abnormal vascular smooth muscle development. Pulmonary hypertension presenting in the newborn period is classified into three separate categories based on the underlying mechanisms for the development of the disorder. The three categories include underdevelopment, maldevelopment, and maladaptive forms. In this classification only underdevelopment and maldevelopment pulmonary hypertension are associated with abnormalities of smooth muscle development. In fetal development, airway branching and smooth muscle development occur in parallel in an environment where pulmonary vascular resistance is high and blood flow is low. In normal lung development, smooth muscle development around the vasculature extends to the level of the respiratory bronchiole. When the fetus is compromised by poor placental function and high placental vascular resistance, smooth muscle development is altered so that it extends further distally in the pulmonary vasculature and is thicker. The thickening occurs as a combination of intimal and adventitial thickening which gives rise to maldevelopment pulmonary hypertension (41). Underdevelopment pulmonary hypertension is associated with pulmonary hypoplasia which leads to a decreased cross-sectional surface area of the pulmonary vascular bed. In addition, underdevelopment pulmonary hypertension is frequently associated with maldevelopment of the pulmonary vasculature (42).

Infants with maldevelopment pulmonary hypertension frequently present with evidence of poor placental function and poor adaptation to their extrauterine environment. Evidence for poor placental function may present as a poorly nourished infant with evidence of fetal weight loss. The perinatal period is often associated with marked fetal distress because labor taxes the function of the compromised placenta. Thick meconium may be noted and the infant may be depressed or asphyxiated at birth. Even without these adverse perinatal events, the abnormal pulmonary vascular bed may not allow the normal rapid initial drop in pulmonary vascular resistance and subsequent increase in pulmonary blood flow which are essential for appropriate cardiopulmonary physiology and adaptation to an adult-type circulation in series with high pulmonary blood flow and air exchange in the lung.

RESPIRATORY PHYSIOLOGY

In the fetus, the organ of respiration is the placenta and the lung is a high resistance, minimal flow, liquid-filled organ. Furthermore, the fetal lung secretes fluid into the airway (43). During late gestation surfactant production increases in preparation for the lung becoming the organ of respiration, and the

molecular processes essential for fluid absorption are induced (44). This induction is enhanced by labor. At delivery with the onset of regular respirations, optimal air exchange physiology occurs when lung volume is adequate and pulmonary vascular resistance drops allowing the resultant increase in blood flow.

Disorders of transition occur when any one of the three critical steps do not occur or are delayed. The three disorders of transition are: (a) transient tachypnea of the newborn, which occurs when the removal of lung water is delayed, (b) RDS, formerly known as hyaline membrane disease, and (c) pulmonary hypertension of the newborn which occurs when the normal drop in pulmonary vascular resistance does not occur or is delayed. Each of these disorders has a characteristic physiology which leads to alterations in air exchange. In most cases, the primary aberration is hypoxemia, even though the physiology by which this aberration occurs is different.

In order to understand respiratory physiology of the newborn it is critical to understand some of the physical properties of the lung that determine ventilation. The equation of motion describes the properties of the lung important for proper ventilation:

$$\Delta P = 1/cV + R\dot{V} + I\ddot{V}$$

where P represents the pressure applied to the respiratory system, C is compliance which is defined as the change in volume divided by the change in pressure, describing the elastance of the respiratory system, V is volume, R is resistance, \dot{V} is the flow, I is inductance, and \ddot{V} is acceleration. Thus, properties of the lung can be divided into the static properties of the lung which are measured when there is no flow and is dependent on the compliance term in the equation of motion, and the resistive properties of the lung, which are measured when there is flow and are dependent on the resistance term in the equation of motion and inductance which, in most cases is thought to be negligible relative to the static and resistive properties and is therefore ignored. In well newborn infants the compliance is normal and the resistance is low so that minimal effort or energy is needed to provide reasonable ventilation to the respiratory system independent of whether the infant is doing the work or if the infant requires mechanical ventilation.

In infants with primary lung disease, the most common biochemical derangement is arterial hypoxemia. The mechanisms for significant hypoxemia in infants with lung disease are primarily ventilation-perfusion abnormalities and/or right-to-left shunting (both intrapulmonary and extrapulmonary). The sum of the shunt fraction and the ventilation-perfusion inequalities is the venous admixture. The venous admixture is higher in newborns even without lung disease (45,46). In parenchymal lung disease, the venous admixture increases dramatically and arterial hypoxemia may become profound. Furthermore, the relative proportion of the shunt fraction and V/Q abnormalities is dynamic such that as ventilation of the lung improves it has been shown that the shunt fraction and low V/Q compartments may be affected independently or in tandem. The primary strategy in infants with lung disease is to improve the function of the low V/Q compartment. Administration of supplemental oxygen may improve the oxygen concentration in the terminal air units and may relieve hypoxic pulmonary vasoconstriction, in which case improvement in oxygenation occurs by decreasing the size of the shunt compartment with no effect on the low V/Q compartment. Improving the ventilation to the low V/Q compartment of the lung frequently addresses both the shunt compartment and the low V/Q compartment. In this case, these strategies may recruit the shunt compartment by improving ventilation, raising the partial pressure of oxygen, and relieving hypoxic pulmonary vasoconstriction. The same

strategies may recruit the former low V/Q compartment into the normal V/Q compartment at the same time. Thus while administration of supplemental oxygen is relatively safe and may decrease the shunt compartment, supportive strategies to safely increase ventilation to the most diseased areas of the lung may affect the shunt compartment and low V/Q compartment simultaneously.

The most appropriate strategy to support the respiratory system in the diseased lung depends on the physical properties of the lung, including the static properties and the resistive properties. It is appropriate to bear in mind that supportive measures which improve the function of the diseased lung do not improve the underlying disorder. In fact, supplemental oxygen is toxic and the application of positive pressure to the lung causes injury (47). When positive pressure is administered the strategy utilized should be tailored to the abnormalities in the lung. In lung diseases dominated by low respiratory system compliance, such as RDS or hyaline membrane disease, the airways and airspaces fill and empty quickly so that if mechanical ventilation is utilized, a fast rate-low tidal volume ventilation strategy should be used and has been associated with better outcomes (48). In diseases dominated by high airway resistance, a ventilator strategy using a slower rate with slightly higher tidal volume ventilation is more successful. Examples of such diseases include meconium aspiration and BPD. In infants with RDS, the safest and most efficient technique to improve lung physiology is by increasing the mean airway pressure and the safest and most efficient technique to increase mean airway pressure is to increase the end pressure (49). In fact, many infants with RDS can be managed with CPAP only which is the preferable mode in relatively mature infants (50,51).

CARDIOPULMONARY INTERACTION

The pulmonary vasculature in the lung of infants is fully recruited at rest and is particularly predisposed to the development of pulmonary edema when flow is increased via anatomic left-to-right shunts. The rate of fluid filtration (Q_f) in the lung or any other organ or vascular bed is governed by the Frank-Starling equation:

$$Q_f = K_f \left[(P_{mv} - P_{pmv}) - \sigma (\pi_{mv} - \pi_{pmv}) \right]$$

where K_f is hydraulic conductance, P_{mv} is hydrostatic pressure in the microvasculature, P_{pmv} is hydrostatic pressure in the peri-microvascular space, σ (sigma) is the reflection coefficient, π_{mv} is oncotic pressure in the microvasculature, and π_{pmv} is oncotic pressure in the perimicrovascular space.

Abnormalities in K_f and P_{mv} are the dominant variables in fluid filtration. K_f is a function of the number and size of the pores in the endothelial cell layer. Disorders that injure endothelial cells markedly increase K_f and fluid filtration (52). When K_f is increased and leads to pulmonary edema, it is characterized as permeability pulmonary edema. There are many disorders that increase K_f and lead to pulmonary edema, but the most common disorders confronted in the newborn period include RDS and sepsis both of which are frequently associated with lung inflammation and a component of lung edema secondary to inflammatory injury (53,54). Unfortunately mechanical ventilation has the potential to induce lung inflammation, thus careful supportive care to limit lung inflammation is imperative.

High pressure pulmonary edema is common in the newborn period, since the lung of the newborn is fully recruited at rest, left-to-right shunts increase fluid filtration substantially

(55,56), and elevations of left atrial pressure also increases filtration. The equation for P_{mv} is:

$$P_{mv} = P_{LA} + c(P_{PA} - P_{LA})$$

where c is equal to a constant between 0 and 1 and PA and LA are pulmonary arterial and left atrial, respectively. This equation illustrates the significant impact of elevated P_{LA} in lung fluid filtration. P_{LA} (or pulmonary venous pressure) can be particularly elevated in some forms of congenital heart disease (e.g., obstructed anomalous pulmonary venous connection, mitral valve disease, or hypoplastic left heart syndrome). Fluid accumulation in the lung can only occur when fluid filtration exceeds lymphatic function which returns filtered fluid to the venous circulation ($Q_f > Q_L$). Q_L is dependent on intrinsic contractility of the lymphatics in the lung and on the right atrial pressure. Right atrial pressure may be elevated in infants with lung disease enhancing fluid accumulation in the lung and the pressures at which lymphatic flow is impaired are lower in the fetus and newborn than in older patients. In summary, infants with lung disease and/or heart diseases are more predisposed to develop pulmonary edema than in any other age-group because increases in flow are invariably associated with increased microvascular pressure and developmentally impaired lymphatic function is frequently incapable of meeting the demands of increased fluid filtration.

The effects of pulmonary edema on respiratory physiology are dependent on the location of the edema fluid. Typically fluid filtration occurs in the alveolar capillary, but hydrostatic forces in the lung favor fluid accumulation in the extra-alveolar interstitium (57). The extra-alveolar interstitium contains airways so that fluid can compress the airways leading to constriction and increased airway resistance (58). This explains the finding of cardiac asthma and increased airway resistance with pulmonary edema. Decreased respiratory system compliance can also occur with pulmonary edema, primarily when accumulation occurs in the alveolar space and impairs surfactant function. It is difficult to filter fluid to the extent that fluid accumulates in the alveolar space because respiratory epithelial cells are excellent barriers to fluid egress and they actively pump fluid from the alveolar space into the interstitium (59). The extra-alveolar interstitium can accumulate excessive fluid before it egresses into the alveolar space. However, the lung is more susceptible to alveolar fluid accumulation when increased fluid filtration is associated with injury to respiratory epithelial cells.

Treatment for pulmonary edema is almost entirely supportive, and includes measures to lower P_{mv} or to support the respiratory system by applying positive pressure. Measures to decrease P_{mv} include reducing pulmonary blood flow by decreasing left-to-right shunts, or by decreasing circulating blood volume. Decreasing fluid administration is a reasonable short-term maneuver to decrease fluid filtration, but only if the fluid restriction does not impair the delivery of adequate nutrition. Therapy with diuretics may also reduce P_{mv} by decreasing circulating blood volume. While equipotent doses of diuretics improve lung function by decreasing lung water, furosemide has the additional effect of pulmonary dilation (60) which lowers P_{mv} further. Thus this diuretic is more effective for pulmonary edema than are equipotent doses of other diuretics. Pulmonary edema may accumulate to the extent that pressure support to the lung is necessary. The delivery of positive pressure does not decrease fluid accumulation in the lung. It simply improves the acute physiology, usually by improving V/Q mismatching (61,62) by improving ventilation to the low V/Q compartment in the lung. Decreasing pulmonary edema by decreasing K_f or by improving lymphatic function would be optimal, but measures to consistently achieve these improvements have not been described.

Abnormalities of pulmonary vascular physiology are confined primarily to inappropriate vasoconstriction. Persistent pulmonary hypertension in the newborn occurs when the normal decrease in pulmonary vascular resistance that occurs at birth does not occur and can be a result of underdevelopment, maldevelopment, or maladaptive forms of pulmonary vascular disease as described previously. Pulmonary hypertension in the newborn frequently presents with significant hypoxia because of right-to-left shunting at the fetal shunt pathways at the atrial and ductal levels. Pulmonary constriction is usually on the arterial side of the circuit so that therapies which dilate the pulmonary circuit may improve hypoxemia without increasing fluid filtration if the venous circuit is normal.

Pulmonary hypertension was the most common reason for placing infants on extracorporeal life support because specific pulmonary vasodilators had not been identified. However, inhaled nitric oxide has unequivocally improved the abnormal pulmonary physiology observed in infants with pulmonary hypertension. In several large randomized trials, nitric oxide was effective at reducing the incidence of death or the need for extracorporeal support (63). Inhaled nitric oxide was approved for utilization in infants with hypoxic respiratory failure in 1997 and was restricted to infants at or beyond 34 weeks of gestation. The utilization of this drug has meant that treatments previously used to support these infants, including high concentrations of oxygen and/or induced alkalosis, are contraindicated. Typical indications for the utilization of inhaled nitric oxide in term or near-term infants are respiratory failure as indicated by an oxygenation index of >20 to 25 ($OI = FiO_2 \times \text{mean airway pressure} \times 100/PaO_2$) and evidence of pulmonary hypertension from Doppler-echocardiography. Supportive efforts with mechanical ventilation and/or administration of surfactant that improve lung inflation improve the efficacy of inhaled nitric oxide (64). Nitric oxide is started at 20 ppm and is decreased in 50% decrements when supplemental oxygen requirements decrease substantially, usually to $<50\%$. When the dose of nitric oxide is 5 ppm, further decrements must be done cautiously as rebound pulmonary hypertension has been described in this range (65). Infants <34 weeks of gestation may also present with hypoxic respiratory failure and recent trials have been published suggesting that these infants may also benefit from treatment with nitric oxide (66–68). However, nitric oxide therapy has not yet been approved for these infants.

HYPERTROPHIC CARDIOMYOPATHY IN INFANTS OF DIABETIC MOTHERS

Maternal diabetes poses several risks to both the fetus and the newborn infant including fetal growth alterations, metabolic derangements, RDS, elevated pulmonary vascular resistance, congenital anomalies, and hypertrophic cardiomyopathy (69). From a cardiovascular standpoint, fetal heart development may be altered with reports of a 15% incidence of congenital heart disease in this population (70). In animal studies involving diabetes during pregnancy, abnormal gene expression has been shown to impair cardiogenesis in the fetus during the first trimester (71,72). During the second and third trimester, maternal diabetes has been associated with the development of hypertrophic cardiomyopathy that generally manifests as asymmetric septal hypertrophy. The incidence of hypertrophic cardiomyopathy has been reported to be approximately 30% to 38% in infants of diabetic mothers (70,73–74). The clinical presentation varies considerably with a spectrum from a limited process that abates within months of birth to severe cardiac compromise leading to mortality (74). Cardiac issues

have been noted in fetuses regardless of type of maternal diabetes. A recent study noted a 50% rate of newborn hypertrophic cardiomyopathy in type 1 diabetic mothers; however, a 25% rate was noted in infants of type 2 diabetic mothers (74). In contrast, an approximate rate of 2% was noted in infants of mothers with gestational diabetes (74). A comparison of those with well-controlled gestational diabetes to normal controls revealed mild hypertrophic changes in the diabetic group. However, these hypertrophic changes were not associated with significant pathology including no left ventricular outflow tract obstruction although minor changes in right ventricular diastolic function were observed (75).

The exact etiology of this hypertrophic change is unknown but plausible evidence suggests that hyperinsulinism triggers hyperplasia and hypertrophy of myocardial cells (76,77). Studies have noted increased maternal serum insulin-like growth factor I (IGF-I) at the time of delivery associated with neonatal hypertrophic cardiomyopathy (78,79). Clinical correlation of the neonatal hypertrophic cardiomyopathy to a history of maternal diabetes is paramount; however if the history is not clear, rare potential associations should be evaluated including Fabry disease, Costello syndrome, and Pompe disease (80–82).

RESPIRATORY SYNCYTIAL VIRUS

Infections caused by respiratory syncytial virus (RSV) create significant morbidity and mortality for patients at high risk including premature infants, infants with BPD, and infants with complicated hemodynamically significant congenital heart disease. The overall hospitalization rate for patients <1 year of age with RSV is 2% annually. Those at high risk experience approximately five times the rate of admissions for RSV-related illness as compared to those not at high risk (83–86). No active immunization program has ever been shown to be efficacious for RSV (87,88); however passive immunity with palivizumab has been shown to decrease RSV infections in high-risk infants. Palivizumab is a monoclonal antibody directed against the F protein of RSV (89,90). Palivizumab has been shown to decrease RSV-related hospitalizations in patients with hemodynamically significant congenital heart disease (91). Monthly intramuscular injections (15 mg/kg) during RSV season in this patient population yielded a 45% reduction in RSV-related hospitalizations, a 56% reduction in total days of RSV-related hospitalizations, and a 73% reduction in RSV hospitalization days with increased supplemental oxygen (91). Evidence exists in patients who receive palivizumab and then undergo surgery involving cardiopulmonary bypass that the levels of monoclonal antibody decrease dramatically. Therefore, after surgery involving cardiopulmonary bypass, dosing should be repeated at a safe time in the postoperative period.

NEUROLOGY

The fetal development of the brain and heart occur simultaneously (92). Therefore, impaired brain maturation and susceptibility to injury has been shown in patients with various forms of congenital heart disease (93,94). A case-control study showed an increased risk of microcephaly, as defined by a head circumference less than the third percentile, in newborns with tetralogy of Fallot, hypoplastic left heart syndrome, and coarctation/arch anomalies (93). Intrauterine hypoxia may lead to central nervous system damage (93). In patients with hypoplastic left heart syndrome and transposition of the great arteries, neonates were found to have smaller and less mature brains

than expected (94). A total maturation score was previously validated and used in this study which is a semiquantitative anatomic scoring system. This score utilizes four parameters to assess whole-brain maturity which include myelination, cortical infolding, involution of the glial cell migration bands, and presence of germinal matrix tissue (94). Magnetic resonance imaging (MRI) and magnetic resonance spectroscopy in neonates with congenital heart disease have shown white matter abnormalities before any cardiac intervention (95,96). Impaired brain maturation may lead to susceptibility to poor neurologic outcomes. Observers have noted that decreased cerebral oxygen delivery perioperatively, as evidenced by near-infrared spectroscopy, is associated with an abnormal psychomotor development index and MRI abnormalities (97).

Many institutions arrange for a head ultrasound study on patients prior to intervention for critical congenital heart disease. The head ultrasound is used to determine anatomical issues, hemorrhage, ischemia, hydrocephalus, and atrophy. Although this test is routinely performed, it is often replaced by other imaging studies if there is an abnormality. Cranial ultrasound in patients with congenital heart disease has shown abnormalities in as high as 42% of those screened (98). Findings included widened ventricular and/or subarachnoid spaces, lenticulostriate vasculopathy, calcification of basal nuclei, and ischemia. Patients with left-sided obstructive lesions seem to have a higher incidence of brain abnormalities (98). There is increasing concern that certain lesions may impact cerebral blood flow not only postnatally but during fetal development. Cerebrovascular resistance is lower than normal in fetuses with hypoplastic left heart syndrome where cerebral perfusion occurs retrogradely via the ductus arteriosus (99). In patients with right-sided lesions, the cerebrovascular resistance is higher than those with left-sided obstructive lesions (99). This may have implications for neurologic development and subsequent susceptibility to adverse sequelae.

A recent study suggested that 19% of neurologic events occur preoperatively in patients with congenital heart disease (100). Predictive factors for a neurologic event, namely seizure, abnormal tone or choreoathetosis include an abnormal preoperative imaging study and an Apgar score of <7 at 5 minutes of life (100). MRI studies performed preoperatively, acutely postoperatively (within weeks of surgery), and then several months postoperatively have shown abnormalities. Preoperatively, patients mainly had periventricular leukomalacia (PVL) and infarct. Shortly after surgery, MRI examinations showed new PVL in 48%, new infarct in 19%, and a new parenchymal hemorrhage in 33% (101). The prevalence of stroke in one series was 10%, half of which occurred preoperatively (102). Lower birth weight, preoperative intubation, lower intraoperative hematocrit, and higher blood pressure at admission postoperatively were associated statistically with stroke (102). The majority were clinically silent with mechanisms felt to be due to either hypoperfusion or thromboembolism (102). Late MRI did show resolution of the findings in a subset of patients (103). Among 82 neonates who had undergone cardiac surgery, 54% had PVL but in older infants the incidence was only 4% (103). Early postoperative hypoxemia and hypotension (mainly diastolic) were noted to be risk factors (103).

Among survivors of congenital heart disease surgery, there are well-known late sequelae that may include learning disabilities, behavioral abnormalities, and attention deficit disorders (104,105). Many issues may lead to these findings including neuroprotection during cardiac surgery, use of deep hypothermic circulatory arrest, and postoperative decreased perfusion from low cardiac output syndrome. With the application of perioperative noninvasive, real-time neurologic monitoring, interdisciplinary teams caring for the patient may be able to intervene and prevent brain injury.

GASTROINTESTINAL SYSTEM

The development of the gastrointestinal system occurs as early as the 4th week of gestation. Mesenteric vascular system development parallels that of the intestine. Regulation of the mesenteric blood flow occurs at the arteriolar and precapillary level. Feeding causes hyperemia and as documented in animal studies (106), the neonate has lower intestinal vascular resistance than the fetus (107). Therefore, mesenteric blood flow is greater in the neonate than in the fetus until the second to fourth postnatal weeks, where intestinal resistance increases, with a corresponding decrease in blood flow and oxygen delivery. Of potential importance to those patients with critical congenital heart disease, mild hypoxia triggers dilation of the vascular bed and perfusion increases whereas severe hypoxia (PO_2 of 40 mmHg or less) causes vasoconstriction, tissue hypoxia, and potential ischemia (108).

The etiology of necrotizing enterocolitis (NEC) remains poorly understood, especially in term infants. Studies have shown that the majority of term newborns who develop NEC have underlying congenital disorders which are commonly either heart disease or endocrine disorders (109). A case control study of neonates with congenital heart disease showed that hypoplastic left heart syndrome (odds ratio 3.8), truncus arteriosus or aortopulmonary window (odds ratio 6.3) were independently associated with development of NEC (82). Additionally, in the same cohort, earlier gestational age at birth ($36.7 \text{ weeks} \pm 2.7 \text{ weeks}$), prematurity, and episodes of shock or low cardiac output were all risk factors (110). There was no documented mortality difference in patients who developed NEC versus those who did not; however the hospital stay was significantly higher in those who developed NEC. In patients with congenital heart disease who develop NEC, it is felt that mesenteric ischemia associated with a low perfusion state is the etiology; however, infectious associations are difficult to elucidate (111). A recent study suggests that patients with congenital heart disease who develop NEC have less risk of major short- and long-term adverse outcomes as compared to patients without heart disease (112). Patients with heart disease and NEC experienced less risk of perforation, need for a bowel operation, strictures, need for a stoma, sepsis, and short bowel syndrome (112). This suggests that NEC in those with cardiac disease may be a distinct entity. Cardiac lesions that elicit a difficult balance between pulmonary and systemic blood flow ($Q_p:Q_s$) whereby systemic perfusion can be limited due to a shift in the systemic and pulmonary vascular resistances pose a difficult dilemma to the intensivist regarding if and when to feed preoperatively and postoperatively.

Many patients with congenital heart disease also have heterotaxy (situs abnormalities). Situs inversus totalis is associated with intra-abdominal anomalies in over half of the patients. These may include duodenal atresia, biliary atresia, gastroschisis with malrotation, and tracheoesophageal fistula. Hiatal and diaphragmatic hernias are commonly noted in patients with right isomerism. Patients with left isomerism may have malrotation and biliary atresia (113). Intestinal malrotation may lead to gastrointestinal complications and require emergent surgery. It is debatable whether an elective Ladd procedure is warranted in all patients with malrotation once the cardiac condition is stabilized or appropriately palliated. Upper gastrointestinal contrast procedures likely should be recommended in all patients with heterotaxy and cardiac lesions to evaluate for intestinal malrotation (114).

RENAL

Glomerular filtration rate (GFR) in term neonates is $20 \text{ mL/min} \times 1.73 \text{ m}^2$ which is generally twice that of premature newborns (115). GFR improves over the first several weeks of life

in all newborns but the velocity at which it improves is less in premature infants. In term newborns, the GFR doubles in the first 2 weeks of life (116,117). These differences in GFR values among varying gestational age newborns impact the administration of medications that are primarily eliminated in the renal system. Digoxin dosages should be decreased for preterm infants. Creatinine is the most commonly used marker for renal function; however in neonates, interpretation must take into account several caveats (118). The creatinine level is falsely elevated at birth, reflecting maternal levels. Over the first several weeks of life in term neonates, creatinine decreases rapidly to expected levels (0.40 mg/dL). In those with extreme prematurity, a transient increase is noted over the first 4 days followed by a steady decrease over the next month of life. In premature infants, the transient rise in creatinine is caused by reabsorption of creatinine across renal tubules (119).

Because of the unique vascular supply of the renal medulla, the kidney is susceptible to hypoxic-ischemic injury. In congenital heart disease that either presents with decreased systemic blood flow in critical left-sided obstructive disease or a shift in $Q_p:Q_s$ with resultant decreased systemic oxygen delivery, renal function may be altered. Prolonged ischemia may result in impairment in sodium and water reabsorption as well as decreased GFR (120). Similarly, use of angiotensin converting enzyme (ACE) inhibitors may lower systemic blood pressure to the extent that hypoperfusion to the kidney occurs (121). Renal perfusion pressure may drop below the autoregulatory threshold and thus promote acute renal failure. Caution in dosing and monitoring of effects of ACE inhibitors in neonates is important to avoid adverse renal effects.

Many institutions advocate the use of umbilical catheters in newborns with critical congenital heart disease for access, monitoring, and acquisition of blood samples. Arterial lines have been associated with aortic and renal arterial complications including thrombosis. No definitive study has shown whether high or low umbilical arterial line placement affects the incidence of thrombotic complications; in fact, conflicting data exist (122,123). Both abdominal coarctation and renal artery stenosis have been reported as long-term complications of umbilical arterial lines. Umbilical venous lines are placed with the tip in the inferior vena cava cephalad to the hepatic and portal veins. Complications of these lines include thrombosis of the portal or hepatic venous systems or inferior vena caval thrombus. Renal vein thrombosis may occur and could manifest itself with symptoms of oliguria, anuria, hematuria, thrombocytopenia, acidosis, and hemolytic anemia (124). Hypertension can occur late after renal vein thrombosis but the magnitude of hypertension is much less than those with umbilical artery thrombosis.

CARDIAC INTERVENTION IN THE PREMATURE OR LOW BIRTH WEIGHT NEONATE

Recent reports suggest that aggressive attempts to treat congenital heart disease in either premature or of low birth weight infants are appropriate. Delaying surgery or cardiac catheter intervention for weight gain lead to longer hospital stays and increased morbidity (125). A meta-analysis of observational studies suggests that diagnosis is the factor that is most predictive of mortality as compared to low birth weight (126). However, data exist that suggest the ideal gestational age for a patient with critical congenital heart disease is 39 to 40 weeks of gestation (127). In 971 consecutive infants, patients born at 37 to 38 weeks of gestation had increased mortality, morbidity, and time on the ventilator as

compared to the reference group, 39 to 40 weeks of gestation (127). Interestingly, in the same analysis, those born before 37 weeks of gestation or after 40 weeks of gestation also had increased morbidity rates and longer ventilatory times (127). Furthermore, in the Pediatric Heart Network single ventricle trial, subanalysis showed that rates of preterm birth (16% vs. 12%, $p < 0.001$), low birth weight (18% vs. 8%, $p < 0.001$), and small for gestational age (22% vs. 10%, $p < 0.001$) were higher in those with single ventricle anatomy as compared to the general population (128).

There are many studies evaluating the subgroup of patients <2,500 g who have congenital heart disease. In one report (129), the mortality rate for closed procedures was 10.4% versus 5.4% for the comparison group. Similarly, the mortality rate for open heart procedures in those <2,500 g was 25.4% versus 10.5% for term counterparts. The actuarial survival rate at 10 years was 51%. Another study examined palliations versus complete biventricular repair in the same weight cutoff and noted that a higher mortality rate was seen in premature infants (vs. low birth weight) and in those who had undergone palliations (130). One study (131) showed that overall surgical mortality in those <2,500 g (either palliation or definitive repair) was 18%. Definitive repair was associated with better outcomes with 13% mortality versus 28% mortality in those who underwent palliative surgery. Medium-term follow-up indicated that survival was 87% in those with corrective surgery and 54% in the palliation group. Obviously, morbidity is higher in the entire low birth weight group compared to term infants. Statistical analysis showed that early outcome was independent of age, weight, prematurity, use of cardiopulmonary bypass, and type of intervention. The authors concluded that primary correction has an early survival benefit over palliation. These results were similarly noted in a series of 60 patients <2,500 g with 35 who had cardiopulmonary bypass (132). Overall results showed acute deaths being 15% and survival at 60 months to be 70% for the entire group. A recent study of 75 consecutive infants weighing <2,500 g who underwent surgical palliation with a heterogeneous set of heart anomalies including single ventricle anatomy and complex cyanotic congenital heart disease revealed a 90% overall 1 year survival and a 88% 5-year survival by Kaplan-Meier analysis (133). Patients in this cohort who had a genetic abnormality had a 28% overall mortality rate as compared to 5.4% in those without a chromosomal issue (133).

Similar conclusions have been made for the very low birth weight infant (<1,500 g). Complete repair has been advocated for these patients since delays for weight gain have been shown to be associated with no long-term benefit and increased preoperative morbidity. Additionally, complete surgical correction is preferred over prolonged medical management or other palliative procedures (134).

Aggressive surgical strategies for the low or very low birth weight neonate have prompted cardiac catheterization in the same group. A recent study compared those <1,500 g who had undergone catheterization in a case-control study with the comparison population weighing between 2 and 3 kg (135). In essence, success rates, complication rates, incidence of blood transfusions, and incidence of major complications were the same for each group. The procedures in the very low birth weight infant are rare, yet pose an impetus for equipment alterations and safety considerations in the catheterization lab for these patients (135). In the past, transcatheter closure of the PDA in low birth weight or preterm infants was felt to be technically challenging and was thus not considered a good option as compared to traditional surgical intervention (136). However, several contemporary reports of catheterization intervention with various devices to occlude the PDA in selected preterm infants have been published (137–142).

INTERDISCIPLINARY APPROACH

This unique patient population merits the same interdisciplinary approach provided to children and adults with congenital heart disease. A firm understanding of neonatal physiology and organ system development is imperative to assure the highest quality of care. The future of this field may involve an evolution of multiple services that may lead to specific neonatal cardiac services that will promote research and enhance care.

REFERENCES

1. Rudolph AM. The changes in the circulation after birth: their importance in congenital heart disease. *Circulation* 1970;41:343–359.
2. Teitel DF, Iwamoto HS, Rudolph AM. Effects of birth related events on central flow patterns. *Pediatr Res* 1987;22:557–566.
3. Gittenberger-De Groot AC. Persistent ductus arteriosus: most probably a primary congenital malformation. *Br Heart J* 1977;39:610–618.
4. Waleh N, Seidner S, McCurnin D, et al. The role of monocyte-derived cells and inflammation in baboon ductus arteriosus remodeling. *Pediatr Res* 2005;57:254–262.
5. Keller RL, Clyman RI. Persistent Doppler flow predicts lack of response to multiple courses of indomethacin in premature infants with recurrent patent ductus arteriosus. *Pediatrics* 2003;112:583–587.
6. Kajino H, Goldbarg S, Roman C, et al. Vasa vasorum hypoperfusion is responsible for medial hypoxia and anatomic remodeling in the newborn lamb ductus arteriosus. *Pediatr Res* 2002;51:228–235.
7. Clyman RI, Seidner SR, Kajino H, et al. VEGF regulates remodeling during permanent anatomic closure of the ductus arteriosus. *Am J Physiol Regul Integr Comp Physiol* 2002;282:R199–R206.
8. Kajino H, Chen YQ, Chemtob S, et al. Tissue hypoxia inhibits prostaglandin and nitric oxide production and prevents ductus arteriosus reopening. *Am J Physiol Regul Integr Comp Physiol* 2000;279:R278–R286.
9. Schmidt B, Roberts RS, Fanaroff A, et al. Indomethacin prophylaxis, patent ductus arteriosus, and the risk of bronchopulmonary dysplasia: further analyses from the Trial of Indomethacin Prophylaxis in Preterms (TIPP). *J Pediatr* 2006;148:730–734.
10. Alpan G, Scheerer R, Bland R, et al. Patent ductus arteriosus increases lung fluid filtration in preterm lambs. *Pediatr Res* 1991;30:616–621.
11. Shimada S, Kasai T, Konishi M, et al. Effects of patent ductus arteriosus on left ventricular output and organ blood flows in preterm infants with respiratory distress syndrome treated surfactant. *J Pediatr* 1994;125:270–277.
12. Laughon MM, Simmons MA, Bose CL. Patency of the ductus arteriosus in the premature infant: is it pathologic? Should it be treated? *Curr Opin Pediatr* 2004;16:146–151.
13. Fowlie PW, Davis PG. Prophylactic intravenous indomethacin for preventing mortality and morbidity in preterm infants. *Cochrane Database Syst Rev* 2002;(3):CD000174.
14. Rojas MA, Gonzalez A, Bancalari E, et al. Changing trends in the epidemiology and pathogenesis of neonatal chronic lung disease. *J Pediatr* 1995;126:605–610.
15. Brooks JM, Travadi JN, Patole SK, et al. Is surgical ligation of patent ductus arteriosus necessary? The Western Australian experience of conservative management. *Arch Dis Child Fetal Neonatal Ed* 2005;90:F235–F239.
16. Clyman RI. Recommendations for the postnatal use of indomethacin: an analysis of four separate treatment strategies [editorial]. *J Pediatr* 1996;128:601–607.
17. Effect of corticosteroids for fetal maturation on perinatal outcomes. NIH Consensus Statement 1994;12:1–24.
18. Antenatal corticosteroids revisited: repeat courses - National Institutes of Health Consensus Development Conference Statement, August 17–18, 2000. *Obstet Gynecol* 2001;98:144–150.
19. Fowlie PW, Davis PG, McGuire W. Prophylactic intravenous indomethacin for preventing mortality and morbidity in premature infants. *Cochrane Database Syst Rev* 2010;7(7):CD000174.
20. Ohlsson A, Walia R, Shah SS. Ibuprofen for the treatment of patent ductus arteriosus in preterm and/or low birth weight infants. *Cochrane Database Syst Rev* 2010;14(4):CD003481.
21. Jones LJ, Craven PD, Attia J, et al. Network meta-analysis of indomethacin versus ibuprofen versus placebo for PDA in preterm infants. *Arch Dis Child Fetal Neonatal Ed* 2011;96:F45–F52.
22. Mosalli R, Alfaleh K. Prophylactic surgical ligation of the patent ductus arteriosus for prevention of mortality and morbidity in extremely low birth weight infants. *Cochrane Database Syst Rev* 2008;23(1):CD006181.
23. Kabra NS, Schmidt B, Roberts RS, et al. Neurosensory impairment after surgical closure of patent ductus arteriosus in extremely low birthweight infants: results from the Trial of Indomethacin Prophylaxis in Preterms. *J Pediatr* 2007;150:229–234.
24. Langston C, Kida K, Reed M, et al. Human lung growth in late gestation and in the neonate. *Am Rev Respir Dis* 1984;129:607–613.

25. Langston C. Normal and abnormal structural development of the human lung. *Prog Clin Biol Res* 1983;140:75–91.
26. Langston C, Thurlbeck WM. Lung growth and development in late gestation and early postnatal life. *Perspect Pediatr Pathol* 1982;7:203–235.
27. Ten Have-Opbroek AA. Lung development in the mouse embryo. *Exp Lung Res* 1991;17:111–130.
28. Northway WH Jr, Rosan RC, Porter DY. Pulmonary disease following respirator therapy of hyaline-membrane disease. Bronchopulmonary dysplasia. *N Engl J Med* 1967;276:357–368.
29. Viscardi RM, Muhumuza CK, Rodriguez A, et al. Inflammatory markers in intrauterine and fetal blood and cerebrospinal fluid compartments are associated with adverse pulmonary and neurologic outcomes in preterm infants. *Pediatr Res* 2004;55:1009–1017.
30. Doyle LW, Faber B, Callanan C, et al. Bronchopulmonary dysplasia in very low birth weight subjects and lung function in late adolescence. *Pediatrics* 2006;118:108–113.
31. Doyle LW. Respiratory function at age 8–9 years in extremely low birth-weight/very preterm children born in Victoria in 1991–1992. *Pediatr Pulmonol* 2006;41:570–576.
32. Liggins GC, Howie RN. A controlled trial of antepartum glucocorticoid treatment for prevention of the respiratory distress syndrome in premature infants. *Pediatrics* 1972;50:515–525.
33. Crowley PA. Antenatal corticosteroid therapy: a meta-analysis of the randomized trials, 1972 to 1994. *Am J Obstet Gynecol* 1995;173:322–335.
34. Wright LL, Verter J, Younes N, et al. Antenatal corticosteroid administration and neonatal outcome in very low birth weight infants: the NICHD Neonatal Research Network. *Am J Obstet Gynecol* 1995;173:269–274.
35. Horbar JD. Antenatal corticosteroid treatment and neonatal outcomes for infants 501 to 1500 gm in the Vermont-Oxford Trials Network. *Am J Obstet Gynecol* 1995;173:275–281.
36. Pollock JS, Forstermann U, Tracey WR, et al. Nitric oxide synthase isozymes antibodies. *Histochem J* 1995;27:738–744.
37. Soll RF. Synthetic surfactant for respiratory distress syndrome in preterm infants. *Cochrane Database Syst Rev* 2000;(2):CD001149.
38. Morley CJ, Davis PG, Doyle LW, et al. Nasal CPAP or intubation at birth for very preterm infants. *N Engl J Med* 2008;358:700–708.
39. Finer NN, Carlo WA, Walsh MC, et al. on behalf of the SUPPORT Study Group. Early CPAP versus surfactant in extremely preterm infants. *N Engl J Med* 2010;362:1970–1979.
40. Bell EF, Acarregui MJ. Restricted versus liberal water intake for preventing morbidity and mortality in preterm infants. *Cochrane Database Syst Rev* 2001;(3):CD000503.
41. Reid LM. Structure and function in pulmonary hypertension. New perceptions. *Chest* 1986;89:279–288.
42. Geggel RL, Murphy JD, Langleben D, et al. Congenital diaphragmatic hernia: arterial structural changes and persistent pulmonary hypertension after surgical repair. *J Pediatr* 1985;107:457–464.
43. Bland RD. Dynamics of pulmonary water before and after birth. *Acta Paediatr Scand Suppl* 1983;305:12–20.
44. Bland RD, Bressack MA, McMillan DD. Labor decreases the lung water content of newborn rabbits. *Am J Obstet Gynecol* 1979;135:364–367.
45. Landers S, Hansen TN, Corbet AJ, et al. Optimal constant positive airway pressure assessed by arterial alveolar difference for CO₂ in hyaline membrane disease. *Pediatr Res* 1986;20:884–889.
46. Hansen TN, Corbet AJ, Kenny JD, et al. Effects of oxygen and constant positive pressure breathing on aADCO₂ in hyaline membrane disease. *Pediatr Res* 1979;13:1167–1171.
47. Hansen TN, Gest AL. Oxygen toxicity and other ventilatory complications of treatment of infants with persistent pulmonary hypertension. *Clin Perinatol* 1984;11:653–672.
48. Multicentre randomised controlled trial of high against low frequency positive pressure ventilation. Oxford Region Controlled Trial of Artificial Ventilation OCTAVE Study Group. *Arch Dis Child* 1991;66:770–775.
49. Stewart AR, Finer NN, Peters KL. Effects of alterations of inspiratory and expiratory pressures and inspiratory/expiratory ratios on mean airway pressure, blood gases, and intracranial pressure. *Pediatrics* 1981;67:474–481.
50. Alba J, Agarwal R, Hegyi T, et al. Efficacy of surfactant therapy in infants managed with CPAP. *Pediatr Pulmonol* 1995;20:172–176.
51. Mandy GT, Moise AA, Smith EO, et al. Endotracheal continuous positive airway pressure after rescue surfactant therapy. *J Perinatol* 1998;18:444–448.
52. Parker JC, Townsley MI. Evaluation of lung injury in rats and mice. *Am J Physiol Lung Cell Mol Physiol* 2004;286:L231–L246.
53. Carlton DP, Albertine KH, Cho SC, et al. Role of neutrophils in lung vascular injury and edema after premature birth in lambs. *J Appl Physiol* 1997;83:1307–1317.
54. Calkins CM, Bensard DD, Partrick DA, et al. Altered neutrophil function in the neonate protects against sepsis-induced lung injury. *J Pediatr Surg* 2002;37:1042–1047.
55. Nelin LD, Wearden ME, Welty SE, et al. The effect of blood flow and left atrial pressure in the DLCO in lambs and sheep. *Resp Physiol* 1992;88:333–342.
56. Means LJ, Hanson WL, Mounts KO, et al. Pulmonary capillary recruitment in neonatal lambs. *Pediatr Res* 1993;34:596–599.
57. Michel RP, Zocchi L, Rossi A, et al. Does interstitial lung edema compress airways and arteries? A morphometric study. *J Appl Physiol* 1987;62:108–115.
58. Sasidharan P, Heimler R. Alterations in pulmonary mechanics after transfusion in anemic preterm infants. *Crit Care Med* 1990;18:1360–1362.
59. Pitkanen OM, O'Brodovich HM. Significance of ion transport during lung development and in respiratory disease of the newborn. *Ann Med* 1998;30:134–142.
60. Demling RH, Will JA. The effect of furosemide on the pulmonary transvascular fluid filtration rate. *Crit Care Med* 1978;6:317–319.
61. Demling RH, Edmunds LH, Jr. Effect of continuous positive airway pressure on extravascular lung water. *Surg Forum* 1973;24:226–228.
62. Wickerts CJ, Berg B, Blomqvist H. Influence of positive end-expiratory pressure on extravascular lung water during the formation of experimental hydrostatic pulmonary oedema. *Acta Anaesthesiol Scand* 1992;36:309–317.
63. Finer NN, Barrington KJ. Nitric oxide for respiratory failure in infants born at or near term. *Cochrane Database Syst Rev* 2006;(4):CD000399.
64. Inhaled nitric oxide in full-term and nearly full-term infants with hypoxic respiratory failure. The Neonatal Inhaled Nitric Oxide Study Group. *N Engl J Med* 1997;336:597–604.
65. Davidson D, Barefield ES, Kattwinkel J, et al. Safety of withdrawing inhaled nitric oxide therapy in persistent pulmonary hypertension of the newborn. *Pediatrics* 1999;104:231–236.
66. Kinsella JP, Cutter GR, Walsh WF, et al. Early inhaled nitric oxide therapy in premature newborns with respiratory failure. *N Engl J Med* 2006;355:354–364.
67. Ballard RA, Truog WE, Cnaan A, et al. Inhaled nitric oxide in preterm infants undergoing mechanical ventilation. *N Engl J Med* 2006;355:343–353.
68. Van Meurs KP, Wright LL, Ehrenkranz RA, et al. Inhaled nitric oxide for premature infants with severe respiratory failure. *N Engl J Med* 2005;353:13–22.
69. Tyralla EE. The infant of the diabetic mother. *Obstet Gynecol Clin North Am* 1996;23:221–241.
70. Abu-Sulaiman RM, Subaih B. Congenital heart disease in infants of diabetic mothers: echocardiographic study. *Pediatr Cardiol* 2004;25:137–140.
71. Molin DG, Roest PA, Nordstrand H, et al. Disturbed morphogenesis of cardiac outflow tract and increased rate of aortic arch anomalies in the offspring of diabetic rats. *Birth Defects Res Part A Clin Mol Teratol* 2004;70:927–938.
72. Siman CM, Gittenberger-De Groot AC, Wisse B, et al. Malformations in offsprings of diabetic rats: morphometric analysis of neural crest-derived organs and effects of maternal vitamin E treatment. *Teratology* 2000;61:355–367.
73. Vural M, Leke L, Mahomedaly H, et al. Should an echocardiographic scan be done routinely for infants of diabetic mothers? *Turk J Pediatr* 1995;37:351–356.
74. Ullmo S, Vial Y, Di Bernardo S, et al. Pathologic ventricular hypertrophy in the offspring of diabetic mothers: a retrospective study. *Eur Heart J* 2007;28:1319–1325.
75. Garcia-Flores J, Janes M, Gonzalez MC, et al. Fetal myocardial morphological and functional changes associated with well-controlled gestational diabetes. *Eur J Obstet Gynecol Reprod Biol* 2011;154:24–26.
76. Mehta A, Hussain K. Transient hyperinsulinism associated with macrosomia, hypertrophic obstructive cardiomyopathy, hepatomegaly and nephromegaly. *Arch Dis Child* 2003;88:822–824.
77. Veille JC, Hanson R, Sivakoff M, et al. Fetal cardiac size in normal, intrauterine growth retarded, and diabetic pregnancies. *Am J Perinatol* 1993;10:275–279.
78. Hayati AR, Cheah FC, Yong JF, et al. The role of serum insulin-like growth factor I (IGF-I) in neonatal outcome. *J Clin Pathol* 2004;57:1299–1301.
79. Hayati AR, Cheah FC, Tan AE, et al. Insulin-like growth factor-1 receptor expression in the placenta of diabetic and normal pregnancies. *Early Hum Dev* 2007;83:41–46.
80. Ackerman MJ, Landstrom AP. Detection of subclinical Fabry disease in patients presenting with hypertrophic cardiomyopathy. *J Am Coll Cardiol* 2007;50:2404–2405.
81. Lo IF, Brewer C, Shannon N, et al. Severe neonatal manifestations of Costello syndrome. *J Med Genet* 2008;45:167–171.
82. Noori S, Acherman R, Siassi B, et al. A rare presentation of Pompe disease with massive hypertrophic cardiomyopathy at birth. *J Perinat Med* 2002;30:517–521.
83. Heilman CA. Respiratory syncytial and parainfluenza viruses. *J Infect Dis* 1990;161:402–406.
84. Hall CB, Kopelman AE, Douglas RG Jr, et al. Neonatal respiratory syncytial virus infection. *N Engl J Med* 1979;300:393–396.
85. Groothuis JR, Gutierrez KM, Lauer BA. Respiratory syncytial virus infection in children with bronchopulmonary dysplasia. *Pediatrics* 1988;82:199–203.
86. MacDonald NE, Hall CB, Suffin SC, et al. Respiratory syncytial virus infection in infants with congenital heart disease. *N Engl J Med* 1982;207:397–400.
87. Kim HW, Canchola JG, Brandt CD, et al. Respiratory syncytial virus disease in infants despite prior administration of antigenic inactivated vaccine. *Am J Epidemiol* 1969;89:422–434.
88. Openshaw PJM, Cully FJ, Olszewska W. Immunopathogenesis of vaccine-enhanced RSV disease. *Vaccine* 2002;20:S27–S31.
89. Prince GA, Hemmin VG, Horswood RL, et al. Immunoprophylaxis and immunotherapy of respiratory syncytial virus infection in the cotton rat. *Virus Res* 1985;3:193–206.

90. Johnson S, Oliver C, Prince GA, et al. Development of a humanized monoclonal antibody (MEDI-493) with potent *in vitro* and *in vivo* activity against respiratory syncytial virus (RSV). *J Infect Dis* 1997;176:1215-1224.
91. Feltes TF, Cabalka AK, Meissner C, et al. Palivizumab prophylaxis reduces hospitalization due to respiratory syncytial virus in young children with hemodynamically significant congenital heart disease. *J Pediatr* 2003;143:532-540.
92. McQuillen PS, Miller SP. Congenital heart disease and brain development. *Ann NY Acad Sci* 2010;1184:68-86.
93. Barbu D, Mert I, Kruger M, et al. Evidence of fetal central nervous system injury in isolated congenital heart defects: microcephaly at birth. *Am J Obstet Gynecol* 2009;201:43.e1-43.e7.
94. Licht DJ, Shera DM, Clancy RR, et al. Brain maturation is delayed in infants with complex congenital heart defects. *J Thorac Cardiovasc Surg* 2009;137:529-536.
95. Miller SP, McQuillen PS, Hamrick S, et al. Abnormal brain development in newborns with congenital heart disease. *N Engl J Med* 2007;357:1928-1938.
96. Shedeed SA, Elfaytouri E. Brain maturity and brain injury in newborns with cyanotic congenital heart disease. *Pediatr Cardiol* 2011;32:47-54.
97. Kussman BD, Wypij D, Laussen PC, et al. Relationship of intraoperative cerebral oxygen saturation to neurodevelopmental outcome and brain magnetic resonance imaging at 1 year of age in infants undergoing biventricular repair. *Circulation* 2010;122:245-254.
98. Te Pas AB, van Wezel-Meijler G, Bokenkamp-Gramann R, et al. Preoperative cranial ultrasound findings in infants with major congenital heart disease. *Acta Pediatr* 2005;94:1597-1603.
99. Kaltman JR, Di H, Tian Z, et al. Impact of congenital heart disease on cerebrovascular blood flow dynamics in the fetus. *Ultrasound Obstet Gynecol* 2005;25:32-36.
100. Chock VY, Reddy VM, Bernstein D, et al. Neurologic events in neonates treated surgically for congenital heart disease. *J Perinatol* 2006;26:237-242.
101. Mahle WT, Tavani F, Zimmerman RA, et al. An MRI study of neurological injury before and after congenital heart surgery. *Circulation* 2002;106:1109-1114.
102. Chen J, Zimmerman RA, Jarvik GP, et al. Perioperative stroke in infants undergoing open heart operations for congenital heart disease. *Ann Thorac Surg* 2009;88:823-829.
103. Galli KK, Zimmerman RA, Jarvik GP, et al. Periventricular leukomalacia is common after neonatal cardiac surgery. *J Thorac Cardiovasc Surg* 2004;127:692-704.
104. McKenzie ED, Andropoulos DB, DiBardino D, et al. Congenital heart surgery 2005: the Brain: it's the heart of the matter. *Am J Surg* 2005;190:289-294.
105. Wernovsky G, Shillingford AJ, Gaynor JW. Central nervous system outcomes in children with complex congenital heart disease. *Curr Opin Cardiol* 2005;20:94-99.
106. Crissinger KD, Burney DL. Influence of luminal nutrient composition on hemodynamics and oxygenation in developing piglet intestine. *Am J Physiol* 1992;263:G254-G260.
107. Martinussen M, Brubakk AM, Vi T, et al. Mesenteric blood flow velocity and its relation to transitional circulatory adaptation in appropriate for gestational age preterm infants. *Pediatr Res* 1996;39:275-280.
108. Nowicki PT, Miller CE, Haun SE. Effects of arterial hypoxia and isoproterenol on *in vitro* postnatal intestinal circulation. *Am J Physiol* 1988;255:H1144-H1148.
109. Bolisetty S, Lui K, Oei J, et al. A regional study of underlying congenital diseases in term neonates with necrotizing enterocolitis. *Acta Paediatr* 2000;89:1226-1230.
110. McElhinney DB, Hedrick HL, Bush DM, et al. Necrotizing enterocolitis in neonates with congenital heart disease: risk factors and outcomes. *Pediatrics* 2000;106:1080-1087.
111. Fatica C, Gordon S, Mossad E, et al. A cluster of necrotizing enterocolitis in term infants undergoing open heart surgery. *Am J Infect Control* 2000;28:130-132.
112. Pickard SS, Feinstein JA, Popat RA, et al. Short- and long-term outcomes of necrotizing enterocolitis in infants with congenital heart disease. *Pediatrics* 2009;123:e901-e906.
113. Lee SE, Kim HY, Jung SE, et al. Situs anomalies and gastrointestinal abnormalities. *J Pediatr Surg* 2006;41:1237-1242.
114. Chang J, Brueckner M, Touloukian RJ. Intestinal rotation and fixation abnormalities in heterotaxia: early detection and management. *J Pediatr Surg* 1993;28:1281-1284.
115. Guignard JP, Torrado A, Da Cunha O, et al. Glomerular filtration rate in the first three weeks of life. *J Pediatr* 1975;87:268-272.
116. Bueva A, Guignard JP. Renal function in preterm neonates. *Pediatr Res* 1994;36:572-577.
117. Vanpee M, Blennow M, Linne T, et al. Renal function in very low birth weight infants: normal maturity reached during early childhood. *J Pediatr* 1992;121:784-788.
118. Guignard JP, Drukker A. Why do newborn infants have a high plasma creatinine? *Pediatrics* 1999;103:e49.
119. Matos P, Duarte-Silva M, Drukker A, et al. Creatinine reabsorption by the newborn rabbit kidney. *Pediatr Res* 1998;44:639-641.
120. Myers BD, Moran SM. Hemodynamically mediated acute renal failure. *N Engl J Med* 1986;314:97-105.
121. Rasoulpour M, Marinelli KA. Systemic hypertension. *Clin Perinatol* 1992;19:121-137.
122. Harris MS, Little GA. Umbilical artery catheters: high, low or no. *J Perinat Med* 1978;6:15-21.
123. Seibert JJ, Northington FJ, Miers JF, et al. Aortic thrombosis after umbilical artery catheterization in newborns: prevalence of complications on long-term follow-up. *Am J Roentgenol* 1991;156:567-569.
124. Mocan H, Beattie TJ, Murphy AV. Renal venous thrombosis in infancy: long-term follow-up. *Pediatr Nephrol* 1991;5:45-49.
125. Ades A, Johnson BA, Berger S. Management of low birth weight infants with congenital heart disease. *Clin Perinatol* 2005;32: 999-1015.
126. Abrishamchian R, Kanhai D, Zwets E, et al. Low birth weight or diagnosis, which is a higher risk? - A meta-analysis of observational studies. *Eur J Cardiothorac Surg* 2006;30:700-705.
127. Costello JM, Polito A, Brown DW, et al. Birth before 39 weeks' gestation is associated with worse outcomes in neonates with heart disease. *Pediatrics* 2010;126:277-284.
128. Williams RV, Ravishanker C, Zak V, et al. Birth weight and prematurity in infants with single ventricle physiology: pediatric heart network infant single ventricle trial screened population. *Congenit Heart Dis* 2010;5: 96-103.
129. Dees E, Lin H, Cotton RB, et al. Outcome of preterm infants with congenital heart disease. *J Pediatr* 2000;137:653-659.
130. Malec E, Werynski P, Mroczek T, et al. Results of surgical treatment of congenital heart defects in infants below 2500 grams. *Przegląd Lekarski* 2000;57:187-190.
131. Bove T, Francois K, De Groote K, et al. Outcome analysis of major cardiac operations in low weight neonates. *Ann Thorac Surg* 2004;78:181-187.
132. Oppido G, Napoleone CP, Formigari R, et al. Outcome of cardiac surgery in low birth weight and premature infants. *Eur J Cardio-thorac Surg* 2004;26:44-53.
133. Azakie A, Johnson NC, Anagnostopoulos PV, et al. Cardiac surgery in low birth weight infants: current outcomes. *Interact Cardiovasc Thorac Surg* 2011;12:409-413.
134. Reddy VM, Hanley FL. Cardiac surgery in infants with very low birth weight. *Semin Pediatr Surg* 2000;9:91-95.
135. Sutton N, Lock JE, Geggel RL. Cardiac catheterization in infants weighing less than 1,500 grams. *Catheter Cardiovasc Interv* 2006;68:948-956.
136. Francis E, Singhi AK, Lakshminenkateshaiah S, et al. Transcatheter occlusion of patent ductus arteriosus in pre-term infants. *J Am Coll Cardiol Interv* 2010;3:550-555.
137. Bentham J, Meur S, Hudsmith L, et al. Echocardiographically guided catheter closure of the arterial ducts in small preterm infants on the neonatal intensive care unit. *Catheter Cardiovasc Interv* 2011;77:409-415.
138. Prsa M, Ewert P. Transcatheter closure of a patent ductus arteriosus in a preterm infant with an Amplatzer Vascular Plug IV device. *Catheter Cardiovasc Interv* 2011;77:108-111.
139. Glatz AC, Petit CJ, Gillespie MJ. Novel use of a modified Amplatzer Vascular Plug to occlude a patent ductus arteriosus in two patients. *Catheter Cardiovasc Interv* 2008;72:82-86.
140. Roberts P, Adwani W, Archer N, et al. Catheter closure of the arterial duct in preterm infants. *Arch Dis Child Fetal Neonatal Ed* 2007;92: F248-F250.
141. Thukaram R, Suarez WA, Sundararaghavan S. Transcatheter closure of the patent arterial duct using the Flipper coil in a premature infant weighing 1,400g: a case report. *Catheter Cardiovasc Interv* 2005;66:18-20.
142. Haneda N, Kato F, Kim SH. Coil closure of a large patent arterial duct in a low-birthweight infant. *Pediatr Int* 2002;44:317-320.

Dean B. Andropoulos ■ Anthony C. Chang

Pediatric cardiovascular intensive care has become increasingly organized as a subspecialty over the past decade, in response to the explosion of knowledge and research in the patient with critical cardiac disease, the increasing complexity of cardiac lesions and procedures to treat them, and the growing numbers of patients of a younger age requiring cardiac intensive care. An international subspecialty society, the Pediatric Cardiac Intensive Care Society, was organized in 2003 to address the issues facing practitioners (1). The consensus that critically ill pediatric patients with acquired or congenital heart disease (CHD) are best cared for in units or systems organized and designed for these patients and by practitioners with specialized training, expertise and skills in this area has dramatically changed the patient care paradigm. The pediatric cardiologist plays a central role in the critical care of these patients. This chapter reviews the organization of Pediatric Cardiac Intensive Care Unit (PCICU) services, as well as continuous quality improvement and family-centered care. Then, evaluation of cardiac output (CO) and treatment of low cardiac output syndrome (LCOS) are addressed. Next, major organ systems as they relate to cardiac intensive care are reviewed. Perioperative care for specific lesions and procedures is next presented. Finally, medical conditions in the PCICU and special considerations for the neonate and adult are reviewed.

ORGANIZATION OF CARDIAC INTENSIVE CARE SERVICES

Despite remarkable progress in the organization of PCICU services, there has been relatively little published information about the optimal delivery of care to this specialized patient population (2–4). Practitioners of the subspecialty may be pediatric cardiologists, pediatric intensivists, pediatric anesthesiologists, or pediatric cardiac surgeons. In a recent survey, 73% of North American and 59% of worldwide PCICUs involved care by pediatric intensivists (5). Specialized training in pediatric cardiac intensive care varies, from a 4th year of training following a standard pediatric cardiology or intensive care fellowship in the United States, to extra dedicated months of training during a pediatric intensive care fellowship, or pediatric cardiovascular anesthesiology fellowship. Many practitioners acquire significant training and experience in PCICU care after formal training is finished. Fellows who cover a PCICU can include those training in pediatric cardiology, intensive care, anesthesia, and congenital heart surgery. As of this writing, there is no formal specialized certificate or board certification in PCICU in the United States. Clearly, the physicians caring for PCICU patients optimally must have special interest, experience, and focus on this patient

population and spend a significant amount of their clinical time caring for them in order to maintain skills, knowledge, and expertise in this complex and rapidly changing field. The projected significant need for PCICU physicians, and the relatively small number of these physicians being trained, means that continued multidisciplinary support of PCICU programs is essential (2,6).

Similarly, the physical organization of PCICU beds varies considerably. In a recent survey of PCICUs in the United States and worldwide, 27 of 29 high-volume centers, defined as >300 open surgical cases per year, cared for patients in dedicated PCICUs. Smaller programs were more likely to care for pediatric cardiac intensive care patients in mixed Pediatric Intensive Care Units (PICUs) or adult cardiac surgical ICUs (5). Designs range from separate, dedicated PCICUs remote from the PICU, to the PCICU having separate beds but being adjacent or in close proximity to the PICU, to a mixed PICU/PCICU with cardiac patients dispersed throughout the unit. Other important design aspects considered optimal include close proximity to cardiac operating rooms (ORs) and catheterization laboratories to account for the frequent patient transfers back and forth for care, and the need for rapid response and frequent communication with the practitioners in these disciplines. Proximity to imaging modalities such as computed tomography and magnetic resonance imaging is highly desirable. Bed space considerations are very important, as PCICU patients often require space for echocardiography, nitric oxide (NO) delivery systems, extracorporeal support, and bedside surgical procedures. Ample space for the OR team, surgical lights, and provision for a sterile surgical field is highly desirable. In addition, space for family is increasingly planned in modern PCICU designs. A minimum standard for bed space per patient in PICUs is 250 square feet (23 m²), but in modern PCICU designs, up to 500 square feet are often planned (7). Bed spaces may be arranged as single room individual beds, as shared spaces divided by movable sliding glass partition doors, or as open-bay design for multiple patients. Careful consideration for visibility of beds and monitors should be made during design of the PCICU. Many PCICUs are designed with rectangular or square pods of 8 to 10 beds for maximum visibility and access. Adherence to local regulatory standards for windows, clean and dirty utility areas, isolation rooms, negative pressure rooms, and nutrition preparation areas is also very important.

Although PCICUs may vary in terms of the type of patients admitted, it is important for each unit to have a specified set of admission criteria. Some units may be limited to postsurgical cardiac patients, but increasingly, PCICUs admit both medical and surgical patients with critical cardiac disease requiring constant monitoring and access to medical, nursing, and ancillary expertise. This often includes the preoperative neonate, patients with severe medical cardiac disease, and even adults with CHD who have had cardiac surgery.

Multidisciplinary Team Approach to Pediatric Cardiac Intensive Care

One of the most important paradigm shifts in PCICU care is the recognition that multidisciplinary care beyond the traditional group of cardiologists, surgeons, intensivists, and anesthesiologists is increasingly important. Additional medical disciplines including adult CHD, neonatology, neurology, gastroenterology and nutrition, general surgery, pulmonology, genetics, nephrology, and others are vitally important to provide consultations and participate in multidisciplinary rounds. Nursing care deserves special emphasis, as the specialized skills and knowledge in PCICU care are critically important to establish and maintain. Nursing staffing ratios must be carefully planned, and nurse-to-patient ratios can vary from 1:3 for less ill, nonventilated patients, to 1:1 for less stable ventilated patients, to 2:1 for extracorporeal membrane oxygenation (ECMO) patients (5). In addition, as trainee duty hours and rotations are restricted by the U.S. Accreditation Council for Graduate Medical Education and other organizations, midlevel practitioners are increasingly employed in PCICUs, including pediatric nurse practitioners and physician's assistants. In some PCICU settings, pediatric hospitalists serve to augment manpower. Other crucial members of the multidisciplinary team (ideally dedicated and with special expertise in PCICU) include respiratory therapists, extracorporeal life support (ECLS) specialists, pharmacists, nutritionists, occupational and physical therapists, social workers, translators, and unit secretaries dedicated to the PCICU (3). Input is sought from all of these stakeholders in the patient's care by the attending PCICU physician, and all members of the team must be given the opportunity to contribute on rounds, and other formats for multidisciplinary collaboration. Multidisciplinary team planning for crises, including cardiopulmonary resuscitation (CPR) and ECMO, which includes simulation scenarios, is important to prepare for the actual events. The parent, patient, and family are also important members of the team (see below). This multidisciplinary approach, with the patient's best possible outcome as the foremost priority, helps eliminate traditional barriers such as "surgical versus medical," "physician versus nursing," and "parent versus caregiver." The director of the PCICU should be a dedicated physician leader who is a seasoned clinician possessing excellent skills in management, organization, and mentorship; these are essential qualities to maintain team cohesion and consistent excellent patient care (3). Managing diverse viewpoints from many disciplines with patience, and having consideration for all stakeholder contributions, are hallmarks of an effective leader.

Night and weekend physician coverage of the PCICU is an important concern, as these commonly unstable patients often are admitted off hours following long surgical procedures, or are transported from outside facilities. It is ideal to provide 24-hour in-hospital presence of an attending cardiac intensivist to assist in dealing with complex management decisions, new admissions, and procedures. This may not be possible in all hospitals; provisions for rapid call-in of the attending physician must be in place in this case. Ideally also, the on-call team of fellows, residents, and midlevel practitioners, as well as the attending physician, should have their duties limited to the PCICU.

Special patient populations being admitted to the PCICU in increasing numbers include low birth weight (LBW) neonates, and adults over the age of 18 years, who have critical cardiac disease. The LBW patients require consultation with neonatologists to optimize management, especially with regard to pulmonary management of immature lungs, feeding and nutrition, infectious issues, and multiple congenital anomalies other than the heart defect. The adult with CHD greatly benefits

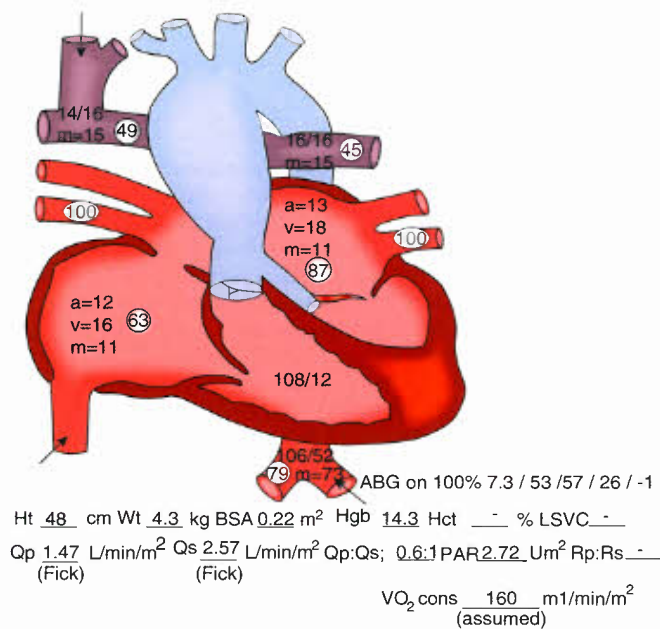
from consultation with adult CHD specialists, who also assist in coordinating other adult consultants who may be needed such as neurologists and nephrologists. Another increasing patient group includes patients requiring ECLS, in the form of ECMO or ventricular assist devices (VADs). The complex problem of anticoagulation regimens to prevent thrombosis while not allowing excessive bleeding requires ready availability of consultants from hematology, or hematopathology services whose specialized knowledge of coagulation issues enhances care of these patients.

Relationship between the PCICU, the Cardiac OR, and the Catheterization Laboratory

An important principle of PCICU care is that the service should be delivered as a continuum of care well in advance of an intervention (3,5). This should begin with the presurgical or catheterization admission to the PCICU, surgical or catheterization planning conference, or even the prenatal multidisciplinary conference where the care and disposition of antenatally diagnosed CHD patients are discussed. Ideally, patients requiring intensive care are admitted preoperatively to the same unit, under care of the same team as they will have postoperatively to facilitate better knowledge of the patient's unique condition and communication with the surgeon, cardiac catheterization team, and family. Colocation of the PCICU near catheterization laboratories and cardiac ORs facilitates communication, rapid transport of very unstable patients, and proximity of skilled assistance during crises in the PCICU, ORs, or catheterization laboratory. The continuum-of-care principle also applies to immediate postoperative, or postcatheterization care, with clear hand-off communication from the procedural teams to the PCICU team and continuing of the support provided in the OR or catheterization laboratory.

Continuous Quality Improvement and Patient Safety in the CICU

Improving patient safety, reducing medical errors, and optimizing outcomes of care have been a priority of the US health care system since the landmark publications of the Institute of Medicine, "To Err is Human" in 1999 (8), and "Crossing the Quality Chasm" in 2001 (9). These issues are particularly important in the PCICU, where complex pathophysiology, invasive procedures, multiple caregivers, multiple physician orders and medications, and the unpredictable nature of events present a multitude of opportunities for errors, both active and latent, which may result in adverse events (10). A culture of patient safety involves change that begins with the PCICU leadership and affects everyone involved in PCICU care, including junior physicians, nurses, and ancillary personnel. Important principles identified to promote a safety culture in complex environments include leadership promoting a safety culture; process design based on human limitations that eliminates unnecessary variability; promoting team work and team functioning; proactive anticipation of unexpected events; and creation of a learning environment that empowers any personnel to report errors and to speak up when unsafe practices are encountered. Care handoffs, whether between nursing or physician shifts, on transfer from OR to PCICU, or transition to a new care team, are frequent sources of error and miscommunication. Protocols for face-to-face handoffs that include a checklist improve consistency of communication and prevent many avoidable errors (11). Communication in the PCICU environment is a key concern. One simple method unique to this environment



DIAGNOSIS

- 1) Hypoplastic left heart syndrome (mitral and aortic stenosis).
- 2) Norwood procedure with a 3.5 mm Blalock-Taussig (BT) shunt.
- 3) Right subclavian artery occlusion.
- 4) Right ventricular dysfunction.
- 5) Bidirectional Glenn
- 6) Poorly controlled atrial tachycardia.

Figure 20.1. Diagram posted on the bed of a patient in the PCICU for rapid identification of cardiac anatomy.

is to place a diagram of the cardiac anatomy of each patient, along with the recent surgical or catheterization procedure, on or near the bed, for easy visibility during an acute event (Fig. 20.1). Other programs with demonstrated effectiveness are central catheter insertion and maintenance “bundles” that include checklists for insertion that guarantee full sterile precautions during insertion, placement of a chlorhexidine disk at the catheter insertion site, regular dressing changes, and daily assessment of the need for the catheter. The PCICU has a particularly high rate of central line-associated blood stream infections (CLABSI), and coordinated efforts have resulted in dramatic reductions in these events by as much as 80% to 90% (12,13).

The electronic medical record (EMR) is increasingly utilized in PCICUs and will become a requirement in the United States in the coming years. The EMR can be an important factor in improving the quality of data recorded that can lead to improved patient outcomes. The EMR can be an important tool for legible, accessible documentation of physician admission and daily progress notes, as well as the electronic nursing PCICU flow sheet that documents not only bedside monitor data but all medications and nursing interventions. The ability to perform bedside echocardiography efficiently, and to review the images at the bedside, is important to optimize PCICU care. Computerized physician order entry can lead to more accurate and timely carrying out of orders, and decision support functions tied to hospital formulary can help avoid medication errors. Implementation of a complete EMR system is costly, and careful planning is needed to ensure the EMR interfaces well with all other electronic systems, such as picture archiving and communicating systems (PACS), and Cardiology databases that display echo and catheterization images. Ample numbers of computer workstations, including

mobile computer carts, are necessary to avoid delays in documentation or physician orders. Processes of care must be understood, and the transition to EMR should be carefully planned to avoid work-arounds that prevent full and effective implementation of the system (14,15).

Databases to measure quality and outcomes in the PCICU, both local internal databases, and national or international multicenter databases, are increasingly recognized as essential functions. It is crucial to have access to the PCICU's basic data, such as number of admissions, type of surgical or catheter procedure, diagnoses, demographics of admitted patients, severity of illness or complexity of surgical procedure, lengths of stay, days on mechanical ventilation, patients receiving mechanical support, and mortality and major morbidity rates. These data are used for internal quality improvement purposes, for comparison to outcomes from other PCICUs, and as the bases for research publications and presentations. Databases available for PCICUs include the Virtual PICU Database Cardiac Module (16), Society of Thoracic Surgeons' Congenital Heart Surgery Database (17), Congenital Cardiac Anesthesia Society Database (18), and IMPACT Registry for catheter interventions (19).

Family-Centered Care

Hospitalization in the PCICU for an intervention or illness, whether known in advance and planned, or emergent and unplanned, is a stressful and emotional experience for the patient, parents, and family. There has been considerable recent progress in involving the family as much as possible in their child's care, and where possible and developmentally appropriate, involving the child in his or her own care. PCICU routines that can involve the parents in the child's care, and reduce stress levels for both parent and patient include a liberal visitation policy that allows the parent to be at bedside with the child whenever possible (20). For times when the child is in surgery or the catheterization laboratory, or when the parent needs a break from the PCICU environment, having comfortable family waiting areas in close proximity to the PCICU is very desirable. Private conference rooms for discussions with the family, away from the unit, are another important feature to allow privacy during critical meetings. Some recent PCICU designs incorporate enough space into individual patient rooms to accommodate parent sleeping in the room. Allowing parents to be present on work rounds, to hear the presentation and discussion of their child's care, has become an important routine in many PCICUs that, if done sensitively, increases the flow of accurate information to the parent and reduces stress. In a recent survey of PCICU physicians and nurses, 77% responded that parents had a right to be present during work rounds, 57% felt parents should be allowed to be present during invasive procedures such as tracheal intubation and arterial and central line placement, and 75% would allow them to be present during CPR. Of these scenarios, parents wanted to be present about 65% of the time for work rounds, but only about 30% of the time for invasive procedures, or for CPR (21). Family-centered care may require a change of culture among the physicians and nurses in the PCICU, and there must be an adequate orientation of the family members as to policies and expectations. With the presence of so many families in the PCICU, strict policies about not disclosing medical information heard about other patients' conditions must be explained and enforced. Despite the occasional inconveniences, or changes in well-established routines, adopting family-centered care fully will result in greater parent and patient satisfaction, and help to reduce the stress, uncertainty, and other negative emotions associated with PCICU admission.

EVALUATION AND MANAGEMENT OF THE CARDIOVASCULAR SYSTEM

The frequent or continual assessment of CO and oxygen delivery, and ensuring that they are optimized, or at least that measures are being undertaken to do so, are the central tenets of cardiac intensive care. This section will review various methods that assess CO.

Physical Examination, Bedside, and Laboratory Data

Despite the availability of many technologically advanced methods, CO should always be assessed by inspection and physical examination in addition to monitoring data, and the invasive and noninvasive methods described below. Poor CO is often heralded by pale or mottled extremities, diminished peripheral pulses, delayed capillary refill (>2 to 3 s), increasing cyanosis, tachycardia, poor heart tones, diminished pulses, cool extremities, presence of third or fourth heart sounds, and evidence of hepatic and pulmonary congestion. Urine output is often decreased. Lethargy or irritability often accompanies low CO. Tachypnea, diaphoresis, and poor feeding are often present. Although these are simple principles, they should not be forgotten in the modern profusion of technology-based monitoring methods.

Routine continuous monitoring of physiologic variables in the PCICU including heart rate, electrocardiogram (ECG), arterial and central venous pressure waveforms, temperature, and end-tidal CO_2 (ETCO_2) can give important information about CO. These include the ECG displaying nonsinus rhythm, elevated filling pressures or lack of an "a" wave on atrial filling pressures, acute decrease in ETCO_2 with increased ETCO_2 to PaCO_2 gradient, blunted arterial waveform upstroke or excessive respiratory variation, and increased core-to-peripheral temperature gradient. Chest radiograph findings include cardiomegaly, pulmonary edema, or, alternately, a paucity of pulmonary vascular markings associated with inadequate pulmonary blood flow. Laboratory data include an increasing calculated base deficit or serum lactate, or persistent lactate above 2 mmol/L (22,23).

Echocardiography

Bedside echocardiography in the PCICU is a very important tool for assessment of CO during a given point in time. Whether formal echocardiogram with complete anatomic and functional assessment, with official interpretation or reporting by an echocardiographer (preferred), or a rapid assessment with portable echocardiography during a crisis, this tool is indispensable for evaluation of CO in the PCICU, yielding information not obtainable by other methods. Besides the obvious measurement of ventricular function by qualitative assessment, ejection fraction or quantitative assessment using shortening fraction, or myocardial performance index, many other important findings are made during low CO states. These include residual anatomic defects such as shunts, outflow tract obstruction, presence and degree of valvular regurgitation or stenosis, pericardial fluid or thrombus leading to a diagnosis of tamponade, assessment of right ventricular function, tricuspid regurgitation jet, and position of the interventricular septum to assess pulmonary hypertension (PH), and many others (24). If standard transthoracic views are not adequate, transesophageal echocardiography can be performed in the intubated, sedated patient. Bedside echocardiography is essential during the performance of balloon atrial septostomy (BAS) (25). Obtaining a bedside echocardiogram the morning after cardiac surgery is routine in many PCICUs. Bedside echocardiography is an excellent modality to define intracardiac anatomy, but extracardiac structures (systemic-pulmonary shunts, pulmonary veins, cavopulmonary anastomoses, aortic arch) are not as

reliably imaged by echocardiography and may require cardiac catheterization (see below).

Venous Oximetry

Measurement of true mixed venous oxygen saturation in the pulmonary artery (PA) of a patient with two ventricles and normal cardiac anatomy is rarely possible in the PCICU; much more useful is the measurement of oxygen saturation in the superior vena cava (SVC), used as a surrogate for mixed venous saturation (26). This technique is used during cardiac catheterization for calculation of CO using the Fick method. Many PCICU patients will have a catheter in the SVC for central venous access. A measured, not calculated, oxygen saturation, or ScvO_2 , can be an important trend monitor to assess CO, and oxygen delivery and consumption. This measurement can be made intermittently, or during changes in patient status, or in response to interventions.

Continuous monitoring of intravascular oxyhemoglobin saturation using reflectance catheters has been used in the umbilical artery, PA, and adult-sized central venous catheters for a number of years, but only recently have standard pediatric-sized 4 and 5 French, double and triple lumen central venous catheters become available for routine use to measure central venous oxygen saturation (ScvO_2) in pediatric patients. In several small studies of pediatric patients undergoing cardiac surgery, good correlation has been demonstrated between ScvO_2 as measured with the catheter, versus blood co-oximetry ($r^2 = 0.8$ – 0.9 , bias -0.03 to $+1.09\%$ with standard deviation 4% to 8%) (27,28). The advantage of this method is that it is continuous, many patients have SVC catheters in place, and the oximetry catheters are of the same diameter as standard central venous catheters. Although assessment of each patient must be individualized, ScvO_2 below 50% in patients with univentricular hearts is often associated with low CO and/or oxygen delivery. For example, in univentricular neonates after Stage I palliation for hypoplastic left heart syndrome (HLHS), low ScvO_2 was associated with death and greater frequency of increased need for ECMO. Goal-directed therapy targeting $\text{ScvO}_2 > 50\%$ is associated with high postoperative survival and low complication rate in this population (29).

Near-Infrared Spectroscopy

Near-infrared spectroscopy (NIRS) is a noninvasive optical technique used to monitor brain and somatic tissue oxygenation. Most devices utilize 2 to 4 wavelengths of infrared light at 700 to 1000 nm, where oxygenated and deoxygenated hemoglobin have distinct absorption spectra (2–4). An oxygen saturation is derived using variants of the Beer-Lambert equation. This saturation is designated a regional oxygen saturation (rSO_2) and is a weighted average of the saturation in venous, arterial, and capillary beds in the light path. Since its now classic description in 1977 by Jobsis (30), this technology has been the subject of over 1000 publications, and because of its noninvasive, compact, portable nature, and potential to measure tissue oxygenation in the brain and other organ systems during surgery and critical illness, it is gaining more widespread clinical use.

In critical care medicine, cerebral NIRS has been used to monitor adequacy of cerebral oxygen delivery and as a surrogate for adequacy of global oxygen delivery in patients after cardiac surgery and in patients on ECMO or VADs (31,32). Changes in rSO_2 have a close correlation with changes in mixed venous saturation (SvO_2) in both single- and two-ventricle patients after congenital cardiac surgery (33,34).

NIRS can be used to measure tissue oxygenation in surgery and critical illness and because of its noninvasive continuous nature has intuitive appeal in conditions where low CO and other causes of shock would benefit from continuous monitoring. Somatic NIRS using a probe placed on the flank at T10-L2 has

been studied by Hoffman et al. (35) in a series of neonates after and during single-ventricle surgical palliation. In nine neonates undergoing cardiopulmonary bypass (CPB) with regional cerebral perfusion (RCP), mean cerebral rSO_2 pre-bypass was 65% and somatic rSO_2 was 59%. During RCP cerebral rSO_2 was 81% versus 41% somatic, signifying relative tissue hypoxia due to lack of perfusion to subdiaphragmatic organs. After CPB, cerebral rSO_2 decreased to 53%, but somatic rSO_2 increased to 76% (35). In 79 postoperative neonates undergoing Norwood Stage I palliation for HLHS, a cerebral–somatic rSO_2 difference of <10% significantly increased the risk for biochemical shock, mortality, or other complications (36). Mean somatic rSO_2 < 70% was associated with a significantly increased risk of prolonged ICU stay, shock, and other complications.

Somatic NIRS has also been used with a probe placed on the abdomen between the umbilicus and symphysis pubis to measure mesenteric rSO_2 in neonates and infants after cardiac surgery. In a study of 20 patients, Kaufman et al. (37) compared mesenteric NIRS and flank NIRS at T10–L2 to gastric pH measured by tonometry and lactate values. In 122 simultaneous measurements made in the first 48 hours after surgery, mesenteric rSO_2 correlated significantly with gastric pH ($r = 0.79$) and serum lactate ($r = 0.77$), SvO_2 ($r = 0.89$). These correlations were all better than those using flank NIRS. The authors concluded that mesenteric NIRS is a sensitive monitor of splanchnic tissue oxygenation and may have utility at managing these patients and improving outcomes. In addition, for infants undergoing biventricular repair, flank (renal) rSO_2 values below 50% for >2 hours in the immediate postoperative period were associated with higher peak creatinine levels, higher incidence of acute kidney injury, greater inotropic support, more days on mechanical ventilation, and higher serum lactate levels (38).

These studies lend credence to the idea that NIRS-directed targeted interventions could be utilized to improve oxy-

gen delivery to tissues and organs and potentially improve outcomes from surgery, anesthesia, and critical illness. To date, there is a lack of such published studies, but more are anticipated given the nature of this modality.

Thermodilution Cardiac Output

Percutaneous PA catheterization has a limited role in the PICU for several reasons. The small size of many patients precludes placement of adequately sized sheaths and catheters, and many patients in whom PA catheter monitoring would be desirable have intracardiac shunting, invalidating results of standard thermodilution CO measurements and confusing mixed venous oxygen saturation (SvO_2) measurements. In addition, right-sided intracardiac surgery makes PA catheterization undesirable. Thus, when pulmonary artery pressure (PAP) or SvO_2 monitoring is indicated, transthoracic PA lines are the most common method used in congenital heart surgery. The availability of continuous central venous oxygen saturation catheters (see below), and the perception that the risk:benefit ratio for PA catheter placement is most often unfavorable, limit indications for this technique (39–42).

Cardiac index may be measured by standard thermodilution methods, with care taken to input the correct calculation constant into the monitor software according to the catheter size and length, and volume and temperature of injectate. The average of three consecutive injections made in rapid succession at the same point in the respiratory cycle, that is, expiration, will optimize conditions to achieve an accurate measurement during steady-state conditions. Vascular resistances and stroke volume can also be calculated, using the formulae shown in Table 20.1 (41,42).

Hemodynamic data represent only a portion of the information available from an oximetric PA catheter. The

TABLE 20.1

Hemodynamic Formulae for Pulmonary Artery Catheter Monitoring

Formula	Normal Values		
	Adult	Infant	Child
$CI = \frac{CO}{BSA}$	2.8–4.2 L/min/m ²	2–4	3–4
$SVI = \frac{SV}{BSA}$	30–65 mL/beat/m ²	40–75	40–70
$LVSWI = \frac{1.36(MAP - PCWP) \times SVI}{100}$	45–60 g · m/m ²	20–40	30–50
$RVSWI = \frac{1.36(PAP - CVP) \times SI}{100}$	5–10 g · m/m ²	5–11	5–10
$SVRI = \frac{(MAP - CVP) \times 80}{CI}$	1500–2400 dyne · s · cm ⁻⁵ m ²	900–1200	1300–1800
$PVRI = \frac{(PAP - PCWP) \times 80}{CI}$	250–400 dyne · s · cm ⁻⁵ m ²	<200	<200

CI, cardiac index; CO, thermodilution cardiac output; BSA, body surface area; SV, stroke volume; SVI, stroke volume index; LVSWI, left ventricular stroke work index; RVSWI, right ventricular stroke work index; SVRI, systemic vascular resistance index; PVRI, pulmonary vascular resistance index.

TABLE 20.2 Oxygen Delivery and Consumption Formulae

Formula	Normal Values		
	Adult	Infant	Child
Arterial O ₂ content: $CaO_2 = (1.39 \times Hb \times SaO_2) + (0.0031 \times PaO_2)$	18–20 mL/dL	15–18	16–18
Mixed venous O ₂ content: $CvO_2 = 1.39 \times Hb \times SvO_2 + 0.0031 \times PvO_2$	13–16 mL/dL	11–14	12–14
Arteriovenous O ₂ content difference: $avDO_2 = CaO_2 - CvO_2$	4–5.5 mL/dL	4–7	4–6
Pulmonary capillary O ₂ content: $CcO_2 = 1.39 \times Hb \times ScO_2 + 0.0031 \times PcO_2$	19–21 mL/dL	16–19	17–19
Pulmonary shunt fraction: $Q_s / Q_t = 100 \cdot (CcO_2 - CaO_2) / (CcO_2 - CvO_2)$	2%–8%	2–8	2–8
O ₂ delivery index: $DO_2I = 10 \cdot CO \cdot CaO_2 / BSA$	450–640 mL/min/m ²	450–750	450–700
O ₂ consumption index: $VO_2I = 10 \cdot CO \cdot (CaO_2 - CvO_2)$	85–170 mL/min/m ²	150–200	140–190

Hb, hemoglobin; SaO₂, measured arterial oxygen saturation; PaO₂, partial pressure of oxygen in arterial blood; SvO₂, measured mixed venous oxygen saturation; PvO₂, partial pressure of oxygen in mixed venous blood; ScO₂, measured pulmonary capillary oxygen saturation; PcO₂, partial pressure of oxygen in pulmonary capillary blood; Q_s, pulmonary shunt blood flow; Q_t, total pulmonary blood flow.

other half consists of oxygen delivery and consumption measurements and calculations, which may also be used to guide therapy in the critically ill patient who has LCOS (41,42) (Table 20.2). They require either measurement of mixed venous and systemic arterial saturations from blood samples from the tip of the PA catheter and arterial line (measured by co-oximetry, not calculated), or substitution of these values with SvO₂ from the oximetric catheter (a valid assumption if properly calibrated), and pulse oximeter value instead of measured systemic saturation. There are data from adult and pediatric critical care literature suggesting that the ability to increase and maximize both oxygen delivery and consumption may improve outcome, and that these are predictors of survival from critical illness, including postoperative cardiac surgery (43–46).

Lithium Dilution and Pulse Contour Analysis Cardiac Output

Because traditional percutaneous, balloon-tipped PA catheterization is limited in small children and those with intracardiac shunting several other recent methods to measure CO and oxygen delivery in patients with CHD have been applied. Lithium dilution cardiac output (LiDCO) uses a standard central line in the SVC or even a peripheral IV catheter, and a special femoral artery catheter equipped with a lithium-detecting electrode. A dilute solution of

lithium chloride is injected into the vein, and arterial blood is withdrawn into the lithium electrode. The cardiac index is related to the area under the curve of the change of lithium concentration. This method has been demonstrated to have reasonable correlation with thermodilution CO in children after congenital heart surgery. In a study of 48 measurements in 17 patients 2.6 to 34 kg, correlation between LiDCO and thermodilution CO was good ($r^2 = 0.96$), mean bias was -0.1 ± 0.31 L/min (47).

Transpulmonary thermodilution CO uses a similar principle as LiDCO, with temperature as the indicator instead of lithium concentration. Cold saline is injected into a central venous catheter, and via a thermistor placed in a femoral artery, a time temperature curve is derived, which correlates reasonably well with standard thermodilution CO as measured by a standard PA catheter (48). Lithium and any thermodilution method are limited to patients without any intracardiac shunting, significantly restricting their use in patients with CHD.

Yet another newer method is pulse contour analysis of the arterial waveform (PiCCO), which relates the contour and area under the curve to the stroke volume, thus the CO. This continuous method is periodically calibrated using transpulmonary thermodilution CO as described above (again making the method invalid in patients with intracardiac shunting), and demonstrate good correlation with transpulmonary thermodilution in a recent study of 24 postoperative pediatric cardiac patients ($r^2 = 0.86$, mean bias:

$0.05 \pm 0.4 \text{ L/min/m}^2$), and in pediatric patients undergoing diagnostic catheterization after cardiac transplantation (49,50). A recent comprehensive review of publications of this method in children and in animal models of pediatric disease, showed agreement that the stroke volume and CO derived with pulse contour analysis are generally accurate and precise, and may be a useful adjunct for measurement of CO in critically ill children (51).

Table 20.3 summarizes physical examination findings and other data associated with low CO.

PREVENTION AND MANAGEMENT OF LOW CARDIAC OUTPUT SYNDROME

Determinants of Cardiac Output and Oxygen Delivery

Besides the unique factors discussed earlier that alter hemodynamic management in patients with CHD, it is important to recognize that alterations of preload, afterload,

TABLE 20.3 Clinical Findings in Low Cardiac Output State

Category	Parameter	Finding/Data
Physical examination		
	Peripheral perfusion	Cool or mottled extremities Diminished peripheral pulses Delayed capillary refill
	Respiratory status	Tachypnea, increased work of breathing, grunting, flaring, retractions
	Cardiac examination	S3 or S4, diminished heart tones, tachycardia or bradycardia
	Other physical examination	Diaphoresis, hepatomegaly, jugular venous distension, increasing cyanosis
	Mental status	Lethargy or irritability
Monitor data		
	Arterial waveform	Diminished pulse pressure, decreased upslope, hypotension, increased variation with respiration
	Atrial filling pressures	Significantly elevated or decreased; lack of "a" wave
	ECG	Nonsinus rhythm, tachycardia, bradycardia, ST-segment depression or elevation, lack of HR variability
	End-tidal CO ₂	Decrease in ETCO ₂ , large end-tidal to arterial CO ₂ difference
	Temperature	Increased core-to-periphery temperature gradient (>5°C core to toe)
	Mixed venous (PA) or central venous (SVC) oxygen saturation	Low SvO ₂ or ScvO ₂ < 50%
	Near-infrared spectroscopy regional oxygen saturation	Low cerebral rSO ₂ < 50%, low somatic (renal) rSO ₂ < 10% above cerebral rSO ₂
Laboratory and radiographic data		
	Serum lactate	Increasing, or persistently elevated over 2 mmol/L
	Calculated base deficit	Increasing or >5 mEq/L
	BNP	Elevated above 100 pg/mL and increasing
	Troponin-I	Elevated above 0.15 ng/mL and increasing
	Chest radiograph	Cardiomegaly, pulmonary edema, or paucity of lung vascular markings
	Renal function	Elevated BUN and creatinine Poor urine output < 0.5 mL/kg/h
Echocardiography		
	LV ejection fraction or shortening fraction; dilated LV	Decreased (EF < 50% or SF < 35%)
Calculated cardiac index		
	Thermodilution, lithium dilution, pulse contour analysis, echocardiographic by VTI method	<2.0 L/min/m ²

S3,S4, third and fourth heart sounds; ETCO₂, end-tidal carbon dioxide; PA, pulmonary artery; SVC, superior vena cava; SvO₂, mixed venous oxygen saturation; ScvO₂, central venous oxygen saturation; rSO₂, regional oxygen saturation; BUN, blood urea nitrogen; EF, ejection fraction; SF, shortening fraction; VTI, velocity time integral method.

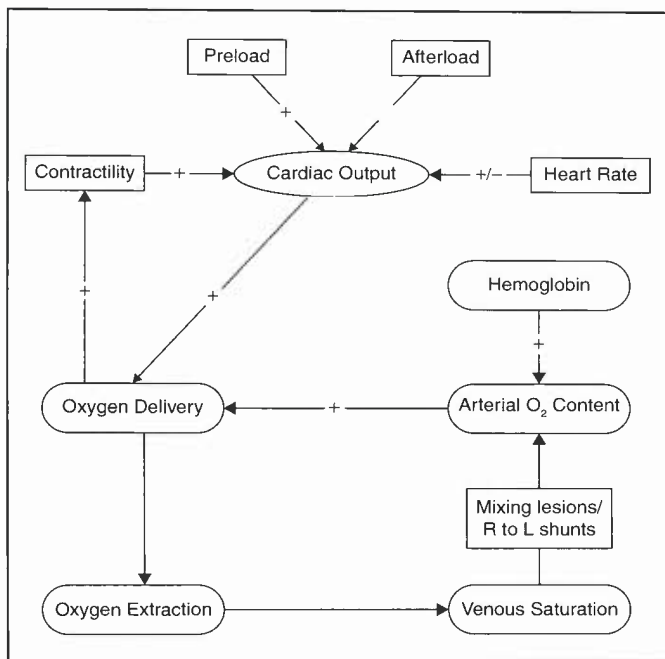


Figure 20.2. Determinants of cardiac output and oxygen delivery.

contractility, and heart rate are four cornerstones that affect CO before and after surgical correction of congenital cardiac disease (Fig. 20.2). In addition, diastolic dysfunction is common in patients with CHD, and measures to improve ventricular compliance are important. The oxygen-carrying capacity of blood is improved by increasing the hemoglobin concentration. Each of these factors should be adjusted for the specific congenital cardiac lesion and the cardiovascular physiology that is associated with the lesion. Figure 20.3 details expected changes in ventricular pressure–volume, and

Starling relationships with manipulation of preload, afterload, contractility, and lusitropy.

Pharmacologic Therapy for Congenital Heart Disease

The goal of drug therapy in an acute setting should be to optimize CO and oxygen delivery; improve perfusion pressure to vital organs such as brain, heart, and kidneys; and maintain an optimal balance between systemic and pulmonary blood flows with an appropriate level of oxygenation. High levels of inotropic and vasoactive infusions in the first 48 hours postoperatively for infants under 6 months of age are associated with poor outcomes including need for mechanical circulatory support, prolonged ventilation, preserved neurologic injury, renal failure, long ICU stays, and death (52). Therefore, it is important to understand the actions of pharmacologic agents and to use them judiciously at the lowest effective doses.

Drugs that may be used in the acute hemodynamic management of patients can be categorized as belonging to one of the following functional classes:

1. Inotropes (epinephrine, dopamine, dobutamine, milrinone, calcium)
2. Chronotropes (isoproterenol)
3. Vasoconstrictors (norepinephrine, phenylephrine, vasopressin, terlipressin)
4. Vasodilators (nitroglycerin, nitroprusside, prostaglandins, NO, nicardipine, fenoldopam)
5. Beta adrenergic antagonists (esmolol)
6. Newer cardiotoxic and vasoactive agents (levosimendan, nesiritide)

The cardiac intensivist must keep in mind that the indications for and doses of these drugs in an individual patient are highly variable. Tables 20.4 and 20.5 summarize the effects and recommended dosages for these drugs. Effects such as age, disease state, and adrenergic receptor up- or down-regulation necessitate frequent titration of drugs to effect.

Preload Recruitment

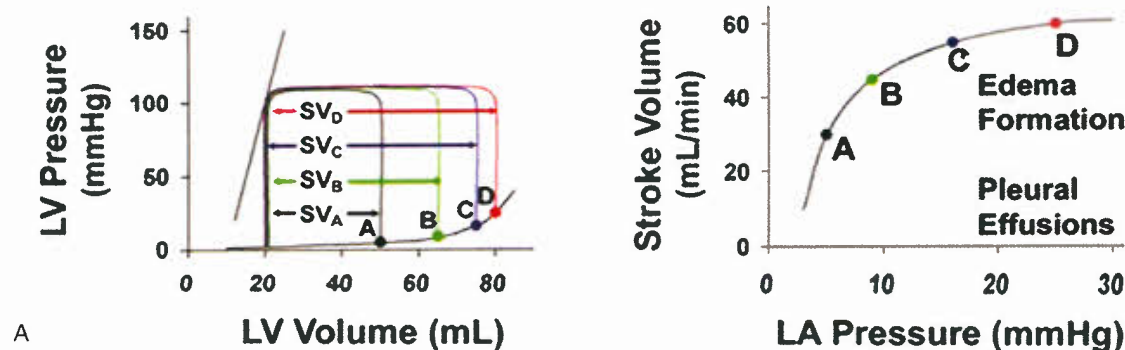
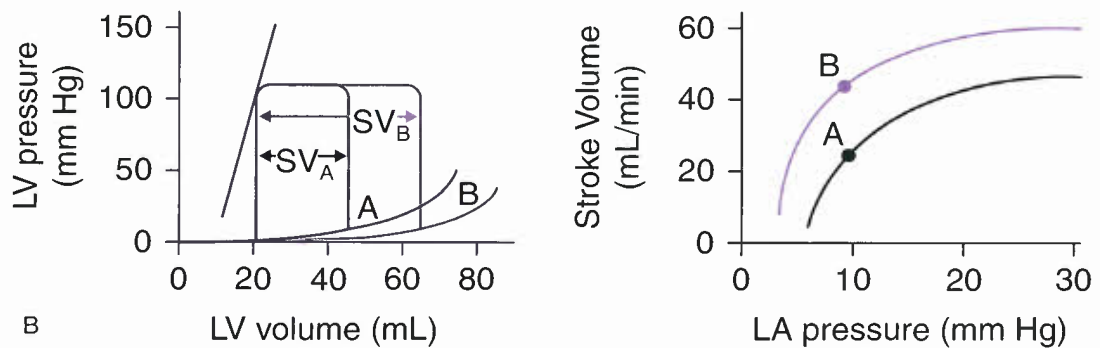
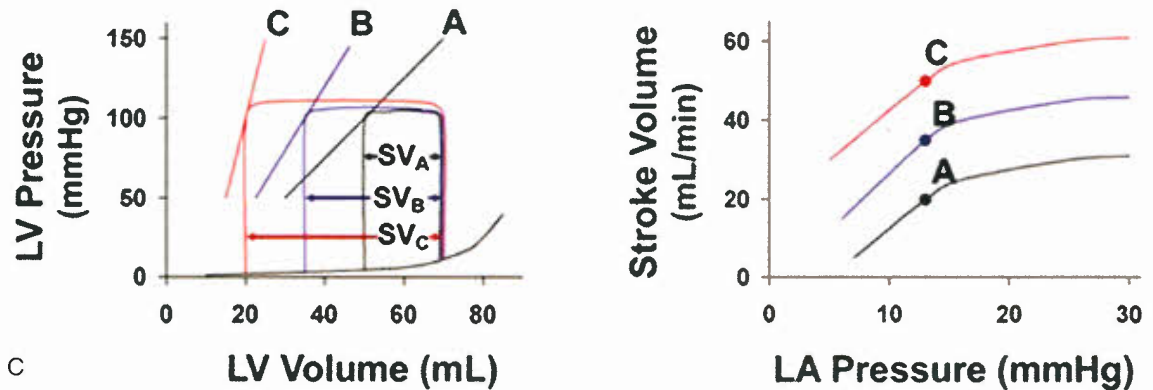


Figure 20.3. Changes in pressure volume and Starling relationships with manipulations of preload (A), diastolic compliance (lusitropy) (B), contractility (inotropic state) (C), and afterload (D). Point A represents baseline end-diastolic volume on the pressure–volume loop on the left of each panel, and baseline stroke volume on the Starling curve on the left of each panel. SV, stroke volume. (A) Effect of increasing preload. With administration of intravascular volume, end-diastolic volume and stroke volume are augmented significantly from point A to point B. However, diastolic compliance is nonlinear, and increases in stroke volume are progressively less with more intravascular volume administration from points B to C, and C to D. At high end-diastolic volumes and pressures, pulmonary capillary leak ensues resulting in pulmonary edema and pleural effusions.

Improve Diastolic Function (Positive Lusitropy)



Increase Contractility (Positive Inotropy)



Afterload Reduction

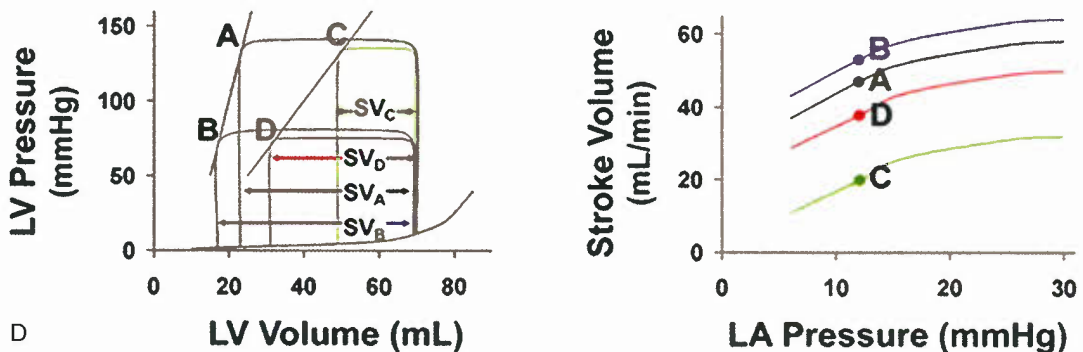


Figure 20.3. (Continued) (B) Effect of improving diastolic function. Enhanced ventricular relaxation and compliance result in an increased end-diastolic volume at the same pressure, point A versus B. This results in an increased stroke volume at the same atrial pressure. Slowing heart rate, or instituting an agent such as milrinone can improve lusitropy. (C) Effect of increased contractility. Increases in the slopes of the pressure-volume loops from points A, to B, to C, represent progressively increased inotropic states. Increased contractility results in a higher stroke volume ejected at the same left atrial pressures. (D) Effect of afterload reduction. At normal inotropic state, represented by the changes from point A to point B, lowering afterload allows the heart to eject to a lower systolic pressure, resulting in a higher stroke volume. With a decreased baseline inotropic state, represented by the changes from point C to point D, the increase in stroke volume with afterload reduction is much greater for a comparable change in afterload. Heart failure patients and neonates are particularly sensitive to changes in afterload.

TABLE 20.4 Inotropic Drugs

Drug	Dose	Receptors	Inotropy	HR	SVR	PVR	Renal Vascular resistance
Epinephrine	0.02–0.2 $\mu\text{g/kg/min}$	$\beta_1, \beta_2 > \alpha_1$ $\alpha_1 > \beta_1, \beta_2$	\uparrow	\uparrow	$\leftrightarrow, \downarrow$	$\leftrightarrow, \downarrow$	\downarrow
	Lower Dose		\uparrow	\uparrow	\uparrow	\uparrow	\uparrow
Norepinephrine	0.02–0.2 $\mu\text{g/kg/min}$	$\alpha_1 > \beta_1, \beta_2$	\uparrow	\uparrow	\uparrow	\uparrow	\downarrow
Dopamine	2–5 $\mu\text{g/kg/min}$	DA_1, DA_2	\leftrightarrow	\leftrightarrow	\leftrightarrow	\leftrightarrow	\downarrow
	5–10 $\mu\text{g/kg/min}$	$\beta_1, \beta_2 > \alpha_1$	\uparrow	\uparrow	$\leftrightarrow, \downarrow$	\leftrightarrow	\uparrow
	> 10 $\mu\text{g/kg/min}$	$\alpha_1 > \beta_1, \beta_2$	\uparrow	\uparrow	\uparrow	\uparrow	\uparrow
Dobutamine	2–20 $\mu\text{g/kg/min}$	$\beta_1 > \beta_2, \alpha_1$	\uparrow	\uparrow	\downarrow	\downarrow	\leftrightarrow
Isoproterenol	0.01–0.2 $\mu\text{g/kg/min}$	β_1, β_2	\uparrow	\uparrow	\downarrow	\downarrow	\downarrow
Milrinone	Loading 25–100 $\mu\text{g/kg}$ Infusion 0.25–0.75 $\mu\text{g/kg/min}$	Phosphodiesterase III inhibitor/ \uparrow cAMP	\uparrow	\uparrow	\downarrow	\downarrow	\downarrow
Calcium chloride	5–10 mg/kg IV bolus; 10 mg/kg/h infusion	Contractile proteins	\uparrow	$\leftrightarrow, \downarrow$	\uparrow	$\leftrightarrow, \uparrow$	\leftrightarrow
Nesiritide	1 $\mu\text{g/kg}$ load; 0.1–0.2 $\mu\text{g/kg/min}$	B-Natriuretic peptide	\leftrightarrow	\leftrightarrow	\downarrow	\downarrow	\uparrow
Levosimendan	6–12 $\mu\text{g/kg}$ load; 0.05–0.1 $\mu\text{g/kg/min}$	Troponin C, increasing Ca^{2+} sensitivity; ATP-sensitive K^+ channels for vasodilation	\uparrow	\leftrightarrow	\downarrow	\downarrow	\downarrow

HR, heart rate; SVR, systemic vascular resistance; PVR, pulmonary vascular resistance; DA, dopamine.

TABLE 20.5 Vasoactive Drugs

Drug	Dose	Receptors	Inotropy	HR	SVR	PVR	Renal Vascular Resistance
Vasopressin	0.01–0.05 U/kg/h	V_1, V_2	\leftrightarrow	$\leftrightarrow, \downarrow$	\uparrow	\uparrow	\uparrow
Phenylephrine	0.02–0.3 $\mu\text{g/kg/min}$	α_1 (Agonist)	\leftrightarrow	\downarrow	\uparrow	\uparrow	\uparrow
Nitroglycerin	0.2–10 $\mu\text{g/kg/min}$	Vascular myocyte/ Guanylyl Cyclase, cGMP \uparrow	\leftrightarrow	$\leftrightarrow, \uparrow$	\downarrow	\downarrow	\downarrow
Nitroprusside	0.2–5 $\mu\text{g/kg/min}$	Vascular myocyte/Guanylyl Cyclase, cGMP \uparrow	\leftrightarrow	$\leftrightarrow, \uparrow$	\downarrow	\downarrow	\downarrow
Inhaled nitric oxide	10–40 ppm	Vascular myocyte/cGMP \uparrow	\leftrightarrow	\leftrightarrow	\leftrightarrow	\downarrow	\leftrightarrow
Prostaglandin E_1	0.01–0.2 $\mu\text{g/kg/min}$	Vascular myocyte/cAMP \uparrow	\leftrightarrow	$\leftrightarrow, \uparrow$	\downarrow	\downarrow	\downarrow
Fenoldopam	0.025–0.3 $\mu\text{g/kg/min}$ initial dose, titrate to maximum dose 1.6 $\mu\text{g/kg/min}$	$\text{DA}-1, \alpha_2$	\leftrightarrow	\leftrightarrow	\downarrow	\leftrightarrow	\downarrow
Nicardipine	0.1–0.3 mg/kg/h; maximum 15 mg/h	Calcium channel antagonist	\leftrightarrow	\uparrow	\downarrow		\downarrow

V, vasopressin; HR, heart rate; SVR, systemic vascular resistance; PVR, pulmonary vascular resistance; DA, dopamine; cAMP, cyclic adenosine monophosphate; cGMP, cyclic guanosine monophosphate.

Inotropes

EPINEPHRINE

Epinephrine is an endogenous catecholamine that is secreted by the adrenal glands and has strong α - and β -adrenergic receptor activation. This action on both types of adrenergic receptors leads to the complexity of response in different organs and tissue beds. The response of exogenously administered epinephrine depends on the ratio of α to β receptors in the individual tissue beds as well as to the dose of epinephrine given. At lower doses ($<0.05 \mu\text{g/kg/min}$), epinephrine causes a moderate increase in systolic blood pressure that is mainly due to the increased ventricular contraction (53). Activation of the β_2 receptors in the vasculature of the skeletal muscles usually leads to a decrease in the systemic vascular resistance (SVR) and the diastolic pressure. As the dose is progressively increased, more prominent peripheral vasoconstriction is seen due to the activation of the α receptors in other vascular beds (54). Renal blood flow is consistently decreased as vascular resistance in all segments of the renal vasculature increases (55). Epinephrine is often used as a strong inotrope for support of the failing myocardium. Epinephrine's action on the predominant β_1 receptors in the heart leads to an increase in contractility and heart rate. Higher doses will lead to a decrease in the refractory period of the atrioventricular (AV) node and an increase in the automaticity of the myocardium, which may predispose to the development of atrial or ventricular arrhythmias.

During CPR, epinephrine is the vasopressor of choice since it has profound α -adrenergic stimulation that aids in maintaining the cerebral and coronary perfusion pressure during cardiovascular collapse (56). The American Heart Association-recommended dose of epinephrine in children for bradycardia, asystolic or pulseless arrest is 0.01 mg/kg intravenously, repeated at 3- to 5-minute intervals. Higher doses of epinephrine are no longer recommended (57,58).

Epinephrine is used as an infusion primarily in the dose range from 0.02 to $0.2 \mu\text{g/kg/min}$, although doses up to $0.5 \mu\text{g/kg/min}$ or higher are occasionally used in the short term for acute severe low CO in situations such as weaning from bypass, or during ECMO cannulation or emergency institution of bypass. Prolonged exposure to high doses of epinephrine, that is, 0.1 to $0.2 \mu\text{g/kg/min}$ or higher for more than several hours, may cause myocardial necrosis in infants, and strong consideration should be given for mechanical circulatory support in this instance (59).

DOPAMINE

Dopamine is a naturally occurring catecholamine that is an immediate precursor of norepinephrine. Most of the functions of endogenously excreted dopamine are as a central neurotransmitter, though it has been found in the peripheral circulation as well. The cardiovascular effects of exogenously administered dopamine are due to the activation of a variety of receptors that have different affinity for the drug (60). At a lower dose ($<5 \mu\text{g/kg/min}$), the primary receptors that are activated are the dopaminergic-1 (DA-1) receptors present in the renal, mesenteric, and coronary vascular beds. Infusion of low-dose dopamine can lead to an increase in renal blood flow and an increase in glomerular filtration rate (GFR) (61). However, "renal dose" dopamine has not been demonstrated to have direct beneficial effects in improving renal function (62). As the dose of the drug is increased, stimulation of the β_1 receptors in the myocardium has inotropic and chronotropic effects (63). At these doses, dopamine causes an increase in CO, decrease in pulmonary capillary wedge pressure, and usually a decrease in SVR with only slight changes in blood pressure. The increase in heart rate is much less than for isoproterenol. Total peripheral resistance is usually unchanged with low or

intermediate doses of dopamine, due to vasodilatory action of dopamine on regional vascular beds. At higher doses ($>10 \mu\text{g/kg/min}$), more α_1 receptors are activated leading to a more intense peripheral vasoconstriction and an increase in vascular resistance. Dopamine causes release of norepinephrine from nerve endings; this also adds to its pharmacologic effect of adrenergic stimulation.

The volume of distribution and the clearance of dopamine are highly variable, underscoring the principle of titrating this drug to effect in the individual patient (64). Dopamine in the dose range 5 to $15 \mu\text{g/kg/min}$ is commonly used as an inotropic support to assist in the weaning from CPB, and in the early postoperative period. In recent years, some practitioners have avoided dopamine because of its role as a neurotransmitter, which can cross the blood brain barrier and is known to suppress pituitary function, particularly thyroid releasing hormone, in infants and children (65). These potential adverse effects are not seen with other natural or synthetic catecholamines (66).

DOBUTAMINE

A synthetic congener of dopamine, dobutamine's pharmacologic actions are due to its activation of α - and β -adrenergic receptors. Dobutamine has not been shown to have any effect on the DA receptors or the release of norepinephrine from nerve endings. The primary action of dobutamine is on β_1 receptors with only a small effect on β_2 or α_1 receptors. This action causes increased inotropy and chronotropy. CO is markedly enhanced and the left-sided filling pressures are decreased. Total peripheral resistance is unchanged or may decrease with the use of dobutamine. This effect may be especially beneficial in treating patients with ventricular dysfunction.

There is little direct increase in renal blood flow as is seen with dopamine. Dobutamine given in doses ranging from 5 to $15 \mu\text{g/kg/min}$ has been shown to be effective in improving depressed cardiac index after CPB in children with CHD (67). Comparison with newer inotropic drugs such as milrinone demonstrates similar improvements in stroke volume but a more profound decrease in left ventricular filling pressures and vascular resistance with the phosphodiesterase inhibitors (68). Increased heart rate is more prominent with dobutamine than with milrinone. At equivalent inotropic doses, dobutamine enhances the automaticity of the sinoatrial (SA) node to a much less extent than isoproterenol (69). Higher doses of dobutamine ($>15 \mu\text{g/kg/min}$) can predispose to the development of atrial or ventricular arrhythmias. Despite the fact that dobutamine will increase CO in neonates by increasing stroke volume, heart rate, and CO, it is frequently used to stress the myocardium, and will increase myocardial oxygen consumption, and produce diastolic dysfunction in some patients with repaired CHD (70,71).

MILRINONE

Milrinone is a bipyridine derivative that induces vasodilation and exerts a positive inotropic effect by inhibiting phosphodiesterase III. This leads to the accumulation of cyclic adenosine monophosphate (cAMP), independent of adrenergic receptor stimulation (72). The increase in cAMP in cardiac myocytes improves systolic and diastolic function by altering calcium influx (73), and by altering uptake and binding of calcium to myofilaments; whereas in vascular smooth muscle, accumulation of cAMP predominantly affects the removal of calcium across sarcolemma and therefore causes vasodilation. The decrease in SVR allows phosphodiesterase inhibitors to increase CO and oxygen delivery without increasing myocardial work and oxygen demand. Because of the dual effects on the inotropic state of the heart and the vascular resistance, milrinone has been used extensively in the treatment of congestive heart failure, PH, and postoperative low CO.

Milrinone has been shown to be an effective inotrope in adults as well as in children with CHD (74,75). Peripheral vasodilation also ensues as a result of vascular smooth muscle relaxation. Chang et al. reported that milrinone (loading 50 $\mu\text{g/kg}$ followed by an infusion of 0.5 $\mu\text{g/kg/min}$), when administered to neonates with low CO after cardiac surgery, lowered filling pressures, systemic and pulmonary vascular resistances (PVRs) (>25%), and improved cardiac index (from 2.1 to 3.1 L/min/m²) (76). Bailey et al. (77) found an increase in CO of 18% after milrinone therapy in 20 children undergoing corrective surgery for congenital cardiac defects. Milrinone also improves diastolic function. Hypotension and reflex tachycardia may result as side effects of milrinone therapy. Mehra et al. (78) reported a 4% incidence of thrombocytopenia in 71 patients who received long-term intravenous milrinone therapy (>3 days). Milrinone is primarily excreted by the kidneys, and higher bolus doses (50 to 75 $\mu\text{g/kg}$) may show prolonged hemodynamic effects in patients with impaired renal function. Serum half-life was found to be 0.8 hours in patients with congestive heart failure (79). Milrinone has also been suggested to have a higher volume of distribution and a faster clearance in infants and children as compared to adults (79). The dose recommended for milrinone therapy in patients with normal renal function is a bolus of 50 $\mu\text{g/kg}$ followed by an infusion of 0.25 to 0.75 $\mu\text{g/kg/min}$. Hypotension seen with a loading dose may be avoided by reducing or eliminating the loading dose and simply beginning the infusion, recognizing that therapeutic plasma levels will not be achieved for several hours.

In recent years, milrinone has gained widespread use in CICUs and is one of the few regimens that have been studied in a prospective, randomized, double-blind, controlled manner. In 227 infants and children undergoing cardiac surgery with bypass, high-dose milrinone (75 $\mu\text{g/kg}$ loading dose after bypass, followed by 0.75 $\mu\text{g/kg/min}$ infusion) reduced the incidence of LCOS by 55% compared to placebo or low-dose milrinone (25 $\mu\text{g/kg}$ load and 0.25 $\mu\text{g/kg/min}$) (80). In a pharmacokinetic study of 16 neonates undergoing Norwood Stage I palliation, a loading dose of 100 $\mu\text{g/kg}$ into the bypass circuit at the start of rewarming provided therapeutic plasma concentrations, but an infusion of 0.5 $\mu\text{g/kg/min}$ caused a significant increase in plasma milrinone concentration over the first 12 hours; impaired renal function was thought to be the cause, and neonates may require lower doses of 0.2 $\mu\text{g/kg/min}$ (81).

CALCIUM

The calcium ion is an integral part of the excitation-contraction coupling and impulse generation in myocardial cells and is a major determinant of vascular smooth muscle tone. Particularly in neonates, where the sarcoplasmic reticulum is not well developed, and the sequestration and release of calcium is thus inefficient, an adequate ionized calcium concentration is important to optimize myocardial contractility. Administration of calcium in the form of calcium chloride or calcium gluconate helps improve the inotropic function of the heart in the presence of hypocalcemia (82). Calcium functions primarily as a vasoconstrictor when the serum ionized calcium levels are normal. Routine administration of calcium salts upon termination of CPB is a subject of debate. The incidence of hypocalcemia during CPB is relatively high, but the ionized calcium levels usually are corrected to normal levels as weaning from CPB is attempted (83); therefore, calcium administration may not be necessary for most patients. Moreover, increasing evidence suggests that elevated intracellular calcium levels are associated with cell death and injury during ischemia and reperfusion injury (84). Murdoch et al. reported an increase in the SVRI (885 to 1,070 dyne/cm⁵/m²) and a decrease in CI (4.44 to 3.85 L/min/m²)

after administration of 10 mg/kg of CaCl₂ in 12 children following cardiac surgery (85). Rapid administration of calcium can slow the heart rate transiently, and it should be used cautiously in patients who are taking digoxin as it may precipitate digoxin toxicity.

Calcium administration is not recommended in severe bradycardia or asystole unless severe hypocalcemia or hyperkalemia coexists or if the arrest is secondary to calcium channel antagonist drugs (57,58).

A higher and more predictable amount of elemental calcium is available from the intravenous administration of calcium chloride than calcium gluconate or gluceptate (86). Because the neonatal myocardial sarcoplasmic reticulum is not well organized, and release and reuptake of Ca²⁺ is not efficient, some anesthesiologists administer a CaCl₂ infusion of 10 mg/kg/h to neonates after CPB, especially when they received citrated blood products for postcardiotomy bleeding. However, a recent retrospective review of infants <1 year of age demonstrated that mortality after cardiac surgery with bypass was correlated with higher Ca²⁺ supplementation, suggesting that this agent should be used only with documented hypocalcemia with associated myocardial dysfunction, or in neonates receiving significant amounts of citrated blood products, and should be discontinued as soon as possible (87).

Chronotropes

ISOPROTERENOL

Isoproterenol is a potent nonselective β -adrenergic agonist with only very minimal actions on α receptors. Due to its vasodilatory β_2 stimulatory actions as well as lack of α -receptor stimulation, isoproterenol leads to lowering of peripheral vascular resistance (53,88). Its vasodilatory actions may be seen in renal, mesenteric, and pulmonary vascular beds. CO is increased in patients with heart failure as a result of the increased inotropy and chronotropy in the face of diminished SVR. An intravenous infusion of isoproterenol has more chronotropic than inotropic effect, as opposed to dopamine or dobutamine. Myocardial oxygen demands are greatly exacerbated by isoproterenol, and this may exacerbate or induce ischemia (89). Higher doses of isoproterenol can be arrhythmogenic and may induce ventricular tachycardia (VT) or ventricular fibrillation (VF). This agent is contraindicated in dynamic obstruction of the right or left outflow tracts.

Isoproterenol has been shown to cause less hyperglycemia than epinephrine, since insulin secretion is stimulated by strong β -adrenergic stimulation. The drug has been shown to be effective in increasing the heart rate in patients with severe bradycardia or a heart block (57,58). This chronotropic effect of isoproterenol remains the principal use of the drug, and it is often used in electrophysiologic studies to increase heart rate and incite atrial and ventricular arrhythmias. Its principal use in the cardiac ICU is in the denervated heart immediately after heart transplant, or in cases of complete AV block. Isoproterenol is generally not used as a first-line drug in the management of myocardial dysfunction or in the treatment of heart failure. The dose for isoproterenol infusion ranges from 0.01 to 0.2 $\mu\text{g/kg/min}$.

Vasoconstrictors

NOREPINEPHRINE

Norepinephrine is an endogenous catecholamine that is primarily released by the postganglionic adrenergic nerve endings. Besides being a major source of epinephrine, the adrenal medulla also contains norepinephrine in a smaller fraction (10% to 20%). The actions of norepinephrine are very similar to epinephrine on the heart with strong stimulation of the β_1 receptors and increase in myocardial contractility (55). There is a substantial difference in the peripheral action of the two drugs (53) accounting for the variation in their clinical

use. Norepinephrine is a potent α_1 agonist at all doses with minimal effects on the vasodilatory β_2 receptors (53). As a result, even low doses of norepinephrine lead to an increase in the systolic and diastolic blood pressure. SVR is increased as a result of the vasoconstriction of most peripheral vascular beds. CO is usually decreased or unchanged, depending upon the increase in total peripheral resistance. Heart rate may be slowed as a result of reflex increase in vagal tone, or may occasionally increase if the β_1 effects predominate in an individual patient. Both of the endogenous catecholamines, epinephrine and norepinephrine, can cause hyperglycemia with prolonged infusions (90). Norepinephrine usually causes these effects at much higher doses than epinephrine.

Norepinephrine functions as a strong vasoconstrictor and is useful in the clinical situation of decreased SVR; however, it is used infrequently in infants and children. Dose range of norepinephrine infusion varies from 0.02 to 0.2 $\mu\text{g/kg/min}$. It is effective in raising SVR in cases of profound vasodilatory shock unresponsive to high doses of dopamine or dobutamine, such as from sepsis in neonates (91).

PHENYLEPHRINE

Phenylephrine is a pure peripheral α_1 -receptor agonist used as a bolus or an infusion where low systemic blood pressure must be treated acutely. The pure α effects often result in reflex slowing of the heart rate, although this is not as pronounced in young infants. Its principal use in CHD is to acutely raise SVR when either ventricle is compromised by outflow obstruction, for example, tetralogy of Fallot (TOF) with low SVR leading to increased right-to-left intracardiac shunting and cyanosis during a "tet Spell," (92) and hypertrophic cardiomyopathy (93) or other left-sided lesions where the gradient across the obstruction is increased by low SVR. It is also useful where an acute increase in SVR is needed to improve oxygenation, that is, partially obstructed systemic-to-pulmonary shunt, or single-ventricle patient with pulmonic stenosis. Infusions can be used when frequent boluses are necessary, such as in the TOF patient whose tetralogy spell is continuous before transfer to the OR. Phenylephrine is very effective at increasing the blood pressure, but its principle adverse effect is vasoconstriction of peripheral tissue beds, including skeletal muscle, skin, renal, and mesenteric. This vasoconstriction may be intense, and theoretically may compromise end-organ blood flow and function, leading many practitioners to limit its use to extreme situations. Extravasation of phenylephrine into the skin and subcutaneous tissues may lead to ischemia, necrosis, and tissue loss. A reflex slowing of heart rate may be observed, and vigilance is necessary with large phenylephrine doses. Bolus dosing of phenylephrine is 0.5 to 5 $\mu\text{g/kg}$ or higher, and infusion dosing ranges from 0.02 to 0.3 $\mu\text{g/kg/min}$ should be administered through a central venous catheter if possible.

VASOPRESSIN

Vasopressin is a neurogenic polypeptide produced by the paraventricular nucleus of the mid-brain in response to low blood pressure and is secreted by the posterior lobe of the pituitary. Vasopressin produces intense vasoconstriction and an antidiuretic effect. Vasopressin exerts these effects via V1 (vasoconstriction) and V2 receptors (antidiuresis). In the past, the most common use of vasopressin was to treat gastrointestinal bleeding. More recently, vasopressin has been used as an alternative to epinephrine in the acute resuscitation; however, the superiority of vasopressin over epinephrine for this indication is not clear. A theoretical advantage of vasopressin is that it does not rely on adrenergic receptors, which may be down-regulated in chronically elevated catecholamine states. In conditions of metabolic acidosis, signal transmission via adrenergic receptors is also ineffective. Some conditions producing low blood pressure (i.e., septic shock) are associated with low plasma vasopressin concentration, suggesting inappropriately low vasopressin

secretion. In some of these patients, hypersensitivity to the administration of vasopressin has been described, possibly due to up-regulation of vasopressin receptors, and is in agreement with studies showing rapid desensitization to vasopressin (94).

Rosenzweig et al. reported their experience with use of vasopressin in moribund pediatric patients after cardiac surgery (95). These patients were classified as unresponsive to standard vasopressors, and the dosage of vasopressin varied from 0.018 to 0.12 U/kg/h. These doses of vasopressin produced an average increase in systolic blood pressure of 22 mm Hg (65 to 87 mm Hg). Measured plasma vasopressin levels were low in the three patients. Patients who had low blood pressure and poor cardiac function before the initiation of vasopressin therapy died. Vasopressin is particularly useful in cases of low SVR induced by excessive α -adrenergic blockade, such as with phenoxybenzamine or phentolamine (96). There are now a number of case series of vasopressin, and its synthetic analog, terlipressin, being used to treat refractory vasodilatory shock in pediatric patients with cardiogenic and septic etiologies (97,98). Vasopressin doses range from 0.01 to a maximum of 0.05 U/kg/h, and should be weaned and discontinued as soon as possible. Hyponatremia is often seen with vasopressin infusions of several days' duration, and serum sodium should be measured at least daily.

Vasodilators

NITROGLYCERIN

Nitroglycerin produces vasodilation by releasing NO. The release of NO from nitroglycerin, unlike that of some other NO donors, is enzymatically mediated. Nitroglycerin is frequently referred to as a venodilator while sodium nitroprusside (SNP) is thought of as a preferential dilator of arteries, although these differences are difficult to demonstrate. The major indications for the use of nitroglycerin are myocardial ischemia, systemic hypertension, PH, volume overload, congestive heart failure, and pulmonary edema. Venodilation associated with nitroglycerin therapy leads to a decrease in venous return. The decrease in preload leads to a lowering of the left ventricular end-diastolic volume and pressure, and therefore decreased wall stress. The net effect is usually an improvement in the ratio of myocardial oxygen demand to delivery. Nitroglycerin also dilates both diseased and normal coronary arteries (99). Hypotension and reflex tachycardia are the potentially undesirable side effects. Nitroglycerin is used in the cardiac surgical patients for the treatment of systemic or pulmonary hypertension, and to decrease filling pressure and improve cardiac index. In a study including 20 pediatric patients with CHD, of whom 14 had preoperative PH, nitroglycerin ($>2 \mu\text{g/kg/min}$) reduced both systemic and PVRs (100). Improved cardiac index was seen only with higher doses. The authors suggested that the effect of the drug on the systemic and pulmonary arteries and on capacitance vessels was dose related. In lower doses ($<2 \mu\text{g/kg/min}$), nitroglycerin mainly produced venodilation, as evidenced by an increased requirement of volume to maintain constant right and left atrial pressures. The usual doses of intravenous nitroglycerin infusion are 0.5 to 5 $\mu\text{g/kg/min}$.

SODIUM NITROPRUSSIDE

The hypotensive properties of SNP were described in the late 1800s; however, the drug was not approved for clinical use until 1974. Frequently, nitroprusside is incorrectly referred to as a "direct, preferential arterial vasodilator." Nitroprusside dilates both arteries and veins by releasing NO in an interaction with tissue compounds containing sulfhydryl groups. The released NO activates soluble guanyl cyclase that increases cGMP. Nitroprusside is most commonly used to control blood pressure in hypertensive patients, and to decrease SVR thereby improving forward flow in patients with poor LV function or

regurgitant lesions (mitral or aortic regurgitation). Because of its short half-life, SNP allows precise control of blood pressure and SVR. In patients with diminished myocardial function, CO is increased from an increased stroke volume as a result of decreased aortic impedance. Despite significant reductions in SVR, the blood pressure decrease is usually modest since an increase in CO compensates for the decrease in SVR. The drop in blood pressure is more dramatic in patients with pre-existing hypovolemia or obstructive cardiac lesions. In patients with hypertrophic cardiomyopathy SNP may increase outflow obstruction, and patients with aortic or mitral stenosis may not be able to compensate with an increase in CO, resulting in profound hypotension. SNP has been used for early postoperative afterload reduction after Norwood Stage I palliation to lower SVR and decrease $Q_p:Q_s$, with excellent early hemodynamics and high early survival rate (101).

One of the dangers associated with the use of nitroprusside is toxicity from the formation of cyanide. Cyanide a by-product of SNP metabolism, is taken up by red cells and inactivated predominantly in the liver by reacting with thiosulfate. This reaction is catalyzed by the enzyme rhodanese, and patients with liver failure are more susceptible to cyanide toxicity. If cyanide toxicity occurs, SNP should be stopped immediately, and after confirmation of diagnosis, the patient should be treated with 3% sodium nitrate followed by administration of sodium thiosulfate. SNP should be used cautiously in patients with renal failure since they may have difficulty metabolizing the thiocyanate produced during breakdown of SNP. In a retrospective review of 63 children receiving SNP after cardiac surgery to control blood pressure, or to lower SVR for hemodynamic purposes, 11% of patients experienced an elevated cyanide concentration. Mean SNP dose was 2.8 $\mu\text{g/kg/min}$ in those patients with elevated cyanide levels, and 1.1 $\mu\text{g/kg/min}$ for those without elevated levels with an increased risk of elevated cyanide levels starting at 1.8 $\mu\text{g/kg/min}$ (102).

The starting dose of SNP is 0.5 to 1 $\mu\text{g/kg/min}$, and the dose can be titrated up to 5 $\mu\text{g/kg/min}$. The high doses pose greater risk for toxicity, so doses exceeding 3 $\mu\text{g/kg/min}$ should not be administered for longer than several hours. Sodium thiosulfate can be added to the infusion to eliminate cyanide, but alternative methods of hypertension treatment should be instituted. In a multicenter study of 118 infants and children receiving esmolol for blood pressure control on admission to the ICU after coarctation repair via thoracotomy, only 15% to 20% of neonates, 50% of patients aged 1 to 24 months, and 80% of patients aged 2 to 6 years were treated with SNP for blood pressure control. The median maximal SNP dose was 3 $\mu\text{g/kg/min}$, and there was no mortality, neurologic complication, or significant acidosis (103).

PROSTAGLANDINS

Prostaglandins such as PGE_1 and PGI_2 are the main metabolites of the arachidonic acid pathway. In the vascular tissues, they are predominantly generated and subsequently released by the endothelium to bind to specific receptors on the underlying smooth muscle cells. This leads to the activation of adenylate cyclase and an increase in cAMP levels, which lowers intracellular Ca^{2+} and produces vascular smooth muscle relaxation.

PGE_1 is used to relax smooth muscle and maintain the patency of the ductus arteriosus in neonates whose systemic or pulmonary circulations are dependent on ductal patency. PGE_1 , when administered to 27 neonates in whom pulmonary or systemic blood flow was entirely or significantly dependent upon ductal patency, led to an improvement in hypoxemia and acidemia, as well as ductus dilation (104). It has been demonstrated to maintain ductal patency for as long as 2 months (105) and to reopen a recently closed ductus. Preoperative drug therapy with PGE_1 has lowered the mortality

and allowed planned surgeries, rather than desperate attempts at emergency palliation, which was frequently the case in the past. Hypotension, apnea, hyperpyrexia, and jitteriness, side effects of PGE_1 therapy, occur in 20% to 40% of patients at higher doses (0.05 to 0.1 $\mu\text{g/kg/min}$), but they are usually reversible upon lowering the dose or discontinuation of the drug.

Besides management of neonatal CHD, PGE_1 has been used to treat PH secondary to mitral valve disease (106), after congenital cardiac surgery (107) and after heart transplantation (108). There has been only limited research conducted in the use of inhaled PGE_1 .

PGI_2 or prostacyclin (epoprostenol) is a relatively recent addition to the drug therapy for the management of pulmonary vascular disease. Even though PGI_2 is probably the most selective pulmonary vasodilator of all the currently available intravenous drugs, administration of PGI_2 via this route will also lower systemic arterial pressure. PGI_2 is spontaneously hydrolyzed to 6-keto-prostaglandin $\text{F}_{1\alpha}$ with a half-life of 1 to 3 minutes. The relatively selective effect on lowering PVR is due to rapid inactivation in the pulmonary vasculature bed during a single circulation time. Intravenous infusions of PGI_2 (epoprostenol) have been shown to be useful in decreasing the PVR in patients with primary PH and after cardiac surgery in neonates (109). Due to its short half-life, aerosolized PGI_2 , like NO, can selectively dilate pulmonary vessels with minimal effects on the systemic arterial pressure. Several anecdotal reports and a few small clinical studies suggest that inhaled PGI_2 can reduce elevated PAPs and PVR. Schulze-Neick et al. reported inhaled PGI_2 and NO to have similar advantageous effects on reducing PVR in patients with CHD after cardiac surgery (110). Another study demonstrated reduction of PAPs and improvement in the right ventricular function following inhaled PGI_2 therapy with bolus dosing (2.5, 5, 10 μg) in nine patients undergoing cardiac surgery including heart transplantation (111). The optimal dosing of epoprostenol remains undefined, and dosing of inhaled PGI_2 ranging from 1 to 50 ng/kg/min has been shown to be efficacious (112). This agent has also been demonstrated to lower elevated PAP and PVR in infants after congenital heart surgery with bypass (113).

SILDENAFIL

Sildenafil is a phosphodiesterase-5 inhibitor, which, in its intravenous form, appears to be a selective and highly effective pulmonary vasodilator in a piglet model of meconium aspiration with severe PH (114). Sildenafil has been shown in case reports to ameliorate the effects of NO withdrawal in a patient after cardiac surgery with persistent PH (115). In doses of 0.5 to 2.0 mg/kg given NG, sildenafil was effective at lowering mean PAP in infants after AV septal defect repairs (116).

INHALED NITRIC OXIDE

A ubiquitous compound in the human body, NO is produced as a result of the conversion of the amino acid arginine to citrulline, a reaction that is facilitated by the enzyme nitric oxide synthase (NOS). NO, being a very small and lipophilic molecule, diffuses into the underlying smooth muscle cells producing an increase in intracellular cGMP levels and subsequent vasodilation (117). NO, when delivered via the inhaled route, readily crosses the alveolar-capillary membrane leading to pulmonary vasodilation and a decrease in PVR. High-affinity binding and immediate inactivation of inhaled nitric oxide (iNO) activity by hemoglobin limits the action of the drug to the pulmonary circulation. iNO therapy has been shown to be useful in the treatment of PH, which is frequently seen in CHD (117,118). PH in patients with CHD is multifactorial, due to chronic hypoxemia or due to chronic elevation of pulmonary blood flow and/or pulmonary venous pressures. PVR

is also increased immediately after CPB due to the endothelial dysfunction. iNO is ideally suited in selectively reducing PVR during this critical period (118). The pulmonary vascular selectivity of iNO may be especially useful in reducing the right ventricular afterload in patients undergoing heart transplant, where the donor hearts may not be accustomed to high PVR of that is usually seen in these patients (119). Several investigators have reported the use of iNO in the preoperative period as a test of reversibility of PVR and in predicting post-CPB PH, as well as using the preoperative evaluation to predict the use of the drug in the immediate post-CPB period (117,120–122).

Others have reported the benefit of iNO in improving oxygenation, likely by improving pulmonary blood flow and ventilation–perfusion balance in congenital cardiac surgery patients (123). Even though iNO has been shown to be effective in a variety of congenital heart lesions, it may not be helpful in reducing PVR in all patients. In a double-blind study, the combination of milrinone 0.5 $\mu\text{g/kg/min}$ and NO 30 ppm was more effective at lowering PAP than either agent alone (124). The nonresponders are usually those who have long-standing PH and extensive remodeling of the pulmonary vasculature. NO also has not been shown to improve postoperative outcome, the cost is prohibitive at several thousand dollars per day of use, the delivery system setup is complex, as is transport with NO, and there are toxicity issues (see below). All of these issues suggest that NO should only be used as a last resort in a patient with known or suspected severe PH resulting in low CO (in two-ventricle patients), or severe desaturation in single-ventricle patients after systemic arterial or venous to PA shunts.

NO can be administered using a face mask in a spontaneously ventilating patient, or added to the inspiratory limb of the breathing circuit in a mechanically ventilated patient. The most commonly used dose range is 10 to 20 ppm, though a decrease in PVR has been demonstrated with doses as low as 2 to 5 ppm. Side effects of iNO at these doses are minimal, even with prolonged therapy.

A novel approach is to administer IV L-citrulline, an amino acid precursor of NO, as a potential therapy to increase NO concentrations and prevent pulmonary hypertensive crises in susceptible patients. Initial phase I and phase II trials have demonstrated predictable pharmacokinetics and no safety issues so far with this approach (125). Abrupt withdrawal of NO or rapid reductions in drug dosage may lead to rebound PH (126). The binding of NO to hemoglobin gives rise to methemoglobin (127), and methemoglobin levels should be routinely monitored especially with prolonged therapy.

Nitrogen dioxide is also formed as a by-product of NO administration, and its levels should be maintained below 5 ppm. Nitrogen dioxide in high concentrations can lead to injury of the lungs (117).

FENOLDOPAM

Fenoldopam is a selective dopamine-1 receptor agonist with moderate affinity for α_2 receptors. Despite its binding to α_2 receptors, fenoldopam has no significant sedative effect. Fenoldopam administration produces dramatic vasodilation of the peripheral vasculature including renal, mesenteric, coronary, and skeletal muscle. The main indication for the use of fenoldopam is in the treatment of hypertensive emergencies and postoperative hypertension (128–130). The theoretical advantage of use of fenoldopam is that it maintains renal perfusion while decreasing blood pressure. This is especially important in patients with decreased renal function, since in rapid drop in blood pressure these patients may lead to decreased renal blood flow, decreased GFR, and even acute renal insufficiency. During prolonged infusion of fenoldopam, there is development of tolerance with a half-life (predicted loss of 50% effectiveness of the drug) of 60 hours, without

a prolonged pharmacodynamic effect or rebound hypertension upon discontinuation of fenoldopam. In a retrospective study of 25 postoperative cardiac neonates with inadequate urine output despite conventional diuretic therapy, fenoldopam increased urine output by 50% and had minimal effect on hemodynamics (131).

NICARDIPINE

Nicardipine is a dihydropyridine calcium channel antagonist that relaxes vascular smooth muscle by inhibiting calcium entry, resulting in decreased systolic, mean, and diastolic blood pressure and SVR (132). Its negative inotropic effects are minimal, and compensatory tachycardia is less than for other direct vasodilators, that is, nitroprusside. It is effective for antihypertensive therapy in postoperative cardiac surgical patients with adequate LV function. Nicardipine has been used successfully for postcoarctectomy hypertension after repair via thoracotomy in children, with significant decreases in mean arterial pressure and minimal increase in heart rate (133). Despite its lack of negative inotropic effect, this agent should not be used in patients with decreased systemic ventricular function, and only should be used with great caution in young infants.

Beta Adrenergic Antagonists

β -Blockers, like angiotensin-converting enzyme (ACE) inhibitors, are more beneficial in the management of chronic heart failure where they have been shown to improve the functional status in both pediatric and adult CHD (134,135). This effect is due to the modulation of the endogenous neurohumoral system. Several studies have demonstrated downregulation of β adrenoceptors in chronic heart failure as a result of elevated sympathetic tone (136,137). Therapy with β -blockers such as propranolol, metoprolol, and carvedilol increase the number of myocardial β adrenoceptors and improve myocardial function in heart failure secondary to CHD (138,139). Responsiveness to catecholamines may be preserved in these patients during the perioperative period as a result of β -blocker therapy. Besides their use in the management of chronic heart failure, these medications have several uses in the acute hemodynamic management of patients with CHD. By reducing the effects of increased sympathetic tone on the right ventricular infundibulum in TOF, β -blockers are effective in the treatment of cyanotic spells (140). Also, a decrease in heart rate allows a longer diastolic filling time and improved preload. The use of esmolol, a short-acting β_1 selective antagonist, is well suited for the hemodynamic management of TOF in the perioperative setting (141). Esmolol in doses of 100 to 700 $\mu\text{g/kg/min}$ has also been successfully used to control postoperative hypertension after repair of aortic coarctation in children (103,142). Labetalol, a combined α - and β -adrenergic receptor blocker with 1:7 α : β blocking effect, is a frequent choice for intermittent IV dosing, during transition from continuous infusion β -blockade to oral therapy. Dosing at 0.1 to 0.2 mg/kg given every 1 to 4 hours is often effective.

Newer Cardiotonic and Vasoactive Agents

Currently, there exists limited scientific literature regarding the use of some new vasoactive drugs in patients with CHD, though a few of them have been well researched in other patient groups. A brief description of some of these newer agents is as follows:

LEVOSIMENDAN

Levosimendan is a positive inotrope and vasodilator. Most other positive inotropes work through stimulation of

adrenergic receptors and increase intracellular calcium that may be already elevated in the failing heart. Unlike these drugs, levosimendan works by causing conformational changes in the myofilaments making them more sensitive to intracellular calcium. The vasodilation produced is mediated by opening of potassium channels. Although drug is not approved for routine clinical use in the United States, there are extensive clinical studies involving large number of patients with end-stage cardiac failure demonstrating that levosimendan is both safe and effective in providing symptomatic relief. Levosimendan was also more effective in decreasing PA wedge pressure and increasing CO (143). Experience with the use of levosimendan in the perioperative period is limited. In a prospective randomized placebo-controlled trial in patients undergoing cardiac surgery, levosimendan given before separation from CPB enhanced cardiac performance, decreased SVR, increased myocardial oxygen consumption, and significantly decreased blood pressure, occasionally leading to hypotension (144). The hypotension was responsive to volume administration and vasoconstrictors were not needed. In 15 children with acute heart failure, levosimendan in doses of 6 to 12 $\mu\text{g/kg}$ load and 0.05 to 0.1 $\mu\text{g/kg/min}$ improved ejection fraction in all while allowing a reduction in dobutamine dose, with other hemodynamics unchanged (145). Despite exhibiting the expected hemodynamic effects, the drug has shown little or no effect on survival in adult patients with heart failure; thus, the drug has not been further developed for use in the United States.

NESIRITIDE (B-NATRIURETIC PEPTIDE)

Nesiritide is a human recombinant form of B-type natriuretic peptide (BNP) that is identical to and has actions that are similar to the endogenous BNP. Human BNP stimulates increases in intracellular cGMP in vascular endothelial cells and smooth muscles. Elevated cGMP levels with nesiritide therapy lead to venodilation and arteriodilation. Nesiritide has natriuretic, diuretic, and vasodilatory properties. Currently, the primary use of nesiritide is for treatment of acute decompensated heart failure where it produces dose-dependent reductions in the pulmonary capillary wedge pressure PCWP and systemic arterial pressure. In addition, vasodilation occurs without a change in heart rate and is associated with increases in stroke volume and CO. In a randomized controlled trial involving 489 subjects, nesiritide, when given as a bolus dose of 2 $\mu\text{g/kg}$ and followed by an infusion at 0.01 to 0.03 $\mu\text{g/kg/min}$, was more effective in lowering PCWP as compared to nitroglycerin (146). In another randomized controlled trial that included 103 patients with heart failure and systolic dysfunction, nesiritide was reported to decrease PCWP by up to 39%. This was accomplished by lowering the right atrial pressure (RAP) and SVR, along with a significant improvement in cardiac index (147). Colucci et al. (148) reported that nesiritide was as effective as standard drug therapies (dobutamine, milrinone, dopamine, or nitroglycerin) in treating heart failure. The renal hemodynamic effects of nesiritide (BNP) appear to be that of arteriolar vasoconstriction, which would likely augment GFR and filtration fraction in the setting of compromised renal perfusion. Additionally, BNP leads to increased urinary sodium excretion and fractional excretion of sodium (FENA) (149). Mild diuretic effect of nesiritide therapy has been reported in a few clinical trials (149,150). In a limited pediatric experience of 17 patients after cardiac surgery, a loading dose of 1 $\mu\text{g/kg}$ was administered on bypass, and then an infusion of 0.1 then 0.2 $\mu\text{g/kg/min}$ was continued. There was a 7% decrease in mean arterial pressure with no adverse effects (151). Use of this agent has been limited in the pediatric population, likely because multiple controlled adult trials have not demonstrated any survival benefit with this agent.

Mechanical Support

Patients who are receiving high-dose inotropic support, considered by many cardiac intensivists to be epinephrine, 0.1 to 0.2 $\mu\text{g/kg/min}$ (or its equivalent) for more than 2 to 4 hours and maintain only marginal CO must be considered for institution of mechanical support in the form of ECMO or VADs. Mechanical support is ideally instituted proactively, rather than after a cardiac arrest or onset of multiorgan failure. (See Chapter 21 for complete discussion of mechanical support therapies.)

ARRHYTHMIAS

Maintenance of normal sinus rhythm, or at least AV synchrony by temporary or permanent pacing, is a goal in every CICU patient. However, arrhythmias are a constant threat, and the intensivist must be ever vigilant to this problem when hemodynamic status is not optimal. This section will summarize the major acute classes of arrhythmia in the CICU; the reader is referred to Chapter 18 for a more extensive discussion.

Etiology and Incidence

In the CICU, postsurgical changes are among the most common causes of arrhythmia, secondary to surgical resection or manipulation of ventricular or atrial tissue. Numerous additional nonsurgical causes of arrhythmia are seen in CICU patients, and the total incidence of arrhythmia is 15% to 30% of CICU admissions (152,153). Junctional ectopic tachycardia (JET), affecting 2% to 5% of postsurgical patients (154), can necessitate mechanical support and can be fatal if not treated effectively. Patients most at risk are infants undergoing ventricular muscle resection, that is, in TOF repairs. This arrhythmia is characterized by impulses arising at or near the AV node, with a discharge rate faster than the atrial rate, loss of AV synchrony, and ventricular rates of 140 to 220 bpm with hypotension and poor CO. Other common arrhythmias include supraventricular tachycardias: atrial tachycardias and AV reentrant nodal tachycardias. These may be caused by intra-atrial interventions including suture lines in the atrium, BAS, or atrial cannulation. SA node injury from SVC cannulation may lead to sinus bradycardia or low atrial rhythm. Ventricular arrhythmias, including isolated premature ventricular contractions (PVCs), multifocal PVCs, VT, and VF, may be seen secondary to myocardial ischemia from aortic crossclamping or acquired coronary artery anatomic obstruction. Second- or third-degree AV block may be seen after surgical manipulation or sutures in the area of the bundle of His, particularly after perimembranous ventricular septal defect VSD repair or subaortic resection. Right bundle branch block is common after right ventricular surgery; left bundle branch block is rare but may be seen in some patients after left ventricular outflow tract surgery.

Sinus bradycardia may be seen after cardiac surgery with SA node injury, hypothermia, or hypoxemia. Sinus tachycardia may be seen with hyperthermia, excessive circulating catecholamines from exogenous (inotropes) or endogenous (inadequate analgesia or uncompensated heart failure) sources, and may significantly impair ventricular filling and ejection times.

Myocardial disease, whether from acute myocarditis, or cardiomyopathy from ischemic or a variety of other causes, may cause any of the above noted arrhythmias. Chronic arrhythmogenic substrates, that is, significant atrial enlargement causing atrial fibrillation, previous lateral tunnel Fontan circulation causing atrioventricular nodal reentrant tachycardia or intra-atrial re-entrant tachycardia (IART) previous Mustard or Senning repairs causing IART-inherited sodium channelopathies causing Long QT syndrome and ventricular

arrhythmias, are other etiologies of arrhythmias observed in CICU patients with hemodynamic compromise.

Diagnosis

Standard 5-lead ECG configuration (right arm, left arm, right leg, left leg, V lead over ventricular apex) for beat-to-beat continuous monitoring of ECG in the CICU is an important modality for arrhythmia diagnosis in every patient. Multilead display allows 8 leads to be displayed simultaneously on the bedside monitor for rapid diagnosis especially during hemodynamic compromise. The capability to electronically archive ECG waveforms, not merely heart rate, is important to retrospectively assess periods of hemodynamic compromise. Standard 12-lead ECG with extended rhythm strip recording in lead II and other leads is important to obtain as soon as possible for diagnosis of arrhythmia. Atrial electrograms, obtained with right and left arm leads connected to temporary atrial pacing wires placed during surgery, are very important tools for diagnosing tachycardias. Information available from implanted pacemakers and defibrillators provides crucial data not obtainable by other bedside means. Assessment of intra-atrial pressure waveforms provides important clues as to whether AV synchrony is preserved in tachycardia when the displayed ECG is ambiguous, as is often the case (Fig. 20.4). Loss of distinct A and V waves is an important sign of supraventricular tachycardia with retrograde conduction to the atrium. In junctional tachycardia, the A waves are not at all synchronized with the V waves. Bedside echocardiography, whether transthoracic or transesophageal, can also allow assessment of AV synchrony, atrial fibrillation, and other features sometimes not discernible by standard ECG methods. Finally, in the case of an open sternum, direct observation of the heart can also assist in the diagnosis of arrhythmia. Consultation from electrophysiology service experts is also highly desirable, particularly in questionable or complex cases.

Prevention and Treatment

Among the most common causes of arrhythmia in the CICU are electrolyte disturbances, particularly hypokalemia for atrial arrhythmias, commonly seen after diuretic use. Maintaining serum potassium values in the 3.5- to 5-mEq/L range is the normal goal for prevention, and IV potassium boluses of 0.5 to 1 mEq/kg over 1 hour are often necessary in the acute setting. Normal serum magnesium levels are an impor-



Figure 20.4. ECG demonstrating normal sinus rhythm the first third of the panel, with onset of supraventricular tachycardia. Note the arterial pressure tracing with a 12 to 15 torr decrease in systolic pressure, and the loss of the A wave on the central venous pressure tracing, with the appearance of large V waves with a systolic pressure increase from 10 to 16 mm Hg.

tant goal to prevent and treat ventricular arrhythmias and JET (155), and normal serum calcium and sodium levels are also desirable. Low serum pH, below 7.25 to 7.30, resulting in myocardial acidosis, promotes arrhythmia risk, particularly ventricular. Correcting acidosis with sodium bicarbonate or increasing minute ventilation are effective.

Excessive circulating catecholamines may contribute to JET, supraventricular tachycardias, ventricular arrhythmias, and sinus tachycardia with undesirable hemodynamic effects. Avoiding unnecessarily high doses of β -adrenergic agonists such as epinephrine and dopamine will decrease risk of such arrhythmias. Other pharmacologic agents such as pancuronium, with its vagolytic effects, or sedation with ketamine, may also contribute. Withdrawal from β -blockade given preoperatively for arrhythmias, prevention of right ventricular outflow tract (RVOT) spasm, or heart failure, is a frequent cause of relative catecholamine excess at the receptor level. Amiodarone is an effective treatment for JET (156). Temperature control is important to decrease the rate of firing of abnormal foci, most particularly JET. Maintaining normothermia is an important preventive measure, and actively cooling the patient to 34°C to 35°C is a cornerstone of JET treatment. Hypothermia is a cause of sinus bradycardia, particularly important in the neonate.

Pharmacologic treatment of acute arrhythmias in the CICU is restricted to a few effective agents. Atrial arrhythmias, including SVT, AVRNT, atrial fibrillation, and atrial flutter, may be treated with *procainamide* loading dose and infusion; effectiveness is variable but this agent can be discontinued with a reasonably short half-life so that other agents, that is, amiodarone can be used. *Amiodarone* load, 5 mg/kg IV over 15 to 30 minutes, can be repeated up to a total loading dose of 15 mg/kg, and is very effective for all atrial arrhythmias. The half-life of this agent is very long; excessive levels or interaction with procainamide may cause refractory ventricular arrhythmias. Rapid amiodarone administration to neonates, or to other very unstable patients, can result in cardiovascular collapse from hypotension due to its acute α -receptor blocking effects. Pretreatment with calcium chloride may prevent this potential disaster. Symptomatic reentrant atrial arrhythmias can be pharmacologically converted with *adenosine*, 50 to 200 μ g/kg pushed IV, which interrupts AV node conduction for up to 5 to 10 seconds (which itself can be problematic). Ectopic supraventricular arrhythmias, that is, atrial ectopic tachycardia and JET, will not respond to adenosine. *Vera-pamil*, the calcium channel-blocking agent, *must not* be used in infants and young children due to its acute effects on myocardial contractility. *Esmolol* infusion is often used in the acute setting and may be very effective, both in controlling the rate response and in suppressing ectopic atrial foci.

In the CICU setting, most cases of symptomatic atrial arrhythmias are treated with synchronized cardioversion, with multifunctional cardioversion/defibrillation/external pacing pads placed on anterior right chest and apex. A current of 0.5 to 1 J/kg is delivered. Sedation and analgesia will be required. If not effective, a second attempt is made, doubling the energy. Repeated failure to convert to sinus rhythm is very unusual; serum electrolytes, pH, and intrinsic myocardial disease are usual causes.

First-line treatment for ventricular arrhythmias often includes lidocaine, 1 to 2 mg/kg loading dose, and 20 to 50 μ g/kg/min. Amiodarone is effective for treating ventricular arrhythmias, again with attention to its acute vasodilating effects in infants, and interactions with other drugs, especially procainamide. For perfusing VT, cardioversion with 1 to 2 J/kg is effective, and for pulseless VT or VF, chest compressions along with immediate defibrillation using 2 to 5 J/kg are necessary. In the case of intractable arrhythmias with severe hemodynamic compromise, ECMO or VAD support may be necessary, until the arrhythmia can be controlled medically, or by ablation in the OR or catheterization laboratory.

TABLE 20.6 Drug Therapy of Acute Hemodynamically Significant Arrhythmias in the CICU

Drug	Dose	Indications	Comments
Adenosine	100 µg/kg rapid bolus, double if ineffective, max 300 µg/kg	SVT	May cause sinus pauses, bradycardia, AV block
Amiodarone	Load 5 mg/kg over 30–60 min; may repeat × 2; infusion 15–20 mg/kg/24 h	Atrial tachycardia, flutter, and fibrillation; JET; VT and VF	May cause sinus bradycardia, AV block, hypotension, drug interactions with procainamide and β-blockers
Atropine	10–20 µg/kg	Sinus bradycardia; Sinus bradycardia	
Epinephrine	1–5 µg/kg	Sinus bradycardia; AV block	
Esmolol	250–500 µg/kg load over 1–2 min; 50–500 µg/kg/min infusion	Sinus tachycardia; atrial and ventricular tachyarrhythmias	May cause negative inotropy, bradycardia, sinus pauses, AV block
Isoproterenol	0.01–0.03 µg/kg/min	Sinus bradycardia in denervated heart; complete AV block	β ₂ effects may decrease diastolic BP
Lidocaine	1–2 mg/kg load over 1 min; may repeat; infusion 20–50 µg/kg/min	PVCs, VT, VF	Toxicity from hepatic/renal failure
Magnesium sulfate	25–50 mg/kg load over 30 min	VT (Torsade de pointes), prevention of JET	May cause muscle weakness, sedation
Procainamide	10–15 mg/kg load over 30–45 min; infusion 20–40 µg/kg/min	Atrial tachycardia; JET; VT	Monitor procainamide and <i>N</i> -acetylprocainamide levels; may cause hypotension; synergistic adverse effects with amiodarone

SVT, supraventricular tachycardia; AV, atrioventricular; JET, junctional ectopic tachycardia; VT, ventricular tachycardia; VF, ventricular fibrillation; PVC, premature ventricular contraction.

Temporary pacing is frequently necessary in the CICU following cardiac surgery, and improves CO in most instances (157). Where there are arrhythmias in the OR, or high risk for arrhythmias exists based on patient history or surgical procedure, the surgeon should place temporary pacing wires at least on the right atrial appendage. Ventricular pacing wires are also placed, along with a ground lead on the skin, for any suspicion or actual disturbance in AV node conduction. Indications for pacing the atrium include sinus bradycardia and junctional rhythms including JET, where AV node conduction is still intact. In cases of actual or suspected risk for AV node or His bundle conduction disturbance, both A and V wires are used. For complete AV block, if no pacing wires are available, pharmacologic treatment with direct-acting β-adrenergic agents such as isoproterenol or epinephrine are used. Temporary external pacing with multifunctional pads is initiated during a crisis when no other means are available. More secure methods are then initiated, such as a transvenous pacing catheter, or emergency sternotomy or subxiphoid incision to place temporary pacing wires. Temporary pacemaker wire thresholds for capture ideally should be tested in the OR, and should be low, that is, 1 to 2 mV for atrial leads, and 2 to 4 mV for ventricular leads. After establishing thresholds, output should be adjusted to equal two times the threshold to establish a margin of safety. Continuous use of temporary wires over a period of days will result in increased thresholds due to damage to the myocardium from the electrical current. If thresholds increase, new temporary wires, or a means of permanent epicardial or transvenous pacing, must be considered. Pacemaker settings must reflect appropriate AV interval and refractory periods for the heart rate of the patient. In addition, in the OR setting pacing is often asynchronous, that is, dual chamber paced, no chamber sensed, no chamber inhibited (DOO); this must be converted to demand, or dual

chamber paced, dual chamber sensed, dual chamber inhibited (DDD) pacing, due to the danger of uncoordinated R on T pacing leading to ventricular fibrillation. Pacemaker thresholds should be checked daily, and pacemaker need should be assessed at least daily. The underlying cardiac rhythm is determined by disconnecting the pacemaker. In the case of surgically induced complete heart block, if there is no recovery after 7 to 10 days, it is highly likely that the condition is permanent, and plans for a permanent pacemaker must be made. Tables 20.6 and 20.7 list the treatment modalities for the most frequent symptomatic arrhythmias encountered in the CICU (158).

PULMONARY HYPERTENSION

PH is commonly encountered in the CICU, and complicates a variety of surgical and medical patients. A high index of suspicion for PH is important to recognize and consider this problem for patients not progressing well in their CICU course. (For a complete discussion of PH, see Chapters 66 and 67.) This section focuses on PH in the acute CICU setting.

Etiologies

In the modern era, the incidence and severity of PH in infants with long-standing left-to-right shunts from lesions such as VSD or AVSD is much lower than in the past, because of early complete correction strategies, now routinely at 2 to 4 months of age. These infants, particularly those with Trisomy 21, may have significant PH, particularly in the immediate postoperative period, when the inflammatory response from bypass,

TABLE 20.7 Pacing/Cardioversion/Defibrillation of Acute Hemodynamically Significant Arrhythmias in the CICU

Treatment	Dose	Indications	Comments
Atrial overdrive pacing	Rate 10%–20% faster than SVT rate for up to 15 s	SVT	
Atrial pacing with temporary wires	Desired rate for optimal hemodynamics	Sinus bradycardia, junctional bradycardia; JET	Output double the capture threshold
AV sequential pacing with temporary wires	Desired rate for optimal hemodynamics	AV block	Output double the capture threshold
Synchronized cardioversion	0.5–1 J/kg	SVT, atrial flutter, atrial fibrillation	Sedation/analgesia needed
Defibrillation	3–5 J/kg	VT/VF	
External transcutaneous pacing	Increase output until capture; desired rate for optimal hemodynamics	Sinus bradycardia, AV block, junctional bradycardia	Temporary therapy in emergencies only
Esophageal pacing	Desired rate for optimal hemodynamics; overdrive for SVT	Sinus bradycardia, SVT	Not effective for AV block
Transvenous pacing	Desired rate for optimal hemodynamics; increase output until capture	AV block, sinus or junctional bradycardia	Temporary therapy; ineffective in single-ventricle patients

SVT, supraventricular tachycardia; AV, atrioventricular; JET, junctional ectopic tachycardia; VT, ventricular tachycardia; VF, ventricular fibrillation; PVC, premature ventricular contraction.

including the increase in endothelin levels, is the highest risk period for a PH crisis (159). In one series from the 1990s, severe PH was seen in 2% of postoperative cardiac patients, and such crises were fatal in almost 10% of such patients (160). This is certainly not the case today, and indeed the severe crises are unusual and accordingly are not recognized promptly. More often in the modern era, the single-ventricle patient, either after systemic-to-pulmonary shunt in the neonatal period, or bidirectional cavopulmonary anastomosis at 2 to 6 months of age, has a relatively subtle degree of elevation of PA pressure and resistance, which by objective criteria such as SVC pressure after surgery, is not impressive; however, the combination of single systemic ventricle that may have impaired systolic or diastolic function, AV valve regurgitation, and hypoplastic PAs, may elevate PAP just enough to cause a marginal patient to decompensate with hypoxemia and further elevations of caval pressures (161). In these patients, PAP can be normal in spite of increased PVR.

Another category of PH patients includes those with left-sided obstructive lesions, including mitral valve stenosis, cor triatriatum, pulmonary vein obstruction, and total anomalous pulmonary venous return (TAPVR) with obstruction. Left ventricular dysfunction such as in cardiomyopathy can also cause significant elevations in PA pressure and resistance. Besides the post-CPB-induced changes, excessive catecholamines, particularly induced by painful or noxious procedures such as tracheal suctioning, can precipitate severe PH crises. Airway and ventilatory problems such as hypoxemia, hypercarbia, and acidosis can also precipitate undesirable PAP elevations. Vigilance to anticipate and prevent PH crises is crucial in such patients.

Diagnosis

Short of a PH crisis (see below), elevated PAPs may cause right or single ventricular dysfunction, increased right-to-left shunting

through atrial or ventricular communications resulting in arterial desaturation, and inability to progress in weaning from mechanical ventilation. Some of these signs may be relatively subtle in the context of a ventilated patient with parenchymal lung disease. Bedside echocardiography is an important tool to assess right ventricular function and estimate PAP from the tricuspid regurgitation velocity, gradient across a VSD, or directionality of shunting at atrial or ventricular level. Position of the inter-ventricular septum is an important component of the examination, with midposition or right-to-left excursion during systole important accompaniments of significant PH. Patients suspected to have PH, and not progressing in their CICU course, should have hemodynamic catheterization to formally assess pulmonary hemodynamics and response to pulmonary vasodilator therapy.

The definition of PH crisis is an acute elevation in PAP to greater than half systemic that results in decreased pulmonary blood flow such that CO is compromised. This is heralded by poor peripheral perfusion, acidosis, and hypotension. Causes of acute PH crises are often inadequate analgesia and sedation before noxious stimulation, that is, tracheal suctioning or painful procedures. Other leading causes include airway and ventilation problems leading to hypoxemia and hypercarbia. If pulmonary blood flow is severely compromised, arterial desaturation will occur, and if an avenue for intracardiac right-to-left shunting exists, hypoxemia can be severe. Decreased blood flow through the lungs can compromise LV filling and coronary perfusion pressure and cause both left and right ventricular dysfunctions. Severe PH can cause acute RV failure. Acute difficulty with ventilation can occur as hypertensive distended pulmonary arterioles compromise small airway lumens. If such a PH crisis is not interrupted, a vicious cycle of hypoxemia and acidosis leads to ongoing severe PH and cardiac arrest. Early intervention is crucial to prevent such a disaster. Figure 20.5 illustrates the pathophysiology of a PH crisis. Echocardiography during an acute crisis will show a dilated poorly functioning RV with the ventricular septum bowing right to left, increased tricuspid

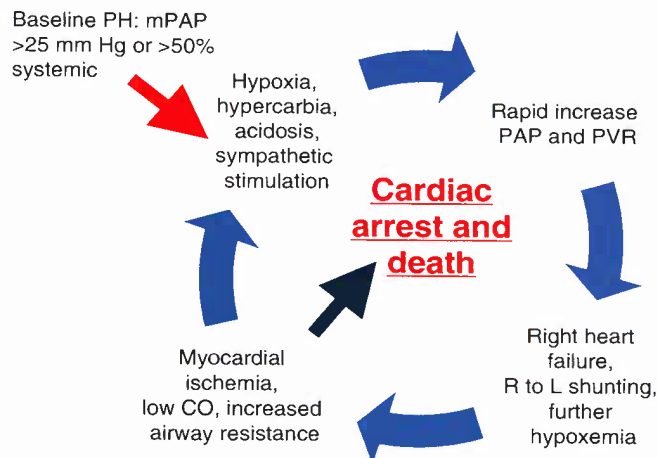


Figure 20.5. Pathophysiology of a pulmonary hypertension crisis. PH, pulmonary hypertension; mPAP, mean pulmonary artery pressure; PAP, pulmonary artery pressure; PVR, pulmonary vascular resistance; CO, cardiac output.

regurgitation velocity, and decreased LV function. In the modern era, direct transthoracic measurement of PAPs or measurement with a Swan Ganz catheter is relatively infrequent, but if these modalities are available elevation to near or systemic suprasystemic pressures will be seen. If SVC pressure line is present in a bidirectional Glenn (BDG) circulation, elevation of this pressure to 20 to 25 mm Hg or higher will be seen.

Treatment

Urgency of treatment depends on the clinical situation but cornerstones of treatment of PH include ensuring an adequate airway to provide oxygenation and ventilation to treat hypoxemia and hypercarbia (162–164). Adequate sedation and analgesia are necessary to reduce endogenous catecholamine secretion. In certain high-risk preoperative patients, prophylactic iNO started during CPB weaning is effective at reducing severity and number of PH crises (165). Assessment of any treatable anatomic causes, that is, pulmonary vein obstruction, PA stenosis, is important. Assessing RV function and providing support for the RV in the form of milrinone to attempt both to lower PAP and improve RV systolic and diastolic function are important (124). iNO is frequently used in the acute setting (166). Sildenafil, administered orally or IV, is often effective at lowering PA resistance enough to improve the patient's condition (167).

Treatment of a PH crisis requires simultaneous institution of multiple modalities to prevent severe cardiovascular compromise. Controlling the airway, hyperventilating with 100% oxygen to achieve alkalosis are crucial, as are sedation and muscle relaxation to facilitate ventilation. Opioids, especially fentanyl, have been proven effective at preventing and treating severe PH. A dose of 5 to 25 $\mu\text{g}/\text{kg}$ is given along with adequate muscle relaxants (168). Volume boluses to increase pulmonary blood flow and LV filling are important. Epinephrine bolus, 1 to 5 $\mu\text{g}/\text{kg}$, is often effective at acutely increasing RV and LV function and increasing systemic blood pressure until other therapies are effective. iNO should be instituted emergently at 20 to 40 ppm; IV sildenafil can be instituted, inhaled nebulized prostacyclin is another alternative (169). In some severe cases of significant cardiopulmonary compromise, or cardiac arrest, ECMO can be used to rescue the patient.

After a PH crisis, weaning from the modalities instituted to lower PAP must be done gradually, and in a staged fashion, with careful assessment of PH at each step. While weaning iNO, administration of IV or oral sildenafil is effective in

preventing rebound PH (170). Although iNO is used very frequently in the CICU, it is a very expensive therapy with side effects such as NO_2 buildup, which is toxic to the lungs, methemoglobinemia, and rebound PH. If iNO is started, its use must be re-evaluated frequently with primary reason to continue being that the patient has responded to the therapy with improved oxygenation, improved CO, or in the case of direct PAP measurement, sustained lowering of PAP.

THE PULMONARY SYSTEM, VENTILATION, AND AIRWAY MANAGEMENT

Endotracheal intubation and mechanical ventilation are most often utilized in the CICU following cardiac surgery to ensure a patent airway and produce adequate oxygenation and ventilation while the patient recovers from the multisystem stresses of CPB. Although an inflammatory capillary leak syndrome is often seen after CPB, severe lung injury similar to adult respiratory distress syndrome (ARDS) is unusual, and most patients can be weaned from the ventilator in a relatively short time as bleeding subsides, cardiac function recovers, and generalized edema improves. Other indications for mechanical ventilation in the CICU are similar to the general PICU population, including cardiac failure with interstitial and alveolar pulmonary edema causing respiratory failure, primary pulmonary disorders such as pneumonia, upper airway obstruction, or central nervous system depression from sedatives or pathologic conditions necessitating control of the airway. Optimizing mechanical ventilation strategies will lead to faster improvement in pulmonary dysfunction, less time on the ventilator, and better overall outcomes (171).

Cardiorespiratory Interactions

Interactions between ventilation techniques and cardiac filling and output are most important in patients with a single functional ventricle (see Chapter 22). Infants with a single ventricle providing both systemic and pulmonary blood flow have complete intracardiac mixing, and manipulation of PVR using ventilator strategies may profoundly affect pulmonary-to-systemic blood flow ratio ($Q_p:Q_s$). This is particularly true with patent ductus arteriosus (PDA)-dependent systemic blood flow such as in HLHS. Hyperoxygenation and hyperventilation may lead to low CO and even cardiovascular collapse by excessively lowering PVR and greatly increasing $Q_p:Q_s$, leading to both ventricular volume overload and steal of blood flow from the systemic circulation (see Chapter 48). After a Stage I palliation, or other surgery replacing the PDA with a modified systemic-to-pulmonary artery shunt, variations in $Q_p:Q_s$ with ventilation are restrained by the fixed small shunt size; but basic physiologic considerations are the same. After the bidirectional cavopulmonary anastomosis, single-ventricle patients are still subject to adverse effects of hyperventilation; in this instance, low PaCO_2 will constrict cerebral arterioles and cerebral blood flow, leading to less pulmonary blood flow and thus less oxygenation (172,173). Finally, in single-ventricle patients after Fontan completion, the total cavopulmonary connection serves as the pulmonary circuit without benefit of a right ventricle contracting and adding kinetic energy to improve pulmonary blood flow. Blood flow depends largely on passive flow from systemic veins and the vena cavae into the thorax, greatly aided by the slightly negative intrathoracic pressure of spontaneous ventilation to provide a pressure drop to promote blood flow. Positive pressure mechanical ventilation presents a significant disadvantage in the Fontan circulation. Thus, minimizing positive pressure, allowing spontaneous breaths as early as possible, and extubating the trachea are important to minimize this disadvantage to pulmonary blood flow (174).

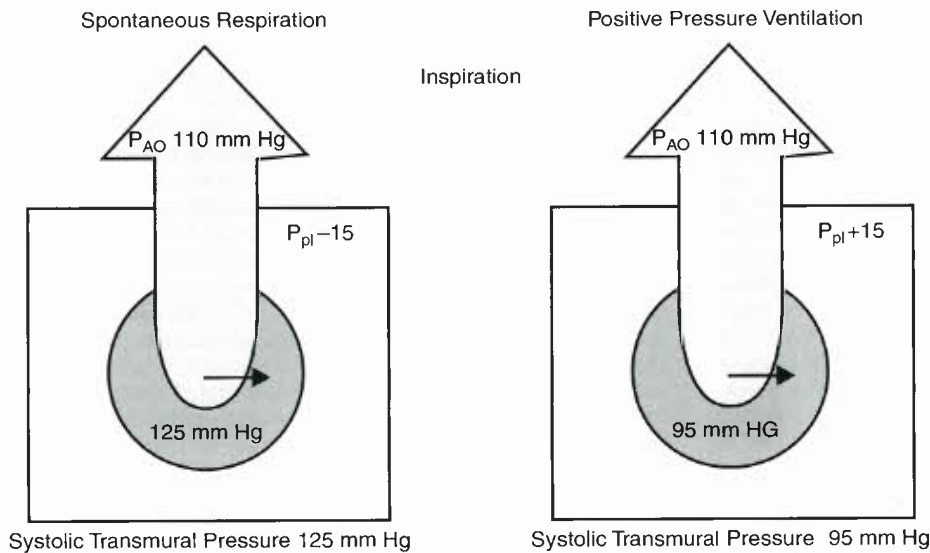


Figure 20.6. The effect of positive pressure ventilation on systemic ventricular transmural pressure. The decreased ventricular wall tension with positive intrapleural pressure will decrease the work of the systemic ventricle. (Reproduced from Stayer SA, Hammer GB. Chapter 18: Ventilatory management. In: Andropoulos DB, Stayer SA, Russell IA, Mossad EB, eds. *Anesthesia for Congenital Heart Disease*. 2nd ed. Oxford, UK: Wiley-Blackwell, 2010:338–354, with permission.)

One pathophysiology where positive pressure ventilation is often advantageous is in left ventricular failure. In this state, the negative pressure surrounding the aorta that accompanies spontaneous respiration increases the pressure gradient thus increasing the ventricular wall tension. Adding positive intrathoracic pressure can reduce this gradient and promote forward flow (Fig. 20.6) (175).

In recent years, emphasis has been placed on gentler mechanical ventilation to reduce the incidence of barotrauma and volutrauma (see below). Excessive tidal volumes and peak pressures may not only injure the lung, but can also elevate PVR as overdistended alveoli compress and occlude small pulmonary arterioles. Excessive ventilation also increases the inflammatory response in patients with PH, presumably from lung injury (176). Conversely, inadequate end-expiratory pressure may lead to collapse of lung units, and similar compression of pulmonary arterioles and elevation of PVR (175) (Fig. 20.7).

Positive pressure mechanical ventilation is frequently needed in the CICU, but the level of mean, peak, and end-expiratory pressure necessary to provide adequate oxygenation and ventilation must always be balanced against the potential negative effects of reducing venous return. Besides the single-ventricle patient, the most common of the dilemmas include the hypovolemic patient and the patient with pericardial effusion or tamponade, where even modest increases in intrathoracic pressure will impede venous return enough to significantly decrease cardiac filling. In general, patients receiving significant amounts of positive pressure ventilation will require higher cardiac filling pressures and intravascular volume status to maintain CO goals. Patients receiving high ventilator pressures that affect CO by conventional ventilation should be considered for alternate strategies such as high-frequency oscillatory ventilation (HFOV) or even ECMO.

Conventional Ventilation Strategies

Large tidal volume ventilation of 10 to 15 mL/kg, and low levels of positive end-expiratory pressure (PEEP 2 to 4 cm H₂O) were often used in the past with the thought that this strategy would lead to better recruitment of inhomogeneous alveolar units throughout the lungs. This strategy is now generally accepted to be a cause of significant lung injury, with both volutrauma and barotrauma occurring from shear stresses in compliant lung units and from high peak airway pressures. Contemporary strategies using tidal volumes of 6 to 8 mL/kg, higher PEEP of 5 to 7 cm H₂O, and limitation of peak pressures to no more than 30 cm H₂O are felt to provide lung recruitment while avoiding lung injury. Pressure limited, or pressure limited-volume controlled modes are often preferred for newly ventilated patients after surgery or intubation for medical illnesses. Inspiratory:expiratory ratios of 1:2 to 1:3 are preferred to allow adequate time for expansion of alveolar units with differing time constants for filling. Excessive inspired oxygen levels are toxic to the lungs causing oxidative damage through generation of oxygen free radicals and toxic oxygen species. FiO₂ should be 1.0 for intubation in most patients, but should be reduced as soon as tolerated to levels below 0.60, a level not generally associated with oxygen toxicity. These strategies have reduced mortality and morbidity, including less days on the ventilator in pediatric patients with acute lung injury (177,178). Obviously, many patients with CHD have right-to-left intracardiac shunting. Thus, they have a ceiling level of PaO₂ or SpO₂ achievable with FiO₂ 1.0, but these patients

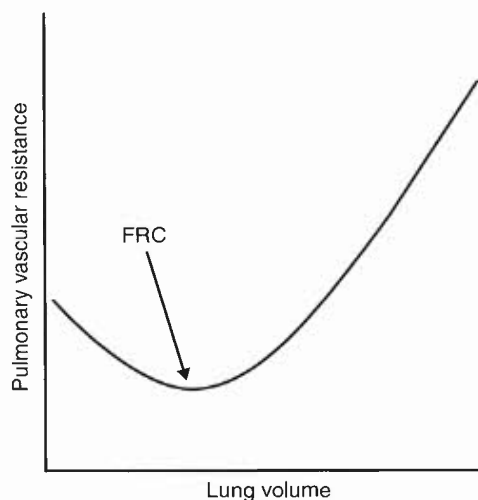


Figure 20.7. Relationship of lung volume to pulmonary vascular resistance. Both low and high lung volumes compress pulmonary arterioles, leading to increased PVR. FRC, functional residual capacity. (Reproduced Stayer SA, Hammer GB. Chapter 18: Ventilatory management. In: Andropoulos DB, Stayer SA, Russell IA, Mossad EB, eds. *Anesthesia for Congenital Heart Disease*. 2nd ed. Oxford, UK: Wiley-Blackwell, 2010:338–354, with permission.)

are still subject to pulmonary injury and fibrosis from excessive oxygen. Patients should be allowed to initiate spontaneous breaths, and to do as much of the work of breathing as they can, assisted by pressure- or volume-supported breaths: 5 to 10 cm H₂O added pressure or 3 to 5 mL/kg added volume. This is necessary to exercise the diaphragm and intercostal muscles, and will also allow lower mean airway pressures and promote venous return to improve CO. Heavy sedation or muscle relaxation that prevents spontaneous breaths can lead to atrophy of these muscles and prolong time on the ventilator. Because the endotracheal tube (ETT) bypasses the natural defenses of the upper airway, and coughing and ciliary function are impaired, ventilator-associated pneumonia (VAP) is a constant threat in the intubated patient. The simple strategy of elevating the head of the bed of a ventilated patient 30 degrees, along with implementation of a relatively simple “bundle” of other strategies will prevent the majority of VAP (179). A defined program of pulmonary toilet, including suctioning, inhaled bronchodilators, chest physiotherapy, and bronchoscopy to open persistent areas of atelectasis, is important to maintain gas exchange and allow progress toward extubation. Daily chest radiographs are indicated in most intubated patients to assess position of endotracheal tube, status of lung parenchyma including atelectasis, pulmonary edema, pleural effusion, pneumothorax, cardiomegaly, and pericardial effusion. These problems should be aggressively treated in order to shorten the period of mechanical ventilation. Multiple studies document that longer duration of mechanical ventilation is associated with worse long-term morbidity, and mortality (180,181).

Monitoring of ventilation includes continuous pulse oximetry and also should include continuous monitoring of ET_{CO}₂. The latter is becoming more frequent in PCI-CUs; the advantages include a continuous assessment of gas exchange with sudden changes and early warning sign of airway obstruction in the case of hypercarbia or low CO and pulmonary blood flow (182). Ventilator disconnection is immediately recognized. Monitoring of ventilatory volumes, pressures, and resistances using sensors inside modern ventilators has limited utility in small pediatric patients. This is because the ventilator tubing itself has a dead space where no gas exchange occurs, and a portion of the tidal volume is absorbed in the mechanical expansion of the tubing with positive pressure ventilation, which is a significant proportion in small infants. Ventilator systems designed for adults cannot adequately compensate or measure pulmonary mechanics in small infants. A much more accurate measurement of pulmonary mechanics is acquired with infant pulmonary function monitors attached directly to the end of the endotracheal tube (183). These devices are integrated into many modern neonatal ventilators, or can be used as stand-alone monitors for intermittent assessment.

Weaning from Mechanical Ventilation

Weaning from mechanical ventilation may be as simple as a brief trial of spontaneous ventilation with continuous positive airway pressure (CPAP) in a postoperative patient with no parenchymal lung disease immediately after surgery, to a prolonged period of gradual weaning ventilator settings, and the patient taking over more and more of the work of breathing, over many days or sometimes weeks (184). To be ready to wean from the ventilator, the patient should have a mental status evaluation done, which assures that after reducing sedation patent airway and protective airway reflexes are maintained. Ventilator settings should be low enough to begin weaning, usually FiO₂ of 0.40 or less acceptable lung compliance and resistance with peak pressures below 25 to 20 cm H₂O and PEEP

5 mm Hg or less. A very effective strategy is to allow the patient periods of spontaneous respiration with volume-supported breaths, of 3 to 6 mL/kg, starting with short periods of 30 to 60 minutes at a time, and gradually lengthening these periods, judged by the patient's work of breathing, and blood gas values at the end of these volume support trials. When the patient is able to sustain adequate arterial blood gases (ABGs) with acceptably low work of breathing, extubation is considered. Quantitative measures for readiness for extubation in infants and children, that is, negative inspiratory force, forced vital capacity, minute ventilation, have limited utility. Clinical examination, chest radiograph, and blood gases are better used to determine readiness. A useful measure is the rapid shallow breathing index (RSBI), which equals respiratory rate/tidal volume (185). Lower RSBI is correlated with readiness for extubation; that is, better lung function indicated by lower respiratory rates and larger tidal volumes. Particularly in small infants, whose small airways are easily traumatized and where even a limited amount of mucosal edema may narrow the subglottic airway considerably, dexamethasone 0.25 mg/kg IV Q 6h for 12 to 24 hours, is effective in preventing upper airway obstruction and nebulized racemic epinephrine treatments are useful for signs of significant upper airway edema (186). Patients who are considered for tracheostomy have prolonged mechanical ventilation from cardiac, pulmonary, and/or airway causes; progress toward extubation is not being made; and need for excessive doses of sedation is interfering with other aspects of general care (187). There are no set guidelines for tracheostomy in pediatric cardiac patients. This is a complex undertaking that complicates future cardiac surgeries because of the proximity of the airway to the sternotomy incision increasing the risk of infection. Patients with CHD, particularly single-ventricle infants on chronic ventilation via tracheostomy, have a high mortality rate (188). Multidisciplinary decision making is necessary, and tracheostomy should be considered a last resort in cardiac patients.

Endotracheal Intubation and Airway Management

The decision to intubate the trachea and institute mechanical ventilation is made when respiratory distress, diagnosed by observing for significant tachypnea, retractions, cyanosis with SpO₂ often 10% or more lower than baseline and significant hypercarbia, is causing low CO, or heralding risk for respiratory arrest. Chest radiographs often show significant pulmonary edema, lobar, or whole-lung infiltration or collapse, or significant cardiomegaly causing airway compression. Short of intubation, noninvasive ventilation methods as outlined below are sometimes useful while other medical therapy is given time to be effective. Arterial blood gases are the gold standard for assessing gas exchange, and often an arterial catheter is present in the CICU patient who is being considered for intubation. If not, capillary blood gas, chest radiography, pulse oximetry, and clinical assessment can give the necessary information. Early intervention before severe cardiopulmonary compromise is the goal. However, intubating the trachea and instituting positive pressure ventilation has potential for severe hemodynamic compromise in the patient with marginal cardiopulmonary status. Emergency tracheal intubation in cardiac patients, as opposed to proactive intubation before the patient is *in extremis*, is associated with higher complication rates, including mortality and need for mechanical support. (189).

Basic equipment and preparations for intubation include laryngoscopes and endotracheal tubes in appropriate sizes, oral airways, working suction immediately at hand, and high-flow oxygen source and manual ventilation bag that is easily operated, either of self-inflating type, or an anesthesia-type

configuration such as a modified Jackson-Rees bag. Methods to detect exhaled CO₂, either colorimetric or continuous monitors, are mandatory to ensure that the tube is in the trachea (190).

In general, FiO₂ of 1.0 is always recommended for pre-oxygenation and initial management immediately after ETT placement. Evaluation of the airway for possible difficult mask ventilation and intubation is mandatory before administering drugs that will render the patient apneic; the most common reason for difficulty in cardiac patients is micrognathia as seen in some patients with craniofacial syndromes that accompany their cardiac disease such as velocardiofacial syndrome or the Pierre-Robin sequence. If difficulty is anticipated, requesting assistance from an anesthesiologist or otolaryngologist is very important to avoid a disastrous “cannot ventilate, cannot intubate” situation. Also, a full stomach mandates suction of gastric contents before intubation where possible and cricoid pressure during mask ventilation before intubation. The infant’s head position is neutral. A small towel is placed under the occiput in an older child to achieve the “sniffing position” during laryngoscopy to align the axes of the pharynx, larynx, and trachea. The patient is preoxygenated with a tight-fitting face mask for 3 to 5 minutes if possible, induction drugs are given, and positive pressure ventilation is instituted early and gently. Jaw thrust or oral airway are used if there is inadequate chest rise with bag and mask ventilation. Cricoid pressure is applied by an assistant in the case of a child who has a full stomach. With loss of consciousness and adequate muscle relaxation, the laryngoscope is inserted into the right side of the mouth, the tongue swept to the left out of the midline, and the blade advanced until the epiglottis is visualized. The blade is advanced further into the vallecula with a curved blade, or under the epiglottis with a straight blade, the handle lifted with a gentle upward motion at a 45 degree angle to the surface of the bed, and position adjusted until the arytenoid cartilages and vocal cords are in view. The “BURP” maneuver (Backward, Upward, Rightward Pressure) on the cricoid cartilage by an assistant often is very effective to improve visualization. The ETT with a stylet bent at a 45 degree angle (“hockey stick” configuration) is inserted by direct visualization, taking care to insert the tube to the correct depth using markings on the tube and guidelines for the tube size. In modern practice, a cuffed ETT is recommended for virtually all CICU patients with the

exception of some small neonates where an uncuffed 3.0- or 3.5-mm ETT is used. A common guide to ETT size selection is:

$$16 + \text{Patient age (years)} / 4$$

For example, 5.0-mm ETT $((16 + 4) / 4 = 5)$ will be used in a 4-year-old patient. Since this formula was developed for uncuffed ETT, many practitioners will use the cuffed ETT 0.5 mm smaller, that is, a 4.5-mm cuffed ETT for a 4-year old.

Ventilation ensues gently; excessive positive pressure in combination with the cardiovascular depression often seen with induction drugs can result in cardiovascular collapse. Breath sounds are auscultated, the stomach is also auscultated to help rule out esophageal intubation. Detection of CO₂ that is persistent for 6 or more breaths is a critical confirmatory step. If there is no ETCO₂, causes include esophageal intubation, poor pulmonary blood flow, cardiac arrest, or severe bronchospasm preventing gas exchange. If this occurs, the first reaction is often to remove the ETT and reinsert; however, strong consideration should be given to having the most experienced airway manager perform a direct laryngoscopy, and often the ETT will indeed be correctly positioned. This avoids the unnecessary situation of the inappropriate removal if the ETT in an arrested patient. Blood pressure, heart rate, and SpO₂ must be followed carefully immediately after tracheal intubation. Patients will sometimes require intravascular volume bolus or pressors, such as a small dose of epinephrine, to restore desirable hemodynamics. In the case of a very tenuous patient, a full cardiac arrest should always be anticipated.

Depth of insertion of the ETT is crucial, especially in small infants where total length of the trachea may be only 4 to 5 cm. Using the depth markings on the tube, the ETT is advanced until the desired mark is at the level of the vocal cords. The chest is auscultated for equal breath sounds. A chest radiograph is obtained as soon as possible after securing the tube. Other methods of estimating proper orotracheal depth of insertion include deliberately placing the tube in the right mainstem bronchus, and then auscultating the left chest during rapid hand ventilation while the tube is being withdrawn. When breath sounds appear, the ETT is at the carina; the tube is then withdrawn another 1 to 1.5 cm for final positioning.

TABLE 20.8 Endotracheal Tube and Laryngoscope Blade Sizes

Age	Weight (kg)	ETT Size (mm)	Laryngoscope Blade
Premature neonate	<2.5	3.0 uncuffed	Miller 0
Full-term neonate	2.5–4	3.5 uncuffed or cuffed	Miller 1
1–6 mo	4–6	3.5 cuffed	Miller 1
6–12 mo	6–8	3.5–4.0 cuffed	Miller 1, Wis-Hipple 1.5
1–2 y	8–10	4.0–4.5 cuffed	Wis-Hipple 1.5
2–3 y	10–12	4.5 cuffed	Wis-Hipple 1.5, MacIntosh 2
4–5 y	12–18	4.5–5.0 cuffed	MacIntosh 2, Miller 2
5–7 y	18–24	5.0–5.5 cuffed	MacIntosh 2, Miller 2
8–10 y	24–35	5.5–6.0 cuffed	MacIntosh 3, Miller 2
11–13 y	35–40	6.0–6.5 cuffed	MacIntosh 3, Miller 2
14–16 y	40–50	6.5 cuffed	MacIntosh 3, Miller 2
16 y and above	50 and over	7.0–7.5 cuffed	MacIntosh 3, Miller 2

TABLE 20.9

Medications for Sedation and Muscle Relaxation for Endotracheal Intubation

Medication	Dose	Comments
Fentanyl	1–5 µg/kg	Titrate to effect; chest wall rigidity
Midazolam	0.025–0.1 mg/kg	
Ketamine	1–2 mg/kg	
Etomidate	0.2–0.4 mg/kg	Best for hemodynamic stability; temporary adrenal suppression
Propofol	1–2.5 mg/kg	Veno- and vasodilator
Vecuronium	0.1–0.2 mg/kg	No hemodynamic effects; muscle relaxation in 2–3 min
Rocuronium	0.6–1.2 mg/kg	Minimal hemodynamic effect; muscle relaxation 1.5–2 min

Also, with an orotracheal tube, an estimate of proper distance is the ETT size multiplied by 3, that is, depth of 12 cm for a 4.0-mm ETT. Tables 20.8 and 20.9 describe ETT, laryngoscope blades, and drugs recommended for endotracheal intubation.

Alternate Ventilation Strategies—Noninvasive Ventilation

With the recognition that mechanical ventilation is a source of barotrauma, volutrauma and infection, recent years have witnessed resurgence in popularity of noninvasive ventilation techniques, either to prevent intubation, or as an immediate postextubation therapy to prevent reintubation. In neonates and small infants, nasal CPAP is often very effective and surprisingly well tolerated, and routine use of this modality after extubation in small infants is used in many PCICUs. CPAP of 5 to 10 cm H₂O for periods of 24 to 72 hours is often utilized (191). High-flow nasal cannula oxygen with humidified gas routed through a heated humidified circuit at flows of 5 to 10 L/min is also an effective therapy for patients of all ages. In older patients unable to tolerate nasal CPAP or where it is not effective, CPAP with a tight-fitting nasal mask or BiLevel Positive airway pressure, where assisted ventilation parameters can be provided, is often very helpful at avoiding intubation (192).

Early Tracheal Extubation

Besides the desirable hemodynamic advantages of negative pressure ventilation in the Fontan circulation, many centers have organized “fast-tracking” programs for early tracheal extubation after simple or even moderately complex cardiac surgery. Cited advantages include less need for sedation; more comfort for the patient, faster progress through the ICU, and avoidance of barotrauma and lower risk of nosocomial pneumonia. Extubation can be accomplished in the OR, or early in the ICU course in the first 1 to 4 hours. Institutional practices vary widely, from no early extubation in any patients, to aggressively extubating all possible patients, even including small infants who underwent moderately complex surgery

(193). Criteria for early extubation include hemodynamic stability on minimal or no inotropes, normal sinus rhythm, minimal bleeding, minimal pulmonary disease, low doses of fixed anesthetic agents, reversal of muscle relaxants allowing appropriate neuromuscular status, and ability of the ICU nursing staff, anesthesiologists, or intensivists to monitor and support the patient airway after extubation, including timely reintubation. A careful and cautious approach is recommended to avoid the situation of having to reintubate a patient who is unstable for 6 to 12 hours after surgery from bleeding, inflammation, and hemodynamic compromise. Multidisciplinary collaboration is important in any early extubation program (194).

High-Frequency Oscillatory Ventilation

When conventional ventilation fails to produce adequate gas exchange despite high ventilator pressures and FiO₂, the ventilator therapy is interfering with CO and/or there is risk for barotrauma, HFOV should be considered. HFOV can be used as a rescue therapy for hypoxemia refractory to conventional mechanical ventilation. It is also used as a means of reducing shear forces the lung is exposed to with conventional ventilation. HFOV uses a rapidly oscillating piston mechanism to actively push gas into the lungs, and remove it by negative pressure with tidal volumes much smaller than conventional ventilation. Oscillation frequency is set at 6 to 14 Hz. The mean airway pressure is generally higher than with conventional ventilation, allowing recruitment of lung units with different time constants. However, the pressure variation, including the peak pressure, is significantly lower, and this often leads to better gas exchange with lower risk of barotrauma. HFOV is often utilized in pediatric patients with ARDS and very noncompliant lungs, and may improve gas exchange. However, conclusive proof is lacking that this strategy improves outcomes, including days ventilated and survival (195,196).

GENERAL POSTOPERATIVE CARE

The majority of admissions to most CICUs are postoperative patients, and a coordinated, multidisciplinary approach to their care is important to facilitate the best outcomes (197,198). Ideally, the care of these patients begins preoperatively, where many CICUs will admit neonatal patients with prenatal diagnoses directly from the delivery room or after transfer when a diagnosis of CHD requiring surgery is made. A multidisciplinary surgery conference greatly facilitates communication among the many disciplines caring for the patient. This should be at least a weekly conference where upcoming patients have their pertinent history, physical examination, radiographic, echocardiographic, catheterization, MRI, and/or CT scan findings presented. This is usually done by a primary cardiologist or fellow. The conference is attended by cardiologists, congenital heart surgeons, intensivists, neonatologists, anesthesiologists, perfusionists, nursing staff from OR and ICU, and trainees from all the services. It serves as both a working conference to plan surgery and as a teaching conference. Findings are discussed, and a surgical plan is decided. The CICU staff has active input into the preoperative decision-making process, is made aware of the planned schedule each week, and can prepare for each patient. The key to successful preoperative planning conferences is concise, organized presentations of each patient with a focused discussion resulting in concrete plans. The postoperative care plan begins with the preoperative conference.

Handoff

The handoff of care from the OR team to the CICU team is an important time where crucial information about the surgery is

CARDIOVASCULAR ANESTHESIA POSTOPERATIVE - ICU Procedure Note

Date: _____ **Time:** _____ **Diagnosis:** HLHS (mitral/aortic atresia)
Procedure: Norwood Stage I palliation; 3.5 mm right modified BT shunt
General Anesthesia: Fentanyl 95 mcg/kg, midazolam 0.75 mg/kg, isoflurane
Muscle Relaxant: vecuronium **Reversed:** No
Regional Anesthesia: NA
Total CPB Time: 161 minutes **Aortic Cross Clamp Time:** 90 minutes
DHCA Time: 10 minutes **Lowest Temp:** 17.6° C
ACP Time: 52 minutes
Phentolamine: 0.3 mg/kg on CPB **Antibiotic:** Cefazolin: Time of last dose: 1310
Post Op Rhythm: NSR Paced: NA—atrial pacing wires x2 Other: NA
Vasoactive Infusions: Epinephrine 0.03 mcg/kg/min, milrinone 0.375 mcg/kg/min (no loading dose); CaCl₂ 10 mg/kg/hr.
Heparin: Yes **Protamine:** Yes **ACT to Baseline:** Yes—123 seconds
Post-CPB Blood Products: PRBC 15 ml, platelets 45 ml; cryoprecipitate 1 unit
Other Fluids: 5% albumin 25 ml; D5W carrier 45 ml
Urine Output: 27 ml **EBL:** NM **Final Hct:** 44% **Final ABG:** 7.37/43/4
1/BE 0
Other Drugs: ε-aminocaproic acid; methylprednisolone
ETT: 3.5 nasal cuffed, taped 11.5 cm; **Drains:** Mediastinal x 2; peritoneal dialysis
leak 25 cm H₂O catheter, foley catheter
Vascular Access: 22 g L radial arterial line; 3.5 Fr UAC; L femoral venous 4 fr double lumen
CVP; 22g PIV R saphenous vein.
Postop TEE: Mildly depressed systolic RV function; minimal tricuspid regurgitation, no
neo-aortic insufficiency; open unrestrictive atrial septum; good flow seen
both pulmonary arteries.
Comments: Generally stable intraoperative course. Weaned from CPB easily, moderate bleeding
responded to platelet and cryoprecipitate infusion. Sternum closed without major
hemodynamic/respiratory change. Transported to CICU, full report given to MD and RN teams, care
transferred.

Figure 20.8. Template for handoff of care from OR to cardiovascular intensive care unit.

communicated in a clear and concise manner (199). Failure to communicate handoff information accurately in a manner that is fully understood by the receiving team is a frequent cause of medical errors that can adversely affect patient outcome (200,201). After transfer of the patient to the CICU transfer of monitors and establishment of ventilation, the handoff report begins. All involved need to be present: CICU attending, fellow, resident, nurse, respiratory therapist, and surgeons should be present. Usually, the anesthesiologist will give a standardized report that summarizes the OR course, including pre-bypass period, surgery done, CPB data including length of CPB, aortic crossclamping, deep hypothermic circulatory arrest (DHCA), and lowest intraoperative temperature. Inotropic support and other vasoactive therapy are detailed, along with results of the postoperative transesophageal echocardiography, including the presence of any residual defects (202). Anesthetic and other drug doses (antifibrinolytics, corticosteroids) are summarized, along with blood gas results, cardiac rhythm and pacing issues, bleeding problems, and blood product administration. Any problems are noted, along with general goals for early postoperative care, that is, early extubation. The timing of the last doses of sedatives and analgesics and antibiotics is reported. Whether the patient's neuromuscular blockade was reversed in the OR should be noted. A member of the surgical team should also be present who details the surgical procedure, and notes any residual lesions, that is, an atrial septal defect (ASD) left intentionally to serve as a pop off after right ventricular reconstructive surgery. The receiving team then has the opportunity to ask questions and formally assumes care of the patient. A

controlled, quiet environment, where all are paying attention to the information being transferred, is very important. A template for the CICU postoperative handoff is displayed in Figure 20.8. This becomes the medical record for the anesthesiologist's handoff report and can easily be adapted for EMR systems.

Effects of Cardiopulmonary Bypass

CPB has made modern congenital heart surgery possible, and the limits of patient size and complexity of surgery are continually expanded to make ever more difficult surgeries feasible. However, a myriad of CPB techniques are utilized, all of them institution or even surgeon specific, the CICU team must be aware of and be prepared to treat any number of sequelae of CPB (203–207). The basic CPB circuit arrangement is depicted in Figure 20.9 (208). The aorta is cannulated for arterial perfusion, and, in most CHD operations, bicaval cannulation of the SVC and IVC is used (Fig. 20.10). Alternately, the right atrium alone can be used for single cannula venous drainage. CPB is instituted after full heparinization, with activated clotting time (ACT) goals of normally 480 seconds to produce profound anticoagulation. CPB suction is used to return shed blood from the pericardial well to the venous reservoir of the CPB machine. Flow is provided by roller pumps, blood is oxygenated, CO₂ is removed, and extracorporeal heating and cooling are provided by a water bath and countercurrent mechanism within an integrated oxygenator/heat exchanger. Monitoring consists of arterial and venous pressures, in-line arterial and

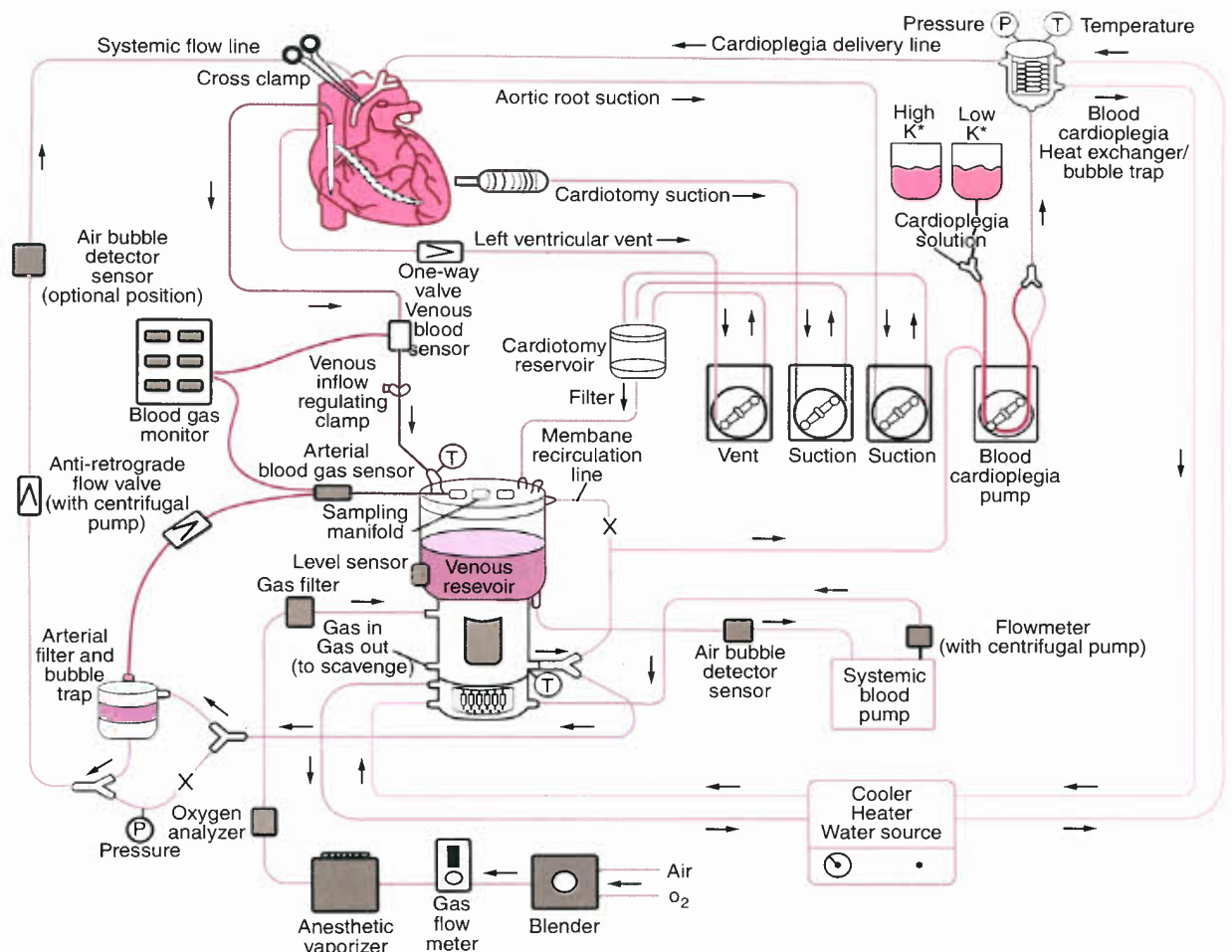


Figure 20.9. CPB basic configuration. (Modified from Hessel EA, Hill AB. Circuitry and cannulation techniques. In: Gravlee GP, Davis RF, Kursz M, Utley JR, eds. *Cardiopulmonary Bypass: Principles and Practice*. Philadelphia, PA: Lippincott, Williams & Wilkins;69–97.)

venous blood gas and saturation sensors and bubble detectors. Modern oxygenators are hollow-fiber membrane designs that allow rapid transfer of oxygen and CO₂ across a very large surface area blood–gas interface with minimal pressure drop across the oxygenator.

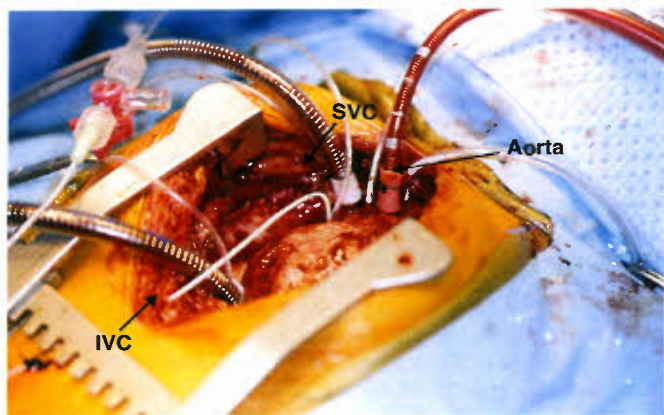


Figure 20.10. Bicaaval cannulation for CPB in a neonate. This allows the surgeon access to intracardiac structures while allowing perfusion to continue, limiting the period of DHCA needed for complex intracardiac repairs.

Choice of CPB flows varies by institution but, in general, for infants is 150 mL/kg/min for full flows, and in older children body in whom surface area is used, full flow is 2.8 L/min/m² for older children, decreasing to 2.4 L/min/m² for larger children and teenagers. Cooling is routinely used for most operations to decrease myocardial, brain, and other organ oxygen consumptions, and preserving function during periods of low CPB flow. The degree of hypothermia is termed mild (30°C to 34°C), moderate (22°C to 30°C), or deep (17°C to 22°C). CPB flow is often decreased during hypothermia in many centers because this decreases blood return into the surgical field from bronchial, thebesian, and intracardiac sources, allowing the surgeon better visibility to perform the surgery. Some surgeons do not reduce CPB flow, reasoning that better blood flow to all organs and tissue beds improve recovery from CPB (209). Some surgery is accomplished with the heart beating; these are extracardiac operations such as bidirectional cavopulmonary anastomoses or simple pulmonary valve replacements. Intracardiac surgery necessitates a period of aortic crossclamping and delivery of high potassium cardioplegia to render the heart asystolic, allowing a near bloodless field. If a period of low flow or DHCA is planned, deep hypothermia is used. DHCA is a period where the CPB flow is stopped completely, the heart and patient are drained completely of blood, and a bloodless field is created to facilitate intracardiac surgery especially in small infants. Because prolonged periods of DHCA are associated with cerebral injury (see below), a recent variation is to use antegrade cerebral perfusion (ACP, also called selective cerebral

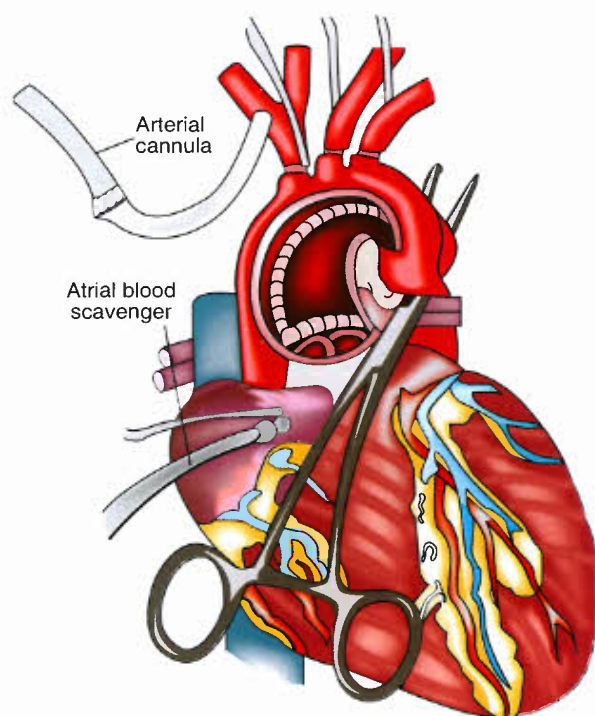


Figure 20.11. Antegrade cerebral perfusion. A graft is sewn to the right innominate artery, the brachiocephalic vessels and descending aorta are snared, and the brain is perfused during aortic arch reconstruction, in lieu of DHCA. (Modified from Pigula FA, Nemoto EM, Griffith BP, et al. Regional low-flow perfusion provides cerebral circulatory support during neonatal aortic arch reconstruction. *J Thorac Cardiovasc Surg* 2000;119:331–339.)

perfusion or RCP), where only the brain is perfused during deep hypothermia such as with aortic arch reconstruction during the Norwood Stage I palliation (210) (Fig. 20.11). Blood gas temperature management during CPB can be either α stat, not correcting for temperature, which causes significant alkalosis at deep hypothermia; or pH stat, in which blood gas values are corrected for temperature, resulting in “normal” pH and PCO_2 at deep hypothermia. Most centers now use hemofiltration, either during CPB or modified ultrafiltration immediately after CPB to remove excess intravascular and interstitial fluid and filter small molecules, including many mediators of inflammation.

CPB induces a number of sequelae that can affect postoperative care. Contact of the patient’s blood with components of the CPB circuit initiates a significant inflammatory response and activation of intrinsic and extrinsic coagulation pathways. Despite this well-known phenomenon, recent studies have not documented that the rate of adverse clinical outcomes is proportional to the magnitude of the inflammatory response (211). Many programs use corticosteroid treatment, usually with methylprednisolone, 10 to 30 mg/kg, given either 4 to 12 hours preoperatively or in the CPB prime to attempt to mitigate this inflammatory response. Despite widespread use and a demonstrated reduction in some of the inflammatory mediators (IL-6, -8, -10), published studies have not demonstrated a difference in outcomes with such treatment (212).

Red blood cells undergo hemolysis from trauma induced by pump suction, oxygenator, and passing through filters in the circuit. Periods of low-flow CPB or DHCA may result in ischemia to end organs such as kidneys, liver, intestines, and brain. The inflammatory response may induce capillary leak, resulting in edema in most tissues and organ systems, including pulmonary interstitial and alveolar edema. Long periods of

aortic crossclamping result in myocardial ischemia reperfusion injury, and myocardial dysfunction manifests in the immediate post-CPB period. Extensive intracardiac surgery, which includes resection of myocardium or long periods of retraction of intracardiac structures, can result in mechanical trauma including tricuspid regurgitation or arrhythmias such as JET or complete AV block. The profound anticoagulation needed for CPB, dilution of clotting factors, hemoglobin, and platelets as well as platelet dysfunction induced by activation from components of the CPB circuit increase the risk of bleeding, particularly in small infants. Extensive high-pressure suture lines, especially with aortic surgery, further increase this risk. Generally speaking, the risk of all of these sequelae increases with longer CPB times, aortic crossclamp times, and DHCA times. It is important to be aware of these issues from the report of the OR team, and to be vigilant for sequelae from long CPB times and complicated surgery. There is a well-documented decrease in CO in infant patients 6 to 12 hours after CPB, thought to be induced by the inflammatory response, which peaks at that time and interferes with intrinsic myocardial function and extrinsic catecholamine effect (213). This period often occurs in the late evening and early morning hours; thus, the overnight team must be vigilant for the possible need for increased support at these times.

Bleeding

As noted above, bleeding after CPB is a constant threat for the newly admitted CICU patient. Antifibrinolytic agents such as ϵ -aminocaproic acid and tranexamic acid are commonly used for complex infant cases or repeat sternotomy and are effective at reducing blood loss and blood transfusion. Heparin effect is reversed with protamine in the OR and is rarely the cause of ongoing bleeding in the CICU. Upon admission, a complete blood count with platelet count, prothrombin time partial thromboplastin time, and fibrinogen concentration should be measured. Some programs will also use thromboelastography as a functional test of coagulation (214).

In infants under 10 kg, the primary defect causing bleeding is poorly functioning platelets and a low platelet count. For these patients, platelet transfusion is the first-line therapy. The second most important defect is low fibrinogen. Thus, cryoprecipitate is often the next line therapy (215). Clotting factors themselves may be affected, but the CPB prime often contains fresh frozen plasma; thus, this is considered third-line therapy. Red blood cells in the form of banked blood or washed cell saver blood from the OR should be immediately available and given as needed to maintain hematocrit in the target range. Whole blood is rarely available. A recent study actually demonstrated worse bleeding when whole blood was used for CPB priming versus using reconstituted fresh whole blood with packed RBC and FFP from the same donor (216). Ongoing bleeding in the face of normal or near-normal coagulation studies usually heralds a surgical source of bleeding, and the surgeon should be consulted early to decide if the patient needs to return to the OR for mediastinal exploration. Blood pressure control is often important early in the postoperative course to limit bleeding from arterial sites and prevent major bleeding from dehiscence of arterial suture lines. Generally, total chest drain output of 10 mL/kg/h for 2 or more hours is considered excessive bleeding and if coagulation studies have been normalized, there should be strong consideration for surgical re-exploration. Early extubation is not advisable in the bleeding patient and the nursing staff must continually strip the chest tubes to ensure adequate drainage. If the chest tubes suddenly cease to drain and the patient has signs of tamponade including low CO and blood pressure, pulsus paradoxus, widened mediastinum on chest radiograph, elevation and equalization of atrial filling pressures, and fluid or thrombus around the heart demonstrated by bedside echocardiography, emergent

mediastinal exploration is indicated to remove thrombus and blood and stop surgical bleeding sources. The intensivist must be vigilant early in the ICU course, particularly in small infants with very limited mediastinal volumes in whom even a small amount of accumulated clot or blood can cause tamponade.

Delayed Sternal Closure

Many infants or other patients who have had extensive surgery causing bleeding, arrhythmias, or hemodynamic instability are candidates to have the sternum left open immediately postoperatively in order to leave maximum space for any bleeding, or mediastinal edema that could adversely affect CO, especially with positive pressure ventilation. Usually, a plastic strut made from a chest tube is sewn to the sternum to hold it open, and covered with a synthetic patch and an iodine impregnated plastic adhesive dressing. This allows rapid access to the mediastinum, and a full mediastinum is easily detected with bulging of the patch. Bedside exploration is often possible. If the patient is very unstable, easy access for ECMO cannulation is possible. When the patient is more stable at 24 to 72 hours postoperatively with no bleeding, acceptable hemodynamic and respiratory status, the sternum is closed at the bedside in the CICU, normally with the OR and anesthesia teams providing support for the surgeon. Sternal closure may induce adverse hemodynamic changes and the intensivist must be vigilant in the early hours after the procedure (217).

PERIOPERATIVE CONSIDERATIONS FOR SPECIFIC LESIONS AND PROCEDURES

This section summarizes the most important perioperative considerations for major lesions encountered in patients admitted to the CICU. The reader is referred to the corresponding chapters for detailed discussion of anatomy, pathophysiology, and diagnostic and treatment considerations for each lesion.

Hypoplastic Left Heart Syndrome

Many HLHS patients are prenatally diagnosed and delivered in a referral center. If there is no perinatal cardiorespiratory depression, the majority of these patients do not need tracheal intubation. PGE₁ is instituted immediately after birth, umbilical vessel catheters are placed, and the patient is transferred to the NICU or CICU while breathing room air. Most of these patients can be managed on room air with spontaneous ventilation before surgery, with careful monitoring of cardiorespiratory status. Arterial blood gas values, along with serum lactate concentration, should be measured at regular intervals. The former practice of tracheal intubation and sedation and ventilation with low FiO₂, including subambient oxygen levels, has been demonstrated to lead to significantly decreased cerebral and somatic oxygen delivery, should be avoided (218). Decreasing PVR in the first several days is heralded by increasing SpO₂, progressive tachypnea, and interstitial edema. Diuretic therapy with furosemide is instituted as needed. Vigilance for signs of decreased systemic perfusion is important, including mesenteric perfusion, which may lead to necrotizing enterocolitis. Feeding is limited to parenteral nutrition and possibly intestinal trophic feeds via nasogastric tube. Tracheal intubation is performed for significant respiratory distress or hemodynamic compromise. The Norwood Stage I palliation or hybrid procedure should be performed in the first week of life if possible. Infants referred with a postnatal diagnosis, especially if late, that is, after 3 to 5 days, may require

resuscitation from shock as the ductus narrows or closes (219). These infants will require mechanical ventilation and inotropic support. End-organ injury, that is, renal, hepatic, gastrointestinal, and CNS, should be investigated and stabilized before proceeding for surgery. Patients with very restrictive or intact atrial septum diagnosed *in utero* require emergent evaluation and intervention immediately after birth, with BAS, atrial septectomy, or the complete Stage I repair (220,221).

The Stage I palliation involves reconstruction of the aorta from native pulmonary valve, native aortic valve and aorta, and homograft material. This is done with DHCA in many centers, or ACP in others. Pulmonary blood flow is provided by a systemic-to-pulmonary artery shunt, normally 3 to 4 mm polytetrafluoroethylene (PTFE) graft, from innominate-subclavian artery to right pulmonary artery, or by a right ventricle to pulmonary artery conduit, usually 5- to 6-mm PTFE graft (Sano modification). Heparin infusion at low doses is begun in most centers after the BT shunt, 6 to 12 hours postoperatively, and continued until the patient is able to take aspirin. Early postoperative hemodynamic stability may be better with the Sano modification, because of higher diastolic blood pressure and thus better coronary perfusion. However, systemic

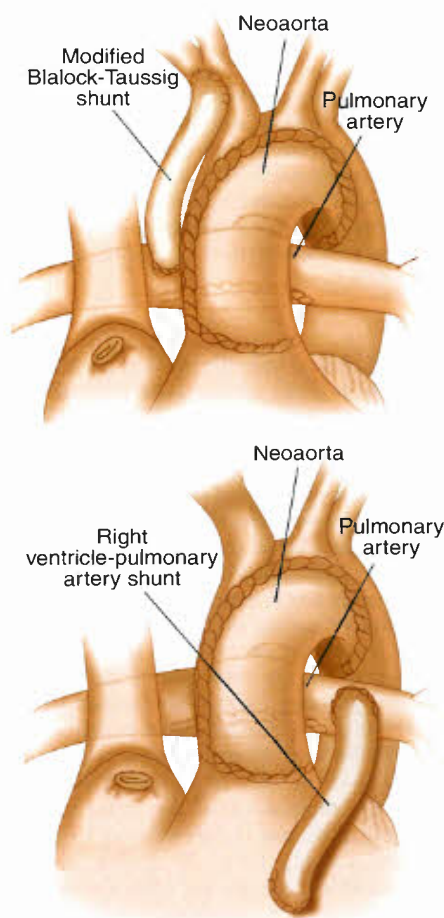


Figure 20.12. Variations in shunt type for hypoplastic left heart syndrome. Classic right modified Blalock-Thomas-Taussig shunt (top), and Sano modification (bottom) that provides pulmonary blood flow via right ventricle to pulmonary artery conduit. (Redrawn from Ohye RG, Sleeper LA, Mahony L, et al. Comparison of shunt types in the Norwood procedure for single-ventricle lesions. *N Engl J Med* 2010;362:1980–1992.)

oxygen saturations are generally lower with the Sano, but cerebral oxygen saturation and diastolic cerebral flow velocities are not different (222). A recent multicenter controlled trial of BT shunt versus RV-PA conduit demonstrated survival advantage with the RV-PA conduit at 12 months of age (223) (Fig. 20.12). However, after age 12 months, the differences in rate of death or transplantation were no longer significant. Early postoperative management involves balancing $Q_p:Q_s$ to be as close to 1:1 as possible; desaturated patients with high PVR may require higher FiO_2 and iNO, or possibly enlargement of the BT shunt (225). Most patients have the problem of PVR that is relatively low, and decreasing FiO_2 and minute ventilation to increase $PaCO_2$ will elevate PVR and help achieve balance, and in severe cases the shunt may require downsizing. Inotropic support with dopamine, epinephrine, or milrinone is usually required, and the sternum is often left open for 24 to 72 hours. Figure 20.13 illustrates priorities in pathophysiologic approach to single-ventricle neonates (224). Bleeding may be significant, and treatment with platelets, cryoprecipitate, red blood cells, and fresh frozen plasma is often necessary. ECMO support is at times necessary, either for low cardiac output or cardiac arrest. HLHS is not a contraindication to mechanical support in most centers. (225)

The hybrid repair of HLHS is performed in a specially designed catheterization laboratory or OR where fluoroscopy is available. This is done without CPB. After sternotomy, the pulmonary arteries are banded by the surgeon and the PDA is stented by the interventional cardiologist, along with a stent in the atrial septum, placed either at the initial operation or later by standard catheterization techniques (226). The advantages of this approach are the avoidance of CPB, DHCA, or ACP in the neonate. However, hybrid HLHS patients are often

hemodynamically unstable in the first 24 to 48 hours with low CO, variable $Q_p:Q_s$, acidosis and need for inotropic support (227,228). The second stage, done at the time of the bidirectional cavopulmonary anastomosis at 3 to 6 months of age, includes the aortic reconstruction.

Despite remarkable improvements in the perioperative mortality of HLHS patients over the past several decades, there is still a high incidence of morbidity in the CICU, and these patients utilize significant resources. Institutions caring for these patients need to plan accordingly (229).

D-Transposition of the Great Arteries

This lesion is often diagnosed prenatally, and delivery should be in a referral center if possible. In the absence of a VSD and inadequate atrial-level shunting, PGE₁ is begun to maintain ductal patency and improve mixing to sustain adequate oxygenation. The approach to BAS is institution dependent, but $SpO_2 < 75\%$, $PaO_2 < 40$ mm Hg are indications for BAS, which can be done at the bedside with echo guidance or in the catheterization laboratory after tracheal intubation with appropriate sedation. Adequate atrial mixing is evident by echocardiography and heralded by immediate increase in oxygenation. Some institutions will electively perform BAS even if SpO_2 is acceptable with a PDA, then extubate the patient, wean off the PGE₁, allow the patient to feed, and schedule repair at 1 to 2 weeks of age. One study demonstrated that BAS is associated with preoperative strokes diagnosed by brain MRI, but studies from two other centers did not find this association (230–232). Preoperative $PaO_2 < 40$ mm Hg and delays in surgery beyond 6 days in these cyanotic patients were associated

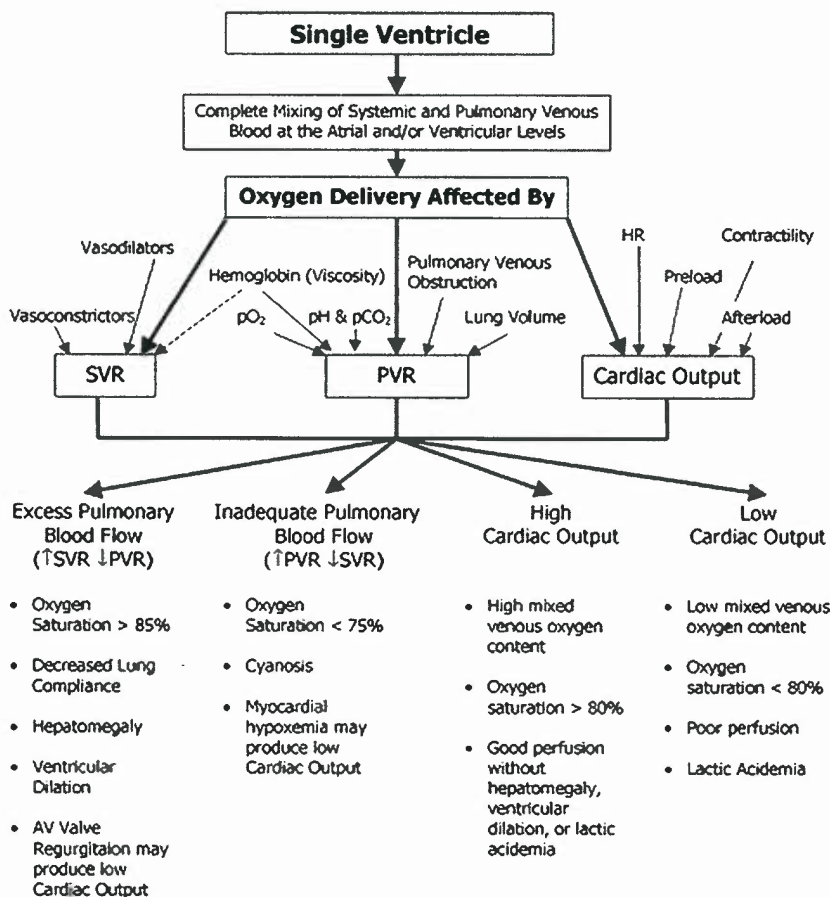


Figure 20.13. Pathophysiologic considerations for patients with a single functional ventricle. (Reproduced from Diaz LK, Nicolson SC, Steven JM. Chapter 24: Anesthesia for the patient with a single ventricle. In: Andropoulos DB, Stayer SA, Russell IA, Mossad EB, eds. *Anesthesia for Congenital Heart Disease*. 2nd ed. Oxford, UK: Wiley-Blackwell, 2010:456–479, with permission.)

with preoperative brain white matter injury. Therefore, TGA patients with significant cyanosis after BAS should be repaired as soon as possible. Significant cyanosis before repair with a preductal SpO₂ significantly lower than postductal SpO₂ may indicate PH and may respond to inhaled NO.

Postoperatively after the arterial switch operation (ASO), understanding of coronary anatomy and details of the repair are important to glean from the surgeon's report. Echocardiography is used to assess ventricular function and any segmental wall motion abnormalities, important for diagnosis of coronary insufficiency from mechanical obstruction (233). Inotropic support in the form of milrinone, low-dose epinephrine, or dopamine is often necessary early in the postoperative period. Nitroglycerin is used in many centers to ensure maximal coronary artery dilation (234). Bleeding from extensive aortic suture lines may be an issue. Transthoracic left atrial catheters are used in many centers and maintaining adequate CO with low LA pressures is important, particularly in the patient with intact ventricular septum in whom there is often some degree of LV deconditioning. The majority of ASO patients have technically adequate repairs, acceptable ventricular function and progress rapidly toward weaning of inotropic and ventilator support in the first 24 to 72 hours. Ventricular dysfunction, ST-segment abnormalities, and ventricular arrhythmias are signs of a coronary artery problem that must be addressed urgently. When ASO is performed relatively late (at age 2 to 4 weeks or later) in the patient with intact ventricular septum, particular attention to LV function is necessary due to possible LV deconditioning.

Truncus Arteriosus

Preoperatively, low diastolic blood pressure from runoff into the pulmonary arteries can be the cause of coronary insufficiency and myocardial dysfunction or poor systemic perfusion that may cause renal or mesenteric ischemia the latter can be heralded by signs of necrotizing enterocolitis. As PVR decreases, these patients are increasingly tachypneic from pulmonary overcirculation. Room air spontaneous ventilation is often a prudent strategy as the patient will control their own minute ventilation. Diuretics are often needed, and tracheal intubation is utilized only for respiratory failure or significant hemodynamic instability. These patients should have repair as soon as possible during the first week of life if they exhibit signs of significant pulmonary overcirculation or decreased systemic perfusion.

Postoperatively, these patients are at risk for hemodynamic compromise from ventricular dysfunction, truncal valve insufficiency, and PH. An understanding of the status in the OR, including echo findings, is important to help direct early postoperative care. Significant inotropic support may be required, along with iNO if PH is an issue affecting CO. Bleeding from extensive suture lines in the aorta, right ventricle, and pulmonary arteries is common.

Total Anomalous Pulmonary Venous Return

The degree of obstruction to pulmonary venous return, including restriction of right-to-left flow at the atrial level, determines preoperative management. Severely obstructed patients require emergent surgery, and every effort should be directed toward the goal of instituting CPB as quickly as possible to provide adequate oxygenation and then proceeding with repair. With significant obstruction, increasing FiO₂ and lowering PVR with iNO is counterproductive; the increased pulmonary blood flow is met with fixed anatomic obstruction, resulting in worsening interstitial and pulmonary edema and paradoxically worsening pulmonary mechanics. In such cases, rapid transport to the OR is essential. In lesser degrees of

obstruction, surgery can be done semiselectively; diuretics are often effective at reducing pulmonary edema. TAPVR repair in infants is usually done with DHCA.

Postoperatively, ongoing PH is frequently problematic and these patients are often admitted to the CICU postoperatively with iNO. The period of maximum increase in PVR due to CPB occurs during the first 6 to 12 h, and adequate sedation and analgesia must be provided during this period. In addition, the small LV is often noncompliant, and heart rate may increase during the early postoperative period to maintain CO. After this time, straightforward two-ventricle TAPVR patients are often relatively stable and can be weaned from iNO, sedation, and ventilation over the next several days with vigilance for pulmonary hypertensive episodes. Complex TAPVR, including mixed lesions, single ventricle with heterotaxy and with additional lesions such as pulmonary atresia or aortic arch anomalies complicate the postoperative care and require frequent individualized adjustments of therapy. Often prolonged periods of mechanical ventilation and inotropic support are necessary.

Systemic-to-Pulmonary Artery Shunts

Preoperatively these patients are usually maintained on PGE₁ for ductal patency. Surgery is performed with a 3 to 4 mm PTFE graft from the innominate or right subclavian artery for pulmonary atresia or significant stenosis. Some centers will place a stent in a PDA with favorable anatomy (235). Surgical approach varies, with some centers preferring a median sternotomy, others a right thoracotomy. A sternotomy is done if CPB is necessary for reconstruction of pulmonary artery. A sternotomy has the advantage that the surgeon can ligate the PDA, leaving only one source of pulmonary blood flow. The PDA cannot be ligated from a right thoracotomy, and there will be two sources of pulmonary blood flow until the PDA closes. This often leads to pulmonary overcirculation. However, a shunt via the innominate artery often can provide excessive pulmonary blood flow. Placement of a shunt from the smaller right subclavian artery via thoracotomy will limit blood flow. These details must be communicated during the surgical hand-off, and the patient managed accordingly. Excessive pulmonary blood flow is heralded by high oxygen saturations even on low FiO₂ and low diastolic blood pressures. Coronary ischemia and cardiovascular collapse are possible. These are managed with manipulation of the FiO₂ and ventilation and with inotropic and vasopressor support to increase the systolic and diastolic blood pressure. This problem usually improves after 24 to 48 hours with closure of the PDA. The problem of excessive pulmonary blood flow is especially prevalent in small neonates under 2.5 kg, where even a 3.0-mm shunt may be relatively large. Downsizing the shunt may be necessary in some circumstances. Maintaining systolic blood pressure at 70 mm Hg or higher is desirable early in the postoperative course to promote pulmonary blood flow. Dopamine, epinephrine, or vasopressin is useful for this purpose. Low-dose heparin infusion is instituted in the first 6 to 12 hours postoperatively. Conversely, severe hypoxemia may be caused by mechanical obstruction of the shunt, PH, or systemic hypotension leading to decreased pulmonary blood flow. This situation must be investigated emergently by echocardiography. Maintaining high systolic blood pressure is crucial if shunt narrowing by thrombosis is suspected. Emergent revision of the shunt may be needed surgically. Alternatively, it is sometimes possible to dilate the shunt in the catheterization laboratory. Complete occlusion of a Blalock-Thomas-Taussig (BTT) shunt in a patient without other sources of pulmonary blood flow results in rapid hypoxemia and cardiac arrest. Resuscitation is instituted but shunt revision must be done immediately. These patients will often need a period of ECMO support after such an incident. Prevention

of shunt thrombosis with low-dose heparin and adequate systolic blood pressure and prevention of PH are key points.

Tetralogy of Fallot

Depending upon surgical results and institutional preference, most centers will perform complete tetralogy repair in infancy, including during the neonatal period for symptomatic RVOT obstruction or pulmonary atresia (236). However, some institutions will perform a systemic-to-pulmonary artery shunt in young infants, preferring to allow the patient to grow to 5 to 10 kg before complete repair (237). Repair in the young infant with pulmonary atresia or significant stenosis involves a Rastelli-type surgery with VSD closure RVOT muscle resection placement of an RV to PA valved conduit. Branch pulmonary arteries are repaired by pericardial or homograft patch if needed. A coronary artery branch from the left anterior descending coronary artery may be present near the site of right ventriculotomy, and coronary ischemia is possible if this structure is injured or distorted by the surgery. In small infants, a 3- to 5-mm ASD is left or created for an atrial level pop off because of the risk of RV systolic and diastolic dysfunction. This is an important piece of information that must be communicated during handoff from the surgical team, as this will often explain the early postoperative arterial desaturations. Older patients often undergo a transatrial transpulmonary repair of the VSD, RVOT resection, and limited incision across the pulmonary valve annulus with transannular pericardial patching if needed (238). Some surgeons will place a monocusp pulmonary valve made from the patient's own pericardium or synthetic material to minimize pulmonary insufficiency in the early postoperative period.

Postoperatively, neonatal TOF repair patients may require significant inotropic support, and be quite unstable early in their course with desaturation from atrial level shunting. Management of such patients can be helped with information gained from using a left atrial catheter. RAP is often increased due to restrictive RV physiology, and high filling pressures are often necessary. Bleeding may be a significant issue and tetralogy patients as a group are at the highest risk for postoperative JET, which can have profound hemodynamic significance and must be addressed promptly.

Ventricular Septal Defect, Atrioventricular Septal Defect

The majority of older patients with small VSD or partial or transitional AVSD undergo straightforward surgery, with little need for inotropic support and minimal bleeding and can be extubated in the OR or shortly after admission to the CICU. Smaller infants with large VSD or AVSD with PH, especially Trisomy 21 patients, require caution and a high degree of vigilance postoperatively for pulmonary hypertensive crises. These patients should have a period of at least moderate sedation, mechanical ventilation, and monitoring for PH crises, usually 12 to 24 hours, before weaning toward extubation. Because of the current practice of routine repair in early infancy in these patients, severe PH is encountered infrequently. When PH is a significant risk, iNO can be effective at preventing crises. Transthoracic pulmonary artery catheters infrequently are used because PAPs are likely to be elevated for days to weeks early after repair, limiting their utility. Bleeding risk is also much higher with these catheters (239,240).

Coarctation of the Aorta, Aortic Arch Hypoplasia, and Interruption

Patients with neonatal coarctation of the aorta, arch hypoplasia, or interruption may present with shock from inadequate

systemic perfusion, when the PDA closes in the first days to several weeks of life (241). PGE₁ infusion and resuscitation, inotropic support, mechanical ventilation, and recovery of end-organ injury should precede repair. Simple juxtaductal coarctation without arch hypoplasia or intracardiac defects is repaired via left thoracotomy, normally using extended end-to-end anastomosis. There is usually 15 to 30 minutes of aortic clamping without CPB. Blood pressure monitoring with an arterial catheter in the right upper extremity is necessary. Most neonates tolerate this surgery well, with minimal need for inotropic support. They are able to wean from mechanical ventilation in 24 to 48 hours after surgery. Older children will often be extubated in the OR. Vasodilators may be necessary in early postoperatively for blood pressure control. Because of the rare complication of paraplegia due to spinal cord ischemia from clamping above the level of the artery of Adamkovich at about the T9 level, all patients should be assessed for lower extremity movement as soon as possible after surgery. Renal or mesenteric ischemia is rare after a short period of crossclamping. The patient is normally cooled in the OR to 34°C to 35°C to afford spinal cord protection.

Significant aortic arch hypoplasia or interruption is repaired via median sternotomy and usually deep hypothermia with a period of DHCA lasting <30 minutes, or ACP. Intracardiac defects, that is, VSD, are repaired at the same time (242). These patients are at significant postoperative bleeding risk due to extensive aortic suture lines, and adequate blood products must be available for hemostasis early in the postoperative course. In addition, uncontrolled blood pressure will increase risk of significant bleeding or dehiscence of the aortic suture lines.

Hypertension is often observed after coarctation repair. The early phase is catecholamine-mediated and usually best treated with β -blocking agents such as esmolol or labetalol. The later phase is mediated by increases in angiotensin and is best treated with ACE inhibitors instituted 24 to 48 hours postoperatively.

Bidirectional Cavopulmonary Connection

The bidirectional cavopulmonary connection, also termed BDG anastomosis, is the common intermediate surgical procedure between the neonatal period and the completion of the total cavopulmonary anastomosis (Fontan operation). The Glenn procedure is performed now for virtually all single-ventricle lesions, normally at 2 to 6 months of age. The SVC is anastomosed to the right PA and the systemic to PA or RV to PA shunt is taken down. The pulmonary arteries are sometimes patch augmented, and any intracardiac issues, that is, significant AV valve regurgitation, or atrial septectomy, are addressed. If a simple BDG is performed, some centers will complete this procedure without CPB (243). Others will use CPB without aortic crossclamping. Intracardiac procedures necessitate at least some crossclamping and if the aortic arch must be repaired, that is, in residual coarctation or hybrid procedure for HLHS, the crossclamp period may be long. These details must be thoroughly communicated at the CICU hand-off from the OR team.

To be candidates for a BDG, PVR cannot be significantly elevated preoperatively. However, as noted above, in these patients, even subtle increases in PVR postoperatively, sometimes with normal PAP, can complicate recovery. In addition, if the patient is hyperventilated, cerebral blood flow will decrease significantly, thereby decreasing SVC flow, thus pulmonary blood flow, and the patient will become hypoxemic (172,173) (Fig. 20.14). PaCO₂ goals early after the BDG are usually 40 to 50 mm Hg, while maintaining pH above 7.30. This will promote cerebral and pulmonary blood flow. If the patient has undergone uncomplicated simple BDG, early extubation in

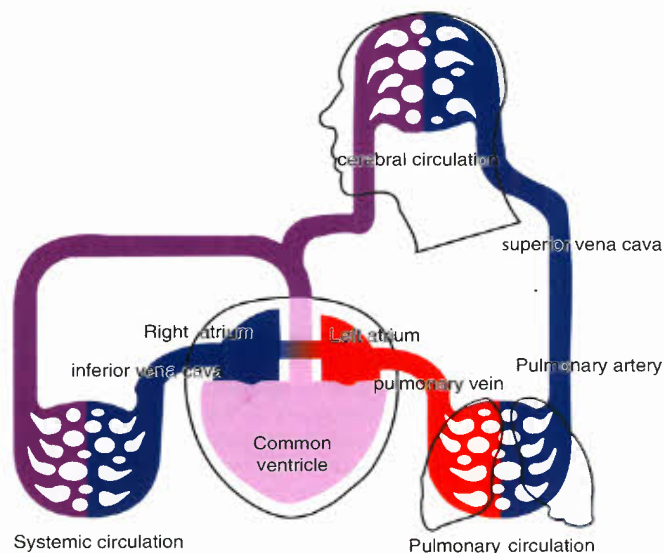


Figure 20.14. The cardio-cerebral-pulmonary circulation after cavopulmonary anastomosis. The relatively large brain of the young infant carries a large percentage of the cardiac output. Hyperventilation will decrease PaCO_2 , constricting the cerebral arterioles and decreasing cerebral blood flow. This in turn decreases superior vena cava flow, decreasing pulmonary artery flow, which will lead to decreased systemic arterial oxygenation. (Figure courtesy of Stephen A. Stayer.)

the OR or CICU is desirable. Positioning the patient in semi-Fowler's position with the head elevated 30 to 45 degrees, and positioned in the midline, will improve cerebral venous drainage and oxygenation. Measurement of transpulmonary pressure gradient, using a small right internal jugular catheter in the SVC, and a catheter in the common atrium, is helpful to guide therapy in the early postoperative period. Some centers use nitroglycerin infused into the SVC catheter as a NO donor for pulmonary vasodilation. The BDG patient who is desaturated can have impedance to pulmonary blood flow from PH, inadequate intravascular volume, poor systemic ventricular

function with or without AV valve regurgitation or stenosis at the surgical anastomosis of SVC and PA. Hypovolemia or anemia can also cause desaturation. PA and atrial pressures and transpulmonary pressure gradient, along with echocardiography are used to elucidate the cause. A summary of the hemodynamic findings and etiologies in the postoperative BDG patient is presented in Table 20.10. Many of these infants are quite irritable and hypertensive after the BDG. This is thought to represent headache from cerebral vascular attempts to reset conditions by autoregulation because of the now higher SVC pressures after the surgery. Analgesics such as morphine, acetaminophen, ibuprofen, and ketorolac are effective. The adjustment of cerebral circulation is accompanied by diminution of these symptoms, usually after 48 to 72 hours.

Fontan Completion

Total cavopulmonary connection is the intended final stage of palliation for most single-ventricle patients. Preoperatively, determination of the anatomy (right or left systemic ventricle), ventricular function, degree of AV valve regurgitation, and presence of pulmonary arteriovenous malformations causing desaturation are important. The surgical procedure itself has undergone many modifications since its original description by Fontan and Baudet in 1971 (244) (Fig. 20.15). In the current era, the extracardiac Fontan consisting of an 18- to 20-mm PTFE graft sewn to the inferior vena cava, with the other end anastomosed to the underside of the right PA, is favored in many centers (245). This can be done without aortic crossclamping or in some cases even without full CPB (246). The lateral tunnel Fontan is also frequently performed in which the atrium is opened and a PTFE patch is sewn inside to create a tunnel for blood flow from the IVC through the top of the atrium to the PA. A fenestration is sometimes created from the Fontan circuit to the left atrium, which is a 3- to 5-mm communication allowing right-to-left shunting, which lowers Fontan circuit pressure and allows greater systemic CO at the expense of some arterial desaturation (247). It should be noted that many Fontan completions, even without fenestration, are not fully saturated due to the opening of the coronary sinus into the left atrium. The details of the surgery, as to what type of Fontan connection, presence of a fenestration, and use of CPB and associated procedures, must be clearly communicated.

TABLE 20.10 Hemodynamic Findings and Etiologies in the Postoperative Bidirectional Cavopulmonary Anastomosis Patient

Profile	PAP (mm Hg)	LAP (mm Hg)	TPG (mm Hg)	SaO ₂ %	Etiology
Normal	10–15	2–6	<10	80 ± 5	Ideal anatomy and physiology
Elevated PAP	>15	2–6	>10	80 ± 5	High PVR; PA or PV obstruction
Elevated LAP	>10–15	>5–8	<10	80 ± 5	Ventricular systolic/diastolic dysfunction; sub-AS; AVVR; tamponade
Cyanosis	10–15	2–6	<10	<75	Decreased CBF; PV desaturation; decompressing veins; hypovolemia; anemia

PAP, pulmonary artery pressure measured in superior vena cava; LAP, left or common atrial pressure; TPG, transpulmonary pressure gradient; PVR, pulmonary vascular resistance; PV, pulmonary vein; AS, aortic stenosis; AVVR, atrioventricular valve regurgitation; CBF, cerebral blood flow.

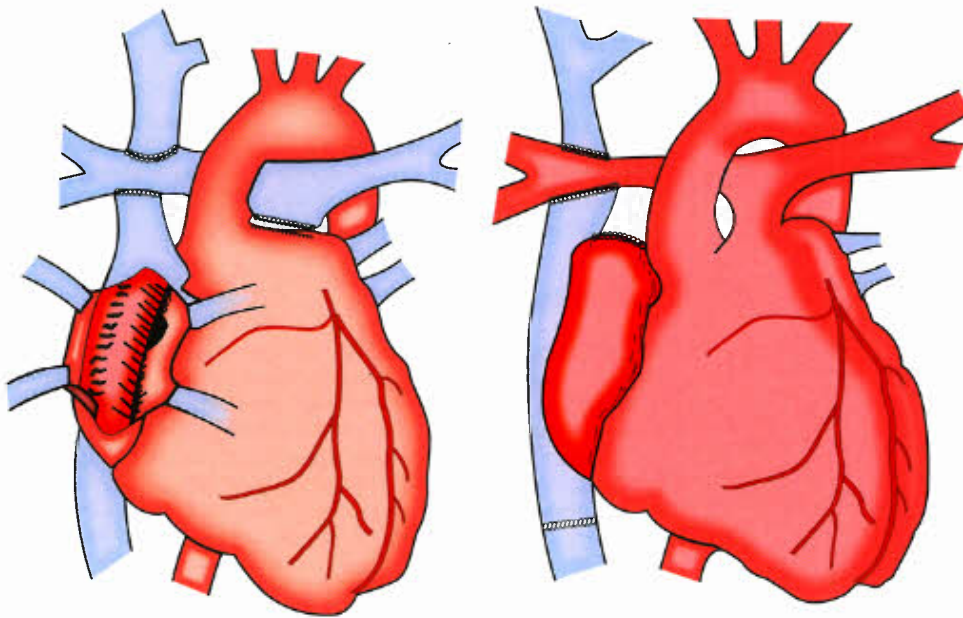


Figure 20.15. Lateral tunnel Fontan (left) and extracardiac Fontan (right). A fenestration can be placed with either of these configurations.

Because the total cavopulmonary connection results in the absence of a pulmonary ventricle to actively pump blood into the lungs, flow into and through this circuit depends in large part on negative intrathoracic pressure creating a gradient from the extrathoracic systemic venous return to the cavae and heart. Therefore, positive pressure ventilation will decrease venous return and CO. Many centers will extubate the Fontan patient in the OR by limiting the dose of opioids to promote this venous return and CO. This requires a patient who is hemodynamically stable on low doses of inotropic support, in normal sinus rhythm or other AV synchrony, not bleeding and making sufficient respiratory effort with adequate gas exchange. In the absence of these conditions, the trachea should be left intubated for CICU transfer.

The Fontan patient is highly dependent on adequate filling volume in the total cavopulmonary connection during the early postoperative period to maintain CO. In the ventilated patient, the effect of the positive pressure can be overcome

with higher filling pressures, that is, 15 to 20 mm Hg. Atrial filling pressures must be maintained at an adequate level. For this reason, an atrial catheter is often placed in Fontan patients. A key point in the early postoperative period is to not get behind in volume replacement. Bleeding from repeat sternotomy and large pleural and mediastinal tube output from increased right-sided pressures often result in significant need for volume replacement. Inotropic support in the form of milrinone and low-dose epinephrine or dopamine is often needed in the early postoperative course. Extubation should be accomplished as early as possible. Close attention to cardiac rhythm and providing AV synchrony with pacing if needed and treating atrial arrhythmias are very important to maximize CO. Nonfenestrated patients especially are prone to high Fontan pressures and pleural effusions. Conversely, they will benefit the most from early extubation. Differential diagnosis of abnormal post-Fontan hemodynamic states is presented in Table 20.11.

TABLE 20.11 Hemodynamic Findings and Etiologies in the Postoperative Fontan Patient

Profile	PAP (mm Hg)	LAP (mm Hg)	TPG (mm Hg)	Systolic BP (mm Hg)	SaO ₂ %	Etiology
Normal	10–15	2–6	<10	85–95	95 ± 5	Ideal anatomy and physiology
Decreased PAP and LAP	8–10	0–4	<10	<80	90 ± 5	Hypovolemia
Elevated PAP	>15	2–6	>10	80 ± 5	90 ± 5	High PVR; PA or PV obstruction
Elevated LAP	>10–15	>5–8	<10	80 ± 5	90 ± 5	Ventricular systolic/diastolic dysfunction; AV dissociation; AVVR; tamponade
Cyanosis	10–15	2–6	<10	85–95	<85%	Excessive fenestration size or baffle leak; PV desaturation; decompressing veins; hypovolemia; anemia

PAP, pulmonary artery pressure measured in superior vena cava; LAP, left or common atrial pressure; TPG, transpulmonary pressure gradient; PVR, pulmonary vascular resistance; PV, pulmonary vein; AV, atrioventricular; AVVR, atrioventricular valve regurgitation.

Other Left-Sided Obstructive Lesions

Aortic stenosis, mitral stenosis, and Shone complex present with a myriad of anatomic variation. The preoperative status of the patient, including ventricular dysfunction and/or hypertrophy and any medications including β -blockade, must be reviewed. Details of the surgery, whether valve repair with subaortic resection or valve replacement, must be communicated. Postoperative transesophageal echocardiographic data should be understood. Residual lesions, that is, stenosis or regurgitation, should be reviewed. With postoperative normal or hyperdynamic left ventricular function, relief of mechanical obstruction will often result in a hypertensive patient, and β -blockade with esmolol should be considered along with other vasodilator therapy, that is, nitroprusside or calcium channel blocker such as nicardipine in older patients. It is important to control blood pressure, as there will frequently be a long aortic suture line and bleeding or dehiscence can accompany uncontrolled high blood pressure. Patients with poor ventricular function may require significant inotropic support. A left atrial catheter is very helpful in these patients to assess the degree of filling of the left ventricle and any residual mitral stenosis or regurgitation.

Other Right-Sided Obstructive Lesions

Pulmonary atresia with intact ventricular septum is a complex lesion with perioperative and catheterization management dependent on details such as the presence of an RVOT, and a reasonably sized RV with thin pulmonary valve leaflets that can be perforated in the catheterization laboratory with radiofrequency energy (248). Other important considerations are the status of the coronary arteries, whether there is proximal coronary artery atresia and right ventricular dependent coronary sinusoids. These patients may be admitted postprocedure to the CICU having undergone one or a combination of RV perforation in the catheterization laboratory or OR, BT shunt, or ductal stenting, and atrial septectomy or septostomy. The details of the procedure should be clearly communicated and CICU care directed accordingly. A common scenario is the creation of RVOT blood flow and then discontinuing PGE₁ postprocedure to assess adequacy of pulmonary blood flow. Vigilance for hypoxemia necessitating restarting of PGE₁ accompanied by echocardiographic evaluation is important.

Pulmonary atresia with VSD and multiple aortopulmonary collaterals (MAPCAs) is another complex lesion, with multi-level preoperative decision making and considerable practice variation among centers. Approaches vary from complete repair via median sternotomy with extensive bilateral unifocalization of MAPCAs, placement of RV to PA conduit, and VSD closure in infants under 6 months (249) to a staged approach that may include thoracotomy for one-sided unifocalization with BT shunt, or central aortopulmonary shunt as a first procedure. Then, thoracotomy on the opposite side may be done for unifocalization followed by a third procedure for a Rastelli-type repair as the intended final stage (250,251). The preoperative anatomy, history of surgery, status of the pulmonary vascular bed, and presence of a residual VSD or ASD are very important to understand.

Ebstein anomaly of the tricuspid valve patients may present to the CICU pre- or postoperatively. Infants with severe malformation are significantly ill with cyanosis and may have SVT or other atrial arrhythmias. The severe TR often results in functional pulmonary atresia. Some patients have anatomic pulmonary atresia. With severe disease, the massive increase in RV size and increase in RV pressure causes impingement on the LV. The interventricular septum is displaced right to left; LV filling and stroke volume are compromised, leading to low

systemic CO. Even after surgery such as valve repair or BT shunt to provide pulmonary blood flow, they will require significant cardiopulmonary support (252).

Tricuspid atresia patients may present in the neonatal period after a BT shunt for pulmonary atresia or stenosis or a PA band for unobstructed pulmonary blood flow. Some patients may have mild-to-moderate pulmonary stenosis and need no intervention in the neonatal period. The BDG usually is performed at 3 to 6 months of age.

Cardiac Transplantation

The preoperative status of the transplantation patient must be thoroughly reviewed and understood, particularly in reference to PH, which can complicate the postoperative course. Intraoperatively, the donor organ ischemic time also should be as short as possible, but given issues with transport of the organ or a complex transplantation procedure such as for cyanotic CHD, ischemic times may be longer. Generally speaking, ischemic times <5 hours are desirable with better myocardial function in the early postoperative period. Details about the donor heart, such as circumstances of the donor's death, cardiac function, level of inotropic support, and any defects such as ASDs are important. Normally, the donor body weight should be 80% to 120% of the recipient's weight. When a small donor heart is placed in a recipient with PH, increased potential for RV dysfunction exists. Additional right ventricular support in the form of milrinone, iNO, or occasional RV assist device may be required in these patients (253). It is also important to understand whether the patient has elevated panel reactive antibodies or a positive crossmatch with the donor heart. In such cases, intraoperative or postoperative plasmapheresis may be instituted to minimize risk of early rejection. ABO-incompatible transplants in infants are increasingly common (254).

The denervated heart after transplantation will not respond to parasympathetic inputs. Therefore, vagolytic agents such as atropine and pancuronium will not increase the heart rate. Many institutions use low-dose isoproterenol immediately postoperatively to maintain heart rate, as there is often slowing of SA node discharge over the initial hours in the ICU. Atrial pacing wires are also placed, and this is another alternative for treatment of slowing HR. Direct-acting adrenergic agents such as epinephrine are also effective. Early in the postoperative period, the same considerations for bleeding, inflammatory response, and pulmonary dysfunction as for standard CHD surgery are followed. It is very important to maintain the patient's corticosteroid, other immunosuppressive agents, and antibiotic regimens exactly according to protocol and schedule and to maintain strict infection prevention precautions in these patients (255). Uncomplicated transplants, that is, first-time sternotomy, no PH, good donor heart function, and minimal bleeding can usually be extubated 12 to 24 hours postoperatively. Transplants complicated by bleeding, PH, complex reconstructions, or in small infants may require prolonged postoperative ventilation and inotropic support.

CENTRAL NERVOUS SYSTEM ISSUES

Sedation and Analgesia

Sedation and analgesia are daily considerations for most CICU patients. Institutional approaches and protocols for sedation and analgesia are highly desirable to standardize care as much as possible and decrease the incidence of undertreated pain and patient distress from anxiety. The ventilated postsurgical

patient will require significant doses of analgesic and sedative drugs, most often in the form of opioids (morphine, fentanyl), which should be given as continuous infusions or on a scheduled basis after major surgery. Similarly, sedation for anxiolysis and to prevent awareness is often provided by benzodiazepines (midazolam, lorazepam). Muscle relaxation is rarely indicated, except where patient movement or coughing will interfere with care, that is, ventilation. Patients with severe lung disease, or at high risk for PH crises who are treated with ECMO or other mechanical support, are often in need of continuous muscle relaxation. A peripheral nerve stimulator, placed over the ulnar nerve, should be used and state of neuromuscular blockade assessed and titrated frequently. Administration of unnecessarily large doses of sedatives, analgesics, and muscle relaxants can lead to a polyneuropathy syndrome characterized by prolonged muscular weakness that may significantly complicate weaning from support (256,257). The minimum effective doses necessary to achieve desired sedation and analgesia should be used. A pain and sedation scale or score with clear goals for each patient, is administered at regular intervals by the bedside nursing staff, and should be part of each institution's protocol (258). Older extubated patients often do very well with patient-controlled analgesia. Neuraxial anesthesia, with continuous local anesthetic infusions with or without opioids, given through thoracic epidural or paravertebral catheters, is often very effective for thoracotomy pain. Parental presence, nursing interventions, and the Child

Life Team are all very important nonpharmacologic strategies for the daily pain and distress that accompany a CICU stay.

Continuous infusions of sedative agents may be necessary for patients who are difficult to sedate. Propofol should never be used for this purpose in children because of its clear association with propofol infusion syndrome that occurs when it is used in large doses over a long time. This syndrome is characterized by mitochondrial failure, severe myocardial dysfunction, acidosis, and cardiovascular collapse leading to death (259,260). The newer IV agent, dexmedetomidine, a centrally acting α_2 antagonist agent with actions similar to clonidine has gained increasing use in CICUs because of its ability to sedate the patient, its additive effects with opioids, its ability to preserve respiratory drive, and its hemodynamic effects including lowering blood pressure and heart rate (261). This agent generally should not be used in infants and in patients with bradycardia or those who are hemodynamically unstable. AV block has been described with this agent (262–264). Despite its potential respiratory benefits, dexmedetomidine was not shown to facilitate early extubation in a recent retrospective review (265). Additional agents that may be used include ketamine, especially for painful procedures barbiturates and chloral hydrate. Table 20.12 summarizes major classes of sedative and analgesic drugs, doses, and side effects.

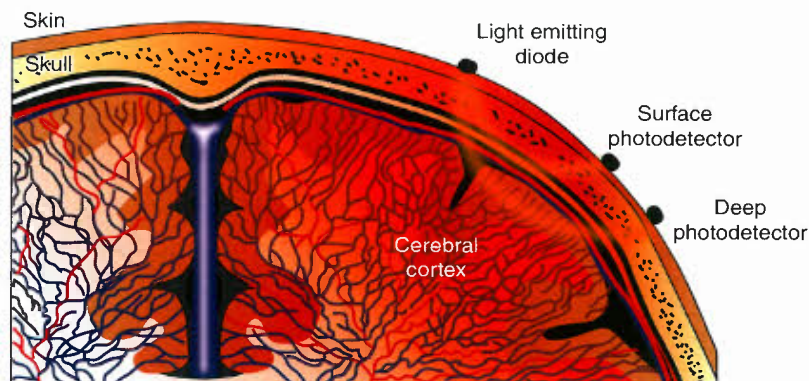
Tolerance; dependence; and a withdrawal syndrome to opioids, benzodiazepines, and other drugs are often observed in CICU patients who receive significant doses and have long ICU

TABLE 20.12 Sedative and Analgesic Drugs

Drug	Class	Dosing	Indications	Comments
Fentanyl	Opioid	Bolus: 1–2 $\mu\text{g/kg}$ Infusion: 1–10 $\mu\text{g/kg/h}$	Analgesia	Chest wall rigidity with rapid bolus; rapid tolerance with infusion
Morphine	Opioid	Bolus: 0.05–0.1 mg/kg Infusion: 0.025–0.1 mg/kg/h	Analgesia	
Methadone	Opioid	0.1–0.2 mg/kg Q8–12h	Analgesia; opioid tolerance	Use for opioid wean protocol
Midazolam	Benzodiazepine	Bolus: 0.025–0.1 mg/kg Infusion: 0.05–0.1 mg/kg/h	Amnesia, sedation, anxiolysis	Rapid tolerance with infusion
Lorazepam	Benzodiazepine	Bolus: 0.025–0.1 mg/kg q 4h	Amnesia, sedation, anxiolysis	
Ketamine	Arylcyclohexylamine	Bolus: 1–2 mg/kg Infusion:	Analgesia, sedation	Hallucinations, dysphoria, excessive salivation, tachycardia
Propofol	Imidazole derivative	Bolus: 1–3 mg/kg Infusion: 100–200 $\mu\text{g/kg/min}$ for procedural sedation	Procedural sedation	Do not use for prolonged ICU sedation, i.e., >4 h
Dexmedetomidine	Central α_2 agonist	0.3–0.7 $\mu\text{g/kg/h}$	Sedation; some analgesia	For short-term ICU sedation; bradycardia and heart block in infants
Acetaminophen	Inhibits prostaglandin synthesis	10–15 mg/kg q 6h	Analgesia	Do not use with significant hepatic disease
Ketorolac	Nonsteroidal anti-inflammatory agent (cyclo-oxygenase-1 and 2 inhibitor)	0.5 mg/kg q 6h; max 30 mg; do not administer for more than 48–72 h	Analgesia	Inhibition of platelet function: bleeding. Renal impairment

All doses are intravenous; see text for details.

Figure 20.16. Principles of NIRS. The sensor is placed on the forehead, and a light- or a laser-emitting diode uses 2 to 4 wavelengths of near infrared light at 700 to 1,000 nm. Oxy- and deoxyhemoglobin have distinct light absorption spectra, and the device calculates the oxyhemoglobin saturation using a modification of the Beer-Lambert Law. Regional oxygen saturation (rSO_2) is reported. Since arterioles, veins, and capillaries are all in the light path, rSO_2 is a venous-weighted oxygen saturation of a tissue sample volume in the frontal cerebral cortex. A subtraction algorithm using surface and deep photodetectors removes signal from shallow tissues, that is, skin, skull, and dura. (Figure courtesy of Covidien-Somanentics Corp.)



stays (266). Risk for this syndrome is generally higher with continuous infusions of large doses of potent synthetic opioids, that is, fentanyl and infusions of short-acting benzodiazepines, that is, midazolam. If these therapies are necessary early after CICU admission, their need should be evaluated daily, minimum effective doses used, and instead of continually escalating doses, adding long-acting scheduled doses of opioids, that is, morphine or methadone, and benzodiazepines, that is, lorazepam, should be considered. Low-dose naloxone infusion may be effective at preventing tolerance syndromes (267). Dexmedetomidine and clonidine have opioid-sparing effects (268). Also, intravenous acetaminophen, ibuprofen, or ketorolac are now available and should be considered for their opioid-sparing effects when no contraindications exist. Patients should be assessed for withdrawal syndromes using the various semi-objective grading scales and if established, a plan to gradually wean the sedative and analgesic drugs, that is, 5% to 10% per day, and substitute long-acting drugs (methadone and lorazepam) or drugs from other classes (barbiturates, transdermal clonidine patch) for withdrawal symptoms. Consultation with an acute pain service expert is recommended for difficult cases.

CNS Injury: Etiologies, Prevention, Evaluation, Treatment

The recognition that patients with CHD who have undergone complex or moderately complex surgery have a significant incidence of long-term, mostly subtle neurodevelopmental problems by the age of school entry has focused attention on the perioperative period as a potential cause of brain injury. In the modern era, gross injuries such as large strokes, seizures, choreoathetosis, and coma are very rare. A myriad of causes of brain injury and abnormal neurodevelopment exists. A recent finding has been that the brains of patients with complex CHD who undergo operation in the neonatal period are very often immature, that is, the full-term infant with complex CHD often has the brain with the morphologic and microcellular characteristics of a premature infant of 32 to 34 weeks' gestational age (269,270). In turn, this brain immaturity leads to higher incidence of brain injury both pre- and postcardiac surgery (232). The falloff in brain growth and maturation begins in the third trimester, and has raised the issue of whether delivery, or CPB surgery before term, is advisable (271,272).

Perioperative etiologies of brain injury include prolonged hypoxemia before repair (231), BAS in some series (230), and prolonged DHCA over about 45 minutes. (206). In addition, hematocrit on CPB below 24% (273) rapid cooling, and α stat management have also been associated with early evidence of CNS injury (207,274). The availability of NIRS to monitor

regional cerebral oxygen saturation (rSO_2) has led to the widespread use of this real-time monitor of cerebral oxygenation in the CICU on many high-risk postoperative patients. These include neonates undergoing complex surgery, patients on mechanical support or older high-risk patients. Prolonged low rSO_2 has been associated with new postoperative brain MRI injury (275,276), need for ECMO and death in HLHS patients (277), and long-term MRI change and lower neurodevelopmental scores (278). To date, there are no published controlled trials of NIRS monitoring and intervention for CHD conclusively demonstrating that this monitoring with intervention protocols improves outcome. However, accumulating evidence of the use of this monitor to maintain a goal rSO_2 (normally $>50\%$) demonstrates its important benefits. In the CICU, NIRS monitoring can help direct therapies to increase oxygen delivery to the brain, including ventilator maneuvers, increasing CO, and hemoglobin. For example, unnecessary or inadvertent hypocarbia significantly affects cerebral blood flow in infants and leads to low rSO_2 (279). In addition, therapies decreasing cerebral oxygen consumption by lowering temperature adding sedative agents or treating seizures, can be directed with NIRS monitoring. The rSO_2 is a noninvasive surrogate for SvO_2 as well and can thus be used to help direct therapy to optimize global oxygen delivery (33). Figure 20.16 illustrates basic principles of NIRS and Table 20.13 summarizes maneuvers to increase rSO_2 . (For a complete discussion of CNS outcomes in CHD, please see Chapter 74.)

THE RENAL SYSTEM

Renal dysfunction is a common problem in CICU patients and frequent causes include LCOS, ischemia from long CPB times, postarrest injury, nephrotoxic drugs, congenital renal malformations, and hemolysis-induced tubular dysfunction from elevated plasma-free hemoglobin. Maintenance of adequate urine output to meet the fluid balance goals for each patient is important. Diuretic therapy, most commonly furosemide, is used for almost all postoperative patients to promote excretion of excess tissue fluid. Furosemide infusion can be an effective approach to the patient in need of maximal diuretic treatment. The incidence of renal dysfunction after congenital heart surgery in the modern era is about 20%, defined as at least a 50% increase in serum creatinine postoperatively (280). Diagnosis is made by noting increased serum creatinine and blood urea nitrogen, decreased urine output, and decreased calculated GFR. Renal ultrasound, including assessment of renal blood flow, may be a useful diagnostic

TABLE 20.13 Measures to Increase Regional Cerebral Oxygen Saturation (rSO₂)

Measures to increase oxygen delivery	
Oxygenation	Increase FiO ₂ ; other means to improve oxygenation
Ventilation	Decrease minute ventilation to increase PaCO ₂
Cardiac output	Volume infusion
	Inotropic, vasodilator support
Oxygen-carrying capacity	Increase hemoglobin by transfusion; diuresis
Relieve SVC obstruction	Head in midline; elevate HOB 30 degrees
Increase cerebral perfusion pressure	Treat hypotension—Increase blood pressure with vasopressors
Measures to decrease oxygen consumption	
Temperature	Cool brain/body temperature to 35°C–36°C
Sedation	Sedate patient to decrease CMRO ₂
Seizures	Treat seizures to decrease CMRO ₂

Measures to increase regional cerebral oxygen saturation (rSO₂). rSO₂ < 50%, or >20% relative below baseline, is a usual indication for treatment. Example: baseline rSO₂ = 65%, a decrease to 52% or lower is treated. SVC, superior vena cava; HOB, head of bed; CMRO₂, cerebral metabolic rate for oxygen.

modality. Temporary renal dysfunction heralded by increase in creatinine and decreased urine output caused by the surge in antidiuretic hormone (ADH) as part of the stress response to major surgery is common in the first 24 to 72 hours. Table 20.14 displays the pediatric RIFLE (pRIFLE), a commonly used scoring system for renal injury in pediatrics (280). When bleeding subsides and hemodynamic stability is achieved, diuretics are often added 12 to 24 hours after admission to the ICU.

Renal Replacement Therapy

The incidence of renal failure requiring renal replacement therapy after CHD surgery is very low, estimated at 1% to 3%, although its precise incidence is difficult to classify (280,281). Peritoneal dialysis is normally used in infants, and the catheter can be inserted at the bedside by the surgeon in the ICU. Normally, hourly cycles of 10 mL/kg of 1.5% to 2.5% Dianeal with 45- to 50-minute dwell time and 10-minute drain time

TABLE 20.14 The Pediatric RIFLE Criteria

Category	GFR Criteria	Urine Output Criteria
Risk	Increased creatinine 1.5 times baseline, or GFR decrease >25%	UO < 0.5 mL/kg/h × 6h
Injury	Increased creatinine 2.0 times baseline, or GFR decrease >50%	UO < 0.5 mL/kg/h × 12h
Failure	Increased creatinine 3.0 times baseline, or GFR decrease >75%	UO < 0.5 mL/kg/h × 24h, or anuria × 12h
Loss	Persistent acute renal failure = complete loss of renal function >4 weeks	
End-Stage Renal Disease	Persistent renal failure = complete loss of renal function >3 months	

GFR can be estimated by the Schwartz method: This equation may not provide an accurate estimation of creatinine clearance for infants <6 mo of age or for patients with severe starvation or muscle wasting.

$eGFR = (k \times \text{Height (cm)}) / \text{Creatinine (mg/dL)}$

where: eGFR = estimated GFR; calculated in mL/min/1.73 m²

k = constant of proportionality that is age-specific:

<1 y preterm: 0.33

<1 y full-term: 0.45

1–12 y: 0.55

>12 y female: 0.55

>12 y male: 0.7

GFR, calculated glomerular filtration rate; UO, urine output.

are very effective at removing excess fluid and balancing electrolyte values, for example, hyperkalemia. Close attention must be paid to hemodynamic and ventilatory status during infusion and draining of peritoneal dialysis fluid the first several cycles in small infants. Some programs routinely place peritoneal dialysis catheters in the OR after complex neonatal and infant surgery (282–284). The catheter is placed via the anterior mediastinum in front of the diaphragm for access to the peritoneal cavity or the catheter can be placed via a small supraumbilical incision and positioned from the incision near the diaphragm. This catheter is easily removed several days postoperatively. Peritoneal dialysis is instituted in the ICU soon after admission to achieve optimal fluid balance during the period of time when kidneys are avidly retaining fluid due to the ADH surge. In addition, mediators of inflammation are filtered in the dialysate reducing plasma levels of these small molecules and possibly reducing the severity of the inflammatory response.

Other forms of renal replacement, such as continuous venovenous hemofiltration continuous arteriovenous hemofiltration or hemodialysis, are reserved for larger patients whose blood vessels can accept the large catheters required for such therapies (285). Patients treated with ECMO or acute VAD therapy normally have a hemofilter placed in the circuit to augment native renal function and to fine tune fluid and electrolyte balances.

FLUIDS, ELECTROLYTES, AND NUTRITION

Intravascular volume and total body fluid status are high-priority issues daily for CICU patients. Most immediate postoperative patients are treated with less than maintenance daily fluid administration, that is, 50% of maintenance levels, with 5% or 10% dextrose and 0.2% to 0.45% normal saline. Potassium is not added to IV fluids initially. Bolus isotonic crystalloids, 5% albumin, or blood products are utilized in the early postoperative period to replace intravascular volume. Fluids are liberalized after 24 to 48 hours and those patients who are extubated and have normal gastrointestinal function will resume feeding shortly thereafter. Frequent measurement of electrolytes and maintenance of normal ranges for serum sodium, potassium, ionized calcium and magnesium are important to optimize end-organ function. Hypokalemia is frequent in patients receiving diuretic therapy and IV replacement over 1 to 2 hours is common. Hyperkalemia is treated first by removing any potassium from IV fluids and then increasing pH with bicarbonate, administering calcium chloride, and giving insulin to promote movement of K⁺ into cells. Kayexelate, a potassium-binding resin, is given per rectum. Hemodialysis is rarely necessary in persistent hyperkalemia. Hyponatremia is a common finding with diuretic therapy; reducing diuretic doses and decreasing the amount of free water intake are the usual approaches. In severe cases, that is, serum sodium <120 mEq/L with seizures, 3% sodium chloride may be necessary, although care must be taken not to correct the serum sodium faster than 10 mEq/L per 24 hours. Hypernatremia is uncommon, but increasing free water and decreasing sodium intake is the usual treatment.

Nutrition in critically ill patients in the CICU is a central issue, and adequate caloric intake is necessary to prevent protein catabolism, maintain energy stores for optimal cardiopulmonary function, promote wound healing, and prevent infection (286). Early complex postoperative patients are given standard IV fluids for 24 to 48 hours and if the GI tract cannot be used for early feeding, central parenteral nutrition should be instituted, increasing dextrose, amino acids, and intralipid infusions to meet goals for calories, protein, and

lipid administration. The gut should be used if at all possible, starting with small-volume continuous feeds of breast milk, fortified if necessary or with age and medical condition appropriate formula. Trophic levels of feeds will prevent involution of intestinal villi and promote higher success rates when full feeds are instituted. The recognition that infants having major cardiac surgery, particularly the Norwood Stage I palliation and other major aortic arch reconstruction, have a significant incidence of recurrent laryngeal nerve injury that affects vocal cord function (10% to 25%) along with a significant incidence of gastroesophageal reflux (GER) (48% to 59%) and aspiration (24% to 35%) (287) has led to institution of refeeding protocols in many centers. This involves an assessment of vocal cord function by nasoendoscopy, assessment of coordination of sucking and swallowing capability by an infant feeding specialist, and possibly barium swallow. Nasogastric or nasoduodenal feeds can be instituted if necessary in cases of vocal cord dysfunction and/or reflux. Persistent dysfunction of vocal cords and GER is an indication for placement of a gastrostomy tube, either surgically or by percutaneous endoscopic gastrostomy. Fundoplication is done less often but can be done via open surgical incision or laparoscopically. Another cause of feeding problems can be intestinal malrotation, frequently seen in patients with heterotaxy syndrome, and a Ladd procedure may be needed in these patients (288,289). Small infants with single-ventricle anatomy are particularly prone to feeding problems, and ICU care is usually necessary after abdominal surgery. Figure 20.17 outlines one approach to refeeding neonates after complex cardiac surgery.

Although not a feeding problem per se, chylothorax often becomes evident when the infant begins full feeding with regular formula and pleural effusion becomes evident on chest radiograph or chylous fluid begins draining from any of the chest tubes. Disruption of the thoracic duct or other lymphatics during surgery can lead to chylothorax, which can significantly complicate the postoperative course. Diagnosis is made by observing a high lymphocyte count and chylomicrons in the fluid. Treatment is initiated by stopping oral intake and starting total parenteral nutrition. When the drainage decreases significantly and is no longer chylous, cautious refeeding with nonfat containing formulae is reinstituted. This therapy may be necessary for weeks afterward until drainage stops. Persistent chylothorax can be treated by continuous infusion of the somatostatin analog octreotide, at 25 to 100 µg/kg/day for 3 to 7 days. Pleurodesis with mechanical methods, talc, or doxycycline is also used for persistent chylothorax. This procedure is extremely painful, initiates a significant inflammatory response, and is not often used. Ligation of the thoracic duct and oversewing of leaking lymphatics is sometimes necessary (290,291).

Glycemic Control

In recent years, an association between hyperglycemia and poor outcomes in ICU patients, particularly in the adult population, has been noted and subsequently an attempt to control glucose concentrations has been made in an attempt to improve these outcomes. The problems with this approach included the fact that it was very difficult to determine whether the hypoglycemia was the cause or the effect of the conditions that led to poor outcomes. In the neonatal and infant cardiac surgery population, hyperglycemia (serum glucose above 180 mg/dL) was not associated with an increased short-term morbidity in one study (292); however, in other studies, either low serum glucose (average below 110 mg/dL) or high serum glucose (average >145 mg/dL, or peak >250 mg/dL) were associated with early morbidity and mortality (293). Longer-term

TCH Evidence-Based Outcomes Center Clinical Algorithm for Feeding the Neonate Post-Cardiac Surgery

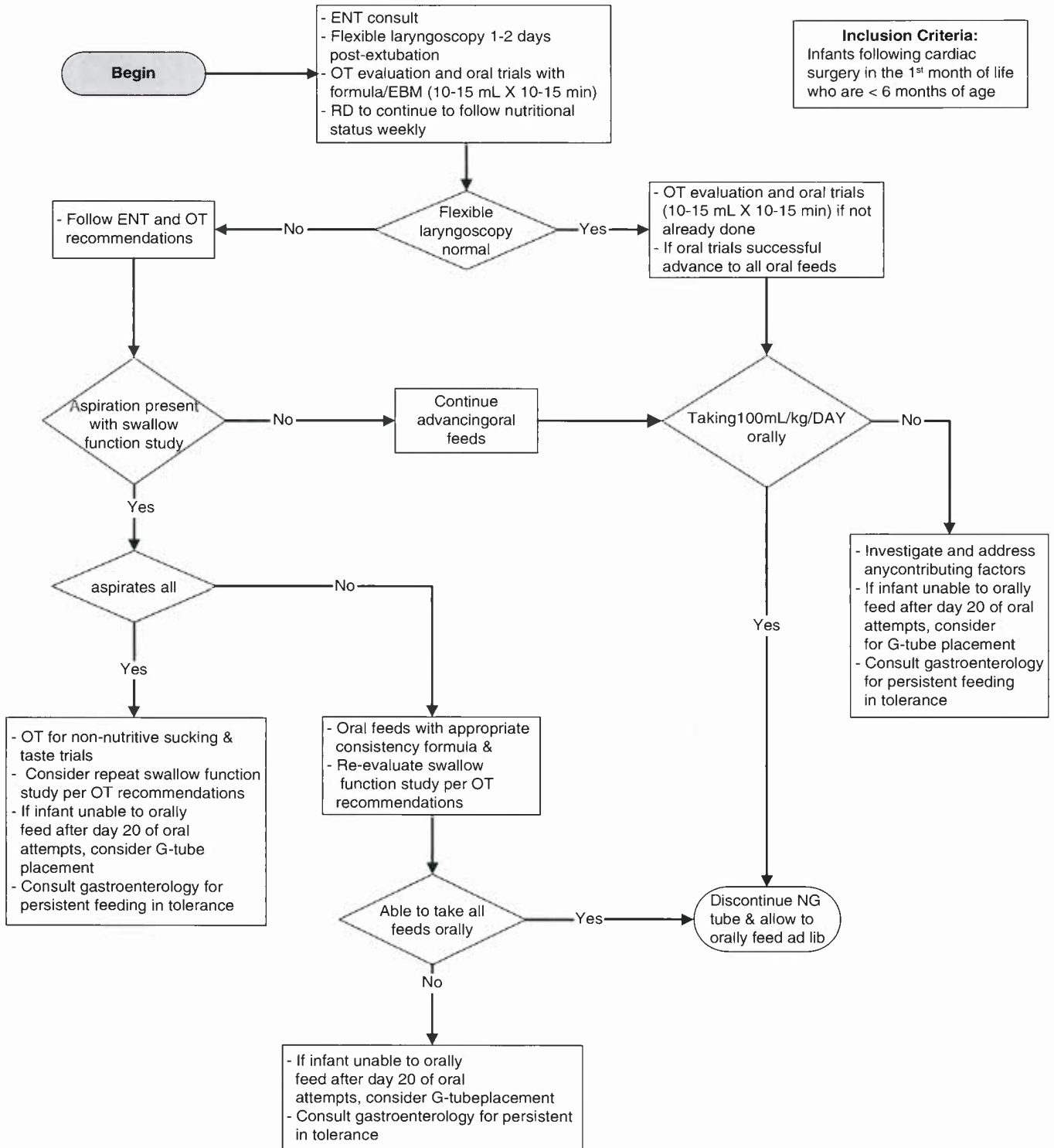


Figure 20.17. Suggested refeeding algorithm for neonates after cardiac surgery. ENT, ear, nose, and throat surgeon; OT, pediatric occupational therapy feeding specialist; EBM, expressed breast milk; RD, pediatric registered dietician; G-tube, gastrostomy tube; NG, nasogastric.

neurodevelopmental outcomes are not affected by hyperglycemia in the perioperative period for infant cardiac surgery (294,295). Both adult (296) and pediatric studies of tight glycemic control (target 81 to 108 mg/dL) versus standard therapy (target <180 mg/dL) demonstrated increased complications, most particularly hypoglycemia, and even death, with tight control (297). Clearly more data are needed in this area. In practice, a target glucose of 80 to 200 mg/dL in most CICU patients is adequate, and short-lived elevations above 200 mg/dL are common perioperatively, particularly if corticosteroids are used. These elevations are normally self-limited and do not necessitate insulin therapy; limiting the glucose infusion rate is sufficient. Insulin therapy is only used for persistent elevations in serum glucose above 300 mg/dL or when osmotic diuresis is complicating fluid therapy. Investigating and treating the underlying cause is important.

INFECTION IN THE PCICU

Prevention of Infection

The PCICU is at particularly high risk for nosocomial infection because of the invasive procedures, and many indwelling vascular catheters and the often-abnormal immune systems of the patients (298). Strict attention to preventing infection by common measures such as hand washing between every patient contact, disinfecting stethoscopes and other equipment and isolation of known or potentially infective patients is of critical importance. In addition, strict adherence to protocols for sterile insertion and maintenance of central venous catheters and protocols to prevent VAP has dramatically reduced such complications in units where they have been implemented (299). For each CICU patient, the treatment team must assess daily whether each indwelling catheter, or the endotracheal tube is necessary, how long it has been in place, whether infection is suspected, what the anticipated duration of placement is, and plans for its removal or replacement. Indwelling catheters and tubes should be removed as soon as possible.

Diagnosis and Treatment: Catheter-Related, Bloodstream, Pulmonary, Urinary, Wound Infections

The signs and symptoms of infection in CICU patients are myriad, and a high index of suspicion necessary in these patients. Fever or hypothermia, leukocytosis, hemodynamic or respiratory compromise, coagulopathy or failure to progress in the expected course of illness are common accompaniments of significant infection. A thorough examination, cultures of blood, endotracheal secretions, urine and imaging studies such as echocardiography to evaluate whether a vegetation is present, are necessary in suspected infection. Empiric antimicrobial therapy, removal of possibly infected catheters, and careful monitoring are first steps in treating significant infection. Therapy is narrowed and promptly directed specifically at any organisms that grow from cultures. Complex patients, that is, infected patients on mechanical support, benefit from consultation by the infectious disease service.

ENDOCRINE ISSUES

Adrenal Insufficiency and Corticosteroids

Some patients in the PCICU experience an acquired adrenal insufficiency from their critical illness or after suppression from chronic steroid administration. In patients suspected of

having adrenal insufficiency, a cosyntropin stimulation test can be done. Nonresponders will frequently benefit from a course of hydrocortisone with improved hemodynamic performance due to increased sensitivity to catecholamines (300,301). Patients with ongoing high inotropic requirements should be suspected of having this acquired adrenal insufficiency. Treatment with hydrocortisone will significantly reduce inotropic requirements in these patients within 6 to 12 hours.

Hypothyroidism

There is a decreased conversion of T4 to T3 after CPB in children, and hypothyroidism may accompany major cardiac surgery with CPB. In addition, many patients with trisomy 21 have either overt or functional hypothyroidism (up to 30%). In these patients and especially infants, T3 infusion can be very effective at improving myocardial function and decreasing the need for high-dose inotropic support (302,303). Patients with refractory LCOS who are receiving high doses of inotropic support should have thyroid function tests measured with consideration for initiation of T3 (triiodothyronine) infusion, 0.05 to 0.15 $\mu\text{g/kg/h}$.

CPR AND ECPR IN THE PCICU

Cardiac arrest is a constant threat in the PCICU and vigilant monitoring and assessment to identify patients at risk and to address treatable causes before an arrest are important tasks in every CICU. Decreasing peripheral perfusion, increasing acidosis and serum lactate, as well as decreasing somatic NIRS values are all used to assess this risk (304). Despite best efforts, sudden arrest from causes such as paroxysmal arrhythmias or PH crises happen all too frequently in the PCICU. Immediate response, institution of effective chest compressions, assuring oxygenation and ventilation, rapid defibrillation or cardioversion, and administering standard resuscitation drugs such as epinephrine and atropine rapidly and prompt cardioversion or defibrillation are very important. However, in the CICU, there are a number of scenarios where standard resuscitative measures will not be effective. Rapid surgical assistance to reopen the sternum of the arrested patient with cardiac tamponade, for instance, is essential. If patients are not responding rapidly to standard measures, rapid institution of ECMO, known as ECPR, is now the standard approach in many centers. Such a system requires considerable institutional resources to equip and train personnel. Survival rates of ECPR are as high as 30% to 40% in experienced programs. Virtually all of these patients would have died without this therapy (305). (See Chapter 21 for a detailed discussion of mechanical support therapies.)

THE CATHETERIZATION LABORATORY AND THE PCICU

Care of Postcatheterization Patients

With increasingly invasive procedures performed in the catheterization laboratory on progressively smaller and sicker patients, a number of these children will need PCICU admission for observation and treatment of postcatheterization issues. These can include low CO after many procedures such as aortic valve balloon angioplasty in the neonate, pulmonary reperfusion injury or hemorrhage after extensive pulmonary artery angioplasty, PH after procedures such as pulmonary vein angioplasty and stenting, severe catheter-induced arrhythmia, or heart block or cardiac arrest after induction of anesthesia

in a patient with preexisting severe myocardial dysfunction. These patients often do not have the same hemodynamic monitoring catheters, that is, arterial, right and left atrial catheters, as postsurgery patients. Their clinical examination parameters are very important. Clear communication between the cardiac catheterization team and the CICU for high-risk patients, identical to that of patients undergoing cardiac surgery, is essential for optimal care of these patients.

Catheterization of ICU Patients

Many PCICU patients undergo preoperative evaluation or interventions in the catheterization laboratory. Patients with known or suspected residual defects who are not progressing in their ICU course in terms of hemodynamic or respiratory support should have serious consideration for thorough hemodynamic and anatomic assessment in the catheterization laboratory. Echocardiographic data are important, but should not be relied upon exclusively for therapeutic decision making in PCICU patients. Not only can residual defects be assessed in detail with catheterization but also pulmonary vein saturations are often helpful to distinguish pulmonary parenchymal disease from other causes of arterial desaturation. This also affords the opportunity for intervention, where additional surgery would be high risk. This includes patients on ECMO. In addition, patients on mechanical support may require catheter therapy to create a larger atrial communication for left heart decompression or correct positioning of intracardiac support catheters. There should be a relatively low threshold for performing cardiac catheterization in PCICU patients.

MEDICAL CONDITIONS IN THE CVICU

Among the most common medical conditions reported in PCICU admission are myocarditis, cardiomyopathies, acute or chronic transplant rejection or graft dysfunction from coronary arteriopathy, and severe infective endocarditis (306). Common pathophysiology often includes a dilated, poorly functioning left ventricle with acute congestive heart failure. Management principles in the acute PCICU setting are the same as noted above, under Prevention and Management of Low Cardiac Output Syndrome. Chapters 55 and 65 contain detailed discussions of these conditions. Diagnosis and specific treatment for the underlying cause of heart failure is of paramount importance. Patients range from those requiring a short PCICU stay for additional diuresis or low-dose inotropic therapy to those who will go on to require mechanical support. A common issue with myocarditis, cardiomyopathy, or transplant rejection patients is when to initiate some form of mechanical support in a marginal patient with established LCOS. Any reversible or treatable causes are addressed. Patients with continued low CO despite significant inotropic support, with respiratory insufficiency, with risk for or experiencing multiorgan failure or cardiac arrest must be strongly considered for such therapy. Serial echocardiograms, serum lactate, mixed venous oxygen saturation measurements, and serum troponin or B-natriuretic peptide levels can be important modalities to assist in decision making.

THE LOW BIRTH WEIGHT INFANT

LBW infants weighing <2,500 g are increasingly admitted to PCICUs, both after and before palliative or corrective cardiac surgery or cardiac catheterization. The emphasis on early total

correction of two-ventricle lesions and on early palliation of single-ventricle lesions had led to the increase in this population. Although complex surgery with CPB can be accomplished in these patients, problems of the premature infant such as intraventricular hemorrhage or bronchopulmonary dysplasia have important implications for these patients (307). Overall survival is lower than for full term and normal birth weight infants. Bloodstream infections are common and a prominent feature for increased mortality (308,309). This problem may be minimized by the routine preoperatively percutaneous placement of central catheters, which have a very low infection rate (310). Alternative approaches to LBW neonates, such as the hybrid Stage I palliation for HLHS, versus conventional Norwood Stage I palliation, have not improved survival in these infants (311). Prolonged treatment with PGE₁ for ductus-dependent lesions has been described as an alternative to early surgical intervention (312). The LBW population in the PCICU must have multidisciplinary consultation, particularly from neonatologists, to assist in identifying and treating conditions unique to this population.

THE ADULT WITH CONGENITAL HEART DISEASE

The issue of critical care for the adult with CHD is a complex one and the setting of care may be in a PCICU in a children's hospital, a general cardiothoracic surgical ICU in an adult hospital, or a specialized unit for adults with CHD (313). Specialized knowledge and experience in caring for the adult with CHD is important for the intensivist involved with these patients. The multiorgan pathophysiology of long-standing CHD is different from the young child and arrhythmias, myocardial failure, renal dysfunction, coagulation abnormalities, and neurologic dysfunction are common in this population. Expert cardiologists specializing in adult CHD are very important for consultation and coordination of the adult subspecialists needed, including neurologists and nephrologists. Each institution must develop a standardized, coordinated, multidisciplinary approach to these patients.

CONCLUSIONS

Cardiac intensive care in infants and children with congenital and acquired heart disease is a rapidly evolving field with a tremendous amount of new knowledge every year. No matter what the exact setting for the care of these patients, whether in the neonatal intensive care unit, within a PICU or in a dedicated cardiac intensive care unit, the institution must provide the adequate resources and support for this very intensive system of care. Multidisciplinary collaboration is key to maximize outcomes. The melding of state-of-the-art knowledge and techniques in Cardiology, Surgery, Intensive Care, Anesthesia, Nursing, Respiratory Therapy, and Perfusion, continually yields new approaches to address the needs of these complicated patients.

REFERENCES

1. Pediatric Cardiac Intensive Care Society. <http://www.pcics.org/>, accessed February 27, 2011.
2. Chang AC. Manpower shortage in pediatric cardiac intensive care: how can we undo this Gordian knot? *Pediatr Crit Care Med* 2004;5:414–415.
3. Chang AC. How to start and sustain a successful pediatric cardiac intensive care program: a combined clinical and administrative strategy. *Pediatr Crit Care Med* 2002;3:107–111.

4. Chang AC. Pediatric cardiac intensive care: current state of the art and beyond the millennium. *Curr Opin Pediatr* 2000;12:238-246.
5. Fraisse A, Le Bel S, Mas B, et al. Paediatric cardiac intensive care unit: current setting and organization in 2010. *Arch Cardiovasc Dis* 2010;103:546-551.
6. Stromberg D. Pediatric cardiac intensivists: are enough being trained? *Pediatr Crit Care Med* 2004;5:391-392.
7. Rosenberg DI, Moss MM. Guidelines and levels of care for pediatric intensive care units. *Pediatrics* 2004;114:1114-1125.
8. Institute of Medicine of the National Academies. To Err Is Human: Building a Safer Healthcare System. <http://www.iom.edu/Reports/1999/To-Err-is-Human-Building-A-Safer-Health-System.aspx>. 1999, accessed February 28, 2011.
9. Institute of Medicine of the National Academies. Crossing the Quality Chasm: A New Health System for the 21st Century. <http://www.iom.edu/Reports/2001/Crossing-the-Quality-Chasm-A-New-Health-System-for-the-21st-Century.aspx>. 2001, accessed February 28, 2011.
10. Thiagarajan RR, Bird GL, Harrington K, et al. Improving safety for children with cardiac disease. *Cardiol Young* 2007;17:127-132.
11. Dracup K, Morris PE. Passing the torch: the challenge of handoffs. *Am J Crit Care* 2008;17:95-97.
12. Costello JM, Graham DA, Morrow DF, et al. Risk factors for central line-associated bloodstream infection in a pediatric cardiac intensive care unit. *Pediatr Crit Care Med* 2009;10:453-459.
13. Ahmed SS, McCaskey MS, Bringman S, et al. Catheter-associated bloodstream infection in the pediatric intensive care unit: a multidisciplinary approach. *Pediatr Crit Care Med* 2012;13:e69-e72.
14. Sittig DF, Singh H. Eight rights of safe electronic health record use. *JAMA* 2009;302:1111-1113.
15. Han YY, Carcillo JA, Venkataraman ST, et al. Unexpected increased mortality after implementation of a commercially sold computerized physician order entry system. *Pediatrics* 2005;116:1506-1512.
16. LaRovere JM, Jeffries HE, Sachdeva RC, et al. Databases for assessing the outcomes of the treatment of patients with congenital and paediatric cardiac disease—the perspective of critical care. *Cardiol Young* 2008;18:130-136.
17. Jacobs JP, Jacobs ML, Lacour-Gayet FG, et al. Stratification of complexity improves the utility and accuracy of outcomes analysis in a Multi-Institutional Congenital Heart Surgery Database: Application of the Risk Adjustment in Congenital Heart Surgery (RACHS-1) and Aristotle Systems in the Society of Thoracic Surgeons (STS) Congenital Heart Surgery Database. *Pediatr Cardiol* 2009;30:1117-1130.
18. Vener DF, Jacobs JP, Schindler E, et al. Databases for assessing the outcomes of the treatment of patients with congenital and paediatric cardiac disease—the perspective of anaesthesia. *Cardiol Young* 2008;18:124-129.
19. Martin GR, Beekman RH, Ing FF, et al. The IMPACT registry: Improving Pediatric and Adult Congenital Treatments. *Semin Thorac Cardiovasc Surg Pediatr Card Surg Annu* 2010;13:20-25.
20. Latour JM, van Goudoever JB, Schuurman BE, et al. A qualitative study exploring the experiences of parents of children admitted to seven Dutch pediatric intensive care units. *Intensive Care Med* 2011;37:319-325.
21. Kuzin JK, Yborra JG, Taylor MD, et al. Family-member presence during interventions in the intensive care unit: perceptions of pediatric cardiac intensive care providers. *Pediatrics* 2007;120:e895-e901.
22. Basaran M, Sever K, Kafali E, et al. Serum lactate level has prognostic significance after pediatric cardiac surgery. *J Cardiothorac Vasc Anesth* 2006;20:43-47.
23. Cheung PY, Chui N, Joffe AR, et al.; Western Canadian Complex Pediatric Therapies Project, Follow-up Group. Postoperative lactate concentrations predict the outcome of infants aged 6 weeks or less after intracardiac surgery: a cohort follow-up to 18 months. *J Thorac Cardiovasc Surg* 2005;130:837-843.
24. Mullen MP. Diagnostic strategies for acute presentation of pulmonary hypertension in children: particular focus on use of echocardiography, cardiac catheterization, magnetic resonance imaging, chest computed tomography, and lung biopsy. *Pediatr Crit Care Med* 2010;11:S23-S26.
25. Martin AC, Rigby ML, Penny DJ, et al. Bedside balloon atrial septostomy on neonatal units. *Arch Dis Child Fetal Neonatal Ed* 2003;88:F339-F340.
26. Martin J, Shekerdemian LS. The monitoring of venous saturations of oxygen in children with congenitally malformed hearts. *Cardiol Young* 2009;19:34-39.
27. Liakopoulos OJ, Ho JK, Yezbick A, et al. An experimental and clinical evaluation of a novel central venous catheter with integrated oximetry for pediatric patients undergoing cardiac surgery. *Anesth Analg* 2007;105:1598-1604.
28. Spenceley N, Krahn G, Skippen PW, et al. Evaluation of a pediatric central venous oximetry catheter in critically ill children. *Pediatr Crit Care Med* 2010;11:26-30.
29. Tweddell JS, Ghanayem NS, Mussatto KA, et al. Mixed venous oxygen saturation monitoring after stage I palliation for hypoplastic left heart syndrome. *Ann Thorac Surg* 2007;84:1301-1310.
30. Jobsis FF. Noninvasive, infrared monitoring of cerebral and myocardial oxygen sufficiency and circulatory parameters. *Science* 1977;198:1264-1267.
31. Rais-Bahrami K, Rivera O, Short BL. Validation of a noninvasive neonatal optical cerebral oximeter in veno-venous ECMO patients with a cephalad catheter. *J Perinatol* 2006;26:628-635.
32. Giacomuzzi C, Heller E, Mejak B, et al. Assessing the brain using near infrared spectroscopy during postoperative ventricular circulatory support. *Cardiol Young* 2005;15:154-158.
33. Tortoriello TA, Stayer SA, Mott AR, et al. A non-invasive estimation of mixed venous oxygen saturation using near infrared spectroscopy by cerebral oximetry in pediatric cardiac surgery patients. *Pediatr Anesth* 2005;15:495-503.
34. Bhutta AT, Ford JW, Parker JG, et al. Non invasive cerebral oximeter as a surrogate for mixed venous saturation in children. *Pediatr Cardiol* 2007;28:34-41.
35. Hoffman GM, Stuth EA, Jacquiss RD, et al. Changes in cerebral and somatic oxygenation during stage I palliation of hypoplastic left heart syndrome using continuous regional cerebral perfusion. *J Thorac Cardiovasc Surg* 2004;127:223-233.
36. Hoffman GM, Ghanayem NS, Mussatto KM, et al. Postoperative two-site NIRS predicts complications and mortality after stage I palliation of hypoplastic left heart syndrome. *Anesthesiology* 2007;107:A234.
37. Kaufman J, Almodovar MC, Zuk J, et al. Correlation of abdominal site near infrared spectroscopy with gastric tonometry in infants following surgery for congenital heart disease. *Pediatr Crit Care Med* 2008;9:62-68.
38. Owens GE, King K, Gurney JG, et al. Low renal oximetry correlates with acute kidney injury after infant cardiac surgery. *Pediatr Cardiol* 2011;32:183-188.
39. Introna RP, Martin DC, Pruett JK, et al. Percutaneous pulmonary artery catheterization in pediatric cardiovascular anesthesia: insertion techniques and use. *Anesth Analg* 1990;70:562-566.
40. Rimensberger PC, Beghetti M. Pulmonary artery catheter placement under transoesophageal echocardiography guidance. *Paediatr Anaesth* 1999;9:167-170.
41. Reich DL, Moskowitz DM, Kaplan JA. Hemodynamic monitoring. In: Kaplan JA, Reich DL, Konstadt SN, eds. *Cardiac Anesthesia*. Philadelphia, PA: W. B. Saunders, 1999:321-358.
42. Vargo TA. Catheterization hemodynamic measurements. In: Garson A, Bricker T, et al., eds. *The Science and Practice of Pediatric Cardiology*. Baltimore, MD: Williams & Wilkins, 1998:961-993.
43. Bishop MH, Shoemaker WC, Appel PL. Prospective, randomized trial of survivor values of cardiac index, oxygen delivery, and oxygen consumption as resuscitation endpoints in severe trauma. *J Trauma* 1995;38:780-787.
44. Velmahos GC, Demetriades D, Shoemaker WC. Endpoints of resuscitation of critically injured patients: normal or supranormal? A prospective randomized trial. *Ann Surg* 2000;232:409-418.
45. Buheitel G, Scharf J, Hofbeck M, et al. Estimation of cardiac index by means of the arterial and the mixed venous oxygen content and pulmonary oxygen uptake determination in the early post-operative period following surgery of congenital heart disease. *Intensive Care Med* 1994;20:500-503.
46. Rossi AF, Seiden HS, Gross RP, et al. Oxygen transport in critically ill infants after congenital heart operations. *Ann Thorac Surg* 1999;67:739-744.
47. Linton RA, Jonas MM, Tibby SM, et al. Cardiac output measured by lithium dilution and transpulmonary thermodilution in patients in a paediatric intensive care unit. *Intensive Care Med* 2000;26:1507-1511.
48. Pauli C, Fakler U, Genz T, et al. Cardiac output determination in children; equivalence of the transpulmonary thermodilution method to the direct Fick principle. *Intensive Care Med* 2002;28:947-952.
49. Fakler U, Pauli C, Balling G, et al. Cardiac index monitoring by pulse contour analysis and thermodilution after pediatric cardiac surgery. *J Thorac Cardiovasc Surg* 2007;133:224-228.
50. Kim JJ, Dreyer WJ, Chang AC, et al. Arterial pulse wave analysis: an accurate means of determining cardiac output in children. *Pediatr Crit Care Med* 2006;7:532-535.
51. Proulx F, Lemson J, Choker G, et al. Hemodynamic monitoring by transpulmonary thermodilution and pulse contour analysis in critically ill children. *Pediatr Crit Care Med* 2011;12:1-8.
52. Gaies MG, Gurney JG, Yen AH, et al. Vasoactive-inotropic score as a predictor of morbidity and mortality in infants after cardiopulmonary bypass. *Pediatr Crit Care Med* 2010;11:234-238.
53. Allwood M, Cobbald A, Ginsburg J. Peripheral vascular effects of noradrenaline, isopropylnoradrenaline and dopamine. *Br Med Bull* 1963;19:132-136.
54. Zaritsky A, Chervon B. Catecholamines in critical care medicine. *Crit Care Med* 1981;9:39-47.
55. Gambos E, Hulet W, Bopp P, et al. Reactivity of renal systemic circulation to vasoconstrictor agents in normotensive and hypertensive subjects. *J Clin Invest* 1962;41:203-217.
56. Michael J, Guerci A, Koehler R, et al. Mechanism by which epinephrine augments cerebral and myocardial perfusion during cardiopulmonary resuscitation in dogs. *Circulation* 1984;69:822-835.
57. International Liaison Committee on Resuscitation. 2005 International Consensus on Cardiopulmonary Resuscitation and Emergency Cardiovascular Care Science with Treatment Recommendation. *Circulation* 2005;112:III-1-III-136.
58. American Heart Association. 2005 American Heart Association (AHA) Guidelines for Cardiopulmonary Resuscitation (CPR) and Emergency Cardiovascular Care (ECC) of Pediatric and Neonatal Patients: Pediatric Advanced Life Support. *Pediatrics* 2006;117:e1005-e1028.

59. Booker PD. Pharmacological support for children with myocardial dysfunction. *Paediatr Anaesth* 2002;12:5-25.
60. Goldberg L, Rajfer E. Dopamine receptors: applications in clinical cardiology. *Circulation* 1985;72:245-248.
61. Parker S, Carlon G, Isaacs M, et al. Dopamine administration in oliguria and oliguric renal failure. *Crit Care Med* 1981;9:630-632.
62. Henderson I, Beattie T, Kennedy A. Dopamine hydrochloride in oliguric renal states. *Lancet* 1980;2:827-828.
63. Goldberg L. Dopamine. Clinical uses of endogenous catecholamine. *N Engl J Med* 1974;291:707-710.
64. Eldadah M, Schwartz P, Harrison R. Pharmacokinetics of dopamine in infants and children. *Crit Care Med* 1991;19:1008-1011.
65. Van den Berghe G, de Zegher F, Lauwers P. Dopamine suppresses pituitary function in infants and children. *Crit Care Med* 1994;22:1747-1753.
66. Filippi L, Pezzati M, Poggi C, et al. Dopamine versus dobutamine in very low birthweight infants: endocrine effects. *Arch Dis Child Fetal Neonatal Ed* 2007;92:F367-F371.
67. Bohn D, Poirier C, Edmonds J, et al. Hemodynamic effects of dobutamine after cardiopulmonary bypass in children. *Crit Care Med* 1980;8:367-371.
68. Gross R, Strain J, Greenberg M, et al. Systemic and coronary effects of intravenous milrinone and dobutamine in congestive heart failure. *J Am Cardiol* 1986;7:1107-1113.
69. Loeb H, Khan M, Saudaye A, et al. Acute hemodynamic effects of dobutamine and isoproterenol in patients with low output cardiac failure. *Circ Shock* 1976;3:55-59.
70. Robel-Tillig E, Knüpfer M, Pulzer F, et al. Cardiovascular impact of dobutamine in neonates with myocardial dysfunction. *Early Hum Dev* 2007;83:307-312.
71. van den Berg J, Wielopolski PA, Meijboom FJ, et al. Diastolic function in repaired tetralogy of Fallot at rest and during stress: assessment with MR imaging. *Radiology* 2007;243:212-219.
72. Kariya T, Willie L, Dage R. Biochemical studies on the mechanism of cardiotonic activity of MDL 17043. *J Cardiovasc Pharmacol* 1982;4:509-514.
73. Benotti J, Grossman W, Braunwald E. Hemodynamic assessment of amrinone: a new inotropic agent. *N Engl J Med* 1978;199:1373-1377.
74. Wright E, Skoyles J, Sherry M. Milrinone in the treatment of low cardiac output states following cardiac surgery. *Eur J Anaesthesiol* 1992;5:21-26.
75. Ramamoorthy C, Anderson G, Williams G, et al. Pharmacokinetics and side effects of milrinone in infants and children after open heart surgery. *Anesth Analg* 1998;86:283-289.
76. Chang A, Atz A, Wernovsky G, et al. Milrinone: systemic and pulmonary hemodynamic effects in neonates after cardiac surgery. *Crit Care Med* 1995;23:1907-1914.
77. Bailey JM, Miller BE, Lu W, et al. The pharmacokinetics of milrinone in pediatric patients after cardiac surgery. *Anesthesiology* 1999;90:1012-1018.
78. Mehra M, Ventura H, Kapoor C, et al. Safety and clinical utility of long term intravenous milrinone in advanced heart failure. *Am J Cardiol* 1997;80:61-64.
79. Edelson J. Pharmacokinetics of bipyridines amrinone and milrinone. *Circulation* 1986;73:145-155.
80. Hoffman TM, Wernovsky G, Atz AM, et al. Efficacy and safety of milrinone in preventing low cardiac output syndrome in infants and children after corrective surgery for congenital heart disease. *Circulation* 2003;107:996-1002.
81. Zuppa AF, Nicolson SC, Adamson PC, et al. Population pharmacokinetics of milrinone in neonates with hypoplastic left heart syndrome undergoing stage I reconstruction. *Anesth Analg* 2006;102:1062-1069.
82. Drop L, Geffin G, O'Keefe D, et al. Relation between ionized calcium concentration and ventricular pump performance in the dog under hemodynamically controlled conditions. *Am J Cardiol* 1981;47:1041-1051.
83. Robertie P, Butterworth J, Royster R, et al. Normal parathyroid hormone responses to hypocalcemia during cardiopulmonary bypass. *Anesthesiology* 1991;75:43-48.
84. Elz J, Panagiotopoulos S, Nayker W, et al. Reperfusion induced calcium gain after ischemia. *Am J Cardiol* 1989;63:7E-13E.
85. Murdoch I, Qureshi S, Huggon I. Perioperative hemodynamic effects of an intravenous infusion of calcium chloride in children following cardiac surgery. *Acta Paediatr* 1983;83:658-661.
86. Broner CW, Stidham GL, Westenkirchner DE, et al. A prospective, randomized, double-blind comparison of calcium chloride and calcium gluconate therapies for hypocalcemia in critically ill children. *J Pediatr* 1990;117:986-989.
87. Dyke PC, Yates AR, Cua CL, et al. Increased calcium supplementation is associated with morbidity and mortality in the infant postoperative cardiac patient. *Pediatr Crit Care Med* 2007;8:254-257.
88. Walters P, Cooper T, Denison A, et al. Dilator responses to isoproterenol in cutaneous and skeletal muscle vascular beds of adrenergic blocking drugs. *J Pharmacol Exp Ther* 1955;115:323-327.
89. Vatner S, Baig H. Comparison of the effects of ouabain and isoproterenol on ischemic myocardium of conscious dogs. *Circulation* 1978;58:654-662.
90. Clutter W, Bier D, Shah S, et al. Epinephrine plasma metabolic clearance rates and physiologic thresholds for metabolic and hemodynamic actions in man. *J Clin Invest* 1980;66:94-101.
91. Tourneux P, Rakza T, Abazine A, et al. Noradrenaline for management of septic shock refractory to fluid loading and dopamine or dobutamine in full-term newborn infants. *Acta Paediatr* 2008;97:177-180.
92. Oshita S, Uchimoto R, Oka H, et al. Correlation between arterial blood pressure and oxygenation in tetralogy of Fallot. *J Cardiothorac Anesth* 1989;3:597-600.
93. Stewart WJ, Schiavone WA, Salcedo EE, et al. Intraoperative Doppler echocardiography in hypertrophic cardiomyopathy: correlations with the obstructive gradient. *J Am Coll Cardiol* 1987;10:327-335.
94. Holmes CL, Patel BM, Russell JA, et al. Physiology of vasopressin relevant to management of septic shock. *Chest* 2001;120:989-1002.
95. Rosenzweig E, Starc T, Chen J, et al. Intravenous arginine-vasopressin in children with vasodilatory shock after cardiac surgery. *Circulation* 1999;100:182-186.
96. O'Blens SB, Roy N, Konstantinov I, et al. Vasopressin reversal of phenoxylbenzamine-induced hypotension after the Norwood procedure. *J Thorac Cardiovasc Surg* 2002;123:1012-1013.
97. Meyer S, Gortner L, McGuire W, et al. Vasopressin in catecholamine-refractory shock in children. *Anaesthesia* 2008;63:228-234.
98. Yildizdas D, Yapicioglu H, Celik U, et al. Terlipressin as a rescue therapy for catecholamine-resistant septic shock in children. *Intensive Care Med* 2008;34:511-517.
99. Strauer B, Scherpe A. Ventricular function and coronary hemodynamics after intravenous nitroglycerin in coronary artery disease. *Am Heart J* 1978;95:210-219.
100. Ilbawi M, Farouk I, Serafin D, et al. Hemodynamic effects of intravenous nitroglycerin in pediatric patients after heart surgery. *Circulation* 1985;72:101-107.
101. Furck AK, Hansen JH, Uebing A, et al. The impact of afterload reduction on the early postoperative course after the Norwood operation—a 12-year single-center experience. *Eur J Cardiothorac Surg* 2010;37:289-295.
102. Moffett BS, Price JF. Evaluation of sodium nitroprusside toxicity in pediatric cardiac surgical patients. *Ann Pharmacother* 2008;42:1600-1604.
103. Tabbutt S, Nicolson SC, Adamson PC, et al. The safety, efficacy, and pharmacokinetics of esmolol for blood pressure control immediately after repair of coarctation of the aorta in infants and children: a multicenter, double-blind, randomized trial. *J Thorac Cardiovasc Surg* 2008;136:321-328.
104. Ohara T, Ogata H, Fujiyama J, et al. Effects of prostaglandin E1 infusion in the pre-operative management of critical congenital heart disease. *Tohoku J Exp Med* 1985;146:237-249.
105. Freed M, Heyman M, Rudolph A, et al. Prostaglandin E1 in ductus arteriosus dependent congenital heart disease. *Circulation* 1981;64:889-905.
106. D'Ambra M, LaRaia P, Philbin D, et al. Prostaglandin E1: a new therapy for refractory right heart failure and pulmonary hypertension after mitral valve replacement. *J Thorac Cardiovasc Surg* 1985;89:567-572.
107. Rubis L, Stephenson L, Johnston M, et al. Comparison of effects of Prostaglandin E1 and Nitroprusside on pulmonary vascular resistance in children after open-heart surgery. *Ann Thorac Surg* 1981;32:563-570.
108. Armitage J, Hardesty R, Griffith B, et al. Prostaglandin E1: an effective treatment of right heart failure after orthotopic heart transplantation. *J Heart Transplant* 1987;6:348-351.
109. Kermode J, Butt W, Shann F. Comparison between prostaglandin E1 and epoprostenol in infants after heart surgery. *Br Heart J* 1991;66:175-178.
110. Schulze-Neick I, Uhlemann F, Nurnberg J, et al. Aerosolized prostacyclin for preoperative evaluation and post-cardiosurgical treatment of patients with pulmonary hypertension. *Z Kardiol* 1997;86:71-80.
111. Haraldsson A, Kieler J, Ricksten S. Inhaled prostacyclin for the treatment of pulmonary hypertension after cardiac surgery or heart transplantation: a pharmacodynamic study. *J Cardiothorac Vasc Anesth* 1996;10:864-868.
112. Zwissler B, Kemming G, Habler O, et al. Inhaled prostacyclin (PGI2) versus inhaled nitric oxide in adult respiratory distress syndrome. *Am J Respir Crit Care Med* 1996;154:1671-1677.
113. Müller M, Scholz S, Kwapisz M, et al. Use of inhaled iloprost in a case of pulmonary hypertension during pediatric congenital heart surgery. *Anesthesiology* 2003;99:743-744.
114. Shekardemian LS, Ravn HB, Penny DJ. Intravenous sildenafil lowers pulmonary vascular resistance in a model of neonatal pulmonary hypertension. *Am J Respir Crit Care Med* 2002;165:1098-1102.
115. Atz AM, Wessel DL. Sildenafil ameliorates effects of inhaled nitric oxide withdrawal. *Anesthesiology* 1999;91:307-310.
116. Raja SG, Danton MD, MacArthur KJ, et al. Effects of escalating doses of sildenafil on hemodynamics and gas exchange in children with pulmonary hypertension and congenital cardiac defects. *J Cardiothorac Vasc Anesth* 2007;21:203-207.
117. Roberts J, Lang P, Bigatello L, et al. Inhaled nitric oxide in congenital heart disease. *Circulation* 1993;87:447-453.
118. Miller O, Celermeyer D, Deanfield J, et al. Very low dose inhaled nitric oxide: a selective pulmonary vasodilator after operations for congenital heart disease. *J Thorac Cardiovasc Surg* 1994;108:487-494.
119. Kieler-Jensen N, Lundin S, Ricksten S. Vasodilator therapy after heart transplantation: effects of inhaled nitric oxide and intravenous prostacyclin, prostaglandin E1 sodium nitroprusside. *J Heart Lung Transplant* 1995;14:436-443.
120. Turanlahti M, Laitinen P, Pesonen E. Preoperative and postoperative response to inhaled nitric oxide. *Scand Cardiovasc J* 2000;34:46-52.

121. Kadosaki M, Kawamura T, Oyama K, et al. Usefulness of nitric oxide treatment for pulmonary hypertensive infants during cardiac anesthesia. *Anesthesiology* 2002;96:835-840.
122. Winberg P, Lundell B, Gustafsson L. Effects of inhaled nitric oxide on raised pulmonary vascular resistance in children with congenital heart disease. *Br Heart J* 1994;71:282-286.
123. Sadao K, Masahiro S, Toshihiko M, et al. Effect of nitric oxide on oxygenation and hemodynamics in infants after cardiac surgery. *Artif Organs* 1997;21:14-16.
124. Khazin V, Kaufman Y, Zabeeda D, et al. Milrinone and nitric oxide: combined effect on pulmonary artery pressures after cardiopulmonary bypass in children. *J Cardiothorac Vasc Anesth* 2004;18:156-159.
125. Barr FE, Tirona RG, Taylor MB, et al. Pharmacokinetics and safety of intravenously administered citrulline in children undergoing congenital heart surgery: potential therapy for postoperative pulmonary hypertension. *J Thorac Cardiovasc Surg* 2007;134:319-326.
126. Miller O, Tang S, Keech A, et al. Rebound pulmonary hypertension on withdrawal from inhaled nitric oxide. *Lancet* 1995;346:51-52.
127. Chiodi H, Mohler J. Effects of exposure of blood hemoglobin to nitric oxide. *Environ Res* 1985;37:355-363.
128. Panacek E, Bednarczyk E, Dunbar L, et al. Randomized, prospective trial of fenoldopam vs sodium nitroprusside in the treatment of acute severe hypertension. Fenoldopam Study Group. *Acad Emerg Med* 1995;2:959-965.
129. Goldberg ME, Cantillo J, Nemiroff MS, et al. Fenoldopam infusion for the treatment of post-operative hypertension. *J Clin Anesth* 1993;5:386-391.
130. Tobias J. Fenoldopam for controlled hypotension during spinal fusion in children and adolescents. *Paediatr Anaesth* 2001;10:261-266.
131. Costello JM, Thiagarajan RR, Dionne RE, et al. Initial experience with fenoldopam after cardiac surgery in neonates with an insufficient response to conventional diuretics. *Pediatr Crit Care Med* 2006;7:28-33.
132. Sahney S. A review of calcium channel antagonists in the treatment of pediatric hypertension. *Paediatr Drugs* 2006;8:357-373.
133. Nakagawa TA, Sartori SC, Morris A, et al. Intravenous nicardipine for treatment of postcoarctectomy hypertension in children. *Pediatr Cardiol* 2004;25:26-30.
134. Buchhorn R, Bartmus D, Siekmeyer W, et al. Beta-blocker therapy of severe congestive heart failure in infants with left to right shunts. *Am J Cardiol* 1998;81:1366-1368.
135. Consensus recommendation for the management of chronic heart failure. *Am J Cardiol* 1999;83:1A-38A.
136. Bristow M, Ginsberg R, Minobe W, et al. Decreased catecholamine sensitivity and beta receptor density in failing human hearts. *N Engl J Med* 1981;307:205-211.
137. Buchhorn R, Hulpke-Wette M, Russchewski W, et al. Beta-receptor down-regulation in congenital heart disease: a risk factor for complications after surgical repair? *Ann Thorac Surg* 2002;73:610-613.
138. Bruns L, Chrisant M, Lamour J, et al. Carvedilol as therapy in pediatric heart failure: an initial multicenter experience. *J Pediatr* 2001;138:505-511.
139. Buchhorn R, Hulpke-Wette M, Hilgers R, et al. Propranolol treatment of congestive heart failure in infants with congenital heart disease: the CHF-PRO-INFANT Trial. *Int J Cardiol* 2001;79:167-173.
140. Garson A, Gillette P, McNamara P. Propranolol: the preferred palliation for tetralogy of Fallot. *Am J Cardiol* 1981;47:1098-1104.
141. Nussbaum J, Zane E, Thys D. Esmolol for the treatment of hypercyanotic spells in infants with tetralogy of Fallot. *J Cardiothorac Anesth* 1989;3:200-202.
142. Wiest D, Garner S, Uber W, et al. Esmolol for the management of pediatric hypertension after cardiac operations. *J Thorac Cardiovasc Surg* 1997;115:890-897.
143. Follath F, Cleland J, Just H, et al. Efficacy and safety of intravenous levosimendan compared with dobutamine in severe low-output heart failure (the LIDO study): a randomised double-blind trial. *Lancet* 2002;360:196-202.
144. Nijhawan N, Nicolosi A, Montgomery M, et al. Levosimendan enhances cardiac performance after cardiopulmonary bypass: a prospective, randomized placebo-controlled trial. *J Cardiovasc Pharmacol* 1999;34:219-228.
145. Namachivayam P, Crossland DS, Butt WW, et al. Early experience with Levosimendan in children with ventricular dysfunction. *Pediatr Crit Care Med* 2006;7:445-448.
146. Young J, Abraham W, Stevenson L, et al. Results of the VMAC trial: vasodilation in the management of acute congestive heart failure. *Circulation* 2000;102:2794.
147. Mills R, LeJemtel T, Horton D, et al. Sustained hemodynamic effects of nesiritide in heart failure: a randomized, double blind, placebo controlled clinical trials. Natreacor study group. *J Am Coll Cardiol* 1999;34:155-162.
148. Colucci W, Elkayam U, Horton D, et al. Intravenous nesiritide, a natriuretic peptide, in the treatment of decompensated congestive heart failure. *N Engl J Med* 2000;343:246-253.
149. Jensen K, Eiskjaer H, Carstens J. Renal effects of brain natriuretic peptide in patients with congestive heart failure. *Clin Sci* 1999;96:5-15.
150. Marcus L, Hart D, Packer M, et al. Hemodynamic and renal excretory effects of human brain natriuretic peptide infusions in patients with congestive heart failure: a double blind, placebo controlled, randomized crossover trial. *Circulation* 1996;94:3184-3189.
151. Simsic JM, Scheurer M, Tobias JD, et al. Perioperative effects and safety of nesiritide following cardiac surgery in children. *J Intensive Care Med* 2006;21:22-26.
152. Hoffman TM, Wernovsky G, Wieand TS, et al. The incidence of arrhythmias in a pediatric cardiac intensive care unit. *Pediatr Cardiol* 2002;23:598-604.
153. Delaney JW, Molledo JM, Dziura JD, et al. Early postoperative arrhythmias after pediatric cardiac surgery. *J Thorac Cardiovasc Surg* 2006;131:1296-1300.
154. Hoffman TM, Bush DM, Wernovsky G, et al. Postoperative junctional ectopic tachycardia in children: incidence, risk factors, and treatment. *Ann Thorac Surg* 2002;74:1607-1611.
155. Manrique AM, Arroyo M, Lin Y, et al. Magnesium supplementation during cardiopulmonary bypass to prevent junctional ectopic tachycardia after pediatric cardiac surgery: a randomized controlled study. *J Thorac Cardiovasc Surg* 2010;139:162-169.
156. Kovacicova L, Hakacova N, Dobos D, et al. Amiodarone as a first-line therapy for postoperative junctional ectopic tachycardia. *Ann Thorac Surg* 2009;88:616-622.
157. Ceresnak SR, Pass RH, Starc TJ, et al. Predictors for hemodynamic improvement with temporary pacing after pediatric cardiac surgery. *J Thorac Cardiovasc Surg* 2011;141:183-187.
158. Kim JJ, Collins KK, Miller-Hance WC. Chapter 17: Arrhythmias: diagnosis and treatment. In: Andropoulos DB, Stayer SA, Russell IA, eds. *Anesthesia for Congenital Heart Disease*. 2nd ed. Oxford, UK: Wiley-Blackwell, 2010:308-337.
159. Kageyama K, Hashimoto S, Nakajima Y, et al. The change of plasma endothelin-1 levels before and after surgery with or without Down syndrome. *Paediatr Anaesth* 2007;17:1071-1077.
160. Lindberg L, Olsson AK, Jögi P, et al. How common is severe pulmonary hypertension after pediatric cardiac surgery? *J Thorac Cardiovasc Surg* 2002;123:1155-1163.
161. Binotto MA, Redington AN. Assessment of the pulmonary circulation in patients with functionally univentricular physiology. *Cardiol Young* 2009;19:35-38.
162. Galante D. Intraoperative management of pulmonary arterial hypertension in infants and children. *Curr Opin Anaesthesiol* 2009;22:378-382.
163. Adatia I, Beghetti M. Early postoperative care of patients with pulmonary hypertension associated with congenital cardiac disease. *Cardiol Young* 2009;19:315-319.
164. Pilchard J, Dadlani G, Andropoulos D, et al. Intensive card and perioperative management of patients with complete atrioventricular septal defect. *World J Pediatr Congenit Heart Surg* 2010;1:105-111.
165. Miller OI, Tang SF, Keech A, et al. Inhaled nitric oxide and prevention of pulmonary hypertension after congenital heart surgery: a randomised double-blind study. *Lancet* 2000;356:1464-1469.
166. Russell IA, Zwass MS, Fineman JR, et al. The effects of inhaled nitric oxide on postoperative pulmonary hypertension in infants and children undergoing surgical repair of congenital heart disease. *Anesth Analg* 1998;87:46-51.
167. Schulze-Neick I, Hartenstein P, Li J, et al. Intravenous sildenafil is a potent pulmonary vasodilator in children with congenital heart disease. *Circulation* 2003;108:II167-II173.
168. Hickey PR, Hansen DD, Wessel DL, et al. Blunting of stress responses in the pulmonary circulation of infants by fentanyl. *Anesth Analg* 1985;64:1137-1142.
169. Carroll CL, Backer CL, Mavroudis C, et al. Inhaled prostacyclin following surgical repair of congenital heart disease—a pilot study. *J Card Surg* 2005;20:436-439.
170. Namachivayam P, Theilen U, Butt WW, et al. Sildenafil prevents rebound pulmonary hypertension after withdrawal of nitric oxide in children. *Am J Respir Crit Care Med* 2006;174:1042-1047.
171. Cooper DS, Costello JM, Bronicki RA, et al. Current challenges in cardiac intensive care: optimal strategies for mechanical ventilation and timing of extubation. *Cardiol Young* 2008;18:72-83.
172. Mott AR, Alomrani A, Tortoriello TA, et al. Changes in cerebral saturation profile in response to mechanical ventilation alterations in infants with bidirectional superior cavopulmonary connection. *Pediatr Crit Care Med* 2006;7:346-350.
173. Li J, Hoskote A, Hickey C, et al. Effect of carbon dioxide on systemic oxygenation, oxygen consumption, and blood lactate levels after bidirectional superior cavopulmonary anastomosis. *Crit Care Med* 2005;33:984-989.
174. Shekerdemian LS, Shore DF, Lincoln C, et al. Negative-pressure ventilation improves cardiac output after right heart surgery. *Circulation* 1996;94:II49-II55.
175. Stayer SA, Hammer GB. Chapter 18: Ventilatory management. In: Andropoulos DB, Stayer SA, Russell IA, Mossad EB, eds. *Anesthesia for Congenital Heart Disease*. 2nd ed. Oxford, UK: Wiley-Blackwell, 2010:338-354.
176. Umenai T, Shime N, Hashimoto S. Hyperventilation versus standard ventilation for infants in postoperative care for congenital heart defects with pulmonary hypertension. *J Anesth* 2009;23:80-86.
177. Albuali WH, Singh RN, Fraser DD, et al. Have changes in ventilation practice improved outcome in children with acute lung injury? *Pediatr Crit Care Med* 2007;8:324-330.

178. Khemani RG, Conti D, Alonzo TA, et al. Effect of tidal volume in children with acute hypoxemic respiratory failure. *Intensive Care Med* 2009;35:1428–1437.
179. Bigham MT, Amato R, Bondurant P, et al. Ventilator-associated pneumonia in the pediatric intensive care unit: characterizing the problem and implementing a sustainable solution. *J Pediatr* 2009;154:582–587.
180. Shi S, Zhao Z, Liu X, et al. Perioperative risk factors for prolonged mechanical ventilation following cardiac surgery in neonates and young infants. *Chest* 2008;134:768–774.
181. Polito A, Paterno E, Costello JM, et al. Perioperative factors associated with prolonged mechanical ventilation after complex congenital heart surgery. *Pediatr Crit Care Med* 2011;12:e122–e126.
182. Kugelman A, Zeiger-Aginsky D, Bader D, et al. A novel method of distal end-tidal CO₂ capnography in intubated infants: comparison with arterial CO₂ and with proximal mainstream end-tidal CO₂. *Pediatrics* 2008;122:e1219–e1224.
183. Nève V, Cremer R, Leclerc F, et al. Measurement of respiratory mechanics in paediatric intensive care: in vitro assessment of a pulmonary function device. *Intensive Care Med* 1998;24:1083–1088.
184. Newth CJ, Venkataraman S, Willson DF, et al. Weaning and extubation readiness in pediatric patients. *Pediatr Crit Care Med* 2009;10:1–11.
185. Yang KL, Tobin MJ. A prospective study of indexes predicting the outcome of trials of weaning from mechanical ventilation. *N Engl J Med* 1991;324:1445–1450.
186. Khemani RG, Randolph A, Markovitz B. Corticosteroids for the prevention and treatment of post-extubation stridor in neonates, children and adults. *Cochrane Database Syst Rev* 2009;CD001000.
187. Hoskote A, Cohen G, Goldman A, et al. Tracheostomy in infants and children after cardiothoracic surgery: indications, associated risk factors, and timing. *J Thorac Cardiovasc Surg* 2005;130:1086–1093.
188. Edwards JD, Kun SS, Keens TG, et al. Children with corrected or palliated congenital heart disease on home mechanical ventilation. *Pediatr Pulmonol* 2010;45:645–649.
189. Carroll CL, Spinella PC, Corsi JM, et al. Emergent endotracheal intubations in children: be careful if it's late when you intubate. *Pediatr Crit Care Med* 2010;11:343–348.
190. American Heart Association. 2005 American Heart Association (AHA) guidelines for cardiopulmonary resuscitation (CPR) and emergency cardiovascular care (ECC) of pediatric and neonatal patients: pediatric basic life support. *Pediatrics* 2006;117:e989–e1004.
191. de Winter JP, de Vries MA, Zimmermann LJ. Clinical practice: noninvasive respiratory support in newborns. *Eur J Pediatr* 2010;169:777–782.
192. Gregoret C, Pelosi P, Chidini G, et al. Non-invasive ventilation in pediatric intensive care. *Minerva Pediatr* 2010;62:437–458.
193. Mittnacht AJ, Thanjan M, Srivastava S, et al. Extubation in the operating room after congenital heart surgery in children. *J Thorac Cardiovasc Surg* 2008;136:88–93.
194. Kin N, Weissmann C, Srivastava S, et al. Factors affecting the decision to defer endotracheal extubation after surgery for congenital heart disease: a prospective observational study. *Anesth Analg* 2011;113:329–335.
195. Turner DA, Arnold JH. Insights in pediatric ventilation: timing of intubation, ventilatory strategies, and weaning. *Curr Opin Crit Care* 2007;13:57–63.
196. Randolph AG. Management of acute lung injury and acute respiratory distress syndrome in children. *Crit Care Med* 2009;37:2448–2454.
197. Gazit AZ, Huddleston CB, Checchia PA, et al. Care of the pediatric cardiac surgery patient—part 1. *Curr Probl Surg* 2010;47:185–250.
198. Gazit AZ, Huddleston CB, Checchia PA, et al. Care of the pediatric cardiac surgery patient—part 2. *Curr Probl Surg* 2011;47:261–376.
199. Zavalkoff SR, Razack SJ, Lavoie J, et al. Handover after pediatric heart surgery: a simple tool improves information exchange. *Pediatr Crit Care Med* 2011;12:309–313.
200. Kitch BT, Cooper JB, Zapol WM, et al. Handoffs causing patient harm: a survey of medical and surgical house staff. *Jt Comm J Qual Patient Saf* 2008;34:563–570.
201. Berkenstadt H, Haviv Y, Tuval A, et al. Improving handoff communications in critical care: utilizing simulation-based training toward process improvement in managing patient risk. *Chest* 2008;134:158–162.
202. Kamra K, Russell I, Miller-Hance WC. Role of transesophageal echocardiography in the management of pediatric patients with congenital heart disease. *Paediatr Anaesth* 2011;21:479–493.
203. Ohye RG, Goldberg CS, Donohue J, et al. The quest to optimize neurodevelopmental outcomes in neonatal arch reconstruction: the perfusion techniques we use and why we believe in them. *J Thorac Cardiovasc Surg* 2009;137:803–806.
204. Fraser CD Jr, Andropoulos DB. Principles of antegrade cerebral perfusion during arch reconstruction in newborns/infants. *Semin Thorac Cardiovasc Surg Pediatr Card Surg Annu* 2008:61–68.
205. Fuller S, Rajagopalan R, Jarvik GP, et al. J. Maxwell Chamberlain Memorial Paper for congenital heart surgery. Deep hypothermic circulatory arrest does not impair neurodevelopmental outcome in school-age children after infant cardiac surgery. *Ann Thorac Surg* 2010;90:1985–1994.
206. Wypij D, Newburger JW, Rappaport LA, et al. The effect of duration of deep hypothermic circulatory arrest in infant heart surgery on late neurodevelopment: the Boston Circulatory Arrest Trial. *J Thorac Cardiovasc Surg* 2003;126:1397–1403.
207. Bellinger DC, Wypij D, du Plessis AJ, et al. Developmental and neurologic effects of alpha-stat versus pH-stat strategies for deep hypothermic cardiopulmonary bypass in infants. *J Thorac Cardiovasc Surg* 2001;121:374–383.
208. Hessel EA, Hill AB. Circuitry and cannulation techniques. In: Gravlee GP, Davis RF, Kursz M, Utley JR, eds. *Cardiopulmonary Bypass: Principles and Practice* 2000. Philadelphia, PA: Lippincott, Williams & Wilkins, 69–97.
209. Dibardino DJ, Allison AE, Vaughn WK, et al. Current expectations for newborns undergoing the arterial switch operation. *Ann Surg* 2004;239:588–596.
210. Pigula FA, Nemoto EM, Griffith BP, et al. Regional low-flow perfusion provides cerebral circulatory support during neonatal aortic arch reconstruction. *J Thorac Cardiovasc Surg* 2000;119:331–339.
211. Allan CK, Newburger JW, McGrath E, et al. The relationship between inflammatory activation and clinical outcome after infant cardiopulmonary bypass. *Anesth Analg* 2010;111:1244–1251.
212. Pasquali SK, Hall M, Li JS, et al. Corticosteroids and outcome in children undergoing congenital heart surgery: analysis of the Pediatric Health Information Systems database. *Circulation* 2010;122:2123–2130.
213. Wernovsky G, Wypij D, Jonas RA, et al. Postoperative course and hemodynamic profile after the arterial switch operation in neonates and infants. A comparison of low-flow cardiopulmonary bypass and circulatory arrest. *Circulation* 1995;92:2226–2235.
214. Miller BE, Guzzetta NA, Tosone SR, et al. Tissue factor-activated thromboelastograms in children undergoing cardiac surgery: baseline values and comparisons. *Anesth Analg* 2003;97:1289–1293.
215. Miller BE, Mochizuki T, Levy JH, et al. Predicting and treating coagulopathies after cardiopulmonary bypass in children. *Anesth Analg* 1997;85:1196–1202.
216. Mou SS, Giroir BP, Molitor-Kirsch EA, et al. Fresh whole blood versus reconstituted blood for pump priming in heart surgery in infants. *N Engl J Med* 2004;351:1635–1644.
217. Vojtovic P, Reich O, Selko M, et al. Haemodynamic changes due to delayed sternal closure in newborns after surgery for congenital cardiac malformations. *Cardiol Young* 2009;19:573–579.
218. Ramamoorthy C, Tabbutt S, Kurth CD, et al. Effects of inspired hypoxic and hypercapnic gas mixtures on cerebral oxygen saturation in neonates with univentricular heart defects. *Anesthesiology* 2002;96:283–288.
219. Dorfman AT, Marino BS, Wernovsky G, et al. Critical heart disease in the neonate: presentation and outcome at a tertiary care center. *Pediatr Crit Care Med* 2008;9:193–202.
220. Petit CJ, Altman CA, Pignatelli RH. Transthoracic echocardiographic assistance for interatrial stenting in low birth-weight neonates with hypoplastic left heart syndrome and intact atrial septum. *Catheter Cardiovasc Interv* 2010;76:425–430.
221. Hill K, Fudge JC, Barker P, et al. Novel transatrial septoplasty technique for neonates with hypoplastic left heart syndrome and an intact or highly restrictive atrial septum. *Pediatr Cardiol* 2010;31:545–549.
222. Kussman BD, Gauvreau K, DiNardo JA, et al. Cerebral perfusion and oxygenation after the Norwood procedure: comparison of right ventricle-pulmonary artery conduit with modified Blalock-Taussig shunt. *J Thorac Cardiovasc Surg* 2007;133:648–655.
223. Ohye RG, Sleeper LA, Mahony L, et al. Comparison of shunt types in the Norwood procedure for single-ventricle lesions. *N Engl J Med* 2010;362:1980–1992.
224. Diaz LK, Nicolson SC, Steven JM. Chapter 24: Anesthesia for the patient with a single ventricle. In: Andropoulos DB, Stayer SA, Russell IA, Mossad EB, eds. *Anesthesia for Congenital Heart Disease*. 2nd ed. Oxford, UK: Wiley-Blackwell, 2010:456–479.
225. Ugaki S, Kasahara S, Kotani Y, et al. Extracorporeal membrane oxygenation following Norwood stage 1 procedures at a single institution. *Artif Organs* 2010;34:898–903.
226. Galantowicz M, Cheatham JP, Phillips A, et al. Hybrid approach for hypoplastic left heart syndrome: intermediate results after the learning curve. *Ann Thorac Surg* 2008;85:2063–2070.
227. Li J, Zhang G, Benson L, et al. Comparison of the profiles of postoperative systemic hemodynamics and oxygen transport in neonates after the hybrid or the Norwood procedure: a pilot study. *Circulation* 2007;116:1179–1187.
228. Caldarone CA, Benson L, Holtby H, et al. Initial experience with hybrid palliation for neonates with single-ventricle physiology. *Ann Thorac Surg* 2007;84:1294–1300.
229. Wernovsky G, Kuijpers M, Van Rossem MC, et al. Postoperative course in the cardiac intensive care unit following the first stage of Norwood reconstruction. *Cardiol Young* 2007;17:652–665.
230. McQuillen PS, Hamrick SE, Perez MJ, et al. Balloon atrial septostomy is associated with preoperative stroke in neonates with transposition of the great arteries. *Circulation* 2006;113:280–285.
231. Petit CJ, Rome JJ, Wernovsky G, et al. Preoperative brain injury in transposition of the great arteries is associated with oxygenation and time to surgery, not balloon atrial septostomy. *Circulation* 2009;119:709–716.
232. Andropoulos DB, Hunter JV, Nelson DP, et al. Brain immaturity is associated with brain injury before and after neonatal cardiac surgery with high-flow bypass and cerebral oxygenation monitoring. *J Thorac Cardiovasc Surg* 2010;139:543–556.
233. Rouine-Rapp K, Rouillard KP, Miller-Hance W, et al. Segmental wall-motion abnormalities after an arterial switch operation indicate ischemia. *Anesth Analg* 2006;103:1139–1146.

234. McGowan FX Jr, Davis PJ, Siewers RD, et al. Coronary vasoconstriction mediated by endothelin-1 in neonates. Reversal by nitroglycerin. *J Thorac Cardiovasc Surg* 1995;109:88–97.
235. Vida VL, Speggorin S, Maschietto N, et al. Cardiac operations after patent ductus arteriosus stenting in duct-dependent pulmonary circulation. *Ann Thorac Surg* 2010;90:605–609.
236. Di Donato RM, Jonas RA, Lang P, et al. Neonatal repair of tetralogy of Fallot with and without pulmonary atresia. *J Thorac Cardiovasc Surg* 1991;101:126–137.
237. Fraser CD Jr, McKenzie ED, Cooley DA. Tetralogy of Fallot: surgical management individualized to the patient. *Ann Thorac Surg* 2001;71:1556–1561.
238. Morales DL, Zafar F, Heinle JS, et al. Right ventricular infundibulum sparing (RVIS) tetralogy of fallot repair: a review of over 300 patients. *Ann Surg* 2009;250:611–617.
239. Gold JP, Jonas RA, Lang P, et al. Transthoracic intracardiac monitoring lines in pediatric surgical patients: a ten-year experience. *Ann Thorac Surg* 1986;42:185–191.
240. Flori HR, Johnson LD, Hanley FL, et al. Transthoracic intracardiac catheters in pediatric patients recovering from congenital heart defect surgery: associated complications and outcomes. *Crit Care Med* 2000;28:2997–3001.
241. Fesseha AK, Eidem BW, Dibardino DJ, et al. Neonates with aortic coarctation and cardiogenic shock: presentation and outcomes. *Ann Thorac Surg* 2005;79:1650–1655.
242. Elgamal MA, McKenzie ED, Fraser CD Jr. Aortic arch advancement: the optimal one-stage approach for surgical management of neonatal coarctation with arch hypoplasia. *Ann Thorac Surg* 2002;73:1267–1272.
243. Azakie A, Johnson NC, Anagnostopoulos PV, et al. Stage II palliation of hypoplastic left heart syndrome without cardiopulmonary bypass. *J Thorac Cardiovasc Surg* 2011;141:400–406.
244. Fontan F, Baudet E. Surgical repair of tricuspid atresia. *Thorax* 1971;26:240–248.
245. Petrossian E, Thompson LD, Hanley FL. Extracardiac conduit variation of the Fontan procedure. *Adv Card Surg* 2000;12:175–198.
246. Petrossian E, Reddy VM, Collins KK, et al. The extracardiac conduit Fontan operation using minimal approach extracorporeal circulation: early and midterm outcomes. *J Thorac Cardiovasc Surg* 2006;132:1054–1063.
247. Salazar JD, Zafar F, Siddiqui K, et al. Fenestration during Fontan palliation: now the exception instead of the rule. *J Thorac Cardiovasc Surg* 2010;140:129–136.
248. Yoshimura N, Yamaguchi M. Surgical strategy for pulmonary atresia with intact ventricular septum: initial management and definitive surgery. *Gen Thorac Cardiovasc Surg* 2009;57:338–346.
249. Malhotra SP, Hanley FL. Surgical management of pulmonary atresia with ventricular septal defect and major aortopulmonary collaterals: a protocol-based approach. *Semin Thorac Cardiovasc Surg Pediatr Card Surg Annu* 2009;145–151.
250. Iyer KS, Mee RB. Staged repair of pulmonary atresia with ventricular septal defect and major systemic to pulmonary artery collaterals. *Ann Thorac Surg* 1991;51:65–72.
251. Watterson KG, Wilkinson JL, Karl TR, et al. Very small pulmonary arteries: central end-to-side shunt. *Ann Thorac Surg* 199;52:1132–1137.
252. Jaquiss RD, Imamura M. Management of Ebstein's anomaly and pure tricuspid insufficiency in the neonate. *Semin Thorac Cardiovasc Surg* 2007;19:258–263.
253. Schure AY, Kussman BD. Pediatric heart transplantation: demographics, outcomes, and anesthetic implications. *Paediatr Anaesth* 2011;21:594–603.
254. Sackowski R, Dacey C, Bernier PL. Does ABO-incompatible and ABO-compatible neonatal heart transplant have equivalent survival? *Interact Cardiovasc Thorac Surg* 2010;10:1026–1033.
255. Denfield SW. Strategies to prevent cellular rejection in pediatric heart transplant recipients. *Paediatr Drugs* 2010;12:391–403.
256. Schweickert WD, Hall J. ICU-acquired weakness. *Chest* 2007;131:1541–1549.
257. Newman AJ, Singer NG. Critical care myopathy in a child. *J Clin Rheumatol* 2005;11:93–97.
258. Boerlage AA, Ista E, de Jong M, et al. The COMFORT behavior scale: is a shorter observation period feasible? *Pediatr Crit Care Med* 2012;13:e124–e125.
259. Laquay N, Pouard P, Silicani MA, et al. Early stages of propofol infusion syndrome in paediatric cardiac surgery: two cases in adolescent girls. *Br J Anaesth* 2008;101:880–881.
260. Jorens PG, Van den Eynden GG. Propofol infusion syndrome with arrhythmia, myocardial fat accumulation and cardiac failure. *Am J Cardiol* 2009;104:1160–1162.
261. Chrysostomou C, Di Filippo S, Manrique AM, et al. Use of dexmedetomidine in children after cardiac and thoracic surgery. *Pediatr Crit Care Med* 2006;7:126–131.
262. Chrysostomou C, Sanchez De Toledo J, Avolio T, et al. Dexmedetomidine use in a pediatric cardiac intensive care unit: can we use it in infants after cardiac surgery? *Pediatr Crit Care Med* 2009;10:654–660.
263. Zhang X, Schmidt U, Wain JC, et al. Bradycardia leading to asystole during dexmedetomidine infusion in an 18 year-old double-lung transplant recipient. *J Clin Anesth* 2010;22:45–49.
264. Jooste EH, Muhly WT, Ibinson JW, et al. Acute hemodynamic changes after rapid intravenous bolus dosing of dexmedetomidine in pediatric heart transplant patients undergoing routine cardiac catheterization. *Anesth Analg* 2010;111:1490–1496.
265. Le KN, Moffett BS, Ocampo EC, et al. Impact of dexmedetomidine on early extubation in pediatric cardiac surgical patients. *Intensive Care Med* 2011;37:686–690.
266. Anand KJ, Willson DF, Berger J, et al. Tolerance and withdrawal from prolonged opioid use in critically ill children. *Pediatrics* 2010;125:e1208–e1225.
267. Cheung CL, van Dijk M, Green JW, et al. Effects of low-dose naloxone on opioid therapy in pediatric patients: a retrospective case-control study. *Intensive Care Med* 2007;33:190–194.
268. Tobias JD. Dexmedetomidine to treat opioid withdrawal in infants following prolonged sedation in the pediatric ICU. *J Opioid Manag* 2006;2:201–205.
269. Miller SP, McQuillen PS, Hamrick S, et al. Abnormal brain development in newborns with congenital heart disease. *N Engl J Med* 2007;357:1928–1938.
270. Licht DJ, Shera DM, Clancy RR, et al. Brain maturation is delayed in infants with complex congenital heart defects. *J Thorac Cardiovasc Surg* 2009;137:529–536.
271. Limperopoulos C, Tworetzky W, McElhinney DB, et al. Brain volume and metabolism in fetuses with congenital heart disease: evaluation with quantitative magnetic resonance imaging and spectroscopy. *Circulation* 2010;121:26–33.
272. Costello JM, Polito A, Brown DW, et al. Birth before 39 weeks' gestation is associated with worse outcomes in neonates with heart disease. *Pediatrics* 2011;126:277–284.
273. Wypij D, Jonas RA, Bellinger DC, et al. The effect of hematocrit during hypothermic cardiopulmonary bypass in infant heart surgery: results from the combined Boston hematocrit trials. *J Thorac Cardiovasc Surg* 2008;135:355–360.
274. Wong PC, Barlow CF, Hickey PR, et al. Factors associated with choreoathetosis after cardiopulmonary bypass in children with congenital heart disease. *Circulation* 1992;86:II118–II126.
275. Dent CL, Spaeth JP, Jones BV, et al. Brain magnetic resonance imaging abnormalities after the Norwood procedure using regional cerebral perfusion. *J Thorac Cardiovasc Surg* 2005;130:1523–1530.
276. McQuillen PS, Barkovich AJ, Hamrick SE, et al. Temporal and anatomic risk profile of brain injury with neonatal repair of congenital heart defects. *Stroke* 2007;38:736–741.
277. Phelps HM, Mahle WT, Kim D, et al. Postoperative cerebral oxygenation in hypoplastic left heart syndrome after the Norwood procedure. *Ann Thorac Surg* 2009;87:1490–1494.
278. Kussman BD, Wypij D, Laussen PC, et al. Relationship of intraoperative cerebral oxygen saturation to neurodevelopmental outcome and brain magnetic resonance imaging at 1 year of age in infants undergoing biventricular repair. *Circulation* 2010;122:245–254.
279. Ghanayem NS, Hoffman GM, Mussatto KA, et al. Perioperative monitoring in high-risk infants after stage 1 palliation of univentricular congenital heart disease. *J Thorac Cardiovasc Surg* 2010;140:857–863.
280. Manrique A, Jooste EH, Kuch BA, et al. The association of renal dysfunction and the use of aprotinin in patients undergoing congenital cardiac surgery requiring cardiopulmonary bypass. *Anesth Analg* 2009;109:45–52.
281. Welke KF, Dearani JA, Ghanayem NS, et al. Renal complications associated with the treatment of patients with congenital cardiac disease: consensus definitions from the Multi-Societal Database Committee for Pediatric and Congenital Heart Disease. *Cardiol Young* 2008;18:222–225.
282. Alkan T, Akçevir A, Türkoglu H, et al. Postoperative prophylactic peritoneal dialysis in neonates and infants after complex congenital cardiac surgery. *ASAIO J* 2006;52:693–697.
283. Dittrich S, Aktuerk D, Seitz S, et al. Effects of ultrafiltration and peritoneal dialysis on proinflammatory cytokines during cardiopulmonary bypass surgery in newborns and infants. *Eur J Cardiothorac Surg* 2004;25:935–940.
284. Sorof JM, Stromberg D, Brewer ED, et al. Early initiation of peritoneal dialysis after surgical repair of congenital heart disease. *Pediatr Nephrol* 1999;13:641–645.
285. Bunchman TE, Brophy PD, Goldstein SL. Technical considerations for renal replacement therapy in children. *Semin Nephrol* 2008;28:488–492.
286. Owens JL, Musa N. Nutrition support after neonatal cardiac surgery. *Nutr Clin Pract* 2009;24:242–249.
287. Skinner ML, Halstead LA, Rubinstein CS, et al. Laryngopharyngeal dysfunction after the Norwood procedure. *J Thorac Cardiovasc Surg* 2005;130:1293–1301.
288. Ferdman B, States L, Gaynor JW, et al. Abnormalities of intestinal rotation in patients with congenital heart disease and the heterotaxy syndrome. *Congenit Heart Dis* 2007;2:12–18.
289. Yu DC, Thiagarajan RR, Laussen PC, et al. Outcomes after the Ladd procedure in patients with heterotaxy syndrome, congenital heart disease, and intestinal malrotation. *J Pediatr Surg* 2009;44:1089–1095.
290. Milonakis M, Chatzis AC, Giannopoulos NM, et al. Etiology and management of chylothorax following pediatric heart surgery. *J Card Surg* 2009;24:369–373.
291. Caverly L, Rausch CM, da Cruz E, et al. Octreotide treatment of chylothorax in pediatric patients following cardiothoracic surgery. *Congenit Heart Dis* 2010;5:573–578.

292. Rossano JW, Taylor MD, Smith EO, et al. Glycemic profile in infants who have undergone the arterial switch operation: hyperglycemia is not associated with adverse events. *J Thorac Cardiovasc Surg* 2008;135:739–745.
293. Polito A, Thiagarajan RR, Laussen PC, et al. Association between intraoperative and early postoperative glucose levels and adverse outcomes after complex congenital heart surgery. *Circulation* 2008;118:2235–2242.
294. de Ferranti S, Gauvreau K, Hickey PR, et al. Intraoperative hyperglycemia during infant cardiac surgery is not associated with adverse neurodevelopmental outcomes at 1, 4, and 8 years. *Anesthesiology* 2004;100:1345–1352.
295. Ballweg JA, Ittenbach RF, Bernbaum J, et al. Hyperglycaemia after Stage I palliation does not adversely affect neurodevelopmental outcome at 1 year of age in patients with single-ventricle physiology. *Eur J Cardiothorac Surg* 2009;36:688–693.
296. NICE-SUGAR Study Investigators, Finfer S, Chittock DR, et al. Intensive versus conventional glucose control in critically ill patients. *N Engl J Med* 2009;360:1283–1297.
297. Faraon-Pogaceanu C, Banasiak KJ, et al. Comparison of the effectiveness and safety of two insulin infusion protocols in the management of hyperglycemia in critically ill children. *Pediatr Crit Care Med* 2010;11:741–749.
298. Costello JM, Graham DA, Morrow DF, et al. Risk factors for surgical site infection after cardiac surgery in children. Risk factors for surgical site infection after cardiac surgery in children. *Ann Thorac Surg* 201;89:1833–1841.
299. Costello JM, Graham DA, Morrow DF, et al. Risk factors for central line-associated bloodstream infection in a pediatric cardiac intensive care unit. *Pediatr Crit Care Med* 2009;10:453–459.
300. Millar KJ, Thiagarajan RR, Laussen PC. Glucocorticoid therapy for hypotension in the cardiac intensive care unit. *Pediatr Cardiol* 2007;28:176–182.
301. Suominen PK, Dickerson HA, Moffett BS, et al. Hemodynamic effects of rescue protocol hydrocortisone in neonates with low cardiac output syndrome after cardiac surgery. *Pediatr Crit Care Med* 2005;6:655–659.
302. Mackie AS, Booth KL, Newburger JW, et al. A randomized, double-blind, placebo-controlled pilot trial of triiodothyronine in neonatal heart surgery. *J Thorac Cardiovasc Surg* 2005;130:810–816.
303. Portman MA, Slee A, Olson AK, et al. Triiodothyronine Supplementation in Infants and Children Undergoing Cardiopulmonary Bypass (TRICC): a multicenter placebo-controlled randomized trial: age analysis. *Circulation* 2010;122:S224–S233.
304. Peddy SB, Hazinski MF, Laussen PC, et al. Cardiopulmonary resuscitation: special considerations for infants and children with cardiac disease. *Cardiol Young* 2007;17:116–126.
305. Kane DA, Thiagarajan RR, Wypij D, et al. Rapid-response extracorporeal membrane oxygenation to support cardiopulmonary resuscitation in children with cardiac disease. *Circulation* 2010;122:S241–S248.
306. Jefferies JL, Hoffman TM, Nelson DP. Heart failure treatment in the intensive care unit in children. *Heart Fail Clin* 2010;6:531–558.
307. McMahon CJ, Penny DJ, Nelson DP, et al. Preterm infants with congenital heart disease and bronchopulmonary dysplasia: postoperative course and outcome after cardiac surgery. *Pediatrics* 2005;116:423–430.
308. Curzon CL, Milford-Beland S, Li JS, et al. Cardiac surgery in infants with low birth weight is associated with increased mortality: analysis of the Society of Thoracic Surgeons Congenital Heart Database. *J Thorac Cardiovasc Surg* 2008;135:546–551.
309. Ades AM, Dominguez TE, Nicolson SC, et al. Morbidity and mortality after surgery for congenital cardiac disease in the infant born with low weight. *Cardiol Young* 2010;20:8–17.
310. Tan LH, Hess B, Diaz LK, et al. Survey of the use of peripherally inserted central venous catheters in neonates with critical congenital cardiac disease. *Cardiol Young* 2007;17:196–201.
311. Pizarro C, Derby CD, Baffa JM, et al. Improving the outcome of high-risk neonates with hypoplastic left heart syndrome: hybrid procedure or conventional surgical palliation? *Eur J Cardiothorac Surg* 2008;33:613–618.
312. Barker CL, Yates RW, Kelsall AW. Prolonged treatment with prostaglandin in an infant born with extremely low weight. *Cardiol Young* 2005;15:425–426.
313. Allan CK. Intensive care of the adult patient with congenital heart disease. *Prog Cardiovasc Dis* 2011;53:274–280.

Elizabeth D. Blume ■ Ravi R. Thiagarajan ■ Peter C. Laussen

Mechanical support of the circulation for infants and children has an important role in providing short-term circulatory support during reversible myocardial failure such as during fulminant myocarditis (1,2), as a means of cardiopulmonary support before and after cardiac surgery (3–7), and as a long-term bridge to cardiac transplantation (8–11). Mechanical circulatory support devices (MCSDs) can be divided by duration of support into short-term support and longer-term support. Short-term support (days to weeks) may be provided by cardiopulmonary bypass (CPB), extracorporeal membrane oxygenation (ECMO), intra-aortic balloon pump (IABP) counterpulsation, or centrifugal ventricular assist devices (VADs). Longer-term support (weeks to months) may be accomplished by pulsatile paracorporeal or implantable VADs or axial flow implantable VADs. Table 21.1 summarizes the types of MCSDs available currently for pediatric patients in the United States.

Selection of the optimal mode of circulatory support is a critical issue in pediatric patients and depends to a great extent upon the anatomy and pathophysiology, patient size, and anticipated duration of support. There are currently no established guidelines for the indications and management of cardiac mechanical support, and there is considerable interinstitutional variability with respect to utility and outcomes. In general, institutions with a well-established ECMO service for either respiratory or cardiac failure are more likely to utilize this form of support for the failing circulation, while institutions with close collaboration with adult VAD programs are more likely to use other forms of MSCD in the older, larger patients. In addition, surgeon preference, case mix, surgical techniques, and CPB management are confounding factors that make institutional comparisons difficult. No prospective randomized trials comparing the indications for and modes of mechanical support have been undertaken although considerable information that has been accumulated in national and international registries for ECMO and VAD provides a framework for decision making. While it could be argued that a MSCD program, including at least ECMO, should be readily available in any center undertaking complex congenital cardiac surgery, it is critical to establish a structured and coordinated team.

ANATOMIC AND PHYSIOLOGIC DIFFERENCES IN CHILDREN

The major consideration in the design and development of safe circulatory support systems for children is the need to accommodate a large range of patient sizes, from newborns to young adults. MCSDs that employ a flexible membrane pump, such as the paracorporeal pneumatic devices, rely on a number of pump sizes to cover the range of patient sizes

encountered in pediatric practice. This adds considerably to the cost of development and patient care. Beyond implications for the pump itself, however, size considerations exist for all aspects of device design for children including cannulas and control systems. Furthermore, the diverse anatomic variations encountered in complex congenital heart disease challenge the design of such devices. For example, abnormalities of viscerotrial situs, such as situs inversus and abnormalities of the location of the cardiac apex (dextrocardia), complicate the application of many existing pump designs.

The design of circulatory support devices for children must take into account other unique physiologic issues. The susceptibility to anticoagulation-related complications is particularly notable in infants and children as evidenced by the important risk of intracranial hemorrhage during infant ECMO support (12,13). Newborns are known to manifest an exaggerated systemic inflammatory response (14–18) following CPB and during ECMO support that may induce multisystem organ dysfunction.

Other factors have developmental components as well such as changes in pharmacokinetics of anticoagulant medications. The ideal mechanical circulatory support system for children, therefore, must provide maximal biocompatibility resulting in minimal activation of systemic inflammatory cascades and avoidance of high-dose, multiagent anticoagulation. Children are also vulnerable to infectious complications during mechanical circulatory support, which are a frequent cause of perisupport mortality (19–21). Thus, choosing an implantable system that does not require multiple skin penetrations for drive lines or other device components is an important goal. Since urgent institution of support may be required to treat cardiac arrest after cardiac surgery or acute myocarditis, some device designs must allow for “rapid deployment” (21,22). Finally, the use of MCSDs in children for long-term permanent use as an alternative to heart transplantation, so-called destination therapy, has not been explored. One could imagine this possibility in the future if technologic advances could overcome the issues of growth and development.

SHORT-TERM MODES OF MECHANICAL CIRCULATORY SUPPORT

Cardiopulmonary Bypass

The first mechanical circulatory support systems for children began in the 1950s shortly after the first successful adult heart-lung machine implementation. In 1954, Gibbon (23) repaired an atrial septal defect using the adult circulatory support system, and at the same time, Lillehei's group (24) began using cross-circulation to repair congenital heart lesions in children. Kirklin et al. (25) developed a pump oxygenator that

TABLE 21.1 Types of Mechanical Circulatory Support for Children

Support Name	Type	Clinical Experience and Age Supported
Short-Term Support		
ECMO	Extracorporeal, centrifugal	Extensive pediatric, all ages
Bio-Pump ^{a,b}	Extracorporeal, centrifugal	Extensive pediatric, all ages
Intra-aortic balloon pump	Extracorporeal, counterpulsation	Limited pediatric, older children
Abiomed BVS 5000 ^{a,c}	Extracorporeal, pneumatic	Limited pediatric, older children
Chronic Support		
Thoratec ^{a,d}	Paracorporeal, pneumatic	Limited pediatric, older children
Heartmate V-E ^{a,e}	Implantable, electric	Limited pediatric, older children
Medos HIA-VAD ^f	Paracorporeal, pneumatic	Increasing pediatric, all ages
Berlin Heart EXCOR ^g	Paracorporeal, pneumatic	Increasing pediatric, all ages
DeBakey VAD Child ^{a,h}	Implantable, axial flow	Limited pediatric, 5–12y

^aFDA approved in the United States.^bBio-Pump (Medtronic Bio-Medicus, Minneapolis, MN).^cABIOMED BVS 5000 (ABIOMED, Inc., Danvers, MA).^dThoratec VAD (Thoratec, Corp., Pleasanton, CA).^eHeartMate LVAS (Thoratec, Corp., Pleasanton, CA).^fMEDOS HIA (MEDOS Medizintechnik AG, Stolberg, Germany).^gBerlin Heart EXCOR (Berlin Heart AG, Berlin, Germany).^hDeBakey VAD Child (MicroMed Technology, Inc., Houston, TX).

required much less prime volume than earlier versions. The next major improvements came in the 1970s with the development of deep hypothermic circulatory arrest in infants by Casteñeda (26) and Barratt-Boyes (27), which allowed surface cooling and shorter CPB times. Over the next several decades, incremental improvements in CPB technology and operative techniques contributed to a significant reduction in mortality rates associated with pediatric cardiac surgery. Nonetheless, the potential morbidity following the use of CPB in infants and children continues to be a significant limitation to this mode of mechanical circulatory support.

Although an in-depth discussion of the mechanisms and techniques of CPB is beyond the scope of this chapter, it is worth understanding the overall principles of CPB in order to assess other MCSs, such as ECMO and VADs, and note specific differences to adult CPB. The CPB circuit has a number of components including arterial and venous cannulae, circuit reservoir, pump, oxygenator, and heat exchanger. CPB is an “open” mechanical support system, allowing for blood, air, and particulate matter to be returned to the circuit reservoir via cardiectomy suckers. This is an important distinction to ECMO and VAD circuits, which are both closed systems; any air entering the closed circuit will cause an airlock and these circuits do not have a reservoir volume to compensate for changes in circulating blood volume. Most pediatric systems use a *roller pump* with flow rates governed by the internal diameter of the tubing, the amount of occlusion of the roller, and the revolutions per minute (rpm) of the pump head. Typically, the membrane-type *oxygenator* systems are used, consisting of microporous membrane with hollow fiber or folded membrane, which must function efficiently at a wide variety of pump flow rates. Some considerations for cannulation for CPB are unique to congenital heart surgery. Venous cannulation in neonates and infants may be single or multiple depending on the anatomy and bypass technique. Obstruction

to venous return is more likely due to the small vessel size and will increase venous pressures, thereby decreasing perfusion pressure to the cerebral and splanchnic circulations. In particular, an elevated SVC pressure will reduce cerebral blood flow, increase the risk of cerebral edema, and reduce the rate of cerebral cooling. Systemic-to-pulmonary shunts such as a patent ductus arteriosus and aortopulmonary collateral vessels must be controlled when initiating CPB to prevent excessive pulmonary flow with resultant increased blood return to the heart, myocardial distention, systemic hypoperfusion, and uneven cooling or rewarming.

Body-indexed pump flow rates are generally higher in neonates and infants reflecting a relatively increased metabolic rate in this age group. During bypass, there is no one measure of index that assures adequate perfusion. Generally flow rates of 100 to 150 mL/kg/min, or indexed flows to 2.2 to 2.5 L/min/m², should provide adequate tissue perfusion at normothermia. Venous oxygen saturation of >75% suggests adequate perfusion. However, these values may be misleading in patients with poor venous drainage, severe hemodilution, or malposition of the aortic cannula or in the presence of a large left-to-right shunt. Online continuous monitoring of blood gas and oxygen saturation is important to identify trends in oxygen extraction.

During hypothermia, there are two broad bypass management strategies. The first strategy is deep hypothermia circulatory arrest (DHCA) (<20°C) with low/intermittent flow or circulatory arrest. DHCA provides optimal operating conditions for intracardiac repairs with an empty, relaxed heart and reduces the duration of bypass and exposure of circulating blood to foreign surfaces. Prolonged brain ischemia is a major disadvantage and risk relates to both DHCA time and temperature. Low-flow deep hypothermic bypass is preferable and offers improved neurologic protection. Flow rates between 30 to 50 mL/kg/min are often referred to as “low flow,” but

the optimal flow rates during low-flow bypass are not firmly established.

The second strategy is moderate hypothermia with normal or increased pump flow. Bicaval cannulation is generally used, the risk of cerebral ischemia is reduced, but CPB is prolonged and operative conditions may not be ideal.

It is well recognized that the exposure of blood elements to the nonepithelialized CPB circuit along with ischemic-reperfusion injury induces a systemic inflammatory response (14–18). The effects of the interactions of blood components with the extracorporeal circuit are magnified in children due to the large bypass circuit surface area and priming volume relative to patient blood volume. Humoral responses include activation of complement, kallikrein, eicosanoid, and fibrinolytic cascades. Cellular responses include platelet activation and an inflammatory response with an adhesion molecule cascade stimulating neutrophil activation and release of proteolytic and vasoactive substances (29,30).

The clinical consequences of CPB include increased interstitial fluid, generalized capillary leak, and potential multiorgan dysfunction. Total lung water is increased with an associated decrease in lung compliance and increase in the alveolar to arterial oxygen ($A-aO_2$) gradient. Myocardial edema results in impaired ventricular systolic and diastolic function. A secondary fall in cardiac output by 20% to 30% is common in neonates in the first 6 to 12 hours following surgery, contributing to decreased renal function and oliguria (31). Sternal closure may need to be delayed due to mediastinal edema and associated cardiorespiratory compromise when closure is attempted. Ascites, hepatic congestion, and bowel edema may affect mechanical ventilation, cause a prolonged ileus, and delay feeding. A coagulopathy post-CPB may contribute to delayed hemostasis. Strategies that have evolved thus far to limit the effect of the endothelial injury resulting from the systemic inflammatory response include limiting both the time spent on CPB and use of DHCA, hypothermia, steroids, and aprotinin (a serine protease inhibitor) may also limit activation of the inflammatory response. Attenuating the stress response, the use of antioxidants such as mannitol, altering prime composition to maintain hematocrit and oncotic pressure, and ultrafiltration during rewarming or immediately after bypass are also used to limit the clinical consequences of the inflammatory response (32–34).

Hypothermia and Cerebral Protection

Techniques of deep hypothermia with or without circulatory arrest have extended the safe duration of CPB in children, particularly neonates and infants, enabling improved surgical conditions and patient outcome. As mortality has decreased, an increasing emphasis has been placed on patient morbidity following repair, and in particular, the consequences of deep hypothermia and low perfusion have become closely scrutinized.

The brain is particularly sensitive to ischemia; therefore, MSCD carries risk for cerebral ischemic injury. Hypothermia is the principle method used for cerebral protection during CPB, effecting both pressure-flow and metabolism-flow cerebral autoregulation (35–37). A reduction in oxygen consumption and metabolic rate during deep hypothermia explains in part the increase in tolerance to cerebral ischemia produced by hypothermia. Other factors possibly contributing to the protective effects of hypothermia include altered cellular metabolism with an increase in high-energy phosphates and intracellular pH, reduced neurotransmitter release, and that the neonatal and infant brain may be more tolerant of cerebral ischemia than the adult brain.

However, diffuse cerebral abnormalities can occur in patients after open heart surgery in children and adults, including global

and watershed injuries related to hypoperfusion or hypoxemia, and multifocal lesions presumed secondary to embolic events (38–40). The early clinical manifestations of neurologic injury in children include seizures, stroke, choreoathetosis (41), and coma. Subtle long-term behavioral, developmental, and motor abnormalities have now been associated with neurologic injury during hypothermic CPB, regardless of strategy, and support the importance of early developmental intervention. The Boston Circulatory Arrest Study (42) demonstrated a strong association between the duration of circulatory arrest and the occurrence of postoperative seizures that become more likely after circulatory arrest duration of 40 minutes. Analysis of developmental outcome at 1 year of age in these patients indicated a significant association between the occurrence of postoperative seizures and a worse than normal outcome for psychomotor development (43). The risk of neurologic abnormalities increased with the duration of circulatory arrest. Data at 4- and 8-year follow-up in these patients indicate a spectrum of both motor and language delays and abnormalities that also correlate with the incidence of postoperative seizures (44,45). Recently, genetic polymorphisms have been recognized that may predispose to impairments in neuronal repair ability (46).

While hypothermia is the principle method for providing protection during CPB, the means by which hypothermia is induced and maintained is critical. Because of the large body surface area (BSA) to mass ratio in neonates and infants, a 2- to 3-degree reduction in core temperature is common prior to bypass. Respiratory alkalosis secondary to mechanical ventilation reduces cerebral blood flow and should be avoided. Cannula position is important as noted above; obstruction to systemic venous return by venous cannula decreases cerebral perfusion pressure, and an obstructive or malpositioned aortic cannula will also decrease cerebral blood flow and effective cooling. Shunts and collateral vessels must be controlled when initiating bypass to prevent excessive runoff to the lungs and return to the heart, resulting in myocardial distention, systemic hypoperfusion, and uneven cooling or rewarming. Once on bypass, rapid cooling should be avoided as this results in uneven cooling of the brain; cooling times of 20 to 25 minutes have been advocated for infants and neonates requiring CPB and DHCA. Possible pharmacologic manipulations include using vasodilation drugs to facilitate cooling and rewarming and steroids are commonly administered to stabilize membranes in an attempt to reduce cerebral edema.

The use of crystalloid pump primes may be associated with an increase in total body water after hypothermic CPB in neonates and infants, secondary to a reduction in plasma oncotic pressure. This will contribute to postoperative capillary leak and can potentially delay recovery. Variability in the target hematocrit during hypothermic CPB remains between centers, but maintaining a hematocrit around 30% appears to be optimal with respect to altered blood viscosity during hypothermia and the maintenance of oncotic pressure and oxygen-carrying capacity (47).

The blood gas strategy during hypothermic CPB is also an important consideration (40,48). Carbon dioxide (CO_2) is a potent cerebral vasodilator in both awake and anesthetized patients with or without CPB. During CPB and hypothermia, cerebral blood flow continues to increase with $PaCO_2$; however, this response is attenuated in neonates and infants with deep hypothermia and reflects cold-induced vasoparesis. During hypothermia, the solubility of CO_2 increases and the neutral pH of both water and blood are reset in the alkaline direction. In the alpha-stat strategy, no compensation is made for the alkaline shift. The alpha-stat strategy theoretically maintains a more normal intracellular pH and therefore electrochemical neutrality with preserved enzymatic function. Further, the uncoupling of flow metabolism is less pronounced, thereby limiting luxuriant cerebral flow during CPB.

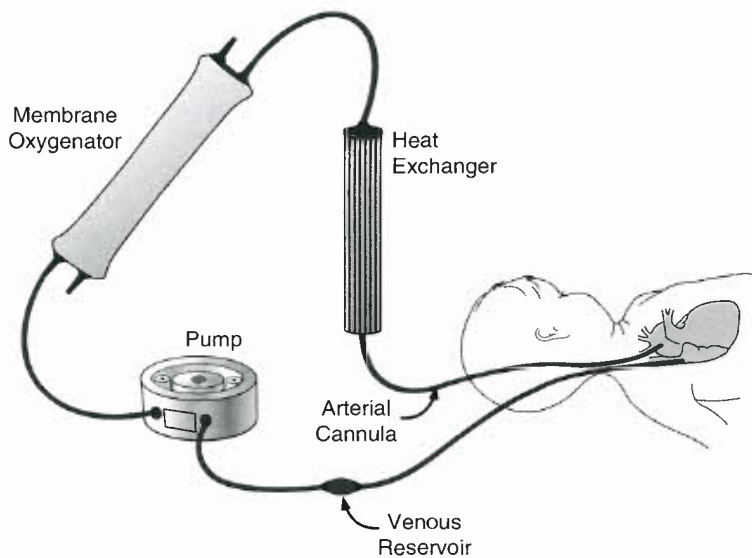


Figure 21.1. Extracorporeal membrane oxygenator circuit with membrane gas exchange device and roller pump.

However, in the context of low mean perfusion pressure, flow, and temperature, cerebral perfusion may be inadequate to meet metabolic demands and cerebral cooling may be nonhomogeneous. In contrast, the pH strategy aims to maintain a normal pH over varying temperatures, and CO₂ must be added to the oxygenator gas mixture during deep hypothermia. The increased cerebral blood flow associated with pH-stat regulation may result in an increase in air or particulate emboli to the brain. Clearly, this is a concern in congenital heart disease with the presence of intra- and extracardiac communications and the need for intracardiac surgical repairs. In addition, pH-stat strategies increase cerebral blood volume, which may result in hyperemia and edema particularly during reperfusion. However, luxuriant cerebral flow and perfusion have the advantage of enhancing global cerebral cooling and reducing cerebral steal from aortopulmonary shunts. Hypothermia causes a left shift of the oxyhemoglobin curve and is further shifted to the left by an alkaline pH. Off-loading of oxygen in the tissues is impaired and the left shift is counteracted by more acidotic pH such as provided by the pH strategy.

Many years of research and understanding of the effects of CPB on the pediatric patient have created a wealth of information that can be extrapolated to the management strategies of other MCSDs, such as ECMO and VAD. Cerebral protection, biocompatibility, and coagulation monitoring continue to be long-term areas of research common to all MCSDs.

Extracorporeal Membrane Oxygenation

ECMO was first introduced as a form of respiratory support in children with severe lung disease and is the most common approach to pediatric mechanical cardiac support today. In venoarterial ECMO (VA ECMO), blood is drained from the venous circulation into the ECMO circuit, pumped into the oxygenator for gas exchange, and returned to the arterial circulation as shown in Figure 21.1. Thus, VA ECMO provides both cardiac and respiratory support and is the most commonly used form of ECMO to support children with cardiac dysfunction (1). In venovenous ECMO (VV ECMO), deoxygenated blood drained from the venous circulation is oxygenated and returned back to the venous circulation and circulation is maintained by native cardiac function. Thus, VV ECMO is commonly used to support those with pure respiratory failure, as it does not provide mechanical circulatory support. The Extracorporeal Life Support Organization (ELSO) collects

data from neonates, children, and adults supported with ECMO for all indications from 140 centers worldwide and has provided important knowledge on outcomes following ECMO that has served as an invaluable guide to the clinical use of ECMO (49).

Indications for ECMO use have evolved over time. Its use in providing biventricular support and oxygenation in pediatric patients with a failing circulation has increased. Reduction in the need for ECMO as respiratory support, particularly in neonates, has occurred as a result of newer therapies such as inhaled nitric oxide, high-frequency oscillatory ventilation, surfactant therapy, and permissive hypercapnia (49–52). As a result, the current patients requiring ECMO for respiratory support are sicker and have usually failed many medical therapies. Consequently, their survival has declined over recent years. Cumulative data reported by the ELSO (49) from 140 centers through to January 2010 provide an important insight into the outcomes and changing landscape of ECMO. In the 2010 report, 75% of all neonates placed on ECMO for respiratory support survived to hospital discharge. The outcome for older patients placed on ECMO for respiratory support is lower than that for children. The reported cumulative survival for pediatric is 56% and for adult patients is 52%. Table 21.2 outlines the survival in the respiratory group by diagnostic category.

TABLE 21.2

Survival Following ECMO Cannulation in Neonates by Respiratory Diagnostic Group Compared with Cardiac Neonates

Diagnosis	Survived (%)
Meconium aspiration syndrome	94
Primary pulmonary hypertension of newborn	78
Sepsis	75
Air leak syndrome	74
Congenital diaphragmatic hernia	51
Cardiac disease	39

Data from Extracorporeal Life Support organization, International Summary 2010.

TABLE 21.3

ECMO Following Cardiectomy in Children with Congenital Heart Disease

Reference	Study Period	Number Needing ECMO (%) of CPB Cases Needing ECMO	Survival Rate (%)
Walters III et al.	1984–1994	66 (3.0)	57.6
Jaggers et al.	1994–1999	35 (3.4)	61
Kolovos et al.	1995–2000	74 (2.2)	50
Aharon et al.	1997–2000	50 (4.0)	50
Chaturvedi et al.	1992–2001	81 (2.5)	49
Morris et al.	1995–2001	89 (3.4)	40
Thourani et al.	2002–2004	17 (1.8)	35

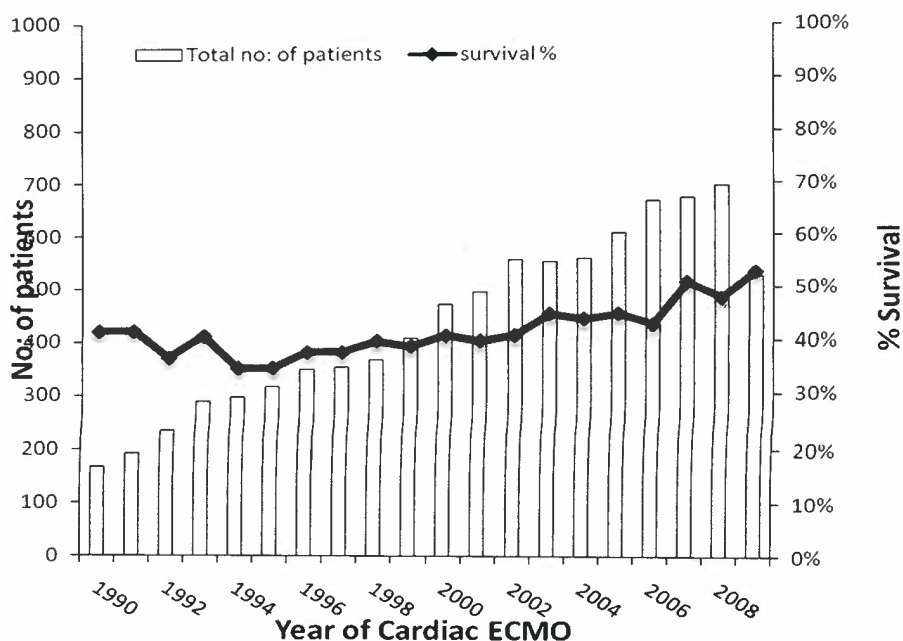
Adapted from Salvin JW, Laussen PC, Thiagarajan RR. Extracorporeal membrane oxygenation for postcardiotomy mechanical cardiovascular support in children with congenital heart disease. *Paediatr Anaesth* 2008;18(12):1157–1162.

In contrast to respiratory ECMO, the use of ECMO for the treatment of circulatory failure following congenital cardiac surgery (Table 21.3) or as a bridge to cardiac transplantation has increased over the past decade (6–11,53–67). However, despite the increased enthusiasm for cardiac ECMO, the survival to hospital discharge as reported by ELSO (49) (39% for neonates and 47% for pediatric patients) has not increased and remains lower than the survival outcomes reported following respiratory ECMO (Fig. 21.2). The average duration for cardiac ECMO runs reported to ELSO over the past 15 years has increased slightly from approximately 4 to 5 days to 5 to 8 days, and the longest reported run has been 93 days (49). These data highlight the fact that ECMO should be viewed as a short-term circulatory support device.

There are significant differences between ECMO for circulatory support compared to respiratory support. Many cardiac ECMO patients are postcardiotomy patients following surgery for congenital heart surgery. A small number of these patients are placed on ECMO after failing to wean from CPB after congenital heart surgery (55). In these cases, severity of organ dysfunction and illness prior to ECMO deployment,

residual hemodynamic lesions, underlying pathophysiology, and end-organ dysfunction prior to ECMO support play an important role in survival following ECMO support. Thus, timing of initiation of ECMO support is important to achieve successful outcomes (57). ECMO facilitates ventricular recovery by reducing myocardial wall tension, increasing coronary perfusion pressure, and providing adequate systemic perfusion with oxygenated blood (60,61,65). In infants, where myocardial failure can be either uni- or biventricular and associated with respiratory insufficiency or pulmonary hypertension, ECMO is the preferred means of mechanical support. In contrast to the concept of “resting the lungs” for patients who are placed on ECMO for respiratory failure and lung injury, it is important that the heart regain contractile function and conduction in order to prevent involution of the myocardial mass. This will require evaluation with echocardiography to prevent overdistension of the heart. As noted above, the ECMO circuit is a “closed” circuit with limited ability to handle any air in the venous limb of the ECMO circuit, and careful de-airing of the venous cannula during initiation is essential.

Figure 21.2. Cardiac ECMO volume and survival outcomes. The use of cardiac ECMO has increased dramatically over time, although survival rates continue to remain stable. (Data from the ELSO International Summary 2010.)



TABLE

21.4

Indications for Mechanical Circulatory Support in Infants and Children

- Preoperative resuscitation
- Inability to wean from CPB
- Postcardiotomy
- Following in-hospital cardiac arrest
- Low output cardiogenic shock
- Myocarditis
- Cardiomyopathy
- Refractory arrhythmia
- Bridge to transplantation

Indications for Cardiac ECMO

Indications for cardiac ECMO are similar to indications for all MCSDs (Table 21.4). It can be an effective bridge to recovery, to transplantation, or to longer term mechanical support.

I. Preoperative Resuscitation and Stabilization:

ECMO may be beneficial for critically ill patients with congenital heart disease prior to cardiac surgery (53,58), enabling resuscitation, optimization, and prevention of end-organ dysfunction. Indications include severe low cardiac output states from left-sided obstructive lesions (e.g., critical aortic stenosis), pulmonary hypertension (e.g., obstructed total anomalous pulmonary venous drainage), or severe hypoxemia (e.g., transposition of the great arteries).

II. Inability to Wean from CPB

There is limited utility for ECMO as a bridge to recovery of ventricular function, and overall survival is poor when patients are placed on ECMO because they cannot be weaned from CPB in the operating room (54–57). Unrecognized residual or irreparable defects are major factors determining successful outcome in this circumstance, and careful assessment in the operating room with a combination with echocardiography and the measurement of oxygen saturations and intracardiac pressures may help identify correctable anatomic defects. Early transport to the cardiac catheterization laboratory may be necessary to diagnose residual defects (67). A major complication in this group transitioned directly to ECMO from CPB is the risk for hemorrhage. A lower activated clotting time (ACT) is used in this circumstance often needing small increments of protamine (1 mg/kg) until a target ACT of 160 to 180 seconds is achieved. Infusions of antifibrinolytic drugs such as aprotinin (bolus 30,000 IU/kg, infusion 10,000 IU/kg/h), tranexamic acid (bolus 100 mg/kg, infusion 10 mg/kg/h), or epsilon aminocaproic acid (bolus 100 mg/kg, infusion 30 mg/kg/h) should also be considered. Exploration of the chest is usually necessary, particularly if the bleeding persists at >10 to 15 mL/kg/h or problems with ECMO flow are encountered from tamponade-like effect.

Ideally, only children with potentially reversible myocardial injury who cannot be weaned from CBP should be considered candidates for ECMO, although this may be extremely difficult to determine in the operating room immediately following cardiac surgery. Considerations include preoperative condition, intraoperative course, and likelihood of becoming a suitable transplant candidate. When a patient is placed on ECMO in the operating

TABLE

21.5

ECMO Survival of Congenital Heart Disease in Infants and Children after Corrective Surgery

Procedure	Total Reported	Survived (%)
Anomalous Venous Return repair (age < 30 d)	286	48
	134	51
Common atrioventricular canal repair	66	41
BDG operation	95	31
Fontan Operation	876	30
Stage 1 palliation (Norwood; age < 30 d)		

Data from Extracorporeal Life Support Organization, International Summary 2010.

room, it is important for discussions with the patient's family to be clear and direct. Recovery of myocardial function should be expected within 2 to 3 days (56,57). If this is not evident, proceeding to transplant evaluation or withdrawal from support must be considered.

III. Postcardiotomy

ECMO is an effective therapeutic option for infants and children who have had a period of relative stability after successful termination of CPB, for whom significant residual cardiac defects are excluded (Table 21.5) (49). Because patients were stable enough to wean off CPB, bleeding is less of an issue. For this group, cannulation can be undertaken through the chest at the bedside; however, if sufficiently stable, neck or femoral sites are preferable. Myocardial or respiratory failure causing a low cardiac output state, hypoxemia or pulmonary hypertension, and cardiac arrest are the major indications in this group, and survival rates as high as 60% to 70% have been reported provided ECMO is instituted rapidly and effectively (49,54–62). Survival for patients with single ventricle lesions supported following surgery (Norwood, Bidirectional Glenn [BDG] or Fontan operations) is lower than those with biventricular circulations requiring ECMO support (59–63).

IV. In-Hospital Cardiac Arrest and Cardiopulmonary Resuscitation (ECPR)

Survival and outcome of in-hospital resuscitation in pediatric patients following a cardiac arrest is extremely poor. Even within a highly monitored environment such as a pediatric intensive care unit, the survival following cardiac arrest has only been reported to be between 9% and 31% (68,71). The duration of cardiac arrest and quality of resuscitation are important determinants of outcome and reports have noted that a critical threshold is 15 minutes for return of circulation for survival to hospital discharge (68). There are a number of reports showing that ECMO can be successfully deployed in children receiving active resuscitation and chest compressions (5,6,22,23,64,69,70), and that the use of ECMO to support failed CPR (ECPR) in some patients can promote survival. Since ECMO deployed during CPR should be conducted expeditiously and avoid significant delays, a "rapid response" ECMO system has been established at some institutions to initiate ECMO during active resuscitation efforts (22,23,70). As a guideline, ECMO should be considered in patients who have suffered a witnessed cardiac arrest and received rapid institution of effective and monitored CPR,

have no or inadequate recovery of cardiac function within 5 to 10 minutes of initiating resuscitation, and have no obvious contraindications for ECMO.

The aim of a rapid-response system is to provide systemic perfusion and oxygen delivery as soon as possible to prevent end-organ injury. Ideally, this should be within 30 minutes of starting resuscitation, although it may take longer if cannulation is complicated. Postcardiotomy cannulation of the atrium is best achieved via a reopened sternotomy, which is usually the access mode of choice. In other patients, experienced practitioners can rapidly gain access via the neck vessels. Groin vessel cannulation has been reported, even in the infant (71). It is important to provide effective and monitored resuscitation during cannulation, and there will be times during cannulation that chest compressions will need to be briefly discontinued. Mild hypothermia should be induced during resuscitation, and should be continued once ECMO has been started to possibly provide end-organ and specifically neurologic protection. Because the aim is to provide systemic perfusion as soon as possible with ECMO flow, there is usually insufficient time to blood prime the ECMO circuit. This means that infants and small children are extremely hemodiluted when ECMO flows are started, but once flow is established, blood products can be added or the priming crystalloid can be removed via hemofiltration.

Determining the relative contraindications to ECMO support during active resuscitation attempts can be difficult. Patients with repaired two-ventricle defects who have a sudden or unexpected event leading to cardiac arrest are good candidates for early initiation of ECMO during resuscitation because effective CPR is more likely to maintain perfusion and oxygen delivery during chest compressions, thereby decreasing the risk for end-organ injury (10,11). In contrast, patients with cavopulmonary connections, that is, Fontan or BDG anastomosis, have been difficult to resuscitate using ECMO for several reasons (59–63). These patients may have occluded or abnormal venous and arterial access, thereby limiting possible cannulation sites. An inability to maintain adequate systemic oxygen delivery during CPR and cerebral venous hypertension during CPR with chest compressions may hinder neurologic outcome. Another complicated group includes patients with pulmonary hypertension and those with systemic outflow obstruction. These patients, similar to the cavopulmonary connection group, are at significant risk for inadequate oxygen delivery during CPR, contributing to subsequent end-organ injury.

V. *Cardiomyopathy, Myocarditis, and Bridge to Cardiac Transplantation*

Patients who present with acute fulminant myocarditis can be successfully managed with ECMO with excellent outcomes (10,11,72–74). They may present with full cardiac arrest, shock from an extreme low cardiac output state, or hemodynamically unstable dysrhythmias including ventricular tachycardia or heart block. The heart is usually distended and contracting very poorly. Prompt institution of ECMO may allow sufficient resuscitation and stabilization to prevent end-organ injury and enable the myocardium to rest while awaiting potential recovery. After instituting ECMO, it is essential that the heart be fully decompressed, and urgent left atrial vent placement may be necessary (67). The heart may not begin to eject for the first 24 to 36 hours after initiating ECMO, although recovery of electrical activity within the first few hours should be expected. If recovery of ventricular ejection is not evident within 2 to 3 days, ECMO can be continued either as a bridge to transplantation or as a bridge to alternative longer-term support with a VAD, if feasible. Transplant-free survival for patients with

acute fulminant myocarditis requiring ECMO support is reported to be >60%.

ECMO should be viewed as a short-term bridge to cardiac transplantation because of the limited donor availability and the time-related risks for complications, such as infection, bleeding, end-organ impairment, problems secondary to immobilization, and difficulties in maintaining adequate nutrition. In our experience at Children's Hospital, Boston, the median time spent on ECMO awaiting heart transplantation has been 140 hours (range 26 to 556 hours), but only 50% of listed patients have been effectively bridged. Our current practice for patient resuscitated with ECMO includes transition to a longer-term MCS to bridge to transplant. The optimal timing for transitioning ECMO patients initially supported with ECMO as a bridge to transplantation to MCSs is unknown but should be considered within 72 to 96 hours if recovery has not occurred prior to the onset of ECMO complications.

ECMO has also been used to effectively support the failing heart after transplantation. This may be necessary immediately after transplantation because of primary graft failure, often in the setting of pulmonary hypertension and acute right ventricular failure of the donor allograft. ECMO is also effective in supporting the transplanted heart during periods of acute rejection (75). The inflammation and myocardial edema are similar to that seen with fulminant myocarditis and lead to a similar spectrum of clinical features. ECMO allows the transplanted heart to decompress with decreased wall tension while antirejection therapy is increased. In our experience, survival to discharge for this indication is 64%, and the median duration of ECMO support has been 4 days.

VI. *ECMO Support during Procedures*

As the complexity and interventions during cardiac catheterization in patients with complex congenital heart disease have continued to expand, patients may be at increased risk for sudden unexpected adverse events. These may range from complications associated with specific intervention to dysrhythmias and low cardiac output state related to wires and catheters within the heart. ECMO support during resuscitation from an acute event during catheterization is beneficial but there are important technical and resuscitative considerations (3,22,76).

Percutaneous cannulation for ECMO can be rapidly achieved using existing catheter access, but staff must be familiar with the technique for upsizing from the catheter sheath to a large-bore ECMO cannula. The catheterization laboratory environment is challenging and resuscitation to ECMO must be well organized to be effective. Often there are conflicting or simultaneous considerations during resuscitation including ongoing chest compressions, cannulation of ECMO, and ongoing efforts by the cath team to stabilize complications such as balloon occlusion of a ruptured vessel.

It is possible to anticipate hemodynamic instability during catheterization in some patients, particularly arrhythmia induction during electrophysiologic studies and radiofrequency ablation (77). The cannulation and support of the circulation using ECMO will enable safe and successful completion of the procedure.

Technical Considerations of ECMO

Children with complex structural cardiac defects may have associated abnormalities with systemic venous damage (e.g., heterotaxy syndromes) or have undergone previous cardiac catheterization or catheter placement that may have caused occlusion of femoral vessels. It is essential, therefore, that the venous and arterial anatomy be well known, including the patency of individual vessels, and be well documented to prevent

inappropriate cannulation attempts. Arteriovenous cannulation is usually employed for cardiac ECMO (78–81), although venovenous bypass can be used in patients who require ventilatory support only. Venous cannulation and ECMO flow via the jugular vein using a double lumen catheter can also provide hemodynamic support in select neonates who have a ductus-dependent circulation, such as hypoplastic left heart syndrome.

The daily management of a patient on ECMO requires attention to cardiorespiratory function, end-organ perfusion and injury, evolving complications such as bleeding or sepsis, and the mechanics of the ECMO circuit (48). Assessing the adequacy of flow and systemic perfusion after initiation of ECMO is essential and well-defined patient and ECMO circuit management protocols must be in place. ECMO flow rates in infants and small children typically range from 100 to 150 mL/kg/min during full circulatory support. Inadequate flow states and/or significant persistent hypotension despite adequate circuit flow may be due to ECMO-related problems with cannula size and position and venous drainage or patient-related factors such as vasodilation and low systemic vascular resistance secondary to sepsis. Venous cannula malposition or inadequate size will limit venous drainage and should be addressed with repositioning or upsizing of existing cannulae, or the addition of a second venous drain. Elevated postmembrane pressures (i.e., >250 mm Hg) may reflect malposition of the arterial cannula or a cannula that is too small and needs to be replaced. Elevated premembrane pressures (i.e., >350 mm Hg) at normal flows without change in postmembrane pressure or evidence of blood-to-gas leak imply membrane oxygenator dysfunction and may need oxygenator replacement. Extensive thrombus evident within the circuit or development of a consumptive coagulopathy with hypofibrinogenemia and thrombocytopenia are indications for circuit replacement. Blood products are administered to keep the hematocrit between 35% and 45% and the platelet count >100,000/mm³. Considerations for cannulation and flow rates once on ECMO may be specific to the underlying cardiac defect or surgical repair. For example, the management of an aortopulmonary shunt in patients with single ventricle physiology may require circuit flows up to 200 mL/kg/min or more to maintain adequate systemic perfusion while accounting for run-off into the pulmonary circulation.

Echocardiography, especially transesophageal imaging, and occasionally cardiac catheterization (67) are used to assess cardiac anatomy and function and to detect residual lesions. In addition, assessment of left atrial hypertension by clinical findings, chest radiograph, and echocardiography is critical. Venting the left atrium may be necessary to lower the left atrial pressure and decrease left ventricular wall stress, thereby minimizing ongoing myocardial injury. Placement of a left atrial vent can be accomplished by direct placement through an open chest or by a transcatheter approach (67). If a patient fails to wean from ECMO or there is delay in anticipated recovery of myocardial function, the possibility of a residual surgical problem must always be considered. This is usually difficult to diagnose by echocardiography alone, and cardiac catheterization (i.e., diagnostic or interventional) should be considered. Safe and successful management of ECMO patients requires a collaborative multidisciplinary team of physicians, surgeons, nurses, and ECMO specialists trained in the management of ECMO patients.

OTHER SHORT-TERM MCS

ECMO has been the mainstay of mechanical circulatory support in infants and children and has been effective in providing circulatory support in the acute setting, especially when

lung disease is also present. However, ECMO has limitations as an effective bridge to transplantation and precludes chronic ambulatory use. In patients unable to be weaned from ECMO who are listed for transplant, transition to a chronic device can be done successfully.

Centrifugal Assist Pump

The centrifugal assist device (BioPump, Medtronic Bio-Medicus, Minneapolis, MN) has historically been the principle means for providing support of the circulation without an oxygenator membrane. This centrifugal pump provides flow by power applied to a rotating magnet coupled to an opposing magnet on a cone-shaped impeller. There are no valves and no obligatory volume displacement by the pump that results in nonpulsatile flow that is both preload and afterload sensitive with priming volumes of 100 mL or less (10,81–85). The various sizes of cone heads available enable this device to be used from infants through to adult sized patients.

Reports using the BioPump predominately as a left ventricular support have demonstrated survival rates of 40% to 70% (10,81–85) when used as a bridge to recovery. Ungerleider (86) reported survival to discharge in an elective strategy following Norwood procedure, with “easier” ICU course. Central nervous system complications, both short and long term, tend to be less prevalent compared to concurrent patients supported with ECMO (82–87). The absence of an oxygenator and reduced lengths of tubing remove an important substrate for cerebral embolic events while the generally reduced level of anticoagulation employed during VAD support may decrease the incidence of hemorrhage. The centrifugal pump VAD enables only short-term support as a bridge to recovery or transplantation. Complications related to this nonpulsatile extracorporeal circuit are similar to those encountered with longer term ECMO use, and patients are unable to ambulate. This is an important consideration, when longer term support allows recovery of end-organ function, improved nutrition, and ability for rehabilitation and ambulation prior to transplantation.

Intra-Aortic Balloon Counter Pulsation

IABP is used for the treatment of left ventricular failure in adults, especially in the postoperative period. Unfortunately, when used in infants and children, results have been disappointing with survival rates <50% (88–93). Many factors contribute to the reduced efficacy of IABP in children. Heart failure in pediatric patients is often due to either right ventricular or biventricular dysfunction, situations where the IABP is less effective. Placement of an IABP in the pulmonary artery has been reported, but is usually problematic, in part because of the small balloon size required and the increased compliance of the pulmonary artery (90). Effective timing of inflation and deflation is more difficult in children because of their relatively rapid heart rates and the variable delay between aortic valve closure and the appearance of the arterial tracing. At heart rates over 160 bpm, the IABP is often reduced to a 1:2 or even 1:4 pumping frequency in order to facilitate cycle timing, at the same time decreasing its effectiveness to 50% to 80% (89–91). The aorta is typically more distensible in infants and in children; therefore, both coronary flow augmentation during diastole (balloon inflation) and afterload reduction during systole (balloon deflation) are likely to be decreased. In addition, the effect of diastolic augmentation of flow to normal coronary arteries, as seen in most pediatric patients, is limited. Severe cyanotic heart disease in children can be accompanied by extensive aortopulmonary collateral vessels, which permit shunting of blood into the pulmonary circulation during balloon inflation, thus reducing augmentation of coronary blood flow.

The smallest balloon system available for children is 2.5 mL, which can be used for neonates as small as 2 kg (92). In general, for children weighing <30 kg, a balloon volume of 0.5 mL/kg is recommended. For balloon inflation, helium is preferred over CO₂, allowing a faster pneumatic response due to its low density. The incidence of vascular complications, such as bleeding, emboli, or limb ischemia, is similar to the adult population where it is reported to be about 10% to 20%. Other potential complications are infection, renal dysfunction, mesenteric occlusion or embolism, and cerebrovascular accidents.

IABP may have a role in the temporary support of the adolescents and adults with single ventricle physiology and poor systolic function during procedures or as a short-term bridge (93). Numerous technical improvements have been made recently to enhance efficacy in the pediatric population. These include modified pumping consoles and small-sized catheters, improved tracking at higher heart rates, more rapid inflation and deflation, and the use of echocardiography for cycle timing. Further studies will be necessary to evaluate the utility of IABP support compared to other techniques for pediatric patients.

LONG-TERM MECHANICAL CIRCULATORY SUPPORT FOR CHILDREN

The use of long-term mechanical circulatory support in children has increased over the past decade as waiting time for pediatric cardiac allografts has increased and understanding of recovery of cardiac function has improved. In adults on chronic term devices, normalization of cardiac output provided by chronic and implantable VADs allows a period of improvement in end-organ function which, combined with patient ambulation and cardiac rehabilitation, optimize patient condition prior to transplant. The use of adult devices in larger children and adolescents has proved successful. In addition, technologic advances have allowed the possibility of mechanical support as a bridge to transplant or recovery for longer periods of time.

The experience with VAD support in infants and children is increasing (94–125); however, it remains challenging due to heterogeneous anatomy and size, anticoagulation strategies, and technical limitations. An important component of these benefits is the ability of the device to allow ambulation and rehabilitation, which cannot be accomplished currently with ECMO and centrifugal VADs. As with ECMO, the selection of appropriate candidates is crucial and surgical problems or residual defects

should be excluded where possible. While ECMO can be instituted by peripheral cannulation of neck or femoral vessels, VADs require direct cannulation of the heart through a sternotomy. Another advantage of VADs is superior ventricular unloading, a prerequisite for myocardial rest and potential recovery.

Clinical Criteria for VAD Placement

VADs can successfully support the circulation and bridge patients to cardiac transplant by improving the patient's cardiac output and oxygen delivery. Therefore, the primary use for VAD is in patients who have unacceptable symptoms or signs of low cardiac output state. In addition to improved oxygen delivery, pulmonary capillary wedge pressure and pulmonary vascular resistance decrease, congestive heart failure symptoms diminish, and nutrition and physical rehabilitation markedly improve in many cases. Thus, VADs have the potential to improve the pretransplant status and to reverse evidence of end-organ dysfunction. Persistent end-organ dysfunction despite maximal medical interventions is the primary indication for VAD in transplant-eligible or listed-patients. These include the obvious symptoms of persistent congestive heart failure and biochemical evidence for renal and hepatic dysfunction. In an attempt to understand the risk factors associated with wait list mortality, Almond et al. (102) analyzed the UNOS database and found that more than 500 children (20% of 1A pediatric candidates) die on the wait list with most being <20 kg (Fig. 21.3A). Risk factor analysis confirmed that wait list mortality was significantly higher for patients who "failed" medical management requiring ECMO or ventilator support (Fig. 21.3B). Subtle symptoms of heart failure such as abdominal pain, vomiting, and anorexia will lead to poor nutrition and should be monitored closely, although no data currently suggest early initiation of VAD support in this population. Early use of VAD, as seen in the current era, with adults (103) in these circumstances may be warranted, although further studies are necessary to understand the true indications for VAD support.

Patients with structurally normal hearts who develop heart failure from acquired heart disease such as myocarditis or who have idiopathic cardiomyopathy are successfully supported and bridged to transplantation with VADs. Compared to patients with structurally normal hearts, the use of chronic MSCD in children with congenital heart disease has not been as favorable with only approximately 30% being successfully bridged to transplant in the congenital group in one study

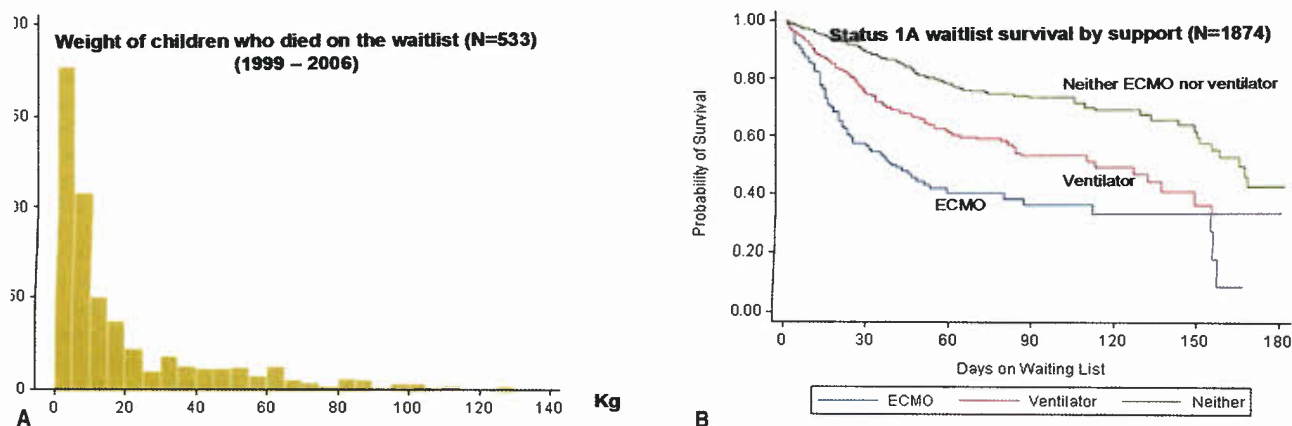


Figure 21.3. A: Almond et al. analyzed the UNOS registry and found that more than 500 children die on the wait list per year (102). B: Risk factor analysis showed that this mortality was significantly higher in children on MCSDs.

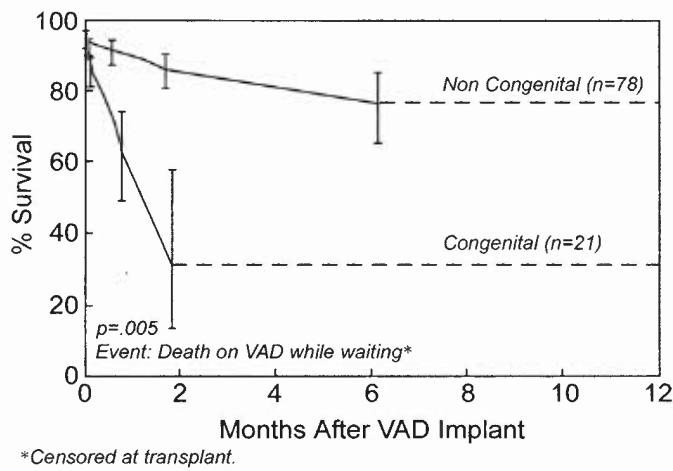


Figure 21.4. Congenital heart disease outcomes are poor. Survival following VAD implantation in pediatric patients with congenital heart disease is significantly worse than in children implanted with structurally normal hearts. (Reproduced from Blume ED, Naftel DC, Bastardi HJ, et al.; for the Pediatric Heart Transplant Study Investigators. Outcomes of children bridged to heart transplantation with ventricular assist devices: a multi-institutional study. *Circulation* 2006;113:2313–2319, with permission.)

(Fig. 21.4). Reoperative status, complex anatomy, nutritional issues, and chronic nature of the diseases are all contributing factors.

In contrast to the ECMO experience, the outcome for children placed on VADs has improved over recent years. Smaller single center studies (106–112) and device registry data (105,113) report approximately a 60% to 70% successful bridge to transplantation in pediatric patients supported with VAD. Improved outcomes in the most recent era (105,111,113) may be related to an increasing experience with the surgical techniques and perioperative care, better patient selection, and earlier introduction of support before irreversible end-organ injury develops, and the application and development of device technology over time.

Adverse Events Related to VAD Support

The adverse event profile and hazard function for death in children are shown in Table 21.6 and Figure 21.5, and are similar

TABLE 21.6		Adverse Events in Pediatric Patients (1993–2003, N = 99) Supported by Short-Term Devices versus Pediatric Patients Implanted with Long-Term Pulsatile Device		
		Chronic	Short Term	p
Adverse Events				
Stroke		9 (13%)	9 (35%)	0.02
Infection		29 (41%)	2 (12%)	0.004
Reoperative bleeding		22 (31%)	11 (42%)	0.32
Hemolysis		13 (19%)	2 (1%)	0.17
Thrombus		8 (11%)	4 (15%)	0.64

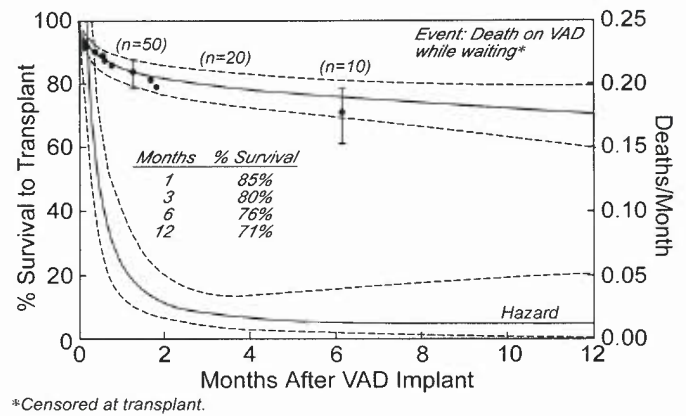


Figure 21.5. Overall survival following VAD implant. Of the 99 pediatric patients implanted with VAD, percent survival to transplant is seen. In addition, hazard curve shows highest risk of death in the first 2 weeks following implantation. (Reproduced from Stein ML, Robbins R, Sabati AA, et al. Interagency Registry for Mechanically Assisted Circulatory Support (INTERMACS)-defined morbidity and mortality associated with pediatric ventricular assist device support at a single US center: the Stanford experience. *Circ Heart Fail* 2010;3:682–688, with permission.)

to those reported from the larger MCSDB database of adult outcomes (99). Adverse events or complications are a major source of morbidity with chronic pediatric VAD support. Prevention requires meticulous attention to detail with the major morbidity related to problems with chronic anticoagulation (114), neurologic complications, and infection (Table 21.6). Neurologic complications in that series (105) include a 20% incidence of stroke, often fatal or leading to withdrawal of support. This rate of stroke was statistically different between short-term devices (35%) and those intended for long-term support (13%, $p = 0.02$). In a single center report (108) of 25 pediatric patients using predetermined Interagency definitions retrospectively, Stein et al. showed a significant number of morbidities following pediatric VAD implant, including 48% neurologic events. Respiratory failure, infection, renal dysfunction, and bleeding were also common and associated with increased mortality.

Protocols for anticoagulation management vary between devices and centers and include a combination of heparin, coumadin, and antiplatelet drugs. Close monitoring of heparin levels, coagulation profiles, and platelet function is critical. In addition, pediatric research efforts must address biocompatibility issues to mitigate the risks arising from blood-prosthetic surface interactions in these devices, which may be unique to children in whom the lower flow rates are necessary. In addition, long-term follow-up of neurocognitive and quality of life issues in these complex patients must be evaluated, monitored, and compared with appropriate peer groups, in order to evaluate the long-term outcomes and utility of VAD successes.

Use of “Adult” VAD Systems in Children

As noted previously and in Figure 21.3, the use of VADs in children has continued to expand. The currently available devices for children and adolescents in the United States are shown in Table 21.1. The Pediatric Heart Transplant Study Group reported the experience from 24 pediatric heart transplant institutions over the decade of 1993 to 2003, in which 99 pediatric patients received VAD support as a bridge to transplantation (105). In this study, which

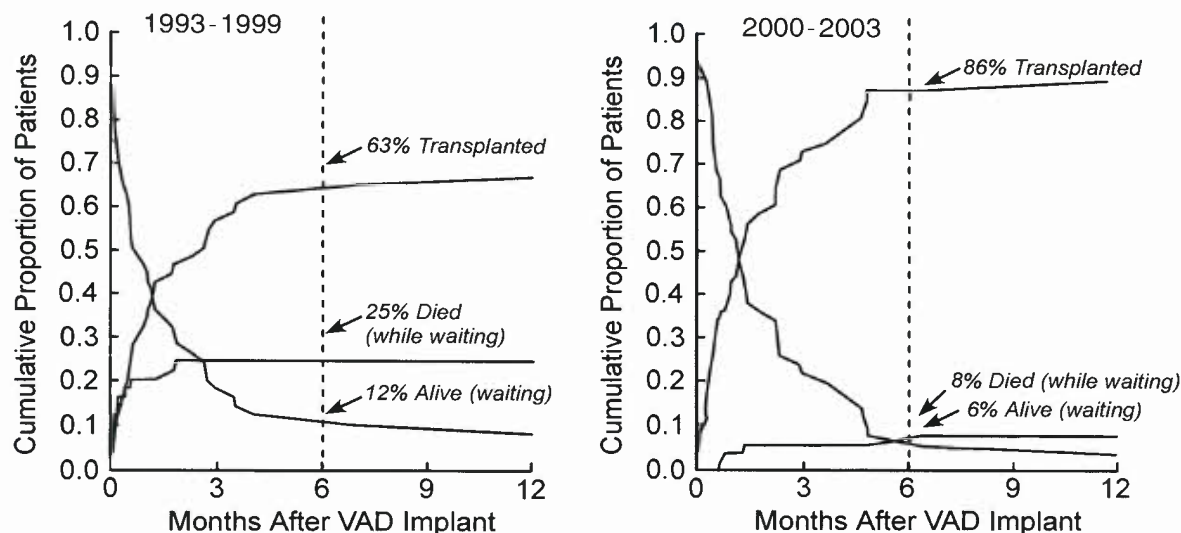


Figure 21.6. Era effect of outcome following pediatric VAD implantation. Competing outcomes analysis shows the early mortality improving over time comparing the 1993–1999 (left) era with the current 2000–2003 era (right). (Reproduced from Blume ED, Naftel DC, Bastardi HJ, et al.; for the Pediatric Heart Transplant Study Investigators. Outcomes of children bridged to heart transplantation with ventricular assist devices: a multi-institutional study. *Circulation* 2006;113:2313–2319, with permission.)

included 2,375 pediatric patients listed for transplant, the percentage of patients transplanted with VAD technology implanted increased from 3.2% of all transplants between 1993 and 1999 to 6.6% of all transplants between 2000 and 2003 (Fig. 21.6). This increase in pediatric patients with VAD implantations is most likely multifactorial, including center experience, regulatory issues, and development of smaller technology. Of the 99 patients retrospectively reviewed with a median age of 13.3 years (range 2 days to 17.9 years), 78% had cardiomyopathy (22 patients had congenital heart disease). They were supported for a mean time of implantation of 70 days (range 1 to 465 days). Status prior to implantation included 34 inotrope dependent, 41 requiring ventilatory support, 26 on another form of mechanical circulatory support including 10 on ECMO, 11 on IABP, and 3 on CPB. Of those 70 children who were supported on an adult pulsatile device, 60 (86%) were successfully bridged to transplant. In comparison of this VAD group with over 1,200 patients listed as Status 1, on inotropic support without mechanical support, outcomes both while awaiting transplant and posttransplant were not statistically different. The 5-year survival following transplant for patients on VAD support at time of transplant is comparable to those not requiring a VAD (77% vs. 73%, $p = 0.8$).

Several adult devices have been used in larger children with continued success. Hill et al. (113) reported on 209 children from the Thoratec Registry who were supported with pulsatile Thoratec device for a mean duration of support of 44 days, with survival to transplant or recovery of 68%. Most recently, as adult pump technology transitions to a greater use of continuous flow pumps, particularly the HeartMate II (Thoratec Corp) with decreased adverse events and improved survival, it is not surprising that there have been recent reports of this device in children (115). The Intermacs registry reports on 74 patients <21 years of age, which improved competing outcomes (Fig. 21.7) of adult VADs in older adolescents and young adults (116). The CentriMag (Levitronix, LLC) has also been approved for temporary support and has been successfully employed in a small number of children (117,118). Other continuous flow pumps that have been used in pediatrics

include the Impella LP 5.0 (119) (Abiomed, Danvers, MA), the TandemHeart (cardiac Assist, Inc.), the Heartware (120) (HeartWare, Inc.), and the DeBakey VAD Child (121) (Micromed, Inc.).

VAD Support for Neonates, Infants, and Small Children

An early development in pediatric circulatory support has been the development of an implantable axial flow device, DeBakey VAD *Child* (MicroMed Technology, Inc., Houston, TX), which was granted Humanitarian Device Exemption (HDE) status by the Food and Drug Administration (FDA) and became available for use in small children in 2004. This pediatric device employs the same continuous axial-flow pump used in the adult version with design modifications aimed at reducing the lateral space requirements for device implantation. Under the current HDE, the VAD *Child* is used to provide temporary left ventricular support as a bridge to cardiac transplantation for children from 5 to 16 years of age with a BSA 0.7 to 1.5 m² and is designed to be fully implantable in this size range. Although the clinical experience has been limited (121,122), this device has been used successfully in a small number of children since its introduction.

Currently, there are two pulsatile VAD systems that are suitable for the entire age range of pediatric patients: MEDOS HIA VAD (MEDOS Medizintechnik AG, Stolberg, Germany) and the Berlin Heart VAD (Berlin Heart AG, Berlin, Germany). Importantly, both devices can be used in neonates and infants, and for this reason, are currently the only alternatives for longer-term VAD support in these patients. Both are paracorporeal systems that employ pneumatically driven, thin membrane pumps to provide pulsatile flow. Both systems are available in a variety of pump sizes (10 to 80 mL), with the smallest pump sizes suitable for infant support. A measured amount of compressed air delivered through a pneumatic line compresses the ventricular chamber or bladder, thereby enforcing ejection of blood (Fig. 21.8). Diastolic pump filling is achieved by negative pressure suction. In general, pump rates are kept

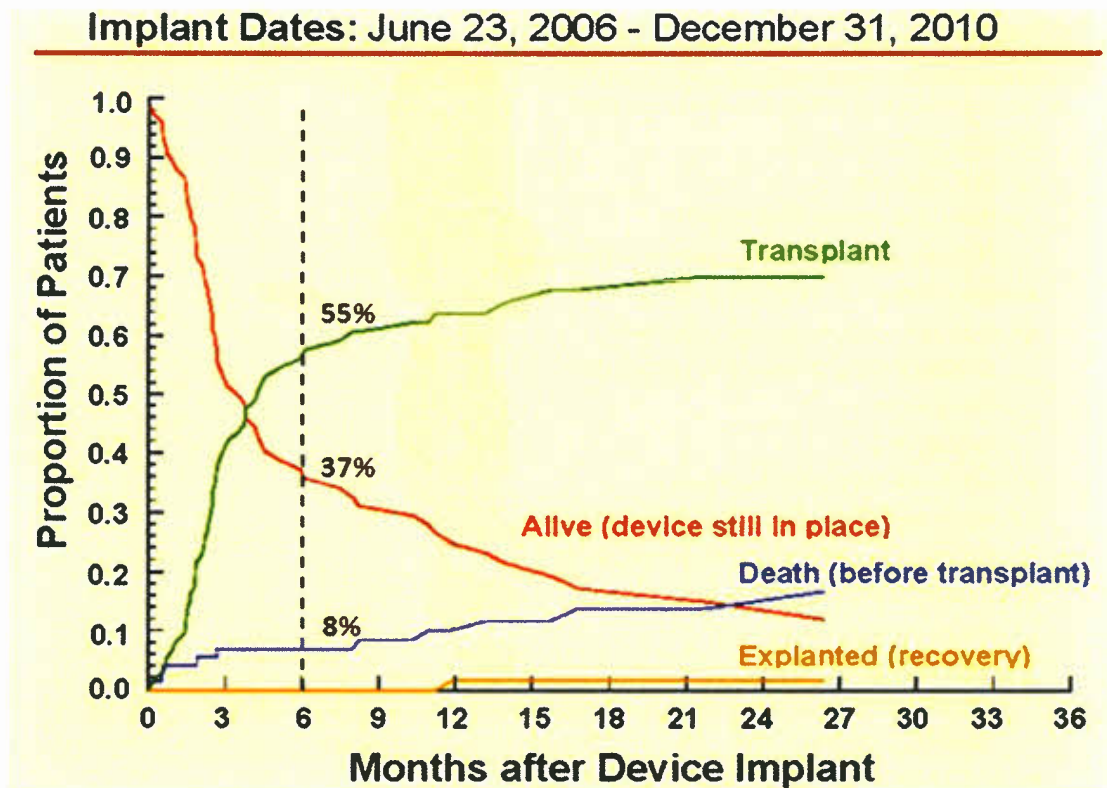


Figure 21.7. Outcomes of pediatric and young adult patients implanted with adult devices in the current era: Intermacs Registry 2011.

low, 60 to 80bpm, and negative pressure 40 to 60mm Hg in order to allow for complete filling. The systolic drive pressure is set at 20 to 30mm Hg more than the patient's systolic pressure. The power source generates positive and negative pressures to move the membrane that separates the blood chamber from the air chamber. This membrane appearance can be evaluated at the bedside to ensure minimal wrinkling

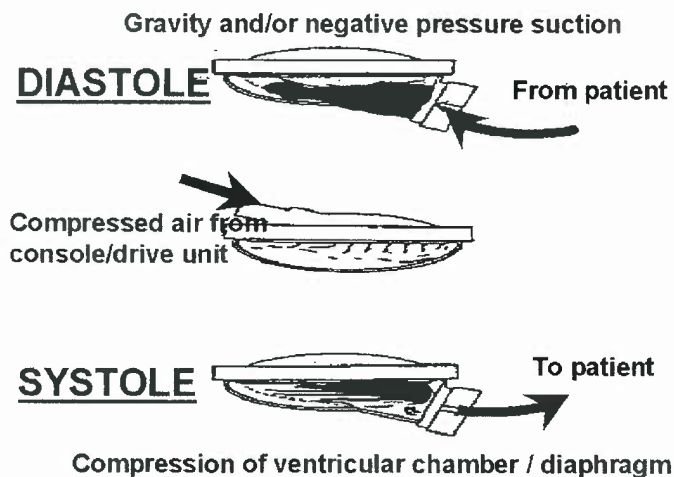


Figure 21.8. Mechanics of pneumatically driven, pulsatile, paracorporeal systems. Blood from the patient enters the pump in diastole, in the presence of gravity and/or negative pressure suction, resulting in a concave membrane. Compressed air from the console then enters from the drive unit, resulting in the convex membrane and resulting in systolic ejection of the blood back to the patient.

(Table 21.7). Insufficient filling (more wrinkles noted in convex position) requires an assessment of preload, intrathoracic pressures, and/or tamponade, or an increase of the diastolic drive pressure (i.e., more negative). In the case of inadequate ejection or stroke volume (wrinkles in concave position), assessment should be made of possible sources of increased pulmonary or systemic vascular resistance (afterload) such as inadequate sedation, ventilatory status, and infection. When this is noted, additional support of the circulation with vasodilators and/or inotropes to augment stroke volume should be considered. Because of the high resistance of the small-bore cannulae in small children, positive pressures up to 350 mm Hg and negative suction of 100 mm Hg at pumping rates of up to 180 bpm may be necessary, increasing the power requirements for the driving unit considerably, although at these maximal settings, there may be considerable blood trauma and hemolysis. In this instance, it may be critical to reevaluate the cannula position and cardiac function either by echocardiography or by cardiac catheterization. The changes in setting of the pulsatile devices need to be reassessed only with changes such as intubation or extubation, and once the patient is ambulatory. Otherwise, settings will remain relatively stable throughout the patient course. Inlet and outlet valves are trileaflet and constructed from polyurethane, and while they function well to prevent regurgitation, they remain a potential nidus for thrombus formation, which requires at least twice-daily assessment.

Reports of the Berlin Heart Institute (123–126) have shown results from 1990 to 2006, with 74 patients supported with a mean age of 7.6 years and an initial mortality of 41%. In this cohort, there was a significant era effect, with 74% survival from 200 onwards. Patients could be mobile with the Berlin Heart but had to manage movement of a large console while ambulating. The first North American use of the Berlin Heart was in 2001,

TABLE 21.7 Algorithm for Pulsatile VAD Pump Troubleshooting**A. Inadequate filling (wrinkles in convex position)**

- Assess preload, monitor:
 - CVP, RAp, LAp
 - Heart rate, arterial blood pressure
 - Maintain adequate preload; volume available at bed space
- Assess changes in intrathoracic pressure with ventilation
- Tamponade: inadequate membrane filling
 - Increased filling pressure (increased CVP)
 - Tachycardia
 - Hypotension
- Consider adjusting diastolic pressure
- Consider adjusting systolic ejection time

B. Inadequate ejection (wrinkles in concave position)

- Increased PVR and SVR (afterload)
 - Assess hemodynamics
 - Consider inotropic support and afterload reduction
 - Consider other factors leading to increased PVR and SVR (i.e., level of sedation, mechanical ventilation, sepsis)
- Consider adjusting systolic drive pressure
- Consider adjusting systolic ejection time

CVP, central venous pressure; RAp, right arterial pressure; LAp, left arterial pressure; PVR, pulmonary vascular resistance; SVR, systemic vascular resistance.

and by 2004, it had gained widespread use. The current North American IDE trial (127) has completed enrollment and awaits FDA decision concerning approval. The North American IDE study included a primary study population of 48 subjects aged 0 to 16 years, divided into 24 younger subjects with BSAs $< 0.7 \text{ m}^2$ and 24 older subjects with a BSA $\geq 0.7 \text{ m}^2$ to $< 1.5 \text{ m}^2$. The primary effectiveness end point compared this study population to a historically matched ECMO control group compiled from the ELSO registry. The purpose of the study was to determine whether use of the EXCOR Pediatric for bridge-to-transplantation is associated with reasonable assurance of safety and probable benefit such that the EXCOR Pediatric merits approval by the FDA under a HDE. In addition, the study was designed to determine whether the EXCOR Pediatric merits continuation with the current trial design and subject population to prove safety and efficacy for premarket approval. Due to the investigational status and while awaiting FDA decisions, few data are available with regards to the IDE trial.

Single center North American experiences have been reported. Fifteen patients from Toronto (112) with a mean age of 8.8 years were on for an average of 29 days, with three being transitioned from ECMO, and 13/15 surviving to transplant. The St. Louis group (107) reported on nine patients with BiVAD support for an average of 35 days, with 8/9 surviving to transplant. The Great Ormond Street group (128) reported on the smallest patients with a group of 11 patients with a median weight of 8 kg and a 91% survival to transplant. Lastly, an Italian group (129) noted 10 patients with a median weight of 6.4 kg and average support time of 61 days with a 40% mortality. The worldwide Berlin Heart EXCOR Pediatric experience now includes >950 patients in 123 centers, in 33 countries, with a median age at implant of 2 years and mean duration of device

support time of 75.5 days. The longest support time worldwide has been 1,131 days (Berlin communication) (116).

Morales et al. (116) reported the most recent nationwide database analysis of children in the United States implanted with MCSDs. They noted that use among pediatric hospitals is growing dramatically and suggested that volume of cases may play a role in overall outcomes. This is an important suggestion that will need further investigation. Other areas requiring further investigation (131–134) include transporting patients on mechanical support, comparing VAD and ECMO outcomes, and understanding the complexities of complex congenital patients.

These data support the use of VAD in children while awaiting transplant. The initial learning curve of the sites appears to be universal, although the North American experience may benefit from the lessons already learned in Europe. The results of the IDE trial will be exciting and well received.

Pediatric Device Initiatives

With the rapid increase in use of the Berlin Heart in North America, pediatric mechanical circulatory support has been recognized as an unmet need by the US HHS. The NHLBI initiative in 2004 awarded \$22 million dollars to promote research and development of mechanical support devices in children. Five awards (130) over 5 years (2004 to 2009) marked significant developments in animal models and *in vitro* testing of infant and pediatric flow dynamics, anticoagulation, and biocompatibility interface technology. The continuation of the Pediatric Mechanical Circulatory Support Program is the PUMPKIN program (2010) that was awarded to four program projects with the intent to move these devices into preclinical

and IDE trial phases. These devices currently include two pediatric VAD devices (PediaFlow and Jarvik child and infant) and two oxygenator devices (Ension (135) and Levotronic). These initiatives and the Berlin Heart IDE trial have led to many more company-led endeavors for pediatric mechanical support.

The future challenge will continue to be the trial design and post market data collection for these new devices. It will be imperative to collect registry data on all children implanted with devices in order to understand patient selection, device specifics, adverse event profiles, and the heterogeneous nature of patient and device-specific variables. Collaboration among clinicians, the FDA, NIH, and industry will be critical in order to continue to move the field forward.

REFERENCES

- Chang AC, Hanley FL, Weindling SN, et al. Left heart support with a ventricular assist device in an infant with acute myocarditis. *Crit Care Med* 1992;20:712-715.
- Kulik TJ, et al. Outcome-associated factors in pediatric patients treated with extracorporeal membrane oxygenator after cardiac surgery. *Circulation* 1996;94:II63-II68.
- Raithel SC, et al. Extracorporeal membrane oxygenation in children after cardiac surgery. *Circulation* 1992;86:II305-II310.
- del Nido PJ, Dalton HJ, Thompson AE, et al. Extracorporeal membrane oxygenator rescue in children during cardiac arrest after cardiac surgery. *Circulation* 1992;86:II-300-II-304.
- Jacobs JP, Ojito JW, McConaghey TW, et al. Rapid cardiopulmonary support for children with complex congenital heart disease. *Ann Thorac Surg* 2000;70:742-750.
- Walters HL, Hakimi M, Rice MD, et al. Pediatric cardiac surgical ECMO: multivariate analysis of risk factors for hospital death. *Ann Thorac Surg* 1995;60:329-337.
- Fiser WP, Yetman AT, Gunselman RJ, et al. Pediatric arteriovenous extracorporeal membrane oxygenation (ECMO) as a bridge to cardiac transplantation. *J Heart Lung Transplant* 2003;22:770-777.
- Gajarski RJ, Mosca RS, Ohye RG, et al. Use of extracorporeal life support as a bridge to pediatric cardiac transplantation. *J Heart Lung Transplant* 2003;22:28-34.
- Levi D, Marelli D, Plunkett M, et al. Use of assist devices and ECMO to bridge pediatric patients with cardiomyopathy to transplantation. *J Heart Lung Transplant* 2002;21:760-770.
- Kirshbom PM, Bridges ND, Myung RJ, et al. Use of extracorporeal membrane oxygenation in pediatric thoracic organ transplantation. *J Thorac Cardiovasc Surg* 2002;123:130-136.
- Ibrahim AE, Duncan BW. Long-term follow-up of children with cardiac disease requiring mechanical circulatory support. In: Duncan BW, ed. *Mechanical Circulatory Support for Cardiac and Respiratory Failure in Pediatric Cardiac Patients*. New York, NY: Marcel Dekker, Inc., 2001:205-220.
- Ibrahim AE, Duncan BW, Blume ED, et al. Long-term follow-up of pediatric cardiac patients requiring mechanical circulatory support. *Ann Thorac Surg* 2000;69:186-192.
- Blume ED, Nelson DP, Gauvreau K, et al. Soluble adhesion molecules in infants and children undergoing cardiopulmonary bypass. *Circulation* 1997;96:II-352-II-357.
- Pasnik J, Siniewicz K, Moll JA, et al. Effect of cardiopulmonary bypass on neutrophil activity in pediatric open-heart surgery. *Arch Immunol Ther Exp (Warsz)* 2005;53:272-277.
- Jensen E, Andreasson S, Bengtsson A, et al. Influence of two different perfusion systems on inflammatory response in pediatric heart surgery. *Ann Thorac Surg* 2003;75:919-925.
- Gessler P, Pfenninger J, Pfammatter JP, et al. Inflammatory response of neutrophil granulocytes and monocytes after cardiopulmonary bypass in pediatric cardiac surgery. *Intensive Care Med* 2002;28:1786-1791.
- Ashraf SS, Tian Y, Zacharias S, et al. Effects of cardiopulmonary bypass on neonatal and paediatric inflammatory profiles. *Eur J Cardiothorac Surg* 1997;12:862-868.
- del Nido PJ, Armitage JM, Fricker FJ, et al. Extracorporeal membrane oxygenation support as a bridge to pediatric heart transplantation. *Circulation* 1994;90:II66-II69.
- Coffin SE, et al. Nosocomial infections in neonates receiving extracorporeal membrane oxygenation. *Infect Control Hosp Epidemiol* 1997;18:93-96.
- Douglass BH, Keenan AL, Purohit DM. Bacterial and fungal infection in neonates undergoing venoarterial extracorporeal membrane oxygenation: an analysis of the registry data of the extracorporeal life support organization. *Artif Organs* 1996;20:202-208.
- Dembitsky WP, et al. Emergency resuscitation using portable extracorporeal membrane oxygenation. *Ann Thorac Surg* 1993;55:304-309.
- Duncan BW, Ibrahim AE, Hraska V, et al. Use of rapid-deployment ECMO for the resuscitation of pediatric patients with heart disease after cardiac arrest. *J Thorac Cardiovasc Surg* 1998;116:305-311.
- Gibbon JH Jr. Application of a mechanical heart and lung apparatus to cardiac surgery. *Minn Med* 1954;37:171-185.
- Lillehei CW, Varco RL, Cohen M, et al. The first open-heart repairs of ventricular septal defect, atrioventricular communis, and tetralogy of Fallot using extracorporeal circulation by cross-circulation: a 30 year follow-up. *Ann Thorac Surg* 1986;41:4-21.
- Kirklin JW, Dushane JW, Patrick RT, et al. Intracardiac surgery with the aid of a mechanical pump-oxygenator system (gibbon type): report of eight cases. *Mayo Clin Proc* 1955;30:201-206.
- Castaneda AR, Lamberti J, Sade RM, et al. Open heart Surgery during the first three months of life. *J Thorac Cardiovasc Surg* 1974;68:719-731.
- Barratt-Boyes B. Complete correction of cardiovascular malformations in the first two years of life using profound hypothermia. In: Barratt-Boyes BG, Neutze JM, Harris EA, eds. *Heart Disease in Infancy*. Edinburgh: Churchill Livingstone, 1973:35.
- Hall RI, Smith MS, Rocker G. Systemic inflammatory response to cardiopulmonary bypass: Pathophysiological, therapeutic and pharmacological considerations. *Anesth Analg* 1997;85:766-782.
- Verrier EW, Boyle EM. Endothelial cell injury in cardiovascular surgery: an overview. *Ann Thorac Surg* 1997;64:S2-S8.
- Wernovsky G, Wypij D, Jonas RA, et al. Postoperative course and hemodynamic profile after the arterial switch operation in neonates and infants: a comparison of low-flow cardiopulmonary bypass versus circulatory arrest. *Circulation* 1995;92:2226-2235.
- Journois D, Israel-Biet D, Pouard P, et al. High-volume, zero-balanced hemofiltration to reduce delayed inflammatory response to cardiopulmonary bypass in children. *Anesthesia* 1996;85:965-976.
- Elliot M. Modified ultrafiltration and open heart surgery in children. *Paediatr Anaesth* 1999;9:1-5.
- Keenan HT, Thiagarajan R, Stephens KE, et al. Pulmonary function after modified venovenous ultrafiltration in infants: a prospective, randomized trial. *J Thorac Cardiovasc Surg* 2000;119:501-505.
- Hickey PR, Andersen NP. Deep hypothermic circulatory arrest: a review of pathophysiology and clinical experience as a basis for anesthetic management. *J Cardiothorac Anesth* 1987;1:137.
- Fox LS, Blackstone EH, Kirklin JW, et al. Relationship of brain blood flow and oxygen consumption to perfusion flow rate during profoundly hypothermic cardiopulmonary bypass. *J Thorac Cardiovasc Surg* 1984;87:658-664.
- du Plessis AJ. Neurologic complications of cardiac disease in the newborn. *Clin Perinatol* 1997;24:807-825.
- Greeley WJ, Kern FH, Ungerleider RM, et al. The effect of hypothermic cardiopulmonary bypass and total circulatory arrest on cerebral metabolism in neonates, infants and children. *J Thorac Cardiovasc Surg* 1991;101:783-794.
- Slogoff ST, Girgis KZ, Keats AS. Etiologic factors in neuro-psychiatric complications associated with cardiopulmonary bypass. *Anesth Analg* 1982;61:903-911.
- du Plessis AJ, Jonas RA, Wypij D, et al. Perioperative effects of alpha-stat versus pH-stat strategies for deep hypothermic cardiopulmonary bypass in infants. *J Thorac Cardiovasc Surg* 1997;114:991-1001.
- Brunberg JA, Doty DB, Reilly EL. Choreoathetosis in infants following cardiac surgery with deep hypothermic and circulatory arrest. *J Pediatr* 1974;84:232s.
- Newburger JW, Jonas RA, Wernovsky G, et al. A comparison of the perioperative neurologic effects of hypothermic circulatory arrest versus low-flow cardiopulmonary bypass in infant heart surgery. *N Engl J Med* 1993;329:1057-1064.
- Bellinger DC, Wernovsky G, Rappaport LA, et al. Cognitive development of children following early repair of transposition of the great arteries using deep hypothermic circulatory arrest. *Pediatrics* 1991;87:701.
- Bellinger D, Jonas RA, Rappaport L, et al. Developmental and neurologic status of children after heart surgery with hypothermic circulatory arrest or low-flow cardiopulmonary bypass. *N Engl J Med* 1995;332:540-555.
- Bellinger DC, Wypij D, duPlessis AJ, et al. Neurodevelopmental status at eight years in children with dextro-transposition of the great arteries: the Boston Circulatory Arrest Trial. *J Thorac Cardiovasc Surg* 2003;126:1385-1396.
- Gaynor JW, Gerdes M, Zackai EH, et al. Apolipoprotein E genotype and neurodevelopmental sequelae of infant cardiac surgery. *J Thorac Cardiovasc Surg* 2003;126:1736.
- Jonas RA, Wypij D, Roth SJ, et al. The influence of hemodilution on outcome after hypothermic cardiopulmonary bypass: results of a randomized trial in infants. *J Thorac Cardiovasc Surg* 2003;126:1765-1774.
- Laussen PC. Optimal blood gas management during deep hypothermic pediatric cardiac surgery: Alpha-stat is easy, but pH-stat may be preferable. *Paediatric Anaesth* 2002;12:199-204.
- Extracorporeal Life Support Organization. ECLS Registry Report: International Summary. July 2010.
- Kennaugh JM, et al. Impact of new treatments for neonatal pulmonary hypertension on extracorporeal membrane oxygenation use and outcome. *J Perinatol* 1997;17:366-369.
- Moront MG, et al. Extracorporeal membrane oxygenation for neonatal respiratory failure. A report of 50 cases. *J Thorac Cardiovasc Surg* 1989;97:706-714.

51. Wilson JM, et al. ECMO in evolution: the impact of changing patient demographics and alternative therapies on ECMO. *J Pediatr Surg* 1996;31:1116–1122; discussion 1122–1123.
52. Hunkeler NM, et al. Extracorporeal life support in cyanotic congenital heart disease before cardiovascular operation. *Am J Cardiol* 1992; 69:790.
53. Walters HL, III et al. Pediatric cardiac surgical ECMO: multivariate analysis of risk factors for hospital death. *Ann Thorac Surg* 1995;60:329–336; discussion 336–337.
54. Flick RP, Sprung J, Gleich SJ, et al. Intraoperative extracorporeal membrane oxygenation and survival of pediatric patients undergoing repair of congenital heart disease. *Paediatr Anaesth* 2008;18:757–766.
55. Duncan BW, et al. Mechanical circulatory support in children with cardiac disease. *J Thorac Cardiovasc Surg* 1999;117:529–542.
56. Chaturvedi RR, Macrae D, Brown KL, et al. Cardiac ECMO for biventricular hearts after paediatric open heart surgery. *Heart* 2004;90:545–551.
57. Bautista-Hernandez V, Thiagarajan RR, Fynn-Thompson F, et al. Preoperative extracorporeal membrane oxygenation as a bridge to cardiac surgery in children with congenital heart disease. *Ann Thorac Surg* 2009;88:1306–1311.
58. Allan CK, Thiagarajan RR, del Nido PJ, et al. Indication for initiation of mechanical circulatory support impacts survival of infants with shunted single-ventricle circulation supported with extracorporeal membrane oxygenation. *J Thorac Cardiovasc Surg* 2007;133:660–667.
59. Ravishankar C, Dominguez TE, Kreutzer J, et al. Extracorporeal membrane oxygenation after stage I reconstruction for hypoplastic left heart syndrome. *Pediatr Crit Care Med* 2006;7:319–323.
60. Booth KL, Roth SJ, Thiagarajan RR, et al. Extracorporeal membrane oxygenation support of the Fontan and bidirectional Glenn circulations. *Ann Thorac Surg* 2004;77:1341–1348.
61. Hoskote A, Bohn D, Gruenwald C, et al. Extracorporeal life support after staged palliation of a functional single ventricle: subsequent morbidity and survival. *J Thorac Cardiovasc Surg* 2006;131:1114–1121.
62. Rood KL, Teele SA, Barrett CS, et al. Extracorporeal membrane oxygenation support after the Fontan operation. *J Thorac Cardiovasc Surg* 2011;Sep;142(3):504–10.
63. Thiagarajan RR, Laussen PC, Rycus PT, et al. Extracorporeal membrane oxygenation to aid cardiopulmonary resuscitation in infants and children. *Circulation* 2007;116:1693–1700.
64. Ishino K, Alexi-Meskishvili V, Hetzer R. Myocardial recovery through ECMO after repair of total anomalous pulmonary venous connection: the importance of left heart unloading. *Eur J Cardio-Thorac Surg* 1997;11:585–587.
65. Alexi-Meskishvili V, et al. Long-term extracorporeal membrane oxygenation in a newborn child after arterial switch operation. *Cardiovasc Surg* 1996;4:258–260.
66. Booth KL, Roth SJ, Perry SB, et al. Cardiac catheterization of patients supported by extracorporeal membrane oxygenation. *J Am Coll Cardiol* 2002;40:1681–1686.
67. Morris MC, Wernovsky G, Nadkarni VM. Survival outcomes after extracorporeal cardiopulmonary resuscitation instituted during active chest compressions following refractory in-hospital pediatric cardiac arrest. *Pediatr Crit Care Med* 2004;5:440–446.
68. Chan T, Thiagarajan RR, Frank D, et al. Survival after extracorporeal cardiopulmonary resuscitation in infants and children with heart disease. *J Thorac Cardiovasc Surg* 2008;136:984–992.
69. Kane DA, Thiagarajan RR, Wypij D, et al. Rapid-response extracorporeal membrane oxygenation to support cardiopulmonary resuscitation in children with cardiac disease. *Circulation* 2010;122: S241–S248.
70. Slomin AD, Patel KM, Ruttimann UE, et al. Cardiopulmonary resuscitation in pediatric intensive care units. *Crit Care Med* 1997;25:1951–1955.
71. Booth KL, Guleserian KJ, Mayer JE, et al. Extracorporeal membrane oxygenation support of a neonate with percutaneous femoral arterial cannulation. *Ann Thorac Surg* 2006;81:1514–1516.
72. Rajagopal SK, Almond CS, Laussen PC, et al. Extracorporeal membrane oxygenation for the support of infants, children, and young adults with acute myocarditis: a review of the Extracorporeal Life Support Organization registry. *Crit Care Med* 2010;38:382–387.
73. Teele SA, Allan CK, Laussen PC, et al. Management and outcomes in pediatric patients presenting with acute fulminant myocarditis. *J Pediatr* 2011;158:638–643 e1.
74. Duncan BW, Bohn DJ, Atz AM, et al. Mechanical circulatory support for the treatment of children with acute fulminant myocarditis. *J Thorac Cardiovasc Surg* 2001;122:440–448.
75. Bae JO, Frischer JS, Waich M, et al. Extracorporeal membrane oxygenation in pediatric cardiac transplantation. *J Pediatr Surg* 2005;40:1051–1056.
76. Allan CK, Thiagarajan RR, Armsby LR, et al. Emergent use of extracorporeal membrane oxygenation during pediatric cardiac catheterization. *Pediatr Crit Care Med* 2006;7:212–219.
77. Carmichael TB, Walsh EP, Roth SJ. Anticipatory use of venoarterial extracorporeal membrane oxygenation for a high-risk interventional cardiac procedure. *Respir Care* 2002;47:1002–1006.
78. Cheung PY, et al. Carotid artery reconstruction in neonates receiving extracorporeal membrane oxygenation: a 4-year follow-up study. Western Canadian ECMO Follow-Up Group. *J Pediatr Surg* 1997;32:560–564.
79. Klein MD, et al. Carotid artery and jugular vein ligation with and without hypoxia in the rat. *J Pediatr Surg* 1997;32:565–570.
80. Karl TR, et al. Infant ECMO cannulation technique allowing preservation of carotid and jugular vessels. *Ann Thorac Surg* 1990;50:488–489.
81. Ashton RC, Oz MC, Michler RE, et al. Left ventricular assist device options in pediatric patients. *ASAIO J* 1995;41:M277–M280.
82. Costa RJ, Chard RB, Nunn GR, et al. Ventricular assist devices in pediatric cardiac surgery. *Ann Thorac Surg* 1995;60:S536–S538.
83. Karl TR, Sano S, Horton S, et al. Centrifugal pump left heart assist in pediatric cardiac operations. Indication, technique, and results. *J Thorac Cardiovasc Surg* 1991;102:624–630.
84. Kesler KA, Pruitt AL, Turrentine MW, et al. Temporary left-sided mechanical cardiac support during acute myocarditis. *J Heart Lung Transplant* 1994;13:268–270.
85. del Nido PJ, et al. Left ventricular assist device improves survival in children with left ventricular dysfunction after repair of anomalous origin of the left coronary artery from the pulmonary artery. *Ann Thorac Surg* 1999;67:169–172.
86. Ungerleider RM, Shen I, Yeh T, et al. Routine mechanical ventricular assist following the Norwood procedure—improved neurologic outcome and excellent hospital survival. *Ann Thorac Surg* 2004;77:18–22.
87. Dela Cruz TV, Stewart DL, Winston SJ, et al. Risk factors for intracranial hemorrhage in the extracorporeal membrane oxygenation patient. *J Perinatol* 1997;17:18–23.
88. Park JK, Hsu DT, Gersony WM. Intraaortic balloon pump management of refractory congestive heart failure in children. *Pediatr Cardiol* 1993;14:19–22.
89. Akomea-Agyin C, Kejriwal NK, Franks R, et al. Intraaortic balloon pumping in children. *Ann Thorac Surg* 1999;67:1415–1420.
90. Moran JM, Opravil M, Gorman AJ, et al. Pulmonary artery balloon counterpulsation for right ventricular failure: II. Clinical experience. *Ann Thorac Surg* 1984;38:254–259.
91. Pantalos GM, Minich LL, Tani LY, et al. Estimation of timing errors for the intraaortic balloon pump use in pediatric patients. *ASAIO J* 1999;45:166–171.
92. del Nido PJ, et al. Successful use of intraaortic balloon pumping in a 2-kilogram infant. *Ann Thorac Surg* 1988;46:574–576.
93. Moran AM, Blume ED, Quinn R. Intra-aortic balloon pump use in the failing Fontan circulation. *Congenit Heart Dis* 2008;3:60–62.
94. Borovetz HS, Badylak S, Boston JR, et al. Towards the development of a pediatric ventricular assist device. *Cell Transplant* 2006;15:S69–S74.
95. Weiss WJ. Pulsatile pediatric ventricular assist devices. *ASAIO J* 2005; 51:540–545.
96. Havemann L, McMahon CJ, Ganame J, et al. Rapid ventricular remodeling with left ventricular unloading postventricular assist device placement: new insights with strain imaging. *J Am Soc Echocardiogr* 2006;19:355. e9–355. e11.
97. Nathan M, Baird C, Fynn-Thompson F, et al. Successful implantation of a Berlin heart biventricular assist device in a failing single ventricle. *J Thorac Cardiovasc Surg* 2006;131:1407–1408.
98. Pekkan K, Frakes D, De Zelicourt D, et al. Coupling pediatric ventricle assist devices to the Fontan circulation: simulations with a lumped-parameter model. *ASAIO J* 2005;51:618–628.
99. Rose EA, Gelijns AC, Moskowitz AJ, et al. Long-term mechanical left ventricular assistance for end-stage heart failure. *N Engl J Med* 2001;345:1435–1443.
100. Hetzer R, et al. Cardiac recovery in dilated cardiomyopathy by unloading with a left ventricular assist device. *Ann Thorac Surg* 1999;68:742–749.
101. Loebe M, Muller J, Hetzer R. Ventricular assistance for recovery of cardiac failure. *Curr Opin Cardiol* 1999;14:234–248.
102. Almond CS, Thiagarajan RR, Piercy GE, et al. Waiting list mortality among children listed for heart transplantation in the United States. *Circulation* 2009;119:717–727.
103. Stevenson LW, Pagani FD, Young JB, et al. INTERMACS profiles of advanced heart failure: the current picture. *J Heart Lung Transplant* 2009;28:S35–S41.
104. Muller, et al. Weaning from mechanical cardiac support in patients with idiopathic dilated cardiomyopathy. *Circulation* 1997;96:542–549.
105. Blume ED, Naftel DC, Bastardi HJ, et al. Outcomes of children bridged to heart transplantation with ventricular assist devices: a multi-institutional study. *Circulation* 2006;113:2313–2319.
106. Arabia FA, Tsau PH, Smith RG, et al. Pediatric bridge to heart transplantation: application of the Berlin Heart, Medos and Thoratec ventricular assist devices. *J Heart Lung Transplant* 2006;25:16–21.
107. Gandhi SK, Huddleston CB, Balzer DT, et al. Biventricular assist devices as a bridge to heart transplantation in small children. *Circulation* 2008;118: S89–S93.
108. Stein ML, Robbins R, Sabati AA, et al. Interagency Registry for Mechanically Assisted Circulatory Support (INTERMACS)-defined morbidity and mortality associated with pediatric ventricular assist device support at a single US center: the Stanford experience. *Circ Heart Fail* 2010;3:682–688.
109. Kaczmarek I, Sachweh J, Groetzner J, et al. Mechanical circulatory support in pediatric patients with the MEDOS assist device. *ASAIO J* 2005;51:498–500.
110. Coskun O, Parsa A, Weitkemper H, et al. Heart transplantation in children after mechanical circulatory support: comparison of heart transplantation with ventricular assist devices and elective heart transplantation. *ASAIO J* 2005;51:495–497.

111. Hetzer R, Potapov EV, Stiller B, et al. Improvement in survival after mechanical circulatory support with pneumatic pulsatile ventricular assist devices in pediatric patients. *Ann Thorac Surg* 2006;82:917–924.
112. Humpl T, Furness S, Gruenwald C, et al. The Berlin heart excor pediatrics-the sick kids experience 2004–2008. *Artif Organs* 2010;Dec;34(12):1082–6.
113. Hill JD, Reinhartz O. Clinical outcomes in pediatric patients implanted with Thoratec ventricular assist device. *Semin Thorac Cardiovasc Surg Pediatr Card Surg Annu* 2006:115–122.
114. Eghtesady P, Nelson D, Schwartz SM, et al. Heparin induced thrombocytopenia complicating support by the Berlin Heart. *ASAIO J* 2005;51:820–825.
115. Owens WR, Bryant R III, Dreyer WJ, et al. Initial clinical experience with the HeartMate II ventricular assist system in a pediatric institution. *Artif Organs* 2010;34:600–603.
116. Morales DL, Almond CS, Jaquiss RD, et al. Bridging children of all sizes to cardiac transplantation: the initial multicenter North American experience with the Berlin Heart EXCOR ventricular assist device. *J Heart Lung Transplant* 2011 Jan;30(1):1–8.
117. Kouretas PC, Kaza AK, Burch PT, et al. Experience with the Levitronix CentriMag in the pediatric population as a bridge to decision and recovery. *Artif Organs* 2009;33:1002–1004. [Epub 2009 Oct 28.]
118. Hirata Y, Charette K, Mosca RS, et al. Pediatric application of the thoratec centrimag bivaid as a bridge to heart transplantation. *J Thorac Cardiovasc Surg* 2008;136:1386–1387.
119. Andrade JG, Al-Saloos H, Jeewa A, et al. Facilitated cardiac recovery in fulminant myocarditis: pediatric use of the Impella LP 5.0 pump. *J Heart Lung Transplant* 2010;29:96–97.
120. Miera O, Potapov EV, Redlin M, et al. First experiences with the HeartWare ventricular assist system in children. *Ann Thorac Surg* 2011;91:1256–1260.
121. Fraser CD Jr, Carberry KE, Owens WR, et al. Preliminary experience with the MicroMed DeBakey pediatric ventricular assist device. *Semin Thorac Cardiovasc Surg Pediatr Card Surg Annu* 2006:109–114.
122. Morales DL, Dibardino DJ, McKenzie ED, et al. Lessons learned from the first application of the debakey VAD Child: an intracorporeal ventricular assist device for children. *J Heart Lung Transplant* 2005;24:331–337.
123. Ishino K, Loebe M, Uhlemann F, et al. Circulatory support with paracorporeal pneumatic ventricular assist device (VAD) in infants and children. *Euro J Cardiothorac Surg* 1997;11:965–972.
124. Stiller B, Weng Y, Hubler M, et al. Pneumatic pulsatile ventricular assist devices in children under 1 year of age. *Eur J Cardiothorac Surg* 2005;28:234–239.
125. Hetzer R, Alexi-Meskishvili V, Weng Y, et al. Mechanical cardiac support in the young with the Berlin Heart EXCOR pulsatile ventricular assist device: 15 years' experience. *Semin Thorac Cardiovasc Surg Pediatr Card Surg Annu* 2006:99–108.
126. Hetzer R, Dandel M, Knosalla C. Left ventricular assist devices and drug therapy in heart failure. *N Engl J Med* 2007;356:869–870.
127. Almond CS, Buchholz H, Massicotte P, et al. Berlin Heart EXCOR Pediatric ventricular assist device Investigational Device Exemption study: Study design and rationale. *Am Heart J* 2011;162:425–435.
128. Karimova A, Van Doorn C, Brown K, et al. Mechanical bridging to orthotopic heart transplantation in children weighing less than 10kg: feasibility and limitations. *Eur J Cardiothorac Surg* 2010;Mar;39(3):304–9.
129. Brancaccio G, Amodeo A, Ricci Z, et al. Mechanical assist device as a bridge to heart transplantation in children less than 10 kilograms. *Ann Thorac Surg* 2010;90:58–62.
130. Baldwin JT, Borovetz HS, Duncan BW, et al. The national heart, lung, and blood institute pediatric circulatory support program: a summary of the 5-year experience. *Circulation* 2011;123:1233–1240.
131. Tissot C, Buchholz H, Mitchell MB, et al. First pediatric transatlantic air ambulance transportation on a Berlin Heart EXCOR left ventricular assist device as a bridge to transplantation. *Pediatr Crit Care Med* 2010;11:e24–e25.
132. Fan Y, Weng YG, Xiao YB, et al. Outcomes of ventricular assist device support in young patients with small body surface area. *Eur J Cardiothorac Surg* 2011;39:699–704.
133. Imamura M, Dossey AM, Prodhan P, et al. Bridge to cardiac transplant in children: Berlin Heart versus extracorporeal membrane oxygenation. *Ann Thorac Surg* 2009;87:1894–901.
134. Lacour-Gayet FG, Lanning CJ, Stoica S, et al. An artificial right ventricle for failing fontan: in vitro and computational study. *Ann Thorac Surg* 2009;88:170–176.
135. Pantalos GM, Horrell T, Merkley T, et al. In vitro characterization and performance testing of the ension pediatric cardiopulmonary assist system. *ASAIO J* 2009;55:282–286.

Cardiopulmonary and Right-Left Heart Interactions

Andrew N. Redington

The singular function of the right ventricle (RV), left ventricle (LV), and the lungs is discussed elsewhere. Nonetheless, particularly in the field of congenital heart disease, we are becoming increasingly aware of the importance of the interactions between them. There is continual cross talk between the two sides of the heart, and in turn, the ventricles are continually responding to subtle changes occurring within the thorax as a whole. In this chapter, these interactions, and their modification by congenital heart disease and its surgical repair, are discussed.

COMPARISON OF RIGHT AND LEFT HEART HEMODYNAMICS

The average cardiac output from the RV must, of course, essentially equal the cardiac output from the left heart. Nonetheless, the mechanism by which this is achieved is very different. The RV performs approximately one quarter of the external mechanical work compared with its left ventricular (LV) counterpart. External mechanical work is a function of stroke volume and developed ventricular pressure, and is more accurately described as the area enclosed by the ventricular pressure–volume curve. Figure 22.1 shows a schematic comparison of left and right ventricular (RV) pressure–volume curves. Not only is the developed pressure substantially lower in the RV but its trapezoidal shape still further reduces the amount of work performed on the circulation to generate the cardiac output. The LV essentially works as a square wave pump, its stroke work being reasonably well represented as a direct product of its stroke volume and developed pressure (stroke work = stroke volume \times peak left ventricular pressure–minimum left ventricular pressure). Because of its ability to eject blood into the pulmonary circulation during both pressure rise and pressure fall (1), the external work performed by the RV cannot be described using such a simple derivation. Furthermore, it can be seen that small changes in hemodynamics might impose a major change to global workload of the RV. Indeed, small changes in RV afterload can lead to major changes in workload and the shape of the pressure–volume characteristics to mirror the LV (2).

The trapezoidal shape of the RV pressure–volume relationship is exquisitely matched to the low hydraulic impedance imposed by the pulmonary vascular bed. Unlike the systemic vascular resistance, which reflects a dynamic balance between vasodilatory and vasoconstrictor influences, the pulmonary vascular bed appears to be maximally vasodilated. The low pulmonary vascular resistance requires a healthy endothelium and normal lung function for its integrity. In health, additional inhaled nitric oxide, for example, fails to lower the pulmonary vascular resistance, suggesting pulmonary endothelial vasodilatory capacity is at its maximum (3). This is a markedly different mechanism to that of the systemic vascular bed where a wide

portfolio of vasodilatory substances can lower its resistance. The pulmonary vascular bed is also uniquely affected by external factors. The status of lung inflation, even the normal circulation, has major effects on the pulmonary vascular resistance and hemodynamic function. Normal respiration, ventilating around functional residual capacity, minimizes the pulmonary vascular resistance. Underinflation of the lungs leads to an increased pulmonary vascular resistance, as a result of atelectasis and secondary alveolar hypoxemia, and overinflation of the lungs leads to an increase, secondary to alveolar stretch and direct vascular compression (Fig. 22.2) (4). Both should be avoided whenever RV afterload needs to be minimized.

CARDIOPULMONARY INTERACTIONS IN THE NORMAL CIRCULATION

Descent of the diaphragm during normal inspiration leads to a modest fall in pleural pressure (3 to 5 cm of water) (5) and a concomitant rise in intra-abdominal pressure. These two changes lead to increased venous return and an increased RV stroke volume, in accord with the Frank Starling mechanism. There is thus a waxing and waning of cardiac output of approximately 10% to 15% during the cardiac cycle (6).

The classic experiments of Cournand in the 1940s (7) were interpreted as confirmation that right heart filling and cardiac output were related to intrathoracic pressure. Positive-pressure ventilation via a mask in conscious volunteers led to a fall in cardiac output of approximately 10% to 15%. This was initially thought to be entirely due to changes in systemic venous return (and reduced ventricular preload) imposed by a raised mean intrathoracic pressure. It has subsequently become clear that reduced preload, as a result of increased airway pressure, is not the whole story. In an elegant series of experiments in dogs, Henning (8) showed that restoration of preload during positive-pressure ventilation failed to restore cardiac output to its baseline levels. The persistent reduction in RV stroke volume, despite normalized preload, suggested an adverse effect on intrinsic RV performance. It was hypothesized that the RV shows signs of reduced systolic function, even under the circumstances of a modest hemodynamic burden imposed by lung hyperinflation, as a result of increased afterload occurring via the mechanism described in Figure 22.2. No matter what the mechanism, however, the functional implications of these changes are not simply theoretic. In a study of children undergoing cardiac catheterization performed by Shekerdemian et al. (9), a negative-pressure cuirass device was used to mimic normal ventilation to compare the effects of positive-pressure and negative-pressure ventilation on cardiac output. In essentially normal children having undergone closure of a small arterial duct, for example, there is an approximate 16% fall in cardiac output, simply as a result of a modest

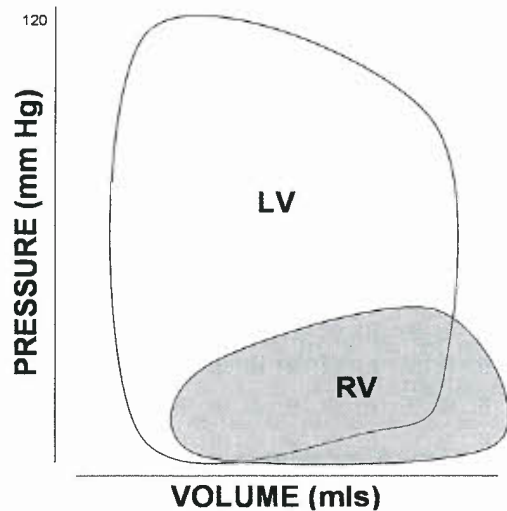


Figure 22.1. Schematic representations of right (shaded) and left ventricular pressure-volume relationships. The external stroke work of the right ventricle (RV; area enclosed by loop) is markedly lower than the left ventricle (LV) (see text for details).

rise in mean airway pressure (to ~8 cm of water) secondary to positive-pressure ventilation. These adverse hemodynamic effects of increased RV afterload (negative cardiopulmonary interactions) become even more important when the right heart circulation is affected by congenital heart disease.

Cardiopulmonary Interactions in Congenital Heart Disease

Given that normal right heart function is dependent on a low RV afterload, normal ventricular preload, and maintained RV systolic function, it would be surprising if congenital heart diseases did not have major effects on its performance. This is indeed the case.

Reduced Right Ventricular Contractile Performance

It has long been known that RV ischemia, in the setting of atherosclerotic coronary disease, is an extremely poorly tolerated hemodynamic burden (10). This, in part, is related to adverse right-left heart interactions (see below), but illustrates the importance of RV contractile performance, even in the presence of a relatively normal pulmonary vascular bed. A more common scenario in congenital heart disease is the adverse effect of cardiopulmonary bypass on right heart function. Brookes et al. (11) showed that even a brief period of cardiopulmonary bypass and cardioplegic arrest, during coronary bypass surgery, leads to a significant decline in RV systolic performance, as assessed by end-systolic elastance. This translates to an even greater dependence on cardiopulmonary interactions in children undergoing congenital heart surgery. Shekerdemian (9), in the study described above, showed that positive-pressure ventilation had an even greater adverse effect in such patients. Compared with negative-pressure ventilation, there was on average a 25% fall in cardiac output with positive-pressure ventilation in children on the intensive care unit after simple right heart surgery (ventricular septal defect [VSD], atrial septal defect [ASD], etc.).

CARDIOPULMONARY INTERACTIONS AND THE ABNORMAL RIGHT HEART

The potential for beneficial and adverse cardiopulmonary interactions is greater when the right heart is intrinsically abnormal because of congenital anomalies or is primarily affected by surgery. There are two circumstances in which these concepts are exemplified, those patients with abnormal RV diastolic function and those with exclusion of the RV from the venopulmonary circulation.

Abnormal Right Ventricular Diastolic Function

It is now known that restrictive RV physiology is a common sequel of surgery for hypoplasia of the right heart, for

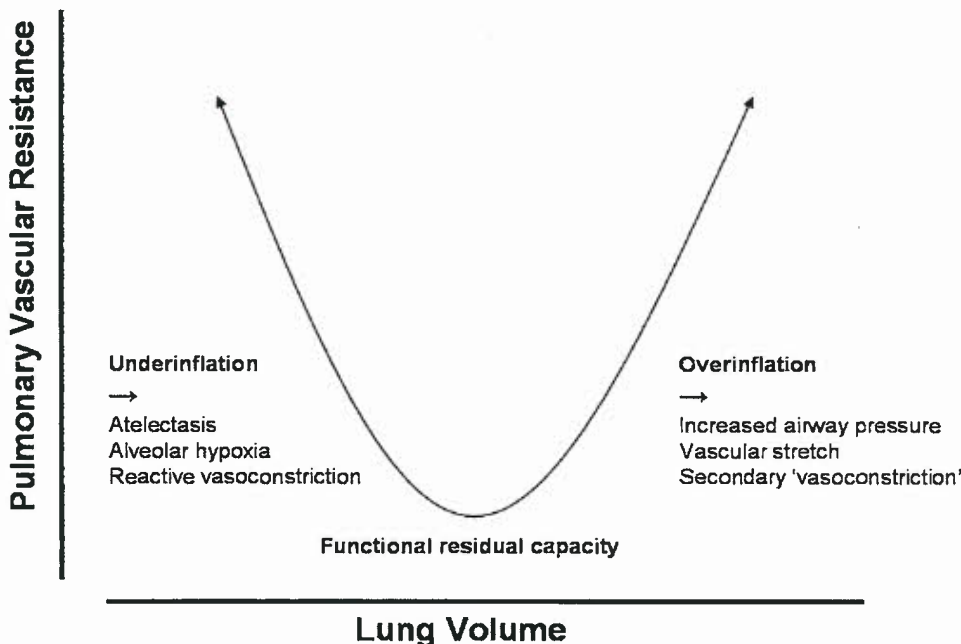


Figure 22.2. Effect of lung inflation on pulmonary vascular resistance. Resistance is at its nadir when the lung is at functional residual capacity.

example, pulmonary atresia with intact ventricular septum (12), and after repair of tetralogy of Fallot, for example. The characteristic physiology of these patients is the presence of antegrade diastolic pulmonary blood flow during atrial systole. This occurs when the resistance to RV filling exceeds the pulmonary vascular resistance. Atrial contraction ejects blood through the tricuspid valve, but there is little or no RV filling as the blood passes through the RV (which acts as a passive conduit) to the pulmonary artery (PA). Consequently, up to one-third of the antegrade pulmonary blood flow, and therefore cardiac output, is dependent on atrial systole. Furthermore, this flow is generated by only modest pressure transients (1 or 2 mm Hg) between the right atrium (RA) and the PA in diastole. Clearly a low pulmonary vascular resistance is crucial for this source of cardiac output to be maintained. An important element of the total pulmonary resistance, as discussed above, is the mean airway pressure. Indeed, antegrade diastolic flow is often entirely abrogated during positive-pressure inspiration. Conversely, negative-pressure ventilation may have a major beneficial effect on cardiac output. In postoperative tetralogy patients, positive-pressure ventilation reduces cardiac output by >30% compared with that achieved during negative-pressure ventilation with a cuirass device (13).

The influence of cardiopulmonary interaction is even more impressive when one considers right heart bypass procedures. Here, resting and exercise pulmonary blood flow is markedly dependent on the work of breathing. In our earlier Doppler studies, the phase relationship between ventilation and pulmonary blood flow was shown clearly in both the venopulmonary and atriopulmonary Fontan circulations (14,15). Subsequently, MRI studies have suggested that well over one-third of the cardiac output occurs as a direct result of the work of breathing (16). This may be even more important during exercise (17), particularly in those with total cavopulmonary anastomosis. Positive-pressure ventilation in the Fontan circulation has long been known to adversely affect cardiac output. In early studies of the use of positive end-expiratory pressure, a linear relationship between positive end-expiratory pressure and cardiac output was demonstrated (18). Unsurprisingly, negative-pressure ventilation under these circumstances can lead to a marked increase in cardiac output compared with positive-pressure ventilation. In a separate series of studies, Shekedemian et al. (19) showed the profound effects of positive and negative pressure ventilation on the pattern of pulmonary blood flow in the Fontan circuit (Fig. 22.3) as

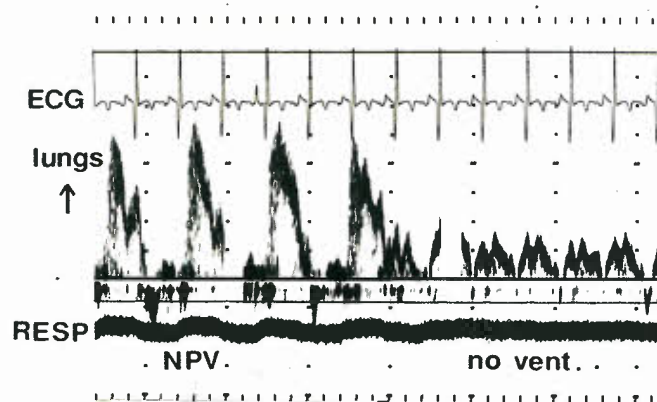


Figure 22.3. The effects of negative-pressure ventilation (NPV) on the pattern of pulmonary blood flow after total cavopulmonary connection. Each negative pressure breath is associated with massive augmentation of pulmonary blood flow, an effect abolished when the ventilator is switched off (no vent).

well as on total cardiac output measured by respiratory mass spectrometry.

These studies and others have reinforced the desirability of normal ventilation in such circulations, and this, wherever possible, should be established as early as possible after surgery. In those requiring positive-pressure ventilation, efforts to reduce the mean airway pressure will reap benefits in terms of changes in cardiac output. Thus, minimizing positive end-expiratory pressure, shortening the inspiratory time, and reducing the airway pressure plateau time will all help to reduce the hemodynamic burden on the right heart. Clearly this must not be at the expense of alveolar ventilation (to avoid hypercapnic pulmonary vasoconstriction) or alveolar inflation (to avoid hypoxemic vasoconstriction).

Exclusion of the Right Ventricle

Because of the very marked changes in RV hemodynamics imposed by progressive pulmonary hypertension or RV outflow tract obstruction, the effects of subtle changes in airway pressure on RV intrinsic contractile performance are much less marked. Indeed, one can consider the pressure-volume relationships of the hypertensive RV to be similar to those of the normal LV (2). Consequently, while changes in preload will continue to occur, the effects of afterload are much less marked. Also, it should not be forgotten that the adverse effects of positive-pressure ventilation on the right heart are in contradistinction to those on the left heart, particularly the failing LV.

CARDIOPULMONARY INTERACTIONS AND THE LEFT HEART

Although the manifestations are different, the LV is also subject to cardiopulmonary interactions and the effect of mean airway pressure on its function. Although in general the effects of increased mean airway pressure are largely adverse on the right heart, they are largely beneficial on the left heart. This is because the total afterload of the LV (transmural pressure) is reduced by increased mean airway pressure (20). Although essentially insignificant to the normal LV, such changes can provide beneficial effects, for example, in dilated cardiomyopathy. Indeed, continuous positive airway pressure (CPAP) has a multitude of beneficial effects to the failing left heart (21). By increasing alveolar pressure, the transalveolar gradient for edema formation is reduced. Furthermore, the afterload of the LV is also reduced, improving its ejection fraction and stroke volume. Although relatively infrequently used in pediatric practice, CPAP masks have proven to be particularly useful in the dilated cardiomyopathy of ischemic and acquired heart disease in adults (22), and such therapy merits further investigation in children.

RIGHT-LEFT HEART INTERACTIONS

It has been traditional to examine LV and RV function as separate entities. Nonetheless, the last two decades have seen an explosion in our understanding of the ways in which the two sides of the heart interrelate and contribute to each other. Not only is this a manifestation of its shared cavity, the pericardium, but also the recognition of shared myofibers that can neither be defined as exclusively LV or RV (23). Thus, the

function of the LV has profound effects on the function of the RV, and vice versa, both in health and disease.

The Effects of the Left Ventricle on the Right Ventricle

The classic experiment of Damiano et al. (24) in 1991 confirmed the presence of substantial cross talk between the ventricles in health. Albeit in an experimental model, the effects of LV performance on RV force generation were clearly demonstrated. In their exquisite study, the electrically isolated but mechanically contiguous ventricles were examined during individual chamber pacing (Fig. 22.4). Under these circumstances, pacing the RV led to virtually no mechanical effects on the left side of the heart. Pacing the electrically isolated LV, however, led to almost normal RV pressure development. It appears, therefore, that the geometric change, consequent on LV shortening, imposes a major mechanical effect on the RV. The crescent-shaped free wall, wrapped around the ventricular septum and contiguous with the LV free wall, is presumably deformed to generate a RV pressure. This effect appears to be largely independent of the RV free wall function. In another set of experiments, Hoffman et al. (25) showed that replacement of the RV free wall with a noncontractile patch was still associated with significant RV pressure generation during LV contraction. Overall, it has been estimated that over one-third of the work performed by the RV is a direct consequence of LV shortening. It might be possible to harness this ventricular-ventricular cross talk to improve biventricular function. In animal experiments, aortic constriction, leading to an increase in LV afterload and work, was shown to increase RV stroke volume, again as a result of the cross talk phenomenon (26).

The Effects of the Right Ventricle on the Left Ventricle

In the experiments by Hoffman et al. (25) described above, the effect of LV shortening on RV pressure development in a model of RV free wall replacement was described. This experiment also showed that as the size of the artificial RV was increased, there appeared to be an adverse effect on LV mechanical function. As the RV dilated, LV pressure development fell. Whether this was a parallel effect (reflecting adverse ventricular cross talk) or a series effect (reflecting reduced cardiac output from the RV and therefore reduced preload to the LV) could not be determined in these experiments. In the mid-1990s, Brookes et al. (27) aimed to dissect out these influences in a porcine model. Isolated RV ischemia was used to induce acute right heart dilation, during which RV and LV contractile performance was measured using end-systolic elastance derived from pressure-volume analysis. It was shown that RV dilation imposes adverse effects on LV mechanical performance directly, presumably owing to geometric changes influencing LV contractile efficiency. These effects were more manifest when the pericardium was intact, supporting this hypothesis.

It would be naive to assume that all of these effects are manifestations purely of systolic interactions. Independent of major changes in contractile performance, adverse diastolic ventricular-ventricular interaction is frequently encountered. Primarily a manifestation of septal shift toward the LV in early diastole, pulmonary hypertension, for example, leads to reduced LV early diastolic filling velocities and increased dependence on atrial systole (28).

The superimposition of congenital heart disease and the effects of surgical correction further amplify these ventricular-ventricular effects and are discussed below.

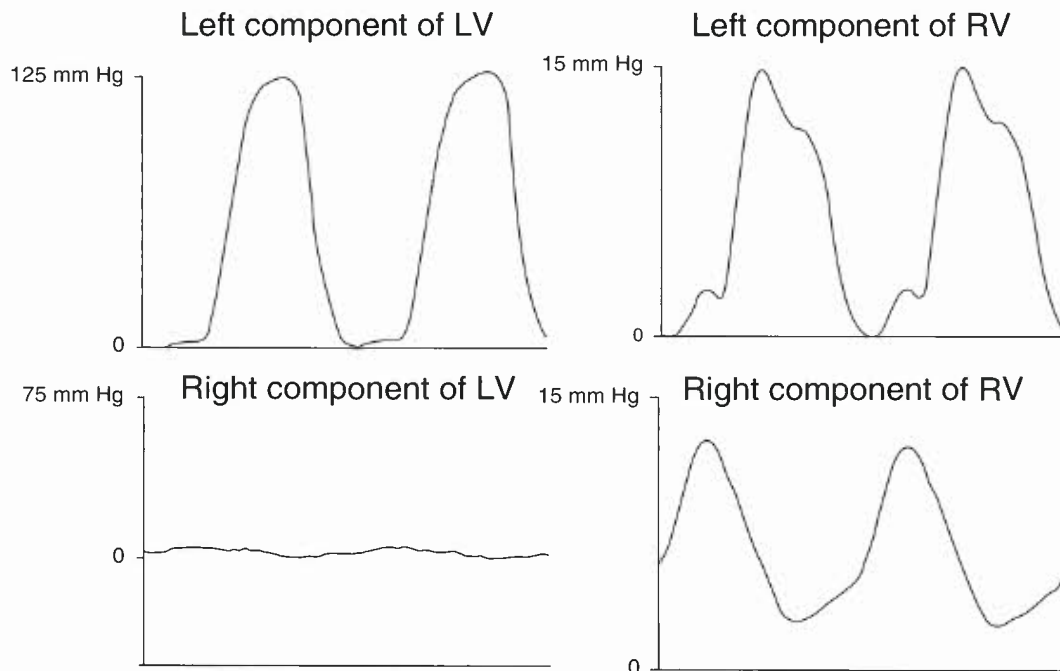


Figure 22.4. This study demonstrates the passive effect of active contraction of the contralateral ventricle (see text for details). Ventricular-ventricular interaction is shown clearly in the **top right-hand panel**. There is almost normal right ventricular pressure development when the left ventricle (LV) contracts, even though the right ventricle (RV) is electrically isolated. (Redrawn from Damiano RJ Jr, La Follette P Jr, Cox JL, et al. Significant left ventricular contribution to right ventricular systolic function. *Am J Physiol* 1991;261:H1514–H1524, with permission.)

Right-Left Heart Interactions in Congenital Heart Disease

It is likely that all congenital heart diseases have more or less subtle abnormalities of ventricular-ventricular interaction. However there are some major, clinically significant interactions that bear more detailed analysis. These can loosely be described as functional and geometric and are discussed in detail below.

Functional Interactions

Surgery to the RV outflow tract almost invariably leads to some degree of residual pulmonary regurgitation, and it is now well known that this ventricular volume load leads to RV dilation in most patients. The effects of pulmonary regurgitation after repair of tetralogy of Fallot are probably the best described examples of this phenomenon. Although our understanding of the effects of right heart dilation under these circumstances has evolved over the last 15 years, it is only in the last 5 years that the biventricular effects of this problem have become apparent. Several studies have now shown a loose but linear relationship between RV ejection fraction and LV ejection fraction late after repair of tetralogy of Fallot (29,30). Furthermore, those with overt biventricular dysfunction have a worse outcome compared with those without (30). Not only are ventricular-ventricular interactions important in terms of global function, but abnormalities of ventricular-ventricular timing may also have significant adverse effects. D'Andrea et al. (31) have explored this phenomenon in a recent study analyzing the dyssynchrony between the ventricles. They studied the onset of RV and LV contraction in patients after repair of tetralogy of Fallot, showing a worse exercise tolerance and an increased frequency of arrhythmia in those with significant ventricular-ventricular delay.

It is likely that subtle regional abnormalities will also have significant biventricular effects. Regional wall motion abnormalities have been described in virtually all congenital heart diseases (32,33). They are also almost always associated with decreased global performance and therefore likely biventricular effects. It remains to be seen whether this intraventricular and interventricular incoordination will be responsive to interventions such as biventricular pacing, but early data appear promising (34).

Geometric Interactions

Unlike the more directly functional interaction described above, acute changes in geometry can modify functional per-

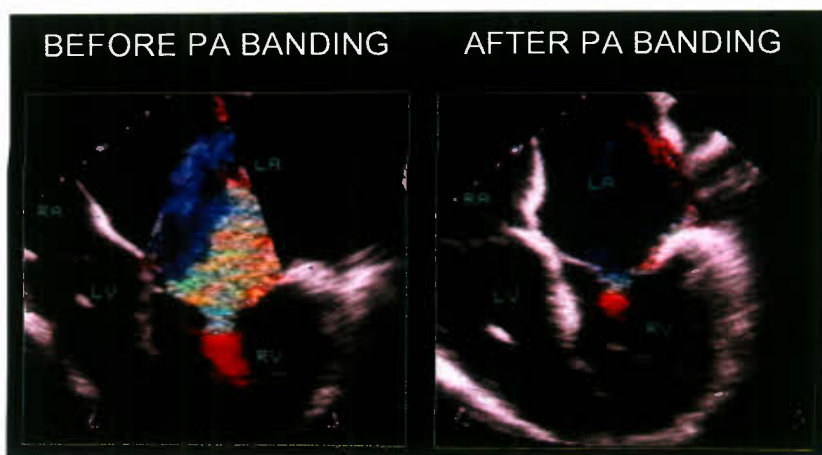
formance of both sides of the heart, particularly in congenital heart disease. Acute right heart dilation not only affects RV performance, but also induces LV dysfunction via systolic and diastolic interactions (see above).

More chronic geometric changes can lead to unique abnormalities in the setting of congenital heart disease. The systemic RV is particularly susceptible to such changes. Here, the morphologic tricuspid valve is the systemic atrioventricular valve and is characterized by its septal papillary muscle and chordal attachments. It is now well recognized both under the circumstances of surgical repair of simple transposition and in the setting of congenitally corrected transposition that septal shift makes a significant contribution to the development of tricuspid regurgitation in these hearts. Conversely, efforts to modify this septal shift can produce profound improvements in the degree of tricuspid incompetence. Figure 22.5 shows just such a change. The right-hand panel from this patient with congenitally corrected transposition shows a dilated RA and hugely dilated morphologic left atrium as a result of severe tricuspid valve incompetence. The left-hand panel shows minimal tricuspid incompetence in the same heart, just 20 seconds later. The reduction in tricuspid regurgitation and the remarkable change in left atrial (LA) size have occurred as a consequence of PA banding. Elevation of LV pressure to modify septal geometry restored tricuspid valve competence in this patient. This phenomenon has been demonstrated in patients after the Mustard procedure (35) as well as in patients undergoing LV retraining in the setting of congenitally corrected transpositions. It is beyond the scope of this chapter to discuss the advisability, prerequisites, and methods for evaluation of LV retraining under such circumstances, but by its effects on tricuspid incompetence, PA banding alone may be destination therapy for some of these patients.

CONCLUSIONS

Important cardiopulmonary and ventricular-ventricular interactions are intrinsic to normal cardiovascular physiology. The consequences of these effects are amplified by disease in the structural normal heart and may be profound when the heart is modified by congenital anomalies. Our understanding of the effects of congenital heart disease on cardiopulmonary and ventricular-ventricular interactions continues to evolve, but we have learned that description of functional performance in any patient is incomplete without their consideration.

Figure 22.5. The acute effects of pulmonary artery (PA) banding on tricuspid valve regurgitation in congenitally corrected transposition. Left ventricular (LV) hypertension induces septal shift toward the systemic right ventricle (RV), leading to restoration of tricuspid leaflet apposition by its effect on its septal attachments. As a result, the left atrial (LA) size is markedly reduced. RA, right atrium.



REFERENCES

1. Redington AN, Gray HH, Hodson ME, et al. Characterisation of the normal right ventricular pressure-volume relation by biplane angiography and simultaneous micromanometer pressure measurements. *Br Heart J* 1988;59:23–30.
2. Redington AN, Rigby ML, Shinebourne EA, et al. Changes in the pressure-volume relation of the right ventricle when its loading conditions are modified. *Br Heart J* 1990;63:45–49.
3. Brett SJ, Chambers J, Bush A, et al. Pulmonary response of normal human subjects to inhaled vasodilator substances. *Clin Sci (Lond)* 1998;95:621–627.
4. Steingrub JS, Tidswell M, Higgins TL. Hemodynamic consequences of heart-lung interactions. *J Intensive Care Med* 2003;18:92–99.
5. Bromberger-Barnea B. Mechanical effects of inspiration on heart functions: a review. *Fed Proc* 1981;40:2172–2177.
6. Norgard G, Vik-Mo H. Effects of respiration on right ventricular size and function: an echocardiographic study. *Pediatr Cardiol* 1992;13:136–140.
7. Cournaud A, Riley RL, Breed ES, et al. Measurement of cardiac output in man using the technique of catheterization of the right auricle or ventricle. *J Clin Invest* 1945;24:106–116.
8. Henning RJ. Effects of positive end-expiratory pressure on the right ventricle. *J Appl Physiol* 1986;61:819–826.
9. Shekerdeman LS, Bush A, Lincoln C, et al. Cardiopulmonary interactions in healthy children and children after simple cardiac surgery: the effects of positive and negative pressure ventilation. *Heart* 1997;78:587–593.
10. Pfisterer M. Right ventricular involvement in myocardial infarction and cardiogenic shock. *Lancet* 2003;362:392–394.
11. Brookes C, Ravn H, White P, et al. Acute right ventricular dilatation in response to ischemia significantly impairs left ventricular systolic performance. *Circulation* 1999;100:761–767.
12. Redington AN, Rigby ML, Hayes A, et al. Right ventricular diastolic function in children. *Am J Cardiol* 1991;67:329–330.
13. Cullen S, Shore D, Redington A. Characterization of right ventricular diastolic performance after complete repair of tetralogy of Fallot: restrictive physiology predicts slow postoperative recovery. *Circulation* 1995;91:1782–1789.
14. Redington AN, Penny D, Shinebourne EA. Pulmonary blood flow after total cavopulmonary shunt. *Br Heart J* 1991;65:213–217.
15. Penny DJ, Redington AN. Doppler echocardiographic evaluation of pulmonary blood flow after the Fontan operation: the role of the lungs. *Br Heart J* 1991;66:372–374.
16. Fogel MA, Weinberg PM, Hoydu A, et al. The nature of flow in the systemic venous pathway measured by magnetic resonance blood tagging in patients having the Fontan operation. *J Thorac Cardiovasc Surg* 1997;114:1032–1041.
17. Rosenthal M, Bush A, Deanfield J, et al. Comparison of cardiopulmonary adaptation during exercise in children after the atriopulmonary and total cavopulmonary connection Fontan procedures. *Circulation* 1995;91:372–378.
18. Williams DB, Kiernan PD, Metke MP, et al. Hemodynamic response to positive end-expiratory pressure following right atrium-pulmonary artery bypass (Fontan procedure). *J Thorac Cardiovasc Surg* 1984;87:856–861.
19. Shekerdeman LS, Bush A, Shore DE, et al. Cardiopulmonary interactions after Fontan operations: augmentation of cardiac output using negative pressure ventilation. *Circulation* 1997;96:3934–3942.
20. Pinsky MR, Summer WR, Wise RA, et al. Augmentation of cardiac function by elevation of intrathoracic pressure. *J Appl Physiol* 1983;54:950–955.
21. Bradley TD, Logan AG, Kimoff RJ, et al.; CANPAP Investigators. Continuous positive airway pressure for central sleep apnea and heart failure. *N Engl J Med* 2005;353:2025–2033.
22. Mehta S, Liu PP, Fitzgerald FS, et al. Effects of continuous positive airway pressure on cardiac volumes in patients with ischemic and dilated cardiomyopathy. *Am J Respir Crit Care Med* 2000;161:128–134.
23. Anderson RH, Ho SY, Sanchez-Quintana D, et al. Heuristic problems in defining the three-dimensional arrangement of the ventricular myocytes. *Anat Rec A Discov Mol Cell Evol Biol* 2006;288:579–586.
24. Damiano RJ Jr, La Follette P Jr, Cox JL, et al. Significant left ventricular contribution to right ventricular systolic function. *Am J Physiol* 1991;261:H1514–H1524.
25. Hoffman D, Sisto D, Frater RW, et al. Left-to-right ventricular interaction with a noncontracting right ventricle. *J Thorac Cardiovasc Surg* 1994;107:1496–1502.
26. Karunanithi MK, Michniewicz J, Young JA, et al. Effect of acutely increased left ventricular afterload on work output from the right ventricle in conscious dogs. *J Thorac Cardiovasc Surg* 2001;121:116–124.
27. Brookes CI, White PA, Bishop AJ, et al. Validation of a new intraoperative technique to evaluate load-independent indices of right ventricular performance in patients undergoing cardiac operations. *J Thorac Cardiovasc Surg* 1998;116:468–476.
28. Stojnic BB, Brecker SJ, Xiao HB, et al. Left ventricular filling characteristics in pulmonary hypertension: a new mode of ventricular interaction. *Br Heart J* 1992;68:16–20.
29. Davlourous PA, Kilner PJ, Hornung TS, et al. Right ventricular function in adults with repaired tetralogy of Fallot assessed with cardiovascular magnetic resonance imaging: detrimental role of right ventricular outflow aneurysms or akinesia and adverse right-to-left ventricular interaction. *J Am Coll Cardiol* 2002;40:2044–2052.
30. Ghai A, Silversides C, Harris L, et al. Left ventricular dysfunction is a risk factor for sudden cardiac death in adults late after repair of tetralogy of Fallot. *J Am Coll Cardiol* 2002;40:1675–1680.
31. D'Andrea A, Caso P, Sarubbi B, et al. Right ventricular myocardial activation delay in adult patients with right bundle branch block late after repair of Tetralogy of Fallot. *Eur J Echocardiogr* 2004;5:123–131.
32. Penny DJ, Redington AN. Angiographic demonstration of incoordinate motion of the ventricular wall after the Fontan operation. *Br Heart J* 1991;66:456–459.
33. Millane T, Bernard EJ, Jaeggi E, et al. Role of ischemia and infarction in late right ventricular dysfunction after atrial repair of transposition of the great arteries. *J Am Coll Cardiol* 2000;35:1661–1668.
34. Dubin AM, Janousek J, Rhee E, et al. Resynchronization therapy in pediatric and congenital heart disease patients: an international multicenter study. *J Am Coll Cardiol* 2005;46:2277–2283.
35. van Son JA, Reddy VM, Silverman NH, et al. Regression of tricuspid regurgitation after two-stage arterial switch operation for failing systemic ventricle after atrial inversion operation. *J Thorac Cardiovasc Surg* 1996;111:342–347.

Gary A. Smith ■ Timothy F. Feltes

Traumatic injury to the heart occurs when energy is transferred to the heart in amounts or at rates that exceed the tissue's threshold to withstand it, resulting in structural damage or functional abnormality. The transfer of injurious energy is most commonly associated with blunt trauma, penetrating trauma, or contact with electrical current. Most medical knowledge about cardiac trauma in children is extrapolated from studies of adults. Relatively little direct information is available regarding cardiac injuries in children.

BLUNT CARDIAC INJURY

Blunt trauma accounts for the vast majority of injuries to children and is the chief cause of cardiac trauma in the pediatric age-group. The incidence of cardiac injury in blunt trauma among children has been reported to be from 0% to 43% (1). Blunt cardiac injuries are often unsuspected injuries associated with multiple system trauma. Clinical manifestations of cardiac trauma vary depending on the location of injury. They are often nonspecific and include shock, cardiovascular instability, dysrhythmias, chest pain, and changes in mentation. In victims of multiple trauma, all of these findings can be easily attributed to other serious injuries to the head, abdomen, or extremities.

Parmley et al. (2) performed autopsies on a large series of motor vehicle crash victims and found that blunt cardiac injury was one of the most frequently missed diagnoses. This finding has been corroborated by others. Having a high level of suspicion for blunt cardiac injury is necessary for early diagnosis and intervention. The autopsy series of Parmley et al. (2) described various mechanisms of nonpenetrating cardiovascular injury (Table 23.1).

Most blunt cardiac injuries from direct chest impact among children are the result of motor vehicle crashes (3). Blunt blows with weapons, fists, and animal kicks; blunt collisions during sports; and falls from heights also cause direct-impact cardiac injuries.

Because the heart is suspended from the great vessels, acceleration-deceleration injuries occur as the heart moves like a pendulum in the thorax. Traction on the great vessels can cause tears at their points of fixation.

Compression of the chest can crush the heart or cause damage through increased intrathoracic and intracardiac pressures. Cardiac rupture is more likely if compression occurs during maximum filling of the chambers. Rib fractures and contusions of the chest wall are not always seen, especially in children owing to their highly compliant chest walls. Abdominal and lower extremity compression also can force blood back to the heart, causing damage through a hydraulic ram effect.

Commotio cordis is a specific form of cardiac trauma that has become an increasingly recognized cause of sudden

cardiac death in otherwise healthy young athletes (4). While the National Commotio Cordis Registry in Minneapolis lists almost 250 cases of commotio cordis, the frequency of such cases is most certainly underestimated (5). Commotio cordis is a form of nonpenetrating chest trauma insufficient to result in significant myocardial or chest wall injury. The most likely mode of death appears to be an induction of a malignant arrhythmia (i.e., ventricular fibrillation) due to the transfer of concentrated mechanical energy (concussion) to the heart resulting in electrical instability. The two critical components appear to be precordial impact location and the timing of the impact occurring during the upstroke of the T wave (6–8). The impact site for victims of commotio cordis is specifically located at or near to the center of the cardiac silhouette. Recent animal model studies suggest that the trauma must occur within an electrical vulnerability period during the cardiac cycle, namely, within 20 milliseconds of the T-wave upstroke.

As reported recently by Maron and Estes (4), commotio cordis is seen most frequently in the second decade of life, peaking at 15 years of age. Baseball is the most common sport in which commotio cordis is observed followed by softball, hockey, and football. It is more commonly experienced during organized sporting events but by no means exclusively. In younger victims (<10 years of age) commotio cordis may occur during activities unrelated to sports.

Victims of commotio cordis most commonly experience instantaneous cardiovascular collapse but in approximately 20% of cases victims are able to stay erect for several seconds after the trauma occurs. Survival from resuscitative efforts is low but has increased to 35% in recent years most likely due to increasing availability of automatic external defibrillators and bystanders knowledgeable in the use of these devices.

According to data from the above-mentioned national registry, nearly one-third of cases of commotio cordis that occurred during competitive sports were victims who were wearing a commercially available chest protector. Many of these devices were not designed to prevent commotio cordis and either expose the precordium or do not adequately absorb the impact from a projectile (9). Efforts have been made to create safer baseballs (aka “safety” baseballs) with some evidence of effectiveness. Some sports now require protective equipment (10). See Table 23.2 for features differentiating cardiac concussion from cardiac contusion (11). It is important that the public and organizers of sporting events be aware of the risk of commotio cordis.

Two other mechanisms of blunt cardiac injury have been described: Blast injury and a combination injury, which involves more than one of the above mechanisms.

The types of anatomic injuries resulting from these various mechanisms in blunt cardiac trauma include pericardial injury, myocardial contusion, cardiac rupture, septal disruption, ventricular aneurysm, injury to the heart valves and supporting

TABLE 23.1 Mechanisms of Blunt Cardiac Trauma

Direct impact
Acceleration–deceleration
Compression
Hydraulic ram effect
Concussion
Blast
Combination

Adapted from Parmley LF, Manion WC, Mattingly TW. Nonpenetrating traumatic injury of the heart. *Circulation* 1958;18:371–396.

structures, and injury to the great vessels, brachiocephalic arteries, venae cavae, and coronary arteries (Table 23.3).

Pericardial Injury

Blunt pericardial injuries range from contusion to rupture and are usually associated with myocardial injury. Isolated pericardial injuries are rare. Pericardial lacerations and pericardial rupture are rarely significant injuries unless cardiac herniation occurs through a pericardial tear. Cardiac herniation can result in severe circulatory compromise and rapid death. Cardiac tamponade is a common complication of myocardial injury but is not likely with isolated pericardial injury.

Traumatic pericarditis can develop after pericardial contusion. A chronic pericarditis after cardiac trauma can last 1 to 4 weeks. The clinical features are single or recurrent pericardial or pleural effusions, similar to the postpericardiotomy syndrome.

The frequency of pericardial injury associated with blunt chest trauma is unknown. Asymptomatic pericardial effusions have been demonstrated by cardiac ultrasonographic examination following blunt chest trauma. Pericardial lacerations were frequently found in dogs following sublethal blunt chest trauma. The most frequent manifestations of traumatic pericarditis include pericardial friction rub and nonspecific electrocardiographic (ECG) ST-T wave changes and diffuse low voltages.

TABLE 23.3 Types of Blunt Cardiac Injuries

Pericardial injury
Myocardial injury
Myocardial contusion
Cardiac rupture
Septal disruption
Ventricular aneurysm
Injury to heart valves and supporting structures
Injury to great vessels, brachiocephalic arteries, vena cavae, and coronary arteries

Adapted from Liedtke AJ, DeMuth WE Jr. Nonpenetrating cardiac injuries: a collective review. *Am Heart J* 1973;86:687–697.

Traumatic cardiac tamponade rarely presents with all the classic Beck triad features of hypotension, distant heart sounds, and elevated central venous pressure with neck vein distension. An echocardiogram is the most sensitive diagnostic test for cardiac tamponade and can be used in the emergency department for selected trauma patients. A diagnostic and therapeutic pericardiocentesis also can be used for patients with suspected cardiac tamponade. However, false-negative pericardiocentesis results have been observed in 25% to 80% of patients who have blood in the pericardium (12).

Treatment of traumatic pericarditis is based on symptoms. If pericardial effusion or associated pleural effusions are clinically significant, pericardiocentesis or thoracocentesis is indicated. Chronic pericarditis or postpericardiotomy syndrome is treated with anti-inflammatory agents.

Most pericardial lacerations are incidentally found during thoracotomy being performed for other indications and are not repaired unless the defect is large enough to pose a risk of cardiac herniation. Large pericardial lacerations that are difficult to repair may be managed by pericardiectomy.

Myocardial Contusion

Myocardial contusion in the general population is most often a result of direct blunt force to the chest during motor vehicle

TABLE 23.2 Differential Features of Cardiac Concussion and Contusion

Feature	Concussion	Contusion
Force	Sharp, not necessarily violent	Generally violent
Direction of force	Sternum to vertebra	Of no significance
Onset	Immediate	Gradual
Course	Transitory	Persisting
Loss of consciousness	Usually	Not characteristic
Disturbances of rhythm and conduction	Characteristic, immediate	Absent or delayed
Changes in ST segment and T waves	Nonspecific	Anatomically localized injury or ischemia

Adapted from Abrunzo TJ. Commotio cordis: the single most common cause of traumatic death in youth baseball. *Am J Dis Child* 1991;145:1279–1282; and Michelson WB. CPK-MB isoenzyme determinations: diagnostic and prognostic value in evaluation of blunt chest trauma. *Ann Emerg Med* 1980;9:562–567.

crashes, industrial injuries, farm injuries, or sports injuries. The reported incidence of myocardial contusion associated with major trauma varies between 3% and 76% depending on the study population and the diagnostic criteria (13,14). Approximately one-third of children with cardiac contusion may have no external evidence of chest injury. ECG abnormalities and dysrhythmias are less common in these children than in adults who have cardiac contusion.

The first reported case of autopsy-proven myocardial contusion was in 1764; it described a boy struck in the chest by a plate (15). Recognition of cardiac contusion is difficult because of nonspecific clinical findings and lack of an accurate diagnostic test (3). The findings of cardiac contusion are easily attributed to other serious injuries that are often present. Predicting which cases will be clinically significant has not been possible, thus complicating the discussion about appropriate management of myocardial contusion. The diagnosis of myocardial contusion should be considered in any child with significant blunt chest or multiple system trauma.

Most cases of myocardial contusion are mild and asymptomatic, and go unrecognized, but complications can be serious. Complications of myocardial contusion include dysrhythmias, conduction disturbances, cardiac failure, aneurysms, pseudoaneurysms, myocardial wall thinning, cardiac rupture, and cardiac arrest. Most are late findings. Underlying cardiac disease, including ischemia, cardiomyopathy, or congenital heart disorders, increases the risk of complications from blunt cardiac injury. The pathologic findings of myocardial contusion include myocardial hemorrhage, myocardial fiber necrosis, and, later, fibrous scar formation.

The diagnosis of myocardial contusion can generally be made in patients with blunt chest trauma if the ECG demonstrates a dysrhythmia or changes compatible with ischemia or contusion, the creatine phosphokinase-muscle band (CPK-MB) fraction is $>5\%$ of the total CPK, and the echocardiogram is abnormal (16). However, ECG findings in cardiac contusion are nonspecific, and false-positive results can occur. Because CPK-MB is also present in skeletal muscle, pancreas, and bowel, extensive skeletal muscle or abdominal trauma can cause elevation of CPK-MB. In addition, CPK-MB has been shown to have a low sensitivity and specificity for cardiac injury in some studies (17,18). Lactate dehydrogenase isoenzymes and serum glutamic oxalotransaminase are of no value in the diagnosis of cardiac contusion. Troponin I and T have been shown to be accurate indicators of myocardial injury that may aid in the diagnosis of myocardial contusion (19–21). In adult studies, the positive predictive value of elevated cardiac troponin T ranges from 20% to 100% and the negative predictive value ranges from 74% to 100% (22–23). Diagnostic sensitivity may be improved by use of recently developed highly sensitive cardiac troponin assays, but validation studies have not yet been reported (24).

The echocardiogram may be more useful than serial ECGs or cardiac isoenzyme measurements in evaluating blunt cardiac injuries because it can detect pericardial effusion, valvular dysfunction, septal defects, enlarging chambers, and wall motion abnormalities and can be used to determine ejection fraction. Echocardiographic abnormalities are detected in 20% to 47% of patients following blunt trauma (25). Transesophageal echocardiography may offer advantages over transthoracic echocardiography, especially in obese patients. The proximity of the esophagus to the thoracic aorta and atrioventricular (AV) valves allows clearer visualization of injuries to these structures. In the absence of ECG abnormalities or cardiac isoenzyme elevation, cardiac dysmotility on echocardiogram is not associated with adverse patient outcome (26).

Gated radionuclide angiography is a useful method for detecting abnormalities of cardiac function. It has been applied in the evaluation of blunt cardiac trauma to detect

diminished ejection fractions, hypokinetic wall segments, and ventricular aneurysms. The most common finding it identified in adult patients with blunt chest trauma was mild hypokinesis of the right ventricular wall with diminished ejection fraction. Unfortunately, gated radionuclide angiography is not predictive of morbidity and mortality in cardiac contusion.

Following blunt chest trauma, patients with abnormal ECGs require admission, continuous cardiac monitoring, and evaluation of cardiac isoenzymes. Cardiac monitoring should continue until abnormal ECGs have reverted to normal for at least 24 hours, cardiac isoenzymes have normalized, and stabilization of other major injuries has been achieved. The main treatment goal is avoidance of death caused by dysrhythmias or hemodynamic compromise.

Cardiac Rupture

Although an uncommon injury, cardiac rupture is estimated to cause 10% to 15% of adult motor vehicular crash fatalities. Two-thirds of deaths owing to cardiac rupture occur at the scene (27). Cardiac rupture occurs most commonly in young male drivers suffering precordial steering wheel impact during a crash (28). Ventricular rupture is more common than atrial rupture, and the thin-walled anteriorly positioned right ventricle is more commonly ruptured than the left ventricle. Multiple chamber rupture is not uncommon in these cases, as is combined cardiac rupture and aortic rupture, reflecting the large amount of force involved in these injuries (2).

Ventricular rupture can result from direct cardiac compression or from an indirect hydraulic ram effect that occurs during abdominal or extremity compression. During late diastole, compressing a distended noncompliant ventricle can tear AV valves, chambers, septa, and other cardiac structures. Atrial rupture appears to involve compression of the filled chamber as well as torsion when the AV valves are closed and the chamber is filled during late systole. The atrial appendages are the thinnest portions and most prone to atrial rupture. Delayed ruptures are extremely rare and may follow infarction associated with trauma and gradual softening of the ischemic tissues or rupture of a myocardial aneurysm or pseudoaneurysm (28).

The clinical manifestation of myocardial rupture is usually tamponade, although approximately one-third of patients will have exsanguinating hemorrhage through associated pericardial lacerations. The association of cardiac tamponade with cardiac rupture limits the rate of exsanguination and increases the chances of survival for these patients.

The first surgical repair of blunt cardiac rupture was reported by Des Forges et al. (29) in 1955 involving a 4-cm right atrial laceration. Until then, cardiac rupture had been considered universally lethal. Surviving ventricular rupture secondary to blunt chest trauma is rare. In 1990 the first pediatric survivor was preceded by only three reported adult cases (30).

Septal Disruption

The interventricular septum ruptures most commonly in the muscular portion near the apex, which is the thinnest area of the septum. Any portion of the muscular septum can rupture, even in multiple sites, with concomitant injury to the conduction system. Echocardiography should demonstrate the abnormality. Cardiac catheterization can be performed to determine the magnitude of left-to-right shunt, measure pulmonary artery pressures, and evaluate ventricular function. Ventricular septal defects with significant left-to-right shunts require surgical closure. Disruption of the atrial septum has also been reported (31). Some attempts to close VSDs by

catheter-delivered devices have met with various levels of success (see Chapter 13).

Ventricular Aneurysm

Posttraumatic ventricular aneurysms usually occur as a complication of coronary artery injury, most commonly to the left anterior descending coronary artery (32). In a world literature review by Grieco et al. (32) in 1989, 32 cases of left ventricular aneurysm following blunt chest trauma were reported. Patients ranged in age from 3 to 59 years. Motor vehicle crashes were the principal mechanism of injury. The most common presenting symptoms were congestive heart failure (10 patients), palpitations or dysrhythmias (9 patients), and arterial embolus (5 patients). Seven patients had mild constitutional complaints or were asymptomatic. Time of diagnosis ranged from 5 days to 18 years (median time 3 months) postinjury. Ventricular aneurysmectomy is recommended to avoid lethal complications (32).

Injury to Heart Valves and Supporting Structures

Heart valve rupture from blunt chest trauma occurs infrequently. Nine percent of adult fatalities from blunt chest trauma had cardiac valve injury in the autopsy series by Parmley et al. (2), and nearly all of these cases had other associated cardiac injuries. The aortic valve is the most frequently injured valve followed by the mitral and tricuspid valves.

Valvular injury results from a rapid increase in intracardiac pressure against a closed valve. During late diastole to early systole, the filled chambers experience their highest normal intraluminal pressures. With additional external pressure from forceful compression of the chest, abnormally high pressure is exerted on a closed heart valve. The timing of chest trauma in the cardiac cycle appears to determine which valve is injured. The greater left heart pressure gradients may contribute to the higher frequency of injury to the aortic and mitral valves. Another mechanism by which the aortic valve can be injured is the hydraulic ram effect that occurs when the aortic blood flow reverses during abdominal and lower extremity compression (33).

Presenting signs and symptoms of valvular injury depend on which valve is involved, the degree of valvular insufficiency, and the presence of other associated cardiac structural damage. Surgical valve replacement is generally required for the more severe injuries. Helpful diagnostic tests are the chest radiograph and ECG. The most useful test is Doppler echocardiography, which can identify disrupted blood flow or valvular dysfunction in addition to other associated structural defects.

Great Vessel Injury

Great vessel injury can occur with blunt trauma. The aorta is the most commonly injured great vessel. Injury to the pulmonary artery is rarely reported. Although aortic rupture from blunt trauma can occur with falls, crush injuries, and blast injuries, nearly 70% of cases in the general population occur with motor vehicle crashes. The mechanism of aortic rupture involves the shearing stress of sudden deceleration or sudden increases in intraluminal pressure. Ejected passengers, pedestrians struck by vehicles, and persons who fall from heights have higher risk for aortic rupture than victims of deceleration vehicular collisions. Aortic injury can occur with either horizontal or vertical deceleration (33).

The aorta most commonly ruptures when acceleration-deceleration forces pull a mobile aortic segment away from a point of fixation. The sites usually ruptured are the aortic

isthmus, fixed by the brachiocephalic arteries; the ascending aorta, fixed to the heart at the aortic root; and the descending aorta, fixed at the diaphragm. Tears of the ascending aorta carry a high risk of immediate mortality and are frequently associated with myocardial contusion and aortic valve injuries (2). Autopsy studies show that tears in the aortic isthmus and ascending aorta occur in 45% and 20% of cases of aortic rupture, respectively, but clinical studies show about 90% of aortic tears at the aortic isthmus. Overall, 80% to 90% of persons with motor vehicle-related aortic rupture are dead at the scene (12). Of the 10% to 20% who survive long enough for diagnosis and intervention, 30% die within 6 hours and 50% within 24 hours.

Fortunately, aortic dissections are rare in pediatric patients and are most commonly associated with trauma or a preexisting medical condition (e.g., Marfan, Loeys-Dietz, or Turner syndrome) (34). Management relies heavily on decision making and treatments established in the adult literature (35–37). Uncomplicated aortic dissections of the descending aorta (Stanford type-B) are typically managed conservatively with close heart rate and blood pressure control with the goal to stabilize the dissection. β -adrenergic blockers are the mainstay in this treatment. In complicated type-B dissections (e.g., impaired organ perfusion, loss of pulses) fenestration should be accomplished in the interventional suite or, in rare instances, surgically considered. Endovascular stent grafting has been reported in some types of aortic disruptions but there is little experience in the pediatric age-group. Dissections of the ascending aorta and/or arch (Stanford type-A) require urgent surgical intervention due to the risk of coronary malperfusion or cerebral embarrassment secondary to a dissection extending into the coronary or carotid arteries, respectively.

More common than aortic rupture and transmural aortic tears are superficial aortic tears into the intima and media with blunt trauma. These are generally without serious consequence and are often undiagnosed. Partial tears are infrequent and usually are located posteriorly. Multiple tears occur in 15% to 20% of cases. Traumatic aortic dissection is rare, occurring when the subadventitial layer remains intact and contains a periaortic hematoma (33).

Presenting complaints and physical findings may not accurately predict the presence or absence of aortic rupture. Symptoms may be absent, and visible external injury is not seen in about one-third of cases. Symptoms of aortic rupture include dyspnea, back pain, dysphagia and hoarseness, upper extremity hypertension, or an upper and lower extremity blood pressure differential similar to that seen with aortic coarctation. An aortic insufficiency heart murmur may be heard.

Chest radiographs may show mediastinal widening, a right-sided aortic root prominence, loss of aortic arch sharpness, or rightward deviation of the trachea. Less common radiographic findings include downward displacement of the left mainstem bronchus, rightward deviation of the esophageal nasogastric tube, left hemothorax, the apical cap sign, and first rib fracture. Aortography is considered to be the gold standard and is indicated in all cases of suspected aortic rupture, even if plane radiographs are normal (12). Transesophageal echocardiography, CT scanning, and magnetic resonance imaging also are useful in diagnosing rupture of the aorta.

Brachiocephalic Arteries

The second most common vascular injury with blunt trauma is injury of the brachiocephalic arteries. The mechanism of injury includes horizontal and vertical deceleration, chest compression, crush, distraction, and hyperextension of the shoulder. The resulting arterial injury is similar to that of the aorta. Massive bleeding or ischemia are rare complications (33).

Vena Caval Injury

Similar to aortic injury, vena caval injury is infrequent with nonpenetrating trauma. The abdominal segment of the inferior vena cava is more frequently injured than the chest segment. Because the thin-walled veins do not vasoconstrict like transected arteries after injury, severe hemorrhage and high mortality are usual with vena caval injuries. Mortality is higher in abdominal than in chest segment vena caval injury. Blunt trauma can cause avulsion or tear of the inferior vena cava near the right atrium that can extend into the right atrium. Therefore, associated cardiac injury is common when inferior vena caval injuries are located near the heart (33).

Plane chest radiography is not helpful. The emergent nature of these injuries does not allow time for venography. Therefore, rapid surgical exploration and repair is indicated when vena caval injury is suspected (33).

Coronary Artery Injury

Coronary artery injury from blunt trauma is rare. The study by Parmley et al. (2) of 547 patients who died from blunt chest trauma reported only 10 coronary artery lacerations and no cases of intraluminal thrombosis, even in areas of cardiac contusion. The incidence of coronary artery injury in nonfatal trauma cases is unknown. The most commonly injured coronary artery is the left anterior descending coronary artery. Consequences of coronary artery injury are myocardial infarction, hemopericardium, cardiac tamponade, and coronary artery and ventricular aneurysms and pseudoaneurysms (33).

A review of the English-language medical literature by Neiman and Hui (38) in 1992 reported 40 cases of myocardial infarction associated with blunt cardiac trauma. The pathophysiologic mechanism underlying acute myocardial infarction following blunt chest injuries has not been clearly established. Suggested mechanisms include transient coronary artery spasm, thrombus formation within the coronary artery, coronary artery dissection, or hemorrhage into an atheromatous plaque.

Definitive diagnosis of coronary artery injury is accomplished by angiography. These injuries are underdiagnosed because chest pain associated with blunt chest injury is often attributed to concomitant chest wall contusion, pericarditis, pulmonary contusion, rib fractures, or other associated injuries that are not routinely evaluated by coronary angiography. Coronary angiography is indicated for all blunt cardiac trauma patients with angina or myocardial infarction to determine the status of the coronary arteries and to locate surgically correctable lesions.

PENETRATING CARDIAC INJURY

Although blunt trauma accounts for most injuries among the pediatric population, penetrating trauma is increasing among young adults, teenagers, and even younger children. The ratio of gunshot to stab wounds is also increasing (39,40). With the concomitant improvement in emergency medical services, more patients with penetrating cardiac wounds are now reaching hospital emergency departments.

The first description of penetrating cardiac wounds is found in the Edwin Smith Papyrus, written in 3000 BC. Homer also described penetrating cardiac trauma in *The Iliad*. Baron Larrey, Napoleon's surgeon, is credited with performing the first pericardiocentesis in 1829. It was common wisdom for years that nothing could be done for wounds to the heart until von Rehn performed the first successful cardiorrhaphy in 1896 for a 22-year-old man with a 1.5-cm stab wound to the right ventricle. This was only 13 years following the statement by

Dr. Theodore Billroth that, "A surgeon who tries to suture a wound of the heart deserves to lose the esteem of his colleagues." (41)

The mortality risk for penetrating cardiac trauma is related to a number of factors, including the cause of injury, size of the wound, location of the wound, any associated noncardiac injuries, and length of time from injury to initiation of resuscitative measures.

Gunshot wounds cause much more extensive tissue destruction than stab wounds owing to transfer of large amounts of kinetic energy to the tissues. Not only does a bullet cause greater disruption of myocardium and internal structures of the heart, but the rent in the pericardium is larger, which makes tamponade less likely and exsanguination more rapid. For these reasons, the mortality rate of gunshot wounds to the heart is approximately twice that of stab wounds.

A stab wound is more likely to result in cardiac tamponade than a gunshot wound. More than 80% of stab wounds to the heart present with cardiac tamponade, whereas only 20% of gunshot wounds present in this fashion. Stab wounds are the most common cause of acute tamponade (41,42). The retention of blood within the pericardial sac prevents rapid exsanguination, providing more time for the patient to reach medical care and receive life-saving cardiorrhaphy. This has led some to consider hemopericardium as a mixed blessing. However, if allowed to progress, hemopericardium can lead to fatal cardiac tamponade. Because of its thicker myocardial wall, stab wounds to the left ventricle that measure <1 cm will often spontaneously seal. Stab wounds to the right ventricular wall, however, usually result in cardiac tamponade because the thinner myocardial wall does not usually spontaneously seal. The thinness of atrial walls decreases the likelihood of spontaneous sealing; however, the low intrachamber pressures counterbalance this factor (41).

As is the case with blunt cardiac trauma, the anatomic position of cardiac structures determines their likelihood of injury owing to penetrating trauma. Those structures located more anteriorly are more likely to be injured. In decreasing order of frequency, penetrating cardiac injuries involve the right ventricle, left ventricle, right atrium, and left atrium. For the same reason, the left anterior descending coronary artery is more frequently injured than the right coronary artery (42). Multiple chamber injury has a high mortality rate (43).

Penetrating cardiac injury can occur owing to iatrogenic causes. These injuries most often occur during diagnostic procedures, invasive monitoring, or other therapeutic interventions (40). Other causes of penetrating injury to the heart include ice picks, nonbullet projectiles, swallowed sewing needles, and inward displacement of fractured ribs with chest trauma (44).

Cardiac injury should be presumed to be present until proven otherwise in patients presenting with penetrating wounds of the precordium, neck, axilla, back, or upper abdomen. Beck triad is frequently absent in patients with cardiac tamponade, and determination of jugular venous distension is particularly difficult in young children because of their short necks. Additionally, if there is hypovolemia owing to acute blood loss, increased central venous pressure may not be seen with cardiac tamponade (41).

Penetrating injuries to the chest are frequently associated with intra-abdominal injury. Ten percent to thirty percent of patients with penetrating cardiac wounds also have intra-abdominal injury. This is important because mortality is greater for patients with penetrating cardiac injury associated with intra-abdominal injury than for those with cardiac injury alone (41).

Approximately 60% to 80% of patients with penetrating cardiac wounds die prior to reaching a hospital. For those who arrive in the emergency department with vital signs, or for those who had vital signs at the scene and lost them en route to the hospital, resuscitative intervention must be immediate (45). Diagnostic tests, such as a chest radiograph, are of little use.

Emergency department echocardiography is available at some trauma centers, which has decreased the time to diagnosis of penetrating cardiac injury and has improved survival. Pericardiocentesis can rule in, but not rule out, cardiac tamponade because of the high frequency of false-negative results. Performing a sub-xiphoid pericardial window has been recommended by some to diagnose hemopericardium in selected stable trauma patients.

Initial emergency management of penetrating cardiac trauma is the same for children and adults, following the principles of (a) maintaining a patent airway with adequate oxygenation and ventilation, (b) preservation of adequate tissue perfusion through rapid intravenous or intraosseous administration of fluids and blood, and (c) control of hemorrhage (12).

As with adults, children with a penetrating cardiac wound should receive emergency thoracotomy in the emergency department whenever they are too unstable to be transported to the operating room. Pericardiocentesis must be viewed as a temporizing measure until thoracotomy and definitive cardiorrhaphy can be performed. Emergency department thoracotomy was first described by Beall et al. (46) in 1966 for immediate resuscitation of moribund patients with penetrating chest injuries. The purpose of emergency department thoracotomy is reversal of cardiac tamponade, control of hemorrhage, open chest cardiac massage, and temporary cross-clamping of the descending aorta to redistribute blood flow to the coronary and cerebral circulations (46). Indications for emergency department thoracotomy in patients with blunt chest trauma are controversial because reported survival rates for both pediatric and adult patients are 0% to 2% with this procedure (47). This is unfortunate, because the vast majority of trauma deaths in the pediatric age group are due to blunt injury.

ELECTRICAL INJURY

The first human fatality caused by alternating current (250 volts) was reported in 1879. Among all age-groups, >1,000 people die each year in the United States because of electrocution on the work site or in the home, and 150 to 300 others die annually from lightning strikes. These deaths are primarily due to fatal cardiac dysrhythmia (48).

Injury from Man-Made Electricity

Ohm's law (amperage = voltage/resistance) describes the inverse relationship between current (A) and tissue resistance (R) and the direct relationship between current (A) and voltage (V). Damage to human tissue from electricity is related to the amount and duration of current that passes through it. In electrical injuries, only voltage is known. The amount of current involved (and resulting tissue damage) is variable, because tissue resistance varies. Overall, bone provides the greatest resistance to current flow, followed in descending order by fat, tendons, skin, muscle, vasculature, and nerves (49). Skin resistance is the most important factor determining the probability of cardiac injury from electrocution. Skin resistance can vary dramatically, depending on skin thickness, vascularity, and, most important, moisture. Although the resistance of dry skin may be 100,000 Ohms, that of moist skin may be as little as 1,000 Ohms. This 100-fold change in skin resistance may mean the difference between a painful electrical shock and the conduction of enough current to cause cardiac dysrhythmia (49).

Alternating current is a greater hazard than direct current. Alternating current can cause tetanic contraction of muscles. Because the forearm flexors are stronger than the extensors, this may prevent the child from being able to let go of an electrical source that he or she has grasped. Additionally,

TABLE 23.4

Factors Affecting Severity of Electrical Injuries

Frequency

Voltage

Amperage

Resistance

Pathway

Duration

Adapted from Cooper MA, Andrews CJ, Holle RL, et al. Lightning injuries. In: Auerbach PS, ed. *Wilderness Medicine*. 4th ed. St. Louis, MO: Mosby, 2001.

the heart is more sensitive to alternating current than direct current. Cardiac dysrhythmias are more likely to occur from household current at 60 Hz than electrical current of higher frequency. The path of the electrical current through the body also is a determinant of the likelihood of cardiac dysrhythmia. Current passing through the thorax is more likely to cause a dysrhythmia (36). See Table 23.4 for factors influencing electrical injury severity (48).

The mechanism by which electricity injures the heart is unknown. Proposed mechanisms include direct myocardial muscle damage, coronary artery endarteritis, and coronary artery spasm. Myocardial ischemia, resulting from decreased coronary perfusion during electrically induced dysrhythmia, also has been proposed as a mechanism of cardiac damage. The only reported pathologic finding at autopsy is petechial hemorrhages in the myocardium (50). Sudden death owing to low-voltage (110 to 380 V) alternating current found in the household is usually secondary to ventricular fibrillation. Following electrical injury, nonspecific ST-segment and T-wave changes are the most common abnormalities observed on ECG (50).

The use of CPK-MB isoenzyme levels in the diagnosis of myocardial infarction after electrical injury is complicated by the extensive skeletal muscle damage that normally occurs with these injuries. Skeletal muscle damaged by electricity will release large amounts of CPK, including the CPK-MB isoenzyme fraction. Skeletal muscle biopsy adjacent to the site of electrical injury demonstrates an increased production of CPK, as well as increased CPK-MB activity. This increased enzymatic activity is hypothesized to have been stimulated by the electrical injury. The utility of troponin levels in lightning injuries is unknown. The effects of cardiopulmonary resuscitation, as well as direct current countershock during resuscitative attempts, also potentially confuse the picture (50).

Initial emergency management of patients injured by electricity includes attention to the airway, breathing, and circulation and treatment of any cardiac dysrhythmias following pediatric advanced life support (PALS) and advanced cardiac life support (ACLS) protocols. Asymptomatic patients with normal ECGs following electrical injury from low-voltage alternating household current do not require routine cardiac monitoring or admission to the hospital (49,51).

Injury from Lightning

Each second, there are an estimated 100 lightning strikes to the earth's surface worldwide. Lightning is responsible for more deaths in the United States than any other natural disaster. Lightning-related injuries are most common during the

TABLE 23.5 Lightning Versus High-Voltage Electrical Injury

Factor	Lightning	High Voltage
Energy level	30,000,000 V, 50,000 A	Usually much lower
Time of exposure	Brief, instantaneous	Prolonged
Pathway	Flashover orifice	Deep, internal
Burns	Superficial, minor	Deep, major injury
Cardiac	Primary and secondary arrest, asystole	Fibrillation
Renal	Rare myoglobinuria or hemoglobinuria	Myoglobinuric renal failure common
Fasciotomy	Rarely if ever necessary	Common, early, and extensive
Blunt injury	Explosive thunder effect	Falls, being thrown

Adapted from Cooper MA, Andrews CJ, Holle RL, et al. Lightning injuries. In: Auerbach PS, ed. *Wilderness Medicine*. 4th ed. St. Louis, MO: Mosby, 2001.

summer, when there is more thunderstorm activity. Only 20% to 30% of people struck by lightning die, and they are usually the ones who experience immediate cardiopulmonary arrest. However, survivors often suffer from serious sequelae (48).

Lightning-related injuries differ in a number of ways from injuries owing to man-made electricity. Lightning strikes involve brief, massive surges of unidirectional current with an associated shock wave. Current magnitude often exceeds 100,000 A, and >30,000,000 V is seen. The 8,000°C temperature of a lightning stroke is threefold to fourfold higher than that seen with high-voltage man-made current, but contact is extremely brief. Lightning typically flashes over the body, causing only minor or superficial burns. This contrasts with the deep and extensive burns associated with high-voltage alternating current. See Table 23.5 for a comparison of electrical injuries owing to lightning and high-voltage current (48).

The electrical surge associated with a lightning strike is thought to cause widespread myocardial depolarization with subsequent asystole. Ventricular fibrillation also has been commonly reported. Respiratory arrest frequently occurs in lightning strike victims, and the associated hypoxia can prevent cardiac recovery from the initial electrically induced cardiac asystole or other dysrhythmia (48,52).

Myocardial necrosis has been found at autopsy following fatal lightning injury. Myocardial damage may be reflected by ECG abnormalities demonstrating an acute myocardial infarction pattern. Nonspecific ST-T wave changes also have been reported. ECG abnormalities may develop up to several days following the injury (52). Resolution of most ECG changes occurs within a few days, although abnormalities have been reported to last for months (48).

Initial emergency management of children struck by lightning is the same as for those with electrical injuries from man-made sources. Maintenance of a patent airway with adequate oxygenation and ventilation is the highest priority, as well as treatment of cardiac dysrhythmias following PALS and ACLS guidelines (48,52). Any child found with linear or punctate burns, clothes exploded off, tympanic membrane rupture, confusion, outdoor location of discovery, or pathognomonic feathering burns should be managed medically as a lightning strike victim. In the case of multiple casualties in a lightning strike, contrary to standard triage guidelines, resuscitation attempts should be directed first toward those who appear dead. Those who are apneic and asystolic may respond to resuscitative efforts, whereas those with spontaneous respirations are likely to already be recovering (48).

REFERENCES

- Baum VC. Cardiac trauma in children. *Paediatr Anaesth* 2002;12:110–117.
- Parmley LF, Manion WC, Mattingly TW. Nonpenetrating traumatic injury of the heart. *Circulation* 1958;18:371–396.
- Dowd MD, Krug S. Pediatric blunt cardiac injury: epidemiology, clinical features, and diagnosis. *J Trauma* 1996;40:61–67.
- Maron BJ, Estes NAM III. Commotio cordis. *N Engl J Med* 2010;362:917–927.
- Maron BJ. Sudden death in young athletes. *N Engl J Med* 2003;349:1064–1075.
- Link MS, Wang PJ, VanderBrink BA, et al. Selective activation of the K_{ATP} channel is a mechanism by which sudden death is produced by low energy chest wall impact (commotio cordis). *Circulation* 1999;100:413–418.
- Link MS, Maron BJ, Wang PJ, et al. Upper and lower limits of vulnerability to sudden arrhythmic death with chest wall impact (commotio cordis). *J Am Coll Cardiol* 2003;41:99–104.
- Garan AR, Maron BJ, Wang PJ, et al. Role of streptomycin-sensitive stretch activated channel in chest wall impact induced sudden death (commotio cordis). *J Cardiovasc Electrophysiol* 2005;16:433–438.
- Classie JA, Distel LM, Borchers JR. Safety baseballs and chest protectors: a systematic review on the prevention of commotio cordis. *Phys Sportsmed* 2010;1:83–90.
- Bliss D, Silen M. Pediatric thoracic trauma. *Crit Care Med* 2002;30:S409–S415.
- Abrunzo TJ. Commotio cordis: the single, most common cause of traumatic death in youth baseball. *Am J Dis Child* 1991;145:1279–1282.
- American College of Surgeons. *Advanced Trauma Life Support Manual*. Chicago, IL: American College of Surgeons, 1993.
- Tenzer ML. The spectrum of myocardial contusion: a review. *J Trauma* 1985;25:620–627.
- Roddy MG, Lange PA, Klein BL. Cardiac trauma in children. *Clin Pediatr Emerg Med* 2005;6:234–243.
- Akenside M. Account of blow upon heart and its effects. *Philos Trans R Soc Lond Biol* 1764:353.
- Fabian TC, Mangiante EC, Patterson CR, et al. Myocardial contusion in blunt trauma: clinical characteristics, means of diagnosis, and implications for patient management. *J Trauma* 1988;28:50–57.
- Bertinchant JP, Polge A, Mohty D, et al. Evaluation of incidence, clinical significance, and prognostic value of circulating troponin I and T elevation in hemodynamically stable patients with suspected myocardial contusion after blunt chest trauma. *J Trauma* 2000;48:924–931.
- Nagy KK, Krosner SM, Roberts RR, et al. Determining which patients require evaluation for blunt cardiac injury following blunt chest trauma. *World J Surg* 2001;25:108–111.
- Towbin JA. Cardiac troponin I: a new diagnostic gold standard of cardiac injury in children? *J Pediatr* 1997;130:853–854.
- Hirsch R, Landt Y, Porter S, et al. Cardiac troponin I in pediatrics: normal values and potential use in the assessment of cardiac injury. *J Pediatr* 1997;130:872–877.
- Rajan GP, Zellweger R. Cardiac troponin I as a predictor of arrhythmia and ventricular dysfunction in trauma patients with myocardial contusion. *J Trauma* 2004;57:801–808.
- Aristomenis E, Thomas S, Heinz A, et al. Highly sensitive cardiac troponin in blunt chest trauma: after the gathering comes the scattering? *J Trauma* 2011;70:766–767.
- Schultz JF, Trunkely DD. Blunt cardiac injury. *Crit Care Clin* 2004;20:57–70.

24. Reichlin T, Hochholzer W, Bassetti S, et al. Early diagnosis of myocardial infarction with sensitive cardiac troponin assays. *N Engl J Med* 2009;361:858–867.
25. Hiatt JR, Yeatman LA Jr, Child JS. The value of echocardiography in blunt chest trauma. *J Trauma* 1988;28:914–922.
26. Turturro MA. Emergency echocardiography. *Emerg Med Clin North Am* 1992;10:47–57.
27. Scorpio RJ, Wesson DE, Smith CR, et al. Blunt cardiac injuries in children: a postmortem study. *J Trauma* 1996;41:306–309.
28. Pevec WC, Udekwa AO, Peitzman AB. Blunt rupture of the myocardium. *Ann Thorac Surg* 1989;48:139–142.
29. Des Forges G, Ridder WP, Lenoci RJ. Successful suture of ruptured myocardium after nonpenetrating injury. *N Engl J Med* 1955;252:567–569.
30. Mozzetti MD, Devin JB, Susselman MS, et al. A pediatric survivor of left ventricular rupture after blunt chest trauma. *Ann Emerg Med* 1990;19:386–389.
31. Thors A, Guarneri R, Costantini EN, et al. Atrial septal rupture, flail tricuspid valve, and complete heart block due to nonpenetrating chest trauma. *Ann Thorac Surg* 2007;83:2207–2210.
32. Grieco JG, Montoya A, Sullivan HJ, et al. Ventricular aneurysm due to blunt chest injury. *Ann Thorac Surg* 1989;47:322–329.
33. Godwin JD, Tolentino CS. Thoracic cardiovascular trauma. *J Thorac Imaging* 1987;2:32–44.
34. Fikar CR, Fikar R. Aortic dissection in childhood and adolescence: an analysis of occurrences over a 10-year interval in New York State. *Clin Cardiol* 2009;32:E23–E26.
35. Bastos Goncalves F, Metz R, Hendriks JM, et al. Decision-making in type B dissection: current evidence and future perspectives. *J Cardiovasc Surg* 2010;51:657–667.
36. Bogdan Y, Hines GL. Management of acute complicated and uncomplicated type B dissection of the aorta. *Cardiol Rev* 2010;18:234–239.
37. Setacci F, Sirignano P, de Donato G, et al. Acute aortic dissection: natural history and classification. *J Cardiovasc Surg* 2010;51:641–646.
38. Neiman J, Hui WKK. Posteromedial papillary muscle rupture as a result of right coronary artery occlusion after blunt chest injury. *Am Heart J* 1992;123:1694–1699.
39. Centers for Disease Control and Prevention. Rates of homicide, suicide, and firearm-related death among children in 26 industrialized countries. *JAMA* 1997;277:289–295.
40. Hall JR, Reyes HM, Meller JL, et al. The new epidemic in children: penetrating injuries. *J Trauma* 1995;39:487–491.
41. Karrel R, Shaffer MA, Franaszek JB. Emergency diagnosis, resuscitation, and treatment of penetrating cardiac trauma. *Ann Emerg Med* 1982;11:504–517.
42. Asfaw I, Arbulu A. Penetrating wounds of the pericardium and heart. *Surg Clin North Am* 1977;57:37–48.
43. Asensio JA, Berne JD, Demetriades D, et al. One hundred five penetrating cardiac injuries: a 2-year prospective evaluation. *J Trauma* 1998;44:1073–1082.
44. Haller JA, Shermeta DW. Major thoracic trauma in children. *Pediatr Clin North Am* 1975;22:341–347.
45. Tyburski JG, Astra L, Wilson RF, et al. Factors affecting prognosis with penetrating wounds of the heart. *J Trauma* 2000;48:587–591.
46. Beall AC Jr, Diethrich EB, Crawford HW, et al. Surgical management of penetrating cardiovascular trauma. *Am J Surg* 1966;112:686–692.
47. Lorenz HP, Steinmetz B, Liberman J, et al. Emergency thoracotomy: survival correlates with physiologic status. *J Trauma* 1992;32:780–788.
48. Cooper MA, Andrews CJ, Holle RL, et al. Lightning injuries. In: Auerbach PS, ed. *Wilderness Medicine*. 4th ed. St. Louis, MO: Mosby, 2001:73–111.
49. Fatovich DM, Lee KY. Household electrical shocks: who should be monitored? *Med J Aust* 1991;155:301–303.
50. Solem L, Fischer RP, Strate RG. The natural history of electrical injury. *J Trauma* 1977;17:487–492.
51. Garcia CT, Smith GA, Cohen DM, et al. Electrical injuries in a pediatric emergency department. *Ann Emerg Med* 1995;26:604–608.
52. Andrews CJ, Cooper MA, Darveniza M, et al. *Lightning Injuries: Electrical, Medical, and Legal Aspects*. Boca Raton, FL: CRC Press, 1992.

From the Gene to the Neonate

Molecular Determinants of Cardiac Development and Disease

Deepak Srivastava ■ H. Scott Baldwin

The heart has for centuries been the fascination of anatomists, embryologists, biologists, and physicians. As the organ most essential for life, the heart is the first organ to form in an embryo and must function to support the rapidly growing embryo before it has the opportunity to shape itself into a four-chambered organ. The combination of the complex morphogenetic events necessary for cardiogenesis and the superimposed hemodynamic influences may contribute to the exquisite sensitivity of the heart to perturbations. This phenomenon is reflected in the estimated 10% incidence of severe cardiac malformations observed in spontaneously aborted fetuses. The fraction of congenital heart malformations that is hemodynamically compatible with the intrauterine circulation (1% of population) composes the spectrum of congenital heart defects (CHDs), which is the subject of this pediatric cardiology textbook.

These defects affect virtually all of the major structures of the mature heart (Fig. 24.1) (1,2). An additional 1% to 2% of the population harbor more subtle cardiac developmental anomalies that become apparent only as age-dependent phenomena reveal the underlying pathology. With >1 million survivors of CHD in the United States, it is becoming apparent that genetic disruptions that predispose to developmental defects can have ongoing consequences in maintenance of specific cell types and cellular processes over decades (3). A more precise understanding of the causes of CHD is imperative for the recognition and potential intervention of progressive degenerative conditions among survivors of CHD.

The anatomic features of most CHD in humans have been carefully catalogued. Although CHD was classified in the 18th and 19th centuries based on embryologic considerations, the advent of palliative procedures and clinical management led to a descriptive nomenclature founded on anatomic and physiologic features that governed surgical and medical therapy. However, seemingly unrelated CHDs could be argued to share common embryologic origins from a mechanistic standpoint, suggesting that the causes of CHDs may be better understood by considering their developmental bases. Advances in genetics and molecular biology have stimulated a renaissance in seeking an embryologic framework for understanding CHDs

as alterations and null mutations in a wide array of genes have targeted the heart and vascular system and established abnormalities in cardiovascular ontogeny as a primary cause of embryonic demise (4). The ability to go beyond descriptions of the anatomic defects to developing an understanding of the genes responsible for distinct steps of cardiac morphogenesis has raised the prospects that the future of pediatric cardiology will involve more directed therapeutic and preventive measures.

Although human genetic approaches have been important in understanding CHDs, detailed molecular analysis of cardiac development in humans has been difficult. The recognition that cardiac genetic pathways are highly conserved across vastly diverse species from flies to man has resulted in an explosion of information from studies in more tractable and accessible biologic models. The fruit fly (*Drosophila*) has been a source of discovery for genes involved in early cardiac determination events. Although no biologic system is ideal for studying human disease, *Drosophila* has several advantages: It has a simple genome and usually has a single copy of genes that often have three or four homologues in vertebrates; genetic studies are facilitated by the rapid breeding times; and, most important, its DNA can be chemically mutated in a random fashion followed by phenotypic analysis and reverse genetics to identify the DNA mutation associated with distinct developmental defects. Similar chemical mutagenesis efforts have been successful in another model system, the zebrafish. Zebrafish have the added advantages of being vertebrates; having a more complex two-chambered heart; and, because the embryos grow in water, having a heart that is easily visible and not necessary for survival during the period of cardiac development. Although genetic approaches are not feasible in chick embryos, they have four-chambered hearts, and the embryos are easily accessible within the egg for surgical and molecular manipulation during cardiogenesis. Such approaches have been useful in cell fate analyses and defining the role of populations of cells during development. Finally, use of the laboratory mouse, a mammal with a cardiovascular system nearly identical to humans, has been invaluable in understanding the mechanisms underlying human disease. Advances in technology have made it possible to mutate or delete specific genes in the

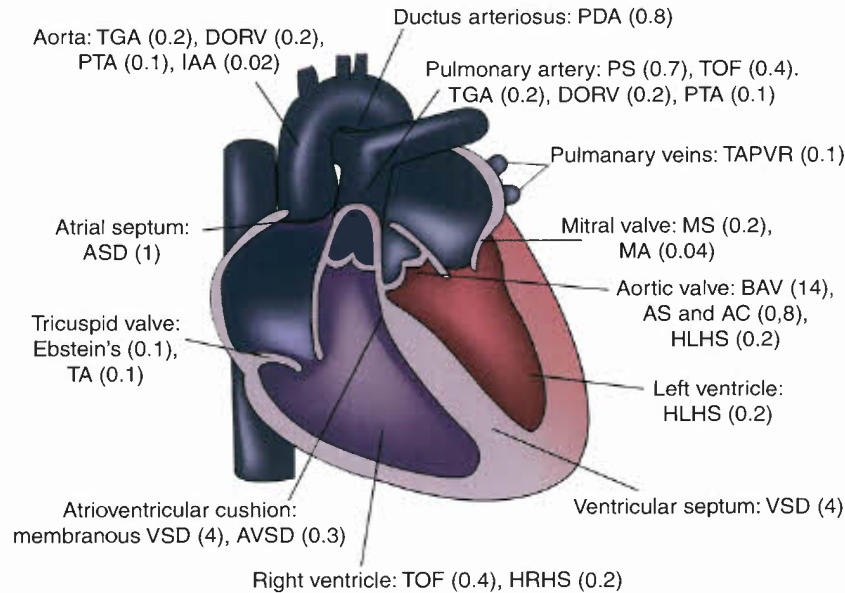


Figure 24.1. Congenital heart defects. This diagram of the adult heart illustrates the structures that are affected by congenital heart diseases, with the estimated incidence of each disease per 1,000 live births indicated in parentheses. AC, aortic coarctation; AS, aortic stenosis; ASD, atrial septal defect; AVSD, atrioventricular septal defect; BAV, bicuspid aortic valve; DORV, double outlet right ventricle; Ebstein, Ebstein anomaly of the tricuspid valve; HLHS, hypoplastic left heart syndrome; HRHS, hypoplastic right heart syndrome; IAA, interrupted aortic arch; MA, mitral atresia; MS, mitral stenosis; PDA, patent ductus arteriosus; PS, pulmonary artery stenosis; PTA, persistent truncus arteriosus; TA, tricuspid atresia; TAPVR, total anomalous pulmonary venous return; TGA, transposition of the great arteries; TOF, tetralogy of Fallot; VSD, ventricular septal defect. (From Bruneau BG. The developmental genetics of congenital heart disease. *Nature* 2008, 451:943–948, with permission.)

mouse genome and study the effects of such mutations in mice heterozygous or homozygous for the disrupted gene of interest. Thus, each biologic system offers unique opportunities to develop a deeper understanding of cardiogenesis.

In adults, heart disease is the number one killer of men and women in the United States, with an additional 5 million people surviving with insufficient cardiac function (5). Deciphering nature's secrets of heart formation might lead to novel approaches to repair or regenerate damaged heart muscle. Recent evidence has begun to support this idea and has led to heightened interest in the early events involved in cardiac cell fate decisions and cardiomyocyte differentiation, migration, and survival. The potential of stem cells in regenerative medicine is enormous, and insights into the natural process of cardiogenesis from progenitor cells during embryogenesis will form the basis of reprogramming cells for therapeutic use (4).

In this chapter, anatomic, molecular, and clinical aspects of cardiac embryology are interwoven to develop a framework in which to consider the causes of human CHDs. Clinical lessons combined with experimental studies in mice, fish, and flies have led to a model suggesting that unique regions of the heart have been added in a modular fashion during evolution. In this model, defects in particular regions of the heart would arise from unique genetic and environmental effects during specific developmental windows of time. To simplify the complex events of cardiogenesis, unique regions of the developing heart are considered individually in the context described above. In addition to the classic review of cardiac development by DeHaan (6) in 1965, more recent publications provide additional details into anatomic events that are required for normal cardiac morphogenesis (7–9). The primary focus of this chapter is to highlight recent work that has identified the molecular processes controlling these critical morphologic events.

ORIGIN OF CARDIAC PRECURSORS

Despite decades of cell lineage tracings and descriptive embryology of the heart's origins, only recently has a more complete and accurate picture of cardiogenesis emerged (8). Recent studies, utilizing careful observation of single embryonic stem (ES) cell differentiation, suggest that the primary cell types that comprise the early heart (myocardial, endocardial, and smooth muscle cells) can be derived from a single mesodermal cardiac progenitor (10–13). Two distinct mesodermal heart fields that share a common origin appear to contribute cells to the developing heart in a temporally and spatially specific manner. The well-studied primary heart field is derived from cells in the anterior lateral plate mesoderm that align in a crescent shape at approximately embryonic (E) day 7.5 in the mouse embryo, roughly corresponding to week 2 of human gestation (Fig. 24.2). By mouse E8.0, or 3 weeks in humans, these cells coalesce along the ventral midline to form a primitive heart tube, which consists of an interior layer of endocardial cells and an exterior layer of myocardial cells, separated by extracellular matrix (ECM) necessary for reciprocal signaling between the two layers.

Previous lineage tracings using dye-labeling techniques suggested that cells along the anterior–posterior (AP) axis of the heart tube were destined to contribute to specific chambers of the future heart (14). However, such studies could not determine the clonal contributions of individual cells (15). More recent studies using Cre-lox technologies to mark progenitor cells and all their descendants indicate—in stark contrast to previous models—that the heart tube derived from the primary heart field may predominantly provide a scaffold that enables a second population of cells to migrate and expand into cardiac chambers (8). These additional cells arise from an area often referred to as the

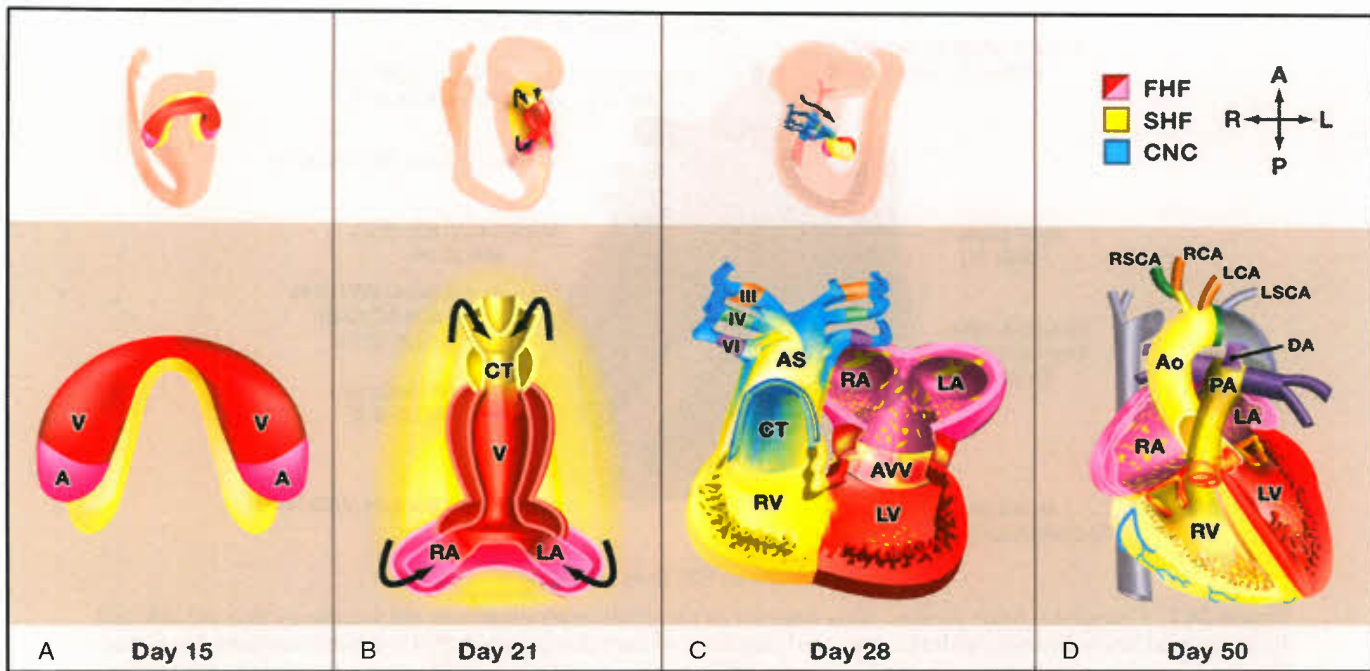


Figure 24.2. Mammalian heart development. Oblique views of whole embryos and frontal views of cardiac precursors during human cardiac development are shown. **A:** First heart field (FHF) cells form a crescent shape in the anterior embryo with second heart field (SHF) cells medial and anterior to the FHF. **B:** SHF cells lie dorsal to the straight heart tube and begin to migrate (arrows) into the anterior and posterior ends of the tube to form the right ventricle (RV), conotruncus (CT), and part of the atria (A). **C:** Following rightward looping of the heart tube, cardiac neural crest (CNC) cells also migrate (arrow) into the outflow tract from the neural folds to septate the outflow tract and pattern the bilaterally symmetric aortic arch arteries (III, IV, and VI). **D:** Septation of the ventricles, atria, and atrioventricular valves (AVV) results in the four-chambered heart. Ao, aorta; AS, aortic sac; DA, ductus arteriosus; LA, left atrium; LCA, left carotid artery; LSCA, left subclavian artery; LV, left ventricle; PA, pulmonary artery; RA, right atrium; RCA, right carotid artery; RSCA, right subclavian artery; V, ventricle.

secondary heart field (SHF), or anterior heart field, based on its location anterior and medial to the crescent-shaped primary heart field (16–18) (Fig. 24.2). Both heart fields appear to be regulated by complex positive and negative signaling networks involving members of the bone morphogenetic protein (Bmp), sonic hedgehog (Shh), fibroblast growth factor (Fgf), Wnt, and Notch proteins. Such signals often arise from the adjacent endoderm, although the precise nature and role of these signals remain unknown (19–22). SHF cells remain in an undifferentiated progenitor state until incorporation into the heart, and this may in part be due to closer proximity to inhibitory Wnt signals emanating from the midline.

As the heart tube forms, the SHF cells also migrate into the midline and position themselves dorsal to the heart tube in the pharyngeal mesoderm. On rightward looping of the heart tube, SHF cells cross the pharyngeal mesoderm into the anterior and posterior portions, populating a large portion of the outflow tract, future right ventricle, and atria (23) (Fig. 24.2). Precursors of the left ventricle are sparsely populated by the SHF and appear to be derived largely from the primary heart field. In contrast to the primary heart field, SHF cells do not differentiate into cardiac cells until they are positioned within the heart. Once within the heart, primary and secondary heart field cells appear to proliferate in response to endocardial-derived signals such as neuregulin and epicardial signals dependent on retinoic acid, although the mechanisms through which these non-cell-autonomous events occur remain poorly understood (24,25).

TRANSCRIPTIONAL REGULATION OF CARDIAC PRECURSORS

Regulation of the SHF involves numerous signaling and transcriptional cascades (Fig. 24.3). Factors secreted from the anterior portion of the heart tube may serve as chemoattractant signals to induce the migration of SHF cells, although the nature of such molecules remains unknown (18). *Isl1* (*Isl1*), a LIM-domain transcription factor involved in pancreatic development, is necessary for development of the SHF (23). Progeny of *Isl1*⁺ cells contribute to most of the heart except the left ventricle, but *Isl1* expression is extinguished as progenitor cells begin to express markers of cardiac differentiation (24). The mechanisms through which *Isl1* regulates SHF progenitor cells are being explored, with a significant advance coming from the discovery that expression of a forkhead protein essential for SHF development, *Foxh1*, is dependent on *Isl1* (26). *Isl1*⁺ cells also mark niches of undifferentiated cardiac progenitor cells in the postnatal heart (27), suggesting that understanding the regulation of SHF-derived progenitor pools may be useful in developing approaches for cardiac repair (discussed below). Interestingly, common mutations in *Isl1* have been shown to confer genetic susceptibility to CHDs (28).

Discovery of the SHF led to the reinterpretation of findings in mice lacking critical regulatory proteins and in transgenic mice harboring enhancers of genes expressed in the heart. As the molecular aspects of cardiogenesis were first being discovered approximately a decade ago, right ventricle-specific enhancers

the heart appear to be regulated by a muscle-specific member of the SWI/SNF complex, Baf60c (60), suggesting that transcriptional activity of cardiac DNA-binding proteins is highly regulated through epigenetic events.

MicroRNA Regulation of Cardiomyocyte Differentiation

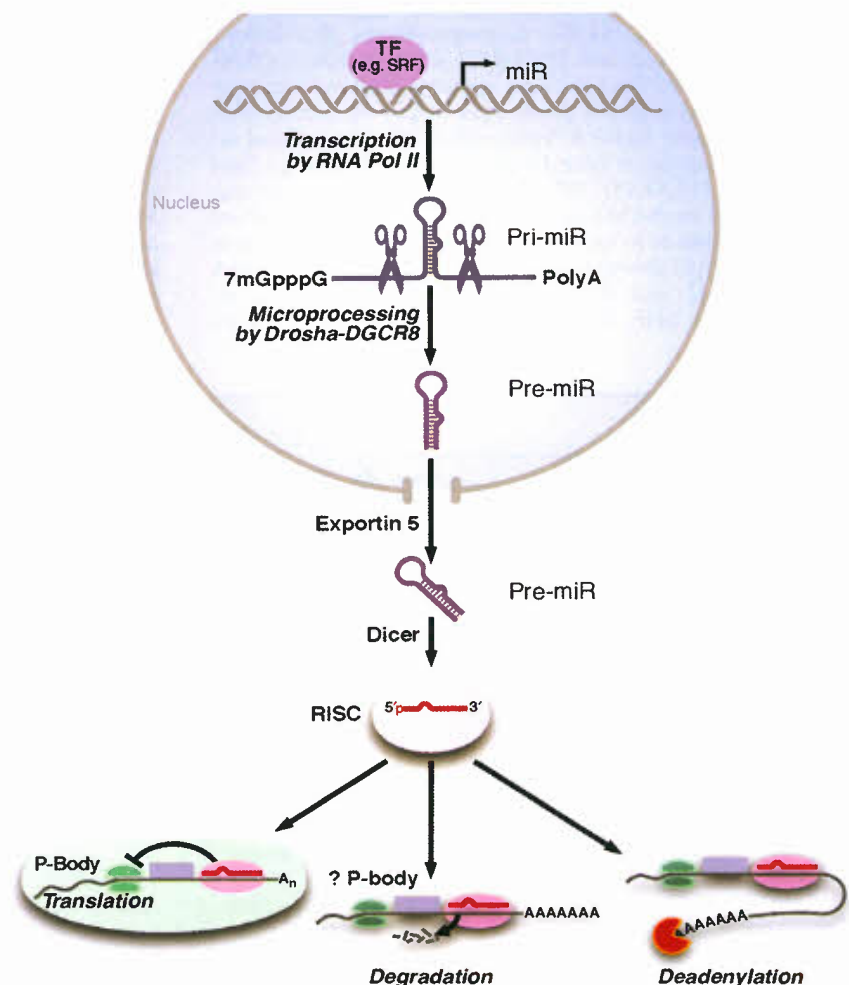
Although transcriptional and epigenetic events regulate many critical cardiac genes, translational control by small noncoding RNAs, such as microRNAs (miRNAs), has recently emerged as another mechanism to fine-tune dosages of key proteins during cardiogenesis (61,62). miRNAs primarily function post-transcriptionally by interacting with the 3' untranslated region (UTR) of specific target mRNAs in a sequence-specific manner (Fig. 24.4). Over 700 miRNAs are encoded in the human genome, and each is thought to target 50 to more than 100 mRNAs, resulting in mRNA degradation or translational inhibition. Interactions between miRNAs and mRNAs are thought to require sequence homology in the 5' end of the miRNA, but significant variance in the degree of complementation in the remaining sequence allows a single miRNA to target a wide range of mRNAs, often regulating multiple genes within a common pathway. miRNAs can often function to influence cell fate decisions including those of the cardiac lineage (63). A common theme has emerged in which miRNAs are often

regulated by the major transcriptional networks controlling cellular decisions and in turn function in positive and negative feedback loops to reinforce and titrate transcriptional decisions through their translational regulation.

Among the first miRNAs to be identified as major regulators of lineage determination were those promoting the formation of muscle (61). Since then, miRNAs have been realized as powerful regulators of cardiac, skeletal, and smooth muscle lineages employing clever regulatory mechanisms impinging on many previously described transcriptional pathways. Two such miRNAs, miR-1 and miR-133, are cotranscribed from a single locus and are uniquely expressed in skeletal and cardiac muscle cells and their progenitors (64,65).

Transcription of the *miR-1/miR-133* bicistronic precursors is directly regulated by the major myogenic differentiation factors, MyoD, myocyte enhancer factor-2 (Mef2), and serum response factor (SRF), early expressed in the muscle mesoderm (61). The influence of miR-1 in promoting the muscle identity is so strong that misexpression of this single miRNA in fibroblasts is sufficient to largely transform their gene program to that of muscle cells (66). Indeed, miR-1 can promote the differentiation of skeletal muscle from myoblast precursors, in part by targeting a repressor of the muscle master regulator Mef2c, which further drives expression of miR-1 (64). Deletion of miR-1 in flies results in a defect in somatic and cardiac muscle differentiation (62,67), where miR-1 regulates Notch signaling and cell polarity (68).

Figure 24.4. Current model of miRNA biogenesis and function. The initial RNA is transcribed by RNA polymerase II as primary miRNAs (pri-miRNAs). These pri-miRNAs range from a few hundred to thousands of nucleotides (nt) in length. The pri-miRNA of each miRNA has a characteristic stem-loop structure that is detected and cleaved by the ribonuclease III (RNase III) endonuclease Drosha within the nucleus. Efficient pri-miRNA cleavage by Drosha requires a protein partner, Pasha/DGCR8, which has a double-stranded RNA-binding domain (dsRBD). The cleavage product, approximately a 70-nt stem-loop RNA called pre-miRNA, is exported from the nucleus to the cytoplasm by Exportin 5/RanGTP. In the cytoplasm, another evolutionarily conserved RNase III enzyme, Dicer, together with its dsRBD protein partner, TRBP and PACT, further process pre-miRNA into mature miRNA approximately 21 nt in length. The mature miRNA is then unwound and a single strand is incorporated into a protein complex known as the RNA-induced silencing complex (RISC), which represses mRNA translation or destabilizes mRNA transcripts through cleavage or deadenylation.



During early cell fate decisions of mouse and human ES cells, *miR-1* and *miR-133* function in concert to promote mesoderm induction, while suppressing differentiation into the ectodermal or endodermal lineages (69). However, *miR-1* and *miR-133* have antagonistic effects on further adoption of muscle lineages: *miR-1* promotes differentiation of mouse and human ES cells toward a cardiac fate, while *miR-133* inhibits differentiation into cardiac muscle. *miR-1* appears to exert this effect, in part, by translationally repressing the mammalian orthologue of *delta*, *Delta-like-1* (*Dll-1*), similar to the repression seen in the fly (69). Thus, the bicistronic *miR-1/miR-133* transcript encodes distinct mature miRNAs that likely share common targets yet complement each other by balancing the differentiation and proliferation of cardiac and skeletal muscle lineages. Interestingly, loss of two alleles of *miR-133* or one allele of *miR-1* causes similar ventricular septal defects (VSDs), consistent with them sharing some common targets (65,70).

Mir208a, contained within the introns of *Myh6* and *Myh7* and highly enriched in embryonic heart, targets *GATA4* and plays a fine tuning role in early cardiac development, although its deletion did not reveal any embryonic cardiac phenotype (71). Wilson et al. (72) reported a cardiac “miRNA-ome,” a miR profile of early cardiomyocytes derived from human ES cells. They found *miR1*, *133* and *208* confirming miRs share their function in mouse embryos and differentiating human ES cells. They further revealed *miR-499* as an upstream regulator of *Mef2c* expression.

Another cotranscribed pair of miRNAs expressed early during cardiogenesis under control of *SRF* and that play a key role in cell fate decision is *miR-143* and *miR-145* (69,73). These two miRNAs are down-regulated during cardiogenesis but are critical regulators of smooth muscle cells, which uniquely oscillate between proliferative or more quiescent, differentiated states. The cotranscribed *miR-143* and *miR-145* cooperatively target a network of transcription factors, including *Klf4* and *Elk-1*, to promote differentiation and repress proliferation of smooth muscle cells in vitro (73). Given their intercalation into these major regulatory pathways, their ability to direct differentiation of multipotent progenitors was also investigated. Indeed, *miR-145* had the unique capacity to induce smooth muscle gene expression and synergize with the smooth muscle master regulator, *Myocardin*. In addition, *miR-145* was able to potently and rapidly direct the differentiation of multipotent neural crest stem cells into smooth muscle (73). Although *miR-145* was not required for smooth muscle differentiation in vivo or in vitro, loss of *miR-145* resulted in a more proliferative, less differentiated state of smooth muscle in vivo (74).

Complex Regulation of Cardiac Morphogenesis

Although the pathways regulating individual cell lineages contributing to the heart are deeply understood, the subsequent complex events involved in integrating multiple cell types, formation of chambers, and patterning of the distinct regions of the heart are also now being elucidated. Major components involving the sequential development of the mouse heart, the primary genetic model for the study of cardiac morphogenesis, have recently been extensively reviewed (75). From an evolutionary standpoint, it appears that as organisms became more complex, a more elaborate cardiovascular system was required. Distinct cardiac chambers began to develop and adopted specialized functions. Fish, which have a circulatory system that functions in series, developed separate atrial and ventricular chambers with a single inflow and outflow tract. The single ventricle pumps blood to the body via the gills, and no separation of deoxygenated and oxygenated blood is necessary. The amphibious frog adopted an intermediate three-chambered heart. In contrast, terrestrial vertebrates required complete separation of oxygenated and deoxygenated blood after birth, necessitating

two separate atrial and ventricular chambers along with two distinct inflow and outflow tracts. These evolutionary observations suggest that the heart was built in modules that were added as they became necessary. The discovery of distinct heart fields as described above and evidence of modular gene expression in the heart supports such a notion.

Dorsal–Ventral Polarity

Beyond the asymmetric addition of SHF cells along the AP axis, a discrete dorsal–ventral (DV) polarity occurs in the primitive heart tube. As the heart tube loops to the right, the ventral surface of the tube rotates to become the outer curvature of the looped heart, and the dorsal surface forms the inner curvature. The outer curvature becomes the site of active growth, whereas remodeling of the inner curvature is essential for the ultimate alignment of the inflow and outflow tracts of the heart. A model in which individual chambers “balloon” from the outer curvature in a segmental fashion has been proposed (76). Consistent with this model, numerous genes, including the transcription factor *Hand1* and the sarcomeric protein *Serca2*, are expressed specifically on the outer curvature of the heart (47,77). *Hand2* is expressed on the inner and outer curvature, but protein production of *Hand2* in the inner curvature may be repressed by miRNA regulation, as *miR-1* is first detected in the inner but not outer curvature at E8.5 (61). Also, through a complex transcriptional network, the unique identity of inner curvature cells is determined by *Tbx2*-mediated repression of genes typically found on the outer curvature (78). Another *Tbox* transcription factor, *Tbx20*, serves to repress *Tbx2* activity in the outer curvature as it expands into the cardiac chambers, thereby establishing the regional patterning of expanding or remodeling myocardium (79–81). Remodeling of the inner curvature allows migration of the inflow tract to the right and the outflow tract to the left, facilitating proper alignment and separation of right- and left-sided circulations. In addition to its role in repressing *Tbx2*, *Tbx20* affects expansion of both the primary and secondary heart field-derived cells and is necessary for outflow tract development, possibly via regulation of *Nkx2.5* and *Mef2c* (79).

Left–Right Asymmetry and Cardiac Looping

Rightward looping of the heart tube with the caudal portion of the tube moving to a more anterior and dorsal position is the first obvious sign of the break in left–right (LR) symmetry. The cellular mechanisms that drive cardiac looping remain poorly understood, but it has been postulated that differential rates of proliferation of cardioblasts, regional differences in intracardiac actin bundles, or altered cell adhesion across the heart tube may be involved. When considering the mechanisms for cardiac looping, it is important to distinguish between the process of looping and the directionality of looping (82). Directionality of looping reflects overall asymmetry throughout the embryo, which is superimposed on the morphogenetic mechanisms for looping.

It has been proposed that abnormalities in the process of cardiac looping underlie a number of CHDs. Folding of the heart tube positions the inflow cushions adjacent to the outflow cushions and involves extensive remodeling of the inner curvature of the looped heart tube. In the primitive looped heart, the segments of the heart are still in a linear pattern and must be repositioned considerably for alignment of the atrial chambers with the appropriate ventricles and the ventricles with the aorta and pulmonary arteries. The atrioventricular septum (AVS) begins to divide the common atrioventricular canal (AVC) into a right and left AVC that subsequently shifts to the right to position the AVS over the ventricular septum (Fig. 24.5). This allows the right AVC and the left AVC to be aligned with the right and left ventricles, respectively. Simultaneously, the conotruncal region becomes septated into the aorta and pulmonary trunks as the conotruncus moves

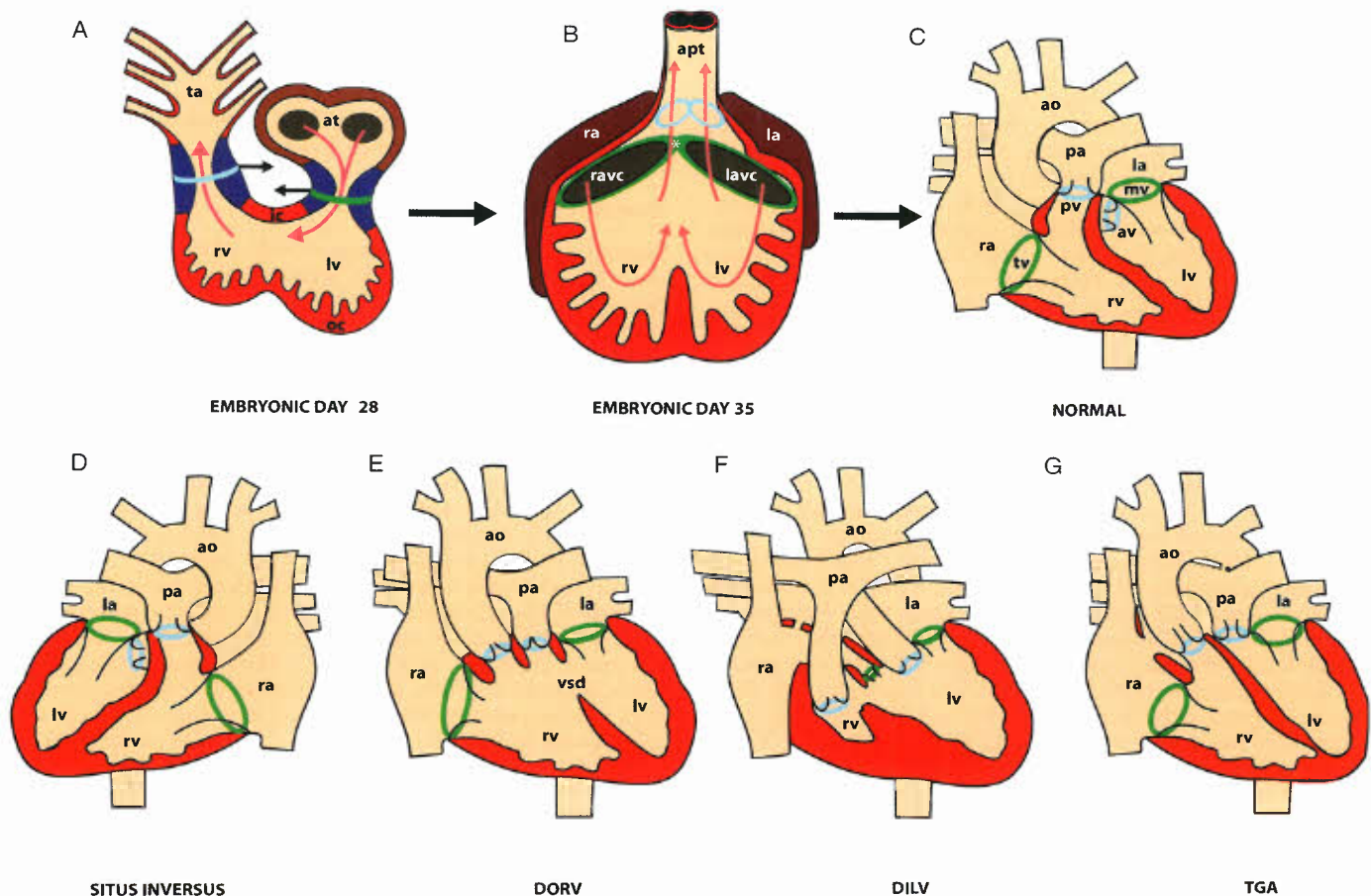


Figure 24.5. Normal and abnormal cardiac morphogenesis associated with LR signaling. **A:** As the linear heart tube loops rightward with inner curvature (ic) remodeling and outer curvature (oc) proliferation, the endocardial cushions (dark blue) of the inflow (green) and outflow (light blue) tracts become adjacent to one another. Subsequently, the AVS shifts to the right, while the aortopulmonary trunk shifts to the left. **B:** The inflow tract is divided into the right (ravc) and left atrioventricular canal (lavc) by the AVS (asterisk). The outflow tract, known as the truncus arteriosus (ta), becomes the aortopulmonary trunk (apt) on septation. **C:** Ultimately, the left (la) and right atrium (ra) are aligned with the left ventricle (lv) and right ventricle (rv), respectively. The lv and rv become aligned with the aorta (ao) and pulmonary artery (pa), respectively, after 180-degree rotation of the great vessels. **D:** If the determinants of the LR axis are coordinately reversed, then a condition known as situs inversus results. **E:** If the apt fails to shift to the left, then a condition known as double-outlet right ventricle (DORV) results, in which the RV is aligned with both the aorta and pulmonary artery. **F:** Likewise, if the AVS fails to shift to the right, both atria communicate with the left ventricle in a condition known as double-inlet left ventricle (DILV). **G:** Transposition of the great arteries (TGA) results if the apt fails to twist, resulting in communication of the rv with ao and lv with pa. av, aortic valve; mv, mitral valve; pv, pulmonary valve; vsd, ventricular septal defect.

toward the left side of the heart such that the conotruncal septum is positioned over the AVS (Fig. 24.5). The rightward shift of the AVS and leftward shift of the conotruncus converts the single-inlet, single-outlet heart into a four-chambered heart that has separate atrial inlets and ventricular outlets (83).

Arrest or incomplete movement of the AVS or conotruncus might result in malalignment of the inflow and outflow tracts (Fig. 24.5). A scenario in which the AVS fails to shift to the right would result in communication of the right and left AVCs with the left ventricle, a condition known as double-inlet left ventricle (DILV). Incomplete shifting may be the basis for “unbalanced” AVC defects where the right AVC only partly communicates with the right ventricle. Similarly, if the conotruncal septum fails to shift to the left, both the aorta and pulmonary artery would arise from the RV causing a double-outlet right ventricle (DORV). From this embryologic perspective, it is not surprising that double-outlet left ventricles and double-inlet right ventricles are rarely, if ever, seen

clinically. In contrast, any abnormality in cardiac looping can be associated with DILV or DORV, along with other manifestations of improper alignment of specific regions of the heart.

The elegant molecular network regulating LR asymmetry of the body plan has been reviewed (84) and is not summarized here. However, it is worth highlighting several clues about the relationship between LR asymmetry and proper alignment of the cardiac chambers. The cascade of LR signals including *Shh* and *Nodal* converge on the transcription factor *Pitx2* (85). *Pitx2* is initially LR asymmetric in the linear heart tube, but this asymmetry is translated into a DV polarity in the looped heart tube. Because *Pitx2* regulates cell proliferation via cyclin D2 and also controls cell migration events (86), it is a potential link between signals regulating the direction and process of cardiac looping. Within certain subdomains, regulation of *Pitx2* by *Tbx1* integrates transcriptional pathways controlling morphogenesis and LR asymmetry (87).

How do the insights into LR asymmetry impact our understanding of CHDs? It is likely that patients with situs inversus totalis have a well-coordinated reversal of LR asymmetry and thus have a lower incidence of defects in visceral organogenesis. However, most patients with LR defects have viscerotaxial heterotaxy and thus have randomization of cardiac, pulmonary, and gastrointestinal situs where coordinated signaling is absent. Such patients can have defects in almost all aspects of cardiogenesis. Often either the right or left side predominates with patients either having bilateral right-sidedness (asplenia syndrome) or bilateral left-sidedness (polysplenia syndrome). In such cases, features of the right or left side of the lungs, heart, and gut are duplicated. Disruption of cascades determining either the left or right side of the embryo might result in asplenia or polysplenia syndromes, respectively. Indeed, mutations in LR pathway members are found in some patients with heterotaxy (88). Familial cases of heterotaxy have also led to identification of mutations in a zinc-finger transcription factor, *ZIC3*, that result in LR axis abnormalities (89).

Cardiac Outflow Tract Regulation

Congenital cardiac defects involving the cardiac outflow tract, aortic arch, ductus arteriosus, and proximal pulmonary arteries account for 20% to 30% of all CHDs. This region of the heart undergoes extensive and rather complex morphogenetic changes with contributions from neural crest cells and the SHF, as discussed above. The cardiac outflow tract can be divided into the muscularized conus and the adjacent truncus arteriosus, collectively termed the conotruncus, as it arises from the primitive right ventricle. The conotruncus normally shifts to the left to override the forming ventricular septum. The truncus arteriosus then becomes septated by mesenchymal cells into the aorta and pulmonary arteries with a muscular ridge forming between the two vessels known as the conotruncal septum (Fig. 24.5). However, at this stage, the aorta communicates with the RV and the pulmonary artery with the left ventricle. Subsequent rotation of the two vessels in a spiraling fashion places the aorta in a more dorsal and leftward position and the pulmonary artery in a more ventral and rightward location. This spiraling event achieves the normal alignment of the aorta and pulmonary artery to the left and right ventricles, respectively.

Abnormalities in septation or incomplete spiraling of the conotruncus result in many CHDs. For example, the

conotruncal septum between the aorta and pulmonary artery forms in tetralogy of Fallot (TOF), but because of malalignment of the great vessels, the conotruncal septum and aorta are shifted to the right. This results in an overriding aorta and failure of the conotruncal septum to connect to the muscular ventricular septum, resulting in a VSD (Fig. 24.5). Similarly, any malalignment of the conotruncus results in an obligatory VSD that, unlike muscular VSDs, does not have the potential to close spontaneously after birth.

A structure referred to as the aortic sac lies distal to the conotruncus and gives rise to six bilaterally symmetric vessels known as aortic arch arteries. The aortic arch arteries arise sequentially along the AP axis, each traversing a pharyngeal arch before joining the paired dorsal aortae (Fig. 24.6). The first and second arch arteries involute, and the fifth arch artery never fully forms. The third, fourth, and sixth arch arteries undergo extensive remodeling to ultimately form distinct regions of the mature aortic arch and proximal pulmonary arteries. Most of the right-sided dorsal aorta and aortic arch arteries undergo programmed cell death leading to a left-sided aortic arch. The third aortic arch artery contributes to the proximal carotid arteries and right subclavian artery (RSCA). The left fourth aortic arch artery forms the transverse aortic arch between the left common carotid (LCC) and left subclavian arteries. Finally, the sixth arch artery contributes to the proximal pulmonary artery and the ductus arteriosus (90). Extrapolating from their embryologic origins, it is believed that aberrant right subclavian arteries and other subtle arch anomalies are the result of third aortic arch defects; interrupted aortic arch (IAA) from fourth arch defects; and patent ductus arteriosus (PDA) and proximal pulmonary artery hypoplasia/discontinuity from defects in sixth arch artery development.

Mesenchyme cells originating from the crest of the neural folds are essential for proper septation and remodeling of the outflow tract and aortic arch (91,196,197). Such neural crest-derived cells migrate away from the neural folds and retain the ability to differentiate into multiple cell types (Fig. 24.6). The migratory path and ultimate fate of these cells depends on their relative position of origin along the AP axis and are partly regulated by the Hox code (92). Neural crest cells differentiate and contribute to diverse embryonic structures, including the cranial ganglia, peripheral nervous system, adrenal glands, and melanocytes. Neural crest cells that arise from the otic placode to the third somite migrate through the developing pharyngeal

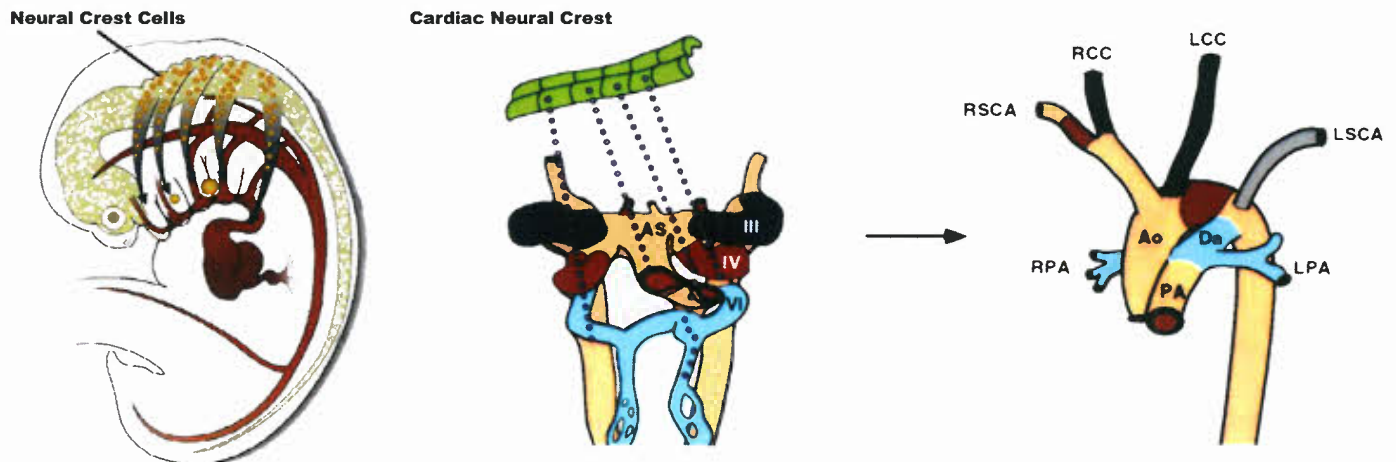


Figure 24.6. Cardiac neural crest contributions to aortic arch development. Cardiac neural crest cells arise from the neural folds and migrate into the outflow tract of the heart and aortic arch arteries. They are involved in remodeling the arch arteries, with derivatives color coded by their arch artery origins. Ao, aorta; AS, atrial septum; Da, descending aorta; LCC, left common carotid; LPA, left pulmonary artery; LSCA, left subclavian artery; RCC, right common carotid; RSCA, right subclavian artery.

arches and populate the mesenchyme of each of the aortic arch arteries and the mesenchyme necessary to septate the outflow tract septum (Fig. 24.6). Because of their migratory path and role, this segment of the neural crest is often referred to as the cardiac neural crest (CNC).

Mutations in many signaling cascades affect neural crest migration or development, including the endothelin and semaphorin pathways, and cause outflow tract defects similar to those observed in humans (91). Embryos deficient in CNC cell migration or differentiation display various cardiac outflow tract and aortic arch defects resembling those in humans. These include TOF, persistent truncus arteriosus (PTA), DORV, VSDs, and defects of aortic arch patterning. Thus, abnormalities in neural crest migration or differentiation likely underlie many of the conotruncal and aortic arch defects seen in humans. Indeed, human mutations of the neural crest-enriched transcription factor *TFAP2 β* result in persistent patency of the ductus arteriosus, a specialized aortic arch vessel essential for fetal cardiac physiology (93) (Fig. 24.6). It is likely that other genetic mutations affect specific regions of the aortic arch.

Disruption of SHF development by mutation of genes such as *Tbx1*, *Fgf8*, and *Isl1* results in defects similar to those observed with neural crest disruption (Fig. 24.3), including PTA (failure of outflow septation), malalignment of the outflow tract of the heart with the ventricular chambers, and VSDs (21,38,44,45). Since SHF-derived myocardial cells neighbor neural crest-derived cells and secrete growth factors such as *Fgf8* in a *Tbx1*-dependent manner that influence neural crest cells (39), reciprocal interactions between the SHF and neural crest-derived cells in the outflow tract are likely essential for normal development. Consistent with this, humans with deletion or mutation of *TBX1* (94), expressed in the SHF, appear to have cell-autonomous defects of SHF development and non-cell-autonomous anomalies of neural crest-derived tissues. It will be interesting to determine if many human cardiac outflow tract defects are a direct result of SHF migration, differentiation, or proliferation.

Cardiac Valve Formation

Critical events regulating cardiac valve development have been recently reviewed (95,96). Appropriate placement and function of cardiac valves is essential for chamber septation and for unidirectional flow of blood through the heart. A molecular network involving *Bmp2* and *Tbx2* defines the position of the valves relative to the chambers (78,97,98). During early heart tube formation, “cushions” of ECM between the endocardium and myocardium presage valve formation at each end of the heart tube. Reciprocal signaling, mediated in part by TGF- β family members, between the myocardium and endocardium in the cushion region induces a transformation of endocardial cells into mesenchymal cells that migrate into the ECM cushion (99–101). These mesenchymal cells differentiate into the fibrous tissue of the valves and are involved in septation of the common AVC into right- and left-sided orifices (102).

Although the processes regulating early epithelial to mesenchymal transition (EMT) in the AVC have been extensively investigated as described above, our understanding of the mechanisms regulating later stages of semilunar valve development are still primarily limited to morphogenic descriptions. This is due, in part, to the fact that this period of development has been essentially inaccessible to experimental manipulation because gene perturbation studies result in embryonic demise in the midgestation mouse embryo. However, based on studies of normal mouse and human embryos (103,104), investigators have demonstrated that the endocardial cushions form condensed mesenchymal protrusions, the primitive valves. These condensed mesenchymal protrusions subsequently elongate to provide the true cardiac valve leaflets (Fig. 24.7). The elongation of primitive valves appears to be a result of restricted proliferation of endocardial cells overlying the mesenchymal projections on the vascular side of the valve and selective cell death under the expanding endocardial rim. The growth of the endocardial edge and evacuation of apoptotic cells underneath the proliferating endocardial rim sculpt the swollen mesenchymal primitive valves into a typical excavated shape and result in morphogenesis of the sinuses of Valsalva.

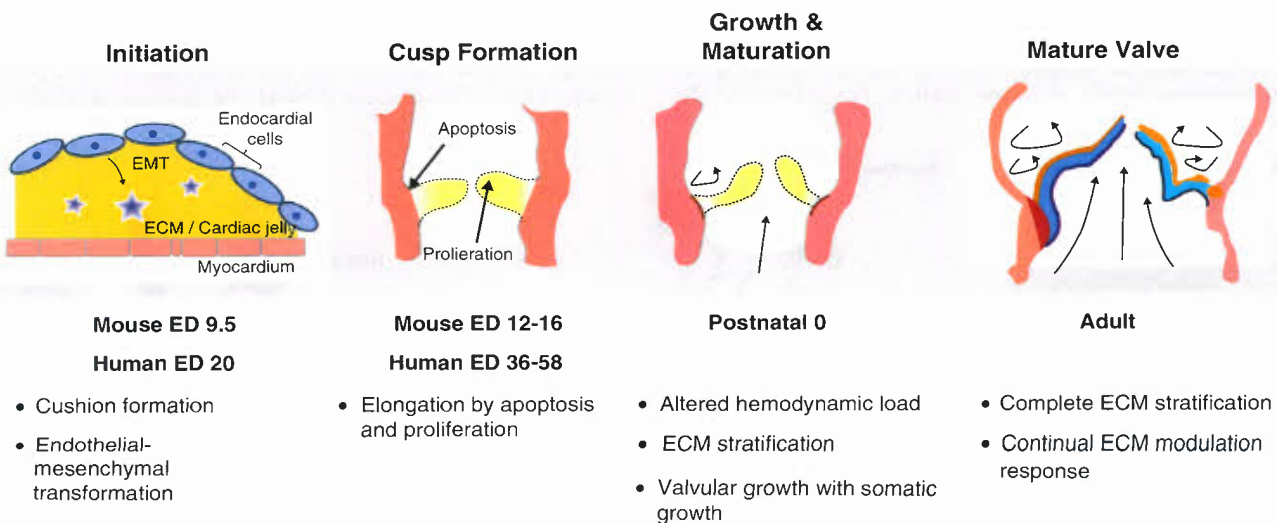


Figure 24.7. Summary of the critical stages in semilunar valve formation. Initially, regional swellings of ECM form the endocardial cushions, which provide valve-like action ensuring that initial blood flow is unidirectional in the developing embryo. Subsequently, endothelial cells undergo a mesenchymal transformation and populate the endocardial cushions. Finally, the endothelial cells on the arterial face proliferate and the ECM is remodeled to begin valve cusp histogenesis. Subsequently, a selected population of mesenchymal cells is thought to undergo apoptosis simultaneously with continued remodeling of the ECM to form the sinuses, which will eventually become the origin of the proximal coronary arteries. The *black arrows* denote the direction of blood flow. (Figure courtesy of Dr. Peggi Angel.)

Recent studies using immunohistochemistry and electron microscopy described late gestational and postnatal valve development in chicken and mouse (105), with a remarkably similar progression of developmental events seen in human fetuses (106) (Fig. 24.8). These studies document progression of remodeling and compartmentalization of the valve leaflet from a disorganized matrix of proteoglycans with little detectable elastin, and small amounts of disorganized collagen and relative uniform distribution of vascular interstitial cells (VICs), to a highly stratified ECM. The ECM contains three organized layers of fibrosa (arterial aspect primarily composed of collagens), spongiosa (central aspect, primarily glycosaminoglycans), and ventricularis (ventricular aspect with elastin fibers) with compartmentalization of VICs resulting in increased cell density in the fibrosa and ventricularis. Notably, this process is not only conserved across species but extends well after birth into postnatal life. Interestingly, the fetal VIC activation that occurs throughout development is similar to the valve changes occurring in pathologic conditions (107,108), suggesting that analogous molecular mechanisms likely direct both normal developmental and pathologic interstitial cell activation (101). Furthermore, recent experiments have suggested that a small population of VICs may reside as a progenitor cell population that retains the ability to differentiate into either endothelial or interstitial cells in the valve leaflet (109).

A few mouse mutants escape early embryonic demise and are thus informative in unraveling the mechanisms of late gestational and early postnatal semilunar valve pathology. Most of these mouse models display normal EMT but then evolve a

hyperplastic valve phenotype that suggests aberrations in valve remodeling. One common feature of many of these defects is perturbations that either enhance or attenuate RAS-MAPK signaling (110,111). Gitler et al. (112) showed that hyperplastic aortic valve defects in neurofibromatosis 1 (NF1) mutant embryos, previously attributed to defects in CNC cells, result from a primary defect in outflow tract and AVC endocardium. These defects were at least partially due to elevations in endocardial MAPK signaling secondary to the loss of NF1 suppression of *Ras-Erk* signaling, resulting in increased proliferation and decreased apoptosis (113). Consistent with this, patients with NF1 mutations develop pulmonary stenosis and hypertension but rarely defects in the AVC (114). NF1 loss of function is mimicked by gain-of-function mutations in the tyrosine phosphatase *Shp2/PTPN11*, which causes an increase in *Ras-Erk* activation, increased proliferation, and decreased apoptosis, resulting in semilunar valve and atrioventricular valve (AVV) hyperplasia (115,116). Autosomal dominant gain-of-function mutations in *Shp2* cause Noonan syndrome, characterized by pulmonary stenosis, hypertrophic cardiomyopathy, and occasional AVV defects (117,118). Most recently, hypomorphic mutations in *SOS1*, an essential RAS guanine nucleotide-exchange factor (*Ras-Gef*), result in enhanced RAS-ERK activation and can account for as many as 20% of the cases of Noonan syndrome not explained by *Shp2* mutations (119,120).

Recent evidence implicates EGF signaling as an important regulator of late valve remodeling. Loss or attenuation of EGFR/Erbb1 signaling results in preferential hypercellularity of semilunar

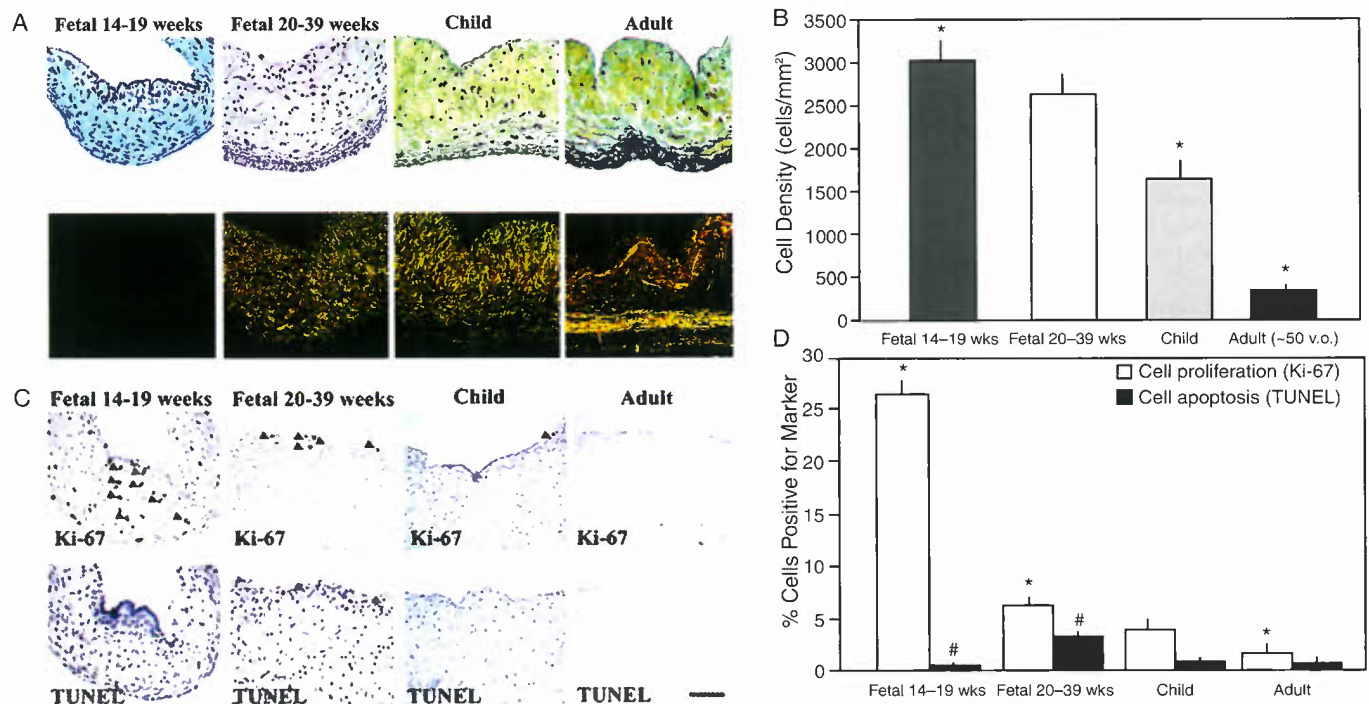


Figure 24.8. A: ECM composition of human cardiac valves from fetus to adult. At 14 to 19 weeks (Top, Movat pentachrome; bottom, picrosirius red under circularpolarized light). Fetal valves were composed mostly of glycosaminoglycans with low elastin and collagen. A trilaminar structure was apparent in children's valves but remained diffuse when compared with normal adult valve collagen in the fibrosa, glycosaminoglycans in the spongiosa, and elastin in the ventricularis. B: Progressive decrease in VIC density throughout life. C: Nuclei staining positively for Ki-67 (MIB-1) to detect proliferation were distributed diffusely through the cusp at 14 to 19 weeks of gestation, whereas Ki-67 and TUNEL-positive cells (marking apoptosis) at 20 to 39 weeks appeared predominantly near the arterial surface. VICs in adult valves showed undetectable levels of proliferating and apoptotic cells. D: Fetal valves at 14 to 19 weeks of gestation had higher VIC proliferation indices, with 90% reduction in adult valves. Apoptosis continued at a low rate throughout life. (Adapted from Aikawa E, Whittaker P, Farber M, et al. Human semilunar cardiac valve remodeling by activated cells from fetus to adult: implications for postnatal adaptation, pathology, and tissue engineering. *Circulation* 2006;113:1344-1352, with permission.)

but not AV valves (121). The hyperplastic semilunar valve phenotype is augmented when crossed to mice heterozygous for a null mutation in *Shp2* (122). Deletion of the EGF ligand, heparin binding (HB)-EGF, results in increased endocardial cushion size and cell proliferation of both semilunar and AV valves (123,124). These mice show prolonged Smad 1/5/8 phosphorylation and loss of phospholipase E (125), a downstream component of EGF and Ras signaling, and are similar to mice with a null mutation in inhibitory Smad6 (126). In contrast, mice lacking the Erb3 receptor die in midgestation of heart failure from hypoplastic semilunar and AV valve primordia (127). Null mutations in other EGFR ligands (EGF, amphiregulin, TGF- α) have no effect on valve formation. Finally, mice lacking Ephrin B2 also have thickened valves, and although the mechanism for this remains unclear, it will be interesting to determine how these signaling pathways intersect (128). The exact mechanism of regulation is likely to be context dependent and receptor specific and may involve the intersection of multiple growth factor signaling pathways.

In contrast to the thickened leaflets described above, disruption of signaling pathways converging on the transcription factor *Nfatc* revealed a requirement of this calcium-activated regulator. *Nfatc* is expressed specifically in the forming embryonic valves, and targeted deletion of *Nfatc* in mice results in absence of cardiac valve formation (129,130). Signaling via the phosphatase, calcineurin, results in nuclear translocation of *Nfatc* and is similarly involved in cardiac valve formation, in part through regulation of vascular endothelial growth factor (Vegf) expression in the endocardium (131).

The Notch signaling pathway is required for cell fate and differentiation decisions throughout the embryo (132), but

only recently have Notch proteins been implicated in vertebrate cardiac development. In fish and frogs, Notch appears to be involved in development of the endocardial cushions that contribute to valve tissue (133). In humans, heterozygous *NOTCH1* mutations disrupt normal development of the aortic valve and occasionally the mitral valve (134) (Fig. 24.9). The severity of valve disease associated with *NOTCH1* mutations in humans varies widely from mild disease in which the aortic valve has two rather than three leaflets (bicuspid aortic valve [BAV]) to severe defects in valve patency in utero, resulting in left ventricular growth failure. Consistent with this genetic finding, 15% of “normal” relatives of children with hypoplastic left heart syndrome (HLHS) have subclinical bicuspid aortic valves (BAVs) (135,136), suggesting that disruption of the NOTCH signaling cascade may underlie a spectrum of aortic valve disease. Although not specifically affecting valves, human mutations in *JAGGED1*, a NOTCH ligand, also cause outflow tract defects associated with the autosomal dominant disease, Alagille syndrome (127–139). The hairy-related family of transcriptional repressors (*Hrt1*, *Hrt2*, and *Hrt3*) may mediate the Notch signal during valve and myocardial development; however, their targets for repression remain unknown (140) (141).

GENETICS OF HUMAN SEPTAL DEFECTS

There has been an explosion in the identification of candidate genes potentially involved in the etiology of CHD and role of these genes impacts virtually every aspect of early cardiac development

Figure 24.9. Origin and genetic etiology of congenital heart disease. Three major classes of developmental defects are indicated: defects in atrial septation, in ventricular or atrioventricular septation, and in the great vessels. The types of congenital heart disease that occur within each class are indicated, with the associated mutated genes listed. Genes for which mutations result in discrete congenital heart diseases are indicated in *black*; genes that are mutated in congenital heart diseases that are part of a wider syndrome (also involving defects that are not associated with congenital heart disease) are indicated in *blue*. *CRELD1*, cysteine-rich with epidermal growth-factor-like domains 1; *KRAS*, ki-Ras; *PTPN11*, protein tyrosine phosphatase, nonreceptor type 11; *SOS1*, son of sevenless homologue 1. (Adapted from Bruneau BG. The developmental genetics of congenital heart disease. *Nature* 2008; 451:943–948, with permission.)

Atrial septation



ASD: *NKX2-5*
GATA4
TBX20
MYH6
TBX5

Ventricular septation and atrioventricular cushion formation



VSD: *NKX2-5*
GATA4
TBX20
TBX1
TBX5
AVSD: *PTPN11*
KRAS
SOS1
RAF1
CRELD1

Ebstein's, TA: *NKX2-5*

Great vessel formation and valvulogenesis



DORV, TGA: *NKX2-5*
THRAP2
PTA: *TBX1*
TOF: *NKX2-5*
NOTCH1
TBX1
JAG1
NOTCH2
AS and AC: *NOTCH1*
PTPN11
PS: *PTPN11*
JAG1
NOTCH2
BAV: *NOTCH*
HLHS: *NOTCH1*
PDA: *TFAP2B*

summarized in Figure 24.9. This has been extensively reviewed elsewhere (2,142–144) and in other chapters of this book. However, we would like to focus on the cardiac transcription factors NKX2.5, TBX5, and GATA4 as they particularly exemplify the synergy between human genetics and studies of model organisms for understanding the etiologic factors of human CHD. Numerous point mutations have been identified in NKX2.5 in families with atrial septal defects (ASDs) and progressive cardiac conduction abnormalities (145). Retrospective analysis of mice heterozygous for *Nkx2.5* disruption revealed a similar phenotype and progressive apoptotic loss of conduction cells, suggesting a likely mechanism for the human phenotype (146,147).

Humans with Holt–Oram syndrome, caused by mutations in *TBX5*, have cardiac anomalies similar to those with NKX2.5 mutations (atrial and ventricular septal defects) as well as limb abnormalities (148,149). Intriguingly, mutations responsible for defects in the heart and limbs are clustered in different regions of the protein, suggesting that TBX5 engages different downstream genes or cofactors in these tissues that depend on unique structural motifs in the protein. One potential cofactor is NKX2-5, as the two physically interact and cooperate to activate common target genes (150).

Like the NKX2.5 and TBX5 mutations, mutations in the zinc-finger-containing protein GATA4 cause similar atrial and ventricular septal defects in autosomal dominant nonsyndromic human pedigrees (151). GATA4 or related proteins are essential for cardiogenesis in flies, fish, and mice (152–155). Like NKX2.5, GATA4 and TBX5 also form a complex to regulate downstream genes, such as myosin heavy chain. Consistent with an important role for such combinatorial interactions, a familial GATA4 point mutation disrupts GATA4's ability to interact with TBX5 (134). Conversely, several human TBX5 mutations disrupt TBX5 interaction with GATA4, suggesting that the two cooperate in cardiac septation events (151). GATA4, TBX5, and NKX2-5 may form a common complex that is necessary for proper cardiac septation (Fig. 24.3). Disruption of any one of the three proteins or their interactions can result in atrial or ventricular septal defects. Although the compendium of septal genes regulated by these transcription factors is unknown, it is intriguing that mutations in human myosin heavy chain (MHC), a direct target of GATA4, TBX5, and NKX2-5, also cause ASDs (156). This observation suggests a possible mechanism by which these genes cause septation defects.

THE EPICARDIUM, CORONARY VASCULARIZATION

The origin of coronary vascular endothelium and formation of the coronary vessels has been an area of intense investigation (157). Several theories have evolved to explain coronary morphogenesis, which range from the sprouting of vessels from the aorta into developing myocardium to outgrowth of the endocardial lining of the heart to the epicardial vessels. Such theories have evolved from descriptive examination of the coronary ontogeny of various animals as well as human embryos. A critical component from most of these reports was the observation that coronary vessel formation was coordinately related to epicardial formation.

Several investigators have demonstrated that the epicardium originates as a villous projection of mesothelial cells in the area of the sinus venosus termed the proepicardial organ. This cluster of cells extends to the AV region and migrates out over the myocardial surface to completely encase the heart (158–162). In vitro data initially suggested that this villous or mesothelial projection might be one possible source of the coronary arteries (163). The correlation between epicardial formation and coronary ontogeny has been clarified in three series of experiments. Using retroviral

tagging of cells initially infected while in the pre-epicardial mesothelium, Mikawa and Fischman (164) were able to document that coronary smooth muscle cells, perivascular fibroblasts, and coronary endothelial cells all derive from independent precursors that arise outside the heart and that the endothelium of the coronary arteries and endocardium have different clonal origins. In complementary experiments, Poelmann et al. (165) used quail epicardial and liver tissue transplanted into chicken so that endothelial cells of quail origin could be identified. These experiments demonstrated that the entire coronary endothelial vasculature originated from an extracardiac source. In addition, this approach suggested that endothelial cells originating from the liver mesenchyme and located within this mesothelial projection or epicardial primordium used the subepicardial matrix to completely vascularize the developing heart. This subepicardial matrix is rich in fibronectin and vitronectin, a conducive ECM for vascular development E104–15. In a definitive set of experiments using retroviral injections directly into the proepicardial organ as well as proepicardial transplants, Mikawa and Gourdie (166) were able to demonstrate that this cluster of extracardiac cells contained differentiated endothelial cells, smooth muscles, and perivascular cells that would ultimately serve as the source of precursors for the coronary vascular bed. These experiments were later confirmed and expanded using a novel in vitro assay of epicardial differentiation (167). All of these experiments provide compelling evidence that coronary artery formation appears to be primarily a vasculogenic process. The coronary angioblasts originate from precursors located within the extracardiac pre-epicardial mesothelium and subsequently organize within the subepicardial matrix into the coronary vascular network. Recently, Red Horse et al. (168) used Cre-lox lineage tracing to confirm that in the mouse, another major contribution of coronary endothelial cells is derived from venous endothelial cells that enter the heart via sinus venosus/SHF and are subsequently reprogrammed to become arterial endothelial cells.

Interestingly, the epicardium is important not only for early developmental cardiac events, but plays a pivotal role in modulating cardiac repair after myocardial injury. Zhou (169) et al. recently demonstrated that while epicardial cells are normally quiescent in the adult, they become “activated” following myocardial injury. Activated epicardial cells undergo proliferation and undergo EMT, forming a layer of cells in the subepicardium that express smooth muscle cell and fibroblast markers and most importantly, secrete angiogenic factors that attenuate infarct size and improve heart function.

Whereas distal coronary development occurs by vasculogenesis, proximal coronary artery morphogenesis appears to result from an angiogenic process. Although traditionally the proximal coronary arteries were described as an outgrowth from the aorta to the epicardial surface of the heart, several investigators have recently shown that in fact the angiogenic process is in the reverse direction. Angiogenic sprouts from the subepicardial endothelial plexus form endothelial strands that grow into the aorta and develop multiple communications with all three cusps of the developing aortic valve (170–172). However, lumens develop only in facing semilunar sinuses with resorption of the strands to the nonfacing or noncoronary cusp (165). These observations have obvious implications for determining the factors that direct coronary artery anatomy in CHDs.

CONDUCTION SYSTEM MORPHOGENESIS

Despite the centrality of electrophysiologic abnormalities to CHDs, very little is known about development of the cardiac conduction system though significant progress has been made recently utilizing both chicken and mouse models (173). A central controversy has revolved around whether primary

conduction tissue differentiates from contractile myocytes or whether it is derived from “invading” neural crest. Using retroviral lineage tracing similar to that described above for defining the source of the coronary vasculature, Gourdie et al. (174) were able to show that pulse-generating conduction cells were derived from local recruitment of differentiated myocytes along the developing coronary artery system. This same group has gone on to demonstrate that endothelin produced by the developing coronary vasculature is a primary mediator of this recruitment of myocytes to the conduction lineage (175). Thus, initial development of the distal conduction system is independent of neural crest. However, the neural crest cells may exert a later, indirect effect on conduction system development via their role in maintaining the coronary vasculature (176,177). Establishment of epicardial to endocardial gradients of key channels is also important for appropriate depolarization and is in part regulated by the transcription factor *Irx5* (178). Networks of transcription factors involving *Nkx*, *T-box*, and *Irx* family members appear to control discrete aspects of the cardiac conduction system and are disrupted in human arrhythmias (55,179). These observations pave the way for a more detailed evaluation of the factors that regulate normal and potentially abnormal development of the conduction system.

ADULT CONSEQUENCES OF CARDIAC MALFORMATIONS

As human survivors of cardiac malformations ranging from simple ASDs to more complex heart disease enter their third and fourth decades of life, new cardiac disease processes are becoming apparent, including abnormal conduction of electricity within the heart and diminished contractile function of the heart. The cause of these secondary defects had in the past been ascribed to abnormal hemodynamics, but recent evidence suggests that the same genes that cause early morphologic defects in heart development might later be directly involved in cardiac dysfunction and cell lineage disturbances in adulthood (3).

For example, human and mouse mutations in *NKX2.5* not only cause a developmental ASD, but also progressively disrupt electrical conduction through the cardiac chambers and can result in sudden death later in life (145,179). The AV node, which serves as the essential site of electrical communication between the atria and ventricles, is smaller than normal in adult *Nkx2.5* mouse mutants; over time, the specialized muscle-derived conduction cells are lost and replaced by fibrotic tissue, resulting in progressive defects in electrical conduction (147).

Another example of a congenital heart malformation causing disease later in life involves the aortic valve. Worldwide, 1% of the population is born with a BAV, typically silent in childhood (1). However, one-third of BAVs develop premature age-dependent calcific stenosis, resulting in poorly mobile, nonfunctioning valves, often in the fifth, sixth, or seventh decades of life (180). As a result, calcific aortic stenosis (AS) is the third leading cause of heart disease in adults and requires >30,000 surgical valve replacements per year in the United States. The recent discovery that *NOTCH1* mutations in humans cause BAVs and later calcification provides firm genetic evidence that the early developmental and later degenerative disease share a common genetic cause (134). Some family members with *NOTCH1* mutations had normal tricuspid aortic valves but still developed calcification, supporting the idea that the premature and severe calcification was primarily due to the genetic mutation itself rather than to hemodynamic effects on the valve leaflets.

Calcified human valves are characterized by ectopic osteoblast-specific gene expression suggesting a cell fate change of mesenchymal or inflammatory cells (180,181). Interestingly,

developing heart valves have a surprisingly similar gene expression profile to osteoblast progenitor cells (182). *Notch1* can repress a central transcriptional regulator of osteoblast cell fate, *Runx2/Cbfa1* (183), suggesting a potential mechanism through which *NOTCH1* normally suppresses calcification in the valve tissue (134). It will be interesting to determine if polymorphisms in *NOTCH1* are associated with altered risk of aortic valve or even vascular calcification, given the similar osteoblast gene expression in atherosclerotic vascular smooth muscle (184). If so, it is attractive to imagine effective preventive interventions over decades with pharmaceuticals, such as statins, to lower levels of cholesterol, a well-known risk factor for calcification (185).

CARDIAC STEM CELL AND REGENERATIVE APPROACHES

The notion that genes involved in the early formation of the heart may be redeployed to help protect, repair, or regenerate cardiac muscle has been a driving force in efforts to understand early developmental pathways (186). Reports describing niches of small, noncardiomyocyte populations in the postnatal heart that on isolation in culture could differentiate into cardiac muscle and endothelial cells initially generated considerable excitement that the heart, like other organs, may have a resident pool of progenitor cells (187–189). A subsequent population of progenitors expressing the developmental transcription factor *Isl1* further suggested an important connection between postnatal progenitor cells and an early developmental pathway regulating cardiomyocyte precursors. As described earlier, *Isl1* is expressed in SHF cells before they differentiate into myocytes and is down-regulated on expression of sarcomeric proteins. Cell fate studies suggest that cells derived from *Isl1*⁺ progenitors populate most of the RV and outflow tract and *Isl1* is required for the formation of these regions; some cells derived from these *Isl1*⁺ cells also contribute to the atria and left ventricle. In mice and humans, niches of *Isl1*⁺ cells are detectable in the early postnatal heart and may be remnants of developmental progenitor cells among terminally differentiated myocytes (27). However, isolation and characterization of these cells has proved elusive and the clinical utility has remained minimal. Interestingly, intrinsic cardiac progenitor cells appear to be much more abundant in neonatal human hearts raising the possibility that utilization of the cells may be particularly advantageous in treating congenital cardiac abnormalities in the early postnatal period (190).

Perhaps the most exciting observation in terms of developing cells that might serve as a source for myocardial regeneration and repair was made by Yamanaka (191), and colleagues, who demonstrated that skin fibroblasts from mice and humans (192) could be reprogrammed or “induced” to form pluripotent cells (iPS) via infection with viruses carrying four transcription factors (*Oct 4*, *Klf4*, *Myc*, *Sox2*) that were known to regulate pluripotency of ES cells. These cells could then be differentiated into various cell types representing derivatives from all three germ layers, including cardiomyocytes. The ability to derive iPS cells from patient that can then be differentiated to specific cell lineages has provided never before realized potential for disease-specific modeling, therapeutic pharmacologic screening, and myocardial-specific regeneration. Exploiting and maximizing the potential of iPS cells will require mining the extensive foundation of knowledge that has resulted from in-depth studies of embryonic cardiac development and ES cell differentiation (193) (Fig. 24.10). Interestingly, recent preliminary studies suggest that it may be possible to derive myocytes directly from fibroblasts (direct reprogramming) without having to first generate a pluripotent intermediate (194). This exciting observation raises the possibility of transforming

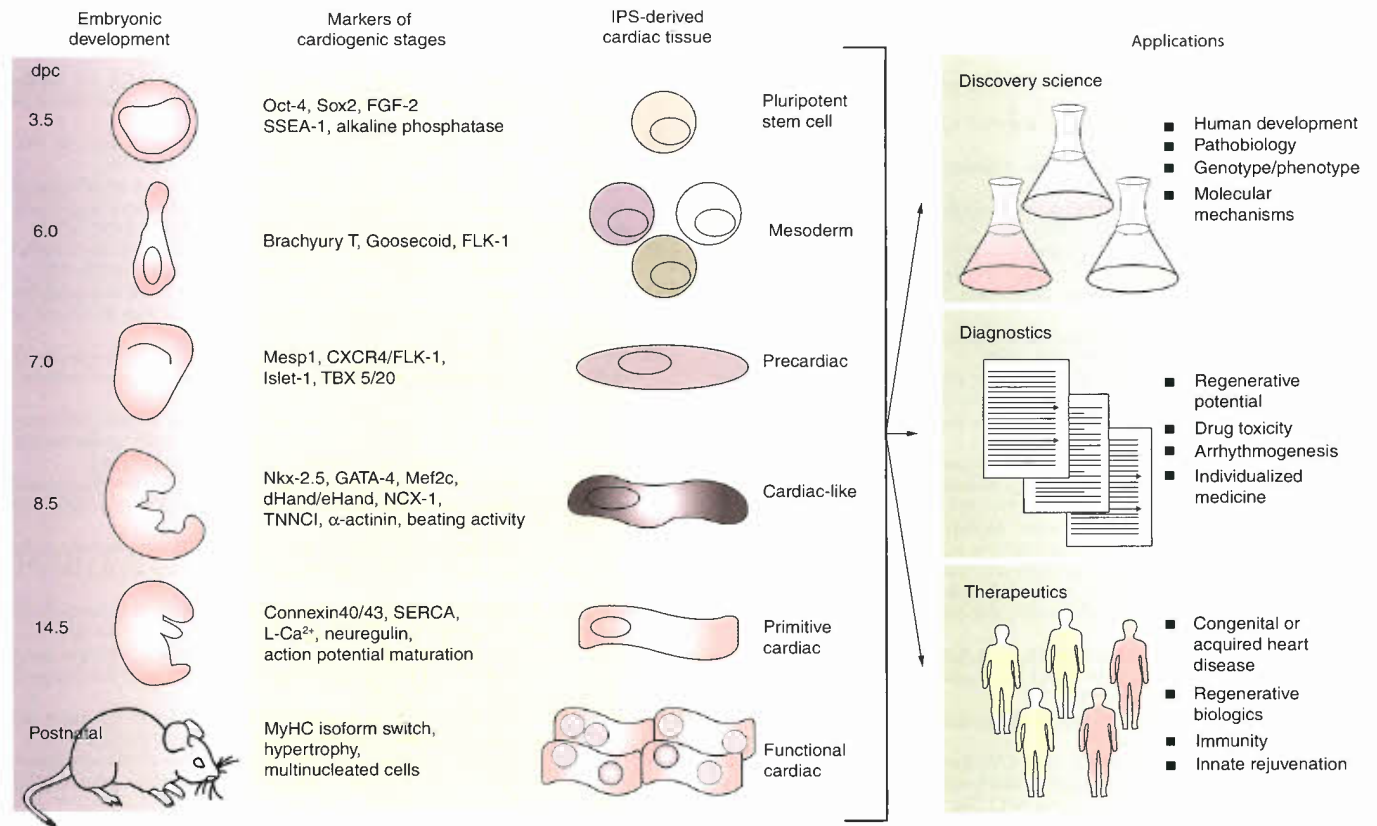


Figure 24.10. The developmental process serves as a guide for stage-specific cardiogenesis, which is characterized by changes in embryonic morphology. The gene-expression profiles that correlate with embryonic stages and differentiation of pluripotent stem cells provide a gauge for acquired cardiogenic potential from mesoderm to cardiac tissues. iPS cells from both humans and mice have the potential to mature through all of the early stages of cardiogenesis. Whether they can reach a mature, differentiated phenotype remains to be determined. iPS cells that can be programmed to distinct stages of cardiogenesis in order to secure reproducible therapeutic outcomes, validate diagnostic criteria, or provide reproducible discovery model systems are critical in order to realize the potential of these cells in discovery, diagnosis, and therapeutic intervention. dpc, days post coitum; iPS, induced pluripotent stem; MyHC, myosin heavy chain. (Adapted from Nelson TJ, Martinex-Fernandez A, Terzic A. Induced pluripotent stem cells: developmental biology to regenerative medicine. *Nat Rev Cardiol* 2010;7:700–710, with permission.)

cardiac fibroblast into myocytes in situ providing a more immediate therapy for injured myocardium.

SUMMARY

The field of cardiac developmental biology has progressed rapidly over the last decade, and the heart is now one of the best understood organs at the molecular, physiologic, and anatomic levels. Advances in human genetic tools have also led to a deeper understanding of the importance of developmental pathways in human disease. CHD can now be conceived as not only a defect of morphogenesis, but in some cases, a failure of differentiation among subsets of lineages that contribute to the heart. We are now embarking on a phase in which knowledge of developmental pathways and high-throughput methods of genotyping rare and common gene variants should allow rigorous investigation into the causes of human heart disease. With the increasing recognition that CHD has a significant genetic contribution, we can now imagine that genetic variation underlies both the morphogenetic defect and the predisposition to long-term consequences that will affect clinical outcomes for the millions of CHD survivors. Thus, vigorous efforts to identify genetic variation associated with CHD and outcome will be essential as therapeutic

or preventive measures to alter the course of disease may be possible throughout childhood and in the adult. It may even be conceivable to eventually predict genetic risk among parents and focus preventive strategies on those at greatest risk to transmit disease vertically. The efficacy of folic acid in prevention of neural tube defects provides hope for similar prevention of congenital heart disease (195,196).

As the next phase of disease-related biology evolves, parallel advances in stem cell biology should usher in an era of new approaches. It is exciting to realize that we are now able to generate disease-specific iPS cell lines for mechanistic studies of disease etiology and development of patient-specific progenitor cells for ultimate treatment modalities. Although it may become possible to guide progenitor cells into a cardiac lineage based on our knowledge of early developmental pathways, many hurdles must be overcome for therapeutic use. Issues such as cell expansion, delivery, incorporation, electrical coupling, and safety remain to be addressed. Despite these significant challenges, there is reason for optimism as we continue to unravel the mysteries surrounding the lineage determination, differentiation, and morphogenesis of cardiac cells. However realization of the potential of these studies will demand a closer collaboration between clinicians and basic scientists and will require the development of physician scientists with an intimate knowledge of developmental biology, genetics, and clinical congenital heart disease.

REFERENCES

- Hoffman JI, Kaplan S. The incidence of congenital heart disease. *J Am Coll Cardiol* 2002;39:1890–1900.
- Bruneau BG. The developmental genetics of congenital heart disease. *Nature* 2008;451:943–948.
- Srivastava D. Heart disease: an ongoing genetic battle? *Nature* 2004;429:819–822.
- Srivastava D, Ivey KN. Potential of stem cell-based therapies for heart disease. *Nature* 2006;441:1097–1099.
- AHA. *Heart Disease and Stroke Statistics—2011 Update*. Dallas, TX: AHA.
- DeHaan RL. Morphogenesis of the vertebrate heart. In: DeHaan RL, Ursprung H, eds. *Organogenesis*. New York, NY: Holt, Reinhart & Winston, 1965:377–420.
- Srivastava D. Making or breaking the heart: from lineage determination to morphogenesis. *Cell* 2006;126:1037–1048.
- Vincen SD, Buckingham ME. How to make a heart: the origin and regulation of cardiac progenitor cells. *Curr Top Dev Biol* 2010;90:1–41.
- Olson EN. Gene regulatory networks in the evolution and development of the heart. *Science* 2006;313:1922–1927.
- Kouskoff V, Lacaud G, Schwantz S, et al. Sequential development of hematopoietic and cardiac mesoderm during embryonic stem cell differentiation. *Proc Natl Acad Sci USA* 2005;102:13170–13175.
- Kattman SJ, Huber TL, Keller GM. Multipotent flk-1⁺ cardiovascular progenitor cells give rise to the cardiomyocyte, endothelial, and vascular smooth muscle lineages. *Dev Cell* 2006;11:723–732.
- Moretti A, Caron L, Nakano A, et al. Multipotent embryonic isl1⁺ progenitor cells lead to cardiac, smooth muscle, and endothelial cell diversification. *Cell* 2006;127:1151–1165.
- Misfeldt AM, Boyle SC, Tompkins KL, et al. Endocardial cells are a distinct endothelial lineage derived from Flk1⁺ multipotent cardiovascular progenitors. *Dev Biol* 2009;333:78–89.
- Srivastava D, Olson EN. A genetic blueprint for cardiac development. *Nature* 2000;407:221–226.
- Meilhac SM, Esner M, Kelly RG, et al. The clonal origin of myocardial cells in different regions of the embryonic mouse heart. *Dev Cell* 2004;6:685–698.
- Kelly RG, Brown NA, Buckingham ME. The arterial pole of the mouse heart forms from Fgf10-expressing cells in pharyngeal mesoderm. *Dev Cell* 2001;1:435–440.
- Waldo KL, Kumiski DH, Wallis KT, et al. Conotruncal myocardium arises from a ventral heart field. *Development* 2001;128:3179–3188.
- Mjaatvedt CH, Nakaoka T, Moreno-Rodriguez R, et al. The outflow tract of the heart is recruited from a novel heart-forming field. *Dev Biol* 2001;238:97–109.
- Zaffran S, Frasch M. Early signals in cardiac development. *Circ Res* 2002;91:457–469.
- Schultheiss TM, Burch JB, Lassar AB. A role for bone morphogenetic proteins in the induction of cardiac myogenesis. *Genes Dev* 1997;11:451–462.
- Schneider VA, Mercola M. Wnt antagonism initiates cardiogenesis in *Xenopus laevis*. *Genes Dev* 2001;15:304–315.
- Marvin MJ, Di Rocco G, Gardiner A, et al. Inhibition of Wnt activity induces heart formation from posterior mesoderm. *Genes Dev* 2001;15:316–327.
- Cai CL, Liang X, Shi Y, et al. Isl1 identifies a cardiac progenitor population that proliferates prior to differentiation and contributes a majority of cells to the heart. *Dev Cell* 2003;5:877–889.
- Martin-Puig S, Wang Z, Chien KR. Lives of a heart cell: tracing the origins of cardiac progenitors. *Cell Stem Cell* 2008;2:320–331.
- Garratt AN, Ozcelik C, Birchmeier C. ErbB2 pathways in heart and neural diseases. *Trends Cardiovasc Med* 2003;13:80–86.
- Stuckmann I, Evans S, Lassar AB. Erythropoietin and retinoic acid, secreted from the epicardium, are required for cardiac myocyte proliferation. *Dev Biol* 2003;255:334–349.
- von Both I, Silvestri C, Erdemir T, et al. Foxh1 is essential for development of the anterior heart field. *Dev Cell* 2004;7:331–345.
- Laugwitz KL, Moretti A, Lam J, et al. Postnatal isl1⁺ cardioblasts enter fully differentiated cardiomyocyte lineages. *Nature* 2005;433:647–653.
- Stevens KN, Hakonarson H, Kim CE, et al. Common variation in ISL1 confers genetic susceptibility for human congenital heart disease. *PLoS One* 2010;5:e10855.
- Firulli AB, Olson EN. Modular regulation of muscle gene transcription: a mechanism for muscle cell diversity. *Trends Genet* 1997;13:364–369.
- Srivastava D. The bHLH proteins, dHAND and eHAND in cardiac development. In: Harvey RP, Olson EN, Schulz RA, et al., eds. *Genetic Control of Heart Development*. Strasbourg: HFSP, 1997.
- Yamagishi H, Yamagishi C, Nakagawa O, et al. The combinatorial activities of Nkx2.5 and dHAND are essential for cardiac ventricle formation. *Dev Biol* 2001;239:190–203.
- Lin Q, Srivastava D, Olson E. A transcriptional pathway for cardiac development. *Cold Spring Harb Symp Quant Biol* 1997;62:405–411.
- Dodou E, Verzi MP, Anderson JP, et al. Mef2c is a direct transcriptional target of ISL1 and GATA factors in the anterior heart field during mouse embryonic development. *Development* 2004;131:3931–3942.
- Zeisberg EM, Ma Q, Jurasek AL, et al. Morphogenesis of the right ventricle requires myocardial expression of Gata4. *J Clin Invest* 2005;115:1522–1531.
- Lindsay EA, Botta A, Jurecic V, et al. Congenital heart disease in mice deficient for the DiGeorge syndrome region. *Nature* 1999;401:379–383.
- Lindsay EA, Vitelli F, Su H, et al. Tbx1 haploinsufficiency in the DiGeorge syndrome region causes aortic arch defects in mice. *Nature* 2001;410:97–101.
- Mersch S, Funke B, Epstein JA, et al. TBX1 is responsible for cardiovascular defects in velo-cardio-facial/DiGeorge syndrome. *Cell* 2001;104:619–629.
- Jerome LA, Papaioannou VE. DiGeorge syndrome phenotype in mice mutant for the T-box gene, Tbx1. *Nat Genet* 2001;27:286–291.
- Hu T, Yamagishi H, Maeda J, et al. Tbx1 regulates fibroblast growth factors in the anterior heart field through a reinforcing autoregulatory loop involving forkhead transcription factors. *Development* 2004;131:5491–5502.
- Xu H, Morishima M, Wylie JN, et al. Tbx1 has a dual role in the morphogenesis of the cardiac outflow tract. *Development* 2004;131:3217–3227.
- Garg V, Yamagishi C, Hu T, et al. Tbx1, a DiGeorge syndrome candidate gene, is regulated by sonic hedgehog during pharyngeal arch development. *Dev Biol* 2001;235:62–73.
- Yamagishi H, Maeda J, Hu T, et al. Tbx1 is regulated by tissue-specific forkhead proteins through a common Sonic hedgehog-responsive enhancer. *Genes Dev* 2003;17:269–281.
- Kume T, Jiang H, Topczewska JM, et al. The murine winged helix transcription factors, Foxc1 and Foxc2, are both required for cardiovascular development and somitogenesis. *Genes Dev* 2001;15:2470–2482.
- Abu-Issa R, Smyth G, Smoak I, et al. Fgf8 is required for pharyngeal arch and cardiovascular development in the mouse. *Development* 2002;129:4613–4625.
- Frank DU, Fotheringham LK, Brewer JA, et al. An Fgf8 mouse mutant phenocopies human 22q11 deletion syndrome. *Development* 2002;129:4591–4603.
- Srivastava D. HAND proteins: molecular mediators of cardiac development and congenital heart disease. *Trends Cardiovasc Med* 1999;9:11–18.
- Biben C, Harvey RP. Homeodomain factor Nkx2-5 controls left/right asymmetric expression of bHLH gene eHand during murine heart development. *Genes Dev* 1997;11:1357–1369.
- Bodmer R. The gene tinman is required for specification of the heart and visceral muscles in *Drosophila*. *Development* 1993;118:719–729.
- Lyons I, Parsons LM, Hartley L, et al. Myogenic and morphogenetic defects in the heart tubes of murine embryos lacking the homeo box gene Nkx2-5. *Genes Dev* 1995;9:1654–1666.
- Tanaka M, Chen Z, Bartunkova S, et al. The cardiac homeobox gene Csx/Nkx2.5 lies genetically upstream of multiple genes essential for heart development. *Development* 1999;126:1269–1280.
- McFadden DG, Barbosa AC, Richardson JA, et al. The Hand1 and Hand2 transcription factors regulate expansion of the embryonic cardiac ventricles in a gene dosage-dependent manner. *Development* 2005;132:189–201.
- Yelon D, Ticho B, Halpern ME, et al. The bHLH transcription factor hand2 plays parallel roles in zebrafish heart and pectoral fin development. *Development* 2000;127:2573–2582.
- Han Z, Yi P, Li X, et al. Hand, an evolutionarily conserved bHLH transcription factor required for *Drosophila* cardiogenesis and hematopoiesis. *Development* 2006;133:1175–1182.
- Pereira FA, Qiu Y, Zhou G, et al. The orphan nuclear receptor COUP-TFII is required for angiogenesis and heart development. *Genes Dev* 1999;13:1037–1049.
- Bruneau BG, Nemer G, Schmitt JP, et al. A murine model of Holt-Oram syndrome defines roles of the T-box transcription factor Tbx5 in cardiogenesis and disease. *Cell* 2001;106:709–721.
- Bao ZZ, Bruneau BG, Seidman JG, et al. Regulation of chamber-specific gene expression in the developing heart by Irx4. *Science* 1999;283:1161–1164.
- Gottlieb PD, Pierce SA, Sims RJ, et al. Bop encodes a muscle-restricted protein containing MYND and SET domains and is essential for cardiac differentiation and morphogenesis. *Nat Genet* 2002;31:25–32.
- Phan D, Rasmussen TL, Nakagawa O, et al. BOP, a regulator of right ventricular heart development, is a direct transcriptional target of MEF2C in the developing heart. *Development* 2005;132:2669–2678.
- Chang S, McKinsey TA, Zhang CL, et al. Histone deacetylases 5 and 9 govern responsiveness of the heart to a subset of stress signals and play redundant roles in heart development. *Mol Cell Biol* 2004;24:8467–8476.
- Lickert H, Takeuchi JK, Von Both I, et al. Baf60c is essential for function of BAF chromatin remodelling complexes in heart development. *Nature* 2004;432:107–112.
- Zhao Y, Samal E, Srivastava D. Serum response factor regulates a muscle-specific microRNA that targets Hand2 during cardiogenesis. *Nature* 2005;436:214–220.
- Kwon C, Han Z, Olson EN, et al. MicroRNA1 influences cardiac differentiation in *Drosophila* and regulates Notch signaling. *Proc Natl Acad Sci USA* 2005;102:18986–18991.
- Ivey KN, Srivastava D. MicroRNAs as regulators of differentiation and cell fate decisions. *Cell Stem Cell* 2010;7:36–41.
- Chen JF, Mandel EM, Thomson JM, et al. The role of microRNA-1 and microRNA-133 in skeletal muscle proliferation and differentiation. *Nat Genet* 2006;38:228–233.
- Zhao Y, Ransom JF, Li A, et al. Dysregulation of cardiogenesis, cardiac conduction, and cell cycle in mice lacking miRNA-1-2. *Cell* 2007;129:303–317.
- Lim LP, Lau NC, Garrett-Engle P, et al. Microarray analysis shows that some microRNAs downregulate large numbers of target mRNAs. *Nature* 2005;433:769–773.

67. Sokol NS, Ambros V. Mesodermally expressed *Drosophila* microRNA-1 is regulated by Twist and is required in muscles during larval growth. *Genes Dev.* 2005;19:2343–2354.
68. King IN, Qian L, Liang J, et al. A genome-wide screen reveals a role for microRNA-1 in modulating cardiac cell polarity. *Dev Cell* 2011;20:497–510.
69. Ivey KN, Muth A, Arnold J, et al. MicroRNA regulation of cell lineages in mouse and human embryonic stem cells. *Cell Stem Cell* 2008;2:219–229.
70. Liu N, Bezprozvannaya S, Williams AH, et al. microRNA-133a regulates cardiomyocyte proliferation and suppresses smooth muscle gene expression in the heart. *Genes Dev.* 2008;22:3242–3254.
71. Han M, Toli J, Abdellatif M. MicroRNAs in the cardiovascular system. *Curr Opin Cardiol* 2011;26:181–189.
72. Wilson KD, Hu S, Venkatasubrahmanyam S, et al. Dynamic microRNA expression programs during cardiac differentiation of human embryonic stem cells: role for miR-499. *Circ Cardiovasc Genet* 2010;3:426–435.
73. Cordes KR, Sheehy NT, White MP, et al. miR-145 and miR-143 regulate smooth muscle cell fate and plasticity. *Nature* 2009;460:705–710.
74. Zhang C. MicroRNA-145 in vascular smooth muscle cell biology: a new therapeutic target for vascular disease. *Cell Cycle* 2009;8:3469–3473.
75. Moon A. Mouse models of congenital cardiovascular disease. *Curr Top Dev Biol* 2008;84:171–248.
76. Moorman AF, Christoffels VM. Cardiac chamber formation: development, genes, and evolution. *Physiol Rev* 2003;83:1223–1267.
77. Tucker A, Matthews K, Sharpe P. Transformation of tooth type induced by inhibition of BMP signaling. *Science* 1998;282:1136–1138.
78. Harrelson Z, Kelly RG, Goldin SN, et al. Tbx2 is essential for patterning the atrioventricular canal and for morphogenesis of the outflow tract during heart development. *Development* 2004;131:5041–5052.
79. Takeuchi JK, Mileikowska M, Koshiba-Takeuchi K, et al. Tbx20 dose-dependently regulates transcription factor networks required for mouse heart and motoneuron development. *Development* 2005;132:2463–2474.
80. Singh MK, Christoffels VM, Dias JM, et al. Tbx20 is essential for cardiac chamber differentiation and repression of Tbx2. *Development* 2005;132:2697–2707.
81. Stennard FA, Costa MW, Lai D, et al. Murine T-box transcription factor Tbx20 acts as a repressor during heart development, and is essential for adult heart integrity, function and adaptation. *Development* 2005;132:2451–2462.
82. Brown NA, Wolpert L. The development of handedness in left/right asymmetry. *Development* 1990;109:1–9.
83. Mjaatvedt CH, Yamamura H, Wessels A, et al. Mechanisms of segmentation, septation, and remodeling of the tubular heart: endocardial cushion fate and cardiac looping. In: Harvey RP, Rosenthal N, eds. *Heart Development*. San Diego, CA: Academic Press, 1999:530.
84. Palmer AR. Symmetry breaking and the evolution of development. *Science* 2004;306:828–833.
85. Piedra ME, Icardo JM, Albajar M, et al. Pitx2 participates in the late phase of the pathway controlling left-right asymmetry. *Cell* 1998;94:319–324.
86. Kiousi C, Briata P, Baek SH, et al. Identification of a Wnt/Dvl/beta-Catenin → Pitx2 pathway mediating cell-type-specific proliferation during development. *Cell* 2002;111:673–685.
87. Nowotschin S, Liao J, Gage PJ, et al. Tbx1 affects asymmetric cardiac morphogenesis by regulating Pitx2 in the secondary heart field. *Development* 2006;133:1565–1573.
88. Kosaki R, Gebbia M, Kosaki K, et al. Left-right axis malformations associated with mutations in ACVR2B, the gene for human activin receptor type IIB. *Am J Med Genet* 1999;82:70–76.
89. Gebbia M, Ferrero GB, Pilia G, et al. X-linked situs abnormalities result from mutations in ZIC3. *Nat Genet* 1997;17:305–308.
90. Sadler TW, ed. *Langman's Medical Embryology*. Baltimore, MD: Williams & Wilkins, 1995.
91. Hutson MR, Kirby ML. Neural crest and cardiovascular development: a 20-year perspective. *Birth Defects Res C Embryo Today* 2003;69:2–13.
92. Le Douarin NM, Creuzet S, Couly G, et al. Neural crest cell plasticity and its limits. *Development* 2004;131:4637–4650.
93. Satoda M, Zhao F, Diaz GA, et al. Mutations in TFAP2B cause Char syndrome, a familial form of patent ductus arteriosus. *Nat Genet* 2000;25:42–46.
94. Yagi H, Furutani Y, Hamada H, et al. Role of TBX1 in human del22q11.2 syndrome. *Lancet* 2003;362:1366–1373.
95. Combs MD, Yutzey KE. Heart valve development: regulatory networks in development and disease. *Circ Res* 2009;105:408–421.
96. Hinton RB, Yutzey KE. Heart valve structure and function in development and disease. *Annu Rev Physiol* 2011;73:29–46.
97. Beis D, Bartman T, Jin SW, et al. Genetic and cellular analyses of zebrafish atrioventricular cushion and valve development. *Development* 2005;132:4193–4204.
98. Ma L, Lu MF, Schwartz RJ, et al. Bmp2 is essential for cardiac cushion epithelial-mesenchymal transition and myocardial patterning. *Development* 2005;132:5601–5611.
99. Gausin V, Van de Putte T, Mishina Y, et al. Endocardial cushion and myocardial defects after cardiac myocyte-specific conditional deletion of the bone morphogenetic protein receptor ALK3. *Proc Natl Acad Sci USA* 2002;99:2878–2883.
100. Kim RY, Robertson EJ, Soloway MJ. Bmp6 and Bmp7 are required for cushion formation and septation in the developing mouse heart. *Dev Biol* 2001;235:449–466.
101. Brown CB, Boyer AS, Runyan RB, et al. Requirement of type III TGF-beta receptor for endocardial cell transformation in the heart. *Science* 1999;283:2080–2082.
102. DeLaughter DM, Saint-Jean L, Baldwin HS, et al. What chick and mouse models have taught us about the role of the endocardium in congenital heart disease. *Birth Defects Res A Clin Mol Teratol* 2011;91:511–525.
103. Hurler JM, Icardo JM, Ojeda JL. Compositional and structural heterogeneity of the cardiac jelly of the chick embryo tubular heart: a TEM, SEM and histochemical study. *J Embryol Exp Morphol* 1980;56:211–223.
104. Maron BJ, Hutchins GM. The development of the semilunar valves in the human heart. *Am J Pathol* 1974;74:331–344.
105. Hinton RB Jr, Lincoln J, Deutsch GH, et al. Extracellular matrix remodeling and organization in developing and diseased aortic valves. *Circ Res* 2006;98:1431–1438.
106. Aikawa E, Whittaker P, Farber M, et al. Human semilunar cardiac valve remodeling by activated cells from fetus to adult: implications for postnatal adaptation, pathology, and tissue engineering. *Circulation* 2006;113:1344–1352.
107. Rabkin E, Aikawa M, Stone JR, et al. Activated interstitial myofibroblasts express catabolic enzymes and mediate matrix remodeling in myxomatous heart valves. *Circulation* 2001;104:2525–2532.
108. Rabkin-Aikawa E, Farber M, Aikawa M, et al. Dynamic and reversible changes of interstitial cell phenotype during remodeling of cardiac valves. *J Heart Valve Dis* 2004;13:841–847.
109. Paruchuri S, Yang JH, Aikawa E, et al. Human pulmonary valve progenitor cells exhibit endothelial/mesenchymal plasticity in response to vascular endothelial growth factor-A and transforming growth factor-beta2. *Circ Res* 2006;99:861–869.
110. Yutzey KE, Colbert M, Robbins J. Ras-related signaling pathways in valve development: Ebb and flow. *Physiology (Bethesda)* 2005;20:390–397.
111. Gelb BD, Tartaglia M. Noonan syndrome and related disorders: dysregulated RAS-mitogen activated protein kinase signal transduction. *Hum Mol Genet* 2006;15:R220–R226.
112. Gitler AD, Zhu Y, Ismat FA, et al. Nf1 has an essential role in endothelial cells. *Nat Genet* 2003;33:75–79.
113. Lakkis MM, Epstein JA. Neurofibromin modulation of ras activity is required for normal endocardial-mesenchymal transformation in the developing heart. *Development* 1998;125:4359–4367.
114. Lin AE, Birch PH, Korf BR, et al. Cardiovascular malformations and other cardiovascular abnormalities in neurofibromatosis 1. *Am J Med Genet* 2000;95:108–117.
115. Tartaglia M, Gelb BD. Noonan syndrome and related disorders: genetics and pathogenesis. *Annu Rev Genomics Hum Genet* 2005;6:45–68.
116. Araki T, Mohi MG, Ismat FA, et al. Mouse model of Noonan syndrome reveals cell type- and gene dosage-dependent effects of Ptpn11 mutation. *Nat Med* 2004;10:849–857.
117. Tartaglia M, Mehler EL, Goldberg R, et al. Mutations in PTPN11, encoding the protein tyrosine phosphatase SHP-2, cause Noonan syndrome. *Nat Genet* 2001;29:465–468.
118. Tartaglia M, Kalidas K, Shaw A, et al. PTPN11 mutations in Noonan syndrome: molecular spectrum, genotype-phenotype correlation, and phenotypic heterogeneity. *Am J Hum Genet* 2002;70:1555–1563.
119. Roberts AE, Araki T, Swanson KD, et al. Germline gain-of-function mutations in SOS1 cause Noonan syndrome. *Nat Genet* 2007;39:70–74.
120. Tartaglia M, Martinelli S, Stella L, et al. Diversity and functional consequences of germline and somatic PTPN11 mutations in human disease. *Am J Hum Genet* 2006;78:279–290.
121. Sibilia M, Wagner B, Hoebertz A, et al. Mice humanised for the EGF receptor display hypomorphic phenotypes in skin, bone and heart. *Development* 2003;130:4515–4525.
122. Chen B, Bronson RT, Klamann LD, et al. Mice mutant for Egfr and Shp2 have defective cardiac semilunar valvulogenesis. *Nat Genet* 2000;24:296–299.
123. Iwamoto R, Yamazaki S, Asakura M, et al. Heparin-binding EGF-like growth factor and ErbB signaling is essential for heart function. *Proc Natl Acad Sci USA* 2003;100:3221–3226.
124. Jackson LF, Qiu TH, Sunnarborg SW, et al. Defective valvulogenesis in HB-EGF and TACE-null mice is associated with aberrant BMP signaling. *EMBO J* 2003;22:2704–2716.
125. Tadano M, Edamatsu H, Minamisawa S, et al. Congenital semilunar valvulogenesis defect in mice deficient in phospholipase C epsilon. *Mol Cell Biol* 2005;25:2191–2199.
126. Galvin KM, Donovan MJ, Lynch CA, et al. A role for smad6 in development and homeostasis of the cardiovascular system. *Nat Genet* 2000;24:171–174.
127. Erickson SL, O'Shea KS, Ghaboosi N, et al. ErbB3 is required for normal cerebellar and cardiac development: a comparison with ErbB2- and heregulin-deficient mice. *Development* 1997;124:4999–5011.
128. Cowan CA, Yokoyama N, Saxena A, et al. Ephrin-B2 reverse signaling is required for axon pathfinding and cardiac valve formation but not early vascular development. *Dev Biol* 2004;271:263–271.
129. Ranger AM, Grusby MJ, Hodge MR, et al. The transcription factor NF-ATc is essential for cardiac valve formation. *Nature* 1998;392:186–190.
130. de la Pompa JL, Timmerman LA, Takimoto H, et al. Role of the NF-ATc transcription factor in morphogenesis of cardiac valves and septum. *Nature* 1998;392:182–186.
131. Chang CP, Neilson JR, Bayle JH, et al. A field of myocardial-endocardial NFAT signaling underlies heart valve morphogenesis. *Cell* 2004;118:649–663.
132. Artavanis-Tsakonas S, Rand MD, Lake RJ. Notch signaling: cell fate control and signal integration in development. *Science* 1999;284:770–776.

133. Timmerman LA, Grego-Bessa J, Raya A, et al. Notch promotes epithelial-mesenchymal transition during cardiac development and oncogenic transformation. *Genes Dev* 2004;18:99–115.
134. Garg V, Muth AN, Ransom JF, et al. Mutations in NOTCH1 cause aortic valve disease. *Nature* 2005;437:270–274.
135. Cripe L, Andelfinger G, Martin LJ, et al. Bicuspid aortic valve is heritable. *J Am Coll Cardiol* 2004;44:138–143.
136. Loffredo CA, Chokkalingam A, Sill AM, et al. Prevalence of congenital cardiovascular malformations among relatives of infants with hypoplastic left heart, coarctation of the aorta, and d-transposition of the great arteries. *Am J Med Genet A* 2004;124:225–230.
137. Li L, Krantz ID, Deng Y, et al. Alagille syndrome is caused by mutations in human Jagged1, which encodes a ligand for Notch1. *Nat Genet* 1997;16:243–251.
138. Oda T, Elkahoul AG, Pike BL, et al. Mutations in the human Jagged1 gene are responsible for Alagille syndrome. *Nat Genet* 1997;16:235–242.
139. Krantz ID, Smith R, Colliton RP, et al. Jagged1 mutations in patients ascertained with isolated congenital heart defects. *Am J Med Genet* 1999;84:56–60.
140. Nakagawa O, Nakagawa M, Richardson JA, et al. HRT1, HRT2, and HRT3: a new subclass of bHLH transcription factors marking specific cardiac, somitic, and pharyngeal arch segments. *Dev Biol* 1999;216:72–84.
141. Kokubo H, Miyagawa-Tomita S, Johnson RL, Hesr, a mediator of the Notch signaling, functions in heart and vessel development. *Trends Cardiovasc Med* 2005;15:190–194.
142. Wessels MW, Williams PJ. Genetic factors in non-syndromic congenital heart malformations. *Clin Genet* 2010;78:103–123.
143. Wolf M, Basson CT. The molecular genetics of congenital heart disease: a review of recent developments. *Curr Opin Cardiol* 2010;25:192–197.
144. Richards AA, Garg V. Genetics of congenital heart disease. *Curr Card Rev* 2010;6:91–97.
145. Schott JJ, Benson DW, Basson CT, et al. Congenital heart disease caused by mutations in the transcription factor NKX2-5. *Science* 1998;281:108–111.
146. Biben C, Weber R, Kesteven S, et al. Cardiac septal and valvular dysmorphogenesis in mice heterozygous for mutations in the homeobox gene *Nkx2-5*. *Circ Res* 2000;87:888–895.
147. Jay PY, Harris BS, Maguire CT, et al. *Nkx2-5* mutation causes anatomic hypoplasia of the cardiac conduction system. *J Clin Invest* 2004;113:1130–1137.
148. Basson CT, Bachinsky DR, Lin RC, et al. Mutations in human *TBX5* cause limb and cardiac malformation in Holt-Oram syndrome. *Nat Genet* 1997;15:30–35.
149. Mori AD, Bruneau BG. *TBX5* mutations and congenital heart disease: Holt-Oram syndrome revealed. *Curr Opin Cardiol* 2004;19:211–215.
150. Hiroi Y, Kudoh S, Monzen K, et al. *Tbx5* associates with *Nkx2-5* and synergistically promotes cardiomyocyte differentiation. *Nat Genet* 2001;28:276–280.
151. Garg V, Kathiriyi IS, Barnes R, et al. *GATA4* mutations cause human congenital heart defects and reveal an interaction with *TBX5*. *Nature* 2003;424:443–447.
152. Molkenstein JD, Lin Q, Duncan SA, et al. Requirement of the transcription factor *GATA4* for heart tube formation and ventral morphogenesis. *Genes Dev* 1997;11:1061–1072.
153. Kuo CT, Morrissey EE, Anandappa R, et al. *GATA4* transcription factor is required for ventral morphogenesis and heart tube formation. *Genes Dev* 1997;11:1048–1060.
154. Reiter JF, Kikuchi Y, Stainier DY. Multiple roles for *Gata5* in zebrafish endoderm formation. *Development* 2001;128:125–135.
155. Gajewski K, Zhang Q, Choi CY, et al. *Pannier* is a transcriptional target and partner of *Tinman* during *Drosophila* cardiogenesis. *Dev Biol* 2001;233:425–436.
156. Ching YH, Ghosh TK, Cross SJ. Mutation in myosin heavy chain 6 causes atrial septal defect. *Nat Genet* 2005;37:423–428.
157. Noden DM, Poelmann RE, Gittenberger-de-Groot AC. Cell origins and tissue boundaries during outflow tract development. *Trends Cardiovasc Med* 1995;5:69–75.
158. Shimada Y, Ho E, Toyota N. Epicardial covering over myocardial wall in the chicken embryo as seen with the scanning electron microscope. *Scan Electron Microsc* 1981;275–280.
159. Viragh S, Challice CE. The origin of the epicardium and the embryonic myocardial circulation in the mouse. *Anat Rec* 1981;201:157–168.
160. Viragh S, Gittenberger-de Groot AC, Poelmann RE, et al. Early development of quail heart epicardium and associated vascular and glandular structures. *Anat Embryol* 1993;188:381–393.
161. Komiyama M, Ito K, Shimada Y. Origin and development of the epicardium in the mouse embryo. *Anat Embryol* 1987;176:183–189.
162. Hiruma T, Hirakawa R. Epicardial formation in embryonic chick heart: computer-aided reconstruction, scanning, and transmission electron microscopic studies. *Am J Anat* 1989;184:129–138.
163. Bolender LM, Olson D, Markwald RR. Coronary vessel vasculogenesis. *Ann N Y Acad Sci* 1990;588:340–344.
164. Mikawa T, Fischman DA. Retroviral analysis of cardiac morphogenesis: discontinuous formation of coronary vessels. *Proc Natl Acad Sci USA* 1992;89:9504–9508.
165. Poelmann RE, Gittenberger-de Groot AC, Mentink MM, et al. Development of the cardiac coronary vascular endothelium, studied with antiendothelial antibodies, in chicken-quail chimeras. *Circ Res* 1993;73:559–568.
166. Mikawa T, Gourdie RG. Pericardial mesoderm generates a population of coronary smooth muscle cells migrating into the heart along with ingrowth of the epicardial organ. *Dev Biol* 1996;174:221–232.
167. Dettman RW, Denerclaw W Jr, Ordahl CP, et al. Common epicardial origin of coronary vascular smooth muscle, perivascular fibroblasts, and intermyocardial fibroblasts in the avian heart. *Dev Biol* 1998;193:169–181.
168. Red Horse K, Ueno H, Weissman IL, et al. Coronary arteries form by developmental reprogramming of venous cells. *Nature* 2010;464:549–553.
169. Zhou B, Honor LB, He H, et al. Adult mouse epicardium modulates myocardial injury by secreting paracrine factors. *J Clin Invest* 2011;121:1894–1904.
170. Bogers AJ, Gittenberger-de Groot AC, Dubbeldam JA, et al. The inadequacy of existing theories on development of the proximal coronary arteries and their connexions with the arterial trunks. *Int J Cardiol* 1988;20:117–123.
171. Bogers AJ, Gittenberger-de Groot AC, Poelmann RE, et al. Development of the origin of the coronary arteries, a matter of ingrowth or outgrowth? *Anat Embryol* 1989;180:437–441.
172. Waldo KL, Willner W, Kirby ML. Origin of the proximal coronary artery stems and a review of ventricular vascularization in the chick embryo. *Am J Anat* 1990;188:109–120.
173. Mikawa T, Hurtado R. Development of the cardiac conduction system. *Semin Cell Dev Biol* 2007;18:90–100.
174. Gourdie RG, Mima T, Thompson RP, et al. Terminal diversification of the myocyte lineage generates Purkinje fibers of the cardiac conduction system. *Development* 1995;121:1423–1431.
175. Gourdie RG, Wei Y, Kim D, et al. Endothelin-induced conversion of embryonic heart muscle cells into impulse-conducting Purkinje fibers. *Proc Natl Acad Sci USA* 1998;95:6815–6818.
176. Waldo KL, Kumiski DH, Kirby ML. Association of the cardiac neural crest with development of the coronary arteries in the chick embryo. *Anat Rec* 1994;239:315–331.
177. Hood LC, Rosenquist TH. Coronary artery development in the chick: origin and deployment of smooth muscle cells, and the effects of neural crest ablation. *Anat Rec* 1992;234:291–300.
178. Costantini DL, Arruda EP, Agarwal P, et al. The homeodomain transcription factor *Irx5* establishes the mouse cardiac ventricular repolarization gradient. *Cell* 2005;123:347–358.
179. Pashmforoush M, Lu JT, Chen H, et al. *Nkx2-5* pathways and congenital heart disease: loss of ventricular myocyte lineage specification leads to progressive cardiomyopathy and complete heart block. *Cell* 2004;117:373–386.
180. Rajamannan NM, Gersh B, Bonow RO. Calcific aortic stenosis: from bench to the bedside—emerging clinical and cellular concepts. *Heart* 2003;89:801–805.
181. Rajamannan NM, Evans FJ, Aikawa E, et al. Calcific aortic valve disease: not simply a degenerative process: a review and agenda for research from the National Heart and Lung and Blood Institute Aortic Stenosis Working Group. Executive summary: calcific aortic valve disease-2011 update. *Circulation* 2011;124:1783–1791.
182. Chakraborty S, Cheek J, Sakthivel B, et al. Shared gene expression profiles I developing heart valve and osteoblast progenitor cells. *Physiol Genomics* 2008;35:75–86.
183. Ducey P, Zhang R, Geoffroy V, et al. *Osf2/Cbfa1*: a transcriptional activator of osteoblast differentiation. *Cell* 1997;89:747–754.
184. Steitz SA, Speer MY, Curinga G, et al. Smooth muscle cell phenotypic transition associated with calcification: upregulation of *Cbfa1* and downregulation of smooth muscle lineage markers. *Circ Res* 2001;89:1147–1154.
185. Rajamannan NM, Subramaniam M, Springett M, et al. Atorvastatin inhibits hypercholesterolemia-induced cellular proliferation and bone matrix production in the rabbit aortic valve. *Circulation* 2002;105:2660–2665.
186. Parmacek MS, Epstein JA. Pursuing cardiac progenitors: regeneration redux. *Cell* 2005;120:295–298.
187. Oh H, Bradfute SB, Gallardo TD, et al. Cardiac progenitor cells from adult myocardium: homing, differentiation, and fusion after infarction. *Proc Natl Acad Sci USA* 2003;100:12313–12318.
188. Beltrami AP, Barlucchi L, Torella D, et al. Adult cardiac stem cells are multipotent and support myocardial regeneration. *Cell* 2003;114:763–776.
189. Martin CM, Meeson AP, Robertson SM, et al. Persistent expression of the ATP-binding cassette transporter, *Abcg2*, identifies cardiac SP cells in the developing and adult heart. *Dev Biol* 2004;265:262–275.
190. Mishra R, Vijayan K, Colletti EJ, et al. Characterization and functionality of cardiac progenitor cells in congenital heart patients. *Circulation* 2011;123:364–373.
191. Takahashi K, Yamanaka S. Induction of pluripotent stem cells from mouse embryonic and adult fibroblast cultures by defined factors. *Cell* 2006;126:663–676.
192. Takahashi K et al. Induction of pluripotent stem cells from adult human fibroblasts by defined factors. *Cell* 2007;131:861–872.
193. Nelson TJ, Martinex-Fernandez A, Terzic A. Induced pluripotent stem cells: developmental biology to regenerative medicine. *Nat Rev Cardiol* 2010;7:700–710.
194. Jeda M, Fu JD, Delgado-Olguin P, et al. Direct reprogramming of fibroblasts into functional cardiomyocytes by defined factors. *Cell* 2010;142:375–386.
195. Mitchell LE, Adzick NS, Melchionne J, et al. Spina bifida. *Lancet* 2004;364:1885–1895.
196. Stoller JZ, Epstein JA. Cardiac neural crest. *Semin Cell Dev Biol* 2005;16:704–715.
197. Brown CB, Baldwin HS. Neural crest contribution to the cardiovascular system. *Adv Exp Med Biol* 2006;589:134–154.

Epidemiology and Prevention of Congenital Heart Defects

Lorenzo D. Botto

FROM EPIDEMIOLOGY TO PREVENTION: INCENTIVE, EVIDENCE, STRATEGIES, TOOLS

Following the birth of a baby with a congenital heart defect, many anxious parents, some sooner and some later, will ask three crucial questions: “What will happen to my child?” (outcomes), “why did this happen?” (causation), and “will it happen again?” (risk).

These three questions—on outcomes, causes, risk—continue to challenge clinicians and public health professionals. While it may not be obvious, these questions are in fact linked, if viewed from the perspective of prevention. For primary prevention, this is clear: by eliminating established causes, primary prevention reduces the risk for affected pregnancies and prevents the associated adverse outcomes through the lifespan. Examples of effective primary prevention abound in pediatrics: immunizations are long-lasting interventions that prevent infectious diseases (including rubella-induced heart defects), whereas daily folic acid use is an ongoing intervention that prevents most cases of spina bifida and anencephaly, two serious birth defects. But prevention is also meaningful for people born with heart defects: by preventing complications and promoting optimal health, this form of prevention (sometimes called secondary prevention) also improves outcomes, though less completely than primary prevention. The main focus of this chapter is primary prevention. It is an overriding goal for pediatric cardiologists and the ideal and fundamental approach to decreasing the personal and societal burden of congenital heart defects. If *primary prevention is the goal, epidemiology is the indispensable tool*. Epidemiology evaluates risk factors, diseases, and outcomes in human populations: it takes the findings from basic research and clinical studies and translates them into meaningful information for populations. Using D-transposition of the great arteries as an example, epidemiologic studies can assess its impact in terms of deaths, hospitalizations, or cost; disparities in outcomes by race-ethnicity or socioeconomic status; and the fraction of cases due to maternal diabetes and preventable by careful metabolic control in the preconceptional period. Epidemiologic studies can also take the causal discoveries in experimental animals, cell cultures, or biochemical pathways and see how they translate into health effects in humans—for example, using population-based case control studies to measure the etiologic impact of specific genetic and environmental factors in human populations.

In this sense, epidemiology, although it has strong theoretical underpinnings, is fundamentally a practical tool. Epidemiology provides data for action and in particular for prevention. Figure 25.1 illustrates this point and provides a roadmap of how the epidemiology of congenital heart defects is discussed in this review. Specifically (Fig. 25.1), epidemiology supports and promotes four interrelated elements of the prevention process: *incentive, evidence, strategies, and tools*.

Incentive refers to the overall impact of heart defects on people and society: persons affected, lives lost, chronic illness, disability, health disparities, decreased quality of life, loss of productivity, and costs. Epidemiologic studies generate many of these metrics, which in turn provide the *policy and moral basis* for prevention. In fact, the current impact of congenital heart defects illustrates the very real cost of doing nothing, or not doing more, to prevent these heart defects. When interventions are implemented, these same metrics provide baselines against which to assess the effectiveness of actions and policies. As will become clear, the current overall impact of congenital heart defects through the lifespan is probably underestimated, mainly because of significant data gaps. Developing more realistic, timely, and population-based estimates of the overall impact of congenital heart defects can help make the case for greater investment into research and prevention.

Once the incentive is documented and understood, the *evidence* for prevention must be robust and convincing (Fig. 25.1). Such evidence provides the *science for action*. Particularly important is the evidence relating to modifiable risk factors, including maternal conditions and environmental exposures. Epidemiologic studies can help build the evidence for prevention: well-designed studies can help identify and characterize risk factors in human populations and generate useful metrics such as relative risks, absolute risks, and attributable fraction (the fraction of cases preventable by reducing the exposure). To be actionable, these data must be authoritatively reviewed and timely, so that interventions can be implemented promptly and improved quickly. Of course, susceptibility genotypes are likely important modifiers of environmental and maternal risk factors; however, the science is still incomplete and its use, particularly in resource-poor countries, will likely continue to be challenging and expensive. Once incentives and evidence are established, prevention needs effective *strategies* and useful *tools* for implementation and evaluation (Fig. 25.1). Effective, high-impact strategies are typically multitiered, from interventions that tackle the global socioeconomic determinants of health to individual health care delivery such as education and counseling. They are typically also person centered, rather than organ specific. One example is preconception care that focuses not only on cardiac risk factors but promotes women's health overall. Strategically, prevention should have maximum population impact for a given amount of resources. For this reason, it also is helpful to assess risk factors by their attributable fraction, as a measure of their contribution to congenital heart defects in the population. This epidemiologic metric is a nonlinear function of the relative risk for congenital heart defects combined with the prevalence of the risk factor in the population. Well-designed epidemiologic studies can provide these estimates and thus help the development of effective and efficient policies.

Finally, effective strategies need to be implemented in ways that are sustainable and pervasive. This requires tools and technologies that are practical and easy to use. A simple example

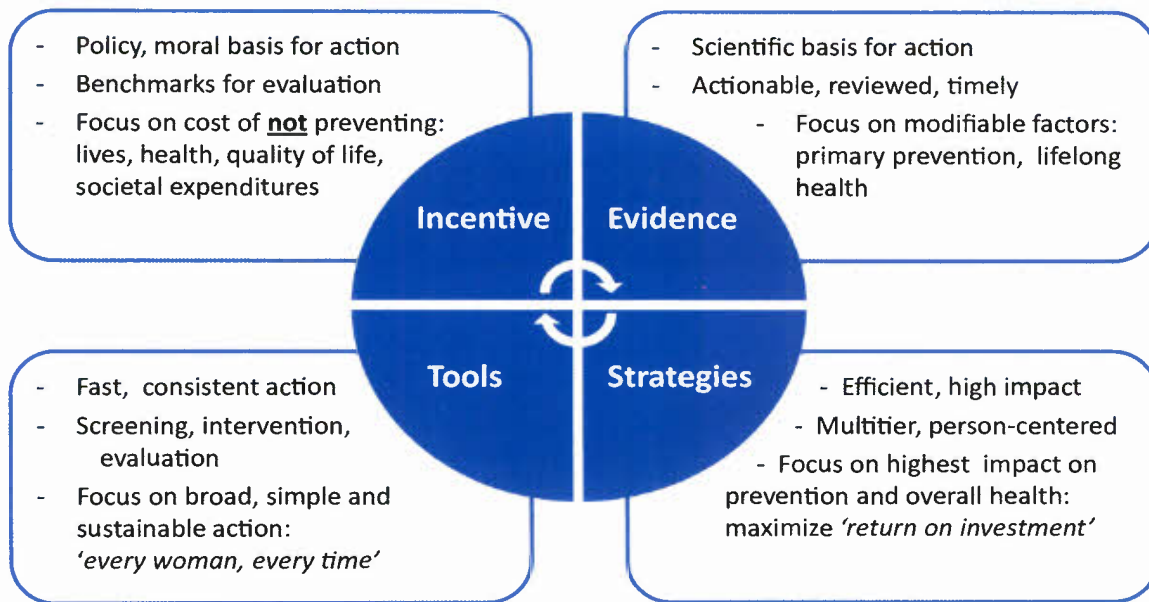


Figure 25.1. From epidemiology to prevention: incentives, evidence, strategies, and tools.

could be a screening questionnaire for use in a busy clinic, to be filled out in the waiting room at every visit, aimed at identifying major risk factors for congenital heart defects in a family. Items flagged in the screening can then prompt further evaluation, education, or referrals. A more complex tool for prevention could be a population-based, country-wide surveillance system, which can be used to assess changes in prevalence, adverse outcomes, or risk factors for congenital heart defects. Such a system would generate timely, ongoing epidemiologic information that will help monitor the effectiveness of prevention. This last example also underscores the circular nature of the four elements of prevention (Fig. 25.1): occurrence and outcomes start out as incentives for prevention, the evidence of causal determinant is generated, effective prevention strategies are developed, tools are designed and used in implementation, and finally occurrence and outcomes are again evaluated to continuously improve prevention, bringing the process to full circle.

In summary, this review focuses on selected epidemiologic aspects of congenital heart defects and discusses their relevance in the broader context of primary prevention (Fig. 25.1). The discussion makes use of material from several reviews, where additional information on epidemiology and risk factors can be found (1–5).

OVERARCHING ISSUES: LIFESPAN PERSPECTIVE AND CODING/CLASSIFICATION

Before examining incentive, evidence, strategies, and tools, it is helpful to address two overarching issues—lifespan perspective and classification/coding—that have important implications for any approach to the epidemiology and prevention of congenital heart defects.

Lifespan, Person-Centered Perspective

A lifespan perspective views a person's life as a continuum, from preconception to adult life and beyond (Fig. 25.2). This perspective provides a helpful framework to assess needs and data gaps for the many issues that arise during the lifespan (1).

Three concepts are particularly important. First, the true impact and relevance of congenital heart defects become clear only when viewed and measured throughout the lifespan. For example, issues such as diagnosis and early treatment are more relevant earlier than later in life, but prevalence remains an important issue for clinical care throughout life. Schooling, employment, and social integration become increasingly important as children grow into adults. At the opposite end of the lifespan, risk assessment and prevention are best assessed in the preconception period. Finally, some issues such as the personal and societal costs, while perhaps high in children, are best evaluated over an entire lifespan, particularly in the current era of improved survival and longer life expectancy. Taking a person-centered, lifespan perspective helps appreciate the many connections among apparently dissimilar issues; for example, quality of life is connected to the quality and timeliness of diagnosis, treatment, and management, and also to the associated complications, disabilities, caregiver stress, cost, and social integration.

Historically the epidemiologic assessment of occurrence and outcomes has focused on newborns and young children, typically looking at one element at the time (e.g., prevalence and mortality). Thus, a second important concept (Fig. 25.2) is that our current view and knowledge are in many ways partial and skewed, with emphasis on the time of birth and early childhood but progressively incomplete and uncertain as the focus shifts backward into pregnancy and preconception (e.g., risk factors) or forward into adult life. In part, this situation is understandable. Birth and infancy are critical periods in life when many diagnoses are made and crucial medical and surgical management is initiated. Also, information on this period is more readily available, because most of these activities take place in hospitals where data on diagnosis, morbidity, and mortality are more easily collected and shared. But—and this is the third important concept—as one moves away from birth and infancy, the issues not only become more complex, but also the data and data systems needed to capture them become more difficult and complicated to acquire. Thus, a major challenge for epidemiology and prevention is that significant data gaps are found precisely for those issues that are more numerous and more complex (Fig. 25.2). Meeting this challenge will require a major, long-term, and coordinated

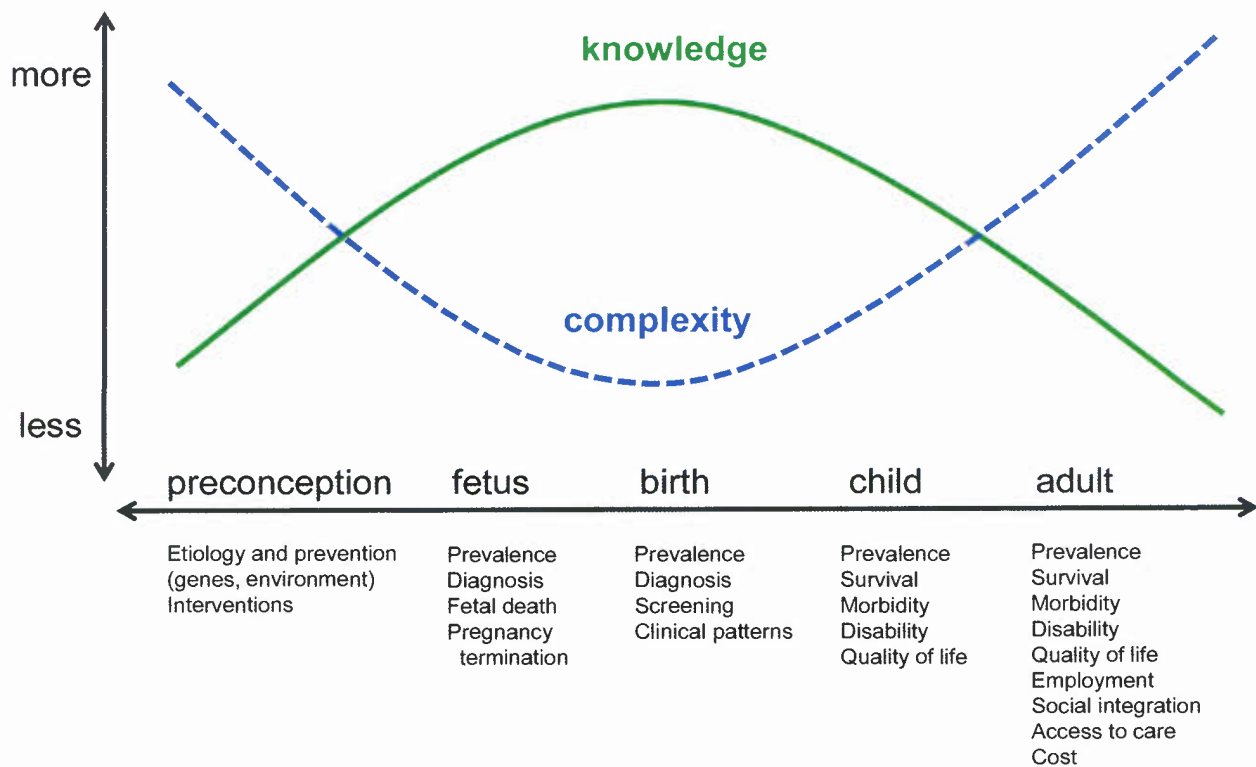


Figure 25.2. Lifespan, person-centered perspective: issues, knowledge, complexity.

effort of epidemiologist, clinicians, and health administrators; the benefits would be considerable, including having global and accurate basis to plan, implement, and evaluate clinical services and prevention.

Coding and Classification

Coding and classification are related but different processes. Typically, coding translates words from a clinical description into well-defined descriptive codes, which then can be used for data sharing and epidemiologic analysis. By moving from description to a limited set of codes, coding usually entails a loss of information. One challenge for a coding system is to retain the essential information while discarding the inessential. However, what is essential in one application may not be essential in others. For example, information on surgical procedures or severity of a valvar stenosis is essential in an outcome study but not as much in an etiologic study.

Classification is typically a higher order process. It can start from descriptions or even codes, and then uses a set of explicit criteria to group cases or phenotypes into meaningful analytic groups. Thus, the same (coded) cases can be classified differently depending on whether the classification emphasizes pathogenetic principles (e.g., neural crest origin), similarities in outcomes (e.g., mortality), or anatomy (e.g., cardiac segment involved). Also, whereas a given person may be assigned multiple descriptive codes, many classification systems try to map each person to one primary group. In practice, many coding systems are designed also with a default classification structure, which is typically hierarchical and based on the code's digits.

Coding and classification are crucial because they are the basis for all epidemiologic analyses: decisions, inconsistencies, or errors in coding and classification can affect findings significantly. In fact, part of the challenge of comparing and aggregating data is the variation or uncertainty in coding and classification among different studies.

To illustrate some of these issues, it is helpful to briefly review two commonly used coding system used for many applications—the World Health Organization (WHO)'s International Classification of Diseases (ICD) system, and the Society of International Surgeons (STS) system—and a classification system based on principles of pathogenesis and implemented in several etiologic studies (Table 25.1).

The WHO's ICD system is used by health care systems worldwide to generate epidemiologic data, including prevalence and mortality, for many diseases. The ICD is now in its 10th edition with the 11th in preparation, though the 9th edition is still widely used in several countries with some clinical modifications. The ICD system for congenital heart defects is mainly based on anatomy. The hierarchy of codes tends to group by regional anatomy. For example, left obstructive heart defects are dispersed across different high-level groups, depending on whether the structure affected is the mitral valve, the aortic valve, or the aorta. As an all-purpose system, the ICD system has known limitations in its ability to code the more complex cardiac defects or to distinguish degrees of severity of a given lesion, and these limitations are particularly felt in studies of etiology and outcomes. Nevertheless, many birth defect registries and epidemiologic studies still use this system, often incorporating the clinical modifications developed for ICD-9 and ICD-10 by the British Paediatric Association (BPA), now the Royal College of Paediatrics and Child Health.

Understanding the limitations of the available systems of coding and nomenclature for congenital heart defects, several leading cardiology organizations have worked to develop new systems that could be used internationally and typically with a focus on supporting large-scale outcome studies with systematic risk stratification. An important step has been the establishment of the International Society for Nomenclature of Paediatric and Congenital Heart Disease (6). One product has been the International Paediatric and Congenital Cardiac Code (7). This coding system is available for free (8) and captures not only the anatomy but also the clinical correlates and procedures.

TABLE 25.1

Coding and Classification Systems for Congenital Heart Defects: Approaches and Examples

	Epidemiologic	Clinical	Etiologic/Pathogenetic
Focus	Coding	Coding	Classification
Example	ICD-International Classification of Diseases and variants (BPA)	International Paediatric and Congenital Cardiac Code	Clark-Pathogenetic Classification and variants
Used by (examples)	Many health systems worldwide, including birth defect registries	STS; EACTS-European Association for Cardiothoracic Surgery; others	NBDPS; BWIS; others
Basis	Anatomy (regional)	Anatomy, severity, procedures	Embryology, developmental mechanisms
Main uses	Assess frequency, patterns, basic outcomes (cause of death)	Evaluate outcomes, treatment, incorporate risk stratification	Find causes, risk factors
Approach	Code each finding, without prioritization	Codes clinically relevant lesions and procedures	Select one main diagnosis per baby; selection is hierarchical, based on earliest developmental event
Strengths	1. International standard, widely used, provides basic metrics for many countries;	1. Incorporates clinically relevant details (e.g., severity, surgery), to improve clinical homogeneity in outcome studies;	1. Incorporates developmental mechanisms and timing, likely relevant in pathogenesis;
	2. Can include clinical modifications;	2. Ongoing efforts for international diffusion and collaborative development	2. Provides a main “pathogenetic” phenotype for each person (one person = one diagnosis);
	3. Updated, maintained by major international body (WHO)	3. Can be mapped to other systems	3. Provides rationale for aggregating (lumping) anatomic phenotypes to increase ability power to detect associations with risk factors (e.g., LVOTO)
Challenges	1. Limited specificity for rare, complex conditions;	1. Required clinical details typically available in medical records but not (yet) in administrative records;	1. Developmental mechanisms still incompletely understood;
	2. Inability to specify degree of severity by lesion	2. Requires careful standardization of description, coding, and reporting across clinical centers	2. Will require revisions as understanding of pathogenesis evolve

LVOTO, left ventricular outflow tract obstruction.

As a dedicated system developed by a team of topic experts, this system has many strengths (Table 25.1) and is used in surgical centers internationally. One caveat is that it could be complex to implement in birth defect registries or administrative settings with limited case information and cardiologic expertise. However, with cardiology expertise, this system could be used in birth defect surveillance, as shown by recent pilot implementation studies (9,10). Finally, interactions between those responsible for the ICD and for the International Nomenclature codes may lead to improvements in the cardiac codes of the next editions of the ICD. Because of the widespread use of the ICD, such changes have the potential to improve the basic epidemiologic information from administrative data bases worldwide (6,7).

By contrast, some systems focus explicitly on classification, rather than coding, and on specific grouping principles. One of these systems (Table 25.1) was developed and updated by Dr. EB Clark (11,12) and is based on pathogenetic and mechanistic considerations, rather than anatomy or clinical

outcomes. Its main use is in etiologic studies. An explicit goal is to improve a study's ability to identify associations between risk factors and congenital heart defects. In such studies, a specific challenge is balancing phenotypic detail with sample size: one must avoid defining groups so narrowly that each group has too few cases (thus losing statistical power and missing associations), while not incurring in the opposite error, making groups so broad that heterogeneous conditions are lumped (thus also underestimating or missing associations). By grouping pathogenetically similar heart defects (e.g., left side obstructive defects), sample size is increased while preserving pathogenetic homogeneity. One important aspect of this system (and of many classification system) is that, to the extent possible, one principal pathogenetic group, the one thought to be more basic or occur earlier in development, is assigned to each affected person, regardless of the number of cardiac malformations (or ICD/STS codes). The groups, mechanism, and hierarchy are summarized in Table 25.2.

TABLE

25.2

Pathogenetic Classification of Heart Defects, with Proposed Hierarchy**Abnormal Situs and Looping**

Heterotaxy, other situs anomalies, L-loop

Ectomesenchymal Tissue Migration*Conotruncal septation defects*

Subarterial ventricular septal defect

Double-outlet right ventricle

Tetralogy of Fallot

Pulmonary atresia with ventricular septal defect

Aortopulmonary window

Truncus arteriosus

Abnormal conotruncal cushion position

D-Transposition of the great arteries

Branchial arch defects

Interrupted aortic arch type B

Double aortic arch

Right aortic arch with mirror-image branching

Extracellular Matrix Abnormalities*Endocardial cushion defects*

Ostium primum atrial septal defect

Inflow/inlet ventricular septal defect

Atrioventricular septal defect

Abnormal Targeted Growth

Anomalous pulmonary venous return

Abnormal Intracardiac Blood Flow

Left heart defects

Bicuspid aortic valve

Aortic valve stenosis

Coarctation of the aorta

Interrupted aortic arch type A

Hypoplastic left heart, aortic atresia/mitral atresia

Right heart defects

Bicuspid pulmonary valve

Secundum atrial septal defect

Pulmonary valve stenosis

Pulmonary valve atresia with intact ventricular septum

Perimembranous ventricular septal defect

Cell Death Abnormalities

Muscular ventricular septal defect

Ebstein malformation (hierarchically placed before intracardiac blood flow defects)

Assigning a principal diagnosis is not always straightforward. One solution in the National Birth Defects Prevention Study (NBDPS) was to create specific groups for common associations, such as atrial septal defects and pulmonic stenosis (13). Other systems assign multiple defect categories to the same baby (14) or add dimensions to the classification scheme (15). Typically, the need to consider multiple diagnoses is more of an issue in outcome studies, where they can be important for risk stratification, than in etiologic research, where in fact having a meaningful principal diagnosis is a methodologic strength.

In its original form or with modifications, the pathogenetic classification has been used in several large epidemiologic studies, including the Baltimore-Washington Infant Study (BWIS) (16,17) and in some analysis of the Atlanta Birth Defects Case Control Study (18,19). Currently it has been incorporated into the cardiac classification of the NBDPS, one of the largest ongoing case control studies on the etiology of birth defects (13). In an extension of the original system, the NBDPS classification system also stratifies phenotypes based on whether the heart defect is simple, an association, or complex (13). The purpose is to identify a subset of “pure” groups of heart defects, defined as simple phenotypes in individuals without extracardiac anomalies. By minimizing anatomic and pathogenetic heterogeneity, this approach aims at improving the ability to find meaningful associations with risk factors. The other cases are still used, but are incorporated later or analyzed separately. This approach is most practical in large studies of cases with accurate clinical description of both the baby and the heart.

Finally, these pathogenetic classifications are best implemented starting from verbatim diagnoses, but, within limits, could be used starting from codes. For example, the International Paediatric and Congenital Cardiac Code/STS codes can be mapped to the NBDPS and Clark Classifications, and such hybrid systems can in principle retain the clinical precision of the former and the pathogenetic perspective of the latter (9).

In summary, this section briefly described two overarching issues—lifespan perspective and classification/coding—that have substantial implications for epidemiology and prevention of congenital heart defects. Embracing a lifespan perspective leads to realizing that our current view of congenital heart defects still misses important aspects in the lives of affected people and their families, and in doing so, underestimates the true impact of such heart defects in people, families, and society. Filling these data gaps is a major undertaking. Classification and coding are foundational elements of epidemiologic studies: they are the basis of any operational definition of what congenital heart defects are and how to group them in studies of occurrence, outcomes, and etiology. Clearly, substantial thought needs to go into their development and use. Also, using well-established coding and classification systems, or systems that can be explicitly mapped to them, will be very helpful when comparing and aggregating data across studies, thus promoting the progress of clinical care, service planning, and prevention. With these considerations in mind, the specific issues of heart defect epidemiology and prevention (Fig. 25.1) can be fruitfully discussed, beginning with “incentive.”

INCENTIVE FOR ACTION: EPIDEMIOLOGY OF OCCURRENCE AND OUTCOMES

The epidemiology of occurrence and outcomes generates key data to assess the true impact of congenital heart defects on individuals and society. Knowing the true impact provides the incentive for action, whether it is in the form of research, primary prevention, or prevention of complications in people

with congenital heart defects. Evaluating occurrence and outcomes, however, can be challenging. Selected issues and key findings are briefly reviewed.

Occurrence

The occurrence of congenital heart defects can be evaluated using incidence and prevalence. Technically, incidence measures the number of new cases among an initially disease-free cohort of at-risk individuals within a specific time frame. Although a good measure of the “force” of disease, incidence is difficult to measure for congenital heart defects. One difficulty is that the disease-free at-risk cohort is formed, strictly, by conceptuses, whose number cannot be estimated with any accuracy (20). Prevalence, on the other hand, reflects the occurrence of disease at a point in time in a defined population. Prevalence therefore can be estimated for fetuses at a certain gestational age, stillbirths, newborns, children, adults, or a combination of these.

Because it can be computed with easily available data, prevalence at birth—the number of babies born with a heart defect divided by the total number of babies (usually live births) in that period—is frequently used as a basic epidemiologic measure of occurrence (20). However, by not including early pregnancy losses, birth prevalence will underestimate the global impact of congenital heart defects.

Published estimates of birth prevalence vary considerably (4,21,22), even in fairly recent studies (14,23–37). A crucial question is to what extent such variation is real or due to methodology. Real variations can provide valuable clues to causation. Variations due to methodology, however, are usually a hindrance: they can complicate many activities, from surveillance to outcome assessment to evaluation of the prevention activities. In practice, methodologic factors certainly play a role in reported rates. To understand the role of these factors, one needs to review carefully aspects such as diagnostic practices, case definitions, case classification, inclusion of pregnancy terminations, timing of diagnosis (fetal, birth, or childhood), length of follow up, and reporting procedures (4,21,22,38). For example, in a recent study from a European network of birth defect registries, birth prevalence varied considerably by country, even with systems using the same central database and procedure protocols (36). These variations are likely systematic rather than due to chance, so that taking the average across programs has limited value (an average is a good approximation when the cause of the variation is random error, not systematic bias).

Several studies published since the 1980s (14,23–36,39) on the prevalence of fetal deaths (stillbirths), newborns/infants, and children with heart defects are illustrated in Figure 25.3.

This figure helps to highlight several points. First, most studies focus on newborns and infants. Limited data are available on fetuses, older children, and adults. While understandable, because of the greater difficulties of population studies outside of the newborn period, this scarcity of data signals an important gap to fill. Second, heart defects appear to be more common among fetal deaths than in other groups. In the three studies, from the United States and France (23–25), the reported prevalence of heart defects among fetal deaths ranged from 13 to 35 per 1,000. The higher figure, from the larger and more recent study (25), is probably closer to reality. Of note, fetal deaths are as common as infant deaths in many developed countries, yet their environmental and genetic determinants are not well characterized. Third, the estimated prevalence in newborns and infants, based on many studies, varies widely by area and reporting program, from approximately 3 to 14 per 1,000. A more detailed analysis of three of these studies (Table 25.3) can help clarify what drives the

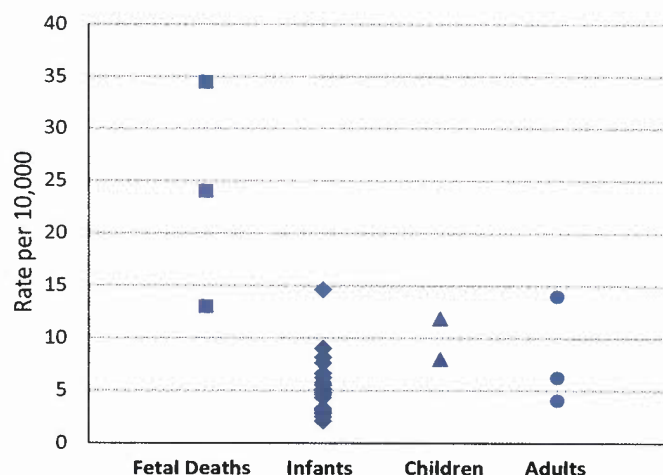


Figure 25.3. Prevalence of congenital heart defects (by 10,000) in different age groups. (Data from Reller MD, Strickland MJ, Riehle-Colarusso T, et al. Prevalence of congenital heart defects in metropolitan Atlanta, 1998–2005. *J Pediatr* 2008; 153:807–813; Wren C, Richmond S, Donaldson L. Temporal variability in birth prevalence of cardiovascular malformations. *Heart* 2000;83:414–419; Ferencz C, Loffredo CA, Rubin JD, et al. *Epidemiology of Congenital Heart Disease: The Baltimore-Washington Infant Study 1981–1989*. Mount Kisco, NY: Futura Publishing Company, Inc., 1993; Ursell PC, Byrne JM, Strobino BA. Significance of cardiac defects in the developing fetus: a study of spontaneous abortuses. *Circulation* 1985;72:1232–1236; Chinn A, Fitzsimmons J, Shepard TH, Fantel AG. Congenital heart disease among spontaneous abortuses and stillborn fetuses: prevalence and associations. *Teratology* 1989;40:475–482; Stoll C, Alembik Y, Roth MP, Dott B, De Geeter B. Risk factors in congenital heart disease. *Eur J Epidemiol* 1989;5:382–391; Fyler DC, Buckley LP, Hellenbrand WE, et al. Report of the New England Regional Infant Cardiac Program. *Pediatrics* 1980;65:376; Grabitz RG, Joffres MR, Collins-Nakai RL. Congenital heart disease: incidence in the first year of life. The Alberta Heritage Pediatric Cardiology Program. *Am J Epidemiol* 1988;128:381–388; Fixler DE, Pastor P, Chamberlin M, Sigman E, Eifler CW. Trends in congenital heart disease in Dallas County births. 1971–1984. *Circulation* 1990;81:137–142; Kidd SA, Lancaster PA, McCredie RM. The incidence of congenital heart defects in the first year of life. *J Paediatr Child Health* 1993;29:344–349; Samanek M. Boy:girl ratio in children born with different forms of cardiac malformation: a population-based study. *Pediatr Cardiol* 1994;15:53–57; Abu-Harb M, Hey E, Wren C. Death in infancy from unrecognized congenital heart disease. *Arch Dis Child* 1994;71:3–7; Tanner K, Sabrine N, Wren C. Cardiovascular malformations among preterm infants. *Pediatrics* 2005;116:e833–8; Roy DL, McIntyre L, Human DG, et al. Trends in the prevalence of congenital heart disease: comprehensive observations over a 24-year period in a defined region of Canada. *Can J Cardiol* 1994;10:821–826; Eichhorn P, Sutsch G, Jenni R. [Congenital heart defects and abnormalities newly detected with echocardiography in adolescents and adults]. *Schweiz Med Wochenschr* 1990;120:1697–700; Tegnander E, Williams W, Johansen OJ, Blaas HG, Eik-Nes SH. Prenatal detection of heart defects in a non-selected population of 30,149 fetuses—detection rates and outcome. *Ultrasound Obstet Gynecol* 2006;27:252–265; Botto LD, Correa A, Erickson JD. Racial and temporal variations in the prevalence of heart defects. *Pediatrics* 2001;107:E32.)

TABLE 25.3 Birth Prevalence of Select Congenital Heart Defects in Three Studies

	BWIS, USA 1981–1989	Atlanta, USA 1998–2005	Trondheim, Norway 1991–2001
	Live Births to 1 y	Live Births to 6 y, Stillbirths, TOP >20 WGA	Fetuses from 18 wks GA to at Least 2 y
	Population-Based, Multiple Ascertainment	Population-Based, Multiple Ascertainment	Area Served by one Major Hospital
	906,646 Births	398,140 Live Births	29,460 Pregnancies
Group	Rate	Rate ^a	Rate
Heterotaxy, L-TGA	1.4	1.7 ^b	1.0
Conotruncal defects			
Tetralogy of Fallot	3.3	4.7	2.4
D-Transposition of the great arteries	2.3	2.3	4.8
Double-outlet right ventricle	0.7		1
Truncus	0.5	0.6	0.3
Atrioventricular septal defect		4.1	
With Down syndrome	2.3		4.8
Without Down syndrome	1.0		3.4
Total anomalous pulmonary venous return	0.7	0.8	0.7
Ebstein anomaly	0.6	0.6	0.3
Right heart defects			0.0
Tricuspid atresia	0.4	0.5	0.7
Pulmonic atresia, intact septum	0.6	0.4	0.0
Pulmonic stenosis, atresia	5.4	5.5	7.8
Peripheral pulmonic stenosis			1.7
Left heart defects			
Hypoplastic left heart	1.8	2.3	3.4
Coarctation of the aorta	1.4	4.4	4.1
Aortic arch atresia/hypoplasia			0.3
Aortic valve stenosis	0.8	1.1	4.4
Septal defects			0.0
Ventricular septal defects	11.2	41.8	83.8
Atrial septal defects	3.2	13.1	19
Patent ductus arteriosus	0.9	2.9	0.0
Other major CHD			2
Total	48.4	81.4	146

Rates are per 10,000 births.

^aMACDP rates by defect are not always mutually exclusive.^bDoes not include L-TGA.

BWIS, Baltimore-Washington Infant Study; TOP, termination of pregnancy; GA, gestational age; WGA, weeks gestational age; L-TGA, L-transposition of the great arteries; CHD, congenital heart disease.

prevalence of congenital heart defects and the variations that are commonly observed.

In the BWIS, investigators in the North-Eastern United States implemented in the 1980s a population-based study of live births with heart defects, with follow-up through 1 year of age. The BWIS was primarily designed as an etiologic case-control study, but because of the high quality of ascertainment, investigators generated a set of birth prevalence estimates that have been often cited since (of note, ventricular septal defects may have been sampled rather than exhaustively included) (16,17). The second study, from the Centers for Disease Control and Prevention (CDC)'s Metropolitan Atlanta Congenital Defects Program (MACDP), reported rates of heart defects from 1998 through 2005 from four counties in a large metropolitan area in the South-Eastern United States (14). BWIS and the MACDP, though not identical, have some broad operational similarities, including active ascertainment from multiple sources, follow-up period through early infancy, and a similar though not identical case classification. MACDP also includes stillbirths and pregnancy terminations. The third study, from Trondheim in northern Norway, combined systematic assessment with prenatal diagnosis to identify heart defects starting from before birth (35). Specifically, these researchers systematically evaluated by prenatal echocardiography a large, unselected cohort of pregnancies from a well-defined geographic area, first at midgestation, then postnatally, with follow-up through 2 years of life.

Side-by-side comparisons are not completely accurate because the defect groups in the MACDP report were not mutually exclusive: approximately 10% of babies were assigned more than one main defect group and are therefore counted multiple times in the categories of Table 25.3 (14). Nevertheless, some broad considerations can be made. First, these three studies report different overall rates of heart defects, with a nearly threefold difference between the lowest (48 per 10,000 in BWIS) and the highest (146 per 10,000 in Trondheim) estimate. Second, these overall differences are largely due to a few common defects, mainly ventricular septal defects and to a lesser degree atrial septal defects and pulmonic or aortic valve stenosis. The potential for variable ascertainment and reporting of these defects, particularly their mild forms, is significant. In fact, in the Norwegian study nearly all (96%) of the ventricular septal defects were considered minor. Other studies support the notion that diagnostic intensity can significantly influence the reported rate of these defects. In one study from Japan (40), for example, 2% of an unselected cohort of newborns had a ventricular septal defect when evaluated sys-

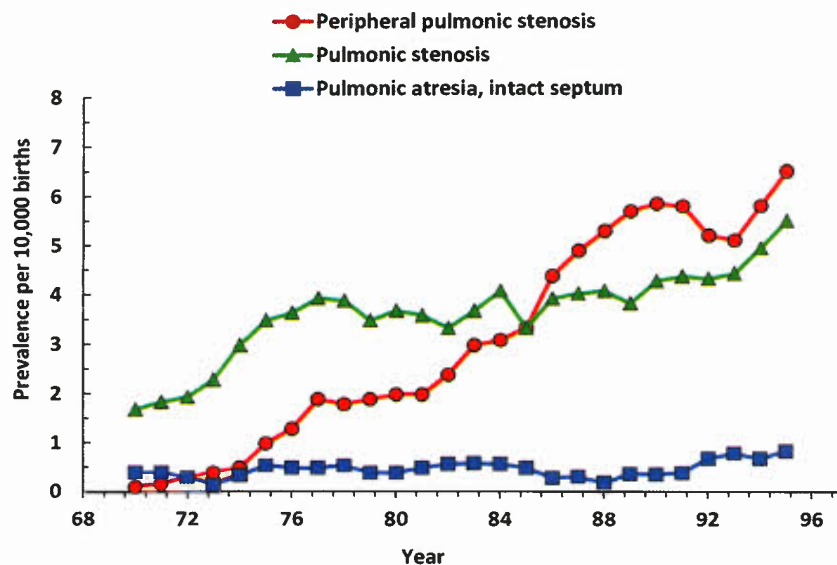
tematically at birth by Doppler ultrasonography. Most of these were small muscular defects, only about half had an associated murmur at hospital discharge, and three-quarters closed spontaneously by 1 year of age (40). A second study also from Japan (41), using similar methods in a cohort of 2,067 newborns in the first 4 days of life, reported a 5% overall birth prevalence of heart defects (503 per 10,000); however, most cases were small ventricular septal defects and patent ductus arteriosus (41), and over half were said to be asymptomatic and did not require intervention. In addition to septal defects, some valvar abnormalities are also variably ascertained and reported. For example, extrapolating from limited data, investigators have estimated that bicuspid aortic valve has a prevalence of about 0.5% in babies (500 per 10,000) (42) and perhaps of 1% to 2% in adults (43). Other defects that can contribute significantly to rate variations include small atrial septal defects (sometimes difficult to differentiate from patent foramen ovale) and patent ductus arteriosus, particularly in preterm infants or in the early newborn period. Although some studies report how these minor defects have been dealt with, this is not always the case, adding to the challenge of interpreting and comparing findings.

In addition to variations by study and program, some temporal trends have been noted in several studies. Many studies (Fig. 25.3) published in the earlier part of the 1980s tended to report a birth prevalence of heart defects between 4 to 6 per 1,000, whereas studies published in more recent years reported rates closer to 8 to 9 per 1,000, sometimes higher (14,28,35,39,44). Direct evidence for time trends within the same reporting program has also been reported in several countries (15,39,45). These studies show two main findings. First, reported rates increased the most for the clinically milder defects, compared to the more severe defects. Second, the time frame of these trends roughly coincides with the increasing use of echocardiography: rates rise quickly in the 1980s and slow considerably, sometimes to a plateau, in the 1990s (15,39,45). An example of such pattern is illustrated in Figure 25.4, focusing on right-sided obstructive defects in Metropolitan Atlanta (39).

In that study, reported rates increased roughly in proportion to the severity of these defects. The rise was sharpest and highest for peripheral pulmonic stenosis, less for valvar stenosis, and minimal for pulmonary atresia with intact septum (39).

These data in the aggregate indicate that most of variations observed between programs is driven by ascertainment and reporting, mainly (but not only) of less severe heart defects. A related factor, now of greater importance than in the past, is prenatal screening and diagnosis. In many developed

Figure 25.4. Trends in birth prevalence of selected right-sided obstructive heart defects, Metropolitan Atlanta. (Data from Botto LD, Correa A, Erickson JD. Racial and temporal variations in the prevalence of heart defects. *Pediatrics* 2001;107:E32.)



countries, most pregnant women undergo a prenatal ultrasound examination, sometimes several times during the pregnancy. Depending on the type and intensity of prenatal examinations, the fraction of congenital heart defects that are diagnosed before birth can be substantial, particularly those that can be detected with simpler screening views (e.g., four-chamber) by practicing obstetricians. In the Norwegian study, for example, the high prevalence of heart defects (Table 25.3) is likely also due to the study's systematic prenatal assessment, possibly augmented by the identification of cases of chromosomal anomalies such as Down and Turner syndromes that have a high fetal mortality and may be overrepresented in fetuses compared to live born infants.

In summary, available data strongly supports that the observed variations in the birth prevalence of heart defects are mainly due to methodology rather than biology. Biology may play a role, but probably a minor one. For example, rates of selected heart defects vary to some degree by race and ethnicity as well as sex: studies from different countries quite consistently document higher rates of D-transposition of the great arteries and aortic stenosis in boys than in girls, and in non-Hispanic whites than in non-Hispanic blacks (14,30,39,46,47). However, these variations, while helpful as clues to etiology, would explain at most a very small fraction of the rate differences among studies.

Prevalence Beyond Infancy and Early Childhood

Compared to birth prevalence, the prevalence of congenital heart defects in older age groups is much less known (Fig. 25.3). For example, an early estimate from the American Heart Association put the number of adults with congenital heart defects at one million adults (or ~1 in 300 people), but was based on very little data. A more formal estimate, published in 2001 by a task force convened by the United States National Institutes of Health (NIH) (48), estimated that in 2000, 1 in 350 people in the United States was an adult with a congenital heart defect (or ~800,000 in total), with about half of these having a moderate or severe heart defect (Fig. 25.5).

These numbers were generated not from direct population surveys of adult patients but from mathematical models that combined birth prevalence data with estimated survival rates to estimate a cross-sectional snapshot of people of different ages living to the year 2000. Of note, these estimates indicated that the number of adults with congenital heart defects surpassed that of children. In fact, using the total United States population as the denominator (275 million people), the data from NIH-convened panel suggested that 1 in 195 people

(children and adult combined) living in the United States in the year 2000 had a congenital heart defect.

These estimates are important for several reasons. Although not based on actual surveys done in the different age groups, the figures generated by mathematical modeling used reasonable assumptions on birth prevalence and survival by broad groups of heart defects. These estimates also tried to incorporate the typical life course of common congenital heart defects; they assumed, for example, that most instances of ventricular septal defect and patent ductus would have resolved by adulthood, thus decreasing their prevalence in adults compared to children. The grouping of heart defects (simple, moderate, and severe) was also meaningful: these categories, based not only on anatomy but also associated procedures and likely outcomes, tried to reflect overall clinical needs, thus providing some basis for planning services for adults with congenital heart defects. Also, as noted, the higher number of adults than children with congenital heart defects emphasizes the need for specialized adult services in the community. Finally, the very fact that modeling was required to generate these estimates highlights the current, significant data gaps and the crucial need to have systems in place to gather valid primary data.

More recently, studies have begun to directly assess the prevalence in older children and adults. Typically, this has been possible in countries other than the United States, with population-based integrated health care systems and databases. For example, researchers in Quebec linked two large provincial healthcare databases (49) to identify people of all ages who had encounters with the health care system for congenital heart defect diagnoses or procedures. The resulting estimates of prevalence in adults and children were in the range of those modeled in the earlier United States study. As a fraction of the overall Quebec population in 2000, 1 in 165 people had a congenital heart defect: 1 in 288 was an adult with a congenital heart defect and 1 in 388 was a child (<18 years) with a congenital heart defect (49). This study also noted an increasing prevalence over time of the prevalence of congenital heart defects in both adults and children. Even taking into account the limitations of administrative databases, this is an important study because it directly evaluated the number of people with congenital heart defects in a population-based setting.

Whereas it is tempting to extrapolate these findings to the United States and other developed countries, it is important that each country develops the resources to perform these studies on an ongoing basis. Also, these estimates, while very important, are only the beginning, as they reflect the past rather than the present. For example, according to both the United States and Quebec studies (48,49), the number of adults with congenital heart defects is projected to increase with time, perhaps by 5% per year (50). Including conditions such as bicuspid aortic valve, the rate of significant disease in adults could be even higher (43,51–53).

In summary, for the first time the high and increasing numbers of adults with congenital heart defects is being actually documented. Significant gaps still remain. Crucial needs include ongoing monitoring of these trends, improving data quality (including validation), and expanding data coverage to the entire population. This information will be extremely helpful in evaluating and meeting clinical needs, particularly in adults, and evaluating prevention—in short, in moving “from numbers to guidelines” (48,49,54,55).

Improving Occurrence Data

This brief review of the occurrence of congenital heart defects, including prevalence at various ages, highlighted several methodologic challenges that can limit the usefulness of the data for planning and prevention. Many of these challenges are solvable in principle (Table 25.4).

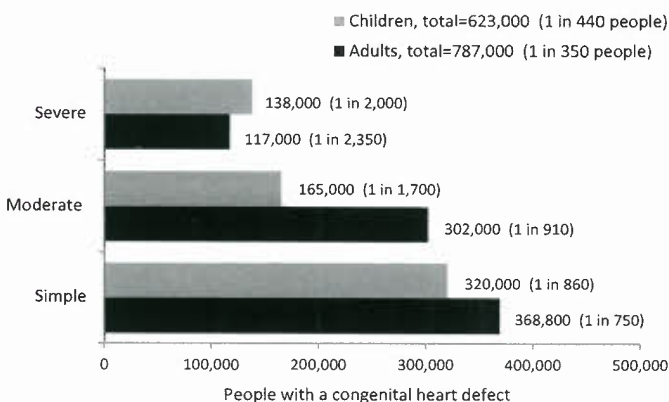


Figure 25.5. Number of adults and children (and rate per total population) estimated to live with a heart defect in the year 2000, by severity of congenital heart defect. (Data from Warnes CA, Liberthson R, Danielson GK, et al. Task force 1: the changing profile of congenital heart disease in adult life. *J Am Coll Cardiol* 2001;37:1170–1175.)

TABLE 25.4

Prevalence of Congenital Heart Defects: Importance of Person, Place, Time, and Implications for Prevention

Issue	Comment and Implications
Defining heart defects	<p>Evaluating heart defects in the aggregate has limited value: rates of clinically minor defects drive overall rates and depend critically on diagnostic and reporting intensity, etiology and prevention are unlikely the same across all types of heart defects, and the benefits of prevention are also a function of clinical severity.</p> <p>More informative to study, report, and monitor specific types of heart defects or, at a minimum, well defined classes of heart defects, defined by severity or pathogenesis, depending on the goal of the study.</p> <p>Exclusions, coding and classification affect findings, sometimes substantially: important to describe completely in report and use consistently.</p> <p>Separate isolated cases from multiple congenital anomalies and genetic syndromes.</p>
Geographic variations	Also driven mostly by clinical practice and reporting methodology. When evaluating trends after interventions, best to use the same area or program as baseline, to minimize the influence of methodologic issues.
Time trends	<p>Baselines and analytic techniques must be chosen carefully when evaluating prevention interventions (e.g., diabetes, flour fortification): preceding time trends need to be identified and adequately incorporated (typically requires statistical modeling).</p> <p>Trends can be valid, even in the presence of incomplete ascertainment, so long as the ascertainment fraction remains constant: methodologic consistency is key in longitudinal assessment.</p>

Briefly, in evaluating prevalence it is very helpful to think in terms of person, place, and time. In practice, this means clearly defining first the “person,” namely, the study population and the heart defects (including method of coding and classification, inclusion, and exclusions) in addition to data sources and reporting procedures. Defining “place” is also important, because of well-known geographic variations in prevalence. One implication of these geographic variations is that when evaluating interventions, it is crucial to have preintervention baselines that are local (this obvious step can be forgotten in the haste of implementing prevention strategies). Finally, the element of “time” is important not only as a reminder to assess temporal trends, but also to highlight the need to expand studies to adolescents, adults, and the elderly, so that their needs are better assessed and met.

WORLD PERSPECTIVE

With the caveats just described, some minimal generalizations can probably be made about the international occurrence of congenital heart defects. The aggregate data described so far (including those in Table 25.3) suggest a birth prevalence of approximately 2 to 3 per 1,000 for the clinically more severe conditions, increasing to 6 per 1,000 when including also moderately serious conditions (21), and summing to 9 per 1,000 to perhaps 15 to 20 per 1,000 when further including smaller septal defects and milder valvar stenoses (35,40). Adding bicuspid aortic valve might add another 5 to 10 per 1,000 cases to these estimates. In numbers, among the estimated 140 million births occurring yearly worldwide, the overall number of babies born with heart defects could be in the order of 1.2 million per year (9 per 1,000), of which approximately 300,000 to 400,000 will have what may be considered severe heart defects (2 to 3 per 1,000).

However, generalizing findings from relatively small study areas in a few developed countries to the rest of the world, while useful as a broad indicator of global impact, requires considerable caution. The best estimates from good studies in developed countries are probably a reasonable starting point (21,56–58), and have been used in the latest March of Dimes

global report on birth defects (59). In fact, because of the challenges of obtaining accurate data on congenital heart defects in resource-poor areas, such extrapolations are probably a better approach than relying on local data of lesser quality. Nevertheless, these extrapolations may underestimate the true numbers. The occurrence of congenital heart defects in developing countries may be higher than in developed countries for several reasons, including higher rates of consanguinity and greater exposure to nutritional, maternal, or environmental risk factors. From a prevention perspective, the large fraction of affected births from developing countries underscores the urgency for effective primary prevention, and in particular prevention that is comprehensive, inexpensive, and focused on modifiable risk factors associated with the largest fraction of disease in the population.

OCCURRENCE: THE FUTURE

As discussed, the prevalence in older children and adults is likely to increase for several years as survival rates improve worldwide. Prevalence at birth may also change over time. Some factors have already been examined, such as the more complete and earlier ascertainment of milder or minor heart defects. Additional factors that could have a significant impact on current rates and trends include pregnancy termination, universal neonatal screening, and changing prevalence of risk factors. A few examples are discussed by way of illustration.

IMPACT OF PRENATAL TERMINATIONS

A major challenge will continue to be the assessment of fetal deaths and pregnancy terminations with congenital heart defects. In some areas, pregnancy terminations account for a substantial fraction of cases of selected congenital heart defects. In a study of a selected group of European birth defect registries, with data through 2005, 6% of all cases of heart defects not associated with chromosomal anomalies were terminations of pregnancy, with variations across registries and type of congenital heart defect (36). In that study, the reported rate of prenatal diagnosis was fairly low (13%), suggesting that terminations of pregnancy could account for a higher fraction

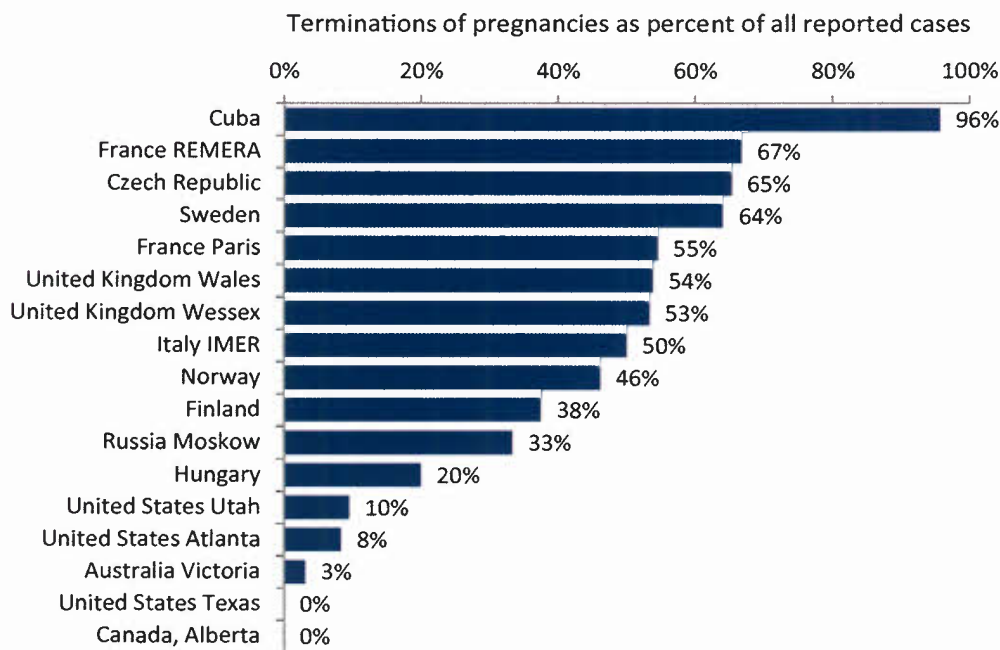


Figure 25.6. Pregnancy terminations as proportion of all cases of hypoplastic left heart syndrome: selected birth defect programs of the International Clearinghouse for Birth Defects Surveillance and Research, 2007. (Data from International Clearinghouse for Birth Defects Surveillance and Research. Annual Report 2009, with data for 2007. In: Mastroiacovo P, ed. Rome, Italy, 2009.)

of cases in the future, as the prenatal diagnosis of severe cases increases. In a related study from the same database, selected heart defects, including hypoplastic left heart syndrome and single ventricle, contributed to late terminations of pregnancy, after 23 weeks of gestation (60).

The impact of pregnancy termination can be considerable in particular for certain heart defects. As an example, Figure 25.6 summarizes the data on hypoplastic left heart syndrome reported to the International Clearinghouse for Birth Defects Surveillance and Research for the 2007 birth cohort, including only programs that ascertain pregnancy terminations, had realistic overall birth prevalence rates (2 per 10,000 or more, see Table 25.3), and at least 10 or more cases of the condition (61).

In some areas, particularly in Europe, pregnancy terminations account for half or more of all cases of hypoplastic left heart syndrome. In North America, this fraction seems to be consistently lower, under 10%. Ascertainment of pregnancy terminations can be difficult and reported rates may vary for methodologic reasons as well. Nevertheless, these findings underscore how studies that fail to incorporate pregnancy terminations will underestimate the overall occurrence and impact of congenital heart defects. In etiologic studies, failure to include pregnancy terminations could introduce potentially significant biases; for example, if an exposure (e.g., smoking or medical use) is associated with the likelihood of a pregnancy termination. Finally, increasing pregnancy termination rates, if unaccounted for, can lead to an apparent drop in birth prevalence, and conversely, with fewer pregnancy terminations, birth prevalence may appear to increase and cause unnecessary community concerns. Systematically including pregnancy terminations in epidemiologic monitoring can help clarify these issues.

NEONATAL SCREENING

Universal neonatal screening by pulse oximetry has been proposed for the early detection of certain critical cyanotic conditions, and is already being implemented either clinically or in pilot studies, mainly in parts of North America and Europe (62–73). Leaving aside the advantages and challenges of this approach, which are still a matter of discussion, universal screening could speed the identification and reporting of selected severe heart defects. High-quality registries with

multiple sources of ascertainment through infancy would be unlikely to miss many such cases; in these areas, the birth prevalence of these heart defects would probably change little if at all, though some cases would be identified and reported earlier than before screening. Advantages for epidemiologic monitoring would be seen mainly in areas with only basic registries or none at all. In fact, universal screening, if properly organized, would create a valuable repository of information on selected major congenital heart defects for the entire screened population. Such population-based data would support some of the key clinical and public health activities on a much larger scale than has been possible so far, including monitoring trends, assessing outcomes, conducting etiologic studies, and evaluating prevention interventions.

CHANGES IN RISK FACTORS

Current population trends suggest that the prevalence of some known risk factors for congenital heart defects is changing. One example is the increasing maternal age in many developed countries. This could lead to an increase in pregnancies with heart defects associated with maternal-age dependent chromosomal syndromes. The increase would likely be small on a yearly basis, and probably undetectable unless the data are examined carefully. The prevalence at birth of these heart defects would also depend on the concurrent use of fetal diagnosis and pregnancy termination. As a risk factor, the population distribution of maternal age is difficult to modify, though education and preconceptional counseling could have an impact in individual situations. A more pervasive concern is the rise of some risk factors such as maternal pregestational diabetes, especially if untreated or unrecognized. As discussed in the section on risk factors, diabetes is already increasing in several countries: the combination of high frequency, increasing trends, and high teratogenic risk makes diabetes a clinical and public health priority in pediatric cardiology.

Detecting the Next Epidemic of Congenital Heart Defects

Several of the potential causes of rate increases so far discussed are to some extent predictable. A different concern is the unexpected, unpredictable introduction of a teratogen that could cause an epidemic of congenital heart defects. Known cardiac

teratogens such as retinoic acid and rubella can and have caused clusters of heart defects. Monitoring for the next unknown teratogen-induced “epidemic” of birth defects is a stated goal for many monitoring programs. Effective monitoring has to balance the ability to detect true changes (high sensitivity, low false-negative rates) with the cost of investigating false alarms (false-positive rates). In practice, this requires continuously discriminating among the multitude of signals to identify those with the greatest epidemiologic and biologic plausibility. Setting the bar too high or too low can lead to missed epidemics, either because these are missed altogether (bar too high) or because so many investigations are started with limited resources (bar too low) that some crucial element could be missed.

A typical challenge, for example, is detecting increases of one type of heart defect because of a teratogenic exposure in one part of a country. The often shifting background rates, the challenges of ascertainment, and the limited resources for population-based surveillance make such ongoing monitoring extremely challenging. Rising to these challenges requires increased resources and innovative approaches, some of which are summarized in Table 25.5.

These approaches strive to improve the quality of clinical description and cardiology expertise available to monitoring programs, and to implement a structured, accurate, and rapid response to a concerning “signal.” Particularly in small clusters and when very difficult to otherwise detect, pediatric cardiologists can play an important role as the “astute clinicians,” who note unusual occurrences (e.g., rare defects clustering in time and space) and activate the public health system for further triaging. The subsequent epidemiologic investigations could identify new or emerging causes of congenital heart defects and prevent further epidemics.

Mortality

Preventing congenital heart defects has a significant potential for decreasing infant deaths. Worldwide, congenital heart defects are the leading cause of infant deaths due to congenital

anomalies (57,74). In the United States, population-based estimates using vital records indicate heart defects as the cause of 1 in 24 neonatal deaths overall (4.2%) and 1 in 4 neonatal deaths due to birth defects (24.5%) (75). In Europe, data from Eurocat registries suggests that heart defects also account for approximately 1 in 4 early neonatal deaths to birth defects (36). Among infants <1 year of age, heart defects may contribute to one-third of infant deaths due to congenital anomalies, and, overall, to approximately one-tenth of all infant deaths (57,74). Data from developing countries is scarce, but the early impact of defects is likely even higher than in developed countries, because of the lack of resources to effectively treat babies with severe heart defects. In one study based on WHO data, infant mortality due to birth defects was roughly in inverse proportion to a country’s per capita gross domestic product (74). From a prevention perspective, these findings underscore the global impact that low-cost, effective strategies of primary prevention may have worldwide.

Mortality on a population level can be monitored, readily but with some limitations, using death certificates. Using this approach, researchers have documented how in the United States, mortality from congenital heart defects has been declining for decades (76,77), and by nearly 2% per year from 1979 through 1997 (76). More recent data (78) continues to show a decline in mortality, at an average rate of 3.6% per year in more recent years. Figure 25.7 combines the data from these two studies (76,78), and shows the overall mortality declining from 2.5 to 1 per 100,000 population from 1979 to 2006, an overall 60% decline in 27 years.

Mortality still remains highest in infancy. Throughout the period shown in Figure 25.7, half of all deaths from congenital heart defects occurred before 1 year of life (76,78). Mortality associated with selected heart defects using the most recent United States data is shown in Figure 25.8 (78).

A few types of heart defects accounted for most infant deaths, with hypoplastic left heart syndrome being by far the major contributor. Of note, mortality due to hypoplastic left heart syndrome decreased between 1999 and 2006, whereas this was not as apparent earlier, from 1979 to 1997 (76).

TABLE 25.5 Detecting the Next Epidemic of Heart Defects: Areas for Improvement

Action	Value
Population-based monitoring	Ensures coverage, decreases likelihood of bias (e.g., referral bias)
Clinical description and classification	High-quality description, coding, and classification, based on verbatim descriptions improves accuracy and precision, allows for monitoring of biologically meaningful groups of defects
Clinical collaboration	Pediatric cardiologist collaborating with public health epidemiologist can provide critical clinical expertise to inform and improve monitoring (case review, coding, classification)
Spatial analysis	Improves detection of spatially confined clusters, such as in agricultural areas (pesticides), near hazardous waste sites (contaminants), or in population areas with disadvantaged socioeconomic status (e.g., border areas) Can be added to temporal analysis (time clustering)
National and international networks	Collaborative monitoring and data sharing allows for “alarms” in one area or country to be quickly examined or tested elsewhere. Networks can also share expertise and protocols (e.g., protocols to investigate apparent clusters)
Concurrent monitoring of risk factors	Monitoring of known or putative risk factors can be done on a population level (e.g., rates of diabetes in a province or country) and also individually (screening questionnaires for parents)
Network of astute clinicians	Promotes timeliness and sensitivity: astute clinicians can detect quickly small clusters, generate accurate clinical information, provide clues to exposures, and facilitate contact with affected families for further investigations. Challenge is minimizing unnecessary alarms (false positives)

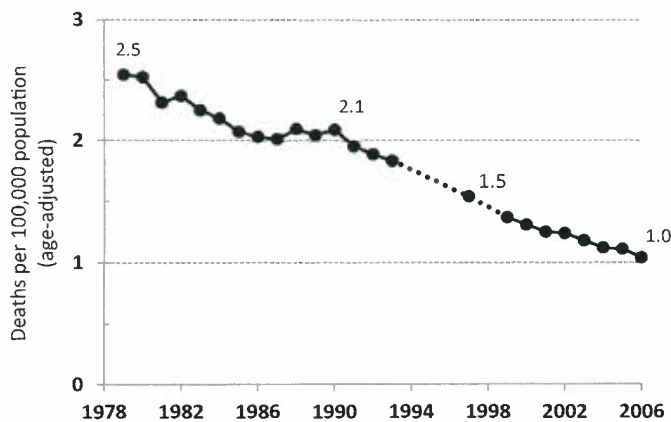


Figure 25.7. Overall mortality from congenital heart defects (age adjusted), calculated as deaths per 100,000 population in the United States from 1979 to 2006. (Data from Boneva RS, Botto LD, Moore CA, et al. Mortality associated with congenital heart defects in the United States: trends and racial disparities, 1979–1997. *Circulation* 2001;103(19):2376–2381; Gilboa SM, Salemi JL, Nembhard WN, et al. Mortality resulting from congenital heart disease among children and adults in the United States, 1999 to 2006. *Circulation* 2010;122(22):2254–2263.)

Some data are emerging also for *older ages*. In the United States, most deaths after infancy (76%) are occurring in adults rather than in older children (78). The declining mortality among adults and their associated findings were also described by other investigators using the same mortality files (79).

These studies using death certificates provide important data. However, because they are based on death records alone, changes in the underlying birth cohort are not accounted for. For example, mortality (deaths per 100,000 population) could decrease not only when survival improves, but also when birth prevalence decreases, either as an effect of primary prevention or of increased pregnancy termination of affected fetuses. These

situations cannot be distinguished based on death certificates alone. For this reason, these data need to be complemented by occurrence studies. Also, studies that follow a well-defined cohort of people with congenital heart defects over time and assess their outcomes are very important. However, such studies typically are difficult and complex, particularly on a population-basis, but can be feasible in countries with robust population-based health registries and universal health care. Nationwide studies have not been done in the United States. However, with the expansion and linkage of clinical, surgical, and birth defect registries, they might be feasible in the future (80). In Denmark, population-based linkage studies were able to estimate mortality in the entire nationwide cohort of people born with heart defects, from 1977 through 2006 (81). A major finding was this cohort's excess risk of death compared to the general population that extended well beyond childhood. It also documented a declining mortality among adults with several types of congenital heart defects. In Quebec, using linked administrative databases, Canadian investigators were able to evaluate mortality in a population-based group of over 70,000 people with congenital heart defects (82). The study documented gains in survival in all age groups, including adults, but particularly among infants with the more severe types of congenital heart defects (82).

Even if not truly population-based, helpful data can also come from networks of hospitals that cover a large fraction of a country. One such study from Belgium documented the improving survival for specific types of congenital heart defects in children followed by the country's seven pediatric cardiology centers (83); by focusing on one center, investigators were also able to demonstrate improved survival for older birth cohorts (84). In the United States, a few population-based cohort studies have been conducted using state registries of birth defects. One such study, from Texas, assessed survival in a cohort of children with functional single ventricle, including hypoplastic left heart syndrome (85). Aside from documenting variations in survival by type of anatomy and presence of extracardiac malformations, the study also confirmed declining mortality in this complex group of conditions, specifically a 47% decline from 1996 through 2003 (85).

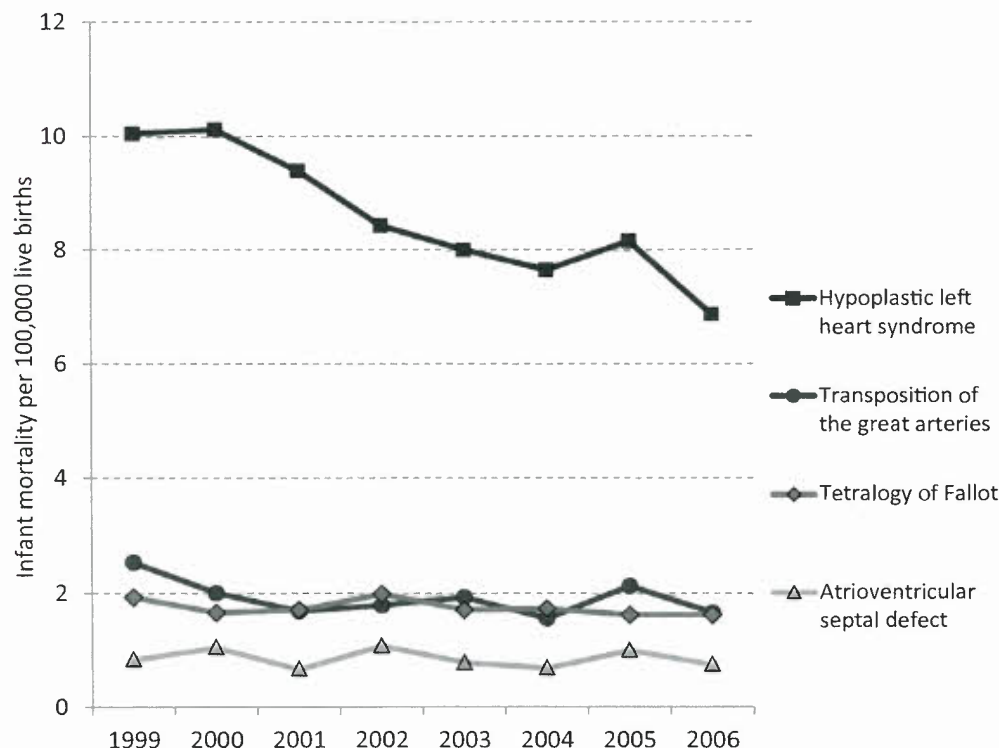


Figure 25.8. Infant mortality from selected congenital heart defects, calculated as deaths per 100,000 livebirths in the United States from 1999 to 2006. (Data from Gilboa SM, Salemi JL, Nembhard WN, et al. Mortality resulting from congenital heart disease among children and adults in the United States, 1999 to 2006. *Circulation* 2010;122(22):2254–2263.)

From a prevention perspective, improving survival is a major goal, ideally through primary prevention, but also through preventing complications and optimizing health in people born with heart defects. Evaluating the effects of prevention will likely require using a combination of epidemiologic approaches. Population-based studies with longitudinal follow up would be of greatest help, particularly, as discussed next, because they would be suited to evaluate not only survival, but also other important outcomes including disabilities, morbidities, and quality of life.

Developmental Disabilities

In estimating the impact of prevention on the life of people with congenital heart defects, it is crucial to include neurodevelopmental outcomes. In one survey, clinicians and parents alike rated neurologic disability a greater concern than cardiac disability when considering quality of life for children with congenital heart defects (86). With improving survival, these outcomes are of increasing relevance and constitute an area of rapidly increasing research (87–89,90,91–96).

Neurodevelopmental outcomes and related clinical issues are discussed in detail elsewhere (see Chapter 73). From an epidemiologic perspective—the focus here—the frequency, range, and causes of neurodevelopmental outcomes associated with congenital heart defects are still incompletely known. Nevertheless, accumulating data suggest the following considerations.

First, neurodevelopmental challenges are common in children with a congenital heart defect who also have an identifiable genetic condition, such as deletion 22q11, or multiple congenital anomalies. In some cases, the genetic condition is undiagnosed at the time of cardiovascular evaluation (97). However, children without syndromes or apparent extracardiac involvement are also at increased risk for adverse neurologic outcomes. Microcephaly, neuronal migration defects and Chiari I malformation have been identified in children with apparently isolated congenital heart defects (98). In some cases, subtle brain anomalies or altered hemodynamics could be present prenatally in fetuses with some heart defects (93,99), as evidenced by small fetal brain volume and signs of impaired brain metabolism on magnetic resonance imaging and spectroscopy (99). After birth, hemodynamics, cyanosis, or the stress and complications of surgery, associated with low birth weight or preterm birth could also play a role (94,97,100–104). It is debated whether children after cardiac transplantation (105) or surgery for single ventricle physiology (100) are at higher risk for adverse neurodevelopmental outcomes.

In general, it appears that in the absence of genetic conditions and severe postnatal complications with brain damage, intellectual disability is probably rare, with overall intelligence typically within the normal range in older children and adolescents. However, deficits in executive function, attention deficit and hyperactivity disorders, and neuropsychiatric conditions such as anxiety and depression could be more common than previously thought. In a systematic review of studies published between 1990 and 2008, Swiss investigators examined 23 studies, including randomized controlled trials, case control, or cohort studies, which evaluated psychological parameters in people with congenital heart defects between 2 and 17 years of age and follow-up of at least 2 years after open heart surgery (106). This review noted the wide range of methodologic quality of the studies, with most studies deemed to be of moderate quality. In their summary of findings, these investigators concluded that according to their parents, a substantial fraction of children experienced psychological maladjustment, particularly in children with

severe heart defects or developmental delay. Nevertheless, studies of long-term psychological adjustment evaluated by self reports tended to indicate good psychological outcomes. The overall conclusion of the review was that a significant fraction of children and young adults who underwent open heart surgery for congenital heart disease (CHD) were at risk for psychological maladjustment but not overt intellectual disability (106).

Such information is useful in planning management and identifying underrecognized issues, such as the need for testing and early intervention. However, with improving prenatal and postnatal management, it is unclear whether what we know now of adolescents and adults, born and treated sometimes decades ago, can be used to counsel the parents of today's babies. For this reason, it is crucial to develop epidemiologically robust, longitudinal studies of developmental outcomes. Studies that follow population-based cohorts would be particularly helpful, as they would capture the entire spectrum of people born with heart defects and would be less prone to biases compared to studies based on one or few referral centers.

Some progress is being made along these lines. In Norway, investigators are utilizing the Norwegian Mother and Child Cohort Study (MoBa), a prospective cohort study conducted by the Norwegian Institute of Public Health, to examine a wide range of outcomes in children with congenital heart defects and their parents. In one such study, investigators linked the cohort of 44,000 children to the Norwegian nationwide heart defect registry. They identified 175 children 3 years of age with congenital heart defects, 60 of whom had severe defects. They then examined the results from maternal questionnaires relative to the child's motor, communication, and social impairment (for this study, investigators used the data collected prospectively at birth, 6, 18, and 36 months). They found that, compared to controls, children with severe heart defects had more than a threefold risk for communication and gross motor impairments, and a twofold increased risk for any developmental impairment. Children with mild and moderate heart defects had a twofold higher risk for gross motor impairment but did not otherwise differ from controls. Of note, impairments were more frequent among children already noted to have developmental delays and a smaller head size at birth (107). The investigators recommended early assessment for motor and communication support provided in children with congenital heart defects, particularly severe types, with the goal of improving long-term outcomes. In a related study (108), investigators from the same group examined whether these same children had a higher risk of internalizing or externalizing emotional problems at 36 months of age compared to controls. They found no evidence of increased risk and speculated this finding could be related to the fact that these children had completed the bulk of their medical and surgical treatment (108). These studies are notable not only for their methodologic strength and results, but also as an example of a systematic, large-scale approach to evaluating health and outcomes over the lifespan. Its ongoing design will hopefully continue to generate additional outcome data on older children and young adults.

In summary, some children with congenital heart defects appear to be at risk for adverse development and psychological outcomes, although their frequency, magnitude of risk, and predictors have not been clearly defined. The impact of these outcomes in terms of use of services, cost, disability, and quality of life for patient and family has not been formally evaluated. Incorporating these outcomes into the "cost" of congenital heart defects would provide a more realistic evaluation of the potential benefits of primary prevention, and a further incentive for research and preventive interventions.

Quality of Life

Health-related quality of life is a focus of increasing interest in pediatric cardiology. By definition, quality of life is a multidimensional construct that integrates an individual's subjective perception of physical, social, emotional, and cognitive functioning. This definition highlights the construct's major strength, namely, bringing to the forefront the subjective perspective of the person with a congenital heart defect (and the family). The need for long-term studies of quality of life is increasingly recognized (90,109). Such studies also try to incorporate dimensions, often missed by other approaches, such as school functioning, social functioning, independent living, and social integration (88). Because such perspectives are not retrievable from clinic and administrative records, quality of life studies require new skill sets as well as novel methods and tools (110–113). In fact, a major challenge has been the scarcity of validated assessment tools targeted at people with congenital heart defects and their families. Because of this, many studies are difficult to compare and summarize: a recent review found that in 12 studies of quality of life studies in people with congenital heart defects (106), eight different assessment tools were used, and only three were used in more than one study. Having common validated tools will help speed progress in this field. With these limitations in mind, it is not surprising that current findings are often inconsistent, as may also be expected for an outcome that depends on a web of factors, including disease severity, surgery, health care support, family support, insurance coverage, income, and societal attitudes toward chronic illness (90,114–118).

For example, one population-based study in Finland found reasonably good outcomes in a group of people with congenital heart defects (mainly mild-to-moderate conditions such as septal defects), including educational attainment, employment level, and frequency of steady relationship (119). By contrast, several studies in North America and Europe reported worse health-related quality of life in people with congenital heart defects compared to reference groups (120–123). Such outcomes in some studies appeared to vary by anatomic lesion and surgeries (116,124), family income (114), and age (125–127). Also, obtaining employment, health insurance, and mortgages were noted as challenges in the United States (128), even for people with mild heart defects (129).

These data should be viewed as exploratory and preliminary, given the heterogeneity in methods and results across studies. A recent systematic review (106) found that in four of the 12 studies analyzed, quality of life of selected congenital heart defects (not always the same across the different studies) was comparable to normative samples according to proxy- (130,131), self- (132) or combined reports (133). One study even observed a better self-reported quality of life compared to healthy norms in a large sample of children with transposition of the great arteries undergoing surgery (116). In contrast, four studies reported an impaired quality of life in many self- and most proxy-reported dimensions (114,120,134,135). Two studies compared quality of life of children with congenital heart defects with that of children with other chronic illnesses: one study found better proxy-reported quality of life among children with congenital heart defects (135), whereas the other study found the converse (131). However, these studies are difficult to compare because they used different tools that tended to measure different dimensions of quality of life (106).

Some studies have tried to identify clinical predictors of quality of life, with inconsistent results. For example, a poorer quality of life was associated only in a minority of studies with the complexity of heart defects, type of surgery, duration of circulatory arrest, and number of surgical procedures (106). In two studies, a poorer quality of life was observed with postoperative complications, length of hospital stay, and current

need for cardiac medication (114,134). Factors that influenced parental quality of life in at least one study included being unemployed or having a low income because of the child's health condition (114), the presence of an adverse family relationship (114), and parental stress at follow up (136). Finally, in two studies, older age at follow-up assessment was associated with a better quality of life (120,135).

In summary, even with incomplete and heterogeneous data, it appears that the quality of life in children and young adults with congenital heart defects seem to be affected, more so when assessed by parental reports than self reports. Also, parent's quality of life appears affected, perhaps even to a higher degree than in their children. The implication for management is that support needs to be aimed not only at the child but also at parents, ideally in an integrated approach. Looking at the future, although the evidence base relative to quality of life is still less than robust, research in this area is expanding rapidly. Specific tools for people with heart defects are being developed and validated, including a cardiac module for the PedsQL (123,137) currently undergoing validation, and a disease-specific Pediatric Cardiac Quality of Life Inventory (138,139) with patient and parent-proxy forms and adapted for a wide age range. These developments should lead to a more extensive and robust body of literature that could be very helpful not only in delivering optimal clinical care but also in providing a more realistic assessment of benefits of prevention that incorporates the quality of life of people with congenital heart defects and their families.

Health Disparities

Health disparities are a primary consideration in implementing and evaluating prevention activities (140). Disparities typically refer to differences in the occurrence, mortality, and burden of disease among groups of people. Disparities may arise because of the unequal distribution in the population of risk factors, including access to care, environmental exposures, low socioeconomic status, compounded or heightened by variations in disease susceptibility (140,141). Identifying and eradicating health disparities are critical steps in pursuing a measure of social justice in community health (140,141).

One example of health disparity is the disproportionate mortality for congenital heart defects (and birth defects in general) in developing countries compared to developed countries, as discussed above. However, health disparities appear also within developed countries, and are a major concern (140). For example, mortality for congenital heart defects in the United States, appears to vary by race and ethnicity and this has been documented for decades (76,78). As illustrated by Figure 25.9, infant mortality in the US, based on death certificate files through 2006, has been consistently higher from black infants than for white infants (78). For Hispanic infants, the pattern is less consistent, and rates are closer to those in white infants than reported previously (76,77).

The potential complexities of these evaluations are highlighted in a recent report on neonatal mortality associated with congenital heart defects in the United States (75). Using vital record data, investigators reported similar overall neonatal mortality between black and white infants. However, these findings changed considerably when stratified by gestational age. For example, among term infants, the neonatal mortality attributable to heart defects was 20% higher among infants of black mothers compared with white mothers, but among preterm infants, the rate was 30% lower among infants of black mothers compared to white mothers (75).

These differences in outcomes by race and ethnicity have been documented independently using different approaches, including follow-up studies after surgery for congenital heart defects using inpatient databases (142) and a population-based

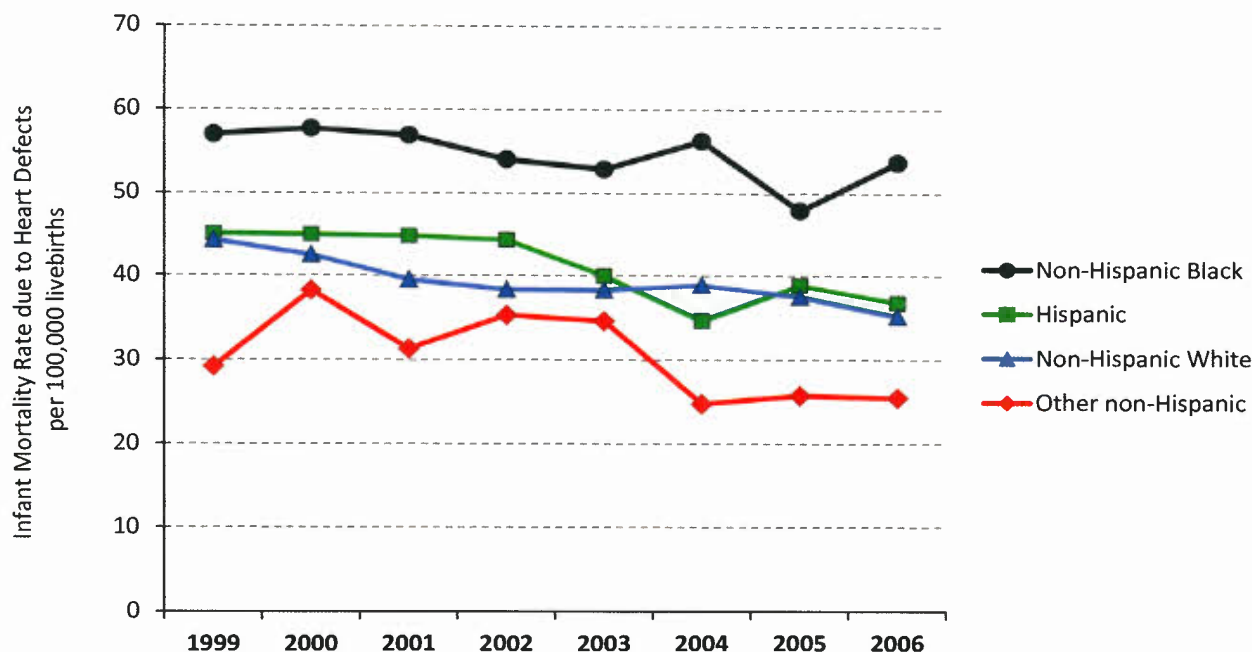


Figure 25.9. Infant mortality from selected congenital heart defects by race-ethnicity, calculated as deaths per 100,000 livebirths in the United States from 1999 to 2006. (Data from Gilboa SM, Salemi JL, Nembhard WN, et al. Mortality resulting from congenital heart disease among children and adults in the United States, 1999 to 2006. *Circulation* 2010;122(22):2254–2263.)

studies of early childhood mortality (143). The latter study identified an approximately twofold higher risk of dying in non-Hispanic black infants with selected severe heart defects compared to white infants, and smaller increased risk for Hispanic infants (143).

Expanding the assessment of potential health disparities over the lifespan (Fig. 25.10), researchers have examined United States death certificate data looking at race-specific mortality by age group (78).

Mortality in blacks compared to whites was disproportionately higher in infants and children (rate ratios of ~1.5 overall), continued to be higher but less so through age 35 years, and became similar or even lower in older adults (perhaps because of fewer survivors or fewer diagnoses at those ages). For Hispanics, the pattern is less consistent, with higher mortality than whites in very young children, but similar and even lower mortality than whites in older age groups. The reasons behind these differences are still unclear (75), and further studies are needed to understand whether they are due to reporting, prenatal diagnosis, prevalence of heart defects, or to differences in risk factors for congenital heart defects or medical treatment.

In general, by reducing occurrence, primary prevention ought to ameliorate such disparities. A mix of targeted and population-based interventions is probably required to ensure that the benefits of prevention accrue equally to all segments of the population. This is particularly important for interventions aimed at exposures that affect the population unequally, such as maternal diabetes, smoking, or lack of preconceptional care. Similar considerations apply also to interventions aimed at improving outcomes among people with heart defects (secondary prevention).

Cost

Cost can be a powerful incentive for prevention. Current cost estimates are particularly important when projecting the future benefits of prevention and comparing these with the investments needed now to make prevention happen (144).

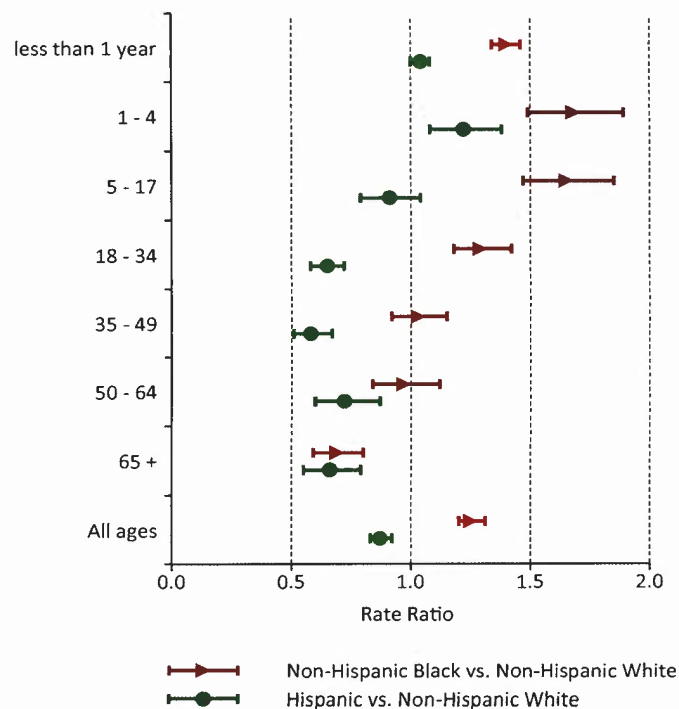


Figure 25.10. Rate ratios comparing mortality from congenital heart defects by race-ethnicity (non-Hispanic black vs. non-Hispanic white, Hispanic vs. non-Hispanic white) in different age groups in the United States from 1999–2006. Lines represent 95% confidence intervals. Rate ratios above 1 suggest increased mortality, and rate ratios below 1 suggest decreased mortality compared to the reference group (non-Hispanic white). (Data from Gilboa SM, Salemi JL, Nembhard WN, et al. Mortality resulting from congenital heart disease among children and adults in the United States, 1999 to 2006. *Circulation* 2010;122(22):2254–2263.)

However, current cost estimates of congenital heart defects in the United States are far from being precise, complete, or timely. Part of the reason lies in the complexity of cost estimation, but a significant part lies also in the fragmentary nature of health care, restricted access to data, and incompleteness of many databases with health expenditure information. Before reviewing the literature on cost estimate, it is helpful to briefly outline the main elements of cost and the related data sources. Further information is available with extensive references in a recent review (144).

COMPONENTS OF COST

To understand the basic aspects of cost, it can be helpful to imagine following a cohort of people with heart defects from birth (or ideally pregnancy) through the lifespan. The cost of congenital heart defects, from a societal perspective, can be defined broadly as the consumption of resources in producing a good outcome, that is, optimal health, in this cohort. (Usually one is interested in incremental cost, which is the cost over and above the cost of people without heart defects). With primary prevention, these incremental costs should be saved. With secondary prevention, which is aimed at improving outcomes through optimal care of people with heart defects, some costs will be saved by preventing complications, whereas others might increase because of prolonged care with longer survival; better cost-effectiveness, if not cost saving, would be the goal.

Viewed as consumption of resources, the cumulative cost of congenital heart defects over the lifespan will have several components, some of which are easier to assess directly, whereas others may require more assumptions and complex statistical modeling. The obvious and most tangible component of cost is the direct medical cost, that is, the health expenditures for providing medical care and other services to people with congenital heart defects. These would include not only inpatient costs (facility as well as professional services costs), but also outpatient costs (office visits, emergency room visits, rehabilitation and early interventions services, etc.) and pharmacy costs. Additional components from a societal perspective are the so-called indirect costs. These include mainly the reduced economic productivity for people with congenital heart defects. Caregiver costs, including lost productivity of caregivers as their activity are diverted to the care of affected family members, are important but rarely incorporated formally into cost estimates.

GOALS OF COST ESTIMATION

Ideally, in estimating cost in a prospective cohort of people with congenital heart defects, several metrics would be derived: incremental cost (rather than charges) due to heart defects, in the aggregate cohort as well in groups of people with specific types of heart defect; direct and indirect costs, separately and combined; cost breakdown by age group as well as longitudinally over the lifespan; national cost; and costs on a yearly basis. These data would be especially valuable if monitored in a timely manner and derived from a population-based, representative cohort of people with congenital heart defects that are accurately diagnosed and well characterized. Having this ideal situation in mind is helpful when evaluating the cost information currently available, which typically lacks several of these attributes. The overall result is that available cost studies likely underestimate, probably by a large margin, the true cost of congenital heart defects. In doing so, they also underestimate the potential benefits of prevention.

ESTIMATING COSTS

In the United States, several health expenditure databases have been used by researchers to estimate cost (144). Some are commercial databases. The MarketScan Commercial Claims

and Encounters database, for example, contains considerable cost information on inpatient admissions and outpatient services. However, this database covers a select population of employees of a set of large self-insured corporations, and is not representative of the general population. Also, researchers are not currently allowed to link these data to outside heart defect registries; to identify and characterize people with congenital heart defects, researchers need to use the ICD codes in the MarketScan database, with well-known problems of miscoding leading to false-positive and false-negative diagnoses. Another resource for cost estimation is the Healthcare Cost and Utilization Project (HCUP), which provides two nationally representative databases: the Nationwide Inpatient Sample (NIS), based on a 20% sample of community-based hospitals, and the Kids Inpatient Database, focusing on pediatric admissions, estimated to cover about 90% of births in the United States. These databases, however, cover only inpatient admissions, and even for these, they include facility costs but no professional service fees, which can be considerable in children with heart defects. Also, no outpatient services are included. Medicaid is a third resource used for cost estimates. It contains comprehensive data, can be linked to birth defect registries, but includes only patients covered by Medicaid and varies in operation between states, limiting extrapolations to the national context.

In summary, in the United States, fairly extensive cost information is typically available only on select, typically nonrepresentative cohorts of people, whose diagnosis is difficult to validate. Conversely, for nationally representative samples only partial cost information, consisting typically of some part of direct medical costs such as inpatient admissions, typically can be obtained. Also, nearly all these data are cross-sectional, rather than longitudinal. With these strengths and limitations in mind, one can now focus on two important metrics of costs for which some data are available, namely, cross-sectional costs and lifetime costs.

CROSS-SECTIONAL COSTS (ANNUAL COSTS)

A helpful estimate for health care professionals and policy makers is the cost of congenital heart defects in a population, in any given year. By providing a cross section of costs in one point in time, these estimates can indicate the immediate short-term cost savings potentially deriving from prevention, particularly primary prevention. Nationally representative estimates of costs (rather than charges) have been produced for people with major congenital heart defects in the aggregate and for specific defects, using the HCUP database (HCUPnet) (144,145). According to these data (Fig. 25.11), the estimated cost of inpatient admissions alone in 2004 for people with congenital heart defects, all ages, was \$1.4 billion.

People with congenital heart defects were identified by ICD codes (745.0 to 747.9) in the principal discharge diagnoses. As high as this figure seems, it still likely underestimates the inpatient cost because, for example, professional services fees during the admission are not included. Nevertheless, it is an important aggregate estimate. An expanded assessment of this dataset (144) provided an additional estimate associated with a subset of severe heart defects. These were defined, based on ICD codes alone, mainly as conotruncal, single ventricle, hypoplastic left heart syndrome, Ebstein anomaly, and endocardial cushion defects. The associated cost, for the same year, and across all age group, was \$511 million (Fig. 25.11). Nearly all admissions for these defects were among infants (95%). However, the study authors noted that admission for heart-defect related causes in older patients could be less likely to be assigned congenital heart defect codes compared to younger patients, leading to an underestimate of costs among adults.

To try and capture not only inpatient admission costs but also outpatient costs, the same investigators also conducted an

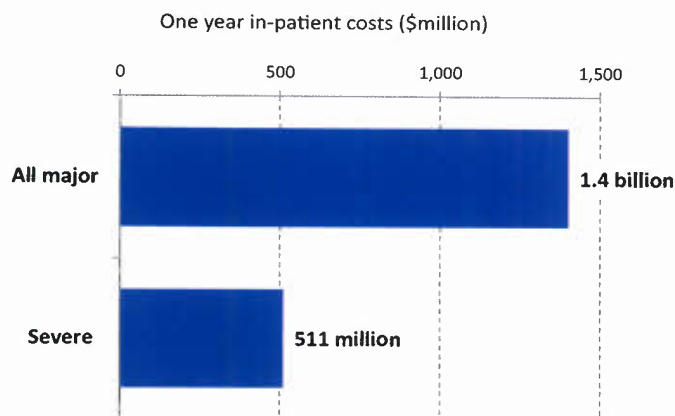


Figure 25.11. Estimated nationwide costs for inpatient admissions for congenital heart defects, overall and in a subset of severe heart defects in the United States in 2004. (Data from Boulet S, Grosse SC, Riehle-Colarusso T, et al. Health care costs of congenital heart defects. In: Wyszynski DF, Correa-Villasenor A, Graham TP, eds. *Congenital Heart Defects: from Origin to Treatment*. New York, NY: Oxford University Press, 2010:493–501; Russo CA, Elixhauser A. Hospitalizations for birth defects, 2004. In: HCUP Statistical Briefs. Rockville MD: U.S. Agency for Healthcare Research and Quality; 2007.)

analysis of MarketScan data (144), focusing on costs for the 2005 for children 0 to 3 years of age with a major congenital heart defect (Fig. 25.12).

The mean cost among infants was estimated at nearly \$100,000 among infants, or 25 times the cost for children without a congenital heart defect (cost ratio). The costs decreased by about one-third among 1-year-olds and again among 2-year-olds, with cost ratios of 12 and 9, respectively. The mean costs were over four times the median costs, indicating that some children contributed disproportionately to the costs. Figure 25.12 also shows the costs associated with by severity. Children with the more complex heart defects were one-tenth of all children with heart defects in the study (153/1,530) but contributed disproportionately to overall costs (Fig. 25.12).

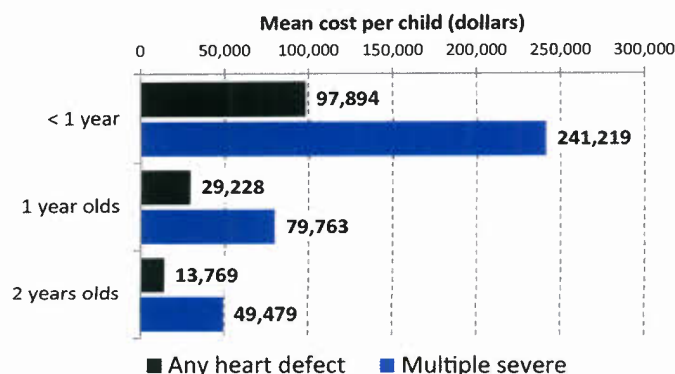


Figure 25.12. Estimated cost (inpatient admission and outpatient services) for 2005 in a select United States population of children under 3 years of age with congenital heart defects. (MarketScan data from reference Boulet S, Grosse SC, Riehle-Colarusso T, et al. Health care costs of congenital heart defects. In: Wyszynski DF, Correa-Villasenor A, Graham TP, eds. *Congenital Heart Defects: from Origin to Treatment*. New York, NY: Oxford University Press, 2010:493–501.)

As noted by its authors (144), this study using MarketScan data has some limitations. The database covers a select, privately insured population, so findings are difficult to generalize. Also, it doesn't capture the switch of some children to state funded programs, such as Medicaid, when costs reach the lifetime limits or parents cannot afford private insurance any longer. Finally, as in other studies without clinical validation, ICD codes may be inaccurate and some cases may have been misclassified. Nevertheless, with its limitations, this is an important study. It examined health expenditures associated with inpatient admissions as well as outpatient and pharmacy services, included a wide variety of congenital heart defects, and assessed the cost variations by age in early childhood and, to the extent possible for ICD codes, also by disease severity.

The cost among adults is unclear and very likely underestimated. One study used the NIS dataset to examine inpatient costs in adults (18 years or older) with a select group of complex congenital heart defects (146). For 2002, a total of 28,072 hospitalizations were identified for adults with these conditions (mean age, 50.8 years), with a mean charge (not cost) per patient of \$31,740. However, the true costs could be higher, as discussed, because ICD codes for congenital heart defects may be underused in older people.

LIFETIME COSTS

Lifetime costs aggregate the costs accumulated by people with congenital heart defects as they progress through life. Ideally, they include not only direct but also indirect costs such as loss of productivity. From a societal perspective, comprehensive lifetime costs are crucial metrics. From a prevention perspective, these lifetime costs provide comprehensive economic estimates of the potential “return on investment” for prevention. For example, the “return on investment” of preventing diabetes-related congenital heart defects in pregnancies occurring in 1 year is the savings gained by not having to expend resources that would have been consumed by affected babies born in 1 year *over their lifetimes*. These lifetime costs, however, are currently complicated to estimate and require assumptions and modeling.

A comprehensive lifetime cost estimate for selected congenital heart defects was reported in a landmark study in the mid-1990s (147,148). In the study, researchers linked the California birth defect registry with health expenditure data and used sophisticated methodology to estimate lifetime cost of illness for babies born each year with four major heart defects. The findings were then extrapolated to the population of the United States at that time. The estimated lifetime cost per *individual new case* is shown in Figure 25.13.

These total costs per case ranged from \$262,000 for tetralogy of Fallot to over \$500,000 for truncus arteriosus. These estimates represent incremental costs for babies born in a single calendar year (1988) with one of the four heart defects, projected through their lifespan. They include not only direct costs (medical, developmental, and special education services) but also some indirect costs (costs of lost work and household productivity). Because these were incremental costs, the cost for general population was subtracted out. Finally, the dollar figure was based on 1992 dollars, obviously a gross underestimate compared to today.

A helpful estimate for national policy is that of total aggregate costs for the nation. These are shown in Figure 25.14, using similar sources and methodology (147,148).

As Figure 25.14 indicates, lifetime costs in the national aggregate are measured in millions of dollars for a single-year cohort, with a combined cost for the four conditions exceeding 1.2 billion in 1992 dollars. A large fraction of these costs were indirect costs, due to loss of productivity because of high early mortality. However, direct medical costs were in the order of 500 million dollars, mainly related to surgical care (147,148).

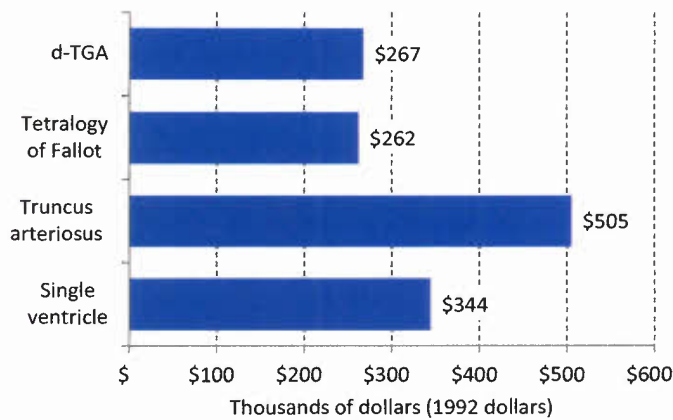


Figure 25.13. Estimated lifetime costs (total costs) per new case, for four major congenital heart defects, in 1992 dollars. (Data from Centers for Disease Control and Prevention, Waitzman NJ, Romano PS, Scheffler RM, Harris JA. Economic Costs of Birth Defects and Cerebral Palsy—United States, 1992. *MMWR Morb Mortal Wkly Rep* 1995;44: 694–699.)

Comparing cost per case (Fig. 25.13) and cost for the national cohort (Fig. 25.14) for the four defects, underscores the impact of birth prevalence on cost. For example, the cost associated with each new case of truncus arteriosus is nearly twice that for d-transposition complex, but the aggregate costs in the United States for truncus arteriosus are less than half that of d-transposition. This is due to the fact (Table 25.3) that the birth prevalence of d-transposition is about four times that of truncus arteriosus, thus driving up the aggregate costs in the population.

In summary, the costs of congenital heart defects are high and increasing. However, the true nationwide cost is difficult to estimate in the United States because of the fragmentation of data and health care and the complexity of how health care

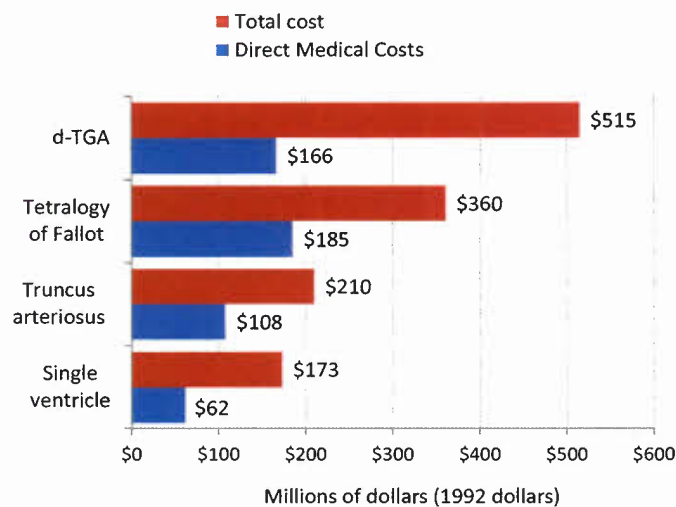


Figure 25.14. Estimated lifetime costs (total costs and medical costs) in 1992 dollars for the cohort of people born in 1 year (1988) in the United States with one of four major congenital heart defects. (Data from Centers for Disease Control and Prevention, Waitzman NJ, Romano PS, Scheffler RM, Harris JA. Economic Costs of Birth Defects and Cerebral Palsy—United States, 1992. *MMWR Morb Mortal Wkly Rep* 1995;44: 694–699.)

is paid. In other countries with national health care systems and comprehensive databases, such costs could be more easily estimated. Nevertheless, even the most basic and conservative costs estimates based on 1 year inpatient care of a decade ago surpass the billion dollar mark. The real costs today are likely even higher, for several reasons: estimates of lifetime costs to date capture only a small fraction of congenital heart defects; medical costs have risen over time; survival has improved, so costs now accrue for more people over a longer period of time; and some components of costs are rarely estimated, including time spent and loss of productivity by family members and costs related to neurodevelopmental disabilities (144,147,148).

Accurate estimates and timely monitoring of costs are crucial in providing services and particularly as an incentive for investing in prevention. As an example, preventing a single case of d-transposition of the great arteries through preconceptional treatment of a diabetic woman would save at least 277,000 dollars (in 1992 United States dollars). These figures should provide powerful financial incentives to invest in preventive services for women of childbearing age (147,148), particularly in times of soaring costs and increasingly limited resources.

EVIDENCE: EPIDEMIOLOGY OF RISK AND CAUSES

The starting point for effective primary prevention is identifying true modifiable causes of congenital heart defects in human populations. Several risk factors, such as diabetes or retinoic acid, reach this level of evidence and are prime candidates for prevention efforts. Others are less well characterized. Causality may be in question (e.g., obesity) or the magnitude of risk may be unclear (e.g., lithium), typically because of inconsistent findings across studies or concerns about bias and confounding.

Part of the challenge of characterizing risk factors has been the near-exclusive reliance on observational studies. For most maternal and environmental factors, randomized clinical trials are out of the question. Exceptions may include factors that are potentially protective, such as folic acid supplementation, where risk reduction is expected and no material side effects are anticipated. But for most other factors, randomization is unethical and even unfeasible (e.g., maternal diabetes). Thus, one is typically left with observational studies, typically case-control studies, and occasionally cohort studies. Because of their complexities, observational studies are seldom consistent and the resulting steady stream of epidemiologic findings may appear disappointingly confusing and difficult to interpret. For this reason, before examining individual risk factors, it is helpful to review some key epidemiologic concepts in risk assessment. These concepts can provide a framework for navigating the complex and ever increasing body of epidemiologic studies on the etiology of congenital heart defects (3,149).

Evaluating Risk Through Epidemiology: Application to Heart Defects

From the perspective of prevention, that is, in order to develop policies and strategies, a risk factor needs to be comprehensively characterized. Some of the important elements in this process are summarized in Table 25.6.

The first element, causality, is perhaps the most challenging. Observational studies typically generate associations. Moving from associations to causality is not simple: causality is a complex concept that requires thoughtful evaluation (150) together with evidential support that goes beyond the

TABLE 25.6 Characterizing Risk Factors: Questions and Epidemiologic Correlates

Questions	Epidemiologic Correlates
Causality: does the factor cause heart defects?	Causality is inferred by finding consistent, plausible associations in multiple, well-designed epidemiologic studies, ideally population based, while controlling for bias and confounding.
Specificity: what types of heart defects does the factor cause?	Establishing specificity requires typically large samples of well-characterized cases of types of heart defects: this implies large, collaborative studies (for sample size) and clinician involvement (for accurate case classification).
Magnitude: how strong is the risk for heart defects?	Magnitude is measured by a study's risk estimates. Relative risk (ratio of disease rate exposed/disease rate in unexposed) can be estimated by cohort and case-control studies; absolute risk (risk of disease when exposed) is readily estimated in cohort studies (can be inferred in population-based case control studies augmented with some external information).
Interactions: what is the risk when exposed to more than one factor?	Interactions may occur between multiple environmental exposures (diabetic women who smoke and drink) or between environmental exposures and genotypes (e.g., MTHFR polymorphisms and folate supplementation). Risks may be combined in an additive, multiplicative, or other scale. Methods are available to determine interactions, but typically require larger, very well designed studies.
Population attributable fraction: what fraction of heart defects in a population is attributable to the factor?	Population attributable risk depends on both the magnitude of risk (relative risk) and the frequency of the factor in the population. The latter can be inferred from surveys, or, in some cases, from the control sample of population-based case control studies. Crude estimates of attributable fraction may be computed easily, but accurate estimations require thoughtful analyses.

results of a single study, however well-conducted. For observational studies, the case for causality can be strengthened by consistent, plausible associations from multiple well-designed studies that stringently control for confounding and convincingly minimize bias. Confounding and bias are significant concerns. For example, an association between maternal smoking and congenital heart defects could be due to confounding by alcohol use, if alcohol causes congenital heart defects and is more common among smokers compared to nonsmokers. The same association could also be spurious because of bias; for example, recall bias can occur in a case control study if mothers of affected babies are more likely than mothers of controls to remember or report smoking during pregnancy. Biases may also hide associations. For example, associations could also be diluted or distorted if exposures are not assigned correctly, as can happen when exposure assessment relies on maternal reports (for smoking but also many factors such as fever, chronic illnesses, medication use) with limited validation or use of biomarkers. Finally, in addition to confounding and bias, associations may be due to also chance. In the case of smoking, this can occur if the excess of smokers among case-mothers in a case-control study is randomly due to sampling. The effect of chance is important but fairly easy to measure and manage, whereas confounding and bias can be difficult to prevent, detect, and eliminate. Specificity (Table 25.6) is important for several reasons. A consistent association can provide clues to pathogenesis and strengthen the case for causality, as in the case of retinoic acid as a specific and consistent cause of complex conotruncal defects, probably through a developmental effect on neural crest cells. However, specificity is not always present, and established teratogens such as maternal diabetes can cause a variety of heart defects. Identifying associations with a specific effect on selected heart defects requires considerable care in study design and ideally the collaboration of expert clinicians in case review and classification. From a prevention perspective, specificity also helps

assess the potential benefits for prevention—a factor causing hypoplastic left heart syndrome would be viewed differently from one causing a small atrial septal defect.

Magnitude of risk can be estimated in case-control and cohort studies, in the form of relative risk of disease, that is, the ratio of disease risk in the exposed divided by the risk in the unexposed. Some relative risks may be low (e.g., smoking), others can be considerable (maternal diabetes), and a few can be extremely elevated (e.g., retinoic acid). Ideally, one would also estimate the absolute risk for congenital heart defects, that is, the absolute rate of disease in those exposed (the numerator of relative risk). This is important information in individual counseling. The relative risk for a specific type of congenital heart defect could be 10 (i.e., 10 times the risk in the unexposed), but if the baseline risk in the unexposed is low, say 1 in 10,000, then the absolute risk, though increased, is still in the order of 1 in 1,000 (or 999 to 1 odds of *not* developing the heart defect).

Interactions (Table 25.6) are potentially important but challenging to identify and characterize precisely. An interaction occurs when the concurrent presence of two factors changes the risk association between each factor alone and disease. These factors can be environmental or genetic. For example, a scenario may occur (not as implausibly as may appear) in which a diabetic woman takes lithium and a folic acid supplement. The question then becomes if and how these individual risks cumulate, and if they do, on which scale (additive, multiplicative, or other). The answers are not just of academic interest. Finding that a vitamin supplement mitigates the risk associated with diabetes or lithium can provide a powerful adjunct tool in clinical management. Also, strong interactions can provide clues to shared pathogenesis and help discover new causes and mechanisms of congenital heart defects. The methodologic challenge, however, is that studying interactions requires stringent precision in assigning exposure and usually much larger sample sizes compared to studies looking at the main effects of risk factors.

Finally, the population attributable fraction (Table 25.6) is particularly helpful in translating measures such as relative risk into estimates of population impact—the number of cases caused by the risk factors. It is intuitive that the more women exposed to a teratogen in a population and the higher the teratogenic risk, the higher the number of affected pregnancies. The population attributable fraction develops this notion rigorously. It is defined as the proportion of cases in a population that can be attributed to a given exposure and is computed as a nonlinear function of disease risk and exposure prevalence, using one of several formulas (151,152). Figure 25.15 illustrates the relation between exposure frequency, disease risk, and population attributable fraction, using a range of plausible values for common risk factors.

This illustration underscores several basic concepts. First, the higher the frequency of exposure to a risk factor, the higher the fraction of cases in the population that is attributable to that factor. The attributable fraction increases as a nonlinear function of the relative risk—the higher the relative risk, the steeper the increase. However, even weak risk factors, with odds ratios of 1.5 to 2, can potentially cause a significant fraction of disease in the population with sufficiently high exposure frequencies. High exposure frequencies are not unrealistic: lack of folic acid supplementation easily exceeds 50% in many developed countries and is probably close to 100% in many developing countries. Smoking rates of 15% to 20% or more in women are not uncommon in some countries or groups in the population.

Whereas attributable fraction may appear to be a straightforward concept (151), in many practical settings it has subtleties that must be appreciated in order to get valid estimates. Such settings include using relative risk estimates derived from multivariable analyses, a common situation in modern epidemiologic studies, or when the exposure has more than two levels rather than being categorized simply as present or absent (153,154). With rare exceptions (155), a systematic assessment of population attributable risk for heart defects has been uncommon. Because of its potential implications for prevention, new rigorous evaluations would be very helpful.

Seeking Candidates for Prevention: Review of Selected Risk Factors

Because of the focus on primary prevention, this review will center on selected modifiable risk factors (Table 25.7), chosen either because they are established risk factors for congenital heart defects (e.g., diabetes, retinoic acid) or because they are so common in many populations (e.g., smoking, obesity) that they should be addressed even if associated with only mildly increased risks for congenital heart defects. The examination of these risk factors is not exhaustive; rather, it focuses on specific aspects relevant to primary prevention, such as the strength of the evidence, the specific outcomes related to the factor, the preventability of the risk factor, and its frequency in the population. Additional data can be found in several reviews (3,149) as well as in the cited primary sources. Because of the continuous stream of studies, the information is to some extent always provisional. Helpful sources for updates, in addition to the published literature, include online databases such as Reprotox and TERIS (156,157), as well as the staff at Teratogen Information Services (TIS) who can provide invaluable summaries and commentary (158,159).

Diabetes

Maternal diabetes is a well-known and established teratogen. It causes heart defects not uncommonly as part of multiple congenital anomaly patterns (16,160–168). Cardiac phenotypes consistently associated with maternal diabetes include laterality defects (heterotaxy) and several conotruncal defects. Less consistently, but still associated with maternal diabetes are left ventricular outflow obstructive defects and septal defects (16,160–164,167,169). Obstructive cardiomyopathy also occurs but typically resolves over time. Estimated relative risks for heart defects in the aggregate range approximately from 3 to 6, though they can be higher for some types of heart defects, especially when associated with extracardiac anomalies (16,160,161,163,164,166,167). Separate risk estimates associated with type 1 and type 2 diabetes are rarely

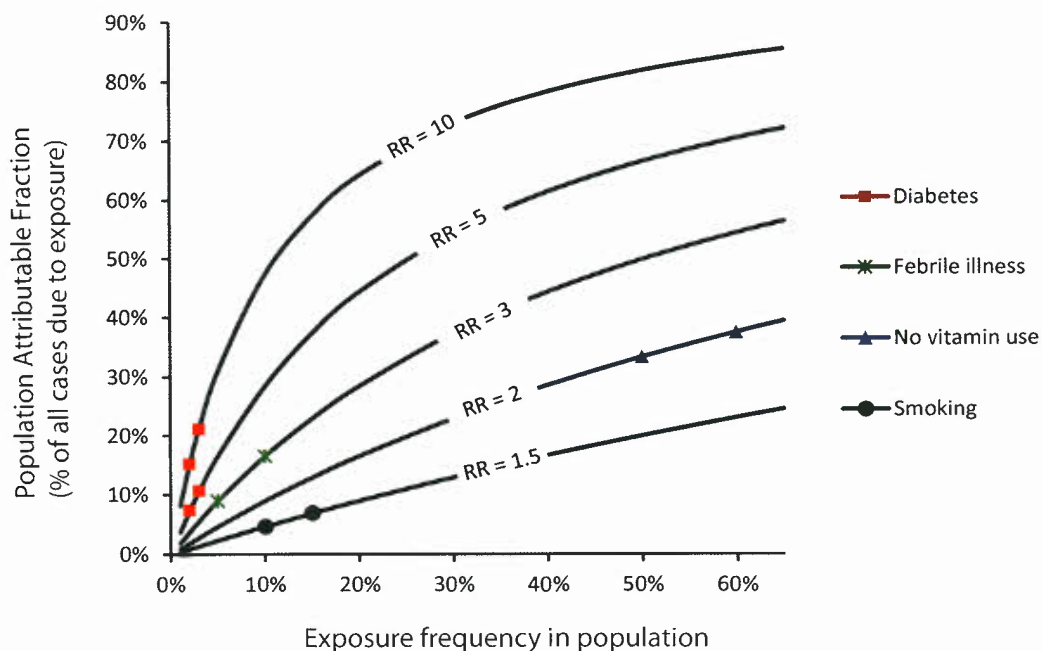


Figure 25.15. Population attributable fraction as a function of relative risk and population exposure frequency, with selected examples of common exposures (see text for details).

TABLE 25.7

Common Exposures Associated with Increased Risk for Congenital Heart Defects: Estimated Effects, Risk, and Prevention

Factor	Congenital Heart Defect	Estimated Risk	Exposure Type and Frequency	Comments
Diabetes	Early developmental CHDs, that is, laterality defects, looping, conotruncal defects, AV septal defects	OR usually 3–10, higher for some phenotypes	Pregestational diabetes	1%–2% of women of childbearing age in United States; increasing in many countries
Febrile illness, influenza	LVOTO, including coarctation of the aorta; tricuspid atresia, dTGA and other conotruncal malformations, VSD, possibly others.	For febrile illness, relative risk between 1.5 and 3 (generally –2), thought possibly higher for tricuspid atresia. For influenza, similar risk estimates	First trimester febrile illness reported in ~6%–9% of pregnancies. Generally associated with respiratory or flu-like symptoms.	Relative contribution of hyperthermia and underlying infection unclear. Risk may be higher when influenza-like illness is associated with high fever.
Maternal phenylketonuria	Tetralogy of Fallot, VSD, PDA, LVOTO	Relative risk up to 6	Frequency of PKU is ~1 in 10,000 among whites	Known teratogen. Relatively rare, but effects preventable with strict dietary compliance from before conception
Retinoic acid	Conotruncal defects	High absolute risk	Isotretinoin, etretinate by mouth are teratogenic, topical tretinoin probably not	Retinoic acid use is subject to rigorous controls in some countries but not others. Exposure is a concern because many users are young women
Lithium	Ebstein anomaly, others	Relative risk likely <10, between 1.5 and 8 in two cohort studies	Use probably infrequent but few systematic studies	Risk lower than originally thought, but likely present. Balance of risk versus benefits of treatments need to be considered.
Obesity	Several heart defects, including conotruncal defects, unclear if specific	Relative risk between one and three, but some studies are negative. Causality not clear	Risks typically associated with BMI > 29, but some studies show risks at BMI 25–29	Causality not clear. Association possibly owing in part to unrecognized diabetes. Important individual and public health concern, as obesity is increasing in many countries
Smoking	Septal defects, others	Relative risk between one and three, but some studies are negative. Causality not clear	In individual studies, risk present if both parents smoke and if father alone smokes (second-hand smoking)	Causality not clear, but preventable. Smoking can cause other adverse pregnancy outcomes
Caffeine	No clear association with structural CHDs	No clear association has been demonstrated	No clear increased risk, no trend for increased risk with increasing amount of caffeine	Caffeine crosses the placenta and can have cardiovascular effects. However, several large studies failed to identify increased risk for heart defects or other malformations
Alcohol	Possibly several heart defects, including conotruncal defects	Inconsistent findings; some studies do not find association	Possible higher risk with high exposure, but not consistent finding	Known teratogen, major effects on central nervous system, association with specific heart defects still being investigated

AV, atrioventricular; OR, odds ratio; LVOTO, left ventricular outflow tract obstruction; dTGA, d-transposition of the great arteries; VSD, ventricular septal defect; PDA, patent ductus arteriosus; BMI, body mass index; CHDs, congenital heart diseases.

available. Some studies have suggested an excess risk also with gestational diabetes, but the literature is inconsistent (162,170–172).

The frequency of diabetes among women of childbearing age varies by country, age, and other factors. According to one estimate, diabetes affects approximately 2% or 1.85 million women of childbearing age in the United States, and preconceptional diabetes management could decrease the risk for pregnancy loss and congenital malformation for approximately 113,000 births per year (141). Rates of diabetes are not only high, but rising in both developed and developing countries (173,174). Of additional concern is that many women could have unrecognized diabetes. One study estimates that in the United States, for every two women of childbearing age diagnosed with diabetes, there is another one with undiagnosed diabetes (175).

Even without considering the overall effect on women's health, these three elements—strong evidence for causation, high relative risk for disease, and comparatively high and rising frequency in the population—combine to make diabetes a clear priority for prevention. Of major importance is therefore the finding that careful metabolic control before conception can reduce considerably the teratogenic risk associated with maternal diabetes (141,176,177). In practice, however, many affected pregnancies continue to occur (141,166,178), highlighting the challenges of implementing optimal preconceptional control (179).

Some findings suggest that birth defect risk may be lower among diabetic women who also took a folic acid-containing multivitamin supplement from before conception (161). If confirmed, taking such a supplement could represent an adjunct prevention strategy for diabetes-associated birth defects. This benefit would add to the established benefit of folic acid in preventing neural tube defects. In summary, maternal diabetes is an established, serious risk for congenital heart defects, and a clear priority target for prevention efforts.

Rubella

The teratogenicity of rubella in pregnancy is well-established. The effectiveness of rubella immunization in decreasing rubella-associated birth defects is testimony to the power of primary prevention worldwide (180–182). Specific heart defects associated with congenital rubella syndrome include pulmonary stenosis, particularly branch pulmonary stenosis (180), patent ductus arteriosus, and, less frequently, other conditions such as tetralogy of Fallot (183).

Through sustained immunization campaigns, congenital rubella syndrome has been nearly eliminated in the United States and some other countries, though continued vigilance is crucial because of lapses in immunization coverage, imported infection, and the challenges of surveillance (182,183). Worldwide, rubella infection and congenital rubella syndrome remain a significant problem, underscoring the need for global eradication of this preventable condition (182,184,185).

Fever and Flu

Fever and hyperthermia are established teratogens in animal models (186–188). However, the extent of cardiac teratogenicity of fever and flu-like illnesses in humans is unclear. The evaluation is made challenging also because reports of febrile illness in pregnancy are difficult to validate, and because the association could be confounded by the underlying infection or use of medications. The balance of the evidence to date suggests that first-trimester febrile or flu-like illnesses are associated with a moderately increased risk for congenital heart defects in the aggregate (relative risks of approximately 1.5 to 3), with perhaps higher relative risks for some right-sided obstructive defects, coarctation of the aorta, aortic stenosis,

ventricular septal defects, and atrioventricular septal defects in children with Down syndrome (18,164,187,189–192). However, these findings are inconsistent across studies.

Data on the frequency in the general population of fever and flu-like illnesses in early pregnancy are difficult to find in national surveys. However, judging by the prevalence among controls in case-control studies (which should represent the underlying population), it appears that approximately 6% to 9% of women experience a respiratory infection (“flu”) or a febrile illness during the first trimester of pregnancy (18,189–191). If this is true, an estimated 250,000 pregnancies or more could be exposed every year in the United States.

If febrile illnesses cause congenital heart defects, prevention strategies may include avoidance of ill contacts and possibly preconceptional immunization before influenza season. The potential effect of antipyretics is unclear. In a reanalysis of the BWIS, use of antipyretics was associated with an attenuation of the fever-associated risk for congenital heart defects (192), but more data are needed to confirm this finding. Finally, two studies reported that periconceptional use of multivitamin supplements among women with febrile illness reduced the fever-associated risk for congenital heart defects (18,189), suggesting a further benefit of supplement use.

Maternal Phenylketonuria

Maternal phenylketonuria (PKU) (women with PKU and high blood phenylalanine levels during pregnancy) is a teratogenic condition, with devastating effects on the fetus's brain and sometimes the heart (193–195). Specific heart defects associated with maternal PKU include left-sided defects (coarctation of the aorta to hypoplastic left heart syndrome), tetralogy of Fallot, septal defects, and possibly patent ductus arteriosus (193–195). Estimated relative risk has been high (6 to 15), and in one study, the absolute risk for heart defects was 14% (34 of 235 pregnancies) among pregnancies exposed to high levels of phenylalanine (193). Strict control of phenylalanine levels from before conception reduces considerably the risk for heart defects and other adverse outcomes in the child (193–195).

The prevalence of women of childbearing age with PKU is unknown. However, assuming an average birth prevalence of PKU of 1 in 20,000 births in the United States (higher in whites, lower in blacks), an estimated 100 girls with PKU are born every year in the United States. With universal newborn screening and appropriate early treatment, essentially all will reach childbearing age and eventually be at risk for having an affected pregnancy. Children of women with uncontrolled PKU continue to be born with a variety of physical and neurodevelopmental disabilities, demonstrating that implementing prevention remains difficult and complex. Many factors influence the desired adherence to the strict metabolic diet needed to control phenylalanine levels, including poor access to medical care, lack of reimbursement for medical foods, practical difficulties with implementing the diet, psychosocial issues, and the need for careful pregnancy planning. A comprehensive treatment approach is required. It should start before conception, and continue through the birth of the child. Proposed elements of the approach include education of girls with PKU from adolescence, preventing unplanned pregnancies, psychosocial support, and improved access to treatment (196). Novel medications such as sapropterin, which can reduce phenylalanine levels in responsive women with PKU, could also help improve metabolic control during pregnancy (196).

Thalidomide and Retinoic Acid Congeners

These medications, quite different in molecular structure and mechanism of action, are grouped here because they are established, potent teratogens associated with some of the highest

teratogenic risk in the literature, including for congenital heart defects (3). In addition to magnitude of risk, these medications are also concerning because of the severity of the heart defects they typically cause, including complex conotruncal anomalies, and the frequent presence of extracardiac defects (197–199). From a prevention perspective, retinoic acid and its congeners, which include isotretinoin and etretinate, are also concerning because they may be used by young women for the treatment of acne and other skin conditions (200). Strict regulatory guidelines have been issued in some but not all countries, and exposures continue to occur (141,200,201).

Epilepsy and Antiepileptic Drugs

Most women with epilepsy have uneventful pregnancies and give birth to healthy newborns. However, considerable data, recently reviewed (202), indicates that some antiepileptic drugs (AEDs) can increase the risk for birth defects. This is particularly clear in experimental animals, in whom congenital heart defects are reported to be among the most common birth defects associated with AEDs, followed by orofacial clefts, hypospadias, skeletal defects, and for valproate in particular, neural tube defects (202).

In human pregnancies, the AEDs, rather than epilepsy itself, seem to be the main, though perhaps not the only determinant of teratogenic risk (202–204). The precise parameters of risk are not clear. Pooling data from different studies is challenging and sometime suspect, because of the heterogeneity in methods and study quality. A more recent approach is the use of networks of pregnancy registries sharing common methods and data (204,205). In a pooled review (206), the absolute risk for congenital malformations as a group among women using AEDs was 7%, about three times higher than the pooled reference group (and the group of women with epilepsy not using AEDs). The risk varied by type of AEDs and appeared to be higher for valproate (206). Risk was also higher with polytherapy and with higher AED doses, possibly with a threshold effect (202,206–210). Medications associated with teratogenic risk include phenytoin, hydantoin, and valproic acid, and among newer agents, carbamazepine and lamotrigine (211–216).

The specific risk for congenital heart defects is not well characterized. For carbamazepine, one study in India suggested an increased risk for congenital heart defects (217), but this was not confirmed in a large cohort study in the United Kingdom (218). For phenobarbital, several studies reported the occurrence of congenital heart defects in exposed pregnancies (203,212,217,219), but the small number of cases and the variability among studies make it difficult to establish conclusively the presence and magnitude of cardiac risk (202).

In the United States, seizure medications are prescribed for an estimated 1 million women (19 per 1,000 population) (141) potentially affecting an estimated 30,000 to 75,000 pregnancies every year (141,204). Prevention requires a joint effort by women and physicians. From a management perspective, withholding AEDs is usually not a realistic option for most women, because many women with epilepsy will need AED treatment during pregnancy to prevent or control seizures (202,204). Preconceptional counseling is crucial, as is the strategy of trying to avoid starting young girls on AEDs with known teratogenic effects or switching to other AEDs before conception (141,214–216,220).

The mechanism of teratogenic action is still unclear. Some AEDs (carbamazepine, phenobarbital, phenytoin and primidone) are known to alter folate metabolism in early pregnancy at least in some women. This finding has led to investigate whether supplementation with folic acid might mitigate the teratogenic risk associated with some AEDs, particularly valproic acid. The overall evidence so far, reviewed by Hill and

collaborators (202) does not suggest that there is a specific protective effect among women on AEDs (202,207,218,221). Nevertheless, folic acid supplementation is still recommended in women on AEDs because AEDs may increase the risk for malformations in women with low blood folate levels (202) and because of the overall benefits of supplementation outside of the specific risk associated with AEDs.

Lithium

Lithium is used for manic-depressive disorders, and has been in clinical practice for decades in many countries. Approval by the United States Food and Drug Administration dates from 1970. Because lithium was found early on to be teratogenic in experimental animals, several studies were initiated to assess the risk for congenital malformations in humans. Data through 1994 have been reviewed in detail (222). An early report from the Danish Lithium Babies Registry, a voluntary reporting system (223), described 188 babies born of exposed pregnancies, of which six (5%) had a congenital heart defect, including two cases (1.7%) of Ebstein anomaly (223). The final report, 3 years later (224), described 225 exposed pregnancies, of which 25 had birth defects (11%), including 18 with congenital heart defects (8%) and six with Ebstein anomaly (2.7%). Using these data together with a base birth prevalence for Ebstein anomaly of 0.6 per 10,000 (Table 25.3), a crude relative risk of about 400 can be calculated. However, such estimates, as noted also in first reports, are unrealistic because of the reporting biases that can affect voluntary registries. In fact, later studies suggested that whereas an excess risk for congenital heart defects probably exists, it is much lower than initially thought (222,225,226). More specifically, a cohort study from Sweden, using a series of data linkages, identified 59 pregnancies exposed to lithium alone and of these seven had birth defects, and four (6.8% overall) had congenital heart defects, for an estimated relative risk of 7.7 (95% confidence interval, 1.5 to 41.2). Notably, none had Ebstein anomaly. Another cohort study, from the United States, evaluated 148 pregnancies of women with first trimester use of lithium, identified through a teratogen information system (225). The women had contacted the service because of concerns about the medication. A matched set of women who contacted the same service but had not been exposed to known teratogens was selected as the reference cohort. Overall birth defect rates in the two groups were similar (four cases in the exposed cohort, three in the reference group). The formal relative risk estimate for congenital heart defects was 1.2 (95% confidence interval, 0.1 to 18.3). However, one of three affected pregnancies in the exposed cohort had Ebstein anomaly. In addition to these two cohort studies, several case-control studies with data on birth defects, some specifically on Ebstein anomaly, are available and have been reviewed in detail (222). Briefly, these studies reported very few exposed pregnancies and the associated odds ratios did not indicate an increased risk for congenital heart defects.

Based on the cohort studies, it appears that the risk associated with first trimester use of lithium is probably increased moderately for birth defects overall, perhaps two- to threefold. The specific risk for congenital heart defects seems to be in the same range or somewhat higher, increased from two- to sevenfold. The risk for Ebstein anomaly in particular is very likely increased but the magnitude is unclear.

These findings can help clinicians assess the use of lithium during pregnancy in an appropriate context of risks and benefits (37,222,226). Women with manic-depressive conditions may benefit from targeted preconceptional counseling and prenatal care, also because they could be at risk for adverse pregnancy outcomes independent of lithium exposure (222,225–227). Some reports suggest that in experimental animals, lithium-induced embryopathy can be prevented by folate supplementation if

administered in doses higher than those provided by a typical multivitamin supplement (228,229). Whether or not this can be extrapolated to women is unknown, but suggests nevertheless that women who need to use lithium in pregnancy should adhere to basic preconceptional care recommendations, including taking folic acid from before conception. Whether or not they could benefit from higher doses of folic acid than the 0.4 mg currently recommended for all women is unknown.

Antidepressants

Antidepressants are a heterogeneous group of medications used for mood disorders. Several have been evaluated for the risk of birth defects. For congenital heart defects, results are often inconsistent and vary across different types and classes of antidepressants. Accumulating data seem to indicate a possible mild to moderate risk for congenital heart defects associated with paroxetine, a selective serotonin reuptake inhibitor (SSRI). Two formal meta-analyses have been published (230, 231). The more recent study (230) generated a summary relative risk estimate for heart defects of 1.24 (95% CI, 1.08–1.43), slightly higher for the group of “combined heart defects.” It is still debated whether such modestly increased risk is entirely driven by medication use or also in part by the underlying risk factors in the select group of women who take the medication (230,232). Studies on paroxetine are also inconsistent regarding the specificity of the association; for example, one study reported an increased risk for right-sided obstructive heart defects (233), another for atrial septal defects but no other heart defect (234), and another still for minor defects such as ventricular septal defects and bicuspid aortic valve (235).

Another antidepressant recently studied for possible cardiac teratogenicity is bupropion, an atypical antidepressant (different from SSRIs) used also for smoking cessation. Studies so far include the pharmaceutical company’s registry data, which showed a potential association, one cohort study (236), reported as negative, and a case-control study (237), which showed a positive association with left-sided obstructive heart defects (odds ratio 2.6, 95% confidence interval 1.2 to 5.7).

Although the magnitude of putative risks seems small, the high prevalence of use of these medications in women of child-bearing age makes them potentially important. In counseling women, the appropriate balance of risk and benefits needs to be reached, taking into account not only the potential risks for some heart defects, but also the serious consequences of untreated or undertreated depression during pregnancy.

ACE Inhibitors

Angiotensin converting enzyme (ACE) inhibitors are medications widely prescribed to control hypertension. They are contraindicated in the second and third trimester of pregnancy because of effects on fetal blood pressure and renal function, leading to fetal toxicity and death (238,239). For this reason, the United States Federal Drug Administration has required warning on ACE inhibitors (currently, category D) since 1992. Questions of cardiac teratogenicity following first trimester were raised by a study in 2006 that reported an increased risk for heart defects in babies of women who had been prescribed ACE inhibitors during pregnancy (240). The study linked coded outcomes with prescription data within the Tennessee Medicaid database and the reported association was based on seven occurrences of atrial or ventricular septal defects and two of patent ductus arteriosus (240). No association was found with the use of other antihypertensive medications, suggesting a specific effect of ACE inhibitors (240). However, such specific association was not found in several subsequent studies, including the population-based National Birth Defect Prevention Study (241), the Swedish Birth Registry (242), a collaboration of Teratogen Information Services in Israel and

Italy (243) and the Kaiser Permanente system in California (244). Some of these studies were also summarized as part of a meta-analysis (245). The pattern that emerges from these studies is that ACE inhibitors are either not a risk factor for congenital heart defects or the associated risk is similar to that present in mothers with untreated hypertension or treated with many other classes of antihypertensive medications. Such a pattern does not support a specific effect with ACE inhibitors. The mild-to-moderate risk associated with antihypertensives could have different causes, including the underlying maternal hypertension. For example, in one study, the exposure to ACE inhibitors was associated with an increased risk for congenital heart defects when compared to normal controls, but not compared to untreated hypertensive controls (244). Bias and confounding could also play a role. Hypertension commonly occurs in women with obesity and diabetes, which are risk factors for congenital heart defects, and these factors have not been consistently accounted for in all studies. In summary, current data does not support the notion that first trimester exposure to ACE inhibitors confers an increased, specific risk for heart defects, above that possibly associated with maternal hypertension (treated or untreated) or with the common comorbidities of hypertension, such as obesity and diabetes. Nevertheless, ACE inhibitors are contraindicated in pregnancy, mainly for their established deleterious effects in the second and first trimester. Women with hypertension should be appropriately counseled, ideally before conception, so they can start pregnancy on a safer medication that appropriately controls hypertension.

Other Medications

Trimethoprim-sulfonamide and sulfasalazine have been associated with a mild-to-moderate increase in risk for congenital heart defects (246,247). In one study, the use of folic acid supplements decreased the excess risk associated with these compounds (247).

Obesity

To date, the evidence for obesity is mixed. Some positive associations have been reported, but it is unclear to what extent they reflect causality or are due to confounding. Both positive and negative findings have been reported for heart defects in aggregate, as well as for specific phenotypes such as septal defects, left- or right-sided obstructive defects, and some conotruncal defects (16,248–255). Among positive studies, the overall magnitude of risk is small, with most odds ratios under 1.5, with both higher and lower risk estimates for specific cardiac phenotypes. Some studies appear to indicate a positive trend of risk with increasing body mass index (255), whereas other did not.

Epidemiologically, it can be very challenging to examine the contribution and interaction of these factors among pregnant women with obesity. For example, obesity may contribute to and be present together with gestational diabetes (256) and perhaps unrecognized type 2 pregestational diabetes. This co-occurrence or confounding could vary by study, depending on the completeness of diabetes screening among study participants. Using appropriate biomarkers could be very helpful, but few are well characterized so far.

Nevertheless, from a prevention perspective, obesity is a significant concern even if the excess teratogenic risks were small, because of its high and rising frequency in many developed and developing countries (174). According to estimates from the United States CDC (257), the overall prevalence of obesity among women aged 20 to 39 years in the United States between 1976 to 1980 and 2007 to 2008 increased from 15% to 34%. These rates varied depending on race-ethnicity, and were higher among non-Hispanic blacks and lower among

non-Hispanic whites (257). Obesity rates also appear to be inversely correlated to education level, with the highest rate among women with less than high school education (258). With such high frequency and complex patterns of exposure, small risks can translate into many affected pregnancies, particularly in groups of the population that are socioeconomically disadvantaged. Interventions will need to take these factors into account, as well as related health issues such as diabetes. Finally, limited evidence suggests a possible mitigating effect of multivitamin supplementation on obesity-related risk for heart defects (251). If confirmed by further research, vitamin supplementation could represent an adjunct approach to reducing the birth defect burden potentially associated with the obesity epidemic.

Caffeine

Caffeine is frequently consumed and has proven cardiovascular effects in mother and fetus. However, the recent literature has been extensively reviewed (259) and did not find strong evidence suggesting an excess risk for congenital heart defects in several larger studies from Finland (260,261), Denmark (262), and the United States (16,263–265).

Alcohol

Alcohol is an established human teratogen, and is known to cause a wide range of structural malformations and neurodevelopmental abnormalities (266,267). The association with heart defects has been less impressive, with inconsistent or negative results in several large studies (16, 260, 261, 268–270), but with some positive associations as well (271–274).

Methodologic issues, including the challenge of documenting exposure reliably and precisely, make studies of alcohol effects in humans especially difficult. In case series with established fetal alcohol syndrome, congenital heart defects and in particular septal defects are common (274). In the context of case-control studies of structural malformations, these findings have been difficult to replicate. In the BWIS, significant associations with alcohol exposure were limited to small ventricular septal defects and only in women who reported heavy consumption (16). In a series of studies from Finland, possible associations were found with ventricular septal defects, atrial septal defects, and possibly conotruncal defects, although dose-response patterns were unimpressive (260,268,269). In the Atlanta population-based case-control study, associations with conotruncal anomalies were evaluated and none were found (270). In two case-control studies from California, alcohol use was reportedly associated with a modestly increased risk for conotruncal heart defects, particularly D-transposition of the great arteries, though the authors noted that the estimates were imprecise and compatible with chance or modest bias (275,276). In the Danish National Birth Cohort study, low-to-moderate levels of alcohol on a weekly basis or occasional binge drinking during the early part of pregnancy was not significantly associated with ventricular or atrial septal defects, with point estimates between 1.1 and 1.4 depending on reported amounts of alcohol use (271). Scarce data are available on possible interactions. In a case-control study in Arkansas, modestly elevated risks for heart defects (odds ratio of 1.7) were found with alcohol use only in women with certain polymorphisms of genes for the folate pathway (273). A case-control study from California that evaluated whether vitamin supplements used in women modified the alcohol-associated risk for congenital heart defects gave inconclusive results, and no specific pattern of risk was found (189).

In summary, although babies with full-blown fetal alcohol syndrome commonly have defects, it is still unclear whether mild-to-moderate alcohol use is associated with an increased

risk for heart defects. However, the global teratogenic effects of alcohol use, particularly on the fetal brain, make prevention of this exposure an important public health priority (141,277). According to one study, approximately seven million women of childbearing age in the United States are frequent drinkers, and without preconception interventions, alcohol misuse might affect approximately 577,000 births per year (141).

Smoking

Although smoking is an established risk factor for low birth weight, preterm birth, and other adverse outcomes, evidence for cardiac teratogenicity is unclear. Some studies suggest a small excess risk (odds ratios, 1.1 to 1.6) for atrial septal defects and pulmonic stenosis (278–281), and perhaps for some conotruncal defects (odds ratio below 2) (16,189,279). Higher risk estimates have been reported with heavier smoking in some, but not in all studies.

As with other common exposures, even a small increased risk for heart defects is of concern because of the high number of women who smoke. In 2003, an estimated 11% of pregnant women in the United States smoked during pregnancy (141). In many countries, rates of smoking in women are high and increasing (282).

In summary, the relative risk for congenital heart defects is probably low and causality is perhaps not entirely established. Nevertheless, smoking is in general bad for the health of women (cancer, heart disease) and their pregnancies (low birth weight, sudden infant death). These reasons strongly support the inclusion of smoking cessation as a priority target for prevention interventions.

Vitamins: Epidemiologic Evidence for Risk and Protection

The interest on the relation between nutrition and congenital heart defects continues to increase. In part, this may be the result of the public health success story of folic acid in preventing neural tube defects. Supplementation campaigns and mandatory food fortification programs have been implemented in several countries, including the United States, Canada, several countries in Latin America, and Australia. Fortification in particular has led to a major population-wide reduction in the prevalence of spina bifida and other neural tube defects (283). From this successful chapter of translating epidemiology into prevention, research has moved in two directions: assessing whether folic acid may prevent other birth defects, including heart defects, and expanding the scope from folic acid to the larger network involving one-carbon metabolism and substrate methylation of which folic acid is part (284). These pathways include several other vitamins, including pyridoxine-B6 and cobalamin-B12, as well as several enzymes and transporters, encoded by genes that often have common functional polymorphisms. Of interest is also the increasing evidence that alterations in folate metabolism and folate levels could be associated with other common maternal risk factors such as smoking. These novel data open the possibility of interactions between multiple genetic and environmental factors. In addition to single nutrient analyses, nutritional epidemiologists increasingly tend also to assess dietary patterns, since people eat foods rather than nutrients. In fact, many nutritional strategies in adult cardiology and medicine to prevent cardiovascular disease and stroke are based on modifying dietary patterns (e.g., with the Mediterranean or the Dietary Approaches to Stop Hypertension-DASH diets), rather than on exclusively controlling a single or a few micronutrients.

Similar approaches to congenital heart defects could prove fruitful (285) but are currently still in their infancy.

For now, most of the published data relate to micronutrients and vitamins. This section will focus on two vitamins in particular, vitamin A and folic acid, with additional discussion on multivitamin supplements.

Vitamin A: Not Too Little, Not Too Much

Vitamin A is an essential vitamin, widely available in over-the-counter supplements. High-dose formulations are easily found. Vitamin A is an important molecule in the synthetic pathway of retinoic acid, a potent transcription factor and established cardiac teratogen, and for this reason it has been assessed in several epidemiologic studies of birth defects.

Vitamin A is typically marketed in one of two forms, beta-carotene and retinol. In all studies that have looked at it, beta-carotene (a provitamin A) has not been associated with increased risks for congenital heart defects (286,287). Retinol, on the other hand, is preformed vitamin A, and has been associated in some studies with an increased risk for congenital heart defects. Specifically, two studies described a moderate to strong association (odds ratios >5) between use of >10,000 IU of retinol and the occurrence of conotruncal heart defects, in particular D-transposition of the great arteries (286,287). Another study, which evaluated the use but not the dose of vitamin A, reported a weaker association (288). In four other reports, however, the association was not confirmed (289–292). Nevertheless, it appears reasonable to recommend avoiding high-dose retinol supplements in the periconceptional period and, if vitamin A is indicated, favor supplements containing beta-carotene.

Folic Acid and Multivitamins: An Evolving Story

Because of its established protective effect on neural tube defects, the use of folic acid for all women of childbearing age or those who do not actively exclude a pregnancy is recommended by medical organizations, public health agencies, and lay organizations in many countries. Thus, assessing whether or not folic acid should be recommended to prevent congenital heart defects could seem a useless exercise. However, this view is simplistic. Identifying a protective effect on heart defects, if indeed one exists, would be beneficial in several ways. It would add to the potential benefits of folic acids, and the associated “return on investment” that could be achieved with more expansive supplementation and fortification programs worldwide. Identifying a protective effect may require approaches and methods that are different from those used to examine neural tube defects. For example, one might need to evaluate higher doses of folic acid or multivitamins rather than folic acid alone, as there is no guarantee that all folic acid-responsive birth defects are as sensitive to folic acid as are neural tube defects. This has implications for research and practice. If preventing congenital heart defects requires high doses of folic acid or multivitamins, then the current fortification programs, which typically use small amounts of folic acid alone, may achieve no or partial results. Also, identifying a role for folic acid or molecules in the broader context of folic acid-related biochemical networks could help understand aspects of the etiology of congenital heart defects, including gene-environment interactions, and ideally open further avenues for prevention. Finally, researching the effect of folic acid in humans has become more complex. Clinical trials comparing folic acid with placebo, now that folic acid is known to protect against serious nervous system defects, would be unethical. Other options would be available, such as evaluating high dose versus standard dose of folic acid/multivitamins, or including in a vitamin trial also a cohort of women who refused taking folic acid, but all these options are imperfect and challenging.

EVIDENCE FROM CLINICAL AND EPIDEMIOLOGIC STUDIES

The main epidemiologic and clinical studies, conducted in the absence of fortification, are described in Table 25.8 together with their main design features and findings.

These studies include one randomized clinical trial from Hungary (293), and four case-control studies from the United States (19,294,295) and the Netherlands (296). All studies were conducted in the absence of universal food fortification.

The randomized clinical trial (293) enrolled women from before conception. Participants were randomized to receive a multivitamin with folic acid or a placebo-like pill containing trace elements. These two cohorts were followed from conception through after the child's birth and their pregnancy outcomes were evaluated. The primary endpoint of the study was the occurrence of neural tube defects. Secondary endpoints included fetal deaths and other structural malformations, including heart defects. The case-control studies evaluated retrospectively the frequency of use of multivitamin supplements, known or presumed to contain folic acid, in case-mothers and control-mothers. Two of the studies evaluated a broad range of heart defects (19,296), whereas the remaining three (294,295,297) were restricted to conotruncal defects (and in one study, also ventricular septal defects).

The findings are illustrated graphically in Figure 25.16.

In the randomized clinical trial (293), fewer women taking the multivitamin with folic acid had a child with a congenital heart defect compared to the reference cohort, for a statistically significant risk reduction of 58%. This finding was driven mainly by the lower rate of conotruncal and septal defects (293,298). However, the available sample size limited the precision of the risk estimates for the subtypes of heart defect.

The case-control studies confirm some of these findings, but not consistently. For example, the two case-control data that assessed heart defects in the aggregate also found an overall reduced risk (19,296), though the magnitude of the apparent protective effect was lower than in the randomized clinical trial (25% vs. >50%). For conotruncal and septal defects, the evidence is mixed. Two case control studies did not show evidence of risk reduction for conotruncal defects (295,297), whereas three others did (19,294,296). For (ventricular) septal defects, one case-control study did not show evidence of risk reduction, (297) whereas two others did (19,296). Why the studies are not entirely consistent is unclear, but methodologic differences as well as varying degrees of bias and confounding could have played a role.

In summary, at this time the preponderance of clinical and epidemiologic data, including findings from a randomized clinical trial, seems to indicate a moderate risk reduction for congenital heart defects in the aggregate with periconceptional use of a multivitamin supplement containing folic acid. However, not all studies are consistent, and more data are needed. Ideally a new, well-designed clinical trial or a large, carefully implemented prospective case-control study, preferably with biologic markers, could provide conclusive data on this important issue.

RATES AFTER FORTIFICATION

Several countries in North and South America and Middle East, as well as Australia (but no countries in Europe yet), have introduced folic acid fortification, that is, have added variable amounts of folic acid to the food supply, typically in cereal grain products that make their way into common staples such as breads and pasta. The main goal was to reduce the occurrence of neural tube defects by increasing folic acid consumption in the population as a whole. Fortification has also allowed the opportunity to examine changes in the rates of major congenital heart defects in response to overall changes in folic acid consumption. Figure 25.17 summarizes the few available population-based studies, all from North America.

TABLE 25.8

Prevention by Vitamin Use: Summary of Studies on Periconceptional Use of Vitamins and Occurrence of Congenital Heart Defects

Type of Study	Year (Reference)	Population-Based	Study Participants	Exposure	Relative Risk (95% Confidence Interval)		Ventricular Septal Defect
					Heart Defects (overall)	Outflow Tract Defects	
Clinical Trials							
Randomized clinical trial	1998 Czeizel et al (293)	—	2,471 women on MV supplements; 2,391 on trace elements	MV pill with 0.8 mg folic acid	0.42 (0.19–0.98)	0.48 (0.04–5.34)	0.24 (0.05–1.14)
Observational Studies							
Case-control	1995 Shaw et al. (294)	Yes	207 with OTD, 481 controls	MV pill	—	0.53 (0.34–0.85)	—
Case-control	1997 Scanlon et al. (295)	Yes	126 with OTD, 679 controls	MV pill with folic acid	—	0.97 (0.6–1.6)	—
Case-control	1999 Werler et al. (297)	No	157 with OTD, 186 with VSD, 521 controls	MV pill	—	1.00 (0.70–1.50)	1.20 (0.80–1.80)
Case-control	2000 Botto et al. (19)	Yes	958 with heart defects, 3,029 controls	MV pill	0.76 (0.60–0.97)	0.46 (0.24–0.86)	0.61 (0.38–0.99)
Case-control	2010 Beynum et al. (296)	Yes	611 with heart defects, 3,343 controls	≥0.4 mg folic acid alone or as MV pill	0.74 (0.62–0.88)	0.69 (0.47–1.03)	0.56 (0.43–0.74) VSD or ASD

MV, multivitamin; OTD, outflow tract defects; VSD, ventricular septal defects; ASD, atrial septal defect.

In the United States, a study using birth defect surveillance data from 23 state programs compared rates of selected congenital heart defects in 1999 to 2000 versus 1994 to 1996 (299). For heart defects, the study reported a modest (12%) but significant decline in D-transposition of the great arteries (12% reduction, rate ratio 0.88 with 95% CI 0.81 to 0.96), but not for tetralogy of Fallot or ventricular septal defects (299). In Canada, studies from two provinces also reported a modest decline in some heart defects after fortification. In Alberta, researchers using data from a well-established population-based birth defect registry reported a 20% decline in secundum atrial septal defects (rate ratio 0.80, 95% CI 0.69 to 0.93), but not for other heart defects (300). In Quebec, researchers using linked administrative databases evaluated trends of a group of severe heart defects, including conotruncal defects (60% of the case group), single ventricle, and endocardial cushion defects (301). They reported a significant decline of these defects, 6% for every year after fortification (yearly rate ratio 0.94, 95% CI 0.90 to 0.97).

Limited additional information is available from Latin America, where several countries, including Chile, Argentina, and Brazil, introduced fortification at different times and levels. Unlike in North America, no population-based studies are available yet. However, researchers from the Latin American Collaborative Study of Congenital Malformations

(ECLAMC) evaluated rates of selected birth defects from a small sample of hospitals in Chile, Argentina, and Brazil before and after fortification (302). For heart defects, they reported a statistically significant reduction of septal defects. This decline was seen in Argentina and Brazil but not in Chile. In a similar pattern, a moderate nonsignificant decline in an aggregate group of severe heart defects (conotruncal defects, single ventricle, endocardial cushion defects) was observed in Argentina (rate ratio, 0.66) and Brazil (rate ratio, 0.77), but not in Chile (rate ratio, 1.28). By contrast, the decline for neural tube defects was marked and consistent across the three countries (302).

In summary, the few postfortification studies available to date do not suggest a marked or consistent decline in congenital heart defects. Some statistically significant reductions have been observed, but so far these have not been consistent across phenotypes and geographic areas, even within the same country. Interpreting these inconsistencies is challenging. Contributing factors could include variations in the effectiveness of fortification (as documented by blood folate levels) and in study methodology (inclusion criteria and classification scheme). In addition, without a concurrent control group, it is difficult to assess the influence of structural changes in reporting and ascertainment, including the influence of elective terminations of pregnancy. Finally, as the ECLAMC researchers note in their report from Latin America (302), studies based

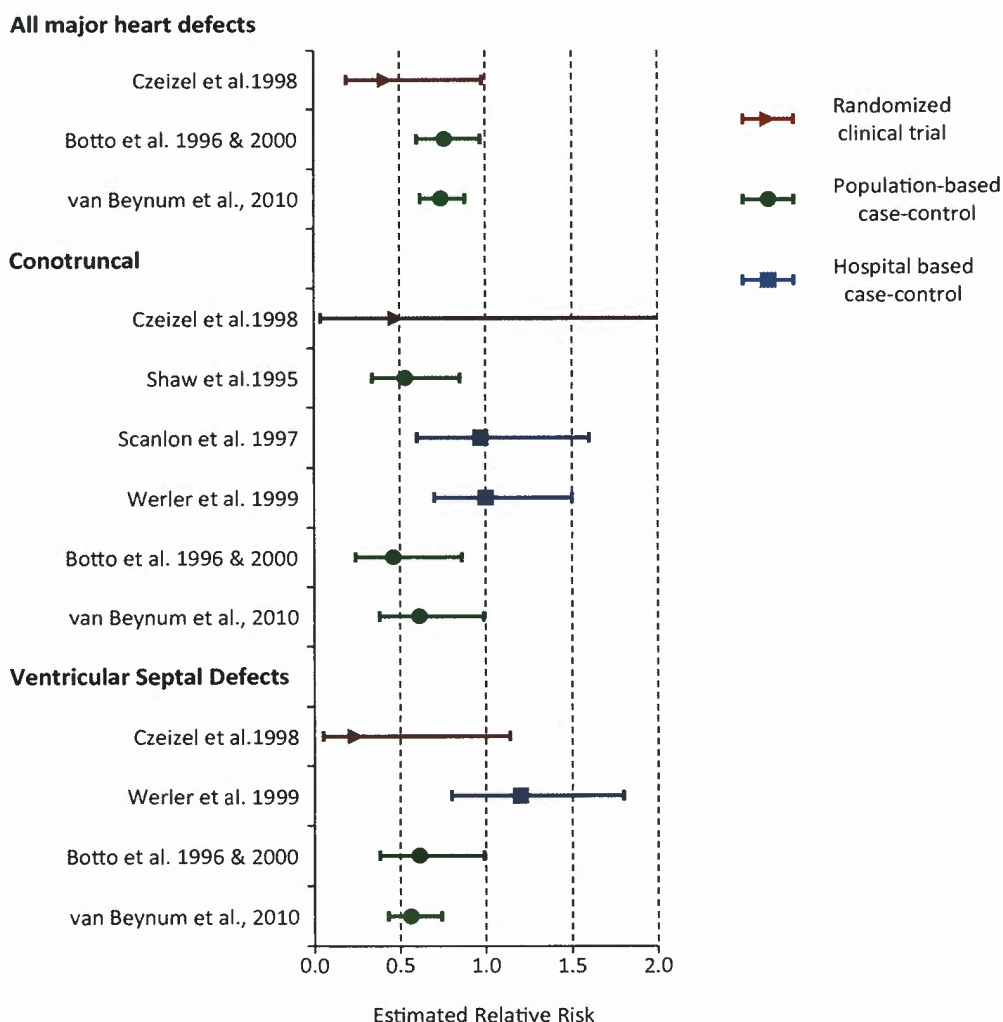


Figure 25.16. Estimated relative risks for congenital heart defects associated with periconceptional use of vitamin supplements with folic acid. Lines represent 95% confidence intervals. Estimated relative risks above 1 suggest increased risk, and relative risks below 1 suggest decreased risk compared to the reference group. (Data from Botto LD, Mulinare J, Erickson JD. Occurrence of congenital heart defects in relation to maternal multivitamin use. *Am J Epidemiol* 2000;151:878–884; Czeizel AE. Periconceptional folic acid containing multivitamin supplementation. *Eur J Obstet Gynecol Reprod Biol* 1998;78:151–161; Shaw GM, O'Malley CD, Wasserman CR, et al. Maternal periconceptional use of multivitamins and reduced risk for conotruncal heart defects and limb deficiencies among offspring. *Am J Med Genet* 1995;59:536–545; Scanlon KS, Ferencz C, Loffredo CA, et al. Preconceptional folate intake and malformations of the cardiac outflow tract. Baltimore-Washington Infant Study Group. *Epidemiology* 1998;9:95–98; van Beynum IM, Kapusta L, Bakker MK, et al. Protective effect of periconceptional folic acid supplements on the risk of congenital heart defects: a registry-based case-control study in the northern Netherlands. *Eur Heart J* 2010;31:464–471; Werler MM, Hayes C, Louik C, et al. Multivitamin supplementation and risk of birth defects. *Am J Epidemiol* 1999;150:675–82.)

on small convenient samples of hospitals can provide detailed data but also be affected by biases, including referral bias.

In general, the data from postfortification studies (Fig. 25.17) are less compelling than those from the clinical trial and observational studies (Fig. 25.16). However, this seems to be true even for neural tube defects, for which the protective effect of folic acid is well established: with fortification, the reduction in occurrence is less and take longer compared to what is seen in observational studies and clinical trials. But the different findings for heart defects and neural tube defects can have other explanations. For example, folic acid may not be effective for heart defects at all; it may be effective only in larger amounts than those typically consumed through fortification or standard folic acid pills (0.4 mg); or it may be effective mainly as part of a multivitamin supplement. In fact,

the reported studies all looked at multivitamin supplement use rather than folic acid alone.

ANCILLARY DATA FROM GENETIC AND ENVIRONMENTAL STUDIES

Potentially relevant data have been generated by studies looking at interactions between multivitamin supplement use and risk factors such as certain medications (247), febrile illnesses (18,189), and pregestational diabetes (161). Findings from one of these studies is illustrated in Figure 25.18 (18).

The odds ratio estimated the relative risk for the different types of heart defects among women reporting a first trimester febrile illness. The figure shows these odds ratios in women who took a multivitamin supplement in the periconceptional period (fever, with MV) and in women who did not take the multivitamin supplement (fever, no MV). Although these risk

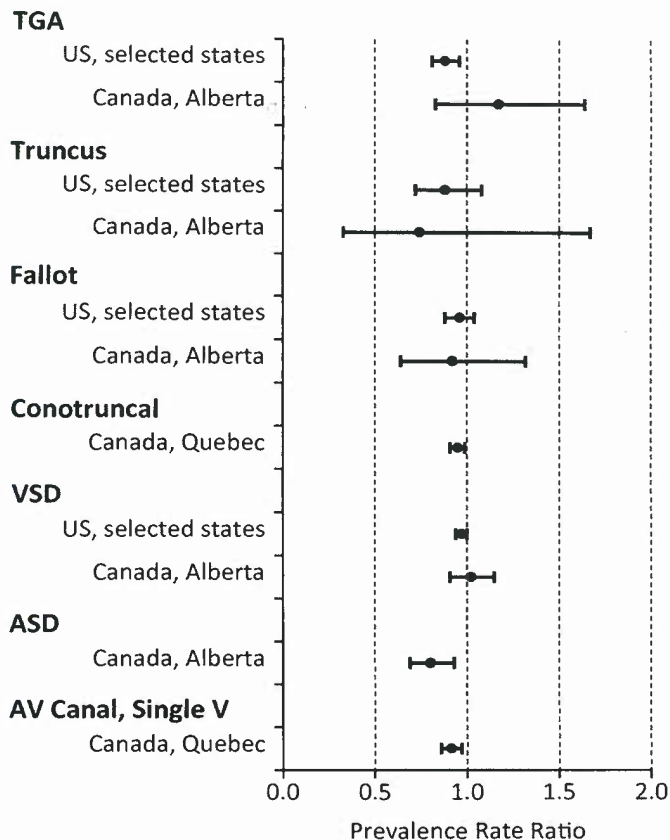


Figure 25.17. Prevalence rate ratios showing changes in reported birth prevalence of selected congenital heart defects in North America after flour fortification with folic acid. Lines represent 95% confidence intervals. Prevalence rate ratios above 1 suggest increased rates after fortification, prevalence rate ratios below 1 suggest decreased rates. (Data from Canfield MA, Collins JS, Botto LD, et al. Changes in the birth prevalence of selected birth defects after grain fortification with folic acid in the United States: findings from a multi-state population-based study. *Birth Defects Res A Clin Mol Teratol* 2005;73:679–689 (US selected states); Godwin KA, Sibbald B, Bedard T, et al. Changes in frequencies of select congenital anomalies since the onset of folic acid fortification in a Canadian birth defect registry. *Can J Public Health* 2008;99:271–275 (Canada Alberta); Ionescu-Ittu R, Marelli AJ, Mackie AS, et al. Prevalence of severe congenital heart disease after folic acid fortification of grain products: time trend analysis in Quebec, Canada. *BMJ* 2009;338:b1673 (Canada Quebec).)

estimates have wide confidence intervals, there appears to be a fairly consistent trend for lower risks among multivitamin users. This would suggest that taking the supplement could mitigate the risk for congenital heart defects associated with fever (18).

Regarding genetic susceptibility in humans, several studies have looked at risk for congenital heart defects in the presence of polymorphisms in several metabolic pathways, but mainly the folate/one-carbon metabolism pathway (303–306). So far, both positive and negative findings have been reported. For folate-related genes, most studies do not show an association with conotruncal or other heart defects (307–312), although some positive associations have been reported (37,313–315). Two studies also suggest a possible gene-nutrient interaction between folate supplementation and presence of a

polymorphism in the reduced folate carrier gene (RFC1). Specifically, these studies found a lower risk for some heart defects associated with the RFC1 polymorphism among mothers who used vitamin supplements in the periconceptional period (316,317).

In summary, folic acid and multivitamin supplementation could have a role in reducing the risk for some congenital heart defects, but evidence, while suggestive, is not conclusive. If confirmed, the impact would be considerable, because the fraction of preventable heart defects may be large. Also, vitamins, including folic acid, are inexpensive and easily transportable, making prevention through vitamin supplementation a viable strategy also in developing countries. Because of the potential implications, a large randomized trial of vitamin supplementation (vs. the recommended dose of folic acid alone) would be very helpful. The resources needed for such study would be considerable, but will likely be minimal compared to the high societal and personal costs of heart defects.

From a practical perspective, however, clinicians need not wait for such a trial. Because of the established protective effect against neural tube defects, daily periconceptional use of folic acid is recommended for all women of childbearing age. By simply promoting periconceptional use of a multivitamin supplement containing folic acid (400 µg), pediatric cardiologists would (and should) provide all women with the benefits of a reduced risk for a neural tube defect-affected pregnancy. The protection against heart defects, to the extent that is present, will be an added benefit, at no additional cost or risk.

STRATEGIES AND TOOLS: EPIDEMIOLOGY OF PREVENTION

Prevention is motivated by incentives and driven by evidence. The next step, implementation, requires strategies to maximize the impact of interventions, and tools to make prevention practical, coherent with the goals, and consistent across practitioners. A broad strategic framework for disease prevention and health promotion is illustrated by the Health Impact Pyramid (Fig. 25.19) (318).

This five-tier model emphasizes that to prevent a large fraction of disease, clinical care and counseling are important, but even more important are interventions that address the broader context of health in society. For example, using diabetes as a model, clinical care and counseling are crucial, but require much individual effort over time by both provider and client and typically reach only a fraction of women with diabetes (318). For maximum effectiveness, diabetes prevention needs to be tackled also through broad societal interventions, such as promoting health education and healthy habits (nutrition, physical activity, obesity prevention), helping make healthy choices the default choices (establishing pedestrian friendly areas, increasing taxes on junk food and beverages), and implementing sustained, long lasting interventions (ad campaigns, including those targeted at youth, screening campaigns) (318). The spectrum of interventions may of course vary depending on the target exposure. For example, to prevent rubella embryopathy, long-lasting interventions (Fig. 25.19) such as immunizations in preteens will play a major role. To decrease smoking, one may need to focus on early education campaigns to reduce the number of first-time smokers and on improvement in socioeconomic conditions, as in many countries socioeconomic status and education levels are inversely related to smoking rates.

This broad strategic framework is crucial not only for primary prevention, but also for reducing complications and optimizing health in people with heart defects

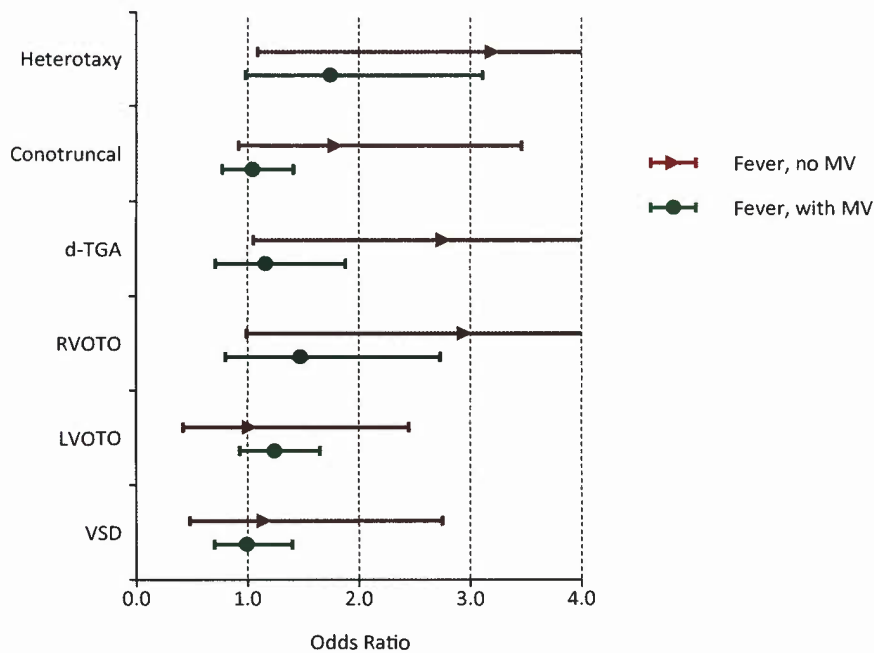


Figure 25.18. Interactions with multivitamin supplement use, possibly mitigating the effect of febrile illness on the risk for selected congenital heart defects. Symbols represent odds ratios for fever, in the absence and in the presence of multivitamin supplement use. Lines represent 95% confidence intervals. Odds ratios above 1 suggest increased risk, odds ratios below 1 suggest decreased risk compared to the reference group. (Data from Botto LD, Erickson JD, Mulinare J, Lynberg MC, Liu Y. Maternal fever, multivitamin use, and selected birth defects: evidence of interaction? *Epidemiology* 2002;13:485–488.)

(secondary prevention), and fits with the increasing attention to prevention throughout the lifespan, from preconception to adults (Fig. 25.2). Clinicians can play a major role not only as providers of individualized clinical care, but also as members of professional organizations that can influence policy making.

Every Woman, Every Time

Moving from this prevention framework to implementation, it is important to characterize the main target population for interventions. Focusing on primary prevention, a preferred target historically have been high-risk families—typically women with family history of congenital heart defects or strong risk factors—and interventions were aimed shortly before conception or in early pregnancy. However, for maximum impact, it is increasingly realized that a more appropriate target is all women of childbearing age. There are several reasons for this shift in focus. First, most babies with heart

defects are born to women and families that are not known to have risk factors, such as having had an affected child. Also, women may not report routinely or even be aware of risk factors, even major ones such as diabetes (175). Second, prevention needs to start before conception. However, most pregnancies worldwide are unplanned (in the United States, over half) and many women find out they are pregnant several weeks after conception. Thus, optimizing women's health before conception requires ongoing attention throughout the childbearing years.

In summary, to maximize the opportunities for prevention, every clinician needs to promote prevention with every woman at every clinical contact—an approach that has been summarized as “every woman, every time.” One significant advantage of this approach is the potential not only to prevent some heart defects, but also improve women's health generally, together with reducing a broad range of adverse pregnancy outcomes. Diabetes, infections, smoking, and lack of folic acid use are risk factors for several types of extracardiac malformations, as well as for preterm birth, intrauterine growth restriction, and infant deaths.

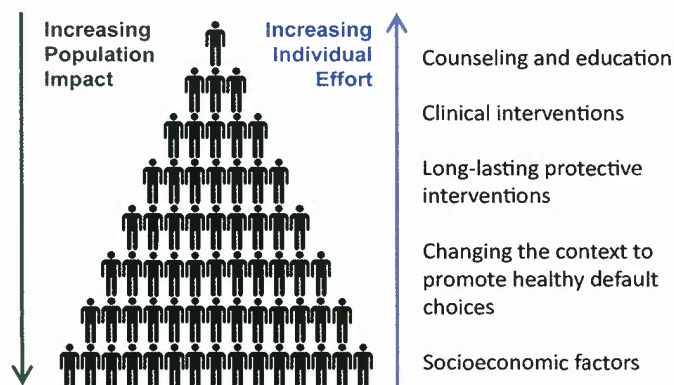


Figure 25.19. The Health Impact Pyramid: designing prevention strategies for maximum population impact. (Modified and redrawn from Frieden TR. A framework for public health action: the health impact pyramid. *Am J Public Health* 2010;100(4):590–595.)

Choosing the Battles: Going for the Greatest Impact

Having broadly identified the target population for prevention (every woman, every time), one is still confronted with a wide range of heterogeneous risk factors (Table 25.7). The final goal is to prevent all preventable congenital heart defects by intervening on all risk factors. However, strategically, it is helpful to reassess these risk factors in terms of their potential for prevention. One useful metric in planning strategies is the attributable fraction of disease, the fraction of cases in the population that is attributable to a risk factor. This is a fraction of disease that could be prevented if the factor was controlled or eliminated. As illustrated previously (Fig. 25.15), the attributable fraction for a risk factor depends not only on its relative risk for disease but also on its frequency in the population.

Risk factors with the highest attributable fraction, assuming that effective prevention strategies exist, would be prime candidates for focused efforts. Factors with low attributable

fraction are not necessarily excluded from prevention efforts, particularly if they are easy to identify and treat, and if they are important for other aspects of population health. For example, even if smoking has a low attributable fraction for congenital heart defects, it is a strong risk factor for many other adverse outcomes, and ought to be included in any comprehensive prevention program. Other considerations, in addition to attributable fraction (and therefore relative risk and exposure frequency), include the strength of the evidence for causality, the severity of the associated heart defects, and, because the final goal is the overall health of woman and child, also the effects on other health outcomes. Table 25.9 summarizes these elements for several of the risk factors that have been reviewed.

As the table illustrates, some risk factors, such as pregestational diabetes, have high potential for prevention, combining strong causal evidence, high relative risks for many congenital heart defects (include severe types), increasing frequency in

the population with increasing attributable fraction, and additional impact on women's health and pediatric outcomes. Others are rare (maternal PKU) but can be easily identified and referred for treatment. For a few, such as folic acid supplementation, the evidence of protective effect for congenital heart defects is not conclusive, but the preventive effect on other adverse outcomes (e.g., spina bifida) is so well established and powerful, that it stands to reason to incorporate these interventions in comprehensive strategies of preconceptional health and prevention. Some of these elements are obviously subject to change, as the prevalence of risk factors increase or decrease, and as the knowledge about causality and specificity improve with new studies.

With these caveats in mind, some guidelines for primary prevention can be suggested (3). With some minor modifications and updates, they are summarized in Table 25.10.

Specifically, all women of childbearing age should be encouraged to take a daily vitamin supplement containing

TABLE 25.9

Selected Risk Factors for Heart Defects by their Potential Global Impact on Primary Prevention and Health Promotion

Factor	Strength of Evidence	Estimated Relative Risk (RR)	Frequency of Exposure (FEP) in Women	Potential Attributable Fraction (%)	Prevention Benefits beyond the Heart
Diabetes (pregestational)	Definite	+++	Common, increasing	7%–15% of more For RR = 4 and FEP = 2.5%–6%	Definite: other birth defects, prematurity and other adverse pregnancy outcomes, maternal health
	Many types	4–10	2%–6%		
Select medications	Definite	++	Varies, but can be common	3% For RR = 4 and FEP = 1%–3%	Definite: neural tube defects and oral clefts (valproic acid), retinoic acid and multiple birth defects
	Many types	2–5 or more			
Phenylketonuria, uncontrolled	Definite	+++	Rare	0.5%	Definite: Mental retardation, microcephaly
	LVOTO	~6	<0.01%		
Non use of folic acid, multivitamin	Possible	+	Very common	33% For RR = 2 and FEP = 50%	Definite: prevent 50%–70% of neural tube defects, possibly other birth defects as well
	Septal, conotruncal	~2	50% to >90%		
Fever/Flu	Possible	+	6 to 10%	4% For RR = 2 and FEP = 6%	Probable/definite: neural tube defects, other adverse outcomes
	Septal, RVOTO	~2			
Smoking	Possible	+	Varies, common	10% For RR = 2 and FEP = 11%	Definite: clefts, low birth weight, intrauterine growth restriction, infant death; maternal health
	Septal	~2	10%–15% or more		
Obesity	Possible	+	Common, increasing	4%–6% For RR = 1.2 and FEP = 20%–30%	Possible: neural tube defects Definite: maternal health, diabetes
	Many types	~1.5	20%–30%		

TABLE 25.10

Improving Health, Decreasing Risk: Seven Steps for Primary Prevention and Health Promotion for Baby and Mother

Action	Comment
1. Take a multivitamin with folic acid daily	Folic acid, 400 µg (0.4 mg) or more Avoid high retinol (>10,000 IU)
2. Promote healthy life and habits	Healthy weight, physical activity, nutrition Preconceptional and early prenatal care
3. Screen/target chronic illnesses	Diabetes (may be unrecognized), epilepsy, PKU
4. Screen/stop smoking, alcohol use	Also second hand smoking
5. Screen/assess medication use	Seizure medications, retinoic acid. Check with physician or teratogen information service (OTIS/ENTIS)
6. Avoid close contact with ill individuals, especially with febrile illnesses	Up-to-date immunizations, including rubella; treat high fever early
7. Avoid exposures to heavy metals, herbicides, pesticides, and organic solvents	At work and at home, self or spouse

folic acid, to reduce the occurrence of neural tube defects and possibly also for some congenital heart defects. They should reevaluate and treat chronic conditions from before conception, especially diabetes. Women diagnosed with PKU as infants should be targeted for interventions aimed at ensuring adherence to a low phenylalanine diet before conception and continue it throughout their pregnancy.

Before conception, women who take potentially teratogenic medications (e.g., valproic acid or lithium) and who are not actively excluding a pregnancy should be counseled about risks and benefits and evaluated for a change in type or dose of medication. Unintended pregnancies need to be avoided particularly among women who use strong teratogens such as retinoic acid medications (e.g., Accutane®). Rubella vaccination provides protective seropositivity and prevents congenital rubella syndrome. Because only 20% of women successfully control tobacco dependence during pregnancy, cessation of smoking is recommended before pregnancy (141), not so much to decrease the potential risk for some congenital heart defects, but to decrease the established risks for preterm birth, low birth weight, and other adverse perinatal outcomes. Alcohol misuse is a significant concern. Although the evidence for specific cardiac teratogenicity is mixed, fetal alcohol syndrome and alcohol-related birth defects can be prevented if women cease intake of alcohol before conception.

With respect to obesity, the risk associated with congenital heart defects is not yet convincingly established. However, obesity is associated with several adverse perinatal outcomes, including neural tube defects, preterm delivery, diabetes,

hypertension, and thromboembolic disease. Appropriate weight loss and improving nutritional health before pregnancy reduces these risks. Additional recommendation for preconception care include vaccination for hepatitis B, identification and treatment of HIV/AIDS and sexually transmitted diseases, treatment of hypothyroidism, and reassessment of oral anticoagulant therapy for warfarin users.

These general guidelines can reasonably apply to all women of childbearing age, to prevent the occurrence of congenital heart defects and other congenital anomalies. Pediatric cardiologists, perhaps more than other specialists, will also see and be called to counsel women who have a congenital heart defect or a previously affected child, and who are contemplating (or not actively excluding) another pregnancy. In this group, the search for modifiable risk factors should be especially rigorous. Also, evaluation for underlying genetic conditions (e.g., deletion 22q11), including referral to an experienced medical geneticists, may be extremely helpful in defining and managing recurrence risk. In the setting of prevention of recurrence of neural tube defects, data from a randomized trial has shown the efficacy of high dose (4 mg) of folic acid, with no adverse effect. No comparable data are available for heart defects.

Ideally, these guidelines would be promoted as an integrated package that emphasizes not only overall preconception care but, broadly, women's health (141). For preconception care in particularly a helpful guiding concept is the 12-month pregnancy, which includes also the trimester *before* conception. This preconceptional period, together with at least the first 2 months of pregnancy, provides a crucial opportunity for promoting healthy cardiac development. Much of cardiac development occurs in the first 7 weeks postconception, at a time that many women may be unaware of the pregnancy, potentially exposed to teratogens, and with limited or no prenatal care. On an individual basis, crucial areas of counseling include screening and managing chronic illnesses or exposures, avoiding exposures to acute illnesses, alcohol and smoking, and taking a daily multivitamin containing folic acid. On a population-basis, effective strategies will have to consider an integrated education campaign for women and providers on common or highly preventable risk factors, increasing access to preconceptional and prenatal care, and reducing disparities in access and care.

Tools

For these interventions, specific tools can be very helpful. Some tools and materials can be found in ongoing prevention initiatives such as "power your life" (319) and through local agencies and organizations. For the busy clinician who wants to promote primary prevention in daily clinical practice, a screening questionnaire could be a helpful adjunct tool to identify major areas for referral or intervention. One possible model (320) is illustrated in Figure 25.20.

Such tools, used regularly ("every woman, every time"), can serve as reminders, as screening tools that can lead to referrals or further management, and as prompts for education.

CONCLUDING COMMENTS

Significant data gaps remain in our understanding of outcomes, risk factors, and best strategies for preventions. However, currently available data is already sufficient to begin a concerted effort to prevent congenital heart defects. Effective prevention requires a combination of incentives that drive policy, evidence based on science, strategies to maximize the effect of interventions, and tools to make these interventions

Health Promotion and Prevention

Date: _____ Patient ID: _____
 Name: _____ Age (years): _____ Date of birth: _____
 Currently Pregnant: N Y Date LMP (day, month, year): _____
 Weight before pregnancy: _____ Current weight (kg): _____ Height (cm): _____

Circle the answer (N=No; Y=Yes; DK=Do not Know). If yes, use the comment/specify section for details

Selected Chronic Conditions	Circle Answer			Comment/Specify
Diabetes (pregestational) type 1	N	Y	DK	
Diabetes (pregestational) type 2	N	Y	DK	
Epilepsy, seizure disorder	N	Y	DK	
Asthma, respiratory disorders	N	Y	DK	
Depression	N	Y	DK	
Thyroid disease	N	Y	DK	
Essential hypertension	N	Y	DK	
Congenital heart disease	N	Y	DK	
Rheumatic heart disease	N	Y	DK	
Chronic renal failure	N	Y	DK	
Sickle cell disease	N	Y	DK	
Other (specify):	N	Y	DK	
Pregnancy and family History				Comment/Specify
Previous babies with birth defects or died in infancy	N	Y	DK	

Legend of timing: BefC = before conception; **P1-2**= month 1-2 of pregnancy; **P3**=month 3 of pregnancy; **T2**=2nd trimester; **T3**=3rd trimester

Selected factors: specify when Yes	Circle Answer			Timing of exposure (circle) See above for legend					Comment/Specify
Smoking	N	Y	DK	BefC	P1-2	P3	T2	T3	
Folic acid or multivitamin (≥3 times/week)	N	Y	DK	BefC	P1-2	P3	T2	T3	
Fever, > 38°C for more than one day	N	Y	DK	BefC	P1-2	P3	T2	T3	
Toxoplasmosis	N	Y	DK	BefC	P1-2	P3	T2	T3	
Rubella (disease)	N	Y	DK	BefC	P1-2	P3	T2	T3	
Rubella immunization	N	Y	DK	BefC	P1-2	P3	T2	T3	
Syphilis	N	Y	DK	BefC	P1-2	P3	T2	T3	
HIV	N	Y	DK	BefC	P1-2	P3	T2	T3	
Medications, specify when Yes									
Seizure medication, type unknown	N	Y	DK	BefC	P1-2	P3	T2	T3	
Carbamazepime (Tegretol)	N	Y	DK	BefC	P1-2	P3	T2	T3	
Valproic acid	N	Y	DK	BefC	P1-2	P3	T2	T3	
Other seizure med (specify):	N	Y	DK	BefC	P1-2	P3	T2	T3	
Antidepressant/Lithium (specify):	N	Y	DK	BefC	P1-2	P3	T2	T3	
Thyroid medications (specify)	N	Y	DK	BefC	P1-2	P3	T2	T3	
Retinoic acid (Accutane)	N	Y	DK	BefC	P1-2	P3	T2	T3	
Warfarin (Cumarin)	N	Y	DK	BefC	P1-2	P3	T2	T3	
Trimethoprim	N	Y	DK	BefC	P1-2	P3	T2	T3	
ACE inhibitors	N	Y	DK	BefC	P1-2	P3	T2	T3	
Others (misoprostol, androgens, corticosteroids, others?): write in below	N	Y	DK	BefC	P1-2	P3	T2	T3	
1.				BefC	P1-2	P3	T2	T3	
2.				BefC	P1-2	P3	T2	T3	
3.				BefC	P1-2	P3	T2	T3	

Additional comments (add a page if needed):

Figure 25.20. Sample questionnaire to screen for common modifiable risk factors for congenital heart defects in clinical practice.

practical, sustainable, and consistent. Epidemiology provides much of the supporting data, from assessing the impact of congenital heart defects (from prevalence to mortality to cost) to evaluating the effects of intervention (by ongoing monitoring of outcomes and risk factors).

In the real world, prevention requires an integrated and sustained effort by the clinical, research, and public health community. This task ought to be tackled with a sense of urgency. Research into new causes and genetic determinants of congenital heart defects needs to go on, to fill the considerable data gaps that still exist on the etiology of heart defects. Yet, even in this stage of incomplete knowledge, some aspects of prevention can and should be implemented today. Pregnancies exposed to known teratogens such as diabetes continue to occur, and affected children continue to be born. To change this, it will be crucial not only to target individual women for preconceptional education and care but also to sustain population-wide interventions that ensure a fair and equitable change for prevention for all groups in the population, so that the benefits of prevention can accrue to all, regardless of education or means.

REFERENCES

1. Botto LD, Goldmuntz E, Lin AE. Epidemiology and prevention of congenital heart defects. In: Allen HD, Driscoll DJ, Shaddy RE, et al., eds. *Moss and Adams' Heart Disease in Infants, Children, and Adolescents, Including the Fetus and Young Adult*. 7th ed. Philadelphia, PA: Lippincott Williams & Wilkins, 2008; pages 524–545.
2. Hoffman JL, Kaplan S, Liberthson RR. Prevalence of congenital heart disease. *Am Heart J* 2004;147:425–439.
3. Jenkins KJ, Correa A, Feinstein JA, et al. Noninherited risk factors and congenital cardiovascular defects: current knowledge: a scientific statement from the American Heart Association Council on Cardiovascular Disease in the Young: endorsed by the American Academy of Pediatrics. *Circulation* 2007;115:2995–3014.
4. McCrindle BW. The prevalence of congenital cardiac lesions. In: Freedom RM, Yoo S-J, Mikailian H, et al., eds. *The Natural and Modified History of Congenital Heart Disease*. New York, NY: Futura, Blackwell Publishing, 2004; pages 8–15.
5. van der Bom T, Zomer AC, Zwinderman AH, et al. The changing epidemiology of congenital heart disease. *Nat Rev Cardiol* 2011;8:50–60.
6. Jacobs JP, Jacobs ML, Mavroudis C, et al. Nomenclature and databases for the surgical treatment of congenital cardiac disease—an updated primer and an analysis of opportunities for improvement. *Cardiol Young* 2008;18:38–62.
7. Franklin RC, Jacobs JP, Krogmann ON, et al. Nomenclature for congenital and paediatric cardiac disease: historical perspectives and The International Pediatric and Congenital Cardiac Code. *Cardiol Young* 2008;18:70–80.
8. International Paediatric and Congenital Cardiac Code. In: available at <http://www.IPCCC.net>.
9. Riehle-Colarusso T, Strickland MJ, Reller MD, et al. Improving the quality of surveillance data on congenital heart defects in the metropolitan Atlanta congenital defects program. *Birth Defects Res A Clin Mol Teratol* 2007;79:743–753.
10. Strickland MJ, Riehle-Colarusso TJ, Jacobs JP, et al. The importance of nomenclature for congenital cardiac disease: implications for research and evaluation. *Cardiol Young* 2008;18:92–100.
11. Clark EB. Pathogenetic mechanisms of congenital cardiovascular malformations revisited. *Semin Perinatol* 1996;20:465–472.
12. Clark EB. Etiology of congenital cardiovascular malformations: epidemiology and genetics. In: Allen HD, Gutgesell HP, Clark EB, et al., eds. *Moss and Adams' Heart Disease in Infants, Children, and Adolescents*. 6th ed. Philadelphia, PA: Lippincott Williams & Wilkins, 2001:64–79.
13. Botto LD, Lin AE, Riehle-Colarusso T, et al. Seeking causes: classifying and evaluating congenital heart defects in etiologic studies. *Birth Defects Res A Clin Mol Teratol* 2007;79(10):714–727.
14. Reller MD, Strickland MJ, Riehle-Colarusso T, et al. Prevalence of congenital heart defects in metropolitan Atlanta, 1998–2005. *J Pediatr* 2008;153:807–813.
15. Wren C, Richmond S, Donaldson L. Temporal variability in birth prevalence of cardiovascular malformations. *Heart* 2000;83:414–419.
16. Ferencz C, Loffredo CA, Correa-Villasenor A, et al. *Genetic and Environmental Risk Factors of Major Congenital Heart Disease: the Baltimore-Washington Infant Study* 1981–1989. Mount Kisco, NY: Futura Publishing Company, Inc., 1997.
17. Ferencz C, Loffredo CA, Rubin JD, et al. *Epidemiology of Congenital Heart Disease: The Baltimore-Washington Infant Study* 1981–1989. Mount Kisco, NY: Futura Publishing Company, Inc., 1993.
18. Botto LD, Erickson JD, Mulinare J, et al. Maternal fever, multivitamin use, and selected birth defects: evidence of interaction? *Epidemiology* 2002;13:485–488.
19. Botto LD, Mulinare J, Erickson JD. Occurrence of congenital heart defects in relation to maternal multivitamin use. *Am J Epidemiol* 2000;151:878–884.
20. Mason CA, Kirby RS, Sever LE, et al. Prevalence is the preferred measure of frequency of birth defects. *Birth Defects Res A Clin Mol Teratol* 2005;73:690–692.
21. Hoffman JL, Kaplan S. The incidence of congenital heart disease. *J Am Coll Cardiol* 2002;39:1890–1900.
22. Rosenthal GL. Prevalence of congenital heart disease. In: Garson AJ, Bricker JT, Fisher DJ, et al., eds. *The Science and Practice of Pediatric Cardiology*. 2 ed. Baltimore, MD: Williams & Wilkins, 1998:1098.
23. Ursell PC, Byrne JM, Strobino BA. Significance of cardiac defects in the developing fetus: a study of spontaneous abortions. *Circulation* 1985;72:1232–1236.
24. Chinn A, Fitzsimmons J, Shepard TH, et al. Congenital heart disease among spontaneous abortions and stillborn fetuses: prevalence and associations. *Teratology* 1989;40:475–482.
25. Stoll C, Alembik Y, Roth MP, et al. Risk factors in congenital heart disease. *Eur J Epidemiol* 1989;5:382–391.
26. Fyler DC, Buckley LP, Hellenbrand WE, et al. Report of the New England Regional Infant Cardiac Program. *Pediatrics* 1980;65:376.
27. Grabitz RG, Joffres MR, Collins-Nakai RL. Congenital heart disease: incidence in the first year of life. The Alberta Heritage Pediatric Cardiology Program. *Am J Epidemiol* 1988;128:381–388.
28. Fixler DE, Pastor P, Chamberlin M, et al. Trends in congenital heart disease in Dallas County births. 1971–1984. *Circulation* 1990;81:137–142.
29. Kidd SA, Lancaster PA, McCredie RM. The incidence of congenital heart defects in the first year of life. *J Paediatr Child Health* 1993;29:344–349.
30. Samanek M. Boy:girl ratio in children born with different forms of cardiac malformation: a population-based study. *Pediatr Cardiol* 1994;15:53–57.
31. Abu-Harb M, Hey E, Wren C. Death in infancy from unrecognised congenital heart disease. *Arch Dis Child* 1994;71:3–7.
32. Tanner K, Sabrine N, Wren C. Cardiovascular malformations among preterm infants. *Pediatrics* 2005;116:e833–8.
33. Roy DL, McIntyre L, Human DG, et al. Trends in the prevalence of congenital heart disease: comprehensive observations over a 24-year period in a defined region of Canada. *Can J Cardiol* 1994;10:821–826.
34. Eichhorn P, Sutsch G, Jenni R. [Congenital heart defects and abnormalities newly detected with echocardiography in adolescents and adults]. *Schweiz Med Wochenschr* 1990;120:1697–1700.
35. Tegnander E, Williams W, Johansen OJ, et al. Prenatal detection of heart defects in a non-selected population of 30,149 fetuses—detection rates and outcome. *Ultrasound Obstet Gynecol* 2006;27:252–265.
36. Dolk H, Loane M, Garne E. Congenital heart defects in Europe: prevalence and perinatal mortality, 2000 to 2005. *Circulation* 2011;123:841–849.
37. van Beynum IM, Kapusta L, den Heijer M, et al. Maternal MTHFR 677C>T is a risk factor for congenital heart defects: effect modification by periconceptional folate supplementation. *Eur Heart J* 2006;27:981–987.
38. Lin AE, Herring AH, Amstutz KS, et al. Cardiovascular malformations: changes in prevalence and birth status, 1972–1990. *Am J Med Genet* 1999;84:102–110.
39. Botto LD, Correa A, Erickson JD. Racial and temporal variations in the prevalence of heart defects. *Pediatrics* 2001;107:E32.
40. Hiraishi S, Agata Y, Nowatari M, et al. Incidence and natural course of trabecular ventricular septal defect: two-dimensional echocardiography and color Doppler flow imaging study. *J Pediatr* 1992;120:409–415.
41. Ishikawa T, Iwashima S, Ohishi A, et al. Prevalence of congenital heart disease assessed by echocardiography in 2067 consecutive newborns. *Acta Paediatr* 2011;100:e55–e60.
42. Tutar E, Ekici F, Atalay S, et al. The prevalence of bicuspid aortic valve in newborns by echocardiographic screening. *Am Heart J* 2005;150:513–515.
43. Ward C. Clinical significance of the bicuspid aortic valve. *Heart* 2000;83:81–85.
44. Oyen N, Poulsen G, Boyd HA, et al. Recurrence of congenital heart defects in families. *Circulation* 2009;120:295–301.
45. Oyen N, Poulsen G, Boyd HA, et al. National time trends in congenital heart defects, Denmark, 1977–2005. *Am Heart J* 2009;157:467.e1–473.e1.
46. Selected birth defects data from population-based birth defects surveillance programs in the United States, 2003–2007. *Birth Defects Res A Clin Mol Teratol* 2010;88:1062–1174.
47. Kornosky JL, Salihu HM. Getting to the heart of the matter: epidemiology of cyanotic heart defects. *Pediatr Cardiol* 2008;29:484–497.
48. Warnes CA, Liberthson R, Danielson GK, et al. Task force 1: the changing profile of congenital heart disease in adult life. *J Am Coll Cardiol* 2001;37:1170–1175.
49. Marelli AJ, Mackie AS, Ionescu-Ittu R, et al. Congenital heart disease in the general population: changing prevalence and age distribution. *Circulation* 2007;115:163–172.
50. Brickner ME, Hillis LD, Lange RA. Congenital heart disease in adults. First of two parts. *N Engl J Med* 2000;342(4):256–263.
51. Chambers J. Aortic stenosis. *BMJ* 2005;330:801–802.
52. Cecconi M, Nistri S, Quarti A, et al. Aortic dilatation in patients with bicuspid aortic valve. *J Cardiovasc Med (Hagerstown)* 2006;7:11–20.

53. Tzemos N, Therrien J, Yip J, et al. Outcomes in adults with bicuspid aortic valves. *JAMA* 2008;300:1317–1325.
54. Williams RG, Pearson GD, Barst RJ, et al. Report of the National Heart, Lung, and Blood Institute Working Group on research in adult congenital heart disease. *J Am Coll Cardiol* 2006;47:701–707.
55. Marelli AJ, Gervitz M. From numbers to guidelines. *Prog Cardiovasc Dis* 2011;53:239–246.
56. Hoffman JL. Incidence of congenital heart disease: I. Postnatal incidence. *Pediatr Cardiol* 1995;16:103–113.
57. Lopez AD, Mathers CD. Measuring the global burden of disease and epidemiological transitions: 2002–2030. *Ann Trop Med Parasitol* 2006;100:481–499.
58. Murray CJL, Lopez AD. *Health Dimensions of Sex and Reproduction: The Global Burden of Sexually Transmitted Diseases, HIV, Maternal Conditions, Perinatal Disorders, and Congenital Anomalies*. Boston, MA: Harvard University Press, 1998.
59. Christianson A, Howson CP, Modell B. *March of Dimes Global Report on Birth Defects: The Hidden Toll of Dying and Disabled Children*. White Plains, NY: March of Dimes Birth Defects Foundation, 2006.
60. Garne E, Khoshnood B, Loane M, et al. Termination of pregnancy for fetal anomaly after 23 weeks of gestation: a European register-based study. *BJOG* 2010;117:660–666.
61. International Clearinghouse for Birth Defects Surveillance and Research. Annual Report 2009, with data for 2007. In: Mastroiacovo P, ed. Rome, Italy, 2009.
62. Walsh W. Evaluation of pulse oximetry screening in Middle Tennessee: cases for consideration before universal screening. *J Perinatol* 2011;31:125–129.
63. Smith AE, Vedder TG, Hunter PK, et al. The use of newborn screening pulse oximetry to detect cyanotic congenital heart disease: a survey of current practice at Army, Navy, and Air Force hospitals. *Mil Med* 2011;176:343–346.
64. Shastri AT, Clarke P, Roy R. Pulse oximetry screening for detection of critical congenital heart disease in newborns: a survey of current practices in the United Kingdom. *Acta Paediatr* 2011;100:636–637.
65. Kang S, Tobin S, Kelsall W. Neonatal pulse oximetry screening: a national survey. *Arch Dis Child Fetal Neonatal Ed* 2011;96:F312.
66. Hoffman JL. It is time for routine neonatal screening by pulse oximetry. *Neonatology* 2011;99:1–9.
67. Tautz J, Merkel C, Loersch F, et al. Implication of pulse oximetry screening for detection of congenital heart defects. *Klin Padiatr* 2010;222:291–295.
68. Riede FT, Worner C, Dahnert I, et al. Effectiveness of neonatal pulse oximetry screening for detection of critical congenital heart disease in daily clinical routine—results from a prospective multicenter study. *Eur J Pediatr* 2010;169:975–981.
69. Kuelling B, Arlettaz Mieth R, Bauersfeld U, et al. Pulse oximetry screening for congenital heart defects in Switzerland: most but not all maternity units screen their neonates. *Swiss Med Wkly* 2009;139:699–704.
70. Meberg A, Andreassen A, Brunvand L, et al. Pulse oximetry screening as a complementary strategy to detect critical congenital heart defects. *Acta Paediatr* 2009;98:682–686.
71. de-Wahl Granelli A, Wennergren M, Sandberg K, et al. Impact of pulse oximetry screening on the detection of duct dependent congenital heart disease: a Swedish prospective screening study in 39,821 newborns. *BMJ* 2009;338:a3037.
72. Koppel RI, Druschel CM, Carter T, et al. Effectiveness of pulse oximetry screening for congenital heart disease in asymptomatic newborns. *Pediatrics* 2003;111:451–455.
73. Hoke TR, Donohue PK, Bawa PK, et al. Oxygen saturation as a screening test for critical congenital heart disease: a preliminary study. *Pediatr Cardiol* 2002;23:403–409.
74. Rosano A, Botto LD, Botting B, et al. Infant mortality and congenital anomalies from 1950 to 1994: an international perspective. *J Epidemiol Community Health* 2000;54:660–666.
75. Centers for Disease Control and Prevention (CDC). Racial differences by gestational age in neonatal deaths attributable to congenital heart defects—United States, 2003–2006. *MMWR Morb Mortal Wkly Rep* 2010;59:1208–1211.
76. Boneva RS, Botto LD, Moore CA, et al. Mortality associated with congenital heart defects in the United States: trends and racial disparities, 1979–1997. *Circulation* 2001;103:2376–2381.
77. Gillum RF. Epidemiology of congenital heart disease in the United States. *Am Heart J* 1994;127:919–927.
78. Gilboa SM, Salemi JL, Nembhard WN, et al. Mortality resulting from congenital heart disease among children and adults in the United States, 1999 to 2006. *Circulation* 2010;122(22):2254–2263.
79. Pillutla P, Shetty KD, Foster E. Mortality associated with adult congenital heart disease: trends in the US population from 1979 to 2005. *Am Heart J* 2009;158:874–879.
80. Morales DL, McClellan AJ, Jacobs JP. Empowering a database with national long-term data about mortality: the use of national death registries. *Cardiol Young* 2008;18:188–195.
81. Olsen M, Christensen TD, Pedersen L, et al. Late mortality among Danish patients with congenital heart defect. *Am J Cardiol* 2010;106:1322–1326.
82. Khairy P, Ionescu-Ittu R, Mackie AS, et al. Changing mortality in congenital heart disease. *J Am Coll Cardiol* 2010;56:1149–1157.
83. Moons P, Sluysmans T, De Wolf D, et al. Congenital heart disease in 111 225 births in Belgium: birth prevalence, treatment and survival in the 21st century. *Acta Paediatr* 2009;98:472–477.
84. Moons P, Bovijn L, Budts W, et al. Temporal trends in survival to adulthood among patients born with congenital heart disease from 1970 to 1992 in Belgium. *Circulation* 2010;122:2264–2272.
85. Fixler DE, Nembhard WN, Salemi JL, et al. Mortality in first 5 years in infants with functional single ventricle born in Texas, 1996 to 2003. *Circulation* 2010;121:644–650.
86. Knowles RL, Griebisch I, Bull C, et al. Quality-of-life and congenital heart defects: comparing parent and professional values. *Arch Dis Child* 2007;92:388–393.
87. Mahle W. Spectrum of heart disease. In: Rubin I, Crocker A, eds. *Medical Care for Children and Adults with Developmental Disabilities*. Baltimore, MD: Paul H Brooks Publishing Co., 2006:379–386.
88. Brown MD, Wernovsky G, Mussatto KA, et al. Long-term and developmental outcomes of children with complex congenital heart disease. *Clin Perinatol* 2005;32:1043–1057, xi.
89. Wernovsky G. Outcomes regarding the central nervous system in children with complex congenital cardiac malformations. *Cardiol Young* 2005;15:132–133.
90. Williams WG. Surgical outcomes in congenital heart disease: expectations and realities. *Eur J Cardiothorac Surg* 2005;27:937–944.
91. von Rhein M, Scheer I, Loenneker T, et al. Structural brain lesions in adolescents with congenital heart disease. *J Pediatr* 2011;158:984–989.
92. Olsen M, Hjortdal VE, Mortensen LH, et al. Educational achievement among long-term survivors of congenital heart defects: a Danish population-based follow-up study. *Cardiol Young* 2011;21:197–203.
93. McQuillen PS, Goff DA, Licht DJ. Effects of congenital heart disease on brain development. *Prog Pediatr Cardiol* 2010;29:79–85.
94. Donofrio MT, Massaro AN. Impact of congenital heart disease on brain development and neurodevelopmental outcome. *Int J Pediatr* 2010;2010.
95. Calderon J, Bonnet D, Courtin C, et al. Executive function and theory of mind in school-aged children after neonatal corrective cardiac surgery for transposition of the great arteries. *Dev Med Child Neurol* 2010;52:1139–1144.
96. Hovels-Gurich HH, Bauer SB, Schnitker R, et al. Long-term outcome of speech and language in children after corrective surgery for cyanotic or acyanotic cardiac defects in infancy. *Eur J Paediatr Neurol* 2008;12:378–386.
97. Fuller S, Nord AS, Gerdes M, et al. Predictors of impaired neurodevelopmental outcomes at one year of age after infant cardiac surgery. *Eur J Cardiothorac Surg* 2009;36:40–47.
98. Limperopoulos C, Majnemer A, Shevell MI, et al. Neurodevelopmental status of newborns and infants with congenital heart defects before and after open heart surgery. *J Pediatr* 2000;137:638–645.
99. Limperopoulos C, Tworetzky W, McElhinney DB, et al. Brain volume and metabolism in fetuses with congenital heart disease: evaluation with quantitative magnetic resonance imaging and spectroscopy. *Circulation* 2010;121:26–33.
100. Hoskoppal A, Roberts H, Kugler J, et al. Neurodevelopmental outcomes in infants after surgery for congenital heart disease: a comparison of single-ventricle vs. two-ventricle physiology. *Congenit Heart Dis* 2010;5: 90–95.
101. Gaynor JW, Wernovsky G, Jarvik GP, et al. Patient characteristics are important determinants of neurodevelopmental outcome at one year of age after neonatal and infant cardiac surgery. *J Thorac Cardiovasc Surg* 2007;133:1344–1353, 1353.e1–1353.e3.
102. Mahle WT, Wernovsky G. Neurodevelopmental outcomes in hypoplastic left heart syndrome. *Semin Thorac Cardiovasc Surg Pediatr Card Surg Annu* 2004;7:39–47.
103. Massaro AN, El-Dib M, Glass P, et al. Factors associated with adverse neurodevelopmental outcomes in infants with congenital heart disease. *Brain Dev* 2008;30:437–446.
104. Mahle WT, Visconti KJ, Freier MC, et al. Relationship of surgical approach to neurodevelopmental outcomes in hypoplastic left heart syndrome. *Pediatrics* 2006;117:e90–e97.
105. Joffe AR, Quinonez LG, Robertson CM, et al. Outcomes after heart transplantation in children under six years of age. *Ann Thorac Surg* 2011;92:174–182.
106. Latal B, Helfrich S, Fischer JE, et al. Psychological adjustment and quality of life in children and adolescents following open-heart surgery for congenital heart disease: a systematic review. *BMC Pediatr* 2009;9:6.
107. Brandlistuen RE, Stene-Larsen K, Holmstrom H, et al. Occurrence and predictors of developmental impairments in 3-year-old children with congenital heart defects. *J Dev Behav Pediatr* 2011;32:526–532.
108. Stene-Larsen K, Brandlistuen RE, Holmstrom H, et al. Longitudinal analysis of emotional problems in children with congenital heart defects: a follow-up from age 6 to 36 months. *J Dev Behav Pediatr* 2011;32(6): 461–464.
109. Schultz AH, Wernovsky G. Late outcomes in patients with surgically treated congenital heart disease. *Semin Thorac Cardiovasc Surg Pediatr Card Surg Annu* 2005;8:145–156.
110. Eiser C, Morse R. Can parents rate their child's health-related quality of life? Results of a systematic review. *Qual Life Res* 2001;10:347–357.
111. Eiser C, Morse R. The measurement of quality of life in children: past and future perspectives. *J Dev Behav Pediatr* 2001;22:248–256.
112. Eiser C, Morse R. A review of measures of quality of life for children with chronic illness. *Arch Dis Child* 2001;84:205–211.

113. Goldbeck L, Melches J. Quality of life in families of children with congenital heart disease. *Qual Life Res* 2005;14:1915–1924.
114. McCrindle BW, Williams RV, Mitchell PD, et al. Relationship of patient and medical characteristics to health status in children and adolescents after the Fontan procedure. *Circulation* 2006;113:1123–1129.
115. Goldbeck L, Melches J. The impact of the severity of disease and social disadvantage on quality of life in families with congenital cardiac disease. *Cardiol Young* 2006;16:67–75.
116. Culbert EL, Ashburn DA, Cullen-Dean G, et al. Quality of life of children after repair of transposition of the great arteries. *Circulation* 2003;108:857–862.
117. Moons P, Van Deyk K, De Geest S, et al. Is the severity of congenital heart disease associated with the quality of life and perceived health of adult patients? *Heart* 2005;91:1193–1198.
118. Rose M, Kohler K, Kohler F, et al. Determinants of the quality of life of patients with congenital heart disease. *Qual Life Res* 2005;14:35–43.
119. Sairanen HI, Nieminen HP, Jokinen EV. Late results and quality of life after pediatric cardiac surgery in Finland: a population-based study of 6,461 patients with follow-up extending up to 45 years. *Semin Thorac Cardiovasc Surg Pediatr Card Surg Annu* 2005;8:168–172.
120. Spijkerboer AW, Utens EM, De Koning WB, et al. Health-related Quality of Life in children and adolescents after invasive treatment for congenital heart disease. *Qual Life Res* 2006;15:663–673.
121. Lane DA, Lip GY, Millane TA. Quality of life in adults with congenital heart disease. *Heart* 2002;88:71–75.
122. Green A. Outcomes of congenital heart disease: a review. *Pediatr Nurs* 2004;30:280–284.
123. Uzark K, Jones K, Slusher J, et al. Quality of life in children with heart disease as perceived by children and parents. *Pediatrics* 2008;121:e1060–e1067.
124. Moons P, De Bleser L, Budts W, et al. Health status, functional abilities, and quality of life after the Mustard or Senning operation. *Ann Thorac Surg* 2004;77:1359–1365; discussion 1365.
125. Rietveld S, Mulder BJ, van Beest I, et al. Negative thoughts in adults with congenital heart disease. *Int J Cardiol* 2002;86:19–26.
126. Lip GY, Lane DA, Millane TA, et al. Psychological interventions for depression in adolescent and adult congenital heart disease. *Cochrane Database Syst Rev* 2003(3):CD004394.
127. Claessens P, Moons P, de Casterle BD, et al. What does it mean to live with a congenital heart disease? A qualitative study on the lived experiences of adult patients. *Eur J Cardiovasc Nurs* 2005;4:3–10.
128. Jefferies JL, Noonan JA, Keller BB, et al. Quality of life and social outcomes in adults with congenital heart disease living in rural areas of Kentucky. *Am J Cardiol* 2004;94:263–266.
129. Crossland DS, Jackson SP, Lyall R, et al. Life insurance and mortgage application in adults with congenital heart disease. *Eur J Cardiothorac Surg* 2004;25:931–934.
130. Spijkerboer AW, Utens EM, Bogers AJ, et al. Long-term behavioural and emotional problems in four cardiac diagnostic groups of children and adolescents after invasive treatment for congenital heart disease. *Int J Cardiol* 2008;125:66–73.
131. Dunbar-Masterson C, Wypij D, Bellinger DC, et al. General health status of children with D-transposition of the great arteries after the arterial switch operation. *Circulation* 2001;104:1138–1142.
132. Mahle WT, Clancy RR, Moss EM, et al. Neurodevelopmental outcome and lifestyle assessment in school-aged and adolescent children with hypoplastic left heart syndrome. *Pediatrics* 2000;105:1082–1089.
133. Ekman-Joelsson BM, Berntsson L, Sunnegardh J. Quality of life in children with pulmonary atresia and intact ventricular septum. *Cardiol Young* 2004;14:615–621.
134. Landolt MA, Valsangiacomo Buechel ER, Latal B. Health-related quality of life in children and adolescents after open-heart surgery. *J Pediatr* 2008;152:349–355.
135. Mussatto K, Tweddell J. Quality of life following surgery for congenital cardiac malformations in neonates and infants. *Cardiol Young* 2005;15:174–178.
136. Majnemer A, Limperopoulos C, Shevell M, et al. Health and well-being of children with congenital cardiac malformations, and their families, following open-heart surgery. *Cardiol Young* 2006;16:157–164.
137. Berkes A, Pataki I, Kiss M, et al. Measuring health-related quality of life in Hungarian children with heart disease: psychometric properties of the Hungarian version of the Pediatric Quality of Life Inventory 4.0 Generic Core Scales and the Cardiac Module. *Health Qual Life Outcomes* 2010;8:14.
138. Marino BS, Shera D, Wernovsky G, et al. The development of the pediatric cardiac quality of life inventory: a quality of life measure for children and adolescents with heart disease. *Qual Life Res* 2008;17:613–626.
139. Marino BS, Tomlinson RS, Wernovsky G, et al. Validation of the pediatric cardiac quality of life inventory. *Pediatrics* 2010;126:498–508.
140. Flores G. Technical report—racial and ethnic disparities in the health and health care of children. *Pediatrics* 2010;125:e979–e1020.
141. Johnson K, Posner SF, Biermann J, et al. Recommendations to Improve Preconception Health and Health Care—United States. *MMWR Morb Mortal Wkly Rep* 2006;55:1–23.
142. Benavidez OJ, Gauvreau K, Jenkins KJ. Racial and ethnic disparities in mortality following congenital heart surgery. *Pediatr Cardiol* 2006;27:321–328.
143. Nembhard WN, Salemi JL, Ethen MK, et al. Racial/ethnic disparities in risk of early childhood mortality among children with congenital heart defects. *Pediatrics* 2011;127:e1128–e1138.
144. Boulet S, Grosse SC, Riehle-Colarusso T, et al. Health care costs of congenital heart defects. In: Wyszynski DF, Correa-Villasenor A, Graham TP, eds. *Congenital Heart Defects: From Origin to Treatment*. New York, NY: Oxford University Press, 2010:493–501.
145. Russo CA, Elixhauser A. Hospitalizations for birth defects, 2004. In: *HCUP Statistical Briefs*. Rockville, MD: U.S. Agency for Healthcare Research and Quality, 2007.
146. Okumura MJ, Campbell AD, Nasr SZ, et al. Inpatient health care use among adult survivors of chronic childhood illnesses in the United States. *Arch Pediatr Adolesc Med* 2006;160:1054–1060.
147. Waitzman NJ, Romano PS, Scheffler RM. *The Cost of Birth Defects*. Lanham, MD: University Press of America, 1996.
148. Centers for Disease Control and Prevention, Waitzman NJ, Romano PS, Scheffler RM, Harris JA. Economic costs of birth defects and cerebral palsy—United States, 1992. *MMWR Morb Mortal Wkly Rep* 1995;44:694–699.
149. Botto LD. Primary prevention of congenital heart defects. In: Wyszynski DF, Correa A, Graham TP, eds. *Congenital Heart Defects: From Origin to Treatment*. New York, NY: Oxford University Press, 2010:462–477.
150. Rothman KJ. What is causation? In: *Epidemiology: An Introduction*. New York, NY: Oxford University Press, 2002.
151. Hanley JA. A heuristic approach to the formulas for population attributable fraction. *J Epidemiol Community Health* 2001;55:508–514.
152. Walter SD. Attributable risk in practice. *Am J Epidemiol* 1998;148:411–413.
153. Benichou J. A review of adjusted estimators of attributable risk. *Stat Methods Med Res* 2001;10:195–216.
154. Rockhill B, Newman B, Weinberg C. Use and misuse of population attributable fractions. *Am J Public Health* 1998;88:15–19.
155. Wilson PD, Loffredo CA, Correa-Villasenor A, et al. Attributable fraction for cardiac malformations. *Am J Epidemiol* 1998;148:414–423.
156. TERIS—Teratogen Information Service and online version of Shepard's Catalog of Teratogenic Agents. In: University of Washington; 2006.
157. REPROTOX—information system on environmental hazards to human reproduction and development. In: www.reprotox.org; 2006.
158. Organization of Teratology Information Specialists. www.otispregnancy.org, 2010.
159. European Network of Teratology Information Services. www.ents-org.com
160. Becerra JE, Khoury MJ, Cordero JF, et al. Diabetes mellitus during pregnancy and the risks for specific birth defects: a population-based case-control study. *Pediatrics* 1990;85:1–9.
161. Correa A, Botto L, Liu Y, et al. Do multivitamin supplements attenuate the risk for diabetes-associated birth defects? *Pediatrics* 2003;111:1146–1151.
162. Correa A, Gilboa SM, Besser LM, et al. Diabetes mellitus and birth defects. *Am J Obstet Gynecol* 2008;199:237.e1–237.e9.
163. Lisowski LA, Verheijen PM, Copel JA, et al. Congenital heart disease in pregnancies complicated by maternal diabetes mellitus. An international clinical collaboration, literature review, and meta-analysis. *Herz* 2010;35:19–26.
164. Loffredo CA. Epidemiology of cardiovascular malformations: prevalence and risk factors. *Am J Med Genet* 2000;97:319–325.
165. Moore LL, Singer MR, Bradlee ML, et al. A prospective study of the risk of congenital defects associated with maternal obesity and diabetes mellitus. *Epidemiology* 2000;11:689–694.
166. Ray JG, O'Brien TE, Chan WS. Preconception care and the risk of congenital anomalies in the offspring of women with diabetes mellitus: a meta-analysis. *QJM* 2001;94:435–44.
167. Wren C, Birrell G, Hawthorne G. Cardiovascular malformations in infants of diabetic mothers. *Heart* 2003;89:1217–1220.
168. Kousseff BG. Diabetic embryopathy. *Curr Opin Pediatr* 1999;11:348–352.
169. Rowland TW, Hubbell JP Jr, Nadas AS. Congenital heart disease in infants of diabetic mothers. *J Pediatr* 1973;83:815–820.
170. Aberg A, Westbom L, Kallen B. Congenital malformations among infants whose mothers had gestational diabetes or preexisting diabetes. *Early Hum Dev* 2001;61:85–95.
171. Martinez-Frias ML, Bermejo E, Rodriguez-Pinilla E, et al. Epidemiological analysis of outcomes of pregnancy in gestational diabetic mothers. *Am J Med Genet* 1998;78:140–145.
172. Sheffield JS, Butler-Koster EL, Casey BM, et al. Maternal diabetes mellitus and infant malformations. *Obstet Gynecol* 2002;100:925–930.
173. Harris MI, Flegal KM, Cowie CC, et al. Prevalence of diabetes, impaired fasting glucose, and impaired glucose tolerance in U.S. adults. The Third National Health and Nutrition Examination Survey, 1988–1994. *Diabetes Care* 1998;21:518–524.
174. Mokdad AH, Ford ES, Bowman BA, et al. Prevalence of obesity, diabetes, and obesity-related health risk factors, 2001. *JAMA* 2003;289:76–79.
175. Cowie CC, Rust KF, Byrd-Holt DD, et al. Prevalence of diabetes and impaired fasting glucose in adults in the U.S. population: National Health And Nutrition Examination Survey 1999–2002. *Diabetes Care* 2006;29:1263–1268.
176. Cousins L. Etiology and prevention of congenital anomalies among infants of overt diabetic women. *Clin Obstet Gynecol* 1991;34:481–493.

177. Suhonen L, Hiilesmaa V, Teramo K. Glycaemic control during early pregnancy and fetal malformations in women with type I diabetes mellitus. *Diabetologia* 2000;43:79–82.
178. Holing EV, Beyer CS, Brown ZA, et al. Why don't women with diabetes plan their pregnancies? *Diabetes Care* 1998;21:889–895.
179. Kitzmiller JL, Wallerstein R, Correa A, et al. Preconception care for women with diabetes and prevention of major congenital malformations. *Birth Defects Res A Clin Mol Teratol* 2010;88:791–803.
180. Oster ME, Riehle-Colarusso T, Correa A. An update on cardiovascular malformations in congenital rubella syndrome. *Birth Defects Res A Clin Mol Teratol* 2010;88:1–8.
181. Forrest JM, Turnbull FM, Sholler GF, et al. Gregg's congenital rubella patients 60 years later. *Med J Aust* 2002;177:664–667.
182. Reef SE, Strebel P, Dabbagh A, et al. Progress toward control of rubella and prevention of congenital rubella syndrome—worldwide, 2009. *J Infect Dis* 2011;204:S24–S27.
183. Reef SE, Plotkin S, Cordero JF, et al. Preparing for elimination of congenital Rubella syndrome (CRS): summary of a workshop on CRS elimination in the United States. *Clin Infect Dis* 2000;31:85–95.
184. Robertson SE, Featherstone DA, Gacic-Dobo M, et al. Rubella and congenital rubella syndrome: global update. *Rev Panam Salud Publica* 2003;14:306–315.
185. Progress toward control of rubella and prevention of congenital rubella syndrome—worldwide, 2009. *MMWR Morb Mortal Wkly Rep* 2010;59:1307–10.
186. Edwards MJ, Shiota K, Smith MS, et al. Hyperthermia and birth defects. *Reprod Toxicol* 1995;9:411–425.
187. Graham JM Jr, Edwards MJ. Teratogen update: gestational effects of maternal hyperthermia due to febrile illnesses and resultant patterns of defects in humans. *Teratology* 1998;58:209–221.
188. Roulston A, Marcellus RC, Branton PE. Viruses and apoptosis. *Ann Rev Microbiol* 1999;53:577–628.
189. Shaw GM, Nelson V, Carmichael SL, et al. Maternal periconceptional vitamins: interactions with selected factors and congenital anomalies? *Epidemiology* 2002;13:625–630.
190. Tikkanen J, Heinonen OP. Maternal hyperthermia during pregnancy and cardiovascular malformations in the offspring. *Eur J Epidemiol* 1991;7:628–635.
191. Zhang J, Cai WW. Association of the common cold in the first trimester of pregnancy with birth defects. *Pediatrics* 1993;92:559–563.
192. Oster ME, Riehle-Colarusso T, Alverson CJ, et al. Associations between maternal fever and influenza and congenital heart defects. *J Pediatr* 2011;158:990–995.
193. Levy HL, Guldberg P, Guttler F, et al. Congenital heart disease in maternal phenylketonuria: report from the Maternal PKU Collaborative Study. *Pediatr Res* 2001;49:636–642.
194. Matalon KM, Acosta PB, Azen C. Role of nutrition in pregnancy with phenylketonuria and birth defects. *Pediatrics* 2003;112:1534–1536.
195. Rouse B, Azen C. Effect of high maternal blood phenylalanine on offspring congenital anomalies and developmental outcome at ages 4 and 6 years: the importance of strict dietary control preconception and throughout pregnancy. *J Pediatr* 2004;144:235–239.
196. Koch R, Trefz F, Waisbren S. Psychosocial issues and outcomes in maternal PKU. *Mol Genet Metab* 2010;99:S68–S74.
197. Smithells RW, Newman CG. Recognition of thalidomide defects. *J Med Genet* 1992;29:716–723.
198. Coberly S, Lammer E, Alashari M. Retinoic acid embryopathy: case report and review of literature. *Pediatr Pathol Lab Med* 1996;16:823–836.
199. Lammer EJ, Chen DT, Hoar RM, et al. Retinoic acid embryopathy. *N Engl J Med* 1985;313:837–841.
200. Honein MA, Paulozzi LJ, Erickson JD. Continued occurrence of Accutane-exposed pregnancies. *Teratology* 2001;64:142–147.
201. Perlman SE, Rudy SJ, Pinto C, et al. Caring for women with childbearing potential taking teratogenic dermatologic drugs. Guidelines for practice. *J Reprod Med* 2001;46:153–161.
202. Hill DS, Wlodarczyk BJ, Palacios AM, et al. Teratogenic effects of antiepileptic drugs. *Expert Rev Neurother* 2010;10:943–959.
203. Holmes LB, Harvey EA, Coull BA, et al. The teratogenicity of anticonvulsant drugs. *N Engl J Med* 2001;344:1132–1138.
204. Meador KJ, Pennell PB, Harden CL, et al. Pregnancy registries in epilepsy: a consensus statement on health outcomes. *Neurology* 2008;71:1109–1117.
205. Tomson T, Battino D, Craig J, et al. Pregnancy registries: differences, similarities, and possible harmonization. *Epilepsia* 2010;51:909–915.
206. Meador K, Reynolds MW, Crean S, et al. Pregnancy outcomes in women with epilepsy: a systematic review and meta-analysis of published pregnancy registries and cohorts. *Epilepsia Res* 2008;81:1–13.
207. Morrow JI, Hunt SJ, Russell AJ, et al. Folic acid use and major congenital malformations in offspring of women with epilepsy: a prospective study from the UK Epilepsy and Pregnancy Register. *J Neurol Neurosurg Psychiatry* 2009;80:506–511.
208. Tomson T, Battino D. Teratogenicity of antiepileptic drugs: state of the art. *Curr Opin Neurol* 2005;18:135–140.
209. Tomson T, Battino D. Teratogenic effects of antiepileptic medications. *Neurol Clin* 2009;27:993–1002.
210. Tomson T, Battino D, Bonizzoni E, et al. Dose-dependent risk of malformations with antiepileptic drugs: an analysis of data from the EURAP epilepsy and pregnancy registry. *Lancet Neurol* 2011;10(7):609–17.
211. Barrett C, Richens A. Epilepsy and pregnancy: report of an Epilepsy Research Foundation Workshop. *Epilepsy Res* 2003;52:147–187.
212. Samren EB, van Duijn CM, Christiaens GC, et al. Antiepileptic drug regimens and major congenital abnormalities in the offspring. *Ann Neurol* 1999;46:739–746.
213. Samren EB, van Duijn CM, Koch S, et al. Maternal use of antiepileptic drugs and the risk of major congenital malformations: a joint European prospective study of human teratogenesis associated with maternal epilepsy. *Epilepsia* 1997;38:981–990.
214. American College of Obstetricians and Gynecologists. Seizure disorders in pregnancy: ACOG educational bulletin number 231. *Int J Gynaecol Obstet* 1997;56:279–286.
215. Crawford P. Best practice guidelines for the management of women with epilepsy. *Epilepsia* 2005;46:117–124.
216. Pschirrer ER. Seizure disorders in pregnancy. *Obstet Gynecol Clin North Am* 2004;31:373–384, vii.
217. Thomas SV, Ajaykumar B, Sindhu K, et al. Cardiac malformations are increased in infants of mothers with epilepsy. *Pediatr Cardiol* 2008;29:604–608.
218. Morrow J, Russell A, Guthrie E, et al. Malformation risks of antiepileptic drugs in pregnancy: a prospective study from the UK Epilepsy and Pregnancy Register. *J Neurol Neurosurg Psychiatry* 2006;77:193–198.
219. Holmes LB, Wyszynski DF, Lieberman E. The AED (antiepileptic drug) pregnancy registry: a 6-year experience. *Arch Neurol* 2004;61:673–678.
220. Tomson T, Battino D. Pregnancy and epilepsy: what should we tell our patients? *J Neurol* 2009;256:856–862.
221. Kjaer D, Horvath-Puho E, Christensen J, et al. Antiepileptic drug use, folic acid supplementation, and congenital abnormalities: a population-based case-control study. *BJOG* 2008;115:98–103.
222. Cohen LS, Friedman JM, Jefferson JW, et al. A reevaluation of risk of in utero exposure to lithium. *JAMA* 1994;271:146–150.
223. Schou M, Goldfield MD, Weinstein MR, et al. Lithium and pregnancy, I: report from the register of lithium babies. *Br Med J* 1973;2:135–136.
224. Weinstein MR. The international register of lithium babies. *Drug Inf J* 1976;94:100.
225. Jacobson SJ, Jones K, Johnson K, et al. Prospective multicentre study of pregnancy outcome after lithium exposure during first trimester. *Lancet* 1992;339:530–533.
226. Warner JP. Evidence-based psychopharmacology 3. Assessing evidence of harm: what are the teratogenic effects of lithium carbonate? *J Psychopharmacol* 2000;14:77–80.
227. Kallen B, Tandberg A. Lithium and pregnancy. A cohort study on manic-depressive women. *Acta Psychiatr Scand* 1983;68:134–139.
228. Linask KK, Huhta J. Folate protection from congenital heart defects linked with canonical Wnt signaling and epigenetics. *Curr Opin Pediatr* 2010;22:561–566.
229. Han M, Serrano MC, Lastra-Vicente R, et al. Folate rescues lithium-, homocysteine- and Wnt3A-induced vertebrate cardiac anomalies. *Dis Model Mech* 2009;2:467–478.
230. Wurst KE, Poole C, Ephross SA, et al. First trimester paroxetine use and the prevalence of congenital, specifically cardiac, defects: a meta-analysis of epidemiological studies. *Birth Defects Res A Clin Mol Teratol* 2010;88:159–170.
231. Bar-Oz B, Einarson T, Einarson A, et al. Paroxetine and congenital malformations: meta-analysis and consideration of potential confounding factors. *Clin Ther* 2007;29:918–926.
232. Reis M, Kallen B. Delivery outcome after maternal use of antidepressant drugs in pregnancy: an update using Swedish data. *Psychol Med* 2010;40:1723–1733.
233. Louik C, Lin AE, Werler MM, et al. First-trimester use of selective serotonin-reuptake inhibitors and the risk of birth defects. *N Engl J Med* 2007;356:2675–2683.
234. Bakker MK, Kerstjens-Frederikse WS, Buys CH, et al. First-trimester use of paroxetine and congenital heart defects: a population-based case-control study. *Birth Defects Res A Clin Mol Teratol* 2010;88:94–100.
235. Merlob P, Birk E, Sirota L, et al. Are selective serotonin reuptake inhibitors cardiac teratogens? Echocardiographic screening of newborns with persistent heart murmur. *Birth Defects Res A Clin Mol Teratol* 2009;85:837–841.
236. Cole JA, Modell JG, Haight BR, et al. Bupropion in pregnancy and the prevalence of congenital malformations. *Pharmacoepidemiol Drug Saf* 2007;16:474–484.
237. Alwan S, Reefhuis J, Botto LD, et al. Maternal use of bupropion and risk for congenital heart defects. *Am J Obstet Gynecol* 2010;203:52.e1–52.e6.
238. Barr M Jr. Teratogen update: angiotensin-converting enzyme inhibitors. *Teratology* 1994;50:399–409.
239. Ratnapalan S, Koren G. Taking ACE inhibitors during pregnancy. Is it safe? *Can Fam Physician* 2002;48:1047–1049.
240. Cooper WO, Hernandez-Diaz S, Arbogast PG, et al. Major congenital malformations after first-trimester exposure to ACE inhibitors. *N Engl J Med* 2006;354:2443–2451.
241. Caton AR, Bell EM, Druschel CM, et al. Antihypertensive medication use during pregnancy and the risk of cardiovascular malformations. *Hypertension* 2009;54:63–70.
242. Lennestall R, Otterblad Olausson P, Kallen B. Maternal use of antihypertensive drugs in early pregnancy and delivery outcome, notably the

- presence of congenital heart defects in the infants. *Eur J Clin Pharmacol* 2009;65:615–625.
243. Diav-Citrin O, Shechtman S, Halberstadt Y, et al. Pregnancy outcome after in utero exposure to angiotensin converting enzyme inhibitors or angiotensin receptor blockers. *Reprod Toxicol* 2011;31:540–545.
 244. Li DK, Yang C, Andrade S, et al. Maternal exposure to angiotensin converting enzyme inhibitors in the first trimester and risk of malformations in offspring: a retrospective cohort study. *BMJ* 2011;343:d5931.
 245. Walfisch A, Al-maawali A, Moretti ME, et al. Teratogenicity of angiotensin converting enzyme inhibitors or receptor blockers. *J Obstet Gynaecol* 2011;31:465–472.
 246. Czeizel AE, Rockenbauer M, Sorensen HT, et al. The teratogenic risk of trimethoprim-sulfonamides: a population based case-control study. *Reprod Toxicol* 2001;15:637–646.
 247. Hernandez-Diaz S, Werler MM, Walker AM, et al. Folic acid antagonists during pregnancy and the risk of birth defects. *N Engl J Med* 2000;343:1608–1614.
 248. Khalil HS, Saleh AM, Subhani SN. Maternal obesity and neonatal congenital cardiovascular defects. *Int J Gynaecol Obstet* 2008;102:232–236.
 249. Mills JL, Troendle J, Conley MR, et al. Maternal obesity and congenital heart defects: a population-based study. *Am J Clin Nutr* 2010;91:1543–1549.
 250. Mikhail LN, Walker CK, Mittendorf R. Association between maternal obesity and fetal cardiac malformations in African Americans. *J Natl Med Assoc* 2002;94:695–700.
 251. Watkins ML, Botto LD. Maternal prepregnancy weight and congenital heart defects in offspring. *Epidemiology* 2001;12:439–446.
 252. Shaw GM, Todoroff K, Schaffer DM, et al. Maternal height and prepregnancy body mass index as risk factors for selected congenital anomalies. *Paediatr Perinat Epidemiol* 2000;14:234–239.
 253. Waller DK, Mills JL, Simpson JL, et al. Are obese women at higher risk for producing malformed offspring? *Am J Obstet Gynecol* 1994;170:541–548.
 254. Oddy WH, De Klerk NH, Miller M, et al. Association of maternal prepregnancy weight with birth defects: evidence from a case-control study in Western Australia. *Aust N Z J Obstet Gynaecol* 2009;49:11–15.
 255. Gilboa SM, Correa A, Botto LD, et al. Association between prepregnancy body mass index and congenital heart defects. *Am J Obstet Gynecol* 2010;202:51 e1–51 e10.
 256. Kim SY, England L, Wilson HG, et al. Percentage of gestational diabetes mellitus attributable to overweight and obesity. *Am J Public Health* 2010;100:1047–1052.
 257. Freedman DS. Obesity—United States, 1988–2008. *MMWR Morb Mortal Wkly Rep* 2011;60:73–77.
 258. Ogden CL, Lamb MM, Carroll MD, et al. Obesity and Socioeconomic Status in Adults: United States, 2005–2008. In: NCHS Data Brief: National Center on Health Statistics, 2010.
 259. Browne ML. Maternal exposure to caffeine and risk of congenital anomalies: a systematic review. *Epidemiology* 2006;17:324–331.
 260. Tikkanen J, Heinonen OP. Risk factors for cardiovascular malformations in Finland. *Eur J Epidemiol* 1990;6:348–356.
 261. Tikkanen J, Heinonen OP. Risk factors for conal malformations of the heart. *Eur J Epidemiol* 1992;8:48–57.
 262. Olsen J, Overvad K, Frische G. Coffee consumption, birthweight, and reproductive failures. *Epidemiology* 1991;2:370–374.
 263. Linn S, Schoenbaum SC, Monson RR, et al. No association between coffee consumption and adverse outcomes of pregnancy. *N Engl J Med* 1982;306:141–145.
 264. Rosenberg L, Mitchell AA, Shapiro S, et al. Selected birth defects in relation to caffeine-containing beverages. *JAMA* 1982;247:1429–1432.
 265. Browne ML, Bell EM, Druschel CM, et al. Maternal caffeine consumption and risk of cardiovascular malformations. *Birth Defects Res A Clin Mol Teratol* 2007;79:533–543.
 266. Hoyne HE, May PA, Kalberg WO, et al. A practical clinical approach to diagnosis of fetal alcohol spectrum disorders: clarification of the 1996 institute of medicine criteria. *Pediatrics* 2005;115:39–47.
 267. Jones KL. *Smith's Recognizable Patterns of Human Malformation*. 6 ed. Philadelphia, PA: Saunders, 2005.
 268. Tikkanen J, Heinonen OP. Risk factors for ventricular septal defect in Finland. *Public Health* 1991;105:99–112.
 269. Tikkanen J, Heinonen OP. Risk factors for atrial septal defect. *Eur J Epidemiol* 1992;8:509–515.
 270. Adams MM, Mulinare J, Dooley K. Risk factors for conotruncal cardiac defects in Atlanta. *J Am Coll Cardiol* 1989;14:432–442.
 271. Strandberg-Larsen K, Skov-Ettrup LS, Gronbaek M, et al. Maternal alcohol drinking pattern during pregnancy and the risk for an offspring with an isolated congenital heart defect and in particular a ventricular septal defect or an atrial septal defect. *Birth Defects Res A Clin Mol Teratol* 2011;91:616–622.
 272. Serrano M, Han M, Brinez P, et al. Fetal alcohol syndrome: cardiac birth defects in mice and prevention with folate. *Am J Obstet Gynecol* 2010;203(1):75.e7–75.e15.
 273. Hobbs CA, Cleves MA, Karim MA, et al. Maternal folate-related gene environment interactions and congenital heart defects. *Obstet Gynecol* 2010;116:316–322.
 274. Burd L, Deal E, Rios R, et al. Congenital heart defects and fetal alcohol spectrum disorders. *Congenit Heart Dis* 2007;2:250–255.
 275. Grewal J, Carmichael SL, Ma C, et al. Maternal periconceptional smoking and alcohol consumption and risk for select congenital anomalies. *Birth Defects Res A Clin Mol Teratol* 2008;82:519–526.
 276. Carmichael SL, Shaw GM, Yang W, et al. Maternal periconceptional alcohol consumption and risk for conotruncal heart defects. *Birth Defects Res A Clin Mol Teratol* 2003;67:875–878.
 277. Institute of Medicine, ed. *Committee to Study Fetal Alcohol Syndrome: Fetal Alcohol Syndrome—Diagnosis, Epidemiology, Prevention and Treatment*. Washington, DC: National Academy Press, 1996.
 278. Kallen K. Maternal smoking and congenital heart defects. *Eur J Epidemiol* 1999;15:731–737.
 279. Alverson CJ, Strickland MJ, Gilboa SM, et al. Maternal smoking and congenital heart defects in the Baltimore-Washington Infant Study. *Pediatrics* 2011;127:e647–e653.
 280. Malik S, Cleves MA, Honein MA, et al. Maternal smoking and congenital heart defects. *Pediatrics* 2008;121:e810–e816.
 281. Woods SE, Raju U. Maternal smoking and the risk of congenital birth defects: a cohort study. *J Am Board Fam Pract* 2001;14:330–334.
 282. Amos A, Haglund M. From social taboo to “torch of freedom”: the marketing of cigarettes to women. *Tob Control* 2000;9:3–8.
 283. Obican SG, Finnell RH, Mills JL, et al. Folic acid in early pregnancy: a public health success story. *FASEB J* 2010;24:4167–4174.
 284. Blom HJ, Smulders Y. Overview of homocysteine and folate metabolism. With special references to cardiovascular disease and neural tube defects. *J Inherit Metab Dis* 2011;34:75–81.
 285. Obermann-Borst S, Vujkovic M, de Vries J, et al. A maternal dietary pattern characterised by fish and seafood in association with the risk of congenital heart defects in the offspring. *BJOG* 2011;118:1205–1215.
 286. Botto LD, Loffredo C, Scanlon KS, et al. Vitamin A and cardiac outflow tract defects. *Epidemiology* 2001;12(5):491–496.
 287. Rothman KJ, Moore LL, Singer MR, et al. Teratogenicity of high vitamin A intake. *N Engl J Med* 1995;333:1369–1373.
 288. Werler MM, Lammer EJ, Rosenberg L, et al. Maternal vitamin A supplementation in relation to selected birth defects. *Teratology* 1990;42:497–503.
 289. Khoury MJ, Moore CA, Mulinare J. Vitamin A and birth defects. *Lancet* 1996;347:322.
 290. Mastroiacovo P, Mazzone T, Addis A, et al. High vitamin A intake in early pregnancy and major malformations: a multicenter prospective controlled study. *Teratology* 1999;59:7–11.
 291. Mills JL, Simpson JL, Cunningham GC, et al. Vitamin A and birth defects. *Am J Obstet Gynecol* 1997;177:31–36.
 292. Shaw GM, Wasserman CR, Block G, et al. High maternal vitamin A intake and risk of anomalies of structures with a cranial neural crest cell contribution. *Lancet* 1996;347:899–900.
 293. Czeizel AE. Periconceptional folic acid containing multivitamin supplementation. *Eur J Obstet Gynecol Reprod Biol* 1998;78:151–161.
 294. Shaw GM, O'Malley CD, Wasserman CR, et al. Maternal periconceptional use of multivitamins and reduced risk for conotruncal heart defects and limb deficiencies among offspring. *Am J Med Genet* 1995;59:536–545.
 295. Scanlon KS, Ferencz C, Loffredo CA, et al. Preconceptional folate intake and malformations of the cardiac outflow tract. Baltimore-Washington Infant Study Group. *Epidemiology* 1998;9:95–98.
 296. van Beynum IM, Kapusta L, Bakker MK, et al. Protective effect of periconceptional folic acid supplements on the risk of congenital heart defects: a registry-based case-control study in the northern Netherlands. *Eur Heart J* 2010;31:464–471.
 297. Werler MM, Hayes C, Louik C, et al. Multivitamin supplementation and risk of birth defects. *Am J Epidemiol* 1999;150:675–682.
 298. Czeizel AE, Dudas I. Prevention of the first occurrence of neural-tube defects by periconceptional vitamin supplementation. *N Engl J Med* 1992;327:1832–1835.
 299. Canfield MA, Collins JS, Botto LD, et al. Changes in the birth prevalence of selected birth defects after grain fortification with folic acid in the United States: findings from a multi-state population-based study. *Birth Defects Res A Clin Mol Teratol* 2005;73:679–689.
 300. Godwin KA, Sibbald B, Bedard T, et al. Changes in frequencies of select congenital anomalies since the onset of folic acid fortification in a Canadian birth defect registry. *Can J Public Health* 2008;99:271–275.
 301. Ionescu-Ittu R, Marelli AJ, Mackie AS, et al. Prevalence of severe congenital heart disease after folic acid fortification of grain products: time trend analysis in Quebec, Canada. *BMJ* 2009;338:b1673.
 302. Lopez-Camelo JS, Castilla EE, Orioli IM. Folic acid flour fortification: impact on the frequencies of 52 congenital anomaly types in three South American countries. *Am J Med Genet A* 2010;152A:2444–2458.
 303. Bailey LB, Berry RJ. Folic acid supplementation and the occurrence of congenital heart defects, orofacial clefts, multiple births, and miscarriage. *Am J Clin Nutr* 2005;81:1213S–1217S.
 304. Daly S, Cotter A, Molloy AE, et al. Homocysteine and folic acid: implications for pregnancy. *Semin Vasc Med* 2005;5:190–200.
 305. Huhta JC, Hernandez-Robles JA. Homocysteine, folate, and congenital heart defects. *Fetal Pediatr Pathol* 2005;24:71–79.
 306. Botto LD, Olney RS, Erickson JD. Vitamin supplements and the risk for congenital anomalies other than neural tube defects. *Am J Med Genet C Semin Med Genet* 2004;125:12–21.

307. Shaw GM, Iovannisci DM, Yang W, et al. Risks of human conotruncal heart defects associated with 32 single nucleotide polymorphisms of selected cardiovascular disease-related genes. *Am J Med Genet A* 2005;138:21–26.
308. Hobbs CA, James SJ, Jernigan S, et al. Congenital heart defects, maternal homocysteine, smoking, and the 677 C>T polymorphism in the methylenetetrahydrofolate reductase gene: evaluating gene-environment interactions. *Am J Obstet Gynecol* 2006;194:218–224.
309. Pereira AC, Xavier-Neto J, Mesquita SM, et al. Lack of evidence of association between MTHFR C677T polymorphism and congenital heart disease in a TDT study design. *Int J Cardiol* 2005;105:15–18.
310. McBride KL, Fernbach S, Meneses A, et al. A family-based association study of congenital left-sided heart malformations and 5,10 methylenetetrahydrofolate reductase. *Birth Defects Res A Clin Mol Teratol* 2004;70:825–830.
311. Shaw GM, Lu W, Zhu H, et al. 118 SNPs of folate-related genes and risks of spina bifida and conotruncal heart defects. *BMC Med Genet* 2009;10:49.
312. Mitchell LE, Long J, Garbarini J, et al. Variants of folate metabolism genes and risk of left-sided cardiac defects. *Birth Defects Res A Clin Mol Teratol* 2010;88:48–53.
313. Junker R, Kotthoff S, Vielhaber H, et al. Infant methylenetetrahydrofolate reductase 677TT genotype is a risk factor for congenital heart disease. *Cardiovasc Res* 2001;51:251–254.
314. Wenstrom KD, Johanning GL, Johnston KE, et al. Association of the C677T methylenetetrahydrofolate reductase mutation and elevated homocysteine levels with congenital cardiac malformations. *Am J Obstet Gynecol* 2001;184:806–812; discussion 812–817.
315. Goldmuntz E, Woyciechowski S, Renstrom D, et al. Variants of folate metabolism genes and the risk of conotruncal cardiac defects. *Circ Cardiovasc Genet* 2008;1:126–132.
316. Shaw GM, Zhu H, Lammer EJ, et al. Genetic variation of infant reduced folate carrier (A80G) and risk of orofacial and conotruncal heart defects. *Am J Epidemiol* 2003;158:747–752.
317. Pei L, Zhu H, Zhu J, et al. Genetic variation of infant reduced folate carrier (A80G) and risk of orofacial defects and congenital heart defects in China. *Ann Epidemiol* 2006;16:352–356.
318. Frieden TR. A framework for public health action: the health impact pyramid. *Am J Public Health* 2010;100:590–595.
319. Utah Department of Health. Power Your Life. In. <http://www.poweryourlife.org/>; Utah Department of Health, 2011.
320. Mastroiacovo P, Botto LD. Surveillance of risk factors for adverse reproductive outcomes in women of childbearing age: report of an international consultation. (unpublished) 2010.

Since the publication of this chapter in the seventh edition of this book, there has been ongoing progress in both the medical and surgical management of children born with congenital heart defects (CHDs) and the genetic technology that has assisted diagnosis, management, and research. Patients with significant heart disease now routinely survive well into adulthood. With these advances come new questions about variability in clinical outcome, long-term survival, fetal intervention, and recurrence risk. Although differences in clinical management affect clinical outcome and survival, evidence suggests that the etiologic basis of these malformations contributes to outcome as well (1–4). These observations highlight the importance of understanding the causes of CHDs.

Environmental, genetic, and stochastic factors contribute to the cause of CHDs (Table 26.1) (5,6); an expanded discussion of environmental risk factors and teratogens can be found in Chapter 25. Evidence for a genetic contribution comes from several observations. First, specific types of CHDs are commonly seen with specific chromosomal abnormalities. For example, atrioventricular septal defects are most commonly diagnosed in patients with trisomy 21, and patients with trisomy 21 are commonly diagnosed with atrioventricular septal defects. Second, similar CHDs can occur in multiple members of a family, suggesting a genetic basis. Recent studies have demonstrated particularly high heritability in certain subsets of CHDs such as left-sided lesions (7–9). Third, epidemiologic studies demonstrate an increased precurrence and recurrence risk for CHDs in families with one affected member (10–13).

These observations also suggest that many CHDs result from complex genetic and environmental interactions rather than simple mendelian inheritance. Although the vast majority of patients with Down syndrome have a complete third copy of chromosome 21, only 40% to 50% of patients have CHD. In contrast to the consistent finding of intellectual disability, the less frequent expression of CHDs suggests that other genetic and/or environmental factors contribute to the risk of CHDs even in the presence of a major chromosomal alteration. Similarly, the likelihood that parents with one child affected with a nonsyndromic CHD will have a second affected child is increased as compared to the baseline risk in the general population, but the recurrence risk is significantly lower than simple mendelian inheritance would predict.

The heterogeneous etiologic factors of CHDs make it more difficult to understand the basis of these disorders. For example, several different genetic alterations are now known to be associated with tetralogy of Fallot including trisomy 21, the 22q11.2 deletion, and *JAG1* mutations (Table 26.1 and see below: Genetics of Specific CHDs). Tetralogy of Fallot is found in many other genetic syndromes and can be associated with maternal exposure to retinoic acid and maternal phenylketonuria (14). Therefore, defining the genetic alterations that contribute to the cause of specific CHDs and identifying those that affect clinical outcome is challenging.

Notable advances have begun to unravel the genetic basis of these disorders. The first edition of this text published in 1968 cited 15 genetic syndromes and conditions, including storage diseases (personal correspondence from Dr. George Emmanouilides, Harbor-UCLA Medical Center). More than 50 years later, this chapter lists 50 of the most familiar or distinctive malformation syndromes characterized in part by CHDs and associated with an identifiable cause. As discoveries are made, the number of children with defined genetic causes of their CHD will increase. The information should help the physician counsel families more accurately about recurrence risks and clinical outcome and, it is hoped, lead to novel medical therapeutics to improve clinical outcomes. Since rapid progress is likely to continue, the medical caregiver will need a firm understanding of this area to anticipate its impact on clinical medicine.

This chapter reviews the genetic basis of CHDs by providing sufficient fundamental concepts to give readers a consistent background, yet remaining a pragmatic “off-the-shelf” handbook in real clinical and educational settings. The term CHDs refers to developmental changes of the intracardiac structures and major vessels and is interchangeable with the terms cardiovascular malformation or congenital heart disease. The genetic basis of cardiomyopathies and arrhythmias, both of which may be associated with a CHD, is discussed in other chapters. Instead of listing all possible genetic syndromes associated with each CHD (which can be found in multiple online and textbook resources listed below), this chapter presents an alternative approach for considering the genetic causes of CHD, ordered by genetic mechanism to help the reader understand and anticipate future developments in this field. In addition, Tables 26.2–26.4 summarize the growing number of syndromes that are either common conditions frequently associated with any type of CHD, or uncommon syndromes associated with a distinctive pattern of CHD. The chapter concludes with suggested guidelines for the genetic evaluation of a child with a CHD.

METHODS AND MECHANISMS

Genetic Testing

In large part, the identification of novel genetic abnormalities associated with disease has been driven by increasingly sensitive methods to detect genetic alterations. The technology to detect structural variation in the human genome (134) has progressed from microscopic to genomic analyses, and is of interest to both clinician and researcher. In the first era of chromosome analysis, the *karyotype* displayed the 23 pairs of human chromosomes and detected changes in chromosome number (such as trisomy 21) or large changes in chromosome architecture such as translocations (the exchange of pieces between two chromosomes). Smaller changes such as

TABLE 26.1 Causes of CHDs

Etiology	Example: Patient with Tetralogy of Fallot (TOF)
Chromosomal change	
Change in chromosome number	Trisomy 18 or 21
Translocation between chromosomes	Translocation 1p36
Deletion of chromosome segment	Deletion 5p or 22q11.2
Duplication of chromosome segment	Partial trisomy 8q
Single gene or gene pair abnormality	
Isolated CHD	Newborn with TOF, whose mother also had TOF repaired in childhood; sister has malalignment-type VSD (probable autosomal dominant inheritance)
Associated with syndrome	<i>JAG1</i> mutation in Alagille syndrome
Mitochondrial defect	None known
Environmental exposure	Fetus found to have TOF, mother known to have maternal phenylketonuria
Multifactorial causation (gene/environmental interaction)	TOF in a child with ectopia cordis
Stochastic events	Isolated TOF

VSD, ventricular septal defect.

a visible *deletion* or *duplication* of chromosomal segments were subsequently detected by new “banding” methods, such as Giemsa staining, which resulted in characteristic dark and light bands for each chromosome. More recently, *fluorescence in situ hybridization* (FISH), multiplex ligation-dependent probe amplification (MLPA), and microarray technologies have been used to detect smaller deletions and duplications of chromosome segments that could not otherwise be seen on a standard or even high-resolution karyotype. Identification of disease-related *mutations* or alterations in the genetic code for a single gene can be detected using various techniques.

Accordingly, changes in chromosome number such as trisomy 21 or Turner syndrome were among the first identified genetic causes of CHDs. Deletion syndromes such as the 22q11.2 deletion or Williams syndromes were subsequently recognized with the advent of new banding techniques and then FISH, MLPA, and now microarrays. The advent of microarray technology has also permitted the characterization of an increasing number of deletion and duplication syndromes such as 1p36 deletion and 8p23 deletion syndromes (Table 26.2) (135,136). Given the ability of microarrays to survey the entire genome for changes in regional chromosomal imbalances, this technology has become the test of choice in many scenarios and centers (137).

Increasingly automated mutation detection and gene sequencing techniques now identify disease-related mutations in single-gene disorders such as Holt-Oram or Alagille syndromes. The growing ability to identify disease-related mutations by gene sequencing has allowed additional clinical genetic testing in individual patients or families.

Investigative Approaches

Investigators have used a variety of approaches to identify the genetic cause of CHDs reflecting advancements made in

molecular genetic technologies. Historically, the identification of a consistent chromosomal alteration on a karyotype focused where investigators might look for the genetic basis of that disease. For example, 5% to 10% of patients with Alagille syndrome were originally noted to have a chromosomal deletion involving the “p” (short) arm of chromosome 20 (see Alagille syndrome). This observation suggested that other patients might have submicroscopic alterations of that region or a mutation in a gene in that region. Further investigations found disease-causing mutations in a gene called *JAG1* that mapped into the region of 20p, thereby establishing *JAG1* as one of the disease genes for Alagille syndrome.

Alternatively, large kindreds with multiple affected members permit a parametric linkage analysis to map the disease gene to a chromosomal position or locus. Informative linkage analyses were responsible for identifying the disease genes in Marfan, Holt-Oram, and Noonan syndromes as well as familial cases of atrial septal defect with atrioventricular conduction blockade (*NKX2.5*), to name a few (see in Single-Gene Disorders). The Human Genome Project has greatly simplified and accelerated the identification of disease genes once a disease locus is defined.

These aforementioned strategies to identify disease-related genes are limited by the relative rarity of large kindred or consistent chromosomal changes. However, emerging chromosome microarray technologies have identified an increasing number of previously unrecognized submicroscopic chromosomal deletions and duplications, thereby defining new genetic syndromes and disease genes (135–138). The advent of “next generation sequencing,” including large-scale gene, whole exome, and whole genome sequencing, promises to identify an increasing number of disease-causing variants as well.

As noted, it is increasingly apparent that a large proportion of CHDs are complex in origin, resulting from a combination of genetic and environmental risk factors in any one patient or family (5,6,13). Studies to date suggest marked genetic heterogeneity in the number of disease genes associated with any one

TABLE 26.2 Chromosome Abnormality Syndromes Associated with CHDs

Syndrome	Reference	Gene(s) ^b	OMIM No.	Frequency of CHD ^a		Distinctive Features ^c
				All (%)	Distinctive or Common	
Changes in chromosome number						
Trisomy 13	(15–17)			50–80	Conotruncal CHDs: DORV, TOF VSD, ASD, PDA AVSD Polyvalvar dysplasia	Polydactyly Cleft lip and palate CNS anomalies (holoprosencephaly) Renal, GU anomalies Scalp cutis aplasia Microphthalmia
Trisomy 18	(15,16,18–21)			95	Polyvalvar dysplasia Conoventricular VSD TOF, DORV AVSD	Overlapping fingers CNS anomalies (posterior fossas) Small facial features Rocker bottom feet Renal, GU anomalies
Down syndrome (trisomy 21 most common)	(22–24)		190685	40	AVSD defects: Complete AVSD Primum ASD VSD, all types Secundum ASD PDA TOF	GI anomalies Endocrine anomalies Fifth finger clinodactyly Leukemoid reaction Microbrachycephaly
Turner syndrome (45,X most common)	(25–32)			25	LVOTO CHDs: BAV ± AS(V) Coarctation MV anomalies, MVP PAPVC, LSVC Aortic dilation, dissection Hypertension Prolonged QTc	Horseshoe kidney Short fourth metacarpal Neck webbing Lymphedema Infertility Short stature Nevi, keloids Hypothyroidism
Chromosome deletion or duplication						
Deletion 1p36	(33–35)		607872	35	Assorted CHD TOF/PA PDA Ebstein DCM, noncompaction	Obesity Cleft lip/palate Epilepsy Hearing loss Brachydactyly
Deletion 3p25	(36–39)			33	Primum ASD, AVSD Assorted CHDs	Ptosis Abnormal ears Hearing loss Postaxial polydactyly Congenital hypothyroidism
Duplication 3q	(40,41)			75	Assorted CHDs	Craniosynostosis Short neck GU anomalies Cleft palate Fifth finger clinodactyly
Deletion 4p16	(42)	WHSC1 WHSC2	194190	30–50	Secundum ASD PS(V) VSD	Abnormal ears Cleft lip/palate GU anomalies Seizures Hearing loss

(Continued)

TABLE 26.2 Chromosome Abnormality Syndromes Associated with CHDs (Continued)

Syndrome	Reference	Gene(s) ^b	OMIM No.	Frequency of CHD ^a		Distinctive Features ^c
				All (%)	Distinctive or Common	
Deletion 4qter	(43,44)			40	RVOTO PS	Abnormal pinnae Cleft palate Pierre-Robin sequence Fifth fingernail tapered, pointed/duplicated
Deletion 5p15	(45)		123450	20	Assorted CHDs VSD PDA TOF	Cat-like cry Cleft lip/palate Abnormal ears Preauricular tags
Williams syndrome Deletion 7p13	(46)	<i>ELN</i>	194050	75 ^d	SVAS ± AS(V) PS PPS Coarctation Coronary artery stenosis	Abnormal calcium levels Hypodontia Characteristic behavior and personality
Deletion 8p23	(47–51)	<i>GATA4</i>	600576	65–80	PS Secundum ASD AVSD VSD Left ventricular noncompaction	GU anomalies Abnormal ears Minor hand anomalies Diaphragmatic hernia
Duplication 8q (recombinant 8)	(52,53)		179613	45	Conotruncal CHDs: TOF, DORV, truncus	Short fifth finger Hypertelorism Hirsutism
Deletion 9p	(54,55)		158170	35	Assorted CHDs	Trigonocephaly Extra flexion creases Hypertelorism Ear anomalies Genital anomalies
Deletion 10p	(56,57)		601362	50	VSD ± ASD PDA	Minor hand/foot anomalies Hearing loss Renal anomalies DiGeorge phenotype
Deletion 11q23 Jacobsen Syndrome	(58)		147791	55	VSD LVOTO: HLHS	Thrombocytopenia or abnormal platelets Undescended testes Renal anomalies
Deletion 17p11.2 Smith-Magenis syndrome	(59,60)	<i>RAI1</i>	182290	10	Assorted CHDs	Brachycephaly Aggressive, self-injurious behavior Sleep disturbances Eye, ear anomalies
Deletion 18q	(61–63)		601808	15–30	PS ASD VSD	Wide-spaced nipples Cleft palate GU anomalies Aural atresia Brain dysmyelination
Tetrasomy 22p Cat eye syndrome	(64)		115470	50	TAVPC PAPVC Assorted CHDs	Rectoanal anomalies Coloboma Preauricular tag/pit GU anomalies

TABLE 26.2 Chromosome Abnormality Syndromes Associated with CHDs (*Continued*)

Syndrome	Reference	Gene(s) ^b	OMIM No.	Frequency of CHD ^a		Distinctive Features ^c
				All (%)	Distinctive or Common	
Derivative 11;22	(65,66)		609029	60	ASD, VSD, PDA LSVC	Preauricular tag/pit Cleft palate Genital anomalies
Deletion 22q11.2	(67–71)	<i>TBX1</i>	192430	75–85	IAA type B	Cleft palate
DiGeorge sequence			602054		Truncus	Hypocalcemia
Velocardiofacial syndrome		<i>CRKL</i> <i>ERK2</i>	602007 176948		TOF VSD	T-cell dysfunction Feeding and speech disorders
Conotruncal anomaly face					Aortic arch anomalies	Psychiatric disorders

^aFrequency figures rounded. When not specified in an article, data were calculated independently. Congenital heart “defects” excluded valve regurgitation, patent foramen ovale, and unspecified murmur, cyanosis, or heart disease. Some syndrome-specific nonstructural anomalies were included.

^bGenes listed map to the disease locus and are specifically associated with the cardiovascular features of the syndrome, though other genes in the chromosomal region may also be related to the syndrome.

^cMost syndromes have growth delay, some degree of developmental delay/mental retardation, and dysmorphic facial features, which can be reviewed in general genetics references (72,73).

^dFrequency reflects cases with molecular confirmation.

ASCA, aberrant subclavian artery; ASD, atrial septal defect; AS(V), aortic stenosis (valvar specified); AVSD, arterioventricular septal defect; BAV, bicuspid aortic valve; CHDs, congenital heart defects; CNS, central nervous system; DCM, dilated cardiomyopathy; DDRV, double-outlet right ventricle; FAVS, facioauriculovertebral spectrum; GI, gastrointestinal; GU, genitourinary; HCM, hypertrophic cardiomyopathy; HLHS, hypoplastic left heart syndrome; IAA, A/B, interrupted aortic arch, type A or B; LSVC, left superior vena cava; LVOTO, left ventricular outflow tract obstruction; MS, mitral stenosis; MVP, mitral valve prolapse; OMIM, on line Mendelian inheritance in man; PA, pulmonary atresia; PAPVC, partial anomalous pulmonary venous connection; PDA, patent ductus arteriosus; (P)PS, (peripheral) pulmonic stenosis; PS(V), pulmonary stenosis (valvar specified); RVOTO, right ventricular outflow tract obstruction; TAVPC, total anomalous pulmonary venous connection; TOF, tetralogy of Fallot; VSD, ventricular septal defect.

lesion, and identify a wide range of genetic alterations ranging from whole chromosome to single nucleotide changes. The extent to which common and/or rare variants, be they single nucleotide polymorphisms (SNPs), deletions, or duplications, contribute to disease risk is a subject of much debate and investigation. In either case, defining disease-associated genetic variants, genes, and developmental pathways provides new opportunities for novel therapeutic and preventive strategies.

PATTERNS OF INHERITANCE AND FAMILIAL RISKS

Assessing the risk of recurrence (the chance that an affected parent will have an affected child or that unaffected parents will have a second affected child) for a patient or their relative is an ongoing challenge (139). Historically, different study designs, variable classification schemes of CHDs, different modes of ascertainment, and evolving methods of diagnosis have made it difficult to compare studies and have complete confidence in the results. Most cases of CHD have been thought to be sporadic. Overall, low recurrence risks of 2% to 4% have been quoted for all types of CHDs with one affected sibling or parent (140–143). Studies suggest that the recurrence risk increases if more than one sibling is affected (13) although it has been unclear if an affected mother confers a greater risk than an affected father (144,145). Recurrent CHDs within a family are often concordant or derive from the same class of defects (140).

Data from these studies are valuable, but must be used with some caution. Earlier studies did not consider the more recently described mendelian syndromes and chromosomal

causes of CHDs, factors that affect the overall recurrence frequency. In addition, familial cases of almost every type of CHD have been observed as has every pattern of inheritance including autosomal dominant, autosomal recessive, X-linked, or complex nonmendelian patterns of inheritance. The observed pattern of inheritance greatly influences the risk of recurrence for any one family and must be considered for counseling purposes.

As an alternative to recurrence risk analysis, investigators from the Baltimore-Washington Infant Study calculated the rate of CHD precurrence (the number of currently affected relatives at the time of birth) (10). Their studies demonstrated increased familial disease, especially left-sided CHDs. Left-sided obstructive defects have also been the subject of several recent large family studies. Echocardiography was performed on first-degree relatives of probands to complement extensive pedigree analysis and better assess the occurrence of CHD in each family. These reports found that 8% to 19% of first-degree relatives of patients with left-sided CHDs had predominantly concordant CHDs, suggesting that left-sided CHDs commonly result from inherited genetic traits (7–9,146). Of note, CHDs were identified with higher frequency in first-degree relatives of probands with hypoplastic left heart syndrome (HLHS) (19.3%) and coarctation of the aorta (9.4%) than in first-degree relatives of probands with D-transposition of the great arteries (2.7%) (9). Most recently, several studies confirm high heritability of left-sided CHDs (implying a strong genetic component to their etiology) and marked genetic heterogeneity with evidence for possible autosomal dominant inheritance in some pedigrees (7,146–149). Studies detailing the heritability of other types or classes of CHDs have not yet been performed to provide similar data.

TABLE 26.3 Single-Gene Disorders Associated with CHDs

Syndrome	Reference	Gene(s)	OMIM No.	Frequency of CHD ^a		Distinctive Features ^b
				All (%)	Distinctive or Most Common	
<i>Autosomal dominant</i>						
Alagille syndrome	(74,75)	<i>JAG1</i> <i>NOTCH2</i>	118450 600275	90 ^c	PPS TOF ± PA ASD, VSD Coarctation	Bile duct paucity Chronic cholestasis Butterfly vertebrae Posterior embryotoxon
Cardiofaciocutaneous syndrome	(76–78)	<i>BRAF</i> <i>MEK1</i> <i>MEK2</i> <i>KRAS</i>	115150	75 ^c	PS(V) Secundum ASD Other valve dysplasia HCM	Sparse, curly hair Low, rotated ears Hyperkeratosis
Char syndrome	(79,80)	<i>TFAP2β</i>	169100	20–70	PDA Muscular VSD	Anomalies of fifth finger Supernumerary nipple
CHARGE syndrome	(81,82)	<i>CHD7</i> <i>SEMA3E</i>	214800	90 ^c	Conotruncal CHDs: TOF, DORV ± AVSD Aortic arch anomalies Assorted CHD	Coloboma Choanal atresia Genital anomalies Ear anomalies Facial asymmetry Cleft lip/palate
Cornelia de Lange syndrome	(83–85)	<i>NIPBL</i> <i>SMC1A</i>	122470 30040	25	VSD, ASD PS HCM	Upper limb deficiency GI anomalies
Costello syndrome	(86)	<i>HRAS</i>	218040	85 ^c	PS(V), other valve dysplasia HCM Atrial tachycardia Aortic dilation	Skin/joint laxity Fine/curly hair Ulnar deviation Papillomata Scoliosis, pectus
Holt-Oram syndrome	(87,88)	<i>TBX5</i>	142900	75 ^c	ASD, VSD PAPVR Assorted CHDs Conduction defect	Upper limb anomalies
Kabuki syndrome	(89–92)	<i>MLL2</i>	147920	45–55	ASD,VSD LVOTO CHDs: BAV, Coarctation, HLHS	Long palpebral fissures Cleft lip/palate Skeletal abnormalities
LEOPARD syndrome	(93–95,102)	<i>PTPN11</i> <i>RAF1</i>	163950	70–100	PS(V) HCM Conduction defect	Café au lait macules Lentigines Deafness, ear anomalies
Neurofibromatosis	(96,97)	<i>NF1</i>	162200	2	PS(V) AS(V), Coarctation HCM	Café au lait macules Optic glioma Scoliosis Pseudarthrosis Neurofibromas
Noonan syndrome	(93,98–104)	<i>PTPN11</i> <i>KRAS</i> <i>SOS1</i> <i>RAF1</i> <i>NRAS</i> <i>BRAF</i> <i>SHOC2</i>	163950	85 ^c	PS(V) ASD AVSD, partial Coarctation HCM	Short, webbed neck Pectus deformity Cryptorchidism
Rubinstein-Taybi syndrome	(105,106)	<i>CREBBP</i> <i>EP300</i>	180849	40	PDA, ASD, VSD Coarctation, HLHS	Broad thumbs, great toes

TABLE 26.3 Single-Gene Disorders Associated with CHDs (Continued)

Syndrome	Reference	Gene(s)	OMIM No.	Frequency of CHD ^a		Distinctive Features ^b
				All (%)	Distinctive or Most Common	
Townes-Brocks syndrome	(107)	<i>SALL1</i>	107480	25 ^c	Truncus, TOF ASD, VSD	Thumb malformations Ear anomalies Imperforate anus
<i>Autosomal recessive</i>						
Ellis-van Creveld syndrome	(108–110)	<i>EVC</i> <i>EVC2</i>	225500 607261	70	AVSD defects: Common atrium Primum ASD, Complete AVSD Secundum ASD	Short limbs Polydactyly Hypoplastic nails Dental anomalies
Keutel syndrome	(111,112)	<i>MGP</i>	245150	70	PS, peripheral	Short digits Mixed hearing loss Cartilage calcification
McKusick-Kaufman syndrome	(113,114)	<i>MKKS</i>	604896	15–50	AVSD defects: Complete AVSD Primum ASD, common atrium	Hydrometrocolpos Postaxial polydactyly
Smith-Lemli-Opitz syndrome	(115,116)	<i>DHCR7</i>	270400	45	Secundum ASD, VSD Complete AVSD TAPVR	2–3 toe syndactyly Cleft palate Lung anomalies Genital anomalies
Simpson-Golabi- Behmel syndrome	(117)	<i>GPC3</i>	312870	25	Secundum ASD, VSD Rare, variable cardiomyopathy	Macrosomia Cleft palate Supernumerary nipples Hypospadias Polysyndactyly

See Table 26.2 for definition of abbreviations.

^aFrequency figures rounded. When not specified in an article, data were calculated independently. Congenital heart “defects” excluded valve regurgitation, patent foramen ovale, and unspecified murmur, cyanosis, or heart disease. Some syndrome-specific nonstructural anomalies were included.

^bMost syndromes have growth delay, some degree of developmental delay or mental retardation, and dysmorphic facial features, which can be reviewed in general genetics references (72,73).

^cFrequency reflects cases with molecular confirmation.

TAPVR, partial anomalous pulmonary venous return; TAPVR, total anomalous pulmonary venous return.

(Adapted from Lin AE, Belmont J, Malik S. Heart. In: Stevenson RE, Hall JG, eds. *Human Malformations and Related Anomalies*. 2nd ed. New York, NY: Oxford University Press, 2006:85–120; Lin AE, Ardinger HH. Genetic epidemiology and an overview of the genetics of congenital heart defects. *Prog Pediatr Cardiol* 2005;20:113–126, Ref. 119.)

Collectively, these findings suggest that precurrence and recurrence rates are likely to vary between specific types of CHD and within different kindred. Therefore, instead of using population-based empiric data alone, counseling for recurrence risk for an individual family requires the consideration of multiple factors including the specific type of CHD, the presence of additional affected family members, and the presence of known genetic or syndromic risk factors.

GENETIC SYNDROMES

Genetic syndromes are defined as a consistent pattern of malformation caused by a genetic alteration. A malformation syndrome consists of multiple structural defects that are thought to be due to a single cause, even if the suspected cause has not yet been identified (72). The cause can include genetic alterations such as changes in chromosome number, translocations

between chromosomes, deletions or duplications of specific chromosomal regions, or single-gene defects, or can involve a teratogen (Table 26.1). The most common genetic syndromes are described in the following sections organized by the type of associated genetic alteration. For each syndrome the genetic basis, clinical and cardiac phenotype, diagnostic testing, natural history, and population frequency are described. A more extensive table of syndromes is provided for reference (Tables 26.2–26.4). In addition to the common conditions summarized in this chapter, there is a constantly enlarging compendium of chromosome regions associated with CHDs that have evolved from cytogenetically visible aberrations (150,151) to complex genomic-based networks (152). Genetic textbooks, chapters, and online services provide extensive descriptions of each syndrome (72,73,153,154). An alternative listing of syndromes by cardiac subclasses may be more practical for the cardiologist searching for information based on the specific type of heart defect, especially when a dysmorphic child lacks a specific syndromic diagnosis (118).

TABLE 26.4

Conditions with Presumed but Unknown Genetic Cause, or Genetic Heterogeneity Associated with CHDs

Syndrome	Reference	Gene(s)	OMIM No.	Frequency of CHD ^a		Distinctive Features ^b
				All (%)	Distinctive or Most Common	
Autosomal dominant						
Adams-Oliver syndrome	(120,121)		100300	20	LVOTO CHDs: Coarctation, parachute MV TOF Pulmonary vascular malformations	Scalp cutis aplasia Terminal transverse limb defect
Autosomal recessive						
Fryns syndrome	(122)		229850	50	Secundum ASD, VSD Conotruncal CHDs	Diaphragmatic hernia Distal digital hypoplasia GU, GI anomalies
Hydrolethalus syndrome	(123,124)	<i>HYLS1</i>	236680 610693	60	AVSD defects: Complete AVSD, common atrium ASD	Hydrocephalus Keyhole occipital defect Polydactyly Cleft lip/palate
Oral-facial-digital syndrome, II	(108)		252100	50	Primum ASD Complete AVSD	Tongue hamartomas Median cleft lip, alveolus Complex polysyndactyly
Ritscher-Schinzel syndrome (3C)	(125)		220210	100	TOF, DORV Complete AVSD, primum ASD ASD, VSD	Dandy-Walker malformation Prominent forehead Cleft palate Coloboma
Etiologic heterogeneity with autosomal gene(s), in some cases						
PHACES syndrome	(126,127)		606519	90	Coarctation IAA type A Right, double, or cervical aortic arch	Posterior fossa malformation Hemangiomas Eye anomalies
HFM,	(128)		164210	30	VSD	
Goldenhar syndrome, oculoauricular vertebral spectrum					Conotruncal CHDs: TOF	Microtia, ear tags, pits Hypoplasia face Epibulbar dermoid Vertebral anomalies Radial deficiency GU anomalies
Heterotaxy	(129–131)	<i>LEFTY2</i> <i>ACVR2B</i> <i>CFC1</i> <i>ZIC3</i>	601877 602730 605376 306955	95	Dextrocardia D-transposition L-transposition AVSD defects TAPVR Interrupted IVC Left SVC	Visceral situs anomalies Lung lobation anomalies Cleft lip, palate GU, brain anomalies Biliary atresia Malrotation, bowel atresia Spleen anomalies
VATER association	(132,133)		192350	50	Assorted CHDs Single umbilical artery	Vertebral anomalies anorectal anomalies Renal anomalies Radial deficiency

See Table 26.2 for definitions of abbreviations.

IVC, inferior vena cava; SVC, superior vena cava; TAPVR, total anomalous pulmonary venous return.

Syndromes Associated with Chromosome Abnormalities

In population-based studies, a chromosome abnormality was detected in approximately 13% of children in the first year (22,155), and in 19% to 36% of miscarriages and stillborn fetuses with a cardiac defect (156). These occurrence data are reviewed in more detail in Chapter 25 of this text. Chromosome abnormalities can be classified according to an increase or decrease in whole chromosome number (aneuploidy), an increase or decrease of part of a chromosome (duplication or deletion, partial trisomy, or partial monosomy), or a more complex rearrangement. More recently, chromosome microarray analysis may be able to detect a causal diagnosis in up to 18% with a “syndromic CHD” (157). Of the many possibilities, Table 26.2 lists the most common syndromes with the most distinctive CHDs, with selected ones discussed below.

Change in Chromosome Number (Aneuploidy)

Down Syndrome

The most familiar syndrome to cardiologists is Down syndrome in which there is trisomy 21 in 94% (a complete extra copy of chromosome 21) (Table 26.2). Less commonly, (6% overall), partial trisomy of chromosome 21 is present owing to a chromosomal translocation or mosaicism. The well-known facial appearance changes with age and varies with ethnic background (Fig. 26.1). Common findings include hypotonia, global developmental delays and moderate intellectual disability, microbrachycephaly, small ears, mouth and nose, protruding tongue, upslanting eyes with epicanthal folds, transverse palmar creases, and sparse hair. Skeletal anomalies include fifth finger clinodactyly, brachydactyly, a gap between first and second toes, atlantoaxial instability, hypoplastic pelvis, and joint laxity. Additional problems involve the visual, auditory, endocrine, hematologic, reproductive, and gastrointestinal systems.

Almost half of liveborn Down syndrome individuals have a CHD, approximately 40% of whom have a complete atrioventricular septal defect (also known as atrioventricular canal defect or endocardial cushion defect) (23). When primum-type atrial septal defect, canal-type ventricular septal defect, and transitional atrioventricular septal defect are included, the frequency of the atrioventricular family of septal defects increases to almost 60% (22–24). The association of Down syndrome and atrioventricular septal defects is underscored by the fact that approximately 75% of patients with a complete atrioventricular septal defect have Down syndrome. Other common CHDs include secundum atrial septal defect, perimembranous and muscular ventricular septal defect, tetralogy of Fallot (with and without atrioventricular septal defect), and hemodynamically significant patent ductus arteriosus.

Mothers older than age 35 years have an increased risk of conceiving a child with aneuploidy (an extra chromosome), including Down syndrome. Cross-sectional data (1979 to 2003) looking at Down syndrome children aged 0 to 19 years in 10 sections of the United States showed a steady increase from 9.0 to 11.8 per 10,000, but was lower among non-Hispanic blacks (158). Overall survival has improved, although prenatally diagnosed CHDs and/or growth retardation may predict a poorer outcome (159). The median age at death increased from 25 to 49 years in the interval from 1983 to 1997 (160). Equivalent if not better surgical results for atrioventricular septal defect repair with similar postoperative residual cardiovascular defects have been reported in Down as compared with non-Down syndrome individuals (161,162).

The largest survey study to date reported that the frequency of CHDs in patients with Down syndrome mosaicism was



Figure 26.1. Down syndrome. A thriving 1-year-old girl with epicanthal folds, small nose, small mouth, small ears, and atrioventricular septal defect. (Courtesy of Sara S. Halbach, MS, CGC; Donna McDonald-McGinn, MS, CGC; Terri Anderson, MD; and Elaine Zackai, MD, The Children's Hospital of Philadelphia.)

similar to the complete trisomy 21 comparison group (~42% and 50%) (163). Atrial septal defect was the most common CHD, with atrioventricular septal defect reported in 11% compared to 22%.

The strong association of Down syndrome and atrioventricular septal defects prompted a search for a cardiac gene on chromosome 21. A Down syndrome critical region on chromosome 21 (21q22) and CHD candidate genes have been proposed, although causation for atrioventricular septal defects has not been demonstrated (164).

The only source of data on Down syndrome adults followed postoperatively (165) recommended monitoring as with any child who had a similar CHD repair. Conduction block with variable escape arrhythmia should be assessed with periodic Holter monitoring.

Trisomy 18

Although most fetuses with trisomy 18 may not survive until livebirth, there are many parents who will seek aggressive support for these seriously affected children, and thus, clinicians should be familiar with their appearance and CHDs (18). These children have short palpebral fissures, small mouth, micrognathia, growth retardation, prominent occiput, clenched hands, disorganized or hypoplastic palmar creases, hyperconvex nails, short sternum, small nipples, radial deficiency, and anomalies of almost every organ system.

CHDs are nearly ubiquitous and include perimembranous ventricular septal defect, tetralogy of Fallot, double-outlet right ventricle, and polyvalvar dysplasia in which two or more valve

leaflets are thickened, myxomatous, or dysplastic (15,19,20). A natural history study of trisomy 18 in the United Kingdom reported that the prevalence at 18 weeks' gestational age was about 1 in 4,000, which decreased to 1 in 8,000 at birth (21). Recent population-based analyses of trisomy 18 (and trisomy 13) born during 1968 to 1999 reaffirmed that the vast majority (91%) die in the first year of life, although CHDs did not seem to affect survival (16). Although the high lethality and obligatory severe mental retardation among survivors is well recognized, some parents of trisomy 18 infants advocate for cardiac surgery, among other procedures.

There is no single trisomy 18 critical region. Instead, analysis of individuals with duplication of distal 18q provides insights into chromosome regions that may contribute to the trisomy 18 phenotype (166).

Turner Syndrome

The liveborn prevalence of Turner syndrome is approximately 1 per 2,000 (167). The phenotype depends on whether the X chromosome is absent (45,X in almost 50% of patients) or structurally abnormal (168). The most common presentation is a spontaneously aborted fetus with hydrops or lymphatic malformation in the neck or mediastinum. Fetal lymphedema produces neck webbing, protruding ears, low hairline, puffy hands and feet, and deep-set nails (Fig. 26.2). Frequent findings include short fourth metacarpals, cubitus valgus, Madelung deformity, osteoporosis, kyphoscoliosis, broad chest with apparently widely spaced nipples, renal anomalies (horseshoe kidney), nevi, hearing loss, infertility, autoimmune diseases, as well as deficits in visual-spatial/perceptual abilities, attention, and social skills. Turner syndrome women with 45,X generally have more malformations as compared to those with only partial deletion of the X chromosome. Mosaicism involving 45,X/46,XX is usually associated with a milder phenotype, and 45,X/46,XY mosaicism increases the risk for gonadoblastoma (168).

Approximately 30% of Turner syndrome women have a CHD, which usually involves the left-sided cardiac structures (25,26,168), and up to 50% of adults have vascular anomalies



Figure 26.2. Turner syndrome. An 11-year-old girl with hyperlordism, facial nevi, and dysplastic right pinnae. She has short stature, normal intelligence, thyroiditis, and no CHDs. (Courtesy of Angela E. Lin, MD.)

detected by magnetic resonance imaging (MRI) (27,169). An asymptomatic bicuspid aortic valve (15%) may progress to aortic stenosis (10%), and coarctation of the aorta (with or without a bicuspid aortic valve) is present in 10% of Turner syndrome patients. Because these findings are significantly associated with the presence of neck webbing, investigators have hypothesized that the altered lymphatic drainage itself causes the associated left-sided obstructive lesions (26,170). It is unproven whether haploinsufficiency for genes on the X chromosome that may impair lymphatic and vascular development represent the underlying cause instead (28). Less common left-sided defects include elongation of the transverse arch and/or pseudocoarctation (almost half of adults with Turner syndrome) (27), various mitral valve anomalies (<5%), and HLHS (rare). Secundum atrial septal defect, perimembranous ventricular septal defect, partial anomalous pulmonary venous connection often involving the upper left pulmonary vein, and persistent left superior vena cava also occur, but complex CHDs, especially conotruncal defects, are noticeably rare (25–27).

Turner syndrome women are at risk for aortic dilation, dissection, and sudden death. Prospective MRI of older patients doubles the echocardiographic detection of aortic dilation (33% vs. 16%) (169). Arterial dilation and arterial wall abnormalities, and cerebral involvement suggest that there may be a more diffuse vasculopathy (171,172). An epidemiologic description of aortic dissection calculated a sixfold population-based risk (36 per 100,000 Turner syndrome years), or an approximate 1.4% risk (29). Aortic dissection in Turner syndrome is almost always associated with a risk factor such as bicuspid aortic valve, coarctation of the aorta or hypertension; the few individuals without an underlying cause may reflect inadequate examination (173,174), although an intrinsic predisposition cannot be excluded. Consensus guidelines (28) for the increasing number of older women with Turner syndrome include baseline imaging of the aorta at the time the condition is diagnosed and ongoing blood pressure monitoring. MRI may provide superior images to echocardiography depending on age, coexisting CHDs, previous surgery, and body habitus (27,169). Repeat imaging should be done every 5 to 10 years, with the appearance of hypertension, or if pregnancy is contemplated (28,175). In general, growth hormone does not appear to promote aortic dilation (30,31). A disturbing number of deaths owing to aortic dissection raises concern about the safety of pregnancy (175,176). For the increasing number of women who consider pregnancy using assisted reproductive technology with oocyte donation, it seems prudent to exclude the women who have risk factors for dissection, and plan pregnancy according to guidelines published in 2007 (28).

Adult women with Turner syndrome require monitoring for postoperative recoarctation and hypertension, and aortic stenosis and regurgitation. Unrepaired bicuspid aortic valve should be monitored for the development of progressive stenosis and aortic dilation. Hypertension and coronary artery disease are more common than in the general population (174,177). Prospective electrocardiogram (ECG) monitoring may also be indicated since data demonstrate conduction and repolarization abnormalities (including prolongation of the QTc interval) (32).

Studies correlating genotype with clinical phenotype suggest that haploinsufficiency of the short stature-homeobox gene on the short arm of the X chromosome leads to short stature and skeletal changes. Genes on both arms of the X chromosome are important for ovarian function. However, there is no known critical region on the X chromosome for CHDs.

Deletion–Duplication Syndromes

Microarray technologies have markedly increased the ability to detect chromosome imbalances along the entire length of

the chromosome, and as such have often become the test of choice to detect deletions and duplications (137). As a result of these rapid technologic advancements, an increasing number of small chromosomal deletions and duplications that are not apparent on a high-resolution karyotype have been identified in patients with various clinical syndromes and multiple congenital anomalies. A chromosomal *deletion* occurs when there is a missing segment of a chromosome on one of the two copies of the same chromosome resulting in one copy, or haploinsufficiency, of that region (partial monosomy). Conversely, a chromosomal *duplication* occurs when there is an extra copy of one segment of a chromosome resulting in three copies of that region (partial trisomy). Research has defined an expanding list of deletion and duplication syndromes over the last decade. Most of these syndromes are characterized by multiple congenital anomalies, presumably because of the number of genes involved in the deleted or duplicated segments. They also display marked clinical variability between individuals. Many of these syndromes are associated with CHDs and thus constitute an increasingly important group of syndromes with which a cardiologist should be familiar. Examples of the most common deletion syndromes with cardiovascular features are described below, and others are highlighted in Table 26.2.

The 22q11.2 Deletion Spectrum (DiGeorge Syndrome, Velocardiofacial Syndrome)

Molecular studies demonstrate that the vast majority of patients with the clinical diagnosis of DiGeorge, velocardiofacial (Shprintzen syndrome), or conotruncal anomaly face syndromes share a common genetic cause, namely, a 22q11.2 deletion (178–180). The 22q11.2 deletion syndrome is currently the most common deletion syndrome known and is estimated to occur in approximately 1 in 6,000 live births (155,181).

The clinical phenotype of the 22q11.2 deletion syndrome is highly variable among related and unrelated individuals (182). The presentation can be severe and easily recognized at birth or subtle and detected late in life. Approximately 6% to 10% of cases are familial, implying that the affected child inherited the chromosomal deletion from a parent. Frequently, the parent is recognized to carry a 22q11.2 deletion only after their more severely affected child is diagnosed. The most common features include CHDs, palate anomalies, feeding disorders, speech and learning disabilities, hypocalcemia, immunodeficiency, renal anomalies, behavioral and psychiatric disorders, and typical facial features (reviewed in Ref. 67) (Fig. 26.3). However, the facial features can be difficult to identify in infants and may be underappreciated in certain populations such as African Americans (183).

CHDs are estimated to occur in 75% to 80% of patients with a 22q11.2 deletion (68,69). The prevalence of CHDs may be overestimated because of increased ascertainment in the pediatric population with CHDs as compared with adults with more subtle features (184). The most common CHDs associated with a 22q11.2 deletion include tetralogy of Fallot, interrupted aortic arch type B, truncus arteriosus, perimembranous ventricular septal defect, and aortic arch anomalies (68,69). It should be noted that a wide range of CHDs has been reported in patients with a 22q11.2 deletion, including pulmonary valve stenosis, atrial septal defect, heterotaxy syndrome, and HLHS.

Because CHDs are common in the 22q11.2 deletion syndrome, several studies have estimated the frequency with which a 22q11.2 deletion is found in patients with CHDs typical of DiGeorge or velocardiofacial syndromes. At least 50% of patients with an interrupted aortic arch type B, 35% with truncus arteriosus, 24% with an isolated aortic arch anomaly, 15% with tetralogy of Fallot, and 10% with a perimembra-



Figure 26.3. 22q11.2 deletion syndrome. A 5-year-old boy with typical facial features of the 22q11.2 deletion syndrome including malar flattening, small mouth, bulbous tipped nose with hypoplastic alae nasi, and micrognathia. He also had tetralogy of Fallot, developmental delay, mild immune suppression, and late emergence of speech. (Courtesy of Donna McDonald-McGinn, MS, CGC; Elaine Zackai, MD; and Elizabeth Goldmuntz, MD, The Children's Hospital of Philadelphia.)

nous ventricular septal defect are found to have a 22q11.2 deletion (70,185–193). In contrast, <1% of patients with double-outlet right ventricle or D-transposition of the great arteries are found to have a 22q11.2 deletion. Several studies have demonstrated that patients with one of these intracardiac anomalies and a concurrent aortic arch anomaly (either abnormal sidedness, cervical location, or abnormal branching pattern) are more likely to have a 22q11.2 deletion. For example, only 3% of patients with a perimembranous ventricular septal defect and a normal left-sided aortic arch with normal branching pattern were diagnosed with the 22q11.2 deletion, whereas 45% with a perimembranous ventricular septal defect and concurrent aortic arch anomaly had a 22q11.2 deletion (192). Therefore, the presence of an aortic arch anomaly increases the risk of finding a 22q11.2 deletion regardless of the intracardiac anatomy. Studies also suggest that the subset of patients with tetralogy of Fallot associated with absent pulmonary valve syndrome or aortopulmonary collaterals are at higher risk of having a 22q11.2 deletion (191,194). Collectively, these findings demonstrate that a 22q11.2 deletion is commonly found in a significant subset of patients with congenital cardiovascular defects.

Identifying the cardiac patient with a 22q11.2 deletion early in life can provide substantial benefits to the child and family. Currently, it is recommended that infants with interrupted aortic arch type B, truncus arteriosus, tetralogy of Fallot, and isolated aortic arch anomalies undergo testing for a 22q11.2 deletion given the high frequency with which these patients are found to harbor a 22q11.2 deletion (5). Likewise, it is

suggested that patients with a perimembranous ventricular septal defect and aortic arch anomaly, or any infant with noncardiac features of the 22q11.2 deletion syndrome (regardless of the CHD) undergo 22q11.2 deletion testing. Although somewhat controversial, current recommendations for testing seek to identify the deletion-bearing patient as early as possible to anticipate associated medical conditions and provide accurate family genetic counseling. Parents found to carry the deletion have a 50% chance of transmitting the deletion-bearing chromosome in subsequent pregnancies.

Although the evaluation must be tailored to each patient's needs, infants or children diagnosed with the 22q11.2 syndrome should be evaluated for associated noncardiac features including hypocalcemia, immunodeficiency, palate anomalies, feeding and speech disorders, renal and skeletal anomalies, cognitive deficiencies, and behavioral issues (67). Parents should be tested for a 22q11.2 deletion as well. A 22q11.2 deletion is now easily detected using FISH, MLPA, or microarray technologies, though the latter is becoming the test of choice in many centers (137).

Many children present with noncardiac symptoms and are diagnosed with a 22q11.2 deletion later in infancy or childhood. Although these patients are unlikely to have major intracardiac anomalies, aortic arch anomalies are commonly identified in this subset of patients. In particular, 38% of patients diagnosed with a 22q11.2 deletion after 9 months of age were found to have an aortic arch anomaly, of whom 27% had a symptomatic vascular ring (195). A remarkable variety of aortic arch anomalies has been found in the 22q11.2-deleted population including absent or isolated subclavian arteries where retrograde flow through the vertebral artery provides flow into the absent or isolated subclavian artery predisposing to a steal phenomenon (196). Since respiratory symptoms including asthma and airway anomalies are commonly diagnosed in the 22q11.2-deleted population, it is important to identify which children have concurrent vascular rings contributing to or causing their respiratory symptoms and which should undergo surgical ligation.

Caring for the CHDs of adults with 22q11.2 deletions is similar to their nonsyndromic counterparts and lesion specific. Aortic root dilation has been observed in a subset of older children without CHD, but its clinical significance is not yet understood (197).

7q11 Deletion (Williams-Beuren Syndrome)

Williams-Beuren syndrome ("Williams syndrome") is another familiar multisystem disorder that occurs in 1 per 20,000 live-births. It is characterized in part by CHDs, hypercalcemia in infancy, skeletal and renal anomalies, cognitive deficits, social personality, and elfin facies (Fig. 26.4). As with other deletion syndromes, children with Williams syndrome can be diagnosed at different ages and present with a broad range of clinical features (reviewed in 206). Early in life, feeding disorders and growth retardation are common. Hypercalcemia is seen in 15% of infants and usually resolves over time (198). The neurocognitive profile of Williams syndrome most commonly includes mild mental retardation, although the full-scale IQ ranges from low normal intelligence to severe mental retardation. Cognitive strengths and weaknesses relative to other patients with mental retardation include relatively good auditory rote memory but extreme difficulty with visuospatial construction tasks (199). The familiar high sociability and overly friendly demeanor seen in some patients with Williams syndrome may be accompanied by substantial behavioral disorders, including inattention and hyperactivity.

Approximately 55% to 80% of patients with Williams syndrome have CHDs, which typically include supravalvar aortic stenosis and/or supravalvar pulmonary stenosis



Figure 26.4. Williams syndrome. A 17-month-old girl with typical facial appearance including flared eyebrows, bright stellate irides, and wide mouth. She has mild supravalvar aortic stenosis. (Courtesy of Amy E. Roberts, MD, Children's Hospital, Boston.)

(200,201). The degree of cardiovascular involvement and the relative involvement of the pulmonic or aortic vessels vary widely. Although supravalvar pulmonary stenosis usually improves with time, supravalvar aortic stenosis progresses in most cases (200,202,203). If significant supravalvar aortic stenosis is left untreated, cardiac hypertrophy followed by cardiac failure can result. Surgical and catheter interventions have met with success in some cases (204). Sudden cardiac death is another reported cardiovascular complication. Sudden death was described in 10 young children with Williams syndrome, seven of whom had coronary artery stenosis along with severe biventricular outflow tract obstruction (205). Presumably, sudden cardiac death resulted from myocardial ischemia, decreased cardiac output, and/or arrhythmias. Finally, patients with Williams syndrome may commonly develop hypertension either because of renal artery stenosis or other undefined mechanisms (201). Because of the generally diffuse arteriopathy and potential for hypertension, lifelong cardiovascular monitoring is recommended for patients with Williams syndrome (206).

Approximately 90% of patients with the clinical diagnosis of Williams syndrome have a deletion at chromosome 7q11.23, which is not generally apparent on a routine karyotype but can be detected by FISH, MLPA, and microarray technologies. Clinical testing is readily available in most standard cytogenetic clinical laboratories. Given the clinical variability of Williams syndrome, it is appropriate to consider testing all patients with supravalvar aortic or pulmonic stenosis for a 7q11.23 deletion.

Most patients with Williams syndrome have a 7q11.23 deletion of the same size. The genes mapping to this region have been defined and include the elastin gene, *ELN*. Mutations within the elastin gene have also been found in patients with isolated supravalvar aortic stenosis (207–209). Therefore, deletion of the elastin gene in patients with Williams

syndrome is thought to account for the cardiovascular phenotype. Molecular studies of rare patients with smaller deletions implicate the gene *LIMK1* in the impaired visuospatial constructive cognition (210). Additional genes mapping into the deleted region are thought to contribute to the neurocognitive features and are under further study. In contrast to the 22q11.2 deletion syndrome, these findings suggest that Williams syndrome is a true contiguous gene deletion syndrome in which the deletion of specific genes corresponds to distinct clinical features.

Studies further suggest that specific types of mutations in the elastin gene result in different clinical syndromes. As noted, a 7q11.23 deletion results in complete loss of one copy of the elastin gene (as well as other genes) and the diffuse arteriopathy seen in Williams syndrome. Disruption or mutation of the elastin gene alone can also result in isolated forms of supravalvar aortic and pulmonic stenosis. Both sporadic cases of supravalvar aortic stenosis and families with autosomal dominant inheritance have been found to have intragenic elastin gene mutations that result in functional hemizyosity (half of the functional gene dosage), similar to deletion of the entire gene (209). Mutations in the elastin gene have been identified in some patients with the autosomal dominant form of cutis laxa, another connective tissue disorder characterized by loose, saggy, inelastic skin. Both autosomal recessive and dominant forms have been observed in this genetically heterogeneous disorder (211,212). Studies suggest that these elastin mutations are functionally distinct from those associated with the diffuse arteriopathy, acting instead as a dominant negative effect. Thus, the specific elastin gene mutation appears to correlate with a specific clinical phenotype. These findings serve to demonstrate the complexity and heterogeneity of even seemingly straightforward genetic syndromes.

Emerging Microdeletion/Microduplication Syndromes

The advent of microarray technologies demonstrated that the human genome exhibits enormous variability both at the level of single nucleotides (so-called SNPs) and large segments of deoxyribonucleic acid (DNA) (deletions and duplications, or so-called copy number variants) (134). These technologies have provided increasingly sensitive means by which to identify cytogenetically undetectable changes in chromosomal copy number, and have therefore been used to identify new potential CHD disease loci. Several studies identify different copy number variants in cardiac patients, particularly in those with multiple congenital anomalies and/or developmental delay (157,213–216). Depending upon the resolution of the array, in these studies nearly 20% of such patients are found to harbor unique or rare copy number variants, though the disease significance of such findings in some cases remains to be demonstrated. These studies nonetheless highlight the potential clinical relevance of screening for submicroscopic alterations. In addition, several new deletion and duplication syndromes have been described, while others are just coming to be recognized. A subset of such syndromes are noted below, though further clinical testing and research will likely identify novel changes and solidify the significance of others.

11q23 Deletion Syndrome (Jacobsen Syndrome)

The 11q terminal deletion syndrome, previously known as Jacobsen syndrome, is thought to be a contiguous gene disorder characterized by distinctive facial features (Fig. 26.5), thrombocytopenia, developmental delay, CHD, short stature, genitourinary anomalies, pyloric stenosis, and ophthalmologic issues. As with other deletion syndromes, the clinical phenotype is highly variable, as is the size of the associated deletion. In a recent study (58), 56% of cases had serious CHDs, of



Figure 26.5. Jacobsen syndrome. An 18-year-old man with a deletion 11q23 (Jacobsen syndrome) who has mild features including short stature, mild intellectual disability, wide-spaced small eyes with mild ptosis, and small ears. (Courtesy of family.)

which approximately one-third had ventricular septal defects, one-third had left-sided anomalies (mitral and aortic valve), and one-third had a range of other types of CHD. Molecular analysis of 110 patients identified potential critical regions for multiple phenotypes. Though a rare diagnosis, it is an area of active research as further molecular analysis may identify specific disease-related genes, and current genetic testing methods may permit the identification of additional cases.

8p23.1 Deletion Syndrome

Numerous patients with interstitial or terminal deletions of 8p23.1 deletion have been reported. In general, such patients are characterized clinically by growth impairment, developmental delay, behavioral problems, microcephaly, diaphragmatic hernia, hypospadias, and CHDs (reviewed in Refs. 47 and 48). The most common CHDs include atrioventricular septal defects, atrial septal defects, ventricular septal defects, and pulmonary valve stenosis. The disease gene, *GATA4*, is often disrupted by these deletions, but cases with a *GATA4* deletion without CHD, as well as cases whose deletion does not encompass *GATA4* but have CHD, have been reported. Other genes disrupted by the deletion have also been implicated, but further studies correlating genotype with phenotype are warranted. More common use of clinical diagnostic array technology will likely identify an increasing number of cases with an 8p23.1 deletion.

1p36 Deletion Syndrome

Monosomy 1p36 is now recognized to be the second most common deletion syndrome with an estimated prevalence of 1 in 5,000 to 10,000 livebirths (33,34). As with other deletion

syndromes, the associated clinical phenotype is variable but notable for characteristic craniofacial features, ocular malformations or visual problems (52%), hearing loss (47%), neurologic abnormalities (44%), skeletal anomalies (41%), renal anomalies (22%), as well as CHDs (71%) (33). The most common CHDs include atrial septal defects, ventricular septal defects, patent ductus arteriosus, valve anomalies, tetralogy of Fallot, and coarctation of the aorta. Of note, many patients with 1p36 deletion syndrome present with cardiomyopathy including noncompaction of the left ventricle or dilated cardiomyopathy. One report described a patient presenting as an adult with noncompaction of the left ventricle, suggesting that lifelong observation for such complications might be warranted (35). As larger patient cohorts are identified with the 1p36 deletion syndrome, the prevalence of CHDs and cardiomyopathy will be better defined.

Genetic Syndromes Caused by Mutations in Single Genes

An increasing number of malformation syndromes has been found to be caused by a mutation of a single gene in contrast to a larger chromosomal abnormality (see Table 26.3). These mutations can be inherited in a mendelian fashion and demonstrate an autosomal dominant pattern of inheritance in families, with a 50% risk of recurrence. As with larger chromosomal alterations, single-gene disorders are characterized by a variable phenotype between related and unrelated affected individuals, suggesting that additional genetic and environmental factors modify the clinical phenotype of any single mutation.

The type of intragenic mutation may be variable (as in Alagille syndrome) or fairly consistent (as in achondroplasia) and may include nonsense, frameshift, missense, or splice site mutations. Specific mutations may result in different biologic consequences and may cause different clinical phenotypes (*variable expression*); mutations in different genes can produce a similar clinical phenotype (*genetic heterogeneity*). These observations have been well characterized in Noonan syndrome and related disorders, and Alagille syndrome (see below). The most common genetic syndromes for which a specific disease gene has been defined are described below. Readers are also referred to GeneReviews.org, a collection of excellent peer-reviewed resources, which are updated periodically.

Alagille Syndrome (*JAG1* and *NOTCH2*)

Alagille syndrome was originally defined as the presence of bile duct paucity on liver biopsy in conjunction with three of the following five findings: cholestasis, CHDs, skeletal or ocular abnormalities, or typical facial features (217,218) (Fig. 26.6). An autosomal dominant disorder, it was noted that a subset of patients with clinical features of Alagille syndrome had deletions of chromosome 20p12 (219–221). The Notch ligand, *JAG1*, was subsequently mapped into the commonly deleted region (222). Two reports identified mutations of *JAG1* in patients with Alagille syndrome and therefore demonstrated that *JAG1* is a disease gene for this disorder (223,224). *JAG1* mutations were also identified in family members with milder presentations or microforms of Alagille syndrome, demonstrating that there is a broad spectrum of clinical phenotypes associated with *JAG1* mutations.

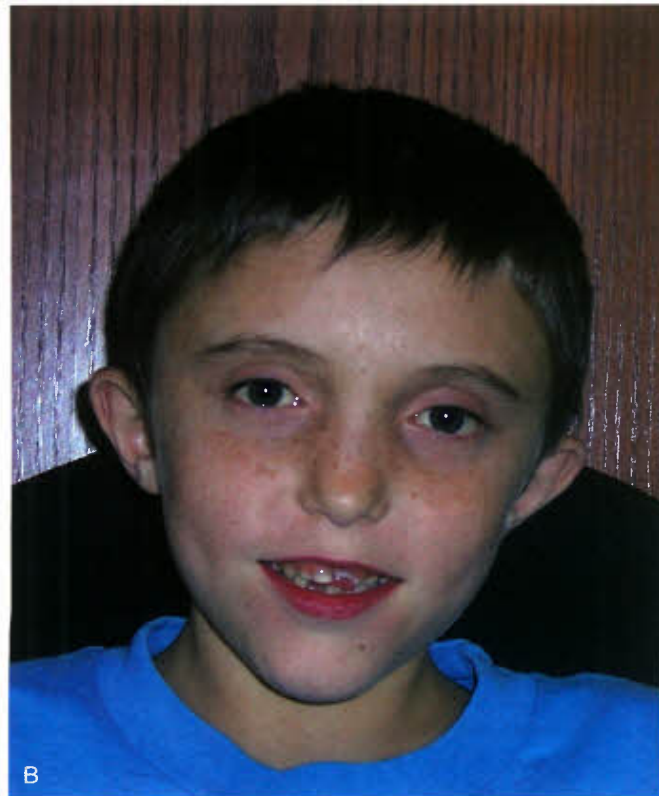


Figure 26.6. Alagille syndrome. Representative facial features of two boys with Alagille syndrome aged 7 months (A) and 9 years (B). Note the broad forehead, deep-set eyes, rounded tip and pear-like shape of the nose, and pointed chin. The features give the face an inverted triangle appearance. (Courtesy of the parents; David Piccoli, MD; and Elizabeth Goldmuntz, MD, The Children's Hospital of Philadelphia.)

Alagille syndrome is now recognized to be a genetically heterogeneous disorder. Approximately 5% of patients will have a chromosomal deletion involving one copy of the entire *JAG1* gene, whereas most will have various intragenic *JAG1* mutations (225,226). Using the most sensitive techniques, *JAG1* mutations can be identified in 94% of patients with features of Alagille syndrome (225,226). A minority of patients will have *NOTCH2* mutations (74). Mutations introducing a shift in the reading frame of the genetic code (so-called frameshift mutations) are the most common type of *JAG1* mutation, but missense mutations that alter only a single amino acid have also been identified. As a result of most *JAG1* deletions and mutations, there is presumably half the amount of functional protein. Therefore, the disease mechanism appears to be that of haploinsufficiency.

Alagille syndrome is characterized by right-sided CHDs including peripheral pulmonary stenosis (diffuse hypoplasia of the pulmonary arterial bed as well as discrete stenosis), pulmonary valve stenosis, and tetralogy of Fallot. Left-sided lesions and septal defects have also been reported (227). Examination of pedigrees of patients with Alagille syndrome and/or *JAG1* mutations suggested that some patients with CHDs without overt hepatic involvement would have *JAG1* mutations. Indeed, *JAG1* mutations have been identified in patients and kindred who do not have overt hepatic disease and therefore do not meet the classic criteria of Alagille syndrome but have CHDs typical of Alagille syndrome and other mild syndromic features (228,229). Therefore, the diagnosis of Alagille syndrome or *JAG1* mutation should be considered in families in which more than one member has a right-sided heart defect. Conversely, patients with right-sided CHDs should be carefully examined for subclinical features of Alagille syndrome and questioned for a relevant family history to identify the patient at risk for Alagille syndrome or a *JAG1* mutation. Patients suspected of having Alagille syndrome should undergo cytogenetic testing including a karyotype and analysis for deletion of chromosomal region 20p12. Testing for intragenic *JAG1* mutations is now clinically available.

Several studies have reported additional vascular anomalies and complications in patients with Alagille syndrome, highlighting the fact that the observed arteriopathy can affect more than the pulmonary arterial bed. In particular, Kamath et al. (230) reported that 9% of their cohort with Alagille syndrome had noncardiac vascular anomalies or events including basilar, internal carotid, and middle cerebral artery aneurysms. Other reported arterial anomalies include renal artery stenosis and moyamoya disease. Vascular events accounted for 34% of the mortality in this cohort. The true prevalence of such arterial anomalies is still unknown; thus, it is not yet clear whether routine screening for other vascular anomalies is clinically warranted. However, these observations point to a diffuse vasculopathy in Alagille syndrome and should heighten the clinician's awareness for these potentially devastating complications.

A small number of patients with clinical features of Alagille syndrome do not have *JAG1* mutations but have mutations in its ligand, *NOTCH2*. In particular, McDaniell et al. (74) identified two unrelated kindred with *NOTCH2* mutations out of 11 *JAG1* mutation-negative patients with the clinical features of Alagille syndrome. Of note, all of the patients with *NOTCH2* mutations had renal manifestations, which are less commonly seen in the cohort of Alagille patients with *JAG1* mutations. These results also further highlight the critical role of the *NOTCH* signaling pathway in cardiovascular development and disease.

Holt-Oram Syndrome (*TBX5*)

Holt-Oram syndrome is the most common “heart–hand” syndrome (upper limb and CHDs) and is estimated to occur in

1 of 100,000 live births. The skeletal anomalies of this autosomal dominant disorder involve the preaxial radial ray and are fully penetrant (i.e., everyone with the diagnosis of Holt-Oram syndrome must have a skeletal anomaly), although they range in severity (231,232). Subclinical changes may include only radiographic evidence of abnormal carpal bone, whereas others have obvious severe manifestations such as phocomelia. The thumb is frequently affected and can be triphalangeal, hypoplastic, or absent. Skeletal anomalies can be seen in one or both upper limbs and may be symmetric or asymmetric.

Approximately 75% of patients diagnosed with Holt-Oram syndrome have CHD (233). Although atrial and ventricular septal defects are most commonly seen (58% and 28%, respectively), additional CHDs including atrioventricular septal defects, conotruncal anomalies, and left-sided defects are also reported. Atrioventricular conduction delay, which can begin as first-degree atrioventricular block and progress to complete heart block, is also an important cardiovascular feature.

Linkage analyses performed on families demonstrating autosomal dominant inheritance identified a disease locus at 12q24 (234,235). Subsequent investigations identified mutations in *TBX5* in patients with Holt-Oram syndrome (236,237). Since the initial discovery, nonsense, frameshift, and missense mutations have been identified in familial and sporadic cases. Mutations of *TBX5* are found in approximately 70% of patients with the clinical features of Holt-Oram syndrome. Presumably those with the correct diagnosis of Holt-Oram syndrome in whom a mutation cannot be readily identified have a mutation in a regulatory domain that is not routinely tested since the disorder is not thought to be genetically heterogeneous. Although in most cases the diagnosis of Holt-Oram syndrome can be reliably made by clinical examination, genetic testing for *TBX5* mutations is clinically available in several specialized laboratories and may be useful in specific situations where the diagnosis is ambiguous or needed for prenatal counseling.

The diagnosis of Holt-Oram syndrome should be considered in the patient with heart and upper limb anomalies. Given the variable phenotype, Holt-Oram syndrome should also be considered in the patient with an apparently isolated septal defect and family history of septal or upper limb anomalies. The patient suspected of having Holt-Oram syndrome should be evaluated for radial ray and cardiac and conduction abnormalities. Although it is most commonly a sporadic rather than familial disorder, selected family members of affected members should be examined for subtle features to allow for appropriate genetic counseling. Some reports have suggested a genotype/phenotype correlation (i.e., certain mutations may be associated with more severe cardiac or skeletal manifestations), but caution must be exercised for the individual when counseling about the implications of each mutation.

Noonan Syndrome Spectrum (Noonan Syndrome, LEOPARD, Cardiofaciocutaneous Syndrome, Costello Syndrome)

Several phenotypically similar, but genetically distinct, multiple anomaly syndromes have been the subject of tremendous clinical and molecular genetic and cardiology research. They are often known collectively by the most common and familiar disorder in the group (“Noonan syndrome spectrum”) or by the Ras/mitogen-activated protein kinase (MAPK) biochemical pathway (“rasopathies”). Noonan syndrome, cardiofaciocutaneous (CFC) syndrome, and Costello syndrome are the result of mutations in the Ras/MAPK pathway (76) and have similar cardiac abnormalities, namely, CHDs, hypertrophic cardiomyopathy (HCM), and arrhythmia (86). Other clinical syndromes in this pathway, broadly defined, such as neurofibromatosis, type 1 and Legius syndrome, are not discussed.



Figure 26.7. Rasopathy syndromes: Noonan syndrome, CFC syndrome, Costello syndrome. A: On the left is a child with Noonan syndrome. B: In the middle is a 12-year-old girl with the CFC syndrome due to the most common *BRAF* mutation (exon 12) without any cardiac disease. C: The right lower panel shows a 16-year-old girl with Costello syndrome due to the typical *HRAS* G12S mutation. She has severe hypertrophy of the left ventricle (HCM) with mitral valve stenosis and sub-aortic obstruction (see [86], Table III, Supplemental patient 6) (Each photo was kindly provided by the family.)

Noonan syndrome occurs in 1 per 1,000 to 1 per 2,500 live births diagnosed clinically (98,238,239) (Fig. 26.7A). There is a characteristic facial appearance (ptosis, hypertelorism, low-set ears, low posterior hairline), webbed neck, pectus excavatum, bleeding diathesis, lymphatic issues, learning disabilities, variable intellectual disability, and cryptorchidism. Noonan syndrome is genetically heterogeneous with at least seven causative genes identified including *PTPN11*, *SOS1*, *KRAS*, *RAF1*, *NRAS*, *BRAF*, and *SHOC2* (98). Linkage analyses and candidate gene studies in patients with Noonan syndrome first identified mutations in the gene *PTPN11*, which encodes the non-receptor-type protein tyrosine phosphatase SHP-2 (src

homology region 2-domain phosphatase-2) that functions in the ras/MAPK pathway (99). Subsequent studies identified additional mutations in genes participating in the same molecular genetic pathway. Approximately half of patients with Noonan syndrome have a mutation in *PTPN11* (99,100,240–242). Genotype-phenotype analyses demonstrate that mutations in specific disease genes correlate with specific clinical features (76,98).

At least 80% of clinically defined Noonan syndrome patients have a cardiovascular abnormality, 60% of which are CHDs and 20% have HCM (98). Pulmonary valve stenosis, often with an atrial septal defect, is most common (25% to 35%) overall and most commonly associated with *PTPN11*

mutations. Additional CHDs include secundum-type atrial septal defect, ventricular septal defect, tetralogy of Fallot, pulmonary artery stenosis, coarctation of the aorta, incomplete atrioventricular septal defect (primum-type atrial septal defect), and polyvalvulopathy (98,101). HCM occurs in approximately 20% of patients with Noonan syndrome, especially those with a *RAF1* mutation and uncommonly with a *PTPN11* mutation. Patients with *KRAS* mutations have the most severe phenotype, and *SOS1* mutations result in a lower prevalence of cognitive delays. *SHOC2* is more likely to have mitral valve prolapse and septal defects, growth hormone deficiency, distinctive hyperactive behavior, hypernasal speech, and the distinctive easily pluckable hair.

Most cases of Noonan syndrome are sporadic, although families with a pattern of autosomal dominant inheritance are well known. There is marked clinical variability among affected individuals, and some parents have been diagnosed with this disorder only after the diagnosis of their more severely affected offspring.

Mutations of *PTPN11* have also been found in syndromes whose features overlap with those of Noonan syndrome, demonstrating that these are allelic disorders sharing a common genetic basis. Mutations of *PTPN11* have been identified in several patients with Noonan-like/multiple giant cell lesion syndrome, a syndrome characterized by features of Noonan syndrome and giant cell lesions of bone and soft tissue (cherubism) (100,102,243,244). A subset of patients with LEOPARD syndrome has also been found to have *PTPN11* mutations (93,245–247). LEOPARD syndrome is an autosomal dominant disorder characterized by multiple lentigines, electrocardiographic conduction abnormalities, ocular hypertelorism, pulmonary valve stenosis, HCM, growth retardation, abnormal genitalia, and sensorineural deafness. LEOPARD syndrome itself appears to be genetically heterogeneous since not all patients with this clinical diagnosis have a *PTPN11* mutation (93,246). Although *PTPN11* mutations resulting in Noonan syndrome are thought to confer a gain in function of the encoded protein, SHP-2 (99), mutations found in LEOPARD syndrome appear to have a dominant negative effect (248), which may explain the distinct phenotype. The ability to induce cardiomyocytes to pluripotent stem cells from a patient with LEOPARD syndrome heralds a new era of research for this group of syndromes (249). The researchers noted in vitro features of sarcomeric organization and preferential localization of *NEATC4* in the nucleus, which correlate with a potential hypertrophic state, thus providing an insight to the disease phenotype.

CFC syndrome and Costello syndrome are usually distinguishable from Noonan syndrome in the older child, but can be quite similar in the fetus, infant, and very young child (Fig. 26.7B,C). Whereas CFC syndrome can be caused by three genes (*BRAF*, *MEK1*, *MEK2*) (76,250), Costello syndrome is defined only by *HRAS* (76). As with Noonan syndrome, children with CFC syndrome also have relative macrocephaly, hypertelorism, and ptosis, but tend to have coarser facial features with sparse eyebrows and eyelashes, and dry skin (follicular hyperkeratosis). Costello syndrome also has coarse facial features, with ulnar deviation of the hand, curly (or very straight) hair, hyperpigmentation, loose skin, deep palmar and plantar creases, papillomata, and premature aging. Posterior fossa crowding can lead to Chiari 1 malformation, hydrocephalus, and syrinx (251). Developmental delays are always present, and intellectual disability is typically in the range of moderate mental retardation. Costello syndrome has a 10% to 15% risk of neoplasia, notably rhabdomyosarcoma.

The overall frequency (~80%) of any cardiovascular abnormality is nearly identical in CFC syndrome, Costello syndrome, and Noonan syndrome (86); HCM is more common (about 60%) in Costello and LEOPARD syndromes. Atrial

tachycardia, especially multifocal atrial tachycardia, is most common in Costello syndrome.

Kabuki Syndrome (*MLL2*)

In the previous edition of this textbook, Kabuki syndrome was listed as a syndrome with a “presumed, but unknown” cause. However, that is no longer the case. Affected patients have a characteristic expressionless facial appearance (reminiscent of the Japanese Kabuki theater actors) including elongated palpebral fissures with everted lower lids, arched eyebrows, sparse lateral brows, large pinnae, and fetal finger pads. Anomalies of the kidney and digits, immunologic and feeding problems, and intellectual disability are common. Because of tremendous phenotypic heterogeneity, the search for a causative gene was elusive until exome sequencing identified *MLL2* (which encodes a Trithorax-group histone methyltransferase) as the gene for Kabuki syndrome (89). Other researchers have described additional mutations and confirmed the original phenotype-genotype correlation that showed classic cases are most likely to be mutation-positive (90).

Atrial and ventricular septal defects are the most common CHDs in Kabuki syndrome. An increased frequency of left-sided CHDs, including HLHS and Shone’s like complexes had been reported in a clinical review (91), and also, in those with molecular confirmation (89,92). This will likely provide valuable information for ongoing candidate gene mapping for this group of CHDs.

CHARGE Syndrome (*CHD7*)

Whether the CHARGE malformation complex should be termed an association or syndrome (252) was resolved after the discovery of causative mutations in the chromodomain helicase DNA-binding gene (*CHD7*) on chromosome 8q12.1 (138). The cause of CHARGE syndrome is likely to be genetically heterogeneous given that *CHD7* mutations have been found in approximately 65% of patients diagnosed clinically (81,138,253–255). The original diagnostic criteria specified coloboma (usually involving the retina or choroid), CHDs, choanal atresia (membranous or bony), retardation of postnatal growth and development (including hypotonia), brain anomalies, genitourinary anomalies (more commonly recognized in males, including hypogonadotropic hypogonadism), and external ear anomalies (small, square, cupped pinnae) and/or deafness (conduction, sensorineural, mixed) (Fig. 26.8). The mnemonic was updated to highlight the diagnostic value of cranial nerve weakness or palsy (especially facial asymmetry) and hypoplasia of the cochlea and semicircular canals. Oral clefts and neurogenic swallowing problems are now appreciated as supportive of the CHARGE syndrome (253,256). The developmental, behavioral, and personality profile is complex since visual and auditory sensory handicaps exaggerate cognitive limitations and may include some features of autism (252).

CHDs have always been part of the core phenotype, and the availability of molecular testing provides more accurate analysis of a core phenotype. A CHD was present in 92% of *CHD7* mutation-positive and 71% *CHD7* mutation-negative individuals (81). Assorted CHDs have been reported, with conotruncal and aortic arch anomalies consistently overrepresented in clinical series. Features of the DiGeorge phenotype have been observed concurrently in patients with CHARGE syndrome (256). A detailed review of the molecular and phenotypic aspects of CHARGE syndrome found a similar occurrence of CHDs among those who were mutation positive and mutation negative; however, more sophisticated analysis was limited by the incomplete molecular typing (82).

The frequency of the CHARGE syndrome has been reported to range from 1 per 10,000 to 1 per 15,000 live births, although one population-based study estimated a frequency of

Figure 26.8. CHARGE syndrome. The characteristic ear anomalies include pinnae that are severely malformed (A), protruding (B), or small (C), as in this 5-year-old girl with very mild facial features and laryngotracheomalacia. She carries the *CHD7* mutation and had a more severely affected brother, presumably representing gonadal mosaicism. (Courtesy of the parents; Margaret A. Hefner, MS, CGS; and the CHARGE Syndrome Foundation, Inc.)



1 in 8,500 live births (257). Most cases of the CHARGE syndrome are sporadic in occurrence, but autosomal dominant inheritance and germline mosaicism, long clinically suspected, have now been confirmed by molecular testing (81).

Other Common Conditions

Table 26.4 lists syndromes that are presumed to be due to a mendelian gene based on observed family inheritance (e.g., affected siblings with Fryns syndrome suggest autosomal recessive inheritance). Also listed are familiar conditions that have more than one cause, such as heterotaxy, and those that are usually not associated with a single genetic cause such as vertebral defects, anal atresia, cardiac defects, tracheoesophageal fistula, renal anomalies, and limb abnormalities (VACTERL) association or hemifacial microsomia (HFM).

Heterotaxy

Heterotaxy is neither a typical genetic syndrome nor an isolated CHD, but a familiar malformation complex involving defects of right–left axis determination (reviewed by 129). The birth prevalence is approximately 1 in 10,000 (130). Heterotaxy implies that the laterality of thoracoabdominal viscera is neither situs solitus (normal position) nor situs inversus (mirror image). Cardiac, pulmonary, renal, gastrointestinal defects, and minor systemic venous anomalies such as interruption of the inferior vena cava (258) may also be accompanied by midline defects of the brain and face (131). Heterotaxy can, thus, be viewed as a developmental field defect or laterality sequence.

Family studies have been invaluable in delineating the genetic basis of heterotaxy. Kindred in which some members had situs inversus and others had heterotaxy, or when some individuals had isolated CHDs such as transposition of the great arteries or double-outlet right ventricle and others had overt heterotaxy syndrome, suggested that laterality defects represent a developmental spectrum. Recognized risk factors for heterotaxy include maternal insulin-dependent diabetes,

but assorted chromosome abnormalities have also been identified (22,130). The first genetic basis of a laterality disorder was observed in Kartagener syndrome in which situs inversus is accompanied by bronchiectasis, chronic sinusitis, nasal polyps, and infertility due to immotile sperm from impaired ciliary function. Autosomal recessive inheritance, and less commonly, autosomal dominant and X-linked recessive inheritance, have been described in Kartagener syndrome. Genetic heterogeneity is supported by the discovery of mutations in the gene encoding axonemal dynein intermediate chain on chromosome 9p21, with additional loci on 7p21 and 5p14 (259,260). The presence of CHD and heterotaxy in a study of primary ciliary dyskinesia confirmed that they are part of a spectrum, and connected by ciliary dysfunction (261).

Pedigrees with X-linked patterns of inheritance for heterotaxy led to the discovery of the first heterotaxy gene, *ZIC3*, which maps to Xq26.2 (262,263). Many genes have also been found in animal models to participate in the establishment of asymmetry and laterality in the embryo. Several of these genes were tested for mutations in patients with heterotaxy and are implicated as potential disease-related genes including *LEFTY A*, *CRYPTIC/CFC1*, *ACVR2 β* , *NKX2.5*, and *CRELD1* (129,264–269). However, such studies were limited and additional research is needed to define the contribution of these candidate genes to the disease spectrum.

VATER/VATERR/VACTERL Association

The VACTERL association is usually a sporadic occurrence of unknown cause. In rare cases as an association, it can occur in a child with an underlying syndrome, such as trisomy 18 (270) or trisomy 21 (132). The original acronym was VATER to include vertebral anomalies, anal atresia (with or without fistula), tracheoesophageal fistula, and renal dysplasia. Later, radial defects including radial or thumb absence or hypoplasia, and preaxial polydactyly expanded the R. The presence of CHDs, a single umbilical artery, and lower spine anomalies were also included. A general diagnostic guideline required three or more defects to establish the diagnosis (133).

Various types of CHDs have been reported in VACTERL association using traditional clinical series, epidemiologic analyses (133,271), and more recent cluster analysis (132). VACTERL is generally a sporadic occurrence. However, when VACTERL occurs with hydrocephalus (especially due to aqueductal stenosis) and/or is associated with a family history of hydrocephalus, it is viewed as a distinct mendelian disorder (272). Autosomal dominant, X-linked recessive, and autosomal recessive inheritance have been described. Because the VACTERL association is not thought to have a single pathogenetic pathway, it would not be suspected of having a single causative gene. When sonic hedgehog signaling is defective in mice, the pattern of defects resembles VACTERL (273), which may provide insights into the human condition.

Hemifacial Microsomia, Facioauriculovertebral Spectrum, and Oculoauriculovertebral Spectrum, Goldenhar Syndrome

Although Goldenhar syndrome is the most familiar eponym, it is perhaps the least accurate description of what is considered a spectrum of craniofacial anomalies (72). Referring to the complex as possible errors in morphogenesis of the first and second branchial arches is cumbersome though accurate. A practical approach using the acronym OMENS is favored by many plastic surgeons and builds on the fundamental HFM; the additional defects of eye, mandible, ear, nerve, and soft tissue involvement are added (274). Many dysmorphologists prefer the literal terms facioauriculovertebral spectrum and oculoauriculovertebral spectrum (OAVS). A few cases are familial, and autosomal dominant inheritance has been reported. Maternal diabetes is a familiar association (275). Other risk factors that have been studied include vasoactive medications and vascular events (276).

Involvement is usually unilateral with variable hypoplasia of facial structures (including bone, soft tissue, ears, eyes, or mouth). Ear tags or ear pits, epibulbar dermoids (characteristic of Goldenhar syndrome), and deafness are also typical. Oral clefts may involve the lip, palate, and corner of the mouth, creating macrostomia. There can be associated vertebral, radial, or rib defects, as well as renal anomalies and midline brain defects (especially agenesis of the corpus callosum, encephalocele, and lipoma). The breadth of associated anomalies has prompted many descriptions of overlapping complexes (277,278).

The largest single-center review noted CHDs in almost one-third of the 87 patients who were defined as having oculoauriculovertebral spectrum (128). The authors acknowledged the wide range of previously reported frequencies (5% to 58%) and attributed this to the selection bias (clinical series, population-based ascertainment) and the variability in case definition. They reported tetralogy of Fallot and ventricular septal defect in about two-thirds of those with a CHD, but many other CHDs were noted. The increased frequency of conotruncal CHDs has led many investigators to suspect a role for neural crest cell migration in producing the head and neck anomalies.

Genetics of Isolated Congenital Heart Defects: *NKX2.5*, *GATA4*, *NOTCH1*

Little is known about the genetic basis of isolated, nonsyndromic CHDs although they constitute the vast majority of clinical cases. The evaluation of kindred with multiple affected members has begun to identify specific disease genes for isolated CHDs in recent years. In particular, the transcription factors *NKX2.5* and *GATA4*, and the regulator of cell fate, *NOTCH1*, have been identified as disease genes for a small subset of patients with specific types of nonsyndromic CHDs. These findings and the remaining questions are described below.

NKX2.5

Schott et al. (279) identified four families whose affected members most commonly had atrial septal defects and atrioventricular conduction disorders. An informative parametric linkage analysis identified a disease locus on chromosome 5q. The gene, *NKX2.5*, mapped into this locus and was already known to participate in cardiovascular development from animal models. Mutations of *NKX2.5* specific to each family were found in the affected members and were not found in any normal control subjects. Each mutation was predicted to alter the encoded protein function, and most mutations disrupted the highly conserved DNA-binding domain. Subsequent reports identified *NKX2.5* mutations in other sporadic and familial cases with atrioventricular conduction abnormalities with or without atrial septal defects (280,281). These studies not only identified the first disease gene for isolated CHD but also made the surprising discovery that *NKX2.5* was critical to atrioventricular nodal development and function over time.

Multiple subsequent studies report additional *NKX2.5* mutations in familial cases with atrial septal defect and atrioventricular block, as well as sporadic cases with atrioventricular block in the absence of CHD. Studies also report missense mutations of *NKX2.5* in sporadic cases with a variety of CHD without atrioventricular block, including some with conotruncal or left-sided defects; the pathologic significance of such mutations remains to be demonstrated (282–284). These studies suggest that *NKX2.5* plays an important role in a range of CHDs and particularly in atrioventricular conduction.

Though investigations continue, it is clear that patients with atrial septal defects and atrioventricular conduction abnormalities are at risk for having a mutation of *NKX2.5*. It is also clear that those patients with *NKX2.5* mutations who present with first-degree atrioventricular block can progress to complete heart block over time and even sudden cardiac death if the conduction abnormality goes undiagnosed (282). These data suggest that patients with an atrial septal defect warrant assessment by ECG for atrioventricular prolongation. If first-degree atrioventricular block is diagnosed, then periodic evaluation for progression to higher grades of atrioventricular block is indicated, even after surgical repair. It is also important to obtain a detailed family history for signs and symptoms of complete heart block and at times, it may be appropriate to screen immediate family members (first-degree relatives) by ECG for subclinical atrioventricular conduction abnormalities to identify underlying familial disease. Likewise, the immediate family members of a patient with atrioventricular conduction abnormalities with or without other CHDs might warrant similar screening. Mutation studies of *NKX2.5* are now clinically available and help identify the subset of patients with an atrial septal defect at risk for progressive conduction abnormalities.

GATA4

Garg et al. (285) first reported mutations in the transcription factor, *GATA4*, in two kindreds with septal defects: members of the first kindred had atrial septal defects, but members of the second kindred displayed a more heterogeneous phenotype with atrial septal defects, ventricular septal defects, and pulmonary valve stenosis. These findings were of particular interest given that *GATA4*, which maps to chromosome 8p22–p23.1, is a molecular partner with *NKX2.5* and is deleted in some patients with CHDs and chromosome 8p23 deletions. Subsequent investigators have reported *GATA4* mutations in familial cases of septal defects (280,281), and less commonly in sporadic cases with septal defects or other conotruncal defects (280,281,286–288). These findings, in conjunction with those

on *NKX2.5*, highlight the significance of this molecular pathway in cardiovascular development and disease.

NOTCH1

Studies of kindred with multiple affected members continue to identify novel molecular developmental pathways that contribute to cardiovascular disease and development. Most recently, Garg et al. (289) identified mutations in *NOTCH1* in two small families with bicuspid aortic valve and aortic valve stenosis. Of particular interest was that some patients did not have congenital bicuspid aortic valves but developed aortic valve calcification in later decades of life. Experiments confirmed that *NOTCH1* was expressed in the developing aortic valve. Experiments also suggested that *NOTCH1* mutations play a role in aortic valve calcification. Subsequent studies of small patient cohorts report rare *NOTCH1* mutations in sporadic cases with a range of left-sided cardiac defects, including aortic valve stenosis, bicuspid aortic valve, coarctation of the aorta, and HLHS (290–292). Though more work remains to be done to define the affected cohort, these studies highlight the important role of the NOTCH pathway in CHD.

GENETICS OF SPECIFIC CARDIAC LESIONS

The growing body of genetic information now allows the clinician to consider whether a patient with a specific type of CHD has an associated genetic alteration (Table 26.5). The clinician needs to consider whether additional genetic consultation or genetic testing is warranted. For example, mutations in *NKX2.5*, *GATA4*, *MYH6*, and *TBX5* have been identified in patients with atrial septal defects (237,279,285,293). Therefore, one can now consider whether a patient with an atrial septal defect has an associated syndrome (such as Holt-Oram syndrome) or mutation in one of these genes. Clinical testing for mutations in these genes is now available, allowing for improved diagnostics, family screening and genetic counseling, and risk assessment for associated features. Similarly, patients with tetralogy of Fallot may be either syndromic or nonsyndromic and are at risk for different genetic alterations accordingly (14) (Tables 26.1 and 26.5). A patient with tetralogy of Fallot should be carefully evaluated for features of one of the known associated syndromes including trisomy 21, 22q11.2 deletions, and *JAG1* mutations. The family history should be carefully reviewed for CHDs or associated syndromic features that might suggest a 22q11.2 deletion or *JAG1* mutation, for example. Table 26.5 lists known genetic alterations associated with specific CHDs to help the clinician move from the cardiac to a concurrent genetic diagnosis. Since all of these CHDs are genetically heterogeneous, this table can list only the currently known associated disease genes. As new diagnostic tests and clinical discoveries are made, this list is likely to become more extensive and clinically relevant. Of course, many other genetic syndromes associated with each CHD are known; only those with recognized specific genetic alterations are listed here.

GENETIC EVALUATION AND COUNSELING

Although most of the care for a patient with CHD focuses on the diagnosis and treatment of the heart itself, it is critical for the referring primary care provider and the cardiologist to consider whether genetic consultation and counseling is warranted both at the time of diagnosis of the CHD and in later years (139). The chances of finding additional congenital anomalies or syndromic features in a patient with a CHD are

high. Approximately 20% to 25% of infants ≤ 1 year of age have a noncardiac malformation, and approximately 5% to 17% have a genetic syndrome (11,22,294–299). The diagnosis of a genetic syndrome is more likely when growth and developmental delay are also present. Therefore, clinicians must examine the patient with a CHD with a critical eye for dysmorphic features, changes in body habitus, other congenital anomalies, neurocognitive deficits, or a family history of these same findings. It is increasingly evident that one should not ascribe neurocognitive deficits to surgery alone and must consider whether they are a symptom of an underlying genetic alteration instead. Even in the apparent absence of dysmorphic features or other congenital anomalies, patients with certain CHDs should be suspect for genetic syndromes based on the known frequency of such associations. For example, the patient with interrupted aortic arch type B is so commonly found to have a 22q11.2 deletion that referral for genetic consultation and testing should be considered even in the absence of overt dysmorphic features. Finally, given the highly variable and often subtle presentation of many genetic syndromes, a concurrent genetic diagnosis can be easily overlooked or delayed if a high level of suspicion and willingness to seek genetic consultation is not maintained.

Importance of Identifying a Genetic Syndrome or Genomic Imbalance

Identifying the underlying genetic syndrome or alteration in a patient with a CHD is of growing clinical importance. First, diagnosing the patient with a genetic syndrome allows for the early identification and treatment of associated *noncardiac* features. For example, the patient found to carry a 22q11.2 deletion can be evaluated and treated for commonly associated noncardiac features such as feeding disorders, palate anomalies, speech disturbances, hypocalcemia, and others. Knowing that a patient with a CHD has a 22q11.2 deletion may help define the cause of feeding disorders and failure to thrive, which might otherwise be accredited to heart failure alone. Second, establishing a specific genetic cause allows for appropriate family counseling regarding risks of recurrence (297). For example, parents of a patient with Alagille syndrome should be tested to determine if one of the parents is a carrier of a *JAG1* mutation since the parent with only subtle syndromic manifestations carrying the mutation has a 50% chance of having a second affected child. Depending on the age of the individual and circumstances, the geneticist may provide information about prenatal diagnosis including options for imaging the fetal heart and obtaining appropriate genetic tests. Third, establishing a genetic diagnosis in the future will most likely allow more accurate counseling regarding cardiac and noncardiac clinical outcome. Several studies already suggest that specific genetic syndromes are associated with a worse clinical cardiac prognosis (1–4). Finally, for many patients and their families, knowing whether a CHD is associated with an identifiable cause such as a chromosome abnormality, gene mutation, or genetic risk factor can be important. Ultimately, determining the patient genetic phenotype is essential to provide more accurate clinical care, estimation of prognosis, and assessment of risk (Table I in (295)). In the future, genotype may influence management strategy.

When to Refer the Cardiac Patient for a Genetics Evaluation

The increasing number of possible genetic diagnoses and the rapid development of new genetic tests necessitate a close collaboration between the referring primary physician,

TABLE 26.5

Disease Loci or Genes Associated with Specific CHDs Known to Date

Congenital Heart Defect	Associated Genetic Loci or Disease Genes^a
Atrial septal defect (with or without atrioventricular conduction blockade)	<i>TBX5</i> (Holt-Oram syndrome) <i>NKX2.5</i>
Atrial septal defect (without atrioventricular conduction blockade)	<i>GATA4</i> <i>MYH6</i>
Perimembranous ventricular septal defect	<i>TBX5</i> (Holt-Oram syndrome) <i>GATA4</i> 22q11.2 deletion Many syndromes including trisomy 21
Tetralogy of Fallot	<i>NKX2.5</i> <i>JAG1</i> (Alagille syndrome) <i>PTPN11</i> (Noonan syndrome) 22q11.2 deletion Many syndromes including trisomy 21
Truncus arteriosus	22q11.2 deletion
Interrupted aortic arch	22q11.2 deletion
Patent ductus arteriosus	<i>TFAP2β</i> (Char syndrome)
Atrioventricular septal defect	<i>CRELD1</i> 1p 8p23 Trisomy 21 (21q22)
Heterotaxy syndrome	<i>ZIC3</i> <i>CFC1</i> <i>ACVR2B</i> <i>Lefty2</i>
Valvar pulmonary stenosis	<i>JAG1</i> (Alagille syndrome) <i>PTPN11</i> <i>KRAS</i> <i>SOS1</i> (Noonan syndrome) <i>HRAS</i> (Costello syndrome) <i>BRAF</i> , <i>MEK1/2</i> (CFC syndrome)
Supravalvar aortic stenosis	<i>ELN</i>
Aortic valve stenosis/Bicuspid aortic valve	<i>NOTCH1</i>

^aSee text for relevant references.

cardiologist, and clinical geneticist (139). Much depends on the cardiologist's diagnostic ability, interest, and time to determine if a CHD is isolated, part of a familial CHD syndrome, or associated with other defects of a known syndrome or as of yet uncharacterized complex (153). Consultation from a clinical geneticist should be sought for the cardiac patient with the following: dysmorphic features, multiple congenital anomalies, neurocognitive deficits, or a family history of CHD, congenital anomalies, or neurocognitive deficits. Although, historically, learning disabilities or developmental delay have often been attributed to the cardiac defect and surgical intervention, these observations may instead prove to be independent problems that may indicate the presence of a genetic syndrome or chromosomal alteration. Families may also benefit from a genetic consultation for counseling purposes, particularly with respect to risks of recurrence. Early referral to a clinical geneticist allows the early diagnosis of associated noncardiac features, as well as early intervention and timely counseling. Finally, sometimes the primary care taker or cardiologist orders the basic genetic tests to screen for abnormalities with the intention

of consulting genetics if an abnormality is discovered. However, this practice may greatly underserve the patient with no detectable chromosomal alteration who nonetheless may have a genetic syndrome or the patient who could benefit from more specialized genetic testing. In addition, the number of clinically available genetic tests has increased remarkably in the last five years, ranging from single-gene mutation studies to genome-wide scans. As such genetic testing has become increasingly complex and requires the ordering physician to be ever more knowledgeable. Thus, genetic consultation should be considered in the suspicious patient to allow for specialized assessment and direction of genetic testing.

The Genetic Evaluation

The goal of the genetic evaluation is to establish a diagnosis and provide information to the patient and family about recurrence risk and expected outcomes that are known (297). The evaluation therefore considers both the patient under

evaluation and the family medical history in detail. Geneticists will first consider the specific type of CHD and associated congenital anomalies present in the patient. The geneticist (or genetic counselor) then obtains a complete family history of malformations and genetic conditions, including malformation syndromes (297). Information is also sought about recurrent miscarriages, sudden death in childhood, developmental delay, and mental retardation.

The geneticist's physical exam begins with an overall appraisal of habitus, facial appearance, and movements. Occasionally when an immediate general impression based on characteristic dysmorphic features provides rapid diagnosis, restraint and confirmation is needed. In addition to height, weight, and head circumference, measurements may be made of facial landmarks and distances, or other body parts to quantify the qualitative sense of hypertelorism, small pinnae, or long fingers. Most geneticists do not perform complete neurodevelopmental examinations, substituting modified office screening tests, reports from family members, previous formal testing, or functional appraisal of the individual's interactions and performance in the office setting.

Depending on whether the consultation is performed during an admission to the hospital or as an outpatient visit, emergently or as a scheduled visit, and whether the location is the tertiary care center or a small satellite clinic, diagnostic testing can be performed at the same time as the initial evaluation or requested to be obtained under the direction of the primary care giver and/or cardiologist. Radiographic and ultrasonographic tests may be ordered to define internal organ structure and function. Medical, educational, and therapeutic specialists may be requested to characterize multisystem involvement and to begin treatment.

Genetic Testing

Historically, the most commonly requested genetics test was a cytogenetic examination ordered as a karyotype of lymphocytes in fresh whole blood. A FISH analysis became complementary to a standard chromosome analysis, which was useful for rapid diagnosis (e.g., amniocentesis diagnosis of trisomy) and the detection of small deletions. Microarray technologies offer the most recent technique for detecting an alteration of DNA quantity and have become the test of choice to detect chromosomal deletions and duplications (137), although a standard karyotype is still necessary to detect mosaicism and chromosomal translocation. More rapid techniques to detect single nucleotide mutation in a panel of genes are also now available.

When a mendelian gene disorder is suspected, geneticists determine if molecular testing is available and whether the testing is being done at a research or clinical lab. Details are sought from the referral laboratory and literature. Before testing can be done, the genetics team needs to know if the laboratory is approved to report clinical results, how specimens are shipped, the cost and potential for reimbursement by insurance, the length of time it takes to complete the test, and how results are communicated. This process can consume as much time as the genetics examination itself.

Practically speaking, the timing and location of having these tests completed may be determined more by medical insurance coverage and less by referring physician or patient preference. Likewise, whether the individual will be permitted to return for a follow-up genetics visit is highly dependent on health care coverage. Regardless of whether the genetics evaluation was conducted on a critically ill neonate on an emergent basis, or during an extensive consultation with the extended family of multiply affected individuals, communication and collaboration with the cardiologist are essential. Of course,

the primary care physician and the individual (and family) should be included in all discussions.

A Partnership

Since approximately 75% of CHDs currently have no identifiable cause (11,22,154,294,296,298,299) or underlying condition, the notion of a formal genetic evaluation may appear to be unnecessary in many cases. However, the list of genetic causes of CHDs is expanding rapidly and is ever more difficult to understand, and many syndromes are now recognized to present with subtle and often unrecognized features. Moreover, options for clinical genetic testing are rapidly evolving and increasingly complicated. As the list of genetic causes and tests for CHDs continues to expand in length and complexity, and the list of genetic syndromes associated with CHDs grows as well, there is clearly a need for clinical partnership between primary caretakers, cardiologists, and geneticists. In many cases, the primary care taker and cardiologist will call on the geneticist for consultation as described in the previous sections. For example, when coarctation is confirmed in a young girl who is noted subsequently to have short stature, redundant neck skin, and low-set ears, the geneticist can confirm the suspected diagnosis of Turner syndrome and provide long-term counseling to the patient and family. In other cases, the geneticist may call upon the cardiologist to define the associated CHD in a patient under consideration for a particular genetic syndrome to assist with the diagnosis. For example, a geneticist may consider the diagnosis of Holt-Oram syndrome in a three-generation family with absent and unusual thumbs. Although *TBX5* mutation studies would be confirmatory, speedier diagnostic support would be provided by two-dimensional echocardiographic detection of a secundum atrial septal defect in mother and son.

It can be difficult to coordinate the cardiology and genetics consultations (295). Instead of being evaluated at different times, some patients are seen in cardiovascular genetics clinics with genetics and cardiology specialists working in tandem. With the assistance of supplemental imaging of other organs; confirmatory cytogenetic, molecular, or metabolic blood tests; and the proven test of time, clinicians may make a unifying diagnosis to enhance each case.

CONCLUSIONS

In concert with the field of human genetics, our understanding of the genetic contribution to CHDs has advanced dramatically over the last 10 years. The field has moved from detailing genetic syndromes to the definition of specific genetic alterations causing those clinical phenotypes. Specific genetic causes of isolated CHDs have also begun to be identified. The remarkable and rapid advancements in human genetics and developmental biology are likely to lead to new discoveries in the field of cardiovascular genetics in the near future. Given these discoveries, an increasing number of patients with a CHD could be given a concurrent genetic diagnosis. It will be of increasing importance for the cardiologist caring for patients with CHDs to have a working knowledge of these discoveries and available genetic testing. It will also be increasingly important for the general pediatrician and cardiologist to work in concert with the clinical geneticists and genetic counselors to identify concurrent genetic diagnoses. The clinical implications of the associated genetic diagnosis, such as associated noncardiac features, will be increasingly important to recognize and address. Already, genotype-specific management strategies have been developed in many fields and will

inform that of pediatric cardiology in the near future. The association between genotype and clinical outcome is also well established (1–4) and will play an increasingly important role in counseling. Most important, understanding the genetic basis of these disorders, in conjunction with advances in developmental biology, will improve our understanding of cardiovascular development and disease and allow for novel, improved management strategies (300).

REFERENCES

- Mahle WT, Crisalli J, Coleman K, et al. Deletion of chromosome 22q11.2 and outcome in patients with pulmonary atresia and ventricular septal defect. *Ann Thorac Surg* 2003;76:567–571.
- Gaynor JW, Mahle WT, Cohen MI, et al. Risk factors for mortality after the Norwood procedure. *Eur J Cardiothorac Surg* 2002;22:82–89.
- Michielon G, Marino B, Formigari R, et al. Genetic syndromes and outcome after surgical correction of tetralogy of Fallot. *Ann Thorac Surg* 2006;81:968–975.
- Anaclerio S, Di Ciommo V, Michielon G, et al. Conotruncal heart defects: impact of genetic syndromes on immediate operative mortality. *Ital Heart J* 2004;5:624–628.
- Pierpont ME, Basson CT, Benson DW Jr, et al. Genetic basis for congenital heart defects: current knowledge: a scientific statement from the American Heart Association Congenital Cardiac Defects Committee, Council on Cardiovascular Disease in the Young: endorsed by the American Academy of Pediatrics. *Circulation* 2007;115:3015–3038.
- Jenkins KJ, Correa A, Feinstein JA, et al. Noninherited risk factors and congenital cardiovascular defects: current knowledge: a scientific statement from the American Heart Association Council on Cardiovascular Disease in the Young: endorsed by the American Academy of Pediatrics. *Circulation* 2007;115:2995–3014.
- Cripe L, Andelfinger G, Martin LJ, et al. Bicuspid aortic valve is heritable. *J Am Coll Cardiol* 2004;44:138–143.
- Lewin MB, McBride KL, Pignatelli R, et al. Echocardiographic evaluation of asymptomatic parental and sibling cardiovascular anomalies associated with congenital left ventricular outflow tract lesions. *Pediatrics* 2004;114:691–696.
- Loffredo CA, Chokkalingam A, Sill AM, et al. Prevalence of congenital cardiovascular malformations among relatives of infants with hypoplastic left heart, coarctation of the aorta, and d-transposition of the great arteries. *Am J Med Genet A* 2004;124:225–230.
- Boughman JA, Berg KA, Astemborski JA, et al. Familial risks of congenital heart defect assessed in a population-based epidemiologic study. *Am J Med Genet* 1987;26:839–849.
- Hanna EJ, Nevin NC, Nelson J. Genetic study of congenital heart defects in Northern Ireland (1974–1978). *J Med Genet* 1994;31:858–863.
- Calzolari E, Garani G, Cocchi G, et al. Congenital heart defects: 15 years of experience of the Emilia-Romagna Registry (Italy). *Eur J Epidemiol* 2003;18:773–780.
- Nora JJ, Nora AH. Update on counseling the family with a first-degree relative with a congenital heart defect. *Am J Med Genet* 1988;29:137–142.
- Rauch R, Hofbeck M, Zweier C, et al. Comprehensive genotype-phenotype analysis in 230 patients with tetralogy of Fallot. *J Med Genet* 2010;47:321–331.
- Musewe NN, Alexander DJ, Teshima I, et al. Echocardiographic evaluation of the spectrum of cardiac anomalies associated with trisomy 13 and trisomy 18. *J Am Coll Cardiol* 1990;15:673–677.
- Rasmussen SA, Wong LY, Yang Q, et al. Population-based analyses of mortality in trisomy 13 and trisomy 18. *Pediatrics* 2003;111:777–784.
- Lehman CD, Nyberg DA, Winter TC III, et al. Trisomy 13 syndrome: prenatal US findings in a review of 33 cases. *Radiology* 1995;194:217–222.
- Muneuchi J, Yamamoto J, Takahashi Y, et al. Outcomes of cardiac surgery in trisomy 18 patients. *Cardiol Young* 2011;21:209–215.
- Balderston SM, Shaffer EM, Washington RL, et al. Congenital polyvalvular disease in trisomy 18: echocardiographic diagnosis. *Pediatr Cardiol* 1990;11:138–142.
- Van Praagh S, Truman T, Firpo A, et al. Cardiac malformations in trisomy-18: a study of 41 postmortem cases. *J Am Coll Cardiol* 1989;13:1586–1597.
- Embleton ND, Wyllie JP, Wright MJ, et al. Natural history of trisomy 18. *Arch Dis Child Fetal Neonatal Ed* 1996;75:F38–F41.
- Ferencz C, Loffredo CA, Correa-Villasenor A, et al. *Genetic and Environmental Risk Factors of Major Congenital Heart Defects: The Baltimore-Washington Infant Study: 1981–1989*. Armonk, NY: Futura Publishing Company Inc., 1997.
- Freeman SB, Bean LH, Allen EG, et al. Ethnicity, sex, and the incidence of congenital heart defects: a report from the National Down Syndrome Project. *Genet Med* 2008;10:173–180.
- McElhinney DB, Straka M, Goldmuntz E, et al. Correlation between abnormal cardiac physical examination and echocardiographic findings in neonates with Down syndrome. *Am J Med Genet* 2002;113:238–241.
- Mazzanti L, Cacciari E. Congenital heart disease in patients with Turner's syndrome. Italian Study Group for Turner Syndrome (ISGTS). *J Pediatr* 1998;133:688–692.
- Loscalzo ML, Van PL, Ho VB, et al. Association between fetal lymphedema and congenital cardiovascular defects in Turner syndrome. *Pediatrics* 2005;115:732–735.
- Ho VB, Bakalov VK, Cooley M, et al. Major vascular anomalies in Turner syndrome: prevalence and magnetic resonance angiographic features. *Circulation* 2004;110:1694–1700.
- Bondy CA. Care of girls and women with Turner syndrome: a guideline of the Turner Syndrome Study Group. *J Clin Endocrinol Metab* 2007;92:10–25.
- Gravholt CH, Landin-Wilhelmsen K, Stochholm K, et al. Clinical and epidemiological description of aortic dissection in Turner's syndrome. *Cardiol Young* 2006;16:430–436.
- van den Berg J, Bannink EM, Wielopolski PA, et al. Aortic distensibility and dimensions and the effects of growth hormone treatment in the turner syndrome. *Am J Cardiol* 2006;97:1644–1649.
- Bondy CA, Van PL, Bakalov VK, et al. Growth hormone treatment and aortic dimensions in Turner syndrome. *J Clin Endocrinol Metab* 2006;91:1785–1788.
- Bondy CA, Ceniceros I, Van PL, et al. Prolonged rate-corrected QT interval and other electrocardiogram abnormalities in girls with Turner syndrome. *Pediatrics* 2006;118:e1220–e1225.
- Battaglia A, Hoyne HE, Dallapiccola B, et al. Further delineation of deletion 1p36 syndrome in 60 patients: a recognizable phenotype and common cause of developmental delay and mental retardation. *Pediatrics* 2008;121:404–410.
- Gajacka M, Mackay KL, Shaffer LG. Monosomy 1p36 deletion syndrome. *Am J Med Genet C Semin Med Genet* 2007;145C:346–356.
- Dod HS, Bhardwaj R, Hummel M, et al. Left ventricular noncompaction: a rare disorder in adults and its association with 1p36 chromosomal anomaly. *Am J Med Genet A* 2010;152:191–195.
- Green EK, Priestley MD, Waters J, et al. Detailed mapping of a congenital heart disease gene in chromosome 3p25. *J Med Genet* 2000;37:581–587.
- Malhotra A, Bergman P, Brown J, et al. Congenital hypothyroidism in association with chromosome 3p25.3-pter deletion. *J Pediatr Endocrinol Metab* 2011;24:787–788.
- Gunnarsson C, Foyn Bruun C. Molecular characterization and clinical features of a patient with an interstitial deletion of 3p25.3-p26.1. *Am J Med Genet A* 2010;152A:3110–3114.
- Shuib S, McMullan D, Rattenberry E, et al. Microarray based analysis of 3p25-p26 deletions (3p- syndrome). *Am J Med Genet A* 2009;149A:2099–2105.
- Faas BH, De Vries BB, Van Es-Van Gaal J, et al. A new case of dup(3q) syndrome due to a pure duplication of 3qter. *Clin Genet* 2002;62:315–320.
- Grossmann V, Muller D, Muller W, et al. "Essentially" pure trisomy 3q27 → qter: further delineation of the partial trisomy 3q phenotype. *Am J Med Genet A* 2009;149:2522–2526.
- Battaglia A, Carey JC, Wright TJ. Wolf-Hirschhorn (4p-) syndrome. *Adv Pediatr* 2001;48:75–113.
- Huang T, Lin AE, Cox GF, et al. Cardiac phenotypes in chromosome 4q-syndrome with and without a deletion of the dHAND gene. *Genet Med* 2002;4:464–467.
- Rossi MR, DiMaio MS, Xiang B, et al. Clinical and genomic characterization of distal duplications and deletions of chromosome 4q: study of two cases and review of the literature. *Am J Med Genet A* 2009;149A:2788–2794.
- Hills C, Moller JH, Finkelstein M, et al. Cri du chat syndrome and congenital heart disease: a review of previously reported cases and presentation of an additional 21 cases from the Pediatric Cardiac Care Consortium. *Pediatrics* 2006;117:e924–e927.
- Smoot L, Zhang H, Klaiman C, et al. Medical Overview and genetics of Williams-Beuren syndrome. *Prog Pediatr Cardiol* 2005;20:195–205.
- Wat MJ, Shchelochkov OA, Holder AM, et al. Chromosome 8p23.1 deletions as a cause of complex congenital heart defects and diaphragmatic hernia. *Am J Med Genet A* 2009;149A:1661–1677.
- Ballarati L, Cereda A, Caselli R, et al. Genotype-phenotype correlations in a new case of 8p23.1 deletion and review of the literature. *Eur J Med Genet* 2011;54:55–59.
- Pehlivan T, Pober BR, Brueckner M, et al. GATA4 haploinsufficiency in patients with interstitial deletion of chromosome region 8p23.1 and congenital heart disease. *Am J Med Genet* 1999;83:201–206.
- Devriendt K, Matthijs G, Van Dael R, et al. Delineation of the critical deletion region for congenital heart defects, on chromosome 8p23.1. *Am J Hum Genet* 1999;64:1119–1126.
- Blinder JJ, Martinez HR, Craigen WJ, et al. Noncompaction of the left ventricular myocardium in a boy with a novel chromosome 8p23.1 deletion. *Am J Med Genet A* 2011;155:2215–2220.
- Digilio MC, Angioni A, Giannotti A, et al. Truncus arteriosus and duplication 8q. *Am J Med Genet A* 2003;121:79–81.
- Wheeler PG. 8q23-q24 duplication—further delineation of a rare chromosomal abnormality. *Am J Med Genet A* 2010;152:459–463.
- Kawara H, Yamamoto T, Harada N, et al. Narrowing candidate region for monosomy 9p syndrome to a 4.7-Mb segment at 9p22.2-p23. *Am J Med Genet A* 2006;140:373–377.

55. Hauge X, Raca G, Cooper S, et al. Detailed characterization of, and clinical correlations in, 10 patients with distal deletions of chromosome 9p. *Genet Med* 2008;10:599–611.
56. Lindstrand A, Malmgren H, Verri A, et al. Molecular and clinical characterization of patients with overlapping 10p deletions. *Am J Med Genet A* 2010;152:1233–1243.
57. Van Esch H, Groenen P, Frys JP, et al. The phenotypic spectrum of the 10p deletion syndrome versus the classical DiGeorge syndrome. *Genet Couns* 1999;10:59–65.
58. Grossfeld PD, Mattina T, Lai Z, et al. The 11q terminal deletion disorder: a prospective study of 110 cases. *Am J Med Genet A* 2004;129:51–61.
59. Edelman EA, Girirajan S, Finucane B, et al. Gender, genotype, and phenotype differences in Smith-Magenis syndrome: a meta-analysis of 105 cases. *Clin Genet* 2007;71:540–550.
60. Girirajan S, Vlangos CN, Szomju BB, et al. Genotype-phenotype correlation in Smith-Magenis syndrome: evidence that multiple genes in 17p11.2 contribute to the clinical spectrum. *Genet Med* 2006;8:417–427.
61. Cody JD, Ghidoni PD, DuPont BR, et al. Congenital anomalies and anthropometry of 42 individuals with deletions of chromosome 18q. *Am J Med Genet* 1999;85:455–462.
62. Linnankivi T, Tienari P, Somer M, et al. 18q deletions: clinical, molecular, and brain MRI findings of 14 individuals. *Am J Med Genet A* 2006;140:331–339.
63. Cody JD, Heard PL, Crandall AC, et al. Narrowing critical regions and determining penetrance for selected 18q- phenotypes. *Am J Med Genet A* 2009;149:1421–1430.
64. Berends MJ, Tan-Sindhunata G, Leegte B, et al. Phenotypic variability of Cat-Eye syndrome. *Genet Couns* 2001;12:23–34.
65. Lin AE, Bernar J, Chin AJ, et al. Congenital heart disease in supernumerary der(22),t(11;22) syndrome. *Clin Genet* 1986;29:269–275.
66. Carter MT, St Pierre SA, Zackai EH, et al. Phenotypic delineation of Emanuel syndrome (supernumerary derivative 22 syndrome): clinical features of 63 individuals. *Am J Med Genet A* 2009;149:1712–1721.
67. Goldmuntz E. DiGeorge syndrome: new insights. *Clin Perinatol* 2005;32:963–978, ix–x.
68. Ryan AK, Goodship JA, Wilson DI, et al. Spectrum of clinical features associated with interstitial chromosome 22q11 deletions: a European collaborative study. *J Med Genet* 1997;34:798–804.
69. McDonald-McGinn DM, LaRossa D, Goldmuntz E, et al. The 22q11.2 deletion: screening, diagnostic workup, and outcome of results; report on 181 patients. *Genet Test* 1997;1:99–108.
70. Goldmuntz E, Clark BJ, Mitchell LE, et al. Frequency of 22q11 deletions in patients with conotruncal defects. *J Am Coll Cardiol* 1998;32:492–498.
71. Momba K. Cardiovascular anomalies associated with chromosome 22q11.2 deletion syndrome. *Am J Cardiol* 2010;105:1617–1624.
72. Jones KL. *Smith's Recognizable Patterns of Human Malformation*. 6th ed. Philadelphia, PA: Elsevier Sanders, 2006.
73. Gorlin RJ, Cohen MM, Hennekam RCM. *Syndromes of the Head and Neck*. 4th ed. Oxford, New York: Oxford University Press, 2001.
74. McDaniel R, Warthen DM, Sanchez-Lara PA, et al. NOTCH2 mutations cause Alagille syndrome, a heterogeneous disorder of the notch signaling pathway. *Am J Hum Genet* 2006;79:169–173.
75. Goldmuntz E, Moore E, Spinner NB. The cardiovascular manifestations of Alagille syndrome and JAG1 mutations. *Methods Mol Med* 2006;126:217–231.
76. Tidyman WE, Rauen KA. Noonan, Costello and cardio-facio-cutaneous syndromes: dysregulation of the Ras-MAPK pathway. *Expert Rev Mol Med* 2008;10:e37.
77. Rodriguez-Viciana P, Tetsu O, Tidyman WE, et al. Germline mutations in genes within the MAPK pathway cause cardio-facio-cutaneous syndrome. *Science* 2006;311:1287–1290.
78. Niihori T, Aoki Y, Narumi Y, et al. Germline KRAS and BRAF mutations in cardio-facio-cutaneous syndrome. *Nat Genet* 2006;38:294–296.
79. Zhao F, Weismann CG, Satoda M, et al. Novel TFAP2B mutations that cause Char syndrome provide a genotype-phenotype correlation. *Am J Hum Genet* 2001;69:695–703.
80. Sweeney E, Fryer A, Walters M. Char syndrome: a new family and review of the literature emphasising the presence of symphalangism and the variable phenotype. *Clin Dysmorphol* 2000;9:177–182.
81. Lalani SR, Safiullah AM, Fernbach SD, et al. Spectrum of CHD7 Mutations in 110 Individuals with CHARGE Syndrome and Genotype-Phenotype Correlation. *Am J Hum Genet* 2006;78:303–314.
82. Zentner GE, Layman WS, Martin DM, et al. Molecular and phenotypic aspects of CHD7 mutation in CHARGE syndrome. *Am J Med Genet A* 2010;152:674–686.
83. Oliver C, Bedeschi MF, Blagowidow N, et al. Cornelia de Lange syndrome: extending the physical and psychological phenotype. *Am J Med Genet A* 2010;152:1127–1135.
84. Limongelli G, Russo S, Digilio MC, et al. Hypertrophic cardiomyopathy in a girl with Cornelia de Lange syndrome due to mutation in SMC1A. *Am J Med Genet A* 2010;152:2127–2129.
85. Jackson L, Kline AD, Barr MA, et al. de Lange syndrome: a clinical review of 310 individuals. *Am J Med Genet* 1993;47:940–946.
86. Lin AE, Alexander ME, Colan SD, et al. Clinical, pathological, and molecular analyses of cardiovascular abnormalities in Costello syndrome: a Ras/MAPK pathway syndrome. *Am J Med Genet A* 2011;155:486–507.
87. Sletten LJ, Pierpont ME. Variation in severity of cardiac disease in Holt-Oram syndrome. *Am J Med Genet* 1996;65:128–132.
88. McDermott DA, Bressan MC, He J, et al. TBX5 genetic testing validates strict clinical criteria for Holt-Oram syndrome. *Pediatr Res* 2005;58:981–986.
89. Ng SB, Bigham AW, Buckingham KJ, et al. Exome sequencing identifies MLL2 mutations as a cause of Kabuki syndrome. *Nat Genet* 2010;42:790–793.
90. Paulussen AD, Stegmann AP, Blok MJ, et al. MLL2 mutation spectrum in 45 patients with Kabuki syndrome. *Hum Mutat* 2011;32:E2018–E2025.
91. Armstrong L, Abd El Moneim A, Aleck K, et al. Further delineation of Kabuki syndrome in 48 well-defined new individuals. *Am J Med Genet A* 2005;132:265–272.
92. Digilio MC, Baban A, Marino B, et al. Hypoplastic left heart syndrome in patients with Kabuki syndrome. *Pediatr Cardiol* 2010;31:1111–1113.
93. Digilio MC, Conti E, Sarkozy A, et al. Grouping of multiple-lentiginos/LEOPARD and Noonan syndromes on the PTPN11 gene. *Am J Hum Genet* 2002;71:389–394.
94. Limongelli G, Sarkozy A, Pacileo G, et al. Genotype-phenotype analysis and natural history of left ventricular hypertrophy in LEOPARD syndrome. *Am J Med Genet A* 2008;146:620–628.
95. Limongelli G, Pacileo G, Marino B, et al. Prevalence and clinical significance of cardiovascular abnormalities in patients with the LEOPARD syndrome. *Am J Cardiol* 2007;100:736–741.
96. Lin AE, Birch PH, Korf BR, et al. Cardiovascular malformations and other cardiovascular abnormalities in neurofibromatosis 1. *Am J Med Genet* 2000;95:108–117.
97. Friedman JM, Arbiser J, Epstein JA, et al. Cardiovascular disease in neurofibromatosis 1: report of the NF1 Cardiovascular Task Force. *Genet Med* 2002;4:105–111.
98. Romano AA, Allanson JE, Dahlgren J, et al. Noonan syndrome: clinical features, diagnosis, and management guidelines. *Pediatrics* 2010;126:746–759.
99. Tartaglia M, Mehler EL, Goldberg R, et al. Mutations in PTPN11, encoding the protein tyrosine phosphatase SHP-2, cause Noonan syndrome. *Nat Genet* 2001;29:465–468.
100. Tartaglia M, Kalidas K, Shaw A, et al. PTPN11 mutations in Noonan syndrome: molecular spectrum, genotype-phenotype correlation, and phenotypic heterogeneity. *Am J Hum Genet* 2002;70:1555–1563.
101. Marino B, Digilio MC, Toscano A, et al. Congenital heart diseases in children with Noonan syndrome: an expanded cardiac spectrum with high prevalence of atrioventricular canal. *J Pediatr* 1999;135:703–706.
102. Sarkozy A, Obregon MG, Conti E, et al. A novel PTPN11 gene mutation bridges Noonan syndrome, multiple lentiginos/LEOPARD syndrome and Noonan-like/multiple giant cell lesion syndrome. *Eur J Hum Genet* 2004;12:1069–1072.
103. Roberts AE, Araki T, Swanson KD, et al. Germline gain-of-function mutations in SOS1 cause Noonan syndrome. *Nat Genet* 2007;39:70–74.
104. Zenker M, Lehmann K, Schulz AL, et al. Expansion of the genotypic and phenotypic spectrum in patients with KRAS germline mutations. *J Med Genet* 2007;44:131–135.
105. Schorry EK, Keddache M, Lanphear N, et al. Genotype-phenotype correlations in Rubinstein-Taybi syndrome. *Am J Med Genet A* 2008;146:2512–2519.
106. Stevens CA, Bhakta MG. Cardiac abnormalities in the Rubinstein-Taybi syndrome. *Am J Med Genet* 1995;59:346–348.
107. Surka WS, Kohlhasse J, Neuner CE, et al. Unique family with Townes-Brocks syndrome, SALL1 mutation, and cardiac defects. *Am J Med Genet* 2001;102:250–257.
108. Digilio MC, Marino B, Ammirati A, et al. Cardiac malformations in patients with oral-facial-skeletal syndromes: clinical similarities with heterotaxia. *Am J Med Genet* 1999;84:350–356.
109. O'Connor MJ, Rider NL, Thomas Collins R, et al. Contemporary management of congenital malformations of the heart in infants with Ellis-van Creveld syndrome: a report of nine cases. *Cardiol Young* 2011;21:145–152.
110. Ulucan H, Gul D, Sapp JC, et al. Extending the spectrum of Ellis van Creveld syndrome: a large family with a mild mutation in the EVC gene. *BMC Med Genet* 2008;9:92.
111. Hur DJ, Raymond GV, Kahler SG, et al. A novel MGP mutation in a consanguineous family: review of the clinical and molecular characteristics of Keutel syndrome. *Am J Med Genet A* 2005;135:36–40.
112. Teebi AS, Lambert DM, Kaye GM, et al. Keutel syndrome: further characterization and review. *Am J Med Genet* 1998;78:182–187.
113. Kumar D, Primhak RA, Kumar A. Variable phenotype in Kaufman-McKusick syndrome: report of an inbred Muslim family and review of the literature. *Clin Dysmorphol* 1998;7:163–170.
114. Slavotinek AM, Biesecker LG. Phenotypic overlap of McKusick-Kaufman syndrome with bardet-biedl syndrome: a literature review. *Am J Med Genet* 2000;95:208–215.
115. Digilio MC, Marino B, Giannotti A, et al. Specific congenital heart defects in RSH/Smith-Lemli-Opitz syndrome: postulated involvement of the sonic hedgehog pathway in syndromes with postaxial polydactyly or heterotaxia. *Birth Defects Res A Clin Mol Teratol* 2003;67:149–153.
116. Lin AE, Ardinger HH, Ardinger RH Jr, et al. Cardiovascular malformations in Smith-Lemli-Opitz syndrome. *Am J Med Genet* 1997;68:270–278.

117. Lin AE, Neri G, Hughes-Benzie R, et al. Cardiac anomalies in the Simpson-Golabi-Beihmel syndrome. *Am J Med Genet* 1999;83:378–381.
118. Lin AE, Belmont J, Malik S. Heart. In: Stevenson RE, Hall JG, eds. *Human Malformations and Related Anomalies*. 2nd ed. New York, NY: Oxford University Press, 2006:85–120.
119. Lin AE, Ardinger HH. Genetic epidemiology and an overview of the genetics of congenital heart defects. *Prog Pediatr Cardiol* 2005;20:113–126.
120. Lin AE, Westgate MN, van der Velde ME, et al. Adams-Oliver syndrome associated with cardiovascular malformations. *Clin Dysmorphol* 1998;7:235–241.
121. Maniscalco M, Zedda A, Faraone S, et al. Association of Adams-Oliver syndrome with pulmonary arterio-venous malformation in the same family: a further support to the vascular hypothesis. *Am J Med Genet A* 2005;136:269–274.
122. Lin AE, Pober BR, Mullen MP, et al. Cardiovascular malformations in Fryns syndrome: is there a pathogenic role for neural crest cells? *Am J Med Genet A* 2005;139:186–193.
123. Mee L, Honkala H, Kopra O, et al. Hydroletharus syndrome is caused by a missense mutation in a novel gene *HYLS1*. *Hum Mol Genet* 2005;14:1475–1488.
124. Visapaa I, Salonen R, Varilo T, et al. Assignment of the locus for hydroletharus syndrome to a highly restricted region on 11q23–25. *Am J Hum Genet* 1999;65:1086–1095.
125. Leonardi ML, Pai GS, Wilkes B, et al. Ritscher-Schinzel cranio-cerebellocardiac (3C) syndrome: report of four new cases and review. *Am J Med Genet* 2001;102:237–242.
126. Bronzetti G, Giardini A, Patrizi A, et al. Ipsilateral hemangioma and aortic arch anomalies in posterior fossa malformations, hemangiomas, arterial anomalies, coarctation of the aorta, and cardiac defects and eye abnormalities (PHACE) anomaly: report and review. *Pediatrics* 2004;113:412–415.
127. Rao RP, Drolet BA, Holland KE, et al. PHACES association: a vasculocutaneous syndrome. *Pediatr Cardiol* 2008;29:793–799.
128. Digilio MC, Calzolari F, Capolino R, et al. Congenital heart defects in patients with oculo-auriculo-vertebral spectrum (Goldenhar syndrome). *Am J Med Genet A* 2008;146:1815–1819.
129. Zhu L, Belmont JW, Ware SM. Genetics of human heterotaxias. *Eur J Hum Genet* 2006;14:17–25.
130. Lin AE, Ticho BS, Houde K, et al. Heterotaxy: associated conditions and hospital-based prevalence in newborns. *Genet Med* 2000;2:157–172.
131. Ticho BS, Goldstein AM, Van Praagh R. Extracardiac anomalies in the heterotaxy syndromes with focus on anomalies of midline-associated structures. *Am J Cardiol* 2000;85:729–734.
132. Solomon BD, Pineda-Alvarez DE, Raam MS, et al. Analysis of component findings in 79 patients diagnosed with VACTERL association. *Am J Med Genet A* 2010;152:2236–2244.
133. Botto LD, Khoury MJ, Mastroiacovo P, et al. The spectrum of congenital anomalies of the VATER association: an international study. *Am J Med Genet* 1997;71:8–15.
134. Feuk L, Carson AR, Scherer SW. Structural variation in the human genome. *Nat Rev Genet* 2006;7:85–97.
135. Ledbetter DH. Cytogenetic technology—genotype and phenotype. *N Engl J Med* 2008;359:1728–1730.
136. Vissers LE, de Vries BB, Veltman JA. Genomic microarrays in mental retardation: from copy number variation to gene, from research to diagnosis. *J Med Genet* 2010;47:289–297.
137. Miller DT, Adam MP, Aradhya S, et al. Consensus statement: chromosomal microarray is a first-tier clinical diagnostic test for individuals with developmental disabilities or congenital anomalies. *Am J Med Genet* 2010;86:749–764.
138. Vissers LE, van Ravenswaaij CM, Admiraal R, et al. Mutations in a new member of the chromodomain gene family cause CHARGE syndrome. *Nat Genet* 2004;36:955–957.
139. Lin AE, Pierpont ME. Genetic counseling for congenital heart defects. In: Wyszynski D, Correa-Villasenor A, Graham TP, eds. *Congenital Heart Defects*. New York, NY: Oxford University Press, 2010:453–461.
140. Gill HK, Splitt M, Sharland GK, et al. Patterns of recurrence of congenital heart disease: an analysis of 6,640 consecutive pregnancies evaluated by detailed fetal echocardiography. *J Am Coll Cardiol* 2003;42:923–929.
141. Burn J, Brennan P, Little J, et al. Recurrence risks in offspring of adults with major heart defects: results from first cohort of British collaborative study. *Lancet* 1998;351:311–316.
142. Nora JJ, Nora AH. Genetic and environmental factors in the etiology of congenital heart diseases. *South Med J* 1976;69:919–926.
143. Pradat P. Recurrence risk for major congenital heart defects in Sweden: a registry study. *Genet Epidemiol* 1994;11:131–140.
144. Nora JJ, Nora AH. Maternal transmission of congenital heart diseases: new recurrence risk figures and the questions of cytoplasmic inheritance and vulnerability to teratogens. *Am J Cardiol* 1987;59:459–463.
145. Whittemore R, Wells JA, Castellsague X. A second-generation study of 427 probands with congenital heart defects and their 837 children. *J Am Coll Cardiol* 1994;23:1459–1467.
146. McBride KL, Pignatelli R, Lewin M, et al. Inheritance analysis of congenital left ventricular outflow tract obstruction malformations: segregation, multiplex relative risk, and heritability. *Am J Med Genet A* 2005;134:180–186.
147. McBride KL, Zender GA, Fitzgerald-Burt SM, et al. Linkage analysis of left ventricular outflow tract malformations (aortic valve stenosis, coarctation of the aorta, and hypoplastic left heart syndrome). *Eur J Hum Genet* 2009;17:811–819.
148. Hinton RB, Martin LJ, Rame-Gowda S, et al. Hypoplastic left heart syndrome links to chromosomes 10q and 6q and is genetically related to bicuspid aortic valve. *J Am Coll Cardiol* 2009;53:1065–1071.
149. Hinton RB Jr, Martin LJ, Tabangin ME, et al. Hypoplastic left heart syndrome is heritable. *J Am Coll Cardiol* 2007;50:1590–1595.
150. van Karnebeek CD, Hennekam RC. Associations between chromosomal anomalies and congenital heart defects: a database search. *Am J Med Genet* 1999;84:158–166.
151. Brewer C, Holloway S, Zawalski P, et al. A chromosomal deletion map of human malformations. *Am J Hum Genet* 1998;63:1153–1159.
152. Barriot R, Breckpot J, Thienpont B, et al. Collaboratively charting the gene-to-phenotype network of human congenital heart defects. *Genome Med* 2010;2:16.
153. Lacro RV. Dysmorphology and genetics. In: Keane JF, Fyler DC, Lock JE, eds. *Nadas' Pediatric Cardiology*. 2nd ed. Philadelphia, PA: Saunders Elsevier, 2006:49–72.
154. Burn J, Goodship J. Congenital heart disease. In: Rimoin DL, Connor JM, Pyritz RE, et al. eds. *Emery and Rimoin's Principles and Practice of Medical Genetics*. 4th ed. London; New York, NY: Churchill Livingstone, 2002:1239–1326.
155. Botto LD, May K, Fernhoff PM, et al. A population-based study of the 22q11.2 deletion: phenotype, incidence, and contribution to major birth defects in the population. *Pediatrics* 2003;112:101–107.
156. Chinn A, Fitzsimmons J, Shepard TH, et al. Congenital heart disease among spontaneous abortuses and stillborn fetuses: prevalence and associations. *Teratology* 1989;40:475–482.
157. Breckpot J, Thienpont B, Peeters H, et al. Array comparative genomic hybridization as a diagnostic tool for syndromic heart defects. *J Pediatr* 2010;156:810–817, 817 e811–e817 e814.
158. Shin M, Besser LM, Kucik JE, et al. Prevalence of Down syndrome among children and adolescents in 10 regions of the United States. *Pediatrics* 2009;124:1565–1571.
159. Wessels MW, Los FJ, Frohn-Mulder IM, et al. Poor outcome in Down syndrome fetuses with cardiac anomalies or growth retardation. *Am J Med Genet A* 2003;116:147–151.
160. Yang Q, Rasmussen SA, Friedman JM. Mortality associated with Down's syndrome in the USA from 1983 to 1997: a population-based study. *Lancet* 2002;359:1019–1025.
161. Reller MD, Morris CD. Is Down syndrome a risk factor for poor outcome after repair of congenital heart defects? *J Pediatr* 1998;132:738–741.
162. Marino B, Diociaiuti L, Calcagni G, et al. Outcome in Down syndrome fetuses with cardiac anomalies. *Am J Med Genet A* 2004;128:101–102; author reply 103.
163. Papavasiliou P, York TP, Gursoy N, et al. The phenotype of persons having mosaicism for trisomy 21/Down syndrome reflects the percentage of trisomic cells present in different tissues. *Am J Med Genet A* 2009;149:573–583.
164. Barlow GM, Chen XN, Shi ZY, et al. Down syndrome congenital heart disease: a narrowed region and a candidate gene. *Genet Med* 2001;3:91–101.
165. Lin AE, Basson CT, Goldmuntz E, et al. Adults with genetic syndromes and cardiovascular abnormalities: clinical history and management. *Genet Med* 2008;10:469–494.
166. Boghosian-Sell L, Mewar R, Harrison W, et al. Molecular mapping of the Edwards syndrome phenotype to two noncontiguous regions on chromosome 18. *Am J Hum Genet* 1994;55:476–483.
167. Nielsen J, Wohler M. Sex chromosome abnormalities found among 34,910 newborn children: results from a 13-year incidence study in Aarhus, Denmark. *Birth Defects Orig Artic Ser* 1990;26:209–223.
168. Sybert VP, McCauley E. Turner's syndrome. *N Engl J Med* 2004;351:1227–1238.
169. Ostberg JE, Brookes JA, McCarthy C, et al. A comparison of echocardiography and magnetic resonance imaging in cardiovascular screening of adults with Turner syndrome. *J Clin Endocrinol Metab* 2004;89:5966–5971.
170. Lacro RV, Jones KL, Benirschke K. Coarctation of the aorta in Turner syndrome: a pathologic study of fetuses with nuchal cystic hygromas, hydrops fetalis, and female genitalia. *Pediatrics* 1988;81:445–451.
171. Ostberg JE, Donald AE, Halcox JP, et al. Vasculopathy in Turner syndrome: arterial dilatation and intimal thickening without endothelial dysfunction. *J Clin Endocrinol Metab* 2005;90:5161–5166.
172. Jagannath AD, Rastogi U, Spooner AE, et al. Aortic dissection and moyamoya disease in Turner syndrome. *Am J Med Genet A* 2010;152:2085–2089.
173. Bondy CA. Aortic dissection in Turner syndrome. *Curr Opin Cardiol* 2008;23:519–526.
174. Gravholt CH, Hansen KW, Erlandsen M, et al. Nocturnal hypertension and impaired sympathovagal tone in Turner syndrome. *J Hypertens* 2006;24:353–360.
175. Karnis MF, Zimon AE, Lalwani SI, et al. Risk of death in pregnancy achieved through oocyte donation in patients with Turner syndrome: a national survey. *Fertil Steril* 2003;80:498–501.
176. Chevalier N, Letur H, Lelannou D, et al. Materno-fetal cardiovascular complications in Turner syndrome after oocyte donation: insufficient

- pregnancy screening and pregnancy follow-up are associated with poor outcome. *J Clin Endocrinol Metab* 2011;96:E260–E267.
177. Elsheikh M, Dunger DB, Conway GS, et al. Turner's syndrome in adulthood. *Endocr Rev* 2002;23:120–140.
 178. Greenberg F. DiGeorge syndrome: an historical review of clinical and cytogenetic features. *J Med Genet* 1993;30:803–806.
 179. Driscoll DA, Spinner NB, Budarf ML, et al. Deletions and microdeletions of 22q11.2 in velo-cardio-facial syndrome. *Am J Med Genet* 1992;44:261–268.
 180. Burn J, Takao A, Wilson D, et al. Conotruncal anomaly face syndrome is associated with a deletion within chromosome 22q11. *J Med Genet* 1993;30:822–824.
 181. Oskarsdottir S, Vujic M, Fasth A. Incidence and prevalence of the 22q11 deletion syndrome: a population-based study in Western Sweden. *Arch Dis Child* 2004;89:148–151.
 182. Digilio MC, Angioni A, De Santis M, et al. Spectrum of clinical variability in familial deletion 22q11.2: from full manifestation to extremely mild clinical anomalies. *Clin Genet* 2003;63:308–313.
 183. McDonald-McGinn DM, Minugh-Purvis N, Kirschner RE, et al. The 22q11.2 deletion in African-American patients: an underdiagnosed population? *Am J Med Genet A* 2005;134:242–246.
 184. Shoener KA, Rope AF, Hopkin RJ, et al. Genetic analyses in two extended families with deletion 22q11 syndrome: importance of extracardiac manifestations. *J Pediatr* 2005;146:382–387.
 185. Amati F, Mari A, Digilio MC, et al. 22q11 deletions in isolated and syndromic patients with tetralogy of Fallot. *Hum Genet* 1995;95:479–482.
 186. Iserin L, de Lonlay P, Vior G, et al. Prevalence of the microdeletion 22q11 in newborn infants with congenital conotruncal cardiac anomalies. *Eur J Pediatr* 1998;157:881–884.
 187. Momma K, Ando M, Matsuoka R. Truncus arteriosus communis associated with chromosome 22q11 deletion. *J Am Coll Cardiol* 1997;30:1067–1071.
 188. Frohn-Mulder IM, Wesby Swaay E, Bouwhuis C, et al. Chromosome 22q11 deletions in patients with selected outflow tract malformations. *Genet Couns* 1999;10:35–41.
 189. Takahashi K, Kido S, Hoshino K, et al. Frequency of a 22q11 deletion in patients with conotruncal cardiac malformations: a prospective study. *Eur J Pediatr* 1995;154:878–881.
 190. Lewin MB, Lindsay EA, Jurecic V, et al. A genetic etiology for interruption of the aortic arch type B. *Am J Cardiol* 1997;80:493–497.
 191. Momma K, Kondo C, Matsuoka R. Tetralogy of Fallot with pulmonary atresia associated with chromosome 22q11 deletion. *J Am Coll Cardiol* 1996;27:198–202.
 192. McElhinney DB, Driscoll DA, Levin ER, et al. Chromosome 22q11 deletion in patients with ventricular septal defect: frequency and associated cardiovascular anomalies. *Pediatrics* 2003;112:e472.
 193. McElhinney DB, Clark BJ III, Weinberg PM, et al. Association of chromosome 22q11 deletion with isolated anomalies of aortic arch laterality and branching. *J Am Coll Cardiol* 2001;37:2114–2119.
 194. Johnson MC, Strauss AW, Dowton SB, et al. Deletion within chromosome 22 is common in patients with absent pulmonary valve syndrome. *Am J Cardiol* 1995;76:66–69.
 195. McElhinney DB, McDonald-McGinn D, Zackai EH, et al. Cardiovascular anomalies in patients diagnosed with a chromosome 22q11 deletion beyond 6 months of age. *Pediatrics* 2001;108:E104.
 196. Johnson TR, Goldmuntz E, McDonald-McGinn DM, et al. Cardiac magnetic resonance imaging for accurate diagnosis of aortic arch anomalies in patients with 22q11.2 deletion. *Am J Cardiol* 2005;96:1726–1730.
 197. John AS, McDonald-McGinn DM, Zackai EH, et al. Aortic root dilation in patients with 22q11.2 deletion syndrome. *Am J Med Genet A* 2009;149:939–942.
 198. Kruse K, Pankau R, Gosch A, et al. Calcium metabolism in Williams-Beuren syndrome. *J Pediatr* 1992;121:902–907.
 199. Mervis CB, Robinson BF, Bertrand J, et al. The Williams syndrome cognitive profile. *Brain Cogn* 2000;44:604–628.
 200. Eronen M, Peippo M, Hiipala A, et al. Cardiovascular manifestations in 75 patients with Williams syndrome. *J Med Genet* 2002;39:554–558.
 201. Kececioglu D, Kotthoff S, Vogt J. Williams-Beuren syndrome: a 30-year follow-up of natural and postoperative course. *Eur Heart J* 1993;14:1458–1464.
 202. Kim YM, Yoo SJ, Choi JY, et al. Natural course of supraaortic stenosis and peripheral pulmonary arterial stenosis in Williams' syndrome. *Cardiol Young* 1999;9:37–41.
 203. Wessel A, Pankau R, Kececioglu D, et al. Three decades of follow-up of aortic and pulmonary vascular lesions in the Williams-Beuren syndrome. *Am J Med Genet* 1994;52:297–301.
 204. Cherniske EM, Carpenter TO, Klaiman C, et al. Multisystem study of 20 older adults with Williams syndrome. *Am J Med Genet A* 2004;131:255–264.
 205. Bird LM, Billman GF, Lacro RV, et al. Sudden death in Williams syndrome: report of ten cases. *J Pediatr* 1996;129:926–931.
 206. Morris CA, Mervis CB. Williams syndrome and related disorders. *Annu Rev Genomics Hum Genet* 2000;1:461–484.
 207. Curran ME, Atkinson DL, Ewart AK, et al. The elastin gene is disrupted by a translocation associated with supraaortic stenosis. *Cell* 1993;73:159–168.
 208. Li DY, Toland AE, Boak BB, et al. Elastin point mutations cause an obstructive vascular disease, supraaortic stenosis. *Hum Mol Genet* 1997;6:1021–1028.
 209. Metcalfe K, Rucka AK, Smoot L, et al. Elastin: mutational spectrum in supraaortic stenosis. *Eur J Hum Genet* 2000;8:955–963.
 210. Frangiskakis JM, Ewart AK, Morris CA, et al. LIM-kinase1 hemizygosity implicated in impaired visuospatial constructive cognition. *Cell* 1996;86:59–69.
 211. Tassabehji M, Metcalfe K, Hurst J, et al. An elastin gene mutation producing abnormal tropoelastin and abnormal elastic fibres in a patient with autosomal dominant cutis laxa. *Hum Mol Genet* 1998;7:1021–1028.
 212. Zhang MC, He L, Giro M, et al. Cutis laxa arising from frameshift mutations in exon 30 of the elastin gene (ELN). *J Biol Chem* 1999;274:981–986.
 213. Goldmuntz E, Paluru P, Glessner J, et al. Microdeletions and microduplications in patients with congenital heart disease and multiple congenital anomalies. *Congenit Heart Dis* 2011;6:592–602.
 214. Erdogan F, Larsen LA, Zhang L, et al. High frequency of submicroscopic genomic aberrations detected by tiling path array comparative genome hybridisation in patients with isolated congenital heart disease. *J Med Genet* 2008;45:704–709.
 215. Richards AA, Santos LJ, Nichols HA, et al. Cryptic chromosomal abnormalities identified in children with congenital heart disease. *Pediatr Res* 2008;64:358–363.
 216. Thienpont B, Mertens L, de Ravel T, et al. Submicroscopic chromosomal imbalances detected by array-CGH are a frequent cause of congenital heart defects in selected patients. *Eur Heart J* 2007;28:2778–2784.
 217. Watson GH, Miller V. Arteriohepatic dysplasia: familial pulmonary arterial stenosis with neonatal liver disease. *Arch Dis Child* 1973;48:459–466.
 218. Alagille D, Odievre M, Gautier M, et al. Hepatic ductular hypoplasia associated with characteristic facies, vertebral malformations, retarded physical, mental, and sexual development, and cardiac murmur. *J Pediatr* 1975;86:63–71.
 219. Spinner NB, Rand EB, Fortina P, et al. Cytologically balanced t(2;20) in a two-generation family with alagille syndrome: cytogenetic and molecular studies. *Am J Hum Genet* 1994;55:238–243.
 220. Krantz ID, Rand EB, Genin A, et al. Deletions of 20p12 in Alagille syndrome: frequency and molecular characterization. *Am J Med Genet* 1997;70:80–86.
 221. Byrne JL, Harrod MJ, Friedman JM, et al. del(20p) with manifestations of arteriohepatic dysplasia. *Am J Med Genet* 1986;24:673–678.
 222. Pollet N, Boccaccio C, Dhorne-Pollet S, et al. Construction of an integrated physical and gene map of human chromosome 20p12 providing candidate genes for Alagille syndrome. *Genomics* 1997;42:489–498.
 223. Li L, Krantz ID, Deng Y, et al. Alagille syndrome is caused by mutations in human Jagged1, which encodes a ligand for Notch1. *Nat Genet* 1997;16:243–251.
 224. Oda T, Elkahoul AG, Pike BL, et al. Mutations in the human Jagged1 gene are responsible for Alagille syndrome. *Nat Genet* 1997;16:235–242.
 225. Warthen DM, Moore EC, Kamath BM, et al. Jagged1 (JAG1) mutations in Alagille syndrome: increasing the mutation detection rate. *Hum Mutat* 2006;27:436–443.
 226. Spinner NB, Colliton RP, Crosnier C, et al. Jagged1 mutations in alagille syndrome. *Hum Mutat* 2001;17:18–33.
 227. McElhinney DB, Krantz ID, Bason L, et al. Analysis of cardiovascular phenotype and genotype-phenotype correlation in individuals with a JAG1 mutation and/or Alagille syndrome. *Circulation* 2002;106:2567–2574.
 228. Krantz ID, Smith R, Colliton RP, et al. Jagged1 mutations in patients ascertained with isolated congenital heart defects. *Am J Med Genet* 1999;84:56–60.
 229. Eldadah ZA, Hamosh A, Biery NJ, et al. Familial Tetralogy of Fallot caused by mutation in the jagged1 gene. *Hum Mol Genet* 2001;10:163–169.
 230. Kamath BM, Spinner NB, Emerick KM, et al. Vascular anomalies in Alagille syndrome: a significant cause of morbidity and mortality. *Circulation* 2004;109:1354–1358.
 231. Basson CT, Cowley GS, Solomon SD, et al. The clinical and genetic spectrum of the Holt-Oram syndrome (heart-hand syndrome). *N Engl J Med* 1994;330:885–891.
 232. Newbury-Ecob RA, Leanne R, Raeburn JA, et al. Holt-Oram syndrome: a clinical genetic study. *J Med Genet* 1996;33:300–307.
 233. Bruneau BG, Logan M, Davis N, et al. Chamber-specific cardiac expression of Tbx5 and heart defects in Holt-Oram syndrome. *Dev Biol* 1999;211:100–108.
 234. Bonnet D, Pelet A, Legeai-Mallet L, et al. A gene for Holt-Oram syndrome maps to the distal long arm of chromosome 12. *Nat Genet* 1994;6:405–408.
 235. Terrett JA, Newbury-Ecob R, Cross GS, et al. Holt-Oram syndrome is a genetically heterogeneous disease with one locus mapping to human chromosome 12q. *Nat Genet* 1994;6:401–404.
 236. Li QY, Newbury-Ecob RA, Terrett JA, et al. Holt-Oram syndrome is caused by mutations in TBX5, a member of the Brachyury (T) gene family. *Nat Genet* 1997;15:21–29.
 237. Basson CT, Bachinsky DR, Lin RC, et al. Mutations in human TBX5 [corrected] cause limb and cardiac malformation in Holt-Oram syndrome. *Nat Genet* 1997;15:30–35.

238. Allanson JE. Noonan syndrome. In: Cassidy SB, Allanson JE, eds. *Management of Genetic Syndromes*. 2nd ed. Hoboken, NJ: Wiley Liss, 2005: 385–398.
239. Noonan JA. Hypertelorism with Turner phenotype. A new syndrome with associated congenital heart disease. *Am J Dis Child* 1968;116: 373–380.
240. Yoshida R, Hasegawa T, Hasegawa Y, et al. Protein-tyrosine phosphatase, nonreceptor type 11 mutation analysis and clinical assessment in 45 patients with Noonan syndrome. *J Clin Endocrinol Metab* 2004;89: 3359–3364.
241. Jongmans M, Otten B, Noordam K, et al. Genetics and variation in phenotype in Noonan syndrome. *Horm Res* 2004;62:56–59.
242. Musante L, Kehl HG, Majewski F, et al. Spectrum of mutations in PTPN11 and genotype-phenotype correlation in 96 patients with Noonan syndrome and five patients with cardio-facio-cutaneous syndrome. *Eur J Hum Genet* 2003;11:201–206.
243. Lee SM, Cooper JC. Noonan syndrome with giant cell lesions. *Int J Paediatr Dent* 2005;15:140–145.
244. Lee JS, Tartaglia M, Gelb BD, et al. Phenotypic and genotypic characterization of Noonan-like/multiple giant cell lesion syndrome. *J Med Genet* 2005;42:e11.
245. Legius E, Schrandt-Stumpel C, Schollen E, et al. PTPN11 mutations in LEOPARD syndrome. *J Med Genet* 2002;39:571–574.
246. Kalidas K, Shaw AC, Crosby AH, et al. Genetic heterogeneity in LEOPARD syndrome: two families with no mutations in PTPN11. *J Hum Genet* 2005;50:21–25.
247. Digilio MC, Sarkozy A, Pacileo G, et al. PTPN11 gene mutations: linking the Gln510Glu mutation to the “LEOPARD syndrome phenotype”. *Eur J Pediatr* 2006;165:803–805.
248. Kontaridis MI, Swanson KD, David FS, et al. PTPN11 (Shp2) mutations in LEOPARD syndrome have dominant negative, not activating, effects. *J Biol Chem* 2006;281:6785–6792.
249. Carvajal-Vergara X, Sevilla A, D’Souza SL, et al. Patient-specific induced pluripotent stem-cell-derived models of LEOPARD syndrome. *Nature* 2010;465:808–812.
250. Roberts A, Allanson J, Jadico SK, et al. The cardiofaciocutaneous syndrome. *J Med Genet* 2006;43:833–842.
251. Gripp KW, Hopkins E, Doyle D, et al. High incidence of progressive postnatal cerebellar enlargement in Costello syndrome: brain overgrowth associated with HRAS mutations as the likely cause of structural brain and spinal cord abnormalities. *Am J Med Genet A* 2010;152:1161–1168.
252. Graham JM Jr. A recognizable syndrome within CHARGE association: Hall-Hittner syndrome. *Am J Med Genet* 2001;99:120–123.
253. Verloes A. Updated diagnostic criteria for CHARGE syndrome: a proposal. *Am J Med Genet A* 2005;133:306–308.
254. Jongmans MC, Admiraal RJ, van der Donk KP, et al. CHARGE syndrome: the phenotypic spectrum of mutations in the CHD7 gene. *J Med Genet* 2006;43:306–314.
255. Aramaki M, Uda K, Kosaki R, et al. Phenotypic spectrum of CHARGE syndrome with CHD7 mutations. *J Pediatr* 2006;148:410–414.
256. Blake KD, Davenport SL, Hall BD, et al. CHARGE association: an update and review for the primary pediatrician. *Clin Pediatr (Phila)* 1998;37: 159–173.
257. Issekutz KA, Graham JM Jr, Prasad C, et al. An epidemiological analysis of CHARGE syndrome: preliminary results from a Canadian study. *Am J Med Genet A* 2005;133:309–317.
258. Prendiville TW, Barton LL, Thompson WR, et al. Heterotaxy syndrome: defining contemporary disease trends. *Pediatr Cardiol* 2010;31:1052–1058.
259. Olbrich H, Haffner K, Kispert A, et al. Mutations in DNAAF5 cause primary ciliary dyskinesia and randomization of left-right asymmetry. *Nat Genet* 2002;30:143–144.
260. Guichard C, Harricane MC, Lafitte JJ, et al. Axonemal dynein intermediate-chain gene (DNAI1) mutations result in situs inversus and primary ciliary dyskinesia (Kartagener syndrome). *Am J Hum Genet* 2001;68:1030–1035.
261. Kennedy MP, Omran H, Leigh MW, et al. Congenital heart disease and other heterotaxic defects in a large cohort of patients with primary ciliary dyskinesia. *Circulation* 2007;115:2814–2821.
262. Casey B, Devoto M, Jones KL, et al. Mapping a gene for familial situs abnormalities to human chromosome Xq24-q27.1. *Nat Genet* 1993;5:403–407.
263. Gebbia M, Ferrero GB, Pilia G, et al. X-linked situs abnormalities result from mutations in ZIC3. *Nat Genet* 1997;17:305–308.
264. Robinson SW, Morris CD, Goldmuntz E, et al. Missense mutations in CRELD1 are associated with cardiac atrioventricular septal defects. *Am J Hum Genet* 2003;72:1047–1052.
265. Kosaki K, Bassi MT, Kosaki R, et al. Characterization and mutation analysis of human LEFTY A and LEFTY B, homologues of murine genes implicated in left-right axis development. *Am J Hum Genet* 1999;64:712–721.
266. Bamford RN, Roessler E, Burdine RD, et al. Loss-of-function mutations in the EGF-CFC gene CFC1 are associated with human left-right laterality defects. *Nat Genet* 2000;26:365–369.
267. Kosaki R, Gebbia M, Kosaki K, et al. Left-right axis malformations associated with mutations in ACVR2B, the gene for human activin receptor type IIB. *Am J Med Genet* 1999;82:70–76.
268. Watanabe Y, Benson DW, Yano S, et al. Two novel frameshift mutations in NKX2.5 result in novel features including visceral inversus and sinus venosus type ASD. *J Med Genet* 2002;39:807–811.
269. Ozcelik C, Bit-Avragim N, Panek A, et al. Mutations in the EGF-CFC Gene Cryptic Are an Infrequent Cause of Congenital Heart Disease. *Pediatr Cardiol* 2006;27:695–698.
270. Weaver DD, Mapstone CL, Yu PL. The VATER association: analysis of 46 patients. *Am J Dis Child* 1986;140:225–229.
271. Kallen K, Mastroiacovo P, Castilla EE, et al. VATER non-random association of congenital malformations: study based on data from four malformation registers. *Am J Med Genet* 2001;101:26–32.
272. Evans JA, Stranc LC, Kaplan P, et al. VACTERL with hydrocephalus: further delineation of the syndrome(s). *Am J Med Genet* 1989;34:177–182.
273. Kim J, Kim P, Hui CC. The VACTERL association: lessons from the Sonic hedgehog pathway. *Clin Genet* 2001;59:306–315.
274. Vento AR, LaBrie RA, Mulliken JB. The O.M.E.N.S. classification of hemifacial microsomia. *Cleft Palate Craniofac J* 1991;28:68–76; discussion 77.
275. Wang R, Martinez-Frias ML, Graham JM Jr. Infants of diabetic mothers are at increased risk for the oculo-auriculo-vertebral sequence: a case-based and case-control approach. *J Pediatr* 2002;141:611–617.
276. Werler MM, Sheehan JE, Hayes C, et al. Vasoactive exposures, vascular events, and hemifacial microsomia. *Birth Defects Res A Clin Mol Teratol* 2004;70:389–395.
277. Kallen K, Robert E, Castilla EE, et al. Relation between oculo-auriculo-vertebral (OAV) dysplasia and three other non-random associations of malformations (VATER, CHARGE, and OEIS). *Am J Med Genet A* 2004;127:26–34.
278. Bergmann C, Zerres K, Peschgens T, et al. Overlap between VACTERL and hemifacial microsomia illustrating a spectrum of malformations seen in axial mesodermal dysplasia complex (AMDC). *Am J Med Genet A* 2003;121:151–155.
279. Schott JJ, Benson DW, Basson CT, et al. Congenital heart disease caused by mutations in the transcription factor NKX2-5. *Science* 1998;281:108–111.
280. Hirayama-Yamada K, Kamisago M, Akimoto K, et al. Phenotypes with GATA4 or NKX2.5 mutations in familial atrial septal defect. *Am J Med Genet A* 2005;135:47–52.
281. Sarkozy A, Conti E, Neri C, et al. Spectrum of atrial septal defects associated with mutations of NKX2.5 and GATA4 transcription factors. *J Med Genet* 2005;42:e16.
282. Benson DW, Silberbach GM, Kavanaugh-McHugh A, et al. Mutations in the cardiac transcription factor NKX2.5 affect diverse cardiac developmental pathways. *J Clin Invest* 1999;104:1567–1573.
283. McElhinney DB, Geiger E, Blinder J, et al. NKX2.5 mutations in patients with congenital heart disease. *J Am Coll Cardiol* 2003;42:1650–1655.
284. Harvey RP, Lai D, Elliott D, et al. Homeodomain factor Nkx2-5 in heart development and disease. *Cold Spring Harb Symp Quant Biol* 2002;67:107–114.
285. Garg V, Kathiriyi IS, Barnes R, et al. GATA4 mutations cause human congenital heart defects and reveal an interaction with TBX5. *Nature* 2003;424:443–447.
286. Rajagopal SK, Ma Q, Obler D, et al. Spectrum of heart disease associated with murine and human GATA4 mutation. *J Mol Cell Cardiol* 2007;43:677–685.
287. Tomita-Mitchell A, Maslen CL, Morris CD, et al. GATA4 sequence variants in patients with congenital heart disease. *J Med Genet* 2007;44: 779–783.
288. Schluterman MK, Krysiak AE, Kathiriyi IS, et al. Screening and biochemical analysis of GATA4 sequence variations identified in patients with congenital heart disease. *Am J Med Genet A* 2007;143A:817–823.
289. Garg V, Muth AN, Ransom JE, et al. Mutations in NOTCH1 cause aortic valve disease. *Nature* 2005;437:270–274.
290. McBride KL, Riley MF, Zender GA, et al. NOTCH1 mutations in individuals with left ventricular outflow tract malformations reduce ligand-induced signaling. *Hum Mol Genet* 2008;17:2886–2893.
291. McKellar SH, Tester DJ, Yagubyan M, et al. Novel NOTCH1 mutations in patients with bicuspid aortic valve disease and thoracic aortic aneurysms. *J Thorac Cardiovasc Surg* 2007;134:290–296.
292. Mohamed SA, Aherrahrou Z, Liptau H, et al. Novel missense mutations (p.T596M and p.P1797H) in NOTCH1 in patients with bicuspid aortic valve. *Biochem Biophys Res Commun* 2006;345:1460–1465.
293. Ching YH, Ghosh TK, Cross SJ, et al. Mutation in myosin heavy chain 6 causes atrial septal defect. *Nat Genet* 2005;37:423–428.
294. Stoll C, Alembik Y, Roth MP, et al. Risk factors in congenital heart disease. *Eur J Epidemiol* 1989;5:382–391.
295. Lin AE, Salbert BA, Belmont J, et al. Total is more than the sum of the parts: phenotyping the heart in cardiovascular genetics clinics. *Am J Med Genet A* 2004;131:111–114.
296. Kramer HH, Majewski F, Trampisch HJ, et al. Malformation patterns in children with congenital heart disease. *Am J Dis Child* 1987;141:789–795.
297. Hoess K, Goldmuntz E, Pyeritz RE. Genetic counseling for congenital heart disease: new approaches for a new decade. *Curr Cardiol Rep* 2002;4:68–75.
298. Eskedal L, Hagemo P, Eskild A, et al. A population-based study of extracardiac anomalies in children with congenital cardiac malformations. *Cardiol Young* 2004;14:600–607.
299. Bosi G, Garani G, Scorrano M, et al. Temporal variability in birth prevalence of congenital heart defects as recorded by a general birth defects registry. *J Pediatr* 2003;142:690–698.
300. Gelb BD, Tartaglia M. RAS signaling pathway mutations and hypertrophic cardiomyopathy: getting into and out of the thick of it. *J Clin Invest* 2011;121:844–847.

Fetal Echocardiography and Fetal Cardiology

Charles S. Kleinman ■ Julie S. Glickstein ■ Ganga Krishnamurthy ■ Jodie K. Votava-Smith

HISTORICAL PERSPECTIVE

In the introduction to his epochal 1974 monograph, "Congenital Diseases of the Heart," Dr. Abraham M. Rudolph (1) emphasized the importance that characterization of the cardiovascular adaptation of the fetus during the months leading to delivery and the postnatal transition of the systemic and pulmonary circulatory system have in improving understanding of the clinical condition of the neonate, and in contributing to the formulation of logical and physiologically based management strategies for various forms of congenital heart disease. Toward this end, Rudolph and Heymann (2) developed techniques for the study of cardiovascular development, using chronically instrumented fetal lambs. Their studies included normal fetal animals, as well as fetuses in which pulmonary artery or ascending aortic banding was used to simulate pulmonary or aortic stenosis (PS or AS). Regional flow within the cardiovascular system was investigated through the use of radionuclide-labeled microspheres (3,4). These observations were extended to include the varied components of the transitional circulation, providing insights into the relative roles played by oxygenation, cord clamping, and the intrinsic fetal shunt pathways in the redistribution of blood flow in the fetus at the time of birth (5–8).

Rudolph's studies of the fetal lamb were postulated as a model for understanding the human fetal and transitional circulation, despite the recognition that the fetal lamb differed in substantial ways from the human fetus. These differences would be reflected in altered regional flow distribution to organs such as the brain, which constitutes a larger fraction of body mass in the primate and human than in the ovine fetus. In addition, the relative difference in the degree of "maturation" of the ovine neonate, compared with the human neonate, could also result in alterations in regional blood flow distribution between the two species.

In 1977, Rudolph's observations of the fetal lamb served as the foundation on which our understanding of the fetal and transitional circulation of the human fetus was based. In 1976, Dr. Frederick Morin completed a doctoral thesis toward his M.D. degree at the Yale University School of Medicine that was, in turn, based on the observations of a 1972 study (9) describing the use of M-mode echocardiographic recordings of fetal cardiac activity in the human fetus. This paper had speculated that fetal cardiac function in normal and abnormal

pregnancies could be analyzed through the use of the measurement of left ventricular ejection fraction from M-mode recordings of cardiac wall motion against time. The same publication predicted that the small size, complex anatomy, and rapid heartbeat of the human fetus would not allow complex congenital cardiac malformations to be diagnosed prenatally.

This served as the intellectual underpinning for the initiation of a clinical research project at the Yale University School of Medicine aimed at applying fetal echocardiography to validate in the human fetus the observations that had been documented in the ovine fetal model. The first findings of significance related to paradoxical motion of the interventricular septum, reminiscent of the findings postnatally in patients with cardiac malformations associated with volume- and pressure-overloaded right ventricles. M-mode echocardiography in the human fetal heart thus provided noninvasive confirmation that the findings that had previously been made in the ovine fetus, where the fetal right ventricle functions as the dominant ventricle, ejecting a larger stroke volume than the left ventricle at systemic blood pressure, held, as well, for the fetal human.

Subsequent studies were undertaken to characterize the development of the human fetal cardiovascular system and were presented at the annual meetings of the Society for Gynecologic Investigation and the Society for Pediatric Research in the spring of 1978. At the latter, Dr. Helen Taussig commented on the importance of these findings, which offered the potential for the diagnosis of congenital heart disease in early gestation, and the potential for termination of such pregnancies, to decrease the individual and societal burden of congenital heart disease in these children.

Thereafter, our attention was turned toward establishing a clinical role for fetal echocardiography. Although we had speculated in 1978 that such studies could be useful for the diagnosis of congenital heart disease, it was not until a year had passed that we were able to prove this. Our first peer-reviewed publication on this topic appeared in 1980 (10). This paper suggested indications for detailed fetal echocardiographic study in pregnancies deemed to be at high risk for congenital heart disease. M-mode and two-dimensional (2-D) echocardiography was used to document atrioventricular septal defect (AVSD) in a patient with left atrial isomerism and complete atrioventricular (AV) block, atrial flutter (AF), and hydrops fetalis. M-mode echocardiography was used to document tricuspid atresia and hypoplastic right ventricle in a second fetus. M-mode echocardiography was used to demonstrate the presence of complete heart block in the fetus of a mother with systemic lupus erythematosus.

This article was reviewed by Dr. Alexander Nadas in the 1981 edition of the Yearbook of Pediatrics (10). Dr. Nadas noted the potential for the use of the technique for research purposes, but he doubted the potential for a clinical role for fetal echocardiography, owing to the improbability of establishing such diagnoses before the legal limits for termination of pregnancy.

During 1980, publications from San Diego (11) and from London (12,13) documented the potential for examination of the fetal heart using sequential, segmental analysis of cardiac

Dr. Kleinman died just after submission of this chapter. His pioneering efforts in fetal echocardiography and physiology have set the stage for perinatal cardiology and innovations in care to the fetus that would not have been possible without his foresight. Charlie was brilliant, always a gentleman, had a fantastic sense of humor, and maintained gentle humility and courage to his last day. 'The professor' will be missed. He was a true friend.

HDA

structure. In 1981, deGeeter et al. from Strasbourg, hosted the first international meeting devoted to fetal echocardiography and clinical fetal cardiology.

In 1984, at the World Congress of Pediatric Cardiology, Fermont et al. (13) from Paris, reported their experience with four-chamber screening of the fetal heart for the detection of congenital heart disease. This was followed by the description provided by Allan et al. (14) of a regional screening program in London. She went on to train ultrasonographers throughout Great Britain and the Continent to participate in similar screening programs throughout Europe.

TABLE 27.1 Indications for Fetal Echocardiography

Familial risk factors

History of congenital heart disease

Previous sibling

Paternal

Mendelian syndromes that include congenital heart disease

Noonan

Tuberous sclerosis

Maternal risk factors

In vitro fertilization

Congenital heart disease

Cardiac teratogen

Isotretinoin

Lithium carbonate

Ethanol

Phenytoin

Valproic acid

Trimethadione

Carbamazepine

Maternal metabolic disorders

Diabetes mellitus

Phenylketonuria

Fetal risk factors

Extracardiac anomalies

Chromosomal

Anatomic

Increased nuchal fold thickness

Fetal cardiac arrhythmia

Irregular rhythm

Tachycardia (>180 bpm) in absence of amnionitis

Fixed bradycardia

Nonimmune hydrops fetalis

Abnormal fetal situs

Suspected fetal heart malformation on screening ultrasound

Lack of reassuring four-chamber view during basic obstetric scan

bpm, beats per minute.

INDICATIONS FOR FETAL ECHOCARDIOGRAPHY

While it must be recognized that most cases of congenital heart disease result from pregnancies in women who are not identified in advance to be at higher-than-average risk for congenital heart disease, most women referred for detailed fetal echocardiographic study have been judged to be at risk according to factors defined as fetal, maternal, or familial risks (Table 27.1).

SCREENING FOR CONGENITAL HEART DISEASE

As noted above, most infants with congenital heart disease are born to women without high-risk indications for congenital heart disease. Fermont et al. (13) documented that the identification of fetuses with abnormal four-chamber views of the heart would improve case findings of major forms of congenital heart disease. The normal four-chamber view of the fetal heart may be obtained in approximately 95% of fetuses examined between the late second and early third trimesters of pregnancy. The fetal heart is normally a midline structure, with the apex pointing leftward toward the fetal stomach. The heart lies in a horizontal orientation, above the transverse liver. By orienting the ultrasound transducer approximately 30 degrees cephalad from the transverse plane where the fetal abdominal circumference is measured, a tomographic view of the fetal heart is obtained (Fig. 27.1) that demonstrates the four-chamber anatomy of the fetal heart. The central fibrous body of the normal fetal heart is intact, with the septal leaflet of the tricuspid valve inserting slightly closer to the cardiac apex than the insertion of the anterior leaflet of the mitral valve. The atrial cavities and the interposed atrial septum are visualized, with the foramen ovale representing the major source of blood flow into the left atrium from the inferior vena cava (IVC). The atrial septum primum undulates in the left atrial flow stream from the IVC and functions as a flap valve that functionally seals

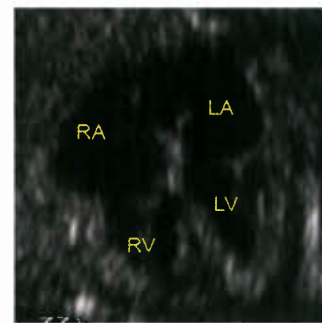
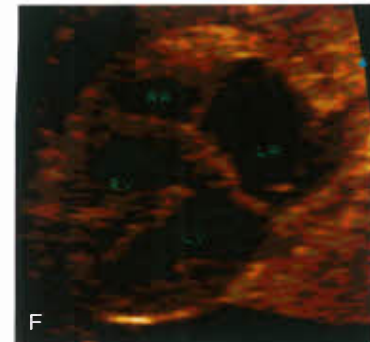
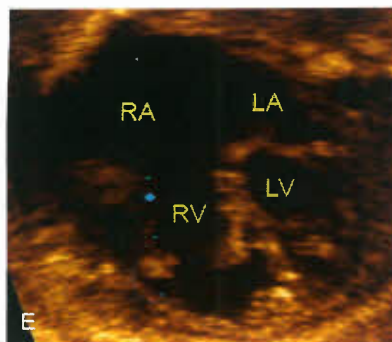
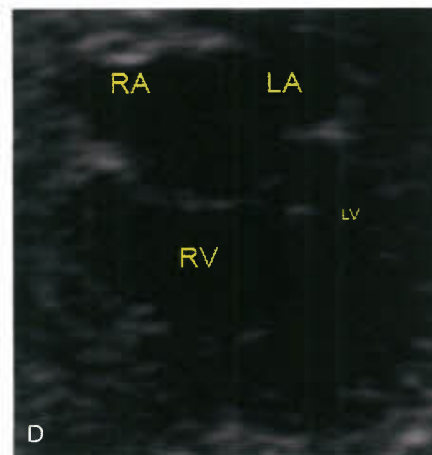
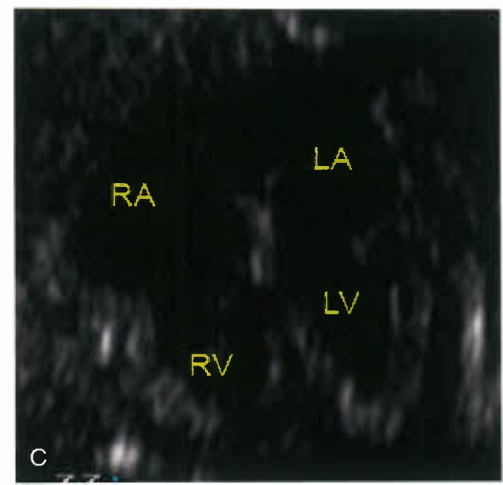
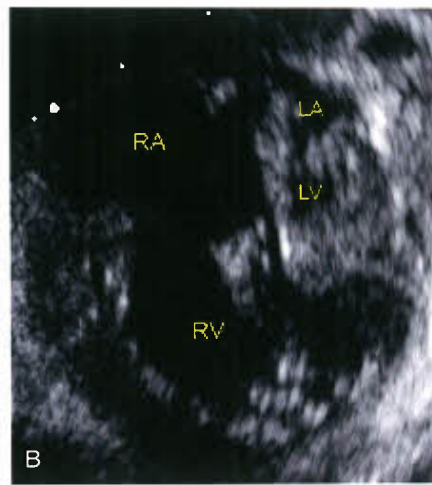
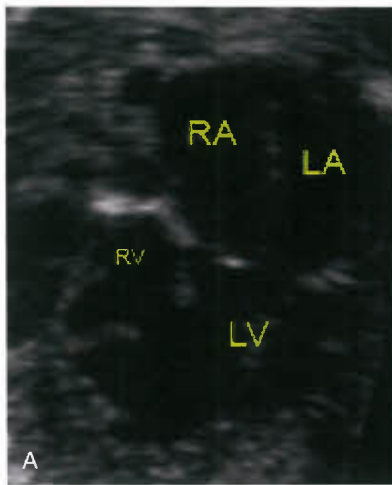


Figure 27.1. Normal four-chamber view of the fetal heart during midtrimester. Note the relatively equal transverse diameters of the right and left atria (RA, LA) and the right and left ventricles (RV, LV). The septal leaflet of the tricuspid valve is inserted into the central fibrous body of the heart in a position that is slightly offset toward the apex of the heart in comparison with the site of insertion of the anterior mitral leaflet to the central fibrous body. The moderator band is seen at the apex of the right ventricle. The posterior inflow portion of the ventricular septum is interposed between the two ventricular chambers. The foramen ovale represents an unrestricted flow orifice between the IVC and the left atrium. Relatively highly oxygenated umbilical venous return from the IVC is preferentially shunted into the left atrium through the left ventricle and into the descending aortic distribution. This provides the most highly oxygenated arterial blood to the fetal coronary arterial and cerebral circulation.

the foramen ovale following birth, owing to increased pulmonary venous return consequent to gaseous expansion of the lungs and postnatal decrease in pulmonary vascular resistance. The atrial chambers are normally symmetrical in appearance as are the ventricular chambers. The right ventricular chamber appears slightly foreshortened owing to the moderator band at the ventricular apex. The right ventricular surface of the ventricular septum is more coarsely trabeculated than the left ventricular septal surface. In the short-axis view, the two papillary muscles of the mitral valve are seen, and neither of these muscles is associated with the ventricular septum, whereas the tricuspid valve characteristically has a chordal insertion to the conal region of the right ventricular outflow tract.

Abnormalities of four-chamber anatomy may characterize certain forms of congenital heart disease. In many cases, the

primary structural abnormality of the heart may be apparent in the view of the central fibrous body. Such defects may include complete atrioventricular septal (canal) defect, hypoplastic left heart syndrome (HLHS), hypoplastic right heart syndrome, Ebstein malformation of the tricuspid valve, and various forms of single ventricle (Fig. 27.2). Disproportion of atrial or ventricular chambers may reflect altered flow patterns through the fetal cardiovascular system (15). In such cases, the four chambers of the heart may change their volume and or wall thickness to reflect the volume and pressure of blood flow through them. Pulmonary valve (PV) stenosis, for example, may be associated with right ventricular wall hypertrophy, with decreased chamber volume secondary to increased right-to-left shunting across the foramen ovale, with right ventricular hypertrophy or with increased chamber



(See legend, following page)

volume if tricuspid regurgitation occurs (16). Similarly, disproportionate development of atria and ventricles may occur in the presence of discrete obstruction to left ventricular outflow (Fig. 27.3) (17–19). The latter findings have served as the foundation for the development of the first programs for fetal intervention.

The sensitivity and specificity of abnormal four-chamber screening for congenital heart disease has been discussed repeatedly in the literature during the past decade, with claims varying from a sensitivity of 0% to 10% (e.g., the RADIUS trial in the United States) (20–22) to a sensitivity of >80%, with most series suggesting a sensitivity in the range of approximately 40% (10,23–49) (Table 27.2).

Based on claims of the utility of four-chamber screening for congenital heart disease, bodies such as the American College of Radiology, the American College of Obstetrics and Gynecology, and the American Institute of Ultrasound in Medicine have recommended that four-chamber screening views of the heart be included in the evaluation of all fetuses undergoing ultrasound examination, regardless of indication.

Views of the ventricular outflow tracts may demonstrate ventriculoarterial connections and allow the integrity of the ventricular septum to be evaluated. The right ventricular outflow through the main pulmonary artery typically proceeds in a posterior sweep to the ductus arteriosus, the descending thoracic aorta, and the pulmonary arterial bifurcation, with the left pulmonary artery continuing posteriorly and the right pulmonary artery arising at a right angle where it passes under the aortic arch. The left ventricular outflow tract (LVOT) continues into the ascending aorta, which ascends vertically toward the head. The ascending aorta and main pulmonary artery crisscross one another after emerging from their respective outflow tracts. Tomographic imaging demonstrates the perpendicular courses of these great arteries by showing one vessel in a longitudinal view while the second vessel is seen as a circular cross section (Fig. 27.4). The presence of subvalvar, valvar, and/or supravulvar obstruction can be detected, and outflow tract abnormalities such as ventricular septal defect (VSD), conal septal malalignment, double-outlet ventricle, or arterial transposition may be documented (Fig. 27.5).

The sensitivity and specificity that are added to four-chamber screening of the fetal heart by the inclusion of long-axis views of the outflow tracts have resulted in revised standards for screening echocardiography by the American College of Radiology, the American College of Obstetrics and Gynecology, and the American Institute of Ultrasound in Medicine.

ECHOCARDIOGRAPHIC ASSESSMENT OF FETAL CARDIOVASCULAR PERFORMANCE

M-mode echocardiographic studies of the human fetus provide insight into the relative size and pressure of the fetal ventricles. The timing of mechanical events during various phases of the cardiac cycle as reflected by wall motion, and motion of the cardiac valves may be used to analyze cardiac rhythm (10) (Fig. 27.6).

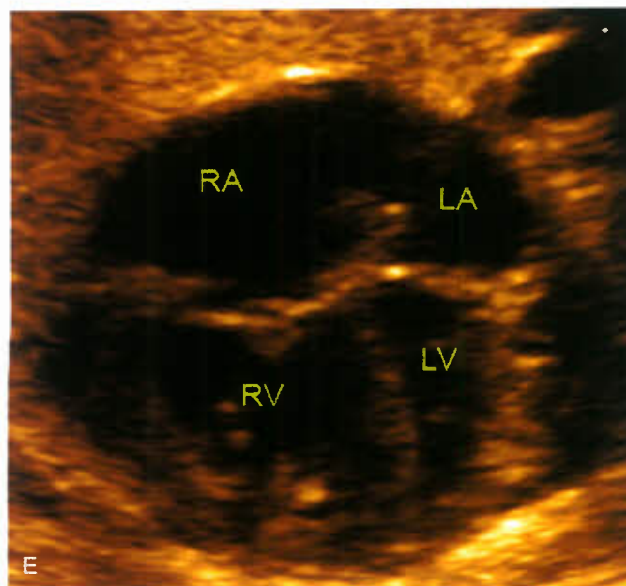
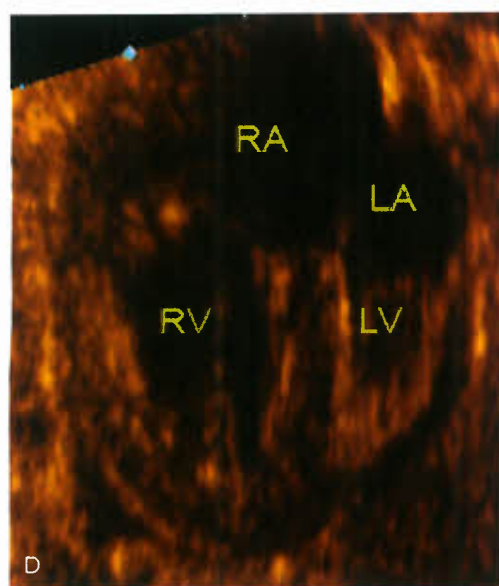
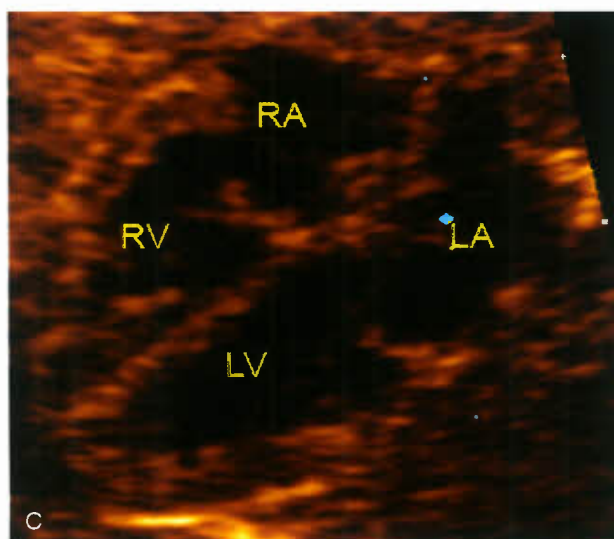
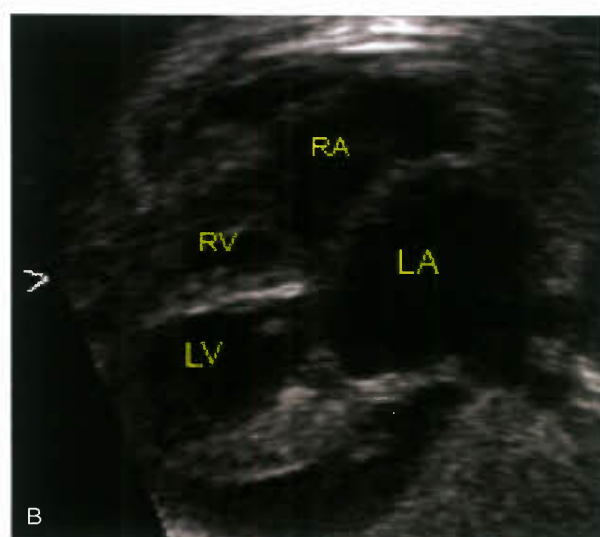
Two-dimensional imaging may provide insight into relative chamber and blood vessel volume and pressure. The addition of color flow Doppler adds further information concerning the function of the AV and semilunar valves and flow within important fetal flow pathways such as the ductus venosus (DV), foramen ovale, and ductus arteriosus (Fig. 27.7).

Feit et al. (50) used 2-D imaging of the fetal foramen ovale to estimate interatrial volume flow and demonstrated that fetuses with left heart obstruction had smaller transatrial flow volumes, whereas patients with right heart obstructive lesions had larger-volume right-to-left interatrial shunts. Berning et al. (51) emphasized the importance of color flow in determining flow volume and direction across the fetal ductus arteriosus and foramen ovale in the diagnosis of left heart hypoplasia and/or obstruction to right ventricular outflow (Fig. 27.8).

Pulsed Doppler flow analysis has been used to estimate regional blood flow distribution within the human fetus during the third trimester of pregnancy. The radionuclide-labeled microsphere studies of Heymann and Rudolph (2) had demonstrated that in the third trimester fetal lamb, the fetal right ventricle ejects 67% of the combined output of the two ventricles, with only approximately 8% of the combined output traversing the high-resistance pulmonary vascular bed. This 8% of combined output enters the fetal left atrium as pulmonary venous return and combines with relatively oxygen-rich pulmonary venous return streaming through the DV and IVC, amounting to approximately 25% of combined ventricular output. Thus, 33% of combined ventricular output crosses the mitral valve and is ejected as left ventricular output. This relatively oxygen-rich blood is preferentially distributed to the coronary arteries and cerebral circulation. In the 1970s, Dr. Rudolph had estimated that the relatively larger brain in the primate and human would probably demand a larger volume of left ventricular output during fetal life. He estimated that the ratio of right-to-left ventricular combined output in the human would be in the range of 55%/45%. Doppler flow studies in the human fetus have confirmed that estimate (52,53).

Friedman et al. (54–56) described studies on isolated strips of myocardium as well as on whole heart preparations

Figure 27.2. Montage of 6 four-chamber views of the fetal heart (A–F). Five cases of congenital heart disease (A–E) involving the central fibrous body of the heart are contrasted with a normal four-chamber view (C). **A:** Four-chamber view of the heart of a fetus with tricuspid atresia and ventricular disproportion favoring a large left ventricle (LV). There is an absent right AV connection, with a solid bar of muscle interposed between the right atrium (RA) and the right ventricle (RV). The sole inflow to the right ventricle is through a small muscular VSD, and the right ventricular cavity is hypoplastic. There is a large, single, mitral AV valve and a large left ventricle. **B:** Marked ventricular disproportion favoring the right ventricle in a patient with hypoplastic left heart. The left atrium (LA) is small and thick walled. The mitral valve is miniscule, and the left ventricle is hypoplastic, with a hypertrophic, fibroelastotic left ventricle. **C:** Normal four-chamber view of the fetal heart with proportionate ventricular and atrial cavities, normal AV valves, and intact central fibrous body. **D:** Unbalanced, right ventricular not dominant, AVSD in a fetus with trisomy 21. Although not visualized in this view, this fetus also had a hypoplastic aortic arch. **E:** Atrial and ventricular disproportion, with enlarged right-sided cardiac chambers in a fetus with the Ebstein malformation of the tricuspid valve. The tricuspid valve leaflets are redundant and thickened, with inferior displacement of the septal (visualized) and posterior (not seen in this view) leaflets. The anterior leaflet (visualized) is redundant and sail-like. A significant portion of the inflow tract of the right ventricle is “atrialized” owing to the apical displacement of the tricuspid valve. **F:** A balanced, complete, AVSD in a hydropic fetus with trisomy 21. The central fibrous portion of the heart is deficient, with a large ostium primum atrial septal defect (ASD), inflow VSD, and a common AV valve.



(See legend, following page)

TABLE 27.2 Prenatal Screening for Congenital Heart Disease

Study	View	GA(Weeks)	Sensitivity
Wylie et al. (1994)	4-Chamber View	18–20	18
Stoll et al. (1993)	4-Chamber View	18–22	9.2
Sharland and Allan (1992)	4-Chamber View	—	69
Vergani et al. (1992)	4-Chamber View	18–20	81
Buskens et al. (1996)	4-Chamber View	16–24	5
Todros et al. (1997)	4-Chamber View	18–22	15
Ott (1995)	4-Chamber View	—	14
Luck (1992)	4-Chamber + outflow	19	33.3
Tegnander et al. (1995)	4-Chamber	16–22	10
Rustico et al. (1995)	Full fetal echo	20–22	35.4
Hafner et al. (1998)	Full fetal echo	16–22	43.8
Achiron et al. (1992)	Extended fetal echo	18–24	78 (48 4-chamber)
Stümpflen et al. (1996)	Extended fetal echo	18–28	88 (47 4-chamber)
Tegnander et al. (2006)	4-Chamber + outflow	18	57

from mature and fetal sheep. These studies demonstrated that mature myocardium generates higher tension (pressure) at any end-diastolic length (volume) than does fetal myocardium. In addition, passive tension (pressure) is higher at any level of diastolic length (volume). These myocardial properties explain the findings of fetal animal studies, suggesting limited afterload and preload reserve. Possible explanations for the intrinsic differences between fetal and mature myocardium have been offered, including a paucity of contractile elements within immature myocytes, the increased amount of nuclear material within mature myocytes, the relatively haphazard orientation of contractile elements within immature myocardium versus the parallel orientation of the contractile elements of mature myocardium, and the relative deficiency of sarcomeres in fetal myocardium versus the rich distribution of sarcomeres and t-tubules that provide intracellular calcium stores to the contractile elements of mature myocardium.

Pulsed Doppler and Doppler tissue imaging studies of biventricular diastolic filling are suggestive of restrictive ventricular diastolic physiology throughout mid and late gestation (57–60) (Fig. 27.9). Recently, normative data have been presented for strain and strain rate analysis of the fetal myocardium (61,62). It is unclear at this point whether this technique will offer a reliable and reproducible means of analyzing fetal systolic and diastolic performance.

Rudolph (1) has summarized the known characteristics of fetal myocardium and the in utero environment to explain the proclivity of fetuses toward the development of interstitial edema and hydrops fetalis (Fig. 27.10). These findings explain the frequent development of hydrops fetalis among fetuses with pressure or volume overload, or sustained bradyarrhythmias or tachyarrhythmias.

Huhta et al. (63,64) have proposed the use of a Cardiovascular Profile Score to determine the overall status of

Figure 27.3. Montage of five four-chamber views of the fetal heart (A–E), including one normal fetal heart (C) and five examples (A,B,D,E) of fetal four-chamber views that are abnormal, owing to perturbed flow distribution, in a setting of a normal central fibrous body. **A:** Four-chamber view of the heart of a fetus with PS. The right ventricle (RV) is thick walled and has a slightly diminutive right ventricular cavity. In the presence of PV stenosis and a competent tricuspid valve, the increased right ventricular afterload results in myocardial hypertrophy, whereas the decreased diastolic compliance of the hypertrophic myocardium results in increased right-to-left shunting at the level of the foramen ovale, with increased left ventricular (LV) diastolic filling volume and diminished right ventricular filling volume. **B:** Four-chamber view of the heart of a hydropic fetus with severe AS, left ventricular dilation, and fibroelastosis, with decreased systolic contraction. Severe mitral regurgitation resulted in marked left ventricular (LV) and left atrial (LA) dilation and premature closure of the foramen ovale. **C:** Normal four-chamber view of fetal heart demonstrating symmetrical right and left atria (RA, LA) and ventricles (RV, LV). **D:** Four-chamber view of fetal heart of a fetus with coarctation of the aorta. The right ventricle is disproportionately enlarged, whereas the left ventricle is relatively volume depleted. This is due to the abnormal distribution of blood flow, favoring outflow from the right ventricle at the expense of outflow from the left ventricle in this fetus with aortic arch hypoplasia. **E:** Four-chamber view of fetal heart near term. This image demonstrates the finding that disproportionate right ventricular dilation, while characteristic of flow redistribution in fetuses with coarctation of the Ao, is sensitive but not specific for this malformation. In this case, the disproportion between ventricular dimensions is not associated with aortic coarctation, but rather, with normal flow redistribution near term in a fetus with mild constriction of the ductus arteriosus, with resulting increased right ventricular afterload. This image was found in one of the patients in our series who was incorrectly suspected to have coarctation of the aorta, based on this finding.

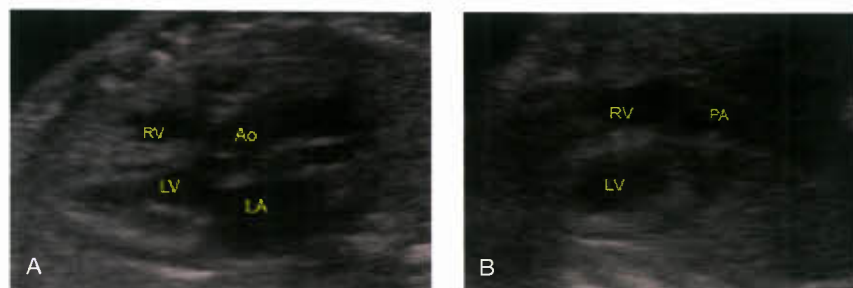


Figure 27.4. A: Long-axis view of the LVOT. The anterior right ventricle (RV) is separated from the posterior left ventricle (LV) by the ventricular septum. The integrity of the anterior ventricular septum can be evaluated. The membranous and conoventricular septa are intact and are in fibrous continuity with the anterior wall of the ascending aorta (Ao). The anterior mitral valve leaflet is in fibrous continuity with the posterior aortic wall, resulting in commitment of the left ventricle to the ascending aorta. The left atrium is posterior to the ascending aorta. The subaortic region is unobstructed. The right pulmonary artery passes beneath the aortic arch. B: Long-axis view of the right ventricular outflow tract. The right and left ventricles (RV, LV) are separated by the intact ventricular septum. The main pulmonary artery (PA) arises above the conus and dives posteriorly to continue into the ductal arch. The main pulmonary artery is perpendicular to the ascending aorta, which passes vertically until the branch point between the innominate artery and the aortic arch.

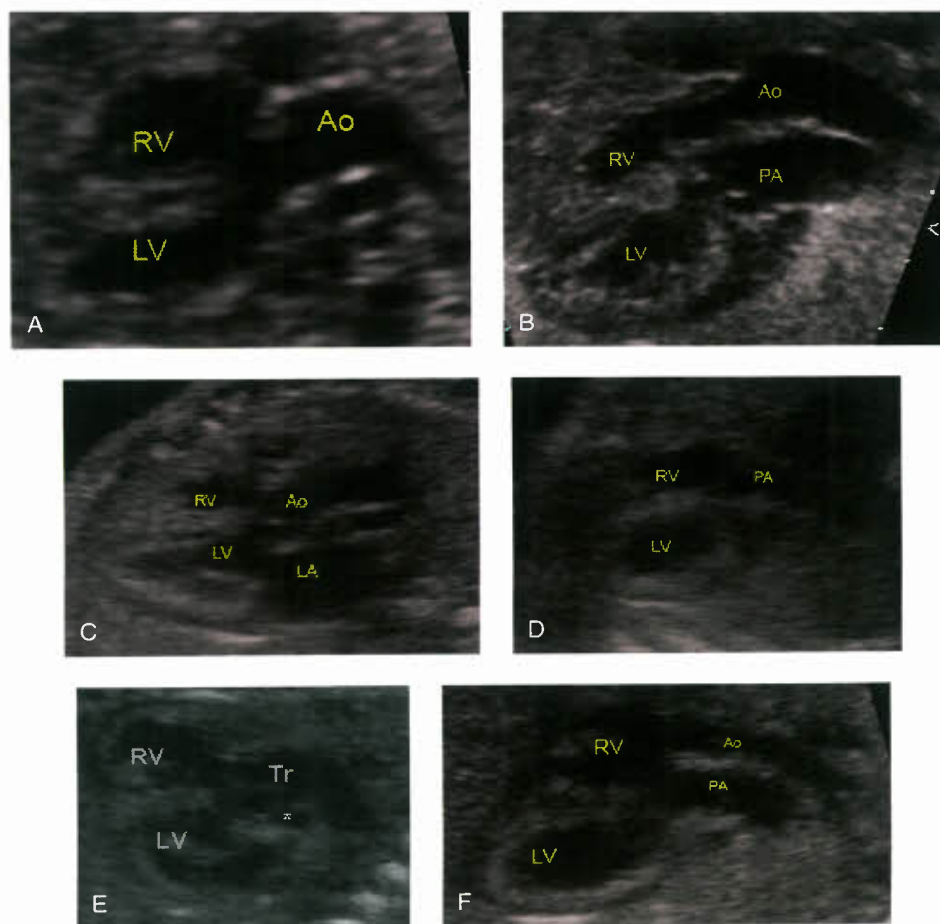


Figure 27.5. Montage of six long-axis views of the fetal heart. A: Long-axis view of the LVOT of a fetus with pulmonary atresia with VSD. The ventricular septum is interposed between the left and right ventricles (LV, RV). The large ascending aorta (Ao) overrides a large, subaortic, conoventricular septal defect. The right ventricular outflow tract is not visualized in this view. B: Long-axis view of the LVOT in a fetus with d-TGA. The interventricular septum is intact. There is ventriculoarterial discordance, with the transposed ascending aorta (Ao) arising anteriorly from the right ventricle (RV) and the main pulmonary artery (PA) arising from the left ventricle. The parallel course of the great arteries is characteristic of transposition or malposition. C,D: Normal left (C) and right (D) ventricular outflow tracts. E: Long-axis view of the LVOT in a fetus with type I persistent truncus arteriosus. The common arterial trunk (Tr) overrides a large conoventricular septal defect. A common pulmonary artery (asterisk) arises from the left and posterior aspect of the common arterial trunk. F: Long-axis view of the LVOT of a fetus with Taussig-Bing double-outlet right ventricle. The parallel, d-malposed great arteries both arise from over the right ventricle, with the pulmonary artery overriding the subpulmonary VSD. The anterior aorta is much smaller than the posterior pulmonary artery. Further investigation demonstrated a hypoplastic aortic arch.

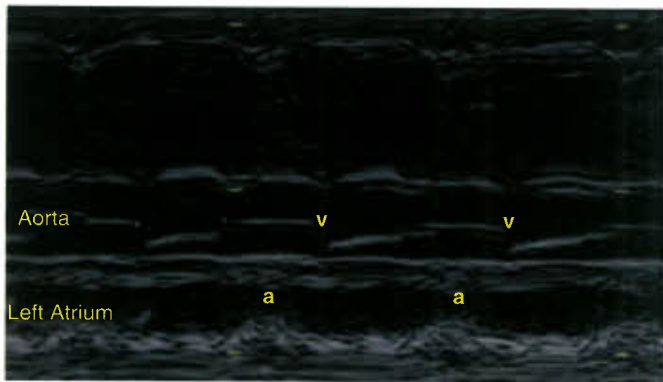


Figure 27.6. M-mode echocardiographic tracing recorded through aortic root of fetus with atrial ectopic tachycardia at 180 beats per minute. The aortic valve opening (v) corresponds to the mechanical response to electrical stimulation leading to ventricular myocardial contraction. Note that there is one atrial undulation (a) for each ventricular contraction.

cardiovascular compensation of given fetuses. They have suggested that this scoring system be used to predict the onset of cardiovascular decompensation in such fetuses (Fig. 27.11).

CONGENITAL HEART DISEASE AND ASSOCIATED ANOMALIES

The association of congenital heart disease with extracardiac malformations of the fetus and neonate is well recognized. In some cases, the genetic basis for these associations has been defined (9,10,65–68).

Increased nuchal fold thickness during the first trimester of pregnancy may be associated with a high incidence of congenital heart disease. In some cases, the increased nuchal thickness is related to karyotypic abnormalities such as Turner (XO) syndrome or trisomy 21 (69–74). In other cases, karyotype may be normal, and increased nuchal thickness is thought to relate to elevated fetal venous pressure from congestive heart failure. Increased first trimester fetal nuchal thickness is another screening method that has been used as an indication for detailed fetal echocardiographic study (17,75–83).

Typical associations do exist between specific congenital heart malformations, extracardiac malformations, and karyotypic abnormalities. These associations include atrioventricular septal (canal) defects, increased nuchal thickness, macroglossia, hypoplastic fifth metacarpal, duodenal atresia,

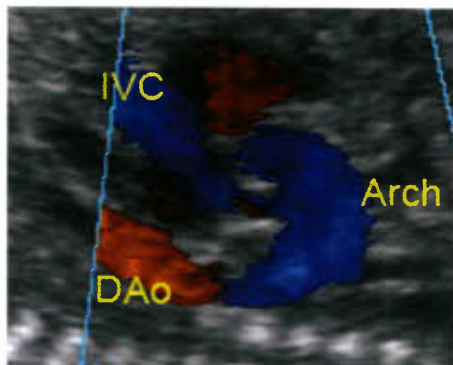


Figure 27.7. Color flow imaging demonstrating inferior vena caval (IVC) return to the fetal right atrium and aortic arch flow (Arch) into the descending thoracic aorta (DAo).

sandal foot, and trisomy 21; double-outlet right ventricle, intrauterine growth restriction, clinodactyly, rocker bottom feet, esophageal atresia, and trisomy 18; VSD, holoprosencephaly, intrauterine growth restriction, cleft lip and palate, and trisomy 13; and coarctation of the aorta, bicommissural aortic valve, cervical cystic hygroma, pedal edema, and Turner syndrome (XO). The association between conotruncal malformations and (del) 22q11.2, DiGeorge syndrome, and/or velocardiofacial syndrome has been well established (84–89).

We have found approximately 60% of fetuses presenting with complete, balanced, AVSD and previously undiagnosed karyotype to have trisomy 21. Approximately 20% of patients with complete AVSD have abnormalities of situs and spleen formation. The association of interrupted IVC, azygous continuation to the superior vena cava, intestinal malrotation, complete heart block, and/or agenesis of the gall bladder and extrahepatic biliary atresia are strongly suggestive of left atrial isomerism and polysplenia. On the other hand, the associated presence of double-outlet right ventricle, AVSD, PS or atresia, totally anomalous pulmonary venous connection, and intestinal malrotation are strongly suggestive of right atrial isomerism with asplenia (90–96). Such fetuses represent some of the most difficult cases to manage postnatally.

The frequent association of karyotypic abnormalities with congenital heart disease diagnosed during the second trimester (30.5%) has led us to recommend genetic diagnosis whenever congenital heart disease is diagnosed in the human fetus (10,65,66,97,98). Although many patients have been reticent to submit to the risks involved with amniocentesis, chorion villus sampling, or fetal umbilical blood sampling, especially if they have no intention of terminating the pregnancy, even if a karyotypic abnormality is found, or if the pregnancy has already progressed past the legal limit for abortion, we have still recommended such testing in selected cases. Although termination of pregnancy is a compelling and common reason for genetic testing, the knowledge of an associated genetic abnormality may serve to change the aggressiveness of tocolytic therapy for the treatment of premature labor or the aggressiveness of fetal monitoring and the use of cesarean delivery for fetal distress during labor in the mothers of such fetuses.

The frequent association of congenital heart disease (C), especially conotruncal malformations and abnormalities of the vertebrae (V), anus (A), trachea (T), esophagus (E), kidneys (R), and limbs (L) (VACTERL) should raise suspicions when congenital heart disease is diagnosed in fetuses with polyhydramnios (e.g., impeded fetal swallowing), oligohydramnios (impeded urine production), scoliosis, or limb reduction (99,100).

Another, increasingly common, indication for targeted echocardiographic imaging is the presence of intensely echogenic foci within the left ventricular cavity (Fig. 27.12). This finding is thought to relate to increased mineralization of the tips of the papillary muscles within the left ventricle and, in and of itself, does not appear to have short- or long-term clinical consequences. Until recently there was some debate about whether these echogenic foci are clinical markers for the presence of trisomy 21. A recent meta-analysis concluded that such foci increase the odds that a given pregnancy is complicated by the Down syndrome by a factor of five to six. It is recommended, therefore, that this factor be included in the risk calculation (e.g., along with traditional serum markers and nuchal translucency evaluation) for consideration of invasive genetic diagnosis for affected fetuses (101–111).

WHAT IS IT THAT PARENTS WANT TO KNOW?

The value of prenatal diagnosis can best be assessed in light of what parents expect from these studies. It would be easier

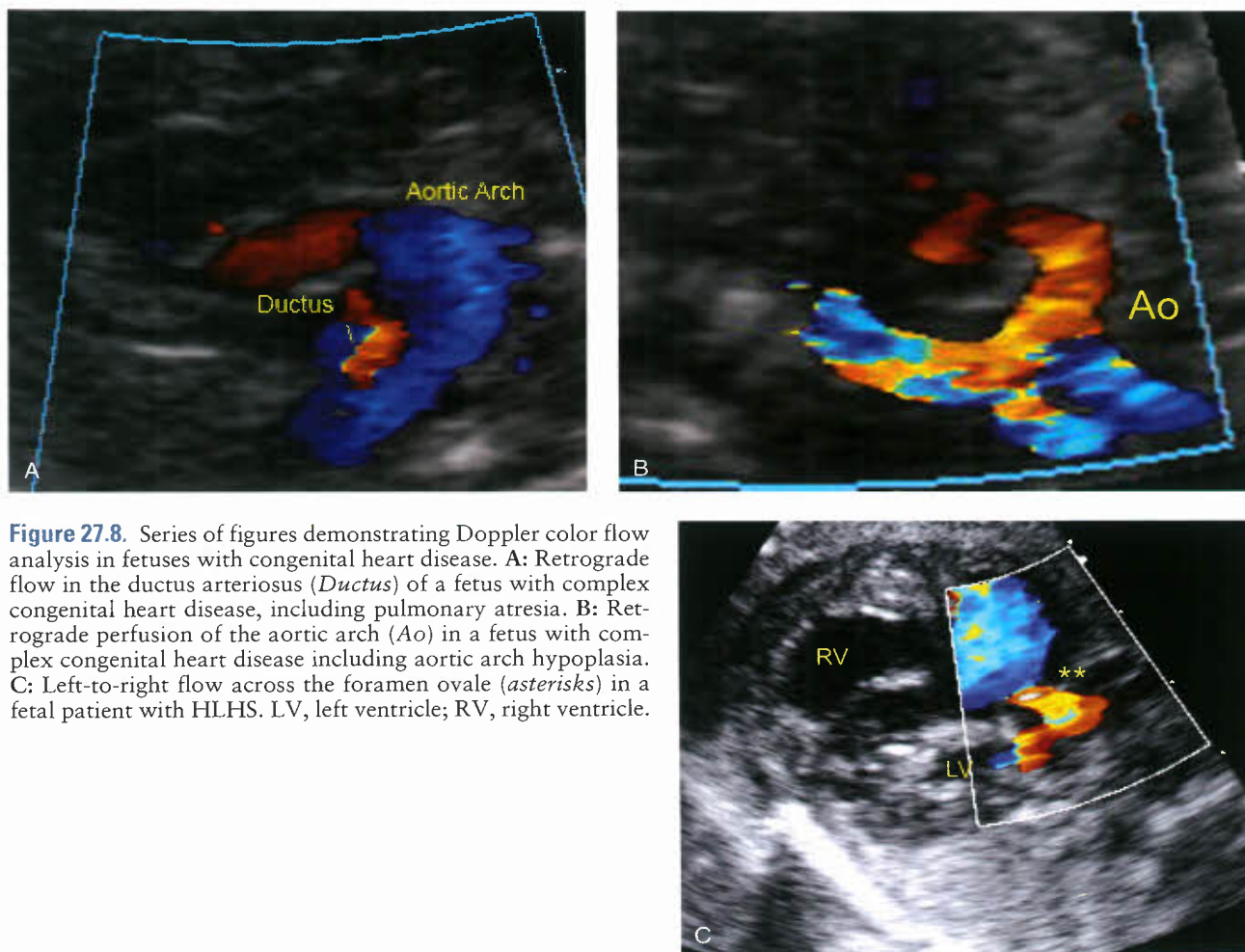


Figure 27.8. Series of figures demonstrating Doppler color flow analysis in fetuses with congenital heart disease. A: Retrograde flow in the ductus arteriosus (*Ductus*) of a fetus with complex congenital heart disease, including pulmonary atresia. B: Retrograde perfusion of the aortic arch (*Ao*) in a fetus with complex congenital heart disease including aortic arch hypoplasia. C: Left-to-right flow across the foramen ovale (*asterisks*) in a fetal patient with HLHS. LV, left ventricle; RV, right ventricle.

to cost account such studies if they had a clear-cut impact on neonatal survival or quality of survival. As we would see below, such an impact is difficult to demonstrate for many of these studies. On the other hand, there is little doubt that detailed prenatal diagnosis has an impact on prenatal counseling and on the process of obtaining informed consent from parents whose fetuses have complex congenital heart disease.

Our counseling process consists of a detailed description of the anatomic abnormalities in the fetus. This includes

abnormalities of the heart and cardiovascular system, as well as extracardiac abnormalities that may have been diagnosed. The details of neonatal care, including the timing, location, and mode of delivery; details of medical support, including the potential need for prostaglandin E_1 infusion for the maintenance of ductal patency; and the potential need for reparative or palliative surgery in the neonatal period are discussed. The details of neonatal and later surgical procedures are discussed, and the parents are given the opportunity to speak

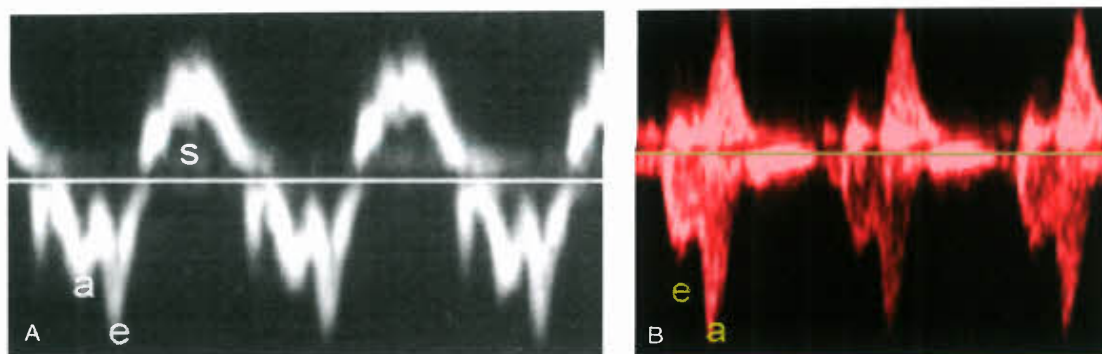


Figure 27.9. Doppler tissue imaging velocities from lateral tricuspid valve ring (A) and Doppler flow-velocity waveforms from right ventricular inflow of normal midtrimester fetus (B). Note dominant a' and a waves. These waveforms are consistent with relatively restrictive fetal ventricular myocardium at this stage of development.

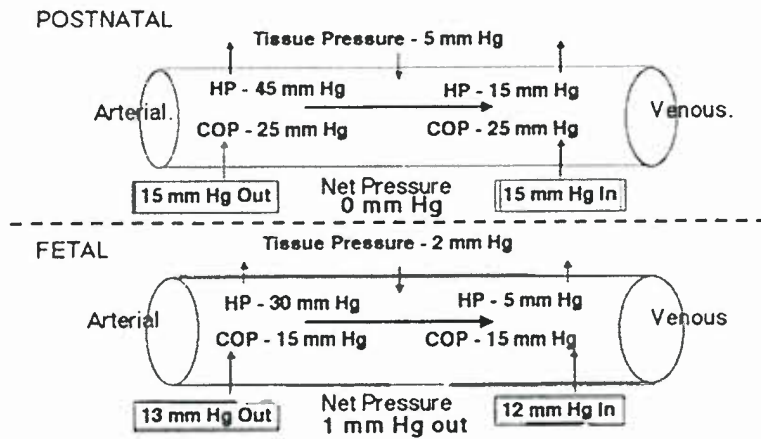


Figure 27.10. Schematic representation of idealized postnatal versus fetal capillary hemodynamics. The relationship between hydrostatic and plasma oncotic pressures and estimated interstitial tissue pressure result in a net outward pressure gradient of 1 mm Hg in the fetus, whereas in the postnatal cardiovascular system the net pressure gradient is 0. This explains the dependency of the fetal cardiovascular system on avid lymphatic drainage to prevent fetal edema and fluid third spacing.

with the pediatric cardiac surgeons, pediatric surgeons, and neonatologists who are likely to be involved in neonatal management.

In large part, parents care little about the detailed name or anatomic description of their child's anomaly. They are, most often, interested in learning what the short-, mid-, and long-term prospects for survival are. These are often related to associated anomalies, genetic syndromes, or underlying anatomy. From a purely anatomic perspective, the breakpoint in the continuum of disease severity, from 1 (minimal) to 10 (most severe), occurs at 8. Eight to ten on this scale represents lesions that are not reparable into a two-ventricular physiology, and will, by definition, require Fontan palliation and/or orthotopic transplantation.

The prospects for cardiac and neurodevelopmental outcome are discussed, and the parents are encouraged to ask questions of the physician management team and/or a team composed of parents of children with similar problems who have consented to be available, as requested.

DOES PRENATAL CARDIAC DIAGNOSIS MAKE A DIFFERENCE?

It has taken approximately a quarter-century of experience with prenatal cardiac diagnosis to demonstrate that such studies have a positive impact on survival (112–114). In fact, multiple studies that focused on the impact of prenatal diagnosis of HLHS appeared to suggest that prenatal diagnosis had a negative influence on short-term survival (49,115–128). This is almost certainly related to a weighting toward prenatal diagnosis in a sicker subpopulation of fetuses. A study undertaken at Yale during the early 1990s failed to demonstrate a survival advantage related to the prenatal diagnosis of congenital heart disease with single-ventricle physiology, whereas fetuses with lesions reparable into two ventricular systems appeared to enjoy a significant enhancement of survival prospects (10). This study also demonstrated a common experience with several other series in which it was noted that prenatal cardiac diagnosis, by facilitating anticipatory use of prostaglandin E_1 to prevent closure of the ductus arteriosus in neonates with critical impairment of systemic or pulmonary blood flow, allows affected fetuses to avoid neonatal acidemia (129–131). Although currently an unproven hypothesis, the potential neurodevelopmental advantage to be derived by the affected neonate who avoids acidemia may, in the long run, prove to be the most important long-term salutary effect of prenatal cardiac diagnosis (132). Among the individual cardiac lesions for which prenatal diagnosis has been suggested to impart a survival advantage are transposition of the great arteries (TGA), coarctation of the aorta, and HLHS. A review

of the experience in the latter series emphasizes the impact of prenatal diagnosis on the parental intention-to-treat decision-making process (10,49,122–124,127,133).

The Impact of Prenatal Cardiac Diagnosis on Planning for Delivery

A relatively unique consideration of the impact of prenatal cardiac diagnosis on outcomes that is not readily appreciated in reviews of surgical outcome for individual lesions relates to the options for site of delivery of these patients. It has been demonstrated that surgical survival for neonates with HLHS is directly related to the surgical volume of the individual surgical center (134). Prenatal diagnosis, by providing parents with the luxury of time to conduct research, may alter survival through alteration of the site of delivery and subsequent surgery. It is possible, if not likely, that the latter will exert a profound impact of prenatal cardiac diagnosis on postnatal survival.

With the possible exception of patients with associated extracardiac lesions (e.g., abdominal wall defects) that necessitate cesarean delivery (135), it is rare for the pediatric cardiologist to become involved in the decision making concerning mode of delivery. Possible exceptions include fetuses with cardiac rhythm disturbances that preclude effective intrapartum fetal heart rate monitoring. Such arrhythmias may include chaotic rhythms that confound the logic of external fetal heart rate monitors that calculate heart rate from instantaneous measurement of R-R intervals or regular tachyarrhythmias or bradyarrhythmias such as AF or complete heart block, where the heart rate may not vary with the alterations in sympathetic and parasympathetic tone that are associated with uterine contraction (10).

Cesarean delivery may be indicated in rare situations in which the coordinated care of the neonate requires the skills of multiple specialists who are assembled specifically at the time of delivery. In the year 2005, at the Morgan Stanley Children's Hospital of New York–Presbyterian we delivered four fetuses by cesarean section specifically for cardiac reasons. Two fetuses were delivered by cesarean section owing to prenatal identification of premature closure of the foramen ovale in fetuses with HLHS with secondary pulmonary venous obstruction, whereas one fetus was delivered by cesarean section to undergo cardiac surgery because of obstructed totally anomalous pulmonary venous return in a setting of right atrial isomerism, AVSD, double-outlet right ventricle with d-malposition of the great arteries, and pulmonary atresia. One fetus, with d-TGA and congenital diaphragmatic hernia, was delivered by cesarean section and immediately placed on extracorporeal membrane oxygenation (ECMO), pending surgical repair of diaphragmatic hernia and subsequent successful arterial switch repair of TGA.

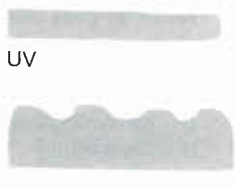




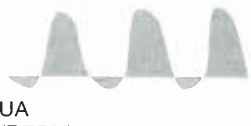
	NORMAL	-1 POINT	-2 POINTS
Hydrops	None (2 pts)	Ascites <u>or</u> Pleural effusion <u>or</u> Pericardial effusion	Skin edema
Venous Doppler (Umbilical vein) (Ductus venosus)	 UV DV (2 pts)	 UV DV	 UV pulsations
Heart Size (Heart Area / Chest Area)	≤ 0.35 (2 pts)	0.35 - 0.50	> 0.50 < 0.20
Cardiac Function	Normal TV & MV RV/LV S.F. > 0.28 Biphasic filling (2 pts)	Holosystolic TR <u>or</u> RV/LV S.F. < 0.28	Holosystolic MR <u>or</u> TR dP/dt < 400 <u>or</u> Monophasic filling
Arterial Doppler (Umbilical artery)	 UA (2 pts)	 UA (AEDV)	 UA (REDV)

Figure 27.11. Huhta's proposed Cardiovascular Profile Score.

It is unusual for neonates with congenital heart disease to require resuscitation in the delivery room. In such cases, there is usually an associated problem that interferes with adequate lung inflation at the time of the first breath. Such issues may arise in fetuses with associated pleural effusions,

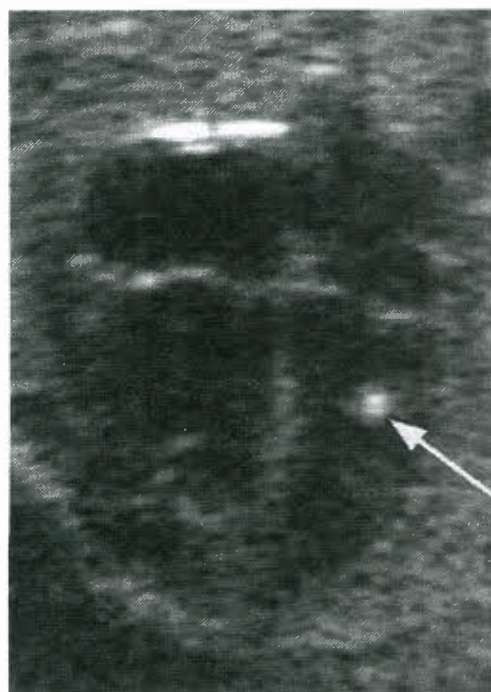


Figure 27.12. Intensely echogenic focus associated with the anterolateral mitral papillary muscle. This does not represent a cardiac neoplasm, nor does it represent a structural malformation of the fetal heart. There has been a suggestion that such foci are associated with an increased odds ratio of associated fetal Down syndrome. The *arrow* points to an echogenic focus in the left ventricle.

in fetuses with associated congenital diaphragmatic hernia, or in fetuses in which marked cardiomegaly results in a mass effect and pulmonary hypoplasia (e.g., occasional cases of Ebstein malformation of the tricuspid valve or AS with marked mitral regurgitation). In fetuses with severe pulmonary venous obstruction, such as those with totally anomalous pulmonary venous drainage with obstruction (particularly common among fetuses with visceral heterotaxy and right atrial isomerism), congenital atresia of the common pulmonary vein, or in fetuses with HLHS and premature closure of the foramen ovale, gas exchange may be rendered inadequate by pulmonary edema. Doppler waveform analysis in the branch pulmonary veins may be predictive of critical pulmonary venous obstruction (Fig. 27.13). Fetuses with tetralogy of Fallot (TOF) and absent PV with aneurysmal pulmonary arteries may have inadequate ventilation owing to external airway compression with secondary tracheomalacia or bronchomalacia (Fig. 27.14).

REGIONAL BLOOD FLOW ANALYSIS AND FETAL CARDIOVASCULAR WELL-BEING

Techniques for the antenatal surveillance of the fetus are aimed at the detection of evidence of cardiovascular compromise secondary to hypoxemia and deterioration of acid-base balance (69,129,136–143). Blood flow within the placental circulation is normally characterized by low placental vascular resistance with no evidence of autoregulation within the placental vascular bed, whereas regional arterial flow in the fetal organ beds is finely tuned through local autoregulation. Impaired forward arterial flow is almost invariably associated with altered preload and with abnormalities of flow within the fetal central venous system, including the inferior vena cava (IVC), ductus venosus (DV), and umbilical vein (UV). Abnormalities of flow in these three locations may be used to predict acid-base status in growth-retarded fetuses (Fig. 27.15). Progressive deterioration in cardiac pump

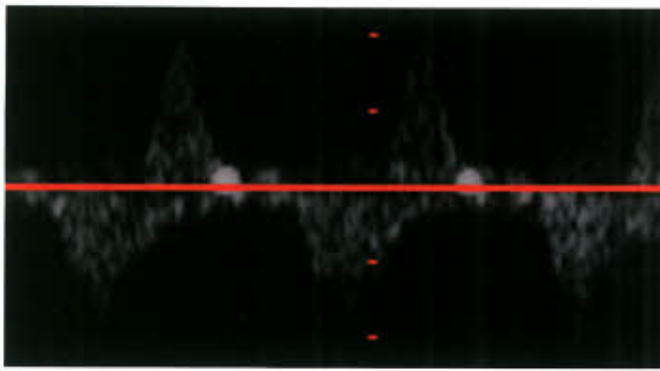


Figure 27.13. To-and-fro flow pattern in pulmonary vein in a fetal patient with obstructed left ventricular inflow and outflow. This pattern is highly suggestive of severe pulmonary venous obstruction. This fetus is likely to have critical pulmonary insufficiency in the neonatal period. Such fetuses may require emergent pulmonary vein decompression in the neonatal period and have been subjected to efforts at atrial septal fenestration in utero.

function is associated with absent forward venous flow during atrial contraction or with atrial flow reversal in the central venous circulation. The finding of retrograde flow in the DV during atrial contraction is almost always associated with fetal acidemia, and diastolic notching of flow within the UV, especially with evidence of absent or reversed end-diastolic flow in the umbilical artery (UA), is a finding that presages fetal death if delivery is not accomplished within the ensuing 72 hours (Fig. 27.16) (144–149).

Ventricular–vascular coupling within a cardiovascular system based largely on massive blood flow through a low-resistance bed such as the placenta, with a propelling pump consisting of fetal myocardium, with limited preload and afterload reserve is markedly sensitive to alterations in placental resistance and/or to altered myocardial performance or intravascular volume (150). Elevation of placental vascular

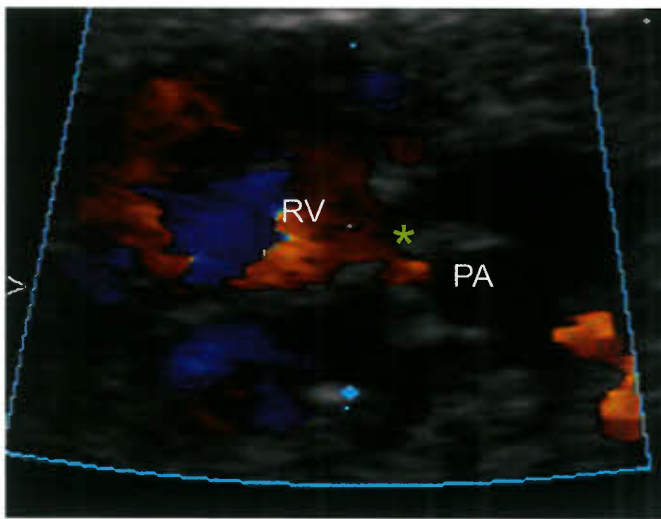


Figure 27.14. Pulmonary regurgitation (asterisk) through the rudimentary PV structure in a fetus with TOF with absent PV results in dilation of the right ventricle (RV) and pulmonary artery (PA). Such fetuses are in danger of pulmonary insufficiency in the delivery room secondary to external compression of the major airways by the aneurysm-dilated main and proximal right pulmonary artery.

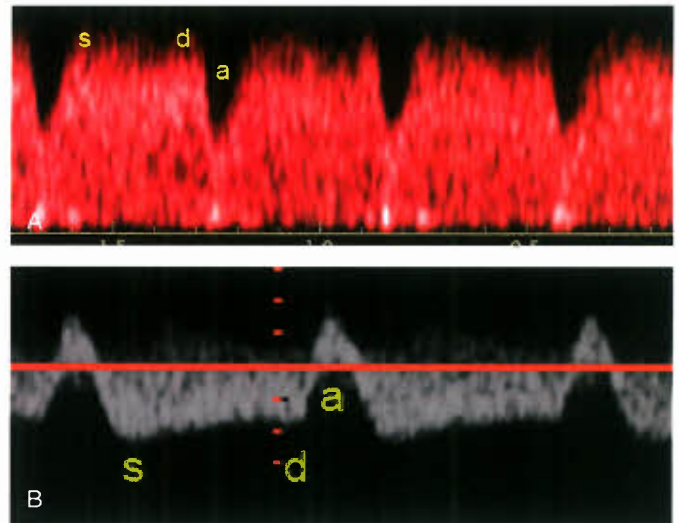


Figure 27.15. DV flow waveforms. A: Normal DV flow demonstrates high continuous antegrade flow during systole (s), diastole (d), and during atrial contraction (a). B: Retrograde DV flow during atrial contraction. This is a finding that is associated with progressive ventricular dysfunction, with increased end-systolic volume, and increased end-diastolic pressure.

resistance is typically accompanied by an increase in umbilical arterial pulsatility (difference between peak arterial and end-diastolic flow velocity), whereas enhanced perfusion (organ-sparing) of fetal organs is associated with decreased local resistance and decreased arterial pulsatility. Brain sparing has been demonstrated to be strongly predictive of perinatal

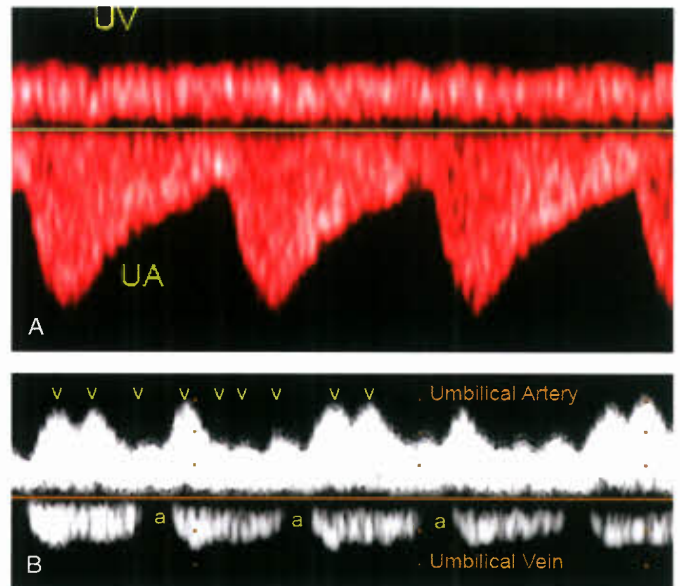


Figure 27.16. A: Simultaneous recording of UA and UV waveforms in normal fetus. Note the high end-diastolic velocity in the UA, characteristic of a low-resistance placental circulation. There is continuous antegrade flow in the UV. B: Umbilical arterial and venous flow in a fetus with paroxysmal polymorphic VT and hydrops fetalis. Note chaotic, rapid, undulating UA flow and marked umbilical venous notching associated with cannon a waves. The latter are associated with elevated systemic venous pressure, hydrops fetalis, and fetal acidosis.

morbidity in fetuses with intrauterine growth retardation and has been correlated with impaired cognitive outcome in children who were born as very preterm infants (151–153). It has been suggested that growth-restricted human fetuses with chronic cerebral hypoxemia and established brain-sparing centralization of blood flow may have limited capacity for further hyperperfusion in response to superimposed acute hypoxemia (154). Fouron et al. (155–157) have focused attention on the direction of blood flow in the aortic isthmus among patients with congenital heart disease. These workers have found that retrograde isthmus blood flow is correlated with impaired neurodevelopmental outcome, perhaps related to limited cerebral oxygen delivery. We have focused our attention on pulsed Doppler evidence of centralization of fetal blood flow as evidence of autoregulation of fetal cerebral blood flow in the presence of congenital cardiac malformations associated with impaired cerebral oxygen delivery owing to impaired cerebral arterial oxygen content or impaired cerebral blood flow volume (158). We have speculated that these alterations in blood flow may be associated with altered neurodevelopmental potential among these fetuses. Kaltman et al. (159) found similar cerebral flow redistribution among fetuses with right ventricular outflow obstruction, whereas Jouannic et al. (160) found similar cerebral flow redistribution among fetuses with TGA.

THE PRENATAL EVOLUTION OF CONGENITAL HEART DISEASE

The principal underlying Rudolph's concept that understanding fetal cardiovascular adaptation to congenital heart disease will provide insight into the transitional and neonatal circulation is that in the fetal heart form follows function. It was postulated for many years prior to the availability of ultrasound for the observation of progressive cardiovascular development in the presence of congenital heart disease that certain congenital cardiac malformations evolve through the course of pregnancy, with a tendency toward progressive chamber and blood vessel disproportion (1).

It has been demonstrated, for example, that pulmonary outflow obstruction in fetuses with TOF may progress in severity, even to the point of acquired pulmonary atresia, over the course of pregnancy (118,161,162). Aortic or pulmonary valvar stenosis may progress over the course of pregnancy into valvar atresia, and ventricular wall thickness may increase in concert with increased ventricular peak systolic pressure. Ventricular chamber development may be stunted by the development of endocardial fibroelastosis and diminished ventricular compliance through pregnancy (163). On the other hand, the onset of AV valve regurgitation, related to papillary muscle dysfunction or chordal rupture, may result in marked progressive ventricular and atrial chamber enlargement.

PRENATAL TREATMENT OF CONGENITAL HEART DISEASE

In 1992, Allan et al. reported an experience with a percutaneous technique for fetal aortic balloon valvuloplasty (164) involving needle puncture of the maternal abdomen, uterus, and fetal thorax, with direct catheterization of the fetal left ventricle by direct apical puncture and subsequent wire and catheter manipulation across the stenotic aortic valve. Four fetuses were subjected to this technique, with a single long-term survivor. That technique was devised against a background of appalling survival figures for neonates who were undergoing surgical

treatment for that lesion at that time. Interestingly, between the announcement of that procedure in the popular press and the appearance of the publication in the scientific literature, that same group declared a moratorium on the procedure, related in part to improved surgical and interventional catheterization results with neonates with AS (120). A subsequent publication described the world's experience with this technique and documented a 100% failure rate at several institutions (165), with the almost inexplicable conclusion that further investigation was merited to determine the potential role for the technique in the management of fetuses with congenital heart disease.

A decade later, the group from Boston Children's Hospital released to the press the results of a preliminary experience with the use of this same technique, which was being proposed as a means of preventing the evolution of severe fetal AS with associated left ventricular fibroelastosis into HLHS. This group has attempted to establish criteria for selection of candidates for this procedure and has preliminary data to suggest that in selected cases fetal balloon valvuloplasty may result in incremental aortic and left ventricular growth, and may result in adequate left heart development to obviate the need for Norwood-type palliation, with subsequent biventricular palliation of these patients. This group has suggested that retrograde perfusion of the aortic arch is one of the criteria that is predictive of hypoplastic left heart in patients who do not undergo palliation. Their experience suggests that successful aortic balloon valvuloplasty results in antegrade perfusion of the aortic arch and isthmus in these fetuses (112,166).

Tulzer et al. (167,168), from Austria, reported an experience with fetal percutaneous pulmonary balloon valvuloplasty, under ultrasound guidance, to alter the natural history of pulmonary atresia with intact ventricular septum. Their initial experience was undertaken to avoid the onset of hydrops fetalis. The potential for hydrops fetalis was assessed on the basis of the Cardiovascular Profile Score that was proposed by Huhta (63). Subsequent experience has suggested that pulmonary outflow obstruction is almost invariably associated with atrial flow reversal in the IVC and DV that may affect the cardiovascular performance score and unduly increase the prediction of subsequent hydrops fetalis. Several centers have subsequently reported successful PV dilation and biventricular management of fetuses who presented with pulmonary atresia and intact ventricular septum (169–171). Rigorous evaluation of the selection criteria and outcome of such fetuses has not been reported at this point.

The Boston Children's Hospital group has also reported a preliminary experience with percutaneous balloon dilation of the atrial septum, in an effort to palliate fetuses with HLHS and pulmonary venous obstruction secondary to premature stenosis or closure of the foramen ovale (112). This technique was devised to improve the results for the palliation of these fetuses, who may present with severe pulmonary hypertension and pulmonary lymphangiectasia. The experience reported to date suggests that needle perforation of the atrial septum, wire passage across the septum, and delivery of an angioplasty catheter with subsequent balloon septoplasty can be accomplished. This preliminary experience suggests that improvement in balloon technology will be required before the technique may be expected to result in a lasting fenestration of the atrial septum that is adequate to effect a positive impact on fetal physiology. This same group has recently reported successful coronary stent placement in the atrial septum of a fetus with HLHS. This fetus survived and subsequently underwent successful Norwood stage I palliation. A recent report describes the use of fetoscopy to place an intracardiac ultrasound catheter into the esophagus of a human fetus with HLHS to provide transesophageal imaging during an unsuccessful attempt to perform balloon septoplasty on a fetus with critical pulmonary venous obstruction (172).

Reports of the use of fetoscopy and laser fenestration of the atrial septum in such fetuses, for the management of AS, have emerged from Tampa (173). Ludomirsky et al. in St. Louis, are investigating the use of targeted ultrasound to create fenestrations of the fetal atrial septum. Scattered anecdotal reports of attempts to perform aortic and pulmonary balloon valvuloplasty procedures have surfaced at national and international cardiology meetings.

The overall results of these procedures ideally should be collected, analyzed, and reported in a critical fashion, lest the pediatric cardiology community repeat the hard lessons learned by the maternal-fetal medicine community during the past 25 years. The latter have had a broad experience with fetal therapy, and have seen several promising techniques capture the imagination of the medical community and the popular press, only to be abandoned later after disappointing functional outcomes were found on follow-up of surviving infants. Such techniques were based on a seemingly sound understanding of physiology and on a genuine desire to be of help to these fetuses. These included procedures for fetal exteriorization for repair of diaphragmatic hernia and for palliation of urinary tract obstruction, and percutaneous cerebral ventriculoamniotic shunting for palliation of obstructive hydrocephalus (113,174–183).

THE CURRENT ROLE OF FETAL ECHOCARDIOGRAPHY

While fetal echocardiography and fetal cardiology have been incorporated into many pediatric cardiology programs during the past two decades, the role of fetal cardiology varies considerably from location to location. In many cases, the role of fetal cardiology is dependent upon the relationship that exists between maternal-fetal medicine and pediatric cardiology in the institution, and whether individual institutions have obstetric and neonatal services housed under the same roof.

We have reviewed the role that prenatal cardiac diagnosis has had during the last 4 calendar years (2007 to 2010) at the Morgan Stanley Children's Hospital of the Columbia University Medical Center campus of New York–Presbyterian Hospital. This service represents a highly evolved fetal cardiology service, with an extremely active Department of Obstetrics and Gynecology, with a maternal-fetal-medicine division that has been actively involved in the performance of detailed fetal echocardiography for many years. Similarly, the Pediatric Echocardiography service of the Morgan Stanley Children's Hospital has been extremely aggressive in its approach to fetal cardiology, and the integration of these patients into the neonatal cardiology and cardiovascular surgery service.

Unlike the case at many centers, where the pediatric cardiology service provides “screening” services for fetal congenital heart disease, the service at our hospital is based on a model in which the pregnant woman is seen, almost exclusively, by the obstetrical service, until a high-risk indication for a targeted fetal echocardiogram is identified (Table 27.1). While services that perform screening studies usually find evidence of fetal cardiovascular disease in approximately 10% to 15% of scans (Table 27.2), with the predominant indication for scan being a previous family history of congenital heart disease, we have a very different experience (270, 271).

In 2007 to 2010, our laboratory detected 615 fetuses with congenital cardiovascular abnormalities among 2,828 fetuses undergoing fetal echocardiography (yield 22%). There were 31 false positives (cases of relative right heart enlargement and suspected coarctation of the aorta including six fetuses with left-sided congenital diaphragmatic hernia with rightward deviation of the heart and mediastinum). Fourteen false-negative cases were documented, including 11 small VSDs

that did not require surgical or medical management and three moderate to large VSDs that required surgery in the first months of life.

Of the 615 patients with congenital heart disease follow-up is complete for 90%. Sixty patients (10%) have been lost to follow-up and an additional 15 were known to have been liveborn at outside hospitals. Of 396 babies known to have been liveborn, 64% (184) underwent surgery during the first 6 months of life (249 at Columbia University Medical Center and 3 at outside hospitals). Ten additional babies underwent interventional catheterization procedures at Columbia. Of these babies 88 (33%) have undergone additional surgery within the first 6 months of life, and nine are <6 months of age as of the time of writing this chapter.

Of the 615 cases of correctly identified congenital heart disease, the “categories” of abnormality, in descending order of frequency, consisted of conotruncal malformations (213 [35%]), left heart obstructive lesions (126 [20%]), left-to-right shunt lesions (106 [17%]), including 29 complete AVSD, right heart obstructions (51 [8%]), visceral heterotaxia (33 [5%]), double-inlet left ventricle (18 [3%]), aortic arch anomalies (27 [4%]), Ebstein malformation of the tricuspid valve (14 [2%]), single ventricle variants (17 [3%]), absent PV syndrome with intact ventricular septum (2 [$<1\%$]), complex conjoined hearts in thoracopagus twins (2 [$<1\%$]), and other, one-of-a-kind anomalies (6 [1%]) (Table 27.3).

One hundred thirty (21%) patients either underwent termination of pregnancy (102) or chose nonintervention (“compassionate care”) (28) for their offspring. The diagnoses of these fetuses, presented in Table 27.4, were weighted toward severe anomalies such as HLHS and visceral heterotaxia, and those with chromosomal and severe extracardiac abnormalities.

Twenty-eight patients suffered intrauterine fetal demise (Table 27.5). These included 10 with documented chromosomal anomalies including five fetuses with trisomy 18, three with trisomy 21, and two with trisomy 13. Two fetuses with demise had additional severe anomalies but no chromosomal study, including one with a complex single ventricle and absent kidneys, and one with double-outlet right ventricle and Pentalogy of Cantrell. Four fetuses who suffered intrauterine demise had normal chromosomes with an extracardiac fetal anomaly or a maternal abnormality, including three fetuses with hypoplastic left heart variants (one with an absent stomach, one with prune belly syndrome, and one with maternal protein S deficiency), and one fetus with persistent truncus arteriosus and placental insufficiency. Three fetuses had intrauterine demise associated with complete AV block, including two with left atrial isomerism, and one with atrial and VSDs. The remaining nine fetuses with intrauterine demise had congenital heart disease but no additional anomalies, including four fetuses with Ebstein malformation of the tricuspid valve (comprising 29% of fetuses with Ebstein malformation seen), two fetuses with pulmonary atresia and intact ventricular septum (one of whom also had left ventricular outflow obstruction and no karyotype, the other with severe cardiomegaly and a normal karyotype), two fetuses with AVSD and hydrops fetalis (one complete AVSD with no chromosomal study and one unbalanced, LV-dominant AVSD with normal chromosomes), and one fetus with absent PV syndrome and intact ventricular septum.

Of the 615 fetuses with congenital cardiac malformations 327 (53%) underwent prenatal karyotyping. Seventy (21%) of these fetuses had identifiable genetic syndromes while 169 patients underwent only postnatal genetic testing, of which 17 (10%) had an abnormality. Chromosomal abnormalities included 39 cases of trisomy 21 (15 with complete AVSD, and 13 with TOF), 13 with trisomy 18 (seven with VSD, four with double-outlet right ventricle, one with complete AVSD, one with AS), four with Turner Syndrome (two with bicommissural aortic valve, one with HLHS, and one with a small VSD).

TABLE 27.3 Congenital Heart Disease Diagnoses in Fetuses 2007–2010 (*n* = 615)

Diagnosis	2007	2008	2009	2010	Total
Conotruncal Malformations					
D-Transposition/IVS	11	12	8	5	36
D-Transposition + VSD, PS, or CoA	6	1	11	3	21
Double-Outlet RV (±Malposition)	12	16	8	9	45
Tetralogy of Fallot	9	15	11	20	55
Pulmonary Atresia/VSD	5	4	3	6	18
Pulmonary Atresia/VSD/MAPCAs	3	3	2	2	10
Tetralogy with Absent PV Syndrome	0	2	3	0	5
TOF/AVSD	1	1	4	1	7
L-TGA (±VSD)	3	1	0	1	5
Truncus Arteriosus	3	2	2	4	11
Left Heart Obstructive Lesions					
HLHS (Mitral/Aortic Atresia)	15	22	16	16	69
HLHS Variant	7	5	0	1	13
Shone's complex	10	10	6	6	32
Isolated mitral valve anomaly	0	2	0	0	2
Aortic stenosis	5	2	2	1	10
Left-to-Right Shunt Lesions					
Atrioventricular Septal Defects					
Complete AVSD	9	10	4	6	29
Ostium Primum ASD	1	3	3	1	8
Ventricular Septal Defect—mod to large	2	10	5	19	36
Ventricular Septal Defect—small	4	9	10	10	33
Right Heart Obstructive Lesions					
Tricuspid Atresia (± d-TGA)	1	6	4	6	16
Pulmonary Atresia + IVS	6	3	5	3	17
Tricuspid Stenosis	0	1	0	1	2
Pulmonary Stenosis	2	4	6	4	16
Visceral Heterotaxia	7	7	9	10	33
Double Inlet LV	5	3	5	5	18
Absent PV/IVS	1	0	1	0	2
Aortic Arch Anomalies					
Isolated Coarctation	1	1	2	0	4
Coarctation + VSD	1	4	4	4	13
IAA + VSD	3	5	1	1	10
Ebstein Malformation of the TV	3	3	5	3	14
Single Ventricle Variants	3	5	6	3	17
Complex conjoined hearts	0	0	2	0	2
Other (1 of a kind)	1	1	2	2	6
TOTAL	140	172	150	153	615

TABLE 27.4

Terminations of Pregnancy or Compassionate Noninterventional Care for Fetuses with Congenital Heart Disease 2007–2010 (*n* = 130)

Terminations of Pregnancy (<i>n</i> = 102)		
Cardiac Lesion	<i>n</i>	Genetic or Extracardiac Abnormality
Hypoplastic Left Heart Syndrome	13	None
Tetralogy of Fallot	13	22q11 deletion (1), Trisomy 21 (1), XYY (1)
VSD	11	Trisomy 18 (3), Trisomy 13 (1), Chromosome 13 deletion (1), Cardiomyopathy (1), CDH (1), CNS (1), skeletal (2), renal (1)
Heterotaxy	9	CDH and renal (1)
Double-outlet right ventricle (DORV)	6	Trisomy 13 (1)
AVSD	5	Trisomy 21 (4)
Complex Single Ventricle	4	CNS (1)
Tricuspid Atresia	4	None
Pulmonary atresia/Intact ventricular septum	4	Cleft lip/palate (1)
Double Inlet LV	4	CDH (1)
Pulmonary atresia/VSD/PDA	4	None
Interrupted arch/VSD	3	22q11 deletion (1)
Truncus arteriosus	3	22q11 deletion (2)
Ebstein's	3	None
HLHS variant	3	CNS and renal (1)
PA/VSD/MAPCAs	2	22q11 deletion (1)
Coarctation/VSD	2	Limb/Body wall complex (1)
TOF/Absent PV syndrome	2	22q11 deletion (1)
d-TGA	1	None
Hypoplastic aortic arch	1	CNS and skeletal (1)
Aortic stenosis	1	Trisomy 18(1)
TOF/AVSD	1	Trisomy 21 (1)
Shones	1	CNS (1)
Absent PV syndrome/IVS	1	None
Complex conjoined hearts	1	Conjoined twins (1)
Total	102	
Compassionate (Hospice) Care (<i>n</i> = 28)		
Cardiac Lesion	<i>n</i>	Genetic or Extracardiac Anomalies or Other Issues
DORV	5	Trisomy 18 (2), CHARGE (1), CNS anomaly (1), Perinatal CNS insult (1)
VSD	4	Trisomy 18 (2), Trisomy 21 + hydrops (1), CHARGE (1)
HLHS variant	3	16q24 deletion (1), Chromosome 8 deletion (1), Abnormal head vessel anatomy (1)
HLHS	3	Intact atrial septum/Premature triplet (1), Poor RV function + TR (1), Compassionate care given at OSH (1)
Heterotaxy	3	Obstructive pulmonary venous return as component of cardiac lesion (2), Heart block + hydrops (1)
Single Ventricle Variant	1	Chromosome 4 deletion
AVSD with coarctation of aorta (CoA)	1	Trisomy 18
Pulmonary atresia/intact ventricular septum	1	Severe cardiomyopathy
PA/VSD/MAPCAs	1	22q11 deletion, premature twin

(continued)

TABLE 27.4

Terminations of Pregnancy or Compassionate Noninterventional Care for Fetuses with Congenital Heart Disease 2007–2010 (*n* = 130) (Continued)

Cardiac Lesion	<i>n</i>	Genetic or Extracardiac Anomalies or Other Issues
TOF	1	Renal disease, anhydramnios
Critical pulmonary stenosis	1	Congenital diaphragmatic hernia
Ebstein anomaly	1	Hydrops
PA/VSD/PDA	1	Trisomy 13
Shone's	1	Restrictive Foramen Ovale
Complex conjoined hearts	1	Thoracopagus twins
Total	28	

Eighteen patients were found to have Chromosome 22q11.2 microdeletion (five with truncus arteriosus communis; four with pulmonary atresia, VSD, and major aortopulmonary collateral arteries (MAPCAs); three with TOF; three with interrupted aortic arch (IAA) with VSD; one with hypoplastic left heart with a cervical aortic arch; one with TOF with absent PV syndrome; and one with pulmonary atresia with VSD and patent ductus arteriosus [PDA]). An additional nine patients had unique abnormalities consisting of a chromosomal deletion, gain, inversion, or translocation. There were two patients who underwent prenatal karyotyping but were not diagnosed to have genetic syndromes until postnatal genetic testing took place (one with a 22q11.2 microdeletion and one with an XrX ring chromosome). Table 27.6 reviews the results of chromosomal testing on this cohort of patients.

One hundred thirty-seven fetuses were identified who had congenital cardiac malformations and associated extracardiac malformations. The latter included 63 fetuses with multiple extracardiac anomalies, and 74 with single extracardiac anomalies, including 6 with congenital diaphragmatic hernia, 18 with central nervous system anomalies, 15 with renal anomalies, 9 with gastrointestinal anomalies, 6 with skeletal anomalies, and 6 with abdominal wall defects.

Indications for detailed fetal echocardiographic study are presented in Table 27.7. Note the marked predominance of “suspected congenital heart disease” in this list, and the relative infrequency of “family history of congenital heart disease.” We attribute this, and the paucity of cases of associated chromosomal abnormalities to the maturity of the screening program within maternal–fetal medicine at our hospital.

In a more recent review of our experience (185), we gained important perspectives that have led us to reexamine our mission. During the 4-year interval from 2004 to 2008, 439 neonates underwent cardiothoracic surgery at our institution. Of these 294 (67%) were diagnosed prenatally. The majority underwent surgery with a Severity Score of 3 to 6. Eighteen of these patients underwent emergency surgery, and a total of three required ECMO support.

A detailed comparison between the prenatally and postnatally diagnosed infants was performed. Not surprisingly, single ventricle variants, including HLHS, were significantly more likely to be diagnosed prenatally. This, alone, was responsible for the significantly higher Surgical Severity Score among the neonates who were diagnosed prenatally. While double-outlet right ventricle was significantly more likely to be diagnosed prenatally, the same did not hold for TOF. TGA was significantly more likely to be diagnosed postnatally, and total

anomalous pulmonary venous connection was, by far, more frequently a postnatal finding than a prenatal diagnosis.

Somewhat surprisingly, we found no difference between arterial pH and highest measured serum lactate between the prenatal and postnatal diagnosis groups. The prenatal diagnosis group was significantly more premature at birth (37.9 ± 2 weeks vs. 38.6 ± 2 weeks). This almost certainly reflects our policy of suggesting elective induction of labor for fetuses with potential ductal dependency who live at any significant distance from our center. This may have deleterious effects on the development of the brain, which has been found to lag in development in many fetuses with severe forms of congenital heart disease. We are reexamining this policy, to avoid elective deliveries prior to 39 weeks gestation. Another finding, which may be unique to our institution, is that the average age at surgery was 6 to 7 days, regardless of whether the infant was diagnosed prenatally or postnatally (in fact, the prenatal group [7 {5 to 8} days] waited significantly longer for surgery than the postnatal diagnosis group [6 {5 to 9} days]). This held, even when the groups were stratified according to cardiac diagnosis. This may be related to the much higher propensity for surgery to be postponed for the infants who were diagnosed prenatally (22.8% vs. 11.7%, $p = 0.006$). The latter is disturbing, and suggests that length of stay and total hospital costs could be impacted significantly for the prenatal group if we are more assiduous in scheduling surgery upon admission for delivery of the prenatal diagnosis group.

FETAL CARDIAC ARRHYTHMIAS

Fetal cardiac arrhythmias have been recognized with increasing frequency during the past several years and in general have been associated with a greater degree of maternal and physician anxiety than they deserve. Most irregularities of fetal cardiac rhythm represent isolated extrasystoles, which frequently present as a perceived skipping of fetal heart beats. Extrasystoles are significant only because of the potential for an appropriately timed extrasystole to initiate sustained reentry tachycardia in the presence of an appropriate anatomic substrate involving an accessory conduction pathway or a region of scar with unidirectional block and decremental conduction. The statistical likelihood of this occurring in the fetal or immediate neonatal period is in the range of 0.5% to 2%. The most common, important, sustained fetal arrhythmias are orthodromic reciprocating supraventricular tachycardia (SVT), AF

TABLE 27.5 Fetal CHD with Intrauterine Fetal Demise 2007–2010 (*n* = 28)

Cardiac Diagnosis	Other Findings	Karyotype
Absent PV Syndrome/IVS	Hydrops fetalis	None
ASD and VSD	Complete heart block	None
AVSD	Hydrops fetalis	None
AVSD	None	Trisomy 21
AVSD	None	Trisomy 21
AVSD	Oligohydramnios	Trisomy 21
AVSD, LV-dominant	Hydrops fetalis	Normal
AVSD, LV-dominant with AS, LA isomerism	Complete heart block	Normal
AVC/DORV/MGV, LA isomerism	Complete heart block, renal anomaly, Hydrops fetalis	Normal
Complex single ventricle	Absent kidneys, anhydramnios	None
DORV	Duodenal atresia	Trisomy 18
DORV	CNS, renal, and skeletal anomalies	Trisomy 18
DORV	Arnold Chiari, neural tube defect, renal and skeletal anomalies, Hydrops fetalis	Trisomy 13
DORV/MA/AA	Absent stomach	Normal
DORV/MGV	Congenital diaphragmatic hernia, skeletal anomalies	Trisomy 18
DORV/PA with Ectopia Cordis	Pentalogy of Cantrell	None
Ebstein malformation	Hydrops fetalis	None
Ebstein malformation	Hydrops fetalis	None
Ebstein malformation	Hydrops fetalis	Normal
Ebstein malformation	None	None
HLHS (Mitral stenosis/Aortic atresia)	Prune belly syndrome	Normal
HLHS (Mitral stenosis/Aortic atresia)	Maternal Protein S deficiency, on Lovenox	Normal
PA/IVS, also LVOT obstruction	Hydrops fetalis	None
PA/IVS	Severe cardiomegaly	Normal
Pulmonary atresia/VSD	Cleft lip and palate, cerebral and genital anomalies, hydrops fetalis	Trisomy 13
Truncus arteriosus	Placental insufficiency	Normal
VSD (large inlet)	Skeletal anomalies	Trisomy 18
VSD (large inlet)	Congenital diaphragmatic hernia, Skeletal anomalies, hydrops	Trisomy 18

with varying degrees of AV block, and severe bradycardia associated with complete AV block (10).

Nineteen patients were found to have sustained fetal arrhythmias during 2004 and 2005. Nine fetuses had sustained atrial premature contractions. None of these fetuses went on to develop sustained SVT, and none received prenatal therapy. Ten patients with sustained arrhythmias received in utero therapy and went on to live birth with normal neonatal cardiovascular function. These included two fetuses with prolonged AV conduction (1) or complete heart block (1) in the presence of positive maternal titers against Ro or La antibodies. The first fetus received dexamethasone as part of a multicenter study and was born with normal AV conduction. The second of these fetuses required cardiac pacing in the neonatal period, owing to recalcitrant complete heart block. Two fetuses, with left atrial isomerism, complete AVSD, hydrops fetalis, and complete heart block were classified as heterotaxy syndrome and were not included in the group presenting with

sustained arrhythmia as the chief complaint. One patient with HLHS and intermittent SVT was classified among fetuses with congenital heart disease as the primary diagnosis.

The other eight fetuses had sustained supraventricular tachyarrhythmias, including AF (1), ectopic atrial tachycardia (EAT) (2), and orthodromic reciprocating tachycardia (5). They responded to antiarrhythmic therapy protocols that contained digoxin, alone or in combination with propranolol, sotalol, or flecainide (Table 27.8).

In the presence of sustained fetal tachyarrhythmia, it is common for the fetus to develop hydrops fetalis (10). The latter arises because of the development of venous hypertension in the presence of significant atrial backflow into the IVC circulation. The increase in hydrostatic pressure results in a net increase in extravasation of fluid into the interstitial space that is not adequately compensated by fetal lymphatic drainage. It is not uncommon, therefore, for hydrops fetalis to develop despite maintenance of normal or nearly normal

TABLE 27.6

Chromosomal Anomalies of Fetuses with Congenital Heart Disease 2007–2010 (*n* = 89)

Chromosomal Defect	Number of Fetuses
Trisomy 21	39
Complete AVSD	15
TOF/AVSD	7
VSD	7
TOF	6
Partial AVSD	2
AVSD—single ventricle variant	2
22q11 Deletion	18
Truncus	5
PA/VSD/MAPCAs	4
TOF	3
IAA/VSD	3
Aortic atresia/cervical arch/VSD	1
TOF/absent PV	1
Pulmonary atresia/VSD/PDA	1
Trisomy 18	13
VSD	7
DORV	4
AVSD	1
AS	1
Trisomy 13	6
Pulmonary atresia/VSD/PDA	3
DORV	2
VSD	1
Turner Syndrome (and similar variants)	4
Bicuspid aortic valve, mild AS	2
Small VSD	1
Hypoplastic left heart	1
Other	9
Total	89

systolic ventricular shortening. Sustained fetal tachycardia and hydrops fetalis have been associated with neonatal hypoalbuminemia and hyperbilirubinemia, even weeks following resolution of the tachycardia and fetal anasarca (186). This is probably attributable to high IVC pressure and associated hepatic dysfunction, with decreased albumin production and biliary stasis. The decreased albumin production, resulting in decreased fetal and neonatal serum oncotic pressure, contributes both to the production of fetal edema and anasarca and to the considerable delay that is often encountered between arrhythmia control and resolution of hydrops fetalis.

Bradycardia associated with complete AV block may result from autoimmune damage to the AV conduction system, related to transplacental passage of anti-Ro (SS-A) or La (SS-B)

TABLE 27.7

Reasons for Referral for Fetal Echocardiogram, 2007–2010 (total *n* = 2,542 Pregnancies)

Reason for Referral	Number of Pregnancies	%
Suspected CHD	965	38%
Subgroup of arrhythmia	129	
Other Fetal Indications:	692	27%
Extracardiac anomaly	495	
Chromosomal anomaly, abnormal quad screen, or nuchal thickness	124	
Two vessel cord	55	
Multiple gestation (not mono/di)	18	
Family History	367	14%
Maternal Indication	323	13%
Maternal diabetes mellitus	236	
Maternal medical issue or medication	84	
Advanced maternal age	3	
Mono/di twins or twin to twin trans-fusion syndrome (TTTS)	139	5%
Other	56	2%
Poor visualization of heart	38	
IVF	7	
Unknown	7	
Research	4	

antibodies. Such mothers may have clinical symptoms of systemic lupus erythematosus or Sjögren syndrome, although in many young women, the detection of fetal heart block may be the first evidence of an elevated antibody titer in an otherwise asymptomatic mother (187–194).

Bradycardia owing to complete AV block may be diagnosed in fetuses with negative maternal antibody titers. Many of these fetuses have complex congenital cardiac disease with malformations involving the development of the central fibrous portion of the heart (e.g., AV discordant connections in congenitally corrected TGA or left atrial isomerism with ambiguous AV connections). Complete heart block must be distinguished from sinus bradycardia, which may be associated with fetal hypoxemia, or from blocked atrial bigeminy, in which every second atrial contraction is so premature that the AV node is still refractory because of the previous sinus beat and therefore unable to conduct the premature contraction (95,195).

These three forms of bradycardia can be distinguished from one another through careful evaluation of atrial rhythm. In sinus bradycardia, there is a one-to-one relationship between the slow atrial rate and the equal ventricular response rate. In complete heart block, the atrial rate is regular and exceeds the slower, regular, idioventricular rhythm. In blocked atrial bigeminy, the atrial rate is regularly irregular, with paired beating between the conducted beat and the blocked premature atrial beat, which is not conducted. Magnetocardiographic

TABLE 27.8 Clinically Important Fetal Arrhythmias Encountered during 2004–2005 (*n* = 13)

Pt. no.	Arrhythmia	Cardiac Structure	Cardiac Function	Medication(s)	Comments	Outcome
1	Orthodromic reciprocating tachycardia (ORT)	Normal	Normal	Digoxin		NSR (A/W)
2	Persistent junctional reciprocating tachycardia (PJRT)	Normal	Decreased (hydrops fetalis)	Digoxin; flecainide; propranolol		NSR Function normalized; hydrops resolved (A/W)
3	ORT (intermittent)	Normal	Normal	Propranolol		NSR (A/W)
4	ORT	Normal	Normal	Digoxin		NSR (A/W)
5	AF	Normal	Decreased (hydrops fetalis)	Digoxin; sotalol		NSR function normalized; hydrops resolved (A/W)
6	EAT	Normal	Decreased	Digoxin; propranolol	In utero control	Neonatal recurrence resolved with amiodarone/propranolol (A/W)
7	ORT	Normal	Decreased (hydrops fetalis)	Digoxin; sotalol		NSR function normalized; hydrops resolved (A/W)
8	ORT	Normal	Normal	Digoxin; flecainide	Therapy started elsewhere	NSR (A/W)
9	ORT	HLHS	Decreased RV function			Termination of pregnancy
10	Complete AV block	LA isomerism complex AVSD	Decreased hydrops fetalis			Termination of pregnancy
11	Complete AV block	LA isomerism complex AVSD	Decreased hydrops fetalis			Termination of pregnancy
12	Complete AV block	Normal	Decreased	Dexamethasone	Maternal lupus	Epicardial VVI pacemaker (A/W)
13	Primary AV block	Normal	Normal	Dexamethasone	Maternal anti-SS-A; anti-SS-B	NSR (A/W)

studies of fetal patients with recurrent episodes of SVT have suggested that many of the premature atrial beats that occur in these fetuses are echo beats that reenter the atrium via accessory pathways but are not conducted back into the ventricle through the AV node (196).

Analysis and Treatment of Fetal Cardiac Arrhythmias

In the absence of reliable electrocardiographic recordings of fetal atrial and ventricular electrical activity, M-mode, pulsed Doppler, and color-encoded M-mode echocardiographic recordings of mechanical and flow events are used to time and sequence the electrical activation underlying these events (Fig. 27.17) (10,52,197–217). Rein et al. (218) described the use of Doppler tissue imaging to time the mechanical activation sequence of the atria and ventricles to analyze cardiac rhythm using a ladder diagram or kinetocardiogram to provide similar information. Recent reports have demonstrated that magnetocardiography may provide important information regarding fetal atrial activation and the morphology of fetal QRS complexes, QT intervals, and T-wave morphology. This procedure is laborious, requires special equipment and magnetic shielding, and is not widely available, but may well emerge as the preferable means of analyzing clinically significant fetal arrhythmias (196,219–223).

Fetal Antiarrhythmic Therapy

The existence of techniques for the analysis and treatment of fetal cardiac arrhythmias is insufficient justification to expose a mother and fetus to the potential hazards of antiarrhythmic therapy. Fetal therapy offers the potential for dramatic success, but also has the potential for catastrophic consequences for two patients at once. The management schema for such patients should be predicated on an understanding of the natural history of the arrhythmia, a precise knowledge of the electrophysiologic basis for the arrhythmia, and a detailed appreciation of the pharmacokinetics and pharmacology of antiarrhythmic agents in the fetus, mother, and placenta. These must be factored in a commonsense risk/benefit analysis. Neonatal risk increases proportionately with the degree of prematurity and lung immaturity at the time of the initial diagnosis. This must be balanced against the degree of cardiovascular compromise accompanying the arrhythmia. In the absence of extreme prematurity, or without evidence of severe fetal hemodynamic compromise (e.g., hydrops fetalis), fetal intervention is difficult to justify.

Analysis of Fetal Tachyarrhythmias

Figure 27.18 presents a suggested algorithm for the analysis and treatment of fetal tachyarrhythmias. If tachycardia is

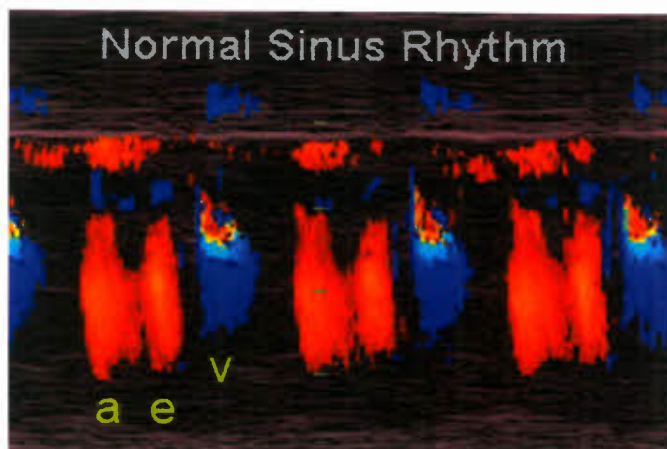


Figure 27.17. Color-encoded M-mode echocardiogram. The M-mode tracing imparts temporal resolution to the color flow recording. In this orientation, diastolic filling of the fetal ventricle is toward the transducer, resulting in the biphasic e and a waves, whereas the ejection into the aorta is away from the transducer and is inscribed as the aliased blue/cyan image.

associated with AV dissociation or is sustained in the presence of varying degrees of AV block, AV reentry tachycardia (AVRT) (either orthodromic or antidromic) or AV nodal reentry tachycardia (AVNRT) cannot be the underlying electrophysiologic mechanism of the tachycardia, since those tachycardias are characterized by a 1:1 AV contraction sequence, driven by a circus movement of electrical energy at the AV junction.

If there is AV dissociation, with a ventricular rate in excess of atrial rate (A:V ratio $<1:1$), one may assume that the tachycardia arises below the bundle of His and does not depolarize the atrium in a retrograde direction with a 1:1 ratio. The latter is characteristic of ventricular tachycardia (VT) or junctional ectopic tachycardia (JET). When there is some degree of AV block with an A:V ratio of $>1:1$, one may be dealing with intra-atrial reentry tachycardia (IART), ectopic atrial tachycardia (EAT), multifocal atrial tachycardia (MAT), atrial flutter (AF), or atrial fibrillation. In the presence of these arrhythmias, the atrial rate exceeds that of the ventricles, with the relationship dictated by the degree of AV block.

In the presence of a strict 1:1 A:V ratio, we evaluate the ventriculoatrial (VA) interval. Using simultaneous recordings of central venous and arterial pulsed Doppler flow waveforms, the time sequence of atrial and ventricular electrical activation can be discerned. Such recordings can be obtained by placement of the Doppler sample volume to overlap the fetal superior vena cava and ascending aorta (224) or fetal right pulmonary artery and right pulmonary vein (Fig. 27.19) (225). The AV mechanical interval may be used as a surrogate of electrocardiographic PR interval, and the VA time interval may also be calculated.

In the presence of a very short VA interval or one slightly >70 ms, the most likely electrophysiologic mechanism of the tachycardia is orthodromic AVRT or AVNRT. If the A:V ratio is $>1:1$ with a regular atrial tachycardia, the likely diagnosis is AF or IART. Depending on gestational age, the likelihood of pulmonary maturity, and the presence or absence of hydrops fetalis, we may or may not consider the use of in utero antiarrhythmic treatment to the fetus. A fetus with unsustained tachycardia or without hydrops fetalis is not in immediate danger and is not likely to be offered prenatal therapy. On the other hand, in the presence of sustained tachyarrhythmia, with hydrops fetalis, the risk/benefit analysis tips in the direction of in utero therapy.

Intrauterine Antitachyarrhythmic Therapy

In the face of severe prematurity, immediate delivery for postnatal treatment may not be a logical option. The frequent association of hydrops fetalis with sustained SVT and the dismal prognosis for such fetuses and neonates in a setting of extreme prematurity may justify vigorous efforts at in utero therapy, if such treatment can be offered at a tolerably low risk to the mother. Even a moderate risk to the fetus could be justified in this setting, in light of the poor prognosis for the neonate if the arrhythmia and hydrops fetalis are unremitting. The decision regarding the institution of fetal treatment should consider the following: (a) the fetal hemodynamic state (Is there hydrops fetalis?), (b) the potential risks to mother and fetus inherent in fetal treatment, (c) availability of facilities for monitoring of mother and fetus, and (d) willingness of the mother to submit to such treatment and monitoring.

Many antiarrhythmic drugs have a narrow therapeutic margin and may be associated with significant toxicity, including proarrhythmic potential. Only the Vaughn-Williams class II (β -blocker) agents appear to lack the potential for late proarrhythmic mortality. Type IA or type III agents, alone or in combination with medications that interfere with drug metabolism through the cytochrome P-450 pathway, may precipitate polymorphic VT (*torsades de pointes*). Type IC agents such as flecainide may cause QRS prolongation and VT that is recalcitrant to treatment. The absence of a readily available technique to monitor fetal QTc or QRS duration during antiarrhythmic therapy constitutes a fundamental hazard associated with fetal antiarrhythmic therapy.

Prior to the initiation of antiarrhythmic therapy, the therapeutic goal should be established. In some circumstances, rate control may provide an adequate opportunity to recover fetal cardiovascular function, whereas in many cases complete control of the arrhythmia is necessary to allow resolution of hydrops fetalis.

The literature is filled with many reports touting the virtues of different antiarrhythmic agents for the control of fetal tachyarrhythmias (10,226–242). Few of these reports discussed medication choices based on a detailed analysis of the electrophysiologic mechanism of the arrhythmia. The algorithm that we present is based on a sequential analysis of arrhythmia mechanism modeled after the framework suggested by Walsh et al. (243). The suggested sequence of drug administration has evolved considerably over the past several years and has been influenced by personal experience and the literature. This is offered as a step-off point for consideration by the reader when fetal antitachycardia treatment is anticipated. Just as different cardiac centers use differing medical regimens for the same arrhythmia in infants and children, it is expected that fetal antiarrhythmic treatment protocols will be individualized, based on local experience with specific antiarrhythmic medications. A rational approach to the treatment of these patients should consider the nature of the arrhythmia, the hemodynamic impact of the rhythm disturbance, and the pharmacology and pharmacokinetics of the maternal-placental-fetal unit. We have settled on a simplified treatment protocol, focusing on the administration of digoxin, propranolol, sotalol, and amiodarone. We have had limited experience with the use of flecainide in the fetus, although some centers have found the latter to be a safe and effective agent for the treatment of some fetal arrhythmias. We have made a team approach to the administration of antiarrhythmic treatment to the pregnant woman. This team includes maternal-fetal medicine, pediatric cardiology, and adult cardiology specialists to focus on the care of these complex patients. Such teams should devise their own treatment plans, which may differ at individual medical centers or for individual patients.

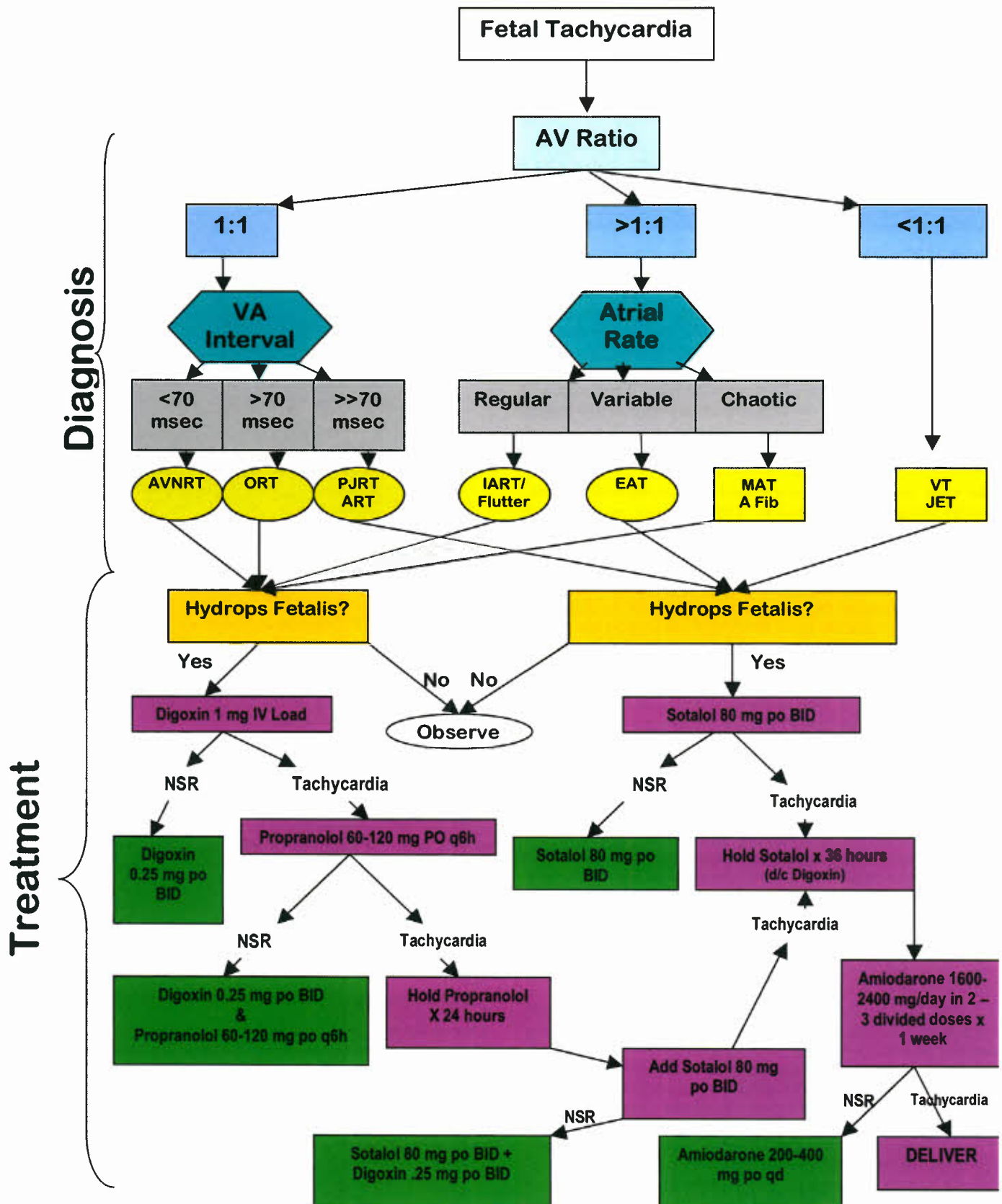


Figure 27.18. Suggested algorithm for the analysis and treatment of fetal tachyarrhythmias.

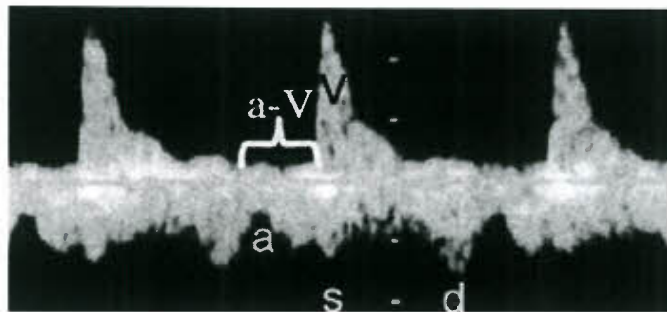


Figure 27.19. Simultaneous inscription of flow waveforms from the right upper pulmonary artery (*above the baseline*) and right upper pulmonary vein (*below the baseline*). The undulations of the pulmonary vein representing atrial contraction (a) are related to the timing of the upstroke of the systolic ejection into the branch pulmonary artery (v). The atrioventricular (a-V) and ventriculoatrial (V-a) conduction times may be measured and related to the electrical events underlying the mechanical responses that result in the flow events recorded in this image.

Treatment of the Fetus with Bradycardia

The most important sustained fetal bradyarrhythmia is congenital complete heart block. These fetuses may develop hydrops fetalis. The latter may occur in the subgroup of fetuses with associated congenital heart disease. The association of fetal heart failure with congenital heart block, with or without congenital heart disease, represents an absolute indication for electrical pacemaker therapy in the neonate. In the fetus, the association of complete heart block and hydrops fetalis is dire. When associated with congenital heart disease, the outcome is almost invariably fatal, with or without fetal therapy (195).

The initial report of the use of electrical pacemaker therapy for the treatment of fetal congenital heart block involved a fetus presenting with heart block in the absence of congenital heart disease (244). This fetus presumably incurred immune complex-mediated damage to the fetal conduction system and myocardium. There was severe bradycardia and hydrops fetalis. In desperation, the treating physicians placed a pacing catheter within the fetal heart via percutaneous puncture of the maternal abdomen, uterus, fetal thorax, and ventricular wall. Fetal ventricular capture was demonstrated, without clinical improvement. Subsequent attempts to use similar pacing systems have been, likewise, unsuccessful.

Laboratory models of complete heart block have been created in fetal lambs, with subsequent resolution of hydrops fetalis following fetal exteriorization and surgical implantation of permanent pacemakers connected to epicardial pacing leads (245). An attempt to implant a pacemaker in this fashion in a human fetus was unsuccessful. Although it may well be that some human fetuses with heart block and hydrops fetalis have deteriorated solely because of bradycardia, we are concerned that some neonates do not respond to pacing alone. This subgroup of patients may have immune-mediated damage to the contractile elements of the heart from the same mechanism that damaged the fetal conduction system (246–250). Although it has been demonstrated that the administration of β -mimetic agents to the pregnant woman may increase the intrinsic ventricular rate of the fetus by 50%, there has been no consistent evidence that such treatment ameliorates hydrops fetalis in affected fetuses (184, 251–253).

A preliminary experience in our laboratory with the administration of absorbable corticosteroid to pregnant women whose fetuses had developed high-grade second-degree or recent-onset third-degree heart block in the presence of high titers of anti-SS-A or SS-B antibodies suggested that such treat-

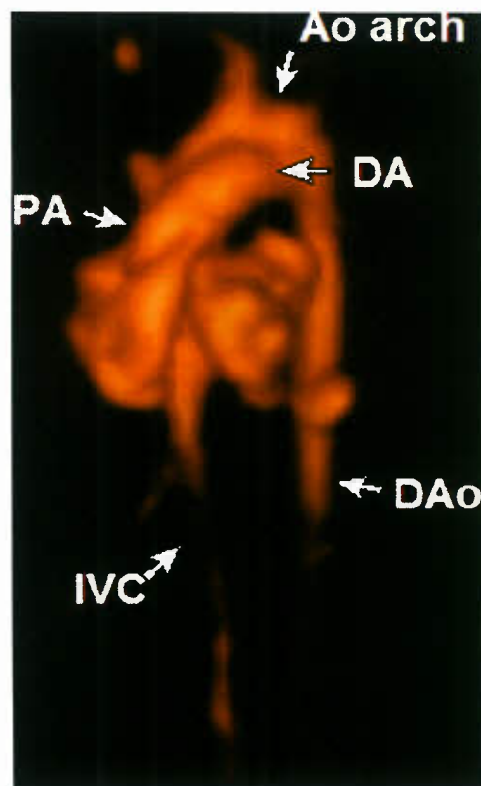


Figure 27.20. Rendered STIC image of aortic and ductal arches obtained from STIC dataset recorded with B-mode documentation of cardiac and vessel blood flow. (Reproduced from Gonçalves LF, Lee W, Espinosa J, et al. How do we do it? Practical advice on imaging-based techniques and investigations. *Ultrasound Obstet Gynecol* 2006;27(3):336–348, with permission from John Wiley and Sons.)

ment might halt the progression or even reverse the damage to the conduction tissue (10). This study spawned a multicenter investigation designed to evaluate the impact of maternally administered corticosteroid on echocardiographically estimated fetal AV conduction intervals (254–261). Some centers have adopted steroid therapy for the routine treatment of fetuses with antibody-mediated congenital complete heart block, based on improved mortality statistics in the current era compared with historical controls (262–265). The results of the multicenter study noted above are likely to provide an important insight into the appropriateness of such therapy (266).

Three-Dimensional Fetal Echocardiographic Imaging

During the few years that have elapsed since the last edition of this textbook, there has been great interest in the use of 3- and 4-D ultrasound for the examination of the fetal heart. Different technologies have evolved for the acquisition of 4-D datasets that allow online and postprocessed images of the cardiac chambers and great vessels. Interest has been expressed by the maternal-fetal-medicine community in the use of such datasets for remote analysis and for automated multislice images of the fetal heart in order to facilitate screening for congenital heart disease. The two most commonly used technologies are Spatiotemporal Image Correlation (STIC) and real-time 4-D imaging using 2-D matrix-array transducers (Fig. 27.20).

STIC imaging requires synchronization of spatial and temporal imaging by serially constructing a 4-D dataset from multiple 2-D images constituting a single cardiac cycle. The 2-D anatomic images may be combined with color or

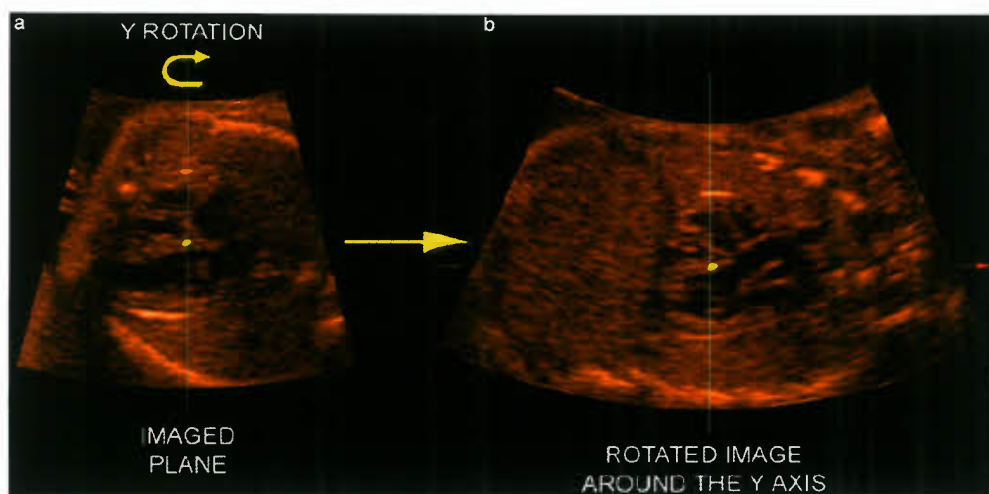


Figure 27.21. STIC image of four-chamber view of fetal heart is seen in the left-sided panel. The yellow dot at the crux of the ventricular septum is the focal point around which the image is “spun” in a clockwise fashion to demonstrate the relationship between the ventricular septum and the anterior wall of the aorta in the left ventricular long-axis view of the outflow tract. (Reproduced from Devore GR, Polanco B, Sklansky MS, et al. The ‘spin’ technique: a new method for examination of the fetal outflow tracts using three-dimensional ultrasound. *Ultrasound Obstet Gynecol* 2004;24(1):72–82, with permission from John Wiley and Sons.)

power Doppler flow information to increase the accuracy of the imaging process.

Using STIC imaging, it is possible to examine the heart in three orthogonal planes and to gradually slice through the azimuthal plane in each view (267). Postprocessing allows rendering, which may view the flow within the heart and great vessels with the body and heart rendered transparent. Using inversion imaging, it is possible to demonstrate B-flow within the heart and blood vessels. Such images may allow detailed evaluation of vascular anomalies (Fig. 27.21). Devore et al. (268) demonstrated the utility of visualizing the outflow tracts in detail in each plane by rotating (“spinning”) the image of the individual 2-D view of the outflow portion of the heart around chosen point within the outflow tract (Fig. 27.22).

It remains to be seen whether STIC imaging fulfills its potential for increasing the sensitivity and specificity of screening programs for fetal congenital heart disease. The automation

of outflow tract imaging is an attractive alternative, but recent studies (269) have suggested that this imaging results in satisfactory views in only 70% to 83% of fetuses at 18 to 22 weeks gestation. Certainly, in order to obtain adequate STIC analysis of the fetal heart, it is essential that satisfactory four-chamber visualization of the heart serve as the foundation for the sequential dissection and rotation of the 4-D dataset.

We have found that 3- and 4-D imaging is particularly useful for evaluating the spatial relationship of the great arteries in fetuses with conotruncal malformations. As noted above, since such fetuses constitute the largest single group of fetal anomalies in our laboratory, we have found ourselves increasingly dependent upon STIC imaging. Another important role for STIC imaging has been for the evaluation of the AV valves and their chordal attachments. The latter are particularly useful in evaluating patients with single ventricular or AVSD variations.

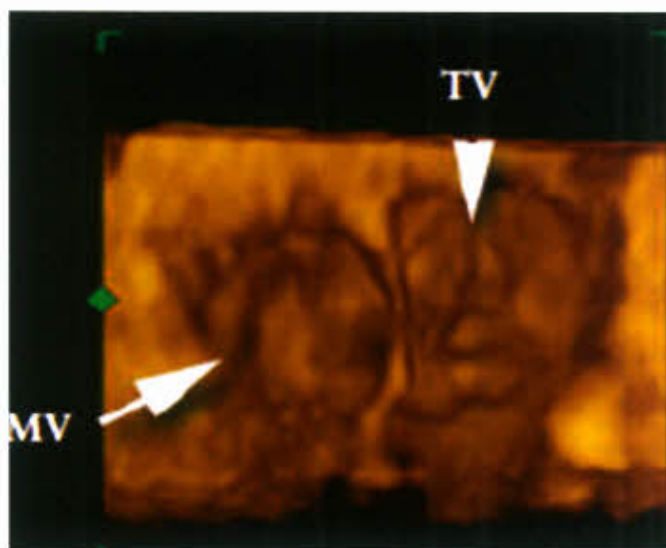


Figure 27.22. Reconstructed 3-D tomogram of the two ventricles. Reconstruction is from STIC 4-D dataset. Mitral valve (MV) and tricuspid valve (TV) are labeled. (Reproduced from Gonçalves LF, Lee W, Espinosa J, et al. How do we do it? Practical advice on imaging-based techniques and investigations. *Ultrasound Obstet Gynecol* 2006;27(3):336–348, with permission from John Wiley and Sons.)

REFERENCES

1. Rudolph AM. *Congenital Diseases of the Heart*. Chicago, IL: Yearbook, 1974.
- 1a. Rudolph AM. *Congenital Diseases of the Heart*. 2nd ed. Armonk, NY: Futura, 2001.
2. Rudolph AM, Heymann MA. The circulation of the fetus in utero: methods for studying distribution of blood flow, cardiac output and organ blood flow. *Circ Res* 1967;21(2):163–184.
3. Heymann MA, et al. Blood flow measurements with radionuclide-labeled particles. *Prog Cardiovasc Dis* 1977;20(1):55–79.
4. Rudolph AM, Heymann MA. Measurement of flow in perfused organs, using microsphere techniques. *Acta Endocrinol (Copenh)* 1972;158:112–127.
5. Rudolph AM, Iwamoto HS, Teitel DF. Circulatory changes at birth. *J Perinat Med* 1988;16:9–21.
6. Teitel DF, Iwamoto HS, Rudolph AM. Effects of birth-related events on central blood flow patterns. *Pediatr Res* 1987;22:557–566.
7. Iwamoto HS, Teitel D, Rudolph AM. Effects of birth-related events on blood flow distribution. *Pediatr Res* 1987;22:634–640.
8. Iwamoto HS, Teitel DF, Rudolph AM. Effect of birth-related events on metabolism in fetal sheep. *Pediatr Res* 1991;30:158–164.
9. Winsberg F. Echocardiography of the fetal and newborn heart. *Invest Radiol* 1972;7:152–158.
10. Kleinman CS, Copel JA. Fetal cardiovascular physiology and therapy. *Fetal Diagn Ther* 1992;7:147–157.
11. Lange LW, et al. Qualitative real-time cross-sectional echocardiographic imaging of the human fetus during the second half of pregnancy. *Circulation* 1980;62:799–806.
12. Allan LD, et al. Echocardiographic and anatomical correlates in the fetus. *Br Heart J* 1980;44:444–451.
13. Kachaner J, Fermont L. Prenatal cardiology [in French]. *Presse Med* 1985;14:517–519.
14. Allan LD, et al. Prenatal screening for congenital heart disease. *Br Med J (Clin Res Ed)* 1986;292:1717–1719.

15. Brown DL, Durfee SM, Hornberger LK. Ventricular discrepancy as a sonographic sign of coarctation of the fetal aorta: how reliable is it? *J Ultrasound Med* 1997;16:95-99.
16. Hornberger LK, Need L, Benacerraf BR. Development of significant left and right ventricular hypoplasia in the second and third trimester fetus. *J Ultrasound Med* 1996;15:655-659.
17. Hornberger LK, et al. Echocardiographic study of the morphology and growth of the aortic arch in the human fetus: observations related to the prenatal diagnosis of coarctation. *Circulation* 1992;86:741-747.
18. Hornberger LK, et al. Antenatal diagnosis of coarctation of the aorta: a multicenter experience. *J Am Coll Cardiol* 1994;23:417-423.
19. Hornberger LK, et al. Left heart obstructive lesions and left ventricular growth in the midtrimester fetus: a longitudinal study. *Circulation* 1995;92:1531-1538.
20. Crane JP, et al. A randomized trial of prenatal ultrasonographic screening: impact on the detection, management, and outcome of anomalous fetuses. The RADIUS Study Group. *Am J Obstet Gynecol* 1994;171:392-399.
21. Ewigman BG, et al. Effect of prenatal ultrasound screening on perinatal outcome. RADIUS Study Group. *N Engl J Med* 1993;329:821-827.
22. LeFevre ML, et al. A randomized trial of prenatal ultrasonographic screening: Impact on maternal management and outcome. RADIUS (Routine Antenatal Diagnostic Imaging with Ultrasound) Study Group. *Am J Obstet Gynecol* 1993;169:483-489.
23. Presbitero P, et al. Fetal echocardiography: diagnosis of congenital cardiomyopathies in a population at risk [in Italian]. *G Ital Cardiol* 1985;15:590-596.
24. Sharland GK, Allan LD. Screening for congenital heart disease prenatally: results of a 2 1/2-year study in the South East Thames Region. *Br J Obstet Gynaecol* 1992;99:220-225.
25. Achiron R, et al. Extended fetal echocardiographic examination for detecting cardiac malformations in low risk pregnancies. *BMJ* 1992;304:671-674.
26. Vergani P, et al. Screening for congenital heart disease with the four-chamber view of the fetal heart. *Am J Obstet Gynecol* 1992;167:1000-1003.
27. Stoll C, et al. Evaluation of prenatal diagnosis of congenital heart disease. *Prenat Diagn* 1993;13:453-461.
28. Hofbeck M, et al. Prenatal findings in patients with prolonged QT interval in the neonatal period. *Heart* 1997;77:198-204.
29. Giancotti A, et al. Prenatal evaluation of congenital heart disease in high-risk pregnancies. *Clin Exp Obstet Gynecol* 1995;22:225-229.
30. Buskens E, et al. Efficacy of fetal echocardiography and yield by risk category. *Obstet Gynecol* 1996;87:423-428.
31. Sinclair BG, Sandor GG, Farquharson DF. Effectiveness of primary level antenatal screening for severe congenital heart disease: a population-based assessment. *J Perinatol* 1996;16:336-340.
32. Kleinert S. Routine prenatal screening for congenital heart disease. *Lancet* 1996;348:836.
33. Stumpflen I, et al. Effect of detailed fetal echocardiography as part of routine prenatal ultrasonographic screening on detection of congenital heart disease. *Lancet* 1996;348:854-857.
34. Alembik Y, Stoll C. Routine fetal echocardiography and detection of congenital heart disease. *Lancet* 1996;348:1732.
35. Buskens E, et al. Routine prenatal screening for congenital heart disease: what can be expected? a decision-analytic approach. *Am J Public Health* 1997;87:962-967.
36. Crane JM, et al. Abnormal fetal cardiac axis in the detection of intrathoracic anomalies and congenital heart disease. *Ultrasound Obstet Gynecol* 1997;10:90-93.
37. Todros T, et al. Accuracy of routine ultrasonography in screening heart disease prenatally: gruppo piemontese for prenatal screening of congenital heart disease. *Prenat Diagn* 1997;17:901-906.
38. Hess DB, et al. Obtaining the four-chamber view to diagnose fetal cardiac anomalies. *Obstet Gynecol Clin North Am* 1998;25:499-515.
39. Stoll C, et al. Evaluation of prenatal diagnosis of congenital heart disease. *Prenat Diagn* 1998;18:801-807.
40. Hafner E, et al. Detection of fetal congenital heart disease in a low-risk population. *Prenat Diagn* 1998;18:808-815.
41. Kirk JS, et al. Fetal cardiac asymmetry: a marker for congenital heart disease. *Obstet Gynecol* 1999;93:189-192.
42. Tometzki AJ, et al. Accuracy of prenatal echocardiographic diagnosis and prognosis of fetuses with conotruncal anomalies. *J Am Coll Cardiol* 1999;33:1696-1701.
43. Paladini D. Prenatal screening of congenital heart disease between ethics and cost-effectiveness: time for a change in current prenatal ultrasound screening policies? *Ultrasound Obstet Gynecol* 1999;14:225-228.
44. Cohen EH, Rein AJ. Antenatal diagnosis of cardiac malformation: a structural study. *Fetal Diagn Ther* 2000;15:54-60.
45. Saxena A, Soni NR. Fetal echocardiography: where are we? *Indian J Pediatr* 1999;72:603-608.
46. Simpsom JM, et al. Accuracy and limitations of transabdominal fetal echocardiography at 12-15 weeks of gestation in a population at high risk for congenital heart disease. *BJOG* 2000;107:1492-1497.
47. Fesslova V, Villa L, Kustermann A. Long-term experience with the prenatal diagnosis of cardiac anomalies in high-risk pregnancies in a tertiary center. *Ital Heart J* 2003;4:855-864.
48. Sharland G. Routine fetal cardiac screening: what are we doing and what should we do? *Prenat Diagn* 2004;24:1123-1129.
49. Sklansky M, et al. Prenatal screening for congenital heart disease using real-time three-dimensional echocardiography and a novel 'sweep volume' acquisition technique. *Ultrasound Obstet Gynecol* 2005;25:435-443.
50. Feit LR, Copel JA, Kleinman CS. Foramen ovale size in the normal and abnormal human fetal heart: an indicator of transatrial flow physiology. *Ultrasound Obstet Gynecol* 1991;1:313-319.
51. Berning RA, et al. Reversed shunting across the ductus arteriosus or atrial septum in utero heralds severe congenital heart disease. *J Am Coll Cardiol* 1996;27:481-486.
52. Reed KL, et al. Cardiac Doppler flow velocities in human fetuses. *Circulation* 1986;73:41-46.
53. Kenny JF, et al. Changes in intracardiac blood flow velocities and right and left ventricular stroke volumes with gestational age in the normal human fetus: a prospective Doppler echocardiographic study. *Circulation* 1986;74:1208-1216.
54. Friedman WF. The intrinsic physiologic properties of the developing heart. *Prog Cardiovasc Dis* 1972;15:87-111.
55. Friedman WF, Kirkpatrick SE. In situ physiological study of the developing heart. *Recent Adv Stud Cardiac Struct Metab* 1975;5:497-504.
56. Sheldon CA, Friedman WF, Sybers HD. Scanning electron microscopy of fetal and neonatal lamb cardiac cells. *J Mol Cell Cardiol* 1976;8:853-862.
57. Harada K, et al. Tissue Doppler imaging in the normal fetus. *Int J Cardiol* 1999;71:227-234.
58. Paladini D, et al. Prenatal diagnosis of congenital heart disease in the Naples area during the years 1994-1999—the experience of a joint fetal-pediatric cardiology unit. *Prenat Diagn* 2002;22:545-552.
59. Paladini D, et al. The association between congenital heart disease and Down syndrome in prenatal life. *Ultrasound Obstet Gynecol* 2000;15:104-108.
60. Jamjureeruk V. Evaluation of ventricular myocardial velocities and heart motion of the fetal heart by tissue Doppler image. *J Med Assoc Thai* 2001;84:1158-1163.
61. Larsen LU, et al. Strain rate derived from color Doppler myocardial imaging for assessment of fetal cardiac function. *Ultrasound Obstet Gynecol* 2006;27:210-213.
62. Di Salvo G, et al. Quantification of regional left and right ventricular longitudinal function in 75 normal fetuses using ultrasound-based strain rate and strain imaging. *Ultrasound Med Biol* 2005;31:1159-1162.
63. Huhta JC. Fetal congestive heart failure. *Semin Fetal Neonatal Med* 2005;10:542-552.
64. Huhta JC. Right ventricular function in the human fetus. *J Perinat Med* 2001;29:381-389.
65. Paladini D, et al. Prenatal diagnosis of congenital heart disease and fetal karyotyping. *Obstet Gynecol* 1993;81:679-682.
66. Fogel M, et al. Congenital heart disease and fetal thoracoabdominal anomalies: Associations in utero and the importance of cytogenetic analysis. *Am J Perinatol* 1991;8:411-416.
67. Fasnacht MS, Jaeggi ET. Fetal and genetic aspects of congenital heart disease [in German]. *Ther Umsch* 2001;58:70-75.
68. Moyano D, Huggon IC, Allan LD. Fetal echocardiography in trisomy 18. *Arch Dis Child Fetal Neonatal Ed* 2005;90:F520-F522.
69. Ghi T, et al. Incidence of major structural cardiac defects associated with increased nuchal translucency but normal karyotype. *Ultrasound Obstet Gynecol* 2001;18:610-614.
70. Hyett JA, et al. Intrauterine lethality of trisomy 21 fetuses with increased nuchal translucency thickness. *Ultrasound Obstet Gynecol* 1996;7:101-103.
71. Cheng PJ, et al. First-trimester nuchal translucency measurement and echocardiography at 16 to 18 weeks of gestation in prenatal detection for trisomy 18. *Prenat Diagn* 2003;23:248-251.
72. Sururus E, Huggon IC, Allan LD. Turner's syndrome in fetal life. *Ultrasound Obstet Gynecol* 2003;22:264-267.
73. Hyett J. Does nuchal translucency have a role in fetal cardiac screening? *Prenat Diagn* 2004;24:1130-1135.
74. Sciarrone A, et al. First-trimester fetal heart block and increased nuchal translucency: an indication for early fetal echocardiography. *Prenat Diagn* 2005;25:1129-1132.
75. Ducarme G, et al. Increased nuchal translucency and cystic hygroma in the first trimester: prenatal diagnosis and neonatal outcome [in French]. *Gynecol Obstet Fertil* 2005;33:750-754.
76. Hyett J, Moscoso G, Nicolaides K. Increased nuchal translucency in trisomy 21 fetuses: relationship to narrowing of the aortic isthmus. *Hum Reprod* 1995;10:3049-3051.
77. Kagan KO, et al. Relation between increased fetal nuchal translucency thickness and chromosomal defects. *Obstet Gynecol* 2006;107:6-10.
78. D'Alton M, Cleary-Goldman J. First and second trimester evaluation of risk for fetal aneuploidy: the secondary outcomes of the FASTER Trial. *Semin Perinatol* 2005;29:240-246.
79. Malone FD, et al. First-trimester or second-trimester screening, or both, for Down's syndrome. *N Engl J Med* 2005;353:2001-2011.
80. Carvalho JS. Nuchal translucency, ductus venosus and congenital heart disease: an important association—a cautious analysis. *Ultrasound Obstet Gynecol* 1999;14:302-306.
81. Devine PC, Simpson LL. Nuchal translucency and its relationship to congenital heart disease. *Semin Perinatol* 2000;24:343-351.

82. Mavrides E, et al. Limitations of using first-trimester nuchal translucency measurement in routine screening for major congenital heart defects. *Ultrasound Obstet Gynecol* 2001;17:106–110.
83. Huggon IC, et al. Fetal cardiac abnormalities identified prior to 14 weeks' gestation. *Ultrasound Obstet Gynecol* 2002;20:22–29.
84. Driscoll DA, et al. Deletions and microdeletions of 22q11.2 in velo-cardio-facial syndrome. *Am J Med Genet* 1992;44:261–268.
85. Kelly D, et al. Confirmation that the velo-cardio-facial syndrome is associated with haplo-insufficiency of genes at chromosome 22q11. *Am J Med Genet* 1993;45:308–312.
86. Goldmuntz E, et al. Microdeletions of chromosomal region 22q11 in patients with congenital conotruncal cardiac defects. *J Med Genet* 1993;30:807–812.
87. Driscoll DA, et al. Prevalence of 22q11 microdeletions in DiGeorge and velocardiocardial syndromes: implications for genetic counselling and prenatal diagnosis. *J Med Genet* 1993;30:813–817.
88. Shprintzen RJ. Velocardiofacial syndrome and DiGeorge sequence. *J Med Genet* 1994;31:423–424.
89. Johnson MC, et al. The genetic basis of paediatric heart disease. *Ann Med* 1995;27:289–300.
90. Phoon CK, et al. Left atrial isomerism detected in fetal life. *Am J Cardiol* 1996;77:1083–1088.
91. Atkinson DE, Drant S. Diagnosis of heterotaxy syndrome by fetal echocardiography. *Am J Cardiol* 1998;82:1147–1149, A10.
92. Berg C, et al. Prenatal diagnosis of cardiopulmonary syndromes: a 10-year experience. *Ultrasound Obstet Gynecol* 2003;22:451–459.
93. Pasquini L, et al. The implications for fetal outcome of an abnormal arrangement of the abdominal vessels. *Cardiol Young* 2005;15:35–42.
94. Tongsong T, et al. Prenatal diagnosis of transposition-like double-outlet right ventricle with mitral valve atresia in heterotaxy syndrome. *J Clin Ultrasound* 2005;33:197–200.
95. Schneider C, et al. Development of Z-scores for fetal cardiac dimensions from echocardiography. *Ultrasound Obstet Gynecol* 2005;26:599–605.
96. Bernasconi A, et al. Fetal dextrocardia: diagnosis and outcome in two tertiary centres. *Heart* 2005;91:1590–1594.
97. Wladimiroff JW, et al. Prenatal diagnosis and management of congenital heart defect: significance of associated fetal anomalies and prenatal chromosome studies. *Am J Med Genet* 1985;21:285–290.
98. Hyett JA, Moscoso G, Nicolaides KH. Cardiac defects in 1st-trimester fetuses with trisomy 18. *Fetal Diagn Ther* 1995;10:381–386.
99. Brons JT, et al. Prenatal ultrasonographic diagnosis of radial-ray reduction malformations. *Prenat Diagn* 1990;10:279–288.
100. Geggel RL. Conditions leading to pediatric cardiology consultation in a tertiary academic hospital. *Pediatrics* 2004;114:e409–e417.
101. Koklanaris N, et al. Isolated echogenic intracardiac foci in patients with low-risk triple screen results: assessing the risk of trisomy 21. *J Perinat Med* 2005;33:539–542.
102. Borgida AF, et al. Frequency of echogenic intracardiac focus by race/ethnicity in euploid fetuses. *J Matern Fetal Neonatal Med* 2005;18:65–66.
103. Finberg HJ. An isolated echogenic heart focus is a low-level risk marker for Down syndrome. *J Ultrasound Med* 2004;23:1008–1009; author reply 1009.
104. Coco C, Jeanty P, Jeanty C. An isolated echogenic heart focus is not an indication for amniocentesis in 12,672 unselected patients. *J Ultrasound Med* 2004;23:489–496.
105. Sotiropoulos A, Makrydimas G, Ioannidis JP. Diagnostic performance of intracardiac echogenic foci for Down syndrome: a meta-analysis. *Obstet Gynecol* 2003;101:1009–1016.
106. Souter VL, et al. Correlation of ultrasound findings and biochemical markers in the second trimester of pregnancy in fetuses with trisomy 21. *Prenat Diagn* 2002;22:175–182.
107. Caughey AB, et al. The impact of the use of the isolated echogenic intracardiac focus as a screen for Down syndrome in women under the age of 35 years. *Am J Obstet Gynecol* 2001;185:1021–1027.
108. Huggon IC, et al. Isolated echogenic foci in the fetal heart as marker of chromosomal abnormality. *Ultrasound Obstet Gynecol* 2001;17:11–16.
109. Wax JR, et al. A preliminary study of sonographic grading of fetal intracardiac echogenic foci: feasibility, reliability and association with aneuploidy. *Ultrasound Obstet Gynecol* 2000;16:123–127.
110. Winter TC, et al. Echogenic intracardiac focus in 2nd-trimester fetuses with trisomy 21: usefulness as a US marker. *Radiology* 2000;216:450–456.
111. Bromley B, et al. Significance of an echogenic intracardiac focus in fetuses at high and low risk for aneuploidy. *J Ultrasound Med* 1998;17:127–131.
112. Tworetzky W, et al. Usefulness of magnetic resonance imaging of left ventricular endocardial fibroelastosis in infants after fetal intervention for aortic valve stenosis. *Am J Cardiol* 2005;96:1568–1570.
113. Franklin O, et al. Prenatal diagnosis of coarctation of the aorta improves survival and reduces morbidity. *Heart* 2002;87:67–69.
114. Bonnet D. Plasticity of the myocardium in pediatric cardiology. *Arch Pediatr* 1996;3:1273–1275.
115. Munn MB, et al. Prenatally diagnosed hypoplastic left heart syndrome—outcomes after postnatal surgery. *J Matern Fetal Med* 1999;8:147–150.
116. Eapen RS, Rowland DG, Franklin WH. Effect of prenatal diagnosis of critical left heart obstruction on perinatal morbidity and mortality. *Am J Perinatol* 1998;15:237–242.
117. Sharland GK, et al. Factors influencing the outcome of congenital heart disease detected prenatally. *Arch Dis Child* 1991;66:284–287.
118. Smythe JF, Copel JA, Kleinman CS. Outcome of prenatally detected cardiac malformations. *Am J Cardiol* 1992;69:1471–1474.
119. Magnier S, et al. Outcome of 77 live born children with cardiac or rhythmic anomalies diagnosed in the prenatal period: apropos of 77 cases [in French]. *Arch Mal Coeur Vaisse* 1995;88:747–752.
120. Simpson JM, Sharland GK. Natural history and outcome of aortic stenosis diagnosed prenatally. *Heart* 1997;77:205–210.
121. Eronen M. Outcome of fetuses with heart disease diagnosed in utero. *Arch Dis Child Fetal Neonatal Ed* 1997;77:F41–F46.
122. Allan LD, Apfel HD, Printz BF. Outcome after prenatal diagnosis of the hypoplastic left heart syndrome. *Heart* 1998;79:371–373.
123. Boldt T, Andersson S, Eronen M. Outcome of structural heart disease diagnosed in utero. *Scand Cardiovasc J* 2002;36:73–79.
124. Brick DH, Allan LD. Outcome of prenatally diagnosed congenital heart disease: An update. *Pediatr Cardiol* 2002;23:449–453.
125. Verheijen PM, et al. Prenatal diagnosis of the fetus with hypoplastic left heart syndrome management and outcome. *Herz* 2003;28:250–256.
126. Fountain-Dommer RR, et al. Outcome following, and impact of, prenatal identification of the candidates for the Norwood procedure. *Cardiol Young* 2004;14:32–38.
127. Simpson JM, et al. Outcome of intermittent tachyarrhythmias in the fetus. *Pediatr Cardiol* 1997;18:78–82.
128. Mellander M. Perinatal management, counselling and outcome of fetuses with congenital heart disease. *Semin Fetal Neonatal Med* 2005;10:586–593.
129. Pattinson RC, et al. Obstetric and neonatal outcome in fetuses with absent end-diastolic velocities of the umbilical artery: a case-controlled study. *Am J Perinatol* 1993;10:135–138.
130. Jouannic JM, et al. Sensitivity and specificity of prenatal features of physiological shunts to predict neonatal clinical status in transposition of the great arteries. *Circulation* 2004;110:1743–1746.
131. Verheijen PM, et al. Prenatal diagnosis of congenital heart disease affects preoperative acidosis in the newborn patient. *J Thorac Cardiovasc Surg* 2001;121:798–803.
132. Lavrijsen SW, et al. Severe umbilical cord acidemia and neurological outcome in preterm and full-term neonates. *Biol Neonate* 2005;88:27–34.
133. Kadar K. Prognosis for the fetus with congenital heart defects in the era of modern diagnostics and therapeutics. *Orv Hetil* 2004;145:849–853.
134. Checchia PA, et al. The effect of surgical case volume on outcome after the Norwood procedure. *J Thorac Cardiovasc Surg* 2005;129:754–759.
135. Hagberg S, et al. Prenatally diagnosed gastroschisis—a preliminary report advocating the use of elective caesarean section. *Z Kinderchir* 1988;43:419–421.
136. Wood C. Fetal scalp sampling: its place in management. *Semin Perinatol* 1978;2:169–179.
137. Woods JR Jr. Birth asphyxia: pathophysiologic events and fetal adaptive changes. *Clin Perinatol* 1983;10:473–486.
138. Low JA. The role of blood gas and acid-base assessment in the diagnosis of intrauterine fetal asphyxia. *Am J Obstet Gynecol* 1988;159:1235–1240.
139. Weiner CP. The relationship between the umbilical artery systolic/diastolic ratio and umbilical blood gas measurements in specimens obtained by cordocentesis. *Am J Obstet Gynecol* 1990;162:1198–1202.
140. Favre R, et al. Standard curves of cerebral Doppler flow velocity waveforms and predictive values for intrauterine growth retardation and fetal acidosis. *Fetal Diagn Ther* 1991;6:113–119.
141. Hata T, et al. Real-time 3-D echocardiographic evaluation of the fetal heart using instantaneous volume-rendered display. *J Obstet Gynaecol Res* 2006;32:42–46.
142. Seelbach-Gobel B, et al. The prediction of fetal acidosis by means of intra-partum fetal pulse oximetry. *Am J Obstet Gynecol* 1999;180:73–81.
143. Baz E, et al. Abnormal ductus venosus blood flow: a clue to umbilical cord complication. *Ultrasound Obstet Gynecol* 1999;13:204–206.
144. Arduini D, Rizzo G, Romanini C. Changes of pulsatility index from fetal vessels preceding the onset of late decelerations in growth-retarded fetuses. *Obstet Gynecol* 1992;79:605–610.
145. Rizzo G, et al. The value of fetal arterial, cardiac and venous flows in predicting pH and blood gases measured in umbilical blood at cordocentesis in growth retarded fetuses. *Br J Obstet Gynaecol* 1995;102:963–969.
146. Reuwer PJ, et al. Feto-placental circulatory competence. *Eur J Obstet Gynecol Reprod Biol* 1986;21:15–26.
147. Carvalho FH, et al. Ductus venosus Doppler velocimetry to predict acidemia at birth in pregnancies with placental insufficiency [in Portuguese]. *Rev Assoc Med Bras* 2005;51:221–227.
148. Kaukola T, et al. Suboptimal neurodevelopment in very preterm infants is related to fetal cardiovascular compromise in placental insufficiency. *Am J Obstet Gynecol* 2005;193:414–420.
149. Baschat AA, et al. Venous Doppler in the prediction of acid-base status of growth-restricted fetuses with elevated placental blood flow resistance. *Am J Obstet Gynecol* 2004;191:277–284.
150. Gardiner HM. Successes and shortcomings of fetal echocardiography. *Hosp Med* 2001;62:634–639.
151. Baschat AA, et al. Doppler and biophysical assessment in growth restricted fetuses: distribution of test results. *Ultrasound Obstet Gynecol* 2006;27:41–47.
152. Harman CR, Baschat AA. Comprehensive assessment of fetal wellbeing: which Doppler tests should be performed? *Curr Opin Obstet Gynecol* 2003;15:147–157.

153. Sterne G, Shields LE, Dubinsky TJ. Abnormal fetal cerebral and umbilical Doppler measurements in fetuses with intrauterine growth restriction predicts the severity of perinatal morbidity. *J Clin Ultrasound* 2001;29:146–151.
154. Fu J, Olofsson P. Restrained cerebral hyperperfusion in response to superimposed acute hypoxemia in growth-restricted human fetuses with established brain-sparing blood flow. *Early Hum Dev* 2006;82:211–216. [Epub 2005 Dec 2.]
155. Fouron JC. The unrecognized physiological and clinical significance of the fetal aortic isthmus. *Ultrasound Obstet Gynecol* 2003;22:441–447.
156. Fouron JC, et al. Correlation between prenatal velocity waveforms in the aortic isthmus and neurodevelopmental outcome between the ages of 2 and 4 years. *Am J Obstet Gynecol* 2001;184:630–636.
157. Sonesson SE, Fouron JC. Doppler velocimetry of the aortic isthmus in human fetuses with abnormal velocity waveforms in the umbilical artery. *Ultrasound Obstet Gynecol* 1997;10:107–111.
158. Donofrio MT, et al. Autoregulation of cerebral blood flow in fetuses with congenital heart disease: the brain sparing effect. *Pediatr Cardiol* 2003;24:436–443.
159. Kaltman JR, et al. Impact of congenital heart disease on cerebrovascular blood flow dynamics in the fetus. *Ultrasound Obstet Gynecol* 2005;25:32–36.
160. Jouannic JM, et al. Middle cerebral artery Doppler in fetuses with transposition of the great arteries. *Ultrasound Obstet Gynecol* 2002;20:122–124.
161. Fesslova V, Nava S, Villa L. Evolution and long term outcome in cases with fetal diagnosis of congenital heart disease: Italian multicentre study. Fetal Cardiology Study Group of the Italian Society of Pediatric Cardiology. *Heart* 1999;82:594–599.
162. Trines J, Hornberger LK. Evolution of heart disease in utero. *Pediatr Cardiol* 2004;25:287–298.
163. Sharland GK, et al. Left ventricular dysfunction in the fetus: relation to aortic valve anomalies and endocardial fibroelastosis. *Br Heart J* 1991;66:419–424.
164. Allan LD, et al. Survival after fetal aortic balloon valvuloplasty. *Ultrasound Obstet Gynecol* 1995;5:90–91.
165. Kohl T, et al. World experience of percutaneous ultrasound-guided balloon valvuloplasty in human fetuses with severe aortic valve obstruction. *Am J Cardiol* 2000;85:1230–1233.
166. Wilkins-Haug LE, et al. In-utero intervention for hypoplastic left heart syndrome—a perinatologist's perspective. *Ultrasound Obstet Gynecol* 2005;26:481–486.
167. Arzt W, et al. Invasive intrauterine treatment of pulmonary atresia/intact ventricular septum with heart failure. *Ultrasound Obstet Gynecol* 2003;21:186–188.
168. Tulzer G, et al. Fetal pulmonary valvuloplasty for critical pulmonary stenosis or atresia with intact septum. *Lancet* 2002;360:1567–1568.
169. Galindo A, et al. Pulmonary balloon valvuloplasty in a fetus with critical pulmonary stenosis/atresia with intact ventricular septum and heart failure. *Fetal Diagn Ther* 2006;21:100–104.
170. Satomi G, et al. Interventional treatment for fetus and newborn infant with congenital heart disease. *Pediatr Int* 2001;43:553–557.
171. Huhta J, et al. Advances in fetal cardiac intervention. *Curr Opin Pediatr* 2004;16:487–493.
172. Kohl T, et al. Fetal transesophageal echocardiography: clinical introduction as a monitoring tool during cardiac intervention in a human fetus. *Ultrasound Obstet Gynecol* 2005;26:780–785.
173. Suh E, et al. How to grow a heart: fiberoptic guided fetal aortic valvotomy. *Cardiol Young* 2006;16:43–46.
174. Harrison MR, et al. Fetal surgical treatment. *Pediatr Ann* 1982;11:896–899, 901–903.
175. Harrison MR, et al. Successful repair in utero of a fetal diaphragmatic hernia after removal of herniated viscera from the left thorax. *N Engl J Med* 1990;322:1582–1584.
176. Lorenz HP, Adzick NS, Harrison MR. Open human fetal surgery. *Adv Surg* 1993;26:259–273.
177. Harrison MR, et al. Correction of congenital diaphragmatic hernia in utero VIII: response of the hypoplastic lung to tracheal occlusion. *J Pediatr Surg* 1996;31:1339–1348.
178. Harrison MR, et al. Correction of congenital diaphragmatic hernia in utero IX: fetuses with poor prognosis (liver herniation and low lung-to-head ratio) can be saved by fetoscopic temporary tracheal occlusion. *J Pediatr Surg* 1998;33:1017–1022; discussion 1022–1023.
179. Harrison MR, et al. Fetoscopic temporary tracheal occlusion by means of detachable balloon for congenital diaphragmatic hernia. *Am J Obstet Gynecol* 2001;185:730–733.
180. Cortes RA, et al. Survival of severe congenital diaphragmatic hernia has morbid consequences. *J Pediatr Surg* 2005;40:36–45; discussion 45–46.
181. Harrison MR, et al. A randomized trial of fetal endoscopic tracheal occlusion for severe fetal congenital diaphragmatic hernia. *N Engl J Med* 2003;349:1916–1924.
182. Clewell WH, et al. Placement of ventriculo-amniotic shunt for hydrocephalus in a fetus. *N Engl J Med* 1981;305:955.
183. Clewell WH. Congenital hydrocephalus: treatment in utero. *Fetal Ther* 1988;3:89–97.
184. Huang HW, et al. Prenatal diagnosis of persistent fetal bradycardia: report of four cases. *Chang Gung Med J* 2001;24:57–61.
185. Levey A, et al. The impact of prenatal diagnosis of complex congenital heart disease on neonatal outcomes. *Pediatr Cardiol* 2010;31:587–597.
186. Vanderhal AL, et al. Conjugated hyperbilirubinemia in a newborn infant after maternal (transplacental) treatment with flecainide acetate for fetal tachycardia and fetal hydrops. *J Pediatr* 1995;126:988–990.
187. Vetter VL, Rashkind WJ. Congenital complete heart block and connective-tissue disease. *N Engl J Med* 1983;309:236–238.
188. Scott JS, et al. Connective-tissue disease, antibodies to ribonucleoprotein, and congenital heart block. *N Engl J Med* 1983;309:209–212.
189. McCue CM, et al. Congenital heart block in newborns of mothers with connective tissue disease. *Circulation* 1977;56:82–90.
190. Veille JC, Sunderland C, Bennett RM. Complete heart block in a fetus associated with maternal Sjogren's syndrome. *Am J Obstet Gynecol* 1985;151:660–661.
191. McCormack GD, Barth WF. Congenital complete heart block with maternal primary Sjogren's syndrome. *South Med J* 1985;78:471–473.
192. Sholler GF, Whight CM, Celemajer JM. Fetal echocardiography: experience and reason. *Med J Aust* 1986;144:250–252.
193. Taylor PV, et al. Maternal antibodies against fetal cardiac antigens in congenital complete heart block. *N Engl J Med* 1986;315:667–672.
194. Horsfall AC, et al. Ro and La antigens and maternal anti-La idiotype on the surface of myocardial fibres in congenital heart block. *J Autoimmun* 1991;4:165–176.
195. Schmidt KG, et al. Perinatal outcome of fetal complete atrioventricular block: A multicenter experience. *J Am Coll Cardiol* 1991;17:1360–1366.
196. Van Leeuwen P. Fetal magnetocardiography: time intervals and heart rate variability. *Neuro Clin Neurophysiol* 2004;46.
197. Herruzo A, et al. Bigeminal fetal rhythm [in Spanish]. *Acta Obstet Ginecol Hisp Lusit* 1979;27:593–600.
198. Martinez J, et al. Ventricular fetal extrasystole [in Spanish]. *Acta Obstet Ginecol Hisp Lusit* 1979;27:579–590.
199. Madison JP, et al. Echocardiography and fetal heart sounds in the diagnosis of fetal heart block. *Am Heart J* 1979;98:505–509.
200. Baumgarten K, Frohlich H. Fetal rhythm disorders during pregnancy and birth [in German]. *Z Geburtshilfe Perinatol* 1972;176:249–265.
201. Chitkara U, et al. Persistent supraventricular tachycardia in utero. *Diagn Gynecol Obstet* 1980;2:291–298.
202. Hawrylyshyn PA, et al. The role of echocardiography in fetal cardiac arrhythmias. *Am J Obstet Gynecol* 1981;141:223–225.
203. DeVore GR, Siassi B, Platt LD. Fetal echocardiography III: the diagnosis of cardiac arrhythmias using real-time-directed M-mode ultrasound. *Am J Obstet Gynecol* 1983;146:792–799.
204. Stewart PA, Tonge HM, Wladimiroff JW. Arrhythmia and structural abnormalities of the fetal heart. *Br Heart J* 1983;50:550–554.
205. Allan LD, et al. Evaluation of fetal arrhythmias by echocardiography. *Br Heart J* 1983;50:240–245.
206. Wester HA, Grimm G, Lehmann F. Echocardiographic diagnosis of fetal heart insufficiency caused by supraventricular tachycardia [in German]. *Z Kardiol* 1984;73:405–408.
207. Shapiro I, Sharf M, Abinader EG. Prenatal diagnosis of fetal arrhythmias: A new echocardiographic technique. *J Clin Ultrasound* 1984;12:369–372.
208. Crowley DC, et al. Two-dimensional and M-mode echocardiographic evaluation of fetal arrhythmia. *Clin Cardiol* 1985;8:1–10.
209. Silverman NH, et al. Recognition of fetal arrhythmias by echocardiography. *J Clin Ultrasound* 1985;13:255–263.
210. Wladimiroff JW, Stewart PA. Treatment of fetal cardiac arrhythmias. *Br J Hosp Med* 1985;34:134–140.
211. Truccone NJ, Mariona FG. Prenatal diagnosis and outcome of congenital complete heart block: the role of fetal echocardiography. *Fetal Ther* 1986;1:210–216.
212. Castillo R, et al. Fetal echocardiography: diagnosis and management of fetal arrhythmias. *J Med Assoc Ga* 1986;75:730–733.
213. Lingman G, Marsal K. Fetal cardiac arrhythmias: doppler assessment. *Semin Perinatol* 1987;11:357–361.
214. Cameron A, et al. Evaluation of fetal cardiac dysrhythmias with two-dimensional, M-mode, and pulsed Doppler ultrasonography. *Am J Obstet Gynecol* 1988;158:286–290.
215. Gembruch U, Bald R, Hansmann M. Color-coded M-mode Doppler echocardiography in the diagnosis of fetal arrhythmia [in German]. *Geburtshilfe Frauenheilkd* 1990;50:286–290.
216. Chaoui R, et al. Fetal echocardiography: part III. Fetal arrhythmia [in German]. *Zentralbl Gynakol* 1991;113:1335–1350.
217. Maeno Y. Fetal arrhythmias; intrauterine diagnosis and treatment. *Kurume Med J* 1991;38:327–336.
218. Rein AJ, et al. Use of tissue velocity imaging in the diagnosis of fetal cardiac arrhythmias. *Circulation* 2002;106:1827–1833.
219. Wakai RT, et al. Magnetocardiographic rhythm patterns at initiation and termination of fetal supraventricular tachycardia. *Circulation* 2003;107:307–312.
220. Comani S, et al. Characterization of fetal arrhythmias by means of fetal magnetocardiography in three cases of difficult ultrasonographic imaging. *Pacing Clin Electrophysiol* 2004;27:1647–1655.
221. Hosono T, et al. Prenatal diagnosis of fetal complete atrioventricular block with QT prolongation and alternating ventricular pacemakers using

- multi-channel magnetocardiography and current-arrow maps. *Fetal Diagn Ther* 2002;17:173–176.
222. Menendez T, et al. Prenatal diagnosis of QT prolongation by magnetocardiography. *Pacing Clin Electrophysiol* 2000;23:1305–1307.
 223. Hamada H, et al. Prenatal diagnosis of long QT syndrome using fetal magnetocardiography. *Prenat Diagn* 1999;19:677–680.
 224. Fouron JC, et al. Management of fetal tachyarrhythmia based on superior vena cava/aorta Doppler flow recordings. *Heart* 2003;89:1211–1216.
 225. DeVore GR, Horenstein J. Simultaneous Doppler recording of the pulmonary artery and vein: a new technique for the evaluation of a fetal arrhythmia. *J Ultrasound Med* 1993;12:669–671.
 226. Lingman G, Ohlander S, Ohlin P. Intrauterine digoxin treatment of fetal paroxysmal tachycardia: case report. *Br J Obstet Gynaecol* 1980;87:340–342.
 227. Kerenyi TD, et al. Transplacental cardioversion of intrauterine supraventricular tachycardia with digitalis. *Lancet* 1980;2:393–394.
 228. Dumesic DA, et al. Transplacental cardioversion of fetal supraventricular tachycardia with procainamide. *N Engl J Med* 1982;307:1128–1131.
 229. King CR, et al. Successful treatment of fetal supraventricular tachycardia with maternal digoxin therapy. *Chest* 1984;85:573–575.
 230. Allan LD, et al. Evaluation and treatment of fetal arrhythmias. *Clin Cardiol* 1984;7:467–473.
 231. Truccone N, Mariona F. Intrauterine conversion of fetal supraventricular tachycardia with combination of digoxin and verapamil. *Pediatr Pharmacol (New York)* 1985;5:149–153.
 232. Lingman G, et al. Fetal cardiac arrhythmia: clinical outcome in 113 cases. *Acta Obstet Gynecol Scand* 1986;65:263–267.
 233. Killeen AA, Bowers LD. Fetal supraventricular tachycardia treated with high-dose quinidine: Toxicity associated with marked elevation of the metabolite, 3(S)-3-hydroxyquinidine. *Obstet Gynecol* 1987;70:445–449.
 234. Allan LD, et al. Flecainide in the treatment of fetal tachycardias. *Br Heart J* 1991;65:46–48.
 235. Perry JC, Ayres NA, Carpenter RJ Jr. Fetal supraventricular tachycardia treated with flecainide acetate. *J Pediatr* 1991;118:303–305.
 236. Pinsky WW, Rayburn WF, Evans MI. Pharmacologic therapy for fetal arrhythmias. *Clin Obstet Gynecol* 1991;34:304–309.
 237. Azancor-Benisty A, et al. Clinical and pharmacologic study of fetal supraventricular tachyarrhythmias. *J Pediatr* 1992;121:608–613.
 238. Parilla BV, Strasburger JF, Socol ML. Fetal supraventricular tachycardia complicated by hydrops fetalis: a role for direct fetal intramuscular therapy. *Am J Perinatol* 1996;13:483–486.
 239. Amano K, et al. Successful treatment of supraventricular tachycardia with flecainide acetate: a case report. *Fetal Diagn Ther* 1997;12:328–331.
 240. Mangione R, et al. Successful treatment of refractory supraventricular tachycardia by repeat intravascular injection of amiodarone in a fetus with hydrops. *Eur J Obstet Gynecol Reprod Biol* 1999;86:105–107.
 241. Schmolling J, et al. Digoxin, flecainide, and amiodarone transfer across the placenta and the effects of an elevated umbilical venous pressure on the transfer rate. *Ther Drug Monit* 2000;22:582–588.
 242. Nakata M, et al. Successful treatment of supraventricular tachycardia exhibiting hydrops fetalis with flecainide acetate: a case report. *Fetal Diagn Ther* 2003;18:83–86.
 243. Walsh EP, Saul JP, Triedman JK. *Cardiac Arrhythmias in Children and Young Adults with Congenital Heart Disease*. Philadelphia, PA: Lippincott Williams & Wilkins, 2001.
 244. Carpenter RJ Jr, et al. Fetal ventricular pacing for hydrops secondary to complete atrioventricular block. *J Am Coll Cardiol* 1986;8:1434–1436.
 245. Crombleholme TM, et al. Complete heart block in fetal lambs. I: technique and acute physiological response. *J Pediatr Surg* 1990;25:587–593.
 246. Herremans G, et al. Fetal death caused by myocarditis and isolated congenital auriculoventricular block [in French]. *Presse Med* 1985;14:1547–1550.
 247. Buyon JP, et al. Intrauterine therapy for presumptive fetal myocarditis with acquired heart block due to systemic lupus erythematosus. Experience in a mother with a predominance of SS-B (La) antibodies. *Arthritis Rheum* 1987;30:44–49.
 248. Buyon JP, Winchester R. Congenital complete heart block: a human model of passively acquired autoimmune injury. *Arthritis Rheum* 1990;33:609–614.
 249. Arroyave CM, et al. Myocardopathy diagnosed in utero in a mother with SS-A antibodies treated with plasmapheresis [in Spanish]. *Ginecol Obstet Mex* 1995;63:134–137.
 250. Udink ten Cate FE, et al. Dilated cardiomyopathy in isolated congenital complete atrioventricular block: early and long-term risk in children. *J Am Coll Cardiol* 2001;37:1129–1134.
 251. Matsushita H, et al. Successful prenatal treatment of congenital heart block with ritodrine administered transplacentally. *Arch Gynecol Obstet* 2002;267:51–53.
 252. Comas C, et al. Complete congenital atrioventricular block. Prenatal diagnosis and perinatal management. *Rev Esp Cardiol* 1997;50:498–506.
 253. Koike T, et al. Fetal ventricular rate in case of congenital complete heart block is increased by ritodrine: case report. *J Perinat Med* 1997;25:216–218.
 254. Friedman DM, Buyon JP. Complete atrioventricular block diagnosed prenatally: anything new on the block? *Ultrasound Obstet Gynecol* 2005;26:2–3.
 255. Buyon JP, et al. Identifying an early marker for congenital heart block: when is a long PR interval too long? Comment on the article by Sonesson et al. *Arthritis Rheum* 2005;52:1341–1342.
 256. Glickstein J, et al. The fetal Doppler mechanical PR interval: a validation study. *Fetal Diagn Ther* 2004;19:31–34.
 257. Buyon JP, Friedman DM. Autoantibody-associated congenital heart block: the clinical perspective. *Curr Rheumatol Rep* 2003;3:374–378.
 258. Brucato A, et al. Proposal for a new definition of congenital complete atrioventricular block. *Lupus* 2003;12:427–435.
 259. Rosenthal D, et al. Validation of the Doppler PR interval in the fetus. *J Am Soc Echocardiogr* 2002;15:1029–1030.
 260. Friedman DM, et al. Congenital heart block in neonatal lupus: the pediatric cardiologist's perspective. *Indian J Pediatr* 2002;69:517–522.
 261. Saleeb S, et al. Comparison of treatment with fluorinated glucocorticoids to the natural history of autoantibody-associated congenital heart block: retrospective review of the research registry for neonatal lupus. *Arthritis Rheum* 1999;42:2335–2345.
 262. Raboisson MJ, et al. Fetal Doppler echocardiographic diagnosis and successful steroid therapy of Luciani-Wenckebach phenomenon and endocardial fibroelastosis related to maternal anti-Ro and anti-La antibodies. *J Am Soc Echocardiogr* 2005;18:375–380.
 263. Jaeggi ET, et al. Is immune-mediated complete fetal atrioventricular block reversible by transplacental dexamethasone therapy? *Ultrasound Obstet Gynecol* 2004;23:602–605.
 264. Jaeggi ET, et al. Transplacental fetal treatment improves the outcome of prenatally diagnosed complete atrioventricular block without structural heart disease. *Circulation* 2004;110:1542–1548.
 265. Jaeggi ET, et al. Outcome of children with fetal, neonatal or childhood diagnosis of isolated congenital atrioventricular block: a single institution's experience of 30 years. *J Am Coll Cardiol* 2002;39:130–137.
 266. Carvalho JS, Shinebourne EA, Kyle P. Efficacy unproved of maternal dexamethasone for fetal heart block. *Am J Obstet Gynecol* 1996;175:502–503.
 267. Goncalves LF, et al. Examination of the fetal heart by four-dimensional (4D) ultrasound with spatio-temporal image correlation (STIC). *Ultrasound Obstet Gynecol* 2006;27:336–348.
 268. DeVore GR, et al. The “spin” technique: a new method for examination of the fetal outflow tracts using three-dimensional ultrasound. *Ultrasound Obstet Gynecol* 2004;24:72–82.
 269. Cohen L, et al. Satisfactory visualization rates of standard cardiac views at 18 to 22 weeks' gestation using spatiotemporal image correlation. *J Ultrasound Med* 2009;28:1645–1650.
 270. Hamar BD, et al. Trends in fetal echocardiography and implications for clinical practice: 1985 to 2003. *J Ultrasound Med* 2006;25:197–202.
 271. Mohan UR, Kleinman CS, Kern JH. Fetal echocardiography and its evolving impact 1992 to 2002. *Am J Cardiol* 2005;96:134–136.

SECTION

VI

Congenital Cardiovascular Malformations

PART

A

Septal Defects

CHAPTER

28

Atrial Septal Defects

Ritu Sachdeva

INTRODUCTION

Atrial septal defects (ASD) originate at particular sites in the atrial septum and are named according to their embryonic origin. The most common occurs in the central part of the atrial septum in the region of fossa ovalis (secundum ASD). Others include those in the region of endocardial cushion (primum ASD), in the sinus venosus septum (sinus venosus ASD), and in the region of ostium of coronary sinus (coronary sinus ASD). In this chapter, we also address patent foramen ovale (PFO), which is a normal interatrial communication present in fetal life that may persist in adults. Ostium primum ASD is discussed in Chapter 29 since it is a part of the spectrum of atrioventricular septal defects (AVSD).

INCIDENCE

ASDs constitute 8% to 10% of congenital heart defects in children. The incidence of ASDs has been estimated to be 56 per 100,000 live births (1). The recent estimates are much higher (100 per 100,000 live births), likely due to increased recognition of ASDs in this era of the common use of echocardiography (2). The female:male ratio for secundum ASDs is 2:1, but for the sinus venosus ASDs it is 1:1 (3,4). Secundum ASDs constitute approximately 75% of ASDs, followed by ostium primum ASD (20%) and sinus venosus ASD (5%) (5). Coronary sinus (CS) ASDs more often are seen in association

with heterotaxy syndromes and systemic venous anomalies, and isolated CS ASDs are rare (<1%).

GENETIC AND ENVIRONMENTAL RISK FACTORS

Although most ASDs occur sporadically, familial modes of inheritance have been reported. The risk of congenital heart disease in offspring of a woman with a sporadic ASD is estimated to be 8% to 10% (6). ASDs may be related to mutations in either regulatory genes or their target sarcomeric genes. Heterozygous mutations in the transcription factor NKX2.5/CSX were among the first found in families with autosomal dominant transmission of secundum ASDs (7). Mutations in other transcription factors such as TBX5, GATA4, GATA6, and TBX20 also have been associated with secundum ASDs (7–11). TBX5 mutations also are responsible for Holt-Oram syndrome, which is an autosomal dominant syndrome characterized by secundum ASD, anomalies of the upper extremities, and atrioventricular (AV) conduction delay (12). A locus on chromosome 14q12 with a missense mutation in alpha-myosin heavy chain (MYH6), a structural protein expressed at high levels in the developing atria, has been linked to dominantly inherited ASD (13). Secundum ASDs also have been reported in association with cardiomyopathies that have resulted from mutations in sarcomeric genes (14,15). In ASDs associated with prolonged AV conduction, an autosomal dominant pattern of inheritance has been reported (16). Secundum ASDs

also are associated with other syndromes such as Noonan, Down, Klinefelter, Williams, Kabuki, Goldenhar, and Ellis-van Creveld. In addition to genetic factors, maternal diseases and exposure to environmental risk factors may play a role in development of ASDs (17). These factors include pregestational diabetes, phenylketonuria, influenza and exposure to retinoids, nonsteroidal anti-inflammatory drugs, anticonvulsants, thalidomide, smoking, and alcohol (17–19).

PATHOGENESIS AND ANATOMIC FEATURES

During embryogenesis, the primitive atrium undergoes a complex septation process (Fig 28.1) (20). In the fourth week of embryonic life, the septum primum appears as a thin-walled sagittal fold in the middle of the common atrium and grows inferiorly toward the endocardial cushion. The opening between the leading edge of the septum primum and the endocardial cushion is called the ostium primum. Before complete closure of the ostium primum, tissue reabsorption occurs in the superior portion of the septum primum resulting in another opening called the ostium secundum. This occurs during the fifth and sixth week of embryonic life. Concurrently, an anterosuperior infolding of the atrial roof develops to the right of the septum primum, called the septum secundum that is concave shaped with a superior and inferior limb. The inferior limb fuses with the lowermost part of the atrial septum to join the endocardial cushion, thus separating the inferior portions of the two atria. The thick muscular ridge of the superior limb forms an incomplete partition that overlies the ostium secundum resulting in an opening called the foramen ovale. The septum secundum thus forms the concave-shaped superior margin of the fossa ovalis, called the limbus of fossa ovalis (annulus ovalis) and the septum primum forms the valve of fossa ovalis. During fetal life, inferior vena caval flow from the placenta is deflected toward the foramen ovale by the eustachian valve, and then blood is

directed from the right atrium to the left atrium via the foramen ovale. This fetal interatrial communication (the PFO) normally closes after birth as a result of fusion of the septum primum and septum secundum. However, it may persist in 25% to 30% of adults where it is probe patent with a competent valve. In some cases, the valve of fossa ovalis is incompetent, either congenitally or acquired due to elevated right or left atrial pressures allowing interatrial shunting across the foramen.

The atrial septal anatomy and location of various types of ASDs are shown in Figure 28.2. Secundum ASDs occur in the central part of the atrial septum (fossa ovalis) as a result of deficient valve tissue, ectopic or excessive resorption of septum primum, or deficient growth of septum secundum (Fig. 28.3). Such defects result in an enlarged ostium secundum. These defects usually are single, but rarely can occur as multiple atrial septal fenestrations.

Sinus venosus defects occur outside the margins of the fossa ovalis, in relation to the venous connections of the right atrium (Fig. 28.4). The right horn of sinus venosus incorporates the right superior vena cava (SVC) and inferior vena cava (IVC) into the right atrium. Ectopic or incomplete resorption of the sinus venosus results in deficiency of the wall that separates the right pulmonary veins from the SVC, IVC, and the right atrium resulting in a sinus venosus ASD (21). Some argue that these should be termed partial anomalous pulmonary venous return to the SVC. The interatrial communication in these defects is, in fact, the orifice of the unroofed right pulmonary vein and is not a true defect in the atrial septum per se. (21) Most commonly, the sinus venosus ASDs are related to the SVC where blood from the right upper and/or middle pulmonary veins is directed into SVC or the right atrium. Less frequently, a similar defect can occur inferior to the fossa ovalis in relation to the IVC and the right lower pulmonary venous orifice. This defect often has been termed an IVC-type sinus venosus ASD, although direct involvement of the IVC almost never occurs. Hence, the term sinus venosus defect of right atrial type is preferred (21).

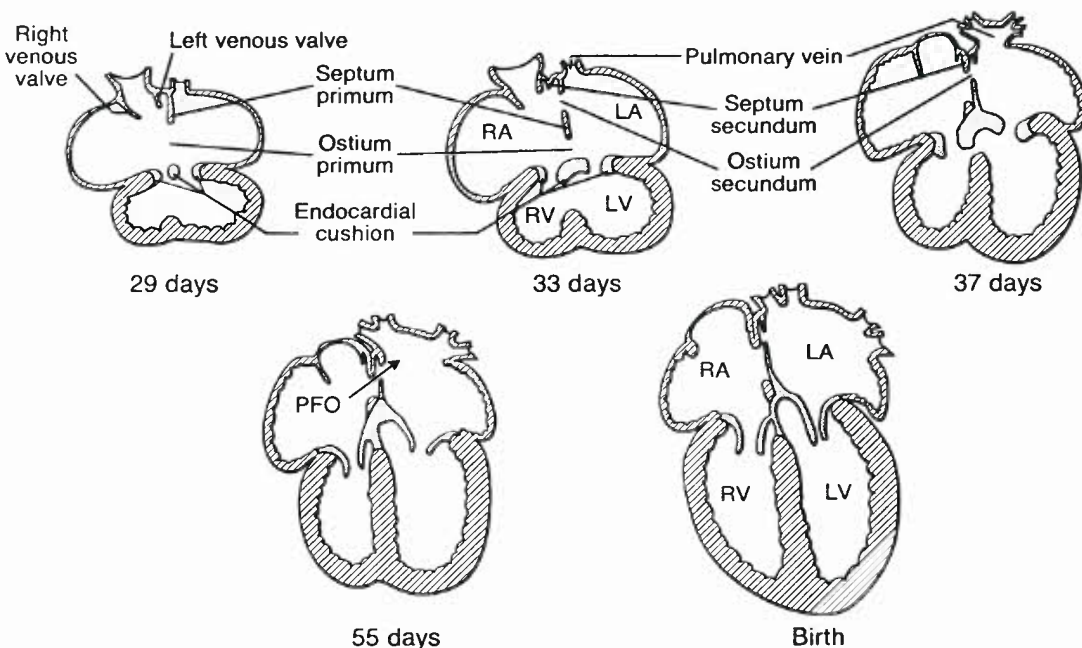


Figure 28.1. Schematic diagram showing embryogenesis of atrial septum. LA, left atrium; LV, left ventricle; PFO, patent foramen ovale; RA, right atrium; RV, right ventricle. (Modified from Van Mierop LHS. Embryology of the atrioventricular canal region and pathogenesis of endocardial cushion defects. In: Feldt RH, McGoon DC, Ongley PA, et al., eds. *Atrioventricular Canal Defects*. Philadelphia, PA: WB Saunders, 1976:1–12, with permission.)

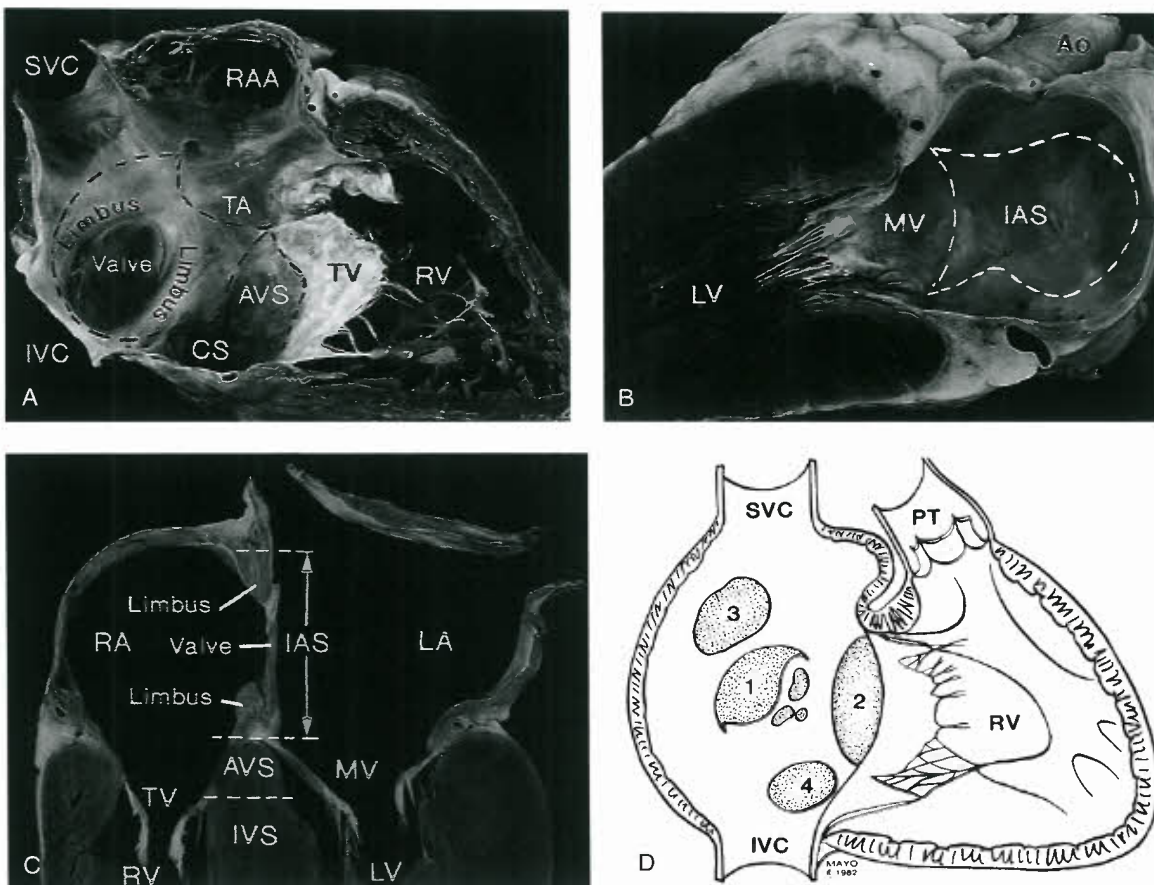


Figure 28.2. A: Anatomy of the atrial septum. View from the right atrial side. B: View from the left atrial side. The interatrial septum (IAS) is outlined by the dotted lines. It is formed by the limbus of the fossa ovalis on the right atrial side and the valve of the fossa ovalis toward the left. The aortic root indents the right atrial free wall anterosuperiorly as the torus aorticus (TA). C: Cross section of the heart in a 4-chamber view. The IAS formed by the limbus and valve of fossa ovalis lies between the right and left atria (RA, LA). The atrioventricular septum (AVS) lies between the RA and left ventricle (LV). D: Schematic diagram showing the location of various types of ASDs: (a) Secundum; (b) Primum; (c) Sinus venosus; (d) Coronary sinus. IVC, inferior vena cava; IVS, interventricular septum; MV, mitral valve; PT, pulmonary trunk; RAA, right atrial appendage; RV, right ventricle; SVC, superior vena cava; TV, tricuspid valve. (Reprinted by permission of the Mayo Foundation.)

The left horn of the sinus venosus forms the CS. The CS defect (unroofed CS) results from failure of the wall between the left atrium and CS to develop. There may be complete or partial unroofing of the CS resulting in direct communication with the left atrium (Fig. 28.5). Almost always, this anomaly is associated with a left SVC. A rare variation consists of complete absence of the CS rather than unroofing, along with a defect in the expected location of the ostium of CS. In such defects, blood from the left SVC directly enters the left atrium. Kirklin and Barratt-Boyes (5) classified the unroofed CS defects as type I, completely unroofed with LSVC; type II, completely unroofed without LSVC; type III, partially unroofed midportion; and type IV, partially unroofed terminal portion.

ASSOCIATED CARDIOVASCULAR ANOMALIES

Interatrial communications can occur in isolation, but often are associated with other congenital heart defects. The presence of an interatrial communication may be crucial for survival in some such defects such as hypoplastic left heart syndrome, D-transposition of great arteries, tricuspid atresia, and total anomalous pulmonary venous return. Partial anomalous pulmonary

venous return is present in almost 90% of patients with sinus venosus ASDs and, more rarely, can occur with secundum ASDs. Although valvular pulmonary stenosis frequently has been associated with ASDs, the increased gradient across the pulmonary valve may be flow related and not necessarily due to an abnormal valve per se. CS ASDs commonly are associated with a persistent left SVC. Aside from congenital heart defects, secundum ASDs also have been reported in association with noncompaction and apical hypertrophic cardiomyopathy (14,15).

Lutembacher Syndrome

Lutembacher syndrome is the association of an ASD with mitral stenosis. Unlike the original description by Lutembacher, where the mitral stenosis was considered to be congenital in origin, the current consensus is that it is of rheumatic origin (22). As a result of the mitral stenosis, the left-to-right shunting across the ASD is augmented. The ASD usually is large and unrestrictive. Therefore, the magnitude of the atrial level shunt is directly related to the degree of obstruction at the mitral valve. Rarely, when the ASD is restrictive, the left-to-right shunt is continuous due to significant pressure difference across the atrial septum during the entire cardiac cycle.

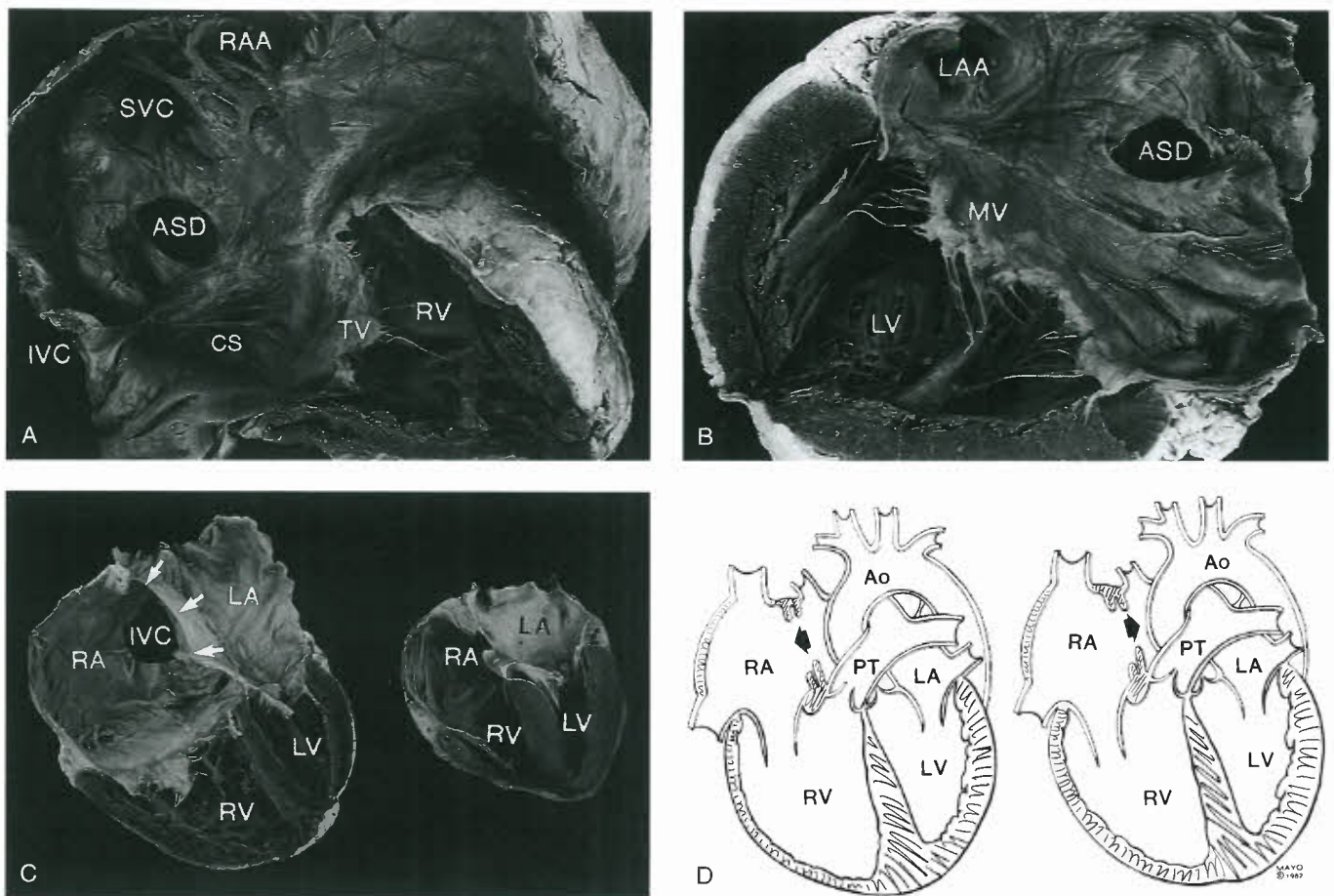


Figure 28.3. Secundum ASD occurs in the region of fossa ovalis. A: Right atrial view. B: Left atrial view. C: Four-chamber view, showing comparison of a heart with large secundum ASD (arrows) with a normal heart (toward the right). The right atrium (RA) and right ventricle (RV) are significantly enlarged in the heart with the ASD. D: Schematic diagram showing a left-to-right shunt across ASD, which becomes right-to-left with development of pulmonary vascular disease. Ao, aorta; LAA, left atrial appendage; IVC, inferior vena cava; MV, mitral valve; PT, pulmonary trunk; RAA, right atrial appendage; RV, right ventricle; SVC, superior vena cava; TV, tricuspid valve. (Reprinted by permission of the Mayo Foundation.)

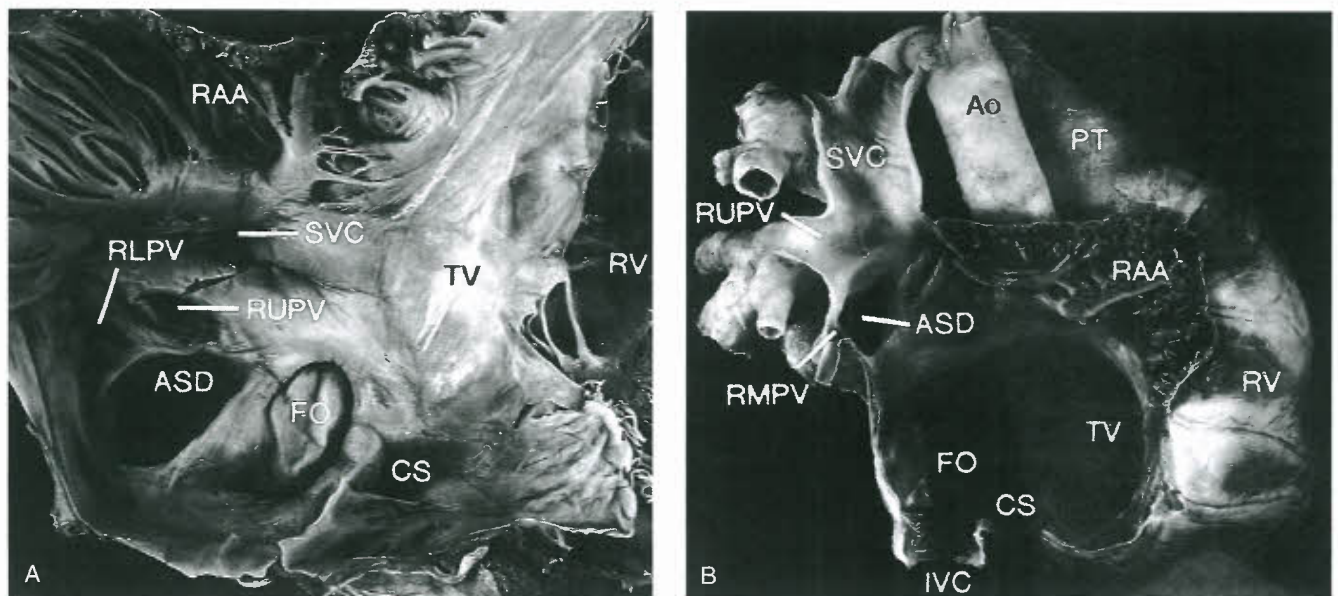


Figure 28.4. Sinus venosus ASD. A: Right atrial view. Right upper (RUPV) and lower (RMPV) pulmonary veins join the right atrium near the site of the ASD, posterior and superior to the fossa ovalis (FO). B: Right atrial view. The ASD is posterior to the FO, and the right upper and middle (RMPV) pulmonary veins are anomalously connected to the SVC. Ao, aorta; IVC, inferior vena cava; PT, pulmonary trunk; RAA, right atrial appendage; RV, right ventricle; SVC, superior vena cava; TV, tricuspid valve. (Reprinted by permission of the Mayo Foundation.)

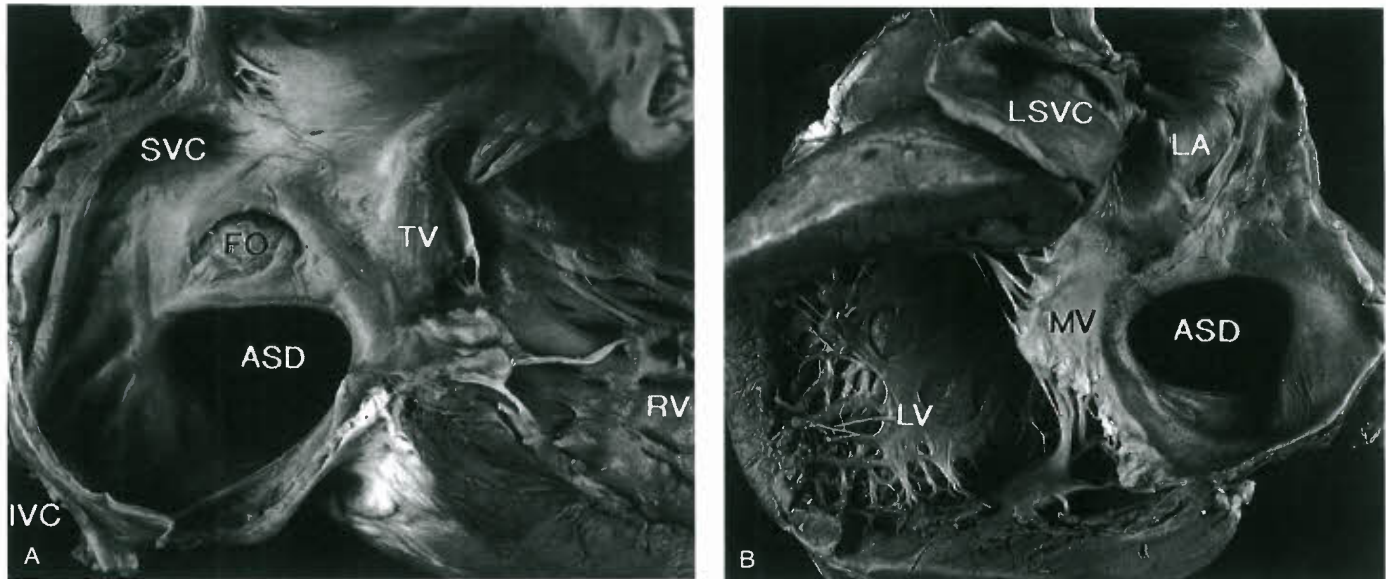


Figure 28.5. Coronary sinus atrial septal defect (ASD). A: Right atrial view. B: Left atrial view. The defect is at the site of the CS ostium, anterior and inferior to the fossa ovalis (FO). A persistent left superior vena cava (LSVC) joins the left atrial wall (LA). IVC, inferior vena cava; MV, mitral valve; RV, right ventricle; SVC, superior vena cava; TV, tricuspid valve. Reprinted by permission of the Mayo Foundation.

PATHOPHYSIOLOGY

During fetal life, the majority of the blood reaching the left atrium comes via the foramen ovale since there is minimal flow to the lungs. After birth, the lungs expand and the pulmonary blood flow increases. The increased pulmonary venous return to the left atrium results in the left atrial pressure exceeding the right atrial pressure causing functional closure of the foramen ovale. Intrauterine physiology is not altered in the presence of an ASD, but unlike the PFO, the ASD does not close with the hemodynamic changes that occur following birth. The physiologic consequences of an ASD depend on the magnitude and duration of the shunt and its interaction with the pulmonary vascular bed. The primary determinant of the magnitude and direction of the shunt is the relative compliance of the ventricles. During the neonatal transition period as the pulmonary vascular resistance drops and the right ventricular wall becomes thinner and hence more compliant than that of the left ventricle, there is an increase in left-to-right shunting. Catheter-based studies on flow dynamics in ASD provide insight into the circulatory pattern during the various phases of cardiac cycle. Maximum left-to-right shunting occurs during diastole when all four cardiac chambers are in communication. Atrial contraction further augments this shunt. A small right-to-left shunt, predominantly from IVC blood can occur during early diastole or during onset of systole. The magnitude and amount of shunting varies with the respiratory cycle. During inspiration when the intrathoracic pressure is decreased, there is a decrease in the left-to-right shunt across the ASD. Conversely, during expiration, when the intrathoracic pressure is increased, there is an increase in the left-to-right shunt.

Moderate-to-large left-to-right shunts across an ASD result in volume overload and dilation of the right atrium and ventricle (Fig. 28.3). The tricuspid and pulmonary annuli may dilate and become incompetent. The volume-overloaded right ventricle alters the diastolic configuration of the left ventricle with septal bowing toward the left. Occasionally, the abnormal left ventricular geometry may result in prolapse of the

mitral valve or superior systolic motion of the mitral leaflet (23). As a result of the increased flow into the lungs, the pulmonary arteries, capillaries, and the veins are dilated and there can be flow-related pulmonary artery hypertension. Over time this can lead to medial hypertrophy of pulmonary arteries and muscularization of the arterioles resulting in pulmonary vascular obstructive disease (24,25). With severe pulmonary vascular obstructive disease, patients develop Eisenmenger syndrome as the atrial level shunt becomes right-to-left, resulting in cyanosis (Fig. 28.3).

CLINICAL PRESENTATION

History

Most patients with ASD are asymptomatic and may remain undiagnosed until later in life. They may come to medical attention due to abnormal auscultatory findings or diagnostic studies such as ECG, chest radiograph, or echocardiogram. Very rarely, some infants with ASD may present with features of pulmonary overcirculation, recurrent respiratory infections, and failure to thrive. The mechanism of heart failure in these infants is not well understood since the hemodynamics are quite similar to those who are asymptomatic. Some have proposed rapid remodeling and thinning of the pulmonary vascular bed to be the reason for this early presentation (26). Additionally, one should carefully evaluate mitral anatomy and function since mitral stenosis or regurgitation can augment atrial shunting. Despite repair of ASD in these patients, there may not be any significant improvement in their symptoms (27). Older children may present with symptoms of mild fatigue and dyspnea that may worsen with age. In adults, worsening of clinical condition has been attributed to various factors such as a decrease in left ventricular compliance secondary to coronary artery disease and hypertension, which, in turn, results in increased left-to-right shunt, right ventricular

failure, atrial arrhythmias, and elevated pulmonary artery pressure. Patients who develop Eisenmenger syndrome (reversal of the left-to-right shunt due to pulmonary hypertension) may present with cyanosis and syncope with exertion.

Physical Examination

Phenotypic features of various syndromes associated with ASD may be notable. The most common syndrome known to be associated with ostium secundum ASD is the Holt-Oram syndrome. In this syndrome, the thumb is hypoplastic and in some cases may be rudimentary or absent. Additionally, the metacarpals may be small or absent and the radius may be absent. The thumb may resemble a finger.

In patients with long-standing large left-to-right shunt, there is a left precordial bulge. Palpation reveals a prominent right ventricular impulse felt along the lower left sternal border and the subcostal area. In normal persons, splitting of S_2 has a normal variation with respiration. During inspiration, negative intrathoracic pressure causes increased venous return into the right side of the heart, which in turn causes the pulmonary valve to stay open for a longer duration in ventricular systole causing a normal delay in the pulmonary valve closure component of S_2 . During expiration, the positive intrathoracic pressure reduces the venous return to the right side of the heart, resulting in an earlier closure of pulmonary valve. The auscultatory hallmark of ASD is wide, fixed splitting of the second heart sound (S_2). This means that the aortic and pulmonary components of S_2 are widely separated during expiration and demonstrate little or no variation in degree of splitting during inspiration or with Valsalva maneuver. S_2 is “widely split” due to a delay in closure of the pulmonary valve resulting from prolonged emptying of the volume-overloaded right ventricle and increased pulmonary vascular capacitance leading to low pulmonary impedance and, therefore, a long “hangout interval” after the end of right ventricular systole. The S_2 is “fixed” since the increased right ventricular stroke volume does not vary much with respiration.

A systolic ejection murmur can be heard in the left upper parasternal area. The murmur is due to increased flow across the pulmonary valve. This murmur begins shortly after S_1 and is crescendo-decrescendo, reaching its peak in early to midsystole and ending before S_2 . When this murmur is loud, it can indicate a large shunt or associated pulmonary valve stenosis

(a systolic ejection click usually is present when the pulmonary valve is truly stenotic). When there is a large left-to-right shunt, a middiastolic murmur can be heard due to excessive flow across the tricuspid valve. This murmur is short, soft, low to medium in frequency, and localized to the left lower parasternal area. Rarely, a diastolic murmur may result from pulmonary regurgitation as a result of an exceptionally large pulmonary trunk that dilates the valve annulus.

Most patients are acyanotic. However, cyanosis can be seen in those with pulmonary hypertension, significant right ventricular outflow tract obstruction, or in rare cases of a large eustachian valve directing IVC blood into the left atrium via the ASD. Patients with pulmonary hypertension and a right-to-left atrial level shunt are cyanotic and have auscultatory findings that are different from those of patients with an ASD without pulmonary hypertension. The jugular venous pulse has a dominant “A” wave resulting from increased force of right atrial contraction. The large “A” waves result in presystolic distention of the right ventricle resulting in a fourth heart sound. The pulmonary component of S_2 is loud and prominent. The wide fixed splitting of S_2 and tricuspid flow murmur disappear and the midsystolic pulmonary flow murmur is replaced by a softer and shorter murmur. A high-frequency early diastolic murmur (Graham Steell murmur) of pulmonary regurgitation can be heard due to pulmonary valve incompetence resulting from pulmonary hypertension. Also, a holosystolic S_1 coincident murmur of tricuspid regurgitation heard best at the right lower sternal border can develop.

DIAGNOSTIC EVALUATION

Electrocardiogram and Electrophysiology

ECG findings depend on the type and size of the ASD. In patients with a small left-to-right shunt and no right atrial or ventricular dilation, the ECG is normal. With a significant left-to-right shunt, an rSR' pattern occurs in the right precordial leads indicating right ventricular volume overload (Fig. 28.6). There often is slight prolongation of the QRS complex with slurring of the terminal R', and the terminal forces are directed to the right, superiorly and anteriorly. Other features include right axis deviation and tall P waves reflecting right atrial enlargement. In almost 50% of patients

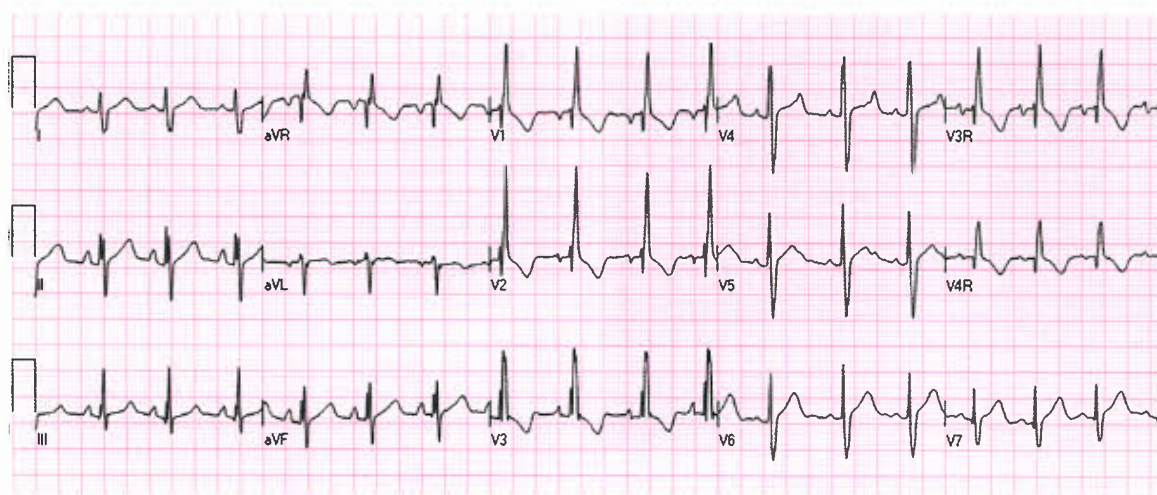


Figure 28.6. ECG in a 4-year-old patient with large secundum ASD showing rSR' pattern in lead V1 and V2 and terminal widening on S in lead V6 indicating right ventricular volume overload.

with sinus venosus ASD, a frontal plane P wave axis of <30 degrees is seen (4). In most patients with ASD, the frontal plane QRS axis is between $+95$ and $+170$ degrees. Ostium primum ASD can be distinguished from other forms of ASDs by the presence of a counterclockwise loop and left axis deviation. Rhythm usually is sinus in children. However, older patients, usually beyond the third decade of life, can have junctional rhythm or atrial arrhythmias such as atrial fibrillation or flutter (28). With the advent of pulmonary hypertension, the rSR' pattern in the right precordial leads is replaced by Q waves and tall monophasic R waves with deeply inverted T waves.

Electrophysiologic studies have demonstrated a significant age-related incidence of sinus node dysfunction that may begin in early childhood (29,30). These patients have prolonged corrected sinus node recovery times and sinoatrial conduction times (31). However, these findings are not significant clinically and the resting and ambulatory ECGs in these patients are normal. AV node dysfunction is less common than sinus node dysfunction. Electrophysiologic studies in such cases show a prolonged A-H interval or an AV node Wenckebach periodicity at slow atrial pacing rates. First-degree AV block can occur in older individuals as a result of intraatrial H-V conduction delay and in patients with a rare autosomal dominant form of secundum ASDs (16).

Chest X-Ray

A small shunt across the ASD generally results in a normal-appearing chest x-ray. Cardiomegaly, due to right atrial and right ventricular enlargement, and increased pulmonary vascular markings extending to the periphery are seen in patients with significant shunts. (Fig. 28.7). The dilated right ventricle occupies the apex and forms an acute angulation with the left hemidiaphragm in the anteroposterior projection and obliterates the retrosternal space in the lateral view. Dilation of the right ventricular outflow tract may cause smooth continuity with the enlarged main pulmonary artery. The proximal branch pulmonary arteries, especially the right pulmonary



Figure 28.7. Chest x-ray of a 5-year-old patient with a sinus venosus ASD. The x-ray shows cardiomegaly with right atrial prominence, increased pulmonary vascular markings, and prominent main pulmonary artery.

artery, also are dilated. The left atrial and left ventricular sizes are normal. If pulmonary hypertension develops, the increased peripheral pulmonary arterial vascularity is replaced by oligemic lung fields.

Echocardiogram

The echocardiogram is instrumental in defining the type of ASD, its size, the degree of shunting, its effect on the right-sided chambers of the heart, associated lesions, and estimations of right ventricular pressure. These echocardiographic findings help in determining the appropriate intervention.

Transthoracic Imaging

TWO-DIMENSIONAL IMAGING AND M-MODE

An ASD can be visualized from the subcostal, parasternal, and apical views. Subcostal views provide the best profile of the atrial septum since the ultrasound beam is perpendicular to it. However, subcostal windows may be suboptimal in older or obese patients. In apical views, a “drop-out” may be seen in the thin septal region of the fossa ovalis since the ultrasound beam is parallel to it. This can give a false appearance of an ASD.

The type of ASD can be determined by defining its location. PFO and secundum ASDs are located in the region of fossa ovalis, that is, the midatrial septal region (Fig. 28.8). A PFO is guarded by a flap valve on the left side and limbus of fossa ovalis to the right. A PFO can be differentiated from a secundum ASD by this overlap of septal tissue. Ostium primum ASDs are located between the anteroinferior margin of the fossa ovalis and AV valves. Sinus venosus defects are seen superiorly at the junction of SVC with the right atrium (Fig. 28.9). These defects are best seen from the subcostal short-axis or high right parasternal views as a communication between the atria where the right upper pulmonary vein and SVC are usually seen. The right pulmonary artery is seen in cross-section immediately above the ASD. Subcostal long-axis and parasternal short-axis views are useful in evaluating sinus venosus ASDs of the right atrial type which appear as a posteroinferior atrial defect with a deficient posterior margin (Fig. 28.9). Anomalous drainage of right middle and lower pulmonary vein can be seen best in the parasternal short-axis view. For CS defects, a large ostium of the CS is seen as an inferior interatrial communication, just above and anterior to the entry of IVC into the right atrium. Absence of the CS indicates complete unroofing. In partial unroofing, parts of the wall between the CS and the left atrium can be identified.

The enlarged right atrium, right ventricle, and pulmonary arteries also are seen on 2-D imaging. The volume-overloaded right ventricle causes diastolic flattening and paradoxical motion of the interventricular septum (Fig. 28.10). Associated anomalies such as pulmonary stenosis, mitral valve prolapse, and anomalous pulmonary venous return also should be evaluated using 2-D imaging. M-mode imaging of the ventricles will show an enlarged right ventricle and paradoxical septal motion (Fig. 28.10).

DOPPLER

Using color Doppler, one can visualize the shunt across the ASD (Fig. 28.8). This shunt usually is left-to-right, but in patients with elevated pulmonary artery pressure, a bidirectional shunt or a right-to-left shunt can be seen. Pulsed-wave Doppler shows interatrial shunting in late systole and early diastole. Since the pressure gradient across the atrial septum is minimal when these defects are nonrestrictive, low-velocity flow is noted using Doppler. Commonly, a qualitative

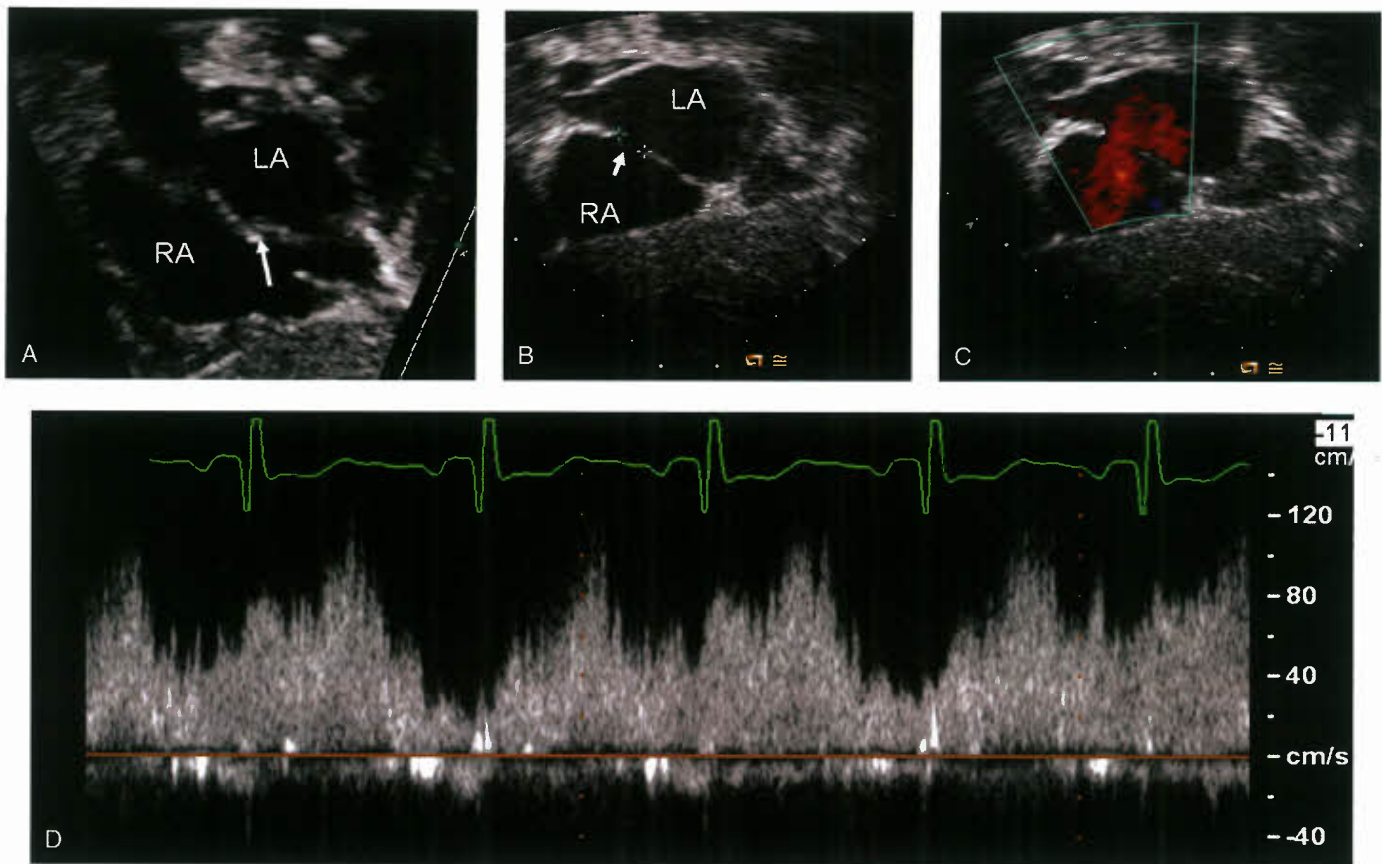


Figure 28.8. Echocardiography delineation of defects in the region of fossa ovalis. A: Subcostal sagittal view showing a PFO (*arrow*), with a flap valve noted on the left atrial side and the limbus of fossa ovalis on the right atrial side. B: Subcostal coronal view showing a large secundum ASD with well-defined rims. C: Color Doppler showing a left-to-right shunt across the ASD. D: A pulsed-wave Doppler showing a left-to-right shunt across the ASD with phasic changes. LA, left atrium; RA, right atrium.

assessment of the shunt across the ASD is done by direct visualization of the shunt using color Doppler and its effect on the right-sided cardiac chambers. However, a quantitative assessment of the pulmonary to systemic blood flow ratio ($Q_p:Q_s$) also can be made. For this, the time velocity integrals obtained by tracing the pulsed-wave Doppler of pulmonary and aortic outflow are multiplied by the area of pulmonary and aortic valve, respectively. This has been shown to have a close correlation with the $Q_p:Q_s$ measured invasively by oximetry during cardiac catheterization (32). Presence of right ventricular outflow tract obstruction, semilunar valve insufficiency, and patent ductus arteriosus limit the use of this method (33).

A large left-to-right shunt may result in a flow-related peak gradient of as much as 30 mmHg across the pulmonary valve. However, with higher gradients, one must suspect associated pulmonary valvular stenosis. Progressive tricuspid regurgitation resulting from tricuspid annular dilation and lack of coaptation of leaflets can be seen with significant right ventricular dilation. Doppler assessment for estimating pulmonary artery pressure can be performed by measuring the tricuspid and pulmonary regurgitant jets and applying the modified Bernoulli equation to calculate transvalve gradients and adding estimated right atrial pressure and right ventricular end-diastolic pressure, respectively. Development of pulmonary hypertension results in worsening of tricuspid and pulmonary regurgitation. In addition, the main and proximal pulmonary arteries further dilate. The right

ventricle becomes hypertrophied, and its systolic function starts deteriorating.

TRANSESOPHAGEAL ECHOCARDIOGRAPHY

A transesophageal echocardiogram (TEE) is useful for evaluation of ASD when transthoracic images are inconclusive due to poor windows or unusual location of the defect. TEE can be particularly useful to detect a sinus venosus ASD, which easily can be missed using transthoracic imaging. In addition, it frequently is used as a monitoring adjunct for operative and percutaneous closure of ASD. Due to the close proximity of the transducer to the cardiac structures, transesophageal imaging allows better spatial resolution and superior images of the atrial septum compared with transthoracic imaging (Fig. 28.11).

CONTRAST ECHOCARDIOGRAPHY

Intravenous contrast using injection of agitated saline during transthoracic or transesophageal echocardiographic imaging can be used to confirm the shunting across an ASD or PFO. A left-to-right shunt is seen as a negative contrast washout into the right atrium, when the right atrium is opacified with contrast. A right-to-left shunt is detected by the presence of microbubbles in the left atrium and ventricle, and this effect can be augmented by performing a simultaneous Valsalva maneuver. In the presence of an unroofed CS, injection of contrast in the left arm will result in microbubbles in the left atrium before it opacifies the right atrium.

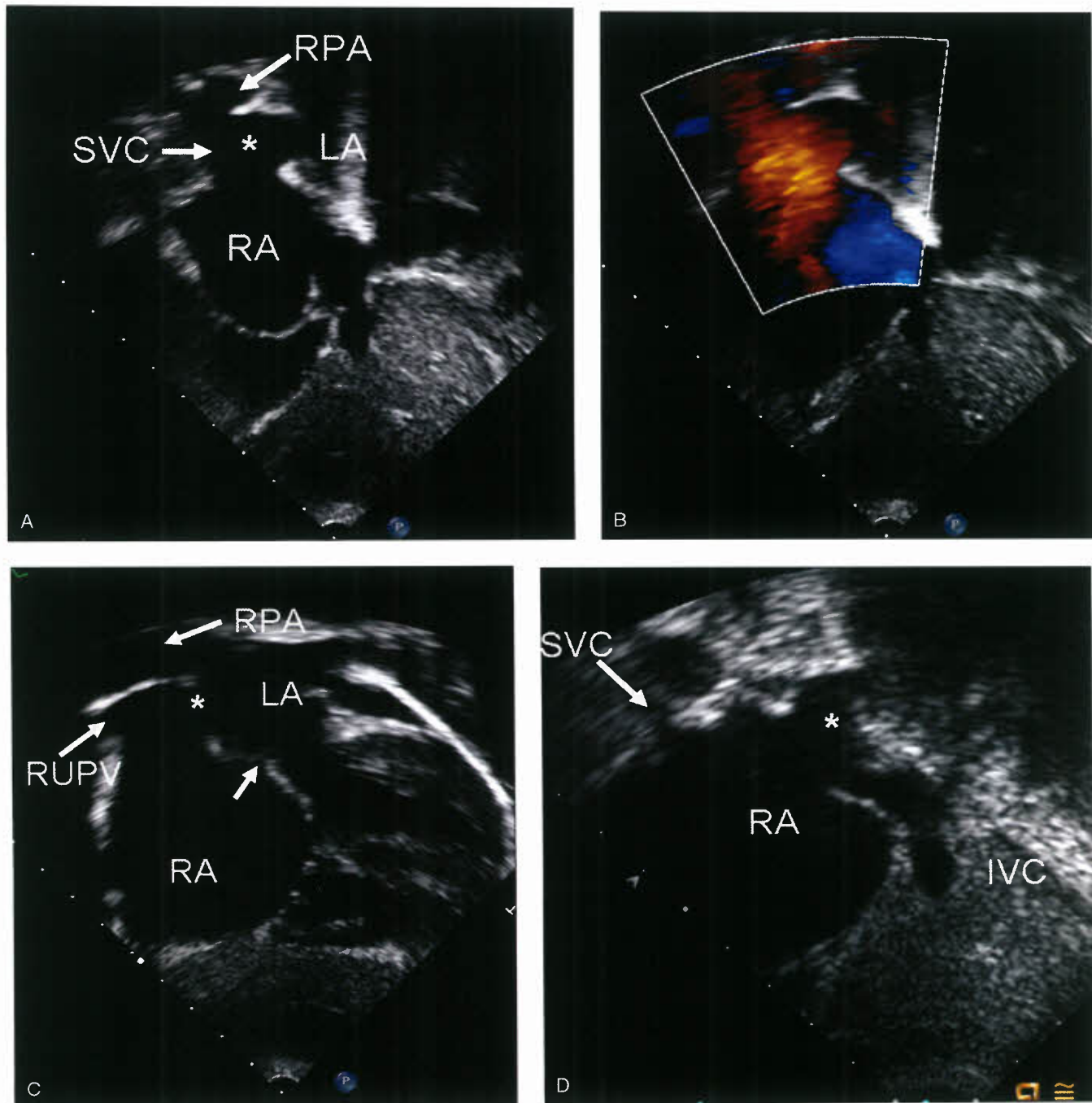


Figure 28.9. Echocardiography of sinus venosus defects: **A:** Subcostal sagittal view showing the SVC-type sinus venosus defect. The defect (*asterisk*) is cranial to the superior limbic band of fossa ovalis and is in communication with the cardiac end of SVC. **B:** Color Doppler image of the same defect shows the blood directed from LA to RA via the left atrial orifice of the right upper pulmonary vein and the sinus venosus defect. **C:** Subcostal coronal view showing the SVC-type sinus venosus defect (*asterisk*), the superior limbic band of fossa ovalis (*arrow*), and orifice of the right upper pulmonary vein (RUPV). **D:** Subcostal coronal views of right atrial type of sinus venosus defect (*asterisk*) showing a large defect in the posterior right atrial wall. IVC, inferior vena cava; LA, left atrium; RA, right atrium; RPA, right pulmonary artery.

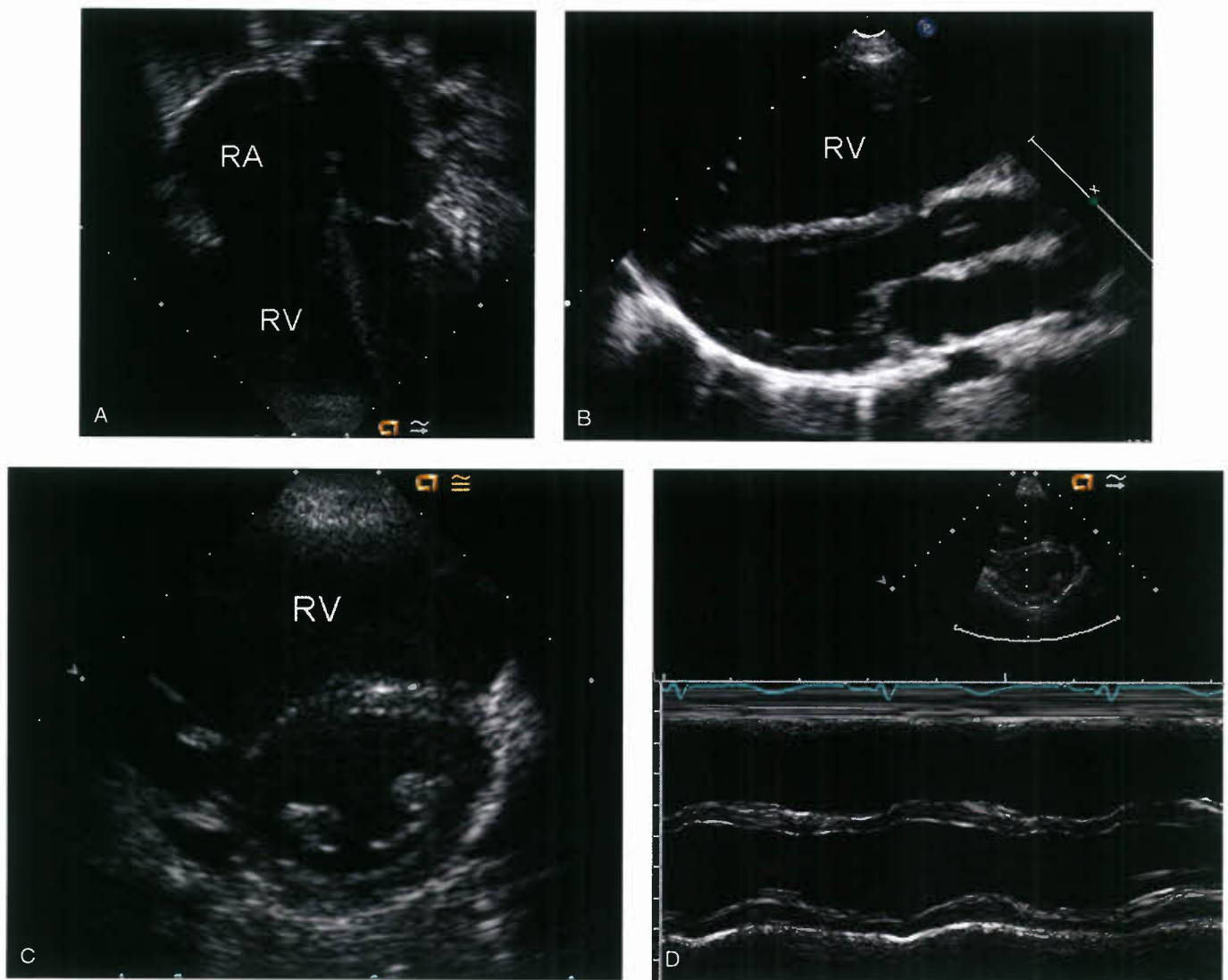


Figure 28.10. Severe right atrial (RA) and right ventricular (RV) dilation seen in a patient with large secundum ASD: **A:** apical view; **B:** Parasternal long-axis view; **C:** Short-axis view. **D:** M mode showing RV dilation and paradoxical motion of the interventricular septum.

THREE-DIMENSIONAL ECHOCARDIOGRAPHY

Imaging the ASD using 2-D echocardiography is based on limited number of orthogonal planes and could result in underestimation of the size of the ASD and its surrounding rims. With the availability of real-time 3-D echocardiography, an en face view of the entire atrial septum can be obtained, thus allowing better morphologic delineation of the ASD and its surrounding structures (34). This information is helpful in determining whether or not closure of the ASD can be accomplished with a transcatheter device (35). Furthermore, 3-D transesophageal echo now is being used not only to delineate anatomic features of ASD but also for guiding device closure during the procedure (Fig. 28.12) (36–38).

INTRACARDIAC ECHOCARDIOGRAPHY

Intracardiac echocardiography using an ultrasound catheter has been shown to be a safe alternative to transesophageal echocardiography for assisting in device closure of ASDs (39–42). It provides excellent 2-D and color-Doppler imaging of the interatrial septum and the surrounding structures. This technique has the advantage of eliminating the need for general anesthesia

and additional personnel to perform transesophageal echocardiography. However, due to the large size of the sheath required to insert the catheter, its use in smaller children is limited (42).

Cardiac Catheterization

In the current era cardiac catheterization seldom is indicated for diagnosis of ASDs unless pulmonary vascular disease is suspected. Angiography can be helpful in diagnosing associated lesions such as partial anomalous pulmonary venous return or mitral stenosis. During catheterization, a step-up in oxygen saturations in the right atrium will be noted in the presence of an atrial level left-to-right shunt. An increase in saturations of 10% or more from SVC and IVC in a single blood sample series or an increase of 5% in two series indicates the presence of an atrial level shunt. Similar results also can be obtained in the presence of a left ventricle to right atrial shunt, a ventricular septal defect-related tricuspid insufficiency, AVSDs, systemic arteriovenous fistula, or anomalous pulmonary venous return to the right atrium. Detection of a CS type of ASD can be challenging. Continuous oximetry using a fiberoptic

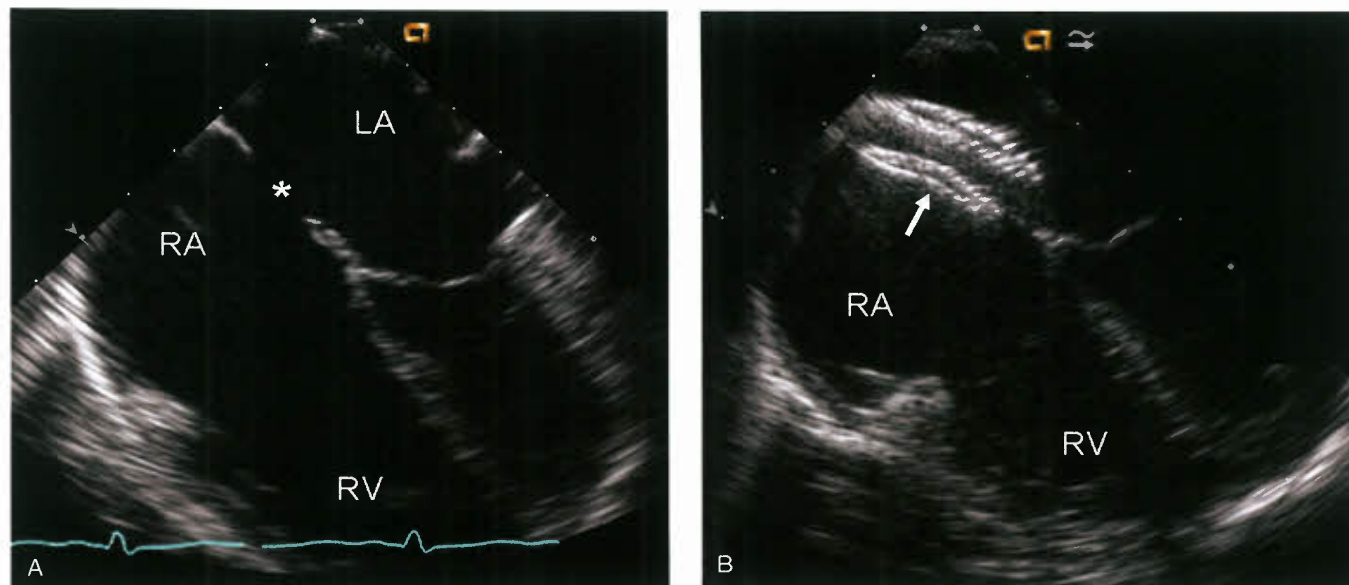


Figure 28.11. A: TEE showing a large secundum ASD (asterisk). B: Amplatzer septal occluder used to close the atrial septal defect (arrow). LA, left atrium; RA, right atrium; RV, right ventricle.

catheter pull-back in the CS has been employed to diagnosis a left-to-right shunting across such ASDs (43).

$Q_p:Q_s$ can be calculated using the standard Fick equation or indicator dilution technique. In the absence of any other major cardiac anomalies, the presence of a small left-to-right shunt ($Q_p:Q_s < 1.5$) is considered hemodynamically insignificant. When the $Q_p:Q_s$ is ≥ 1.5 , the shunt is considered significant.

Direct measurement of intracardiac and pulmonary artery pressure can be performed during catheterization, and pulmonary vascular resistance can be calculated. In the presence of a large defect, there is minimal gradient between the two atria and there can be a flow-related gradient across the pulmonary valve as high as 30 mm Hg. In cases of pulmonary hypertension, acute response to pulmonary vasodilators such as nitric oxide and oxygen generally has been used to assess the reversibility and make decisions regarding closure.

Angiography just outside the orifice of right upper pulmonary vein in a cranially angulated left anterior oblique projec-

tion is ideal for optimal visualization of location of the ASD (44). Injection into the main pulmonary artery will demonstrate pulmonary venous anatomy and shunt across the atrial septum, but is not ideal for determining the size and location of the ASD. A CS type of ASD can be diagnosed by injecting contrast selectively into the left SVC, pulmonary vein, or left atrium (45).

Other Imaging Modalities: CT/MRI

If the findings on echocardiography are uncertain, computerized tomography (CT) or magnetic resonance imaging (MRI) can be used to define the anatomy of an ASD and its influence on the right-sided cardiac chambers and associated anomalies (Fig. 28.13) (46,47). Both CT and MRI also have been used to define the CS type of ASD, which can be particularly challenging to recognize using routine echocardiography (48). Multislice CT has a high spatial and temporal resolution and

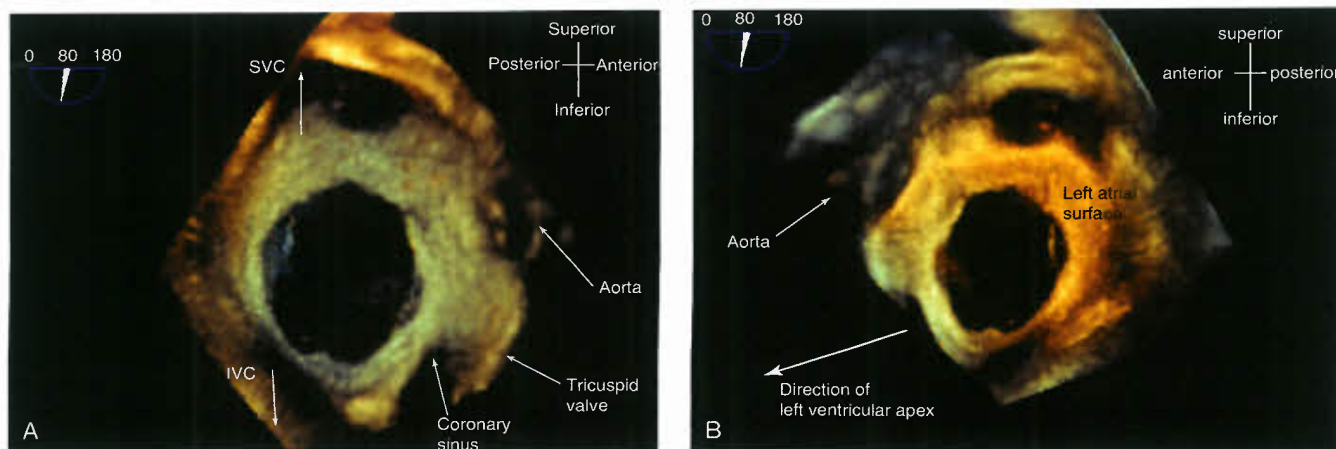


Figure 28.12. Three-Dimensional transesophageal echocardiogram. A: Right atrial view of secundum ASD. B: Left atrial view of secundum ASD. IVC, inferior vena cava; SVC, superior vena cava. (From Pushparajah K, Miller OI, Simpson JM. 3D echocardiography of the atrial septum: anatomical features and landmarks for the echocardiographer. *JACC Cardiovasc Imaging*. 2010;3:981–984, with permission).

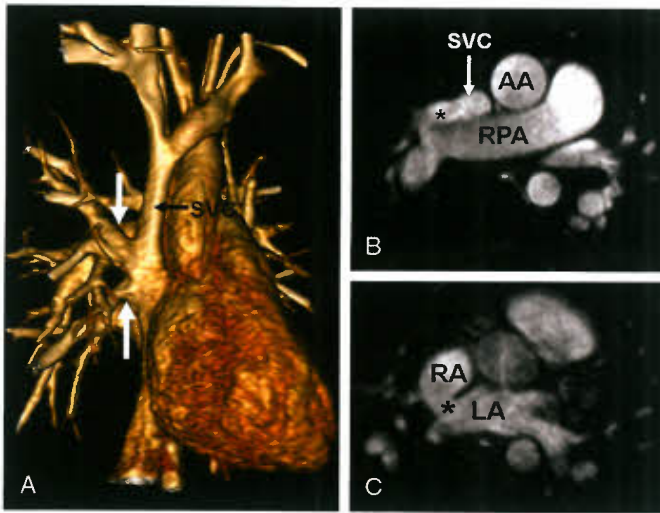


Figure 28.13. A: Gadolinium-enhanced magnetic resonance angiogram showing anomalous drainage of right upper and middle pulmonary veins (arrows) into the SVC. B: Bright blood image in axial plane showing drainage of right upper pulmonary vein (asterisk) to the SVC. C: Bright blood image showing a sinus venosus defect (asterisk). AA, ascending aorta; LA, left atrium; RA, right atrium; RPA, right pulmonary artery.

multiplanar reconstruction capabilities to characterize ASDs and pulmonary venous anomalies, though at the cost of radiation exposure (49). MRI is being used increasingly in adults since the transthoracic echocardiographic images can be quite limited. MRI has been shown to have a good correlation with TEE in assessing the size and rims of the defect (47). Velocity-encoded, phase-difference MRI measurements of flow in the proximal great vessels has been used to noninvasively measure $Q_p:Q_s$ with results comparable to those obtained by oximetry and indicator dilution techniques (50).

Exercise Testing

Even though most patients with ASD are asymptomatic, their exercise capacity may be decreased. Closure of an ASD may improve exercise capacity in adults who were asymptomatic or mildly symptomatic prior to closure (51). Exercise capacity is uniformly low in patients with ASD and pulmonary hypertension. In cases where the symptoms are discordant with the clinical findings, it can be useful to document the exercise capacity. Exercise testing can be helpful in documenting oxygen saturations during exertion in patients with pulmonary hypertension, though maximal exercise is not recommended in the presence of severe pulmonary hypertension (52).

Natural History of ASDs

While secundum ASDs can spontaneously close over time, other types of ASDs do not. In a report on the natural history of unrepaired ASD, Campbell (53) noted that the mean age of death was 37.5 ± 4.5 years with 75% dying by 50 years and 90% dying by 60 years of age. This was in the era prior to echocardiography where reports regarding outcome of ASDs obviously were skewed toward clinically recognizable defects. Since the advent of echocardiography, it is possible to report data from serial echocardiographic evaluations estimating the change in the size of the defect and the rate of spontaneous closure (54–56). In general, most defects <5 mm that were recognized during infancy are likely

to spontaneously close, while those larger than 8 to 10 mm are unlikely to do so.

In a report of 30 children with secundum ASDs (mean age at diagnosis 1.3 years) that were considered hemodynamically insignificant during infancy, Brassard et al. (57) noted that 17 children had spontaneous closure of the defect at a mean age of 8.4 years. In seven asymptomatic patients, the defect size was 1 to 6 mm at a mean follow-up of 13.2 years. In the remaining six patients, the defect had become larger and closure was performed since the patients were symptomatic or the defect was determined to be hemodynamically significant (57). Radzik et al. (58) evaluated the predictive factors for spontaneous closure of ASDs diagnosed in infants <3 months. They reported that the frequency and timing of closure were inversely related to the diameter of the ASD. At a mean follow-up of about 14 months, spontaneous closure occurred in all the defects that were <3 mm at diagnosis, in 87% of defects that were 3 to 5 mm, in 80% of defects that were 5 to 8 mm, and in none of the defects that were ≥ 8 mm. In a longitudinal study of 200 children with isolated secundum ASDs diagnosed at a median age of 5 months, Hanslik et al. (59) reported spontaneous closure in 34% and a decrease in size to ≤ 3 mm in another 28%. ASD diameter and age at diagnosis were noted to be independent predictors of spontaneous closure or regression to ≤ 3 mm defect size. None of the ASDs >10 mm at diagnosis closed spontaneously (59). In contrast to the above studies, a study by McMahon et al. (60) of 104 patients with isolated secundum ASDs reported that the diameter of ASDs increased in 65% of their cohort, with a >50% increase in 30% of their patients. Spontaneous closure occurred in only 4%, and 12% reached a size of ≥ 20 mm. The mean age at diagnosis in this study was much older (4.5 years, range 0.1 to 71 years) than in the previously mentioned studies, and the mean interval between echocardiograms was 3.1 years (0.7 to 8.1 years), which may contribute to the differences reported in the natural history of secundum ASDs (60).

Pulmonary vascular obstructive disease may develop in patients with large left-to-right shunts during adulthood, though it occurs much later with ASDs compared to high-pressure left-to-right shunts such as ventricular septal defects or patent ductus arteriosus. According to Craig and Selzer (3), young adults with ASD have about a 14% chance of developing progressive pulmonary hypertension. Eventually, when there is reversal of the left-to-right shunt, these patients become progressively cyanotic and symptomatic. They eventually die of cardiac failure or pulmonary artery thrombosis (3). Their pulmonary vascular disease usually is progressive and becomes irreversible. Acute response to vasodilators during cardiac catheterization is helpful to determine reversibility, though some cases may still fall into an indeterminate zone where it is difficult to differentiate between a reversible and an irreversible state. In patients with advanced pulmonary vascular disease, closure of the ASD can result in further deterioration of the patient and decreased survival compared to patients with unrepaired ASDs (61). In most of these patients there is right ventricular failure, and the right-to-left shunt across the ASD provides increased cardiac output albeit at the cost of cyanosis.

Chronic volume overload, elevated pulmonary artery pressures, ventricular dysfunction, and AV valve regurgitation can contribute to atrial stretching, which in turn predisposes to atrial arrhythmias. Late in the natural history of ASDs, atrial arrhythmias in the form of atrial fibrillation, flutter, or less commonly, paroxysmal supraventricular tachycardia contribute to morbidity and mortality.

Management

Most children with an ASD are asymptomatic. In rare cases when they are symptomatic, anticongestive therapy with diuretics may be indicated until closure is accomplished. Closure

of an ASD is indicated if there is a large shunt, that is, $Q_p:Q_s \geq 1.5$. Other indicators of a large shunt include a diastolic flow rumble in the tricuspid area, ECG evidence of right ventricular hypertrophy, chest x-ray evidence of cardiomegaly or increased pulmonary vascular markings, or echocardiographic evidence of right ventricular enlargement and/or paradoxical septal motion (62). In asymptomatic patients with a large shunt, elective closure between 2 and 5 years of age is recommended (62). Even though most children with large defects may be asymptomatic, elective closure is recommended to prevent long-term complications such as atrial arrhythmias, paradoxical embolism, pulmonary hypertension, severe right ventricular dilation and dysfunction with overt symptoms of congestive heart failure, and hemodynamically significant mitral and tricuspid insufficiency. If large ASDs are identified later in life, it is important to have evidence of pulmonary vascular reactivity and a net left-to-right shunt prior to considering closure. Those with irreversible pulmonary hypertension are not candidates for ASD closure and warrant medical therapy for treatment of pulmonary hypertension.

Closure of small defects without any right-sided cardiac enlargement is controversial. While these patients may remain asymptomatic well into their fourth and fifth decades of life, there is concern about increase of the left-to-right shunt at an older age due to reduced left ventricular compliance as a result of CAD, systemic hypertension, or valvular disease (52). Routine follow-up of these patients during adulthood should include assessment for atrial arrhythmias and paradoxical embolic events and an echocardiogram every 2 to 3 years to evaluate right atrial and ventricular size and pressures (52).

Although closure of secundum ASDs can be performed with percutaneous devices or surgically, surgical closure is the only option for sinus venosus, CS, and primum ASDs. ASDs with multiple fenestrations and atrial septal aneurysm (ASA) require careful evaluation before proceeding with device closure.

Secundum ASDs

Surgical Closure: Surgical closure of an ASD was first performed by Murray in 1948 using an external suture technique without directly visualizing the defect. With development of the pump oxygenator, in 1953 Gibbon performed closure of ASD using the open technique that allowed complete visualization of the defect. For small to moderate ASDs direct suture closure can be accomplished. If the ASD is too large to allow direct suture closure, patch closure is performed. Use of autologous pericardial patch has eliminated the need to use prosthetic material, thereby theoretically, minimizing the risks of thromboembolism and endocarditis. In adult patients with atrial arrhythmias, a concomitant Maze procedure can be performed. Conventionally, median sternotomy approach has been used for surgical repair of ASD. More recently, partial

lower sternotomy has been used particularly in children below 3 years of age (63,64).

Surgical mortality and morbidity for secundum ASDs with normal pulmonary vascular resistance are negligible. The majority of patients who had closure of secundum ASDs during childhood have had an uncomplicated course with a normal cardiac rhythm and exercise capacity. Rarely, there may be inadvertent attachment of the eustachian valve to the atrial septum, thereby diverting blood from inferior vena cava to the left atrium and causing a right-to-left shunt, necessitating surgical reintervention.

The long-term outcome following surgical repair of ASD primarily depends on the age at surgery and pulmonary artery pressures prior to surgery. Several investigators have reported the outcome in patients with pulmonary hypertension who have undergone surgical closure of ASD. In 1960, Rahimtoola et al. (65) reported that the outcome in those who had a peak pulmonary artery pressure of more than 60 mm Hg is poor. In 1973, Dave et al. (66) reported that surgical outcome is adversely affected when the mean pulmonary artery pressure was more than 40 mm Hg. In 1987, Steele et al. (25) reported that in patients with pulmonary hypertension, total pulmonary resistance, pulmonary arteriolar resistance, pulmonary-to-systemic resistance ratio, and systemic and pulmonary arterial oxygen saturation were all predictors of surgical outcome, with total pulmonary resistance being the best one. In 1990, Murphy et al. reported the long-term postoperative outcomes of 123 patients at Mayo Clinic between 1956 and 1960 who had surgical repair of secundum or sinus venosus ASDs. The overall 30-year actuarial survival rate among survivors of the perioperative period was 74%, compared to 85% among age- and sex-matched controls (67). The late survival in patients undergoing surgery below 24 years of age was similar to that of the control population. However, survival is significantly decreased in those repaired between 25 and 41 years when compared to the controls (84% and 91%, respectively). There was a further decline in late survival in those repaired after 41 years of age to 40% versus 59% in controls (67). Independent predictors for long-term survival were younger ages at operation and lower preoperative pulmonary artery systolic pressures (67). Late repair was associated with significant morbidity including atrial fibrillation, stroke, and cardiac failure.

Device Closure

Transcatheter device closure of secundum ASDs has significantly altered the management of ASDs. The first transcatheter device closure was reported by King et al. (68) in 1976. Following that, several modifications in devices as well as delivery systems have been made. Various devices such as Amplatzer septal occluder, CardioSEAL, Gore HELEX septal occluder,

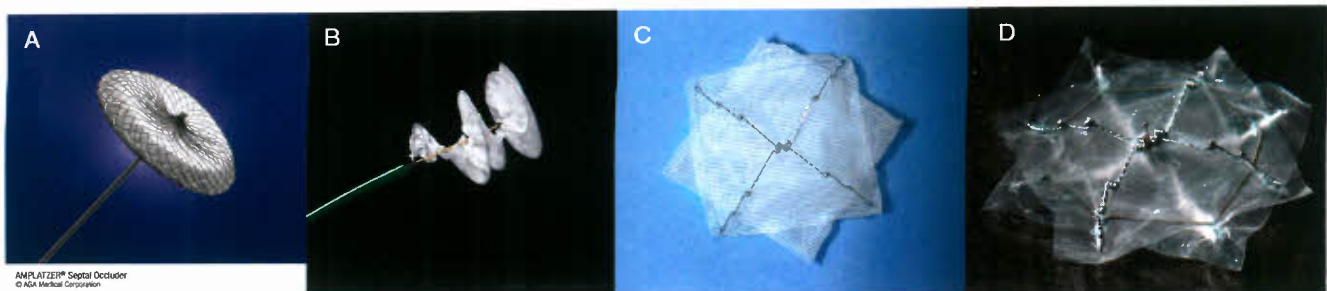


Figure 28.14. Various devices used for transcatheter closure of ASD. A: Amplatzer septal occluder (Illustration courtesy of AGA Medical Corp.). B: Gore Helix septal occluder (Illustration courtesy of W.L. Gore & Associates, Inc). C: CardioSEAL device. D: BioSTAR device. (Illustrations C and D courtesy of NMT Medical, Inc.)

Clamshell occluder, Sideris Buttoned device, Das-Angel Wings occlusion device, and BioSTAR are now available (Fig. 28.14). The Amplatzer septal occluder is currently the most widely used device. Some of the advantages of this device include relatively easy deployment, easy retrievability (until released from the delivery system), ability to close large defects, and the relatively larger left atrial disc to close additional atrial fenestrations.

While device closure has proven to be technically safe and feasible and has the obvious advantage of being a nonsurgical technique, it is not free of complications. These complications include fracture or embolization of the device, device malalignment, residual shunts, device thrombosis, and impingement of adjacent structures such as valves, SVC, CS, pulmonary veins, or aorta (69–71). Also, long-term problems such as late erosion of the atrial wall or aorta, inaccessibility of the left atrium if needed, and artifact during MRI can be encountered (72). A partially biodegradable device (BioSTAR) made of collagen discs and metallic arm and rings has been developed to overcome some of these problems. This device has been used in Europe since 2006 for PFO and ASD closure (73). The closure rates are comparable to the Amplatzer device with very little foreign material left over at 6 months' follow-up (74). A fully absorbable transcatheter device (BioTREK) is currently undergoing experimental trials.

In the current era of ASD device closure, several studies have evaluated outcomes of ASD closure using this technique in patients with pulmonary hypertension. In 2008, Balint et al. (75) reported the outcome of device closure of ASD with moderate or severe pulmonary arterial hypertension. They noted that at a mean follow-up of 31 months, although there was a decrease in the mean right ventricular systolic pressures as determined by echocardiography, it normalized in only 44%, while 15% had persistence of severe pulmonary hypertension. In 2009, Yong et al. (76) reported a longitudinal study evaluating pulmonary hypertension in 215 adults with attempted device closure of ASDs. Independent predictors of moderate or severe pulmonary hypertension were older age, larger ASD, female sex, and presence of at least moderate tricuspid regurgitation (76). Among patients with moderate or severe pulmonary hypertension, independent predictors of normalization of pulmonary pressure were lower baseline pulmonary artery pressure and no more than mild tricuspid regurgitation (76). In a study of 236 adults who had device closure of ASD at a mean age of 49 ± 18 years, Humenberger et al. (77) found that ASD closure at any age was followed by improvement in symptoms and decrease in pulmonary artery pressures and right ventricular size, but the best outcome was in patients with less functional impairment and lower baseline pulmonary artery pressures. These studies indicate that, similar to surgical closure of ASDs, the outcome following device closure is influenced by age at closure and the presence of pulmonary hypertension.

Sinus Venosus ASD

In the rare case where the sinus venosus ASD is not associated with anomalous pulmonary venous return, an autologous pericardial patch closure of the ASD is performed. However, in more than 90% of cases, anomalous pulmonary venous return to the SVC is present. In such cases, surgical correction involves closure of ASD and redirection of anomalous pulmonary veins into the left atrium. While the surgery for superior, posterior, and inferior sinus venous ASD with anomalous veins draining directly into the right atrium is associated with minimal complications, that for anomalous pulmonary veins connected to SVC is complex and can be associated with long-term complications such as obstruction of the pulmonary vein orifice, SVC stenosis, sinus node dysfunction, and

atrial arrhythmias, including atrial flutter or atrial fibrillation depending on the surgical technique used. In the intracaval baffle technique the anomalous pulmonary venous return is redirected through the sinus venosus defect by baffling these structures with a pericardial or synthetic patch with or without performing a patch cavoplasty as needed (78). The transcaval technique uses a lateral incision in the SVC and a single-patch closure of the ASD along with baffling of anomalous pulmonary veins into the left atrium (79). When the right pulmonary venous insertion into the SVC is high (more than 2 cm above the atriocaval junction), the Warden procedure is used, in which the SVC is transected above the site of the anomalous pulmonary veins and connected to the right atrial appendage. The cardiac end of the SVC along with the anomalous pulmonary venous flow is baffled into the left atrium with a patch (80).

Coronary Sinus ASD

In a partially unroofed CS defect, repair can be performed using a roofing procedure (81). If there is redundant tissue, primary closure of the defect can be performed. If that is not feasible, a roof can be created using a pericardial patch.

Most cases of CS ASD are associated with a left SVC which is dealt with on its own merits. If the left SVC is small and there is a bridging vein, it can be ligated. If it is large and is the only source of systemic venous drainage from the head and upper extremities, an intraatrial baffle can be performed.

Management Issues During Follow-Up

Patients who had surgical closure of ASD during childhood have an excellent outcome. In general, they have decrease in or resolution of preoperative symptoms, an increase in exercise capacity, and are free of significant cardiac rhythm abnormalities. However, the outcome in those who had surgery during adulthood is significantly different due to pulmonary hypertension, atrial arrhythmias, and cardiac failure. Device closure is also associated with early and long-term complications as mentioned above which warrant long-term surveillance. Specific issues that need attention during follow-up are discussed below.

Postpericardiotomy Syndrome

During the first few weeks postoperatively, patients may present with fever, chest pain, abdominal pain, emesis, and fatigue. These symptoms should alert one to the diagnosis of postpericardiotomy syndrome, and an echocardiogram should be performed to exclude pericardial effusion and cardiac tamponade.

Pulmonary Hypertension

It is well established that the outcome of patients with repaired or unrepaired ASD and pulmonary hypertension is not favorable compared to those with normal pulmonary artery pressure. Despite closure of the defect, pulmonary vascular disease may progress in some patients. Therefore, periodic surveillance along with serial Doppler echocardiograms is recommended to estimate pulmonary artery pressures. Medical therapy using pulmonary vasodilators should be instituted if indicated.

Atrial Arrhythmias

Atrial fibrillation and flutter are uncommon in patients with ASD before the age of 40 years with a prevalence of <1% (82). Beyond 40 years of age, the prevalence increases significantly compared to that of the general population: 15% and 61% at 40 to 60 years and beyond 60 years, respectively (82). Patients

with atrial arrhythmias also are more likely to have higher pulmonary artery pressures and worse functional class (83). Patients older than 40 years at the time of ASD closure are more likely to have new-onset atrial arrhythmias. Those with atrial arrhythmias before and soon after ASD closure are more likely to have persistent arrhythmias (83). In patients predisposed to atrial arrhythmias, periodic follow-up with ECG and Holter monitoring is recommended. Atrial arrhythmias should be appropriately treated to restore and maintain sinus rhythm. If sinus rhythm cannot be restored with medical or interventional means, then rate control and anticoagulation are recommended (52).

Right Atrial and Ventricular Size and Function

Following ASD closure, there is regression of right atrial and ventricular size in the majority of patients, irrespective of the technique used for closure (46,84). Most of the regression occurs within the first year following closure (85). While significant changes in the right atrial size may not be observed acutely, that too decreases over time (86). Regression in right heart size is less in patients repaired at an older age and in those with pulmonary hypertension. Right ventricular systolic function is normal to hyperdynamic in those with unrepaired ASDs, but chronic volume overload can result in reduced right ventricular systolic and diastolic dysfunction in adults, which may or may not improve following closure of the defect.

Left Ventricular Function

Although earlier reports indicated that left ventricular function was normal in patients with ASD, there is now evidence that both systolic and diastolic function can be influenced adversely by severe chronic right ventricular volume overload (87–89). Therefore, monitoring of both right and left ventricular function during follow-up is advisable.

Mitral Regurgitation

Patients with ASD may develop mitral valve prolapse and insufficiency, presumably from leftward shifting of the ventricular septum due to an enlarged right ventricle (90). This may persist after successful closure of the defect (90,91). While the etiology of mitral regurgitation has been ascribed to mechanical ventricular dysfunction, the valve itself often is noted to be morphologically abnormal with myxomatous changes and prolapse (92).

Bacterial Endocarditis

Patients with isolated ASDs are not predisposed to endocarditis unless there is an associated valvular lesion such as cleft mitral valve with mitral valve regurgitation. There are rare reports of bacterial endocarditis following uncomplicated surgical or device closure of ASD. Endothelialization of prosthetic material or devices usually occurs within the first 6 months after the procedure. Therefore, antibiotic prophylaxis is recommended for the first 6 months following such a procedure and is then discontinued (93).

ASD in Adults

ASD is the most common congenital heart disease in adults accounting for up to 30% of congenital heart defects in this age-group. Patients with ASD may survive into adulthood without being diagnosed. Although many come to attention due to abnormal physical findings, chest x-ray, or ECG, some may present with a cerebrovascular event due to paradoxical embolism or signs and symptoms related to cardiac failure,

arrhythmias, or pulmonary hypertension. Dyspnea on exertion is the most prevailing symptom present in symptomatic adults with ASD. Other symptoms include fatigue, palpitations, and rarely, chest pain (3). The development of these symptoms can be attributed to multiple factors. In older patients, left ventricular compliance may be reduced due to systemic hypertension or CAD, which in turn increases the left-to-right shunt across the ASD. Chronic right ventricular volume overload ultimately results in right ventricular failure and progressive tricuspid valve insufficiency. Survival into adulthood is quite common with infrequent deaths during the first two decades of life. Symptoms of progressive pulmonary hypertension can begin in the third decade. The mortality rate is significant after the fourth decade, around 6% per year (53).

Adults who had surgical repair of secundum ASDs during childhood are usually symptom free, but rarely can have atrial arrhythmias and sick sinus syndrome (94). When surgery is performed in adults, the outcome primarily depends on the age at repair and the pulmonary artery pressures. Konstantinides et al. (95) compared outcomes of 179 patients ≥ 40 years with secundum ASD who were treated either medically or surgically. The 10-year survival in the medically managed group was 84% compared to 95% in surgically managed group. The functional status of one-third of the medically managed patients deteriorated, but improved in those who had surgical repair, though the incidence of atrial arrhythmias and cerebrovascular events was similar in both groups (95). Horvath et al. (96) reported early and long-term follow-up of surgical repair of secundum and sinus venosus ASDs in 166 adults repaired at Brigham and Women's Hospital at a mean age of 44 years. The 5- and 10-year survival rates were 98% and 94%, respectively. There were two operative deaths and six late deaths. Those with a systolic pulmonary artery pressure of >30 mm Hg had significantly higher late mortality. St John Sutton et al. (97) reported patients who had surgical closure of ASD between 60 and 78 years. There was improved survival in patients discharged from the hospital following surgery compared to age- and sex-matched medically treated controls. In this study, the majority of patients showed symptomatic improvement irrespective of preoperative pulmonary vascular resistance and functional class (97). Based on these studies and several others in the literature, there is general agreement that symptomatic adult patients improve after closure of ASD; the only contraindication for closure is severe pulmonary hypertension. There is some controversy over management of asymptomatic adults, but closure can be performed with minimal risk with the advantage of reducing overload of right ventricle and progression of tricuspid insufficiency and in many cases reducing progression of pulmonary hypertension. Moreover, there is improvement in functional capacity even in asymptomatic patients following ASD closure (51). Given the low mortality and morbidity associated with closure of ASD within the first two decades of life, these patients have no cardiac restrictions and can have less frequent follow-up provided there is no cardiac rhythm or hemodynamic concerns. Patients repaired in their third decade and beyond require regular surveillance for atrial arrhythmias, cardiac failure, stroke, and pulmonary vascular disease (52,98).

In general, pregnancy in patients with ASD is well tolerated as the increase in the left-to-right shunt across the atrial septum is balanced by the decrease in peripheral vascular resistance. Paradoxical embolism may occasionally occur unrelated to the size of the ASD. Pregnancy is not recommended in patients with ASD and severe pulmonary artery hypertension due to very high maternal and fetal mortalities (52). Such patients may develop arrhythmias, ventricular dysfunction, and progressive pulmonary hypertension during pregnancy.

Atrial Septal Aneurysm

An ASA is a saccular deformity of the atrial septum with a reported prevalence of 0.22% to 1.9% (99,100). Although in most cases the aneurysm is limited to the region of the fossa ovalis, it occasionally can involve the entire septum (Fig. 28.15D). ASA may protrude into the left or the right atrium or have a bidirectional excursion. Various classifications of ASA based upon its excursion have been proposed (99,100). Hanley et al. (99) suggested diagnostic criteria for ASA based on transthoracic echocardiograms that include (a) protrusion of the aneurysm at least 15 mm beyond the plane of the atrial septum or when the atrial septum shows a phasic excursion of ≥ 15 mm during the cardiorespiratory cycle and (b) the base amplitude (width) of the aneurysm ≥ 15 mm. Although ASAs may occur in isolation, they commonly are associated with congenital or acquired heart disease. The most commonly associated cardiac lesion is ASD, though other lesions such as ventricular septal defects, pulmonary stenosis, patent ductus arteriosus, coarctation, and interrupted aortic arch can occur (101). ASAs also have been associated with atrial arrhythmias, AV valve prolapse, and systemic and pulmonary embolism (99). The association of ASA with cerebrovascular events, in particular cryptogenic strokes has been reported. The coexistence of a PFO with an ASA further increases the risk of stroke. The potential source of embolization in these cases could be a primary thrombus in the aneurysm or paradoxical embolization through interatrial

shunting (102,103). TEE provides superior images for morphologic characterization of ASA. It also is helpful in defining interatrial shunting and the presence of multiple fenestrations and thrombi within the aneurysm (102,104).

Management of patients with ASA and stroke includes medical therapy with aspirin or warfarin or closure by surgical or transcatheter technique (105).

Patent Foramen Ovale

A PFO is a normal interatrial communication present in fetal life that persists in many adults (Fig. 28.15). Based on transesophageal echocardiography, it is present in up to 24% of healthy adults (106). A Mayo Clinic study based on 965 autopsy specimens of human hearts reported the incidence and size of the PFO during the first 10 decades of life (107). While the overall incidence was 27.3%, it progressively declined with increasing age from 34.3% during the first three decades of life to 25.4% during the fourth through eighth decades and to 20.2% during the 9th and 10th decades (107). Furthermore, the PFO size increased from a mean of 3.4 mm in the first decade to a mean of 5.8 mm in the 10th decade, likely due to stretching of the fossa ovalis over time. The incidence and size of PFO were reported to be similar in males and females (107).

In the current era, transcatheter closure of PFOs is performed using a wide variety of devices such as Amplatzer, CardioSEAL-STARflex, Helex occluder, and BioSTAR, a new

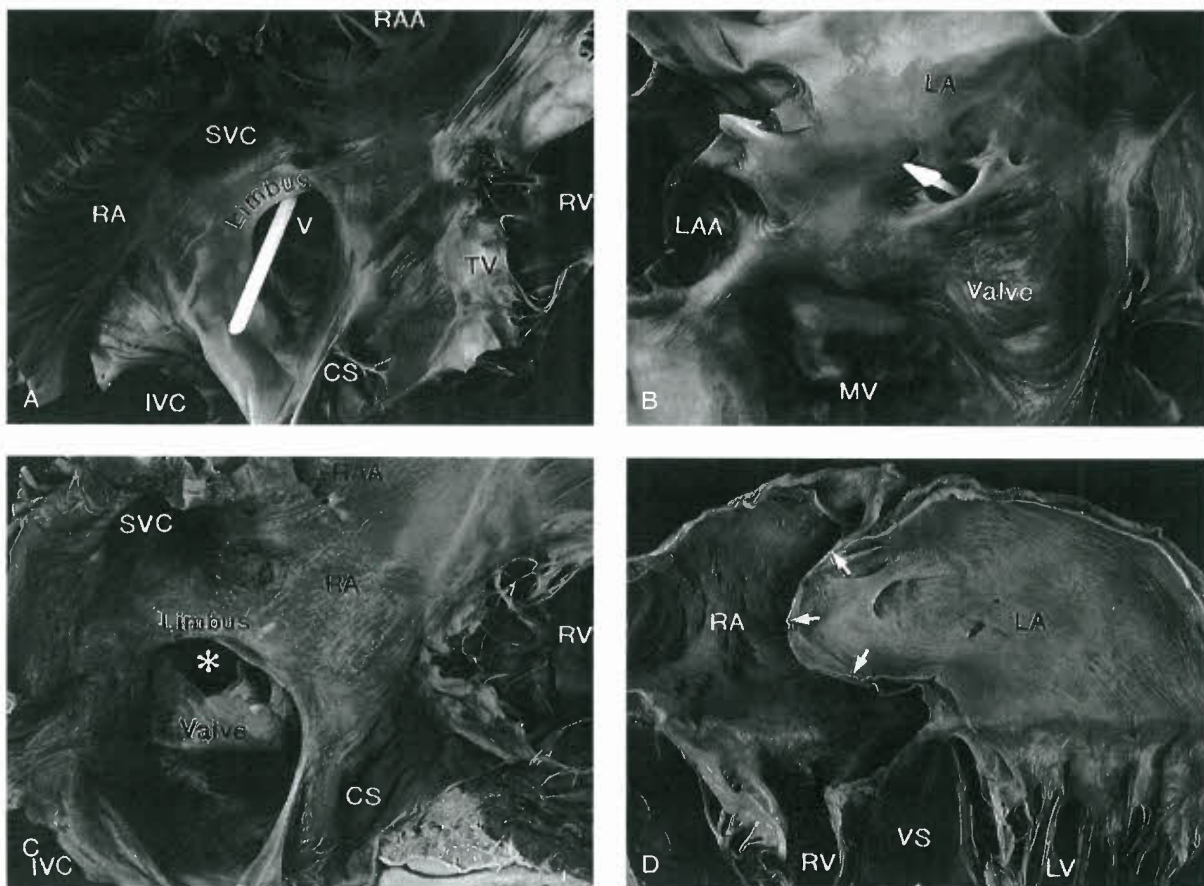


Figure 28.15. Patent foramen ovale. A: Right atrial view. B: Left atrial view. A white probe is seen between the limbus and valve (V) of the fossa ovalis and enters the left atrium (LA) through the ostium secundum (white arrow). C: Right atrial view. Atrial dilation has resulted in a valvular-incompetent PFO, that is, an acquired ASD (asterisk). D: Atrial septal aneurysm. Four-chamber view showing aneurysm of the fossa ovalis (arrows) bulging toward the right. LAA, left atrial appendage; VS, ventricular septum. (See Fig. 28.2 for other abbreviations.)

bioabsorbable implant (108,109). While the safety and efficacy of these devices has been reported in many studies, complications are similar to those with the devices used for ASD closure and include device embolization, hemopericardium, device thrombosis, residual shunts, and paroxysmal atrial fibrillation (108).

PFO has been associated with cryptogenic strokes, transient ischemic attacks, and migraine headaches (110). Systemic, noncerebral paradoxical embolism also rarely can occur in the form of myocardial infarction, renal infarction, or limb ischemia (111). The prevalence of PFO has been noted to be higher in patients with cerebrovascular events than in those without cerebral vascular events ranging from 40% to 70%. Therefore, a potential etiologic role has been suggested. These patients have been treated with antithrombotic drugs like warfarin and aspirin, or closure has been performed to prevent future events (105,112,113). The recurrence of these events is not completely eliminated following surgical or transcatheter closure of PFO (113). Similar to studies in patients with stroke, some studies have reported relief of migraine with aura following closure of PFO (114–116). However, a recent population-based study of 1,100 stroke-free patients with self-reported migraines did not find any significant associations between PFO and migraine (117). Direct documentation of paradoxical embolization through the PFO resulting in cerebrovascular events obviously is challenging. Hence, the role of closure of PFO in such patients remains controversial. In the current era of device closure, there has been a dramatic increase in the rate of PFO closure in these patients in light of some observational studies reporting reduced incidence of recurrence. However, there are no randomized control trials as yet to prove the benefit of closing PFOs (105,118,119).

REFERENCES

- Hoffman JI, Kaplan S. The incidence of congenital heart disease. *J Am Coll Cardiol* 2002;39:1890–1900.
- Botto LD, Correa A, Erickson JD. Racial and temporal variations in the prevalence of heart defects. *Pediatrics* 2001;107:E32.
- Craig RJ, Selzer A. Natural history and prognosis of atrial septal defect. *Circulation* 1968;37:805–815.
- Davia JE, Cheitlin MD, Bedynek JL. Sinus venosus atrial septal defect: analysis of fifty cases. *Am Heart J* 1973;85:177–185.
- Kirklin JW, Barratt-Boyes BG. *Cardiac Surgery*. New York, NY: John Wiley & Sons, 1986.
- Siu SC, Colman JM, Sorensen S, et al. Adverse neonatal and cardiac outcomes are more common in pregnant women with cardiac disease. *Circulation* 2002;105:2179–2184.
- Stallmeyer B, Fenge H, Nowak-Gottl U, et al. Mutational spectrum in the cardiac transcription factor gene NKX2.5 (CSX) associated with congenital heart disease. *Clin Genet* 2010;78(6):533–40.
- Posch MG, Perrot A, Berger F, et al. Molecular genetics of congenital atrial septal defects. *Clin Res Cardiol* 2010;99:137–147.
- Posch MG, Gramlich M, Sunde M, et al. A gain-of-function TBX20 mutation causes congenital atrial septal defects, patent foramen ovale and cardiac valve defects. *J Med Genet* 2010;47:230–235.
- Chen Y, Han ZQ, Yan WD, et al. A novel mutation in GATA4 gene associated with dominant inherited familial atrial septal defect. *J Thorac Cardiovasc Surg* 2010;140:684–687.
- Lin X, Huo Z, Liu X, et al. A novel GATA6 mutation in patients with tetralogy of Fallot or atrial septal defect. *J Hum Genet* 2010;55:662–667.
- Basson CT, Huang T, Lin RC, et al. Different TBX5 interactions in heart and limb defined by Holt-Oram syndrome mutations. *Proc Natl Acad Sci U S A* 1999;96:2919–2924.
- Ching YH, Ghosh TK, Cross SJ, et al. Mutation in myosin heavy chain 6 causes atrial septal defect. *Nat Genet* 2005;37:423–428.
- Monserat L, Hermida-Prieto M, Fernandez X, et al. Mutation in the alpha-cardiac actin gene associated with apical hypertrophic cardiomyopathy, left ventricular non-compaction, and septal defects. *Eur Heart J* 2007;28:1953–1961.
- Budde BS, Binner P, Waldmuller S, et al. Noncompaction of the ventricular myocardium is associated with a de novo mutation in the beta-myosin heavy chain gene. *PLoS One* 2007;2:e1362.
- Pease WE, Nordenberg A, Ladda RL. Familial atrial septal defect with prolonged atrioventricular conduction. *Circulation* 1976;53:759–762.
- Jenkins KJ, Correa A, Feinstein JA, et al. Noninherited risk factors and congenital cardiovascular defects: current knowledge: a scientific statement from the American Heart Association Council on Cardiovascular Disease in the Young: endorsed by the American Academy of Pediatrics. *Circulation* 2007;115:2995–3014.
- Tikkanen J, Heinonen OP. Risk factors for atrial septal defect. *Eur J Epidemiol* 1992;8:509–515.
- Torfs CP, Christianson RE. Maternal risk factors and major associated defects in infants with Down syndrome. *Epidemiology* 1999;10:264–270.
- Van Mierop LH, Alley RD, Kausel HW, et al. The anatomy and embryology of endocardial cushion defects. *J Thorac Cardiovasc Surg* 1962;43:71–83.
- Van Praagh S, Carrera ME, Sanders SP, et al. Sinus venosus defects: unroofing of the right pulmonary veins—anatomic and echocardiographic findings and surgical treatment. *Am Heart J* 1994;128:365–379.
- Perloff JK. Lutembacher's syndrome. A contemporary appraisal. *Med Ann Dist Columbia* 1970;39:71–77.
- Schreiber TL, Feigenbaum H, Weyman AE. Effect of atrial septal defect repair on left ventricular geometry and degree of mitral valve prolapse. *Circulation* 1980;61:888–896.
- Haworth SG. Pulmonary vascular disease in secundum atrial septal defect in childhood. *Am J Cardiol* 1983;51:265–272.
- Steele PM, Fuster V, Cohen M, et al. Isolated atrial septal defect with pulmonary vascular obstructive disease—long-term follow-up and prediction of outcome after surgical correction. *Circulation* 1987;76:1037–1042.
- Borow KM, Karp R. Atrial septal defect—lessons from the past, directions for the future. *N Engl J Med* 1990;323:1698–1700.
- Mainwaring RD, Mirali-Akbar H, Lamberti JJ, et al. Secundum-type atrial septal defects with failure to thrive in the first year of life. *J Card Surg* 1996;11:116–120.
- Garson A, Jr, Bink-Boelkens M, Hesslein PS, et al. Atrial flutter in the young: a collaborative study of 380 cases. *J Am Coll Cardiol* 1985;6:871–878.
- Clark EB, Kugler JD. Preoperative secundum atrial septal defect with coexisting sinus node and atrioventricular node dysfunction. *Circulation* 1982;65:976–980.
- Karpawich PP, Antillon JR, Cappola PR, et al. Pre- and postoperative electrophysiologic assessment of children with secundum atrial septal defect. *Am J Cardiol* 1985;55:519–521.
- Bink-Boelkens MT, Bergstra A, Landsman ML. Functional abnormalities of the conduction system in children with an atrial septal defect. *Int J Cardiol* 1988;20:263–272.
- Kitabatake A, Inoue M, Asao M, et al. Noninvasive evaluation of the ratio of pulmonary to systemic flow in atrial septal defect by duplex Doppler echocardiography. *Circulation* 1984;69:73–79.
- Sanders SP, Yeager S, Williams RG. Measurement of systemic and pulmonary blood flow and Q_p/Q_s ratio using Doppler and two-dimensional echocardiography. *Am J Cardiol* 1983;51:952–956.
- van den Bosch AE, Ten Harkel DJ, McGhie JS, et al. Characterization of atrial septal defect assessed by real-time 3-dimensional echocardiography. *J Am Soc Echocardiogr* 2006;19:815–821.
- Morgan GJ, Casey F, Craig B, et al. Assessing ASDs prior to device closure using 3D echocardiography. Just pretty pictures or a useful clinical tool? *Eur J Echocardiogr* 2008;9:478–482.
- Pushparajah K, Miller OL, Simpson JM. 3D echocardiography of the atrial septum: anatomical features and landmarks for the echocardiographer. *JACC Cardiovasc Imaging* 2010;3:981–984.
- Saric M, Perk G, Purgess JR, et al. Imaging atrial septal defects by real-time three-dimensional transesophageal echocardiography: step-by-step approach. *J Am Soc Echocardiogr* 2010;23:1128–1135.
- Lodato JA, Cao QL, Weinert L, et al. Feasibility of real-time three-dimensional transesophageal echocardiography for guidance of percutaneous atrial septal defect closure. *Eur J Echocardiogr* 2009;10:543–548.
- Bartel T, Konorza T, Arjmand J, et al. Intracardiac echocardiography is superior to conventional monitoring for guiding device closure of interatrial communications. *Circulation* 2003;107:795–797.
- Bartel T, Konorza T, Neudorf U, et al. Intracardiac echocardiography: an ideal guiding tool for device closure of interatrial communications. *Eur J Echocardiogr* 2005;6:92–96.
- Hijazi Z, Wang Z, Cao Q, et al. Transcatheter closure of atrial septal defects and patent foramen ovale under intracardiac echocardiographic guidance: feasibility and comparison with transesophageal echocardiography. *Catheter Cardiovasc Interv* 2001;52:194–199.
- Earing MG, Cabalka AK, Seward JB, et al. Intracardiac echocardiographic guidance during transcatheter device closure of atrial septal defect and patent foramen ovale. *Mayo Clin Proc* 2004;79:24–34.
- Franz C, Mennicken U, Dalichau H, et al. Abnormal communication between the left atrium and the coronary sinus. Presentation of 2 cases and review of the literature. *Thorac Cardiovasc Surg* 1985;33:113–117.
- Barger LM, Jr, Elliott LP, Soto B, et al. Axial cineangiography in congenital heart disease. Section I. Concept, technical and anatomic considerations. *Circulation* 1977;56:1075–1083.
- Freedman RM, Culham JA, Rowe RD. Left atrial to coronary sinus fenestration (partially unroofed coronary sinus). Morphological and angiographic observations. *Br Heart J* 1981;46:63–68.
- Berbarie RE, Anwar A, Dockery WD, et al. Measurement of right ventricular volumes before and after atrial septal defect closure using multislice computed tomography. *Am J Cardiol* 2007;99:1458–1461.

47. Teo KS, Disney PJ, Dundon BK, et al. Assessment of atrial septal defects in adults comparing cardiovascular magnetic resonance with transtoesophageal echocardiography. *J Cardiovasc Magn Reson* 2010;12:44.
48. Kim H, Choe YH, Park SW, et al. Partially unroofed coronary sinus: MDCT and MRI findings. *AJR Am J Roentgenol* 2010;195:W331-W336.
49. Rajiah P, Kanne JP. Computed tomography of septal defects. *J Cardiovasc Comput Tomogr* 2010;4:231-245.
50. Hundley WG, Li HF, Lange RA, et al. Assessment of left-to-right intracardiac shunting by velocity-encoded, phase-difference magnetic resonance imaging. A comparison with oximetric and indicator dilution techniques. *Circulation* 1995;91:2955-2960.
51. Brochu MC, Baril JF, Dore A, et al. Improvement in exercise capacity in asymptomatic and mildly symptomatic adults after atrial septal defect percutaneous closure. *Circulation* 2002;106:1821-1826.
52. Warnes CA, Williams RG, Bashore TM, et al. ACC/AHA 2008 guidelines for the management of adults with congenital heart disease: a report of the American College of Cardiology/American Heart Association Task Force on Practice Guidelines (Writing Committee to Develop Guidelines on the Management of Adults With Congenital Heart Disease). Developed in Collaboration With the American Society of Echocardiography, Heart Rhythm Society, International Society for Adult Congenital Heart Disease, Society for Cardiovascular Angiography and Interventions, and Society of Thoracic Surgeons. *J Am Coll Cardiol* 2008;52:e1-e121.
53. Campbell M. Natural history of atrial septal defect. *Br Heart J* 1970;32:820-826.
54. Giardina AC, Raptoulis AS, Engle MA, et al. Spontaneous closure of atrial septal defect with cardiac failure in infancy. *Chest* 1979;75:395-397.
55. Dimich I, Steinfeld L, Park SC. Symptomatic atrial septal defect in infants. *Am Heart J* 1973;85:601-604.
56. Mahoney LT, Truesdell SC, Krzmarzick TR, et al. Atrial septal defects that present in infancy. *Am J Dis Child* 1986;140:1115-1118.
57. Brassard M, Fourn JC, van Doesburg NH, et al. Outcome of children with atrial septal defect considered too small for surgical closure. *Am J Cardiol* 1999;83:1552-1555.
58. Radzik D, Davignon A, van Doesburg N, et al. Predictive factors for spontaneous closure of atrial septal defects diagnosed in the first 3 months of life. *J Am Coll Cardiol* 1993;22:851-853.
59. Hanslik A, Pospisil U, Salzer-Muhar U, et al. Predictors of spontaneous closure of isolated secundum atrial septal defect in children: a longitudinal study. *Pediatrics* 2006;118:1560-1565.
60. McMahon CJ, Feltes TF, Fraley JK, et al. Natural history of growth of secundum atrial septal defects and implications for transcatheter closure. *Heart* 2002;87:256-259.
61. Somerville J. How to manage the Eisenmenger syndrome. *Int J Cardiol* 1998;63:1-8.
62. Driscoll D, Allen HD, Atkins DL, et al. Guidelines for evaluation and management of common congenital cardiac problems in infants, children, and adolescents. A statement for healthcare professionals from the Committee on Congenital Cardiac Defects of the Council on Cardiovascular Disease in the Young, American Heart Association. *Circulation* 1994;90:2180-2188.
63. Gundry SR, Shattuck OH, Razzouk AJ, et al. Facile minimally invasive cardiac surgery via ministernotomy. *Ann Thorac Surg* 1998;65:1100-1104.
64. Del Nido PJ, Bichell DP. Minimal-access surgery for congenital heart defects. *Semin Thorac Cardiovasc Surg Pediatr Card Surg Annu* 1998;1:75-80.
65. Rahimtoola SH, Kirklin JW, Burchell HB. Atrial septal defect. *Circulation* 1968;38:2-12.
66. Dave KS, Pakrashi BC, Wooler GH, et al. Atrial septal defect in adults. Clinical and hemodynamic results of surgery. *Am J Cardiol* 1973;31:7-13.
67. Murphy JG, Gersh BJ, McGoon MD, et al. Long-term outcome after surgical repair of isolated atrial septal defect. Follow-up at 27 to 32 years. *N Engl J Med* 1990;323:1645-1650.
68. Mills NL, King TD. Nonoperative closure of left-to-right shunts. *J Thorac Cardiovasc Surg* 1976;72:371-378.
69. Babic UU, Grujicic S, Popovic Z, et al. Double-umbrella device for transvenous closure of patent ductus arteriosus and atrial septal defect: first experience. *J Interv Cardiol* 1991;4:283-294.
70. Chan KC, Godman MJ, Walsh K. Transcatheter closure of atrial septal defect and interatrial communications with a new self expanding nitinol double disc device (Amplatzer septal occluder): multicentre UK experience. *Heart* 1999;82:300-306.
71. Prieto LR, Foreman CK, Cheatham JP, et al. Intermediate-term outcome of transcatheter secundum atrial septal defect closure using the Bard Clamshell Septal Umbrella. *Am J Cardiol* 1996;78:1310-1312.
72. Amin Z, Hijazi ZM, Bass JL, et al. Erosion of Amplatzer septal occluder device after closure of secundum atrial septal defects: review of registry of complications and recommendations to minimize future risk. *Catheter Cardiovasc Interv* 2004;63:496-502.
73. Mullen MJ, Hildick-Smith D, De Giovanni JV, et al. BioSTAR Evaluation Study (BEST): a prospective, multicenter, phase I clinical trial to evaluate the feasibility, efficacy, and safety of the BioSTAR bioabsorbable septal repair implant for the closure of atrial-level shunts. *Circulation* 2006;114:1962-1967.
74. Morgan G, Lee KJ, Chaturvedi R, et al. A biodegradable device (BioSTAR) for atrial septal defect closure in children. *Catheter Cardiovasc Interv* 2010;76:241-245.
75. Balint OH, Samman A, Haberer K, et al. Outcomes in patients with pulmonary hypertension undergoing percutaneous atrial septal defect closure. *Heart* 2008;94:1189-1193.
76. Yong G, Khairy P, De Guise P, et al. Pulmonary arterial hypertension in patients with transcatheter closure of secundum atrial septal defects: a longitudinal study. *Circ Cardiovasc Interv* 2009;2:455-462.
77. Humenberger M, Rosenhek R, Gabriel H, et al. Benefit of atrial septal defect closure in adults: impact of age. *Eur Heart J* 2011;32:553-560.
78. Trusler GA, Kazenelson G, Freedom RM, et al. Late results following repair of partial anomalous pulmonary venous connection with sinus venosus atrial septal defect. *J Thorac Cardiovasc Surg* 1980;79:776-781.
79. Nicholson IA, Chard RB, Nunn GR, et al. Transcaval repair of the sinus venosus syndrome. *J Thorac Cardiovasc Surg* 2000;119:741-744.
80. Warden HE, Gustafson RA, Tarnay TJ, et al. An alternative method for repair of partial anomalous pulmonary venous connection to the superior vena cava. *Ann Thorac Surg* 1984;38:601-605.
81. Takahashi H, Kaminishi Y, Saito T, et al. Anatomical repair of partially unroofed coronary sinus syndrome through the coronary sinus orifice. *Ann Thorac Cardiovasc Surg* 2005;11:208-210.
82. Berger F, Vogel M, Kramer A, et al. Incidence of atrial flutter/fibrillation in adults with atrial septal defect before and after surgery. *Ann Thorac Surg* 1999;68:75-78.
83. Gatzoulis MA, Freeman MA, Siu SC, et al. Atrial arrhythmia after surgical closure of atrial septal defects in adults. *N Engl J Med* 1999;340:839-846.
84. Berger F, Vogel M, Alexi-Meskishvili V, et al. Comparison of results and complications of surgical and Amplatzer device closure of atrial septal defects. *J Thorac Cardiovasc Surg* 1999;118:674-678; discussion 678-680.
85. Veldtman GR, Razack V, Siu S, et al. Right ventricular form and function after percutaneous atrial septal defect device closure. *J Am Coll Cardiol* 2001;37:2108-2113.
86. Kort HW, Balzer DT, Johnson MC. Resolution of right heart enlargement after closure of secundum atrial septal defect with transcatheter technique. *J Am Coll Cardiol* 2001;38:1528-1532.
87. Popio KA, Gorlin R, Teichholz LE, et al. Abnormalities of left ventricular function and geometry in adults with an atrial septal defect. Ventriculographic, hemodynamic and echocardiographic studies. *Am J Cardiol* 1975;36:302-308.
88. Satoh A, Katayama K, Hiro T, et al. Effect of right ventricular volume overload on left ventricular diastolic function in patients with atrial septal defect. *Jpn Circ J* 1996;60:758-766.
89. St John Sutton MG, Tajik AJ, Mercier LA, et al. Assessment of left ventricular function in secundum atrial septal defect by computer analysis of the M-mode echocardiogram. *Circulation* 1979;60:1082-1090.
90. Toyono M, Pettersson GB, Matsumura Y, et al. Preoperative and postoperative mitral valve prolapse and regurgitation in adult patients with secundum atrial septal defects. *Echocardiography* 2008;25:1086-1093.
91. Speechly-Dick ME, John R, Pugsley WB, et al. Secundum atrial septal defect repair: long-term surgical outcome and the problem of late mitral regurgitation. *Postgrad Med J* 1993;69:912-915.
92. Joy J, Kartha CC, Balakrishnan KG. Structural basis for mitral valve dysfunction associated with ostium secundum atrial septal defects. *Cardiology* 1993;82:409-414.
93. Wilson W, Taubert KA, Gewitz M, et al. Prevention of infective endocarditis: guidelines from the American Heart Association: a guideline from the American Heart Association Rheumatic Fever, Endocarditis, and Kawasaki Disease Committee, Council on Cardiovascular Disease in the Young, and the Council on Clinical Cardiology, Council on Cardiovascular Surgery and Anesthesia, and the Quality of Care and Outcomes Research Interdisciplinary Working Group. *Circulation* 2007;116:1736-1754.
94. Meijboom F, Hess J, Szatmari A, et al. Long-term follow-up (9 to 20 years) after surgical closure of atrial septal defect at a young age. *Am J Cardiol* 1993;72:1431-1434.
95. Konstantinides S, Geibel A, Olschewski M, et al. A comparison of surgical and medical therapy for atrial septal defect in adults. *N Engl J Med* 1995;333:469-473.
96. Horvath KA, Burke RP, Collins JJ, Jr, et al. Surgical treatment of adult atrial septal defect: early and long-term results. *J Am Coll Cardiol* 1992;20:1156-1159.
97. St. John Sutton MG, Tajik AJ, McGoon DC. Atrial septal defect in patients ages 60 years or older: operative results and long-term postoperative follow-up. *Circulation* 1981;64:402-409.
98. Humenberger M, Rosenhek R, Gabriel H, et al. Benefit of atrial septal defect closure in adults: impact of age. *Eur Heart J* 2011;32:553-560.
99. Hanley PC, Tajik AJ, Hynes JK, et al. Diagnosis and classification of atrial septal aneurysm by two-dimensional echocardiography: report of 80 consecutive cases. *J Am Coll Cardiol* 1985;6:1370-1382.
100. Olivares-Reyes A, Chan S, Lazar EJ, et al. Atrial septal aneurysm: a new classification in two hundred five adults. *J Am Soc Echocardiogr* 1997;10:644-656.
101. Brand A, Keren A, Branski D, et al. Natural course of atrial septal aneurysm in children and the potential for spontaneous closure of associated septal defect. *Am J Cardiol* 1989;64:996-1001.

102. Schneider B, Hanrath P, Vogel P, et al. Improved morphologic characterization of atrial septal aneurysm by transesophageal echocardiography: relation to cerebrovascular events. *J Am Coll Cardiol* 1990;16:1000–1009.
103. Ueno Y, Shimada Y, Tanaka R, et al. Patent foramen ovale with atrial septal aneurysm may contribute to white matter lesions in stroke patients. *Cerebrovasc Dis* 2010;30:15–22.
104. Mugge A, Daniel WG, Angermann C, et al. Atrial septal aneurysm in adult patients. A multicenter study using transthoracic and transesophageal echocardiography. *Circulation* 1995;91:2785–2792.
105. Wahl A, Krumdort U, Meier B, et al. Transcatheter treatment of atrial septal aneurysm associated with patent foramen ovale for prevention of recurrent paradoxical embolism in high-risk patients. *J Am Coll Cardiol* 2005;45:377–380.
106. Meissner I, Whisnant JP, Khandheria BK, et al. Prevalence of potential risk factors for stroke assessed by transesophageal echocardiography and carotid ultrasonography: the SPARC study. Stroke Prevention: Assessment of Risk in a Community. *Mayo Clin Proc* 1999;74:862–869.
107. Hagen PT, Scholz DG, Edwards WD. Incidence and size of patent foramen ovale during the first 10 decades of life: an autopsy study of 965 normal hearts. *Mayo Clin Proc* 1984;59:17–20.
108. Taaffe M, Fischer E, Baranowski A, et al. Comparison of three patent foramen ovale closure devices in a randomized trial (Amplatzer versus CardioSEAL-STARflex versus Helex occluder). *Am J Cardiol* 2008;101:1353–1358.
109. Van den Branden BJ, Post MC, Jaarsma W, et al. New bioabsorbable septal repair implant for percutaneous closure of a patent foramen ovale: short-term results of a single-centre experience. *Catheter Cardiovasc Interv* 2009;74:286–290.
110. Lechat P, Mas JL, Lascault G, et al. Prevalence of patent foramen ovale in patients with stroke. *N Engl J Med* 1988;318:1148–1152.
111. Rigatelli G, Giordan M, Braggion G, et al. Incidence of extracerebral paradoxical embolisms in patients with intracardiac shunts. *Cardiovasc Revasc Med* 2007;8:248–250.
112. Homma S, Sacco RL, Di Tullio MR, et al. Effect of medical treatment in stroke patients with patent foramen ovale: patent foramen ovale in Cryptogenic Stroke Study. *Circulation* 2002;105:2625–2631.
113. Dearani JA, Ugurlu BS, Danielson GK, et al. Surgical patent foramen ovale closure for prevention of paradoxical embolism-related cerebrovascular ischemic events. *Circulation* 1999;100:II171–175.
114. Reisman M, Christofferson RD, Jesurum J, et al. Migraine headache relief after transcatheter closure of patent foramen ovale. *J Am Coll Cardiol* 2005;45:493–495.
115. Anzola GP, Frisoni GB, Morandi E, et al. Shunt-associated migraine responds favorably to atrial septal repair: a case-control study. *Stroke* 2006;37:430–434.
116. Azarbal B, Tobis J, Suh W, et al. Association of interatrial shunts and migraine headaches: impact of transcatheter closure. *J Am Coll Cardiol* 2005;45:489–492.
117. Rundek T, Elkind MS, Di Tullio MR, et al. Patent foramen ovale and migraine: a cross-sectional study from the Northern Manhattan Study (NOMAS). *Circulation* 2008;118:1419–1424.
118. Windecker S, Wahl A, Chatterjee T, et al. Percutaneous closure of patent foramen ovale in patients with paradoxical embolism: long-term risk of recurrent thromboembolic events. *Circulation* 2000;101:893–898.
119. Paciaroni M, Agnelli G, Bertolini A, et al. Risk of Recurrent Cerebrovascular Events in Patients with Cryptogenic Stroke or Transient Ischemic Attack and Patent Foramen Ovale: The FORI (Foramen Ovale Registro Italiano) Study. *Cerebrovasc Dis* 2011;31:109–116.

Frank Cetta ■ L. Luann Minich ■ Joseph J. Maleszewski ■ Joseph A. Dearani ■ Harold MacDonald Burkhart

INTRODUCTION AND NOMENCLATURE

Atrioventricular septal defects (AVSDs) are a group of anomalies that share a defect of the atrioventricular (AV) septum and abnormalities of the AV valves. The terms “AV canal defects” or “endocardial cushion defects” also describe these lesions but, for the purposes of this chapter, the term *atrioventricular septal defect* is used. These lesions are divided into partial and complete forms. In partial AVSD, a primum atrial septal defect (ASD) always is present and there are two distinct, but focally contiguous, right and left AV valve annuli. The left AV valve invariably is cleft. The complete form also includes a primum ASD, but it is contiguous with an inlet ventricular septal defect (VSD), and the common AV valve has a single annulus. Similarly, the clinical manifestations and management of these patients depend on the extent and severity of the lesions present.

Several classifications have been used to describe AVSDs. *Transitional AVSD* is a subtype of partial AVSD. This term is used when a partial AVSD also has a *small* inlet VSD that is partially occluded by dense chordal attachments to the ventricular septum. *Intermediate AVSD* is a subtype of complete AVSD that has distinct right and left AV valve orifices despite having only one common annulus. These separate orifices are referred to as right and left AV valve orifices rather than tricuspid and mitral. This also is true when describing the valves after repair of complete AVSD. The VSD in intermediate AVSD is large similar to other forms of complete AVSD. Unfortunately, the terms “transitional” and “intermediate” have been confused and are used synonymously in the literature. Because of the conflicting and confusing terminology of these subtypes, the clinician, echocardiographer, and surgeon should communicate by simply describing AV valve morphology, cardiac chamber sizes, and magnitude of shunting observed. Complete and intermediate AVSDs have the physiology and clinical features of a combined ASD and VSD, whereas partial and transitional AVSDs have the clinical picture of a large ASD (Fig. 29.1). Anatomic features shared by all forms of AVSD are summarized in Table 29.1.

Surgical repair of AVSDs has been one of the great successes of the last several decades of congenital cardiac surgery. Recently, the Pediatric Heart Network (PHN) reported AVSD outcome data from seven North American centers demonstrating an overall operative mortality of 3% (1,2). Long-term survival has been excellent. Cumulative 20-year survival of 95% has been reported (3). This success has been tempered by the relatively large number of patients (~25%) who await reoperation, most commonly because of progressive left AV valve regurgitation or for relief of left ventricular outflow tract (LVOT) obstruction. Unfortunately, the prevalence of postoperative left AV valve regurgitation has remained the most common sequel of repair for decades. The PHN study found that 26% of patients had more than moderate left AV regurgitation 6 months after “repair” (1,2).

DEMOGRAPHICS

AVSDs account for 4% to 5% of congenital heart defects and the estimated occurrence is 0.19 in 1,000 live births (4,5). In a large fetal echocardiography experience, AVSD was the most common anomaly detected, constituting 18% of abnormal fetal hearts (6). In utero diagnosis of an AVSD is made on routine fetal four-chamber imaging. Gender distribution is approximately equal or may show a slight female preponderance (4).

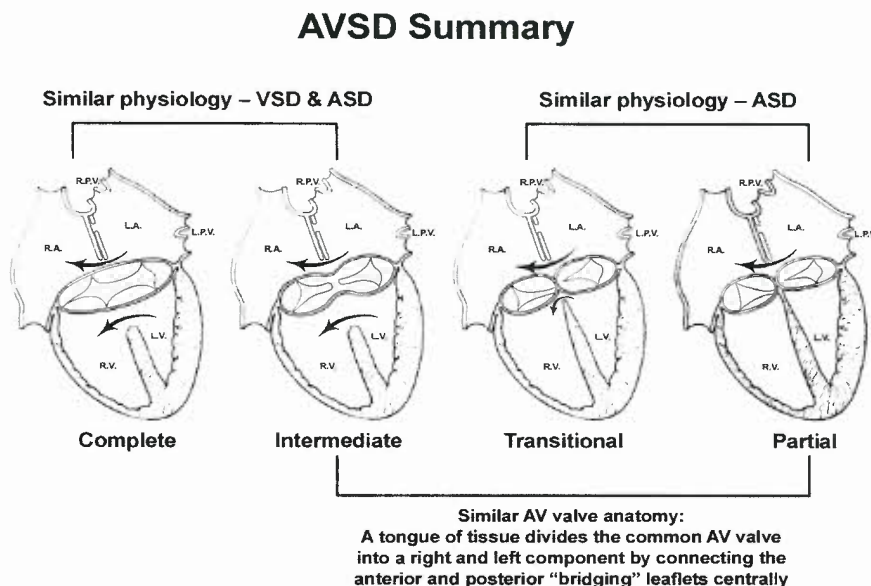
About 40% to 45% of children with Down syndrome have congenital heart disease, and among these, approximately 45% have an AVSD. In more than 75% of patients with Down syndrome, it is the complete form of AVSD (7). Conversely, approximately 50% of patients with AVSD have Down syndrome. Race and ethnicity may factor into prevalence of AVSD in patients with Down syndrome. Patients of Black African ancestry with Down syndrome have AVSD more commonly than do whites. Familial occurrence of AVSD is rare. Complete AVSDs also occur in patients with heterotaxy syndromes (more common with asplenia than with polysplenia). Common atrium has been associated with Ellis-van Creveld and heterotaxy syndromes (8–11).

EMBRYOGENESIS

The etiology of AVSDs has traditionally been considered as faulty development of the AV endocardial cushions. However, recent studies have illustrated additional pathways involving the “dorsal mesenchymal protrusion” that may act alone or in concert with development of the endocardial cushions to create AVSDs (12). In partial AVSDs, incomplete fusion of the superior and inferior endocardial cushions results in a cleft in the midportion of the left AV valve anterior leaflet often associated with regurgitation. In contrast, complete AVSD is associated with lack of fusion between the superior and inferior cushions and, consequently, with the formation of separate anterior and posterior bridging leaflets along the subjacent ventricular septum (Fig. 29.2).

Failure of the endocardial cushions to fuse creates a defect in the AV septum. The primum atrial septal component of this defect usually is large. This results in downward displacement of the anterior left AV valve leaflet to the level of the septal right AV valve leaflet (13). In AVSDs, the AV valves have the same septal insertion level in contrast to the leaflet arrangement in the normal heart (Fig. 29.3). The distance from the cardiac crux to the left ventricular apex is foreshortened, and the distance from the apex to the aortic valve is increased. This is in contrast to the normal heart, in which the two distances are roughly equal (Fig. 29.4). In AVSDs, the disproportion between the two distances causes anterior displacement of

Figure 29.1. Summary of AVSD. Anatomic and physiologic similarities between the different forms of AVSD are illustrated. Complete AVSDs have one annulus with large interatrial and interventricular communications. Intermediate defects (one annulus, two orifices) are a subtype of complete AVSD and have a large ventricular septal defect (VSD). Complete AVSDs have physiology of VSDs and ASDs. In contrast, partial AVSDs have physiology of ASDs. Transitional defects are a form of partial AVSD in which a *small* inlet VSD is present. Partial AVSD and the intermediate form of complete AVSD share a similar anatomic feature: A tongue of tissue divides the common atrioventricular valve into distinct right and left orifices. LA, left atrium; LPV, left pulmonary vein; LV, left ventricle; RA, right atrium; RPV, right pulmonary vein; RV, right ventricle. (With permission of Patrick O’Leary, MD.)



the LVOT resulting in elongation and narrowing of the LVOT producing the characteristic “goose-neck” deformity. After surgical repair of the defect, progressive subaortic stenosis still may develop (14).

Since the dextrodorsal conus cushion contributes to the development of the right AV valve and the outflow tracts lie adjacent to their respective inflow tracts, AVSDs may be associated with conotruncal anomalies, such as tetralogy of Fallot and double-outlet right ventricle (RV). In addition, shift of the AV valve orifice may result in connection of the valve primarily to only one ventricle, creating disproportionate or unbalanced ventricles.

PARTIAL ATRIOVENTRICULAR SEPTAL DEFECT

Pathology

In partial AVSD, the right and left AV valve annuli are separate. The most frequent form of partial AVSD consists of a primum ASD and a cleft left AV valve anterior leaflet (Figs. 29.5 and 29.6). Most primum ASDs are large and located anterior and inferior to the fossa ovalis. The defect is bordered by a crescentic rim of atrial septal tissue posterosuperiorly and by AV valve continuity anteroinferiorly. These defects are not amenable to transcatheter device closure because of their proximity to the AV valves.

TABLE 29.1

Anatomic Features Shared by All Forms of AVSD

- AV valve leaflets insert at the same level at the cardiac crux
- Absence of the AV septum
- Unwedged and anterior displacement of the aortic valve
- Elongated LVOT
- Counterclockwise rotation of the LV papillary muscles
- Cleft left AV valve component, directed toward the ventricular septum

The right and left AV valves have the same septal insertion level because the left AV valve annulus is displaced toward the ventricular apex. As a result, the deficient AV septum is associated with an interatrial communication rather than an interventricular or right atrial to left ventricular communication. Nonetheless, the defect imparts a scooped-out appearance to the inlet ventricular septum, and the distance from the left AV valve annulus to the left ventricular apex is less than the distance from the aortic annulus to the apex (Fig. 29.4).

The cleft in the left AV valve anterior leaflet is directed toward the midportion of the ventricular septum, along the anteroinferior rim of the septal defect (Fig. 29.7). In contrast, isolated mitral valve clefts (not associated with AVSD) are directed toward the aortic valve annulus (15). The left AV valve orifice is triangular rather than elliptical (as in a normal heart) and resembles a mirror-image tricuspid valve orifice. The cleft left AV valve usually is regurgitant and, with time, becomes thickened and exhibits histologic alterations that resemble myxomatous mitral valve prolapse.

The most common associated anomalies with partial AVSD are a secundum ASD, patent ductus arteriosus (PDA), and a persistent left superior vena cava connecting to the coronary sinus (1). Less frequently, pulmonary stenosis, tricuspid stenosis or atresia, cor triatriatum, coarctation of the aorta, membranous VSD, pulmonary venous anomalies, and hypoplastic right or left ventricle (LV) have been reported (16–18).

Clinical Manifestations

Although patients with partial AVSD may be asymptomatic until adulthood, symptoms of excess pulmonary blood flow typically occur in childhood. Tachypnea and poor weight gain occur most commonly when the defect is associated with moderate or severe left AV valve regurgitation or with other hemodynamically significant cardiac anomalies. Patients with primum ASDs usually have earlier and more severe symptoms, including growth failure, than patients with secundum ASDs.

An uncomplicated primum ASD often is discovered in young children when echocardiography is performed to investigate a murmur. The murmur has typical systolic ejection qualities and is best heard over the upper left sternal border with radiation to the lung fields. The murmur is caused by turbulent flow across the pulmonary valve (not flow through the ASD). The second heart sound is widely split and fixed during respiration. An S1-coincident

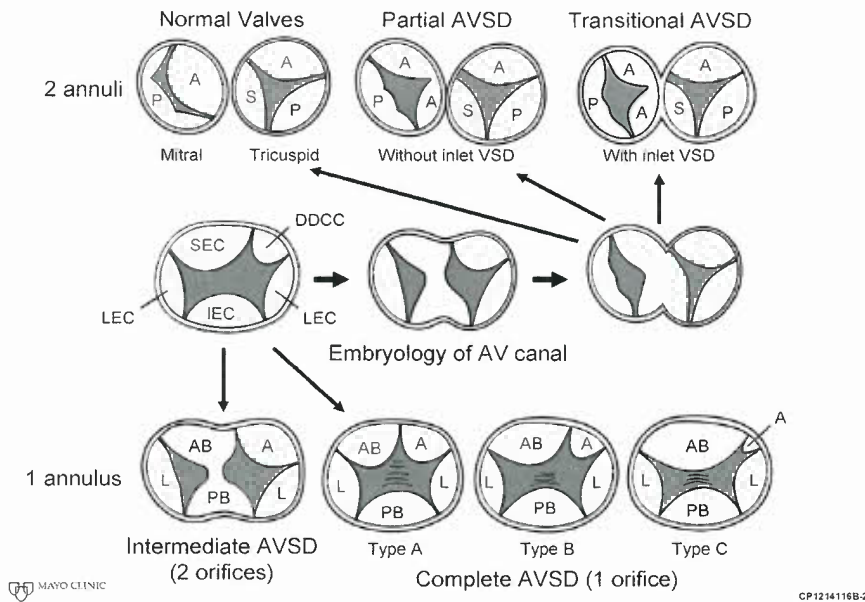


Figure 29.2. Diagram of the embryologic development of the AV canal region and the spectrum of AVSD, including partial, transitional, complete, and intermediate forms. A, anterior leaflet; AB, anterior bridging leaflet; DDCC, dextrodorsal conus cushion; IEC, inferior endocardial cushion; LEC, lateral endocardial cushion; P, posterior leaflet; PB, posterior bridging leaflet; S, septal leaflet; SEC, superior endocardial cushion; L, lateral leaflet.

holosystolic murmur due to left AV valve regurgitation through the cleft may also be heard at the apex. A low-pitched middiastolic murmur heard at the left lower sternal border may be present if the shunt is large or if significant left AV valve regurgitation is present.

Echocardiography

Two-dimensional echocardiography is the primary imaging technique for diagnosing AVSDs (19–21). It is useful particularly for delineating the morphology of the AV valves.

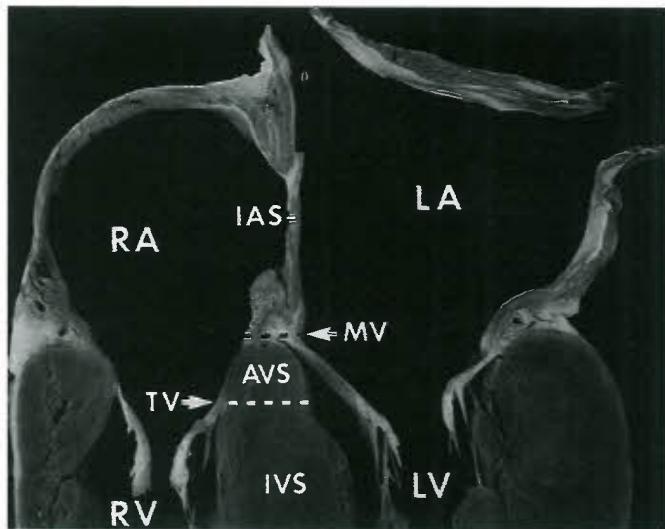


Figure 29.3. AV septum in the normal heart (four-chamber view). The atrioventricular septum (AVS) lies between the RA and the left ventricle (LV) with the interatrial septum (IAS) above and the interventricular septum (IVS) below. The septal tricuspid leaflet (TV—right AV valve) normally inserts at a lower (more apical) level than the anterior mitral leaflet (MV—left AV valve). LA, left atrium; RV, right ventricle. (From Edwards WD. Applied anatomy of the heart. In: Brandenburg RO, Fuster V, Giuliani ER, et al., eds. *Cardiology: Fundamentals and Practice*. Vol. 1. Chicago, IL: Year Book Medical, 1987:47–109, with permission of Mayo Foundation.)

Transesophageal echocardiography (TEE) can provide incremental diagnostic information in larger patients or in patients with associated complex abnormalities.

The internal cardiac crux is the most consistent echocardiographic imaging landmark (19). The apical four-chamber imaging plane clearly allows visualization of the internal crux where the primum ASD is seen as an absence of the lower atrial septum. The size of the primum ASD is made reliably from this imaging position (Fig. 29.8) or from the subcostal four-chamber (frontal) projection. Accurate visualization of the cardiac crux also permits assessment of the AV valves. Several 2-D echocardiographic features are shared by all forms of AVSD: deficiency of a portion of the inlet ventricular septum, inferior displacement of the AV valves, and attachment of a portion of the left AV valve to the septum. The AV valves are displaced toward the ventricles, with the septal portions inserting at the same level onto the crest of the ventricular septum. Therefore, in these defects, the two separate AV valve orifices are equidistant from the cardiac apex.

In the transitional form of partial AVSD, there is aneurysmal replacement of a portion of the inlet ventricular septum (21) (Fig. 29.9A,B). Small shunts may occur through this so-called “tricuspid pouch.” However these dense chordal attachments eventually obstruct flow. Spectral and color flow Doppler hemodynamic assessments are useful to determine the severity of AV valve stenosis or insufficiency and to quantitate right ventricular systolic pressure. Doppler echocardiography often is not useful for evaluating the degree of left AV valve stenosis in the setting of a primum ASD because the ASD will decompress the left atrium (LA).

Other left AV valve abnormalities are typical with both the partial and complete forms of AVSD (Fig. 29.10A). The most common abnormality, a cleft, is best visualized from the parasternal and subcostal short-axis imaging planes. Careful 2-D and color Doppler assessment of the left AV valve cleft needs to be performed since multiple jets of regurgitation may be present. LV to right atrium (RA)-directed left AV valve regurgitation is usually remedied during surgery with successful repair of the cleft and closure of the primum ASD. LV to LA regurgitation may not be completely eliminated with cleft repair and may signify other intrinsic abnormalities with the valve. An important factor that predicts the amount of residual postoperative left AV valve regurgitation is the degree of preoperative regurgitation. Rarely, other abnormalities of the left AV valve occur such as a parachute or a double-orifice valve.

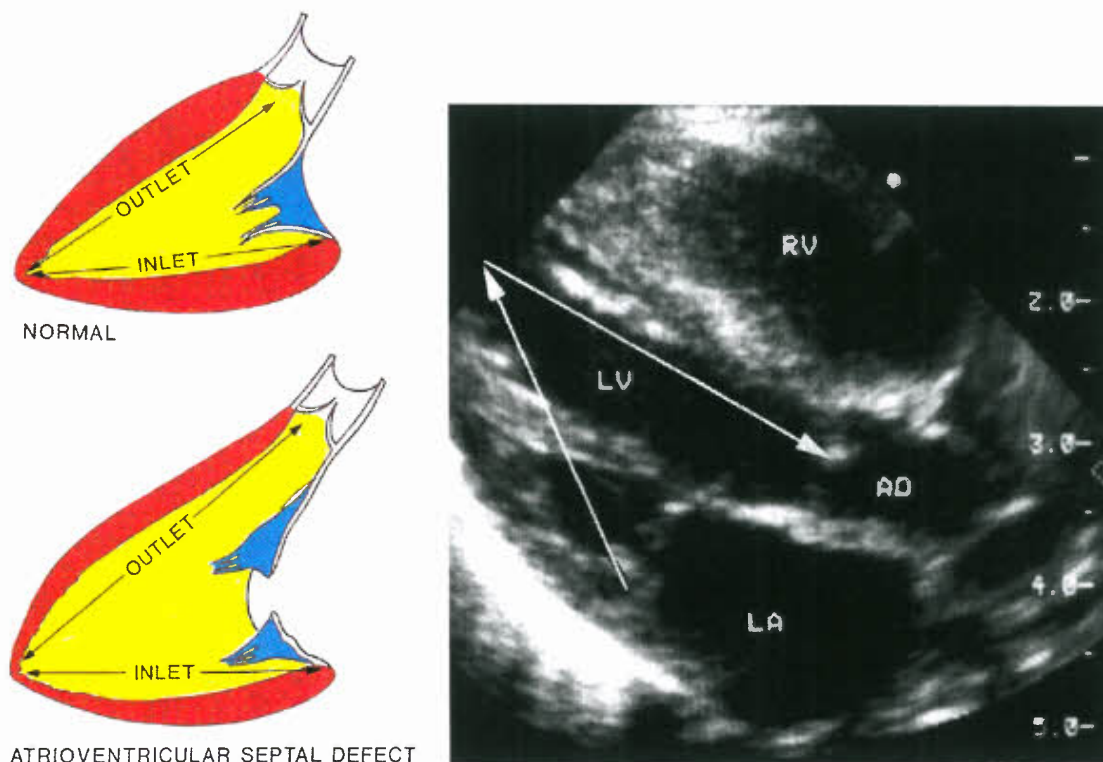


Figure 29.4. Elongate LVOT in AVSD: Because of deficiency of the ventricular component of the AV septum and the “sprung” AV junction, the distance from the LV apex to the posterior left AV valve annulus is 20% to 25% shorter than the distance from the apex to the aortic annulus. Ao, aorta; LA, left atrium; LV, left ventricle; RV, right ventricle. (With permission of Robert H. Anderson, MD.)

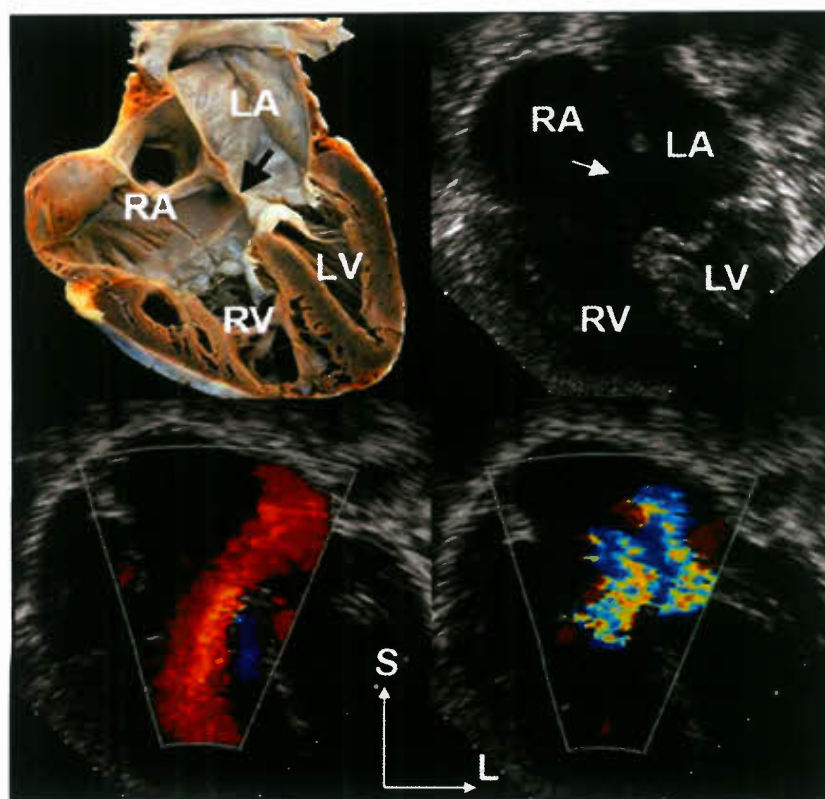


Figure 29.5. Top left: Four-chamber anatomic specimen demonstrating a large primum ASD (arrow), severe RA and RV dilation, and connection of both AV valves to the septum at the same level. Top right: Corresponding apical four-chamber diastolic image demonstrating severe RA and RV dilation owing to a large primum ASD (arrow). Bottom left: Color Doppler scan from the apex, demonstrating a large left-to-right shunt crossing the primum ASD in diastole (red flow jet). Bottom right: Systolic color flow Doppler displaying moderate right and left AV valve regurgitation. LA, left atrium.

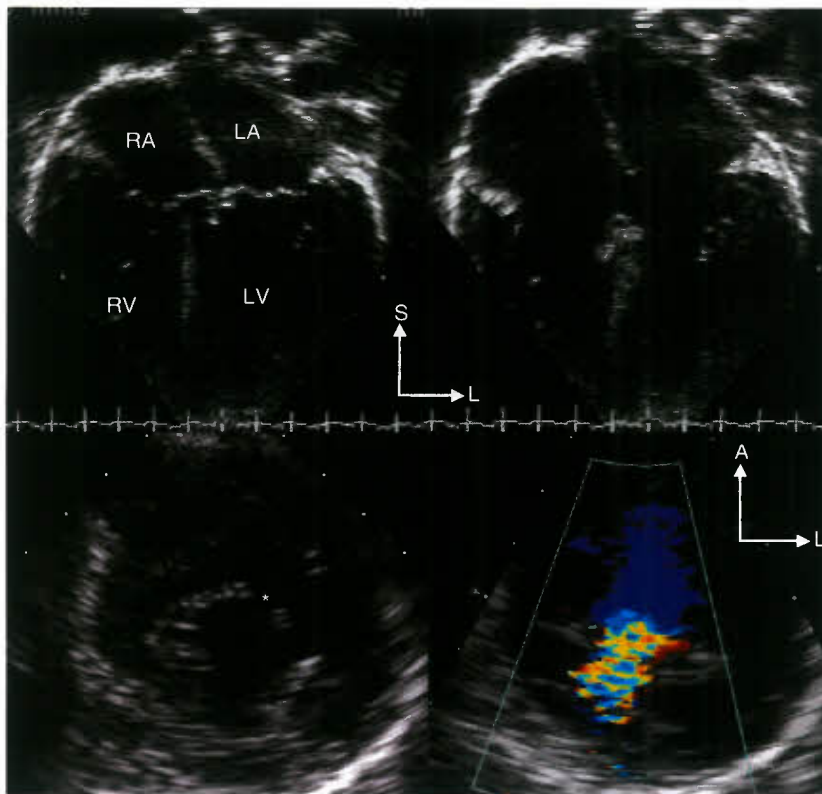


Figure 29.6. Partial AVSD: AV valve anatomy. **Top left:** Systolic apical four-chamber image demonstrating that both right and left AV valves insert onto the crest of the ventricular septum at the same level. **Top right:** Corresponding diastolic frame showing a large primum ASD. Systolic frames often understate the size of the interatrial communication. There is significant RA and RV enlargement. **Bottom panels:** These are parasternal short-axis scans focused at the valve leaflet level in the left ventricular inflow. The **left panel** demonstrates the cleft in the anterior leaflet of the left AV valve (*asterisk*). The anterior leaflet is made of two separate components that move independently. This creates the diastolic gap in the leaflet (*asterisk*). Color Doppler on the **right panel** shows considerable regurgitation through the cleft. LA, left atrium; LV, left ventricle.

Double-orifice left AV valve occurs in 3% to 5% of AVSDs (22). This abnormality is more common when two distinct right and left AV valve orifices are present. A tongue of tissue may divide the left AV valve into two orifices. The combined effective valve area of a double-orifice valve always is less than the valve area of a single-orifice valve. This predisposes the valve to postoperative stenosis. Standard subcostal and parasternal short-axis views usually demonstrate the double-orifice valve characteristics (Fig. 29.10B,C). However, in the setting of a common AV valve, the diagnosis may be challenging. Double-orifice left AV valve rarely occurs in hearts that do not have AVSD. In contrast to AVSD, in the otherwise normal

heart, double-orifice mitral valves have complete duplication of the valve structure.

In the normal heart, the aortic valve is wedged between the mitral and tricuspid annuli. In AVSD, the aortic valve is displaced or “sprung” anteriorly (Fig. 29.11). This anterior displacement creates an elongate, so-called gooseneck deformity of the LVOT (Fig. 29.12) that predisposes the patient to progressive subaortic obstruction. LVOT obstruction may occur in all subtypes of AVSD. It is more frequent when two distinct AV valve orifices are present rather than when there is a common orifice. But whenever the superior bridging leaflet attaches to the crest of the ventricular septum,

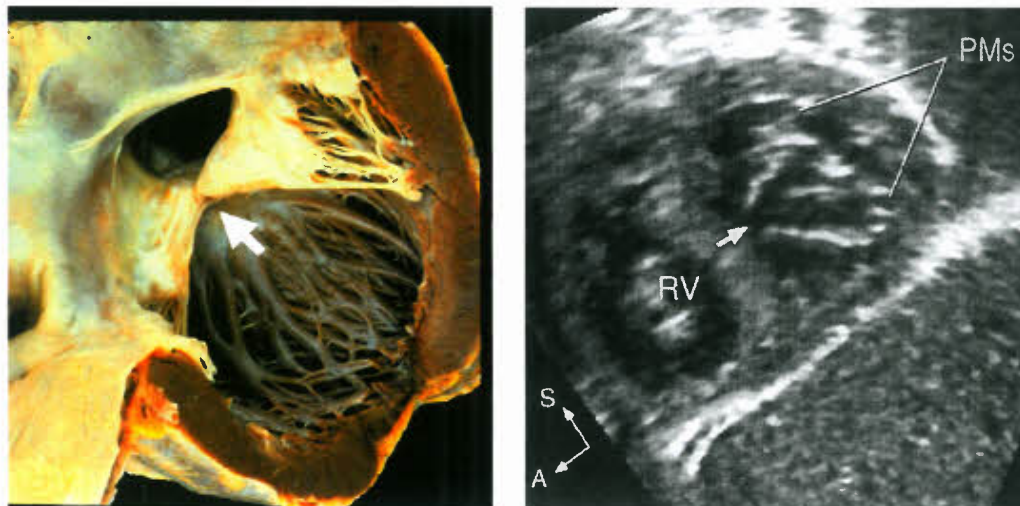


Figure 29.7. Cleft left AV valve: **Left:** In AVSD, the cleft in the anterior leaflet of the left AV valve is typically oriented toward the midportion of the ventricular septum (*arrow*) along the anterior–inferior rim of the septal defect. **Right:** Subcostal sagittal image demonstrating the septal orientation of the cleft. A, anterior; PMS, papillary muscles; RV, right ventricle; S, superior.

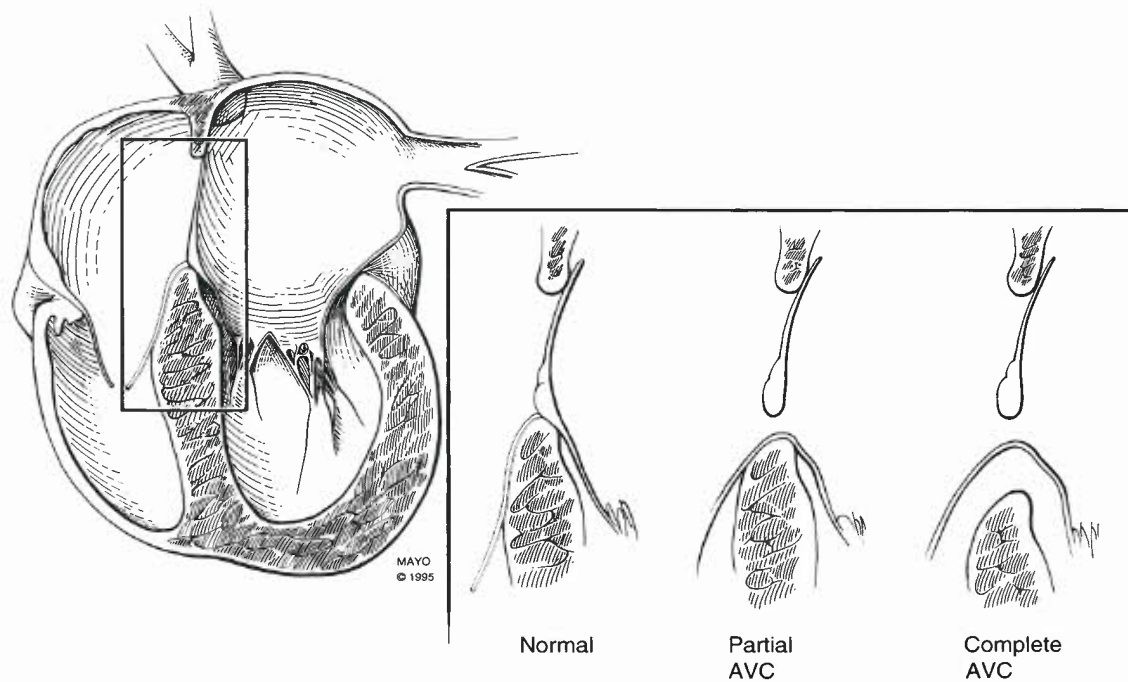


Figure 29.8. AVSD and the internal cardiac crux. The internal cardiac crux is best visualized in the apical four-chamber imaging plane. In the normal heart, the anterior leaflet of the mitral insertion is more superiorly fixed than the corresponding tricuspid septal leaflet. In all forms of AVSD, both right and left AV valve components insert at the same level on the crest of the inflow ventricular septum. A cleft in the left AV valve occurs in conjunction with the downward displacement of the anterior leaflet. In partial AVSD, there is a defect in the lower fatty portion of the atrial septum (i.e., within the atrial ventricular septum). In complete AVSD, there is a defect beneath the AV valves in the inflow ventricular septum. In general, these easily recognized anatomic features distinguish normal from partial and complete AVSD. AVC, atrioventricular canal.

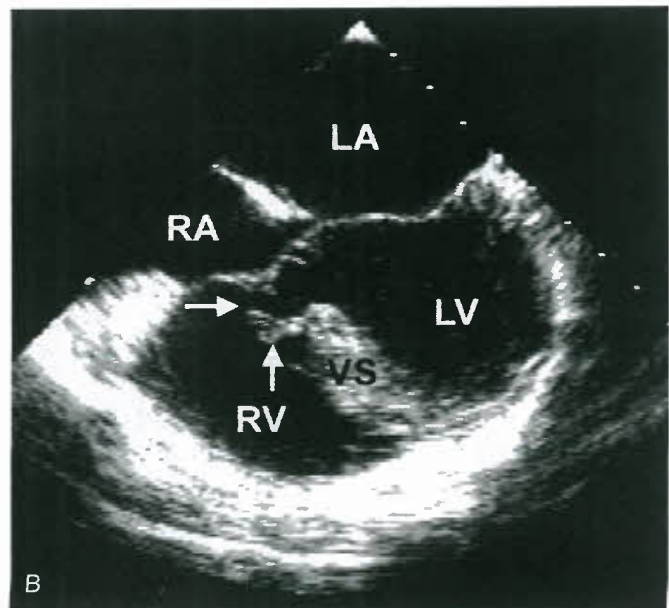


Figure 29.9. A: Transesophageal echocardiogram in a four-chamber projection demonstrating a typical primum ASD in a 20-year-old patient with partial AVSD. No VSD is present. B: In contrast to image 9A, this patient has a transitional AVSD. Note the membranous aneurysm in the inflow ventricular septum (arrows). There is a primum ASD; clinically, it presents as a partial AVSD. There can be restrictive VSDs in the inflow aneurysmal membrane. LA, left atrium; LV, left ventricle; RA, right atrium; RV, right ventricle; VS, ventricular septum.

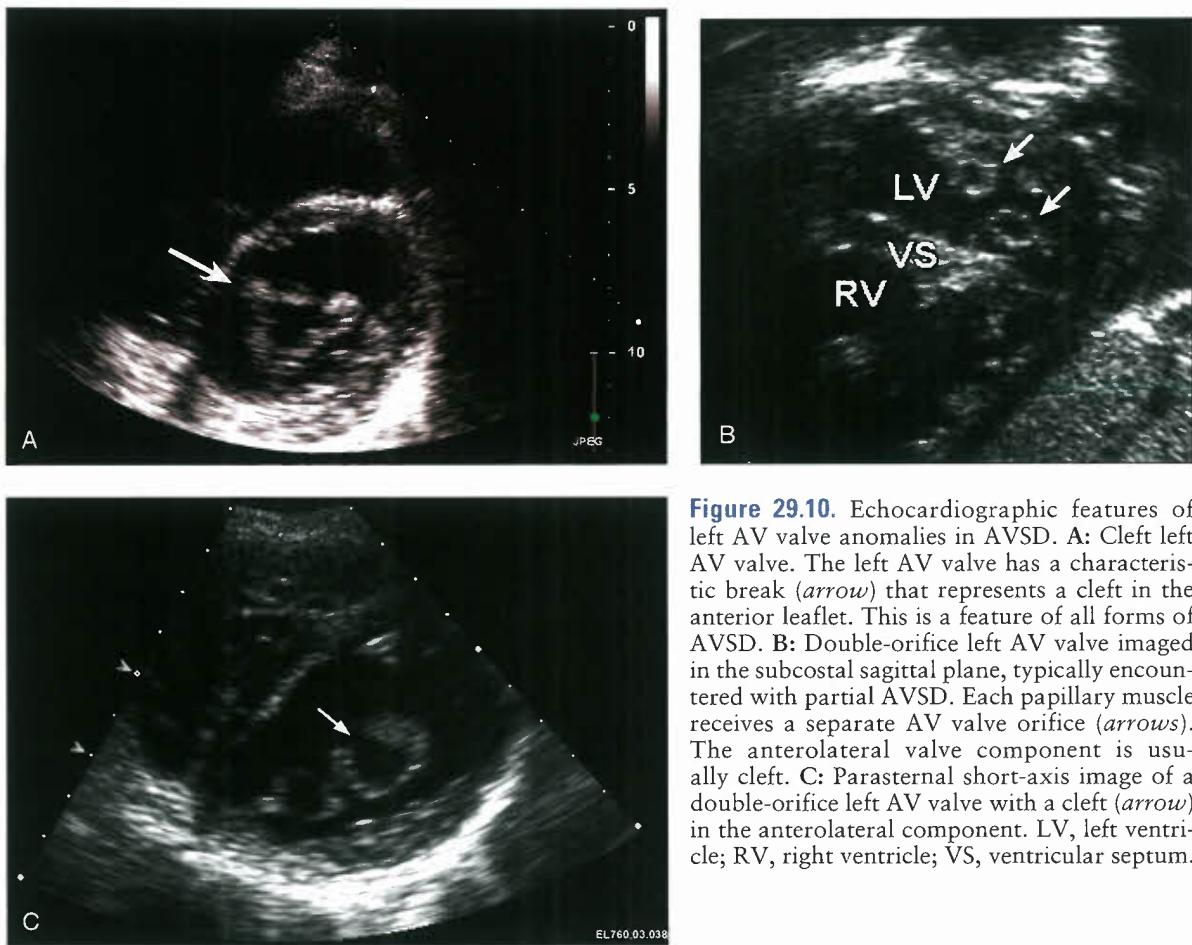


Figure 29.10. Echocardiographic features of left AV valve anomalies in AVSD. **A:** Cleft left AV valve. The left AV valve has a characteristic break (*arrow*) that represents a cleft in the anterior leaflet. This is a feature of all forms of AVSD. **B:** Double-orifice left AV valve imaged in the subcostal sagittal plane, typically encountered with partial AVSD. Each papillary muscle receives a separate AV valve orifice (*arrows*). The anterolateral valve component is usually cleft. **C:** Parasternal short-axis image of a double-orifice left AV valve with a cleft (*arrow*) in the anterolateral component. LV, left ventricle; RV, right ventricle; VS, ventricular septum.

creating two orifices, this further elongates and narrows the LVOT. In addition, discrete subaortic fibromuscular ridges, septal hypertrophy, abnormal left AV valve chordal attachments, and abnormally oriented papillary muscles can further exacerbate the subaortic narrowing. LVOT obstruction may be subtle and therefore not appreciated during the preoperative echocardiographic assessment. LVOT obstruction may

develop de novo after initial repair of AVSD (23) (Fig. 29.13). The LVOT obstruction often is progressive. Even after primary repair of partial AVSD in adulthood, de novo LVOT obstruction may occur. The Mayo Clinic has reported the case of a 58-year-old woman who had reoperation for LVOT obstruction after primary repair of partial AVSD at age 45 years (24).

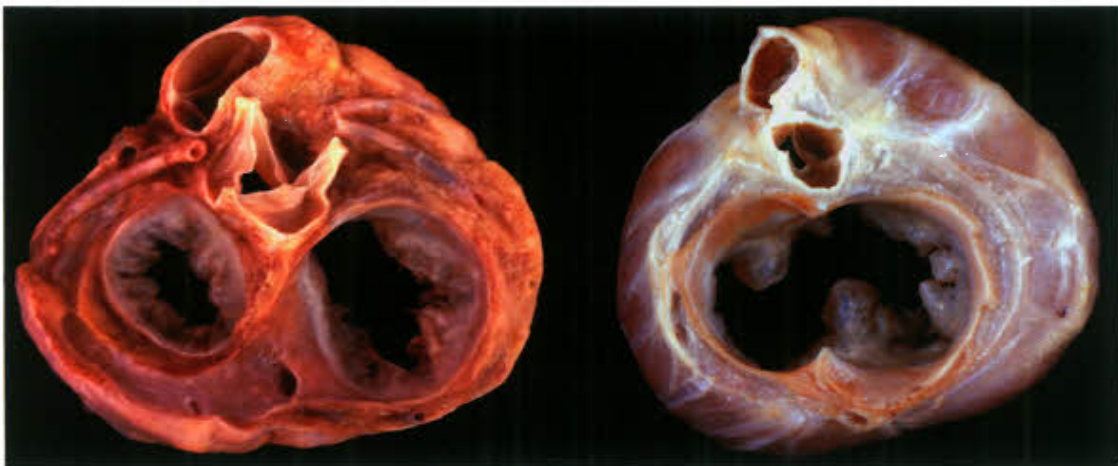


Figure 29.11. Sprung aortic valve: **Left:** Normal heart pathologic specimen cut in short axis at the base demonstrating where the AV junction has a figure-of-8 configuration. **Right:** Similar projection in an AVSD heart where the AV junction is “sprung.” The aortic valve is anterior of the AV junction instead of being wedged between the AV valve annuli.



Figure 29.12. Because of the anterior displacement of the LVOT in AVSD, the elongate LVOT has been described as a “goose neck” with echocardiographic and angiographic imaging. **Left:** subcostal frontal view of the LVOT. **Middle:** pediatric and adult goose necks in Minnesota. **Right:** Prograde LV angiograph demonstrating elongate LVOT.

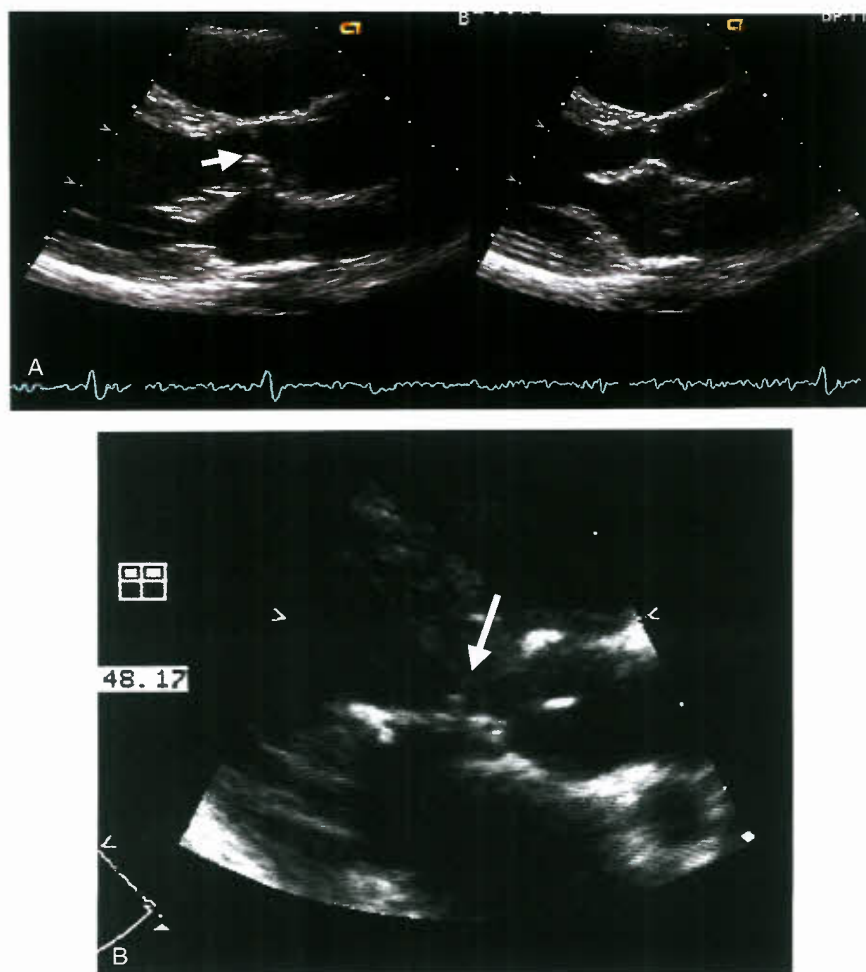


Figure 29.13. **A:** LVOT obstruction: systolic (left) and diastolic (right) echocardiograms demonstrating LVOT obstruction in a 17-year-old who had repair of a partial AVSD at age 15 months. LVOT obstruction (arrow) is usually progressive and may be undetected at time of initial repair. **B:** LVOT obstruction: parasternal long-axis projection demonstrating left AV valve attachments (arrow) to the septum in a patient after repair of partial AVSD. 10% to 15% of patients with AVSD require reoperation to relieve LVOT obstruction. Progressive LVOT obstruction is more common in partial than in complete AVSD. Mechanisms of LVOT obstruction include attachments of superior bridging leaflet to ventricular septum, extension of the anterolateral papillary muscle into the LVOT, discrete fibrous subaortic stenosis, tissue from an aneurysm of the membranous septum bowing into the LVOT.

Detailed and comprehensive echocardiographic assessment is required to evaluate associated lesions and determine their significance. Tetralogy of Fallot, double-outlet RV, and pulmonary valve atresia are associated with all forms of AVSDs but are less frequent with partial AVSD. In contrast, AV valve abnormalities and left ventricular hypoplasia are more frequent in two-orifice AV connections. Coarctation of the aorta occurs with equal frequency in partial and complete AVSD.

Radiography

Typically, chest radiography demonstrates cardiomegaly and prominent pulmonary vascular markings. Because the jet of mitral regurgitation often is directed into the RA, right atrial enlargement rather than left atrial enlargement may be apparent.

Electrocardiography and Electrophysiology

The position of the AVSD dictates the position of the AV conduction tissues. Accordingly, the AV node is displaced posteriorly, near the orifice of the coronary sinus, and the His bundle is displaced inferiorly, along the inferior rim of the septal defect. The displacement of the AV conduction tissues, in conjunction with loss of ventricular septal myocardium, results in left axis deviation in the frontal plane QRS.

Sinus rhythm is present in most patients with a primum ASD. Prolongation of the P-R interval, in relation to patient age and heart rate, is seen in approximately 25% of patients. It is due primarily to increased conduction time from the high RA to the low septal RA (25). P-wave changes indicating right atrial, left atrial, or biatrial enlargement are seen in approximately half of patients. The mean QRS axis in the frontal plane ranges from -30 degrees to -120 degrees, with most axes between -30 degrees and -90 degrees. Anatomic and electrophysiologic studies show that this abnormal vectorcardiographic pattern is associated with a specific anomaly of the conduction system (26). Right ventricular volume overload results in right ventricular hypertrophy and some variation of the rsR' or RSR' pattern in the right precordial leads in 80% of patients; 10% of patients have a qR pattern. Patients with significant left AV valve regurgitation may have evidence of left ventricular hypertrophy.

Except for prolonged intra-atrial conduction time, other intracardiac electrophysiologic measurements usually are normal, including sinus node function, AV node function, His-Purkinje conduction time, and refractory periods (25).

Cardiac Catheterization and Angiography

Cardiac catheterization and angiography rarely are necessary for diagnosis or management of patients with a partial AVSD. Current echocardiographic techniques accurately define the anatomy and physiology of this lesion. In an older patient, cardiac catheterization may have a role in assessing the degree of pulmonary vascular obstructive disease or coronary artery disease.

A large left-to-right shunt can be demonstrated at atrial level by a higher oxygen saturation sampled from the RA compared with the blood in the inferior and superior vena cavae. Because of the anatomic position of the ASD, blood samples taken from the inflow portion of the RV may have elevated oxygen saturation. The calculated left-to-right shunt often exceeds 50%. In most patients, right ventricular pressure is $<60\%$ of systemic pressure. A significant increase in

calculated pulmonary vascular resistance is unusual in infants. Left ventricular angiography will demonstrate the elongate gooseneck deformation of the LVOT (Fig. 29.12).

Special Forms of Partial Atrioventricular Septal Defect

Malaligned Atrial Septum or Double-Outlet Right Atrium

Deviation of the atrial septum to the left of the AV junction has been reported rarely (27,28). When this occurs, both the right and left AV valves are visualized from the RA, which is connected to both ventricles through a large primum ASD. If deviation of the atrial septum to the left is extreme, the pulmonary veins may be isolated and obstructed, simulating cor triatriatum. Although the term "double-outlet" RA has been applied to this lesion (29), it is truly a form of AVSD.

Common Atrium

Common atrium is characterized by near absence of the atrial septum. In the presence of two ventricles, it always is associated with an AVSD (30). Cases of common atrium typically are syndromic. The most common syndromes are asplenia, polysplenia, and Ellis-van Creveld (9–11). The pathologic spectrum of this lesion ranges from patients with coexistent primum and secundum ASDs to others who lack the entire septum except for a small muscular cord. Patients with syndromes and common atrium frequently have concomitant complex congenital heart disease. In these cases, transposition of the great arteries, double-outlet RV, univentricular AV connection, and anomalous pulmonary venous connections often are encountered. Patients with common atrium frequently have anomalies of cardiac and abdominal situs as well as asplenia.

Clinical Manifestations. Most patients with common atrium present in infancy with symptoms of excess pulmonary blood flow, fatigue, tachypnea, and failure to thrive. However, if increased pulmonary vascular resistance develops, the left-to-right shunt decreases and somatic growth improves. In general, these patients are symptomatic earlier in life than patients with only a primum ASD. The radiographic and electrocardiographic characteristics of patients with common atrium are indistinguishable from those with other forms of AVSD.

Echocardiography. The subcostal four-chamber imaging plane is most suitable for accurate diagnosis. A muscle bundle or band coursing through the atrium should not be misinterpreted as an atrial septum.

Cardiac Catheterization and Angiography. The hemodynamic diagnosis of common atrium depends on the demonstration of complete mixing of systemic and pulmonary venous blood. The oxygen saturations of pulmonary and systemic arterial blood are nearly identical. Pulmonary blood flow exceeds systemic flow, except in patients with severe pulmonary vascular obstructive disease. Right ventricular pressure is increased more often than in secundum ASD or partial AVSD. If definitive repair is delayed, significant pulmonary vascular obstructive disease may develop at an earlier age than in patients with isolated secundum ASD or partial AVSD.

Treatment. Prior to surgical repair, medical therapy usually is instituted when signs and symptoms of excess pulmonary blood flow and failure to thrive are present. Digoxin and diuretic therapy are traditional forms of therapy. Common atrium requires surgical repair, which should be performed early in life because patients usually have symptoms and there is a risk for early development of pulmonary vascular obstructive disease.

COMPLETE ATRIOVENTRICULAR SEPTAL DEFECT

Pathology

The complete form of AVSD is characterized by a large septal defect with interatrial and interventricular components and a common AV valve that spans the entire septal defect (30) (Fig. 29.14). The septal defect extends to the level of the membranous ventricular septum, which is usually deficient or absent.

The common AV valve has five leaflets. The posterior bridging leaflet drapes over the inlet ventricular septum and conceptually represents fusion of the septal tricuspid leaflet and the inferior half of the anterior mitral leaflet. Two lateral leaflets correspond to the posterior tricuspid and posterior mitral leaflets in a normal heart. The right-sided anterior leaflet, in essence, represents the normal anterior tricuspid leaflet, and the so-called anterior bridging leaflet corresponds to the superior half of the anterior mitral leaflet. The extent to which the anterior bridging leaflet actually straddles into the RV varies considerably and has formed the basis for a classification system of complete AVSD into types A, B, and C (see below). The common AV valve may be divided into distinct right and left orifices by a tongue of tissue that connects the two bridging leaflets, representing the rare intermediate form of complete AVSD.

Beneath the five commissures are five papillary muscles. The two left-sided papillary muscles are oriented closer together than in a normal heart, such that the lateral leaflet is smaller than a normal posterior mitral leaflet. In addition, the two papillary muscles often are rotated counterclockwise, such that the posterior muscle is farther from the septum than normal and the anterior muscle is closer to the septum. This papillary muscle arrangement, in conjunction with prominence of an anterolateral muscle bundle, may contribute to progressive LVOT obstruction. Moreover, the leaflets are prone to develop progressive regurgitation and, with time, they become thickened and exhibit hemodynamic and structural changes similar to that associated with mitral valve prolapse (31).

The potential for interventricular shunting exists along the septal surface between the two bridging leaflets and at the interchordal spaces beneath the leaflets. The posterior bridging leaflet characteristically overhangs the ventricular septum and has extensive septal chordal attachments. Occasionally, chordal fusion obliterates the interchordal spaces beneath this leaflet. The anatomic relationship between the anterior bridging leaflet and the ventricular septum is variable and forms the basis for a classification described by Rastelli et al. (32) (Fig. 29.15).

Rastelli Classification for Complete Atrioventricular Septal Defect

Giancarlo Rastelli died in 1970 at 36 years of age (33). During his abbreviated life and brilliant but short career, he made many landmark contributions to the field of congenital heart disease. In the 1960s, he devoted much of his time to obtaining a better understanding of the morphology of the common AV valve in patients with AVSD. The classification scheme that now bears his name was based on the morphology of the anterior bridging leaflet. The improved understanding of the AV valve diversity aided surgeons and improved operative mortality for these patients. Prior to 1964, hospital mortality for patients with AVSD was 60%. Rastelli et al. (34) from the Mayo Clinic published their work in 1968 and operative mortality between 1964 and 1967 decreased to 20%. The classification scheme that Rastelli described is listed below and summarized in Table 29.2.

In type A (most common), the anterior bridging leaflet inserts entirely along the anterosuperior rim of the ventricular

septum. It forms a true commissure with the right-sided anterior leaflet. Beneath this commissure is either a distinct medial papillary muscle or, more commonly, multiple direct chordal insertions along the septum. Interventricular communication beneath the anterior bridging leaflet may be minimal or absent in some cases owing to extensive interchordal fusion.

In type B (least common), the anterior bridging leaflet is larger and the right-sided anterior leaflet is smaller than in type A. As a result, the bridging leaflet straddles the septum and is associated with papillary muscle attachment along the septal or moderator band in the RV. Because chordal anchors are not present between the anterior bridging leaflet and the underlying ventricular septum, free interventricular communication exists.

In type C, the anterior bridging leaflet is larger than in type B, and its medial papillary muscle attachments fuse to the right-sided anterior papillary muscle. As a result, this leaflet is generally very small. Because the anterior bridging leaflet is not attached to the ventricular septum, free interventricular communication is possible, and the leaflet has been described as “free floating.”

The subtype of complete AVSD has some bearing on the likelihood of associated lesions. Type A usually is an isolated defect and is frequent in patients with Down syndrome. In contrast, type C is encountered with other complex anomalies, such as tetralogy of Fallot, double-outlet RV, complete transposition of the great arteries, and heterotaxy syndromes (35,36). Coronary artery anomalies, when they occur, tend to be associated with coexistent conotruncal malformations rather than the AVSD. The combination of type C complete AVSD with tetralogy of Fallot is observed in patients with Down syndrome, whereas double-outlet RV is a feature of patients with asplenia.

Clinical Manifestations

Tachypnea and failure to thrive invariably occur early in infancy as a result of excessive pulmonary blood flow. Virtually all patients with complete AVSD have symptoms by 1 year of age. If these symptoms do not develop early on, the clinician should suspect premature development of pulmonary vascular obstructive disease. AV valve regurgitation compounds these problems. After surgical repair, left AV valve regurgitation is the most common reason for reoperation. A recent study demonstrated that 22% of patients who had undergone repair of complete AVSD had more than moderate left AV valve regurgitation at 6 month follow-up (2). Although single-center reports have identified preoperative AV valve regurgitation as an important risk factor for reoperation (37), it failed to predict greater than moderate postoperative AV regurgitation in the PHN study (2). Greater than moderate AV valve regurgitation within 1 month of surgery was a strong predictor of persistent AV regurgitation at 6 month follow-up. Regression of postoperative left AV valve regurgitation was not demonstrated in that study (2) in contrast to anecdotes that this occurs.

If severe pulmonary vascular obstructive disease is absent, there may be no systemic arterial oxygen desaturation. The physical examination demonstrates a hyperactive precordium and an accentuated first sound, and the second sound may move with respiration but it is quite variable. Because of elevated pulmonary artery pressures, the pulmonary closure sound is accentuated. A loud S1-coincident holosystolic murmur can be heard along the lower left sternal border and at the cardiac apex if left AV valve regurgitation is present. A separate crescendo-decrescendo systolic ejection murmur is heard over the upper left sternal border as a result of increased pulmonary blood flow. A middiastolic murmur can be heard along the lower left sternal border and frequently at the apex

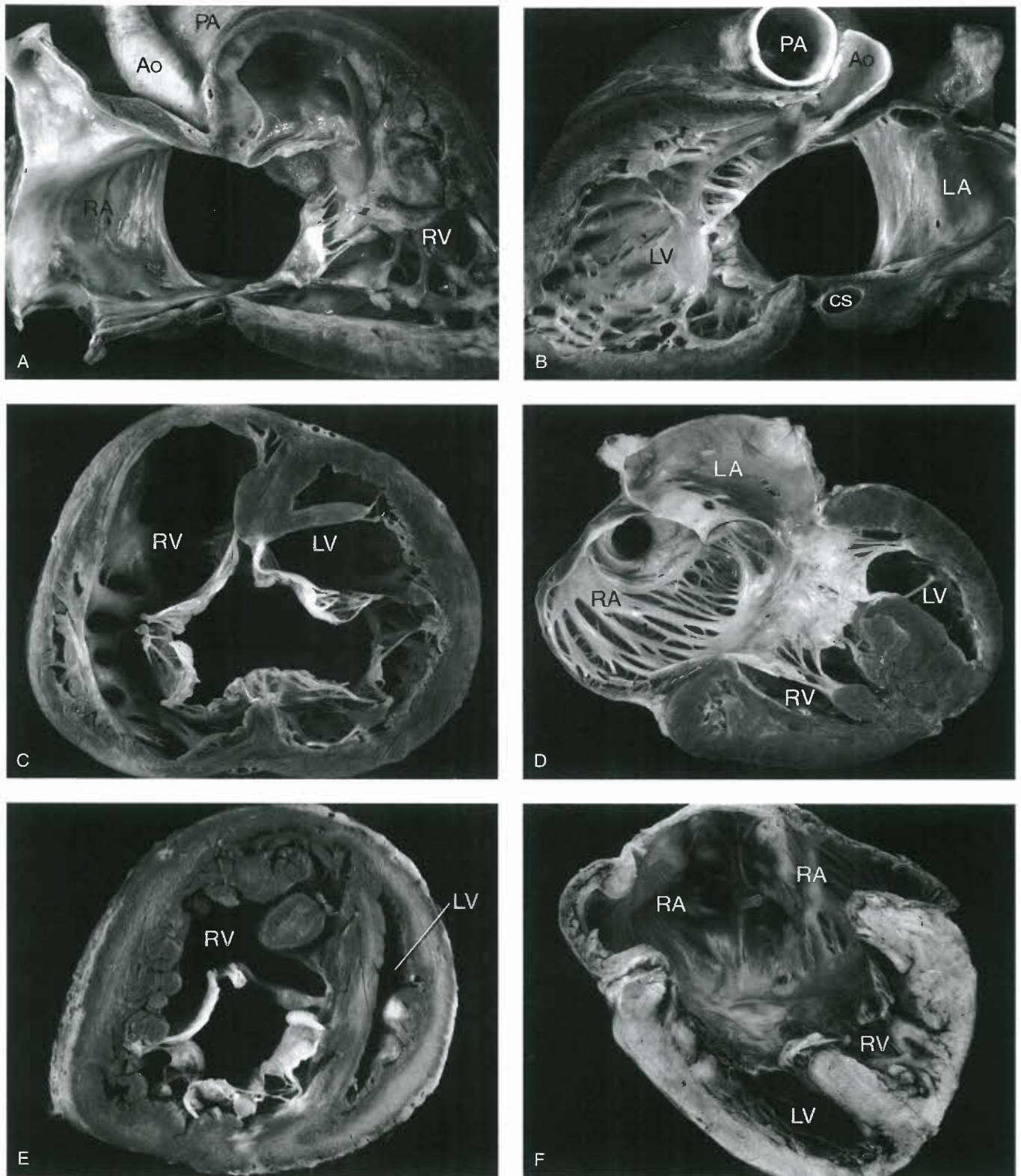


Figure 29.14. Complete AVSD. **A:** Right anterior oblique view with right atrial and right ventricular free walls removed, demonstrating a large septal defect. **B:** Left posterior oblique view (same specimens as in **A**) with left atrial and left ventricular free walls removed, showing the same septal defect. **C:** Short-axis view, illustrating a type A common AV valve with five leaflets. **D:** Four-chamber view, showing secondary right ventricular hypertrophy and right atrial dilation. **E:** Short-axis view of a biventricular specimen removed during cardiac transplantation, showing an unbalanced form of AVSD with dilation of a common inlet RV, leftward septal bowing, and a hypoplastic LV. **F:** Four-chamber view of a complete AVSD associated with right atrial isomerism, mirror-image ventricles (L-loop ventricular inversion), and asplenia. Ao, aorta; CS, coronary sinus; LA, left atrium; LV, left ventricle; PA, pulmonary artery; RA, right atrium; RV, right ventricle.

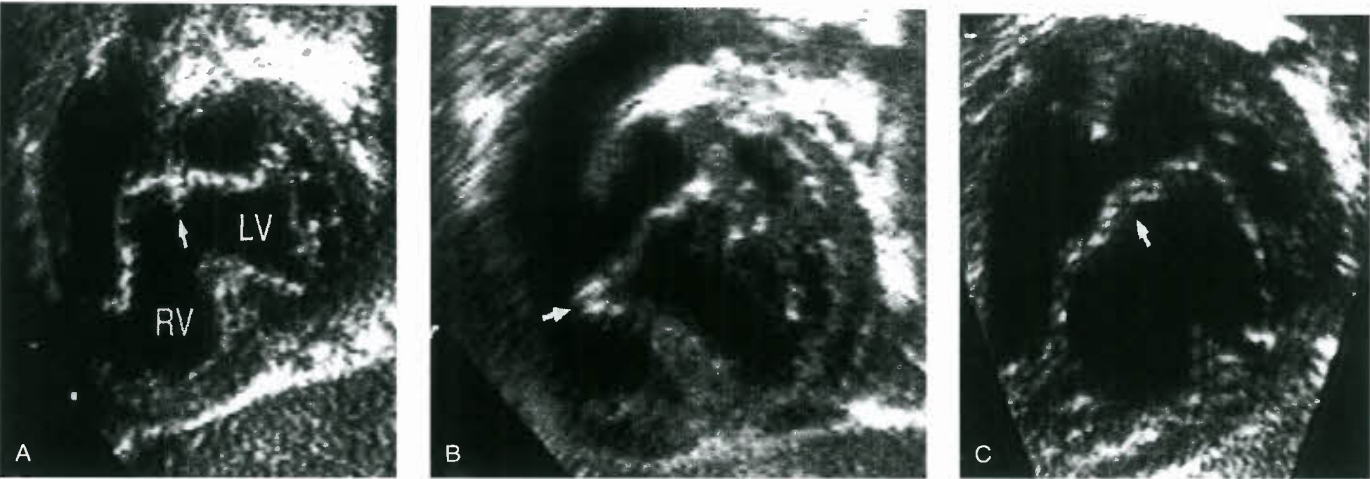


Figure 29.15. Anatomic and echocardiographic features of complete AVSD based on the Rastelli Classification. A: Type A complete AVSD. The defect is characterized by insertion of the anterior bridging leaflet to the crest of the ventricular septum (VS). B: Type B complete AVSD. The defect is characterized by dominant insertion of the anterior leaflets into papillary muscles in the RV. In this example, the anterior bridging leaflet inserts onto the crest of the ventricular septum, as well as onto a large ventricular papillary muscle (P) (arrow in echocardiogram). C: Type C AVSD. The anterior leaflet is unattached (arrow) and overrides the crest of the ventricular septum. The free anterior leaflet does not insert onto the crest of the ventricular septum. A, anterior; P, posterior; L, left; LA, left atrium; LV, left ventricle; R, right; RA, right atrium; S, superior. (Modified from Seward JB, Tajik AJ, Edwards WD, et al. *Two-Dimensional Echocardiographic Atlas. Vol. 1. Congenital Heart Disease.* New York, NY: Springer-Verlag, 1987:270–292, with permission.)

as a result of increased blood flow across the common AV valve. However, the physical examination findings of complete AVSD may be indistinguishable from those of an uncomplicated large VSD or partial AVSD.

Echocardiography

Two-dimensional echocardiography is the primary diagnostic tool for evaluation of complete AVSD (19,20,38). As described earlier, assessment of the internal cardiac crux from the apical and subcostal four-chamber projections provides excellent detail of the size and locations of defects in both the atrial and ventricular septa (Fig. 29.16). Additional secundum ASD, a fairly common associated finding, can be detected from the subcostal four-chamber coronal view and with clockwise rota-

tion of the transducer from the subcostal sagittal imaging plane (21). The VSD is located posteriorly in the inlet septum. Both right- and left-sided components of the common AV valve are displaced toward the ventricles and are associated with variable deficiency of the inflow ventricular septum. A PDA is a common associated finding. In the PHN report, 44% of patients had PDA ligation at the time of AVSD repair. Suprasternal notch and high left parasternal imaging should be performed to evaluate the PDA. However, in the setting of massive pulmonary blood flow from a complete AVSD, aliased color Doppler signals in the branch pulmonary arteries may make small PDAs difficult to appreciate. Fortunately, surgeons routinely check for ductal patency at the time of AVSD repair. Spectral and color Doppler serve as adjuncts to assess the sites of shunting, severity of AV valve regurgitation, and connections of the pulmonary veins. Fetal echocardiography readily detects complete AVSD in standard four-chamber views (Fig. 29.17).

When communicating with a surgeon, the echocardiographer must describe the morphology of the AV valve in precise detail. The surgeon needs to know the competence and ventricular commitment of the AV valve orifices and whether a tongue of tissue connects the superior and inferior bridging leaflets to form two distinct orifices. The subcostal *en face* view is essential for this determination. This view is obtained with counterclockwise rotation from the four-chamber coronal view until the AV valve leaflets appear *en face* (Fig. 29.18). Deliberate superior and inferior angulation of the probe will permit inspection of the cross section of all five valve leaflets. The valve is inspected from the inferior margin of the atrial septum to the superior margin of the ventricular septum (38). In the operating room, the TEE transgastric short-axis view will aid in this assessment.

A single left ventricular papillary muscle may occur in complete AVSD. Similar to the double-orifice valve, a single papillary muscle will reduce the effective valve area and complicate the surgical repair. Left AV valve repair may be

TABLE 29.2 Rastelli Classification for Complete AVSD	
Rastelli Type	Anterior Bridging Leaflet and Chordae
A	Divided and attached to crest of ventricular septum. Multiple chordae.
B	Partly divided, not attached to crest of the septum. Chordae attach to papillary muscle in RV usually on septal surface
C	Not divided and not attached to the crest of the septum (“free floating”). Chordae attach to papillary muscle on RV free wall

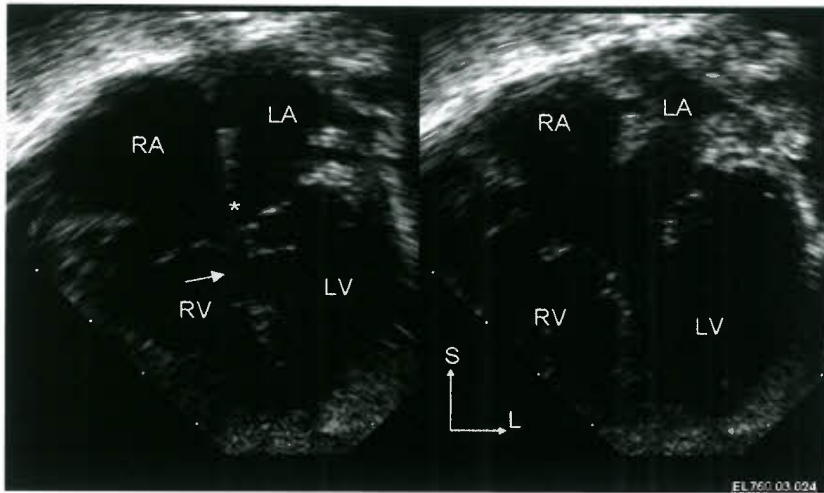


Figure 29.16. Complete AVSD: Apical four-chamber images in systole (left) and diastole (right) demonstrating a complete AVSD with large primum ASD (*asterisk*), large inlet VSD (*arrow*), and common single-orifice AV valve. The **right panel** demonstrates the valve opening as a single unit with only lateral “hinge points” visible in this image. Biventricular volume overload and a small secundum ASD are present in this patient.

compromised further by relative leaflet hypoplasia. Echocardiographic imaging techniques for this abnormality are similar to those for double-orifice left AV valve.

The Concept of “Balance”

Two-dimensional echocardiography is essential for determining the relative sizes of the ventricles. In AVSD, the AV valves (regardless of number of orifices) may be more committed to one ventricle at the expense of flow into the other. This will lead to relative hypoplasia of the underperfused ventricle. Both partial and complete AVSDs can be “balanced” or “unbalanced” based on how the AV junction is shared by the ventricles. If the AV inlet is equally shared by both ventricles, then this is consistent with a “balanced” AVSD.

In *unbalanced* AVSD, one ventricle is typically hypoplastic, although the common AV valve is its usual size (Fig. 29.19). The larger ventricle is termed the “dominant” ventricle. Unbalanced AVSD occurs in approximately 10% of all AVSDs. Two-thirds of unbalanced AVSDs are right ventricular dominant. When the RV is dominant, the LV is hypoplastic, and more than half of the AV junction is committed to the RV. These patients frequently have severe coarctation of the aorta and aortic arch anomalies. Conversely, unbalanced AVSD with a dominant LV has a hypoplastic RV and is associated with

pulmonary valve stenosis or atresia. Interestingly, in children with Down syndrome and unbalanced AVSD, left ventricular dominance is common.

With standard 2-D echocardiographic imaging, both ventricles are appreciated from the apical four-chamber view. This imaging plane allows visualization of malalignment between the atrial and ventricular septa. This can be a clue to an unbalanced AVSD. The subcostal sagittal view gives an estimate of the proportion of the AV valve committed to each ventricle. Determining “balance” with echocardiographic imaging is important as it forms the basis for deciding single-ventricle versus biventricular surgical repair. Modest degrees of right ventricular hypoplasia also may be addressed with a “1.5-ventricle repair.” In this situation, intracardiac shunts are repaired and the RV is unloaded by performing a bidirectional cavopulmonary connection.

Cohen et al. (39) (Fig. 29.20) proposed a quantitative approach using the subcostal sagittal view to delineate cases with significant left ventricular hypoplasia that may be better treated with a single-ventricle approach. They measured the area of the AV valve apportioned over each ventricle and calculated an AV valve index (AVVI). This serves as an LV/RV area ratio. The AVVI may be used as the basis for an algorithm to stratify patients into a single-ventricle versus a two-ventricle surgical pathway. Those with an AVVI <0.67 who have a large VSD would be considered for the single-ventricle pathway.



Figure 29.17. A 31-week gestation fetal echocardiogram with severe common AV valve regurgitation: four-chamber images in diastole (left), systole (center), and systole with color Doppler (right) demonstrating a common atrium, common AV valve, and common ventricle. After delivery, this child was found to also have asplenia.

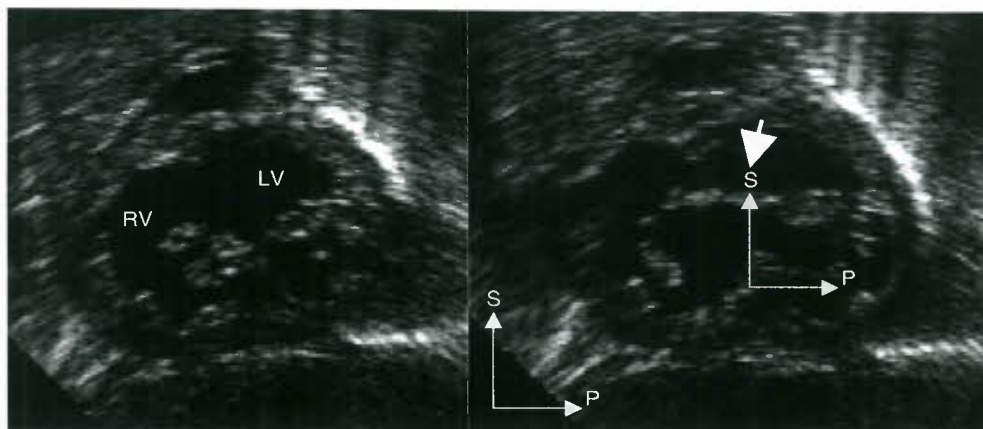
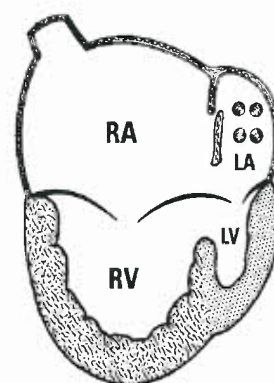
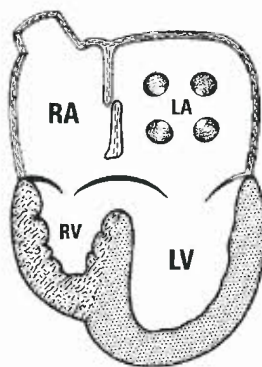


Figure 29.18. Subcostal sagittal imaging of common AV valve: Subcostal sagittal images in systole (left) and diastole (right) in a patient with complete AVSD. The right panel demonstrates the anterior bridging leaflet (arrow) of the common AV valve. This leaflet crosses (bridges) the VSD anteriorly and is shared by both ventricles. It is not divided into right and left components and has no attachments to the ventricular septum. This morphology is also called free floating or Rastelli type C. During repair, unlike the naturally divided anterior bridging leaflet (type A), this leaflet must be incised into right and left components before attachment to the VSD patch.

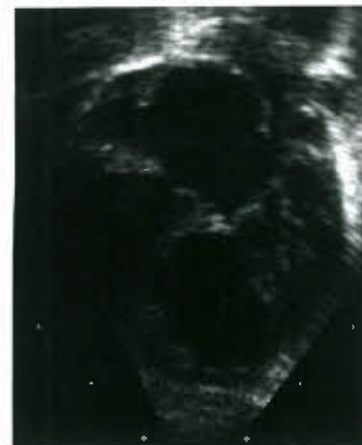
The clinician must be aware of several caveats that may make interpretation of “ventricular balance” less straightforward. For example, the severity of valve malalignment may not necessarily correlate with the degree of ventricular hypoplasia. Moreover, pulmonary venous blood preferentially crosses the ASD causing underfilling of the LV. Finally,

the presence of a large left-to-right shunt may cause severe right ventricular enlargement with bowing of the septum to the left. This will lend an appearance of “hypoplasia” to the LV. van Son et al. (40) attempted to estimate the “potential volume” of the LV preoperatively by using a theoretical model that calculates the relative areas of the LV and

Figure 29.19. Right versus left ventricular dominance, based on a classification scheme from Bharati and Lev: Left ventricular dominance (left panels) and right ventricular dominance (right panels) are demonstrated. In the LV-dominant case, the common AV valve opens predominantly into the LV. Conversely, in the RV-dominant case, the common AV valve opens predominantly into the RV. LA, left atrium; LV, left ventricle; RA, right atrium; RV, right ventricle.



LV Dominant



RV Dominant

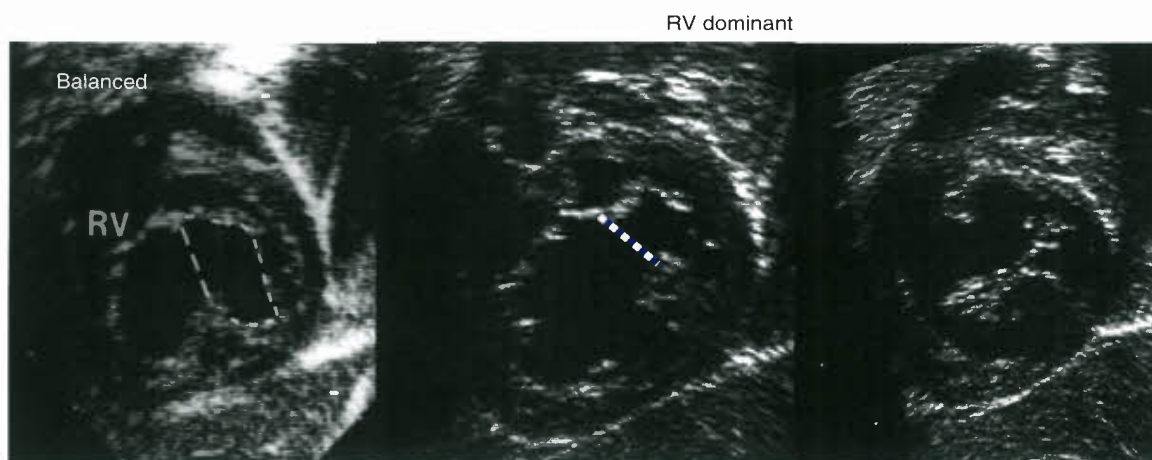


Figure 29.20. Echocardiographic assessment of ventricular dominance: Assessing unbalanced AVSDs using AV valve area measurements. **Left panel:** Diastolic frame from the subcostal sagittal plane demonstrating an en face view of the common AV valve. The planimetry demonstrates relative balance between the right and left portions of the common valve. **Center panel:** Diastolic frame demonstrating an RV-dominant unbalanced AVSD with relative dominance of the right portion of the common AV valve. **Right panel:** Companion systolic frame of an RV-dominant AVSD. (From Cohen M, Jacobs ML, Weinberg PM, et al. Morphometric analysis of unbalanced common atrioventricular canal using two-dimensional echocardiography. *J Am Coll Cardiol* 1996;28:1017, with permission.)

RV in short axis after assuming normal septal configuration (Fig. 29.21).

All of these methods should be employed when assessing a patient with an unbalanced AVSD. One must realize that none of these methods factor in patient/cardiac growth. It also is important to know if the LV is apex forming. Generally patients with

unbalanced AVSD may present many challenges both from the echocardiographic imaging and clinical management perspectives.

Radiography

The heart usually is enlarged in patients with complete AVSD. Enlargement of the RA is suggested by increased convexity of the right heart border, and left atrial enlargement may produce a characteristic flattening of the left heart border. The pulmonary artery is prominent, and the pulmonary vascular markings are increased.

Electrocardiography

Prolongation of the P-R interval is observed in approximately 25% of patients with AVSD (25). Intracardiac studies have revealed increased intra-atrial or AV node conduction times as the cause of P-R prolongation. More than 50% of patients meet voltage criteria for atrial enlargement. A superior or northwest QRS axis is common (Fig. 29.22). The QRS axis in the frontal plane lies between -60 degrees and -135 degrees, with most patients having an axis between -90 degrees and -120 degrees. Most patients have an rsR, RSR', or Rr' in lead V1, and others have a qR or R pattern in the same chest lead, all indicating right ventricular hypertrophy. Left ventricular hypertrophy may also be present.



Figure 29.21. Short-axis assessment of septal flattening in unbalanced AVSD. Due to right ventricular volume overload, the septum bows toward the LV. This may provide the misperception that the LV is hypoplastic. However, if one assumes normalization of septal position, the potential volume of the LV after repair may be predicted. (From van Son JAM, Phoon CK, Silverman NH, et al. Predicting feasibility of biventricular repair of right-dominant unbalanced atrioventricular canal. *Ann Thorac Surg* 1997;63:1657, with permission.)

Cardiac Catheterization and Angiography

Cardiac catheterization and angiography rarely are needed for management of infants with complete AVSD. In an older child, when pulmonary vascular obstructive disease is suspected, there is a role for determining pulmonary vascular resistance. Severe pulmonary vascular obstructive disease (pulmonary vascular resistance of >10 U·m²) is rare but has been reported in infants <1 year of age.

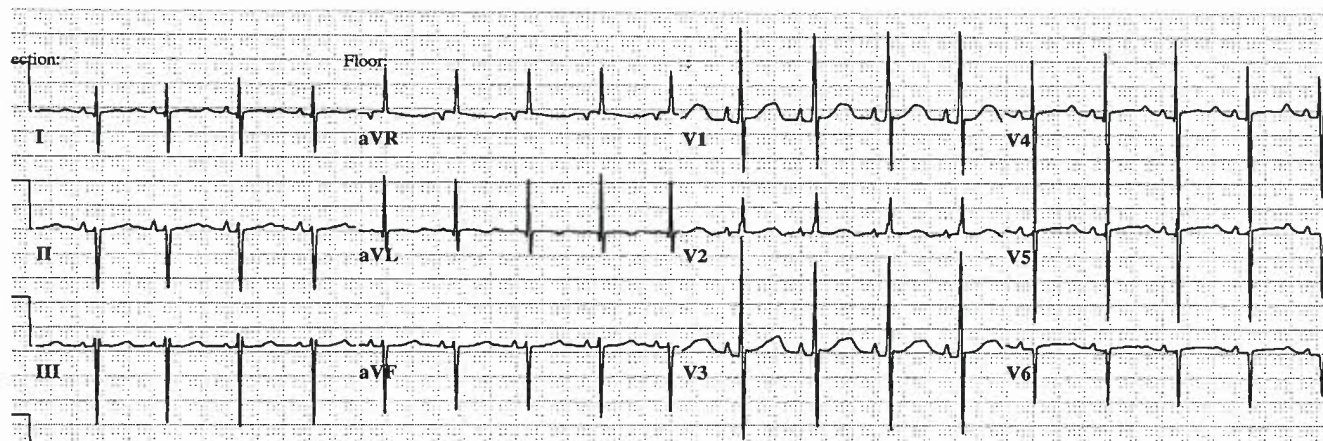


Figure 29.22. A 12-lead ECG from a 3-month-old with complete AVSD. Left axis deviation and right ventricular hypertrophy are present.

Cardiac catheterization demonstrates increased oxygen saturation at both the right atrial and the right ventricular levels. In complete AVSD, pulmonary artery systolic pressure invariably is at or near systemic level. However, in partial AVSD, pulmonary artery systolic pressure usually is <60% of systemic pressure. Pulmonary blood flow is increased as a result of left-to-right shunting at both atrial and ventricular sites, and the degree of shunting depends upon the relationship of pulmonary to systemic vascular resistance. The hemodynamic abnormality in complete AVSD may be complicated by severe common AV valve regurgitation, allowing blood to shunt freely among all cardiac chambers. Left ventricular angiography rarely is required but reveals the typical LVOT gooseneck deformity and varying severity of left AV valve regurgitation.

Clinical Course

Infants with complete AVSD typically will require medical therapy with diuretics, sometimes augmented with digoxin or angiotensin-converting-enzyme inhibitors depending on the specific clinical situation. The timing of surgical intervention must take into account the propensity of pulmonary vascular disease to develop in these patients at an early age. The decision for operation is usually made in the first 6 months of life. Children with complete AVSD frequently have surgical repair between 3 and 6 months of age. But, children with Down syndrome may require surgical intervention at an earlier age due to their propensity to develop pulmonary vascular obstructive changes.

Special Forms of Complete Atrioventricular Septal Defect

Intermediate Defect

A rare subtype of complete AVSD occurs when the anterior and posterior bridging leaflets are fused atop the ventricular septum and the common AV valve is divided into distinct right and left orifices. This defect usually has a large primum ASD and a large inlet VSD. Patients present in the same manner as with other forms of complete AVSD. Surgical repair does not have to include division of separate right

and left AV valve components (this has occurred naturally). The cleft in the left AV valve is closed, but the bridging leaflets often have insufficient tissue to reconstruct a competent anterior leaflet.

Down Syndrome and Atrioventricular Septal Defect

Down syndrome occurs in more than half of patients with complete AVSD. Children with Down syndrome and complete AVSD also are more likely to have associated tetralogy of Fallot (41,42). In contrast, sidedness (situs) and splenic anomalies are rare in patients with Down syndrome. Patients with Down syndrome usually do not have associated LVOT obstruction, left ventricular hypoplasia, coarctation of the aorta, or additional muscular VSDs (43,44). In cases with unbalanced AVSD, patients with Down syndrome have LV dominant morphology more frequently than RV dominance.

The extent and progression of pulmonary vascular changes in children with Down syndrome and complete AVSD remain controversial. Histologic studies (45) have failed to show any differences in the extent of pulmonary vascular changes when patients with Down syndrome were compared with normal children who also had AVSD. Other studies (46,47) have suggested that children with Down syndrome have relative pulmonary parenchyma hypoplasia and develop pulmonary vascular obstructive disease appreciably earlier than patients with normal chromosomes and complete AVSD.

The hemodynamic assessment of children with Down syndrome must take into account that these patients may have chronic nasopharyngeal obstruction, relative hypoventilation, and sleep apnea. These factors contribute to carbon dioxide retention, relative hypoxia, and elevated pulmonary vascular resistance.

Patients with Down syndrome have a higher ratio of pulmonary to systemic resistance than patients without Down syndrome (48). This difference resolves with administration of 100% oxygen, suggesting that apparent hypoxia and hypoventilation are factors that can be corrected during hemodynamic study. Fixed and elevated pulmonary vascular resistance has been demonstrated in 11% of Down syndrome patients <1 year of age (48). In the current era, timing of repair and surgical outcome for patients with Down syndrome are similar to those of the general population (2,49).

INITIAL SURGICAL TREATMENT OF AVSD

Partial Atrioventricular Septal Defect

The objectives of surgical repair include closure of the interatrial communication and restoration and preservation of left AV valve competence. These objectives can be accomplished by careful approximation of the edges of the valve cleft with interrupted nonabsorbable sutures. On occasion, it is necessary to add eccentric annuloplasty sutures, typically in the area of the commissures to correct persistent central leaks. The repair is completed by closure of the interatrial communication (usually with an autologous or bovine pericardial patch), avoiding injury to the conduction tissue (50). This repair results in a two-leaflet valve. Rarely, if the left AV valve is considered a trileaflet valve, with the cleft viewed as a commissure, the commissure may be left unsutured and annuloplasty sutures can be placed to promote coaptation of the three leaflets. In the recent PHN study, the cleft was closed in 98% of cases (1).

However, the morphologic concepts and surgical methods favored by Carpentier (51) and Piccoli et al. (52) continue to be debated. The PHN investigators could not demonstrate that annuloplasty decreased the prevalence of left AV valve regurgitation 6 months after surgery. In that study, 18 of 59 patients (31%) who had 6 month postoperative echocardiography data available demonstrated moderate or greater left AV valve regurgitation (1). Because the details of annuloplasty were not available in all operative reports, the PHN study loosely defined “annuloplasty” as any additional intervention on the left AV valve beyond cleft closure. This limits the ability to assess specific surgical techniques. At Mayo Clinic, the left AV valve cleft is usually closed and, if needed, limited annuloplasty sutures are placed near the commissures to improve valve competence.

The risk of hospital death after surgical repair of partial AVSD is approximately 1% (1). The timing of repair for partial AVSD trended to an earlier age in the PHN study. The median age of repair for patients with partial AVSD was 1.8 years. Long-term survival after repair of partial AVSD is good. In a series of 334 patients from Mayo Clinic, 20- and 40-year survivals after repair of partial AVSD were 87% and 76%, respectively (53). Closure of the left AV valve cleft and age <20 years at time of operation were associated with improved survival. Reoperation was performed for 11% of these patients. Repair of residual/recurrent left AV valve regurgitation or stenosis was the most common reason for reoperation (53). In the PHN study, residual ASD shunts (<1%) and left AV valve stenosis (1%) were rare (1). Residual left AV regurgitation remains the major reason for reoperation. In that study, 31% of patients had at least moderate regurgitation 6 months after surgery for partial AVSD repair. Repair after age 4 years was a risk factor for residual moderate-severe left AV valve regurgitation (1).

A low frequency of postoperative arrhythmias has been noted. The finding of surgical complete heart block has been uncommon and would require permanent pacemaker implantation. Late onset of atrial flutter has been rarely encountered.

Complete Atrioventricular Septal Defect

Surgical repair of complete forms of AVSD is indicated early in life. The median age at time of repair in the recent multicenter report was 3.6 months (2). Repair of complete AVSD must be performed prior to the development of irreversible pulmonary vascular obstructive disease. Repair typically is performed between 3 and 6 months of age. Earlier repair should be considered for infants with failure to thrive.

For the symptomatic infant, surgical options include palliative pulmonary artery banding or complete repair of the anomaly. Silverman et al. (54) reported excellent results of pulmonary artery banding in 21 infants with complete AVSD who were <1 year of age. In that series, there was one surgical death (5%), and the remaining patients had excellent palliation. Williams et al. (55) recommended pulmonary artery banding for infants weighing <5 kg who were unresponsive to medical treatment or had significant associated anomalies. In the modern era, most centers perform complete repair in small infants who fail to thrive. This approach has largely obviated the need for pulmonary artery band placement. Investigators in the PHN study found that age at repair <2.5 months frequently was associated with concurrent procedures that likely drove the early timing of surgery. In that study, infants who required early repair had similar outcomes in respect to residual shunts and severity of left AV valve regurgitation, but they were more likely to require circulatory arrest, prolonged intensive care unit stays, and increased duration of hospitalization due to their comorbidities (2).

The objectives of surgical repair include closure of interatrial and interventricular communications, construction of two separate and competent AV valves from available leaflet tissue, and repair of associated defects. Techniques for the surgical repair of complete AVSD have been standardized and are based on the use of a single patch or double patch (separate atrial and ventricular patches) to close the ASD and VSD and then reconstruction of the left AV valve as a bileaflet valve. (Figs. 29.23, 29.24) Puga and McGoon (56) have described these techniques in detail. Piccoli et al. (52) and Studer et al. (57) consider the cleft of the left AV valve to be a true commissure and envisioned this valve as a trileaflet valve. On the basis of these concepts, Carpentier (51) preferred the two-patch technique and the left AV valve remained a trileaflet structure (Fig. 29.25). More recently, the “Australian” single-patch technique with primary suture closure of the VSD and pericardial patch closure of the ASD has been described (58,59).

Investigators in the PHN study evaluated the various surgical techniques utilized to repair complete AVSD (2). In that study, the cleft was closed in 93% of cases. The two-patch technique was used in 72% of cases, the single-patch technique in 18%, and the Australian repair in 10%. Choice of repair depended on surgeon/center preference. The Australian technique was used in younger patients and required return to cardiopulmonary bypass (CPB) more frequently than the single- or two-patch techniques. The single-patch technique had longer CPB and aortic cross-clamp times but no patients repaired with this technique needed to return to CPB. Operative mortality, hospital stay, residual shunt, and significant left AV valve regurgitation were similar with all techniques (2).

In the modern era, hospital mortality was 2.5% (2). Left AV valve regurgitation was the most common reason for reoperation and occurred in 4% of cases within 6 months of initial repair. Similar to previous reports, approximately 25% of patients had at least moderate residual left AV valve regurgitation. Residual shunts were rare and usually closed spontaneously within 6 months.

At most centers, the current approach is to offer repair for complete AVSD at age 3 to 6 months. If a child is failing to thrive or has excessive pulmonary blood flow or heart failure, repair is offered at an earlier age. Surgeons at many North American centers prefer to utilize a two-patch technique thereby avoiding division of the bridging leaflets (60) (Figs. 29.23 and 29.24). If the VSD is shallow, a single-patch technique is considered with primary VSD closure (Australian technique) (Fig. 29.25). The left AV valve cleft typically is closed and eccentric annuloplasty sutures are utilized to gain valve competence. Intraoperative TEE is utilized in all AVSD cases. If TEE demonstrates more than mild left AV valve regurgitation, then CPB is resumed and aggressive attempts are made to improve valve competency (61).

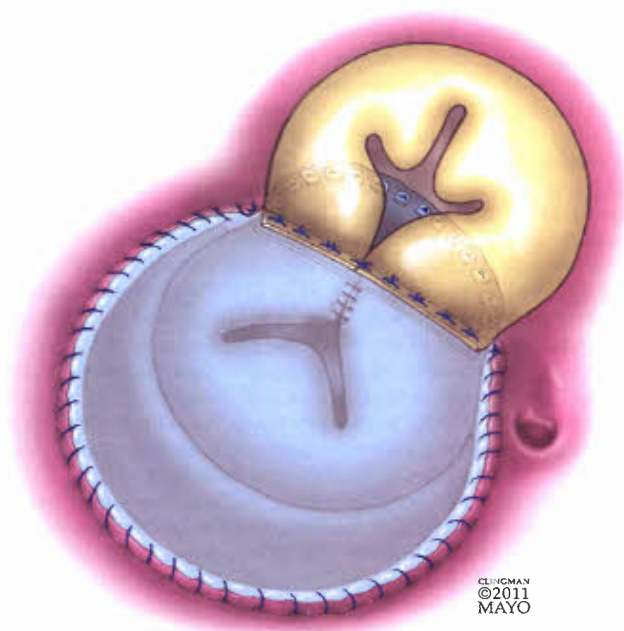


Figure 29.23. The traditional *single-patch* repair of complete AVSD (surgical view from the RA). Note that one patch is utilized to close both the VSD and ASD. The ventricular component of the single patch is seen deep to the AV valves. This patch is positioned by dividing the bridging leaflets. Once the patch is sutured into place, the bridging leaflets are resuspended to the patch. The cleft in the left AV valve has been closed.

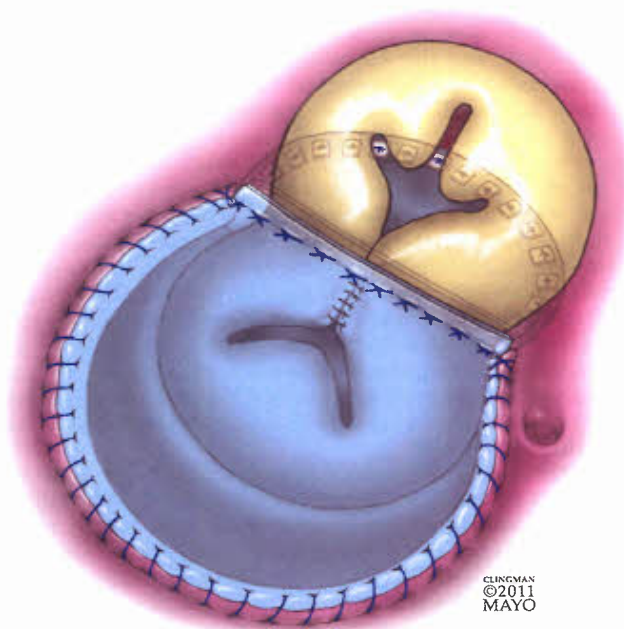


Figure 29.24. The *two-patch* technique for complete AVSD (surgical view from the RA). The first patch is utilized to close the VSD and is demonstrated deep to the AV valves. The bridging leaflets are *not* divided. Once the VSD patch is placed and the cleft is repaired, a second patch is utilized for ASD repair.

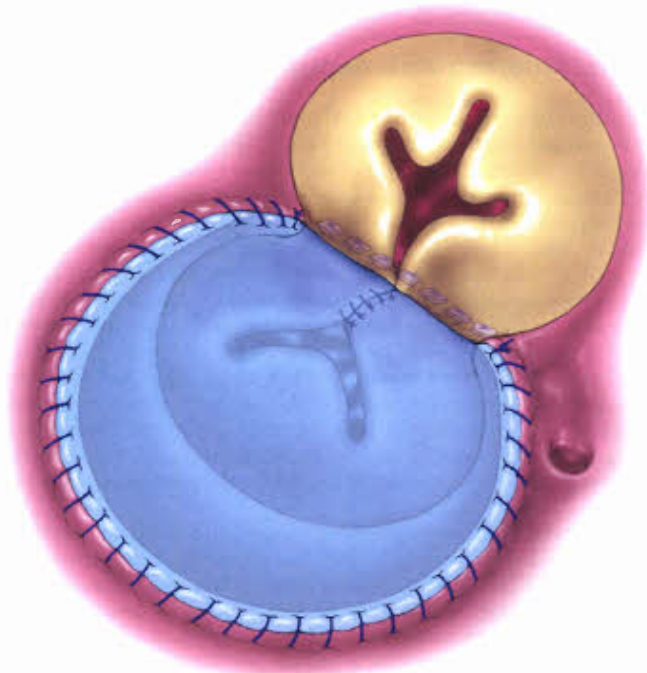


Figure 29.25. The modified single-patch or *Australian technique* (surgical view from the RA). The bridging leaflets are sutured down directly to the VSD crest. Note that the AV valve leaflets appeared "tucked" to the crest of the septum. Once this is performed, a single patch is utilized to repair the remaining ASD.

Special Problems in Complete AVSD Surgery

Parachute Deformity of the Left AV Valve. This problem has been addressed by David et al. (62). With such a deformity, closure of the cleft at the time of repair may result in an obstructed orifice. If the patient has significant left AV valve regurgitation with a parachute deformity, then valve replacement may be the only suitable option.

Double-Orifice Left AV Valve. The surgeon must resist the temptation to join the two orifices by incising the intervening leaflet tissue. The combined opening of both orifices is satisfactory for adequate left AV valve function (63).

Right or Left Ventricular Hypoplasia. These anomalies may be severe enough to preclude septation. The only option for definitive surgical treatment is the modified Fontan procedure preceded by adequate pulmonary artery banding in infancy (64).

Tetralogy of Fallot. In patients with this anomaly, all of whom have complete AVSD, the infundibular septum is displaced anteriorly, so that the inlet VSD extends anteriorly and superiorly toward the perimembranous area. In tetralogy of Fallot, there is obstruction of the right ventricular outflow tract. These cyanotic infants often initially are treated with a systemic-to-pulmonary artery shunt and then with "complete repair" at 2 to 4 years of age. The intracardiac repair of these hearts is best accomplished through a combined right atrial and right ventricular approach (42).

Subaortic Stenosis. If discovered at the time of initial preoperative evaluation, subaortic stenosis tends to be of the fibromuscular membrane type and should be treated by appropriate resection during surgical repair. However, subaortic stenosis may appear late after surgical repair of AVSD. The

stenosis may be related to the uncorrected deficiency in the inlet septum. The obstruction usually is due to the formation of endocardial fibrous tags and fibromuscular ridges. Usually it can be treated by local resection, although in some patients, a modified Konno procedure may be necessary (65–68).

REOPERATION AFTER REPAIR OF ATRIOVENTRICULAR SEPTAL DEFECT

Partial Atrioventricular Septal Defect

Late reoperation following repair of partial AVSD may be required for regurgitation or stenosis of the left AV valve, subaortic stenosis, regurgitation of the right AV valve, or residual ASD. Reoperation for left AV valve regurgitation occurs in 10% to 15% of survivors of primary repair of partial AVSD. Risk factors for reoperation include significant residual left AV valve regurgitation as assessed intraoperatively at the time of initial repair, the presence of a severely dysplastic valve, and failure to close the cleft in the anterior (septal) leaflet. Repeat valve repair is possible if the dysplasia is not severe or when the mechanism of regurgitation is through a residual cleft. Eccentric commissural annuloplastic sutures often are needed to correct central regurgitation. Replacement of the valve may be required in the presence of a severe dysplasia.

Reoperation for left AV valve stenosis may be necessary if the valve orifice is hypoplastic, or if the orifice is restricted owing to a parachute deformity of the subvalvular apparatus. Patient–prosthetic mismatch in patients who required valve replacement during infancy or early childhood will merit valve re-replacement. Relief of prosthetic left AV valve stenosis resulting from a small annulus is technically challenging. The small valve requires replacement with a larger prosthesis, and there are no reliable techniques for annular enlargement. Thorough debridement and excision of fibrous scar and old prosthetic material is necessary. In rare circumstances, the new larger prosthesis is sewn into the LA in a supra-annular position.

Late LVOT obstruction owing to subaortic stenosis occurs more frequently after correction of partial AVSD than with complete AVSD. This is likely due to the fact that during the conventional repair, the deficient portion of the inlet ventricular septum is not reconstructed so that the anterior (septal) leaflet of the left AV valve hinges on the line of fibrous fusion to the crest of the ventricular septum. Thus, the standard surgical repair does not modify the elongated and potentially narrowed LVOT. This is in contrast to complete AVSD in which the deficient inlet septum is reconstructed with the subvalvular patch that effectively widens the outflow tract. Relief of LVOT obstruction can be accomplished in several ways, including transaortic resection of the fibrous or fibromuscular membrane

and patch enlargement of the LVOT with a transaortic and right ventricular approach (modified Konno procedure). Others have described alternative approaches, including reconstruction of the deficient inlet septum, septal myectomy, and apicoaortic conduits (65–68). Reoperation for an isolated residual or recurrent ASD is rare after repair of partial AVSD.

Stulak et al. (69) recently reported the Mayo Clinic experience with 93 patients who had reoperation after initial repair of partial AVSD. Average time to reoperation was 10 years. The most common indications for reoperation were left AV valve regurgitation (67%), subaortic stenosis (25%), right AV valve regurgitation (22%), and residual ASD (11%). Reoperations included left AV valve repair or replacement, subaortic resection, and right AV valve repair. There was no difference in survival when comparing left AV valve repair (38 patients) with replacement (35 patients).

Complete Atrioventricular Septal Defect

Late reoperation following repair of complete AVSD occurs in approximately 20% of patients during the first 20 years after surgical repair. Lesions requiring reoperation include left and right AV valve regurgitation, left AV valve stenosis (native and prosthetic), and residual ASDs or VSDs.

Residual left AV valve regurgitation may result from inadequate surgical reconstruction. Intraoperative TEE helps guide the surgical repair thereby preventing patients from leaving the operating room with significant residual left AV valve regurgitation. Right AV valve regurgitation requiring reoperation is rare after repair of complete AVSD. It occurs in the presence of pulmonary hypertension or in association with tetralogy of Fallot with right ventricular dysfunction and pulmonary valve regurgitation or stenosis. Residual shunts are rare causes for late reoperation after initial repair of complete AVSD.

Investigators at the Mayo Clinic recently assessed reoperation in 50 patients after repair of complete AVSD (70). The most common indication for reoperation was left AV valve regurgitation (41 patients). Similar to the PHN data, left AV valve stenosis was rare (1 patient). Half of this cohort underwent left AV valve re-repair and the other half had valve replacement. Long-term survival was 86% at 15 years after the reoperation.

POSTOPERATIVE ECHOCARDIOGRAPHIC ASSESSMENT

Echocardiographic assessment of the patient after repair of an AVSD includes evaluation of the morphology of the AV valves (Fig. 29.26) and determination of right and left AV valve stenosis or regurgitation (71). A search for residual shunts should be performed. Doppler evaluation of the velocity profiles across a ventricular level shunt and right AV valve regurgitation can

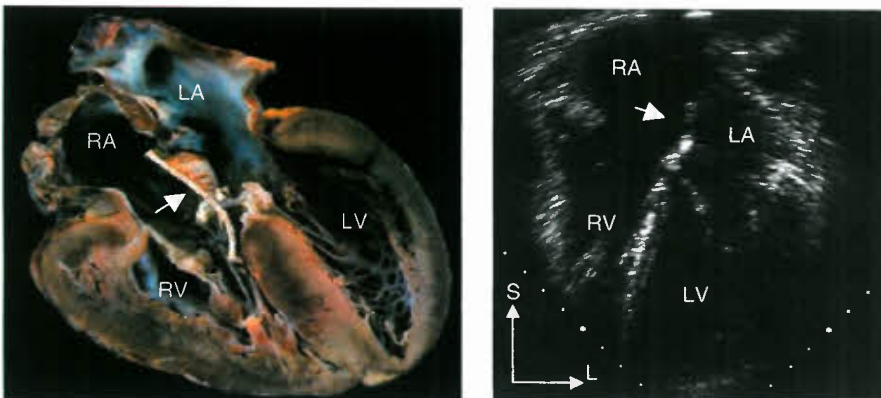


Figure 29.26. Left: Four-chamber anatomic specimen of a patient with partial AVSD after patch closure of a primum ASD and repair of a cleft mitral valve. The patch (arrow) is attached to the right side of the atrial septum and the right AV valve to avoid damage to the conduction tissue and left AV valve. Right: corresponding apical four-chamber echocardiograph. L, left; LA, left atrium; LV, left ventricle; RA, right atrium; RV, right ventricle; S, superior.

provide accurate determination of right ventricular systolic pressure. However, in the setting of a residual VSD, the VSD jet may contaminate the right AV valve regurgitation signal and preclude accurate quantification of right ventricular systolic pressure. In that setting, the echocardiographer should use indirect techniques such as assessment of ventricular septal flattening or bowing, right ventricular size and function, and Doppler interrogation of the pulmonary regurgitation velocity waveforms to assess pulmonary artery diastolic pressure. Meticulous assessment of progressive left AV valve regurgitation and progression of LVOT obstruction must be performed during serial postoperative evaluations.

THE ADULT WITH ATRIOVENTRICULAR SEPTAL DEFECT

Previously Undiagnosed Adults with Atrioventricular Septal Defect

When discovered in adulthood, patients with partial AVSD will present with symptoms of exercise intolerance, dyspnea on exertion, or palpitations from a new atrial arrhythmia. These patients may exhibit the typical physical exam findings of an ASD (systolic ejection murmur at the left upper sternal border, widely split and fixed second heart sound, and a diastolic rumble along the left sternal border due to increased flow across the right AV valve). Adults with previously undiagnosed partial AVSD may come to diagnosis when a chest x-ray or electrocardiogram is performed for other reasons. The chest x-ray may demonstrate cardiomegaly, and the electrocardiogram often shows left axis deviation. A regurgitant S1-coincident holosystolic murmur (due to the cleft in the anterior leaflet of the left AV valve) may also prompt echocardiographic evaluation. Left AV valve stenosis is a rare finding in adults with unrepaired partial AVSD. If left AV stenosis is present, these patients usually have a single papillary muscle and morphology of a parachute valve. Surgical repair of partial AVSD is recommended if discovered in adulthood in the absence of significant pulmonary hypertension.

Echocardiography of adults with AVSD should be performed in an imaging laboratory with extensive congenital heart disease experience. The role of cardiac catheterization for some patients is to evaluate coronary artery anatomy or for calculation of pulmonary vascular resistance. One would prefer the pulmonary arteriolar resistance (rPa) to be <7 units- m^2 to safely consider repair of a partial AVSD in adulthood. If the rPa is elevated above this level, then provocative testing in the catheterization laboratory with the use of pulmonary vasoactive agents such as nitric oxide is indicated. That said, patients with rPa as high as 15 units- m^2 have undergone successful surgery for isolated ASD (72). In this select group of patients, one would consider pre- and postoperative treatment with pulmonary vasoactive agents such as bosentan, sildenafil, or Flolan and documentation via hemodynamic catheterization of a substantial improvement in rPa during this therapy. In patients older than age 40 years, regardless of symptoms, noninvasive assessment of coronary artery disease typically is performed prior to surgery. Selective coronary angiography or CT angiography may be indicated if noninvasive coronary assessment is abnormal. Primum ASDs are not amenable to closure with commercially available transcatheter devices. Minimally invasive robotic techniques have been used to repair isolated mitral valve clefts but, thus far, not in the setting of AVSD.

Adults with Previously Repaired Atrioventricular Septal Defect

Surgery for the repair of partial AVSD should be performed by surgeons with training and expertise in congenital heart

disease (73). Surgical reoperation is recommended in adults with previously repaired AVSD for the following reasons:

1. Need for left AV valve repair or replacement due to symptomatic regurgitation or stenosis, arrhythmia, increase in LV dimensions, or LV dysfunction
2. LVOT obstruction with a mean gradient >50 mm Hg or a Doppler-derived maximum instantaneous gradient >70 mm Hg. LVOT obstruction with a mean gradient <50 mm Hg but associated with significant mitral or aortic valve regurgitation
3. Residual or recurrent ASD or VSD with a significant left-to-right shunt

Reoperation on the left AV valve does not necessarily dictate that valve replacement will be needed. In the recent study from the Mayo Clinic, only half of the patients required left AV valve replacement at the time of the second operation (70). Interestingly, left AV valve replacement did not preclude further reoperation in these patients.

Recommendations for Pregnancy

All women with a history of AVSD should be evaluated when first contemplating pregnancy to ensure that there are no significant residual hemodynamic problems that may complicate their management. Pregnancy usually is well tolerated by women who have had successful repair of AVSD. In addition, for women with unrepaired partial AVSD, the left-to-right shunt and the left AV valve regurgitation usually are well tolerated during pregnancy. The data from the CARPREG study (74) and a more recent follow-up to that database (75) demonstrated that women with repaired and unrepaired left-to-right shunt lesions generally tolerated pregnancy well, except for a few cases of arrhythmia.

However, for women with pulmonary vascular obstructive disease and severe pulmonary artery hypertension (pulmonary artery systolic pressure > 60 mm Hg), pregnancy is not advised. Adult patients with unrepaired complete AVSD typically have Eisenmenger physiology. Fortunately with the advances in surgical techniques and improved outcomes over the last four decades, presentation in adulthood with unrepaired AVSD and Eisenmenger physiology is rare.

Patients who had repair of partial or complete AVSD require lifelong cardiology follow-up. Preferably, this should be at centers that specialize in the care of adults with congenital heart disease. At least 15% to 20% of these patients will come to reoperation because of progressive left AV valve regurgitation or LVOT obstruction. LVOT obstruction may occur de novo even if the patient had undergone primary repair of partial AVSD as an adult (24).

Endocarditis prophylaxis is not generally advised based on the 2007 AHA guidelines for uncomplicated vaginal delivery in woman with unrepaired partial AVSD. For women who had repair of AVSD, one would expect to utilize endocarditis prophylaxis only in those who had valve replacement. Fetal echocardiography is recommended at approximately 20 weeks' gestation due to the 3% to 5% recurrence risk of congenital heart disease in offspring when either parent had AVSD.

CONCLUSIONS

The repair of AVSD has been one of the success stories in the field of congenital heart surgery over the last four decades. The pioneering work performed by Giancarlo Rastelli in the 1960s is but one of these accomplishments. In the modern era, adult survival with excellent quality of life is expected for children

born with AVSD. However, 15% to 20% of these patients may face reoperation in their lifetime. All of these patients require lifelong surveillance for development of LVOT obstruction and left AV valve regurgitation.

ACKNOWLEDGMENTS

The authors acknowledge the contributions of the former authors of this chapter (Drs. William Edwards, Francisco Puga, and Robert Feldt). They participated in the landmark research that formed the cornerstone of this chapter during several editions of the textbook. We also appreciate the constructive review of this chapter by Drs. Bryan Cannon and Patrick O'Leary.

REFERENCES

- Minich LL, Atz AM, Colan SD, et al. Partial and transitional atrioventricular septal defects outcomes. *Ann Thorac Surg* 2010;89:530–536.
- Atz AM, Hawkins JA, Lu M, et al. Surgical management of complete atrioventricular septal defect: associations with surgical technique, age, and trisomy 21. *J Thorac Cardiovasc Surg* 2010;141:1371–1379.
- McGrath LB, Gonzalez-Lavin L. Actuarial survival, freedom from reoperation, and other events after repair of atrioventricular septal defects. *J Thorac Cardiovasc Surg* 1987;94:582.
- Fyler DC, Buckley LP, Hellenbrand WE, et al. Endocardial cushion defect. Report of the New England Regional Infant Cardiac Program. *J Pediatr* 1980;65:441–444.
- Samanek M. Prevalence at birth, “natural” risk and survival with atrioventricular septal defect. *Cardiol Young* 1991;1:285–289.
- Allan LD, Sharland GK, Milburn A, et al. Prospective diagnosis of 1006 consecutive cases of congenital heart disease in the fetus. *J Am Coll Cardiol* 1994;23:1452–1458.
- Freeman SB, Taft LF, Dooley KJ, et al. Population-based study of congenital heart defects in Down syndrome. *Am J Med Genet* 1998;80:213–217.
- Freeman SB, Bean LH, Allen EG, et al. Ethnicity, sex and the incidence of congenital heart defects: a report from the National Down Syndrome Project. *Genet Med* 2008;10:173–180.
- Lynch JL, Perry LW, Takakuwa T, et al. Congenital heart disease and chondroectodermal dysplasia. Report of two cases, one in a Negro. *Am J Dis Child* 1968;115:80–87.
- Phoon CK, Neill CA. Asplenia syndrome: insight into embryology through an analysis of cardiac and extracardiac anomalies. *Am J Cardiol* 1994;73:581–587.
- Peoples WM, Moller JH, Edwards JE. Polysplenia: a review of 146 cases. *Pediatr Cardiol* 1983;4:129–137.
- Goddeeris MM, Rho S, Petier A, et al. Intracardiac septation requires hedgehog-dependent cellular contributions from outside the heart. *Development* 2008;135:1887–1895.
- Gugesell HP, Huhta JC. Cardiac septation in atrioventricular canal defect. *J Am Coll Cardiol* 1986;8:1421–1424.
- Taylor NC, Somerville J. Fixed subaortic stenosis after repair of ostium primum defects. *Br Heart J* 1981;45:689–697.
- di Segni E, Edwards JE. Cleft anterior leaflet of the mitral valve with intact septa: a study of 20 cases. *Am J Cardiol* 1983;51:919–926.
- Goel AK, Ganesan L, Edelstein M. Atrioventricular septal defect with cor triatriatum: case report and review of the literature. *Pediatr Cardiol* 1998;19:243–245.
- LaCorte MA, Cooper RS, Kauffman SL, et al. Atrioventricular canal ventricular septal defect with cleft mitral valve: angiographic and echocardiographic features. *Pediatr Cardiol* 1982;2:289–295.
- Silverman NH, Ho SY, Anderson RH, et al. Atrioventricular septal defect with intact atrial and ventricular septal structures. *Int J Cardiol* 1984;5:567–572.
- Seward JB, Tajik AJ, Hagler DJ. Two-dimensional echocardiographic features of atrioventricular canal defect. In: Lundström N-R, ed. *Pediatric Echocardiography: Cross Sectional, M-Mode and Doppler*. New York, NY: Elsevier/North Holland, 1980:197–206.
- Snider RA, Serwer GA, Ritter SA. Defects in cardiac septation. *Echocardiography in Pediatric Heart Disease*. 2nd ed. St. Louis, MO: Mosby-Year Book, 1997:277–289.
- Seward JB, Tajik AJ, Edwards WD, et al. Congenital heart disease. *Two-Dimensional Echocardiographic Atlas*. Vol. 1. New York, NY: Springer-Verlag, 1987.
- Warnes CA, Somerville J. Double mitral valve orifice in atrioventricular defects. *Br Heart J* 1983;49:59–64.
- Reeder GS, Danielson GK, Seward JB, et al. Fixed subaortic stenosis in atrioventricular canal defect: a Doppler echocardiography study. *J Am Coll Cardiol* 1992;20:386–394.
- Cetta F. Atrioventricular septal defects. In: Warnes CA, ed. *Adult Congenital Heart Disease. AHA Clinical Series*, 2009, Wiley-Balckwell, Hoboken, NJ.
- Fournier A, Young M-L, Garcia OL, et al. Electrophysiologic cardiac function before and after surgery in children with atrioventricular canal. *Am J Cardiol* 1986;57:1137–1141.
- Feldt RH, DuShane JW, Titus JL. The atrioventricular conduction system in persistent common atrioventricular canal defect: correlations with electrocardiogram. *Circulation* 1970;42:437–444.
- Alivizatos P, Anderson RH, Macartney FJ, et al. Atrioventricular septal defect with balanced ventricles and malaligned atrial septum: double-outlet right atrium. *J Thorac Cardiovasc Surg* 1985;89:295–297.
- Corwin RD, Singh AK, Karlson KE. Double-outlet right atrium. A rare endocardial cushion defect. *Am Heart J* 1983;106:1156–1157.
- Horiuchi T, Saji K, Osuka Y, et al. Successful correction of double outlet left atrium associated with complete atrioventricular canal and l-loop double outlet right ventricle with stenosis of the pulmonary artery. *J Cardiovasc Surg (Torino)* 1976;17:157–161.
- Titus JL, Rastelli GC. Anatomic features of persistent common atrioventricular canal. In: Feldt RH, McGoon DC, Ongley PA, et al., eds. *Atrioventricular Canal Defects*. Philadelphia, PA: WB Saunders, 1976.
- Fugelstad SJ, Danielson GK, Puga FJ, et al. Surgical pathology of the common atrioventricular valve: a study of 11 cases. *Am J Cardiovasc Pathol* 1988;2:49–55.
- Rastelli GC, Kirklin JW, Titus JL. Anatomic observations on complete form of persistent common atrioventricular canal with special reference to atrioventricular valves. *Mayo Clin Proc* 1966;41:296–308.
- Konstantinov IE, Rosapepe F, Dearani JA, et al. A tribute to Giancarlo Rastelli. *Ann Thorac Surg* 2005;79:1819–1823.
- Rastelli GC, Ongley PA, Kirklin JW, et al. Surgical repair of the complete form of persistent common atrioventricular canal. *J Thorac Cardiovasc Surg* 1968;55:299–308.
- Sridaromont S, Feldt RH, Ritter DG, et al. Double-outlet right ventricle associated with persistent common atrioventricular canal. *Circulation* 1975;52:933–942.
- Bharati S, Kirklin JW, McAllister HA Jr, et al. The surgical anatomy of common atrioventricular orifice associated with tetralogy of Fallot, double outlet right ventricle and complete regular transposition. *Circulation* 1980;61:1142–1149.
- Ten Harkel ADJ, Cromme-Dijkhuis AH, Heinerman BCC, et al. Development of left atrioventricular valve regurgitation after correction of atrioventricular septal defect. *Ann Thorac Surg* 2005;79:607–612.
- Minich LL, Snider AR, Bove EL, et al. Echocardiographic evaluation of atrioventricular orifice anatomy in children with atrioventricular septal defect. *J Am Coll Cardiol* 1992;19:149–153.
- Cohen M, Jacobs ML, Weinberg PM, et al. Morphometric analysis of unbalanced common atrioventricular canal using two-dimensional echocardiography. *J Am Coll Cardiol* 1996;28:1017–1023.
- van Son JAM, Phoon CK, Silverman NH, et al. Predicting feasibility of biventricular repair of right-dominant unbalanced atrioventricular canal. *Ann Thorac Surg* 1997;63:1657–1663.
- Vet TW, Ottenkamp J. Correction of atrioventricular septal defect: results influenced by Down syndrome? *Am J Dis Child* 1989;143:1361–1365.
- Uretzky G, Puga FJ, Danielson GK, et al. Complete atrioventricular canal associated with tetralogy of Fallot: morphologic and surgical considerations. *J Thorac Cardiovasc Surg* 1984;87:756–756.
- De Biase L, Di Ciommo V, Ballerini L, et al. Prevalence of left-sided obstructive lesions in patients with atrioventricular canal without Down syndrome. *J Thorac Cardiovasc Surg* 1986;91:467–472.
- Marino B. Atrioventricular septal defect—atomic characteristics in patients with and without Down syndrome. *Cardiol Young* 1992;2:308–310.
- Newfeld EA, Sher M, Paul MH, et al. Pulmonary vascular disease in complete atrioventricular canal defect. *Am J Cardiol* 1977;39:721–726.
- Cooney TP, Thurlbeck WM. Pulmonary hypoplasia in Down syndrome. *N Engl J Med* 1982;307:1170–1173.
- Clapp S, Perry BL, Farooki ZQ, et al. Down's syndrome, complete atrioventricular canal, and pulmonary vascular obstructive disease. *J Thorac Cardiovasc Surg* 1990;100:115–121.
- Hals J, Hagemo PS, Thaulow E, et al. Pulmonary vascular resistance in complete atrioventricular septal defect: a comparison between children with and without Down syndrome. *Acta Paediatr* 1993;82:595–598.
- Rizzoli G, Mazzucco A, Maizza F, et al. Does Down syndrome affect prognosis of surgically managed atrioventricular canal defects? *J Thorac Cardiovasc Surg* 1992;104:945–953.
- Thiene G, Wenink ACG, Frescura C, et al. Surgical anatomy and pathology of the conduction tissues in atrioventricular defects. *J Thorac Cardiovasc Surg* 1981;82:928–937.
- Carpentier A. Surgical anatomy and management of the mitral component of atrioventricular canal defects. In: Anderson RH, Shinebourne EA, eds. *Paediatric Cardiology*. Edinburgh: Churchill Livingstone, 1978:477–490.

52. Piccoli GP, Wilkinson JL, Macartney FJ, et al. Morphology and classification of complete atrioventricular defects. *Br Heart J* 1979;42:633–639.
53. El-Najdawi E, Driscoll D, Puga F, et al. Operation for partial atrioventricular septal defect: a 40-year review. *J Thorac Cardiovasc Surg* 2000;119:880–889.
54. Silverman N, Levitsky S, Fisher E, et al. Efficacy of pulmonary artery banding in infants with complete atrioventricular canal. *Circulation* 1983;68:II148–II153.
55. Williams WH, Guyton RA, Michalik RE, et al. Individualized surgical management of complete atrioventricular canal. *J Thorac Cardiovasc Surg* 1983;86:838–844.
56. Puga FJ, McGoon DC. Surgical treatment of atrioventricular canal. *Mod Technics Surg* 1980;26:1–13.
57. Studer M, Blackstone EH, Kirklin JW, et al. Determinants of early and late results of repair of atrioventricular septal (canal) defects. *J Thorac Cardiovasc Surg* 1982;84:523–542.
58. Wilcox BR, Jones DR, Frantz EG, et al. Anatomically sound, simplified approach to repair of “complete” atrioventricular septal defect. *Ann Thorac Surg* 1997;64:487–493.
59. Nicholson IA, Nunn GR, Sholler GF, et al. Simplified single patch technique for the repair of atrioventricular septal defect. *J Thorac Cardiovasc Surg* 1999;118:642–646.
60. Backer CL, Stewart RD, Bailliard F, et al. Complete atrioventricular canal: comparison of modified single-patch technique with two-patch technique. *Ann Thorac Surg* 2007;84:2038–2046.
61. Cohen GA, Stevenson JG. Intraoperative echocardiography for atrioventricular canal: decision-making for surgeons. *Semin Thorac Cardiovasc Surg Pediatr Card Surg Annu* 2007;47–50.
62. David I, Castaneda AR, van Praagh R. Potentially parachute mitral valve in common atrioventricular canal: pathological anatomy and surgical importance. *J Thorac Cardiovasc Surg* 1982;84:178–186.
63. Lee C-N, Danielson GK, Schaff HV, et al. Surgical treatment of double-orifice mitral valve in atrioventricular canal defects. *J Thorac Cardiovasc Surg* 1985;90:700–705.
64. De Oliveira NC, Sittiwangkul R, McCrindle BW, et al. Biventricular repair in children with atrioventricular septal defects and a small right ventricle: anatomic and surgical considerations. *J Thorac Cardiovasc Surg* 2005;130:250–257.
65. Mace L, Dervanian P, Folliguet T, et al. Atrioventricular septal defect with subaortic stenosis; extended valvular detachment and leaflet augmentation. *J Thorac Cardiovasc Surg* 1997;113:615–616.
66. van Son JA, Schneider P, Falk V. Repair of subaortic stenosis in atrioventricular canal with absent or restrictive interventricular communication patch augmentation of ventricular septum, resuspension of atrioventricular valves, and septal myectomy. *Mayo Clin Proc* 1997;72:220–224.
67. Van Ardsell GS, Williams WG, Boutin C, et al. Subaortic stenosis in the spectrum of atrioventricular septal defects. Solutions may be complex and palliative. *J Thorac Cardiovasc Surg* 1995;110:1534–1541.
68. DeLeon SY, Ilbawi MN, Wilson WR Jr, et al. Surgical opinions in subaortic stenosis associated with endocardial cushion defects. *Ann Thorac Surg* 1991;52:1082–1083.
69. Stulak JD, Burkhart HM, Dearani JA, et al. Reoperations after repair of partial atrioventricular septal defect: a 45-year single-center experience. *Ann Thorac Surg* 2010;89:1352–1359.
70. Stulak JM, Burkhart HM, Dearani JA, et al. Reoperations after initial repair of complete atrioventricular septal defects. *Ann Thorac Surg* 2009;87:1872–1877;discussion 1877–1878.
71. El Yaman M, Edwards WD, Cetta F. Atrioventricular septal defects. In: Eidem BW, Cetta F, O’Leary PW, eds. *Echocardiography in Pediatric and Adult Congenital Heart Disease*. Philadelphia, PA: Lippincott Williams and Wilkins, 2010.
72. Steele PM, Fuster V, Cohen M, et al. Isolated atrial septal defect with pulmonary vascular obstructive disease—long-term follow-up and prediction of outcome after surgical correction. *Circulation* 1987;76:1037–1042.
73. Warnes CA, et al. ACC/AHA 2008 guidelines for adults with congenital heart disease. *J Am Coll Cardiol* 2008;52:1890–1947.
74. Siu SC, Sermer M, Colman JM, et al. Prospective multicenter study of pregnancy outcomes in women with heart disease. *Circulation* 2001;104:515–521.
75. Balint OH, Siu SC, Mason J, et al. Cardiac outcomes after pregnancy in women with congenital heart disease. *Heart* 2010;96:1656–1661.

Agustin E. Rubio ■ Mark B. Lewin

Except for bicuspid aortic valve, ventricular septal defects (VSDs) are the most common congenital heart lesions in infancy, childhood, and adolescence.

PREVALENCE

Historically, VSDs constituted 20% to 30% of congenital heart defects. They occur in 1.35 to 3.5/1,000 live births (1,2). The incidence of spontaneous closure of isolated VSDs approximated 45% during the first 12 months of life and 22% during childhood. A study of neonates followed for 15 years showed a spontaneous closure rate of 31% uniformly over the first 10 years of follow-up (3). This explains why the diagnosis of VSDs in adulthood is distinctly rare (4).

With the advent of echocardiography, the recognition of VSDs has increased to 5 to 50/1,000 live births (5,6). A recent review of the incidence of congenital heart disease in metropolitan Atlanta between 1998 and 2005 demonstrated a prevalence of muscular VSDs as detected by physical examination and confirmed by echocardiography to be 2.75/1,000 live births for infants (7). VSD is the most common cardiovascular manifestation associated with aneuploidies (trisomy 21, trisomy 18, and trisomy 13). Although there has not been a clear genetic link put forth, it is theorized that multifactorial causality is present (8).

PATHOLOGY

Multiple classification systems have been proposed for the description of VSDs. The classification system described in the subsequent sections utilizes the description of the ventricular anatomy as per Soto et al. and Anderson et al. (9,10). The ventricular septum is separated into three separate components—an inlet septum, an apical trabecular septum, and an outlet or infundibular septum.

The inlet septum separates the mitral and the tricuspid valves. The trabecular portion extends from the chordal attachments of the tricuspid valve into the apex and superiorly to the crista supraventricularis. The outlet or infundibular segment is the smooth-walled portion which is in continuity with the crista supraventricularis and the pulmonary valve. The membranous septum is small and often is divided by the septal leaflet of the tricuspid valve.

The defects that extend into the membranous, inlet, or outlet septum have been termed perimembranous VSDs. This term also has been used to describe defects that lie in the outflow tract of the left ventricle (LV) just under the aortic valve. A descriptive synonym used for this particular location is an infracristal or membranous VSD. Inspection from the right

ventricle (RV) demonstrates that this defect is beneath the crista supraventricularis and posterior to the papillary muscle of the conus. Surgical and autopsy case series have shown that possibly 80% of the VSDs noted were within this region (11,12). It is common for these defects to extend into portions of the inlet, outlet, or muscular aspects of the septum and be classified as perimembranous. The perimembranous defect also may accompany abnormalities of the tricuspid valve, most often the septal leaflet. The abnormality of the tricuspid valve leaflet may be secondary to damage from the left-to-right shunt. One of those anomalies is the presence of septal leaflet tissue that can partially or completely obstruct the defect, otherwise known as an aneurysm of the ventricular septum. Another important characteristic of the perimembranous defect is the potential for malalignment. Anterior malalignment of the infundibular septum and the anterior ventricular septum have been associated with the aortic valve overriding the septal defect (9). A less commonly observed phenomenon is a posterior malalignment of the ventricular septum that could cause left ventricular outflow tract obstruction, specifically subaortic narrowing. Posterior malalignment commonly is associated with the VSD associated with aortic arch interruption. In the presence of a deficient tricuspid valve septal leaflet, a LV-right atrial (RA) shunt can occur. This more commonly occurs with the presence of both an LV-RV and LV-RA shunt. If there is no LV-RV shunt, delineation of tricuspid valve abnormalities should be sought, some of which include septal perforation, a deficient leaflet, or a tricuspid valve cleft. Rarely, the absence of atrioventricular septal tissue will result in an isolated LV-RA shunt (Gerbode defect).

Using surgical and autopsy case series, investigators have estimated that outlet-type VSDs constitute 5% to 7% of VSDs. These outlet type VSDs have been labeled suprastal, infundibular, conal, subpulmonary, or doubly committed subarterial defects. Population studies show that patients from Japan and other Far East nations have a much higher incidence of this type of VSD than Occidental populations. In Japan, outlet septal defects comprise 30% of all VSDs (9,11,13).

One type of inlet VSD, located posterior and inferior to the perimembranous region, has been mislabeled as an atrioventricular septal defect. The true atrioventricular septal defect is one in which there are abnormalities of the mitral and/or the tricuspid valve and the course of the conduction system is displaced. The inlet-type VSD has neither mitral nor tricuspid valve abnormalities and no evidence of displacement of the conduction system. From a surgical/autopsy case series review these VSDs comprised 3% to 8% of the total cases (11,12).

The incidence of muscular VSDs ranges from 5% to 20% in surgical and autopsy case series. These defects effectively can be described as either apical or central. The apical defects, as seen from the RV, can have multiple orifices and therefore present with multiple jets. Often, when evaluated from the left

ventricular aspect, these have a single point of origin from the LV. This type of defect can be quite large. The central-type defect, located in the midportion of the septum and posterior to the septal band of the crista, often can be hidden from the right ventricular view and can have multiple jets. As with the apical VSD, the left ventricular view can demonstrate a single well-circumscribed VSD that is away from the anterior and posterior walls of the LV. Another muscular type of VSD is the marginal or anterior septal wall defect. This type of defect commonly is described as a "Swiss-cheese" type septum comprised of multiple small, tortuous marginal defects. This type of VSD also can be associated with other muscular as well as perimembranous defects (10,14).

Patients with either outlet-type or perimembranous defects are at risk of developing aortic valve insufficiency. It is hypothesized that the outlet-type defect involves a deficiency of the muscular or fibrinous support underneath the aortic valve that may contribute to prolapse of an aortic valve cusp. The right coronary cusp most commonly prolapses into this type of defect. In contrast, the perimembranous defect more often is associated with prolapse of the right or noncoronary cusps. Generally, inlet-type and muscular-type defects are unassociated with prolapse of the aortic valve. According to a recent review, aortic insufficiency, caused by VSD flow disturbances is due to a lack of the necessary support for the aortic valve causing prolapse of the aortic valve cusp (15).

Identification of the nature of the defect also will allow an understanding of the course of the conduction system. In perimembranous defects, the bundle of His travels along the posterior and inferior rim of the defect as opposed to the inlet-type of defect in which it will be anterior and superior to the defect (10). Surgically induced atrioventricular block is less likely with an isolated muscular trabecular defect or an outlet-type defect because they are distant from the atrioventricular node and the bundle of His.

PHYSIOLOGY

The clinical manifestations of an interventricular ventricular left-to-right shunt largely are dependent on the size of the defect and the pulmonary and systemic vascular resistances. With small defects, the volume of the left-to-right shunt is limited by the resistance of the small defect. With larger defects, the volume of the left-to-right shunt depends upon the relative pulmonary and systemic vascular resistances.

Transition from fetal to extrauterine existence is associated with changes in the pulmonary vascular resistance. The small highly muscularized medial layer of the pulmonary arteries undergoes physiologic changes that result in a larger lumen and thinner-walled pulmonary artery. These changes result in declining right ventricular systolic pressure. By 7 to 10 days of life, the right ventricular pressure should have declined to normal. Infants born with large VSDs have a delayed decline in pulmonary vascular resistance that serves as a protective mechanism to prevent massive pulmonary overcirculation. Thus, it mainly is the pulmonary vascular resistance that determines the magnitude of the left-to-right shunt associated with large VSDs (16–18).

The size of the VSD can be compared to the aortic valve. This concept was proposed years ago by Dr. Nadas. Those defects that are less than one-third the diameter of the aortic valve are considered small and therefore restrict the amount of left-to-right shunting via the defect. For most of these restrictive defects, catheter-based data have demonstrated near-normal right ventricular pressure, pulmonary arterial pressure, and near-normal pulmonary vascular resistance

(19). The high resistance at the VSD results in a large difference of systolic pressure between the right and LVs. The peak gradient between the two occurs during systole. However, due to the large pressure difference, a continuous left-to-right shunt can be appreciated by color-flow Doppler interrogation.

Perimembranous and outlet defects often can have flow directed toward the right ventricular outflow tract and to the pulmonary artery. The moderate-sized defect (defined as >33% of the aortic valve annulus but <50% of the annulus) will offer some pressure restriction. Continuous-wave Doppler interrogation often will demonstrate a >20 mm Hg gradient through the defect. Most of these patients will have mildly elevated right ventricular pressure as well as mild elevation of the pulmonary arterial pressure. Typically, they have normal to near-normal pulmonary vascular resistance. Yet, there is a greater degree of volume overload, which explains, in part, the dilation of the left atrium and the LV.

A large VSD (>50% of the aortic valve annulus and a Doppler flow interrogation predicting <20 mm Hg gradient between the left and RVs) results in nearly systemic systolic pulmonary arterial pressures. As the infant ages, the pulmonary vascular resistance will continue to decline and the degree of pulmonary overcirculation will increase. The further rise in pulmonary pressures will be transmitted to the pulmonary veins and the left atrium causing pulmonary venous hypertension and left atrial hypertension and eventually an increase of LV muscle mass (20). As the pulmonary vascular resistance declines by 2 to 8 weeks of age, the pulmonary blood flow increases resulting in increased sympathetic tone and dilation of the left atrium and ventricle. The latter results in a shift in position along the Frank-Starling curve that can adversely affect ventricular mechanics. The ability of the infant to tolerate a large shunt is dependent upon the interplay between these competing factors.

As pulmonary vascular disease develops, the pulmonary vascular resistance increases and the left-to-right shunt reverses, and the presence of a right-to-left shunt will result in cyanosis (Eisenmenger complex or syndrome). Cyanosis will be accompanied by a right ventricular heave with a short or no systolic murmur. In this situation, other murmurs may be heard. A holosystolic murmur coincident with S1 from tricuspid valve insufficiency along with an early diastolic murmur of pulmonary valve insufficiency may be heard. The second heart sound will become loud, single or narrowly split. A third heart sound due to right ventricular filling may be appreciated (21,22). Wood described the clinical features of Eisenmenger syndrome including squatting and hemoptysis. Hemoptysis occurred in 33% of patients after 24 years of age and 100% of patients by 40 years of age. Early mortality was estimated to be 29%.

Pathologic analysis of patients with nonrestrictive pulmonary blood flow demonstrates that excessive pulmonary blood flow is deleterious to the small branch pulmonary arteries. Recent investigations have shown that chronic exposure to increased blood flow and pressure in the distal pulmonary arteries result in thickened adventitia, muscular medial hypertrophy, and potential intimal injury that can lead to thrombosis, ultimately causing pulmonary vascular obstructive disease (23,24). Patients with congenital heart disease and pulmonary vascular obstructive disease have plexiform lesions that express polyclonal endothelial cell proliferation as opposed to those with familial pulmonary artery hypertension that expresses monoclonal proliferating endothelial cells (25,26). Furthermore, genetic and molecular mechanisms currently are being elucidated to provide a better understanding of the changes that occur secondary to the abnormal flow and pressure patterns that occur in patients with large left-to-right shunts.

DIAGNOSTIC EVALUATION

Physical Examination

The physical findings for a patient with a VSD depend upon the size of the VSD, the magnitude of the left-to-right shunt, and the level of right ventricular and pulmonary artery hypertension and the balance of systemic and pulmonary resistances.

A small VSD with a $Qp/Qs < 1.5$ and normal or only slightly elevated right ventricular and pulmonary artery pressure is characterized by normal precordial impulses and normal first and second heart sounds. The murmur is S_1 coincident and holosystolic. In muscular VSDs, this murmur may be best heard over the lower sternal area. If the jet of blood through the VSD is directed toward the pulmonary artery, as is the case with many perimembranous and supracristal VSDs, the murmur radiates to the upper left sternal border. Frequently a precordial thrill is palpable.

For moderate and large VSDs, the right ventricular impulse, felt at the lower left sternal border or the subxiphoid region, is prominent. In addition, the left ventricular impulse will be displaced laterally and have increased activity. The first heart sound will be normal. As the degree of pulmonary hypertension increases, the intensity of the pulmonary component of S_2 will increase. There will be an S_1 -coincident holosystolic mid-frequency murmur. In patients with $Qp/Qs > 2$, in addition to the systolic murmur, there will be a middiastolic mitral flow murmur as a result of increased volume of blood flowing from the left atrium to the LV. A precordial thrill may be palpable and closure of the pulmonary and aortic valves may be palpable. Infants with a large VSD will be tachypneic. In addition, infants with severe congestive heart failure may have pallor, poor feeding, and failure to gain weight.

Electrocardiography

Small VSDs will have little effect on the QRS axis but large defects can be associated with left- or right-axis deviation. This may make it difficult to differentiate between a large VSD and an atrioventricular septal defect.

Moderate-sized defects are associated with chronic volume overload of the left atrium and ventricle resulting in left ventricular dilation and hypertrophy. Hypertrophy of both the right and the LVs is common (27). A moderate-sized VSD may or may not have electrocardiographic evidence of RVH.

Large VSDs in infants are difficult to diagnose solely using the ECG. Infants with moderate-sized VSDs often will demonstrate a counterclockwise frontal plane QRS axis. Patients with a large VSD have equalization of the ventricular pressures and, thus, have right ventricular hypertrophy. Patients with excessive pulmonary blood flow often will develop left atrial dilation, manifested by biphasic P waves in leads I, AVR, and V6. Prominent negative deflection of the P wave also can be seen in V1.

Patients with markedly elevated pulmonary vascular resistance in the setting of a large VSD rarely have evidence of left ventricular hypertrophy or left atrial dilation using ECG criteria. These patients will exhibit evidence of RVH.

Chest Radiography

Characteristic findings on chest radiographs vary depending upon the size of the VSD. Small defects with restrictive left-to-right shunting often will have a normal cardiac silhouette and normal pulmonary vascular markings. In contrast, patients with moderate to large VSDs will have cardiomegaly, increased pulmonary vascular markings centrally and peripherally,

possibly a dilated main pulmonary arterial segment, and/or elongation of the cardiac silhouette in a downward and leftward direction. Lateral projections may show upward deviation of the left main bronchus due to left atrial dilation. The standard posteroanterior projection also will demonstrate a change in the plane of the left main bronchus because of left atrial dilation.

Children with large VSDs and marked elevation of pulmonary vascular resistance can have normal cardiac size. Due to the frequent presence of right ventricular hypertrophy the cardiac apex is slightly rotated upward, leftward, and posteriorly. There often is marked dilation of the central branch pulmonary arteries as well as the main pulmonary artery segment. There will be increased peripheral vascular markings. For patients with Eisenmenger complex, the heart may not be enlarged and the pulmonary vascular markings may not be increased. The main pulmonary artery is enlarged.

Echocardiography

Transthoracic echocardiography is the mainstay for the definitive diagnosis of VSDs. It allows delineation of the location of the defect, associated cardiac lesions, pulmonary artery pressure, and degree of cardiac heart dilation.

In order to determine the anatomic site of the VSD, multiple echocardiographic imaging planes must be used. From the parasternal long-axis view data can be obtained regarding perimembranous, malalignment (Fig. 30.1), and muscular VSDs. Additional information is obtained via the parasternal long- and short-axis plane including the relationship of the perimembranous VSD to the septal tricuspid valve leaflet, secondary to flow disturbance that might distort the aortic valve's right coronary cusp (Fig. 30.2A,B), and the location and size of muscular defects (Fig. 30.3). The parasternal short-axis view also allows location of the position of the supracristal (subpulmonic) VSD (Fig. 30.4). The apical four-chamber view allows assessment of the isolated inlet VSD (Fig. 30.5), the muscular VSD, and the VSD associated with a complete atrioventricular septal defect. In addition, assessment of the left ventricular outflow tract allows evaluation of the perimembranous VSD. Aortic insufficiency can be quantified and billowing of the tricuspid valve septal leaflet through the VSD can be appreciated (Fig. 30.6). The subcostal short-axis plane is well suited for assessment of the common atrioventricular valve.

The subcostal as well as apical planes allow assessment of anterior deviation of the conal septum in the malalignment VSD associated with tetralogy of Fallot, the posterior mala-

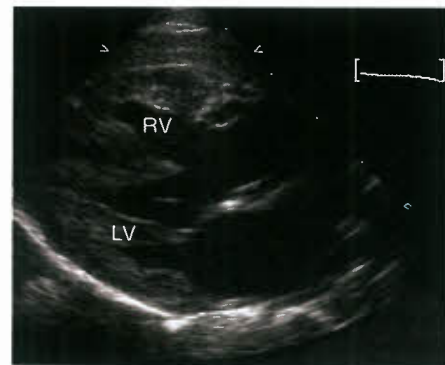


Figure 30.1. Parasternal long-axis view demonstrating a malalignment VSD associated with tetralogy of Fallot. There is anterior deviation of the interventricular septum resulting in aortic override of the VSD.

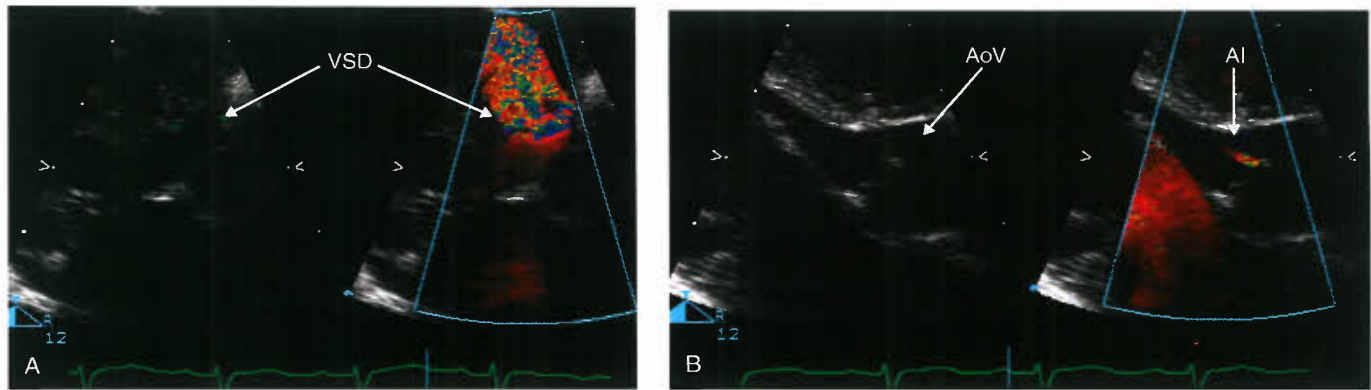


Figure 30.2. A: Parasternal long-axis imaging plane demonstrating aliased color Doppler left-to-right flow across a perimembranous VSD. B: Parasternal long-axis imaging plane color Doppler demonstration of aortic insufficiency associated with distortion of the right coronary cusp caused by a perimembranous VSD.

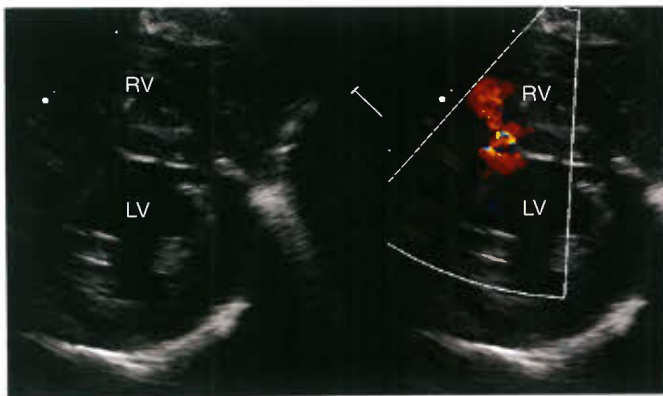


Figure 30.3. Parasternal short-axis imaging plane at the level of the papillary muscles demonstrating two-dimensional and color Doppler left-to-right flow across a midmuscular VSD.

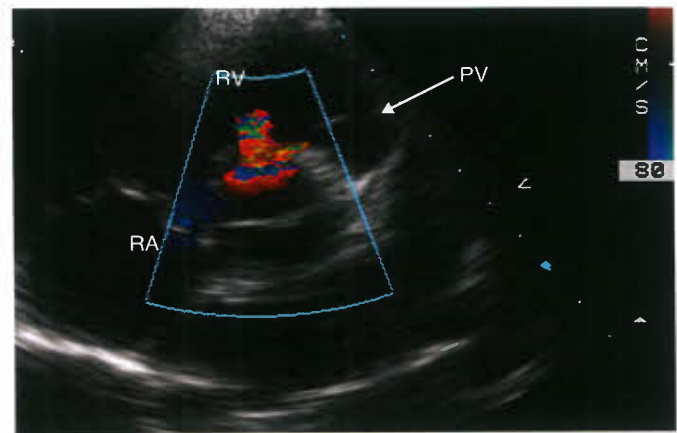


Figure 30.4. Parasternal short-axis imaging plane at the level of the aortic and pulmonic valves demonstrating color Doppler left-to-right flow across a supracristal VSD.

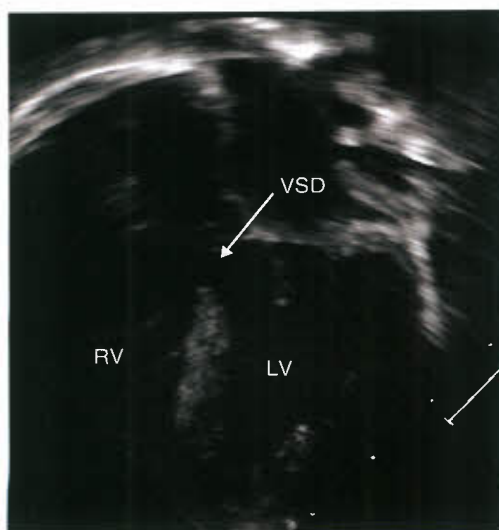


Figure 30.5. Apical four-chamber view at the level of the tricuspid and mitral valves demonstrating a moderate-sized isolated inlet VSD.

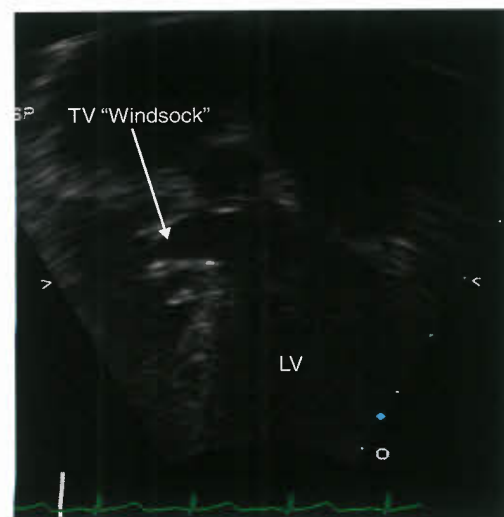


Figure 30.6. Apical long-axis view at the level of the aortic valve demonstrating a moderate-sized perimembranous VSD, which is partially occluded by a tricuspid valve septal leaflet aneurysm resulting in a "windsock" deformity.

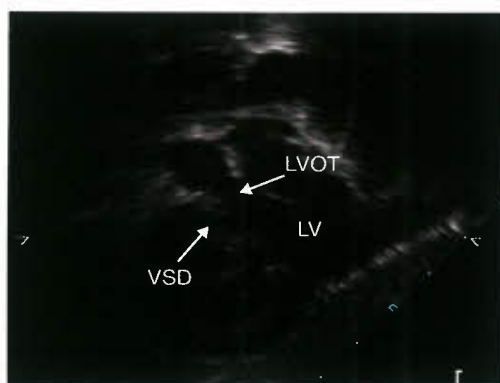


Figure 30.7. Subcostal short-axis view at the level of the left ventricular outflow tract demonstrating posterior malalignment of the interventricular septum resulting in narrowing of the left ventricular outflow tract.

alignment VSD associated with interrupted aortic arch and subaortic membrane (Figs. 30.7 and 30.8A,B), and further delineation of the size and number of multiple muscular VSDs (Fig. 30.9).

Using the modified Bernoulli equation (pressure gradient in mm Hg = $4 \times \text{jet velocity}^2$) the gradient between LV and RV can be calculated. In some circumstances, right ventricular and pulmonary artery systolic pressure can be calculated. For example, with a systolic systemic blood pressure = 100 mm Hg, and a velocity across the VSD = 2 m/s, the right ventricular/pulmonary artery pressure can be calculated as $100 - 4(2)^2 = 84$ mm Hg.

The presence of left atrial or left ventricular dilation suggests that the VSD is hemodynamically important. Left-sided cardiac dilation correlates with a $Q_p:Q_s > 2:1$. The presence of significant chamber enlargement of or greater than one-half of systemic right ventricular pressure suggests the need for VSD closure.

Intraoperative transesophageal echocardiography (TEE) is utilized to clarify anatomic and physiologic details (Fig. 30.10). For example, the surgeon may want additional details about the anterior mitral valve cleft associated with complete atrioventricular septal defect. With aortic insufficiency, additional data can be obtained regarding the anatomy of the aortic valve, which might allow prediction of the likelihood of valve

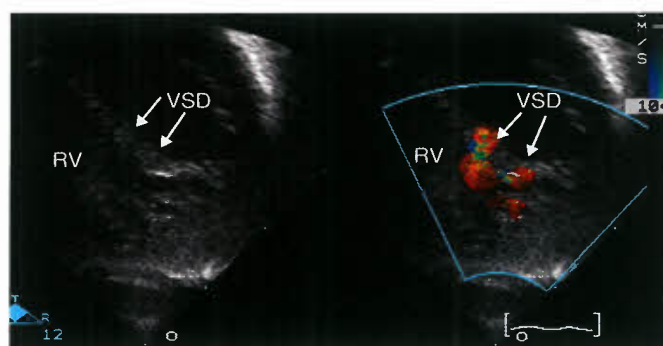


Figure 30.9. Subcostal short-axis view at the level of the midinterventricular septum demonstrating color Doppler interrogation of a moderate-sized as well as a smaller low-muscular VSD.

repair. Postoperatively, one can ascertain the presence of residual ventricular-level shunting and pulmonary artery pressures.

TEE is useful to guide the implantation of an occlusion device during cardiac catheterization (Fig. 30.11). In addition, one can detect residual shunts, predict pulmonary artery pressure, and delineate problems such as distortion of the tricuspid valve as a result of device impingement upon the valve.

Magnetic Resonance Imaging

Didier et al. (28) demonstrated the use of MRI to determine the presence and location of VSD by voltage-gated imaging. Several investigators have quantitated pulmonary blood flow in the setting of left-to-right shunts (29). Most recently, investigators have correlated Q_p/Q_s by phase-contrast MRI and oxygen saturation measurement (30) (see Chapter 10).

Cardiac Catheterization

The primary indication for cardiac catheterization is to determine (a) the presence or absence of additional smaller defects and abnormalities, (b) quantitate the volume of shunting, (c) determine pulmonary vascular resistance, and (d) establish landmarks for possible transcatheter or surgical procedures.

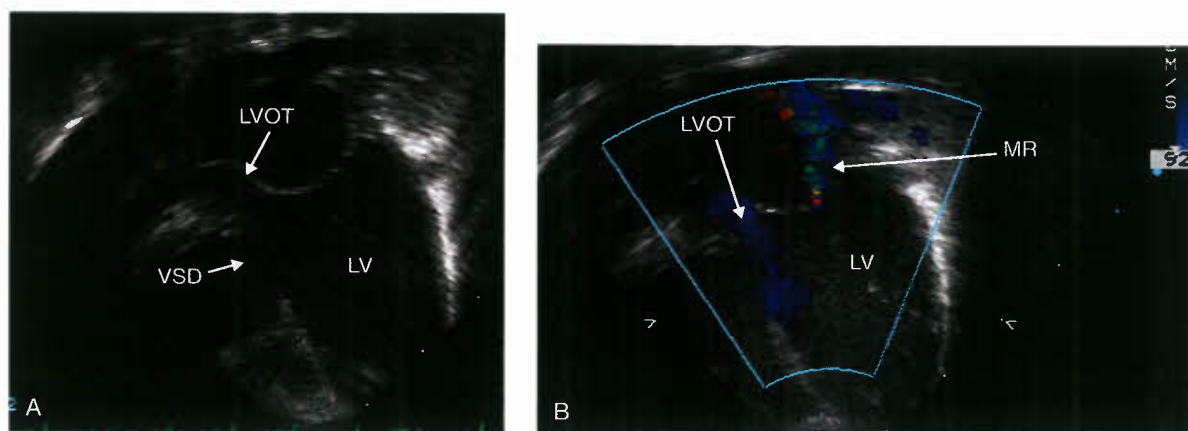


Figure 30.8. A: Apical long-axis view of a large posteriorly malaligned VSD. Note the resultant narrowing of the left ventricular outflow tract. The LV is dilated due to pulmonary overcirculation. B: Apical long-axis view demonstrating color Doppler flow through an unobstructed, but narrowed left ventricular outflow tract due to posterior deviation of the interventricular septum in the setting of a malalignment VSD. Note the presence of mitral regurgitation.

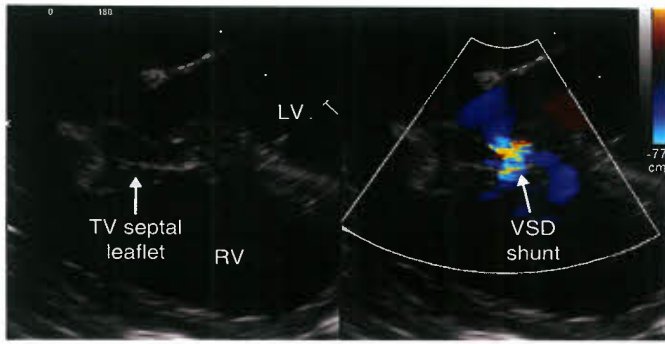


Figure 30.10. Transesophageal echo long-axis view of a perimembranous VSD interrogation prior to surgical closure. The left image demonstrates the relationship of the VSD to the aortic and tricuspid valves. The right image demonstrates left-to-right color Doppler flow.

Right ventricular angiography allows one to determine the size and presence of muscle hypertrophy of the RV, evaluate pulmonary venous return, and assess intra-atrial shunting. Left ventriculography will demonstrate the presence or absence of left ventricular outflow tract anomalies, and the size, location, and number of VSDs (Fig. 30.12). To delineate the interventricular septum, the AP camera should be oriented to obtain a right-axial oblique view at about 30 degrees angulation and the lateral camera should be oriented to obtain a 60-degree long-axial oblique view with cranial angulation (31,32) (Fig. 30.13). If this view fails to adequately define the VSD, the “hepatoclavicular” or “four-chamber view” could allow for better delineation of those defects. This view is useful to delineate the course of the left ventricular outflow tract and demonstrate left ventricular–RA shunts (Gerbode defect).

Retrograde aortography can be used to determine the presence and degree of semilunar valve insufficiency, the coronary artery anatomy, the presence or absence of the ductus arteriosus, arch sidedness, and the presence or absence of a coarctation of the aorta.

If there is elevated pulmonary vascular resistance, one should perform a provocative test to evaluate pulmonary vascular reactivity. This is performed using 100% oxygen to produce pulmonary vasodilation. In addition, inhaled nitric oxide can be used if there is little or no decline with 100% oxygen. Additional drugs such as epoprostenol sodium (PGI_2) have

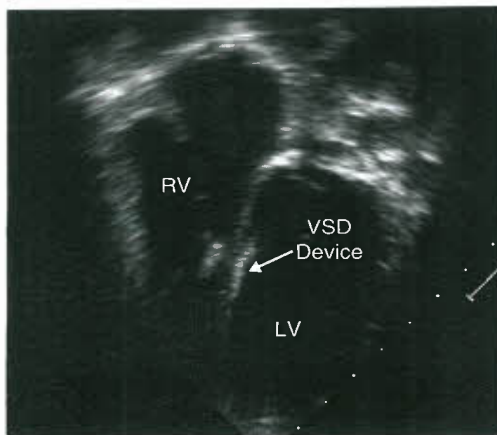


Figure 30.11. Transesophageal echo four-chamber view demonstrating successful Amplatzer VSD occlusion device deployment across a midmuscular VSD.



Figure 30.12. Retrograde pigtail catheter in the LV with the cameras in left anterior oblique with cranial angulation. This view demonstrates the interventricular septum and left-to-right shunt through a perimembranous VSD with aneurismal tissue obstructing some of the left-to-right flow. Mild mitral valve insufficiency is also noted.

been used to determine the degree of pulmonary vasoreactivity (33,34). Historically, patients who have irreversible elevation of PVR were considered to be poor candidates for surgical correction. Although the level of pulmonary vascular resistance that is considered incompatible with successful cardiothoracic

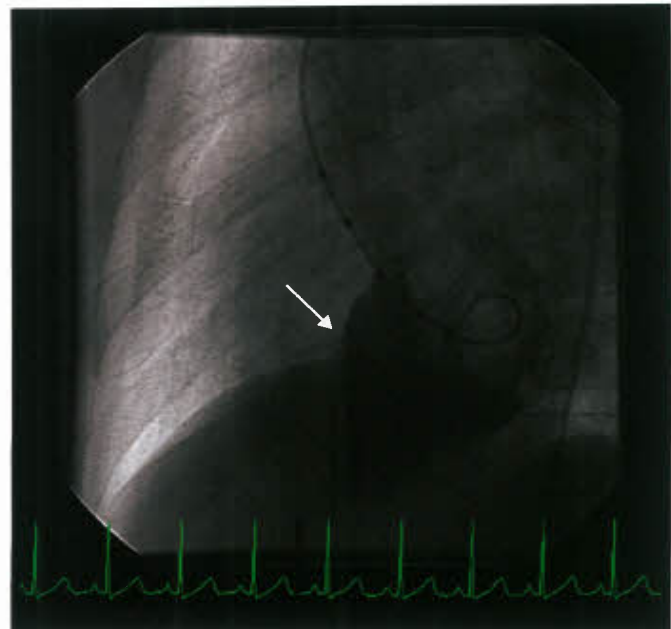


Figure 30.13. Retrograde catheter coursing through the aortic valve and into the LV. Left anterior oblique view with cranial angulation demonstrating a midmuscular VSD prior to muscular device occlusion.

surgery has not been determined, a nonmodifiable pulmonary vascular resistance >6 to 8 Woods units \times m^2 has been considered predictive of reduced postoperative survival (35,36).

DIFFERENTIAL DIAGNOSIS

The differential diagnosis of a large left-to-right shunt and pulmonary overcirculation includes atrioventricular septal defect with unrestricted pulmonary blood flow, double outlet RV, LV-RA shunts (Gerbode), patent ductus arteriosus, aorticopulmonary window, truncus arteriosus, congenitally corrected transposition of the great arteries with a VSD, and functional single ventricle without pulmonary stenosis among others.

Atrioventricular septal defects are differentiated from isolated VSDs using echocardiography and electrocardiography (see Chapter 29). Although atrioventricular septal defects typically have a northwest axis on the surface ECG, this can also be seen in an isolated VSD.

Patients with double outlet RV also may present with significant pulmonary overcirculation. One can differentiate an isolated malalignment VSD from double-outlet RV using echocardiography (see Chapter 51).

VSDs typically present with an S_1 -coincident holosystolic murmur that can sometimes be confused with the ejection murmur of pulmonary valve or subpulmonary or subaortic stenosis. Sometimes the ejection murmur of aortic stenosis in patients with high heart rates can be confused with that of a VSD. However, the murmur of aortic stenosis is ejection in timing, radiates into the neck, and usually is associated with an ejection click. The click is sometimes so prominent that the examiner thinks it is the first sound. It is important to listen “behind” the click to hear the softer S_1 . VSD can be associated with subaortic stenosis. Identification of associated anomalies is important when considering operation.

TREATMENT

Medical Therapy

Small VSDs do not cause significant pulmonary overcirculation. The outcome of these patients is excellent and medical therapy, surgical, or percutaneous closure of these defects are unnecessary.

Medical treatment of patients with large VSDs involves the use of diuretics, afterload reduction, and maximizing caloric intake. Diuretics are the first line of medical therapy. Furosemide (1 mg/kg to 3 mg/kg per day) divided into two or three doses relieves some of the increased preload and will reduce tachycardia and tachypnea. The use of furosemide may be complicated by hypokalemia, hypercalcemia, hearing loss, and possible renal toxicity. Spironolactone can be used as adjunctive therapy to prevent hypokalemia. A third line of medical therapy is afterload reduction. The concept behind afterload reduction is to shift the Qp/Qs more toward the systemic circulation and therefore reduce pulmonary blood flow (37). The efficacy of this approach has been documented in case-control trials from the late 1980s and early 1990s (38–40). Because angiotensin-converting enzyme inhibitors may cause potassium retention, spironolactone must be used carefully in conjunction with them.

The use of digoxin has gradually diminished over time. Hougren et al. (41) summarized the basic mechanisms of cardiac glycosides and their clinical use in heart failure in children. He noted that most pediatric patients with large left-to-right shunts have normal systolic ventricular function and

that these patients benefit little from the addition of digoxin. Others have made similar observations (42,43). However, digoxin continues to be used by some clinicians (44).

Over time, with medical therapy one may observe reduction in the volume of the left-to-right shunt due to spontaneous closure of the defect, increasing pulmonary vascular resistance, or hypertrophy of the right ventricular outflow tract portion of the right ventricle.

Patients with Eisenmenger complex will exhibit increasing cyanosis, decreasing exercise tolerance, and polycythemia (or erythrocythemia). Polycythemia can cause headaches and extreme fatigue. Relative iron deficiency is common in these patients and should be avoided or treated if it occurs. Symptomatic headaches and exhaustion can be ameliorated with partial exchange transfusion. Heart–lung transplantation may be a consideration for some of these patients. However, in the Second Natural History Study of Congenital Heart Disease, the 25-year survival for patients with Eisenmenger complex was 40%, which is superior to the 25-year survival after heart–lung transplantation. Often, these patients will need oxygen therapy and should be advised against living at high altitude due to the lower FiO_2 . If air travel is unavoidable, supplemental oxygen therapy should be provided since commercial aircraft often pressurize the cabin at 5,000 to 7,000 ft, lowering the FiO_2 accordingly.

SURGICAL THERAPY

Infants with a large shunt, congestive heart failure, and failure to thrive despite optimal medical therapy should have repair prior to 12 months of age both to eliminate congestive heart failure and to prevent the development of pulmonary vascular disease. For older children and adolescents with normal or reversible pulmonary vascular resistance but with a $Qp/Qs >2:1$, closure of the defect is indicated. Progressive aortic valve insufficiency associated with a supracristal (outlet) VSD is an indication for VSD closure. The surgical mortality in children is $<1\%$ to 3% (45).

Current practice guidelines suggest that adult patients with a Qp/Qs ratio >2 and echocardiographic evidence of volume overload of the left side of the heart or a history of infective endocarditis should have surgical closure (46,47).

Most perimembranous and inlet-type defects are closed using a transatrial approach. In contrast, defects that are associated with the outlet septum are best visualized and closed through the pulmonary valve. The approach more commonly used in the 1960s and 1970s employed staged palliation with the initial placement of a pulmonary artery band and subsequent debanding with VSD closure. The complications of pulmonary artery banding include inadequate or poorly controlled pulmonary blood flow, distortion of the main pulmonary arterial segment, and encroachment of the band on the proximal branch pulmonary arteries as well as possible interference of the band with pulmonary valve function including development of pulmonary valve stenosis. Because of these problems and because of improvements in infant surgery, pulmonary artery banding rarely is done in the modern era. Pulmonary artery banding may have a role in management of the premature or smaller infant (<3 kg) and patients with multiple VSDs (so-called Swiss cheese septum).

Another approach to patients with a “Swiss cheese” septum has incorporated the use of percutaneous or hybrid catheter (see Chapter 13) techniques to close one or more of the larger defects. Closure of large muscular defects from a left ventricular approach has been effective albeit with the potential for long-term adverse effect upon left ventricular function and the development of ventricular arrhythmias (48,49). Some investigators

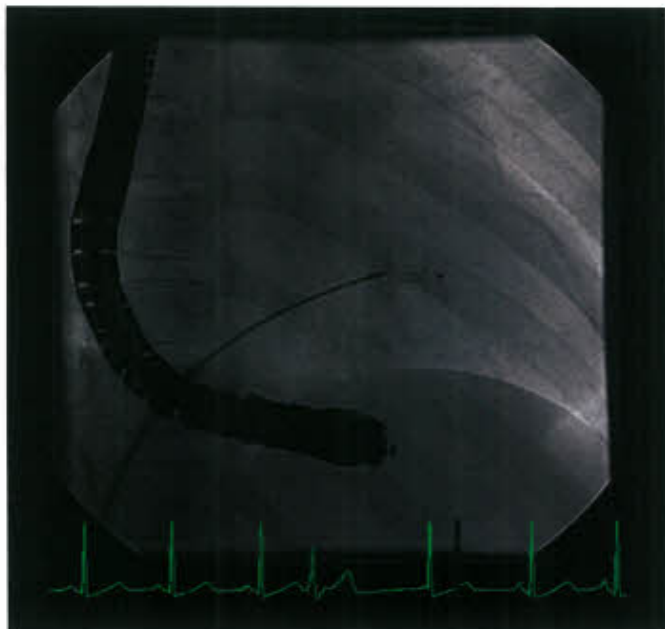


Figure 30.14. Right anterior oblique orientation of anterior-posterior camera demonstrating the TEE probe and the prograde deployment of an Amplatzer muscular VSD device occluder.

have described the feasibility of percutaneous device closure of perimembranous and muscular VSDs (Fig. 30.14) (48,49) (see Chapter 13). Percutaneous techniques have been used to close postmyocardial infarction VSDs. The attractiveness of percutaneous closure lies in the avoidance of cardiopulmonary bypass and sternotomy, a shorter hospital stay, and decreased cost. The major drawback has been creation of atrioventricular conduction block. Follow-up studies of patients who have had percutaneous VSD closure have been limited to <10 years in contrast to the follow-up of surgical closure of the VSDs, which is now reaching 57 years. Early and delayed atrioventricular block occurs in fewer than 1% of patients after surgical closure of an isolated VSD, whereas atrioventricular block ranges from 3% to 20% after percutaneous closure (50,51,52).

In summary, use of percutaneous device occlusion has an increasing role in interventional pediatric and adult cardiology. However, investigators have demonstrated that surgical closure has excellent outcomes with low early and late postoperative complications as compared to patients who have had percutaneous occlusion. As techniques and materials improve, the outcomes of patients who have percutaneous occlusion undoubtedly will improve.

Postoperative sequelae

The presence of residual defects after surgical or percutaneous closure have been well documented (53,54). Postoperative evaluation should include a surface electrocardiogram, an echocardiogram to determine presence or absence of residual shunts, presence or absence of pericardial effusions, and a chest x-ray to evaluate heart size and presence or absence of pleural effusions. Common postoperative findings include right bundle branch block, especially if a right ventriculotomy was performed. Although rare, delayed complete heart block can occur after surgical VSD closure. Patients who have had a left ventriculotomy for either surgical or percutaneous access to muscular VSDs may exhibit abnormal left

ventricular wall motion, elevated left ventricular end-diastolic pressure, and or left ventricular systolic dysfunction. Small residual VSDs can occur. Most often, these are small defects either around the device or around the surgical patch; they may close spontaneously during the first year after closure. Repeat surgical intervention rarely is needed for small residual defects (<2 mm) (54).

CLINICAL OUTCOMES AND PROGNOSIS

The prognosis is good for most patients with small VSDs. They are at very low risk for the development of elevated pulmonary vascular resistance (27,55). Long-term studies have demonstrated that those patients have excellent outcomes and that mortality has been linked to the presence of associated semilunar valve problems (most commonly aortic valve insufficiency) or bacterial endocarditis (56). Kidd et al. concluded that the majority of patients fared well. Long-term survival at 25 years was approximately 87%. Despite this, there was a higher than normal 15-year prevalence of serious arrhythmia and sudden death among patients managed either medically or surgically (57). Similar findings were reported by Roos-Hesselink et al. in their review of 22- to 34-year postoperative outcomes of patients who had surgical repair of VSDs. A review of 176 consecutive patients between 1968 and 1980 at a single institution showed a survival rate of 92%. A 4% incidence of sinus node dysfunction requiring pacemaker implantation was noted. The incidence of pulmonary hypertension was 4% and the incidence of aortic valve insufficiency was 16%. The need for surgical reintervention was 6% (58).

Most (75% to 80%) small perimembranous-type defects and small muscular-type VSDs will close spontaneously within the first 2 years of life. However, untreated patients with large VSDs in infancy can die from congestive heart failure during the first 6 weeks to 6 months of life. With proper medical and surgical management, however, these patients should have an excellent outcome (59–65).

ACKNOWLEDGMENTS

We would like to thank the echocardiography staff at Seattle Children's Hospital for their tireless dedication to our patients and for their assistance in collecting the images presented in this chapter. Special thanks to Heidi Borchers, RDCS, Raylene Choy, RDCS, and Colleen Cailles, RDCS, RCS.

REFERENCES

1. Hoffman JJ, Rudolph AM. The natural history of ventricular septal defects in infancy. *Am J Cardiol* 1965;16:634–653.
2. Graham TP, Bender HW, Spach MS. Ventricular septal defect. In: Adams FH, Emmanouilides GC, eds. *Moss; Heart Disease in Infants, Children and Adolescents*. 3rd ed. Baltimore, MD: Williams & Wilkins, 1983:134.
3. Dickinson D, Arnold R, Wilkinson J. Ventricular septal defect in children born in Liverpool: 1960–1969. *Br Heart J* 1981;46:47–54.
4. Hoffman JJ, Kaplan S, Liberthson RR. Prevalence of congenital heart disease. *Am Heart J* 2004;147:425–439.
5. Tikanoja T. Effect of technical development on the apparent incidence of congenital heart disease. *Pediatr Cardiol* 1995;16:100–101.
6. Roguin N, Du Z-D, Barak M, et al. High prevalence of muscular ventricular septal defects in neonates. *J Am Coll Cardiol* 1995;26:1545–1548.
7. Reller MD, Strickland MJ, Riehle-Colarusso T, et al. Prevalence of congenital heart defects in metropolitan Atlanta, 1998–2005. *J Pediatr* 2008; 153: 807–813.
8. Nora JJ, Fraser FLC. *Medical Genetics*. Philadelphia, PA: Lea & Febiger, 1974:334.

9. Soto B, Becker AE, Moulart AJ, et al. Classification of ventricular septal defects. *Br Heart J* 1980;43:332-343.
10. Anderson RH, Wilcox BR. The surgical anatomy of the ventricular septal defect. *J Cardiac Surg* 1992;7:17-34.
11. Lincoln C, Jamieson S, Joseph M, et al. Transatrial repair of ventricular septal defects with reference to their anatomic classification. *J Thorac Cardiovasc Surg* 1977;74:183-190.
12. Scully BB, Morales DLS, Zafar F, et al. Current expectations of surgical repair of isolated ventricular septal defects. *Ann Thorac Surg* 2010;89:544-551.
13. Tatsuno K, Ando M, Takan A, et al. Diagnostic importance of aortography in conal ventricular septal defect. *Am Heart J* 1975;89:171-177.
14. Wennik ACG, Oppenheimer-Dekker A, Moulart AJ. Muscular ventricular septal defects: a reappraisal of the anatomy. *Am J Cardiol* 1979;43:259-264.
15. Anderson RH, Leval MR. The morphology of ventricular septal defects as related to the mechanics associated with aortic regurgitation. *Semin Thorac Cardiovasc Surg Pediatr Card Surg Annu* 2006;140-146.
16. Rudolph AM. The effects of postnatal circulatory adjustments in congenital heart disease. *Pediatrics* 1965;36:763-772.
17. Dammann JF Jr, Thompson WM Jr, Sosa O, et al. Anatomy, physiology and natural history of simple ventricular septal defects. *Am J Cardiol* 1960;5:136-166.
18. Ritter DG, Feldt RH, Weidman WH, et al. Ventricular septal defect. *Circulation* 1965;32:III42-III52.
19. Bloomfield DK. The natural history of ventricular septal defects in patients surviving infancy. *Circulation* 1964;29:914-955.
20. Jarmakani MM, Graham TP Jr, Canent RV Jr, et al. Effect of site of shunt on left heart volume characteristics with ventricular septal defect and patent ductus arteriosus. *Circulation* 1969;40:411-418.
21. Wood P. Eisenmenger syndrome or pulmonary hypertension with reversed central shunt. *BMJ* 1958;1:298.
22. Abbott ME. Congenital heart disease. In: *Nelson's Loose-leaf Medicine*. Vol. 5. New York, NY: Thomas Nelson & Sons, 1932:207.
23. Rabinovitch M, Keane JF, Norwood WI, et al. Vascular structure in lung tissue obtained at biopsy correlated with pulmonary hemodynamic findings after repair of congenital heart defects. *Circulation* 1984;69:655-667.
24. Weidman WH, DuShane JW, Kirklin JW. Observations concerning progressive pulmonary vascular obstruction in children with ventricular septal defects. *Am Heart J* 1963;65:148-154.
25. Lee S-D, Shroyer KR, Markham NE, et al. Monoclonal endothelial cell proliferation is present in primary but not secondary pulmonary hypertension. *J Clin Invest* 1998;101:927-934.
26. Adatia I, Kothari SS, Feinstein JA. Pulmonary hypertension associated with congenital heart disease: pulmonary vascular disease: the global perspective. *Chest* 2010;137:525-615.
27. Van Hare GF, Soffer LJ, Sivakoff MC, et al. Twenty-five-year experience with ventricular septal defect in infants and children. *Am Heart J* 1987;114:606-614.
28. Didier D, Higgins CB. Identification and localization of ventricular septal defect by gated magnetic resonance imaging. *Am J Cardiol* 1986;57:1363-1368.
29. Beerbaum P, Körperich H, Barth P, et al. Noninvasive quantification of left-to-right shunt in pediatric patients: phase-contrast cine magnetic resonance imaging compared with invasive oximetry. *Circulation* 2001;103:2476-2482.
30. Debl K, Djavidani B, Buchner S, et al. Quantification of left-to-right shunting in adult congenital heart disease: phase-contrast cine MRI compared with invasive oximetry. *Br J Radiol* 2009;82:386-391.
31. Barger LM Jr, Elliott LP, Soto B, et al. Axial cineangiography in congenital heart disease Section I Concept, technical and anatomic considerations. *Circulation* 1977;56:1075-1083.
32. Elliott LP, Barger LM Jr, Bream PR, et al. Axial cineangiography in congenital heart disease Section II Specific lesions. *Circulation* 1977;56:1048-1093.
33. Taylor MB, Laussen PC. Fundamentals of management of acute postoperative pulmonary hypertension. *Pediatr Crit Care Med* 2010;11:S27-S29.
34. Atz AM, Adatia I, Lock JE, et al. Combined effects of nitric oxide and oxygen during acute pulmonary vasodilator testing. *J Am Coll Cardiol* 1999;33:813-819.
35. Day RW, Lynch JM, Shaddy RE, et al. Pulmonary vasodilatory effects of 12 and 60 parts per million inhaled nitric oxide in children with ventricular septal defect. *Am J Cardiol* 1995;75:196-198.
36. Neutze JM, Ishikawa T, Clarkson PM, et al. Assessment and follow-up of patients with ventricular septal defect and elevated pulmonary vascular resistance. *Am J Cardiol* 1989;63:327-331.
37. Boucek MM, Chang RL. Effects of captopril on the distribution of left ventricular output with ventricular septal defect. *Pediatr Res* 1988;24:499-503.
38. Shaw NJ, Wilson N, Dickinson DE. Captopril in heart failure secondary to a left to right shunt. *Arch Dis Child* 1988;63:360-363.
39. Montigny M, Davignon A, Fouron JC, et al. Captopril in infants for congestive heart failure secondary to a large ventricular left-to-right shunt. *Am J Cardiol* 1989;63:631-633.
40. Webster MW, Neutze JM, Calder AL. Acute hemodynamic effects of converting enzyme inhibition in children with intracardiac shunts. *Pediatr Cardiol* 1992;13:129-135.
41. Hougren TJ. Digitalis use in children: an uncertain future. *Prog Pediatr Cardiol* 2000;12:37-43.
42. Berman W, Yabek SM, Dillon T, et al. Effects of digoxin in infants with a congested circulatory state due to a ventricular septal defect. *N Engl J Med* 1983;308:363-366.
43. Kimball TR, Daniels SR, Meyer RA, et al. Effect of digoxin on contractility and symptoms in infants with a large ventricular septal defect. *Am J Cardiol* 1991;68:1377-1382.
44. Stewart JM, Hintze TH, Woolf PK, et al. Nature of heart failure in patients with ventricular septal defect. *Am J Physiol* 1995;269:H1473-H1480.
45. Jonas R. Ventricular septal defect. In: Jonas R, ed. *Comprehensive Surgical Management of Congenital Heart Disease*. London, UK: Hooper Arnold Publication, 2004:242-255.
46. Kidd L, Driscoll DJ, Gersony WM, et al. Second natural history study of congenital heart defects Results of treatment of patients with ventricular septal defects. *Circulation* 1993;87:I38-I51.
47. Warnes CA, Williams RG, Bashore TM, et al.; on behalf of American Society of Echocardiography, Heart Rhythm Society, International Society for Adult Congenital Heart Disease, Society for Cardiovascular Angiography and Interventions, Society of Thoracic Surgeons. ACC/AHA 2008 guidelines for the management of adults with congenital heart disease: a report of the American College of Cardiology/American Heart Association Task Force on Practice Guidelines (Writing Committee to Develop Guidelines on the Management of Adults With Congenital Heart Disease). *J Am Coll Cardiol* 2008;52:e1-e121.
48. Hannan RL, McDaniel NL, Kron IL. Repair of large muscular ventricular septal defects in infants employing left ventriculotomy. *Ann Thorac Surg* 1997;63:288-289.
49. Michel-Behnke I, Ewert P, Koch A, et al.; Investigators of the Working Group Interventional Cardiology of the German Association of Pediatric Cardiology. Device closure of ventricular septal defects by hybrid procedures: a multicenter retrospective study. *Catheter Cardiovasc Interv* 2011;77:242-251.
50. Lin A, Mahle WT, Frias PA, et al. Early and delayed atrioventricular conduction block after routine surgery for congenital heart disease. *J Thorac Cardiovasc Surg* 2010;140:158-160.
51. Butera G, Carminati M, Chessa M, et al. Transcatheter closure of perimembranous ventricular septal defects: early and long-term results. *J Am Coll Cardiol* 2007;50:1189-1195.
52. Predescu D, Chaturvedi RR, Friedberg MK, et al. Complete heart block associated with device closure of perimembranous ventricular septal defects. *J Thorac Cardiovasc Surg* 2008;136:1223-1228.
53. Sommer RJ, Golinko RJ, Ritter SB. Intracardiac shunting in children with ventricular septal defect: evaluation with Doppler color flow mapping. *J Am Coll Cardiol* 1990;16:1437-1444.
54. Muhiudeen IA, Roberson DA, Silverman NH, et al. Intraoperative echocardiography in infants and children with congenital cardiac shunt lesions: transeptophageal versus epicardial echocardiography. *J Am Coll Cardiol* 1990;16:1687-1695.
55. Moller JH, Patton C, Varco RL, et al. Late results (30 to 35 years) after operative closure of isolated ventricular septal defect from 1954 to 1960. *Am J Cardiol* 1991;68:1491-1497.
56. Corone P, Doyon F, Gaudeau S, et al. Natural history of ventricular septal defect: a study involving 790 cases. *Circulation* 1977;55:908-915.
57. Yacoub MH, Khan H, Stavri G, et al. Anatomic correction of the syndrome of prolapsing right coronary aortic cusp, dilation of the sinus of Valsalva, and ventricular septal defect. *J Thorac Cardiovasc Surg* 1997;113:253-261.
58. Roos-Hesselink JW, Meijboom FJ, Spitaels SE, et al. Outcome of patients after surgical closure of ventricular septal defect at young age: longitudinal follow-up of 22-34 years. *Eur Heart J* 2004;25:1057-1062.
59. Cordell D, Graham TP Jr, Atwood GE, et al. Left heart volume characteristics following ventricular septal defect closure in infancy. *Circulation* 1976;54:294-298.
60. Graham TP Jr, Jarmakani JM, Canent RV Jr, et al. Left heart volume estimations in infancy and childhood: re-evaluation of methodology and normal values. *Circulation* 1971;43:895-904.
61. Kogon B, Butler H, Kirshbom P, et al. Closure of symptomatic ventricular septal defects: how early is too early? *Pediatr Cardiol* 2008;29:36-39.
62. Nadas AS, Thilenius OG, LaFarge CG, et al. Ventricular septal defect with aortic regurgitation: medical and pathologic aspects. *Circulation* 1964;29:862-873.
63. McDaniel N, Gutgesell HP, Nolan SP, et al. Repair of large muscular ventricular septal defects in infants employing left ventriculotomy. *Ann Thorac Surg* 1989;47:593-594.
64. Oses P, Hugues N, Dahdah N, et al. Treatment of isolated ventricular septal defects in children: amplatzer versus surgical closure. *Ann Thorac Surg* 2010;90:1593-1598.
65. Dodge-Khatami A, Knirsch W, Tomaske M, et al. Spontaneous closure of small residual ventricular septal defects after surgical repair. *Ann Thorac Surg* 2007;83:902-905.

Patent Ductus Arteriosus and Aortopulmonary Window

Phillip Moore ■ Michael M. Brook

PATENT DUCTUS ARTERIOSUS

Anatomy

The ductus arteriosus, a large channel normally found in all mammalian fetuses, develops from the distal portion of the left sixth aortic arch and connects the main pulmonary trunk with the descending aorta, 5 to 10 mm distal to the origin of the left subclavian artery in a full-term infant. With a right aortic arch, the ductus arteriosus may be on the right, joining the right pulmonary artery and the right aortic arch just distal to the right subclavian artery; more commonly, it is on the left, joining the left pulmonary artery and the proximal portion of the left subclavian artery. Rarely, the ductus arteriosus may be bilateral. It varies in length and in the term fetus has a diameter of approximately 10 mm, similar to that of the descending aorta (1). The ductus is a tube with a relatively uniform diameter prior to closure; however when it remains patent postnatally it changes shape dramatically. Closure usually begins at the pulmonary artery end, so most often a patent duct is conical in shape, large at the aortic ampulla and narrowing toward the pulmonary artery entrance; however, there is great variability in the anatomical shape of the persistent ductus.

The microscopic structure of the ductus arteriosus differs from that of the adjacent pulmonary trunk or aorta. Although wall thicknesses are similar, the media of the latter are composed mainly of circumferentially arranged layers of elastic fibers, whereas the media of the ductus arteriosus consist largely of layers of smooth muscle arranged spirally in both leftward and rightward directions together with increased amounts of hyaluronic acid. The intimal layer of the ductus arteriosus is thicker than that of the adjoining arteries and contains an increased amount of mucoid substance. There are also small, thin-walled vessels in its subendothelial region (2,3).

Important associated structures to the ductus arteriosus include the recurrent laryngeal nerve, the phrenic nerve, and the thoracic duct. The recurrent laryngeal nerve arises from the vagus nerve anteriorly and caudally, coursing around the duct to ascend posteriorly to the larynx. It can be injured during surgical ligation as well as interventional treatment with devices and stents (4,5).

Physiology

Role in the Fetus

By 6 weeks of gestation, the ductus arteriosus is developed sufficiently to carry most of the right ventricular output. The relative sizes of the great arteries and the ductus arteriosus reflect the

proportions of cardiac output (combined ventricular output) carried by them (1). The right ventricle ejects about two-thirds of combined ventricular output, and because lung flow is only 6% to 8%, the ductus arteriosus carries 55% to 60% of combined ventricular output (6). The ductus arteriosus permits flow to be diverted away from the high-resistance pulmonary circulation to the descending aorta and the low-resistance placental circulation. A large pulmonary blood flow during fetal life would represent wasted circulation, and the ductus arteriosus therefore reduces the total workload of the fetal ventricles (6).

Whether the ductus arteriosus plays an active physiologic role during fetal life is unknown. It had been considered a relatively passive structure until it was shown that prostaglandin E_2 (PGE_2) and prostacyclin (PGI_2) produce and maintain active relaxation (7–11).

Normal Postnatal Closure

Postnatal closure of the ductus arteriosus is effected in two phases. Immediately after birth, contraction and cellular migration of the medial smooth muscle in the wall of the ductus arteriosus produce shortening, increased wall thickness, and protrusion into the lumen of the thickened intima (intimal cushions or mounds), resulting in functional closure (3). This commonly occurs within 12 hours after birth in full-term human infants (12). The second stage usually is completed by 2 to 3 weeks in human infants, produced by infolding of the endothelium, disruption and fragmentation of the internal elastic lamina, proliferation of the subintimal layers, and hemorrhage and necrosis in the subintimal region. The mounds enlarge progressively, and there is connective tissue formation and replacement of muscle fibers with fibrosis and permanent sealing of the lumen to produce the ligamentum arteriosum (2).

The exact mechanisms responsible for the initial postnatal closure of the ductus arteriosus are not fully understood. During fetal life, the partial pressure of oxygen (pO_2) to which the ductus arteriosus is normally exposed is 18 to 28 mm Hg (6). An increase in pO_2 , as it occurs with ventilation after birth, constricts the ductus arteriosus in mature fetal animals (6,7,9,10,13); however, at about 0.6 gestation (term = 150 days), although capable of contracting, the ductus arteriosus is not constricted by increased oxygen even at high concentrations. With advancing gestation, the amount of constriction in response to increasing pO_2 is greater and the level of pO_2 required to initiate a response decreases (11,13). Other factors, such as the release of vasoactive substances (e.g., acetylcholine, bradykinin, or endogenous catecholamines), may contribute to postnatal closure of the ductus arteriosus under physiologic conditions (6,13).

Of greater importance is the role of prostaglandins, the cyclooxygenase-mediated products of arachidonic acid metabolism, in the ontogenic and overall physiology of the ductus arteriosus. Exogenous PGE₁, PGE₂, and PGI₂ dilate isolated ductus arteriosus strips or rings from term fetal lambs (7,8,10). Inhibitors of prostaglandin synthesis, either *in vitro* or when administered *in vivo* to pregnant animals near term, produce constriction of the ductus arteriosus (7,8,10), reversible by PGE₁ infusion (8), indicating that prostaglandins play an active role in maintaining the ductus arteriosus in a dilated state during normal fetal life. The exact sites of production of these prostaglandins *in vivo* are unclear. PGE₂ and PGI₂ are formed intramurally in the ductus arteriosus and may exert their action locally on muscle cells (7–9). Endogenous PGI₂ production is about tenfold that of PGE₂; however, PGE₂ is three orders of magnitude more potent than PGI₂ as a relaxer of the ductus arteriosus (7,9). Prostaglandins are detectable only in very low concentrations in adult plasma, and most are not thought to act as circulating hormones because of their rapid catabolism in the lung (9). The fetus, however, has high circulating concentrations of prostaglandins, particularly PGE₂, probably owing to low fetal pulmonary blood flow and therefore decreased prostaglandin catabolism in the lungs, as well as to the fact that the placenta produces prostaglandins (7–9).

The effects of prostaglandins, as well as of inhibitors of prostaglandin synthesis, vary at different gestational ages (7,9,11). Indomethacin constricts rings of ductus arteriosus from immature fetal lambs more than it does rings from close-to-term lambs. Both PGE₂ and PGI₂ relax the ductus arteriosus from immature lambs more than that from mature animals, reflecting the significantly greater sensitivity to PGE₂ and PGI₂ of the immature ductus arteriosus. This change in sensitivity is influenced by the increase in endogenous cortisol toward term. Thus, patency or closure of the ductus arteriosus represents a balance between the constricting effects of oxygen, and perhaps certain vasoconstrictive substances, and the relaxing effects of several prostaglandins (9,10). At birth, the placental source is removed, and the marked increase in pulmonary blood flow allows effective removal of circulating PGE₂ tipping the balance in favor of ductal closure.

Physiology of Patency

Ontogenic differences in physiologic factors almost certainly account for the higher incidence of persistent patency of the ductus arteriosus (PDA) in preterm infants (11). Sensitivity of ductus arteriosus smooth muscle to PGE₂ is highest in immature animals and decreases with advancing gestation. In term infants, responsiveness is lost shortly after birth; this does not occur in the immature ductus. Pulmonary metabolism is important in reducing circulating concentrations of PGE₂; because this function is significantly reduced in immature lungs, increased circulating concentrations of PGE₂ as well as increased sensitivity are important contributors to persistent patency in preterm infants.

Physiology of the Left-to-Right Shunt

As with all left-to-right shunts, with PDA three major, interrelated factors control the magnitude of shunting: the diameter and length of the ductus arteriosus, which governs the resistance offered to flow; the pressure difference between the aorta and the pulmonary artery; and the systemic and pulmonary vascular resistances.

Normally after birth, systemic vascular resistance (afterload) is high, whereas pulmonary vascular resistance decreases when ventilation begins. As a result, systemic arterial blood pressure becomes higher than that in the pulmonary artery. With a small PDA, a high resistance to flow is offered by the small cross-sectional opening of the ductus arteriosus, so that

the left-to-right shunt will be small despite the large pressure difference. However, with a large communication, pressures tend to become equal, and the magnitude of shunting is then determined by the relationship of the systemic and pulmonary vascular resistances. For this reason left-to-right shunting through a PDA has been defined as dependent shunting (14). Because systemic vascular resistance does not change significantly after birth, changes in pulmonary vascular resistance are the major determinants in regulating the left-to-right shunting through a PDA. This is particularly important in the first 2 months after birth, when pulmonary vascular resistance normally is decreasing.

The physiologic features associated with left-to-right shunting through a PDA depend on the magnitude of the left-to-right shunt and the ability of the infant to handle the extra volume load (15). The volume shunted left to right through the PDA increases left ventricular output (16) that normally is high in the immediate newborn period (17). The resultant increase of pulmonary venous return to the left atrium and left ventricle (LV) increases ventricular diastolic volume (preload) and thereby LV stroke volume (Frank-Starling mechanism). LV dilation will result in an increased LV end-diastolic pressure with secondary increase in left atrial (LA) pressure. This may lead to signs of overt left heart failure with LA dilation and pulmonary edema. Right ventricular failure may occur if there is a large PDA with pulmonary hypertension or pulmonary edema and an elevated LA pressure, in which case pulmonary vascular resistance may be increased. The net result of both these situations is an increased pressure load for the right ventricle. Left-to-right shunting through a stretched, incompetent foramen ovale secondary to LA dilation is a fairly common association (15).

Several compensatory physiologic mechanisms help to improve myocardial performance and thereby maintain a normal systemic output. In addition to the Frank-Starling mechanism, the sympathetic adrenal system is stimulated, as is the development of myocardial hypertrophy. Increased sympathetic stimulation leads to direct stimulation of nerve fibers within the myocardium, with local norepinephrine release as well as an increase in circulating catecholamines released from the adrenal glands. As a result, both the force of contraction and the heart rate are increased. These mechanisms are responsible for the rapid heart rate and the sweating often seen in infants with heart failure. If the increased volume load persists, hypertrophy of the ventricular myocardium will develop. Because of the diastolic runoff through the PDA, the overall resistance to the LV is low facilitating increased total LV output.

These compensatory mechanisms are ordinarily well developed in older children or adults; however, they are not as well developed in newborn infants and are even less so in prematurely born infants. It is most important, therefore, to consider the state of maturity (i.e., gestational age at time of birth) of an infant who has a PDA with left-to-right shunting. Many physiologic functions that are present in older children reach full maturation at different rates and periods of gestation. For example, sympathetic nervous innervation of the LV myocardium may be completed only at term, or even after term (18), so that in an infant born prematurely, sympathetic stimulation of the LV myocardium likely would be incomplete. Likewise, the myocardium in an immature animal responds less to stretch (Frank-Starling mechanism) than does that in a more mature animal (19). The structure of the immature myocardium, too, is quite different from that at term in that there are far fewer contractile elements (19). Premature infants often have lower than normal serum Ca²⁺ concentrations, and this too may affect myocardial performance (20). Probably for one or all of these reasons, premature infants with left-to-right shunts through a PDA develop LV failure earlier than their full-term counterparts and, in addition, with a smaller volume

load. Of considerable importance as well is maintenance of myocardial perfusion. Because coronary arterial blood flow to the LV occurs mainly during diastole and depends on the systemic arterial–intramyocardial diastolic pressure differences as well as the duration of diastole, alterations in either can affect coronary blood flow (21). A reduction in aortic diastolic pressure occurs in a large PDA, and with a significant shunt, LV end-diastolic pressure may be increased and cause an increase in subendocardial intramyocardial pressure. The development of tachycardia will reduce the diastolic period. All three factors may result in decreased myocardial perfusion in the presence of a large PDA.

Delivery of oxygen to the myocardium depends on not only the coronary blood flow, but also the oxygen content of arterial blood and the ability of arterial blood to deliver oxygen at the tissue sites. A low hemoglobin concentration caused by physiologic anemia in the newborn period, particularly in premature infants, or by repeated blood sampling as it occurs with intensive neonatal care, jeopardizes oxygen delivery to the myocardium as well as to other organs. A further important factor, particularly in premature infants, is the amount of fetal hemoglobin present. Because fetal hemoglobin has a low affinity for the organic phosphates such as 2,3-diphosphoglycerate, the facilitation of oxygen delivery to peripheral tissues is reduced. This effect is greater with higher amounts of fetal hemoglobin (22).

Effects on the Pulmonary Circulation and Lungs

A small communication has little or no effect on the pulmonary arterial circulation. However, with a large communication, systemic and pulmonary arterial pressures will equalize, and because of the high flow and pressure, the small pulmonary arteries may not undergo their normal postnatal maturational changes. The medial smooth muscle does not regress as rapidly as normal or to the same extent, so that pulmonary vascular resistance falls more slowly and less completely than usual.

Initially the increase in pulmonary vascular resistance is associated only with an increased amount of medial smooth muscle. However, true pulmonary vascular disease (23) may occur subsequently, manifested by intimal damage with cellular proliferation, hyalinization, and finally thrombosis and fibrosis of the small pulmonary arteries. As more small pulmonary arteries become involved in this process, the pulmonary vascular resistance increases, the left-to-right shunt diminishes, and eventually a right-to-left shunt occurs. In severe pulmonary vascular obstructive disease, arteriovenous malformations may form with resultant hemoptysis.

Pulmonary edema occurs commonly in premature infants with only a moderate shunt and without severe heart failure. Capillary permeability in newborn animals is greater than in adults, and may be even more pronounced in premature infants. A small elevation in pulmonary venous pressure therefore can produce significant pulmonary edema.

Physiology of Delayed Closure in Term Infants

Although functional closure of the ductus arteriosus typically is completed on the first day after birth, it may be delayed for several days. Because pulmonary vascular resistance decreases normally, flow will occur from the aorta into the pulmonary artery throughout this period of functional patency. On careful auscultation, therefore, a murmur may be heard in the first few hours of life in many infants (24). Two particular murmurs have been described: a crescendo systolic murmur and a continuous murmur with a crescendo systolic and diminuendo diastolic component. Neither murmur is very loud (grade 1 to 2 on a scale of 1 to 6), and

both may be accentuated, or possibly only heard, during inspiration; the murmurs are heard best in the second to third left intercostal space and do not radiate widely. Because pulmonary arterial pressure is normal, the pulmonic component of the second sound is of normal intensity and the second sound is often well split (24). As the ductus arteriosus constricts, the diastolic component becomes inaudible and leaves only a crescendo systolic murmur that usually disappears by the 2nd to 3rd day of life. The electrocardiogram (ECG) and chest roentgenogram in these infants are normal. Real-time two-dimensional echocardiography shows normal intracardiac structures, and the ductus arteriosus generally is visualized directly. Doppler and color Doppler evaluation invariably detect and delineate the flow patterns of the shunt across the ductus arteriosus into the main pulmonary artery (25–27). Retrograde aortic flow is not seen in these infants with a small ductus. Hemodynamic studies performed in these infants have shown small left-to-right shunts with normal arterial pressures.

During the initial hours of constriction, any condition that lowers arterial blood pO_2 or increases circulating blood PGE_2 concentrations may delay normal closure (28). Likewise, before true anatomic closure occurs, the functionally closed ductus arteriosus may dilate with a reduced arterial blood pO_2 (29) or increased PGE_2 concentration. This may occur in asphyxial states and in the presence of any one of many different pulmonary diseases (e.g., meconium aspiration). Residing at a high-altitude location, a nonpulmonary cause of arterial hypoxemia, has been shown to produce delayed closure of the ductus arteriosus. The incidence of PDA is about 30 times greater at high altitude (4,500 to 5,000 m) than at sea level (30). With severe pulmonary disease or persistent pulmonary hypertension syndrome of the newborn, when there is an increase in pulmonary vascular resistance, no shunt or even a right-to-left shunt through the PDA may occur. This leads to a lower pO_2 in the lower extremities than in the upper. This difference in pO_2 may persist for many days, and with pulmonary disease the ductus arteriosus may remain patent for several weeks.

The initial constriction of the ductus arteriosus is most prominent at its pulmonary arterial end and extends progressively toward the aorta, thus accounting for the predominant cone shape of the small PDA in which the diameter at the aortic end is considerably larger than at the pulmonary end. Even after the pulmonary arterial end has closed completely, the dilated aortic end of the ductus arteriosus may persist. This ductus ampulla, or ductus bump, may be evident on the chest roentgenogram (Fig. 31.1A,B) for several weeks (31).

Pathologic States

Premature Closure *in Utero*

In utero closure of the duct is well described. It can occur spontaneously, but is also associated with maternal use of nonsteroidal anti-inflammatory agents (NSAIDs) (32–34). Indomethacin appears to have the greatest effect, with the risk 15-fold higher than that of other NSAIDs (34). Interestingly aspirin does not appear to be associated with a significant risk for ductal closure (35), and no information exists about the risk of closure after ibuprofen exposure.

Premature closure of the duct *in utero* results in increased afterload on the right ventricle and increase pulmonary blood flow. This can lead to right ventricular failure, hydrops, and postnatal pulmonary hypertension (36). These can lead to increased risk for premature delivery, need for postnatal ventilation or extracorporeal support, and death. Fortunately, in the setting of NSAID usage, the effect on the duct is generally

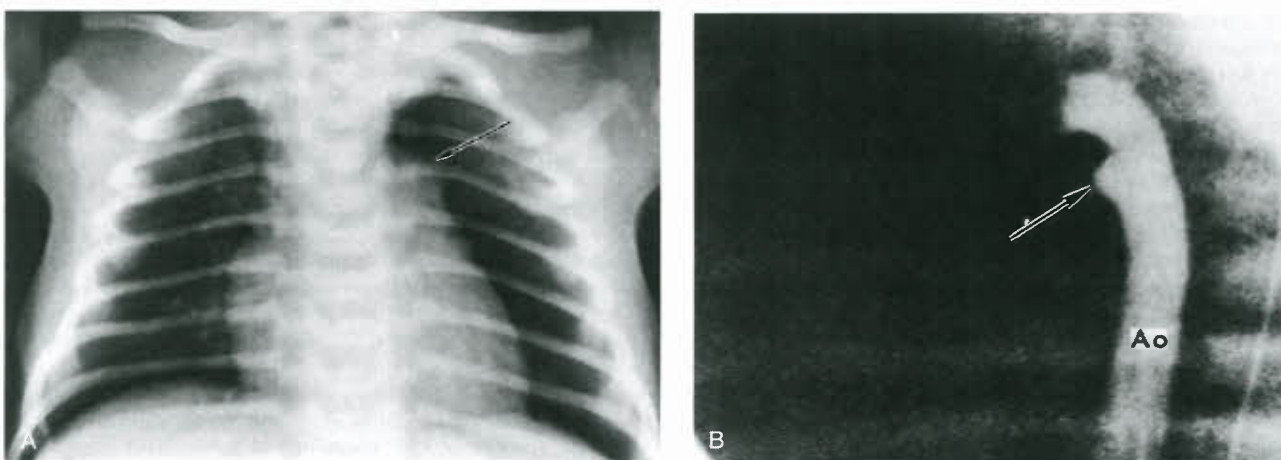


Figure 31.1. A: Posterior-anterior chest roentgenogram of a 2-day-old infant demonstrating the ductus bump (arrow). B: Angiogram in the lateral position of a 5-day-old infant demonstrating the ampulla of the ductus arteriosus (arrow). Ao, aorta.

short lived and reversible when the medication is discontinued (37). The finding is easily seen using fetal echocardiography, which shows an increased diastolic velocity through the duct (38,39) (Fig. 31.2A,B).

Persistent Patency in Premature Infants

Delayed closure of the ductus arteriosus in preterm infants is well recognized (12,40–44). With the advent of techniques for maintenance of ventilation in premature infants, survival, particularly of small premature infants, has improved dramatically. Improvement of lung function with surfactant replacement therapy, by decreasing pulmonary vascular resistance, has led to the clinical emergence of PDA earlier and more frequently in preterm infants (45). Because the constrictor response of the ductus arteriosus to oxygen and the dilator effect of PGE_2 are closely related to gestational age (7,9,13), it is not surprising that there is an extremely high incidence of PDA in low-birth-weight preterm infants, particularly the very low-birth-weight infant (<1,000 g) and those with pulmonary disease. Approximately 45% of infants <1,750 g birth weight have clinical evidence of PDA, and infants <1,200 g birth weight have a prevalence closer to 80%. Overall, the incidence of PDA in preterm infants is about 8 per 1,000 of all live births.

The presence of a significant PDA in premature infants is associated with lower regional cerebral oxygen saturation (46) that implies reduced cerebral blood flow. In addition, studies have shown an elevated cardiac troponin T that normalizes after closure (47). These elevations are associated with increased morbidity and mortality (47) and worse 2-year neurodevelopmental outcome (48). These findings imply an inability of the immature myocardial and vascular systems to accommodate the increased volume load produced by the left-to-right shunt.

The clinical features depend on the magnitude of left-to-right shunt through the PDA and the ability of the infant to initiate compensatory mechanisms to handle the extra volume load. Because many premature infants have respiratory distress syndrome, the stage of development of this disease and the use of surfactant replacement therapy will determine the pulmonary vascular resistance and therefore the shunt. The maturity of the infant and the stage of myocardial development determine the ability to handle the shunt.

Three fairly distinct patterns of clinical presentation are recognized in these infants.

Patent Ductus Arteriosus with Little or No Lung Disease. In the first group, there is little or no underlying pulmonary disease (usually infants whose birth weight exceeds 1,500 g). However, smaller infants are encountered, and in many instances, their mothers have received steroid or other therapy prior to delivery,

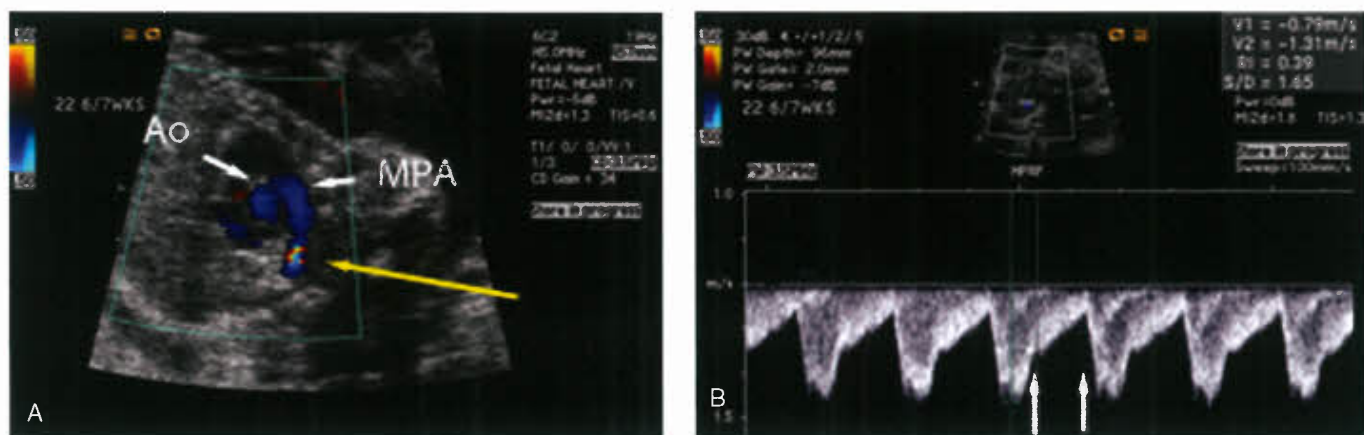


Figure 31.2. A: Fetal echocardiogram with color-flow mapping showing constriction of the ductus. B: Spectral Doppler image of a fetal ductus showing continuous right-to-left flow with abnormally high diastolic velocities.

or the infants have received surfactant replacement therapy. A systolic murmur is first heard 24 to 72 hours after birth, and as the left-to-right shunt increases, this murmur becomes louder and more prolonged, extending to and often beyond the second heart sound into early diastole. The murmur commonly is heard best at the left sternal border in the second and third intercostal spaces. The classic continuous machinery murmur, described for older children with PDA, is not usual in premature infants, in whom the murmur generally has a high-frequency “rocky” quality. The pulmonic component of the second sound may become moderately accentuated. In the most mature infants in this group, a middiastolic flow rumble owing to increased diastolic flow across the normal mitral valve may be heard at the apex. If the shunt becomes large enough, a third heart sound due to rapid ventricular filling during diastole may be heard at the apex. The precordium becomes increasingly more hyperactive, the pulse pressure widens, and the peripheral pulses become more prominent and bounding as the left-to-right shunt increases. Increased peripheral pulses are best appreciated by the presence of palmar or forearm pulses.

If the shunt is allowed to become sufficiently large, clinical evidence of LV failure may appear. This includes tachycardia, tachypnea, and rales on auscultation of the lung fields. Associated with the development of pulmonary edema, there may be a decrease in arterial blood pO_2 . If LV failure were allowed to progress, a significant number of these infants might develop episodes of apnea, often associated with severe bradycardia. Enlargement of the liver will occur, but usually quite late.

The ECG is not helpful early in the disease, but if a moderately large shunt persists for several weeks, LV hypertrophy

and LA enlargement may become evident. The chest roentgenogram may show enlargement of both the left atrium and LV if there is a moderately large shunt, but heart size commonly is normal. Pulmonary vascularity is often increased. Dilation of the ascending aorta usually is not seen in premature infants, but may occur with a protracted moderately severe shunt.

A full echocardiographic and Doppler evaluation has become essential in the clinical management of PDA and in assessing the magnitude of the shunt (25,26,49,50). This also will exclude congenital heart lesions with similar clinical findings as well as LV failure owing to poor intrinsic myocardial function. LA diameter varies with the size of the infant, so the ratio of the LA diameter to the aortic root (Ao) diameter, as measured from the parasternal long-axis echocardiographic view of the heart, can be used to determine LA enlargement. The normal LA:Ao ratio in infants is between 0.8 and 1. A ratio >1.2 suggests LA enlargement, which, in the absence of LV failure due to some other cause (such as aortic or mitral valve abnormalities or volume overload), most often indicates a significant left-to-right shunt. In the premature infant this is likely to be through a PDA. Two-dimensional echocardiography is now used to accurately assess LA and ventricular size directly. The dynamics of both LV and descending aortic wall motion also indicate the magnitude of shunt. Direct visualization of the ductus arteriosus (Fig. 31.3A) confirms the diagnosis. Doppler techniques (pulsed, continuous wave, and color) are applied to the evaluation of flow patterns in infants with PDA and are most helpful (26) (Fig. 31.3B). Flow from the aorta into the pulmonary artery can be detected, and velocity profiles of flow in the main pulmonary artery, ductus arteriosus, and descending aorta

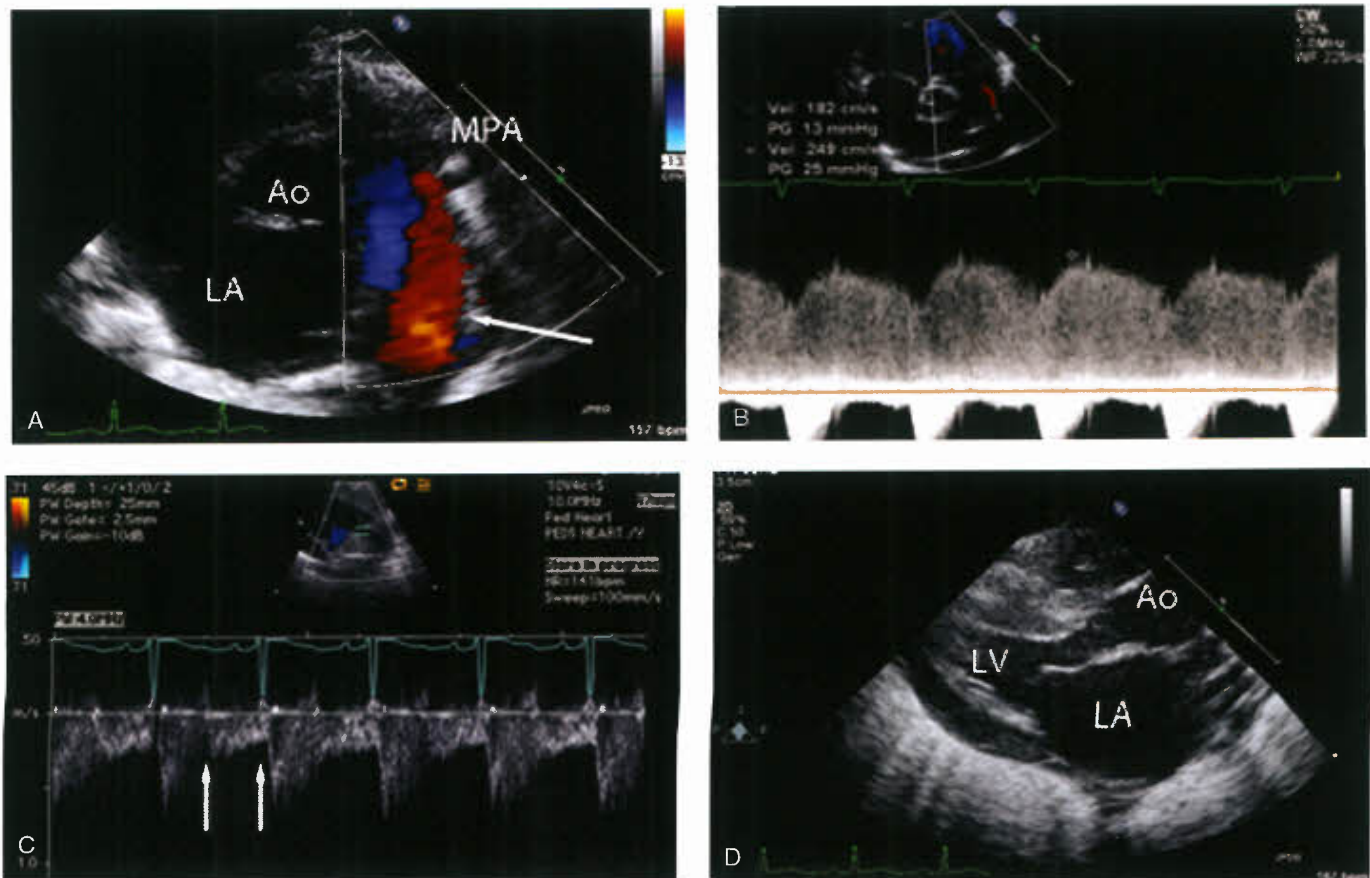


Figure 31.3. A: Echocardiogram in parasternal short axis demonstrating a patent ductus arteriosus with color-flow mapping indicating reversed flow. B: Continuous wave Doppler echocardiogram positioned through the PDA, showing retrograde flow throughout the cardiac cycle. C: Pulsed-Doppler echocardiogram shows increased diastolic flow in the branch pulmonary artery. D: Parasternal long axis showing LA and left ventricular enlargement.

in infants with PDA have been characterized. Doppler color-flow mapping (27) also allows visualization of the extent of flow disturbance in the main pulmonary artery and the direction of the flow jet. Estimates of pulmonary arterial pressure also can be made if systemic arterial blood pressure is known (51).

Cardiac catheterization and angiography in these infants now is unnecessary because of the complete diagnostic information obtained by echocardiography. If performed, catheterization reveals moderate elevation of pulmonary arterial pressures and left-to-right shunting through the ductus arteriosus (40).

The use of biomarkers in the presence of PDA has been evaluated. As early as 1987, it was known that natriuretic peptide levels were abnormally elevated in the presence of a PDA (52). More recently, B-type natriuretic peptide (BNP) has been studied in the presence of a PDA in premature infants. BNP has been shown in adults to correlate with LV volume overload and LV failure (53). Small studies have shown that BNP levels are elevated in the presence of a large ductal shunt in premature infants (54,55). BNP levels decrease in both term and preterm infants rapidly after birth (56,57). In patients with a significant ductal shunt and elevated BNP levels, closure of the PDA results in a fall in BNP levels (58,59). BNP therefore, may be helpful in the screening and evaluation of newborn premature infants with a suspected ductal shunt, but its role in older infants (>2 weeks) or in asymptomatic patients has yet to be investigated.

Many infants in this group do not develop severe LV failure and ordinarily are easily managed with specific medical therapy to constrict the ductus arteriosus or conventional medical therapy of mild heart failure in preterm infants, fluid intake restriction, diuretics, and maintenance of hematocrit above 45%. Very rarely, intractable heart failure develops, necessitating urgent surgical closure. More often existing premature lung disease, active or resolving, adds to respiratory and feeding difficulties, which prompt treatment. If left alone, the ductus arteriosus closes spontaneously in most of these infants, commonly within 2 to 3 months after birth.

Patent Ductus Arteriosus in Infants Recovering from Lung Disease. The second and most common group of infants develops left-to-right shunting while recovering from severe or moderately severe respiratory distress syndrome. These infants usually weigh 1,000 to 1,500 g at birth. The idiopathic respiratory distress syndrome usually is evident within a few hours after birth, and if it follows the usual course, starts to improve after 3 to 4 days. As this improvement continues, early clinical evidence of a left-to-right shunt through a PDA appears. In addition, at about this age, fluid administration generally is increased to deliver adequate calories; this often aggravates the volume-loading effects of the left-to-right shunt on LV function. Probably the ductus arteriosus has been patent since birth and the pulmonary disease with a resultant increase in pulmonary vascular resistance has prevented a detectable left-to-right shunt. As the pulmonary disease improves, oxygenation increases and the ductus arteriosus should constrict. However, most of these infants are quite immature, so a good constrictor response may not occur. Many of these infants are still maintained on mechanical ventilators or continuous positive airway pressure (CPAP), so that careful clinical assessment is required to establish the presence of a shunt through the ductus arteriosus. In many instances the murmurs are not audible until the infant is briefly detached from the ventilator or CPAP system. Because recovery from the respiratory distress syndrome often is not continuously progressive but is interspersed with periods of deteriorating lung function, left-to-right shunting (and therefore the murmur) may be intermittent for several days. The murmur commonly disappears and reappears several times within short periods of time. Initially a systolic murmur alone is heard; however, as the shunt

increases, the murmur extends into diastole. The murmur is similar in distribution and quality to that in the first group of premature infants with PDA. Because infants in the second group are usually more immature than those in the first, LV failure may occur in them when clinically there seems to be less left-to-right shunting. A third sound often is heard, but a mid-diastolic flow rumble is uncommon. The pulmonic component of the second sound ordinarily is already accentuated because of the pulmonary disease but may become louder as the shunt increases. Increasing precordial activity is a good clinical indication of the magnitude of shunting in these infants, and increased heart rate, pulse pressure, and bounding pulses with a rapid upstroke are often detectable early. Palmar or forearm pulses are often palpable. Because most of these infants have indwelling umbilical arterial catheters, careful monitoring of the umbilical arterial blood pressure often shows a widening pulse pressure and a decrease in diastolic pressure as left-to-right shunting develops.

Rales are unreliable as an index of pulmonary edema and LV failure because they may be suppressed by positive pressure ventilation used in these infants. However, in those extubated who have recovered sufficiently from their respiratory distress syndrome, rales may be heard. Apneic episodes are also common in this group and may be associated with short periods of bradycardia.

Deterioration in the ventilatory status of an infant recovering from respiratory distress syndrome is often a strong indication of a significant left-to-right shunt through a PDA. However, other causes, such as recurring lung disease and pneumothorax or sepsis, should be actively excluded. Deterioration of the ventilatory status is manifested by the requirement for an increasing concentration of inspired oxygen, alterations in ventilator rate or pressure settings, increased requirements of CPAP, and assisted ventilation and increasing arterial blood $p\text{CO}_2$. The ECG often shows increased right ventricular forces owing to the underlying pulmonary disease but generally is of little help. A chest roentgenogram will show the parenchymal changes of respiratory distress syndrome, and increased pulmonary vascularity therefore may be extremely difficult to assess. Cardiomegaly is variable, particularly if the infant is being artificially ventilated; however, increasing cardiomegaly may indicate an increasing shunt.

Because many of the changes described may be due to deterioration resulting from underlying pulmonary disease, it is important to be able to assess the contribution to the clinical picture of a PDA. For this purpose, the echocardiogram usually is very helpful. An increasing LA:Ao ratio will be produced by increasing left-to-right shunting, whereas a ratio that remains constant and within normal limits may indicate non-cardiac causes of deterioration. Changes in the LV, left atrium, and PDA size assessed reliably by two-dimensional Doppler echocardiography will determine the role of shunting through the PDA. It should be emphasized that very early diagnosis is possible with two-dimensional Doppler echocardiography, which is completely noninvasive and safe. In addition, BNP can be quite useful in these patients to indicate significant overcirculation. This, coupled with current, more aggressive management approaches, has altered the natural history of PDA so that infants rarely are allowed to develop many of the signs described above.

Patent Ductus Arteriosus Associated with Lung Disease. The third group consists of infants who have severe respiratory distress syndrome from birth. Because many of these are very low-birth-weight infants (<1,000 g), the likelihood of a PDA being present is very high (>80%). A few show no clinical signs even when carefully evaluated—the “silent” ductus arteriosus (60). Many do show clinical evidence of a left-to-right shunt through the PDA, or fail to show improved respiratory status at an age when they should start to recover from the primary

pulmonary disease. They too are extremely sensitive to small increases in Na^+ and fluid administration. They require ventilatory assistance by mechanical respirators or CPAP. Deterioration commonly is manifested by the need for increasing ventilator pressure, rate, or oxygen, or CPAP support. Failure to improve is manifested by the inability to wean the infant from ventilatory support. An increase in arterial blood $p\text{CO}_2$ is common. Murmurs may be difficult to hear, and in some of these infants, the ductus arteriosus may be so widely patent that a murmur is not produced (61). Changes in the ventilatory status may be due to progression of the primary pulmonary disease, and it is often even more difficult to separate LV failure from increasing pulmonary problems than in the previous group. Increasing precordial activity, bounding pulses, and a widening arterial pulse pressure suggest the development of left-to-right shunting. When present, the murmur is usually only systolic, the pulmonic component of the second sound is accentuated, and a gallop rhythm is often heard. The ECG and chest radiograph usually are not helpful, but as outlined above, the two-dimensional Doppler echocardiographic evaluation is diagnostic even before clinical signs are apparent.

Persistent Patency in Term Infants, Children, and Adults

The incidence of isolated PDA in full-term infants is about 1 in 2,000 live births (62), accounting for about 5% to 10% of all types of congenital heart disease. Unlike the ductus arteriosus in premature infants, in whom failure of closure is due to physiologic developmental retardation, the ductus arteriosus in full-term infants is abnormal, and failure to constrict is probably related to a significant structural abnormality.

PDA may occur in more than one member of a family, suggesting possible genetic factors in certain instances. PDAs have been produced by genetic inbreeding in poodles (63). Gene linkage and chromosome analysis studies in humans have shown abnormalities on chromosome 12 in isolated PDA patients in Iran (64) and on chromosome 16 in association with aortic aneurysm (65).

In mature infants, older children, and adults, the factors determining the clinical features are the same as in premature infants, namely, the size of the communication, the relationship

between pulmonary and systemic vascular resistances, and the ability of the myocardium to handle the extra volume load.

Small Ductus Arteriosus. With a small communication, pulmonary vascular resistance and therefore pulmonary arterial pressure normally decrease after birth. However, because the resistance to flow across the ductus arteriosus is high, only a small left-to-right shunt develops. Pulmonary blood flow is increased only minimally, and LV failure does not occur. Therefore, few patients are symptomatic, and attention is often brought to this condition only by the murmur detected at a routine physical examination.

Physical growth is normal except in those children who are otherwise predisposed to poor growth, such as those in whom maternal rubella was present. The peripheral pulses may be full, and the arterial pulse pressure is slightly increased unless the shunt is very small. Precordial activity usually is normal with no increased apical impulse. First and second heart sounds are normal, and the only significant abnormal auscultatory finding may be the presence of a murmur. In early infancy, before pulmonary vascular resistance has decreased completely, there may be a short period in which no murmur is heard. A short systolic murmur may then be heard, which may progress to the typical, continuous murmur heard in older children. This murmur is heard best in the second left intercostal space and often is accentuated when the patient is recumbent or during inspiration. Administration of a vasoconstrictor agent such as phenylephrine raises systemic vascular resistance and increases left-to-right shunt, and the murmur will become longer and louder. The important features of the characteristic continuous murmur first described by Gibson (66) are the late systolic accentuation and continuation through the second sound into diastole. The murmur ordinarily starts shortly after the first sound, peaks at the second heart sound, and fades away, ending in the last third of diastole.

The ECG and chest roentgenogram are usually normal in these children; however, slight prominence of the main and peripheral pulmonary arteries may be seen on the roentgenogram (Fig. 31.4A). The two-dimensional echocardiogram Doppler study will delineate the PDA size and flow patterns as described before.

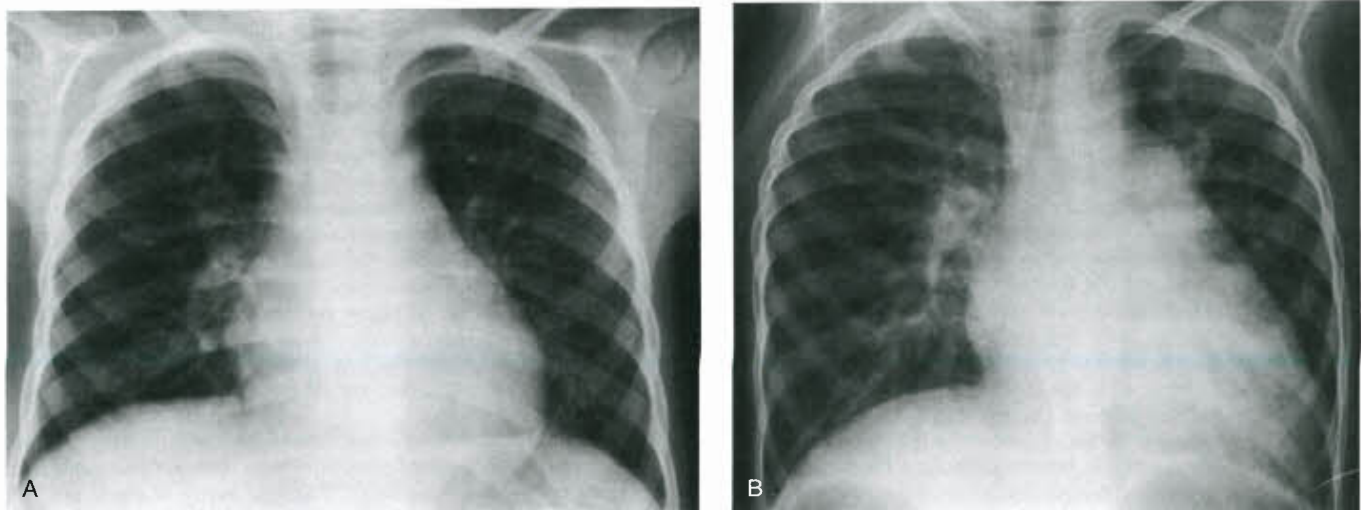


Figure 31.4. Posterior–anterior chest roentgenograms in two children each with a patent ductus arteriosus. A: A 4-year-old child with a small left-to-right shunt. Slight cardiomegaly and prominence of the pulmonary vasculature are present. B: A 4-year-old child with a very large left-to-right shunt. A double density and elevation of the left mainstem bronchus are present owing to LA enlargement. The LV, main and peripheral pulmonary arteries, and ascending aorta are prominent. Pulmonary venous congestion is also present.

Moderate Ductus Arteriosus. In infants, a moderate left-to-right shunt may produce symptomatology related to LV failure. Poor feeding, irritability, and tachypnea may be present, and weight gain is often slow. The symptoms ordinarily increase until about the 2nd to 3rd month of age. If the LV failure does not produce severe disease at this stage, compensatory myocardial hypertrophy occurs, and in many instances these infants improve considerably. Some, in fact, are detected only on subsequent routine physical examination, but close questioning will yield the previous abnormal history. General physical development can be slightly retarded, and easy fatigability may be present in the older child. The pulse rate is often increased, with the peripheral pulses full and bounding. The systemic arterial pressure is widened with a low diastolic pressure. The precordium is hyperdynamic, and LV enlargement produces a thrusting apical impulse. A systolic thrill may be palpable at the upper left sternal border. Both the first and second sounds may be difficult to hear, because they often are masked by a loud murmur. A third heart sound is often heard at the apex. The progression from a systolic murmur to a continuous murmur is considerably more rapid in these infants than in those with a small shunt. The continuous murmur is more intense, has more extensive radiation, and generally is well heard posteriorly. It has a much harsher quality with low-frequency components, and because of the large flow and great turbulence, eddy sounds that vary from beat to beat give the murmur a machinery quality.

If heart failure occurs, the murmur may lose its continuous character and occupy only systole. A middiastolic, low-frequency, rumbling murmur is ordinarily heard at the apex. Early pulmonic or aortic ejection sounds may occur. The increased LV stroke may produce a functional systolic pressure difference across the aortic valve that may be manifested by a soft ejection systolic murmur. In early infancy, LV failure with increased LA size and pressure often induces a left-to-right shunt through a stretched and incompetent foramen ovale (15). Depending on the magnitude of left-to-right atrial shunting, right ventricular hyperactivity may become evident and the right ventricular outflow murmur typical of atrial left-to-right shunting may be heard. In addition, a middiastolic flow rumble owing to the increased flow across the tricuspid valve may be audible at the lower left sternal border.

The ECG may be relatively normal during infancy, but LV hypertrophy is usual in older infants and children. The mean frontal plane axis usually is normal. LV hypertrophy is manifested by a deep Q wave and a tall R wave in leads II, III, aVF, and the left precordial leads V5 and V6. The T waves in these leads ordinarily are upright and show increased amplitude. A pattern compatible with left bundle branch block also has been described in some children. A widened P wave indicating LA enlargement may be present. If there is a left-to-right atrial shunt as well as mild pulmonary hypertension, right ventricular hypertrophy may increase the amplitude of the R waves in the right precordial leads. Right atrial enlargement may increase the height of the P wave.

The chest roentgenogram shows an enlarged heart with prominence of the LV and the typical signs of LA enlargement (Fig. 31.4B). The main pulmonary artery segment is prominent, and the pulmonary vascular markings in the peripheral lung fields are increased. The ascending aorta is often very prominent. The two-dimensional echocardiogram demonstrates increased LA and ventricular diameters, hypertrophy if present, and the PDA itself. Doppler evaluation will demonstrate flow and velocity patterns and will allow for an estimate of pulmonary arterial pressure (51).

Large Ductus Arteriosus. Infants with a large PDA are invariably symptomatic. They are irritable, feed poorly, fail to gain weight normally, tire easily—particularly while feeding—and sweat excessively. They have increased respiratory effort

and respiratory rates, also aggravated by feeding, and are prone to develop recurrent upper respiratory infections and pneumonia. These symptoms indicative of severe LV failure with pulmonary edema may occur early in infancy.

Many of the typical physical signs may be absent when there is severe LV failure. However, tachycardia and tachypnea are present, and if there is pulmonary edema, rales will be heard throughout the lung fields. The respiratory signs may be suggestive of pneumonia. The peripheral pulses are bounding with a rapid upstroke and a wide pulse pressure unless there is severe LV failure when the pulse volume decreases. The precordium is markedly hyperdynamic, and clinical evidence of cardiac enlargement is present. The LV apical impulse is thrusting and, if right ventricular enlargement occurs, may be accompanied by a left parasternal impulse. A systolic thrill is often palpable. The first and second heart sounds are accentuated, and a third sound ordinarily is heard at the apex. Occasionally no murmur is heard, especially with severe failure. When LV failure is controlled, a moderately loud systolic murmur is heard best in the pulmonary area or occasionally in the third or fourth intercostal space. The murmur peaks late in systole, and the prolongation into diastole is variable; the murmur commonly ends within the first third of diastole. The typical continuous murmur heard with a small or moderate-sized PDA may be heard but is less usual. A prominent middiastolic mitral flow rumble commonly is audible at the apex.

The ECG shows more prominent LV hypertrophy, with deep Q and taller R waves than in the previous group. The T waves may be diphasic or even inverted. Right ventricular hypertrophy may be evident, with upright T waves in the right precordial leads and increased R-wave amplitude in the right precordial leads. LA enlargement, as demonstrated by a widened P wave, also will be seen. The chest roentgenogram shows striking enlargement of the heart with predominant LA and LV enlargement. The main pulmonary artery segment usually is markedly enlarged, and the peripheral pulmonary vascular markings are markedly accentuated. Evidence of LV failure with increased pulmonary venous markings and interstitial fluid also may be seen. With an enlarged left atrium or pulmonary arteries, lobar collapse or emphysema owing to bronchial compression may occur. The two-dimensional echocardiogram/Doppler study is as described for the previous group.

Infants with large left-to-right shunts through a PDA may not survive the resultant heart failure without treatment. However a certain proportion of those capable of compensating adequately survive the initial period. A moderate or large left-to-right shunt either undetected in infancy or treated but allowed to persist eventually leads to the development of obstructive pulmonary vascular disease. As pulmonary vascular resistance increases, pulmonary hypertension increases until systemic levels are reached. The left-to-right shunting decreases and this leads to improvement in the infant's symptomatology and signs, usually 8 to 15 months after birth. Feeding problems, poor weight gain, and the increased sweating previously present disappear, with far fewer episodes of respiratory infection. The murmur becomes shorter, and the diastolic component may be completely lost. The middiastolic rumble decreases and disappears, and the first heart sound becomes softer. The second heart sound remains markedly accentuated, but the third heart sound disappears. Precordial hyperactivity diminishes, and the pulses become less bounding. The chest roentgenogram shows decreasing pulmonary vascularity, and a decrease in heart size also may be noted. The period of time over which these changes occur varies and may last several years, but irreversible changes are common after 15 to 18 months of age.

As the increased pulmonary vascular resistance progresses to irreversible pulmonary vascular disease, the symptoms and

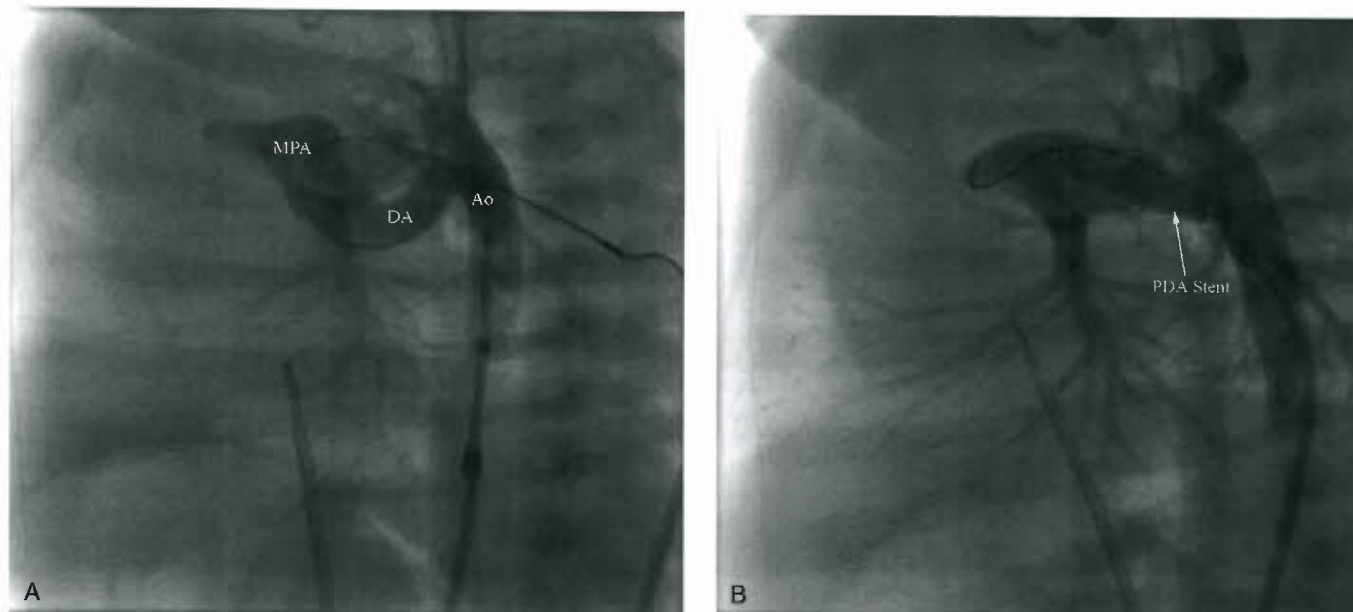


Figure 31.5. A: Angiogram in the lateral position in a newborn infant with pulmonary atresia. The typical anatomy associated with right ventricular outflow obstruction is demonstrated. The aorta is widely dilated, and the aortic isthmus is wider than the descending aorta. The typical tortuous ductus arteriosus with an acute rather than the normal obtuse inferior angle with the aorta is present. This orientation is consistent with aorto-to-pulmonary arterial blood flow in fetal life. Ao, aorta; DA, ductus arteriosus; MPA, main pulmonary artery. B: Lateral distal transverse angiogram in an infant with pulmonary atresia after placement of a ductal stent to maintain patency.

clinical features change even further. The murmur continues to shorten until eventually it disappears. The second sound becomes single and progressively louder, an ejection systolic click occurs, and a faint blowing early-diastolic regurgitant murmur owing to pulmonary incompetence may be heard at the upper left sternal edge. LV hyperactivity disappears, and the right ventricular parasternal impulse increases. The ECG shows increasing right ventricular hypertrophy with dominant R waves in the right precordial leads. Peaked P waves indicative of right atrial enlargement also may occur. The chest roentgenogram shows increasing right ventricular enlargement with decreasing LV size, a large main pulmonary artery, and progressive decrease in peripheral vascular markings.

Cyanosis, often more pronounced in the lower than in the upper limbs, begins to appear, initially only with exertion, but eventually becoming continuous as persistent right-to-left shunting across the ductus arteriosus occurs. The final picture, if allowed to progress, is one of irreversible pulmonary vascular disease with marked right-to-left shunting. The precordial activity is now dominantly right ventricular, and the pulses are either of normal or small volume. The second heart sound typically is palpable in the pulmonic area, and a diastolic thrill also may be felt. The first heart sound is slightly accentuated, and the pulmonic component of the second heart sound is markedly accentuated. A harsher and longer early diastolic blowing murmur caused by pulmonary incompetence is heard at the left sternal border. A blowing systolic murmur owing to secondary tricuspid insufficiency may be heard at the lower left sternal border. The ECG shows right-axis deviation in the frontal plane with marked right ventricular hypertrophy and eventually T wave inversion in older patients. The chest roentgenogram shows moderate cardiomegaly with predominant enlargement of the right ventricle and a markedly enlarged main pulmonary artery with prominence of the central vessels but no peripheral plethora. Right atrial enlargement may be evident.

Role of the Ductus Arteriosus in Complex Congenital Cardiac Malformations

In right ventricular outflow obstruction lesions such as pulmonary atresia, the normal flow patterns in fetal life are altered, and development of the ductus arteriosus is probably abnormal (1,67). The diameter is large and orientation is vertical from the underside of the aortic arch (Fig. 31.5A). Because patency of a PDA is essential for maintenance of pulmonary blood flow, the constrictor response to an increase in pO_2 is undesirable. Despite the hypoxemia in these infants, the ductus arteriosus closes, resulting in cessation of pulmonary blood flow, progressive hypoxia, acidosis, and death. PGE_1 is currently used as pharmacologic prevention of this closure before the creation of a surgical aortopulmonary communication. PGE_1 produces dilation of the ductus arteriosus with a significant increase in systemic arterial pO_2 (68). Systemic oxygenation is markedly improved, acidemia reversed, and the infants ordinarily can be stabilized for days to weeks before palliative surgery. Maintenance of patency for a more prolonged period has been produced by placement of a metal intravascular stent in the PDA (69–73) (Fig. 31.5B). Early results are encouraging with excellent pulmonary artery growth (74) but technical issues may favor use in less tortuous ducts found most commonly in lesions such as pulmonary atresia with intact ventricular septum.

Maintenance of systemic blood flow in hypoplastic left heart lesions such as aortic or mitral atresia or in interrupted aortic arch depends on PDA. PGE_1 has proved extremely valuable in improving lower body perfusion in these infants. Acidemia is often reversed and renal function markedly improved so that the infants can be stabilized and returned to electrolyte and hemodynamic balance before corrective surgery is undertaken (68). More recent developments in the initial palliative treatment of hypoplastic left heart syndrome have included the placement of a metal stent in the ductus arteriosus and banding of the pulmonary arteries (hybrid approach) to stabilize systemic and pulmonary

blood flow until infants reach the age of 4 to 6 months at which time surgical Glenn shunt with arch reconstruction is performed. It has yet to be shown whether this new approach will have significant advantages, but early results show a potential for decreased early mortality in high-risk patients with comparable late mortality in experienced centers (75–77). There is a significant incidence of transverse aortic arch obstruction after PDA stenting (>25%) that may require additional intervention (78).

It has been shown that the ductus arteriosus plays an important role in the presentation of infants with juxtaductal aortic coarctation. Localized coarctation ordinarily is produced by a well-circumscribed posterior shelf protruding into the aortic lumen at a point opposite the insertion of the ductus arteriosus (1). If the ductus arteriosus remains patent or if there is a well-formed ductus ampulla even when the ductus arteriosus is closed, obstruction by the juxtaductal coarctation may not occur. However, as the ductus arteriosus closes and the ampulla retracts, progressive interference with flow occurs, and clinical symptoms and signs will develop. The sudden occurrence of acute LV failure in infants with juxtaductal coarctation of the aorta may be produced by rapid constriction of the ductus arteriosus in the postnatal period. PGE₁ has been of great benefit in the management of these infants as well (75). In the rare child or adult with a persistent PDA in the setting of coarctation, covered stent repair has been shown to be an effective nonsurgical treatment alternative (Fig. 31.6A,B).

Clinical Differential Diagnosis

Venous Hum

The continuous bruit produced by flow through the large veins in the neck is often confused with the continuous murmur of a PDA. The venous hum varies in intensity with head and neck position as well as the phase of respiration and is usually obliterated by firm pressure over the neck, by turning the head to one side, or by lying flat.

Total Anomalous Pulmonary Venous Connection

Unobstructed total anomalous pulmonary venous connection to the innominate vein occasionally produces a continuous

murmur very much like a venous hum. The other features of this lesion serve to differentiate it from a PDA.

Ruptured Sinus of Valsalva

Rupture of one of the sinuses of Valsalva into either the right atrium or right ventricle is accompanied by a continuous murmur. However, onset of symptoms and signs in this condition is usually abrupt and often follows trauma to the chest. The murmur is usually heard lower in the precordium.

Arteriovenous Communications

Arteriovenous fistulas involving one of the coronary arteries, an intercostal artery, or an internal mammary artery may be associated with continuous murmurs similar to those occurring in PDA. The murmurs typically are more superficial and sound extracardiac in origin. Origin of one of the pulmonary arteries from the aorta (hemitruncus arteriosus) also may produce a continuous murmur, as may lobar sequestration, in which an anomalous artery arising from the aorta supplies one or more pulmonary lobes. Pulmonary arteriovenous fistulas may produce a continuous murmur, but when large enough to do so are usually associated with cyanosis and classical radiographic findings.

Anomalous Origin of the Left Coronary Artery from the Pulmonary Artery

In this lesion, retrograde flow occurs from the right coronary artery into the pulmonary artery. If this retrograde flow is sufficiently large, a continuous murmur may be heard, but this is rare. The clinical presentation and ECG are diagnostic of this condition.

Absent Pulmonary Valve

This lesion is associated invariably with massive dilation of the pulmonary arteries and almost always with a ventricular septal defect. The murmur has been described as “sawing wood” in character and is not really continuous, but has more of a to-and-fro character. The massively dilated pulmonary artery

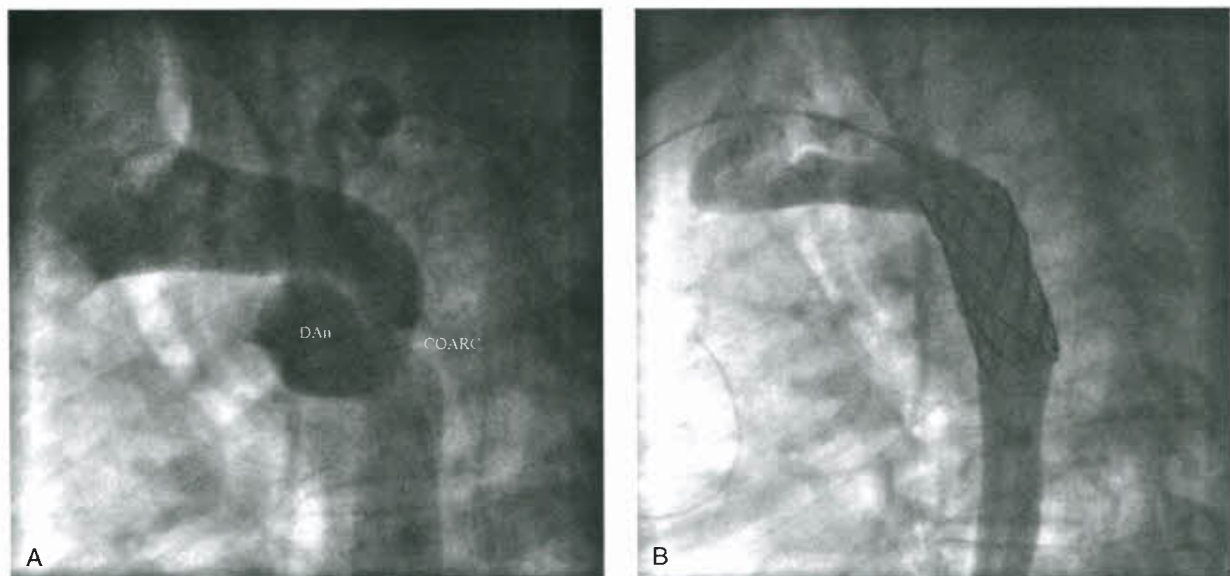


Figure 31.6. A: Lateral angiogram of a patient confirming a large ductal aneurysm (DAn) associated with a coarctation (Coarc). B: Lateral transverse aortic angiogram immediately after placement of covered stent for treatment of PDA aneurysm with associated coarctation.

evident on chest roentgenogram ordinarily allows for accurate differentiation.

Aortic Insufficiency Associated with a Ventricular Septal Defect

Prolapse of one aortic sinus complicates ventricular septal defects, particularly supracristal defects. The murmur is not strictly continuous, and the systolic murmur produced by the ventricular septal defect and the blowing regurgitant diastolic murmur produced by the incompetence are usually separated. However, accurate clinical differentiation may be difficult.

Peripheral Pulmonary Stenosis

Although commonly associated with a PDA, peripheral pulmonary stenosis may occur as an isolated defect and give rise to a soft, continuous murmur heard best in the infraclavicular areas and conducted to the axillae. Stenosis may occur in only one pulmonary artery, producing a unilateral murmur. This lesion may be difficult to distinguish clinically from a PDA.

Truncus Arteriosus

Truncus arteriosus may not be accompanied by cyanosis in early infancy, and with a low pulmonary vascular resistance and increased pulmonary blood flow, there may be a continuous murmur. Absence of the pulmonary artery segment on the posterior–anterior chest roentgenogram suggests this diagnosis; furthermore, the relatively common occurrence of right aortic arch with truncus arteriosus excludes the diagnosis of isolated PDA.

Aortopulmonary Window

This defect may be extremely difficult to differentiate from a PDA. The murmur commonly is heard best lower down the left sternal border and is often mistaken for the murmur of a high ventricular septal defect.

Pulmonary Atresia

When pulmonary atresia is accompanied by markedly enlarged bronchial arteries supplying pulmonary blood flow, a continuous murmur may be heard. However, cyanosis is present, and the peripheral pulses are not bounding as in PDA. The chest roentgenogram also shows absence of the pulmonary artery segment.

Complications

Endarteritis

Bacterial endarteritis has become extremely uncommon in developed countries, although it remains a serious complication of PDA. Because of the advent of surgical correction of many congenital heart defects, the prevalence of endocarditis, particularly in defects associated with left-to-right shunts, has declined dramatically (79). In one survey of major congenital heart defects, PDA had the lowest frequency, which was attributed to early surgical closure (80). In undeveloped countries PDA accounts for $\leq 15\%$ of all endocarditis cases and for 4.8 of 1,000 hospital admissions at a tertiary cardiac referral center (81). Organisms are typical with *Streptococcus viridans* and *Staphylococcus aureus* being the most common. Vegetations occur in $>80\%$ and are always seen on the pulmonary artery end of the duct.

Aneurysm/Calcification Formation

Marked dilation of a PDA or of the ampulla of the closed ductus arteriosus has been described (Fig. 31.7). The massive dilation that occurs may be diagnosed as a mediastinal mass.

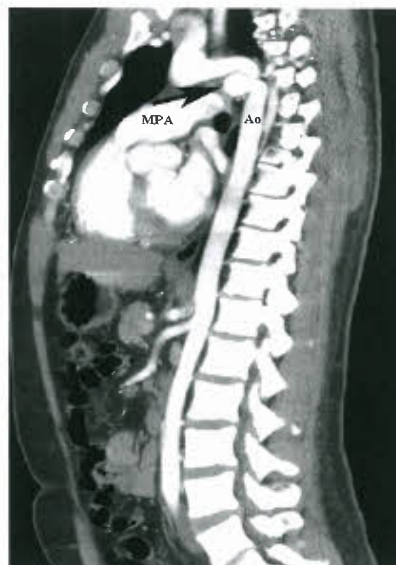


Figure 31.7. CT scan of a young adult showing a large ductal aneurysm.

It also has been found as an incidental finding at autopsy. It occurs in $\leq 1.5\%$ of normal births (82). In adults calcification of the PDA is frequent and may increase the surgical risk (83).

Diagnostic Testing

Echocardiography

Two-dimensional echocardiography, combined with Doppler echocardiography and color-flow mapping is the primary imaging technique for evaluating the patient with a suspected PDA. A complete echocardiogram is particularly important prior to initiation of treatment to exclude any ductal-dependent congenital heart lesions.

In addition to directly demonstrating the presence of a PDA, echocardiography is used to evaluate the physiology. Features that are associated with an increased shunt through the PDA include the presence of LA dilation as demonstrated by an increased LA:Ao ratio as previously described. In addition, the presence of holodiastolic flow reversal in the abdominal aorta indicates a significant runoff through the PDA. This runoff is also demonstrated by increased diastolic flow in the branch pulmonary arteries. Finally, pulmonary artery pressure can be determined by the systolic and diastolic gradients through the PDA.

The parasternal short- and long-axis views and the suprasternal notch views are of particular use in evaluating the patient with a suspected PDA. The parasternal views demonstrate the size and anatomy of the PDA, the anatomy of the branch pulmonary arteries, and evaluate the LA and LV size (Fig. 31.3A–D). Doppler echocardiography can show the flow through the PDA as well as the increased flow in the branches. The suprasternal notch view shows a second view of the PDA, determines the patency of the aortic arch to exclude coarctation, and demonstrates the increased diastolic flow in the arch (Fig. 31.8A,B). Finally, the subcostal sagittal views demonstrate the abdominal aorta and show the diastolic runoff present due to ductal shunting.

Echocardiography can both predict and demonstrate the presence of low cardiac output in the premature infant who has undergone ductal ligation. PDA size prior to ligation directly correlates with the likelihood of postoperative low cardiac output (39).

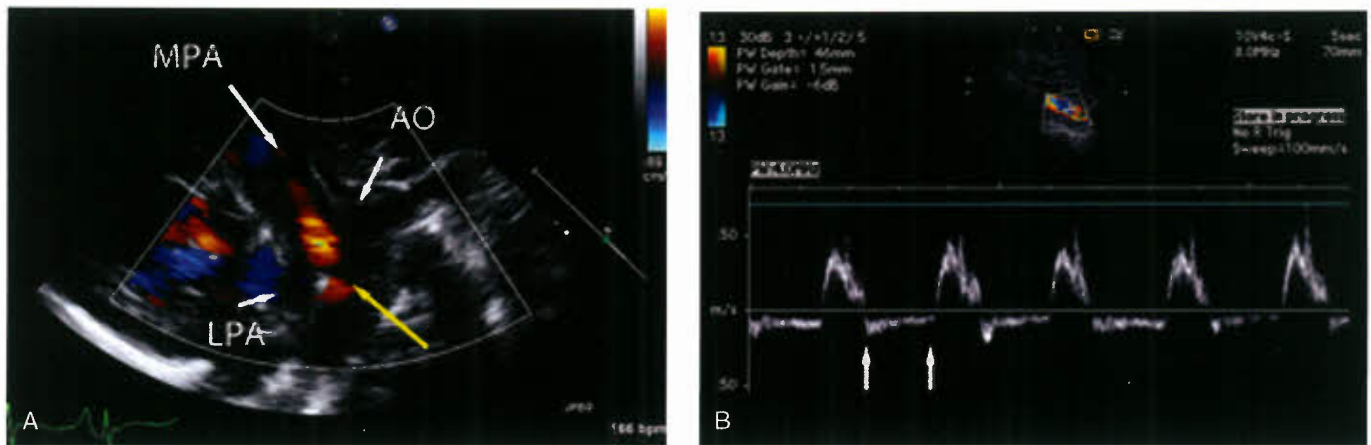


Figure 31.8. A: Echocardiogram in suprasternal view showing patent distal aortic arch and reversed ductal flow (red) from the ductal ampulla into the main pulmonary artery. B: Subcostal sagittal view showing holodiastolic flow reversal in the abdominal aorta.

Cardiac Catheterization with Angiography

Based on careful clinical evaluation—principally the characteristic continuous murmur, together with the ECG, chest roentgenogram, and two-dimensional echocardiogram Doppler study—diagnosis of PDA (and any associated defects) does not require catheterization. Color Doppler flow mapping is as sensitive as cardiac catheterization for detecting even a small PDA. In children with pulmonary hypertension, determining the exact location of the shunt can be more difficult. Contrast echocardiography can assist in the localization, but patients will require catheterization to determine the severity of pulmonary hypertension, reactivity to pulmonary vasodilators, and determine if closure is indicated.

Right heart catheterization alone usually suffices to confirm the diagnosis. However, if an additional lesion such as ventricular septal defect is suspected, retrograde catheterization may be required if the interatrial septum is intact and the LV cannot be entered prograde. The venous catheter usually can be passed from the main pulmonary artery through the PDA into the descending aorta. If the venous catheter cannot be passed through the PDA, retrograde aortic catheterization is indicated to define the anatomy with an aortic angiogram.

An increase of pulmonary arterial blood oxygen content of >0.5 mL/dL or a saturation increase of $>4\%$ to 5% from that in right ventricular blood indicates a significant left-to-right shunt at the pulmonary arterial level. Occasionally, an increase in oxygen saturation is noted in blood just below the pulmonary valve owing to pulmonary regurgitation. Because preferential streaming of oxygenated blood from the PDA into one or another of the branch pulmonary arteries is common, a sample from either one does not reflect mixed pulmonary arterial blood oxygen saturation (15). Measuring pulmonary blood flow accurately from the blood oxygen data is therefore difficult, making an accurate calculation of the true magnitude of left-to-right shunting impossible. In the presence of LV failure with pulmonary edema, pulmonary venous blood oxygen saturation may be reduced. If the foramen ovale is incompetent, a left-to-right atrial shunt may be detected by an increase in oxygen saturation in the right atrial blood. A large increase in oxygen saturation at the right atrial level may mask a smaller rise of saturation in the pulmonary artery, even though the increase represents a significant shunt at the pulmonary arterial level. With significant pulmonary hypertension and right-to-left shunting

through the PDA, oxygen saturation of blood in the descending aorta will be lower than that obtained in the ascending aorta. Bidirectional shunting may be present until pulmonary vascular disease is severe, when right-to-left shunting alone occurs.

A small left-to-right shunt may not be detected by blood oxygen saturation data alone. An increase in oxygen saturation in pulmonary arterial blood is not diagnostic of a PDA, but may be present in lesions such as aortopulmonary window or a high ventricular septal defect (supracristal), in which streaming may direct the highly saturated blood into the pulmonary artery.

With a small communication, pulmonary arterial blood pressures are normal, but systemic arterial pulse pressure may be slightly widened owing to a low diastolic pressure. With a moderate-sized defect, pulmonary arterial systolic, diastolic, and mean blood pressures may be slightly elevated. Systemic arterial diastolic blood pressure falls, whereas systemic arterial pulse pressure increases. Both left and right atrial mean pressures are moderately elevated in the presence of a moderate shunt. With a large shunt, pulmonary and systemic arterial pressures are equal (Fig. 31.9A,B), LA mean pressure may be increased substantially, and a prominent V wave is seen. LV end-diastolic pressure may be elevated, and with a large flow, a diastolic pressure gradient between the left atrium and LV is demonstrated. A small systolic pressure difference between the LV and aorta is also encountered occasionally when there is a large shunt. Because calculation of pulmonary blood flow in PDA is often inaccurate, the calculation of pulmonary vascular resistance is also inaccurate (15).

Angiography. Although angiography cannot accurately measure the magnitude of left-to-right shunting, it is the most effective test for defining the anatomy of the PDA. Contrast medium is injected into a catheter passed through the PDA into the aorta from the pulmonary artery or into the aorta retrogradely from the femoral artery. As shown in Figure 31.10A, the aortic end of the PDA usually is widely dilated, and the ductus narrows down at the pulmonary arterial end. This is the usual shape in most children, but occasionally other shapes are observed, including tubular (long ductus arteriosus of similar diameter throughout), complex (narrowing at both the pulmonary artery and aortic end), and short (window-like PDA) (84) (Fig. 31.10 A–E). In most instances the lateral projection, or occasionally the left anterior oblique projection, demonstrates the anatomy most clearly. The AP camera can be positioned in the right anterior

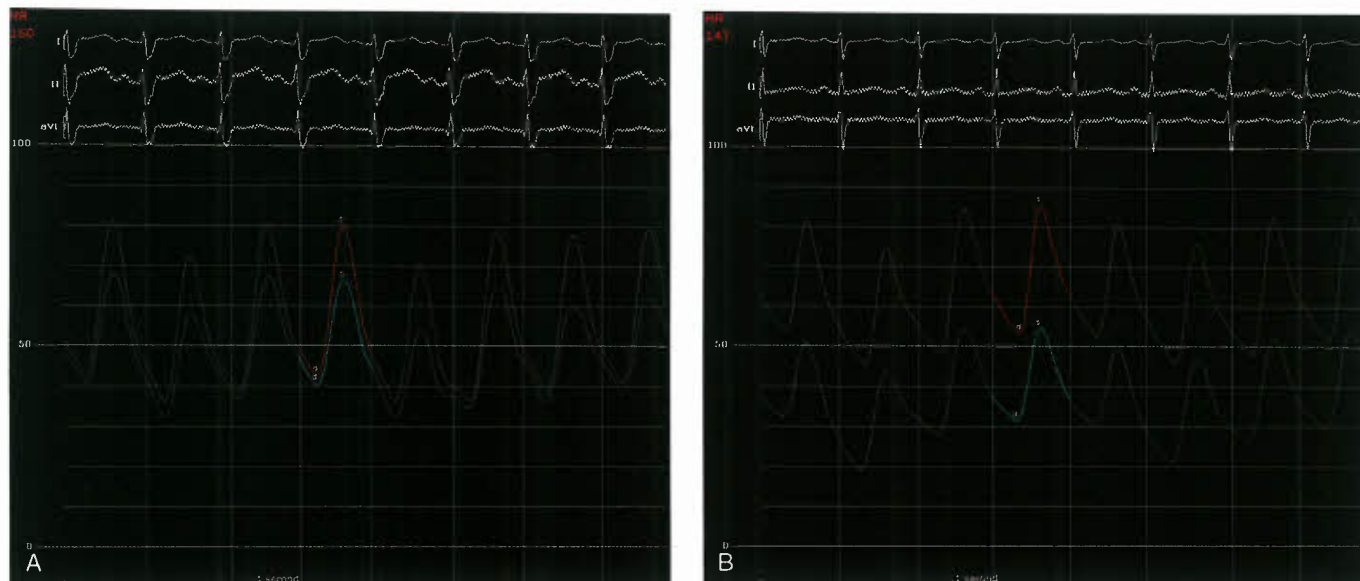


Figure 31.9. A: Simultaneous descending aortic (Ao) (red) and main pulmonary artery (MPA) (blue) pressure tracings in an infant with a large patent ductus arteriosus. Notice the resting tachycardia, elevated PA pressures, and low Ao diastolic pressure. B: Immediately after ductal closure with a vascular plug, repeat measurements show a marked reduction in heart rate, PA pressures, and an elevation in Ao diastolic pressure.

oblique caudal position to demonstrate the PDA. One should remember that in infants with severe heart failure associated with a ventricular septal defect or interatrial communication, a PDA may coexist; selective descending aortography is essential in these infants to exclude a PDA if not defined clearly by echocardiography.

Magnetic Resonance Imaging or Computed Tomography Scan

Although simpler techniques such as two-dimensional echocardiography Doppler evaluation accurately define the anatomy and flow patterns of the ductus arteriosus, nuclear magnetic resonance imaging (MRI) or computed tomography (CT) scan can clearly delineate the anatomy (85,86). These studies can be of use in adolescents or adults with poor echo windows where the diagnosis is suspected but not anatomically confirmed (Fig. 31.11), or in patients with associated aortic pathology such as a ductal aneurysm or coarctation. Velocity-encoded cine MRI imaging for estimation of left-to-right shunting may have additional clinical utility (87).

Treatment

Overview

All symptomatic PDAs with left-to-right shunting and those that are asymptomatic but causing LA or LV enlargement should be closed regardless of age. Management strategies are different for the preterm infant compared to the term infant, older child, and adult as described below. Prophylactic closure of hemodynamically insignificant PDAs for prevention of late complications such as endocarditis, aneurysm, and rupture remains controversial although is rarely considered, if at all before late toddler or school age. Patients with significant pulmonary vascular disease and right-to-left ductal shunting at rest should not have their PDA closed. Closure in these patients can be considered if aggressive treatment of their pulmonary vascular disease reverses their shunt.

Treatment of Preterm Infant with PDA

Aggressive, urgent treatment of a significant PDA in a preterm infant is required if signs of progressive respiratory distress or evidence of low cardiac output develop. This is particularly true if signs of necrotizing enterocolitis develop, including persistent abdominal distention, increasing residuals before feedings, blood in the stools or gastric aspirate, decreasing bowel sounds, and, particularly, intramural air. Immediate supportive medical management includes optimizing the hematocrit, limiting sodium and fluid intake, and the use of diuretics. If systemic output is quite poor, intravenous inotropic support with dopamine has been used. Maintenance of an adequate hematocrit and hemoglobin is an important consideration in a preterm infant with a PDA. A reduction in hemoglobin requires an increased cardiac output to maintain peripheral oxygenation, and with a left-to-right shunt and an already compromised myocardium, anemia may further impair cardiac function. In addition, because myocardial oxygen delivery depends on blood oxygen content, low hemoglobin exacerbates tissue ischemia, particularly in the abdomen and lower body where blood flow is reduced. Because arterial blood gas sampling is common, the hematocrit often decreases and care must be taken to maintain it >45%. Because peripheral tissue oxygen delivery is retarded by fetal hemoglobin, exchange transfusion replacing fetal hemoglobin with adult hemoglobin may help to facilitate peripheral oxygenation (22). Electrolyte, glucose, and nutritional requirements must be carefully maintained. Caloric intake is often a major problem, and intravenous hyperalimentation may be required. Because volume overload may precipitate LV failure, Na⁺ and fluid administration commonly are restricted to low maintenance amounts. Increased interstitial lung water related to pulmonary overcirculation results in tachypnea and increased work of breathing that should be acutely treated with diuretics, most commonly furosemide. All of the above are aimed at supportive treatment of a left-to-right shunt in anticipation of directly removing the shunt and its effects by closing the PDA. Options for closure include medical treatment, surgical division and ligation, and more recently catheter device closure.

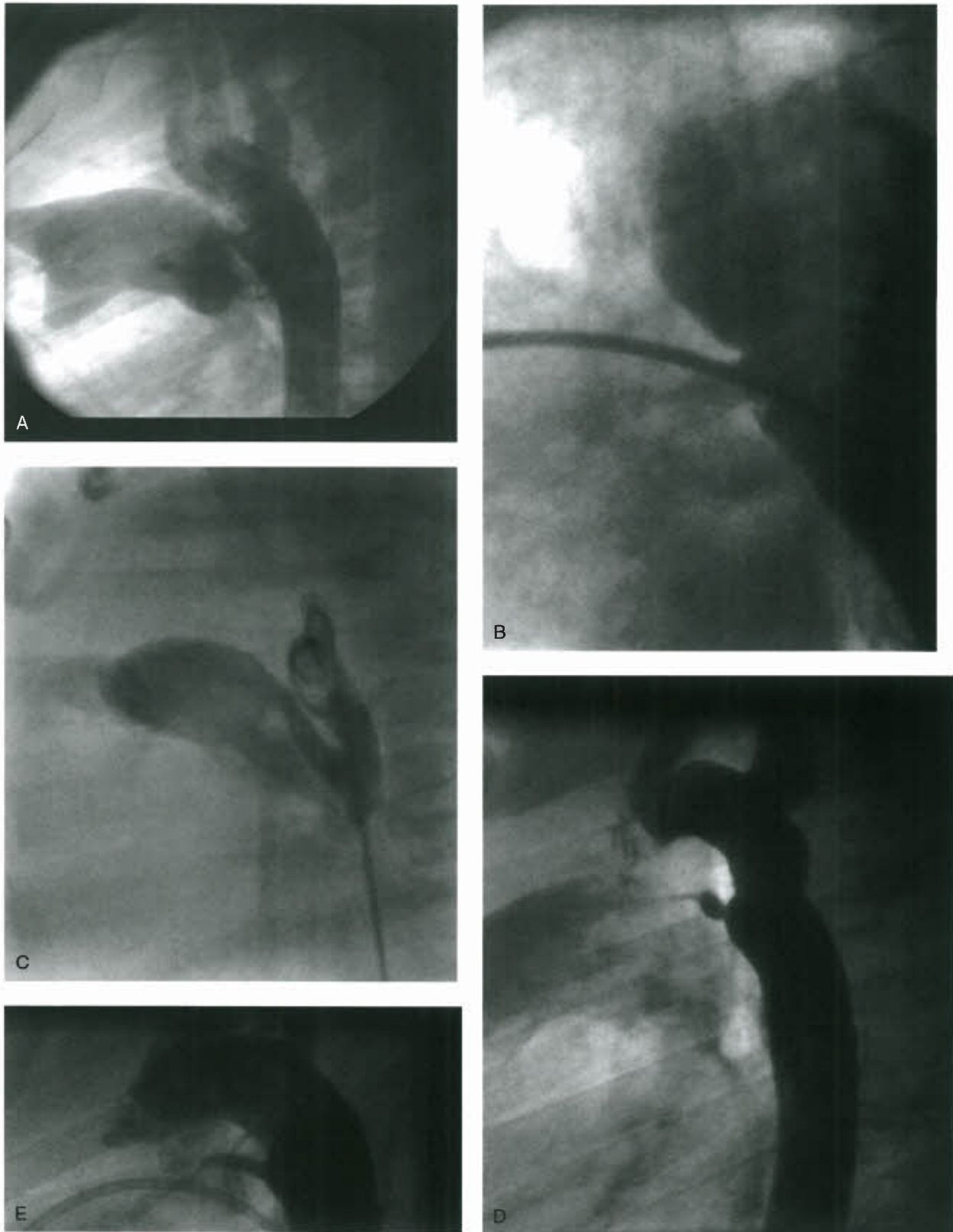
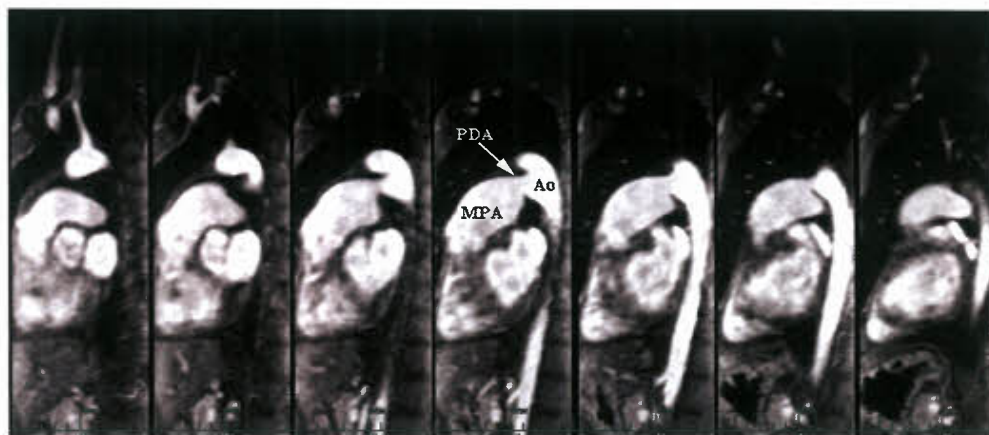


Figure 31.10. Common angiographic ductal morphologies. **A:** Conical with narrowing at the pulmonary artery end, by far the most common. **B:** Window. **C:** Tubular. **D:** Complex. **E:** Elongated.

Figure 31.11. Serial sagittal MRI images in a young adult showing a large patent ductus arteriosus (PDA). Ao, aorta; MPA, main pulmonary artery.



Medical Closure. The use of oral or, preferably, intravenous (lyophilized) indomethacin to constrict the PDA has led to successful nonsurgical closure in a large proportion of treated infants (88–90); the effects of indomethacin apparently are best when it is administered before 10 days of age and in less mature infants. Originally, indomethacin was administered only to infants in whom standard medical management had failed and surgery was contemplated (88); however, it is now considered first line of therapy unless renal dysfunction or necrotizing enterocolitis is present. Dose schedules vary, but commonly a first dose of 0.2 mg/kg is given by nasogastric tube or intravenously. For intravenous indomethacin, subsequent doses depend on the age at initial treatment—if <48 hours, the subsequent two doses are 0.10 mg/kg; if 2 to 7 days, 0.20 mg/kg; and if >7 days, 0.25 mg/kg. A total of three doses usually are given 12 to 24 hours apart depending on urinary output; if urine flow decreases, fewer doses may be used or the time between doses may be extended. If clinical signs reappear after an initially successful course of therapy, a second course may be considered. Because signs of a shunt reappear in some infants, a more prolonged initial course of therapy has been suggested. Indomethacin should not be administered to infants with renal dysfunction (serum creatinine > 1.6 mg/dL or blood urea nitrogen > 20 mg/dL), overt bleeding, shock, necrotizing enterocolitis, or any suspicion thereof, or if there is ECG evidence of myocardial ischemia (91). The renal side effects of oliguria and hyponatremia do not always occur, and when they do they usually are transient; no obvious long-term adverse effects have been experienced (92). These renal side effects are more common, and often more severe, when significant fluid restriction precedes therapy. Administration to infants with PDA before they show obvious major hemodynamic complications has been used with good success, particularly in infants with birth weight <1,000 g (89). In this group of infants, the initiation of therapy is suggested immediately on diagnosis, which ordinarily is before 72 hours of age. True prophylactic therapy on the first day after birth appears to have no advantage, and because not all infants develop a PDA, a certain number would receive indomethacin unnecessarily.

Some studies have investigated combined treatment with indomethacin and inhibition of the nitric oxide pathway for very premature infants refractory to indomethacin alone (93). The combination of L-NMMA and indomethacin improved the closure rate, but the use adversely affected the creatinine and produced systemic hypertension, limiting its usefulness.

More recently, ibuprofen has also been evaluated as a possible alternative to indomethacin in preterm infants (94–99). In addition, meta-analysis of the available studies has shown a comparable rate of ductal closure after ibuprofen treatment (100–102). Some evidence exists that there may be less effect

of ibuprofen on renal function and urine output (94,95). In addition, ibuprofen has less effect on cerebral vasculature and cerebral blood flow but has not shown a decreased risk for intraventricular hemorrhage (96,98,99). However, in trials using ibuprofen for prophylaxis, there has been an increased incidence of pulmonary hypertension (103) such that this trial was ended prematurely. More recently, there is evidence that oral paracetamol may be an alternative to intravenous therapy (104).

In premature baboons, PDA ligation results in improved lung mechanics and ventilation at 14 days; however, there is no effect on histologic progression of chronic lung injury (105). Improved lung mechanics have been confirmed in premature infants at 26 to 29 weeks of gestation after ligation showing an increase in dynamic compliance, tidal volume, and minute ventilation (106). The benefit of treatment in premature infants with lung disease has been confirmed in a retrospective study showing a fourfold mortality risk for infants <28 weeks with persistent PDA after medical treatment as compared with those without PDA or those successfully closed (107). However, the timing of treatment remains controversial, because there is no demonstrated long-term benefit to early treatment (108).

Surgical Closure. If medical treatment is unsuccessful or not possible, surgical or catheter device closure can be performed. Surgical closure before 10 days of age reduces the duration of ventilatory support and hospital stay and lowers morbidity (109). Despite the small risk of recanalization, ligation rather than division of the ductus arteriosus has been recommended, although many surgeons still clip ligate to minimize the need for dissection and associated injury. Surgery now can be performed with minimal morbidity and mortality (110). Thoracoscopic surgery is used at some centers to minimize the effect on chest wall mechanics (111). A recent comparative study confirms both excellent safety, with 0% mortality, and success, with 100% complete closure, with both techniques although it suggests a potential advantage for the thoracoscopic approach with less morbidity and cost (112). However, some infants do develop acute low cardiac output after ductal ligation thought to be due to the acute increase in afterload with a concomitant decrease in LV preload, more pronounced with a larger PDA (39).

Catheter Device Closure. Technological advances have reduced the size of catheter PDA closure devices to allow delivery through 4 French catheters, outer diameter < 1.3 mm, making device closure a possibility for even small preterm infants (Fig. 31.12 A,B). Although not common practice, there is increasing use of these devices, with reports of successful implants in infants < 1.5 kg (113,114). The devices are delivered antegrade from the femoral vein. Ongoing concerns with

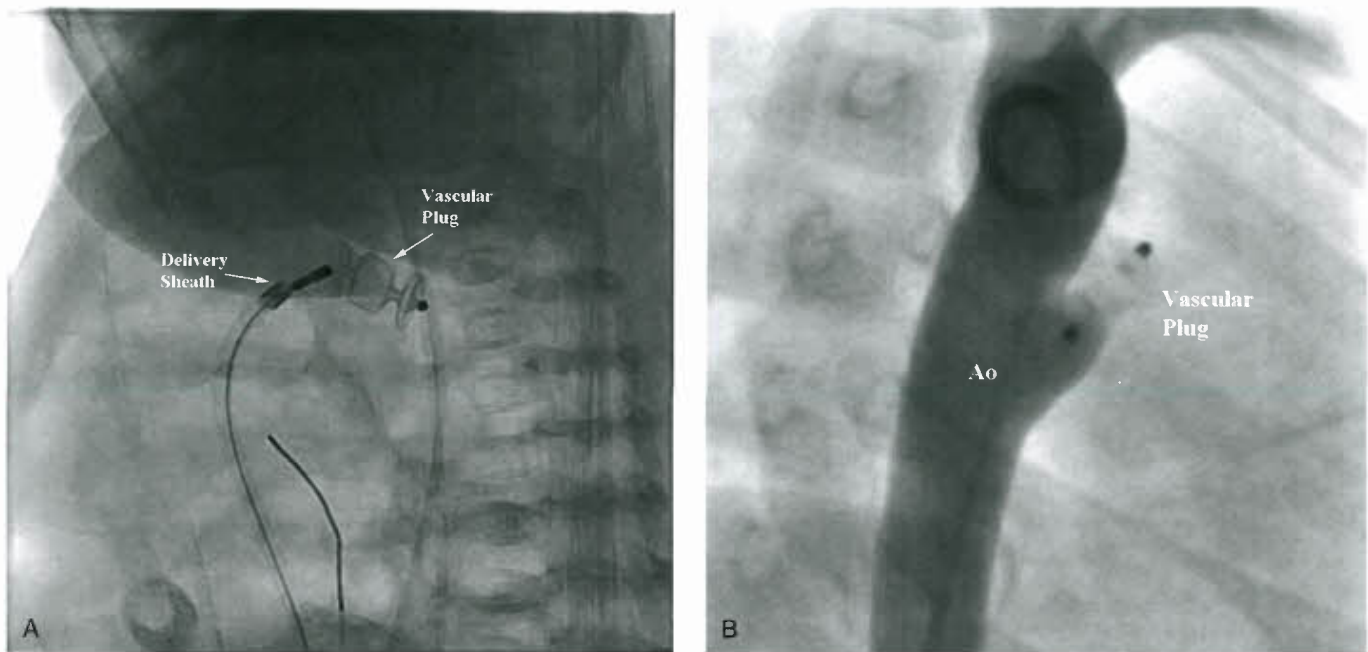


Figure 31.12. A: Lateral fluoroscopy image of delivery of a vascular plug into the tubular PDA of a 2.3 kg infant through a 4 French (1.3-mm-diameter) long sheath. B: Right anterior oblique aortic angiogram after release of the vascular plug showing complete closure of the PDA.

this technique include late femoral vein thrombosis and risk of device embolization with potential severe sequelae. Experience is too small at this time to quantify these risks accurately, so at present time, this has been used in patients at increased risk for either medical or surgical closure. As experience and improvements continue, this may become appropriate therapy for many preterm infants.

Prophylactic Closure. Despite the efficacy of treatment of the PDA in preterm infants, significant morbidity remains. Therefore it would seem that early closure before the development of clinical symptoms may reduce associated morbidity. Indeed, prophylactic administration of indomethacin in preterm infants prior to 28 weeks of gestation decreases the incidence of serious pulmonary hypertension, grade III/IV intraventricular hemorrhage, and need for surgical closure, but has not been shown to alter mortality (115). Prophylactic ibuprofen also decreases the need for symptomatic treatment but has not yet been shown to alter the incidence of intraventricular hemorrhage (116). In addition, one trial reported an incidence of significant pulmonary hypertension after prophylactic ibuprofen administration (103). Although the issue has not been put to rest, current practice is not to prophylactically close PDAs in preterm infants, even extremely low-birth-weight ones.

Treatment of Term Infants, Children, and Adults with PDA

In term infants or children, the complications resulting from isolated PDA, including failure to grow, recurrent respiratory infections, cardiac enlargement and failure, lobar emphysema or collapse, bacterial endarteritis, and the development of pulmonary hypertension are all indications for early correction. In adults, indications are more typically left heart enlargement, exercise intolerance, or bacterial endarteritis. Because treatment of an uncomplicated PDA is accompanied by minimal risk, closure should be recommended soon after the diagnosis is made. There is a small chance of spontaneous closure during the first 6 months of life so most pediatric cardiologists wait until about 9 months of age in asymptomatic infants. Treatment options

currently include catheter coil or device closure or surgery, with catheter closure having become the treatment of choice in most patients due to equal efficacy, fewer complications, and shorter recovery times (117). Indomethacin is ineffective in term infants and older children and therefore should not be used. If severe heart failure is present, medical management with intravenous diuretics, inotropes, and mechanical ventilation may be beneficial (118) prior to immediate catheter or surgical closure.

Catheter Coil/Device Closure. Catheter closure with occluding coils has become the treatment of choice for a small PDA (<2.5 mm in diameter). This 2- to 3-hour outpatient procedure is performed in the catheterization laboratory using conscious sedation, allowing discharge the same day with return to full activity the next day. A catheter is advanced from the femoral artery or vein across the PDA. An occluding coil is placed in the PDA with a single coil loop on the pulmonary artery side and the remaining three to four loops in the aortic ductal ampulla (Fig. 31.13A,B). Occasionally, immediate placement of a second or third coil is needed to achieve complete closure. This procedure is >97% successful with no mortality and minimal significant morbidity (119,120). Catheter technology has advanced so that coils currently used are made of platinum or a metal composite that is MRI compatible, resolving the previous issue of chest MRI artifact due to stainless steel PDA coils. For PDAs larger than a few mm but <12 mm in diameter, specialized devices, such as the Amplatzer duct occluder or the PFM Duct-Occlud coil (Fig. 31.14A–D) are available for catheter-based repair. The procedure is similar in duration, risk, and recovery time to the coil closure procedure. The devices are implanted antegrade from the femoral vein or retrograde from the femoral artery using long catheters through sheaths sized 4 to 8 French (1.3 to 2.5 mm outer diameter) (Fig. 31.15A–C). There is a >98% complete closure rate at 6 months with minimal complications and no reported mortality (121–123). PDAs larger than 12 mm have been closed using septal closure devices (AGA septal occluder, AGA VSD device, NMT CardioSEAL device) (Fig. 31.16A,B) or covered stents in select cases (124).

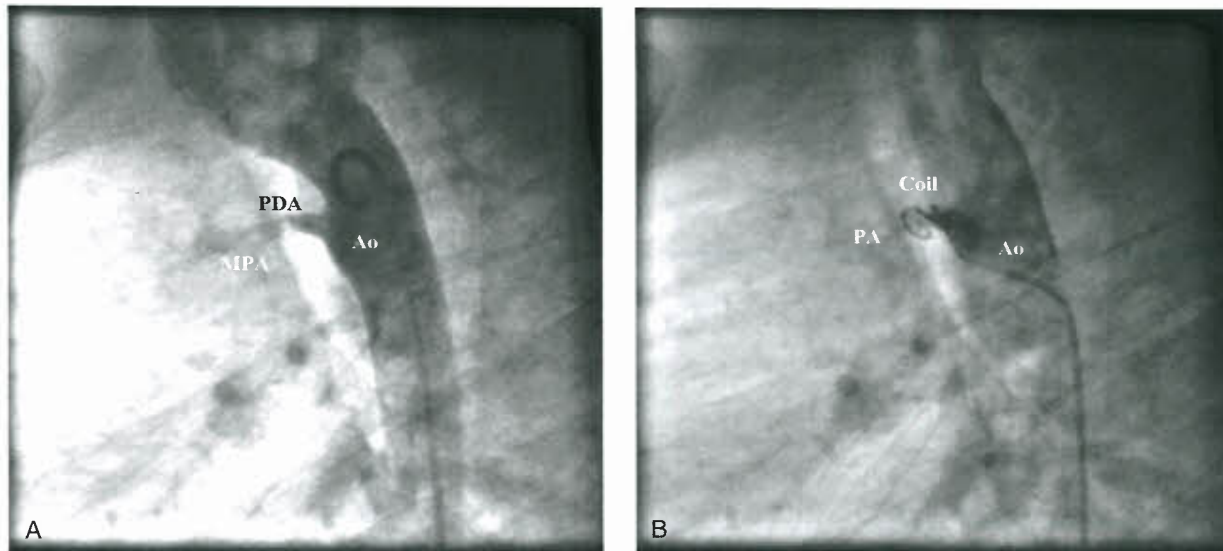


Figure 31.13. A: Lateral descending aortic angiogram showing a typical small (1.5 mm) patent ductus arteriosus (PDA) in a child. MPA, main pulmonary artery, Ao, aorta. B: Lateral descending aortogram after placement of a single 0.038" coil with a single loop of coil in the pulmonary artery (PA), and the remaining loops in the aorta (Ao).

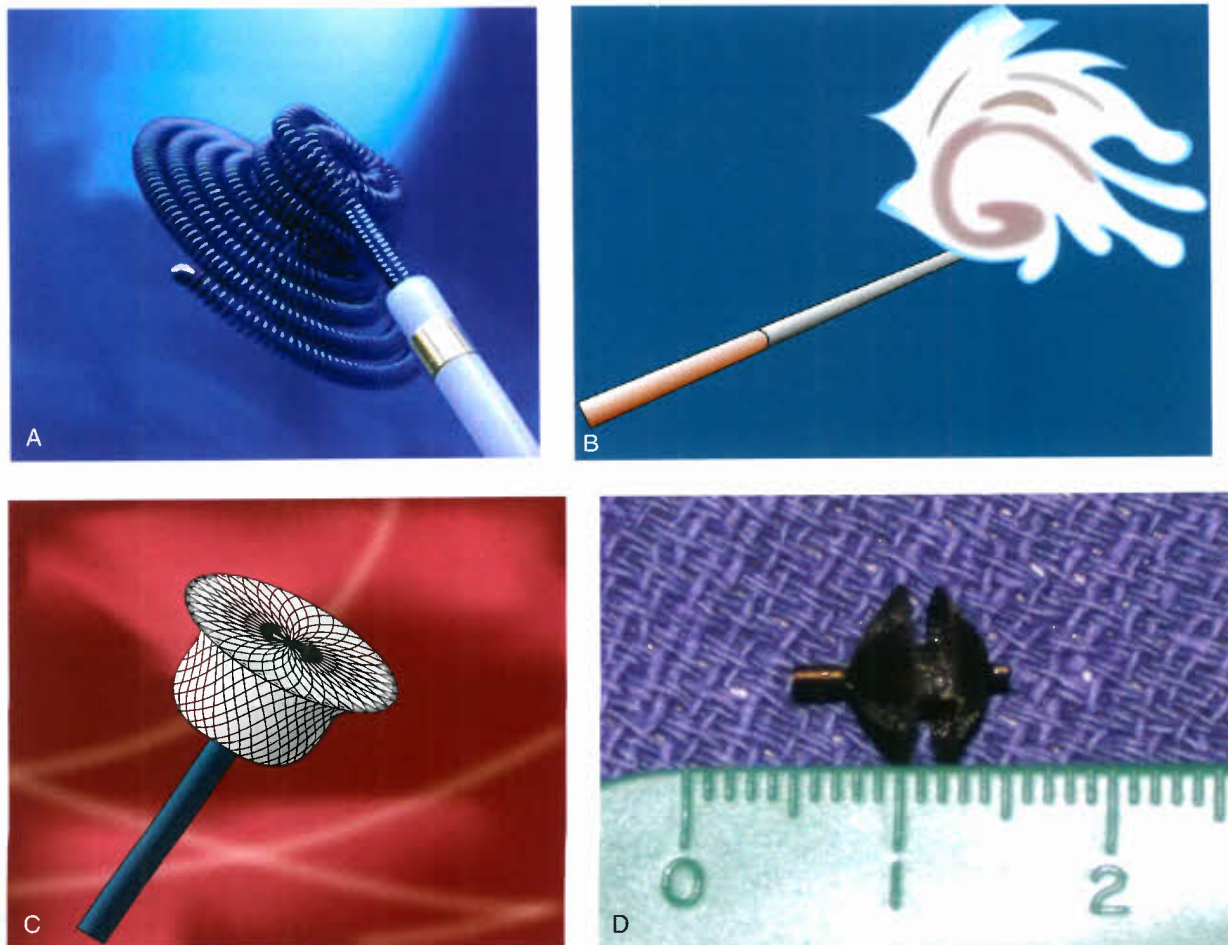


Figure 31.14. PDA occlusion devices. A: PFM Duct-Occlud coil. B: Cook MREYE coil. C: Amplatzer ADO I. D: Amplatzer ADO II.

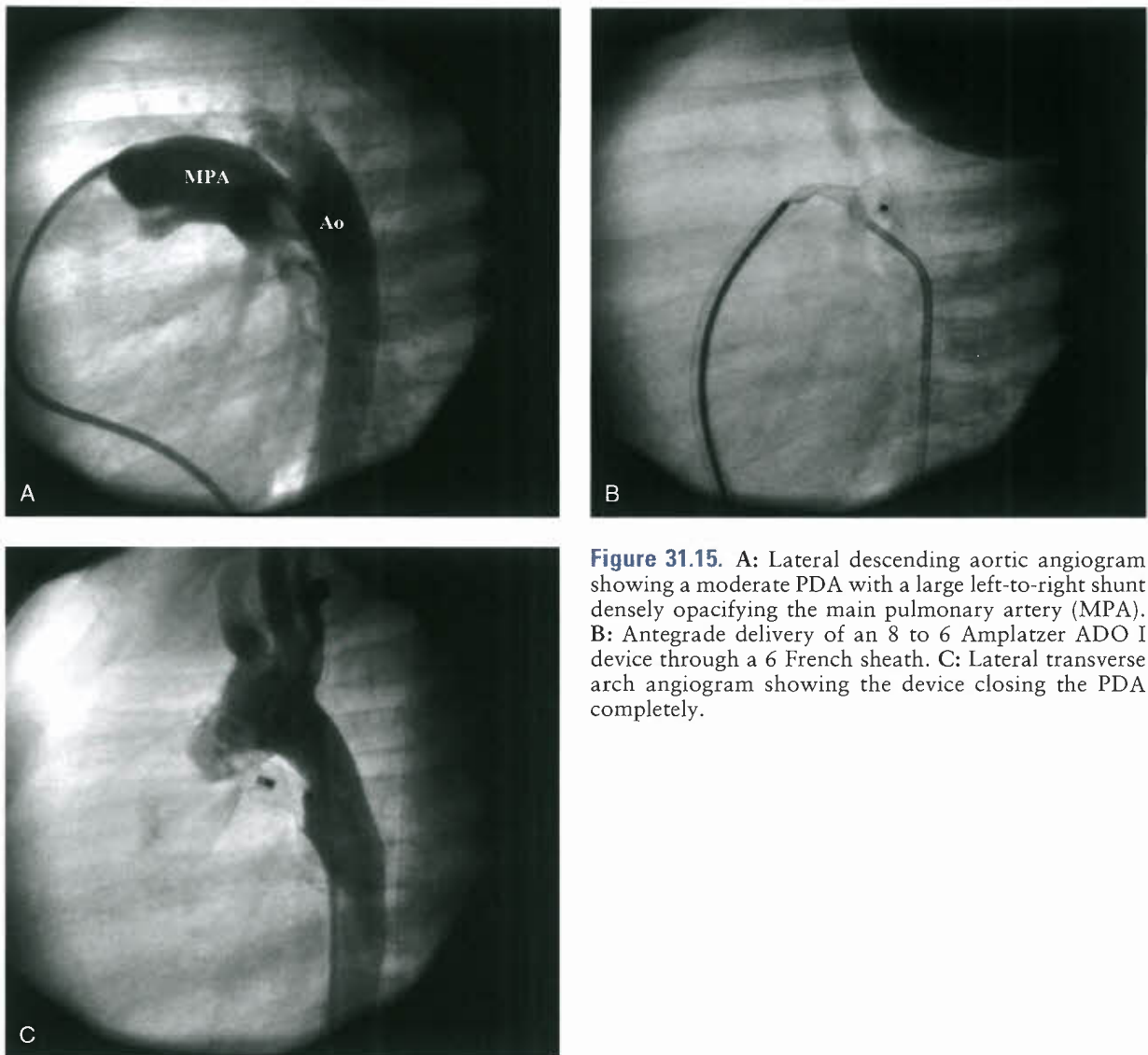


Figure 31.15. A: Lateral descending aortic angiogram showing a moderate PDA with a large left-to-right shunt densely opacifying the main pulmonary artery (MPA). B: Antegrade delivery of an 8 to 6 Amplatzer ADO I device through a 6 French sheath. C: Lateral transverse arch angiogram showing the device closing the PDA completely.

Surgical Closure. Surgery remains the treatment of choice for PDAs too large for catheter closure. The traditional surgical approach to closure of the PDA involves division or transection of the PDA through a lateral thoracotomy. Suture ligation without division has the potential for recanalization, particularly following single-suture ligation. Surgery is extremely safe with minimal mortality and morbidity. Hospital stays can be as short as 3 days, with return to full activity within 3 weeks. A recent surgical advance is thoracoscopic surgical closure. In this technique, three small 1.5-in incisions are made in the lateral thorax through which a thoracoscope and several surgical tools are inserted. Several surgical clips are placed on the PDA under direct visualization through the scope. Obvious advantages of this technique include less operative lung manipulation, less chest wall pain, faster recovery, and a smaller scar. Some critics of this new technique have raised concerns regarding the potential for tearing and hemorrhage with clipping of large PDAs, particularly in adults in whom the PDA may be calcified. This technique is increasing in use; early results show similar efficacy, shorter hospital stay, and lower cost but in at least one study a higher rate of laryngeal nerve injury compared with standard thoracotomy (112,125,126).

Treatment of Children and Adults with PDA and Pulmonary Hypertension

The decision to recommend closure of a PDA in a child or young adult with significantly elevated pulmonary vascular resistance is not simple. Catheterization is recommended in these patients to evaluate the pulmonary vascular bed's response to test occlusion with a balloon catheter and pulmonary vasodilators, such as oxygen and nitric oxide. If there is a good response, whereby a significant decrease in pulmonary artery diastolic pressure and decrease in calculated pulmonary vascular resistance occurs, closure is advised. Device closure should be considered in this setting if the surgical risk is increased because of significant pulmonary hypertension (127). However, if the response to test occlusion with pulmonary vasodilators is equivocal, the decision is considerably more difficult. Aggressive treatment with pulmonary vasodilators including home oxygen, sildenafil, bosentan, and/or inhaled iloprost should be considered with repeat catheterization in 4 to 9 months with repeat evaluation and consideration for device closure (128). Some patients respond extremely well and show significant improvement after PDA closure,

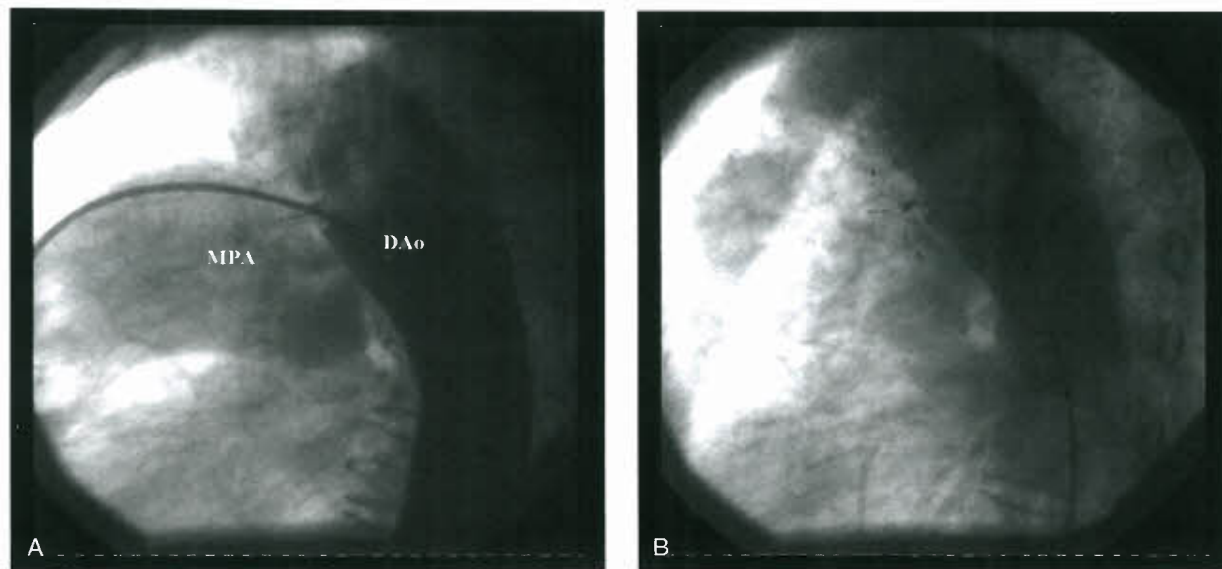


Figure 31.16. A: Lateral proximal descending aortic angiogram in an elderly patient showing a large window-type patent ductus arteriosus with marked dilation of both the main pulmonary artery (MPA) and descending aorta (DAo). B: Lateral proximal descending aortic angiogram after closure with a 28 mm CardioSEAL device showing an immediate small residual shunt.

whereas others show a progressive increase in pulmonary vascular resistance after closure. Therefore, careful monitoring and use of pulmonary vasodilators after closure is needed. The only contraindication to closure of an isolated PDA is severe pulmonary hypertension with irreversible pulmonary vascular disease and baseline right-to-left ductal shunting despite maximal medical pulmonary vasodilation. If the PDA is closed in these patients, they are incapable of maintaining an adequate systemic output in response to stress, and rapid deterioration and death frequently occur.

AORTOPULMONARY WINDOW

Aortopulmonary window, or aortopulmonary septal defect, is a relatively rare cardiac malformation. Since first described by Elliotson (129) nearly two centuries ago, just over 300 cases have been reported (129–143). It accounts for 0.2% to 0.6% of all cases of congenital heart disease (139). Nearly half of all patients have associated cardiac lesions, including aortic origin of the right pulmonary artery (131,134,141,144), type A interruption of the aortic arch (132,134,139,142), tetralogy of Fallot (130,133,139), and anomalous origin of the right or left coronary artery from the pulmonary artery and right aortic arch (135,139,145). More rarely, it is associated with ventricular septal defect (131,143), pulmonary (143) or aortic atresia (142), D-transposition of the great arteries (146,147), and tricuspid atresia (136).

The aortopulmonary septum is formed by the two opposing truncal cushions, which appear at the 9-mm stage, then rapidly enlarge and fuse, dividing the truncus arteriosus into separate aortic and pulmonary channels (148). Cells that migrate from the neural crest influence this division. Removal of neural crest tissue results in various arterial abnormalities including truncus arteriosus, transposition of the great arteries, and aortic interruption. However, aortopulmonary window is not seen when neural crest tissue is removed (149). In addition, unlike truncus arteriosus, aortopulmonary window has not been reported in association with DiGeorge syndrome

(150). In contrast to other conotruncal abnormalities, there is no known association with 22Q11 deletion (147,151,152). Finally, whereas type B aortic interruption is associated with truncus arteriosus, type A is seen more frequently with aortopulmonary window (134,139). Thus, although these anomalies involve the same region of the heart, they appear to be unrelated embryologically, not variants of the same disease.

In most cases, there is a defect in the proximal portion of the aortopulmonary septum, midway between the semilunar valves and the pulmonary bifurcation. The defect is variable in size, but most defects result in a large, generally continuous left-to-right shunt when the pulmonary vascular resistance falls, similar to other interarterial communications such as PDA or truncus arteriosus. Without corrective surgery, irreversible obstructive changes in the pulmonary vascular bed develop early, followed by death in the second decade, although patients surviving into the fourth decade have been reported (133).

Pathology

Following the immediate perinatal period, once hemodynamic changes have occurred, the heart is large, owing primarily to an enlarged, volume-loaded left atrium and LV. The branch pulmonary arteries are usually enlarged because of the increased pulmonary flow. The ascending aorta is often small, particularly in cases with a very proximal defect or with associated aortic arch anomalies. The aortopulmonary defect is a discrete area, variable in size, usually positioned midway between the semilunar valves and the pulmonary bifurcation. It has a regular edge and is usually circular, although a form has been described with a border that is not continuous but describes slightly more than one turn of a spiral (139).

Although several classifications have been presented, the one proposed by Mori et al. (141) is most commonly used (Fig. 31.17). It describes three types of aortopulmonary connection. Type I is the most common type described earlier: a small defect midway between the semilunar valves and the pulmonary bifurcation. Type II is a more distal defect, the distal

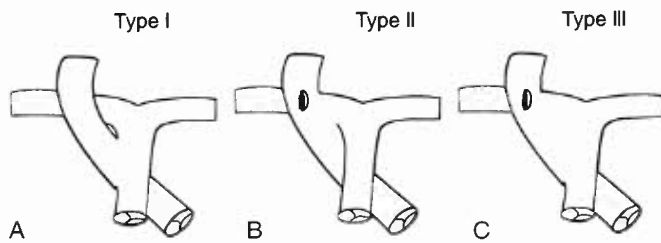


Figure 31.17. Classification of aortopulmonary window. A: Type I, proximal defect, midway between the semilunar valves and pulmonary bifurcation. B: Type II, distal defect, with posterior border absent and aortic origin of right pulmonary artery. C: Type III, total defect, incorporating defects present in both types I and II. (From Mori K, Ando M, Takao A, et al. Distal type of aortopulmonary window. Report of 4 cases. *Br Heart J* 1978;40:681–689, with permission.)

border of which is formed by the pulmonary bifurcation. This type is more commonly associated with aortic origin of the right pulmonary artery (131,134,141). Type III, a large, confluent defect involving essentially the entire aortopulmonary septum, is the most rare.

Manifestations

Clinical Features

The clinical features of aortopulmonary window are not specific but are those of a large left-to-right shunt, and clinically this lesion often mimics either a ventricular septal defect or a PDA or both. Signs of congestive heart failure (tachypnea, diaphoresis, failure to thrive, and recurrent respiratory difficulty) usually begin in the first weeks of life (133,135,141). Cyanosis usually is not present, although large defects can produce desaturation owing to bidirectional shunting and mixing at the arterial level. When aortic arch anomalies are present, the presenting symptoms may be those of metabolic acidosis when the PDA closes, and the aortopulmonary window may be masked.

Physical examination shows tachypnea, abdominal breathing, and overexpansion of the lungs with intercostal retractions. There may be a prominent right ventricular impulse at the left sternal border. The pulses may be bounding, indicating arterial runoff into the lungs. On auscultation, the second heart sound generally is accentuated and narrowly split, suggesting pulmonary hypertension. In some patients a prominent ejection click is heard in the pulmonic area (133,141). There is either a loud systolic ejection murmur at the left upper sternal border or a machinery-type murmur similar to that found with a PDA (141). Often a middiastolic rumbling murmur is present at the apex, indicating increased flow across the mitral valve.

Patients with very small defects may be asymptomatic. In these patients, the second heart sound may be normal, with only a systolic ejection murmur and possibly a middiastolic murmur audible at the apex. The defect in these patients may be mistaken clinically for a small ventricular septal defect and may be diagnosed accurately only during routine echocardiography.

Electrocardiographic Features

There are no characteristic ECG findings in patients with aortopulmonary window. Evidence of right ventricular hypertrophy usually is present, although biventricular hypertrophy may be present when the defect is large or has been present for some time (135,141). Rarely, the ECG is normal or shows only a mild degree of right ventricular hypertrophy suggested by an rsR' pattern in the right precordial leads.

Radiologic Features

The chest roentgenogram is indicative of a large left-to-right shunt. A moderately enlarged heart with prominent pulmonary vascular markings is usually present. The main pulmonary artery segment is usually pronounced, as are the LA and LV borders. The aortic knuckle usually is not prominent. The lung fields frequently show hyperinflation, and pulmonary edema may be present.

Echocardiographic Features

Two-dimensional echocardiography can accurately diagnose aortopulmonary window and generally describe any associated anomalies (Fig. 31.18). In addition, the lesion is readily diagnosed *in utero* using fetal echocardiography (153). The left atrium and LV are dilated owing to the large left-to-right shunt. The right ventricle may be hypertrophied, although not always. The semilunar valves usually are normal in both position and motion. The pulmonary arteries are significantly enlarged. The aortopulmonary window can usually be seen directly, but dropout is often seen in the aortopulmonary septal area of normal patients. Balaji et al. (130) described a “T” artifact at the edges of the defect to help distinguish it from normal dropout. In addition, color Doppler flow mapping demonstrates flow through the defect.

Doppler echocardiography is helpful in the diagnosis of aortopulmonary window, with findings similar to that seen in a PDA. Abnormal, continuous forward flow in the pulmonary arteries indicates the presence of an aortopulmonary communication (130) (Fig. 31.3C). Significant retrograde descending aortic diastolic flow is found in both the proximal aortic arch and the abdominal aorta (Fig. 31.8B); this is also in contrast to a PDA where the proximal arch has diastolic prograde flow. Doppler echocardiography also demonstrates the presence of pulmonary hypertension when pulmonary or tricuspid insufficiency is present.

Cardiac Catheterization

With current echocardiographic techniques, cardiac catheterization usually is not required. The right ventricular and pulmonary arterial pressures usually are at systemic levels (135,141). The LA pressure may be elevated from the left-to-right shunt and increased pulmonary venous return, whereas the LV pressure is usually normal. Aortic pressure usually is normal, but in the presence of large defects may have a decreased diastolic and widened pulse pressure owing to runoff into the pulmonary vascular bed. The catheter often can be manipulated directly from the main pulmonary artery through the defect into the ascending aorta.

Either an ascending aorta or main pulmonary angiogram will demonstrate the defect. An ascending aorta angiogram shows filling of the pulmonary arteries, including the pulmonary valve sinuses, and main and branch pulmonary arteries (141). It also will demonstrate associated aortic arch anomalies. A main pulmonary arterial angiogram shows filling of the ascending aorta, and when present, also can demonstrate anomalous origin of a coronary artery from the pulmonary artery (135).

Differential Diagnosis

Because aortopulmonary window is an extremely rare defect, the clinical features are often ascribed to a large ventricular septal defect, a large PDA, or persistent truncus arteriosus. The bounding pulses, wide pulse pressure, and continuous murmur, if present, indicate the presence of an arterial communication (133). Distinguishing aortopulmonary window from

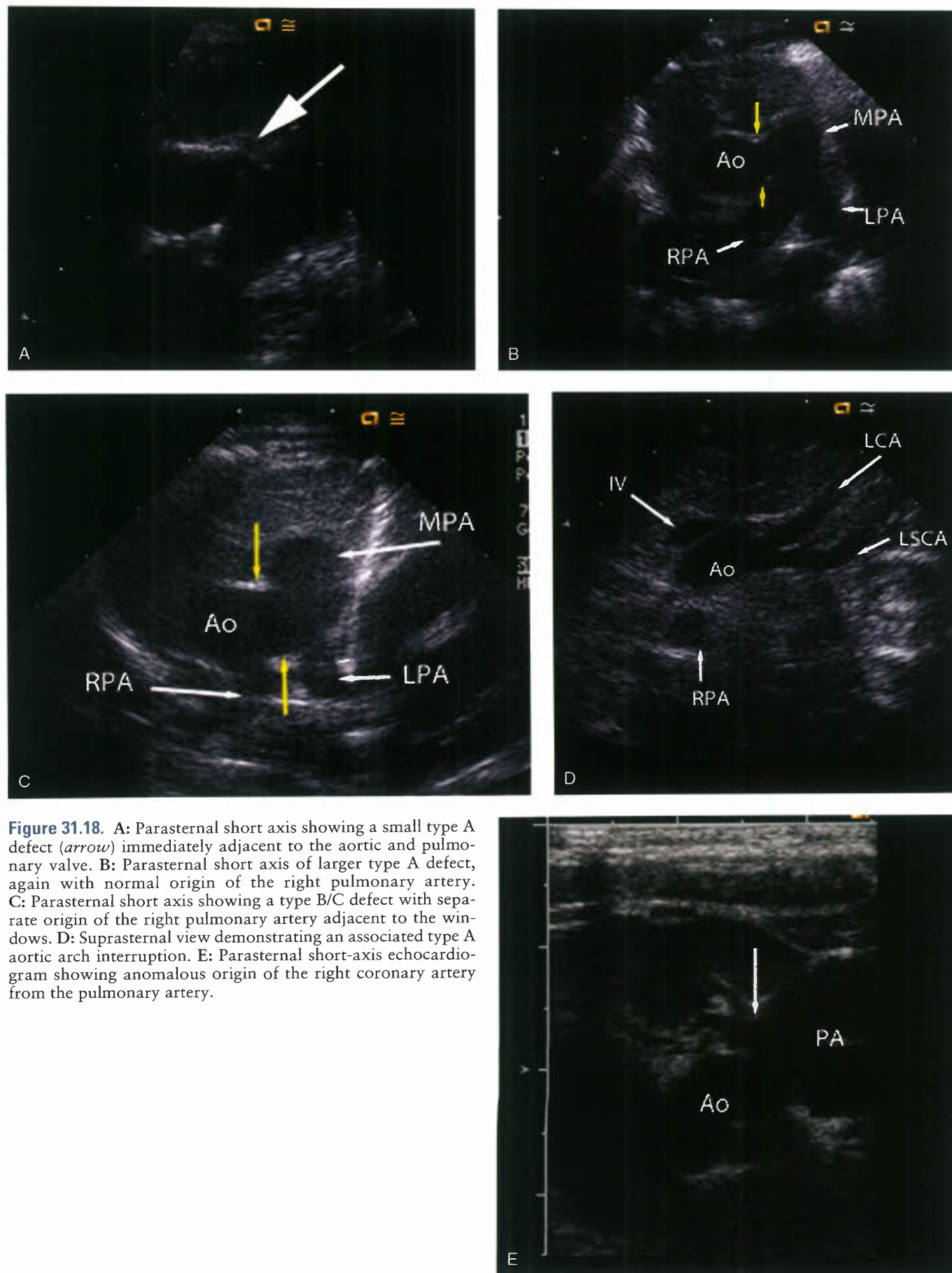


Figure 31.18. A: Parasternal short axis showing a small type A defect (arrow) immediately adjacent to the aortic and pulmonary valve. B: Parasternal short axis of larger type A defect, again with normal origin of the right pulmonary artery. C: Parasternal short axis showing a type B/C defect with separate origin of the right pulmonary artery adjacent to the windows. D: Suprasternal view demonstrating an associated type A aortic arch interruption. E: Parasternal short-axis echocardiogram showing anomalous origin of the right coronary artery from the pulmonary artery.

either a large PDA or from persistent truncus arteriosus often is extremely difficult by physical examination alone. A systolic ejection or continuous murmur is also present in patients with PDA; however, significant clinical symptoms in the first weeks of life are very unusual. Patients with persistent truncus arteriosus usually have more arterial desaturation than patients with aortopulmonary window and the same degree of congestive heart failure, as the common ventricular outlet results in complete mixing. They often also have a diastolic murmur indicative of regurgitation of the truncal valve. The murmur of a ventricular septal defect usually is heard toward the base of the sternum, and the pulses are not bounding.

Treatment

Closure of the defect is indicated in essentially all patients with aortopulmonary window. The classical treatment is surgical closure of the defect. Since the first reported correction by Gross (137), several types of surgical correction have been attempted. Simple ligation (135) and division with suture closure of the defect (133) both have met with poor results. Although exposure and patch closure of the defect from the pulmonary artery is possible (135,137), most authors recommend a transaortic approach using a median sternotomy and cardiopulmonary bypass (135,141,154). This approach provides optimal exposure of the defect and also allows access for correction of associated defects, particularly arch anomalies and anomalous origin of either the right pulmonary artery or right coronary artery. In patients with aortic origin of the right pulmonary artery, the patch closure can be tunneled to include the right pulmonary artery in the repair (134). Some revisions have used a pulmonary artery flap to close the defect (155–157). This technique avoids the use of prosthetic material. More recently, several patients have undergone closure using various catheter-delivered devices (158–161), although this approach is likely not applicable for larger defects or those with anomalous right pulmonary artery origin.

The prognosis of patients with aortopulmonary window is excellent if surgical correction is performed early in life, before irreversible pulmonary vascular changes occur (154). Although long-term follow-up is limited, late complications of the defect in patients adequately repaired are unlikely to be significant. Patients with associated anomalies will likely be limited more by the associated anomaly than by the repaired aortopulmonary window.

REFERENCES

- Rudolph AM, Heymann MA, Spitznas U. Hemodynamic considerations in the development of narrowing of the aorta. *Am J Cardiol* 1972;30:514–525.
- Fay FS, Cooke PH. Guinea pig ductus arteriosus. II. Irreversible closure after birth. *Am J Physiol* 1972;222:841–849.
- Gittenberger-de Groot AC, Van Erbruggen I, Moulart AJMG, et al. The ductus arteriosus in the preterm infant: histologic and clinical observations. *J Pediatr* 1980;96:88–93.
- Liang CD, Ko SF, et al. Vocal cord paralysis after transcatheter coil embolization of patent ductus arteriosus. *Am Heart J* 2003;146:367–371.
- Benjamin JR, Smith PB, et al. Long-term morbidities associated with vocal cord paralysis after surgical closure of a patent ductus arteriosus in extremely low birth weight infants. *J Perinatol* 2010;30:408–413.
- Heymann MA, Rudolph AM. Control of the ductus arteriosus. *Physiol Rev* 1975;55:62–78.
- Clyman RI. Ontogeny of the ductus arteriosus response to prostaglandins and inhibitors of their synthesis. *Semin Perinatol* 1980;4:115–124.
- Cocconi F, Olley PM. Role of prostaglandins, prostacyclin, and thromboxanes in the control of prenatal patency and postnatal closure of the ductus arteriosus. *Semin Perinatol* 1980;4:109–113.
- Clyman RI, Heymann MA. Pharmacology of the ductus arteriosus. *Pediatr Clin North Am* 1981;28:77–93.
- Clyman RI. Ductus arteriosus: Current theories of prenatal and postnatal regulation. *Semin Perinatol* 1987;11:64–71.
- Clyman RI. Developmental physiology of the ductus arteriosus. In: Long W, ed. *Fetal and Neonatal Cardiology*. Philadelphia, PA: WB Saunders, 1990:64–75.
- Rudolph AM, Drorbaugh JE, Auld PAM, et al. Studies on the circulation in the neonatal period. The circulation in the respiratory distress syndrome. *Pediatrics* 1961;27:551–566.
- McMurphy DM, Heymann MA, Rudolph AM, et al. Developmental changes in constriction of the ductus arteriosus: responses to oxygen and vasoactive substances in the isolated ductus arteriosus of the fetal lamb. *Pediatr Res* 1972;6:231–238.
- Rudolph AM. *Congenital Diseases of the Heart: Clinical-Physiologic Considerations in Diagnosis and Management*. Chicago, IL: Year Book Medical, 1974.
- Rudolph AM, Mayer FE, Nadas AS, et al. Patent ductus arteriosus. A clinical and hemodynamic study of patients in the first year of life. *Pediatrics* 1958;22:892–904.
- Baylen BG, Ogata H, Oguchi K, et al. The contractility and performance of the pre-term left ventricle before and after early patent ductus arteriosus occlusion in surfactant-treated lambs. *Pediatr Res* 1985;19:1053–1058.
- Lister G, Walter TK, Versmold HT, et al. Oxygen delivery in lambs: Cardiovascular and hematologic development. *Am J Physiol* 1979;237:H668–H675.
- Lebowitz EA, Novick JS, Rudolph AM. Development of myocardial sympathetic innervation in the fetal lamb. *Pediatr Res* 1972;6:887–893.
- Friedman WF. The intrinsic physiologic properties of the developing heart. In: Friedman WF, Lesch M, Sonnenblick EH, eds. *Neonatal Heart Disease*. New York, NY: Grune & Stratton, 1973:21–49.
- Tsang RC, Light IJ, Sutherland JM, et al. Possible pathogenetic factors in neonatal hypocalcemia of prematurity. *J Pediatr* 1973;82:423–429.
- Hoffman JIE, Buckberg GD. Regional myocardial ischemia—causes, prediction and prevention. *Vasc Surg* 1974;8:115–131.
- Delivoria-Papadopoulos M, Roncovic NP, Oski FA. Postnatal changes in oxygen transport of term, premature, and sick infants: the role of red cell 2,3-diphosphoglycerate and adult hemoglobin. *Pediatr Res* 1971;5:235–245.
- Hoffman JIE, Rudolph AM, Heymann MA. Pulmonary vascular disease with congenital heart lesions: pathologic features and causes. *Circulation* 1981;64:873–877.
- Braudo M, Rowe RD. Auscultation of the heart: early neonatal period. *Am J Dis Child* 1961;101:575–586.
- Huhta JC, Cohen M, Gutgesell HP. Patency of the ductus arteriosus in normal neonates: two dimensional echocardiography vs Doppler assessment. *J Am Coll Cardiol* 1984;4:561–564.
- Silverman NH. Patent ductus arteriosus. In: *Pediatric Echocardiography*. Baltimore, MD: Williams & Wilkins, 1993:167–177.
- Liao PK, Su WJ, Hung JS. Doppler echocardiographic flow characteristics of isolated patent ductus arteriosus: better delineation by Doppler color flow mapping. *J Am Coll Cardiol* 1988;12:1285–1291.
- Clyman RI, Brett C, Mauray F. Circulating prostaglandin E2 concentrations and incidence of patent ductus arteriosus in preterm infants with respiratory distress syndrome. *Pediatrics* 1980;66:725–729.
- Moss AJ, Emmanouilides GC, Adams FH, et al. Response of ductus arteriosus and pulmonary and systemic arterial pressure to changes in oxygen environment in newborn infants. *Pediatrics* 1964;33:937–944.
- Alzamora-Castro V, Battilana G, Abugattas R, et al. Patent ductus arteriosus and high altitude. *Am J Cardiol* 1960;5:761–763.
- Baden M, Kirks DR. Transient dilation of the ductus arteriosus—the “ductus bump.” *J Pediatr* 1974;84:858–860.
- Koren G, Florescu A, Costei AM, et al. Nonsteroidal antiinflammatory drugs during third trimester and the risk of premature closure of the ductus arteriosus: a meta-analysis. *The Ann Pharmacother* 2006;40:824–829.
- Sawdy RJ, Lye S, Fisk NM, et al. A double-blind randomized study of fetal side effects during and after the short-term maternal administration of indomethacin, sulindac, and nimesulide for the treatment of preterm labor. *Am J Obstet Gynecol* 2003;188:1046–1051.
- Stika CS, Gross GA, Leguizamon G, et al. A prospective randomized safety trial of celecoxib for treatment of preterm labor. *Am J Obstet Gynecol* 2002;187:653–660.
- de Swiet M, Fryers G. Review: the use of aspirin in pregnancy. *J Obstet Gynecol* 1990;10:467–482.
- Gewillig M, Brown SC, De Catte L, et al. Premature foetal closure of the arterial duct: clinical presentations and outcome. *Eur Heart J* 2009;30:1530.
- Noori S, Friedlich P, Seri I. Changes in myocardial function and hemodynamics after ligation of the ductus arteriosus in preterm infants. *J Pediatr* 2007;150:597–602.
- Respondek M, Weil SR, Huhta JC. Fetal echocardiography during indomethacin treatment. *Ultrasound Obstet Gynecol* 1995;5:86–89.
- Huhta JC, Moise KJ, Fisher DJ, et al. Detection and quantitation of constriction of the fetal ductus arteriosus by Doppler echocardiography. *Circulation* 1987;75:406–412.
- Danilowicz D, Rudolph AM, Hoffman JIE. Delayed closure of ductus arteriosus in premature infants. *Pediatrics* 1966;37:74–78.
- Siassi B, Emmanouilides GC, Cleveland RJ, et al. Patent ductus arteriosus complicating prolonged assisted ventilation in respiratory distress syndrome. *J Pediatr* 1969;74:11–19.
- Kitterman JA, Edmunds LH Jr, Gregory GA, et al. Patent ductus arteriosus in premature infants: incidence, relation to pulmonary disease, and management. *N Engl J Med* 1972;287:473–477.

43. Clyman RI. The role of the patent ductus arteriosus in respiratory distress syndrome. *Semin Perinatol* 1984;8:293-299.
44. Strauss HW, Wagner HN Jr, Wesselhoeft H, et al. Radionuclide angiocardigraphy in pediatrics. In: James AE, Wagner HN, Cooke RE, eds. *Pediatric Nuclear Medicine*. Philadelphia, PA: WB Saunders, 1974:219-231.
45. Clyman RI, Jobe A, Heymann MA, et al. Increased shunt through the patent ductus arteriosus after surfactant replacement therapy. *J Pediatr* 1982;100:101-107.
46. Lemmers PMA, Molenschot MC, Evens J, et al. Is cerebral oxygen supply compromised in preterm infants undergoing surgical closure for patent ductus arteriosus? *Arch Dis Child Fetal Neonatal Ed* 2010;95:F429-F434.
47. El-Khuffash AF, Slevin M, McNamara PJ, et al. Troponin T, N-terminal pro natriuretic peptide and a patent ductus arteriosus scoring system predict death before discharge or neurodevelopmental outcome at 2 years in preterm infants. *Arch Dis Child Fetal Neonatal Ed* 2011;96:F133-F137.
48. El-Khuffash AF, Molloy EJ. Influence of a patent ductus arteriosus on cardiac troponin T levels in preterm infants. *J Pediatr* 2008;153:350-353.
49. Serwer GA, Armstrong BE, Anderson PAW. Noninvasive detection of retrograde descending aortic flow in infants using continuous wave Doppler ultrasonography. *J Pediatr* 1980;97:394-400.
50. Smallhorn JE, Gow R, Olley PM, et al. Combined noninvasive assessment of the patent ductus arteriosus in the preterm infant before and after indomethacin treatment. *Am J Cardiol* 1984;54:1300-1304.
51. Houston AB, Lim MK, Doig WB, et al. Doppler flow characteristics in the assessment of pulmonary artery pressure in ductus arteriosus. *Br Heart J* 1989;62:284-290.
52. Fyhrius F, Tikkanen J, Totterman KJ, et al. Plasma atrial natriuretic peptide in health and disease. *Eur Heart J* 1987;8:117-122.
53. Doust JA, Glasziou PP, Pietrzak E, et al. A systematic review of the diagnostic accuracy of natriuretic peptides for heart failure. *Arch Intern Med* 2004;164:1778-1784.
54. Holmstrom H, Omland T. Natriuretic peptides as markers of patent ductus arteriosus in preterm infants. *Clin Sci (Lond)* 2002;103:79-80.
55. Puddy VF, Amirmansour C, Williams AF, et al. Plasma brain natriuretic peptide as a predictor of haemodynamically significant patent ductus arteriosus in preterm infants. *Clin Sci (Lond)* 2002;103:75-77.
56. Yoshibayashi M, Kamiya T, Saito Y, et al. Plasma brain natriuretic peptide concentrations in healthy children from birth to adolescence: marked and rapid increase after birth. *Eur J Endocrinol* 1995;133:207-209.
57. da Graca RL, Hassinger DC, Flynn PA, et al. Longitudinal changes of brain-type natriuretic peptide in preterm neonates. *Pediatrics* 2006;117:2183-2189.
58. Sanjeev S, Pettersen M, Lua J, et al. Role of plasma B-type natriuretic peptide in screening for hemodynamically significant patent ductus arteriosus in preterm neonates. *J Perinatol* 2005;25:709-713.
59. Eerola A, Jokinen E, Boldt T, et al. The influence of percutaneous closure of patent ductus arteriosus on left ventricular size and function: a prospective study using two- and three-dimensional echocardiography and measurements of serum natriuretic peptides. *J Am Coll Cardiol* 2006;47:1060-1066.
60. McGrath RL, McGuinness GA, Way GL, et al. The silent ductus arteriosus. *J Pediatr* 1978;93:110-113.
61. Thibeault DW, Emmanouilides GC, Nelson RJ, et al. Patent ductus arteriosus complicating the respiratory distress syndrome in preterm infants. *J Pediatr* 1975;86:120-126.
62. Mitchell SC, Korones SB, Berendes HW. Congenital heart disease in 56,109 births: incidence and natural history. *Circulation* 1971;43:323-332.
63. Knight DH, Patterson DF, Melbin J. Constriction of the fetal ductus arteriosus induced by oxygen, acetylcholine and norepinephrine in normal dogs and those genetically predisposed to persistent patency. *Circulation* 1973;47:127-132.
64. Mani A, Meraji SM, Houshyar R, et al. Finding genetic contributions to sporadic disease: a recessive locus at 12q24 commonly contributes to patent ductus arteriosus. *Proc Natl Acad Sci USA* 2002;99:15054-15059.
65. Khau Van Kien P, Mathieu F, Zhu L, et al. Mapping of familial thoracic aortic aneurysm/dissection with patent ductus arteriosus to 16p12.2-p13.13. *Circulation* 2005;112:2000-2006.
66. Gibson GA. Persistence of the arterial duct and its diagnosis. *Edinburgh Med J* 1900;8:1-5.
67. Santos MA, Moll JN, Drumond C, et al. Development of the ductus arteriosus in right ventricular outflow tract obstruction. *Circulation* 1980;62:818-822.
68. Freed MD, Heymann MA, Lewis AB, et al. Prostaglandin E1 in infants with ductus arteriosus-dependent congenital heart disease. *Circulation* 1981;64:899-905.
69. Gibbs JL, Uzun O, Blackburn ME, et al. Fate of the stented arterial duct. *Circulation* 1999;99:2621-2625.
70. Michel-Behnke I, Akintuerk H, Thul J, et al. Stent implantation in the ductus arteriosus for pulmonary blood supply in congenital heart disease. *Catheter Cardiovasc Interv* 2004;61:242-252.
71. Gewillig M, Boshoff DE, Dens J, et al. Stenting the neonatal arterial duct in duct-dependent pulmonary circulation: new techniques, better results. *J Am Coll Cardiol* 2004;43:107-112.
72. Hussain A, Al-Zharani S, et al. Midterm outcome of stent dilatation of patent ductus arteriosus in ductal-dependent pulmonary circulation. *Congenit Heart Dis* 2008;3:241-249.
73. Schranz D, Michel-Behnke I, Hayer R, et al. Stent implantation of the arterial duct in newborns with a truly duct-dependent pulmonary circulation: a single-center experience with emphasis on aspects of the interventional technique. *J Interv Cardiol* 2010;23:581-588.
74. Santoro G, Palladino MT, et al. Pulmonary artery growth following arterial duct stenting in congenital heart disease with duct-dependent pulmonary circulation. *Catheter Cardiovasc Interv* 2009;74:1072-1076.
75. Lim DS, Peeler BB, Matherne GP, et al. Risk-stratified approach to hybrid transcatheter-surgical palliation of hypoplastic left heart syndrome. *Pediatr Cardiol* 2006;27:91-95.
76. DiBardino DJ, McElhinney DB, et al. A review of ductal stenting in hypoplastic left heart syndrome: bridge to transplantation and hybrid stage I palliation. *Pediatr Cardiol* 2008;29:251-257.
77. Galantowicz M, Cheatham JP, et al. Hybrid approach for hypoplastic left heart syndrome: intermediate results after the learning curve. *Ann Thorac Surg* 2008;85:2063-2070; discussion 2070-2071.
78. Egan MJ, Hill SL, Boettner BL, et al. Predictors of retrograde aortic arch obstruction after hybrid palliation of hypoplastic left heart syndrome. *Pediatr Cardiol* 2011;32:67-75.
79. Morris CD, Reller MD, Menashe VD. Thirty-year incidence of infective endocarditis after surgery for congenital heart defect. *JAMA* 1998;279:599-603.
80. Johnson DH, Rosenthal A, Nadas AS. A forty-year review of bacterial endocarditis in infancy and childhood. *Circulation* 1975;51:581-588.
81. Sadiq M, Latif F, Ur-Rehman A. Analysis of infective endarteritis in patent ductus arteriosus. *Am J Cardiol* 2004;93:513-515.
82. Jan SL, Hwang B, Fu YC, et al. Isolated neonatal ductus arteriosus aneurysm. *J Am Coll Cardiol* 2002;39:342-347.
83. Celermajer DS, Sholler GF, Hughes CF, et al. Persistent ductus arteriosus in adults. A review of surgical experience with 25 patients. *Med J Aust* 1991;155:233-236.
84. Krichenko A, Benson LN, Burrows P, et al. Angiographic classification of the isolated, persistently patent ductus arteriosus and implications for percutaneous catheter occlusion. *Am J Cardiol* 1989;63:877-880.
85. Higgins CB, Silverman NH, Kersting-Sommerhoff BA, et al. Left-to-right shunt lesions. In: *Congenital Heart Disease: Echocardiography and Magnetic Resonance Imaging*. New York, NY: Raven Press, 1990:99-133.
86. Morgan-Hughes GJ, Marshall AJ, Roobottom C. Morphologic assessment of patent ductus arteriosus in adults using retrospectively ECG-gated multidetector CT. *AJR Am J Roentgenol* 2003;181:749-754.
87. Brenner LD, Caputo GR, Mostbeck G, et al. Quantitation of left to right atrial shunts with velocity-encoded cine nuclear magnetic resonance imaging. *J Am Coll Cardiol* 1992;20:1246-1250.
88. Heymann MA, Rudolph AM, Silverman NH. Closure of the ductus arteriosus in premature infants by inhibition of prostaglandin synthesis. *N Engl J Med* 1976;295:530-533.
89. Mahony L, Carnero V, Brett C, et al. Prophylactic indomethacin therapy for patent ductus arteriosus in very-low-birth-weight infants. *N Engl J Med* 1982;306:506-510.
90. Gersony WM, Peckham GJ, Ellison RC, et al. Effects of indomethacin in premature infants with patent ductus arteriosus: results of a national collaborative study. *J Pediatr* 1983;102:895-906.
91. Way GL, Pierce JR, Wolf RR, et al. ST depression suggesting subendocardial ischemia in neonates with respiratory distress syndrome and patent ductus arteriosus. *J Pediatr* 1979;95:609-611.
92. Merritt TA, White CL, Jacob J, et al. Patent ductus arteriosus treated with ligation or indomethacin: a follow-up study. *J Pediatr* 1979;95:588-594.
93. Keller RL, Tacy TA, Fields S, et al. Combined treatment with a nonselective nitric oxide synthase inhibitor (L-NMMA) and indomethacin increases ductus constriction in extremely premature newborns. *Pediatr Res* 2005;58:1216-1221.
94. Lago P, Bettiol T, Salvadori S, et al. Safety and efficacy of ibuprofen versus indomethacin in preterm infants treated for patent ductus arteriosus: a randomised controlled trial. *Eur J Pediatr* 2002;161:202-207.
95. Mosca F, Bray M, Lattanzio M, et al. Comparative evaluation of the effects of indomethacin and ibuprofen on cerebral perfusion and oxygenation in preterm infants with patent ductus arteriosus. *J Pediatr* 1997;131:549-554.
96. Patel J, Roberts I, Azzopardi D, et al. Randomized double-blind controlled trial comparing the effects of ibuprofen with indomethacin on cerebral hemodynamics in preterm infants with patent ductus arteriosus. *Pediatr Res* 2000;47:36-42.
97. Pezzati M, Vangi V, Biagiotti R, et al. Effects of indomethacin and ibuprofen on mesenteric and renal blood flow in preterm infants with patent ductus arteriosus. *J Pediatr* 1999;135:733-738.
98. Su PH, Chen JY, Su CM, et al. Comparison of ibuprofen and indomethacin therapy for patent ductus arteriosus in preterm infants. *Pediatr Int* 2003;45:665-670.
99. Van Overmeire B, Smets K, Lecoutere D, et al. A comparison of ibuprofen and indomethacin for closure of patent ductus arteriosus. *N Engl J Med* 2000;343:674-681.
100. Thomas RL, Parker GC, Van Overmeire B, et al. A meta-analysis of ibuprofen versus indomethacin for closure of patent ductus arteriosus. *Eur J Pediatr* 2005;164:135-140.
101. Aranda JV, Thomas R. Systematic review: intravenous Ibuprofen in preterm newborns. *Semin Perinatol* 2006;30:114-120.

102. Ohlsson A, Walia R, Shah S. Ibuprofen for the treatment of patent ductus arteriosus in preterm and/or low birth weight infants. *Cochrane Database Syst Rev* 2005;CD003481.
103. Gournay V, Roze JC, Kuster A, et al. Prophylactic ibuprofen versus placebo in very premature infants: a randomised, double-blind, placebo-controlled trial. *Lancet* 2004;364:1939–1944.
104. Hammerman C, Bin-Nun A, Markovitch E, et al. Ductal closure with paracetamol: a surprising new approach to patent ductus arteriosus treatment. *Pediatrics* 2011;128:e1618–e1621.
105. McCurnin DC, Yoder BA, Coalson J, et al. Effect of ductus ligation on cardiopulmonary function in premature baboons. *Am J Respir Crit Care Med* 2005;172:1569–1574.
106. Szymankiewicz M, Hodgman JE, Siassi B, et al. Mechanics of breathing after surgical ligation of patent ductus arteriosus in newborns with respiratory distress syndrome. *Biol Neonate* 2004;85:32–36.
107. Brooks JM, Travadi JN, Patole SK, et al. Is surgical ligation of patent ductus arteriosus necessary? The Western Australian experience of conservative management. *Arch Dis Child Fetal Neonatal Ed* 2005;90:F235–F239.
108. Steer P, Woodgate P. Indomethacin for asymptomatic patent ductus arteriosus in preterm infants—Cochrane Database of Systematic Reviews—Cooke-Wiley Online Library. *Cochrane Database Syst Rev* 2003.
109. Cotton RB, Stahlman MT, Berder HW, et al. Randomized trial of early closure of symptomatic patent ductus arteriosus in small preterm infants. *J Pediatr* 1978;93:647–651.
110. Wagner HR, Ellison RC, Zierler S, et al. Surgical closure of patent ductus arteriosus in 268 preterm infants. *J Thorac Cardiovasc Surg* 1984;87:870–875.
111. Hines MH, Raines KH, Payne RM, et al. Video-assisted ductal ligation in premature infants. *Ann Thorac Surg* 2003;76:1417–1420.
112. Chen H, Weng G, Chen Z, et al. Comparison of posterolateral thoracotomy and video-assisted thoracoscopic clipping for the treatment of patent ductus arteriosus in neonates and infants. *Pediatr Cardiol* 2011;32:386–390.
113. Roberts P, Adwani S, Archer N, et al. Catheter closure of the arterial duct in preterm infants. *Arch Dis Child Fetal Neonatal Ed* 2007;92:F248–F250.
114. Benthani J, Meur S, Hudsmith L, et al. Echocardiographically guided catheter closure of arterial ducts in small preterm infants on the neonatal intensive care unit. *Catheter Cardiovasc Interv* 2011;77:409–415.
115. Fowlie PW, Davis PG. Prophylactic indomethacin for preterm infants: a systematic review and meta-analysis. *Arch Dis Child Fetal Neonatal Ed* 2003;88:F464–F466.
116. Van Overmeire B, Allegaert K, Casaer A, et al. Prophylactic ibuprofen in premature infants: a multicentre, randomised, double-blind, placebo-controlled trial. *Lancet* 2004;364:1945–1949.
117. Chen ZY, Wu LM, et al. Comparison of long-term clinical outcome between transcatheter Amplatzer occlusion and surgical closure of isolated patent ductus arteriosus. *Chin Med J* 2009;122:1123–1127.
118. Rudolph AM, Mesel E, Levy JM. Epinephrine in the treatment of cardiac failure due to shunts. *Circulation* 1963;28:3–13.
119. Patel HT, Cao QL, Rhodes J, et al. Long-term outcome of transcatheter closure of small to large patent ductus arteriosus. *Catheter Cardiovasc Interv* 1999;47:457–461.
120. Alwi M, Kang LM, Samion H, et al. Transcatheter occlusion of native persistent ductus arteriosus using conventional Gianturco coils. *Am J Cardiol* 1997;79:1430–1432.
121. Masura J, Tittel P, Gavora P, et al. Long-term outcome of transcatheter patent ductus arteriosus closure using Amplatzer duct occluders. *Am Heart J* 2006;151:755.e7–755.e10.
122. Masura J, Walsh KP, Thanopoulos B, et al. Catheter closure of moderate- to large-sized patent ductus arteriosus using the new Amplatzer duct occluder: immediate and short-term results. *J Am Coll Cardiol* 1998;31:878–882.
123. Cuaso CC, Tan RB, Del Rosario JD, et al. Update on the Amplatzer Duct Occluder: a 10-year experience in Asia. *Pediatr Cardiol* 2012;33:533–538.
124. Hazama S, Sakamoto I, Yamachika S, et al. Endovascular surgery using an original occluder for patent ductus arteriosus in an adult patient. *Jpn J Thorac Cardiovasc Surg* 2005;53:58–61.
125. Laborde F, Folliquet TA, Etienne PY, et al. Video-thoracoscopic surgical interruption of patent ductus arteriosus. Routine experience in 332 pediatric cases. *Eur J Cardiothorac Surg* 1997;11:1052–1105.
126. Vanamo K, Berg E, Kokki H, et al. Video-assisted thoracoscopic versus open surgery for persistent ductus arteriosus. *J Pediatr Surg* 2006;41:1226–1229.
127. Roy A, Juneja R, Saxena A. Use of Amplatzer duct occluder to close severely hypertensive ducts: utility of transient balloon occlusion. *Indian Heart J* 2005;57:332–336.
128. Beghetti M, Galie N. Eisenmenger syndrome a clinical perspective in a new therapeutic era of pulmonary arterial hypertension. *J Am Coll Cardiol* 2009;53:733–740.
129. Elliotson J. Case of malformation of the pulmonary artery and aorta. *Lancet* 1830;1:247.
130. Balaji S, Burch M, Sullivan ID. Accuracy of cross-sectional echocardiography in diagnosis of aortopulmonary window. *Am J Cardiol* 1991;67:650–653.
131. Berry TE, Bharati S, Muster AJ, et al. Distal aortopulmonary septal defect, aortic origin of the right pulmonary artery, intact ventricular septum, patent ductus arteriosus and hypoplasia of the aortic isthmus: a newly recognized syndrome. *Am J Cardiol* 1982;49:108–116.
132. Bertolini A, Dalmonte P, Bava GL, et al. Aortopulmonary septal defects. A review of the literature and report of ten cases. *J Cardiovasc Surg* 1994;35:207–213.
133. Blieden LC, Moller JH. Aorticopulmonary septal defect. An experience with 17 patients. *Br Heart J* 1974;36:630–635.
134. Boonstra PW, Talsma M, Ebels T. Interruption of the aortic arch, distal aortopulmonary window, arterial duct and aortic origin of the right pulmonary artery in a neonate: report of a case successfully repaired in a one-stage operation. *Int J Cardiol* 1992;34:108–110.
135. Deverall PB, Lincoln JC, Aberdeen E, et al. Aortopulmonary window. *J Thorac Cardiovasc Surg* 1969;57:479–486.
136. Geva T, Ott DA, Ludomirsky A, et al. Tricuspid atresia associated with aortopulmonary window: controlling pulmonary blood flow with a fenestrated patch. *Am Heart J* 1992;123:260–262.
137. Gross RE. Surgical closure of an aortic septal defect. *Circulation* 1952;5:858–863.
138. Johnsson L, Michaelsson M, Westerholm CH, et al. Aortopulmonary window: a new operative approach. *Ann Thorac Surg* 1978;25:564–567.
139. Kutsche LM, Van Mierop LHS. Anatomy and pathogenesis of aorticopulmonary septal defect. *Am J Cardiol* 1987;59:443–447.
140. McElhinney DB, Reddy VM, Tworetzky W, et al. Early and late results after repair of aortopulmonary septal defect and associated anomalies in infants <6 months of age. *Am J Cardiol* 1998;81:195–201.
141. Mori K, Ando M, Takao A, et al. Distal type of aortopulmonary window. Report of 4 cases. *Br Heart J* 1978;40:681–689.
142. Redington AN, Rigby ML, Ho SY, et al. Aortic atresia with aortopulmonary window and interruption of the aortic arch. *Pediatr Cardiol* 1991;12:49–51.
143. Shore DF, Yen Ho S, Anderson RH, et al. Aortopulmonary septal defect coexisting with ventricular septal defect and pulmonary atresia. *Ann Thorac Surg* 1983;35:132–137.
144. Richardson JV, Doty DB, Rossi NP, et al. The spectrum of anomalies of aortopulmonary septation. *J Thorac Cardiovasc Surg* 1979;78:21–27.
145. McMahon CJ, DiBardino DJ, Undar A, et al. Anomalous origin of left coronary artery from the right pulmonary artery in association with type III aortopulmonary window and interrupted aortic arch. *Ann Thorac Surg* 2002;74:919–921.
146. Duca V, Sullioti G, Maggio C, et al. Transposition of the great arteries and aortopulmonary window in the same patient: clinical report and follow-up. *Pediatr Cardiol* 2002;23:474–475.
147. Takahashi K, Kido S, Hoshino K, et al. Frequency of a 22q11 deletion in patients with conotruncal cardiac malformations: a prospective study see comments. *Eur J Pediatr* 1995;154:878–881.
148. Van Mierop LHS, Kutsche LM. Embryology of the heart. In: Hurst JW, ed. *The Heart*. 6th ed. New York, NY: McGraw-Hill, 1986.
149. Kirby ML, Gale TF, Stewart DE. Neural crest cells contribute to normal aorticopulmonary septation. *Science* 1983;220:1059–1061.
150. Marmon LM, Balsara RK, Chen R, et al. Congenital cardiac anomalies associated with the DiGeorge syndrome: a neonatal experience. *Ann Thorac Surg* 1984;38:146–150.
151. Iserin L, de Lonlay P, Viot G, et al. Prevalence of the microdeletion 22q11 in newborn infants with congenital conotruncal cardiac anomalies. *Eur J Pediatr* 1998;157:881–884.
152. Webber SA, Hatchwell E, Barber JC, et al. Importance of microdeletions of chromosomal region 22q11 as a cause of selected malformations of the ventricular outflow tracts and aortic arch: a three-year prospective study see comments. *J Pediatr* 1996;129:26–32.
153. Valsangiacomo ER, Smallhorn JF. Images in cardiovascular medicine. Prenatal diagnosis of aortopulmonary window by fetal echocardiography. *Circulation* 2002;105:E192.
154. Bagtharia R, Trivedi KR, Burkhart HM, et al. Outcomes for patients with an aortopulmonary window, and the impact of associated cardiovascular lesions. *Cardiol Young* 2004;14:473–480.
155. Di Bella I, Gladstone DJ. Surgical management of aortopulmonary window. *Ann Thorac Surg* 1998;65:768–770.
156. Matsuki O, Yagihara T, Yamamoto F, et al. New surgical technique for total-defect aortopulmonary window. *Ann Thorac Surg* 1992;54:991–992.
157. Messmer BJ. Pulmonary artery flap for closure of aortopulmonary window. *Ann Thorac Surg* 1994;57:498–501.
158. Atiq M, Rashid N, Kazmi KA, et al. Closure of aortopulmonary window with Amplatzer duct occluder device. *Pediatr Cardiol* 2003;24:298–299.
159. Jureidini SB, Spadaro JJ, Rao PS. Successful transcatheter closure with the buttoned device of aortopulmonary window in an adult. *Am J Cardiol* 1998;81:371–372.
160. Naik GD, Chandra VS, Shenoy A, et al. Transcatheter closure of aortopulmonary window using Amplatzer device. *Catheter Cardiovasc Interv* 2003;59:402–405.
161. Tulloh RM, Rigby ML. Transcatheter umbrella closure of aorto-pulmonary window. *Heart* 1997;77:479–480.

Congenital Anomalies of the Coronary Vessels and the Aortic Root

D. Scott Lim ■ G. Paul Matherne

Coronary and aortic root anomalies represent a small but interesting group of malformations that may occur alone or in association with structural heart disease (1–3). Recognizing and identifying these anomalies has become an important part of the evaluation of complex congenital heart disease. In the absence of structural heart disease, coronary anomalies are also important in certain clinical situations such as dilated cardiomyopathy (4), hypertrophic cardiomyopathy (5), and sudden cardiac events in older children (6). This chapter reviews coronary artery development and anatomy, coronary anomalies in the absence of structural heart disease, coronary anomalies in the presence of structural heart disease, and aortic root anomalies. Coronary arteriovenous malformations are covered in Chapter 37.

CORONARY VASCULAR ANOMALIES

Embryology

The cells of the developing myocardium initially receive nourishment directly from circulating blood in the ventricular cavity. As the myocardium thickens and develops, the presence of multiple trabeculations allows close proximity of the myocardial cells to the ventricular cavity. These trabeculations then develop into a sinusoidal system that continues to minimize diffusion distance between myocytes and the circulation. It was previously thought that these sinusoids were the forerunners of the coronary vascular system, but new data have provided evidence for an epicardial origin of the coronary vascular system (7).

The new model of coronary vascular development (7) begins with formation of a proepicardial protrusion by cells of the primordial liver. These cells establish the proepicardium and epicardial cells and then migrate over the surface of the heart. The epicardial cells invade the forming subepicardial matrix and form the coronary vascular plexus. The epicardial cells then undergo epithelial mesenchymal transformation by an as yet undefined mechanism that probably involves multiple growth factors. Nascent capillaries then are associated with subepicardial mesenchymal cells to form mature vessels. It has now been shown that small vessels on the surface of the heart fuse and grow inward to penetrate the aorta rather than coronary buds from the aortic sinuses fusing with the coronary vessels (8).

New experimental data on the development of the coronary system implicate multiple growth factors as well as adhesion molecules and chemotactic factors in this complicated coordinated migration and transformation of cells to form coronary vessels. The presence of congenital anomalies of coronary arteries suggests abnormalities in these signaling pathways or alterations in local factors that direct coronary vessel development.

Anatomy

Coronary Arteries

Normal coronary artery anatomy is briefly reviewed, but for a complete discussion on this subject the reader is referred to Dr. Frank Netter's diagrams in the *CIBA Collection of Medical Illustrations* (9). The entire blood flow to the myocardium is derived from two main coronary arteries arising from the right and left aortic sinuses of Valsalva (Fig. 32.1). The left main coronary artery is about 13 mm long in adults (range 2 to 40 mm) and gives rise to the circumflex branch, which courses posteriorly in the atrioventricular groove; the left main coronary then continues as a left anterior descending branch. The right coronary artery gives rise to a small conal branch and then courses posteriorly in the opposite direction along the atrioventricular groove. There is no separate septal branch, the septum being supplied by perforating branches that enter the septum from the anterior and posterior descending coronary arteries. In 69% of the population, the right coronary artery is dominant (10), giving rise to the posterior descending coronary artery, which extends to the apex and supplies the posterior part of the ventricular septum, the inferior wall of the left ventricle, and the atrioventricular node (11). In 11%, the left coronary artery is dominant, thereby giving rise to the posterior descending coronary artery, and in 20% there is codominance (10). The left coronary artery supplies the free wall of the left ventricle. Interestingly, many patients with bicuspid aortic valves or aortic stenosis (20% to 57%) have left-dominant systems and a short left main coronary artery (10,12,13).

Within the myocardium, small arteries branch repeatedly until they reach the endocardium. Normally, there are connections between coronary arterial branches that are 25 to 200 mm in diameter and are known as collaterals. They may be superficial or subendocardial, and they are capable of enlarging if pressure gradients develop between branches. These collateral arteries become significant in cases of primary arterial occlusion, in which cases they may allow reperfusion of affected myocardium.

Cardiac Veins

The coronary sinus arises from the proximal portion of the left sinus horn and the common cardinal vein. The great cardiac vein begins at the apex and runs up the anterior interventricular groove to enter the coronary sinus just below the left lower pulmonary vein. The coronary sinus then courses around the left edge of the heart in the posterior atrioventricular groove until it enters the right atrium near the atrioventricular node. The middle cardiac vein runs up in the posterior atrioventricular groove to enter the coronary sinus. The posterior ventricular vein drains the free wall of the left ventricle up to the coronary sinus. The small cardiac vein runs with the right

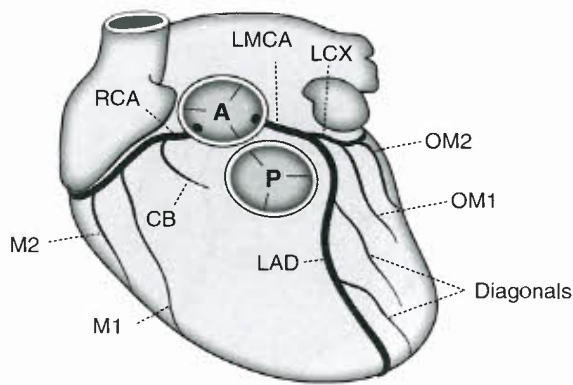


Figure 32.1. Normal anatomy of the coronary arteries. A, aortic valve; CB, conus branch of the right coronary artery; Diagonals, first and second diagonal branches of the left anterior descending coronary artery; LAD, anterior descending branch of left coronary artery; LCX, circumflex branch of the left coronary artery; LMCA, left main coronary artery; M1/2, first and second marginal branches of the right coronary artery; OM1/2, first and second obtuse marginal branches of the left coronary artery; P, pulmonic valve; RCA, right coronary artery.

coronary artery in the right posterior part of the atrioventricular groove; it drains into the coronary sinus or directly into the right atrium, as do the small veins draining the right ventricular free wall (14,15).

ANOMALIES OF CORONARY ARTERIES IN THE ABSENCE OF STRUCTURAL HEART DISEASE

Normal Variations

The right and left coronary arteries arise from the right and left aortic sinuses of Valsalva (Fig. 32.1). Usually they come from the middle of the sinuses, but they may arise from the sinotubular junction or even above it. The position of the ostium does not appear to affect the flow through it. The ostia may be round, oval, or elliptical. The arteries are usually perpendicular to the aortic wall; that is, they are radially arranged relative to the center of the aorta.

Separate origin of the conus branch of the right coronary artery commonly occurs (11). The corresponding anomaly on the left side—separate origins of the left anterior descending and left circumflex coronary arteries—occurs in about 1% of the population and is more frequent with bicuspid aortic valves (11). Neither of these anomalies appears to have any clinical consequence.

Abnormal Origin of Right or Left Coronary Artery from Inappropriate Sinus

Anomalous Origin of Left Coronary Arterial Branches from Right Sinus of Valsalva

The most common anomaly, accounting for about one-third of all major coronary arterial anomalies, is origin of the left circumflex coronary artery from the right main coronary artery (Fig. 32.2A) (2,3,16,17). The left circumflex coronary artery passes behind the aorta to reach its normal territory of supply. This anomaly has no general clinical significance, but the artery may be compressed if both mitral and aortic

prosthetic fixation rings are implanted. These anomalous arteries may have an unusually high incidence of coronary atheroma (2).

Much less common, accounting for 1% to 3% of major coronary arterial anomalies (2,16), but of greater clinical significance is origin of the left main coronary artery from the right sinus of Valsalva (1,16,18). There are four pathways that the left main coronary artery can take after leaving the sinus: posterior to the aorta (Fig. 32.2B), anterior to the right ventricular outflow tract (RVOT) (Fig. 32.2C), within the ventricular septum beneath the right ventricular infundibulum (Fig. 32.2D, the most common variant), and between the aorta and the RVOT (Fig. 32.2E). With rare exceptions, the first three courses have not been associated with sudden death or premature myocardial ischemia. The course that passes between the two great arteries, however, has often been associated with sudden death in people during or just after vigorous exercise. Several of these patients had had episodes of syncope or chest pain during previous exercise. In most of these patients, the ostium of the left main coronary artery was slit-like, with an intramural course within the aortic root and adherent to it for about 1.5 cm (18).

In some patients, the left anterior descending coronary artery originates in the right sinus of Valsalva or from the right main coronary artery (Fig. 32.2F). This anomaly is rare in the absence of congenital heart disease (2,18) but is common in tetralogy of Fallot. The artery usually passes in front of the RVOT or through the interventricular septum but has rarely been seen to pass between the aorta and RVOT. Should there be atheroma near the ostium of the common arterial trunk, most of the heart will become ischemic, so that the lesion is the equivalent of a left main coronary stenosis.

Anomalous Origin of Right Coronary Arterial Branches from the Left Sinus of Valsalva

Origin of the right main coronary artery from the left sinus of Valsalva, first described by White and Edwards (19) in 1948, is relatively common, making up about 30% of all major coronary arterial anomalies (2,18), and has a significantly higher incidence in Asians and Hispanics (20). The right coronary artery then courses between the aorta and the RVOT to reach the right side of the atrioventricular groove, after which it is distributed normally (Figs. 32.3 and 32.4). This anomaly was once thought to be benign, but there are now many reports of myocardial ischemia, infarction, or sudden death (21–23). In many of the autopsies, the origin of the right main coronary artery was angulated and the ostium was described as slit-like.

Single Coronary Artery

In 5% to 20% of major coronary arterial anomalies, a single coronary artery arises from the aorta and then branches (17,24). Sometimes an atretic cord connects part of the artery to a sinus of Valsalva that has no ostium. About 40% of these anomalies are associated with other cardiac malformations, including transposition of the great vessels, tetralogy of Fallot, truncus arteriosus, coronary-cameral fistulas, and bicuspid aortic valves. The single artery can arise from either the right (Fig. 32.5A–C) or the left sinus of Valsalva (Fig. 32.5D–F) with many variations (24). The single coronary artery on either side can follow its usual course and then continue on to supply the other side of the heart, or separate branches can arise from a main coronary artery and course posteriorly or anteriorly to supply the other side of the heart. Branches also can pass between the great vessels.

For the single coronary arteries arising from the right side, the right coronary can follow the course of the normal right

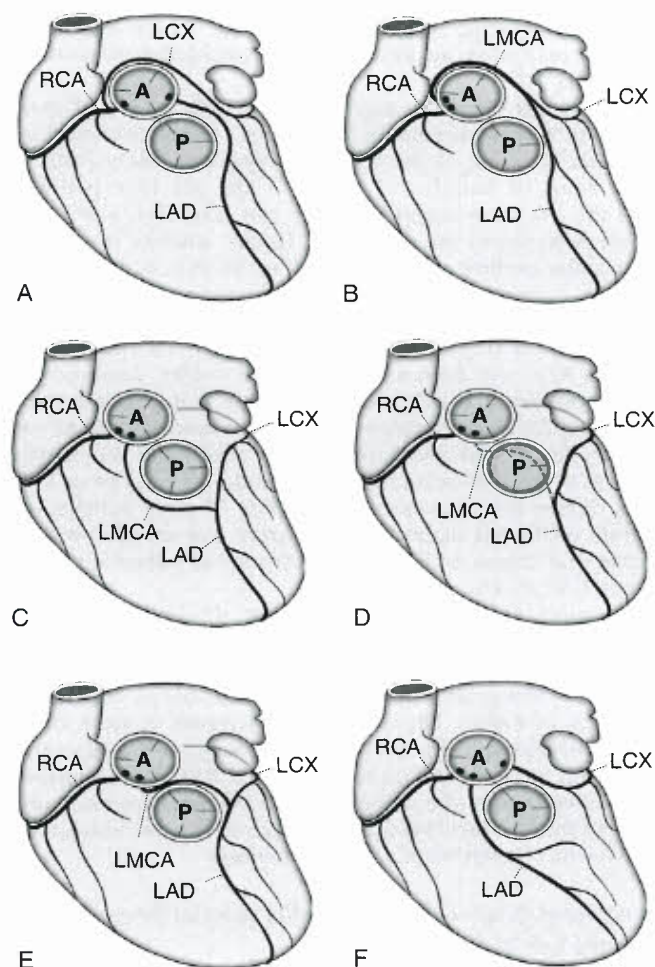


Figure 32.2. Anomalous origin of the left main coronary artery from the right sinus of Valsalva. A: Left circumflex coronary artery arising from the right coronary artery. B: Left main coronary artery arising from the right sinus of Valsalva (posterior course). C: Left main coronary artery arising from the right sinus of Valsalva (anterior course). D: Left main coronary artery arising from the right sinus of Valsalva (interventricular septal course). E: Left main coronary artery arising from the right sinus of Valsalva, and with a course between the two great arteries. Note the oblique origin of left main coronary artery (LMCA). F: Separate origin of the left anterior descending coronary artery (LMCA). A, aorta; LAD, left anterior descending coronary artery; LCX, left circumflex coronary artery; LMCA, left main coronary artery; P, pulmonary outflow; RCA, right coronary artery.

coronary artery and continue as the left circumflex artery, which then gives off the left anterior descending coronary artery (Fig. 32.5A). Alternatively, after the right coronary artery arises, a separate branch to the left side can arise that passes posterior to the aorta and gives rise to a circumflex vessel and a left anterior descending coronary artery (Fig. 32.5B), or the separate branch can follow a course anterior to the right ventricular infundibulum, giving rise to the anterior descending coronary artery before continuing on as the circumflex (Fig. 32.5C).

A single left coronary artery can display branching patterns similar to those on the right. A single left coronary artery can branch into the left anterior descending and left circumflex coronary arteries with the circumflex continuing across the crux to form the right coronary artery (Fig. 32.5D). A separate right coronary vessel also can arise from the single left coronary artery

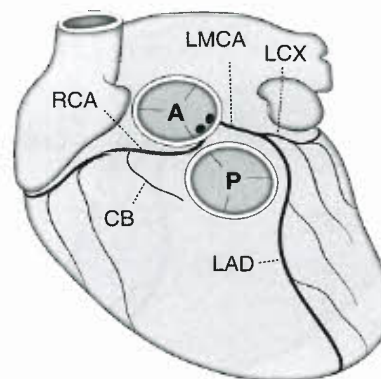


Figure 32.3. Anomalous origin of the right coronary artery from the left sinus of Valsalva, with oblique origin and course between the great arteries. A, aorta; CB, conal branch of the right coronary artery; LAD, left anterior descending coronary artery; LCX, left circumflex coronary artery; LMCA, left main coronary artery; P, pulmonary outflow; RCA, right coronary artery.

and pass posterior to the aorta (Fig. 32.5E) to reach the opposite side of the heart or the vessel can pass anterior to the right ventricular infundibulum (Fig. 32.5F). Most single coronary arteries produce no symptoms in the absence of severe atheroma (which is clearly more serious when there is only one main artery supplying the whole heart), but a few premature deaths have been reported with this anomaly (24). It is usually those variants in which a major branch passes between the aorta and the right ventricular infundibulum that are at greatest risk for sudden death (24), but other patterns can cause myocardial ischemia.

Left or Right Coronary Arterial Branches Arising from the Posterior Sinus of Valsalva

These are very rare (18) and have not been associated with premature or sudden death.

Pathology and Clinical Features of Abnormal Origin of Right or Left Coronary Artery from Inappropriate Sinus

Pathology

In about 20% of autopsies there are subendocardial scars, and occasionally a major myocardial territory infarction is reported. However, the suddenness of death in most of these patients prevents large scar from occurring. Occasionally, severe atherosclerosis has been seen in a segment of the abnormal vessels, even in children (25). In some of the anomalies, the initial few millimeters of artery may run within the aortic wall. Finally, the anomalous artery may arise tangentially from the aorta, and its ostium may be slit-like and partly covered by a valve-like flap.

Mechanisms of Death

Death is almost certainly due to myocardial ischemia, but the exact mechanism is unknown. The left ventricular myocardium has a huge demand for oxygen during strenuous exercise. Systolic pressure increases during strenuous exercise, and there is activation of the sympathetic nervous system. The root of the aorta therefore distends in systole. If part of the anomalous artery runs within the wall, it may be compressed, and if the artery runs adjacent to the wall, it may be stretched, compressed, or both. Presumably, the severe myocardial ischemia

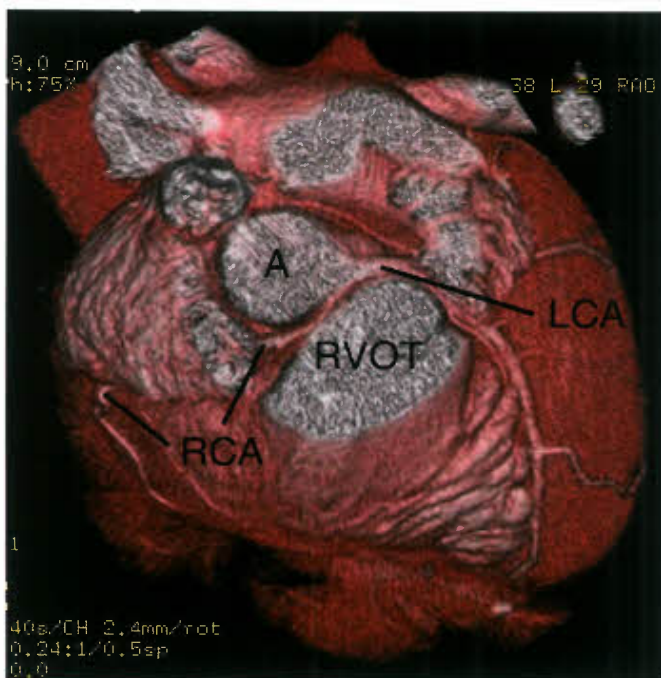


Figure 32.4. Three-dimensional reconstruction from computed tomographic imaging of the coronary arteries demonstrating anomalous origin of the right coronary artery from the left sinus of Valsalva, with oblique origin and course between the great arteries. Note the oblique origin of the right coronary artery, which then runs between the two great arteries. A, aorta; LCA, left coronary artery; RCA, right coronary artery; RVOT, right ventricular outflow tract.

that occurs from any of these mechanisms produces either ventricular fibrillation or electromechanical dissociation. In those with previous syncope, the severe ischemia might have produced transient ventricular tachycardia or fibrillation or else suddenly impaired ventricular function might have decreased cardiac output catastrophically. Why some patients with apparently identical anomalies survive without ischemia until their 70s and 80s is unknown.

Clinical Features

Most of these anomalous arteries do not cause myocardial ischemia, particularly if the anomalous branch does not pass between the aorta and the right ventricular infundibulum. Even those that do run between these structures do not always lead to sudden or premature death. However, this is the group that accounts for symptoms and sudden death in children, adolescents, and young adults. Although the first sign of the anomaly is sometimes sudden death or a fatal myocardial infarction, in many of these patients, there may be a history of syncope or prolonged chest pain before the fatal event. These symptoms almost invariably come on during or just after strenuous exercise, and many of the victims have been athletes.

Diagnosis

Any episode of syncope or of severe chest pain during or after exercise calls for intensive investigation. The standard clinical examination usually shows no abnormalities. A resting electrocardiogram should be performed to evaluate ventricular hypertrophy, evidence of prior infarction, and persistent arrhythmia. An echocardiogram should be performed to exclude persisting ventricular dysfunction, hypertrophic cardiomyopathy, and proximal coronary anatomy. Careful

attention should be directed to the origins of the coronary arteries because most of the anomalies affect the origins of the major arteries or their major branches and therefore may be detectable by echocardiography. Following the course of the coronary vessels is also important because the lesions with the highest risk of sudden death are associated with a major branch passing between the great vessels. Proving that a coronary artery passes between the great vessels can be difficult by angiography and may be easier by echocardiography. Because most patients are older children or adults, the resolution of the transthoracic echocardiogram may be inadequate to show the anomalies, and transesophageal echocardiography (26), magnetic resonance imaging (27), or computed tomographic scans (28) (Fig. 32.4) may be more sensitive.

Evaluating blood pressure and the electrocardiogram or injecting thallium at near-maximal exercise can be useful. However, a normal near-maximal stress test result has been reported in patients who subsequently died suddenly and had an anomalous left main coronary artery (29). Because of this, exertional syncope or severe exertional chest pain in a child or young adult warrants further investigation if the echocardiogram is inconclusive.

Anomalous Left Coronary Artery from the Pulmonary Artery

In this anomaly, the left coronary artery arises from the pulmonary artery, usually from the left posterior facing sinus (Fig. 32.6). This anomaly was first described by pathologists in 1866 (30), and by 1962 Fontana and Edwards (31) had collected descriptions of 58 necropsies with this anomaly. Most of these patients died at <13 months of age. The first report relating clinical and autopsy findings in a 3-month-old boy was by Bland et al. (32). The anomaly has thus been called the Bland-White-Garland syndrome.

Pathophysiology

In fetal life, this anomaly probably has no harmful effect: Pressures and oxygen saturations are similar in the aorta and pulmonary artery. Myocardial perfusion is presumably normal, and there is no stimulus to collateral formation (Fig. 32.6A). After birth, however, the pulmonary artery contains desaturated blood at pressures that rapidly fall below systemic pressures. Therefore, the left ventricle, with its huge demand for oxygen, is perfused with desaturated blood at low pressures. Collateral flow is initially low. The left ventricular myocardial vessels dilate to reduce their resistance and increase flow, but soon coronary vascular reserve becomes exhausted and myocardial ischemia ensues. At first, ischemia is transient and occurs only with exertion such as during feeding or crying, but further increases in myocardial oxygen demand lead to infarction of the anterolateral left ventricular free wall (Fig. 32.6B), with resultant compromise of left ventricular function. This causes congestive heart failure, which is often made worse by mitral regurgitation secondary to a dilated mitral valve annulus or infarction and dysfunction of the anterolateral papillary muscle. Collateral vessels between the normal right and abnormal left coronary artery enlarge, and with the increased flow, so does the right coronary artery itself (Fig. 32.6C). However, because the left coronary artery is connected to the low-pressure pulmonary artery, the collateral flow tends to pass into the pulmonary artery rather than into the high-resistance myocardial blood vessels. There is a pulmonary-coronary steal with a left-to-right shunt. The shunt is usually relatively small in terms of cardiac output but relatively large in terms of coronary flow. In about 15% of these patients, myocardial blood flow can sustain myocardial function at rest or even during exercise. These are the patients who reach adult life (33).

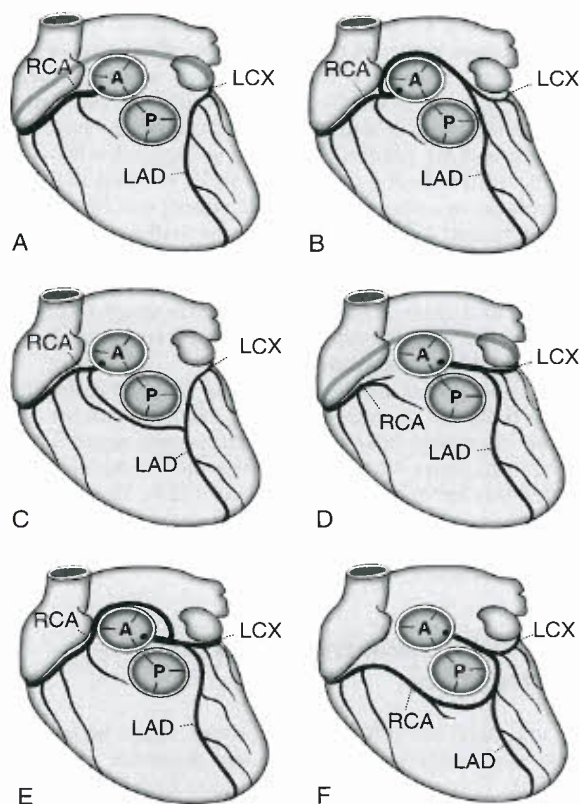


Figure 32.5. Single coronary artery variants. A to C: Single coronary artery originating from right sinus of Valsalva. A: Right coronary continuation to the left circumflex coronary artery (LCX) and left anterior descending coronary artery (LAD). B: Posterior course of separate LCX giving off the LAD. C: Anterior course of a separate LAD branch feeding back to the LCX. D to F: Single coronary artery originating from the left sinus of Valsalva. D: Left coronary artery giving rise to the LAD and the LCX, which then continues as the right coronary artery. E: Posterior course of separate right coronary branch off the left main coronary artery. F: Anterior course of separate right coronary artery coming off of the LAD. Variants passing between great vessels are not illustrated. A, aorta; P, pulmonary artery; RCA, right coronary artery.

Pathology

This anomaly is usually isolated but has been associated with patent ductus arteriosus (17,33), ventricular septal defect, tetralogy of Fallot, or coarctation of the aorta (33). If there is pulmonary hypertension, as with a large ventricular septal defect, left ventricular perfusion may be adequate to prevent ischemia. Under these circumstances, closure of the defect with a decrease in pulmonary arterial pressure is catastrophic.

The right coronary artery is greatly dilated, and large collaterals may be visible on the surface of the heart. The left coronary artery is seen entering the main pulmonary artery, usually into the left pulmonary sinus, but rarely enters a branch pulmonary artery. It is usually only 2 to 5 mm long before it branches.

In infancy, the heart is large, with the left ventricle and atrium in particular being dilated and hypertrophied. The anterolateral papillary muscle may be atrophic and scarred, and the chordae attached to it may be shortened. In some studies, the posterior papillary muscle has been similarly affected (33). There may be diffuse endocardial fibroelastosis of the left ventricle, and the anterior mitral valve leaflet is

often thickened. Thinning and scarring of the anterolateral left ventricular wall and apex owing to infarction are noted, and there are often mural thrombi.

In adults, the left coronary artery is thin-walled, resembling a vein. The heart is usually enlarged, but relatively not as much as in infants, and there is usually no endocardial fibroelastosis. However, there is usually scarring and calcification of the anterolateral papillary muscle and occasionally even of the adjacent left ventricle (18,34).

Clinical Features

For infants, the description by Bland et al. (32) still applies:

Nothing remarkable was noted about the patient until the tenth week; while nursing from the bottle, the onset of an unusual group of symptoms occurred which consisted of paroxysmal attacks of acute discomfort precipitated by the exertion of nursing. The infant appeared at first to be in obvious distress, as indicated by short expiratory grunts, followed immediately by marked pallor and cold sweat with a general appearance of severe shock. Occasionally, with unusually severe attacks, there appeared to be a transient loss of consciousness. The eructation of gas at times seemed to relieve the discomfort and to shorten the duration of the attack which usually lasted from 5 to 10 minutes, and following which the infant might proceed to nurse without difficulty and remain free of symptoms for several days.... It seems probable that in this infant, the curious attacks of paroxysmal discomfort... were those of angina pectoris. If this is true, it represents the earliest age at which this condition has been recorded.

These patients with angina can be misdiagnosed as having either colic or reflux. Not all infants present in this way. Many present with the signs and symptoms of congestive heart failure. A few children have severe difficulties in infancy and then gradually improve until they are asymptomatic. Older children and adults may be asymptomatic or may have dyspnea, syncope, or angina pectoris on effort. Sudden death after exertion has been common (35). However, typical myocardial infarctions or congestive heart failure are rare in adults.

On physical examination, there may be signs of congestive heart failure. In infants, the heart is usually enlarged, the left ventricle being the predominant ventricle affected. However, there may be right ventricular enlargement and a loud pulmonary component of the second heart sound if left ventricular failure has caused considerable pulmonary hypertension. The first heart sound may be soft or absent (if there is mitral regurgitation), and apical gallop rhythms are common. There may be no murmurs or they may have a murmur of mitral regurgitation. At times, there is a soft continuous murmur at the upper left sternal border that is similar to the murmur of a small patent ductus arteriosus, which is due to the continuous flow from the anomalous coronary artery into the pulmonary artery.

Electrocardiography

Classically, because there is an anterolateral infarct by the time the infant presents for diagnosis, there will be abnormal Q waves in leads I, aVL, and precordial leads V4 to V6. There also may be abnormal R waves or R-wave progression in the left precordial leads. Although this pattern is not pathognomonic for this anomaly (it is seen in myocardial infarcts from other causes or occasionally in cardiomyopathies), if it is found, the diagnosis of this anomaly should be considered and evaluated by other means. Even in asymptomatic adults, the resting electrocardiogram is abnormal, and abnormal ischemic responses occur with exercise (34).

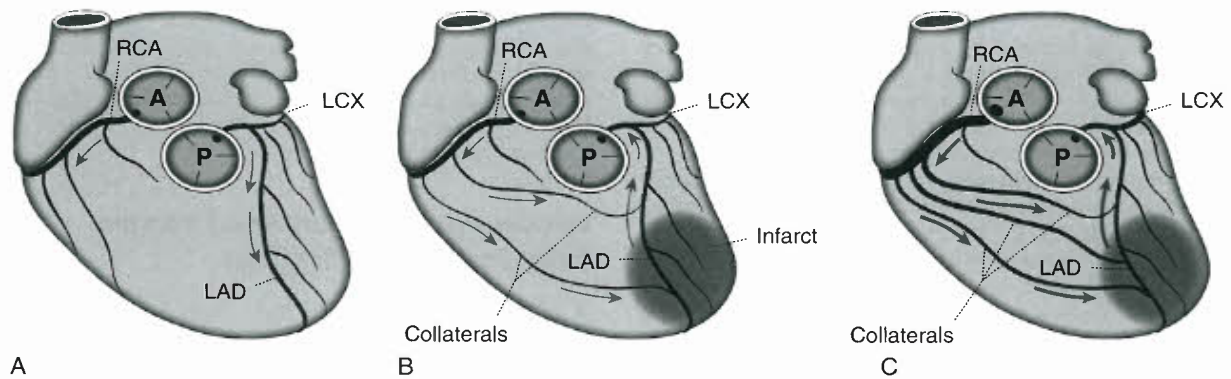


Figure 32.6. Anomalous origin of the left main coronary artery from the pulmonary artery. **A:** In the fetus, both right and left coronary arteries receive forward flow from the great arteries. **B:** Early after birth, before collaterals are well developed, there may be an anterolateral infarct and slight retrograde flow from the left coronary artery to the pulmonary artery. **C:** After collaterals have enlarged, there is high flow in the enlarged right coronary artery and the collaterals and significant retrograde flow into the pulmonary artery. Arrows indicate direction and approximate magnitude of flow in the right and left coronary arteries and the collaterals between them. A, aorta; LAD, left anterior descending coronary artery; LCX, left circumflex coronary artery; P, pulmonary artery; RCA, right coronary artery.

Noninvasive Imaging

On the chest film in affected infants, there is marked cardiomegaly, predominantly of the left atrium and ventricle, and evidence of pulmonary edema. These features are similar to those of many forms of cardiomyopathy, with which this anomaly is often confused.

Nuclear myocardial perfusion imaging is quite sensitive, showing reduced uptake in the anterolateral ischemic region. However, this finding is not specific because it has been seen in cardiomyopathies as well.

Echocardiography with Doppler color flow mapping has replaced cardiac catheterization as the standard method of diagnosis (36). The improved resolution of current echocardiographic equipment often allows the abnormal attachment of the origin of the left coronary artery to be seen. Color Doppler interrogation shows that flow passes from the coronary artery into the pulmonary artery. Therefore, even if the attachment of the coronary artery to the great artery is uncertain by 2-D imaging, the presence of diastolic flow into the pulmonary artery will be informative. An enlarged right coronary artery should also raise suspicion of the diagnosis. The study also will show the size and function of the cardiac chambers, particularly the left ventricle as well as regional left ventricular wall motion abnormalities and mitral regurgitation. There may be increased echogenicity of the papillary muscle and adjacent endocardium due to fibrosis and fibroelastosis.

Computed tomography scans have shown high resolution for defining coronary artery anatomy and origination in most older patients. The main advantage of this technique is rapid acquisition times and, particularly with the 32- and 64-detector scanners, high resolution. However, ECG gating of the scans requires heart rates to be slow or, in the younger child, pharmacologically slowed. There remains a significant radiation exposure with this technique, but its ability to define coronary artery abnormalities is excellent (Fig. 32.4) (see Chapter 11).

Cardiac Catheterization and Angiography

Although previously, cardiac catheterization and angiography were commonly used in the diagnosis of congenital coronary abnormalities, currently they are used only if the results of noninvasive imaging are uncertain. In symptomatic infants, diagnostic cardiac catheterization demonstrates a low cardiac

output and high filling pressures and usually some degree of pulmonary hypertension. In asymptomatic older patients, output and pressures are usually normal, except for a slight increase in left ventricular end-diastolic pressure. There may be a left-to-right shunt at the pulmonary arterial level, but because the shunt may be small, its absence does not rule out the diagnosis. Ventriculography demonstrates the dilated left ventricle and atrium with dysfunction of the anterolateral left ventricular free wall and the presence and severity of mitral regurgitation. Aortic root angiography will show the dilated right coronary artery and, if there are large collaterals, will show filling of the left coronary artery and passage of contrast material from the left coronary to the main pulmonary artery. Although main pulmonary arterial angiography may show reflux of contrast medium into the origin of the left coronary artery, neither this nor left ventriculography can reliably exclude the diagnosis.

Natural History

Of all children born with this rare anomaly, approximately 87% present in infancy (33), and of these, 65% to 85% die before 1 year of age from intractable congestive heart failure (37), usually after 2 months of age. A few children improve spontaneously (38). Others never have symptoms, perhaps because of extensive collaterals and even a restrictive opening between the origin of the left coronary artery and the pulmonary trunk. Nevertheless, even these people are at high risk of sudden death (35), especially during exercise. Some present as adults with exercise-induced angina (34) or with congestive heart failure owing to mitral regurgitation (18).

Treatment

The first effective surgical treatment was ligation of the left coronary artery at its origin from the pulmonary artery to prevent the steal. Most older children benefit from this procedure, especially if they have extensive coronary-to-pulmonary arterial shunting, but late sudden death can still occur (34,39).

Ligation of the origin of the left coronary artery and reconstitution of flow through it with an internal mammary arterial or saphenous venous graft has been successful (40,41), although graft thrombosis and stenosis has occurred, particularly with vein grafts. Late obliterative changes in saphenous

vein grafts have been seen (41), which can seriously complicate the patient's course because by approximately 3 years after successful revascularization, there is usually marked reduction of collaterals from the right coronary artery (16). Grafts using the internal mammary artery have a longer survival and are preferred when coronary reimplantation cannot be done.

Direct reimplantation of the origin of the left coronary artery into the aorta (with a button of pulmonary artery around the origin) has been proven successful and is considered the standard approach in many centers (42–45). An alternative approach is the Takeuchi et al. (46) procedure, in which an aortopulmonary window is created and a tunnel is fashioned that directs blood from the aorta to the left coronary ostium.

In the past, it was recommended that, because surgical mortality is high in the sickest infants, surgery should be delayed until after 18 to 24 months of age (47). More recently, as surgical experience has accrued, early surgical intervention to establish a two-coronary system has been found to have significantly improved outcomes (45,48). However, because of papillary muscle infarction and dysfunction, significant preoperative mitral insufficiency has been found to be a risk factor for both mortality and need for late mitral valve surgery. Additionally, it has been reported that a two-vessel repair is feasible even in the sickest infants if postoperative support with a left ventricular assist device is used (49).

RARE CORONARY ANOMALIES

Coronary Atresia

Total absence of the extramural coronary arteries is rare and occurs most often with pulmonary atresia and aortic atresia. In both these anomalies, pressure in the small but hypertrophied right or left ventricle is at or above aortic pressure and enlarged sinusoids carry blood from the ventricle to be distributed in the distal coronary arterial branches.

Stenosis or Atresia of a Coronary Ostium

Stenosis or atresia of the ostium or first few millimeters of the left main coronary artery is one of the rarest of the congenital coronary anomalies. The more distal branches are normal and develop multiple collaterals from the right coronary artery. Patients may present from 3 months to 60 years of age with sudden death, angina pectoris, myocardial infarction, or congestive heart failure.

All Coronary Arteries from Pulmonary Artery

Rarely, both right and left coronary arteries, or a single coronary artery, comes from the pulmonary trunk. Unless there is a cardiac lesion causing pulmonary hypertension, these children do not survive infancy without surgical intervention. More recently, these rare patients who have had dual coronary surgical reimplantation have survived (50).

Left Anterior Descending Coronary Artery from the Pulmonary Artery

This is a very rare anomaly (18), with few patients having been described. Apart from a 7-month-old child who died with an anterior myocardial infarct, all the others have been 18 to 55 years of age. Five had angina pectoris, one an anterior myocardial infarct, and one had mitral regurgitation from papillary muscle dysfunction. Precordial murmurs were

common. Most had electrocardiographic evidence of ischemia. Chest radiographs were normal in three and showed cardiomegaly in three. Angiography was diagnostic. Echocardiographic findings have not been reported. Surgical treatment by ligation of the anomalous artery or connecting it to the aorta has been recommended (18).

Left Circumflex Coronary Artery from the Pulmonary Artery or Branches

A few of these anomalies have been reported (18), and in many patients, the circumflex coronary artery was attached to a branch pulmonary artery rather than to the main pulmonary trunk. All have been in children, and all but one had other congenital cardiac lesions.

Right Coronary Artery from the Pulmonary Artery

This anomaly is rare, only about one-tenth as common as the left main coronary artery coming from the pulmonary artery (17,31,33). The anomaly was initially known only as an incidental finding at autopsy (18), but recently, it has been associated with ischemia, syncope, cardiomyopathy, and sudden death (51,52).

Diagnosis

There may be a continuous murmur at the left sternal border. The electrocardiogram and chest radiograph are usually normal. Echocardiography with Doppler examination or cineangiography demonstrates the abnormal attachment of the right coronary artery to the pulmonary trunk and the retrograde flow from the right coronary artery to pulmonary artery. If echocardiography is nondiagnostic, definitive imaging of the anomalous right coronary artery origin can be obtained by computed tomography scan (28) or from angiography using the left coronary artery to fill the right by collaterals.

Treatment

Because most patients are asymptomatic and remain so, there is no way to determine which patients are at risk of dying without surgical correction of this defect. Nevertheless, because sudden death is a risk, many cardiologists recommend surgical correction, which has been done by reimplanting the right coronary artery into the aortic root (51).

MISCELLANEOUS ANOMALIES

Myocardial Bridges

The large epicardial coronary arteries run on the surface of the heart, with only their terminal branches penetrating the muscle, but it is very common for part of the epicardial artery to dip beneath the epicardial muscle for several millimeters so that there is a muscle bridge over the large artery (53). Most of these bridges are not functionally important, particularly if they are superficial. There are, however, documented examples of myocardial ischemia (54) or infarction associated with these bridges, including relief of ischemia after myotomy. During coronary angiography, a portion of the coronary artery appears to be narrowed in systole but widely patent in diastole, distinguishing it from a partially occlusive lesion of the artery (53).

Because myocardial bridges are so common and do not necessarily indicate present or future coronary arterial disease, the decision about myotomy to relieve anginal symptoms must

carefully be made. Not only should there be a well-defined muscle bridge, but there should be ischemia, based on electrocardiography or documented by nuclear scan or stress echocardiography, in the region supplied by the artery with the bridge. Ischemia may be due to long, thick bridges that compress the artery and relax unusually slowly, so that diastolic filling of the coronary artery beyond the bridge is impaired. Under these circumstances, disappearance of symptoms and of signs of ischemia may follow myotomy (54).

Although myocardial bridges causing ischemia are rare in children with normal hearts, they may represent a significant cause of morbidity and mortality in children with hypertrophic cardiomyopathy (see Chapter 54) (55), although this is also debated. Myocardial bridges with hypertrophic cardiomyopathy have been associated with chest pain, exercise intolerance, ventricular arrhythmias, and cardiac arrest in some, but debated in other studies (5,56). Unroofing the myocardial bridge has been reported to reduce the incidence of sudden death and arrhythmias in these patients (55). Children with hypertrophic cardiomyopathy and the above symptoms should be evaluated for bridges by stress perfusion imaging and selective coronary arteriography, and consideration should be given for unroofing the bridges if detected and felt to be causative.

CORONARY ARTERY PATTERNS WITH CONGENITAL HEART DEFECTS

Complete Transposition of the Great Arteries

Anomalies of the coronary arteries in transposition of the great arteries are important to identify because some patterns have been more difficult to transfer with the arterial switch operation. Anomalies occur in both the origin and distribution, with further anomalies secondary to intramural coursing of some vessels. This topic is briefly reviewed in this chapter, and a more complete review can be found in Chapter 49.

Terminology of the anomalies has been controversial because the aorta and main pulmonary artery are abnormally related in complete transposition of the great arteries and the aortic sinuses do not have their normal positions. The two sinuses adjacent to the pulmonary artery are termed facing sinuses (57). The nomenclature of the facing sinuses depends on the relationship of the great vessels. If the vessels are side by side, then the sinuses are termed anterior or posterior. If the great vessels are oblique, the sinuses are left anterior or right posterior. If the vessels are anterior-posterior, the sinuses are right or left (57).

The presence of a ventricular septal defect or of side-by-side great vessels should alert the cardiologist to an increased likelihood of coronary anomalies. In almost all patients, the coronary arteries arise from the facing sinuses (57,58). In 60%, the coronary arteries come from their appropriate sinuses and branch normally, a pattern seen most often with the aorta anterior and to the right of the pulmonary artery. The coronary arteries usually take the shortest course to reach their distribution, and because the aorta is anterior, the left main and circumflex coronary arteries pass anterior and leftward to the RVOT (Fig. 32.7A). The next most common variation is the left circumflex arising from the right coronary artery and coursing posterior to the pulmonary artery, which is seen in about 20% of patients, usually with side-by-side great vessels (Fig. 32.7B). The coronary arteries also may be completely inverted, with the right coronary artery arising from a left anterior sinus and the left coronary artery arising from the right posterior sinus (Fig. 32.7C). The coronary vessels also may be partially inverted, with the left circumflex arising from

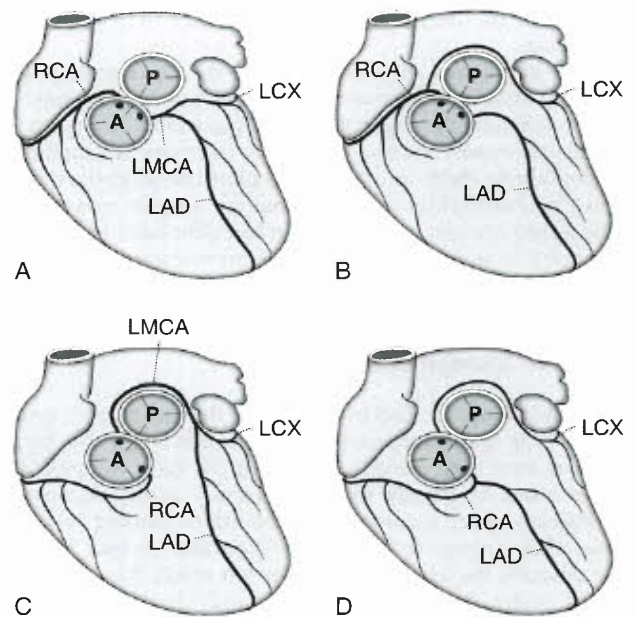


Figure 32.7. Coronary arteries in complete transposition of the great arteries. **A:** Most common variant (60%). **B:** Next most common variant, with left circumflex coronary artery (LCX) coming from the right coronary artery (RCA) (20%), which is seen most often with side-by-side great arteries. **C:** Inverted arteries coming from the inappropriate sinuses (4%). **D:** Inverted arteries with the left anterior descending coronary artery (LAD) coming from the right coronary artery (RCA) (4%). Variants with single (8%) and intramural (5%) coronary arteries are not illustrated. A, aorta; LMCA, left main coronary artery P, pulmonary artery.

the right posterior sinus and the left anterior descending arising with the right coronary artery from the left anterior sinus (Fig. 32.7D).

Finally, various single coronary anomalies may occur, and intramural coursing of any of the variants may occur, usually with branches passing between the great vessels. These variations affect the planning and conduct of the arterial switch operation because it may be difficult to move the coronary arterial origins to the neo-aortic root without creating excessive tension.

Tetralogy of Fallot

About 40% of tetralogy patients have an abnormally long, large conus artery that supplies a significant mass of myocardium. In 4% to 5%, the left anterior descending coronary artery arises from the right coronary artery and passes across the RVOT (Fig. 32.2F) (59). Occasionally, a single coronary artery comes from either the right or left sinus and the major branch that crosses the heart may pass across the RVOT (Fig. 32.4C,F) or pass behind the aorta and so avoid the outflow tract (Fig. 32.4B,E). Rarer variations also occur (33,59).

If major arteries cross the RVOT, it makes surgery with the traditional transannular incision more difficult. To avoid cutting the artery and infarcting part of the myocardium supplied by it (60), the surgeon may make incisions parallel to the artery, make incisions above and below the artery, tunnel underneath the artery, or bypass the stenotic region with a conduit (59). All these approaches interfere with the effectiveness of the surgery and in the small infant

may lead to the decision to palliate rather than perform a total repair.

These anomalies may be detected by echocardiography and if the anatomy is uncertain, aortic root angiography or selective coronary angiography is necessary (59). Although the surgeon can usually see the anomalies, there are advantages in knowing about them in advance to plan the procedure more effectively. Furthermore, the anomalous arteries may not be visible if they are obscured by epicardial adhesions from previous surgery or if they run deep in the myocardium.

Congenitally Corrected Transposition of the Great Arteries (L-Transposition)

The aorta is anterior and to the left of the pulmonary artery, and the two main coronary arteries come from the facing sinuses as seen with D-transposition of the great arteries. The anterior sinus is usually the noncoronary sinus. Because of this anatomy, there is some confusion about naming coronary arteries that appear to arise from incorrect sinuses (58,61). Some describe the vessels as right or left sided, based on their sinus of origin (61), whereas others (62) describe the arteries based on their territory of supply, and that terminology is used here. The left coronary artery supplies the left ventricle but arises in the right facing sinus. It passes in front of the pulmonary annulus and divides into left anterior descending and circumflex branches, the latter passing in front of the right atrial appendage in the atrioventricular groove. The right coronary artery supplies the systemic right ventricle. It arises from the left facing sinus and runs in the atrioventricular groove in front of the left atrial appendage to terminate as the posterior descending artery. The most common variant is a single coronary artery coming from the right facing sinus.

Double-Inlet Left Ventricle (Univentricular Heart)

Because there is no true ventricular septum and there is no typical interventricular groove, the arterial branches that run along the borders of the rudimentary outlet chamber are referred to as delimiting arteries (33,63) rather than as anterior descending arteries.

When the outlet chamber is anterior and to the right, the aorta and pulmonary artery are related as in complete transposition. The right coronary artery arises from the right facing aortic sinus and runs along the right atrioventricular sulcus. The left main coronary artery comes from the left facing sinus and continues around the left atrioventricular groove as the circumflex artery. The left and right coronary arteries give off the left and right delimiting arteries, respectively. When the outlet chamber is anterior and to the left, the great vessels are related like those in congenitally corrected transposition of the great arteries (CCTGV) (L-transposition). The right and left main coronary arteries arise from their respective facing sinuses, and the "anterior descending" coronary artery may come from the left or the right coronary arteries or there may be two delimiting arteries that border the rudimentary outlet chamber (63). With any of these variants, there may be several large diagonal arterial branches that run parallel to the delimiting branches and cross the outflow tract of the right ventricle, making septation difficult.

Double-Outlet Right Ventricle

The coronary artery origins are usually normal in most forms of this group of anomalies, but because the aortic sinuses are rotated clockwise, the right coronary artery arises anteriorly and the left coronary artery arises posteriorly (58). When the

aorta is anterior and to the right, the coronary pattern is similar to that in CCTGV, with the right coronary artery arising from the right facing sinus. In 15%, there may be a single coronary artery arising anteriorly or posteriorly (64). Occasionally, the left anterior descending coronary artery comes from the right coronary artery and crosses the RVOT, as in tetralogy of Fallot (64). When the aorta is to the left, the right coronary artery passes to the right from the anterior sinus of the leftward aorta in front of the pulmonary artery to reach the atrioventricular groove.

Truncus Arteriosus

The right and left coronary arteries usually arise normally from their appropriate sinuses (65). If, however, the valve has more than three cusps, conventional descriptions must be abandoned. What is most consistent is that the left main coronary artery arises from the posterior sinus. Major variants include unusually high ostia, closely approximated ostia, or a single ostium (65). Large diagonal branches of the right coronary artery may cross over the anterior surface of the right ventricle and contribute to flow to the ventricular septum and even part of the left ventricular free wall (65).

CONGENITAL ANOMALIES OF THE AORTIC ROOT

Aortic–Left Ventricular Defect (Tunnel)

This rare lesion is a vascular connection between the aorta and the left ventricle (Fig. 32.8). Some describe it as a tunnel that begins above the right coronary ostium, usually separated from it by a ridge, and passes behind the right ventricular infundibulum and through the anterior upper part of the ventricular septum to enter the left ventricle just below the right and left aortic cusps (66). It is usually short and direct but may be aneurysmal. Levy et al. (66) attributed the tunnel to a congenital endothelialized connection between the aorta and

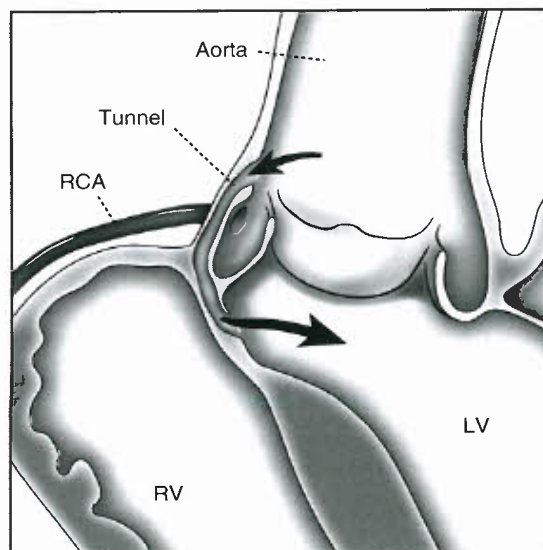


Figure 32.8. Aortic–left ventricular tunnel. Sagittal section showing the tunnel burrowing through the septal wall to enter the left ventricle. The proximal opening of the tunnel is superior to the right coronary ostium. LV, left ventricle; RCA, right coronary artery; RV, right ventricle.

the left ventricle. Others (67) have considered the lesion to be a congenital defect associated with the thinned-out anterior wall of the left ventricular outflow tract where the right aortic sinus meets the membranous septum.

Many of these patients present in infancy with congestive heart failure. They have signs resembling marked aortic valve regurgitation: a wide pulse pressure with a low diastolic blood pressure, a hyperactive dilated left ventricle and enlarged left atrium, and a loud to-and-fro murmur at the base. The electrocardiogram shows varying degrees of left ventricular and atrial hypertrophy. The chest radiograph shows variable cardiomegaly, possibly signs of congestive heart failure, but in all patients there is a dilated ascending aorta and in some a bulge of the enlarged right aortic sinus. Echocardiography with Doppler color flow mapping and aortography serve to separate this lesion from aortic valve regurgitation by the absence of retrograde flow through the aortic valve, from a coronary artery–left ventricular fistula by the finding of normal right and left main coronary arteries, from an associated ventricular septal defect by the absence of a left-to-right shunt through the defect, and from a ruptured sinus of Valsalva by the anterior position of the tunnel and the absence of a dilated sinus of Valsalva (68). Treatment has been surgical, but there is a high incidence of aortic incompetence after surgery. Alternative treatment options include transcatheter occlusion in selected patients.

Aneurysms of the Sinus of Valsalva

A localized weakness of the wall of a sinus of Valsalva, a relatively rare lesion reported in the 19th century (69), leads to aneurysmal bulging and even rupture. It is to be distinguished from diffuse dilation of all the sinuses as is seen in Marfan syndrome. The localized aneurysms are usually congenital, with thinning just above the annulus at the leaflet hinge owing to absence of normal elastic and muscular tissue (70). These aneurysms can follow infective endocarditis. At times, deciding if the endocarditis is the cause or the consequence of the aneurysm is impossible.

Pathologic Anatomy and Physiology

About 75% of the patients are male. Two-thirds of the aneurysms are located in the right aortic sinus, one-fourth in the noncoronary sinus, and the rest in the left aortic sinus (71). The aneurysms may be isolated or in 30% to 50% may be associated with ventricular septal defects, especially defects of the outlet septum. The proportion of patients with ventricular septal defects is higher when the aneurysm arises from the right sinus. With an associated ventricular septal defect, particularly if subpulmonic, there is often prolapse of the aortic valve cusp and aortic incompetence. The aortic incompetence tends to be progressive as the valve prolapses farther and becomes fibrous and stiff. Coarctation of the aorta, atrial septal defect, tetralogy of Fallot, and patent ductus arteriosus also may be associated with these aneurysms. Because the aortic root is central, the aneurysms can rupture into any cardiac chamber, and virtually all combinations of sinus and chamber fistulas have been described. Rupture is most often of the right sinus aneurysm into the right ventricle, particularly if there is an outlet ventricular septal defect. The next most frequent site of rupture is into the right atrium from an aneurysm in the noncoronary sinus. Rupture into the pericardium is rare. At surgery, most fistulas resemble wind socks projecting from the sinus into the chamber of entry, with one or more openings near the end of the wind sock.

These aneurysms do not always rupture but may cause symptoms by obstructing the RVOT, distorting the aortic valve and causing aortic incompetence, compressing the left

coronary artery and causing myocardial ischemia, or causing conduction disturbances or even complete heart block by compressing the conduction system. Because all complications of these aneurysms are functions of their size, and because they grow slowly, they seldom present in infancy and early childhood. The mean age for the onset of symptoms owing to sudden rupture of the aneurysms was 31 years (71). Rupture can follow acute chest trauma or severe exertion.

If the aneurysm ruptures, the size of the fistula determines the amount of shunting and its site of entry into the heart often determines its specific features. Thus, aneurysmal rupture into the left heart does not produce signs of a left-to-right shunt, whereas rupture into the right heart produces a left-to-right shunt of variable size.

Infective endocarditis is an important complication of the smaller fistulas. It may occur in 5% to 10% of patients with these congenital aneurysms (71).

Clinical and Laboratory Features

Before rupture, these aneurysms are diagnosed only incidentally during imaging for other lesions (72). Rupture may be accompanied by a tearing pain in the chest or upper abdomen. If a huge shunt develops rapidly, the symptoms of congestive heart failure appear almost immediately, but with smaller fistulas, it may take several months for heart failure to develop (71). About 20% of patients are asymptomatic.

With a small fistula, there may be only a continuous murmur like that of a ductus arteriosus, but with its maximal intensity in the third or fourth intercostal space near the sternal edge. If the fistula enters the right atrium, the murmur may be maximal to the right of the sternum. With larger fistulas, there will be a wide pulse pressure, a collapsing pulse, and left ventricular hyperactivity. If the fistula enters the right side, there will be right ventricular hyperactivity as well. A large fistula entering the left ventricle may display a to-and-fro murmur and simulate aortic incompetence. Occasionally, there is only a diastolic murmur in fistulas entering the left ventricle (71) or the high-pressure right ventricle in a neonate. If a ventricular septal defect is present, especially with infundibular obstruction, the combined murmurs can be confusing.

With a large chronic fistula, the electrocardiogram will show hypertrophy of the appropriate chambers. Occasionally, signs of myocardial ischemia or conduction defects occur because of compression of the coronary artery or the conduction system.

The chest roentgenogram will show enlargement of the appropriate chambers as well as pulmonary overcirculation if there is a large left-to-right shunt. Evidence of congestive heart failure may be seen. The aortic root is not enlarged, although in the rare aneurysms of the left sinus of Valsalva there may be a bulge on the left aortic root border.

Two-dimensional echocardiography with Doppler color flow mapping shows the aneurysmal dilation, even before rupture (73), but transesophageal echocardiography may give information not obtainable by routine transthoracic echocardiography (74), including information on degree and mechanism of associated aortic insufficiency. Further noninvasive imaging with computed tomography or magnetic resonance scans has been shown to provide excellent definition of the aneurysm and the tissue planes involved (75).

Cardiac Catheterization and Angiography

Previously, cardiac catheterization was used for diagnostic purposes in this entity, to define the magnitude of any left-to-right shunt, ventricular systolic and diastolic pressures, pulmonary hypertension, and any infundibular obstruction. However, its diagnostic use has been largely supplanted by

noninvasive imaging with CT or MRI. More recently, in highly selected cases, percutaneously delivered devices have been used to occlude the ruptured aneurysm (76), but caution must be advised so as to not cause future aortic valvar insufficiency by the device.

Management

While previously, some authors have advocated treatment of congestive heart failure, with emphasis on afterload reduction to minimize runoff through the fistula, current definitive therapy is surgical anatomic correction.

REFERENCES

- Alexander RW, Griffith GC. Anomalies of the coronary arteries and their clinical significance. *Circulation* 1956;14:800-805.
- Click RL, Holmes DR Jr, Vlietstra RE, et al. Anomalous coronary arteries: location, degree of atherosclerosis and effect on survival—a report from the Coronary Artery Surgery Study. *J Am Coll Cardiol* 1989;13:531-537.
- Liberthson RR, Zaman L, Weyman A, et al. Aberrant origin of the left coronary artery from the proximal right coronary artery: diagnostic features and pre- and postoperative course. *Clin Cardiol* 1982;5:377-381.
- Chang RR, Allada V. Electrocardiographic and echocardiographic features that distinguish anomalous origin of the left coronary artery from pulmonary artery from idiopathic dilated cardiomyopathy. *Pediatr Cardiol* 2001;22:3-10.
- Mohiddin SA, Begley D, Shih J, et al. Myocardial bridging does not predict sudden death in children with hypertrophic cardiomyopathy but is associated with more severe cardiac disease. *J Am Coll Cardiol* 2000;36:2270-2278.
- Davis JA, Cecchin F, Jones TK, et al. Major coronary artery anomalies in a pediatric population: incidence and clinical importance. *J Am Coll Cardiol* 2001;37:593-597.
- Tomanek RJ. Formation of the coronary vasculature: a brief review. *Cardiovasc Res* 1996;31:E46-E51.
- Tomanek RJ. Formation of the coronary vasculature during development. *Angiogenesis* 2005;8:273-284.
- Netter FJ. *A Compilation of Paintings on the Normal and Pathologic Anatomy and Physiology, Embryology, and Diseases of the Heart*. The CIBA Collection of Medical Illustrations. Caldwell, NJ: CIBA Pharmaceutical Company, 1978.
- Hutchins GM, Nazarian JH, Bulkley BH. Association of left dominant coronary arterial system with congenital bicuspid aortic valve. *Am J Cardiol* 1978;42:57-59.
- Baroldi G, Scmazzone G. *Coronary Circulation in the Normal and the Pathologic Heart*. Washington, DC: Office of the Surgeon General, 1967.
- Johnson AD, Detwiler JH, Higgins CB. Left coronary artery anatomy in patients with bicuspid aortic valves. *Br Heart J* 1978;40:489-493.
- Scholz DG, Lynch JA, Willerscheidt AB, et al. Coronary arterial dominance associated with congenital bicuspid aortic valve. *Arch Pathol Lab Med* 1980;104:417-418.
- Gensini GG, Giorgi S, Coskun O. Anatomy of the coronary circulation in living man: coronary venography. *Circulation* 1965;31:778-784.
- Gillard M, Mansourati J, Etienne Y, et al. Angiographic anatomy of the coronary sinus and its tributaries. *Pacing Clin Electrophysiol* 1998;21:2280-2284.
- Donaldson RM, Raphael MJ, Yacoub MH, et al. Hemodynamically significant anomalies of the coronary arteries. Surgical aspects. *Thorac Cardiovasc Surg* 1982;30:7-13.
- Ogden JA. Congenital anomalies of the coronary arteries. *Am J Cardiol* 1970;25:474-479.
- Roberts WC. Major anomalies of coronary arterial origin seen in adulthood. *Am Heart J* 1986;111:941-963.
- White NK, Edwards JE. Anomalies of the coronary arteries. Report of four cases. *Arch Pathol* 1948;45:766-771.
- Ho JS, Strickman NE. Anomalous origin of the right coronary artery from the left coronary sinus: case report and literature review. *Tex Heart Inst J* 2002;29:37-39.
- Brandt B III, Martins JB, Marcus ML. Anomalous origin of the right coronary artery from the left sinus of Valsalva. *N Engl J Med* 1983;309:596-598.
- Taylor AJ, Byers JR, Cheitlin MD, et al. Anomalous right or left coronary artery from the contralateral coronary sinus: "high-risk" abnormalities in the initial coronary artery course and heterogeneous clinical outcomes. *Am Heart J* 1997;133:428-435.
- Taylor AJ, Rogan KM, Virmani R. Sudden cardiac death associated with isolated congenital coronary artery anomalies. *J Am Coll Cardiol* 1992;20:640-647.
- Shirani J, Roberts WC. Solitary coronary ostium in the aorta in the absence of other major congenital cardiovascular anomalies. *J Am Coll Cardiol* 1993;21:137-143.
- Jim MH, Siu CW, Ho HH, et al. Anomalous origin of the right coronary artery from the left coronary sinus is associated with early development of coronary artery disease. *J Invasive Cardiol* 2004;16:466-468.
- Dawn B, Talley JD, Prince CR, et al. Two-dimensional and Doppler transesophageal echocardiographic delineation and flow characterization of anomalous coronary arteries in adults. *J Am Soc Echocardiogr* 2003;16:1274-1286.
- Casolo G, Del Meglio J, Rega L, et al. Detection and assessment of coronary artery anomalies by three-dimensional magnetic resonance coronary angiography. *Int J Cardiol* 2005;103:317-322.
- Schmitt R, Froehner S, Brunn J, et al. Congenital anomalies of the coronary arteries: imaging with contrast-enhanced, multidetector computed tomography. *Eur Radiol* 2005;15:1110-1121.
- Barth CW III, Roberts WC. Left main coronary artery originating from the right sinus of Valsalva and coursing between the aorta and pulmonary trunk. *J Am Coll Cardiol* 1986;7:366-373.
- Brooks HSJ. Two cases of an abnormal coronary artery of the heart, arising from the pulmonary artery; with some remarks upon the effect of this anomaly in producing cirroid dilatation of the vessels. *J Anat Physiol* 1885;20:26-29.
- Fontana RS, Edwards JE. *Congenital Cardiac Disease: A Review of 357 Cases Studied Pathologically*. Philadelphia, PA: WB Saunders, 1962.
- Bland EF, White PD, Garland J. Congenital anomalies of the coronary arteries: report of an unusual case associated with cardiac hypertrophy. *Am Heart J* 1933;8:787-801.
- Neufeld HN, Schneeweiss A. *Coronary Artery Disease in Infants and Children*. Philadelphia, PA: Lea & Febiger, 1983.
- Moodie DS, Fyfe D, Gill CC, et al. Anomalous origin of the left coronary artery from the pulmonary artery (Bland-White-Garland syndrome) in adult patients: long-term follow-up after surgery. *Am Heart J* 1983;106:381-388.
- George JM, Knowlan DM. Anomalous origin of the left coronary artery from the pulmonary artery in an adult. *N Engl J Med* 1959;261:993-998.
- King DH, Danford DA, Huhta JC, et al. Noninvasive detection of anomalous origin of the left main coronary artery from the pulmonary trunk by pulsed Doppler echocardiography. *Am J Cardiol* 1985;55:608-609.
- Wesselhoeft H, Fawcett JS, Johnson AL. Anomalous origin of the left coronary artery from the pulmonary trunk. Its clinical spectrum, pathology, and pathophysiology, based on a review of 140 cases with seven further cases. *Circulation* 1968;38:403-425.
- Liebman J, Hellerstein HK, Ankeney JL, et al. The problem of the anomalous left coronary artery arising from the pulmonary artery in older children. Report of three cases. *N Engl J Med* 1963;269:486-494.
- Shrivastava S, Casteneda AR, Moller JH. Anomalous left coronary artery from pulmonary trunk. Long-term follow-up after ligation. *J Thorac Cardiovasc Surg* 1978;76:130-134.
- Cooley DA, Hallman GL, Bloodwell RD. Definitive surgical treatment of anomalous origin of left coronary artery from pulmonary artery: indications and results. *J Thorac Cardiovasc Surg* 1966;52:798-808.
- El-Said GM, Ruzyllo W, Williams RL, et al. Early and late result of saphenous vein graft for anomalous origin of left coronary artery from pulmonary artery. *Circulation* 1973;48:III2-III6.
- Grace RR, Angelini P, Cooley DA. Aortic implantation of anomalous left coronary artery arising from pulmonary artery. *Am J Cardiol* 1977;39:609-613.
- Huddleston CB, Balzer DT, Mendeloff EN. Repair of anomalous left main coronary artery arising from the pulmonary artery in infants: long-term impact on the mitral valve. *Ann Thorac Surg* 2001;71:1985-1988; discussion 1988-1989.
- Jin Z, Berger F, Uhlemann F, et al. Improvement in left ventricular dysfunction after aortic reimplantation in 11 consecutive paediatric patients with anomalous origin of the left coronary artery from the pulmonary artery. Early results of a serial echocardiographic follow-up. *Eur Heart J* 1994;15:1044-1049.
- Schwartz ML, Jonas RA, Colan SD. Anomalous origin of left coronary artery from pulmonary artery: recovery of left ventricular function after dual coronary repair. *J Am Coll Cardiol* 1997;30:547-553.
- Takeuchi S, Imamura H, Katsumoto K, et al. New surgical method for repair of anomalous left coronary artery from pulmonary artery. *J Thorac Cardiovasc Surg* 1979;78:7-11.
- Driscoll DJ, Nihill MR, Mullins CE, et al. Management of symptomatic infants with anomalous origin of the left coronary artery from the pulmonary artery. *Am J Cardiol* 1981;47:642-648.
- Ando M, Mee RB, Duncan BW, et al. Creation of a dual-coronary system for anomalous origin of the left coronary artery from the pulmonary artery utilizing the trapdoor flap method. *Eur J Cardiothorac Surg* 2002;22:576-581.
- Del Nido PJ, Duncan BW, Mayer JE Jr, et al. Left ventricular assist device improves survival in children with left ventricular dysfunction after repair of anomalous origin of the left coronary artery from the pulmonary artery. *Ann Thorac Surg* 1999;67:169-172.
- Ochoa-Ramirez E, Valdez-Garza HE, et al. Double anomalous coronary origin from the pulmonary artery: successful surgical correction in an infant. *Tex Heart Inst J* 2005;32:348-350.

51. Coe JY, Radley-Smith R, Yacoub M. Clinical and hemodynamic significance of anomalous origin of the right coronary artery from the pulmonary artery. *Thorac Cardiovasc Surg* 1982;30:84–87.
52. Yao CT, Wang JN, Yeh CN, et al. Isolated anomalous origin of right coronary artery from the main pulmonary artery. *J Card Surg* 2005;20:487–489.
53. Angelini P, Trivellato M, Donis J, et al. Myocardial bridges: a review. *Prog Cardiovasc Dis* 1983;26:75–88.
54. Hill RC, Chitwood WR Jr, Bashore TM, et al. Coronary flow and regional function before and after supraarterial myotomy for myocardial bridging. *Ann Thorac Surg* 1981;31:176–181.
55. Yetman AT, McCrindle BW, MacDonald C, et al. Myocardial bridging in children with hypertrophic cardiomyopathy—a risk factor for sudden death. *N Engl J Med* 1998;339:1201–1209.
56. Sorajja P, Ommen SR, Nishimura RA, et al. Myocardial bridging in adult patients with hypertrophic cardiomyopathy. *J Am Coll Cardiol* 2003;42:889–894.
57. Wernovsky G, Sanders SP. Coronary artery anatomy and transposition of the great arteries. *Coron Artery Dis* 1993;4:148–157.
58. Elliott LP, Amplatz K, Edwards JE. Coronary arterial patterns in transposition complexes. Anatomic and angiographic studies. *Am J Cardiol* 1966;17:362–378.
59. Fellows KE, Freed MD, Keane JF, et al. Results of routine preoperative coronary angiography in tetralogy of Fallot. *Circulation* 1975;51:561–566.
60. Berry BE, McGoon DC. Total correction for tetralogy of Fallot with anomalous coronary artery. *Surgery* 1973;74:894–898.
61. Lev M, Rowlatt UF. The pathologic anatomy of mixed levocardia. A review of thirteen cases of atrial or ventricular inversion with or without corrected transposition. *Am J Cardiol* 1961;8:216–263.
62. Kirklin JW, Barratt-Boyes BG. Congenitally corrected transposition of the great arteries. In: Barratt-Boyes B, Kirklin JW. *Cardiac Surgery*. New York, NY: John Wiley and Sons, 1993.
63. Lev M, Liberthson RR, Kirkpatrick JR, et al. Single (primitive) ventricle. *Circulation* 1969;39:577–591.
64. Gomes MM, Weidman WH, McGoon DC, et al. Double-outlet right ventricle without pulmonic stenosis. Surgical considerations and results of operation. *Circulation* 1971;43:131–136.
65. Anderson KR, McGoon DC, Lie JT. Surgical significance of the coronary arterial anatomy in truncus arteriosus communis. *Am J Cardiol* 1978;41:76–81.
66. Levy MJ, Lillehei CW, Anderson RC. Aortico-left ventricular tunnel. *Circulation* 1963;27:841–853.
67. Serino W, Andrade JL, Ross D, et al. Aorto-left ventricular communication after closure. Late postoperative problems. *Br Heart J* 1983;49:501–506.
68. Frapp RR, Werner JC, Whitman V, et al. Pulsed Doppler and two-dimensional echocardiographic findings in aortico-left ventricular tunnel. *J Am Coll Cardiol* 1984;4:1012–1014.
69. Hope J. *A Treatise of Diseases of the Heart and Great Vessels*. London: John Churchill, 1839.
70. Edwards JE, Burchell HB. The pathological anatomy of deficiencies between the aortic root and the heart, including aortic sinus aneurysms. *Thorax* 1957;12:125–139.
71. Norwick ER, Aberdeen E, Friedman S, et al. Congenital left aortic sinus-left ventricle fistula and review of aortocardiac fistulas. *Ann Thorac Surg* 1977;23:378–388.
72. Mayer JH 3rd, Holder TM, Canent RV. Isolated, unruptured sinus of Valsalva aneurysm: serendipitous detection and correction. *J Thorac Cardiovasc Surg* 1975;69:429–432.
73. Hands ME, Lloyd BL, Hung J. Cross-sectional echocardiographic diagnosis of unruptured right sinus of Valsalva aneurysm dissecting into the interventricular septum. *Int J Cardiol* 1985;9:380–383.
74. Abdelkhirane C, Roudaut R, Dallochio M. Diagnosis of ruptured sinus of Valsalva aneurysms: potential value of transesophageal echocardiography. *Echocardiography* 1990;7:555–560.
75. Noji Y, Hifumi S, Nagayoshi T, et al. Sixteen-slice computed tomography, transthoracic real-time 3-dimensional echocardiography and magnetic resonance imaging assessment of a long-term survivor of rupture of sinus of Valsalva aneurysm. *Intern Med* 2005;44:513–515.
76. Abidin N, Clarke B, Khattar RS. Percutaneous closure of ruptured sinus of Valsalva aneurysm using an Amplatzer occluder device. *Heart* 2005;91:244.

Paul M. Weinberg ■ Shobha Natarajan ■ Lindsay S. Rogers

Congenital abnormalities of the aortic arch have been known at least since the anatomical reports of anomalous right subclavian artery by Hunauld (1) in 1735, double aortic arch by Hommel (2) in 1737, right aortic arch by Fioratti and Aglietti (3) in 1763, and interrupted aortic arch by Steidele (4) in 1788. While the clinicopathologic correlation of swallowing difficulty with anomalous right subclavian artery was made by Bayford (5) in 1789, it was not until the 1930s and the use of barium esophagography that some arch anomalies were diagnosed during life. Since that time, clinical interest has generally paralleled surgical capability. The first division of a vascular ring was performed by Gross (6) in 1945, and the first successful repair of interrupted aortic arch was accomplished by Merrill et al. (7) in 1957. In the current era with the advent of minimally invasive surgery (8,9) and robotically assisted surgery (10), precise definition of aortic arch anatomy, preferably by noninvasive means, is essential.

ANATOMICAL CLASSIFICATION

Aortic arch anomalies can be thought of as falling into one or a combination of the following anatomical categories: abnormalities of branching, abnormalities of arch position including right aortic arch and cervical aortic arch, supernumerary arches including double aortic arch and persistent fifth aortic arch, interrupted aortic arch, and anomalous origin of a pulmonary artery branch from the ascending aorta or from the contralateral pulmonary artery branch.

LEFT AND RIGHT ARCH DEFINITION

Left and right aortic arch refer to which bronchus is crossed by the arch, not to which side of the midline the aortic root ascends. This is particularly important to remember when looking at projection images from angiography where it may be difficult to make the determination directly without significant cranial angulation. Practically, the sidedness of the aortic arch is usually determined indirectly with echocardiography or angiography by the branching pattern of the brachiocephalic vessels. As a rule, the first arch vessel contains the carotid artery opposite the side of the arch. However, caution must be exercised in using this indirect method, particularly when surgical decisions, such as the approach to repair of esophageal atresia, hinge on this determination. Three very rare anomalies are categorical exceptions to this rule: retroesophageal innominate artery, isolated innominate artery, and congenital absence of the carotid artery contralateral to the arch. But by far the most common source of error in the use of this rule is when it is difficult to decide which of two carotid arteries is the *first*. A more reliable rule, but one that may be difficult to apply with ultrasound imaging, is that retroesophageal vessels and

isolated vessels, that is, arising only from a ductus or ligamentum (without connection to the aorta), are *always* opposite the side of the aortic arch. Magnetic resonance imaging (MRI) or computed tomography (CT) shows the relationship of the arch to the trachea and bronchi *directly*, thus eliminating ambiguity when atypical branching patterns are encountered.

Embryology

The specific anomalies can better be understood through an appreciation of their embryologic origins. Development of the aortic arch system can best be described as a sequential appearance and persistence or dissolution of six paired vessels connecting the trunco-aortic sac of the embryonic heart tube with the paired dorsal aortae, which fuse to form the definitive descending aorta. Each arch corresponds to a branchial pouch derived from embryonic foregut. While the mechanism for determining persistence or dissolution of aortic arch components is not completely known, migration of neural crest cells into the pharyngeal arches (11) may play a significant role. In addition, the association of various arch anomalies such as right aortic arch, cervical aortic arch, aberrant and isolated subclavian or innominate arteries, and certain vascular rings, with microdeletions of chromosome 22q11 (12) implies a genetic component to the derivation of at least some arch anomalies. The fact that neural crest cells are also involved in development of the conotruncus and that conotruncal anomalies also occur in chromosome 22q11-deleted patients provides a further etiologic link to aortic arch anomalies.

The normal left aortic arch as shown by Congdon (13) is derived from the aortic portion of the embryonic truncus arteriosus, the left branch of the trunco-aortic sac, the left fourth arterial arch, the left dorsal aorta between the fourth and sixth embryonic arches, and the left dorsal aorta distal to the sixth arch. The three brachiocephalic branches of the arch are derived from the following: the innominate artery from the right branch of the trunco-aortic sac with the right common carotid artery from right third embryonic arch and right subclavian from right fourth arch and (proximal) right dorsal aorta proximally and right seventh intersegmental artery distally; left carotid artery from left third aortic arch; and left subclavian artery from left seventh intersegmental artery. While the appearance and loss of vessels as arches or portions of the brachiocephalic vasculature is sequential, Edwards (14) proposed the concept of a "hypothetical double aortic arch" that is, in essence, the potential contribution of nearly all embryonic arches to components of the definitive arch system. These diagrams are used extensively in the excellent monograph by Stewart et al. (15). They are invaluable not only to demonstrate possible embryologic explanations for each arch anomaly but also to help the diagnostician determine possible and probable arch anomalies and their corresponding sequences of arch vessels. We have adopted a simplified schematic version of the Edwards diagrams, which is feasible for those who are less

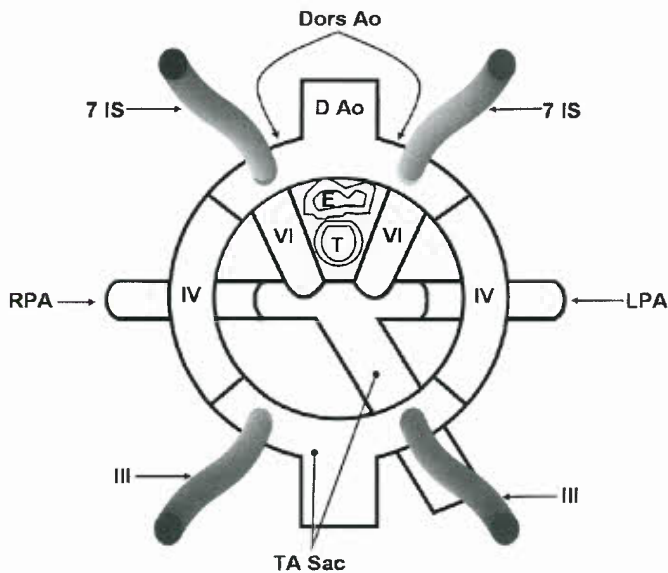


Figure 33.1. Totipotential aortic arch from embryonic contributions. D Ao, descending aorta; Dors Ao, dorsal aorta(e); E, esophagus; LPA, left pulmonary artery; RPA, right pulmonary artery; T, trachea; TA Sac, truncus aortic and pulmonary components; III, IV, VI refer to third, fourth, sixth embryonic arches, respectively, 7 IS, seventh intersegmental artery. (Modified from hypothetical double aortic arch diagrams of Edwards JE. *Anomalies of the derivatives of the aortic arch system.* *Med Clin North Am* 1948;32:925–949, as if viewed from overhead.)

artistically inclined, to provide similar information (Fig. 33.1). This can easily be drawn at the bedside or in the patient chart to diagram almost any arch anomaly and is used throughout this chapter to illustrate many of the abnormalities.

Diagnostic Methods

Beginning in the 1930s, barium esophagography was the primary method for diagnosing arch anomalies. In the 1960s and 1970s, angiography became the gold standard and remained so even in the face of echocardiography. While the branching pattern may be determined by careful examination of arch vessels in the suprasternal short- and long-axis views (16), arch sidedness is often inferred from the branching pattern and in some cases may be inconclusive or even lead to erroneous deduction. However, in the last 20 years, MRI and CT, where available, have supplanted angiography as the gold standard for definitive diagnosis of arch anomalies. Both modalities have the advantages of large fields of view and simultaneous visualization of vessels and airways, and both are minimally invasive. While CT usually has shorter scan times, that advantage is disappearing as MRI sequences become faster. MRI has the advantage of no ionizing radiation—still a significant problem with CT even with the reduced dosage strategies employed in some centers. Furthermore, MRI has capabilities for physiologic measurements, which are particularly helpful in patients with associated intracardiac disease.

There is still a role for ultrasonography in the diagnosis of arch anomalies, and, in particular, vascular rings. That is in the fetus where the fluid-filled trachea does not hamper visualization the way the air-filled trachea does after birth. Furthermore, the ductus arteriosus is virtually always patent, so that nearly all rings can be seen completely encircling the trachea with blood-filled vessels. Specific strategies for recognizing vascular rings in the fetus have been reported by several authors (17–19).

However, one study (20) found a different distribution of rings in fetuses (predominantly diverticulum of Kommerell) from what has been observed by others postnatally (predominantly double aortic arch), and with most of the fetal-diagnosed cases being asymptomatic through infancy.

CLINICAL CLASSIFICATION

In addition to the anatomic categorization of aortic arch anomalies discussed above, one can subdivide arch anomalies according to clinical features as follows: vascular rings; nonring vascular compression of the trachea, bronchi, or esophagus; noncompressive arch malformations; and ductal-dependent arch anomalies including interrupted aortic arches and isolated subclavian, carotid, or innominate arteries. In addition, genetic syndromes represent an important group of patients from the standpoint of diagnostic criteria and associated abnormalities.

Chromosome 22q11.2 Deletion Syndromes

Chromosome 22q11.2 microdeletions are seen in more than 80% of patients with DiGeorge, velocardiofacial, and conotruncal anomaly face syndromes. The combination has been referred to collectively with the acronym CATCH 22 (Cardiac defects, Abnormal facies, Thymic hypoplasia, Cleft palate, and Hypocalcemia together with microdeletion of chromosome 22) (21). Most of these patients have conotruncal anomalies: either subaortic stenosis with posterior malalignment of the infundibular septum, often associated with interrupted aortic arch, type B; truncus arteriosus communis; or tetralogy of Fallot, with or without pulmonary atresia. More than two-thirds of these have aortic arch anomalies (22). What is more, nearly one-fourth of patients with arch anomalies but without intracardiac defects have 22q11 deletion (23). While a wide variety of arch anomalies has been noted in these patients, there is a predilection for anomalies involving absence of one or both embryonic fourth aortic arches, as seen most notably in abnormalities of the subclavian arteries: aberrant, isolated, or cervical origin (22,24,25). When all three types of subclavian artery anomaly are included, more than 80% of patients with both conotruncal and arch anomalies involving the subclavian artery have 22q11 deletion compared to only 17% of patients with conotruncal anomaly and normal subclavians (24). Other fourth arch anomalies occurring in chromosome 22q11 deletion syndromes include type B interrupted aortic arch, cervical aortic arch with separate origins of internal and external carotid arteries from the arch (26), and possibly “stenosis” in the middle of the right aortic arch between right carotid and subclavian arteries along with a diverticulum of Kommerell (27). The pathogenesis of these fourth arch anomalies may be mediated by transforming growth factor- β 2 (TGF- β 2) as demonstrated in TGF- β 2 knockout mice (28,29).

Vascular Rings

A vascular ring is an aortic arch anomaly in which the trachea and esophagus are completely surrounded by vascular structures. The vascular structures need not be patent, for example, a ligamentum arteriosum or atretic segment of aortic arch may complete a ring. The clinical picture typically includes stridor, though pneumonia, bronchitis, or cough may characterize the presentation. Infants may demonstrate a posture of hyperextension of the neck. Less commonly, patients exhibit reflex apnea associated with eating. A common history is that of a 1- to 3-month-old with “noisy breathing since birth” who develops more significant respiratory distress in association with an intercurrent upper

TABLE 33.1

Three “D”s Indicating Vascular Rings When Not All Vessels Are Patent

<ul style="list-style-type: none"> ■ Diverticulum ■ Dimple ■ Descending aorta 	}	Opposite the side of the arch
--	---	-------------------------------

respiratory infection. Less commonly and usually in toddlers or older children, the presentation will be swallowing difficulty or choking on food. These patients tend to have looser rings, but careful questioning of parents will sometimes reveal the history of stridor in infancy, which was passed off as “recurrent bronchitis.” Some infants will have wheezing and may be mistaken for having asthma or bronchiolitis. In general, such patients will have normal oxygen saturations and in severe cases, elevated $p\text{CO}_2$, whereas patients with bronchiolar obstruction will tend to have hypoxemia with normal $p\text{CO}_2$ (30). Some asymptomatic patients will be discovered incidentally while imaging for another reason (31). Occasionally, in patients with associated intracardiac abnormalities, respiratory symptoms may mistakenly be attributed to the cardiac disease when, in fact, they are in part or completely due to the vascular ring. Older children and adults are occasionally followed for many years with a diagnosis of “asthma” only to have a vascular ring diagnosed and surgically treated with resolution of symptoms (32,33). However, respiratory symptoms may persist for months or years after surgical relief of the ring due to the presence of tracheomalacia. Fetal echocardiography is one such source of discovery of vascular rings. Many cases found by this modality may be asymptomatic after birth (20) but knowledge of the ring can lead to prompt treatment if symptoms do occur later (34). In general, asymptomatic patients do not require surgery, but if associated with congenital heart disease that requires surgery, it should be addressed at the time of the cardiac surgery. The diagnosis may be suspected from the combination of history and plain chest film; however, if symptomatic, the patient should have definitive study.

When all elements of the ring are patent, visualization, especially by tomographic imaging, is straightforward. In cases where the ring is completed by an atretic segment of aorta or ligamentum arteriosum, those segments cannot be visualized with current imaging technologies. However, these rings are recognizable by the presence of one of three “D”s *opposite* the side of the aortic arch: Diverticulum, Dimple, or Descending aorta (Table 33.1). A diverticulum is a large vessel arising from the descending aorta that gives rise to a smaller-caliber vessel or vessels with a *sudden* taper beyond the trachea and esophagus. A dimple is a small tapered, blindly ending outpouching from the aorta. Descending aorta opposite the side of the aortic arch refers to the location of the descending aorta in the upper thorax with a dramatic angulation between the transverse arch and descending aorta. (This is distinct from the typical right aortic arch that begins its descent on the right but in most cases gradually moves to the left by the point where it reaches the diaphragm.) These three “D”s *only* occur when connected by a ligamentum arteriosum or an atretic segment of aortic arch and *always* indicate a vascular ring.

NORMAL LEFT AORTIC ARCH AND VARIANTS

The normal left aortic arch crosses the left mainstem bronchus at the level of thoracic vertebra T5 and descends left of the midline to the diaphragm and beyond in cases of visceral situs solitus. The normal branching pattern has the right

innominate artery first, which, in turn, branches into right common carotid and right subclavian arteries, the left carotid artery second, and the left subclavian artery third. Typically, the ductus arteriosus or the ligamentum arteriosum joins the aorta distal to the takeoff of the left subclavian artery but can insert more proximally, as in some cases of tetralogy of Fallot.

There are two frequent variants of the left aortic arch. One is common brachiocephalic trunk, in which the right innominate and left carotid arteries arise from a single origin. This is present in 10% of otherwise normal left arches (35) and usually is of no consequence, although some have suggested that innominate artery compression of the trachea (discussed below) is more frequent when common brachiocephalic trunk is present. The other variant is separate origin of the left vertebral artery from the aortic arch proximal to the takeoff of the left subclavian artery rather than from the subclavian artery (Fig. 33.2A). This too is seen in 10% of normal left arches (35) and is important only in the fact that it should not be confused angiographically or echocardiographically with anomalous right subclavian artery in which there are also four brachiocephalic vessels (see below). The distinguishing feature here is the normal appearance of the first arch vessel (right innominate artery), being larger than the second (left carotid), and the third (left vertebral) being smaller than the fourth (left subclavian). Again, no functional significance attends this common variant.

Embryology

Using the totipotential aortic arch diagram (Fig. 33.1), one envisions the normal left arch resulting from dissolution of the right sixth aortic arch (ductus) and the right dorsal aorta distal to the origin of the seventh intersegmental artery (distal subclavian artery precursor). Thus the right fourth arch, rather than remaining an arch (connecting trunco-aortic sac to descending aorta), becomes the proximal right subclavian artery as it arises from the innominate artery. The left fourth arch becomes the definitive aortic arch.

ABNORMAL LEFT AORTIC ARCH

Left Aortic Arch with Retroesophageal Right Subclavian Artery

This anomaly was first described anatomically by Hunauld (1) in 1735. Bayford (5) linked the postmortem discovery of such a case with the history of swallowing difficulty during life and coined the term “dysphagia lusoria” (from the Latin, *lusus naturae*, trick of nature). This is the most common arch anomaly, occurring in 0.5% of the general population (demonstrated in a large adult autopsy series [36]). The incidence in Down syndrome patients with congenital heart disease is very high at 38% (37).

This is the most common form of anomalous or aberrant right subclavian artery (another is described below under left arch, right descending aorta) with the following branching pattern being usual: the first branch is the right carotid artery, the second the left carotid, third the left subclavian, and fourth a retroesophageal right subclavian artery arising from the posteromedial aspect of the distal aortic arch (Fig. 33.1). Of note is the fact that 20% of cases have a bicarotid trunk (i.e., common origin of both carotid arteries) and 14% have right vertebral origin from the right carotid so that the carotid artery bifurcates even though there is no innominate artery (38). Most cases of left aortic arch with retroesophageal right subclavian artery are asymptomatic, with the diagnosis made while imaging for another condition or at autopsy. In a large pediatric echocardiographic series (16), nearly one-third of patients with aberrant right subclavian artery

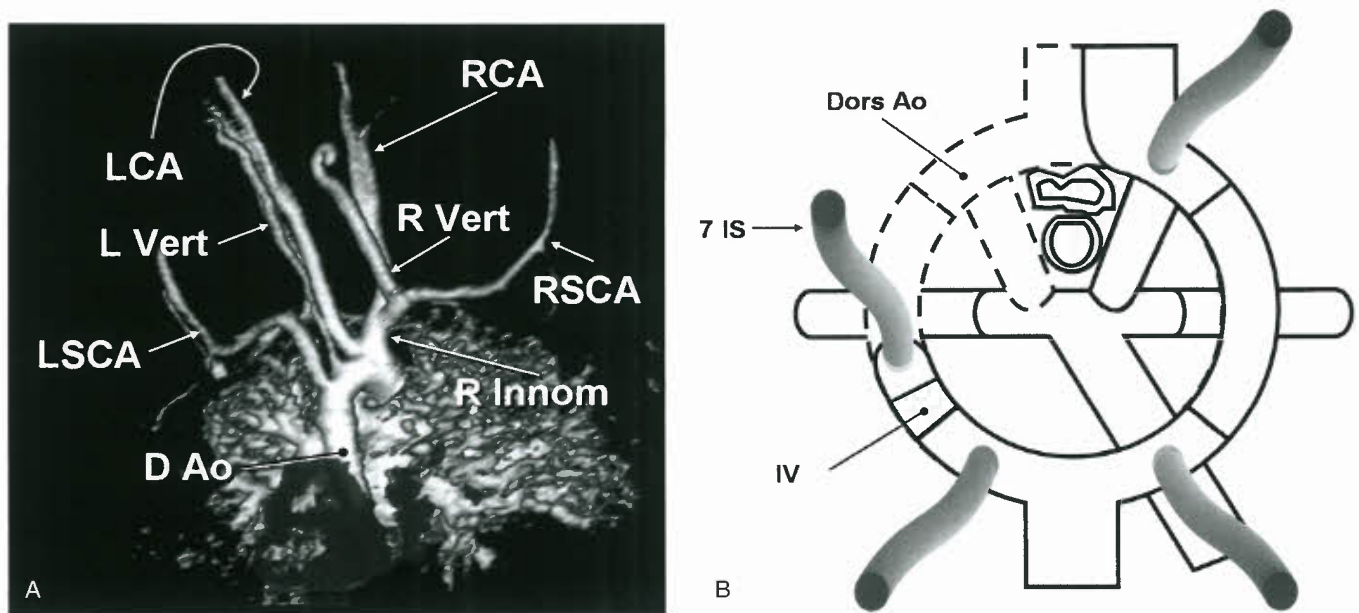


Figure 33.2. Normal left arch. **A:** Right posterior oblique view of 3-D shaded surface display from MRI of normal left aortic arch variant with separate origin of left vertebral artery (L Vert) from aortic arch. It shows origin of right innominate artery (R Innom), which gives rise to right carotid (RCA) and right subclavian (RSCA) arteries, left carotid (LCA), L Vert, and left subclavian (LSCA). Note the relatively short length of R innom and the relatively distant division of RCA into internal and external carotid arteries (*above arrow*). **B:** Presumptive embryonic arch diagram of normal left arch. *Dotted lines* indicate dissolution or disappearance of portions of embryonic arch system—right sixth arch and right dorsal aorta distal to right subclavian artery.

had no intracardiac abnormality, while 18% had conotruncal anomalies—especially tetralogy of Fallot and interrupted aortic arch, 11% had left-sided obstructive lesions such as hypoplastic left heart syndrome and coarctation, and 10% had common atrioventricular septal defect. In that study, the highest incidence of aberrant right subclavian artery amongst the various lesions was interrupted aortic arch at 28%, followed by hypoplastic left

heart syndrome at 10%, common atrioventricular septal defect at 8%, and tetralogy of Fallot with pulmonary atresia at 7%.

Embryology

This can be envisioned as a disappearance of the right fourth aortic arch (Fig. 33.3F). The distal right dorsal aorta (rather

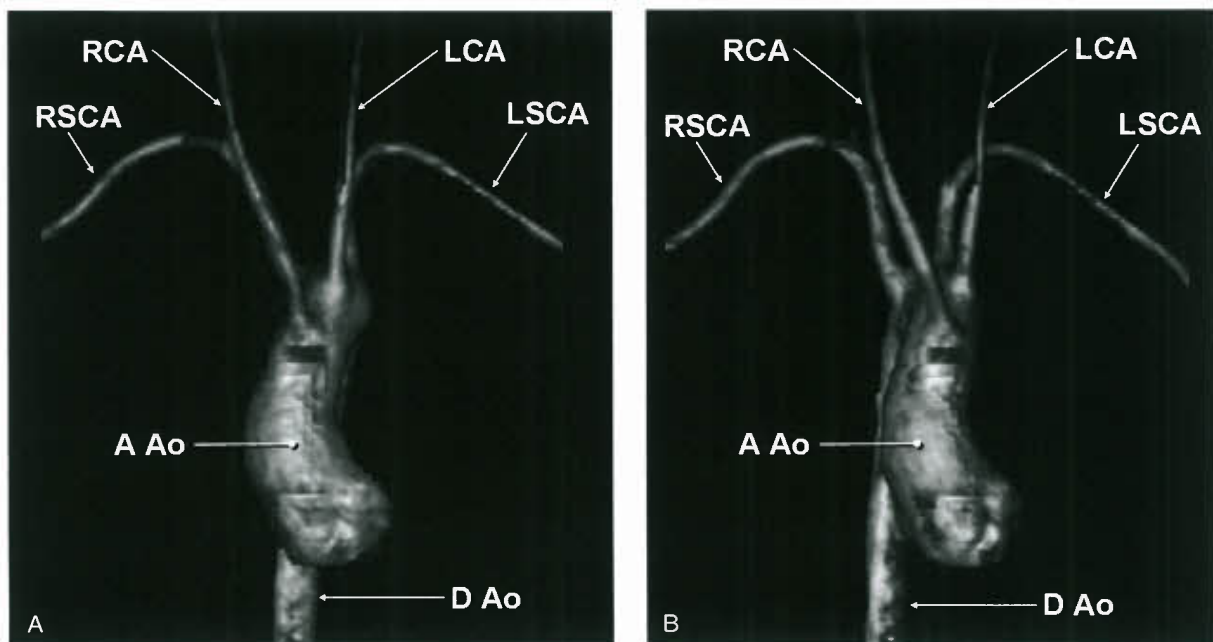


Figure 33.3. Left arch, retroesophageal right subclavian artery. **A:** Anterior view of 3-D shaded surface display from MRI. Note that RCA is superimposed on RSCA in this view. **B:** RCA and RSCA separated in slightly right anterior oblique view showing sequence of arch vessels: RCA, LCA, LSCA, and RSCA.

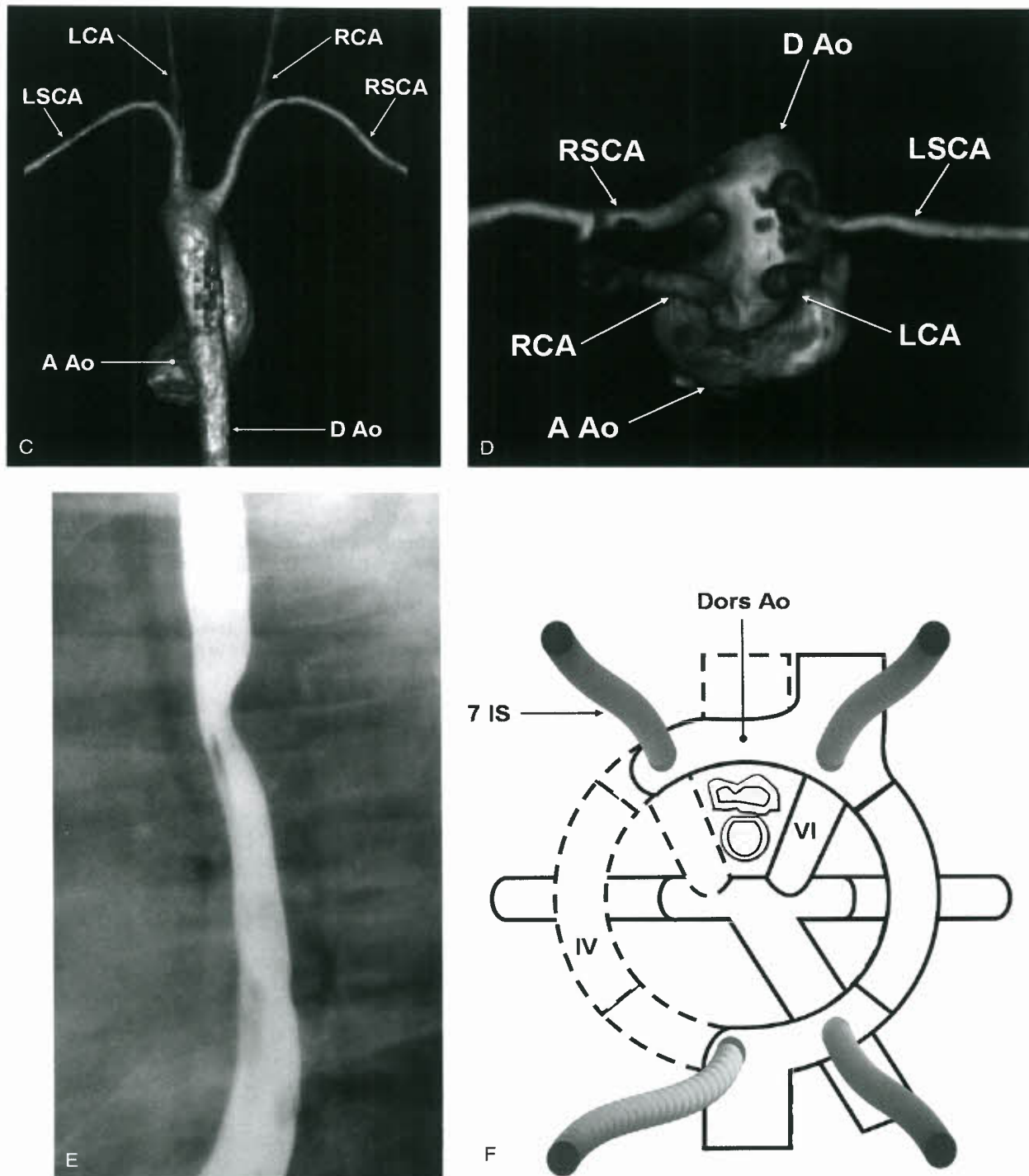


Figure 33.3. (Continued) C: Posterior view. Note virtually uniform caliber of RSCA from origin to peripheral extent. D: Overhead view showing proximity of RCA and RSCA. A Ao, ascending aorta; D Ao, descending aorta; RCA, right carotid artery; RSCA, right subclavian artery; LCA, left carotid artery; LSCA, left subclavian artery. E: Barium esophagram showing small posterior indentation by retroesophageal subclavian artery. F: Presumptive embryonic arch diagram showing dissolution of right fourth and sixth aortic arches.

than the right fourth arch) becomes the proximal right subclavian artery forming its retroesophageal portion. The right sixth arch (ductus) also involutes.

Diagnosis and Management

Since there is no innominate artery, the first and second branches from the aortic arch, the right and left carotid arteries respectively,

tend to be similar in size as are the last two branches, the left and right subclavian arteries. Barium esophagography is usually specific for the diagnosis with a fixed filling defect usually slanting upward to the right and best appreciated with fluoroscopy. The defect is relatively small (Fig. 33.3E) compared to that seen in other anomalies where an aortic arch, or diverticulum, impinges on the esophagus (see Fig. 33.11). With angiography, the diagnosis may sometimes be missed in the anteroposterior

(AP) projection since the right subclavian may be superimposed on the right carotid artery in the usual position (Fig. 33.3A). However, careful single-frame analysis will demonstrate the earlier filling of the right carotid on an aortic root injection or the earlier filling of the right subclavian on a descending aortic injection. This arch anomaly is usually recognized with echocardiography by the branching pattern discussed above, namely, a nonbifurcating first branch that ascends toward the right, followed by two successive left-sided vessels (left carotid and left subclavian arteries), followed by a fourth branch that heads toward the right but may disappear behind the trachea. The retroesophageal course of the subclavian artery is shown by MRI on transverse (axial) cuts, and the largest expanse from aortic origin to the thoracic apex is usually seen on coronal sections.

Left Aortic Arch with Right-Sided Retroesophageal Diverticulum of Kommerell

This very rare arch anomaly was actually the first vascular ring to be diagnosed in life with barium esophagography by

Kommerell (39) whose name is associated with this diverticulum. Although, the name is usually used in reference to the much more common mirror image of this anomaly, viz., a left-sided diverticulum associated with a right aortic arch (discussed below). The branching pattern in left arch with retroesophageal diverticulum is identical to that of the more common left arch with retroesophageal right subclavian artery discussed above, which is not a vascular ring. The difference is in the caliber of the proximal subclavian artery (Fig. 33.1). The significance of this is that the abrupt change of vessel size always indicates the presence of a ligamentum arteriosum, which completes a vascular ring.

Embryology

This anomaly exhibits embryology similar to that of left arch, retroesophageal right subclavian artery described above, that is, involution of the right fourth aortic arch. The difference is that unlike the aforementioned anomaly, the right sixth (ductal) arch persists and completes the ring (Fig. 33.4C).

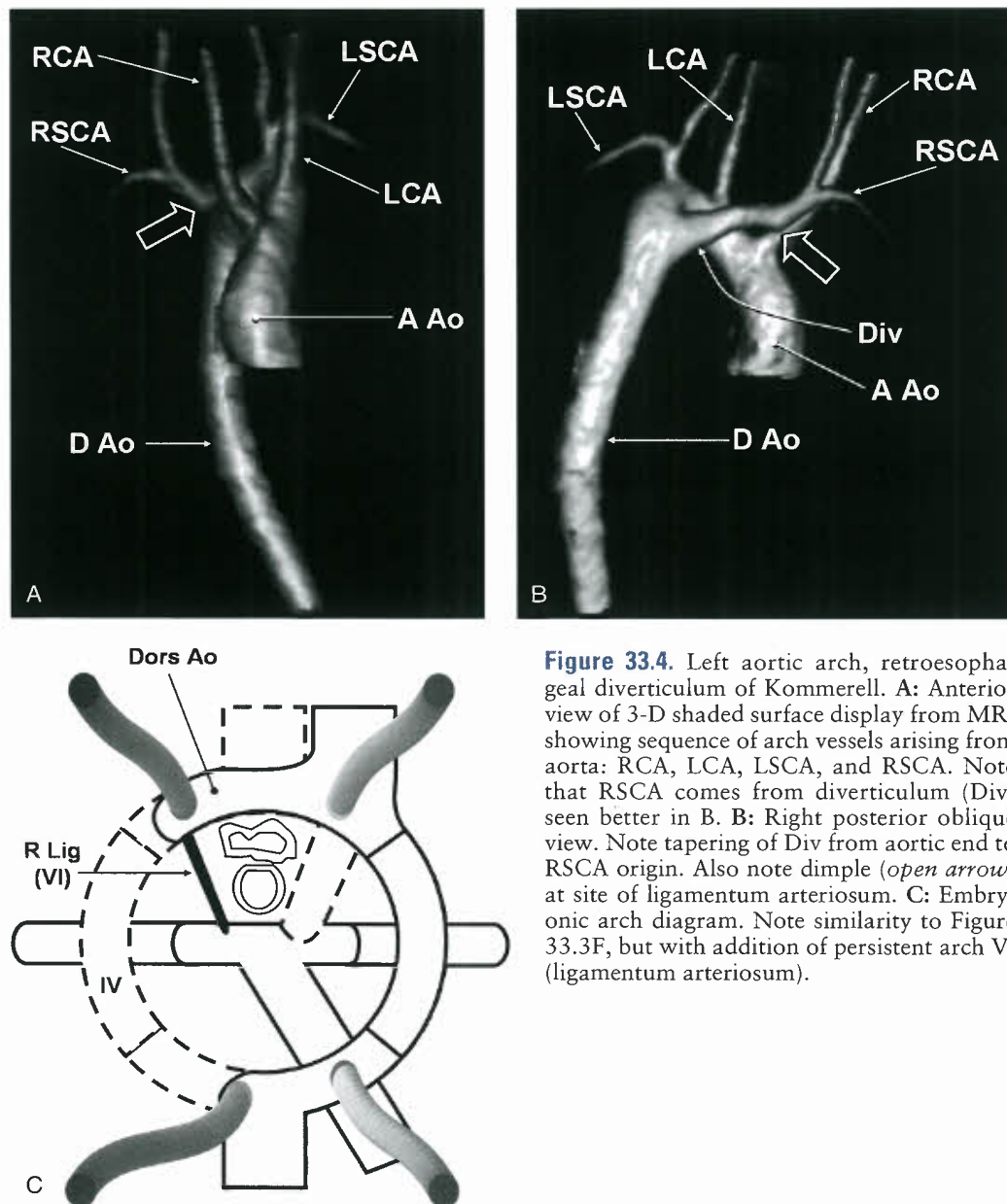


Figure 33.4. Left aortic arch, retroesophageal diverticulum of Kommerell. **A:** Anterior view of 3-D shaded surface display from MRI showing sequence of arch vessels arising from aorta: RCA, LCA, LSCA, and RSCA. Note that RSCA comes from diverticulum (Div) seen better in B. **B:** Right posterior oblique view. Note tapering of Div from aortic end to RSCA origin. Also note dimple (open arrow) at site of ligamentum arteriosum. **C:** Embryonic arch diagram. Note similarity to Figure 33.3F, but with addition of persistent arch VI (ligamentum arteriosum).

Left Aortic Arch with Right Descending Aorta and Right Ductus (or Ligamentum)

This is a rare arch anomaly, also known as circumflex aortic arch, with branching pattern similar to left arch with retroesophageal right subclavian artery. However the arch itself is retroesophageal; hence the right subclavian artery, while it may arise as the last arch vessel, that is, aberrant subclavian, is not retroesophageal (Fig. 33.1). The descending aorta is connected by a ductus or ligamentum to the right pulmonary artery (RPA) forming a vascular ring.

Embryology

The embryology of this anomaly, also similar to left arch with retroesophageal subclavian artery, can be thought of as

a disappearance of the right fourth aortic arch but with the distal left dorsal aorta forming the definitive distal aortic arch and passing retroesophageally to a descending aorta beginning to the right of the vertebral column (Fig. 33.5D). Thus the right seventh intersegmental artery arises from the right-sided descending aorta. There is also persistence of the right sixth (ductal) arch connecting the RPA portion of the trunco-aortic sac with the distal right dorsal aorta similar to the also rare left arch diverticulum of Kommerell (above).

Diagnosis and Management

This diagnosis can be suspected if a patient who presents with symptoms suggestive of a vascular ring has findings of a left aortic arch without evidence of a right aortic arch. Plain chest roentgenogram can show the left-sided arch and

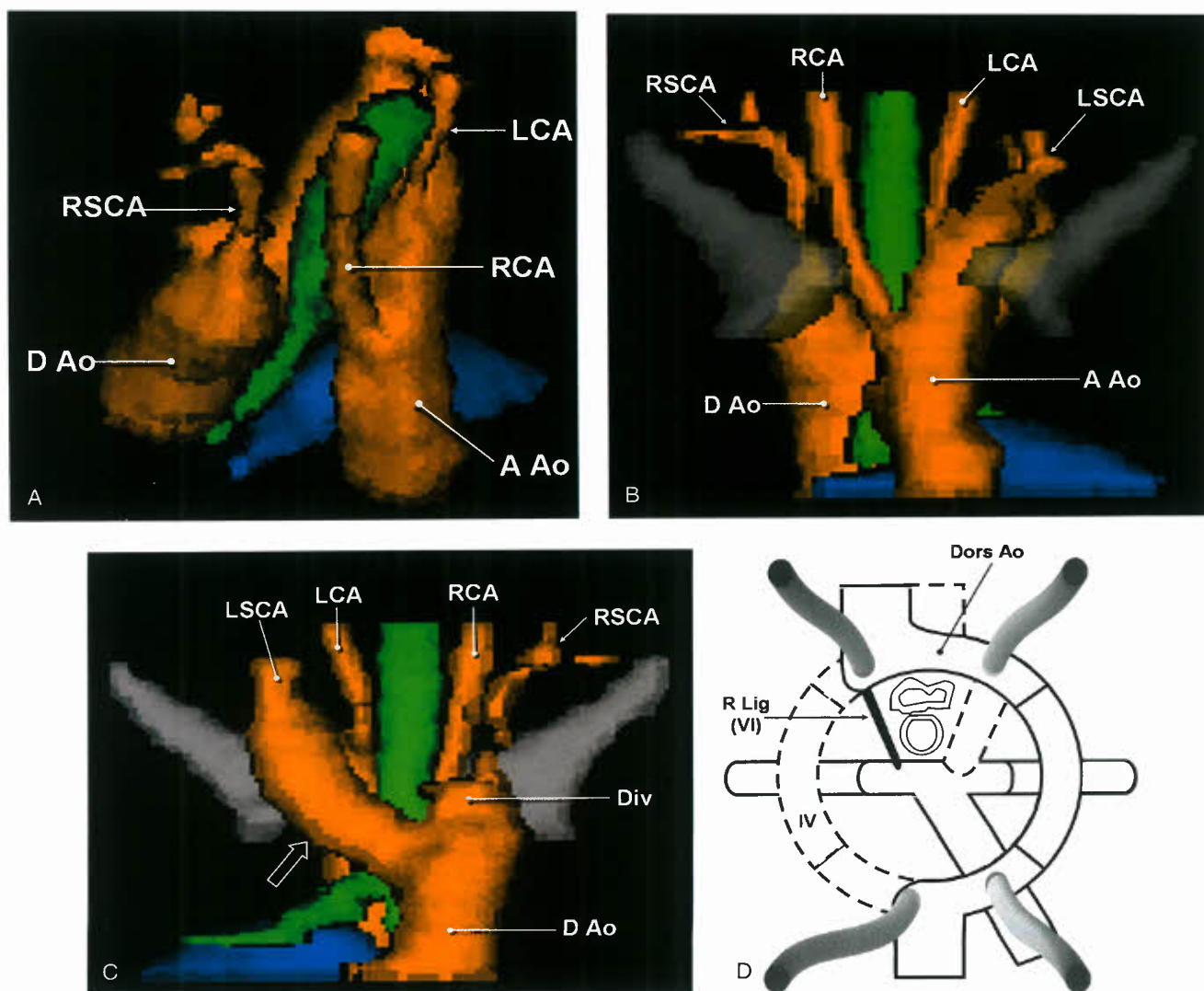


Figure 33.5. Cervical left arch, right descending aorta. **A:** Right lateral view with slight cranial angulation of 3-D shaded surface display from MRI. Trachea (green) trapped by ligamentum arteriosum (not visualized) between D Ao and RPA (blue). **B:** AP view of same reconstruction showing arch extending above level of clavicles (grey). Hairpin appearance of cervical arch is seen through translucent rendering of left clavicle. **C:** Posterior view of same 3-D reconstruction. Circumflex aortic arch (open arrow) passes behind trachea and esophagus (not shown) to D Ao, from which arises a diverticulum (Div) that gives rise to RSCA and ligamentum arteriosum. **D:** Embryonic arch diagram showing dissolution of right fourth arch and left sixth arch and persistence of right sixth arch remnant, namely, right ligamentum (R Lig [VI]). Note similarity to Figure 33.4C but with right descending aorta instead of left. In both cases, the retroesophageal portion is derived from embryonic dorsal aorta.

the right-sided upper descending aorta, particularly in adults. The addition of barium esophagography can demonstrate the large posterior indentation from the retroesophageal aorta; however, the course of this vessel, upward to the left, is indistinguishable from the much more frequently occurring right aortic arch with retroesophageal diverticulum (see below). In both cases the upper descending aorta is right sided. While the aortic knob on chest roentgenogram would be left sided, this is not always evident, especially in infants with a prominent thymus. Angiography will show the course of the aorta from left arch to retroesophageal segment to right upper descending. The subclavian artery can be seen arising from the descending aorta as it turns from its transverse to more nearly vertical course. This pattern can also be demonstrated by MRI with the addition of direct imaging of the aortic position relative to the trachea. *While most vascular*

rings can be divided through a left thoracotomy, this type and the rare diverticulum of Kommerell noted above are usually approached by a right thoracotomy (40), so that the ligamentum can be reached, although a midline approach may also be employed.

Left Aortic Arch with Isolated Right Subclavian Artery

Another rare anomaly, isolated subclavian artery means that the subclavian artery arises only from the ductus arteriosus. As with the previous two anomalies, the left arch version is much less common than the right arch form. The branching pattern is right carotid artery, left carotid artery or bicarotid trunk, and left subclavian artery (Fig. 33.6). According to a recent case report and review of the literature (41), five of

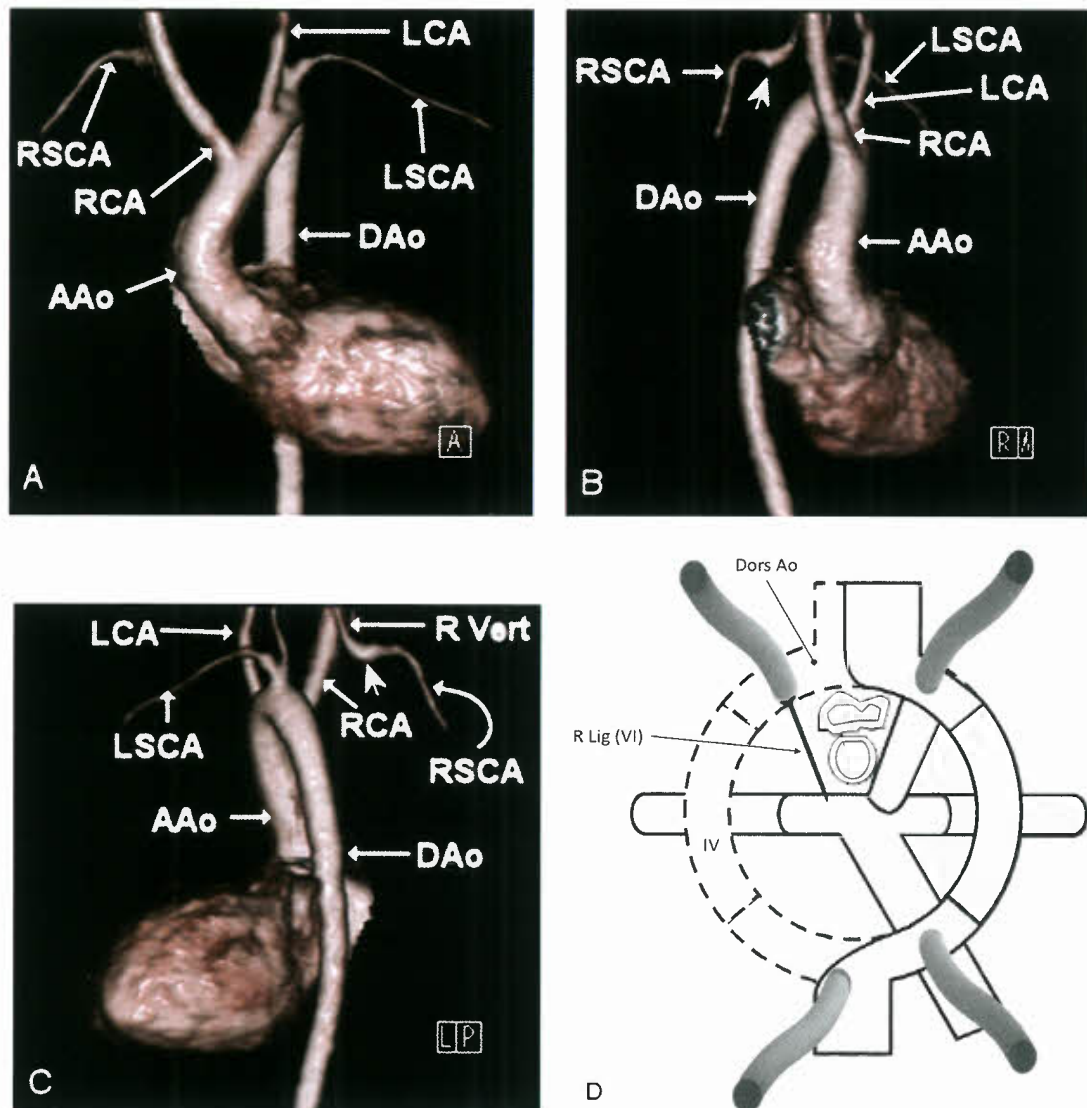


Figure 33.6. Left aortic arch with isolated right subclavian artery. Shaded surface display from gadolinium-enhanced 3-D MRI dataset. **A:** Straight AP view showing left aortic arch. In this view, the right carotid (RCA) and right subclavian (RSCA) arteries are superimposed giving the false impression of a normal right innominate artery (compare with Fig. 33.3 with retroesophageal right subclavian). Aao, ascending aorta; Dao, descending aorta; LCA, left carotid artery; LSCA, left subclavian artery. **B:** Steep right anterior oblique view shows the separation between the RSCA and the RCA. Arrowhead shows dimple where right ligamentum arteriosum is attached. **C:** Steep left posterior oblique view better demonstrates the isolated right subclavian artery (RSCA) and right vertebral artery (R Vert) through which blood flows to the subclavian from the circle of Willis. **D:** Embryonic arch diagram showing ipsilateral loss of right fourth arch and dorsal aorta with persistence of ipsilateral sixth arch.

14 cases had D-transposition of the great arteries (15,42–45) (Fig. 33.1), five had no intracardiac anomaly (in two of those (42,46) the ductus remained patent) (15,47,48), two (including their own case with a patent ductus) had tetralogy of Fallot (49), and one each had ventricular septal defect (VSD) (50) and interrupted aortic arch (51).

Embryology

This occurs with dissolution of the right fourth arch and right dorsal aorta but persistence of the right sixth arch.

Diagnosis and Management

If the ductus remains patent with high pulmonary resistance, the subclavian and vertebral arteries are supplied from the pulmonary artery resulting in decreased oxygen saturation in the right arm compared with the head (earlobe) except in transposition when the arm saturation would be higher than the head. Assuming bilateral ductus, the left arm and lower body would be expected to have saturations similar to the right arm, whereas the head, receiving blood from the ascending aorta would be different. When the ductus closes, the subclavian is typically supplied by retrograde flow from the vertebral artery via the circle of Willis. When this occurs in the absence of other anomalies it may go unrecognized or may cause vertebral insufficiency with so-called congenital subclavian steal. In many cases, there may be no symptoms or simply absence of the right arm pulse. This may be recognized with angiography by delayed filling of the subclavian artery after aortic root injection. With phase-encoded velocity mapping, retrograde flow in the vertebral artery can be detected on MRI. Symptomatic patients are treated by implantation of the subclavian artery into the ipsilateral carotid artery or the aorta.

Left Aortic Arch with Cervical Origin of the Right Subclavian Artery

This rare anomaly was first reported by Kutsche and Van Mierop (52) in association with type B interrupted aortic arch. It was subsequently found in patients with tetralogy of Fallot, with or without pulmonary atresia, and has only been seen in patients with 22q11 deletion (25). This is an abnormality whose clinical significance appears to be that it is a marker for CATCH 22. Normally, the right innominate artery bifurcates into a common carotid and subclavian artery near its origin from the aorta (see Fig. 33.2A). However, in this anomaly, the innominate trifurcates in the neck, giving rise to external and internal carotids and the subclavian artery, which then travels caudally back to the thorax before heading out to the arm (Fig. 33.1).

Embryology

The presumptive embryology has been elegantly described by Kutsche and Van Mierop (52). This together with the observation of Rauch et al. (25) that abnormalities of subclavian artery origin are frequently associated with 22q11 deletion sheds light on an important pathway in the pathogenesis of arch anomalies in CATCH 22 patients. There appears to be a predilection for unilateral or bilateral absence or atresia of the embryonic fourth arch. When this occurs on the side opposite the definitive arch, there are three main variations in the fate of the subclavian artery: (a) origin from the descending aorta, that is, from the dorsal aorta distal to the seventh intersegmental artery—retroesophageal subclavian artery or circumflex aortic arch as described above (b) origin from the sixth arch—isolated subclavian artery, also described above, and (c) origin from the third arch, which, being more cephalad than

the fourth, gives origin to the subclavian artery in the neck rather than in the thorax.

When the fourth arch is absent or atretic ipsilateral to the definitive aortic arch, there are also three possibilities, which are elaborated upon below: (a) interrupted aortic arch, in which the sixth arch replaces the fourth, (b) persistent fifth aortic arch with atresia of the distal fourth, and (c) cervical aortic arch, in which the third arch replaces the fourth, analogous to cervical origin of the subclavian artery on the side opposite the arch. Of note is the fact that all of these have been seen in association with 22q11 deletion, and collectively are more common than cases with normal origin of the subclavian arteries and well developed fourth arches (22,24).

RIGHT AORTIC ARCH

Right aortic arches have in common (by definition) a single aortic arch that crosses over the right mainstem bronchus, passing to the right of the trachea. There are four major types of right arch: (a) with mirror-image branching and right descending aorta, (b) with retroesophageal left subclavian artery, (c) with retroesophageal diverticulum of Kommerell, and (d) with left descending aorta. There are also several infrequently occurring variations.

The incidence of right aortic arch among patients with tetralogy of Fallot has been reported to be anywhere from 13% to 34% (53); however studies vary as to the source of the material (chest roentgenogram, angiography, surgery, or postmortem examination) and frequently do not distinguish between specific types of right arch. The incidence in truncus arteriosus is generally higher than in tetralogy. An overall incidence of 8% in patients with D-transposition of the great arteries, compared to 16% in those with transposition, VSD, and pulmonary stenosis has been reported (54).

A relatively rare but important subset of right aortic arch is that with coarctation of the aorta. Pooling the results of two large series, one from our institution (55) and one from Shanghai Children's Medical Center (56), coarctation in right aortic arch represented only 1.7% of all coarctations and 2.9% of right aortic arches. Of interest is the high incidence of aberrant left subclavian artery—65% compared with only 25% of all right arches (16), and the similarly high incidence of vascular rings—70%. Most of these were long-segment coarctations.

Right Aortic Arch with Mirror-Image Branching

Mirror-image right arch has the first branch as a *left* innominate artery which, in turn, divides into left carotid and left subclavian arteries, the second as the right carotid, and the third as a right subclavian (Fig. 33.1). This is the left–right mirror of a normal left aortic arch. However, frequently that is the end of the symmetry, since the ductus arteriosus (or ligamentum arteriosum) is usually the left-sided one, arising from the base of the innominate artery rather than from the aortic arch. Therefore, typical mirror-image right aortic arch with left ductus or ligamentum *does not form a vascular ring*. This arch anomaly is almost always associated with congenital intracardiac disease. The most common association is with tetralogy of Fallot (48% in a series of 74 postmortem cases [57]), but truncus arteriosus communis, other conotruncal anomalies including transposition of the great arteries, double-outlet right ventricle, right ventricular aorta with pulmonary atresia, and anatomically corrected malposition were also seen. In addition, lesions not usually considered conotruncal anomalies such as pulmonary atresia with intact ventricular septum, conoventricular VSD

with anomalous muscle bundle of the right ventricle, and isolated VSD are occasionally found to have mirror-image right arch.

A rare variation of mirror-image right aortic arch has a left ductus or ligamentum arising from a retroesophageal dimple pointing toward the left from the right-sided descending aorta. This does form a vascular ring (Fig. 33.1). This is different from right arch with diverticulum of Kommerell in that no arch vessel arises from the dimple. Unlike other patients with mirror-image right aortic arch, the few reported cases with retroesophageal ductus dimple appear not to have associated congenital heart disease (58). Because of the directly AP arrangement of the ascending and descending aorta in right arches, the right mainstem bronchus is subject to compression between the RPA and the descending aorta. In one case, this compression was exaggerated by a unique ligamentum arteriosum passing beneath the right bronchus in a patient with discontinuous branch pulmonary arteries with a thrombosed left pulmonary artery arising exclusively from a left ductus off the left innominate artery (59). Watanabe et al. (60) demonstrated that a right aortic arch with L-transposed or malposed aorta can cause tracheal compression because of elongation of the aortic arch.

Embryology

The presumptive pattern of mirror-image right arch development includes dissolution of the left dorsal aorta distal to the origin of the seventh intersegmental artery (distal subclavian artery precursor) so that the left fourth arch becomes the proximal subclavian artery rather than remaining as an aortic arch (Fig. 33.7). Typically, the right sixth (ductal) arch involutes

while the left sixth persists. However, with disappearance of the left dorsal aorta distal to the left seventh intersegmental artery, the sixth arch usually connects to the proximal or subclavian artery side of the disruption. Thus, in the definitive arch the left ductus arises from the underside of the left innominate artery and passes to the left pulmonary artery appearing as a congenital modified left Blalock-Thomas-Taussig shunt. Alternatively, the left sixth arch will disappear and the right persist giving a true mirror image of normal, that is, a ductus connecting the underside of the right-sided arch with the RPA. Other cases, particularly when associated with tetralogy of Fallot, may have dissolution of both ductus. Finally, in those with retroesophageal ductus dimple the left sixth arch connects left pulmonary artery with the distal left dorsal aorta (Fig. 33.8).

Diagnosis and Management

Since this type of right arch usually produces no retroesophageal compression or vascular ring, there are, with rare exceptions, no symptoms produced by the arch itself. Therefore, the diagnosis is usually made during imaging of the associated congenital intracardiac disease. The distinctive branching pattern can be used for echocardiographic and angiographic diagnosis, while the appearance of a right-sided indentation of trachea and esophagus on plain radiograph and barium esophagography, respectively, but without posterior impression on the esophagram, permits the diagnosis to be made with those modalities. The presence of a left innominate artery in a patient with symptoms suggestive of a vascular ring and in the absence of cyanotic congenital heart disease should suggest the differential diagnosis of the rare right arch, retroesophageal ductus or the more common right arch, or left descending aorta or double aortic arch with atretic left arch distal to the subclavian artery (discussed below) (differentiated by presence of a left upper descending aorta).

No treatment of right aortic arch per se is required; however, it may be helpful for surgeons to know the sidedness of the aortic arch in certain circumstances. For systemic-to-pulmonary shunts, the classical Blalock-Thomas-Taussig (subclavian artery to pulmonary artery, direct end-to-side) anastomosis or the modified form (polytetrafluoroethylene [Gore-Tex] tube graft interposition side-to-side anastomosis of subclavian artery to pulmonary artery) is best carried out using the side with an innominate artery. With the classical form, the more nearly horizontal takeoff of the subclavian artery makes kinking of the vessel less likely when the cut end is brought down to the level of the pulmonary artery than with the subclavian artery arising directly from the arch. Even with Gore-Tex tube graft interposition, the innominate is a more favorable site of origin since the overall diameter of the innominate is greater, making the proximal anastomosis easier. Furthermore, the angle of takeoff is less acute, making kinking of the vessel of origin less likely even if there is some downward traction after completion of the anastomosis. Another situation in which knowledge of the side of the aortic arch may be useful is in the repair of esophageal atresia and tracheoesophageal fistula where it may be desirable to avoid having the arch obscure the view of the fistula (Fig. 33.9).

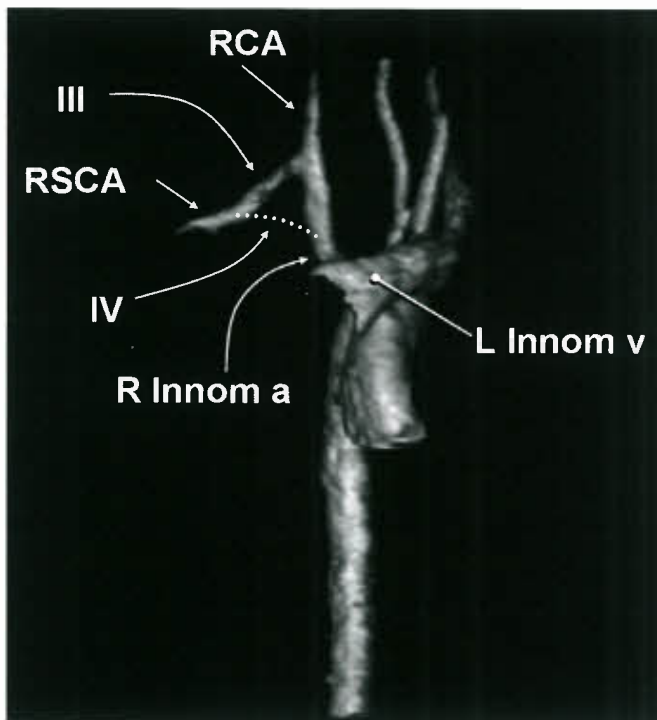


Figure 33.7. Cervical origin of the right subclavian artery. Slightly right anterior oblique view of 3-D shaded surface display from MRI. Note the high (i.e., cervical) origin of the RSCA from the right innominate artery (R Innom a) and the downward course into the thorax. Compare with Figure 22.2A. Dotted line shows expected location of absent embryonic fourth arch (IV). Note superior location of embryonic third arch (III) component of RSCA. L innom v, left innominate vein.

Right Aortic Arch with Retroesophageal Left Subclavian Artery

Right aortic arch with retroesophageal left subclavian artery (the nonvascular-ring form of anomalous or aberrant subclavian) consists of an arch passing to the right of the trachea with the following sequence of brachiocephalic arteries: left carotid, right carotid, right subclavian, and retroesophageal

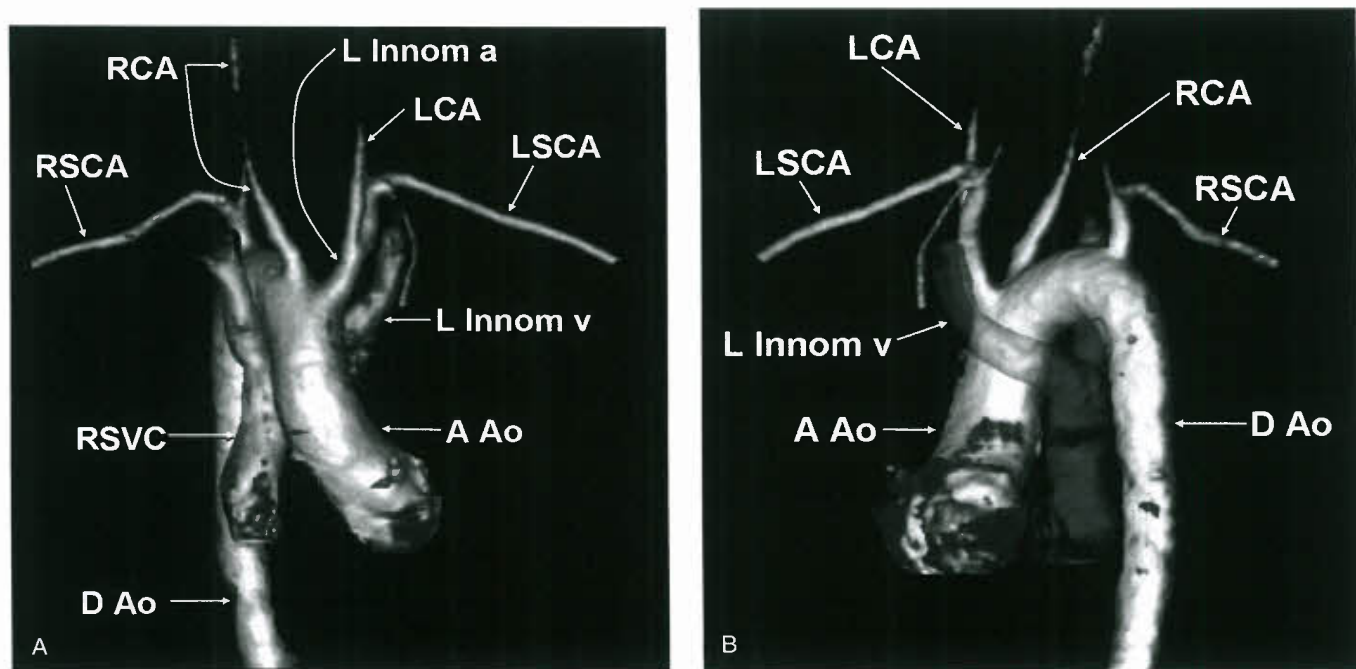


Figure 33.8. Right aortic arch, mirror-image type. **A:** Anterior view of 3-D shaded surface display from MRI. Sequence of arch vessels is L Innom a, RCA, RSCA. **B:** Left posterior oblique view. Note incidental retroaortic L Innom v. There was no ductus arteriosus in this case. **C:** Embryonic arch diagram showing dissolution of left dorsal aorta after proximal migration of left subclavian artery. Note that left fourth arch forms proximal left subclavian artery and left sixth (ductal) arch (if present) extends from underside of left innominate artery to left pulmonary artery.

left subclavian arteries (Fig. 33.1). This differs from the arch anomaly described below in that the proximal left subclavian artery is not significantly larger in caliber than its more distal portion (i.e., no aortic diverticulum). Therefore, there is no left-sided ductus arteriosus or ligamentum arteriosum and thus no vascular ring. Many of these patients have associated conotruncal anomalies. As has been noted previously, aberrant subclavian artery has a higher incidence of 22q11 deletion than does mirror-image right aortic arch (22).

Embryology

This is similar to the right arch with retroesophageal diverticulum with involution of the left fourth aortic arch, but with loss of the left sixth (ductal) arch as well (Fig. 33.10C). In this way, the left dorsal aorta becomes *only* the proximal left subclavian artery and not the “beginning” of the descending aorta.

A right sixth arch, if present, connects RPA with right dorsal aorta, which is part of the definitive right arch.

Diagnosis and Management

The diagnosis may be suspected from barium esophagography with a relatively small posterior indentation on the esophagus passing upward to the left. Since there is no vascular ring, the trachea is unaffected except for the slight leftward deviation seen with virtually all right aortic arches. As noted above, echocardiography may be expected to identify the first branch of the aorta as a left carotid artery (since it does not bifurcate proximally like an innominate artery and is similar in caliber to the second branch—right carotid artery), but appreciation of the size of the retroesophageal vessel itself may be difficult. Both MRI and angiography can demonstrate the size of the left subclavian artery that distinguishes this lesion from right

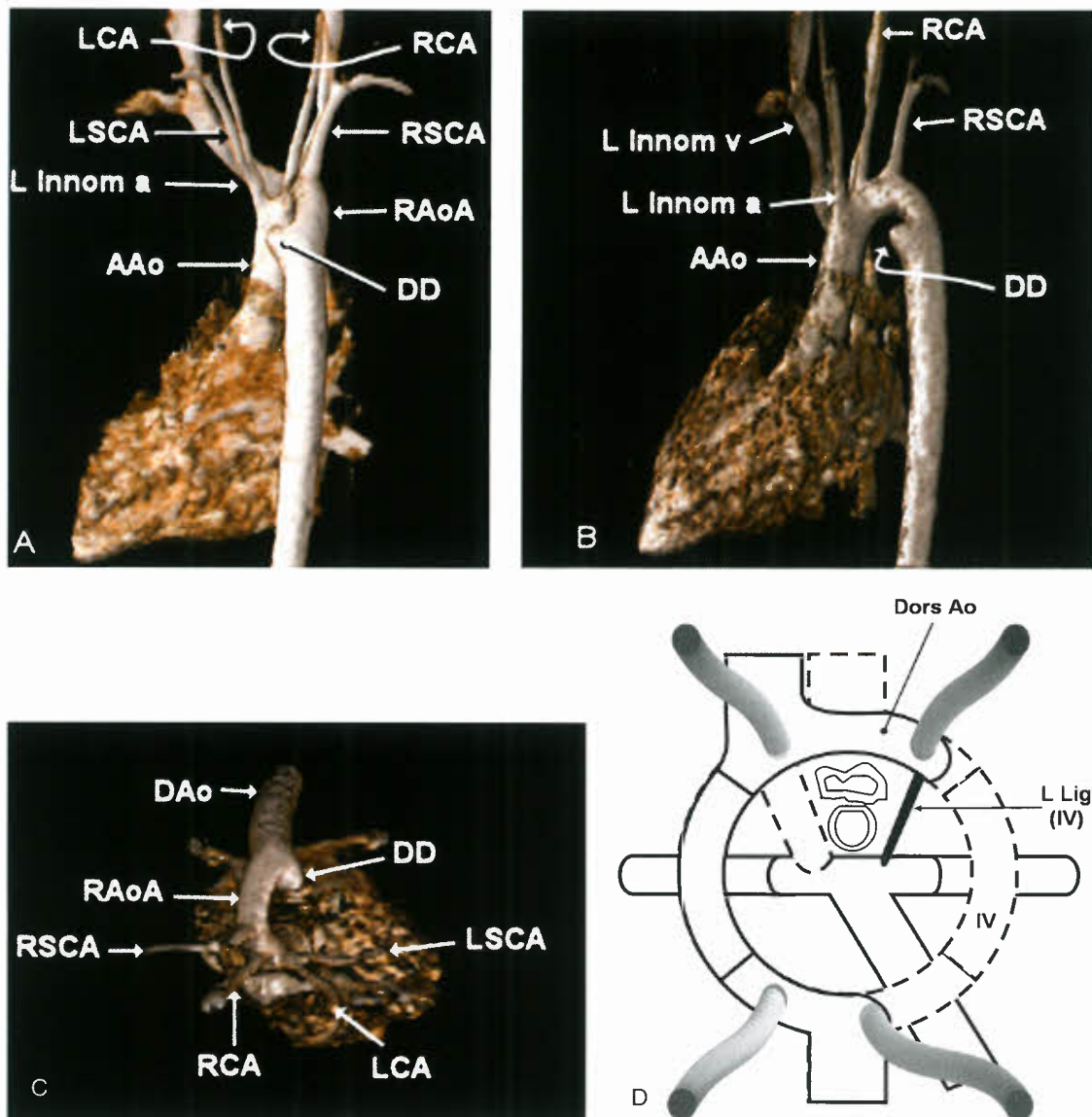


Figure 33.9. Right aortic arch with retroesophageal left ligamentum arteriosum. Shaded surface display from gadolinium-enhanced 3-D MRI dataset. **A:** Posterior view showing mirror-image branching pattern—first arch vessel being left innominate artery (L Innom a) giving rise to left subclavian (LSCA) and carotid (LCA) arteries, second is right carotid (RCA), then right subclavian (RSCA)—of right aortic arch (RAoA) but with ductus dimple (DD) pointing toward the left. **B:** Left posterior oblique view showing no posterior tethering of the left innominate artery indicating that this is not a double aortic arch with atretic left arch (compare with Fig. 33.18A). Left carotid and subclavian arteries superimposed in this view. Left innominate vein (L Innom v) is seen anterior to L Innom a. **C:** Overhead view showing the right aortic arch (RAoA) and right descending aorta (DAo) with the DD pointing toward the left, indicating a vascular ring. **D:** Embryonic arch diagram shows mirror-image right arch branching pattern with LPA connected by left sixth arch (ligamentum) to dimple formed by remnant of left dorsal aorta.

aortic arch with retroesophageal diverticulum. Since there is no vascular ring, there is usually no need for treatment other than that of associated anomalies.

Right Aortic Arch with Retroesophageal Diverticulum of Kommerell

Right arch with diverticulum of Kommerell is the second most common vascular ring after double aortic arch. It is far more

common than its mirror image described above. It has as its first branch the left carotid artery, second the right carotid artery, third the right subclavian artery, and finally a retroesophageal vessel from which the left subclavian artery arises and the left ductus arteriosus or ligamentum arteriosum connects (Fig. 33.1). This combination of vessels produces a vascular ring. The true incidence of this lesion is more difficult to obtain than that of mirror-image right arch where virtually all patients have associated intracardiac disease. However, of 26 consecutive patients undergoing surgical division of vascular rings at

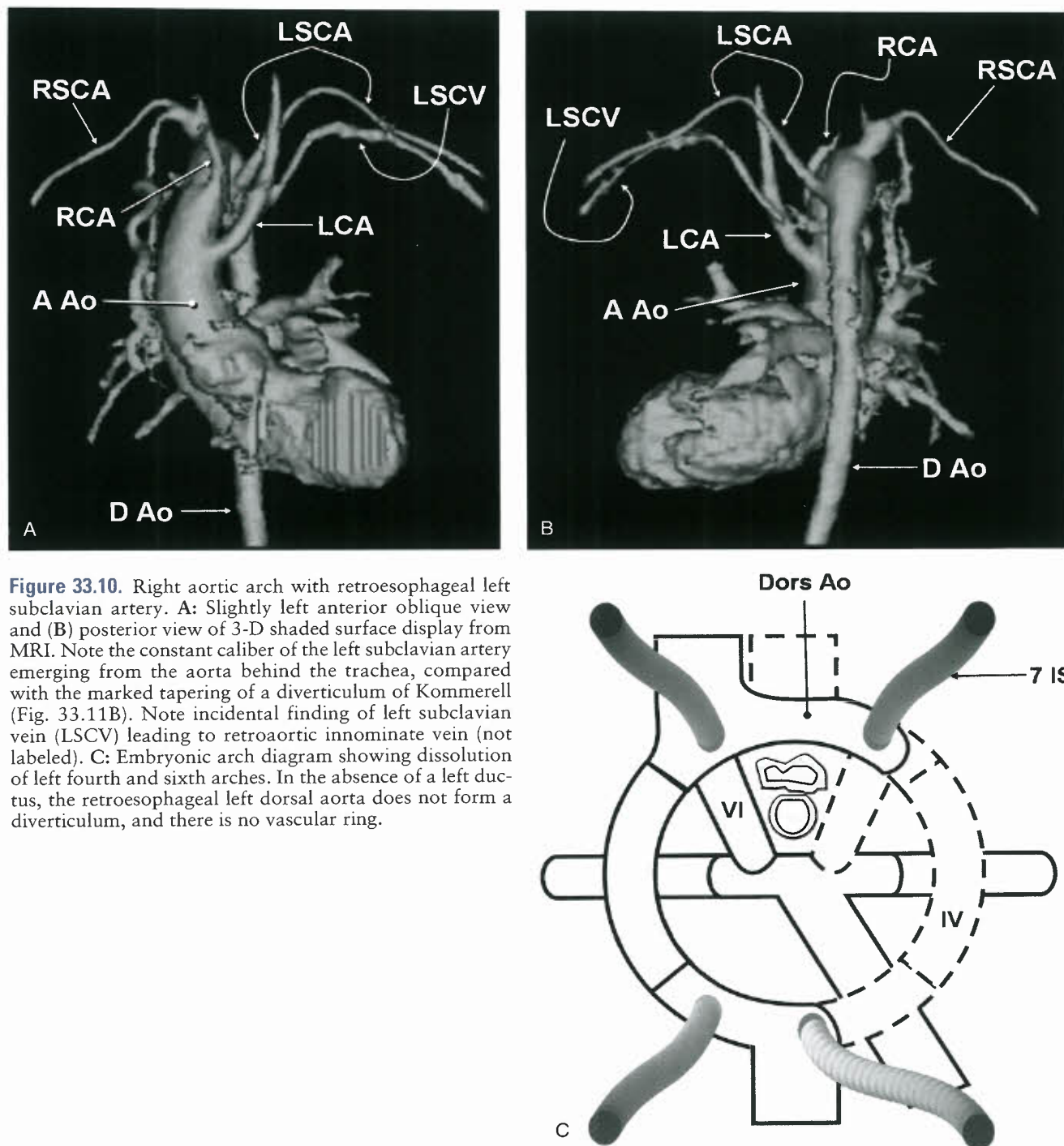


Figure 33.10. Right aortic arch with retroesophageal left subclavian artery. A: Slightly left anterior oblique view and (B) posterior view of 3-D shaded surface display from MRI. Note the constant caliber of the left subclavian artery emerging from the aorta behind the trachea, compared with the marked tapering of a diverticulum of Kommerell (Fig. 33.11B). Note incidental finding of left subclavian vein (LSCV) leading to retroaortic innominate vein (not labeled). C: Embryonic arch diagram showing dissolution of left fourth and sixth arches. In the absence of a left ductus, the retroesophageal left dorsal aorta does not form a diverticulum, and there is no vascular ring.

our institution, five (19%) had right arch, retroesophageal diverticulum, and most of them had no other heart defect. What is more, many people with this arch anomaly are asymptomatic and therefore go unrecognized except for incidental discovery.

If the ductus arteriosus is patent, it is easy to understand how one might visualize the complete ring formed by the aortic arch on the right, retroesophageal vessel supplying the left subclavian posteriorly, the ductus on the left, and the pulmonary artery anteriorly. However, if the ductus is closed, it is not intuitive that one could distinguish this from the more benign right arch with retroesophageal subclavian artery (non-ring) discussed above. The difference is the diverticulum of

Kommerell, which is a much larger vessel than the subclavian artery itself. Typically, the origin of the diverticulum is equal in diameter to the descending aorta and tapers to the subclavian artery caliber at the site of juncture with the left ligamentum after passing behind the trachea and esophagus.

Congenital absence of the left carotid artery is a rare association with right arch, diverticulum of Kommerell (61). Its importance lies in the fact that it is one of three exceptions to the general rule that the first arch vessel contains a carotid artery *opposite* to the side of the arch. Furthermore, if resection of the diverticulum is contemplated, the subclavian must be connected to the ascending aorta or to the right carotid.

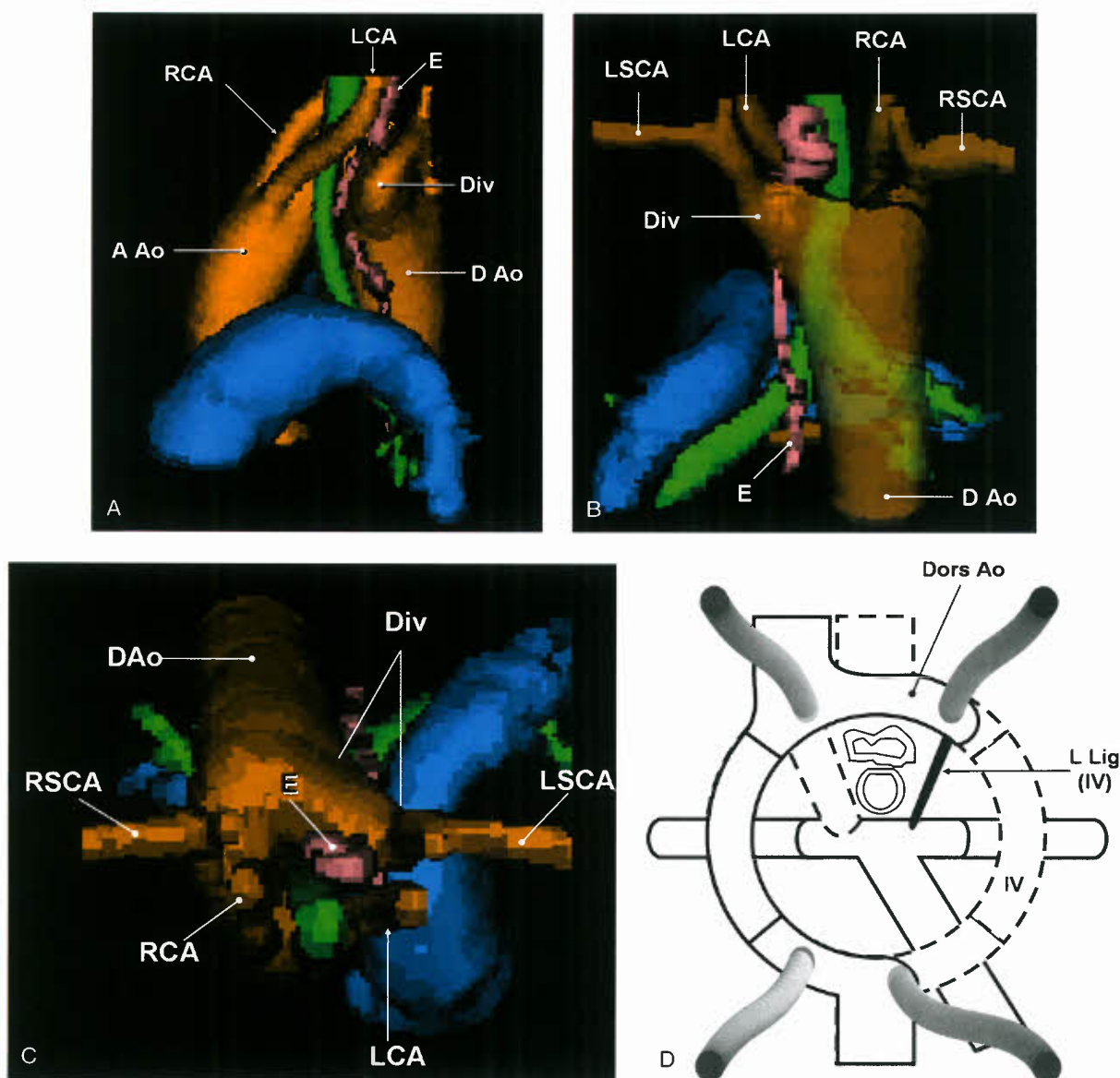


Figure 33.11. Right aortic arch, retroesophageal diverticulum of Kommerell. **A:** Left anterior oblique view of 3-D shaded surface display from MRI. Trachea (green) and esophagus (E) are compressed by diverticulum (Div) tethered by ligamentum arteriosum (not visualized) to pulmonary artery (blue). **B:** Posterior view shows tapered Div behind esophagus giving rise to LSCA. The tracheal deviation to the left is seen through the translucent D Ao. Compare with Figure 33.9A. **C:** Cranial view shows trachea (green) and esophagus (E) compressed between Div and LCA and pulmonary artery (blue). **D:** Embryonic arch diagram showing dissolution of left fourth arch and formation of retroesophageal diverticulum from left dorsal aorta in the presence of a left sixth arch—left ligamentum (L Lig [IV]).

Embryology

Disappearance of the left fourth embryonic arch with persistence of the left sixth (ductal) arch between the truncal aortic sac (pulmonary artery precursor) and left dorsal aorta accounts for the findings in this arch anomaly (Fig. 33.11D). Note that the left dorsal aorta is not merely the proximal left subclavian artery but is also the continuation of the left sixth aortic arch leading to the fused dorsal aortae. Since the normal fetal ductus carries nearly the entire output of the right ventricle, the left dorsal aorta would also carry that amount and would become significantly larger than the subclavian artery. This size discrepancy persists after ductal closure, giving the diverticulum its characteristic appearance. In the rare variant with absence of the left carotid, there is absence of both the

left fourth embryonic arch and the truncal aortic sac connection to the left third.

Diagnosis and Management

The presentation in symptomatic patients is usually that of a vascular ring. With that history, the appearance of a right aortic arch on a plain chest roentgenogram should raise the question of this anomaly and prompt further, more specific evaluation. Barium esophagram reveals a large posterior indentation on the esophagus similar to that seen in Figure 33.11E, F (in contrast to the smaller defect seen with simple retroesophageal subclavian artery [Fig. 33.3E]). However, rare vascular rings such as left aortic arch with right descending aorta and right ligamentum can give similar findings on barium study, and since the

surgical approach is different, this form of imaging should not be considered definitive. While the ligamentum arteriosum is not visualized with any of the current imaging modalities, its presence is guaranteed by the characteristic appearance of the abruptly tapered diverticulum. Echocardiography will show the left carotid artery arising alone as the first arch vessel, but definitive diagnosis requires that the diverticulum be followed out to the point at which the caliber changes to that of the smaller subclavian artery. This is usually not possible since the trachea itself and nearby lung may thwart attempts to see this area. Angiography demonstrates the characteristic branching pattern but more importantly shows the abrupt change in caliber from diverticulum to subclavian artery. As mentioned previously under left aortic arch with retroesophageal right subclavian artery, angiography in the straight AP view may produce superimposition of the posterior subclavian artery on the more anterior left carotid giving the appearance of a left innominate artery as in mirror-image right aortic arch and therefore not a ring. However, careful single-frame viewing of cineangiography will confirm the separate origins. Contrast injection in the more distal portion of the arch will better delineate the plump aortic diverticulum giving rise to the noticeably smaller subclavian artery. Angiography while definitive, showing both the characteristic branching pattern and the typical appearance of the aortic diverticulum requires arterial catheterization, less desirable in the young infant. MRI is ideal for making this diagnosis, being noninvasive and having the ability to display both vascular and airway structures. Axial or transverse imaging demonstrates the aortic arch to the right of the trachea and the diverticulum posterior to it. Coronal imaging shows the V-shaped juncture of the aortic diverticulum and the more right-sided descending aorta. However, computer-generated shaded surface displays (3-D representations) permit viewing of the entire aortic arch at once and in relationship to trachea and pulmonary artery (Fig. 33.11A–C) and give the surgeon a clear anatomical image with which to proceed.

The majority of people with this arch anomaly are asymptomatic. Treatment is surgical division of the ductus or ligamentum in those patients who are symptomatic. This is usually performed through a left thoracotomy. Video-assisted thoracoscopic surgery, or VATS, has been shown to be effective and comparable in procedure time and length of stay to open thoracotomy (62). Some surgeons prefer a median sternotomy approach, particularly if an intracardiac defect will also be addressed in the same operation. Some surgeons advocate not only division of the ligamentum but also resection of the diverticulum and transfer of the left subclavian artery to the left carotid artery because of the recurrence of symptoms in some patients due to compression from an aneurysmal diverticulum and traction by the subclavian artery (63). In adult cases where the diverticulum has become aneurysmal, there is a significant risk of dissection or rupture (64,65); the usual treatment is resection. A novel hybrid approach in which both subclavian arteries are connected by grafts to their respective carotid arteries by minimally invasive surgery followed by covered stent placement in the aortic arch to exclude the aneurysmal diverticulum has also been employed (66).

In those patients undergoing surgery for another lesion such as an intracardiac abnormality or repair of tracheoesophageal fistula, even an “asymptomatic” ligamentum should be divided. With esophageal atresia, a symptomatic ring may be avoided when repairing the esophagus outside the ring.

Right Aortic Arch with Left Descending Aorta and Left Ductus (Ligamentum) Arteriosus(um)

Right arch, left descending aorta, also known as right aortic arch with retroesophageal segment or circumflex right aortic

arch, is similar in presentation to right arch with retroesophageal diverticulum (above), but it is less common. Unlike cases with retroesophageal diverticulum in which the aorta after passing over the right mainstem bronchus descends for some distance on the right, then gradually crosses to the left before reaching the level of the diaphragm, right arch left descending (aorta) has the aortic arch itself cross the midline to the left at the level of the T4 or T5 vertebral body at which point it gives rise to the left ductus (ligamentum) arteriosus(um). Another difference is that some of these cases have a mirror-image branching pattern—left innominate, right carotid, right subclavian (Fig. 33.1)—and can therefore be erroneously misdiagnosed as a nonring, while others have left carotid, right carotid, right subclavian, and finally the left subclavian (Fig. 33.1). Yet another pattern has an aberrant left innominate artery—right carotid, right subclavian, left innominate as the last vessel (67), sometimes with coarctation of the right arch (68). However, in all of these it is the aortic arch that is retroesophageal, not the subclavian artery, innominate artery, or an aortic diverticulum.

Embryology

Two forms exist with dissolution of either the left dorsal aorta distal to the takeoff of the left subclavian artery (Fig. 33.12G) or the left fourth arch (Fig. 33.13E). The distal portion of the definitive arch is comprised of the retroesophageal right-sided dorsal aorta. The persistent left sixth arch connects to the left-sided dorsal aorta completing a vascular ring.

Diagnosis and Management

The findings on chest roentgenogram and barium esophagography (Fig. 33.12E) may be similar to those findings in right arch with retroesophageal diverticulum. Differences include a downward to the left instead of upward to the left orientation of the esophageal indentation (Fig. 33.12F). Furthermore, in some cases the descending aorta itself can be seen on the left of the spine instead of the right, but this is not a consistent finding. When associated with a hypoplastic arch (69), this anomaly can be mistaken for interrupted aortic arch (70).

With a projection image such as angiography it may not be clear whether the aorta passes anterior to the trachea as it courses from right ascending to left descending, as is seen with a normal left aortic arch, or posterior to the trachea, that is, a right aortic arch with left descending. A clue to which is the case (without attempting steep cranial angulation—usually more confusing than helpful because of overlapping shoulder, head, liver) is the order of brachiocephalic artery branching. In the case of right aortic arch with left descending aorta the first vessel contains the left carotid artery, whereas in normal left arches, a vessel containing a right carotid is first. MRI can avoid some of the pitfalls seen with projection images and can delineate the entire aorta, not only in its normal rightward ascending and leftward descending segments, but definitively in its relationship to the trachea (Fig. 33.12A,B).

Division of the vascular ring is indicated when patients are symptomatic, although these are typically loose rings. However, an adult with dysphagia may require more than simple division of the ligamentum. Actual division of the aortic arch with mobilization of the retroesophageal portion and reanastomosis of ascending and descending aorta using a tube graft may be necessary to relieve the esophageal compression (71,72). Alternatively, resection of the retroesophageal portion, advancement of the aortic arch, and direct end-to-side anastomosis of the descending aorta to the ascending to the left of the trachea has also been used (73,74).

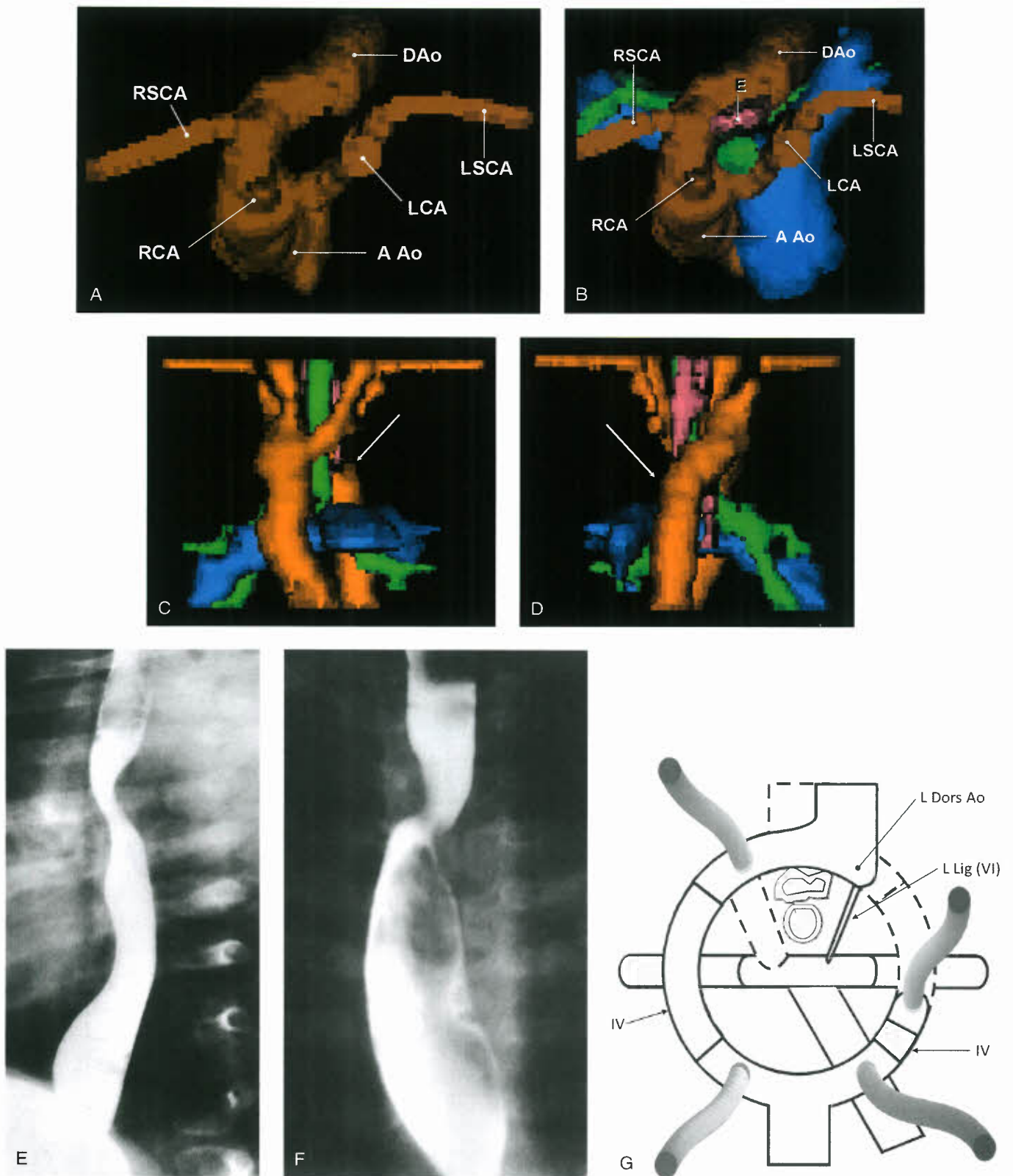


Figure 33.12. Right aortic arch, left descending aorta, left innominate artery. **A:** Cranial view of 3-D shaded surface display from MRI showing takeoff of brachiocephalic arteries: left innominate artery giving rise to LCA and LSCA, RCA, and RSCA. **B:** Same view as (A) but with trachea (green), esophagus (blue), and pulmonary artery (red) showing further crowding. Anterior (C) and posterior (D) of same reconstruction showing retroesophageal course of circumflex aortic arch with sharp turn inferiorly at point of attachment of ligamentum arteriosum (arrow) to descending aorta. Barium esophagram in lateral view (E) showing large posterior indentation, and AP view (F) showing bilateral indentations on the esophagus. Similar patterns are seen with double arch and right arch with diverticulum. **G:** Embryonic arch pattern similar to Figure 33.9D above but with left descending aorta instead of right.

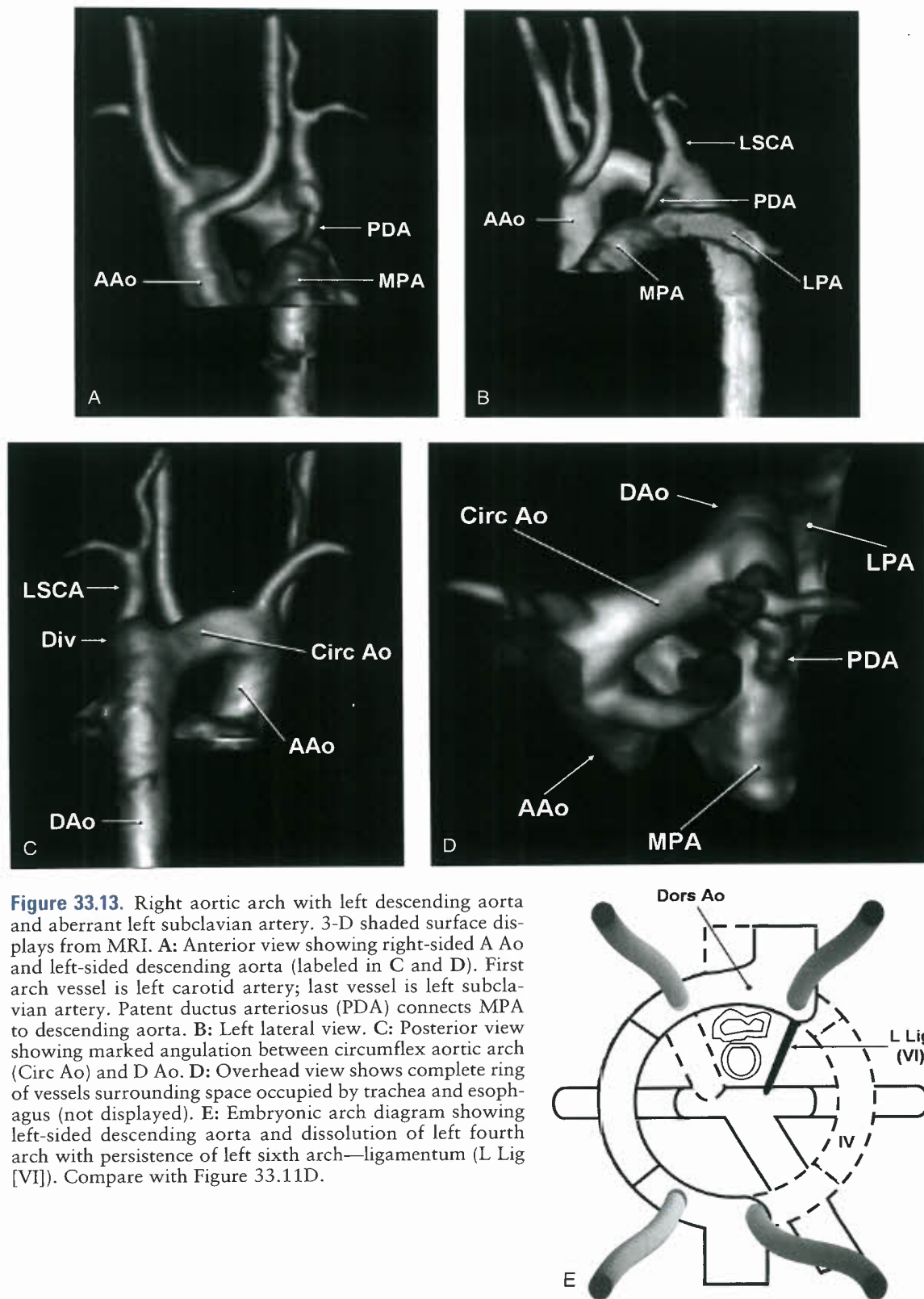


Figure 33.13. Right aortic arch with left descending aorta and aberrant left subclavian artery. 3-D shaded surface displays from MRI. **A:** Anterior view showing right-sided AAo and left-sided descending aorta (labeled in C and D). First arch vessel is left carotid artery; last vessel is left subclavian artery. Patent ductus arteriosus (PDA) connects MPA to descending aorta. **B:** Left lateral view. **C:** Posterior view showing marked angulation between circumflex aortic arch (Circ Ao) and DAo. **D:** Overhead view shows complete ring of vessels surrounding space occupied by trachea and esophagus (not displayed). **E:** Embryonic arch diagram showing left-sided descending aorta and dissolution of left fourth arch with persistence of left sixth arch—ligamentum (L Lig [VI]). Compare with Figure 33.11D.

Right Aortic Arch with Retroesophageal Innominate Artery

Right aortic arch with retroesophageal innominate artery is another rare abnormality of the aortic arch system. Contrary to the general rule that the first arch vessel contains a carotid artery contralateral to the aortic arch, in these cases the sequence of brachiocephalic vessels is right carotid, right

subclavian, retroesophageal left innominate artery (Fig. 33.1). The ductus (or ligamentum) arteriosus(um) completes a vascular ring as it connects the left pulmonary artery with the base of the so-called innominate artery.

Embryology

The apparent site of arch dissolution is between the left branch of the trunco-aortic sac and the third arch (Fig. 33.14D) with

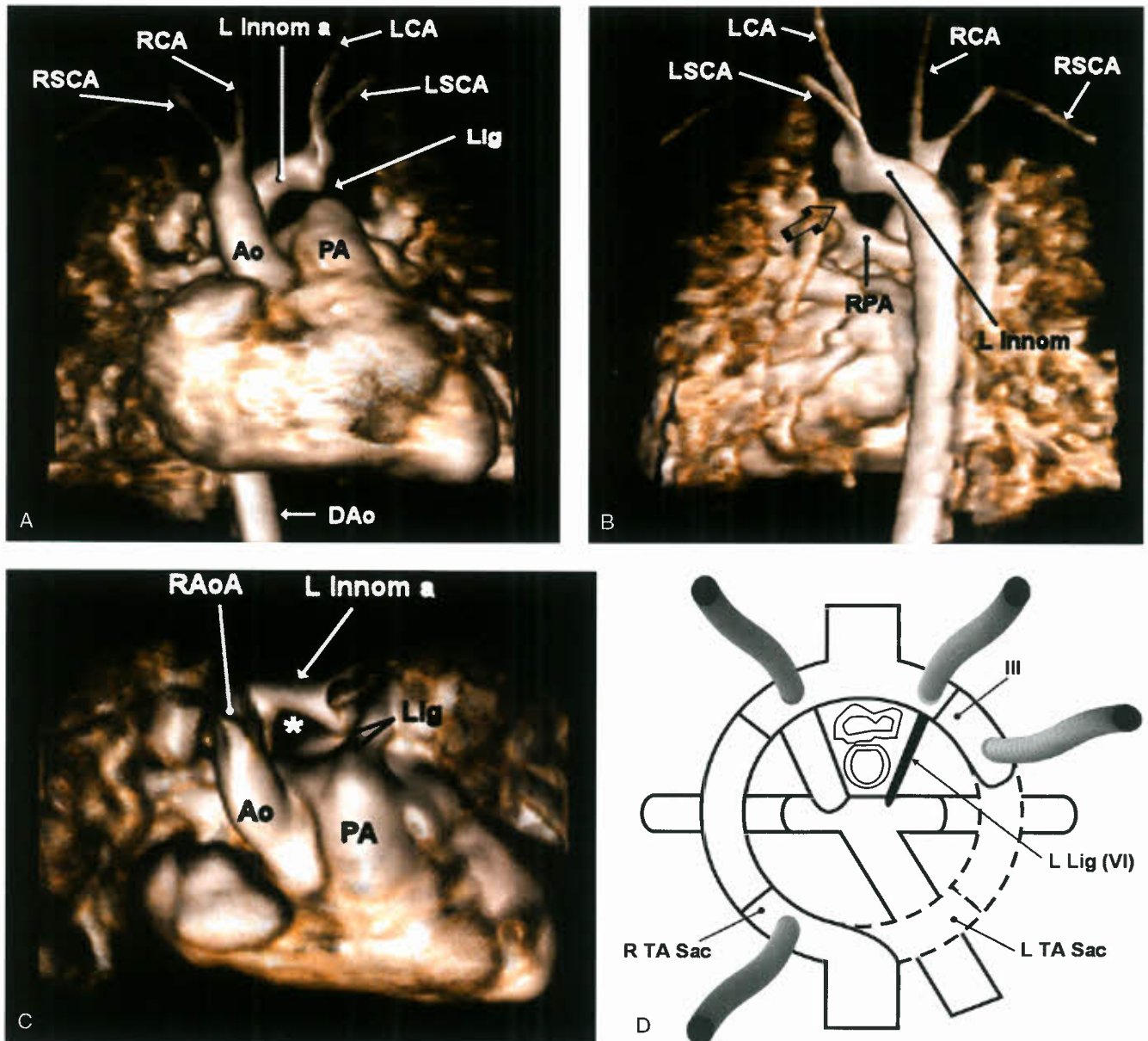


Figure 33.14. Right aortic arch with retroesophageal left innominate artery (L Innom). Shaded surface display from gadolinium-enhanced 3-D MRI dataset. **A:** Anterior view showing ascending aorta (Ao) superimposed on right aortic arch giving rise to right carotid (RCA) and right subclavian (RSCA) arteries. There is a retroesophageal diverticulum that acts as a left innominate artery (L Innom a) giving rise to left carotid (LCA) and left subclavian (LSCA) arteries. The very large caliber diverticulum is connected to the pulmonary artery (PA) by way of a left ligamentum arteriosum (Lig), which is not visualized. Dao, descending aorta. **B:** Posterior view showing same arch vessels as in (A). RPA forms anterior portion of vascular ring. Open arrow indicates left pulmonary artery end of ligamentum connecting pointed portion of left innominate artery (L Innom). **C:** Cranially angulated view showing vascular ring formed by right aortic arch (RAoA) on the right, left innominate artery (L Innom a) posteriorly, left ligamentum arteriosum (Lig) to the left, and pulmonary artery (PA) anteriorly. The location of the trachea and esophagus is indicated by asterisk. Ao, ascending aorta. **D:** Diagram of embryonic arch contributions. Dissolution of left limb of trunco-aortic sac (L TA Sac) connection to third arch (III); persistence of left third arch (instead of fourth arch) connection to left dorsal aorta. R TA Sac, right limb of trunco-aortic sac.

absence of the fourth arch. Thus the definitive aortic arch is formed by the right branch leading to the right fourth arch, which, in turn, connects to the right dorsal aorta. The left dorsal aorta supplies the left seventh intersegmental artery (distal left subclavian) and the distal connection to the left third arch (common carotid artery).

Diagnosis and Management

With so few cases in the literature (75), it is difficult to draw conclusions about presentation and management. Tracheal compression seems to be the rule, though the degree of symptomatology varies considerably. The important anatomical clues to the diagnosis by any imaging modality are the presence of a single carotid artery arising from the proximal aorta. The other anomalies with that finding are also rare: interrupted aortic arch with interruption between the two carotid arteries and isolated left carotid or innominate artery, as well as congenital absence of the carotid artery contralateral to the side of the arch (see below). The differentiating feature is the presence of a normal-sized (right) aortic arch—missing in arch interruption—and the distal origin of the carotid artery from that arch—not present with isolated carotid or innominate or in congenital absence of the contralateral carotid. If symptomatic from the vascular ring, division of the ductus or ligamentum is in order. Conceivably in the adult, detachment of the innominate artery from the distal arch and reimplantation in the ascending aorta might be necessary based on similar arch anomalies mentioned above in which the retroesophageal vessel continued to cause dysphagia even after relief of the ring by division of the ligamentum.

Right Aortic Arch with Isolation of Contralateral Arch Vessel

Isolation of brachiocephalic vessels is relatively uncommon. The term isolation means that the particular vessel arises exclusively from the pulmonary artery via the ductus arteriosus (or ligamentum) but without connection to the aorta. Three different forms have been noted: isolation of the left subclavian

artery (Fig. 33.1), isolation of the left carotid, and isolation of the left innominate artery. Isolated left subclavian is by far the most common of the three. Luetmer and Miller (76) reviewed the literature to 1990 describing 39 cases demonstrated by angiography or at postmortem examination. Congenital heart disease was found in more than half the cases with two-thirds of those having tetralogy of Fallot. There are sporadic reports of isolated left innominate artery (77). A very rare example associated with single left ventricle with L-loop ventricular arrangement and aortic atresia is shown in Figure 33.1. A forme fruste is shown in Figure 33.16A with a small innominate artery and larger subclavian and carotid, suggesting that during fetal life they had been fed by a left ductus that had since closed. A unique case of isolated subclavian artery in a patient with tetralogy of Fallot had a collateral vessel from the abdominal aorta fill the subclavian in addition to the usual retrograde flow from the vertebral artery (78).

Embryology

All cases of isolated arch vessels derive from two ipsilateral breaks in the aortic arch system (Fig. 33.15B). In isolated subclavian artery, the distal left dorsal aorta involutes after cephalad migration of the left seventh intersegmental (subclavian) artery to the level where left sixth (ductal) arch normally joins the proximal dorsal aorta. This together with involution of the left fourth arch leaves the subclavian isolated from the aortic arch but connected to the pulmonary artery via the ductus. In similar fashion one could imagine the disappearance of the left fourth arch and the left branch of the aortic sac with the sixth arch connecting the pulmonary artery portion of the trunco-aortic sac to the third arch (common carotid artery precursor). With disruption of the left fourth arch, the left seventh intersegmental artery remains connected to the descending aorta via the left dorsal aorta producing a retroesophageal left subclavian artery. It is postulated that isolated innominate artery (see Figs. 33.15B and 33.16D) derives from dissolution of the left branch of the trunco-aortic sac connection to the third arch, loss of the fourth arch, and dissolution of the connection of distal left dorsal aorta with the left sixth (ductal)

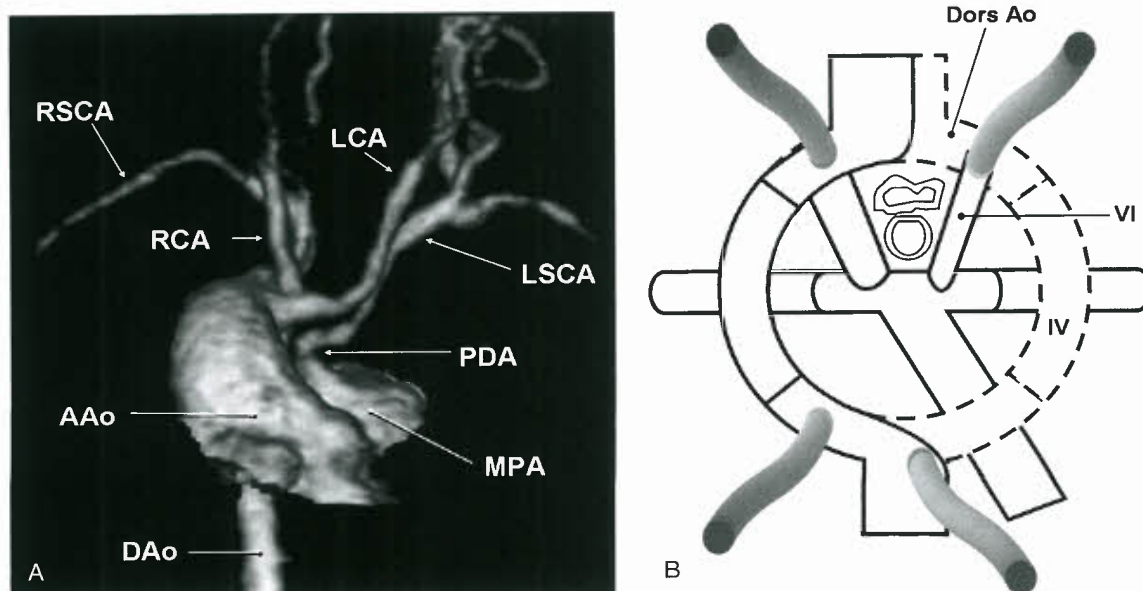


Figure 33.15. Right aortic arch with isolation of left subclavian artery. **A:** Anterior view of 3-D shaded surface display from MRI shows exclusive origin of LSCA from left PDA. Sequence of arch vessels arising from aorta is LCA, RCA, and RSCA. **B:** Embryonic arch diagram showing ipsilateral loss of left fourth arch and dorsal aorta with persistence of ipsilateral sixth arch.

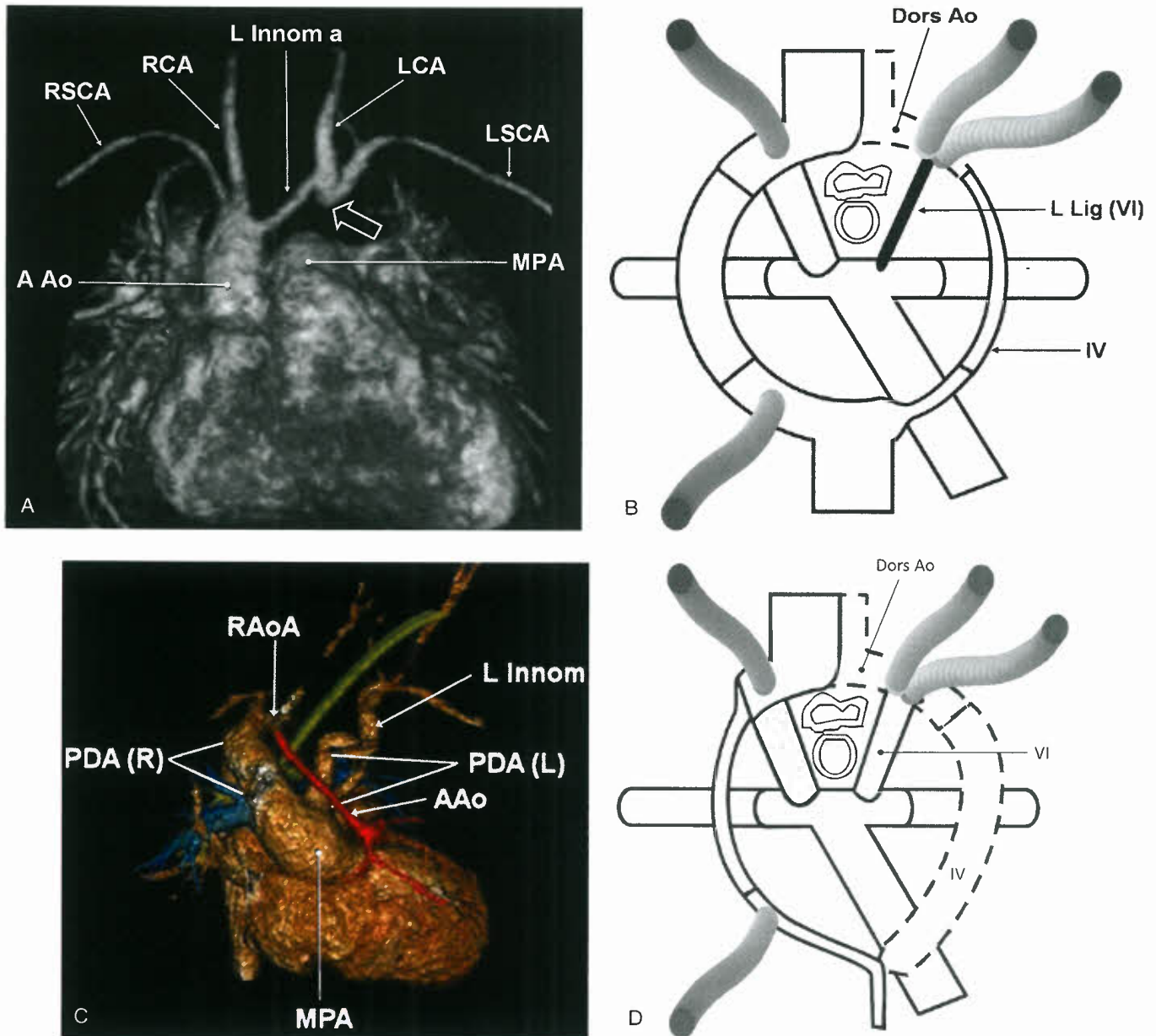


Figure 33.16. Isolated left innominate artery. **A:** *Forme fruste*. Anterior view of 3-D shaded surface display from MRI. Note small left innominate artery (L Innom a) giving rise to larger caliber LSCA and LCA. These latter two appear to arise from a point consistent with a ligamentum arteriosum (*open arrow*) and apparently received more flow from that vessel than from the aorta during fetal development. **B:** Embryonic arch diagram showing hypoplasia of left limb of truncus aortic sac and left fourth arch with dissolution of connections to left Dors Ao and persistence of left sixth arch. **C:** Completely isolated left innominate artery (L Innom). Slightly left anterior oblique and slightly cranially angulated view of shaded surface display from CT scan of infant with single left ventricle and diminutive right ventricular outflow chamber with L-transposition of the great arteries and aortic atresia. The L Innom is fed by the left patent ductus arteriosus (PDA[L]) and possibly retrograde from circle of Willis via left vertebral and carotid arteries. There is a right aortic arch (RAoA) and markedly hypoplastic ascending aorta (AAo) fed exclusively from the main pulmonary artery (MPA) via the right patent ductus (PDA[R]). Branch pulmonary arteries shown in *blue*, trachea in *green*, ascending aorta and coronary arteries in *red*. **D:** Embryonic arch diagram showing dissolution of left limb of truncus aortic sac and left fourth arch with dissolution of connections to left Dors Ao and persistence of left sixth arch supplying left carotid (distal third arch) and left subclavian (left seventh intersegmental artery).

arch. Thus the pulmonary portion of the truncus aortic sac feeds the left seventh intersegmental (subclavian) artery via the sixth and the carotid artery in turn via the distal left third arch similar to retroesophageal innominate artery described above. The resulting confluence of carotid and subclavian arteries is

analogous to an innominate artery. An alternative mechanism based on identification of a pulmonary-to-brachiocephalic artery connection proximal to or upstream from the ductus in chick embryos is explained by an abnormal partition of the truncus aortic sac (79).

Diagnosis and Management

Cases of isolated brachiocephalic arteries may have diminished pulses or lower blood pressure in the affected artery. When the subclavian and vertebral arteries are involved, the possibility of subclavian steal syndrome exists in which blood flows down the vertebral artery into the subclavian, particularly when the arm is exercised. In 13% of cases reviewed by Luetmer and Miller (76), this produced cerebral insufficiency. Another 13% showed signs of left arm ischemia. If the ductus remains patent, pulmonary artery steal can occur with flow down the vertebral artery through the ductus into the low-resistance pulmonary artery (80). One case of underdevelopment of the left arm with isolated subclavian artery showed catch-up growth after reimplantation in the left carotid. Another case with left hemisphere atrophy associated with global developmental delay and bulbar dysfunction in the face of isolated left innominate artery with a patent ductus and retrograde left carotid flow was found (77). The diagnosis should be suspected in any patient with right aortic arch and diminished pulse amplitude or blood pressure in the left arm, although coarctation of a right arch with aberrant left subclavian artery could also produce these findings. Contrast injection in the aortic arch shows delayed filling of the subclavian artery via the vertebral and various collateral arteries (81). Barium esophagography is not helpful in making this diagnosis other than demonstration of the right aortic arch. Doppler echocardiography may be able to demonstrate the reversal of flow in the vertebral artery that would corroborate this diagnosis, but phase-encoded velocity mapping on MRI can also be definitive.

Surgical management in children consists of repair of the accompanying heart disease and ligation of the ductus, if patent, to prevent pulmonary steal. Patients with central nervous system symptoms or claudication of the left arm should have surgical reimplantation of the subclavian artery into the carotid or aorta. Some have advocated this approach in asymptomatic cases to avoid subclavian steal later in life (82).

CERVICAL AORTIC ARCH

Cervical aortic arch is a rare anomaly in which the arch is found above the level of the clavicle (as high as the C2 vertebral body). There are two main subcategories of cervical arch: those with anomalous subclavian artery and vascular ring, with either descending aorta contralateral to the arch (see Fig. 33.5) or retroesophageal diverticulum and those with a virtual normal branching pattern. The first and larger group usually has a right aortic arch. This group is further subdivided into those with separate origins of the internal and external carotid arteries from the arch and those with a common carotid artery or a bicarotid trunk in which both common carotid arteries arise from a single vessel and the subclavian arteries both arise separately from the distal arch (83). Separate origin of the vertebral artery from the arch can be seen in each of the groups. While most of the patients with contralateral descending aorta have an anatomical vascular ring from the aortic arch on the right, retroesophageal segment of aorta posteriorly, ligamentum arteriosum to the left, and pulmonary artery anteriorly, only about half are symptomatic from the ring. When a bicarotid trunk accompanies the contralateral descending aorta form of cervical arch, tracheal or esophageal compression between the "V" of the bicarotid trunk and the retroesophageal aorta may occur without a complete vascular ring.

The second group (with ipsilateral descending aorta—nonring) typically has a left aortic arch. Aortic arch obstruction due to a long, tortuous, hypoplastic retroesophageal segment is an uncommon but well-documented association (84). More discrete

coarctations have been reported in both the ring and nonring groups (85). For reasons that are not clear, stenosis or atresia of the origin of the left subclavian artery is sometimes seen in either group (86).

Embryology

It would appear that the embryologic explanations for the various subgroups mentioned above are different. The normal common carotid artery comes about from the dissolution of the segment of dorsal aorta between the third and fourth embryonic arches, the so-called ductus caroticus. Both internal and external carotid arteries arise from the third arch. If the ductus caroticus were to persist while the embryonic fourth arch involutes, the embryonic third arch would become the definitive arch with separate internal and external carotid arteries arising from it (as they had when the third arch was, in part, the common carotid artery) (87). The third arch being one branchial pouch higher than the fourth arch would be expected to be more cephalad after completion of arch development. This type of cervical arch (i.e., with separate internal and external carotid arteries arising directly from the arch) due to persistent ductus caroticus and absent fourth arch has been described in chromosome 22q11 deletion as previously mentioned (88).

An alternative explanation for this subgroup and more plausible for the other groups that have normal common carotid arteries is a failure of the normal descent of the aortic arch system from its cephalic location at 3 weeks to its normal intrathoracic location by 7 weeks' gestation (89). The etiology of this failure of caudal migration is not known.

Diagnosis and Management

Cervical arches may present as pulsatile masses in the supraclavicular fossa or in the neck. In infants, prior to the appearance of a mass, the presenting signs may be those of a vascular ring, namely, stridor, dyspnea, or repeated lower respiratory infections. In the adult, the most likely symptom from a vascular ring is dysphagia. In those patients with stenosis or atresia of the left subclavian artery and origin of the ipsilateral vertebral artery distal to the obstruction, a subclavian steal may exist with central nervous system symptomatology. In the presence of a pulsatile neck mass, a presumptive diagnosis can be made by notation of loss of femoral pulses during brief compression of the mass (86).

The diagnosis of cervical arch may be suspected on plain chest roentgenogram by the presence of a widened upper mediastinum and the absence of the aortic knob. Evidence of anterior deviation of the trachea is in favor of the diagnosis. In the past, angiography has been the standard diagnostic imaging tool, and in those cases with intracardiac anomalies, probably remains so. However, in those without congenital heart disease, the diagnosis of cervical aortic arch can be made by echocardiography. Treatment is necessary if the cervical arch is complicated by arch hypoplasia, symptomatic vascular ring, or rarely aneurysm of the cervical arch itself (90). In these cases, the surgical approach is dictated by the specific complicating feature. In some cases with cervical right aortic arch and a tortuous, hypoplastic retroesophageal segment, repair is accomplished by left-sided ascending-to-descending aorta anastomosis or tube graft interposition (91). Separate origin of external and internal carotid arteries from the arch warrants screening for 22q11 deletion.

DOUBLE AORTIC ARCH

Double aortic arch, as the name implies, is an anomaly in which both right and left aortic arches are present. Several

variations on this basic theme occur: both arches of similar size (Fig. 33.1), hypoplasia of one arch (Fig. 33.16) (usually the left), and atresia of one arch (Fig. 33.1) (usually the left). In addition, a ductus arteriosus or ligamentum may be present. Typically, the right arch is the more superiorly located.

While all double aortic arches technically form complete vascular rings around the trachea and esophagus, the branching pattern evident from various imaging modalities is determined by the patency of the various arch components and the side of the descending aorta. For example, while a double arch with both arches patent will show relatively symmetrical origins of each of the four major brachiocephalic arteries from their respective arches (Fig. 33.17K,L), double arch with atretic left arch distal to the origin of the left subclavian artery (Fig. 33.18) will have a branching pattern similar to a mirror-image right aortic arch, that is, an apparent left innominate artery,

followed by a right carotid and right subclavian, but with a left descending aorta. In fact, this pattern in conjunction with signs of tracheal compression, may be indistinguishable (except at surgery) from the rare anomaly right aortic arch with left descending aorta, unless, as in Figure 33.18A, a distal left arch stump is present. Similarly, double arch with atretic left arch between left carotid and left subclavian can mimic right aortic arch with retroesophageal diverticulum of Kommerell. Atretic right arch is quite rare (92) but can simulate left arch variants. Of 17 patients at one institution undergoing division of the vascular ring, 11 had a left descending aorta, six, a right (93). A review of 26 patients undergoing surgical division of vascular rings over an 8-year period at The Children's Hospital of Philadelphia showed 20 to have double aortic arches. Seventeen had both arches patent with the right arch larger in 16. The other three patients had an atretic left arch.

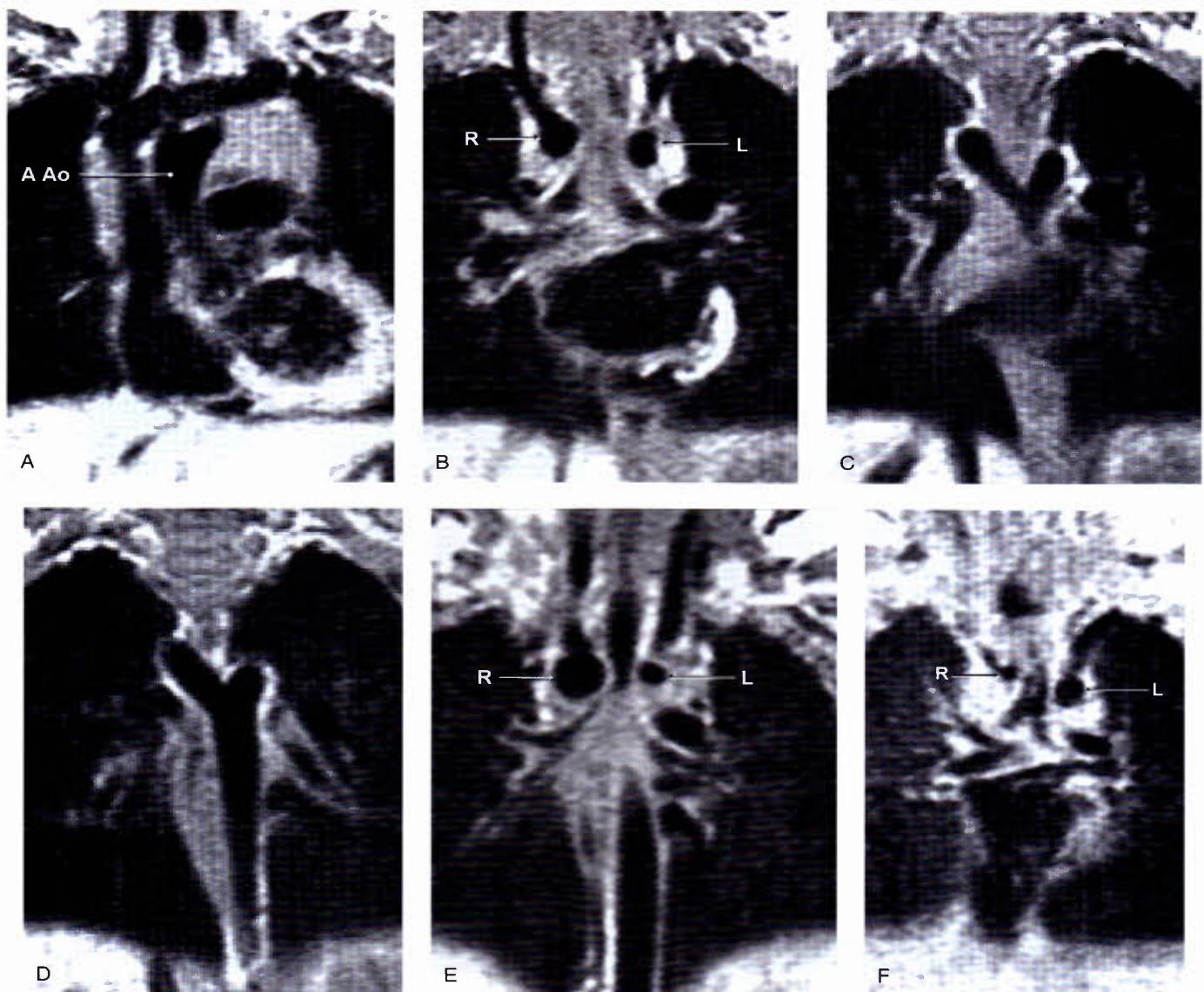


Figure 33-17 Double aortic arch, both patent. A–D: Spin echo MRI (coronal cuts, anterior to posterior) showing ascending aorta (A Ao) dividing into equal-sized right (R) and left (L) aortic arches reuniting posteriorly as the descending aorta. Coronal images of patients having double arch with (E) dominant right and (F) rare case of dominant left.

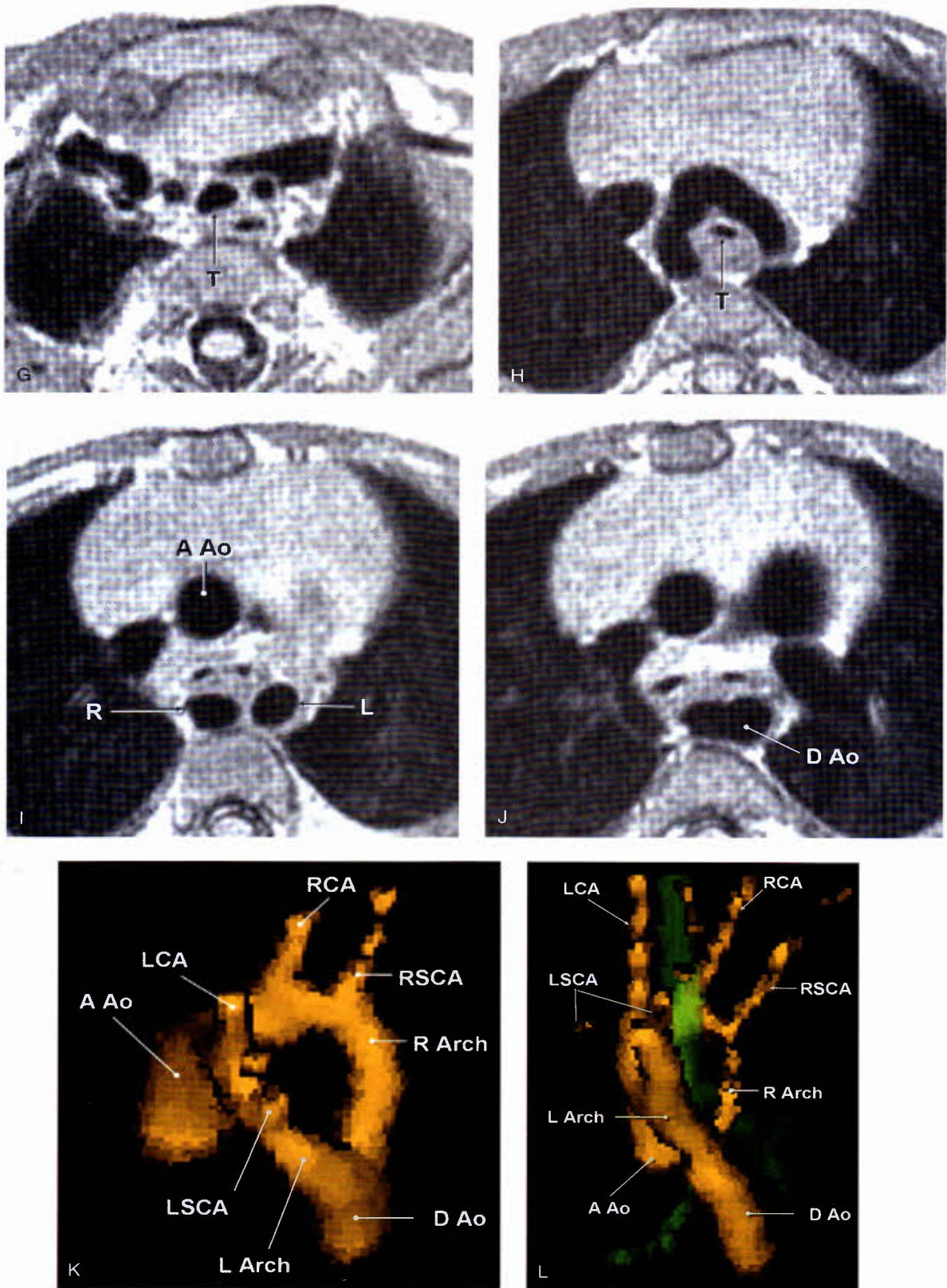


Figure 33-17 (Continued) G–J: transverse cuts, cranial to caudal, from same patient as (A–D). Note marked decrease in caliber of trachea (T) from (G–H), indicative of tracheal compression. K: Left posterior oblique with cranial angulation view of 3-D shaded surface display from MRI in same patient as (A–D) and (G–J). Note double aortic arch with nearly equal-sized right (R arch) and left (L arch) distal aortic arch components. L: Similar view of patient with rare dominant left arch.

Double aortic arch is rarely associated with congenital heart disease, but when present, tetralogy of Fallot is most common (94), with transposition of the great arteries a distant second (94,95), and a single reported case of congenitally corrected transposition (96). Infrequent associated arch abnormalities including coarctation of the left (97) or both arches (98) and cervical left aortic arch (99) have been noted.

Embryology

Double aortic arch represents a persistence of both right and left embryonic fourth branchial arches joining the aortic portion of the trunco-aortic sac to their respective dorsal aortae, both of which persist as well. Thus double aortic arch with both arches patent appears as persistence of the entire hypothetical double arch (Fig. 33.1) though usually with only one sixth (ductal) arch, whereas double arch with atretic left arch has patterns similar to either right arch with retroesophageal diverticulum or right arch, left descending aorta (compare Fig. 33.18B with Fig. 33.13E or Fig. 33.18C with Fig. 33.12G).

In keeping with the theme of absent or atretic fourth arches in 22q11 deletions, double arch with atretic left arch is more commonly associated with those syndromes than double arch with both widely patent.

Diagnosis and Management

The clinical manifestations of double aortic arches, as with the other vascular rings, are related to the tightness of the ring. With both arches widely patent, the rings are typically tight, and patients present with stridor in the first weeks of life, whereas with double arch and atretic left arch, the rings are usually looser, with presentations at 3 to 6 months of age or later. Rarely, double aortic arches present in adulthood with swallowing or respiratory symptoms (100). Even rarer is the case of an 85-year-old woman with an asymptomatic double aortic arch—both patent—who presented with back pain from an aortic dissection of an aneurysmal left arch (101). At the other extreme of age is a 22-week fetus with echocardiographic findings of congenital high airway obstruction

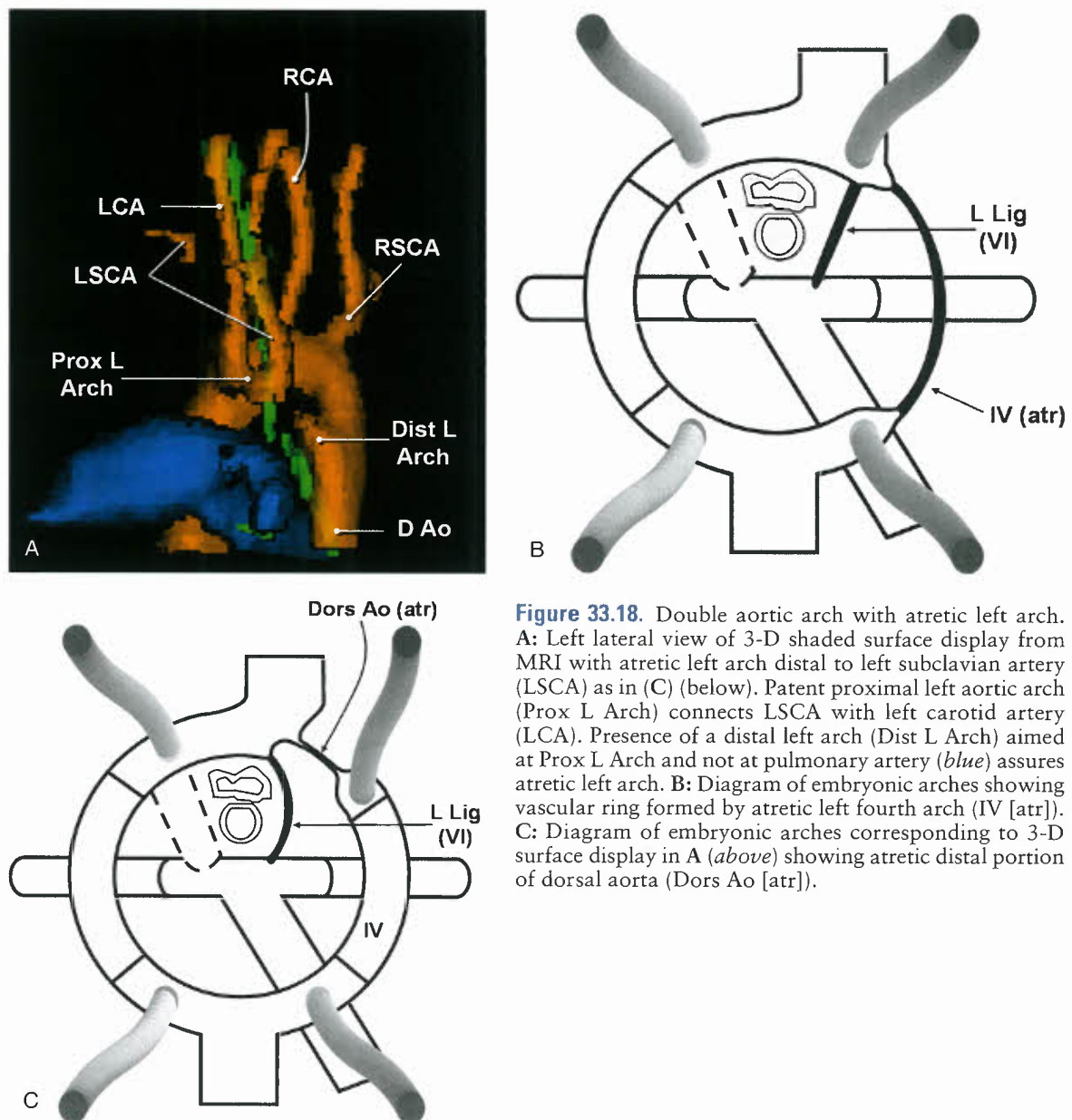


Figure 33.18. Double aortic arch with atretic left arch. A: Left lateral view of 3-D shaded surface display from MRI with atretic left arch distal to left subclavian artery (LSCA) as in (C) (below). Patent proximal left aortic arch (Prox L Arch) connects LSCA with left carotid artery (LCA). Presence of a distal left arch (Dist L Arch) aimed at Prox L Arch and not at pulmonary artery (blue) assures atretic left arch. B: Diagram of embryonic arches showing vascular ring formed by atretic left fourth arch (IV [atr]). C: Diagram of embryonic arches corresponding to 3-D surface display in A (above) showing atretic distal portion of dorsal aorta (Dors Ao [atr]).

syndrome with fetal ascites and enlarged echogenic lungs subsequently found by fetal echocardiography to be due to a right dominant double aortic arch (102).

The diagnosis of double arch with both arches patent can sometimes be made convincingly from the plain chest roentgenogram. The tracheal air column is indented by the more superior, right-sided arch and the more inferior left arch. In the lateral view, the right arch can be seen to indent the trachea posteriorly. These findings may be more obvious with barium esophagography. However, confirmation by echocardiography, angiography, or MRI is desirable because the two arches may be unequal in caliber and it is important to identify the hypoplastic segment in order to divide it. In addition, a web-like coarctation of one arch may not be detectable by the surgeon from the external appearance of the vessel (103). Suprasternal imaging (104) permits the most extensive echocardiographic visualization of the two arches; whereas subcostal (105) and high parasternal imaging (106) rely more on deductive interpretation. While statistically the left arch is much more likely to be hypoplastic than the right, numerous exceptions to that rule necessitate detailed evaluation of each case. MRI provides information both noninvasively and together with the important spatial relationships of the vessels, trachea, and esophagus to better permit surgical planning (107). Furthermore, when both arches are widely patent, velocity mapping permits quantification of flow in the two distal arches to determine which arch should be divided.

Surgical division of the vascular ring is indicated in any patient who is symptomatic with airway or esophageal compression or in a patient undergoing surgery for intracardiac disease. The ring should be divided in its smaller limb, usually but not always the left. The decision to divide between left carotid and left subclavian or distal to the left subclavian is usually determined by accessibility and the length of the particular segment. In the absence of an accompanying conotruncal anomaly with a large VSD, a ductus arteriosus must have been present prenatally. While the presence of a ductus or ligamentum does not appear to contribute to the

severity of tracheal compression by the vascular ring, its importance lies in the surgical management. If the arch is divided but the ligamentum remains intact, there may still be a vascular ring. Thus the surgeon must dissect down to the level of the trachea to be sure that all vascular contributors to a ring have been divided.

PERSISTENT FIFTH AORTIC ARCH

Persistent fifth aortic arch was first reported in man by Van Praagh and Van Praagh (108) in 1969 as a double-lumen aortic arch in which both arches appear on the same side of the trachea, as opposed to double aortic arch in which the two are on opposite sides of the trachea. Since the initial report at least one other variation has been noted resulting in the following subcategorization of this rare anomaly: 1) double-lumen aortic arch with both lumina patent (Figs. 33.1C and 33.2) atresia or interruption of the superior arch with patent inferior (persistent fifth) arch—common origin of all brachiocephalic vessels from the ascending aorta (Fig. 33.19A). More recently, an intermediate form has been recognized with a hypoplastic but patent superior arch (109). Double-lumen aortic arch, in which a “subway” vessel occurs beneath the normal aortic (embryonic fourth) arch, appears to be the more common of the two types (110). This inferior arch extends from the innominate artery to a point opposite the takeoff of the left subclavian artery, just proximal to the ductus arteriosus or its remnant. While frequently associated with major cardiac anomalies, it can be an incidental finding without clinical significance (111,112). Cases of atresia or interruption of the superior arch, with a single arterial trunk giving rise to all four brachiocephalic arteries, have had coarctation of the aorta as the cause for presentation (110). Similarly, the intermediate type with superior arch hypoplasia also presented with coarctation of the inferior arch (109), although we have seen a case with a widely patent inferior arch.

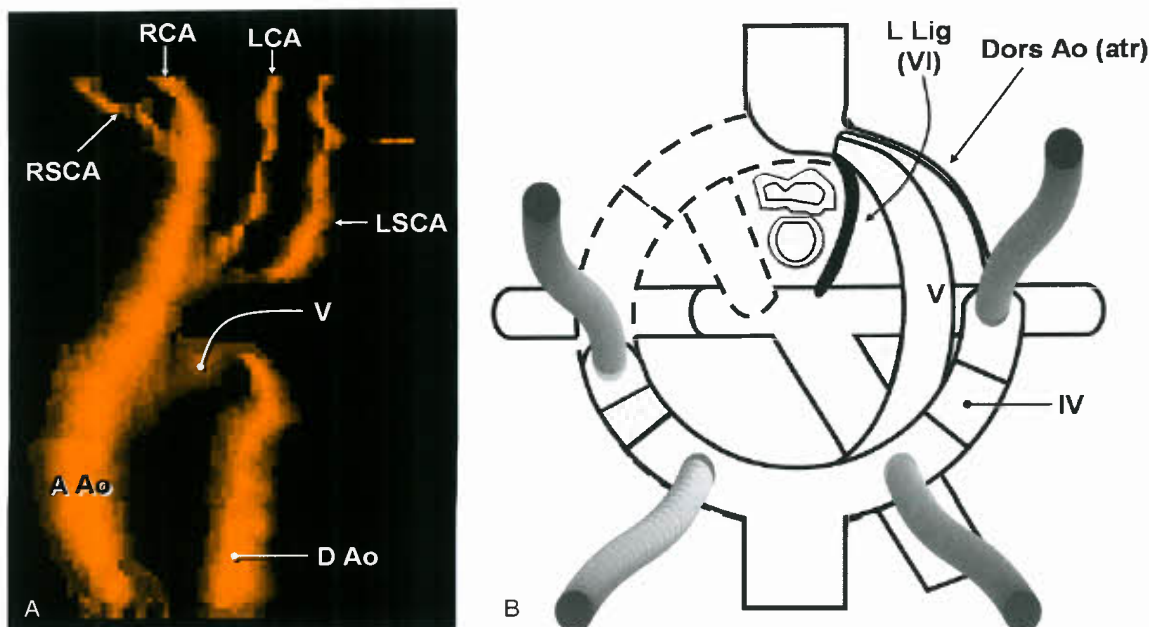


Figure 33.19. Persistent fifth aortic arch. A: Left lateral view of 3-D shaded surface display from MRI of atretic fourth arch type. Note coarctation of fifth arch distally. At surgery, an atretic strand attaching the inferior aspect of the left subclavian artery (LSCA) to descending aorta (D Ao) beyond the coarctation was found. B: Embryonic arch diagram of the case in (A).

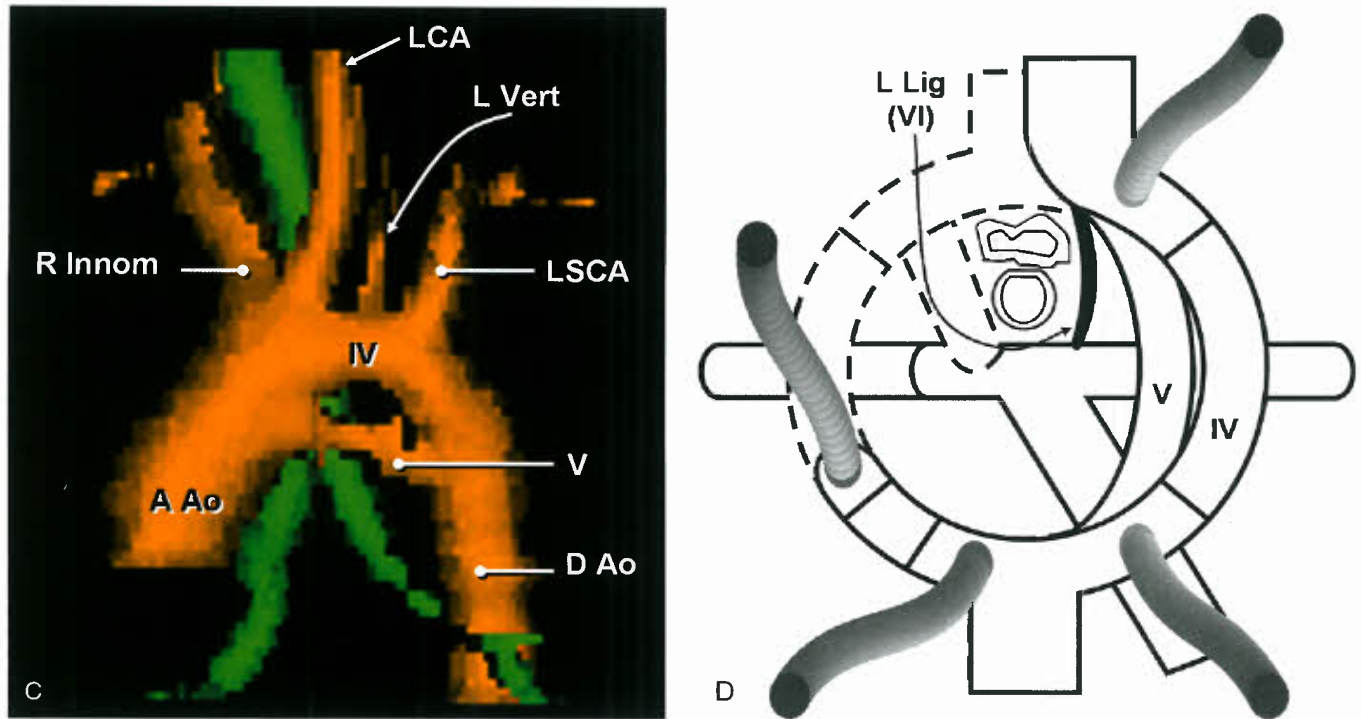


Figure 33.19. (Continued) C: Left lateral view of 3-D shaded surface display from MRI of double-lumen-type persistent fifth aortic arch. Note the trachea (T) behind both the embryonic fourth (IV) and fifth (V) arches. Incidentally, there is separate origin of the left vertebral artery (L Vert) from the normal fourth arch. D: Embryonic arch diagram of case in (C).

Embryology

While some animals have been noted to have all six pairs of branchial arches during embryonic development, the fifth pair is often seen as only incomplete arches in man (13), implying a brief appearance with no remnant in the definitive arch system. In order to understand the contribution of a persistent fifth arch to the development of the definitive arch, a modification to the hypothetical double arch is necessary (Fig. 33.19B,D). In cases of double-lumen aortic arch, the fourth arch persists as the superior arch connecting trunco-aortic sac to dorsal aorta, and the fifth (inferior) arch does the same (Fig. 33.19D). With atresia or interruption of the superior arch, the fourth arch serves as the connection between carotid and subclavian artery, similar to an innominate artery, but ipsilateral to the definitive arch, which is the fifth arch. The portion of the dorsal aorta between the entrance of the fourth and fifth arches is atretic or disappears completely (Fig. 33.19B).

Diagnosis and Management

Double-lumen aortic arch has been recognized by angiography, by echocardiography, or at postmortem examination, with the appearance of a subway vessel beneath the normal arch. This can be seen with MRI as well, in coronal or off-axis sagittal (candy cane) sections, since axial slices have to be thin enough to resolve the small gap between the two arches (112). In atresia or interruption of the superior arch, there is the appearance of a truly common brachiocephalic trunk in which all four arch vessels, including the left subclavian artery, arise from a single vessel (Fig. 33.19A). In this situation, the branching pattern alone is the indication of a persistent fifth arch since the atretic dorsal aortic extension of the fourth arch cannot be visualized. However, at surgery for repair of coarctation of

the aorta (distal to the fifth arch), an atretic strand connecting the left subclavian artery to the descending aorta may be seen. There appears to be no other plausible explanation for such a branching pattern. Without additional coarctation of the existing aorta, these two arch anomalies alone have no physiologic significance.

INTERRUPTED AORTIC ARCH

Interrupted, or congenitally absent, aortic arch is defined as a complete separation of ascending and descending aorta. It comprises several different anomalies that generally relate to the pattern of branching of the brachiocephalic arteries. There are at least nine theoretically possible branching patterns. Celoria and Patton (113) classified these as type A if the interruption were distal to the left subclavian artery, type B if between carotid and subclavian arteries, and type C if between carotid arteries. However, these types may be further subcategorized (114) and definitions generalized to include both right and left arch patterns as follows:

- A. Interruption distal to that subclavian artery that is ipsilateral to second carotid artery (i.e., if first carotid right, interruption distal to left subclavian artery)
 1. Without retroesophageal or isolated subclavian artery
 2. With retroesophageal subclavian artery
 3. With isolated subclavian artery
- B. Interruption between second carotid and ipsilateral subclavian artery.
 1. Without retroesophageal or isolated subclavian artery
 2. With retroesophageal subclavian artery (i.e., both carotid arteries proximal, both subclavians distal) (Fig. 33.1)
 3. With isolated subclavian artery

C. Interruption between carotid arteries

1. Without retroesophageal or isolated subclavian artery
2. With retroesophageal subclavian artery
3. With isolated subclavian artery

The order of brachiocephalic artery branching suggests a right or left aortic arch pattern following the conventions of noninterrupted arches: in general, the first branch of the aorta proximal to the interruption contains the carotid artery *opposite* the side of the presumptive arch; a retroesophageal or isolated subclavian artery is always *opposite* the side of the presumptive arch. The significance of sidedness of the presumptive arch in cases of interruption is the finding that interrupted “right” aortic arch is apparently seen only in association with DiGeorge syndrome (115).

Type A interruptions tend to occur with aorticopulmonary septal defect and intact ventricular septum (116); they are seen in a disproportionately large subgroup of patients with transposition of the great arteries and interrupted aortic arch (114). Type B interruptions are much more common than type A and usually have a conotruncal anomaly with normally aligned great arteries in which there is a large malalignment-type VSD associated with posterior displacement of the infundibular septum and subaortic obstruction. Those patients with DiGeorge syndrome and interruption have type B. Type C interruption is quite rare, permitting no general conclusions about associations.

Embryology

The etiology of interrupted aortic arches can be thought of in terms similar to those that describe the formation of the other arch anomalies discussed above. Type A interruptions show involution of both dorsal aortae distal to the fourth arches and proximal to the persistent sixth arch that supplies the descending aorta in place of the fourth arch (Fig. 33.20C). Type B interruptions show involution of one fourth arch and one dorsal aorta between arches four and six (Fig. 33.20D), or, in the frequent variant with both subclavian arteries distal to the interruption, involution of both fourth arches and the sixth arch contralateral to the descending aorta (Fig. 33.20B). Type C interruption entails involution of one limb of the truncus arteriosus and its associated proximal third arch and entire fourth arch with persistence of the normally involuted dorsal aorta between arches three and four, the so-called ductus caroticus (Fig. 33.20E).

Virtually all cases of interruption between carotid and subclavian arteries (type B) are associated with a conotruncal anomaly in which hypoplasia of the subaortic region causes subaortic obstruction and a conal septal malalignment type of VSD (117). The pathophysiology of the interruption is thought to be an absolute decrease in left ventricular output to the ascending aorta (due to the combination of outflow obstruction and VSD) with maintenance of normal fetal cerebral perfusion resulting in a relatively large decrease in flow through the aortic arches beyond the takeoff of one or both carotid arteries. The contributing factors that determine precisely which combination of arch involutions occur in each case are not understood. In a large series of cases with DiGeorge syndrome (118), 43% were found to have type B interrupted aortic arch, and 68% of interrupted arch patients had DiGeorge syndrome. This contrasts with truncus arteriosus communis in which comparable figures were 34% and 33%, respectively. Again, we see the predisposition to fourth arch abnormality in 22q11 patients. Cases in which subaortic obstruction is not present to explain arch involution are not well understood but may well relate to primary neural crest cells' direct influence on the aortic arches themselves.

Diagnosis and Management

These patients typically present, like other ductal-dependent left heart obstructive lesions, with acute cardiovascular collapse or heart failure after spontaneous closure of the ductus arteriosus in the first days of life. Initial management entails fluid resuscitation, induction and maintenance of ductal patency with prostaglandin E₁, and establishment of stable hemodynamics, with inotropic support if necessary. Physical findings of pulse discrepancy, depending upon branching pattern, are only helpful after restoration of satisfactory cardiac output. Absence of all limb pulses suggests interruption type B with anomalous subclavian artery, that is, both carotid arteries proximal, both subclavians distal to the interruption. Strong carotid pulses help to differentiate interrupted arch from critical aortic stenosis in which all pulses are diminished. Differential cyanosis (pink upper body, blue lower body) while theoretically possible is uncommonly seen since pulmonary arterial blood (hence ductal blood) is relatively highly saturated due to the large left-to-right shunt through the VSD. Currently, 2-D echocardiography is the most important tool for diagnostic imaging of interrupted arch. The diagnosis should be suspected from the marked discrepancy in size between ascending aorta and main pulmonary artery (119) with subcostal frontal imaging, in the presence of the typical malalignment-type VSD with posterior deviation of the infundibular (conal) septum, best visualized in the parasternal long-axis view. Imaging of the arch entails determination of the branching pattern and notation of patency of the arch from suprasternal or high parasternal imaging (120). The smooth superior course of the carotid artery origins, especially in type B interruptions, in contrast to the usual posterior course of an intact aortic arch, is a further clue to the presence of interruption. Angiography is still used in many centers to confirm the diagnosis of interrupted aortic arch; however, torrential flow through a VSD makes it difficult to obtain high-quality imaging of the ascending aorta in order to distinguish between interruption and severe arch hypoplasia. Interruption can be diagnosed consistently by angiography when both carotid arteries arise proximal to and both subclavian arteries distal to the interruption (and ductus). The wide separation of carotid arteries from descending aorta unequivocally demonstrates interruption. Three-dimensional reconstruction from MRI can demonstrate the branching pattern and the separation between proximal and distal aorta (Fig. 33.20A).

The surgical approach to treatment depends on the degree of subaortic obstruction. Subaortic diameters of 5 to 6 mm or greater seem to be compatible with primary intracardiac repair, namely patch closure of the VSD and plus aortic arch reconstruction. Subaortic regions of 3 mm or less are inadequate to support normal cardiac output in a full-term infant. In the case of normally aligned great arteries the subaortic obstruction must be bypassed. The preferred method is to associate the proximal main pulmonary artery with ascending aorta using homograft augmentation to complete the aortic reconstruction, similar to that employed for hypoplastic left heart syndrome (Norwood operation) (121,122). Pulmonary blood flow is provided by a Gore-Tex tube graft from the reconstructed aorta if the VSD is left open, or by a right ventricle-to-pulmonary artery confluence conduit if the ventricles are separated by a baffle from left ventricle to pulmonary valve via the VSD. When interrupted aortic arch is associated with transposition of the great arteries, arterial switch operation is combined with transannular patch across the neopulmonary outflow. Pulmonary artery banding is not a satisfactory palliation of VSD with interrupted aortic arch, because it frequently results in biventricular hypertrophy with progressive subaortic stenosis thus complicating definitive repair by any method at a later date.

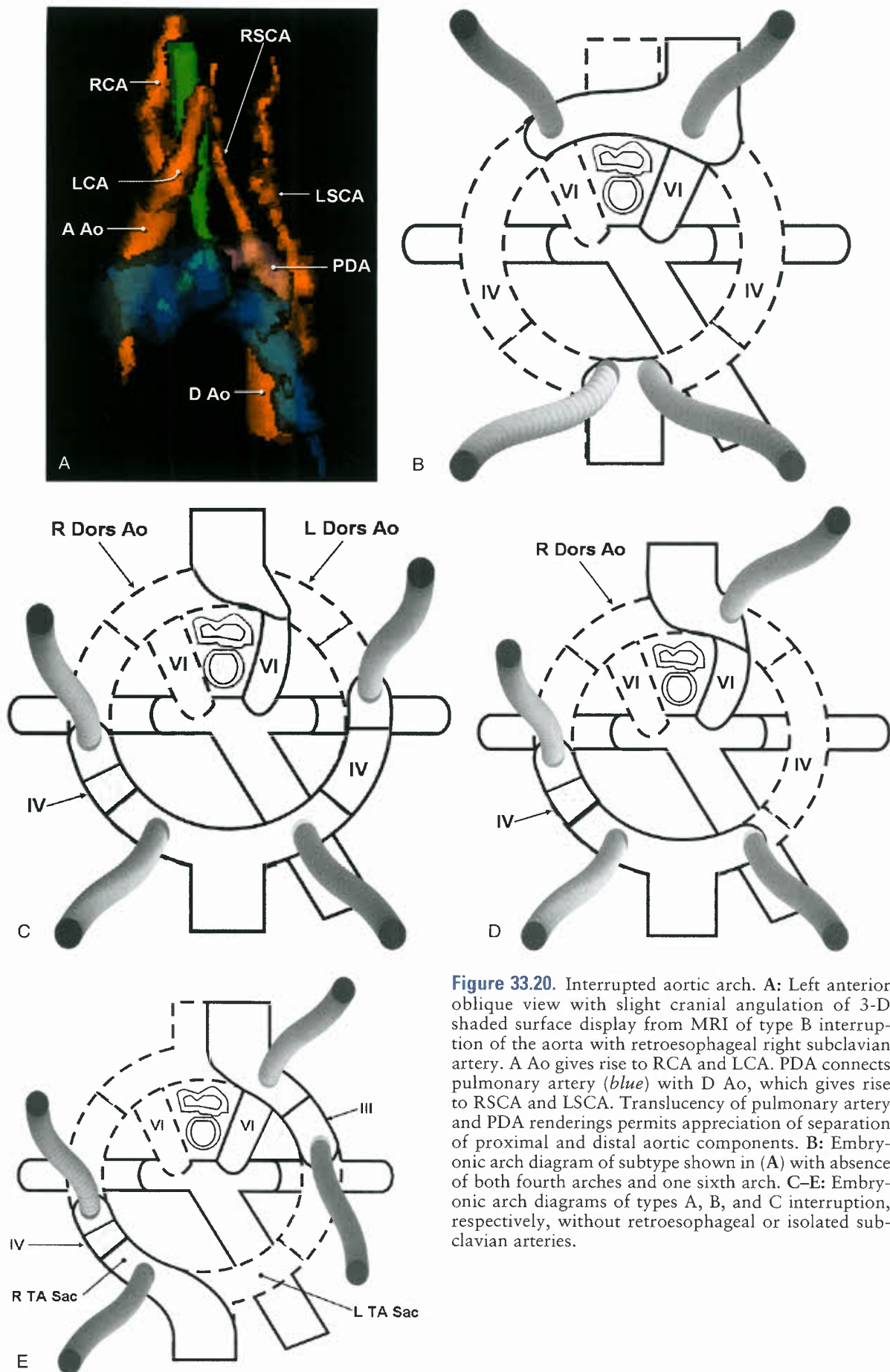


Figure 33.20. Interrupted aortic arch. **A:** Left anterior oblique view with slight cranial angulation of 3-D shaded surface display from MRI of type B interruption of the aorta with retroesophageal right subclavian artery. A Ao gives rise to RCA and LCA. PDA connects pulmonary artery (blue) with D Ao, which gives rise to RSCA and LSCL. Translucency of pulmonary artery and PDA renderings permits appreciation of separation of proximal and distal aortic components. **B:** Embryonic arch diagram of subtype shown in (A) with absence of both fourth arches and one sixth arch. **C–E:** Embryonic arch diagrams of types A, B, and C interruption, respectively, without retroesophageal or isolated subclavian arteries.

The aortic arch itself can almost always be reconstructed by liberal dissection around the two arch components with direct anastomosis of the two ends (123) plus homograft augmentation of the reconstructed arch when necessary to achieve adequate arch size. Artificial tube grafts connecting proximal and distal aorta should be avoided in the initial operation in infancy, if possible, since they are rapidly outgrown, and with fibrous tissue encasement of the native aorta, complicate primary end-to-end anastomosis at a later date.

OTHER ANOMALIES OF THE AORTIC ARCH SYSTEM

Anomalous Origin of the Pulmonary Artery from the Ascending Aorta

Anomalous pulmonary artery branch arising from the ascending aorta in the presence of a main pulmonary artery arising separately from the heart is a rare anomaly. While the term “hemitruncus” has been used, this lesion should be distinguished from true truncus arteriosus communis with only one pulmonary artery branch arising in common with the ascending aorta, and the other arising from a ductus or systemic collateral vessel from the descending aorta.

By far the more common form is anomalous origin of the RPA, seen in 82% of 108 cases of an excellent review by Kutsche and Van Mierop (124). All had left aortic arch; many had patent ductus arteriosus; few had tetralogy of Fallot. Interrupted aortic arch distal to the left subclavian artery or coarctation of the aorta was present in 14% of those where the pulmonary artery arose just above the aortic valve, and 8/11 of those had an aorticopulmonary septal defect. In contrast, anomalous origin of the left pulmonary artery was associated with tetralogy of Fallot in 74%, and in all cases had either tetralogy or right aortic arch or both. No cases of aorticopulmonary septal defect or interrupted aortic arch were present.

Embryology

The rather dramatic difference in associations between anomalous left and RPA origins suggests different embryologic mechanisms. Kutsche and Van Mierop (124) propose that in anomalous origin of the RPA, the embryonic branch pulmonary artery joins the trunco-aortic sac (at its right side) but fails in leftward migration to reach the main pulmonary artery portion before septation occurs. They point out that this probably accounts for the significant incidence of aorticopulmonary septal defect. The mechanism of anomalous origin of the left pulmonary artery may be failure of the embryonic branch pulmonary artery to join the trunco-aortic sac (or subsequent separation from it) in association with absence of the left sixth (ductal) arch and perhaps persistence of the left fifth arch, whereby the left pulmonary artery becomes associated with the ascending aorta.

Diagnosis and Management

The clinical presentation of anomalous origin of a pulmonary artery branch from the ascending aorta is predominantly that of congestive heart failure (CHF) in infancy followed by the development of pulmonary vascular disease as early as 6 months of age, if unrepaired. In some patients, there may be an abbreviated (or no) period of clinical heart failure, in which case they may go on to develop pulmonary vascular obstructive disease without warning. While many have a significant systolic murmur from turbulent, increased pulmonary blood flow, some have little or no murmur and only a loud, narrowly

split or single second heart sound to suggest the abnormality. The above findings may be tempered by the relatively infrequent association with other major anomalies such as tetralogy of Fallot or interrupted aortic arch.

The chest roentgenogram may show differential pulmonary blood flow, especially when superimposed on decreased flow in association with tetralogy of Fallot. Echocardiography is diagnostic, but one must be aware of the potential for mistaking RPA merging posteriorly with aorta for normal confluence with main pulmonary artery when using a subcostal frontal sweep. Imaging in multiple views including parasternal short axis permits differentiation of the pulmonary artery bifurcation from the juncture of RPA with ascending aorta. In the case of the very uncommon origin of left pulmonary artery, the rule of thumb is to carefully search for all possible origins of both pulmonary artery branches in the face of tetralogy of Fallot. The more lateral origin of the left pulmonary artery from the ascending aorta also makes imaging of this abnormality easier. Cardiac catheterization usually shows pulmonary hypertension in both pulmonary arteries, though only one can be entered from the right ventricle via the main pulmonary artery. Angiographic demonstration is possible with a left ventriculogram but requires an ascending aortogram if there is a VSD. In patients with unexplained pulmonary hypertension, aortic root injection to rule out origin of a pulmonary artery branch from the ascending aorta or the physiologically similar aorticopulmonary septal defect should be considered. While MRI can be diagnostic, at present it cannot be used to quantify pulmonary vascular resistance. Treatment consists of surgical division of the anomalously connected pulmonary artery branch and anastomosis directly, or with a graft, to the main pulmonary artery. This should be carried out as early as possible to avoid the development of pulmonary vascular disease.

Anomalous Origin of the Left Pulmonary Artery from the Right Pulmonary Artery

Origin of the left pulmonary artery from the RPA, also known as anomalous left pulmonary artery, or pulmonary artery sling (125), is a rare anomaly in which the lower trachea is partially surrounded by vascular structures: the left pulmonary artery arising as a very proximal branch of the right loops around the trachea. It is the only situation in which a major vascular structure passes between the trachea and esophagus. Pulmonary sling is frequently associated with complete cartilaginous rings in the distal trachea (126) resulting in tracheal stenosis that may require direct surgical treatment in addition to relief from vascular compression. It usually appears as an isolated abnormality but can be associated with other congenital cardiac defects, including tetralogy of Fallot (127).

Embryology

The distal pulmonary arteries normally arise from their respective lung buds and join the pulmonary artery portion of the trunco-aortic sac separately. If the two distal arteries join each other by incorporation of potential vascular islets from the splanchnic bed before becoming incorporated into the trunco-aortic sac, one possibility is that the left pulmonary artery would pass behind the trachea before making this juncture. This would result in pulmonary artery sling. If it passed in front of the trachea, this would be indistinguishable from the normal situation.

Diagnosis and Management

These patients typically present with severe respiratory distress and stridor although milder forms do exist and may be identified incidentally during imaging for another cardiovascular

anomaly. Sometimes, the respiratory distress can be exaggerated by right lung emphysema (128). Barium swallow, when classical (Fig. 33.1), is diagnostic if one can rule out mediastinal tumor. However, nondiagnostic barium swallows are common, and more definitive testing with echocardiography, angiocardiology, CT, or MRI (Fig. 33.21B–E) is usually necessary to ensure the accuracy of the diagnosis. Symptomatic patients should be evaluated by bronchoscopy at the time of surgical repair because of the frequent association of complete cartilaginous rings. The usual surgical approach is division of the left pulmonary artery from the right and reanastomosis in front of the trachea. Alternatively, Jonas et al. (129) have recommended leaving the pulmonary artery and its branches intact while transecting the trachea, mobilizing it behind the pulmonary artery bifurcation and reanastomosing it. If complete cartilaginous tracheal rings are present, tracheal reconstruction may also be necessary. The latter approach is more amenable in that case since the trachea is already opened.

Innominate Artery Compression of the Trachea

Innominate artery compression of the trachea or so-called anomalous innominate artery is a poorly understood abnormality in which there is anterior compression of the trachea at the point where it is crossed by the innominate artery (Fig. 33.22). Some have thought this to be due to a more distal, that is, leftward, takeoff of the innominate artery from the aortic arch; however, 3-D reconstructions from MRI have not demonstrated any consistent abnormality of the aorta or its branching pattern. The presumed abnormality is tracheomalacia, whether idiopathic or in association with tracheoesophageal fistula (130), with the innominate artery in the vicinity of the malacic segment of trachea. The diagnosis is suspected when signs of severe inspiratory and expiratory stridor, usually in a 2- to 6-month-old child, are associated with anterior indentation of the tracheal air column on lateral chest roentgenogram. However, vascular rings should

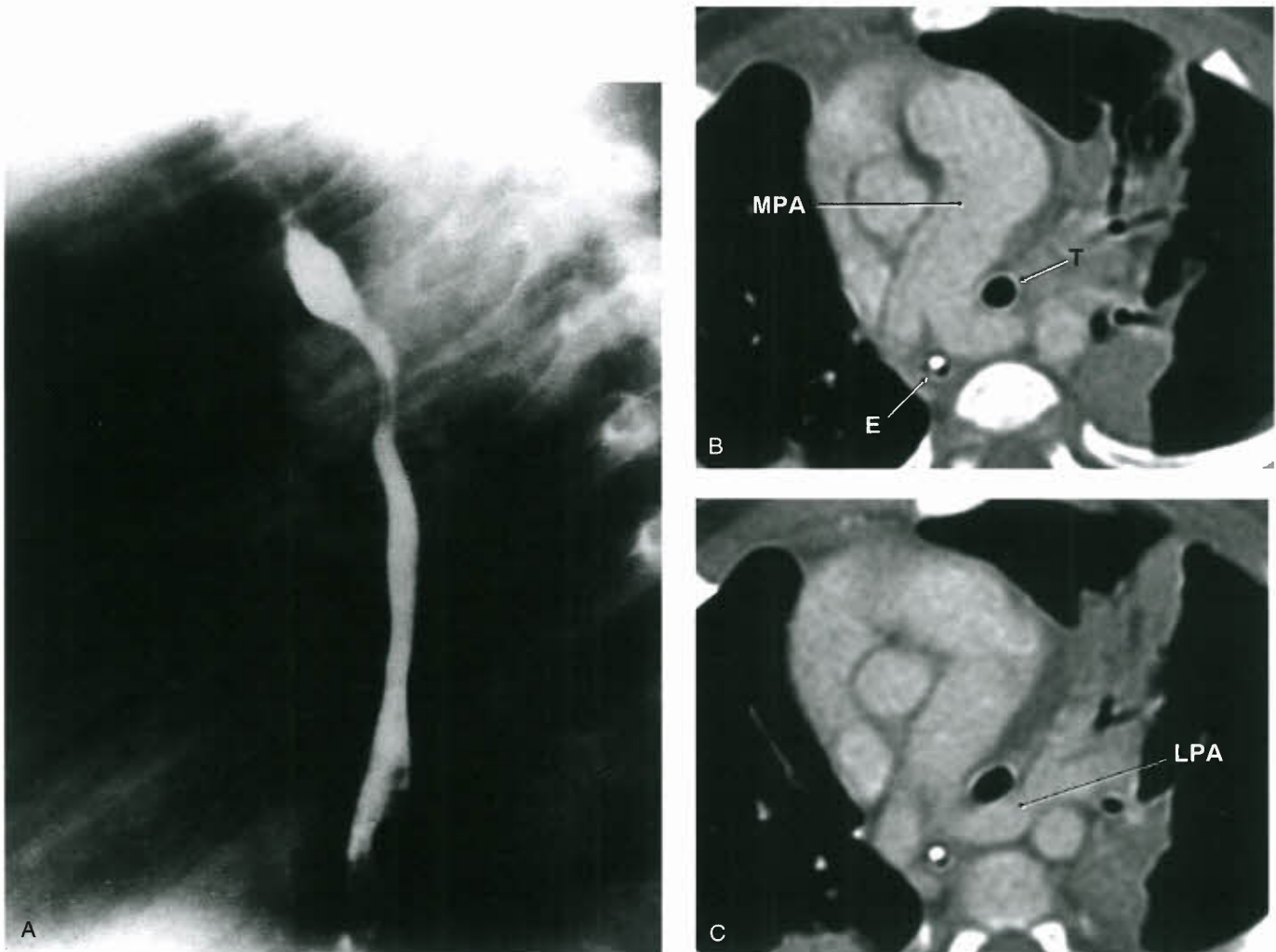


Figure 33.21. Anomalous origin of left pulmonary artery from RPA (sling). **A:** Barium esophagram showing classical anterior indentation. **B,C:** Consecutive images from CT scan of another patient, showing left pulmonary artery (LPA) looping around a small distal trachea (T) but anterior to the esophagus (E) with high signal from a nasogastric tube. (*Continued*)

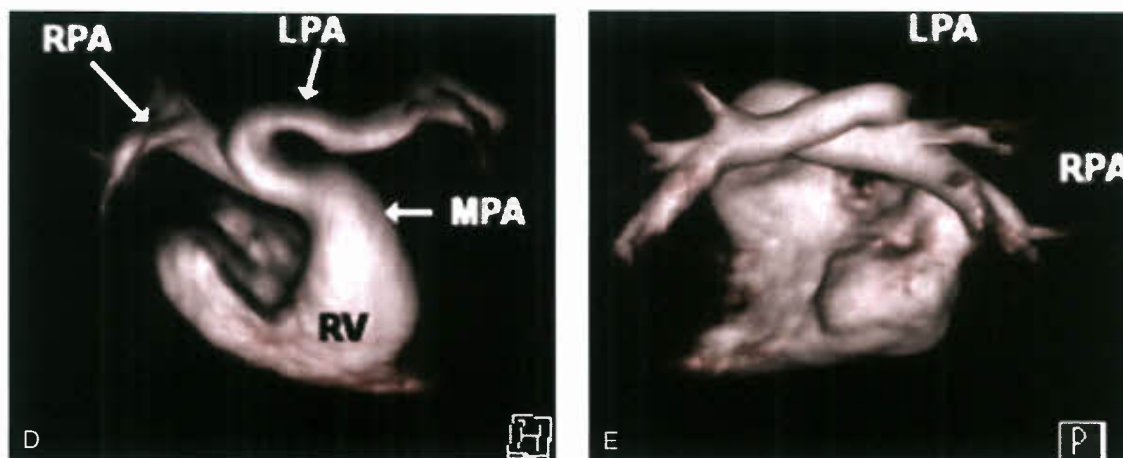


Figure 33.21. (Continued) D: 3-D surface display from gadolinium-enhanced MRI of the right heart from a different patient than (A–C). Direct cranial view showing the right ventricle (RV) and main pulmonary artery (MPA) giving rise to the RPA. Note the left pulmonary artery (LPA) taking off from the RPA and looping back around the trachea in a tight hairpin turn. E: Posterior view of the same patient as in (D). Again it is clear that the LPA arises from the RPA.

be ruled out with at least a barium esophagram. Simultaneous visualization of the innominate artery and the trachea is afforded by MRI and is shown dramatically with 3-D reconstruction (Fig. 33.1). Treatment usually entails waiting for the tracheomalacia to resolve, typically by age 2 years; however, in cases associated with apnea or repeated lower respiratory infections, surgical sectioning of the innominate artery and reimplantation more proximally, that is, rightward in the aorta may be helpful. In limited cases, suspension from the sternum has been used, but there is often little room behind the sternum to relieve pressure on the trachea because of decreased AP dimension of the chest.

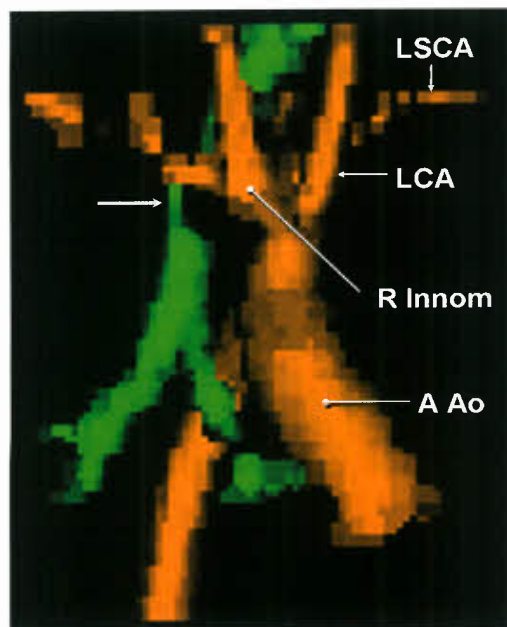


Figure 33.22. Innominate artery compression of the trachea. Right anterior oblique view of 3-D shaded surface display from MRI showing severely compressed midtrachea (arrow) adjacent to right innominate artery (R Innom).

VASCULAR ANOMALIES

Descriptions of some vascular anomalies refer to Greek mythology as *caput medusae*, or a radial orientation of small blood vessels that resemble the hair of Medusa. Writings of Greek and Arab physicians dating back to the 6th century include surgical descriptions of arterial aneurysms in the setting of trauma (131). In 1761, Hunter described two cases of arteriovenous (AV) connections and the physical exam auscultation finding as “as if there was a blast of air through a small hole and interrupted, answering precisely and constantly to the stroke of the heart or diastole of the artery” (132). Following these descriptions, numerous case reports and case series presented arteriovenous malformations (AVMs) in various organ systems, including the liver, brain, and lungs and their physiologic effects (133–136). Elaborate, often confusing nomenclature developed. More recently, detailed investigations into the genetics, physiology, and natural history of vascular anomalies have broadened our understanding of the wide array of defects and have led to clinically applicable classification systems.

EMBRYOLOGY AND PATHOGENESIS

The vascular system is formed well before the heart starts beating in the embryo. Vasculogenesis begins with angioblast formation from mesoderm. These angioblasts differentiate into endothelial cells that then form blood vessels including the dorsal aorta (137). Thus, differences between arteries and veins exist early on in embryogenesis. Studies on tumor angiogenesis (formation of new vessels from existing vasculature) in the 1970s led to the discovery of critical proteins that stimulate vascular development, including basic fibroblast growth factor (bFGF) and vascular endothelial growth factor (VEGF), among others (138). Members of the fibroblast growth factor family stimulate angioblast formation from mesoderm. Disruption of receptors for VEGF and deficiency of VEGF appears to interfere with late stage of vascular development with abnormal vessel wall development and with differentiation of endothelial cells leading to impaired capillary vessel formation (139–141). Tyrosine kinases are believed to aid in the assembly

of nonendothelial components of the blood vessel wall (142). Interestingly, genetic mapping in two families with venous malformations revealed mutations in tyrosine receptors (143).

CLASSIFICATION

There were several reports dating back to the 1800s (Virchow [1863] and Wegner [1877]) that described various features of vascular anomalies but many of them had inconsistent terminology (144). A distinct classification system was described in 1982 based on the biologic behavior and histopathology (145). In this system, vascular malformations are differentiated from hemangiomas. Vascular malformations are usually recognized at birth, have a normal endothelial cell cycle, grow with the child, and show no signs of spontaneous regression. Within the classification of vascular malformations, there are fast flow lesions (arterial malformations, AVMs, and fistulas) and slow flow lesions (venous, capillary, lymphatic, and glomuvenous malformations) (Table 33.2) (146). Hemangiomas, in contrast, are vascular “tumors” with proliferating, involuting, and involuted phases. Only a certain percentage of hemangiomas are present at birth, but they do grow rapidly over the first 2 years of life.

Although there are several types of vascular anomalies that can occur, this chapter emphasizes the abnormalities that typically have cardiovascular manifestations: (a) systemic arterial malformations (b) pulmonary arterial malformations, (c) hemangiomas, and other vascular malformations.

SYSTEMIC ARTERIAL MALFORMATIONS

Systemic arterial malformations include AVMs and arteriovenous fistulas (AVFs). These malformations can develop in various organ systems including the brain, liver, skin, and extremities. Systemic arterial malformations are most often congenital but acquired lesions can develop from trauma, infection, and surgery (147–150). Clinical presentation depends on the location and degree of shunting. The Schobinger staging system has been used to describe the four stages through which AVMs progress (Table 33.3) (151). In large, fast-flow lesions, signs and symptoms of heart failure can develop (Stage 4) and can mimic congenital heart disease. Specific malformations where heart

TABLE 33.3 Clinical Staging of AV Malformations Schobinger Staging (151)

Stage	Description (Typical Age)
1	Asymptomatic (birth—adolescence)
2	Expansion with invasion of deep structures (begins during adolescence)
3	Deep destruction: necrosis, ulceration, pain, and hemorrhage (years after progressive worsening)
4	High-output cardiac failure

failure has been described include vein of Galen malformations, hepatic AVMs, thoracic AVMs, and lower extremity AVMs.

Prevalence

There are numerous types of systemic arterial malformations with varying prevalence, but in general these defects are rare. Vein of Galen malformations occur in <1 in 25,000 live births (152). In adults, the prevalence of brain AVMs vary between 15 and 18 per 100,000 per person years (153,154). Most arterial malformations are sporadic, but there are particular syndromes associated with certain types of AVMs. Hereditary hemorrhagic telangiectasia (HHT) and hereditary neurocutaneous angiomatous malformations, for example, are associated with brain AVMs (155).

Pathology and Pathogenesis

The formation of blood and lymphatic vessels involve vasculogenesis, angiogenesis, and lymphangiogenesis. Although the exact mechanisms of AVM formation are largely unknown, studies of the gene defects of inherited diseases associated with AVMs have provided valuable insight into the pathogenesis of these malformations (156). See section on embryology and pathogenesis for further details.

Pathologic findings in AVMs include a nidus of tortuous vessels that connect feeding arteries to veins without a capillary bed interface. These vessels appear to have chronic changes and are nonfunctioning. Both the connecting arteries and veins demonstrate muscularization of the walls (157).

HHT is highly associated with AVMs in many organ systems and provides insight into the molecular changes leading to AVM formation. Endoglin, a receptor for the TGF- β family of ligands, is found on endothelial cells. Patients with HHT-1 have mutations in endoglin. Deficiency in endoglin along with angiogenic stimulus promotes an abnormal increase in endothelial cell proliferation and resultant AVM formation in a mouse model (158). This mechanism has also been implicated in sporadic cerebral AVMs (159). A high-flow state and resultant shear forces also promote muscularization of the veins within the AVMs, contributing further to the starkly abnormal appearance of these blood vessels (160).

AVMs can be found in the brain, head/neck, limbs, trunk, and viscera. These are fast-flow malformations and can lead to high-output heart failure, which is an indication for treatment.

In infants and children, central nervous system AVMs include the vein of Galen malformation, now commonly referred to as vein of Galen aneurysmal malformations (VGAM). This malformation can cause significant morbidity and mortality related to the neurologic and cardiovascular effects. One of the highest-risk groups are neonates with VGAM that present

TABLE 33.2 Types of Vascular Malformations

Vascular Malformations		
	Slow-Flow	Fast-Flow
Simple	Capillary	Arterial
	Lymphatic	
	Venous	
	Glomuvenous	
Combined	Lymphatic venous	AV
	Capillary-lymphatic-venous	Capillary-AV
	Capillary-venous	AVF

Adapted from Huang JT, Liang MG. Vascular malformations. *Pediatr Clin North Am* 2010;57:1091–1110.

with high-output heart failure that can progress to multiorgan system failure and death. VGAM has been associated with congenital heart defects. Published reports note sinus venosus atrial septal defects and coarctation of the aorta to be relatively more prevalent than other cardiac defects in patients with VGAM. The association of these defects to VGAM may be due to (a) the relatively increased blood flow returning from the superior vena cava (SVC) and possible interruption of the formation of the sinus venosus septum and (b) increased flow across the ductus arteriosus and decreased flow across the isthmus (161,162).

Thoracic AVF/AVMs have only been described in the literature as case reports. Connections between the subclavian artery and innominate vein, the internal carotid arteries, the aorta, and hemiazygos vein and between the subclavian artery and the SVC have all been reported (163–167).

Arterial malformations of the lower extremity can be high-flow lesions, as is the case with Parkes Weber Syndrome. This syndrome is defined by overgrowth of the extremity with multiple AV fistulas along that extremity. The fistulas usually develop around puberty or after trauma and can be complicated by CHF (168).

Physiology and Clinical Manifestations

Clinical manifestations of AVMs are largely dependent on the size of the malformation and degree of left-to-right shunting. The more extensive the AV connections, the greater the amount of shunting and the larger the hemodynamic burden on the cardiopulmonary system. For the purposes of this section, we focus on the diagnosis of patients with large systemic AV shunts who are experiencing high-output cardiac failure.

The VGAM can produce significant morbidity and mortality related to neurologic and cardiovascular manifestations. In utero, fetuses can experience a range of hemodynamic effects due to VGAM including mild cardiac insufficiency to fetal hydrops. While the placenta provides a low resistance circuit to redirect blood flow away from the AVM, after birth, elimination of the placenta redistributes blood flow. Now, the obligatory (independent of pulmonary vascular resistance) VGAM shunt increases SVC flow and right atrial and right ventricular enlargement soon develop. There can be a right-to-left atrial shunt, a poorly contracting and dilated right ventricle, and antegrade systolic flow in the ductus arteriosus shortly after birth due to a high pulmonary vascular resistance (169,170).

Neonates and young infants with these cardiovascular changes present with a history of respiratory distress, failure to thrive, and sometimes lethargy or seizure. In particular, cyanosis and pulmonary hypertension can complicate the heart failure symptoms and may mimic a significant congenital heart defect, potentially delaying the diagnosis of VGAM. Physical exam reveals tachypnea, tachycardia, and cardiac murmur, and auscultation over the anterior fontanelle sometimes reveals a continuous murmur due to the increased blood flow through the AVM (169,171).

Older infants may present with macrocephaly, leading to hydrocephalus and seizures. Long-standing cerebral venous hypertension can lead to developmental delay. Older children and adults present with headaches or intracranial hemorrhage (172).

Thoracic AVMs present either in childhood with a continuous murmur or with symptoms and signs of high-output heart failure due to a significant left-to-right shunt. In addition to the murmur, a widened pulse pressure, bounding pulses, hyperdynamic precordium, and prominent S_2 can be found. There have been reports of fetal presentation of large thoracic AVMs with hydrops and high-output failure (173).

Electrocardiogram and Radiography

Electrocardiographic findings of infants with large AVMs are nonspecific and may show sinus tachycardia, right ventricular

or biventricular hypertrophy. Occasionally signs of ischemia, with ST segment changes are present (152,174). In older children who present with systemic AVMs, the electrocardiogram (ECG) may be normal or demonstrate ventricular hypertrophy. Infants with large systemic AVMs will have cardiomegaly on chest radiography, especially marked right atrial and right ventricular enlargement.

Ultrasound

Ultrasound is extremely helpful in the diagnosis of systemic AVMs. These malformations appear heterogeneous with large feeding vessels often seen by 2-D imaging. Color Doppler interrogation shows high vessel density with high-velocity systolic flow and low resistance. Draining veins appear dilated and pulsatile (175).

Echocardiography

Echocardiographic findings include cardiomegaly with markedly enlarged right heart with leftward displacement of the interventricular and atrial septae. There is often tricuspid valve regurgitation with a high-velocity jet, consistent with elevated right-ventricular pressure. Flow across the patent foramen ovale is often right-to-left. In the cases of VGAM, the proximal aorta and its branches are dilated and retrograde diastolic flow can be seen in the descending thoracic aorta. High-velocity flow is observed in the SVC, main pulmonary artery, and ascending aorta secondary to the large volume of blood flow from the shunt (169).

Cardiac Catheterization and Angiography

Patients do not commonly undergo diagnostic cardiac catheterization in the presence of systemic AVMs. Those who do, have oximetry data that shows a high-cardiac output state (low arterial venous oxygen difference) and can have a difference in saturation between the inferior vena cava (IVC) and SVC depending on the site of the AVM (176,177). Hemodynamic measurements can show elevated ventricular end-diastolic pressure in presence of CHF and elevated pulmonary arterial pressure in neonates with large AVMs.

Angiography is important in definition and management of systemic AVM. Angiograms show enlarged arterial feeding vessels with rapid transit time across the AVM, followed by dilated venous drainage of the malformation (178). (Fig. 33.1) Selective angiography at the site of the AVM can define size, number, and location of feeding vessels to plan for possible intervention.

Other Imaging

By CT, AVMs appear as enhancing lesions with several afferent and efferent vessels without persistent tissue staining. MRI shows low signal intensity secondary to a flow void phenomenon of the rapid/turbulent flow (178). Magnetic resonance venograms are an accurate, noninvasive method of imaging systemic AVMs and can be a desirable alternative to angiography if immediate intervention is not needed (Fig. 33.23).

Differential Diagnosis

In the setting of heart failure symptoms with cardiac enlargement on adjunct testing and without evidence of an intracardiac shunt, an AVM must be considered. The differential diagnosis of systemic AVM includes congenital heart defects, other vascular malformations, vascular tumors, and rarely other neoplasms. Auscultation and noninvasive imaging can aid in differentiating the above diagnoses (179).

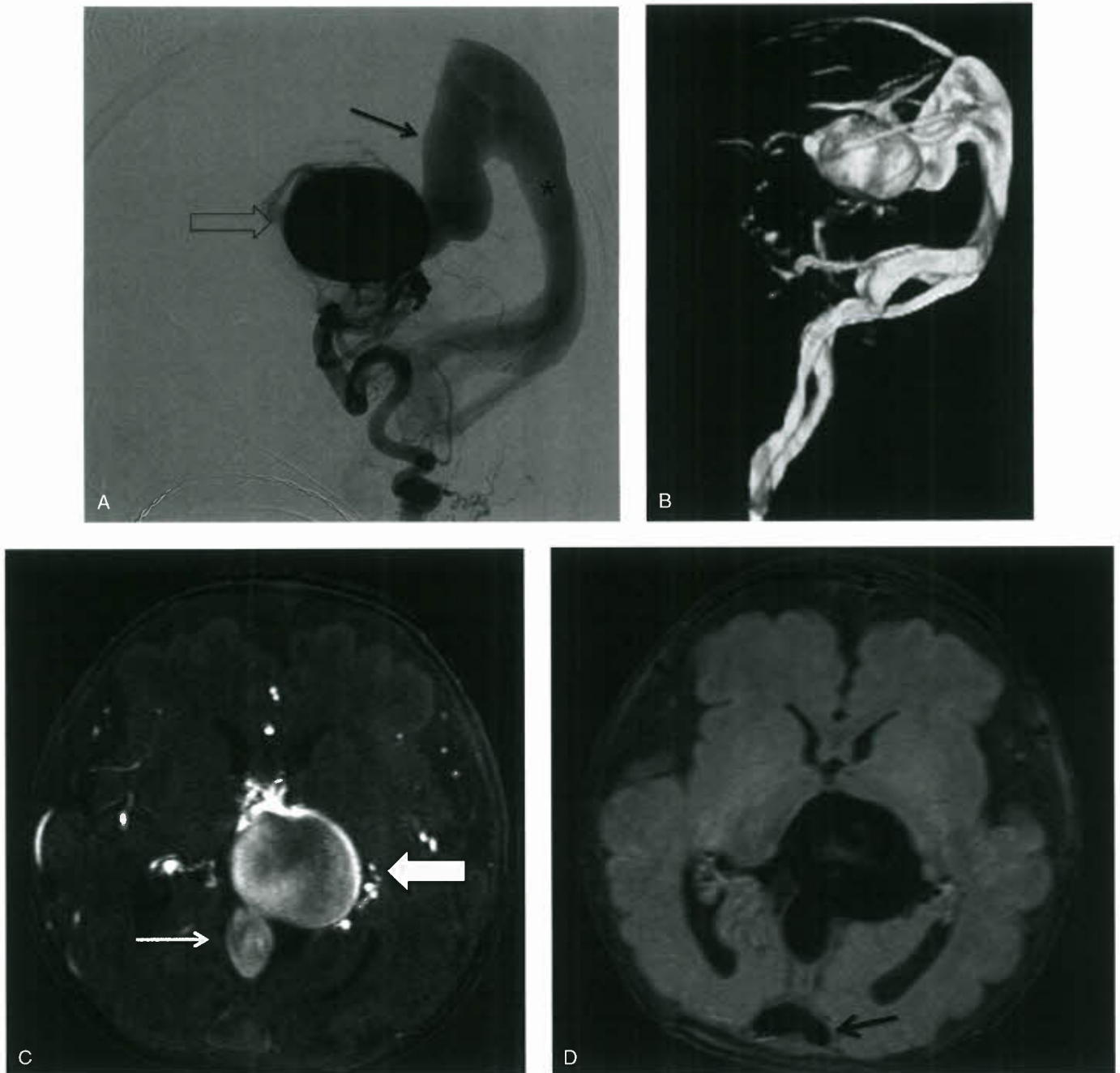


Figure 33.23. Systemic arterial malformations. **A:** Lateral view of a left vertebral angiogram. There is a large tortuous vertebral artery supplying branches to fill the aneurysmal vein (*unfilled arrow*). The enlarged VGAM (*filled arrow*) drains into a dilated straight sinus (*asterisk*). **B:** Three-Dimensional time-of-flight MR venogram without contrast demonstrating a similar image to (**A**). Large venous aneurysm is seen draining into dilated vein of Galen, which drains via the dilated venous sinuses to the jugular veins. **C:** Axial source image for 3-D time-of-flight MR. Mixed bright signal is seen within the aneurysm (*thick arrow*). A slice of the dilated vein of Galen is seen (*thin arrow*). Brain and fluid are deemphasized to display high-flow areas as bright signal intensity. **D:** Axial image at same level as (**C**). T1 weighted with high signal intensity within the brain parenchyma. Flow void seen within the venous aneurysm and vein of Galen. The straight sinus (*arrow*) is also dilated secondary to increased venous return. (Images courtesy of Marc Keller, MD, Department of Interventional Radiology, The Children's Hospital of Philadelphia.)

Treatment/Natural history

Initial management of neonates often includes minimizing the cardiovascular effects and damage to other end organs while awaiting more definitive treatment. Inotropic support with

dopamine or dobutamine can worsen cardiac output, but low-dose dopamine has been shown to improve systemic perfusion (152). Administration of milrinone can also be considered as there is evidence that it promotes cerebral vasodilation as well as systemic vasodilation (180). However, there have been

no studies in VGAM. There is also some evidence that prostaglandin administration improves systemic perfusion from systemic vasodilation (170). Failure of intensive care management to stabilize the neonate often leads to early embolization to attempt to reduce the shunt. Even with aggressive management, severe heart failure requiring intubation in the newborn period is usually associated with a poor outcome (172,181).

Although prompt neonatal diagnosis and management of significant VGAM has reduced early mortality, the general prognosis for infants with large cerebral arterial malformations is grave. These patients not only can suffer from heart failure due to a large shunt but also can have significant neurologic sequelae, including seizures, intracranial hemorrhage, and developmental delay.

Surgical excision of systemic AVMs is only possible if the malformation is well circumscribed and accessible. For significant cerebral AVMs, neurosurgical techniques carry mortality between 30% and 90% depending on the age of the patient (182,183). Recently, surgical intervention is reserved for evacuation of intracranial hematomas, treatment of hydrocephalus, and surgical ligation of vessels when transcatheter embolization is not possible.

Transcatheter embolization is now the therapy of choice for significant systemic arterial malformations, including cerebral AVMs. There is a wide variety of agents to treat these malformations depending on the location. For VGAM, chemical agents such as ethanol, *N*-Butyl-2-cyanoacrylate, and ethylene-vinyl alcohol have been most successful. This sclerosant technique targets the high-flow, low-resistance nidus between the arterial and venous system (184). In a large study of 216 patients, utilizing a transfemoral arterial approach to deliver this glue in the fistulous zone, 23 died (10.6%), 20 of the surviving 193 patients (10.4%) were severely delayed, and 143 (74%) were neurologically normal on follow-up (185). Other, smaller series reported similar data (—186–188). Intervention on the feeding arteries by surgical ligation or mechanical agents, such as coils, provides only temporary relief, as collateral vessels ultimately form to continue to feed the direct AV connection (175). Stereotactic radiotherapy also only has a limited role, especially in the neonate.

PULMONARY ARTERIOVENOUS MALFORMATIONS

Pulmonary arteriovenous malformations (PAVMs) are vascular lesions defined by abnormal connections between pulmonary arteries and pulmonary veins (Fig. 33.24). Patients with PAVMs often have systemic AVMs as well. The most common associated diagnosis is HHT, otherwise known as Osler-Weber-Rendu Syndrome. PAVMs can also be seen in patients with pulmonary hypertension, congenital heart defects with single-ventricle physiology and palliation, cystic fibrosis, and severe liver disease (189).

Prevalence

HTT affects about 1 in 5,000 people overall (190). About 15% to 33% of patients with HHT have PAVMs (191). Patients with congenital heart disease defined by single-ventricle physiology and palliated with superior cavopulmonary connection (bidirectional Glenn, BDG) can also develop PAVMs. The overall incidence of PAVM in this population is 15% to 25% and is seen more commonly in patients with heterotaxy and interrupted IVC with azygos continuation (192,193). In addition, patients with complete cavopulmonary connections (Fontan palliation) who have preferential hepatic flow to one lung can manifest PAVMs in the opposite lung (194).

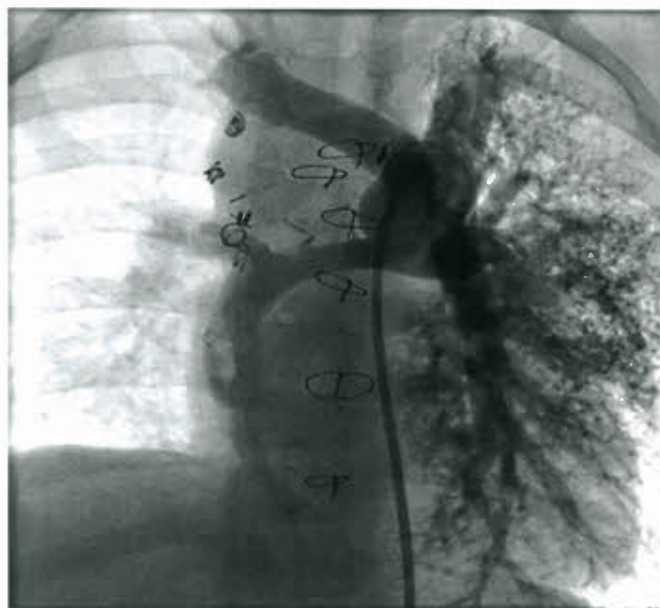


Figure 33.24. Pulmonary AVM. Angiogram in the AP projection in a patient with heterotaxy syndrome who is status post superior cavopulmonary connection. An antegrade catheter courses through the interrupted IVC with azygos continuation and is positioned in the main pulmonary artery (MPA). Injection of contrast into the MPA demonstrates a reticular appearance of the left lung. In addition, there is contrast seen in the left pulmonary veins, while the right lung contrast is still in the arterial phase, indicating decreased transit time in the left lung. Both angiographic findings are consistent with left lung PAVMs.

Pathology and Pathogenesis

The pathologic appearance of PAVMs is similar to AVMs seen elsewhere in the body. Pathology and pathogenesis of AVMs in HHT is outlined above.

PAVMs in the setting of single-ventricle heart defects were initially reported as a late complication after SVC-RPA anastomosis (classic Glenn shunt) (195). In the current era, even with varied surgical approaches to the cavopulmonary anastomosis, some patients continue to develop PAVMs. There is growing evidence that a yet unidentified “hepatic factor” is the putative agent that, when absent in the pulmonary circulation, predisposes to the development of PAVMs (196). Hepatopulmonary syndrome is a condition associated with cirrhotic liver disease where PAVMs can develop. Once patients undergo liver transplantation to resolve their liver failure, the PAVMs have been shown to regress. Similarly, in single-ventricle heart disease palliated by a cavopulmonary anastomosis, PAVMs tend to resolve once hepatic venous flow is directed to the affected lung segments, suggesting a pathophysiology similar to that of hepatopulmonary syndrome. Nonpulsatile flow and preferential blood flow to the lower lobes of the lung are thought to be additional contributors to the development of PAVMs in patients with superocavopulmonary connections (197).

Physiology and Clinical Manifestations

PAVMs promote varying degrees of shunting of deoxygenated blood to the systemic circulation. These abnormal vessels in the lungs bypass the pulmonary capillary bed and hence, oxygenation does not occur. Systemic arterial desaturation

and compensatory polycythemia develop depending on the extent of the PAVMs.

Clinical manifestations of PAVMs include dyspnea, cyanosis, and occasionally hemoptysis. The most common complaint in HHT patients is epistaxis, either spontaneous or with minor trauma (198). Patients with HHT also commonly present with dyspnea on exertion but a large number of patients with HHT may tolerate long-standing hypoxemia without dyspnea (191). Platypnea (improvement in dyspnea when lying supine) has been described and is thought to be secondary to redistribution of pulmonary flow to nondependent regions, away from the regions of the AVMs (198). On physical exam, patients are desaturated by pulse oximetry or can appear cyanotic. These patients can have an audible bruit over the lung fields, which is louder with inspiration and may have clubbing of the extremities.

In the absence of congenital heart disease, the majority of patients with PAVMs can remain asymptomatic until the fourth decade of life. There have been some series that have shown a correlation between symptoms and lesion size (<2cm being asymptomatic) or number, with multiple PAVMs causing more severe symptoms. However, reports have been inconsistent, despite trends supporting that correlation (198). In addition, there have been rare reports of infants presenting with profound cyanosis who are found to have direct RPA to left atrial connections (199). In adults, severe cases can present with massive hemoptysis, hemothorax, or neurologic events (transient ischemic attack, stroke, or cerebral abscess) secondary to right-to-left shunting of septic emboli (200).

Patients with single-ventricle cardiac defects and cavopulmonary anastomosis are asymptomatic initially after their surgery and become progressively cyanotic with decreased arterial oxygen saturation as PAVMs develop. Their chest radiographs show no evidence of parenchymal disease. This constellation of findings should prompt screening for PAVMs in this group of patients (see below) (193,197).

Electrocardiography

ECGs are usually normal in patients with PAVMs. Occasionally, left atrial enlargement and left ventricular hypertrophy can occur, especially in the setting of a direct RPA to left-atrial connection (199).

Radiography

Chest radiographs show abnormalities in the majority of patients with PAVM. The malformations usually appear as discrete, 1- to 5-cm, round or oval masses with uniform density. These masses can be lobulated but have well-defined borders and are more common in the lower lobes. Feeding vessels can also be seen on chest radiography and can range in size from 4 to 7 mm, being as large as 20 mm in some cases (198).

Echocardiography

Based on adult data in patients with HHT, the current recommendation for screening of PAVMs is transthoracic contrast echocardiography with agitated saline (201). During echocardiography, agitated saline is injected in a peripheral vein while imaging the atria and ventricles on apical four-chamber view, for example. Normally, on imaging, acoustic signals (or bubbles) from the agitated saline appear in the right atrium and ventricle immediately after injection and do not appear on the left side of the heart in the absence of a right-to-left shunt because the bubbles dissolve in the pulmonary capillary bed. The appearance of bubbles in the left atrium after several beats indicates the passage of blood through the lungs and into the left atrium without interfacing with the pulmonary capillary

bed and confirms the presence of pulmonary AVMs. This finding also differentiates pulmonary AVMs from an atrial shunt where saline contrast would appear in the left atrium immediately after injection (202). If contrast echocardiography is positive, the diagnosis can be confirmed by CT scan or angiography.

Cardiac Catheterization and Angiography

Although the diagnosis of PAVMs can be made by angiography, cardiac catheterization is usually not the initial diagnostic test of choice in this era of accurate noninvasive diagnostic testing. However, in patients with congenital heart disease and new-onset cyanosis, hemodynamic catheterization and angiography provides important data and can afford a means of treatment.

Hemodynamic assessment of patients with PAVMs reveals pulmonary vein desaturation in the affected lung. It is important to obtain oximetry data from all pulmonary veins to localize the PAVMs. Typically, pulmonary artery pressure, resistance, and output are normal, even in the setting of profound cyanosis and polycythemia (203). Angiographic appearance of PAVMs include rapid transit time from pulmonary arteries to pulmonary veins with a reticular appearance of the lung parenchyma (204) (Fig. 33.1).

Other Imaging

Helical multidetector CT scan of the chest is emerging as the preferred technique for diagnosis and characterization of PAVMs. Intravenous contrast enhances PAVMs and allows differentiation from other lung nodules and characterization of perfusion. Nuclear medicine scans can also be diagnostic. Intravenous injection of radiolabeled albumin particles collect in normal lung: areas not opacified after IV injection represent areas of lung with AV connection. This technique is no longer widely used (191).

Differential Diagnosis

The differential diagnosis of PAVMs includes many forms of cyanotic congenital heart disease, especially those having anomalous return to systemic veins to the left atrium. In single-ventricle heart disease after cavopulmonary connection, increased cyanosis can also occur with systemic venovenous connections that develop from the Glenn pathway and connect either to vessels that drain to the IVC or to the pulmonary veins. The formation of these connections is thought to occur in the setting of elevated pressure in the Glenn connection.

Treatment/Natural History

Growth rates are variable and appear faster in those with HHT than in those without that diagnosis (205). However, the morbidity of untreated AVMs is also significant and include incidence of stroke of 11%, 6.8% incidence of brain abscess, and total morbidity and mortality of 23% (205,206). Definitive indications for treatment of pulmonary arterial malformations include cyanosis, exertional dyspnea, or systemic emboli. Some experts advocate for prophylactic treatment of all PAVMs to prevent potential systemic embolization if the vessel is >3 mm in diameter (197,207). Treatment of PAVMs with smaller feeding vessels (1.5 to 2 mm) can be undertaken if a right-to-left shunt is present and vessels are easily accessible.

Currently, the most widely used therapy is transcatheter embolization of the feeding arteries to the PAVM using coils or detachable balloons. Malformations with large feeding arteries may require device occlusion (191). Surgical treatment for PAVMs has become increasingly uncommon, as catheter-based

techniques have evolved. Surgical lobectomy, segmentectomy, or pneumonectomy is currently reserved for patients with extensive PAVMs that are not amenable to catheter embolization or as an emergent procedure for hemothorax (208).

In patients with single-ventricle heart defects and superior cavopulmonary connections, inclusion of hepatic venous blood to the pulmonary circulation will often cause regression of PAVMs. This resolution occurs after completing the Fontan procedure, hepatic vein inclusion in patients with heterotaxy syndrome and interrupted IVC with azygos continuation, correction of pulmonary artery discontinuity in a Fontan where IVC blood is directed to one lung and PAVMs develop in the other, creation of a brachial AVF, or cardiac transplantation (209–213). Patients with heterotaxy syndrome with interrupted IVC and azygos continuation have been shown to more commonly develop PAVMs after superior cavopulmonary connection (Kawashima) (214). In addition, there is some evidence that patients with interrupted IVC who have hepatic vein inclusions, with conduits on the contralateral side of SVC, are less likely to have resolution of PAVMs. This phenomenon is likely secondary to streaming of hepatic venous blood preferentially to one lung (212). There are efforts to derive computer models of all the possible types of Fontan connections to optimize surgical planning in these patients and reduce the likelihood of persistent PAVMs (215).

HEMANGIOMAS AND OTHER VASCULAR MALFORMATIONS

Historically, the field of vascular anomalies has grappled with classification and nomenclature of very disparate lesions (216). More recently, a biologic classification system has appropriately divided vascular anomalies into vascular tumors, lesions that arise from endothelial hyperplasia, and vascular malformations, lesions that arise by dysmorphogenesis and normal endothelial cell turnover. This system appears to better guide diagnosis, prognosis, and treatment (216). Vascular tumors include hemangiomas, while vascular malformations encompass venous, capillary, and lymphatic malformations.

Prevalence and Pathogenesis

Hemangiomas are the most common vascular tumor, occurring in 4% to 10% of infants. It is a tumor of the endothelium and a model for angiogenesis. These tumors are more common in Caucasians and more frequent in females (3:1). Sixty percent of tumors occur in the head and neck, 25% are found on the trunk, and 15% occur in the extremities. While 80% are single lesions, approximately 20% of hemangiomas are located in multiple cutaneous sites and in other organ systems, specifically the liver, gastrointestinal tract, and brain (144).

Hemangiomas appear a few weeks after birth and grow rapidly. The proliferative phase is highlighted by plump endothelial cells with frequent mitosis and lasts until 1 year of life. bFGF and VEGF are angiogenic proteins that stimulate this endothelial proliferation. Spontaneous slow involution follows from approximately 1 to 7 years of life with normal-appearing endothelial cells in a matrix of “fibrous fatty tissue.” This phase involves endothelial apoptosis and down regulation of angiogenesis. The life cycle of this tumor ends with the involuted phase. Fifty percent of hemangiomas have complete regression by the age of 5 years and 90% by the age of 9 years (217). There are many classification systems based on location and color of hemangiomas (145,218).

As discussed above, vascular malformations are classified according to the type of blood vessel involved: arterial,



Figure 33.25. Cutaneous hemangioma. Large cutaneous hemangiomas on forehead of an infant with multiple cutaneous hemangiomas. The lesion is *bright red, nodular*, and well circumscribed with normal surrounding skin.

AV, capillary, venous, or lymphatic. These malformations are present at birth but may not be clinically evident until later in life depending on the type; they occur equally in males and females (144). In contrast to hemangiomas, vascular malformations enlarge by hypertrophy. Histologic appearance includes normal-appearing endothelial cells and ecstasic vessels (145). These malformations can be classified by their hemodynamic characteristics on angiography (see Table 33.2) as high-flow lesions (arterial, AV) and low-flow lesions (capillary, venous, lymphatic) (144). Syndromes associated with slow-flow vascular malformations include Sturge-Weber, Klippel-Trenaunay, Rubinstein-Taybi, thrombocytopenia-absent radius, Beckwith-Wiedemann, and others. Those associated with fast-flow lesions are Parkes Weber, capillary malformation-AVM, and Cobb syndrome (Fig. 33.25).

Clinical Manifestations

It is often difficult to distinguish hemangiomas from vascular malformations because it is not always apparent whether or not the lesion was present at birth. Vascular lesions, which are not present at birth and show signs of either proliferation or involution are typically hemangiomas. The typical superficial hemangiomas are red and raised (Fig. 33.1). Deeper hemangiomas can be confused with a vascular malformation or other rare tumors. There have been documented cases of hemangiomas diagnosed prenatally and a few cases with hydrops fetalis and heart failure (173). In addition, infants with multiple cutaneous hemangiomas (≥ 5) are more likely to have hepatic hemangiomas (16%). Hepatic hemangiomas can have a variable course from asymptomatic to high-output cardiac failure in rare cases (219). Venous and lymphatic malformations are compressible but high-flow lesions such as arterial or AVMs are typically firm to the touch and do pulsate.

Diagnosis and Treatment

The diagnosis of hemangiomas and vascular malformations can generally be made on history and physical exam. However, noninvasive imaging with ultrasound or MRI should be performed when deeper lesions are suspected to outline the extent of the lesion(s) and ensure there is no organ system involvement.

In most cases, hemangiomas are followed closely and allowed to regress naturally without need for treatment. After regression, a minor blemish may be all that remains. Only

about 10% of hemangiomas are associated with significant symptoms and require treatment. These high-risk lesions tend to occur in the areas of head, neck, airway, eye, lumbosacrum, or liver (220). Treatment is indicated in children with compromised airways, neurologic changes, digestive tract obstruction, bleeding, or ulceration. Medical treatment options include oral corticosteroids, tapered over infancy with 80% to 90% response rate. Interferon- α is a second-line agent for life-threatening hemangiomas (216).

Treatment of cutaneous hemangiomas with the beta-blocker, propranolol was first noted in 2008. An infant, being treated with propranolol for hypertrophic cardiomyopathy, was noted to have coincidental improvement in a

nasal hemangioma (221). This case prompted a study of 11 patients, describing significant improvement in hemangioma appearance 24 hours after initiating propranolol treatment (221). Propranolol is a nonselective β -receptor antagonist, having effect on both β_1 and β_2 receptors. The proposed mechanism of action of propranolol in the setting of hemangiomas is threefold: (a) vasoconstriction, secondary to the blocking of vasodilatory properties of epinephrine, allowing unopposed α_1 stimulation, (b) inhibition of angiogenesis, by blocking of angiogenic growth factors important to hemangioma proliferation, and (c) induction of apoptosis, thought to be regulated through β_1 receptor pathways (217,222).

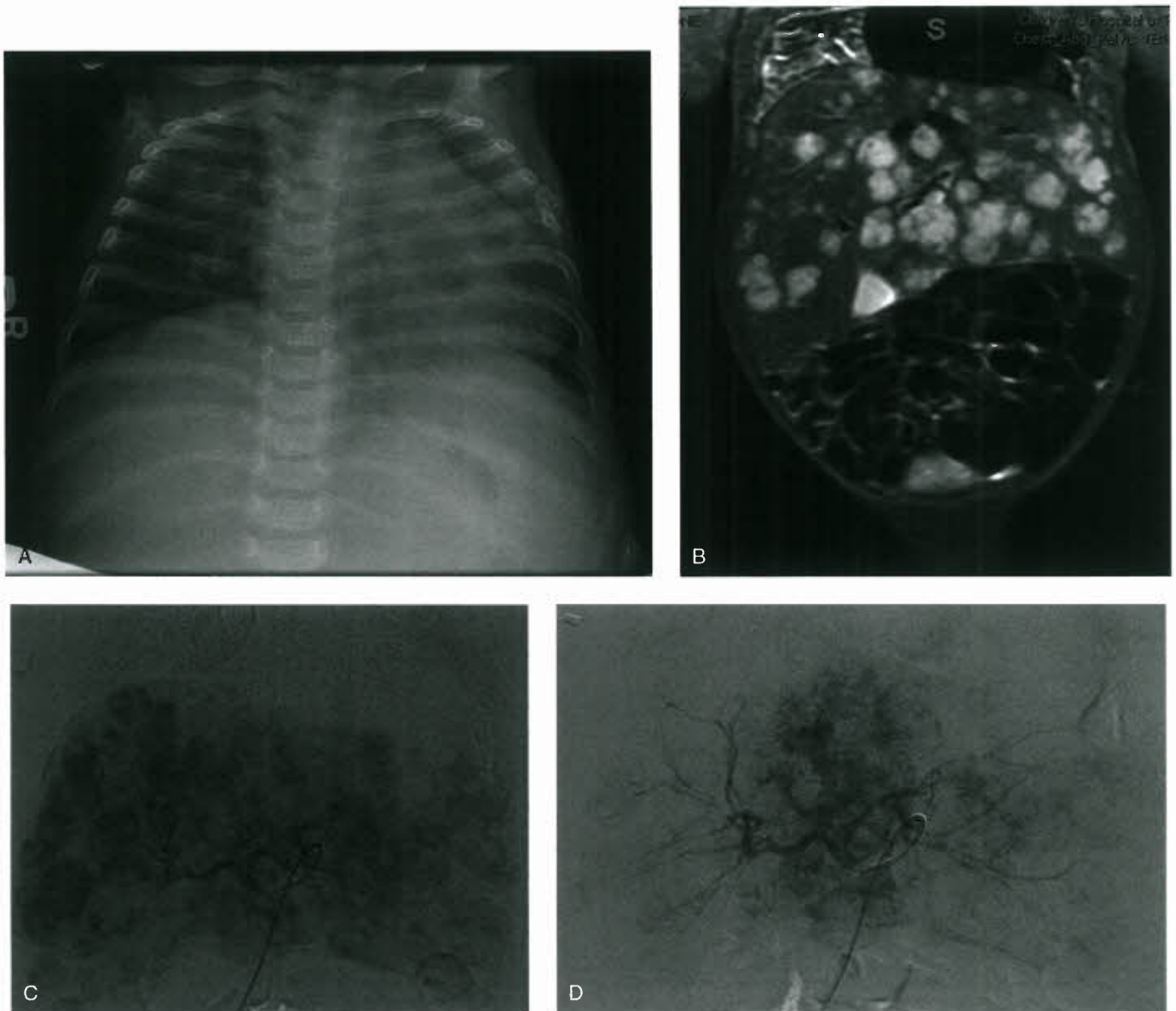


Figure 33.26. Hepatic hemangiomas. **A:** Chest radiograph of 5-month old with multiple hepatic hemangiomas and high cardiac output state. There is marked cardiomegaly with increased pulmonary vascular markings and hepatomegaly. **B:** Coronal section of T2-weighted abdominal MRI showing multiple homogenous, circular hemangiomas throughout the liver. **C:** Selective angiography of the hepatic artery prior to intervention, demonstrating multiple hemangiomas throughout both lobes of the liver. **D:** Selective angiography of the hepatic artery after particle embolization of liver hemangiomas in the right lobe. There is significant improvement with little contrast seen outside of the normal liver vasculature of the right lobe. The left lobe hemangiomas remain prominent. (Images courtesy of Anne Marie Cahill, M.D. Department of Interventional Radiology, The Children's Hospital of Philadelphia.)

More recent studies have shown propranolol to be effective treatment for complex infantile hemangiomas. These patients are often treated in conjunction with a pediatric cardiologist, given propranolol's potential to cause bradycardia and hypotension, although these side-effects are rare (222). Hypoglycemia is a more commonly observed side effect of propranolol therapy, especially in younger infants (223). Evidence on outcomes after propranolol treatment is lacking given the small studies and case reports available (221,222,Starkey, 2011 #262).

Other modalities for treatment of hemangiomas include cryotherapy, sclerotherapy, surgical resection, and laser therapy. Embolization therapy may be utilized to control heart failure symptoms. This therapy is most often used for hepatic hemangiomas as they have a higher incidence of CHF (216). (Fig. 33.1)

In contrast to hemangiomas, vascular malformations do not generally resolve spontaneously and treatment is less controversial. Laser treatment, embolization therapy, and surgical excision have all been used and the choice depends on the location and extent of the malformation. Low-flow capillary and venous malformations can be addressed with laser therapy, whereas surgery may be indicated in lymphatic malformations. Transcatheter embolization therapy is indicated in high-flow, arterial or arteriovenous malformations.

ACKNOWLEDGMENTS

We would like to thank our colleagues Mark A. Fogel, M.D., Matthew Harris, M.D., and Kevin Whitehead, M.D., Ph.D. for their contribution of many of the 3-D shaded surface displays from MRI; Marc Keller, MD for angiogram and MR images in Figure 33.23; Anne Marie Cahill, M.D. for chest radiograph, MRI, and angiograms in Figure 33.26; and William M. Gottliebson, MD, MS, Division of Cardiology, Cincinnati Children's Hospital Medical Center for the 3-D CT image in Figure 33.16C.

REFERENCES

- Hunault F. Examen de quelques parties d'un singe. *Hist Acad roy d sc* 1735;2:516–523.
- Hommel W. *Commercium literarium norimbergae. Hebdom* 1737;21:162.
- Fioratti G, Aglietti F. Osservazione anatomica. *Saggi scientif e letterari dell'acad di Padova* 1763;1:69–72.
- Steidele R.J. Sammlg verschiedner in der chirurg prakt. *Lehrschule Gemahlen Beob* 1777;2:114–116.
- Bayford D. An account of a singular case of obstructed deglutition. *Mem Med Soc London* 1794;2:275–286.
- Gross RE. Surgical relief for tracheal obstruction from a vascular ring. *N Engl J Med* 1945;233:586–590.
- Merrill DL, Webster CA, Samson PC. Congenital absence of the aortic isthmus. *J Thorac Surg* 1957;33:311–320.
- Burke RP, Chang AC. Video-assisted thoracoscopic division of a vascular ring in an infant: a new operative technique. *J Cardiac Surg* 1993;8:537–540.
- Koontz CS, Bhatia A, Forbess J, et al. Video-assisted thoracoscopic division of vascular rings in pediatric patients. *Am Surg* 2005;71:289–291.
- Mihaljevic T, Cannon JW, del Nido PJ. Robotically assisted division of a vascular ring in children. *J Thorac Cardiovasc Surg* 2003;125:1163–1164.
- Kuratani S, Kirby ML. Initial migration and distribution of the cardiac neural crest in the avian embryo: an introduction to the concept of the circumpharyngeal crest. *Am J Anat* 1991;191:215–227.
- Momma K. Cardiovascular anomalies associated with chromosome 22q11.2 deletion syndrome. [Review] [97 refs]. *Am J Cardiol* 2010;105:1617–1624.
- Congdon ED. Transformation of the aortic-arch system during the development of the human embryo. *Contrib Embryol* 1922;14:47–110.
- Edwards JE. Anomalies of the derivatives of the aortic arch system. *Med Clin North Am* 1948;32:925–949.
- Stewart JR, Kincaid OW, Edwards JE. *An Atlas of Vascular Rings and Related Malformations of the Aortic Arch System*. Springfield, IL: Charles C. Thomas, 1964.
- Ramaswamy P, Lytrivi ID, Thanjan MT, et al. Frequency of aberrant subclavian artery, arch laterality, and associated intracardiac anomalies detected by echocardiography. *Am J Cardiol* 2008;101:677–682.
- Bronshtein M, Lorber A, Berant M, et al. Sonographic diagnosis of fetal vascular rings in early pregnancy. *Am J Cardiol* 1998;81:101–103.
- Achiron R, Rotstein Z, Heggesh J, et al. Anomalies of the fetal aortic arch: a novel sonographic approach to in-utero diagnosis. *Ultrasound Obstet Gynecol* 2002;20:553–557.
- Yoo SJ, Min JY, Lee YH, et al. Fetal sonographic diagnosis of aortic arch anomalies. *Ultrasound Obstet Gynecol* 2003;22:535–546.
- Galindo A, Nieto O, Nieto MT, et al. Prenatal diagnosis of right aortic arch: associated findings, pregnancy outcome, and clinical significance of vascular rings. *Prenat Diagn* 2009;29:975–981.
- Wilson DJ, Burn J, Scambler P, et al. DiGeorge syndrome: part of CATCH 22. *J Med Genet* 1993;30:852–856.
- Goldmuntz E, Clark BJ, Mitchell LE, et al. Frequency of 22q11 deletions in patients with conotruncal defects. *J Am Coll Cardiol* 1998;32:492–498.
- McElhinney DB, Clark BJ III, Weinberg PM, et al. Association of chromosome 22q11 deletion with isolated anomalies of aortic arch laterality and branching. *J Am Coll Cardiol* 2001;37:2114–2119.
- Rauch R, Rauch A, Koch A, et al. Laterality of the aortic arch and anomalies of the subclavian artery—reliable indicators for 22q11.2 deletion syndromes? *Eur J Pediatr* 2004;163:642–645.
- Rauch R, Rauch A, Koch A, et al. Cervical origin of the subclavian artery as a specific marker for monosomy 22q11. *Am J Cardiol* 2002;89:481–484.
- Kazuma N, Murakami M, Suzuki Y, et al. Cervical aortic arch associated with 22q11.2 deletion. *Pediatr Cardiol* 1997;18:149–151.
- Momma K, Kondo C, Matsuoka R, et al. Cardiac anomalies associated with a chromosome 22q11 deletion in patients with conotruncal anomaly face syndrome. *Am J Cardiol* 1996;78:591–594.
- Molin DG, DeRuiter MC, Wisse LJ, et al. Altered apoptosis pattern during pharyngeal arch artery remodelling is associated with aortic arch malformations in Tgfbeta2 knock-out mice. *Cardiovasc Res* 2002;56:312–322.
- Bergwerff M, DeRuiter MC, Hall S, et al. Unique vascular morphology of the fourth aortic arches: possible implications for pathogenesis of type-B aortic arch interruption and anomalous right subclavian artery. *Cardiovasc Res* 1999;44:185–196.
- Clark J. Wheezing child. *Clin Pediatr* 2008;47:191–198.
- Kindler H, Bagger JP, Tait P, et al. A vascular ring without compression: double aortic arch presenting as a coincidental finding during cardiac catheterisation. *Heart* 2005;91:773.
- Stoica SC, Lockowandt U, Couden R, et al. Double aortic arch masquerading as asthma for thirty years. *Respiration* 2002;69:92–95.
- Uchida DA. Late presentation of double aortic arch in school-age children presumed to have asthma: the benefits of spirometry and examination of the flow-volume curve. *Respir Care* 2009;54:1402–1404.
- Tuo G, Volpe P, Bava GL, et al. Prenatal diagnosis and outcome of isolated vascular rings. *Am J Cardiol* 2009;103:416–419.
- Edwards JE. *An Atlas of Acquired Diseases of the Heart and Great Vessels*. Philadelphia, PA: WB Saunders, 1961.
- Edwards JE. Malformations of the aortic arch system manifested as “vascular rings.” *Lab Invest* 1953;2:56–75.
- Goldstein WB. Aberrant right subclavian artery in mongolism. *AJR Am J Roentgenol* 1965;95:131–134.
- Tsai IC, Tzeng WS, Lee T, et al. Vertebral and carotid artery anomalies in patients with aberrant right subclavian arteries. *Pediatr Radiol* 2007;37:1007–1012.
- Kommerell B. Verlagerung der oesophagus durch eine abnorm verlaufende arteria subclavia dextra (Arteria lusoria). *Fortschr Geb Rontgenstr* 1936;54:590–595.
- Whitman G, Stephenson LW, Weinberg P. Vascular ring: left cervical aortic arch, right descending aorta, and right ligamentum arteriosum. *J Thorac Cardiovasc Surg* 1982;83:311–315.
- Turkvatan A, Pac A, Kiziltepe U, et al. MDCT angiography of isolated right subclavian artery. *Turk J Pediatr* 2010;52:668–672.
- Nath PH, Castaneda-Zuniga W, Zollikofer C, et al. Isolation of a subclavian artery. *AJR Am J Roentgenol* 1981;137:683–688.
- Paquet M, Williams RL, Paquet M, et al. Origin of the right subclavian artery from the right pulmonary artery in a newborn with complete transposition of the great arteries. *Can J Cardiol* 1994;10:932–934.
- Mosieri J, Chintala K, Delius RE, et al. Abnormal origin of the right subclavian artery from the RPA in a patient with D-transposition of the great vessels and left juxtaposition of the right atrial appendage: an unusual anatomical variant. *J Cardiac Surg* 2004;19:41–44.
- Marin C, Sanchez ML, Fernandez-Velilla M, et al. MR imaging of isolated right subclavian artery. *Pediatr Radiol* 2008;38:216–219.
- Keagy KS, Schall SA, Herrington RT, et al. Selective cyanosis of the right arm. Isolation of right subclavian artery from aorta with bilateral ductus arteriosus and pulmonary hypertension. *Pediatr Cardiol* 1982;3:301–303.
- Garti IJ, Aygen MM, Garti IJ, et al. Left aortic arch with congenital isolation of the right subclavian artery. *Pediatr Radiol* 1980;9:241–243.
- Baudet E, Roques XF, Guibaud JP, et al. Isolation of the right subclavian artery. *Ann Thorac Surg* 1992;53:501–503.
- Mathieson JR, Silver SF, Culham JA, et al. Isolation of the right subclavian artery. *AJR Am J Roentgenol* 1988;151:781–782.
- Brill CB, Peyster RG, Keller MS, et al. Isolation of the right subclavian artery with subclavian steal in a child with Klippel-Feil anomaly: an example of the subclavian artery supply disruption sequence. *Am J Med Genet* 1987;26:933–940.

51. Barger JD, Creasman RW, Edwards JE, et al. Bilateral ductus arteriosus associated with interruption of the aortic arch. *Am J Clin Pathol* 1954;24:441-444.
52. Kutsche LM, Van Mierop LH. Cervical origin of the right subclavian artery in aortic arch interruption: pathogenesis and significance. *Am J Cardiol* 1984;53:892-895.
53. Hastreiter AR, DCruz IA, Cantez T, et al. Right-sided aorta. I. Occurrence of right aortic arch in various types of congenital heart disease. II. Right aortic arch, right descending aorta, and associated anomalies. *Br Heart J* 1966;28:722-739.
54. Mathew R, Rosenthal A, Fellows K. The significance of right aortic arch in D-transposition of the great arteries. *Am Heart J* 1974;87:314-317.
55. Ismat FA, Weinberg PM, Rychik J, et al. Right aortic arch and coarctation: a rare association. *Congenit Heart Dis* 2006;1:217-223.
56. Ming Z, Aimin S. Right aortic arch with coarctation in Chinese children. *Pediatr Radiol* 2008;38:511-517.
57. Knight L, Edwards JE. Right aortic arch: types and associated cardiac anomalies. *Circulation* 1974;50:1047-1051.
58. Garti IJ, Aygen MM, Vidne B, et al. Right aortic arch with mirror-image branching causing vascular ring: a new classification of the right aortic arch patterns. *Br J Radiol* 1973;46:115-119.
59. Bethuyne N, Proesmans M, Daenen W, et al. Vertical vascular ring around right mainstem bronchus. *Eur J Cardiothorac Surg* 2007;31:952-954.
60. Watanabe N, Hayabuchi Y, Inoue M, et al. Tracheal compression due to an elongated aortic arch in patients with congenital heart disease: evaluation using multidetector-row CT. *Pediatr Radiol* 2009;39:1048-1053.
61. Nakahira A, Hirai H, Sasaki Y, et al. Agenesis of the left carotid artery in the right aortic arch with Kommerell diverticulum. *J Thoracic Cardiovasc Surg* 2010;140:e5-e7.
62. Kogon BE, Forbess JM, Wulkan ML, et al. Video-assisted thoracoscopic surgery: is it a superior technique for the division of vascular rings in children? *Congenit Heart Dis* 2007;2:130-133.
63. Backer CL, Hillman N, Mavroudis C, et al. Resection of Kommerell's diverticulum and left subclavian artery transfer for recurrent symptoms after vascular ring division. *Eur J Cardiothorac Surg* 2002;22:64-69.
64. Austin EH, Wolfe WG, Austin EH, et al. Aneurysm of aberrant subclavian artery with a review of the literature. [Review] [39 refs]. *J Vasc Surg* 1985;2:571-577.
65. Cina CS, Althani H, Pasenau J, et al. Kommerell's diverticulum and right-sided aortic arch: a cohort study and review of the literature. [Review] [47 refs]. *J Vasc Surg* 2004;39:131-139.
66. Frigatti P, Grego F, Deriu GP, et al. Hybrid endovascular treatment of aneurysm degeneration in a rare right-aortic arch anomaly with Kommerell diverticulum. *J Vasc Surg* 2009;50:903-906.
67. Barcudi S, Sanders SP, Di Donato RM, et al. Aberrant left innominate artery from the left descending aorta in right aortic arch: echocardiographic diagnosis. *J Am Soc Echocardiogr* 2010;23:e5-e7.
68. Ahn KS, Yong HS, Lee JW, et al. Right circumflex retro-oesophageal aortic arch with coarctation of a high-positioned right arch. *Pediatr Radiol* 2007;37:584-586.
69. Stos B, Adler G, Lebreit E, et al. Vascular ring and coarctation of the aorta associated with oesophageal atresia. *Eur J Cardiothorac Surg* 2008;34:1110.
70. Knight WB. Hypoplastic right retro-oesophageal aortic arch: similarities to interrupted aortic arch. *Br Heart J* 1989;62:477-481.
71. Drucker MH, Symbas PN. Right aortic arch with aberrant left subclavian artery: symptomatic in adulthood. *Am J Surg* 1980;139:432-435.
72. Konstantinov IE, Puga FJ, Konstantinov IE, et al. Surgical treatment of persistent esophageal compression by an unusual form of right aortic arch. *Ann Thorac Surg* 2001;72:2121-2123.
73. Bleakney CA, Zafar F, Fraser CD, Jr. Circumflex right aortic arch with associated hypoplasia and coarctation: repair by aortic arch advancement and end-to-side anastomosis. *Ann Thorac Surg* 2011;91:624-626.
74. Hilmes M, Hernandez R, Devaney E. Markedly hypoplastic circumflex retroesophageal right aortic arch: MR imaging and surgical implications. *Pediatr Radiol* 2007;37:63-67.
75. Garti IJ, Aygen MM. Right aortic arch with aberrant left innominate artery. *Pediatr Radiol* 1979;8:48-50.
76. Luetmer PH, Miller GM. Right aortic arch with isolation of the left subclavian artery: case report and review of the literature. *Mayo Clin Proc* 1990;65:407-413.
77. Reeves BM, Colen TM, Sheridan BJ, et al. Isolated innominate artery as a cause of subclavian steal and cerebral hemisphere atrophy. *Pediatric Cardiol* 2010;31:1083-1085.
78. Ming Z, Qian W. An isolated left subclavian artery supplied by a collateral artery from the abdominal aorta. *Pediatr Radiol* 2009;39:857-859.
79. Manner J, Seidl W, Steding G, et al. The formal pathogenesis of isolated common carotid or innominate arteries: the concept of malseptation of the aortic sac. *Anat Embryol* 1997;196:435-445.
80. Killen DA, Battersby EJ, Klatte EC. Subclavian steal syndrome due to anomalous isolation of the left subclavian artery. *Arch Surg* 1972;104:342-344.
81. Shuford WH, Sybers RG, Schlant RC. Subclavian steal syndrome in right aortic arch with isolation of the left subclavian artery. *Am Heart J* 1971;82:98-104.
82. Konstantinov IE, Saxena P, d'Udekem Y, et al. Isolated subclavian artery: anatomical and surgical considerations. *Ann Thorac Surg* 2009;88:1685-1687.
83. Haughton VM, Fellows KE, Rosenbaum AE. The cervical aortic arches. *Radiology* 1975;114:675-681.
84. Kveselis DA, Snider AR, Dick M, et al. Echocardiographic diagnosis of right aortic arch with a retroesophageal segment and left descending aorta. *Am J Cardiol* 1986;57:1198-1199.
85. Tiraboschi R, Crupi G, Locatelli G, et al. Cervical aortic arch with aortic obstruction: report of two cases. *Thorax* 1980;35:26-30.
86. Mullins CE, Gillette PC, McNamara DG. The complex of cervical aortic arch. *Pediatrics* 1973;51:210-215.
87. Harley HR. Development and anomalies of aortic arch and its branches with report of case of right cervical aortic arch and intrathoracic vascular ring. *Br J Surg* 1956;46:561-573.
88. Kumar A, McCombs JL, Sapire DW, et al. Deletions in chromosome 22q11 region in cervical aortic arch. *Am J Cardiol* 1997;79:388-390.
89. Beaven TED, Fatti L. Ligature of aortic arch in the neck. *Br J Surg* 1947;34:414-416.
90. Cooley DA, Mullins CE, Gooch JB. Aneurysm of right-sided cervical arch: surgical removal and graft replacement. *J Thorac Cardiovasc Surg* 1976;72:106-108.
91. Hellenbrand WE, Kelley MJ, Talner NS, et al. Cervical aortic arch with retroesophageal aortic obstruction: report of a case with successful surgical intervention. *Ann Thorac Surg* 1978;26:86-92.
92. Burrows PE, Moes CA, Freedom RM. Double aortic arch with atretic right dorsal segment. *Pediatr Cardiol* 1986;6:331-334.
93. Han MT, Hall DG, Manche A, et al. Double aortic arch causing tracheoesophageal compression. *Am J Surg* 1993;165:628-631.
94. Higashino SM, Ruttenberg HD. Double aortic arch associated with complete transposition of the great vessels. *Br Heart J* 1968;30:579-581.
95. Cui W, Patel D, Husayni TS, et al. Double aortic arch and d-transposition of the great arteries. [Review] [9 refs]. *Echocardiography* 2008;25:91-95.
96. Goldberg DJ, Glatz J, Weinberg PM, et al. A novel case of L-transposition with a right-dominant double aortic arch. *Congenit Heart Dis* 2009;4:278-280.
97. Etedgui JA, Lorber A, Anderson D. Double aortic arch associated with coarctation. *Int J Cardiol* 1986;12:258-260.
98. Singer SJ, Fellows KE, Jonas RA. Double aortic arch with bilateral coarctations. *Am J Cardiol* 1988;61:196-197.
99. Cornali M, Reginato E, Azzolina G. Cervical aortic arch and a new type of double aortic arch: report of a case. *Br Heart J* 1976;38:993-996.
100. Kron IL, Mappin G, Nolan SP, et al. Symptomatic double aortic arch causing tracheal and esophageal compression in the adult. *Ann Thorac Surg* 1987;43:105-106.
101. Higuchi S, Takahashi T, Yamasaki Y, et al. Complete vascular ring with aortic dissection in an octogenarian. *Intern Med* 2010;49:1043.
102. Shum DJ, Clifton MS, Coakley FV, et al. Prenatal tracheal obstruction due to double aortic arch: a potential mimic of congenital high airway obstruction syndrome. *AJR Am J Roentgenol* 2007;188:W82-W85.
103. Raju S, Ratliff J, Timmis H, et al. "Internal coarctation" associated with double aortic arch. *J Thorac Cardiovasc Surg* 1973;66:192-195.
104. Enderlein MA, Silverman NH, Stanger P, et al. Usefulness of suprasternal notch echocardiography for diagnosis of double aortic arch. *Am J Cardiol* 1986;57:359-361.
105. Sahn DJ, Valdes Cruz LM, Ovitt TW, et al. Two dimensional echocardiography and intravenous digital video subtraction angiography for diagnosis and evaluation of double aortic arch. *Am J Cardiol* 1982;50:342-346.
106. Kan MN, Nanda NC, Stopa AR. Diagnosis of double aortic arch by cross sectional echocardiography with Doppler colour flow mapping. *Br Heart J* 1987;58:284-286.
107. Johnson TR, Goldmuntz E, McDonald-McGinn DM, et al. Cardiac magnetic resonance imaging for accurate diagnosis of aortic arch anomalies in patients with 22q11.2 deletion. *Am J Cardiol* 2005;96:1726-1730.
108. Van Praagh R, Van Praagh S. Persistent fifth arterial arch in man: congenital double-lumen aortic arch. *Am J Cardiol* 1969;24:279-282.
109. Santoro G, Caianiello G, Palladino MT, et al. Aortic coarctation with persistent fifth left aortic arch. *Int J Cardiol* 2009;136:e33-e34.
110. Gerlis LM, Dickinson DE, Wilson N, et al. Persistent fifth aortic arch: a report of two new cases and a review of the literature. *Int J Cardiol* 1987;16:185-192.
111. Geva T, Ray RA, Santini F, et al. Asymptomatic persistent fifth aortic arch (congenital double-lumen aortic arch) in an adult. *Am J Cardiol* 1990;65:1406-1407.
112. Yang SG, Fogel MA, Stephens P Jr, et al. Noninvasive imaging of isolated persistent fifth aortic arch. *Pediatr Cardiol* 2003;24:179-181.
113. Celoria GC, Patton RB. Congenital absence of the aortic arch. *Am Heart J* 1959;58:407-413.
114. Oppenheimer Dekker A, Gittenberger de Groot AC, Roozendaal H. The ductus arteriosus and associated cardiac anomalies in interruption of the aortic arch. *Pediatr Cardiol* 1982;2:185-193.
115. Moerman P, Dumoulin M, Lauweryns J, et al. Interrupted right aortic arch in DiGeorge syndrome. *Br Heart J* 1987;58:274-278.
116. Braunlin E, Peoples WM, Freedom RM, et al. Interruption of the aortic arch with aorticopulmonary septal defect: an anatomic review. *Pediatr Cardiol* 1982;3:329-335.
117. Van Praagh R, Bernhard WF, Rosenthal A, et al. Interrupted aortic arch: surgical treatment. *Am J Cardiol* 1971;27:200-211.
118. Van Mierop LH, Kutsche LM. Cardiovascular anomalies in DiGeorge syndrome and importance of neural crest as a possible pathogenetic factor. *Am J Cardiol* 1986;58:133-137.

119. Smallhorn JF, Anderson RH, Macartney FJ. Cross-sectional echocardiographic recognition of interruption of aortic arch between left carotid and subclavian arteries. *Br Heart J* 1982;48:229-235.
120. Riggs TW, Berry TE, Aziz KU, et al. Two-dimensional echocardiographic features of interruption of the aortic arch. *Am J Cardiol* 1982;50:1385-1390.
121. Yasui H, Kado H, Nakano E, et al. Primary repair of interrupted aortic arch and severe aortic stenosis in neonates. *J Thorac Cardiovasc Surg* 1987;93:539-545.
122. Rychik J, Murdison KA, Chin AJ, et al. Surgical management of severe aortic outflow obstruction in lesions other than the hypoplastic left heart syndrome: use of a pulmonary artery to aorta anastomosis. *J Am Coll Cardiol* 1991;18:809-816.
123. Norwood WI, Lang P, Castaneda AR, et al. Reparative operations for interrupted aortic arch with ventricular septal defect. *J Thorac Cardiovasc Surg* 1983;86:832-837.
124. Kutsche LM, Van Mierop LH. Anomalous origin of a pulmonary artery from the ascending aorta: associated anomalies and pathogenesis. *Am J Cardiol* 1988;61:850-856.
125. Contro S, Miller RA, White H, et al. Bronchial obstruction due to pulmonary artery anomalies. I. vascular sling. *Circulation* 1958;17:418-423.
126. Berdon WE, Baker DH, Wung JT, et al. Complete cartilage-ring tracheal stenosis associated with anomalous left pulmonary artery: the ring-sling complex. *Radiology* 1984;152:57-64.
127. Murdison KA, Weinberg PM. Tetralogy of Fallot with severe pulmonary valvar stenosis and pulmonary vascular sling (anomalous origin of left pulmonary artery from right pulmonary artery): a case report. *Pediatr Cardiol* 1991;12:189-191.
128. Oppido G, Pace NC, Gargiulo G. Neonatal right lung emphysema due to pulmonary artery sling. *Pediatr Cardiol* 2008;29:469-470.
129. Jonas RA, Spevak PJ, McGill T, et al. Pulmonary artery sling: primary repair by tracheal resection in infancy. *J Thorac Cardiovasc Surg* 1989;97:548-550.
130. Fearon B, Shortreed R. Tracheo-bronchial compression by congenital cardiovascular anomalies in children. *Ann Otol Rhinol Laryngol* 1963;72:949-969.

Matina Prapa ■ John Pepper ■ Michael A. Gatzoulis

INTRODUCTION

Progressive aortic root dilation has been reported in a number of congenital heart defects, both repaired and unrepaired (1). Following extensive research in this field in the past decades, the thoracic aortic wall is no longer considered as a simple tube but rather a highly sophisticated structure responsive to local hemodynamic changes (2). Inherited connective tissue disorders, such as Marfan disease and bicuspid aortic valve (BAV), have served as aortopathy models, both in terms of pathogenesis and medical management. However, similar aortic wall abnormalities have been reported in a wider range of disparate congenital heart defects, including coarctation of the aorta, tetralogy of Fallot (TOF), and complete transposition of the great arteries (TGA) (Table 34.1). Aortic dilation is usually silent but may produce symptoms of acute aortic dissection or rupture as aneurysm formation progresses. Thus, early identification of aortopathy is important for appropriate follow-up and timely intervention. As life expectancy of patients with congenital heart disease (CHD) increases, several cardiovascular risk factors superimpose on inherent wall abnormalities, and may increase the incidence of aortic complications. The following sections review the most prevalent CHD lesions associated with aortic root abnormalities and the underlying pathology, diagnostic evaluations, and treatment options.

MARFAN SYNDROME

Marfan syndrome (MFS) is a heritable connective tissue disorder resulting from mutations in the fibrillin-1 (FBN1) gene located on chromosome 15 (15q21.1). The estimated prevalence of MFS is 1 in 5,000 to 10,000 live births, affecting both sexes equally (3). Up to 95% of individuals fulfilling the clinical criteria for MFS have a FBN1 mutation (4). Approximately a quarter of affected individuals have *de novo* mutations, with absence of family history of the disease. MFS has an autosomal dominant pattern of inheritance with a high penetrance, affecting almost all allele carriers, but marked phenotypic variability. The syndrome has several manifestations from the skin and the skeletal, cardiovascular, and ocular systems and is considered a prototype model for aortic pathology; practically all affected patients present with aortic dilation or dissection during their lifetime (5). Underlying histologic abnormalities of the aneurysmal aortic wall have been described applying the term “cystic medial necrosis,” characterized by elastic fiber fragmentation, noninflammatory loss of vascular smooth muscle cells (VSMCs), and accumulation of basophilic ground substance within cell-depleted areas in the aortic media (3). However, as described later, these changes are not unique to MFS but can be found in other causes of nonsyndromic thoracic aortic aneurysms (TAA) (6).

Despite the identified causative role of FBN1 mutations, the exact sequence of molecular changes leading to MFS continues to be under investigation. FBN1 is a main structural component of the extracellular microfibrillar network that connects VSMCs to the surrounding elastic fibers, facilitating tissue elasticity (7). At present, more than 1,000 mutations have been described in the FBN1 gene without a clear genotype–phenotype association (3). Mutations in exons 24–32 may be indicators of earlier onset of morbidity in MFS although the latter were not associated with a higher risk of aortic dissection in patients with aortic dilation (8). Due to the established weakness of connective tissue, early theories on the pathogenesis of MFS focused on the structural properties of FBN1. A dominant negative effect was initially suggested, where the mutant allele gives rise to abnormal FBN1 that in turn disrupts the assembly of normal fibrillin polymers (9,10). However, a different study in transgenic mice has exhibited that the mutated protein participates in productive microfibrillar formation (8). Moreover, the addition of a normal allele in the same animal model rescued the aortic phenotype, highlighting the contribution of haploinsufficiency to the disease (11). This raises the possibility that the normal aortic wall lamellar structure can be restored.

More recently, the importance of transforming growth factor beta (TGFβ) in the pathogenesis of MFS has emerged. The TGFβ family of cytokines plays a central role in vascular remodeling and aneurysm formation (2). Mouse models of the disease have shed light on the regulatory functions of fibrillin 1, which controls the bioavailability of TGFβ by binding a latent form of the cytokine. Excessive TGFβ signaling has been shown to play a causal role in aortic root enlargement, mitral valve abnormalities, and emphysema associated with MFS (12–14). More importantly, the administration of TGFβ-neutralizing antibody has led to reversal of the above manifestations (3). The general mechanistic hypothesis for the above findings is that fibrillin 1 deficiency makes sequestered TGFβ more accessible to activation, although mutated forms of the protein can also stimulate TGFβ release (15). The significance of the TGFβ pathway was confirmed with the discovery of a second locus for MFS, termed as Marfan syndrome type II (MFS2), associated with mutations in the transforming growth factor-beta type II receptor (TGFB2) (16). Overall, it is hypothesized that FBN1 deficiency results in altered homeostasis of the extracellular matrix and subsequent increase of TGFβ activity. The exact sequence of succeeding mechanisms leading to aortic wall degeneration remains elusive. However, it has been established that increased elastolysis occurs, with activation of matrix metalloproteinases (MMP-2 and MMP-9), apoptosis of VSMC, and abnormal cell migration (17).

Diagnosis

The diagnosis of MFS is largely based on clinical grounds. Due to the wide range of clinical manifestations, a multidisciplinary approach is required. A definite diagnosis can be made

TABLE 34.1 Commonest Congenital Heart Disease Lesions Associated with Aortic Root Abnormalities

Heart Defect	Location of AoD	Incidence of AoD	Incidence of Dissection	Recommendations for Ao Replacement
MFS	Sinuses of Valsalva (typical location)	<ul style="list-style-type: none"> ■ 35% by 5 y (24) ■ 68% by 19 y (24) 	<ul style="list-style-type: none"> ■ 4.3% in childhood (26) ■ 20% in adolescence (26) 	<ul style="list-style-type: none"> ■ >50 mm ■ accelerated aortic growth (>10 mm/y) ■ Development of aortic regurgitation ■ Need for mitral valve surgery
BAV	Ao root and ascending aorta	<ul style="list-style-type: none"> ■ <19 y, isolated BAV (64) ■ 12% marked AoD ■ 25% moderate AoD 	<ul style="list-style-type: none"> ■ Case reports in adolescents (65) 	<ul style="list-style-type: none"> ■ >50 mm ■ accelerated aortic growth (>10 mm/y) ■ Need for aortic valve surgery with AoD > 45 mm
TOF	Ao root and ascending aorta	<ul style="list-style-type: none"> ■ <19 y, repaired TOF (89) ■ 87% at sinus of Valsalva ■ 63% at ascending aorta 	<ul style="list-style-type: none"> ■ two case reports in adults with repaired TOF (84,85) 	<ul style="list-style-type: none"> ■ ≥ 55 mm, especially when there is an indication for pulmonary valve implantation ■ Development of aortic regurgitation with AoD > 50 mm
CoA	Ascending aorta and site of previous surgical repair	<ul style="list-style-type: none"> ■ Pediatric and adult population (100) ■ 9% after surgical repair 	<ul style="list-style-type: none"> ■ Pediatric and adult population (100) ■ <1% after surgical repair 	<ul style="list-style-type: none"> ■ ~50 mm ■ Accelerated aortic growth (>10 mm/y) ■ Development of aortic regurgitation
Arterial switch	Neo-aortic root dilation	<ul style="list-style-type: none"> ■ 33.4% after surgical repair (106) 	<ul style="list-style-type: none"> ■ No reports 	<ul style="list-style-type: none"> ■ Severe neo-aortic root dilation (≥55 mm)

Ao, aortic; AoD, aortic dilation; BAV, bicuspid aortic valve; CoA, coarctation of the aorta; TOF, Tetralogy of Fallot.

TABLE 34.2 Revised Ghent Nosology for the Diagnosis of Marfan Syndrome

Revised Ghent Criteria for the Diagnosis of Marfan Syndrome (19)

In the Absence of Family History of MFS:

- (1) Ao ($z \geq 2$) and ectopia lentis
- (2) Ao ($z \geq 2$) and FBN1 mutation
- (3) Ao ($z \geq 2$) and systemic features (≥ 7 points)^a
- (4) Ectopia lentis and FBN1 mutation previously associated with aortic root aneurysm/dissection

In the Presence of Family History of MFS:

- (5) Ectopia lentis
- (6) Systemic features (≥ 7 points)^a
- (7) Ao ($z \geq 2$ above 20 y old, ≥ 3 below 20 y old)

^aNew Scoring of Systemic Features (≥ 7 Points Indicates Systemic Involvement):

- Wrist and thumb sign—3 (wrist or thumb sign—1)
- Pectus carinatum deformity—2 (pectus excavatum or chest asymmetry—1)
- Hindfoot deformity—2 (plain pes planus—1)
- Pneumothorax—2
- Dural ectasia—2
- Protrusio acetabuli—2
- Reduced upper segment/lower segment ratio and increased arm/height and no severe scoliosis—1
- Scoliosis or thoracolumbar kyphosis—1
- Reduced elbow extension—1
- Facial features (3/5)—1 (dolichocephaly, enophthalmos, downslanting palpebral fissures, malar hypoplasia, retrognathia)
- Skin striae—1
- Myopia >3 diopters—1
- Mitral valve prolapse (all types)—1

Special Considerations for Young Individuals (<20 y old):

- (1) Use term “nonspecific connective tissue disorder” in sporadic cases with insufficient systemic features (<7 points) and/or borderline aortic root measurements ($z < 3$) without FBN1 mutation, until follow-up echocardiographic evaluation shows aortic root dilation ($z \geq 3$)
- (2) Use term “potential MFS” in sporadic or familial cases with a FBN1 mutation and Ao $z < 3$, until the aorta reaches threshold
- (3) Neonatal MFS is not considered as a separate category, but represents the severe end of the MFS spectrum

Ao, aortic diameter at the sinuses of Valsalva above indicated z-score or aortic root dissection; FBN1, fibrillin-1 gene mutation; MFS, Marfan syndrome; z, z-score.

^aNew scoring of systemic features.

Modified from Loeys BL, Dietz HC, Braverman AC, et al. The revised Ghent nosology for the Marfan syndrome. *J Med Genet* 2010;47:476–485.

applying the Ghent criteria, which are based on demonstration of symptoms from different organ systems and family history of MFS (3). However, Ghent nosology cannot exclude MFS in children, due to the variability in onset and severity of symptoms in this age group (18). Consequently, long-term follow-up is required in younger patients before a diagnosis can be established. Recently, an international expert board has published a revised Ghent nosology, in which aortic root aneurysm and ectopia lentis are the cardinal features of MFS with a new scoring system for other systemic features of the disease (19) (Table 34.2). Genetic screening can be adjunctive to clinical evaluation, in cases with suspected MFS or where other family members carry an identified causal mutation. However, FBN1 mutations are not specific to MFS and can be found in a wide range of phenotypes including mitral valve, aorta, skeleton, and skin (MASS) syndrome; familial mitral valve prolapse; and familial ectopia lentis (16). Mutations in TGFBR2 can be found in up to 21% of MFS patients who are FBN1 negative (20,21). Conversely, the above type of the disorder, termed as MFS type 2, has a phenotype overlapping with that of Loeys-Dietz syndrome, a dominant disease that is similar to MFS, but patients have bifid uvula and widely spaced eyes, and some have cleft palate (5). The presence of ectopia lentis, which is absent in the latter, can be useful in the differential diagnosis between the two syndromes (22).

The most characteristic and troublesome features of MFS involve the cardiovascular system and include TAA formation, aortic regurgitation owing to an enlarged aortic root, and mitral valve prolapse (5). Aortic enlargement is typically located at the level of sinuses of Valsalva and may eventually extend to the sinotubular junction and proximal ascending aorta (Fig. 34.1B) (23). Approximately 35% of MFS patients develop aortic root dilation by the age of 5 years and 68% by the age of 19 years (24). Dilation is progressive although its rate is unpredictable and can vary even in the same patient (25). The incidence of serious cardiovascular complications, including aortic dissection or rupture, has been estimated to be around 4.3% in childhood with a rise to approximately 20% in adolescence (26). Aortic regurgitation may develop in 15% to 44% of MFS patients during childhood and adolescence, and has been strongly associated with acute cardiovascular events (27). Additional predictors of aortic complications include younger age at presentation and a family history of severe aortic disease (26). Patients diagnosed with MFS during childhood have significantly fewer adverse cardiac events compared to those diagnosed during adulthood, highlighting the importance of early identification of the disease (28).

Following diagnosis of MFS, an echocardiogram is recommended at 6-month intervals to assess the progression of aortic disease. If measurements remain stable, echocardiographic follow-up can be performed on an annual basis (5). However, those guidelines refer to adult patients, and it has been suggested that younger patients should be monitored every 6 months, particularly during accelerated growth phases (29). Children who do not meet the full diagnostic criteria of the disease should be screened at least every 5 years until they reach adulthood (29). Baseline echocardiographic imaging requires diameter measurement at the level of the sinuses of Valsalva, which is the typical affected aortic segment in MFS. Of note, aortic root diameters should be indexed to age and body surface area (30). It has been suggested that an adjusted nomogram with higher upper limits should be used for the diagnosis of aortic dilation in children with MFS, as they tend to be taller compared to their peers (31). In the instance of poor echocardiographic windows, magnetic resonance imaging (MRI) or computed tomography (CT) angiograms should be performed (Fig. 34.2A). Importantly, both of the above modalities measure external diameter, which is

Different patterns of aortopathy in CHD

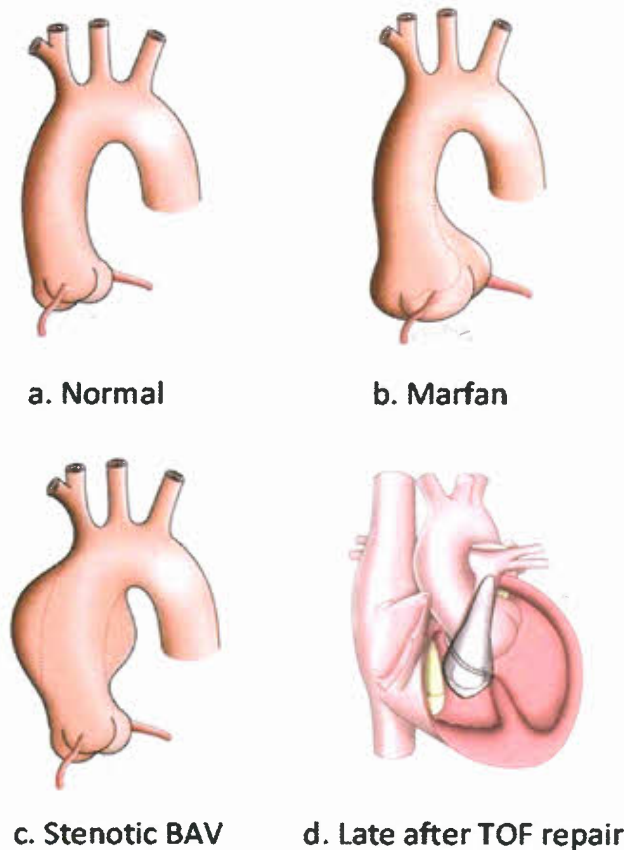
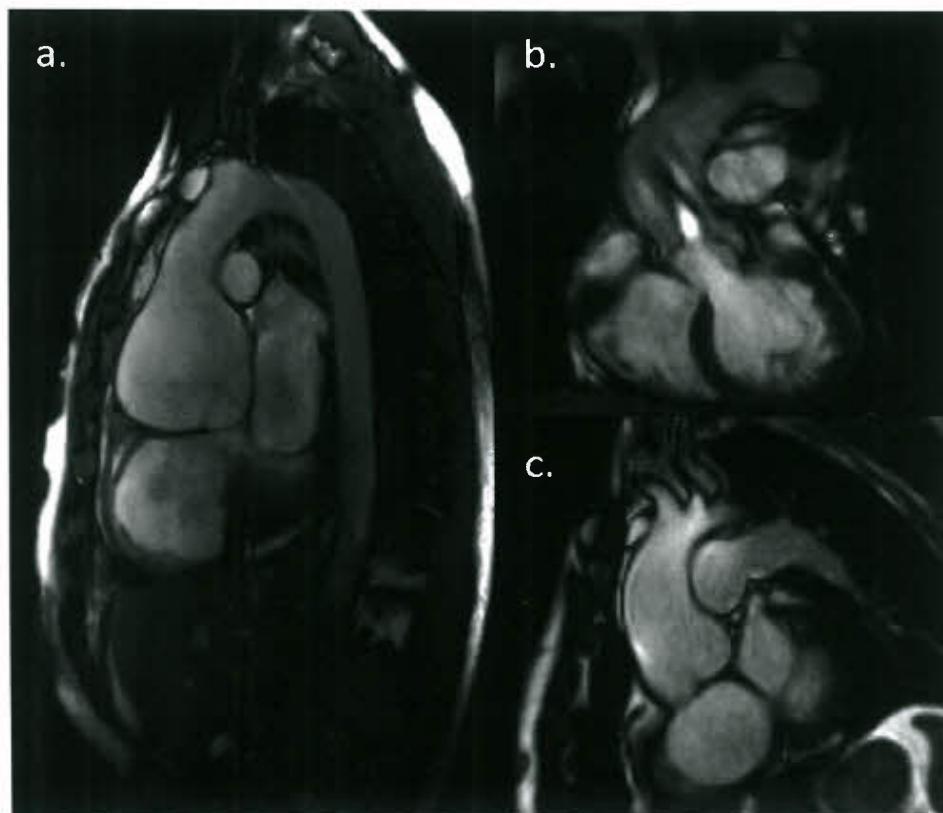


Figure 34.1. Different patterns of aortopathy seen in congenital heart disease (CHD). **A:** Anterior view of a normal aortic root, ascending aorta, and aortic arch. **B:** Typical location of aortic dilation at the level of sinuses of Valsalva in patients with Marfan syndrome. **C:** Asymmetric pattern of ascending aortic dilation encountered in stenotic bicuspid aortic valve (BAV) disease. **D:** Uniform dilation of aortic root and ascending aorta following repair of Tetralogy of Fallot (TOF).

0.2 to 0.4 cm higher compared to the internal diameter measured by echocardiography (5). Precise measurements are difficult due to movement of the ascending aorta in three planes and the difficulty of obtaining a true cross-sectional diameter of the aorta. Therefore, recommendations in asymptomatic patients based on diameter values in guidelines should be made with caution.

Routine CT or MRI imaging of the entire thoracic aorta is recommended in patients who present with descending aortic dilation, with type B aortic dissection, or following ascending aortic aneurysm repair (32). The vast majority of MFS patients present with dilation of the ascending aorta or type A dissection (5). However, in a smaller subset of patients, the disease initially involves the distal thoracic aorta with reported poor outcomes in cases of acute type B aortic dissection (33). Moreover, up to 52.6% of MFS patients who underwent initial repair of the ascending aorta had subsequent vascular procedures involving portions of their descending thoracic aortas (34), prompting comprehensive imaging follow-up. Increased regional wall stiffness assessed by MRI may be an additional marker for extensive screening, as it has been shown to be a predictor of progressive descending aortic dilation in MFS (35).

Figure 34.2. Magnetic resonance images of different types of aortic dilation. **A:** Still frame from steady-state free precession image showing the “pear-shaped” aortic dilation seen in Marfan syndrome. A jet of mild aortic regurgitation is seen. **B:** Jet lesion directed to the anterior–lateral portion of the ascending aorta in a stenotic bicuspid aortic valve with asymmetrical dilation of the vessel wall at the same level. **C:** Dilation of the aortic root extending to the sinotubular junction and proximal ascending aorta in a patient with repaired Tetralogy of Fallot.



Therapy

Both medical and surgical treatments have substantially increased life expectancy in MFS, extending it up to 70 years compared to 40 years in the 1970s (34). Conservative treatment consists of use of β -blockers and exercise limitation, with an aim to reduce arterial stress in MFS. Beta-blockade may be initiated at the time of diagnosis or in the presence of significant aortic dilation (32). Dosage must be closely monitored during accelerated growth phases and adjusted in case of adverse effects, such as asthma aggravation. If not well tolerated, medical treatment can be substituted with a calcium channel blocker. A protective effect of both agents has been reported on aortic growth rate in children and adolescents with MFS (36). Recently, in a pilot study including 18 children with MFS, the use of angiotensin II–receptor blockers (ARBs) significantly slowed the rate of progressive aortic root dilation (37). However, these data are preliminary, and the efficacy of ARB therapy in MFS is being investigated by two ongoing prospective randomized trials: one in the United States, coordinated by the Pediatric Heart Network of the National Heart Lung and Blood Institute (NHLBI), and the other in Europe, run by the Clinical Trials and Evaluation Unit (CTEU) of the Royal Brompton and Harefield National Health Service (NHS) Foundation Trust (38,39). Despite long-term treatment, major cardiovascular complications may still develop (36). Therefore, pharmacologic therapy can be used to delay surgical treatment in affected children, but the need for close follow-up is fundamental. Avoidance of maximal and isometric exertion is also recommended, although exercise restrictions may not always be applicable in younger children. An American Heart Association consensus document published in 2004 offers recommendations for physical activity in young patients with genetic cardiovascular diseases, including MFS (40).

Surgery for aortic root aneurysm in children with MFS has been reported to be safe with good long-term results (41). If the aortic valve is affected, a composite replacement of the valve and ascending aorta is performed. In cases with no substantial aortic valve disease, valve-sparing techniques can be applied, including remodeling of the aortic root or reimplantation of the aortic valve (Fig. 34.3). Creation of neo-aortic sinuses in the reimplantation technique is thought to enhance the durability of repair in MFS (42). Current recommendations for elective aortic root surgery in adults with MFS are based on the positive correlation between aortic diameters and risk of dissection. Nonetheless, there is a lack of similar data in children owing to the rarity of aortic complications in this age group. Due to the absence of general consensus in the pediatric population, most centers advise prophylactic surgery using the diameter criterion for adults (~ 50 mm) but also take into consideration the presence of accelerated aortic growth (>10 mm/year), development of aortic regurgitation, or need for mitral valve surgery (29). Following aortic root surgery, close follow-up and continuation of medical therapy is necessary, since distal segments of the aorta may also be affected (32).

BICUSPID AORTIC VALVE

BAV is the commonest congenital cardiac malformation with a prevalence of 0.5% to 2% (44,45). The term BAV has been used to describe a broad spectrum of malformations, including “true” BAV, denoting the presence of two fully developed valve leaflets, and “functional” BAV, with presence of three leaflets, two of which have been fused together. The disease is a heritable condition with familial studies demonstrating the occurrence of a BAV in approximately 9% of first-degree relatives of affected individuals (46). In some instances, the pattern

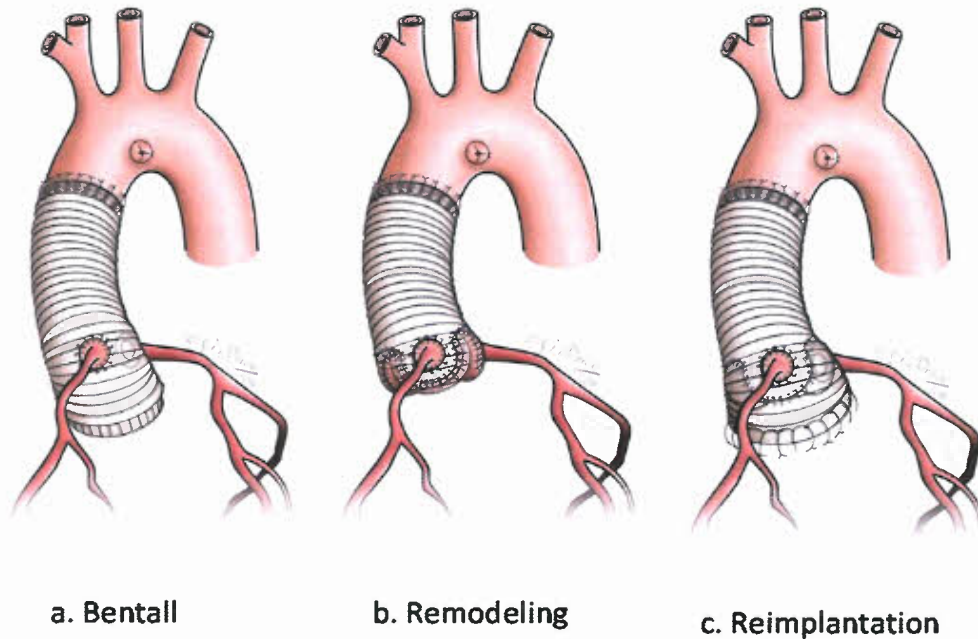


Figure 34.3. A: Bentall procedure, composite graft replacement of the aortic valve and the ascending aorta. The aortic cusps and sinuses are excised completely. A valved conduit is sutured to the aortic annulus, and the coronary arteries are reimplanted into the graft. B: Aortic root replacement with remodeling of the aortic root. A tubular Dacron graft is used with the proximal end tailored to reconstruct the aortic sinuses. The coronary arteries are reimplanted into their respective neo-aortic sinuses. C: Aortic root replacement with reimplantation of the aortic valve. The aortic sinuses are excised leaving a rim of aortic tissue attached to the aortic annulus and around the coronary artery orifices. The aortic valve is reimplanted inside a tubular Dacron graft using two suture lines, one below and one above the aortic annulus. The coronary arteries are reimplanted into their respective aortic sinuses, and the graft is anastomosed to the distal ascending aorta. (Mulder BJ, Webb GD. Marfan syndrome: a cardiovascular perspective. In: Gatzoulis MA, Webb GD, Daubeney P, eds. *Diagnosis and Management of Adult Congenital Heart Disease*. 2nd ed. Philadelphia, PA: Elsevier, Ref. 43).

of inheritance is autosomal dominant with variable penetrance and a male/female ratio of 3:1 (46,47). Development of a bile-alet aortic valve predisposes to several complications, including valvular dysfunction and infective endocarditis (48–51). Moreover, BAV is associated with structural pathologies of the aortic wall, including coarctation of the aorta, dilation of the ascending aorta, and TAA formation (52,53). As a result, BAV is considered as a continuum of a disease process affecting the entire aortic root and ascending aorta (54). Despite the lower incidence of aortic dissection compared to MFS (5% vs. 40%),

BAV disease is overall responsible for a larger number of dissections due to its higher prevalence (47).

The pathogenesis of vessel wall remodeling leading to aortic dilation in patients with BAV remains unclear and may be related to mechanical responses to local hemodynamics or to intrinsic structural abnormalities of the aortic wall. The latter is supported by evidence of cystic medial necrosis in the aortic media of BAV patients (Fig. 34.4). Fedak et al. (7) have proposed a defect of FBN1 synthesis as the culprit lesion for aneurysm development, having observed a reduction of expression

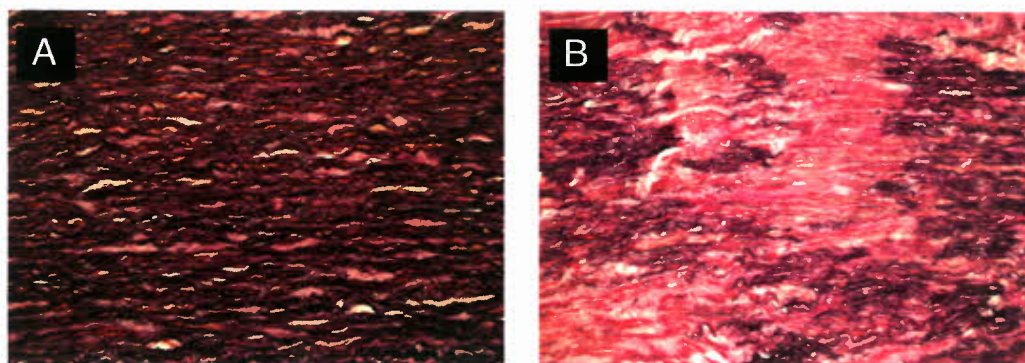


Figure 34.4. Histologic abnormalities in the aortic wall of patients with congenital heart disease. Image (A) is from a normal aorta and (B) from a patient with a bicuspid aortic valve (BAV): (A) shows normal distribution of the elastic lamellae (purple), and (B) shows severe medial wall degeneration with elastic fiber fragmentation and accumulation of basophilic ground substance (pink). Both images are stained in elastic van Gieson. Magnification $\times 20$.

of this protein in the extracellular matrix of dilated aortas with BAVs (7). Deficiency of FBN1 leads to detachment of VSMCs from elastin and collagen and activation of MMPs, inducing accelerated apoptosis. Despite the similar underlying pathology with MFS, BAV patients are negative for mutations in the FBN1 gene (55). Notch homolog 1 (NOTCH1) gene may have a key role in BAV disease as mutations within this gene have been associated with both sporadic and familial BAV and TAA as well as increased calcium deposition on the aortic valve (56). The NOTCH1 gene encodes a transmembrane protein activating a signaling pathway in cardiac embryogenesis, involved in the development of the great vessels and the aortic and pulmonary valves (56). Mutations in the ACTA-2 gene, encoding VSMC α -actin, have been associated with familial thoracic aortic aneurysm and dissection (TAAD) disease and concomitant BAV (57). Endothelial nitric oxide synthase (eNOs) is another candidate gene product, as murine studies have exhibited a strong association between eNOs deficiency and the development of BAV (58). Finally, an X-linkage has been hypothesized due to association of BAV with Turner syndrome (45XO) and the male predominance of the disease (54).

While structural abnormalities of the aortic wall have been identified, local hemodynamic factors may also be operative in TAA formation. In vitro experiments have shown that cultured human endothelial cells respond to different levels of wall shear stress (59). Morphologic variations in BAV carry different risks of aortic dilation, which could be related to their different hemodynamic effect: anteroposteriorly oriented BAVs are more likely to develop regurgitation, whereas right-left oriented BAVs are more prone to stenosis, resulting in different flow patterns in the aorta (60,61). Stenotic BAVs create a high-velocity jet, which imposes increased shear stress on the right anterolateral portion of the ascending aorta, whereas regurgitant BAVs increase wall tension, due to higher stroke volumes, and correlate with aortic root dilation (Fig. 34.2B) (54). The hemodynamic effect has been investigated in collected tissue specimens from BAV patients, exhibiting different patterns of stress-induced vascular remodeling in the convexity versus the concavity of the enlarged aorta (62).

Aortic dilation has been shown to be present in the early stages of life and progressive throughout childhood in BAV disease. In a pediatric population of 107 patients with normally functioning BAVs, aortic root diameters assessed by echocardiography were significantly larger in BAV compared to controls (63). However, the greatest discrepancy was noticed at the level of the ascending aorta, with a faster rate of annual growth in BAV patients than controls. In a different study, the rate of ascending aortic dilation was reported to increase even further when children with BAV reach adolescence (64). Reported risk factors for ascending aortic dilation in BAV include aortic valve morphology, severity of outflow gradient and aortic regurgitation, and systolic left ventricular outflow jet angles (65). Despite the above findings, the incidence of aortic dissection is rare in children with BAV and only reported in isolated cases of adolescent patients (65). In a cohort of 981 children with BAV followed up in a single center, the incidence of primary cardiac events was approximately threefold lower than in young adults and was largely related to aortic stenosis with no cases of aortic dissection (65). Of note, the above study was restricted to isolated BAV disease, whereas Turner syndrome and prior coarctation repair are identified risk factors of aortic dissection in the adult BAV population (66,67).

Diagnosis

In view of the silent nature of aortic enlargement and the high mortality rates of aortic dissection, annual imaging has been recommended for BAV patients until the rate of progressive

enlargement has been established (1). In contrast with MFS, the location of maximal dilation is more distal and therefore, echocardiographic imaging may not provide complete assessment of aortopathy in BAV (Fig. 34.1C) (1). Compared to CT, MRI has the advantages of simultaneous evaluation of aortic valve pathology and left ventricular dysfunction without exposure to radiation (5). Moreover, the elastic properties of the ascending aorta can be assessed and may be used analogously to MFS in risk stratification for progressive dilation (68). Of note, recent AHA recommendations include echocardiographic screening of first-degree relatives of patients with BAV, as affected members may have isolated thoracic aortic dilation or increased aortic stiffness in the absence of BAV (5,69). Those findings suggest that BAV and TAA may share a common genetic background, as variable expressions of the same disease.

Therapy

Prophylactic β -blockade in BAV disease is based on consensus opinion and is recommended in patients with aortic dilation (>40 mm) without significant aortic regurgitation (70). Extrapolation of data on pharmacologic therapy in MFS cannot be made, due to the lack of clinical trials in BAV patients (54). Timing of surgical treatment in young patients with a BAV and dilated ascending aorta remains a challenge. Similar to children with MFS, diameter measurements cannot be associated with the risk of aortic dissection due to the rarity of such events in this age group. Therefore, the traditional threshold of 50 mm for aortic repair is used along with aortic growth rate exceeding 10 mm/year, and an aortic diameter of more than 45 mm for aortic valve surgery (71). Valve-sparing procedures are favorable in children with an aortic annulus >18 mm. The presence of a bileaflet aortic valve is not necessarily a contraindication to a valve-sparing operation unless there is significant valve regurgitation, leaflet distortion, or calcification (71). Use of a composite valve graft is preferable in cases of acute aortic dissection and abnormal aortic valve leaflets. Homografts can be used as an alternative in children with an annulus of <18 mm. However, their durability is limited leading to a reoperation rate of approximately 40% in several pediatric series (41,72–74). Finally, pulmonary valve autotransplantation (Ross procedure) remains a source of controversy in young patients with BAV who need an aortic valve replacement. Despite the satisfactory results of the procedure, durability limitations have been reported by the end of the first postoperative decade in younger patients (75). Pulmonary autograft dilation may occur following the Ross procedure with described intrinsic histologic abnormalities of the pulmonary root similar to those of the aorta in BAV disease (76). Predictors of autograft failure in children include the presence of preoperative aortic regurgitation and aortic root dilation (75).

TETRALOGY OF FALLOT

TOF is the most frequently encountered cyanotic heart lesion accounting for nearly 10% of all congenital heart defects (77). Approximately 7% of affected individuals have a deletion on chromosome 22q11 with important implications in terms of genetic counseling and family screening, due to the associated 50% risk of transmission (78). Aortic root dilation is a known feature of unrepaired TOF and has been attributed to increased aortic blood flow due to right to left shunting (79). However, progressive dilation also occurs in 15% to 48% of TOF patients following reparative surgery (79,80). The overall survival in repaired TOF has increased dramatically, with a reported 85% survival rate over a 36-year follow-up (81).

Excessive development of aortic enlargement is one of the contributing factors to late morbidity in this patient cohort (82). Aortic root dilation may lead to aortic regurgitation due to incomplete leaflet coaptation, necessitating aortic valve replacement (83). Moreover, aortic enlargement imposes the risk of aortic dissection and rupture in patients with TOF (83–85).

Aortic wall pathology in TOF has been postulated to occur due to the influence of increased blood flow from both ventricles to the overriding aorta, prior to anatomical repair (79). This is further supported by the fact that dilation is greatest in patients with pulmonary atresia, the extreme end of the morphologic spectrum of TOF, where volume load through the aorta is maximal (79). However, intrinsic histologic abnormalities are also present in the aortic media of TOF patients, similar to the processes of cystic medial necrosis described in MFS and BAV disease (6,82). Those structural changes can be seen not only in the aorta of adult TOF patients, where the hemodynamic component has been removed, but also in infants and neonates, only a few days old (82). It remains unknown whether hemodynamic stress, even present before birth, is the causal mechanism for the structural changes in the aorta. Even if that is the case, progressive aortic dilation only takes place in a subset of TOF patients, where a genetic component could be equally operative. A recent study reported the vasoprotective role of an MMP-9 genetic polymorphism in TOF patients, which was associated with lower aortic stiffness and smaller z score of the aortic sinotubular junction (86).

Dilated aortic segments in TOF patients include the aortic root and ascending aorta (Fig. 34.1D) (82). Among unoperated patients, those with TOF and pulmonary atresia have greater aortic enlargement (87,88). Aortic root dilation has been described in children following TOF repair with a prevalence of 88%, 87%, 61%, and 63% at the annulus, sinus of Valsalva, sinotubular junction, and ascending aorta, respectively (89). A different study reported similar findings with increased diameters in the first 3 to 6 months after palliative shunt surgery (90). Interestingly, root dimensions “normalized” by 7 years of age in TOF patients who had undergone repair in infancy, whereas aortic dilation persisted into adulthood in those repaired after 1 year of age (90). Identified risk factors for progressive aortic dilation in repaired TOF include male sex, longer time interval from palliation to repair, and presence of pulmonary atresia and right aortic arch (79). Aortic wall stiffness may be an additional risk stratifier, as it was found to be increased in both children and adults with repaired TOF and was closely associated with aortic root dilation (91).

In case of progressive dilation, imaging of the aorta is recommended on an annual basis (Fig. 34.2C) (1). Similar to BAV disease, there is currently no consensus on prophylactic β -blocker treatment in TOF patients with aortic root dilation. Moreover, no guidelines for timing of aortic root surgery have been reported. Despite the increased recognition of aortic pathology in this patient cohort, aortic dissection has only been reported in a few isolated cases with an aortic diameter of ≥ 55 mm with additional risk factors (84,85). Therefore, it may be that aortic root replacement should be considered in TOF patients when aortic diameter exceeds 55 mm, especially when there is an indication for pulmonary valve implantation (79). Additional soft indications may include the development of aortic regurgitation with a root diameter of more than 50 mm, similar to patients with MFS (79). However, these are all arbitrary and clearly merit further investigation.

COARCTATION OF THE AORTA

Coarctation of the aorta has an incidence of 0.3 to 0.4 in 1,000 live births, accounting for 5% to 7% of all CHD (92,93). More than 50% of affected patients have a BAV with

similar underlying structural abnormalities in the aortic media (6). Aneurysm formation is a known clinical feature of the disease and may occur at the site of previous surgical repair or in the proximal aorta (94). Natural history studies report dissection of the aorta as the cause of death in 19% of patients with coarctation, reaching 50% in the presence of a concomitant bileaflet aortic valve (95). The disease is associated with significant cardiovascular morbidity, even following surgical repair, with survival rates of 72% at 30 years (96). The commonest cause of late death is coronary artery disease followed by sudden death, heart failure, cerebrovascular accidents, and ruptured aortic aneurysm (96).

Structural abnormalities of the aortic media in coarctation patients have been reported within 24 hours after birth, implying an intrinsic underlying cause (97). Moreover, medial wall abnormalities were identical at sites subjected to high and low pressure (proximal and distal ends of the coarctation site), eliminating the influence of hemodynamics in the described pathology (6). Nevertheless, it has been hypothesized that hemodynamics in the form of systemic hypertension in patients with coarctation and BAV may trigger apoptotic mechanisms in the latter, due to the higher incidence of ascending aortic dissection when the two entities coexist (95). Interestingly, both BAV and coarctation have a known male predominance as well as an association with Turner syndrome, leading to the hypothesis that a common genetic substrate may be located on the X chromosome (95). Finally, approximately 10% of patients with coarctation and 10% of patients with isolated BAV have concurrent intracranial aneurysms (98). Cardiac structures derived from neural crest cells include the outflow tract of the heart and the aortic arch system, as well as the cervicocephalic arteries. Maldevelopment of the neural crest may lead to vascular fragility, supporting the concept that BAV and coarctation may belong to a spectrum of diffuse aortopathy (98,99).

Despite successful surgical repair of coarctation, approximately 9% of patients develop aortic aneurysms late after the operation, with potential aortic rupture and death (100). Development of aneurysm at the site of surgical repair is associated with the patch graft technique and repair of coarctation before the age of 14 (100). Predictors of ascending aortic aneurysm formation include the coexistence of a BAV and advanced age, with a 1.4 risk ratio per decade of age at follow-up (94). As such, coarctation is considered to be a lifelong disease and requires close surveillance of the aortic sequelae, especially in patients with concomitant BAV. Imaging follow-up of both the ascending and descending thoracic aorta is recommended in coarctation patients, irrespective of previous repair, for early detection of aortic wall complications (94,101). Prophylactic treatment with β -blockade as well as appropriate timing of surgical intervention on the dilated ascending aorta in this patient cohort remain uncertain. Most centers use the criteria applied for aortic surgery in MFS, whereas novel surgical techniques may be required in patients with coarctation and a BAV (95,102).

TRANSPOSITION OF THE GREAT ARTERIES

Complete TGA is the second most common cyanotic heart defect, accounting for 5% of all congenital heart defects (103). TGA has a prevalence of 20 to 30 in 100,000 live births, with a 2:1 male predominance (103). Arterial switch operation (ASO) has become the preferred technique for anatomic correction of TGA, offering the advantage of a systemic left ventricle over the Mustard procedure. However, ASO is not without late complications, including development of neo-aortic dysfunction, with dilatation of the proximal ascending aorta resulting in aortic regurgitation (104). At a median follow-up of

4.9 years following ASO, the incidence of neo-aortic regurgitation of all grades was 16% (104). Nonetheless, the cumulative incidence of grade 2 or higher regurgitation was 9% at 15 years, with pulmonary outflow obstruction reported as the main cause for reoperation. To date, no cases of neo-aortic dissection or rupture have been reported although, taking into consideration the relative young age of the ASO, the magnitude of aortic complications cannot be fully appreciated. In the largest published series of 1,200 infants who underwent ASO between 1982 and 1999 in a single center, only a substrate of 1,095 survivors is currently reaching adulthood (104).

Histologic abnormalities, similar to those seen in MFS and BAV, have been described in normal-sized ascending aortas of neonates with TGA undergoing arterial switch (6). These findings may imply an inherent structural weakness of the aortic wall in patients with TGA. Interestingly, aortic root pathology has also been described in this lesion following the Mustard procedure, but may be largely underestimated due to other serious complications of the technique, such as right ventricular dysfunction, arrhythmias, and sudden cardiac death (1). Despite the evidence of intrinsic abnormalities, hemodynamics may also have a causal role in aortic dilation in TGA. Sharper angulation of the aortic arch in patients with TGA has been associated with greater pulse wave reflection, dilation of the ascending aorta, and aortic regurgitation late after the ASO (105).

During echocardiographic assessment of TGA patients who had undergone ASO, neo-aortic root dilation, defined as a z-score ≥ 3 , was reported in 33.4% at a median follow-up of 5 years (106). Importantly, in the majority of patients with neo-aortic dilation, a stabilization of z-scores was observed during late follow-up, suggestive of absence of progressive dilation. Risk factors for neo-aortic dilation included previous pulmonary artery banding and older age at operation. Freedom from reoperation on the neo-aortic valve or root was 95% at 10 years. According to current recommendations, annual follow-up is suggested for TGA patients undergoing ASO with root intervention in the instance of severe neo-aortic root dilation (>55 mm) (103). Longer term follow-up will be available for ASO patients in the future and may further elucidate the mechanisms of neo-aortic dilation in this cohort.

OTHER LESIONS

Structural abnormalities of the aortic media have been documented in a wide range of congenital heart defects, including ventricular septal defect, truncus arteriosus, double outlet right ventricle, tricuspid atresia, and double aortic arch (6). These changes may be present as early as the neonatal period, raising the question of a common genetic substrate that is yet to be elucidated.

CONCLUSIONS

Increasing recognition of aortic complications in patients with CHD has led to a significant change in our perception of aortic enlargement from a model of "poststenotic dilation" to a co-existent intrinsic aortopathy. Despite the exponential research in this field during the last decade, there is a paucity of data in terms of available genetic screening and development of new therapies. Following the paradigm of FBN1 mutations in MFS, complete sequencing of the gene currently incurs a prohibitive cost, and no clear genotype-phenotype correlation exists. Similarly, despite our deeper understanding of the pathogenetic mechanisms implicated in aneurysm formation in MFS, β -blockers remain the mainstay of pharmacologic therapy.

However, recently recognized molecules promoting aneurysm formation are being targeted in animal models. Such examples include angiotensin receptor drugs, which reduce TGF β activity as well as doxycycline, which acts as an MMP inhibitor (29). Likewise, genetic sequencing is a useful tool for screening of first-degree relatives of patients who are positive for a mutation associated with aortic aneurysm formation, such as FBN1 and ACTA2 (5). Overall, the prognosis of patients with aortic root abnormalities and CHD has improved substantially over the past decades, mainly as a result of early diagnosis and timely intervention. As life expectancy of patients with CHD increases, so will our understanding of the pathogenetic mechanisms implicated in aortic disease.

REFERENCES

1. Yetman AT, Graham T. The dilated aorta in patients with congenital cardiac defects. *J Am Coll Cardiol* 2009;53:461-467.
2. El-Hamamsy I, Yacoub MH. Cellular and molecular mechanisms of thoracic aortic aneurysms. *Nat Rev Cardiol* 2009;6:771-786.
3. Canadas V, Vilacosta I, Bruna I, et al. Marfan syndrome. Part 1: pathophysiology and diagnosis. *Nat Rev Cardiol* 2010;7:256-265.
4. Keane MG, Pyeritz RE. Medical management of Marfan syndrome. *Circulation* 2008;117:2802-2813.
5. Hiratzka LF, Bakris GL, Beckman JA, et al. 2010 ACCF/AHA/AATS/ACR/ASA/SCA/SCAI/SIR/STS/SVM guidelines for the diagnosis and management of patients with Thoracic Aortic Disease: a report of the American College of Cardiology Foundation/American Heart Association Task Force on Practice Guidelines, American Association for Thoracic Surgery, American College of Radiology, American Stroke Association, Society of Cardiovascular Anesthesiologists, Society for Cardiovascular Angiography and Interventions, Society of Interventional Radiology, Society of Thoracic Surgeons, and Society for Vascular Medicine. *Circulation* 2010;121:e266-e369.
6. Niwa K, Perloff JK, Bhuta SM, et al. Structural abnormalities of great arterial walls in congenital heart disease: light and electron microscopic analyses. *Circulation* 2001;103:393-400.
7. Fedak PW, de Sa MP, Verma S, et al. Vascular matrix remodeling in patients with bicuspid aortic valve malformations: implications for aortic dilatation. *J Thorac Cardiovasc Surg* 2003;126:797-806.
8. Faivre L, Collod-Beroud G, Loeys BL, et al. Effect of mutation type and location on clinical outcome in 1,013 probands with Marfan syndrome or related phenotypes and FBN1 mutations: an international study. *Am J Hum Genet* 2007;81:454-466.
9. Dietz HC, McIntosh I, Sakai LY, et al. Four novel FBN1 mutations: significance for mutant transcript level and EGF-like domain calcium binding in the pathogenesis of Marfan syndrome. *Genomics* 1993;17:468-475.
10. Eldadah ZA, Brenn T, Furthmayr H, et al. Expression of a mutant human fibrillin allele upon a normal human or murine genetic background recapitulates a Marfan cellular phenotype. *J Clin Invest* 1995;95:874-880.
11. Judge DP, Biery NJ, Keene DR, et al. Evidence for a critical contribution of haploinsufficiency in the complex pathogenesis of Marfan syndrome. *J Clin Invest* 2004;114:172-181.
12. Neptune ER, Frischmeyer PA, Arking DE, et al. Dysregulation of TGF-beta activation contributes to pathogenesis in Marfan syndrome. *Nat Genet* 2003;33:407-411.
13. Ng CM, Cheng A, Myers LA, et al. TGF-beta-dependent pathogenesis of mitral valve prolapse in a mouse model of Marfan syndrome. *J Clin Invest* 2004;114:1586-1592.
14. Habashi JP, Judge DP, Holm TM, et al. Losartan, an AT1 antagonist, prevents aortic aneurysm in a mouse model of Marfan syndrome. *Science* 2006;312:117-121.
15. Carta L, Smaldone S, Zilberberg L, et al. p38 MAPK is an early determinant of promiscuous Smad2/3 signaling in the aortas of fibrillin-1 (Fbn1)-null mice. *J Biol Chem* 2009;284:5630-5636.
16. Boileau C, Jondeau G, Mizuguchi T, et al. Molecular genetics of Marfan syndrome. *Curr Opin Cardiol* 2005;20:194-200.
17. Nagashima H, Sakomura Y, Aoka Y, et al. Angiotensin II type 2 receptor mediates vascular smooth muscle cell apoptosis in cystic medial degeneration associated with Marfan's syndrome. *Circulation* 2001;104:I282-I287.
18. Pyeritz RE, McKusick VA. The Marfan syndrome: diagnosis and management. *N Engl J Med* 1979;300:772-777.
19. Loeys BL, Dietz HC, Braverman AC, et al. The revised Ghent nosology for the Marfan syndrome. *J Med Genet* 2010;47:476-485.
20. Mizuguchi T, Collod-Beroud G, Akiyama T, et al. Heterozygous TGFBR2 mutations in Marfan syndrome. *Nat Genet* 2004;36:855-860.
21. Sakai H, Visser R, Ikegawa S, et al. Comprehensive genetic analysis of relevant four genes in 49 patients with Marfan syndrome or Marfan-related phenotypes. *Am J Med Genet A* 2006;140:1719-1725.
22. Loeys BL, Schwarze U, Holm T, et al. Aneurysm syndromes caused by mutations in the TGF-beta receptor. *N Engl J Med* 2006;355:788-798.

23. Pyeritz RE. Marfan syndrome: 30 years of research equals 30 years of additional life expectancy. *Heart* 2009;95:173–175.
24. Aburawi EH, O'Sullivan J. Relation of aortic root dilatation and age in Marfan's syndrome. *Eur Heart J* 2007;28:376–379.
25. Sisk HE, Zahka KG, Pyeritz RE. The Marfan syndrome in early childhood: analysis of 15 patients diagnosed at less than 4 years of age. *Am J Cardiol* 1983;52:353–358.
26. Groenink M, Rozendaal L, Naeff MS, et al. Marfan syndrome in children and adolescents: predictive and prognostic value of aortic root growth for screening for aortic complications. *Heart* 1998;80:163–169.
27. Mulder BJ. The distal aorta in the Marfan syndrome. *Neth Heart J* 2008;16:382–386.
28. Willis L, Roosevelt GE, Yetman AT. Comparison of clinical characteristics and frequency of adverse outcomes in patients with Marfan syndrome diagnosed in adulthood versus childhood. *Pediatr Cardiol* 2009;30:289–292.
29. Canadas V, Vilacosta I, Bruna I, et al. Marfan syndrome. Part 2: treatment and management of patients. *Nat Rev Cardiol* 2010;7:266–276.
30. Roman MJ, Devereux RB, Kramer-Fox R, et al. Two-dimensional echocardiographic aortic root dimensions in normal children and adults. *Am J Cardiol* 1989;64:507–512.
31. Rozendaal L, Groenink M, Naeff MS, et al. Marfan syndrome in children and adolescents: an adjusted nomogram for screening aortic root dilatation. *Heart* 1998;79:69–72.
32. Milewicz DM, Dietz HC, Miller DC. Treatment of aortic disease in patients with Marfan syndrome. *Circulation* 2005;111:e150–e157.
33. Umana JR, Miller DC, Mitchell RS. What is the best treatment for patients with acute type B aortic dissections—medical, surgical, or endovascular stent-grafting? *Ann Thorac Surg* 2002;74:S1840–S1843; discussion S1857–S1863.
34. Finkbohner R, Johnston D, Crawford ES, et al. Marfan syndrome: long-term survival and complications after aortic aneurysm repair. *Circulation* 1995;91:728–733.
35. Nollen GJ, Groenink M, Tijssen JG, et al. Aortic stiffness and diameter predict progressive aortic dilatation in patients with Marfan syndrome. *Eur Heart J* 2004;25:1146–1152.
36. Rossi-Foulkes R, Roman MJ, Rosen SE, et al. Phenotypic features and impact of beta blocker or calcium antagonist therapy on aortic lumen size in the Marfan syndrome. *Am J Cardiol* 1999;83:1364–1368.
37. Brooke BS, Habashi JP, Judge DP, et al. Angiotensin II blockade and aortic root dilation in Marfan's syndrome. *N Engl J Med* 2008;358:2787–2795.
38. Lacro RV, Dietz HC, Wruck LM, et al. Rationale and design of a randomized clinical trial of beta-blocker therapy (atenolol) versus angiotensin II receptor blocker therapy (losartan) in individuals with Marfan syndrome. *Am Heart J* 2007;154:624–631.
39. <http://www.rbht.nhs.uk/research/cteu/projects/congenital-heart-disease/aims/>
40. Maron BJ, Chaitman BR, Ackerman MJ, et al. Recommendations for physical activity and recreational sports participation for young patients with genetic cardiovascular diseases. *Circulation* 2004;109:2807–2816.
41. Cattaneo SM, Bethea BT, Alejo DE, et al. Surgery for aortic root aneurysm in children: a 21-year experience in 50 patients. *Ann Thorac Surg* 2004;77:168–176.
42. David TE, Ivanov J, Armstrong S, et al. Aortic valve-sparing operations in patients with aneurysms of the aortic root or ascending aorta. *Ann Thorac Surg* 2002;74:S1758–S1761; discussion S1792–S1759.
43. Mulder BJ, Webb GD. Marfan syndrome: a cardiovascular perspective. In: Gatzoulis MA, Webb GD, Daubeney P, eds. *Diagnosis and Management of Adult Congenital Heart Disease*. 2nd ed. Philadelphia, PA: Elsevier.
44. Basso C, Boschello M, Perrone C, et al. An echocardiographic survey of primary school children for bicuspid aortic valve. *Am Cardiol* 2004;93:661–663.
45. Braverman AC, Guven H, Beardslee MA, et al. The bicuspid aortic valve. *Curr Prob Cardiol* 2005;30:470–522.
46. Huntington K, Hunter AG, Chan KL. A prospective study to assess the frequency of familial clustering of congenital bicuspid aortic valve. *J Am Coll Cardiol* 1997;30:1809–1812.
47. Fedak PW, Verma S, David TE, et al. Clinical and pathophysiological implications of a bicuspid aortic valve. *Circulation* 2002;106:900–904.
48. Mack G, Silberbach M. Aortic and pulmonary stenosis. *Pediatr Rev/Am Acad Pediatr* 2000;21:79–85.
49. Roberts WC, Ko JM. Frequency by decades of unicuspid, bicuspid, and tricuspid aortic valves in adults having isolated aortic valve replacement for aortic stenosis, with or without associated aortic regurgitation. *Circulation* 2005;111:920–925.
50. Mills P, Leech G, Davies M, et al. The natural history of a non-stenotic bicuspid aortic valve. *Br Heart J* 1978;40:951–957.
51. Ward C. Clinical significance of the bicuspid aortic valve. *Heart (British Cardiac Society)* 2000;83:81–85.
52. Lindsay J, Jr. Coarctation of the aorta, bicuspid aortic valve and abnormal ascending aortic wall. *Am J Cardiol* 1988;61:182–184.
53. Edwards WD, Leaf DS, Edwards JE. Dissecting aortic aneurysm associated with congenital bicuspid aortic valve. *Circulation* 1978;57:1022–1025.
54. Tadros TM, Klein MD, Shapira OM. Ascending aortic dilatation associated with bicuspid aortic valve: pathophysiology, molecular biology, and clinical implications. *Circulation* 2009;119:880–890.
55. Robinson PN, Godfrey M. The molecular genetics of Marfan syndrome and related microfibrilopathies. *J Med Genet* 2000;37:9–25.
56. Niessen K, Karsan A. Notch signaling in cardiac development. *Circ Res* 2008;102:1169–1181.
57. Guo DC, Pannu H, Tran-Fadulu V, et al. Mutations in smooth muscle alpha-actin (ACTA2) lead to thoracic aortic aneurysms and dissections. *Nat Genet* 2007;39:1488–1493.
58. Lee TC, Zhao YD, Courtman DW, et al. Abnormal aortic valve development in mice lacking endothelial nitric oxide synthase. *Circulation* 2000;101:2345–2348.
59. Topper JN, Cai J, Falb D, et al. Identification of vascular endothelial genes differentially responsive to fluid mechanical stimuli: cyclooxygenase-2, manganese superoxide dismutase, and endothelial cell nitric oxide synthase are selectively up-regulated by steady laminar shear stress. *Proc Natl Acad Sci U S A* 1996;93:10417–10422.
60. Sonoda M, Takenaka K, Uno K, et al. A larger aortic annulus causes aortic regurgitation and a smaller aortic annulus causes aortic stenosis in bicuspid aortic valve. *Echocardiography* 2008;25:242–248.
61. Hope MD, Hope TA, Meadows AK, et al. Bicuspid aortic valve: four-dimensional MR evaluation of ascending aortic systolic flow patterns. *Radiology* 2010;255:53–61.
62. Della Corte A, Quarto C, Bancone C, et al. Spatiotemporal patterns of smooth muscle cell changes in ascending aortic dilatation with bicuspid and tricuspid aortic valve stenosis: focus on cell-matrix signaling. *J Thorac Cardiovasc Surg* 2008;135:8–18, 18 e11–e12.
63. Beroukhi RS, Roosevelt G, Yetman AT. Comparison of the pattern of aortic dilation in children with the Marfan's syndrome versus children with a bicuspid aortic valve. *Am J Cardiol* 2006;98:1094–1095.
64. Holmes KW, Lehmann CU, Dalal D, et al. Progressive dilation of the ascending aorta in children with isolated bicuspid aortic valve. *Am J Cardiol* 2007;99:978–983.
65. Mahle WT, Sutherland JL, Frias PA. Outcome of isolated bicuspid aortic valve in childhood. *J Pediatr* 2010;157:445–449.
66. Friedman T, Mani A, Elefteriades JA. Bicuspid aortic valve: clinical approach and scientific review of a common clinical entity. *Expert Rev Cardiovasc Ther* 2008;6:235–248.
67. Matura LA, Ho VB, Rosing DR, et al. Aortic dilatation and dissection in Turner syndrome. *Circulation* 2007;116:1663–1670.
68. Grotenhuis HB, Ottenkamp J, Westenberg JJ, et al. Reduced aortic elasticity and dilatation are associated with aortic regurgitation and left ventricular hypertrophy in nonstenotic bicuspid aortic valve patients. *J Am Coll Cardiol* 2007;49:1660–1665.
69. Loscalzo ML, Goh DL, Loey B, et al. Familial thoracic aortic dilation and bicommissural aortic valve: a prospective analysis of natural history and inheritance. *Am J Med Genet A* 2007;143A:1960–1967.
70. Bonow RO, Carabello BA, Chatterjee K, et al. ACC/AHA 2006 guidelines for the management of patients with valvular heart disease: a report of the American College of Cardiology/American Heart Association Task Force on Practice Guidelines (writing Committee to Revise the 1998 guidelines for the management of patients with valvular heart disease) developed in collaboration with the Society of Cardiovascular Anesthesiologists endorsed by the Society for Cardiovascular Angiography and Interventions and the Society of Thoracic Surgeons. *J Am Coll Cardiol* 2006;48:e1–e148.
71. Zanotti G, Vricella L, Cameron D. Thoracic aortic aneurysm syndrome in children. *Semin Thorac Cardiovasc Surg Pediatr Card Surg Annu* 2008:11–21.
72. Anttila V, Piasczynski M, Mora B, et al. Improved outcome with composite graft versus homograft root replacement for children with aortic root aneurysms. *Eur J Cardiothorac Surg* 2005;27:420–424.
73. Clarke DR. Invited letter concerning: accelerated degeneration of aortic allografts in infants and young children. *J Thorac Cardiovasc Surg* 1994;107:1162–1164.
74. Kirklin JK, Smith D, Novick W, et al. Long-term function of cryopreserved aortic homografts: a ten-year study. *J Thorac Cardiovasc Surg* 1993;106:154–165; discussion 165–156.
75. Takkenberg JJ, Klieverik LM, Schoof PH, et al. The Ross procedure: a systematic review and meta-analysis. *Circulation* 2009;119:222–228.
76. de Sa M, Moshkovitz Y, Butany J, et al. Histologic abnormalities of the ascending aorta and pulmonary trunk in patients with bicuspid aortic valve disease: clinical relevance to the Ross procedure. *J Thorac Cardiovasc Surg* 1999;118:588–594.
77. Therrien J, Webb G. Clinical update on adults with congenital heart disease. *Lancet* 2003;362:1305–1313.
78. Rauch R, Hofbeck M, Zweier C, et al. Comprehensive genotype-phenotype analysis in 230 patients with tetralogy of Fallot. *J Med Genet* 2010;47:321–331.
79. Niwa K, Siu SC, Webb GD, et al. Progressive aortic root dilatation in adults late after repair of tetralogy of Fallot. *Circulation* 2002;106:1374–1378.
80. Jonsson H, Ivert T, Brodin LA. Echocardiographic findings in 83 patients 13–26 years after intracardiac repair of tetralogy of Fallot. *Eur Heart J* 1995;16:1255–1263.
81. Nollert G, Fischlein T, Bouterwek S, et al. Long-term survival in patients with repair of tetralogy of Fallot: 36-year follow-up of 490 survivors of the first year after surgical repair. *J Am Coll Cardiol* 1997;30:1374–1383.
82. Tan JL, Davlouros PA, McCarthy KP, et al. Intrinsic histological abnormalities of aortic root and ascending aorta in tetralogy of Fallot: evidence of causative mechanism for aortic dilatation and aortopathy. *Circulation* 2005;112:961–968.

83. Dodds GA III, Warnes CA, Danielson GK. Aortic valve replacement after repair of pulmonary atresia and ventricular septal defect or tetralogy of Fallot. *J Thorac Cardiovasc Surg* 1997;113:736–741.
84. Kim WH, Seo JW, Kim SJ, et al. Aortic dissection late after repair of tetralogy of Fallot. *Int J Cardiol* 2005;101:515–516.
85. Rathi VK, Doyle M, Williams RB, et al. Massive aortic aneurysm and dissection in repaired tetralogy of Fallot; diagnosis by cardiovascular magnetic resonance imaging. *Int J Cardiol* 2005;101:169–170.
86. Cheung YF, Hong WJ, Chan KW, et al. Modulating effects of matrix metalloproteinase-3 and -9 polymorphisms on aortic stiffness and aortic root dilation in patients after tetralogy of Fallot repair. *Int J Cardiol* 2011;151:214–217.
87. Bull K, Somerville J, Ty E, Spiegelhalter D. Presentation and attrition in complex pulmonary atresia. *J Am Coll Cardiol* 1995;25:491–499.
88. Marelli AJ, Perloff JK, Child JS, et al. Pulmonary atresia with ventricular septal defect in adults. *Circulation* 1994;89:243–251.
89. Chong WY, Wong WH, Chiu CS, et al. Aortic root dilation and aortic elastic properties in children after repair of tetralogy of Fallot. *Am J Cardiol* 2006;97:905–909.
90. Bhat AH, Smith CJ, Hawker RE. Late aortic root dilatation in tetralogy of Fallot may be prevented by early repair in infancy. *Pediatr Cardiol* 2004;25:654–659.
91. Senzaki H, Iwamoto Y, Ishido H, et al. Arterial haemodynamics in patients after repair of tetralogy of Fallot: influence on left ventricular after load and aortic dilatation. *Heart* 2008;94:70–74.
92. Mitchell SC, Korones SB, Berendes HW. Congenital heart disease in 56,109 births. Incidence and natural history. *Circulation* 1971;43:323–332.
93. Rosenthal E. Coarctation of the aorta from fetus to adult: curable condition or life long disease process? *Heart* 2005;91:1495–1502.
94. Oliver JM, Gallego P, Gonzalez A, et al. Risk factors for aortic complications in adults with coarctation of the aorta. *J Am Coll Cardiol* 2004;44:1641–1647.
95. Warnes CA. Bicuspid aortic valve and coarctation: two villains part of a diffuse problem. *Heart* 2003;89:965–966.
96. Cohen M, Fuster V, Steele PM, et al. Coarctation of the aorta: long-term follow-up and prediction of outcome after surgical correction. *Circulation* 1989;80:840–845.
97. Isner JM, Donaldson RF, Fulton D, et al. Cystic medial necrosis in coarctation of the aorta: a potential factor contributing to adverse consequences observed after percutaneous balloon angioplasty of coarctation sites. *Circulation* 1987;75:689–695.
98. Schievink WI, Raissi SS, Maya MM, et al. Screening for intracranial aneurysms in patients with bicuspid aortic valve. *Neurology* 2010;74:1430–1433.
99. Kappetein AP, Gittenberger-de Groot AC, Zwinderman AH, et al. The neural crest as a possible pathogenetic factor in coarctation of the aorta and bicuspid aortic valve. *J Thorac Cardiovasc Surg* 1991;102:830–836.
100. von Kodolitsch Y, Aydin MA, Koschyk DH, et al. Predictors of aneurysmal formation after surgical correction of aortic coarctation. *J Am Coll Cardiol* 2002;39:617–624.
101. Grotenhuis HB, de Roos A. Structure and function of the aorta in inherited and congenital heart disease and the role of MRI. *Heart* 2011;97:66–74.
102. Alegria JR, Burkhart HM, Connolly HM. Coarctation of the aorta presenting as systemic hypertension in a young adult. *Nat Clin Pract Cardiovasc Med* 2008;5:484–488.
103. Baumgartner H, Bonhoeffer P, De Groot NM, et al. ESC Guidelines for the management of grown-up congenital heart disease (new version 2010). *Eur Heart J* 2010;31:2915–2957.
104. Losay J, Touchot A, Serraf A, et al. Late outcome after arterial switch operation for transposition of the great arteries. *Circulation* 2001;104:1121–1126.
105. Agnoletti G, Ou P, Celermajer DS, et al. Acute angulation of the aortic arch predisposes a patient to ascending aortic dilatation and aortic regurgitation late after the arterial switch operation for transposition of the great arteries. *J Thorac Cardiovasc Surg* 2008;135:568–572.
106. Schwartz ML, Gauvreau K, del Nido P, et al. Long-term predictors of aortic root dilation and aortic regurgitation after arterial switch operation. *Circulation* 2004;110:1128–1132.

David W. Brown ■ Tal Geva

Anomalies of the pulmonary veins vary widely in their anatomic spectrum and clinical presentation, course, and outcome. As with other types of congenital heart disease, advances in diagnosis, cardiovascular surgery in newborns and infants, and transcatheter therapy have heightened the importance of early recognition, accurate diagnosis, and better understanding of abnormalities of the pulmonary veins.

ANATOMY

Pulmonary venous anomalies may be categorized as anomalous connections, anomalous drainage with normal connections, stenotic connections, and abnormal numbers of pulmonary veins.

Anomalous Connections and Drainage

One or more of the pulmonary veins may connect anomalously to one or more of the systemic veins. The condition is termed totally anomalous pulmonary venous connection (TAPVC) if all the veins connect anomalously, and partially anomalous pulmonary venous connection (PAPVC) if one or more, but not all, of the veins connect anomalously.

The physiologic consequence of anomalous pulmonary venous connection is usually anomalous pulmonary venous drainage. It is also possible, however, to have normal pulmonary venous connections with abnormal drainage. Examples of this condition include a common atrium and malposition of the septum primum. Although the pulmonary veins in these anomalies connect normally (e.g., into the back wall of the atria between the right and left horns of the sinus venosus), either complete absence of the interatrial septum or malattachment of the septum primum can lead to anomalous drainage into the morphologic right atrium (RA). When some or all of the pulmonary veins drain anomalously into the RA or its tributaries without being abnormally connected, the terms partially anomalous pulmonary venous drainage (PAPVD) or totally anomalous pulmonary venous drainage (TAPVD) with normal pulmonary venous connections are used. Therefore, the terms pulmonary venous connections and pulmonary venous drainage should not be used synonymously.

We dedicate this chapter to the late Dr. Stella Van Praagh who was a coauthor in the sixth and seventh editions of this textbook.

Stenotic Connections

Stenosis in one or more of the pulmonary veins or in the common pulmonary vein may occur. Veins with normal connections may exhibit stenoses, varying from stenosis of one or more of the individual pulmonary veins to cor triatriatum. These produce obstruction to pulmonary venous return to the left atrium (LA). Anomalous connected veins may be stenosed, resulting in obstruction to pulmonary venous return to the RA. The physiologic feature common to these stenotic connections is obstruction of egress of pulmonary venous blood.

Abnormal Numbers of Pulmonary Veins

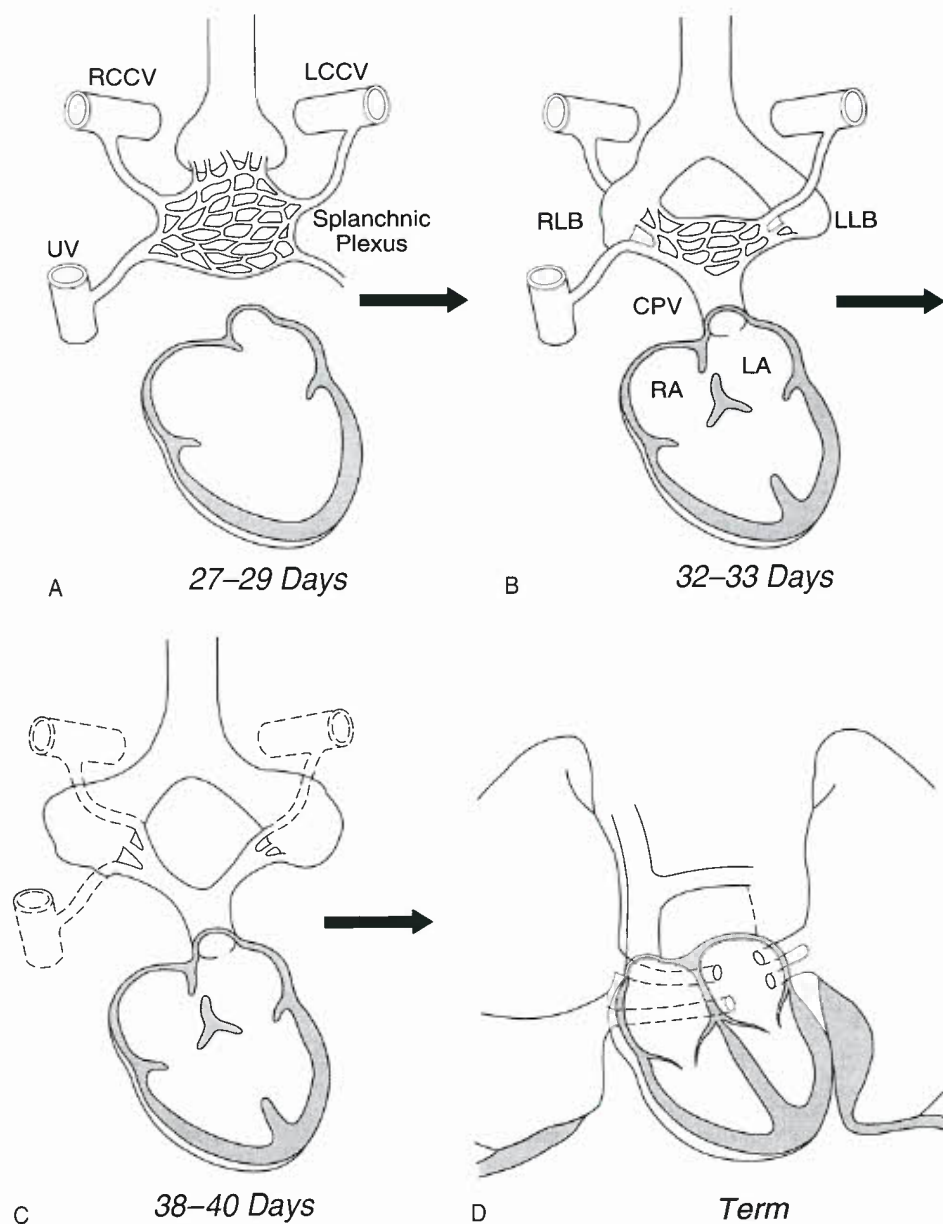
Normally, there are two right and two left pulmonary veins. The most common variation is the presence of a single pulmonary vein on either the right or left side, with a prevalence of about 24% in anatomic studies (1). Rarely, all pulmonary veins enter a common pulmonary vein that drains into the LA. A single left pulmonary vein was found more frequently than a single right (1). A single common pulmonary vein, usually without stenosis, occurs almost exclusively in cases of visceral heterotaxy with asplenia. It also is possible to have an increased number of normally connecting pulmonary veins. The prevalence of a third pulmonary vein on either the right or left side is 1.6% to 2% (1). A fourth or even a fifth vein infrequently is present. An abnormal number of pulmonary veins imposes no physiologic handicap.

EMBRYOLOGY

A classification of pulmonary venous anomalies based on embryologic principles introduces a unifying concept to the consideration of these anatomically and physiologically diverse conditions. Review of the embryologic development of the pulmonary venous system is a prerequisite.

In the human embryo, the primordia of the lungs, larynx, and tracheobronchial tree are derived by a division of the foregut. In their early stages of development, the lungs are enmeshed by the vascular plexus of the foregut, the splanchnic plexus. As pulmonary differentiation progresses, part of the splanchnic plexus forms the pulmonary vascular bed. At this stage, there is no direct connection to the heart. Instead, the pulmonary vascular bed shares the routes of drainage of the splanchnic plexus (i.e., umbilicovitelline and cardinal systems

Figure 35.1. Development of the pulmonary veins. **A:** At 27 to 29 days of gestation, the primordial lung buds are enmeshed by the vascular plexus of the foregut (the splanchnic plexus). At this stage, there is no direct connection to the heart. Instead, there are multiple connections to the umbilico-vitelline and cardinal venous systems. A small evagination can be seen in the posterior wall of the left atrium to the left of the developing septum secundum. **B:** By the end of the first month of gestation, the common pulmonary vein establishes a connection between the pulmonary venous plexus and the sinoatrial portion of the heart. At this time, the connections between the pulmonary venous plexus and the splanchnic venous plexus are still patent. **C:** Next, the connections between the pulmonary venous plexus and the splanchnic venous plexus involute. **D:** The common pulmonary vein (CPV) incorporates into the left atrium, so that the individual pulmonary veins connect separately and directly to the left atrium. LA, left atrium; LCCV, left common cardinal vein; LLB, left lung bud; RA, right atrium; RCCV, right common cardinal vein; RLB, right lung bud; UV, umbilical vein. (Adapted from Lucas RV Jr, Anderson RC, Amplatz K, et al. Congenital causes of pulmonary venous obstruction. *Pediatr Clin North Am* 1963;10:781–836.)



of veins) (Fig. 35.1A). Subsequently, the intraparenchymal pulmonary veins connect with the LA by establishing a connection with the common pulmonary vein, which evaginates from the LA (2).

No unanimous opinion about the site of development of the common pulmonary vein has been attained. Some investigators believe the common pulmonary vein originates from an evagination in the sinoatrial region of the heart (3). Others believe that the common pulmonary vein starts from a confluence of vessels from the pulmonary plexus (1). According to a third opinion, the beginning of the common pulmonary vein occurs by the confluence of capillaries that grow into the mesocardium, located between the lung buds and the heart. Nevertheless, it is generally accepted that, by the end of the first month of gestation, the common pulmonary vein can be identified as a vessel draining the pulmonary plexus and entering the sinoatrial portion of the heart. The site of entry is cephalad to the junction of the left and right horns of the sinus venosus and to the left of the developing septum primum (Fig. 35.1B) (3,4).

When the direct connection to the heart is established, the initial communications between the pulmonary portion of the

splanchnic plexus and the cardinal and umbilicovitelline systems are, for the most part, obliterated. The pulmonary vascular bed then drains via four individual major pulmonary veins into the common pulmonary vein, which in turn empties into the LA (Fig. 35.1C). The common pulmonary vein is a transient anatomic structure. By a process of differential growth, it becomes incorporated into the LA, resulting in the ultimate anatomic arrangement wherein the four individual pulmonary veins connect separately and directly to the LA (Fig. 35.1D).

Imperfect development of the common pulmonary vein provides embryologic basis for most anomalies of the pulmonary veins. The following aberrations of development of the common pulmonary vein explain these anomalies and are used as a means of classifying them (Table 35.1).

Early Atresia of the Common Pulmonary Vein while Pulmonary–Systemic Venous Connections are Still Present

If the common pulmonary vein fails to develop or becomes atretic early in its development, collateral channels for

TABLE 35.1 Embryologic Classification of Pulmonary Venous Anomalies

- I. Normal absorption of the common pulmonary vein associated with defects that result in abnormal pulmonary venous drainage
 - A. Sinus venosus defect
 - B. Malposition of septum primum
- II. Atresia of the common pulmonary vein (early) while pulmonary-to-systemic venous connections are still present
 - A. Partially anomalous pulmonary venous connection
 - B. Totally anomalous pulmonary venous connection
 1. Without pulmonary venous obstruction
 2. With pulmonary venous obstruction
- III. Atresia of the common pulmonary vein (late) after pulmonary-to-systemic venous connections are obliterated
 - A. Atresia of the common pulmonary vein
- IV. Stenosis of the common pulmonary vein
 - A. Cor triatriatum
- V. Abnormal absorption of the common pulmonary vein into the LA
 - A. Stenosis of the individual pulmonary veins
 - B. Abnormal number of pulmonary veins

pulmonary venous drainage are available in the form of primitive connections between the splanchnic plexus and the cardinal or umbilicovitelline systems of veins (Fig. 35.2). Any one of these collateral channels may persist and enlarge, resulting in TAPVC. If only the right or left portion of the common pulmonary vein becomes atretic, persistence of the pulmonary venous–systemic venous connections of that side provides the etiologic basis for PAPVC (5) (Fig. 35.2).

Late Atresia of the Common Pulmonary Vein after Pulmonary–Systemic Connections Are Obliterated

When atresia of the common pulmonary vein occurs late, the collateral venous channels already are obliterated. The resulting anomaly has been termed atresia of the common pulmonary vein. The individual pulmonary veins empty into a blind cul-de-sac that has no direct connection to the LA or to the systemic venous systems (Fig. 35.3A).

Stenosis of the Common Pulmonary Vein

Cor triatriatum is the result of stenosis of the common pulmonary vein (Fig. 35.3B and 35.4). In the usual case, the stenosis occurs late, after collateral venous connections have been lost, or else the severity of the obstruction produced by

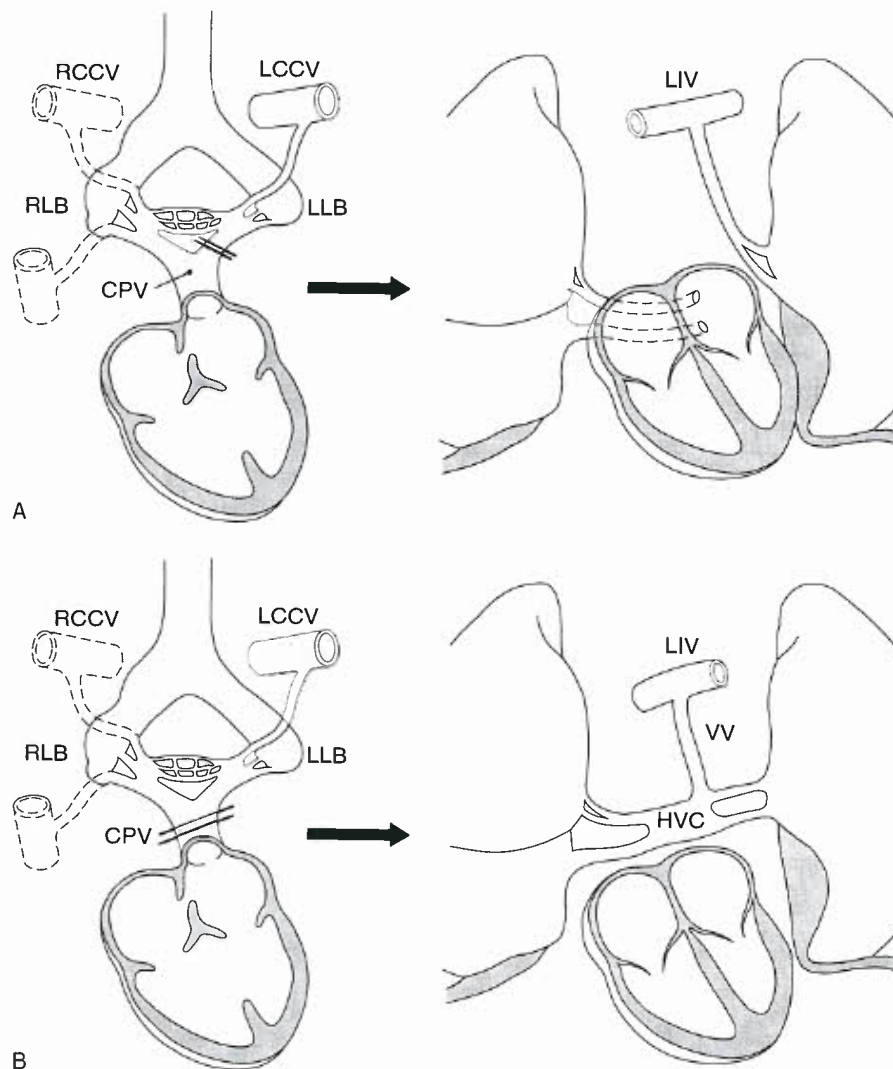


Figure 35.2. Embryologic basis of partially and totally anomalous pulmonary venous connections. **A:** Partially anomalous pulmonary venous connection results from failure to establish a normal connection between one or more of the pulmonary veins with the common pulmonary vein (CPV) before the connections with the splanchnic venous system have regressed. **B:** Totally anomalous pulmonary venous connection results from failure to establish a normal connection between the pulmonary venous plexus and the common pulmonary vein before the connections with splanchnic venous system have regressed. HVC, horizontal pulmonary venous confluence; LCCV, left common cardinal vein; LIV, left innominate vein; LLB, left lung bud; RCCV, right common cardinal vein; RLB, right lung bud; VV, vertical vein. (From Edwards JE. Symposium on anomalous pulmonary venous connection (drainage): pathologic and developmental considerations in anomalous pulmonary venous connection. *Proc Staff Meetings Mayo Clin* 1953;28:441–452, with permission.)

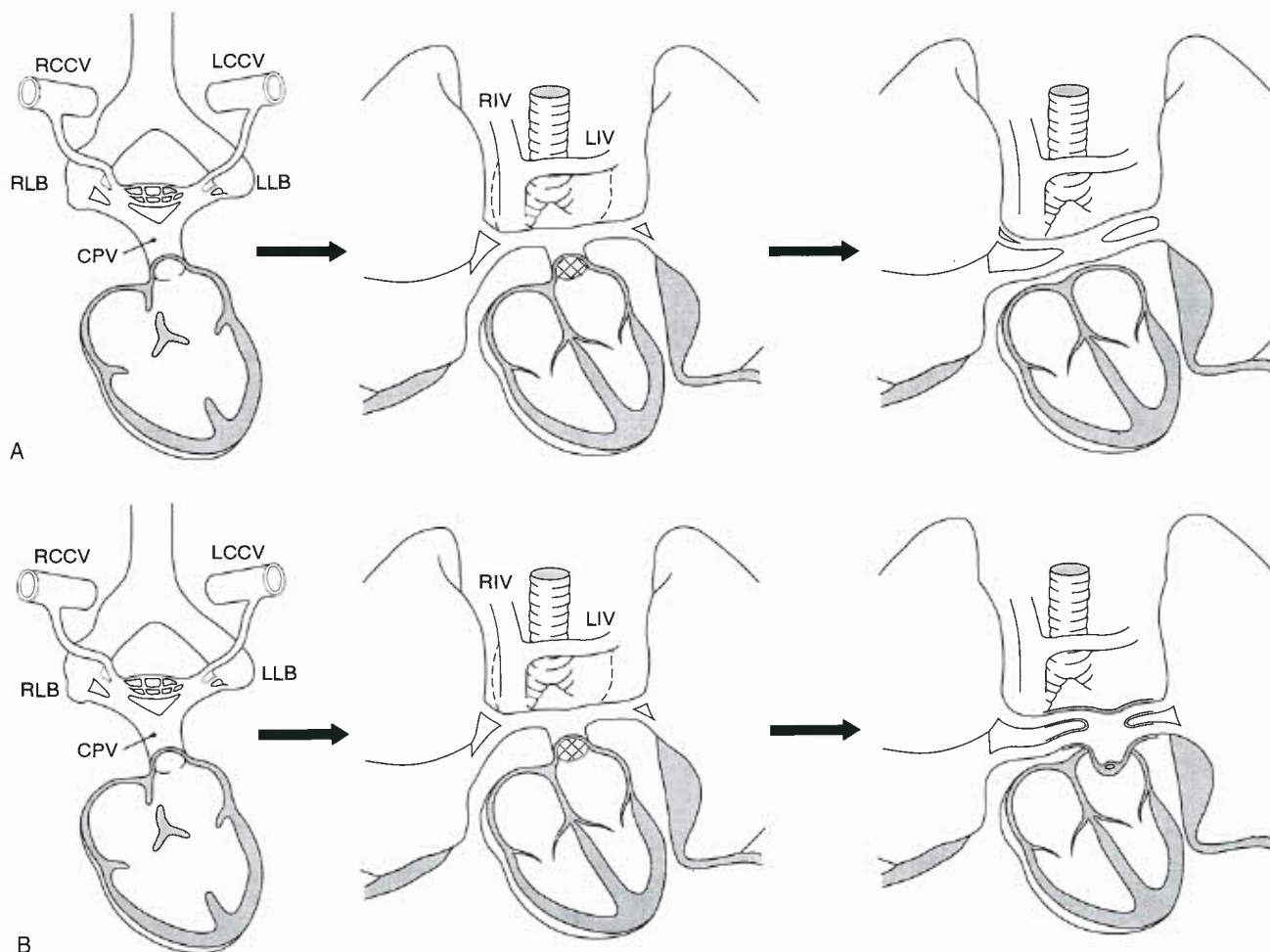


Figure 35.3. Embryologic basis of atresia of the common pulmonary vein and cor triatriatum. **A:** The common pulmonary vein (CPV) has established a connection with the left atrium, and the primitive venous connections have regressed (**center panel**). Normally, the connection between the common pulmonary vein and the left atrium enlarges. If the normal connection between the common pulmonary vein and the left atrium fails, the pulmonary veins drain into a blind cul-de-sac without a significant alternative egress for pulmonary venous blood (atresia of the common pulmonary vein). **B:** The connection between the common pulmonary vein and the left atrium is stenotic, and the common pulmonary vein dilates (cor triatriatum). LCCV, left common cardinal vein; LIV, left innominate vein; LLB, left lung bud; RCCV, right common cardinal vein; RIV, right innominate vein; RLB, right lung bud.

cor triatriatum is insufficient to stimulate maintenance of the primitive routes of venous drainage. Occasionally, however, cor triatriatum may be associated with anomalous pulmonary venous connection, implying that in such cases, the obstruction was early enough and sufficient to favor persistence of one of the primitive drainage channels such as a levoatriocardinal vein.

Anomalous Incorporation of the Common Pulmonary Vein into the Left Atrium

Abnormal numbers of pulmonary veins are the result of imperfect incorporation of the common pulmonary vein into the LA. Incomplete absorption of the common pulmonary vein results in fewer than the normal number of pulmonary veins (1). Rarely, in the mature heart, a common pulmonary vein draining both lungs empties into the LA. More commonly, a single pulmonary vein drains one lung. If more than the usual

absorption takes place, there will be an increased number of pulmonary veins.

Stenosis in individual pulmonary veins at their junction with the LA may or may not be a consequence of abnormal incorporation of the common pulmonary vein. One or more of the veins may be affected. Trauma, inflammation, proliferative disorder, or other yet unidentified mechanism(s) may cause stenosis of the individual pulmonary veins.

Early Atresia of the Common Pulmonary Vein while Pulmonary–Systemic Venous Connections Are Still Present

Partially Anomalous Pulmonary Venous Connection

PAPVC is the congenital anomaly in which one or more, but not all, of the pulmonary veins are connected to a systemic vein. Winslow is credited with the first description of



Figure 35.4. Cor triatriatum sinister. Echocardiogram in the apical four-chamber view showing “classic” cor triatriatum sinister. The cor triatriatum membrane (arrow) separates the pulmonary venous confluence (PVC) from the low-pressure left atrial (LA) chamber, which includes the left atrial appendage. The only egress for pulmonary venous blood is through the membrane orifice. LV, left ventricle; RA, right atrium.

this anomaly in 1739 (6). By 1942, Brody (7) collected 65 cases from the literature. The advent of surgical correction of cardiac defects necessitated a more critical approach to diagnosis and resulted in the identification and description of hundreds of cases.

Hughes and Rumore (8) found PAPVC in 0.7% of a series of 280 anatomic dissections, and Healy (1) found 0.6% in a series of 801 anatomic dissections. Both figures are higher than those deduced from clinical studies, which implies that some patients with PAPVC are not recognized during life. The most common type of PAPVC is to the right superior vena cava (SVC), and the second most common is to the RA. In Healy's material, the incidence of those two sites together was 55% of the total number of 86 cases (1).

Our present understanding of the normal connections of the right pulmonary veins (RPV) in sinus venosus defects of the SVC or the right atrial type and in the cases of malposition of the septum primum explains why PAPVD occurs mostly into the right SVC and the RA (see sections on sinus venosus defects and malposition of the septum primum). In both anomalies, the common pulmonary vein developed normally and is incorporated normally into the LA. The abnormal drainage of the RPVs is due to defects other than abnormal development of the common pulmonary vein. Hence, the actual incidence of partial obliteration of the common pulmonary vein resulting in PAPVC is much lower than thought in the past.

If one considers the cases of sinus venosus defects with the RPVs draining into the SVC or RA, the cases of malposition of the septum primum with drainage of part or all the pulmonary veins into the RA, and cases with partially or totally anomalous pulmonary venous drainage but normal pulmonary venous connections, the incidence of PAPVC to a systemic vein is quite low.

Normal Absorption of the Common Pulmonary Vein with Partially or Totally Abnormal Pulmonary Venous Drainage and Normal Connection of the Pulmonary Veins

Sinus Venosus Defects

Sinus venosus defects allow an atrial-level or a supratratrial-level shunt, but they are not atrial septal defects (ASDs). Specifically, these defects do not involve the fossa ovale, septum primum, or septum secundum. They always are associated with drainage of some or all the RPVs into the right SVC or the RA, but the pulmonary veins are normally connected with the LA.

Van Praagh et al.'s study (9) of these defects based on post-mortem specimens and echocardiographic studies supports the following conclusions. The true defect is the deficiency of the common wall between the right SVC and the right upper pulmonary vein or the wall between the RA and the right upper and lower pulmonary veins (Fig. 35.5). The result of these deficiencies is the unroofing of the right upper pulmonary vein and its branches into the right SVC (sinus venosus defects of the SVC type) or the unroofing of the right upper and lower pulmonary veins into the RA (sinus venosus defect of the right atrial type) (9).

The interatrial communication is not a defect. It is the left atrial orifice of the unroofed pulmonary veins, as in cases of an unroofed coronary sinus (CS) where the interatrial communication is not a defect; rather, it represents the right atrial orifice of the CS.

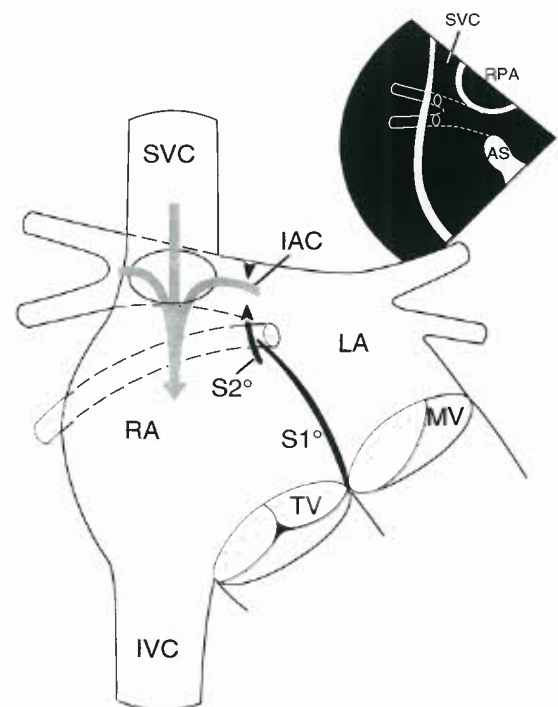


Figure 35.5. Diagrammatic representation of sinus venosus defect. Unroofing of the common wall between the right superior vena cava (SVC) and the right upper pulmonary vein allows drainage of blood from the right upper pulmonary vein into the SVC and right atrium (RA). The interatrial communication (IAC) is not a defect. It is the native orifice of the right upper pulmonary vein (arrowheads), and it allows flow from the LA into the right atrium. Inset shows the normal course of the right upper pulmonary vein behind the superior vena cava. AS, atrial septum; IVC, inferior vena cava; MV, mitral valve; RPA, right pulmonary artery; S1°, septum primum; S2°, septum secundum; TV, tricuspid valve.

When the interatrial communication in sinus venosus defects is viewed from the LA, it is located posterosuperiorly to the upper border of septum primum, exactly in the position of the orifice of the RPVs. In the SVC type of sinus venosus defects, the true defect is much larger than

the interatrial communication (the orifice of the right upper pulmonary vein) and occupies all the area where the orifices of the branches of the right upper pulmonary vein are seen to enter the right SVC (Fig. 35.6A). In the right atrial type of sinus venosus defects, the interatrial communication

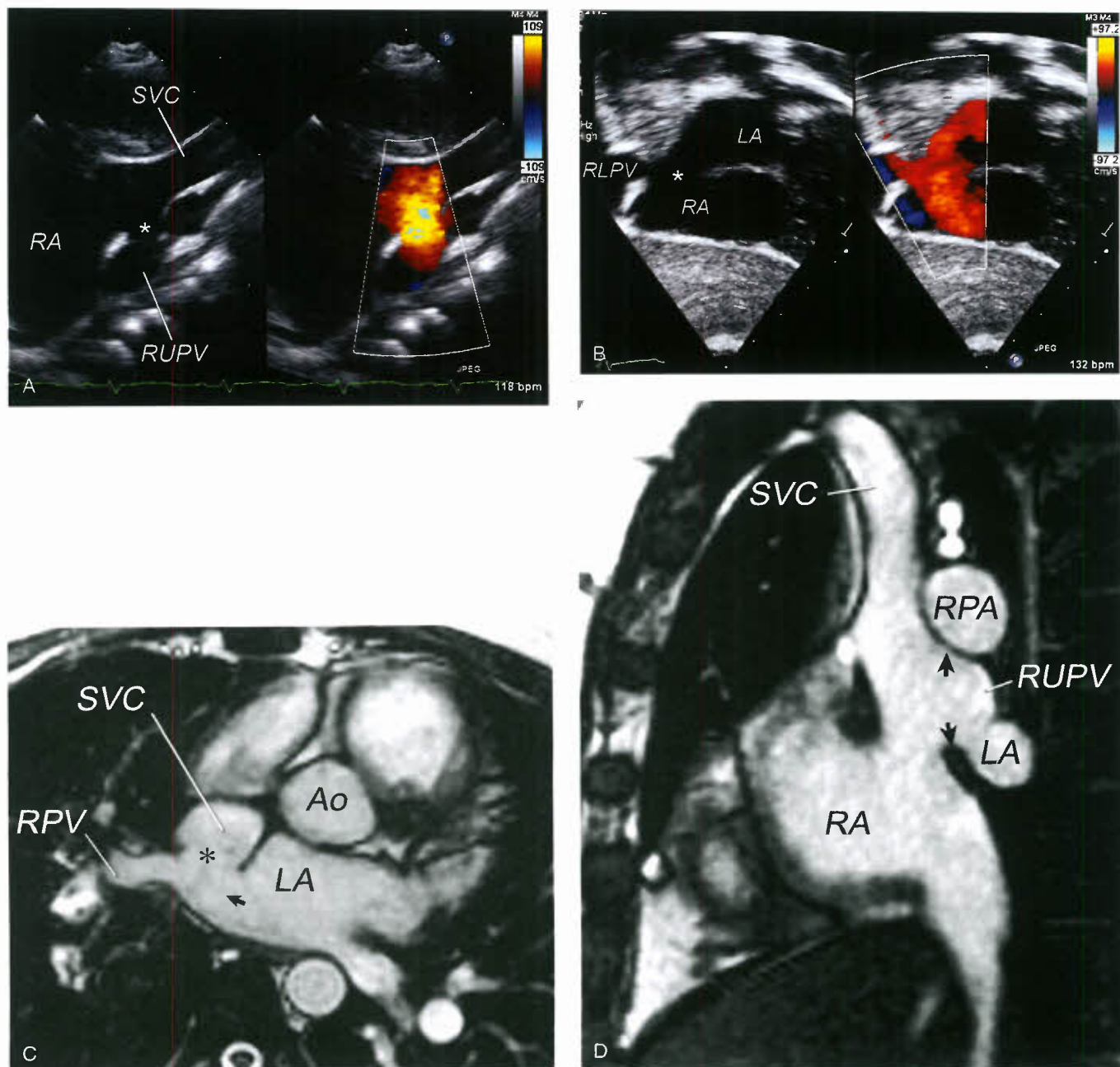


Figure 35.6. Sinus venosus defect. Echocardiogram (A,B) and MRI (C,D) of sinus venosus defect. **A:** Transthoracic right sternal border view in a patient with SVC-type sinus venosus defect. The deficiency in the wall between the right upper pulmonary vein (RUPV) and the SVC is the sinus venosus defect. The interatrial communication is the orifice of the right upper pulmonary vein (asterisk). **B:** Subcostal oblique view in a patient with inferior-type sinus venosus defect with color Doppler comparison. Note the absence of tissue (asterisk) between the right lower pulmonary vein (RLPV) and right atrium (RA), with flow directed into the right atrium (red flow) from both the RLPV and the LA through the RLPV's normally connecting orifice. **C:** Axial plane cine MRI image showing the defect (asterisk) in the tissue that separates the posterior wall of the SVC and the anterior wall of the right upper pulmonary vein (RPV). The arrow indicates the left atrial orifice of the right upper pulmonary vein, which serves as a communication between the LA and the SVC (Ao, aorta). **D:** Sagittal plane cine MRI: The arrows indicate the sinus venosus defect between the right upper pulmonary vein (RUPV) and the SVC. LA, left atrium; RA, right atrium; RPA, right pulmonary artery.

from the left atrial view is again in the position of the orifice of the RPVs. From the right atrial view, the missing partition between the RPVs and the RA can be imaged clearly by echocardiography (Fig. 35.6B). In both types of sinus venosus defects, the surgeon does not close the interatrial communication. Instead, the operation aims to restore the original function of the interatrial communication as the left atrial orifice of the RPVs (9), which can be accomplished by “reroofing” the pulmonary veins, that is, by patching the missing wall between the SVC and the pulmonary veins or between the RA and the pulmonary veins. The true nature of the interatrial communication, the left atrial orifice of the RPV(s), is thus restored.

Malposition of Septum Primum

Edwards (2) and Moller et al. (10) observed that, when the septum secundum is absent (usually in cases of visceral heterotaxy with polysplenia), septum primum may be displaced toward the anatomic LA (left sided or right sided, depending on the type of atrial situs). This displacement

of the upper border of the septum primum will result in the incorporation of some or even all the pulmonary veins into the morphologically RA. Although this malformation differs from sinus venosus defects, here also the normally connected pulmonary veins will drain into the RA. The two-dimensional (2-D) echocardiograms of such patients will show the change in the plane of the septum primum and the normal connection of the pulmonary veins in the back wall of the atrium (Fig. 35.7). The displaced septum primum may not reach the posterior wall of the LA. In such cases, there will be a small interatrial communication that is not an ASD or a patent foramen ovale; rather, it is a septum primum malposition defect. If the septum primum has some fenestrations (foramina secunda), multiple small interatrial communications will be present. Finally, in cases where septum primum fuses with the posterior left atrial wall, there is no interatrial communication. Supporting evidence for the conclusion that the pulmonary veins are connected normally to the atrial wall is that they are located between the right and left SVCs (when two SVCs are present). This is the normal location for the atrial con-



Figure 35.7. Malposition of septum primum.

A: Subcostal long-axis echocardiographic view showing leftwardly malattached septum primum (arrow), which results in anomalous drainage of the right pulmonary veins (RPV) into the right atrium (RA). The left pulmonary veins drain normally in this patient. **B:** Systolic frame of cine MRI in the axial plane in a 6-month-old infant with visceral heterotaxy and polysplenia showing leftward malposition of septum primum leading to drainage of the right pulmonary veins into the RA. Notice the dilated left-sided azygous vein (Az), which carries the blood from an interrupted inferior vena cava to the left superior vena cava (LSVC). DAo, descending aorta; LA, left atrium; RLPV, right lower pulmonary vein.

nection of the common pulmonary vein (i.e., between the two horns of the sinus venosus just above the CS). The absence of septum secundum makes it possible to visualize the attachments of septum primum from the right atrial side in heart specimens, a unique finding of this malformation. The echocardiographic appearance of the displaced mobile upper border of the septum primum helps to establish the diagnosis *in vivo*.

The essential anatomic elements that make possible the malposition of the septum primum toward the anatomic LA include absence of septum secundum and a well-developed septum primum. Those two elements often are present in patients with visceral heterotaxy and polysplenia. Patients with asplenia, however, seldom have a well-developed septum primum that could become malpositioned. Instead, they often exhibit TAPVC to a systemic vein above or below the diaphragm.

PARTIALLY ANOMALOUS PULMONARY VENOUS CONNECTIONS

Anatomy

PAPVCs exhibit a wide anatomic spectrum. Almost every conceivable connection between the pulmonary veins, on the one hand, and the various systemic venous tributaries, on the other hand, has been reported (Fig. 35.8). Left-sided pulmonary veins usually connect anomalously to derivatives of the left cardinal system (i.e., the CS and the left innominate vein [LIV]). Anomalous connections of the RPVs usually are to derivatives of the right cardinal system (i.e., the SVC or inferior vena cava [IVC]). The embryologic splanchnic plexus is a midline structure, thus explaining the developmental possibility for crossed drainage of left-sided pulmonary veins to derivatives of the right cardinal system and vice versa. Excluding the cases previously considered

PAPVC to the right SVC and to the RA (now considered under sinus venosus defect and malposition of the septum primum), the most common type of PAPVC is of the left pulmonary veins to the LIV. The second most common types are anomalous connections of pulmonary veins from the right lung to the IVC.

Right Pulmonary Veins to Superior Vena Cava

As outlined in the section on sinus venosus defects, the RPVs may drain into the right SVC or into the RA without being abnormally connected with them. The upper lobe drains by one large or two or three smaller veins into the SVC below the azygous vein. The multiple orifices indicate that the unroofing of the right upper pulmonary veins extends into their branches. The vein from the right lower lobe usually enters the LA. The lower part of the SVC, between the azygous vein and RA, is dilated. An interatrial communication (the left atrial orifice of the unroofed pulmonary veins) usually is present. Occasionally, a secundum ASD also is present. Rarely an ostium primum ASD also exists. When the orifice of the right upper pulmonary vein is atretic, the atrial septum is intact. Persistence of a left SVC is an occasional accompanying finding.

Anomalous connection of a single pulmonary vein to the right SVC as an isolated lesion or in combination with a sinus venosus defect is possible. The anomalously connected pulmonary vein in such a case originates from the right upper lobe and enters the right SVC either through the azygous vein or cranial to the insertion of the azygous vein to the SVC.

Gross examination of the heart reveals features common to all cases, regardless of the specific site of anomalous connection. These include mild to moderate dilation and hypertrophy of the RA and right ventricle and dilation of the pulmonary artery. The left-sided chambers are normal. Specific anatomic features vary according to the site of connection.

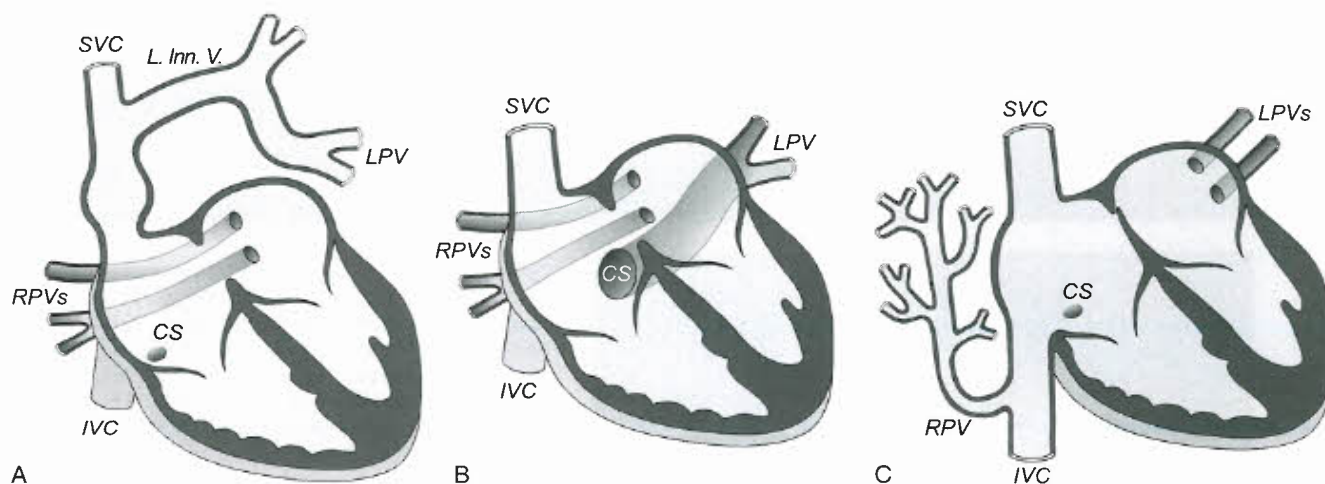


Figure 35.8. Partially anomalous pulmonary venous connection: variants. **A:** Anomalous connection of the two left pulmonary veins (LPVs) to the left innominate vein to the SVC; the right pulmonary veins (RPVs) connect normally to the left atrium. **B:** Anomalous connection of the left pulmonary veins to the CS. **C:** Anomalous connection of the right pulmonary veins to the inferior vena cava (IVC) to right atrium junction; in association with right lung hypoplasia this is termed “scimitar syndrome.” (From Brown DW. Pulmonary venous anomalies. In: Lai WW, Mertens LL, Cohen MS, et al., eds. *Echocardiography in Pediatric and Congenital Heart Disease: From Fetus to Adult*. 1st ed. United Kingdom: Wiley-Blackwell, 2009:119–142, with permission.)

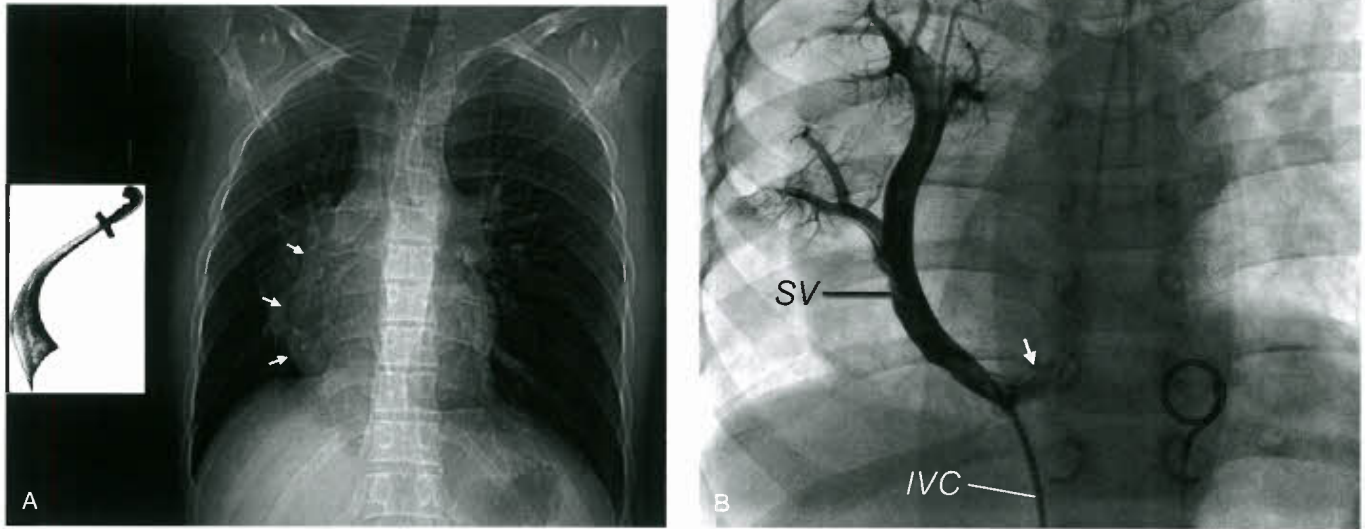


Figure 35.9. Scimitar syndrome. **A:** Chest radiogram in the posteroanterior projection showing the scimitar sign (arrowheads). Note the rightward shift of the cardiac silhouette. The inset shows a Turkish sword called scimitar. **B:** Catheter angiogram with catheter advanced from IVC up the SV in the same patient. Note the connection with the IVC close to the right atrial junction (arrow). **C:** 3-D lung surface volume rendering derived from computed tomography imaging in the same patient as (A). Note the degree of right lung hypoplasia.

Right Pulmonary Veins to Inferior Vena Cava

All the RPVs or occasionally the veins draining the right middle and right lower lobes enter the IVC either just above or below the diaphragm (Fig. 35.9). The normal pulmonary venous pattern of the right lung is altered in this condition, resulting in a “fir tree” configuration. The atrial septum is usually intact. This malformation, termed the scimitar syndrome by Neill et al. (5), frequently is associated with other anomalies, including hypoplasia of the right lung, anomalies of the bronchial system, horseshoe lung, secondary dextrocardia, hypoplasia of the right pulmonary artery, anomalous arterial connection to the right lung from the aorta, and pulmonary sequestration (11). Neill et al. (5) considered this a more primitive anomaly compared with other instances of PAPVC and suggested that it represents an anomaly of development of the right lung.

Left Pulmonary Veins to Inferior Vena Cava

Rarely, some or all of the left pulmonary veins can drain into the IVC. Juraszek et al. observed a case in which all the left pulmonary veins connected to the IVC below the diaphragm in association with an ostium secundum defect (Fig. 35.10). There was no additional heart defect, and both lungs were normal (12). Others also have reported cases of left-sided scimitar syndrome (13,14).

Left Pulmonary Veins to Left Innominate Vein

The LIV is the usual site of anomalous connection of the left pulmonary veins (Fig. 35.10A). The veins from the left upper lobe or from the whole left lung connect to the LIV via a persistent early embryonic pathway, which, because of its orientation, has been termed a vertical vein. An interatrial communication in the form of a secundum ASD or a patent foramen ovale is common.

The connecting vein between the left pulmonary veins and the LIV also has been called a persistent left superior vena cava (LSVC). This term is incorrect both embryologically and anatomically. Embryologically, the vertical vein represents a persistent early embryonic connection between the

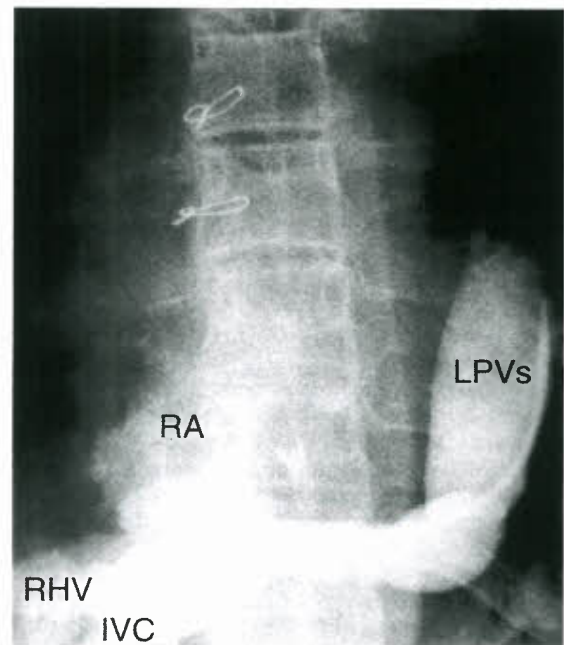


Figure 35.10. Partially anomalous pulmonary venous connection. Catheter angiogram showing PAPVC of the LPVs to the inferior vena cava. IVC, inferior vena cava; RA, right atrium; RHV, right hepatic vein.

splanchnic plexus of the lung buds and the cardinal veins. Anatomically, it is positioned more posteriorly than the LSVC, which is located immediately behind the left atrial appendage. An LSVC connects either with the CS or with the LA when the CS is unroofed. When an left pulmonary vein drains into the LSVC, the LSVC also should connect with the CS or with the LA. In a rare case (1), the left upper pulmonary vein (LUPV) joined the left superior intercostal vein, which in turn joined the LSVC. The confluence of those three veins entered the LIV. The proximal segment of the LSVC was atretic (ligament of Marshall) but present. To avoid inadvertent occlusion of pulmonary venous drainage, it is important that the differential diagnosis between a vertical vein and persistent LSVC be made before performance of any surgical or transcatheter intervention.

Other Sites of Partially Anomalous Pulmonary Venous Connection

Uncommon sites of PAPVC of the left pulmonary veins are to the CS (Fig. 35.8), IVC, right SVC, left subclavian vein, and azygous vein. In rare cases, veins of both lungs connect anomalously to systemic veins, while some of the pulmonary veins connect normally to the LA. Functionally, these patients resemble patients with TAPVC.

Physiology

The fundamental physiologic disturbance of PAPVC is similar to that in ASD, that is, increased pulmonary blood flow (PBF) as a consequence of recirculation of oxygenated blood through the lungs. The factors that determine the hemodynamic state include the number of anomalously connected veins, the cross-sectional area of the anomalously draining pulmonary vascular bed, the site of the anomalous connections, the presence or absence of an ASD, and the size of the ASD.

Partially Anomalous Pulmonary Venous Connection with Intact Atrial Septum

When the atrial septum is intact, factors that determine the proportion of blood that drains through the anomalously connected veins include the number of veins that are anomalously connected and the amount of lung tissue involved, the relative resistance of the vascular beds normally and anomalously connected, compliance of the respective atria into which the normally and anomalously connected veins empty, and the presence and degree of obstruction to pulmonary arterial blood flow.

When a single pulmonary vein is anomalously connected, the anomalously draining blood flow is about 20% to 25% of the total PBF (6). It is of such slight hemodynamic significance that the lesion is rarely recognized clinically. Hughes and Rumore (8) found neither dilation nor hypertrophy of the right heart in two patients with a single-lobe PAPVC who died at middle age of rheumatic heart disease. When all but one of the pulmonary veins drain anomalously, the anomalously draining blood approximates 80% of the PBF. The physiology and clinical presentation of these patients are comparable to those of the patient with TAPVC.

When the veins of one lung drain anomalously, the factors of relative pulmonary resistance and relative receiving chamber compliance modify the relative blood flows. In one study of patients with PAPVC of the RPVs to the IVC with intact atrial septum (scimitar syndrome), calculated PBF to the anomalously connected vein was 24% to 32% of the PBF (15). This low flow is related to abnormalities of the right lung parenchyma and the frequently associated anomalies of arterial supply that are seen in the scimitar syndrome

(17). On the other hand, when anomalous connection of one lung is the sole abnormality, the anomalously draining blood flow approximates 66% of the PBF as a result of the greater compliance of the RA, to which the anomalous veins drain, and the lesser compliance of the LA, the chamber receiving the normally draining blood. Thus, in patients in whom partially anomalous venous connection is the sole abnormality, the right atrial pressure is usually lower than left atrial pressure. As long as pulmonary vascular resistance remains equal in both lungs and there is no pulmonary arterial stenosis, blood flow is greater in the anomalously connected lung.

The lobe or lobes drained by the anomalously connecting pulmonary vein also affect the magnitude of the left-to-right shunt. In the upright position at rest, PBF is distributed preferentially to the middle and lower lobes. In supine position and during exercise, PBF is redistributed to the upper lobes. Hence, the magnitude of the left-to-right shunt in a patient with PAPVC from one of the upper lobes may vary according to body position and level of activity.

Partially Anomalous Pulmonary Venous Connection with Atrial Septal Defect

When the ASD is small, the hemodynamic state closely resembles that of PAPVC with an intact septum. On the other hand, a large ASD significantly influences the hemodynamic picture. It is pertinent to review briefly the physiology of uncomplicated ASD, in particular, the preferential shunting that occurs in this anomaly.

Using indicator-dye dilution techniques, Burchell et al. (16) evaluated the relative contribution of each lung to the left-to-right shunt in patients with ASD. The average ratio of pulmonary blood flow (PBF) to systemic blood flow (SBF) was 3.5:1. The proportion of blood from the right lung that was shunted left-to-right averaged 84%, whereas the proportion of blood from the left lung that was shunted averaged 54%. Thus, blood from both lungs drained anomalously, but the right lung contributed more than the left lung to left-to-right shunt. This preferential shunting from the right lung in ASD has been shown experimentally to result from the proximity of the right pulmonary venous orifices to the ASD.

When PAPVC and ASD coexist, the hemodynamic picture may be similar to that of uncomplicated ASD. The left-to-right shunt may be large. This shunt is the result of anomalous drainage of most of the blood from the anomalously connected lung and of anomalous drainage of half or more of the blood from the normally connected lung via the ASD (16).

A small right-to-left shunt from the SVC (both systemic venous blood and anomalously draining pulmonary venous blood) is usual in the presence of a sinus venosus defect. Likewise, a small right-to-left shunt from the IVC is commonly seen in a secundum ASD. Pulmonary vascular disease has been reported in older patients with uncomplicated PAPVC (17). Although pulmonary hypertension is thought to be rare, its prevalence is unknown.

Clinical Features

The anomalous connection of one pulmonary vein usually is not apparent clinically. If all but one of the veins connect anomalously (subtotal TAPVC), the clinical features mimic those of TAPVC. The following features occur when the veins of one lung connect anomalously. Symptoms are uncommon in childhood, but some dyspnea may occur on exertion. Cyanosis is unusual during childhood, even though a small right-to-left shunt may exist, depending on the location of the PAPVC.

The frequency of patients presenting with cyanosis increases during the third and fourth decades as a result of changes in the pulmonary vascular bed, pulmonary hypertension, and increasing right-to-left shunt.

The clinical presentation of patients with the scimitar syndrome varies widely. Dupuis et al. (18) reported on 25 infants with the scimitar syndrome, and Gao et al. (11) reviewed the data of 13 such patients. All but two patients presented with severe symptoms in early infancy. Pulmonary hypertension was common and was secondary to a combination of conditions, including arterial blood supply from the descending aorta, stenosis of the anomalously connecting RPVs, pulmonary parenchymal abnormalities, and associated obstructive anomalies of the left heart and aorta. Hypoplasia of the right lung with secondary dextrocardia was common. In contrast, in a study of 122 patients with scimitar syndrome who presented later in life (the adult form of scimitar syndrome), symptoms were rare, the left-to-right shunt was <50% in 100 of the 122 patients, the pulmonary artery pressure was normal in 94 and mildly elevated in 28 patients, and the clinical outcome was good in most of these patients (19).

In the presence of an associated ASD, the physical findings are identical to those noted in uncomplicated ASD. When the atrial septum is intact, splitting of the second sound is not marked, and there is normal variation of splitting with respiration. A pulmonary outflow murmur is usually present, and a diastolic tricuspid flow murmur may be present.

Associated Cardiac Defects and Syndromes

PAPVC or drainage has been associated with other congenital cardiac defects and syndromes. Most notably, patients with visceral heterotaxy and polysplenia have a high incidence of PAPVD secondary to malposition of the septum primum, and patients with asplenia have a high incidence of TAPVC. Recent reports described a significant incidence of PAPVC in association with Turner and Noonan syndromes. A prospective evaluation of 21 patients with Turner syndrome by Moore et al. (20) showed three cases of PAPVC with intact atrial septum (14.3%). Of these 21 patients, 12 had the 45 XO karyotype. PAPVC was seen only in this latter population (incidence of 25%) but did not occur in the nine patients who had Turner syndrome of the mosaic type. Additionally, van Wassenaer et al. (21) reported the association of PAPVC with intact atrial septum in three patients with Turner syndrome. Hence, the possibility of PAPVC should be considered in any patient with either Turner or Noonan syndrome.

A rare but clinically important association is that of anomalous pulmonary venous connections with tetralogy of Fallot. A review of 1,183 patients with tetralogy of Fallot (22) described seven patients with anomalous pulmonary venous connections (0.6%). PAPVC was present in four patients, whereas the other three patients had TAPVC.

Diagnostic Features

Electrocardiographic Features

The electrocardiographic (ECG) findings are comparable to those seen in uncomplicated ASD. The rR' pattern and the rSR' pattern are most commonly seen; the ECG is occasionally normal. Peaked P waves and right ventricular hypertrophy of the systolic overload pattern occur in older patients exhibiting pulmonary hypertension. A frontal P-wave axis of $\leq 15^\circ$ (inverted P wave in lead III) has been described with sinus venosus defect. The ECG is often normal in the patient with intact atrial septum.

Radiologic Features

The routine chest radiogram reflects the increased PBF and right ventricular dilation. Additionally, there may be distinctive features dependent on the site of anomalous connection.

The patient with anomalous connection of the RPVs to the IVC has a crescent-like shadow in the right lower lung field (Fig. 35.9B). This characteristic shadow prompted Neill et al. (5) to coin the term scimitar syndrome for this group of patients. Hypoplasia of the right lung (Fig. 35.9D) and chest, mesocardia or dextrocardia, and pulmonary parenchymal abnormalities also may be seen on the chest radiogram when drainage is into the IVC.

When the SVC is the site of the anomalous connection, dilation of the lower portion of the SVC is often recognized just above the right atrial contour or as a double density just inside the upper atrial border. When the anomalous connection is to the azygous vein, this structure is enlarged and can be recognized on the chest radiogram as a rounded bulge in the right superior mediastinum at the right cardiac border.

When the LIV is the site of connection of the left pulmonary veins, the chest radiogram shows a prominent supracardiac shadow composed of the vertical vein on the left, the innominate vein above, and the SVC at the right (Fig. 35.11). These structures are the same ones that account for the characteristic "snowman" appearance when there is a TAPVC to the innominate vein, but the enlargement is not as prominent.

Echocardiographic Features

The key to accurate echocardiographic diagnosis of PAPVC and PAPVD is detailed comprehensive imaging of all cardiovascular structures. The individual pulmonary veins should be examined in every patient, particularly at the time of the first echocardiographic evaluation. The size and course of the individual pulmonary veins must be determined both by 2-D

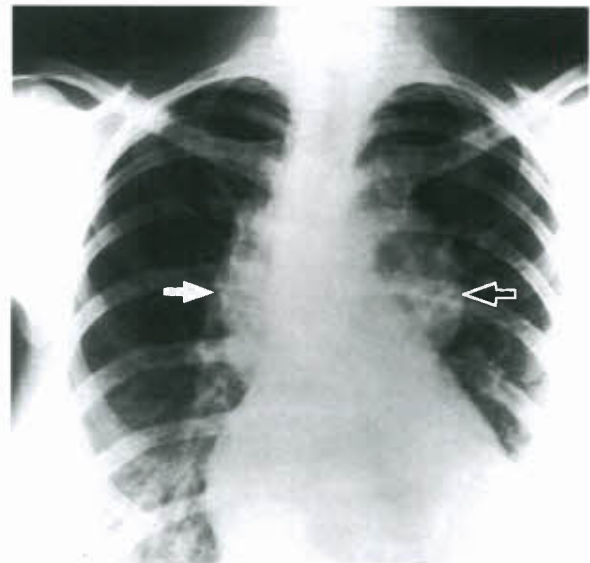


Figure 35.11. Supracardiac totally anomalous pulmonary venous connection. Chest radiogram in the posteroanterior projection in a patient with totally anomalous pulmonary venous connection to the innominate vein showing the typical "snowman" appearance of the mediastinum. The *solid arrow* points to the shadow of the ascending vertical vein. The *white arrow* points to the shadow of the dilated right superior vena cava. Note the cardiomegaly secondary to right heart volume overload and the congested right pulmonary veins.

imaging and by color Doppler flow mapping. The connection and drainage of the right upper and right lower and the left upper and left lower pulmonary veins with the LA should be demonstrated unequivocally. This can be achieved from the subcostal, apical, parasternal, and suprasternal notch windows. The subcostal window is ideal for evaluating the pulmonary veins in infants and young patients with good subcostal acoustic windows. The parasternal, subclavicular, and suprasternal windows are used in older patients. Transesophageal echocardiography is useful in patients with suboptimal transthoracic acoustic windows. Magnetic resonance imaging (MRI) is a preferred noninvasive alternative to transesophageal echocardiography (see later discussion). The presence of right ventricular volume overload, manifested as right ventricular enlargement with flattening of the ventricular septum during diastole, is a useful clue for the presence of a left-to-right shunt but is not specific for PAPVC. The finding of right ventricular volume overload in the absence of an ASD should prompt a careful search for PAPVC.

The echocardiographic diagnosis of PAPVC is based on the demonstration of a connection between one or more of the pulmonary veins with a systemic vein. Typically, the systemic vein distal to the connection of the pulmonary vein is dilated, reflecting the increased flow. Anomalous connection of pulmonary veins to the SVC is best imaged from the suprasternal notch or high parasternal long-axis of the SVC. Similarly, high parasternal short- and long-axis views allow visualization of the anomalous connection of the pulmonary veins to the LIV (Fig. 35.12). The diagnosis can be made from the subcostal window in infants and young children. Enlargement of the LIV and the SVC associated with evidence of increased flow by Doppler are clues to the diagnosis.

The anomalous pulmonary venous connection to the CS is best imaged by scanning the posterior left atrioventricular

(AV) groove from the subcostal, apical, and parasternal windows. The dilated CS in this condition should be distinguished from the more common persistent LSVC.

Imaging of the anomalous connection of one or more of the RPVs with the IVC establishes the diagnosis of scimitar syndrome. The subcostal window is most useful in this condition. The presence of mesocardia or dextrocardia in 70% of patients and a smaller-caliber right pulmonary artery compared with the left pulmonary artery are useful clues. Other findings include blunting of the right border of the LA when both RPVs do not connect with the LA and demonstration of aortopulmonary collaterals by color Doppler flow mapping.

Sinus venosus defect of the inferior type can be a challenging diagnosis to make by echocardiography, particularly in distinguishing this entity from a posteriorly located secundum ASD. Banka et al. (23) demonstrated in a group of 45 patients with inferior-type sinus venosus defect that the rate of accurate preoperative diagnosis was only 36% and that patients with incorrect diagnoses had worse technical outcome scores postoperatively compared with those with the correct preoperative diagnosis (23).

Magnetic Resonance Imaging

Cardiac MRI is suited ideally for evaluation of pulmonary venous anomalies (Fig. 35.13). The wide field of view, excellent spatial orientation, and its inherent three-dimensional (3-D) nature allow unambiguous delineation of the course, connections, and drainage of the pulmonary veins independent of body size and acoustic windows. Also, the ability to depict noncardiovascular structures such as lung parenchyma, airways, bones, and soft tissue offer an advantage over

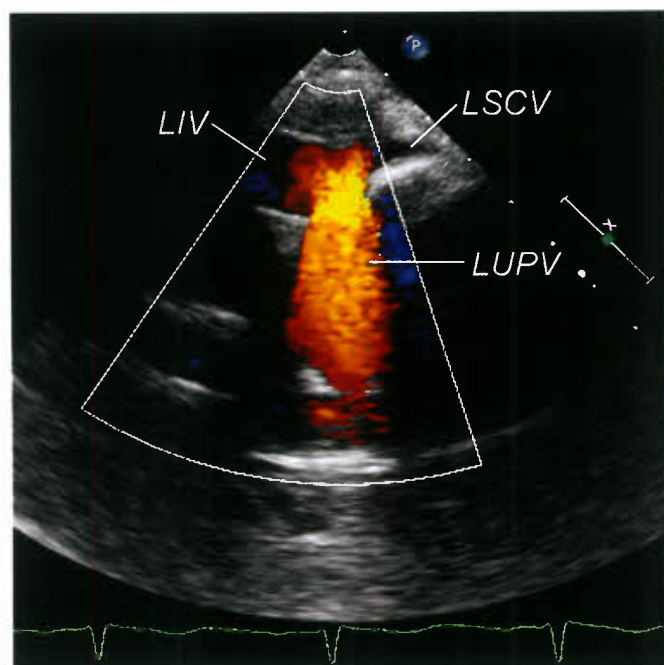


Figure 35.12. Partially anomalous pulmonary venous connection. Echocardiogram from the high left parasternal window in the transverse plane with color Doppler imaging showing partially anomalous pulmonary venous connection of the left upper pulmonary vein (LPV) to the LIV. Note the prominent jet of red (antegrade) flow into the inferior aspect of the LIV. LSCV, left subclavian vein.

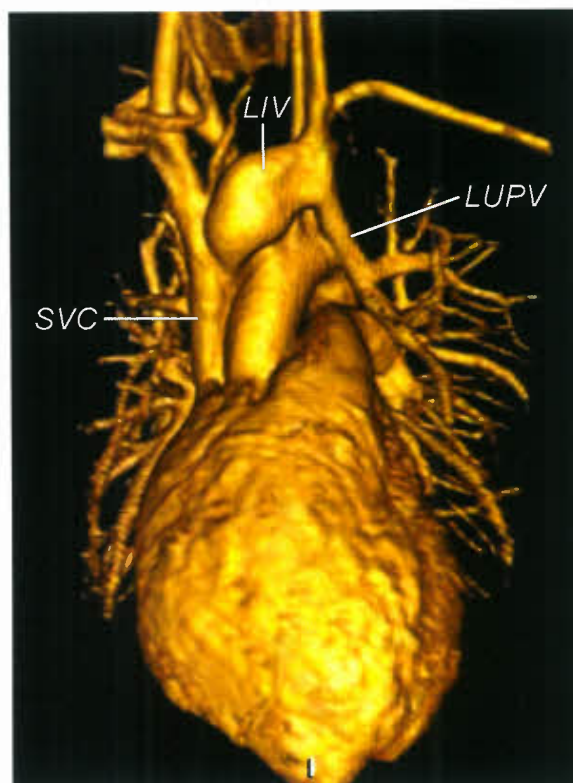


Figure 35.13. Partially anomalous pulmonary venous connection. Three-dimensional reconstruction of gadolinium-enhanced magnetic resonance angiogram with an anterior view showing partially anomalous pulmonary venous connection of the left upper pulmonary vein (LUPV) to the left innominate vein (LIV), which then drains into the SVC.

echocardiography and angiocardiology. Another advantage of MRI is its ability to measure the hemodynamic consequences of anomalous pulmonary venous connections and drainage, including the pulmonary-to-systemic flow ratio and right ventricular size and function.

The anatomy of the pulmonary veins can be evaluated by a series of T1-weighted spin echo images in the axial (transverse), coronal, or oblique planes. This sequence offers excellent spatial resolution but provides only one image in each location. The use of ECG-gated cine MRI sequence allows rapid acquisition of multiple contiguous cine MRI slabs that cover the chest. Cine steady-state free precession MRI clearly depicts the size, course, and drainage of the pulmonary veins and their relations to neighboring structures. Turbulent flow is seen clearly by this sequence. The advent of magnetic resonance angiography (MRA) added a powerful tool that allows fast 3-D imaging of cardiovascular structures (Figs. 35.13 and 35.14). Phase-contrast cine MRI allows quantification of



Figure 35.14. Scimitar syndrome. Three-dimensional reconstruction of gadolinium-enhanced magnetic resonance angiogram in a posterior view in a 20-year-old male with scimitar syndrome. Most of the pulmonary venous return from the right lung enters into the inferior vena cava through the scimitar vein (arrow), and a large collateral artery from the abdominal aorta enters the right lower lobe (asterisk). A small right upper pulmonary vein connects normally to the left atrium with a small intrapulmonary connection (not shown). At cardiac catheterization, the scimitar vein was occluded near its junction with the inferior vena cava, thus diverting the venous return from the entire right lung into the left atrium. The arterial collateral vessel was occluded as well. L, left; R, right.

blood flow through the pulmonary veins, determination of systemic and pulmonary flow ($Q_p:Q_s$), and flow to the left and right lungs. Experience with MRI and MRA in the evaluation of anomalous pulmonary venous connections indicates that it is superior to echocardiography and angiocardiology (24,25).

Cardiac Catheterization

Cardiac catheterization usually is not necessary for the diagnosis of PAPVC, its differentiation from secundum ASD, or estimation of the magnitude of the left-to-right shunt. Clinical features, echocardiography, and MRI provide sufficient anatomic and hemodynamic preoperative data. Cardiac catheterization is still useful in selected cases, especially if pulmonary hypertension is suspected. Interventional catheterization is indicated to occlude aortopulmonary collaterals in scimitar syndrome.

When cardiac catheterization is performed, frequent oximetry sampling usually allows identification of anomalous pulmonary venous connection to the CS, to the azygous vein, and to the SVC. Oximetry is usually of little value when the anomalous connection is to the IVC because blood flow through the right lung is diminished and also because of the contribution of highly oxygenated blood to the IVC by the renal veins. Inability to pass the catheter from the RA to the LA or a difference between the right atrial pressure and the pulmonary wedge pressure is suggestive of PAPVC with intact atrial septum.

Selective angiography is of limited value if the anomalously draining veins enter the RA or close to it. When the anomalous connections are to more peripheral vessels, however, angiography usually can define the site of anomalous connection, for example, PAPVC to the IVC, SVC, LIV, and azygous vein. Performing selective pulmonary arteriography and watching the levophase for pulmonary venous return may image the connections. If the anomalous connection is entered, direct injection of radiographic contrast dye will delineate the anatomy.

Differential Diagnosis

The distinction between ASD and PAPVC by clinical evaluation is difficult to make but is academic. The capabilities of today's noninvasive imaging techniques (echo and MRI) allow accurate preoperative diagnosis. Ostium primum ASD and single atrium also result in left-to-right shunt at the atrial level; these may be differentiated on the basis of their characteristic ECG pattern (i.e., counterclockwise frontal vector loop and left axis deviation). TAPVC presents a strikingly different clinical picture, with severe pulmonary congestion and cardiac failure, usually leading to death prior to 6 months of age if not treated. Cyanosis is an additional distinguishing feature.

Treatment

Medical Management

When heart failure occurs, either as a result of increased PBF or as a consequence of pulmonary vascular disease, the usual measures are indicated. When pulmonary parenchymal anomalies are associated, as in anomalous connection to the IVC, medical measures may be of temporary benefit. The only definitive therapy in PAPVC, however, is surgical correction.

Surgical Treatment

Surgical treatment of PAPVC is indicated when patients exhibit evidence of pulmonary overcirculation or respiratory insufficiency. Some of the surgical techniques are summarized briefly in the following sections.

MALPOSITION OF SEPTUM PRIMUM WITH PARTIALLY ANOMALOUS PULMONARY VENOUS DRAINAGE TO THE RA

Because many patients with malposition of septum primum and PAPVD draining to the RA have additional cardiovascular malformations, surgical treatment must be individualized. In general, patients may be divided into the following three groups:

1. Patients with atrioventricular concordance in whom a biventricular repair can be achieved. In these patients, the atrial septum is excised, and a new septum is constructed so that the systemic and pulmonary veins drain into their corresponding atria.
2. Patients with atrioventricular discordance and two well-developed ventricles. In these patients, the pulmonary veins are baffled into the systemic ventricle and the systemic veins and then drain into the pulmonary ventricle.
3. Patients in whom a biventricular repair cannot be achieved. In this group, the malposition of the septum primum is usually not relevant to the modified Fontan operation or to the bidirectional Glenn shunt (26).

SINUS VENOSUS DEFECT

Van Praagh et al. (27) described four surgical techniques, which have been used in 44 patients with superior-type sinus venosus defects:

1. Patch closure of the defect between the SVC and the RPVs baffling the right upper pulmonary vein to the LA through its native orifice.
2. In addition to the patch closure of the defect in the wall between the SVC and the RPVs, a second patch was used to enlarge the SVC (double patch technique).
3. This technique, described by J. Lewis and first performed by Warden et al. (28), involves division of the SVC and azygous vein superior to the entrance of the pulmonary veins. The cranial end of the SVC is sewn to an incision in the right atrial appendage. The cardiac end of the divided SVC is oversewn, and a patch diverts the right pulmonary venous blood into the LA through the interatrial communication.
4. Enlargement of the interatrial communication and baffling the RPVs to the LA via the enlarged interatrial communication are used for the inferior (right atrial) sinus venosus defects.

PAPVC TO INFERIOR VENA CAVA

Repair has been accomplished in the presence of an ASD by dividing the anomalously connecting vein at its IVC junction and anastomosing it to the LA (29). Repair then can be continued as in PAPVC to the RA. When the atrial septum is intact, as is usually the case, the anomalously connected vein is transplanted to the right atrial wall, and then an ASD is created and made contiguous to the anomalously connected vein by patching. A third technique is to baffle the anomalously connecting scimitar vein through the IVC and RA to the LA via a surgically created ASD. All of the above techniques carry a substantial risk of postoperative stenosis of the RPV.

PAPVC TO CORONARY SINUS

When this anomaly is present, it may be repaired using the technique described for repair of TAPVC to the CS.

PAPVC OF LEFT PULMONARY VEINS TO INNOMINATE VEIN

Kirklin (30) corrected this anomaly by anastomosing the common left pulmonary vein to the base of the amputated left atrial appendage.

Prognosis

Untreated

There is a paucity of information on which to base a prognosis in this defect. Studies based on anatomic material (8) indicate that patients with one pulmonary vein connected anomalously and with an intact septum have an excellent prognosis and rarely present with cardiorespiratory symptoms. It would be erroneous, however, to apply this excellent prognosis to patients who present with symptoms. The natural history in these patients appears comparable to that in uncomplicated ASD.

Postoperative Course

The impact of operative intervention of PAPVC depends in part on the state of the pulmonary vascular bed at the time of surgery. In patients with high PBF, symptoms are reduced dramatically, postoperative studies reflect a normal physiology, and a near-normal longevity may be assumed. These favorable results cannot be anticipated in the patient who has developed pulmonary vascular disease.

Long-term follow-up of repair of PAPVC has been reported in few series. Gustafson et al. (31) operated on 38 patients with sinus venosus defect. They had one early operative death in a 31-year-old patient with severe pulmonary hypertension. Symptomatic SVC obstruction occurred in one patient. Sick sinus syndrome was present in one patient. Of the surviving 30 patients, all remained well over a 1-year to 24-year period of follow-up. Van et al. (32) reported on the follow-up of PAPVC of the left pulmonary veins to left SVC, innominate vein, or CS in 13 patients. They reported no operative deaths, and one patient developed postpericardiotomy syndrome. Clinical follow-up of these patients 1.5 to 8 years after surgical repair demonstrated no evidence of pulmonary hypertension or pulmonary venous obstruction. A recent multicenter study of long-term outcomes after surgical treatment of scimitar syndrome from the European Congenital Heart Surgeons Association (33) found an early postoperative mortality of 5.9% in 68 patients and two late deaths resulting from severe pulmonary arterial hypertension. There was a relatively high incidence of residual scimitar drainage stenosis (freedom from scimitar vein stenosis was 85% at 13 years) that did not appear to vary by surgical approach (33). Sick sinus syndrome has been reported after repair of sinus venosus defect. Postoperative arrhythmias are infrequent with other forms of PAPVC.

The postoperative patient should be monitored periodically for development of pulmonary venous obstruction and for arrhythmias. The obstruction can result from occlusion of the anomalous pulmonary veins and can result in no blood flow to the affected lung. This can be detected by ventilation perfusion scintigraphy, echocardiography, MRI, or angiography. The pulmonary venous obstruction also can be secondary to stenosis of the SVC or IVC, which could be relieved with balloon angioplasty or placement of a stent.

TOTALLY ANOMALOUS PULMONARY VENOUS CONNECTION OR DRAINAGE

TAPVC defines the anomaly in which the pulmonary veins have no connection with the LA. Rather, the pulmonary veins connect directly to one of the systemic veins (TAPVC) or drain into the RA (TAPVD) (Fig. 35.15).

The frequency of TAPVC is difficult to define. In Abbott's (34) series of 1,000 cases of congenital heart disease, there

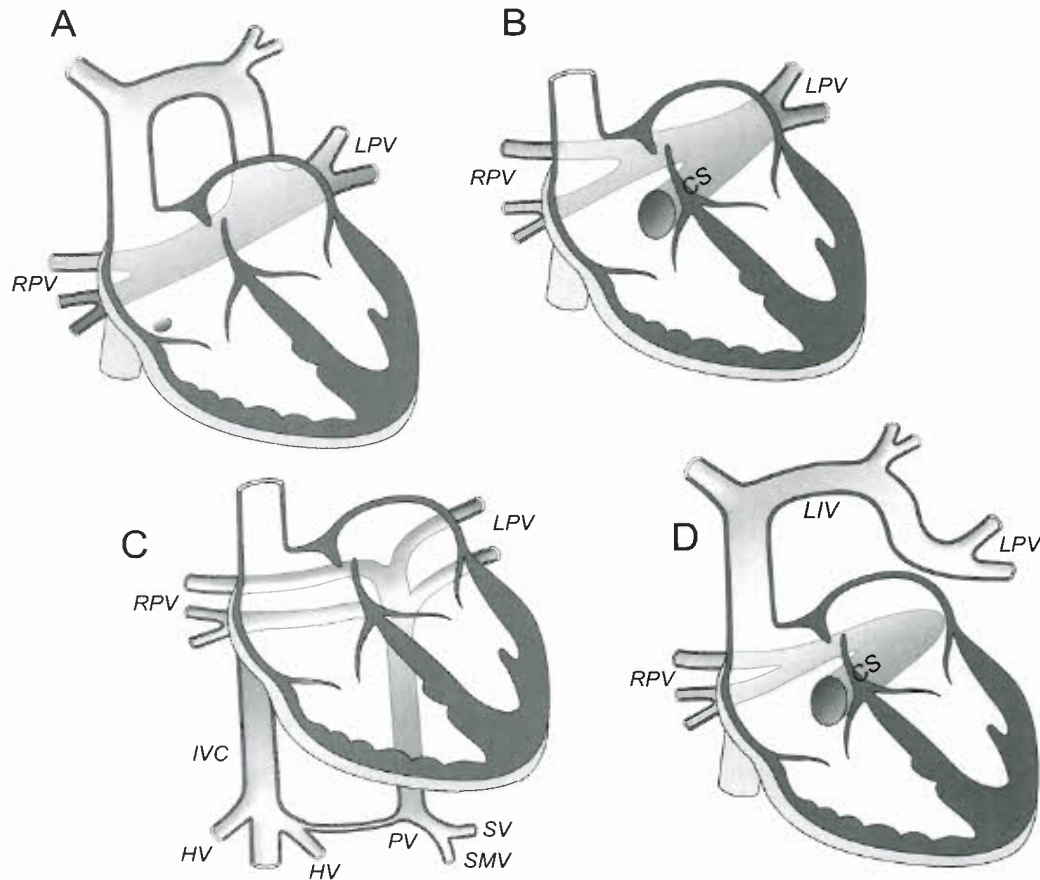


Figure 35.15. Totally anomalous pulmonary venous connection. **A: Supracardiac.** Both right (RPV) and left (LPV) pulmonary veins join a common pulmonary venous confluence behind the heart that drains via a vertical vein to the undersurface of the left innominate vein and thence to the right atrium. **B: Cardiac.** The pulmonary venous confluence connects to the coronary sinus (CS), and thence to the right atrium via the coronary sinus ostium. **C: Infradiaphragmatic.** The pulmonary venous confluence drains inferiorly via a vertical vein to the portal vein (PV) or hepatic veins (HVs) and thence to the right atrium. **D: Mixed Connections.** Left pulmonary veins drain to the LIV, and right pulmonary veins to the coronary sinus in this example. SV, splenic vein; SMV, superior mesenteric vein. (From Brown DW. Pulmonary venous anomalies. In: Lai, WW, Mertens LL, Cohen MS, et al., eds. *Echocardiography in Pediatric and Congenital Heart Disease: From Fetus to Adult*. United Kingdom: Wiley-Blackwell, 2009:119–142, with permission).

were 4 instances of TAPVC. Another study recorded 2% of 800 autopsied cases of congenital cardiac disease in the first year of life (35). There is a marked male preponderance in TAPVC to the portal vein (3.6:1) (36), whereas there appears to be no sex prevalence in the other sites of connection.

Genetics and Epidemiology

The mechanism of transmission of TAPVC has not been elucidated. The Baltimore-Washington Infant Study, however, showed a possible association with exposure to lead, paint or paint-stripping chemicals, and pesticides (35,37).

Although there is no known genetic pattern of transmission of TAPVC, a monogenic pattern of inheritance has been suggested from the number of reported family cases in the literature among siblings (38). Among the affected families, the common denominator was the anomalous pulmonary venous connection; the site of the anomalous venous connection was usually not concordant. TAPVC and TAPVD have been associated with a few syndromes, most notably asplenia, polysplenia, and cat's-eye syndrome.

Anatomy

Numerous classifications of TAPVC have been advanced. Craig et al. (39) divided TAPVC as follows: (a) anomalous connection at the supracardiac level, (b) anomalous connection at the cardiac level (to the CS), (c) anomalous connection at the infracardiac level, and (d) anomalous connection at two or more of the above levels (mixed type). This classification is the most commonly used approach to date. Burroughs and Edwards (40) suggested a classification with prognostic implications based on the length of the anomalous channel (i.e., long, intermediate, or short); however, the prognostic and physiologic implications suggested by these classifications are not always true. Smith et al. (41) provided an alternative classification for TAPVC: Supracardiac (without pulmonary venous obstruction) and infradiaphragmatic (with pulmonary venous obstruction).

Earlier in this chapter, TAPVD to the RA secondary to malposition of the septum primum was discussed. This kind of TAPVD usually is associated with visceral heterotaxy and additional heart defects (30).

The frequencies of the various sites of TAPVC or drainage are shown in Table 35.2. More than one-third of the cases had the anomalous connection to the LIV.

TABLE 35.2 Comparison of Anatomic Site of Connection of TAPVC and TAPVD in Three Autopsy Series

Site of Connection or Drainage	Burroughs and Edwards (40) (% , N = 113)	Lucas et al. (36) (% , N = 71)	Delisle et al. (42) (% , N = 93)
Left innominate vein	36	35	26
Coronary sinus	16	16	1
Right atrium	15	2	8
Right superior vena cava	11	12	15
Portal system	13	23	24
Multiple sites	7	10	5
Unknown or other	2	0	4

TAPVC, totally anomalous pulmonary venous connection; TAPVD, totally anomalous pulmonary venous drainage.

The presence of an interatrial communication is necessary to sustain life; therefore, an ASD or patent foramen ovale is considered part of the complex. Also, the young age of the patients makes the presence of a PDA usual, and this is not considered a complicating defect. A rare exception was a case of TAPVC to the CS with intact atrial septum, multiple VSDs, and a persistent LSV to the CS who survived to the age of 11 years (42).

Gross examination of the heart shows several features common to all cases, regardless of the site of the anomalous connection. These include dilation and hypertrophy of the right ventricle and RA and dilation of the pulmonary artery. The left ventricle is of normal size, and left ventricular volume measured in life is usually within the normal limits. Left atrial size

usually is diminished because it lacks the contribution of the common pulmonary vein. In addition to these findings, specific anatomic features vary as to the site of the anomalous connection as follows.

Connection to the Right Superior Vena Cava or the Right Azygous Vein

The pulmonary veins from each lung join to form a confluence posterior to the LA. An anomalous vessel originating from the right side of this confluence ascends, passes anterior to the hilum of the right lung, and enters the posterior aspects of the right SVC (Fig. 35.16A). In a rare case, the right-sided ascending pulmonary venous vessel connects to the azygous vein.

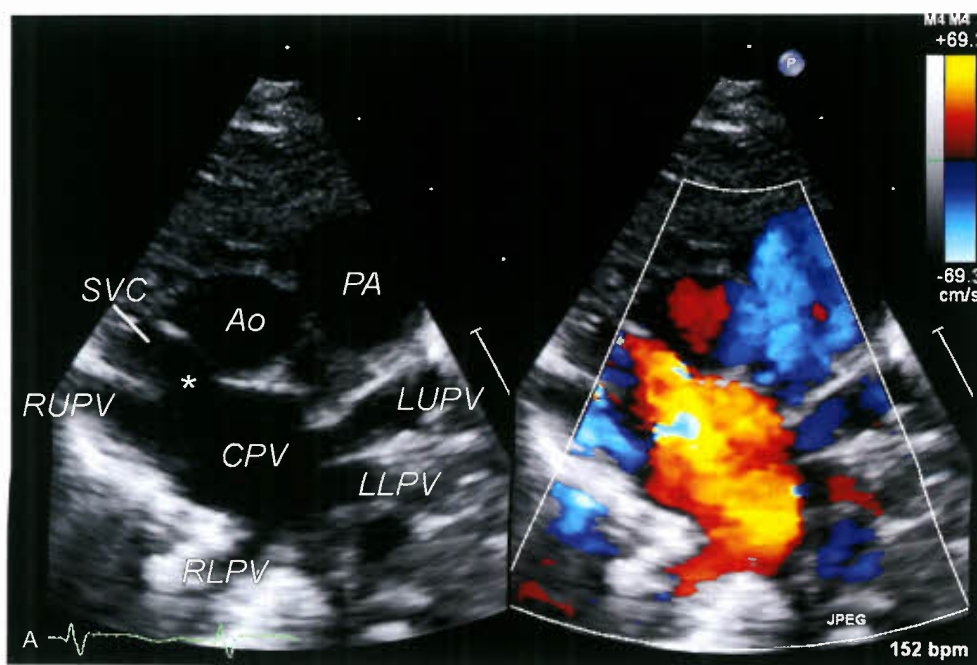


Figure 35.16. Echocardiographic delineation of totally anomalous pulmonary venous connection. A: High left parasternal transverse view of TAPVC to the right superior vena cava (SVC). The right upper pulmonary vein (RUPV), right lower pulmonary vein (RLPV), left upper pulmonary vein (LUPV) and left lower pulmonary vein (LLPV) are seen joining a horizontal pulmonary venous confluence (PVC). The vertical vein (asterisk) ascends rightward and anteriorly to join the posterior aspect of the SVC. The pulmonary artery (PA) is dilated secondary to the volume load. Ao, aorta.

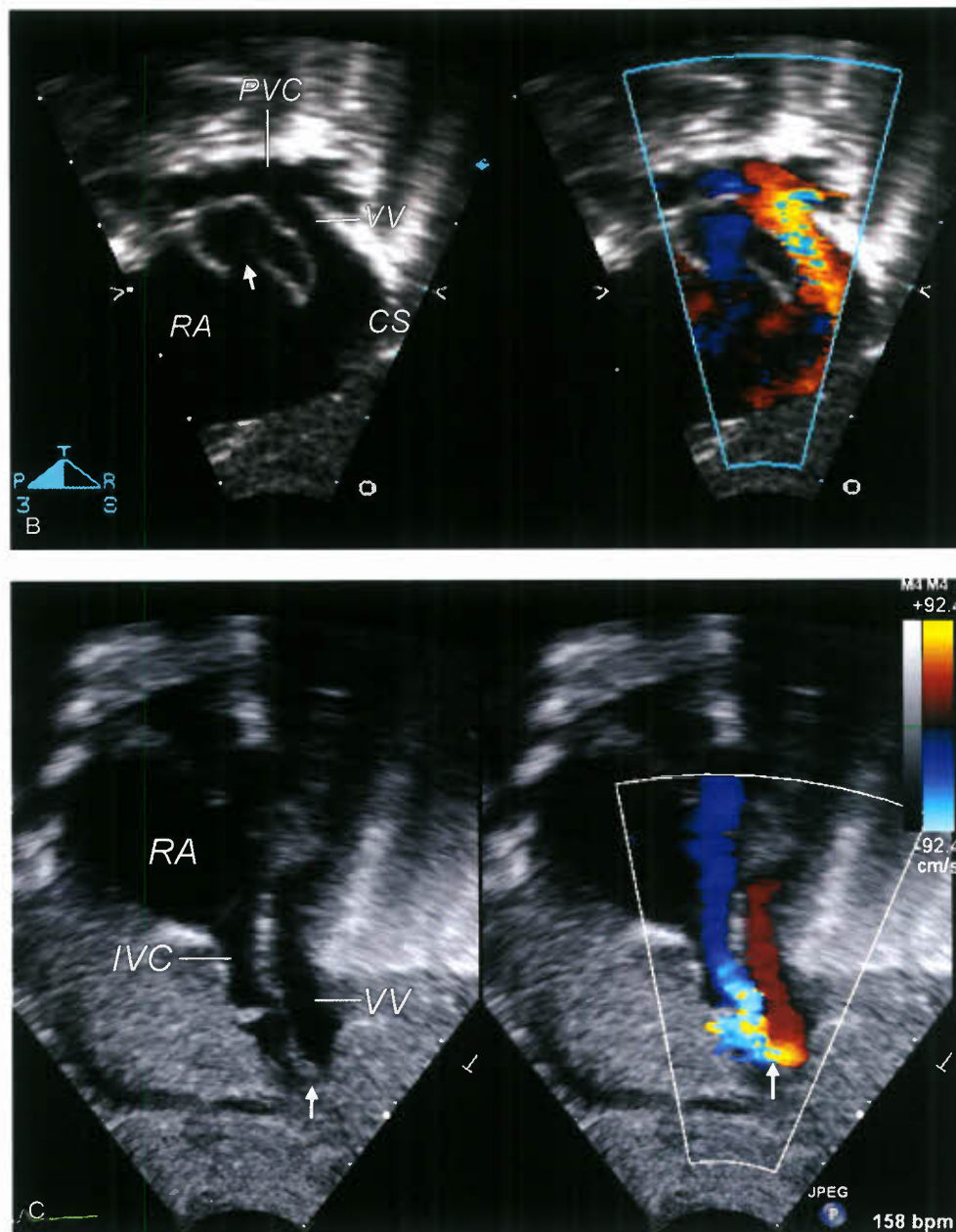


Figure 35.16. (Continued) **B:** Subcostal oblique view with color Doppler comparison of TAPVC to the coronary sinus (CS), which is markedly dilated. The image depicts the typical “whale’s tail” appearance of the pulmonary venous confluence (PVC) and connection of the vertical vein (VV) to the CS. Note the obligate right-to-left shunt across the patent foramen ovale (PFO, arrow) and the small left atrium. (RA, right atrium.) **C:** Subcostal short-axis view with color Doppler comparison of infradiaphragmatic TAPVC in a patient with congenital absence of the left lung. From this view, the descending VV flow is demonstrated (red), with obstruction (arrow) at the point of connection with the IVC.

Connection to the Left Cardinal System

CONNECTION TO THE LEFT INNOMINATE VEIN

In this, the most common site of TAPVC, the pulmonary veins from both lungs form a confluence immediately posterior to the LA (Fig. 35.15A). A venous channel originates from the left portion of the confluence, usually passes anterior to the left pulmonary artery and mainstem bronchus, ascends into the superior mediastinum, passes anterior to the aortic arch, and joins the LIV proximal to its origin from the left jugular and subclavian veins (Fig. 35.17). The LIV then joins the right SVC in normal fashion. Less commonly, the ascending vein passes between the left pulmonary artery and left main

stem bronchus; the latter structures produce an extrinsic obstruction to pulmonary venous flow. The venous channel connecting the pulmonary vein to the LIV is an anomalous vertical vein that represents an embryonic channel between the splanchnic and the cardinal venous systems. Therefore, the term persistent LSVC should not be used for this venous channel (a persistent LSVC connects with the CS or with the LA when the CS is unroofed).

CONNECTION TO THE CORONARY SINUS

The entire anomalous pathway is situated within the pericardium. The pulmonary veins join a common vessel that connects to the CS in the region of the AV groove (Figs. 35.15B

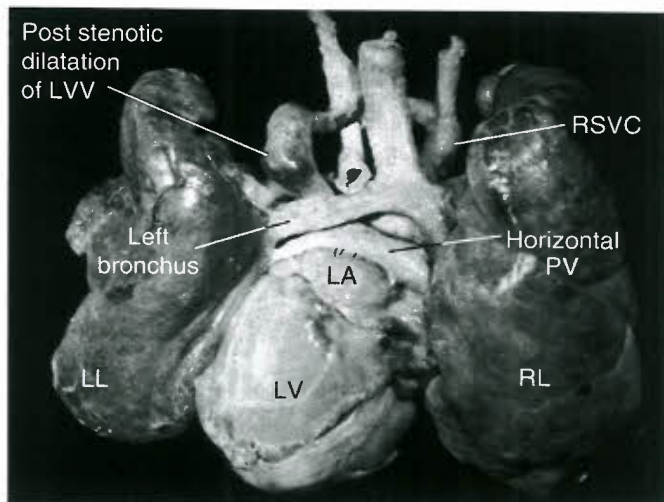


Figure 35.17. Posterior view of heart and lungs specimen showing supracardiac totally anomalous pulmonary venous connection. The individual pulmonary veins form a horizontal confluence (Horizontal PV) behind the left atrium (LA). The left vertical vein (LVV) connects to left innominate vein, which continues into the right superior vena cava (RSVC). The VV is “sandwiched” between the left main stem bronchus posteriorly and the left pulmonary artery anteriorly. Note the poststenotic dilatation of the LVV. LL, left lung; LV, left ventricle; RL, right lung.

and 35.16B). The CS then follows its normal course to the RA. The enlarged orifice of the CS is either normally placed between the orifices of the IVC and tricuspid valve or is displaced posterior to the orifice of the IVC. The cardiac veins drain normally into the CS, which shares a common wall with the LA throughout the greater portion of its length. Stenosis at the junction of the common pulmonary vein with the CS or within the CS is rare but can occur.

Connection to the Umbilicovitelline System

This distal site of connection is situated below the diaphragm. The pulmonary veins from both lungs join to form a confluence immediately behind the LA. A common vessel originates from this confluence, descends immediately anterior to the esophagus, and penetrates the diaphragm through the esophageal hiatus. Most commonly, the anomalous descending vessel then joins the portal vein at the confluence of the splenic and superior mesenteric veins (Figs. 35.15C and 35.18). Less often, the anomalous vessel connects to the ductus venosus, to one of the hepatic veins, or to the IVC. When the anomalous connection is to the umbilicovitelline system, pulmonary venous obstruction is usually present.

Anatomic Sites of Obstruction to Pulmonary Venous Drainage

The presence of an obstructive lesion in the anomalous pulmonary venous channel profoundly influences the hemodynamic state and clinical features in a case of TAPVC. Some of the anatomic causes of obstruction are listed in the following sections.

Obstruction at the Interatrial Septum

Burroughs and Edwards (40) clearly related longevity in TAPVC to the size of the ASD. Those patients with large defects survived longer than did patients with restricted interatrial openings.

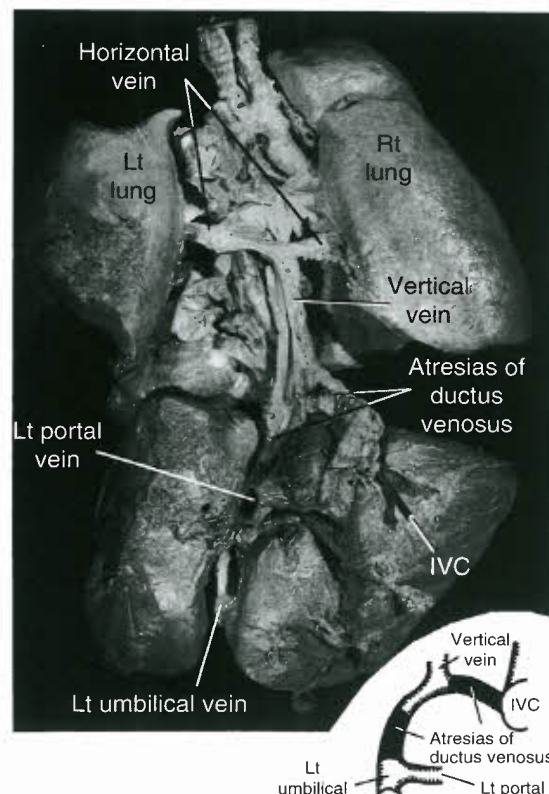


Figure 35.18. Posterior view of heart and lung specimen showing totally anomalous pulmonary venous connection to the portal vein. The ductus venosus is atretic at two locations (Inset) between the vertical vein and the suprahepatic segment of the inferior vena cava (IVC), and between the vertical vein and the confluence of the left umbilical and left portal veins. (From Delisle G, Ando M, Calder AL, et al. Total anomalous pulmonary venous connection: Report of 93 autopsied cases with emphasis on diagnostic and surgical considerations. *Am Heart J* 1976;91:99–122, with permission from Elsevier).

Obstruction in the Anomalous Venous Channel

Obstruction in the anomalous venous channel may be caused by several factors. Intrinsic narrowing in the walls of the anomalous vessels frequently occurs. Extrinsic pressure also results in narrowing of the venous structure. For example, when the vertical vein in TAPVC to the innominate vein passes between the left main pulmonary artery and left mainstem bronchus, the latter structures may obstruct the former (Fig. 35.17). Similarly, the anomalous pulmonary vein in TAPVC to the SVC may be obstructed by the right pulmonary artery and trachea. The ductus venosus normally undergoes constriction, and therefore anomalous connection to this structure results in pulmonary venous obstruction. Finally, when the anomalous connection is to the portal vein or one of its tributaries, the hepatic sinusoids are interposed in the pulmonary venous channel and result in increased resistance to pulmonary venous return. Another factor that may contribute to impedance of pulmonary venous return is the length of the ascending or descending vertical venous pathway.

Associated Cardiac Anomalies

Frequently, TAPVD occurs as an isolated anomaly in patients with normal viscerotransposition. It has been reported, however, to be associated with transposition of the great arteries,

tetralogy of Fallot, single ventricle, truncus arteriosus, tricuspid atresia, hypoplastic left heart syndrome, pulmonary atresia, multiple VSDs, coarctation of the aorta, vascular sling, and other anomalies (42). In contrast, TAPVD to the RA occurs, as a rule, in patients with visceral heterotaxy and polysplenia. Rarely, it is found in patients with visceral heterotaxy and asplenia as well. Hence, TAPVD may be associated with the various defects characterizing the heterotaxic patients, such as common AV canal, conotruncal anomalies, septal defects, pulmonary stenosis or atresia, mitral atresia, systemic venous anomalies, and others.

Microscopic Anatomy

Anomalous Vessels

Sherman and Bauersfeld (43) examined the anomalous venous vessels in eight patients and reported each to be altered by scarring. Fibrosis was abundant in the adventitia, and in some cases, there were focal areas of severe medial fibrosis. An intimal fibrous layer was noted in one. Unobstructed veins often exhibited vein wall atrophy or hypertrophy of intima, media-adventitia, or both. Obstructed veins usually have media-adventitial thickening and often have intimal proliferation.

Left Atrium

Sherman and Bauersfeld (43) reported that the histologic picture of the LA in 13 patients was atrophy. Although the muscle fibers were narrow with scanty cytoplasm, they had abundant nuclei. These investigators found that the number of muscle fibers in the LA in TAPVC approximated controls.

Lungs

The microscopic findings in the lungs vary depending on whether pulmonary venous obstruction is present.

TAPVC without Obstruction

In the absence of pulmonary venous obstruction, the muscular arteries and arterioles generally have prominent medial hypertrophy. Intimal lesions in the arterioles are uncommon in the infant but usual in the older child and adult.

TAPVC with Obstruction

In TAPVC with obstruction, there is medial hypertrophy within the anomalous venous channels, the extrapulmonary veins, and the small veins of the lungs. Pulmonary edema and extravasation of red cells into the alveolar spaces are pronounced. Prominent dilation of the subpleural and interlobular lymphatics is present, and medial hypertrophy of the pulmonary arterioles and pulmonary arteries is pronounced. Intimal proliferation within the arterioles is common, and necrotizing arteritis rarely is seen.

Physiology

All venous blood returns to the RA. Some form of communication between the right and left sides of the heart is essential for survival in TAPVC. The physiologic features depend on the distribution of this mixed venous blood between the pulmonary and systemic circulations. The state of the interatrial septum is of primary importance in this distribution. During fetal life, PBF is small, and the combined systemic and pulmonary venous return to the RA is only minimally increased. Hence, the stimulus for the development of a large interatrial communication is minimal. Some degree of restriction to

flow across a patent foramen ovale (found in 70% to 80% of cases) is common. In patients with a restrictive interatrial communication, the amount of blood reaching the LA is limited and systemic output is reduced. As pulmonary vascular resistance gradually decreases after birth and as demands for SBF increase with the rapid growth of the infant, massive pulmonary overcirculation ensues. Pulmonary and systemic venous blood return is to the RA; therefore, increased right atrial pressure results in pressure elevation and congestion in both venous circuits.

On the other hand, the presence of a widely patent foramen ovale or ASD allows free communication between the two atria. In this circumstance, the distribution of mixed venous blood depends on the relative compliance of the atria and ventricles and the relative resistance imposed by the pulmonary and systemic arterial circuits. The major variable is the state of the pulmonary vascular bed, which initially depends on the presence or absence of pulmonary venous obstruction.

TAPVC without Pulmonary Venous Obstruction

At birth, the distribution of blood between the pulmonary and systemic circuits is approximately equal because the resistance in these two vascular beds is nearly equal. In the first few weeks of life, maturation of the pulmonary vascular bed produces a decrease in pulmonary vascular resistance, and a progressively larger proportion of the mixed venous blood traverses the pulmonary circuit. PBF is commonly three to five times SBF. SBF is usually normal. Because the mixed venous pool receives three to five parts of fully saturated blood for each part of desaturated systemic venous blood, oxygen saturation in the RA may be $\geq 90\%$. Adequate mixing in the RA is the rule. Thus, oxygen saturation in the right ventricle, pulmonary artery, LA, left ventricle, and aorta is expected to be equal to that in the RA. Oxygen saturation in the systemic arteries may vary considerably, depending on the type of TAPVC (i.e., supracardiac, to the CS, or infradiaphragmatic), presumably as a result of the streaming of the mixed venous blood. Progressive dilation and hypertrophy of the right ventricle and dilation of the pulmonary artery usually occur.

Pulmonary artery pressure in infants ranges from slightly elevated to systemic. The state of the interatrial communication in patients with TAPVC without pulmonary venous obstruction has a major impact on PBF, pressure, and resistance. In the few patients who survive to older childhood or early adulthood, the pulmonary artery pressure is only slightly elevated. As time goes on, medial hypertrophy and intimal proliferation occur in the pulmonary arterioles, resulting in more severe pulmonary hypertension in the third and fourth decades.

TAPVC with Pulmonary Venous Obstruction

Elevated pressure in the pulmonary venous channels is transmitted to the pulmonary capillary bed. Pulmonary edema results when the hydrostatic pressure in the capillaries exceeds the osmotic pressure of the blood. Mechanisms that tend to prevent pulmonary edema include increased pulmonary lymphatic flow, alternative pulmonary venous bypass channels, altered permeability of the pulmonary capillary wall, and reflex pulmonary arteriolar constriction. The last mechanism results in a decrease in pulmonary flow, pulmonary hypertension, right ventricular hypertension and hypertrophy, and, ultimately, right heart failure.

The right ventricular volume and pressure overload result in a leftward shift of the interventricular septum that, together with the decreased inflow from the LA, lead to a decrease in left ventricular volume. Systemic output usually is low because of the inadequate filling volume.

Clinical Manifestations

The signs and symptoms in TAPVC are variable, depending on the underlying hemodynamics. When the interatrial communication is inadequate, symptoms occur at birth or shortly thereafter. The hemodynamic consequences of inadequate interatrial communication include pulmonary venous obstruction. The presence of intrinsic or extrinsic narrowing in the connecting vein also produces pulmonary venous obstruction. Thus, the manifestations may be divided according to whether pulmonary venous obstruction is absent or present.

TAPVC without Pulmonary Venous Obstruction

CLINICAL FEATURES

Patients are usually asymptomatic at birth. Seventy-four patients with TAPVC without pulmonary venous obstruction are present in the files of the Northern Great Plains Registry of Congenital Heart Disease (44). Of these, 56% had symptoms in the first month of life and the remainder in the first year. Tachypnea and feeding difficulties were the initial symptoms, usually manifested by the first few weeks of life. From that point on, the infants did not thrive, were subject to repeated respiratory infections, and usually had cardiorespiratory failure by 6 months of age.

Cyanosis may be so mild as to be clinically inapparent, except in the presence of cardiac failure and in the patient who survives long enough to acquire secondary pulmonary vascular changes. Of these infants, 75% to 85% die by 1 year of age, most in the first 3 months of life (40). The infants are thin and irritable and may exhibit slight duskeness on crying and exertion. Dyspnea, tachypnea, tachycardia, and poor feeding are almost always present.

A prominent right ventricular heave is a typical finding. A characteristic feature is the presence of multiple cardiac sounds. The first sound is loud and distinct and often is followed by a systolic ejection click. The second sound is widely split and does not vary with respiration. The pulmonary component of the second sound is accentuated. A third heart sound, maximal at the apex almost always, is present. A fourth heart sound is frequently heard in older patients. A cardiac murmur is occasionally absent. Characteristically, a grade 2/6 soft, blowing, systolic ejection murmur is heard in the pulmonary area. This murmur often is heard well over the xiphoid and at the lower left sternal border; in this case, it is S1 coincident secondary to tricuspid regurgitation. Turbulence in the pulmonary outflow tract or tricuspid valve insufficiency, or both, account for the systolic murmurs. A diastolic tricuspid flow murmur at the lower left sternal border occurs frequently. When the anomalous connection is to the LIV, a venous hum at the left or right base may be heard. Unlike the “innocent” venous hum, this murmur is not louder during diastole and is not altered by change in position or pressure on the neck veins.

Cardiac failure occurs in most patients prior to 6 months of age. In cardiac failure, hepatomegaly is always present, and peripheral edema is present in about half of the cases. Clubbing occasionally is seen in the patient who survives infancy.

ELECTROCARDIOGRAPHIC FEATURES

A tall peaked P wave in lead II or the right precordial leads characteristic of right atrial enlargement is a constant finding. Right-axis deviation is usual. Right ventricular hypertrophy invariably is present, usually manifested by high voltage in the right precordial leads and occasionally as an incomplete right bundle branch block pattern.

RADIOLOGIC FEATURES

Certain features are common to all cases. The lung fields reflect increased PBF. The RA and right ventricle are enlarged, and the pulmonary artery segment is prominent. The left-sided chambers are not enlarged. In addition, the specific site of anomalous connection may result in characteristic signs. A figure-of-8 or “snowman” appearance of the cardiac shadow is seen in patients with TAPVC to the LIV (Fig. 35.11). The upper portion of the figure-of-8 is composed of the anomalous vertical vein on the left, the LIV superiorly, and the SVC on the right. This diagnostic sign usually is not present in the first few months of life but often is present in the older child and adult. When the anomalous connection is to the right SVC, dilation of this structure results in a prominence at the upper right cardiac border.

ECHOCARDIOGRAPHIC FEATURES

The goals of the echocardiographic examination in TAPVC are (a) to establish the diagnosis; (b) to image and determine the size of the individual pulmonary veins; (c) to ascertain that all four major pulmonary veins join the pulmonary venous confluence and that no additional pulmonary veins drain separately; (d) to image and determine the size of the pulmonary venous confluence and its relation to the LA; (e) to image the course of the pulmonary venous channel (usually the vertical vein), its connection with the systemic vein, and its relation to neighboring structures (i.e., pulmonary arteries and airways); (f) to determine whether there is obstruction to pulmonary venous flow and its mechanism; (g) to evaluate the interatrial communication for obstruction; and (h) to perform a complete anatomic and functional survey of all cardiovascular structures and to exclude additional structural cardiac anomalies. These goals are achieved by performing a complete step-by-step echocardiographic examination from multiple windows.

The features common to all forms of TAPVC are signs of right ventricular volume overload. The right-sided heart structures are dilated. The RA is enlarged, and the atrial septum bows toward the left. The right ventricle appears to compress the left ventricle, the interventricular septum deviates leftward, and left ventricular volume is decreased. The interventricular septum may move paradoxically. The pulmonary arteries are dilated.

Aside from the features of right ventricular volume overload, the first echocardiographic suspicion that supports the diagnosis of TAPVC is the inability to image the pulmonary veins entering the LA. The LA is small. The pulmonary venous confluence usually is easy to recognize as an echo-free space behind the LA. Next, the individual pulmonary veins are sought. Once identified, each individual pulmonary vein is imaged by 2-D and is interrogated by color Doppler flow mapping. The course and diameter of each vein then should be determined. Jenkins et al. (45) showed that the size of the individual pulmonary veins at the time of initial diagnosis is a strong, independent predictor of survival in TAPVC. Smaller pulmonary veins were associated with poorer prognosis. Based upon a recent multicenter study from Europe investigators similarly found hypoplastic/stenotic pulmonary veins to be an independent risk factor for death (46). The individual pulmonary veins should be imaged from multiple windows, but the parasternal, subclavicular, and suprasternal notch views mostly are used (Fig. 35.16).

The size and orientation (i.e., horizontal or vertical) of the pulmonary venous confluence and its relationship with the LA are important for surgical planning. When all pulmonary veins connect to a horizontal confluence at approximately the same level, anastomosis of this confluence to the back wall of the LA is relatively straightforward. In contrast, when the pulmonary veins connect to a vertical confluence at different levels,

the repair is more challenging. The subcostal, parasternal, and suprasternal notch windows are most useful. Once the pulmonary venous confluence is characterized, the venous channel that connects with the systemic vein is followed by 2-D imaging and color Doppler flow mapping. In general, the venous channel in supracardiac TAPVC is best imaged from the precordial windows (Fig. 35.16A), and the venous channel in infradiaphragmatic TAPVC is best evaluated from the subcostal view (Fig. 35.16C). In supracardiac TAPVC, the venous channel should be examined for its relation with the branch pulmonary arteries and the bronchi. Obstruction may be caused by external compression or by intrinsic stenosis. The site of connection with the systemic vein, most frequently the LIV, is a common site of narrowing. In infradiaphragmatic TAPVC, the most common site of obstruction is at its connection with the portal or the hepatic vein. Often the pulmonary venous channel dilates proximal to the site of stenosis, a finding that should prompt a careful search for obstruction. Luminal narrowing associated with flow acceleration and turbulence by color Doppler characterizes pulmonary venous obstruction, regardless of its mechanism. Spectral Doppler is most useful. Pulmonary venous flow in an unobstructed vessel is characterized by a low-velocity, phasic laminar flow pattern with brief flow reversal during atrial systole. An increased flow velocity disturbed (turbulent) flow pattern, and loss of the phasic variations characterize obstructed pulmonary venous flow.

When TAPVC connects to the CS, the sinus is dilated and can be imaged easily from the subcostal, parasternal long-axis, or apical four-chamber view (Fig. 35.16B). The dilated CS bulges anterosuperiorly into the LA. Dilation of the CS also occurs in other conditions (persistent left SVC draining to CS); hence, imaging of the pulmonary veins draining into the CS is key to the diagnosis.

Infradiaphragmatic TAPVC usually connects to the portal venous system but can connect to the hepatic veins or to the IVC. The pulmonary veins converge into a common channel, which is located inferior to the LA immediately above the diaphragm. The common pulmonary venous channel may appear as a distinct chamber. It is best imaged from the subcostal short- and long-axis windows, with scanning from left to right and superior to inferior to identify the abdominal connection of the anomalously connecting vein (Fig. 35.16C). In a transverse plane, the descending aorta lies to the left and posteriorly, the IVC to the right and anteriorly, and the anomalous pulmonary venous channel in an intermediate position. The descending anomalous vein may be missed if it is compressed by a congested liver. Doppler interrogation is used to differentiate flow characteristics among the various abdominal vessels. Flow in the descending aorta has a systolic laminar profile in a direction away from the heart. Flow in the IVC is nearly continuous, phasic, and toward the heart. Flow in the common pulmonary vein is characteristic of the venous flow pattern, except the direction is away from the heart toward the abdomen.

In mixed TAPVC, multiple windows must be used to image the connections of at least four individual pulmonary veins. Suprasternal, parasternal, and subcostal windows, as described previously, should be used. The most common type of mixed drainage is connection to both the CS and the LIV.

With each type of TAPVC, a thorough echocardiographic study is necessary to identify coexisting cardiac anomalies. Errors in the identification of TAPVC are more frequent when there are coexisting mixed connection of the pulmonary veins and associated cardiac lesions.

Transesophageal echocardiography provides an alternative approach in patients with poor transthoracic windows. The need for transesophageal imaging in the newborn and young infant, however, is minimal because the transthoracic windows

are usually adequate. Transesophageal echocardiography has a greater role in the evaluation of patients after TAPVC repair, especially in an acute-care circumstance. MRI provides superior diagnostic capabilities in the evaluation of pulmonary veins and should be considered in patients who can be safely imaged by this modality.

Prenatal diagnosis of TAPVC is important for counseling parents, determining prognosis, and planning delivery at a center with facilities and expertise in neonatal pediatric cardiac surgery. Identification of the pulmonary venous connections is one goal of a fetal echocardiographic examination. The normal connection of some of the pulmonary veins to the LA is apparent from the four-chamber view of the fetal heart as well as from short-axis views. Because fetal PBF is less *in utero* than postnatally, it can be difficult to identify anomalous pulmonary venous connections. If one sees right ventricular and pulmonary artery enlargement out of proportion to the left ventricular and aortic size *in utero*, one should consider the diagnosis of TAPVC, especially when other cardiac lesions that can produce the same picture have been excluded (i.e., coarctation, left-sided obstructive lesions, arteriovenous malformations). The prerequisite to the prenatal diagnosis of TAPVC is a high index of suspicion and good-quality imaging of the pulmonary veins; clues to the prenatal diagnosis in one study of 11 cases included visualization of a pulmonary venous confluence behind the LA and a vertical vein (47). Unambiguous identification of a normal connection of some of the pulmonary veins to the LA excludes the diagnosis. The diagnosis of heterotaxy syndrome should prompt a meticulous evaluation of the pulmonary veins.

MAGNETIC RESONANCE IMAGING

The advent of new MRI and MRA techniques in recent years brings this diagnostic modality to the forefront of imaging of pulmonary venous anomalies (24). MRI provides a wide-field imaging of the pulmonary veins and blood flow within them as well as adjacent cardiovascular structures. Noncardiac structures, such as airways, lungs, spine, and abdominal organs, are also seen. MRA provides a 3-D dataset that encompasses all cardiovascular and noncardiac structures (Fig. 35.19). Multilevel steady-state free precession cine MRI in axial, coronal, and oblique planes is performed across the chest and demonstrates the dynamic nature of blood flow, cardiac chambers, and AV and semilunar valves. Cine PC is used to determine flow direction and to quantify flow velocity and flow rate.

Usually, MRI is not necessary in the initial evaluation of newborns and in the infant with TAPVC because echocardiography is accurate, portable, and readily available. MRI is indicated in infants with TAPVC only when echocardiography is inconclusive. In older patients and elective circumstances, MRI provides a superior alternative to ultrasound.

CARDIAC CATHETERIZATION

The accuracy of 2-D and Doppler echocardiography in identifying the presence and type of TAPVC nearly has eliminated the need for diagnostic cardiac catheterization and angiography in the diagnosis of TAPVC. Ninety-seven percent sensitivity and 99% specificity have been reported in the echocardiographic diagnosis of TAPVC, even before color Doppler became available (48). Diagnostic cardiac catheterization now rarely is performed to clarify problems unresolved by 2-D and Doppler echocardiography. The advent of MRI in recent years may obviate the need for diagnostic catheterization even further.

The venous site of anomalous connection may be identified if highly saturated blood is obtained from the LIV, right SVC, or CS. In TAPVC, the oxygen saturation in the RA usually

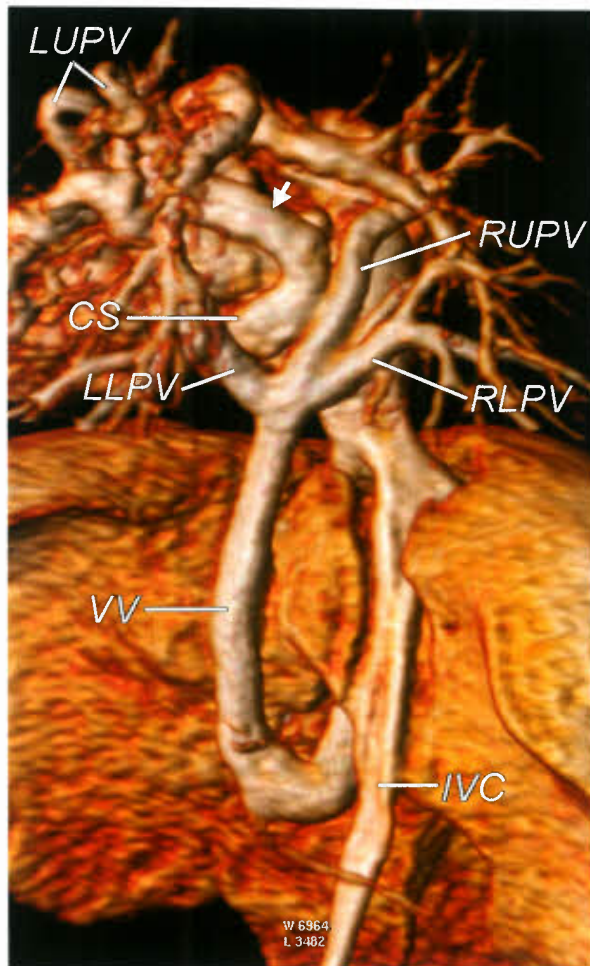


Figure 35.19. Mixed-type totally anomalous pulmonary venous connection (TAPVC). Maximal-intensity projection image from a gadolinium-enhanced 3-D magnetic resonance angiogram viewed from posterior in a 1-day-old newborn with mixed-type TAPVC. The left lower (LLPV), right upper (RUPV), and right lower (RLPV) pulmonary veins drain into a large pulmonary venous confluence that drains via a large vertical vein (VV) below the diaphragm to join the portal vein into the inferior vena cava (IVC). The left upper pulmonary veins (LUPVs) join a separate VV that drains into the coronary sinus (CS). The MRI examination was requested as an alternative to cardiac catheterization and angiography because of the complexity of the pulmonary venous anatomy and acoustic shadowing from the right lung. The MRI examination delineated the anatomy of all pulmonary veins as well as the intra-cardiac and extracardiac anatomy, and these findings were subsequently confirmed at surgery.

ranges between 80% and 95%, and saturations in the RA, right ventricle, pulmonary artery, LA, left ventricle, and systemic arteries are nearly identical. When TAPVC is to the LIV or right SVC, SVC blood preferentially flows into the tricuspid orifice and IVC blood preferentially shunts into the LA, resulting in a pulmonary artery oxygen saturation that may be higher than that in the systemic artery.

Pressure in the right ventricle and pulmonary artery ranges from slightly elevated to equal or higher than systemic pressure. Interpretation of atrial pressures, particularly in an attempt to determine the adequacy of the interatrial communication, is difficult. The presence of equal pressures in the two atria is probably an unreliable sign of a nonobstructive intera-

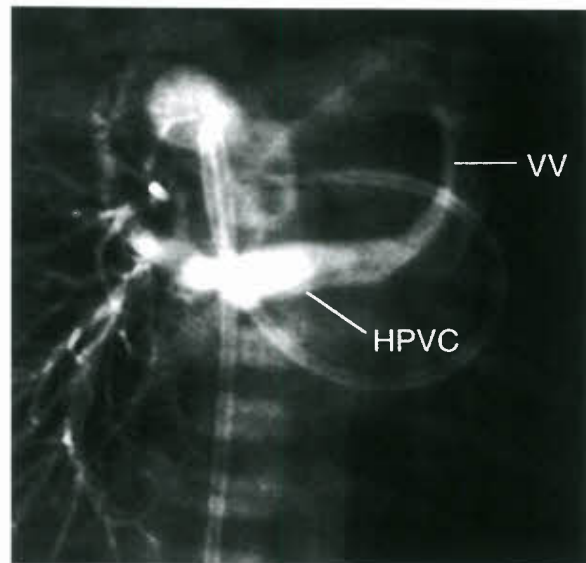


Figure 35.20. Catheter angiography of totally anomalous pulmonary connection. Levophase of a right pulmonary artery angiogram showing supracardiac TAPVC to the left innominate vein. HPVC, horizontal pulmonary venous confluence; VV, vertical vein.

trial communication. This phenomenon is most likely attributable to the fact that the compliances of the two ventricles are usually comparable, and their filling pressures are thus equal even in the face of a restrictive interatrial communication. A right atrial pressure ≥ 2 mm Hg in excess of left atrial pressure is more reliable in predicting a restrictive interatrial communication, but too often it occurs in the face of free communication between the atria. The only reliable way to assess the size of the interatrial communication is to measure it with a balloon catheter.

Selective pulmonary arteriography usually is diagnostic. Following injection and passage of opaque dye through the pulmonary fields, the dye collects in the pulmonary venous channels and clearly outlines the anomalous connection (Fig. 35.20). In TAPVC to the LIV, the vertical vein can be seen to originate from the area of the common pulmonary vein and to ascend to join the LIV. The latter is outlined in its course to the SVC.

TAPVC with Pulmonary Venous Obstruction

CLINICAL FEATURES

Pulmonary venous obstruction is usual when the venous connection is to the umbilicovitelline venous system. Pulmonary venous obstruction is present in about 50% of cases when the connection is to supracardiac structures (49). Obstruction in the anomalous venous channel occurs but is less common in patients with anomalous connection to the CS. Regardless of the site of pulmonary venous obstruction, the clinical profile is the same.

There were 43 cases of TAPVC with obstruction in the files of the Northern Great Plains Registry of Congenital Heart Disease (44). Of these patients, 72% presented in the first month of life and the remainder presented early in the first year. Symptoms usually did not appear in the first 12 hours of life, a finding that helped differentiate these patients from patients with respiratory distress syndrome. Once symptoms began, there was rather rapid progression to dyspnea, feeding difficulties, and cardiorespiratory failure.

Age at death ranged from 2 days to 4.5 months (36). When the anomalous connection is below the diaphragm, cyanosis

and dyspnea may be accentuated by straining and swallowing as a consequence of interference of pulmonary venous outflow by increased intra-abdominal pressure or impingement of the esophagus on the common pulmonary vein as it exits through the esophageal hiatus. The clinical course in patients with severely obstructed infradiaphragmatic TAPVC might be stormy with rapid development of severe respiratory distress and acidosis in the first hours of life.

Despite the alarming symptoms, the cardiovascular findings may be minimal. The heart is not enlarged and has no significant right ventricular heave. The second sound usually is split, and the pulmonary component is accentuated. A cardiac murmur often is absent, but, when present, it is usually a soft, blowing, systolic ejection murmur in the pulmonary area. Moist rales are usual at the lung bases. Hepatomegaly is almost always present, and peripheral edema often is associated.

ELECTROCARDIOGRAPHIC FEATURES

Right ventricular hypertrophy is invariably present. Unlike TAPVC without obstruction, however, right atrial enlargement is not a usual feature.

RADIOLOGIC FEATURES

The cardiac size is normal or nearly so. The lung fields have abnormal pulmonary vascular markings, characterized by diffuse, stippled densities that form a reticular pattern that fans out from the hilar regions. The cardiac borders often are obscured. Kerley B lines have been described, and prominence of the superior pulmonary veins is usual. The radiographic appearance is not diagnostic of TAPVC with obstruction because it also is associated with other causes of pulmonary venous obstruction.

ECHOCARDIOGRAPHIC FEATURES

The 2-D and Doppler findings are as described in the previous section on TAPVC without obstruction. It is important to perform a thorough Doppler interrogation of the individual pulmonary veins, the pulmonary venous confluence, and its insertion into the right-sided cardiac structure to look for the presence of obstruction. This is characterized by a high-velocity, continuous, and nonphasic venous flow profile.

MAGNETIC RESONANCE IMAGING

In the uncommon circumstance when echocardiography cannot provide all diagnostic information required for surgical planning, MRI provides an excellent complementary option. Given that infants with obstructed TAPVC are often in cardiorespiratory distress, the MRI examination should be streamlined to quickly provide the essential diagnostic information. The fastest approach is to obtain only a contrast-enhanced 3-D MRA, a procedure that requires only several minutes of scan time and can be accomplished in < 15 minutes “door-to-door” time. In stable patients, a more comprehensive examination is performed as described in the previous section on TAPVC without obstruction.

CARDIAC CATHETERIZATION

Diagnostic cardiac catheterization in patients with obstructed TAPVC rarely is indicated because of the accuracy of echocardiography. The procedure should be avoided as much as possible because it may aggravate the already compromised clinical condition of these patients and delay operation.

Oximetry may be helpful if fully saturated blood is obtained from the IVC or the SVC. Interpretation of oximetry must be cautious, however. On the one hand, PBF is decreased and its volume may not be sufficient to allow a high oxygen saturation when mixed with systemic venous blood. On the other hand, streaming of renal venous blood may result

in the appearance of highly oxygenated blood in the IVC. In a newborn with TAPVC to the portal venous system, blood obtained from the umbilical vein is fully saturated, confirming the diagnosis.

Right ventricular pressures usually are systemic or higher. Pressures in the RA usually are normal. Left atrial pressure also is normal but contrasts strikingly with the elevated pulmonary artery wedge pressure.

When the pulmonary arteriogram demonstrates TAPVC to the portal venous system, pulmonary venous obstruction may be assumed. Sites of obstruction also may be outlined when the anomalous connection is to other venous channels. If the cardiac catheter enters the anomalous venous channel, it may traverse the area of obstruction, thereby creating high-grade or complete obstruction to venous return. If selective injection of contrast material into the anomalous venous channel is contemplated in the patient with TAPVC with obstruction, the injection should be done by hand.

Differential Diagnosis

TAPVC without Pulmonary Venous Obstruction

In the infant with this condition, the differential diagnosis must include large VSD, PDA, truncus arteriosus, common atrioventricular (canal) septal defect (AVSD), and functional single ventricle without pulmonary stenosis. Unlike TAPVC, all these anomalies have radiographic and ECG evidence of left atrial and left ventricular hypertrophy. Multiple heart sounds are not usual, and the cardiac murmur is harsher and may be associated with a thrill. The counterclockwise frontal vector loop identifies common AVSD, as does the murmur of mitral regurgitation. The severity of the illness in the infant with suspected TAPVC warrants prompt echocardiographic examination, which will provide a definite diagnosis.

In the older child or adult with TAPVC, the differential diagnosis must include ASD, common atrium, and PAPVC. Common atrium and ostium primum ASD may be differentiated on the basis of a counterclockwise frontal vector loop. In the older patient, at least mild cyanosis is usually present in TAPVC, and this feature is absent in the usual case of secundum ASD or PAPVC unless pulmonary hypertension coexists. Nonetheless, a clinical distinction may be difficult in the older patient and will require special studies.

TAPVC with Pulmonary Venous Obstruction

Differential diagnosis in these infants includes the other causes of pulmonary venous obstruction as well as persistence of the fetal circulation. An accurate diagnosis should be achieved with a timely echocardiogram.

Treatment

Corrective surgery for the infant or child with TAPVC should be performed as soon as possible. In the sickest infants, the patient's clinical condition should be optimized, including the cardiorespiratory and metabolic states. Measures may include mechanical ventilation, inotropic support, diuresis, and correction of acidosis and other metabolic problems. When possible, surgery should be done on the basis of echocardiography because omitting cardiac catheterization speeds the time to operation, spares the infant the stress of this invasive procedure, and may reduce mortality.

Balloon atrial septostomy and blade atrial septostomy have been used as palliative procedures. Septostomy no longer seems appropriate because it delays the definitive procedure and is of little value when an anomalous venous channel

also is obstructed. Balloon dilation of obstructed anomalous venous channels was unsuccessful in the patients described by Lock et al. (50).

Operation for correction of TAPVC in infants < 1 year of age was associated with a mortality of about 50% through the early 1970s (49) and fell to 30% in the late 1970s (51). Bando et al. (52) reported the results of surgical repair of TAPVC in 105 infants from 1966 through 1995. Over time, the age at surgical repair has gradually decreased, as did operative mortality. From 1991 through 1995, none of the 31 operated infants died. Multivariate analysis showed that the only independent risk factor for death was a small pulmonary venous confluence. A more recent, larger multicenter cohort of 422 cases from European centers found the 3-year survival for those operated between 1998 and 2004 to be 85%, with independent risk factors for death in multivariate analysis comprised of earlier age at surgery, hypoplastic/stenotic pulmonary veins, associated complex cardiac lesions, postoperative pulmonary hypertension, and postoperative pulmonary venous obstruction (46). The surgical techniques for the specific anomalies are indicated in the following sections.

TAPVC to Coronary Sinus

The surgical technique for correction of TAPVC to the CS was described by Van Praagh et al. (27) in 1972. The common wall of the CS and LA is excised through a right atriotomy approach. This allows drainage of the pulmonary venous flow into the LA. The orifice of the CS is then closed either by direct suture or with the use of a patch. If present, an ASD should be closed as well. Rarely, the junction between the pulmonary veins and the CS can be stenotic. In such a case, the pulmonary venous obstruction must be addressed.

TAPVC to Left Innominate Vein

The basis of this correction is the creation of a large side-to-side anastomosis between the LA and the pulmonary venous confluence. Subsequent to the creation of the anastomosis, the ASD is closed, and the site of anomalous connection is ligated. Usually, a patch is used for ASD closure to ensure that the postoperative left atrial volume is normal. With minor modifications, this technique is used in correcting the TAPVC to the right SVC and TAPVC to the umbilicovitelline system.

An end-to-side anastomosis of the pulmonary venous confluence to LA often kinks. Use of the stump of the amputated left atrial appendage as a site for anastomosis often results in an inadequate opening because the diameter of the waist of the left atrial appendage is smaller than the diameter of the common pulmonary venous confluence (49).

Prognosis

Untreated

The prognosis in TAPVC is influenced by the size of the interatrial communication and by the presence of obstructing lesions in the anomalous venous pathways. The state of the pulmonary vascular bed, by determining the magnitude of the PBF, also plays a significant role in the prognosis.

In the survey by Keith et al. (53) involving TAPVC of all types, 50% were dead at age 3 months and 80% had died by 1 year of age. The figures reported by Burroughs and Edwards (40) are comparable. Patients with inadequate interatrial communication had an even poorer prognosis (40,52). When obstruction exists in the anomalous venous channel, the prognosis is grim. Death usually occurs within the first few weeks of life. In a series of patients with TAPVC with obstruction, the oldest survivor was 4.5 months old (36). The patients who

survive infancy often do so as a consequence of the protection provided by increased pulmonary vascular resistance, which is a mixed blessing and may jeopardize subsequent attempts at surgical repair. Far advanced intimal lesions in the pulmonary arterioles have been described as early as 8 months of age.

Postoperative Course

The long-term prognosis appears to depend mainly on the state of the pulmonary vascular bed at the time of operation and the adequacy of the pulmonary venous–left atrial anastomosis. In a series of 30 infants with TAPVC operated on between 1981 and 1991 (54) with a mean follow-up of 47 months, two late deaths and two reoperations occurred for pulmonary venous obstruction proximal to the anastomosis. The late deaths were due to persistent pulmonary hypertension in one and recurrent pulmonary venous obstruction in the other.

A similar hospital mortality rate of 13% was reported by Serraf et al. (55) in 30 infants with TAPVC operated on between 1985 and 1988. The cause of death was pulmonary hypertension in all four patients who died. The type of TAPVC, patient's age or weight, duration of cardiopulmonary bypass time, aortic cross-clamp time, or use of circulatory arrest did not affect the operative mortality. The mortality rate was affected by the preoperative status of the infant and the postoperative pulmonary artery pressure. Late pulmonary venous obstruction occurred in four patients for whom further therapy was advised. Reoperation was performed in two patients with one death, balloon dilation was successful in one patient, and the fourth patient died before reoperation. Residual stenosis at the left atrial–pulmonary venous anastomosis created at surgery was present in 8 of 68 patients (12%) reported by Yee et al. (56). These obstructions were relieved by patch plasty 1 to 24 months following the initial operation.

Sano et al. (57) operated on 44 infants with TAPVC. One operative death occurred secondary to postoperative suprasystemic pulmonary artery pressures. Of the remaining 43 patients, three developed recurrent pulmonary venous obstruction, and one developed SVC obstruction requiring reoperation within 2 months of the initial operation. Two of the three patients with recurrent pulmonary venous obstruction were found to have diffuse fibrosis of all lobar pulmonary veins as the cause rather than obstruction at the left atrial–pulmonary venous anastomosis. The patient with SVC obstruction had surgery and postoperatively developed bradycardia and sick sinus syndrome necessitating placement of a pacemaker. Lamb et al. (58) reported a series of 80 patients with TAPVC undergoing surgery. They noted the development of postoperative pulmonary venous obstruction in five patients (6%) 1.5 to 3 months after the initial operation. Five other children (6%) had reoperations, for residual shunts in four and for SVC obstruction in one.

Seale et al. (46) recently reported the results of an international, multicenter study of 422 patients with TAPVC, with an overall 3-year mortality of 15%; independent risk factors for death in multivariable analysis included earlier age at surgery, hypoplastic/stenotic pulmonary veins, associated complex cardiac lesions, postoperative pulmonary hypertension, and postoperative pulmonary venous obstruction. Sixty (15%) of these infants developed postoperative pulmonary venous obstruction, with 3-year mortality of 41% in this subgroup; risk factors for the development of postoperative pulmonary venous obstruction included hypoplastic/stenotic pulmonary veins at presentation and the absence of a common pulmonary venous confluence.

The postoperative development of pulmonary venous obstruction can be delineated with 2-D echocardiography combined with the use of spectral and color flow Doppler to identify and localize the area of obstruction. MRI and CT may

be particularly useful in the evaluation of pulmonary venous obstruction after TAPVC repair.

Late arrhythmias may develop in a small number of these patients. Atrial arrhythmias are most common and include sinus bradycardia, atrial flutter, and supraventricular tachycardia. Ventricular rhythm problems are unusual.

ATRESIA OF THE COMMON PULMONARY VEIN AFTER THE PULMONARY SYSTEMIC CONNECTIONS ARE OBLITERATED

Atresia of the Common Pulmonary Vein

In this anomaly, no communication exists between the normally formed pulmonary veins and the LA. In addition, there is no anomalous connection between the confluence of the pulmonary veins, on the one hand, and the heart or any systemic vein on the other hand. The physiologic consequence is severe obstruction to PBF. The condition appears to be rare. A pathologic review by Deshpande and Kinare (59) revealed three cases of atresia of the common pulmonary vein in a study of 1,326 autopsied hearts with congenital heart disease. Dudell et al. (60) diagnosed five cases in a 5-year period and documented 26 cases in the literature. Seale et al. (46) noted two cases of common pulmonary vein atresia in a study of 422 live-born infants with TAPVC.

Anatomy

The characteristic anatomic feature is the absence of a functional connection between the pulmonary veins and the LA or any other cardiac chamber or systemic vein. The normally formed pulmonary veins converge immediately behind the LA to form a blind cul-de-sac that has no outlet for pulmonary venous blood. Minor anatomic variations in the pulmonary venous system exist in some cases, including an atretic strand of tissue that may extend from one of the pulmonary veins to the RA or LA or an atretic fibrous strand that may connect the pulmonary venous confluence to a systemic vein. The lungs are firm and congested, and their pleural surfaces are remarkable in that the lobules are prominently outlined by edematous interlobular tissue and dilated lymphatic channels.

On microscopic examination, the pulmonary veins are thick-walled as a result of medial hypertrophy. The pulmonary arteries also reflect medial hypertrophy. The subpleural and interlobular lymphatics are markedly dilated, and the interlobular connective tissue is edematous. Large, dilated, irregular venous channels are also present in the parenchyma and interlobular areas. The alveoli contain many erythrocytes and iron-containing macrophages. Among the three cases reported by Deshpande and Kinare (59), there were two cases of atresia of the common pulmonary vein seen in association with asplenia syndrome, and one case had truncus arteriosus.

Physiology

Severe obstruction to pulmonary venous flow is present in this anomaly. PBF is markedly decreased and is even diverted away from the lungs by the right-to-left shunting at the atrial and the ductus arteriosus levels. Because these patients can live a few days to a few weeks, some means of blood flow from the lungs must exist. One must assume that an exit, however restricted, is provided by the bronchopulmonary veins carrying blood from the lungs to the systemic venous system. The features of severe pulmonary venous obstruction are comparable to those in TAPVC with venous obstruction.

Manifestations

Dyspnea and cyanosis appear shortly after birth. Death occurs in the first month. A thrill is not present. A grade 1 to 2 soft systolic ejection murmur along the left sternal border is usual, although a murmur may be absent. The ECG may be normal or show evidence of right ventricular hypertrophy. The usual chest radiographic picture of severe pulmonary venous obstruction is present. The pulmonary vascular markings have a diffuse reticular character. Cardiomegaly is minimal or absent.

Echocardiography

Echocardiographic demonstration of atresia of the common pulmonary vein was reported in three of five infants with this anomaly. We would anticipate that the echocardiographic findings would include right atrial, right ventricular, and pulmonary artery dilation and a small LA. Individual pulmonary veins would not return to the LA, and the common pulmonary venous confluence may be imaged behind the LA. The confluence would not connect to a right-sided cardiac structure. If PBF is limited, the ability to detect pulmonary venous flow by Doppler will be hampered. If the cardiac output is diminished, the Doppler flow in the aortic arch may be retrograde in systole. As a result of the pulmonary hypertension, a right-to-left shunt would be detected through the foramen ovale and ductus arteriosus by Doppler.

Cardiac Catheterization

Cardiac catheterization demonstrates severe pulmonary hypertension and marked systemic desaturation. Selective injection of contrast material into the right ventricle results in persistence of the contrast material in the pulmonary vascular bed and failure of opacification of the LA. Only rarely does contrast opacify the pulmonary venous confluence. If pulmonary arteriography is performed, the dye is shunted through the PDA into the thoracic aorta and usually does not opacify the pulmonary veins and the confluence.

Treatment

Some factors seem to favor successful surgical intervention. The anatomic problems are similar to those in cases of TAPVC, and anastomosis of the confluence of the pulmonary veins and the LA would afford a direct route for pulmonary venous drainage. The confluence of pulmonary veins is ample in size and is located directly behind the LA. The LA and left ventricle seem to be of adequate size, and complex cardiac anomalies are not present. Five infants have had successful surgical anastomosis of the common pulmonary venous confluence to the LA (60–62). Extracorporeal membrane oxygenation was an essential postoperative supportive measure in two of these patients (60).

Prognosis

Symptoms occur on the first day of life, and these patients follow a progressive downhill course to death within the first month of life when there is no surgical intervention. In too few cases has surgery been performed, usually with no follow-up period, to know the long-term outcome.

STENOSIS OF THE COMMON PULMONARY VEIN

Cor Triatriatum

In cor triatriatum, the pulmonary veins enter a pulmonary venous chamber that joins the LA through a narrow opening.

Alternatively, the pulmonary venous chamber may communicate with the RA directly or indirectly by way of an anomalous channel. Cor triatriatum is an unusual congenital anomaly, but it is probably not as rare as some reports indicate. The variety of anatomic expressions of cor triatriatum defeats an attempt to define a unified embryogenesis for all of them. The theory that abnormal growth of the septum primum accounts for cor triatriatum is difficult to reconcile with the observations of most workers in this field. Failure of incorporation of the common pulmonary vein into the LA is the most widely accepted theory of the embryogenesis of cor triatriatum. Some variants of cor triatriatum did not appear to be consistent with this theory, however. Other reports highlighted the embryogenetic complexities of this group of cardiac defects (63).

So-called cor triatriatum dexter is usually a persistence of the right valve of the sinus venosus. This section deals only with what is sometimes called cor triatriatum sinister.

Anatomy

The number of variants of cor triatriatum demands an inclusive classification (Table 35.3, Fig. 35.21).

PULMONARY VENOUS CHAMBER RECEIVES ALL PULMONARY VEINS AND COMMUNICATES WITH LEFT ATRIUM WITH NO OTHER CONNECTIONS

In classic cor triatriatum (Figs. 35.21A and 35.4), a membranous partition that has the shape of a windsock separates the more proximal chamber, which receives the pulmonary veins, from the more distal LA, which communicates with the mitral valve. The windsock is directed toward the mitral valve. The diameter of the orifice ranges from <3 mm to about 1 cm. There may be several small defects in the obstructive membrane (64). Histologically, the anomalous membrane contains cardiac muscle fibers and is occasionally calcified.

The more distal, true LA communicates with the left atrial appendage and in almost all cases has the fossa ovale lying between it and the RA. In many patients, no communication exists between either of the left atrial chambers to the RA (64).

TABLE 35.3 Anatomic Classification of Cor Triatriatum	
I. Pulmonary venous chamber receives all pulmonary veins and communicates with LA	
A. No other connections: classic cor triatriatum	
B. Other anomalous connections:	
1. To RA directly	
2. With totally anomalous pulmonary venous connection	
II. Pulmonary venous chamber receives all pulmonary veins and does not communicate with LA	
A. Anomalous connection to RA directly	
B. With totally anomalous pulmonary venous connection	
III. Subtotal cor triatriatum	
A. Pulmonary venous chamber receives part of pulmonary veins and connects to LA	
1. Remaining pulmonary veins connect normally	
2. Remaining pulmonary veins connect anomalously	
B. Pulmonary venous chamber receives part of pulmonary veins and connects to RA	
1. Remaining pulmonary veins connect normally	

Occasionally, a patent foramen ovale or an ASD allows the lower left atrial chamber to communicate with the RA. Right ventricular hypertrophy and dilation are found almost invariably, and right atrial hypertrophy and dilation are present in about 25% of cases (64).

Other Anomalous Connections

In a few cases, the pulmonary venous chamber communicates with the more distal true LA via a stenotic opening in the interatrial membrane and, additionally, with the RA through a defect between the RA and the pulmonary venous chamber (Fig. 35.21B). The pulmonary venous chamber may communicate indirectly with the RA through anomalous venous connections (Fig. 35.21C). Marin-Garcia et al. (65) reported findings on 20 patients with complete cor triatriatum communicating with the LA. In 12 patients, a classic diaphragm divided the LA. In three patients, an extrinsic constriction separated the pulmonary venous chamber from the LA (hourglass type), and in three there was obstructive tubular narrowing of the channel connecting the common venous confluence with the LA (tubular type). The hourglass and tubular types were all associated with complex cardiac lesions.

PULMONARY VENOUS CHAMBER RECEIVES ALL PULMONARY VEINS AND DOES NOT COMMUNICATE WITH LEFT ATRIUM

In this anomaly, the tissue separating the pulmonary venous chamber from the LA is intact and prevents the direct flow of pulmonary venous blood to the LA. A defect exists between the pulmonary venous chamber and the RA, and a patent foramen ovale allows communication between the RA and the lower, true LA (Fig. 35.21D). Pulmonary venous blood thus enters the pulmonary venous chamber, crosses the defect into the RA, and then traverses the foramen ovale to reach the true LA. In three of the six cases reported by Lam et al. (66), the defect was successfully corrected by excising the anomalous left atrial membrane and closing the ASD.

When there is no direct communication between the pulmonary venous chamber and the true LA, one of the alternatives for egress of pulmonary venous blood flow is TAPVC (Fig. 35.21E). Pulmonary venous blood entering the pulmonary venous chamber reaches the RA through the anomalous connecting vein and then enters the LA through a patent foramen ovale or ASD.

Subtotal Cor Triatriatum

The pulmonary venous chamber receives part of the pulmonary veins and connects to the LA. In this anomaly, the veins from one lung empty into a small pulmonary venous chamber that communicates with the true LA through a stenotic opening. The remaining pulmonary veins may connect normally to the LA (Fig. 35.21F) or they may connect anomalously to a systemic vein (Fig. 35.21G). Distinction of this anomaly from stenosis of individual pulmonary vein(s) at the left atrial junction can be challenging.

In another variant, the pulmonary venous chamber receives part of the pulmonary veins and connects to the RA (Fig. 35.21H). In this circumstance, the pulmonary veins from one lung empty into a small pulmonary venous chamber that communicates via a stenotic opening with the RA. The remaining pulmonary veins connect normally to the LA.

Microscopic Anatomy

When cor triatriatum obstructs pulmonary venous flow, the lungs reflect varying degrees of pulmonary edema and intraalveolar hemorrhage. There is medial hypertrophy of the pulmonary veins, and lymphatic channels are dilated. Pulmonary arterial lesions range from medial hypertrophy alone, to

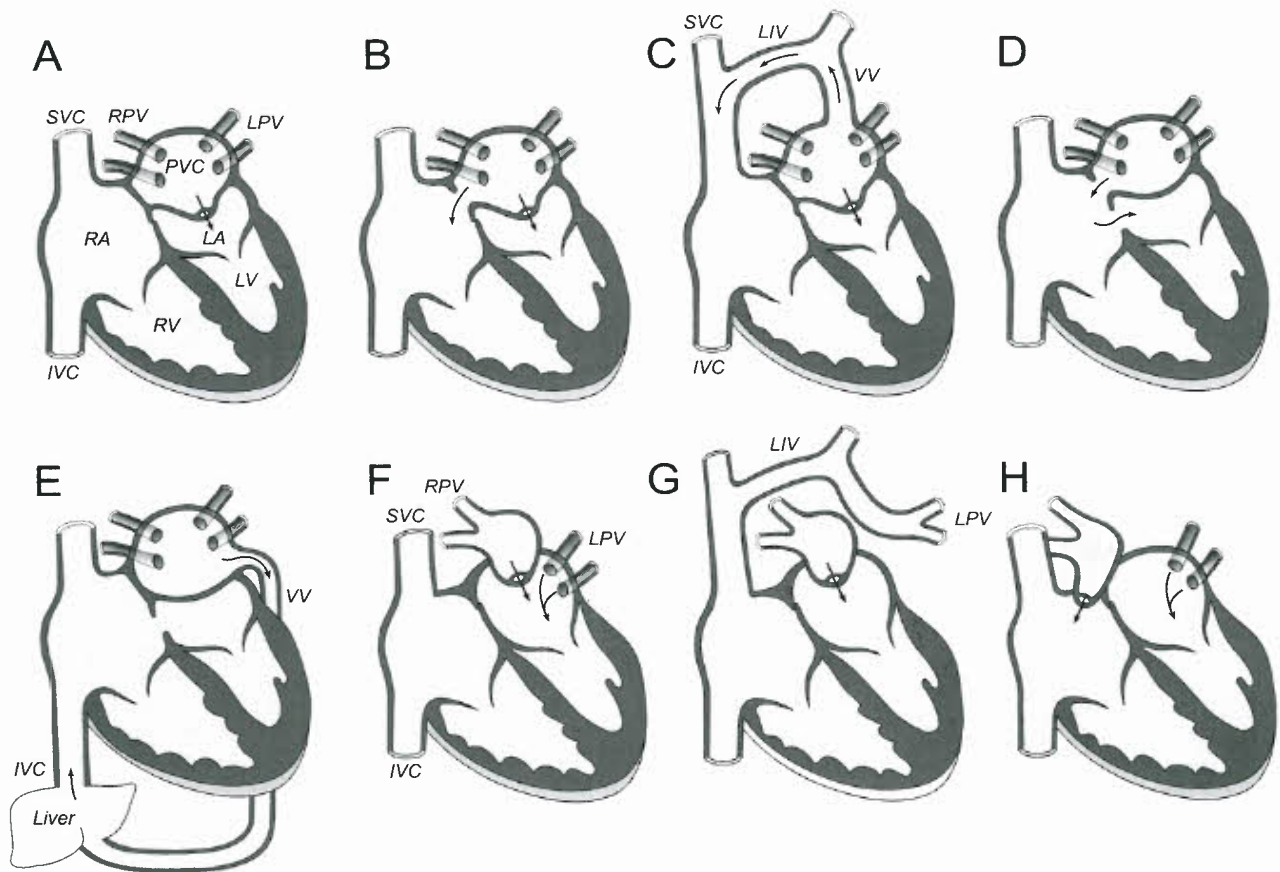


Figure 35.21. Cor triatriatum variants. **A:** Classic cor triatriatum. Right and left pulmonary veins (RPVs and LPVs) drain to the pulmonary venous confluence (PVC), with discrete membrane between the PVC and true left atrium (LA); the only egress for blood is through the opening in the membrane. **B:** Cor triatriatum with defect between the PVC and the right atrium (RA), which allows for decompression of pulmonary venous blood. **C:** Cor triatriatum with decompressing vertical vein (VV) to the left innominate vein (LIV), which allows for decompression of the PVC. **D:** Pulmonary venous return decompresses via a communication between the PVC and right atrium, and then crosses to the true left atrium via a patent foramen ovale. **E:** Decompressing vertical vein that descends below the diaphragm to connect to the systemic venous circulation via the hepatic or portal veins. **F:** "Partial" or subtotal cor triatriatum with normally draining left pulmonary veins; the right pulmonary veins communicate with the true left atrium via a stenotic orifice. **G:** Subtotal cor triatriatum of the right pulmonary veins along with partially anomalous venous return of the left pulmonary veins via the left innominate vein. **H:** Subtotal cor triatriatum of the right pulmonary veins to the right atrium (RA) with normal drainage of the left pulmonary veins to the left atrium. (From Brown DW. Pulmonary Venous Anomalies. In: Lai, WW, Mertens LL, Cohen MS, Geva T, et al., eds. *Echocardiography in Pediatric and Congenital Heart Disease: From Fetus to Adult*. United Kingdom: Wiley-Blackwell, 2009:119–142, with permission).

medial hypertrophy with intimal proliferation, to necrotizing arteriolitis.

Physiology

In defects where the blood from the pulmonary venous chamber drains either directly or indirectly to the RA, the hemodynamic features are comparable to those seen in TAPVC and will not be considered further here. On the other hand, when there is no alternative pathway for pulmonary venous blood, the stenotic opening in the intra-atrial membrane dividing the pulmonary venous chamber from the LA results in elevated pressure in the former, which is transmitted to the pulmonary veins. The features of pulmonary venous obstruction pertain.

In the patient with subtotal cor triatriatum, the obstructive phenomenon affects only one lung. Reflex pulmonary arterial constriction in the affected lung will result in diminished flow through that lung; however, the remaining unobstructed lung

is usually capable of accepting increased blood flow, and thus pulmonary arterial pressure is not elevated.

Manifestations

The following sections consider the features of only classic cor triatriatum.

CLINICAL FEATURES

Most patients with classic cor triatriatum have onset of symptoms within the first few years of life. Nonetheless, some patients are asymptomatic until the second or third decade of life. Usually, the patients present with a history of breathlessness, frequent respiratory infections, and pneumonia.

The signs of pulmonary hypertension, including loud pulmonary component of the second heart sound, right ventricular heave, and pulmonary systolic ejection click, are most characteristic. The usual cardiac murmur is a soft, blowing, systolic

murmur along the left sternal border. Less often, a diastolic murmur is detected at the mitral area, or a continuous murmur is heard. Pulmonary rales are frequent. Right-sided heart failure is common in severe, untreated cor triatriatum.

ECCHOCARDIOGRAPHIC FEATURES

The advances in 2-D and Doppler echocardiography have simplified the noninvasive diagnosis of causes of pulmonary venous obstruction and increased its accuracy (Fig. 35.4). Cor triatriatum, by producing venous obstruction, results in dilation of the RA, right ventricle, and pulmonary artery. Imaging from the parasternal, apical, and subcostal windows allows assessment of the size of these cardiac chambers. These are nonspecific findings, also associated with TAPVC, coarctation, hypoplastic left heart syndrome, and critical aortic stenosis.

Two anomalies, cor triatriatum and supraventricular stenosing ring of the LA, create pulmonary venous obstruction by the presence of a membrane within the left atrial cavity. In both conditions, the membrane can be imaged as a linear echo-bright structure above the mitral valve in the LA. The membrane in cor triatriatum usually is curvilinear and may have the appearance of a windsock. A supramitral stenosing ring is located on the atrial surface of the base of the mitral valve leaflets and is relatively immobile. During diastole, the cor triatriatum membrane moves toward the mitral valve. The motion and appearance of the mitral valve are usually normal. The left atrial appendage and foramen ovale are located distal to the membrane of cor triatriatum, and the pulmonary veins insert into the proximal chamber. In contrast, the membrane in supraventricular stenosing ring of the LA is usually adherent to the mitral valve, moves away from the valve in diastole, and has the left atrial appendage and foramen ovale located proximal to the membrane. The mitral valve domes during diastole and has decreased excursion of the posteromedial leaflet.

Doppler interrogation of left atrial membranes may reveal disturbed diastolic flow profiles that may be best appreciated by color flow Doppler mapping. The flow profiles may mimic mitral stenosis.

ELECTROCARDIOGRAPHIC FEATURES

The typical finding is right ventricular hypertrophy. Right atrial hypertrophy results in tall, peaked P waves in some of the cases. Broad, notched P waves are present in some cases, presumably as a consequence of the dilated pulmonary venous chamber, but are absent in others.

RADIOLOGIC FEATURES

The routine chest radiogram reflects pulmonary venous obstruction. Fine, diffuse, reticular pulmonary markings fan out from the pulmonary hilum to involve the lower lung fields. Kerley B lines may be present. Prominent venous engorgement of the upper pulmonary veins results in the staghorn sign. The chest radiogram also reveals enlargement of the main pulmonary artery, right ventricular hypertrophy, and signs of "left atrial" enlargement, including posterior deviation of the barium-filled esophagus and a double density at the right cardiac border. These latter features are due to the dilated pulmonary venous chamber.

MAGNETIC RESONANCE IMAGING

This is another noninvasive imaging modality that can delineate the left atrial membrane of cor triatriatum. MRI may be helpful in defining the cause of pulmonary hypertension when echocardiography is not diagnostic.

CARDIAC CATHETERIZATION

Pulmonary hypertension routinely is found. Using oximetry one can exclude a left-to-right shunt. Thus, pulmonary hypertension is either caused by primary pulmonary vascular

disease or secondary to pulmonary venous obstruction. The pulmonary arterial wedge pressure is elevated, and left atrial pressure is normal.

Selective pulmonary arteriography usually demonstrates cor triatriatum. Pulmonary transit time is prolonged. As the pulmonary veins opacify, they drain into an accessory left atrial chamber. There is usually a delay between the opacification of this chamber and the opacification of the true LA and left ventricle. Moreover, in some cases, the intra-atrial membrane can be identified as a linear or cone-shaped filling defect between the pulmonary venous chamber and the true LA. The pulmonary venous chamber remains opacified for some time and does not change size or contour with cardiac contractions as does a normal LA (67).

Differential Diagnosis

The differential diagnosis differs depending upon the age of the patient. In the infant or young child, the differential diagnosis lies within the group of cardiac anomalies that produce pulmonary venous obstruction.

In the adult, cor triatriatum should be distinguished from primary pulmonary hypertension. In addition, the differential diagnosis includes congenital and acquired mitral stenosis, supramitral stenosing ring, left atrial tumor, and left atrial thrombus. In the adults with cor triatriatum reviewed by McGuire et al. (68), four of eight had a mitral diastolic murmur, but none had the typical presystolic crescendo rumble of mitral stenosis. Likewise, no case had an opening snap. The absence of broad and notched P waves was another feature distinguishing cor triatriatum from mitral stenosis. Atrial fibrillation, commonly seen in mitral stenosis of comparable severity, was observed in only one of eight patients with cor triatriatum.

Treatment

Surgical resection of the obstructive membrane is indicated in patients with cor triatriatum and elevated pulmonary artery pressure.

Prognosis

The prognosis of cor triatriatum is related to the size of the orifice in the obstructing membrane. In Niwayama's survey (64), average survival was 3 1/3 months when the opening was <3 mm, and 16 years when the opening was >3 mm. When pulmonary edema and right heart failure occur, survival is usually only a matter of months.

In patients who survive operative correction, the prognosis seems excellent. The severe pulmonary arterial changes that result in pulmonary hypertension have been reversible in the patients studied postoperatively (26,27).

ABNORMAL ABSORPTION OF THE COMMON PULMONARY VEIN INTO LEFT ATRIUM

Stenosis of the Individual Pulmonary Veins

Two varieties of this unusual cardiac anomaly are recognized. In localized stenosis of the pulmonary veins, one or more of the pulmonary veins has a localized stenosis at its junction with the LA. The other variety is characterized by narrowing of the lumen of the pulmonary veins for a considerable distance in their intrapulmonary and extrapulmonary portions; this condition may be termed diffuse pulmonary veins stenosis or hypoplasia.

Localized stenosis of the individual pulmonary veins may be an isolated phenomenon, or it may be associated with a

minor or major cardiac anomaly. Reye (69) first described this anomaly in 1951. Shone et al. (70) have defined a characteristic angiographic feature that should allow a premortem diagnosis of this condition.

Diffuse stenosis or hypoplasia of the individual pulmonary veins is occasionally present in patients with pulmonary artery atresia or hypoplastic left heart syndrome. Seale et al (71) reported a series of 58 cases of pulmonary vein stenosis, with a history of prematurity found in 38%, and associated cardiac lesions in 79%. A significant extracardiac anomaly or syndrome was present in 28% of this cohort. The majority (62%) presented with unilateral pulmonary venous involvement, of which 86% was on the left.

The factors that favor a congenital cause were summarized by Shone et al. (70). The embryologic basis for stenosis of the individual pulmonary veins appears to be abnormal incorporation of the common pulmonary vein into the LA.

Anatomy

Krabbil and Lucas (72) studied examples of stenosis, hypoplasia, or atresia of individual pulmonary veins found in the Jesse Edwards Registry of Cardiovascular Pathology. After excluding complex left-sided obstructive lesions, mitral valve abnormalities, and cor triatriatum, eight examples remained. All pulmonary veins entered the LA in each case. Two cases had an associated common AVSD, one had Ebstein anomaly of the tricuspid valve, and the five remaining cases had no associated congenital cardiac anomalies. All pulmonary veins were obstructed in two cases, three of four pulmonary veins were obstructed in three specimens, and the veins of only one lung were obstructed in three specimens. Obstruction was produced by three different mechanisms. In four cases, the obstruction was due to a discrete area of medial hypertrophy or intimal proliferation of the affected pulmonary vein at its left atrial junction. Atresia of the pulmonary vein at its junction with the LA occurred in two cases. Hypoplasia of the pulmonary vein, which extended from the hilum of the lung to the LA, was present in two cases.

In addition to the extraparenchymal pulmonary vein obstruction, seven of eight cases had intimal proliferation involving the intraparenchymal pulmonary veins. In two of these, small veins in the unobstructed lung, as well as the veins in the obstructed lung, were stenotic. Others have noted the association of intimal proliferation in the small intraparenchymal pulmonary veins in both obstructed and unobstructed lobes. Sadr et al. (73) found abnormal intimal spindle-shaped cellular proliferation in all tissue specimens from 10 patients with pulmonary veins stenosis. In three of the four patients in whom immunohistochemical staining was available, there was evidence that the proliferating cells were myofibroblasts. Subsequent work by Riedlinger et al. (74) with autoantibodies directed against multiple cellular proteins and signaling ligands in intimal cells from seven patients with pulmonary vein stenosis demonstrated strong diffuse immunoreactivity for smooth muscle markers, as well as expression of receptor tyrosine kinases and other ligands. This work suggests an autocrine or paracrine role of these proteins in the pathogenesis of this disease.

The frequent occurrence of small pulmonary vein obstructive lesions may be responsible in part for the poor operative results in patients with stenosis of the individual pulmonary veins. In most of the cases reported in the literature, medial hypertrophy of the pulmonary arterioles is present. These pulmonary arteriolar changes occur in both the obstructed and unobstructed lung.

Manifestations

Clinical Features

Patients present with history of persistent tachypnea and recurrent pneumonia, ultimately progressing to right-sided

heart failure. They frequently exhibit failure to thrive and have hemoptysis. Most are cyanotic. The physical examination is consistent with signs of pulmonary hypertension, including a right ventricular heave and accentuation of the pulmonary component of the second heart sound. A short systolic murmur is the usual finding, and in the case reported by Shone et al. (70), a pulmonary systolic click was heard.

Echocardiographic Features

The distal portions of the pulmonary veins and their insertion into the LA are best imaged from suprasternal, high parasternal, or subcostal windows. The reflective nature of the air in the lungs limits the ability of ultrasound to image more proximal portions of the pulmonary veins. Discrete areas of narrowing or areas of hypoplasia may be noted in the distal pulmonary vein and at the pulmonary vein-LA junction. When pulmonary venous obstruction or stenosis of individual pulmonary veins is in the differential diagnosis, identification of each pulmonary vein is necessary. Normally, pulmonary vein flow is nearly continuous and phasic, with a short period of flow reversal following atrial contraction. In contrast, stenotic pulmonary veins have a continuous, high-velocity turbulent flow pattern without phasic variation.

Electrocardiographic Features

Right ventricular hypertrophy is usual, and right atrial enlargement may be present.

Radiologic Features

The heart is not greatly enlarged but reflects right ventricular hypertrophy. The pulmonary artery segment is enlarged, and the characteristic reticular markings of pulmonary venous obstruction are usual (70). The heart shifts toward the side of major involvement with pulmonary venous stenosis. The pulmonary vascularity will be asymmetric, with increased vascularity seen in the unaffected lung segments. Technetium-99m lung perfusion scans will show absence or diminished perfusion of the lung segments with pulmonary vein stenosis.

Magnetic Resonance Imaging and Computed Tomography

Both MRI and CT are ideally suited to evaluating pulmonary veins stenosis (Fig. 35.22A). CT is particularly helpful in the evaluation of abnormalities of the lung parenchyma.

Cardiac Catheterization

Right-sided heart catheterization reflects pulmonary hypertension. If the pulmonary veins are obstructed from only one lung, there will be an elevation of the pulmonary capillary wedge on that side. Angiography demonstrates prolonged transit time of opaque dye through the lung. The angiogram in the case reported by Shone et al. (70) clearly demonstrated the constriction at the pulmonary vein-left atrial junction and delayed emptying of the pulmonary veins (Fig. 35.22B).

Treatment

Operative management of stenosis of the individual pulmonary veins is disappointing, which may be related to the coexistence or progression of obstruction into the intraparenchymal pulmonary vein (long-segment stenosis/hypoplasia). An occasional patient with stenosis of the individual pulmonary veins involving only one lung has had successful reanastomosis of the stenotic veins to the LA, and some have benefited from pneumonectomy. The poor results of operation in stenosis of the individual pulmonary veins led to attempts to improve obstruction with transcatheter approaches, from simple balloon angioplasty (75,76) to cutting balloon dilation (77,78), and stent placement (79), including drug eluting stents. Several series have demonstrated effective short-term relief of stenosis with transcatheter techniques, but nearly universal recurrence

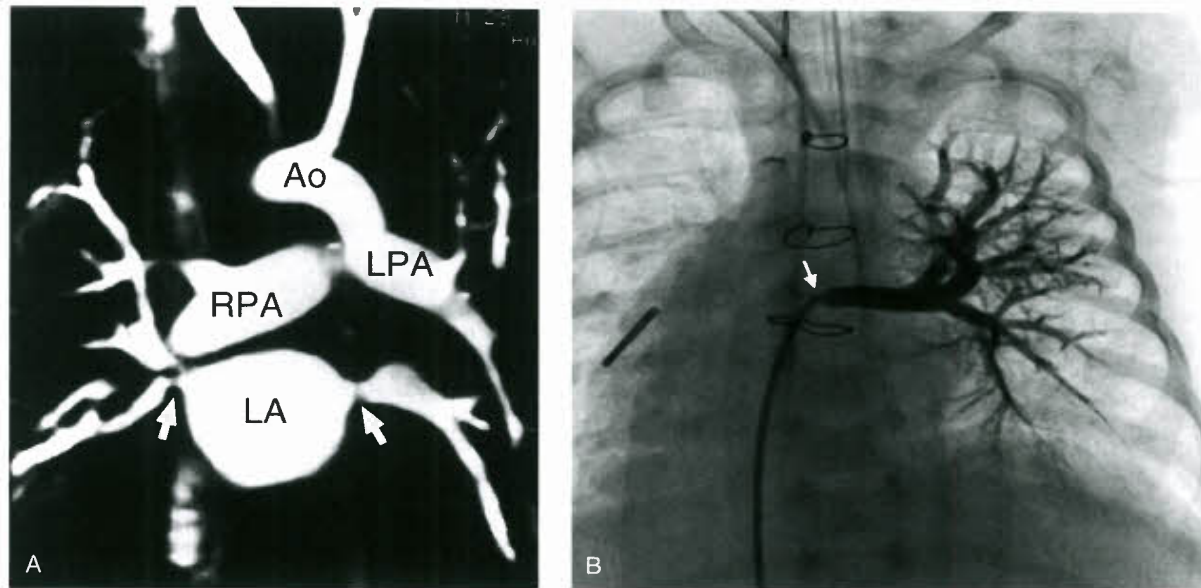


Figure 35.22. Pulmonary vein stenosis. **A:** Maximal-intensity projection image from a gadolinium-enhanced 3-D magnetic resonance angiogram (MRA) in a 21-year-old man with severe bilateral pulmonary vein stenoses (arrow). The patient was referred for MRI examination to rule out constrictive pericardial process after an evaluation by echocardiography and cardiac catheterization at another institution did not find a cause for the patient's severe pulmonary hypertension. The MRI findings were subsequently confirmed at cardiac catheterization in which balloon dilations of the pulmonary veins stenoses were performed. **B:** Catheter angiogram in a 3-month-old infant with heterotaxy syndrome, dextrocardia, and supracardiac TAPVC that had been repaired with anastomosis of the pulmonary venous confluence to the posterior aspect of the common atrium. Angiogram with catheter in the left upper pulmonary vein (LUPV) demonstrates the severe, discrete narrowing of the LUPV at the junction with the pulmonary venous confluence (arrow), with narrowing to the diameter of the catheter (1.2 mm). Note the lack of involvement of the proximal LUPV in the obstruction.

of obstruction. Newer surgical techniques including “sutureless” procedures to unroof the pulmonary veins at the junction with the LA may be slightly more successful than previous techniques (80), but the long-term prognosis for patients with pulmonary vein stenosis remains poor. Lung transplantation has been reported as well and may be curative (81).

REFERENCES

- Healy J Jr. An anatomic survey of anomalous pulmonary veins: their clinical significance. *J Thorac Cardiovasc Surg* 1952;23:433–444.
- Edwards JE. Pathologic and developmental considerations in anomalous pulmonary venous connection. *Proc Staff Meet Mayo Clin* 1953;28:441–452.
- Neill CA. Development of the pulmonary veins; with reference to the embryology of anomalies of pulmonary venous return. *Pediatrics* 1956;18:880–887.
- Streeter GL. Developmental horizons in human embryos: description of age group XV, XVI, XVII, XVIII. *Contrib Embryol Carnegie Inst* 1948;32:145–146.
- Neill CA, Ferencz C, Sabiston DC. The familial occurrence of hypoplastic right lung with systemic arterial supply and venous drainage: “scimitar syndrome.” *J Johns Hopkins Med J* 1960;107:1–21.
- Tajik AJ, Gau GT, Ritter DG, et al. Echocardiographic pattern of right ventricular diastolic volume overload in children. *Circulation* 1972;46:36–43.
- Brody H. Drainage of the pulmonary veins into the right side of the heart. *Arch Pathol* 1942;33:221–240.
- Hughes C, Rumore P. Anomalous pulmonary veins. *Arch Pathol* 1944;37:364–366.
- Van Praagh S, Carrera ME, Sanders SP, et al. Sinus venosus defects: unroofing of the right pulmonary veins—atomic and echocardiographic findings and surgical treatment. *Am Heart J* 1994;128:365–379.
- Moller JH, Nakib A, Anderson RC, et al. Congenital cardiac disease associated with polysplenia. A developmental complex of bilateral “left-sidedness.” *Circulation* 1967;36:789–799.
- Gao YA, Burrows PE, Benson LN, et al. Scimitar syndrome in infancy. *J Am Coll Cardiol* 1993;22:873–882.
- Juraszek AL, Cohn H, Van PR, et al. Isolated left-sided scimitar vein connecting all left pulmonary veins to the right inferior vena cava. *Pediatr Cardiol* 2005;26:846–847.
- Mardini MK, Sakati NA, Nyhan WL. Anomalous left pulmonary venous drainage to the inferior vena cava and through the pericardiophrenic vein to the innominate vein: left-sided scimitar syndrome. *Am Heart J* 1981;101:860–863.
- Rutledge JM, Hiatt PW, Wesley VG III, et al. A sword for the left hand: an unusual case of left-sided scimitar syndrome. *Pediatr Cardiol* 2001;22:350–352.
- Fiandra O, Barcia A, Cortes R, et al. Partial anomalous pulmonary venous drainage into the inferior vena cava. *Acta Radiol* 1962;57:301–310.
- Burchell HB, Hetzel PS, Swan HJ, et al. Relative contribution of blood from each lung to the left-to-right shunt in atrial septal defect; demonstration by indicator dilution techniques. *Circulation* 1956;14:200–211.
- Saalouke MG, Shapiro SR, Perry LW, et al. Isolated partial anomalous pulmonary venous drainage associated with pulmonary vascular obstructive disease. *Am J Cardiol* 1977;39:439–444.
- Dupuis C, Charaf LA, Breviere GM, et al. “Infantile” form of the scimitar syndrome with pulmonary hypertension. *Am J Cardiol* 1993;71:1326–1330.
- Dupuis C, Charaf LA, Breviere GM, et al. The “adult” form of the scimitar syndrome. *Am J Cardiol* 1992;70:502–507.
- Moore JW, Kirby WC, Rogers WM, et al. Partial anomalous pulmonary venous drainage associated with 45,X Turner's syndrome. *Pediatrics* 1990;86:273–276.
- van Wassenae AG, Lubbers LJ, Losekoot G. Partial abnormal pulmonary venous return in Turner syndrome. *Eur J Pediatr* 1988;148:101–103.
- Redington AN, Raine J, Shinebourne EA, et al. Tetralogy of Fallot with anomalous pulmonary venous connections: a rare but clinically important association. *Br Heart J* 1990;64:325–328.
- Banka P, Bacha E, Powell AJ, et al. Outcomes of inferior sinus venosus defect repair. *J Thorac Cardiovasc Surg* 2011;142:517–522.
- Greil GF, Powell AJ, Gildein HP, et al. Gadolinium-enhanced three-dimensional magnetic resonance angiography of pulmonary and systemic venous anomalies. *J Am Coll Cardiol* 2002;39:335–341.
- Valente AM, Sena L, Powell AJ, et al. Cardiac magnetic resonance imaging evaluation of sinus venosus defects: comparison to surgical findings. *Pediatr Cardiol* 2007;28:51–56.

26. Van Praagh S, Carrera ME, Sanders S, et al. Partial or total direct pulmonary venous drainage to right atrium due to malposition of septum primum. Anatomic and echocardiographic findings and surgical treatment: a study based on 36 cases. *Chest* 1995;107:1488–498.
27. Van PR, Harken AH, Delisle G, et al. Total anomalous pulmonary venous drainage to the coronary sinus. A revised procedure for its correction. *J Thorac Cardiovasc Surg* 1972;64:132–135.
28. Warden HE, Gustafson RA, Tarnay TJ, et al. An alternative method for repair of partial anomalous pulmonary venous connection to the superior vena cava. *Ann Thorac Surg* 1984;38:601–605.
29. Brown JW, Ruzmetov M, Minnich DJ, et al. Surgical management of scimitar syndrome: an alternative approach. *J Thorac Cardiovasc Surg* 2003;125:238–245.
30. Kirklin JW. Surgical treatment of anomalous pulmonary venous connection (partial anomalous pulmonary venous drainage). *Mayo Clin Proc* 1953;28:476–479.
31. Gustafson RA, Warden HE, Murray GF, et al. Partial anomalous pulmonary venous connection to the right side of the heart. *J Thorac Cardiovasc Surg* 1989;98:861–868.
32. Van MC Jr, LeBlanc JG, Culpepper WS III, et al. Partial anomalous pulmonary venous return. *Circulation* 1990;82:IV195–IV198.
33. Vida VL, Padalino MA, Boccuzzo G, et al. Scimitar syndrome: a European Congenital Heart Surgeons Association (ECHSA) multicentric study. *Circulation* 2010;122:1159–1166.
34. Abbott ME. *Atlas of Congenital Heart Disease*. New York, NY: American Heart Association, 1936.
35. Mehrizi A, Hirsch MS, Taussig HB. Congenital heart disease in the neonatal period: autopsy study of 170 cases. *J Pediatr* 1964;65:721–726.
36. Lucas RV Jr, Adams P Jr, Anderson RC. Total anomalous pulmonary venous connection to the portal venous system: a cause of pulmonary venous obstruction. *AJR Am J Roentgenol* 1961;86:561–575.
37. Ferencz C, Rubin JD, McCarter RJ, et al. Congenital heart disease: prevalence at livebirth. The Baltimore-Washington Infant Study. *Am J Epidemiol* 1985;121:31–36.
38. Solymar L, Sabel KG, Zetterqvist P. Total anomalous pulmonary venous connection in siblings. Report on three families. *Acta Paediatr Scand* 1987;76:124–127.
39. Craig JM, Darling RC, Rothney WB. Total pulmonary venous drainage into the right side of the heart; report of 17 autopsied cases not associated with other major cardiovascular anomalies. *Lab Invest* 1957;6:44–64.
40. Burroughs JT, Edwards JE. Total anomalous pulmonary venous connection. *Am Heart J* 1960;59:913–931.
41. Smith B, Frye TR, Newton WA Jr. Total anomalous pulmonary venous return: diagnostic criteria and a new classification. *Am J Dis Child* 1961;101:41–51.
42. Delisle G, Ando M, Calder AL, et al. Total anomalous pulmonary venous connection: report of 93 autopsied cases with emphasis on diagnostic and surgical considerations. *Am Heart J* 1976;91:99–122.
43. Sherman FE, Bauersfeld SR. Total, uncomplicated, anomalous pulmonary venous connection; morphologic observations on 13 necropsy specimens from infants. *Pediatrics* 1960;25:656–668.
44. Moller JE. Northern Great Plains Regional Cardiac Program. Bureau of Maternal and Child Health, 1981.
45. Jenkins KJ, Sanders SP, Orav EJ, et al. Individual pulmonary vein size and survival in infants with totally anomalous pulmonary venous connection. *J Am Coll Cardiol* 1993;22:201–206.
46. Seale AN, Uemura H, Webber SA, et al. Total anomalous pulmonary venous connection: morphology and outcome from an international population-based study. *Circulation* 2010;122:2718–2726.
47. Valsangiacomo ER, Hornberger LK, Barrea C, et al. Partial and total anomalous pulmonary venous connection in the fetus: two-dimensional and Doppler echocardiographic findings. *Ultrasound Obstet Gynecol* 2003;22:257–263.
48. Huhta JC, Gutgesell HP, Nihill MR. Cross sectional echocardiographic diagnosis of total anomalous pulmonary venous connection. *Br Heart J* 1985;53:525–534.
49. Norwood WI, Hougen TJ, Castaneda AR. Total anomalous pulmonary venous connection: surgical considerations. *Cardiovasc Clin* 1981;11:353–364.
50. Lock JE, Bass JL, Castaneda-Zuniga W, et al. Dilation angioplasty of congenital or operative narrowings of venous channels. *Circulation* 1984;70:457–464.
51. Whight CM, Barratt-Boyes BG, Calder AL, et al. Total anomalous pulmonary venous connection. Long-term results following repair in infancy. *J Thorac Cardiovasc Surg* 1978;75:52–63.
52. Bando K, Turrentine MW, Ensing GJ, et al. Surgical management of total anomalous pulmonary venous connection. Thirty-year trends. *Circulation* 1996;94:II12–II16.
53. Keith JD, Rowe RD, Vlad P. Complete anomalous pulmonary venous drainage. *Am J Med* 1954;16:23–38.
54. Cobanoglu A, Menashe VD. Total anomalous pulmonary venous connection in neonates and young infants: repair in the current era. *Ann Thorac Surg* 1993;55:43–48.
55. Serraf A, Bruniaux J, Lacour-Gayet F, et al. Obstructed total anomalous pulmonary venous return. Toward neutralization of a major risk factor. *J Thorac Cardiovasc Surg* 1991;101:601–606.
56. Yee ES, Turley K, Hsieh WR, et al. Infant total anomalous pulmonary venous connection: factors influencing timing of presentation and operative outcome. *Circulation* 1987;76:III83–III87.
57. Sano S, Brawn WJ, Mee RB. Total anomalous pulmonary venous drainage. *J Thorac Cardiovasc Surg* 1989;97:886–892.
58. Lamb RK, Qureshi SA, Wilkinson JL, et al. Total anomalous pulmonary venous drainage. Seventeen-year surgical experience. *J Thorac Cardiovasc Surg* 1988;96:368–375.
59. Deshpande JR, Kinare SG. Atresia of the common pulmonary vein. *Int J Cardiol* 1991;30:221–226.
60. Dudell GG, Evans ML, Krous HF, et al. Common pulmonary vein atresia: the role of extracorporeal membrane oxygenation. *Pediatrics* 1993;91:403–410.
61. Shimazaki Y, Yagihara T, Nakada T, et al. Common pulmonary vein atresia: a successfully corrected case. *J Cardiovasc Surg (Torino)* 1987;28:395–397.
62. Suzuki T, Sato M, Murai T, et al. Successful surgical repair of common pulmonary vein atresia in a newborn. *Pediatr Cardiol* 2001;22:255–257.
63. Gharagozloo F, Bulkley BH, Hutchins GM. A proposed pathogenesis of cor triatriatum: impingement of the left superior vena cava on the developing left atrium. *Am Heart J* 1977;94:618–626.
64. Niwayama G. Cor triatriatum. *Am Heart J* 1960;59:291–317.
65. Marin-Garcia J, Tandon R, Lucas RV Jr, et al. Cor triatriatum: study of 20 cases. *Am J Cardiol* 1975;35:59–66.
66. Lam CR, Green E, Drake E. Diagnosis and surgical correction of 2 types of triatrial heart. *Surgery* 1962;51:127–137.
67. Hernandez RJ, Aisen AM, Foo TK, et al. Thoracic cardiovascular anomalies in children: evaluation with a fast gradient-recalled-echo sequence with cardiac-triggered segmented acquisition. *Radiology* 1993;188:775–780.
68. McGuire LB, Nolan TB, Reeve R, et al. Cor triatriatum as a problem of adult heart disease. *Circulation* 1965;31:263–272.
69. Reye RD. Congenital stenosis of the pulmonary veins in their extrapulmonary course. *Med J Aust* 1951;1:801–802.
70. Shone JD, Mplat K, Anderson RC, et al. Congenital stenosis of individual pulmonary veins. *Circulation* 1962;26:574–581.
71. Seale AN, Webber SA, Uemura H, et al. Pulmonary vein stenosis: the UK, Ireland and Sweden collaborative study. *Heart* 2009;95:1944–1949.
72. Krabill KA, Lucas RV, Jr. Abnormal pulmonary venous connections. In: Emmanouilides GC, Reimenschneider TA, eds. *Heart Disease in Infants, Children, and Adolescents*. Baltimore, MD: Williams & Wilkins, 1995:839–874.
73. Sadr IM, Tan PE, Kieran MW, et al. Mechanism of pulmonary vein stenosis in infants with normally connected veins. *Am J Cardiol* 2000;86:577–579.
74. Riedinger WF, Juraszek AL, Jenkins KJ, et al. Pulmonary vein stenosis: expression of receptor tyrosine kinases by lesional cells. *Cardiovasc Pathol* 2006;15:91–99.
75. Driscoll DJ, Hesslein PS, Mullins CE. Congenital stenosis of individual pulmonary veins: clinical spectrum and unsuccessful treatment by transvenous balloon dilation. *Am J Cardiol* 1982;49:1767–1772.
76. Singh H, Singh C, Aggarwal N, et al. Angioplasty of congenital pulmonary vein stenosis. *Indian Heart J* 2005;57:709–712.
77. Seale AN, Daubeny PE, Magee AG, et al. Pulmonary vein stenosis: initial experience with cutting balloon angioplasty. *Heart* 2006;92:815–820.
78. Peng LF, Lock JE, Nugent AW, et al. Comparison of conventional and cutting balloon angioplasty for congenital and postoperative pulmonary vein stenosis in infants and young children. *Catheter Cardiovasc Interv* 2010;75:1084–1090.
79. Tomita H, Watanabe K, Yazaki S, et al. Stent implantation and subsequent dilatation for pulmonary vein stenosis in pediatric patients: maximizing effectiveness. *Circ J* 2003;67:187–190.
80. Spray TL, Bridges ND. Surgical management of congenital and acquired pulmonary vein stenosis. *Semin Thorac Cardiovasc Surg Pediatr Card Surg Annu* 1999;2:177–188.
81. Mendeloff EN, Spray TL, Huddleston CB, et al. Lung transplantation for congenital pulmonary vein stenosis. *Ann Thorac Surg* 1995;60:903–906.

Tal Geva

The word *vein* stems from the Latin *vena* (from the Latin verb *venio*, “to come”). Hence, a vein is a passage, a conduit, a vessel that brings blood to the heart regardless of the consistency of the blood it carries. A single exception is the portal vein, which carries blood from the intestine to the liver before its return to the heart through the hepatic veins. The spectrum of systemic venous anomalies varies widely from minor asymptomatic anatomic variations to complex abnormalities that can lead to cyanosis or that might complicate surgical repair of congenital heart disease. Clinically significant abnormalities of the systemic veins are infrequent when viscerotransposition is lateralized (either situs solitus or situs inversus). In contrast, the incidence of systemic venous anomalies in patients with heterotaxy syndrome exceeds 90% (1,2). The advent of pediatric cardiac surgery and interventional cardiology heightened interest in these anomalies. Consequently, in-depth understanding and accurate diagnosis of abnormal systemic venous connections have become essential for successful management of many congenital cardiovascular anomalies.

As with all congenital heart disease, understanding the anatomy of the systemic veins and its variations is greatly facilitated by reviewing its embryology. In considering the wide range of abnormalities of the systemic veins, an anatomic classification based on developmental principles provides a solid framework. In this chapter, the embryology of the systemic veins is reviewed first to provide a background for further discussion of specific venous anomalies. These have been categorized into the following groups: anomalies of the superior vena cavae, anomalies of the coronary sinus, anomalies of the inferior vena cava (IVC), anomalies of the ductus venosus, and anomalies of the sinoatrial valves.

EMBRYOLOGY

There are three basic venous systems in the human embryo: (a) the cardinal veins and their tributaries, which form the superior and inferior caval systems; (b) the umbilical, vitelline, and omphalomesenteric veins, which carry the blood from the placenta, yolk sac, and intestine; and (c) the pulmonary veins, which return the blood from the lungs.

The age of human embryos cannot be estimated reliably on the basis of their length, which may vary greatly (3), or on the number of somites, which are visible for only a limited time. In 1942, therefore, Streeter (4) proposed classifying human embryos into 25 age groups, or horizons, each representing 2 days of embryonic life. He later omitted the last two stages because he thought that stage XXIII could be considered the last stage of embryonic development. This approach generally has been accepted.

This chapter is dedicated to the late Dr. Stella Van Praagh, my teacher, mentor, and friend, who coauthored this chapter in the sixth and seventh editions of this textbook.

Normal Development of the Cardinal and Umbilicovitelline Venous Systems

The sinus venosus, that is, the cavity into which all veins eventually drain, develops by enlargement of the confluence of the umbilical veins and joins the atrial segment of the heart through a slit-like opening, the sinoatrial foramen. It already is present in the 20 somite embryo (horizon XI) (Fig. 36.1). It is composed of a middle section, which has been called the transverse sinus, and right and left sections, which have been named the right and left horns of the sinus venosus. The three main paired venous systems of the embryo—the cardinal, the umbilical, and the vitelline veins—drain into the ipsilateral horns of the sinus venosus.

The right and left umbilical veins develop first. They can be recognized during the third week of gestation in embryos of 13 somites (Fig. 36.1). At the same time, the vitelline plexus of the liver is formed and soon becomes more prominent on the right side. It will connect with the sinus venosus through the right hepatocardiac channel, which drains into the right horn of the sinus venosus and with the yolk sac via the left omphalomesenteric vein (Fig. 36.1).

The anterior cardinal veins make their appearance shortly after the umbilical and the vitelline veins (horizon XI, 22 to 24 days of gestation) (Fig. 36.2A,B). They drain blood from the fused neural folds that form the central nervous system. Soon after, the posterior cardinal veins appear lateral to the spinal cord. They join the anterior cardinals to form the right and left common cardinals (ducts of Cuvier) and drain together with the umbilical and vitelline veins into the right and left horns of the sinus venosus. Each horn of the sinus venosus drains for a short time into its respective sides of the common atrium (Fig. 36.1, stage of 20 somites).

At the beginning of the fourth week of embryonic life, an invagination appears between the left horn of the sinus venosus and the left atrium (LA) and ultimately separates the left horn from the LA. A rightward shift of the transverse portion of the sinus venosus that follows the appearance of the aforementioned invagination will complete the anatomic isolation of the LA from the three pairs of veins that enter the sinus venosus (cardinals, umbilicals, and vitellines). These veins will now drain into the right atrium (RA) through the sinoatrial foramen (Fig. 36.1, stage of 28 somites).

Normal Development of the Right Superior Vena Cava and the Coronary Sinus

The right superior vena cava (RSVC) extends from the confluence of the right and left innominate veins (RIV, LIV) to the RA. It is composed of the most proximal part of the right anterior cardinal vein and the right common cardinal vein. The development of the LIV at the seventh week of gestation usually is followed by the involution of the left SVC (LSVC),

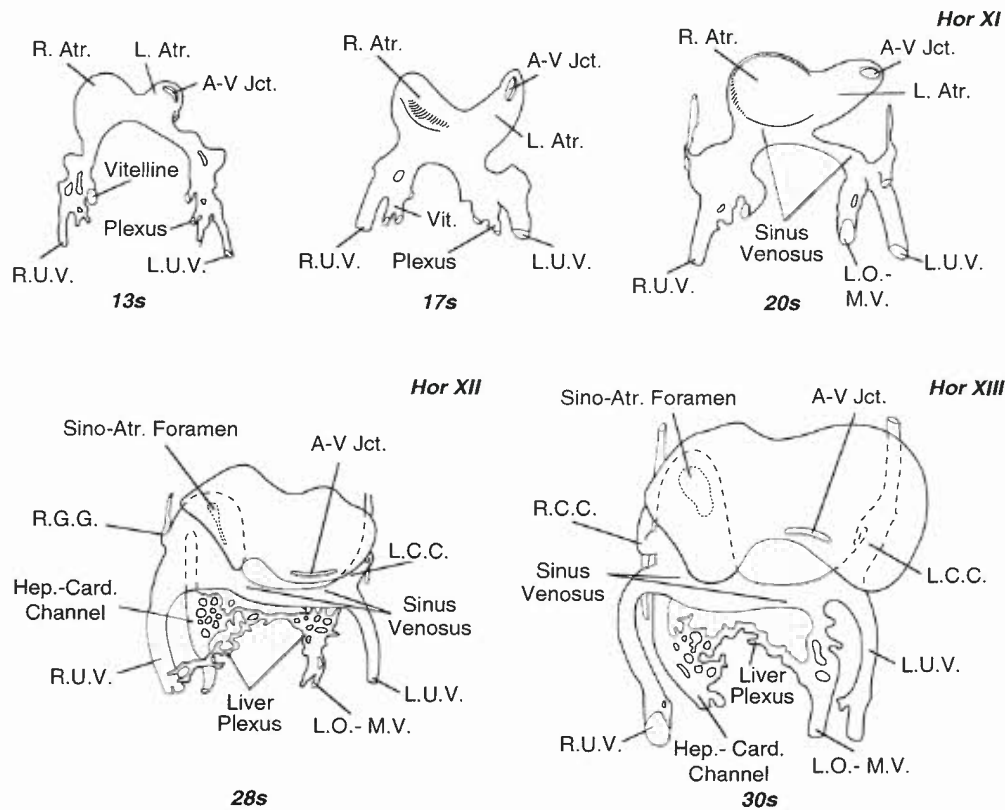


Figure 36.1. Drawings made from models of human embryos (horizons XI–XIII, 13–30 somites [S]) showing the venous end of the heart viewed from the front. The ventricular part of the heart is removed at the atrioventricular junction (A-V Jct.). It can be seen that the atria are new formations, superimposed on the vitelline plexus (Vit. Plexus). The sinus venosus retains more definitely its identity with the vitelline plexus, taking on the character of a reservoir into which all the veins of the embryo drain. The venous blood then flows into the right atrium through the sinoatrial foramen (Sino-Atr. Foramen). This foramen marks the boundary between veins and heart proper. L. Atr., left atrium; L.C.C., left common cardinal vein; L.O.-M.V., left omphalomesenteric vein; L.U.V., left umbilical vein; R. Atr., right atrium; R.C.C., right common cardinal vein; R.U.V., right umbilical vein. (Modified from Streeter GL. Developmental horizons in human embryos: description of age group XI, 13 to 20 somites, and age group XXII, 21 to 29 somites. *Carnegie Inst Contrib Embryol* 1942;30:211–245.)

which becomes the ligament of Marshall (5). As the transverse segment of the sinus venosus shifts rightward, it pulls the left horn of the sinus venosus along the posterior atrioventricular groove. The left horn of the sinus venosus and the adjacent part of the common cardinal vein receive the cardiac veins and form the coronary sinus. The mode of formation of the coronary sinus is responsible for the following anatomic observations, which are helpful in making a diagnosis of certain congenital heart defects:

1. The orifice of a normally formed coronary sinus is always in the anatomically right atrium.
2. A persistent LSVC always continues with the coronary sinus since the left common cardinal vein is part of the coronary sinus and of the LSVC.
3. Functional connection (i.e., drainage) of a persistent LSVC or any other vein with the anatomically LA can occur only if the coronary sinus is partly or completely unroofed.

Normal Development of the Inferior Vena Cava

The IVC, the largest vein of the human body, is formed by the contribution of five different venous systems. The following description is a simplified version of a rather complex process. The posterior cardinal veins appear first, shortly after the establishment of the anterior cardinal veins. They

develop as longitudinal vessels running in the dorsolateral portion of the urogenital fold and are associated primarily with the mesonephroi (wolffian bodies) (Figs. 36.2 and 36.3) (6). The subcardinal veins are a new venous plexus, which initiates the diversion of the venous drainage of the mesonephroi and the developing urogenital system of the embryo. They are established along the ventromedial borders of the mesonephroi medial and ventral to the posterior cardinals (Fig. 36.3) (6). They have many channels connecting them with the posterior cardinals. As the mesonephroi increase in size and bulge toward the midline, the subcardinals are brought closer together. In the midmesonephric region, they establish communications with each other by several small vessels, which become confluent to form intersubcardinal anastomoses and eventually a large medial venous space, the subcardinal sinus (Figs. 36.2C and 36.3). When the subcardinal sinus is established, the small vessels that connect the subcardinals with the posterior cardinals drain medially into the subcardinal sinus rather than laterally toward the posterior cardinals. This will result in the diminution and the later disappearance of the posterior cardinals at the level of the subcardinal sinus.

The blood from the posterior part of the body is still collected by the distal part of the postcardinals but returns to the heart by way of the subcardinal sinus (Figs. 36.2C and 36.3). As the embryo grows, the blood volume that enters the

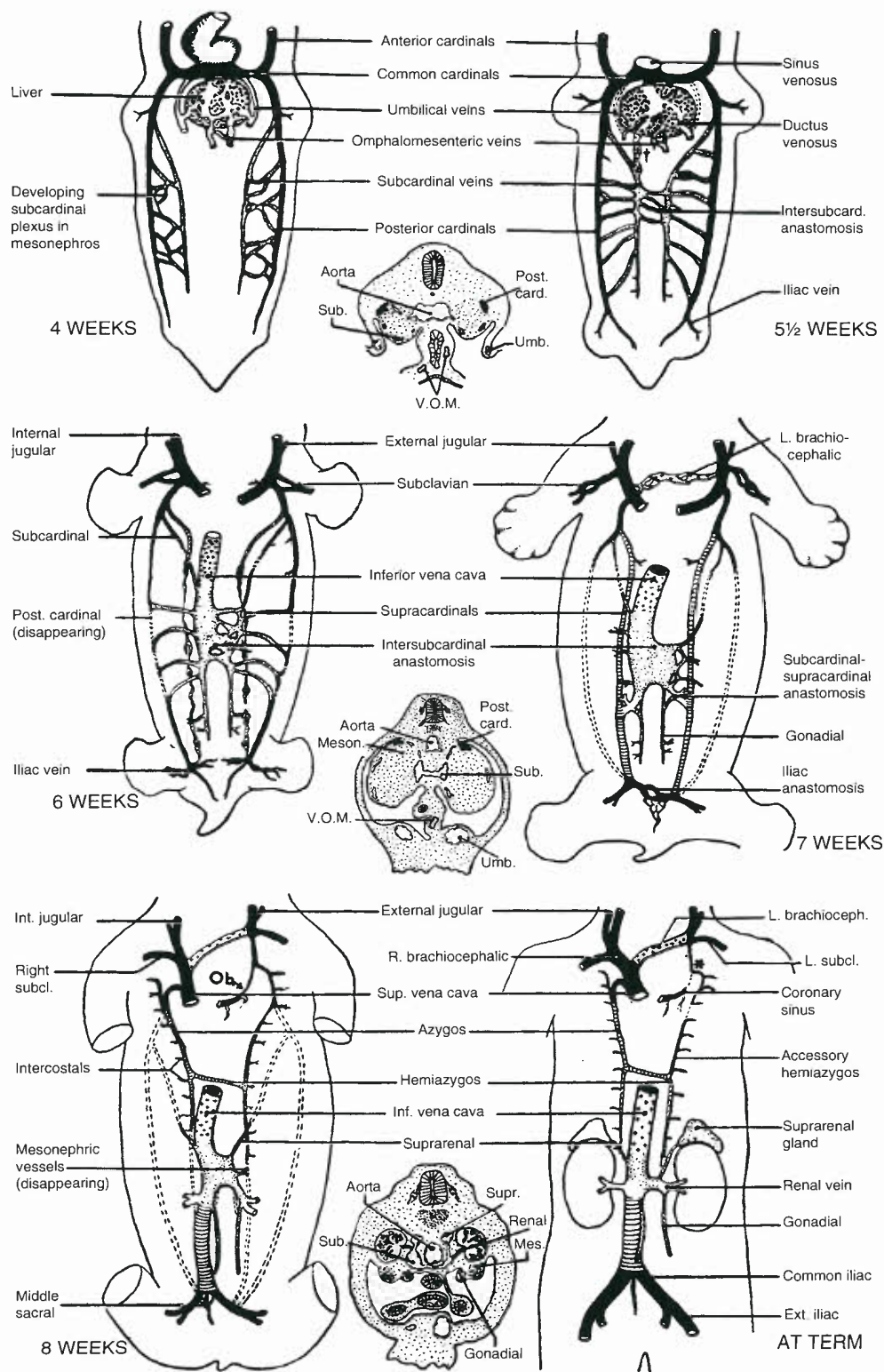


Figure 36.2. Schematic diagram showing some steps in the development of the IVC. Cardinal veins are shown in *black*; subcardinal veins are *stippled*; supracardinal veins are *horizontally hatched*. Vessels arising independent of these three systems are indicated by *small crosses*. Ext., external; inf., inferior; int., internal; L, left; ob, oblique vein of left atrium; Post. card., posterior cardinal; R, right; subcl., subclavian; sup, superior; Sub., subcardinal; Umb., umbilical; V.O.M., ventral omphalomesenteric vein; *, left superior intercostal vein. (From Patten BM. *Human Embryology*. 2nd ed. New York, NY: McGraw-Hill, 1953:637–681, with permission.)

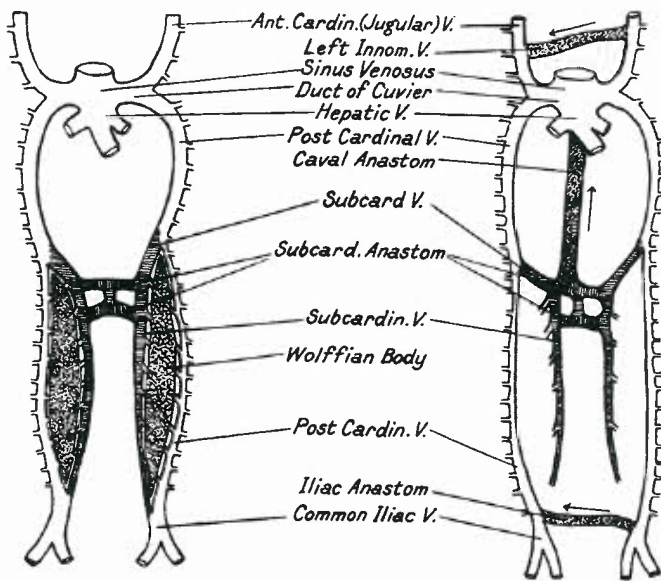


Figure 36.3. Diagram showing the anterior and posterior cardinal veins (Post Cardinal V.), the subcardinal veins (Subcardin. V., shaded), and the position of the wolffian bodies (mesonephroi) in the fifth week of gestation (left panel). The right panel shows the anastomoses between the anterior cardinal (Ant. Cardin.) veins (left innominate vein [left Innom. V.]), the inferior end of the posterior cardinal veins (left common iliac vein), and the intersupracardinal anastomosis with the hepatic veins (caval anastomosis [Caval Anastom.]) in the seventh week of gestation. (From Keith A. *Human Embryology and Morphology*. Baltimore, MD: Williams & Wilkins, 1948;433.)

subcardinal sinus increases and stimulates development of a new unpaired venous channel. This large unpaired venous channel, called the hepatic segment of the IVC, lies in a notch along the dorsal aspect of the liver (Fig. 36.2C,D). It is formed by a confluence of the small vessels that appear in a fold of the dorsal body wall just to the right of the dorsal mesentery. This fold is known as the caval fold of the mesentery. Connections of these small vessels with the plexus of the liver cephalically and the mesonephroi via the subcardinal sinus caudally allows the blood to flow from the mesonephroi to the liver plexus, resulting in rapid enlargement of this channel (6). By the seventh week of gestation, this new unpaired venous channel connects the subcardinal sinus with the confluence of the hepatic veins and the ductus venosus. The resulting large vessel constitutes the suprahepatic segment of the IVC, which enters the RA (Fig. 36.4).

At this stage, the posterior cardinals have involuted to the level of the common cardinals proximally and the iliac veins distally. Dorsal to the subcardinal sinus, a new set of paired veins appear: the supracardinal veins (Fig. 36.2D). These veins connect the subcardinal sinus with the cephalic remnant of the posterior cardinals via the azygos and hemiazygos veins. They also connect the subcardinal sinus with the iliac veins via the caudal remnant of the posterior cardinal veins. Eventually, the infrarenal portion of the left supracardinal vein will involute, and the infrarenal portion of the right supracardinal vein will become the infrarenal portion of the IVC (Fig. 36.2E,F).

By the seventh week of gestation, venous channels have been established to connect the left side with the right side of the paired veins. Proceeding from cephalad to caudad, these channels are the LIV, the hemiazygos, the left renal vein, and the left common iliac (Fig. 36.2F). The development of the

connecting channels is followed by partial involution of the left side of the paired veins. All venous blood, with the exception of the pulmonary venous return, now enters the right-sided SVC and IVC, which bring it to the RA.

In summary, the five venous systems that contribute to the formation of the IVC, from distal to proximal, are the posterior cardinals, the right supracardinals, the subcardinals, the hepatic segment of the IVC, and the hepatic (former vitelline) veins. Four of these five venous systems begin as bilateral venous channels, a fact that makes possible the existence of partly bilateral IVCs above the liver or below the kidneys (Fig. 36.5).

Normal Development of the Ductus Venosus

The paired umbilical veins, when first established, connect the placenta with the right and left horns of the sinus venosus. As the liver grows, it fuses with the lateral body wall. At the site of this fusion, multiple vessels develop, connecting the umbilical veins with the liver plexus (6). The umbilical stream tends to pass by way of these vessels into the liver, and the early direct connections of the umbilical veins with the sinus venosus involute. Distal to their entrance into the body of the embryo, the umbilical veins fuse. Consequently, there is only one vein in the umbilical cord. Inside the embryo, the right umbilical vein involutes except for a small segment that drains the body wall (Fig. 36.4). As the embryo grows and the volume of the umbilical venous blood increases, a new large channel is created through the liver substance, the ductus venosus, which connects the left umbilical vein with the right hepatic veins (Fig. 36.4). By the seventh week of gestation, placental blood finds its way to the RA by way of the left umbilical vein, the ductus venosus, and the suprahepatic segment of the IVC (Fig. 36.4). As it passes through the liver, the ductus venosus receives blood flow from the right and left hepatic veins and delivers it into the RA. After birth, the ductus venosus becomes the ligamentum venosum and the left umbilical vein becomes the ligamentum teres (round ligament of liver).

Azygos and Hemiazygos Veins

The azygos (“unpaired,” Greek) vein connects the suprarenal segment of the IVC with the right SVC (RSVC). It is formed by the suprarenal segment of the right supracardinal vein and the cephalic remnant of the right posterior cardinal vein (Fig. 36.2D–F). In the older literature, it was referred to as the vena azygos major. It commences from the right lumbar or the right renal vein or the IVC and passes through the aortic opening of the diaphragm to enter the thorax. It runs up medial to the thoracic vertebrae, to the right of the aorta and the thoracic duct, and receives the lower ten right intercostal veins. At the level of the fourth thoracic vertebra, it arches anteriorly to connect with the posterior surface of the SVC (Fig. 36.6) (7).

The hemiazygos (“half azygos”) vein has two parts: The first is the left lower, or smaller, azygos vein (vena azygos minor), which starts at the lumbar region from one of the lumbar veins or from the left renal vein, passes through the left crus of the diaphragm, and ascends on the left side of the spine up to the level of the ninth thoracic vertebra (Fig. 36.6). It then turns to the right behind the aorta and the thoracic duct to terminate into the azygos vein. The left upper hemiazygos varies inversely with the size of the left superior intercostal vein. It receives the left intercostal veins that did not drain into the left superior intercostal vein and the lower hemiazygos and terminates in the right azygos or the lower hemiazygos. In some cases with bilateral SVCs, bilateral azygos veins

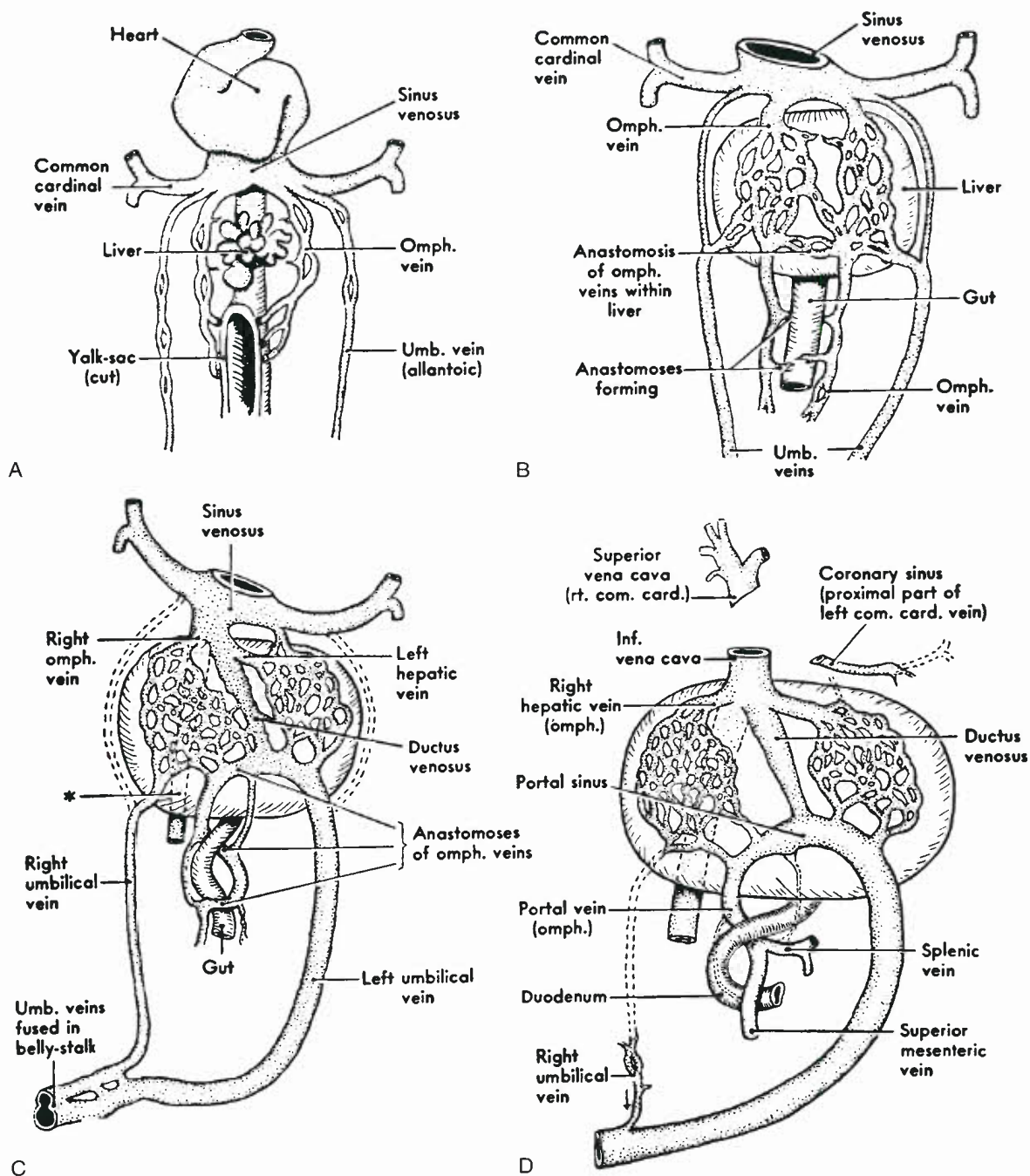


Figure 36.4. Diagrams showing development of the hepatic and portal circulations from omphalomesenteric veins and the changes by which blood returning from the placenta by way of umbilical veins is rerouted through the liver. **A:** Based on conditions in pig embryos of 3 to 4 mm, applicable to human embryos of fourth week. **B:** Based on conditions in pig embryos of 6 mm, applicable to human embryos of fifth week. **C:** Based on conditions in pig embryos of 8 to 9 mm, applicable to human embryos of sixth week; (*, inferior vena cava.) **D:** Based on conditions in pig embryos of 20 mm, applicable to human embryos of seventh week and older. (Com. card, common cardinal; Inf., inferior; omph, omphalomesenteric; Umb., umbilical.) (From Patten BM. *Human Embryology*. 2nd ed. New York, NY: McGraw-Hill, 1953;637-681, with permission.)

may be present. It is obvious that the term bilateral azygos (i.e., bilaterally unpaired veins) is literally incorrect. It is also incorrect to use the term hemiazygos (i.e., half azygos) for a vein that extends from the suprarenal segment of the IVC to the LSVC. In current literature, both terms are used according to individual preference. We prefer to use the term left azygos vein rather than hemiazygos to indicate the course and length of this vein.

Normal Development of the Portal Vein

Venous return of the primitive gut circulation is by way of the vitelline veins of the yolk sac that become confluent with the right and left omphalomesenteric veins, which enter the sinus venosus posteriorly (Fig. 36.4). As the omphalomesenteric veins approach the heart, they lie adjacent to the developing liver. The proximal portion of the omphalomesenteric veins breaks

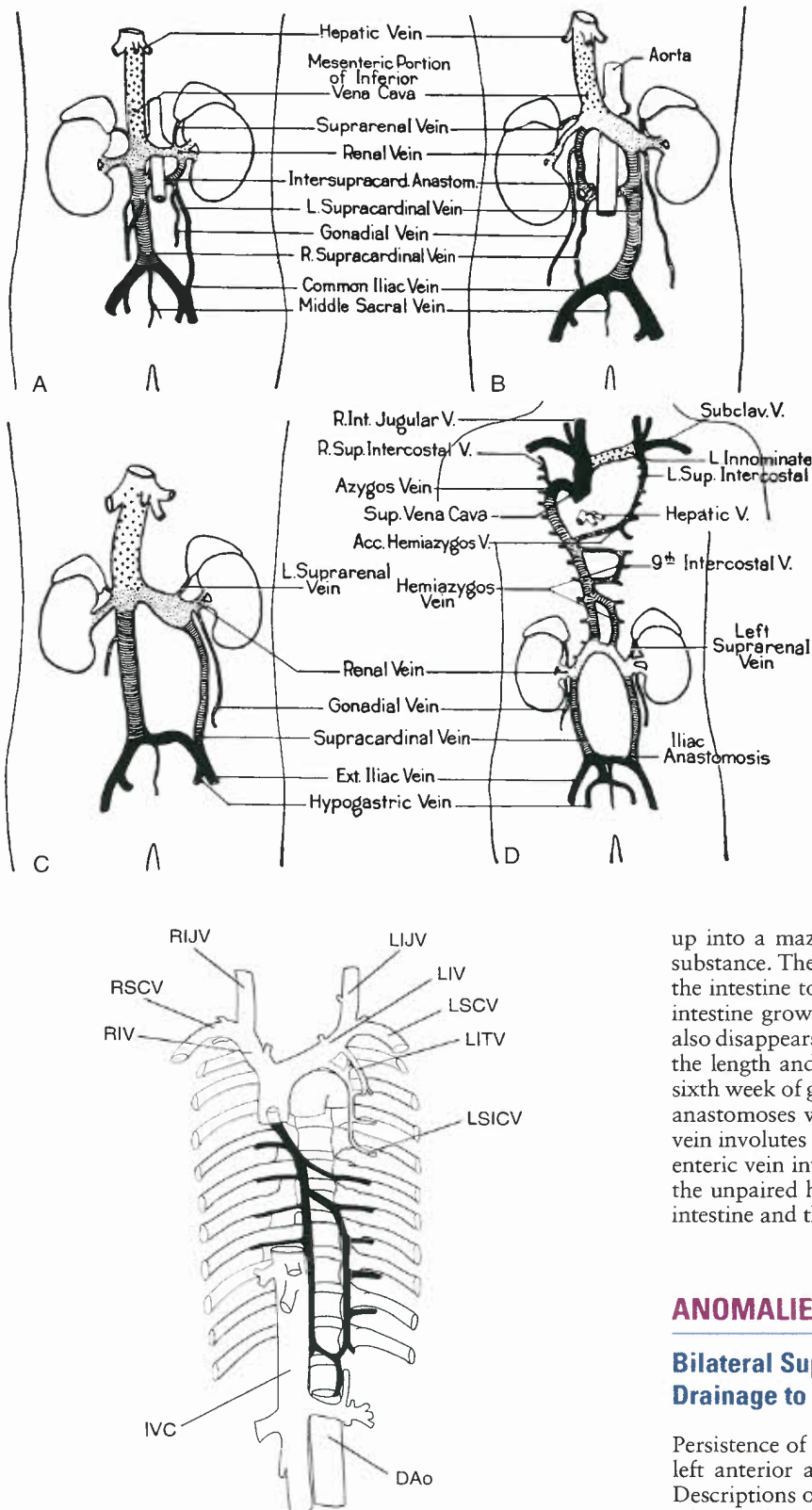


Figure 36.5. Variations in the formation of the IVC without abnormal systemic venous drainage. Drawings have been schematized as in Figure 36.2. A: Renal collar formed by persistent intersupracardinal anastomosis. B: Renal collar formed by a lumbar channel from left supracardinal. C: Double cava at lumbar level owing to persistent supracardinal veins on both sides. D: Absence of the hepatic segment of the IVC with azygos continuation into the right SVC. Acc., accessory; Ext., external; Int., internal; Subclav., subclavian; Sup., superior; V., vein. (From Patten BM. *Human Embryology*. 2nd ed. New York, NY: McGraw-Hill, 1953:637–681, with permission.)

Figure 36.6. Schematic diagram of the azygos and hemiazygos veins (solid black) and their relations to the venae cavae. DAo, descending aorta; IVC, inferior vena cava; LIJV, left internal jugular vein; LITV, left internal thoracic vein; LIV, left innominate vein; LSCV, left subclavian vein; LSICV, left superior intercostal vein; RIJV, right internal jugular vein; RIV, right innominate vein; RSCV, right subclavian vein. (Modified from Gray H. *Anatomy: Descriptive and Surgical*. New York, NY: Bounty Books, 1977:610.)

up into a maze of small channels ramifying through the liver substance. The distal portion brings blood from the yolk sac and the intestine to the liver. When the yolk sac disappears and the intestine grows, the omphalic (yolk sac) portion of these veins also disappears. The mesenteric part persists and grows to match the length and complexity of the growing intestine (6). By the sixth week of gestation, the paired mesenteric veins have formed anastomoses with each other. A week later, the left mesenteric vein involutes cephalad to the anastomosis, while the right mesenteric vein involutes caudal to the anastomosis. This results in the unpaired hepatic portal vein that connects the veins of the intestine and the spleen with the circulation of the liver.

ANOMALIES OF THE SUPERIOR VENAE CAVAE

Bilateral Superior Venae Cavae with Normal Drainage to the Right Atrium

Persistence of the LSVC is thought to result from failure of the left anterior and left common cardinal veins to involute (5). Descriptions of persistent LSVC date back to 1787 (8). In 92% of cases, the LSVC drains into the RA through the coronary sinus (9). In the remainder, it drains into the LA by means of a partially or completely unroofed coronary sinus. The incidence of persistent LSVC in two large autopsy series was approximately 0.3% (10,11). Among patients with congenital heart disease, the prevalence of LSVC is much higher (12). Congenital heart malformations that show a high frequency of persistent LSVC are tetralogy of Fallot (11%), atrioventricular septal defects (19%), mitral atresia (17%) (13), and juxtaposition of the right atrial appendage (RAA) (34%) (14). Whereas persistent LSVC

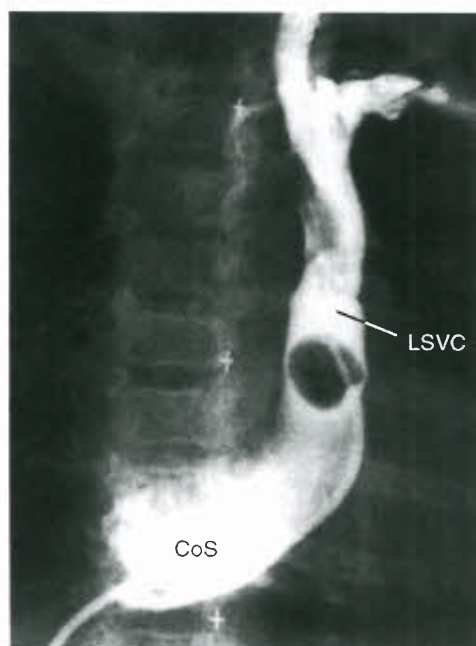


Figure 36.7. Venogram of a 4-month-old girl with absent RSVC and persistent LSVC draining into the coronary sinus (CoS) and right atrium.

to coronary sinus results in normal return of systemic venous blood to the RA, this anomaly may have clinical implications for patients with associated cardiac malformations.

Anatomy

The size of the LSVC varies. It may be smaller than, equal to, or larger than the size of the RSVC. An LIV of variable size may be present in 60% of cases (15). The LSVC starts at the junction of the left jugular and left subclavian veins. It descends in front of the aortic arch and the left pulmonary vessels and, after receiving the left superior intercostal vein, it penetrates the pericardium. It then proceeds obliquely along the posterior wall of the LA and joins the coronary sinus in the posterior left atrioventricular groove (5,10). The flow of the LSVC blood into the coronary sinus results in its enlargement and posterior displacement of its orifice on the floor of the RA (Figs. 36.7 and 36.8). The thebesian valve seldom, if ever, is present.

Clinical Manifestations

When the LSVC drains into the RA through the coronary sinus, physiology is normal and there are no clinical manifestations. When this anomaly accompanies other congenital cardiac malformations, it may pose diagnostic and technical difficulties during catheterization and cardiac surgery (16). Enlargement of the coronary sinus resulting from a persistent LSVC may interfere with blood flow from the LA into the left ventricle. An increase in the magnitude of the left-to-right shunt at the atrial level was found in patients with secundum atrial septal defects (ASDs), persistent LSVC, and dilated coronary sinus (17,18).

Diagnostic Features

The presence of an LSVC can be suspected on a chest radiogram based on a shadow along the left upper border of the mediastinum. Echocardiography is the most widely used non-invasive method to detect an LSVC (19). Huhta et al. (20), before color Doppler became available, demonstrated that detection of LSVC by 2-D echocardiography had a specificity of 100% and a sensitivity of 96%.

Imaging of a dilated coronary sinus is often the first clue to the diagnosis of an LSVC during the course of an echocardiographic examination. The coronary sinus can be imaged from the subcostal, apical, and parasternal windows (Fig. 36.9). It appears as a tubular structure in the posterior left atrioventricular groove with an opening into the postero-inferior aspect of the RA adjacent to the orifice of the IVC. The LSVC and its drainage into the coronary sinus can be imaged from the subcostal short-axis view in patients with adequate acoustic windows. In most patients, the LSVC can be imaged from the suprasternal notch or from the high left parasternal/subclavicular windows (Fig. 36.9D). From these windows, the presence and size of the LIV can be imaged. In general, there is an inverse relationship between the caliber of the LSVC and the LIV. Pulsed and color Doppler flow mapping are useful in demonstrating typical systemic venous flow patterns in the LSVC. Flow mapping by Doppler also is important in differentiating between an LSVC and other veins that may connect with the LIV. These include partial or total anomalous pulmonary venous connection, a left superior intercostal vein, and a levoatrialcardinal vein (LACV). In contrast to an LSVC to an intact coronary sinus, however, the direction of blood flow in these veins is expected to be into the LIV.

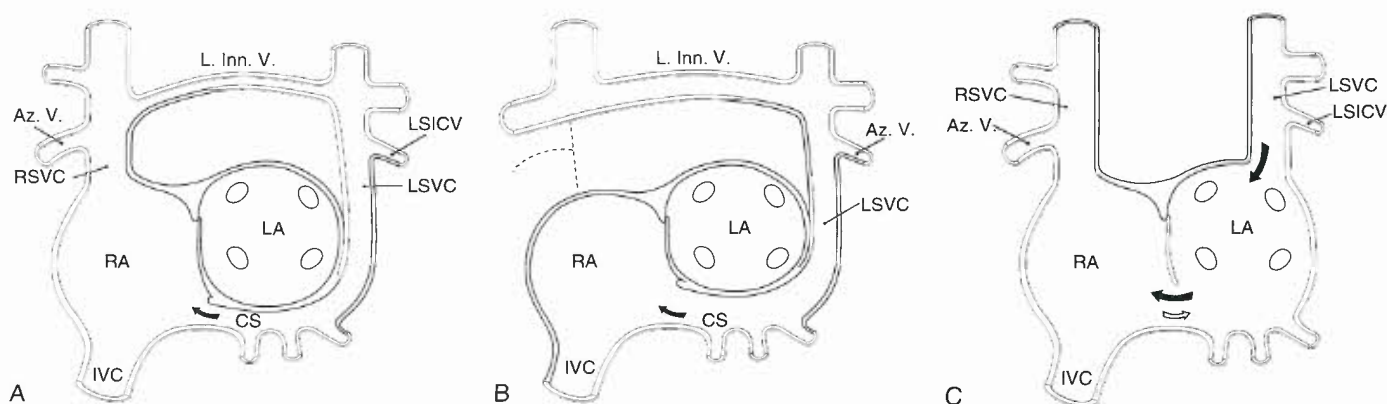


Figure 36.8 Persistent left superior vena cava (LSVC). **A:** LSVC drains via coronary sinus (CS) into right atrium (RA). The diameters of the LSVC and the left innominate vein (L. Inn. V.) vary inversely; the latter may be absent. **B:** Absence of the right superior vena cava. **C:** Bilateral superior venae cavae associated with unroofed coronary sinus and drainage of LSVC into left atrium (LA); the right atrial orifice of the coronary sinus is enlarged and allows an interatrial communication. Az. V., azygos vein; IVC, inferior vena cava; LSICV, left superior intercostal vein; RSVC, right superior vena cava.

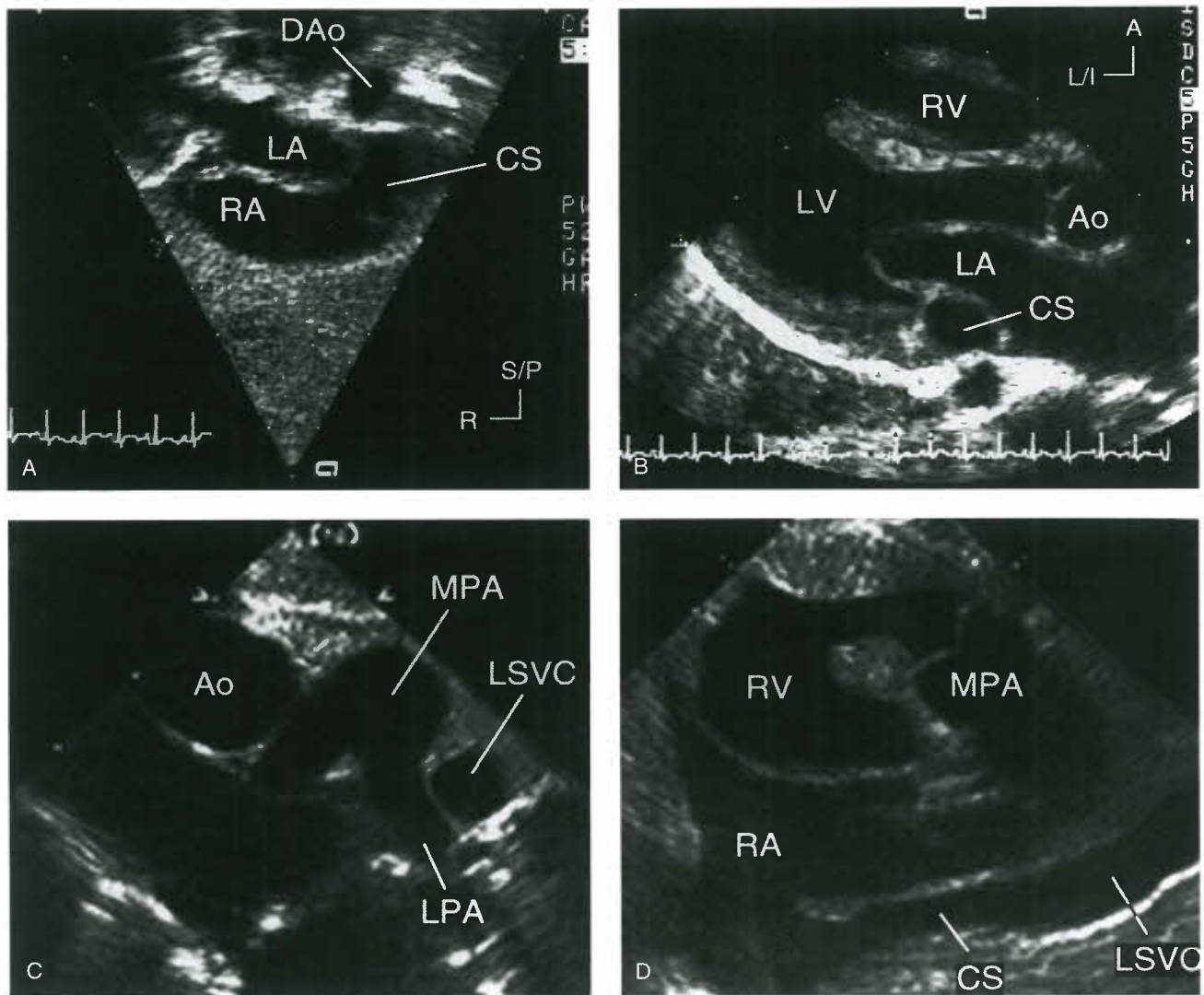


Figure 36.9. Echocardiographic features of persistent left superior vena cava (LSVC). **A:** Dilated coronary sinus (CS) imaged from the subcostal long-axis view. **B:** The dilated coronary sinus is seen in the posterior left atrio-ventricular groove from the parasternal long-axis view. **C:** The LSVC is seen anterior to the left pulmonary artery (LPA) in the parasternal short-axis view. **D:** The drainage of the LSVC to the coronary sinus (CS) and to the right atrium (RA) is seen from the high left parasternal sagittal view. A, anterior; Ao, aorta; DAo, descending aorta; LA, left atrium; L/I, left inferior; LV, left ventricle; MPA, main pulmonary artery; R, right; RV, right ventricle; S/P, superoposterior.

An anomalously connecting pulmonary vein can be diagnosed by following the vein into the lung hilum, by the Doppler flow pattern, and by the absence of normal connection of the involved pulmonary vein to the LA. The left superior intercostal vein is a small systemic vein that can be followed toward the anterior chest wall. An LACV is a remnant of an early embryonic venous channel that connects the splanchnic plexus of the lungs with the cardinal system. In the mature heart, it connects the LA or a pulmonary vein with the left innominate or other systemic veins (Fig. 36.10). Typically, it is associated with severe left atrial outlet obstruction, such as mitral stenosis or atresia with a restrictive patent foramen ovale or an intact atrial septum, and provides an alternative egress for pulmonary venous blood (21). The diagnosis can be established by following the anomalous vein from its origin (either from the LA or from one of the pulmonary veins) to its termination in a systemic vein. Unlike persistent LSVC that

courses anterior to the left pulmonary artery (LPA), an LACV typically ascends posterior to it (22). The different positions of an LSVC and an LACV in relation to the LPA are important for distinguishing between these venous structures. Although in some patients the levoatrialcardinal vein can be ligated safely or closed in the catheterization laboratory, inadvertent obstruction to venous drainage from the left lung can occur. Demonstration of retrograde flow in an LSVC toward the LIV indicates that the LSVC is venting obstructed coronary sinus flow, usually owing to stenosis or atresia of the coronary sinus orifice.

Persistent LSVC can be diagnosed by magnetic resonance imaging (MRI) either by spin echo or by gradient echo sequences. Magnetic resonance angiography (MRA) is particularly suitable for rapid noninvasive delineation of systemic venous anatomy (Fig. 36.10). By cardiac catheterization, LSVC can be suspected by the presence of

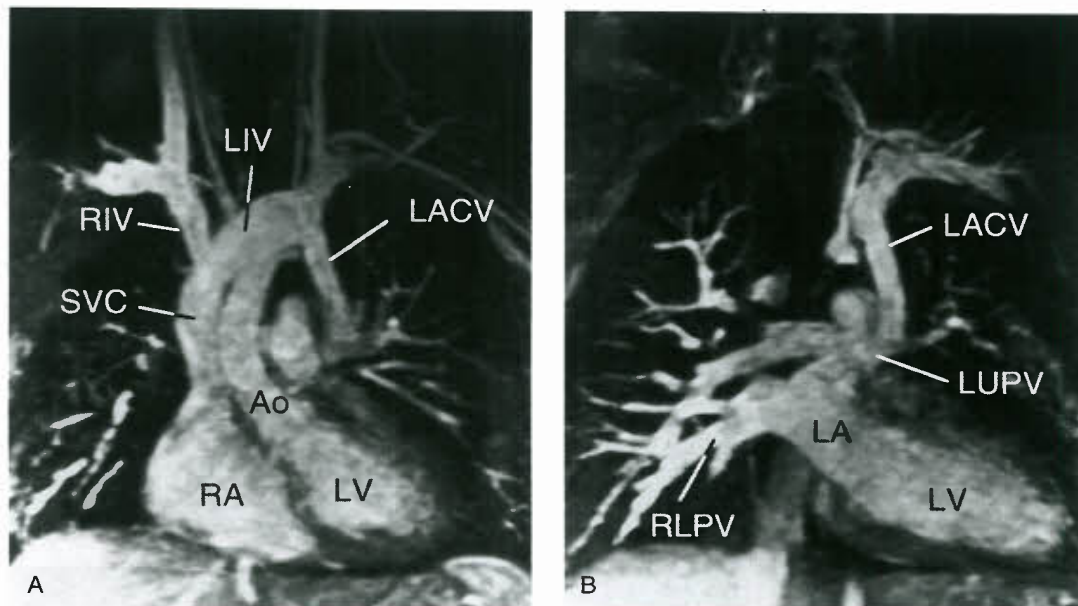


Figure 36.10. Three-dimensional magnetic resonance angiogram of a levoatriocardinal vein (LACV) in an asymptomatic 13-year-old boy with mild pulmonary valve stenosis and single right coronary artery. **A:** The levoatriocardinal vein is seen as a venous channel between the left upper pulmonary vein and the left innominate vein (LIV). The dilated left innominate vein is joined by the right innominate vein (RIV) to form the superior vena cava (SVC), which drains into the right atrium (RA). **B:** The connection of the left upper pulmonary vein (LUPV) with the levoatriocardinal vein (LACV) and with the left atrium (LA). Ao, aorta; LV, left ventricle; RLPV, right lower pulmonary vein.

higher-than-expected coronary sinus oxygen saturation. LIV angiography with balloon occlusion proximal to the injection site is diagnostic. The LSVC can be approached either through the right SVC (when the innominate vein is present) or through the coronary sinus (Fig. 36.7). The diagnosis of systemic venous anomalies can be established reliably by echocardiography and MRI. Cardiac catheterization is unnecessary in most patients.

Treatment

No treatment is necessary for an isolated LSVC to an intact coronary sinus.

Bilateral Superior Venae Cavae with an Unroofed Coronary Sinus

Anatomy

Partial or complete absence of the common wall between the LA and the coronary sinus has been termed partial or complete unroofing of the coronary sinus. In hearts with partial or complete unroofing of the coronary sinus, a persistent LSVC drains into the LA. In patients with a normal septum primum and septum secundum, the orifice of the unroofed coronary sinus will function as an interatrial communication. This type of interatrial communication has been erroneously diagnosed as a posterior ASD occurring in association with a persistent LSVC and unroofed coronary sinus (23).

Bilateral SVC with an unroofed coronary sinus may occur in association with other congenital heart defects and rarely as an isolated lesion (24). Visceral heterotaxy with asplenia exhibits the highest incidence of bilateral SVCs with a completely unroofed coronary sinus. In a study of

58 postmortem cases of visceral heterotaxy with asplenia, the incidence was 67%, and in 46 postmortem cases of polysplenia, the incidence was 13% (1). The reason for the high frequency of an unroofed coronary sinus in asplenia is not known. The high frequency of bilateral SVCs in asplenia probably represents a remnant of the normal early embryonic symmetry of the systemic veins that is characteristic of visceral heterotaxy.

As mentioned, a persistent LSVC entering the LA when the coronary sinus is unroofed should be distinguished from persistence of an embryonic connection between the LA and a systemic vein (LACV) or between the left pulmonary veins and a systemic vein (vertical vein) (25). Almost all cases of LACV have been associated with severe left atrial outlet stenosis or atresia (21). Rarely, a normally connected left upper pulmonary vein to the LA may maintain the early embryonic connection with the LIV without left atrial outflow stenosis or atresia (21). We also encountered such a case (Fig. 36.10). It is interesting to note that both cases had coarctation of the aorta.

Clinical Manifestations

Most patients with an isolated persistent LSVC to a partially or completely unroofed coronary sinus also have a large coronary sinus ostium that functions as an interatrial communication (Raghib syndrome) (Fig. 36.8C). The hemodynamic consequences of the Raghib syndrome are cyanosis and left-to-right shunting through the “ASD.” Systemic arterial desaturation is caused by mixing of LSVC blood with pulmonary venous blood in the LA. The degree of arterial desaturation is related to the net right-to-left shunt, which, in turn, depends on the amount of systemic venous blood carried by the LSVC and the proportion of systemic venous blood that crosses the atrial septum and reaches the pulmonary circulation. In most

patients, the arterial oxygen saturation ranges between 85% and 95%. These patients exhibit varying degrees of cyanosis, clubbing of the nail beds, and polycythemia. They are at risk for complications of right-to-left shunting, including paradoxical emboli, brain abscess, strokes, and death. In some patients, the coronary sinus ostium is atretic and there is no significant interatrial communication. The only clinical manifestations in these patients are cyanosis and its sequelae. Patients with a significant interatrial communication exhibit signs and symptoms related to left-to-right shunting as well as cyanosis. When a persistent LSVC to an unroofed coronary sinus is associated with complex congenital heart disease (often in the context of heterotaxy syndrome), the clinical features of LSVC drainage to the LA are obscured by manifestations of the associated anomalies. When right atrial outflow stenosis or atresia coexists with a persistent LSVC to an unroofed coronary sinus, the shunt is exclusively from right to left.

Diagnostic Features

The LSVC may appear as a shadow along the left upper border of the mediastinum on the chest radiogram. The electrocardiographic features of isolated LSVC to an unroofed coronary sinus are similar to those in patients with uncomplicated secundum ASD. The frontal axis of the P wave may be abnormal in patients with heterotaxy syndrome, reflecting a left sinoatrial node or an ectopic atrial rhythm.

Echocardiography is the definitive imaging modality in most patients (26). The LSVC and its drainage into the LA can be imaged from the subcostal window in young patients and from the precordial and suprasternal notch windows in most patients. The posterior left atrioventricular groove is examined in detail to ascertain the extent of deficiency of the coronary sinus septum. When the coronary sinus septum is completely unroofed, the LSVC terminates in the upper left posterior corner of the LA between the left upper pulmonary vein posteriorly and the left atrial appendage anteriorly. Flow mapping with color Doppler is useful in demonstrating flow from the LSVC into the LA. If the diagnosis is still in doubt, a contrast injection in a left arm vein establishes the diagnosis by demonstration of microbubbles in the LA before they appear in the RA. MRI is increasingly used to establish the diagnosis, especially when technical limitations compromise the quality of echocardiography or when the anatomy has not been completely delineated. By cardiac catheterization, the diagnosis is established by demonstration of a step-down in oxygen saturation between the pulmonary veins and the LA and by LSVC-selective angiocardiography (Fig. 36.11).

Treatment

The coronary sinus defect of a partially or completely unroofed coronary sinus that receives an LSVC must be repaired to avoid complications of cyanosis and its sequelae and of chronic left-to-right shunting. Accurate preoperative diagnosis is essential to avoid inadvertent closure of an enlarged coronary sinus orifice that is mistaken for a secundum ASD. Such an error will result in significant postoperative cyanosis.

If the LSVC is relatively small and there is an adequate-sized LIV, the LSVC can be ligated and the interatrial communication closed, leaving the coronary sinus blood to drain into the LA. In the absence of an adequate-sized bridging LIV, the coronary sinus is “reroofed” (27). This is achieved by baffling the LSVC along the posterior wall of the LA into the RA. Care is taken to avoid the orifices of the pulmonary veins. A coronary sinus defect also can be closed in the catheterization laboratory with an ASD device.

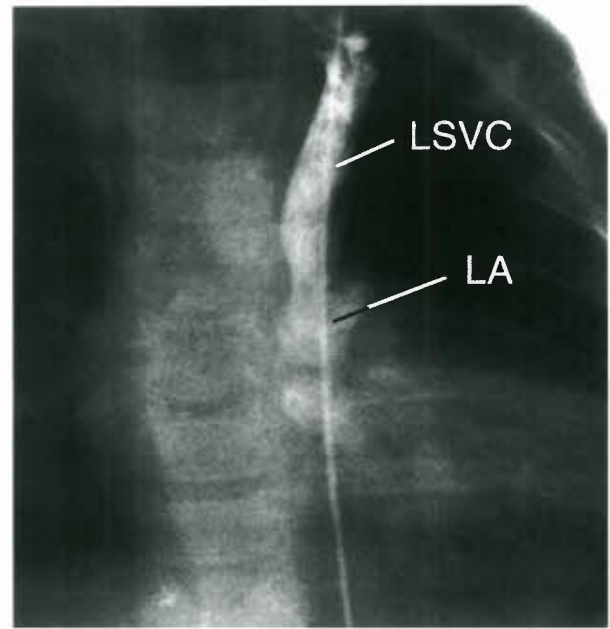


Figure 36.11. Venogram of a left superior vena cava (LSVC) entering the left side of a common atrium via an unroofed coronary sinus in a 15-month-old boy with visceral heterotaxy. A catheter inserted into the right femoral vein entered a left venous channel that crossed the diaphragm and entered the left side of a common atrium. LA, left atrium. The additional venous anomalies of this case are presented in Figure 36.20. (The angiocardiogram of this patient was kindly provided by Dr. John Murphy, duPont Hospital for Children, Wilmington, DE.)

Absent Right Superior Vena Cava in Visceroatrial Situs Solitus

Anatomy

Absent or atretic right SVC in viscerotaxial situs solitus is rare, occurring in 0.07% to 0.13% of patients with cardiovascular malformations (28,29). In a study of 121 cases, we found that this anomaly occurred both in patients with structurally normal hearts (54%) and in patients with congenital heart defects (46%) (30). This anomaly is characterized by persistence of the LSVC draining to the RA via the coronary sinus and by left-sided azygos vein draining into the LSVC (Fig. 36.8B). Less constant features were additional cardiovascular malformations (46%) and rhythm abnormalities (35%) that usually appeared related to complications of old age. In seven cases (6%), the coronary sinus was unroofed; hence, the LSVC drained into the LA (30). The LSVC, in cases of atretic or absent right SVC, should not be considered an inverted SVC. The origin and course of this LSVC are exactly the same as the origin and course of the LSVC, which may be present when the right SVC is normal (30).

Clinical Manifestations

In the absence of additional cardiovascular malformations, absence of the right SVC with drainage of the LSVC into the RA via the coronary sinus is asymptomatic. Of the 121 cases reviewed by Bartram et al. (30), 36 (30%) had no associated anomalies, and the systemic venous anomaly was an incidental finding. Rhythm disturbances without additional structural heart disease were reported in 29 patients (24%), including atrioventricular block, sinoatrial node dysfunction, ventricular tachycardia, left and right bundle-branch block,

supraventricular tachycardia, and sudden death. A range of associated cardiovascular malformations with or without arrhythmia were found in 56 patients (46%). When the only associated cardiac anomaly is partial or complete unroofing of the coronary sinus (found in four patients), cyanosis dominates the clinical picture.

Diagnostic Features

The clinical relevance of establishing the diagnosis of absent right SVC with a persistent LSVC to the coronary sinus in viscerotransposition is mainly to avoid difficulties during the following procedures: transvenous pacemaker implantation, venous cannulation for cardiopulmonary bypass or extracorporeal membrane oxygenator, and placement of a right ventricular or pulmonary arterial monitoring line through the subclavian or jugular veins. Precise preoperative knowledge of the systemic venous anatomy is also crucial before surgery that includes cavopulmonary anastomosis and orthotopic heart transplantation. The diagnosis can be established by echocardiography, MRI, CT, or angiography (Fig. 36.12).

Treatment

No intervention is indicated when the physiology is normal.

Left Atrial or Biatrial Drainage of Right Superior Vena Cava

Anatomy

Left atrial drainage of the RSVC is a rare malformation that typically manifests itself as unexplained cyanosis and clubbing in patients who do not have any other signs of a heart defect (31). A variation of this malformation is an RSVC draining into both atria (32). Van Praagh et al. (31) recently reported two cases of biatrial drainage of the RSVC and one case of left atrial drainage of the RSVC and reviewed 26 previously published cases. Nutzel described the earliest reported cases of biatrial

drainage of the RSVC in a 47-year-old man (reference 18 in Van Praagh et al. [31]). The earliest reported case in the English literature of left atrial drainage of the RSVC involved a 10-year-old girl described by Wood (33). At least 18 additional cases have been published in English since then (31,34); 10 of these patients underwent surgery, and in all but one, the right upper lobe pulmonary veins usually drained into the RSVC (35). A persistent left SVC was present in three cases (31,35,36). In several of the operated cases, the diagnosis of pulmonary veins draining into the RSVC was missed preoperatively.

Based on our understanding of the nature of sinus venosus defects (31,37), we believe this malformation represents a sinus venosus defect of the SVC type in association with atresia of the RSVC orifice (Fig. 36.13). A sinus venosus defect of the SVC type results from the deficiency of the common wall between the SVC and the right upper pulmonary vein (RUPV) (37). This defect unroofs the RUPV and its branches into the RSVC. The unroofed RUPV then drains into the SVC, and its left atrial orifice becomes the interatrial communication. This interatrial communication is not a defect; like the right atrial orifice of an unroofed coronary sinus, it functions as an interatrial communication but is not an ASD. Depending on the pressure and compliance differences between the two atria, left atrial blood can be shunted into the SVC–right atrial junction, or RSVC blood can enter the LA. We suspect that if the RSVC-to-LA shunt predominates during early fetal life, the blood flow toward the RA through the right atrial orifice of the SVC will be diminished or completely eliminated. Lack of blood flow will result in gradual involution of the proximal segment of the SVC and stenosis or atresia of its orifice. In cases of stenosis of the SVC orifice, the SVC will drain into both atria (31,32), whereas in cases of SVC orifice atresia, the SVC will drain only into the LA (Fig. 36.14) (31). The true nature of the interatrial communication was fully understood by Hackensellner (38), who reported the postmortem findings in a 72-year-old man with biatrial drainage of the RSVC. A similar view was expressed by Shapiro et al. (32), who also realized that if the shunt from the RSVC to the LA was large

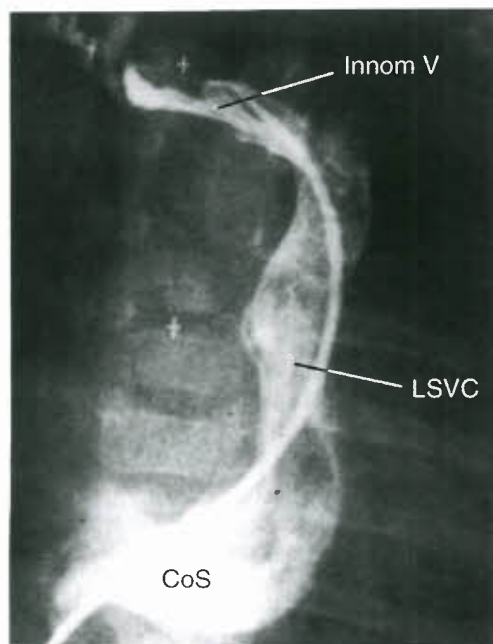


Figure 36.12. Venogram of the innominate vein (Innom V) in a patient with absence of the right superior vena cava and persistence of the left superior vena cava (LSVC), which drains into the right atrium via the coronary sinus (CoS).

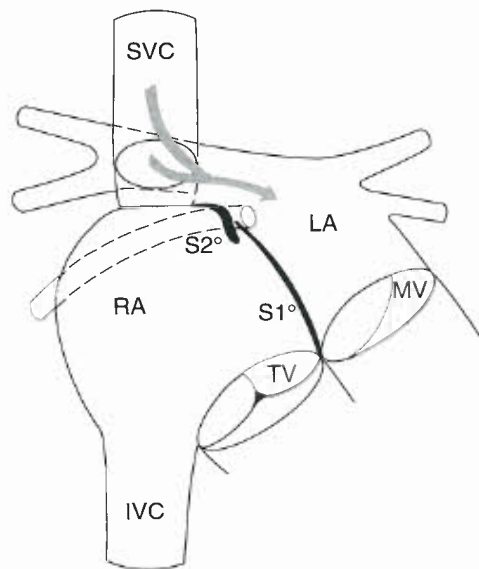


Figure 36.13. Diagrammatic representation of the anatomy of right superior vena cava (SVC) drainage into left atrium (LA). A combination of sinus venosus defect and atresia of the right atrial orifice of the superior vena cava results in drainage of the right upper pulmonary vein and SVC into the left atrium via the left atrial orifice of the right upper pulmonary vein (see text for details). IVC, inferior vena cava; MV, mitral valve; RA, right atrium; S1, septum primum; S2, septum secundum; TV, tricuspid valve.

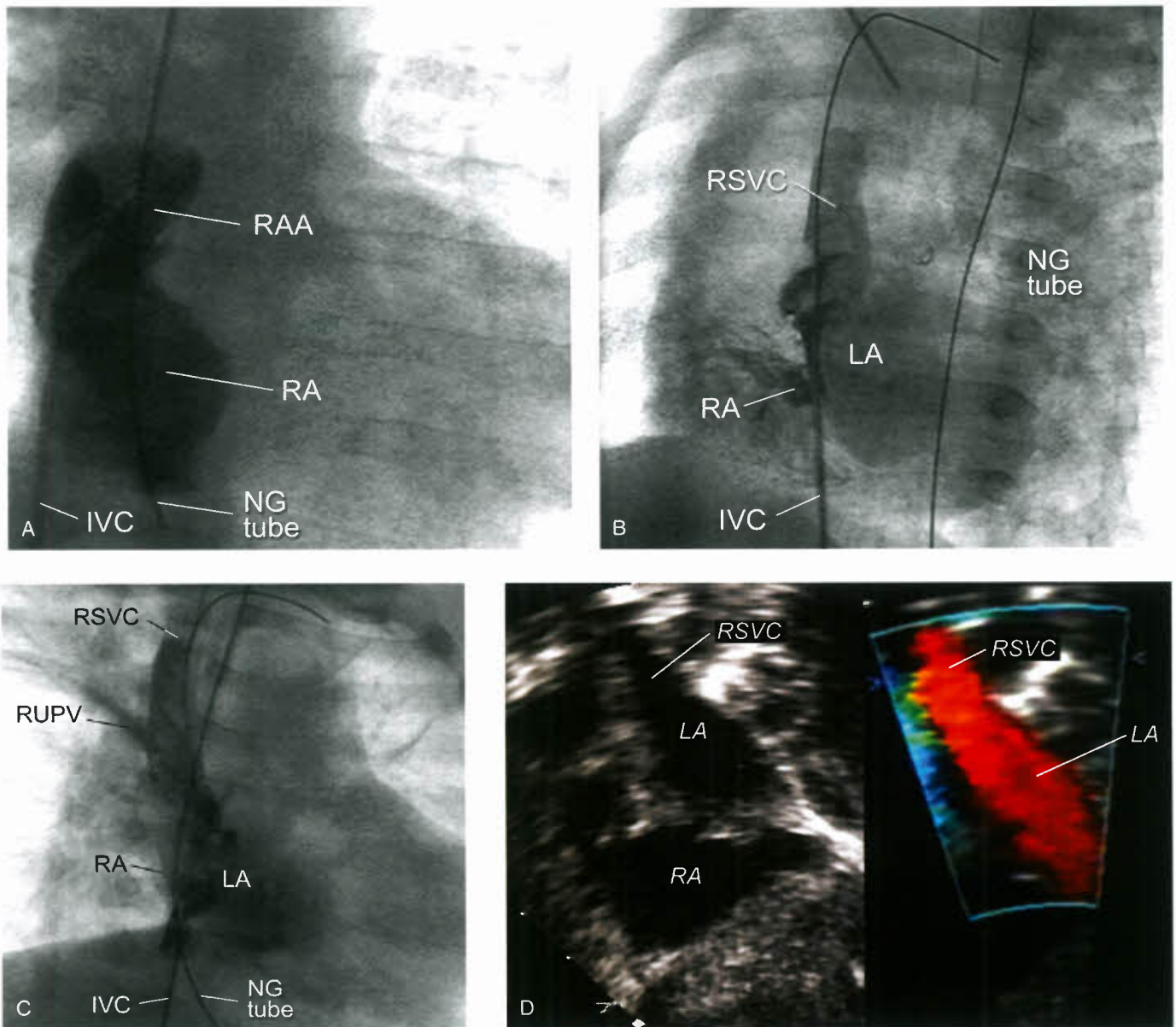


Figure 36.14. Drainage of right superior vena cava (RSVC) to left atrium (LA). **A:** Right atrial angiogram showing catheter course from the inferior vena cava (IVC) to the right atrium (RA). The contrast fills the RA and right atrial appendage (RAA) but not the superior vena cava. **B:** The catheter crosses the foramen ovale to the left atrium (LA) and is advanced into the RSVC. The RSVC-to-LA drainage is seen with contrast entering the RA through the foramen ovale. **C:** Drainage of the right upper pulmonary vein (RUPV) into the RSVC is seen on a later frame. **D:** Echocardiogram from the subcostal short-axis view showing the RSVC-to-LA drainage. NG, nasogastric.

enough, “the normal SVC channel to the RA became relatively hypoplastic.” We had reached the same conclusion prior to our knowledge of these two reports.

Clinical Manifestations

Cyanosis is the dominant clinical feature in patients with drainage of the RSVC to the LA. The degree of cyanosis may be mild, and symptoms may not develop until late childhood or adolescence (31,39) and rarely until adulthood (40). The risks of polycythemia, shortness of breath, decreased exercise tolerance, systemic emboli, brain abscess, and other cerebrovascular complications increase with age. The echocardiogram or

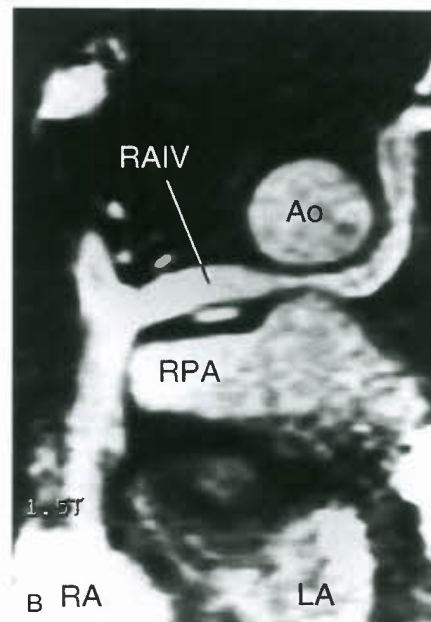
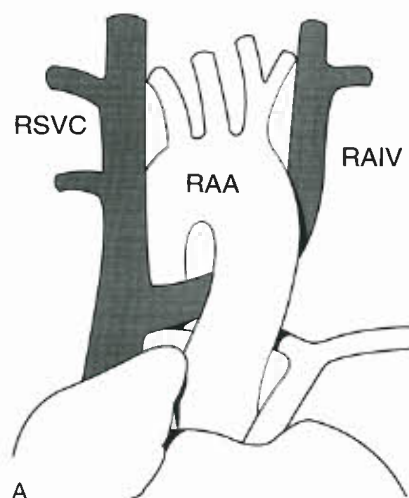
angiocardiogram of such patients shows a common entrance site of the RSVC and the RUPV in the roof of the LA (36).

Treatment

The RSVC flow is surgically diverted into the RA. In the past, this was done by creating an ASD and redirecting SVC flow into the RA and the pulmonary blood flow into the LA (41). More recently, the preferred surgical approach has involved transection of the RSVC above the entrance of the RUPV(s) and anastomosis of the transected caval end to the RAA (31). A surgical technique without the use of cardiopulmonary bypass was reported by Nazem and Sell (42).

Figure 36.15. Retroaortic innominate vein.

A: Diagram showing a retroaortic innominate vein (RAIV) associated with a right aortic arch (RAA) in a patient with tetralogy of Fallot. RSVC, right superior vena cava. **B:** Gadolinium-enhanced magnetic resonance angiogram showing a retroaortic innominate vein. Ao, aorta; LA, left atrium; RA, right atrium; RPA, right pulmonary artery.



Retroaortic Innominate Vein

Anatomy

Retroaortic innominate vein (RAIV), also known as postaortic innominate vein, is a rare systemic venous anomaly characterized by an abnormal position of the LIV behind the ascending aorta (Fig. 36.15). The normal course of the LIV is from left to right, anterior to the aortic arch in the superior mediastinum. It then joins the RIV to form the RSVC. In RAIV, the confluence of the left subclavian and left common jugular veins forms the LIV, which then turns inferiorly to run a course that

is initially similar to that of a persistent LSVC. After passing anterior to the LPA and before reaching the LA, the LIV turns rightward and courses horizontally behind the ascending aorta to reach the SVC below the insertion of the azygos vein (Fig. 36.15). The insertion of the RAIV into the SVC is only a short distance above the SVC–RA junction. We encountered a heart specimen in which the RAIV also communicated with an LSVC that drained into a partially unroofed coronary sinus. Another rare anatomic variation is *duplication of the left innominate vein*—defined as the coexistence of a retroaortic LIV and a normally positioned LIV (Fig. 36.16).

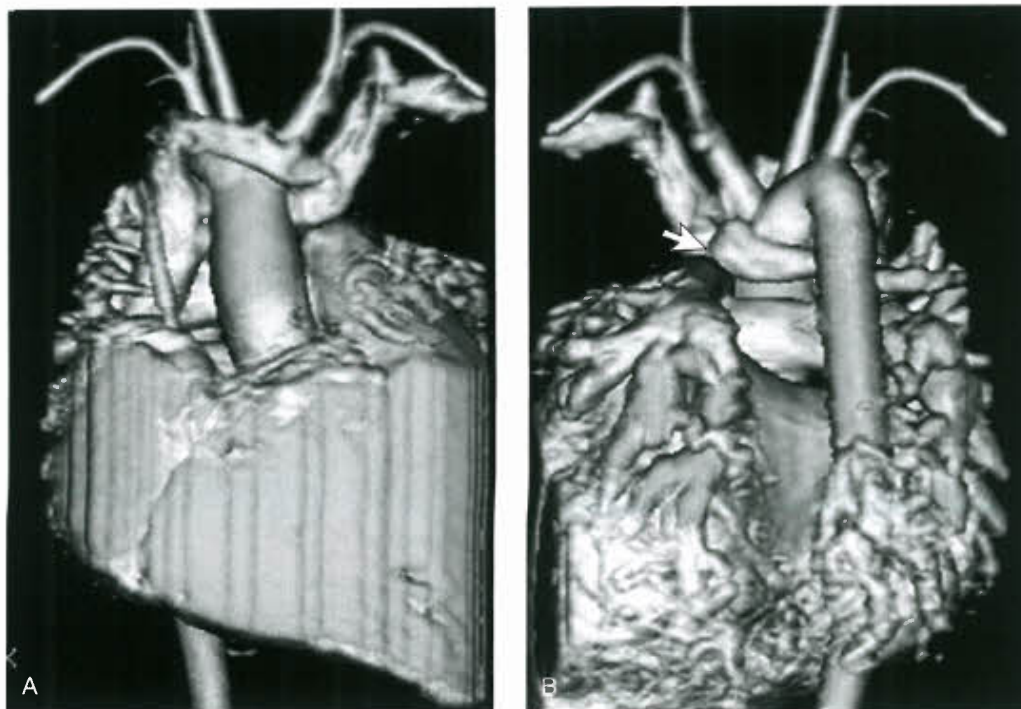


Figure 36.16. Duplication of the left innominate vein. Anterior (**A**) and posterior (**B**) views of volume reconstruction of gadolinium-enhanced 3-D magnetic resonance angiogram. The anterior (normal position) and posterior (retroaortic; *arrow*) left innominate veins form a ring that encircles the aorta.

This rare anomaly was first reported in 1888 (43), and 62 cases have been reported to date. Choi et al. (44) reported 24 patients with RAIV among 2,457 patients with congenital heart disease (0.98%). Of the 35,000 persons who underwent an echocardiographic examination at Children's Hospital in Boston from 1980 through 1997, 31 patients were diagnosed with RAIV (0.09%). Most patients with RAIV have associated congenital cardiac malformations, including tetralogy of Fallot with or without pulmonary atresia, truncus arteriosus, atrioventricular septal defect, heterotaxy syndrome, hypoplastic left heart syndrome, pulmonary atresia with intact ventricular septum, coarctation of the aorta, and others (44–46). In some patients, RAIV is an incidental finding not associated with other congenital cardiac anomalies. Based on autopsy findings, Gerlis and Ho (46) and Kitamura et al. (47) distinguished between RAIV that courses ventral to or dorsal to the ligamentum arteriosum. This distinction, however, cannot be made in living patients unless the ductus arteriosus is patent. The cause and embryogenesis of RAIV are unknown. Gerlis and Ho (46) suggested that the anomaly results from failure of the high transverse capillary plexus that forms the LIV to develop at a time when the lower portion of the left anterior cardinal vein atrophies. In such circumstance, venous blood returning from the left side of the head and the left arm may drain through a lower venous plexus that communicates between the left and right anterior cardinal veins. This lower venous plexus then forms the RAIV.

Clinical Manifestations

RAIV is widely considered an anatomic variant without clinical ramifications. In 3 of the 31 patients with RAIV diagnosed at Children's Hospital in Boston, the anomaly was associated with defects that required a cavopulmonary anastomosis as part of their surgical repair. The abnormal connection of the RAIV to the SVC at or below the level of the right pulmonary artery hindered the surgical mobilization of the SVC and necessitated modifications of the surgical technique.

Diagnostic Features

The anomaly can be identified readily by echocardiography, angiocardiology, and MRI (Figs. 36.15B and 36.16). Accurate echocardiographic diagnosis is based on tracking the LIV

from its origin through its retroaortic course to the SVC (45). The imager must be careful not to confuse a RAIV with a persistent LSVC. The latter will connect with the coronary sinus or with the LA if the coronary sinus is unroofed. Cine MRI and 3-D MRA are particularly useful in depicting the anatomy.

Treatment

No treatment is necessary because blood flow is normal.

ANOMALIES OF THE CORONARY SINUS

Coronary Sinus Defect and Unroofed Coronary Sinus

Anatomy

Unroofed coronary sinus almost always is associated with a persistent LSVC. This condition was discussed earlier in this chapter. A coronary sinus defect without an associated LSVC is rare, and the physiology is the same as in ASD. The interatrial communication, however, is through the mouth of the coronary sinus, which is located below and posterior to the fossa ovale. It also has been observed in patients with isolated secundum ASD (48). When unroofing of the coronary sinus occurs in cases with an intact atrial septum, its orifice takes the form and function of an interatrial communication (Fig. 36.8C). When unroofed coronary sinus is associated with an ostium primum defect, a complete common atrioventricular septal defect, or a common atrium, the orifice of the coronary sinus merges with the atrial septal deficiency and becomes unrecognizable. In some patients, the coronary sinus ostium is atretic and the coronary sinus defect is the only egress for coronary venous blood (Fig. 36.17A). A coronary sinus defect also may be an alternate or an accessory route for blood flow from an atrium that has no other functional outlet (Fig. 36.17C).

A left or a right hepatic vein may drain separately from the other hepatic veins into the coronary sinus (49). When the orifice of the coronary sinus is enlarged as a result of a persistent LSVC, it may incorporate into its territory the orifice of the IVC. In a recently reported case of absent RSVC and persistent LSVC, the entire systemic venous return entered the heart by way of the coronary sinus orifice (50).

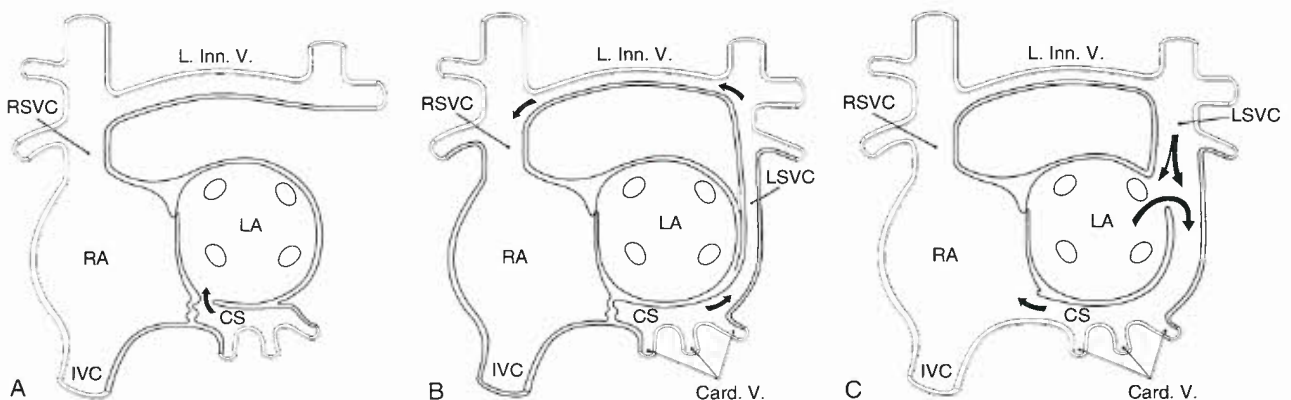


Figure 36.17. Anomalies of the coronary sinus. Atrisia of the ostium of the coronary sinus (CS). **A:** Drainage of coronary sinus blood into the left atrium (LA) through a coronary sinus septal defect. **B:** Drainage of coronary sinus blood in a retrograde direction into a persistent left superior vena cava (LSVC), to left innominate vein (L. Inn. V.), and to right atrium (RA). **C:** Coronary sinus septal defect associated with a persistent LSVC (Raghib syndrome). Card. V., cardiac vein; IVC, inferior vena cava; RSVC, right superior vena cava.

Clinical Manifestations

The clinical manifestations of an unroofed coronary sinus associated with a persistent LSVC were discussed earlier in this chapter. Patients with partial or complete unroofing of the coronary sinus without an LSVC exhibit signs and symptoms identical to those with a secundum ASD.

Diagnostic Features

Echocardiographic diagnosis can be made by imaging the coronary sinus septum in the posterior left atrioventricular groove. Color Doppler flow mapping is useful in demonstrating blood flow through a defect identified by 2-D imaging. In the presence of an associated LSVC, left-arm contrast injection will result in the appearance of bubbles in the LA before they appear in the RA. In the absence of an associated LSVC, contrast injection can aid only in demonstrating the atrial-level shunt. Surgery is usually performed for associated malformations.

Coronary Sinus Orifice Atresia

Anatomy

Atresia or severe stenosis of the right atrial orifice of the coronary sinus is rare (51). The coronary sinus is usually well formed, and the orifice is covered by a thin membrane-like tissue that appears to be related to the thebesian valve. In 13 of the 15 heart specimens described by Lucas and Krabill (52), an alternative exit for coronary venous blood return was identified. A small LSVC was found in six cases, a large thebesian vein in five, a coronary sinus septal defect in one, and a connection with the IVC in one case. No alternative outlet for coronary sinus blood flow was identified in the remaining two heart specimens. In 12 of the 15 cases, associated congenital cardiac anomalies were found.

Clinical Manifestations

Myocardial ischemia is unlikely as long as there is an alternate egress for the coronary sinus blood. Myocardial ischemia, infarction, and death have been reported in several patients in whom there was no alternative exit for the coronary sinus blood. Two patients with coronary sinus orifice atresia died of myocardial ischemia following ligation of a small LSVC (52,53). Two neonates without anatomic evidence of an egress route for the coronary sinus blood died at 6 and 10 days, respectively. Both had myocardial hemorrhage and necrosis at autopsy.

Diagnostic Features

The demonstration of a persistent LSVC to an intact coronary sinus with retrograde flow toward the innominate vein should prompt a careful examination of the coronary sinus ostium. Angiographic demonstration of retrograde flow in the coronary sinus and a small-caliber LSVC is suggestive of the diagnosis (Fig. 36.18) (51,54).

Coronary Sinus Aneurysm or Diverticulum

Anatomy

Congenital diverticulum of the coronary sinus was first described in 1983 by Ho et al. (55) in a 1-year-old child by angiography and in a 23-year-old man with tachycardia and sudden death. Gerlis et al. (56) described two patients who died of malignant arrhythmia associated with posteroseptal accessory atrioventricular pathways. Each had a coronary sinus aneurysm.

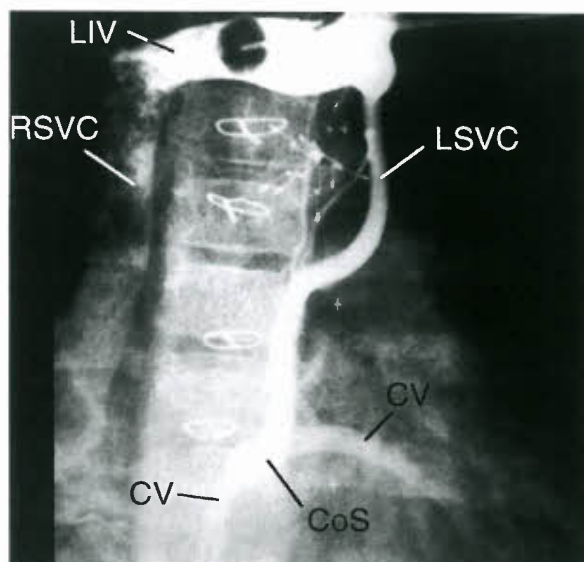


Figure 36.18. Coronary sinus orifice atresia. Selective balloon occlusion angiogram in the left innominate vein (LIV) in an 8-year-old girl with mitral atresia and a large left ventricle. Contrast material fills the innominate vein, left superior vena cava (LSVC), part of the coronary sinus (CoS), and two large cardiac veins (CV). Blood flows in a retrograde direction from the coronary sinus to the LSVC, to the left innominate vein, to the right superior vena cava (RSVC), and, finally, into the right atrium. (Reprinted from Shinpo H, Van Praagh S, Parness I, et al. Mitral atresia with a large left ventricle and an underdeveloped or absent right ventricular sinus: clinical profile, anatomic data and surgical considerations. *J Am Coll Cardiol* 1992;19: 1561–1576, with permission from Elsevier.)

Guiraundon et al. (57) described the entity of coronary sinus diverticulum associated with Wolff-Parkinson-White syndrome in a study of 65 patients with posteroseptal accessory pathways. Intraoperatively, six were found to have coronary sinus diverticula in the posteroseptal region. The coronary sinus diverticulum is a pouch with its neck originating in the coronary sinus proximal to the entrance of the middle cardiac vein. The pouch, 2 to 5 cm in diameter, extends into the left ventricular wall.

Similar coronary sinus diverticula or aneurysms have been observed in children without the presence of Wolff-Parkinson-White syndrome or tachycardia. One case of a 20-month-old girl (58) involved a fistulous connection between the coronary sinus and the left ventricle without any other cardiac defects. Di Segni et al. (59) described a coronary sinus diverticulum that penetrated the right ventricular posterior wall in a newborn with mitral atresia and hypoplastic left heart syndrome. Conduction studies indicated that the accessory pathway is closely associated with the diverticulum and that the conduction abnormality disappears only after separation or ablation of the coronary sinus diverticulum neck.

Diagnostic Features

Coronary sinus diverticulum has been diagnosed by echocardiography (58). The coronary sinus is first imaged from the subcostal, apical, and parasternal windows. The aneurysm is seen as an outpouch, typically with a distinct neck, which extends behind the left ventricle or into the ventricular myocardium. Color Doppler flow mapping is helpful in making the diagnosis and in delineating the connection into the aneurysm by displaying a jet from the coronary sinus (59). Other sites of

connection may be demonstrated with color Doppler. Many of the reported cases, however, have been defined during intra-cardiac electrophysiologic mapping and ablation of supraventricular tachycardia as well as during surgical dissection at the time of operative ablation of the accessory pathway (57).

Treatment

The six patients of Guiraundon et al. (57), four men and two women aged 19 to 67 years, all had surgical treatment of the diverticulum. They also had dissection of the posterior canal region. The coronary sinus was dissected away from the left ventricle and the arteriovenous junction and that site was cryoablated. No postoperative recurrences or complications occurred. The indication for intervention in cases with a coronary sinus aneurysm or diverticulum who do not have associated tachycardia is unclear.

ANOMALIES OF THE INFERIOR VENA CAVA

Interrupted Inferior Vena Cava

Anatomy

Absence of the hepatic segment of the IVC with azygos continuation into the right or left SVC is referred to as an interrupted IVC. In rare cases, the infrahepatic segment of the IVC may continue to both right and left SVC via bilateral azygos veins (Fig. 36.19). Interrupted IVC was reported as an incidental autopsy finding as early as 1793 (60). Although the presence of multiple spleens and abnormalities of the visceral situs were mentioned in the earliest reported cases (1,61–63), their relation to interrupted IVC was not appreciated. It was not until 1967 that Moller et al. (64), studying the anatomic data of 12 cases with visceral heterotaxy and polysplenia, concluded that interrupted IVC represents one of the characteristics of the polysplenia syndrome. Since then, many publications confirmed this association (65). In our study of 46 postmortem cases of visceral heterotaxy with polysplenia, the incidence of interrupted IVC was 86% (1). Although as a rule interrupted IVC occurs in patients with situs abnormalities and congenital heart defects, it also has been reported in patients with normal hearts (66,67) and rarely in patients with asplenia (68).

Clinical Manifestations

Because interrupted IVC with azygos continuation usually does not result in a physiologic abnormality, this venous abnormality does not result in clinical manifestations. Its clinical importance is due to its frequent association with the heterotaxy syndrome and polysplenia. Interrupted IVC with azygos continuation can complicate cardiac catheterization and interventional procedures such as radiofrequency catheter ablation. In patients whose associated cardiovascular anomalies require surgical therapy that involves redirection of the systemic venous return to the pulmonary arteries (bidirectional Glenn and modified Fontan procedures), awareness of the anomaly and appropriate surgical planning are important.

Diagnostic Features

Interruption of the IVC with azygos continuation to the SVC can be diagnosed readily by echocardiography (69,70). The diagnosis is based on imaging of the size, location, and course of the IVC and the azygos vein from the subcostal window. Normally, in the subcostal short-axis view, the renal-to-hepatic segment of the IVC is seen as an oval blood vessel located anterior and to the right of the abdominal aorta. The azygos vein is a much smaller vessel seen beside the vertebral bodies. In patients with heterotaxy syndrome, the IVC may be juxtaposed to the abdominal aorta either to the left or to the right of the spine (26,69). An intact IVC can be seen throughout most or all of its length from the subcostal parasagittal plane. When the renal-to-hepatic segment of the IVC is absent, no IVC is seen below the liver. Care must be taken not to confuse a hepatic vein with the IVC. The azygos vein is enlarged and can be followed cranially until its connection with a SVC (which may be right-sided, left-sided, or there may be bilateral azygos with connections to the left and right SVCs). The drainage of the azygos vein to the SVC also can be imaged from the parasternal and suprasternal windows.

An interrupted IVC with azygos continuation can be diagnosed readily by MRI. In particular, 3-D MRA is accurate and effective in delineating normal and abnormal systemic venous anatomy. During cardiac catheterization, venous angiography from the lower extremity is diagnostic.

Treatment

No specific treatment of an interrupted IVC with azygos continuation is indicated. Inadvertent ligation of the azygos vein can lead to death (66).

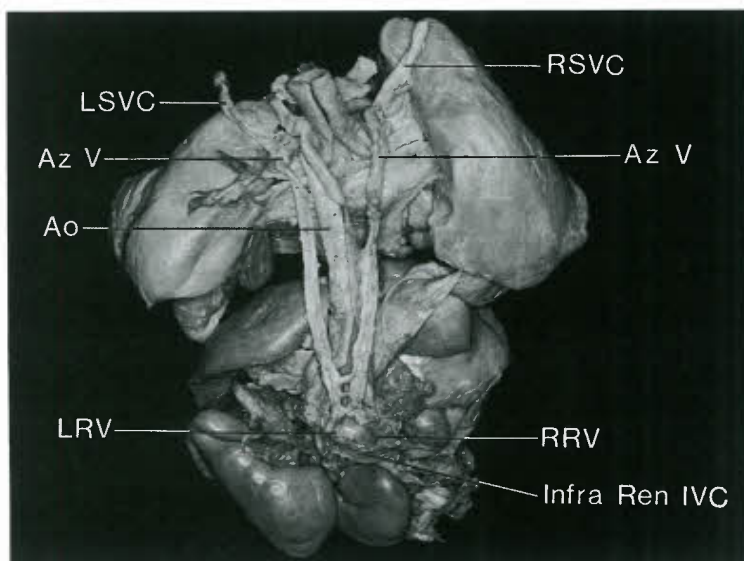


Figure 36.19. Posterior view of the heart, lungs, liver, and kidneys of a 6 1/2-month-old boy with visceral heterotaxy and left-sided polysplenia. There is interruption of the right-sided inferior vena cava (IVC) with bilateral azygos veins (Az V) connecting with bilateral superior venae cavae (RSVC, LSVC). The RSVC entered the right atrium directly. The LSVC continued into the coronary sinus, which drained normally into the right atrium. Ao, aorta; LRV, left renal vein; Ren, renal; RRV, right renal vein. (From Van Praagh S, Santini F, Sanders SPJ. Cardiac malpositions with special emphasis on visceral heterotaxy [asplenia and polysplenia syndromes]. In: Nadas AS, Fyler DC, eds. *Nadas' Pediatric Cardiology*. 4th ed. Philadelphia, PA: Hanley & Belfus, 1992: 589–608, with permission.)

Bilateral Inferior Venae Cavae

Anatomy

The bilateral nature of four of the five venous systems that contribute to the formation of the IVC can easily explain the presence of bilateral IVCs above and below the liver (Fig. 36.5). Bilateral suprahepatic IVCs (i.e., a normal IVC and a contralateral hepatic vein) are a frequent finding in cases of visceral heterotaxy with asplenia. In our study of 109 postmortem cases of visceral heterotaxy, bilateral suprahepatic IVC was present in 28% of the asplenia group and in 6% of the polysplenia group (1). Bilateral suprahepatic IVCs also can occur rarely in patients with normal visceral situs. The left-sided hepatic vein in those cases drains into a normal coronary sinus.

Bilateral infrarenal IVCs, in their entire length or in some of their segments, can occur in patients with normal or abnormal visceral situs and have been described in several reports (71). They do not produce any hemodynamic disturbance. The same is true for the suprahepatic duplication of the IVC if a normal coronary sinus is present.

The bilaterality of four of the five components of the IVC explains the cases where a left-sided IVC may become right-sided at the level of the liver and at its suprahepatic segment. Similarly, a right-sided IVC may become left-sided at the level of the liver and at its suprahepatic segment. The same is true in cases of interrupted IVC.

The existence of an unpaired segment of the IVC (the hepatic segment) does not permit the formation of truly complete bilateral IVC. Nevertheless, in rare cases of absent ductus venosus, it is possible to have two venous channels mimicking bilateral IVCs (Fig. 36.20). In the case described by Lucas and Krabill (52), the right-sided venous channel was the true IVC.

The left-sided venous channel is composed of the left umbilical vein, the left portal vein, and the left hepatic vein, which enter the LA through an unroofed coronary sinus (see section on anomalies of the ductus venosus).

Inferior Vena Cava Drainage to the Left Atrium

Anatomy

During fetal life, about half of the IVC blood that enters the RA is directed toward the LA with the help of two venous valves: the eustachian valve (which is part of the embryonic right venous valve) and the valve of the foramen ovale (i.e., septum primum). The eustachian valve usually involutes by the time of birth and is represented by a ridge a few millimeters high, located between the mouth of the IVC and the tricuspid valve orifice. In some cases, however, for unknown reasons, the eustachian valve may persist with little or no change from its fetal size and attachments. If the foramen ovale is patent or if there is an ostium secundum defect, the IVC blood will continue to drain into both atria. Contrast injected into the IVC will appear into the LA and may create the erroneous impression that the IVC is connected with the LA. This has occurred in several cases reported as "left atrial IVC". (52).

A left atrial IVC also was thought to occur in cases in which all the systemic and all the pulmonary veins drained into a left-sided atrium. Present-day understanding makes it clear that this atrium is a left-sided RA. We now understand that it is impossible for the right horn of the sinus venosus (i.e., the IVC and the SVC) to be incorporated fully into the morphologically left atrium. By contrast, it is not unusual in patients with visceral heterotaxy and absence of septum secundum, for

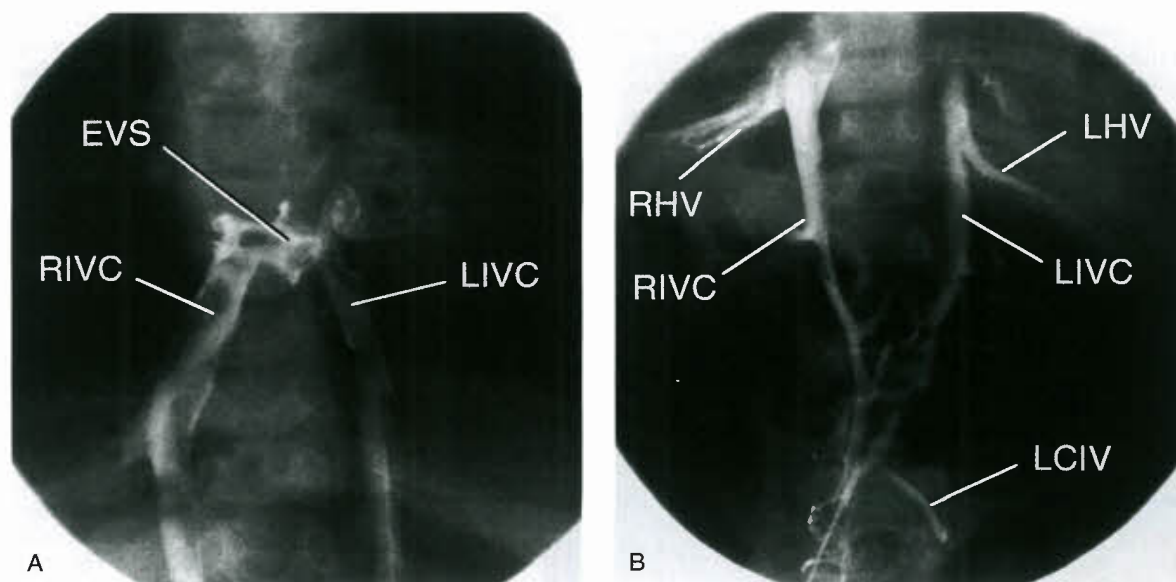


Figure 36.20. Anteroposterior venogram in a 15-month-old boy with visceral heterotaxy, asplenia, bilateral IVCs, bilateral SVCs, common atrium, common atrioventricular septal defect, d-transposed aorta, and pulmonary atresia. **A:** Frame showing the cardiac end of the systemic venous return from the lower part of the body. **B:** Frame showing the inferior part of the systemic veins. Contrast material injected into the right iliac vein filled two venous pathways. The right-sided pathway represents a right-sided inferior vena cava (RIVC), which receives the right hepatic vein (RHV) and then enters the right side of the common atrium. The left venous channel appears to represent a left-sided IVC (LIVC), which connects with the left hepatic vein (LHV) and then joins the RIVC and drains into the common atrium via a common orifice. The two venous pathways connect by way of an extracardiac venous sinus (EVS) just before their entry into the common atrium. We think this case represents a rare variation of the venous pathways observed in cases of visceral heterotaxy. The right renal vein drained into the RIVC, and the left renal vein drained into the LIVC (not shown). LCIV, left common iliac vein. (This angiogram was kindly provided by Dr. John Murphy, duPont Hospital for Children, Wilmington, DE.)

half or all of the pulmonary veins to drain into the morphologically right atrium, which may be right- or left-sided (72). These well-documented possibilities can explain the reported cases of left atrial IVC except for the case reported by Gardner and Cole in 1955 (73).

This case concerned a woman who “at the age of 4 years had pneumonia and was subsequently noticed to be cyanosed.” She had a succession of three miscarriages, but at the age of 24 years she gave birth to a full-term normal infant. “She led a comparatively active life until the age of 32 years. Then one day while stretching up to a high shelf she collapsed suddenly and died.” According to the report by Gardner and Cole, postmortem examination of the heart revealed a normal coronary sinus and an intact atrial septum. The IVC was thought to drain directly into the LA. If the postmortem findings were correct, this case would defy what is known about the development of the atria, the sinus venosus, and the systemic veins of the human heart. We thought that, if possible, it was essential to reexamine this heart specimen, and this became possible thanks to the kindness and cooperation of Dr. Gardner, now professor of pathology in Edinburgh, Scotland.

Reexamination of this heart specimen revealed that a large segment of the posterior wall of the RA was missing. Consequently, no remnant of the IVC itself connecting with the RA could be found. Nevertheless, a small eustachian valve (right venous valve remnant) and a left venous valve with multiple fenestrations were easily identified (Fig. 36.21). The posteroinferior wall of the LA was also missing as a result of a postmortem artifact that was produced when the heart was removed from the chest by the prosector. This incision was made too high, above the IVC, removing a portion of the posteroinferior walls of both the right and left atria (Fig. 36.21). The defect in the left atrial wall was approximated by a stitch postero-

inferiorly, which inadvertently changed this defect into an approximately circular orifice thought to represent the orifice of the IVC. On reexamination, however, it was noted that the margins of this putative left atrial IVC consisted not of thin venous tissue, consistent with the wall of the IVC. Instead, it consisted of the left atrial myocardium, 3 mm in thickness, that lay outside of an approximately 1-mm-thick layer of fibrous tissue representing the left atrial endocardium (Fig. 36.21). Examination of the pulmonary histology by Dr. Reid revealed “large size and increased density of the arteries and veins consistent with the presence of arteriovenous communications sufficiently big or numerous to produce the effect of arterial-to-venous shunting.” Hence the cyanosis of the patient was explained with the histologic findings of the lungs.

This extraordinary case quoted repeatedly in the literature of the last 44 years was the result of an unintended misinterpretation of the anatomic findings of a heart specimen not examined in situ but brought to Professor Gardner’s attention “as a Coroner’s autopsy.” According to Professor Gardner, “diagrams were made much later. They were of the heart only.” “You have to recognize,” he wrote to us, “that the diagnosis of an IVC anomaly was not made at the time of the autopsy but only after subsequent examination of the heart.” Hence, we can now conclude that there has not been a documented case of the IVC connecting directly with the LA. The present knowledge of the embryology and possible connections of the IVC remains unchallenged.

Clinical Manifestations

Partial or complete drainage of the IVC into the LA results in cyanosis. The clinical manifestations are the result of right-to-left shunting, including polycythemia, brain abscess, and paradoxical emboli.

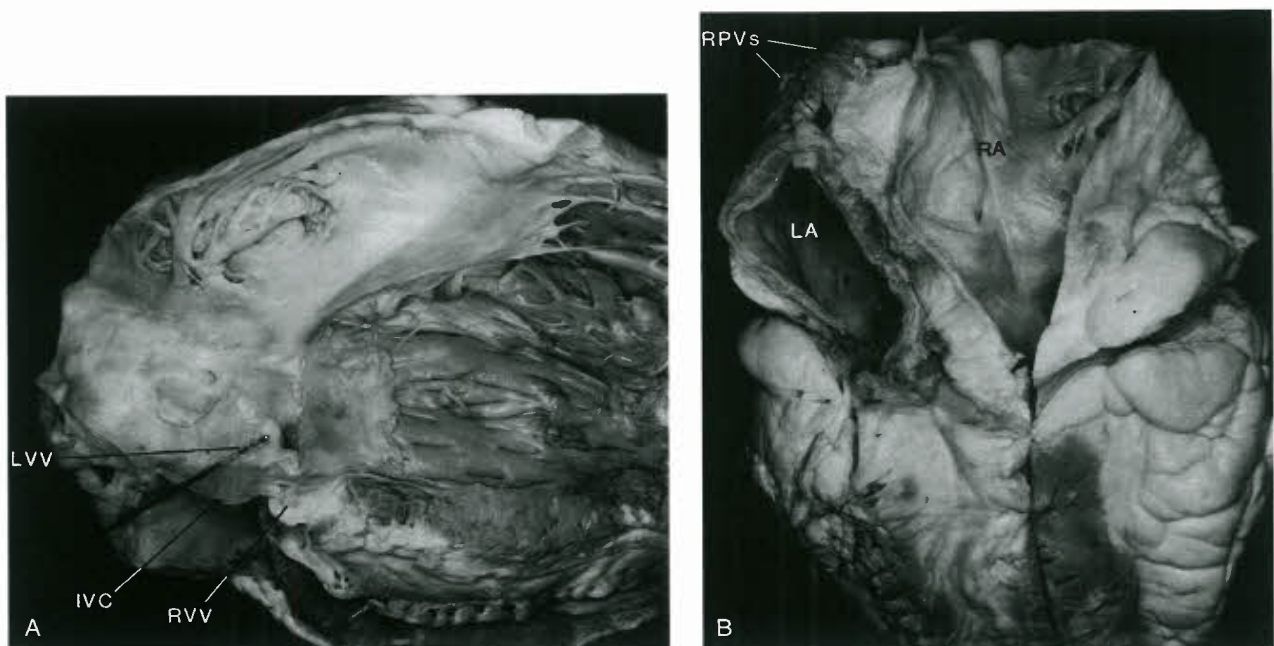


Figure 36.21. A: Opened right atrium and right ventricle of a 32-year-old woman. There is a small remnant of the right venous valve (RVV) separating the eustachian valve and a multiperforated remnant of the left venous valve (LVV). Between these two venous valves is the entry of the transected inferior vena cava (IVC). B: The posterior view of the atria and part of the ventricles of the same heart. Part of the posterior wall of the right atrium (RA) and of the left atrium (LA) has been transected by the prosector during the removal of the heart from the thoracic cavity. Note the thickness of the transected posterior wall of the left atrium. RPVs, right pulmonary veins. (These photographs were obtained with the kind permission of Professor D. L. Gardner.)

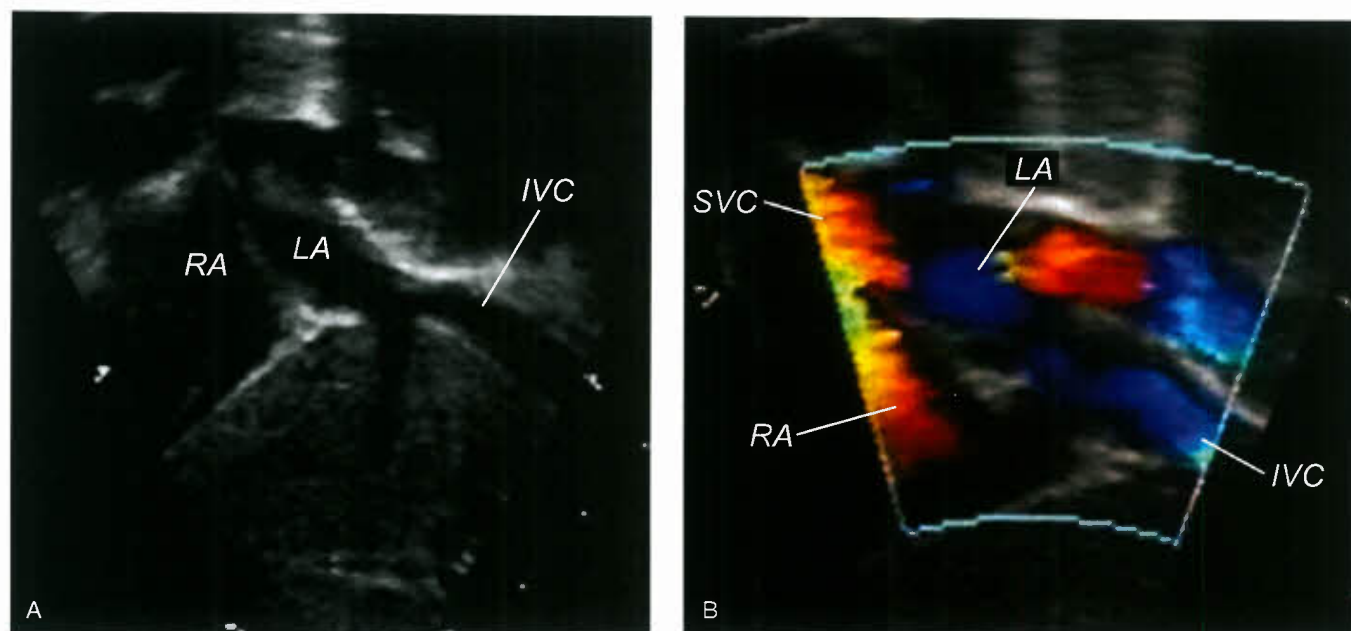


Figure 36.22. Echocardiogram in a 7-year-old boy with cyanosis. **A:** Subcostal short-axis image showing drainage of the inferior vena cava (IVC) to the left atrium (LA). **B:** Color Doppler flow mapping confirms flow from the inferior vena cava (IVC) to the left atrium (LA) and from the superior vena cava (SVC) to the right atrium (RA). At surgery, the atrial septum was resected, and an autologous pericardial patch was placed to the left of the inferior vena cava, thus incorporating it into the right atrium.

Diagnosis

The diagnosis can be established by echocardiography (Fig. 36.22), cardiac MRI, computed tomography, or cardiac catheterization.

Treatment

IVC blood is surgically redirected into the RA (74,75).

ANOMALIES OF THE DUCTUS VENOSUS

Anomalous Termination of the Umbilical Veins and Absent Ductus Venosus

Anatomic descriptions of abnormal termination of umbilical veins with absence of ductus venosus are rare. Recently, abnormal termination of umbilical veins and absence of ductus venosus were recognized clinically during umbilical vein cannulation of the newborn, during cardiac catheterization and angiography, during fetal or postnatal echocardiography, and at operation. Many of these clinical observations have been confirmed at autopsy. Usually, the absence of the ductus venosus and abnormal termination of the umbilical veins do not produce symptoms; however, two cases of intrauterine obstruction of the umbilical vein flow and three patients who required operation for postnatal intestinal obstructions secondary to the anomalous termination of the umbilical veins have been reported (76–80). The major clinical importance of these anomalies is the need to recognize them during prenatal and postnatal diagnostic studies and at the time of cannulation or catheterization of the umbilical vein in sick neonates.

Anatomy

Lucas and Krabill (52) reported autopsy findings of four specimens in the Jesse Edwards Registry of Cardiovascular

Pathology as well as 18 cases reviewed in the literature. The ductus venosus was confirmed to be absent in 18 of these 23 cases and presumed to be absent in the remainder.

The left umbilical vein persisted in five patients, terminating directly into the coronary sinus in one (Fig. 36.23A), into the coronary sinus by way of the left portal vein in two patients (Fig. 36.23B), and into the iliac vein in two. In our case shown in Figure 36.20, the left umbilical vein connected with the left common iliac vein. The right umbilical vein persisted in 11 patients and terminated directly into the RA in five (Fig. 36.23C), into the IVC in two (Fig. 36.23D), into the right portal vein in two, and into the RSVC in one.

Both the right and left umbilical veins persisted in three patients. In the first, the umbilical veins entered the right and left iliac veins, respectively; in the second, into the right and left portal veins, respectively; and in the third, the right umbilical vein entered the RA, and the left umbilical vein entered the left portal vein.

In four patients, the persisting umbilical vein could not be identified as either right or left. In three of these, the umbilical vein terminated into a right or left iliac vein, and in the fourth it communicated with the portal vein.

Clinical Manifestations

Of the 23 collected cases, 10 patients were male, 10 were female, and in 3 the gender was unknown or ambiguous. Only four patients had clinical evidence of abnormal physiology as a result of the abnormal termination of the umbilical vein; one had anatomic evidence of severe intrauterine obstruction of umbilical vein flow (77). Intestinal obstruction requiring surgical intervention was present as a result of the anomalous termination of the umbilical vein in three patients (78–80). These were females of ages 13 days, 27 years, and 31 years at the time of operation.

The number of umbilical arteries was identified in 16 patients; one umbilical artery was present in nine patients, two in the remainder. Thirteen of the twenty-three patients had

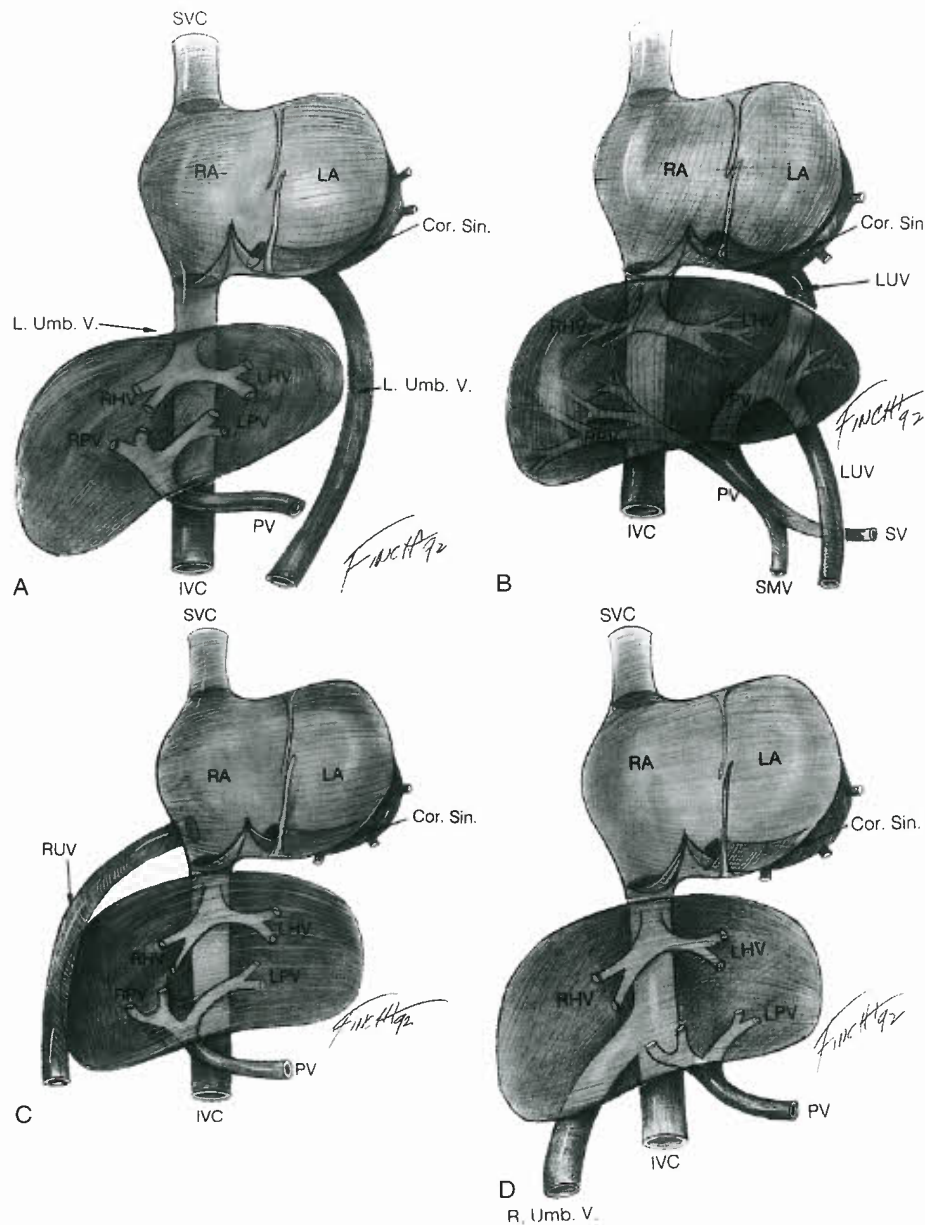


Figure 36.23. Diagram of absent ductus venosus and anomalous termination of an umbilical vein. **A:** Left umbilical vein (L. Umb. V.) terminates in coronary sinus (Cor. Sin.). **B:** Left umbilical vein (LUV) connects to left portal vein (LPV) and then continues to termination in coronary sinus. **C:** right umbilical vein (RUV) terminates in right atrium (RA). **D:** Right umbilical vein (R. Umb. V.) terminates in inferior vena cava (IVC). (LA, left atrium; LHV, left hepatic vein; LPV, left portal veins; PV, portal veins; RHV, right hepatic vein; RPV, right portal veins; SMV, superior mesenteric vein; SV, splenic vein; SVC, superior vena cava.)

no additional cardiac anomalies. Of the 10 patients with associated cardiac anomalies, two had tetralogy of Fallot, two had ectopia cordis, two had total anomalous pulmonary venous connections, and one each atrioventricular canal defect, mitral valve atresia, parachute mitral valve, and hypertrophic cardiomyopathy.

Diagnostic Features

Definitive anatomic diagnosis was accomplished by the following methods: catheterization of the umbilical vein, dye injection plus local surgical dissection of the umbilical vein, car-

diac catheterization, cardiac catheterization plus angiography, prenatal echocardiography, postnatal echocardiography, and at the time of operation for intestinal obstruction.

The major clinical importance of these cases is the potential for confusion and misinterpretation during catheterization of the umbilical vein in the neonate or abnormal course of the catheter in newborns undergoing cardiac catheterization by way of the umbilical vein; however, the increasing use of fetal echocardiography as well as echocardiography early in the postnatal period makes the noninvasive recognition of these anomalies of termination of the umbilical veins possible.

Postnatal Persistence of the Ductus Venosus

Horiguchi et al. (81) reported four cases of intrahepatic portosystemic shunt and reviewed six other cases from the literature.

Anatomy

These cases may have been congenital postnatal persistence of the ductus venosus because the shunt was away from the portal venous septum proximally to the distal hepatic veins or IVC distally. These intrahepatic portosystemic shunts are due to abnormal persistence of elements of the omphalomesenteric system (Fig. 36.4).

Clinical Manifestations

Three of the ten cases reported (82) resulted in portal-systemic encephalopathy. Hepatic function and liver histology were normal in some patients.

Diagnosis

Ultrasound or computed tomography delineated the diagnosis in most cases by demonstrating a large tortuous vessel originating from the portal vein that connected to the hepatic vein or IVC (82,83).

Treatment

We are not aware of successful treatment of the abnormality. In the absence of encephalopathy, treatment may not be indicated. If ligation of the ductus venosus is contemplated, one should establish the integrity of the portal system. If it is not intact, ligation could lead to mesenteric venous congestion and ultimately bowel ischemia.

PERSISTENT VALVES OF THE SINUS VENOSUS

This section is based on the excellent description of Lucas and Krabill (52). In the normal heart, remnants of the valves of the sinus venosus are the eustachian and thebesian valves and crista terminalis. Minor abnormal persistence of the valves of the sinus venosus results in larger-than-usual eustachian and thebesian valves and in Chiari networks. The latter are fine, filamentous structures that may represent persistence of either the right or left valves. Usually, Chiari networks are persistent right valves and extend from the crista terminalis to eustachian or thebesian valves. Networks derived from the left valves are inconspicuously located at the posterior rim of the limbus fossa ovalis and on the medial wall of the IVC as it enters the RA. None of these is of hemodynamic consequence.

In past years, pathologic persistence of the right valve of the sinus venosus was an anatomic phenomenon occasionally observed at autopsy. Recent developments in noninvasive imaging have resulted in clinical recognition of numerous instances of persistence of the right valve of the sinus venosus.

At one point in embryologic development, the right valve of the sinus venosus almost completely divides the RA into the sinus venosus portion and the muscular portion, and so abnormal persistence of the right valve may result in obstruction of blood flow into the RA or through the RA.

Cardiac anomalies attributable to maldevelopment of the right valve of the sinus venosus have been identified by various terms, including cor triatriatum dextrum, right atrial flap, right atrial spinnaker, right atrial sail, right atrial windsock, persistent eustachian valve, persistent thebesian valve, IVC connecting to LA, atresia of the right atrial ostium of the coronary sinus, supra-avalvular tricuspid stenosis, tricuspid

valve "stopper," IVC obstruction, and others. Knowledge of normal fetal development of the sinoatrial valves is helpful in understanding these cardiac derangements.

Persistence of the right sinus venosus valve has been seen in isolation and in association with hypoplastic right heart syndrome and ventriculocoronary artery communications (84), Ebstein malformation (85), and tricuspid atresia (86).

Embryology of the Valves of the Sinus Venosus

In the 3-week-old (4 mm) human embryo, the sinus venosus is external to the primitive RA. The right horn of the sinus venosus receives the hepatic vein (precursor to the IVC) and the anterior cardinal vein (precursor to the superior vena cava). The left horn of the sinus venosus is the embryologic precursor of the coronary sinus.

The right and left valves of the sinus venosus separate the sinus venosus from the primitive RA. The sinus venosus septum has already formed and joins the right and left valves of the sinus venosus (87).

In the 4-week-old (6 mm) human embryo, the septum primum appears and begins to septate the common atrium. At this stage, the opening of the sinus venosus into the common atrium is well guarded by the right and left valves of the sinus venosus (88).

In the 5- to 6-week-old (9 mm) human embryo, the sinus venosus has been absorbed into the common atrium. The right and left valves of the sinus venosus join cranially to form the septum spurium (23), which maintains the valves in a state of tension but plays no role in further embryogenesis. The septum secundum has begun to divide the common atrium from posterosuperior to anteroinferior. In subsequent embryologic development, the left valve of the sinus venosus retrogresses and is absorbed into the limbus region of the septum secundum. The right valve of the sinus venosus begins to enlarge.

By the time the human embryo reaches 3 months' gestation (36 mm), the right valve of the sinus venosus almost completely divides the RA into the sinus portion (sinus venosus) receiving the SVC, IVC, coronary sinus, and foramen ovale, and the muscular portion of the RA communicating with the tricuspid valve and the RAA (89).

At this point in embryologic development, the right valve of the sinus venosus almost completely segregates all systemic venous blood exiting the SVC, IVC, and coronary sinus from the tricuspid valve and tends to shunt it into the LA. One can predict the physiologic abnormalities of blood flow that might occur if there is partial or complete persistence of the right valve of the sinus venosus (Fig. 36.24).

In the great majority of humans, the right valve of the sinus venosus almost completely regresses by the time of birth. The remnant of the right valve of the sinus venosus where it separated the RA into two portions persists as the crista terminalis. In the normal human heart, the crista terminalis separates the anterior, muscular portion of the RA from the posterior, sinus venosus, or sinus portion of the RA. The superior portion of the right valve of the sinus venosus plus a portion of the sinus venosus septum persists as the eustachian valve guarding the inferior vena caval orifice. The inferior portion of the right valve of the sinus venosus plus a portion of the sinus venosus septum persists as the thebesian valve guarding the orifice of the coronary sinus (Fig. 36.24) (87).

Right Ventricular Outflow Tract Obstruction

This defect has been identified at echocardiography (90), on angiography (91), at operation, and at postmortem (92). By any of these methods, it appears as a windsock, parachute,

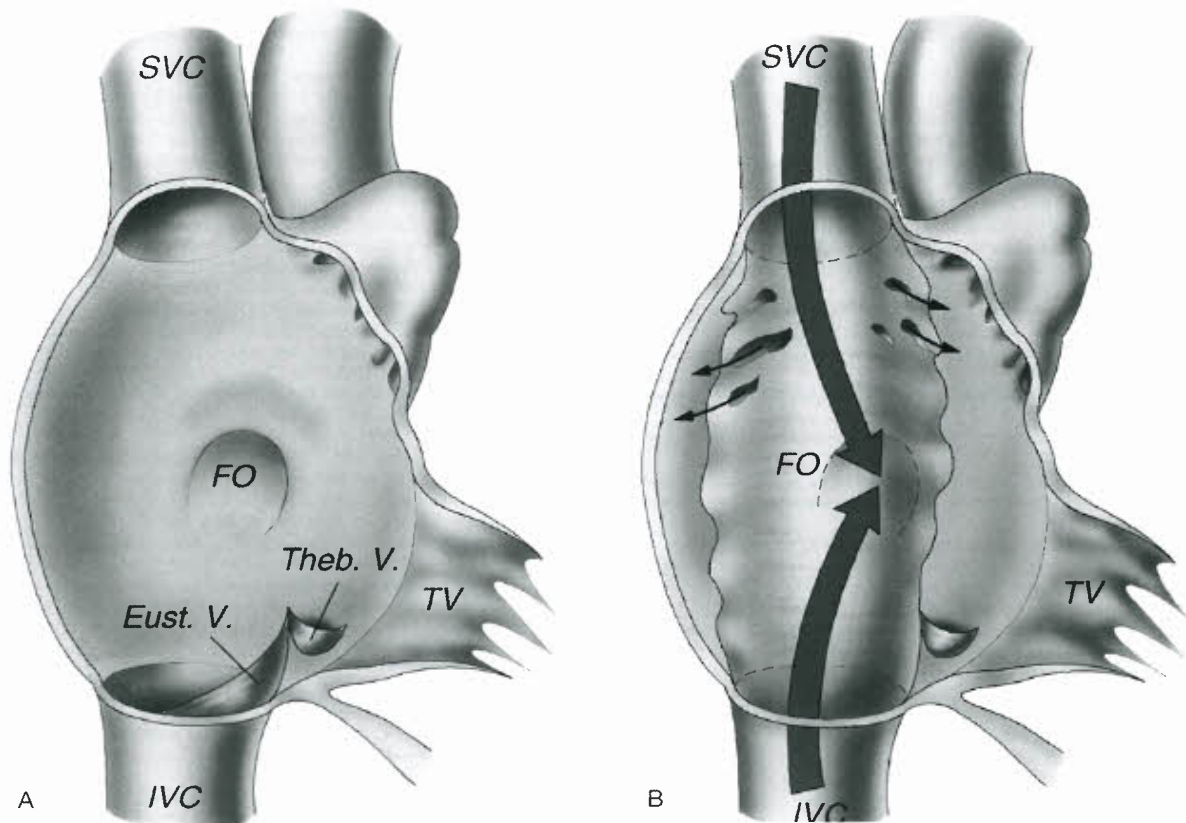


Figure 36.24. A: Diagram showing the normal appearance of the remnants of the right venous valve in the right atrium. The eustachian valve (Eust. V.) is seen at the entrance of the inferior vena cava (IVC) into the right atrium. The thebesian valve (Theb. V.) is seen at the right atrial orifice of the coronary sinus. B: Persistence of the embryonic right venous valve leads to diversion of the entire systemic venous return into the left atrium through the foramen ovale (FO). Multiple fenestrations of varying extent and size are often present (Chiari network) and allow some systemic venous blood to flow into the right ventricle through the tricuspid valve (TV). SVC, superior vena cava.

or spinnaker-like sack that originates in the RA and traverses the tricuspid valve, right ventricle, and pulmonary valve to obstruct either partially or nearly completely the blood flow to the pulmonary artery. On echocardiography, it can be imaged as a thin, mobile, linear structure originating in the RA and traversing the tricuspid valve to obstruct pulmonary flow.

Failure to recognize the nature of the windsock obstructing the pulmonary artery at operation can lead to death (92). On the other hand, successful resection of the pulmonary artery windsock results in return of normal physiology (90,91).

Tricuspid Valve Obstruction

This is a relatively more common anatomic abnormality. Lucas and Krabill (52) reviewed five autopsied cases from the material in the Jesse Edwards Registry of Cardiovascular Pathology and added five well-described cases from the literature.

Anatomy

Typically, in these cases, the orifice of the tricuspid valve is nearly occluded by a “windsock” or “stopper.” The windsock appears to be persistence of the right valve of the sinus venosus.

Associated Cardiac Anomalies

These 10 cases included four males and six females with an age range of newborn to 58 years. All cases had a patent foramen ovale or ASD. Two had significant associated congenital cardiac defects, one had D-transposition of the great vessels, and the other had L-loop (congenitally corrected) transposition of the great vessels, Ebstein anomaly of the left-sided tricuspid valve, and heart block. Two other cases had hemodynamically insignificant VSDs.

Clinical Features

Nine of these ten patients were cyanotic, and seven had significant right-sided heart failure. Echocardiographic imaging from a high right parasternal longitudinal view demonstrated an echo-reflective linear structure anchored to the RA near the IVC at one end and near the foramen ovale at the other side (93). A four-chamber view of the heart demonstrated a linear, mobile, echo-reflective structure moving toward the tricuspid valve in diastole and toward the posterior right atrial wall in systole.

Treatment

Operative resection of the windsock and closure of the ASD were attempted in four patients. All four survived and had no symptoms and normal physiology postoperatively (94).

REFERENCES

- Van Praagh S, Santini F, Sanders SP. Cardiac malpositions with special emphasis on visceral heterotaxy (asplenia and polysplenia syndromes). In: Nadas AS, Fyler DC, eds. *Nadas' Pediatric Cardiology*. 4th ed. Philadelphia, PA: Hanley & Belfus, 1992:589–608.
- Van Mierop LHS, Gessner IH, Schiebler GL. Asplenia and polysplenia syndromes. *Birth Defects* 1972;8:36–44.
- Van Mierop LHS. Morphologic development of the heart. In: Berne RN, ed. *Handbook of Physiology*. Baltimore, MD: Williams & Wilkins, 1979:1–28.
- Streeter GL. Developmental horizons in human embryos: description of age group XI, 13 to 20 somites, and age group XXII, 21 to 29 somites. *Carnegie Inst Contrib Embryol* 1942;30:211–245.
- Marshall J. On the development of the great anterior veins in man and mammalia. *Philos Trans R Soc Lond* 1850;140:133–170.
- Patten BM. *Human Embryology*. 2nd ed. New York, NY: McGraw-Hill, 1953:637–681.
- Gray H. *Anatomy: Descriptive and Surgical*. New York, NY: Bounty Books, 1977:611–612.
- McCotter RE. Three cases of persistent left superior vena cava. *Anat Rec* 1916;10:371–383.
- Meadows WR, Sharp JT. Persistent left superior vena cava draining into the left atrium without arterial oxygen unsaturation. *Am J Cardiol* 1965;16:273–279.
- Sanders JM. Bilateral superior vena cava. *Anat Rec* 1946;94:657–662.
- Geissler W, Albert M. Persistent left superior vena cava and mitral stenosis [in German]. *Z Gesamte Inn Med* 1956;11:865–874.
- DeLeval MR, Ritter DG, McGoon DC, et al. Anomalous systemic venous connection—surgical considerations. *Mayo Clinic Proc* 1975;50:599–610.
- Nash EN, Moore GW, Hutchins GM. Pathogenesis of persistent left superior vena cava with coronary sinus connection. *Pediatr Pathol* 1991;11:261–269.
- Van Praagh S, O'Sullivan J, Brili S, et al. Juxtaposition of the morphologically right atrial appendage in solitus and inversus atria: a study of 35 postmortem cases. *Am Heart J* 1996;132:382–390.
- Winter FS. Persistent left superior vena cava: survey of world literature and report of thirty additional cases. *Angiology* 1954;5:90–132.
- Hardey DW, White MS, Malloy KP, et al. Persistent left superior vena cava: review of embryologic anatomy and considerations for cardiopulmonary bypass. *Tex Heart Inst J* 1980;7:433–441.
- Cochrane AD, Menahem S, Mee RBB. Divided left atrium with absence of the interatrial septum in monozygotic twins. *Cardiol Young* 1993;3:51–54.
- Byerregaard P, Laursen HB. Persistent left superior vena cava. *Acta Paediatr Scand* 1980;69:105–108.
- Sanders SP. Echocardiography and related techniques in the diagnosis of congenital heart disease. I. Veins, atria and interatrial septum. *Echocardiography* 1984;1:185–217.
- Huhta JC, Smallhorn JF, Macartney FJ. Cross-sectional echocardiographic diagnosis of systemic venous return. *Br Heart J* 1982;48:388–403.
- Bernstein HS, Moore P, Stanger P, et al. The levoatrialcardinal vein: morphologic and echocardiographic identification of the pulmonary-systemic connection. *J Am Coll Cardiol* 1995;26:995–1001.
- Lucas RV Jr, Lester RG, Lillehei CW, et al. Mitral atresia with levoatrial cardinal vein: a form of congenital pulmonary venous obstruction. *Am J Cardiol* 1964;2:607–613.
- Raghib G, Ruttenbert HD, Anderson RC, et al. Termination of left superior vena cava in left atrium, atrial septal defect, and absence of coronary sinus: a developmental complex. *Circulation* 1965;31:906–918.
- Davis WH, Jordaan FR, Snyman HW. Persistent left superior vena cava draining into the left atrium as an isolated anomaly. *Am Heart J* 1959;57:616–622.
- Edwards JE. Malformation of the atrial septal complex. In: Gould SE, ed. *Pathology of the Heart*. Springfield, IL: Charles C. Thomas Publisher, 1960:260–293.
- Geva T. Echocardiography and Doppler ultrasound. In: Garson A Jr, Bricker JT, Fisher DJ, et al., eds. *The Science and Practice of Pediatric Cardiology*. Baltimore, MD: Williams & Wilkins, 1997:789–843.
- Castaneda AR, Jonas RA, Mayer JE Jr, et al. *Cardiac Surgery of the Neonate and Infant*. Philadelphia, PA: WB Saunders, 1994:152–153.
- Irllich TN, Herzer JA, Schulte HD, et al. Left persisting, singular superior vena cava and pacemaker electrode implantation by right cephalic vein [in German]. *Z Kardiol* 1976;65:575–582.
- Lenox CC, Zuberhuhler JR, Park SC, et al. Absent right superior vena cava with persistent left superior vena cava: implications and management. *Am J Cardiol* 1980;45:117–122.
- Bartram U, Van Praagh S, Levine JC, et al. Absent right superior vena cava in viscerotransposition situs solitus. *Am J Cardiol* 1997;80:175–183.
- Van Praagh S, Geva T, Lock JE, et al. Biatial or left atrial drainage of the right superior vena cava: anatomic, morphogenetic, and surgical considerations report of three new cases and literature review. *Pediatr Cardiol* 2003;24:350–363.
- Shapiro EP, Al-Sadir J, Campbell NPS, et al. Drainage of the right superior vena cava into both atria. *Circulation* 1981;63:712–717.
- Wood P. *Diseases of the Heart and Circulation*. 2nd ed. London: Eyre and Spottiswood, 1957:457–458.
- Alday LE, Maisuls H, De Rossi R. Right superior caval vein draining into the left atrium—diagnosis by color flow mapping. *Cardiol Young* 1995;5:345–349.
- Akalin H, Uysalel A, Ozyurda U, et al. The triad of persistent left superior vena cava connected to the coronary sinus, right superior vena cava draining into the left atrium, and atrial septal defect: report of a successful operation for a rare anomaly. *J Thorac Cardiovasc Surg* 1987;94:151–153.
- Chin AJ. Subcostal two-dimensional echocardiographic identification of right superior vena cava connecting to left atrium. *Am Heart J* 1994;127:939–941.
- Van Praagh S, Carrera ME, Sanders SP, et al. Sinus venosus defects: unroofing of the right pulmonary veins—anatomic and echocardiographic findings and surgical treatment. *Am Heart J* 1994;128:365–379.
- Hackensellner H. Abnormal drainage of the pulmonary vein into the superior vena cava. *Virchows Arch* 1955;327:603–606.
- Vasquez-Perez J, Frontera-Izquierdo P. Anomalous drainage of the right superior vena cava into the left atrium as an isolated anomaly. Rare case report. *Am Heart J* 1979;97:89–91.
- Ezekowitz MD, Alderson PO, Bulkley BH, et al. Isolated drainage of the superior vena cava into the left atrium in a 52-year-old man. *Circulation* 1978;58:751–756.
- Braudo M, Beanlands DS, Trusler G. Anomalous drainage of the right superior vena cava into the left atrium. *Can Med Assoc* 1968;99:715–719.
- Nazem A, Sell JE. Closed technique for repair of right superior vena cava draining to left atrium. *Ann Thorac Surg* 1993;55:1568–1570.
- Kershner L. Zur Morphologie der Vena Cava Inferior. *Anat Anz* 1888;3:808–823. (Cited in Gerlis LM, Ho SY. Anomalous subaortic position of the brachiocephalic (innominate) vein: a review of published reports and report of three new cases. *Br Heart J* 1989;61:540–545.)
- Choi JY, Jung MJ, Kim YH, et al. Anomalous subaortic position of the brachiocephalic vein (innominate vein): an echocardiographic study. *Br Heart J* 1990;64:385–387.
- Smallhorn JF, Zielinsky P, Freedom RM, et al. Abnormal position of the brachiocephalic vein. *Am J Cardiol* 1985;55:234–236.
- Gerlis LM, Ho SY. Anomalous subaortic position of the brachiocephalic (innominate) vein: a review of published reports and report of three new cases. *Br Heart J* 1989;61:540–545.
- Kitamura S, Sakai A, Nishiguchi T. A case of the left innominate vein passing behind the ascending aorta. *Anat Rec* 1981;201:567–572.
- Freedom RM, Culham JAG, Rowe RD. Left atrial to coronary sinus fenestration (partially unroofed coronary sinus): morphologic and angiographic observations. *Br Heart J* 1981;46:63–68.
- Sanders SP. Anomalous hepatic venous connection to the coronary sinus diagnosed by two-dimensional echocardiography. *Am J Cardiol* 1984;54:458–459.
- Kadletz M, Black MD, Smallhorn J, et al. Total anomalous systemic venous drainage to the coronary sinus in association with hypoplastic left heart disease: more than a mere coincidence. *J Thorac Cardiovasc Surg* 1997;114:282–284.
- Prows MS. Two cases of bilateral superior vena cava, one draining a closed coronary sinus. *Anat Rec* 1943;87:99–106.
- Lucas RV Jr, Krabill KA. Abnormal systemic venous connections. In: Emmanouilides GC, Reimenschneider TA, Allen HD, eds. *Heart Disease in Infants, Children, and Adolescents*. 5th ed. Baltimore, MD: Williams & Wilkins, 1995:874–902.
- Yokoto M, Kyota I, Kitano M, et al. Atresia of the coronary sinus orifice: fatal outcome after intraoperative division of the drainage left superior vena cava. *J Thorac Cardiovasc Surg* 1980;98:30–32.
- Yeager SD, Balian AA, Gustafson RA, et al. Angiographic diagnosis of coronary sinus ostium atresia. *Am J Cardiol* 1985;56:996.
- Ho SY, Gupta I, Anderson RH, et al. Aneurysm of the coronary sinus. *Thorax* 1983;38:686–689.
- Gerlis LM, Davies MJ, Boyle R, et al. Pre-excitation due to accessory sinoventricular connexions associated with coronary sinus aneurysm. A report of two cases. *Br Heart J* 1985;53:314–322.
- Guiraundon GM, Guiraundon CM, Klein GJ, et al. The coronary sinus diverticulum: a pathologic entity associated with the Wolff-Parkinson-White syndrome. *Am J Cardiol* 1988;62:733–735.
- Gnanapragasam JP, Houston AB, Lilley S. Congenital fistula between left ventricle and coronary sinus: elucidation by colour Doppler flow mapping. *Br Heart J* 1989;62:406–408.
- Di Segni E, Seigel A, Katzenstein M. Congenital diverticulum of the heart arising from the coronary sinus. *Br Heart J* 1986;56:380–384.
- Abernathy J. Account of two instances of uncommon formations in the viscera of the human body. *Philos Trans R Soc Lond B Biol Sci* 1793;83:59–66.
- Griffith TW. A case of transposition of the thoracic and abdominal viscera with congenital malformation of the heart and certain abnormalities of the arterial and venous systems. *J Anat Physiol* 1892;26:117–129.
- Carpentier C, Bertaux A. Anomalie des systemes de la veine cave inferieure et des veines azgos. *Arch Physiol Norm Pathol* 1888;20:79–89.
- Dwight T. Absence of the inferior vena cava below the diaphragm. *J Anat Physiol* 1901;35:7–21.
- Moller JH, Nakib A, Anderson RC, et al. Congenital cardiac disease associated with polysplenia: a developmental complex of bilateral “left-sidedness.” *Circulation* 1967;36:789–799.

65. Van Praagh S, Kreutzer J, Alday L, et al. Systemic and pulmonary venous connections in visceral heterotaxy, with emphasis on the diagnosis of the atrial situs: a study of 109 postmortem cases. In: Clark EB, Takao A, eds. *Developmental Cardiology: Morphogenesis and Function*. Mt Kisco, NY: Futura Publishing, 1990:671–727.
66. Effler DB, Greer AE, Sifers AE. Anomaly of the vena cava inferior: report of fatality after ligation. *JAMA* 1951;146:1321–1323.
67. Latimer HB, Virden HH. A case of complete absence of the inferior vena cava. *J Kansas Med Soc* 1944;45:346–353.
68. Ruscazio M, Van Praagh S, Marras AR, et al. Interrupted inferior vena cava in asplenia syndrome and a review of the hereditary patterns of visceral situs abnormalities. *Am J Cardiol* 1998;81:111–116.
69. Huhta JC, Smallhorn JF, Macartney FJ. Cross sectional echocardiographic diagnosis of azygous continuation of the inferior vena cava. *Cathet Cardiovasc Diagn* 1984;10:221–232.
70. Garris JB, Kangaroo H, Sample WF. Ultrasonic diagnosis of infrahepatic interruption of the inferior vena cava with azygous (hemiazzygous) continuation. *Radiology* 1980;134:179–183.
71. Gladstone RJ. Development of the inferior vena cava in the light of recent research, with special reference to certain abnormalities, and current description of the ascending lumbar and azygos veins. *J Anat* 1929;64:70–93.
72. Van Praagh S, Carrera ME, Sanders SP, et al. Partial or total direct pulmonary venous drainage to right atrium due to malposition of septum primum. *Chest* 1995;107:1488–1498.
73. Gardner DL, Cole L. Long survival with inferior vena cava draining into left atrium. *Br Heart J* 1955;17:93–97.
74. Licata RH. The human embryonic heart in the ninth week. *Am J Anat* 1954;94:73–125.
75. Yater WM. Variations and anomalies of the venous valves of the right atrium of the human heart. *Arch Pathol* 1929;7:418–441.
76. White JJ, Brenner H, Avery ME. Umbilical vein collateral circulation: the caput medusae in a newborn infant. *Pediatrics* 1969;43:391–395.
77. MacMahon HE. The congenital absence of the ductus venosus: report of a case. *Lab Invest* 1960;9:127–131.
78. Hoffert PW, Strackman J. Intestinal obstruction due to an aberrant umbilical vein and hypertrophic pyloric stenosis in a 2 week old infant. *Bull NY Acad Med* 1960;36:475–477.
79. Prust FW, Eskandari F. Intestinal obstruction due to an aberrant umbilical vein: a case report. *Ann Surg* 1967;165:464–465.
80. Svendsen LB, Johansen TS, Kristensen P. Intestinal obstruction caused by an aberrant umbilical vein. *Acta Chir Scand* 1977;143:191–192.
81. Horiguchi Y, Kitano T, Imai H, et al. Intrahepatic portal-systemic shunt: its etiology and diagnosis. *Gastroenterol Jpn* 1987;22:496–502.
82. Wittich G, Jantsch H, Dimiter D. Congenital portosystemic shunt diagnosed by combined real-time and Doppler sonography. *J Ultrasound Med* 1985;4:315–318.
83. Neumaier CE, Cicio GR, Derchi LE, et al. The patent ductus venosus: an additional ultrasonic finding in portal hypertension. *J Clin Ultrasound* 1983;11:231–233.
84. Kauffman SL, Andersen DH. Persistent venous valves, maldevelopment of the right heart, and coronary artery-ventricular communications. *Am Heart J* 1963;66:664–669.
85. Trakhtenbroit A, Majid P, Rokey R. Cor triatriatum dexter: antemortem diagnosis in an adult by cross sectional echocardiography. *Br Heart J* 1990;63:314–316.
86. Jones RN, Niles NR. Spinnaker formation of sinus venosus valve: case report of a fatal anomaly in a ten-year-old boy. *Circulation* 1968;38:468–473.
87. Steding G, Jinwen X, Seidl W, et al. Developmental aspects of the sinus valves and the sinus venosus septum of the right atrium in human embryos. *Anat Embryol* 1990;181:469–475.
88. Arey LB. *Developmental Anatomy*. 7th ed. Philadelphia, PA: WB Saunders, 1965:382–384.
89. Licata RH. The human embryonic heart in the ninth week. *Am J Anat* 1954;94:73–125.
90. Gussenhoven WI, Essed CE, Bos E. Persistent right sinus venosus valve. *Br Heart J* 1982;47:183–185.
91. Thomta I, Bending L, Szente A, et al. Cor triatriatum dextran simulating right ventricular myxoma and pulmonary stenosis. *Thorac Cardiovasc Surg* 1983;31:114–116.
92. Sutherland RD, Stanger P, Chimie ARW, et al. Large anomalous fibrous sac in the right side of the heart. *Circulation* 1969;399:837–840.
93. Alboliras ET, Edwards WD, Driscoll DJ, et al. Cor triatriatum dexter: two-dimensional echocardiographic diagnosis. *J Am Coll Cardiol* 1987;9:334–337.
94. Mazzucco A, Bortolotti U, Gallucci V, et al. Successful repair of symptomatic cor triatriatum dexter in infancy. *J Thorac Cardiovasc Surg* 1983;85:140–145.

Ahmad I. Alomari

INTRODUCTION

Vascular anomalies are relatively common heterogeneous disorders characterized by developmentally abnormal blood vessels including the venous, arterial, and lymphatic lineages. These anomalies may overlap clinically and radiologically creating considerable confusion in the clinical practice and published research. Nevertheless, the diagnosis and management of the vast majority of vascular anomalies fundamentally can be simplified if the proper nomenclature and classification are applied. Commonly used inaccurate terms such as lymphangioma, cystic hygroma, cavernous hemangioma, hemangioma, strawberry hemangioma, hemangiolymphangioma, and cavernoma should be abandoned for the more representative designation.

The binary classification proposed by Mulliken and Glowacki in 1982 (1) divides vascular anomalies into two major categories: (i) vascular tumors and (ii) vascular malformations. Vascular malformations can be either of the slow-flow (venous, capillary, and lymphatic) or fast-flow type (arteriovenous malformations (AVMs) and fistulas). The correct diagnosis and appropriate therapy require proper awareness of the clinical and imaging features of different types of vascular anomalies. Improper terminology can lead to the wrong diagnosis, mistreatment, and misdirected research efforts (2).

Unfortunately, terminological imprecision is still prevalent in the published literature. "Hemangioma," according to Hasanein et al. (1b) was used incorrectly in 228 of 320 of the publications (71.3%) analyzed. The authors also demonstrated that inaccurate designation of the vascular anomaly was associated with an increased risk of erroneous management.

EMBRYOLOGY AND GENETICS

The embryonic vascular network primarily is created via two major, distinct mechanisms: vasculogenesis and angiogenesis (3,4). The differentiation and growth of blood vessels from hemangioblasts of mesodermal origin forming the heart and the primitive vascular plexus is called "vasculogenesis," while the subsequent process of remodeling and expanding this network is referred to as "angiogenesis" (5). The distinction between arteries and veins is an early developmental process (6) with molecular differences between arterial and venous channels prior to the establishment of the circulation (7,8).

Due to the extensive, complex biologic pathways involved in the formation of normal blood vessels, developmental anomalies of the vasculature (both idiopathic and those caused by specific defects) are frequently seen.

Most vascular anomalies are sporadic with no identifiable familial or genetic predisposition. Nevertheless, specific mutations have been identified in many vascular anomalies and

syndromes. Inherited disorders of vessels include hemorrhagic telangiectasia (HHT, ENG, ALK1, or SMAD4 mutations), capillary malformation–arteriovenous malformation (CM-AVM, RASA1 mutation), cutaneomucosal venous malformation (VMCM, TIE2 mutations), glomuvenous malformation (GVM, GLOMULIN mutation), PTEN hamartoma tumor syndromes (PTEN mutation), Ataxia-telangiectasia (ATM mutation), cerebral cavernous malformation (CCM, CCM1-4 mutations), primary congenital lymphedema (Milroy disease, VEGFR3 mutation), among others (9a).

Several sporadic, complex syndromes are known to be associated with fast-flow vascular anomalies. Parkes Weber syndrome and CLOVES syndrome, two rare overgrowth syndromes, are associated with AV shunts and hypervascularity. AVMs and fistulas also have been reported in Noonan syndrome (bilateral multiple pulmonary arteriovenous fistulas [AVF] and duplicated renal collecting (9)), Ehlers-Danlos syndrome (10,11), VACTERL association and fibromuscular dysplasia (12), and liver hemangioma (13), among others.

Infantile hemangioma and rapidly involuting congenital hemangioma (RICH) are probably the most common vascular pediatric tumors and occasionally can be associated with arteriovenous shunts. For instance, hepatic RICH is typically a large solitary mass and might be associated with various types of transhepatic vascular shunts and high-output heart failure (14).

CLASSIFICATION

The well-known classification of vascular anomalies, proposed by Mulliken and Glowacki (1), divided them into two distinct types: tumors and malformations. This classification is based on clinical, histopathologic, and imaging differences (Tables 37.1 and 37.2).

Infantile hemangiomas (IHs), the prototype of vascular tumors, are common endothelial tumors that present in early infancy and spontaneously involute later in childhood. Congenital hemangiomas, a less common lesion, are present at birth. Endothelial cell tumors also include a spectrum of uncommon hemangioendotheliomas (such as kaposiform hemangioendotheliomas (KHEs) and epithelioid hemangioendotheliomas) and angiosarcoma.

Vascular malformations typically are present at birth and grow with the patient. Based on the cellular lineage and flow pattern, malformations are divided into slow-flow (including venous malformations [VMs], lymphatic malformations [LMs], capillary malformations [CMs] or combined malformations) and high-flow malformations (arteriovenous malformations [AVMs] and arteriovenous fistulae [AVF]).

Out of 375 pediatric vascular anomalies reviewed by Finn et al. (15), 96% of these lesions can be classified as tumors or malformations.

TABLE 37.1 Vascular Tumors

Hemangiomas	Angiosarcoma
Infantile (Glut-1 +)	
Congenital (Glut-1 -)	
Rapidly involuting ("RICH")	
Noninvoluting ("NICH")	
Tufted angioma ^a	Spindle cell hemangioendothelioma
Kaposiform hemangioendothelioma ^a	Infantile hemangioendothelioma

^aAssociated with Kasabach Merritt syndrome.

CLINICAL MANIFESTATIONS

Vascular Tumors

Infantile Hemangiomas

IHs are the most common tumors of infancy that present in the first few months of infancy or at birth in 4% to 5% of infants (16). IH is not fully developed at birth, though earlier signs (such as faint macular or telangiectatic stain) may herald the definitive manifestation of the lesion. Typically, IH undergoes rapid growth (proliferative phase) over a few months, then regresses spontaneously over years (involuting phase). IH, like many other vascular anomalies, has a predilection to affect the cervicofacial region. The lesions are known to disproportionately affect Caucasians, females, and premature infants.

Histologically, IH shows lobules and sheets of tightly packed, mostly capillary-sized vascular channels.

The tumor initially manifests as a well-margined reddish-purple lesion with variable size, shape, and depth of tissue involvement (Fig. 37.1). Superficial hemangiomas are limited to the skin and subcutis. Deep lesions affect the subcutis and adjacent anatomical spaces, typically sparing the skin and bone. Combined (deep and superficial) and multiple IHs are not uncommon. IHs also can be solitary (focal) or multiple (multifocal). Hemangiomas are usually rubbery, warm, and can be pulsatile.

TABLE 37.2 Vascular Malformations

Telangiectasia	Combined vascular malformations (CVM)
Capillary (Port wine stain)	Klippel-Trenaunay syndrome (CLVM)
Venous (VM)	Parks Weber syndrome (PWS)
Lymphatic (LM)	Servelle Martorell syndrome
Arterial-venous (fast flow) (AVM)	Proteus syndrome
Arterial	Capillary malformation-AVM
	Glomovenous malformation
	Clove syndrome
	Maffucci syndrome



Figure 37.1. Infantile hemangiomas of the face. The raised, well-margined reddish lesions have superficial (cutaneous) and deep portions.

In most patients with IHs, no treatment is necessary because most lesions regress over years without leaving significant scarring (17a). Nevertheless, complications of hemangiomas such as ulcers, bleeding, amblyopia (periorbital), airway obstruction (subglottic), and heart failure (liver) require prompt intervention (17a,17b).

The combination of posterior fossa malformations, cervicofacial, hemangiomas, arterial anomalies, cardiac defects, eye anomalies, and sternal clefting, or supraumbilical raphe, is referred to as "PHACES" Association (17).

PELVIS (or SACRAL) association is composed of a perineal hemangioma, external genitalia malformations, lipomyelomeningocele, vesicorenal abnormalities, imperforate anus, and skin tag (18,19).

Congenital Hemangiomas

Congenital hemangiomas are present and fully mature at birth. Rapidly involuting congenital hemangioma (RICH) and noninvoluting congenital hemangioma (NICH) demonstrate marked similarities in appearance, location, size, and equal sex ratio (20). RICH regresses in the first year of life while NICH persists. Glucose transporter protein (GLUT1), an immunohistochemical marker for IH, is not expressed in congenital hemangioma (21,22).

Liver hemangiomas represent a spectrum of lesions with variable clinical and imaging features. The large, solitary liver hypervascular tumors are RICHs, while the multifocal and diffuse types are histopathologically IHs (23) (Fig. 37.2). Hepatic hemangiomas typically are asymptomatic. However, they can cause high-output cardiac failure, liver dysfunction, hypothyroidism, coagulopathy, and abdominal compartment syndrome.

KHE is an infiltrative tumor with clinical and imaging features distinct from IHs. KHE typically is present at birth or appears shortly thereafter in early infancy, though they rarely can develop in adults. Histologically, KHE is characterized by a predominant Kaposi sarcoma-like, fascicular spindle cell growth pattern of epithelial cells, infiltrating nodules with slit-like, or crescentic vessels that are poorly canalized (26).

The tumor presents clinically with thickened, purple-ecchymotic skin discoloration (Fig. 37.3). KHE commonly is associated with Kasabach-Merritt phenomenon (KMP)

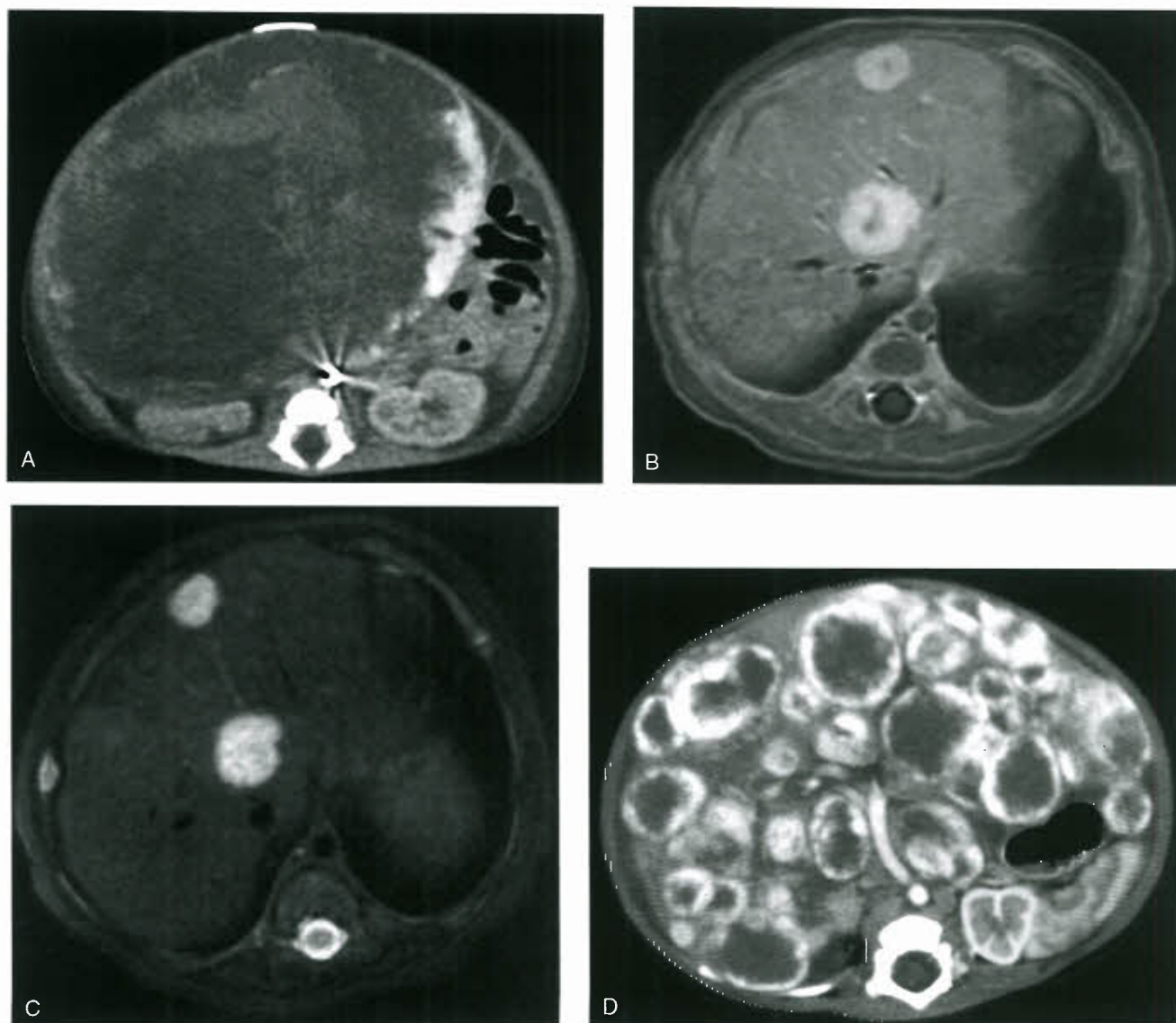


Figure 37.2. Liver hemangiomas. **A:** Hepatic RICH. Enhanced CT scan shows huge hypodense mass in the right lobe of the liver. Note peripheral enhancement and subcapsular locations. **B,C:** Multifocal hepatic infantile hemangioma. T2 and postcontrast T1 sequences demonstrate two focal, well-defined T2 hyperintense lesions that enhance following contrast administration. **D:** Diffuse hepatic infantile hemangioma. Enhanced CT scan reveals numerous, hypodense masses with peripheral enhancement almost completely replacing the liver parenchyma.

with platelet entrapment within the tumor leading to severe thrombocytopenia (24). KHE, unlike IH, is a solitary lesion, affects both genders equally, and has predilection for the trunk, extremities, retroperitoneum, and head and neck (26). It is locally invasive.

On imaging, the affected area exhibits thickening of skin with reticular infiltration of the skin, subcutis, and deeper tissue planes. The infiltrate is hyperintense on T2-WI and enhances on T1-WI following contrast administration (Fig. 37.4).

Imaging of Vascular Tumors

Ultrasonography is the initial, simple, and reliable imaging modality for many vascular tumors.

For infantile hemangioma, ultrasound images typically depict a solid, hypervascular mass with well-defined margins (Fig. 37.5). The feeding arteries and draining veins are enlarged. The former displays a low-resistance arterial spectral waveform.

Magnetic resonance imaging (MRI) is superior to CT scan in demonstrating the characteristic features of hemangiomas. On both modalities, IHs are well-defined, lobulated solid masses with homogeneous enhancement following contrast administration. The tumor demonstrates a homogeneously low or moderate intensity on T1-WI and high intensity on T2-WI magnetic resonance (MR) images. Flow voids within or around the lesion are caused by the dilated feeding arteries and draining veins (Fig. 37.6).

Angiography rarely is needed for diagnostic purposes. Angiography is an integral part of therapeutic embolization for the rare hemangiomas that are associated with heart failure. Typically, IHs demonstrate a hypervascular well-marginated mass with dense, prolonged capillary blush, enlarged feeding arteries, and draining veins (Fig. 37.7).

Congenital hemangioma usually displays a discoid cutaneous-subcutaneous well-defined mass with large feeding arteries and superficial vessels (Fig. 37.8). Angiographic findings of



Figure 37.3. Kaposiform hemangioendothelioma. Irregular patch of purple-ecchymotic skin thickening with overgrowth of the right thigh.

congenital hemangioma include inhomogeneous parenchymal staining, large, and irregular feeding arteries in disorganized patterns, arterial aneurysms, and direct arteriovenous shunts (25).

KHE characteristically demonstrates a network of subcutaneous reticular pattern in the subcutis and confluent intensities along the fascial planes. The infiltrate is hyperintense on T2-WI with thickening of the skin, underlying subcutaneous tissue, and involved deeper spaces. The lesion enhances homogeneously following contrast administration (Fig. 37.9).

Management of Vascular Tumors

Asymptomatic, nondisfiguring IHs can be monitored clinically without treatment. If treatment is indicated, successful medical management typically is achieved using systemic corticosteroids or propranolol. Alternatively, intralesional

corticosteroids can be used for IHs in critical locations where accelerated response is needed (e.g., periorbital, nasal tip).

Embolization of large arterial feeders and intratumoral shunts is reserved for hemangiomas causing high-flow heart failure. Typically, these lesions are hepatic and manifest early in infancy.

Single-agent chemotherapy currently is the mainstay treatment for KHE-associated KMP including the use of vincristine, cyclophosphamide, corticosteroids, interferon alfa-2a, and other agents (26).

Vascular Malformations

Slow-Flow Types

VENOUS MALFORMATIONS

VMs are the most common vascular malformations with a predilection for the cervicofacial region (27). VMs are typically solitary lesions, though a minority of patients have a genetic predisposition (such as in cutaneomucosal venous malformation and glomuvenous malformation). Blue rubber bleb nevus syndrome (Bean syndrome) is a rare sporadic disorder with soft tissue and gastrointestinal multiple VMs.

The classic histological features of VMs are irregular, venous-type channels lined by flat endothelium surrounded by scant (or absent) smooth muscles (28).

VMs are bluish, soft, and compressible masses. Lesions can be flat, slightly raised, or even exophytic. Calcified old clots (phleboliths) can be palpated and occasionally are tender (Fig. 37.10). As the solid component of VMs, composed of venous walls, membranes, and clots, is negligible, the size of the lesion predominantly is composed of stagnant blood. Hence, the volume of the VM increases with dependent positions and/or compression of the draining veins. Pain in VM is multifactorial. Clot formation is almost universal to VMs and some of the thrombosis episodes can incite swelling and pain. Pain also can be attributed to joint, muscle, and tendon involvement and weakening. Recurrent hemarthrosis, particularly of the knee joint, is predisposed by synovial involvement and usually results in chronic pain and joint degenerative changes.

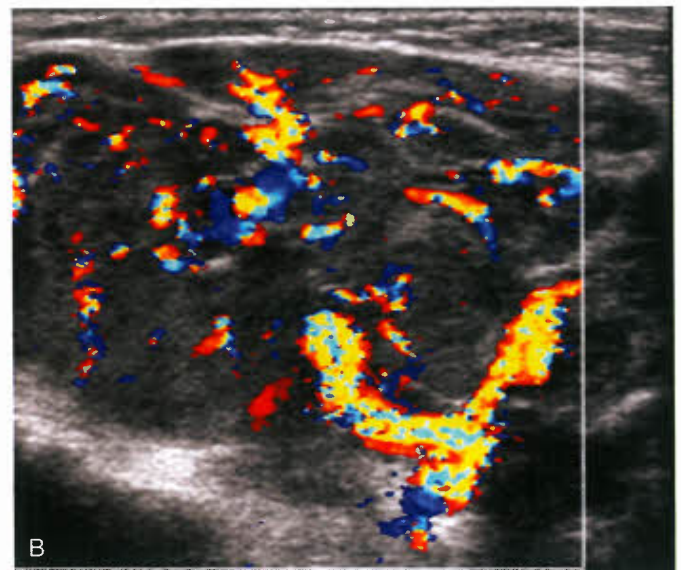


Figure 37.4. Ultrasonography of infantile hemangiomas. A: Diffuse enlargement of the right parotid gland caused by an infantile hemangioma. B: Marked hypervascularity of the lesion with enlarged feeding arteries.

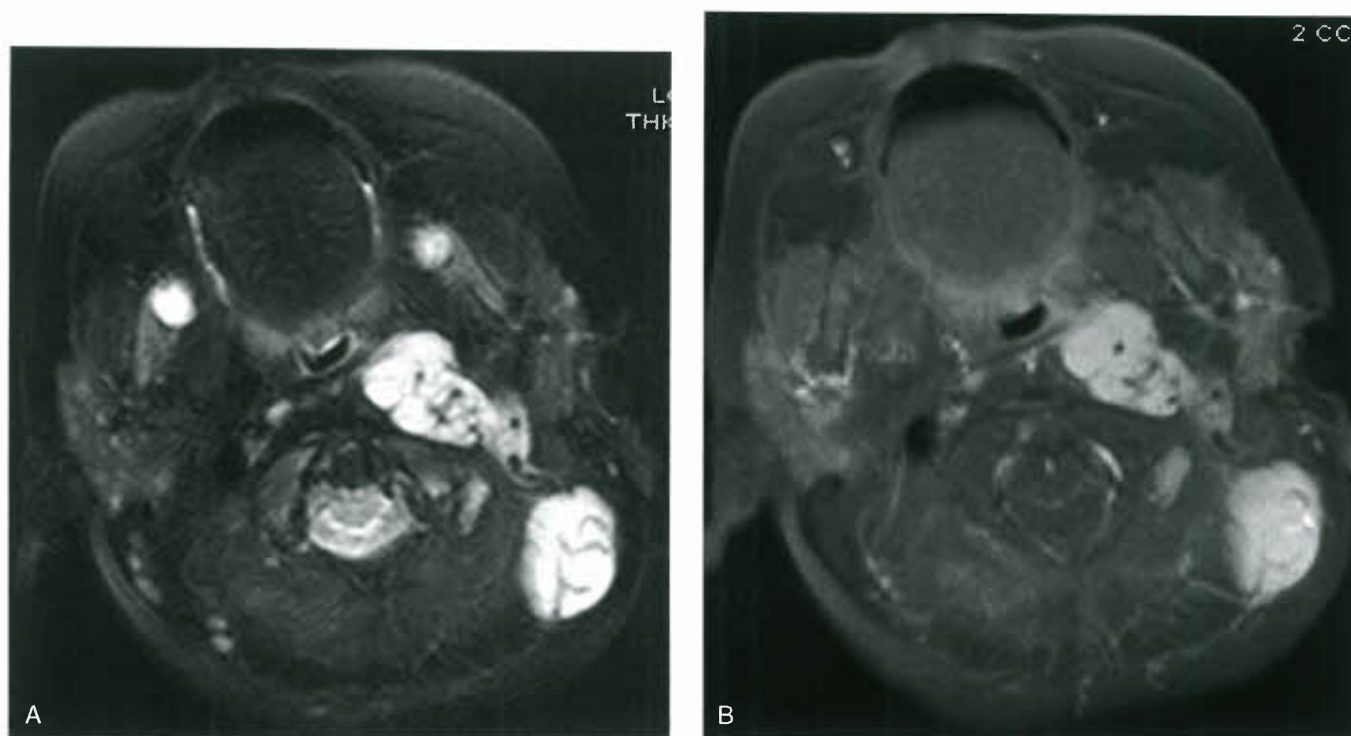


Figure 37.5. MRI of infantile hemangiomas. Two well-defined, lobulated soft tissue masses in the left occipital and parapharyngeal spaces. Note the hyperintense signal and flow voids (enlarged vessels) on axial T2 sequence (A) and strong enhancement following contrast administration on axial T1 sequence (B).

Symptoms may worsen with menses, pregnancy, and use of oral contraceptive pills. Specific locations of VMs can result in additional morbidity: joints (e.g., hemarthrosis), extensive osseous involvement (bone deformity and fracture), airways (obstruction), and intestines (chronic bleeding).

Localized intravascular coagulation (LIC) commonly occurs with large VMs. This typically asymptomatic phenomenon is

characterized by elevated D-dimer and hypofibrinogenemia with normal or slightly decreased platelet counts (29). These changes are due to constant intralesional thrombosis. Therefore, basic coagulation parameters (CBC, PT/INR, PTT, fibrinogen, and D-dimers) are obtained prior to major interventions.

IMAGING OF VASCULAR TUMORS

Most VMs can be diagnosed clinically and small, superficial lesions may require no further evaluation. Nevertheless, larger lesions can be characterized by ultrasonography and MRI in terms of the actual size, extension, and confirmation of the diagnosis, particularly for deeper lesions.

Sonographic findings of VMs are compressible, blood-filled masses surrounded and internally septated by thin venous walls (Fig. 37.11). Clots or phleboliths are typically incompressible, hyperechoic oval or round filling defects. Color and spectral Doppler interrogation typically shows no flow within the venous spaces. Ultrasonography is invaluable to guidance guiding image-guided treatment.

Recommended MRI sequences for VMs (and essentially all other vascular anomalies) include pre- and postcontrast T1-WI and T2-WI, all with fat saturation. MR venography may demonstrate the local venous system and provide spatial information, especially for phlebectasia of the extremities (Fig. 37.12), but is not routinely needed.

Typical MRI appearances of VMs are hyperintense masses on T2-WI containing thin curvilinear network of septations with focal hypointense lesions corresponding to phleboliths (Fig. 37.13). VMs enhance heterogeneously on T1-WI following contrast administration. Intralesional or ascending venography is not typically needed as a diagnostic study. Venography shows amorphous, spongiform spaces with stagnant flow and variable types of draining veins (Fig. 37.14). CT scan is particularly useful in assessing osseous VMs.



Figure 37.6. Rapidly involuting congenital hemangioma (RICH). Large, solid hypervascular lesion of the right thigh with red-purple overlying skin. The lesion was present at birth and regressed rapidly within months.

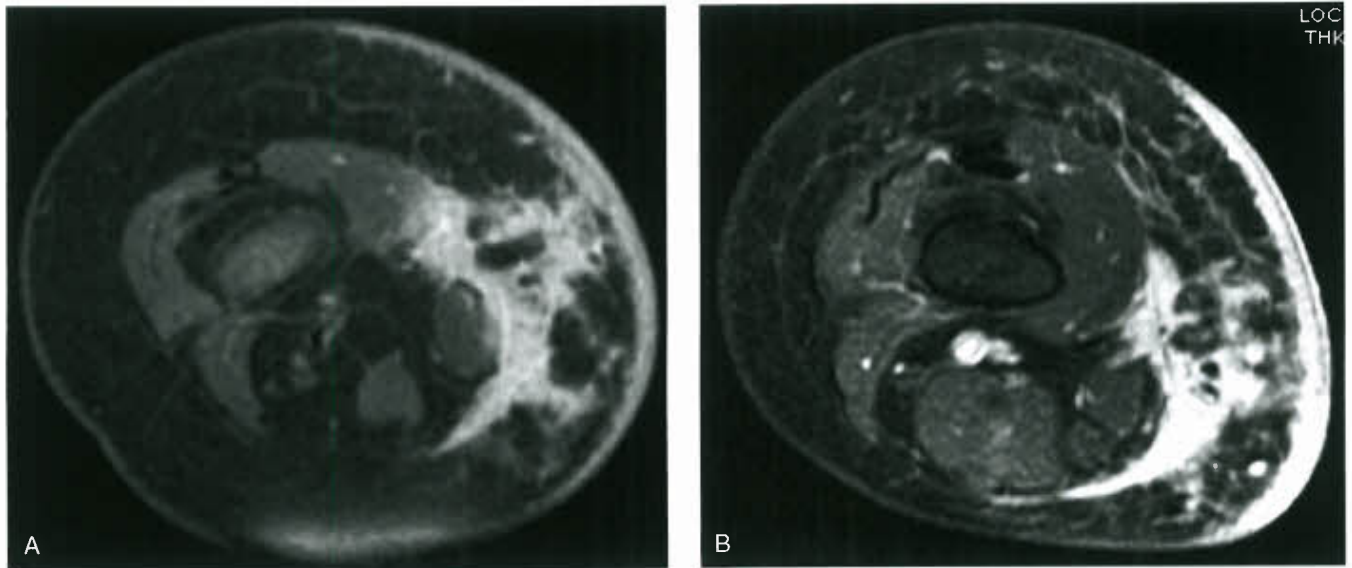


Figure 37.7. Kaposiform hemangioendothelioma of the thigh. Axial T2 sequence (A) shows skin thickening, reticular subcutaneous infiltrate, and epifascial confluence of signal. Following contrast administration, the lesion enhances strongly (B).

Other less frequent types of VMs include phlebectasia (congenital varicosity), persistent embryonic veins, and venous aneurysms. These less common venous anomalies can be isolated or syndromic (e.g., Klippel-Trenaunay and CLOVES syndromes).

TREATMENT OF VENOUS MALFORMATIONS

VMs can be minor, asymptomatic, and require no immediate treatment. Nevertheless, the natural history of VMs is progressive growth and potential symptoms. VMs causing disfigurement or located within sensitive areas (e.g., joints, airways) may necessitate preemptive therapy earlier in childhood.

Compression stocking for VMs of the extremities, particularly the superficial ones, may reduce the blood contents of the VMs and control symptoms. Minimally invasive treatment approaches to VMs include sclerotherapy, laser, and photodynamic therapy.

Sclerotherapy is widely accepted as the initial treatment of choice at many specialized centers. Proper preoperative imaging (typically an MRI) is paramount to planning and performing the procedure. Sclerotherapy, particularly for extensive lesions, is performed under general anesthesia. We do not routinely treat mild forms of coagulopathy prophylactically. Ultrasound guidance using a high-resolution probe

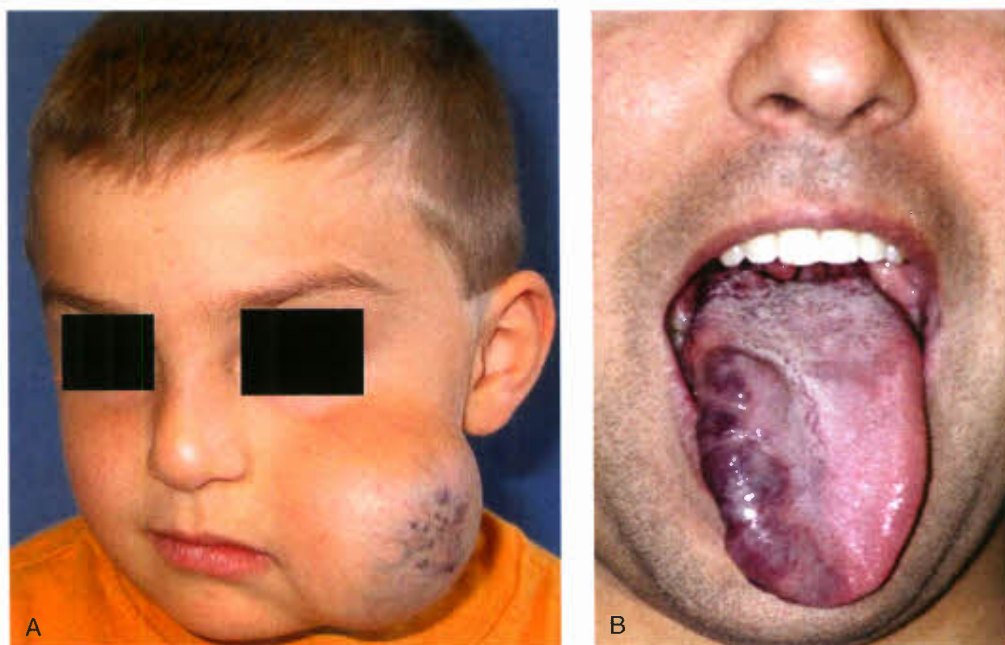


Figure 37.8. Venous malformation. A: Left cheek exophytic VMs with limited cutaneous involvement. B: Tongue VMs with slightly raised contour.



Figure 37.9. Ultrasonography of venous malformation. VMs of the chest wall with fluid-filled compressible spaces and compartmentalization by thin septa. Note the fluid-fluid levels.

is essential for locating the lesions and directing the needles. The tools required for sclerotherapy generally are inexpensive and simple.

Access needles of variable gauges and lengths (e.g., 20- to 21-gauge angiocatheters or micropuncture needles) are placed within the VMs under sonographic guidance. Intralesional placement is confirmed by free blood return and intralesional venography. The latter is performed to delineate the size of the opacified portion and the draining veins as well as to exclude extravasation outside the VMs (Fig. 37.15).

It is crucial to implement x-ray dose reduction techniques such as proper collimation, filtration, and last image hold. Complex anatomical location, such as the head and neck, may require biplane imaging for adequate visualization of the VMs. Ascending venography of the entire limb is helpful in delineating the deep venous system that should be protected and observed throughout the procedure. Contrast material should be diluted with saline without jeopardizing the imaging quality. After confirming the proper position of the needle, the lesion is injected with the sclerosant under fluoroscopic and/or sonographic guidance (Fig. 37.16). Dual-needle technique is useful in focal lesions where two needles (or more) are simultaneously placed within the lesions. The sclerosant is injected through one needle displacing blood via the other (draining) needle. No attempt is made to aspirate the sclerosant. Whenever possible, blood is aspirated or compressed out of the VM immediately prior to the injection of the sclerosant. The volume of the sclerosant typically is equal to (or more than) the

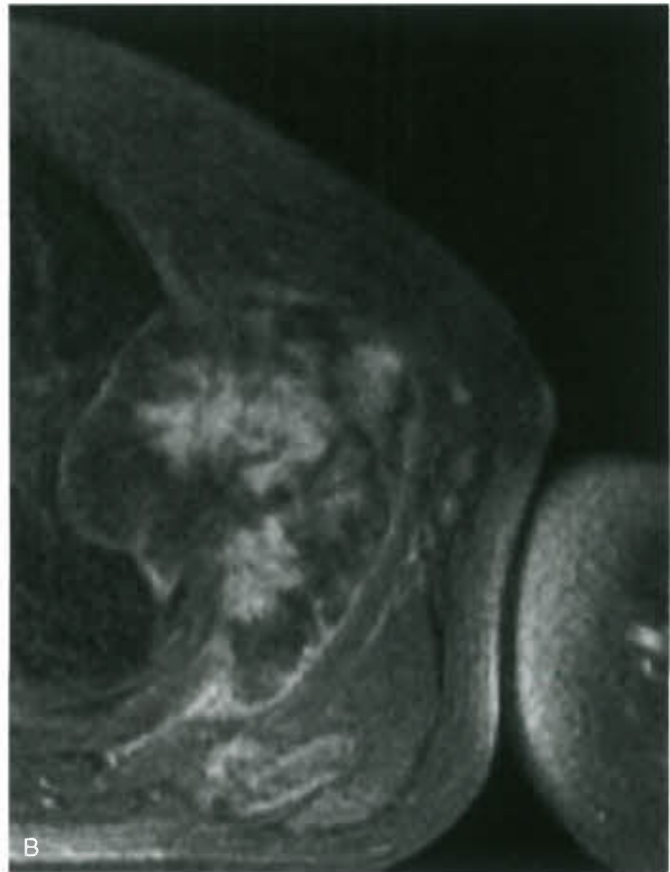
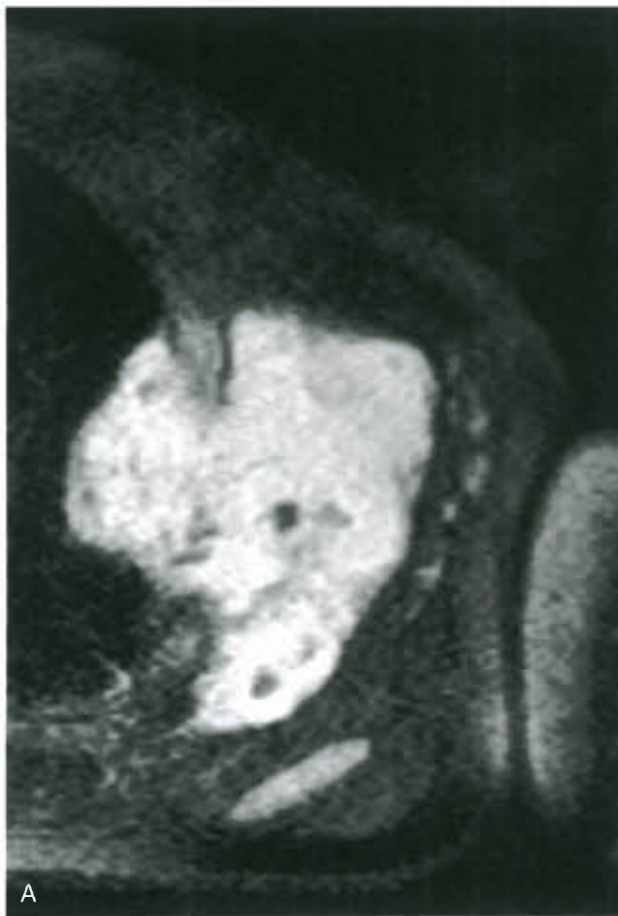


Figure 37.10. MRI of venous malformation. **A:** Axial T2 sequence showing the hyperintense signal of the VMs of the chest wall with herniation into the thoracic cavity. The signal reflects the dominant fluid (blood) component. Note multiple hypointense foci representing phleboliths. **B:** Partial, heterogeneous enhancement on axial T1 sequence following contrast administration.

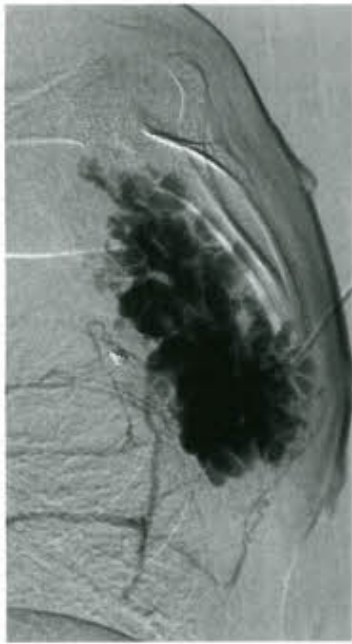


Figure 37.11. Intralesional venography of the VMs. The amorphous, spongiform communicating venous spaces are opacified with direct injection of contrast. The small draining veins communicate with the intercostal veins.

volume of contrast required to opacify the lesion. The rest of the lesion is then treated similarly.

Extralesional extravasation of sclerosant likely is the cause of most of complications. Problematic or positional accesses should be abandoned for safer ones. On venography, extravasation is manifested as geometric, smooth, or lenticular contrast collection around the tip of the needle, expansion artifacts, and persistent tissue infiltration. Cessation of blood return from the access needle and resistance for further

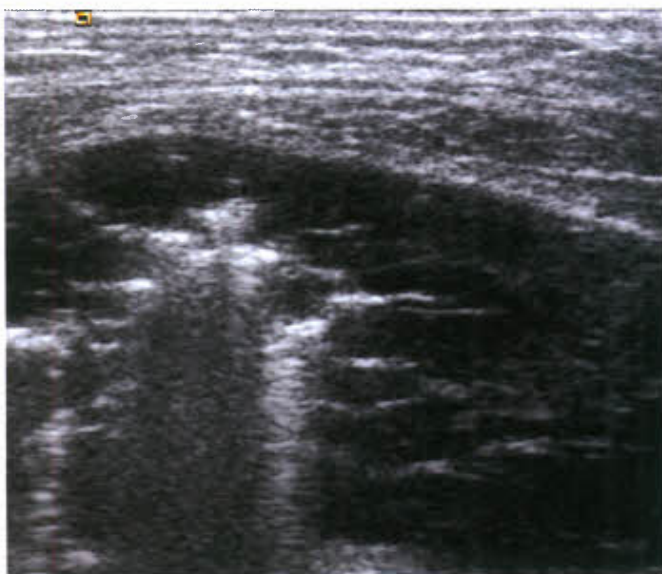


Figure 37.12. Sclerotherapy of VMs with sodium tetradecyl sulfate foam. Ultrasonography reliably differentiates between the portion of the VMs injected with the foam (hyperechoic signal with air artefact) and the untreated portions.



Figure 37.13. Embolization of congenital phlebectasia of the right lower extremity. **A:** MRV of the leg demonstrating the extensive superficial phlebectasia superimposed over the patent deep venous system. **B:** Multiple glue casts permanently occluded the anomalous, ectatic superficial veins and diverted the flow into the deep venous system.

injection should not be overlooked as they may represent extravasation.

The overlying skin may demonstrate immediate changes during injection of the sclerosant into superficial lesions.

Control of the drainage veins, when needed for large VMs, can be achieved with direct pressure (manual or with an ultrasound probe or clamp), positioning, or by using a tourniquet. The latter should be inflated for a short period (typically a few minutes) so it does not cause unnecessary stagnation and accumulation of sclerotherapy by-products in the normal deep veins. Ultrasound and fluoroscopy can be used complementarily to confirm that the treatment covered the intended parts of the lesions.

Due to hemolysis of blood within the VM, hemoglobinuria and oliguria may develop. Perioperative hydration is necessary. A urinary catheter is inserted to observe for these complications. Following the treatment, the treated site is elevated and pain is prophylactically controlled. We do not routinely administer antibiotics or steroids. Prolonged intubation in the ICU is mandatory for critical airway VMs. Alternatively, tracheostomy may be placed.

Blistering and ulceration of the overlying skin are managed with standard wound care. Hemoglobinuria and oliguria are common and are managed successfully with hydration and diuresis. Compartment syndrome and neuropathy are often avertable by avoiding extravasation and excessive therapy.

The commonly used sclerosants for VMs are dehydrated ethanol, sodium tetradecyl sulfate (STS), polidocanol, sodium morrhuate, ethanolamine oleate bleomycin, and alcohol solution of zein. Ethanol can be injected pure or opacified with ethiodized oil contrast (e.g., Ethiodol). The mixture is injected under digital subtraction fluoroscopy and caution is exercised to avoid extravasation (Fig. 37.17). Injection of ethanol can be very painful and irritating causing transient tachycardia



Figure 37.14. Macrocystic lymphatic malformation of the base of the neck. **A:** The photograph shows a left cervical mass with normal skin. **B:** Sonographic image reveals the cystic nature of the mass with thin walls and septa. Fat saturated axial T2 (**C**) and postcontrast T1 (**D**) MRI sequences show a simple cystic lesion with no solid component. The thin walls and septations enhance after contrast injection.

and tachypnea. Large volumes of ethanol and hemolysis by-products entering into the systemic veins can cause life-threatening pulmonary hypertension and cardiopulmonary arrest. The maximum amount of ethanol typically is limited to 0.5 to 1.0 mL/kg per session (30). Elevated serum ethanol can cause respiratory depression, arrhythmias, seizures, rhabdomyolysis, and hypoglycemia (31).

STS 3% () is a widely used sclerosant which can be used in foam or liquid forms. The foam form is likely to be more effective and can be reconstituted by mixing STS with an equal volume (or more) of air (or CO₂) through a three-way stopcock. Ethiodol can be added to the mixture (1:10) to stabilize the foam. Visualization of the foam is superior with sonography.

Embolic agents such as *N*-butyl cyanoacrylate glue, ethylene vinyl alcohol (Onyx), and coils can be used as adjuvant tools, particularly for filling huge anomalous venous spaces, to control draining veins, or preoperatively. These agents are not bioabsorbable and typically are not used as primary treatment

for VMs. Endovenous laser photocoagulation, in combination with sclerotherapy and venous embolization, can be useful in selective cases of phlebectasia of the extremities (Fig. 37.18).

The two major factors to gauge the response to sclerotherapy are pain relief and size reduction. While pain control is achieved in the vast majority of patients, shrinkage of the VM usually requires multiple procedures. For large and disfiguring VMs, sclerotherapy can be combined with surgical resection. When multiple treatments are required, procedures are scheduled 6 to 8 weeks apart.

For diffuse involvement of the limb or organ, “targeted” sclerotherapy of the painful portions may offer symptomatic relief.

LYMPHATIC MALFORMATIONS

LMs are divided into several main subtypes, namely, the macrocystic, microcystic, combined form, and anomalies of the central conducting lymphatics. Lymphedema also falls within the spectrum of LM. Erroneous names are still widely used (such as cystic hygroma, lymphangioma, and hemangiolymphangioma)



Figure 37.15. Microcystic lymphatic malformation of cervicofacial region with macroglossia.

and should be abandoned. Macrocystic LMs are composed of lymph-filled cysts and microcystic LMs consist of microscopic lymphatic spaces not identifiable with imaging tools. Microcystic LMs tend to be extensive and infiltrative through the tissue planes with associated bony overgrowth, particularly in maxillofacial area. The overlying skin is usually intact though capillary stains or lymphatic vesicles are occasionally encountered.

Histopathologically, LMs have a thick myxoid fibrous wall containing myofibroblasts and smooth muscle cells with abnormal channels which can be empty, contain lymph, proteins, or blood (28).

Symptoms related to LMs can vary from mild disease to significant pain, recurrent infection, lymphatic or chylous leak, mass effect, and deformities. LMs rarely involute spontaneously. Hence, early and appropriate treatment of LM to provide symptomatic, functional, and cosmetic improvement is recommended. Spontaneous painful swelling (flare-ups) is commonly predisposed by systemic or local infections such as viral illnesses. Intralesional bleeding also is common, particularly with flare-ups. LMs most commonly affect the cervicofacial, axillary, and pelvic regions.

Sclerotherapy is the first-line management for LMs. Most procedures are performed with general anesthesia. In general, fluid-filled spaces are cannulated with 21- or 20-gauge needles using ultrasound guidance, fluid is aspirated, and the sclerosant is injected into the macrocysts under sonographic or fluoroscopic guidance. Sclerosants generally are not removed

after injection (32–34). Large cysts can be drained with a pig-tail catheter and sclerosed repeatedly.

Ultrasound-guided procedures may not need any contrast opacification.

Commonly used sclerosing agents for LMs include ethanol, doxycycline, STS, bleomycin, and OK-432 (35). Doxycycline is a broad-spectrum antibiotic from the tetracycline class. It is used for pleurodesis in pediatric patients. A report of its use in a small group of patients with unresectable LMs concluded that doxycycline is a safe and, to a varying degree, effective sclerosing agent (24). We usually add 10 mL of half strength contrast medium to 100 mg of lyophilized doxycycline powder (Doxo 100 and 200, American Pharmaceutical Partners, Inc., Los Angeles, CA). The resulting opacified solution of 10 mg/mL is then injected directly into the malformation under fluoroscopic and/or sonographic guidance. OK-432 is packaged as a powder in 0.1- or 0.5-mg vials. The OK-432 solution is prepared by dissolving 0.1 mg of OK-432 in 10 mL of normal saline.

CAPILLARY MALFORMATIONS

CMs are pink-red skin macules with a tendency to affect the cervicofacial region. Extensive CMs can be occasionally associated with hypertrophy of the affected region. CMs also occur in several syndromes with complex vascular anomalies such as Sturge-Weber syndrome, Klippel-Trenaunay syndrome, Parkes Weber syndrome, CLOVES syndrome, and CM-AVM (RASA-1 mutation).

IMAGING OF VASCULAR ANOMALIES

Focal VMs are hyperintense on T2-weighted MRI sequences with thin linear septations. VMs enhance heterogeneously and partially following contrast administration and fluid–fluid levels are common. MR venography may demonstrate the local venous system but is not routinely needed to establish the diagnosis. Conventional venography rarely is utilized for diagnosis but is an integral part of percutaneous treatment. CT scan can provide some additional information for bone or deep mesenteric VMs, but generally is less helpful with the soft tissue lesions. Focal intralesional hypointense foci are caused by phleboliths. Phleboliths also can be detected on CT scan and plain radiographs. Ultrasonography demonstrates the compressible blood-filled spaces with internal septations and phleboliths. Venous flow typically is not visualized due to extremely sluggish flow of blood within VMs.

On MRI, lymphatic macrocysts are similar to any other simple cysts with thin walls. Internal septations or a conglomeration of multiple cysts is common. Macrocysts typically demonstrate enhancement of wall and/or internal septa following the administration of contrast but not of the fluid contents. The microcystic LM appears as an ill-defined soft tissue thickening on sonography. Evidence of intralesional bleeding is common and causes the typical fluid–fluid level. Microcystic LMs typically are solid T2 hyperintense lesions with a poorly defined, infiltrating nature with some heterogeneous postcontrast enhancement and overgrowth of the affected tissue. For CMs, imaging is not usually required to establish the diagnosis except if there is an associated malformation, overgrowth, or syndrome.

FAST-FLOW VASCULAR MALFORMATIONS

An AVM is composed of a primitive network of connecting channels (nidus) bypassing the capillary bed. There is no associated mass. AVMs are rare lesions and are congenital though typically stay dormant during childhood.

AVMs result in major local and sometime systemic hemodynamic disturbances. The arterial flow preferentially is diverted through the AV shunt and into the draining veins that may result in tissue ischemia and venous hypertension. These hemodynamic changes manifest clinically as tissue overgrowth,

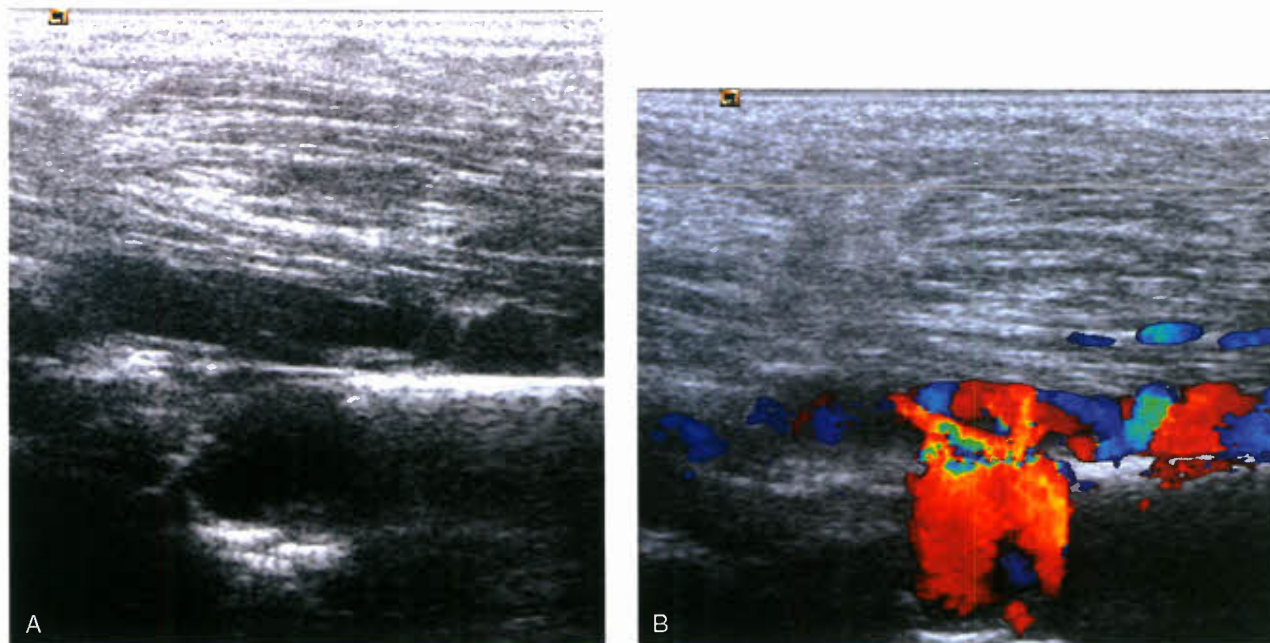
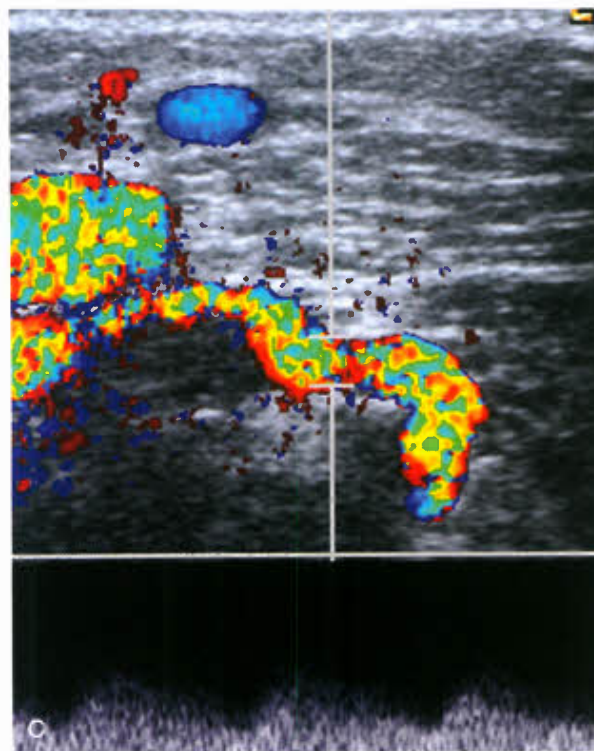


Figure 37.16. Ultrasonography of arteriovenous malformation of the left upper extremity. Images (A and B) showing increased blood vessels around the eroded bony cortex with turbulent flow and intraosseous dilated draining sac. C: Doppler spectral wave with low-resistance pattern (increased diastolic flow).



hyperemia, pain, pulsatility, tissue loss, bleeding, and, infrequently, high-output heart failure.

Direct simpler shunts between an artery and a vein are called AVFs, such as seen in pulmonary AVFs in HHT and vein of Galen malformation. AVFs commonly are acquired related to traumatic and iatrogenic causes. Congenital AVF may present early in infancy with high-output heart failure.

Schobinger staged AVMs and described the natural progression of these lesions from quiescence (stage 1) to expansion (stage 2) to destruction: pain, bleeding, ulceration (stage 3), and in major AV shunts to stage 4 (decompensated heart failure) (36).

CT and MRI studies demonstrate dilated feeding arteries and draining veins without a discrete mass. On MRI, signal

abnormalities may be present in the surrounding tissue representing fibrofatty changes, edema, and disorganized overgrowth. Osseous involvement manifest as overgrowth and lytic changes with diffuse abnormal marrow signal.

Angiography demonstrates dilation of the feeding arteries with tortuosity, AV shunting, and even greater dilation of draining veins. In a diffuse or early-stage AVM, a blush with early venous opacification may be seen rather than a discrete nidus.

Arterial and venous embolization are preferred to surgical resection and often are performed in a staged fashion. Arteries supplying the nidus are selectively embolized at the nidus level, not proximally, via microcatheter access and high-quality selective angiography. Permanent liquid or semiliquid agents

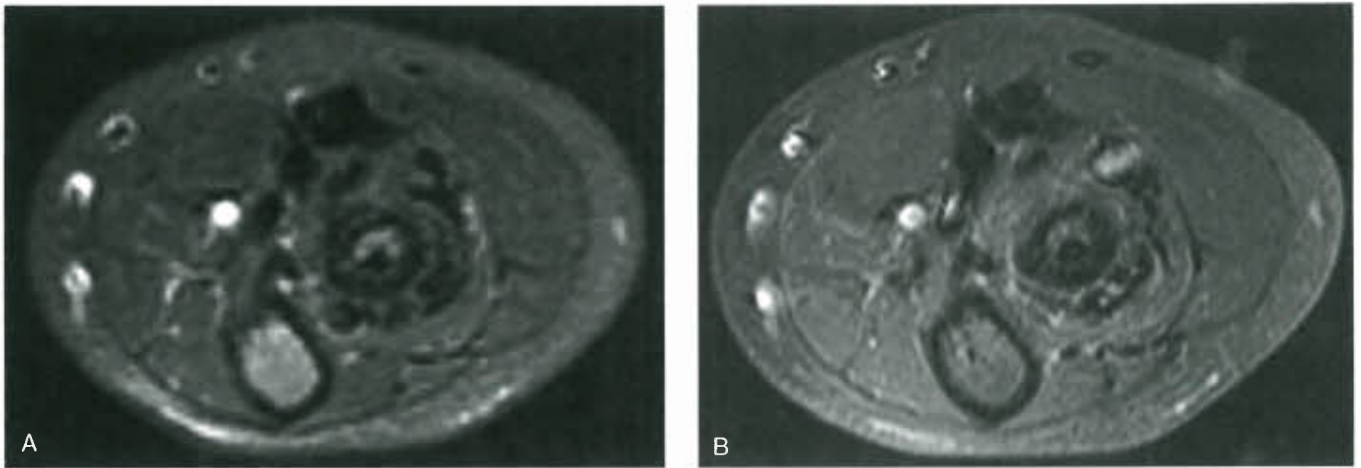


Figure 37.17. MRI of arteriovenous malformation. Axial T2 (A) and postcontrast T1 (B) MRI sequences show a tangle of flow voids (enlarged blood vessels) around the proximal aspect of the radius bone. Note lack of soft tissue mass.

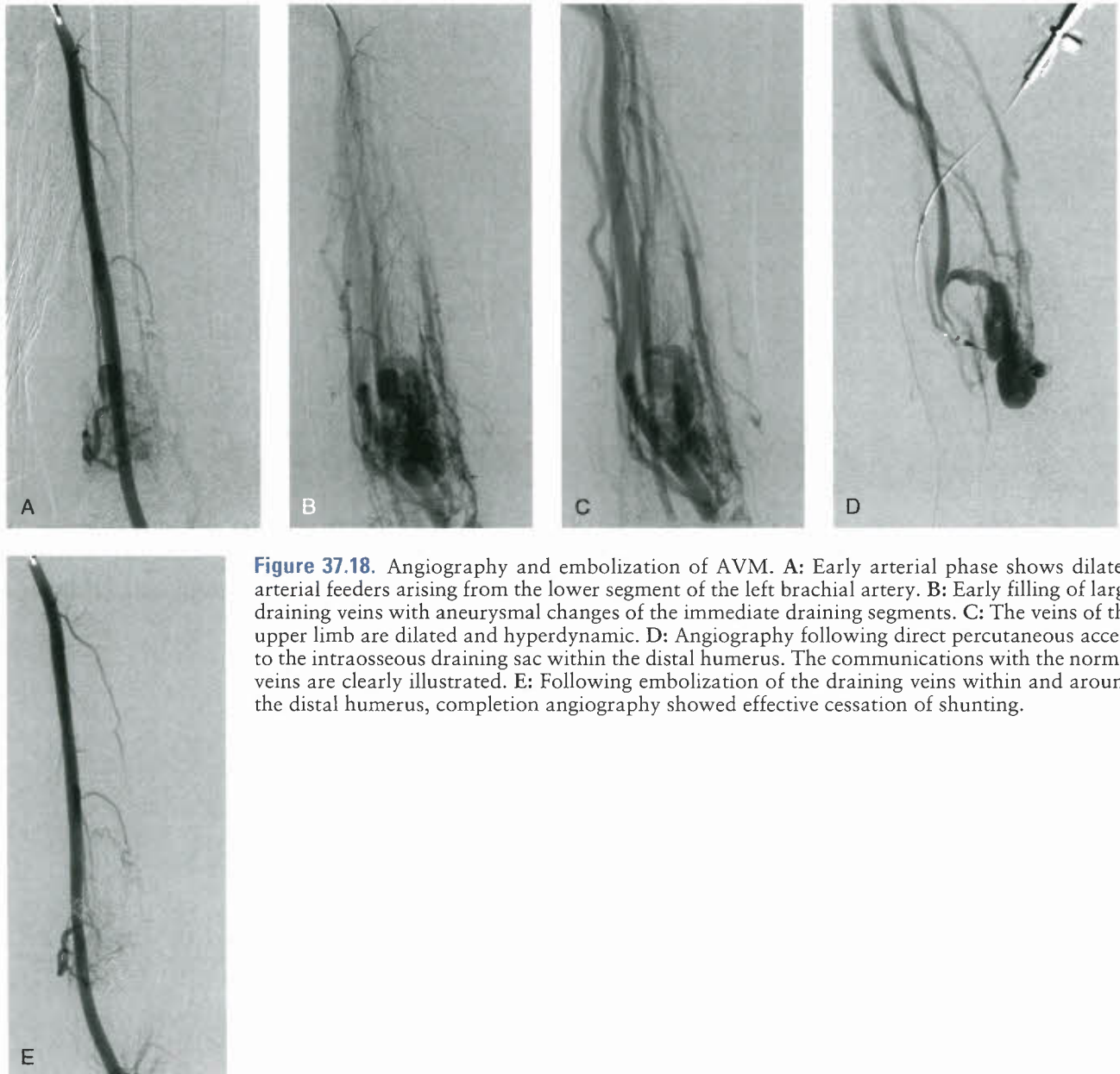


Figure 37.18. Angiography and embolization of AVM. A: Early arterial phase shows dilated arterial feeders arising from the lower segment of the left brachial artery. B: Early filling of large draining veins with aneurysmal changes of the immediate draining segments. C: The veins of the upper limb are dilated and hyperdynamic. D: Angiography following direct percutaneous access to the intraosseous draining sac within the distal humerus. The communications with the normal veins are clearly illustrated. E: Following embolization of the draining veins within and around the distal humerus, completion angiography showed effective cessation of shunting.

(ethanol, glue and Onyx) are injected under fluoroscopy into the nidus and immediate draining vein.

Temporary embolic agents, such as particles, can be used preoperatively to devascularize a selective focal lesion with tiny channels.

For AVMs with dominant draining veins, transvenous embolization, typically done with coils and other permeant agents, may provide superior results to transarterial embolization, particularly with numerous feeding arteries.

REFERENCES

- Mulliken JB, Glowacki J. Hemangiomas and vascular malformations in infants and children: a classification based on endothelial characteristics. *Plast Reconstr Surg* 1982;69:412–422.
- Hassanein AH, Mulliken JB, Fishman SJ, et al. Evaluation of terminology for vascular anomalies in current literature. *Plast Reconstr Surg* 2011;127:347–351.
- Mulliken JB, Fishman SJ, Burrow PE. Vascular anomalies. *Curr Probl Surg* 2000;37:517–584.
- Patan S. Vasculogenesis and angiogenesis as mechanisms of vascular network formation, growth and remodeling. *J Neurooncol* 2000;50:1–15.
- Glottzbach JP, Levi B, Wong VW, et al. The basic science of vascular biology: implications for the practicing surgeon. *Plast Reconstr Surg* 2010;126:1528–1538.
- Folkman J. Angiogenesis: an organizing principle for drug discovery? *Nat Rev Drug Discov* 2007;6:273–286.
- Zhong TP, Childs S, Leu JP, et al. Gridlock signalling pathway fashions the first embryonic artery. *Nature* 2001;414:216–220.
- Yamamizu K, Yamashita JK. Roles of cyclic adenosine monophosphate signaling in endothelial cell differentiation and arterial-venous specification during vascular development. *Circ J* 2011;75:253–260.
- Rocha SF, Adams RH. Molecular differentiation and specialization of vascular beds. *Angiogenesis* 2009;12:139–147.
- Brouillard P, Viskula M. Genetic causes of vascular malformations. *Hum Mol Genet* 2007;16:R140–R149.
- Semizel E, Bostan OM, Saglam H. Bilateral multiple pulmonary arteriovenous fistulas and duplicated renal collecting system in a child with Noonan's syndrome. *Cardiol Young* 2007;17:229–231.
- Lynch HT, Larsen AL, Wilson R, et al. Ehlers-Danlos syndrome and "congenital" arteriovenous fistulae. A clinicopathologic study of a family. *JAMA* 1965;194:1011–1014.
- Behjati S, Knight Y, Borgstein R, et al. A life-threatening complication of Ehlers-Danlos syndrome. *Br J Hosp Med (Lond)* 2009;70:360.
- Alomari AK, Alomari AI. A Rare Association of Fibromuscular Dysplasia, Renal Agenesis, Renal Arteriovenous Fistulae and Vertebral Anomalies: expanding the "V" in VACTERL Association. *Am J Med Genet A* [in press]
- Christison-Lagay ER, Burrows PE, Alomari A, et al. Hepatic hemangiomas: subtype classification and development of a clinical practice algorithm and registry. *J Pediatr Surg* 2007;42:62–67.
- Zenzen W, Perez-Atayde AR, Elisofon SA, et al. Hepatic failure in a rapidly involuting congenital hemangioma of the liver: failure of embolotherapy. *Pediatr Radiol* 2009;39:1118–1123.
- Finn MC, Glowacki J, Mulliken JB. Congenital vascular lesions: clinical application of a new classification. *J Pediatr Surg* 1983;18:894–900.
- Kilcline C, Frieden IJ. Infantile hemangiomas: how common are they? A systematic review of the medical literature. *Pediatr Dermatol* 2008;25:168–173.
- Maguiness SM, Frieden IJ. Current management of infantile hemangiomas. *Semin Cutan Med Surg* 2010;29:106–114.
- Greene AK. Management of hemangiomas and other vascular tumors. *Clin Plast Surg* 2011;38:45–63.
- Oza VS, Wang E, Berenstein A, et al. PHACES association: a neuroradiologic review of 17 patients. *AJNR Am J Neuroradiol* 2008;29:807–813.
- Girard C, Bigorre M, Guillor B, et al. PELVIS Syndrome. *Arch Dermatol* 2006;142:884–888.
- Bourrat E, Lemarchand-Venencie F, Jacquemont ML, et al. PELVIS/SACRAL syndrome with livedoid haemangioma and amniotic band. *Ann Dermatol Venereol* 2008;135:855–859.
- Mulliken JB, Enjolras O. Congenital hemangiomas and infantile hemangioma: missing links. *J Am Acad Dermatol* 2004;50:875–882.
- Berenguer B, Mulliken JB, Enjolras O, et al. Rapidly involuting congenital hemangioma: clinical and histopathologic features. *Pediatr Dev Pathol* 2003;6:495–510.
- North PE, Waner M, Mizeracki A, et al. GLUT1: a newly discovered immunohistochemical marker for juvenile hemangiomas. *Hum Pathol* 2000;31:11–22.
- Christison-Lagay ER, Burrows PE, Alomari A, et al. Hepatic hemangiomas: subtype classification and development of a clinical practice algorithm and registry. *J Pediatr Surg* 2007;42:62–67.
- Gruman A, Liang MG, Mulliken JB, et al. Kaposiform hemangioendothelioma without Kasabach-Merritt phenomenon. *J Am Acad Dermatol* 2005;52:616–622.
- Konec O, Burrows PE, Mulliken JB, et al. Angiographic features of rapidly involuting congenital hemangioma (RICH). *Pediatr Radiol* 2003;33:15–19.
- Enjolras O, Mulliken JB, Wassef M, et al. Residual lesions after Kasabach-Merritt phenomenon in 41 patients. *J Am Acad Dermatol* 2000;42:225–235.
- Berenguer B, Burrows PE, Zurakowski D, et al. Sclerotherapy of craniofacial venous malformations: complications and results. *Plast Reconstr Surg* 1999;104:1–11.
- Gupta A, Kozakewich H. Histopathology of vascular anomalies. *Clin Plast Surg* 2011;38:31–44.
- Mazoyer E, Enjolras O, Laurian C, et al. Coagulation abnormalities associated with extensive venous malformations of the limbs: differentiation from Kasabach-Merritt syndrome. *Clin Lab Haematol* 2002;24:243–251.
- Alomari AI, Karian VE, Lord DJ, et al. Percutaneous sclerotherapy for lymphatic malformations: a retrospective analysis of patient-evaluated improvement. *J Vasc Interv Radiol* 2006;17:1639–1648.
- Mason KP, Michna E, Zurakowski D, et al. Serum ethanol levels in children and adults after ethanol embolization or sclerotherapy for vascular anomalies. *Radiology* 2000;217:127–132.
- Molitch HI, Unger EC, Witte CL, et al. Percutaneous sclerotherapy of lymphatic malformations. *Radiology* 1995;194:343–347.
- Greene AK, Perlyn CA, Alomari AI. Management of lymphatic malformations. *Clin Plast Surg* 2011;38:75–82.
- Alomari AI, Karian VE, Lord DJ, et al. Percutaneous sclerotherapy for lymphatic malformations: a retrospective analysis of patient-evaluated improvement. *J Vasc Interv Radiol* 2006;17:1639–1648.
- Burrows PE, Mitri RK, Alomari A, et al. Percutaneous sclerotherapy of lymphatic malformations with doxycycline. *Lymphat Res Biol* 2008;6:209–216.
- Greene AK, Orbach DB. Management of arteriovenous malformations. *Clin Plast Surg* 2011;38:95–106.

Tricuspid Atresia, Stenosis, Regurgitation and Uhl's Anomaly

Michael L. Epstein

Diseases of the tricuspid valve are relatively rare. This chapter deals with the more common forms of congenital malformations. Acquired disease of the tricuspid valve is extremely uncommon, other than infections (endocarditis) associated with illicit drug use or long-term use of indwelling intravenous catheters. These issues are not discussed in this chapter, but can be found elsewhere in this textbook.

TRICUSPID ATRESIA

The congenital heart defect known as tricuspid atresia can be defined as a complete absence of the tricuspid valve with no direct communication between the right atrium and right ventricle. This defect invariably leads to some degree of hypoplasia of the right ventricle. As a result of the absence of flow from the right atrium into the right ventricle, there is an obligatory right-to-left shunt at the atrial level, through either an atrial septal defect or a widely patent foramen ovale. There also must be a communication between the systemic circulation and the pulmonary circulation, usually in the form of a ventricular septal defect (VSD). Occasionally, however, there is associated pulmonary atresia, and pulmonary blood flow is supplied by a patent ductus arteriosus. This cardiac malformation, first described by Kreysig in 1817 (1), is uncommon and was found in fewer than 3% (0.056 per 1,000 live births) of patients reported in the New England Regional Infant Cardiac Program between 1968 and 1974 (2). Although tricuspid atresia usually occurs as an isolated defect, multiple cardiac anomalies have been reported in $\leq 20\%$ of patients. The cause of this defect is unknown. To date, no specific genetic marker responsible for this defect has been found (3).

Pathology

Because development of the tricuspid valve is related to the inflow (sinus) portion of the right ventricle, in patients with tricuspid atresia, the inlet portion of the right ventricle is absent. The right ventricle is composed largely of the infundibular portion and an incompletely formed trabecular portion. If a large VSD is present, the trabecular portion of the right ventricle may be better developed, resulting in a larger right ventricular cavity. On the other hand, if no VSD is present, the right ventricle is rudimentary or may be absent entirely. In this circumstance, the pulmonary valve also will be atretic.

The atretic tricuspid valve is represented by a dimple in the floor of the right atrium (Fig. 38.1). The resulting membrane is usually muscular but may be fibrous. The interatrial communication is usually a widely patent foramen ovale but may be a secundum atrial septal defect or, rarely, an ostium primum defect associated with an atrioventricular septal defect. When a VSD is present, it is usually perimembranous but also

may occur in the muscular septum or as a component of an atrioventricular septal defect, although the latter is rare. In the presence of a large VSD, the pulmonary flow is unobstructed. On the other hand, pulmonary blood flow can be restricted by the presence of a small VSD, pulmonary valve stenosis or pulmonary annular hypoplasia, or severe hypoplasia of the right ventricular outflow tract.

Tricuspid atresia may occur with normally related great arteries or in association with d-transposition of the great arteries (Fig. 38.2). In patients with associated transposition, the right ventricle forms a subaortic chamber, and there may be restriction to blood flow into the systemic circulation if the VSD is small. The clinical presentation of infants with tricuspid atresia often depends on associated anomalies, such as the presence of transposition of the great arteries, VSD coarctation, or pulmonary stenosis.

The various forms of tricuspid atresia usually are classified in a manner initially proposed by Kuhne (4) and later modified (5). Type I describes patients with normally related great arteries and occurs in 70% to 80% of patients with tricuspid atresia. Type II refers to patients with D-transposition of the great arteries and occurs in 12% to 25% of patients. Type III, a relatively uncommon form of tricuspid atresia occurring in only 3% to 6% of patients, is used by some authors for those patients born with more complex associated lesions such as congenitally corrected transposition or malposition of the great arteries. Perhaps type III might best be used to identify patients with all forms of more complex associated lesions, such as truncus arteriosus or atrioventricular septal defect.

Types I and II have been subclassified (Table 38.1). The subclassification for type I patients relates to the presence or size of a VSD. Type Ia refers to patients with no VSD and associated pulmonary atresia. Type Ib patients have a small VSD and some degree of restriction to pulmonary blood flow. Type Ic patients have large VSDs and no pulmonary stenosis. Obviously, there may be some overlap in classification in a particular patient. It is common for the VSD to decrease in size, thereby changing a patient's classification (6). In type II patients, the subclassifications relate to the degree of restriction of pulmonary blood flow directly from the left ventricle. Type IIa refers to patients with pulmonary atresia, type IIb refers to patients with pulmonary stenosis, and type IIc refers to patients with no obstruction into the transposed pulmonary artery. The physiology in type II patients may vary considerably, depending on the size of the VSD, but the subclassification does not consider this variation. Type III patients are uncommon, and subclassifications generally are not used.

Additional cardiovascular abnormalities are present in $\leq 20\%$ of all patients but are less common in those with normally related great arteries. Coarctation of the aorta is the most significant associated cardiac abnormality and occurs in approximately 8% of patients with tricuspid atresia. Other cardiac lesions include persistent left superior vena cava (SVC), juxtaposition of the atrial appendages, and right aortic arch.



Figure 38.1. Pathology specimen seen through an opened right atrium. The *arrowhead* indicates the muscular membrane in place of the tricuspid valve. The *arrow* indicates the patent foramen ovale.

Physiology

Normally Related Great Arteries

Because the only egress of blood from the right atrium occurs through the atrial septum, systemic venous return mixes completely with pulmonary venous return in the left atrium and subsequently flows across the mitral valve into the left ventricle. In patients with a VSD and a patent right ventricular outflow tract, blood is ejected directly into the normally arising aorta as well as through the VSD and the hypoplastic right ventricle into the pulmonary artery. The amount of pulmonary blood flow depends on the size of the VSD and the presence or absence of obstruction into the pulmonary artery. As the pulmonary vascular resistance decreases in the newborn infant, pulmonary overcirculation may develop.

Cyanosis is invariably present to some extent because of complete mixing of the pulmonary and systemic venous returns. The degree of cyanosis depends on the magnitude of pulmonary blood flow. Pulmonary overcirculation will not

Figure 38.2. Diagram depicting anatomy of tricuspid atresia type I (normally related great arteries) and type II (D-transposition of the great arteries). In these figures, both the atrial and ventricular septal defects are shown to be large. Ao, aorta; LV, left ventricle; PA, pulmonary artery; RA, right atrium; RV, right ventricle.

TABLE 38.1 Classification of Tricuspid Atresia

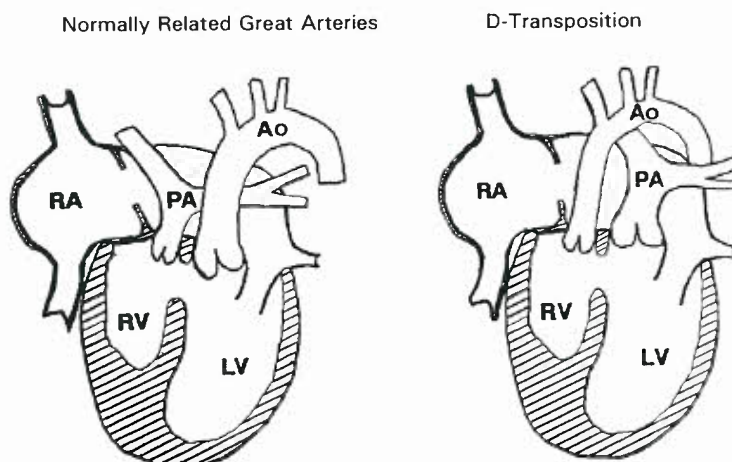
Type I	Normally related great arteries
	a. Intact ventricular septum with pulmonary atresia
	b. Small VSD and pulmonary stenosis
	c. Large VSD without pulmonary stenosis
Type II	Transposition of the great arteries
	a. VSD with pulmonary atresia
	b. VSD with pulmonary stenosis
	c. VSD without pulmonary stenosis
Type III	Transposition or malposition of the great arteries. Associated complex lesions, that is, truncus arteriosus, atrioventricular septal defect

occur when the pulmonary vascular resistance decreases in patients with a restrictive VSD or some form of pulmonary stenosis, but the degree of cyanosis is likely to be greater. In patients with an intact ventricular septum or pulmonary valve atresia, pulmonary blood flow is supplied through a patent ductus arteriosus. The size of the ductus arteriosus will determine the degree of pulmonary blood flow and consequently the degree of cyanosis.

Transposed Great Arteries

Pulmonary overcirculation occurs within the first few weeks of life in most patients with tricuspid atresia and D-transposition of the great arteries because obstruction to flow into the transposed pulmonary artery, which arises directly from the left ventricle, is uncommon. In these type II patients, the presence of a restrictive VSD or infundibular narrowing results in obstruction to systemic blood flow. If the obstruction is severe with resultant diminished systemic circulation, the infant may present with hypotension or shock and metabolic acidosis.

Other abnormalities of physiology may be present, depending on associated defects. For example, in a patient with a restrictive interatrial communication, marked hepatomegaly would be present with signs of diminished cardiac output as well as diminished pulmonary blood flow. In the presence of an associated coarctation of the aorta, the physiology of the type of tricuspid atresia would be present along with associated



findings of the coarctation, most notably diminished lower-extremity pulses and perfusion.

Clinical Features

Systemic arterial desaturation is present to some extent in every patient with tricuspid atresia because of complete admixture of the systemic and pulmonary venous returns (6). Although cyanosis may not be perceived immediately, most patients with tricuspid atresia are noted to be cyanotic by 1 week of age. Heart murmurs are almost always present. If there is no significant obstruction to pulmonary blood flow, cyanosis may not be apparent for some time. Symptoms of pulmonary overcirculation and resultant heart failure are likely to develop in these patients as the pulmonary vascular resistance diminishes. Cyanosis will be more apparent in patients with diminished pulmonary blood flow, but they will not develop pulmonary overcirculation. Hypercyanotic spells can occur in patients with tricuspid atresia as a result of either a decrease in the size of the VSD or infundibular narrowing (7). The physiology of these spells is similar to that seen in patients with tetralogy of Fallot and indicates the need for urgent surgery.

Patients with D-transposition of the great arteries usually present with pulmonary overcirculation; pulmonary stenosis is rare. When these patients have large VSDs, it is difficult to distinguish clinically between these patients (type IIc) and those with normally related great arteries and unobstructed pulmonary blood flow (type Ic).

On physical examination, newborn infants with tricuspid atresia are usually of normal size and demonstrate varying degrees of cyanosis. A left ventricular impulse is likely to be more prominent than a right ventricular impulse. A thrill may be palpable if the VSD is restrictive. The first heart sound is single and often accentuated. The second heart sound is often single, but two components may be heard, especially in infants with normally related great arteries and minimal pathology of the pulmonary valve. A holosystolic murmur may be heard as a result of flow through the VSD, or an ejection murmur may be more prominent because of obstruction through the right ventricular outflow tract. If pulmonary blood flow is increased significantly, a third heart sound and middiastolic rumble may be heard at the apex. The liver may be enlarged, especially in infants with a restrictive interatrial communication. Pulses are readily palpable in all extremities unless an associated coarctation of the aorta is present.

In older patients who either have not undergone any surgery or have had only a palliative aortopulmonary shunt, cyanosis will be more apparent and clubbing of the digits will develop. Additional physical findings will be present depending on the type of surgical intervention. For example, pulses in an arm will be diminished or absent if a previous classic Blalock-Thomas-Taussig shunt has been performed on that side.

Electrocardiographic Features

The electrocardiogram (ECG) from patients with tricuspid atresia is often helpful in the differential diagnosis of a cyanotic newborn (7–9). Right atrial enlargement may or may not be present at birth but often develops in older infants and children. Interestingly, there is no relationship between the amplitude of the P wave and the presence or absence of restriction at the interatrial communication. In patients with increased pulmonary blood flow, combined atrial enlargement may be present. The PR interval is normal in most patients with tricuspid atresia.

In most infants with cyanotic heart disease, the mean QRS frontal plane axis is rightward and inferior with prominent right ventricular forces. The ECG from a patient with tricuspid atresia, on the other hand, usually demonstrates a frontal plane QRS axis that is leftward and superior, and the anterior rightward forces are diminished (Fig. 38.3). This is especially true for type I patients, in whom about 85% of the ECGs demonstrate left-axis deviation. In patients with associated D-transposition of the great arteries (type II), the frontal plane QRS axis is evenly divided between a leftward superior axis and an axis that is directed inferiorly and to the left. In either event, right ventricular forces are usually diminished. Patients with tricuspid atresia and increased pulmonary blood flow often have ECGs demonstrating tall R waves and deep Q waves in lead V6. The ECG in patients with diminished pulmonary blood flow often shows small R waves with shallow Q waves (9).

In some patients, especially older patients, biphasic or inverted T waves may be present in the left precordial leads (V5, V6), with or without associated ST-segment depression (Fig. 38.4). The significance of this finding is unclear because these patients often have no myocardial dysfunction.

The cardiac rhythm is generally sinus. Atrial tachyarrhythmias, such as atrial flutter or fibrillation, may occur in older patients, especially those with restrictive atrial communications

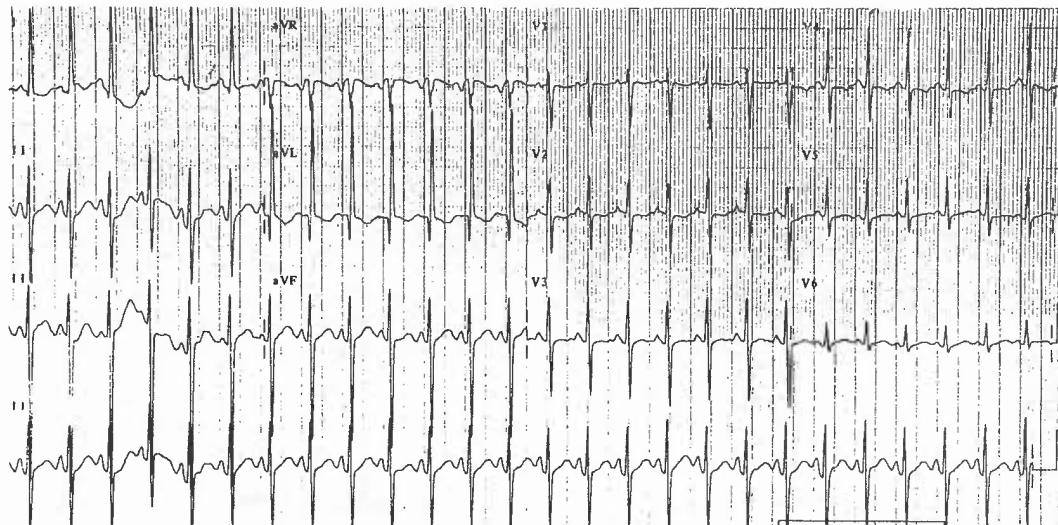


Figure 38.3. Standard 12-lead ECG and lead II rhythm strip from an infant with tricuspid atresia and normally related great arteries. Note right atrial enlargement, leftward superior QRS axis, and diminished right ventricular forces. The precordial leads are recorded at half standard.

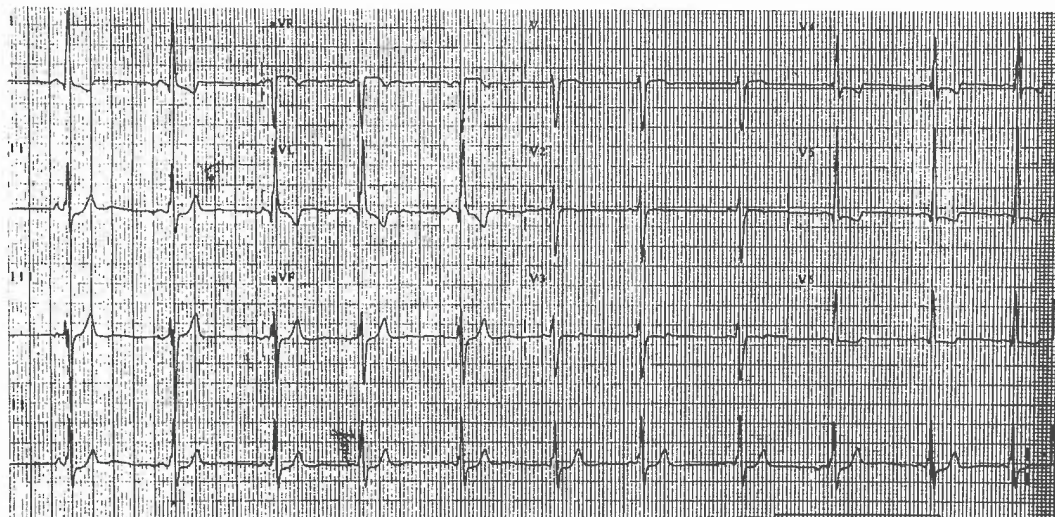


Figure 38.4. Standard 12-lead ECG and lead II rhythm strip from an older child with tricuspid atresia and normally related great arteries. Note leftward superior QRS axis, diminished right ventricular forces, left ventricular hypertrophy or enlargement, and T-wave changes. Precordial leads are recorded at half standard.

and dilated hypertensive right atria. Following completion of surgery to separate the systemic and pulmonary circulations (modified Fontan procedure), arrhythmias are relatively common and occur in $\leq 48\%$ of patients (10). Atrial tachyarrhythmias are encountered most commonly, but bradyarrhythmias and ventricular arrhythmias may occur.

Radiographic Features

The heart size is usually normal in infants with tricuspid atresia. In patients with no obstruction to pulmonary blood flow (types Ic and IIc), cardiomegaly is likely to develop from the increased volume load on the left cardiac chambers as pulmonary resistance decreases. In this circumstance, the pulmonary vascular markings will be prominent. Patients with obstruction to pulmonary blood flow will have normal or diminished pulmonary vascular markings, and heart size will remain normal. The cardiac silhouette is often globular shaped with a concavity in the region of the main pulmonary artery (MPA). The right-sided heart border may appear prominent as a result of dilation of the right atrium, especially in older infants and children.

Echocardiographic Features

Echocardiography has become the diagnostic procedure of choice. This noninvasive diagnostic modality has markedly diminished the need for cardiac catheterization for this lesion. The anatomy of tricuspid atresia is easily defined with two-dimensional echocardiography (11). Indeed, this technique has proven so accurate that most details of the anatomy are easily determined on fetal echocardiographic studies (12,13). M-mode echocardiography is of limited usefulness. Its value is mainly for quantitating the size and function of the left ventricle. The left ventricular cavity may be dilated, especially in patients with increased pulmonary blood flow. Ventricular function is usually normal but may become depressed because of chronic volume overload and hypoxemia, especially in older patients who have not undergone surgery or who have undergone only a palliative shunt.

In the vast majority of patients, all cardiac anatomic details are easily defined. Because the tricuspid valve is easily visualized by echocardiography, the presence of an imperforate linear echo density in the location of the normal tricuspid valve

confirms the diagnosis (Fig. 38.5). Unless pulmonary atresia is a concomitant defect, echocardiography also can demonstrate the presence of two semilunar valves and great arteries. Initial management may be different, depending on the great artery relationship; therefore, it is especially important to confirm the relationship of the great arteries by imaging techniques such as identifying the bifurcation of the pulmonary artery or origin of the coronary arteries. Determining the presence and size of a VSD is almost always possible. It is also important to visualize the atrial septum to evaluate the size of the interatrial communication. If there is restriction to flow between the atria, cardiac catheterization and balloon septostomy may be necessary. Finally, echocardiography usually shows major associated lesions, such as coarctation of the aorta.

The color Doppler portion of the echocardiogram will confirm the absence of a direct communication from the right atrium into the right ventricle and will demonstrate the right-to-left shunt at the atrial level. This portion of the echocardiographic study will define the physiology of pulmonary blood flow, such as restriction through the VSD, narrowing of the right ventricular outflow tract, or obstruction to pulmonary blood flow at the pulmonary valve annulus. It also is important to identify the presence and severity of mitral valve regurgitation, which is an important consideration for subsequent intervention.

Serial echocardiograms are important to evaluate the hemodynamic status of a patient following an initial surgical palliation (aortopulmonary shunt or pulmonary artery banding). Using the Doppler technique, pulmonary artery pressure can be estimated by determining the pressure gradient through the shunt or across the band. Following a more definitive surgical palliation, such as a modified Fontan procedure, echocardiography is the most effective means of monitoring these patients for the development of complications, such as ventricular dysfunction, mitral valve insufficiency, or obstruction to flow from the right atrium into the pulmonary arteries. These patients have a sluggish flow pattern through the right side of the heart and are at risk of developing thrombi in the right atrium. Echocardiography is an excellent means by which thrombi can be detected. For patients with recurrent atrial tachyarrhythmias, especially atrial flutter or fibrillation, transesophageal echocardiography may be necessary to rule out the possibility of a thrombus being present.

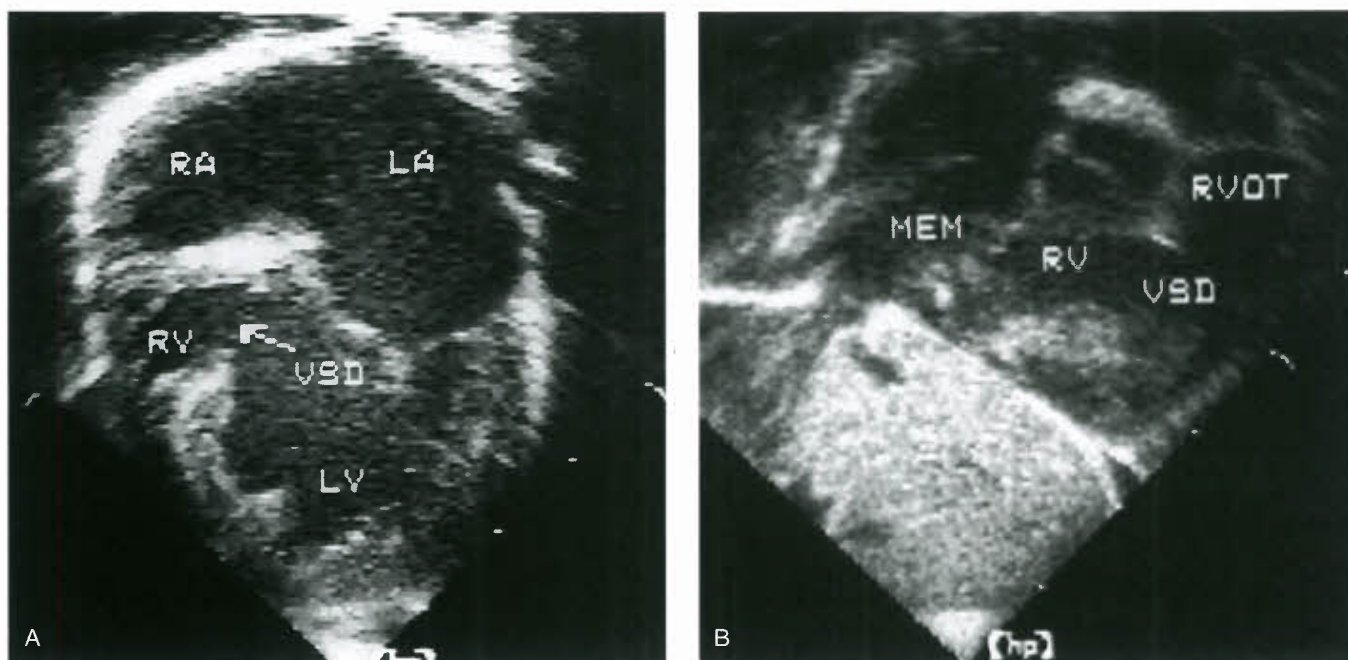


Figure 38.5. Echocardiographic views of an infant with tricuspid atresia and normally related great arteries. **A:** Apical four-chamber view demonstrating a thick linear echo-dense membrane in place of the tricuspid valve. There is a large communication between the right atrium and the left atrium. The arrow indicates a ventricular septal defect that measures 7 mm in this view. Note the hypoplastic right ventricle. **B:** A modified subcostal short-axis view demonstrating the membrane replacing the tricuspid valve. The hypoplastic right ventricle and ventricular septal defect are visualized. The right ventricular outflow tract is widely patent. LA, left atrium; LV, left ventricle; MEM, membrane; RA, right atrium; RV, right ventricle; RVOT, right ventricular outflow tract; VSD, ventricular septal defect.

Cardiac Catheterization

The need for cardiac catheterization has diminished substantially with the development of echocardiography. Catheterization is indicated in specific clinical instances. In the newborn, there may be a need to define sources of pulmonary blood flow and associated cardiac anomalies not clearly defined by echocardiography. Although most patients with tricuspid atresia have large defects in the atrial septum, a restrictive interatrial communication may be present. In these patients, a balloon septostomy may be necessary to relieve any obstruction to egress of blood flow from the right atrium. Occasionally, a large atrial septal defect will become restrictive with time. A balloon septostomy in older patients will often be inadequate, necessitating a blade septostomy or, rarely, surgical intervention (14).

During catheterization, a venous catheter introduced through the groin can be manipulated easily from the right atrium into the left atrium. Indeed, because there is no direct communication from the right atrium to the right ventricle, advancing the venous catheter into the left atrium is the only available pathway. The catheter then can be manipulated easily into the left ventricle. If necessary, the catheter can be advanced, often with the help of a tip-deflector wire, into the posterior great artery, which arises directly from the left ventricle. This may be necessary especially in patients with associated D-transposition of the great arteries in whom the echocardiogram suggests obstruction into the posterior pulmonary artery. It is usually difficult to advance the catheter from the left ventricle into the right ventricle and then into the anterior great artery unless the VSD is large. Fortunately, clinical and echocardiographic findings usually obviate the need to enter the right ventricle and pulmonary artery during catheterization.

Hemodynamic data during the catheterization in infants will show that the right atrial pressure is slightly higher than the left atrial pressure (7). There is likely to be a prominent a wave in the right atrium, especially if the interatrial communication is restrictive. Left ventricular systolic and end-diastolic pressures are likely to be normal, although the end-diastolic pressure may increase in patients with large VSDs as the pulmonary vascular resistance drops and left heart volume overload develops. In patients with associated D-transposition of the great arteries, pulmonary arterial hypertension will be present if there is no pulmonary stenosis. It is especially important in these infants to determine whether there is obstruction through the VSD or at the infundibulum that will result in obstruction to systemic blood flow.

Oxygen saturation in the systemic venous return will be lower than normal as a result of diminished oxygen saturation in the systemic arterial blood. In the absence of associated pulmonary disease, oxygen saturation of pulmonary venous return will be normal, but because of the obligatory right-to-left atrial-level shunt, left atrial and left ventricular saturations will be diminished.

Cardiac catheterization may be indicated to determine the hemodynamics following palliative surgical intervention prior to consideration for the next operation. The most critical determination is that of pulmonary vascular resistance because the eventual plan is creation of a complete systemic venous to pulmonary arterial communication. For patients with decreased pulmonary blood flow who have undergone placement of a shunt, a catheter usually can be manipulated through the shunt into the pulmonary artery. If this is not possible, obtaining a pulmonary venous wedge pressure can accurately reflect pulmonary artery pressure. In patients who have undergone placement of a pulmonary artery band (usually type IIc), a catheter can be advanced from the left ventricle across the band into the pulmonary artery.

Cardiac catheterization might be especially helpful in patients with associated cardiac malformations, especially type III patients. In patients with associated congenitally corrected transposition of the great arteries and ventricular inversion, atresia of the tricuspid valve and a restrictive interatrial communication will result in symptoms of pulmonary venous congestion. It is important to determine pulmonary artery pressure and to define sources of pulmonary blood flow in more complex patients, such as those with associated truncus arteriosus, so that appropriate initial steps can be taken to optimize chances for successful subsequent surgeries.

Finally, in patients who have undergone an intermediate surgical procedure anastomosing the SVC to the pulmonary artery (bidirectional Glenn), a catheter must be introduced through a vein in the upper part of the body (i.e., internal jugular, subclavian, brachial) to enter the pulmonary artery. This maneuver is important to measure pulmonary artery pressure and to estimate pulmonary vascular resistance.

Angiocardiography

The diagnosis of tricuspid atresia can be confirmed at catheterization by performing a right atriogram or superior vena cava-gram that demonstrates absence of flow directly from the right atrium to the right ventricle. This type of angiographic study is rarely necessary, however. Angiography may be useful to define more fully the location and size of a VSD and the source of pulmonary blood flow (Fig. 38.6). Angiography occasionally can document a right ventricular cavity that is larger than that suggested by echocardiography. This difference is not likely to be of clinical significance, however. Because the size of the pulmonary arteries is important for the eventual systemic venous-to-pulmonary artery anastomosis, angiography may be important not only to evaluate pulmonary artery size but also to determine the presence or absence of pulmonary artery distortion that may have been caused by previous surgery. These distortions may be caused by aortopulmonary shunts created in patients with normally related great arteries and

restricted pulmonary blood flow (type Ia and Ib) or patients with d-transposition of the great arteries who have undergone pulmonary artery banding (type IIc).

Angiography may be particularly important in patients with more complex associated cardiac lesions (type III) to define associated anomalies such as anomalous pulmonary venous drainage or coarctation of the aorta. In older patients, especially those who have not yet undergone a more definitive palliation, angiography is extremely important to define the presence or absence of collateral arteries from the descending aorta supplying portions of the lungs. Patients who have undergone a complete systemic venous-to-pulmonary arterial anastomosis, especially if marginally increased pulmonary vascular resistance is present, may require angiography to determine whether collateral venous channels resulting in a functional right-to-left shunt are present (*infra vide*). Angiography in these patients must be obtained using a venous approach from the upper part of the body as described above.

Recent advances in CT and MR imaging have obviated many of the imaging issues that previously required angiography. Catheterization is mainly used for therapeutic rather than diagnostic reasons in the recent era.

Treatment

Patients with tricuspid atresia will undergo one or more surgical procedures to achieve the eventual goal of separation of the systemic and pulmonary circuits. Because of the single-ventricle physiology, separation of the circuits will ultimately include a complete systemic venous-to-pulmonary artery anastomosis with elimination of the right-to-left atrial level shunt. The goal of surgery in the newborn infant is to (a) provide pulmonary blood flow adequate to avoid extreme hypoxemia; (b) prevent pulmonary overcirculation and pulmonary hypertension, which can lead to left ventricular failure or pulmonary vascular disease; and (c) preserve pulmonary artery anatomy for later surgery.

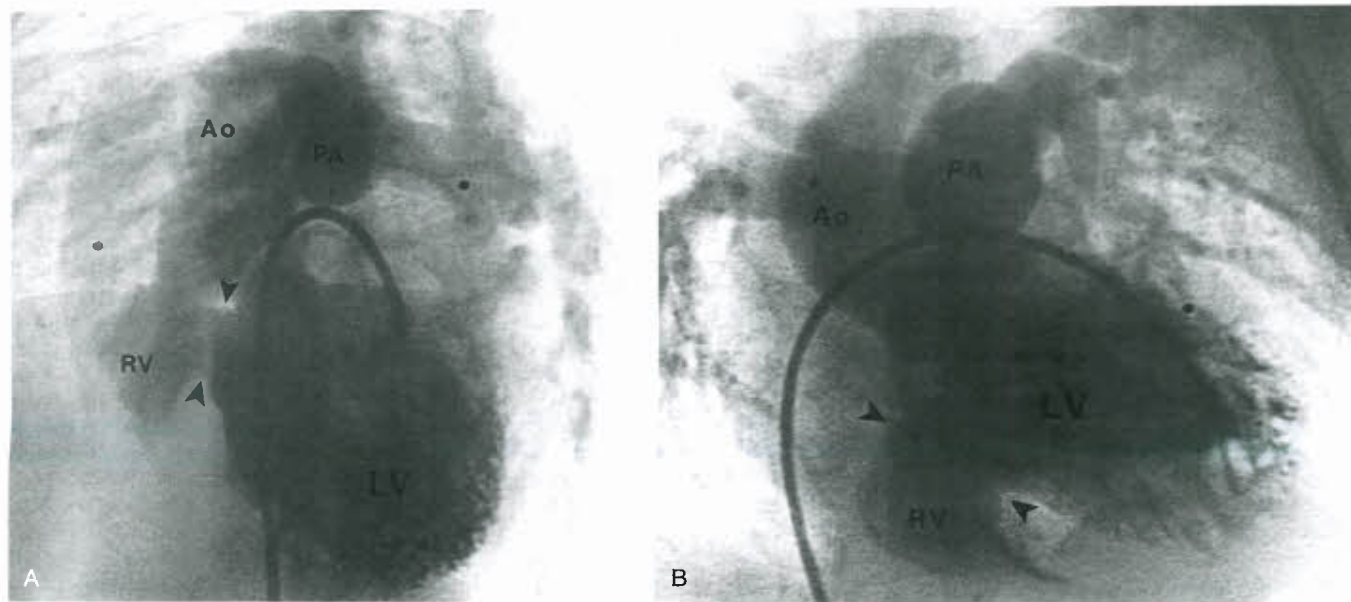


Figure 38.6. Views of a left ventriculogram from an infant with tricuspid atresia type Ic. **A:** A left anterior oblique view demonstrating a dilated left ventricle. Note the dense opacification of both the aorta and the pulmonary artery. The arrowheads outline the VSD. The hypoplastic right ventricle is well seen. **B:** A right anterior oblique view of the same ventriculogram shown in (A). The large ventricular septal defect is outlined by arrowheads. Ao, aorta; LV, left ventricle; PA, pulmonary artery; RV, right ventricle.

If severe restriction to pulmonary blood flow is present at birth, an infusion of prostaglandin E_1 (0.025 to 0.1 mg/kg/min) will maintain patency of the ductus arteriosus and ensure adequate pulmonary blood flow until surgery can be performed. Intubation and mechanical ventilation may become necessary because of the potential apnea caused by prostaglandin in a small percentage of patients. Other side effects for which these patients must be monitored include seizures, fever, and hypotension resulting from peripheral vasodilation.

The newborn with tricuspid atresia and normally related great arteries will have either an aortopulmonary shunt or pulmonary arterial banding procedure if there is diminished pulmonary blood flow (types Ia and Ib). If there is no obstruction between the left ventricle and the pulmonary circulation (type Ic), initial palliative treatment is either pulmonary artery detachment and central shunting or a pulmonary artery band. Occasionally, a type I patient will have enough obstruction to pulmonary blood flow that overcirculation will not occur, but pulmonary blood flow will be adequate enough that an initial shunt is not necessary. These patients must be monitored closely for reduction in VSD size and resultant inadequate pulmonary circulation.

Various shunts have been used in the past to provide adequate pulmonary blood flow for types Ia and Ib. The initial aortopulmonary shunt to be developed was the Blalock-Thomas-Taussig shunt, which anastomosed the subclavian artery to the ipsilateral pulmonary artery in an end-to-side fashion (15). This shunt fell out of favor because of the difficulty in maintaining patency in the early postoperative period. Other shunts then were developed, including the Potts shunt (16) (creation of a window between the descending aorta and the distal left pulmonary artery [LPA]) and the Waterston shunt (17) (creation of a window between the ascending aorta and the proximal right pulmonary artery [RPA]). These latter two operations resulted in various complications, including distortion of the pulmonary arteries, congestive heart failure with subsequent left ventricular dysfunction, and pulmonary hypertension with subsequent development of pulmonary vascular disease. As surgical techniques improved, the modified Blalock-Thomas-Taussig shunt, using prosthetic material (e.g., Gore-Tex tube), became the procedure of choice. Although distortion of the pulmonary artery still can occur, the more serious complications of left ventricular dysfunction and pulmonary vascular disease are rarely seen. A central shunt, which interposes a prosthetic tube between the ascending aorta and the MPA through a sternotomy, occasionally is used.

In patients with D-transposition of the great arteries and no obstruction to pulmonary blood flow (type IIc), a pulmonary artery band will be necessary not only to prevent pulmonary overcirculation but also to eliminate pulmonary hypertension and possible pulmonary arteriolar damage. An additional important consideration in patients with associated transposition is the size of the VSD. If there is obstruction to flow into the transposed ascending aorta, the options are to try to enlarge the VSD directly or to create an anastomosis between the MPA and ascending aorta, similar to the procedure described by Damus (18), Kaye (19), and Stansel (20). In this operation, the MPA is anastomosed to the ascending aorta. The branch pulmonary arteries usually are detached from the MPA, and pulmonary blood flow is supplied by an aortopulmonary shunt. Left ventricular output then will flow both through the restrictive VSD into the transposed aorta and directly into the MPA and subsequently into the ascending aorta. Other more complex surgery may be necessary, depending on associated lesions, especially in type III patients. The exact surgery to be performed depends on the specific details of the cardiac anatomy.

In 1965, Glenn et al. (21) described an operation that created an anastomosis between the SVC and the distal RPA.

This operation was performed by detaching the SVC from the right atrium and the RPA from the MPA. The SVC and RPA then were anastomosed in an end-to-end fashion. In this situation, the RPA blood flow was composed entirely from the systemic venous return, but the LPA was supplied by mixed systemic and pulmonary venous return traveling through the heart into the MPA. This operation was used successfully for many forms of cyanotic heart disease, including tricuspid atresia. The Glenn anastomosis was an attractive surgical option because it provided enough pulmonary blood flow to prevent severe hypoxemia and its consequences and, because the flow into the RPA was venous, there was no risk of developing pulmonary hypertension. Patients undergoing a Glenn anastomosis still had persistent right-to-left shunting from the inferior vena caval blood and its associated potential complications. Additionally, some patients develop pulmonary arteriovenous malformations many years after the Glenn shunt, which then worsens the cyanosis.

In 1971, Fontan and Baudet (22) described an operation that resulted in complete separation of the systemic and pulmonary circuits. The superior vena caval blood was directed to the RPA (Glenn shunt), and the right atrial appendage was anastomosed to the LPA system, which directed all the inferior vena caval blood into the LPA, interposing an aortic homograft valve. The atrial septal defect then was closed, completing separation of the systemic venous return and the pulmonary venous return (Fig. 38.7A). A similar operation was described by Kreutzer et al. (23) in which the right atrium was anastomosed directly to the MPA with an interposed semilunar valve. In this procedure, the branch pulmonary arteries remained in continuity with each other.

It has become convention to refer to any operation that reroutes systemic venous return into the pulmonary arteries without passing through a ventricle as a Fontan operation or its modifications. Over the ensuing years, completion of a Fontan procedure has become the eventual goal for all patients with tricuspid atresia. In 1978, Choussat et al. (24) described 10 criteria for optimal results following the Fontan procedure. These criteria included (a) age at operation between 4 and 15 years; (b) the presence of normal sinus rhythm; (c) normal systemic venous connections; (d) normal right atrial size; (e) normal pulmonary arterial pressure (mean ≤ 15 mm Hg); (f) low pulmonary vascular resistance (4 Woods units/m²); (g) adequate-sized pulmonary arteries with diameter $\geq 75\%$ of the aortic diameter; (h) normal left ventricular ejection fraction ($\geq 60\%$); (i) an absence of mitral valve insufficiency; and (j) absence of complicating factors from previous surgeries, such as pulmonary artery distortion. Today, the classic Fontan procedure is rarely, if ever, performed, but many modifications can accomplish the same physiologic result. Additionally, some of the criteria listed by Choussat et al. are no longer considered necessary to achieve an excellent result. Whereas it is still important that pulmonary vascular resistance (and therefore pulmonary pressure) is low, a modified Fontan procedure is routinely done in children younger than 4 years of age, many of whom had abnormal systemic venous connections. Diminished left ventricular function and the presence and degree of mitral valve insufficiency have become only relative contraindications. Nevertheless, with the exception of the age and size of the patient, a better outcome can be expected if all or most of the other criteria listed above are present.

Creation of the physiology of a Fontan procedure or one of its modifications results in marked changes in systemic venous hemodynamics. In the best of circumstances, the systemic venous or right atrial pressure rises significantly, equaling the mean pulmonary artery pressure. This sudden change in right-sided hemodynamics can cause early complications, such as persistent pleural effusions, in part because of altered lymphatic drainage. If the pulmonary vascular resistance is

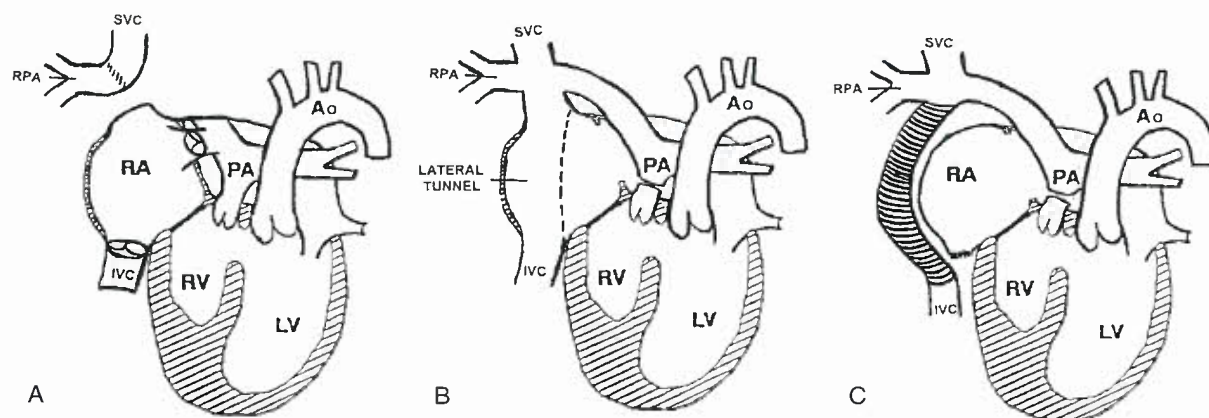


Figure 38.7. Diagrams depicting the original Fontan procedure and two subsequent modifications. **A:** The original procedure included (i) SVC to RPA anastomosis (Glenn shunt) and anastomosis of the right atrial appendage to the left pulmonary artery system directing IVC flow through a valved homograft, (ii) placement of a valved homograft at the IVS-RA junction, and (iii) closure of the atrial septal defect. **B:** Modified Fontan directing IVC flow through the lateral portion of the RA into the pulmonary artery system via an anastomosis to the underside of the RPA. The SVC flow is already directed into the RPA by a previous bidirectional Glenn shunt. **C:** Modification of the Fontan procedure using an extracardiac conduit. Ao, aorta; IVC, inferior vena cava; LV, left ventricle; PA, pulmonary artery; RA, right atrium; RPA, right pulmonary artery; RV, right ventricle; SVC, superior vena cava.

elevated or there is any impediment to forward flow through the pulmonary vascular tree, filling of the left heart will be compromised, resulting in low cardiac output.

In many cardiac centers performing these kinds of operations, an intermediate step has been developed between the newborn physiology and the Fontan procedure. A bidirectional Glenn anastomosis creates a communication between the SVC and the RPA that allows blood to go both into the RPA and LPA (25) (Fig. 38.8). The inferior vena caval blood

continues to flow right to left at the atrial level. The bidirectional Glenn anastomosis has the advantage of providing an adequate amount of effective pulmonary blood flow, diminishing the volume load on the left ventricle and preventing distortion of the pulmonary artery. Depending on the anatomy of the branch pulmonary arteries (e.g., stenosis resulting from previous surgery), differential blood flow can occur which may have to be addressed at later surgical intervention. Indeed, some studies suggest differential flow occurs simply due to the physiology of the venous return from either side of the body, and this differential flow may affect interpretation of studies that evaluate surgical results (26).

At a later date, after the patient has accommodated to the partial change in physiology, a complete cavopulmonary anastomosis can be accomplished by directing the inferior vena caval blood into the pulmonary artery. This procedure usually is performed by creating a tunnel within the right atrium, directing the inferior vena caval blood into the pulmonary artery through an anastomosis on the underside of the RPA (Fig. 38.7B). The portion of the right atrium not included within the tunnel remains part of the pulmonary venous atrium. Some investigators believe that loss of energy can be minimized with careful attention to the details of the anastomosis and/or type of procedure such that the direction of flow into each pulmonary artery avoids sharp turns and obstructions, thereby optimizing the fluid dynamics (27,28). The total cavopulmonary anastomosis has an additional advantage over the classic Fontan procedure in that it eliminates the dilated systemic venous reservoir with elevated pressure (right atrium) in which the blood flow is sluggish, predisposing to the development of thrombus formation and arrhythmias, especially atrial flutter. This physiology also can be accomplished by using an external conduit directing the inferior vena caval blood into the right pulmonary without using any of the right atrium (Fig. 38.7C).

In the best of circumstances, the force with which blood flows through the right side of the heart will be less than normal. It is imperative, therefore, that any impediment be relieved as much as possible. Interventional catheterization techniques (angioplasty with or without stent implantation) may be useful in alleviating obstruction to forward flow secondary to pulmonary artery distortion. In some cases surgical

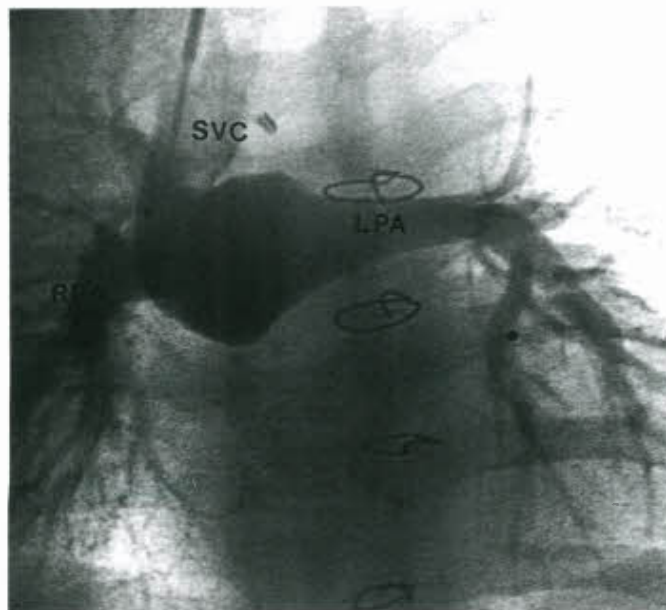


Figure 38.8. Pulmonary angiogram from a patient with tricuspid atresia who has undergone creation of a bidirectional Glenn anastomosis. The catheter was introduced through the internal jugular vein and superior vena cava (SVC). The tip is at the SVC-RPA junction. The pulmonary arterial tree is well visualized, and there is no distortion of the branch pulmonary arteries. LPA, left pulmonary artery; RPA, right pulmonary artery.

intervention might be necessary. The optimal timing of completion of a total cavopulmonary anastomosis is not established, but most investigators agree that earlier completion is better if circumstances permit. There is evidence that excessive volume overload on the left ventricle for a prolonged period can have detrimental effects on ventricular performance years later (29). In addition, patients having undergone completion of a total cavopulmonary anastomosis before 3 years of age were shown in one study to have better exercise tolerance up to 10 years after surgery than a group who underwent repair at a later age (30).

For patients having undergone a modification of Fontan procedure, arrhythmias can be particularly troublesome. It is important to try to maintain sinus rhythm. Depending on the exact type of surgical repair (e.g., intra-atrial baffling, external conduit, etc.), patients may have a greater propensity toward arrhythmias due to abnormalities in electrical dispersion (31). If appropriate drug treatment is unsuccessful, more aggressive therapy may be necessary. Electrophysiology study and catheter ablation may be helpful in controlling some tachyarrhythmias (32). However, because the right atrial wall thickness is considerably greater than in normal hearts, the success rate is lower than that in patients with normal anatomy and physiology. Surgical techniques to control arrhythmias, especially atrial flutter, have proven useful in patients with more recalcitrant problems.

For patients with marginally elevated pulmonary vascular resistance, a technique was developed to place a small fenestration between the systemic venous atrium and the pulmonary venous atrium. The presence of the fenestration allows a "safety valve" so that some flow can bypass the lungs and help to ensure adequate filling of the left ventricle. The disadvantage, of course, is that some degree of cyanosis will persist. If the hemodynamics allow, the fenestration may be closed in the early postoperative period (33) or later at cardiac catheterization (34).

Prognosis

Patients born with tricuspid atresia who have not undergone a surgical palliation have a 1-year survival rate as low as 10%, depending on the type of tricuspid atresia and associated lesions (7). Before the widespread use of the modified Fontan procedure, the likelihood of a patient born with tricuspid atresia surviving into young adulthood was still quite low (~50%). Today, the outlook is much improved. Patients who undergo complete separation of the pulmonary and systemic venous returns by a modified Fontan procedure have widely varying outcomes, depending on details of the preoperative hemodynamic status (35–37). The overall mortality rate of patients undergoing the Fontan procedure in recent series is between 7% and 11% (38–40); however, most of the larger series include patients with many forms of single-ventricle physiology, and so these results must be reviewed carefully for the outcome of patients with tricuspid atresia.

Although some patients undergoing a modified Fontan procedure have excellent outcomes, others develop major clinical complications, including development of collateral (both arterial and venous) vessels. Because of the elevated systemic venous pressure, it is not unusual for small venous channels from the right atrium or the venae cavae to dilate and create right-to-left shunting. If the amount of shunting is substantial, resulting in significant systemic desaturation, some of these channels can be occluded using catheterization techniques. Unfortunately, other channels are likely to develop unless the underlying physiology is corrected. On the other hand, systemic arterial collateral vessels may develop from the descending aorta. These collaterals communicate with the pulmonary arterial tree, and the flow from these vessels competes

with the low-pressure pulmonary blood flow created by the modified Fontan procedure. This can result in increased volume load on the left ventricle. The collateral artery can usually be occluded later at catheterization.

A particularly bothersome long-term complication that develops in some patients having undergone a Fontan procedure is protein-losing enteropathy (PLE) (41,42). The exact mechanism of this condition, which includes hypoproteinemias, ascites, and peripheral edema, is not known, but elevated mean pulmonary artery pressure preoperatively has been shown to increase the likelihood of development of PLE postoperatively (43). The marked change in right atrial pressure and subsequent disturbance in lymphatic drainage and hydrostatic pressure, however, are likely to be involved. Various treatment modalities, including administration of corticosteroids or heparin, have been tried with varying success (44–46). Because of hypoalbuminemia, administration of parenteral albumin and a diet including medium-chain triglycerides may be helpful. No treatment has been found to have long-term benefit.

Compared with the pre-Fontan condition, exercise tolerance is improved after surgery; however, exercise capacity is diminished in patients who have undergone a Fontan procedure or one of the modifications compared with normal (47,48). Even in patients who are asymptomatic at rest, there is compromise of the response to exercise. Causes for this decreased response include lack of a right ventricle, depressed left ventricular function, impaired chronotropic response, conduit obstruction, or abnormal pulmonary vascular resistance. Because of the compromise in right heart flow even in the best results, most cardiologists now recommend anticoagulation. In addition, afterload reduction using angiotensin-converting enzyme inhibitors is becoming more commonplace, especially in patients who have any degree of left ventricular dysfunction.

It remains to be seen whether operating on younger children who have experienced fewer years of chronic hypoxemia and left ventricular volume overload will have a better long-term prognosis than patients who were operated on between the mid-1970s and mid-1980s; this population of patients was older when they underwent the final Fontan modification.

Cardiac transplantation remains an option for patients with tricuspid atresia who either have such complex associated anatomy that conventional palliation is not likely to be successful or for those who had undergone palliation and have developed long-term complications. Transplant is the only option for patients with severe left ventricular dysfunction or PLE unresponsive to medical management.

TRICUSPID STENOSIS

Congenital tricuspid stenosis usually is associated with other anomalies, especially right ventricular outflow tract obstruction or atresia with secondary hypoplasia of the right ventricle (49). Some investigators differentiate tricuspid valvar stenosis from hypoplasia of the valve (50). In the former condition, the annulus may be relatively large, but the leaflets are thickened with commissural fusion and shortened chordae tendineae. In the latter condition, the valve annulus is small, and the leaflets and chordae may be diminutive but otherwise normal.

Isolated tricuspid stenosis is extremely rare. When described in adults, it is highly likely that this finding is secondary to rheumatic heart disease rather than being a congenital anomaly. Familial occurrences of tricuspid stenosis have been described (51).

Clinical manifestations of isolated congenital tricuspid stenosis resemble those seen in tricuspid atresia, and the two conditions may be difficult to differentiate, even with cardiac

catheterization (49). Not only is the clinical presentation similar in these two lesions, but the ECG in isolated tricuspid stenosis may demonstrate the typical left-axis deviation, right atrial enlargement, and prominent left ventricular forces typical for tricuspid atresia. Some investigators have suggested, therefore, that isolated tricuspid stenosis is merely a mild form of tricuspid atresia. Differentiating between the two is important because better options for surgical intervention may exist in patients with tricuspid stenosis compared with those with tricuspid atresia.

Early reports of tricuspid stenosis were made from autopsy examinations (52). The first description in a living patient reported clinical and catheterization data and reviewed previously published reports (53). Surgery has been attempted in some patients with mixed results. Infants requiring intervention are likely to have more severe lesions, and the results are likely to be worse (49). Older patients would be expected to fare better, with commissurotomy or valve replacement being the main option.

TRICUSPID VALVE INSUFFICIENCY

Isolated congenital tricuspid valve insufficiency, other than that associated with Ebstein anomaly, is rare. Various anatomic abnormalities of the tricuspid valve have been described, accounting for some of these cases. Tricuspid valve insufficiency also may be associated with other lesions, especially severe stenosis or atresia of the right ventricular outflow tract. In this situation, however, the tricuspid insufficiency, in all likelihood, is a secondary phenomenon. Occasionally, tricuspid valve insufficiency may occur with a structurally normal valve in the absence of associated lesions. Usually, there is a history of an intrauterine or perinatal event resulting in right ventricular and especially papillary muscle dysfunction (54).

Anatomic abnormalities resulting in tricuspid valve insufficiency have been well described. In some cases, one or more of the valve leaflets may show nodular thickening with shortened chordae tendineae and hypoplastic or absent papillary muscles (55,56). Although there may be no downward displacement of the valve leaflets and the leaflets themselves are not adherent to the right ventricular myocardium, some investigators believe this form of tricuspid valve dysplasia represents a mild form of Ebstein anomaly. Interestingly, similar nodules are often also found on the mitral valve, although mitral insufficiency is infrequent. Other structural abnormalities of the tricuspid valve have been described, including an isolated cleft of a valve leaflet and absence of valve tissue altogether with a relatively normal valve annulus (unguarded tricuspid orifice).

Patients who have isolated tricuspid valve insufficiency usually present in the newborn period but also may present later in infancy and childhood or even in adulthood. Age at presentation obviously depends on several factors, the most important of which is the degree of valve dysfunction, which may be exaggerated in a newborn in the presence of elevated pulmonary vascular resistance and particularly following a complicated perinatal course. In neonates and infants with severe tricuspid insufficiency, cyanosis and clinical findings of congestive cardiac failure appear early. Cardiac examination includes a pansystolic murmur loudest at the left lower sternal border, often with a precordial thrill.

The chest radiograph is likely to demonstrate marked cardiomegaly with diminished pulmonary vascular markings. The ECG is likely to be relatively unhelpful, although in cases with a perinatal insult, ST-segment depression may be prominent in the anterior precordial leads (54). Echocardiography may or may not demonstrate dysplasia of the tricuspid valve, but Doppler and color flow examinations will provide a

definitive diagnosis while ruling out the presence of associated lesions. Careful ultrasound evaluation of the pulmonary valve is likely to differentiate between functional and anatomic atresia of the right ventricular outflow tract (55,56). Cardiac catheterization, therefore, is unlikely to be necessary. In the event it is undertaken, findings are likely to include elevated right atrial pressure with a right-to-left atrial-level shunt. Right ventricular systolic pressure may be elevated, but in the case of severe insufficiency, it may be normal. Angiocardiography will demonstrate dense opacification of the right atrium. The degree of pulmonary artery opacification will depend on whether the right ventricle can generate enough forward flow to open the pulmonary valve in the face of elevated neonatal pulmonary vascular resistance.

The prognosis for newborns with tricuspid insufficiency depends on the extent of valve dysfunction, associated cardiac lesions, and cause of the insufficiency. Resolution of neonatal tricuspid insufficiency has been described, presumably in patients with relatively normal tricuspid valve structure and insufficiency owing to papillary muscle dysfunction (54). Early attempts at surgical intervention have been largely unsuccessful. With improved surgical techniques, the prognosis is likely to be improved, but there are no reports of successes thus far in infants with *severe* tricuspid insufficiency attributable to valve dysplasia. For patients who survive the newborn period and live into childhood, adolescence, or adulthood, the surgical options are likely to be greater, with a higher likelihood of success.

UHL ANOMALY

In 1952, a report published by Uhl (57) described an unusual congenital cardiac malformation consisting of an almost total absence of the right ventricular myocardium, although this condition was described years earlier by Sir William Osler (58). Uhl anomaly, as it has come to be known, is extremely rare, and by 1979, <20 cases had been reported, each individually as a case report (59). Some investigators have suggested that this condition is related to other conditions that affect the right ventricular myocardium, such as arrhythmogenic right ventricular dysplasia (60). Although some cases of Uhl anomaly presented with clinical findings consistent with tricuspid valve insufficiency, tricuspid valve abnormalities have not been universally reported.

The typical anatomic findings of Uhl anomaly have been described on prenatal ultrasound examination (61). Ages at postnatal presentation ranged between 1 day and 57 years, with equal gender distribution. Because each of these patients was reported as an isolated case without much family history, there is nothing to suggest a specific inheritance pattern. Most patients were clinically cyanotic, and, except for the presence of an atrial septal defect or patent foramen ovale, other associated congenital heart defects were rare. Clinical signs of right heart failure are almost universally present.

At physical examination, along with cyanosis, hepatomegaly is often present as well as jugular venous distension with a dominant "a" wave. Surprisingly, in view of gross right ventricular dilation found at autopsy, the precordium usually is described as being quiet, and peripheral pulses often are diminished in amplitude. Cardiac auscultation usually reveals a decrease in the intensity of the heart tones, especially the first heart sound. A typical pansystolic murmur of tricuspid insufficiency may be present, but patients may have other nonspecific murmurs or indeed no murmur at all.

Electrocardiography usually shows prominent right atrial enlargement with P waves often larger than the markedly diminished QRS amplitude, especially in the right precordial

leads. The chest radiograph demonstrates cardiomegaly, often of impressive degree, and normal to diminished pulmonary vascularity, often leading to the mistaken diagnosis of Ebstein anomaly of the tricuspid valve.

Echocardiography demonstrates marked dilation of the right-sided cardiac chambers. Although detailed echocardiographic investigation of Uhl anomaly using present-day instrumentation has not been described, an important finding is the presence of the tricuspid valve leaflets arising appropriately from the annulus, differentiating this lesion from Ebstein anomaly. Recently, newer techniques have been used to help characterize this lesion and to aid in planning treatment (62).

At cardiac catheterization, a typical finding is the similarity of pressure wave contours obtained from the pulmonary artery, right ventricle, and right atrium. The right atrial wave is dominant. There is usually systemic desaturation. Endocardial potentials, if recorded during catheterization, show normal transition between the ventricular and atrial complexes, helping to rule out Ebstein anomaly (59). Angiocardiology demonstrates dilated right cardiac chambers with delayed filling of the pulmonary artery and also may demonstrate a small right-to-left atrial shunt.

Although a few patients have been described who lived into adulthood, most patients die in infancy or childhood. The typical pathologic finding is the markedly dilated right ventricle, which is described as parchment-like. Histologically, the endocardium is thickened, and there are few if any true myocardial cells in the right ventricular free wall. Indeed, the right atrial wall may be thicker than the right ventricular anterior wall. The tricuspid valve arises normally from a dilated valve annulus and may be dysplastic but is not displaced into the right ventricular cavity as is typical for Ebstein anomaly.

Medical management has been of limited value. Various surgical procedures have been performed, including atrial septal defect closure, Potts anastomosis, and Glenn anastomosis. Most attempts at surgical intervention have failed to prolong life to any extent. However, procedures that create total cavopulmonary anastomosis and right ventricular exclusion, with or without resection of the dilated right ventricular anterior wall, have resulted in survival into later years (63–65). Although this lesion is extremely rare, at least one patient has undergone successful heart transplantation (66) and it has been considered in others (67). This form of treatment seems to be an option for long-term survival in symptomatic patients with findings of Uhl anomaly.

REFERENCES

- Kreysig EL. *Die Krankheiten des Herzens: Systematisch Bearbeitet und Durchzählige Beobachtungen Erläutert*. Berlin: Dritten Theil, 1817:104–109.
- Fyler DC, Buckley LP, Hellenbrand WE, et al. Report of the New England Regional Infant Cardiac Program. *Pediatrics* 1980;65:388–461.
- Sarkozy A, Conti E, D'Agostino R, et al. ZFPM2/FOG2 and HEY2 genes analysis in nonsyndromic tricuspid atresia. *Am J Med Genet* 2005;113A:68–70.
- Kuhne M. Über zwei fälle kongenitaler atresie des ostium venosum dextrum. *Jahrb F Kinderh* 1906;63:235–249.
- Tandon R, Edwards JE. Tricuspid atresia: a re-evaluation and classification. *J Thorac Cardiovasc Surg* 1974;67:530–542.
- Rao PS. Natural history of the ventricular septal defect in tricuspid atresia and its surgical implications. *Br Heart J* 1977;39:276–288.
- Dick M, Fyler DC, Nadas AS. Tricuspid atresia: clinical course in 101 patients. *Am J Cardiol* 1975;36:327–337.
- Gamboa R, Gersony WM, Nadas AS. The electrocardiogram in tricuspid atresia and pulmonary atresia with intact ventricular septum. *Circulation* 1966;34:24–37.
- Davachi F, Lucas RV Jr, Moller JH. The electrocardiogram and vectorcardiogram in tricuspid atresia. Correlation with pathologic anatomy. *Am J Cardiol* 1970;25:18–27.
- Weber HS, Hellenbrand WE, Kleinman CS, et al. Predictors of rhythm disturbances and subsequent morbidity after the Fontan operation. *Am J Cardiol* 1989;64:762–767.
- Silverman NH, Snider AR. Two-dimensional echocardiography in tricuspid atresia. In: Giuliani ER, ed. *Two-Dimensional Real-Time Ultrasonic Imaging of the Heart*. Boston: Martinus-Nijhoff, 1985:359–366.
- Berg C, Lachmann R, Kaiser C, et al. Prenatal diagnosis of tricuspid atresia: intrauterine course and outcome. *Ultrasound Obstet Gynecol* 2010;35:183–190.
- Wald RM, Tham EB, McCrindle BW, et al. Outcome after prenatal diagnosis of tricuspid atresia: a multicenter experience. *Am Heart J* 2007;153:772–778.
- Park SC, Neches WH, Mullins CE, et al. Blade atrial septostomy: collaborative study. *Circulation* 1982;66:258–266.
- Blalock A, Taussig HB. The surgical treatment of malformations of the heart in which there is pulmonary stenosis or pulmonary atresia. *JAMA* 1945;128:189–202.
- Potts WJ, Smith S, Gibson S. Anastomosis of the aorta to a pulmonary. Certain types in congenital heart disease. *JAMA* 1946;132:627–631.
- Waterston DJ. The treatment of Fallot's tetralogy in children under one year of age. *Rozhl Chir* 1962;41:181–183.
- Damus PS. Correspondence. *Ann Thorac Surg* 1975;20:724–725.
- Kaye MP. Anatomic correction of transposition of great arteries. *Mayo Clin Proc* 1975;50:638–640.
- Stansel HC Jr. A new operation for d-loop transposition of the great vessels. *Ann Thorac Surg* 1975;19:565–567.
- Glenn WWL, Ordway NK, Talner NS, et al. Circulatory bypass of the right heart. VI. Shunt between superior vena cava and distal right pulmonary artery: Report of clinical application in thirty-eight cases. *Circulation* 1965;31:172–190.
- Fontan F, Baudet E. Surgical repair of tricuspid atresia. *Thorax* 1971;26:240–248.
- Kreutzer G, Galindez E, Bono H, et al. An operation for correction of tricuspid atresia. *J Thorac Cardiovasc Surg* 1973;66:613–621.
- Choussat A, Fontan F, Besse P, et al. Selection criteria for Fontan procedure. In: Anderson RH, Shinebourne EA, eds. *Pediatric Cardiology* 1977. Edinburgh: Churchill Livingstone, 1978;559–566.
- Norwood WL, Jacobs ML. Fontan procedure in two stages. *Am J Surg* 1993;166:548–551.
- Fukuda Y, Momoi N, Mitomo M, et al. Increasing the accuracy of lung perfusion scintigraphy in children with bidirectional Glenn circulation. *Pediatr Radiol* 2010;40:1890–1894.
- Sharma S, Goudy S, Walker P, et al. In vitro flow experiments for determination of optimal geometry of total cavopulmonary connection for surgical repair of children with functional single ventricle. *J Am Coll Cardiol* 1996;27:1264–1269.
- Bove EL, de Laval MR, Migliavacca F, et al. Computational fluid dynamics in the evaluation of hemodynamic performance of cavopulmonary connections after the Norwood procedure for hypoplastic left heart syndrome. *J Thorac Cardiovasc Surg* 2003;126:1040–1047.
- Adachi I, Ueno T, Ichikawa H, et al. Effect of ventricular volume before unloading in a systemic ventricle supporting the Fontan circulation. *Am J Cardiol* 2011;107:459–465.
- Shiraishi S, Yagihara T, Kagisaki K, et al. Impact of age at Fontan completion on postoperative hemodynamics and long-term aerobic exercise capacity in patients with dominant left ventricle. *Ann Thorac Surg* 2010;87:555–560.
- Koh M, Uemura H, Kada A, et al. Chronologic changes in P-wave characteristics after the Fontan procedure: the effect of surgical modification. *J Thorac Cardiovasc Surg* 2010;140:137–143.
- Weipert J, Noebauer C, Schreiber C, et al. Occurrence and management of atrial arrhythmia after long-term Fontan circulation. *J Thorac Cardiovasc Surg* 2004;127:457–464.
- Laks H, Pearl JM, Haas GS, et al. Partial Fontan: advantages of an adjustable interatrial communication. *Ann Thorac Surg* 1991;52:1084–1094.
- Bridges ND, Lock JE, Castaneda AR. Baffle fenestration with subsequent transcatheter closure: modification of the Fontan operation for patients at increased risk. *Circulation* 1990;82:1681–1689.
- Gale AW, Danielson GK, McGoon DC, et al. Fontan procedure for tricuspid atresia. *Circulation* 1980;62:91–96.
- Stanton RE, Lurie PR, Lindesmith GG, et al. The Fontan procedure for tricuspid atresia. *Circulation* 1981;64:140–146.
- Sanders SP, Wright GB, Keane JF, et al. Clinical and hemodynamic results of the Fontan operation for tricuspid atresia. *Am J Cardiol* 1982;49:1733–1740.
- Jacobs ML, Norwood WI. Fontan operation: influence of modifications on morbidity and mortality. *Ann Thorac Surg* 1994;58:945–952.
- Sharma R, Iyer KS, Airan B, et al. Univentricular repair: early and midterm results. *J Thorac Cardiovasc Surg* 1995;110:1692–1701.
- Gentles TL, Mayer JE Jr, Gauvreau K, et al. Fontan operation in five hundred consecutive patients: factors influencing early and late outcome. *J Thorac Cardiovasc Surg* 1997;114:376–391.
- Crupi G, Locatelli G, Tiraboschi R, et al. Protein-losing enteropathy after Fontan operation for tricuspid atresia (imperforate tricuspid valve). *J Thorac Cardiovasc Surg* 1980;28:359–363.
- Hess J, Kruijzinga K, Bijleveld CMA, et al. Protein-losing enteropathy after Fontan operation. *J Thorac Cardiovasc Surg* 1984;88:606–609.
- Mascio CE, Wayment M, Colaizy TJ, et al. The modified Fontan procedure and prolonged pleural effusions. *Am Surg* 2009;75:175–177.
- Rothman A, Snyder J. Protein-losing enteropathy following the Fontan operation: resolution with prednisone therapy. *Am Heart J* 1991;121:618–619.

45. Rychik J, Riccoli DA, Barber G. Usefulness of corticosteroid therapy for protein-losing enteropathy after Fontan operation. *Am J Cardiol* 1991;68:819-821.
46. Donnelly JP, Rosenthal A, Castle VP, et al. Reversal of protein-losing enteropathy with heparin therapy in three patients with univentricular hearts and Fontan palliation. *J Pediatr* 1997;130:474-478.
47. Ben Shachar G, Fuhrman BP, Wang Y, et al. Rest and exercise hemodynamics after the Fontan procedure. *Circulation* 1982;65:1043-1048.
48. Driscoll DJ, Danielson GK, Puga FJ, et al. Exercise tolerance and cardiorespiratory response to exercise after the Fontan operation for tricuspid atresia or functional single ventricle. *J Am Coll Cardiol* 1986;7:1087-1094.
49. Shore DF, Rigby ML, Lincoln C. Severe tricuspid stenosis presenting as tricuspid atresia: echocardiographic diagnosis and surgical management. *Br Heart J* 1982;40:404-406.
50. Svane S. Congenital tricuspid stenosis: a report on six autopsied cases. *Scand J Thorac Cardiovasc Surg* 1971;5:232-238.
51. Davachi F, McLean RH, Moller JH, et al. Hypoplasia of the right ventricle and tricuspid valve in siblings. *J Pediatr* 1967;71:869-874.
52. Lewis T. Congenital tricuspid stenosis. *Clin Sci* 1945;5:261-271.
53. Calleja HB, Hosier DM, Kissane RW. Congenital tricuspid stenosis: the diagnostic value of cineangiography and hepatic pulse tracing. *Am J Cardiol* 1960;6:821-829.
54. Bucciarelli RL, Nelson EM, Egan EA, et al. Transient tricuspid insufficiency of the newborn: a form of myocardial dysfunction in stressed newborns. *Pediatrics* 1977;59:330-337.
55. Barr PA, Celermajor JM, Bowdler JD, et al. Severe congenital tricuspid incompetence in the neonate. *Circulation* 1974;49:962-967.
56. Becker AE, Becker MJ, Edwards JE. Pathologic spectrum of dysplasia of the tricuspid valve: features in common with Ebstein's malformation. *Arch Pathol* 1971;91:167-178.
57. Uhl HSM. A previously undescribed congenital malformation of the heart: almost total absence of the myocardium of the right ventricle. *Bull Johns Hopkins Hosp* 1952;91:197-205.
58. Osler WM. *The Principles and Practice of Medicine*. 6th ed. New York: D. Appleton, 1905:280.
59. Vecht RJ, Carmichael DJS, Gopal R, et al. Uhl anomaly. *Br Heart J* 1979;41:676-682.
60. Pamuru PR, Dokuparthi MV, Remersu S, et al. Comparison of Uhl's anomaly, right ventricular outflow tract ventricular tachycardia (RVOT VT) and arrhythmogenic right ventricular dysplasia/cardiomyopathy (ARVD/C) with an insight into genetics of ARVD/C. *Ind J Med Res* 2010;131:35-45.
61. Wager GP, Couser RJ, Edwards OP, et al. Antenatal ultrasound findings in a case of Uhl anomaly. *Am J Perinatol* 1988;5:164-167.
62. Cheng JF, Mohammed TL, Griffith BP, et al. CT of Uhl's anomaly in an adult. *Int J Cardiovasc Imaging* 2005;21:663-666.
63. Takizawa K, Suzuki S, Honda Y, et al. Long-term survival of Uhl's anomaly with total cavopulmonary conversion. *Asian Cardiovasc Thorac Ann* 2009;17:203-205.
64. Azhari N, Assaqqat M, Bulbul Z. Successful surgical repair of Uhl's anomaly. *Cardiol Young* 2002;12:192-195.
65. Tanoue Y, Kado H, Shiokawa Y. Uhl's anomaly complicated with critical ventricular arrhythmia in a 2-month-old infant. *Eur J Cardiothorac Surg* 2003;24:1040-1042.
66. Ikari NM, Azeka E, Aiello VD, et al. Uhl's anomaly. Differential diagnosis and indication for cardiac transplantation in an infant. *Arq Bras Cardiol* 2001;77:73-76.
67. Gilljam T, Bergh C-H. Right ventricular cardiomyopathy: timing of heart transplantation in Uhl's anomaly and arrhythmogenic right ventricular cardiomyopathy. *Eur J Heart Failure* 2008;11:106-109.

Ebstein's Anomaly, Congenital Tricuspid Valve Regurgitation, and Dysplasia

Sameh M. Said ■ Joseph A. Dearani

EBSTEIN'S ANOMALY

History

Wilhelm Ebstein (1836–1912) who was a German physician, described in a report titled, “Concerning a very rare case of insufficiency of the tricuspid valve caused by a congenital malformation” in 1866 the unusual cardiac findings in a 19-year-old laborer who had died of cyanotic heart disease (1). He accurately described the characteristic anatomic and the hemodynamic abnormalities of Ebstein anomaly (Fig. 39.1). By 1950, only three case reports of this anomaly had been published.

Prevalence

Ebstein's anomaly is a rare congenital heart defect, which occurs in about 1/200,000 live births. It accounts for almost 1% of all cases of congenital heart disease (2,3).

Pathologic Anatomy

Normally, the tricuspid valve (TV) has three leaflets: anterior, inferior (posterior), and septal. The leaflets of the TV develop equally from the endocardial cushion tissues and the myocardium (7). The leaflets and tensile apparatus of the atrioventricular (AV) valves are formed by a process of delamination of the inner layers of the inlet zone of the ventricles. In Ebstein's anomaly, delamination of the TV leaflets fails to occur, but the mechanism is not entirely understood.

Ebstein's anomaly is a malformation of the TV and right ventricle (RV) characterized by (4):

1. Adherence of the septal and inferior leaflets to the underlying myocardium (failure of delamination)
2. Downward (apical) displacement of the functional annulus (septal > inferior > anterior)
3. Dilation of the “atrialized” portion of the RV, with variable degrees of thinning of the free wall
4. Redundancy, fenestrations, and tethering of the anterior leaflet
5. Dilation of the right AV junction (true tricuspid annulus) (5,6)

Tricuspid Valve

TV morphology in Ebstein's anomaly is highly variable. The leaflets are malformed and are attached to both the TV annulus and to the right ventricular endocardium.

It may be funnel shaped, incompetent, or rarely stenotic.

■ Leaflets:

- The anterior leaflet:
 - Usually large and is attached to the TV annulus.
 - Generally redundant and may contain several fenestrations (8) (Fig. 39.2A and B).

- Chordae tendineae generally are short and poorly formed.

- It may be severely deformed, so that the only mobile leaflet tissue is displaced into the right ventricular outflow tract (RVOT), where it may form a sail-like intracavitary curtain.

- The inferior and septal leaflet development is variable and most often rudimentary and may even be absent due to failure of the delamination process.
- Leading edges may be freely mobile with chordal and/or papillary muscular support, or may be tethered (adherent) to the endocardium.
- The apical displacement of the hinge point of the valve from the AV ring is shown in (Fig. 39.3) (7,8). The point of maximal displacement is at the commissure between the inferior and septal leaflets (11). In normal hearts, the downward displacement of the septal and posterior leaflets in relation to the anterior mitral valve leaflet is <8 mm/m² body surface area (8). The spectrum of the malformation in Ebstein's anomaly may range from only minimal displacement of the septal and inferior leaflets to an imperforate membrane or muscular shelf between the inlet and trabecular zones of the RV. The range of variability is infinite. Typical autopsy examples of Ebstein's anomaly are shown in Figures 39.4 and 39.5.
- TV annulus
 - There often is marked dilatation of the true TV annulus, which is not displaced, and a large chamber separating the true annulus from the functional RV is the “atrialized” portion of the RV(8) (Fig. 39.3).

Right Coronary Artery

The right coronary artery (RCA) demarcates the level of the true annulus. The thin nature of the atrial and ventricular tissue at the level of the AV groove makes the RCA vulnerable to kinking or distortion during RV plication, annuloplasty procedure (Figure 39.6), or TV replacement.

Right Ventricle

- In Ebstein's anomaly, the RV is divided into two regions: the area involved with the malformation (i.e., the inlet portion) that is functionally integrated with the right atrium (RA), and the area that is not involved by the anomaly and consists of the other two components of the RV—the trabecular and outlet portions, which constitute the functional RV. The “atrialized” portion of the RV (i.e., the inlet component) can become disproportionately dilated and may account for more than half of the RV volume instead of the usual one-third of the total right ventricular volume (Fig. 39.7A and B).
- The majority (>2/3) of hearts with Ebstein's anomaly have RV dilatation. Dilatation often involves not only the atrialized inlet portion of the RV but also the functional right ventricular apex and outflow tract. In some cases,



Figure 39.1. Figure from Ebstein's original case report. The RA and RV are shown opened along the right border beginning at the superior vena cava. A, RA; B, RV; b, valve; I, rudimentary septal leaflet of TV with its chordae tendineae, which insert on the endocardium of the ventricular septum; r, opening through which one can get into the right conus arteriosus, and in the opposite direction, one can get into the sac that is formed by membrane h, h', and posterior part of endocardium of ventricular septum o. (From Mann RJ, Lie JT. The life story of Wilhelm Ebstein (1836–1912) and his almost overlooked description of a congenital heart disease. *Mayo Clin Proc* 1979;54:197–204, used with permission of the Mayo Foundation for Medical Education and Research.).

right ventricular dilatation is so marked that the ventricular septum is deviated leftward, compressing the left ventricular chamber (8). In such cases, the short-axis view demonstrates a circular RV and a D-shaped or crescent-shaped left ventricle (LV). In extreme cases, episodic left ventricular outflow tract obstruction (LVOTO) can occur (Fig. 39.8).

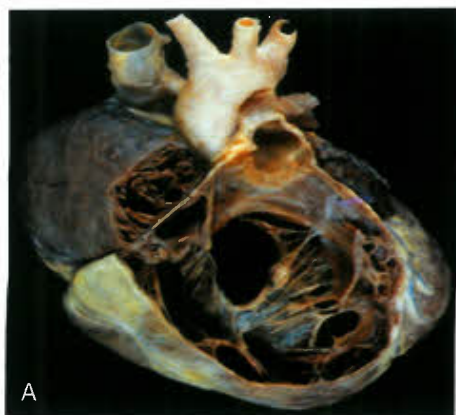


Figure 39.2. A,B: Ebstein's heart: marked fenestrations, and tethering of the TV anterior leaflet. (Used with permission of the Mayo Foundation for Medical Education and Research.)

Classifications

- A. Based on the echocardiographic appearance, Ebstein's anomaly can be classified as mild, moderate, or severe (9) according to:
 - Extent of the apical displacement of the TV leaflets
 - Degree of tricuspid regurgitation (TR)
 - Degree of RV dilatation and dysfunction
- B. Four types of Ebstein's anomaly were proposed based on the anatomic findings during surgery (10) (Table 39.1). This is our preferred approach, which is to describe the exact anatomy of each of the involved structures of the heart as visualized at operation. This nomenclature system emphasizes characteristics that surgeons find important when considering repair of the TV. In general, classification systems of Ebstein's anomaly are difficult since there are infinite variations in the anatomy and no two hearts are alike.
- C. In 1988, Carpentier et al. (11) proposed the following classification of Ebstein's anomaly (Fig. 39.9):
 - Type A: the volume of the true RV is adequate
 - Type B: a large atrialized component of the RV exists, but the anterior leaflet of the TV moves freely
 - Type C: the anterior leaflet is severely restricted in its movement and may cause significant obstruction of the RVOT
 - Type D: almost complete atrialization of the ventricle except for a small infundibular component.
- D. Celermajor et al. (12) described an echocardiographic grading score for neonates with Ebstein's anomaly, the Great Ormond Street Echocardiography (GOSE) score, with grades 1 to 4. The ratio of the combined area of the RA and atrialized RV is compared to the functional RV and left heart. This classification is particularly helpful with neonatal Ebstein's anomaly.
 - Grade 1: ratio <0.5
 - Grade 2: ratio of 0.5 to 0.99
 - Grade 3: ratio of 1.0 to 1.49
 - Grade 4: ratio ≥ 1.5

Genetic Factors

There are heterogeneous genetic factors in Ebstein's anomaly. Case-control studies suggest genetic, reproductive, and environmental risk factors (e.g., the anomaly is more common in twins, in those with a family history of congenital heart disease, and in those with maternal exposure to benzodiazepines) (13). Most cases are sporadic; familial Ebstein's anomaly is rare. In a genetic study of 26 families with Ebstein's anomaly, 93

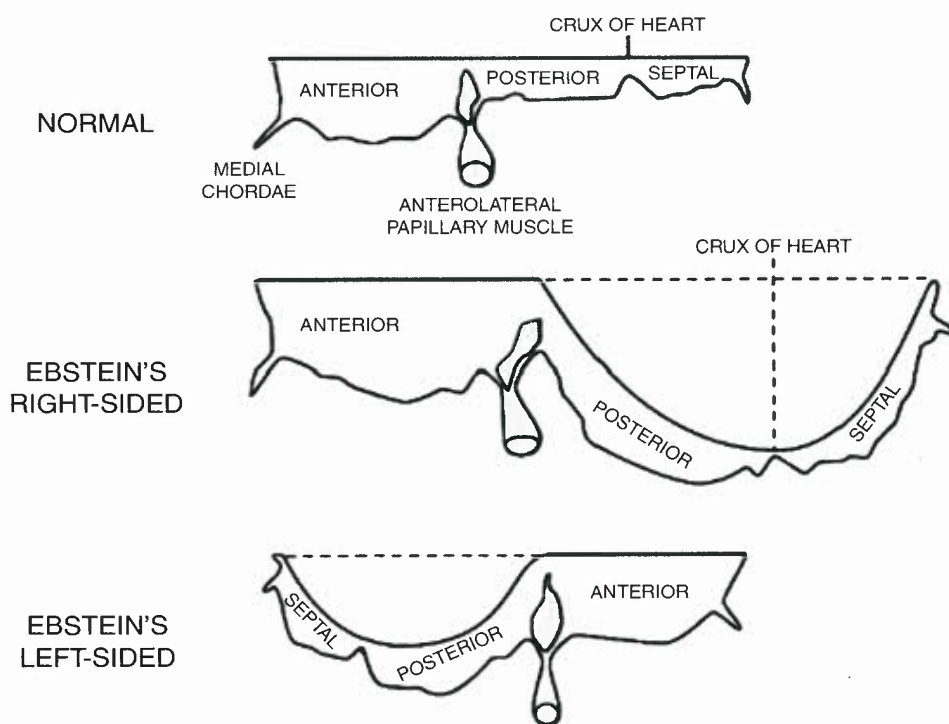


Figure 39.3. Top: Normal TV with anterior, posterior, and septal leaflets in one plane. Middle: TV in right-sided Ebstein's anomaly showing displacement of posterior and septal leaflets; maximal displacement is at the crux of the posterior and septal leaflets. Bottom: TV in left-sided Ebstein's anomaly; the displacement of leaflets is similar to that in the right-sided anomaly. (From Anderson KR, Zuberbuhler JR, Anderson RH et al., Morphologic spectrum of Ebstein's anomaly of the heart: a review. *Mayo Clin Proc* 1979;54(3):174–180, with permission.)

of 120 first-degree relatives were evaluated (14). No case of the anomaly was found, but two first-degree relatives had ventricular septal defects (VSDs), and another, who died at seven months, was said to have had congenital heart disease. Rare cases of cardiac transcription factor NKX2.5 mutations, 10p13-p14 deletion, and 1p34.3-p36.11 deletion have been described in the anomaly (15,16). Recently, Postma et al. (17) reported the results of a mutational analysis in a cohort of 141 unrelated probands with Ebstein anomaly. Eight were found to have a mutation in the gene MYH7 and six of the eight patients also had left ventricular noncompaction. This may warrant genetic testing and family evaluation in this subset of patients.

Associated Cardiac Defects

The most common associated cardiac defects include (18,19):

- Interatrial septal defects:
 - Patent foramen ovale (PFO) or an atrial septal defect (ASD), mostly secundum, is present in 80% to 94% of the patients (20).
- VSD with or without pulmonary atresia.
- RVOT obstruction
 - Due to structural abnormalities (pulmonic valve stenosis or pulmonary atresia), branch pulmonary artery stenosis, and, rarely, the displaced TV.
- Patent ductus arteriosus.

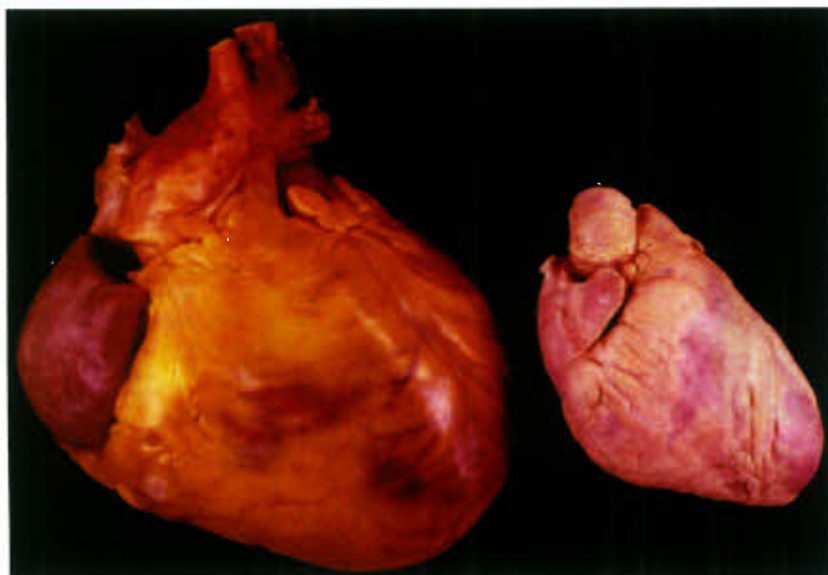


Figure 39.4. Marked cardiomegaly caused by right-sided chamber dilatation in a 67-year-old man with severe Ebstein's anomaly, with normal heart at right for comparison (anterior view). (Used with permission of the Mayo Foundation for Medical Education and Research.)

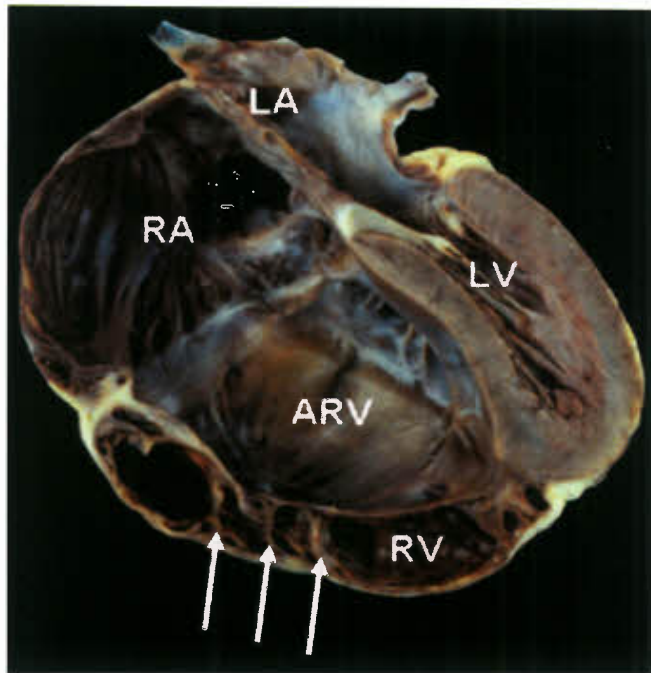


Figure 39.5. Severe Ebstein's malformation of TV (*four-chamber view*) showing marked downward displacement of shelf-like posterior leaflet with attachment to underlying free wall by numerous muscular stumps (*arrows*), markedly dilated atrialized portion of right ventricle (ARV), small functional portion of RV, leftward bowing of ventricular septum, and marked dilatation of RA. LA, left atrium; LV, left ventricle. (Used with permission of the Mayo Foundation for Medical Education and Research.)

- Coarctation of the aorta.
- One or more accessory conduction pathways are present in up to 15% to 20% of patients with Ebstein's anomaly, predisposing patients to arrhythmias. The majority of these pathways are located around the orifice of the malformed TV (7,21).

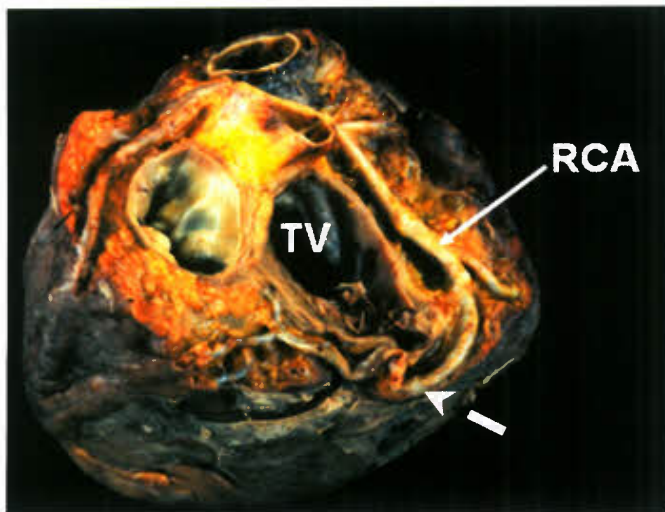


Figure 39.6. Pathologic specimens showing: the close relation between the RCA and the TV annulus. RCA (*arrow*) can be easily kinked (*dashed arrow*) during TV repair procedure. RCA, right coronary artery; TV, tricuspid valve. (Used with permission of the Mayo Foundation for Medical Education and Research.)

- Left sided heart lesions:
 - Diastolic and systolic dysfunction
 - Mitral valve prolapse
 - Accessory mitral valve tissue
 - Subaortic stenosis
 - Bicuspid or atretic aortic valve
 - Muscle bands of the LV
 - Myocardial changes resembling left ventricular non-compaction (22)

We recently reported features resembling noncompaction in three patients with Ebstein's anomaly (25). Since then, we have analyzed 106 consecutive patients who had Ebstein's anomaly and found left-sided heart abnormalities in 39%; 18% of these patients had left ventricular dysplasia resembling noncompaction (21).

- Congenitally corrected transposition of the great arteries (cc-TGA):

Most patients with cc-TGA have an abnormal systemic AV valve (morphologic TV) that fulfills the criteria for Ebstein's anomaly in 15% to 50% of cases (23). The Ebsteinoid displacement (Fig. 39.10) of the TV into the morphologic RV is different from the classic right-sided Ebstein malformation in that there is usually a lack of atrialization of the RV free wall (24). In addition, when functioning at lower pulmonary pressures after a double-switch procedure, the regurgitation is reduced markedly; that is, it tends to be a high-pressure regurgitant valve rather than a low-pressure regurgitant valve (25). The morphological RV (systemic ventricle) is rarely dilated in cc-TGA.

Pathophysiology

Due to the wide spectrum of anatomic severity, there is a wide spectrum of pathophysiology and associated symptoms. The functional impairment of the RV and TV regurgitation retard forward flow of blood through the right side of the heart. In addition, during contraction of the atrium, the atrialized portion of the RV balloons out and acts as a passive reservoir, decreasing the volume of ejected blood. The overall effect on the RA is dilatation, increasing the size of an interatrial communication. TR increases with progressive annular dilatation. Associated heart disease in Ebstein's anomaly has an additional detrimental effect on cardiopulmonary physiology. Symptomatic neonates have massive cardiac enlargement with associated hypoplasia of the lungs. Due to the absence of forward flow from the ineffective RV, there can be physiologic pulmonary atresia, and the child is dependent on ductal patency for survival. All systemic venous return must pass from right to left, across a PFO or ASD. The enormous capacitance of the RA and the inefficiency of the RV prevent adequate filling of the LV. LV output also is compromised in sick neonates, and these neonates are severely cyanotic and acidotic. Those with less severe atrialization of the RV may have adequate pulmonary blood flow that will further improve with the decrease in pulmonary vascular resistance. At the other end of the spectrum, there may be only a mild degree of cyanosis, which may not be noted until adult life and may result in few, if any, symptoms.

Clinical Presentation

Presentation varies widely and can range from the severely symptomatic neonate to an incidental finding in an

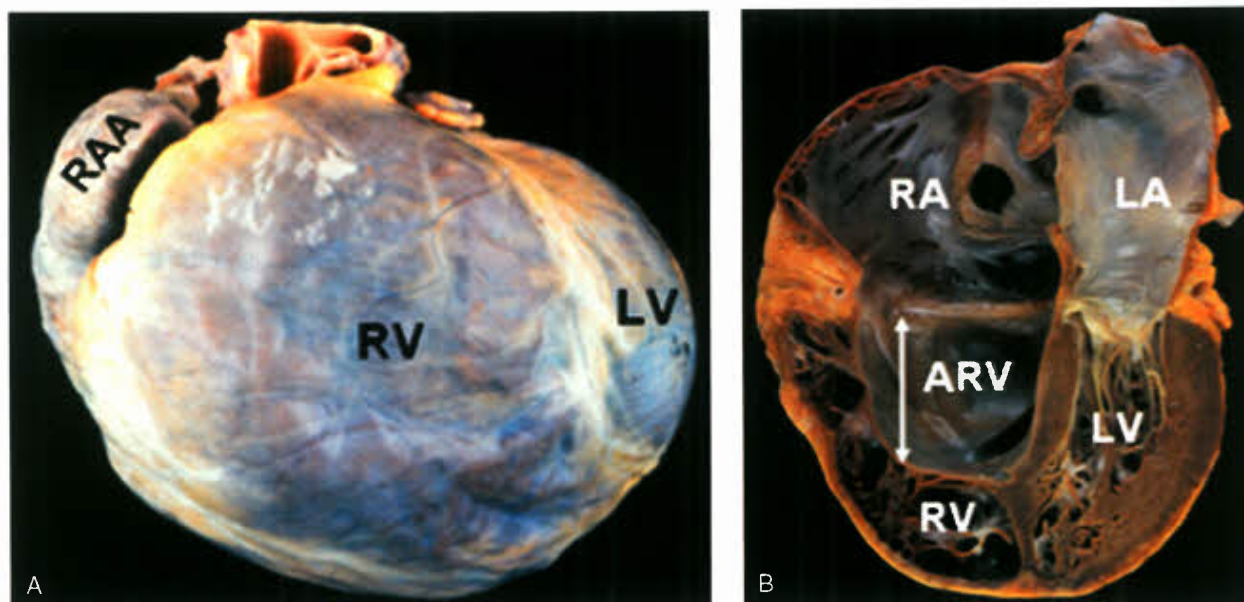


Figure 39.7. A: Ebstein's heart with marked dilatation of the RV. B: Severe apical displacement of the TV apparatus is shown (*double-headed arrow*), the RV in Ebstein's anomaly is divided into two regions: the RV proper and the atrialized portion, which can become disproportionately dilated and may account for more than half of the RV volume in extreme cases instead of the usual one-third of the total right ventricular volume. RA, right atrium; LA, left atrium; LV, left ventricle; RV, right ventricle; RAA: right atrial appendage; aRV, atrialized right ventricle. (Used with permission of the Mayo Foundation for Medical Education and Research.)

octogenarian. In general, symptoms are related to the anatomic severity. Patients with mild apical displacement and normal function of the TV may remain asymptomatic for years (26). In the presence of marked tricuspid leaflet displacement or abnormal leaflet attachment and severe valvular regurgitation, patients will have elevated right atrial pressure, and significant right-to-left interatrial shunting with arterial desaturation. The anomaly may be fatal shortly after birth if severe heart failure is present (15).

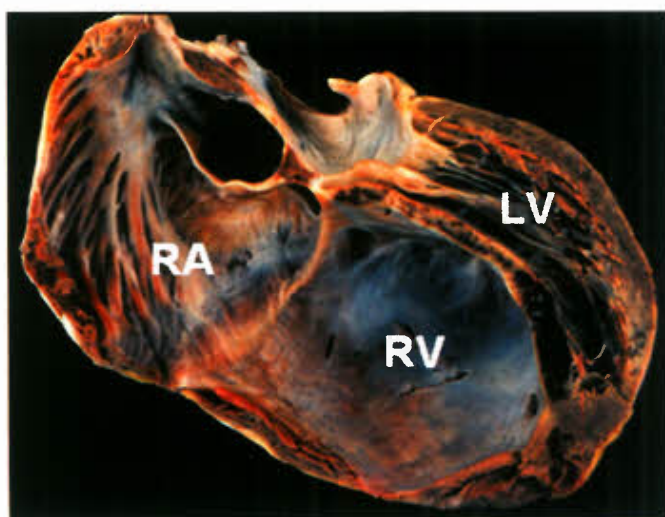


Figure 39.8. Ebstein's heart showing marked dilatation of the RV. In extreme cases, episodic LVOTO can occur with marked interventricular septal shift. RA, right atrium; RV, right ventricle; LV: left ventricle. (Used with permission of the Mayo Foundation for Medical Education and Research.)

In a review of 220 patients with Ebstein's anomaly, the most common presentation varied with age at presentation (10):

- Fetuses—an abnormal routine prenatal scan (86%)
- Neonates—cyanosis (74%)
- Infants—heart failure (43%)
- Children—an incidental murmur in children (63%)
- Adolescents and adults—arrhythmia (42%), decrease exercise tolerance, fatigue, or right-sided heart failure.

Early age at presentation frequently was associated with other cardiac lesions, particularly pulmonary stenosis or atresia. Ebstein's anomaly is a common lesion referred for fetal echocardiography because severe forms may lead to cardiomegaly, hydrops, and tachyarrhythmias (27,28).

Symptoms

CYANOSIS AND HEART FAILURE

- From significant TR
- May appear soon after birth, because of high pulmonary vascular resistance (10).
- Often improves as pulmonary vascular resistance decreases.

EXERTIONAL DYSPNEA, FATIGUE, CYANOSIS, AND PALPITATIONS

- May occur at a later age
- May recur; and may be insidious in onset.

PALPITATIONS

- Due to atrial tachyarrhythmia
- Present in 20% to 30% of cases (10,29)
- Some of these arrhythmias may be due to Wolff-Parkinson-White syndrome (WPW).

PARADOXICAL EMBOLIZATION

- In the presence of an interatrial communication, patients with Ebstein's anomaly are at risk for paradoxical embolization, brain abscesses, and sudden death.

TABLE 39.1 Types of Ebstein's Valve Based on the Anatomic Findings During Surgery

Type	Anterior Leaflet		Posterior Leaflet	Septal Leaflet	Atrialized RV Chamber Size
	Size	Mobility			
I	Larger	Mobile	Apically displaced, dysplastic, or absent.		Varies from relatively small to large.
II	Relatively small and displaced in a spiral fashion toward the apex.				Moderately large.
III		Restricted motion Shortened, fused, and tethered chordae. Direct insertion of papillary muscles into the anterior leaflet is frequently present.	Displaced, dysplastic, and usually not reconstructible.		Large
IV		Severely deformed Few or no chordae. Direct insertion of the papillary muscles into the leading edge of the valve is common.	Typically dysplastic or absent	Represented by a ridge of fibrous material descending apically from the membranous septum.	Nearly the entire RV cavity is atrialized. TV tissue is displaced into the RVOT and may cause obstruction of blood flow (functional tricuspid stenosis).

Physical Examination

Findings vary with the severity of pathology and the magnitude of right-to-left interatrial shunting.

- Murmur and click; commonly mistaken for mitral valve prolapse (11).
- Cyanosis
 - May be severe in infants.
 - Mild in older children.
 - Digital clubbing will depend on the degree of cyanosis (30).
- Prominent “a” wave in the distended jugular veins.
- Hepatomegaly:
 - Represents passive hepatic congestion resulting from TR and elevated right atrial pressure.
 - Hepatomegaly becomes pulsatile due to systolic expansion of the liver.
- Palpable prominent diffuse apical impulse
- Systolic thrill at the left lower sternal border.
- Widely split first and second heart sounds, resulting from right bundle branch block.
- A prominent S3 and/or a loud S4 give the impression of multiple heart sounds (triple or quadruple gallop).
- A systolic murmur
 - From TR
 - Increases in intensity with inspiration and may be associated with a mid-diastolic murmur due to high diastolic flow volume across the tricuspid annulus.
 - May be very soft or absent in adults because the low velocity of to- and-fro flow and rapid equalization of pressure across the TV does not result in blood flow turbulence.

- The jugular venous pulse rarely shows a large V wave despite severe regurgitation of the TV because the large RA engulfs the increased volume.

Diagnostic Evaluation

Chest Radiography

The cardiac silhouette varies from almost normal to a markedly enlarged globe-shaped heart with a narrow waist (Fig. 39.11) similar to that seen with pericardial effusion. The vascular pedicle is narrow because the pulmonary trunk is not border forming and the ascending aorta, with rare exception, often is small and inconspicuous or absent. Symptomatic neonates can have massive heart size (Fig. 39.12) and outcome is poor if the cardiothoracic ratio is >0.65 . The infundibulum either straightens the left cardiac border or forms a convex border. The most consistent and dramatic feature is the enlarged right atrial silhouette; this is seldom normal even if the cardiac silhouette is otherwise normal. Lung fields may be normal or decreased due to hypoplasia from severe cardiomegaly.

Electrocardiography

Ebstein's anomaly may be diagnosed using the electrocardiogram. It is rarely normal even with a mild anomaly. The major physiologic changes include the following (31) (Fig. 39.13):

- Intra-atrial conduction disturbance including PR interval prolongation and tall P waves.
- Right bundle branch block

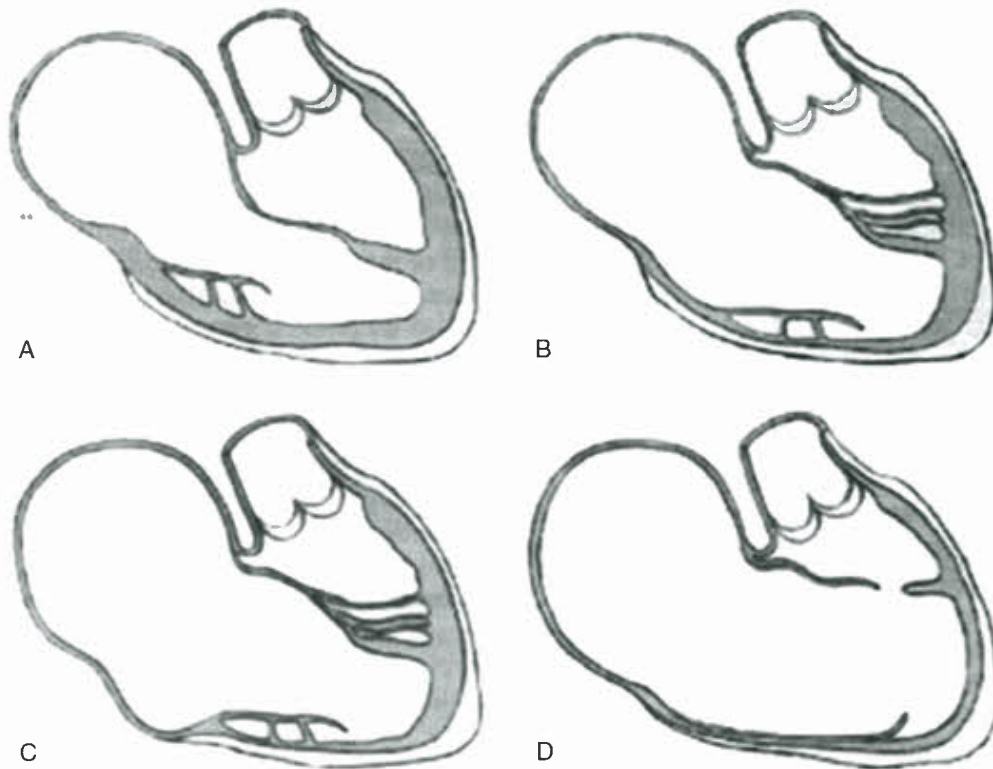


Figure 39.9. Carpentier classification: Type A = minor anomaly: the ARV is small. Type B = intermediate: the displacement of the septal leaflet is 2 to 3 cm, the ARV is normally contracting. Type C = severe form: the septal leaflet is severely displaced, the posterior leaflet is adherent to the ventricular wall or absent, the ARV is huge with hypo or akinetic motion. Type D = tricuspid sac: the leaflet tissue, even the anterior one is adherent to the RV wall. The contractility of the RV is globally impaired. (From Chauvaud S, Carpentier A. Ebstein's anomaly: the Broussais approach. *Multimedia Manual of Cardiothoracic Surgery (Internet)* June 26, 2008, with permission.)

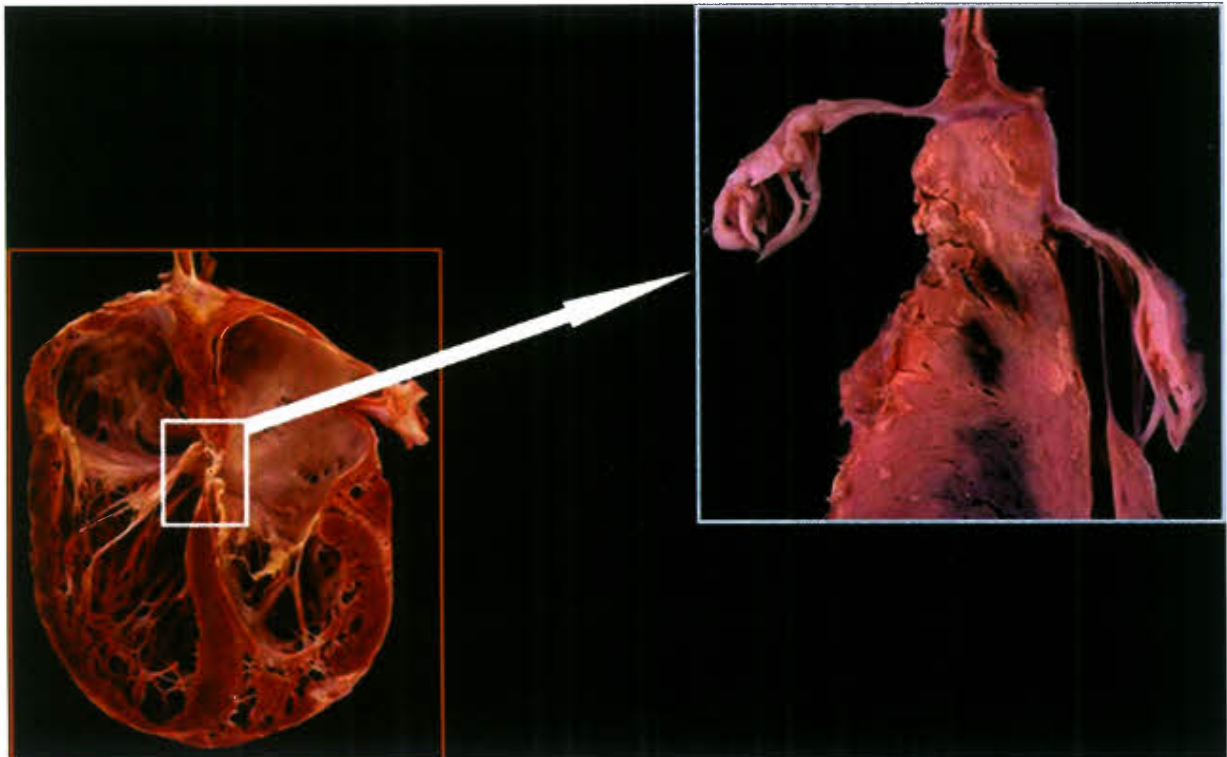


Figure 39.10. Ebsteinoid displacement of the TV (*inset*) in congenitally corrected transposition of great arteries (cc-TGA). This is different from the typical right-sided Ebstein TV. There is little if any atrialization of the RV free wall in cc-TGA. (Used with permission of the Mayo Foundation for Medical Education and Research.)

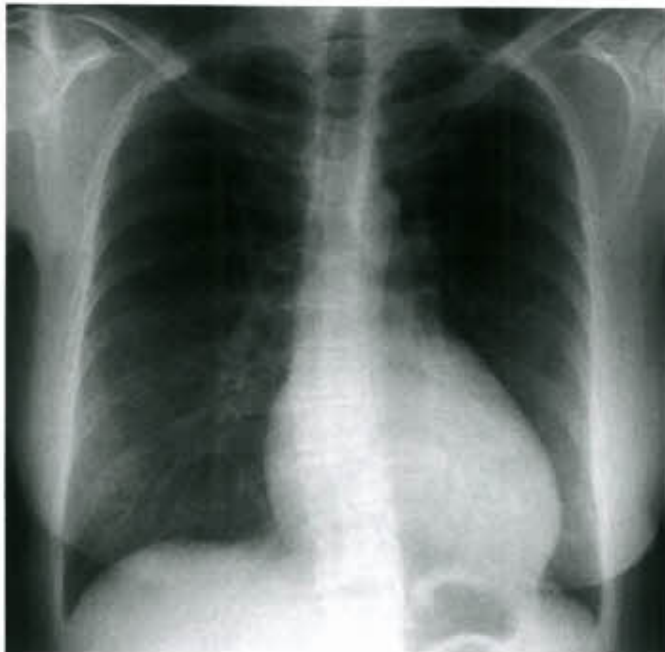


Figure 39.11. Chest radiograph: of a patient who had Ebstein's anomaly with severe TR and a small ASD before TV surgery. This typical image shows cardiomegaly, a narrow waist, and a cardiothoracic ratio of 0.56. (Used with permission of the Mayo Foundation for Medical Education and Research.)

- WPW preexcitation (Fig. 39.14)
- Supraventricular tachycardia
- Atrial flutter or fibrillation
- Arrhythmogenic atrialized RV
- Deep Q waves in leads V_{1-4} and in inferior leads

Complete AV block is rare but first-degree AV block occurs in 42% of patients due to right atrial enlargement and the



Figure 39.12. Chest radiograph: of a neonate with Ebstein's anomaly showing massive cardiomegaly. (Used with permission of the Mayo Foundation for Medical Education and Research.)

structural abnormalities of the AV conduction system (32). The AV node may be compressed but is in the normal location. Apical displacement of the septal leaflet is associated with discontinuity of the central fibrous body and the septal AV ring with direct muscular connections, creating a substrate for accessory pathways and pre-excitation (33).

More than one accessory pathway is present in 6% to 36% of cases (34); most of them are located around the orifice of the malformed TV (35). It is essential to correctly identify and treat these accessory pathways to prevent sudden cardiac death. Paroxysmal tachyarrhythmias in Ebstein's anomaly are based on typical, fast-conducting AV accessory pathways with both antegrade and retrograde conduction properties in most patients (37). In addition, wide QRS tachycardia over a septal accessory AV pathway, ventricular tachycardia, or flutter, as well as ectopic atrial tachycardia, atrial flutter, and atrial fibrillation, can occur (36).

Atrial fibrillation and atrial flutter are most likely caused by secondary alterations of the right atrial myocardium (dilatation), or may occur postoperatively and related to the atriotomy scar resulting in an incisional atrial tachycardia (37).

Echocardiography

2-D echocardiography is the diagnostic test of choice (Fig. 39.15) (37). More recently, 3-D echocardiography is also being used as an adjunct for additional details about TV anatomy. It accurately evaluates the TV and the size and function of different cardiac chambers.

Apical displacement of the septal leaflet by at least 8 mm/m² body surface area is considered a diagnostic feature of Ebstein's anomaly (8). The presence of at least three accessory attachments of the leaflet to the ventricular wall confirms leaflet tethering that causes restricted motion of the leaflet (30). Marked enlargement of the RA and atrialized RV is present when the combined area of the RA and atrialized RV is larger than the combined area of the functional RV, left atrium (LA), and LV in the apical 4-chamber view at end-diastole (15). Echocardiography allows assessment of the site and degree of TV regurgitation and the feasibility of valve repair (9). Ebstein's anomaly can be diagnosed in utero using fetal echocardiography in as early as the 18th week of pregnancy (38). Fetal echocardiography remains a challenge because of the small size of the heart, and it may be difficult to distinguish Ebstein's anomaly from pulmonary atresia or other causes of TR. Important features that can be determined echocardiographically and that can predict outcome in neonates with Ebstein's anomaly include the patency of the RVOT, and the GOSE score (39). The GOSE score, as described by Celermajer, is calculated in the four-chamber view to create a ratio of the combined areas of the RA and atrialized RV compared with the functional RV, LA, and the left ventricular areas. Patients who have the most severe GOSE score (grades 3 and 4) have a very poor prognosis (Table 39.2).

Cardiac Catheterization

This rarely is necessary, apart from preoperative coronary angiography in older patients. Pulmonary artery pressure usually is normal, although the right ventricular end-diastolic pressure may be elevated. Despite severe TV regurgitation, the right atrial pressure may be normal, especially with marked right atrial dilatation. Hemodynamic catheterization can also be performed in selected situations when there is left ventricular dysfunction and suspected elevated pulmonary artery pressures or elevated left ventricular end-diastolic pressure. This is particularly important if a bidirectional cavopulmonary anastomosis (BDCPA) is being considered.



Figure 39.13. ECG of a patient with severe Ebstein's anomaly showing the typical changes, with prolongation of the PR interval (226 ms), right bundle-branch block, and somewhat bizarre configuration of the QRS complex. (Used with permission of the Mayo Foundation for Medical Education and Research.)

Magnetic Resonance Imaging

Recently, cardiac magnetic resonance (CMR) imaging has emerged as another tool for evaluation of Ebstein's patients (Fig. 39.16). It provides quantitative measurement of right atrial and ventricular size and systolic function even in the presence of significant distortion of right ventricular anatomy. Axial imaging provides more reliable analysis and new expressions of disease severity, such as the atrialized right ventricular volume. The ability to create 3-D images (Fig. 39.17) may provide greater delineation of disease severity (40).

NATURAL HISTORY

It is not uncommon for Ebstein's anomaly to be undiagnosed until adulthood. The oldest patient in the Mayo surgical series was 79 years of age at time of diagnosis and subsequent surgery. However, late diagnosis is associated with reduced survival. The mean age of diagnosis in a study of the natural history of 72 unoperated patients, was 23.9 ± 10.4 years. In this group of patients, arrhythmias were the most common clinical presentation (51%) (41). The estimated cumulative overall survival rates were 89%, 76%, 53%, and 41% at 1, 10, 15, and 20 years of follow-up, respectively. Predictors of cardiac-related death on univariate analysis included: (a) cardiothoracic ratio of ≥ 0.65 , (b) increasing severity of TV displacement on echocardiography, (c) New York Heart Association (NYHA) class III or IV, (d) cyanosis, (e) severe TR, and

(f) younger age at diagnosis. In a multivariate model, younger age at diagnosis, male sex, cardiothoracic ratio of ≥ 0.65 , and the severity of TV leaflet displacement on echocardiography were predictors of late cardiac mortality.

MANAGEMENT

Neonatal Ebstein

Neonatal Ebstein's anomaly carries a poor prognosis, with reported survival of only 68% in one series (15). Surgery is required in the presence of heart failure or profound cyanosis. The surgical options include: (a) biventricular repair (Knott-Craig approach), (b) single ventricle pathway with right ventricular exclusion (Starnes' approach), and, rarely, (c) cardiac transplantation.

Biventricular Repair (Knott-Craig Approach)

This approach (Figure 39.18A–D) has been popularized by Knott-Craig (42) in which the TV is repaired and the atrial septum is partially closed. This repair is typically a monocusp type based on a satisfactory anterior leaflet (43). It is important in the early postoperative period to allow some right-to-left shunting across the atrial septum, especially in the presence of elevated pulmonary vascular resistance and right ventricular dysfunction. Routine right atrial reduction is important to reduce the size of the markedly enlarged heart to allow room for the lungs.

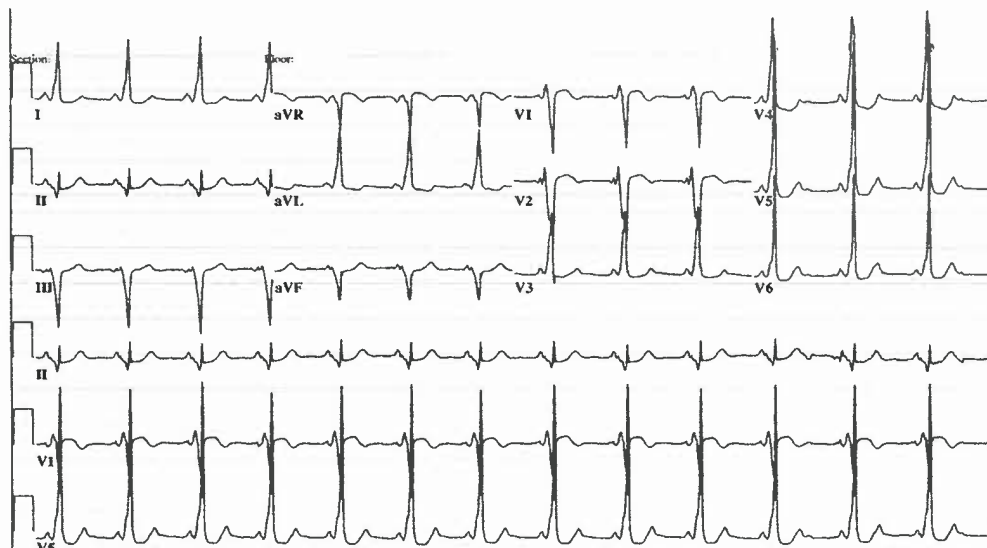
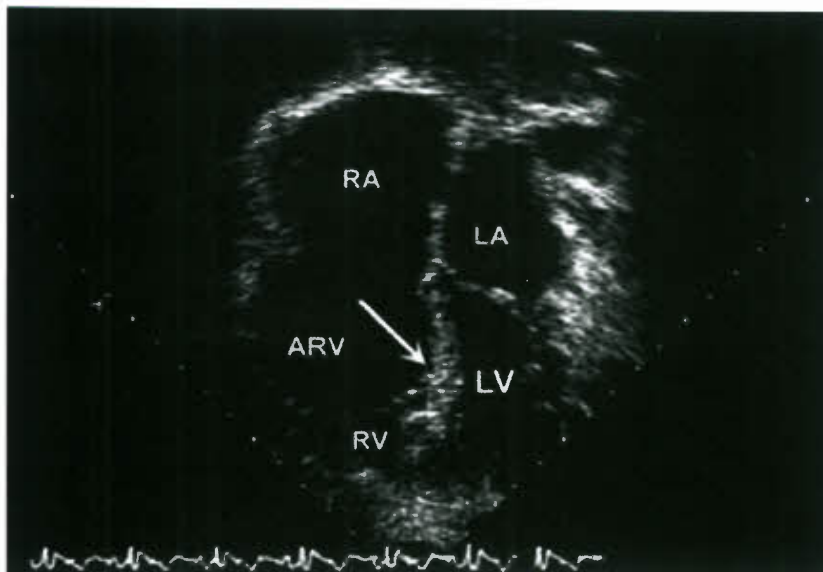


Figure 39.14. ECG of a patient with severe Ebstein's anomaly: showing sinus rhythm with pre-excitation (Wolf-Parkinson-White syndrome). (Used with permission of the Mayo Foundation for Medical Education and Research.)

Figure 39.15. Example of an echocardiogram (four-chamber view, apex down): of a patient with severe Ebstein's anomaly showing a grossly displaced septal leaflet (arrow). The anterior leaflet is severely tethered and nearly immobile. The functional RV is small. RV, right ventricle; aRV, atrialized right ventricle. LA, left atrium. LV, left ventricle; RA, right atrium. (Used with permission of the Mayo Foundation for Medical Education and Research.)



Postoperative care in these patients is challenging, and delayed sternal closure should be performed liberally. Inhaled nitric oxide may be helpful to decrease the pulmonary vascular resistance. Early arterial desaturation is not uncommon. Peritoneal dialysis catheters are helpful to ensure complete decompression of the abdomen. Although early mortality is high (about 25%), the intermediate outcome appears to be promising. In 2007, Knott-Craig et al. (44) reported their experience with 27 neonates and young infants. Associated anatomic or functional pulmonary atresia was present in 18 neonates, while VSDs, hypoplastic branch pulmonary arteries, and small LV were each present in three neonates. Biventricular approach was performed in 25 neonates with tricuspid repair in 23 of them. Survival to hospital dismissal was 74% with no late mortality. The median follow-up was 5.4 years with a maximum of 12 years. Despite high early mortality compared to many other neonatal anomalies corrected in the first month of life, these results have become a benchmark for a very difficult problem.

Right Ventricular Exclusion

■ Starnes Approach (Fig. 39.19)

Starnes et al. (45) pioneered the right ventricular exclusion approach, which involves: (a) fenestrated patch closure of the TV orifice, (b) enlarging the interatrial communication, (c) right atrial reduction, and (d) placing a systemic-to-pulmonary artery shunt. This approach is particularly useful when there is anatomic RVOT obstruction. Right ventricular decompression is required as it passively fills from Thebesian venous drainage;

this is usually accomplished with a 4- to 5-mm punch fenestration in the TV patch (46,47). This allows progressive involution of the enlarged, dysfunctional RV, which will be helpful at the time of Fontan completion. If the pulmonary valve is not competent, this will lead to right ventricular distension and in these situations, ligation or closure of the main pulmonary artery is required. Significant right ventricular dilatation can lead to left ventricular dysfunction, and the above mentioned issues must be considered at the time of initial surgery in order to optimize Fontan candidacy down the road.

■ Modified Starnes Repair (Total Ventricular Exclusion)

Sano et al. (48) modified the Starnes single-ventricle approach by performing a total right ventricular exclusion in which the free wall of the RV is resected and closed primarily (Fig. 39.20) or with a polytetrafluoroethylene patch (51). This simulates a large right ventricular plication, which may improve the left ventricular filling and provide adequate decompression to the lungs and LV.

The postoperative care is similar to any shunt-palliated patient with a univentricular heart. The primary goal is to optimize systemic perfusion while obtaining adequate oxygenation. Delayed sternal closure and peritoneal drainage also are helpful. Close surveillance is required between the first and second stage procedure (BDCPA), which usually is performed between 3 and 6 months of age.

Reemtsen et al. (49) reported the results of the single-ventricle pathway in 16 neonates; two patients underwent TV repair, one patient had heart transplantation, 10 patients had a right ventricular exclusion procedure with a fenestrated TV patch, and three patients had a right ventricular exclusion with a nonfenestrated patch. Operative survival was 80% in those with a fenestration versus 33% without. All survivors had a successful BDCPA (second stage), and three patients had Fontan completion.

Cardiac Transplantation

With the improved results of the biventricular and single ventricle approaches, transplantation rarely is performed in the current era. Cardiac transplantation remains an option in the most severe forms of Ebstein's anomaly, particularly when there is significant left ventricular dysfunction. Scarcity of organ donors and the side effects of immunosuppression are the main limitations. The availability of smaller ventricular

TABLE 39.2 Mortality Risk by GOSE Score

GOSE Score	Ratio	Mortality
1–2	<1.0	8%
3 (acyanotic)	1.1–1.4	10% early, 45% late
3 (cyanotic)	1.1–1.4	100%
4	>1.5	100%

GOSE 1: <0.5, GOSE 2: 0.5–1.0, GOSE 3, 1.1–1.4, GOSE 4: >1.5.

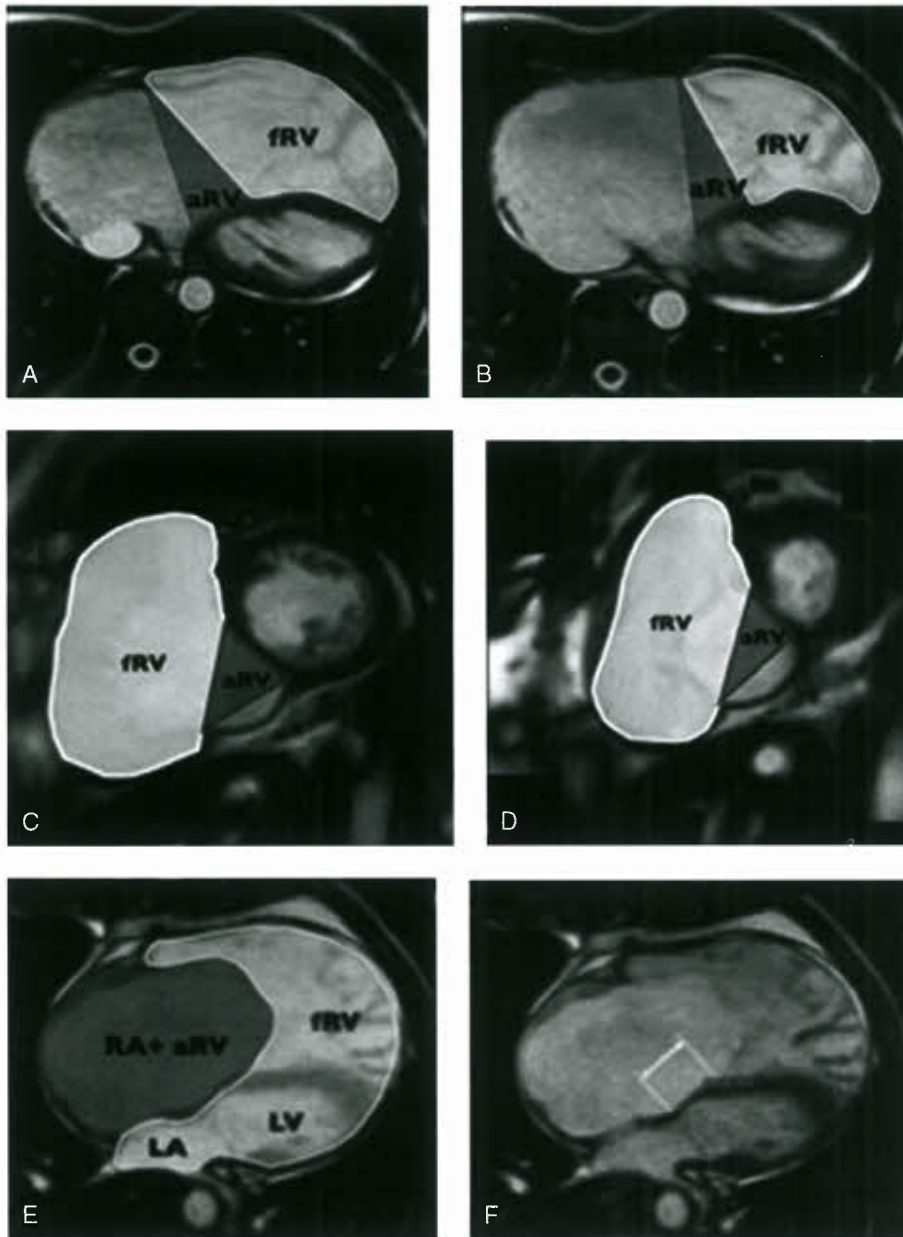


Figure 39.16. A–F: Cardiac MRI showing: Systolic and diastolic contours of functional RV and ARV in (A,B) axial and (C,D) short-axis views. E: Severity index representing ratio of areas of RA and ARV in numerator and summation of functional RV and left atrium and left ventricular areas in denominator (i.e., severity index = [right atrial area + atrialized right ventricular area]/[functional right ventricular area + left atrial area + left ventricular area]). F: Degree of apical displacement of septal leaflet of TV (in millimeters) measured in ventricular diastole. fRV, functional RV; aRV, atrialized right ventricle; RA, right atrium; LA, left atrium; LV, left ventricle. (Reprinted from Yalonetsky S, et al. Cardiac magnetic resonance imaging and the assessment of ebstein anomaly in adults. *Am J Cardiol* 2011;107(5):767–773, Epub 2011 Jan 19, with permission from Elsevier.)

support devices and advances in neonatal extracorporeal membrane oxygenation have provided mechanical support options in the perioperative period for these infants undergoing conventional operation.

Children and Adults

Medical

Regular congenital cardiology evaluations for patients with Ebstein's anomaly are essential. Bacterial endocarditis prophylaxis may be required in the presence of prosthetic materials or patches that were used for the repair. Recommendations for physical activity are summarized by Task Force 1 on Congenital Heart Disease. In mild Ebstein's anomaly, with nearly normal heart size, and in absence of arrhythmias, athletes can participate in all sports. However, in severe Ebstein's anomaly, activity is restricted unless it has been optimally repaired with near normal heart size and no arrhythmias. Although rare in the current era, those who are not candidates for surgery are treated with standard heart failure regimens.

Angiotensin-converting enzyme inhibitors have unproven efficacy in cases of right-sided failure, but they are used frequently as part of a heart failure regimen. Individualized management of arrhythmias with medical treatment combined with operative or catheter-based intervention is recommended.

Catheter Ablation

Patients with tachyarrhythmias should undergo electrophysiologic evaluation with mapping and radiofrequency ablation of accessory pathways. The success rate of catheter ablation in Ebstein's patients is lower than in those with structurally normal hearts, and there is an increased risk of recurrence (50,51). Atrial tachyarrhythmias (fibrillation and flutter) are treated surgically at the time of operation.

Surgery

INDICATIONS FOR SURGERY

Apart from asymptomatic patients with no right-to-left shunting, and mild cardiomegaly, most patients require surgical intervention. The current indications for surgery include: presence

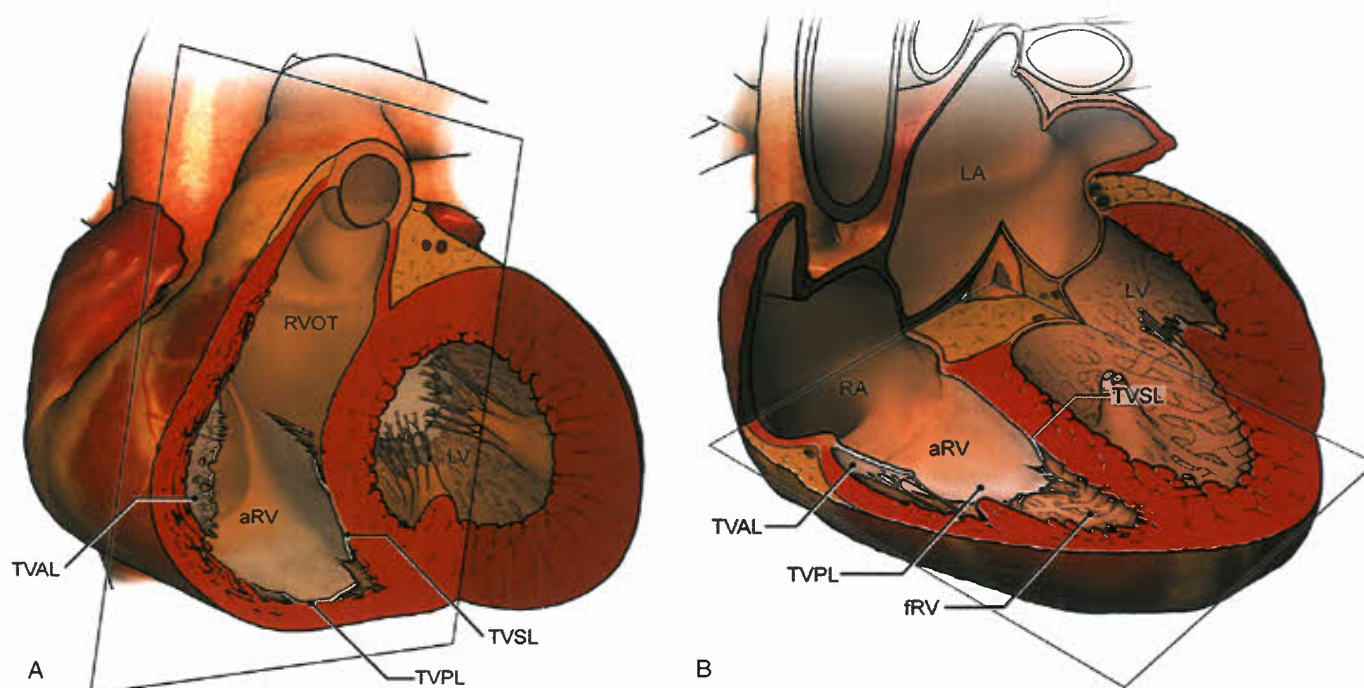


Figure 39.17. A,B: Three-dimensional reproduction of heart with Ebstein anomaly demonstrating: views of TV from (A) short axis and (B) axial imaging. aRV, atrialized right ventricle; fRV, functional right ventricle; LA, left atrium. LV; left ventricle; RA, right atrium; RVOT, right ventricular outflow tract. TVAL, TV anterior leaflet; TVPL, TV posterior leaflet; TVSL, TV septal leaflet. (Reprinted from Yalonetsky S, et al. Cardiac magnetic resonance imaging and the assessment of ebstein anomaly in adults. *Am J Cardiol* 2011;107(5):767–773. Epub 2011 Jan 19, with permission from Elsevier.)

of symptoms, cyanosis, and paradoxical embolization. Patients who have decreased exercise performance, progressive increase in cardiothoracic ratio, progressive right ventricular dilatation and dysfunction, onset or progression of arrhythmias, will benefit from surgical intervention. In the presence of class III or IV NYHA or significant symptoms, medical treatment has little to offer and the surgery will be the best chance for improvement. Echocardiographic assessment of the TV plays a key role in decision making regarding valve repair versus replacement. High probability of successful valve repair supports earlier operation.

PRINCIPLES OF SURGERY FOR EBSTEIN'S ANOMALY

The following principles are the goals of surgery: (a) closure of any intracardiac communications, (b) TV repair or replacement, (c) ablation of arrhythmias, (d) selective plication of the atrialized RV from apex to base, (e) reduction right atrio- plasty, and (f) repair of associated defects (e.g., closure VSD).

Tricuspid Valve Repair

The goal of operation is to obtain a competent TV, preserve right ventricular contractility, and to decrease the risk of late rhythm disturbances.

HISTORY

Repair of the TV was reported in 1959 in two patients who had Ebstein's anomaly; both died (52). In 1962, the TV was replaced, which was a successful operative intervention for the regurgitant valve (53). Several other methods for TV repair were described but they were associated with high early mortality and unsatisfactory late results (54) in this early era.

THE MAYO CLINIC EXPERIENCE

Danielson Repair

This repair technique was reported in 1979 and was based on the creation of a monocusp valve using the anterior leaflet.

This consisted of plication of the free wall of the atrialized RV, posterior tricuspid annuloplasty, and right reduction atrio- plasty (55).

Modified Danielson Repair

We have incorporated various modifications since then, depending on the numerous variants encountered with Ebstein's hearts (56). One of these modifications involves bringing the anterior papillary muscle(s) toward the ventricular septum, which facilitates coaptation of the leading edge of the anterior leaflet with the ventricular septum (Fig. 39.21A–C). Generally, an anteroposterior tricuspid purse-string or ringed annuloplasty is used, and atrialized right ventricular plication is performed selectively. This results in a TV repair at the level of the functional annulus, in contrast to the original repair, which brought the hinge point of the functional annulus up to the true annulus. A more recent modification includes patch augmentation of the mid-anterior leaflet with surgical delamination of attachments to the anterior and/or inferior leaflets.

In a recent review of 539 patients with Ebstein anomaly that had 604 cardiac operations, the mean age was 24 years (range, 8 days to 79 years) and 317 were female. One hundred and forty-three (26.5%) patients had a prior invasive cardiac procedure. At the time of the first operation, 182 patients had TV repair, and 337 had TV replacement. The 30-day mortality was 5.9% for the entire cohort (2.7% after 2001). Late survival was 84.7% at 10 years and 71.2% at 20 years (57).

THE BRAZIL EXPERIENCE (da SILVA APPROACH)

Recently, we have adopted the cone repair described by Dr. da Silva from Brazil when the anatomy allows, as this technique is the most anatomic of all the repair techniques described (details of cone technique are described below) (Fig. 39.22 A–J). Specifically, some septal leaflet should be present, which facilitates this repair technique. As noted above with the modified

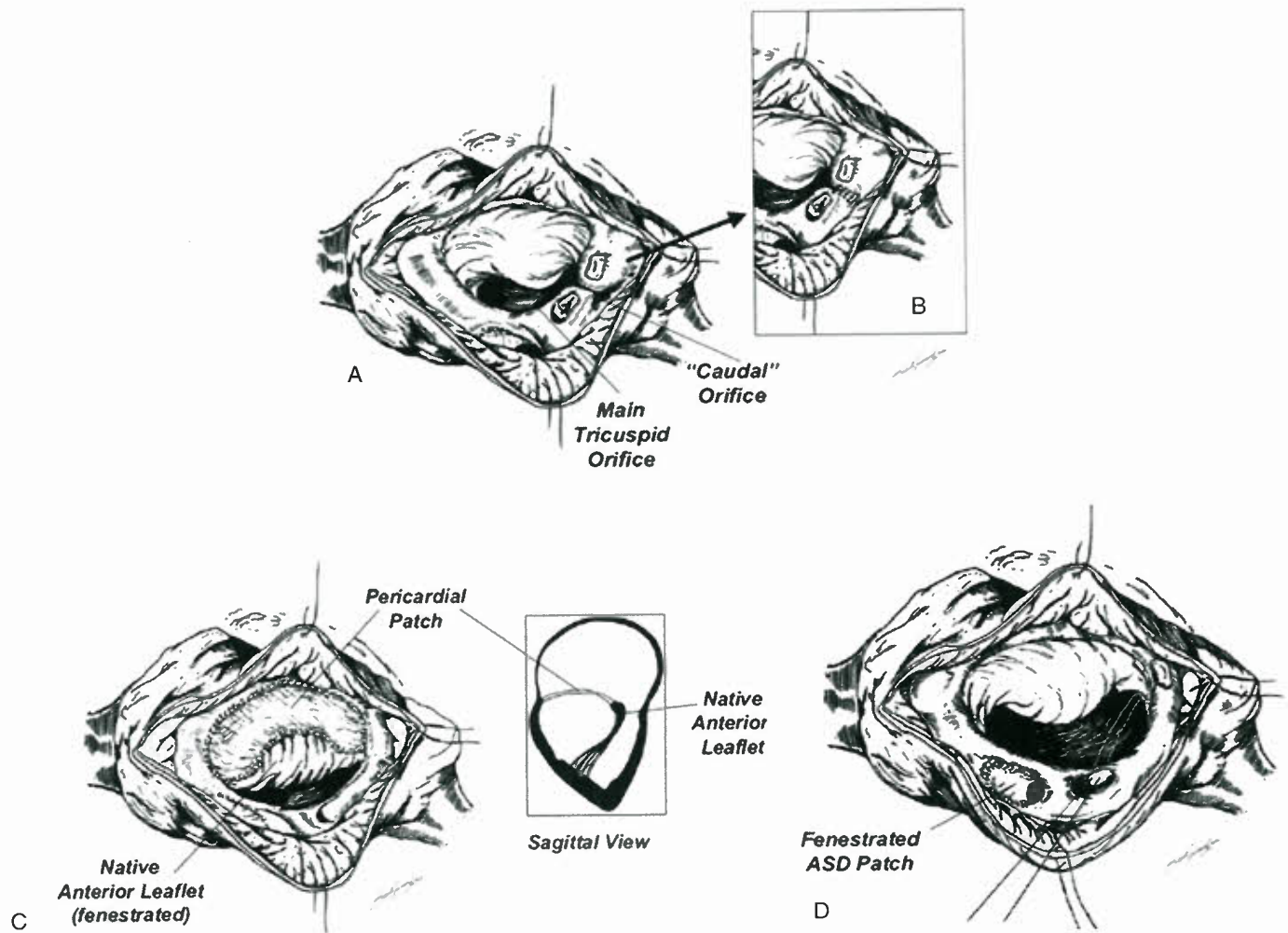


Figure 39.18. A–D: Biventricular repair of neonatal Ebstein (Knott-Craig): A: Partition of the TV orifice into two openings by approximation of the annuloplasty stitch. B: Once the valve is judged to be competent, the “caudal” orifice is closed, thereby plicating the atrialized portion of the RV. C: Creation of a competent monocuspid valve by taking down the anterior leaflet from the annulus, fenestrating it, and augmenting it with a pericardial patch. D: The ASD is closed with a fenestrated patch, and an annuloplasty stitch is placed with one pledgetted end in the coronary sinus and the other pledgetted end at the location of the commissure between anterior and posterior leaflets. ASD, atrial septal defect. (Reprinted from Knott-Craig CJ, Goldberg SP. Management of neonatal Ebstein’s anomaly. *Semin Thorac Cardiovasc Surg Pediatr Card Surg Annu* 2007;112–116, with permission from Elsevier.)

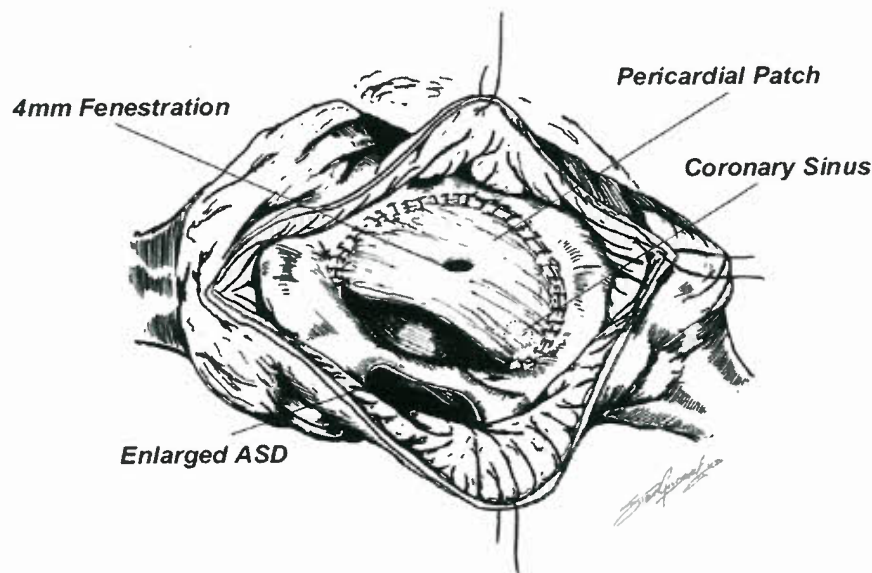
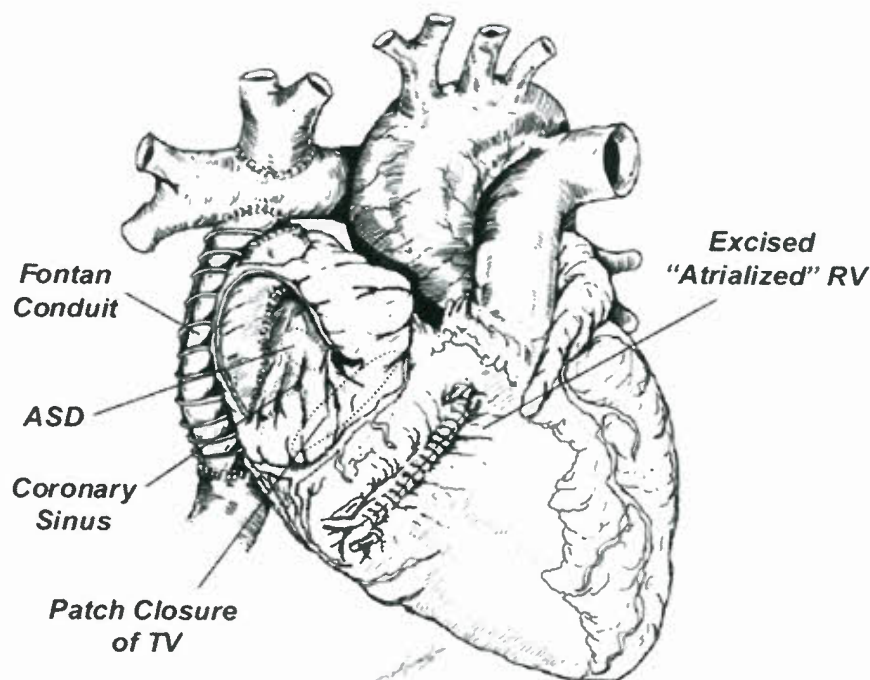


Figure 39.19. Starnes repair of neonatal Ebstein anomaly (EA). (Reprinted from Knott-Craig CJ, Goldberg SP. Management of neonatal Ebstein’s anomaly. *Semin Thorac Cardiovasc Surg Pediatr Card Surg Annu* 2007;112–116, with permission from Elsevier.)

Figure 39.20. Sano “RV exclusion” procedure. ASD, atrial septal defect. RV, right ventricle. TV, tricuspid valve. (Reprinted from Knott-Craig CJ, Goldberg SP. Management of neonatal Ebstein’s anomaly. *Semin Thorac Cardiovasc Surg Pediatr Card Surg Annu* 2007;10:112–116, with permission from Elsevier.)



monocusp technique, we also have a low threshold to augment anterior leaflet size to facilitate leaflet coaptation. The cone technique represents the most anatomic repair by completion of the delamination process of the TV, providing 360 degrees of leaflet tissue around the AV junction with its hinge point at the AV groove (true annulus). Although not initially described with this technique, we do supplement the repair with a flexible anterior annuloplasty band from anteroseptal commissure to inferoseptal commissure whenever possible.

THE FRENCH EXPERIENCE (BROUSSAIS APPROACH)

In 1988, Carpentier et al. (11) proposed a repair that used mobilization of the anterior leaflet of the TV. For their types B and C, temporary detachment of the anterior leaflet and adjacent part of the posterior leaflet was followed by longitudinal plication of the atrialized ventricle and adjacent RA, repositioning of the anterior and posterior leaflets to cover the orifice area at the normal level, and remodeling and reinforcement of the tricuspid annulus with a prosthetic ring.

From 1980 to 2007, 269 patients were operated on with this technique. The mean age was 25 ± 16 years (1 to 70 years). Forty-two percent and sixteen percent were in functional class III and IV, 39% were cyanotic and 58% with permanent sinus rhythm. Ninety-eight percent underwent TV repair and 2% (five patients) had replacement. The overall hospital mortality was 9% (24 patients). Actuarial survival at 20 years was $80 \pm 5\%$. Eighty-four percent were in functional class I or II. Residual TV insufficiency (grade 3+) was present in 7%, but it was usually well tolerated when a bidirectional shunt was performed. Reoperations occurred in 9% (20 pts), two were transplanted, 12 patients had a second repair and six patients a valve replacement. Eighty-four percent remained in sinus rhythm, 5% experienced supraventricular tachycardia (usually well tolerated), and 6% had a persistent atrial fibrillation. Seven patients (5%) had an AV block and a pacemaker was implanted. It is unclear whether late problems will develop because of devitalized TV tissue related to reattachment.

THE CONE RECONSTRUCTION (da SILVA)

In 2007, da Silva et al. (58) published a series of 40 patients who had repair with the cone reconstruction (Fig. 39.22A–J). The

operative mortality was 2.5%. Mean follow-up was 4 years (range, 3 months to 12 years), only one patient died and two patients required late TV rerepair. The cone technique has the potential to cause TV stenosis, although no patient in his series had this complication. Additional follow-up is required to determine the long-term durability of this method of repair.

We consider the following as relative contraindications to the cone reconstruction technique: (a) age >50 years, (b) moderate pulmonary hypertension, (c) significant left ventricular dysfunction: ejection fraction <30%, (d) complete failure of delamination of the septal and posterior leaflets with poor delamination of the anterior leaflet (<50%), (e) severe right ventricular enlargement, and (f) severe TV annular dilatation (right AV junction)

THE VENTRICULIZATION PROCEDURE

Ullmann et al. (59) published their results with the ventricularization procedure in 2004. This is characterized by reintegration of the atrialized portion of the RV into the right ventricular cavity (ventricularization). This can be obtained by orthotopic transposition of the detached septal and posterior leaflets of the TV. The reimplanted septal leaflet serves as an opposing structure for coaptation of the reconstructed AV valve (59). Between March 1993 and April 2003, they performed this technique in 23 patients aged 13.6 (4.1 to 52.6) years. One early death (4.4%) occurred and was caused by right heart failure. Follow-up was 4.6 (0.5 to 10.9) years. Rupture of the fixation sutures occurred in three patients (13%) causing significant AV valve regurgitation, which required reintervention at 3 (0.03 to 4) months postoperatively, with rerepair of the valve in two patients and replacement in the other one (51).

OTHER REPORTED TECHNIQUES

Many others, including Hetzer et al. (60) and Quaegebeur et al. (61), have reported their repair techniques for Ebstein’s anomaly in older children and adults. Wu and Huang (62) reported a series of 34 consecutive patients who underwent removal and reattachment of the posterior and septal leaflets with or without pericardial reconstruction of the septal leaflet. There were no operative mortality and there was only mild or no TR in all patients at time of hospital dismissal. Mean

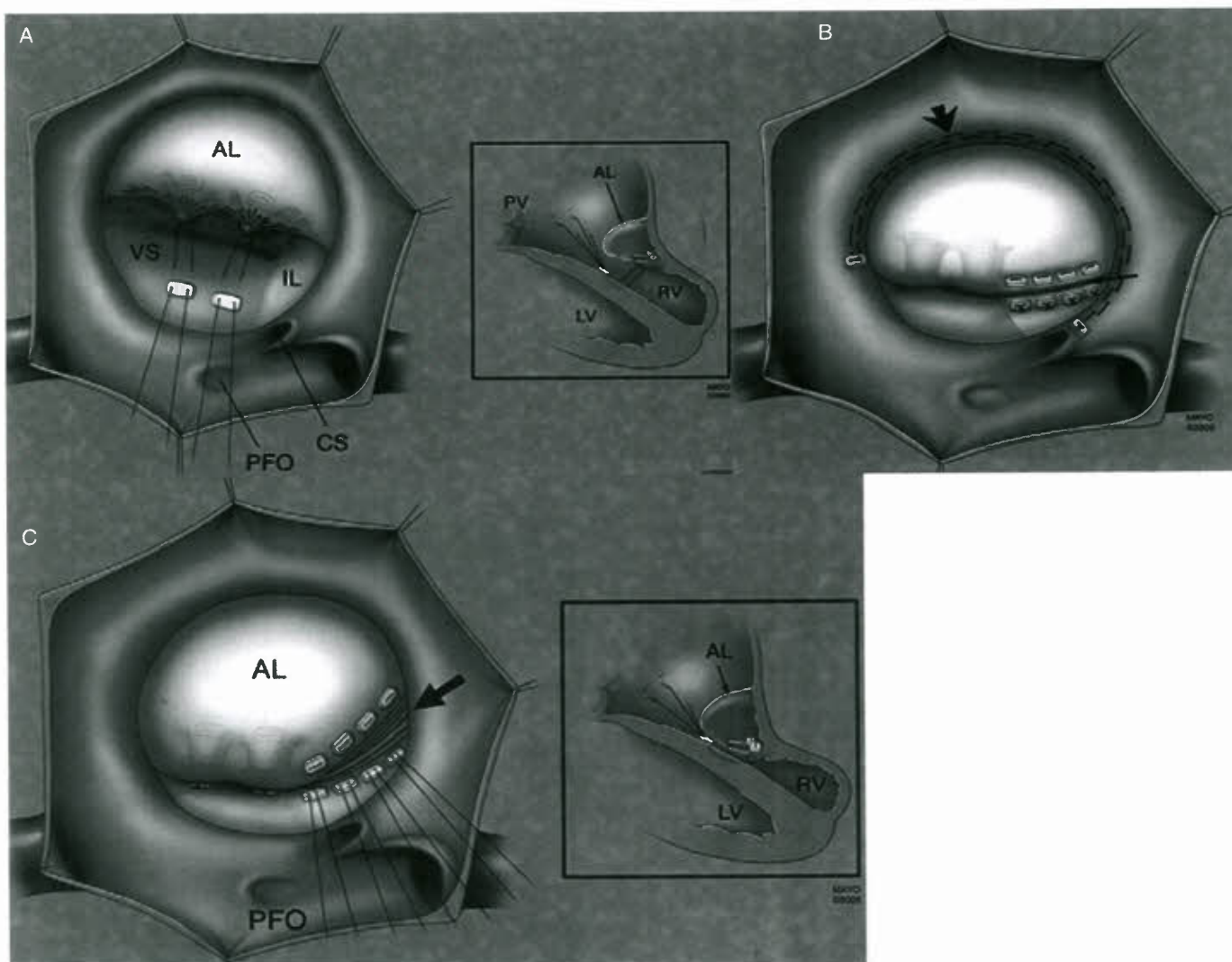


Figure 39.21. A: Basic principles of one of the modified Danielson technique for repair of the TV. The maneuvers are designed to progressively bring the leading edge of the anterior leaflet closer to the ventricular septum, or septal leaflet to optimize leaflet coaptation and establish competence of the valve. The base of the intact major papillary muscle, which arises from the free wall of the RV, is moved toward the ventricular septum at the appropriate level with pledgeted horizontal mattress sutures. **Inset:** Coronal view of the RV and RA demonstrating a small dimple effect that occurs in the anterior free wall of the RV after this maneuver is completed. **B:** The inferior angle of the tricuspid orifice is closed by bringing the right side of the anterior leaflet down to the septum and plicating the nonfunctional inferior leaflet in the process (arrow). **Inset:** After all of the mattress sutures are secured, improved proximity of the leading edge of the anterior leaflet with the ventricular septum is noted. **C:** Plication of the inferior angle of the annulus with pledgeted mattress sutures (arrow). An anterior pursestring annuloplasty (arrowhead) may be performed to further narrow the tricuspid annulus. This annuloplasty may begin at the anterosseptal commissure, anterior to the membranous septum, and end beyond the inferoseptal commissure, adjacent to the coronary sinus. Alternatively, the annuloplasty can be performed posterolaterally to reduce the size of the annulus, which also brings the free wall closer to the septum. CS, coronary sinus; AL, anterior leaflet; IL, inferior leaflet; PFO, patent foramen ovale; VS, ventricular septum; LV, left ventricle; RV, right ventricle. PV, pulmonary valve. (Copyrighted and used with permission of Mayo Foundation for Medical Education and Research.)

follow-up was 25 months (range, 1 to 55 months), with no evidence of TR in 28 patients (82%), mild regurgitation in three patients (9%), and moderate regurgitation in three (9%). Chen et al. (63) published their results of vertical plication and valve leaflet reimplantation in 2004. Twenty-five patients, with a mean age of 14 years, had TV repair. The majority of patients did well, with good functional outcomes, but 40% of them had moderate to severe TR postoperatively, and three patients required reoperation at an average follow-up of

4.1 years. Thus, TV repair techniques continue to evolve, and there is not one universally correct repair technique because of the variations in anatomy of patients with Ebstein's anomaly.

Tricuspid Valve Replacement

Every effort should be made to repair the TV rather than replacing it, but if TV repair is not feasible, then porcine bioprosthetic valve replacement remains a good alternative. We prefer

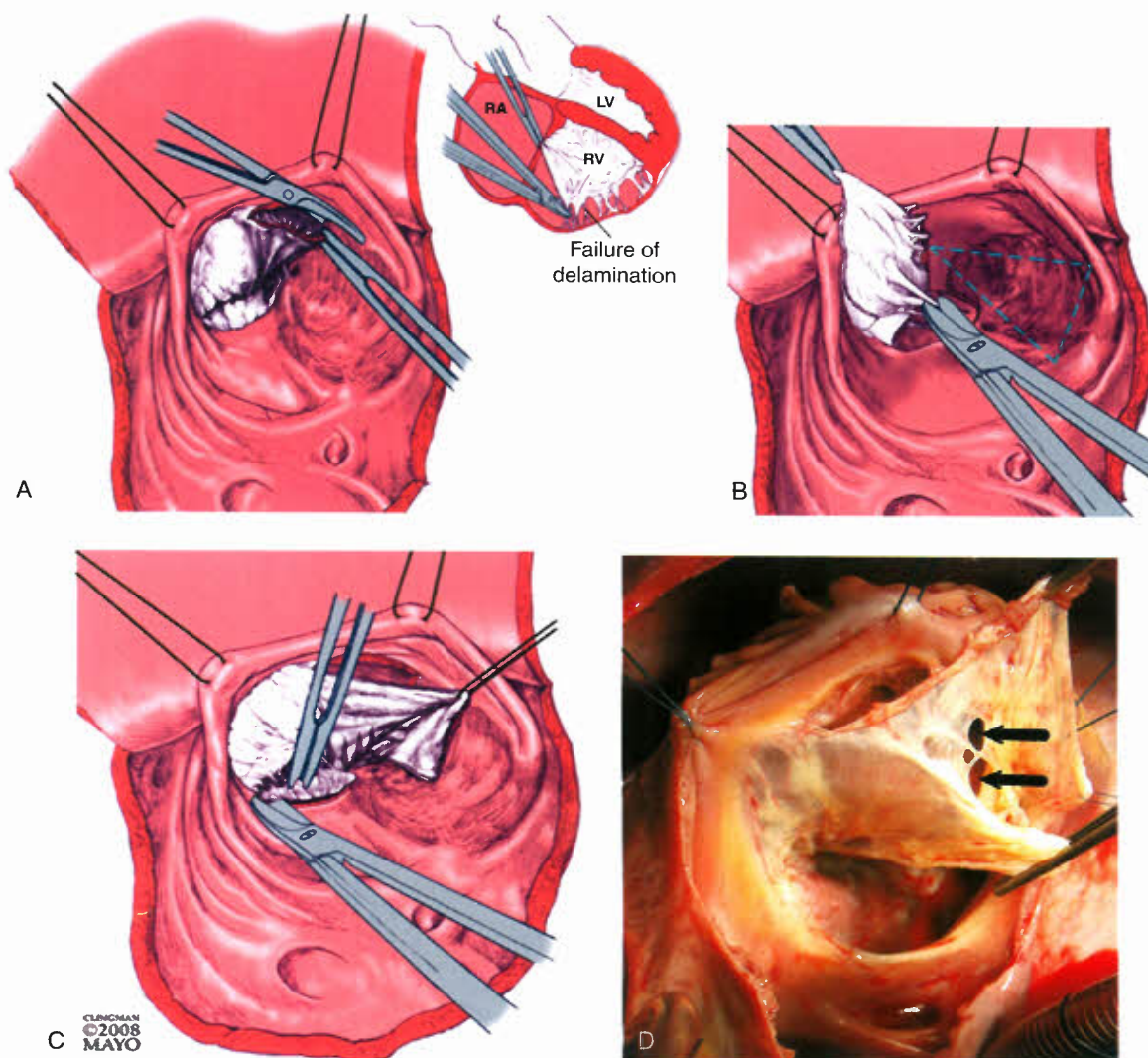


Figure 39.22 A–J: Operative steps for “da Silva technique” for Ebstein’s anomaly repair: A: The first incision is made with a no. 15 blade in the anterior leaflet at 12:00; the incision is a few millimeters away from the true annulus. The incision is then extended rightward in a clockwise fashion using a scissors. It is common for there to be a true space between the anterior leaflet and the RV in this region (i.e., normally delaminated leaflet). However, when the transition is met between the anterior and inferior (*posterior*) leaflets, it is common for there to be failure of delamination (inset) resulting in fibrous and muscular attachments between the leaflet and myocardium. The diagram demonstrates the scissors approaching the area where there is some adherence of leaflet tissue to the underlying myocardium. The dissection continues in a way that a portion of distal anterior leaflet and some inferior leaflet tissue is “surgically delaminated.” The most important aspect of this surgical delamination is to incise all fibrous and muscular attachments between the body of the leaflet and the right ventricular myocardium, but to maintain intact all fibrous and (and occasionally muscular) attachments of the leading edge of the leaflet to the underlying myocardium. Importantly, do not disrupt chordal attachments to the leading edge of any leaflet. LV, left ventricle; RA, right atrium; RV, right ventricle. (Copyrighted and used with permission of Mayo Foundation for Medical Education and Research.) B: As the anterior and surgically delaminated inferior leaflet is reflected away from the right ventricular myocardium, all fibrous and muscular attachments into the body of the underside of the leaflet are incised as shown with the scissors. It is important to keep all attachments of the leading edge of the leaflet intact; if the edge is linearly attached, then surgical fenestrations are created as depicted earlier. The dotted triangle represents the atrialized RV. (Copyrighted and used with permission of Mayo Foundation for Medical Education and Research.) C: Dissection is continued with a scissors with the goal of taking down all attachments between the septal leaflet and myocardium but preserving all attachments of the leading edge to the endocardium as described above. The dissection should proceed medially all the way to the antero-septal commissure. The leaflet tissue is typically very fragile and thin in this area. There can be marked variability in the status of the leading edge of the septal leaflet as was described for the anterior and inferior leaflets. If there is a linear attachment, then surgically created fenestrations are also made in this leaflet (not shown). (Copyrighted and used with permission of Mayo Foundation for Medical Education and Research.) D: Intraoperative photo demonstrating the mobilized anterior and inferior (*posterior*) leaflets. Natural fenestrations are shown at the junction of the anterior and inferior leaflets (arrows). (Copyrighted and used with permission of Mayo Foundation for Medical Education and Research.)

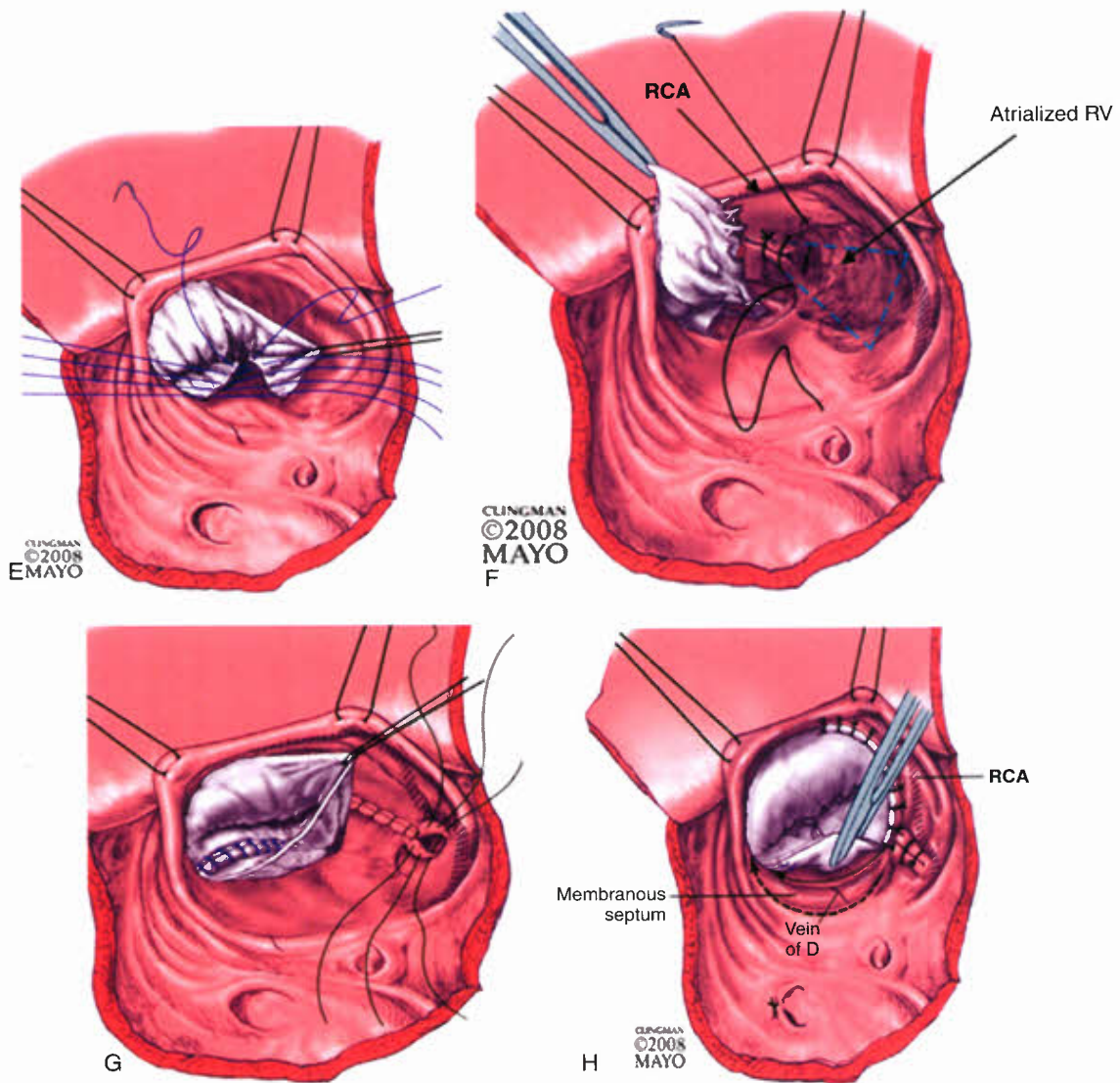


Figure 39.22. (Continued) **E:** After the anterior, inferior, and septal leaflets have been completely mobilized, the cut edge of the inferior leaflet is rotated clockwise to meet the proximal edge that has been prepared of the septal leaflet. The two are approximated with interrupted 6-0 monofilament sutures completing the cone reconstruction. This results in 360 degree of leaflet tissue that will make up the new TV orifice. (Copyrighted and used with permission of Mayo Foundation for Medical Education and Research.) **F:** After the cone reconstruction is completed, the atrialized RV is examined to determine if plication is necessary. Note the position of the RCA in the true TV annulus and keep in mind that there are acute marginal branches of the RCA that can be compromised with plication. This figure demonstrates the technique for internal plication of the atrialized RV. Monofilament 5-0 is utilized and the suture is begun distally, that is, closest to the apex of the RV. It is important to frequently examine the outside of the inferior wall of the RV to insure that inadvertent compromise of branches of the RCA is avoided. (Copyrighted and used with permission of Mayo Foundation for Medical Education and Research.) **G:** The suture line is advanced toward the base of the heart, that is, toward the AV groove. As the dotted lines of the triangle are effectively approximated, the atrialized RV is excluded. It is important for this suture line to stop approximately 1 cm before reaching the AV groove to avoid injury or distortion of the RCA. After the sides of the triangle are approximated, the entrance into the excluded atrialized segment of the RV is then closed to eliminate the “blind pouch.” (Copyrighted and used with permission of Mayo Foundation for Medical Education and Research.) **H:** After the plication or resection is completed, the newly constructed TV is then reattached at the level of the true tricuspid annulus. Because the neoTV will have an orifice that is smaller than the original dilated AV junction, a plication of the inferior annulus is necessary to meet the size of the neoTV. The inferior annulus is usually plicated with two to four simple or figure-of-eight 5-0 monofilament sutures. Proper placement of these sutures is critical to the success of this repair. The sutures need to be deep enough to maintain the integrity of the new annulus intact *without* compromising or significantly distorting the RCA. If the size discrepancy between the true tricuspid annulus and the neoTV is large, smaller annular plication sutures should be placed in multiple areas around the true annulus to avoid distortion of the RCA by a large plication in a single area. To avoid heart block, the suture line is deviated slightly cephalad to the membranous septum and AV node, which is marked by the previously mentioned vein and fatty tissue. RCA, right coronary artery. (Copyrighted and used with permission of Mayo Foundation for Medical Education and Research.)

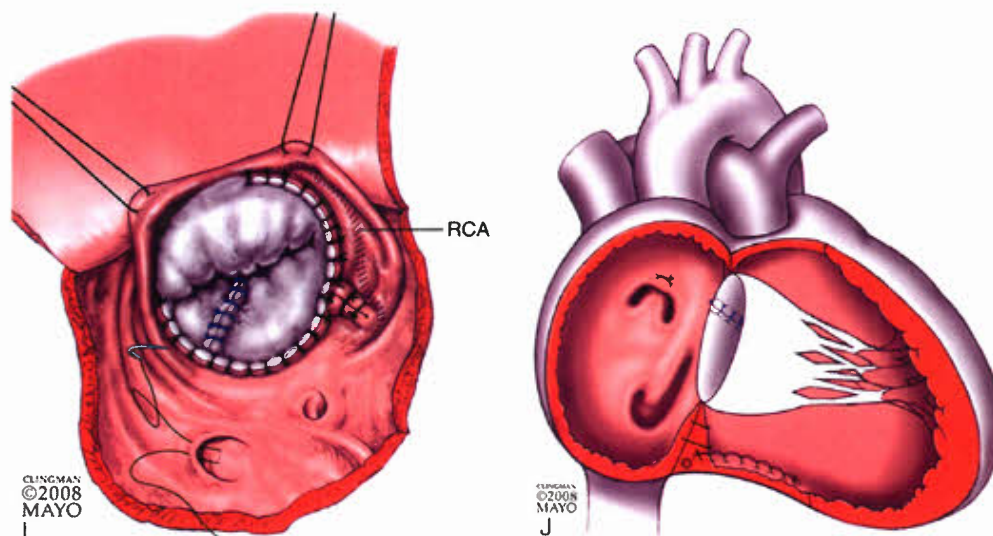


Figure 39.22. (Continued) **I:** The completed cone reconstruction of the TV. Saline is injected via bulb syringe into the RV to examine competency of the TV. Any residual fenestrations or areas of leak are repaired as needed. A subtotal closure of the PFO or ASD is usually performed. If it is felt that a bidirectional Glenn shunt is needed because of a small effective orifice of the neoTV, or because of severely depressed RV function; then the intra-atrial communication may be closed completely. Redundant RA is excised from each side of the atriotomy and then the atriotomy is closed. RCA, right coronary artery. (Copyrighted and used with permission of Mayo Foundation for Medical Education and Research.) **J:** The completed cone reconstruction of the TV for Ebstein's anomaly. This represents an "anatomic repair" because there is 360 degrees of tricuspid leaflet tissue that surrounds the orifice of the TV and it is anchored at the level of the normal right AV junction (true TV annulus). Extreme forms of thinned, atrialized RV are plicated and redundant RA is excised. (Copyrighted and used with permission of Mayo Foundation for Medical Education and Research.)

bioprostheses to mechanical valves due to the relatively good durability (Fig. 39.23) and the lack of need for anticoagulation (64,65). However, bioprosthetic valves are less durable and are more prone to structural valve deteriorations in infants and young children than in adults with a high likelihood of reoperation (66,67). This decreased durability in young children is related to increased calcification and also to rapid somatic growth that results in patient-prosthesis mismatch. On the other hand, mechanical valves in the tricuspid position are associated with higher frequency of thromboembolic complications especially in the presence of right ventricular dysfunction (68).

To avoid the potential for RVOT obstruction during TV replacement, the anterior leaflet tissue toward the RVOT is excised. The suture line is deviated to the atrial side of the AV node and membranous septum to avoid injury to the conduction tissue (Fig. 39.24). The AV node location usually is marked by a small vein crossing the tricuspid annulus adjacent to the membranous septum. The suture line should be deviated toward the atrial side of the TV annulus anteriorly and posterolaterally where the tissues frequently are very thin to avoid injury to the vulnerable RCA. The coronary sinus, can be left to drain into the RA if there is a sufficient distance between it and the AV node; but if the distance is short, then it can be

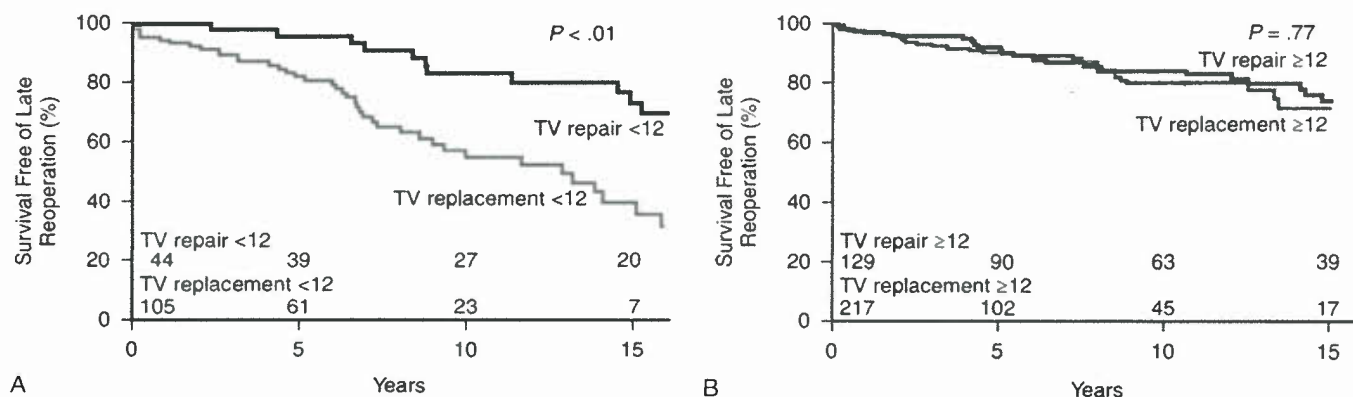


Figure 39.23. A,B: Patients were divided into two groups (<12 years old, and ≥12 years old) and stratified into patients who had TV repair or replacement. The age cutoff was chosen because an adult-sized TV prosthesis can generally be inserted into a 12-year-old patient. In survival free from late reoperation on the TV, there was no difference between repair and replacement in adult patients (≥12 years old). However, there was a significant advantage for young patients (<12 years old) who had a TV repair versus TV replacement ($p < 0.001$). (Copyrighted and used with permission of Mayo Foundation for Medical Education and Research.)

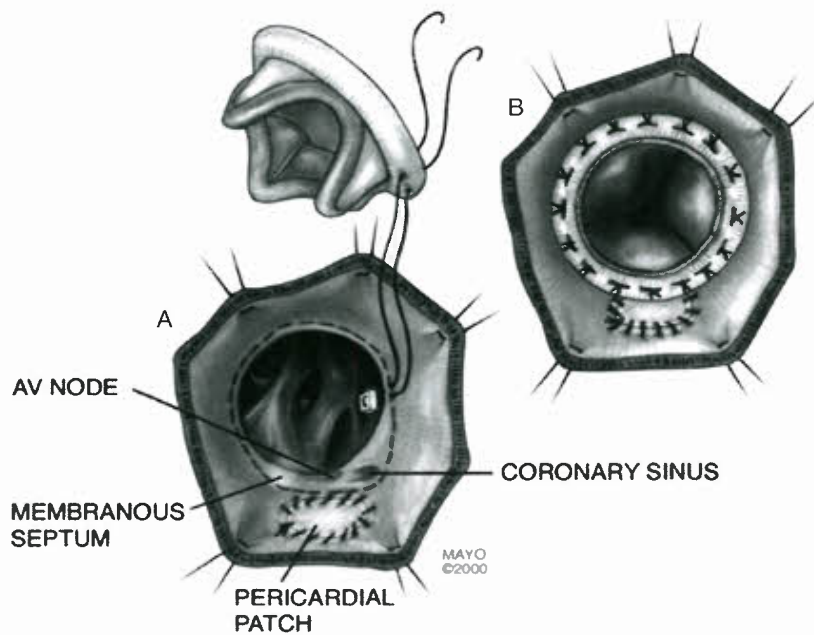


Figure 39.24. A,B: Diagram for TV replacement technique; in Ebstein's anomaly. A: The valve suture line is placed on the atrial side of the membranous septum and AV node to avoid injury to the conduction system. The suture line is also deviated cephalad to the tricuspid annulus posterolaterally when the tissues are thin, to avoid injury to the RCA. When there is sufficient distance between the coronary sinus and the AV node, the coronary sinus may be left on the atrial side of the suture line. B: The sutures are tied with the heart perfused and beating to ensure that a conducted rhythm is preserved. (Copyrighted and used with permission of Mayo Foundation for Medical Education and Research.)

left to drain into the RV in order to avoid AV block by sutures placed too close to the conduction tissue. The struts of the porcine bioprosthesis should straddle the area of the membranous septum and conduction tissue also as an effort to avoid AV block. After septal defects are closed, tricuspid replacement can be performed on bypass without aortic clamping, which also can be helpful when there is significant ventricular dysfunction because it reduces the ischemic time. It is advisable to tie the sutures while the heart is beating, to detect any rhythm disturbance that may happen.

We prefer mild or less regurgitation after repair but accept moderate regurgitation to delay the time of valve replacement as much as we can in young children. In our experience in both pediatric and adult populations, bioprostheses in the tricuspid position have greater durability than bioprostheses in other cardiac positions, even when compared with tricuspid bioprostheses for non-Ebstein cases (57). This may be due, in part, to the large size of bioprosthesis that can be implanted relative to the patient somatic size and, the other factor may be the low right ventricular systolic pressure that is almost always present in Ebstein's anomaly. Both of these factors decrease turbulence and stress on the bioprosthesis. We avoid the use of mechanical valves in the tricuspid position in the presence of significant right ventricular dysfunction, as the discs may not open and close properly, which will increase the chance of valve thrombosis despite adequate anticoagulation. Mechanical valve replacement can be considered for adult patients who are taking warfarin anticoagulation for other indications and who want to potentially minimize the need for a subsequent reoperation for bioprosthetic deterioration provided right ventricular function is reasonable.

One and Half Ventricle Repair

The BDCPA has been used in selected patients with Ebstein's anomaly. The BDCPA does two important things in the setting of Ebstein's anomaly. First, it reduces venous return to the enlarged, dysfunctional RV by approximately one-third, and second, it provides sufficient preload to the LV to sustain adequate systemic perfusion when right-sided output is low. While some surgeons apply the BDCPA to repair of Ebstein's anomaly routinely (French reference), it has been our approach to utilize it selectively (Quinnonez and Hanley reference).

Indications for the BDCPA include: (a) severe RV enlargement and/or dysfunction, (b) a squashed LV (D-shaped LV), (c) moderate degree of TV stenosis (mean gradient >6 mm Hg) as a result of reduction in the valve orifice area after repair, and (d) RA:LA pressure ratio >1.5 , which indicates poor RV function. Other indications include preoperative cyanosis at rest or with exercise, which also indicates decreased RV function.

The BDCPA has the following disadvantages: (a) pulsations of the head and neck veins, (b) facial swelling, (c) development of pulmonary arteriovenous fistulae (69) and, (4) compromised access to the heart from the internal jugular vein approach for electrophysiologic studies or for pacemaker placement, if needed in the future.

Left ventricular dysfunction may be present in Ebstein's anomaly especially when there is a significant right ventricular dilatation or dysfunction. Whether this is due to a change in the geometry of the LV because of RV enlargement or whether it is due to an actual reduction in LV function is not known. However, it is important to document by direct pressure measurements the pulmonary arterial and left atrial pressures (LAP) before committing to a BDCPA. We prefer that the left ventricular end-diastolic pressure (LVEDP) is <12 mm Hg, the transpulmonary gradient <10 mm Hg, and the mean pulmonary arterial pressure <16 mm Hg, before considering a BDCPA. LV dysfunction can cause an increase in LVEDP, LAP, and pulmonary artery pressures. However, it often is still feasible to perform BDCPA in the presence of moderate left ventricular dysfunction (ejection function of 35% to 40%) in the setting of Ebstein's anomaly, but permissible hemodynamics should be confirmed. The BDCPA also may allow greater amounts of residual TR to be tolerated. The smaller regurgitant volume and the unloading of the RV may allow patients to tolerate longer intervals between repeat TV operations performed for failing TV prostheses or progressive valve regurgitation. Finally, if the repair has resulted in mild or moderate tricuspid stenosis (mean gradient 5 to 10 mm Hg) the gradient will be reduced by reduction in systemic venous return with the BDCPA (70). Chavaud et al. (71,72) and Quiñonez et al. (73) have proposed that the use of a bidirectional cavopulmonary shunt may decrease operative mortality and facilitate postoperative management when there is severe right ventricular dysfunction. The application of the BDCPA in patients with Ebstein's anomaly is increasing: in a

series of 150 patients in a European registry, approximately 26% underwent a 1.5-ventricle repair (74). The late results of the BDCPA approach are unknown.

We believe that the use of cavopulmonary anastomosis in Ebstein's anomaly should be reserved for selected patients until the late outcomes are well described, but it is considered a promising option especially in the presence of right heart failure.

Plication of Atrialized Right Ventricle

Plication (Fig. 39.22F and G) or resection of the atrialized portion of the RV in Ebstein's anomaly is controversial. The theoretical advantages may include: (a) decreasing the size of the nonfunctioning portion of the RV, which may speed the exit of blood from the right side of the heart, (b) minimizing the pancake effect of the RV on the LV, which may improve the left ventricular contractility and cardiac output, (c) eliminating tension on the TV repair, especially with a complex repair that incorporates multiple suture lines (e.g., cone reconstruction), and (d) allowing more space for the lung since the RV is reduced in size. The potential risk with the plication or resection process is the interruption of some coronary arterial supply to the RV, and the risk of RCA injury, both of which will predispose to ventricular arrhythmias and compromise ventricular function.

In our practice, plication of the atrialized RV is done selectively. We plicate the atrialized RV if it is thin, transparent, and dyskinetic intraoperatively. We always inspect the right coronary and posterior descending coronary arteries during the plication process to insure that it is not kinked or compromised during the course of plication.

Right Reduction Atrioplasty

There is almost always a significant right atrial dilatation in Ebstein's anomaly; so we perform right reduction atrioplasty routinely at the time of atriotomy closure. We take great care to avoid suture placement in the crista terminalis at the time of atriotomy closure in order to decrease the incidence of atrial tachyarrhythmias (75,76).

Surgical Treatment of Arrhythmias

The most common atrial tachyarrhythmias in Ebstein's anomaly are atrial fibrillation and flutter. We have used successfully the right-sided cut-and-sew lesions of Cox-maze III procedure in Ebstein's anomaly. With the availability of newer devices such as radiofrequency or cryoablation, the procedure time for maze procedure is shortened significantly. Consequently, our current preference is to perform a biatrial maze procedure, particularly when there is chronic atrial fibrillation, left atrial dilatation, or concomitant mitral regurgitation. We follow the lesions in both atria that have been previously described (77,78) (Fig. 39.25). In the presence of atrial flutter, we prefer to add a "right atrial isthmus" lesion, which is the posterolateral TV annulus to the coronary sinus to the inferior vena cava. We also make an effort to close the left atrial appendage.

In patients with AV nodal re-entrant tachycardia who underwent unsuccessful ablation in the electrophysiologic laboratory preoperatively, we perform perinodal cryoablation on cardiopulmonary bypass after opening the RA and closure of the intracardiac shunt. This involves multiple applications of the cryoprobe around and in the ostium (os) of the coronary sinus, which is then carried anteriorly toward the proximal AV node until temporary complete heart block is noted, at which time the rewarming is begun; normal AV conduction returns shortly thereafter. In case of accessory conduction pathway as in WPW syndrome, mapping and ablation is performed routinely preoperatively. Intraoperative mapping and ablation is rarely performed in the current era.

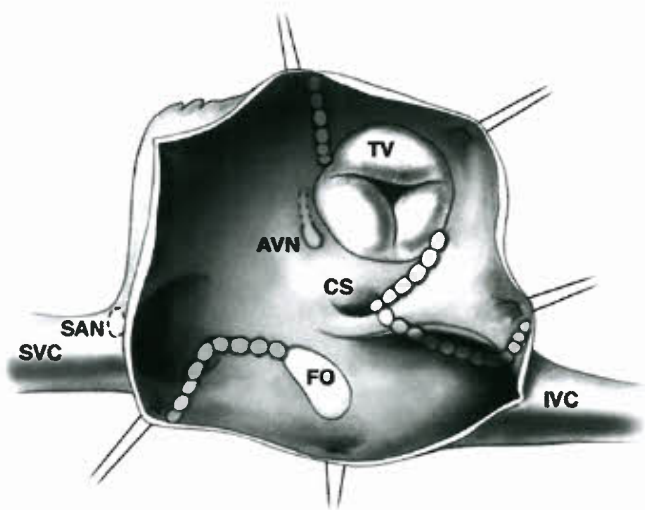


Figure 39.25. Diagram showing: location of cryoablation blocking lines for atrial flutter/fibrillation. TV, Tricuspid valve; AVN, AV node; CS, coronary sinus; SAN, sinoatrial node; SVC, superior vena cava; FO, foramen ovale; IVC, inferior vena cava. (Copyrighted and used with permission of Mayo Foundation for Medical Education and Research.)

Heart Transplantation

Heart transplantation rarely is necessary for Ebstein's anomaly. In our experience, the indication for transplantation is usually the presence of severe biventricular dysfunction (left ventricular ejection fraction <25%). On the other hand, patients with severe right ventricular dysfunction and normal or mild to moderately depressed left ventricular dysfunction are better served with a BDCPA at the time of TV repair or replacement. Other indications for transplantation include patients with significant left ventricular dilation and dysfunction and those with severe mitral regurgitation with significant left ventricular dysfunction. To determine the feasibility of transplantation versus conventional surgery, hemodynamic cardiac catheterization to ascertain left-sided filling pressures and pulmonary artery pressures is recommended.

PREGNANCY AND EBSTEIN'S ANOMALY

Pregnancy in the presence of Ebstein's anomaly always poses a challenge. Fertility is not affected, but close observation always is required by the treating obstetrician and cardiologist to optimize the best outcome. In an analysis of pregnancy outcome in four females, Chopra et al. (79) reported that pregnancy was well tolerated and there were eight vaginal deliveries with two premature ones. The mean birth weight was 2.54 ± 0.88 kg. No cardiac anomaly was found in six babies, but there was an unexplained death in one and no data was available in the other one. One patient had right heart failure during early pregnancy, and another one had an arrhythmia during labor, which was managed medically. Among the Mayo Clinic experience (80), we recorded a total of 275 pregnancies among 82 women. The incidence of congenital heart disease in children of a parent with Ebstein anomaly was 3.9%, which is significantly higher than the expected incidence of 0.75% in the general population. However, it is nearly identical to the 4% incidence in Ebstein anomaly reported by Drenthen et al. (81) and previous reports from our institution (82). In addition, it is consistent, with the incidence in children born

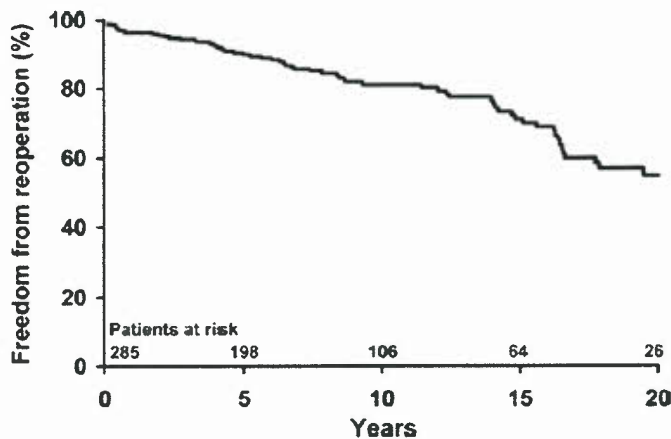


Figure 39.26. Freedom from any reoperation is shown with the time zero being the first operation at Mayo Clinic. (Copyrighted and used with permission of Mayo Foundation for Medical Education and Research.)

to a parent with aortic stenosis, pulmonary stenosis, or VSD (1.2% to 3.9%, CI 0.01% to 7.5%) (81)."

FUNCTIONAL OUTCOME AFTER SURGERY

Most of the literature focuses on survival and reoperation with very little discussion about the functional outcome for patients with Ebstein's anomaly after surgery. We recently reported our experience of 539 patients with Ebstein's anomaly who underwent 604 cardiac operations (80). The mean age at the initial operation was 24 years (range 8 days to 79 years) and 53% were female. Survival at 5, 10, 15, and 20 years was 94%, 90%, 86%, and 76%, respectively. Survival free of late reoperation (Fig. 39.26) was 86%, 74%, 62%, and 46% at 5, 10, 15, and 20 years, respectively. Two hundred and thirty-seven (83%) patients were in NYHA functional class I or II, and 34% were taking no cardiac medication. The reported exercise tolerance was comparable to that of the patients' peers. In a small subset of these patients, formal exercise testing

was conducted (83,84). There was improvement in exercise tolerance (Fig. 39.27) after operation, but this improvement was believed to be a result of the elimination of the right-to-left shunt at the atrial level rather than improvement in ventricular function. Late reoperation, rehospitalization, and atrial tachyarrhythmias continue to be a problem, with a rate of freedom from rehospitalization (for cardiac causes including reoperation) of 91%, 79%, 68%, 53%, and 35% at 1, 5, 10, 15, and 20 years, respectively (72). Thus, further improvements in the durability of TV repair and replacement, as well as improved control of atrial arrhythmias, may lead to improved quality of life in patients with Ebstein's anomaly.

CONGENITAL NON-EBSTEIN TRICUSPID VALVE REGURGITATION

Congenital TV regurgitation is a relatively uncommon condition that includes a heterogeneous group of lesions with a unique management strategy. There are wide anatomical variations that lead to TR in patients without Ebstein malformation. Possible etiologies may include primary valve abnormalities, for example, congenital absence of chordae (85) or TV dysplasia in congenitally unguarded TV orifice (86), and patients with pulmonary atresia and intact ventricular septum (87), which can be similar to the valves of Ebstein's anomaly, or secondary regurgitation in association with other anomalies as in atrio VSDs (88), cc-TGA (24), congenital coronary arterial fistula with secondary right ventricular enlargement (89), and Uhl's anomaly (90). Iatrogenic causes in infants, children, and adolescents include TR secondary to previous VSD closure (chordal or leaflet injury), pacemaker or internal cardioverter-defibrillator lead-induced TR (91), and traumatic TR (ruptured chordae) (92). The presentations depend on the severity of the disease and it may be apparent in infancy, childhood, or adulthood (93).

In general, there are two categories of TV dysplasia—those with and those without downward displacement. Cases with downward displacement, which is due to failure of delamination of valve leaflets from underlying myocardium, are by definition, Ebstein malformation. Although downward displacement often is given as the sole feature of Ebstein malformation, dysplasia of the leaflets and subvalvar apparatus are

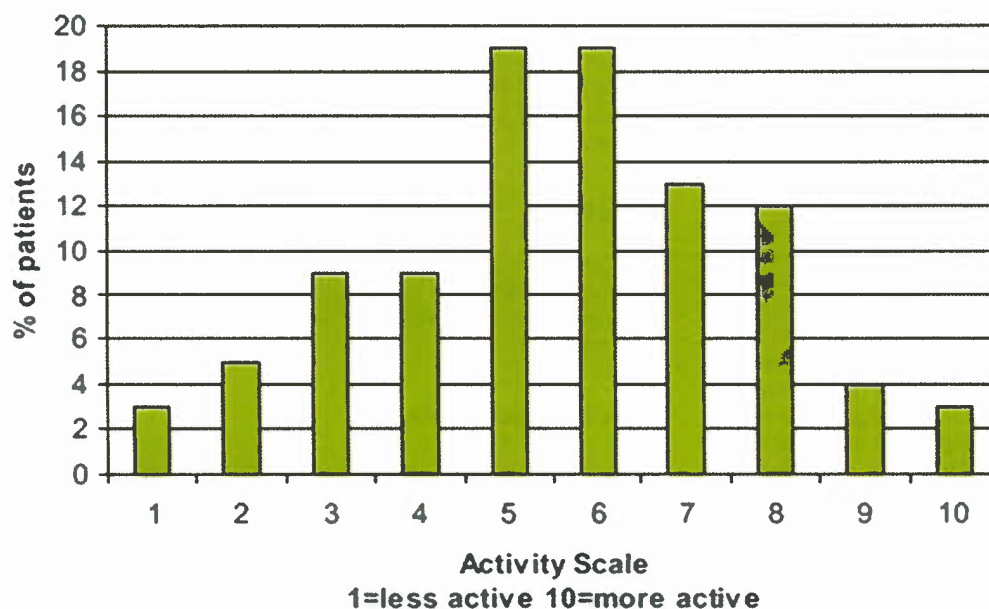


Figure 39.27. Self-reported activity scale after operation for Ebstein anomaly is shown with the percentage of survey responders who rated their exercise tolerance related to other people their own age on a scale of 1 to 10. (Copyrighted and used with permission of Mayo Foundation for Medical Education and Research.)

an almost universal feature as well. The pathognomic findings of Ebstein malformation are downward displacement, whether or not features of dysplasia are present, and a myopathy of the RV as a result of failure of delamination. When downward displacement is absent, then the anatomic entity is referred to as “tricuspid valvular dysplasia (94).”

Echocardiography confirms the diagnosis, determines the degree of TR, allows accurate evaluation of the tricuspid leaflets and subvalvar apparatus (displacement, tethering, dysplasia, etc.), size and function of the RV and LV, and detection of an ASD.

Magnetic resonance imaging (MRI) is being used increasingly in all types of patients with cardiac disease, including those with Ebstein's anomaly and other forms of congenital TR. Functional assessment can be made including quantitative measurements of left and right ventricular size and function. At the present time, we utilize echocardiography (2- and 3-D) for evaluation of TV anatomy and MRI for assessment of right ventricular size and function.

TR has been considered a benign lesion for a long time, but recent studies suggest that irrespective of pulmonary artery pressure or left ventricular ejection fraction, TR negatively affects long-term survival (95). The reported 2-year postoperative event-free survival in the presence of severe preoperative right ventricular dysfunction is 57% (96). Severe TR induces chronic right ventricular volume overload, which leads to progressive ventricular dilatation, dysfunction, and eventually right-sided heart failure. Timely correction of TR will preserve right ventricular function, improve functional capacity, and improve long-term survival. TV repair is the preferred treatment strategy when it is feasible, particularly in children. Optimal timing is now recommended before the onset of right ventricular dysfunction even in asymptomatic patients (97,98). The surgical indications in TR are not clearly identified, but generally include symptoms or cyanosis (when ASD is present), decreased exercise tolerance, progressive cardiomegaly on chest x-ray, progressive right ventricular dilatation or reduction of right ventricular systolic function by echocardiography, or appearance of atrial or ventricular arrhythmias. In borderline situations, the echocardiographic determination of high probability of TV repair makes the decision to proceed earlier with operation easier. This may be explained by the following: few data exist on postoperative outcomes; and the overall prevalence of TR as compared with left-sided valvular disease is low.

The goal of operation is repair of the TV whenever possible. In order to increase the number of successful TV repairs, particularly in children, we have been utilizing a cone-type reconstruction (58,99), which results in 360 degrees of tricuspid leaflet tissue surrounding the right AV junction. This allows leaflet tissue to coapt with leaflet tissue, similar to what occurs with normal TV anatomy. The hinge point of the reconstructed TV is at the true TV annulus (AV junction). Alternatively, a monocusp-type repair based on a large anterior leaflet has also been successful (57,64). It is important that the repair is tension free. In order to facilitate this, augmentation of the mid-anterior leaflet with an ellipse of autologous pericardium or other pliable synthetic material can increase the height of the anterior leaflet, which facilitates coaptation with the ventricular septum while minimizing tension at an inferior annuloplasty line. Importantly, we avoid the creation of complete pericardial leaflets (from annulus to leading edge) because of poor durability. We use *flexible* annuloplasty C-shaped rings (from anteroseptal commissure to inferoseptal commissure) liberally since significant tricuspid annular dilation is often present and the possibility of iatrogenic tricuspid stenosis is low. Finally, closure of intra-atrial shunts and right reduction atriotomy are routine, and the maze procedure is performed when atrial tachyarrhythmias are present.

Prosthetic TV replacement remains a good alternative for the treatment of TR when valve repair is not feasible. Porcine bioprosthetic valve replacement, as opposed to mechanical valve replacement, is generally preferred because of relative good durability of the porcine bioprosthesis in the tricuspid position and the lack of need for chronic warfarin anticoagulation. Mechanical TV replacement should be advised in selected circumstances since there is a higher frequency of prosthetic valve dysfunction (thrombosis) compared to mechanical valves in other cardiac positions, particularly when right ventricular function is poor. In general, postoperative management includes short term (3 months) warfarin anticoagulation for porcine bioprostheses and life long aspirin, 81 mg daily. When a mechanical valve is used, the target international normalized ratio (INR) is 3 to 3.5 in addition to aspirin, 81 mg daily.

The wide and infinite variability of anatomic abnormality with Ebstein malformation and congenital TV dysplasia demonstrate that every valve is a little different and no two hearts are alike...illustrating why this lesion continues to be one the most challenging valve lesions for the surgeon. There have been more reports in the literature of tricuspid valvuloplasty techniques for Ebstein malformation and congenital tricuspid dysplasia than any other valve lesion in the cardiac arena. While the ability to obtain a competent, durable tricuspid repair has improved in recent years, the surgical treatment of the congenitally abnormal TV is still considered palliative since the many patients will require more than one operation in their lifetime.

UHL'S ANOMALY

History

William Osler in 1905 described the term “parchment heart,” but Henry Uhl reported the first case in 1952 (100).

Pathology

In Uhl's anomaly, there is complete or partial absence of the myocardial layer of the RV and the endocardium and the epicardium become opposed, but the septal component, septomarginal trabeculation, and the papillary muscles of the TV are normally muscularized (101). The absence of myocardium may be the result of primary nondevelopment of myocytes or a form of selective apoptosis. Most cases are sporadic and Feucht et al. (102) suggested the role of vascular endothelial growth factor in the induction of this cardiovascular malformation.

Prevalence

Uhl's anomaly is extremely rare. Gerlis et al. (103) in 1993 reported only 84 cases since the beginning of the 20th century. It is mainly sporadic although some familial occurrences have been reported.

Clinical Presentation

Congestive heart failure with associated peripheral edema and pleural effusion is the most frequent symptom. Arrhythmias and conduction disturbances are not common in Uhl's anomaly as in arrhythmogenic right ventricular dysplasia due to the absence of foci that transmit abnormal electrical activity (103).

Associated Anomalies

Pulmonary atresia with intact ventricular septum

Differential Diagnosis

- Ebstein's anomaly
- Arrhythmogenic right ventricular dysplasia:

In arrhythmogenic right ventricular dysplasia, there is a patchy replacement of the right ventricular muscle with fibrofatty tissue. Arrhythmia, palpitations, syncope, or sudden death are common presentations.

Treatment

Treatment includes medical management of congestive heart failure, and drainage of pleural effusions. Surgical options include:

- Right ventricular exclusion (104): with atrial septectomy, BDCPA, and closure of the TV orifice.
- One-and-half ventricle repair (105): with BDCPA and partial right ventriculectomy and atrial septectomy.
- Cardiac transplantation (106).

REFERENCES

1. Ebstein W. Ueber einen sehr seltenen Fall von Insufficienz der Valvula tricuspidalis, bedingt durch eine angeborene hochgradige Missbildung derselben. *Arch Anat Physiol* 1866;238–254.
2. Mann RJ, Lie JT. The life story of Wilhelm Ebstein (1836–1912) and his almost overlooked description of a congenital heart disease. *Mayo Clin Proc* 1979;54:197–204.
3. van Son JA, Konstantinov IE, Zimmermann V. Wilhelm Ebstein and Ebstein's malformation. *Eur J Cardiothorac Surg* 2001;20:1082–1085.
4. Lamers WH, Viragh S, Wessels A, et al. Formation of the tricuspid valve in the human heart. *Circulation* 1995;91:111–121.
5. Edwards WD. Embryology and pathologic features of Ebstein's anomaly. *Prog Pediatr Cardiol* 1993;2:5–15.
6. Dearani JA, Danielson GK. Ebstein's anomaly of the tricuspid valve. In: Mavroudis C, Backer CL, eds. *Pediatric Cardiac Surgery*. 3rd ed. Philadelphia, PA: Mosby, 2003:524–536.
7. Lev M, Liberthson RR, Joseph RH, et al. The pathologic anatomy of Ebstein's disease. *Arch Pathol* 1970;90:334–343.
8. Anderson KR, Zuberbuhler JR, Anderson RH, et al. Morphologic spectrum of Ebstein's anomaly of the heart: a review. *Mayo Clin Proc* 1979;54:174–180.
9. Attenhofer Jost CH, Connolly HM, Dearani JA, et al. Ebstein's anomaly. *Circulation* 2007;115:277–285.
10. Dearani JA, Danielson GK. Congenital heart surgery nomenclature and database project: Ebstein's anomaly and tricuspid valve disease. *Ann Thorac Surg* 2000;69:S106–S117.
11. Carpentier A, Chauvaud S, Mace L, et al. A new reconstructive operation for Ebstein's anomaly of the tricuspid valve. *J Thorac Cardiovasc Surg* 1988;96:92–101.
12. Celermajer DS, Bull C, Till JA, et al. Ebstein's anomaly: presentation and outcome from fetus to adult. *J Am Coll Cardiol* 1994;23:170–176.
13. Correa-Villasenor A, Ferencz C, Neill CA, et al. For the Baltimore-Washington infant study group. Ebstein's malformation of the tricuspid valve: genetic and environmental factors. *Teratology* 1994;50:137–147.
14. Emanuel R, O'Brien K, Ng R. Ebstein's anomaly: genetic study of 26 families. *Br Heart J* 1976;38:5–7.
15. Benson DW, Silberbach GM, Kavanaugh-McHugh A, et al. Mutations in the cardiac transcription factor NKX2.5 affect diverse cardiac developmental pathways. *J Clin Invest* 1999;104:1567–1573.
16. Yatsenko SA, Yatsenko AN, Szigeti K, et al. Interstitial deletion of 10p and atrial septal defect in DiGeorge 2 syndrome. *Clin Genet* 2004;66:128–136.
17. Postma AV, van Engelen K, van de Meerakker J, et al. Mutations in the sarcomere gene MYH7 in Ebstein anomaly. *Circ Cardiovasc Genet* 2011;4:43–50.
18. Attenhofer Jost CH, Connolly HM, O'Leary PW, et al. Left heart lesions in patients with Ebstein anomaly. *Mayo Clin Proc* 2005;80:361–368.
19. Sumner RG, Jacoby WJ Jr, Tucker DH. Ebstein's anomaly associated with Cardiomyopathy and Pulmonary Hypertension. *Circulation* 1964;30:578–587.
20. Danielson GK, Driscoll DJ, Mair DD, et al. Operative treatment of Ebstein's anomaly. *J Thorac Cardiovasc Surg* 1992;104:1195–1202.
21. Lev M, Gibson S, Miller RA. Ebstein's disease with Wolff-Parkinson-White syndrome; report of a case with a histopathologic study of possible conduction pathways. *Am Heart J* 1955;49:724–741.
22. Attenhofer Jost CH, Connolly HM, Warnes CA, et al. Noncompacted myocardium in Ebstein's anomaly: initial description in three patients. *J Am Soc Echocardiogr* 2004;17:677–680.
23. van Son JA, Danielson GK, Huhta JC, et al. Late results of systemic atrioventricular valve replacement in corrected transposition. *J Thorac Cardiovasc Surg* 1995;109:642–652.
24. Said SM, Burkhardt HM, Schaff HV, et al. Congenitally corrected transposition of great arteries: surgical options for the failing right ventricle and/or severe tricuspid regurgitation. *World J Pediatr Congenit Heart Surg* 2011;2:64–79.
25. Anderson KR, Danielson GK, McGoon DW, et al. Ebstein's anomaly of the left-sided tricuspid valve: pathological anatomy of the valvular malformation. *Circulation* 1978;58:87–91.
26. Adams JC, Hudson R. A case of Ebstein's anomaly surviving to the age of 79. *Br Heart J* 1956;18:129–132.
27. Roberson DA, Silverman NH. Ebstein's anomaly: echocardiographic and clinical features in the fetus and neonate. *J Am Coll Cardiol* 1989;14:1300–1307.
28. Oberhoffer R, Cook AC, Lang D, et al. Correlation between echocardiographic and morphological investigations of lesions of the tricuspid valve diagnosed during fetal life. *Br Heart J* 1992;68:580–585.
29. Watson H. Natural history of Ebstein's anomaly of tricuspid valve in childhood and adolescence. An international co-operative study of 505 cases. *Br Heart J* 1974;36:417–427.
30. Giuliani ER, Fuster V, Brandenburg RO, et al. Ebstein's anomaly: the clinical features and natural history of Ebstein's anomaly of the tricuspid valve. *Mayo Clin Proc* 1979;54:163–173.
31. Perloff JK. Ebstein's anomaly of the tricuspid valve. In: Perloff JK, ed. *Clinical Recognition of Congenital Heart Disease*. 5th ed. Philadelphia, PA: Saunders, 2003:194–215.
32. Silverman NH, Gerlis LM, Horowitz ES, et al. Pathologic elucidation of the echocardiographic features of Ebstein's malformation of the morphologically tricuspid valve in discordant atrioventricular connections. *Am J Cardiol* 1995;76:1277–1283.
33. Frescura C, Angelini A, Daliento L, et al. Morphological aspects of Ebstein's anomaly in adults. *Thorac Cardiovasc Surg* 2000;48:203–208.
34. Hebe J. Ebstein's anomaly in adults: arrhythmias: diagnosis and therapeutic approach. *Thorac Cardiovasc Surg* 2000;48:214–219.
35. Ho SY, Goltz D, McCarthy K, et al. The atrioventricular junctions in Ebstein malformation. *Heart* 2000;83:444–449.
36. Smith WM, Gallagher JJ, Kerr CR, et al. The electrophysiologic basis and management of symptomatic recurrent tachycardia in patients with Ebstein's anomaly of the tricuspid valve. *Am J Cardiol* 1982;49:1223–1234.
37. Shina A, Seward JB, Edwards WD, et al. Two dimensional echocardiographic spectrum of Ebstein's anomaly: detailed anatomic assessment. *J Am Coll Cardiol* 1984;3:356–370.
38. Hornberger LK, Sahn DJ, Kleinman CS, et al. Tricuspid valve disease with significant tricuspid insufficiency in the fetus: diagnosis and outcome. *J Am Coll Cardiol* 1992;17:167–173.
39. Celermajer DS, Cullen S, Sullivan ID, et al. Outcome in neonates with Ebstein's anomaly. *J Am Coll Cardiol* 1992;19:1041–1046.
40. Yalonsky S, Tobler D, Greutmann M, et al. Cardiac magnetic resonance imaging and the assessment of Ebstein anomaly in adults. *Am J Cardiol* 2011;107:767–773.
41. Attie F, Rosas M, Rijlaarsdam M, et al. The adult patient with Ebstein anomaly. Outcome in 72 unoperated patients. *Medicine (Baltimore)* 2000;79:27–36.
42. Knott-Craig CJ, Overholt ED, Ward KE, et al. Repair of Ebstein's anomaly in the symptomatic neonate: an evolution of technique with 7-year follow-up. *Ann Thorac Surg* 2002;73:1786–1793.
43. Knott-Craig CJ. Management of neonatal Ebstein's anomaly. *Oper Tech* 2008;13:101–108.
44. Knott-Craig CJ, Goldberg SP, Overholt ED, et al. Repair of neonates and young infants with Ebstein's anomaly and related disorders. *Ann Thorac Surg* 2007;84:587–593.
45. Starnes VA, Pitlick PT, Bernstein D, et al. Ebstein's anomaly appearing in the neonate. A new surgical approach. *J Thorac Cardiovasc Surg* 1991;101:1082–1087.
46. Reemtsen BL, Starnes VA. Fenestrated right ventricular exclusion (Starnes' procedure) for severe neonatal Ebstein's anomaly. *Oper Tech* 2008;13:91–100.
47. Reemtsen BL, Polimenakos AC, Fagan BT, et al. Fate of the right ventricle after fenestrated right ventricular exclusion for severe neonatal Ebstein anomaly. *J Thorac Cardiovasc Surg* 2007;134:1406–1412.
48. Sano S, Ishino K, Kawada M, et al. Total right ventricular exclusion procedure: an operation for isolated congestive right ventricular failure. *J Thorac Cardiovasc Surg* 2002;123:640–647.
49. Reemtsen BL, Fagan BT, Wells WJ, et al. Current surgical therapy for Ebstein anomaly in neonates. *J Thorac Cardiovasc Surg* 2006;132:1285–1290.
50. Graham TP Jr, Bricker JT, James FW, et al. Twenty-Sixth Bethesda Conference: recommendations for determining eligibility for competition in athletes with cardiovascular abnormalities: Task Force 1: congenital heart disease. *Med Sci Sports Exerc* 1994;26: S246–S253.

51. Reich JD, Auld D, Hulse E, et al. For the Pediatric Electrophysiology Society. The Pediatric Radiofrequency Ablation Registry's experience with Ebstein's anomaly. *J Cardiovasc Electrophysiol* 1998;9:1370-1377.
52. Schiebeler GL, Adams P Jr, Anderson RC, et al. Clinical study of twenty-three cases of Ebstein's anomaly of the tricuspid valve. *Circulation* 1959;19:165-187.
53. Barnard CN, Schrire V. Surgical correction of Ebstein's malformation with prosthetic tricuspid valve. *Surgery* 1963;54:302-308.
54. Hardy KL, May IA, Webster CA, et al. Ebstein's anomaly: a functional concept and successful definitive repair. *J Thorac Cardiovasc Surg* 1964;48:927-940.
55. Danielson GK, Maloney JD, Devloo RA. Surgical repair of Ebstein's anomaly. *Mayo Clin Proc* 1979;54:185-192.
56. Dearani JA, Danielson GK. Tricuspid valve repair for Ebstein's anomaly. *Oper Tech Thorac Cardiovasc Surg* 2003;8:188-192.
57. Brown ML, Dearani JA, Danielson GK, et al. The outcomes of operations for 539 patients with Ebstein anomaly. *J Thorac Cardiovasc Surg* 2008;135:1120-1136.
58. da Silva JP, Baumgratz FJ, Fonseca L, et al. The cone reconstruction of the tricuspid valve in Ebstein's anomaly. The operation: early and midterm results. *J Thorac Cardiovasc Surg* 2007;133:215-223.
59. Ullmann MV, Born S, Sebening C, et al. Ventricularization of the atrialized chamber: a concept of Ebstein's anomaly repair. *Ann Thorac Surg* 2004;78:918-924.
60. Hetzer R, Nagdyman N, Ewart P, et al. A modified repair technique for tricuspid incompetence in Ebstein's anomaly. *J Thorac Cardiovasc Surg* 1998;115:857-868.
61. Quaegebeur JM, Sreeram N, Fraser AG, et al. Surgery for Ebstein's anomaly: the clinical and echocardiographic evaluation of a new technique. *J Am Coll Cardiol* 1991;17:722-728.
62. Wu Q, Huang Z. A new procedure for Ebstein's anomaly. *Ann Thorac Surg* 2004;77:470-776.
63. Chen JM, Mosca RS, Altman K, et al. Early and medium-term results for repair of Ebstein's anomaly. *J Thorac Cardiovasc Surg* 2004;127:990-999.
64. Boston US, Dearani JA, O'Leary PW, et al. Tricuspid valve repair for Ebstein's anomaly in young children: a 30-year experience. *Ann Thorac Surg* 2006;81:690-695.
65. Kiziltan HT, Theodoro DA, Warnes CA, et al. Late results of bioprosthetic tricuspid valve replacement in Ebstein's anomaly. *Ann Thorac Surg* 1998;66:1539-1545.
66. Geha AS, Laks H, Stansel HC, et al. Late failure of porcine valve heterografts in children. *J Thorac Cardiovasc Surg* 1979;78:351.
67. Williams DB, Danielson GK, McGoon DC, et al. Porcine heterograft valve replacement in children. *J Thorac Cardiovasc Surg* 1982;84:446-450.
68. Sanfelippo PM, Giuliani ER, Danielson GK, et al. Tricuspid valve prosthetic replacement: early and late results with the Starr-Edwards prosthesis. *J Thorac Cardiovasc Surg* 1976;71:441-445.
69. Kopf GS, Laks H, Stansel HC, et al. Thirty-year follow-up of superior vena cava-pulmonary artery (Glenn) shunts. *J Thorac Cardiovasc Surg* 1990;117:662-670.
70. Marianeschi SM, McElhinney DB, Reddy VM, et al. Alternative approach to the repair of Ebstein's malformation: intracardiac repair with ventricular unloading. *Ann Thorac Surg* 1998;66:1546-1550.
71. Chauvaud S, Fuzellier JF, Berrebi A, et al. Bi-directional cavopulmonary shunt associated with ventriculo and valvuloplasty in Ebstein's anomaly: benefits in high risk patients. *Eur J Cardiothorac Surg* 1998;13:514-519.
72. Chauvaud S. Ebstein's malformation. Surgical treatment and results. *J Thorac Cardiovasc Surg* 2000;48:220-223.
73. Quiñonez LG, Dearani JA, Puga FJ, et al. Results of the 1.5-ventricle repair for Ebstein anomaly and the failing right ventricle. *J Thorac Cardiovasc Surg* 2007;133:1303-1310.
74. Sarris GE, Giannopoulos NM, Tsoutsinos AJ, et al. Results of surgery for Ebstein anomaly: a multicenter study from the European Congenital Heart Surgeons Association. *J Thorac Cardiovasc Surg* 2006;132:50-57.
75. Gandhi SK, Bromberg BI, Rodefeld MD, et al. Spontaneous atrial flutter in a chronic canine model of the modified Fontan operation. *J Am Coll Cardiol* 1997;30:1095.
76. Durongpisitkul K, Porter CJ, Cetta F, et al. Predictors of early- and late-onset supraventricular tachyarrhythmias after Fontan operation. *Circulation* 1998;98:1099.
77. Mavroudis C, Deal BJ, Back CL, et al. Arrhythmia surgery in patients with and without congenital heart disease. *Ann Thorac Surg* 2008;86:857-868.
78. Cox JL, Jaquiss RD, Schuessler RB, et al. Modification of the maze procedure for atrial flutter and atrial fibrillation. II. Surgical technique of the maze III procedure. *J Thorac Cardiovasc Surg* 1995;110:485-495.
79. Chopra S, Suri V, Aggarwal N, et al. Ebstein's anomaly in pregnancy: maternal and neonatal outcomes. *J Obstet Gynaecol Res* 2010;36:278-283.
80. Brown ML, Dearani JA, Danielson GK, et al. Functional status after operation for Ebstein anomaly: the Mayo Clinic experience. *J Am Coll Cardiol* 2008;52:460-466.
81. Drenthen W, Pieper PG, Roos-Hesselink JW, et al.; For the ZAHARA Investigators. Outcome of pregnancy in women with congenital heart disease: a literature review. *J Am Coll Cardiol* 2007;49:2303-2311.
82. Connolly HM, Warnes CA. Ebstein's anomaly: outcome of pregnancy. *J Am Coll Cardiol* 1994;23:1194-1198.
83. MacLellan-Tobert SG, Driscoll DJ, Mottram CD, et al. Exercise tolerance in patients with Ebstein's anomaly. *J Am Coll Cardiol* 1997;29:1615-1622.
84. Driscoll DJ, Mottram C, Danielson G. Spectrum of exercise intolerance in 45 patients with Ebstein's anomaly and observations on exercise tolerance in patients after surgical repair. *J Am Coll Cardiol* 1988;11:831-836.
85. Shikata F, Nagashima M, Nishimura K, et al. Repair of congenitally absent chordae in a tricuspid valve leaflet with hypoplastic papillary muscle using artificial chordae. *J Card Surg* 2010;25:737-739.
86. Mohan JC, Passey R, Arora R. Echocardiographic spectrum of congenitally unguarded tricuspid valve orifice and patent right ventricular outflow tract. *Int J Cardiol* 2000;74:153-157.
87. Bautista-Hernandez V, Hasan BS, Harrild DM, et al. Late pulmonary valve replacement in patients with pulmonary atresia and intact ventricular septum: a case-matched study. *Ann Thorac Surg* 2011;91:555-560.
88. Ando M, Takahashi Y. Variations of atrioventricular septal defects predisposing to regurgitation and stenosis. *Ann Thorac Surg* 2010;90:614-621.
89. El Watidy AM, Ismail HH, Calafore AM. Surgical management of right coronary artery-coronary sinus fistula causing severe mitral and tricuspid regurgitation. *Interact Cardiovasc Thorac Surg* 2010;10:110-112.
90. Vaidyanathan K, Agarwal R, Johari R, et al. Isolated congenital pulmonary regurgitation with right ventricular outflow tract aneurysm-a rare variant of Uhl's anomaly. *J Card Surg* 2010;25:415-417.
91. Lin G, Nishimura RA, Connolly HM, et al. Severe symptomatic tricuspid valve regurgitation due to permanent pacemaker or implantable cardioverter-defibrillator leads. *J Am Coll Cardiol* 2005;45:1672-1675.
92. Messika-Zeitoun D, Thomson H, Bellamy M, et al. Medical and surgical outcome of tricuspid regurgitation caused by flail leaflets. *J Thorac Cardiovasc Surg* 2004;128:296-302.
93. Gupta A, Grover V, Gupta VK. Congenital tricuspid regurgitation: review and a proposed new classification. *Cardiol Young* 2010;22:1-9.
94. Becker AE, Becker MJ, Edwards JE. Pathologic spectrum of dysplasia of the tricuspid valve. Features in common with Ebstein's malformation. *Arch Pathol* 1971;91:167-178.
95. Koelling TM, Aaronson KD, Cody RJ, et al. Prognostic significance of mitral regurgitation and tricuspid regurgitation in patients with left ventricular systolic dysfunction. *Am Heart J* 2002;144:524-529.
96. Kim YJ, Kwon DA, Kim HK, et al. Determinants of surgical outcome in patients with isolated tricuspid regurgitation. *Circulation* 2009;120:1672-1678.
97. Lee JW, Song JM, Park JP, et al. Long-term prognosis of isolated significant tricuspid regurgitation. *Circ J* 2010;74:375-380.
98. Shibata Y, Sato M, Chanda J, et al. Isolated tricuspid regurgitation due to atypical morphology of anteriorposterior leaflets in an adult: a case report and review of the literature. *J Cardiovasc Surg (Torino)* 1999;40:527-530.
99. Brown ML, Dearani JA. Ebstein malformation of the tricuspid valve: current concepts in management and outcomes. *Curr Treat Options Cardiovasc Med* 2009;11:396-402.
100. Uhl HS. A previously undescribed congenital malformation of the heart: total absence of the myocardium of the right ventricle. *Bull Johns Hopkins Hosp* 1952;91:197-209.
101. Gould L, Guttman B, Carrasco J, et al. Partial absence of the right ventricular musculature. A congenital lesion. *Am J Med* 1967;42:636-641.
102. Feucht M, Christ B, Wilting J. VEGF induces cardiovascular malformation and embryonic lethality. *Amer J Pathol* 1997;151:1407-1416.
103. Gerlis LM, Schmidt-Ott SC, HO SY, et al. Dysplastic conditions of the right ventricular myocardium: Uhl's anomaly versus arrhythmogenic right ventricular dysplasia. *Br Heart J* 1993;69:142-150.
104. Azhari N, Assaqqat M, Bulbul Z. Successful surgical repair of Uhl's anomaly. *Cardiol Young* 2002;12:192-195.
105. Yoshii S, Suzuki S, Hosaka S, et al. A case of Uhl's anomaly treated with a one and a half ventricle repair combined with partial right ventriculectomy in infancy. *J Thorac Cardiovasc Surg* 2001;122:1026-1028.
106. Ikari NM, Azeka E, Aiello VD, et al. Uhl's anomaly. Differential diagnosis and indications for cardiac transplantation in an infant. *Arq Bras Cardiol* 2001;77:69-76.

Lourdes R. Prieto ■ Larry A. Latson

Congenital obstruction to right ventricular outflow is most commonly due to pulmonary valve stenosis, but may also be intracavitary or supra-valvar and involve the main and branch pulmonary arteries. Pulmonary stenosis at some level, with and without other associated lesions, occurs in 25% to 30% of all patients with congenital heart disease. This chapter discusses all levels of pulmonary stenosis with intact ventricular septum.

ISOLATED VALVAR PULMONARY STENOSIS

Isolated pulmonary valve stenosis is found in 80% to 90% of all patients with right ventricular outflow obstruction. It was described in 1761 by John Baptist Morgagni (1) and initially was thought to be rare. With improved diagnostic capability, however, pulmonary valve stenosis has been found in 8% to 10% of patients with congenital heart disease.

Familial occurrence of pulmonary stenosis has been reported. Campbell (2) found a 2.1% incidence of cardiac disease, usually pulmonary stenosis or tetralogy of Fallot, in siblings of patients with pulmonary stenosis. In the Second Natural History Study of Congenital Heart Defects, the occurrence of definite and possible congenital cardiac defects in 1,356 siblings of 449 patients with valvar pulmonary stenosis was 1.1% and 2.1%, respectively (3).

Embryology and Pathology

The process of cardiac valve development begins with migration of a subset of endothelial cells lining the inner layer of the developing heart tube into the extracellular matrix that separates the inner endothelial layer from the outer layer of myocardium, forming cardiac cushions precisely in the areas overlying the future atrioventricular canal and outflow tract. The cells forming these cushions continue to proliferate and differentiate into mesenchymal cells. Whereas the mitral and tricuspid valves are derived only from endocardial cushion tissue, the final development of the aortic and pulmonary valves involves migration of neural crest cells from the branchial arches to the distal outflow tract where aortopulmonary septation will take place (4,5). Further remodeling of these cushions culminate in the formation of thin, tapered leaflets with a single endothelial cell layer and a central matrix of collagen, elastin, and glycosaminoglycans.

Normal valve development involves several signaling pathways that tightly regulate endothelial cell differentiation and remodeling, and is also dependent on the interaction between these endothelial cells, the extracellular matrix, and the surrounding myocardium (6). The complex interaction between

these pathways can be disrupted at various levels, resulting in a malformed valve. For example, deletion of CXCR7, a G-protein-coupled receptor found in cushion mesenchymal cells in the developing heart, resulted in aortic and pulmonary valve stenosis in mouse embryos due to excessive proliferation of mesenchymal valve cells associated with increased bone morphogenetic protein signaling (7). Deletion of Ptpn11 exon 2, which encodes the protein tyrosine phosphatase SHP-2 involved in another signaling pathway, results in dysplastic outflow valves (8). Notably, PTPN11 mutations are found in patients with Noonan syndrome and LEOPARD syndrome, both manifesting pulmonary valve stenosis (9–11). Research to date has elucidated disruptions that affect the development of both the pulmonary and aortic valves, but factors resulting specifically in pulmonary valve abnormalities have yet to be recognized. The pathways controlling the later stages of valve remodeling that would affect one or the other semilunar valve are not yet known.

In the classic form of pulmonary valve stenosis, the valve is conical or dome shaped, and two to four raphe may be visible, but there is no separation into valve leaflets (12) (Fig. 40.1). Less commonly, the valve may be diffusely thickened with one, two, or three leaflets and commissural fusion. A distinct pathology termed pulmonary valve dysplasia has been described in 10% to 20% of patients (13). Dysplastic valves are trileaflet with markedly thickened cusps composed of disorganized myxomatous tissue and little, if any, fusion (Fig. 40.2). The valve annulus is usually hypoplastic. This entity is found in most patients with Noonan syndrome and may be seen in nonfamilial cases.

Secondary changes in the right ventricle (RV) and pulmonary arteries can occur as a result of pulmonary valve obstruction. The RV, particularly the infundibular region, becomes diffusely hypertrophied. Hypertrophy of the infundibulum can produce dynamic subvalvar obstruction (Fig. 40.1). At autopsy, small myocardial infarctions frequently have been seen in the subendocardium of the right ventricular free wall and papillary muscles in patients with severe pulmonary stenosis. Thickening of the tricuspid valve and chordal attachments may be present, and the valve may become regurgitant. The right atrium may be thick and dilated as a result of the increased pressure necessary to fill the hypertrophic RV. In many cases, a patent foramen ovale or, less often, an atrial septal defect is seen.

Most patients develop poststenotic dilation of the pulmonary artery trunk, sometimes extending to the proximal left pulmonary artery (LPA). One notable exception to this finding is in patients with dysplastic pulmonary valves. The degree of dilation is not necessarily proportional to the severity of obstruction, often being more pronounced in mild cases. Poststenotic dilation may result from the high-velocity jet of flow ejected through the small valve orifice.

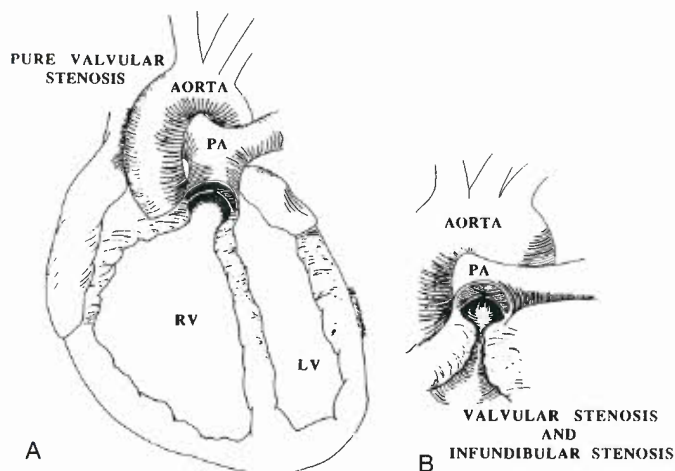


Figure 40.1. A schematic illustration of pulmonary valve stenosis with intact ventricular septum. A: Valvular stenosis with “doming” of the pulmonary valve. B: The secondary infundibular hypertrophy can be seen. LV, left ventricle; PA, pulmonary artery; RV, right ventricle.

Physiology

The main physiologic effect of valvar pulmonary stenosis is a rise in right ventricular pressure proportional to the severity of obstruction. This elevation of right ventricular pressure is accompanied by an increase in muscle mass that occurs by one of two mechanisms, depending on the stage of development. Work in animal models has shown that the fetal and neonatal myocardium responds to increased afterload by hyperplasia of the muscle cells with a concomitant increase in

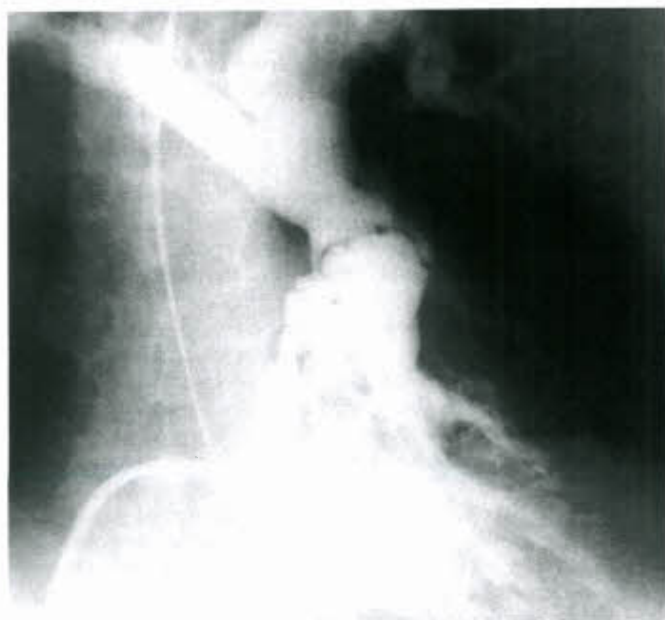


Figure 40.2. Right ventricular angiogram of a child with dysplastic pulmonary valve stenosis. The view is anteroposterior with cranial angulation. Note the thickened, irregular leaflets and relatively small annulus. Supravalvar narrowing is present, and the main pulmonary artery is not dilated.

the number of capillaries (14). In contrast, the adult myocardium responds with hypertrophy of the existing fibers, with no change in the capillary network. Thus, the neonatal myocardium may be better adapted to generate the high pressures necessary to overcome severe obstruction. Increased muscle mass may enable the hypertensive RV to maintain a normal stroke volume. If the size of the stenotic orifice remains fixed, however, the degree of obstruction becomes relatively more severe as the patient grows. The RV eventually may dilate and fail. This process is exacerbated by the development of tricuspid insufficiency in many patients with severe pulmonary stenosis. Right ventricular failure may occur in infancy if severe neonatal obstruction is present. As right ventricular output decreases with a failing ventricle, adequate tissue oxygenation can be maintained only by increasing tissue oxygen extraction. Any increase in oxygen demand, such as during exercise, may result in frank peripheral cyanosis. In patients with a patent foramen ovale or atrial septal defect, central cyanosis is observed as a result of right-to-left atrial shunting when the right atrial pressure exceeds the left atrial pressure. Progressive hypertrophy and decreased compliance of the RV, or myocardial failure with subsequent dilation, may lead to central cyanosis in some initially well-compensated patients.

When the degree of valvar pulmonary stenosis is severe enough to cause a decrease in fetal right ventricular output, a larger-than-normal atrial right-to-left shunt is established in utero. This condition has been termed critical pulmonary stenosis (15). The RV is often hypoplastic because of severe hypertrophy and the effects of reduced flow through the RV during development (Fig. 40.3). At birth, affected infants are cyanotic and have systemic or suprasystemic right ventricular pressure. Even if the stenosis is relieved, right-to-left atrial shunting and cyanosis often persist for months after the stenosis is relieved, until there is a decrease in the right ventricular hypertrophy and an increase in right ventricular size.

Manifestations

Clinical Features

Most patients with valvar pulmonary stenosis are asymptomatic, and the diagnosis usually is made when a pathologic murmur is detected on routine examination. Symptoms are rarely present in childhood but become more common with increasing age in patients with moderate to severe stenosis. Initial symptoms usually consist of exertional dyspnea and fatigue due to inability of the RV to increase its output in response to exertion. If the stenosis is not relieved, right heart failure may ensue. Cyanosis may be observed in patients with an atrial communication. Occasionally, patients with moderate to severe stenosis may experience chest pain, syncope, and even sudden death with strenuous exercise. Decreased myocardial perfusion caused by inadequate cardiac output during exercise, leading to ischemia and ventricular arrhythmias, is thought to be the mechanism for these events.

Children with valvar pulmonary stenosis usually exhibit normal growth and development regardless of the severity of obstruction. Squatting is extremely rare even in patients with significant central cyanosis. If squatting is present, other diagnoses, especially tetralogy of Fallot, should be sought.

Infants with critical pulmonary stenosis are cyanotic at birth, and the cyanosis may be severe enough to be life threatening (15). Although the right ventricular cavity is often relatively hypoplastic, the atrial communication is usually large enough to maintain cardiac output and prevent right heart failure at the expense of cyanosis. Symptoms

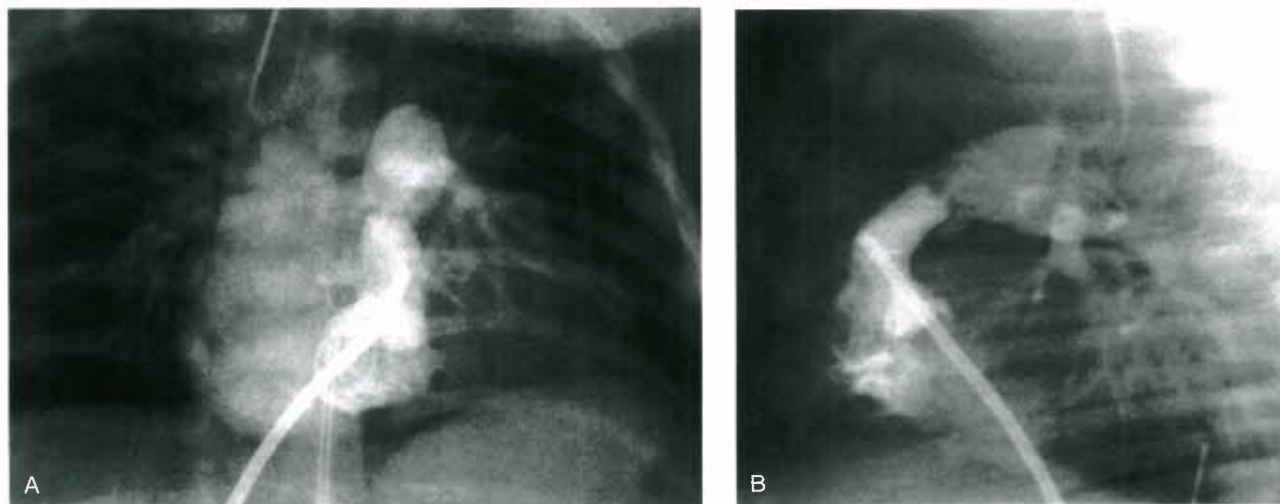


Figure 40.3. Right ventricular angiogram of a 1-day-old infant with critical pulmonary valve stenosis and intact ventricular septum. Right ventricular pressure was suprasystemic. **A:** The anterior view with cranial angulation shows a hypoplastic RV and a small, regurgitant tricuspid valve. **B:** The same findings are demonstrated in the corresponding lateral view. The pulmonary valve annulus is mildly hypoplastic, and the leaflets are thickened and “domed.” A thin jet of flow directed anteriorly is seen, and the main pulmonary artery is dilated.

of right-sided heart failure may be seen in some newborns with significant tricuspid insufficiency or may develop in untreated infants if the atrial communication becomes inadequate with growth.

The auscultatory findings in valvar pulmonary stenosis are quite distinctive, often allowing the diagnosis to be made based only on the physical examination (16) (Fig. 40.4). The first heart sound is normal, and in patients with mild or moderate stenosis, it is followed by a pulmonary ejection click. The click corresponds to the time when the doming pulmonary valve reaches its open position. The more severe the stenosis, the earlier in systole the click occurs, until it merges with the first heart sound and becomes inaudible. The intensity of the click varies with respiration, decreasing during inspiration and increasing during expiration.

The systolic murmur of valvar pulmonary stenosis is ejection in quality and maximal at the upper left sternal border. It may radiate over the entire precordium and neck, but characteristically is heard in the back. In general, the intensity of the murmur increases with the severity of obstruction. Mild stenosis is associated with murmurs of grade 3 or lower, and moderate to severe stenosis with grade 4 or louder. Patients with severe stenosis and right heart failure may have an unusually soft murmur because of low cardiac output. The length of the murmur is proportionately related to the duration of right ventricular ejection, which is determined primarily by the severity of obstruction. With more severe obstruction, the murmur peaks later in systole. In mild stenosis, the murmur is relatively short and peaks at or before midsystole (Fig. 40.4). In moderate stenosis, the murmur ends at or slightly after the aortic component of the second heart sound, which remains audible. With severe obstruction, the murmur extends beyond the aortic closure sound, which may become inaudible. A soft, early diastolic murmur of mild pulmonary insufficiency is rarely heard and usually results from progressive pulmonary trunk dilation.

Patients with mild pulmonary valve stenosis have normal “a” waves and therefore normal jugular venous pulsations.

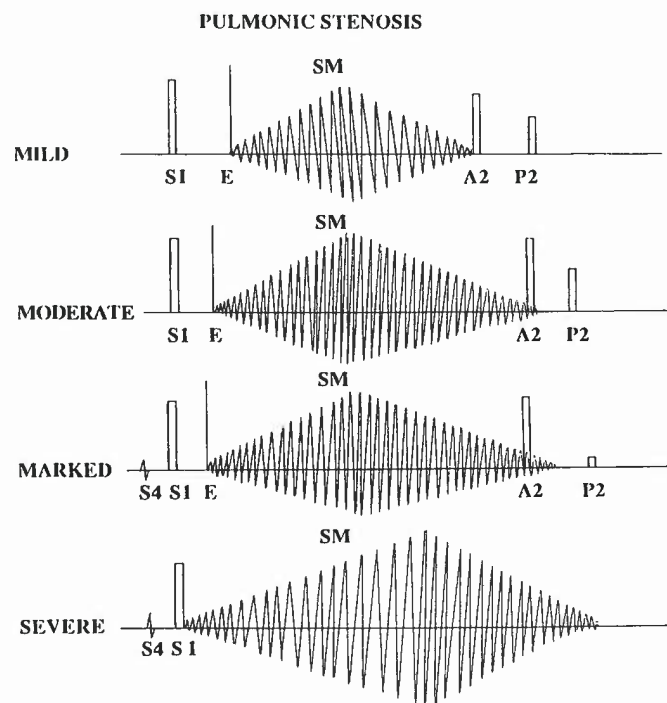


Figure 40.4. Schematic illustration of phonocardiograms in mild to severe valvular pulmonary stenosis. S1, first heart sound; E, ejection sound; SM, systolic murmur; A2, aortic component of the second heart sound; P2, pulmonic component of the second heart sound; S4, fourth heart sound. (Modified from Vogelpoel L, Schrire L. Auscultatory and phonocardiographic assessment of pulmonary stenosis with intact ventricular septum. *Circulation* 1960;22:55; Perloff JK. Congenital pulmonic stenosis. In: *The Clinical Recognition of Congenital Heart Disease*. 4th ed. Philadelphia, PA: WB Saunders, 1994:209.)

With more severe obstruction, the “a” wave becomes progressively larger, and abnormal pulsations may be felt both in the jugular venous pulse and in the liver. In infants and children, jugular venous pulsations are often difficult to appreciate, even in the presence of large “a” waves.

A prominent right ventricular systolic impulse and a systolic thrill almost always can be palpated in patients with severe pulmonary stenosis. Typically, the thrill is located at the second to third intercostal space, but it may also be felt at the suprasternal notch. The thrill may be absent in young infants with severe stenosis and in patients with congestive heart failure and low cardiac output. When the stenosis is mild, the precordium is quiet and a thrill is not present.

The second heart sound in pulmonary stenosis is usually split, and the degree of splitting is proportional to the degree of stenosis. The split may become fixed in severe stenosis as a result of a fixed stroke volume. The intensity of the pulmonary component of the second heart sound typically decreases with increasing obstruction, which may make the splitting difficult to appreciate. Occasionally, in mild stenosis, the pulmonary closure sound is louder than normal because of marked dilation of the pulmonary artery trunk. A fourth heart sound often is heard at the lower left sternal border in patients with severe stenosis. When a third heart sound is heard, the presence of an atrial septal defect should be suspected.

The cardiac examination in infants with critical pulmonary stenosis may differ from that of older patients with severe obstruction. The systolic murmur of pulmonary stenosis may be deceptively soft as a result of decreased flow across the pulmonary valve in the presence of an atrial right-to-left shunt. A holosystolic murmur of tricuspid insufficiency may be present lower along the left sternal border, or a patent ductus murmur may be audible along the mid to upper sternal border. Either of these may be the predominant murmur. The pulmonary closure sound is typically absent. Significant cardiomegaly may be detected by precordial palpation, most commonly due to right atrial enlargement.

Electrocardiographic Features

The electrocardiogram can be somewhat useful in assessing the severity of obstruction in patients with pulmonary valve stenosis. As many as 40% to 50% of patients with mild stenosis have a normal electrocardiogram. Slight rightward deviation of the QRS frontal axis is often the only abnormality. The R-wave amplitude in the right precordial leads rarely exceeds 10 to 15 mm. A right ventricular conduction delay is commonly present.

In moderate pulmonary stenosis, the electrocardiogram is almost always abnormal, with only 10% of patients having a normal tracing. Right axis deviation is usually present. The R:S ratio in V1 is usually >4:1, and the R wave is typically <20 mm. The T waves in the right precordial leads are upright in approximately 50% of patients.

In severe pulmonary stenosis, the electrocardiogram is rarely normal (Fig. 40.5). The mean frontal QRS axis is usually >110 degrees, and not uncommonly, extreme right axis deviation is seen. A pure R, RS, or QR is the usual pattern in the right precordial leads, and the R wave is usually >20 mm. The R:S ratio in V6 may be <1.0. The T waves may be upright or inverted in the right precordial leads, and the P waves are abnormally tall and peaked in lead 2 and in the right precordial leads, indicating right atrial enlargement.

It is possible to estimate the right ventricular pressure in patients between 2 and 20 years of age if a pure R wave is present in lead V4R or V1. The height of the R wave in millimeters, multiplied by 5, approximates the right ventricular systolic pressure in millimeters of mercury (14). Occasionally, infants with severe stenosis, in whom the RV may be

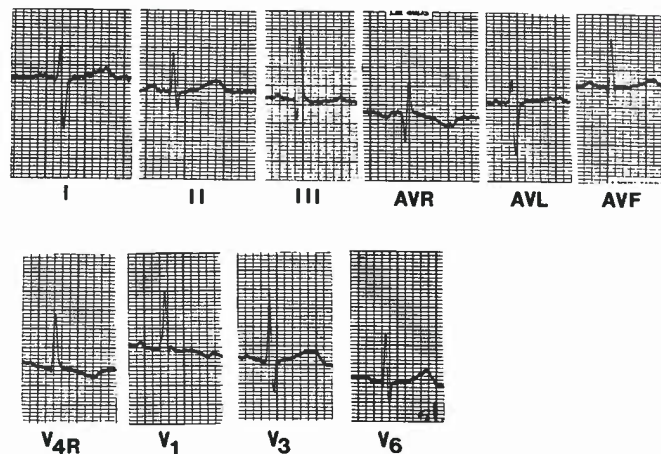


Figure 40.5. Electrocardiogram of a child with severe valvular pulmonary stenosis. Note the qR complex and inverted T in V4R.

hypoplastic, have a more leftward axis than expected (in the range of +30 to +70 degrees) as well as evidence of left ventricular hypertrophy. A superior axis, sometimes accompanied by a conduction abnormality of the left bundle, also has been described in some patients with pulmonary stenosis. There may be a correlation between these findings and Noonan syndrome, with its associated cardiomyopathy.

Radiographic Features

The most distinctive feature in valvular pulmonary stenosis is a prominent main pulmonary artery segment resulting from poststenotic dilation of the pulmonary trunk and sometimes the LPA (Fig. 40.6). This finding is present in 80% to 90% of cases, but it may be absent in infants, in patients with dysplastic pulmonary valve, and in cases of rubella syndrome. The apex of the heart is usually rounded and points downward. The right atrial segment may be prominent, more commonly in patients with associated tricuspid insufficiency or atrial septal defect. A left aortic arch is virtually always present.

Heart size and pulmonary vascularity are usually normal in patients with mild to moderate stenosis. In the absence of right ventricular failure, even with severe obstruction, only mild cardiomegaly is seen. When heart failure develops, marked cardiomegaly results due to right atrial and right ventricular enlargement, and pulmonary vascularity is decreased as a result of a reduction in pulmonary flow. Cardiomegaly is commonly present in infants with severe or critical pulmonary stenosis, and pulmonary vascularity is severely reduced because of the large atrial right-to-left shunt (Fig. 40.7).

Two-Dimensional Echocardiography

The 2-D echocardiogram clearly demonstrates the typical features of the stenotic pulmonary valve from the standard and high parasternal short-axis and long-axis views as well as the subcostal sagittal views (Fig. 40.8). The valve leaflets usually appear prominent because of thickening. Systolic motion is restricted, with inward curving of the tips of the leaflets, known as doming. Associated features, such as poststenotic dilation of the main and branch pulmonary arteries, also are easily recognized. Right ventricular hypertrophy, contractility of the RV, as well as anatomy and function of the tricuspid valve should be assessed. Evidence of dynamic subpulmonary stenosis should be sought, but the severity may be impossible to estimate in the presence of more than mild valvular stenosis.

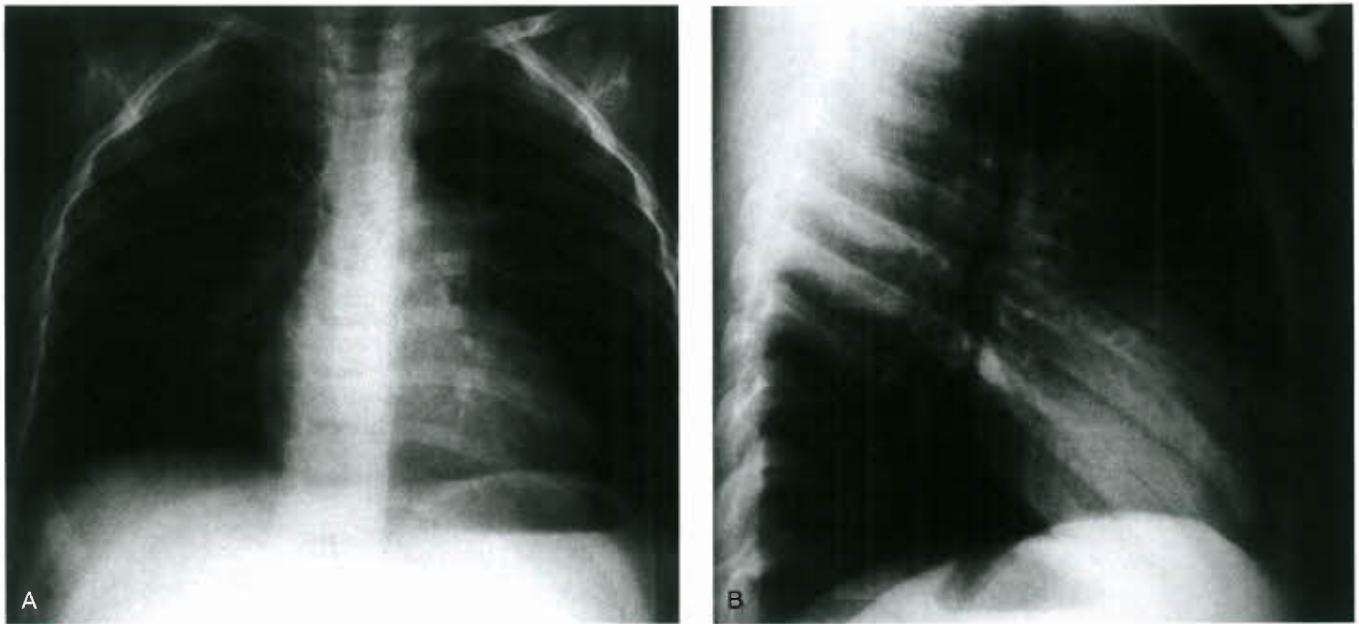


Figure 40.6. Roentgenogram of a boy with severe valvar pulmonary stenosis and suprasystemic right ventricular pressure. **A:** Anteroposterior view. Note the prominent right cardiac border and rounded apex pointing downward. The main pulmonary artery segment is dilated. Pulmonary vascularity is normal. **B:** The lateral view demonstrates prominence of the RV with increased filling of the space between the thoracic wall and anterior border of the heart.

The diagnosis of dysplastic pulmonary valve usually can be ascertained by echocardiography. The leaflets appear thickened and immobile, without the characteristic doming seen in typical cases. The pulmonary valve annulus is hypoplastic, and supraannular narrowing of the proximal main pulmonary artery is often present. The poststenotic pulmonary artery dilation seen in classic cases is absent.



Figure 40.7. Roentgenogram of a 1-day-old infant with critical pulmonary stenosis and congestive heart failure. The heart is markedly enlarged. The right heart border is due to severe right atrial enlargement. The pulmonary vascularity is diminished as a result of right-to-left shunting at the atrial level.

Doppler Evaluation

The Doppler echocardiogram allows quantitative assessment of severity of pulmonary valve stenosis by estimating the pressure drop across the pulmonary valve (Fig. 40.9). The simplified Bernoulli equation $P = 4V^2$ is used, where P is the peak instantaneous pressure gradient (mm Hg), across the obstructed pulmonary valve, and V is the peak flow velocity (m/s), distal to the obstructive orifice. If significant subpulmonary stenosis coexists, V_1 (the peak flow velocity proximal to the obstruction) must be taken into account. The Doppler beam must be aligned parallel with the main pulmonary artery trunk or the direction of the flow jet as seen on color Doppler. If tricuspid insufficiency is present, the Doppler technique can be used to calculate the pressure difference (P) between the right atrium and RV by measuring the peak flow velocity (V) of the tricuspid insufficiency jet. Right ventricular pressure then can be estimated by adding the pressure gradient to the estimated right atrial pressure.

Several studies have documented excellent correlation between the Doppler-derived gradient and that obtained by direct pressure measurement at catheterization (17,18). It should be recognized, however, that the Doppler-derived peak instantaneous pressure gradient exceeds the peak-to-peak pressure gradient measured at catheterization by a small amount. In pulmonary valve stenosis, this difference is clinically insignificant, and the two measurements are close enough to obviate the need for diagnostic catheterization in most patients until intervention becomes necessary.

The development of color Doppler 2-D echocardiography has contributed to the diagnostic accuracy of pulmonary valve stenosis by demonstrating an abnormal flow pattern originating at the stenotic valve (Fig. 40.8). Normal flow is coded as red or blue, depending on whether it is directed toward or away from the transducer, respectively. High-velocity, turbulent flow through stenotic lesions appears as a mosaic jet with green, yellow, and other shades. Visualization of the jet by

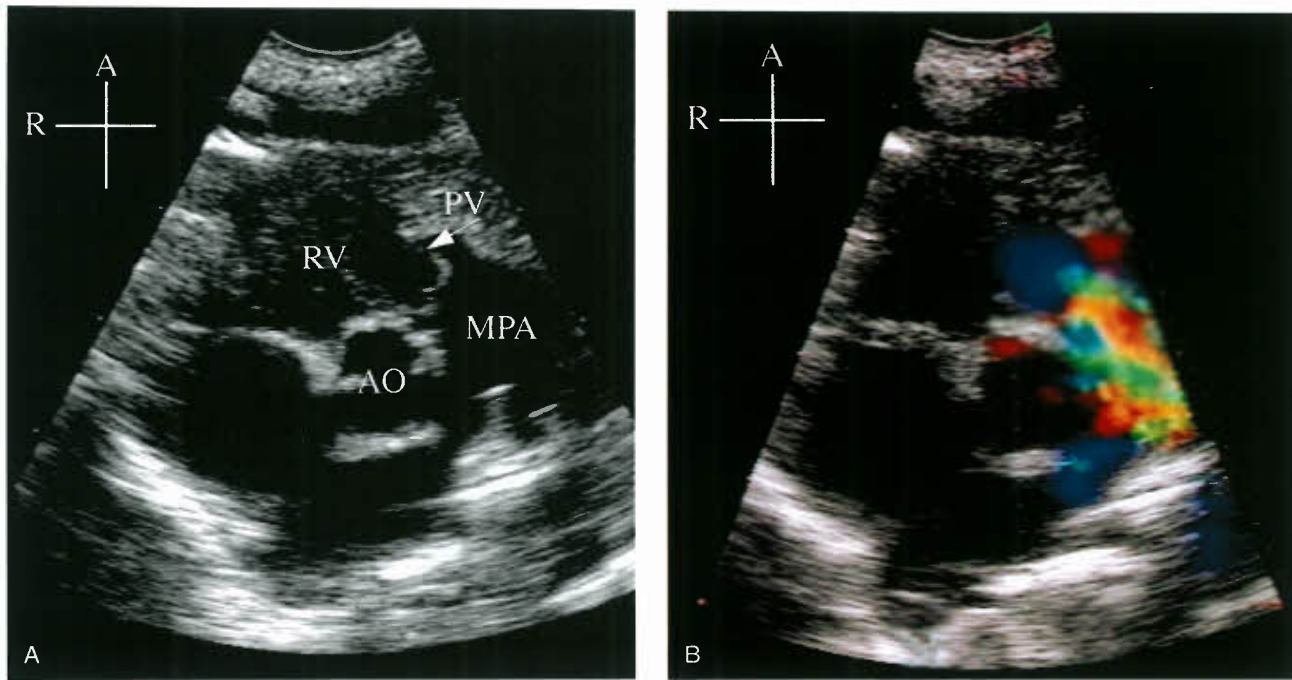


Figure 40.8. A: Parasternal short-axis view from a 1-day-old infant with critical pulmonary valve (PV) stenosis (same patient as in Fig. 40.3). Note the thickened, “doming” leaflets in systole. The PV annulus is hypoplastic compared with the aortic valve annulus. There is poststenotic dilation of the main pulmonary artery (MPA). B: Color Doppler through the stenotic PV shows a mosaic pattern indicating high-velocity, turbulent flow originating at the level of the PV. A, anterior; AO, aorta; R, right; RV, right ventricle.

color also facilitates optimization of the alignment between the Doppler sample volume and the direction of flow, increasing the accuracy of the measured gradient.

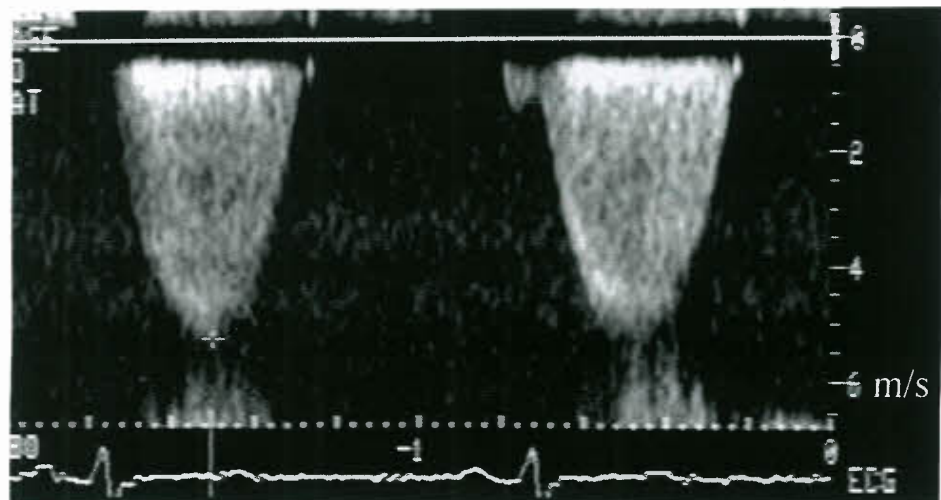
Cardiac Catheterization

The refinement of 2-D and Doppler echocardiography over the past three decades has had a dramatic impact on the use of cardiac catheterization in the management of pulmonary valve stenosis. Because diagnosis and exclusion of other significant lesions can now be accomplished noninvasively, the role of catheterization has become largely therapeutic. Balloon pulmonary valvuloplasty has supplanted surgical valvotomy as the treatment of choice for this lesion (19).

Hemodynamics

The most important measurements made at catheterization are the right ventricular pressure compared with systemic arterial pressure and the pressure gradient across the pulmonary valve. A resting right ventricular pressure >30 to 35 mm Hg and a pressure gradient across the pulmonary valve of >10 mm Hg are considered abnormal. An end-hole catheter is used to obtain carefully the withdrawal pressure recordings from the pulmonary artery to the body of the RV to assess the severity and location of any stenoses. In the presence of associated infundibular obstruction, pressure gradients are encountered across the pulmonary valve and also across the infundibulum. In the infundibular chamber, the pressure curve is usually

Figure 40.9. Continuous-wave Doppler recording from the parasternal short-axis view of a patient with severe pulmonary valve stenosis. The high-velocity systolic flow with a negative deflection from the baseline results from a jet directed away from the transducer from the RV to the main pulmonary artery. The peak velocity of the jet is 5.2 m/s, equivalent to a peak pressure gradient of 110 mm Hg across the pulmonary valve.



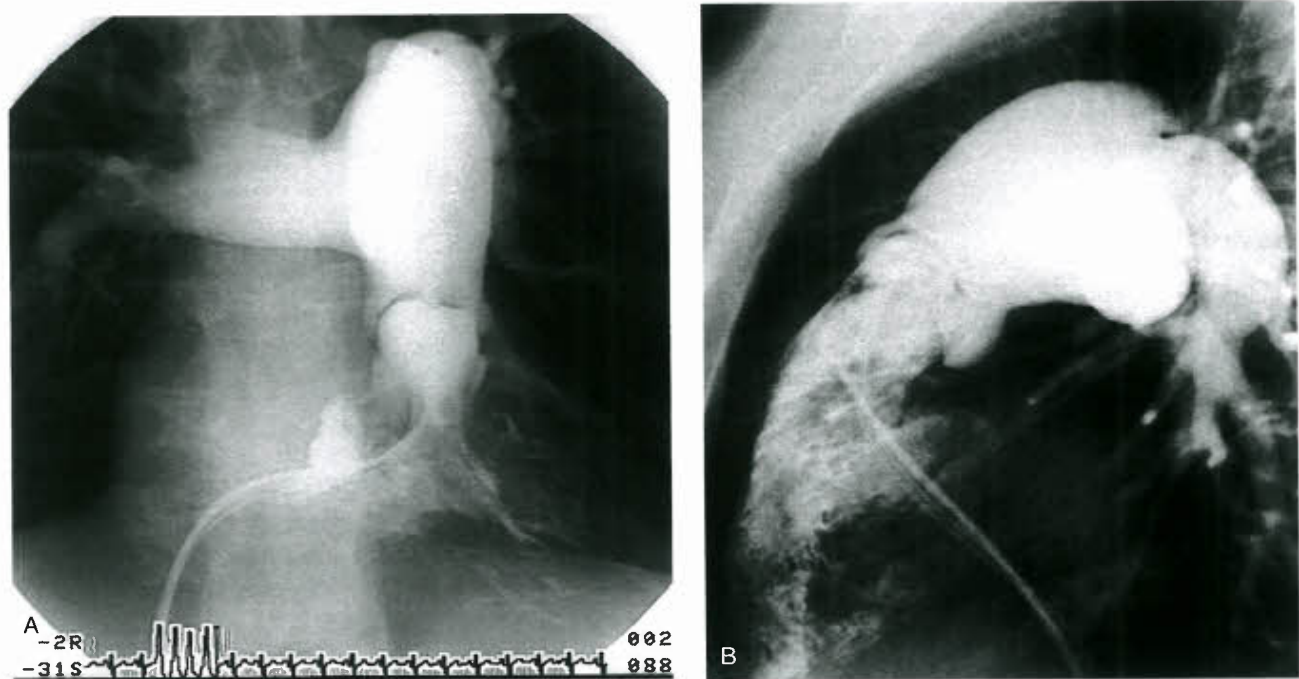


Figure 40.10. Right ventricular angiogram of a 17-year-old girl with severe pulmonary valve stenosis (RV pressure 122/16 mm Hg). A: Anteroposterior view with cranial angulation shows a thickened, “domed” pulmonary valve and poststenotic dilation of the main pulmonary artery. B: Lateral projection with similar findings.

triangularly shaped, with a fall in the late systolic pressure resulting from progressive narrowing of the outflow tract during ventricular contraction (20). The right ventricular end diastolic pressure may be normal, but usually it is elevated with severe obstruction or right ventricular failure. The right atrial pressure is normal in mild to moderate obstruction, but tall right atrial “a” waves usually are seen with severe obstruction. Pulmonary artery pressure is normal in mild cases, but it is decreased and dampened in severe cases. This depression of pulmonary artery pressure is more marked in the main pulmonary artery just beyond the valve than further distally because of the Bernoulli effect. The increase in flow velocity across the stenotic valve causes more of the total energy to be expressed as kinetic energy, necessitating a drop in pressure to maintain the total energy constant. As blood velocity decreases further downstream, pressure recovery is observed.

In patients with relatively normal cardiac output, classification of severity of pulmonary stenosis is routinely based on measurements of right ventricular pressure and valve gradient. Mild stenosis is characterized by a right ventricular pressure less than half the left ventricular pressure or a valve gradient <35 to 40 mm Hg. In moderate stenosis, the right ventricular pressure is greater than half but <75% of the left ventricular pressure, or the gradient is 40 to 60 mm Hg. Severe stenosis is defined as a right ventricular pressure $\geq 75\%$ of the left ventricular pressure or a gradient >60 to 70 mm Hg.

During exercise, an increase in the pressure gradient across the stenotic valve occurs primarily because an increase in the volume of flow and the rate of contraction of the RV leads to an increase in flow velocity across the obstruction. Patients with severe stenosis are unable to increase their stroke volume and rely solely on an increase in heart rate to augment cardiac output during exercise. A marked increase in heart rate can be detrimental in patients with severe obstruction because of the resultant shortening of diastolic filling time. The impedance to filling of the hypertrophied, stiff RV can

lead to a decrease in cardiac output and systolic blood pressure when marked tachycardia develops. Decreased right ventricular compliance is further evidenced by elevated right ventricular end diastolic pressure at rest and abnormal increase with exercise observed in patients with severe obstruction (21).

Angiocardiography

Angiocardiography provides information about the location and severity of pulmonary stenosis that is invaluable for diagnostic and therapeutic purposes. The anatomy of the pulmonary valve and associated features can be shown best by right ventricular angiography in the anteroposterior view with the tube angled cephalad and in the lateral view (Fig. 40.10, Video 40.1). Characteristically, the pulmonary valve leaflets are mildly thickened and dome in systole, returning to the normal position in diastole. A narrow jet of contrast is seen crossing the valve, usually along the anterosuperior margin of the main pulmonary artery, resulting in poststenotic dilation of this vessel. The pulmonary valve annulus is typically of normal size, but it may be hypoplastic in infants with severe stenosis. The right ventricular cavity is usually of normal size, but it may be hypoplastic in newborns with critical pulmonary stenosis, or it may be dilated in the presence of congestive heart failure. The walls usually are thickened with prominent trabeculations. Narrowing of the right ventricular outflow tract (RVOT) as a result of infundibular hypertrophy is usually seen in severe obstruction. Right ventricular function is normal except in severe cases with ventricular failure.

The angiographic features of dysplastic pulmonary valve stenosis differ in several ways from those of typical pulmonary valve stenosis (Fig. 40.2, Video 40.2). The valve leaflets are markedly thickened and relatively immobile, with little excursion during the cardiac cycle. The annulus is hypoplastic, and this hypoplasia usually extends to the

proximal main pulmonary artery. There is often the appearance of tethering of the valve leaflets to the main pulmonary artery wall at the sinotubular junction. Poststenotic dilation of the main or branch pulmonary arteries usually is not seen. Often the origin of the right pulmonary artery (RPA) from the main pulmonary artery has a more proximal than normal position.

Differential Diagnosis

The diagnosis of pulmonary valve stenosis with intact ventricular septum is usually readily made by careful auscultation and supportive electrocardiographic and radiographic features, but certain conditions must be considered in the differential diagnosis. Mild pulmonary stenosis should be differentiated from idiopathic dilation of the main pulmonary artery, atrial septal defect, peripheral pulmonary arterial stenosis, mitral valve prolapse, straight back syndrome, mild aortic stenosis, and innocent murmurs. Moderate to severe pulmonary stenosis without cyanosis should be distinguished from ventricular septal defect (VSD) with or without associated pulmonary stenosis and moderate aortic stenosis. When cyanosis is present in severe stenosis, tetralogy of Fallot and pulmonary atresia with intact ventricular septum must be excluded. Ebstein anomaly of the tricuspid valve occasionally mimics severe pulmonary stenosis in the newborn.

PULMONARY STENOSIS ASSOCIATED WITH SYSTEMIC DISEASES

Congenital heart disease is seen in approximately 50% of patients with Noonan syndrome (10). The most common lesion is pulmonary stenosis due to pulmonary valve dysplasia. Hypertrophic cardiomyopathy of the left ventricle with or without pulmonary stenosis is also found in up to 25% of cases. The cardiac examination in these patients is often atypical and does not reflect the severity of the pulmonary stenosis. The ejection click is usually absent, and a soft, relatively short murmur may be heard despite severe stenosis. The electrocardiogram usually shows superior axis deviation even in patients without apparent cardiomyopathy.

Intracardiac tumors or extrinsic lesions compressing cardiac structures are rare causes of pulmonary stenosis. Echocardiography or magnetic resonance imaging (MRI) usually can establish the diagnosis. Multiple lentiginos syndrome, or LEOPARD syndrome, has been associated with pulmonary or pulmonary artery stenosis. Neurofibromatosis rarely causes right ventricular outflow obstruction, as can deposits from glycogen storage diseases and gout. Carcinoid disease of the bowel may be associated with endocardial fibroelastosis of the RV with involvement of the pulmonary and tricuspid valves, leading to stenosis.

Treatment

Balloon Valvuloplasty

The technique of percutaneous balloon pulmonary valvuloplasty was described initially by Kan et al. (19). Since then, many other workers have reported the successful application of this technique to treat patients with moderate to severe pulmonary valve stenosis. This procedure led the way to the era of pediatric catheter intervention, which has been expanded to a multitude of other lesions over the past three decades.

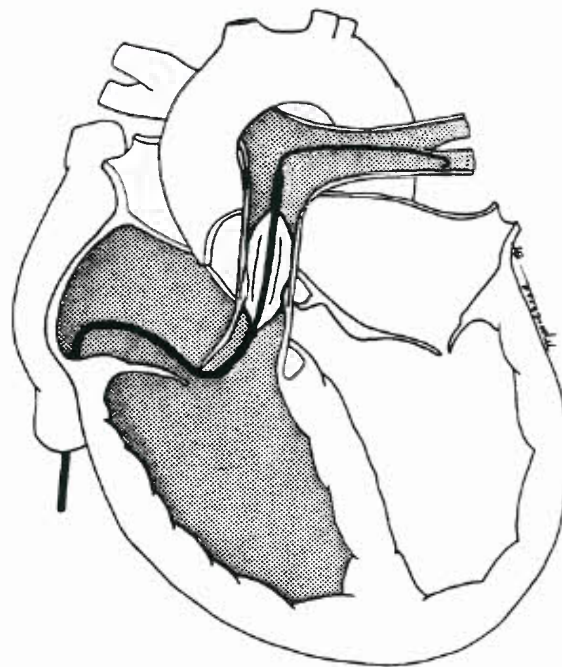


Figure 40.11. Schematic illustration of the balloon valvuloplasty catheter positioned across the pulmonary valve. The wire should be positioned in the distal left or right pulmonary artery.

The technique of balloon valvuloplasty is relatively straightforward (Fig. 40.11). After obtaining appropriate hemodynamic and angiographic information about severity and location of obstruction, an exchange guidewire is introduced through an end-hole catheter and positioned in the distal left or RPA. A balloon is chosen that is 20% to 30% larger than the angiographically measured pulmonary valve annulus, and it is positioned over a guidewire with the valve at its midpoint. As the balloon is inflated, a waist from the stenotic valve should be observed initially and disappear at full inflation (Fig. 40.12). In larger patients with an annulus diameter of more than 20 mm, the double-balloon technique may be necessary, with simultaneous inflation of two angioplasty balloons. A method to calculate the effective diameter of two balloons was described by Radtke et al. (22). Following balloon dilation, a careful pullback with an end-hole catheter is performed to evaluate the degree and site of any residual obstruction. Not infrequently, a gradient is measured across the infundibulum that may have been masked before valvuloplasty by the distal valvar obstruction. This type of dynamic infundibular stenosis typically resolves over time as the hypertrophied muscle regresses.

Shortly after the introduction of pulmonary valvuloplasty in children, the procedure was performed successfully in neonates with critical pulmonary valve stenosis (23). Before catheterization, these patients usually require stabilization and initiation of a prostaglandin E1 infusion to maintain ductal patency. Several of technical advances, such as the introduction of low-profile balloons, have increased the success and safety of balloon dilation in this group of patients, such that it is now considered the treatment of choice (24–26). The use of angled-tip catheters and high-torque wires has facilitated crossing the tiny pulmonary valve orifice. Initial dilation with a small coronary angioplasty balloon to enlarge the orifice and subsequent dilations with progressively larger balloons allow adequate relief of obstruction in most neonates (27). Placement of the guidewire through the patent ductus into

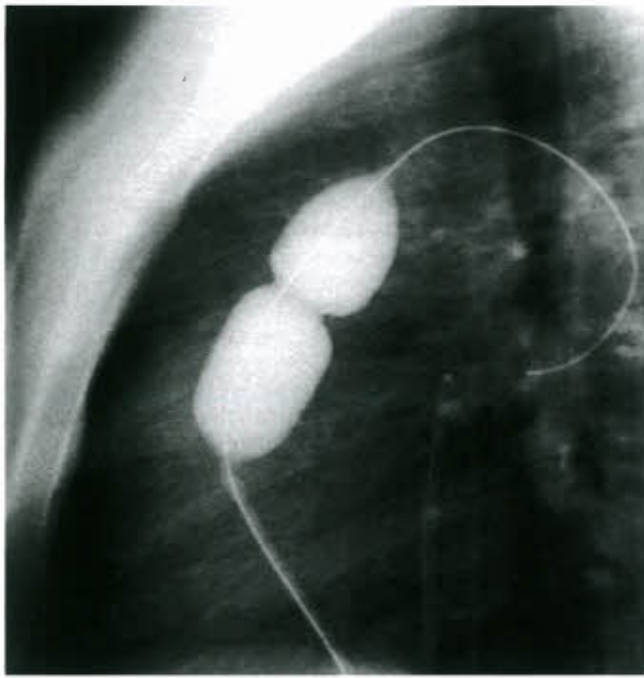


Figure 40.12. Lateral view of a partially inflated valvuloplasty catheter positioned across the pulmonary valve. As the balloon is inflated, a “waist” appears at the site of the pulmonary valve. This waist should be centered in the mid portion of the balloon.

the descending aorta, rather than in the LPA, allows a more stable wire position. Creating a “rail” by snaring the wire in the descending aorta can facilitate introduction of the desired balloon catheter through the orifice (Fig. 40.13) (28).

The short- and intermediate-term results of pulmonary valvuloplasty in children and adults with typical pulmonary valve stenosis have been excellent (29–33). The most comprehensive series to date reported on 533 patients with a median follow-up of 33 months and a maximum follow-up of 8.7 years (33). The morphology of the pulmonary valve was typical in 82% of patients, dysplastic in 13%, and complex (postsurgical valvotomy, associated with other significant lesions) in 5%. A good outcome, defined as a residual Doppler gradient at follow-up of 36 mm Hg or lower without the need for repeat procedures, was achieved in 77% of the total group and in 85% of those with typical valve morphology. In contrast, 65% of patients with dysplastic pulmonary valve had a suboptimal outcome. Independent predictors of suboptimal intermediate-term outcome were a small annular size (characteristic of patients with dysplastic valves), a higher immediate residual gradient, an earlier year of the initial valvuloplasty, and smaller balloon:annulus ratio (BAR) in those with typical valves. Balloons used in this study were a mean of $112\% \pm 20\%$ of the annular diameter. The latter two predictors suggest that gradient reduction, at least for typical pulmonary valve morphology, could be improved by greater experience and the use of BARs > 1.2 , as has been borne out by smaller studies (31,32). The use of excessively large balloons, however, has been associated with a higher rate of late severe pulmonary insufficiency (32,34).

Long-term outcomes have been reported on smaller series of patients with a mean follow-up of 11.9 years and a range up to 19.3 years (35). In this group of 134 patients, in whom the average BAR was 1.3, the results have been similar with persistent gradient reduction in the majority of patients and a lower success rate in those with dysplastic valves. Freedom

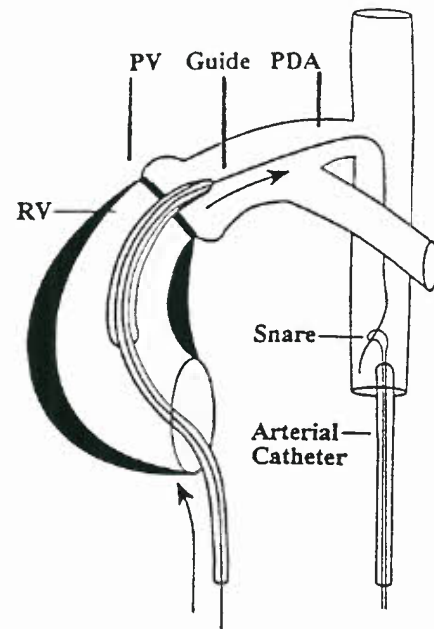


Figure 40.13. Schematic illustration of the technique of pulmonary valvuloplasty in a neonate as seen from the lateral projection. The guidewire was placed in the descending aorta through the patent ductus arteriosus. If necessary, the guidewire can be snared in the descending aorta to facilitate introduction of the balloon through the tiny orifice. PDA, patent ductus arteriosus; PV, pulmonary valve; RV, right ventricle. (Modified from Latson L, Cheatham J, Froemming S, et al. Transductal guidewire “rail” for balloon valvuloplasty in neonates with isolated critical pulmonary valve stenosis or atresia. *Am J Cardiol* 1994;73:713–714, with permission.)

from any reintervention at 1, 5, 10, and 15 years were 90%, 83%, 83%, and 77%, respectively. Only 17 patients had surgical intervention at some point during follow-up to relieve valvar, subvalvar, or supra-valvar obstruction, and 11 of those had dysplastic valves. Two additional children had surgical intervention for severe tricuspid regurgitation at 11 and 12 years of age. At operation, a flail anterior leaflet was found in both, possibly caused by a tear at the time of valvuloplasty. Repeat balloon valvuloplasty was performed in 11 children, 2 of whom eventually underwent surgery due to the development of subpulmonary stenosis. Risk factors for reintervention were younger age and lower body surface area, a smaller pulmonary valve annular diameter Z-score, a higher pulmonary valve gradient at the initial procedure, and the presence of Noonan syndrome. Clinical status for the entire cohort was excellent at a mean follow-up of 11.9 years, with no reported arrhythmias and only two patients in New York Heart Association (NYHA) class II.

The significantly lower success rate for patients with dysplastic pulmonary valves is not surprising given the anatomic features of these valves. The mechanism of obstruction relief in patients with typical, doming pulmonary valves has been shown to be commissural splitting in the majority of cases (36,37). In dysplastic valves, the leaflets may be markedly thickened and myxomatous with little commissural fusion. In addition, the annulus and main pulmonary artery are usually hypoplastic, further limiting the effectiveness of valvuloplasty. Several studies, however, documented adequate relief of obstruction in 35% to 65% of patients with dysplastic valves (30,32,33). Accurate predictors of success before valvuloplasty have not been identified. Thus, although controversy remains, the usual practice is to offer balloon valvuloplasty as a first

line of treatment and proceed to surgical valvotomy if balloon valvuloplasty is unsuccessful. In neonates with critical pulmonary valve stenosis, the success of pulmonary valvuloplasty at intermediate-term follow-up also has been lower than in older patients, regardless of valve morphology (24–26,34,38,39). With a mean follow-up of approximately 3 to 6 years for most studies, varying success rates have been reported, depending on how success is defined. Early in the experience, procedural failure was often due to an inability to cross the severely stenotic pulmonary valve, but with the availability of preformed catheters, better wires, and lower profile balloons, dilation can now be accomplished in nearly 100% of patients. If dilation was accomplished, immediate effective gradient reduction usually was achieved in more than 90% of patients. Despite successful relief of obstruction, 5% to 10% of these patients were unable to sustain sufficient forward flow through the pulmonary valve to maintain adequate saturations because of their severely hypertrophic, noncompliant, and sometimes hypoplastic RVs.

If discontinuation of prostaglandin E1 and subsequent ductal constriction are not tolerated immediately after valvuloplasty, these infants can be maintained on prostaglandin for as long as 2 to 3 weeks while intermittently assessing whether constriction of the ductus is tolerated with O₂ saturations remaining 70% or greater. If ductal dependency persists after that time, a surgical aortopulmonary shunt is placed. In rare instances, balloon atrial septostomy is also necessary to ensure adequate cardiac output. Neonates who remain cyanotic following valvuloplasty, with or without a surgical shunt, often demonstrate progressive resolution of their cyanosis over weeks to months as right ventricular compliance improves and the atrial right-to-left shunt diminishes. Ultimately, those in whom a shunt was created can undergo shunt closure either surgically or by transcatheter techniques. Atrial septal defect closure also may be necessary, depending on the size of the atrial communication. Recurrent valvar stenosis necessitating repeat valvuloplasty may occur within months of the initial procedure in about 10% of these patients and subsequently may afford long-term relief of obstruction.

Stenting of the ductus can be considered as an alternative to a surgical shunt in patients who remain ductal dependant following valvuloplasty. The use of a stent to maintain ductal patency was first reported in the early 1990s (40,41). Available data document gradual narrowing of the stent lumen over a period of months, during which time there is typically sufficient growth of the right heart and improved right ventricular compliance to obviate the need for ductal flow (42,43). Transcatheter techniques can also be used to close the atrial septal defect when necessary, potentially eliminating the need for any surgical intervention.

Maintaining an unobstructed pulmonary valve is important in these infants to optimize forward flow through the RV as a stimulus for growth and to allow resolution of the right ventricular hypertrophy. About 15% to 20% of neonates with critical pulmonary stenosis ultimately undergo surgical intervention to relieve either valvar stenosis resistant to dilation or subvalvar obstruction (25,26,39,44). The strongest determinant of the need for surgical intervention has been found to be the presence of subvalvar stenosis, followed by the annular dimension and morphology of the pulmonary valve. A smaller indexed tricuspid valve annulus also confers a higher risk of surgical intervention (39). In a small minority, persistent right ventricular hypoplasia precludes a two-ventricle repair.

The incidence of major complications from pulmonary valvuloplasty is exceedingly low in children and adults but is higher in infants and neonates. The largest study to date from the Valvuloplasty and Angioplasty Registry reported only two deaths from a total of 822 patients (0.2%) (29). The causes of death were laceration of the inferior vena

cava–iliac vein junction during balloon withdrawal in a 5-day-old infant and tearing of the pulmonary valve annulus during balloon inflation with a reportedly properly sized balloon in a 12-month-old infant. Other major complications occurred in three patients, including perforation of the RVOT resulting in tamponade and tricuspid regurgitation requiring surgical intervention. The incidence of minor complications was 1.3%, including vein thrombosis, vein tears, and arrhythmias. In neonates, mortality was approximately 3% and was due to various causes, including venous injury, myocardial dissection, and development of necrotizing enterocolitis. The incidence of significant morbidity in neonates was on average around 10%. Specific complications reported include wire perforation of the RVOT with or without tamponade, stroke, seizures, necrotizing enterocolitis, endocarditis, septic shock, and abrupt closure of the ductus despite prostaglandin infusion requiring urgent aortopulmonary shunt placement.

Most patients who have been treated with pulmonary valvuloplasty have some degree of pulmonary regurgitation (PR) (31–33). The incidence of moderate PR early after valvuloplasty has been variably reported as <5% to as much as 24% at intermediate-term follow-up. This relatively wide range is at least partially a result of the lack of standardized grading criteria for severity of PR. Longer follow-up and improved grading methods have shown greater degrees of PR (35,45), particularly in patients undergoing the procedure as neonates. PR has been shown to progress over time in the same group of patients (35). At a mean follow-up of 0.9 years, 22% of patients had moderate and 2% had severe PR, while at 11.9 years of follow-up, the percentage of patients with moderate PR increased to 40%, and with severe PR to 17%. Severe PR was diagnosed by echocardiogram when there was reverse flow in the branch pulmonary arteries and a nonrestrictive regurgitant Doppler signal across the RV outflow tract. Right ventricular enlargement was significantly greater in children with severe PR. Multivariate analysis identified only smaller body surface area at the time of intervention as being significantly associated with moderate or severe PR in follow-up. Moderate or severe PR developed in 74% of patients who underwent the procedure as neonates, in contrast to 44% of all other patients. Using cardiac MRI to obtain RV volumes, Harrild et al. (45) found that 34% of patients at a median follow-up of 13 years after pulmonary valvuloplasty had a PR fraction >15%, while in 17% of the cohort, the PR fraction was >30%. In this series, PR fraction was associated with younger age at dilation and with BAR, particularly when the BAR was ≥ 1.4 . The median PR fraction in patients with a BAR ≥ 1.4 was 26%. Other series have also found that a larger BAR and a higher degree of obstruction before dilation, in addition to younger age, are associated with the development of severe PR (32,44).

Compared with surgical valvotomy, patients treated with valvuloplasty appear to have less regurgitation with clinically equivalent relief of obstruction, although duration of follow-up is significantly longer for the surgical patients (31,46), and there is no contemporaneous surgical series. It is well known that significant degrees of PR with no other hemodynamically significant lesions are well tolerated for long periods. However, moderate degrees of surgically induced pulmonary insufficiency affect the normal hemodynamic response to exercise, resulting in decreased exercise capacity (47). Similarly, it has been found that patients with a PR fraction >15% following balloon dilation have decreased exercise capacity when compared to those with a PR fraction $\leq 15\%$ (percent predicted peak VO₂ $85 \pm 17\%$ vs. $96 \pm 16\%$) (45). It would seem prudent to accept mild degrees of residual stenosis as opposed to complete relief of obstruction in exchange for avoiding significant PR.

No patient outside of the neonatal group has been reported to have had pulmonary valve replacement following balloon dilation. In contrast, severe PR requiring surgery has been

reported in a handful of patients who underwent balloon valvuloplasty as neonates (34,44). In a series of 107 patients, 6 had severe PR at a mean follow-up of 7.2 years (34). All were under 2 months of age at the time of valvuloplasty and had severe or critical obstruction. The postdilation gradient was significantly lower in these six patients (8 mm Hg) than in the whole group (19 mm Hg). One underwent pulmonary valve replacement, and the remaining five are likely to have surgery during childhood. The average BAR used in these six patients was 1.44, in comparison to 1.08 for the group as a whole. Perhaps even greater caution against overly aggressive dilation should be exercised in neonates than in their older counterparts, aiming for a BAR closer to 1.2, and not exceeding 1.3 (48). This approach may lead to repeat balloon valvuloplasty in a slightly larger number of patients with critical pulmonary stenosis, but this is preferable to the need for eventual pulmonary valve replacement.

Surgical Valvotomy

Since the advent of pulmonary balloon valvuloplasty, surgical valvotomy is reserved for patients with dysplastic pulmonary valves resistant to dilation or patients with multiple levels of fixed obstruction. Valvotomy can be achieved using either a closed or open technique through the main pulmonary artery. There is often a persistent pressure gradient immediately after surgery in patients with isolated valvar pulmonary stenosis attributable to dynamic narrowing of the hypertrophied infundibulum (as also observed following balloon valvuloplasty). A reduction in this gradient occurs in the first 24 hours after surgery, and continues at a slower rate as the hypertrophy resolves over the subsequent months. In rare cases, fatal right ventricular failure occurs (suicidal RV) in the immediate postoperative period. Propanolol may be given and may differentiate dynamic from fixed obstruction. When infundibular resection is necessary, it may be accomplished through a transatrial route via the tricuspid valve.

Simple valvotomy is ineffective when the pulmonary valve is dysplastic. Partial or more often total removal of the pulmonary valve may be necessary. In addition, insertion of a transannular patch may be necessary to enlarge the hypoplastic annulus and main pulmonary artery. These patients are usually left with at least moderate PR, which is well tolerated in medium-term follow-up. However, it is now increasingly recognized that the long-term effects of significant PR are more harmful than previously suspected (44–47,49).

Long-term relief of obstruction after pulmonary valvotomy is excellent, and restenosis is uncommon (50). The second natural history study of patients with pulmonary stenosis demonstrated that 96% of surgically treated patients remained free of reoperation for 10 years. The incidence of postoperative PR is between 57% and 90% (50–52) and is classified as moderate to severe in 28% by echocardiographic estimation (50). Despite the presence of PR in most patients, 25-year survival is excellent at 97%, and 97% of surviving patients are in NYHA class I (50). As mentioned previously, formal exercise testing has shown a tendency toward mildly decreased exercise tolerance. There is also a higher incidence of ventricular ectopy associated with exercise for postoperative pulmonary stenosis patients when compared to age-matched normal subjects (53).

Longer-term follow-up has been reported in a smaller group of 53 patients followed at a large tertiary care center, but not necessarily operated at that same institution (46). At a mean follow-up of 33 years, 53% of patients underwent reintervention, most commonly pulmonary valve replacement for free PR. A significant increase in the percentage of patients needing reintervention was noted after 25 years of follow-up. Though 50% of patients were free from reintervention at 40 years, 80% required repeat surgery by 45 years of follow-up.

Univariate analysis identified closed pulmonary valvotomy at initial repair as the only factor predictive of the need for reintervention. Overall 40% of patients underwent pulmonary valve replacement at a mean interval of 33 years after the initial surgery. All of the remaining patients who had not undergone reoperation had PR, graded as moderate or severe in 70%. The unoperated group had a shorter duration of follow-up, suggesting that with longer follow-up, many more would also require pulmonary valve replacement.

The incidence of arrhythmias in postoperative pulmonary stenosis patients was higher with longer follow-up than previously reported, with 38% of patients suffering from atrial arrhythmias and 6% with ventricular arrhythmias (46). Survival at a mean follow-up of 33 years was excellent with only two patients (3.8%) dying suddenly. Both had untreated atrial fibrillation, but neither had significant right ventricular dilation or a prolonged QRS complex on electrocardiography. Functional status was quite good, although again there was some decline with longer-term follow-up. Of the 53 patients, 82% were in NYHA class I, 16% in class 2, and 2% in class III at last follow-up. These findings must take into consideration the possibility of referral bias in this large tertiary care center.

Indications for Either Pulmonary Valvotomy or Pulmonary Balloon Valvuloplasty

Pulmonary valvuloplasty is currently the first line of treatment for pulmonary valve stenosis at any age and, most would agree, for any valve morphology. Valvuloplasty should be performed in any symptomatic patient as soon as the diagnosis is made. Infants with critical pulmonary valve stenosis also should undergo immediate valvuloplasty, but, if this is unsuccessful, surgery should be performed without delay.

Even asymptomatic patients with severe obstruction should be treated semiselectively with valvuloplasty shortly after diagnosis. With the currently available low-profile balloons, there is little benefit to waiting for the patient to reach a certain size. On the contrary, the progression of infundibular hypertrophy that may occur while waiting could make the procedure technically more difficult and prolong the duration of right ventricular hypertension following relief of the valve stenosis. Patients with moderate obstruction should undergo elective valvuloplasty if the right ventricular pressure is 50% systemic or higher. No intervention is necessary for patients with mild obstruction. They should not be restricted in their physical activity and should be treated like normal children. Endocarditis prophylaxis is not recommended for patients with pulmonary valve stenosis (54).

Assessment of Severity, Course, and Prognosis

The course and prognosis of patients with valvar pulmonary stenosis and intact ventricular septum are determined primarily by the severity of the obstruction. Symptoms are unreliable in reflecting hemodynamic severity because they usually are seen only in patients with severe or critical obstruction. Severity of stenosis is best determined noninvasively by 2-D echo-Doppler techniques. Cardiac catheterization is performed when the obstruction is deemed severe enough to require balloon valvuloplasty.

Mild pulmonary valve stenosis is generally defined as a gradient of <30 to 35 mm Hg across the valve and a right ventricular pressure less than half the left ventricular pressure. The course of mild stenosis is benign, and no intervention is required. The hemodynamic response to exercise in these patients is normal (55). No deaths occurred during a 4- to 8-year follow-up of 214 patients with mild pulmonary stenosis (56). Of 261 patients with gradients <40 mm Hg included in

the First Natural History Study, only three had progression of gradients to 60 mm Hg or more after a 4- to 8-year follow-up (51). The Second Natural History Study documented that patients with gradients <25 mm Hg do not experience an increase in gradient (50). One exception to these findings is in young infants with mild pulmonary stenosis, defined as an echo gradient of <40 mm Hg (57). Of 56 patients younger than 1 month of age with mild obstruction, 16 (29%) progressed to moderate or severe stenosis, and half of those did so in the first 6 months of life. Although in some of those neonates, the physiologic decrease in pulmonary vascular resistance may have accounted for the perceived progression, worsened anatomic obstruction seemed to occur in some.

Controversy exists over the course and prognosis of patients with moderate pulmonary valve stenosis. Most available data suggest that infants and children with moderate stenosis may develop progressively greater outflow tract obstruction, especially during periods of rapid growth (51,56). Patients with gradients between 50 and 79 mm Hg enrolled in the First Natural History Study (51) had excellent survival when evaluated as part of the Second Natural History Study (50) 20 years later, whether managed medically or surgically. By completion of the Second Natural History Study, most of these patients had surgery. In the same study, the likelihood of having surgery for patients with gradients of 25 to 49 mm Hg was about 20%. Despite the absence of symptoms in most patients with moderate pulmonary valve stenosis, formal exercise testing demonstrated subnormal cardiac output response and abnormal increase in right ventricular end-diastolic pressure, especially in adult patients, suggesting that both systolic and diastolic dysfunction may be caused by long-standing moderate obstruction (55). Currently, most centers recommend elective balloon valvuloplasty for patients with Doppler gradients of 40 mm Hg or greater.

Children with severe stenosis commonly develop increasingly severe obstruction, which may result from disproportionate growth of the child relative to the pulmonary valve. Exercise hemodynamics in children and adults with severe obstruction before and after valvotomy suggest that irreversible changes in cardiac function can develop if treatment is delayed beyond childhood. Children and adults with severe stenosis have a lower stroke index at rest and during exercise than patients with milder disease. They also have higher right ventricular end diastolic pressure at rest that abnormally increases with exercise (55). Following valvotomy in young patients, there is an improvement in stroke index and reduction in right ventricular end diastolic pressure at rest and during exercise within 1 year of operation. In contrast, this improvement is not observed in older patients, implying that permanent changes, such as myocardial fibrosis, have occurred (58,59). Hence, relief of severe pulmonary valve stenosis without undue delay is recommended.

The incidence of morbid events, such as bacterial endocarditis, in patients with pulmonary valve stenosis is quite low (50). Of 592 patients enrolled in the First Natural History Study and followed through the Second Natural History Study, only 1 patient developed endocarditis (60). Antibiotic prophylaxis is no longer recommended regardless of treatment, unless a prosthetic valve has been implanted. In such a case, prophylaxis should be used during any episodes of probable bacteremia for life (54).

Indications for Pulmonary Valve Replacement for Induced Pulmonary Insufficiency Following Relief of Pulmonary Valve Stenosis

The indications for pulmonary valve replacement for induced PR remain controversial, but most would agree that selected patients benefit from insertion of a competent pulmonary

valve (61,62). Most of the available data on the effects of long-standing PR, and the outcomes after pulmonary valve replacement, have been derived from patients with repaired tetralogy of Fallot (63–66). Limited information on the natural history of isolated congenital pulmonary valve regurgitation also documents eventual development of symptoms, particularly after age 40, as well as premature death from pulmonary valve regurgitation in a handful of patients (49). Current criteria for intervention typically include (a) the presence of symptoms such as progressive decrease in exercise tolerance or functional class or evidence of right heart failure; (b) progressive right ventricular enlargement, often accompanied by increasing tricuspid insufficiency due to annular dilation; and (c) development or progression of atrial and/or ventricular arrhythmias (46,61). Most would agree that intervention should precede significant right ventricular systolic dysfunction, which would likely be irreversible despite pulmonary valve replacement. The argument against prophylactic early replacement of the pulmonary valve centers primarily on the lack of an excellent, long-lasting prosthetic valve. Because of the eventual need for reoperation after surgical insertion of a prosthetic valve in the majority of patients, the aim is to wait as long as possible before replacing the valve, but not so long that irreversible injury to the RV has occurred.

Until recently, pulmonary valve replacement required open heart surgery under cardiopulmonary bypass. Various prosthetic valves have been used including homograft valves, xenograft valves, pericardial valves, and mechanical valves. All of these have been shown to have a limited life span due to calcification or intimal proliferation causing stenosis and/or regurgitation (64,67). Percutaneous pulmonary valve replacement with a bovine jugular venous valve sutured inside a stent was first described in a human in 2000 (68), and after refinements in the valve design and delivery system over the past decade, the procedure can now be offered to a subset of patients with an already existing prosthetic RV to pulmonary artery conduit (Video 40.3). It is not suitable for patients with a native or patched RVOT at the time of this writing. The Melody percutaneous pulmonary valve (Medtronic Inc., Minneapolis, Minnesota), as the prosthesis is named, consists of a bovine jugular venous valve sawn to a platinum-iridium balloon expandable stent that can be dilated to a diameter of 18, 20, or 22 mm. Children weighing at least 20 kg can undergo implantation of the valve, which requires a 22 Fr delivery system. In order to accommodate the valve and ensure proper function, the conduit must have a waist of 14 to 20 mm on balloon sizing in the catheterization laboratory prior to valve insertion.

At the time of this writing, over a thousand Melody valves have been implanted worldwide, and the valve is approved in the United States under HDE guidelines. The largest group of patients undergoing the procedure is postoperative tetralogy of Fallot patients who have had one or more surgical pulmonary valve replacement(s) (69). The valve has performed well with 70% freedom from reoperation at 70 months in a series that includes the learning curve from the first 50 patients (70). Further improvement in these results is expected with better patient selection and modifications in the valve design. A potentially lethal though rare complication is coronary artery compression by the valve stent. Careful assessment of the coronary anatomy in the catheterization laboratory while maintaining a fully inflated balloon at the site of planned implantation should identify patients at risk, in which case the valve would not be implanted. Conduit rupture may also occur in rare cases, and can be treated with insertion of either a covered stent or the Melody valve itself that is a covered stent, but urgent surgical intervention may be required (71). Very few deaths have occurred with Melody valve insertion and most have been related to coronary artery compression, which should be avoidable with the currently recommended protocol.

A mild increase in pressure gradients has been observed over time, while the valve has remained remarkably competent even in patients followed as long as 5 to 10 years. Fractures of the valve stent felt to be due to compressive forces can result in stenosis (72,73). This problem is likely to be reduced by the current practice of pretesting the conduits prior to valve implantation when recoil is observed during balloon dilation (74,75). A second Melody valve can be implanted in patients who develop obstruction requiring reintervention (72,76).

The Edwards SAPIEN valve, which is the same device as the Cribier Edwards transcatheter aortic valve, is another percutaneous pulmonary valve for which there is a much smaller clinical experience at this time (77). This valve consists of three bovine pericardial leaflets sawn to a stainless steel balloon expandable stent, and is available in 23- and 26-mm diameters. It also requires implantation within a prosthetic conduit. At a median follow-up of 10 months for seven patients reported in 2010, the valves were functioning well with no stent fractures (78). A feasibility trial has been completed in the United States, but HDE status has not yet been granted.

Currently, only about 15% of patients with pulmonary valve dysfunction can benefit from transcatheter pulmonary valve insertion, namely those with prosthetic conduits that meet the size requirements described previously. New technology in valve design will hopefully make the procedure available to the larger group of patients with native outflow tracts in need of a functional pulmonary valve (79,80).

To date, surgical pulmonary valve replacement for induced PR has not universally been shown to improve right ventricular hemodynamics or functional capacity, and there are no data addressing long-term survival (63,65). Similarly, following percutaneous pulmonary valve implantation, RV end diastolic volume decreased significantly in patients who underwent the procedure for either pulmonary stenosis or regurgitation, but RV ejection fraction improved only in the group with pulmonary stenosis. In those with regurgitation, the RV ejection fraction did not change either at 1 month or at 1 year of follow-up. Moreover, functional capacity measured by cardiopulmonary stress testing improved significantly in the pulmonary stenosis group by 1 month after valve implantation, and the improvement was sustained at 1 year. Patients with PR had no improvement in their functional capacity at either 1 month or 1 year after valve insertion (81). It has been argued that the current criteria for intervention may be too conservative, with some patients already having irreversible disease. The availability of a percutaneous method to replace the pulmonary valve may allow a more aggressive approach, and result in improved outcomes in selected patients.

Recently published guidelines recommend endocarditis prophylaxis after either surgical or percutaneous pulmonary valve replacement (54).

PULMONARY VALVE STENOSIS IN YOUNG ADULTS

The vast majority of patients with pulmonary valve stenosis present during childhood. If the diagnosis is not made in childhood, adult patients with hemodynamically significant pulmonary valve stenosis tend to be more symptomatic than their younger counterparts (82). Not infrequently, there is concomitant infundibular stenosis due to muscular hypertrophy in response to long-standing valvar obstruction. There may also be tricuspid insufficiency with severe pulmonary valve stenosis and right ventricular failure. In such cases, and in any symptomatic patient, intervention should be performed at lower gradients than generally accepted, since decreased flow through the valve from low cardiac output may mask severe stenosis.

As in children, balloon dilation of the pulmonary valve is the treatment of choice (83). In patients with a large annulus, the double-balloon technique may be utilized, but it is not always necessary to use a balloon larger than the annular diameter when the annulus is very large. A 25-mm-diameter balloon should suffice for most patients with typical pulmonary valve morphology. Acutely, right ventricular hypertension may persist due to infundibular hypertrophy and/or spasm after dilation, and some operators favor temporary treatment with beta-blockers in severe cases (84). Long-term results are excellent, and regression of infundibular stenosis over time is well documented (83,85,86). PR has not been reported to be a significant issue, but rigorous long-term assessment is lacking. Percutaneous pulmonary valve implantation can now be performed in adults with stenotic or regurgitant RV to pulmonary artery conduits following the guidelines described previously.

SUBVALVULAR RIGHT VENTRICULAR OUTFLOW TRACT OBSTRUCTION

Primary subpulmonary stenosis with intact ventricular septum, described by Elliotson (87) in 1830, accounts for only about 5% of all cases of RVOT obstruction. This entity has been separated into two types. One type consists of an obstructive fibrous band or bands at the junction of the main right ventricular cavity and the proximal infundibulum, often referred to double-chambered RV or right ventricular muscle bundles. In the second type, narrowing of the infundibulum itself is due to fibromuscular thickening of the infundibular wall, which may extend from immediately below the pulmonary valve to the proximal infundibulum. Infundibular stenosis is more commonly associated with tetralogy of Fallot or pulmonary valve stenosis. The physiologic and clinical manifestations of infundibular stenosis are almost identical to those for double-chambered RV. Infundibular stenosis associated with pulmonary valve stenosis may improve spontaneously over time after balloon pulmonary valvuloplasty but double-chambered RV tends to worsen with age (86).

RIGHT VENTRICULAR OBSTRUCTION

Double-Chambered Right Ventricle

This congenital malformation, known as “double-chambered RV,” is characterized by aberrant hypertrophied muscular bands that divide the right ventricular cavity into a proximal high-pressure chamber and a low-pressure chamber distal to the hypertrophied muscle bands.

Pathology

Anatomically, the anomalous hypertrophied muscle bundles constitute a pyramidal mass of muscle that runs between the ventricular septum inferior to the insertion of the septal leaflet of the tricuspid valve to the anterior wall of the RV. There are usually two bundles: the ventral bundle, which attaches to the wall of the RV adjacent to the septum, and the dorsal bundle, which is larger and attaches to the base of the anterior papillary muscle (Fig. 40.14). The right ventricular cavity is divided into a proximal chamber, which consists of the sinus portion of the RV, and a distal chamber, which consists of the infundibulum. In tetralogy of Fallot, the obstruction involves the infundibular area, but the anomalous muscle bundles in double-chambered RV cross the right ventricular cavity and lie proximal to the infundibulum. The orientation of these

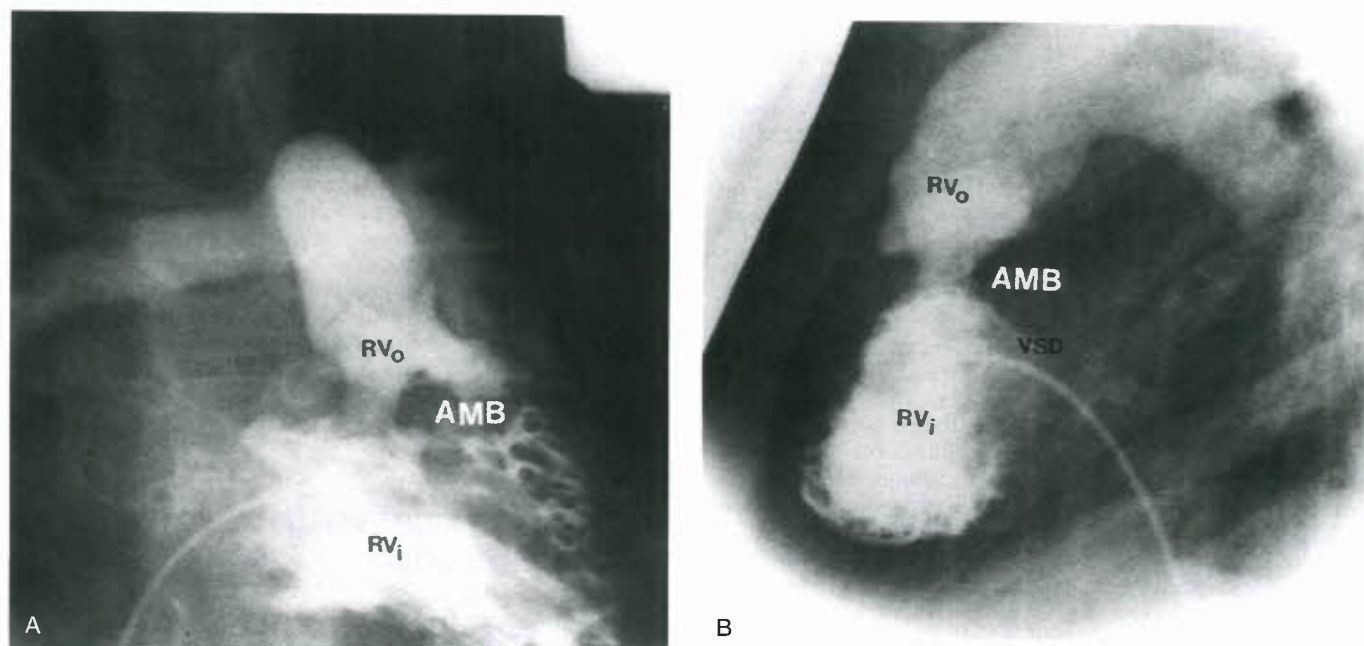


Figure 40.14. Right ventricular angiogram of a child with double-chambered RV. **A:** Anteroposterior projection demonstrates the anomalous muscle bundle (AMB) dividing the RV horizontally into inflow (RV_i) and outflow (RV_o) portions. **B:** The anomalous muscle bundle and inflow and outflow chambers also are well seen on the lateral projection. A small VSD is faintly opacified.

bundles differs from that of the moderator band. The septal attachment of the moderator band is usually in the apical third of the ventricular septum, whereas in anomalous muscle bundles, the septal attachments are near the base of the tricuspid valve ring. Although both types of muscle bundles attach to the anterior wall of the RV, the moderator band lies toward the septum and does not ordinarily obstruct the cavity.

The origin of these anomalous bundles is unknown. It is believed that they may be due to a localized growth of the trabeculated myocardium early in development. It also has been suggested that the right ventricular subdivision and obstruction in this malformation represent an arrested incorporation of the primitive bulbus cordis into the right ventricular body (88). The improper expansion of the bulboventricular junction would therefore result in incomplete fusion of the bulbar and endocardial cushion elements that normally close the superior portion of the ventricular septum, which could explain the frequent association of a VSD with this malformation. The VSD is most frequently found in the perimembranous septum and occasionally in a subarterial location (89). Discrete subaortic stenosis also can occur with this lesion, supporting the concept of inadequate bulbar incorporation as an etiologic mechanism.

Physiology

The anomalous muscle bundles may cause varying degrees of obstruction within the RV, and the severity of obstruction often will increase with time (90). Often nonobstructive anomalous muscle bundles in infancy become obstructive later. For blood to pass from the right ventricular inflow to the right ventricular outflow, it must course either above the muscle bundles, between the muscle bundles and the tricuspid valve, or through the narrow channel between the bundles and septal wall. During ventricular systole, the diameter of these channels is usually markedly reduced. The hemodynamic consequence of the obstruction is an elevated pressure within the proximal or sinus portion of the RV.

Manifestations

Clinically, patients with anomalous muscle bundles and intact ventricular septum closely resemble patients with isolated pulmonary valvar stenosis. When a VSD is present, the clinical features may be dominated by the ventricular septal defect.

A loud pansystolic crescendo-decrescendo murmur, often accompanied by a thrill, is heard at the left sternal border. The murmur may be indistinguishable from that of isolated valvar pulmonary stenosis, but a click is not audible, and the pulmonary valve closure sound may not be as delayed or as soft as one would expect with a murmur of similar intensity in valvar pulmonary stenosis. The chest radiograph is similar to that from other types of RVOT obstruction, unless a significant VSD is present. In most patients, the electrocardiogram shows right ventricular hypertrophy, but may show evidence of diminished terminal right ventricular forces. In a report involving 30 patients with double-chambered RV, an upright T wave in V3R was the only finding suggestive of right ventricular hypertrophy in approximately 40% of the cases (91).

Two-dimensional echocardiography is usually diagnostic in this lesion. The anomalous muscle bundles can be visualized best from either the subcostal or parasternal views (Fig. 40.15). Severity of obstruction can be assessed by the degree of anatomic narrowing and by Doppler interrogation of the obstructed region. Color-flow Doppler identifies the site of obstruction by the appearance of a mosaic pattern where the high-velocity flow originates (Fig. 40.15). In addition, the presence or absence of a VSD can be documented. Abnormal fluttering of the pulmonary valve is often a concomitant finding.

Cardiac Catheterization

Cardiac catheterization is sometimes performed to confirm the diagnosis of double-chambered RV. The catheter must be placed in the inflow portion of the right ventricular cavity, and

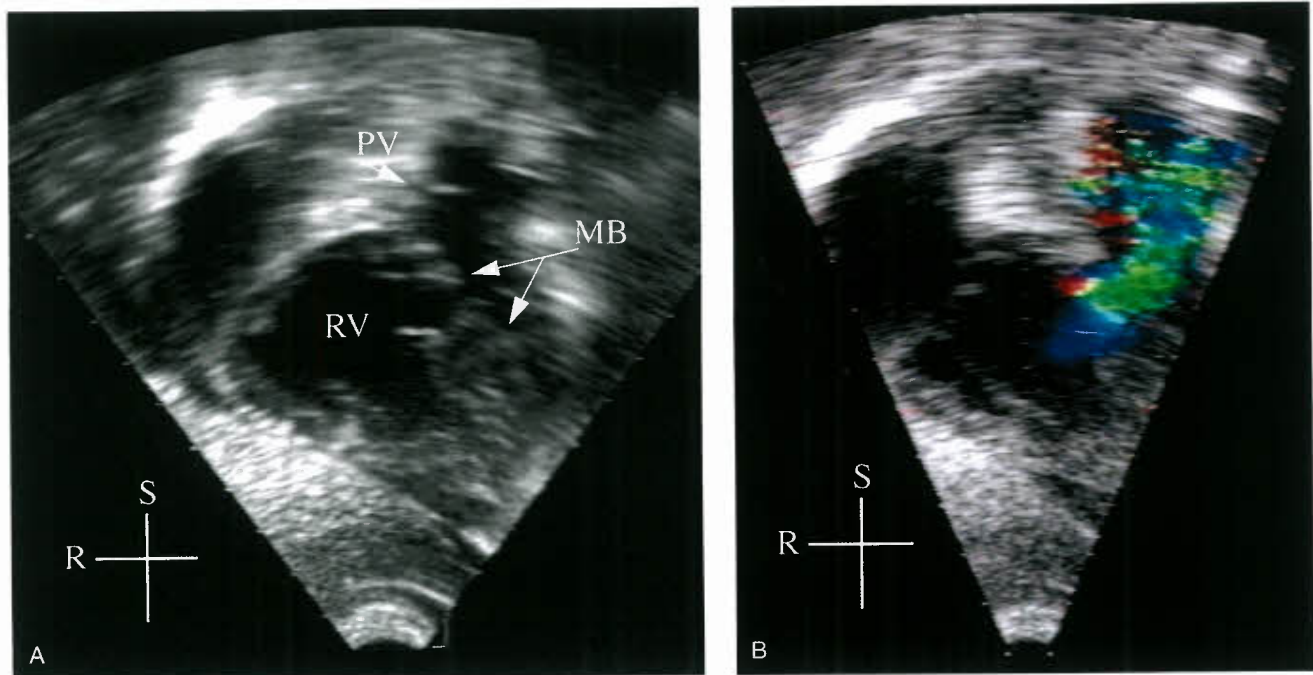


Figure 40.15. A: Subcostal view of the RV from a patient with double-chambered RV. The anomalous muscle bundle (MB) courses obliquely across the RV. B: Color-flow Doppler through the obstructing MB has a mosaic pattern consistent with high-velocity flow. PV, pulmonary valve; R, right; S, superior.

a pressure gradient is demonstrated as the catheter is further advanced into the distal, low-pressure chamber. The pressure in the distal chamber is usually equal to that in the pulmonary artery unless there is associated pulmonary valve stenosis. Care must be taken first to place the catheter into the right ventricular apex, because it is relatively easy to advance the catheter from the right atrium directly to the RVOT and “miss” the gradient. If a VSD is present, the location and resultant shunt should be determined.

Angiocardiography

Right ventricular angiography is an excellent method to demonstrate the anatomy of this lesion and always should be performed when a significant intraventricular pressure gradient is detected. Anterior and lateral projections demonstrate filling defects within the RV below the crista supraventricularis, between the outflow and inflow areas (Fig. 40.14). Left ventriculography also can be performed if there is a question about an associated VSD or, less commonly, subaortic stenosis.

Magnetic Resonance Imaging

The role of MRI as a diagnostic tool in congenital heart disease has increased significantly over the past decade. Its role is particularly important in adult patients, in whom echocardiographic views are often limited, and who can best cooperate with the testing requirements of MRI to obtain optimal images. The anatomic features of double-chambered RV can be readily recognized by MRI (92), and it is even possible to obtain a quantitative assessment of the severity of obstruction by measuring flow velocities. MRI is likely to be superior to echocardiography in the older patient, and may obviate the need for cardiac catheterization in most patients.

Treatment

The treatment of this type of obstruction is usually surgical. Every effort should be made to define the anatomy correctly before surgery. Certain characteristic features of this condition seen at surgery have been described (93). During ventricular contraction, a visible “dimple” in the ordinarily smooth right ventricular surface strongly suggests the presence of an obstructing muscle bundle. The dimple deformity usually is found near the anterior intraventricular groove about midway between the base and the apex of the heart, and it corresponds to the parietal attachment of the ventral limb of the anomalous muscle bundle. A right ventriculotomy is usually not necessary to visualize the obstructing muscle mass adequately. The best approach is typically through the tricuspid valve. The papillary muscle attachments to one or the other end of the trabeculum can be fully defined. Usually, one end or the other of the trabeculum can be divided. Occasionally, it must be left intact and channels in front and behind enlarged. A search for a VSD always should be carried out because of the frequent association of these two lesions (89). Stenting of the stenotic region in two high-surgical-risk patients with comorbidities has been reported. Results were favorable in the short term, but concerns about long-term stent integrity will need to be evaluated in a larger group of patients before this approach can be considered a reasonable alternative to surgery in standard risk patients (94).

Course and Prognosis

Double-chambered RV appears to be a progressive disease with gradually increasing severity of obstruction from the anomalous muscle bundles. As the obstruction worsens, an associated VSD may become progressively smaller or close spontaneously. Cases presenting with intact ventricular septum may in fact have had spontaneous closure of a ventricular septal defect. Long-term follow-up to 20 years after repair

of double-chambered RV demonstrated only mild residual sequelae, and serious cardiac compromise has been infrequent (89,90,95). The residual lesions have included mild right ventricular outflow obstruction, insignificant residual VSDs, tricuspid regurgitation, and the presence of aortic valve regurgitation. The need for reoperation for recurrent obstruction is exceedingly uncommon if adequate resection of the anomalous bundles is achieved (89).

DOUBLE-CHAMBERED RIGHT VENTRICLE IN ADULTS

Double-chambered RV is usually diagnosed and surgically corrected in childhood because patients come to medical attention with a loud systolic murmur. Left untreated, the severity of the obstruction in double-chambered RV tends to become progressively worse into adulthood. Patients with this lesion who first come to attention as adults tend to have higher pressure gradients than children and are very frequently symptomatic (96,97). The most common symptom is dyspnea on exertion, but angina, syncope, and right heart failure have been reported. Many adult patients have a perimembranous VSD but little left-to-right shunting because the VSD connects to the high-pressure inflow part of the RV. The systolic murmur in these patients is therefore predominately due to the right ventricular outflow narrowing rather than the VSD. Up to 40% of adults may have mild aortic insufficiency secondary to either aortic valve prolapse into the VSD or mild subaortic stenosis (which can create turbulence and deformity of the aortic valve). Endocarditis has been reported in a number of older patients with this condition. Surgical repair in adults may be more likely to require a transventricular incision. Surgery usually improves the clinical status of symptomatic adults, and later development of recurrence, worsening aortic regurgitation, or arrhythmias is rare (96,97). Patients who undergo surgical repair in childhood appear to do very well as adults, but infrequent follow-up is recommended with surveillance for arrhythmias, valve dysfunction, and ventricular dysfunction.

PERIPHERAL PULMONARY ARTERY STENOSIS WITH INTACT VENTRICULAR SEPTUM

Stenosis of the pulmonary arteries, isolated or in association with other cardiac defects, occurs in 2% to 3% of all patients with congenital heart disease. The stenosis may be single, involving the main pulmonary artery or either of its branches, or multiple, involving both the main and several smaller peripheral pulmonary artery branches (98).

Isolated peripheral pulmonary artery stenosis was described first by Maugars (99) and later by Schwalbe (100), and numerous reports have followed since. Other associated cardiac defects, most commonly valvar pulmonary stenosis and VSD, are present in about two-thirds of the cases. Hypoplasia of the pulmonary arteries also is seen frequently with tetralogy of Fallot. Peripheral pulmonary stenosis is often seen as a feature of several congenital syndromes. In the syndrome of congenital rubella, peripheral pulmonary artery stenosis typically is associated with patent ductus arteriosus and atrial septal defect. The association of supravalvar aortic stenosis, multiple peripheral pulmonary artery stenosis, mental retardation, and peculiar facies has been described as Williams syndrome (101). Peripheral pulmonary artery stenosis also is associated with Noonan syndrome, Alagille syndrome, cutis

laxa, Ehlers-Danlos syndrome, and Silver-Russell syndrome. Although rare, familial and nonfamilial cases of isolated peripheral pulmonary stenosis with no underlying syndrome also have been described (102).

Embryology and Pathology

The pulmonary artery and its branches developmentally have their origin from three separate vascular components. The proximal portion of the main pulmonary artery just above the semilunar valve probably is derived from the bulbus cordis. The remainder of the trunk of the main pulmonary artery arises from the common truncus arteriosus. The proximal segments of the right and left branch pulmonary arteries are derived from the sixth branchial arches on either side. The distal portion of the right sixth arch disappears completely, whereas the one on the left persists as the ductus arteriosus and later as the ligamentum arteriosus. The peripheral portions of the pulmonary artery branches derive from the postbranchial pulmonary vascular plexus, which lies in close relationship to the growing lung buds.

The pathogenesis of peripheral pulmonary artery stenosis is not completely understood but probably differs with the underlying process. It appears that multiple factors and many types of pathologic changes may produce narrowing of the branch pulmonary artery. When pulmonary artery stenosis is associated with significant intracardiac anomalies, the pathogenesis is likely to be developmental in origin. Certain teratogenic agents may interfere with the development of any of the components of the pulmonary arterial tree and may lead to atresia, hypoplasia, or stenosis. At least one such agent, the rubella virus, appears to exert its teratogenic effect by interfering with the normal formation of the elastic tissues. Relatively discrete branch stenosis can be seen in association with ductal closure, especially in cyanotic heart disease.

Specific genetic abnormalities underlying many of the syndromes associated with isolated peripheral pulmonary artery stenosis are being increasingly recognized. A genetic deletion mapped to chromosome 7 resulting in abnormal elastin production was found in most patients with Williams syndrome (103). A deletion in chromosome 20 appears to be responsible for Alagille syndrome, but the resulting biochemical abnormality has not been identified (104). Several families with multiple relatives affected with Noonan syndrome have had the genetic mutation mapped to chromosome 12, and missense mutations in a specific gene on this chromosome are now known to account for more than 50% of cases (9,105). These genetic abnormalities can arise as sporadic mutations or can be familial with autosomal dominant inheritance.

A useful classification of peripheral pulmonary artery stenosis was proposed by Gay et al. (98) (Fig. 40.16). They classified the stenoses into four types: stenoses involving the main pulmonary trunk or the right and left branches, stenoses involving the bifurcation of the pulmonary artery extending into both branches, multiple peripheral stenoses, and a combination of main and peripheral stenoses. In approximately two-thirds of cases, the stenoses involved the main pulmonary trunk, its bifurcation, or its main branches. When the stenosis is localized, dilation of the vessel distal to the narrowing is usually present. With long segment constrictions, only minimal poststenotic dilation, if any, is seen, and no dilation at all is noted with the hypoplastic form. The main pulmonary trunk usually is not dilated, even with severe stenosis involving its distal portions or with bifurcation and branch stenosis. Mild degrees of prestenotic dilation are seen occasionally, but never to the extent seen in obstructive pulmonary hypertension.

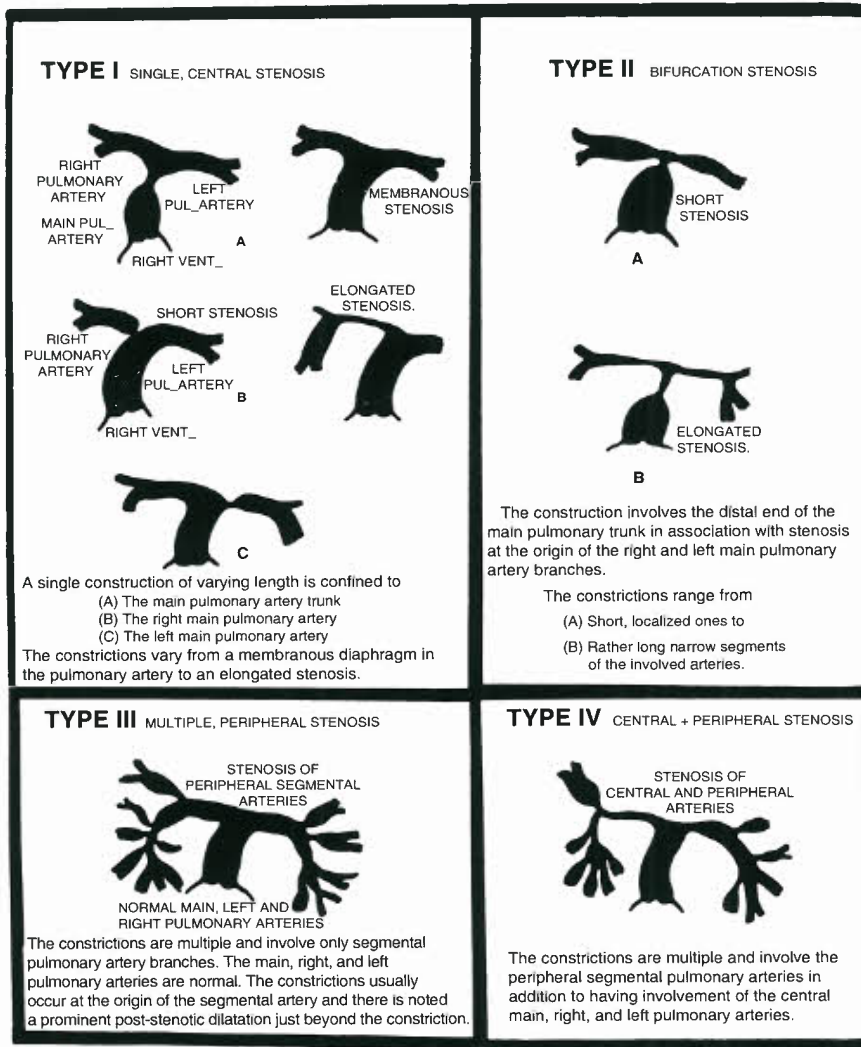


Figure 40.16. Classification of pulmonary artery stenosis. (From Gay BB, Franch RH, Shuford WH, et al. Roentgenologic features of simple and multiple coarctations of the pulmonary artery and branches. *Am J Roentgenol* 1963;90:599, with permission.)

Physiology

The physiology associated with peripheral pulmonary artery stenosis results in elevations of right ventricular and pulmonary artery (proximal to stenosis) systolic pressure that depends on the severity and distribution of the stenoses. In most cases, the obstruction is central and results in a limited volume capacity of the pulmonary trunk proximal to the obstruction. When the obstruction is severe, right ventricular ejection is prolonged, and the pulmonary artery trunk proximal to the obstruction behaves as an extension of the RVOT. The pulmonary arterial pressure proximal to the obstruction is the same as that of the RV, and the pulmonary valve remains open as long as there is a systolic pressure gradient between the RV and the distal pulmonary artery. This explains the delay in pulmonary valve closure despite the high systolic pressure in the pulmonary tree. The pressure tracing proximal to the stenosis resembles that of the RV, with high systolic and low diastolic pressure. In cases of severe multiple peripheral pulmonary stenoses involving many small branches, closure of the pulmonary valve occurs early and approximates closure of the aortic valve. When the stenosis is unilateral and there is no left-to-right shunt, resting right ventricular pressure remains normal. In such cases, the normal contralateral pulmonary arterial tree can accommodate the cardiac output without an increase in pressure. Because flow to the stenotic side is lower than normal, the systolic pressure difference tends to underestimate the severity of obstruction;

however, the diastolic pressure difference between the main pulmonary artery and the stenotic branch is proportional to the severity of obstruction. Measurement of flow distribution, rather than pressure gradients, is the best way to assess relative stenosis in the pulmonary branches. Relative flow to the various regions of the lungs can most easily be measured by quantitative radionuclide pulmonary perfusion scans or by MRI.

Manifestations

Clinical Features

Patients with mild or moderate bilateral pulmonary artery stenosis, as well as those with unilateral stenosis, are usually asymptomatic. Dyspnea on exertion, easy fatigability, and signs of right heart failure may occur in patients with severe obstruction. Several auscultatory findings differentiate pulmonary artery stenosis from other right-sided obstructive lesions. The first heart sound is usually normal, and there is no ejection click. The second sound is usually normally split and of normal or slightly increased intensity. There is a systolic ejection murmur in the pulmonary area that is well transmitted to the axilla and back. A continuous murmur occasionally may be present, indicating that the diastolic gradient across the obstruction is significant. In patients with multiple peripheral pulmonary artery stenoses, the second sound in the pulmonary area may be so loud that pulmonary hypertension is suspected.

The presence of soft, blowing systolic or continuous murmurs typically heard over both lung fields and in the back should point to the correct diagnosis.

Electrocardiographic Features

The electrocardiogram is normal in patients with mild stenosis and demonstrates right ventricular hypertrophy in those with moderate to severe obstruction. A relatively high frequency of left axis deviation has been noted in infants with the rubella syndrome and peripheral pulmonary artery stenosis, as well as in infants with Noonan syndrome.

Radiologic Features

The chest radiograph in patients with unilateral or bilateral pulmonary artery stenosis is almost always normal. There must be severe unilateral stenosis, and often an associated left-to-right shunt lesion, for there to be a detectable difference in the degree of vascularity between the two lung fields. When the stenosis is bilateral and severe, right atrial and right ventricular enlargement may be seen. MRI is becoming increasingly useful in detailing pulmonary artery anatomy. It is superior to echocardiography and complementary to angiography for the detection of pulmonary artery abnormalities. Radionuclide lung perfusion scans are very useful in quantifying flow to each lung before and after surgical or transcatheter therapy.

Echocardiographic Features

The anatomy of the proximal pulmonary arteries usually can be delineated fairly well by echocardiography, but the distal pulmonary arteries cannot be imaged reliably. The parasternal short axis view and suprasternal views are the most helpful (Fig. 40.17). Color-flow Doppler can contribute to the qualitative assessment of stenosis by the appearance of turbulence at

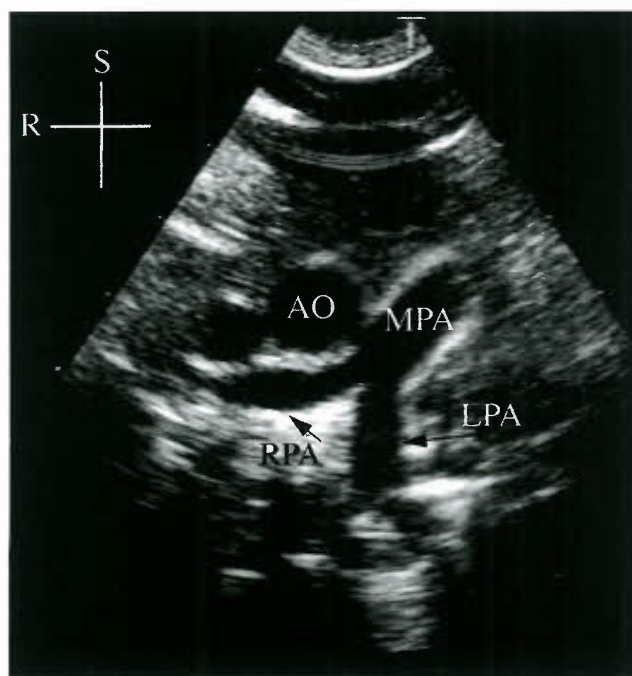


Figure 40.17. Suprasternal notch short-axis view from an infant with Williams syndrome and mild proximal right pulmonary artery (RPA) and left pulmonary artery (LPA) stenosis. The proximal branches are well seen, but the peripheral branches cannot be well imaged. AO, aorta; MPA, main pulmonary artery; R, right; S, superior.

the area of obstruction. The pressure gradient can be estimated by Doppler but not always accurately. The echocardiogram is useful in detecting secondary manifestations of right ventricular hypertension, such as right ventricular hypertrophy, tricuspid insufficiency, or enlargement of the right-sided chambers.

Cardiac Catheterization

The clinical suspicion of peripheral pulmonary stenosis may require cardiac catheterization to confirm the diagnosis and determine the severity and exact anatomy. Carefully obtained withdrawal pressure tracings from the distal branches will demonstrate pressure gradients across the stenotic segments (Fig. 40.18). Systolic pressure gradients higher than 10 mm Hg should be considered abnormal in the absence of a left-to-right shunt with increased pulmonary blood flow. When the stenosis is unilateral, a pressure gradient is present at the site of obstruction, but the proximal pulmonary artery pressure is normal. The measured gradient may underestimate the severity of angiographic obstruction as a result of preferential flow to the unobstructed side. Physiologic gradients >10 mm Hg may be recorded in young infants, especially premature infants, between the pulmonary branches and the main trunk due to the size discrepancy between the two. Artifactual gradients may be created by an overly large catheter in a small vessel.

With bilateral pulmonary artery stenosis, the pressure tracing proximal to the obstruction has characteristic features (Fig. 40.18). The systolic portion of the tracing is identical to that of the RV. The diastolic notch is usually quite low with a slow descent, followed by low diastolic pressure similar to that distal to the obstruction. The pulse pressure is wide and increases with increasing severity of obstruction. These characteristics are attributed to the altered function of the pulmonary trunk, which becomes an extension of the RVOT. The wall of the pulmonary trunk is usually thick and fibrotic with reduced elasticity. As long as pulmonary artery pressure distal to the obstruction is lower than the right ventricular pressure, the pulmonary valve remains open. Closure of the valve occurs during the early phase of isometric relaxation of the ventricle, which results in a sudden increase in the volume capacity of the pulmonary trunk with a corresponding fall in pressure and formation of the diastolic notch. The slow descent of the diastolic pressure is a consequence of the distal obstruction and the impaired elastic recoil of the main pulmonary trunk. When there is associated valvular stenosis, the severity of peripheral pulmonary artery stenosis may be difficult to determine by pressure measurements but can be assessed by angiography and flow scans.

Angiocardiography

Angiocardiography is the best tool for the assessment of anatomic features of peripheral pulmonary artery stenosis. The exact location, extent, and distribution of the lesions can be easily visualized with selective injections proximal to the site of obstruction (Fig. 40.19). The anterior view with cranial angulation and straight lateral views usually show the anatomy of the RPA and of the peripheral branches bilaterally (Fig. 40.20). The proximal left main branch can be well visualized in the hemiaxial left anterior oblique and sometimes lateral views. The main pulmonary trunk is usually normal or hypoplastic. In severe unilateral obstruction, delayed filling of the respective pulmonary vein may be noted.

Noninvasive Imaging: Magnetic Resonance Imaging and Computed Tomography

Advances in noninvasive radiologic imaging modalities in the last decade have allowed excellent visualization of the pulmonary artery anatomy by these techniques, often complementing,



Figure 40.18. Pressure tracing during withdrawal of an end-hole catheter from distal right pulmonary artery (RPA) to proximal right pulmonary artery in a child with severe RPA stenosis. The pressure increases abruptly as the stenotic segment is crossed. Note the slow terminal descent and low diastolic pressure in the proximal RPA. Note also that there is no gradient between the proximal RPA pressure and right ventricle pressure (RVP).

and sometimes replacing, angiography. Gadolinium-enhanced 3-D magnetic resonance angiography (MRA) has been shown to correlate with angiographic findings with 100% sensitivity and specificity when assessing pulmonary artery stenosis or hypoplasia, absent or discontinuous pulmonary arteries (106). Measurements of pulmonary artery diameter also showed excellent correlation, with a mean difference of 0.5 ± 1.5 mm between the two modalities. A limitation of MRA for pediatric patients is motion artifact requiring breath-holding for optimal image acquisition. General anesthesia and suspending mechanical ventilation may be necessary in very

young patients. Anatomic delineation of the more peripheral branches, typically beyond the third and fourth generation, is not adequately achieved by MRA. Advantages of MRA over angiography include reduced risk, avoidance of radiation, and preservation of vascular access for future interventional procedures. Electron-beam computed tomography (CT) has also shown excellent correlation with angiography (107). It is less sensitive to motion artifact and can often be performed with sedation alone, even in small infants. CT is more suited for the unstable patient because of the short time needed to acquire the information, and has better spatial resolution than MRA.

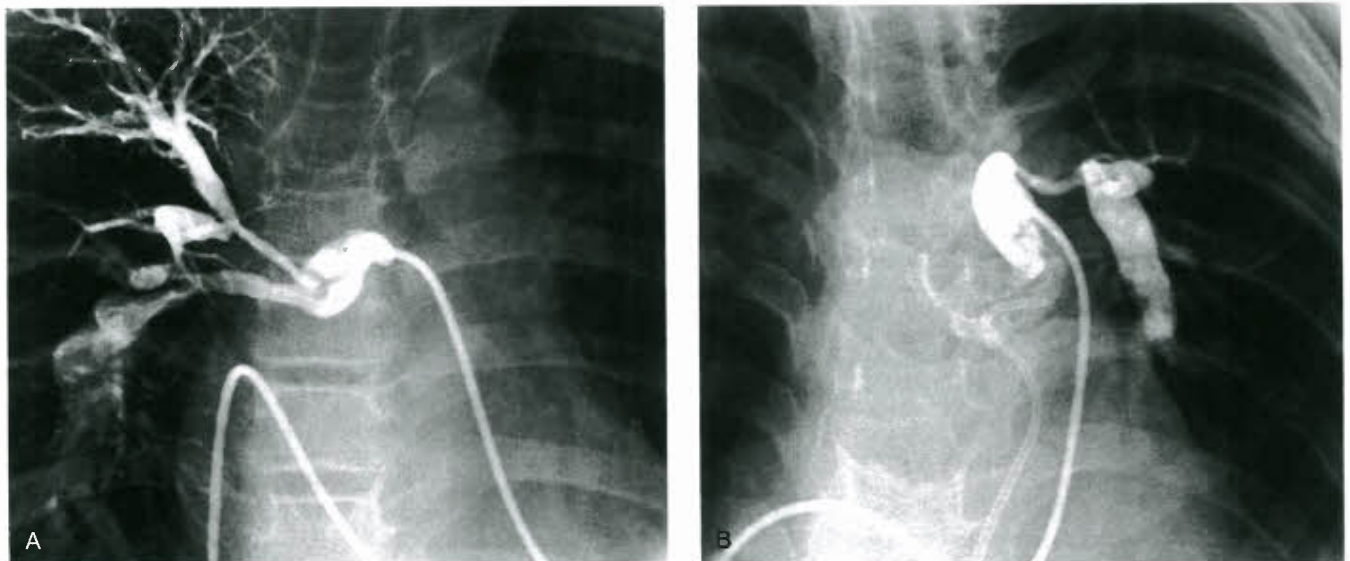


Figure 40.19. Selective right and LPA angiograms of an 8-year-old girl with severe bilateral pulmonary artery stenosis and no other associated cardiac or systemic disease. **A:** Anterior view of the right pulmonary artery demonstrates long-segment severe hypoplasia of the first-order branches. Some of the more peripheral branches also appear small. Note the lack of significant prestenotic and poststenotic dilation. **B:** Long axial oblique view with cranial angulation of the LPA also demonstrates long segment hypoplasia of its mid portion and small peripheral vessels.

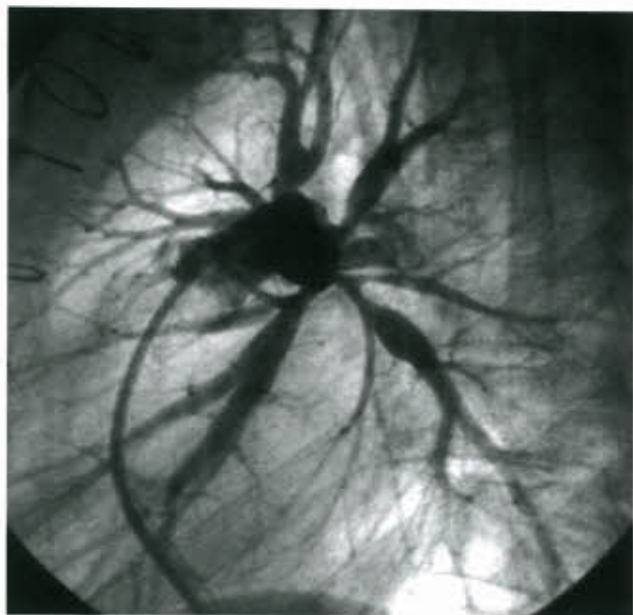


Figure 40.20. Lateral projection of a selective right pulmonary artery angiogram in a 23-year-old woman with bilateral pulmonary artery stenosis and supra-valvar aortic stenosis, but without the phenotype for Williams syndrome. Note the “starburst” appearance with origin stenosis of multiple peripheral branches.

Radiation exposure and contrast administration are necessary, but the dose of both is typically lower than needed for angiography to obtain the same information if study protocols are carefully chosen. Exact hemodynamic measurements still require cardiac catheterization. Judicious use of these different modalities should result in increased safety and efficiency for the patient.

Differential Diagnosis

The differential diagnosis of isolated peripheral pulmonary artery stenosis is similar to that of pulmonary valve stenosis. The characteristic systolic murmur that is widely transmitted to the axilla and the back should suggest the diagnosis. Because peripheral pulmonary artery stenosis is commonly associated with other intracardiac and extracardiac malformations, the features of the predominant lesion will determine the clinical picture. A history of maternal rubella, familial congenital heart disease, prolonged neonatal jaundice, and the finding of facies or features suggesting Noonan syndrome or Williams syndrome should suggest the diagnosis of peripheral pulmonary artery stenosis in a patient with a pathologic murmur. Pulmonary artery stenosis should be considered in patients with tetralogy of Fallot and other complex cyanotic congenital cardiac lesions.

Treatment

Mild to moderate isolated unilateral or bilateral peripheral pulmonary artery stenosis usually does not require treatment, but severe cases do require some form of therapy. Prior to 1981, surgical reconstruction was attempted, but the results were suboptimal, prompting the development of catheter therapy. Despite significant improvements in surgical techniques, access to distal vessels remains difficult, and catheter treatment is sometimes the only option.

Balloon Angioplasty

The first use of percutaneous transluminal angioplasty for peripheral pulmonary arterial stenosis was described by Martin et al. (108) in 1980. Subsequently, Lock et al. (109) used the technique in newborn lambs with experimentally produced branch pulmonary arterial stenosis. These investigators demonstrated histologically that successful dilations resulted from intimal and medial tearing of the pulmonary artery wall. These experiments led to the initiation of clinical trials in the early 1980s.

The technique for angioplasty consists of positioning a balloon dilation catheter across the stenotic segment of the pulmonary artery. The balloon diameter usually must be three to four times the narrowest pulmonary artery segment to be effective. Initially, the balloon is inflated to low pressure (1 to 2 atm) while confirming proper position, indicated by a “waist” representing the stenotic segment centered on the balloon. If the diameter of the waist in the balloon is <70% of the balloon nominal diameter at this pressure, the initial dilation should be performed with a different, slightly smaller balloon. Overstretching a tight, noncompliant lesion increases the risk of potentially catastrophic rupture. Under continuous fluoroscopic monitoring, the appropriate balloon is inflated further to higher pressure for a variable period (10 to 60 seconds) until the waist disappears or the maximum pressure is reached. A postdilation angiogram should be performed either just proximal to the dilated area or by advancing an end-hole angiographic catheter over a guidewire left in place across the dilated segment (Fig. 40.21).

Percutaneous balloon angioplasty of peripheral pulmonary artery stenosis has met with a significantly lower success rate than pulmonary valvuloplasty. The criteria used to determine success has been described arbitrarily as an increase of 50% or more in vessel diameter, an increase of more than 20% in flow to the affected lung, or a decrease of more than 20% in systolic right ventricular to aortic pressure ratio (110). The overall acute success rate for patients with varying diagnoses, most commonly tetralogy of Fallot with and without pulmonary atresia, has been reported as 50% to 60% and appears to be similar in the small subset of patients with isolated peripheral pulmonary artery stenosis and intact ventricular septum (110,111). Hosking et al. (111) examined the clinical impact of balloon angioplasty using relatively low-pressure balloons on subsequent management and found that only 35% of patients were favorably influenced by the procedure, with no patient previously considered inoperable becoming operable following angioplasty. A similar study by Zeevi et al. (112) found a 50% rate of favorable clinical impact using more stringent criteria for technical success and high-pressure balloons on some patients. The rate of recurrent stenosis has been 15% to 20% in short to midterm follow-up (110,111); long-term follow-up is unknown.

Because of the disappointing results obtained with low-pressure balloons, high-pressure balloons that can be inflated up to 20 to 25 atm are being used increasingly to dilate pulmonary arteries. The overall acute success rate, defined as 50% or greater increase in vessel diameter or a >20% decrease in right ventricular to aortic pressure ratio, is around 70% to 80%, but still only 50% in patients with isolated peripheral pulmonary artery stenosis (113,114). Limited information is available regarding the frequency of restenosis, but it may be higher than had been previously suspected. Using high-pressure balloons whenever necessary and defining restenosis as >50% decrease in the gain in diameter achieved at the initial successful angioplasty, a restenosis rate of 35% was found at follow-up angiography in a group of 48 patients (115). The only statistically significant variable associated with the occurrence of restenosis was weight at the time of follow-up.

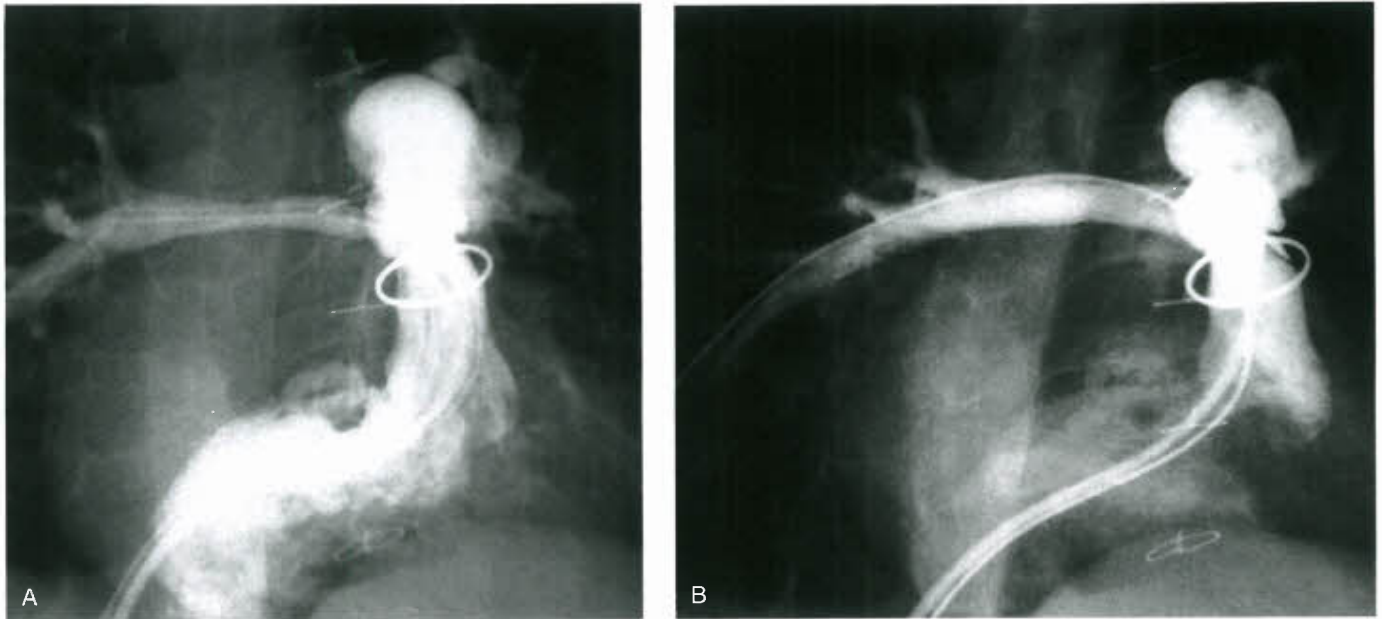


Figure 40.21. Right ventricular angiogram of a 3-year-old boy with truncus arteriosus and right pulmonary artery stenosis before and after balloon angioplasty. A: Stenosis of the right pulmonary artery at its origin and at its midportion is visualized. B: Following angioplasty, the stenotic areas have increased in diameter and the caliber of the vessel is uniformly larger. The systolic pressure gradient from the distal right pulmonary artery to the main pulmonary artery decreased from 36 to 18 mm Hg.

The continued effort to improve on the success rate of balloon angioplasty for resistant pulmonary artery stenosis has recently brought about the use of cutting balloons in this setting (116). These balloons have three or four microsurgical blades with a cutting depth of 0.15 mm mounted longitudinally at 90 degree angles to the balloon. The technique is best suited for small, lobar pulmonary artery branches not amenable to stenting. Vessels resistant to high-pressure balloon angioplasty have been shown to respond to either cutting balloon angioplasty alone or cutting balloon angioplasty followed by high-pressure ballooning (117,118). The longitudinal cuts made by the blades create sites for the tear to propagate when further dilated with a high-pressure balloon. Successful dilation, defined as >50% increase in vessel diameter, has been achieved in 92% of resistant vessels (118). Follow-up data are still very limited, but encouraging (119,120). Much further in the future is the possibility of gene transfer to the pulmonary artery vessel wall via balloon angioplasty techniques, which could result in the expression of angiogenic factors and vessel growth (121).

Significant complications have been reported in 5% to 15% of patients following percutaneous balloon dilation of peripheral pulmonary arterial stenosis (110–113). These complications include exsanguination from a ruptured pulmonary artery either by the dilating balloon or by the guide-wire, hemoptysis, ipsilateral pulmonary edema, obstruction of dilated vessels by intimal flaps, pulmonary artery aneurysms, and clotted iliac veins. Aneurysms typically occur in small distal vessels spanned by the balloon during dilation of a more proximal stenosis. Thus, it is recommended that the balloon be positioned in the largest available distal vessel. A high incidence of aneurysms due to lack of technical control led to abandonment of intraoperative pulmonary artery dilations in many centers (110). Limited midterm angiographic follow-up of these aneurysms showed that they tend to remain unchanged or decrease slightly in size over time, but late enlargement and catastrophic rupture have rarely been seen.

Transient arrhythmias, cyanosis, and hypotension also may occur during pulmonary artery angioplasty.

Special mention should be made of the experience with balloon angioplasty in patients with Williams syndrome (114). Despite a success rate of approximately 50% as defined by a >50% increase vessel diameter, it has been noted that the decrease in right ventricular to aortic pressure ratio is often disappointing. Diffuse hypoplasia of the pulmonary vascular bed, stenoses distal to the dilated segment, and difficulty in dilating central portions of the pulmonary arteries have been implicated. The complication rate is substantially higher than encountered in other subsets of patients with pulmonary artery stenosis, and the incidence of aneurysms has been reported to be as high as 18%. The mortality rate, measured at 7.7% in one series (114), is more than twice that reported in other settings. Interestingly, the cause of death was not associated with pulmonary artery trauma in any of the patients in this study, but rather occurred in patients with significant coronary artery stenosis or ventricular hypertrophy and concomitant subendocardial ischemia with transient hemodynamic perturbations. These findings, coupled with the recognition that spontaneous improvement is often seen in patients with Williams syndrome and pulmonary artery stenosis, have led most investigators to recommend watchful waiting, particularly in young, asymptomatic children, despite significant elevation of the right ventricular pressure. When necessary, a combined approach with distal balloon angioplasty and proximal surgical reconstruction may be the best therapy in this difficult group of patients.

Balloon-Expandable Intravascular Stents

The lack of response to balloon dilation in a substantial number of patients led to the search for more effective transcatheter treatment. The stainless steel balloon-expandable stent developed by Palmaz et al. (122) dramatically improved the effectiveness of balloon angioplasty in a selected group of patients (123,124). Stent placement is accomplished by positioning

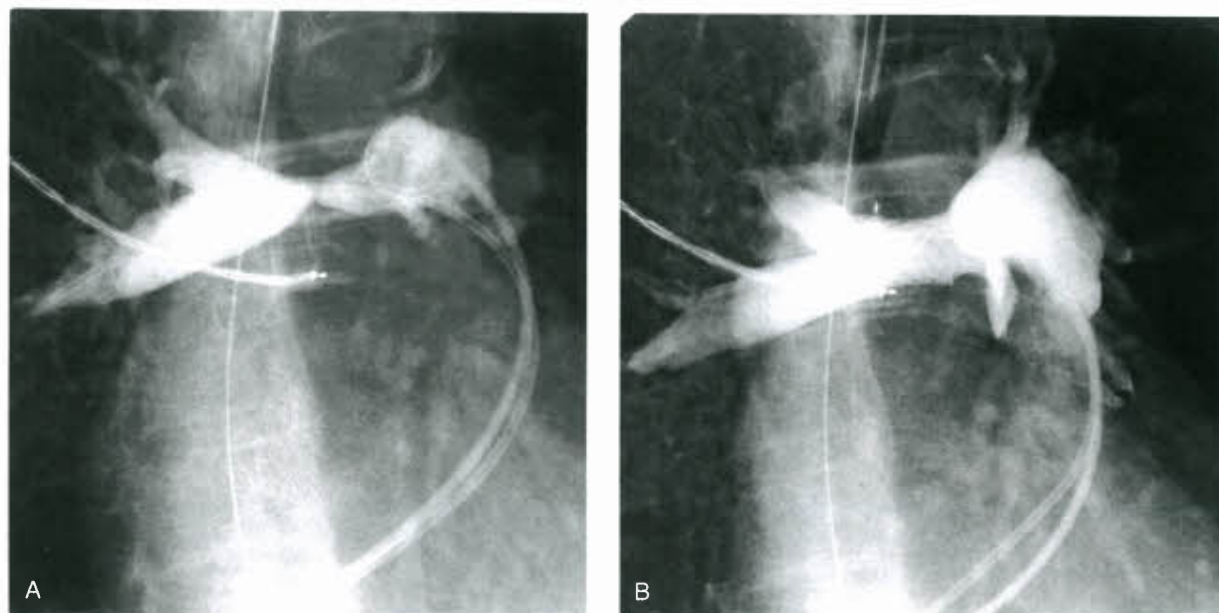


Figure 40.22. Right pulmonary artery angiogram of an adult patient with isolated bilateral pulmonary artery stenosis and right heart failure before and after stent placement. **A:** Right axial oblique view demonstrates severe stenosis in the midportion of the right pulmonary artery. **B:** Following stent placement, there is marked improvement in vessel caliber. The proximal LPA was also stented with a similar result. Right ventricular pressure decreased from 55/16 to 42/8 mm Hg with no significant gradients across the stents. Cardiac index increased from 1.9 to 2.7 L/min/m². The patient's symptoms of right heart failure resolved following the procedure.

the stent, mounted on an appropriately sized balloon angioplasty catheter, across the stenotic segment via a long sheath. The sheath then is withdrawn off the stent–balloon angioplasty catheter assembly, and the balloon is inflated to its recommended pressure, expanding the stent and anchoring it in place (Fig. 40.22). Premounted stents may be held securely enough to the balloon to negate the need for advancement through a protective long sheath. Because of the often tortuous course in patients with congenital heart defects, however, dislodgement of the stent can occur, so placement without a long sheath must be done cautiously.

Several investigators reported excellent results acutely as well as in midterm follow-up of stent implantation for pulmonary artery stenosis (123–125), with an increase of more than 100% in stenosis diameter and a >75% reduction in gradient. Most of the patients in these studies had associated congenital heart disease, such as tetralogy of Fallot with and without pulmonary atresia and truncus arteriosus, and a smaller number had isolated congenital pulmonary artery stenosis. Shaffer et al. (124) reported on a group of 15 patients with isolated pulmonary artery stenosis. There was a dramatic immediate decrease in the gradient across the stenotic areas but a less significant decrease in right ventricular pressure than seen in the rest of the group as well as an increase in the right ventricular pressure at midterm follow-up not seen in the other patients. The largest series to date evaluating the immediate and midterm results of stent placement for pulmonary artery stenosis also documents less optimal outcome in this subgroup acutely as well as at a mean follow-up of 5.6 years (125). In a group of 61 patients with isolated congenital pulmonary artery stenosis who underwent placement of 115 stents, the pressure gradient across the stenosis decreased from 50 to 8 mm Hg, on par with the decrease observed in patients with other types of pulmonary artery stenosis. There was also a decrease in the right ventricular to aortic pressure ratio acutely from 0.59 to 0.45. On follow-up, the gradient had increased to 19 mm Hg, similar to the increase observed in the other groups. However, the right

ventricular to aortic pressure ratio had risen to 0.59 (the same ratio as before stenting), while the increase was less significant in other groups. In contrast, follow-up data for the entire cohort of 338 patients, in whom 664 stents were implanted, showed persistent reduction in right ventricular to aortic pressure ratio from 0.66 before stenting, to 0.45 immediately after stenting, and to 0.50 at a mean follow-up of 5.6 year. The rate of restenosis and the incidence of nonphysiologic neointimal proliferation (>1 mm lining on either side of the stent) were only 2% each. The difference in outcome between patients with isolated congenital pulmonary artery stenosis and others, such as patients with tetralogy of Fallot, is felt to be related to the underlying elastin arteriopathy in the former group, rendering the reaction of the vessel wall to the stent less optimal, and resulting in early restenosis (125). These patients are also at higher risk of complications from either balloon angioplasty or stenting of their pulmonary arteries. Of 5 deaths reported by McMahon et al. in their 338 patients, 2 occurred in patients with congenital pulmonary artery stenosis. One patient died of fulminant pulmonary edema after placement of two stents in the left lower lobe, and the other developed massive hemoptysis, a bronchopleural fistula, and died despite lobectomy to control the bleeding.

Complications from stent implantation include incorrect stent positioning or embolization, sometimes requiring surgical removal; thrombosis of the pulmonary artery within the stent (mostly seen in patients with systemic vein to pulmonary artery anastomosis); and all the complications associated with balloon angioplasty alone, including pulmonary edema and pulmonary hemorrhage. Operator experience and technologic advances over the past two decades have been shown to significantly reduce the incidence of complications (125). Lessons learned have led to changes in practice, including avoidance of overdistention and conservative serial dilations in patients with isolated congenital pulmonary artery stenosis, and simultaneous stenting of several branches, or of the right and left pulmonary arteries where applicable, in those with systemic or

suprasystemic right ventricular pressure to avoid flooding a single segment. Technologic advances include shorter stents, improved balloon profiles, central inflation of the stents preventing protrusion of the stent struts into the vessel wall, refinements in techniques to assure stable positioning of the stent over the balloon as it is advanced to the lesion, and more recently, the introduction of premounted stents. These latter stents can be advanced over a wire even without the protection of a long sheath without slippage of the stent off the balloon (126).

At follow-up catheterization, a small and usually hemodynamically insignificant decrease in diameter of the stented vessel has been noted that resulted from neointimal proliferation. McMahon et al. (125) noted an increase in luminal diameter from 5.4 to 11.2 mm immediately after stent placement, and a decrease to 9.3 mm after 5.6 years of mean follow-up. More significant narrowings can develop in areas of diameter mismatch between the stented and nonstented vessel (123) or in between nonoverlapping serial stents. In the majority of cases, the gradient measured on follow-up was due to growth of the vessel wall adjacent to the stent despite the absence of significant restenosis within the stent (125). Stent redilation has been performed safely and effectively in midterm follow-up (127); however, concerns about the unknown long-term effects of stent implantation and about the potential limitations of redilation prompted several investigators to recommend withholding stent placement in very young children (124). In very small patients, stents should be avoided unless the stent utilized has the capacity to later be enlarged to adult diameter. For older children and adult patients, in whom stents can be dilated at the initial or subsequent catheterizations to the required adult size of the vessel, stent placement has become the preferred therapy for refractory branch pulmonary stenosis. Future technologic advances such as biodegradable stent designs may further expand the indications for pulmonary artery stent implantation to all age groups (128).

Surgery

Early attempts to relieve pulmonary artery stenosis were confined to the main pulmonary artery or origin of the branch pulmonary arteries with varying success. Multiple peripheral stenoses were first tackled by McGoon et al. (129) using an azygous vein graft to patch over the incised stenotic segments. Further surgical experience with pulmonary artery reconstruction was gained primarily in patients with tetralogy of Fallot with pulmonary atresia and aortopulmonary collateral arteries. When native arterioplasty is not sufficient, stenotic segments are enlarged, preferably with autologous pericardium and occasionally with azygous vein grafts. Isolated congenital peripheral pulmonary artery stenosis, often accompanied by long-segment hypoplasia, is difficult to treat successfully with either balloon angioplasty or surgery. In our institution, various techniques are used to deal with this lesion, including excision of stenotic segments, augmentation of stenotic branching points using cutback angioplasty, and use of an autologous pericardial roll to restore arterial continuity when direct anastomosis is not possible. At least one patient with severe bilateral branch pulmonary artery stenosis was treated surgically with near normalization of right ventricular pressure (130) (Fig. 40.23). A combined approach, with surgical reconstruction followed by transcatheter pulmonary artery intervention, is often the best form of treatment.

Course and Prognosis

Routine prophylaxis against endocarditis in patients with peripheral pulmonary stenosis is not recommended. Most patients with mild or moderate stenosis remain stable, and pressure gradients recorded early in life often decrease with growth.



Figure 40.23. Pulmonary artery angiogram of the same patient depicted in Figure 40.19 following surgical reconstruction. The right ventricular pressure decreased from 102/6 to 40/5 mm Hg.

This is particularly true in patients with associated syndromes such as Williams, Noonan, or congenital rubella; however, multiple peripheral pulmonary stenosis of severe degree may be progressive (102,131), and the prognosis is poor unless angioplasty, stent placement, or surgery is successful. Complications include right ventricular failure, pulmonary artery thrombosis, and poststenotic aneurysmal dilation with pulmonary artery hemorrhage. Death in childhood has been reported (131).

PULMONARY ARTERY STENOSIS IN YOUNG ADULTS

Isolated peripheral pulmonary artery stenosis is rarely seen in adult patients, and often is misdiagnosed as chronic pulmonary thromboembolic disease (132). These patients typically present with exertional dyspnea and fatigue, and symptomatic improvement has been seen following balloon angioplasty. Systemic vasculitis with pulmonary arterial involvement should be excluded. The presence of murmurs consistent with pulmonary artery stenosis in many of these patients in childhood or adolescence suggests a congenital etiology with slow progression. Inadequately repaired pulmonary artery branch stenosis may be seen in patients who underwent childhood repairs of lesions such as tetralogy of Fallot, truncus arteriosus, or transposition of the great arteries (if arterial switch procedure was utilized). Abnormal distribution of pulmonary blood flow has been associated with reduced exercise capacity (133).

REFERENCES

1. Morgagni JB. De Sedibus et Causis Morborum (The Seats and Causes of Diseases). Venice: Remondini, 1761.
2. Campbell M. Factors in the aetiology of pulmonary stenosis. *Br Heart J* 1962;24:625–632.
3. Driscoll DJ, Michels VV, Gersony WM, et al. Occurrence risk for congenital heart defects in relatives of patients with aortic stenosis, pulmonary stenosis, or ventricular septal defect. *Circulation* 1993;87:1114–1120.

4. Hutson MR, Kirby ML. Model systems for the study of heart development and disease. Cardiac neural crest and conotruncal malformations. *Semin Cell Dev Biol* 2007;18:101–110.
5. Snarr BS, Kern CB, Wessels A. Origin and fate of cardiac mesenchyme. *Dev Dyn* 2008;237:2804–2819.
6. Armstrong EJ, Bischoff J. Heart valve development: endothelial cell signaling and differentiation. *Circ Res* 2004;95:459–470.
7. Yu S, Crawford D, Tsuchihashi T, et al. The chemokine receptor CXCR7 functions to regulate cardiac valve remodeling. *Dev Dyn* 2011;240:384–393.
8. Chen B, Bronson RT, Klamon LD, et al. Mice mutant for *Egfr* and *Shp2* have defective cardiac semilunar valvulogenesis. *Nat Genet* 2000;24:296–299.
9. Tartaglia M, Mehler EL, Goldberg R, et al. Mutations in *PTPN11*, encoding the protein tyrosine phosphatase SHP-2, cause Noonan syndrome. *Nat Genet* 2001;29:465–468.
10. Noonan JA. Hypertelorism with Turner phenotype. A new syndrome with associated congenital heart disease. *Am J Dis Child* 1968;116:373–380.
11. Digilio MC, Conti E, Sarkozy A, et al. Grouping of multiple-lentiginos/LEOPARD and Noonan syndromes on the *PTPN11* gene. *Am J Hum Genet* 2002;71:389–394.
12. Edwards J. Congenital malformations of the heart and great vessels. In: Gould S, ed. *Pathology of the Heart*. Springfield, IL: Charles C. Thomas, 1953.
13. Koretzky ED, Moller JH, Korn ME, et al. Congenital pulmonary stenosis resulting from dysplasia of valve. *Circulation* 1969;40:43–53.
14. Rudolph A. *Congenital Diseases of the Heart*. Chicago: Yearbook Medical, 1974.
15. Freed MD, Rosenthal A, Bernhard WF, et al. Critical pulmonary stenosis with a diminutive right ventricle in neonates. *Circulation* 1973;48:875–881.
16. Vogelpoel L, Schrire V. Auscultatory and phonocardiographic assessment of pulmonary stenosis with intact ventricular septum. *Circulation* 1960;22:55–75.
17. Lima CO, Sahn DJ, Valdes-Cruz LM, et al. Noninvasive prediction of transvalvular pressure gradient in patients with pulmonary stenosis by quantitative two-dimensional echocardiographic Doppler studies. *Circulation* 1983;67:866–871.
18. Currie PJ, Hagler DJ, Seward JB, et al. Instantaneous pressure gradient: a simultaneous Doppler and dual catheter correlative study. *J Am Coll Cardiol* 1986;7:800–806.
19. Kan JS, White RI Jr, Mitchell SE, et al. Percutaneous balloon valvuloplasty: a new method for treating congenital pulmonary-valve stenosis. *N Engl J Med* 1982;307:540–542.
20. Watson H, Lowe KG. Ventricular pressure flow relationships in isolated valvular stenosis. *Br Heart J* 1962;24:431–440.
21. Lewis JM, Montero AC, Kinard SA Jr, et al. Hemodynamic response to exercise in isolated pulmonic stenosis. *Circulation* 1964;29:854–861.
22. Radtke W, Keane JF, Fellows KE, et al. Percutaneous balloon valvotomy of congenital pulmonary stenosis using oversized balloons. *J Am Coll Cardiol* 1986;8:909–915.
23. Tynan M, Jones O, Joseph MC, et al. Relief of pulmonary valve stenosis in first week of life by percutaneous balloon valvuloplasty. *Lancet* 1984;1:273.
24. Colli AM, Perry SB, Lock JE, et al. Balloon dilation of critical valvar pulmonary stenosis in the first month of life. *Cathet Cardiovasc Diagn* 1995;34:23–28.
25. Gournay V, Piechaud JF, Delogu A, et al. Balloon valvotomy for critical stenosis or atresia of pulmonary valve in newborns. *J Am Coll Cardiol* 1995;26:1725–1731.
26. Tabatabaei H, Boutin C, Nykanen DG, et al. Morphologic and hemodynamic consequences after percutaneous balloon valvotomy for neonatal pulmonary stenosis: medium-term follow-up. *J Am Coll Cardiol* 1996;27:473–478.
27. Ali Khan M, Al Yousef A, Sawyer W. Graduated sequential balloon dilatation as a treatment for severe pulmonary valve stenosis in infants and children. *Pediatr Cardiol* 1987;8:212.
28. Latson L, Cheatham J, Froemming S, et al. Transductal guidewire “rail” for balloon valvuloplasty in neonates with isolated critical pulmonary valve stenosis or atresia. *Am J Cardiol* 1994;73:713–714.
29. Stanger P, Cassidy SC, Girod DA, et al. Balloon pulmonary valvuloplasty: results of the Valvuloplasty and Angioplasty of Congenital Anomalies Registry. *Am J Cardiol* 1990;65:775–783.
30. McCrindle BW, Kan JS. Long-term results after balloon pulmonary valvuloplasty. *Circulation* 1991;83:1915–1922.
31. O’Connor BK, Beekman RH, Lindauer A, et al. Intermediate-term outcome after pulmonary balloon valvuloplasty: comparison with a matched surgical control group. *J Am Coll Cardiol* 1992;20:169–173.
32. Masura J, Burch M, Deanfield JE, et al. Five-year follow-up after balloon pulmonary valvuloplasty. *J Am Coll Cardiol* 1993;21:132–136.
33. McCrindle BW. Independent predictors of long-term results after balloon pulmonary valvuloplasty. Valvuloplasty and Angioplasty of Congenital Anomalies (VACA) Registry Investigators. *Circulation* 1994;89:1751–1759.
34. Berman W Jr, Fripp RR, Raisher BD, et al. Significant pulmonary valve incompetence following oversize balloon pulmonary valvuloplasty in small infants: a long-term follow-up study. *Catheter Cardiovasc Interv* 1999;48:61–65; discussion 66.
35. Garty Y, Veldtman G, Lee K, et al. Late outcomes after pulmonary valve balloon dilatation in neonates, infants and children. *J Invasive Cardiol* 2005;17:318–322.
36. Ettedgui JA, Ho SY, Tynan M, et al. The pathology of balloon pulmonary valvuloplasty. *Int J Cardiol* 1987;16:285–293.
37. Medina A, Bethencourt A, Olalla E, et al. Intraoperative balloon valvuloplasty in pulmonary valve stenosis. *Cardiovasc Intervent Radiol* 1989;12:199–201.
38. Weber HS. Initial and late results after catheter intervention for neonatal critical pulmonary valve stenosis and atresia with intact ventricular septum: a technique in continual evolution. *Catheter Cardiovasc Interv* 2002;56:394–399.
39. Karagoz T, Asoh K, Hickey E, et al. Balloon dilation of pulmonary valve stenosis in infants less than 3 kg: a 20-year experience. *Catheter Cardiovasc Interv* 2009;74:753–761.
40. Gibbs JL, Rothman MT, Rees MR, et al. Stenting of the arterial duct: a new approach to palliation for pulmonary atresia. *Br Heart J* 1992;67:240–245.
41. Rosenthal E, Qureshi SA, Tynan M. Percutaneous pulmonary valvotomy and arterial duct stenting in neonates with right ventricular hypoplasia. *Am J Cardiol* 1994;74:304–306.
42. Schneider M, Zartner P, Sidiropoulos A, et al. Stent implantation of the arterial duct in newborns with duct-dependent circulation. *Eur Heart J* 1998;19:1401–1409.
43. Gewillig M, Boshoff DE, Dens J, et al. Stenting the neonatal arterial duct in duct-dependent pulmonary circulation: new techniques, better results. *J Am Coll Cardiol* 2004;43:107–112.
44. Fedderly RT, Lloyd TR, Mendelsohn AM, et al. Determinants of successful balloon valvotomy in infants with critical pulmonary stenosis or membranous pulmonary atresia with intact ventricular septum. *J Am Coll Cardiol* 1995;25:460–465.
45. Harrild DM, Powell AJ, Tran TX, et al. Long-term pulmonary regurgitation following balloon valvuloplasty for pulmonary stenosis risk factors and relationship to exercise capacity and ventricular volume and function. *J Am Coll Cardiol* 2010;55:1041–1047.
46. Earing MG, Connolly HM, Dearani JA, et al. Long-term follow-up of patients after surgical treatment for isolated pulmonary valve stenosis. *Mayo Clin Proc* 2005;80:871–876.
47. Marx GR, Hicks RW, Allen HD, et al. Noninvasive assessment of hemodynamic responses to exercise in pulmonary regurgitation after operations to correct pulmonary outflow obstruction. *Am J Cardiol* 1988;61:595–601.
48. Latson LA. Critical pulmonary stenosis. *J Interv Cardiol* 2001;14:345–350.
49. Shimazaki Y, Blackstone EH, Kirklin JW. The natural history of isolated congenital pulmonary valve incompetence: surgical implications. *Thorac Cardiovasc Surg* 1984;32:257–259.
50. Hayes CJ, Gersony WM, Driscoll DJ, et al. Second natural history study of congenital heart defects. Results of treatment of patients with pulmonary valvar stenosis. *Circulation* 1993;87:128–137.
51. Nugent EW, Freedom RM, Nora JJ, et al. Clinical course in pulmonary stenosis. *Circulation* 1977;56:138–147.
52. McNamara DG, Latson LA. Long-term follow-up of patients with malformations for which definitive surgical repair has been available for 25 years or more. *Am J Cardiol* 1982;50:560–568.
53. Driscoll DJ, Wolfe RR, Gersony WM, et al. Cardiorespiratory responses to exercise of patients with aortic stenosis, pulmonary stenosis, and ventricular septal defect. *Circulation* 1993;87:1102–1113.
54. Wilson W, Taubert KA, Gewitz M, et al. Prevention of infective endocarditis: guidelines from the American Heart Association: a guideline from the American Heart Association Rheumatic Fever, Endocarditis and Kawasaki Disease Committee, Council on Cardiovascular Disease in the Young, and the Council on Clinical Cardiology, Council on Cardiovascular Surgery and Anesthesia, and the Quality of Care and Outcomes Research Interdisciplinary Working Group. *J Am Dent Assoc* 2007;138:739–745, 747–760.
55. Krabill KA, Wang Y, Einzig S, et al. Rest and exercise hemodynamics in pulmonary stenosis: comparison of children and adults. *Am J Cardiol* 1985;56:360–365.
56. Levine OR, Blumenthal S. Pulmonic stenosis. *Circulation* 1965;32:III33–III41.
57. Rowland DG, Hammill WW, Allen HD, et al. Natural course of isolated pulmonary valve stenosis in infants and children utilizing Doppler echocardiography. *Am J Cardiol* 1997;79:344–349.
58. Johnson AM. Impaired exercise response and other residua of pulmonary stenosis after valvotomy. *Br Heart J* 1962;24:375–388.
59. Stone FM, Bessinger FB Jr, Lucas RV Jr, et al. Pre- and postoperative rest and exercise hemodynamics in children with pulmonary stenosis. *Circulation* 1974;49:1102–1106.
60. Gersony WM, Hayes CJ, Driscoll DJ, et al. Bacterial endocarditis in patients with aortic stenosis, pulmonary stenosis, or ventricular septal defect. *Circulation* 1993;87:1121–1126.
61. Gaynor JW. Severe pulmonary insufficiency should be conservatively treated. *Cardiol Young* 2005;15:68–71.
62. Backer CL. Severe pulmonary valvar insufficiency should be aggressively treated. *Cardiol Young* 2005;15:64–67.
63. Carvalho JS, Shinebourne EA, Busst C, et al. Exercise capacity after complete repair of tetralogy of Fallot: deleterious effects of residual pulmonary regurgitation. *Br Heart J* 1992;67:470–473.
64. Warner KG, Anderson JE, Fulton DR, et al. Restoration of the pulmonary valve reduces right ventricular volume overload after previous repair of tetralogy of Fallot. *Circulation* 1993;88:III189–III197.

65. Therrien J, Siu SC, McLaughlin PR, et al. Pulmonary valve replacement in adults late after repair of tetralogy of fallot: are we operating too late? *J Am Coll Cardiol* 2000;36:1670-1675.
66. Hazekamp MG, Kurvers MM, Schoof PH, et al. Pulmonary valve insertion late after repair of Fallot's tetralogy. *Eur J Cardiothorac Surg* 2001;19:667-670.
67. Razzouk AJ, Williams WG, Cleveland DC, et al. Surgical connections from ventricle to pulmonary artery. Comparison of four types of valved implants. *Circulation* 1992;86:II154-III158.
68. Bonhoeffer P, Boudjemline Y, Saliba Z, et al. Percutaneous replacement of pulmonary valve in a right-ventricle to pulmonary-artery prosthetic conduit with valve dysfunction. *Lancet* 2000;356:1403-1405.
69. Asoh K, Walsh M, Hickey E, et al. Percutaneous pulmonary valve implantation within bioprosthetic valves. *Eur Heart J* 2010;31:1404-1409.
70. Lurz P, Coats L, Khambadkone S, et al. Percutaneous pulmonary valve implantation: impact of evolving technology and learning curve on clinical outcome. *Circulation* 2008;117:1964-1972.
71. Kostolny M, Tsang V, Nordmeyer J, et al. Rescue surgery following percutaneous pulmonary valve implantation. *Eur J Cardiothorac Surg* 2008;33:607-612.
72. Nordmeyer J, Khambadkone S, Coats L, et al. Risk stratification, systematic classification, and anticipatory management strategies for stent fracture after percutaneous pulmonary valve implantation. *Circulation* 2007;115:1392-1397.
73. Schievano S, Taylor AM, Capelli C, et al. Patient specific finite element analysis results in more accurate prediction of stent fractures: application to percutaneous pulmonary valve implantation. *J Biomech* 2010;43:687-693.
74. Lurz P, Gaudin R, Taylor AM, et al. Percutaneous pulmonary valve implantation. *Semin Thorac Cardiovasc Surg Pediatr Card Surg Annu* 2009:112-117.
75. Nordmeyer J, Lurz P, Khambadkone S, et al. Pre-stenting with a bare metal stent before percutaneous pulmonary valve implantation: acute and 1-year outcomes. *Heart* 2011;97:118-123.
76. Nordmeyer J, Coats L, Lurz P, et al. Percutaneous pulmonary valve-in-valve implantation: a successful treatment concept for early device failure. *Eur Heart J* 2008;29:810-815.
77. Webb JG, Pasupati S, Humphries K, et al. Percutaneous transarterial aortic valve replacement in selected high-risk patients with aortic stenosis. *Circulation* 2007;116:755-763.
78. Boone RH, Webb JG, Horlick E, et al. Transcatheter pulmonary valve implantation using the Edwards SAPIEN transcatheter heart valve. *Catheter Cardiovasc Interv* 2010;75:286-294.
79. Moller A, Basquin A, Stos B, et al. Off-pump replacement of the pulmonary valve in large right ventricular outflow tracts: a transcatheter approach using an intravascular infundibulum reducer. *Pediatr Res* 2007;62:428-433.
80. Capelli C, Taylor AM, Migliavacca F, et al. Patient-specific reconstructed anatomies and computer simulations are fundamental for selecting medical device treatment: application to a new percutaneous pulmonary valve. *Philos Transact A Math Phys Eng Sci* 2010;368:3027-3038.
81. Lurz P, Nordmeyer J, Giardini A, et al. Early versus late functional outcome after successful percutaneous pulmonary valve implantation are the acute effects of altered right ventricular loading all we can expect? *J Am Coll Cardiol* 2011;57:724-731.
82. Meadows J, Landzberg MJ. Advances in transcatheter interventions in adults with congenital heart disease. *Prog Cardiovasc Dis* 2011;53:265-273.
83. Chen CR, Cheng TO, Huang T, et al. Percutaneous balloon valvuloplasty for pulmonic stenosis in adolescents and adults. *N Engl J Med* 1996;335:21-25.
84. Thapar MK, Rao PS. Use of propranolol for severe dynamic infundibular obstruction prior to balloon pulmonary valvuloplasty (a brief communication). *Cathet Cardiovasc Diagn* 1990;19:240-241.
85. Kaul UA, Singh B, Tyagi S, et al. Long-term results after balloon pulmonary valvuloplasty in adults. *Am Heart J* 1993;126:1152-1155.
86. Fawzy ME, Hassan W, Fadel BM, et al. Long-term results (up to 17 years) of pulmonary balloon valvuloplasty in adults and its effects on concomitant severe infundibular stenosis and tricuspid regurgitation. *Am Heart J* 2007;153:433-438.
87. Elliottson J. *The Recent Improvements in the Art of Distinguishing the Various Diseases of the Heart*. London: Longman & Company, 1830.
88. Keith A. The Hunterian lectures on malformations of the heart. *Lancet* 1909;2:359.
89. Hachiro Y, Takagi N, Koyanagi T, et al. Repair of double-chambered right ventricle: surgical results and long-term follow-up. *Ann Thorac Surg* 2001;72:1520-1522.
90. Telagh R, Alexi-Meskishvili V, Hetzer R, et al. Initial clinical manifestations and mid- and long-term results after surgical repair of double-chambered right ventricle in children and adults. *Cardiol Young* 2008;18:268-274.
91. Li MD, Coles JC, McDonald AC. Anomalous muscle bundle of the right ventricle. Its recognition and surgical treatment. *Br Heart J* 1978;40:1040-1045.
92. Ibrahim T, Dennig K, Schwaiger M, et al. Images in cardiovascular medicine. Assessment of double chamber right ventricle by magnetic resonance imaging. *Circulation* 2002;105:2692-2693.
93. Warden HE, Lucas RV Jr, Varco RL. Right ventricular obstruction resulting from anomalous muscle bundles. *J Thorac Cardiovasc Surg* 1966;51:53-65.
94. Steadman CD, Clift PF, Thorne SA, et al. Treatment of dynamic subvalvar muscular obstruction in the native right ventricular outflow tract by percutaneous stenting in adults. *Congenit Heart Dis* 2009;4:494-498.
95. Kveselis D, Rosenthal A, Ferguson P, et al. Long-term prognosis after repair of double-chamber right ventricle with ventricular septal defect. *Am J Cardiol* 1984;54:1292-1295.
96. McElhinney DB, Chatterjee KM, Reddy VM. Double-chambered right ventricle presenting in adulthood. *Ann Thorac Surg* 2000;70:124-127.
97. Nagashima M, Tomino T, Satoh H, et al. Double-chambered right ventricle in adulthood. *Asian Cardiovasc Thorac Ann* 2005;13:127-130.
98. Gay BB Jr, French RH, Shuford WH, et al. The roentgenologic features of single and multiple coarctations of the pulmonary artery and branches. *Am J Roentgenol Radium Ther Nucl Med* 1963;90:599-613.
99. Maugars A. Description d'une artere pulmonaire considerable naissant de l'aorte abdominale. *Rec Period Soc Med Paris* 1802;13:74.
100. Schwalbe E. *Morphologie Der Missbildungen Des Menschen Und Der Tiere*. Jena, Germany: Fisher, 1909.
101. Beuren AJ, Schulze C, Eberle P, et al. The syndrome of supra-aortic aortic stenosis, peripheral pulmonary stenosis, mental retardation and similar facial appearance. *Am J Cardiol* 1964;13:471-483.
102. Matsumoto AH, Delany DJ, Parker LA, et al. Massive hemoptysis associated with isolated peripheral pulmonary artery stenosis. *Cathet Cardiovasc Diagn* 1987;13:313-316.
103. Nickerson E, Greenberg F, Keating MT, et al. Deletions of the elastin gene at 7q11.23 occur in approximately 90% of patients with Williams syndrome. *Am J Hum Genet* 1995;56:1156-1161.
104. Oda T, Elkhouloun AG, Pike BL, et al. Mutations in the human Jagged1 gene are responsible for Alagille syndrome. *Nat Genet* 1997;16:235-242.
105. Legius E, Schollen E, Matthijs G, et al. Fine mapping of Noonan/cardiofacio cutaneous syndrome in a large family. *Eur J Hum Genet* 1998;6:32-37.
106. Geva T, Greil GF, Marshall AC, et al. Gadolinium-enhanced 3-dimensional magnetic resonance angiography of pulmonary blood supply in patients with complex pulmonary stenosis or atresia: comparison with x-ray angiography. *Circulation* 2002;106:473-478.
107. Westra SJ, Hurteau J, Galindo A, et al. Cardiac electron-beam CT in children undergoing surgical repair for pulmonary atresia. *Radiology* 1999;213:502-512.
108. Martin EC, Diamond NG, Casarella WJ. Percutaneous transluminal angioplasty in non-atherosclerotic disease. *Radiology* 1980;135:27-33.
109. Lock JE, Niemi T, Einzig S, et al. Transvenous angioplasty of experimental branch pulmonary artery stenosis in newborn lambs. *Circulation* 1981;64:886-893.
110. Rothman A, Perry SB, Keane JF, et al. Early results and follow-up of balloon angioplasty for branch pulmonary artery stenoses. *J Am Coll Cardiol* 1990;15:1109-1117.
111. Hosking MC, Thomaidis C, Hamilton R, et al. Clinical impact of balloon angioplasty for branch pulmonary arterial stenosis. *Am J Cardiol* 1992;69:1467-1470.
112. Zeevi B, Berant M, Bliden LC. Midterm clinical impact versus procedural success of balloon angioplasty for pulmonary artery stenosis. *Pediatr Cardiol* 1997;18:101-106.
113. Gentles TL, Lock JE, Perry SB. High pressure balloon angioplasty for branch pulmonary artery stenosis: early experience. *J Am Coll Cardiol* 1993;22:867-872.
114. Geggel RL, Gauvreau K, Lock JE. Balloon dilation angioplasty of peripheral pulmonary stenosis associated with Williams syndrome. *Circulation* 2001;103:2165-2170.
115. Bush DM, Hoffman TM, Del Rosario J, et al. Frequency of restenosis after balloon pulmonary arterioplasty and its causes. *Am J Cardiol* 2000;86:1205-1209.
116. Magee AG, Wax D, Saiki Y, et al. Experimental branch pulmonary artery stenosis angioplasty using a novel cutting balloon. *Can J Cardiol* 1998;14:1037-1041.
117. Rhodes JF, Lane GK, Mesia CI, et al. Cutting balloon angioplasty for children with small-vessel pulmonary artery stenoses. *Catheter Cardiovasc Interv* 2002;55:73-77.
118. Bergersen LJ, Perry SB, Lock JE. Effect of cutting balloon angioplasty on resistant pulmonary artery stenosis. *Am J Cardiol* 2003;91:185-189.
119. Bergersen L, Jenkins KJ, Gauvreau K, et al. Follow-up results of Cutting Balloon angioplasty used to relieve stenoses in small pulmonary arteries. *Cardiol Young* 2005;15:605-610.
120. Suda K, Matsumura M, Hayashi H, et al. Comparison of efficacy of medium-sized cutting balloons versus standard balloons for dilation of peripheral pulmonary stenosis. *Am J Cardiol* 2006;97:1060-1063.
121. Keller LH, Vander Heide R, Pebbles KA, et al. Percutaneous pulmonary artery gene transfer in pigs using naked plasmid DNA delivered during angioplasty. *Pediatr Cardiol* 2000;21:223-227.
122. Palmaz JC, Sibbitt RR, Tio FO, et al. Expandable intraluminal vascular graft: a feasibility study. *Surgery* 1986;99:199-205.
123. Fogelman R, Nykanen D, Smallhorn JF, et al. Endovascular stents in the pulmonary circulation. Clinical impact on management and medium-term follow-up. *Circulation* 1995;92:881-885.
124. Shaffer KM, Mullins CE, Grifka RG, et al. Intravascular stents in congenital heart disease: short- and long-term results from a large single-center experience. *J Am Coll Cardiol* 1998;31:661-667.

125. McMahon CJ, El Said HG, Vincent JA, et al. Refinements in the implantation of pulmonary arterial stents: impact on morbidity and mortality of the procedure over the last two decades. *Cardiol Young* 2002;12:445–452.
126. Trivedi KR, Benson LN. Interventional strategies in the management of peripheral pulmonary artery stenosis. *J Interv Cardiol* 2003;16:171–188.
127. Ing FF, Grifka RG, Nihill MR, et al. Repeat dilation of intravascular stents in congenital heart defects. *Circulation* 1995;92:893–897.
128. Zartner P, Cesnjevar R, Singer H, et al. First successful implantation of a biodegradable metal stent into the left pulmonary artery of a preterm baby. *Catheter Cardiovasc Interv* 2005;66:590–594.
129. McGoon DC, Kincaid OW. Stenosis of branches of the pulmonary artery: surgical repair. *Med Clin North Am* 1964;48:1083–1088.
130. Fraser CD Jr, Latson LA, Mee RB. Surgical repair of severe bilateral branch pulmonary artery stenosis. *Ann Thorac Surg* 1995;59:738–740.
131. Papadopoulos GS, Folger GM Jr. Progressive pulmonary arterial stenosis. *Am J Cardiol* 1983;51:1462–1463.
132. Kreutzer J, Landzberg MJ, Preminger TJ, et al. Isolated peripheral pulmonary artery stenoses in the adult. *Circulation* 1996;93:1417–1423.
133. Giardini A, Khambadkone S, Taylor A, et al. Effect of abnormal pulmonary flow distribution on ventilatory efficiency and exercise capacity after arterial switch operation for transposition of great arteries. *Am J Cardiol* 2010;106:1023–1028.

Pulmonary Atresia and Intact Ventricular Septum

David G. Nykanen

A discussion of pulmonary atresia (PA) and intact ventricular septum (IVS) would be incomplete without acknowledging the legacy of Robert M. Freedom. As a clinical cardiac morphologist, his monograph described the diversity of this malformation, emphasizing the complexity of a disorder that appears so simple on the surface (1). His understanding of the nature of this condition has endured the test of time and continues to influence our treatment strategies today. To those who were fortunate to know him, he was a passionate, tireless teacher dedicated to the concept that the practice of knowledge-based medicine incorporates observations gained from both an understanding of the literature and the recognition of the value of cumulative experience. Scholars of pediatric cardiology will continue to identify Robert Freedom's contributions to our understanding of PA and IVS for decades to come. It is appropriate that many of his insights continue to be reflected in the pages that follow.

PA and IVS was first described in 1783 by Hunter (2) and then revisited 86 years later by Peacock in 1869 (3). While its name focuses primarily on membranous or muscular atresia of the right ventricular outflow tract, this disorder is characterized by striking heterogeneity of the right ventricle, its inlet, and its functional size. Furthermore, many of these patients have connections between the right ventricle and subepicardial coronary arteries and a predisposition for an unusual coronary circulation. These connections were originally a pathologic curiosity; however, management can be dictated by their nature. Prognosis appears to relate to the nature of the coronary circulation in the right ventricle at high pressure or, alternatively, the presence of severe tricuspid regurgitation in the setting of a low-pressure right ventricle (4–6). It is truly a complex, diverse disorder that challenges surgical and catheter-based interventional strategies. Current interventional algorithms range from achieving a biventricular circulation and variations of the cavopulmonary circulation (Fontan operation or 1.5-ventricle repair) to cardiac transplantation.

EPIDEMIOLOGY

Data obtained from the New England Regional Infant Cardiac Program identified 75 patients with this disorder, accounting for 3.1% of all infants enrolled in the study. The Baltimore-Washington Infant Study defined the prevalence for this disorder as 0.083 per 1,000 live births (7). Despite being uncommon, when integrated into the overall statistics of congenital heart disease, PA/IVS is one of the more common cardiac etiologies of cyanotic congenital heart disease in the neonate, along with transposition of the great arteries and PA with ventricular septal defect. A published study from the United Kingdom and Eire defined the incidence of PA and IVS to be 4.1 per 100,000 live births (8). Overall, by the best estimates, PA and IVS occurs at a rate of 0.6/10,000 live births. However, if one includes

pregnancies that are aborted spontaneously or electively after 20 weeks' gestational age with live births, the rate has been reported as much as 10 times higher at 0.6/1,000.

Fetal echocardiography provides a unique window to study the later phases of the fetal heart development recognizing that cardiac organogenesis is complete by about 8 weeks' gestation. There is increasing evidence that fetuses with severe tricuspid regurgitation may not fare well. Such fetuses are known to develop right-sided heart failure with pleural and pericardial effusions, ascites, pulmonary hypoplasia, and fetal death. Thus, fetal loss might be anticipated in a specific subset of patients with PA, IVS, extremely severe tricuspid regurgitation, and a low-pressure right ventricle. The data collected from the United Kingdom and Eire also showed that termination of pregnancy once this diagnosis was established led to an important reduction in live-born incidence in mainland Britain (8). Prenatal echocardiography is becoming an important predictor of postnatal management of this patient population and likely will grow to include strategic application of in utero intervention (9–13).

DEFINITION

The usual form of PA and IVS occurs in a left-sided heart with normal atrial relations, concordant atrioventricular connections, and concordant ventriculoarterial connections. As its name implies, the right ventricular outflow tract is imperforate and this can be either membranous or represented by a longer segment of muscular atresia. The ventricular septum functionally is intact. A patent arterial duct usually mediates pulmonary blood flow. Very rarely, multiple direct aortopulmonary collaterals originating from the descending thoracic aorta are the sole sources of pulmonary arterial supply. Nonconfluent pulmonary arteries, each supplied by a patent arterial duct, also have been recognized, but this situation also is uncommon (14).

MORPHOGENESIS

Kutsche and Van Mierop (15) suggested that PA with ventricular septal defect occurs earlier in cardiac morphogenesis than PA and IVS. This conclusion is based on an analysis of a number of morphologic factors, including the diameter of the pulmonary trunk, the morphology of the pulmonary valve, and the morphology and topography of the ductus arteriosus. They postulated that PA and ventricular septal defect occur early in cardiac morphogenesis at or shortly after partitioning of the truncoconal part of the heart but before closure of the ventricular septum. Conversely, they suggest that PA and IVS probably occur after cardiac septation. For some forms of hearts with PA and IVS, it is possible that their conclusions about the timing of maturational arrest are correct, specifically

for patients with PA and IVS, a nearly normal-sized right ventricle, and an imperforate “tricuspid” pulmonary valve whose commissures are completely fused.

Embryologically, this defect must occur after ventricular septation is complete as the septum is, by definition, intact. An abnormality of intracardiac blood flow may result in atresia of the valve, thus further altering blood flow and ventricular growth. Animal experiments have demonstrated that reduced flow to a heart structure, even late in gestation, can have devastating effects on the development of associated structures (16,17). The concept is further evidenced by current (as yet unproven) experimental fetal interventional strategies for treatment during pregnancies that are aimed at restoring normal flow patterns in an effort to promote growth or prevent regression of cardiac chamber size. While human fetuses with PA and IVS demonstrate abnormalities in intracardiac blood flow, the specific etiology of the blood flow abnormality remains unknown.

The tricuspid valve in this condition usually is abnormal. This makes intuitive sense as any blood entering the fetal right ventricle has no egress; hence it must regurgitate. The annulus may become hypoplastic, the leaflets of the valve abnormal, and the chords supporting the valve malformed or damaged due to the high pressures in the ventricle created by the lack of an egress of blood from the right heart. Once the valve begins to leak, it is further altered structurally by turbulent flow.

Another very important prognostic feature concerns the presence or absence of ventriculocoronary connections and coronary artery abnormalities. Conceptually, if the pressure is very high in the right ventricle and the blood has nowhere to go, the ventricle can develop these connections to partially decompress in fetal life. Once these connections have formed, they have not been demonstrated to disappear. Shear forces created by blood flowing at high pressure within these connections can result in progressive stenosis and interruption of the coronary arteries that effectively renders the circulation of major portions of heart muscle dependent on flow from the right ventricle. This is recognized after birth as a “right ventricular-dependent coronary circulation” and in its worst form is an absolute contraindication to decompressing the right ventricle by surgery or transcatheter methods.

The pulmonary valve is derived from endocardial tissue within the conotruncus. Abnormalities in morphology of the pulmonary valve can result from failure of normal development of the valve itself. In this setting, the valve consists of the usual three leaflets, but they have markedly thickened abnormal cusps of myxomatous tissue. It often is accompanied by abnormalities of the valve annulus and the sinotubular junction. These types of valve abnormalities have been linked to genetic conditions such as Noonan syndrome and Williams syndrome as well as environmental exposures such as rubella. Here the problem clearly occurs early as a result of abnormal formation of the valve itself. This is in contrast to the valve that has been subject to abnormalities of flow after it has developed where the leaflets are thickened and fused together with a near-normal-appearing sinotubular junction.

PATHOLOGY AND PHYSIOLOGY

Gross External Inspection

The heart may be only mildly enlarged, or it may be massively enlarged, with a hugely dilated right atrium occupying much of the right hemithorax. In this latter situation, the lungs may be compressed by the enlarged heart and may exhibit a varying degree of hypoplasia. When the heart is only mildly enlarged, the course of the anterior descending coronary artery in the anterior interventricular sulcus outlines a smaller than normal

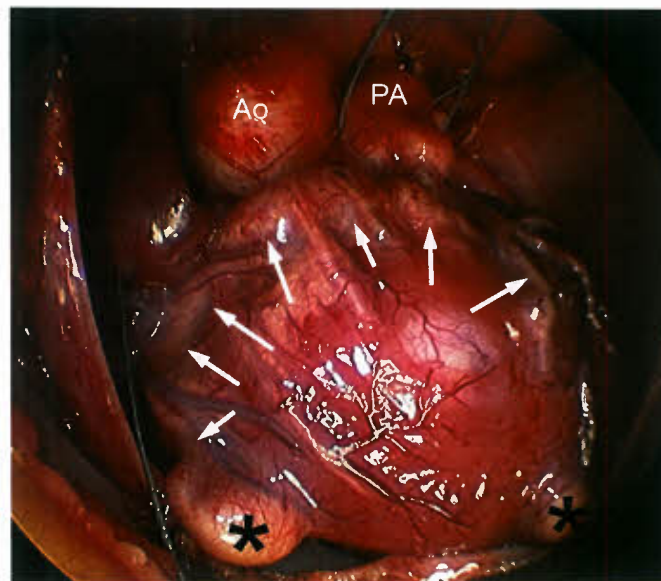


Figure 41.1. Intraoperative photograph of the epicardial surface of the heart of a patient with pulmonary atresia and intact ventricular septum with right ventricle to coronary connections. The coronary arteries are dilated (arrows) with aneurysmal dilation (asterisk).

right ventricle. The right atrium usually is somewhat enlarged, accounting for the cardiomegaly. The right ventricle may be profoundly thinned, and this may be apparent even with the heart in situ.

From external inspection of the heart, there may be obvious clues that there are significant abnormalities of the coronary artery circulation. The coronary arteries may be obviously thickened and nodular, and rarely the coronary arteries may be seen connecting with the pulmonary trunk. Severe abnormalities may be readily apparent with epicardial aneurysmal dilation (Fig. 41.1). So-called dimples may be observed on the epicardial surface of the heart, usually, but not exclusively, in association with the subepicardial coronary arteries. Such dimples may be considered the external stigmata of ventriculocoronary connections and may indicate the site of such connections.

Nature of the Pulmonary Atresia

Braunlin et al. (18) documented the morphologic bases for PA in this disorder, correlating the type of imperforate pulmonary valve with the character of the right ventricle and its infundibulum. In patients with a well-formed infundibulum, the imperforate pulmonary valve exhibits three semilunar cusps with complete fusion of the commissures (Fig. 41.2). The pulmonary valve is primitive in patients with a diminutive right ventricle and a severely narrowed or atretic infundibulum. The muscular nature of the infundibulum has received both morphologic and clinical and angiocardiographic attention, and the nature of those right ventricular muscle bundles contributing to the infundibular atresia has been described.

Great Veins, Atrial Septum, Coronary Sinus, and Venous Valves

A peculiar relationship exists between persistent right venous valve, ventriculocoronary connections, and PA/IVS. It would be too simplistic, indeed incorrect, to speculate that a persistent venous valve is causal to right-sided heart hypoplasia. The

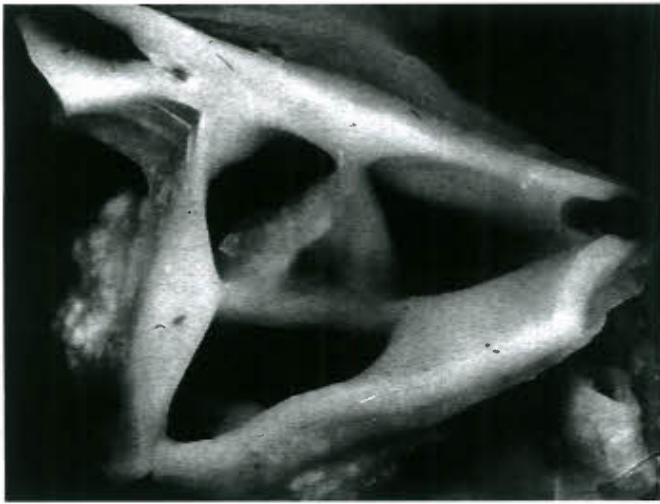


Figure 41.2. Appearance of pulmonary valve in a patient with pulmonary atresia and intact ventricular septum. The valve leaflets are reasonably well identified.

coronary sinus usually terminates in the right atrium. Stenosis and atresia of the coronary sinus ostium have been observed, with decompression through an unroofed coronary sinus–left atrium fenestration.

Because of the obligatory right-to-left shunt at atrial level, with rare exception, there is either a patent foramen ovale or true secundum atrial septal defect. Premature closure of the foramen has been observed in this disorder, usually with fetal death. Rarely, if the interatrial septum is intact or nearly so, alternative pathways for systemic venous return have been recognized, including coronary sinus–left atrial fenestration. The septum primum may assume aneurysmal proportions in patients with a restrictive atrial septal defect, and its herniation through or obstruction of left ventricular inflow has been observed.

Tricuspid Valve

The tricuspid valve rarely is normal in patients with PA and IVS. This atrioventricular valve demonstrates the continuum of abnormalities and a functional impact that ranges from extreme stenosis to profound regurgitation (19) (Fig. 41.3). The stenotic valve can demonstrate a hypoplastic obstructive annulus that may be muscularized with a very abnormal valve apparatus consisting of a thickened free valve margin, shortened dysplastic chordae, and papillary muscle abnormalities. The severely regurgitant valve can be characterized by a dilated annulus. In this situation, the valve exhibits both profound displacement similar to the severest form of Ebstein anomaly and dysplasia. In some severely regurgitant valves, the valve is not displaced but it is extremely dysplastic. Rarely, the valve orifice may be virtually unguarded, a situation similar to profound Ebstein anomaly (20). The most severely stenotic and obstructive tricuspid valve is observed in patients with the most hypoplastic of right ventricles. Conversely, patients with a large right ventricle usually have severe tricuspid regurgitation with a valve exhibiting features of Ebstein anomaly and dysplasia. This latter malformation represents a major management challenge with a poor overall prognosis.

Right Ventricle

Clinicians and pathologists have attempted to characterize the size of the right ventricle in this disorder for decades.

Methodologies have included angiocardiographic volumetric analysis, a variety of measurements of the inlet/outlet axis, and the convention advocated by the Congenital Heart Surgeons Study (CHSS), that is, the use of the so-called tricuspid diameter Z value (5). This is the diameter of the tricuspid valve normalized to body surface area and was based on an early pathologic study of the normal quantitative anatomy. Data from the CHSS showed that the Z value of the tricuspid valve was correlated with the size of the right ventricular cavity ($r = 0.68$, $p < 0.0001$), and this relationship has been confirmed in more recent studies as well (21). This continues to be referenced to the present day.

Others have advocated a semimorphologic approach to the right ventricle. Although there is no consensus as to whether the morphologically right ventricle is embryologically a bipartite or tripartite structure, there are examples of congenitally malformed hearts that may support the view of the right ventricle as a tripartite structure. Taking this latter approach, the normal right ventricle can be considered to be composed of confluent inlet, apical trabecular, and outlet components. This approach has been used widely in the categorization of patients with PA and IVS. Thus, some patients have PA and IVS, wherein the right ventricle is particularly well formed and all three components are well represented. In others, the right ventricle is extremely underdeveloped and seemingly limited to an inlet only (22) (Figs. 41.3C–E and 41.4). Attempts to characterize the size of the right ventricle are plagued by difficulty in assessing the contribution of muscular hypertrophy of the apical and outlet myocardium (23). This has tremendous impact on clinical management as it appears that relief of outflow tract obstruction with associated pulmonary insufficiency may result in remodeling with regression of hypertrophy that can result in real or perceived growth of the right ventricle (23–30).

Left Atrium, Left Ventricle, and Aortic Valve

The left atrium usually receives the pulmonary veins in a normal fashion, although one or more pulmonary veins may connect anomalously to the systemic circulation. The left ventricle may exhibit variable degrees of hypertrophy, especially in patients who survive past infancy. Some years ago, attention was given to a convexity of the outlet portion of the interventricular septum that occurred in those patients with small and extremely hypertensive right ventricles (Fig. 41.5). In this setting, severe left ventricular outflow tract obstruction resulting in death occurring after surgical creation of a cavopulmonary connection has been observed when there is an unfavorable change in the ratio between left ventricular mass and end-diastolic volume (31,32). Aortic valve stenosis has been described in patients with PA and IVS, including the neonate with critical aortic stenosis and the somewhat older child with severe aortic valve stenosis (33). With rare exceptions, the aortic arch is left sided.

Pulmonary Circulation

Confluent pulmonary arteries usually receive flow from a left-sided ductus arteriosus. Rarely, nonconfluent pulmonary arteries are supported by bilateral ductus arteriosus or aortopulmonary collaterals (34). A main pulmonary trunk almost always is present. Unlike the patient with PA *with* ventricular septal defect, the caliber of the pulmonary arteries in patients with PA and *intact* ventricular septum is rarely a major determinant of outcome. This may be in part mediated by the observation that the arterial duct tends to close earlier in patients with PA and intact septum than it does in patients with PA and ventricular septal defect (35). More recently, transcatheter

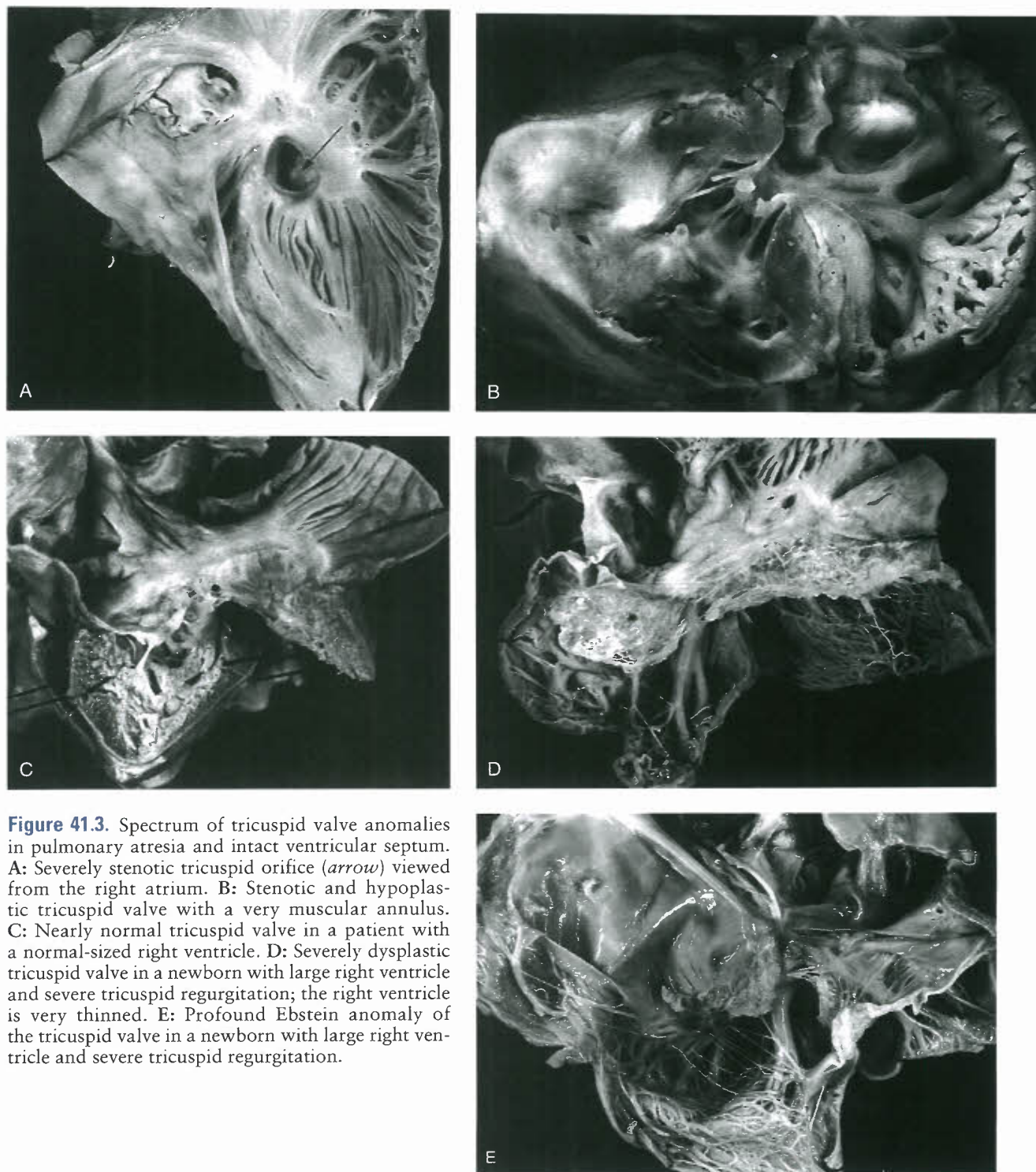


Figure 41.3. Spectrum of tricuspid valve anomalies in pulmonary atresia and intact ventricular septum. **A:** Severely stenotic tricuspid orifice (*arrow*) viewed from the right atrium. **B:** Stenotic and hypoplastic tricuspid valve with a very muscular annulus. **C:** Nearly normal tricuspid valve in a patient with a normal-sized right ventricle. **D:** Severely dysplastic tricuspid valve in a newborn with large right ventricle and severe tricuspid regurgitation; the right ventricle is very thinned. **E:** Profound Ebstein anomaly of the tricuspid valve in a newborn with large right ventricle and severe tricuspid regurgitation.

means of maintaining pulmonary blood flow such as stenting of the arterial duct have necessitated increased awareness of the assessment of the neonatal anatomic details of the pulmonary artery at the insertion of the patent ductus arteriosus (36–39).

Myocardial Abnormalities

The myocardium of patients with PA and IVS can demonstrate a wide range of abnormalities. Ischemia, fibrosis, infarction,

and myocardial rupture have been observed in these patients (40–45) (Fig. 41.6). Other abnormalities include myocardial disarray, the appearance of so-called spongy myocardium, and ventricular endocardial fibroelastosis. In this regard, an inverse relationship exists between ventricular endocardial fibroelastosis and extensive ventriculocoronary communications. Perhaps this observation is fundamental to the frequent finding of ventriculocoronary connections in PA and IVS: dense, “sugar-coated” right ventricular endocardial sclerosis is uncommon. Conversely, dense, sugar-coated left ventricular

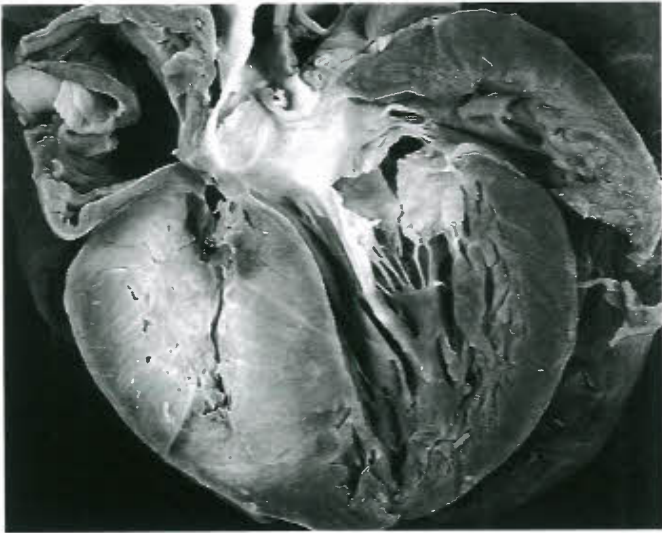


Figure 41.4. Severe right ventricular underdevelopment in a patient with pulmonary atresia and intact ventricular septum. Severely hypoplastic right ventricle with free-wall and septal hypertrophy (see also Fig. 41.2C–E).

endocardial sclerosis is common in patients with a hypoplastic left heart syndrome; but a perforate mitral valve, and thus ventriculocoronary connections, is uncommon. The right ventricular myocardium may be particularly thinned in babies with severe tricuspid regurgitation.

Coronary Arteries

It is important to gain an understanding of the status of the coronary circulation in patients with PA and IVS prior to proceeding with an interventional algorithm because myocardial ischemia may be related to the presence and extent of these ventriculocoronary connections. An extensive literature has documented the vast array of changes in the coronary arteries among some patients with PA and IVS (46–50). Several articles have characterized the histopathologic

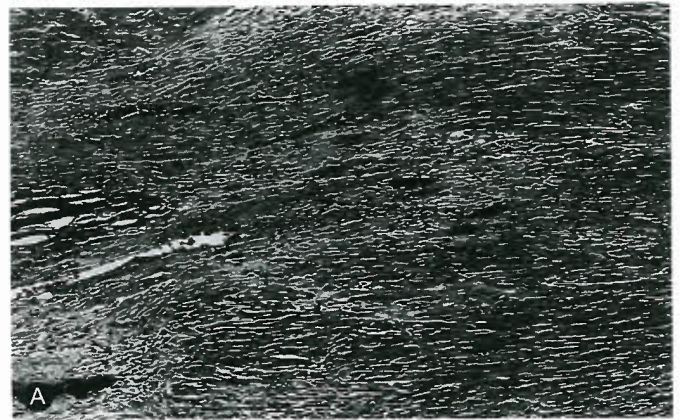


Figure 41.6. Myocardial abnormalities seen in some patients with pulmonary atresia and intact ventricular septum. A: Acute myocardial infarction with rich inflammatory infiltrate and loss of cellular integrity. B: So-called spongy myocardium with endothelial-lined vascular lakes.

alterations of the involved coronary arteries. This process is not characterized by inflammation, as once thought, but more appropriately as myointimal hyperplasia with a rich background of glycosaminoglycans. There is a wide spectrum of histopathologic lesions of both the extramural and intramural coronary arteries. These lesions range from mild degrees of intimal and medial thickening in which a continuous internal elastic lamina and normal lumen is present to a loss of normal arterial wall morphology with replacement of the arterial wall by fibrocellular tissue containing irregular, unorganized elastin strands and severe stenosis or obliteration of the arterial lumen. Some have designated these changes as fibroelastosis of the coronary arteries, but emphasis would be more appropriately focused on myointimal hyperplasia. Staining for glycosaminoglycans shows the prominence of ground substance formation by the activated smooth-muscle cells rather than the reduplicated elastica and collagen characteristic of fibroelastosis (Fig. 41.7). This pathologic process leads to a profound distortion of the normal architecture, eventuating in endothelial irregularity, stenosis, or interruption. Such coronary arterial involvement occurs only in patients with ventriculocoronary connections and, by inference, with a hypertensive right ventricle. The pathogenesis of these arterial lesions likely is predicated on the repeated and sustained injury to the coronary arterial intima from high-pressure right ventricular systolic turbulent blood flow mediated by the presence of the ventriculocoronary connections. Intramural or extramural coronary arteries remote



Figure 41.5. Note septal convexity (*asterisk*) in a patient with pulmonary atresia and intact ventricular septum. It has the potential for promoting left ventricular outflow tract obstruction after Fontan repair.



Figure 41.7. Spectrum of severe coronary arterial lesions in infants with pulmonary atresia and intact ventricular septum. **A:** Virtual obliteration of coronary arterial lumen by a rich cellular process. **B:** Obliteration of extramural coronary arteries in a different patient with a right ventricular–dependent coronary circulation.

from the ventriculocoronary connections do not demonstrate these arterial lesions, nor do hearts not exhibiting ventriculocoronary connections. These lesions have been found in fetal hearts with PA and IVS and in hearts of the immediate newborn. Ventriculocoronary connections do not occur in thin-walled, low-pressure right ventricles.

The coronary abnormalities in patients with PA and IVS embrace the same spectrum of abnormalities as those seen in patients with otherwise normal hearts, including abnormalities of origin, epicardial course, and number. A single coronary artery may originate from the aorta or, rarely, from the pulmonary trunk. Many congenital and acquired conditions of the coronary circulation are specific to PA and IVS and impact surgical management. These conditions include an absence of a proximal aortocoronary connection between one or both coronary arteries, coronary arterial stenosis or interruption, or a so-called coronary–cameral fistula with a major fistula between the right or left coronary artery and the right ventricle. Peculiar arterial connections such as those from the descending thoracic aorta or the gastric artery to the coronary circulation very rarely have been described.

Right Ventricular–Dependent Coronary Artery Circulation

Intrinsic to awareness of ventriculocoronary connections in this disorder and their impact on the myocardium is the concept of a right ventricular–dependent coronary artery

TABLE 41.1 **A Right Ventricular–Dependent Coronary Circulation**

Coronary artery abnormalities requiring right ventricular blood flow:

- Absent aortocoronary connections
- Coronary artery interruption or stenosis
- Profound coronary–cameral steal or fistula

circulation (Table 41.1). In the normal circulation, it is in large part the aortic diastolic pressure that is the driving pressure for coronary blood flow. Factors that reduce aortic diastolic pressure or shorten diastole will compromise coronary blood flow. The presence of ventriculocoronary artery connections may promote coronary artery stenosis and interruption, and aortic diastolic pressure may not be sufficient to drive coronary blood flow when obstructive lesions are present within the coronary circulation. It is important to remember that these infants are hemodynamically fragile, tachycardic, and often receiving prostaglandin or palliated with a systemic-to-pulmonary artery shunt to augment pulmonary blood flow. Notably these therapeutic maneuvers also will reduce aortic diastolic pressure. Therefore, retrograde coronary blood flow from the hypertensive right ventricle occurring during systole and mediated by the ventriculocoronary connections may be necessary to sustain adequate myocardial perfusion. In a coronary circulation that is wholly or in part right ventricular dependent, it is the blood that gets into the right ventricle at systemic or above-systemic right ventricular systolic pressure that supplies the dependent myocardium in a retrograde fashion. Unfortunately, this process can lead to further coronary arterial distortion. The management corollary to this is clear: interference with blood flow into the right ventricle or reduction of right ventricular systolic pressure in situations in which the coronary circulation is right ventricular dependent may result in myocardial ischemia, infarction, and death.

There is unequivocally a predisposition to ventriculocoronary connections among patients who have the smallest right ventricles. Thus, it is unlikely but not impossible to define such abnormal communications in patients with a normal-sized right ventricle or with a nearly normal right ventricle (51). It is much more likely to observe ventriculocoronary communications in patients whose ventricles have been categorized as unipartite or bipartite. Using the convention of the tricuspid Z value, data from the CHSS demonstrated a positive correlation with ventriculocoronary connections: a negative tricuspid Z value correlates with the presence of ventriculocoronary connections. Data from this study support the observation that the smallest tricuspid valve (i.e., the most negative Z value) is observed in patients with the smallest right ventricle (5). Data provided by the CHSS indicated that, of the 145 patients for whom this information was available, ventriculocoronary connections were observed in 45%. In 9% of the 145 patients, the coronary circulation was considered wholly right ventricular dependent. Ventriculocoronary connections may involute after successful right ventricular decompression (whether by pulmonary valvotomy or tricuspid valve excision or avulsion). Such involution has been demonstrated in the newborn and in the older patient. With reduction in right ventricular pressure, there is always the possibility that flow from the coronary artery to the right ventricle might occur or become exaggerated, and this phenomenon has been recognized.

Perhaps of more concern is determination of the timing of the occurrence of coronary arterial obstructive lesions, coronary artery stenosis, or interruption. Such coronary arterial obstructive lesions can occur in fetal tissues, and these lesions have been identified clinically by both angiography and histopathology in hearts from patients who die in the first few hours and days after birth. Thus, such changes should not be interpreted as a later, acquired postnatal phenomenon (47). Obviously, some changes may be acquired late, but clearly obstructive coronary arterial lesions may be identified in the immediate newborn.

CLINICAL FEATURES

Physical Examination

Newborns with PA and IVS become cyanotic and hypoxemic coincident with functional and anatomic closure of the patent arterial duct. In the rare patient in whom the interatrial communication is truly restrictive, the cardiac output may be affected as well by restricting the obligatory right-to-left shunt.

There is no known sex predilection, and there is no identified genetic predisposition, although familial cases have been described as well as an occurrence in monozygotic twins (52). It has been assigned to a single gene theory in at least one instance (53). Infants typically are born at term. Cyanosis usually is apparent within hours of birth and is progressive. Dyspnea is not conspicuous without significant acidosis, reduced cardiac output, or pulmonary hypoplasia, but tachypnea may be prominent.

In the absence of profound cardiac enlargement, the left precordium will not bulge. The left ventricle may be enlarged, and at the apex, its impulse may be forceful. The first and second heart sounds are single. A pansystolic murmur often is audible at the left lower sternal border, consistent with tricuspid regurgitation. In infants with severe tricuspid regurgitation, the murmur of tricuspid regurgitation is conspicuous, sometimes associated with a thrill, and a tricuspid diastolic rumble may be audible. A murmur of the arterial duct may be distinguished in the second and third left intercostal space, especially after prostaglandin has been administered to promote ductal patency. Unless the atrial septum is profoundly restrictive, affecting cardiac output, the caliber of the arterial pulses is normal. The liver is not particularly enlarged unless there is severe tricuspid insufficiency or a restrictive foramen ovale.

The most striking and consistent finding before prostaglandins are administered is hypoxemia refractory to increased inspired oxygen concentration and a mild degree of hypocarbia, reflecting the tachypnea. Significant metabolic acidosis usually indicates progressive hypoxic cellular damage signifying imminent death in the absence of intervention.

Radiographic Features

The chest radiograph may demonstrate a heart that is only mildly enlarged or one that fills the entire chest cavity. In the former, the pulmonary vascular markings are reduced, which may be confirmed on the lateral radiograph, where hilar pulmonary arterial markings are sparse. In the latter situation, with massive cardiomegaly, it may be difficult to define enough pulmonary parenchyma to evaluate the lung markings. The differential radiographic diagnosis of extreme cardiomegaly in the newborn includes the conditions shown in Table 41.2.

TABLE 41.2 Differential Diagnosis of Massive Cardiomegaly in the Newborn

Pulmonary atresia and Ebstein anomaly
Ebstein and functional pulmonary atresia
Aortic atresia, AV and VA discordance, and severe left AV valve regurgitation
Functional aortic atresia, AV and VA discordance, and severe left AV valve regurgitation
Intrapericardial teratoma

AV, atrioventricular; VA, ventriculoarterial.

Electrocardiographic Features

The classic electrocardiogram shows normal sinus rhythm, a frontal QRS axis of +30 to +90, a paucity of right ventricular forces, left ventricular dominance or left ventricular hypertrophy, and right atrial enlargement. There frequently are abnormalities of the ST-T segments, consistent with some degree of subendocardial ischemia. The differential diagnosis based on the electrocardiogram is shown in Table 41.3. The differential diagnosis of a cyanotic baby with a soft systolic murmur, mild cardiac enlargement, and oligemic lungs is fairly extensive (Table 41.4).

Echocardiographic Features

Although echocardiography has been advocated as the imaging modality for the diagnosis and treatment of many forms of neonatal congenital heart disease, both echocardiography and angiocardiology are often required for a complete evaluation of this disorder. It is not that echocardiographer cannot make the diagnosis of PA and IVS. Rather, important consideration in the treatment algorithm of neonates with PA and IVS is given to the presence of right ventricular to coronary artery connections and a right ventricular-dependent coronary circulation, especially if one is considering decompressing the right ventricle by creating continuity between the right ventricle and the pulmonary circulation. Identification of the extent of ventriculocoronary connections can be difficult by echocardiography. Echocardiographic imaging has not allowed one to identify reliably coronary arterial stenosis or interruption in neonates. As a result of these limitations, angiocardiology can be very important in infants with severe hypoplasia of the right ventricle, in whom a high incidence of ventriculocoronary artery connections is anticipated. Because ventriculocoronary connections have been observed in the

TABLE 41.3 Differential Diagnosis of Paucity of Right Ventricular Forces and LV Dominance/LVH on Scalar Electrocardiogram

Pulmonary atresia and intact ventricular septum
Tricuspid atresia
Double-inlet left ventricle

LV, left ventricular; LVH, left ventricular hypertrophy.

TABLE 41.4

Differential Diagnosis of a Cyanotic Neonate with Soft Systolic Murmur, Mild Cardiomegaly, and Oligemic Lungs

Pulmonary atresia and intact ventricular septum
Critical pulmonary stenosis
Tetralogy of Fallot
Pulmonary atresia with ventricular septal defect
Tricuspid and pulmonary atresia
Complex univentricular atrioventricular connection and pulmonary atresia
Hearts with right atrial isomerism and pulmonary atresia or pulmonary stenosis

patient even with a normal-sized right ventricle, all patients should undergo angiocardigraphic imaging prior to ventricular decompression. This is not intended to underestimate the importance of echocardiography as a primary diagnostic tool in those neonates with PA and IVS. Indeed, the initial therapeutic plan often is dictated by echocardiographic findings (Figs. 41.8–41.13).

It is important to ascertain the functional status of the interatrial septum as the neonate relies on obligatory right-to-left shunting to maintain cardiac output. The interatrial communication can be assessed readily by the subcostal approach with a combination of imaging and Doppler interrogation. The atrial septum rarely may assume aneurysmal proportions, with septum primum herniating through the mitral valve. The size and morphology of the tricuspid valve must be assessed. It may be difficult to detect forward flow across an extremely stenotic, obstructive tricuspid valve and patency may be determined best by the identifying tricuspid regurgitation. In the absence of Doppler detection of tricuspid regurgitation, the question of patency cannot always be resolved. The right ventricular size, which usually corresponds to the dimension of the tricuspid annulus, can be imaged by a combination of subcostal and precordial views. Absolute volume measurements are of limited value at the present time, although in the future,

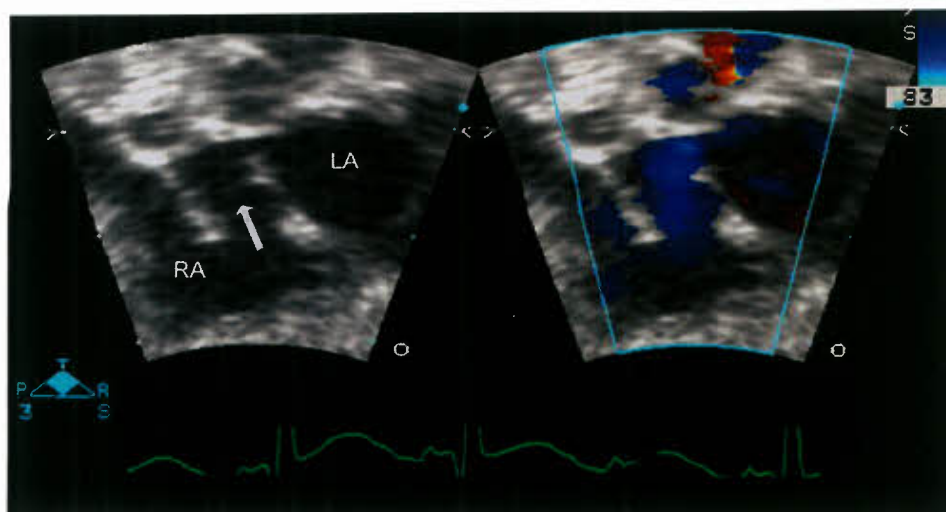
three-dimensional echocardiography may provide further insights. Hypoplasia, if present, may involve all components of the right ventricle. Although the noninvasive identification of pulmonary infundibular and valve atresia is recognized readily (Figs. 41.9 and 41.11), it may be difficult to distinguish isolated valve atresia from extremely severe stenosis. Even with the application of Doppler echocardiography, this issue remains a problem because ductal flow potentially can mask a small jet of forward flow.

It is important to distinguish anatomic from functional PA. In the former, the pulmonary valve is anatomically imperforate, whereas in the latter, the lack of forward flow is due to high pulmonary artery pressure with poor right ventricular function or very severe tricuspid insufficiency. In general, the pulmonary valve is morphologically normal but functionally closed. As discussed previously, it also is possible to have anatomic valve atresia with extreme tricuspid regurgitation and a low right ventricular pressure, hence the importance of differentiating the two conditions. With the use of Doppler echocardiography, it is possible to do this by detecting systolic regurgitation of the pulmonary valve, which is caused by a jetting effect of the patent ductus arteriosus against the valve (Fig. 41.12). This is not observed in patients with anatomic pulmonary valve atresia. Another technique is through the use of Doppler echocardiography during positive pressure ventilation, which transiently results in opening of the pulmonary valve and forward Doppler flow. Finally, an attempt to document coronary artery connections from the right ventricle should be made, recognizing that this can be difficult (Fig. 41.13) (54).

Cardiac Catheterization

If one is considering decompression of the right ventricle, then a full hemodynamic and angiocardigraphic investigation is required for the interventional management of the neonate with PA and IVS. Although one can recognize echocardiographically the presence of large ventriculocoronary connections or fistulae, this technique does not allow for the recognition of coronary artery stenosis or interruption, both of which have been documented in the newborn. Significant coronary artery abnormalities with a right ventricle dependence for myocardial flow has been predicted by an evaluation of the size of the tricuspid valve relative to the patient size with a Z-score of < -2.5 predicting clinically important

Figure 41.8. Subcostal echocardiographic view in pulmonary atresia and intact ventricular septum demonstrating an interatrial communication with an aneurysmal flap; color Doppler (right panel) shows right-to-left shunting in blue. LA, left atrium; RA, right atrium; arrow, patent foramen ovale.



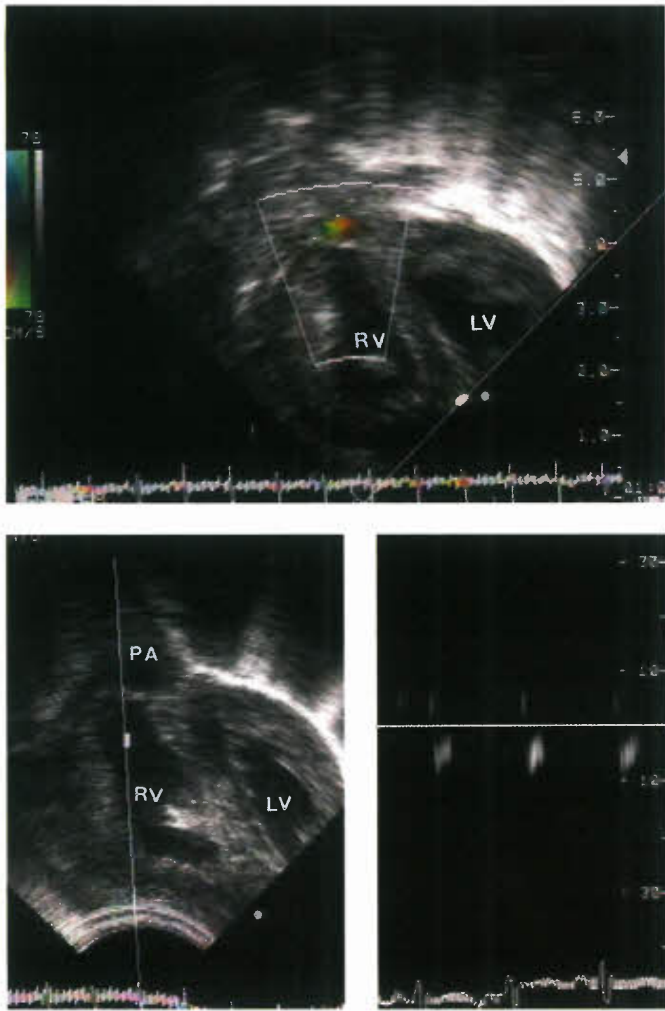


Figure 41.9. Subcostal view demonstrating an imperforate valve that was subsequently dilated at cardiac catheterization. Note the lack of forward flow in the infundibular region. **Upper panel:** Color flow Doppler. **Lower panel:** Confirmed with pulsed Doppler LV, left ventricle; PA, pulmonary artery; RV, right ventricle. (Figs. 41.8 through 41.11 kindly provided by Dr. Jeffrey Smallhorn, Director of Echocardiography, Division of Cardiology, University of Alberta, Canada.)

abnormalities (51). Furthermore, using echocardiography, it may be difficult to document without any doubt those patients with tenuous proximal aortocoronary connections (55).

The level of systemic arterial oxygen saturation data reflects the magnitude of pulmonary blood flow. Before the era of routine administration of prostaglandin, these infants became progressively hypoxemic coincident with functional and anatomic closure of the arterial duct. All these infants experience an obligatory right-to-left shunt at the atrial level. Unless there is pulmonary disease, the pulmonary venous saturation is normal, or nearly so. The administration of prostaglandin, by virtue of its action on the arterial duct and the pulmonary vascular resistance, augments pulmonary blood flow, and thus arterial saturation increases.

The hemodynamic evaluation of the patient with the hypertensive right ventricle establishes right ventricular pressure at or above systemic levels. When dealing with the patient with massive cardiac enlargement, right ventricular pressure may be substantially less than systemic. These patients raise the possibility that the obstruction to pulmonary blood flow reflects functional rather than anatomic PA.

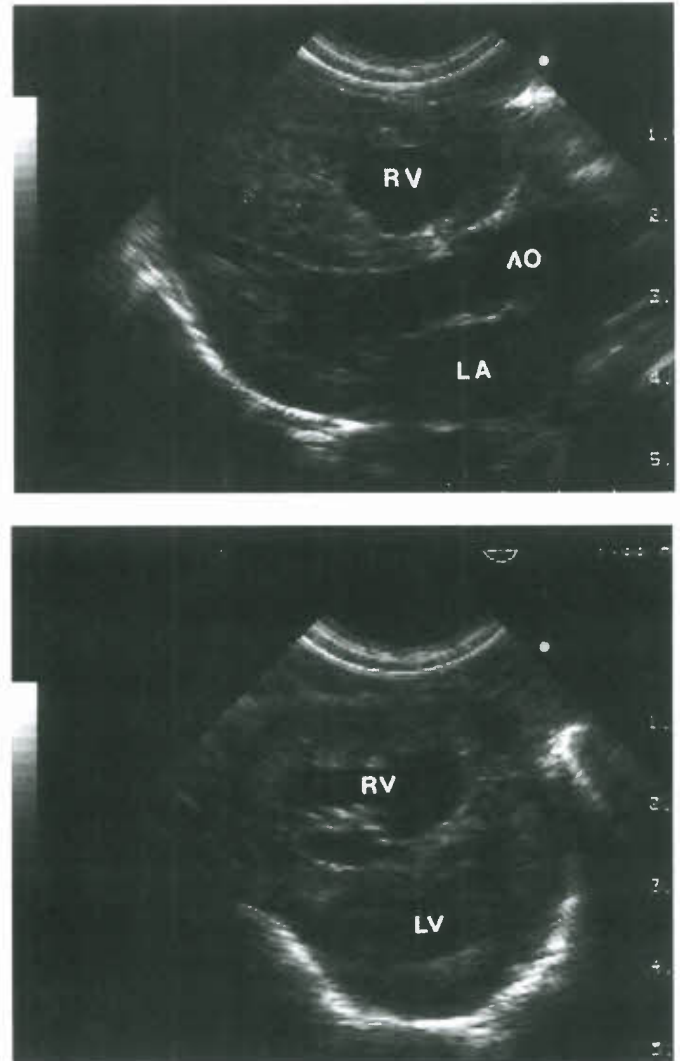


Figure 41.10. The topography of the interventricular septum bowing into the left ventricular outflow tract. **Upper panel:** A precordial long-axis view. **Lower panel:** Short-axis view. AO, aorta; LA, left atrium; LV, left ventricle; RV, right ventricle (see also Fig. 41.4).

In the presence of nonrestrictive interatrial communication, the atrial mean pressures equalize, although there is often a small “a” wave gradient from the right to the left atrium. If true restriction to atrial flow is demonstrated then it is important to consider a balloon atrial septostomy at catheterization to avoid a low cardiac output syndrome, especially if decompression of the right ventricle is not to be included in the therapeutic track. The right ventricle is at systemic levels of pressure or higher, and the end-diastolic pressure may be abnormally high, consistent with a noncompliant ventricular chamber. Alternatively the right-to-left ventricular pressure ratio may be <1 . The finding of a subsystemic right ventricular pressure is consistent with a globally disadvantaged right ventricle. The right ventricle is usually thinned, and severe tricuspid regurgitation often is present. The functional disturbance of severe tricuspid regurgitation correlates with an Ebstein-like abnormality of the tricuspid valve or severe tricuspid valve dysplasia. Rarely, the tricuspid valve may be unguarded, or nearly so.

Angiocardiography remains an important imaging modality in patients with PA and IVS (Figs. 41.14–41.18). Although much of the intracardiac anatomy can be determined from a

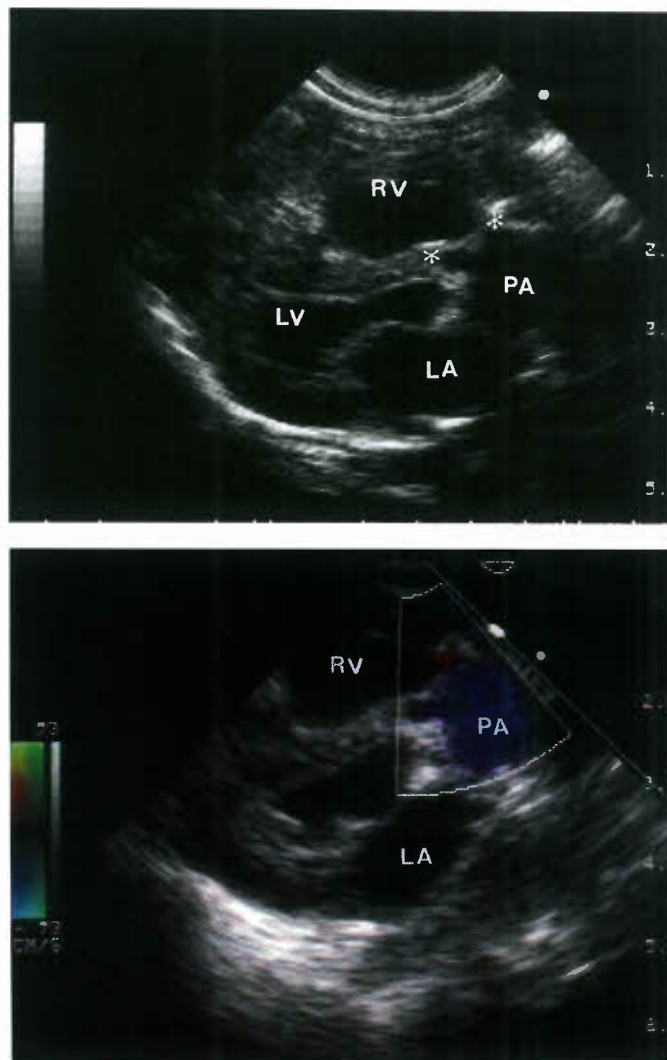


Figure 41.11. The pulmonary outflow tract in this patient with valvar atresia is imaged in the precordial short-axis view with slight clockwise rotation. **Upper panel:** Anatomic pulmonary “annulus”. **Lower Panel:** The possibility of pulmonary insufficiency (red flow) raises the possibility that the valve is severely stenotic and not atretic. LA, left atrium; LV, left ventricle; PA, pulmonary artery; RV, right ventricle; *asterisk*, atretic pulmonary valve.

systematic approach to echocardiography, right ventricular angiocardiography provides information about the form and function of the tricuspid valve, the size of the morphologically right ventricle, the extent of the apical trabecular zone, and the dimensions and degree of expansion of the infundibulum of the right ventricle. Most importantly, right ventricular angiography will define the presence or absence of ventriculocoronary connections. Selective injection of the right ventricular outflow tract can differentiate severe stenosis of the pulmonary valve from membranous atresia (56). Selective left ventricular angiocardiography provides information about the form and function of the left ventricle and aortic valve, and this certainly complements echocardiographic imaging. Aortography in the neonate defines the laterality of the aortic arch, the caliber of the subclavian arteries, the site of insertion of the arterial duct, the caliber of the pulmonary arteries, and coarctation of the pulmonary artery at the insertion of the arterial duct that may preclude treatment with a stent to permanently maintain its patency or require a surgical patch at the time of placing a

systemic-to-pulmonary artery shunt. A balloon occlusion technique performed in the newborn's ascending aorta will allow imaging of the coronary arteries, their origin, epicardial distribution, and caliber changes indicative of stenosis or interruption. In some patients, including newborns, selective coronary arteriography may be necessary to characterize fully the coronary arterial involvement. When right ventricular angiography does not demonstrate ventriculocoronary connections, one can be reasonably certain that coronary arterial stenosis or interruption or major fistulae with coronary–cameral flow will not be evident. In some patients with ventriculocoronary connections, a balloon catheter inflated in the right ventricle or catheter-induced tricuspid insufficiency with concurrent observation of the simultaneous electrocardiographic tracing may unmask a right ventricular–dependent coronary circulation.

The angiocardiographic investigation of the patient with the hypertensive right ventricle requires right ventricular angiocardiography in frontal and lateral projections (Figs. 41.14 and 41.16). Further information can be obtained with angulated views of the right ventricular angiogram in the setting of ventriculocoronary communications (Fig. 41.17). It remains to be seen whether advanced imaging techniques such as three-dimensional rotational angiography will augment the evaluation of coronary pathology in this condition (Fig. 41.19).

TREATMENT

Medical

Immediate attention must be paid to maintaining ductal patency, which can be accomplished by the systemic administration of prostaglandin. The reported surgical survival of 27% prior to the availability of prostaglandins was poor (57). Rarely an urgent balloon atrial septostomy may be required for a restrictive septum as pulmonary flow improves and should be considered in any neonate that demonstrates persistent low cardiac output with the usual therapeutic maneuvers. For the premature infant or the extremely small-for-gestational-age infant, a prolonged course of an E-type prostaglandin may be necessary before surgery is undertaken, although this is unusual in the current surgical era. Once pulmonary blood flow is established, it is important to recognize that systemic oxygen saturation is related to the amount of flow into the pulmonary circulation. A very low pulmonary vascular resistance and conversely high systemic vascular resistance can result in low cardiac output despite a high saturation. The patient has an obligatory right-to-left shunt at atrial level, hence a very high saturation usually reflects an enormous amount of pulmonary flow. The resulting low diastolic pressure and low cardiac output syndrome can result in compromised splanchnic and renal flow as well as ongoing acidosis and, in the extreme, cardiogenic shock. In addition, this physiology can compromise oxygen delivery to the aortocoronary circulation resulting in myocardial ischemia.

Surgical

Surgical and other catheter-based interventional therapies have continued to change with an understanding of the heterogeneity of this disorder. The diagnostic and therapeutic algorithms are now quite diverse, depending on a wide number of morphologic variables (5,58–62). Among some centers, primary cardiac transplantation also is considered particularly when the coronary artery anatomy is complex. In evaluating an individual patient with this disorder and assuming a neonatal presentation, different surgical strategies will be derived for the patient with massive cardiomegaly and a right-to-left

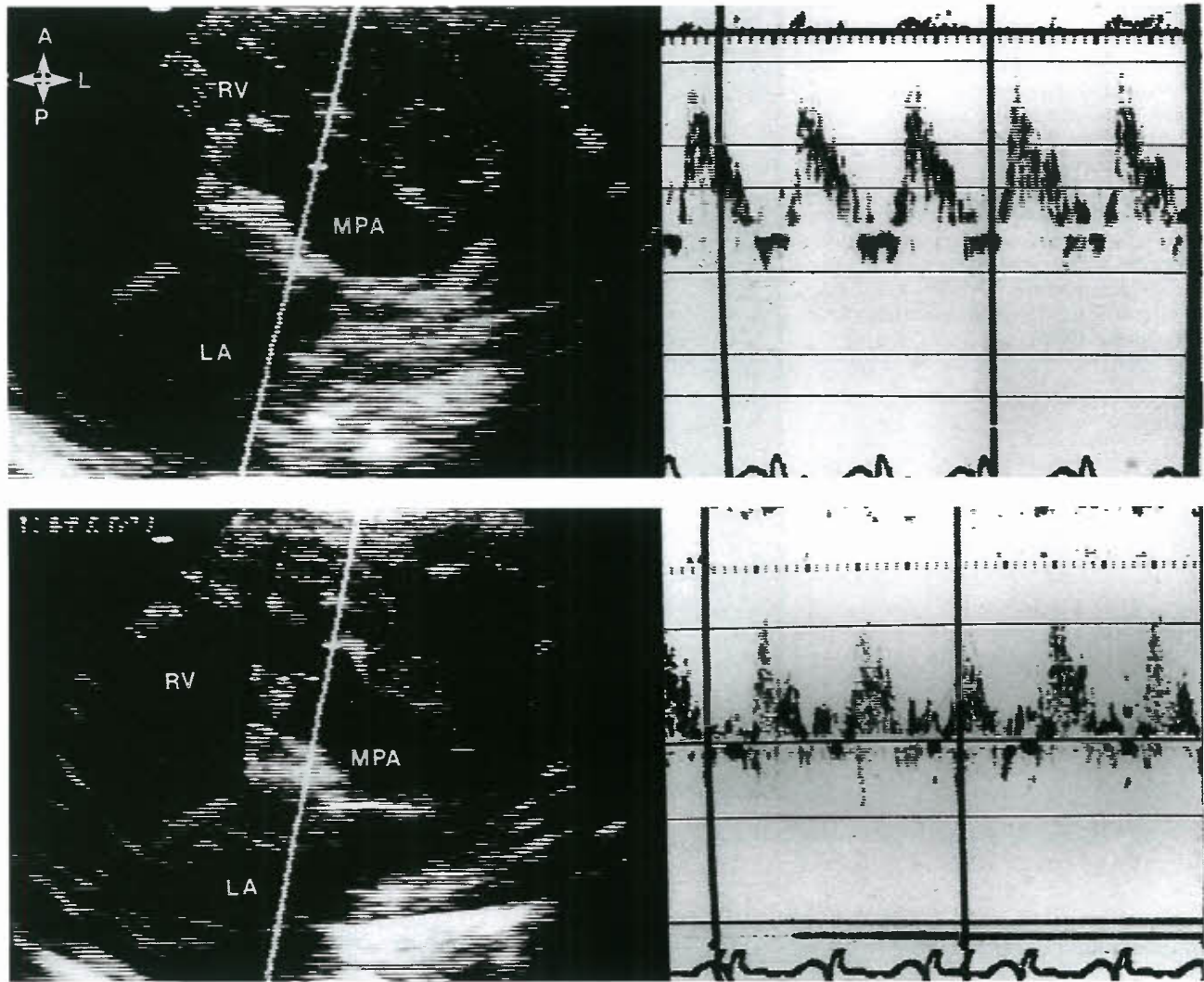


Figure 41.12. Functional pulmonary atresia in a newborn with pulmonary atresia and intact ventricular septum. The upper panel demonstrates retrograde systolic flow in the main pulmonary artery (MPA); the lower panel shows the systolic regurgitation through the pulmonary valve. LA, left atrium; RV, right ventricle.

ventricular pressure ratio below 1.0 than for the neonate with a diminutive right ventricle and ventriculocoronary connections as the former carries with it very poor outcomes.

Most infants with PA and IVS will have some degree of right ventricular hypoplasia and hypertension, and thus the initial surgical considerations should include the following:

1. Is the patient ultimately a candidate for a complete biventricular (including the so-called one-and-a-half ventricle) repair or a univentricular total cavopulmonary (Fontan) palliation?
2. Does the patient have ventriculocoronary connections? If so, how much of the myocardial perfusion is right ventricular dependent?
3. Does the patient have an infundibulum? Is there a main pulmonary trunk in continuity with the imperforate pulmonary valve?
4. Is left ventricular function preserved?

Ideally, one would like to achieve a biventricular repair in these patients, and the initial approach should allow right ventricular decompression by some form of right ventricular outflow tract reconstruction, whether surgical pulmonary valvotomy,

outflow tract patch, or catheter-based perforation and dilation of the pulmonary valve. If there are ventriculocoronary connections and the majority or the entirety of the coronary circulation is right ventricular dependent, clearly the patient should be placed on a univentricular palliation algorithm (63–65).

Data in a small number of patients have suggested that the right ventricle can enlarge if it is satisfactorily decompressed; however, no single institution has a sufficient number of contemporarily treated patients in the current era to provide consistent therapeutic recommendations. When evaluating the literature, it is important to consider whether growth is measured in terms of absolute changes in size or normalized to growth of the individual. Conventional wisdom has suggested that if the right ventricle outlet remains atretic, growth of the right ventricle is unlikely to occur, and thus a two-ventricle heart is unlikely to be achieved (61).

In a prospective, multi-institutional investigation, 171 neonates with PA and IVS were studied between January 1, 1987, and January 1, 1991 (5). Multivariable analysis of the data showed that small diameter of the tricuspid valve, a coronary circulation that was severely right ventricular dependent, birth weight, and date and type of initial surgical procedures were

Figure 41.13. A: Four-chamber apical view depicting a dilated right coronary artery (RCA) in the atrioventricular groove. B: Color flow Doppler of the same image confirms flow within the vessel. C: Sub-costal imaging of the epicardial right coronary artery confirms dilation to suggest increased flow. D: Pulsed Doppler confirms systolic retrograde flow with diastolic antegrade flow in the coronary vessel with connections to the hypertensive right ventricle. LA, left atrium; LV, left ventricle; RA, Right atrium; RV, right ventricle. Red arrows: dilated RCA.

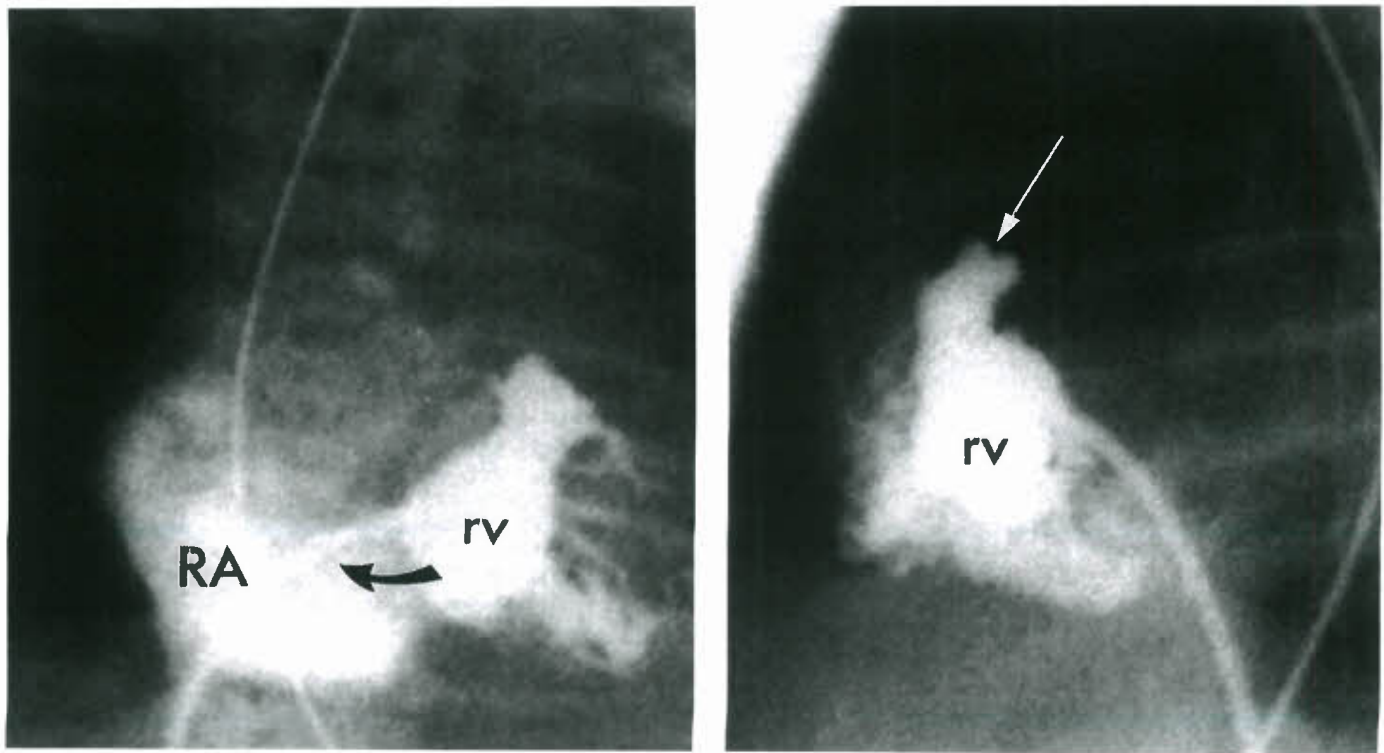
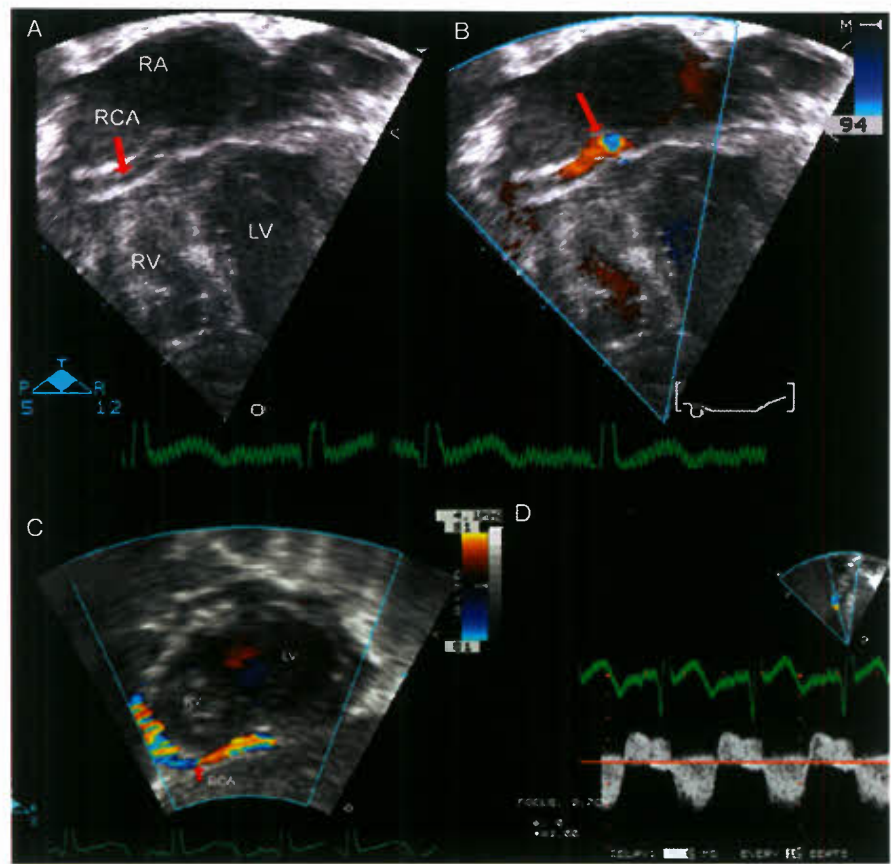


Figure 41.14. Mild right ventricular hypoplasia, but the inlet, trabecular, and outlet zones of the right ventricle are well represented. Note the tricuspid insufficiency (black arrow) and the atretic pulmonary valve (white arrow). Systole (right), diastole (left). RA, right atrium; RV, right ventricle.

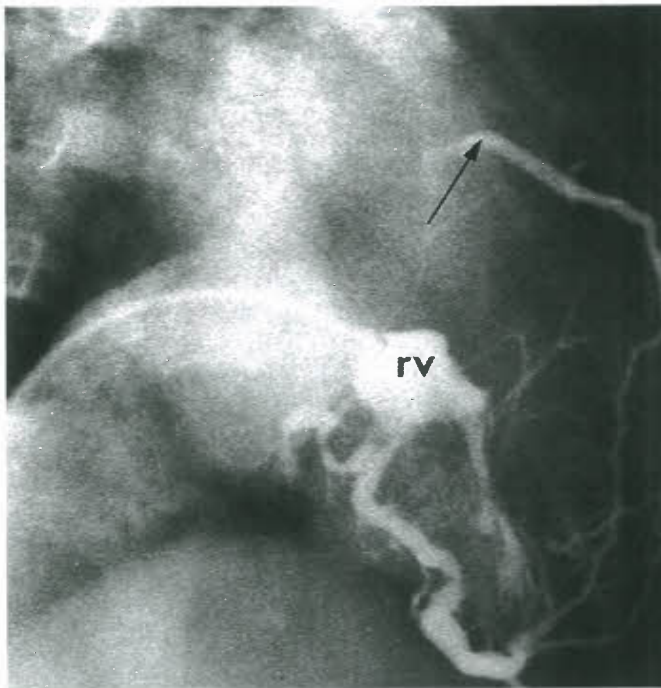


Figure 41.15. This right ventricle (RV) angiogram demonstrates dense opacification of the left anterior descending coronary artery (*arrow*) but no filling of the aortic root. This should be interpreted as consistent with lack of a proximal aortocoronary connection. The diminutive right ventricle is unipartite.

risk factors for time-related death. Data from this study indicated that 49 patients had a surgical valvotomy with or without systemic-to-pulmonary artery shunt as the initial procedure, 42 had a transannular patch, and 71 had only a systemic-to-pulmonary artery shunt. Survival for all procedures was 81% at 1 month after the first intervention and 64% at 4 years. Eighteen percent of living patients had received univentricular palliation within 3 years and 32% a two-ventricle repair. The remainder, 50%, had still incompletely separated pulmonary and systemic circulations. What, then, is the optimal initial surgical therapy? A systemic-to-pulmonary artery shunt has a low initial surgical mortality, but this procedure does not promote the possibility of ventricular growth. Ideally, one would like to perform a valvotomy alone, but many, especially those with a small right ventricle and tricuspid valve, will require a systemic shunt as well. Even many patients treated by initial surgical transannular pulmonary outflow tract repair required an additional shunt.

To survive, some patients will require a combination of a transannular right ventricular outflow tract patch and an arterial shunt as the initial surgical procedures. A proportion of these patients will go on to successful closure of the interatrial communication as well as closure of the shunt, thus resulting in a two-ventricle repair. In others, the tricuspid valve may not grow and repair will have to be combined with a bidirectional cavopulmonary connection, perhaps in concert with pulmonary valve replacement (66,67). In this latter group of patients, it may be necessary to try to balloon-occlude the atrial septal defect temporarily and to measure cardiac output as well as right atrial pressures before, during, and after occlusion. It is likely that a proportion of these patients can be treated in the cardiac catheterization laboratory with

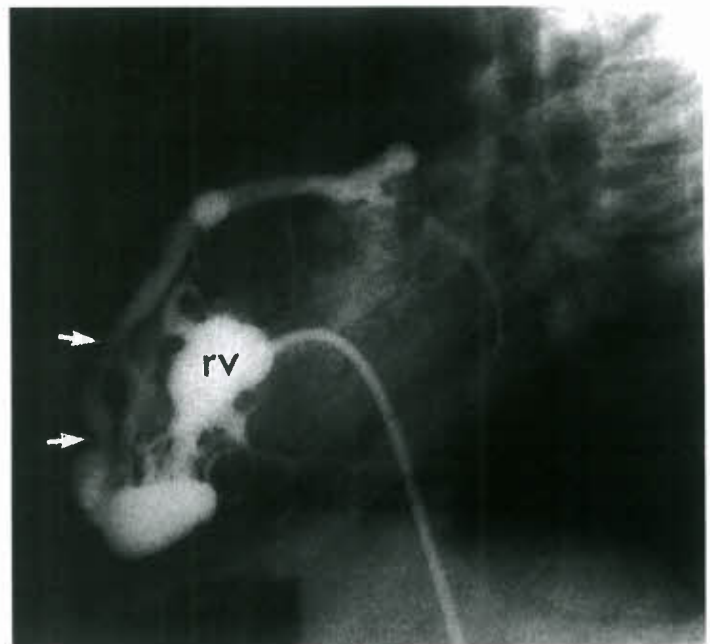
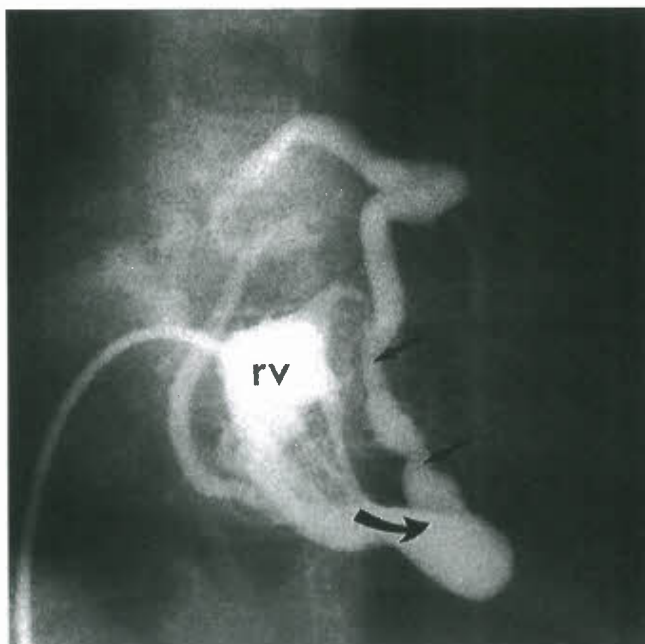
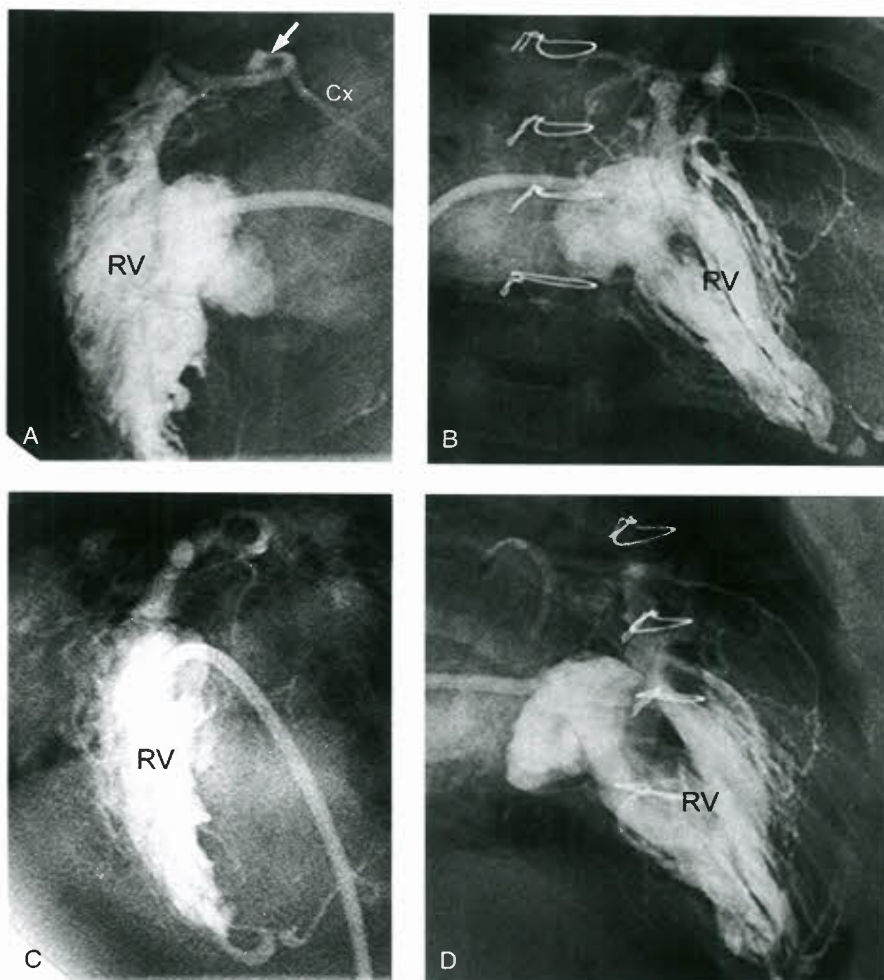


Figure 41.16. A unipartite right ventricle (RV) whose tricuspid Z value was -3.5 . Extensive ventriculocoronary connections are demonstrated by frontal and lateral right ventriculograms. The anterior descending coronary artery demonstrates numerous caliber changes (*arrows*) consistent with arterial obstructions. (See also Fig. 41.6.) The connection from RV to the coronary circulation is noted by the *curved arrow*. Left: anteroposterior view. Right: lateral view.

Figure 41.17. Right ventricular angiograms in a patient with pulmonary atresia and absence of an anterior descending coronary artery. **A:** The lateral projection demonstrates the presence of a communication between the right ventricle and the coronary artery. Unlike Figure 41.14, the ostium of the coronary artery is not atretic (*arrow*). The left main coronary artery continues posteriorly as the circumflex vessel (Cx). **B:** In the frontal projection, the aortic origin of the left coronary artery is obscured; however, a network of fine vessels within the leftward and anterior myocardium is delineated. Left (**C**) and right (**D**) axially angulated projections fail to demonstrate an anterior descending vessel. This was confirmed on subsequent selective angiography.

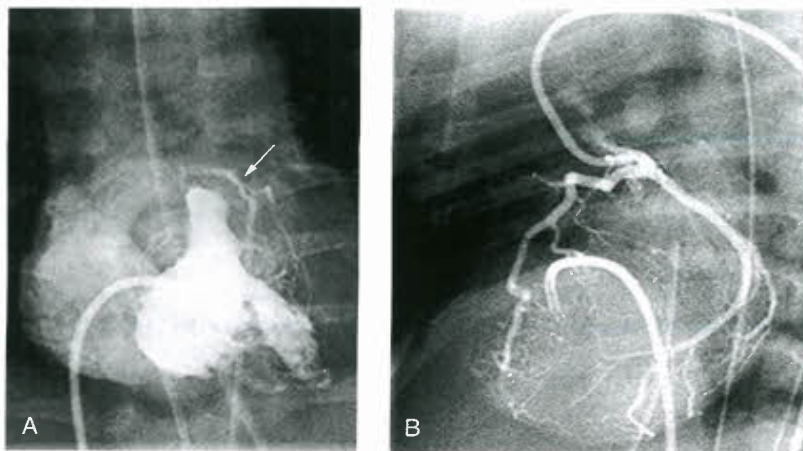


catheter occlusion of the atrial septal defect and occlusion of the systemic-to-arterial shunt. Some patients likely will require a so-called one-and-a-half ventricle repair, with the bidirectional cavopulmonary shunt effectively unloading the small right ventricle and potentially obstructive tricuspid valve. Decompression of the hypertensive right ventricle can be accomplished by removing the tricuspid valve or performing a pulmonary valvotomy. Although both these maneuvers usually are considered within the domain of surgical influence, both can now be accomplished in the cardiac

catheterization laboratory. Most centers have abandoned tricuspid valve avulsion or excision and right ventricular thromboexclusion.

The CHSS database was reviewed for 408 neonates with PA and IVS from 33 institutions (68). Survival for the cohort was 77% at 1 month, 70% at 6 months, 60% at 5 years, and 58% at 15 years. The morphologic heterogeneity is illustrated by the prevalence of described end points at 15 years with 33% achieving a biventricular repair, 20% a univentricular Fontan, 5% a one-and-a-half ventricular palliation, and 2%

Figure 41.18. **A:** Right ventricular angiogram demonstrates the presence of a left coronary artery fistulous connection (*arrow*); however, the extent to which the right ventricle provides exclusive myocardial perfusion is not delineated. **B:** Retrograde selective injection of the left coronary artery in a long-axis oblique projection in the same patient clearly demonstrates the left ventricular myocardium perfused by the aortocoronary supply without significant coronary artery stenosis or occlusion.



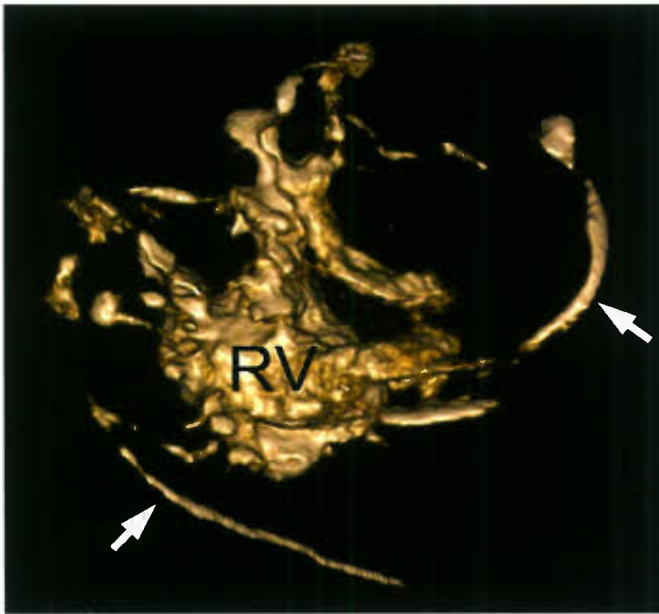


Figure 41.19. Three-dimensional rotational right ventricular angiogram depicting coronary artery connections for the right ventricle (RV). Epicardial coronary arteries (*arrows*) demonstrate interruptions.

a transplantation. A further 2% were alive without definitive repair or palliation, and the remaining 38% died before achieving definitive repair or palliation. Not surprisingly, the end state was predicted by the adequacy of the right-sided structures, the degree of aberrancy of the coronary circulation, a low birth weight, and the degree of tricuspid regurgitation. An important observation was the improved 5-year survival with surgical era reflected by an increase from 49% born to 1987, to 63% in 1992, and to 79% in 1992 to 1997. This improvement in surgical era is also supported by single institutional reviews (69,70). The documented improvement in outcome over time is, most likely, a reflection of improved understanding of neonatal and pediatric physiology and intensive care in the pre- and postoperative management of these medically complex patients and is important to consider when considering the literature.

Management of the Patient Whose Coronary Circulation Is in Large Part Right Ventricular Dependent

Decompression of the right ventricle in the setting of a significantly dependent myocardial circulation is unwise as any procedure that reduces right ventricular systolic pressure or blood entering the right ventricle will unmask any right ventricle-dependent coronary circulation with massive, if not fatal, myocardial ischemia. These maneuvers include pulmonary valvotomy or right ventricular outflow tract reconstruction, tricuspid valve excision or catheter avulsion, and right ventricle thromboexclusion. These patients should undergo a ductal stent or a systemic-to-pulmonary artery shunt as the initial procedure, with a balloon atrial septostomy given consideration in the cardiac catheterization laboratory. The patient should be placed on a program eventuating in a one-ventricle total cavopulmonary (Fontan) palliation. In some centers, these patients are considered for primary cardiac replacement, especially if the coronary anomalies are particularly severe.

The lateral-tunnel or extracardiac modifications of the total cavopulmonary (Fontan) principle with pulmonary venous blood having access to the tricuspid valve, right ventricle, and thus in a retrograde fashion to the coronary arteries have been applied to patients with an extremely disordered coronary circulation (71,72). It is probable that this approach is ultimately a bridge to cardiac transplantation. Indeed, some patients exhibit globally reduced left ventricular function that cannot be improved by a variety of medical and surgical maneuvers and are destined for cardiac replacement. Table 41.5 outlines some approaches to the management of patients with PA and IVS and an abnormal coronary circulation.

Extreme Ebstein-like/Dysplastic Tricuspid Valve and Organic Pulmonary Atresia

The previous conventional therapies of attempting to repair or replace the tricuspid valve and pulmonary valvotomy with or without a surgical shunt have carried a poor prognosis. Contemporary approaches include cardiac transplantation and conversion to tricuspid atresia and construction of a systemic-to-pulmonary artery shunt with a later cavopulmonary palliation. Relatively little experience has been gained in the transplantation of infants with this particular variety of the lesion, but Starnes et al. (73) prepared an interesting

TABLE 41.5 Current Surgical Strategies Based on Abnormal Coronary Artery Anatomy

Coronary Artery Anomaly	Surgical Strategy
Absence of bilateral proximal coronary-aorto connections	Consider transplant versus high-risk shunt or ductal stent
Absence of aorto-left coronary artery connection	Consider transplant versus high-risk shunt or ductal stent
Severe coronary-cameral steal	Consider fistula occlusion with RV decompression
Ventriculocoronary connections with no stenosis or interruption	Decompress RV
Mild distal stenoses or ectasia in presence of ventriculocoronary connections	Decompress RV (but at higher risk than in absence of stenoses/interruption)
Proximal LAD interruption, proximal RCA stenosis, significantly RV-dependent myocardial perfusion	Shunt or ductal stent, univentricular track

LAD, left anterior descending; RCA, right coronary artery; RV, right ventricle.

alternative to conventional surgical wisdom with their surgical conversion of these patients to tricuspid atresia, construction of a systemic-to-pulmonary arterial anastomosis with a later Fontan.

Transcatheter Techniques in the Management of Pulmonary Atresia and Intact Ventricular Septum

Surgical algorithms for patients with PA and an IVS focus on the probability of avoiding the total cavopulmonary (Fontan) circulation. Many clinicians advocate establishing continuity from right ventricle to pulmonary artery with a right ventricular outflow tract patch or valvotomy early in the patient's course to encourage growth of the hypoplastic ventricle as a means of achieving a biventricular or so-called one-and-one-half ventricle repair in carefully selected patients. This approach mandates prediction of the ventricle with the potential for growth and exclusion of patients with a right ventricle-dependent coronary circulation who are at risk for

ischemic myocardial injury following ventricular decompression. Initial results have been encouraging, but surgical mortality remains relatively high. The ideal patient would have a tripartite right ventricle of near normal size with valvar PA and a well-developed pulmonary arterial circulation (Fig. 41.20).

Whereas several factors may contribute to high surgical mortality, myocardial insult incurred at surgery with ventriculotomy and reperfusion injury in the setting of preexisting myocardial fiber disarray and diffuse fibrosis may play an important role. This has encouraged some centers to complement the surgical algorithm with interventional catheterization techniques to achieve right ventricular to pulmonary artery continuity. Transcatheter perforation of the atretic pulmonary valve with subsequent balloon dilation can be employed as an alternative to surgical valvotomy in selected patients. Laser energy applied to the tip of a small wire has allowed controlled perforation of the atretic valve tissue and has been achieved in several patients with good results in short-term follow-up (74); however, laser therapy carries the disadvantages of increased risk to staff, the requirement for protective goggles, limited

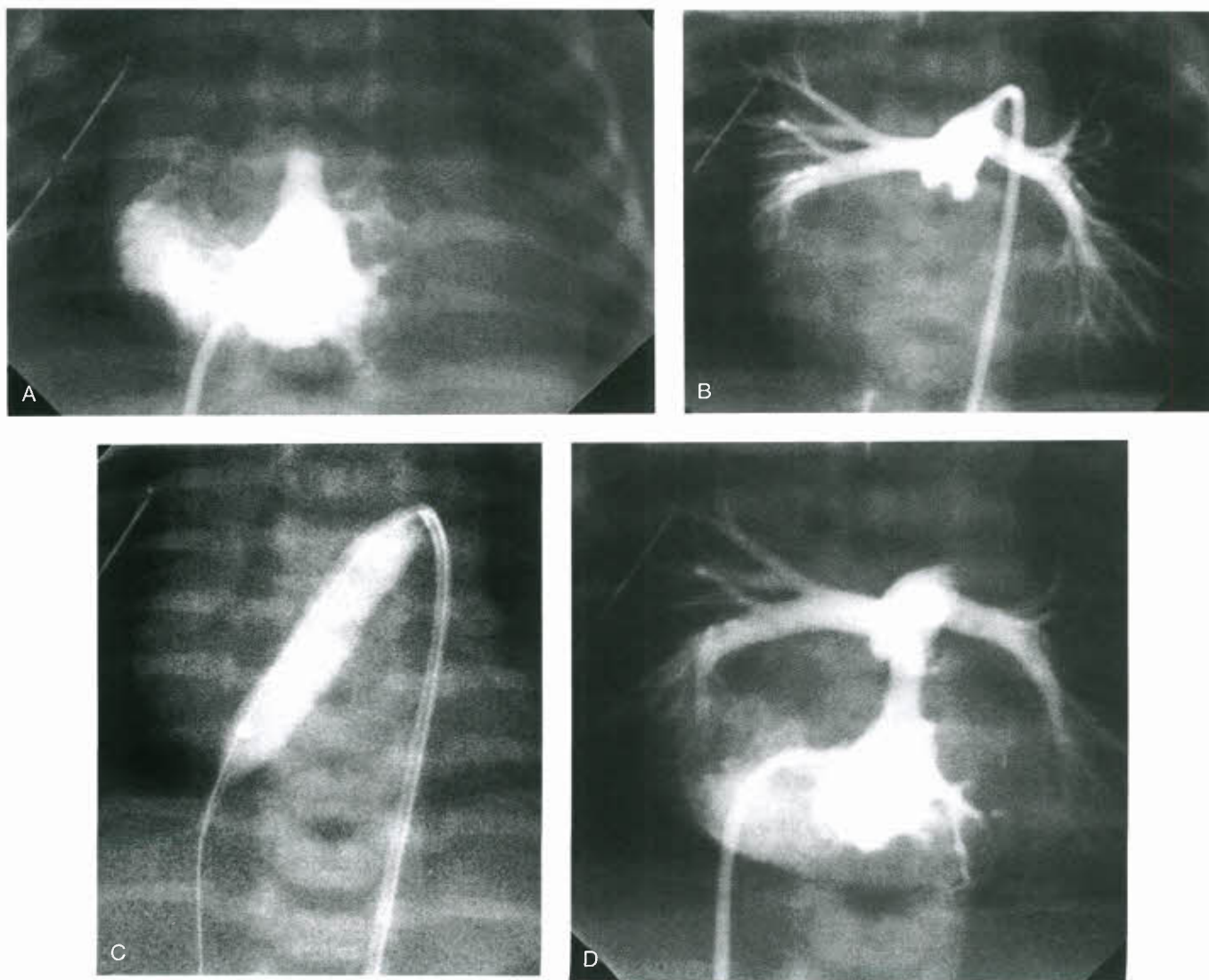


Figure 41.20. A: Right ventricular angiogram in frontal projection confirms a hypoplastic tripartite right ventricle with pulmonary atresia. B: Retrograde injection into the main pulmonary artery confirms membranous atresia of the pulmonary valve. C: Perforation of the membranous valve is achieved (in this case assisted by radiofrequency energy), thus allowing a balloon catheter to be positioned across the valve and inflated. D: Repeat angiography immediately following balloon valvotomy demonstrates a patent right ventricular outflow tract.

portability, and considerable capital expense in the setting of an uncommon defect.

Radiofrequency energy, which can safely achieve well-defined lesions of coagulation necrosis, is now widely applied in the treatment of many cardiac dysrhythmias. Use of this energy source to perforate atretic valve tissue has the advantages of being considerably less expensive, more portable, and less hazardous to staff. Radiofrequency wires capable of confining the energy to the tip have been developed for this lesion based on proven utility in recanalization of arterial occlusions, and results have been encouraging. Where radiofrequency or laser wires have not been available, other means of attaining perforation have been used, including mechanical wire perforation and standard electrode catheters.

The reported literature attests to the fact that it is possible to establish continuity from right ventricle to the pulmonary artery in the catheter laboratory and thus avoid the need for cardiopulmonary bypass in many patients (21,38,74–96). The long-term results of the procedure remain largely unknown. Although early success defined by the ability to achieve perforation has been demonstrated in >80% of patients reported, controversy remains regarding the growth of the right ventricle and outflow tract over time. In evaluating the literature, one must be careful to distinguish an absolute increase in the size of an anatomic structure such as the tricuspid valve from that of the indexed size. As an example, the tricuspid valve appears to enlarge over time with transcatheter perforation of the tricuspid valve (97); however, the indexed Z value does not appear to change significantly (21). In addition, the need for prolonged prostaglandin infusion, creation of a systemic-to-pulmonary artery shunt, or implantation of a stent in the ductus arteriosus to achieve the same end is a common occurrence in this group of patients and occurs in 33% to 58%. Notably, however, these secondary interventions do not require the use of cardiopulmonary bypass that may be important when one considers the influence of myocardial abnormalities on outcome. To further frustrate clinicians, the timing of secondary intervention to increase pulmonary blood flow can be difficult to assess after transcatheter valvotomy as it appears that days to weeks are required for the decompressed right ventricular compliance to improve. If a systemic-to-arterial shunt is created too early, one can be in the paradoxical situation of embolizing the same shunt in the future once the ventricular compliance has improved. To further complicate matters, a systemic shunt in the setting of severe pulmonary insufficiency and tricuspid insufficiency can result in an ineffective “circular” circulation where flow of systemic arterial blood courses through the shunt to the right ventricle, regurgitates through the tricuspid valve to the right atrium, and courses across the atrial septum to the left atrium where the process repeats. Effective pulmonary blood flow is decreased, and the left ventricle is exposed to physiology similar to a large arteriovenous fistula. Myocardial oxygen demand is increased, diastolic aortic pressure is borderline, and the patient is cyanotic, all of which contribute to progressively worsening myocardial performance. Indeed, this circulation may be more likely to occur with a stented ductus arteriosus as the flow through the shunt is directed through the perforated valve to the ventricle as opposed to the modified Blalock-Thomas-Taussig shunt where flow to the ventricle must take a more indirect path through the pulmonary artery to the right ventricle. Still, consideration may be given to stenting the ductus concurrent with valve perforation in selected cases (98). It seems that the best outcomes are clearly achieved with an individualized cooperative creative transcatheter surgical approach including so-called hybrid interventions (99–101).

The role of transcatheter techniques in the management continuum of these patients is in evolution; however, com-

parison to surgical outflow tract reconstruction is, at least in one series, favorable (75). With a relatively small number of patients affected by this condition, there is much to be learned from a multicentered approach to collecting a longitudinal experience in a combined transcatheter and surgical approach to a challenging clinical problem. Whereas a percutaneous approach may avoid or delay the use of cardiopulmonary bypass in the newborn period, it remains to be seen whether it results in a decrease in long-term morbidity or mortality.

TREATMENT OF THE ADULT

It should be clear from the preceding discussions that there is a great anatomic and physiologic diversity of patients surviving into adulthood with PA and IVS. Patients may have achieved a biventricular circulation, a univentricular circulation in the form of a total cavopulmonary circulation, or a permanently palliated shunted state. Outcome data for the adult population are few, and reported results may even be counterintuitive. For instance, it is unclear whether a biventricular circulation holds advantage over a univentricular circulation in the assessment of exercise capacity and indeed may be more influenced by pulmonary than cardiac issues as aerobic capacity appears to decrease in both groups (102). Myocardial perfusion abnormalities persist well beyond definitive repair (palliation) (103). In the adult with a biventricular repair, right ventricular restriction may favor better physiologic status; however, many patients will go on to require a pulmonary valve replacement to restore competency of the right ventricular outflow tract (104,105). In a recent study (106) of 20 survivors into adulthood (19 to 39 years old) with Fontan ($n = 7$), biventricular ($n = 8$), and palliated shunts ($n = 5$), there were 5 deaths at a mean age of 32 years. All patients required interventions in adulthood with tricuspid and pulmonary valve replacements being very common in the biventricular group. Atrial arrhythmias occurred frequently in the cohort (80%) but ventricular arrhythmias were not uncommon (15%). Although the literature is sparse, it is clear that all of these patients will require continued specialized tertiary and quaternary follow-up, specialized intervention, arrhythmia management, and ancillary support as they reach adulthood. The value of registry data to guide the care of the growing population of adults with congenital heart disease cannot be overstated.

SUMMARY

Congenitally malformed hearts with PA/IVS demonstrate clinically important heterogeneity of the right-sided cardiac structures, the coronary circulation, and the myocardium. Fetal recognition of this condition will affect newborn epidemiology due to the influence of elective termination of pregnancy (8,107,108). Rarely, survival beyond the neonatal period has been documented due to persistent patency of the arterial duct or more rarely by associated conditions that preserve pulmonary blood flow such as an aortopulmonary window or coronary to pulmonary artery connections. A variety of surgical and transcatheter interventions exist that culminate in eventual biventricular repair or in the univentricular total cavopulmonary circulation. An intermediate form of palliation exists in the form of the so-called one-and-a-half ventricle repair where the right ventricle with a patent outflow tract is effectively unloaded with a bidirectional cavopulmonary connection, although the long-term advantage of this circulation remains to be seen (66,109–112). Where some have questioned whether it is possible to improve outcomes, the literature

supports cautious optimism by demonstrating improved survival with more recent era of intervention. Understanding the nature of the coronary artery circulation, the application of a one ventricle or one-and-a-half ventricle repair, and the application of radiofrequency catheter perforation of the imperforate pulmonary valve all have contributed to increased salvage of these infants, although there is still much to be achieved. Intrinsic, indeed congenital, abnormalities in the vascular supply and myocardial architecture ultimately may argue for a poor outcome in at least some of these patients. Sudden coronary death remains a worrisome long-term concern, but establishing risk is unclear (113). The role for cardiac transplantation of the neonate is unclear; however, consideration should be given to the patient with severe Ebstein-like malformation and severe tricuspid insufficiency as these patients continue to represent the worst surgical outcomes. Adult survivors will require specialized follow-up and frequent reintervention. It is clear that the anatomic and physiologic diversity of this patient population represented by the neonate will continue to challenge treatment strategy into adulthood.

REFERENCES

- Freedom RM. *Pulmonary Atresia with Intact Ventricular Septum*. Mount Kisco, NY: Futura Pub. Co., 1989.
- Hunter J. *Medical Observations and Inquiries* by a Society of physicians in London. Vol VI. (Read July 28, 1783). London. Printed for T. Cadell 1784: 291–299. 1783:291.
- Peacock T. Malformations of the heart: atresia of the orifice of the pulmonary artery. *Trans Pathol Soc Lond* 1869;61–86.
- Coles JG, Freedom RM, Lightfoot NE, et al. Long-term results in neonates with pulmonary atresia and intact ventricular septum. *Ann Thorac Surg* 1989;47:213–217.
- Hanley FL, Sade RM, Blackstone EH, et al. Outcomes in neonatal pulmonary atresia with intact ventricular septum: a multiinstitutional study. *J Thorac Cardiovasc Surg* 1993;105:406–423, 424–407; discussion 423–404.
- Lightfoot NE, Coles JG, Dasmahapatra HK, et al. Analysis of survival in patients with pulmonary atresia and intact ventricular septum treated surgically. *Int J Cardiol* 1989;24:159–164.
- Ferencz C, Rubin JD, McCarter RJ, et al. Congenital heart disease: prevalence at livebirth. The Baltimore-washington infant study. *Am J Epidemiol* 1985;121:31–36.
- Daubeney PE, Sharland GK, Cook AC, et al. Pulmonary atresia with intact ventricular septum: impact of fetal echocardiography on incidence at birth and postnatal outcome. UK and Eire collaborative study of pulmonary atresia with intact ventricular septum. *Circulation* 1998;98:562–566.
- Gomez-Montes E, Herraiz I, Mendoza A, et al. Pulmonary atresia/critical stenosis with intact ventricular septum: prediction of outcome in the second trimester of pregnancy. *Prenat Diagn* 2011;31:372–379.
- Kawazu Y, Inamura N, Kayatani F. Prediction of therapeutic strategy and outcome for antenatally diagnosed pulmonary atresia/stenosis with intact ventricular septum. *Circ J* 2008;72:1471–1475.
- Peterson RE, Levi DS, Williams RJ, et al. Echocardiographic predictors of outcome in fetuses with pulmonary atresia with intact ventricular septum. *J Am Soc Echocardiogr* 2006;19:1393–1400.
- Roman KS, Fouron JC, Nii M, et al. Determinants of outcome in fetal pulmonary valve stenosis or atresia with intact ventricular septum. *Am J Cardiol* 2007;99:699–703.
- Salvin JW, McElhinney DB, Colan SD, et al. Fetal tricuspid valve size and growth as predictors of outcome in pulmonary atresia with intact ventricular septum. *Pediatrics* 2006;118:e415–e420.
- Mildner RJ, Kiraly L, Sreeram N. Pulmonary atresia, “intact ventricular septum”, and aortopulmonary collateral arteries. *Heart* 1997;77:173–175.
- Kutsche LM, Van Mierop LH. Pulmonary atresia with and without ventricular septal defect: a different etiology and pathogenesis for the atresia in the 2 types? *Am J Cardiol* 1983;51:932–935.
- deAlmeida A, McQuinn T, Sedmera D. Increased ventricular preload is compensated by myocyte proliferation in normal and hypoplastic fetal chick left ventricle. *Circ Res* 2007;100:1363–1370.
- Fishman NH, Hof RB, Rudolph AM, et al. Models of congenital heart disease in fetal lambs. *Circulation* 1978;58:354–364.
- Braunlin EA, Formanek AG, Moller JH, et al. Angio-pathological appearances of pulmonary valve in pulmonary atresia with intact ventricular septum: interpretation of nature of right ventricle from pulmonary angiography. *Br Heart J* 1982;47:281–289.
- Choi YH, Seo JW, Choi JY, et al. Morphology of tricuspid valve in pulmonary atresia with intact ventricular septum. *Pediatr Cardiol* 1998;19:381–389.
- Anderson RH, Silverman NH, Zuberbuhler JR. Congenitally unguarded tricuspid orifice: its differentiation from ebstein's malformation in association with pulmonary atresia and intact ventricular septum. *Pediatr Cardiol* 1990;11:86–90.
- Humpl T, Soderberg B, McCrindle BW, et al. Percutaneous balloon valvotomy in pulmonary atresia with intact ventricular septum: impact on patient care. *Circulation* 2003;108:826–832.
- Daubeney PE, Delany DJ, Anderson RH, et al. Pulmonary atresia with intact ventricular septum: range of morphology in a population-based study. *J Am Coll Cardiol* 2002;39:1670–1679.
- Zuberbuhler JR, Anderson RH. Morphological variations in pulmonary atresia with intact ventricular septum. *Br Heart J* 1979;41:281–288.
- Freedom R. How can something so small cause so much grief? Some thoughts about the underdeveloped right ventricle in pulmonary atresia and intact ventricular septum. *J Am Coll Cardiol* 1992;19:1038–1040.
- Giglia TM, Jenkins KJ, Matitau A, et al. Influence of right heart size on outcome in pulmonary atresia with intact ventricular septum. *Circulation* 1993;88:2248–2256.
- Lewis AB, Wells W, Lindesmith GG. Right ventricular growth potential in neonates with pulmonary atresia and intact ventricular septum. *J Thorac Cardiovasc Surg* 1986;91:835–840.
- Mainwaring RD, Lamberti JJ. Pulmonary atresia with intact ventricular septum. Surgical approach based on ventricular size and coronary anatomy. *J Thorac Cardiovasc Surg* 1993;106:733–738.
- Patel RG, Freedom RM, Moes CA, et al. Right ventricular volume determinations in 18 patients with pulmonary atresia and intact ventricular septum: analysis of factors influencing right ventricular growth. *Circulation* 1980;61:428–440.
- Pawade A, Capuani A, Penny DJ, et al. Pulmonary atresia with intact ventricular septum: surgical management based on right ventricular infundibulum. *J Card Surg* 1993;8:371–383.
- Schmidt KG, Cloez JL, Silverman NH. Changes of right ventricular size and function in neonates after valvotomy for pulmonary atresia or critical pulmonary stenosis and intact ventricular septum. *J Am Coll Cardiol* 1992;19:1032–1037.
- Razzouk AJ, Freedom RM, Cohen AJ, et al. The recognition, identification of morphologic substrate, and treatment of subaortic stenosis after a fontan operation: an analysis of twelve patients. *J Thorac Cardiovasc Surg* 1992;104:938–944.
- Amin P, Levi DS, Likes M, et al. Pulmonary atresia with intact ventricular septum causing severe left ventricular outflow tract obstruction. *Pediatr Cardiol* 2009;30:851–854.
- Patel RG, Freedom RM, Bloom KR, et al. Truncal or aortic valve stenosis in functionally single arterial trunk: a clinical, hemodynamic and pathologic study of six cases. *Am J Cardiol* 1978;42:800–809.
- Luciani GB, Swilley S, Starnes VA. Pulmonary atresia, intact ventricular septum, and major aortopulmonary collaterals: morphogenetic and surgical implications. *J Thorac Cardiovasc Surg* 1995;110:853–854.
- Marino B, Guccione P, Carotti A, et al. Ductus arteriosus in pulmonary atresia with and without ventricular septal defect: anatomic and functional differences. *Scand J Thorac Cardiovasc Surg* 1992;26:93–96.
- Alwi M, Choo KK, Latiff HA, et al. Initial results and medium-term follow-up of stent implantation of patent ductus arteriosus in duct-dependent pulmonary circulation. *J Am Coll Cardiol* 2004;44:438–445.
- Gibbs JL, Rothman MT, Rees MR, et al. Stenting of the arterial duct: a new approach to palliation for pulmonary atresia. *Br Heart J* 1992;67:240–245.
- Rosenthal E, Qureshi SA, Tynan M. Percutaneous pulmonary valvotomy and arterial duct stenting in neonates with right ventricular hypoplasia. *Am J Cardiol* 1994;74:304–306.
- Schneider M, Zartner P, Sidiropoulos A, et al. Stent implantation of the arterial duct in newborns with duct-dependent circulation. *Eur Heart J* 1998;19:1401–1409.
- Arcilla RA, Gasul BM. Congenital aplasia or marked hypoplasia of the myocardium of the right ventricle (uhl's anomaly): clinical, angiographic, and hemodynamic findings. *J Pediatr* 1961;58:381–388.
- Bulkley BH, D'Amico B, Taylor AL. Extensive myocardial fiber disarray in aortic and pulmonary atresia: relevance to hypertrophic cardiomyopathy. *Circulation* 1983;67:191–198.
- Fyfe DA, Edwards WD, Driscoll DJ. Myocardial ischemia in patients with pulmonary atresia and intact ventricular septum. *J Am Coll Cardiol* 1986;8:402–406.
- Hausdorf G, Gravinghoff L, Keck EW. Effects of persisting myocardial sinusoids on left ventricular performance in pulmonary atresia with intact ventricular septum. *Eur Heart J* 1987;8:291–296.
- Hubbard JF, Girod DA, Caldwell RL, et al. Right ventricular infarction with cardiac rupture in an infant with pulmonary valve atresia with intact ventricular septum. *J Am Coll Cardiol* 1983;2:363–368.
- Oosthoek PW, Moorman AF, Sauer U, et al. Capillary distribution in the ventricles of hearts with pulmonary atresia and intact ventricular septum. *Circulation* 1995;91:1790–1798.
- Calder AL, Co EE, Sage MD. Coronary arterial abnormalities in pulmonary atresia with intact ventricular septum. *Am J Cardiol* 1987;59:436–442.
- Gittenberger-de Groot AC, Erulp I, Lie-Venema H, et al. Development of the coronary vasculature and its implications for coronary abnormalities in general and specifically in pulmonary atresia without ventricular septal defect. *Acta Paediatr Suppl* 2004;93:13–19.

48. Gittenberger-de Groot AC, Sauer U, Bindl L, et al. Competition of coronary arteries and ventriculo-coronary arterial communications in pulmonary atresia with intact ventricular septum. *Int J Cardiol* 1988;18:243-258.
49. Kasznica J, Ursell PC, Blanc WA, et al. Abnormalities of the coronary circulation in pulmonary atresia and intact ventricular septum. *Am Heart J* 1987;114:1415-1420.
50. MacMahon HE, Dickinson PC. Occlusive fibroelastosis of coronary arteries in the newborn. *Circulation* 1967;35:3-9.
51. Sarou GM, Perry SB, Gauvreau K, et al. Echocardiographic predictors of coronary artery pathology in pulmonary atresia with intact ventricular septum. *Am J Cardiol* 2000;85:1319-1324.
52. De Stefano D, Li P, Xiang B, et al. Pulmonary atresia with intact ventricular septum (pa-ivs) in monozygotic twins. *Am J Med Genet A* 2008;146A:525-528.
53. Chitayat D, McIntosh N, Fouron JC. Pulmonary atresia with intact ventricular septum and hypoplastic right heart in sibs: a single gene disorder? *Am J Med Genet* 1992;42:304-306.
54. Garcia JA, Zellers TM, Weinstein EM, et al. Usefulness of doppler echocardiography in diagnosing right ventricular coronary arterial communications in patients with pulmonary atresia and intact ventricular septum and comparison with angiography. *Am J Cardiol* 1998;81:103-104.
55. Selamet SE, Hsu DT, Thaker HM, et al. Complete atresia of coronary ostia in pulmonary atresia and intact ventricular septum. *Pediatr Cardiol* 2004;25:67-69.
56. Walsh KP, Abdulhamed JM, Tometzki JP. Importance of right ventricular outflow tract angiography in distinguishing critical pulmonary stenosis from pulmonary atresia. *Heart* 1997;77:456-460.
57. Aziz KU, Olley PM, Rowe RD, et al. Survival after systemic to pulmonary arterial shunts in infants less than 30 days old with obstructive lesions of the right heart chambers. *Am J Cardiol* 1975;36:476-483.
58. Amodeo A, Keeton BR, Sutherland GR, et al. Pulmonary atresia with intact ventricular septum: is neonatal repair advisable? *Eur J Cardiothorac Surg* 1991;5:17-21.
59. Hawkins JA, Thorne JK, Boucek MM, et al. Early and late results in pulmonary atresia and intact ventricular septum. *J Thorac Cardiovasc Surg* 1990;100:492-497.
60. McCaffrey FM, Leatherbury L, Moore HV. Pulmonary atresia and intact ventricular septum: definitive repair in the neonatal period. *J Thorac Cardiovasc Surg* 1991;102:617-623.
61. Shaddy RE, Sturtevant JE, Judd VE, et al. Right ventricular growth after transventricular pulmonary valvotomy and central aortopulmonary shunt for pulmonary atresia and intact ventricular septum. *Circulation* 1990;82:IV157-IV163.
62. Williams WG, Burrows P, Freedom RM, et al. Thromboexclusion of the right ventricle in children with pulmonary atresia and intact ventricular septum. *J Thorac Cardiovasc Surg* 1991;101:222-229.
63. Calder AL, Peebles CR, Ocleshaw CJ. The prevalence of coronary arterial abnormalities in pulmonary atresia with intact ventricular septum and their influence on surgical results. *Cardiol Young* 2007;17:387-396.
64. Cleuziou J, Schreiber C, Eicken A, et al. Predictors for biventricular repair in pulmonary atresia with intact ventricular septum. *Thorac Cardiovasc Surg* 2010;58:339-344.
65. Liava'a M, Brooks P, Konstantinov I, et al. Changing trends in the management of pulmonary atresia with intact ventricular septum: the Melbourne experience. *Eur J Cardiothorac Surg* 2011;40:1406-1411.
66. Miyaji K, Shimada M, Sekiguchi A, et al. Pulmonary atresia with intact ventricular septum: long-term results of "one and a half ventricular repair". *Ann Thorac Surg* 1995;60:1762-1764.
67. Van Arsdel GS, Williams WG, Maser CM, et al. Superior vena cava to pulmonary artery anastomosis: an adjunct to biventricular repair. *J Thorac Cardiovasc Surg* 1996;112:1143-1148; discussion 1148-1149.
68. Ashburn DA, Blackstone EH, Wells WJ, et al. Determinants of mortality and type of repair in neonates with pulmonary atresia and intact ventricular septum. *J Thorac Cardiovasc Surg* 2004;127:1000-1007; discussion 1007-1008.
69. Dyamenahalli U, McCrindle BW, McDonald C, et al. Pulmonary atresia with intact ventricular septum: management of, and outcomes for, a cohort of 210 consecutive patients. *Cardiol Young* 2004;14:299-308.
70. Rychik J, Levy H, Gaynor JW, et al. Outcome after operations for pulmonary atresia with intact ventricular septum. *J Thorac Cardiovasc Surg* 1998;116:924-931.
71. Mair DD, Julsrud PR, Puga FJ, et al. The fontan procedure for pulmonary atresia with intact ventricular septum: operative and late results. *J Am Coll Cardiol* 1997;29:1359-1364.
72. Najm HK, Williams WG, Coles JG, et al. Pulmonary atresia with intact ventricular septum: results of the fontan procedure. *Ann Thorac Surg* 1997;63:669-675.
73. Starnes VA, Pitlick PT, Bernstein D, et al. Ebstein's anomaly appearing in the neonate: a new surgical approach. *J Thorac Cardiovasc Surg* 1991;101:1082-1087.
74. Qureshi SA, Rosenthal E, Tynan M, et al. Transcatheter laser-assisted balloon pulmonary valve dilation in pulmonic valve atresia. *Am J Cardiol* 1991;67:428-431.
75. Alwi M, Geetha K, Bilkis AA, et al. Pulmonary atresia with intact ventricular septum percutaneous radiofrequency-assisted valvotomy and balloon dilation versus surgical valvotomy and blalock taussig shunt. *J Am Coll Cardiol* 2000;35:468-476.
76. Cheatham JP, Coe JY, Kugler JD, et al. Successful transcatheter perforation of the atretic pulmonary valve membrane in a newborn using the new coe radiofrequency end hole catheter. *Cathet Cardiovasc Diagn* 1998;45:162-166.
77. Fedderly RT, Lloyd TR, Mendelsohn AM, et al. Determinants of successful balloon valvotomy in infants with critical pulmonary stenosis or membranous pulmonary atresia with intact ventricular septum. *J Am Coll Cardiol* 1995;25:460-465.
78. Gibbs JL, Blackburn ME, Uzun O, et al. Laser valvotomy with balloon valvoplasty for pulmonary atresia with intact ventricular septum: five years' experience. *Heart* 1997;77:225-228.
79. Hausdorf G, Schulze-Neick I, Lange PE. Radiofrequency-assisted "reconstruction" of the right ventricular outflow tract in muscular pulmonary atresia with ventricular septal defect. *Br Heart J* 1993;69:343-346.
80. Justo RN, Nykanen DG, Williams WG, et al. Transcatheter perforation of the right ventricular outflow tract as initial therapy for pulmonary valve atresia and intact ventricular septum in the newborn. *Cathet Cardiovasc Diagn* 1997;40:408-413.
81. Latson LA. Nonsurgical treatment of a neonate with pulmonary atresia and intact ventricular septum by transcatheter puncture and balloon dilation of the atretic valve membrane. *Am J Cardiol* 1991;68:277-279.
82. Latson LA, Fleming WH, Hofschire PJ, et al. Balloon valvuloplasty in pulmonary valve atresia. *Am Heart J* 1991;121:1567-1569.
83. Leung MP, Lo RN, Cheung H, et al. Balloon valvuloplasty after pulmonary valvotomy for babies with pulmonary atresia and intact ventricular septum. *Ann Thorac Surg* 1992;53:864-870.
84. Park IS, Nakanishi T, Nakazawa M, et al. Radiofrequency pulmonary valvotomy using a new 2-french catheter. *Cathet Cardiovasc Diagn* 1998;45:37-42.
85. Parsons JM, Rees MR, Gibbs JL. Percutaneous laser valvotomy with balloon dilation of the pulmonary valve as primary treatment for pulmonary atresia. *Br Heart J* 1991;66:36-38.
86. Radtke WA. Interventional pediatric cardiology: state of the art and future perspective. *Eur J Pediatr* 1994;153:542-547.
87. Rosenthal E, Qureshi SA, Chan KC, et al. Radiofrequency-assisted balloon dilatation in patients with pulmonary valve atresia and an intact ventricular septum. *Br Heart J* 1993;69:347-351.
88. Rosenthal E, Qureshi SA, Kakadekar AP, et al. Technique of percutaneous laser-assisted valve dilatation for valvar atresia in congenital heart disease. *Br Heart J* 1993;69:556-562.
89. Schneider M, Schranz D, Michel-Behnke I, et al. Transcatheter radiofrequency perforation and stent implantation for palliation of pulmonary atresia in a 3060-g infant. *Cathet Cardiovasc Diagn* 1995;34:42-45.
90. Siblini G, Rao PS, Singh GK, et al. Transcatheter management of neonates with pulmonary atresia and intact ventricular septum. *Cathet Cardiovasc Diagn* 1997;42:395-402.
91. Veldtman GR, Hartley A, Visram N, et al. Radiofrequency applications in congenital heart disease. *Expert Rev Cardiovasc Ther* 2004;2:117-126.
92. Wang JK, Wu MH, Chang CI, et al. Outcomes of transcatheter valvotomy in patients with pulmonary atresia and intact ventricular septum. *Am J Cardiol* 1999;84:1055-1060.
93. Weber HS. Initial and late results after catheter intervention for neonatal critical pulmonary valve stenosis and atresia with intact ventricular septum: a technique in continual evolution. *Catheter Cardiovasc Interv* 2002;56:394-399.
94. Wright SB, Radtke WA, Gillette PC. Percutaneous radiofrequency valvotomy using a standard 5fr electrode catheter for pulmonary atresia in neonates. *Am J Cardiol* 1996;77:1370-1372.
95. Agnoletti G, Piechaud JF, Bonhoeffer P, et al. Perforation of the atretic pulmonary valve. Long-term follow-up. *J Am Coll Cardiol* 2003;41:1399-1403.
96. Marasini M, Gorrieri PF, Tuo G, et al. Long-term results of catheter-based treatment of pulmonary atresia and intact ventricular septum. *Heart* 2009;95:1520-1524.
97. Ovaert C, Qureshi SA, Rosenthal E, et al. Growth of the right ventricle after successful transcatheter pulmonary valvotomy in neonates and infants with pulmonary atresia and intact ventricular septum. *J Thorac Cardiovasc Surg* 1998;115:1055-1062.
98. Alwi M, Choo KK, Radzi NA, et al. Concomitant stenting of the patent ductus arteriosus and radiofrequency valvotomy in pulmonary atresia with intact ventricular septum and intermediate right ventricle: early in-hospital and medium-term outcomes. *J Thorac Cardiovasc Surg* 2011;141:1355-1361.
99. Burke RP, Hannan RL, Zabinsky JA, et al. Hybrid ventricular decompression in pulmonary atresia with intact septum. *Ann Thorac Surg* 2009;88:688-689.
100. Hannan RL, Zabinsky JA, Stanfill RM, et al. Midterm results for collaborative treatment of pulmonary atresia with intact ventricular septum. *Ann Thorac Surg* 2009;87:1227-1233.
101. Li S, Chen W, Zhang Y, et al. Hybrid therapy for pulmonary atresia with intact ventricular septum. *Ann Thorac Surg* 2011;91:1467-1471.
102. Sanghavi DM, Flanagan M, Powell AJ, et al. Determinants of exercise function following univentricular versus biventricular repair for pulmonary atresia/intact ventricular septum. *Am J Cardiol* 2006;97:1638-1643.

103. Ekman-Joelsson BM, Berggren H, Boll AB, et al. Abnormalities in myocardial perfusion after surgical correction of pulmonary atresia with intact ventricular septum. *Cardiol Young* 2008;18:89–95.
104. Bautista-Hernandez V, Hasan BS, Harrild DM, et al. Late pulmonary valve replacement in patients with pulmonary atresia and intact ventricular septum: a case-matched study. *Ann Thorac Surg* 2011;91:555–560.
105. Liang XC, Lam WW, Cheung EW, et al. Restrictive right ventricular physiology and right ventricular fibrosis as assessed by cardiac magnetic resonance and exercise capacity after biventricular repair of pulmonary atresia and intact ventricular septum. *Clin Cardiol* 2010;33:104–110.
106. John AS, Warnes CA. Clinical outcomes of adult survivors of pulmonary atresia with intact ventricular septum. *Int J Cardiol* 2011. [Epub ahead of print.]
107. Maeno YV, Boutin C, Hornberger LK, et al. Prenatal diagnosis of right ventricular outflow tract obstruction with intact ventricular septum, and detection of ventriculocoronary connections. *Heart* 1999;81:661–668.
108. Sharland G. Pulmonary valve abnormalities. In: Allan L, Hornberger L, Sharland G, eds. *Textbook of Fetal Cardiology*. London, UK: Greenwich Medical Media, 2000:333–347.
109. Gentles TL, Keane JF, Jonas RA, et al. Surgical alternatives to the fontan procedure incorporating a hypoplastic right ventricle. *Circulation* 1994;90:II1–II6.
110. Kreutzer C, Mayorquim RC, Kreutzer GO, et al. Experience with one and a half ventricle repair. *J Thorac Cardiovasc Surg* 1999;117:662–668.
111. Muster AJ, Zales VR, et al. Biventricular repair of hypoplastic right ventricle assisted by pulsatile bidirectional cavopulmonary anastomosis. *J Thorac Cardiovasc Surg* 1993;105:112–119.
112. Takayama H, Sekiguchi A, Chikada M. 1995. Pulmonary atresia with intact ventricular septum: long-term results of “one and a half ventricular repair”. Updated in 2001. *Ann Thorac Surg* 2001;72:2178–2179.
113. Leonard H, Derrick G, O’Sullivan J, et al. Natural and unnatural history of pulmonary atresia. *Heart* 2000;84:499–503.

Pulmonary Atresia and Ventricular Septal Defect

Patrick W. O'Leary ■ William D. Edwards ■ Paul R. Julsrud ■ Harold MacDonald Burkhart

The combination of pulmonary valve atresia and ventricular septal defect (PA-VSD) can be considered to be the most severe form of tetralogy of Fallot (TOF). However, unlike TOF, the right ventricular outflow tract (RVOT) ends blindly, and all of the right ventricular stroke volume is directed to the aorta via the ventricular septal defect (VSD). In addition, the pulmonary arterial architecture is much more complex in PA-VSD than in TOF. As a result, delineating these arterial complexities and planning the most effective management strategy are more difficult for this lesion than for TOF. Although the pulmonary arteries in TOF occasionally are hypoplastic and can show anomalies of peripheral arborization, more commonly they are normal. Also, in TOF, systemic-to-pulmonary collateral vessels are extremely unusual. In PA-VSD, however, often there are severe abnormalities in the size and distribution of the pulmonary arterial branches and well-developed systemic collateral vessels that supply all or portions of the lung parenchyma. In extreme cases, the pulmonary vascular tree can even be composed of discontinuous segments, each with an independent source of flow.

PA-VSD accounts for about 2% of congenital heart disease (CHD). It is one of the common causes of cyanosis and hypoxemia in the neonate. PA-VSD is slightly more prevalent in male than in female infants. In the Baltimore-Washington Infant Study (BWIS), a prevalence of 0.07 per 1,000 live births was observed for PA-VSD (1,2), and PA-VSD accounted for 20.3% of all forms of TOF.

Although corrective operation was first performed >30 years ago for patients with well-developed pulmonary arteries, patients with severe abnormalities of the pulmonary arteries initially were considered inoperable or only as candidates for surgical palliation. Surgical techniques have evolved to a stage that correction (with VSD closure) is possible for steadily increasing numbers of these patients.

ENVIRONMENTAL FACTORS AND GENETICS

Maternal diabetes, maternal phenylketonuria (PKU), and maternal exposure to retinoic acids and to trimethadione are associated with an increased risk of conotruncal defects in the infant (2–5). Investigators in the BWIS found that infants of diabetic women had nearly a 10-fold increased risk of developing PA-VSD (2).

Investigators have described families with multiple members with PA-VSD (6–11). In some families, each affected person has PA-VSD, whereas in other families, various types of conotruncal defects, or CHDs, occurred. Wulfsberg et al. (12) described one family in which two siblings from nonconsanguineous parents had PA-VSD. Der Kaloustian et al. (13) described two siblings of first cousins with PA-VSD. Other families had members with TOF and a spectrum of pulmonary valvular abnormalities or conotruncal defects. These reports

support different modes of inheritance and support a role for genetic factors in the etiology of PA-VSD. The recurrence risk for any individual family can vary tremendously, depending on the number of affected persons and whether the CHD is associated with a single gene defect or a chromosomal deletion.

Many patients with PA-VSD have genetic syndromes and extracardiac anomalies. In the BWIS, 8.3% of cases with PA-VSD had chromosomal anomalies; 11.7% were syndromic (mendelian and nonmendelian), and 6.7% had other single organ defects (2). Thus, only 73.3% of patients with PA-VSD had no recognized associated anomalies.

Investigators have identified the genetic cause of the DiGeorge/velocardiofacial syndrome (DGS/VCFS). The phenotype associated with the 22q11.2 deletion syndrome (or DGS/VCFS) is highly variable and includes CHD, palatal anomalies, hypocalcemia, immunodeficiency, speech and learning disabilities, renal anomalies, psychiatric problems, and distinct facial features (14,15). The clinical features vary, not only among unrelated persons, but also among family members sharing the same 22q11.2 deletion. Furthermore, the clinical features can be subtle and go unrecognized. Eight percent to twenty-three percent of patients with TOF have a 22q11.2 deletion (16–19).

In a European collaborative study, 10% of patients with a 22q11 deletion had PA-VSD (20). In two studies, it was found that a 22q11.2 deletion occurred in patients with PA-VSD more frequently than in patients with TOF (21,22). In a third study, however, no statistical difference in the frequency of a 22q11.2 deletion in patients with PA-VSD was found compared with TOF/pulmonary stenosis (PS) (19). Additional vascular anomalies, such as aortopulmonary collaterals, right aortic arch, or aberrant subclavian artery, occur more frequently in patients with PA-VSD and a 22q11.2 deletion than in those without a deletion (19,23). Branch pulmonary arteries are smaller in patients with a 22q11.2 deletion than in those without the deletion (22,24). Clinical outcomes have been worse for patients with PA-VSD and the 22q11.2 deletion (25).

EMBRYOLOGY

During early gestation, the lungs develop from the foregut, and therefore their nutrient blood supply arises initially from the paired dorsal aortas. About day 27, the arterial branches of the paired sixth aortic arches form an anastomosis with the pulmonary vascular plexus. As a result, the lungs initially have a dual blood supply. During normal development, the branches from the sixth aortic arches enlarge, and those from the descending thoracic aorta become smaller. The larger vessels will form the true pulmonary arteries and deliver blood to the alveoli or capillaries that are derived from the pulmonary vascular plexus. The smaller vessels form the nutrient

bronchial arteries. Bronchopulmonary anastomoses persist but are of small caliber and tend to disappear postnatally. In the normal heart, supply to the derivatives of the sixth aortic arches (the true pulmonary arteries) will be the right ventricle (RV). However, in PA/VSD there is complete discontinuity of the RV and the central pulmonary arteries (Fig. 42.1). Therefore, the source of pulmonary blood supply is variable (26,27).

In a sense, the embryologic development of the pulmonary arteries is analogous to that of the pulmonary veins. Thus, the variable origins of pulmonary blood supply in cases of PA-VSD are analogous to the variable sites of drainage in total anomalous pulmonary venous connection. When the normal connection between the heart and pulmonary arteries does not develop, the alternate blood supply to the lungs can be from the ductus arteriosus, bronchial arteries, or other systemic-to-pulmonary collateral arteries.

PATHOLOGY

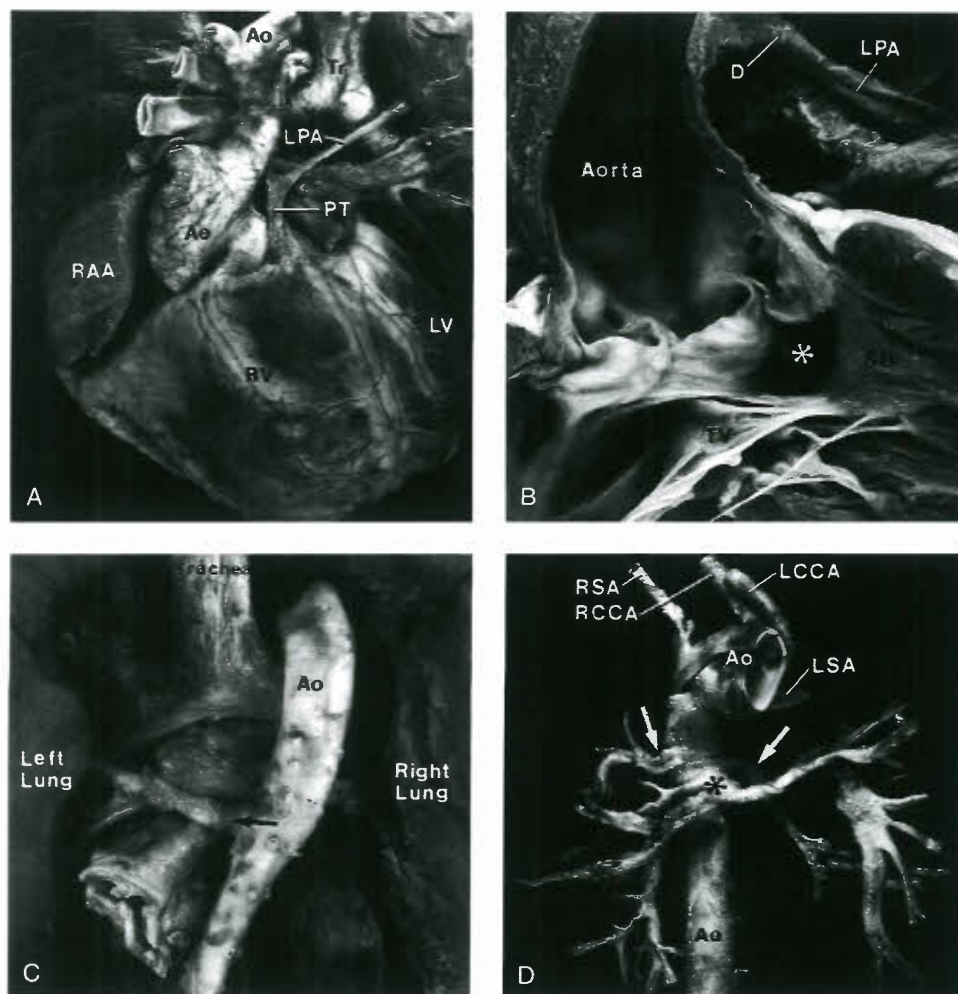
The extent of pulmonary artery atresia is quite variable and involves the central pulmonary arteries (i.e., those outside the lungs) either proximally and/or distally. The atretic arterial segment can be recognized as a solid elastic cord in about 75% of the cases but is unidentifiable in the other cases. Most commonly, the pulmonary valve and the proximal portion of the pulmonary trunk (PT) are involved. Rarely, only the

pulmonary valve is imperforate. The central right and left pulmonary arteries and/or the segmental pulmonary arteries can be confluent or nonconfluent. In PA-VSD, the blood supply to the lungs is entirely from the systemic arterial circulation. The sources are the ductus arteriosus, systemic-to-pulmonary collateral arteries (henceforth designated simply as collateral arteries), occasionally a coronary artery, and plexuses of bronchial or pleural arteries (26). Ductal and collateral sources may coexist in the same patient but only rarely coexist in the same lung (26). A single systemic arterial source to a lung is termed a unifocal blood supply, whereas multiple sources are termed multifocal blood supply.

The caliber of the central pulmonary arteries varies considerably and appears to be directly related to the amount of blood flow (26). When the ductus or collateral arteries connect proximally to the central pulmonary arteries or their lobar branches, the central vessels may be only mildly hypoplastic or even normal in size. In contrast, when multiple collateral arteries are anastomosed more distally at segmental or subsegmental levels, the central pulmonary arteries tend to be quite hypoplastic. Furthermore, stenosis of the systemic arterial channels, either congenital or acquired, can be associated with hypoplasia of the central pulmonary arteries (26).

The various patterns of intrapulmonary arterial distribution may be quite complex and are determined primarily by the types of systemic arterial blood supply (26). When a ductus supplies confluent central pulmonary arteries, the intrapulmonary arteries of both lungs are normal. When nonconfluent central pulmonary arteries are present, however, the lung

Figure 42.1. Pulmonary atresia and ventricular septal defect. **A:** Anterior view of unopened specimen from an 18-year-old patient shows dextroposed aorta (Ao), right aortic arch, and severely hypoplastic pulmonary trunk (PT) and left pulmonary artery (LPA). **B:** Opened right ventricle from a 1-year-old patient shows VSD (asterisk) cradled by limbs of septal band (SB) and left ductal origin (D) of the left pulmonary artery (LPA). **C:** Posterior view of mediastinal structures from a 4-year-old child with pulmonary situs inversus, right aortic arch, and right atrial isomerism shows origin of large systemic collateral artery (arrow) to left lung from descending thoracic aorta. **D:** Anterior view of right aortic arch from an 8-year-old child shows mirror-image brachiocephalic branching, aberrant retroesophageal left subclavian artery (LSA), and origin of two small collateral arteries (arrows) and one large trifurcating collateral artery (asterisk). (LCCA, left common carotid artery; LV, left ventricle; RAA, right atrial appendage; RCCA, right common carotid artery; RSA, right subclavian artery; RV, right ventricle; Tr, trachea; TV, tricuspid valve.)



supplied by a ductus will have a unifocal blood supply and a normal arterial distribution, but the contralateral lung usually has a multifocal blood supply and a fragmented pulmonary arterial distribution (so-called *arborization abnormality*) (26). When both lungs are supplied by multiple collateral channels, intrapulmonary arborization abnormalities are the rule (26), and a ductus is absent.

The ductus arteriosus, when present, usually is a unilateral structure and is associated with confluent pulmonary arteries in >80% of cases (26). Rarely, bilateral ductus may occur with nonconfluent pulmonary arteries. Unlike collateral arteries, the ductus does not branch before joining the central pulmonary arteries, and it tends to be less tortuous than collaterals. Because the ductus is widely patent during fetal life, the pulmonary arteries may be of normal size at birth. However, normal postnatal ductal narrowing usually occurs and produces distal stenosis in 35% to 50% of cases (26). As a result, blood flow to the lungs is diminished, and relative hypoplasia of the pulmonary arteries becomes more severe as the child grows.

Collateral arteries, when present, arise most commonly from the descending thoracic aorta, less commonly from the subclavian arteries, and rarely from the abdominal aorta or its branches or from the coronary arteries (26–28). Their number varies from 1 to 6, and their diameter ranges from 1 to 20 mm (26). Stenoses are present in nearly 60% of collateral arteries and tend to occur near the aortic or intrapulmonary anastomoses. The stenoses may be discrete or segmental, congenital or acquired (26). Anastomoses between the central pulmonary arteries (or their branches) and the collateral arteries are observed in about 40% of patients and may occur at the hilum or within the lung (26,29). In the remaining 60%, the collateral arteries enter the pulmonary hilum, travel with the bronchi as pulmonary arteries, and supply a variable number of bronchopulmonary segments (26). Although the central pulmonary arteries are confluent in about two-thirds of the cases, they usually supply only a portion of each lung owing to the coexistence of multiple collateral arteries and arborization abnormalities (26).

Small arterial plexuses that follow the bronchi or spread over the pleural surfaces may be apparent angiographically in more than half of the patients (26). They may arise from the aorta and its thoracic branches or from the systemic collateral arteries (26). It is thought that these vessels enlarge and proliferate postnatally in response to regional reductions in blood flow.

The ductus arteriosus is a precarious sole source of pulmonary blood supply, and its tendency to close necessitates surgical intervention in early infancy in more than half of the cases. Collateral arteries appear to be a more stable source of pulmonary blood flow, presumably because of multiple numbers. However, stenosis of collaterals may develop progressively, and they may become inadequate as the patient grows. Furthermore, because of hyperperfusion of some bronchopulmonary segments and hypoperfusion of others in the same patient, the pulmonary vascular bed may exhibit various histopathologic lesions, ranging from hypertensive pulmonary vascular disease to stasis thrombosis (26).

The VSD may be membranous or infundibular. Because it is also a malignancy defect with an overriding aorta, it tends to be larger than isolated membranous or infundibular defects. Rarely, the VSD can be obstructed partially by accessory tricuspid valvular tissue (30).

Although equal biventricular origin may occur, the aorta usually arises predominantly from the RV (31). The ascending aorta characteristically is dilated, but the degree of dextroposition usually is less than with TOF (31). Aortic valve insufficiency may result from annular dilation or infective endocarditis. A right aortic arch is present in 26% to 50% of the cases (31).

The right atrium tends to be dilated and hypertrophied, and the left atrium usually is normal. A secundum atrial septal defect (ASD) or patent foramen ovale is present in about half of the cases (31). Generally, the tricuspid orifice is of normal size, but minor leaflet abnormalities occur commonly. The mitral valve orifice tends to be normal or mildly hypoplastic (31).

Right ventricular hypertrophy is moderate to severe. The infundibulum ends blindly and may range in length from normal to very short. In many instances, the displaced infundibular septum is fused to the right ventricular wall. The left ventricular wall thickness generally is normal, and the chamber size tends to be normal or somewhat small (31). Occasionally (usually in older patients), the left ventricle (LV) is hypertrophied and dilated.

In most cases, the origin and distribution of the coronary arteries are normal. However, the conus artery tends to be quite prominent (31). Coronary anomalies include high origin of the coronary ostia, coronary-to-pulmonary artery fistulas, and origin of the right coronary artery from the left anterior aortic sinus, coursing across the right ventricular infundibulum (31).

The sinus node is normal. The atrioventricular node occupies its normal position within the triangle of Koch. The non-branching proximal portion of the His bundle penetrates the central fibrous body and lies along the left ventricular aspect of the posteroinferior rim of the VSD. The His bundle is related closely to the rim of membranous VSD, but is relatively remote from the border of infundibular defects. The sheet-like left bundle branch spreads along the ventricular septal endocardium in a relatively normal fashion. However, the cord-like right bundle branch must travel through the septal musculature to reach its subendocardial position along the septal band (SB) (septomarginal trabecula). It may be bifid or form several aberrant branches (32). Pulmonary atresia and VSD may be associated with other anomalies, including a persistent left superior vena cava to the coronary sinus, anomalies of the coronary sinus, partial or total anomalous pulmonary venous connection, tricuspid stenosis or atresia, complete atrioventricular septal defect, D- or L-transposition of the great arteries, dextrocardia, and heterotaxia syndromes (31).

Clinical Features

A patient with PA-VSD often presents as a cyanotic newborn. The infant may do well for a day or two, as long as there is substantial blood flow through a patent ductus arteriosus (PDA), but then becomes increasingly hypoxemic as the ductus constricts. If there are insufficient systemic-to-pulmonary artery collateral vessels, closure of the ductus will be lethal. Use of prostaglandin E₁ is critical in the early neonatal period to maintain ductal patency and stabilize the patient prior to surgery.

Some neonates with PA-VSD are not severely hypoxemic, either because the ductus arteriosus remains patent or because systemic collateral vessels are sufficiently developed to provide adequate pulmonary blood flow. These babies may maintain good oxygenation for some time. However, over time, hypoxemia and cyanosis increase as the patient outgrows the relatively fixed sources of pulmonary blood flow.

On rare occasions, an infant with PA-VSD may have heart failure and signs of increased pulmonary blood flow. This occurs most commonly at 4 to 6 weeks of age after the pulmonary arteriolar resistance has decreased. The increased pulmonary flow can be due to a large PDA or large systemic-to-pulmonary artery collateral vessels. This may be difficult to control medically, and surgical intervention may be necessary. In patients with a large PDA, the pulmonary arteries usually are well developed, and early complete repair may be feasible.

In the group of patients with large collateral vessels, however, the true pulmonary arteries frequently are hypoplastic with arborization abnormalities making definitive correction more difficult.

Patients with microdeletion of 22q11.2 tend to have more complex collateral and pulmonary arterial anatomy than patients without this genetic abnormality. Absence or severe hypoplasia of the central pulmonary arteries and the presence of multiple major collateral arteries reduces the likelihood of successful biventricular repair in these patients (22).

The presentation of patients with PA-VSD who have had palliative surgical procedures is quite variable. In the absence of significant valve regurgitation, heart failure is uncommon. Most patients are somewhat cyanotic, and some patients may be severely hypoxemic. As patients outgrow shunts performed early in life, they become increasingly cyanotic. These shunts usually improve oxygenation, but complications of shunts include distortion and stenosis of pulmonary arteries and occasionally lead to pulmonary vascular obstructive disease. These vascular complications are common, particularly in patients who have had either a Waterston (the ascending aorta to the right pulmonary artery connection) or Potts shunt (descending aorta to the left pulmonary artery [LPA] connection). As a result, these procedures, for the most part, have been abandoned. The classic or modified Blalock-Thomas-Taussig shunt is the preferred palliative shunt. Alternatively, initial palliation can be accomplished by establishing a direct connection between the ascending aorta and the remnant of the main pulmonary artery (33) or creating a nonvalved connection between the RV and hypoplastic confluent pulmonary arteries leaving the VSD open. These procedures produce more rapid enlargement of the central pulmonary arteries than systemic-to-peripheral pulmonary artery shunts and also produce less distortion of the peripheral pulmonary arterial architecture. However, in patients with inadequate distal distribution from the central confluence or those with significant peripheral stenosis, these large central connections may produce segmental pulmonary hypertension. Due to the fact that all palliative approaches are associated with potential complications, a substantial number of older patients will have arterial beds damaged by these procedures. The frequency of late arterial distortion also emphasizes the need to obtain a detailed understanding of the pulmonary vascular architecture prior to planning an interventional strategy.

Physical Examination

Profound cyanosis usually is present in the early neonatal period. The rare exception is the patient with a large PDA or well-developed systemic-to-pulmonary artery collaterals. Cyanosis may be mild immediately after birth, but it increases in severity during the first several days of life as the PDA closes. It is common for the degree of cyanosis and the arterial oxygen tension to fluctuate considerably during the first several days as the ductus arteriosus constricts and relaxes. After the neonatal period, the degree of cyanosis in these patients usually increases gradually as the patient's growth outstrips the pulmonary blood flow.

Growth and development can be delayed, but if pulmonary flow is adequate and systemic hypoxemia is only mild, this may not be the case. If growth is delayed, one should suspect the presence of a 22q11.2 microdeletion. Heart failure caused by excessive pulmonary blood flow is uncommon in these patients; therefore, growth failure on this basis is infrequent.

The peripheral pulses and blood pressure usually are normal in the neonatal period, even with a PDA, because the runoff into the lungs is not excessive during the first few weeks of life. In cyanotic patients, the pulses are normal.

However, in patients beyond the first 4 to 6 weeks of age in whom pulmonary blood flow through a PDA, collaterals, or surgically created shunt is substantial, the pulses can be bounding, and only minimal cyanosis may be present. The cardiac impulse usually is most prominent at the lower left sternal border. The heart size is normal for patients with normal or decreased pulmonary blood flow.

There is a normal first heart sound and a single loud second heart sound. A systolic murmur may be audible along the lower left sternal border but usually is not more than grade 3/6 in intensity. Because the RVOT is atretic, there is no separate loud systolic ejection murmur at the upper left sternal border. This is in contrast to the finding in TOF with antegrade pulmonary blood flow. If a PDA is present, a continuous murmur usually is heard after the first 4 to 6 weeks of life. If systemic-to-pulmonary collateral vessels are present, continuous murmurs can be heard. These may be multiple and often are most prominent over the back because these vessels usually originate from the descending aorta.

Electrocardiographic Features

Right ventricular hypertrophy and right-axis deviation are the rule. In patients with increased pulmonary blood flow (a small subgroup), combined ventricular hypertrophy and left atrial enlargement may occur. Electrocardiography often helps to differentiate this condition from pulmonary atresia with intact ventricular septum (VS), in which right ventricular hypoplasia usually is present and diminutive anterior QRS forces with left ventricular preponderance occur.

Radiographic Features

The heart frequently has a characteristic appearance likened to the shape of a boot (*coeur en sabot*). This is due to levorotation of the heart, which produces a prominent, upturned cardiac apex, secondary to right ventricular hypertrophy. There is also a concavity in the region of the main pulmonary artery produced by underdevelopment of the subpulmonary infundibulum. The frequency of a right-sided aortic arch is greater in patients with PA-VSD (26% to 50% of these patients) than in those with TOF (20% to 25%). The pulmonary vascular markings usually have a heterogeneous reticular appearance that does not conform to the usual arborization pattern of pulmonary vessels. This appearance is caused by collateral arteries from the systemic circulation that frequently are quite large and supply blood to the pulmonary artery. In patients with small systemic collaterals, the lung fields may have diminished vascular markings. In the patient with a large PDA and normally developed central pulmonary arteries, chest radiography shows enlarged central pulmonary arteries with increased peripheral vascularity.

Echocardiographic Features

Echocardiography usually provides the initial diagnosis, can determine the presence (and size) of a central pulmonary arterial confluence, can detect large collateral vessels, and can define many associated cardiovascular malformations. Echocardiographic techniques cannot completely delineate the distal pulmonary arterial tree or the sources of pulmonary arterial supply. Therefore, cardiac catheterization is necessary prior to definitive repair.

The 2-D echocardiographic appearance of PA-VSD is similar to that of TOF. Parasternal long-axis scans in both malformations show a large aortic valve that overrides a malaligned VSD (Fig. 42.2). The infundibular portion of the

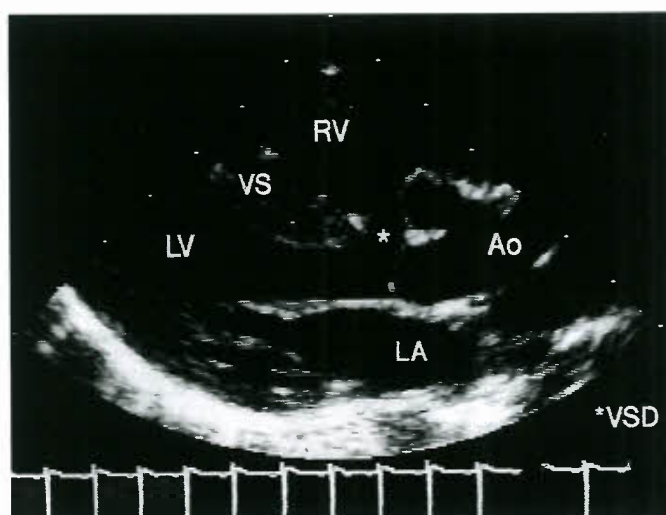


Figure 42.2. This parasternal long-axis image from a patient with PA-VSD demonstrates a large malalignment VSD (*VSD) and an overriding aortic valve. These features are also present in tetralogy of Fallot and truncus arteriosus. (Ao, aortic root; LA, left atrium; LV, left ventricle; RV, right ventricle; VS, ventricular septum.)

VS is anteriorly malpositioned. The difference between these malformations is that the patient with TOF has a patent, although hypoplastic, RVOT anterior to the malaligned infundibular septum. This outflow tract is in continuity with the main pulmonary artery. In contrast, the infundibular septum has fused with the right ventricular free wall in patients with PA-VSD, and there is no separate outflow from the RV. All of the RV stroke volume enters the overriding aorta via the VSD. Another malformation that shares some characteristics with PA-VSD is truncus arteriosus. The distinguishing feature between these two anomalies is that in truncus arteriosus, the pulmonary arteries arise directly from the posterolateral aspect of the truncal root prior to the arch.

Echocardiographic scans from the suprasternal notch and high parasternal windows (both right and left) frequently provide important information about the size and status of the proximal pulmonary arteries. When the pulmonary arteries are confluent and clearly identified by echocardiography, newborns with ductal-dependent pulmonary blood flow can undergo a palliative systemic-to-pulmonary artery shunt procedure without cardiac catheterization (34,35). The 2-D echocardiographic evaluation of these features can be difficult when the pulmonary arteries are nonconfluent, the pulmonary arteries are extremely hypoplastic, or multiple collateral arteries are present in the area of the confluence. In these situations, color flow imaging markedly enhances evaluation of the pulmonary and collateral arteries (35). This technique has been especially helpful in neonates with hypoplastic but confluent pulmonary arteries (35,36). Regardless of the quality of echocardiographic data available, we believe that angiography is required for a complete assessment of the pulmonary arterial tree in most patients with PA-VSD prior to attempting definitive biventricular repair with VSD closure.

Although all collateral arteries cannot be defined using echocardiography, their presence should be noted and their origins delineated as precisely as possible. Knowledge of an unusual origin of a collateral vessel (such as from the abdominal aorta, a brachiocephalic artery, or a coronary artery) (Fig. 42.3) can simplify subsequent cardiac catheterization and angiocardiographic procedures.



Figure 42.3. This modified parasternal short-axis scan demonstrates an unusual origin of a collateral artery. The right coronary artery gave rise to a large coronary-to-pulmonary artery fistula (*Fistula). This fistula supplied most of the flow to the pulmonary artery confluence. Ao, aortic root; LA, left atrium; RA, right atrium.

Echocardiographic examinations can define many of the other abnormalities associated with conotruncal malformations. The position of the malalignment VSD, usually either membranous or infundibular, can be determined. ASDs and additional muscular VSDs can be detected with 2-D and color flow imaging. Short-axis parasternal and subcostal scans have been helpful in detecting coronary artery abnormalities, especially in neonates. Color flow imaging and continuous wave Doppler techniques allow serial noninvasive assessments of surgically created shunts and right ventricular-to-pulmonary artery conduits (37,38). Suprasternal notch scans define the sidedness and branching pattern of the aortic arch.

Cardiac Catheterization and Angiocardiography

Patients with small central pulmonary arteries or multiple sources of pulmonary flow should have cardiac catheterization for pulmonary angiographic mapping before definitive repair. For the neonate undergoing palliation, it is our policy to refer patients with small, but echocardiographically detectable, centrally confluent pulmonary arteries for a shunt to establish a reliable source of pulmonary blood flow without catheterization. These patients, who often have hypoxemia and cyanosis in the first few days of life, are treated with prostaglandin E₁ to maintain ductal patency until they can have an operation. In infants who require more pulmonary blood flow and in whom no proximal pulmonary arteries can be visualized echocardiographically, catheterization and angiography are performed to determine the source of pulmonary blood flow and to define the possible surgical options to increase pulmonary blood flow.

Before a patient with PA-VSD and complex arterial anatomy can be considered for a definitive operation, cardiac catheterization is mandatory to delineate the size and distribution

of the true pulmonary arteries and to ascertain the extent of collateral blood supply to the lungs. Right atrial pressures are normal unless tricuspid regurgitation is present, and there is no increase of oxygenation at the atrial level unless an associated ASD is present. RV pressure is equal to the LV pressure because of the large VSD. Since the RVOT is atretic, the catheter cannot be advanced into the pulmonary arteries from the RV, but can be manipulated easily from the RV through the VSD into the aorta. Aortic pressure is normal if pulmonary blood flow is normal or decreased. Widened pulse pressure may be present if there is a large runoff into the lungs through a PDA or a previously constructed shunt. Systemic arterial blood oxygen desaturation is present, and the degree depends on the volume of pulmonary blood flow.

The true pulmonary artery pressure and resistance are normal in most instances. In a few cases, however, patients with a large PDA, a large communication between a systemic collateral vessel and the true pulmonary arteries, a large fistula connecting the coronary artery to the pulmonary artery, or a shunt anastomosis that is too large (particularly common in Waterston and Potts shunts) have increased pulmonary artery pressure. These patients are at risk for developing pulmonary vascular obstructive disease. In such cases, usually it is easy to enter the true pulmonary arteries through the large communication, measure the pressure, and estimate pulmonary flow by the Fick principle. With this information, pulmonary arteriolar resistance can be calculated.

Angiocardiography is useful during the preoperative evaluation of these patients. Documenting the existence of multiple VSDs and anatomy of the coronary arteries is extremely important, particularly in infants. Ventricular and aortic root angiography should be done if this information is unavailable from noninvasive imaging studies. Compound angulated views greatly enhance the angiographer's ability to demonstrate this anatomy (39). Ventriculography should be performed with an injection into the left ventricular cavity while the cameras are positioned to record a 70-degree left anterior oblique view with 20 degrees of cranial angulation. This projection displays the middle portion and most of the upper interventricular septum tangentially. Figure 42.4 illustrates this view and demonstrates the superiorly located malaligned VSD and exclusion of additional septal defects. Although the coronary artery anatomy can be visualized during a ventricular injection, it is better defined by an aortic root angiogram and a 70-degree left anterior oblique view (with or without 20 degrees of cranial angulation). This projection identifies the relevant coronary artery anatomy. Of surgical importance is the origin of the left anterior descending coronary artery from the right coronary artery, which occurs in approximately 5% of patients (39). It is particularly important to define the coronary artery preoperatively if there have been previous surgical procedures resulting in pericardial adhesions that obscure the coronary anatomy. We found it necessary to do selective injection of individual coronary arteries only in patients with large aortic roots and high rates of flow (particularly in patients with Waterston shunts).

Angiographic delineation of the anatomy of pulmonary blood supply is of critical importance. Although it may be possible to accomplish this from a venous approach by crossing the VSD, the retrograde arterial approach is used most often because it allows easier access to surgically created shunts or systemic collateral vessels. A large-field radiographic format using biplane angiocardiography is advantageous in this situation. The image should provide a large field of view, ideally visualizing both lung fields simultaneously. Subtraction techniques have also proved useful in demonstrating the anatomy of interest.

Determining the presence or absence of a central pulmonary arterial confluence is of paramount importance. In addition,



Figure 42.4. Long-axis oblique view of left ventriculogram. Note single large VSD just inferior to aortic valve.

a detailed analysis of the systemic arterial collateral blood supply to the pulmonary arterial tree, which includes identification of the degree of intercommunication among the various vascular pathways, must be done. If a pulmonary artery confluence is present, the systemic-to-pulmonary collateral vessels may communicate directly with it or connect to it indirectly by a connection to a peripheral branch of the pulmonary artery. In addition, systemic collaterals may not communicate with central pulmonary arteries at all, instead terminating by connections to peripheral pulmonary artery branches that are separate from the confluence (noncommunicating) (29).

Angiographic evaluation should be tailored to the type of systemic-to-pulmonary collateral artery anatomy found in each patient. Historically, an initial aortogram was necessary to demonstrate the number and location of the systemic-to-pulmonary collateral arteries (Fig. 42.5). However, prior delineation of at least the origins of collateral vessels by echocardiography or other imaging studies allows one to proceed directly to selective injections in some cases. This avoids the larger-volume contrast injection used during nonselective aortography. Thus, nonselective injections now more frequently are performed later in a catheterization, if the pulmonary segmental arterial anatomy has not been defined completely by selective injections. The purpose of selective injections in the systemic-to-pulmonary collateral arteries usually is to delineate the extent of the pulmonary arterial tree supplied by each collateral vessel and to determine which type of pulmonary artery connection is present (Fig. 42.6). Such collateral injections can be enhanced by selective balloon occlusion techniques (40).

Both the central and the peripheral pulmonary arteries must be demonstrated. This allows detection of discrete stenoses or tubular hypoplasia involving the pulmonary arteries as well as the degree to which the central and peripheral pulmonary arteries communicate (41). Both the size and the peripheral distribution of the pulmonary arteries are important in planning the surgical treatment of these patients.

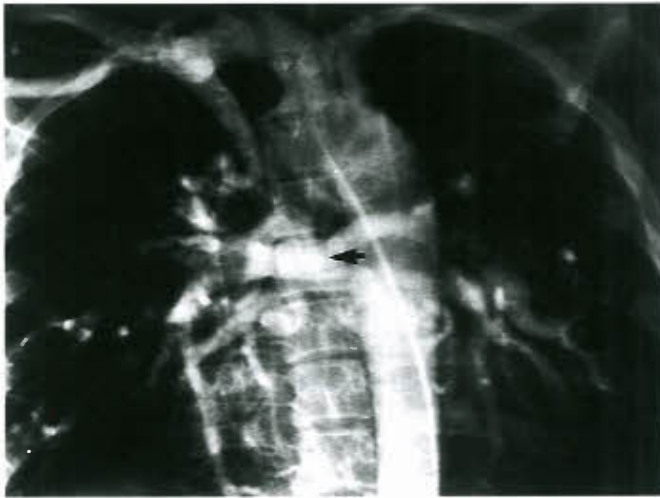


Figure 42.5. Aortogram demonstrates relatively large pulmonary confluence (arrow) but fails to define connections of individual, systemically derived collateral arteries.

Identifying communications between adjacent areas of the peripheral pulmonary arterial tree is particularly important and requires close attention to the sequential flow of contrast medium. Occasionally, an evanescent negative washout pattern can be appreciated that is due to a stream of unopacified blood from a connecting pulmonary artery flowing into an area of opacified pulmonary arterial tree. This may be the only indication of an existing communication (Fig. 42.6). If the initial echocardiogram or aortogram does not allow identification of a pulmonary artery confluence and selective injection of systemic-to-pulmonary collateral arteries fails to identify such a confluence, a retrograde pulmonary vein wedge injection may be helpful to identify hypoplastic central pulmonary arteries (Fig. 42.7).

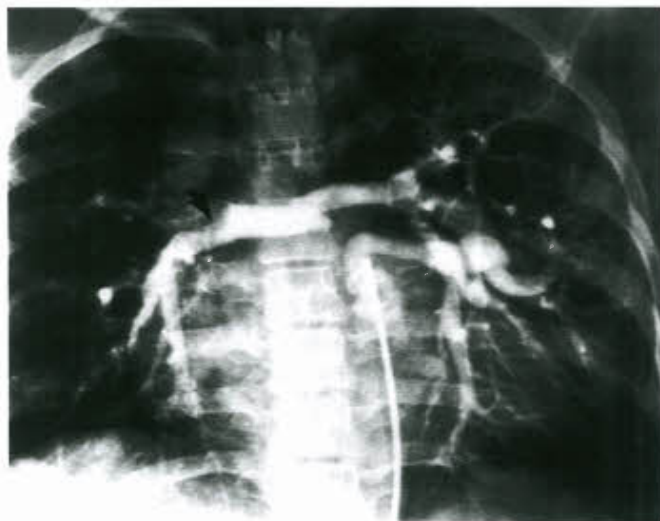


Figure 42.6. Selective injection into a collateral artery arising from middle portion of descending thoracic aorta (same patient as in Fig. 42.5). Opacification of a pulmonary artery confluence by contrast medium indicates that a direct communication exists between the pulmonary artery confluence and the systemic collateral. Note stream of unopacified blood (arrow) washing out contrast medium in right pulmonary artery, an indication of competitive blood flow from a connecting vessel (see text).

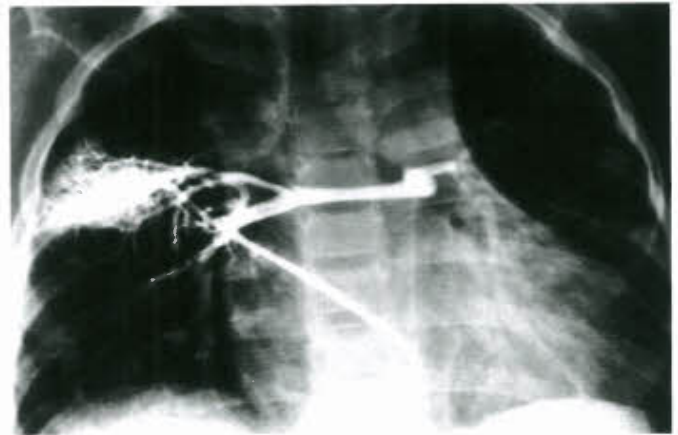


Figure 42.7. Pulmonary vein wedge angiogram demonstrating a hypoplastic pulmonary artery confluence.

Some patients with complex patterns of pulmonary blood supply may require multiple injections of contrast material before the pulmonary vascular supply is documented. Because these patients often are hypoxemic and polycythemic, our policy is to inject a total dose of not more than 5 to 6 mL of contrast material per kilogram of body weight during any single procedure. This approach occasionally necessitates that the patient's diagnostic catheterization be divided into two sessions separated by at least 24 hours. Adequate hydration of these patients before, during, and after the study is mandatory to prevent thromboembolic complication or a potential complication secondary to hyperosmolality caused by the contrast material. Magnetic resonance imaging of sources of pulmonary blood can reduce the amount of contrast material needed at the time of angiographic examination (42).

DIFFERENTIAL DIAGNOSIS

The differential diagnosis of the cyanotic infant includes TOF, transposition of the great arteries, tricuspid atresia, double-outlet RV with severe PS or PA, single ventricle with severe PS or PA, and total anomalous pulmonary venous connection with pulmonary venous obstruction. In the patient with PA-VSD in whom the pulmonary blood supply is normal or increased, the differential diagnosis includes lesions in which cyanosis is minimal and evidence of heart failure may be present. Such lesions include VSD, large PDA, atrioventricular septal defect, double-outlet RV or single ventricle without significant PS, persistent truncus arteriosus, and total anomalous pulmonary venous connection without pulmonary venous obstruction.

Physical examination often gives important clues to the correct diagnosis. When the physical examination is complemented by an electrocardiogram and chest radiograph, an accurate clinical diagnosis often can be established. Echocardiography is the noninvasive means to make an accurate diagnosis.

NATURAL HISTORY

The natural history of PA-VSD depends primarily on the adequacy of the pulmonary blood supply. Infants in whom a PDA is the primary source of pulmonary blood supply may become critically hypoxemic within the first few days of life as the PDA begins to close. In patients in whom the pulmonary blood

supply primarily is through systemic-to-pulmonary collaterals, the natural history can vary greatly because it depends on the adequacy of pulmonary blood supply by these channels. Most patients would have had an operation to increase pulmonary blood flow; however, some patients can reach adulthood without having undergone palliative surgery.

TREATMENT

Medical treatment for heart failure may be indicated for the rare patient with PA-VSD who has excessive pulmonary flow. Phlebotomy may occasionally offer relief from the side effects of extreme polycythemia in extremely hypoxemic patients. However, the treatment of the vast majority of PA-VSD patients is surgical.

It is critical to map the pulmonary artery architecture and sources of pulmonary blood supply. In addition, the degree of communication between the central pulmonary arteries and the major aortopulmonary collateral arteries (MAPCAs) must be determined preoperatively.

The goals of operation can be palliative for those patients whose pulmonary artery anatomy precludes complete repair. Depending on the clinical presentation, palliation can be accomplished by procedures designed to augment pulmonary arterial blood flow (systemic-pulmonary artery shunts, unifocalization) or by procedures designed to reduce pulmonary blood flow (interruption of unnecessary MAPCAs, unifocalization). In contrast, for patients whose pulmonary artery anatomy appears amenable to reconstruction, procedures leading to complete repair are indicated. Such procedures have included right ventricular outflow reconstruction for inducement of central pulmonary artery growth. This involves connecting the RV to the central pulmonary artery using a conduit. Such a connection can promote growth of the hypoplastic central pulmonary arteries so that they are adequate for complete repair (43). Unifocalization procedures involve disconnecting MAPCAs from their aortic origins, so that they can be positioned in the vicinity of the heart (or the central confluence) for final connection to the RV (Fig. 42.8). Connections between non-communicating segments are created, and a single source of flow is provided to the unifocalized lung. These unifocalizations are designed to incorporate the maximum number of pulmonary artery segments into the eventual right ventricular outflow reconstruction. The ultimate goal of such reconstructions is complete repair, defined as closure of all septal defects, interruption of all extracardiac sources of pulmonary arterial blood flow, and incorporation of at least 14 pulmonary arterial segments in a connection to the RV (44,45). Additionally, the central pulmonary artery size should be at least 50% of normal. At the end of operation, the right ventricular pressure should be $\leq 70\%$ that measured in the LV (some evidence suggests that pressure ratios of $< 60\%$ may offer a better long-term outlook). If higher, the VSD is fenestrated.

Historically, a staged reconstructive surgical approach was applied in patients who did not meet the criteria for complete repair at presentation (46). This involved lateral thoracotomies for “unifocalization” procedures to deal with significant arborization abnormalities of the pulmonary arteries and to create a single, central arterial source for each lung. If these operations were successful, the two reconstructed central pulmonary arteries were connected. Complete repair was performed at a later date.

Cho et al. (47) reported their experience with 495 patients treated with this approach. One hundred and sixty patients had preliminary surgical staging, including systemic-to-pulmonary artery shunts, right ventricular outflow reconstruction, and/or unifocalization procedures. Actuarial survival data are shown in

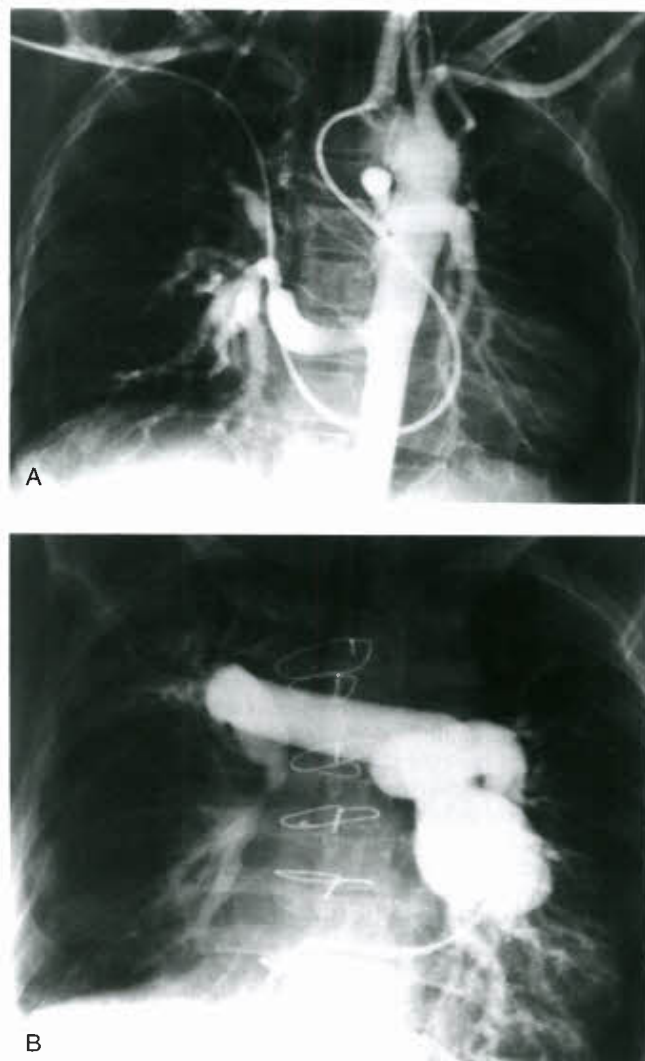


Figure 42.8. A: Preoperative aortogram. Note two large systemic-to-pulmonary collateral arteries, absence of a pulmonary artery confluence, and abnormal branching pattern of right pulmonary artery. B: Postoperative angiogram with an injection of contrast medium in right ventricular outflow tract demonstrates establishment of continuity between the branches of the right pulmonary arterial tree and creation of a pulmonary artery confluence.

Figure 42.9. The presence of MAPCAs was a significant factor associated with late mortality ($p = 0.0182$). Most of the patients (68%, $n = 335$) eventually underwent complete repair. Age at the time of complete repair ranged from 1 day to 54.6 years (mean, 11.3 years). Surgical mortality was 4.5%. Twenty-four patients had repair during the first year of life. There were two surgical deaths in this group (8.3%). At the end of the operation, the systolic pressure ratio between the RV and LV was 0.66 (SD = 0.180). The VSD was reopened in 22 patients who had excessively high right ventricular pressure (RV/LV systolic pressure > 0.85). Follow-up of 320 patients ranged from 1 month to 23 years (mean, 11.4 years). Fifty-two (16.3%) early survivors died during the follow-up period. Actuarial survival data are shown in Figure 42.10. The major predictor for late mortality was the need for reopening the VSD. Other investigators have reported similar results with the staged approach (48,49). We currently use this approach only in select patients.

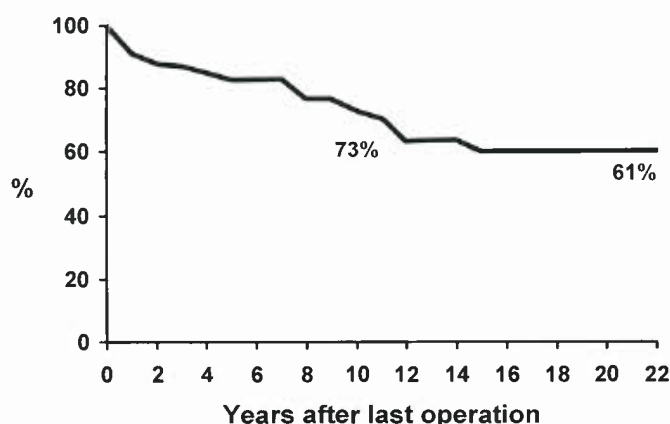


Figure 42.9. Actuarial survival of patients who underwent palliative or reconstructive procedures, but had not yet undergone or were turned down for complete intracardiac repair. (From Cho JM, Puga FJ, Danielson GK, et al. Early and long-term results of the surgical treatment of tetralogy of Fallot with pulmonary atresia, with or without major aortopulmonary collateral arteries. *J Thorac Cardiovasc Surg* 2002;124:70–81, with permission.)

McElhinney et al. (50) and Reddy et al. (51,52) have proposed an alternative single-stage unifocalization/complete repair approach for previously unoperated patients with PA-VSD. Using a median sternotomy and cardiopulmonary bypass, both the right and left pulmonary arteries and MAP-CAs are unifocalized directly to the RVOT. A valved conduit is used to reconstruct the atretic RVOT. Malhorta and Hanley (53) have reported that a “complete” unifocalization could be accomplished in 76% of 464 patients managed in this way. Immediate closure of the VSD was possible in 56% of their patients. Over time, VSD closure was performed in 90% of the initial cohort (within 5 years of the midline, “single-stage” unifocalization). Overall surgical mortality for the series was 5.9%. The RV/LV systolic pressure ratio after VSD closure was <50% in over two-thirds of cases, and was stable during early follow-up (mean, 7 years). The earlier interventions inherent in this more aggressive approach may reduce the occurrence of segmental pulmonary vascular disease and progressive “loss”

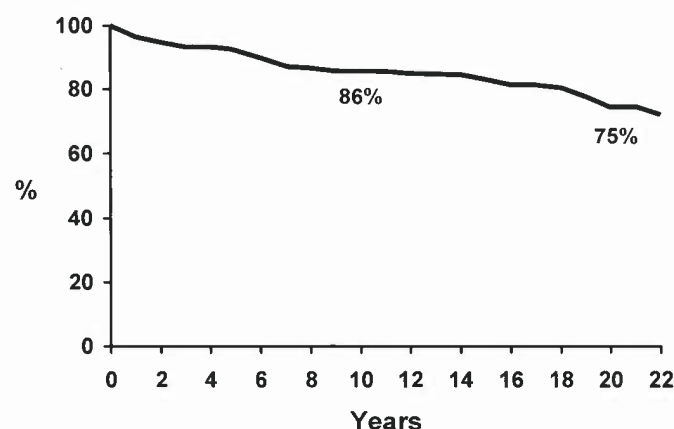


Figure 42.10. Actuarial survival of patients who underwent complete repair in a single setting or after preliminary surgical stages. (From Cho JM, Puga FJ, Danielson GK, et al. Early and long-term results of the surgical treatment of tetralogy of Fallot with pulmonary atresia, with or without major aortopulmonary collateral arteries. *J Thorac Cardiovasc Surg* 2002;124:70–81, with permission.)

of segmental pulmonary arteries. However, longer duration of follow-up is needed to be certain of these benefits. Restenosis of both the reconstructed pulmonary arterial tree and the RV outflow conduit continue to pose late problems for these patients regardless of the initial surgical approach.

Our current approach at Mayo Clinic is similar favoring complete unifocalization via median sternotomy at 4 to 8 months of age in newly diagnosed patients. When an acceptable bilateral unifocalization can be achieved, the VSD is closed and right ventricular pressure is measured intraoperatively. An RV/LV ratio of >0.7 prompts VSD patch fenestration. In patients who require patch fenestration or in those who do not have VSD closure, the reconstructed RVOT allows pulsatile flow to the central pulmonary arteries as a stimulus for growth and catheter access for subsequent interventions in anticipation of eventual complete repair.

REPRODUCTIVE ISSUES

Patients with PA-VSD who become parents run a higher-than-normal risk that their children will have a congenital heart lesion. Women who have had correction and who have pulmonary artery pressures that are normal or only slightly increased should tolerate pregnancy well. For women in whom significant pulmonary artery hypertension persists after correction, pregnancy probably is not advisable. Likewise, in palliated patients who remain hypoxemic, pregnancy carries a risk to both the mother and the fetus (54).

REFERENCES

- Perry LW, Neill CA, Ferencz C, et al. Infants with congenital heart disease: the cases. In: Ferencz C, Rubin JD, Loffredo CA, et al., eds. *Perspectives in Pediatric Cardiology: Epidemiology of Congenital Heart Disease. The Baltimore-Washington Infant Study 1981–1989*. Armonk, NY: Futura Publishing, 1993:33–62.
- Ferencz C, Loffredo CA, Correa-Villasenor A, et al. eds. *Malformations of the Cardiac Outflow Tract in Genetic and Environmental Risk Factors of Major Cardiovascular Malformations. The Baltimore-Washington Infant Study 1981–1989*. Armonk, NY: Futura Publishing, 1997:59–102.
- Lammer EJ, Chen DT, Hoar RM, et al. Retinoic acid embryopathy. *N Engl J Med* 1985;313:837–841.
- Koch R, Levy HL, Matalon R, et al. The North American collaborative study of maternal phenylketonuria. *Am J Dis Child* 1993;147:1224–1230.
- Feldman GL, Weaver DD, Lovrien EW. The fetal trimethadione syndrome. *Am J Dis Child* 1977;131:1389–1392.
- Ando M, Takao A, Mori K. Genetic and environmental factors in congenital heart disease. In: Inouye E, Nishimura H, eds. *Gene-Environmental Interaction in Common Diseases*. Baltimore, MD: Baltimore University Park Press, 1977:71–88.
- Sanchez-Cascos A. The recurrence risk in congenital heart disease. *Eur J Cardiol* 1978;7:197–210.
- Dennis NR, Warren J. Risks to the offspring of patients with some common congenital heart defects. *J Med Genet* 1981;18:8–16.
- Nora JJ, Nora AH. Genetics and environmental factors in the etiology of congenital heart disease. *South Med J* 1976a;69:919–926.
- Zellers TM, Driscoll DJ, Michels VV. Prevalence of significant congenital heart defects in children of parents with Fallot's tetralogy. *Am J Cardiol* 1990;65:523–526.
- Burn J, Brennan P, Little J, et al. Recurrence risks in offspring of adults with major heart defects: results from first cohort of British collaborative study. *Lancet* 1998;351:311–316.
- Wulfsberg EA, Zintz EJ, Moore JW. The inheritance of conotruncal malformations: a review and report of two siblings with tetralogy of Fallot with pulmonary atresia. *Clin Genet* 1991;40:12–16.
- Der Kaloustian VM, Ratl H, Malouf J, et al. Tetralogy of Fallot with pulmonary atresia in siblings. *Am J Med Genet* 1985;21:119–122.
- Thomas JA, Graham JM. Chromosome 22q11 deletion syndrome: an update and review for the primary pediatrician. *Clin Pediatr* 1997;36:253–266.
- Emanuel BS, Budarf ML, Scrambler PJ. The genetic basis of conotruncal cardiac defects: the chromosome 22q11.2 deletion. In: Harvey RP, Rosenthal N, eds. *Heart Development*. New York, NY: Academic Press, 1999:463–478.

16. Amati F, Mari A, Digilio MC, et al. 22q11 deletions in isolated and syndromic patients with tetralogy of Fallot. *Hum Genet* 1995;95:479-482.
17. Takahashi K, Kido S, Hoshino K, et al. Frequency of a 22q11 deletion in patients with conotruncal cardiac malformations: a prospective study. *Eur J Pediatr* 1995;154:878-881.
18. Trainer AH, Morrison N, Dunlop A, et al. Chromosome 22q11 microdeletions in tetralogy of Fallot. *Arch Dis Child* 1996;74:62-63.
19. Goldmuntz E, Clark BJ, Mitchell LE, et al. Frequency of 22q11 deletions in patients with conotruncal defects. *J Am Coll Cardiol* 1998;32:492-498.
20. Ryan AK, Goodship JA, Wilson DI, et al. Spectrum of clinical features associated with interstitial chromosome 22q11 deletions: a European collaborative study. *J Med Genet* 1997;34:798-804.
21. Digilio MC, Marino B, Grazioli S, et al. Comparison of occurrence of genetic syndromes in ventricular septal defect with pulmonic stenosis (classic tetralogy of Fallot) versus ventricular septal defect with pulmonic atresia. *Am J Cardiol* 1996;77:1375-1376.
22. Chessa M, Butera G, Bonhoeffer P, et al. Relation of genotype 22q11 deletion to phenotype of pulmonary vessels in tetralogy of Fallot and pulmonary atresia-ventricular septal defect. *Heart* 1998;79:186-190.
23. Momma K, Kondo C, Matsuoka PR, et al. Tetralogy of Fallot with pulmonary atresia associated with chromosome 22q11 deletion. *J Am Coll Cardiol* 1996;27:198-202.
24. Hofbeck M, Rauch A, Buheite G, et al. Monosomy 22q11 in patients with pulmonary atresia, ventricular septal defect, and major aortopulmonary collateral arteries. *Heart* 1998;79:180-185.
25. Mahle WT, Crisalli J, Coleman K, et al. Deletion of chromosome 22q11.2 and outcome in patients with pulmonary atresia and ventricular septal defect. *Ann Thorac Surg* 2003;76:567-571.
26. Liao PK, Edwards WD, Julsrud PR, et al. Pulmonary blood supply in patients with pulmonary atresia and ventricular septal defect. *J Am Coll Cardiol* 1985;6:1343-1350.
27. Ramsay JM, Macartney FJ, Haworth SG. Tetralogy of Fallot with major aortopulmonary collateral arteries. *Br Heart J* 1985;53:167-172.
28. Rabinovitch M, Herrera-deLeon V, Castaneda AR, et al. Growth and development of the pulmonary vascular bed in patients with tetralogy of Fallot with or without pulmonary atresia. *Circulation* 1981;64:1234-1249.
29. Faller K, Haworth SG, Taylor JFN, et al. Duplicate sources of pulmonary blood supply in pulmonary atresia with ventricular septal defect. *Br Heart J* 1981;46:263-268.
30. Fisher EA, Thanopoulos BD, Eckner FAO, et al. Pulmonary atresia with obstructed ventricular septal defect. *Pediatr Cardiol* 1980;1:209-217.
31. Bharati S, Paul MH, Idriss FS, et al. The surgical anatomy of pulmonary atresia with ventricular septal defect: pseudotruncus. *J Thorac Cardiovasc Surg* 1975;69:713-721.
32. Davies MJ, Anderson RH, Becker AE. *The Conduction System of the Heart*. Stoneham, MA: Butterworth-Heinemann, 1983:121-124.
33. Watterson KG, Wilkinson JL, Karl TR, et al. Very small pulmonary arteries: central end to side shunt. *Ann Thorac Surg* 1991;52:1132-1137.
34. Marino B, Pasquini L, Guccione P, et al. Pulmonary atresia with ventricular septal defect: selection of patients for systemic-to-pulmonary artery shunt based on echocardiography. *Chest* 1991;99:158-161.
35. Acherman RJ, Smallhorn JF, Freedom RM. Echocardiographic assessment of pulmonary blood supply in patients with pulmonary atresia and ventricular septal defect. *J Am Coll Cardiol* 1996;28:1308-1313.
36. Smyllie JH, Sutherland GR, Keeton BR. The value of Doppler color flow mapping in determining pulmonary blood supply in infants with pulmonary atresia with ventricular septal defect. *J Am Coll Cardiol* 1989;14:1759-1765.
37. Reeder GS, Currie PJ, Fyfe DA, et al. Extracardiac conduit obstruction: initial experience in the use of Doppler echocardiography for noninvasive estimation of pressure gradient. *J Am Coll Cardiol* 1984;4:1006-1011.
38. Silvilairat S, Cabalka AK, Cetra F, et al. Outpatient echocardiographic assessment of complex pulmonary outflow stenosis: Doppler mean gradient is superior to the maximum instantaneous gradient. *J Am Soc Echocardiogr* 2005;18:1143-1148.
39. Elliott LP, Bargerion LM Jr, Bream PR, et al. Axial cineangiography in congenital heart disease. II: specific lesions. *Circulation* 1977;56:1084-1093.
40. Hrudka J, Julsrud PR. Diagnostic selective balloon occlusion technique in pulmonic valve atresia and ventricular septal defect. *Am J Cardiol* 1989;63:1408-1409.
41. Mair DD, Julsrud PR. Diagnostic evaluation of pulmonary atresia and ventricular septal defect: Cardiac catheterization and angiography. *Prog Pediatr Cardiol* 1992;1:23-36.
42. Rees RSO, Somerville J, Underwood SR, et al. Magnetic resonance imaging of the pulmonary arteries and their systemic connections in pulmonary atresia: comparison with angiographic and surgical findings. *Br Heart J* 1987;58:621-626.
43. Puga FJ, Uretzky G. Establishment of right ventricle-hypoplastic pulmonary artery continuity without the use of extracorporeal circulation. *J Thorac Cardiovasc Surg* 1982;83:74-80.
44. Puga FJ, Leoni FE, Julsrud PR, et al. Complete repair of pulmonary atresia, ventricular septal defect, and severe peripheral arborization abnormalities of the central pulmonary arteries: experience with preliminary unifocalization procedures in 38 patients. *J Thorac Cardiovasc Surg* 1989;98:1018-1028.
45. Matsuda H, Hirose H, Nakano S, et al. Management of large aortopulmonary collateral arteries in patients with ventricular septal defect and pulmonary atresia: simultaneous ligation through median sternotomy during intracardiac repair. *Ann Thorac Surg* 1985;40:593-598.
46. Millikan JS, Puga FJ, Danielson GK, et al. Staged surgical repair of pulmonary atresia, ventricular septal defect, and hypoplastic, confluent pulmonary arteries. *J Thorac Cardiovasc Surg* 1986;91:818-825.
47. Cho JM, Puga FJ, Danielson GK, et al. Early and long-term results of the surgical treatment of tetralogy of Fallot with pulmonary atresia, with or without major aortopulmonary collateral arteries. *J Thorac Cardiovasc Surg* 2002;124:70-81.
48. Iyer KS, Mee RBB. Staged repair of pulmonary atresia with ventricular septal defect and major systemic to pulmonary artery collaterals. *Ann Thorac Surg* 1991;51:65-72.
49. Gupta A, Odum J, Levi D, et al. Staged repair of pulmonary atresia with ventricular septal defect and major aortopulmonary collateral arteries: experience with 104 patients. *J Thorac Cardiovasc Surg* 2003;126:1746-1752.
50. McElhinney DB, Reddy VM, Hanley FL. Tetralogy of Fallot with major aortopulmonary collaterals: early total repair. *Pediatr Cardiol* 1998;19:289-296.
51. Reddy VM, Petrossian E, McElhinney DB, et al. One-stage complete unifocalization in infants: when should the ventricular septal defect be closed? *J Thorac Cardiovasc Surg* 1997;113:858-868.
52. Reddy VM, McElhinney DB, Amin Z, et al. Early and intermediate outcomes after repair of pulmonary atresia with ventricular septal defect and major aortopulmonary collateral arteries: experience with 85 patients. *Circulation* 2000;101:1826-1832.
53. Malhorta SP, Hanley FL. Surgical management of pulmonary atresia with ventricular septal defect and major aortopulmonary collaterals: a protocol-based approach. *Semin Thorac Cardiovasc Surg Pediatr Card Surg Annu* 2009;12:145-151.
54. Atanassoff PG, Schmid ER, Jenni R, et al. Epidural anesthesia for a cesarean section in a patient with pulmonary atresia and ventricular septal defect. *J Clin Anesth* 1991;3:399-402.

Tetralogy of Fallot with Pulmonary Stenosis and Tetralogy of Fallot with Absent Pulmonary Valve

S. Lucy Roche ■ Steven C. Greenway ■ Andrew N. Redington

In many ways, tetralogy of Fallot (TOF) could be considered the archetype congenital heart disease (CHD); setting a pattern for the evolution of anatomical description, surgical management, pathophysiological understanding, and the appreciation of late outcomes in adult life. The origins of congenital cardiac surgery can be traced back to the early palliative procedures for TOF, and the triumph of efforts toward its surgical “correction” were quickly replicated in other conditions. Over the past 60 years, outcomes for patients with TOF have been transformed, so that now (assuming they have access to surgery) almost all infants born with TOF are expected to survive. Through the careful long-term study of these patients, TOF has become a model for late pathophysiology after CHD repair, and as we have learned more, our approach to surgical correction has adapted and changed. The late outcomes of patients with repaired TOF taught us the importance of providing lifelong follow-up for patients with CHD, and at the other end of the spectrum, TOF is leading the way in elucidating the genetic causes of CHD. In this chapter, we review not just the epidemiology, anatomy, and treatment of TOF, but its history. We hope to highlight just how much progress has been made and how the contributions of many have revolutionized outcomes for patients with this condition and developed our understanding of CHD as a whole.

EPIDEMIOLOGY

TOF is the commonest form of cyanotic CHD. A 2002 meta-analysis of the incidence of CHD, which included 41 studies pertaining to TOF, suggested that the best estimate of incidence would be 577 cases of TOF per million live births (1). The prevalence of TOF (number of patients living with the diagnosis at any given time) has significantly increased since the introduction of successful surgical repair. In the year 2000, the prevalence of TOF in the adult population of Quebec was $\approx 0.17/1,000$, and in Quebec’s children, the prevalence was $\approx 0.49/1,000$ (2). Consequently, it has been suggested that for many countries there are now numerically more adults with TOF than children.

TOF has a nearly equal sex distribution with perhaps a slight predominance in males. In a study that included information from 2.5 million live born infants and stillborn fetuses over a 10-year period, the Californian Birth Defects Monitoring Program reported a 1.1 relative risk of TOF in males compared to females (CI 0.9 to 1.3) (3). Maternal race seems to have little effect on incidence (4). Several studies have considered recurrence risk. Several studies have considered recurrence risk, both in siblings and offspring of the proband. A patient with TOF has approximately 2% to 3% chance of

having a sibling with CHD, although not necessarily TOF (5,6). Recurrence risk in the offspring of patients with TOF is undoubtedly affected by whether or not the proband has 22q.11.2 deletion. In the absence of 22q.11.2 deletion, prospective parents might expect 3% to 4% risk of having a child with CHD (5,7).

ETIOLOGY (GENETIC AND ENVIRONMENTAL FACTORS)

Although familial disease contributes only a small fraction to the overall incidence of TOF, its increased frequency in consanguineous populations (8) and markedly increased recurrence risk in some pedigrees (9) allude to a central role for genetics in the underlying etiology. While a chromosomal duplication or a microdeletion at the 22q11.2 locus occurs in approximately 20% of patients with TOF and single gene mutations have been identified in others, in at least 50% to 60% of patients with TOF the causal genetic influences remain unknown (Fig. 43.1). However, this is a rapidly advancing field and with advances in both genomics and our understanding of human cardiogenesis, this percentage is likely to decrease. The relatively large number of distinct genetic loci that have been associated with TOF highlights the complexity and apparent genetic heterogeneity of cardiovascular development.

TOF is found in two broad categories of patients: *syndromic* TOF, which occurs in the presence of additional noncardiac congenital anomalies and, the more common, *nonsyndromic* TOF, which occurs in apparent isolation, usually appearing sporadically in families with no history of CHD. Even within these two distinct classes, there is significant genetic overlap with mutations having been identified in the same gene in both syndromic and nonsyndromic patients (Fig. 43.2).

Syndromic Tetralogy of Fallot

To date, TOF is associated with 96 entries in the Online Mendelian Inheritance in Man (OMIM) database (<http://www.ncbi.nlm.nih.gov/omim>), and there are 32 listed syndromes that include the presence of TOF as a characteristic feature. Furthermore, there are many case reports and series of TOF in association with other syndromes in which the presence of a heart defect is more variable. The best known syndrome and most frequently identified cause of TOF occur as a result of a 22q11.2 microdeletion. This deletion has a prevalence of approximately 1 per 6,000 to 10,000 live births, with males

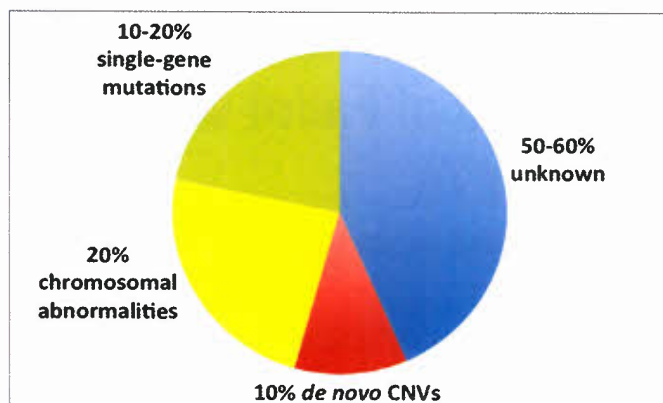


Figure 43.1. An illustration of the genetic causes of TOF.

and females equally affected (10–12), although frequencies as high as 1 per 3,000 to 1 in 6,000 live births have been cited in some populations (13). A hemizygous deletion of chromosome 22q11.2 or, rarely, point mutations within *TBX1* itself cause haploinsufficiency of the transcription factor *TBX1* and result in the 22q11.2 microdeletion syndrome also known as DiGeorge syndrome, the velocardiofacial syndrome, or by several other names (14–18). Today, the recommendation is that the syndrome be described using molecular terminology, that is, 22q11.2 microdeletion with the term DiGeorge syndrome reserved for those rare patients who have the clinical features but with no identified mutation (13).

The most common mutation at the 22q11.2 locus is a 3 megabase (Mb) deletion responsible for 90% of cases (19). Atypical deletions have also been described and increasing use of SNP arrays as an alternative to fluorescent in situ hybridization (FISH) for molecular diagnosis may enhance our knowledge regarding the frequency and effect of these atypical mutations (13). While most cases of 22q11.2 deletion arise sporadically as the result of de novo mutations, the inheritance of defects at this locus is autosomal dominant. Currently, 6% to 10% of new cases are familial, a percentage that is likely to increase due to the survival of individuals with previously lethal CHD (13). Since the phenotype is highly variable, even within families, it is not uncommon that genetic screening of a proband's family identifies the microdeletion in parents or siblings with mild or no clinical evidence of the disorder.

22q11.2 microdeletion syndrome is characterized by the presence of a conotruncal defect (TOF, pulmonary atresia with ventricular septal defect [VSD], persistent arterial trunk, interrupted aortic arch, isolated arch anomalies, and VSD), immunodeficiency, neonatal hypocalcemia, developmental or psychiatric abnormalities, facial dysmorphisms, and palatal defects (13). However, its precise features are highly variable. In a cohort of 251 patients with conotruncal lesions, a chromosome 22q11.2 deletion was found in 16% of TOF patients, 50% of patients with interrupted aortic arch type B, 35% of patients with persistent arterial trunk, and 33% of patients with an outlet (malalignment) VSD (20). The likelihood of finding a 22q11.2 deletion in the presence of a conotruncal defect is further increased by the presence of anomalies of the aortic arch (right-sided or high arch), subclavian artery, pulmonary artery (PA) (atresia, absent central confluence, absent pulmonary valve, or multiple aortopulmonary collateral arteries), or absence of the arterial duct (14,21). Interestingly, 22q11.2 deletion is very rarely found in association with other forms of CHD, such as transposition of the great arteries and hypoplastic left heart syndrome (10).

The next most common causes of syndromic TOF are those associated with major chromosomal abnormalities including Down syndrome (Trisomy 21), Edward syndrome (Trisomy 18),

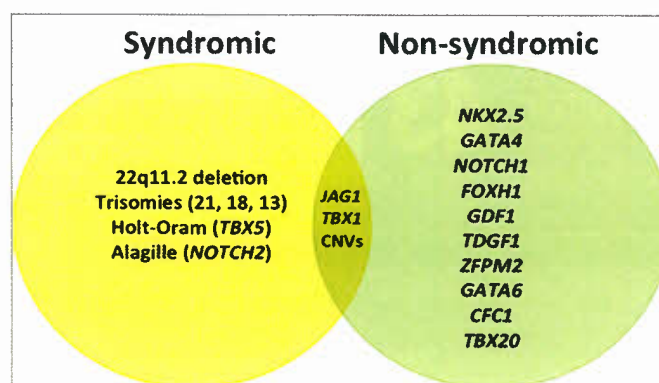


Figure 43.2. Genetic mutations identified in patients with syndromic and nonsyndromic TOF.

and Patau syndrome (Trisomy 13). These trisomies are estimated to cause 5% to 7% of syndromic TOF with Trisomy 21 responsible for most cases (22).

Smaller deletions and duplications have also been described as causes of syndromic TOF. These copy number variants (CNVs) are larger than 1,000 base pairs but are submicroscopic and, therefore, not detected on a routine karyotype. The importance of these rare variants in human disease has recently been appreciated due to technologic advances allowing genome-wide surveys at greater resolution than previously possible. These CNVs identify known or candidate TOF disease genes (23,24). At the current time, these CNVs account for only a small fraction of syndromic TOF but, with increasing use of microarrays and high-throughput DNA sequencing, we can expect to identify genetic abnormalities in a larger proportion of TOF patients. Microarray testing for CNVs in the population of syndromic TOF patients may have a relatively high yield since approximately 25% of patients with syndromic CHD have an identifiable mutation (24,25).

Single gene causes of syndromic TOF have been described and include mutations in *TBX5* causing Holt-Oram syndrome, which manifests most commonly as forearm and thumb anomalies with atrial septal defect (26). Mutations in *JAG1* and *NOTCH2* cause Alagille syndrome, a disorder characterized by cholestasis, CHD, skeletal and ocular anomalies, and characteristic dysmorphic features (27–29).

Nonsyndromic Tetralogy of Fallot

Mutations in many genes have been linked with nonsyndromic TOF (Fig. 43.2). In some cases, gene discovery in syndromic patients has been helpful in identifying the cause of nonsyndromic TOF. For example, 22q11.2 deletion may be present in up to 6% of patients with nonsyndromic TOF and appears more frequently in those with pulmonary atresia (30). In addition, mutations in *JAG1*, initially identified in Alagille syndrome, have been found in patients with isolated TOF (31–34), and mutations causing nonsyndromic TOF have also been identified in *TBX1*, which is deleted in the 22q11.2 microdeletion syndrome (22,31). Few studies of nonsyndromic TOF have considered inheritance; in those that have, mutations were inherited from phenotypically normal parents. This observation suggests reduced penetrance and/or the presence of additional cofactors and has led to the proposal that nonsyndromic TOF may fit a “multiple-hit” model of etiology (5,35). A variety of environmental exposures have been identified that contribute a modest increased risk for TOF or other conotruncal defects and include maternal pregestational diabetes, febrile or viral illnesses, vitamin A exposure, and exposure to organic solvents (36). Perhaps the development

of nonsyndromic TOF requires both genetic susceptibility and one or more environmental insults. However, to date, evidence supporting this hypothesis remains weak and anecdotal.

The contribution of CNVs to nonsyndromic TOF has also been examined (33,37). Similar to the loci identified in syndromic TOF, these CNVs identify known and putative TOF disease genes. Of the 12 CNVs identified, there were only three loci affecting known disease genes (*JAG1*, *NOTCH1*, and *TBX1*). Furthermore, several of these loci affected regions of DNA that did not contain any known genes, suggesting that mutations in non-protein coding DNA may contribute to the development of disease. The most common CNV affected the 1q21.1 locus, which accounted for 1% of TOF cases in this study (33). This locus has been identified by other groups and has been associated with psychiatric and neurologic disease as well as TOF and other CHD (38–47). This potential link between “nonstructural” nervous system disease and TOF is certainly intriguing since it parallels the findings for the 22q11.2 deletion and syndromic TOF.

To date, mutations in 12 single genes have been associated with nonsyndromic TOF but, thus far, each mutation appears to contribute to only a tiny percentage of cases. The disease genes identified primarily consist of transcription factors (*NKX2.5* [48,49], *GATA4* [50–52], *ZFPM2* [53,54], *GATA6* [55,56], *TBX1* [22,57], and *TBX20* [58]) and receptors or ligands in the NOTCH (*NOTCH1* [59] and *JAG1* [22,32]) or NODAL (*FOXH1* [60], *TDGF1* [60], *GDF1* [61], and *CFC1* [60]) pathways.

Current and Future Roles of Genetic Testing and Counseling in Tetralogy of Fallot

The potential genetic links and implications of genetic testing in TOF should be discussed with the parents of each newly diagnosed patient, whether a diagnosis of TOF has been made in a fetus or postnatally. There is also a role for genetic counseling in older patients, who may have been diagnosed with TOF at a time before much was known about its potential genetic etiology. In each case, the patient or parents should decide whether or not genetic testing is appropriate after considering the potential benefits and disadvantages. When combined with adequate resources for counseling, genetic testing can provide useful information for physicians, the parents of children with TOF, and the patients themselves.

For physicians, genetic testing of patients with TOF may identify a syndrome associated with other abnormalities that should be considered when planning management and discussing prognosis. For instance, there are potentially important reasons to identify a 22q11.2 deletion in infants with TOF before they undergo cardiac surgery (62). First, at the time of surgery and during the postoperative period, it is useful to anticipate and correct hypocalcemia, which can result as a consequence of the hypoparathyroidism seen in over 50% of patients with 22q11.2 deletion (63). Second, a small percentage of infants with 22q11.2 deletion exhibit complete T-cell deficiency, a condition known as “complete DiGeorge syndrome.” Such patients are at risk of iatrogenic graft-versus-host disease (GVHD), which may occur due to transfusion of lymphocyte-containing blood components and is a potentially fatal, but preventable, complication (64). Transfusion-associated GVHD is usually only a risk if CD4 and CD8 T-cell counts are below 1,000 and 800 cells/mm³, respectively (65). Guidelines suggest that infants with known or suspected 22q11.2 deletion should receive irradiated blood products at the time of cardiac surgery unless T-cell lymphocyte deficiency has been specifically excluded (66).

For the parents of a child with TOF, and for the patients themselves, another possible benefit of genetic counseling and testing is the provision of information that might inform future reproductive decisions. In addition, genetic testing may iden-

tify a condition that is associated with learning difficulties. In such cases, obtaining a genetic diagnosis may help the family of a patient with TOF obtain additional educational support from an early age. As they age, patients with 22q11.2 microdeletion remain at risk of symptomatic hypocalcemia and may also develop psychiatric disorders that would benefit from early recognition and treatment (67).

Recommendations for genetic testing in TOF and other forms of CHD have been developed (21). Currently, these guidelines advocate genetic testing only in children with syndromic TOF (21). However, many centers have already adopted routine genetic screening for all patients with TOF. Although routine clinical genetic testing is currently limited to the detection of large chromosomal abnormalities either through karyotyping or through FISH, advances in technology and decreasing costs in DNA sequencing may lead to an increased prevalence of this approach together with improved diagnostic yields. Furthermore, approximately 6% to 10% of children with a 22q11.2 deletion will have no other features of the disorder and will be missed if screening is confined to those only with obvious external abnormalities.

ANATOMY (MORPHOLOGIC, ECHOCARDIOGRAPHIC, AND ANGIOGRAPHIC CORRELATIONS)

The journey towards anatomic understanding of this complex heart defect began well before the time of Etienne-Louis Arthur Fallot and continues to this day. In his 1888 papers concerning “la maladie bleue,” Fallot acknowledged earlier reports of patients with the same pathology, including the paper by Danish anatomist and Bishop, Niels Stenson, which is considered to be the earliest description (68). In 1671, Stenson reported his pathologic findings in a fetus with multiple abnormalities, including cardiac features we would now recognize as TOF (69). One hundred years later, Eduard Sandifort, an anatomist at the University of Leiden, published the first clinical-anatomical correlate of this condition when he described the life and subsequent autopsy findings of a 12-year-old boy who had suffered from progressive cyanosis and breathlessness despite being “perfectly normal at birth” (70). Detailed anatomical diagrams accompanied his report and, unlike others present at the autopsy, Sandifort realized that the condition must have been congenital (70). In the 1800s, there were other reports including 15 cases published in John Farre’s textbook on cardiac malformations (71) and 64 cases referenced by Thomas Bevil Peacock (72). Fallot’s important contribution was to clearly define the clustering of four distinct anatomical features as a frequent cause of cardiac cyanosis and to introduce the term “tetralogy.” This defining contribution was forever acknowledged when Maude Abbott gave the disease its eponym. Fallot also dispelled the widely held belief that the blue discoloration of these patients was due to patency of the oval fossa (73). Fallot’s tetralogy, as described by him, is: stenosis of the PA, a VSD, hypertrophy of the right ventricle (RV), and rightwards deviation of the origin of the aorta (68); and, for over 120 years, generations of medical students have memorized these cardinal features.

More recently, increasing knowledge of embryonic growth, understanding of cardiac morphology, and the development of rigorous nomenclature systems have resulted in a search for the pathognomonic features unique to a diagnosis of TOF. In today’s perception, TOF is generally considered a “monology” from which all four characteristic features result. The two great schools of cardiac morphology have somewhat different perspectives on this matter but the areas of controversy are relatively minor. In Anderson’s view, the characteristic abnormalities of TOF occur because the components that normally unite to form the outlet of the RV remain separate during development. He maintains



Figure 43.3. Parasternal short axis view of an infant with TOF demonstrating: (1) anterior and cephalad deviation of the outlet septum, (2) the VSD, and (3) narrowing of the subpulmonary RV outflow tract.

that the defining morphology is anterior-cephalad deviation of the outlet (infundibular) septum (which may sometimes be only a fibrous remnant) relative to the septomarginal trabeculation (SMT) together with malformation of the SMTs (74,75). In contrast, the Van Praags judge underdevelopment of the subpulmonary infundibulum to be the primary pathology; with all characteristics of TOF (including anterior-cephalad deviation of the outlet septum) being sequelae of this one pathologic feature (76,77). Whichever abnormality ultimately proves to be defining, anterior-cephalad deviation of the outlet septum (which is a much larger structure in TOF than in the normal heart) is certainly a cardinal feature. Since deviation of the outlet septum is often easily appreciated by echocardiography, identification of this anatomy is key to diagnosis (Fig. 43.3).

The most frequent segmental anatomy in patients with TOF is normal abdominal situs with the heart located in the left chest, its apex pointing to the left (levocardia) and usual atrial arrangement with concordant atrioventricular and ventriculoarterial connections. By contrast, the intracardiac anatomy is highly variable (78) and surgical planning for individual patients is facilitated by establishing the precise configuration of each of the cardinal anatomical components. Furthermore, it should be emphasized that TOF may coexist with other connections (e.g., double outlet RV) and indeed may be the underlying diagnosis even when there is complete atresia of the right ventricular outflow tract (RVOT) with or without the presence of major aortopulmonary collateral arteries.

The Interventricular Communication

The large, unrestrictive interventricular communication of TOF is always “roofed” by the aortic valve (Fig. 43.4) but its remaining borders are somewhat variable and complicated to define since they depend on the tissue planes considered. In general, the defect is described from its RV aspect (which is the aspect the surgeon encounters when closing it). The crest of the ventricular septum usually terminates with the

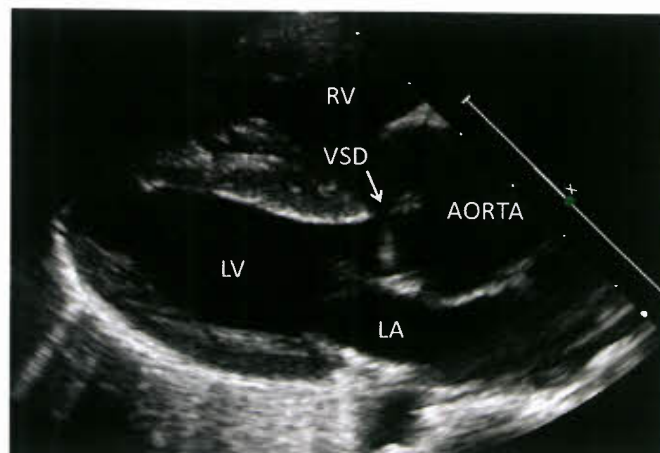


Figure 43.4. Typical parasternal long axis view in a patient with TOF. The aorta overrides the crest of the ventricular septum. VSD, ventricular septal defect; LV, left ventricle; RV, Right ventricle; LA, left atrium.

Y-shaped division of the anterior and posterior limbs of the SMT. In approximately one-fifth of Caucasian patients, a muscular rim, formed by the limbs of the SMT, the ventriculo-infundibular fold (VIF) and the muscular outlet septum, encircles the RV side of the VSD posteroinferiorly and thus protects the conduction axis from damage (74). More commonly, the VIF fails to reach the SMT and an area of fibrous continuity exists between the aortic cusps and the septal leaflet of the tricuspid valve to form the posteroinferior margin of the defect. In these cases, the defect incorporates a remnant of the membranous septum and is perimembranous (74). Its superior margin is usually formed by the deviated muscular outlet (or infundibular) septum. In some patients, there is absence, or near absence, of the infundibular septum, and the cusps of the aortic and pulmonary valves are in fibrous continuity and together form the superior border of the VSD. In these cases, the VSD is described as both doubly committed and subarterial, and while usually there is a muscular posteroinferior rim, the defect may also be perimembranous. This variant

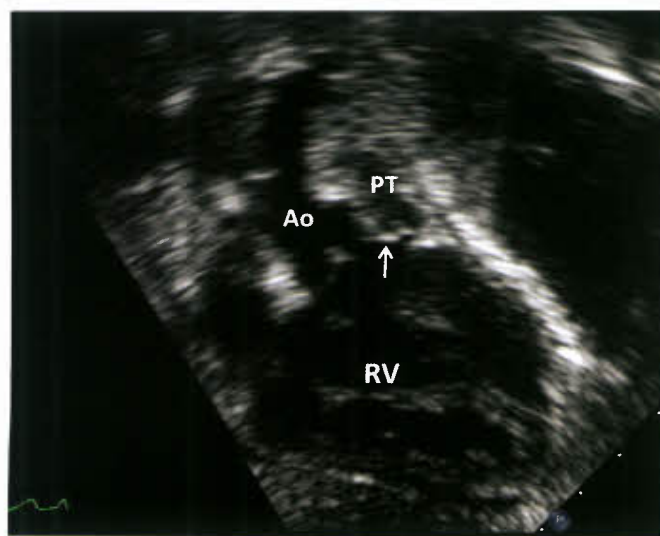


Figure 43.5. Subcostal right oblique section of TOF with a doubly committed VSD. The arrow points to point of fibrous continuity between the leaflets of the aortic valve and the hypoplastic pulmonary valve. RV, Right ventricle; Ao, Aorta; PT, Pulmonary trunk.

is rare in some populations, but relatively frequent in those of South American or South-East Asian descent (Fig. 43.5). In the past, it was argued that such patients should not be classified as having TOF since they have no muscular infundibular septum. It has been argued, however, that the outlet septum is present, albeit in the form of a fibrous remnant or raphe (79) and, since postnatally these patients exhibit all four classical features, this entity is now accepted to be a variant of TOF (75,80). TOF with a doubly committed VSD may be diagnosed preoperatively by echocardiography or angiography (79,81). Compared to the majority of patients with TOF, those with a doubly committed VSD are at higher risk for the development of aortic regurgitation, both before and after repair, and have a higher incidence of residual postoperative RVOT obstruction (RVOTO) (82).

The large outlet VSD seen in TOF can extend into the inlet component of the ventricle, either with or without an associated common atrioventricular valve, and there may be additional muscular VSDs that can be difficult to image by echocardiography because of the equalization of RV and left ventricle (LV) pressures. In each case, effort should be made to exclude additional muscular defects by imaging the ventricular septum with reduced Doppler color scale.

Aortic Position

In TOF, if an imaginary line were drawn perpendicular to the long axis of the heart, upwards from the crest of the ventricular septum, it would transect the cusps of the closed aortic valve and, when the valve opened, this line would extend

onwards into the aortic root. This is what is meant by the term “overriding aorta.” In patients with TOF, the aorta overrides the VSD, a relationship best appreciated by echocardiography from the parasternal long-axis view (Fig. 43.4). The degree of aortic override varies significantly between 15% and 95% (83), a feature which has created some confusion. Contention remains as to whether or not hearts in which there is >50% aortic override should be classified as double outlet RV, irrespective as to whether there is a bilateral infundibulum. The precise mechanics underlying aortic override in TOF remain incompletely understood. However, most authorities agree that, compared to normal, there is rightwards malposition and clockwise rotation of the aortic root (76,77,84–86).

Right Ventricular Outflow Tract Obstruction

Multilevel obstruction to pulmonary blood flow is a hallmark of TOF although the severity of obstruction varies considerably from patient to patient (Fig. 43.6). In TOF, the length of the infundibular region is similar to that of normal hearts (76,84), but its diameter is usually significantly reduced. Whether this reduction in diameter is primarily due to developmental hypoplasia (76,77) or is caused by anterior cephalad deviation of the outlet septum combined with hypertrophy of the SMTs (74) remains of academic interest but, from the patients' perspective, it is the effect of this narrowing that is important. The degree of narrowing of the subpulmonary infundibulum is variable in extent and timing. Progression from a patent RVOT to atresia during fetal life is well described, resulting in TOF with PA (also termed pulmonary

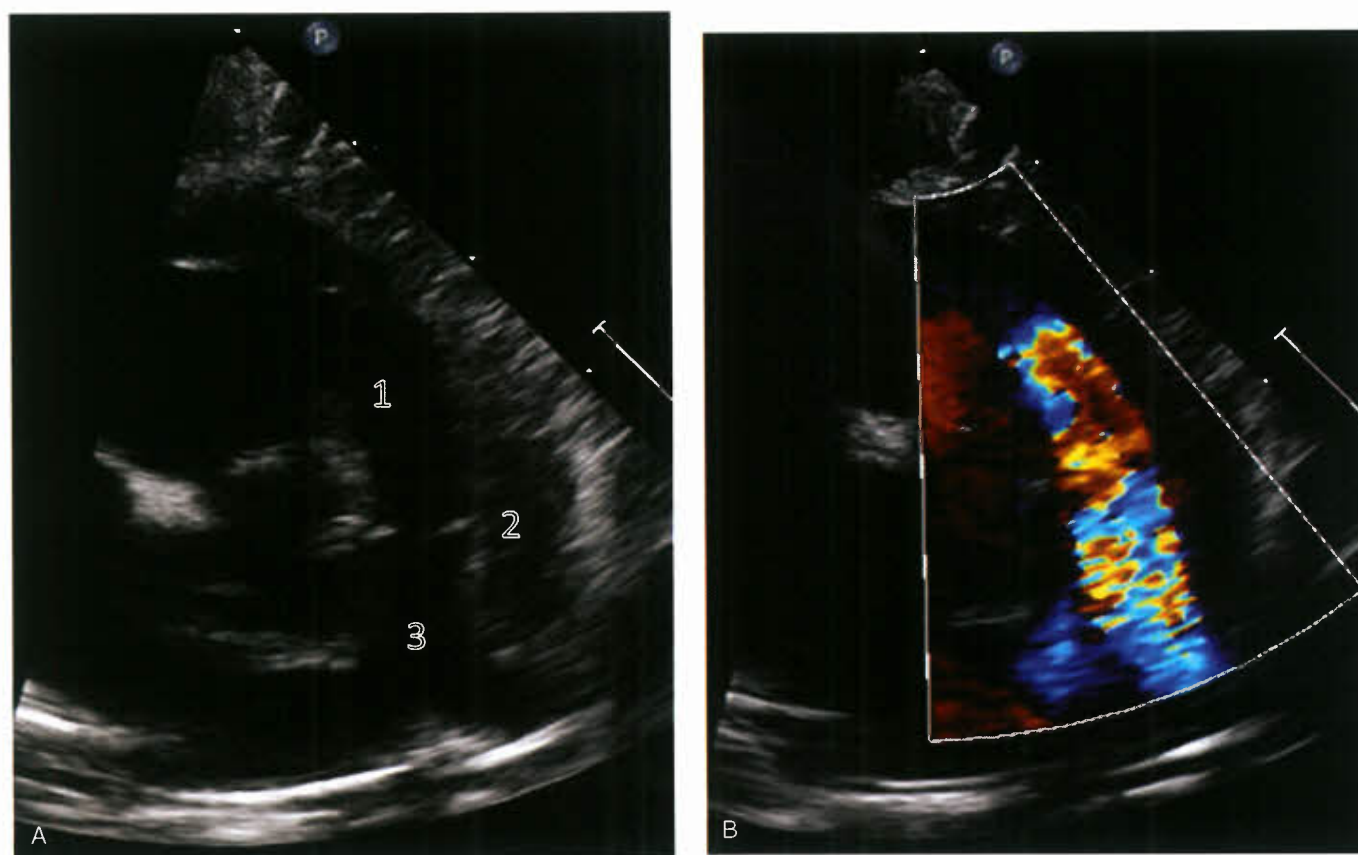


Figure 43.6. There is potential for multilevel obstruction of the RV outflow tract. This can occur because of (1) subpulmonary infundibular obstruction, (2) valvular pulmonary stenosis, and (3) branch PA stenosis. The RVOT is best imaged in a parasternal short axis view. Color flow Doppler can be used to demonstrate both the location and severity of obstruction.

atresia with VSD) (87) and, postnatally, the development of increasing obstruction leading to symptomatic cyanosis is commonplace. The typical pulmonary valve in TOF is thickened and obstructive, and is frequently bicuspid. The main PA and its branches exhibit highly variable anatomy with important abnormalities in up to 40% of patients (88,89). The high incidence of discrete stenosis at the origin of the left PA is related to constriction of a sling of ductal tissue at the site of its insertion (88).

Coronary Arteries

The prevalence of coronary artery abnormalities in TOF varies somewhat between surgical, pathologic, and angiographic series but is approximately 5% to 7% (90). The significance lies mainly in an increased vulnerability of the anomalous vessels to injury during surgical repair, particularly if they cross the RVOT (91–93). In approximately 4% of TOF patients, the left anterior descending artery (LAD), or an accessory LAD, takes origin from the right coronary artery (RCA) or right coronary sinus and crosses the RVOT in its course towards the LV (90). A single coronary artery (more often from the left coronary sinus) is the second most frequent variant and occurs in ≈1% of patients (90). The solitary artery usually divides early into left and right branches, one of which may pass behind or in front of the RVOT. When a single coronary arises from the left sinus, it is the right branch that lies in a vulnerable position, whereas when the single coronary arises from the right sinus, it is the left branch that is vulnerable (94). In patients with significant RV hypertrophy, there may be enlargement of the infundibular (or conal) branch of the RCA. Strictly speaking, this is not anomalous anatomy but, since this branch supplies the musculature of the subpulmonary infundibulum, its prominence may nonetheless challenge the surgeon.

In previous eras, when ventriculotomy and transannular patching were frequent components of TOF repair, the risk of transecting an anomalous coronary vessel was high and patients with abnormal coronary anatomy had increased operative mortality. Preoperative coronary angiography became routine and, if anomalies were suspected, corrective surgery was delayed until midchildhood by use of a palliative shunt procedure (93). Today, there are several surgical techniques for dealing with anomalous coronaries in patients with TOF and it is rarely necessary to delay surgery, even for abnormalities that might previously have precluded repair. For the majority of patients who have a reasonably sized pulmonary valve annulus, the now standard transatrial-transpulmonary approach (see below) can be used successfully, even in the presence of coronary artery anomalies (95). Several options exist for infants who have both a coronary artery that crosses the RVOT and severe pulmonary annulus hypoplasia. These include RVOT reconstruction with single or separated patches (96,97), placement of an RV-to-PA conduit (96), and use of a native PA flap to protect the anomalous coronary by placing a glutaraldehyde-treated patch between a low ventriculotomy and the PA (98). The technique employed usually depends on surgical preference. It is not always possible to directly identify anomalous coronaries at the time of surgery, so it is important that the coronary anatomy be delineated by careful preoperative echocardiography.

Aortic Arch

In 20% to 25% of patients with TOF, the aortic arch is right-sided with mirror image branching (i.e., it crosses over the right main bronchus and the first branch is a left-sided brachiocephalic artery, which divides into the left subclavian and left carotid arteries [76,99,100]). In isolation, a right-sided aortic

arch in TOF causes no additional symptoms, since it does not produce a complete vascular ring. A right-sided aortic arch may be diagnosed on plain chest x-ray by the absence of the expected left-sided aortic knuckle. By echocardiogram, a right aortic arch is best diagnosed from the suprasternal notch. The standard suprasternal view (in which the scanning plane extends from the right nipple to left scapula with the probe's marker directed towards the patient's back) will demonstrate only part of a right aortic arch (101). To obtain a full arch image, the transducer must be rotated clockwise from the standard position, so that the marker faces away from the patient and the plane of ultrasound extends from the left border of the sternum to an area just right of the spine (101). From this position, the first branch of a right aortic arch can be traced coursing leftward (in contrast to a left aortic arch where this vessel would course rightwards before bifurcating). A right-sided aortic arch may also be diagnosed by fetal echocardiography, when, in a transverse view, the "sausage-shaped" arch is located to the right of the trachea, rather than its usual left-sided position (102).

Aortopulmonary Collaterals

Collateral vessels from the aorta to the pulmonary arteries are unusual in TOF in the absence of pulmonary atresia but approximately 6% of patients have a patent arterial duct (88,89).

Other Associated Cardiac Abnormalities

Important variants of TOF exist and the different anatomy may impact differently on the patient's physiology, clinical presentation, and surgical management.

Tetralogy of Fallot with Pulmonary Atresia

Morphologically, many clinicians (including the authors of this chapter) consider the combination of a VSD with aortic override and pulmonary atresia, to be part of the spectrum of TOF, albeit with the most extreme form of RVOT. Others believe this condition to be a separate entity. Regardless of the formal classification, this variant has such marked variability in pulmonary blood supply, clinical presentation, and surgical management strategies that it warrants special consideration. In this textbook, this entity is described in detail in the Chapter 42 titled "Pulmonary Atresia and Ventricular Septal Defect," and is not discussed further here.

Tetralogy of Fallot with Origin of One Pulmonary Artery from the Right Ventricle and One from the Ascending Aorta

In this rare variant, there is discontinuity of the branch pulmonary arteries with one PA (more often the left) originating from the ascending aorta (103–107). Although use of the term is generally discouraged (because it is teleologically incorrect), this anatomy is sometimes known as a "hemitruncus." It is important to identify patients with this abnormality (which may be overlooked initially) and undertake surgical repair early, so as to prevent the development of left lung pulmonary arterial hypertension.

Occasionally, there may be apparent complete absence of the left PA in the setting of TOF (108–110), although such cases (particularly if recognized in early infancy) should be investigated for possible origin of the left PA from a left-sided arterial duct (commonly arising from the base of the left brachiocephalic or subclavian artery), as this can sometimes be probed, dilated, stented, and rehabilitated, even after complete closure of the duct.

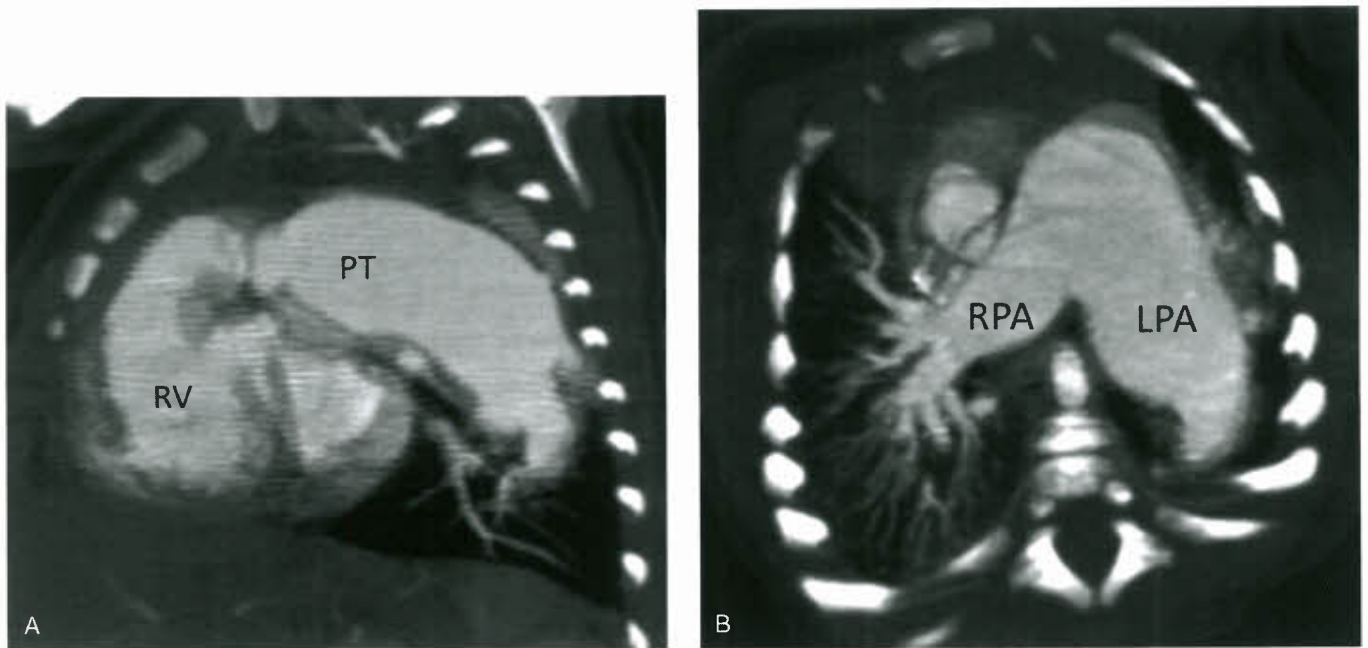


Figure 43.7. MRI of infant with TOF with absent pulmonary valve. Note the massive dilatation of main and branch pulmonary arteries. RV, Right ventricle; PT, Pulmonary trunk; LPA, Left pulmonary artery; RPA, Right pulmonary artery. (Images courtesy of Dr. Shi-Joon Yoo at The Hospital for Sick Children, Toronto.)

Tetralogy of Fallot with Absence of the Pulmonary Valve Leaflets

In approximately 3% to 6% of patients with TOF, the pulmonary valve leaflets are absent (78,100) or only a rudimentary ridge of tissue is present. This variant is associated with significantly aneurysmal main and branch pulmonary arteries that may compromise the airways and respiratory function (Fig. 43.7). The first description of this anomaly is attributed to Chevers (111) in 1847 and the first detailed case report was published in 1927 by Kurtz et al. (112) who described the clinical features and postmortem findings of an 11-year-old boy. Despite an absence of pulmonary valve tissue, these patients usually exhibit some degree of RVOTO. This is almost always caused predominantly by a ring of tissue present at the level where the pulmonary valve leaflets would be expected, rather than by infundibular stenosis (113,114). An anatomical peculiarity of TOF with absent pulmonary valve is that the arterial duct is nearly always absent (113,115). In about 50% of patients with TOF and absent pulmonary valve, there is also a right-sided aortic arch, and the condition may also be associated with absent or aortic origin of a branch PA.

Discussion continues as to whether the massive PA dilation already present by the time of birth is primarily attributable to an abnormality of pulmonary vessel tissue, the orientation of the subpulmonary infundibulum, or severe in utero pulmonary regurgitation (PR) (consequent to absence of the arterial duct and pulmonary valve leaflets) (Fouron, 1990:829). Free PR makes the aneurysmal pulmonary arteries highly pulsatile and they often cause external compression of the airways, sometimes completely obliterating the bronchial lumens during systole. This leads to varying degrees of tracheobronchial malacia and air trapping. Rabinovitch et al. (116) described abnormal branching of the pulmonary arteries with “tufts” of arteries that entwined and compressed the intrapulmonary bronchi on autopsy of two patients with TOF and absent pulmonary valve. The authors suggested that their findings might explain why some patients continue to experience respiratory

problems, despite relief of compression of the main stem bronchus by surgical repair (114).

On examination, newborns with TOF and absent pulmonary valve exhibit “to-and-fro” systolic and diastolic murmurs and a single second heart sound, whereas patients with isolated TOF rarely have a diastolic murmur. Most are initially cyanotic, but this usually becomes less apparent during the first week of life (114). Around 40% of patients have some degree of respiratory distress at birth (113). Since there is usually less RVOTO than in other forms of TOF, as pulmonary vascular resistance falls, infants usually develop signs of increased pulmonary blood flow. The chest x-ray of these patients is distinctive and is characterized by a moderately enlarged cardiac silhouette that has a prominent bulge at the upper left cardiac border, caused by the massively dilated proximal pulmonary arteries, and usually normal peripheral vascular markings. Some infants also demonstrate lobar emphysema (117). MRI or CT scanning may add further information about the extent and severity of airway disease (118).

The clinical course and prognosis of patients with TOF and absent pulmonary valve is variable. Although there is probably a spectrum of disease, general consensus divides patients into two groups: those who exhibit severe respiratory problems in early in life and those who do not. Patients who present with severe respiratory compromise immediately after birth or in the first weeks of life will generally require urgent intervention and have a worse outcome than those who escape early intervention with relatively minor respiratory involvement. For severely affected infants, some clinical improvement may be gained by prone positioning, which allows the pulmonary arteries to fall forward and away from the bronchi. Otherwise, these patients usually require prompt intubation and positive airway pressure ventilation to maintain their airway. It is clear from early surgical series that infants who present with severe respiratory distress and require preoperative ventilation have the highest surgical mortality (119). However, modern surgical strategies and improvements in intensive care management may have improved outcomes in this group. The authors of a 2007 publication reported successful weaning

from ventilation and survival to eventual hospital discharge in all 61 consecutive neonates with TOF and absent pulmonary valve surgically repaired in the preceding 12 years (120).

Several surgical options have been suggested for management of TOF with absent pulmonary valve and, to date, no clear consensus exists as to which is best. Strategies usually focus on intracardiac TOF repair in conjunction with plication and reduction of the pulmonary arteries where necessary. The pulmonary arteries can be reduced by removal of tissue from either their anterior or posterior walls. Some surgeons also suspend the left PA to the anterior chest wall on closing the chest, hoping to further release pressure on the bronchi (119,120). An alternative is to perform the LeCompte maneuver, that is, transect the ascending aorta during repair and move the right PA anterior to it, away from the tracheobronchial tree (121). The surgeon must also decide whether or not to implant a pulmonary valve at the time of the primary procedure, which usually requires placement of a valved RV-to-PA conduit. Some groups also advocate stenting the airway at the time of surgical repair. However, there is no clear consensus about the best approach (122). Even after complete surgical repair with apparent relief of airway obstruction, patients may suffer long-term problems such as recurrent respiratory tract infection, wheezing, and reactive airways disease; some require reintervention for such symptoms (119).

Tetralogy of Fallot with an Atrioventricular Septal Defect

Around 2% of patients with TOF also have an associated atrioventricular septal defect (AVSD) (123). These patients usually present more like patients with isolated TOF than they do like patients with isolated AVSD, since the RVOT limits pulmonary overcirculation and prevents symptoms of heart failure. Furthermore, they will often have left axis deviation on the electrocardiogram. The association should be actively excluded in children with Down syndrome and apparently isolated TOF. It is important to remember in this regard that a primum component may not always be present in such cases, and the presence of an associated AVSD may only be indicated by the presence of a trifoliate ("cleft") left atrioventricular valve component of a divided common atrioventricular junction (which should be repaired at the time of correction, to avoid later valvar regurgitation). The restriction to pulmonary blood flow protects the pulmonary arteries, and these patients can usually be repaired somewhat later than those with an isolated AVSD. Since surgical repair involves division of the inlet valve as well as closure of the interatrial and interventricular septal defects and reconstruction of the RVOT, this combination of cardiac defects is a particular surgical challenge. Nonetheless, it has been shown that primary repair of both the AVSD and TOF may be performed in the first few months of life and produces better outcomes than an initial palliative approach with full repair delayed until 4 to 6 years of age (123).

CLINICAL FEATURES AND INVESTIGATION

Prenatal Diagnosis

Advances in fetal echocardiography, the development of structured screening programs, and increasing sonographer experience have resulted in increased prenatal diagnosis of CHD, including TOF and its variants (124,125). In expert hands, the prenatal diagnosis rate for TOF may be as high as 70% and the diagnostic accuracy can be as high as 90% (124,126). The main source of diagnostic inaccuracy results from diagnosing TOF with pulmonary stenosis in fetuses that are then postnatally found to have TOF with pulmonary atresia (124,126).

To some extent, this may be unavoidable since there is good evidence that the outflow tract obstruction seen in TOF may be progressive during fetal life and that some fetuses with patent pulmonary valves early in pregnancy will have developed complete pulmonary atresia by the time of birth (87,127). In 2008, Kaguelidou et al. (128) examined outcomes for 238 fetuses diagnosed with either TOF ($n = 153$) or TOF with pulmonary atresia ($n = 65$). The median gestational age at diagnosis was 24 weeks, with 45% of cases diagnosed before 24 weeks. Ultrasonography detected coexisting extracardiac anomalies in 70/153 fetuses with TOF. Fetal karyotyping results were available in 132/153 TOF cases and 106/153 fetuses were screened for a 22q11.2 deletion. Of those screened, Trisomy 21 was diagnosed in 4.5%, Trisomy 13 in 0.8%, and other rare (often sex chromosomal) abnormalities in 6%. A 22q11.2 deletion was found in 15% of the 106 fetuses with TOF that were screened. As a result of the antenatal screening, 24% of parents with fetus diagnosed with TOF decided to terminate their pregnancy (a lower proportion than in cases where the diagnosis was TOF with pulmonary atresia). The authors reported that the presence of associated chromosomal abnormalities or severe extracardiac abnormalities were factors that determined parental choice (128).

Postnatal Presentation and Natural History

The clinical signs and symptoms seen in infants born with TOF generally vary in accordance with the degree of RVOTO and frequently the diagnosis will be made following neonatal detection of an asymptomatic murmur. Infants with the most severe obstruction shunt right-to-left across the VSD and have reduced pulmonary blood flow. They often present with cyanosis in the first days of life. Cyanosis may be recognized at the time of delivery, during routine measurement of newborn oxygen saturation or perhaps only during episodes of crying. Infants with minimal RVOTO usually have a normal, or near normal, oxygen saturation after birth. These babies ("pink tets") may present with heart failure symptoms (poor feeding, tachypnea, diaphoresis, and failure to thrive) at 4 to 6 weeks of age due to increasing pulmonary blood flow as their pulmonary vascular resistance drops and they shunt left-to-right across the VSD.

Typical auscultatory findings in a newborn with TOF include a normal first heart sound, a single second heart sound, and a loud systolic ejection murmur most clearly audible at the left lower sternal border that radiates to the back. This murmur originates from turbulent blood flow across the narrowed RVOT and not from blood flow across the large nonrestrictive VSD, which produces equalization of ventricular pressures. Generally speaking, the loudness of the murmur is proportional to, and the length of the murmur inversely proportional to, the degree of RVOTO (i.e., a loud short murmur indicates significant RVOTO). However, in those patients with severe RVOTO or who are actively spelling, the murmur may be both short and soft or virtually inaudible.

Fallot's three patients died at the ages of 19, 26, and 36 years; interestingly not from their CHD but of tuberculosis (68). At the time, adult survivors of TOF would have been unusual since, without surgical intervention, the outcome from TOF is poor. There are two retrospective studies that considered autopsy data from fixed geographical populations during time periods prior to the availability of any cardiac surgery and, as such, describe the natural history of TOF. The first, conducted in Denmark, found that without surgical intervention only 66% of babies born with TOF survived to 1 year of age, 49% until 3 years of age, and only 24% lived to the age of 10 years (129). Similar statistics were seen in the population of Central Bohemia where 64% survived the first year of life

but only 14% of children with unpalliated or unrepaired TOF survived beyond 15 years of age (130).

Not only is the mortality from untreated TOF high but the child's quality of life is also poor and the distress caused to families great. Although two-thirds of newborns with TOF are acyanotic and appear healthy at birth, by 6 months of age over half will have become desaturated at rest (131). This clinical progression occurs because of worsening infundibular stenosis and RV hypertrophy, which further reduces pulmonary blood flow and increases right-to-left shunting across the VSD. Intermittent hypercyanotic episodes ("tet spells") are one of the defining features of TOF, now seen less frequently due to earlier recognition and intervention. During hypercyanotic spells, which are often provoked by crying but then associated with a quite different frantic cry during the episode that is probably due to the pain of skeletal muscle and myocardial ischemia, the patient develops abruptly worsening cyanosis and breathlessness that may ultimately lead to loss of consciousness and, in severe untreated cases, death. In milder cases, postspell somnolence is characteristic. The mechanism for cyanotic spells remains unknown but the previous assumption that they were related to "infundibular spasm" is difficult to reconcile with the lack of a "sphincter" function of the subpulmonary infundibulum and the frequent recognition of identical clinical features in those lacking a subpulmonary infundibulum (e.g., tetralogy with a doubly committed VSD). Rather, the physiology is more likely related to acute changes in inotropy (endogenous catecholamine release in response to pain), increased systemic oxygen consumption (secondary to pain and anxiety) leading to reduced mixed venous oxygen content, acute reduction in systemic vascular resistance (they are more frequent during febrile illness), and with decreased RV preload associated with tachycardia (they can be induced by atrial tachycardias), and this understanding underpins their treatment (see below).

ECG Findings

Preoperatively, the electrocardiogram in TOF characteristically shows sinus rhythm with normal or rightward axis deviation and right ventricular hypertrophy. As previously mentioned, there may be left axis deviation in TOF associated with AVSD. Surgical repair of TOF often disrupts the electrical conduction pathways and afterwards >90% of patients exhibit right bundle branch block (RBBB) (Fig. 43.8) (132–135), although this has become less marked with the transatrial and transpulmonary repair. As discussed below, in patients left with residual PR, the QRS duration (QRSd) tends to increase over time and may have prognostic implications (136,137).

Chest X-Ray Findings

The typical chest radiograph findings in TOF are well known and consist of a normal cardiac size but with an abnormal morphology characterized by an upturned apex ("boot-shaped" heart) related to RV hypertrophy, deficiency of the main PA segment ("PA bay" visualized as a notch in the upper left cardiac border), and reduced pulmonary vascularity (138). However, historically, an upturned apex was only actually present in two-thirds of cases and a more consistent sign of RV hypertrophy was said to be increased proximity of the anterior cardiac border to the sternum on a lateral film (139). Today, since most patients are operated during infancy and before they develop significant RV hypertrophy, the typical "boot-shaped heart" is much less commonly seen. It is usually possible to diagnose a right-sided aortic arch from the chest x-ray by absence of the usual left-sided aortic knuckle, a bulge to the right of the upper mediastinum, and an impression to the right of the trachea (139).

Echocardiography

Echocardiography is one of the most important tools in the diagnosis and follow-up of patients with TOF. Obtaining images of intracardiac anatomy, as described above, can make the diagnosis of TOF and it is important to specifically check for associated abnormalities. Echocardiography (either epicardial or transesophageal) also plays a role at the time of corrective surgery, particularly in checking the completeness of VSD closure and relief of RVOTO. During the immediate postoperative phase, echocardiography is routinely used to assess LV and RV function, atrioventricular valve function, and the status of the RVOT. Its role in postoperative follow-up is primarily in the surveillance for late complications, particularly in patients with important PR (see the following section).

Angiography and Magnetic Resonance Imaging

Preoperative cardiac catheterization and invasive angiography for TOF have been almost entirely supplanted by other imaging modalities, most commonly echocardiography. In rare circumstances, angiography may still be useful for imaging abnormal coronary artery or peripheral PA anatomy but, even in this situation, a high-resolution CT scan may be preferable since it is noninvasive and results in less radiation exposure.

The use of cardiac MRI is limited in the preoperative evaluation of TOF patients, and is largely reserved for those



Figure 43.8. Typical ECG after TOF repair. Note the RBBB with QRSd of 180 milliseconds.

with vascular abnormalities, in particular those with major aortopulmonary collateral arteries. However, MRI has become an important component of postoperative follow-up, particularly in the older adolescent and adult with repaired TOF. The poor acoustic windows generally found in adults do not limit MRI and, furthermore, the ability to quantify RV volumes and PR is an important advantage. MRI can also be used to quantify RV (and LV) systolic function, assess differential pulmonary blood flow, quantify PR, and define the presence of restrictive RV physiology.

MRI may be particularly important in the serial follow-up of TOF patients to monitor the potentially deleterious effects of chronic PR on RV volume and function and to identify patients whose RV compensatory mechanisms are failing even before symptoms develop (140). Sufficient data have accumulated that MRI measurements are routinely applied in clinical decision making regarding interventions such as pulmonary valve replacement (PVR) (see later section). The avoidance of ionizing radiation is another important advantage of MRI, particularly if patients are to be followed regularly over decades. However, MRI is contraindicated in patients with pacemakers or defibrillators and may be limited by arrhythmia, patient claustrophobia, and the need to breath-hold effectively. In our experience, children under the age of 7 or 8 years of age usually require sedation or general anesthesia for MRI in order to prevent movement artifact during a study that may take 60 to 90 minutes.

MEDICAL TREATMENT

As will be discussed, surgical strategies for the management of patients with TOF have changed remarkably over the past few decades. In many centers, a move towards earlier corrective surgery has obviated the need for medical management in this condition. However, in some circumstances, a limited period of medical management may still be appropriate and, in the instance of an acute hypercyanotic spells, medical management can be lifesaving. Depending on the nature of their outflow tract obstruction, infants with TOF may develop symptoms related to either too little or too much pulmonary blood flow. Those who develop heart failure usually derive some benefit from pharmacotherapy (141–143), and caloric supplementation with nasogastric tube feeds allows continued weight gain (144). Infants who develop gradual, but consistent, worsening of cyanosis usually do so as a result of increasing RVOTO and will benefit little from medical therapy. In contrast, infants who develop episodic cyanosis during hypercyanotic spells usually do respond to medical therapy, both as prophylaxis and for acute treatment.

As discussed above, the pathophysiology of hypercyanotic spells should be thought of as an acute imbalance between systemic and pulmonary blood flow resulting from a vicious spiral of changes in inotropy secondary to endogenous catecholamine release, increased systemic oxygen consumption, reduced systemic vascular resistance, and reduced RV preload due to increased heart rate. The aim of therapy is to redress this imbalance and disrupt the pathophysiologic spiral by relieving pain and anxiety (to reduce heart rate and systemic oxygen consumption), increase systemic vascular resistance, and increase pulmonary blood flow. Since most hypercyanotic spells are provoked, or worsened, by crying, the infant should be picked up and comforted as soon as an episode begins, ideally while being held in a position of flexed knees and hips that kinks or compresses the femoral arteries and increases peripheral systemic vascular resistance. If no improvement is seen within a few minutes, oxygen should be administered and intravenous access obtained.

The following measures (in order of increasing intensity of intervention) can then be tried, any of which may terminate the spell (145):

- An intravenous bolus of colloid or crystalloid fluid will increase intravascular volume, maximize preload, and improve cardiac output (thereby increasing mixed venous O₂ content) and may help prevent hypotension caused by other therapeutic interventions below.
- Intravenous (or intramuscular) morphine (0.1 to 0.2 mg/kg) should be given to relieve pain and anxiety, thereby reversing endogenous catecholamine release, reducing heart rate, and lowering respiratory rate.
- Intravenous propranolol (0.015 to 0.02 mg/kg) or the shorter-acting esmolol (0.5 mg/kg given over 1 minute, thereafter continued as an infusion). Beta-receptor antagonists lower heart rate and improve diastolic ventricular filling thus increasing preload and probably also act acutely to increase systemic vascular resistance.
- Intravenous sodium bicarbonate (1 mEq/kg) may be required if there is evidence of worsening acidosis despite the measures above.
- In unremitting cases, intravenous systemic vasoconstrictors, for example, phenylephrine (boluses of 0.005 to 0.001 mg/kg), or norepinephrine (0.05 to 1.0 µg/kg/min) may be required.
- Anesthesia, intubation, and ventilation may ultimately be required to reduce the work of breathing and reduce oxygen consumption and improve mixed venous oxygen content.
- Very occasionally, severe life-threatening spells may require emergent surgical intervention or mechanical circulatory support.

Most spells are self-limiting and do not require intensive medical therapy. Many groups consider their onset as an indication for surgical correction, but interval prophylaxis with beta-receptor antagonists (oral propranolol in a dose of 0.25 to 1 mg/kg, 2 to 3 times per day) may be helpful if surgery is delayed (146).

PERCUTANEOUS PALLIATION

In an era when primary repair can be achieved in almost all infants, even during the neonatal period, with low operative mortality (147), the role of percutaneous palliation is yet to be fully determined. However, it is possible to palliate cyanotic neonates and young infants with TOF by percutaneous placement of a stent across the stenosed RVOT, which improves pulmonary blood flow and allows growth of the native pulmonary arteries (148,149). However, the procedure destroys the native pulmonary valve and so this technique should be reserved for the limited number of, usually very young, premature or small, infants in whom a transannular patch will almost certainly be necessary in any case, or in whom the pulmonary arteries are diminutive and would increase surgical mortality or morbidity (150).

THE EVOLUTION OF SURGICAL TREATMENT

Palliative Procedures

In 1930, Dr. Helen Taussig was put in charge of the newly founded Pediatric Cardiac Clinic at Johns Hopkins Hospital and, although rheumatic fever was the biggest problem

of the time, she had a keen interest in the “little cyanotic babies (referred) to the clinic as nothing could be done for them” (151). It was not long before Dr. Taussig had an idea that would change not just the outlook for her own cyanotic patients but the face of CHD forever. It was the clinical and autopsy findings of two patients that brought Dr. Taussig to the realization that infants with severe pulmonary stenosis and right heart hypoplasia died not, as was widely believed, from heart failure but because of the sudden cessation of pulmonary blood flow that occurred with closure of their arterial duct (151). After realizing the importance of a patent arterial duct to patients with limited pulmonary blood flow, Taussig recognized the potential benefit that might be possible from creation of an artificial duct. When, in 1939, Drs. Robert Gross and John Hubbard successfully ligated a persistently patent arterial duct (152), Taussig made the leap of imagination to think it “ought also to be possible to build one” (151). Subsequently (after she failed to interest Gross in the idea) she worked together with her surgical colleague in Baltimore, Dr. Alfred Blalock, and his technician, Vivian Thomas, to develop a surgically created shunt that would siphon blood from the aorta into the pulmonary arteries (151). After trialing several different techniques, the team ultimately settled on a operation performed via a thoracotomy on the opposite side to that of the patient’s aortic arch, where a direct anastomosis was formed between the subclavian branch of the innominate artery and the PA on that side (151). The first clinical shunt procedure, successfully performed in 1945, was a monumental advance and the true beginning of surgical therapy for CHD (153). Dr. Denton Cooley, who at the time was a surgical intern present in the operating room, has provided a detailed description of this first procedure and an explanation of its significance in his 2010 “Reflections of the Pioneers” essay (154). In recognition of their vital contributions, this arterial-pulmonary shunt bears both the surgeon and cardiologist’s names: the Blalock-Taussig (BT) shunt. Recognizing Dr. Thomas’ contribution, this text calls it the Blalock-Thomas-Taussig shunt (ed.). A shunt formed in this original manner (making use the native subclavian artery) is now known as a “classical” B-T-T-shunt; but in the current era, when this procedure is required, the preference is to use a prosthetic tube graft interposed between the subclavian and pulmonary arteries forming a “modified” B-T-T-shunt. Within a short period of time, other systemic-to-PA shunts were devised and used successfully: the Potts shunt (connection between the descending aorta and left PA) in 1946 (155) and the Waterston shunt (connection between the ascending aorta and right PA) in 1962 (156). Although these procedures proved useful in specific anatomical circumstances, their use never overtook that of the B-T-T shunt due to complications related to technical issues and pulmonary hypertension.

Systemic-to-PA shunts dramatically improved a patient’s clinical condition and provided reasonable mid- to long-term palliation (157–159) but, since the intracardiac defects remained, the surgery could not be considered definitive therapy. Follow-up studies of TOF patients with shunts demonstrated gradual attenuation of the initial symptomatic improvement and the late occurrence of complications such as bacterial endocarditis, cerebral abscesses, and heart failure (157–159). In 1948, Dr. Russell Brock developed a technique for direct intracardiac relief of valvar pulmonary stenosis with a knife that was passed through an incision in the RVOT and onwards, across the stenosed valve to free its leaflets (160). Dr. Brock’s technique was quickly adopted for use in TOF (162) and, since it bestowed a degree of anatomical correction, some groups favored it over shunt palliation. However, as acknowledged by all, the Brock procedure fell short of a full correction and was not without complications such as

infundibular aneurysm (163), pulmonary edema (164), and recurrent RVOTO (165).

“Complete” Surgical Repair

In 1954, Dr. C. Walton Lillehei and his colleagues repaired a VSD in an 11-year-old boy using the boy’s father’s circulation to take over the pumping and oxygenating capacity of the patient’s heart and lungs (166). “Cross-circulation” opened the doors to corrective surgery for complex CHD and, later that same year, 10-year-old Michael Eugene Shaw became the first patient with TOF to undergo successful surgical repair (167). Mr. Shaw survived to adulthood and had a successful career as a professional musician (168). Nevertheless, cross-circulation carried considerable risk to both the donor and the patient and work continued on the development of a completely artificial means of supporting the circulation during surgery; a task that had occupied John H. Gibbon and others since the 1930s (169). In 1955, Dr. John Kirklin (170) of the Mayo Clinic reported the use of a modified Gibbon heart-bypass machine in the repair of complex CHDs, including TOF. Initial mortality was high, but as early as 1959, Dr. Kirklin (171) managed to achieve postoperative survival rates as high as 83% in young children and adults with TOF. By 1964, this figure had reached 93% (172) and results from the Cleveland Clinic depicted a similar rate of progress (173). Dr. Kirklin (171,173) published a series of detailed papers explaining the developments that had contributed to these improved outcomes. He particularly commented on the need for “vigorous pursuit” of normalized postoperative blood gases and volume status, reduced use of outflow tract patches, myocardial protection strategies, and close attention to hemostasis (171,172).

During this first epoch of cardiac surgery, TOF repair was performed via either a longitudinal or transverse incision in the RV. Through this, the hypertrophied subpulmonary musculature was resected and any valvar pulmonary stenosis was relieved. Patients with an insufficiently sized pulmonary annulus were managed by extending the ventriculotomy across the valve into the main PA, so that a pericardial patch could be used to augment the outflow tract and, where necessary, the pulmonary arteries. These “transannular” patches provided complete relief of outflow tract obstruction but at the cost of destroying competency of the pulmonary valve leaflets. The VSD was closed via the ventriculotomy after reconstruction of the outflow tract. During the 1960s, most centers reserved this type of full repair for TOF patients over 4 to 6 years of age. Since attempts at full repair in infants had accrued a high mortality (174,175), cardiologists and surgeons favored a staged approach, with initial palliation by B-T-T-shunt, for those who developed severe and early cyanosis (174,176). The first successful repair of TOF in a patient <1 year-of-age was achieved by a group from Guy’s Hospital, London in 1962 (177). However, the techniques used by this group varied little from those used in previous unsuccessful attempts and throughout the 1960s; infant survivors of TOF repair remained a rare curiosity.

In the late 1960s, groups from Japan reported remarkable results from their attempts to correct CHD during the first year of life; with only 6 deaths in 78 infants, 9 of whom had undergone TOF repair (178,179). The key change was the use of deep hypothermic circulatory arrest, a technique developed by the Canadian surgeon, Dr. Bigelow (180), in the 1950s, reintroduced in Japan (178) and then popularized for use in infants and neonates with CHD by Dr. Barratt-Boyes (181) in New Zealand. However, it should be mentioned that, at the same time, Rees and Starr (182) also achieved excellent results from infant repair of TOF employing only modest hypothermia. By 1972, Dr. Barratt-Boyes’ group (183) had completely corrected the cardiac defects of 12 infants with TOF

and, of those, 11 survived to hospital discharge. In the light of his results, Dr. Barratt-Boyes (181,184) questioned whether symptomatic infants with TOF continued to be best served by a staged repair and suggested that complete primary repair might be a better option. Comparison of mortality rates before and after the introduction of complete repair during infancy lent strength to his argument (185). In New Zealand, during the era of staged palliation, survival to hospital discharge after complete repair of TOF was <50% if an infant required a shunt under the age of 4 months, and 85% if palliation was required between 4 months and 2 years (185). After changing to a strategy of complete primary repair rather than palliative shunting, mortality in the first 25 children aged under 2 years at the time of repair was only 4% (185). Impressed, Dr. Kirklin and the team at University of Alabama Medical Center completely changed their view about the timing of intracardiac TOF repair and, in 1971, all but abandoned the staged approach (186). Other centers followed suit, including the team at Boston Children's Hospital who, up until 1972, had firmly believed palliative shunts to be the preferred option for symptomatic infants but later, after Dr. Castañeda's arrival, became staunch proponents of neonatal primary repair for all infants with TOF (not just those who become symptomatic) (187–189). When follow-up studies suggested that early repair might carry hemodynamic and anatomical advantages, Dr. Castañeda and others at Boston Children's Hospital came to believe that early primary repair for all patients would not only avoid risks associated with a shunt procedure but might also reduce RV hypertrophy and promote pulmonary blood vessel growth (190,191).

Today, most centers perform elective repair of TOF in asymptomatic infants between 3 and 12 months of age (with a trend towards the lower end of the range in many large centers). For patients who become symptomatic earlier than this practice continues to vary. Some groups are staunch advocates of complete primary repair in all patients, regardless of the age at which symptoms develop, believing that the benefits of avoiding a shunt include promotion of PA growth, elimination of chronic hypoxemia, and reduced need for extensive RV muscle resection (147,192,193). Others remain concerned about the neurologic effects of neonatal cardiopulmonary bypass and hypothermic circulatory arrest and the possible increased incidence of transannular patching when operating on a very small and young baby and continue to prefer the staged (surgical or catheter-based) approach for very young symptomatic infants, with later full repair.

Coincidental to the move towards earlier complete repair, but occurring over a similar time course, surgeons also changed their operating techniques. During the earliest era of TOF repair, it was noted that residual VSDs and pulmonary stenosis were predictors of postsurgical mortality and the main causes of reoperation. Accordingly, surgeons considered the complete elimination of RVOT obstruction one of the primary aims of repair (91,171,194) and they liberally applied transannular patches to achieve this end (171). In 1963, Hudspeth et al. (195) were the first to suggest that a transatrial approach (with an atriotomy and exposure of the VSD and subpulmonary infundibulum after detachment of the septal leaflet of the tricuspid valve) might permit total correction of TOF without risk of coronary artery division, need for ventriculotomy, or external enlargement of the RVOT. Initially, Hudspeth's technique was little adopted but the method was reintroduced by Edmunds (196) in 1976 and was popularized during the 1980s with growing understanding of the long-term effects of ventriculotomy and destruction of the pulmonary valve. By the early 1990s, most centers preferentially performed TOF repair via a transatrial and transpulmonary approach, with transannular patching avoided whenever possible (95,186,197,198).

Surgical Outcomes

Since the development of the B-T-T shunt, outcomes for infants with TOF who are born in countries that can provide neonatal and infant congenital cardiac surgery and postoperative intensive care have been revolutionized. Parents of a child born with TOF can now be reassured that their baby's cardiac defect will be repaired in the first 6 months of life and that there is a >96% chance of survival to hospital discharge (132,134,199–201). Furthermore, of the surviving infants, >90% are expected to be alive 30 years after repair (202). During childhood, approximately 5% of patients require reoperation and a further 6% require catheter intervention (134). Late follow-up studies suggest a 0.8% risk per year of requiring PVR, with the highest incidence of this reintervention in patients with TOF and pulmonary atresia or TOF with absent pulmonary valve (203). This impressive subversion of natural history means that there is a large, and growing, cohort of adult TOF survivors, and for these patients (many with families of their own) and their care providers, focus has switched to late outcomes.

It is important to note that although TOF repair is now associated with little short- or medium-term mortality, long-term survival is not equal to that of the general population (197). For the 30-year-old with repaired TOF, there is a 0.5% annual risk of death (203), while according to the United States Social Security Ministry's 2006 actuarial periodic life tables (www.ssa.gov), the baseline annual probability of death for a 30-year-old male is 0.15% and for a female is 0.06%. Therefore, a 30-year-old man with TOF faces a yearly risk of death threefold higher than baseline, while a woman's risk is approximately eightfold higher. Furthermore, this increased risk of mortality increases with age (204). The most recent data suggest that the annual mortality risk for patients with TOF increases by 0.1% per decade (203). The reason that patients with TOF experience increasing adverse outcomes with age is the presence of a slowly evolving postoperative pathophysiology, which although it remains incompletely understood, has certainly become better recognized.

POSTOPERATIVE PATHOPHYSIOLOGY

While it dramatically alters a patient's life expectancy, surgical repair of TOF is not a cure and the hearts of patients with repaired TOF remain anatomically, physiologically, and electrically abnormal. Potential anatomical problems include incomplete relief of RVOTO, residual VSDs, tricuspid regurgitation, and RVOT aneurysms. Pulmonary insufficiency is probably the most important physiologic disturbance and electric problems may stem either from the RBBB or patchy ventricular fibrosis. Such abnormalities are usually well tolerated during childhood and early adult life, but extended follow-up of patients with repaired TOF has revealed the presence of a slowly progressive postoperative pathophysiology that has a pervasive influence on late outcome, with effects seen decades after repair. Adults with repaired TOF demonstrate a high frequency of exercise impairment and a small, but increasing, risk of arrhythmia, biventricular dysfunction, and premature cardiac death; outcomes that can all be related to the evolving postoperative pathophysiology (130,134,198,200–204).

Pulmonary Regurgitation and the Fate of Right Ventricle

Although many factors impact late outcomes after TOF repair, chronic PR is widely recognized as a key pathophysiological

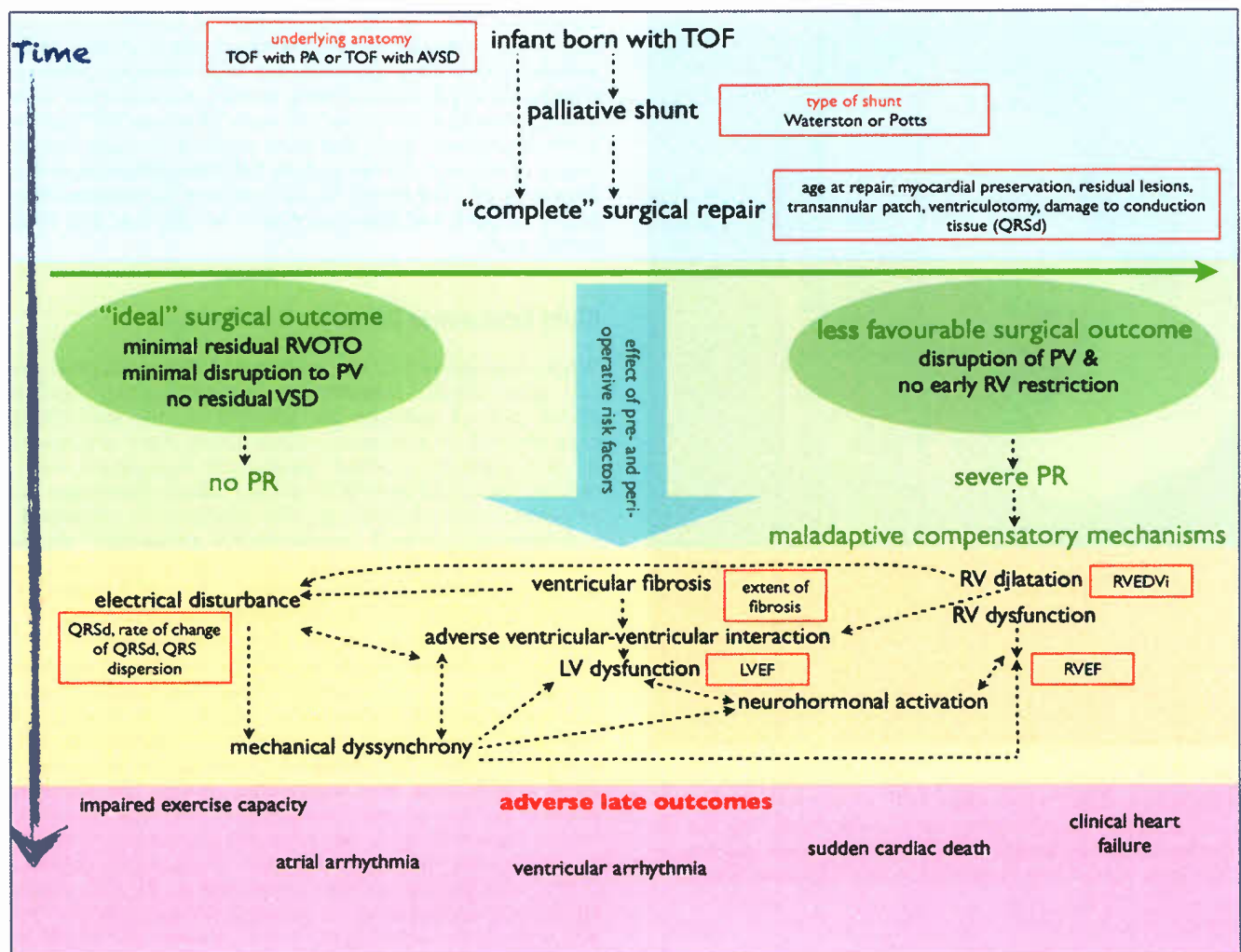


Figure 43.9. Pathophysiology after TOF repair—red boxes indicate known risk factors for late outcomes.

driver (Fig. 43.9) (210–215). A common sequel of TOF repair, PR is especially likely, and most severe in patients with a transannular patch. Unfortunately, PR tends to increase with time (216,217) and places a volume load on the RV that is exacerbated by any distal PA stenosis (217,218). It has come to be understood that the RV responds to chronic volume loading with an adaptive remodeling, which while initially compensatory, ultimately proves detrimental. In the face of chronic PR, compensatory RV dilation and hypertrophy maintain forward flow and wall stress (Fig. 43.10). An association between pulmonary insufficiency and RV end-diastolic volumes in patients with TOF was first recognized in the 1980s (219,220) and the strong positive relationship became easier to demonstrate with the advent of MRI (221). RV dilation is not initially associated with a reduction in RV ejection fraction (219,221) and stroke volume is maintained, so that patients experience a long preclinical compensated phase during which they rarely report symptoms (Fig. 43.9). Nevertheless, formal testing during these decades often reveals impaired exercise capacity (222) and neurohormonal activation that correlates with RV volumes (223–225). Ultimately, RV compensatory adaptations become inadequate and TOF patients with severe PR begin to develop RV contractile dysfunction (210,211,215). Pathophysiologic progression can be exacerbated by coexisting abnormalities. For example, tricuspid regurgitation (present in around 30% of patients [226]) produces a cycle of worsening RV

dilation, leading to worsening tricuspid regurgitation, leading to worsening RV dilation etc. (227). For a period of time, RV dysfunction remains reversible with intervention to abolish PR (140,227–230) but, eventually, the damage progresses and permanent myocardial injury ensues. This manifests as an inability of the RV to regain normal dimensions, even after PVR (231) and as overt RV failure with increased risk of ventricular arrhythmia and sudden cardiac death (203,204,232).

Ventricular Fibrosis

Many studies have demonstrated ventricular fibrosis in patients with repaired TOF and several have linked the extent of fibrosis to late complications such as arrhythmia, systolic dysfunction, exercise intolerance, and neurohormonal activation (233–236). It seems that almost all adults with repaired TOF exhibit markers of RVOT fibrosis (whether or not a transannular patch has been placed) and this correlates with both regional and global abnormalities of RV function (233,235,236). Over half of the patients also have patchy LV fibrosis; sometimes correlating with the site of an apical vent from the time of cardiopulmonary bypass (233). Those repaired at older ages have the most fibrosis, suggesting that pre- and perioperative factors are the most important insults (233). The extent to which ongoing pathophysiologic processes (i.e., severe PI)

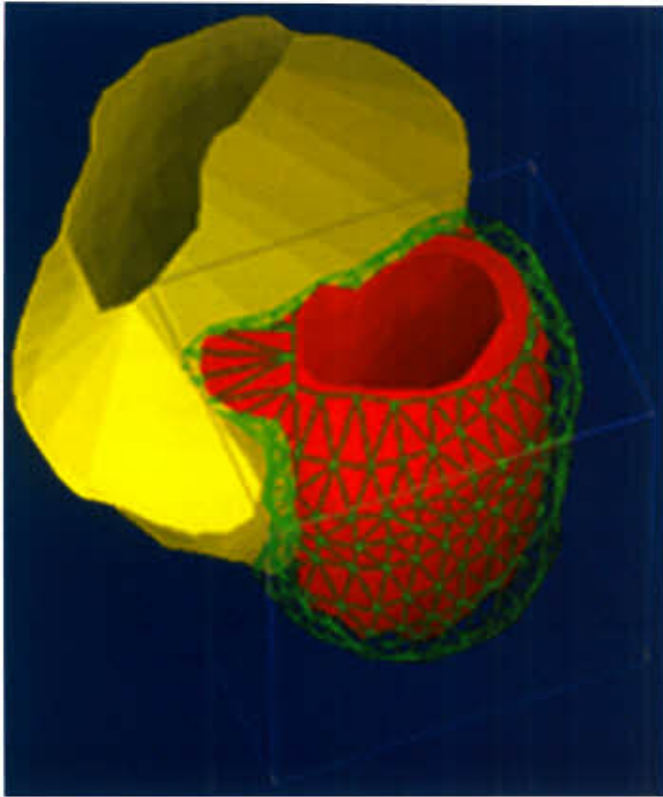


Figure 43.10. Three dimensional MRI rendered image of left and right ventricle 8 years after TOF repair. RV shaded yellow, LV shaded red. Note the size disproportion between the ventricles caused by severe RV dilatation. (Image courtesy of Dr. Shi-Joon Yoo of The Hospital for Sick Children, Toronto.)

cause the further development of postoperative fibrosis is not yet known.

Mechanoelectrical Interactions

A leap forward in understanding the late outcomes after TOF repair occurred with the realization that, along with direct mechanical effects, chronic PR also causes electrical deterioration of the heart and that the two are pathophysiologically linked (136,237). In 1995, Gatzoulis et al. (237) correlated RV dilation with QRS prolongation and identified QRSd as an important predictor of adverse outcomes late after TOF repair. The group studied 41 randomly selected TOF patients 15 or more years after repair, then tested their findings in a second group of 178 patients (237). They found a QRSd of ≥ 180 milliseconds to be a sensitive and specific predictor of later symptomatic ventricular tachycardia and/or sudden cardiac death (237). Patients with a QRSd of ≥ 180 milliseconds also had increased cardiothoracic ratio (a surrogate for RV size) and increased longitudinal RV dimensions, whereas those without PR consistently demonstrated a QRSd of < 180 milliseconds (237). Several years later, in collaboration with others, the same group conducted a multicenter investigation of nearly 800 TOF patients that confirmed the importance of adverse mechanoelectrical interactions (136). Increased cardiothoracic ratio, QRSd prolongation, and the requirement for TAP were each associated with adverse outcomes and both a QRSd ≥ 180 milliseconds and the rate of QRSd progression (> 5 milliseconds per year over a 10 year period) were predictive of sudden cardiac death (136). These studies changed not just the way the postoperative pathophysiology of TOF is

understood but also the management of patients, since most centers now consider absolute or rapid rate of change of QRS prolongation in their algorithm for PVR. However, when considering the implications of these studies, it is important to note that it followed patients repaired in an earlier era (91% of those in the multicenter study had been repaired via right ventriculotomy [136]) and did not include MRI quantification of either RV size or PR. The thresholds for intervention in more contemporary cohorts will almost certainly be different and deserve further study.

Right Ventricular Diastolic Dysfunction

While disruption of the pulmonary valve during surgical repair usually initiates the pathophysiology described above, not all patients are affected in this way. Despite near absence of pulmonary valve tissue, there is a minority of TOF patients in whom pulmonary regurgitant volumes remain low and whose RVs do not dilate during the years of postoperative follow-up. The difference is explained by a phenomenon termed “restrictive RV physiology” that was first identified in infants during the immediate postoperative period but has also been seen in adults and children late after TOF repair (215). In the mid-1990s, Cullen et al. (238) identified a group of infants with postoperative RV diastolic dysfunction set apart by their more difficult postoperative course and a set of specific echocardiographic findings. When studied with pulsed-wave Doppler echocardiography, these patients demonstrated antegrade diastolic blood flow in the PA (238). The timing of PA antegrade flow matched atrial systole and was augmented during the expiratory phase of positive pressure ventilation (238). For reasons that remain incompletely understood but are suspected to relate to inadequate intraoperative RV myocardial protection (239), such patients exhibit restriction to RV late diastolic filling as a consequence of reduced RV compliance (240). When the atria contract, the pressure wave and blood flow are transmitted directly to the PA, because the resistance to pulmonary flow is less than the resistance to RV stretch. In the mid-term (2 years postrepair) postoperative restriction predicts later restrictive physiology (241) but long-term prospective studies with serial follow-up are lacking.

A stiff RV resists not only filling through the tricuspid valve but also filling from PR theoretically limiting RV volume loading and its subsequent deleterious effects. To this end, while restrictive RV physiology is disadvantageous in the early postoperative period, because it causes low cardiac output, it may be protective in the longer term. Gatzoulis et al. (237) demonstrated that adult TOF patients with restrictive physiology have a smaller cardiothoracic ratio, an improved exercise capacity, and a shorter QRSd than those without RV restriction. Interestingly, groups that used MRI to determine the presence of restrictive physiology have found results somewhat at odds with those of Gatzoulis et al. (240,242). For example, Helbing et al. (242) found their patients with restrictive physiology to have reduced, rather than improved, exercise tolerance and, although Apitz et al. (240) were the first to demonstrate that TOF patients have increased RV stiffness, they found no difference in MRI measurements of RV volume between the “restrictive” and “nonrestrictive” groups. Their results might be explained by the fact that children were studied rather than adults (perhaps there had been insufficient time to detect the RV effects of chronic volume loading) but the discrepancies between Gatzoulis’ and Helbing’s results are more difficult to explain. The answer may lie in the differences in the methodologies used to determine RV restriction. Indeed, this may go some way towards explaining the wide range of prevalence for restriction reported by the various studies, since

the reported prevalence of restrictive physiology in patients with TOF varies from 28% to 67% (238,242–245).

The Role of Pulmonary Valve Replacement

PVR is one of the commonest procedures performed in adults with CHD (246) with a risk of operative mortality generally quoted at around 1% (140). Today, given suitable anatomy, PVR can even be achieved without recourse to open heart surgery using percutaneous techniques (247,248), although this technique is currently largely reserved for those with an RV-PA conduit or previous stenting of the RVOT. Given the long-term adverse influences of chronic PR, insertion of a competent pulmonary valve is clearly an attractive option. However, no replacement valve has an infinite lifespan and PVR usually commits patients to at least one additional operation or procedure during their lifetime. In addition, PVR remains a relatively expensive and invasive procedure and, while the risk of procedural complications is low, it is not zero. So, before recommending PVR to an individual, the physician must first consider whether the benefits outweigh the risks and, if so, determine optimal timing for the procedure. These have become central questions for those caring for patients with repaired TOF. Unfortunately as yet, the literature contains no definite answers.

Although two studies have made attempts at retrospective case–control “matching” (249,250), to date, there have been no randomized controlled trials examining the impact of PVR. It is fairly clear that PVR improves exercise tolerance and symptoms in patients with PR after TOF repair (230,231,249,251–253) but there are no definitive data as to whether PVR also favorably modifies late clinical outcomes. For this reason, while most centers recommend PVR for TOF patients complaining of symptoms related to their hemodynamic load, criteria vary widely when considering PVR in asymptomatic patients. The key considerations are usually RV size, QRSd, formally documented exercise capacity, and biventricular function.

There is evidence that RV dilation reaches a threshold, beyond which reverse remodeling is unlikely even after PVR (228,254,255). Consequently, most centers consider PVR in patients with progressive RV dilation or RV end-diastolic volumes that approach 160 to 180 mL/m², with the exact number dependent on local policies. However, these thresholds are somewhat arbitrary since MRI methods for measuring RV volumes are not standardized, studies from which the cutoffs are drawn include fewer than 100 patients, and no study has shown that clinical outcomes are worse in patients whose RV volumes fail to normalize after PVR.

Given the evidence that prolonged QRSd increases the risk of life-threatening arrhythmia and sudden cardiac death late after TOF repair, most centers consider a QRSd of ≥ 180 milliseconds, or one that is rapidly increasing, an indication for PVR. Studies that have specifically considered the electrical implications of PVR do suggest it reduces QRSd in association with a reduction in RV size and that PVR reduces the incidence of arrhythmia in individual patients (255–257). However, most studies included some patients who underwent electrophysiologic ablation in conjunction with PVR and it is difficult to tease out which procedure had the most effect (257,258). Certainly patients who undergo ablation as well as PVR seem most likely to remain arrhythmia-free, with ablation particularly effective against SVT (257,258).

Ventricular–Ventricular Interactions and the Fate of the Left Ventricle

Of the thousands of papers published regarding TOF, hundreds discuss the RV, its outflow tract, and the pulmonary arteries.

In contrast, fewer than 40 papers consider the effects TOF might have on the LV. In the minds of many, TOF remains a disease entirely of the right heart. This is a perception that needs to change, since it has become increasingly evident that the LV is intimately involved in the postoperative pathophysiology of TOF and plays an important role in long-term clinical outcomes.

Apart from a few conflicting studies during the earliest era of TOF repair (259–261) and a handful from the 1980s and 1990s (262–265), the fate of the LV after TOF repair received little attention until 2002, when Ghai et al. (206) discovered LV dysfunction late after TOF repair to be a risk factor for sudden cardiac death (201). Several years later, the same group used MRI to conduct a more quantitative study in an attempt to uncover the mechanisms of LV dysfunction (266). The investigators found that in a group of 75 adult patients with TOF, prolonged QRSd was associated with increased size and decreased ejection fraction of both ventricles (266). The QRSd was also associated with heterogeneous LV contraction, presumably induced by RBBB, and the authors proposed that, in combination with RV dysfunction, LV dyssynchrony and adverse LV mechanics might explain the link between QRSd and adverse clinical outcomes (266). Geva et al. (267) also highlighted the importance of the LV in patients with repaired TOF when they found LV ejection fraction (LVEF) to be a primary determinant of late clinical status. The group’s results seem to suggest that although RV mechanics relate to functional status late after repair, moderate or severe LV impairment might yet be the strongest determinant of clinical symptoms (267).

Since the right and left ventricles share common myocardial strands (268,269), an interventricular septum and pericardium, it is to be expected that processes affecting the RV may also impact the LV, a concept known as ventricular–ventricular interaction (see Chapter 22). As well as anatomical considerations, there are physiologic factors linking the ventricles. Blood moved through the lungs by the RV immediately becomes LV preload, so that problems such as pulmonary stenosis or regurgitation threaten LV preload and cardiac output. Furthermore, when the RV changes shape and/or size, it alters the shape and size of the LV. Even in health, the filling of one ventricle influences the compliance and filling of the other (diastolic ventricular–ventricular interaction). For instance, an elevation of RV end-diastolic pressure increases LV end-diastolic pressure (270) and shifts the septum towards the left. In 1983, Kingma et al. (271) demonstrated in an animal model that it is the transseptal pressure gradient that determines the position of the ventricular septum at end-diastole. Thus, if RV end-diastolic pressure is higher than LV end-diastolic pressure (as occurs with either RV volume or pressure overload), the septum flattens at end-diastole and moves towards the LV cavity that affects LV filling. In the subsequent systole, initial movement of the septum is back towards the neutral position (to the right) and this creates paradoxical septal motion. Ventricular–ventricular interactions (both systolic and diastolic) are certainly relevant to the postoperative pathophysiology of patients with repaired TOF as evidenced by several studies that demonstrate a strong positive correlation between RVEF and LVEF (266,267,272). However, the clinical meaning and the mechanisms underlying this relationship remain uncertain. Does it imply that intrinsic contractile function of the myocardium in each ventricle is interdependent? Or rather, given the known load dependency of ejection fraction, does it tell us more about the effects of a dilated RV and paradoxical septum on LV filling? In patients with impaired LVEF and severe PR, demonstrable improvements in LVEF are seen after PVR supporting the concept that adverse ventricular–ventricular interactions may be reversible (273).

Quite separate from the potential for adverse ventricular–ventricular interactions are the unique anatomical

and perioperative factors that might directly affect the left ventricular myocardium of individual patients. For instance, it is conceivable that abnormal coronary artery anatomy, prolonged periods of deep cyanosis (hypercyanotic spells), and LV volume overloading as a result of palliative shunting might cause LV hypoxic or ischemic damage. Davlouros et al. (267) found three independent predictors of LVEF, measured by MRI at a mean of 24 years after complete TOF repair, including RVEF, duration of palliation prerepair, and aortic regurgitation.

If we are to understand the true mechanisms by which this primarily “right-sided” CHD is able to affect the LV and thereby increase the risk of sudden death and symptomatic heart failure, investigators must consider both the significance of perioperative and patient-specific factors as well as the role of adverse ventricular–ventricular and diastolic–systolic interactions.

The Aortic Root

In fetuses with TOF, the diameter of the ascending aorta is usually normal for gestational age at the time of diagnosis but serial measurements reveal accelerated growth during fetal life, particularly in those with most severe RVOTO (87). By the time of birth, the ascending aorta of infants with TOF is not just increased relative to the PA, its absolute diameter is enlarged (87). It is presumed that this enlargement occurs as a result of the increased volume load on the developing aorta, which must carry more of the blood ejected from both ventricles than in fetuses with a normal unobstructed RVOT. However, there are also aortic root histologic (274) and elastic (275) abnormalities in these patients, and it seems likely that these, too, play a role. While rarely a problem in childhood, dilation of the aortic root can cause clinical problems in adults with TOF. The most frequent issue is aortic insufficiency, with a reported prevalence of more than mild aortic regurgitation in 6.6% of patients 15 years postrepair (271) and the occasional requirement for aortic valve replacement (272). There are case reports of aortic dissection in patients with TOF and severe aortic dilation (278,279), but this is an extremely rare complication. In the two published reports of dissection, one patient's aortic root measured 6.5 cm and his ascending aorta 7.1 cm in diameter (278) and the other's ascending aorta measured 9.3 × 8.3 cm (279). In 2010, François et al. (280) reported serial aortic root measurements adjusted for body surface area in 88 children who underwent TOF repair at a median age of 7 months. All aortic root measurements were enlarged at the time of repair, but within 7 years, the annulus and sinotubular Z-scores had returned to normal and the aortic sinus measurements showed significant regression (280). These retrospective data are interesting because they suggest that early repair might prevent aortic dilation; however, given the known abnormalities of aortic tissue in patients with TOF, further follow-up will be required before definite conclusions can be drawn.

OTHER ISSUES FOR ADULT LIFE

Monitoring for Late Complications

Since the 1960s, after undergoing surgical intervention, most infants born with TOF have survived into adulthood. As a result, there are large numbers of adults living with this condition and, since several programs have reported their long-term outcome data, much is known about what those born with this CHD might expect to face as they move through adult life. The European, American, and Canadian guidelines for the

care of adults with CHD all recommend lifelong follow-up of patients with TOF in a specialist center by physicians with expertise in adult CHD. These guidelines suggest that for the majority of patients, the frequency of review should be annual, but those with an excellent surgical outcome or who remain stable might be followed less frequently.

The purpose of routine follow-up is to anticipate and monitor potential complications and, when necessary, to intervene before these become clinically important. Regular visits also provide an opportunity for patient education and advice on maintaining a healthy lifestyle. In addition to an assessment of a patient's general wellbeing, routine follow-up visits should specifically evaluate the presence and effects of: PR, residual RVOTO including branch pulmonary arteries, residual VSD, RV dysfunction, aortic root dilation, aortic insufficiency, and LV dysfunction. An ECG should be recorded at each visit, so that the QRSd can be recorded and any progression can be monitored over time. Routine Holter monitoring has not proven useful for predicting clinically important arrhythmias but patients should be asked about symptoms of palpitations and syncope. Echocardiography should be performed at each visit and regular cardiopulmonary exercise testing is useful to formally document changes in exercise capacity. Cardiac MRI should be performed at regular intervals, particularly in patients with severe PR to quantify RV volumes and biventricular function. Cardiac tomography (CT) is an alternative for patients with pacemakers/defibrillators. The frequency of cardiopulmonary studies and MRI/CT is determined on an individual patient basis. In patients for whom further interventions are planned, cardiac catheterization is sometimes necessary to assess hemodynamics and anatomy and, in middle-aged patients, to exclude atherosclerotic coronary artery disease.

The Timing of Pulmonary Valve Replacement

Patients with moderate to severe PR clearly need monitoring for possible PVR. However, as discussed earlier, at present there is no consensus as to the indications and optimal timing of this procedure. Decisions surrounding PVR remain one of the biggest challenges in this population, with each adult CHD center having their own policies. Most centers would intervene in patients with symptoms attributable to PR, and in asymptomatic patients, RV size, exercise capacity, and QRSd are important factors in decision making.

Monitoring after Pulmonary Valve Replacement

Since no artificial valve has an indefinite lifespan, after PVR patients require regular (every 1 to 2 years) echocardiograms to monitor the function of their new bioprosthetic valve or RV-to-PA conduit. If they become significantly stenosed or regurgitant, surgically placed valves can often be re-replaced nonsurgically with the previous percutaneously implanted valve providing support for the new valve. A metallic valve is rarely chosen for PVR but, if it is, patients will require anticoagulation and appropriate monitoring.

Endocarditis

Endocarditis is rare after TOF repair but increases in frequency after PVR. At clinic visits, patients should be reminded of the symptoms of endocarditis and of the importance of maintaining excellent oral hygiene. Current guidelines should be consulted but, in general, antibiotic prophylaxis is only recommended for those patients with conduits and prosthetic valves.

Contraception and Pregnancy after Tetralogy of Fallot Repair

Issues surrounding contraception and pregnancy should be introduced early to female adolescents with TOF and discussed regularly. Issues regarding genetics, recurrence risk, and fetal screening should also be discussed with male TOF patients. The majority of women with repaired TOF will be able to choose from the full range of available contraceptive options. Caution with combined hormonal preparations is required in women with significant ventricular dysfunction or atrial arrhythmias because of the associated thromboembolic risks of estrogen (281,282). In general, pregnancy is well tolerated in women with repaired TOF. For any individual patient, the risks of pregnancy depend on the severity of any residual lesions, the degree of any ventricular dysfunction, and the likelihood of developing an arrhythmia. The long-term effects of pregnancy on women with TOF (if any) are, as yet, unknown. Ideally, all women with CHD who are considering pregnancy should be directed to specialists with expertise and experience in managing such patients, so as to discuss their individual risks and optimize their care through pregnancy and delivery. For further information, see this book's chapter on pregnancy in CHD and other specialist resources, for example, www.heartdiseaseandpregnancy.com.

REFERENCES

- Hoffman JIE, Kaplan S. The incidence of congenital heart disease. *J Am Coll Cardiol* 2002;39:1890–1900.
- Marelli AJ, et al. Congenital heart disease in the general population: changing prevalence and age distribution. *Circulation* 2006;115:163–172.
- Shaw GM, et al. Differential risks to males and females for congenital malformations among 2.5 million California births, 1989–1997. *Birth Defect Res A Clin Mol Teratol* 2003;67:953–958.
- Nembhard WN, et al. Variation in the prevalence of congenital heart defects by maternal race/ethnicity and infant sex. *J Pediatr* 2010;156:259–264.
- Burn J, et al. Recurrence risks in offspring of adults with major heart defects: results from first cohort of British collaborative study. *Lancet* 1998;351:311–316.
- Nora JJ, Nora AH. Recurrence risks in children having one parent with a congenital heart disease. *Circulation* 1976;53:701–702.
- Dilgilio MC, et al. Recurrence risk figures for isolated tetralogy of Fallot after screening for 22q.11 microdeletion. *J Med Genet* 1997;34:188–190.
- Chehab G, et al. Congenital cardiac disease and inbreeding: specific defects escape higher risk due to parental consanguinity. *Cardiol Young* 2007;17:414–422.
- Øyen N, et al. Recurrence of congenital heart defects in families. *Circulation* 2009;120:295–301.
- Botto LD, et al. A population-based study of the 22q11.2 deletion: phenotype, incidence, and contribution to major birth defects in the population. *Pediatrics* 2003;112:101–107.
- Goodship J, et al. A population study of chromosome 22q11 deletions in infancy. *Arch Dis Child* 1998;79:348–351.
- Tézenas Du Montcel S, et al. Prevalence of 22q11 microdeletion. *J Med Gen* 1996;33:719.
- McDonald-McGinn DM, Sullivan KE. Chromosome 22q11.2 Deletion Syndrome (DiGeorge Syndrome/Velocardiofacial Syndrome). *Medicine* 2011;90:1–18.
- Momma K. Cardiovascular anomalies associated with chromosome 22q11.2 deletion syndrome. *Am J Cardiol* 2010;105:1617–1624.
- Shprintzen RJ, et al. A new syndrome involving cleft palate, cardiac anomalies, typical facies, and learning disabilities: velo-cardio-facial syndrome. *Cleft Palate J* 1978;15:56–62.
- Wilson DI, et al. DiGeorge syndrome: part of CATCH 22. *J Med Genet* 1993;30:852–856.
- Yagi H, et al. Role of TBX1 in human del22q11.2 syndrome. *Lancet* 2003;362:1366–1373.
- Zweier C, et al. Human TBX1 missense mutations cause gain of function resulting in the same phenotype as 22q11.2 deletions. *Am J Hum Genet* 2007;80:510–517.
- Edelmann L, Pandita RK, Morrow BE. Low-copy repeats mediate the common 3-Mb deletion in patients with velo-cardio-facial syndrome. *Am J Hum Genet* 1999;64:1076–1086.
- Goldmuntz E, et al. Frequency of 22q11 deletions in patients with conotruncal defects. *J Am Coll Cardiol* 1998;32:492–498.
- Pierpont ME, et al. Genetic basis for congenital heart defects: current knowledge: a scientific statement from the American Heart Association Congenital Cardiac Defects Committee, Council on Cardiovascular Disease in the Young; endorsed by the American Academy of Pediatrics. *Circulation* 2007;115:3015–3038.
- Rauch R, et al. Comprehensive genotype-phenotype analysis in 230 patients with tetralogy of Fallot. *J Med Genet* 2010;47:321–331.
- Costain G, et al. 13q13.1-q13.2 deletion in tetralogy of Fallot: clinical report and a literature review. *Int J Cardiol* 2011;146:134–139.
- Thienpont B, et al. Submicroscopic chromosomal imbalances detected by array-CGH are a frequent cause of congenital heart defects in selected patients. *Eur Heart J* 2007;28:2778–2784.
- Richards AA, et al. Cryptic chromosomal abnormalities identified in children with congenital heart disease. *Pediatr Res* 2008;64:358–363.
- Mori AD, Bruneau BG. TBX5 mutations and congenital heart disease: Holt-Oram syndrome revealed. *Curr Opin Cardiol* 2004;19:211–215.
- Li L, et al. Alagille syndrome is caused by mutations in human Jagged1, which encodes a ligand for Notch1. *Nat Genet* 1997;16:243–251.
- McDaniell R, et al. NOTCH2 mutations cause Alagille syndrome, a heterogeneous disorder of the notch signaling pathway. *Am J Hum Genet* 2006;79:169–173.
- Oda T, et al. Mutations in the human Jagged1 gene are responsible for Alagille syndrome. *Nat Genet* 1997;16:235–242.
- Giol-Pereira L, et al. Frequency of 22q11.2 microdeletion in sporadic non-syndromic tetralogy of Fallot cases. *Int J Cardiol* 2008;126:374–378.
- Bauer RC, et al. Jagged1 (JAG1) mutations in patients with tetralogy of Fallot or pulmonary stenosis. *Hum Mutat* 2010;31:594–601.
- Eldadah ZA, et al. Familial Tetralogy of Fallot caused by mutation in the jagged1 gene. *Hum Mol Genet* 2001;10:163–169.
- Greenway SC, et al. De novo copy number variants identify new genes and loci in isolated sporadic tetralogy of Fallot. *Nat Genet* 2009;41:931–935.
- Krantz ID, et al. Jagged1 mutations in patients ascertained with isolated congenital heart defects. *Am J Med Genet* 1999;84:56–60.
- Nora JJ. Multifactorial inheritance hypothesis for the etiology of congenital heart diseases. The genetic-environmental interaction. *Circulation* 1968;38:604–617.
- Jenkins KJ, et al. Noninherited risk factors and congenital cardiovascular defects: current knowledge: a scientific statement from the American Heart Association Council on cardiovascular disease in the young; endorsed by the American Academy of Pediatrics. *Circulation* 2007;115:2995–3014.
- Erdogan F, et al. High frequency of submicroscopic genomic aberrations detected by tiling path array comparative genome hybridisation in patients with isolated congenital heart disease. *J Med Genet* 2008;45:704–709.
- Brunetti-Pierri N, et al. Recurrent reciprocal 1q21.1 deletions and duplications associated with microcephaly or macrocephaly and developmental and behavioral abnormalities. *Nat Genet* 2008;40:1466–1471.
- Christiansen J. Chromosome 1q21.1 Contiguous gene deletion is associated with congenital heart disease. *Circ Res* 2004;94:1429–1435.
- De Vries BBA, et al. Diagnostic genome profiling in mental retardation. *Am J Hum Genet* 2005;77:606–616.
- Mefford HC, et al. Recurrent rearrangements of chromosome 1q21.1 and variable pediatric phenotypes. *New Engl J Med* 2008;359:1685–1699.
- Redon R, et al. Global variation in copy number in the human genome. *Nature* 2006;444:444–454.
- Sharp AJ, et al. Discovery of previously unidentified genomic disorders from the duplication architecture of the human genome. *Nat Genet* 2006;38:1038–1042.
- Stefansson H, et al. Large recurrent microdeletions associated with schizophrenia. *Nature* 2008;455:232–236.
- Stone JL, et al. Rare chromosomal deletions and duplications increase risk of schizophrenia. *Nature* 2008;455:237–241.
- Walsh T, et al. Rare structural variants disrupt multiple genes in neurodevelopmental pathways in schizophrenia. *Science* 2008;320:539–543.
- Xu B, et al. Strong association of de novo copy number mutations with sporadic schizophrenia. *Nat Genet* 2008;40:880–885.
- Benson DW, et al. Mutations in the cardiac transcription factor NKX2.5 affect diverse cardiac developmental pathways. *J Clin Invest* 1999;104:1567–1573.
- Schott JJ, et al. Congenital heart disease caused by mutations in the transcription factor NKX2-5. *Science* 1998;281:108–111.
- Nemer G, et al. A novel mutation in the GATA4 gene in patients with Tetralogy of Fallot. *Hum Mutat* 2006;27:293–294.
- Tomita-Mitchell A, et al. GATA4 sequence variants in patients with congenital heart disease. *J Med Genet* 2007;44:779–783.
- Zhang W, et al. GATA4 mutations in 486 Chinese patients with congenital heart disease. *Eur J Med Genet* 2008;51:527–535.
- De Luca A, et al. New mutations in ZFPM2/FOG2 gene in tetralogy of Fallot and double outlet right ventricle. *Clin Genet* 2010;80:184–190.
- Pizzuti A, et al. Mutations of ZFPM2/FOG2 gene in sporadic cases of tetralogy of Fallot. *Hum Mutat* 2003;22:372–377.
- Lin X, et al. A novel GATA6 mutation in patients with tetralogy of Fallot or atrial septal defect. *J Hum Genet* 2010;55:662–667.

56. Maitra M, et al. Identification of GATA6 sequence variants in patients with congenital heart defects. *Pediatr Res* 2010;68:281–285.
57. Griffin HR, et al. Systematic survey of variants in TBX1 in non-syndromic tetralogy of Fallot identifies a novel 57 base pair deletion that reduces transcriptional activity but finds no evidence for association with common variants. *Heart* 2010;96:1651–1655.
58. Liu C, et al. T-box transcription factor TBX20 mutations in Chinese patients with congenital heart disease. *Eur J Med Genet* 2008;51:580–587.
59. Garg V, et al. Mutations in NOTCH1 cause aortic valve disease. *Nature* 2005;270–274.
60. Roessler E, et al. Reduced NODAL signaling strength via mutation of several pathway members including FOXH1 is linked to human heart defects and holoprosencephaly. *Am J Hum Genet* 2008;83:18–29.
61. Karkera JD, et al. loss-of-function mutations in growth differentiation factor-1 (gdf1) are associated with congenital heart defects in humans. *Am J Hum Genet* 2007;81:987–994.
62. Jatana V, et al. Deletion 22q11.2 syndrome—implications for the intensive care physician. *Pediatr Crit Care Med* 2007;8:459–463;quiz 464.
63. Ryan AK, et al. Spectrum of clinical features associated with interstitial chromosome 22q11 deletions: a European collaborative study. *J Med Genet* 1997;34:798–804.
64. Parshuram C, et al. Transfusion-associated graft versus host disease. *Pediatr Crit Care Med* 2002;3:57–62.
65. Shinebourne EA. Tetralogy of Fallot: from fetus to adult. *Heart* 2006;92:1353–1359.
66. Treleaven J, et al. Guidelines on the use of irradiated blood components prepared by the British Committee for Standards in Haematology blood transfusion task force. *Br J Haematol* 2010;152:35–51.
67. Philip N, Bassett A. Cognitive, behavioural and psychiatric phenotype in 22q.11.2 deletion syndrome. *Behav Genet* 2011;41:403–412.
68. Fallot A. Contribution à l'anatomie pathologique de la maladie bleue. *Marseille-Medical* 1888;25:77–93, 138–158, 207–223, 270–286, 341–354, 403–420.
69. Steno N. Embryo monstro affinis Parissis dissectus. *Acta Hafniensia* 1673;1:300–303.
70. Sandifort E. in *Observations Anatomico-Pathologicae*. 1777.
71. Farre JR. *Pathological Researches: Essay on the Malformations of the Heart, or of its Arteries*. London: Longman, Hurst, Rees, Orm and Brown, 1814.
72. Peacock T. *Malformations of the Heart*. 2nd ed. London: Churchill, 1866.
73. Van Praagh R. Etienne-Louis Arthur Fallot and his tetralogy: a new translation of Fallot's summary and a modern reassessment of this anomaly. *Eur J Cardiothorac Surg* 1989;3:381–386.
74. Anderson RH, Jacobs ML. The anatomy of tetralogy of Fallot with pulmonary stenosis. *Cardiol Young* 2008;18:12.
75. Anderson RH, Weinberg PM. The clinical anatomy of tetralogy of fallot. *Cardiol Young* 2005;15:38–47.
76. Van Praagh R. The first Stella Van Praagh memorial lecture: the history and anatomy of tetralogy of Fallot. *Semin Thorac Cardiovasc Surg Pediatr Card Surg Ann* 2009;12:19–38.
77. Van Praagh R, et al. Tetralogy of Fallot: underdevelopment of the pulmonary infundibulum and its sequelae. *Am J Cardiol* 1970;26:25–33.
78. Lev M, Eckner FAO. The pathologic anatomy of tetralogy of Fallot and its variations. *Chest* 1964;45:251–261.
79. Griffin ML, et al. Doubly committed subarterial ventricular septal defect: new morphological criteria with echocardiographic and angiographic correlation. *Br Heart J* 1988;59:474–479.
80. Jacobs ML. Congenital heart surgery nomenclature and database Project: tetralogy of Fallot. *Ann Thorac Surg* 2000;69:S77–S82.
81. Goel PK, et al. Absent conal septum in tetralogy of Fallot. An angiographic study. *Angiology* 1997;48:643–647.
82. Ando M, et al. Tetralogy of Fallot with subarterial ventricular septal defect. *Ann Thorac Surg* 2003;76:1059–1064; discussion 1064–1065.
83. Anderson RH, et al. Surgical anatomy of tetralogy of Fallot. *J Thorac Cardiovasc Surg* 1981;81:887–896.
84. Becker AE, Connor M, Anderson RH. Tetralogy of Fallot: a morphometric and geometric study. *Am J Cardiol* 1975;35:402–412.
85. Chiu IS, et al. Influence of aortopulmonary rotation on the anomalous coronary artery pattern in tetralogy of fallot. *Am J Cardiol* 2000;85:780–784, A9.
86. Isaz K, et al. Is the aorta truly dextroposed in tetralogy of Fallot? A two-dimensional echocardiographic answer. *Circulation* 1986;73:892–899.
87. Hornberger LK, et al. In utero pulmonary artery and aortic growth and potential for progression of pulmonary outflow tract obstruction in tetralogy of Fallot. *J Am Coll Cardiol* 1995;25:739–745.
88. Harikrishnan S, et al. Central pulmonary artery anatomy in right ventricular outflow tract obstructions. *Int J Cardiol* 2000;73:225–230.
89. Saeed S, Hyder SN, Sadiq M. Anatomical variations of pulmonary artery and associated cardiac defects in Tetralogy of Fallot. *J Coll Physicians Surg Pak* 2009;19:211–214.
90. Gupta D, et al. Detection of coronary artery anomalies in tetralogy of Fallot using a specific angiographic protocol. *Am J Cardiol* 2001;87:241–244, A9.
91. Kirklin JW, et al. Surgical treatment for the tetralogy of Fallot by open intracardiac repair. *J Thorac Surg* 1959;37:22–31.
92. Landolt CC, et al. Importance of coronary artery anomalies in operations for congenital heart disease. *Ann Thorac Surg* 1986;41:351–355.
93. McManus BM, et al. The case for preoperative coronary angiography in patients with tetralogy of Fallot and other complex congenital heart diseases. *Am Heart J* 1982;103:451–456.
94. White RI, et al. The nature and significance of anomalous coronary arteries in tetralogy of Fallot. *Am J Roentgenol Radium Ther Nucl Med* 1972;114:350–354.
95. Brizard CP, et al. Transatrial-transpulmonary tetralogy of Fallot repair is effective in the presence of anomalous coronary arteries. *J Thorac Cardiovasc Surg* 1998;116:770–779.
96. Humes R, et al. Tetralogy of Fallot with anomalous origin of left anterior descending coronary artery. Surgical options. *J Thorac Cardiovasc Surg* 1987;94:784–787.
97. Ruzmetov M, et al. Repair of tetralogy of Fallot with anomalous coronary arteries coursing across the obstructed right ventricular outflow tract. *Pediatr Cardiol* 2005;26:537–542.
98. van Son JAM. Repair of tetralogy of Fallot with anomalous origin of left anterior descending coronary artery. *J Thorac Cardiovasc Surg* 1995;110:561–562.
99. Dabizzi RP, et al. Associated coronary and cardiac anomalies in the tetralogy of Fallot. An angiographic study. *Eur Heart J* 1990;11:692–704.
100. Nagao GI, et al. Cardiovascular anomalies associated with tetralogy of Fallot. *Am J Cardiol* 1967;20:206–215.
101. Celano V, et al. Two-dimensional echocardiographic recognition of the right aortic arch. *Am J Cardiol* 1983;51:1507–1512.
102. Yoo SJ, et al. Fetal sonographic diagnosis of aortic arch anomalies. *Ultrasound Obstet Gynecol* 2003;22:535–546.
103. Diab K, et al. Left hemitruncus associated with tetralogy of Fallot: fetal diagnosis and postnatal echocardiographic and cardiac computed tomographic confirmation. *Pediatr Cardiol* 2010;31:534–537.
104. Duncan WJ, et al. Two-dimensional echocardiographic identification of hemitruncus: anomalous origin of one pulmonary artery from ascending aorta with the other pulmonary artery arising normally from right ventricle. *Am Heart J* 1981;102:892–896.
105. Kutsche LM, Van Mierop LH. Anomalous origin of a pulmonary artery from the ascending aorta: associated anomalies and pathogenesis. *Am J Cardiol* 1988;61:850–856.
106. Robin E, et al. Aortic origin of the left pulmonary artery. Variant of tetralogy of Fallot. *Am J Cardiol* 1975;35:324–329.
107. Soyul M, et al. Left hemitruncus associated with tetralogy of fallot: a case report. *Catheter Cardiovasc Interv* 2000;51:58–60.
108. Halit V, et al. Tetralogy of fallot and absence of left pulmonary artery. *Thorac Cardiovasc Surg* 2008;56:430–432.
109. Pool PE, Voge JH, Blount SG. Congenital unilateral absence of a pulmonary artery. The importance of flow in pulmonary hypertension. *Am J Cardiol* 1962;10:706–732.
110. Talwar S, et al. Absent left pulmonary artery and double aortic arch in tetralogy of Fallot: reconstruction using homograft saphenous vein or iliac artery. *Interact Cardiovasc Thorac Surg* 2009;8:277–279.
111. Chevers N. Recherches sur les maladies de l'artere pulmonaire. *Arch Gen Med* 1847;15:488–508.
112. Kurtz C, Sprague H, White P. Interventricular septal defects with associated anomalies in a series of three cases examined postmortem, and a living patient fifty-eight years old with cyanosis and clubbing of the fingers. *Am Heart J* 1927;3:77–90.
113. Donofrio MT, Jacobs ML, Rychik J. Tetralogy of Fallot with absent pulmonary valve: echocardiographic morphometric features of the right-sided structures and their relationship to presentation and outcome. *J American Soc Echocardiogr* 1997;10:556–561.
114. Lakier JB, et al. Tetralogy of Fallot with absent pulmonary valve. Natural history and hemodynamic considerations. *Circulation* 1974;50:167–175.
115. Emmanouilides GC, et al. "Agenesis" of ductus arteriosus associated with the syndrome of tetralogy of Fallot and absent pulmonary valve. *Am J Cardiol* 1976;37:403–409.
116. Rabinovitch M, et al. Compression of intrapulmonary bronchi by abnormally branching pulmonary arteries associated with absent pulmonary valves. *Am J Cardiol* 1982;50:804–813.
117. Owens CM, et al. Plain chest radiographic changes of the absent pulmonary valve syndrome. *Br J Radiol* 1994;67:248–251.
118. Taragin BH, Berdon WE, Htmilz B. MRI assessment of bronchial compression in absent pulmonary valve syndrome and review of the syndrome. *Pediatr Radiol* 2005;36:71–75.
119. McDonnell BE, et al. Outcome after repair of tetralogy of Fallot with absent pulmonary valve. *Ann Thorac Surg* 1999;67:1391–1395; discussion 1395–1396.
120. Watterson KG, et al. Absent pulmonary valve syndrome: operation in infants with airway obstruction. *Ann Thorac Surg* 1992;54:1116–1119.
121. Hraska V. Repair of tetralogy of Fallot with absent pulmonary valve using a new approach. *Semin Thorac Cardiovasc Surg Pediatr Card Surg Ann* 2005:132–134.
122. Sakamoto T, et al. One-stage intracardiac repair in combination with external stenting of the trachea and right bronchus for tetralogy of Fallot with an absent pulmonary valve and tracheobronchomalacia. *J Thorac Cardiovasc Surg* 2005;130:1717–1718.
123. Najm HK, et al. Primary repair is superior to initial palliation in children with atrioventricular septal defect and tetralogy of Fallot. *J Thorac Cardiovasc Surg* 1998;116:905–913.
124. Khoshnood B, et al. Trends in prenatal diagnosis, pregnancy termination, and perinatal mortality of newborns with congenital heart disease in France, 1983–2000: a population-based evaluation. *Pediatrics* 2005;115:95–101.

260. Miller GA, et al. Volume of the left ventricle in tetralogy of Fallot. *Am J Cardiol* 1965;16:488–493.
261. Sunderland CO, et al. Total correction of tetralogy of Fallot in infancy. Postoperative hemodynamic evaluation. *Circulation* 1973;48:398–405.
262. Borow KM, et al. Left ventricular function after repair of tetralogy of fallot and its relationship to age at surgery. *Circulation* 1980;61:1150–1158.
263. Hausdorf G, et al. Left ventricular contractile state after surgical correction of tetralogy of Fallot: risk factors for late left ventricular dysfunction. *Pediatr Cardiol* 1990;11:61–68.
264. Kondo C, et al. Left ventricular dysfunction on exercise long term after total repair of tetralogy of fallot. *Circulation* 1995;92:250–255.
265. Waien SA, et al. Serial follow-up of adults with repaired tetralogy of Fallot. *J Am Coll Cardiol* 1992;20:295–300.
266. Tzemos N, et al. Adverse left ventricular mechanics in adults with repaired tetralogy of fallot. *Am J Cardiol* 2009;103:420–425.
267. Geva T, et al. Factors associated with impaired clinical status in long-term survivors of tetralogy of Fallot repair evaluated by magnetic resonance imaging. *J Am Coll Cardiol* 2004;43:1068–1074.
268. Greenbaum RA, et al. Left ventricular fibre architecture in man. *Br Heart J* 1981;45:248–263.
269. Ho SY. Anatomy and myoarchitecture of the left ventricular wall in normal and in disease. *Eur J Echocardiogr* 2009;10:III3–III7.
270. Bemis CE, et al. Influence of right ventricular filling pressure on left ventricular pressure and dimension. *Circ Res* 1974;34:498–504.
271. Kingma I, Tyberg JV, Smith ER. Effects of diastolic transseptal pressure gradient on ventricular septal position and motion. *Circulation* 1983;68:1304–1314.
272. Davlourous PA, et al. Right ventricular function in adults with repaired tetralogy of Fallot assessed with cardiovascular magnetic resonance imaging: detrimental role of right ventricular outflow aneurysms or akinesia and adverse right-to-left ventricular interaction. *J Am Coll Cardiol* 2002;40:2044–2052.
273. Tobler D, et al. The left heart after pulmonary valve replacement in adults late after tetralogy of Fallot repair. *Int J Cardiol* 2011.
274. Niwa K, et al. Structural abnormalities of great arterial walls in congenital heart disease: light and electron microscopic analyses. *Circulation* 2001;103:393–400.
275. Chong W, et al. Aortic root dilation and aortic elastic properties in children after repair of tetralogy of Fallot. *Am J Cardiol* 2006;97:905–909.
276. Ishizaka T, et al. Prevalence and optimal management strategy for aortic regurgitation in tetralogy of Fallot. *Eur J Cardiothorac Surg* 2004;26:1080–1086.
277. Dodds GA, Warnes CA, Danielson GK. Aortic valve replacement after repair of pulmonary atresia and ventricular septal defect of tetralogy of Fallot. *J Thorac Cardiovasc Surg* 1997;113:734–736.
278. Kim W, et al. Aortic dissection late after repair of tetralogy of Fallot. *Int J Cardiol* 2005;101:515–516.
279. Rathi VK, et al. Massive aortic aneurysm and dissection in repaired tetralogy of Fallot; diagnosis by cardiovascular magnetic resonance imaging. *Int J Cardiol* 2005;101:169–170.
280. Francois KF, et al. The fate of the aortic root after early repair of tetralogy of Fallot. *Eur J Cardiothorac Surg* 2010;37:1254–1258.
281. Silversides CK, Sermer M, Siu SC. Choosing the best contraceptive method for the adult with congenital heart disease. *Curr Cardiol Rep* 2009;11:298–305.
282. Thorne S. Risks of contraception and pregnancy in heart disease. *Heart* 2006;92:1520–1525.

Allison K. Cabalka ■ William D. Edwards ■ Joseph A. Dearani

Persistent truncus arteriosus is an uncommon congenital cardiovascular malformation. There is not a striking gender difference in frequency, although most series contained more male than female subjects. Truncus arteriosus usually occurs as an isolated cardiovascular malformation, although on occasion it has been reported in association with anomalies of other systems, particularly the DiGeorge or velocardiofacial syndrome (microdeletion chromosome 22q11.2) (1–4). Maternal diabetes has been implicated as a risk factor for truncus arteriosus. The anomaly has occurred in dizygotic twins (5) and siblings, and there is an increased incidence of cardiac malformations in relatives of children with this lesion (6–8). Because corrective operation for this malformation was first performed more than 30 years ago (9), ever-increasing numbers of postoperative patients now are reaching adolescence and adulthood. Patients who have had truncus arteriosus corrected need continued follow-up care throughout life. During the last 25 years, surgical correction of truncus arteriosus during infancy has become routine (10,11).

EMBRYOLOGY

The embryonic truncus arteriosus lies between the conus cordis proximally and the aortic sac and aortic arch system distally. Partitioning of the truncus arteriosus, which is intimately associated with conal and aortopulmonary septation, was reviewed by Van Mierop et al. (12) and more recently by Bartelings and Gittenberger-de Groot (13). Truncus swellings, similar in appearance to endocardial cushions, divide the truncal lumen into two channels: the proximal ascending aorta and the pulmonary trunk. As the proximal portion of this truncal septum fuses with the developing conal septum (derived from conal swellings), the right ventricular origin of the pulmonary trunk and the left ventricular origin of the aorta are established. Valve swellings develop from truncal tissue at this line of fusion, and the excavation of these swellings leads to formation of the aortic and pulmonary valves in their respective sinuses. Along the aortic sac, the paired sixth aortic arches (primitive pulmonary arteries) migrate leftward, and the paired fourth aortic arches shift rightward. Invagination of the aortic sac roof thereby forms an aortopulmonary septum that eventually fuses with the distal extent of the truncal septum. Accordingly, the right and left pulmonary arteries originate from the pulmonary trunk, and the aortic arch emanates from the ascending aorta. The spiral course of the trunco-aortic partition produces the normal intertwining of the great arteries.

When conotruncal or trunco-aortic septation does not proceed normally, various congenital ventriculoarterial anomalies may result (12). One of these anomalies is truncus arteriosus, in which a single arterial trunk exits from the heart. Also, either deficiency or absence of the conal (infundibular) septum produces a large ventricular septal defect. Because the conal septum also contributes to the development of the anterior tricuspid leaflet and the medial tricuspid papillary muscle, these structures may be malformed. The single truncal valve may be deformed and functionally insufficient or, less commonly, stenotic (14). If vestiges of distal trunco-aortic septation develop, the pulmonary arteries may arise together from a short pulmonary trunk; otherwise, they arise separately from the truncal root.

PATHOLOGY

Truncus arteriosus is characterized by a single arterial vessel that arises from the base of the heart and gives origin to the coronary, pulmonary, and systemic arteries (Fig. 44.1). Origin of the pulmonary arteries from this single artery serves to differentiate truncus arteriosus from pulmonary valve atresia, a condition in which a single arterial vessel also receives the entire output of both ventricles but in which the pulmonary arteries do not arise directly from the ascending portion of this single great artery. Collett and Edwards (15) recognized four types of truncus arteriosus on the basis of the anatomic origin of the pulmonary arteries. In type I, a short pulmonary trunk originating from the truncus arteriosus gives rise to both pulmonary arteries. When both pulmonary arteries separate from the truncus arteriosus, with no vestige of a main pulmonary artery (MPA), they may arise close to one another (type II) or at some distance from one another (type III). The type IV truncus arteriosus is now considered to represent a form of pulmonary atresia with ventricular septal defect and is not discussed further in this chapter.

Van Praagh and Van Praagh (16) have proposed an expanded classification system that also includes two commonly associated abnormalities of the great arteries. Their type A1 corresponds to type I of Collett and Edwards, and type A2 encompasses types II and III (Fig. 44.2). Type A3 includes cases with absence of truncal origin of one pulmonary artery, with blood supply to that lung from the ductus arteriosus or from a collateral artery. Last, type A4 is associated with underdevelopment of the aortic arch, including tubular hypoplasia, discrete coarctation, or complete interruption.

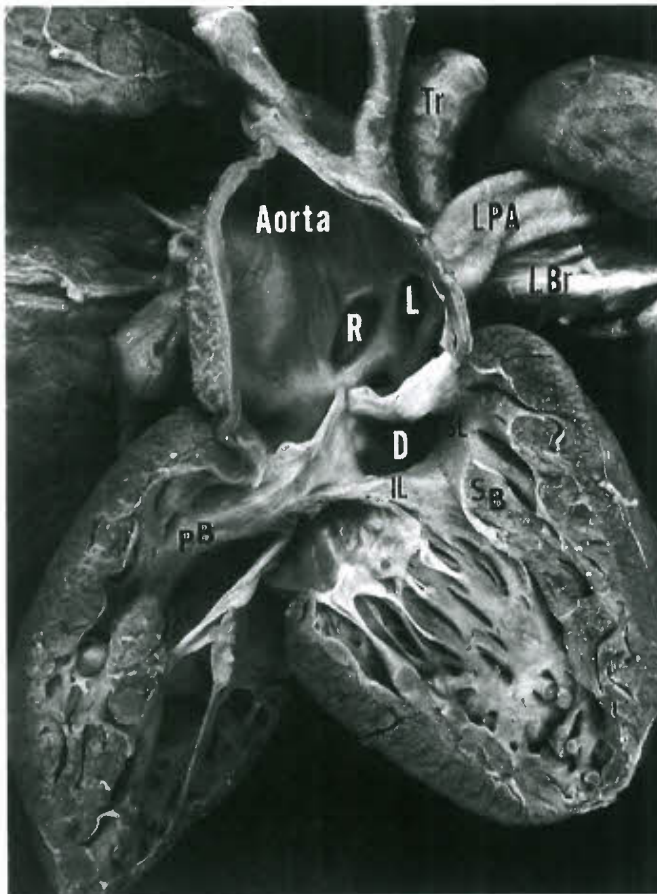


Figure 44.1. Pathology of truncus arteriosus: Right ventricular view showing truncal origin of aorta, right (R) and left (L) pulmonary arteries (type II), and coronary arteries. Ventricular septal defect (D) is cradled between superior (SL) and inferior (IL) limbs of septal band (SB). Fusion of inferior limb with parietal band (PB) separates tricuspid valve from bicuspid truncal valve and mitral valve. Infundibular septum and medial tricuspid papillary muscle are absent. Aortic arch is right-sided. LBr, left bronchus; LPA, left pulmonary artery; Tr, trachea.

The ventricular septal defect in truncus arteriosus is generally large and results from either absence or pronounced deficiency of the infundibular septum. The defect is cradled between the two limbs of the septal band and is roofed by the truncal valve cusps (Fig. 44.1). In most instances, fusion of the inferior limb and the parietal band causes muscular discontinuity between the tricuspid valve and the truncal valve (15). Accordingly, the membranous septum is intact, and the defect is of the infundibular type. When such fusion fails to occur, tricuspid–truncal valvular continuity is present, and the defect (which now involves the membranous septum) is of combined membranous and infundibular types. Rarely, the ventricular septal defect in truncus arteriosus may be small and restrictive or even absent (17).

Among 400 cases of truncus arteriosus from four publications reviewed by Fuglestad et al. (14), the truncal valve was tricuspid in 277 (69%), quadricuspid in 86 (22%), bicuspid in 35 (9%), pentacuspid in 1 (0.3%), and unicommissural in 1 (0.3%). The semilunar valve is in fibrous continuity with the mitral valve in all patients but is continuous with the tricuspid valve in only a minority. By overriding the ventricular septum, the truncus arteriosus has a biventricular origin

in 68% to 83% of patients (15,18). In 11% to 29% of patients, the truncal valve arises entirely from the right ventricle, whereas in 4% to 6% of patients, it emanates entirely from the left ventricle.

The anatomic cause for truncal valve insufficiency is variable and includes thickened and nodular dysplastic cusps, prolapse of unsupported cusps or of conjoined cusps with only a shallow raphe, inequality of cusp size, minor commissural abnormalities, and annular dilation (14,19). Truncal valve stenosis, when present, usually is associated with nodular and dysplastic cusps (19). The truncal root frequently is dilated, and the truncal sinuses often are poorly developed.

A right aortic arch with mirror-image brachiocephalic branching, occurring in 21% to 36% of patients (19,20), is associated more commonly with truncus arteriosus than with any other congenital cardiac malformation except pulmonary atresia with ventricular septal defect. Rarely, a double aortic arch persists. Hypoplasia of the arch, either with or without coarctation of the aorta, occurs in 3% of patients (18). Interrupted aortic arch occurs relatively frequently (11% to 19% of patients) (19,21) and is accompanied by ductal continuity of the descending thoracic aorta. It frequently is associated with the DiGeorge syndrome.

The ductus arteriosus is absent in approximately half of patients with truncus arteriosus, but it remains patent postnatally in nearly two-thirds of patients in whom it is present. The relative sizes of the aorta and the ductus arteriosus tend to vary inversely, such that the ductus arteriosus is particularly large in patients with underdevelopment of the aortic arch (type A4 truncus).

The pulmonary arteries most commonly arise from the left posterolateral aspect of the truncus arteriosus, a small distance above the truncal valve. Type I truncus arteriosus is observed in 48% to 68% of patients, type II in 29% to 48% (18), and type III in 6% to 10% (15,18). In type II, the left pulmonary artery ostium generally is somewhat higher than that of the right pulmonary artery. Rarely, in the setting of interrupted aortic arch, this ostium may arise to the right of the right pulmonary artery ostium and cause crossing of the pulmonary arteries posterior to the truncus arteriosus (19).

Stenosis of the pulmonary artery ostia or arteries is uncommon. In rare instances, deformed truncal valvular tissue may obstruct the pulmonary ostia during ventricular systole. In general, however, unless pulmonary arterial banding is performed, the pulmonary vascular bed will be exposed to systemic arterial pressure.

In truncus arteriosus, one pulmonary artery may be absent. Of the Mayo Clinic's previously published series of patients with truncus arteriosus, 16% (11 of 70) had only a single pulmonary artery (22). In 9 of the 11 patients, the pulmonary artery was absent on the side of the aortic arch. Thus, in truncus arteriosus, the pulmonary artery most frequently is absent on the side of the aortic arch, in contrast to tetralogy of Fallot, in which the pulmonary artery more frequently is absent on the side opposite the aortic arch.

This chapter does not consider either so-called pseudotruncus arteriosus, which is actually a form of pulmonary valve atresia with ventricular septal defect, or "hemitruncus," in which one pulmonary artery arises from the ascending aorta and the other emanates from the right ventricle and clearly has a well-developed pulmonary valve at its origin. The embryologic basis for these deformities appears to be different from that for true persistent truncus arteriosus.

Knowledge of variations in coronary arterial origin and distribution, which are common in truncus arteriosus, is important to the surgeon. Because the left anterior descending coronary artery frequently is relatively small and displaced leftward, the conus branch of the right coronary artery, in a compensatory manner, is usually prominent and supplies several large branches to the right ventricular outflow tract

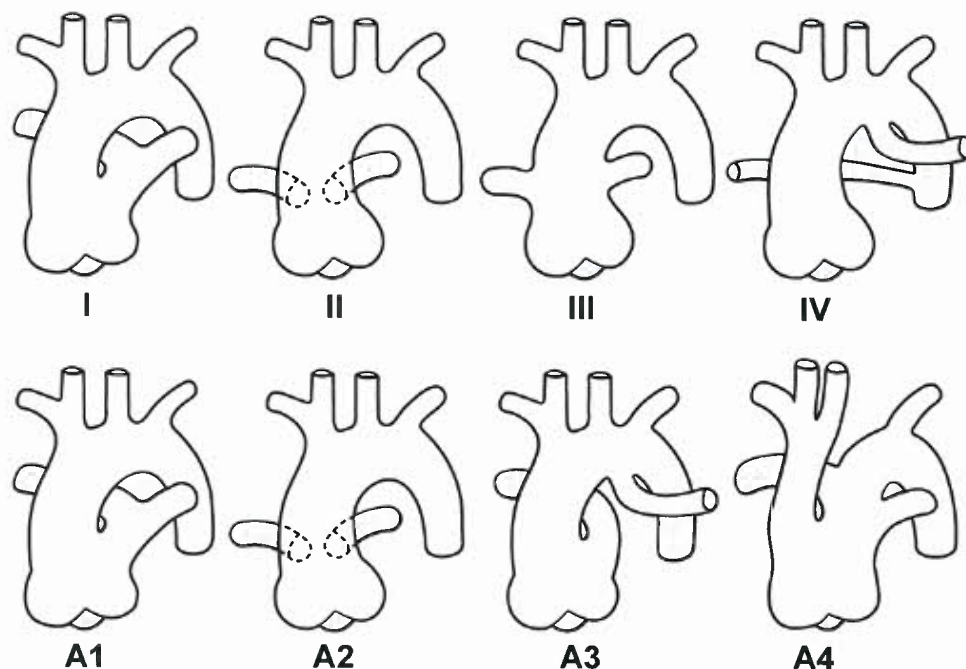


Figure 44.2. Classification systems for persistent truncus arteriosus. **Top:** Type I to IV. (Collett RW, Edwards JE. Persistent truncus arteriosus: a classification according to anatomic types. *Surg Clin North Am* 1949;29:1245–1270.) **Bottom:** Types A1 to A4. (Van Praagh R, Van Praagh S. The anatomy of common aorticopulmonary trunk (truncus arteriosus communis) and its embryologic implications: a study of 57 necropsy cases. *Am J Cardiol* 1965;16:406–425.) (See text for description for each type.)

(23,24). The posterior descending coronary artery arises from the left circumflex artery (left coronary dominance) in 27% of patients with truncus arteriosus (25), which is about three times the frequency of this variation in the normal population. Anomalies of coronary ostial origin, involving 37% to 49% of patients with truncus arteriosus (25), are common, regardless of the number of truncal valve cusps. In general, however, the left coronary artery tends to arise from the left posterolateral truncal surface and the right coronary artery from the right anterolateral surface (18,25).

In the setting of a single coronary ostium, frequently associated with left coronary dominance, all three major epicardial branches originate from this common site, or the right coronary artery may be absent (19). When two ostia exist, both may arise from the same truncal sinus; one may take origin from the expected site of the noncoronary sinus, or both may arise normally. High ostial origin, above the truncal sinotubular junction, occurs often, but when the origin is at or slightly above a truncal valve commissure, the involved ostium (most commonly the left) may be slit-like and functionally stenotic. Conceivably, dysplastic valvular tissue also could obstruct an otherwise normal coronary ostium. Rarely, the left coronary artery originates from the pulmonary trunk (18,26). Combinations of the aforementioned coronary anomalies frequently are observed.

The location of the conduction tissue in truncus arteriosus is also of surgical importance. The sinus node and the atrioventricular node are normal in location and structure. The atrioventricular bundle courses to the left of the central fibrous body, and the left bundle branch emanates along the left ventricular septal subendocardium, just beneath the membranous septum (27). The right bundle branch travels within the myocardium of the ventricular septal summit, attaining a subendocardial course at the level of the moderator band. In most instances in which the ventricular septal defect is truly infundibular and the membranous septum is intact, the

atrioventricular conduction tissue is somewhat distant from the rim of the defect. In patients with combined membranous-infundibular ventricular septal defect, however, the conduction tissue passes along the left aspect of the posterior-inferior rim of the defect.

The anomalies most commonly associated with truncus arteriosus are right aortic arch, interrupted aortic arch, absent ductus arteriosus, patent ductus arteriosus, unilateral absence of a pulmonary artery, coronary ostial anomalies, and an incompetent truncal valve. A secundum atrial septal defect has been noted in 9% to 20% of patients, an aberrant subclavian artery in 4% to 10%, a persistent left superior vena cava draining into the coronary sinus in 4% to 9%, and mild tricuspid stenosis in 6% (18,20). Total or partial anomalous pulmonary venous connection in association with truncus arteriosus also has been described (22,28). Rare associated anomalies that have been reported include tricuspid atresia, mitral atresia, ventricular inversion, and association with the asplenia complex. We have encountered one patient with both truncus arteriosus and complete atrioventricular septal defect. Extracardiac anomalies, present in 21% to 30% of autopsy cases of truncus arteriosus, include skeletal deformities, hydroureter, bowel malrotation, and multiple complex anomalies.

Among the secondary complications of truncus arteriosus, biventricular hypertrophy is frequent, and dilation of ventricular chambers is prominent when truncal valve insufficiency exists. If there is massive cardiac hypertrophy, chronic subendocardial myocardial ischemia may develop (even with normal epicardial coronary arteries). As a result of chronic exposure of the pulmonary vasculature to systemic arterial pressure, hypertensive pulmonary vascular disease (plexogenic pulmonary arteriopathy) may develop. The arteriolar lesions often develop more rapidly and to a more severe extent in truncus arteriosus than in isolated ventricular septal defect. With chronic truncal valve insufficiency, pulmonary venous hypertension also may develop.

As patients with surgical repair survive into adulthood, progressive dilation of their aorta (original truncal artery) often occurs but is rarely associated with complications, including dissection or rupture (29).

MANIFESTATIONS

Clinical Features

In most patients with truncus arteriosus, congenital heart disease is recognized during early infancy, often during the neonatal period. During the 1990s, intrauterine diagnosis became possible with fetal echocardiography (30). The clinical features depend largely on the volume of pulmonary blood flow and whether associated significant truncal valve insufficiency is present.

During the first weeks of life, persistence of increased pulmonary arteriolar resistance present during fetal life may cause mild cyanosis with little evidence of cardiac decompensation, unless severe truncal valve insufficiency also is present. As pulmonary resistance gradually decreases and flow through the lungs increases, the cyanosis may disappear. However, tachypnea, tachycardia, excessive sweating, poor feeding, and other signs of pulmonary overcirculation may appear. If truncal valve insufficiency is severe, the signs and symptoms of heart failure may appear shortly after birth. The additional volume load produced by this associated problem always adds to the increasing demands placed on the heart as pulmonary flow increases.

In the uncommon situation in which the infant has naturally occurring stenosis of the pulmonary arteries, cyanosis may be present at birth and may intensify with increasing age. However, such stenosis protects the child from pulmonary overcirculation that would otherwise occur with falling pulmonary resistance. Severe cyanosis, in addition to the signs of heart failure, may be present early if the child has both naturally occurring stenosis of the pulmonary artery and severe insufficiency of the truncal valve.

Physical Examination

Physical findings are related primarily to the volume of pulmonary blood flow and the presence or absence of truncal valve insufficiency. Patients with increased pulmonary blood flow have little or no cyanosis. The peripheral pulses are accentuated and may be bounding. The pulse pressure usually is increased owing to runoff into the pulmonary vascular bed during diastole and is accentuated in the setting of truncal valve insufficiency. A left precordial bulge may be noted, and a systolic thrill often is palpable along the left sternal border. The heart usually is overactive. The first heart sound is normal and frequently followed by an ejection click, which echocardiographic studies have shown to coincide with maximal opening of the truncal valve. The second heart sound usually is loud and single. The occasional auscultatory or phonocardiographic observation of a split second sound in these patients with a single semilunar valve may be caused by delayed closure of some of the cusps of the abnormal truncal valve. An apical third heart sound often is present. A loud pansystolic murmur maximal at the lower left sternal border and radiating to the entire precordium most often is heard. An apical diastolic low-pitched murmur caused by increased flow across the normal mitral valve frequently is audible.

The patient with truncal valve insufficiency usually has a diastolic high-pitched murmur that is heard best along the left sternal border. A truly continuous murmur is uncommon in

truncus arteriosus and, when present, is usually suggestive of pulmonary artery ostial stenosis. Continuous murmurs are common in patients with pulmonary valve atresia/ventricular septal defect, however, where either a patent ductus arteriosus or systemic collateral arteries provide pulmonary blood flow. Because the differential diagnosis of truncus arteriosus includes this lesion, a continuous murmur is strongly suggestive of pulmonary atresia rather than of truncus arteriosus. Patients in heart failure may exhibit the additional signs of tachypnea, crepitant rales, hepatomegaly, and neck-vein distension.

Cyanosis is present, and clubbing of the fingers and toes may be seen in patients with decreased pulmonary blood flow caused by naturally occurring pulmonary artery stenosis, pulmonary artery banding, or pulmonary vascular disease. If there is no associated truncal valve insufficiency, the peripheral pulses and pulse pressure are nearly normal. The apical diastolic murmur often is not present. These patients are less likely to have signs and symptoms of cardiac decompensation.

Electrocardiographic Features

The electrocardiogram (ECG) usually shows a normal frontal plane QRS axis or minimal right-axis deviation. Generally, normal sinus rhythm is present, and the conduction times are not prolonged. Combined ventricular hypertrophy occurs frequently. Left ventricular forces are particularly prominent in patients with increased pulmonary blood flow. Left atrial enlargement also is common in this group. Patients with normal or decreased pulmonary flow may exhibit right ventricular hypertrophy only.

Radiologic Features

Typically, radiography of the chest shows moderate cardiomegaly and increased pulmonary vascular markings (Fig. 44.3). The aortic arch is right-sided in approximately one-third



Figure 44.3. Radiograph demonstrating typical features of truncus arteriosus in newborn with significant truncal valve insufficiency. Note the cardiomegaly and pulmonary vascular congestion.

of patients, and the combination of a right aortic arch and increased pulmonary vascularity is strongly suggestive of truncus arteriosus. Type I truncus arteriosus frequently is associated with a relatively superiorly located proximal left pulmonary artery, which usually can be distinguished on a frontal chest radiograph. A dilated truncal root is common. Although the pulmonary vascular markings typically are increased, variation in the pulmonary vascular pattern can be seen. In truncus arteriosus with unilateral absent pulmonary artery, the pulmonary vascular markings are markedly diminished on the side without the pulmonary artery (usually the left side). In addition, pulmonary vascular obstructive disease is common in patients with truncus arteriosus and is reflected in the chest radiograph by disproportionate enlargement of the central pulmonary arteries associated with accentuated tapering of the distal pulmonary arterial tree.

Echocardiographic Features

The use of 2-D, Doppler, and color Doppler echocardiography has greatly increased the ability to determine accurately the cardiac anatomy and, in most cases, the hemodynamics in truncus arteriosus (31,32). Subcostal windows are used to document abdominal visceral situs and atrial situs, in addition to the position of the cardiac apex. A single great vessel arising from the heart typically is seen from a subcostal image (Fig. 44.4A), and assessment of the atrial septum is performed best from this location as well. Subcostal windows provide additional views for evaluation of the truncal valve function, truncal root, and pulmonary artery branch anatomy. The parasternal long-axis view demonstrates the deficiency in the ventricular septum and the overriding great artery, with continuity between the truncal valve and the mitral valve. Slightly higher position in the parasternal long-axis view can be used to visualize the origin of the pulmonary trunk or branches (Fig. 44.4B). Further imaging is required to document the presence of a single arterial trunk and lack of a pulmonary outflow tract from the ventricle. High parasternal short-axis views will provide visualization of the pulmonary arteries arising directly from the posterolateral aspect of the truncal root, typically bifurcating into the right and left pulmonary arteries.

Persistence of a short MPA segment is seen in truncus arteriosus type I (Van Praagh type A1, Fig. 44.5). Separate origins of the pulmonary branches are seen in type II (type A2). When only one pulmonary artery is present, as in type III truncus (type A3), the remaining pulmonary artery origin must be documented, typically originating from the aortic arch or ductus arteriosus. The short-axis view is also useful in evaluating the anatomy of the truncal valve leaflets (number and morphology), as well as visualization of the coronary arteries and their origins, and the location and extension of the ventricular septal defect. Suprasternal notch imaging is critical for evaluation of the aortic arch anatomy, as interruption of the aortic arch may be associated with truncus arteriosus (type A4). Right-sided aortic arch also is common in truncus arteriosus and can be determined from short-axis imaging of the arch branching pattern. In addition, the pulmonary artery branches also can be visualized from the suprasternal notch, excluding any important branch stenoses (33).

Aortopulmonary window is in the differential diagnosis of truncus arteriosus and angiographically may be confused with truncus arteriosus. Echocardiographically, however, these two entities easily can be differentiated. Aortopulmonary window usually is not associated with a ventricular septal defect, and the right ventricular outflow tract and pulmonary valve are in the expected positions. These features usually are recognized easily by 2-D echocardiography. Moreover, in aortopulmonary window, use of a high parasternal short-axis view usually allows its direct visualization. In patients with truncal valve stenosis, Doppler echocardiography usually enables an estimation of this gradient. In patients with significant truncal valve insufficiency, the systolic Doppler gradient may overestimate the degree of valve stenosis owing to the volume of flow across the valve (2-D morphology must be correlated with the Doppler findings). Truncal valve incompetence also can be delineated and quantitated by Doppler technique; the color flow Doppler examination has been particularly helpful in this assessment. Doppler flow reversal in the abdominal descending aorta may be due to either pulmonary artery runoff, truncal valve insufficiency, or both. In the rare patient with a pulmonary artery band(s) in place, Doppler evaluation also permits assessment of the pressure gradient between the truncal root and the pulmonary arteries beyond the band.

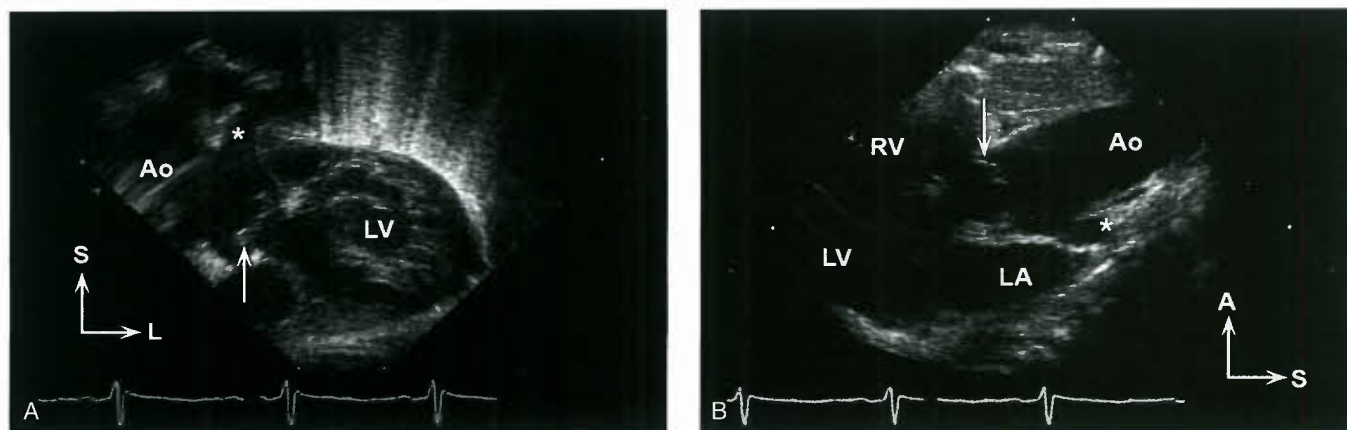


Figure 44.4. A: Subcostal coronal view with anterior angulation in newborn with truncus arteriosus type I and moderately severe truncal regurgitation. Arrow indicates doming, thickened truncal valve; aortic root (Ao) continues anteriorly/superiorly. Origin of the pulmonary trunk indicated by the asterisk. L, left; LV, left ventricle; S, superior. B: High parasternal long-axis view in same newborn with truncus arteriosus type I, with the doming truncal valve (arrow) and posterior origin of the pulmonary trunk (asterisk). A, anterior; LA, left atrium; LV, left ventricle; RV, right ventricle; S, superior.

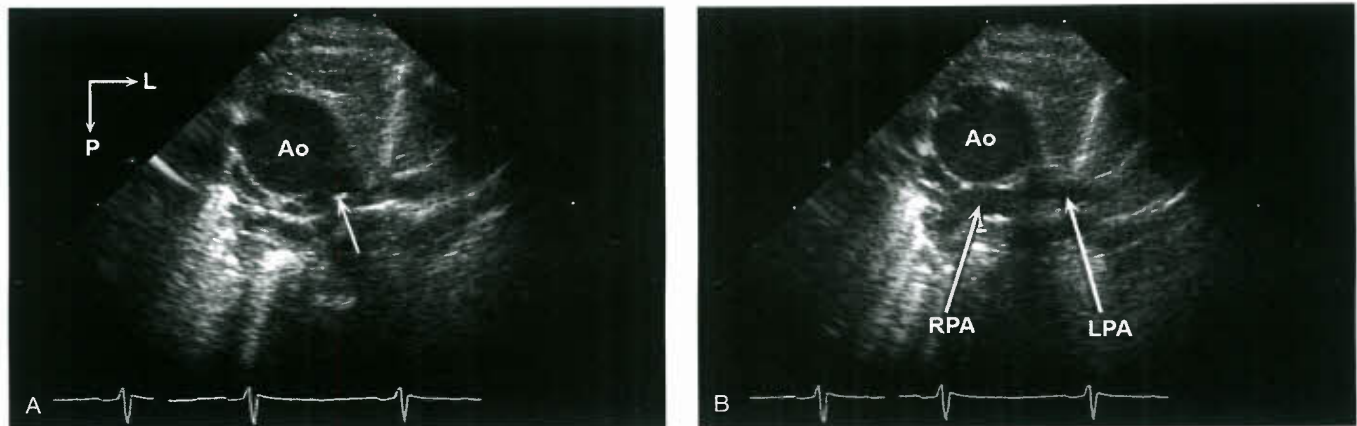


Figure 44.5. A: High parasternal short-axis view above the level of the truncal valve demonstrating posterior origin of pulmonary branches with very short main pulmonary artery segment (*short arrow*) and normal left and right pulmonary origins. Ao, aorta; L, leftward; P, posterior. B: Slightly higher short-axis view with same orientation as (A) illustrates central pulmonary artery confluence. RPA, right pulmonary artery; LPA, left pulmonary artery.

Truncus arteriosus may be diagnosed in utero with fetal echocardiography. The echocardiographer must be certain to identify the central MPA origin or proximal branch origin from the ascending truncal root to differentiate this condition from pulmonary atresia/ventricular septal defect. Associated interruption of the aortic arch also may be recognized in the fetus with truncus arteriosus. Severe truncal valve dysfunction (stenosis typically in combination with regurgitation) in utero may lead to fetal hydrops (30).

Cardiac Catheterization and Angiocardiography

With the introduction and advancement of accurate echocardiographic diagnosis and the advent of surgical correction during early infancy, before irreversible pulmonary vascular disease is a concern, diagnostic cardiac catheterization and angiography usually are unnecessary in the patient with truncus arteriosus (32). Rarely, the patient with truncus

arteriosus with associated interruption at the aortic arch or single pulmonary artery will need angiography to delineate aortic arch anatomy or the anatomy of the pulmonary arterial tree precisely. An example of a truncal root angiogram is seen in Figure 44.6. Magnetic resonance imaging (MRI), magnetic imaging angiography (MRA), or computed tomography (CT) scanning may be adequate to delineate this anatomy (see below).

Patients with truncus arteriosus are at risk of having pulmonary vascular obstructive disease develop at an early age, and this has driven the major impetus for early surgical correction (10). Even more uncommonly in this era, a patient with truncus arteriosus will still present initially beyond early infancy for consideration of surgical correction, and cardiac catheterization may be necessary to assess the status of the pulmonary vascular bed (22). Although direct measurement of pulmonary resistance is not possible, the calculated indirect value, obtained by dividing the mean driving pressure across the pulmonary bed (in mm Hg) by the total pulmonary flow

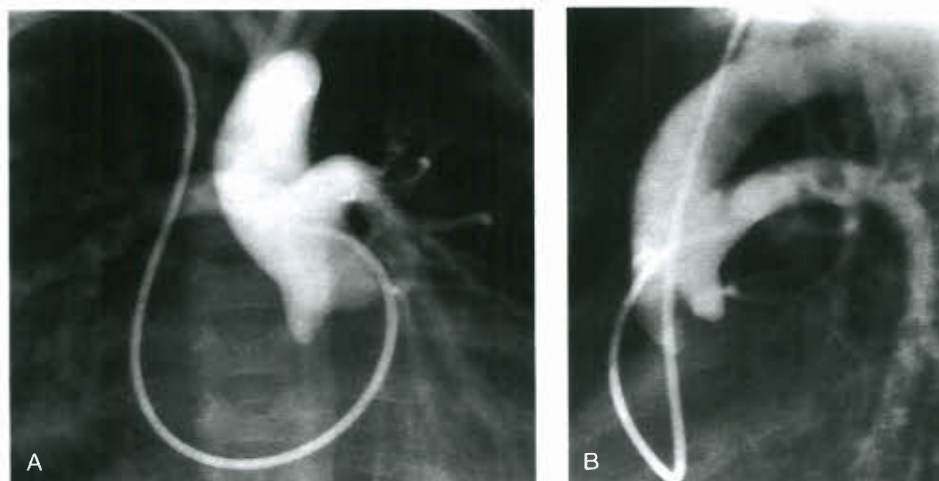


Figure 44.6. Anteroposterior (A) and lateral (B) views of truncal root angiogram in 10-month-old patient with truncus arteriosus, type I. Note common pulmonary trunk originating from posterolateral aspect of truncal root and bifurcating into right and left pulmonary arteries. Truncal valve is competent.

index (in liters per minute per square meter), provides a reliable estimation of the status of the pulmonary arterioles.

Patients with truncus arteriosus who have two pulmonary arteries and a pulmonary arteriolar resistance >8 units m^2 are at higher operative risk than patients with resistances below that level (20,22). Among the group with resistances >8 units m^2 , late deaths were due to progression of pulmonary vascular obstructive disease with secondary severe pulmonary hypertension and right ventricular failure. Among the survivors of operation in the group with preoperative resistance <8 units m^2 , no late deaths occurred secondary to progressive pulmonary hypertension.

Fortunately, the trend toward early corrective surgery has reduced the number of patients who are inoperable because of pulmonary vascular obstructive disease. Our current policy is not to offer corrective surgery to patients with truncus arteriosus who have two pulmonary arteries and whose pulmonary arteriolar resistance is >8 units m^2 . The exceptions are children younger than 2 years of age whose resistance decreases to <8 units m^2 , when 100% oxygen is breathed or after administration of a pharmacologic vasodilator such as inhaled nitric oxide. In such young patients, surgery still may be offered if the parents are willing to accept a higher surgical risk because it is possible that the increased resistances may result from arteriolar or medial smooth muscle hypertrophy and vasoconstriction rather than advanced intimal occlusive disease. These changes potentially may be reversible, and such patients can be treated with pulmonary vasodilator therapy after surgical repair is undertaken.

Different criteria must be used to assess the feasibility of operation in patients with unilateral absence of a pulmonary artery (34). Severe pulmonary vascular disease is particularly likely to develop at an early age in patients with a single pulmonary artery (22,35). To achieve good surgical results in this subgroup, corrective surgery should be performed in the neonatal period. Even in patients who survive corrective operation, however, pulmonary vascular disease tends to progress postoperatively more often than it does in patients with

corrected truncus arteriosus who have two pulmonary arteries (35). This difference may be related to the fact that the entire cardiac output still must pass through one lung so that the rate of flow through each arteriole remains approximately double. This may be a potential stimulus for the progression of pulmonary vascular changes.

An accurate preoperative catheterization laboratory assessment of truncal valve insufficiency may be difficult because of contrast runoff into the pulmonary artery bed.

Magnetic Resonance Imaging

Cardiac MRI and MRA can provide additional noninvasive anatomic and hemodynamic information in the patient with truncus arteriosus (36,37). Visualization of the conotruncus and pulmonary artery anatomy is accomplished by multiple techniques, including black blood and white blood imaging techniques with gating, and with the use of gadolinium contrast-enhanced MRA (Figs. 44.7 and 44.8).

DIFFERENTIAL DIAGNOSIS

In infants with truncus arteriosus and increased pulmonary blood flow, the differential diagnosis includes the other congenital cardiac conditions that cause early heart failure and are associated with either mild or no cyanosis. Such malformations include ventricular septal defect, patent ductus arteriosus, aorticopulmonary window, pulmonary atresia with ventricular septal defect, and patent ductus arteriosus, or large collateral arteries, double-outlet right ventricle, univentricular heart, and total anomalous pulmonary venous connection. In truncus arteriosus with decreased pulmonary flow, other conditions to be considered include pulmonary atresia, tricuspid atresia, tetralogy of Fallot, univentricular heart with pulmonary stenosis, and double-outlet right ventricle with

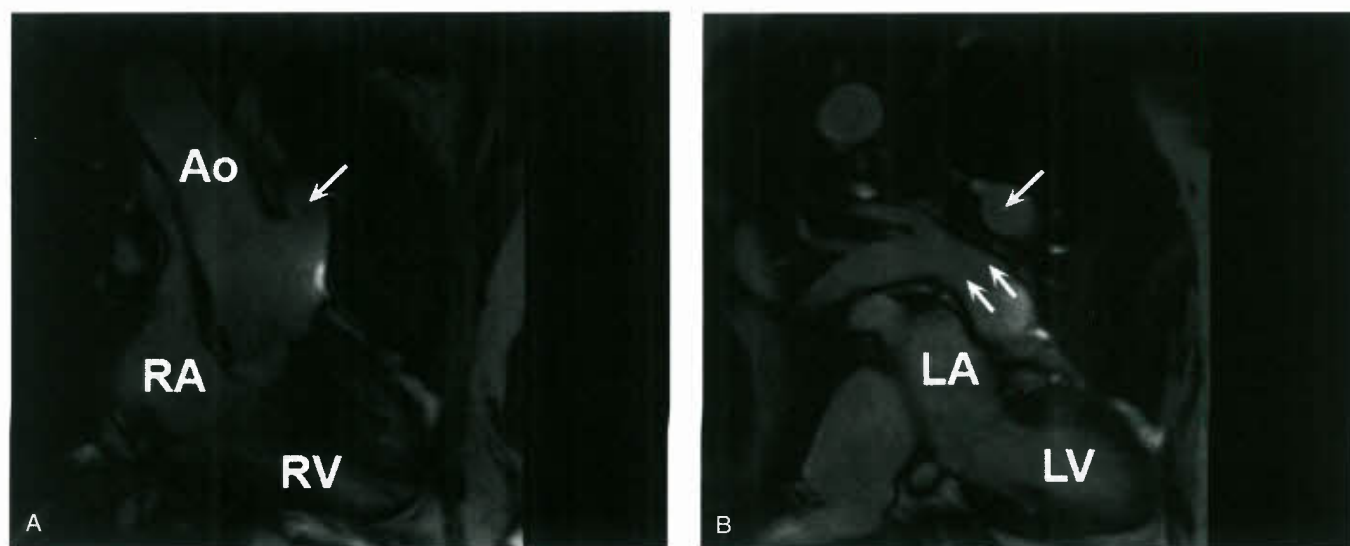


Figure 44.7. Magnetic resonance noncontrast (bright blood) imaging in adult patient with untreated truncus arteriosus, type II, with separate pulmonary artery branch origins. **A:** Anterior sagittal oblique image demonstrating the trunco-aortic root with origin of the left pulmonary artery depicted by *arrow*, leftward and superiorly, and continuation of the right aortic arch (Ao). RA, right atrium; RV, right ventricle. **B:** Slightly more posterior angulated view showing origin of the right pulmonary artery (*double arrow*) and continuation of the left pulmonary artery (*single arrow*). LA, left atrium; LV, left ventricle.

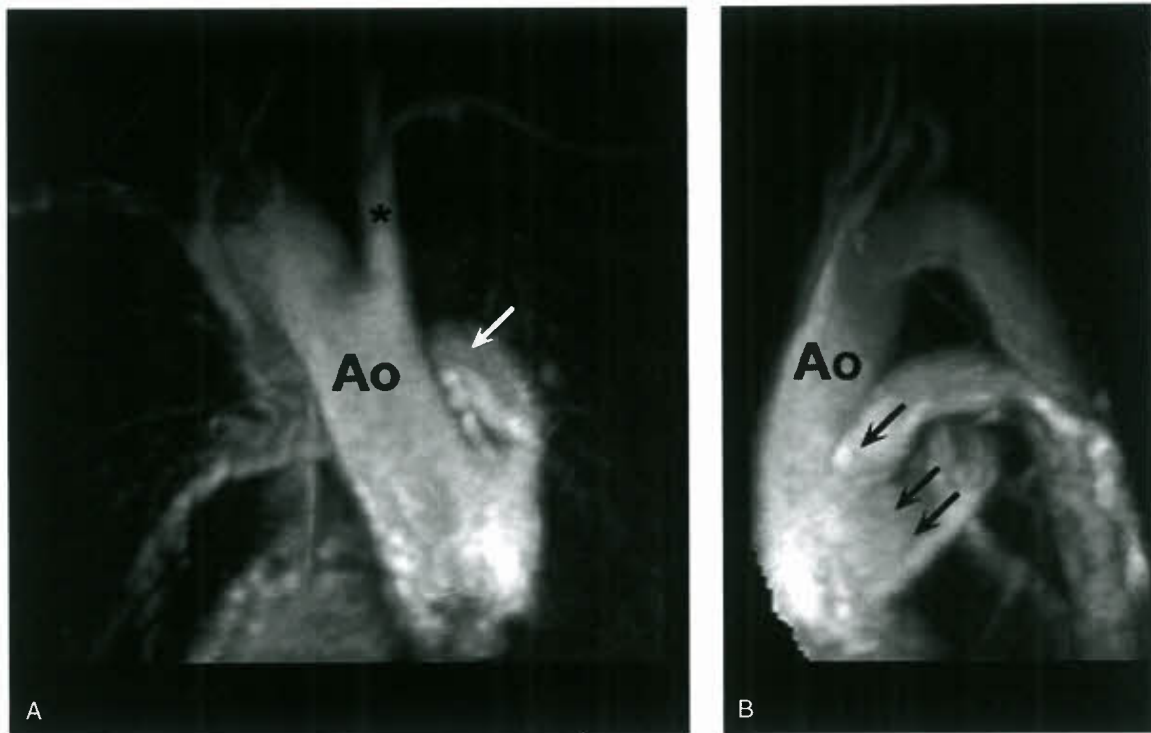


Figure 44.8. Magnetic resonance angiography with gadolinium contrast in same adult patient with unrepaired truncus arteriosus, type II. **A:** Anteroposterior view with the proximal leftward origin of the left pulmonary artery (*single white arrow*) and continuation of the right aortic arch (Ao). First arch branch coursing leftward (*asterisk*). **B:** Lateral view shows the posterior/inferior origin of the right pulmonary artery (*double dark arrows*) and leftward/superior origin of the left pulmonary artery (*single dark arrow*).

pulmonary stenosis. Although certain physical findings, chest radiographic evidence, and electrocardiographic features may suggest the increased likelihood of a particular lesion, echocardiography is necessary to establish the diagnosis definitively.

NATURAL HISTORY

Although patients with truncus arteriosus occasionally survive to adulthood without surgery, the natural history of this condition is generally dismal. In one autopsy series, the mean age of death was 5 weeks. Another series reported a survival of only 15% beyond the age of 1 year. Death in infancy most commonly is caused by heart failure. In patients who survived the first 4 years, death may occur from heart failure, but more frequently it results from the complications of hypertensive pulmonary vascular disease and infective endocarditis.

Once severe pulmonary vascular disease is present (38), deterioration often is rapid, with severe morbidity and death frequently occurring in late childhood or early adolescence. This dismal natural history was the main factor that gave rise to the approach of early surgical repair that is now advocated for these patients.

TREATMENT

The diagnosis of truncus arteriosus, itself, is an indication for operation. Diagnosis ideally is made prenatally or soon after birth. Medical stabilization is performed in the intensive care unit, and operation with complete repair is preferred in

the first weeks of life. Delay of operation results in chronic ischemia of the hypertrophied ventricle, which is perfused by desaturated blood at a low diastolic perfusion pressure caused by runoff through the pulmonary arteries, and, when present, “aortic” insufficiency. This hazard of ventricular dysfunction may explain, in part, the observation that repair of truncus at 6 to 12 months of age is associated with mortality twice that for repair between 6 weeks and 6 months of age (10). Pulmonary vascular obstructive disease also can develop early, which provides additional impetus for correction in the first few months of life. Pulmonary vascular obstructive disease, no doubt, also is partly responsible for the increased surgical mortality in infants who undergo repair after 6 months of age.

The preferred operation is complete repair during the neonatal period. Although pulmonary artery banding may provide palliation for young patients with truncus arteriosus, there are well-documented risks and potential complications of banding for this condition. In addition, successful banding has not guaranteed that these patients will be good candidates for later correction (39). During the past 15 years, improved surgical techniques and postoperative care have made correction of truncus arteriosus during infancy possible at an operative risk less than that previously reported for banding.

SURGICAL CORRECTION

Successful definitive surgical correction in a patient with truncus arteriosus was first accomplished by McGoon et al. in 1967 (9). In the original operation, based on the experimental work of Rastelli et al. (40), continuity between the right ventricle and

the pulmonary arteries was established with an aortic homograft. Cryopreserved homograft tissue continues to be the conduit of choice for repair of this defect in early infancy (41).

The early and late results experienced by the initial 92 patients who had correction at the Mayo Clinic were reported in 1977 (20). Although overall hospital mortality was 25%, the operative mortality decreased to 9% in the 33 patients operated on during the last 2.5 years of this early series. Since that time, an operative mortality of 5% was achieved in patients without severe associated abnormalities who subsequently have undergone correction of truncus arteriosus. In 1984, Ebert et al. (10) reported results of 100 infants repaired prior to 6 months of age, emphasizing the importance of early repair to prevent the development of pulmonary vascular obstructive disease. Early mortality was 11%. At this time, the importance of complete repair in early infancy to prevent the development of pulmonary vascular obstructive disease was also emphasized.

During the last three decades, there has been great progress in the surgical management of infants (42). In the current era, excellent results have been obtained with corrective operation during infancy (42–48). In patients who undergo successful correction during early infancy, the small right ventricular to

pulmonary artery conduit eventually must be replaced with a larger one, but reoperation for conduit replacement alone carries a low risk (49–52). A 1993 late follow-up of 137 patients with truncus arteriosus corrected at the Mayo Clinic between 1967 and 1992 showed no perioperative deaths in 39 patients who underwent reoperation for isolated conduit replacement. One death occurred in 15 patients who had isolated conduit replacement performed elsewhere (53).

Although techniques of repair that do not include an extracardiac conduit also have been described (54), most surgeons prefer a valved conduit when complete repair is performed because of the presence of pulmonary hypertension. Techniques for conduit replacement have evolved over the last two decades (49,55). It is our current preference to use the autologous tissue reconstruction (“peel operation”) to reconstruct the right ventricular outflow tract when conduit replacement is required (Fig. 44.9). The technique includes placement of a prosthetic roof (usually bovine pericardium) over the fibrous bed of the explanted conduit with insertion of a prosthetic valve (usually bioprosthesis). Early mortality has been low for conduit replacement, in our experience, even after multiple conduit revisions (49,55). Early mortality was

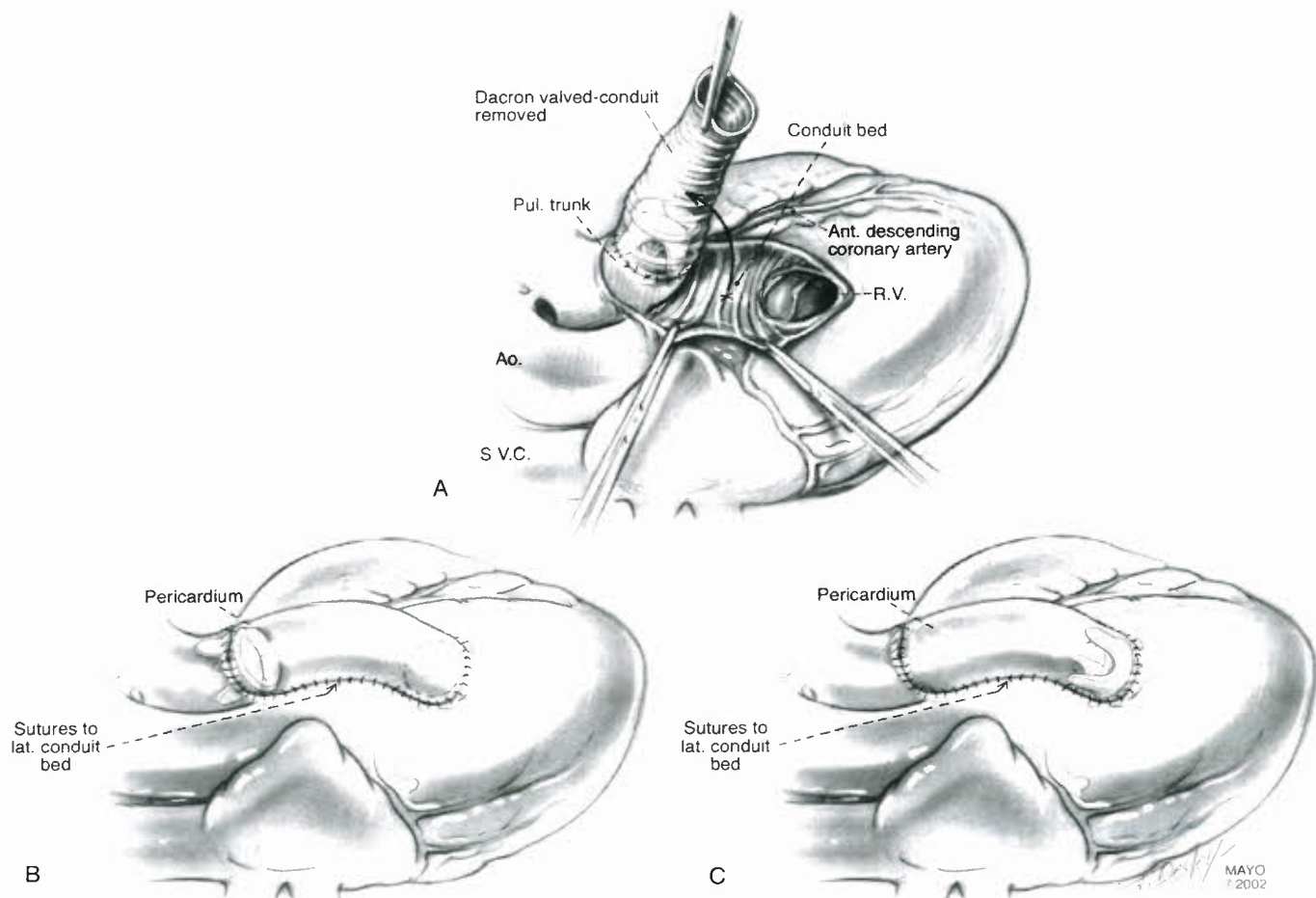


Figure 44.9. Technique of peel operation. A: Illustration depicting the obstructed extracardiac Dacron conduit being removed from the thick fibrous peel that surrounds it. Illustrations of the pericardial roof constructed and sewn to the lateral edges of the fibrous tissue bed. The routinely inserted porcine bioprosthesis is positioned either distally (B) or proximally (C), depending on the cardiac diagnosis, the anatomy, and the discretion of the operating surgeon (see text). Ant, anterior; Ao, aorta; lat, lateral; Pul, pulmonary; RV, right ventricle; SVC, superior vena cava. (Reprinted from Dearani J, Danielson G, Puga F. Late follow-up of 1095 patients undergoing operation for complex congenital heart disease utilizing pulmonary ventricle to pulmonary artery conduits. *Ann Thorac Surg* 2003;75:339–411, with permission from the Society of Thoracic Surgeons.)

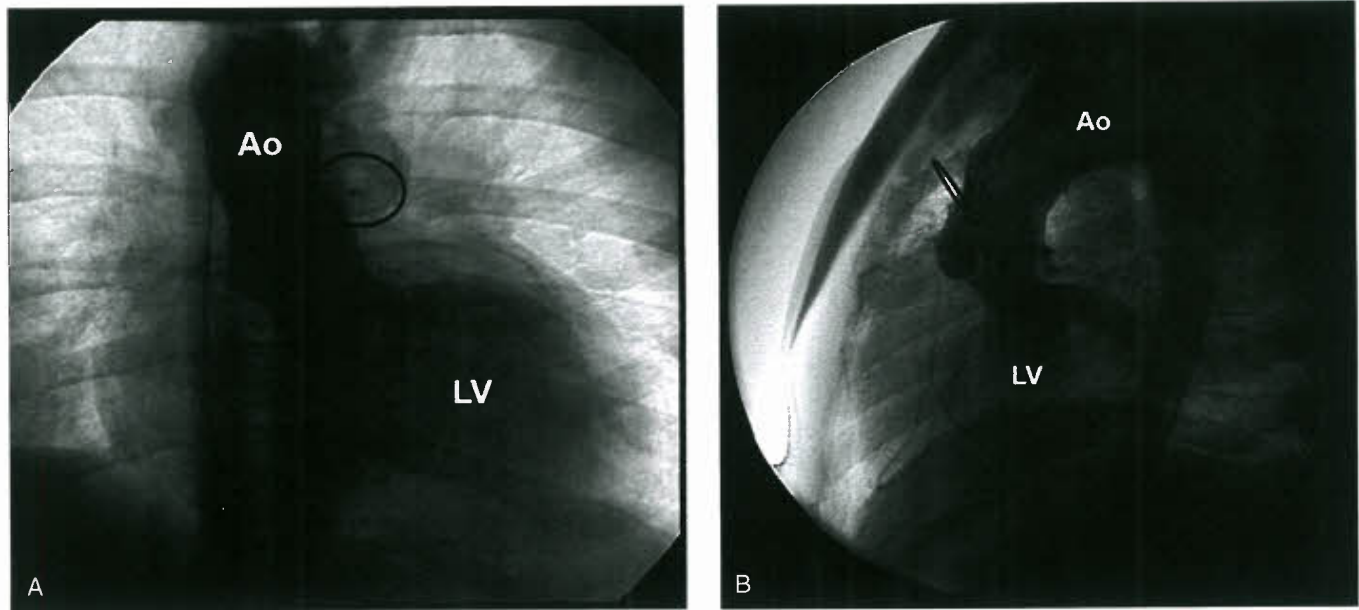


Figure 43.10. Postoperative aortic root angiogram from a 7-year-old patient with severe aortic valve regurgitation following truncal (aortic) valvuloplasty in infancy at the time of complete repair. Anteroposterior (A) and lateral (B) views show dense opacification of the left ventricle following injection in the ascending aorta. Ao, aorta; LV, left ventricle.

2% but was 0% for isolated conduit replacement. Overall survivorship free of reoperation for the peel reconstruction at 10 and 15 years was 90.7% and 82%, respectively.

The presence of a regurgitant truncal valve almost always is amenable to various repair techniques, and replacement is rarely, if ever, done in the neonatal period. Numerous authors have described various truncal valvuloplasty techniques (43,56–62). Frequently used techniques include suturing of the prolapsing leaflet to adjacent leaflets. The prolapsing leaflet usually is thickened and adjacent leaflet edges also are thickened, which facilitates suture placement. The tops of the commissures often are splayed from dilation of the sinotubular junction. This can be corrected by wedge excisions of the aorta. If recurrent truncal valve incompetence occurs, our policy is to repair or replace the truncal valve at the time of reoperation for conduit replacement.

Late results following complete repair are determined by the degree of truncal valve regurgitation and the need for conduit replacement. The need for truncal valve repair at the time of complete repair is low (63). If reoperation is required for truncal valve regurgitation, intermediate-term results favor repair of the truncal valve (43,62). Serial echocardiographic examinations are essential during lifelong follow-up. Recurrent truncal valve regurgitation may necessitate repair or replacement at a subsequent operation (Fig. 44.10). In our follow-up of 137 patients with truncus arteriosus who were operative survivors in our initial 25-year experience, no one underwent truncal valve replacement when trivial or no truncal valve incompetence was present at the time of correction. In patients who had mild, moderate, or severe truncal incompetence, the eventual need for truncal valve replacement was high. The difference between the two groups was highly significant ($p < 0.001$, Fig. 44.11).

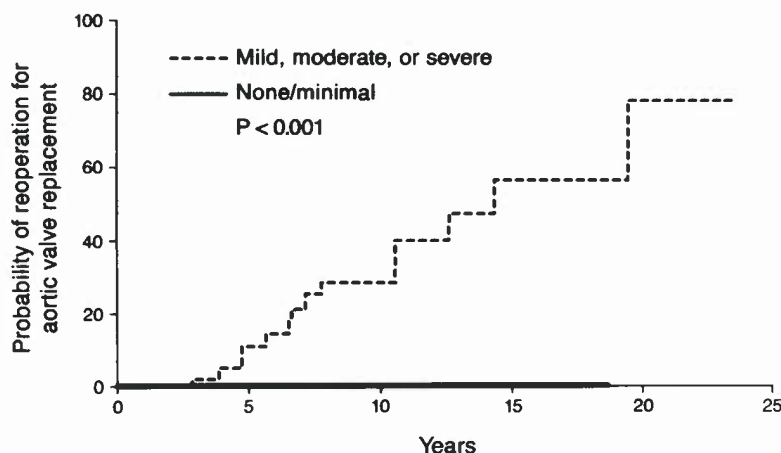


Figure 44.11. Probability of late aortic (truncal) valve replacement after corrective operation: late survivors according to degree of assessed immediate post correction aortic valve insufficiency. All reoperations for valve replacement were in patterns judged to have mild, moderate, or severe insufficiency.

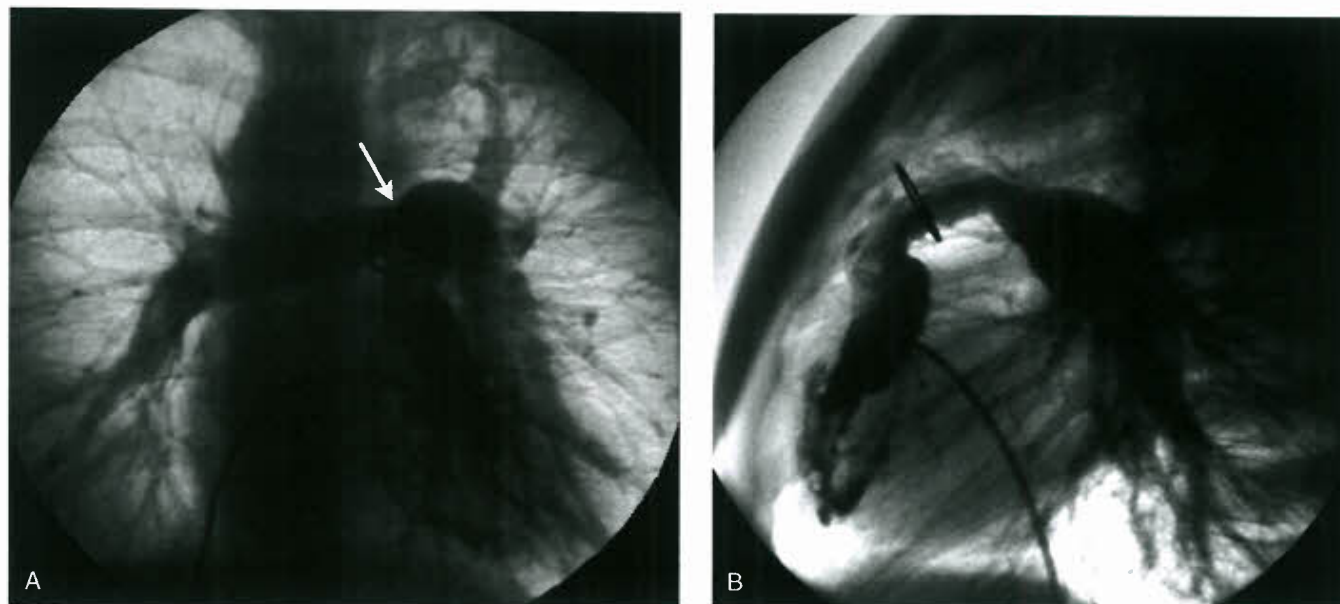


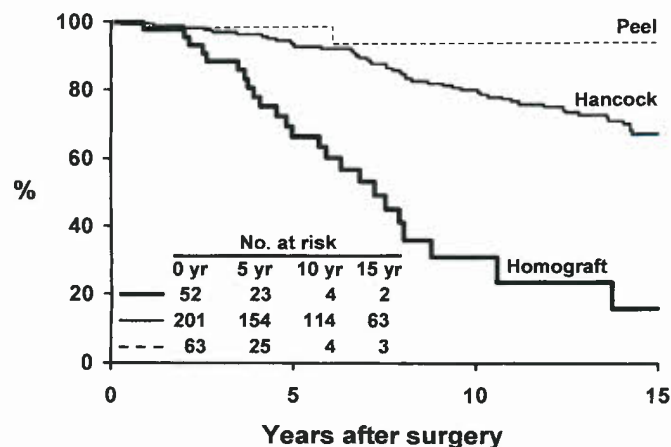
Figure 44.12. Postoperative right ventricular angiogram from the same 7-year-old patient as in Figure 44.10 who underwent truncus arteriosus repair as neonate, followed by re-replacement of the original pulmonary homograft in the first year of life. Anteroposterior (A) and lateral (B) views show heavily trabeculated right ventricle (RV) with diffuse narrowing of the heterograft conduit. In addition, there is mild proximal right pulmonary artery narrowing seen in the AP projection (arrow). No significant tricuspid regurgitation is seen.

The primary late problem related to extracardiac conduit operations is the need for conduit replacement because of somatic growth or progressive deterioration and calcification of the conduit (Fig. 44.12). Numerous reports have focused on issues of conduit size, valve degeneration, and conduit degeneration (49–52,64–80). Late outcome of homograft (41,49,81–84) and prosthetic (49,85,86) conduits has been reported with variable results. Our attempt to reduce the incidence of late conduit failure was the construction of an autologous tissue conduit, with or without a valve. Advantages of this technique include an autogenous floor with a pericardial roof that does not form obstructive peels, and the diameter of the pathway can be as large as desired, allowing a large bioprosthetic valve to be inserted. We have examined the freedom from reoperation for conduit failure in an age-matched group of patients who have received a Hancock conduit, a homograft conduit,

and a valved peel reconstruction (Fig. 44.13). The peel operation had statistically significant better freedom from reoperation compared with the homograft ($p = 0.001$). Although the peel operation had more favorable durability than the Hancock conduit, this did not reach statistical significance ($p = 0.19$) owing to the small numbers in the peel operation group at late follow-up. Percutaneous pulmonary valve therapy is now an alternative and complementary therapy for the postoperative truncus patient with a failing conduit (87–90).

The search continues for the ideal extracardiac conduit. Although the need for reoperation is inevitable for most patients, the risk of reoperation is low and most patients enjoy a good quality of life. Presently, the peel operation provides the most favorable freedom from reoperation and is our procedure of choice when conduit replacement is required.

Figure 44.13. Survival freedom from reoperation for conduit failure in an age-matched population, stratified according to conduit type (peel operation vs. Hancock, $p = 0.19$; peel operation vs. homograft, $p = 0.0001$). (Reprinted from Bermudez C, Dearani J, Puga F. Late results of the peel operation for replacement of failing extracardiac conduits. *Ann Thorac Surg* 2004;77:881–888, with permission from the Society of Thoracic Surgeons.)



CARE OF THE ADULT PATIENT WITH REPAIRED TRUNCUS ARTERIOSUS

The adult patient with repaired truncus arteriosus will require lifelong follow-up by experienced adult congenital heart disease cardiologists. Truncus arteriosus is considered to be a complex form of congenital heart disease so that care of these patients in an experienced regional center is preferred (91). The primary issues for these patients include long-term function of the right ventricular-to-pulmonary artery conduit and of the truncal (aortic) valve, the potential for branch pulmonary artery abnormalities, development of significant tricuspid regurgitation, and aortic root dilation. In addition, genetic testing should be considered in patients who have not had evaluation for 22q11 microdeletion syndrome (92).

Follow-up of such patients generally is performed every 1 to 2 years, and should include a thorough clinical examination, chest radiogram, and ECG. Echocardiography is recommended to assess the function of the right ventricle-to-pulmonary artery conduit and valve, paying close attention to stenosis and/or regurgitation. A peak gradient of over 50 mm Hg in the pulmonary conduit generally is considered to be indicative of severe stenosis, as is a right ventricular systolic pressure over 75 mm Hg (91). There may be evidence of decreased right ventricular function and/or an increase in the degree of tricuspid regurgitation concurrent with a deterioration of conduit valve function. One should assess the degree of truncal or aortic valve insufficiency and consider replacing this valve if significantly incompetent. Aortic root dilation may occur. Pulmonary artery branch abnormalities may be difficult to image with echocardiography, so that ancillary imaging techniques such as cardiac MRI often are helpful in the assessment and management of these patients (93).

Cardiac catheterization generally is reserved for assessment of abnormalities detected by noninvasive imaging techniques and may involve additional interventions, such as balloon angioplasty of pulmonary branch stenosis or implantation of endovascular stents in the branch pulmonary arteries. Percutaneous implantation of a bioprosthetic pulmonary valve now is available for appropriate patients (88–90). Any surgical intervention should be carried out in an institution that specializes in the care of adults with congenital heart disease and performed by a surgeon trained in congenital heart disease (91).

LONG-TERM ISSUES

In summary, patients with repaired truncus arteriosus will need lifelong cardiovascular follow-up. Infective endocarditis precautions are warranted. Primary issues that will require attention, ongoing evaluation, and potentially further treatment after neonatal repair include truncal valve dysfunction (stenosis and/or insufficiency), function of the pulmonary homograft/conduit in the right ventricular outflow tract, and the development of branch pulmonary artery stenosis. Left and right ventricular function, both systolic and diastolic, must be evaluated in an ongoing fashion. Echocardiography and cardiac MRI/MRA are useful tools for ongoing noninvasive evaluation of the patient with repaired truncus arteriosus (37). Seamless transition from the pediatric cardiologist to the adult congenital heart disease specialist is clearly warranted as this patient group ages.

REFERENCES

1. Van Mierop LHS, Kutsche LM. Cardiovascular anomalies in digeorge syndrome and importance of neural crest as a possible pathogenetic factor. *Am J Cardiol* 1986;58:133–137.
2. Lupski JR, Langston C, Friedman R. Digeorge anomaly associated with a de novo y; 22 translocation resulting in monosomy del(22)(q11.2). *Am J Med Genet* 1991;40:196–198.
3. McElhinney DB, Driscoll DA, Emanuel BS, et al. Chromosome 22q11 deletion in patients with truncus arteriosus. *Pediatr Cardiol* 2003;24:569–573.
4. Goldmuntz E, Clark BJ, Mitchell LE, et al. Frequency of 22q11 deletions in patients with conotruncal defects. *J Am Coll Cardiol* 1998;32:492–498.
5. Lang MJ, Aughton DJ, Riggs TW. Dizygotic twins concordant for truncus arteriosus. *Clin Genet* 1991;39:75–79.
6. Pierpont ME, Gobel JW, Moller JH, et al. Cardiac malformations in relatives of children with truncus arteriosus or interruption of the aortic arch. *Am J Cardiol* 1988;61:423–427.
7. Digilio MC, Marino B, Musolino AM, et al. Familial recurrence of nonsyndromic interrupted aortic arch and truncus arteriosus with atrioventricular canal. *Teratology* 2000;61:329–331.
8. Brizard C, Cochrane A, Austin C, et al. Management strategy and long-term outcome for truncus arteriosus. *Eur J Cardiothorac Surg* 1997;11:687–695.
9. McGoon DC, Rastelli GC, Ongley PA. An operation for the correction of truncus arteriosus. *J Am Med Assoc* 1968;205:69–73.
10. Ebert PA, Turley K, Stanger P. Surgical treatment of truncus arteriosus in the first 6 months of life. *Ann Surg* 1984;200:451–456.
11. Urban A, Sinzobahamvya N, Brecher A, et al. Truncus arteriosus: ten-year experience with homograft repair in neonates and infants. *Ann Thorac Surg* 1998;66:S183–S188.
12. Van Mierop L, Patterson D, Schnaar W. Pathogenesis of persistent truncus arteriosus in light of observations made in a dog embryo with the anomaly. *Am J Cardiol* 1978;41:755–762.
13. Bartelings N, Gittenberger-de Groot A. Morphogenetic considerations on congenital malformations of the outflow tract. I. common arterial trunk and tetralogy of fallot. *Int J Cardiol* 1991;32:213–230.
14. Fuglestad SJ, Puga FJ, Danielson GK. Surgical pathology of the truncal valve: a study of 12 cases. *Am J Cardiovasc Pathol* 1988;2:39–47.
15. Collett RW, Edwards JE. Persistent truncus arteriosus: a classification according to anatomic types. *Surg Clin North Am* 1949;29:1245–1270.
16. Van Praagh R, Van Praagh S. The anatomy of common aorticopulmonary trunk (truncus arteriosus communis) and its embryologic implications: a study of 57 necropsy cases. *Am J Cardiol* 1965;16:406–425.
17. Rosenquist GC, Bharati S, McAllister HA. Truncus arteriosus communis: truncal valve anomalies associated with small conal or truncal septal defects. *Am J Cardiol* 1976;37:410–412.
18. Bharati S, McAllister HA, Rosenquist GC. The surgical anatomy of truncus arteriosus communis. *J Thorac Cardiovasc Surg* 1974;67:501–510.
19. Butto F, Lucas RV, Edwards JE. Persistent truncus arteriosus: pathologic anatomy in 54 cases. *Pediatr Cardiol* 1986;7:95–101.
20. Marcelletti C, McGoon DC, Danielson GK. Early and late results of surgical repair of truncus arteriosus. *Circulation* 1977;55:636–641.
21. Nath P, Zollhofer C, Castaneda-Zuniga W. Persistent truncus arteriosus associated with interruption of the aortic arch. *Br J Radiol* 1980;53:853–859.
22. Mair DD, Ritter DG, Davis GD. Selection of patients with truncus arteriosus for surgical correction: anatomic and hemodynamic considerations. *Circulation* 1974;49:144–151.
23. Dickinson DF, Arnold R, Wilkinson JL. Congenital heart disease among 160,480 liveborn children in liverpool 1960 to 1969: implications for surgical treatment. *Br Heart J* 1981;46:55–62.
24. de la Cruz MV, Cayre R, Angelini P. Coronary arteries in truncus arteriosus. *Am J Cardiol* 1990;66:1482–1486.
25. Shrivastava S, Edwards JE. Coronary arterial origin in persistent truncus arteriosus. *Circulation* 1977;55:551–554.
26. Daskalopoulos DA, Edwards WD, Driscoll DJ. Fatal pulmonary artery banding in truncus arteriosus with anomalous origin of circumflex coronary artery from right pulmonary artery. *Am J Cardiol* 1983;52:1363–1364.
27. Thiene G, Bortolotti U, Gallucci V. Anatomical study of truncus arteriosus communis with embryological and surgical considerations. *Br Heart J* 1976;38:1109–1123.
28. Lotvinsky SH, Ostfeld I, Bjornstad PG, et al. Truncus arteriosus with anomalous pulmonary venous connection. *Am J Cardiol* 1999;83:801–804.
29. Stulak JM, Dearani JA, Burkhardt HM, et al. Does the dilated ascending aorta in an adult with congenital heart disease require intervention? *J Thorac Cardiovasc Surg* 2010;140:S52–S57.
30. Tometzki AJP, Suda K, Koh T, et al. Accuracy of prenatal echocardiographic diagnosis and prognosis of fetuses with conotruncal anomalies. *J Am Coll Cardiol* 1999;33:1696–1701.
31. Rice MJ, Seward JB, Hagler DJ. Definitive diagnosis of truncus arteriosus by two-dimensional echocardiography. *Mayo Clin Proc* 1982;57:476–481.
32. Tworetzky W, McElhinney DB, Brook MM, et al. Echocardiographic diagnosis along for the complete repair of major congenital heart defects. *J Am Coll Cardiol* 1999;33:228–233.
33. Snider AR, Serwer GA, Ritter SB. *Echocardiography in Pediatric Heart Disease*. 2nd ed. St Louis, MO: Mosby, 1997.
34. Mair DD, Ritter DG, Danielson GK. Truncus arteriosus with unilateral absence of pulmonary artery: criteria for operability and surgical results. *Circulation* 1977;55:641–647.
35. Fyfe DA, Driscoll DJ, Di Donato RM. Truncus arteriosus with single pulmonary artery: influence of pulmonary vascular obstructive disease on early and late operative results. *J Am Coll Cardiol* 1985;5:1168–1172.

36. Didier D, Ratib O, Beghetti M, et al. Morphologic and functional evaluation of congenital heart disease by magnetic resonance imaging. *J Magn Reson Imaging* 1999;10:639-655.
37. Frank L, Dillman JR, Parisk V, et al. Cardiovascular mr imaging of conotruncal anomalies. *RadioGraphics* 2010;30:1069-1094.
38. Danielson GK, Anderson BJ, Schleck CD. Late results of pulmonary ventricle to pulmonary artery conduits. *Semin Thorac Cardiovasc Surg* 1995;7:162-167.
39. McFaul RC, Mair DD, Feldt RH. Truncus arteriosus and previous pulmonary arterial banding: clinical and hemodynamic assessment. *Am J Cardiol* 1976;38:626-632.
40. Rastelli GC, Titus JL, McGoon DC. Homograft of ascending aorta and aortic valve as a right ventricular outflow: an experimental approach to the repair of truncus arteriosus. *Arch Surg* 1967;95:698-708.
41. Gerestein CG, Takkenberg JM, Oei FB. Right ventricular outflow tract reconstruction with an allograft conduit. *Ann Thorac Surg* 2001;71:911-918.
42. Pearl JM, Laks H, Drinkwater DC. Repair of truncus arteriosus in infancy. *Ann Thorac Surg* 1991;52:780-786.
43. Jahangiri M, Zurakowski D, Mayer JE. Repair of the truncal valve and associated interrupted arch in neonates with truncus techniques. *J Thorac Cardiovasc Surg* 2000;119:508-514.
44. Bove EL, Lupinetti FM, Pridjian AK. Results of a policy of primary repair of truncus arteriosus in the neonate. *J Thorac Cardiovasc Surg* 1993;105:1057-1065.
45. Pearl JM, Laks H, Drinkwater DC. Repair of conotruncal abnormalities with the use of the valved conduit: improved early and midterm results with the cryopreserved homograft. *J Am Coll Cardiol* 1992;20:191-196.
46. Hanley FL, Heinemann MK, Jonas RA. Repair of truncus arteriosus in the neonate. *J Thorac Cardiovasc Surg* 1993;105:1047-1056.
47. Rajasinghe HA, McElhinney DB, Reddy VM. Long-term follow-up of truncus arteriosus repaired in infancy: a twenty-year experience. *J Thorac Cardiovasc Surg* 1997;113:869-878.
48. McKay R, Miyamoto S, Pearl I. Truncus arteriosus with interrupted aortic arch: successful correction in a neonate. *Ann Thorac Surg* 1989;48:587-589.
49. Dearani JA, Danielson GK, Puga FJ. Late follow-up of 1095 patients undergoing operation for complex congenital heart disease utilizing pulmonary ventricle to pulmonary artery conduits. *Ann Thorac Surg* 2003;75:399-411.
50. Reddy VM, Rajasinghe HA, McElhinney DB. Performance of right ventricle to pulmonary artery conduits after repair of truncus arteriosus: a comparison of dacron-housed porcine valves and cryopreserved allografts. *Semin Thorac Cardiovasc Surg* 1995;7:133-138.
51. Chan KC, Fyfe DA, McKay R. Right ventricular outflow reconstruction with cryopreserved homografts in pediatric patients: intermediate term follow-up with serial echocardiographic assessment. *J Am Coll Cardiol* 1994;24:483-489.
52. Lange R, Weipert J, Homann M. Performance of allografts and xenografts for right ventricular outflow tract reconstruction. *Ann Thorac Surg* 2001;71:365-367.
53. Mair DD, Sim EK, Danielson GK. Long term follow-up of surgically corrected patients with truncus arteriosus. *Prog Pediatr Cardiol* 2002;15:65-71.
54. Barbero-Marcial M, Riso A, Atik E. A technique for correction of truncus arteriosus type i and ii without extracardiac conduits. *J Thorac Cardiovasc Surg* 1990;99:364-369.
55. Bermudez CA, Dearani JA, Puga FJ. Late results of the peel operation for replacement of failing extracardiac conduits. *Ann Thorac Surg* 2004;77:881-888.
56. Imamura M, Drummond-Webb JJ, Saris GE. Improving early and intermediate results of truncus arteriosus repair: a new technique of truncal valve repair. *Ann Thorac Surg* 1999;67:1142-1146.
57. McElhinney DB, Reddy VM, Rajasinghe HA. Trends in management of truncal valve insufficiency. *Ann Thorac Surg* 1998;65:517-524.
58. Black MD, Adatia I, Freedom RM. Truncal valve repair: initial experience in neonates. *Ann Thorac Surg* 1998;65:1737-1740.
59. Elami A, Laks H, Pearl JM. Truncal valve repair: initial experience with infants and children. *Ann Thorac Surg* 1994;57:397-402.
60. Mavroudis C, Backer CL. Surgical management of severe truncal valvular regurgitation. *Ann Surg* 2001;72:396-400.
61. de Leval MR, McGoon DC, Wallace RB. Management of truncal valvular regurgitation. *Ann Surg* 1974;180:427-432.
62. Kaza AK, Burch PT, Pinto N, et al. Durability of truncal valve repair. *Ann Thorac Surg* 2010;90:1307-1312.
63. Bove EL, Beekman RH, Snider AR. Repair of truncus arteriosus in the neonate and young infant. *Ann Thorac Surg* 1989;47:499-506.
64. Agarwal KC, Edwards WD, Feldt RH. Pathogenesis of nonobstructive fibrous peels in right-sided porcine-valved extracardiac conduits. *J Thorac Cardiovasc Surg* 1982;83:584-589.
65. Bisset GS, III, Schwartz DC, Benzing G, III. Late results of reconstruction of the right ventricular outflow tract with porcine xenografts in children. *Ann Thorac Surg* 1981;31:437-443.
66. Jonas RA, Freed MD, Mayer JE. Long-term follow-up of patients with synthetic right heart conduits. *Circulation* 1985;72:77-83.
67. Kay PH, Ross DN. Fifteen years' experience with the aortic homograft: the conduit of choice for right ventricular outflow tract reconstruction. *Ann Thorac Surg* 1985;40:360-364.
68. Kirklin JW, Blackston EH, Maehara T. Intermediate term fate of cryopreserved allograft and xenograft valved conduits. *Ann Thorac Surg* 1987;44:598-606.
69. Edwards WD, Agarwal KC, Feldt RH. Surgical pathology of obstructed, right-sided, porcine-valved extracardiac conduits. *Arch Pathol Lab Med* 1983;107:400-405.
70. Bull C, Macartney FJ, Horvath P, et al. Evaluation of long-term results of homograft and heterograft valves in extracardiac conduits. *J Thorac Cardiovasc Surg* 1987;94:12-19.
71. Weipert J, Meisner H, Mendler N. Allograft implantation in pediatric cardiac surgery: surgical experience from 1982 to 1994. *Ann Thorac Surg* 1995;60:S101-S104.
72. Perron J, Maron AM, Gauvreau K, et al. Valved homograft conduit repair of the right heart in early infancy. *Ann Thorac Surg* 1999;68:542-548.
73. Wells WJ, Arroyo H, Bremner RM, et al. Homograft conduit failure in infants is not due to somatic outgrowth. *J Thorac Cardiovasc Surg* 2002;124:88-96.
74. Schlichter AJ, Kreutzer C, Mayorquim RC. Five to fifteen year follow-up of fresh autologous pericardial valved conduits. *J Thorac Cardiovasc Surg* 2000;119:869-879.
75. Danton MH, Barron DJ, Stumper O, et al. Repair of truncus arteriosus: a considered approach to right ventricular outflow tract reconstruction. *Eur J Cardiothorac Surg* 2001;20:95-103.
76. Chard RB, Kang N, Andrews DR, et al. Use of the medtronic freestyle valve as a right ventricular to pulmonary artery conduit. *Ann Thorac Surg* 2001;71:361-364.
77. Aupechle B, Serraf A, Belli E. Intermediate follow-up of a composite stentless porcine valved conduit of bovine pericardium in the pulmonary circulation. *Ann Thorac Surg* 2001;74:127-132.
78. Brown JW, Ruzmetov M, Okada Y, et al. Truncus arteriosus repair, outcomes, risk factors, reoperation and management. *Eur J Cardiothorac Surg* 2001;20:221-227.
79. Allen BS, El-Zein C, Cunico B, et al. Pericardial tissue valves and gore-tex conduits as an alternative for right ventricular outflow tract replacement in children. *Ann Thorac Surg* 2002;74:771-777.
80. Powell AJ, Lock JE, Keane JF, et al. Prolongation of rv-pa conduit life span by percutaneous stent implantation: intermediate term results. *Circulation* 1995;92:3282-3288.
81. Brando K, Danielson GK, Schaff HV, et al. Outcome of pulmonary and aortic homografts for right ventricular outflow tract reconstruction. *J Thorac Cardiovasc Surg* 1995;109:509-518.
82. Niwaya K, Knott-Craig CJ, Lane MM, et al. Cryopreserved homograft valves in the pulmonary position: risk analysis for intermediate term failure. *J Thorac Cardiovasc Surg* 1999;117:141-147.
83. Clarke DR, Bishop DA. Ten year experience with pulmonary homografts in children. *J Heart Valve Dis* 1995;4:384-391.
84. Lamberti JJ, Angell WW, Waldman JD, et al. The cryopreserved homograft valve in the subpulmonary position: early results and technical consideration. *J Card Surg* 1988;3:247-251.
85. Calderone CA, McCrindle BW, Van Ardsell GS. Independent factors associated with longevity of prosthetic pulmonary valves and valved conduits. *J Thorac Cardiovasc Surg* 2000;120:1022-1031.
86. Klovekorn WP, Meisner H, Paek SU, et al. Long-term results after right ventricular outflow tract reconstruction with porcine and allograft conduits. *J Thorac Cardiovasc Surg* 1991;39:225-227.
87. Khambadkone S, Coats L, Taylor A, et al. Percutaneous pulmonary valve implantation in humans: Results in 59 consecutive patients. *Circulation* 2005;112:1189-1197.
88. Lurz P, Coats L, Khambadkone S, et al. Percutaneous pulmonary valve implantation: impact of evolving technology and learning curve on clinical outcome. *Circulation* 2008;117:1964-1972.
89. Coats L, Tsang V, Khambadkone S, et al. The potential impact of percutaneous pulmonary valve stent implantation on right ventricular outflow tract re-intervention. *Eur J Cardiothorac Surg* 2005;27:536-543.
90. Zahn EM, Hellenbrand WE, Lock JE, et al. Implantation of the melody transcatheter pulmonary valve in patients with a dysfunctional right ventricular outflow tract conduit. *J Am Coll Cardiol* 2009;54:1722-1729.
91. Warnes CA, Williams RG, Bashore TM, et al. ACC/AHA 2008 guidelines for the management of adults with congenital heart disease: a report of the American college of cardiology/American heart association task force on practice guidelines (writing committee to develop guidelines on the management of adults with congenital heart disease): Developed in collaboration with the American society of echocardiography, heart rhythm society, international society for adult congenital heart disease, society for cardiovascular angiography and interventions, and society of thoracic surgeons. *J Am Coll Cardiol* 2008;52:e1-e121.
92. Beauchesne LM, Warnes CA, Connolly HM, et al. Prevalence and clinical manifestations of 22q11.2 microdeletion in adults with selected conotruncal anomalies. *J Am Coll Cardiol* 2005;45:595-598.
93. Baumgartner H, Bonhoeffer P, De Groot N, et al. ESC guidelines for the management of grown-up congenital heart disease. *Eur Heart J* 2010;31:2915-2957.

Anatomical and Functional Mitral Valve Abnormalities in the Pediatric Population

Andrew S. Mackie ■ Jeffrey F. Smallhorn

This chapter deals with mitral valve (MV) abnormalities that are encountered in the pediatric population. We include abnormalities of the morphologic MV in corrected transposition, but exclude abnormalities in the setting of a univentricular atrioventricular connection, left side atrioventricular valve in atrioventricular septal defect, and MV abnormalities in rheumatic heart disease. As well, we exclude hearts with hypoplastic left heart syndrome, as these patients follow a different clinical pathway. Although some MV abnormalities occur in isolation, many are part of a spectrum of left-sided congenital abnormalities. If missed, these associated lesions often have profound implications with regard to patient outcome, and hence a high index of suspicion is essential when evaluating a patient with abnormalities of the MV.

Although clinical signs and symptoms are important, noninvasive imaging, in particular echocardiography, is the current cornerstone to detailed anatomical and physiologic assessment and subsequent management implications of congenital MV disease. Three-dimensional echocardiography provides novel anatomical and functional information above and beyond 2-D echocardiography and is emphasized throughout this chapter.

MITRAL VALVE DEVELOPMENT

Following rightward looping of the heart tube, the atrioventricular junction becomes prominent around the 25th day of gestation (1,2). The future left ventricle (LV) supports the larger part of the circumference of the atrioventricular canal by the end of the 5th week. The atrioventricular canal is occupied by the inferior and superior endocardial cushions that fuse during the 6th week, producing separate right and left atrioventricular junctions. Parts of these fused cushions remain on the left side of the muscular septum, forming the scaffold of the anterior or aortic leaflet of the MV.

The normal MV proceeds when the aorta becomes committed to the LV, permitting the development of fibrous continuity between one of the leaflets of the MV and two of the leaflets of the aortic valve. Initially, there is a cleft at the site of fusion of the superior and inferior cushions within the LV. The mural leaflet or posterior leaflet is formed by protrusion and growth of a sheet of atrioventricular myocardium into the ventricular lumen, with subsequent formation of valvar mesenchyme on its surface (3). The myocardial layer is then removed by apoptosis. The aortic leaflet of the MV develops from the mesenchyme of the superior and inferior atrioventricular cushions and is never attached to, or supported by, the myocardium apart from its attachment to the papillary muscles. The inferior quadrants of the left atrioventricular junction expand involving growth of the parietal wall of the LV, with comparable growth of the lateral cushion. This results in the lateral cushion occupying

two-thirds of the circumference of the developing mitral valvar orifice, hence the larger mural or posterior leaflet that is seen during clinical or pathologic assessment. The papillary muscles develop from compacting columns in the trabecular layer of the ventricular muscle. Importantly, the MV develops and functions as a unit, which has profound implications during life. With the advent of 3-D echocardiography, we are moving away from thinking of the MV as independent units, but rather as units that interact with each other and with the left ventricular myocardium.

Reciprocal signaling between the endocardial and myocardial cell layers in the cushion is mediated in part by members of the TGF- β family, and induces a transformation of endocardial cells into mesenchymal cells. Sox 9 is activated when endocardial cells undergo mesenchymal transformation and Sox-9-deficient mesenchymal cells fail to express ErbB3, which is required for proliferation of the cells within the endocardial cushions. The mesenchymal cells migrate into the cushions and differentiate into the fibrous tissue of the valves. Several genes play a role in formation of the valvar leaflets, with signaling and downstream activation dependent on the NF-AT family of transcription factors. Absence of any of these genes results in fatal defects of valvar formation (4–6).

INCIDENCE OF MITRAL VALVE ABNORMALITIES

Congenital MV abnormalities are rare. Congenital mitral stenosis (MS) accounts for 0.6% of congenital heart disease (CHD) in postmortem studies and 0.21% to 0.42% when examined in clinical series (7). Isolated congenital MV regurgitation is even rarer and indeed if encountered should be considered as potentially being secondary to another process such as rheumatic fever or in the younger patient, anomalous left coronary artery from the pulmonary artery (8). The male to female ratio of congenital MS is of the order of 1.5:1. It is important to consider associated MV pathology in any child presenting with a left-sided obstructive lesion, such as coarctation of the aorta or aortic valve stenosis. As well, MS may be associated with many other congenital lesions. Therefore, assessment of MV morphology and function should be part of the evaluation of all patients with CHD.

MITRAL VALVE MORPHOLOGY AND FUNCTION

Although the morphologist has previously been the master in this area, that role has now fallen to the echocardiographer, who can evaluate both morphology and function.

MITRAL ANNULUS

The mitral annulus is mostly a muscular structure that is attached to the left atrium by fibrous connections. Three-dimensional imaging has demonstrated that it is saddle shaped (9), with two high and two low points (Fig. 45.1A). The high points are at the site of aortic–mitral continuity and at the posterior aspect of the valve, while the two low points are along the lines of the commissure between the aortic and mural leaflets. The region of the mitral annulus that is not

muscular is the site of aortic–mitral fibrous continuity. This is an important component, since changes in the mitral annulus during the cardiac cycle are heterogeneous, such that the outlet maintains maximum dimension during contraction to prevent any impediment to flow (10,11).

The saddle shape of the mitral annulus has significant implications with regard to leaflet stress. If the annulus is more planar in shape, this increases leaflet stress, which has negative implications with regard to MV function (12,13). This in part explains why standard MV rings fail, as they do not address the primary problem, and flatten the MV annulus as well.

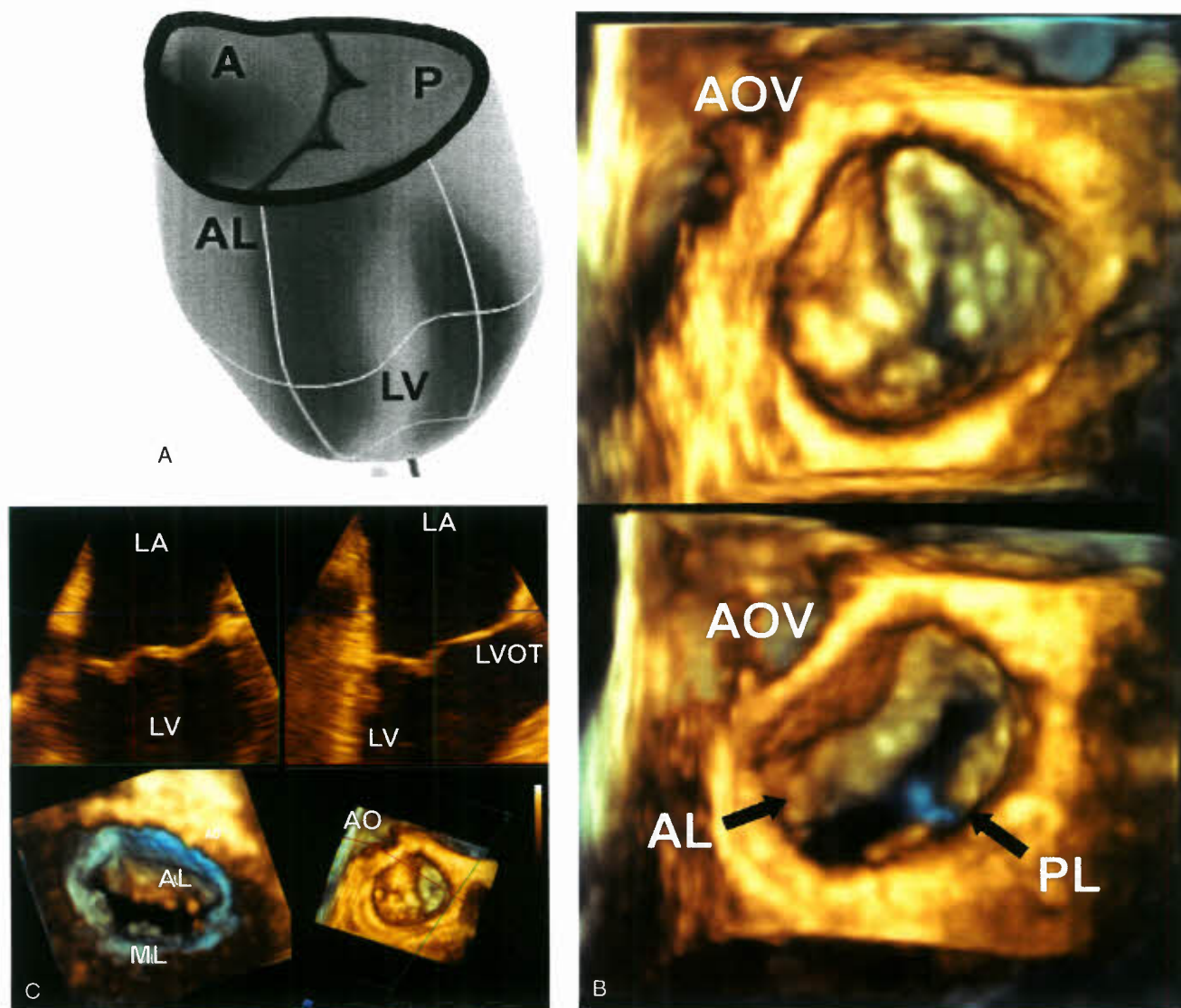


Figure 45.1. A: Schematic diagram demonstrating the saddle shape of the mitral annulus with two high points, one at the aortic–mitral continuity end and the other posterior. The two low points are along the commissure lines of the anterior and posterior leaflets. The maximum bending of the MV occurs along the commissure line. A, aortic leaflet; AL, anteriolateral; LV, left ventricle; P, posterior or mural leaflet. B: This montage demonstrates the normal features of the MV, as seen by 3-D echocardiography. Note the scalloped appearance of the posterior or mural leaflet. The commissures are seen in the image. Three-dimensional echocardiography shows the true features of the MV with its undulations that are readily appreciated in this *en face* view. The upper panel is taken in systole, while the lower one is in diastole. AL, aortic or anterior leaflet; AOV, aortic valve; PL, posterior or mural leaflet. C: These images demonstrate a normal MV seen in a 3-D and an MPR (multiplane reformatting) mode obtained from a full-volume data set. The upper two images are the 2-D views of the MV, taken at right angles to each other. The lower right hand image shows the reconstructed image of the valve and the two planes (red and green) can be seen. The lower left hand panel shows the MV from below. The commissures are well seen, as are the two leaflets. Note the detail in the 3-D image that is lacking in its 2-D counterpart. AL, aortic or anterior leaflet; AO, aorta; LA, left atrium; LV, left ventricle; LVOT, left ventricular outflow tract.

Starting at end diastole and with atrial contraction the annulus begins to contract, attaining its smallest area just before ventricular systole, presumably to aid in leaflet closure. During midventricular systole there is a dominant inward motion of the annulus in an anterior–posterior direction. This helps maintain an oval shape just when the orifice area is at its greatest, with the added advantage of helping to keep the leaflets together. During ventricular contraction, the annulus descends with a gradual increase in annular area, height, and bending angle. This reaches its maximum at end systole and during the period of isovolumic relaxation. With rapid ventricular filling there is a rapid reduction in MV area (14–17), more so in children, which may be related to their superior ventricular relaxation (14–17). These changes are most likely related to the torsional deformation of the LV from base to apex, demonstrating the importance of thinking of the MV as one unit, with important interactions with the LV.

MITRAL VALVE LEAFLETS AND SUPPORTING APPARATUS

The normal MV has two leaflets, the anterior or aortic and the posterior or mural (Fig. 45.1B). The anterior leaflet is in fibrous continuity with the noncoronary cusp of the aortic valve and hinges from the annulus with support at two commissures by the anterior and posterior papillary muscles (1,18). The anterior leaflet has been arbitrarily divided into

three components, A1 to A3, which is a useful description for both the echocardiographer and the surgeon. The mural or posterior leaflet is anchored along the parietal part of the left atrioventricular junction. As with its anterior counterpart, this is divided into three components, P1 to P3. As with the anterior leaflet, it is supported by the two papillary muscles. The posterior or mural leaflet frequently has a series of scallops, which are supported by chordal structures (Fig. 45-1B,C).

Three-dimensional echocardiography has provided the ability to assess not only the morphology but also the dynamic changes that are seen in the MV. This technique emphasizes that the leaflets are not flat, but consist of a series of undulations, which are in part related to the chordal attachments (13) (Fig. 45-1A). There are several chordal support mechanisms that can be appreciated in pathologic specimens (19), as well as by real-time 3-D echocardiography. The strut chordae insert into the undersurface of the anterior leaflet and in part result in the appearance of a series of peaks and valleys in the anterior leaflet when seen in real time from the left atrial view (Fig. 45.2A). These chordae run onto the belly of the leaflet, whereas the rough zone chordae insert into the tip of the anterior leaflet (Fig. 45.2A). These latter chordae are responsible for preventing leaflet prolapse. The strut chordae are important in situations of ischemic MV regurgitation where they are displaced, resulting in leaflet tethering and regurgitation (20). Next, there are commissural chords, which by definition support the two MV commissures, while the cleft chordae support the scallops of the posterior or mural leaflet. When viewed from above by 3-D echocardiography during systole,

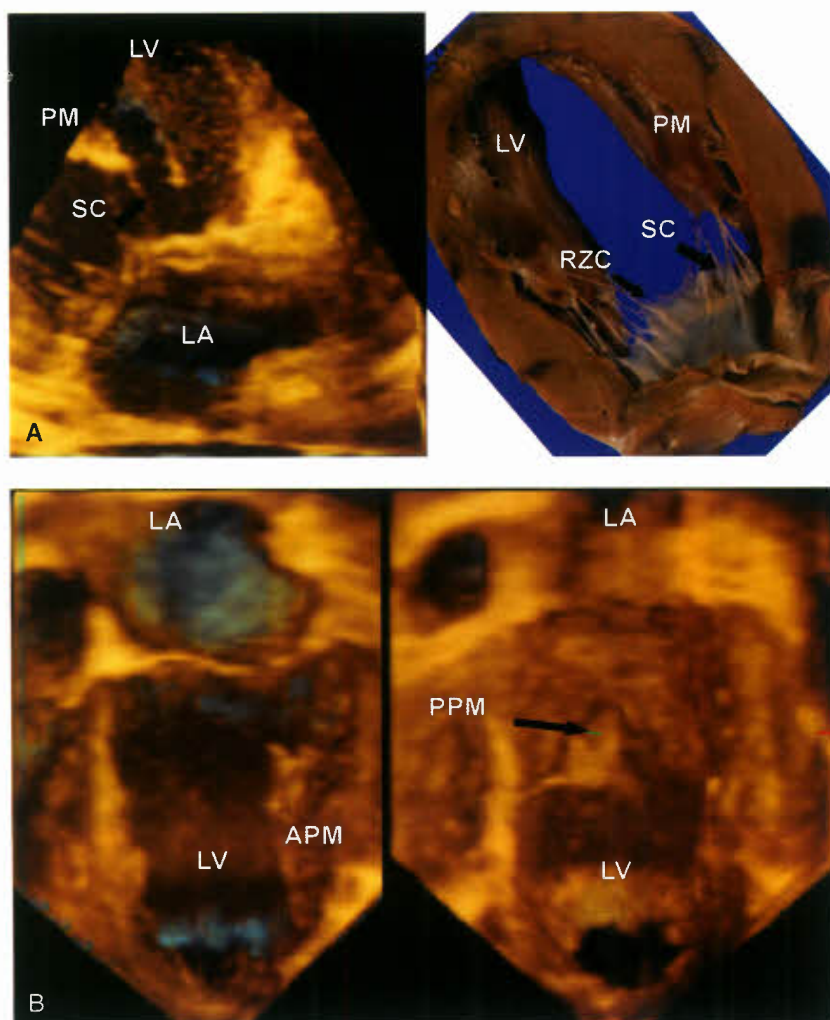


Figure 45.2. A: These figures demonstrate the chordal structures of the MV in a specimen, as well as by 3-D echo. Note the thicker strut chordae that are indicated by the *black arrow*. These insert into the belly of the aortic leaflet of the MV. The thinner rough zone chordae insert into the edges of the leaflet. LA, left atrium; LV, left ventricle; PM, papillary muscle; RZC, rough zone chordae; SC, strut chordae. B: This montage shows the normal papillary muscle arrangement of the MV. The image on the left demonstrates the anterior papillary muscles with mitral chordal insertion. The image on the right shows the posterior papillary muscle and shows how it is blended in the posterior wall of the LV. APM, anterior papillary muscle; LA, left atrium; LV, left ventricle; PPM, posterior papillary muscle.

the leaflets appear to be a series of peaks and valleys, the coaptation of which prevents regurgitation (13). The zones of coaptation of the leaflets roll over each other, providing the maximum area of contact, which maintains valve competence. It is when pathologic processes disturb this relationship that regurgitation is seen. Pathologic specimens and surgical inspection, along with saline testing of the valve provide a sub-optimal assessment of the functional nature of the MV; 3-D echocardiography overcomes this limitation (21).

The two papillary muscles are evenly placed such that they maintain constant tension on the leaflets throughout systole (Fig. 45.2B). The angle between the papillary muscle tips and the mitral annulus is about 70 to 80 degrees, as determined by 3-D echocardiography. This is achieved by the ability to map the coordinates of all of the components of the MV throughout the cardiac cycle and relate them to each other. This papillary muscle angle does not change throughout the cardiac cycle, despite the influence of ventricular contraction and torsion of the LV. The chordae fan out as they insert into the leaflets, but the direction of pull on the leaflets is relatively vertical, avoiding tension on the leaflets. The papillary muscle morphology is also variable, in particular with regard to the number of heads. The papillary muscles are derived from left ventricular myocardium and blend in with the wall of the LV, playing an important role in maintaining normal left ventricular function (Fig. 45.2B). Indeed if they are removed during valve replacement, then this results in left ventricular dysfunction (22).

MITRAL VALVE PATHOLOGY: AN INTEGRATED MORPHOLOGIC AND HEMODYNAMIC APPROACH

Although it is tempting to divide pathology into regurgitant and stenotic lesions, this is artificial, since congenital MV

abnormalities can result in both. We therefore describe the types of pathology and their echocardiographic appearances together.

Mitral Valve Dysplasia and Hypoplasia

In MV dysplasia, the leaflets are thickened, the interchordal spaces obliterated, and the papillary muscles deformed (7,23,24). The valve often shows global hypoplasia and is the most common lesion associated with isolated congenital MS, though this may occur in conjunction with regurgitation. The free edges of the dysplastic leaflets are thickened and rolled. Therefore, when viewed as a functional unit, the thickened leaflets and obliterated interchordal spaces result in tethering and deficient zones of coaptation. These features are readily appreciated by 3-D echocardiography, both from a left atrial and left ventricular view (Fig. 45.3A,B). As well, additional images can be obtained by cropping the heart from above, which demonstrate the MV and its support apparatus. This is of particular value for imaging the chordal apparatus, as they are imaged in the axial plane that provides optimal resolution. The left ventricular view is of particular importance for imaging the commissures, because they are imaged more reliably from below than from the left atrial view. This is due to the fact that the normal mitral leaflets billow toward the left atrium, just as a parachute does when seen from the sky.

With the addition of color Doppler, sites of mitral regurgitation (MR) can be identified and related to valve pathology (Fig. 45.3A). It is possible to image the vena contracta, which represents the *en face* view of the regurgitant jet. The area of this jet correlates well with absolute volume regurgitation, providing a semiquantitative assessment of the degree of regurgitation (Fig. 45.4A). As well, it provides an accurate road map to the location of the regurgitation, providing vital information for the surgeon when contemplating repair. With the addition of pulsed or continuous wave Doppler the hemodynamic mean gradient can be determined. Recall that this is

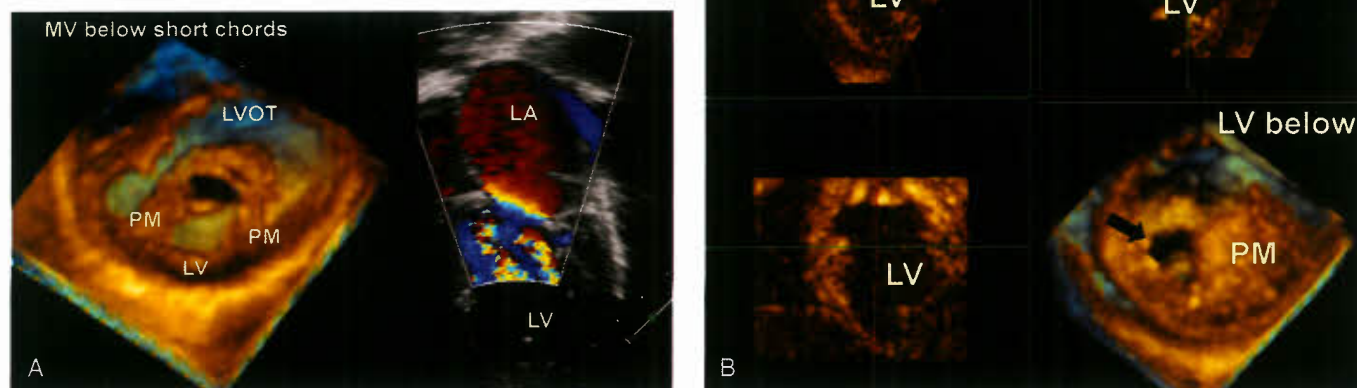


Figure 45.3. A: These images are from a case with MS due to shortened chordae and thickened leaflets. The 3-D image from below shows the thickened leaflets with shortened chordae. Note the orifice of the MV. The image on the right is a 2-D Doppler and shows the turbulent jet through the valve. LV, left ventricle; LVOT, left ventricular outflow tract; PM, papillary muscle. B: This montage is from a case with MV stenosis due to thickened chordae, with virtual fusion of the anterior papillary muscle to the leaflets, as seen by the lower right hand 3-D echo. The upper left hand image shows the 2-D appearance of the anterior papillary muscle and leaflet. The restrictive functional orifice is clearly seen in the lower right hand panel (black arrow). LV, left ventricle; PM, papillary muscle.

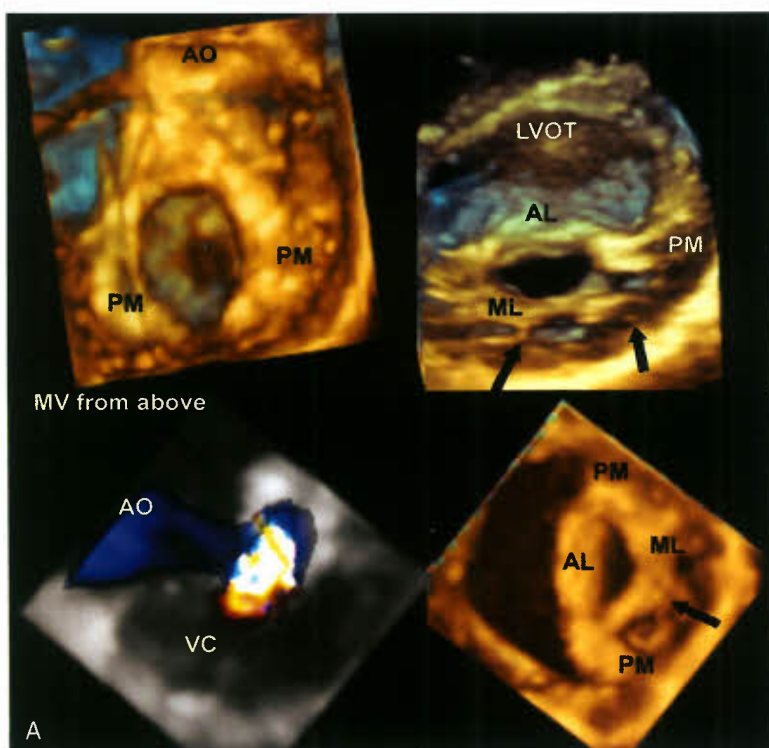
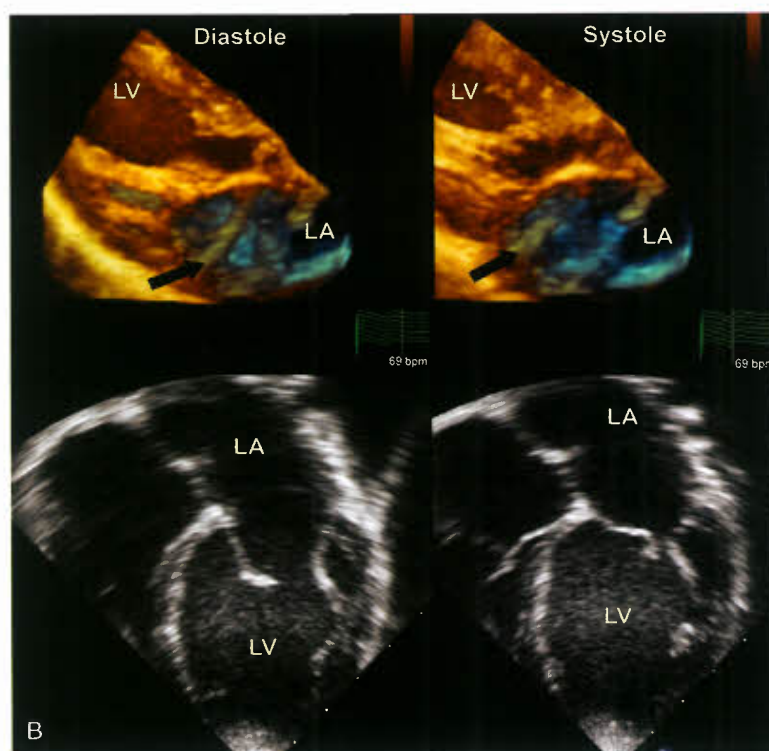


Figure 45.4. A: This montage is from a case with a tethered mural leaflet of the MV, associated with thickening of both that leaflet and its aortic counterpart. The upper left image is viewed from front, looking down on top of the MV. Note that it is difficult to see separate chordae. The lower left hand picture shows the vena contracta from the MV regurgitation. Note that the relationship of this to the valve can be appreciated from this image. The upper right hand picture views the MV from the left ventricular aspect and shows the tethering of the mural leaflet as indicated by the *black arrows*. The lower right hand picture is a view of the MV from above at a level just below the mitral annulus. The mitral orifice and the thickened leaflets can be seen, as well as the tethering of the mural leaflet (*black arrow*). AL, aortic leaflet; AO, aorta; LVOT, left ventricular outflow tract; ML, mural leaflet; PM, papillary muscle; VC, vena contracta. B: This is from the same case as Figure 45.4A and shows the 2-D echo appearance of the tethered mural leaflet, as well as a 3-D long-axis view of the MV. The upper left hand image is taken in diastole and the right one in systole. The *black arrow* points to the annulus of the MV and shows that during systole the leaflets are tethered below the annulus. This appearance cannot be appreciated in 2-D images. LA, left atrium; LV, left ventricle.



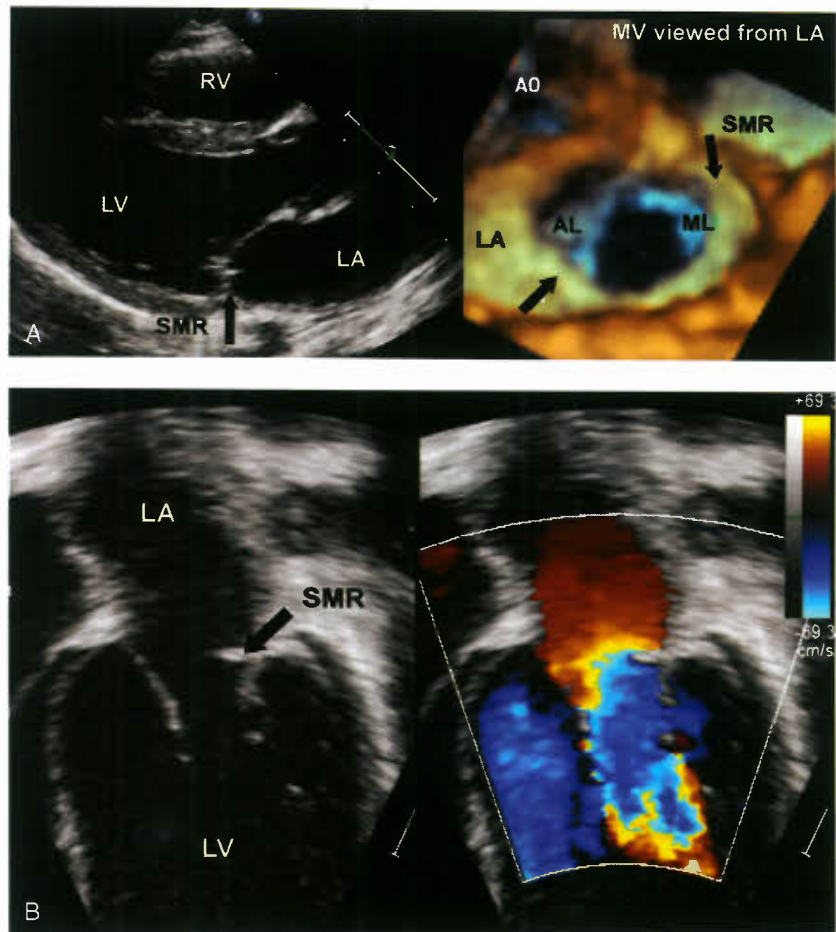
directly related to cardiac output, with an underestimation in states of low output. Unfortunately, in the majority of children, it is not possible to calculate a pressure halftime that can provide an absolute valve area in adults.

Dysplasia of the Posterior or Mural Leaflet

Occasionally, a young child is seen who has significant MV regurgitation secondary to dysplasia of the posterior or mural

leaflet (25). The leaflet is invariably tethered by shortened chordae, preventing normal coaptation with the anterior leaflet (Fig. 45.4A,B). The regurgitant jet invariably extends along the total length of the valve orifice and may respond to surgical repair by leaflet extension. Three-dimensional echocardiography provides optimal imaging of this entity, as well as an accurate assessment of the severity of regurgitation. Although the mural leaflet is tethered, the aortic leaflet of the MV is usually thickened (Fig. 45.4A,B).

Figure 45.5 A: This montage shows a mild case of supramitral stenosis, which is more difficult to appreciate in the 2-D image in the left hand panel, compared to the 3-D image on the right viewed from the left atrium. B: The color Doppler image on the right shows that the flow acceleration is starting just above the annulus, consistent with supravale stenosis. LA, left atrium; LV, left ventricle; SMR, supramitral ridge.



Supravale Mitral Stenosis

Although this is often considered as a separate entity (Fig. 45.5A,B), it invariably coexists with associated abnormalities of the leaflets and subvalve apparatus (26,27) (Fig. 45.6). Therefore, in the majority of cases, surgical intervention does not cure the problem, but simply provides some relief of the associated stenosis. The membrane starts at the annulus of the MV, thus differentiating it from cor triatriatum, which sits above the left atrial appendage. It may or may not be circumferential and in some cases extends into the orifice of the MV, providing the appearance of subvalve MS. Physiologically, it usually results in MS, the hemodynamic consequence that can be determined by a Doppler assessment of the MV in conjunction with an assessment of pulmonary artery pressure from the tricuspid regurgitation and/or pulmonary insufficiency jets. This entity therefore has a physiologic impact on the mitral annulus, as well as the leaflets and subvalve apparatus.

Mitral Arcade

This is a rare entity, however one that has a significant impact on outcome. The morphologic and echocardiographic features are of muscularization of the chordal apparatus, such that it is difficult to differentiate between the leaflets, chordae, and their supporting papillary muscles (Fig. 45.7). The functional result is often regurgitation, which is due to a tethered valve with deficient zones of leaflet coaptation. This lesion usually presents early on in life and invariably results in a poor outcome (28,29).

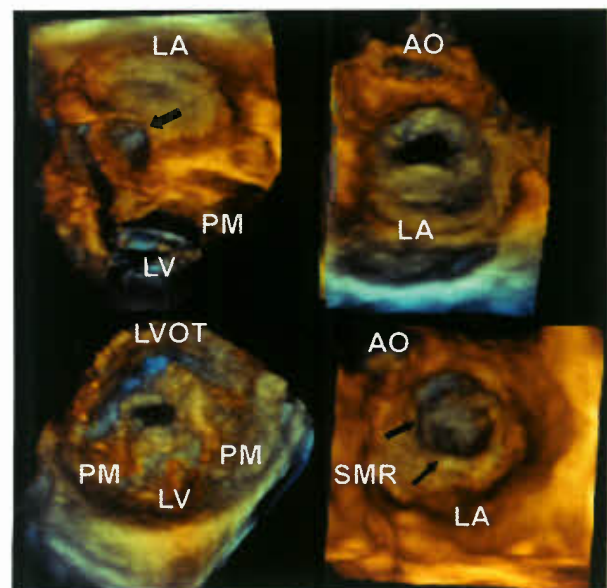


Figure 45.6. This is from a case with supramitral valve stenosis and associated significant pathology of the leaflets and subvalve apparatus of the MV. The upper left hand and lower right hand panels show the ring as indicated by the black arrows. The upper left hand and lower right hand demonstrate the thickened leaflets and chordae. The upper right hand panel shows the orifice of the MV as seen from the left atrium. AO, aorta; LA, left atrium; LV, left ventricle; LVOT, left ventricular outflow tract; PM, papillary muscle; SMR, supramitral ridge.

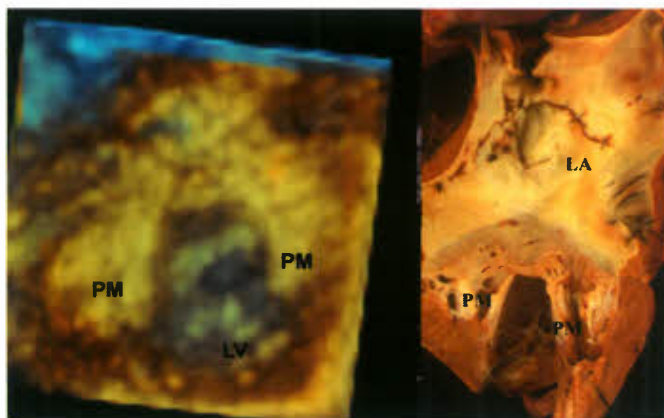


Figure 45.7. This montage shows a specimen with a mitral arcade with muscularization of the subvalve apparatus and a 3-D echocardiogram showing similar features, but from a different case. LA, left atrium; LV, left ventricle; PM, papillary muscle.

Cleft Mitral Valve

This involves the anterior or aortic leaflet of the MV and varies in degree with some hearts having a complete cleft, whereas in others it involves only the tip of the leaflet. The cleft points towards the left ventricular outflow tract, which differentiates it from that seen in an atrioventricular septal defect (30–35) (Fig. 45.8). The supporting papillary muscles are in the normal location, again which differs from an atrioventricular septal defect where the posterior muscle is rotated laterally (36). MV regurgitation is usually seen when the edges of the cleft are unsupported by chordae. In other cases, the edges of the cleft are supported by chordae without evidence of associated MV regurgitation (Fig. 45.9). The chordae invariably insert into the crest of the interventricular septum, while in other cases they may straddle an anterior ventricular septal defect. The degree of MV regurgitation is usually dictated by the extent of the cleft, with greater severity in those where the cleft extends along the whole length of the anterior leaflet. While 2-D echocardiography is helpful in the diagnosis, it does not permit a complete evaluation of the

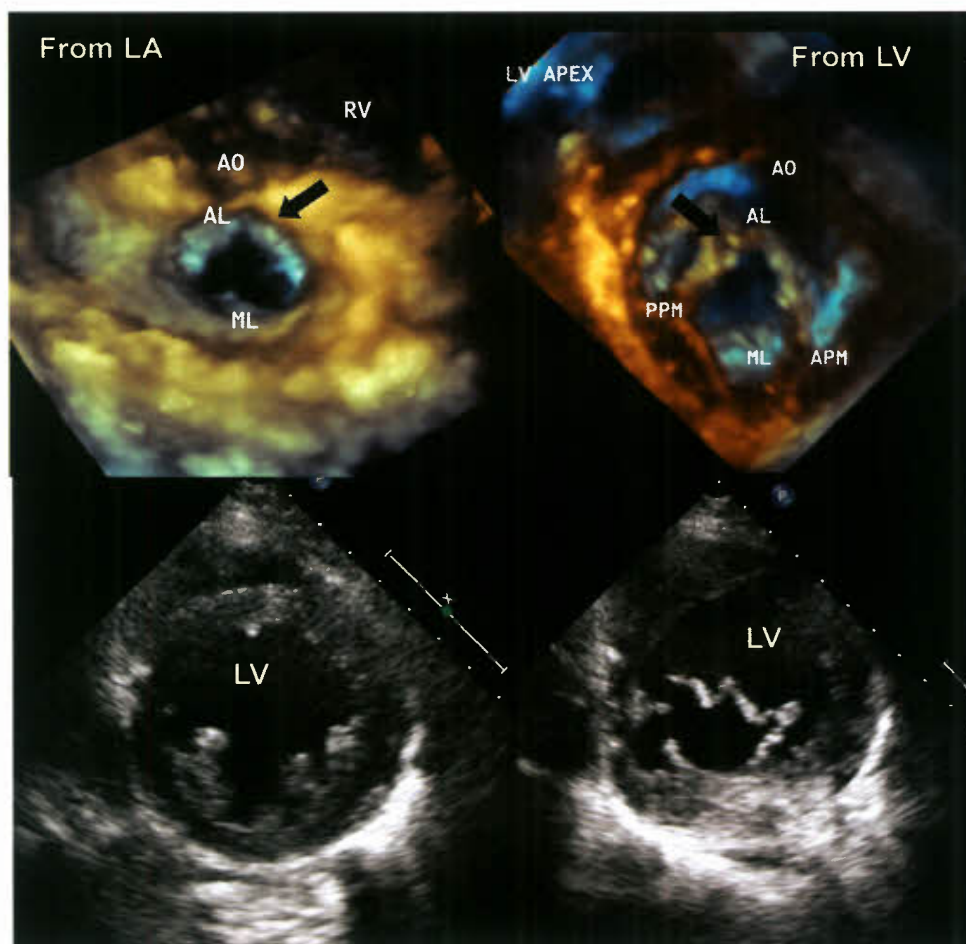
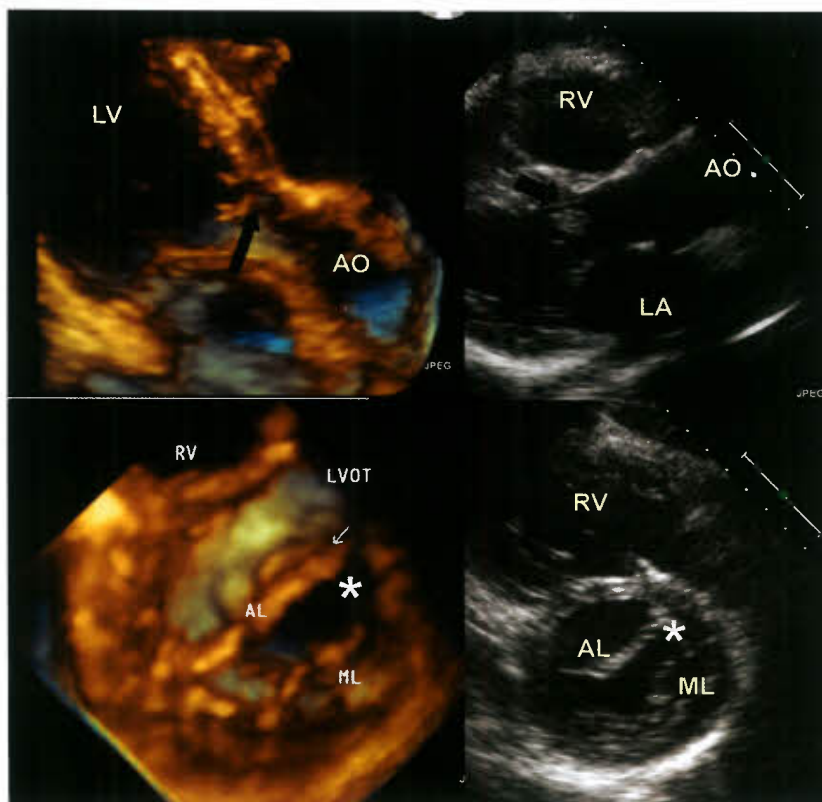


Figure 45.8. These images are from a case with a cleft in the anterior leaflet of the MV, with the cleft pointing toward the left ventricular outflow tract. The upper left hand image is a 3-D echocardiogram seen from the left atrium, with the cleft being indicated by the *black arrow*. The upper right hand picture is from the same case, but viewed from the left ventricular aspect. The lower two images are from the same case, with the left one showing the papillary muscle distribution and the right one the 2-D appearance of the cleft. The extent of the cleft is better appreciated in the 3-D images. AL, aortic leaflet; AO, aorta; APM, anterior papillary muscle; LV, left ventricle; ML, mural leaflet; PPM, posterior papillary muscle; RV, right ventricle.

Figure 45.9. These images are from a case with postoperative tetralogy of Fallot and an eccentric MV cleft associated with accessory chordal apparatus that inserts from the cleft into the interventricular septum. The eccentric cleft is indicated by the *asterisk*. AL, aortic leaflet; AO, aorta; LA, left atrium; LVOT, left ventricular outflow tract; ML, mitral leaflet; RV, right ventricle.



extent of the cleft: 3-D echocardiography does. Imaging the MV from the left atrial or left ventricular aspect provides a complete assessment of the extent of the cleft, the supporting apparatus, and the commissures. The site and degree of regurgitation can be determined by an *en face* view of the valve using color Doppler.

Parachute Mitral Valve

Although cases exist with a solitary papillary muscle, the initial description by Shone (26) included hearts with a dominant papillary muscle, which supported most of the chordal apparatus and a smaller secondary rudimentary muscle. The presence of a parachute MV does not infer stenosis or regurgitation, as medium-term data would suggest that many require no intervention (37). In general, it is the associated leaflet dysplasia and chordal tethering that result in valve failure. This entity is readily recognized by 2-D echocardiography; however, its 3-D counterpart permits a more detailed assessment of the valve leaflets and chordal apparatus.

Double-Orifice Mitral Valve

This entity is seen more frequently in hearts with an atrioventricular septal defect; however it is occasionally encountered in an otherwise normal heart (38,39). In this setting, it is more common for each orifice to be supported by chordal apparatus and papillary muscle (Fig. 45.10A). This may be discovered as an incidental finding during an echocardiogram for another reason, while in other cases one of the functional orifices is regurgitant. These valves are rarely stenotic and in most cases never require any intervention. In general, this entity is readily recognized by both two and three-dimensional echocardiography. In some instances, one of the orifices is

imperforate, and the supporting tension apparatus can be appreciated from the left ventricular aspect (Fig. 45.10B).

Ebstein's-Like Anomaly of the Mitral Valve

This is a rare entity that involves displacement of the posterior or mural leaflet without thinning of the atrialized portion of the LV.

The Mitral Valve in Corrected Transposition

Although the major atrioventricular valve pathology involves the morphologic tricuspid valve, abnormalities of the MV are encountered fairly frequently (40). It is important to recognize these abnormalities, as they can have a profound effect on outcome when a double switch or atrial switch and Rastelli pathway is chosen. There may be MV leaflet dysplasia, multiple papillary muscles, an associated cleft, or a straddling MV (Fig. 45.11A,B). Three-dimensional echocardiography provides superior evaluation of the morphologic MV. The cleft, shortened chordae, and multiple papillary muscles are readily identified. In some cases, the valve is competent at presentation; however, when an anatomical repair is performed, the MV is unable to accommodate the associated systemic pressure. Unlike the normal MV that can cope with left ventricular dilation in the setting of normal left ventricular function many of these valves cannot due to the pathologic abnormalities mentioned above.

Straddling of the Mitral Valve

This is an important lesion to identify and invariably occurs in hearts with an abnormal ventriculoarterial connection,

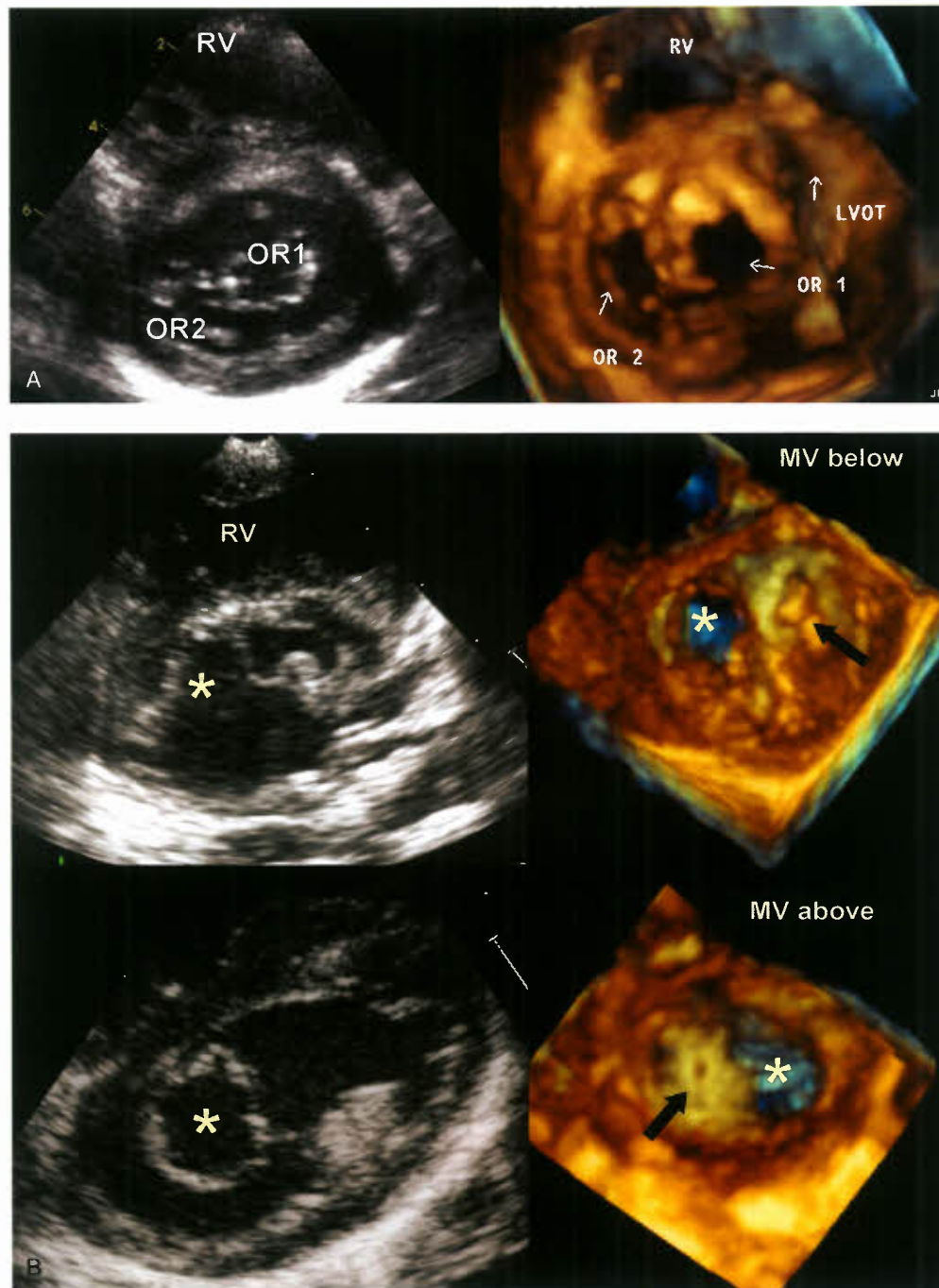


Figure 45.10. A: These two images are from a double-orifice left atrioventricular valve, where both orifices are of a similar size. The 3-D image is from the left ventricular aspect. OR, orifice; LVOT, left ventricular outflow tract; RV, right ventricle. B: These images are from a double-orifice MV with an imperforate anterior orifice. The 2-D echo images on the left show the large posterior orifice and what appears to be a large separate anterior papillary muscle. The upper right hand panel is a 3-D image from below and shows the main orifice indicated by the *asterisk*, and the tension apparatus that supports the imperforate anterior orifice. The lower right hand panel views the MV from above and shows the imperforate anterior orifice indicated by the *black arrow*. MV, mitral valve; RV, right ventricle.

in particular ventriculoarterial discordance or double outlet right ventricle with an anterior aorta. The aortic or anterior leaflet is always involved with chordal apparatus from that leaflet having variable attachments within the right ventricle. In some instances, they insert into the crest of the interventricular septum while in others, they insert into a papillary

muscle on the proximal or distal interventricular septum (Fig. 45.12A,B). Of note, there is invariably an associated cleft in the MV with an eccentric orifice, pointing more toward the ventricular septal defect. The MV is usually competent due to the chordal support; however, recognition is important, because if the chordae are inadvertently cut during repair, the

Figure 45.11. A: This montage is from a case with corrected transposition after a double switch. There is significant MV regurgitation that is seen in the right hand color Doppler panel. The left hand panel shows the thickened leaflets, but the precise mechanism is unclear. MLV, morphologic left ventricle; MRV, morphologic right ventricle; PVA, pulmonary venous atrium. **B:** This montage is from the same patient as in Figure 45.11A. This shows the 3-D appearance of the morphologic MV. The image on the left shows the two atrioventricular valves from above during systole, while the one on the right shows the MV from below. The MV is trileaflet due to a cleft in the anterior leaflet. The *black asterisk* indicates the three components of the MV. AO, aorta; MLV, morphologic left ventricle; MMV, morphologic MV; MTV, morphologic tricuspid valve.

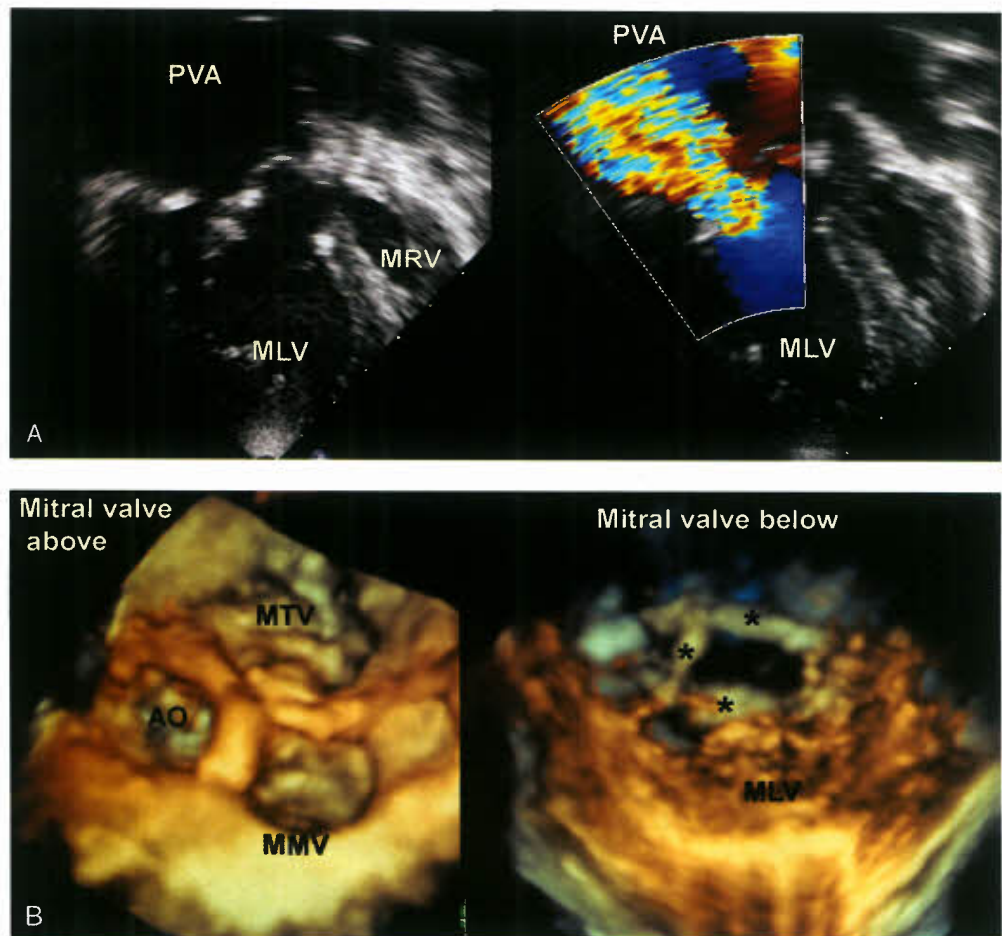
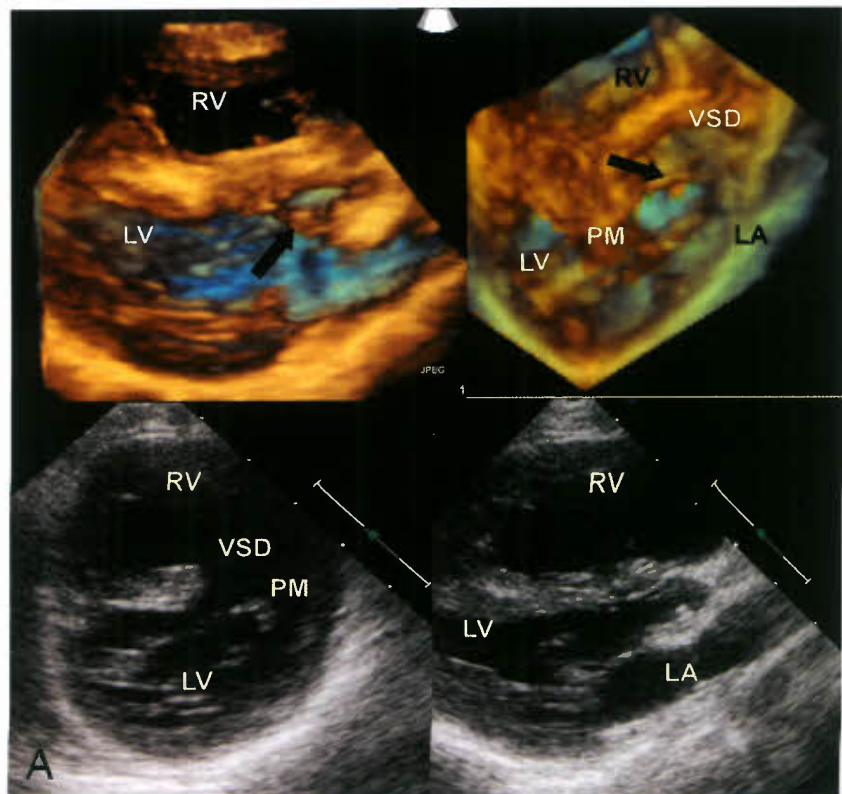


Figure 45.12. A: This montage shows a straddling MV as seen by two and three-dimensional echocardiography. The two lower images show the mitral chords inserting into a papillary muscle; however, the precise location is unclear. The upper right hand image is similar to the upper left one, but with slight angulation to show the anterior muscular ventricular septal defect with the chordae from the MV inserting into it. LA, left atrium; LV, left ventricle; PM, papillary muscle; RV, right ventricle; VSD, ventricular septal defect.



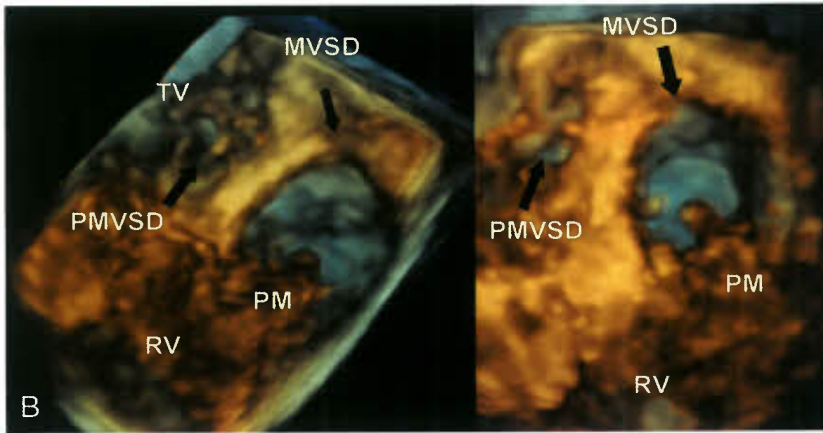


Figure 45.12. (Continued) B: This is from the same case as Figure 45.12A and shows the anterior muscular ventricular septal defect, as well as a second smaller perimembranous defect. The image on the left is with partial cropping of the heart, while the one on the right views the ventricular septal defect in front from the right ventricle. The precise location of the papillary muscle to which the MV is attached in the right ventricle is seen. MVSD, muscular ventricular septal defect; PM, papillary muscle; PMVSD, perimembranous ventricular septal defect; RV, right ventricle; TV, tricuspid valve.

valve will become regurgitant. Although 2-D echocardiography has superior temporal resolution making identification of fine chordal structures more accurate, inferior spatial resolution can impede precise location of the abnormal chordae. Three-dimensional echocardiography, by combining the multiplanar reformatting (MPR) mode, with volume rendering overcomes this limitation. The MPR mode permits navigation through the full-volume data set, making it possible to relate the chords to their anatomical location (Fig. 45.13). As the MV and its straddling chords insert in an anterior location, they are readily identified in a full-volume data set obtained from the parasternal long-axis view. Precise location of the straddling MV at its site of insertion is important, as this dictates whether a biventricular or single ventricle pathway is followed (41).

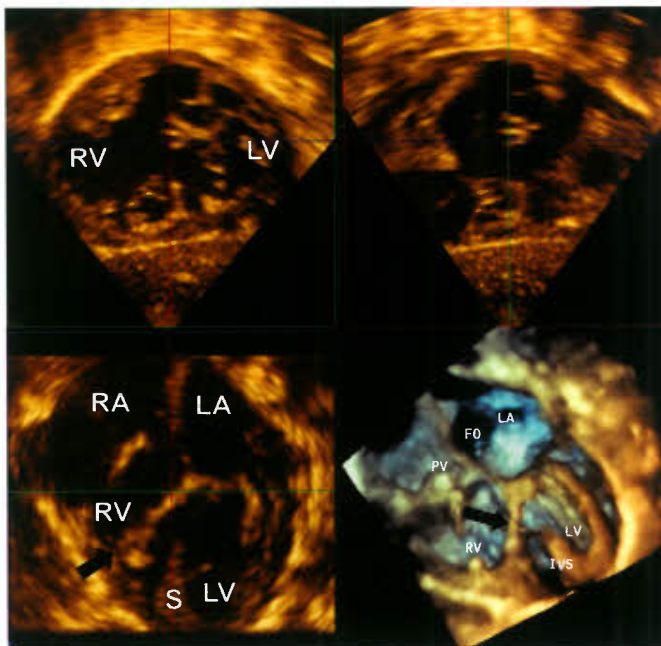


Figure 45.13. This set of images shows the use of the MPR mode for imaging the thin chords in a straddling MV. The lower right hand image shows the component of the MV, which inserts into the right ventricle (black arrow). The lower right hand image is the reconstructed 3-D view that shows the straddling component of the MV as well. FO, foramen ovale; IVS, interventricular septum; LA, left atrium; LV, left ventricle; PV, pulmonary valve; RV, right ventricle.

HEMODYNAMIC ASSESSMENT OF THE MITRAL VALVE

In the current era, echocardiography provides most of the hemodynamic information that is necessary to make a clinical decision with regard to intervention and its timing. Many MV abnormalities have a combination of stenosis and regurgitation. This impacts on mean gradient evaluation, which is also dependent on cardiac output. Despite this, it is an invaluable measurement in pediatric patients, whereas pressure halftime is difficult to interpret due to the higher heart rates of children compared to adults (42). The advantage of pressure halftime (Fig. 45.14A) is that it is not dependent on cardiac output, but will be affected by moderate or severe aortic regurgitation that causes the MV to close prematurely (43). It is also possible to obtain an estimation of MV area by planimetry from 3-D echocardiography (Fig. 45.14B), with this being shown to be of value in adult patients (44). As well, tricuspid or pulmonary regurgitation jets can be used to assess right ventricular and pulmonary artery pressure, which is often increased due to left atrial hypertension.

ASSESSMENT OF MITRAL VALVE REGURGITATION

Vena Contracta Size

We have already discussed the role of 3-D echocardiography in the evaluation of both the site and severity of MV regurgitation. Certainly, this technique provides superior data with regard to the site of regurgitation and can be incorporated into surgical decision making. The advantage is that the valve can be seen as a whole, and commissural and central regurgitant jets pinpointed (Fig. 45.4A). In adult patients, there appears to be a good correlation with effective regurgitant orifice area (EROA) measured by 2-D color Doppler techniques in those with circular orifices, with a weaker relationship when the jets are eccentric (45,46). This is understandable as 2-D color techniques presume that the jets are circular in shape. Of interest, for the tricuspid valve, although there is a good correlation between vena contracta width by 2-D echocardiography and vena contracta area by 3-D echocardiography, only the latter has been shown to be predictive of outcome using multivariate analysis (47). Despite this, it is still not widely utilized and clinical utility needs to be established in large adult series where it can be related to outcome and volumetric

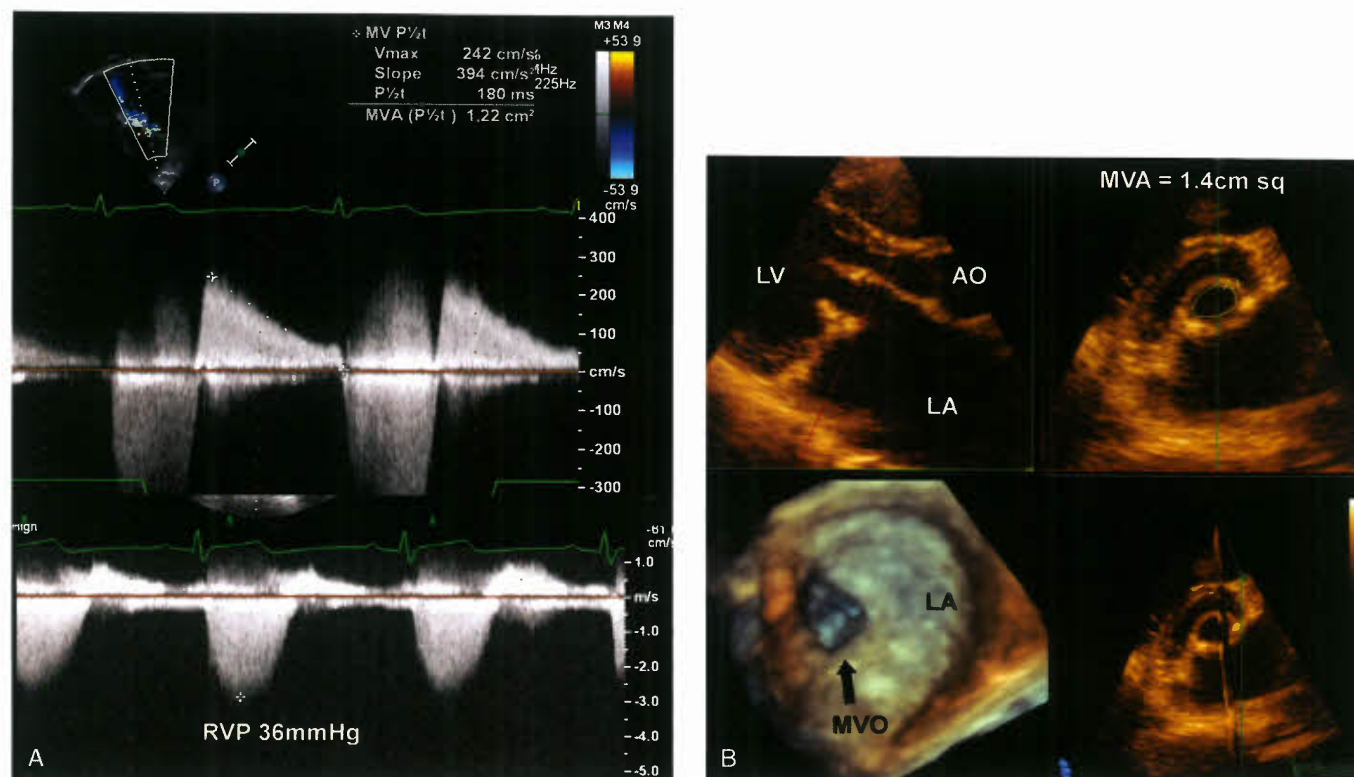


Figure 45.14. A: The upper Doppler trace is from an adolescent with a slower heart rate so that the pressure halftime could be used to calculate MV area (1.22 cm^2). The lower trace shows the right ventricular pressure from tricuspid valve regurgitation. RVP, right ventricular pressure. B: This is from the same case as Figure 45.14A and shows MV area calculation from 3-D echocardiography using the MPR mode. Note that the planimetered area of the MV is 1.4 cm^2 , which is similar to the pressure halftime calculation. The lower right hand panel shows the true MV orifice as seen from the left atrium with 3-D echocardiography. AO, aorta; LA, left atrium; LV, left ventricle; MVA, mitral valve area; MVO, mitral valve orifice.

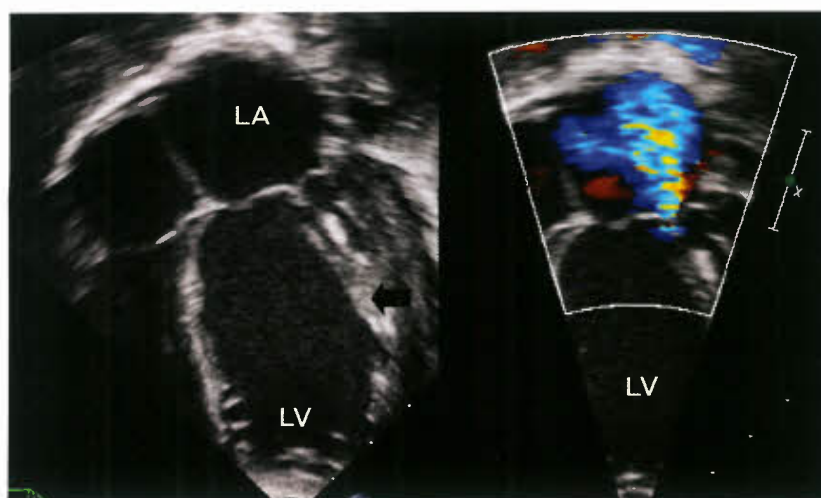
measurements of regurgitation. Therefore, we still have to rely on other methods, as outlined below.

Left Atrial and Left Ventricular Size

These are good indicators of the severity of regurgitation, and indeed, left ventricular end-systolic dimension is considered when determining optimal timing for surgical intervention in those with primary MV disease (48). This is not the case in

patients with associated left-to-right shunt lesions such as a ventricular septal defect or patent arterial duct, which affect not only chamber size but also flow dynamics through the MV. The main lesion that might be confused with primary MV regurgitation in the young population is regurgitation associated with anomalous left coronary artery, which results in subendocardial ischemia and papillary muscle dysfunction. In that setting, the papillary muscles are invariably sclerotic, and abnormal flow from associated coronary collaterals also can be identified (Fig. 45.15).

Figure 45.15. These images are from a child with anomalous left coronary artery from the pulmonary artery with sclerotic papillary muscles resulting in MV regurgitation. The image on the left shows the sclerotic anterior papillary muscle, indicated by the black arrow. The image on the right shows the MV regurgitation. LA, left atrium; LV, left ventricle.



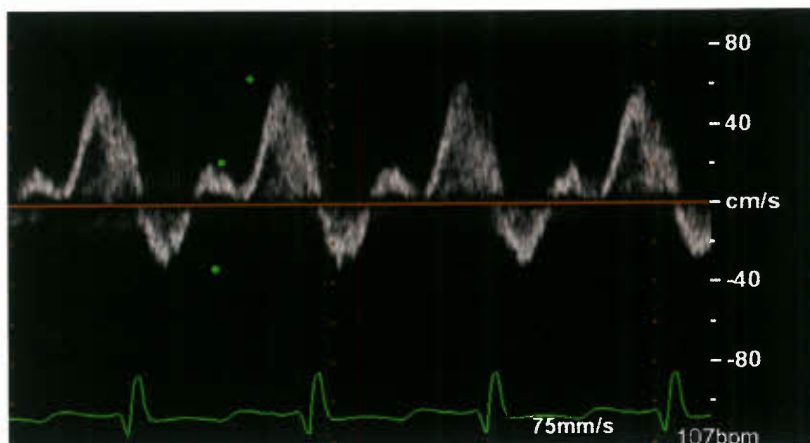


Figure 45.16. This Doppler profile is from a child with significant MV regurgitation in the presence of normal left ventricular function. Note the flow reversal in the pulmonary vein profile during ventricular systole.

Pulmonary Venous Doppler Pattern

Systolic flow reversal can be seen in cases with significant regurgitation; however, it is important that more than one pulmonary vein is sampled, as a jet may be directed into one particular pulmonary vein (49) (Fig. 45.16). Limitations to this approach relate to the presence of diastolic dysfunction with raised left atrial pressure and blunted systolic forward flow.

Continuous Doppler Regurgitant Jet Profile

The more severe the regurgitation, the denser the continuous-wave Doppler profile (Fig. 45.14A). This must be taken in context as increased gain settings can enhance a Doppler signal.

Mitral E Velocity Dominance

A dominant pulsed Doppler E profile is seen in those with severe MV regurgitation. Once again, this will be affected by those cases with associated diastolic dysfunction (Fig. 45.17).

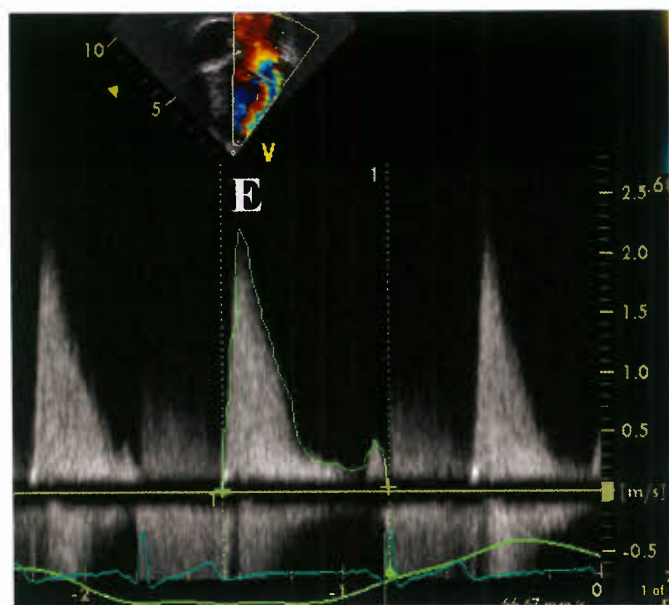


Figure 45.17. This figure demonstrates the E wave dominance of mitral inflow Doppler in a case with significant mitral valve regurgitation and no associated stenosis.

QUANTITATIVE ASSESSMENT OF MITRAL REGURGITATION BY DOPPLER

Pulsed Doppler Assessment of Regurgitant Fraction, Volume, and Effective Regurgitant Orifice Area

This technique measures the stroke volume (SV) through the mitral valve (MV) and aorta, the difference of which represents the volume of regurgitation: $SV = CSA \times VTI = \pi d^2/4 \times VTI = 0.785d^2 \times VTI$ (CSA = cross-sectional area, SV = stroke volume, VTI = velocity time integral). Regurgitant volume (mL) = $SV_{MV} - SV_{LVOT}$. Regurgitant fraction = $(SV_{MR} - SV_{LVOT})/SV_{MV}$. These are techniques that are widely utilized in adult populations and indeed play an important role in decision making (50). Limitations relate to CSA measurements in children, because any errors are squared. Similar measurements can be made by calculating the left ventricular SV by biplane Simpson's rule and subtracting the left ventricular outflow SV determined by Doppler; however, reproducibility of the SV measurements is the main problem.

Proximal Isovelocity Surface Area or Flow Convergence

Proximal isovelocity surface area (PISA) is based on the principle that as blood approaches an orifice, it forms a series of concentric, roughly hemispheric shells that increase in velocity, but decrease in area. In practical terms, the color Doppler Nyquist limit is set to a value at which aliasing occurs near the regurgitant orifice. From this the regurgitant flow is calculated as: $2\pi r^2 \times V_a$ where r = radius of aliasing velocity, V_a = velocity at which aliasing occurs. From this EROA can be calculated as: Regurgitant flow/peak velocity of regurgitation. Limitations of this technique are related to the shape of the PISA shell which may not be semicircular, multiple jets, and the effect of adjacent boundaries as well as determining the precise location of the regurgitant orifice (51). Compared to real-time 3-D echocardiography the PISA technique underestimates the true volume in comparison to the actual volume (46).

MITRAL VALVE PROLAPSE

In the pediatric population MV prolapse is infrequently encountered in patients who do not have connective tissue disorders such as Marfan syndrome. Prior to the understanding of the 3-D aspects of the mitral annulus with its two

high and two low points, the diagnosis of MV prolapse was overestimated by M-mode and in part by 2-D echocardiography (8). It was finally resolved that if the parasternal long-axis view was used then this could be used to make the diagnosis, because this view images the mitral annulus at its two

high points (Fig. 45.18). On the other hand, the apical four-chamber view should not be used, because it images the valve at the two low points (52). Using such criteria, a report from the Framington study demonstrated an incidence of 2.4% in an adult population (53).

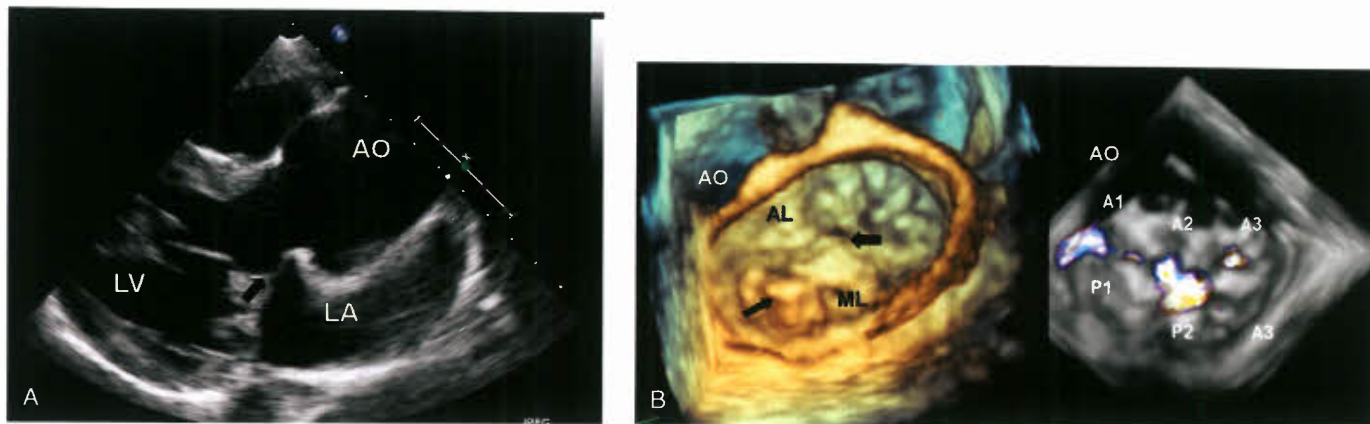
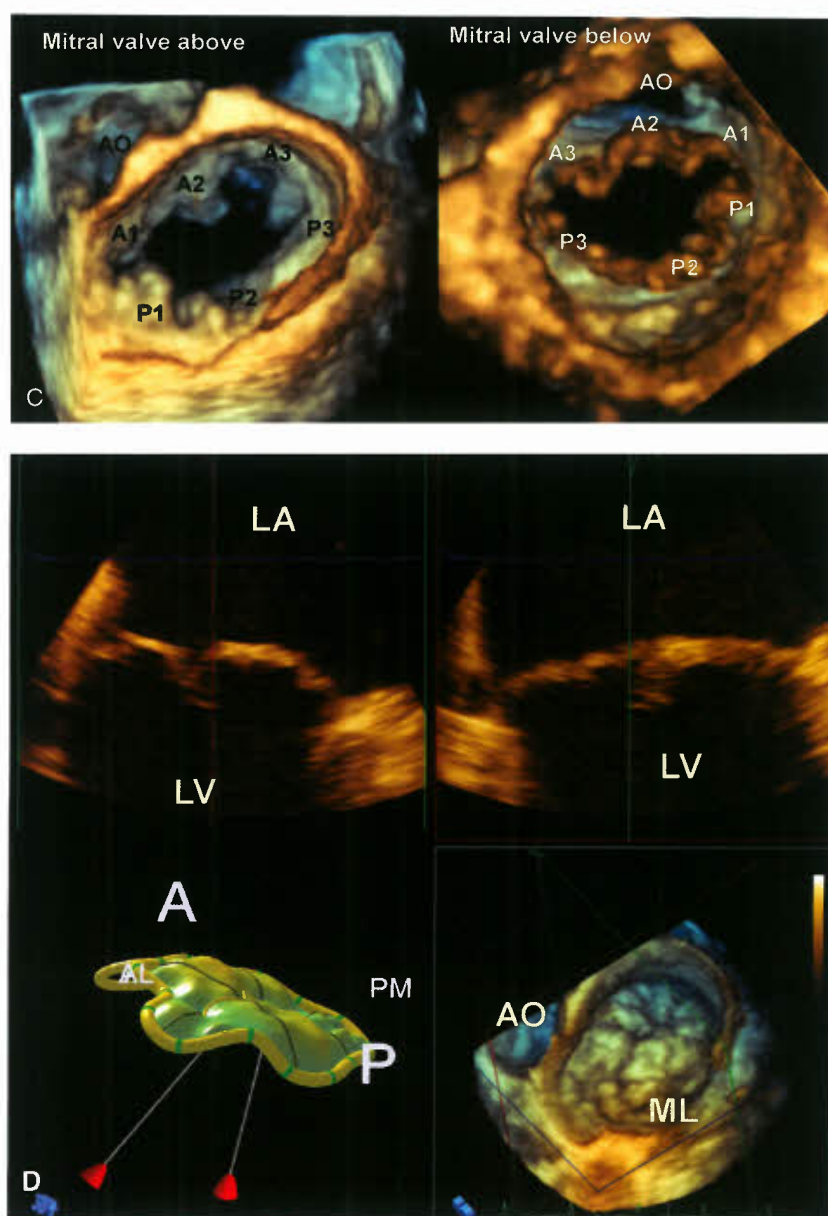


Figure 45.18. A: This parasternal long-axis view demonstrates the 2-D features of mitral valve prolapse, with part of the anterior leaflet being behind the high point of the mitral annulus (black arrow). LA, left atrium; LV, left ventricle. B: This 3-D image of mitral valve prolapse was taken using transesophageal echocardiography. It is the same case as Figure 45.18A and shows the detail that is possible by this technique. The prolapsing segments of the valve can be seen, with the right hand panel showing the sites of regurgitation. The image with the color Doppler assessment also shows the division of the valve into segments A1-A3 and P1-P3. The mitral valve is viewed from the left atrium. AL, aortic leaflet; AO, aorta; ML, mural leaflet. C: These two images show the mitral valve from above and below, demonstrating the individual scallops of the leaflets, as well as their dysplastic nature and the commissures. AO, aorta; A1, A3, and P1-P3 represent the individual segments of the aortic and mural leaflets and is the nomenclature that is used to describe them for surgical management. D: This series of images is obtained from a MPR format and represents the reconstructed 3-D image as seen in the lower right hand panel, with the 2-D images in the upper two panels, with each being at right angles to each other. The lower left hand panel is a reconstructed image that shows how the relationship of the annulus to the prolapsing segments can be calculated using QLab software. AO, aorta; LA, left atrium; LV, left ventricle; ML, mural leaflet; PM, papillary muscle.



The posterior or mural leaflet is involved more frequently in hearts with MV prolapse and may affect a single scallop or the entire leaflet. Annular dilation depends on the presence and severity of associated MV regurgitation. Histologically, there is obvious myxomatous proliferation of the spongy layer of the leaflet. The spongiosa layer is increased with an increase in glycosaminoglycans. In this setting, myxomatous valves show disorganization in their collagen content and elastin fibers (54–56). Their chordae show an increase in glycosaminoglycans, in particular, chondroitin dermatan 6 sulphate and hyaluronan, which have the ability to bind more water, resulting in the gelatinous appearance of the leaflets and their supporting chordae.

MV prolapse that is not syndromal may well be autosomal dominant with variable penetrance. It appears that there is a linkage of myxomatous MV prolapse to chromosome 16 (MMVP1) in cases with an autosomal dominant form, while in others, there is a linkage to MMVP2 on chromosome 11p15.4 and 13q31.3-q32.1 (57,58). It may turn out that MV prolapse is similar to hypertrophic cardiomyopathy with multiple genetic abnormalities responsible for a common phenotype (4).

ECHOCARDIOGRAPHIC ASSESSMENT OF MITRAL VALVE PROLAPSE

Three-dimensional echocardiography is currently the reference standard for this entity, as it provides instantaneous recognition of not only the diagnosis but also the components of the leaflet involved (59–61). In the past, this role belonged to 2-D transthoracic and transesophageal echocardiography; however, these provided a series of snap-shot views of the MV, rather than an overall picture (at 20 degrees, scallops A3-P1 are seen; at 60 degrees scallops P3-A2-P1; at 90 degrees, scallops P3-A1; at 120–160 degrees scallops A2-P2 are seen) (62).

In the pediatric population, transthoracic 3-D echocardiography is usually adequate; however, as patients move into their teenage and young adult years, transesophageal echocardiography is superior. The transesophageal approach is helpful as with the zoom mode a real-time evaluation is possible, which overcomes the problem with stitch artifacts seen from multiple slices (Fig. 45.18B,C). The disadvantage is that the frame rate is lower, but as the MV is in the near field, the resolution is usually adequate. Importantly, it permits a precise identification of the component(s) that are prolapsing, as well as the relationship to the site and degree of regurgitation (Fig. 45.18B). More recently, with the advent of newer analysis packages it is possible to quantify the degree of MV prolapse and relate it to annular height, coaptation, and annular and leaflet area (Fig. 45.18D). This can be performed pre- and postoperatively, providing objective data regarding the quality of the surgical repair and the relationship to any persistent MV regurgitation.

It is possible to obtain multiple views of the MV leaflets and the annulus from a single four-chamber data set. This provides optimal resolution as the leaflets are imaged in the axial plane. In other cases, if the four-chamber view is inadequate, a full-volume data set can be acquired from the parasternal long-axis view; however, this images the leaflets in a lateral plane, which provides lower image resolution.

CLINICAL PRESENTATION

The clinical presentation of MV disease in children is highly variable and is influenced not only by the degree of stenosis and/or regurgitation but also by the presence and severity of

associated lesions when present. At one end of the spectrum are asymptomatic infants or children who have a heart murmur detected on routine examination. At the other end of the spectrum are infants who present early in life with poor feeding, growth failure, tachypnea, diaphoresis with feeds, and recurrent respiratory tract infections. Cardiogenic shock is typically a consequence of associated lesions such as coarctation of the aorta rather than due to intrinsic abnormalities of the MV.

Physical findings of MS include a middiastolic murmur and a late diastolic murmur during atrial systole. These murmurs are low pitched and better appreciated with the bell rather than the diaphragm of the stethoscope. They are often quiet and therefore easily missed unless there is a high clinical suspicion of MV disease. Unlike adults with rheumatic mitral stenosis S1 invariably is not increased in intensity. The pulmonary component of the second heart sound may be loud if there is pulmonary hypertension. Determining the contribution of a stenotic MV to clinical symptoms is difficult in the presence of an associated left-to-right shunting ventricular septal defect or patent ductus arteriosus, which by its very nature increases the flow across the valve if the atrial septum is intact. If an associated diastolic murmur is louder than expected for the size of the associated defect, then suspect associated MV stenosis.

Mitral regurgitation results in a high-pitched pansystolic S1-coincident murmur that may make it difficult to appreciate the first and second heart sounds. This murmur is best appreciated at the left lower sternal border and apex and may radiate to the left axilla and back. The murmur of MR may be associated with a third heart sound or even a flow rumble due to increased diastolic inflow into the LV. Hepatomegaly and increased work of breathing are other physical findings that may be present in children with either MS or regurgitation.

MV prolapse is characterized by the presence of one or more midsystolic clicks. These are believed to be caused by sudden tensing of the mitral apparatus as the leaflets prolapse into the left atrium during systole. Clicks may be followed by a high-pitched late systolic murmur of mitral regurgitation, heard best at the left lower sternal border or apex. Rarely this murmur may be “honking” in quality. The timing of the click(s) and subsequent murmur of MR depends on left ventricular loading. For example, standing results in decreased left ventricular preload, resulting in prolapse that occurs earlier in systole with a click(s) that are close to S1. However, squatting increases preload and delays the prolapse, resulting in the click moving closer to S2. Decreased left ventricular contractility or increased afterload will also delay the click. Note that not all patients with MV prolapse (MVP) have these classic auscultatory findings.

Electrocardiography

The electrocardiogram (ECG) in children with isolated MV disease may be normal if the hemodynamic consequence of the stenosis and/or regurgitation is mild. In children with moderate or severe lesions, the ECG is not diagnostic but may be an early clue to the presence of MV disease on the basis of left atrial enlargement (LAE). Criteria for LAE include a broad, biphasic P wave in one or more of leads I, II aVF, V5, and V6 and in V1 a terminal component of the P wave that is at least 40 ms in duration and at least 1 mm below the baseline (Fig. 45.19). There may also be evidence of right ventricular hypertrophy, right axis deviation, and right atrial enlargement if pulmonary hypertension is a complicating feature.

Radiography

Chest radiography is not sufficiently sensitive for the detection of heart disease in children and should not be routinely performed as part of the initial investigation of children with



Figure 45.19. Electrocardiographic findings in a 12-year-old with MS. Note the broad, notched P waves (in leads II and V1), the P wave below the baseline (V1), and the prominence of right ventricular forces (V1) consistent with pulmonary hypertension.

possible heart disease. Even among children with MV disease confirmed by echocardiography, chest radiography is not routinely necessary, as the findings often do not influence clinical management. However, chest radiography is reasonable prior to surgical or catheter interventions. Findings among patients with MS or regurgitation include straightening of the left heart border, splaying of the carina, and pulmonary venous congestion.

Magnetic Resonance Imaging

Although MRI has a valuable role in the evaluation of some CHD lesions, MV morphology is better evaluated by echocardiography than MRI due to superior spatial resolution. However, MRI may contribute to hemodynamic assessment in some patients. For example, MRI is an accurate and robust technique for measuring mitral regurgitant volume, done by subtracting aortic flow volume from left ventricular SV. Further, ventricular volumes as measured by MRI show a stronger correlation with regurgitant volumes than echocardiography-derived linear dimensions (63). Although the 2008 American Heart Association/American College of Cardiology guidelines for management of valvular heart disease in adults only describe left ventricular size in terms of linear dimensions, MRI-derived ventricular volumes (indexed to body surface area in children) may be of increasing value to guide the timing of surgical intervention. MRI can also determine anatomic regurgitant orifice area using planimetry, which in adults correlates well with MRI-derived regurgitant fraction and with catheterization and echocardiographic assessment of regurgitation severity (64).

Hemodynamic Evaluation

Diagnostic cardiac catheterization is not routinely indicated in children with MV disease, even among those with severe lesions undergoing surgical intervention, because echocardiography as an imaging modality of the MV is superior to angiography and the correlation between mean transmitral pressure gradients obtained by Doppler echocardiography and catheterization is acceptable (42). However, hemodynamic assessment may be valuable in children with mitral disease associated with other lesions. For example, in a symptomatic child with LAE, MS, and a ventricular septal defect, catheterization to calculate Qp:Qs may clarify the relative contribution

toward left atrial hypertension of the MS versus the volume load of the left-to-right shunt.

Findings at catheterization of a child with pure MS include the following. Oximetry may show mild desaturation in the setting of pulmonary edema or may indicate the presence of a left-to-right shunt (e.g., through a patent foramen ovale) in the setting of severe obstruction. Hemodynamic assessment may show pulmonary hypertension, elevated pulmonary capillary wedge pressures, and left atrial hypertension with elevated “A” waves. One exception is with supra-annular prosthetic stenosis, where the “V” wave is larger than the “A” wave and the left ventricular end-diastolic pressure is often elevated (65). Simultaneous pulmonary capillary wedge pressures and left ventricular pressures will demonstrate diastolic pressure gradients between the two. Angiography is associated with significant risk in patients with pulmonary hypertension and should be avoided unless balloon valvuloplasty is planned.

Catheterization of a child with mitral regurgitation, even severe regurgitation, is not routinely indicated prior to surgical intervention but may be helpful in patients with pulmonary hypertension or mixed obstruction and regurgitation. Findings will include elevated left ventricular end diastolic pressure, elevated left atrial pressure with large “V” waves, and increased pulmonary capillary wedge pressure. Angiography will show left atrial opacification that varies from minimal (grade I) in mild MR to complete opacification of the left atrium including the pulmonary veins with delayed emptying (grade IV) in severe mitral regurgitation. However, angiography poses the risk of a pulmonary hypertensive crisis in children with pre-existing pulmonary hypertension and therefore warrants great caution.

MANAGEMENT AND PROGNOSIS OF CONGENITAL MITRAL VALVE STENOSIS

Management of patients with congenital MS is influenced by the severity and mechanism of the obstruction and the presence of associated lesions, if any. Patients with mild or moderate stenosis typically do not warrant surgical or catheter intervention but may benefit from diuretic therapy. Patients with severe stenosis require relief of the obstruction. Interventions for relief of MS include balloon mitral valvuloplasty by cardiac catheterization, surgical mitral valvuloplasty, or MV replacement (MVR).

Medical Management

All patients with congenital MS require regular and lifelong cardiology follow-up to monitor for progression of the mitral inflow gradient, for reassessment of MR and other associated lesions, and for monitoring of possible secondary complications. Secondary complications include failure to thrive, increasing right ventricular and pulmonary artery pressures, atrial fibrillation, respiratory infections, and endocarditis. Children <2 years of age should be considered for monthly prophylaxis against respiratory syncytial virus (RSV) infection with palivizumab (66) during times of the year when community RSV infection is prevalent. Influenza vaccine should be given annually. Endocarditis prophylaxis is not required unless the patient has a prosthetic valve (67) but good dental hygiene and regular dental follow-up are important.

Balloon versus Surgical Management

McElhinney et al. (68) recently reviewed their experience of 108 children with severe congenital MS at Children’s Hospital

in Boston who underwent intervention between 1985 and 2003. The initial MV intervention was balloon valvuloplasty in 64 (59%), and was typically done in children with typical MS, double-orifice MV, or parachute MV. Balloon dilation resulted in a decrease in peak and mean transmitral gradients by a median of 33% and 38%, respectively. However, significant MR developed as a complication of this procedure in 28% of the subjects. Surgical mitral valvuloplasty was the initial intervention in 33 (31%) and these patients were more likely to have a supralvalvar mitral ring as the anatomic substrate of their MS or significant MR at baseline; the majority also underwent surgical intervention for other indications such as ventricular septal defect closure. Initial MVR was performed in 11 (10%), with the decision between surgical mitral valvuloplasty and MVR based on intraoperative assessment of the reparability of the MV. MVR was performed in an additional 24 patients after primary balloon valvuloplasty ($n = 18$) or surgical valvuloplasty ($n = 6$). Approximately, three-fourths of subjects had the prosthesis placed in the supra-annular position. Due to significant baseline differences between patients in each of these three initial treatment groups, conclusions cannot be drawn about the relative outcome benefit of one treatment strategy over another.

The surgical management of obstructive MV disease is challenging. The heterogeneous nature of congenital MS, the presence of associated lesions, and rarity of this clinical problem are likely contributing factors. Surgical, rather than balloon intervention is appropriate when the predominant mechanism of obstruction is a supralvalvar mitral ring, when there are associated lesions that warrant surgical intervention (e.g., subaortic stenosis, coarctation of the aorta) or when significant MR is also present. Surgery may be in the form of chordal fenestration when fusion is an issue, resection of subannular accessory tissue, or splitting of a solitary papillary muscle.

Recent retrospective cohorts published by large centers show that surgical intervention results in a 60% to 70% reduction in transmitral Doppler gradients and can be achieved with in-hospital mortality of 10% or less (68,69). However, moderate or severe mitral insufficiency remains a postoperative challenge. Repeat surgical mitral valvuloplasty or MVR as a follow-up procedure is necessary in 10% to 25% (68,69). Supramitral rings in the absence of other anomalies of the MV have an excellent prognosis, with only 10% having significant postoperative MR and rarely needing reintervention (68,70). One of the problems with surgical intervention in the infant is that failure to relieve the stenosis is associated with increased morbidity and less than ideal options. These children often have associated pulmonary hypertension, which makes them a poor candidate for transplantation, and MVR is challenging due to the small annular size. Therefore, it is preferable to identify those cases with significant MV stenosis early on in life when other options are more likely to result in a successful outcome. If recognized in the neonatal period, a Norwood/Hybrid approach can be undertaken, thus abandoning the left side of the heart. Also, cardiac transplantation is more likely to lead to success prior to developing sustained changes in the pulmonary vascular bed.

Mitral Valve Replacement

MVR should be avoided as initial intervention for congenital MS where possible. In young children, MVR is limited by the lack of small prostheses and the need for supra-annular implantation in some patients. However, supra-annular placement impairs left atrial compliance and results in pulmonary hypertension, even in the absence of significant prosthetic obstruction (65). The limited lifespan of prostheses, particularly bioprostheses, requiring repeated reinterventions later in

life (71,72), is an additional drawback. The Pediatric Cardiac Care Consortium reported on 102 survivors of mechanical MVR in children <5 years of age, of whom 29 (28%) underwent a second MVR a mean of 4.8 years later (72). The most common indication for second MVR was prosthetic valve stenosis (83%). Highest-risk patients for second MVR were those who were <2 years of age with prosthesis <20 mm at first MVR (72). The need for anticoagulation with warfarin for mechanical prostheses is also a major challenge, particularly in young children. Finally, operative mortality, while improving, remains a significant issue, particularly in young children (71,73). In a 30-year review of 118 children undergoing MVR at 5 years of age or less, factors associated with worse survival included MVR at <1 year of age, earlier need for redo MVR, and additional procedures at the time of MVR (74). Supra-annular placement was associated with a reduced likelihood of needing subsequent pacemaker placement, but in the latter half of the cohort (1991 to 2006) it was associated with worse survival (74).

Patient-prosthesis mismatch is also a significant consideration with respect to MVR in children. Eble et al. (75) found that compared to nonsurvivors of MVR, survivors had placement of a prosthetic valve within one z-score of the echocardiographically measured mitral annulus, while those with an oversized prosthesis had more adverse outcomes. Caldaroni et al. (76) similarly reported that an increased ratio of prosthetic valve size to patient weight was an independent predictor of death among children undergoing MVR before 5 years of age. Alsoufi et al. (77) also found that greater prosthesis size to body surface area-predicted mitral annulus ratio was an independent risk factor for death following MVR. Prostheses that are too large may contribute to left ventricular outflow tract obstruction, impaired prosthetic valve mobility, and conduction system injury. These data suggest that attempts to oversize prostheses in the hope of delaying second MVR are of little to no benefit. MVR may be particularly problematic in patients with a hypoplastic mitral annulus in which case an annular-enlarging operation may be necessary.

The use of tissue prostheses in children is limited by lack of availability of small sizes, limiting their use in young children, and also by more rapid degeneration compared to mechanical prostheses resulting in a very high rate of reoperation (78). However, unlike mechanical prostheses, tissue prostheses do not require anticoagulation with warfarin and therefore may be a good option in female adolescents and in those who are unlikely to be compliant with oral anticoagulation. Pregnancy appears safe with a tissue bioprosthesis and the low rate of valve-related complications and good functional class of this patient population is such that bioprosthesis remains a good option in some patients. Homografts have rarely been used in the mitral position and are associated with a higher reoperation risk when compared to other bioprostheses.

In summary, the management of severe congenital MS is challenging, and is associated with high reintervention rates and significant mortality. However, among children with mild to moderate MV obstruction, the prognosis is much better. In a recent review by Tierney et al. (79) of all comers diagnosed with MS before 6 months of age and managed with a biventricular strategy, independent predictors of MV intervention (catheter or surgery) or death were higher initial mean mitral inflow gradient and lower left ventricular diastolic length Z-score. Among those with an initial mean mitral gradient of <2 mm Hg, none had an intervention or died, whereas among those with an initial mean mitral gradient of >5.5 mm Hg, 85% had MV intervention or died. MV morphology was not predictive of outcome, though this study excluded those with a supramitral ring (79). Among patients with a parachute MV or a parachute-like asymmetric MV, approximately 60% maintain a biventricular circulation, but >90% require

catheter or surgical intervention, predominantly for associated lesions (80), and of those with a biventricular circulation, only about half have MS at follow-up and one-third have MR at follow-up (80). Need for intervention among children with a parachute MV is rare (37,80).

MANAGEMENT AND PROGNOSIS OF CONGENITAL MITRAL REGURGITATION

As with congenital MS, infants and children with congenital MR should be managed “medically” delaying surgical MV intervention beyond the first year of life if possible in order to avoid the complications of MVR that are associated with small patient size, should MV repair not be feasible. However, elimination of any large left-to-right shunts may be of benefit early on, should left ventricular and mitral annular dilation be contributing to the severity of MR (81). Medical management includes optimizing caloric intake and weight gain, monitoring for the possible development of pulmonary hypertension and atrial arrhythmias, aggressive management of respiratory infections, influenza vaccinations, and prophylaxis against respiratory syncytial virus infection with palivizumab for children <2 years of age. Afterload reduction and use of diuretics may be of value, though data in children are limited.

Surgical Management

The goal of surgical management of congenital MR should be to restore normal valve function rather than normal valve anatomy (81,82). Mitral reconstruction for MR has been described by Carpentier et al. (83). Stellin and colleagues recently described 48 children undergoing MV surgery for mitral regurgitation, of whom only 2 were infants, reflecting the potential to delay surgery beyond the first year of life in many cases. Surgical techniques used were cleft closure (this study excluded atrioventricular septal defects), annuloplasty, chordal shortening, commissuroplasty, and accessory orifice closure. Freedom from reintervention was 80% at 10 years, and survival was approximately 95% at 15 years and approximately 85% at 20 years. These excellent results demonstrate the feasibility of a conservative surgical approach (i.e., MV repair rather than replacement) in carefully selected patients, avoiding the complications of MVR as discussed above. Furthermore, delay of surgery in children with significant MR until the onset of severe symptoms is not associated with late left ventricular dysfunction (84), supporting the practice of delaying any surgical intervention as long as possible.

MANAGEMENT AND PROGNOSIS OF MITRAL VALVE PROLAPSE

Surgical management of MVP may be appropriate in patients with severe MR, for example, in those with a flail mitral leaflet due to rupture or severe elongation of chordae tendineae. Surgical repair of MVP is associated with excellent outcomes and is recommended over MVR, though it should be performed in centers experienced in MV repair (85). Anterior leaflet repair is associated with a higher risk of reoperation than posterior leaflet repair. Factors to consider when contemplating surgical intervention include not only the severity of the regurgitation but also left ventricular systolic function (usually normal in children and adolescents with MVP), left ventricular end-systolic and end-diastolic volumes, pulmonary artery pressure,

symptoms if any, and presence or absence of atrial fibrillation, though atrial fibrillation is unusual in the pediatric age range. Well-accepted indications for MV surgery in adolescents with MVP are the same as for those with other causes of MR, and include (a) the symptomatic patient with severe MR and NYHA class III or IV symptoms or (b) the asymptomatic adolescent with severe MR and left ventricular systolic dysfunction (ejection fraction <0.60) (48). In the unusual situation of a symptomatic patient with MR and severe LV dysfunction, cardiac transplantation may be preferable to either MV repair or replacement.

Medical management of MVP primarily involves reassurance, as most patients with MVP have mild disease and no intervention is needed. Regular exercise is recommended for most subjects. Restriction from competitive sports is prudent for those with moderate or severe left ventricular enlargement and those with aortic root dilation. The presence of a connective tissue disorder such as Marfan syndrome or Ehlers-Danlos syndrome should be considered in all patients with MVP. Metabolic and storage disorders may also be associated with MVP. Asymptomatic patients with no significant MR can be seen infrequently (every 2 to 5 years), whereas those with moderate-severe MR, symptoms, or associated aortic root dilation should be seen more often. The potential for familial inheritance of MVP should be explained, and echocardiography of first-degree family members should be considered.

Prevention of embolic complications is also a responsibility of the cardiologist. Fortunately, these are very rare in children but may infrequently be observed in adolescents. Aspirin therapy (75 to 325 mg/day) is recommended in those with MVP who experience transient cerebral ischemic attacks or who have atrial fibrillation. Warfarin therapy is recommended in those with MVP who have a history of stroke (48) in the setting of mitral regurgitation, atrial fibrillation, or left atrial thrombus (Class I indications), in which case the international normalized ratio should be kept between 2.0 and 3.0.

REFERENCES

1. Kanani M, Moorman AFM, Cook AC, et al. Development of the atrioventricular valves: clinicomorphological correlations. *Ann Thorac Surg* 2005;79:1797-1804.
2. Wenink ACG, Gittenberger-de Groot AC, Brom AG. Developmental considerations of mitral valve anomalies. *Int J Cardiol* 1986;11:85-98.
3. De Lange FJ, Moorman AFM, Anderson RH, et al. Lineage and morphogenetic analysis of the cardiac valves. *Circ Res* 2004;95:645-654.
4. Levine RA, Slaughter SA. Molecular genetics of mitral valve prolapse. *Curr Opin Cardiol* 2007;22:171-175.
5. Ranger AM, Grusby MJ, Hodge MR, et al. The transcription factor NF-ATc is essential for cardiac valve formation. *Nature* 1998;392:186-190.
6. Hurlstone AFL, Haramis AG, Wienholds E, et al. The Wnt/ β -catenin pathway regulates cardiac valve formation. *Nature* 2003;425:633-637.
7. Collins-Nakai RL, Rosenthal A, Castaneda AR. Congenital mitral stenosis. A review of 20 years' experience. *Circulation* 1977;56:1039-1047.
8. Karr SS, Parness IA, Spevak PJ, et al. Diagnosis of anomalous left coronary artery by Doppler color flow mapping: distinction from other causes of dilated cardiomyopathy. *J Am Coll Cardiol* 1992;19:1271-1275.
9. Levine RA, Triulzi MO, Harrigan P, et al. The relationship of mitral annular shape to the diagnosis of mitral valve prolapse. *Circulation* 1987;75:756-767.
10. Salgo IS, Gorman III JH, Gorman RC, et al. Effect of annular shape on leaflet curvature in reducing mitral leaflet stress. *Circulation* 2002;106:711-717.
11. Lansac E, Lim KH, Shomura Y, et al. Dynamic balance of the aortomitral junction. *J Thorac Cardiovasc Surg* 2002;123:911-918.
12. Veronesi F, Corsi C, Sugeng L, et al. A study of functional anatomy of aortic-mitral valve coupling using 3D matrix transesophageal echocardiography. *Circ Cardiovasc Imaging* 2009;2:24-31.
13. Watanabe N, Ogasawara Y, Yamaura Y, et al. Quantitation of mitral valve tenting in ischemic mitral regurgitation by transthoracic real-time three-dimensional echocardiography. *J Am Coll Cardiol* 2005;45:763-769.
14. Tsakiris AG, Von Bernuth G, Rastelli GC, et al. Size and motion of the mitral valve annulus in anesthetized intact dogs. *J Appl Physiol* 1971;30:611-618.

15. Karlsson MO, Glasson JR, Bolger AF, et al. Mitral valve opening in the ovine heart. *Am J Physiol Heart Circ Physiol* 1998;274:H552-H563.
16. Kwan J, Qin JX, Popović ZB, et al. Geometric changes of mitral annulus assessed by real-time 3-dimensional echocardiography: becoming enlarged and less nonplanar in the anteroposterior direction during systole in proportion to global left ventricular systolic function. *J Am Soc Echocardiogr* 2004;17:1179-1184.
17. Carlhäll C, Wigström L, Heiberg E, et al. Contribution of mitral annular excursion and shape dynamics to total left ventricular volume change. *Am J Physiol Heart Circ Physiol* 2004;287:H1836-H1841.
18. Asante-Korang A, O'Leary PW, Anderson RH. Anatomy and echocardiography of the normal and abnormal mitral valve. *Cardiol Young* 2006;16:27-34.
19. Lam JH, Ranganathan N, Wigle ED, et al. Morphology of the human mitral valve. I. Chordae tendineae: a new classification. *Circulation* 1970;41:449-458.
20. Orsui Y, Gilon D, Jiang L, et al. Restricted diastolic opening of the mitral leaflets in patients with left ventricular dysfunction: evidence for increased valve tethering. *J Am Coll Cardiol* 1998;32:398-404.
21. Takahashi K, Mackie AS, Rebeyka IM, et al. Two-dimensional versus transthoracic real-time three-dimensional echocardiography in the evaluation of the mechanisms and sites of atrioventricular valve regurgitation in a congenital heart disease population. *J Am Soc Echocardiogr* 2010;23:726-734.
22. Björk VO, Björk L, Malers E. Left ventricular function after resection of the papillary muscles in patients with total mitral valve replacement. *J Thorac Cardiovasc Surg* 1964;48:635-639.
23. Daliento L, Thiene G, Chirillo F, et al. Congenital malformations of the mitral valve: clinical and morphological aspects. *G Ital Cardiol* 1991;21:1205-1216.
24. Ruckman RN, Van Praagh R. Anatomic types of congenital mitral stenosis: report of 49 autopsy cases with consideration of diagnosis and surgical implications. *Am J Cardiol* 1978;42:592-601.
25. Oberhansli I, Baldovinos A, Beghetti M, et al. Hypoplasia of the posterior leaflet as a rare cause of congenital mitral insufficiency. *J Cardiac Surg* 1997;12:339-342.
26. Shone JD, Sellers RD, Anderson RC, et al. The developmental complex of "parachute mitral valve," supra-aortic ring of left atrium, subaortic stenosis, and coarctation of aorta. *Am J Cardiol* 1963;11:714-725.
27. Sullivan ID, Robinson PJ, De Leval M, et al. Membranous supra-aortic mitral stenosis: a treatable form of congenital heart disease. *J Am Coll Cardiol* 1986;8:159-164.
28. Pacileo G, Russo MG, Calabro R. Anomalous mitral arcade: echocardiographic and color flow findings. *Echocardiography* 1991;8:657-659.
29. Layman TE, Edwards JE. Anomalous mitral arcade. A type of congenital mitral insufficiency. *Circulation* 1967;35:389-395.
30. Coto EO, Jimenez MQ, Deverall PB, et al. Anomalous mitral "cleft" with abnormal ventriculo-arterial connection: anatomical findings and surgical implications. *Pediatr Cardiol* 1984;5:1-5.
31. Di Segni E, Bass JL, Lucas Jr. RV, et al. Isolated cleft mitral valve: a variety of congenital mitral regurgitation identified by 2-dimensional echocardiography. *Am J Cardiol* 1983;51:927-931.
32. Fraisse A, Massih TA, Kreitmann B, et al. Characteristics and management of cleft mitral valve. *J Am Coll Cardiol* 2003;42:1988-1993.
33. Kohl T, Silverman NH. Comparison of cleft and papillary muscle position in cleft mitral valve and atrioventricular septal defect. *Am J Cardiol* 1996;77:164-169.
34. Timóteo A, Galrinho A, Fiarresga A, et al. Isolated cleft of the anterior mitral valve leaflet. *Eur J Echocardiogr* 2007;8:59-62.
35. Tamura M, Menahem S, Brizard C. Clinical features and management of isolated cleft mitral valve childhood. *J Am Coll Cardiol* 2000;35:764-770.
36. Sittiwangkul R, Ma RY, McCrindle BW, et al. Echocardiographic assessment of obstructive lesions in atrioventricular septal defects. *J Am Coll Cardiol* 2001;38:253-261.
37. Schaverien M, Freedom RM, McCrindle BW. Independent factors associated with outcomes of parachute mitral valve in 84 patients. 2004;109:2309-2313.
38. Scardi S, Pandullo C, Poletti A. Isolated double orifice mitral valve. *G Ital Cardiol* 1994;24:1007-1010.
39. Trowitzsch E, Bano-Rodrigo A, Burger BM. Two-dimensional echocardiographic findings in double orifice mitral valve. *J Am Coll Cardiol* 1985;6:383-387.
40. Gerlis LM, Wilson N, Dickinson DF. Abnormalities of the mitral valve in congenitally corrected transposition (discordant atrioventricular and ventriculoarterial connections). 1986;55:475-479.
41. Aeba R, Katogi T, Takeuchi S, et al. Surgical management of the straddling mitral valve in the biventricular heart. *Ann Thorac Surg* 2000;69:130-134.
42. Banerjee A, Kohl T, Silverman NH. Echocardiographic evaluation of congenital mitral valve anomalies in children. *Am J Cardiol* 1995;76:1284-1291.
43. Hatle L, Brubakk A, Tromsdal A, et al. Noninvasive assessment of pressure drop in mitral stenosis by doppler ultrasound. *Br Heart J* 1978;40:131-140.
44. Pérez de Isla L, Casanova C, Almería C, et al. Which method should be the reference method to evaluate the severity of rheumatic mitral stenosis? Gorlin's method versus 3D-echo. *Eur J Echocardiogr* 2007;8:470-473.
45. Yosefy C, Hung J, Chua S, et al. Direct measurement of vena contracta area by real-time 3-dimensional echocardiography for assessing severity of mitral regurgitation. *Am J Cardiol* 2009;104:978-983.
46. Altioek E, Hamada S, van Hall S, et al. Comparison of direct planimetry of mitral valve regurgitation orifice area by three-dimensional transesophageal echocardiography to effective regurgitant orifice area obtained by proximal flow convergence method and vena contracta area determined by color Doppler echocardiography. *Am J Cardiol* 2011;107:452-458.
47. Takahashi K, Inage A, Rebeyka IM, et al. Real-time three-dimensional echocardiography provides new insight into the mechanisms of tricuspid valve regurgitation in patients with hypoplastic left heart syndrome. *Circulation* 2009;120:1091-1098.
48. 2006 Writing Committee Members; Bonow RO, Carabello BA, Chatterjee K, et al. 2008 Focused update incorporated into the ACC/AHA 2006 guidelines for the management of patients with valvular heart disease: a report of the American College of Cardiology/American Heart Association Task Force on Practice Guidelines (Writing Committee to Revise the 1998 Guidelines for the Management of Patients With Valvular Heart Disease): endorsed by the Society of Cardiovascular Anesthesiologists, Society for Cardiovascular Angiography and Interventions, and Society of Thoracic Surgeons. *Circulation* 2008;118:e523-e661.
49. Passafium A, Shiota T, Depp M, et al. Factors influencing pulmonary venous flow velocity patterns in mitral regurgitation: an in vitro study. *J Am Coll Cardiol* 1995;26:1333-1339.
50. Zoghbi WA, Enriquez-Sarano M, Foster E, et al. Recommendations for evaluation of the severity of native valvular regurgitation with two-dimensional and Doppler echocardiography. *J Am Soc Echocardiogr* 2003;16:777-802.
51. Yosefy C, Levine RA, Solis J, et al. Proximal flow convergence region as assessed by real-time 3-dimensional echocardiography: challenging the hemispheric assumption. *J Am Soc Echocardiogr* 2007;20:389-396.
52. Angelini A, Siew Yen Ho, Anderson RH, et al. A histological study of the atrioventricular junction in hearts with normal and prolapsed leaflets of the mitral valve. *Br Heart J* 1988;59:712-716.
53. Feigenbaum H. Echocardiography in the management of mitral valve prolapse. *Aust N Z J Med* 1992;22:550-555.
54. Freed LA, Benjamin EJ, Levy D, et al. Mitral valve prolapse in the general population: the benign nature of echocardiographic features in the Framingham Heart Study. *J Am Coll Cardiol* 2002;40:1298-1304.
55. Grande-Allen KJ, Griffin BP, Calabro A, et al. Myxomatous mitral valve chordae. II: selective elevation of glycan content. *J Heart Valve Dis* 2001;10:325-333.
56. King BD, Clark MA, Baba N. "Myxomatous" mitral valves: Collagen dissolution as the primary defect. *Circulation* 1982;66:288-296.
57. Nesta F, Leyne M, Yosefy C, et al. New locus for autosomal dominant mitral valve prolapse on chromosome 13: clinical insights from genetic studies. *Circulation* 2005;112:2022-2030.
58. Freed LA, Acierno JS Jr, Dai D, et al. A locus for autosomal dominant mitral valve prolapse on chromosome 11p15.4. *Am J Hum Genet* 2003;72:1551-1559.
59. Levine RA, Stathogiannis E, Newell JB, et al. Reconsideration of echocardiographic standards for mitral valve prolapse: lack of association between leaflet displacement isolated to the apical four chamber view and independent echocardiographic evidence of abnormality. *J Am Coll Cardiol* 1988;11:1010-1019.
60. Müller S, Müller L, Laufer G, et al. Comparison of three-dimensional imaging to transesophageal echocardiography for preoperative evaluation in mitral valve prolapse. *Am J Cardiol* 2006;98:243-248.
61. Patel V, Hsiung MC, Nanda NC, et al. Usefulness of live/real time three-dimensional transthoracic echocardiography in the identification of individual segment/scallop prolapse of the mitral valve. *Echocardiography* 2006;23:513-518.
62. Pepi M, Tamborini G, Maltagliati A, et al. Head-to-head comparison of two- and three-dimensional transthoracic and transesophageal echocardiography in the localization of mitral valve prolapse. *J Am Coll Cardiol* 2006;48:2524-2530.
63. Uretsky S, Supariwala A, Nidadovolu P, et al. Quantification of left ventricular remodeling in response to isolated aortic or mitral regurgitation. *J Cardiovasc Magn Reson* 2010;12:32.
64. Buchner S, Debl K, Poschenrieder F, et al. Cardiovascular magnetic resonance for direct assessment of anatomic regurgitant orifice in mitral regurgitation. *Circ Cardiovasc Imaging* 2008;1:148-155.
65. Adatia I, Moore PM, Jonas RA, et al. Clinical course and hemodynamic observations after supraannular mitral valve replacement in infants and children. *J Am Coll Cardiol* 1997;29:1089-1094.
66. Feltes TF, Cabalka AK, Meissner HC, et al. Palivizumab prophylaxis reduces hospitalization due to respiratory syncytial virus in young children with hemodynamically significant congenital heart disease. *J Pediatr* 2003;143:532-540.
67. Wilson W, Taubert KA, Gewitz M, et al. Prevention of infective endocarditis: guidelines from the American Heart Association: a guideline from the American Heart Association Rheumatic Fever, Endocarditis, and Kawasaki Disease Committee, Council on Cardiovascular Disease in the Young, and the Council on Clinical Cardiology, Council on Cardiovascular Surgery and Anesthesia, and the Quality of Care and Outcomes Research Interdisciplinary Working Group. *Circulation* 2007;116:1736-1754.
68. McElhinney DB, Sherwood MC, Keane JF, et al. Current management of severe congenital mitral stenosis: outcomes of transcatheter and surgical therapy in 108 infants and children. *Circulation* 2005;112:707-714.
69. Hoashi T, Bove EL, Devaney EJ, et al. Mitral valve repair for congenital mitral valve stenosis in the pediatric population. *Ann Thorac Surg* 2010;90:36-41.

70. Toscano A, Pasquini L, Iacobelli R, et al. Congenital supra-annular mitral ring: an underestimated anomaly. *J Thorac Cardiovasc Surg* 2009;137:538–542.
71. Beierlein W, Becker V, Yates R, et al. Long-term follow-up after mitral valve replacement in childhood: poor event-free survival in the young child. *Eur J Cardiothorac Surg* 2007;31:860–865.
72. Raghuvver G, Caldarone CA, Hills CB, et al. Predictors of prosthesis survival, growth, and functional status following mechanical mitral valve replacement in children aged <5 years, a multi-institutional study. *Circulation* 2003;108:II174–II179.
73. Alexiou C, Galogavrou M, Chen Q, et al. Mitral valve replacement with mechanical prostheses in children: improved operative risk and survival. *Eur J Cardiothorac Surg* 2001;20:105–113.
74. Selamet Tierney ES, Pigula FA, Berul CI, et al. Mitral valve replacement in infants and children 5 years of age or younger: evolution in practice and outcome over three decades with a focus on supra-annular prosthesis implantation. *J Thorac Cardiovasc Surg* 2008;136:954–961.e3.
75. Eble BK, Fiser WP, Simpson P, et al. Mitral valve replacement in children: predictors of long-term outcome. *Ann Thorac Surg* 2003;76:853–859.
76. Caldarone CA, Raghuvver G, Hills CB, et al. Long-term survival after mitral valve replacement in children aged <5 years: a multi-institutional study. *Circulation* 2001;104:i143–i147.
77. Alsoufi B, Manlhiot C, Al-Ahmadi M, et al. Outcomes and associated risk factors for mitral valve replacement in children. *Eur J Cardiothorac Surg* 2011.
78. Alsoufi B, Manlhiot C, McCrindle BW, et al. Aortic and mitral valve replacement in children: is there any role for biologic and bioprosthetic substitutes? *Eur J Cardiothorac Surg* 2009;36:84–90.
79. Selamet Tierney ES, Graham DA, McElhinney DB, et al. Echocardiographic predictors of mitral stenosis-related death or intervention in infants. *Am Heart J* 2008;156:384–390.
80. Marino BS, Kruger LE, Cho CJ, et al. Parachute mitral valve: morphologic descriptors, associated lesions, and outcomes after biventricular repair. *J Thorac Cardiovasc Surg* 2009;137:385–393.e4.
81. Ganeshalingham A, Finucane K, Hornung T. Isolated congenital mitral valve regurgitation presenting in the first year of life. *J Paediatr Child Health* 2010;46:159–165.
82. Stellin G, Padalino MA, Vida VL, et al. Surgical repair of congenital mitral valve malformations in infancy and childhood: a single-center 36-year experience. *J Thorac Cardiovasc Surg* 2010;140:1238–1244.
83. Carpentier A, Branchini B, Cour JC. Congenital malformations of the mitral valve in children. Pathology and surgical treatment. *J Thorac Cardiovasc Surg* 1976;72:854–866.
84. Krishnan US, Gersony WM, Berman-Rosenzweig E, et al. Late left ventricular function after surgery for children with chronic symptomatic mitral regurgitation. *Circulation* 1997;96:4280–4285.
85. Mohy D, Orszulak TA, Schaff HV, et al. Very long-term survival and durability of mitral valve repair for mitral valve prolapse. *Circulation* 2001;104:i1–i7.

Douglas J. Schneider ■ John W. Moore

INTRODUCTION

The clinical spectrum of congenital aortic stenosis ranges from a nonstenotic bicuspid aortic valve to severe aortic stenosis in fetal life leading to hypoplastic left heart syndrome. Congenital aortic stenosis occurs in different forms, usually classified with respect to the location of the obstruction relative to the aortic valve: valvular, subvalvular, or supra-valvular. Because the clinical features and treatment of these forms of aortic stenosis differ, they are discussed separately in this chapter. Although this chapter deals primarily with congenital aortic stenosis and not hypoplastic left heart syndrome, the infant with severe aortic stenosis and small left ventricle presents important therapeutic issues that justify separate discussion (see Chapter 48).

VALVULAR AORTIC STENOSIS

Prevalence and Etiology

The true incidence of congenital aortic valve abnormalities is not precisely known because minor malformations of the aortic valve (primarily bicuspid aortic valves) are common, and these abnormalities clinically are frequently unapparent during infancy and childhood. Autopsy studies have reported that congenital bicuspid aortic valve occurs in approximately 1.3% of the population (1,2), and therefore is one of the most common congenital heart malformations. Given that the overall prevalence of congenital heart disease in infants is approximately 0.8% (3–5), with aortic stenosis accounting for 3% to 8% of these lesions (5–7), it is clear that minor malformations of the aortic valve are frequently undetected early in life. Only 2% of patients with congenitally abnormal aortic valve will develop significant stenosis or regurgitation by adolescence (8). Although such valves usually function well during early life, a high percentage will develop progressive valve dysfunction (stenosis and/or regurgitation) over time (9,10) and may require surgical intervention during adult life (11,12).

About 60% to 75% of cases of congenital aortic stenosis are valvular aortic stenosis (13,14). Males are affected more frequently than females, with a ratio reported to be in the range of 3:1 to 5:1 (14,15). Associated congenital heart defects occur in approximately 20% of patients with congenital aortic stenosis (16). The most common associated lesions are ventricular septal defect (VSD), coarctation of the aorta, and patent ductus arteriosus.

There is compelling evidence for an important genetic component in the etiology of aortic stenosis (17,18). Valvular aortic stenosis is known to occur in human genetic syndromes such as Turner syndrome (19) and Jacobsen syndrome (20). Non-syndromic aortic stenosis occurs sporadically or in familial

patterns compatible with autosomal dominant or multifactorial inheritance (20–22). Affected individuals within the same family can have a spectrum of cardiovascular malformations ranging from isolated bicuspid aortic valve to hypoplastic left heart syndrome. This observation not only suggests that at least some cases are caused by single-gene defects, but also that the anomalies in the spectrum of left ventricular outflow tract obstruction lesions are developmentally related. A study of first-degree relatives of 38 patients with hypoplastic left heart demonstrated that 19% had congenital cardiovascular malformations, 72% of which were left heart obstructive lesions (23). Because the recurrence risk in offspring appears to be less if the father is affected than if the mother is affected, a role for cytoplasmic inheritance of congenital aortic stenosis has been suggested as well (24).

Autosomal dominant transmission of *NOTCH-1* gene mutations has been shown to be associated with bicuspid aortic valve in some families (25). *NOTCH* genes encode transmembrane receptor proteins that are important regulators of cellular differentiation, proliferation, and specification. Genetic linkage analyses have identified several chromosomal loci associated with bicuspid aortic valve and other left ventricular outflow obstructions within pedigrees (26). Specific genes at these loci that are responsible for aortic valve development are yet to be identified. It is likely that multiple genes at different loci are involved, coding for transcription factors, extracellular matrix proteins, and signaling pathway elements that regulate cell proliferation and apoptosis.

Mechanical factors, including abnormal fluid forces, have also been implicated in the etiology of anomalies in the spectrum of left ventricular outflow tract obstruction (27). Premature closure of the foramen ovale, with resultant diminution of fetal left heart flow volume, has been associated with hypoplastic left heart syndrome (28). Manipulation of left heart flow in chick embryos leads to various forms of left ventricular outflow tract obstruction (29). It appears, then, that congenital aortic stenosis may arise from a complex interaction of genetic factors, with influence of environmental factors as well. These factors and mechanisms are not fully elucidated to date.

Approximately one-half of patients with normally functioning but abnormal bicuspid aortic valves have significant aortic root dilation (30). Mechanical factors and genetic factors have been implicated. Even without clinical stenosis, the flow velocity distribution in the ascending aorta is asymmetrical and eccentric in patients with bicuspid aortic valve, with uneven stress distribution on the aortic wall (31). The rightward anterior aspect of the ascending aorta is typically subject to increased stress, and this area has been shown to exhibit pathologic changes in the vascular smooth muscle (32). Further evidence that abnormal flow patterns contribute to aortic root dilation is the fact that patients with fusion of the left and right valve cusps usually have normal-shaped aortic roots, whereas those with right and noncoronary cusp fusion more often have a dilated ascending aorta (33). However, aortic

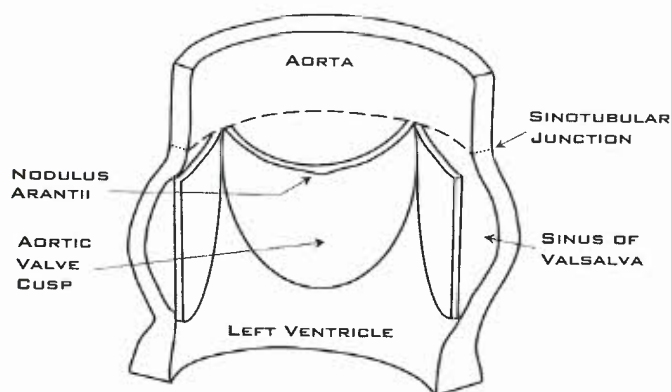


Figure 46.1. Diagram of aortic valve anatomy.

dilation is not strongly correlated with the degree of valve stenosis (34), suggesting a genetic basis. Pedigree analysis of relatives of patients with bicuspid aortic valve and dilated ascending aorta demonstrated a clear genetic link (35). Interestingly, a significant number of relatives had dilated ascending aortas in the absence of bicuspid aortic valve, suggesting a common genetic etiology of these different phenotypes, but specific genes have not been identified. NOTCH-1 mutations, associated with bicuspid aortic valve in some pedigrees, do not correlate with ascending aortic aneurysms (25). Mutations in fibrillin and transforming growth factor-beta genes are associated with ascending aorta dilation and other connective tissue disease manifestations in Marfan and Loeys-Dietz syndromes (see Chapter 34). However, studies have not shown an association of these gene defects with bicuspid aortic valve (36,37).

Embryology and Pathology

The aortic valve develops from three swellings, or ridges, of subendocardial tissue that form when the aortopulmonary septum divides the bulbus cordis and truncus arteriosus into aortic and pulmonary trunks. Cavitation, or “hollowing out,” of these swellings results in transformation into thin and smooth pliable leaflets and the sinuses of Valsalva (Fig. 46.1). The normal aortic valve has three pocket-like cusps, which are approximately equal in size (Fig. 46.2). At the center of the free edge of each semilunar cusp is a fibrous nodule, the

nodule(s) of Arantius, which meet in the center when the valve closes. The valve is surrounded by a fibrous ring, to which the cusps are attached.

The normal aortic valve is composed of three layers (38). The ventricular aspect of the valve leaflets is termed the ventricularis, and is composed of radially oriented elastin fibers. The aortic surface, the fibrosa, is composed of fibroblasts and circumferentially oriented collagen fibers. Between these two layers, at the base of the leaflets, is the spongiosa, a matrix composed primarily of fibroblasts, mesenchymal cells, and mucopolysaccharides.

Stenosis of the aortic valve is due to decreased orifice size that results from cusp fusion and thickening and increased rigidity of the valve leaflets. The most common malformation is the bicuspid aortic valve (Fig. 46.3), with presence of only two cusps. Bicuspid aortic valve results from partial or complete fusion of two of the aortic valve cusps, with or without a central fibrous bridge (raphé) at the site of fusion, resulting in absence of a functional commissure between the fused cusps (1). Enormous variation exists in the morphology of individual bicuspid aortic valves (11). The relative sizes of the conjoined and nonconjoined cusps may be equal or markedly asymmetrical, and the valve orifice may be central or eccentric. Most commonly, in approximately 75% of cases, the right and left cusps are conjoined. Most of the remainder have fusion of the right and noncoronary cusps, and a small minority have fusion of the left and noncoronary cusps. A raphé can be identified in approximately 75% of bicuspid aortic valves, and the raphé can be short or long, cord-like or shallow, and solid or fenestrated.

Although the majority of congenitally malformed aortic valves are bicuspid, other morphologic abnormalities account for some cases of congenital aortic valve stenosis. A unicuspid valve may result from fusion of more than one cusp, resulting in a single slit-like opening that extends to the annulus. All three cusps may be partially fused, resulting in a small central orifice. Rarely, the aortic valve cusps are relatively normal, but hypoplasia of the annulus results in stenosis (39). Myxoid dysplasia of a tricuspid nonfused valve is another uncommon pathologic substrate for congenital aortic stenosis (40).

In addition to the primary morphologic abnormality of the valve cusps, other pathologic features play a significant role in aortic valve dysmorphology and dysfunction. These factors include myxomatous degeneration, fibrosis, inflammatory changes, lipid accumulation, calcification, annular dilatation, and “acquired” fibrotic fusion of true commissures (41).

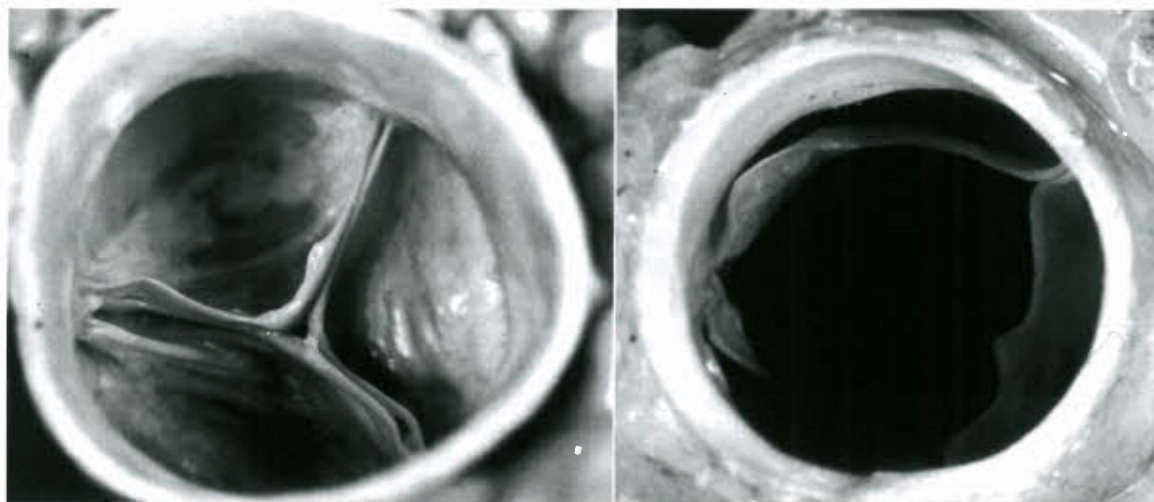


Figure 46.2. Normal aortic valve, as viewed from above. Left panel: Closed. Right panel: Open.

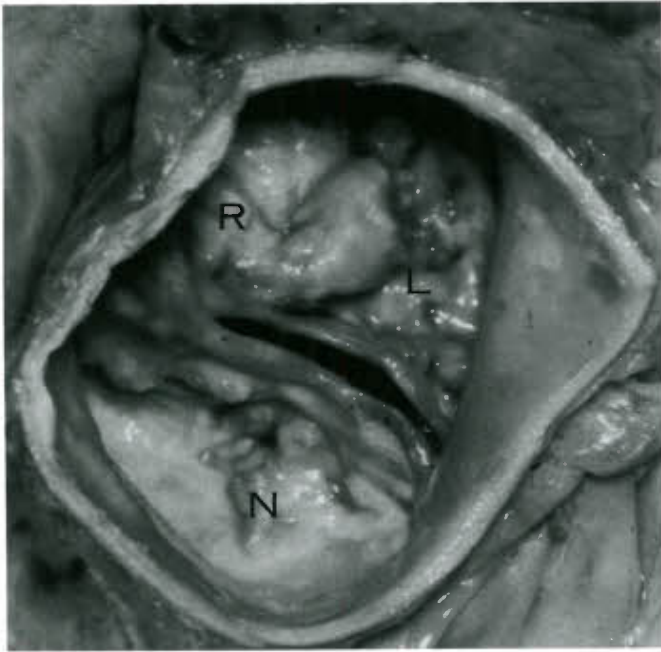


Figure 46.3. Stenotic bicuspid aortic valve. Note fusion of the small right coronary cusp (R) and left coronary cusp (L), with thickened and dysplastic-appearing raphe. N, noncoronary cusp.

These changes progress gradually over time, resulting in cusp thickening, stiffening, and progressive stenosis. Calcification is a rare finding in childhood and adolescence, but is almost universal in older adults with aortic valve stenosis. Calcific aortic stenosis is the third leading cause of adult heart disease (38). Progression of calcification, fibrosis, and degree of stenosis is more rapid in valves with unequal cusp sizes (11) and those with fusion of the right and noncoronary cusps (42). These progressive changes in the valve tissue are in part modulated by mechanical forces (43) and inflammatory processes (44). The mechanical stresses on the leaflets of a nonstenotic, clinically “normal,” bicuspid aortic valve are abnormal due to excessive folding and creasing, extended areas of leaflet contact, significant “morphologic” stenosis, and asymmetrical flow patterns with turbulence (31). Calcification of valve leaflets results from differentiation of mesenchymal cells into bone progenitor cells (45), but the triggers and mechanism of this osteogenic process are not fully elucidated. Increased biomechanical stress has been shown to initiate osteoblastic activity in cultured human aortic valve interstitial cells (46), and may be a major factor in the development of aortic valve calcification. Research is ongoing to delineate the molecular mechanisms that link mechanical stretch and shear stress to fibrosis and calcification of aortic valve leaflet tissue (47).

In some patients with congenitally abnormal aortic valve, cystic medial necrosis leads to an inherently weaker ascending aorta compared to normal (2,3). The media is also thinner than in normal aortas. Patients with congenital aortic valve malformation, therefore, may develop annular dilation as well as dilation or aneurysm of the ascending aorta, with risk of dissection or rupture. These findings are independent of the degree of aortic stenosis (34), but aortic regurgitation is more frequently present in patients with annular dilation. Extracellular matrix protein changes have been demonstrated in the aortas of patients with ascending aorta dilation, but whether these changes represent cause or effect is not known. Metalloproteinase activity is increased (48), and changes in collagen, laminin, and fibronectin have been demonstrated (32,49).

Left ventricular hypertrophy and myocardial fibrosis are seen in some patients with aortic stenosis. These changes may be profound with endomyocardial fibroelastosis and papillary muscle infarction that may be present in infants with severe aortic stenosis. Myocardial fibrosis may also be present in asymptomatic children with hemodynamically moderate congenital aortic stenosis (50). These findings are probably secondary changes resulting from pressure overload, and there is evidence to suggest that they may be at least partially reversible after resolution of pressure overload (51).

Physiology

The fundamental physiologic impact of aortic stenosis is obstruction of left ventricular outflow, resulting in increased afterload. Whereas in patients with normal aortic valves the systolic pressure in the left ventricle approximates the systolic pressure in the aorta, in patients with aortic stenosis the left ventricular pressure exceeds the aortic pressure during ejection. If the stroke volume is normal, the magnitude of the pressure difference reflects the severity of the stenosis.

Despite the elevation in left ventricular peak systolic pressure, the development of wall hypertrophy results in maintenance of normal wall stress, even in relatively severe aortic stenosis (52). Stroke volume, cardiac output, baseline heart rate, and ejection fraction generally remain normal, although in patients with severe symptomatic aortic stenosis, indices of contractility are decreased, and left ventricular end diastolic volume and pressure are increased.

Left ventricular subendocardial ischemia and infarction may occur in patients with valvular aortic stenosis and unobstructed coronary arteries (53). The cause of this ischemia appears to be an imbalance between coronary blood flow to the hypertrophic left ventricle and myocardial oxygen demand that increases due to pressure overload. Because intramyocardial compressive forces are greatest in the subendocardium, and this region is farthest from the epicardial coronary arteries, the subendocardium and papillary muscles are the most vulnerable myocardial regions. Patients with severe aortic stenosis and normal coronary arteries have near-maximum coronary vasodilation at rest (54). Therefore, the principal determinants of subendocardial blood flow, which occurs almost exclusively during diastole, are the length of diastole and the coronary artery driving pressure. Accordingly, the diastolic pressure time index (DPTI), which is the mean diastolic gradient between the left ventricle and aorta multiplied by the length of diastole, is an index of subendocardial blood flow (55). Mathematically, this is represented by the area between the aortic and left ventricular pressure curves during diastole (Fig. 46.4). Similarly, myocardial oxygen demand can be estimated by the systolic pressure time index (SPTI), which is the area under the left ventricular pressure curve during systole. The ratio of DPTI to SPTI has been used to quantify the oxygen supply/demand ratio of the left ventricle (56).

Although, at rest, subendocardial perfusion may be adequate to meet demand, the effects of exercise promote the development of subendocardial ischemia. Since patients with severe aortic stenosis have near-maximal coronary artery vasodilation at rest (54), there is little coronary reserve during stress. Heart rate is a critical factor in the development of a reduction in the oxygen supply/demand ratio. Although exercise stroke volume increases minimally, increased heart rate leads to shortening of both the systolic and diastolic periods. Since the left ventricle has to eject this stroke volume over a shorter time period, the left ventricular systolic pressure increases (57), and this results in increased oxygen demand. The diastolic period shortens even more than the systolic

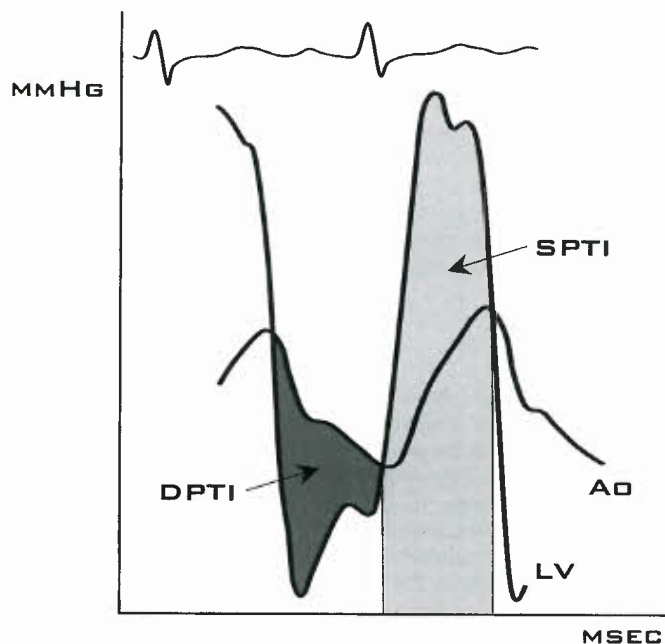


Figure 46.4. Simultaneous pressure tracings from the left ventricle (LV) and aorta (Ao). The systolic pressure time interval (SPTI) is the area under the LV pressure curve during systole, and is a measure of myocardial oxygen demand. The diastolic pressure time index (DPTI) is the area between the aortic pressure and the left ventricular pressure during diastole, and is a measure of myocardial perfusion.

period, resulting in decreased coronary perfusion. In addition, systemic vasodilation that occurs with exercise may result in decreased diastolic blood pressure, also impairing coronary perfusion. Therefore, the effects of exercise decrease the oxygen supply/demand ratio, leading to subendocardial ischemia and even infarction.

Clinical Features and Diagnostic Methods

Symptoms

Outside of patients with symptomatic infantile aortic stenosis (discussed below), most patients with congenital aortic valve stenosis are asymptomatic during childhood. Normal growth and development are the rule. When symptoms occur, those most commonly reported are fatigability, exertional dyspnea, angina pectoris, and syncope (16). Easy fatigability is the most commonly reported symptom. This symptom has been reported by about 15% of patients with mild aortic stenosis and 31% of patients with severe aortic stenosis (58). Interpretation of the clinical significance of this symptom therefore may be difficult. Even in severe aortic stenosis, angina or syncope is uncommon, reported to occur in <10% of patients even with peak-to-peak pressure gradients >80 mm Hg (59). However, when present, angina or syncope suggests severe stenosis and mandates prompt evaluation and treatment.

Physical Exam

Except in children with severe aortic stenosis and congestive heart failure, vital signs are normal. In mild aortic stenosis the apical impulse is usually normal, but with increasing severity of stenosis, the apical cardiac impulse becomes more forceful. The presence of a presystolic tap indicates forceful atrial

contraction and suggests elevated left ventricular end-diastolic pressure. A thrill is palpable in the suprasternal notch in as many as 85% of patients with valvular aortic stenosis. A precordial thrill is also usually present in patients with moderate or severe obstruction.

The first heart sound is usually normal. Splitting of the second heart sound may not be present in severe stenosis due to prolongation of left ventricular ejection, but in most patients even with severe stenosis the second heart sound splitting is normal. In exceptionally severe cases, there may be paradoxical splitting of the second heart sound. A fourth heart sound may be present, indicating severe stenosis with diastolic dysfunction of the left ventricle and high end-diastolic pressure. Although the presence of a third heart sound is common in children and adolescents with normal hearts, it is more frequent in aortic stenosis.

The systolic crescendo-decrescendo murmur of aortic stenosis usually follows an early systolic ejection click, which is loudest at the left lower sternal border or apex, and unlike a pulmonary valve ejection click, the timing and intensity of the click do not vary with the respiratory cycle. The presence of an ejection click and suprasternal notch thrill strongly suggest that the stenosis is valvular rather than subvalvular or supraventricular. The ejection murmur is generally loudest at the upper right sternal border, or in younger children at the upper left sternal border, and it radiates into the neck over the carotid arteries bilaterally. Increasing severity of stenosis is accompanied by a louder, harsher, and later-peaking ejection murmur. In patients with aortic regurgitation, an early diastolic decrescendo murmur may also be present.

Electrocardiography

The resting electrocardiogram usually demonstrates voltage criteria for left ventricular hypertrophy if the aortic stenosis is severe. However, even in patients with peak-to-peak gradient >80 mm Hg, the ECG may be normal in up to one-third of patients (59). In patients with aortic stenosis, ECG criteria for left ventricular hypertrophy do not correlate well with left ventricular mass computed by magnetic resonance imaging (MRI) (60). The resting ECG therefore appears to be a poor discriminator of aortic stenosis severity. The presence of left ventricular hypertrophy with ST segment depression and T-wave inversion in the left precordial leads ("strain" pattern), however, is fairly specific for severe stenosis despite the relatively poor sensitivity.

Twenty-four-hour ambulatory ECG monitoring may demonstrate ventricular dysrhythmias in asymptomatic patients, and there is evidence of a strong relationship between ventricular arrhythmia and sudden death in patients with aortic stenosis (61).

Radiology

In children with aortic stenosis, the heart size on chest radiograph is usually normal or minimally enlarged. In patients with left ventricular hypertrophy, the cardiac apex may be "rounded" in the frontal projection and there may be posterior displacement of the cardiac silhouette in the lateral projection. Left atrial enlargement, if present, strongly suggests a severe degree of stenosis. Pulmonary venous congestion and other signs of congestive heart failure may be present in patients with severe stenosis and left ventricular dysfunction. Enlargement of the ascending aorta is a common finding in older children and adolescents with valvular aortic stenosis. Cardiac MRI or computed tomography (CT) scanning accurately delineates the anatomy of the ascending aorta (Fig. 46.5). Although rarely seen in children, adults with congenital aortic valve stenosis frequently have radiographic evidence of calcification of the valve.

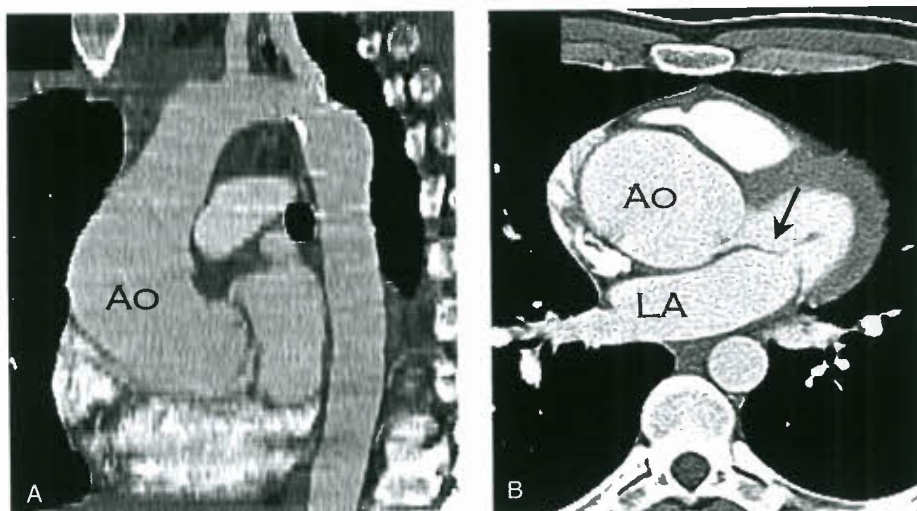


Figure 46.5. Computed tomography images of dilated aortic root in a patient with bicuspid (but not stenotic or regurgitant) aortic valve. The patient has had repair of coarctation of the aorta. **A:** Sagittal view. **B:** Axial view. Ao, aorta; LA, left atrium; black arrow, anterior mitral valve leaflet.

Exercise Testing

The severity of aortic stenosis has been correlated with exercise capacity, systolic blood pressure response, and significant ST segment depression during exercise testing (62–65). Unfortunately, the relatively poor sensitivity and specificity of these findings limit clinical utility. However, exercise testing is usually safe, and in many cases of moderate to severe aortic stenosis may add important and useful information to the clinical evaluation. Exercise-induced ischemic ST segment changes likely reflect subendocardial ischemia due to an imbalance in the oxygen supply/demand ratio precipitated by exercise but not evident at rest (66). Successful gradient reduction by balloon valvuloplasty results in resolution of exercise-induced ischemic ST segment changes (67). In patients felt to have borderline indications for intervention, the exercise test findings may help guide management decisions. As many as 40% of “asymptomatic” aortic

stenosis patients will develop symptoms for the first time during exercise testing (68). Exercise Doppler echocardiography may provide additional information; patients with an 18 mm Hg or greater increase in the mean Doppler gradient during exercise (compared to rest) may have higher risk of cardiac events than those who have <18 mm Hg increase (69).

Echo Doppler

Echocardiography with Doppler evaluation remains the most commonly utilized modality in defining the anatomy and assessing the severity of aortic stenosis. The normal aortic valve has three thin and mobile cusps that open and close symmetrically (Fig. 46.6). Imaging of the aortic valve in different planes allows characterization of the valve anatomy and mechanisms of dysfunction. The long-axis view of the left ventricular outflow tract demonstrates decreased

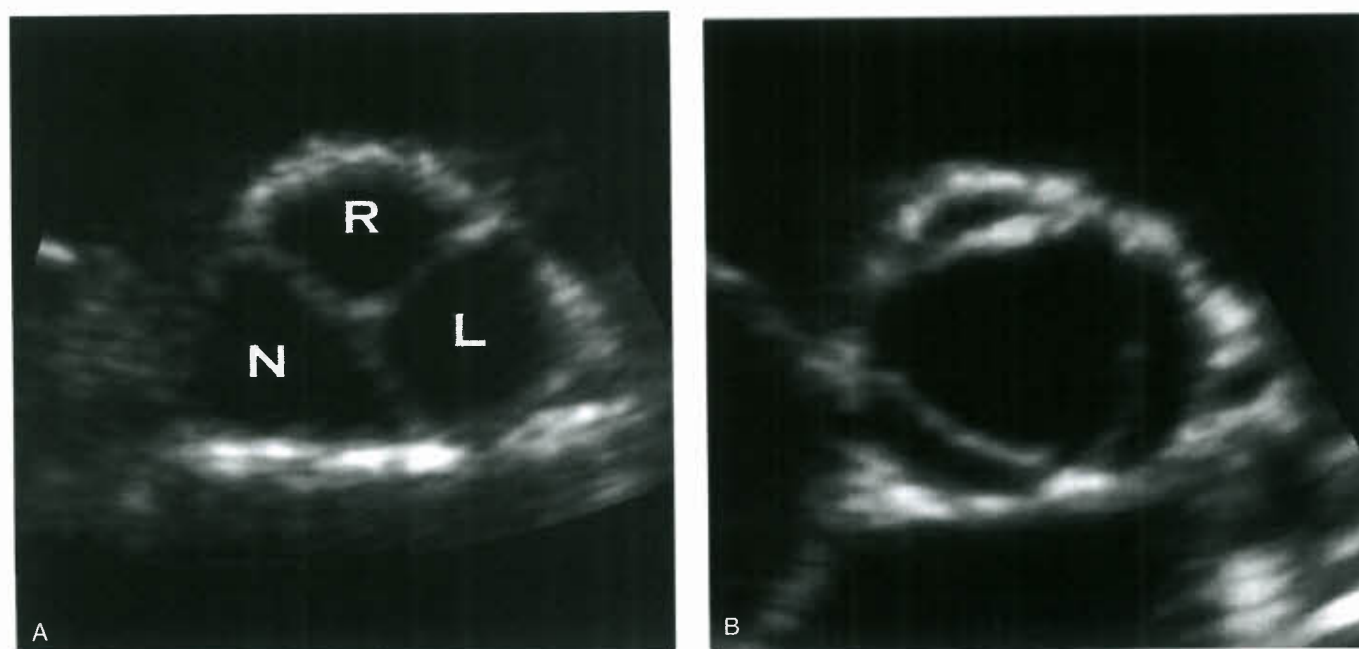


Figure 46.6. Echocardiographic parasternal short-axis views of a normal tricuspid aortic valve. **A:** Diastole. **B:** Systole. R, right coronary cusp; L, left coronary cusp; N, noncoronary cusp.

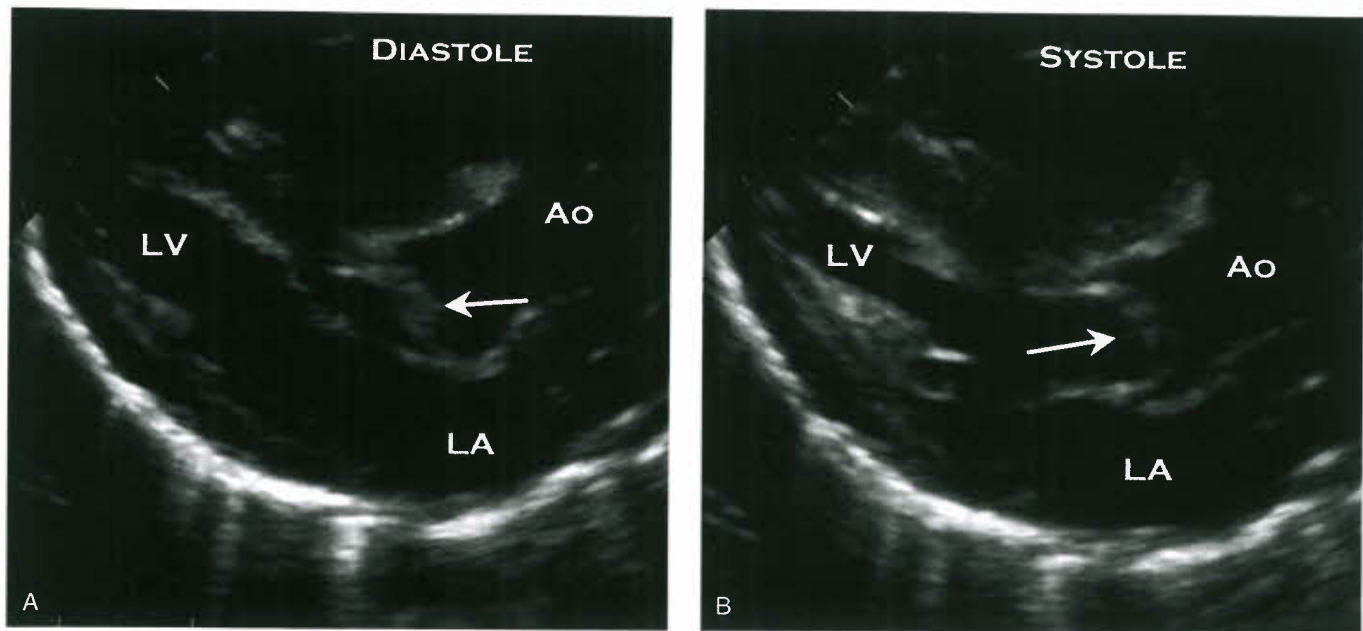


Figure 46.7. Echocardiographic parasternal long-axis views of a stenotic aortic valve. A: Diastole. B: Systole. LV, left ventricle; LA, left atrium; Ao, aorta; arrow, thickened valve leaflets that dome during systole.

valve mobility and systolic doming of the cusps (Fig. 46.7). The aortic valve annulus dimension is best measured in the long-axis view. Imaging in the short axis demonstrates the anatomy of the valve cusps and commissures. Many bicuspid aortic valves have a raphé between the conjoined cusps, and during diastole the valve may appear tricuspid (Fig. 46.8). Careful analysis of the valve motion, however, frequently demonstrates that the valve opens and closes with the “fish mouth” appearance of a bicuspid valve. In addition to details of the aortic valve pathology, evaluation

of left ventricular mass and systolic function are performed, as well as evaluation for other associated defects including other sites of left-sided obstruction. M-mode and two-dimensional measurements are performed to quantitate left ventricular dimensions and shortening fraction. Unfortunately, direct measurement of the orifice area from two-dimensional images has not proven accurate (70,71). Three-dimensional echocardiography may provide more detailed anatomical imaging of the valve morphology and more accurate measurement of the orifice area (72).

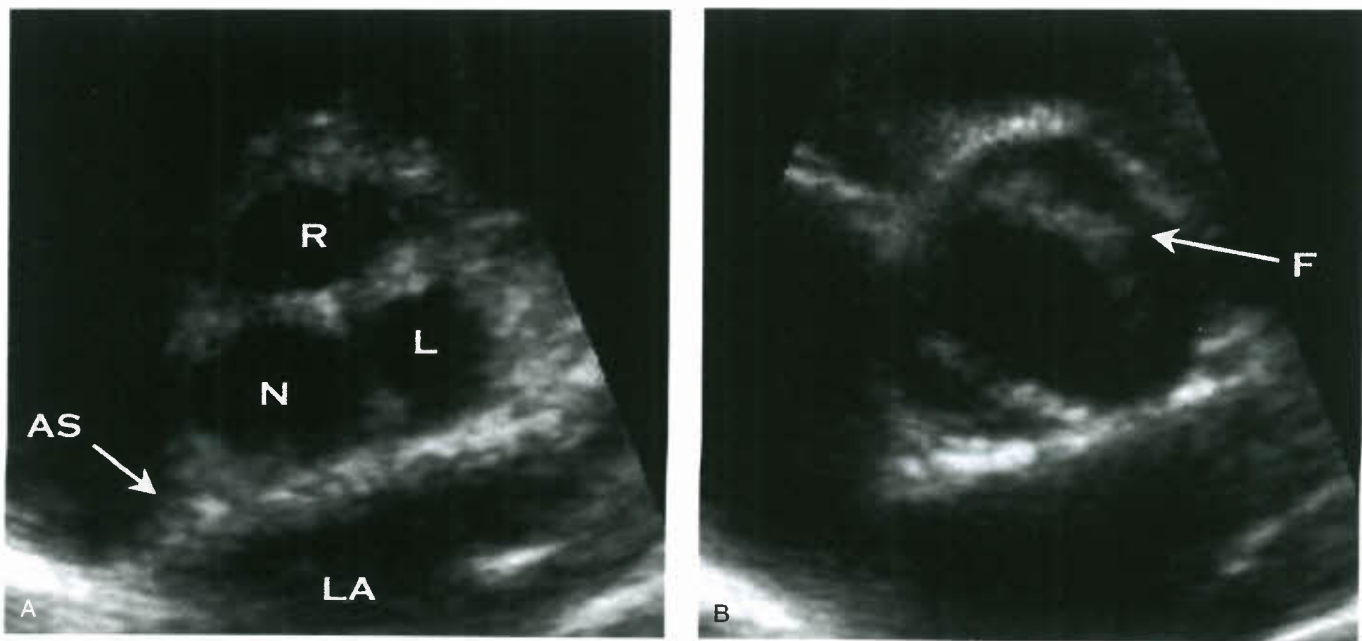


Figure 46.8. Echocardiographic parasternal short-axis views of a bicuspid aortic valve. A: Diastole, with cusps closed and appearance of three separate cusps. B: Valve opening during systole, with fusion of the right and left coronary cusps (F) evident. R, right coronary cusp; L, left coronary cusp; N, noncoronary cusp; AS, atrial septum; LA, left atrium.

Although in most children the acoustic windows allow very good transthoracic imaging of the aortic valve, transesophageal echocardiography (TEE) is useful in patients whose transthoracic imaging is suboptimal. TEE is more sensitive than transthoracic echocardiography for evaluation of vegetations in patients with endocarditis. TEE is also helpful in the perioperative setting to evaluate valve morphology and mechanism of dysfunction prior to repair or replacement, and to evaluate the status of the valve (repaired, autograft, or prosthesis) immediately after weaning from cardiopulmonary bypass.

Color Doppler and spectral pulse and continuous wave Doppler are performed to confirm localization of the obstruction and to quantitate the degree of stenosis. Injecting a fixed stroke volume through a small valve orifice results in rapid flow velocity; this relationship is quantitated by the modified Bernoulli equation, which states that the instantaneous pressure gradient across the valve (in mm Hg) is equal to the flow velocity (m/s) squared multiplied by four (73). The peak instantaneous pressure gradient is calculated using the maximum Doppler velocity, usually obtained by continuous wave Doppler interrogation. The angle of incidence of the Doppler interrogation is important; multiple tracings should be recorded from different views (suprasternal notch, right parasternal, apical, subcostal) and the maximum velocity should be used to calculate the peak instantaneous pressure gradient.

Traditionally, the catheter-derived peak-to-peak pressure gradient has been used to estimate clinical severity of aortic valve stenosis and to guide management decisions. Because the peak pressure in the aorta occurs after the peak pressure is reached in the left ventricle, the Doppler-derived peak instantaneous pressure gradient represents a different physiologic parameter than the catheter-derived peak-to-peak pressure gradient (74) (Fig. 46.9). The peak instantaneous gradient is higher than the peak-to-peak gradient (75), and these two different measurements of pressure gradient are not

interchangeable. In addition, the peak instantaneous Doppler gradient obtained from different echocardiographic windows are not equivalent; the suprasternal notch gradient was significantly higher than the gradient obtained from the apical position in a study designed to evaluate the predictive value of Doppler-derived gradients with respect to those measured in the catheterization laboratory (76). The mean systolic pressure gradient can be calculated from the Doppler spectral profile, and this correlates fairly well with the mean pressure gradient derived from simultaneous catheter recordings (75,77). Some investigators favor using mean pressure gradient to guide clinical decision making (78).

The 2006 American College of Cardiology/American Heart Association Task Force Report Guidelines for the Management of Patients with Valvular Heart Disease (8) recommends the guidelines for grading the severity of aortic stenosis according to the Doppler-derived gradients. Mild stenosis is present when the peak instantaneous gradient is <36 mm Hg (jet velocity 3 m/s) or the mean gradient is <25 mm Hg. Moderate stenosis is present when the peak instantaneous gradient is between 36 and 64 mm Hg (jet velocity between 3 and 4 m/s) or the mean gradient is between 25 and 40 mm Hg. Severe stenosis is present when the peak gradient is >64 mm Hg (jet velocity 4 m/s) or the mean gradient is >40 mm Hg. These guidelines, of course, are valid only in patients with normal ventricular function and absence of other defects, such as a VSD, which can result in a measured gradient that underestimates the true severity of the stenosis due to “pop off” of left ventricular ejection through the VSD.

All pressure gradient estimations depend not only on the severity of the obstruction, but also on underlying hemodynamic conditions, which may vary significantly at different times in the same patient. States of increased contractility or stroke volume will result in higher pressure gradients than states of decreased contractility or stroke volume, and for a given stroke volume, a faster heart rate (decreased ejection time) results in a higher pressure gradient. The same patient may have significantly different gradient measurements during general anesthesia as compared to an alert and anxious state. In addition, patients with severe obstruction may have abnormally low myocardial systolic performance and low cardiac output, resulting in low pressure gradients. For this reason, many clinicians advocate using valve area calculations rather than pressure gradient measurements to gauge the severity of obstruction and guide management decisions.

The most commonly used method to calculate aortic valve area using echocardiography with Doppler involves use of the continuity equation, which simply states that the volume of flow per cardiac cycle is the same at the aortic valve orifice as it is at the mitral valve annulus (79) or in the left ventricular outflow tract below the valve (80). Using the left ventricular outflow tract, one may calculate the aortic valve area (cm^2) by multiplying the LVOT cross-sectional area (cm^2) and the mean velocity in the LVOT (cm/s) and then dividing this by the mean velocity through the valve orifice (cm/s). In children, the aortic valve area should be indexed to body surface area. In full-grown adolescents and adults, the normal aortic valve area is 3.0 to 4.0 cm^2 . The following guidelines classify the degree of stenosis based on valve area: area >1.5 cm^2 (mild stenosis), area between 1.0 and 1.5 cm^2 (moderate stenosis), and area <1.0 cm^2 (severe stenosis). In children, the normal aortic valve area is approximately 2 cm^2/m^2 ; area <0.6 cm^2/m^2 represents severe stenosis (8).

Tissue Doppler imaging may be helpful in assessment of diastolic and systolic left ventricular myocardial dysfunction in patients with aortic stenosis. The presence of symptoms in patients with preserved ejection fraction has been attributed to diastolic dysfunction, with associated elevated filling pressures and increased myocardial stiffness (81). Traditionally,

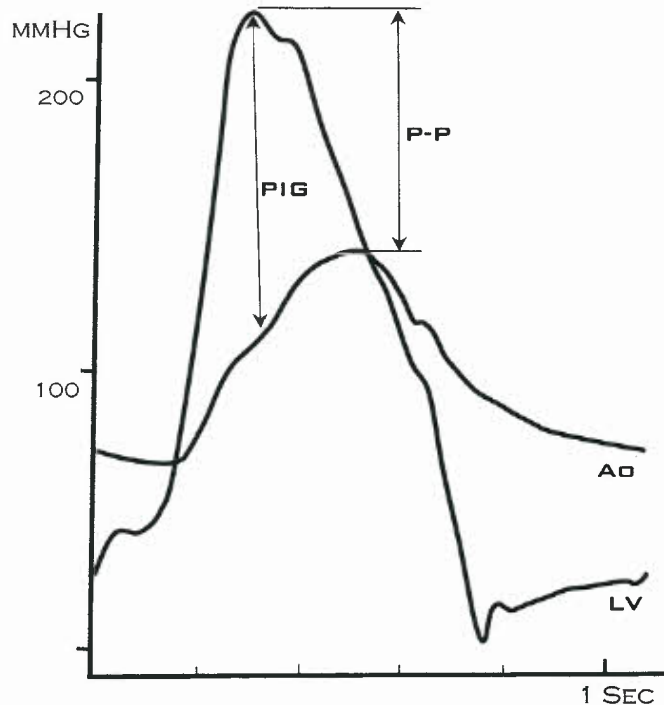
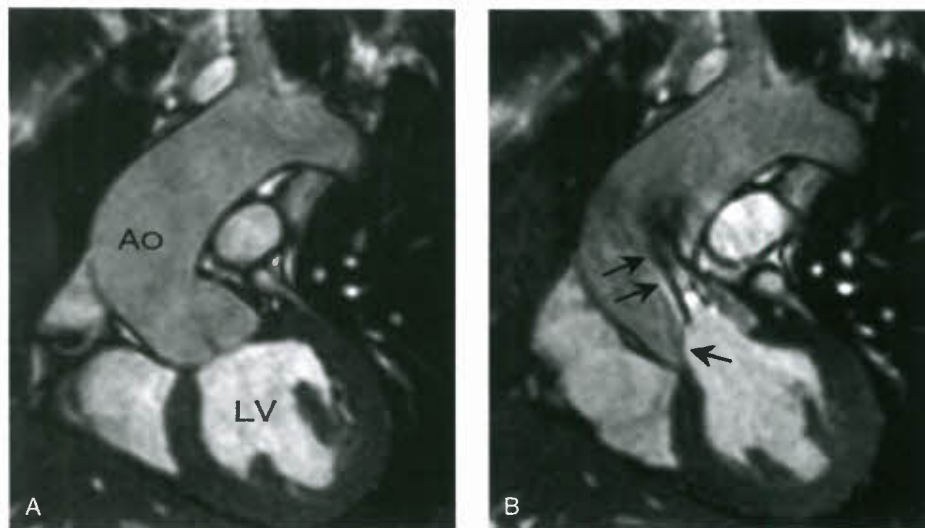


Figure 46.9. Simultaneous left ventricular (LV) and aortic (Ao) pressure tracings demonstrating the difference between peak instantaneous pressure gradient (PIG) and peak-to-peak pressure gradient (P-P).

Figure 46.10. MRI angiogram in a patient with valvular aortic stenosis. **A:** Diastole, with closed valve. The aortic root is dilated. Ao, aorta; LV, left ventricle. **B:** Systole. Doming of the valve leaflets (*single arrow*) and high-velocity jet (*double arrows*) is demonstrated. (Courtesy of E.S. Rivera and T. Geva.)



Doppler parameters derived from mitral or pulmonary vein flow have been used for estimation of left ventricular filling pressure, but these measurements are dependent on loading conditions, heart rate, and other factors that limit clinical usefulness. Use of tissue Doppler imaging to measure systolic and diastolic mitral annular velocities allows quantification of systolic long-axis function and diastolic function. In patients with aortic stenosis, the ratio of early mitral inflow velocity (E) to early diastolic mitral annular velocity (E') correlates with the left ventricular end diastolic pressure (82), thereby providing a clinically useful noninvasive method of assessing diastolic dysfunction. In addition, measurement of the mitral annular systolic velocity (S') by tissue Doppler imaging may demonstrate systolic long-axis dysfunction in patients with aortic stenosis even in the presence of normal ejection fraction and normal indexes of transverse function (82). Because longitudinally oriented fibers are present in the subendocardial region, and the subendocardium is most susceptible to ischemia in patients with aortic stenosis, these fibers are at greater risk than the circumferentially oriented fibers (83). Long-axis dysfunction therefore might be expected to precede transverse axis dysfunction.

Cardiac Magnetic Resonance Imaging

Cardiac MRI (Fig. 46.10) is a useful noninvasive tool for assessment of left ventricular mass and function, and velocity-encoded MRI techniques allow quantification of pressure gradients and aortic valve area. Such measurements have been shown to correlate well with Doppler measurements of the same parameters (84). Cardiac MRI may also accurately define the anatomy of the valve morphology (Fig. 46.11), ascending aorta, annulus size, and coronary artery origins.

Cardiac Catheterization

Due to the evolution of noninvasive techniques that accurately diagnose and evaluate the anatomy and severity of aortic valve stenosis, cardiac catheterization is generally undertaken primarily for the purpose of therapeutic balloon valvuloplasty in patients with known aortic valve stenosis and noninvasive evidence of severe obstruction. However, diagnostic catheterization may still be indicated if the clinical data and noninvasive evaluation are not consistent. Information obtained from cardiac catheterization has been considered to be the “gold standard” to which traditional and emerging noninvasive modalities have been compared. Complete hemodynamic assessment in the catheterization laboratory

includes measurement of cardiac output (Fick technique and/or thermodilution), left ventricular end-diastolic pressure, and pressure gradients (mean and peak to peak). Access to the left ventricle may be either transeptal or retrograde. Angiography of the left ventricle permits evaluation of left ventricular cavity size and function, aortic valve annulus size, degree of leaflet thickening and cusp mobility, patency and origin of the coronary arteries, and the size and contour of the ascending aorta.

Hemodynamic measurements can be used to calculate the effective valve orifice area by the method of Gorlin (85). The aortic valve area is calculated by dividing the aortic valve flow (AVF) by the product of 44.3 and the square root of the mean pressure gradient across the valve.

$$\text{Aortic valve area (cm}^2\text{)} = \frac{\text{AVF}}{44.3 \sqrt{\text{mean pressure gradient}}}$$

The AVF, which occurs during systole, is determined from the cardiac output and systolic ejection period (SEP). The systolic ejection time (SET) for a single cardiac cycle is measured

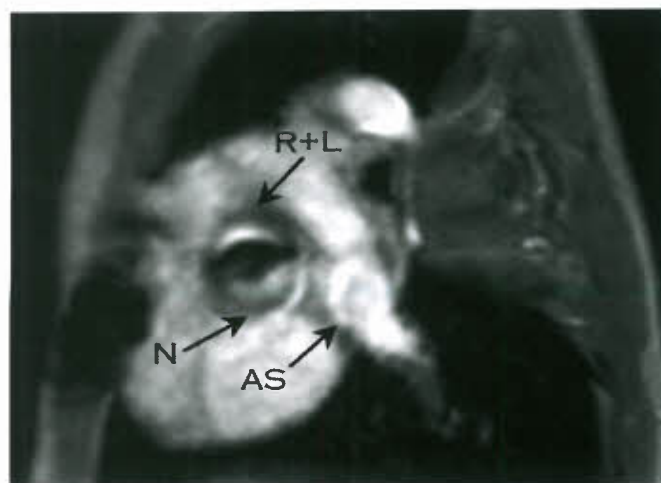


Figure 46.11. MRI image of bicuspid aortic valve. Although a raphe is not visualized, there is fusion of the right and left coronary cusps (R+L). N, noncoronary cusp; AS, atrial septum. (Courtesy of E.S. Rivera and T. Geva.)

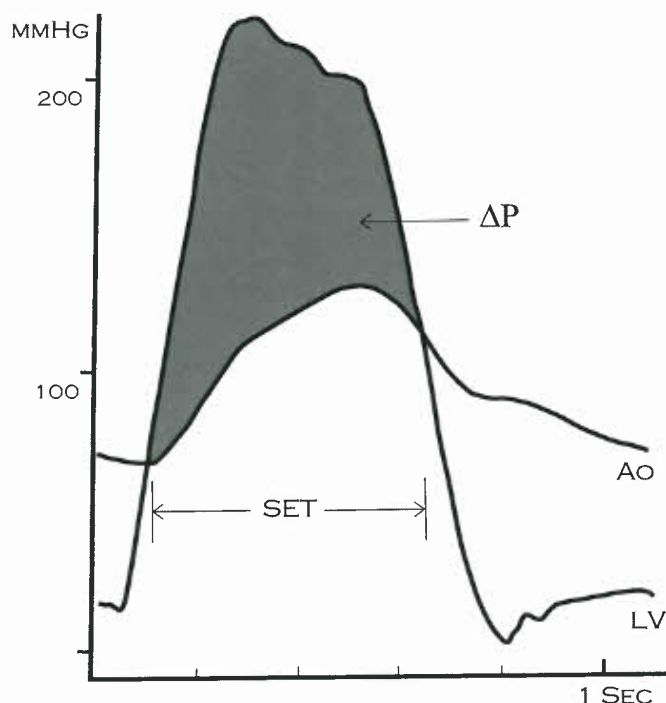


Figure 46.12. Pressure tracings from the aorta (Ao) and left ventricle (LV) used for calculation of the aortic valve area using the Gorlin equation. The systolic ejection time (SET) is the time period during which there is flow through the valve orifice into the aorta, and this occurs during the period of time when the left ventricular pressure is greater than the aortic pressure. The shaded area (ΔP) represents the pressure gradient, from which the mean pressure gradient during systole can be calculated using planimetry.

from simultaneous pressure tracings from the aorta and left ventricle (Fig. 46.12), which by multiplying by the heart rate gives the SEP per minute (s/min).

$$\text{SEP (s/min)} = \text{SET (s/beat)} \times \text{HR (beats/min)}$$

The AVF (mL/s) is then determined by dividing the cardiac output (mL/min) by the SEP (s/min).

$$\text{AVF (mL/s)} = \frac{\text{Cardiac output (mL/min)}}{\text{SEP (s/min)}}$$

The mean pressure gradient (mm Hg) is determined by planimetry using simultaneous pressure tracings from the aorta and left ventricle. The aortic valve area (cm^2), then, is calculated by taking the square root of the mean pressure gradient and multiplying this by 44.3, then dividing this into the AVF. In theory, the aortic valve orifice area represents the most reliable index of stenosis severity, more reliable than other parameters (such as pressure gradients) that are dependent on loading conditions and heart rate. Unfortunately, the calculation of the valve area may not always accurately reflect the degree of obstruction seen clinically. Measurements used in calculation of aortic valve area must be made with extreme care and precision, and the calculated aortic valve area should be considered along with the entire body of clinical data when formulating management decisions.

Natural History

The natural history of aortic stenosis is not completely known, due largely to the fact that techniques for diagnosing and quantitating aortic stenosis have developed simultaneously with the evolution of surgical and transcatheter treatment modalities. The 1993 Report from the Second Joint Study on the Natural History of Congenital Heart Defects (NHS-2) represents the study with the largest number of patients and longest follow-up period. However, this report still only provides complete data on 235 patients (51% of the original NHS-1 cohort) with median follow-up of 22.5 years (range 17 to 29 years; ages 17 to 49 years) (86). In addition, congenital aortic valve disease encompasses a wide spectrum from critical infantile aortic stenosis to normal functioning bicuspid aortic valve. Only about 1 in 50 of the 1.3% of the population with congenitally bicuspid aortic valves will develop significant valve dysfunction by adolescence (8).

Despite the lack of very long-term intervention-free data, natural history studies have provided important information. Patients who present in infancy with aortic valve stenosis generally have more severe stenosis and higher mortality with or without treatment (87–89). Twenty-five of the patients in the original NHS-1 cohort (90) were <2 years old; the 1-year survival rate was 64%, and most had undergone surgical intervention. In contrast, the 25-year survival in patients who were 2 years of age or greater at the time of original enrollment was 85%. An older study by Campbell (14), published in 1968, found that the mean age of death in patients with aortic stenosis was 35 years, with 40% mortality by age 30 and 60% mortality by age 40. Over half of the patients who died had sudden unexpected death, whereas most of the remaining deaths were due to progressive congestive heart failure. The notion that sudden death is extremely rare in the absence of preceding symptoms has been challenged by several recent studies including NHS-2 (86,91,92). About half of sudden death cases from aortic stenosis occur during or immediately after exercise (93). In the current era, children with aortic stenosis treated by balloon valvuloplasty have an extremely low risk of sudden unexpected death (94).

Although mild aortic stenosis may remain mild for many years (86), progression over time is the rule (14,91,95–97). The rate of progression is highly variable in individual patients. The rate of progression may be greater in children than in adolescents and adults due to inability of the valve orifice to increase in proportion to somatic growth (98). Outcome is highly correlated with the initial gradient, with those having higher gradients at the time of diagnosis developing symptoms, dying, or requiring valve replacement sooner than those with lower gradients (86,91). In addition to the progression of aortic stenosis, many patients will develop significant and progressive aortic valve regurgitation over time, particularly if they have had surgical valvotomy or percutaneous balloon valvuloplasty (86). Patients with fusion of the right and noncoronary cusps are at risk of more rapid progression of valve dysfunction (99).

Risk of bacterial endocarditis has been reported to be as high as 1% per year (14), but the risk is probably less based on the data from NHS-2, where the incidence rate was 27.1 cases per 10,000 person-years (100) (0.27% per year). Although bacterial endocarditis risk is present even in patients with bicuspid aortic valve without stenosis, the incidence of endocarditis is higher in patients with more severe stenosis.

Treatment

Medical Treatment and Balloon Valvuloplasty

Because progression of valve dysfunction is the rule, medical management is essentially expectant, with timing of intervention being the primary focus. There are currently no medical

therapies known to alter the progression of aortic valve dysfunction. Because adult aortic stenosis is a progressive process that resembles atherosclerosis, the effect of lipid-lowering medical therapy with statins has been studied, but has not been shown to be helpful in curbing the progression of aortic valve changes (101). In contrast to older adults with aortic stenosis, for whom intervention is recommended only when symptoms develop or are considered imminent (8,102), indication for intervention in children and adolescents is more liberal. Whereas for older adults 20-year survival is considered long-term, in children and adolescents the goal is survival for many decades. In asymptomatic patients with severe congenital aortic stenosis, relief of the obstruction likely reduces the risk of sudden cardiac death and decreases the extent of subtle and progressive myocardial injury and interstitial myocardial fibrosis (91,92,103,104).

Although surgical valvotomy may still be performed, balloon valvuloplasty (105) has generally supplanted open surgical valvotomy as initial treatment for congenital aortic valve stenosis in infants, children, and adolescents. Both procedures are generally safe and effective in relieving the obstruction (106), but in either case, subsequent progression of stenosis and/or valve regurgitation is anticipated (88,107–112), with valve replacement considered to be the eventual definitive treatment. Nevertheless, balloon aortic valvuloplasty in many cases postpones the need for surgery by several years, even decades (111,112). A retrospective study of late outcomes after balloon aortic valvuloplasty in children (109) showed a freedom from reintervention rate of 46% at 12 years. In infants and children, delaying the need for valve replacement can allow for growth, permitting insertion of a larger replacement valve when valve replacement becomes necessary. Predictors of less favorable outcome and need for early reintervention or surgery include small aortic annulus, depressed left ventricular function, and mitral valve dysfunction (110).

Adults with congenital aortic valve stenosis generally have developed valve calcification, diminishing the chances of good results from either surgical valvotomy or balloon valvuloplasty, and therefore valve replacement is the primary treatment beyond young adulthood. In older patients with severe aortic stenosis who are not surgical candidates, balloon valvuloplasty is associated with poor survival (113), but has been shown to be a successful bridge to transcatheter aortic valve implantation (114). Children and adolescents with aortic stenosis who have significant aortic valve regurgitation (either native disease or after previous valvotomy or balloon valvuloplasty) also require valve replacement therapy (or surgical repair) rather than valvotomy or balloon valvuloplasty.

The American Heart Association 2011 Scientific Statement on Indications for Cardiac Catheterization and Intervention in Pediatric Cardiac Disease (115) provides guidelines for the management of infants and children with congenital aortic valve stenosis. Given the absence of clinical trial data, these recommendations are based on nonrandomized studies and expert opinion rather than data from randomized prospective clinical trials. For infants with isolated critical ductal-dependent valvular aortic stenosis, or any infant or child with isolated aortic stenosis with left ventricular systolic dysfunction, balloon valvuloplasty is indicated regardless of the measured pressure gradient. Most infants and children with aortic stenosis are asymptomatic, however, and the guidelines recommend that the catheter gradient should be measured. If the catheter-measured peak-to-peak gradient is ≥ 50 mm Hg, then balloon valvuloplasty is indicated. If the patient desires to play competitive sports, become pregnant, has ischemic or repolarization changes on rest or exercise ECG, or has symptoms of angina or syncope, then balloon valvuloplasty is justified if the peak-to-peak gradient is ≥ 40 mm Hg. Other causes of the symptoms or ECG changes should be sought if the gradient is

<40 mm Hg. Valvuloplasty is not recommended for asymptomatic patients with peak-to-peak gradient <40 mm Hg unless cardiac output is impaired, in which case, the gradient underestimates the true severity of the obstruction.

These guidelines are intended for patients under conscious sedation. For patients under deep sedation or general anesthesia, the measured gradients are likely to be lower, and the guidelines state that it is reasonable to consider balloon valvuloplasty in asymptomatic patients if the mean Doppler gradient when not sedated is >50 mm Hg, even if the measured catheterization-derived peak-to-peak gradient is <50 mm Hg. However, given the relatively slow rate of progression of stenosis outside of infancy (86), caution should be exercised in borderline cases due to the risk of introducing significant aortic regurgitation that might progress and necessitate valve replacement sooner than might have occurred without intervention.

For patients with milder degrees of aortic stenosis, periodic follow-up with interval medical history, physical examination, 12-lead ECG, and echo Doppler study is recommended (8). According to the American College of Cardiology/American Heart Association 2006 Guidelines for the Management of Valvular Heart Disease (8), for adolescents and young adults with peak Doppler gradients <50 mm Hg or mean gradients <30 mm Hg, follow-up is recommended every 2 years. For those with peak Doppler gradients >50 mm Hg or mean gradients >30 mm Hg, follow-up should be yearly. These guidelines seem reasonable for most children as well, although infants and young children should be followed more closely as progression of aortic valve dysfunction may be more rapid. Exercise ECG testing should be considered for patients who are interested in athletic participation. If the clinical findings and the echo-Doppler evaluation are disparate, then cardiac catheterization may be indicated for complete hemodynamic assessment including direct measurement of the peak-to-peak gradient.

The 36th Bethesda Conference Task Force recommendations for competitive athletics (116) defines patients to have mild aortic stenosis if the catheter-derived peak-to-peak gradient is <30 mm Hg, the mean Doppler gradient is <25 mm Hg, or the peak instantaneous Doppler gradient is <40 mm Hg. Such patients are permitted to participate in all competitive sports if they are asymptomatic and have normal exercise tolerance. Asymptomatic patients with moderate aortic stenosis (peak-to-peak gradient 30 to 50 mm Hg, mean Doppler gradient 25 to 40 mm Hg, or peak Doppler gradient 40 to 70 mm Hg) may participate in sports with a low static component and low-to-moderate dynamic component (such as golf, bowling, baseball/softball, and volleyball) so long as they have only mild or absent left ventricular hypertrophy, absence of repolarization abnormality on ECG, and a normal exercise test. In addition, if such patients also have no history of supraventricular tachycardia or ventricular tachyarrhythmia at rest or with exercise, then they may participate in sports with moderate static component and low dynamic component (such as diving, archery, equestrian, and motorcycling). Patients with severe aortic stenosis (peak-to-peak gradient >50 mm Hg, mean Doppler gradient >40 mm Hg, or peak Doppler gradient >70 mm Hg) should not participate in any competitive sports. For aortic valve stenosis patients who also have significant aortic regurgitation, these recommendations must be considered in concert with the Task Force recommendations for aortic regurgitation.

Even in the absence of stenosis or significant regurgitation, patients with bicuspid aortic valve are at risk of progressive aortic root dilation and aortic dissection; the mortality risk is as high in younger patients as in those over 40 years old (117). The risk of aortic dissection is nine times greater in patients with a bicuspid aortic valve compared to those with

a tricuspid aortic valve (10). Because of the high prevalence of bicuspid aortic valve, it is a more common etiology of aortic dissection than Marfan syndrome (118). In children, dilation is usually mild and aortic complications are rare (119). However, approximately half of young adults with a bicuspid aortic valve have significant aortic root dilation (30). Most patients with aortic dissection have hypertension (120,121), and this helps to explain the strong association of aortic dissection with bicuspid aortic valve and aortic coarctation (10). Aggressive and meticulous management of hypertension is therefore the mainstay of medical treatment. Although the benefit of prophylactic β -blocker or angiotensin converting enzyme (ACE) inhibitor therapy has not been proven in normotensive patients with aortic root dilation associated with congenitally abnormal aortic valve, such treatment is reasonable for those patients who tolerate β -blockers or ACE inhibitors. The angiotensin receptor blocker losartan is an antihypertensive medication that also inhibits transforming growth factor- β signaling, and is now frequently used in this setting. Increased transforming growth factor- β signaling has been implicated as an important factor in aortic root dilation in Marfan syndrome, Loeys-Dietz syndrome, and some patients with familial thoracic aneurysm and dissection (122), but this mechanism has not been demonstrated in patients with bicuspid aortic valve-associated aortic dilation. Nevertheless, the potential association in some patients may justify the use of losartan as the antihypertensive medication of choice in this setting. Because aortic root dilation is a precursor of aortic dissection, careful surveillance with serial noninvasive imaging examinations is warranted to detect progressive aortic root dilation so that prophylactic surgery can be performed preemptively before aortic dissection occurs. Prophylactic surgery is sometimes recommended in asymptomatic adolescents or young adults if the aortic diameter reaches 4.5 cm (or 2.5 cm/m²) in diameter (123), or if the rate of growth of the aorta is rapid and out of proportion to somatic growth (124).

Pregnancy can be managed conservatively in women with mild aortic stenosis and normal left ventricular function (8). In women with moderate to severe aortic stenosis, pregnancy should be deferred until the stenosis is successfully treated by valvuloplasty or valve replacement. Women with moderate to severe aortic stenosis who become pregnant should be followed closely. If symptoms develop or left ventricular dysfunction develops, consideration should be given to either balloon valvuloplasty or surgery (8). If significant aortic root dilation is present, there is risk of aortic dissection, particularly in the third trimester, and the aortic root size should be followed closely along with careful attention to blood pressure control.

Infective endocarditis prophylaxis precautions are no longer recommended for patients with congenital aortic valve stenosis (125). However, those with prosthetic valves or surgically repaired valves with prosthetic material remain candidates for premedication with antibiotics in the event of a procedure expected to induce bacteremia.

Aortic Valve Surgery

Aortic valve replacement is usually required in patients who develop progressive aortic valve regurgitation or recurrent stenosis refractory to balloon valvuloplasty. Surgical repair of the aortic valve (126) may be possible in some cases, although generally such repairs are considered palliative, as with balloon valvuloplasty, with eventual expectation of valve replacement. Replacement with a mechanical prosthesis currently provides the most durable result, but the patient must be anticoagulated and there is no growth potential, both of which are very significant problems in small children. Use of bioprosthetic valves, either homograft or heterograft, prevents the need for anticoagulation, but growth potential is still a major issue, and

the longevity of these valves is frequently poor, particularly in small children. In some centers, the Ross procedure (127) is the preferred procedure, particularly in infants and small children. In this procedure, the patient's pulmonary valve is translocated to the aortic position, and a pulmonary homograft is implanted in the pulmonary valve position. The need for anticoagulation is avoided, and importantly the autograft (neo-aortic valve) has growth potential. The major disadvantage of the Ross procedure is that pulmonary homograft dysfunction is universal, frequently relatively early in children. Given current technology, children who undergo a Ross procedure can expect several additional procedures over their lifetime for recurrent pulmonary homograft dysfunction. In addition, progressive neo-aortic valve dysfunction, with or without dilation of the neo-aortic root, is not uncommon over time. However, modifications of the Ross operation have reduced the incidence of these complications, and in many cases, the function of the autograft valve remains excellent for many years (128–130).

Percutaneous aortic valve implantation is a promising new technique that has been developed as an alternative to surgical valve replacement in adult patients with severe aortic stenosis who are deemed inoperable (131). Currently, this procedure is not an option for children and adolescents with congenital aortic stenosis, but results in inoperable elderly patients and in patients with high surgical risk have shown significant improvement in survival compared to medical treatment (132) and similar rates of survival at 1 year compared to surgical replacement (133). As advances are made in device materials and design, and implantation techniques are refined, transcatheter aortic valve replacement may be a viable option for children and adolescents in the future.

Long-Term Outcome

Congenital aortic valve disease is a lifetime disease. Although interventional and surgical techniques have resulted in marked improvement in the prognosis of this disease, there is no currently available medical, interventional, or surgical approach that renders the aortic valve normal. Given the relatively high incidence of congenitally abnormal aortic valve and the likelihood of eventually developing clinically important complications, this condition may be responsible for more deaths and morbidity than all other forms of congenital heart disease combined (10,134). Lifelong follow-up of these patients is mandatory. As new valve replacement technologies and techniques evolve, continued improvement in outcomes should follow.

VALVULAR AORTIC STENOSIS IN INFANCY

Clinical Features

Although the majority of patients with congenital aortic valve stenosis are asymptomatic in childhood, approximately 10% present during infancy with symptoms and signs of congestive heart failure (89). Improvements in fetal imaging and diagnosis have led to prenatal diagnosis of severe aortic valve stenosis in many cases (135). Anatomically, the valve may be bicuspid or unicuspid, with thickening and myxoid dysplasia. In some patients, there may be no identifiable cusps or commissures.

In utero, the presence of mild or moderate aortic stenosis results in increased left ventricular pressure and possibly left ventricular hypertrophy, which may be well tolerated. With more severe stenosis, the left ventricular hypertrophy is more severe, and the resultant decrease in left ventricular compliance may lead to decreased flow through the left heart and ultimately in hypoplasia of the left ventricle, mitral valve, aortic

valve annulus, and left ventricular outflow tract. Coarctation of the aorta may also be present, with or without hypoplasia of the ascending aorta. Endomyocardial fibroelastosis and/or papillary muscle infarction may occur due to oxygen supply/demand mismatch, and severe fetal aortic stenosis may evolve into hypoplastic left heart syndrome (136). The fetus usually tolerates severe aortic stenosis, even in cases of severe left ventricular hypoplasia, since the right ventricle is capable of handling the entire cardiac output. Once the fetus is born and separated from the placental circulation, however, symptoms may develop rapidly.

If the left ventricular size and function are adequate to handle the entire cardiac output, symptoms and signs may be mild or absent even after closure of the ductus arteriosus. However, poor feeding, tachypnea, and growth failure may occur. A systolic murmur is usually present, and gallop rhythm may be noted. Hepatomegaly may be present, and peripheral pulses may be weak.

In more severe cases of neonatal aortic stenosis, the left heart may not have the capacity to handle the entire cardiac output and closure of the ductus arteriosus may result in circulatory collapse. Such infants are pale and poorly perfused, with poor pulses, hepatomegaly, tachycardia, gallop rhythm, hyperdynamic right ventricular impulse, tachypnea with retractions, and usually (but not always) a systolic heart murmur (88). Such infants may appear well prior to closure of the ductus arteriosus, which may not occur for several days after birth. Careful attention to the neonatal physical exam findings, such as hyperdynamic right ventricular impulse and differential cyanosis, is necessary to avoid presentation in extreme cardiovascular collapse after discharge from the hospital. Routine neonatal screening with upper and lower extremity pulse oximetry has been recommended by some for early detection of ductal-dependent left heart obstructive lesions.

Evaluation and Management

Echocardiography with Doppler evaluation confirms the diagnosis and delineates the details of the anatomy in infants with critical aortic stenosis. The aortic valve is frequently thickened with reduced mobility and a small orifice. The left ventricle is usually hypertrophic with relatively small cavity size, but it may be dilated and poorly contractile. Abnormally increased echogenicity of the endomyocardium and/or mitral valve papillary muscles may be present (Fig. 46.13), representing endomyocardial fibroelastosis and/or papillary muscle infarction. The right ventricle is frequently enlarged. Careful assessment of the size and function of the left ventricle and mitral valve is imperative, as is evaluation for other left-sided obstructions such as aortic coarctation, cor triatriatum, supraannular mitral stenosis, and pulmonary vein stenosis. The ascending aorta may be hypoplastic or dilated.

Doppler interrogation of flow in the proximal ascending aorta demonstrates increased velocity and turbulence. The calculated gradient, however, may underestimate the severity of the stenosis if left ventricular function is depressed, a significant portion of the systemic cardiac output is provided by the right ventricle via the patent ductus arteriosus, and/or there is significant left ventricular ejection ("pop off") through a VSD. The status of the ductus arteriosus and the direction and magnitude of ductal flow is an essential part of the evaluation, including the direction of flow in the distal aortic arch.

Initial management of neonatal critical aortic stenosis consists of maintaining ductal patency with prostaglandin E₁ infusion, inotropic support if the left ventricular function is impaired, and avoidance of supplemental oxygen if the systemic circulation is ductal dependent. If mechanical ventilation is necessary, hyperventilation should be avoided.

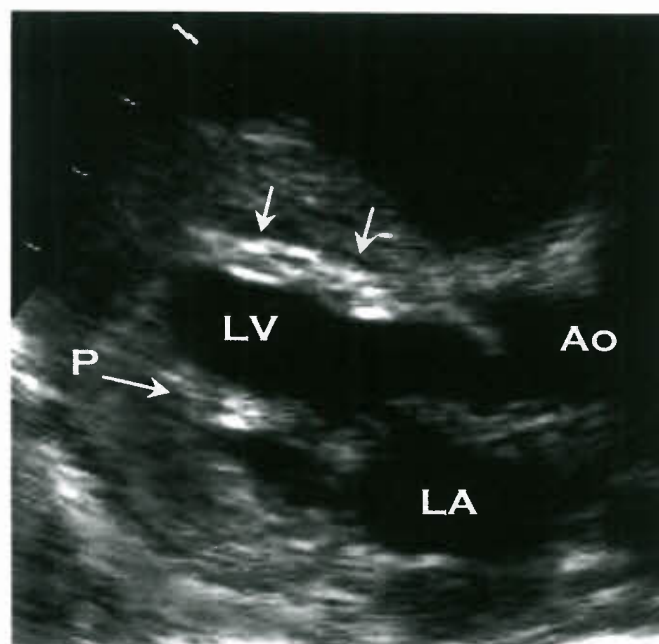


Figure 46.13. Echocardiographic parasternal long-axis image in an infant with critical aortic stenosis demonstrating severe endomyocardial fibroelastosis (double arrows) and infarcted papillary muscle (P). LA, left atrium; LV, left ventricle; Ao, aorta.

In neonates with critical aortic stenosis and small left ventricle, more definitive management involves a decision regarding adequacy of the left heart to support a two-ventricle circulation. Several studies have addressed methods of quantitatively assessing the adequacy of the left heart to handle the entire systemic circulation. Infants with non-apex-forming left ventricle, small aortic annulus (<5 mm), and small mitral valve annulus (<9 mm) may have improved survival with Norwood-type palliation or cardiac transplant than with treatment strategies to achieve a two-ventricle circulation (137). Rhodes et al. (138) developed a predictive equation for success of two-ventricle management plan in neonates with isolated critical aortic stenosis. The parameters that were most predictive of success or failure included aortic root dimension indexed to body surface area, the ratio of the long axis of the left ventricle to the long axis of the heart, and the indexed mitral valve area. In a prospective multicenter analysis performed by the Congenital Heart Surgeons Society (139), a regression equation was used to predict 5-year survival probability with Norwood-type palliation versus two-ventricle approach. Discriminating parameters included age, z-score of aortic valve, grade of endomyocardial fibroelastosis, diameter of ascending aorta, presence of significant tricuspid valve regurgitation, and z-score of left ventricular length. Significant retrograde flow in the distal aortic arch via the patent ductus arteriosus is also associated with lower likelihood of success with a two-ventricle approach (140). Cardiac MRI may provide more accurate quantification of left ventricular size, morphology, and function than echocardiography, and therefore might improve decision making regarding the choice of treatment approach (141).

For infants with severe or critical isolated aortic valve stenosis deemed to have adequate left heart structures for two-ventricle circulation, initial therapy usually entails balloon valvuloplasty or surgical valvotomy (open or transventricular). Although some advocate open surgical valvotomy as the treatment of choice for critical neonatal aortic stenosis (142), studies have demonstrated similar outcomes with the less invasive percutaneous

balloon valvuloplasty procedure (143,144), which in most centers is the preferred procedure in the majority of cases. It appears that open surgical valvotomy may result in higher likelihood of residual or recurrent stenosis, whereas balloon valvuloplasty may be associated with a higher incidence of important aortic regurgitation (145). Techniques for balloon aortic valvuloplasty include antegrade approach via the foramen ovale from venous access, as well as retrograde approach via femoral, umbilical, or carotid artery access (146). As with children and adolescents, balloon valvuloplasty is considered palliative. In a retrospective review of 113 neonates who underwent balloon aortic valvuloplasty, the reintervention-free survival was 48% at 5 years (147). The goal is to postpone the need for surgery, which likely is inevitable in the vast majority of patients.

Given the issue of growth, as well as the poor durability of tissue valves in the aortic position in infants, aortic valve replacement with mechanical or bioprosthetic valves is an undesirable option in neonates and infants with congenital aortic stenosis. The Ross procedure (pulmonary autograft), with Konno-type enlargement of the aortic annulus, may offer a durable aortic valve with growth potential and is thus a viable option as primary therapy for severe aortic stenosis in infants (148). Resection of endomyocardial fibroelastosis may increase growth potential of the borderline left ventricle. Although the results of this technique have not been systematically compared with surgical valvotomy or balloon valvuloplasty, anecdotal success has been reported (149). Another surgical approach in neonates with critical aortic stenosis and borderline left ventricle is to perform a stage I Norwood operation with subsequent reoperation to achieve a two-ventricle repair (150). More recently, temporary palliation has been accomplished by the stage I hybrid procedure (bilateral pulmonary artery band placement and stenting of the ductus arteriosus) (151). Determination of left ventricular adequacy may be more reliable after this period of temporary palliation, and successful outcome may be enhanced when definitive surgery is postponed to outside of the neonatal period.

Balloon dilation of aortic stenosis in the unborn fetus may prevent or reverse left heart hypoplasia in the fetus (135). Early attempts resulted in limited success with high mortality, but more recent advancements in patient selection and techniques offer the prospect that fetal intervention may one day have a role in the management of critical congenital aortic stenosis and possible prevention of hypoplastic left heart syndrome.

SUBVALVULAR AORTIC STENOSIS

Prevalence and Etiology

Fixed subvalvular aortic stenosis accounts for approximately 10% to 20% of cases of aortic stenosis in children, and the male to female ratio is 2:1 to 3:1 (152,153). Associated cardiac defects are present in more than half of cases (152,154). Common associated defects include VSD, coarctation of the aorta, atrioventricular septal defect, and valvular aortic stenosis. Mitral valve anomalies are also frequently present, and likely play a role in the pathophysiology of the obstruction in some patients (155,156).

Except for cases of malalignment VSD with posterior deviation of the outlet septum into the left ventricular outflow tract, subvalvular aortic stenosis is rare in infants. Most cases seem sporadic, although familial subaortic stenosis has been reported (157,158). Although most cases appear to develop postnatally, there may be a genetic substrate in many cases, and interestingly, this genetic substrate appears to not be specific for subaortic stenosis but rather also includes lesions of right ventricular outflow tract obstruction (159).

Despite the evidence for genetic etiology in some cases (160), the fact that discrete fixed subaortic stenosis is rarely seen in the fetal or neonatal heart has led many investigators to regard it as an acquired rather than a congenital lesion (161–165). The development and subsequent progression of fixed subaortic stenosis in children without previous evidence of left ventricular outflow tract obstruction supports this notion (166). It is likely that fixed subaortic stenosis develops due to an abnormal endothelial substrate that undergoes abnormal proliferation due to some stimulus. One such stimulus might be abnormal shear stresses caused by abnormal flow patterns that result from variations in geometric and anatomical features of the left ventricular outflow tract (167,168), such as increased mitral–aortic separation (161) and steeper aortoseptal angle (169–171). The tissue substrate for development of subaortic stenosis remains uncertain, although maldevelopment or persistence of embryonal endocardial cushion tissue has been hypothesized (153,172).

Pathology

The obstruction in fixed subvalvular aortic stenosis usually consists of a collar or ridge of membranous and/or fibromuscular tissue encircling the left ventricular outflow tract, or in some cases it may be diffuse and tunnel-like (152,173). The membranous curtain may arise from a thicker, muscular base. Histology of the fibrous tissue demonstrates dense collagen fibers, elastic fibers, and myocytes (174). Fibrous tissue may be closely related or “tethered” to the aortic valve or to the anterior mitral leaflet (165). Mitral valve anomalies are common, and these include insertion of a papillary muscle or chordal tissue into the septum or aortic leaflet, accessory mitral valve tissue, and “muscularization” of the subaortic portion of the anterior leaflet (155). The aortic valve may be thickened, and is usually tricuspid. The aortic valve abnormality appears to be acquired, and may be a consequence of the turbulent flow jet damaging the aortic valve cusps (175–178), but might also result from progression of the underlying disease substrate.

Physiology

The physiology of fixed subaortic stenosis is similar to valvular aortic stenosis, with pressure overload of the left ventricle resulting in hypertrophy. In most cases, the amount of hypertrophy correlates with the degree of obstruction, but in some cases, it may be out of proportion to the degree of obstruction (179). As with valvular aortic stenosis, in severe cases, subendocardial oxygen demand may exceed supply and result in subendocardial ischemia and fibrosis.

Clinical Features and Diagnostic Method

The diagnosis of subaortic stenosis frequently surfaces during echocardiographic evaluation at the time of diagnosis or follow-up of associated congenital heart disease, such as VSD or coarctation of the aorta. Patients with isolated subaortic stenosis usually present with an asymptomatic heart murmur. Commonly, the patient initially is thought to have an innocent murmur, and as the stenosis progresses, the murmur becomes more typical of pathologic left ventricular outflow tract obstruction. As in the case of valvular aortic stenosis, chest pain and syncope may occur, but generally only when the stenosis is severe.

The systolic ejection murmur is loudest at the mid left sternal border, and radiates to the upper sternal borders and into

the suprasternal notch. A systolic click is rare, and this helps to differentiate subvalvular aortic stenosis from valvular aortic stenosis. The left ventricular impulse may be hyperdynamic, and the associated findings of aortic regurgitation and/or mitral valve regurgitation may be present. The ECG usually demonstrates left ventricular hypertrophy, even in many cases with mild stenosis (179), although the ECG may occasionally be normal even in severe subaortic stenosis (152,153). Chest radiograph is generally normal, and dilation of the ascending aorta is much less common than in valvular aortic stenosis (153,154).

Echocardiography with Doppler evaluation is highly sensitive and specific for making the diagnosis of subaortic stenosis and to define the anatomy of the lesion (180,181). Early systolic partial closure and "fluttering" of the aortic leaflets may be present (182). Careful evaluation of the aortic and mitral valve anatomy and function is mandatory, as is a thorough search for other associated lesions. Pulsed Doppler demonstrates velocity acceleration and aliasing in the outflow tract beneath the valve, and continuous wave Doppler allows accurate calculation of the peak instantaneous and mean pressure gradients (183). Coexistent valvular aortic stenosis is confirmed by an additional velocity increase above the aortic valve by pulsed Doppler. TEE may be helpful in further defining the anatomy of the left ventricular outflow tract, and is commonly performed intraoperatively to assist in the repair by evaluating the anatomy and valve function pre- and post-operatively.

Diagnostic cardiac catheterization is not mandatory in the evaluation of subaortic stenosis, but may provide useful information in cases where the clinical data and noninvasive evaluation are not consistent. Peak-to-peak and mean pressure gradients can be determined, and left ventricular end diastolic pressure can be measured. In the case of coexistence of valvular and subvalvular aortic stenosis, slow and careful pullback across the left ventricular outflow tract using an end-hole catheter will quantitate the degree of obstruction across both sites (Fig. 46.14). Angiography in the right anterior oblique and long axial oblique views may clearly demonstrate the anatomy of the lesion, but echocardiography (particularly TEE) also reliably delineates the anatomy of subaortic stenosis (181) (Fig. 46.15–46.17).

Natural History

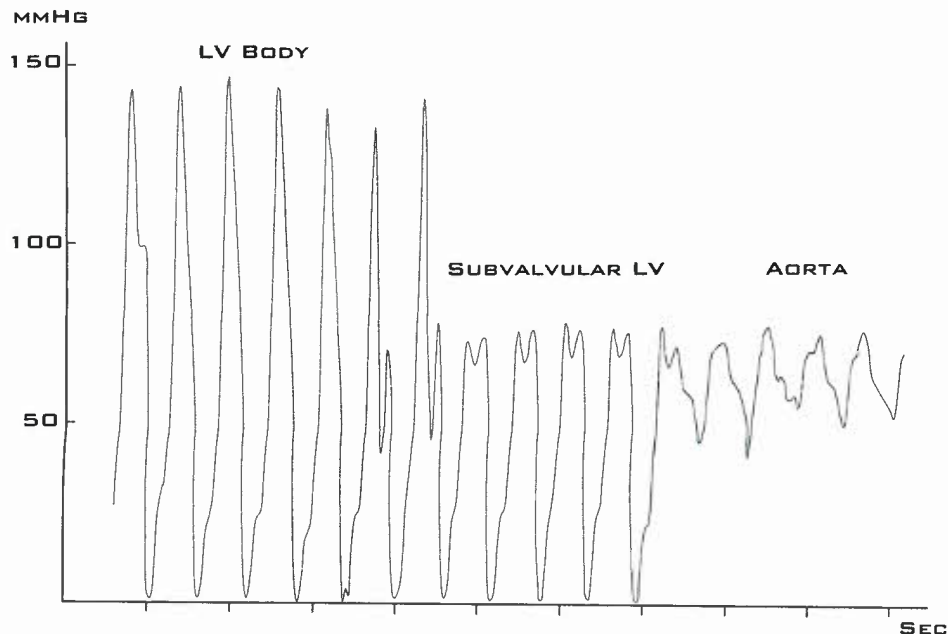
In infants and children with associated cardiac malformations, the natural history is influenced significantly by the coexisting disease. In general, subaortic stenosis is a progressive lesion (98,152,184) and occasionally progressive obstruction occurs rapidly (166). However, rate of progression of mild subvalvular aortic stenosis is variable, and the obstruction may remain mild and stable for many years in children and adults (185–187). Factors associated with more rapid progression of obstruction include higher initial pressure gradient, short distance between the obstructive lesion and the aortic valve, and anterior mitral valve leaflet involvement (188,189).

Aortic regurgitation is a frequent finding in subaortic stenosis, most commonly mild but occasionally moderate or severe (176,190). Doppler peak instantaneous gradient >50 mm Hg and increased age at diagnosis are risk factors for moderate or severe aortic regurgitation, but these parameters are not sensitive and prediction of development and progression of aortic regurgitation in patients with subaortic stenosis is difficult (178). Aortic regurgitation is common in adults with unoperated subaortic stenosis, but is rarely hemodynamically significant (186). Children at low risk for aortic valve dysfunction are those with mild gradient, thin, and mobile aortic valve leaflets, and subaortic lesion not in close proximity to the aortic valve (178).

Treatment

Although balloon dilation has been reported, long-term success is limited, and treatment for subaortic stenosis is surgical. The indications for surgery are not universally agreed upon. Because obstruction can be rapidly progressive, and because aortic regurgitation may be the result of progressive damage to the aortic leaflets by turbulent flow, there is rationale for early intervention (191–193). The increased probability of aortic regurgitation at follow-up in patients with higher preoperative gradient and older age of operation supports this approach (194). However, in the era of echocardiography, patients are frequently diagnosed with very mild subvalvular aortic stenosis, and it is clear that progression of disease is highly variable.

Figure 46.14. Pressure recording from an end-hole catheter as it is pulled back slowly from the body of the left ventricle (LV body) to the aorta. The left ventricular systolic pressure immediately beneath the valve is equal to the systolic pressure in the aorta, indicating absence of valvular aortic stenosis.



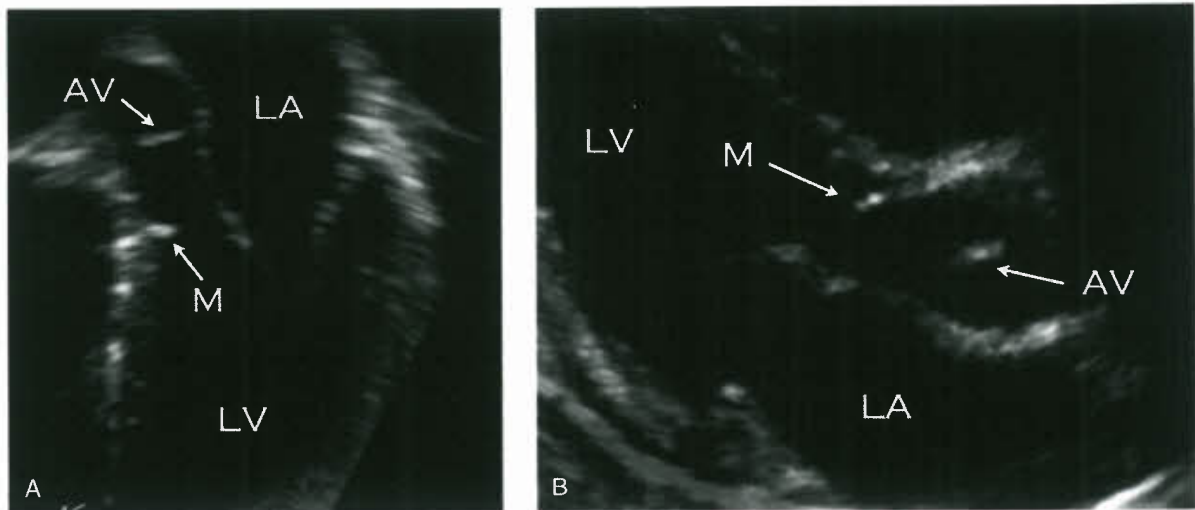


Figure 46.15. Echocardiographic images of discrete membranous subaortic stenosis. A: Apical five-chamber view. B: Parasternal long-axis view. (M, subaortic membrane; LA, left atrium; LV, left ventricle; AV, aortic valve.)

Many patients with mild subaortic stenosis remain stable for many years, without progression and without aortic regurgitation (185,186). In addition, there is evidence that aortic regurgitation may develop in operated and nonoperated patients (190), and in fact may be more prominent after surgical

intervention than in nonoperated patients (186,195). It appears that children with subaortic lesions not in close proximity to the aortic valve, mild obstruction (peak Doppler gradient <30 mm Hg), and aortic valve cusps that are thin and mobile may be managed conservatively, with close follow-up to detect

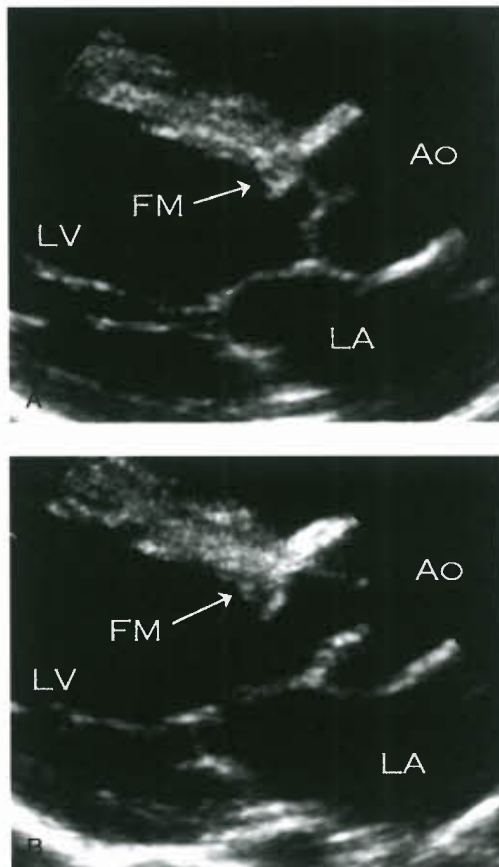


Figure 46.16. Echocardiographic parasternal long-axis views of fibromuscular subaortic stenosis, with broad-based subaortic fibromuscular ridge. A: Diastole, with aortic valve closed. B: Systole, with aortic valve open.

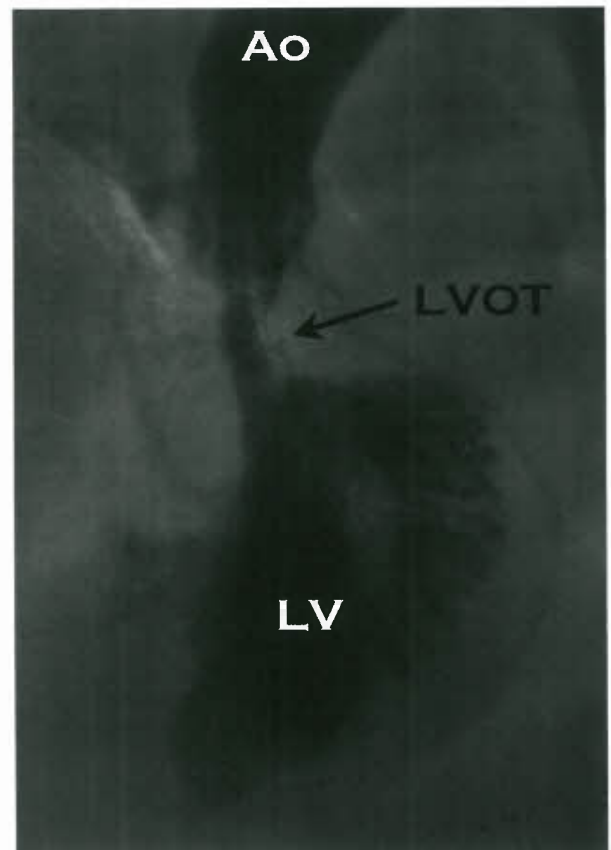


Figure 46.17. Left ventricular angiogram demonstrating tunnel-like subaortic stenosis. Note the symmetrically narrowed long-segment narrowing of the left ventricular outflow tract (LVOT). (LV, left ventricle; Ao, aorta.)

significant progression (178,195). Patients with progressive obstruction should have surgical relief of obstruction.

Surgical management consists of resection of obstructive tissue in the left ventricular outflow tract. Muscle resection in addition to membrane excision may decrease the risk of recurrent subaortic stenosis (196), which may be as frequent as 20%. Some recurrences may be cases of inadequate relief of obstruction at the time of initial surgery (176). Surgical correction of mitral valve abnormalities that contribute to the subaortic obstruction, such as anomalous papillary muscle insertion, should also be performed to reduce the risk of residual or recurrent stenosis (155). In addition to residual obstruction, complications of surgery include heart block, worsening of aortic or mitral valve regurgitation, and inadvertent creation of a VSD. Patients with tunnel-like left ventricular outflow tract obstruction have highest risk of complications, including inadequate relief of obstruction. In some cases of severe subaortic stenosis, particularly if the aortic annulus is small, more extensive tissue resection is necessary to achieve adequate relief of obstruction, and a Konno procedure (197) or Ross/Konno procedure (148) may be utilized.

Long-Term Outcome

Many patients with isolated membranous discrete subaortic stenosis have complete and lasting surgical relief of obstruction without aortic or mitral valve dysfunction. However, many have mild aortic valve dysfunction, which may progress despite adequate relief of obstruction, and recurrence or incomplete relief of subaortic stenosis is not uncommon. Periodic long-term follow-up is prudent for all patients with subaortic stenosis. In postoperative patients, further intervention may be indicated if recurrent stenosis or aortic regurgitation progresses. In addition, patients frequently require follow-up care for other associated cardiac defects. Some feel that endocarditis prophylaxis precautions are advisable indefinitely in most patients due to aortic valve thickening and regurgitation (even if very mild) and/or residual turbulence in the left ventricular outflow tract; however, the revised AHA guidelines do not recommend prophylaxis.

SUPRAVALVULAR AORTIC STENOSIS

Prevalence and Etiology

Supravalvular aortic stenosis is the least common type of aortic stenosis. It is rare, estimated to occur in approximately 1 of 25,000 live births (198), which accounts for approximately 0.5% of congenital heart disease cases. Approximately 30% to 50% of patients with supravalvular aortic stenosis have Williams-Beuren syndrome (199,200), features of which include supravalvular aortic stenosis, peripheral pulmonary stenosis, mental retardation, and characteristic facial appearance. About 20% of cases are familial but without other features of Williams-Beuren syndrome, and the remaining cases, about half, appear to be sporadic.

The etiology of supravalvular aortic stenosis is reduced or abnormal expression of the elastin gene on chromosome 7q11.23 (201). Familial "isolated" supravalvular aortic stenosis appears to result from a discrete mutation involving the elastin gene (202,203), whereas other features of Williams-Beuren syndrome result from disruption of the elastin gene together with other neighboring genes (204). Genetic transmission is autosomal dominant, with heterozygotes expressing only 50% of the normal amount of elastin, resulting in reduced arterial elastin content and abnormal elastin fiber geometry. Sporadic cases of

supravalvular aortic stenosis appear to be from either new mutations of the elastin gene or possibly from variable expression of the autosomal dominantly transmitted mutation (205,206). Large arteries such as the aorta and proximal pulmonary arteries have high elastin content in the media, and therefore are more commonly affected than smaller arteries (207).

Pathology

Reduced elastin in the arterial media results in reduced elasticity and markedly thickened media with smooth muscle hypertrophy, disorganization, and increased collagen deposition (208). Most commonly, the stenosis is localized primarily to the sinotubular junction, but approximately one-fourth of patients have diffuse narrowing of the entire ascending aorta and in some cases the transverse aorta (209). The main and/or proximal branch pulmonary arteries are frequently stenotic (210,211), and branches of the aortic arch may be involved (212). Stenoses of the renal and mesenteric arteries may also be present in as many as 30% of patients with supravalvular aortic stenosis (210–212).

The peripheral attachment of the aortic valve commissures is at the level of the sinotubular junction, and in patients with supravalvular aortic stenosis the aortic valve cusps may be thickened and adherent to the narrowed sinotubular junction (213,214). Abnormalities of the aortic valve may be present in as many as half of patients with supravalvular aortic stenosis (207). Coronary blood flow may be impaired by adhesion of an aortic valve leaflet to the sinotubular junction, or by thickening of the aortic wall, especially if the orifice is located close to the sinotubular junction (209,215). The coronary arteries may also manifest primary structural changes related to the underlying elastin arteriopathy as well as secondary hypertensive changes resulting from the fact that they originate proximal to the obstruction (216,217).

Physiology

Although the physiology of supravalvular aortic stenosis is similar to that of valvular and subvalvular aortic stenosis, the manifestations are exacerbated by the fact that the coronary arteries orifices are proximal to the obstruction. Not only does this expose the coronary arteries to high pressure during systole, with resultant secondary effects on the coronary vasculature, but also the stenosis may limit diastolic flow into the coronary arteries. Given that coronary ostial abnormalities are not uncommon as well, patients with supravalvular aortic stenosis are at significant risk of subendocardial ischemia, fibrosis, papillary muscle infarction, and sudden death due to oxygen supply/demand mismatch (56,218,219).

Clinical Features and Diagnostic Method

The majority of patients with supravalvular aortic stenosis are diagnosed during evaluation of an asymptomatic heart murmur. Published surgical series, which probably include the more severe spectrum of patients, report a high incidence of symptoms, which are present in more than half of cases (220,221). Symptoms include angina, syncope, cardiac arrest, and dyspnea on exertion.

The systolic murmur is similar to that of valvular aortic stenosis, most prominent at the upper right sternal border with radiation into the suprasternal notch and into the neck. Frequently, a suprasternal notch thrill is palpable. A systolic click is uncommon. Blood pressure in the right arm is frequently greater than that in the left arm due to the Coanda effect (222). Differences in upper extremity blood pressures

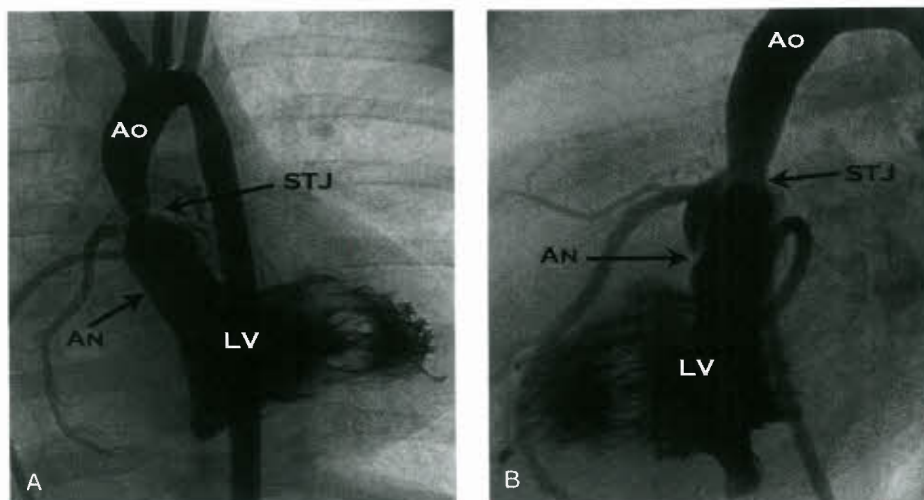


Figure 46.18. Left ventricular angiogram in a patient with elastin arteriopathy demonstrating supravalvular aortic stenosis. **A:** AP projection. **B:** Lateral projection. The diameter at the sinotubular junction (STJ) is considerably smaller than the diameter of the aortic annulus (AN), and the entire aorta (Ao) is small. Note the origin of the coronary arteries in close proximity to the sinotubular junction. (LV, left ventricle.)

and carotid artery pulses may also result from stenosis of the aortic arch branches.

Findings of associated cardiovascular anomalies are frequently present, and these include branch pulmonary artery stenosis, coarctation of the aorta, patent ductus arteriosus, mitral regurgitation, VSD, atrial septal defect, and tetralogy of Fallot (223–226). Patients with Williams-Beuren syndrome have “elfin” facies and other characteristic features. Many are musical savants.

The ECG may be normal or demonstrate left ventricular hypertrophy, T-wave abnormalities, and/or ST segment depression. These findings are not specific. The chest radiograph is usually normal. Echocardiography with Doppler is highly sensitive in making the diagnosis of supravalvular aortic stenosis, but at times does not completely delineate the anatomy of the ascending aorta, aortic arch, and aortic branches. Cardiac catheterization with angiography will define the anatomy and physiology in detail (Fig. 46.18), particularly in cases where aortic valve disease coexists, but MRI (227) and multidetector CT scanning are less invasive, lower risk methods of accurately defining the anatomy. The risk of cardiac catheterization is significant (212,220), with cardiac arrest presumably resulting from impairment of coronary flow from contrast injection and/or catheter manipulation near the coronary ostia at the site of severe supravalvular stenosis.

In addition to carefully delineating the anatomy of the supravalvular aortic stenosis, it is imperative that other sites of possible elastin vasculopathy are also thoroughly evaluated. Noninvasive imaging of the aortic arch branches, pulmonary arteries, and renal arteries is mandatory prior to embarking on surgical treatment for supravalvular aortic stenosis.

Natural History

The natural history of supravalvular aortic stenosis is not well known, in part due to the rarity of the disease and also because of the rapid evolution of diagnostic modalities and surgical techniques over the past few decades. In general, supravalvular aortic stenosis tends to progress, whereas coexistent pulmonary artery stenosis tends to improve over time (224,228). Sudden cardiac death has been reported (212,214).

Treatment

Although balloon dilation (229) and stent treatment (230) of supravalvular aortic stenosis have been reported, the close proximity to the aortic valve and coronary artery orifices are

significant obstacles and currently, surgical management is the treatment of choice. Indications for surgery are not clearly defined, but most centers use pressure gradient criteria similar to those in valvular aortic stenosis. Certainly, the presence of symptoms warrants prompt consideration for surgery. Some feel that bacterial endocarditis prophylaxis precautions are advisable, but AHA guidelines do not include this lesion.

Surgical techniques include simple patch enlargement of the sinotubular junction above the noncoronary sinus (231), extended aortoplasty with an inverted bifurcating patch into the noncoronary and right coronary sinuses (232), and Brom’s technique with insertion of separate patches in all three sinus after transecting the aorta (233). Any obstruction to coronary blood flow should be surgically corrected at the time of supravalvular aortic stenosis repair, and this may include patch enlargement of coronary ostial stenosis and/or internal mammary artery bypass grafting (234,235). If there is diffuse stenosis of the ascending and/or transverse aorta, the most common surgical technique is augmentation using an elongated patch, with the use of deep hypothermic circulatory arrest if necessary to extend the patch far enough to adequately relieve the obstruction (207).

Long-Term Outcome

Long-term outcome after surgical repair of supravalvular aortic stenosis is not known, but it appears that with current surgical techniques the rate of restenosis is very low (220,233). Because of the high likelihood of aortic valve abnormality, though usually mild, and other vascular lesions associated with elastin vasculopathy, long-term monitoring of the cardiovascular status in patients with supravalvular aortic stenosis is prudent.

REFERENCES

1. Roberts WC. The congenitally bicuspid aortic valve. A study of 85 autopsy cases. *Am J Cardiol* 1970;26:72–83.
2. Larson EC, Edwards WD. Risk Factors for aortic dissection: a necropsy study of 161 cases. *Am J Cardiol* 1984;53:849–855.
3. Hoffman JIE, Kaplan S. The incidence of congenital heart disease. *J Am Coll Cardiol* 2002;39:1890–1900.
4. Mitchell SC, Korones SB, Berendes HW. Congenital heart disease in 56,109 births. *Circulation* 1971;43:323–332.
5. Hoffman JI, Christianson R. Congenital heart disease in a cohort of 19,502 births with long-term follow-up. *Am J Cardiol* 1978;42:641–647.
6. Serratto M, Hastreiter AR, Miller RA. Management of congenital aortic stenosis in children and young adults. *Prog Cardiovasc Dis* 1965;8:78–99.

7. Fukuda T, Tadavarthi SM, Edwards JE. Dissecting aneurysm of aorta complicating aortic valvular stenosis. *Circulation* 1976;53:169-175.
8. Bonow RO, Carabello B, de Leon AC JR, et al. ACC/AHA guidelines for the management of patients with valvular heart disease: a report of the American College of Cardiology/American Heart Association Task Force on Practice Guidelines (Writing Committee to Revise the 1998 Guidelines for the Management of Patients With Valvular Heart Disease). *J Am Coll Cardiol* 2006;48:598-675.
9. Fenoglio JJ, McAllister HA, DeCastro CM, et al. Congenital bicuspid aortic valve after age 20. *Am J Cardiol* 1977;39:164-169.
10. Ward C. Clinical significance of the bicuspid aortic valve. *Heart* 2000;83:81-85.
11. Sabet HY, Edwards WD, Tazelaar HD, et al. Congenitally bicuspid aortic valves: a surgical pathology study of 542 cases (1991 through 1996) and a literature review of 2,715 additional cases. *Mayo Clin Proc* 1999;74:14-26.
12. Lewin MB, Otto CM. The bicuspid aortic valve: adverse outcomes from infancy to old age. *Circulation* 2005;111:832-834.
13. Roberts WC. Valvular, subvalvular, and supra-aortic stenosis: morphologic features. *Cardiovasc Clin* 1973;5:97-126.
14. Campbell M. The natural history of congenital aortic stenosis. *Br Heart J* 1968;30:514-526.
15. Frank S, Johnson A, Ross J. Natural history of valvular aortic stenosis. *Br Heart J* 1973;35:41-46.
16. Braunwald E, Goldblatt A, Aygen MM, et al. Congenital aortic stenosis. I. Clinical and hemodynamic findings in 100 patients. II. Surgical and the results of operation. *Circulation* 1963;27:426-462.
17. Lewin MB, McBride KL, Pignatelli R, et al. Echocardiographic evaluation of asymptomatic parental and sibling cardiovascular anomalies associated with congenital left ventricular outflow tract lesions. *Pediatrics* 2004;114:691-696.
18. Cripe L, Andelfinger G, Martin LJ, et al. Bicuspid aortic valve is heritable. *J Am Coll Cardiol* 2004;44:138-143.
19. Mazzanti L, Cacciari E. Congenital heart disease in patients with Turner's syndrome. Italian Study Group for Turner Syndrome (ISGTS). *J Pediatr* 1998;133:688-692.
20. Grossfeld PD, Mattina T, Lai Z, et al. The 11q terminal deletion disorder: a prospective study of 110 cases. *Am J Med Genet A* 2004;129:51-61.
21. Nora JJ. Causes of congenital heart diseases: old and new modes, mechanisms, and models. *Am Heart J* 1993;125:1409-1419.
22. Wessels MW, Berger RM, Frohn-Mulder IM, et al. Autosomal dominant inheritance of left ventricular outflow tract obstruction. *Am J Med Genet A* 2005;134:171-179.
23. Loffredo CA, Chokkalingam A, Sill AM, et al. Prevalence of congenital cardiovascular malformations among relatives of infants with hypoplastic left heart, coarctation of the aorta, and d-transposition of the great arteries. *Am J Med Genet A* 2004;124A:225-230.
24. Nora JJ, Nora AH. Maternal transmission of congenital heart disease: new recurrence risk figures and the questions of cytoplasmic inheritance and vulnerability to teratogens. *Am J Cardiol* 1987;59:459-463.
25. Garg V, Muth AN, Ransom JF. Mutations in NOTCH1 cause aortic valve disease. *Nature* 2005;437:270-274.
26. Martin JL, Ramachandran V, Cripe LH, et al. Evidence in favor of linkage to chromosomal regions of 18q, 5q, and 13q for bicuspid aortic valve and associated cardiovascular malformations. *Hum Genet* 2007;121:275-284.
27. Hove JR, Koster RW, Forouhar AS, et al. Intracardiac fluid forces are an essential epigenetic factor for embryonic cardiogenesis. *Nature* 2003;421:172-177.
28. Lev M, Arcilla R, Rimoldi HJ, et al. Premature narrowing or closure of the foramen ovale. *Am Heart J* 1963;65:638-647.
29. Harh JY, Paul MH, Gallen WJ, et al. Experimental production of hypoplastic left heart in the chick embryo. *Am J Cardiol* 1973;31:51-56.
30. Nistri S, Sorbo MD, Marin M, et al. Aortic root dilatation in young men with normally functioning bicuspid aortic valves. *Heart* 1999;82:19-22.
31. Robicsek F, Thubrikar MJ, Cook JW, et al. The congenitally bicuspid aortic valve: how does it function? Why does it fail? *Ann Thorac Surg* 2004;77:177-185.
32. Della Corte A, Quarto C, Bancone C, et al. Spatiotemporal patterns of smooth muscle changes in ascending aortic dilatation with bicuspid and tricuspid aortic valve stenosis: focus on cell matrix signaling. *J Thorac Cardiovasc Surg* 2008;135:8-18.
33. Shafer BM, Lewin MB, Stout KK, et al. The bicuspid aortic valve: an integrated phenotypic classification of leaflet morphology and aortic root shape. *Heart* 2008;94:1634-1638.
34. Pachulski RT, Weinberg AL, Chan KL. Aortic aneurysm in patients with functionally normal or minimally stenotic bicuspid aortic valve. *Am J Cardiol* 1991;67:781-782.
35. Loscalzo ML, Goh DL, Loeys B, et al. Familial thoracic aortic dilation and bicuspid aortic valve: a progressive analysis of natural history and inheritance. *Am J Med Genet A* 2007;143A:1960-1967.
36. Notatmadja M, West M, West J, et al. Abnormal extracellular matrix protein transport associated with increased apoptosis of vascular smooth muscle cells in Marfan Syndrome and bicuspid aortic valve thoracic aortic aneurysm. *Circulation* 2003;108:II329-II334.
37. Arrington CB, Sower CT, Chuckwuk N, et al. Absence of TGFB1 and TGFB2 mutations in patients with bicuspid aortic valve and aortic dilatation. *Am J Cardiol* 2008;102:629-631.
38. Freeman RV, Otto CM. Spectrum of calcific aortic valve disease: pathogenesis, disease progression, and treatment strategies. *Circulation* 2005;111:3316-3326.
39. Reeve J, Robinson SJ. Hypoplastic annulus: an unusual type of aortic stenosis: a report of three cases in children. *Dis Chest* 1964;45:99-102.
40. Bharati S, Lev M. Congenital polyvalvular disease. *Circulation* 1973;47:575-586.
41. Subramanian R, Olson LJ, Edwards WD. Surgical pathology of pure aortic stenosis: a study of 374 cases. *Mayo Clin Proc* 1984;59:683-690.
42. Fernandes SM, Sanders SP, Khairi P, et al. Morphology of bicuspid aortic valve in children and adolescents. *J Am Coll Cardiol* 2004;44:1648-1651.
43. Thubrikar MJ, Aouad J, Nolan SP. Patterns of calcific deposits in operatively excised stenotic or purely regurgitant aortic valves and their relation to mechanical stress. *Am J Cardiol* 1986;58:304-308.
44. Olsson M, Dalsgaard CJ, Haegerstrand A, et al. Accumulation of T lymphocytes and expression of interleukin-2 receptors in nonrheumatic stenotic aortic valves. *J Am Coll Cardiol* 1994;23:1162-1170.
45. Jajamann NM, Subramaniam M, Rickard O, et al. Human aortic valve calcification is associated with an osteoblast phenotype. *Circulation* 2003;107:2181-2184.
46. Lehmann S, Walther T, Kempfert J, et al. Mechanical strain and the aortic valve: influence on fibroblasts, extracellular matrix, and potential stenosis. *Ann Thorac Surg* 2009;88:1476-1483.
47. Nagam V, Srivastava D. Notch1 represses osteogenic pathways in aortic valve cells. *J Mol Cell Cardiol* 2009;47:828-834.
48. Fedak PW, de Sa MP, Verma S, et al. Vascular matrix remodeling in patients with bicuspid aortic valve malformations: implications for aortic dilatation. *J Thorac Cardiovasc Surg* 2003;126:797-806.
49. Paloschi V, Curtovic S, Folkerson L, et al. Impaired splicing of fibronectin is associated with thoracic aortic aneurysm formation in patients with bicuspid aortic valve. *Arterioscler Thromb Vasc Biol* 2001;31:691-697.
50. Pacileo G, Calabro P, Limongelli G, et al. Left ventricular remodeling, mechanics, and tissue characterization in congenital aortic stenosis. *J Am Soc Echocardiogr* 2003;16:214-220.
51. Pacileo G, Pisacane C, Russo MG, et al. Left ventricular remodeling and mechanics after successful repair of aortic coarctation. *Am J Cardiol* 2001;87:748-752.
52. Donner R, Carabello BA, Black I, et al. Left ventricular wall stress in compensated aortic stenosis in children. *Am J Cardiol* 1983;51:946-951.
53. Moller JH, Nakeb A, Edwards JE. Infarction of papillary muscles and mitral insufficiency associated with congenital aortic stenosis. *Circulation* 1966;34:87-91.
54. Fallen EL, Elliott WC, Gorlin R. Mechanisms of angina in aortic stenosis. *Circulation* 1967;36:480-488.
55. Buckberg GD, Fixler DE, Archie JR, et al. Experimental subendocardial ischemia in dogs with normal coronary arteries. *Circ Res* 1972;30:67-81.
56. Vincent WR, Buckberg GD, Hoffman JI. Left ventricular subendocardial ischemia in severe valvar and supra-aortic stenosis. A common mechanism. *Circulation* 1974;49:326-333.
57. Cueto L, Moller JH. Haemodynamics of exercise in children with isolated aortic valvular disease. *Br Heart J* 1973;35:93-98.
58. Ellison RC, Wagner HR, Weidman WH, et al. Congenital valvular aortic stenosis: clinical detection of small pressure gradient. Prepared for the Joint Study on the Natural History of Congenital Heart Defects. *Am J Cardiol* 1976;37:757-761.
59. Wagner HR, Weidman WH, Ellison RC, et al. Indirect assessment of severity in aortic stenosis. *Circulation* 1977;56:120-123.
60. Beyerbach HP, Bax JJ, Lamb HJ, et al. Evaluation of ECG criteria for left ventricular hypertrophy before and after aortic valve replacement using magnetic resonance imaging. *J Cardiovasc Magn Reson* 2003;5:465-474.
61. Wolfe RR, Driscoll DJ, Gersony WM, et al. Report from the Second Joint Study on the Natural History of Congenital Heart Defects (NHS-2): arrhythmias in patients valvar aortic stenosis, pulmonary stenosis, and ventricular septal defects: results of twenty-four ECG monitoring. *Circulation* 1993;87:1189-1101.
62. Driscoll DJ, Wolfe RR, Gersony WM, et al. Report from the Second Joint Study on the Natural History of Congenital Heart Defects (NHS-2): cardiorespiratory responses to exercise of patients with aortic stenosis, pulmonary stenosis, and ventricular septal defect. *Circulation* 1993;87:1102-1113.
63. Holloran KH. The telemetered exercise electrocardiogram in congenital aortic stenosis. *Pediatrics* 1971;47:31-39.
64. Alpert BS, Moes DM, Durant RH, et al. Hemodynamic response to ergometer exercise in children and young adults with left ventricular pressure or volume overload. *Am J Cardiol* 1983;52:563-567.
65. James FW, Schwartz DC, Kaplan S, et al. Exercise electrocardiogram, blood pressure, and working capacity in young patients with valvar or discrete subvalvar aortic stenosis. *Am J Cardiol* 1982;50:769-775.
66. Lewis AB, Heymann MA, Stanger P, et al. Evaluation of subendocardial ischemia in valvar aortic stenosis in children. *Circulation* 1974;49:978-984.
67. Latta L, Schneider D, Sokoloski M, et al. Use of exercise testing in patients with aortic stenosis. *Pediatr Exerc Sci* 2003;17:100A.
68. Das P, Rimington H, McGrane K, et al. The value of treadmill exercise testing in apparently asymptomatic aortic stenosis. *J Am Coll Cardiol* 2001;37:489A.

69. Lancellotti P, Lebios F, Simon M, et al. Prognostic importance of quantitative exercise Doppler echocardiography in asymptomatic valvular aortic stenosis. *Circulation* 2005;112:1377-1382.
70. Huhta JC, Gutgesell HP, Latson LA, et al. Two-dimensional echocardiographic assessment of the aorta in infants and children with congenital heart disease. *Circulation* 1984;70:417-424.
71. DeMaria AN, Bommer W, Joye J, et al. Value and limitations of cross-sectional echocardiography in the diagnosis and quantification of the aortic valve in the diagnosis and quantification of valvular aortic stenosis. *Circulation* 1980;62:304-312.
72. Sadagoban SA, Veldtman GR, Sivaprakasam MC, et al. Correlations with operative anatomy of real time three-dimensional echocardiographic imaging of congenital aortic valve stenosis. *Cardiol Young* 2006;16:490-494.
73. Hatle L, Angelsen BA, Tromsdal A. Noninvasive assessment of aortic stenosis by Doppler ultrasound. *Br Heart J* 1980;43:284-292.
74. Beekman RH, Rocchini AP, Gillon JH, et al. Hemodynamic determinants of the peak systolic left ventricular-aortic pressure gradient in children with valvular aortic stenosis. *Am J Cardiol* 1992;69:813-815.
75. Currie PJ, Seward JB, Reeder GS, et al. Continuous-wave Doppler echocardiographic assessment of severity of calcific aortic stenosis: a simultaneous Doppler-catheter correlative study in 100 adult patients. *Circulation* 1985;71:1162-1169.
76. Vlahos AP, Marx GR, McElhinney D, et al. Clinical utility of Doppler echocardiography in assessing aortic stenosis severity and predicting need for intervention in children. *Pediatr Cardiol* 2008;29:507-514.
77. Teien D, Karp K, Eriksson P. Non-invasive estimation of the mean pressure difference in aortic stenosis by Doppler ultrasound. *Br Heart J* 1986;56:450-454.
78. Bengur AR, Snider AR, Serwer GA, et al. Usefulness of the Doppler mean gradient in evaluation of children with aortic valve stenosis and comparison to gradient at catheterization. *Am J Cardiol* 1989;64:756-761.
79. Richards KL, Cannon SR, Miller JF, et al. Calculation of aortic valve area by Doppler echocardiography: a direct application of the continuity equation. *Circulation* 1986;73:964-969.
80. Skjaerpe T, Hegrenaes L, Hatle L. Noninvasive estimation of valve area in patients with aortic stenosis by Doppler ultrasound and two-dimensional echocardiography. *Circulation* 1985;72:810-818.
81. Hess OM, Villari B, Krayerbuehl HP. Diastolic dysfunction in aortic stenosis. *Circulation* 1993;87:IV73-IV76.
82. Bruch C, Stypmann J, Grude M, et al. Tissue Doppler imaging in patients with moderate to severe aortic valve stenosis: clinical usefulness and diagnostic accuracy. *Am Heart J* 2004;148:696-702.
83. Henein MY, Gibson DG. Long axis function in disease. *Heart* 1999;81:229-231.
84. Caruthers SD, Lin SJ, Brown P, et al. Practical value of cardiac magnetic resonance imaging for clinical quantification of aortic valve stenosis: comparison with echocardiography. *Circulation* 2003;108:2236-2243.
85. Gorlin R, Gorlin SG. Hydraulic formula for calculation of area of stenotic mitral valve, other cardiac valves, and central circulatory shunts. *Am Heart J* 1951;41:1-29.
86. Keene JF, Driscoll DJ, Gersony WM, et al. Report from the Second Joint Study on the Natural History of Congenital Heart Defects (NHS-2): results of treatment of patients with aortic valvular stenosis. *Circulation* 1993;87:116-127.
87. Serratto M, Hastreiter AR, Miller RA. Management of congenital aortic stenosis in children and young adults. *Prog Cardiovasc Dis* 1965;8:78-99.
88. Moller JH, Nakib A, Eliot RS, et al. Symptomatic congenital aortic stenosis in the first year of life. *J Pediatr* 1966;69:728-734.
89. Harstreiter AR, Oshima M, Miller RA, et al. Congenital aortic stenosis syndrome in infancy. *Circulation* 1963;28:1084-1095.
90. Nadas AS. Report from the Joint Study on the Natural History of Congenital Heart Defects. IV. Clinical course. Introduction. *Circulation* 1977;56:136-138.
91. Otto CM, Burwash IG, Legget ME, et al. Prospective study of asymptomatic valvular aortic stenosis. Clinical, echocardiographic, and exercise predictors of outcome. *Circulation* 1997;95:2262-2270.
92. Pellikka PA, Sarano ME, Nishimura RA, et al. Outcome of 622 adults with asymptomatic, hemodynamically significant aortic stenosis during prolonged follow-up. *Circulation* 2005;111:3290-3295.
93. Lambert EC, Menon VA, Wagner HR, et al. Sudden unexpected death from cardiovascular disease in children. A cooperative international study. *Am J Cardiol* 1974;34:89-96.
94. Brown DW, Dipilato AE, Chong EC, et al. Sudden unexpected death after balloon valvuloplasty for congenital aortic stenosis. *J Am Coll Cardiol* 2010;56:1939-1946.
95. Cohen LS, Friedman WF, Braunwald E. Natural History of mild congenital aortic stenosis elucidated by serial hemodynamic studies. *Am J Cardiol* 1972;30:1-5.
96. Davies SW, Gershlick AH, Balcon R. Progression of valvular aortic stenosis: a long-term retrospective study. *Eur Heart J* 1991;12:10-14.
97. Rosenhek R, Klaar U, Schemper M, et al. Mild and moderate aortic stenosis: natural history and risk stratification by echocardiography. *Eur Heart J* 2004;25:199-205.
98. El-Said G, Galioto FM, Mullins CE, et al. Natural hemodynamic history of congenital aortic stenosis in childhood. *Am J Cardiol* 1972;30:6-12.
99. Fernandes SM, Khairy P, Sanders SP, et al. Bicuspid aortic valve morphology and interventions in the young. *J Am Coll Cardiol* 2007;49:2211-2214.
100. Gersony WM, Hayes CJ, Driscoll DJ, et al. Report from the Second Joint Study on the Natural History of Congenital Heart Defects (NHS-2): bacterial endocarditis in patients with aortic stenosis, pulmonary stenosis, or ventricular septal defect. *Circulation* 1993;87:1121-1126.
101. Parolari A, Tremoli E, Cavallotti L, et al. Do statins improve outcomes and delay the progression of non-rheumatic calcific aortic stenosis? *Heart* 2011;97:523-529.
102. Carabello BA. Evaluation and management of patients with aortic stenosis. *Circulation* 2002;105:1746-1750.
103. Lund O, Flo C, Jensen FT, et al. Left ventricular systolic and diastolic function in aortic stenosis. Prognostic value after valve replacement and underlying mechanisms. *Eur Heart J* 1997;18:1977-1987.
104. Villari B, Vassalli G, Monrad E, et al. Normalization of diastolic dysfunction in aortic stenosis late after valve replacement. *Circulation* 1995;91:2353-2358.
105. Lababidi Z. Aortic balloon valvuloplasty. *Am Heart J* 1983;106:751-752.
106. Rocchini AP, Beekman RH, Ben Shachar G, et al. Balloon aortic valvuloplasty: results of the valvuloplasty and angioplasty of congenital anomalies registry. *Am J Cardiol* 1990;65:784-789.
107. Jones M, Barnhart GR, Morrow AG. Late results after operations for left ventricular outflow tract obstructions. *Am J Cardiol* 1982;50:569-579.
108. Hsieh KS, Keane JF, Nadas AS, et al. Long-term follow-up of valvotomy before 1968 for congenital aortic stenosis. *Am J Cardiol* 1986;58:338-341.
109. Pedra CA, Sidhu R, McCrindle BW, et al. Outcomes after balloon dilation of congenital aortic stenosis in children and adolescents. *Cardiol young* 2004;14:315-321.
110. Reich O, Tax P, Marek J, et al. Long term results of percutaneous balloon valvuloplasty of congenital aortic stenosis: independent predictors of outcome. *Heart* 2004;90:70-76.
111. Fratz S, Gildein HP, Balling G, et al. Aortic valvuloplasty in pediatric patients substantially postpones the need for aortic valve surgery: a single-center experience of 188 patients after up to 17.5 years of follow-up. *Circulation* 2008;117:1201-1206.
112. Brown DW, Dipilato AE, Chong EC, et al. Aortic valve reinterventions after balloon aortic valvuloplasty for congenital aortic stenosis. Intermediate and late follow-up. *J Am Coll Cardiol* 2010;56:1740-1749.
113. Klein A, Keane L, Atul G, et al. Long-term mortality, cause of death, and temporal trends in complications after percutaneous aortic balloon valvuloplasty for calcific aortic stenosis. *J Interv Cardiol* 2006;19:269-275.
114. Tissot CM, Attias D, Himbert D, et al. Reappraisal of percutaneous aortic balloon valvuloplasty as a preliminary treatment strategy in the transcatheter aortic valve implantation era. *Eurointervention* 2011;7:49-56.
115. Feltes TF, Bacha E, Beekman RH III, et al. on behalf of the American Heart Association Congenital Cardiac Defects Committee of the Council on Cardiovascular Disease in the Young, Council on Clinical Cardiology, and Council on Cardiovascular Radiology and Intervention. Indications for cardiac catheterization and intervention in pediatric cardiac disease: a scientific statement from the American Heart Association. *Circulation* 2011;123:2607-2652.
116. Maron BJ, Zipes DP. 36th Bethesda Conference: eligibility recommendations for competitive athletes with cardiovascular abnormalities. *J Am Coll Cardiol* 2005;45:1313-1375.
117. Januzzi JL, Isselbacher EM, Fattori R, et al. Characterizing the young patient with aortic dissection: results from the International Registry of Aortic Dissection (IRAD). *J Am Coll Cardiol* 2004;43:655-659.
118. Spittell PC, Spittell JA, Joyce JW, et al. Clinical features and differential diagnosis of aortic dissection. *Mayo Clin Proc* 1993;68:642-651.
119. Mahle WT, Sutherland JL, Frias PA. Outcome of bicuspid aortic valve in childhood. *J Pediatr* 2010;157:445-449.
120. Roberts CS, Roberts WC. Dissection of the aorta associated with congenital malformation of the aortic valve. *J Am Coll Cardiol* 1991;17:712-716.
121. Elsheikh M, Casadei B, Conway GS, et al. Hypertension is a major risk factor for aortic root dilatation in women with Turner's syndrome. *Clin Endocrinol* 2001;54:69-73.
122. Pannu H, Fadulu VT, Chang J, et al. Mutations in transforming growth factor-beta receptor type II cause familial thoracic aortic aneurysms and dissections. *Circulation* 2005;112:513-520.
123. Davies RR, Goldstein LJ, Coady MA, et al. Yearly rupture or dissection rates for thoracic aortic aneurysms: simple prediction based on size. *Ann Thorac Surg* 2002;73:17-27.
124. Boyer JK, Gutierrez F, Braverman AC. Approach to the dilated aortic root. *Curr Opin Cardiol* 2004;19:563-569.
125. Nishimura RA, Carabello GA, Faxon DP, et al. ACC/AHA 2008 guideline update on valvular heart disease: focused update on infective endocarditis: a report of the American College of Cardiology/American Heart Association Task Force on Practice Guidelines. *J Am Coll Cardiol* 2008;52:676-685.
126. Backer CL. Techniques for repairing the aortic and truncal valves. *Cardiol Young* 2005;15:125-131.
127. Elkins RC, Knott-Craig CJ, Razook JD, et al. Pulmonary autograft replacement of the aortic valve in the potential parent. *J Card Surg* 1994;9:198-203.
128. Hazekamp MG, Grotenhuis HB, Schoof PH, et al. Results of the Ross operation in a pediatric population. *Eur J Cardiothorac Surg* 2005;27:975-979.

129. Slater M, Shen I, Welke K, et al. Modification to the Ross procedure to prevent autograft dilatation. *Semin Thorac Cardiovasc Surg Pediatr Card Surg Annu* 2005;181-184.
130. Luciani GB, Favaro A, Casali G, et al. Ross operation in the young: a ten-year experience. *Ann Thorac Surg* 2005;80:2271-2277.
131. Cribier A, Elchaninoff H, Tron C, et al. Early experience with percutaneous transcatheter implantation of heart valve prosthesis for the treatment of end-stage inoperable patients with aortic stenosis. *J Am Coll Cardiol* 2004;43:698-703.
132. Leon MB, Smith CR, Mack M, et al. PARTNER Trial Investigators. Transcatheter aortic valve implantation for aortic stenosis in patients who cannot undergo surgery. *N Engl J Med* 2010;363:1597-1607.
133. Smith CR, Leon MB, Mack MJ, et al. Partner trial investigators. Transcatheter vs surgical aortic-valve replacement in high-risk patients. *N Engl J Med* 2011;364:2187-2198.
134. Fedak PW, Verma S, David TE, et al. Clinical and pathophysiological implications of a bicuspid aortic valve. *Circulation* 2002;106:900-904.
135. Tworetzki W, Wilkins-Haug L, Jennings RW, et al. Balloon dilation of severe aortic stenosis in the fetus: potential for prevention of hypoplastic left heart syndrome: candidate selection, technique, and results of successful intervention. *Circulation* 2004;110:2125-2131.
136. Hornberger LK, Sanders SP, Rein AJ, et al. Left heart obstructive lesions and left ventricular growth in the midtrimester fetus: a longitudinal study. *Circulation* 1995;92:1531-1538.
137. Leung MP, McKay R, Smith A, et al. Critical aortic stenosis in early infancy: anatomic and echocardiographic substrates of successful open valvotomy. *J Thorac Cardiovasc Surg* 1991;101:526-535.
138. Rhodes LA, Colan SD, Perry SB, et al. Predictors of survival in neonates with critical aortic stenosis. *Circulation* 1991;84:2325-2335.
139. Lofland GK, McCrindle BW, Williams WG, et al. Critical aortic stenosis in the neonate: a multi-institutional study of management, outcomes, and risk factors. *J Thorac Cardiovasc Surg* 2001;121:10-27.
140. Kovalchin JP, Brook MM, Rosenthal GL, et al. Echocardiographic hemodynamic and morphometric predictors of survival after two-ventricle repair in infants with critical aortic stenosis. *J Am Coll Cardiol* 1998;32:237-244.
141. Grosse-Wortmann L, Yun TJ, Al-Radi O, et al. Borderline hypoplasia of the left ventricle in neonates: insights for decision-making from functional assessment with magnetic resonance imaging. *J Thorac Cardiovasc Surg* 2008;136:1429-1436.
142. Alexiou C, Langley SM, Dalrymple-Hay MJ, et al. Open commissurotomy for critical isolated aortic stenosis in neonates. *Ann Thorac Surg* 2001;71:489-493.
143. Zeevi B, Keane JF, Castaneda AR, et al. Neonatal critical valvar aortic stenosis: a comparison of surgical and balloon dilation therapy. *Circulation* 1989;80:831-839.
144. Gatzoulis MA, Rigby ML, Shinebourne EA, et al. Contemporary results of balloon valvuloplasty and surgical valvotomy for congenital aortic stenosis. *Arch Dis Child* 1995;73:66-69.
145. McCrindle BW, Blackstone EH, Williams WG, et al. Are outcomes of surgical versus transcatheter balloon valvotomy equivalent in neonatal critical aortic stenosis? *Circulation* 2001;104:152-158.
146. Pass RH, Hellenbrand WE. Catheter intervention for critical aortic stenosis in the neonate. *Cathet Cardiovasc Intervent* 2002;55:88-92.
147. McElhinney DB, Lock JE, Keane JF, et al. Left heart growth, function, and reintervention after balloon aortic valvuloplasty for neonatal aortic stenosis. *Circulation* 2005;111:451-458.
148. Ohye RG, Gomez CA, Ohye BJ, et al. The Ross/Konno procedure in neonates and infants: intermediate-term survival and autograft function. *Ann Thorac Surg* 2001;72:823-830.
149. Van Son JA, Falk V, Mohr FW. Ross-Konno operation with resection of endocardial fibroelastosis for critical aortic stenosis with borderline-sized left ventricle in neonates. *Ann Thorac Surg* 1997;63:112-116.
150. Nurozler F, Bradley SM. Considerations in biventricular repair after the Norwood procedure. *Eur J Cardiothorac Surg* 2000;18:540-544.
151. Davis CK, Pastuszko P, Lamberti J, et al. The hybrid procedure for the borderline left ventricle. *Cardiol Young* 2011;21:26-30.
152. Newfeld EA, Muster AJ, Paul MM, et al. Discrete subvalvar aortic stenosis in childhood. Study of 51 patients. *Am J Cardiol* 1976;38:53-61.
153. Kelly DT, Wulfsberg E, Rowe RD. Discrete subaortic stenosis. *Circulation* 1972;46:309-322.
154. Reis RL, Peterson LM, Mason DT, et al. Congenital fixed subvalvular aortic stenosis. An anatomical classification and correlations with operative results. *Circulation* 1971;43:111-118.
155. Cohen L, Bennani R, Hulin S, et al. Mitral valvar anomalies and discrete subaortic stenosis. *Cardiol Young* 2002;12:138-146.
156. Marasini M, Zannini L, Ussia GP, et al. Discrete subaortic stenosis: incidence, morphology and surgical impact of associated subaortic anomalies. *Ann Thorac Surg* 2003;75:1763-1768.
157. Urbach J, Glaser J, Balkin J, et al. Familial membranous subaortic stenosis. *Cardiology* 1985;72:214-217.
158. Petsas AA, Anastassiades LC, Constantinou EC, et al. Familial discrete subaortic stenosis. *Clin Cardiol* 1998;21:63-65.
159. Pyle RL, Patterson DF, Chacko S. The genetics and pathology of discrete subaortic stenosis in the Newfoundland dog. *Am Heart J* 1976;92:324-334.
160. Fatimi SH, Ahmad U, Javed MA. Familial membranous subaortic stenosis: review of familial inheritance pattern and a case report. *J Thorac Cardiovasc Surg* 2006;132:1484-1486.
161. Rosenquist GC, Clark EB, McAllister HA, et al. Increased mitral-aortic separation in discrete subaortic stenosis. *Circulation* 1979;60:70-74.
162. Freedom RM, Pelech A, Brand A, et al. The progressive nature of subaortic stenosis in congenital heart disease. *Int J Cardiol* 1985;8:137-143.
163. Vogt J, Dische R, Rupprath G, et al. Fixed subaortic stenosis: an acquired secondary obstruction? A twenty-seven year experience with 168 patients. *Thorac Cardiovasc Surg* 1989;37:199-206.
164. Lampros TD, Cobanoglu A. Discrete subaortic stenosis: an acquired heart disease. *Eur J Cardiothorac Surg* 1998;14:296-303.
165. Choi JY, Sullivan ID. Fixed subaortic stenosis: anatomical spectrum and nature of progression. *Br Heart J* 1991;65:280-286.
166. Freedom RM, Fowler RS, Suncan WJ. Rapid evolution from "normal" left ventricular outflow tract to fatal subaortic stenosis in infancy. *Br Heart J* 1981;45:605-609.
167. Gilliers AM, Gewillig M. Rheology of discrete subaortic stenosis. *Heart* 2002;88:335-336.
168. Cape EG, Vanauker MD, Sigfussen G, et al. Potential role of mechanical stress in the etiology of pediatric heart disease: septal shear stress in subaortic stenosis. *J Am Coll Cardiol* 1997;30:247-254.
169. Sigfussen G, Tracy T, Vanauker MD, et al. Abnormalities of the left ventricular outflow tract associated with discrete subaortic stenosis in children: an echocardiographic study. *J Am Coll Cardiol* 1997;30:255-259.
170. Tutar HE, Aralay S, Turkyay S, et al. Echocardiographic, morphologic, and geometric variations of the left ventricular outflow tract: possible role in the pathogenesis of discrete subaortic stenosis. *Angiology* 2000;51:213-221.
171. Kleinert S, Geva T. Echocardiographic morphometry and geometry of the left ventricular outflow tract in fixed subaortic stenosis. *J Am Coll Cardiol* 1993;22:1501-1508.
172. Van Praagh R, Corwin RD, Dahlquist EH, et al. Tetralogy of Fallot with severe left ventricular outflow tract obstruction due to attachment of the mitral valve to the ventricular septum. *Am J Cardiol* 1970;26:93-101.
173. Deutsch V, Shem-Tov AA, Yahini JH, et al. Subaortic stenosis (discrete form). Classification and angiocardiac features. *Radiology* 1971;101:275-286.
174. Ferrans VJ, Muna WF, Jones M, et al. Ultrastructure of the fibrous ring in patients with discrete subaortic stenosis. *Lab Invest* 1978;39:30-40.
175. Sung CS, Price EC, Cooley DA. Discrete subaortic stenosis in adults. *Am J Cardiol* 1978;42:283-290.
176. Wright GB, Keane JF, Nadas AS, et al. Fixed subaortic stenosis in the young: medical and surgical course in 83 patients. *Am J Cardiol* 1983;52:830-835.
177. Champsaur G, Trusler GA, Mustard WT. Congenital discrete subvalvar aortic stenosis. Surgical experience and long-term follow-up in 20 paediatric patients. *Br Heart J* 1973;35:443-446.
178. McMahon CJ, Gauvreau K, Edwards JC, et al. Risk factors for aortic valve dysfunction in children with discrete subvalvar aortic stenosis. *Am J Cardiol* 2004;94:459-464.
179. Shem-Tov A, Schneeweiss A, Motro M, et al. Clinical presentation and natural history of mild discrete subaortic stenosis. Follow-up of 1-17 years. *Circulation* 1982;66:509-512.
180. Vogt J, Rupprath G, De Vivie R, et al. Discrete subaortic stenosis: the value of cross-sectional sector echocardiography in evaluating different types of obstruction. *Pediatr Cardiol* 1983;4:253-258.
181. Wilcox WD, Plauth WH, Williams WH, et al. Discrete subaortic stenosis. Two-dimensional echocardiographic features with angiographic and surgical correlation. *Mayo Clin Proc* 1980;55:425-433.
182. Sabbah HN, Stein PD. Mechanism of early systolic closure of the aortic valve in discrete membranous subaortic stenosis. *Circulation* 1982;65:399-402.
183. Kinney EL, Machado H, Cortada X, et al. Diagnosis of discrete subaortic stenosis by pulsed and continuous wave echocardiography. *Am Heart J* 1985;110:1069-1071.
184. Mody MR, Mody GT. Serial hemodynamic observations in congenital valvular and subvalvular aortic stenosis. *Am Heart J* 1975;89:137-143.
185. Rohlicek CV, Del Pino SF, Hosking M, et al. Natural history and surgical outcomes for isolated discrete subaortic stenosis in children. *Heart* 1999;82:708-713.
186. Oliver JM, Gonzalez A, Gallego P, et al. Discrete subaortic stenosis in adults: increased prevalence and slow rate of progression of the obstruction and aortic regurgitation. *J Am Coll Cardiol* 2001;38:835-842.
187. deVries AG, Hess J, Witsenburg M, et al. Management of fixed subaortic stenosis: a retrospective study of 57 cases. *J Am Coll Cardiol* 1992;19:1013-1017.
188. Bezold LI, Smith EO, Kelly K, et al. Development and validation of an echocardiographic model for predicting progression of discrete subaortic stenosis in children. *Am J Cardiol* 1998;81:314-320.
189. Hwang MS, Chu JJ, Su WJ, et al. Natural history and risk stratification of discrete subaortic stenosis in children: an echocardiographic study. *J Formos Med Assoc* 2004;103:17-22.
190. Firpo C, Maitre Azcarate MJ, Quero Jimenez M, et al. Discrete subaortic stenosis (DSS) in childhood: a congenital or acquired disease? Follow-up in 65 patients. *Eur Heart J* 1990;11:1033-1040.

191. Brown J, Stevens L, Lynch L, et al. Surgery for discrete subvalvular aortic stenosis: actuarial survival, hemodynamic results, and acquired aortic regurgitation. *Ann Thorac Surg* 1985;40:151–155.
192. Douville EC, Sade RM, Crawford FA, et al. Subvalvar aortic stenosis: timing of operation. *Ann Thorac Surg* 1990;50:29–33.
193. Brauner R, Laks H, Drinkwater DC, et al. Benefits of early surgical repair in fixed subaortic stenosis. *J Am Coll Cardiol* 1997;30:1835–1842.
194. Rizzoli G, Tiso E, Mazzucco A, et al. Discrete subaortic stenosis. Operative age and gradient as predictors of late aortic valve incompetence. *J Thorac Cardiovasc Surg* 1993;106:95–104.
195. Gersony WM. Natural history of discrete subvalvar aortic stenosis: management implications. *J Am Coll Cardiol* 2001;38:843–845.
196. Lupinetti FM, Pridjian AK, Callow LB, et al. Optimum treatment of discrete subaortic stenosis. *Ann Thorac Surg* 1992;54:467–470.
197. Konno S, Imai Y, Iida Y, et al. A new method for prosthetic valve replacement in congenital aortic stenosis associated with hypoplasia of the aortic valve ring. *J Thorac Cardiovasc Surg* 1975;70:909–917.
198. Ewart AK, Morris CA, Ensing GJ, et al. A human vascular disorder, supravalvular aortic stenosis, maps to chromosome 7. *Proc Natl Acad Sci U S A* 1993;90:3226–3230.
199. Williams JC, Barratt-Boyes BH, Lowe JB. Supravalvar aortic stenosis. *Circulation* 1961;24:1311–1318.
200. Beuren AJ, Schulze C, Eberle P, et al. The syndrome of supravalvular aortic stenosis, peripheral pulmonary stenosis, mental retardation and similar facial appearance. *Am J Cardiol* 1964;13:471–483.
201. Nickerson E, Greenberg F, Keating MT, et al. Deletions of the elastin gene at 7q11.23 occur in approximately 90% of patients with Williams syndrome. *Am J Hum Genet* 1995;56:1156–1161.
202. Eward AK, Jin W, Atkinson D, et al. Supravalvular aortic stenosis associated with a deletion disrupting the elastin gene. *J Clin Invest* 1994;93:1071–1077.
203. Li DY, Toland AE, Boak BB, et al. Elastin point mutations cause an obstructive vascular disease, supravalvular aortic stenosis. *Hum Mol Genet* 1997;6:1021–1028.
204. Meng X, Lu X, Li Z, et al. Complete physical map of the common deletion region in Williams syndrome and identification and characterization of three novel genes. *Hum Genet* 1998;103:590–599.
205. Keating MT. Genetic approaches to cardiovascular disease. Supravalvular aortic stenosis, Williams syndrome, and Long-QT syndrome. *Circulation* 1995;92:142–147.
206. Boeckel T, Dierks A, Vergopoulos A, et al. A new mutation in the elastin gene causing supravalvular aortic stenosis. *Am J Cardiol* 1999;83:1141–1143.
207. Stamm C, Friehs I, Ho SY, et al. Congenital supravalvar aortic stenosis: a simple lesion? *Eur J Cardiothorac Surg* 2001;19:195–202.
208. O'Connor WN, Davis JB, Geissler R, et al. Supravalvular aortic stenosis. Clinical and pathological observations in six patients. *Arch Pathol Lab Med* 1985;109:179–185.
209. Stamm C, Li J, Ho SY, et al. The aortic root in supravalvular aortic stenosis: the potential surgical relevance of morphologic findings. *J Thorac Cardiovasc Surg* 1997;114:16–24.
210. McDonald AH, Gerlis LM, Somerville J. Familial arteriopathy with associated pulmonary and systemic arterial stenosis. *Br Heart J* 1969;31:375–385.
211. Zalstein E, Moes CA, Musewe NN, et al. Spectrum of cardiovascular anomalies in Williams–Beuren syndrome. *Pediatr Cardiol* 1991;12:219–223.
212. Bleiden LC, Lucas RV, Carter JB, et al. A developmental complex including supravalvar stenosis of the aorta and pulmonary trunk. *Circulation* 1974;49:585–590.
213. Peterson TA, Todd DB, Edwards JE. Supravalvular aortic stenosis. *J Thorac Cardiovasc Surg* 1965;50:734–741.
214. Flaker G, Teske D, Kilman J, et al. Supravalvular aortic stenosis. A 20-year clinical perspective with patch aortoplasty. *Am J Cardiol* 1983;51:256–260.
215. Bonnet D, Cormier V, Villain E, et al. Progressive left main coronary artery obstruction leading to myocardial infarction in a child with Williams syndrome. *Eur J Pediatr* 1997;156:751–753.
216. Schmidt RE, Gilbert EF, Amend TC, et al. Generalized arterial fibromuscular dysplasia and myocardial infarction in familial supravalvular aortic stenosis syndrome. *J Pediatr* 1969;74:576–584.
217. van Son JA, Edwards WD, Danielson GK. Pathology of coronary arteries, myocardium, and great arteries in supravalvular aortic stenosis. *J Thorac Cardiovasc Surg* 1994;108:21–28.
218. Terhune PE, Buchino JJ, Rees AG, et al. Myocardial infarction associated with supravalvular aortic stenosis. *J Pediatr* 1985;106:251–255.
219. Conway EE, Noonan J, Marion RW. Myocardial infarction leading to sudden death in Williams syndrome: report of three cases. *J Pediatr* 1990;117:593–595.
220. Stamm C, Kreutzer C, Zurakowski D, et al. Forty-one years of surgical experience with congenital supravalvular aortic stenosis. *J Thorac Cardiovasc Surg* 1999;118:874–885.
221. Keane JF, Fellows KE, LaFarge CG, et al. The surgical management of discrete and diffuse supravalvar aortic stenosis. *Circulation* 1976;54:112–117.
222. French JW, Guntheroth WB. An explanation of asymmetric upper extremity blood pressures in supravalvular aortic stenosis. The Coanda effect. *Circulation* 1970;52:31–36.
223. Hallidie-Smith KA, Karas S. Cardiac anomalies in Williams–Beuren syndrome. *Arch Dis Child* 1988;63:809–813.
224. Kim YM, Yoo SJ, Choi JY, et al. Natural course of supravalvar aortic stenosis and peripheral pulmonary stenosis in Williams syndrome. *Cardiol Young* 1999;9:37–41.
225. Wessel A, Pankau R, Kececioğlu D, et al. Three decades of follow-up of aortic and pulmonary vascular lesions in the Williams–Beuren syndrome. *Am J Med Genet* 1994;52:297–301.
226. Wren C, Oslizlok P, Bull C, et al. Natural history of supravalvular aortic stenosis and pulmonary artery stenosis. *J Am Coll Cardiol* 1990;15:1625–1630.
227. Boxer RA, Fishman MC, La Corte MA, et al. Diagnosis and post-operative evaluation of supravalvular aortic stenosis by magnetic resonance imaging. *Am J Cardiol* 1986;58:367–368.
228. Giddins NG, Finley JP, Nanton MA, et al. The natural course of supravalvar aortic stenosis and peripheral pulmonary artery stenosis in Williams syndrome. *Br Heart J* 1989;62:315–319.
229. Jacob JL, Coelho WM, Machado NC, et al. Initial experience with balloon dilatation of supravalvar aortic stenosis. *Br Heart J* 1993;70:476–478.
230. de Lezo JS, Pan M, Medina A, et al. Acute aortic insufficiency complicating stent treatment of supravalvular aortic stenosis: successful release of trapped leaflets by wiring the stent. *Cathet Cardiovasc Intervent* 2004;61:537–541.
231. McGoon DC, Mankin HT, Vlad P, et al. The surgical treatment of supravalvular aortic stenosis. *J Thorac Cardiovasc Surg* 1961;41:125–133.
232. Doty DB, Polansky DB, Jenson CB. Supravalvular aortic stenosis. Repair by extended aortoplasty. *J Thorac Cardiovasc Surg* 1977;74:362–371.
233. Hazekamp MG, Kappetein A, Schoof PH, et al. Brom's three-patch technique for repair of supravalvular aortic stenosis. *J Thorac Cardiovasc Surg* 1999;118:252–258.
234. Rosenkranz ER, Murphy DJ, Cosgrove DM. Surgical management of left coronary artery ostial atresia and supravalvar aortic stenosis. *Ann Thorac Surg* 1992;54:779–781.
235. Matsuda H, Miyamoto Y, Takahashi T, et al. Extended aortic and left main coronary angioplasty with a single pericardial patch in a patient with Williams syndrome. *Ann Thorac Surg* 1991;52:1331–1333.

Robert H. Beekman, III

In its simplest form, coarctation of the aorta is a discrete stenosis of the proximal thoracic aorta (Fig. 47.1). However, considerable variation exists in coarctation anatomy as well as in its pathophysiology, clinical presentation, treatment options, and outcomes. For example, although often a discrete stenosis, coarctation may be a long segment in nature, may be associated with hypoplasia of the transverse aortic arch (common in infancy), or may be abdominal in location. The pathophysiology of coarctation varies with the severity of the stenosis, and also is affected by the presence of associated lesions, such as patent ductus arteriosus, ventricular septal defect, or left ventricular outflow obstruction. The clinical presentation of coarctation also varies, ranging from heart failure in infancy to asymptomatic hypertension and/or a murmur in an older child or adult. Treatment options include surgery (most commonly resection and end-to-end anastomosis) and percutaneous balloon angioplasty and stenting. Finally, clinical outcomes and long-term prognosis after treatment vary widely and are not entirely benign. In many patients, the late prognosis is affected by residual coarctation stenosis or arch hypoplasia, associated intracardiac pathology, and resting or exercise hypertension. It is correct to conclude that coarctation of the aorta is not the simple lesion it often appears to be.

PREVALENCE AND ETIOLOGY

Coarctation of the aorta occurs in approximately 6% to 8% of patients with congenital heart disease. The New England Regional Infant Cardiac Program (NERICP) (1) identified coarctation of the aorta as the fourth most common lesion requiring cardiac catheterization or surgery during the first year of life. Coarctation accounted for 7.5% of infants encountered in the program between 1969 and 1974. The prevalence is actually higher because the NERICP reported only infants having intervention during the first year of life. As with most left-sided obstructive lesions, coarctation occurs more commonly in males than in females, with a male:female ratio ranging from 1.27 to 1.74 (1,2).

A genetic influence on the development of coarctation has long been recognized in patients with Turner XO syndrome, in whom about 35% are affected. More recent data suggest that there is an important genetic influence on the development of left-sided obstructive lesions (3–8). For example, linkage studies have identified multiple overlapping genetic loci for left-sided obstructive lesions, including coarctation, strongly supporting the notion that these lesions are causally related (6,7). NOTCH1 mutations have been identified in some patients with bicuspid aortic valve, aortic valve stenosis, coarctation, and hypoplastic left heart syndrome (8). Environmental influence on the development of coarctation also has been suggested by a study detecting a seasonal

variation, with the incidence of coarctation peaking in the late fall and winter (9).

PATHOLOGY

Coarctation of the aorta is typically a discrete stenosis in the upper thoracic aorta, at or near the point of the insertion of the ductus arteriosus (Fig. 47.2). Most coarctations, therefore, are properly described as juxtaductal in location. The gross morphology of coarctation includes an intimal and medial malformation and a prominent posterior infolding (the posterior shelf), which, in some cases, extends around the entire circumference of the aorta (10). In fact, the gross pathology of coarctation varies considerably. Coarctation is most often a discrete stenosis (Fig. 47.3), but may be associated with isthmus and transverse arch hypoplasia (Fig. 47.4), or may be long segment and/or tortuous. In infants, particularly those with associated left-ventricular outflow obstruction or a ventricular septal defect, there may be diffuse hypoplasia of the transverse aortic arch (Fig. 47.5) and isthmus proximal to a discrete coarctation (11,12). Less commonly, coarctation of the aorta occurs in other locations, such as the ascending aorta or the abdominal aorta. Coarctation of the abdominal aorta is a complex long-segment stenosis that typically is associated with renal artery stenosis.

Histologic examination reveals thick intimal and medial ridges that protrude posteriorly and laterally into the aortic lumen (Fig. 47.2). Associated intimal thickening and hyperplasia are particularly prominent in older patients (10). The ductus or ligamentum arteriosus inserts at the same level anteromedially. Intimal proliferation and disruption of elastic tissue may occur distal to the coarctation (the jet lesion), at a site where high-velocity flow impacts the arterial wall. It is this distal site where infective endarteritis, intimal dissections, or aneurysms may occur. Cystic medial necrosis, consisting of depletion and disarray of medial elastic tissue, occurs commonly in the aorta adjacent to the coarctation site (13) and in the ascending aorta as well. In some patients, cystic medial necrosis provides the histologic substrate for late aortic aneurysm formation or dissection.

Coarctation of the aorta may be associated with intracardiac pathology in some patients. Children who present in infancy are much more likely than older patients to have an associated ventricular septal defect and/or left ventricular outflow obstruction. Ventricular septal defects associated with coarctation include the perimembranous, muscular, or malalignment types. With a malalignment ventricular septal defect, posterior deviation of the conal septum may cause significant left ventricular outflow tract obstruction (14,15). A bicuspid aortic valve occurs in up to 85% of patients with a coarctation, and the valve may be stenotic or the annulus hypoplastic. Mitral

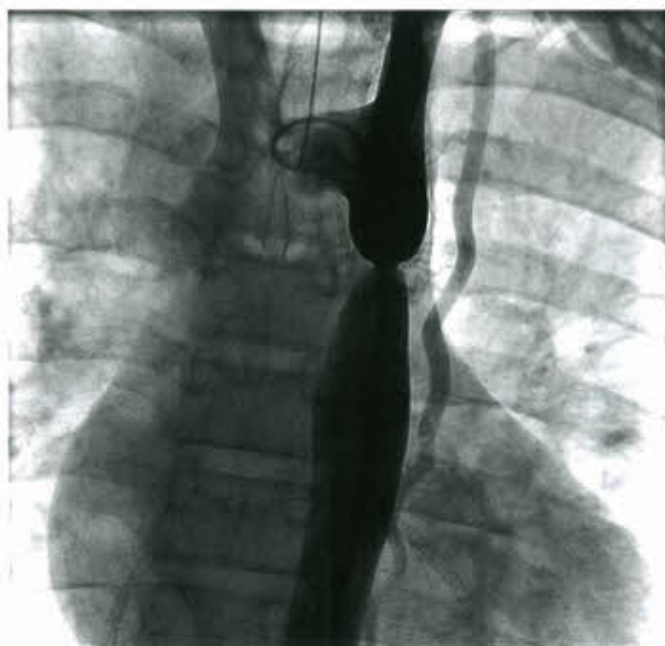


Figure 47.1 Aortogram demonstrating a discrete coarctation of the thoracic aorta. A somewhat tortuous left internal mammary artery is apparent.

stenosis also occurs in patients with coarctation and may be caused by a supravalvar mitral ring, thickening and dysplasia of the mitral leaflets, short dysplastic chordae tendineae, or the presence of a single “parachute” papillary muscle (16). The association of multiple left-sided obstructive lesions with

coarctation has been referred to as Shone syndrome (17), and constitutes a challenging group of lesions when treatment is required in infancy. Other intracardiac anomalies that may be associated with coarctation include atrioventricular septal defects, D-transposition with or without tricuspid atresia, the Taussig-Bing type of double-outlet right ventricle, and congenitally corrected transposition of the great arteries. Coarctation also is an important component of the hypoplastic left heart syndrome.

Extracardiac vascular anomalies are present in many patients with coarctation and include variations in brachiocephalic artery anatomy, a collateral arterial circulation, and aneurysms of the circle of Willis. Thoracic coarctation usually occurs just beyond the origin of the left subclavian artery, but variations in the brachiocephalic arterial vessels may occur. The left subclavian artery may arise at the site of coarctation and may be stenotic at its origin. The right subclavian artery arises anomalously below the coarctation as the last brachiocephalic branch in 4% to 5% of cases. Reversed vertebral artery flow to a subclavian artery arising at or below a coarctation may produce the subclavian steal syndrome. A collateral arterial circulation, augmenting perfusion to the descending aorta, may develop by childhood or adolescence but is rarely present in infancy. This collateral system has two components: an anterior and a posterior collateral circulation. The anterior circulation develops between internal mammary arteries and the external iliac arteries via the epigastric arterial system. The posterior collateral circulation develops between the thyrocervical arteries and the descending aorta via retrograde flow through enlarged intercostal arteries. These intercostal arteries may become dilated and tortuous, producing palpable thoracic thrills, continuous murmurs, and rib notching on the chest roentgenogram. Finally, saccular (“berry”) aneurysms occur in the circle of Willis in 3% to 5% of patients with coarctation. These may be responsible

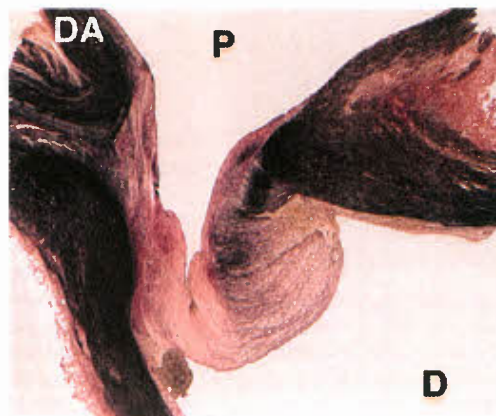
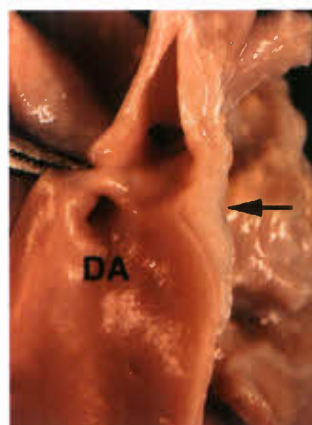
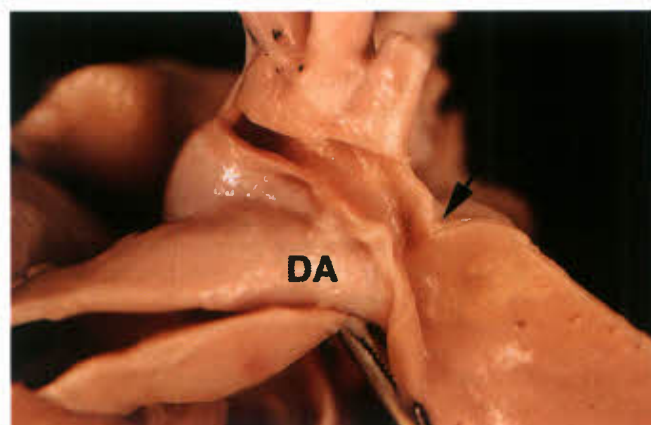


Figure 47.2 Upper left: Autopsy findings in a typical juxtaductal coarctation. The posterior shelf (arrow) is seen opposite a patent ductus arteriosus (DA). Upper right: Discrete coarctation (arrow) with DA distally. Lower left: DA inserts distal to a hypoplastic transverse aortic arch. There is poststenotic dilation of the aorta distally. Lower right: Elastic stain demonstrating disorganized media and intimal proliferation on the discrete “posterior shelf” on the right, opposite the DA; P, proximal aortic lumen; D, distal aortic lumen.

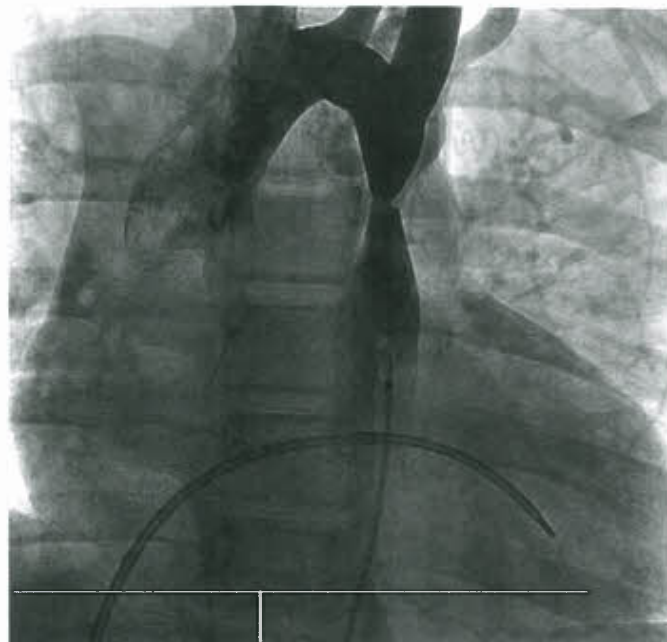


Figure 47.3 Aortogram demonstrating a discrete coarctation of the thoracic aorta in a 12-year-old child. The transverse arch and isthmus are well developed. A catheter is positioned in the left ventricle via an atrial transeptal puncture.

for cerebral vascular accidents in some patients with arterial hypertension.

Extracardiac nonvascular anomalies are also common in patients with coarctation of the aorta. In addition to Turner XO syndrome, abnormalities of the musculoskeletal system, genitourinary system, gastrointestinal system, or respiratory

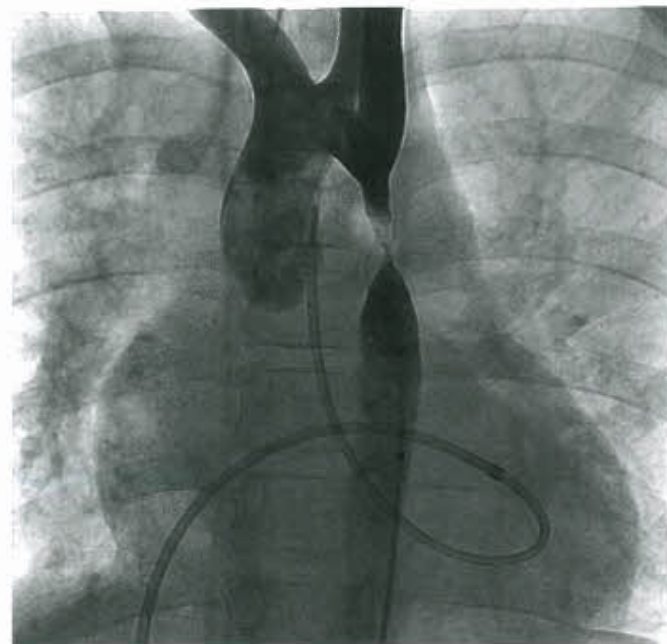


Figure 47.4 Aortogram demonstrating a very severe coarctation with hypoplasia of the aortic isthmus and transverse arch. A tiny ductus is seen entering at the site of the coarctation. A catheter is positioned in the ascending aorta via an atrial transeptal puncture.



Figure 47.5 Left ventricular angiogram (lateral projection) in an infant with coarctation of the aorta and hypoplasia of the transverse aortic arch. The transverse arch is moderately between the carotids and the left subclavian artery. There is a patent ductus arteriosus which inserts beyond the coarctation.

system are present in as many as 25% of children with coarctation (1,18). There is also an increased incidence of head and neck abnormalities in patients with coarctation, raising the possibility that a neural crest abnormality may be involved in the embryogenesis of coarctation (19).

EMBRYOLOGY

The aortic arch and its branches develop during the sixth to eighth week of human gestation. The embryologic third aortic arches persist as the common carotid arteries. The left fourth aortic arch forms the thoracic aortic arch and isthmus, and the right fourth arch normally involutes. The embryologic sixth aortic arches persist as the proximal pulmonary arteries, with the left sixth aortic arch developing distally into the ductus arteriosus. Thoracic coarctation is, therefore, a manifestation of abnormal development of the embryologic left fourth and sixth aortic arches (20). The underlying cause is not well understood. Two concepts have been advanced, neither of which is entirely satisfactory: the ductus tissue theory and the hemodynamic theory.

Coarctation occurs most commonly at the site of insertion of the ductus arteriosus. The ductus tissue theory proposes that coarctation develops as the result of migration of ductal smooth muscle cells into the periductal aorta, with subsequent constriction and narrowing of the aortic lumen (21). This concept is concordant with the clinical observations that coarctation often becomes manifest after ductus closure and that it may be palliated in the newborn with prostaglandin E_1 infusion. However, the ductal tissue theory does not adequately explain aortic coarctation that occurs distant from the insertion of the ductus arteriosus, such as in the transverse arch or abdominal aorta.

The hemodynamic theory proposes that coarctation develops because of hemodynamic disturbances that reduce the volume of blood flow through the fetal aortic arch (22). In the normal fetus, the aortic isthmus receives only 10% of the combined ventricular output, which explains the observation that

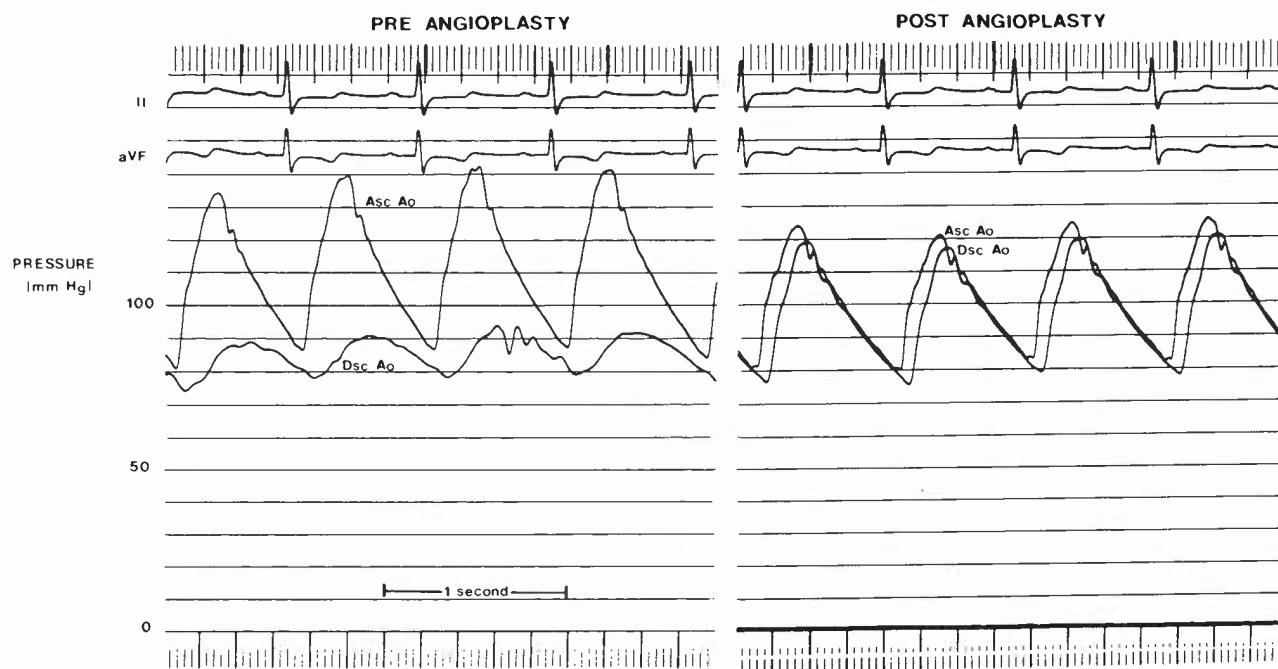


Figure 47.6 Simultaneous pressure recordings from the ascending and descending aorta in a child with coarctation, before and immediately after balloon angioplasty. Prior to angioplasty (**left panel**) typical pressure contours are demonstrated: The systolic and pulse pressures are elevated in the ascending aorta and diminished in the descending aorta. A pressure gradient is present throughout systole and diastole. After angioplasty (**right panel**), the pressure contours are normalized, with the peak systolic gradient decreasing from 50 to 5 mm Hg.

the normal isthmus diameter is only about 70% to 80% of the diameter of the neonatal ascending aorta (22). According to the hemodynamic theory, intracardiac lesions that diminish the volume of left ventricular outflow promote development of coarctation in the fetus by reducing flow through the aortic isthmus. This theory does help to explain the common association of coarctation with ventricular septal defect, aortic stenosis, and hypoplasia of the transverse aortic arch. It is also consistent with fetal echocardiographic studies demonstrating that hypoplasia of the transverse arch and isthmus are common in fetuses with coarctation (23). An interesting variation of the hemodynamic theory has been proposed to account for the occurrence of coarctation in girls with Turner syndrome. It is suggested that fetal lymphatic obstruction, which may cause the webbed neck in Turner syndrome, also leads to distended thoracic ducts that compress the fetal ascending aorta and promote the development of coarctation (24).

HEMODYNAMICS

Fetal hemodynamics are rarely disturbed by the presence of a coarctation because normally only 10% of the combined ventricular output traverses the aortic isthmus in utero. After birth, with closure of the foramen ovale and ductus arteriosus, a substantially larger volume flow must cross the stenotic aortic segment. Therefore, important hemodynamic disturbances may occur postnatally. Depending on the severity of coarctation and the presence of associated cardiac lesions, these hemodynamic changes range from mild systolic hypertension to severe heart failure and shock.

Coarctation of the aorta increases impedance to left ventricular outflow and elevates systolic pressure in the left ventricle, the ascending aorta, and its branches. Depending on the severity of the stenosis, the cardiac output, and the extent of

the collateral circulation, the systolic pressure gradient generated across a coarctation may be as high as 50 to 60 mm Hg at rest. In many patients, a pressure gradient from ascending to descending aorta exists throughout systole and diastole (Fig. 47.6). Multiple compensatory mechanisms assist the left ventricle in response to the increase in outflow impedance. Left ventricular myocardial hypertrophy is perhaps the most important. Myocardial hypertrophy tends to normalize myocardial wall stress and ventricular afterload (25) and helps maintain normal systolic ventricular function. In isolated coarctation, left ventricular end-diastolic volume is typically normal, and the end-systolic volume may be reduced. Thus, left ventricular ejection fraction is normal to increased in most children with coarctation of the aorta (in the absence of heart failure).

If a coarctation is severe or develops rapidly, as in a newborn upon ductal closure, left ventricular systolic dysfunction and heart failure may ensue. The hemodynamic consequences include diminished stroke volume, increased left ventricular end-diastolic pressure, elevated left atrial pressure, pulmonary venous congestion, and pulmonary artery hypertension. If cardiac output is severely compromised, diminished myocardial perfusion and the development of acidosis further depress myocardial contractility. This clinical scenario is particularly common in the first weeks of life. Compensatory mechanisms include activation of the sympathetic nervous system (to increase heart rate and enhance myocardial contractility) and the Frank-Starling mechanism (to increase left ventricular end-diastolic volume and help maintain a normal stroke volume). The immature myocardium, however, is relatively ineffective in using these compensatory responses (26). The neonatal myocardium lacks mature sympathetic innervation as a result, in part, of a decrease in sympathetic beta-receptor density. Further, compared with the adult myocardium, the neonatal left ventricular myocardium is poorly compliant and less able to enlist the Frank-Starling mechanism to preserve ventricular stroke volume. Finally, with severe coarctation in

the newborn, left ventricular pressure overload occurs rapidly upon closure of the ductus arteriosus, without time for myocardial hypertrophy to develop. Thus, left ventricular afterload and wall stress increase in a relatively uncompensated fashion. Many factors, therefore, make the immature myocardium of infancy particularly vulnerable to the hemodynamic disturbances imposed by severe coarctation and explain the observation that systolic dysfunction and heart failure in coarctation are confined primarily to the first weeks of life.

Coarctation also may cause left ventricular diastolic dysfunction. Echocardiographic studies have demonstrated a decreased rate of early left ventricular diastolic relaxation, with consequent abnormalities in diastolic filling characterized by a shift of left ventricular filling into late diastole (27). These abnormalities in diastolic function are believed to relate to diminished left ventricular compliance caused by myocardial hypertrophy, myocardial fibrosis, and, in some patients, an increase in the inotropic state of the myocardium. An important functional consequence is an increase in left ventricular end-diastolic pressure at any given filling volume. Thus, left atrial hypertension and pulmonary venous congestion may occur, particularly in patients with an increased left ventricular end-diastolic volume.

The presence of an associated cardiovascular defect compounds the hemodynamic burden in some patients with a coarctation. Valvar or subvalvar aortic stenosis will increase the left ventricular systolic pressure and ventricular afterload further. A large ventricular septal defect, patent ductus arteriosus, or mitral regurgitation will increase left ventricular end-diastolic volume and ventricular preload. In concert with diminished left ventricular compliance, the augmented diastolic volume leads to an increase in left ventricular end-diastolic pressure. Subsequently, left atrial pressure will rise, and pulmonary venous and arterial hypertension may develop. Therefore, heart failure and pulmonary artery hypertension are relatively common in children with coarctation and associated aortic stenosis and/or ventricular septal defect as a consequence of disturbances in left ventricular preload, afterload, and diastolic function.

Abnormalities in vascular physiology also occur in patients with coarctation of the aorta. Systolic arterial hypertension is a manifestation of the aortic constriction, but it also reflects changes in vascular reactivity, arterial wall compliance, and baroreceptor reflex function. Studies of patients after coarctation repair have demonstrated abnormal arterial vascular function (28–30), as well as resetting of the baroreceptor reflex in some patients with persistent hypertension (31). Such abnormalities in arterial physiology, which may be present after successful anatomic relief of coarctation, help to explain the occurrence of systolic hypertension in some patients many years after coarctation repair.

CLINICAL FEATURES

The clinical presentation of coarctation generally follows one of three patterns: an infant with congestive heart failure, a child with a heart murmur, or a child or adolescent with systemic arterial hypertension. When coarctation manifests in infancy, it often presents as a catastrophic illness. Congestive heart failure and shock often occur suddenly as the ductus arteriosus closes. A large proportion of these infants have coarctation with important associated lesions such as a ventricular septal defect or aortic stenosis. In an infant with severe coarctation and a large ventricular septal defect, acute heart failure, shock, and acidosis classically develop suddenly around 8 to 10 days of life. Multiorgan system failure, particularly renal failure and/or necrotizing enterocolitis and death occur rapidly unless definitive medical and surgical interventions are provided immediately.

Coarctation of the aorta may present later in childhood as systolic upper extremity hypertension or as a heart murmur. Delayed diagnosis beyond infancy is common as physical findings may be subtle, and most of these patients are asymptomatic. On careful investigation, some will report lower extremity claudication with exercise or frequent headaches. In a review of children (older than 1 year) presenting with coarctation at Columbia University between 1969 and 1978, the median age at diagnosis was 10 years (32). The most common causes for referral were hypertension or a heart murmur. The correct diagnosis of coarctation was made by the referring physician in only 14% of cases.

Physical Examination

The general appearance of a child with coarctation will vary depending on the mode of presentation. In an infant with heart failure, one encounters a pale, irritable child in respiratory distress. Tachycardia, dyspnea, diaphoresis, hepatomegaly, and poor perfusion signal the presence of congestive heart failure and low cardiac output. Differential cyanosis may be observed (cyanosis confined to the lower extremities) if a right-to-left ductal shunt is present. In contrast, an older child with coarctation may appear entirely healthy. The characteristic findings of Turner syndrome are evident in some girls, and include short stature, widely spaced nipples, and a webbed neck. Not all girls with the Turner genotype manifest the phenotype.

The hallmark physical findings in coarctation consist of discrepant arterial pulses and systolic blood pressures in the upper and lower extremities. Arterial pulses below the coarctation are diminished in amplitude and delayed in timing compared with the proximal pulses (*pulsus parvus et tardus*). Systolic blood pressure is elevated proximal to the coarctation, and a systolic pressure gradient is present between the arm and leg. Several clinical circumstances may make detection of arterial pulse and pressure discrepancies difficult. First, the coarctation pressure gradient may be minimal, sometimes as a result of a mild coarctation, but also with heart failure and diminished cardiac output or with a large patent ductus arteriosus. Descending aorta flow may be maintained by a right-to-left ductal shunt and, in the presence of a large ventricular septal defect, the perfusion may be well oxygenated and pulsatile. Second, detection of arterial pulse and pressure differences may be difficult because of variations in brachiocephalic artery anatomy. An anomalous right subclavian artery arises distal to the coarctation in approximately 3% to 4% of cases. In these patients, the arterial pulse and blood pressure are identical in the right arm and leg, and discrepancies are detected only in the left arm. In other patients, the left subclavian artery arises adjacent to the coarctation, and its orifice may be stenotic. In such patients, a bounding arterial pulse and elevated systolic pressure will be detected only in the right arm. Rarely, patients may present with an anomalous right subclavian artery and a stenotic left subclavian artery. In these patients, arterial differences in the four extremities will not be detected, although carotid artery pulsations will be bounding.

Several findings may be noted on palpation of the precordium. Left ventricular pressure and volume overload may produce a prominent, heaving ventricular impulse at the apex. A prominent right ventricular impulse at the lower left sternal border or xiphoid area occurs if there is associated pulmonary hypertension. A systolic thrill may be palpable in the suprasternal notch, but the presence of a precordial thrill is unusual in isolated coarctation and should raise suspicion of an associated intracardiac lesion. If a robust collateral system exists, a common occurrence in older children and adolescents, prominent collateral artery pulsations may be palpable in the intercostal areas and/or between the scapulae posteriorly.

Auscultation generally reveals normal first and second heart sounds. A constant systolic ejection click may be heard at the apex, signaling the presence of a bicuspid aortic valve. Several murmurs may be present, depending on the nature of the coarctation, associated intracardiac lesions, and the arterial collateral system. A grade 2–3/6 systolic ejection murmur originating from the coarctation itself is usually best heard at the upper left sternal border, at the base, and in the left interscapular area posteriorly. If the coarctation is severe, this systolic murmur may be long and spill into diastole. The interscapular location of the murmur helps to identify the site of coarctation as the upper thoracic aorta. Continuous murmurs may be prominent throughout the chest anteriorly, laterally, and posteriorly in patients with a well-developed arterial collateral system. Associated intracardiac lesions create other murmurs. Aortic valve stenosis will produce a systolic ejection murmur at the upper right sternal border. A ventricular septal defect or mitral regurgitation will produce an S1-coincident holosystolic murmur at the lower left sternal border or apex. Associated mitral stenosis or a large left-to-right ventricular shunt will give rise to a mid-diastolic rumble at the apex. Finally, a gallop rhythm may be heard in an infant with congestive heart failure. If the cardiac output is severely diminished, murmurs may be subtle and the gallop rhythm may be the most prominent auscultatory finding.

Electrocardiographic Features

An infant presenting with coarctation of the aorta generally has a normal electrocardiogram (33). The finding of left ventricular hypertrophy in infancy, particularly with a strain pattern of ST segment and T-wave depression, strongly suggests associated aortic stenosis or primary myocardial disease. The electrocardiogram of older children and adolescents will reflect the effects of long-standing left ventricular pressure overload. Left ventricular hypertrophy and left atrial enlargement may be present. Associated intracardiac lesions will affect the electrocardiographic findings. The frontal-plane QRS axis may be left and anterior with associated atrioventricular septal defects, double-outlet right ventricle, or primary myocardial disease. Left ventricular hypertrophy with strain may indicate the presence of severe valvar or subvalvar aortic stenosis. Right ventricular hypertrophy that persists beyond infancy may indicate the presence of pulmonary hypertension resulting from associated lesions, such as a ventricular septal defect or mitral stenosis.

Radiologic Features

The chest roentgenogram of an infant with coarctation who presents with congestive heart failure is nonspecific. Moderate to severe cardiomegaly is evident, and the pulmonary vascular markings are increased. Pulmonary vascular congestion may be indistinct and passive in nature, related to left ventricular failure or mitral stenosis with pulmonary venous hypertension, or it may be active and related to increased pulmonary blood flow from a large left-to-right shunt. Rib notching is not present in infants because the collateral circulation is not yet well developed.

In older children and adolescents with coarctation of the aorta, the chest roentgenogram typically shows normal or only mildly enlarged heart size. The pulmonary vascular markings are normal unless there is an associated defect present. An abnormal contour of the aortic arch is common on the frontal film and consists of a localized indentation of the aorta at the site of coarctation (3 sign). Immediately below the 3 sign, the descending aorta may be prominent due to poststenotic dilation. Rib notching may be found in older patients. It is caused by erosion of the inferior surfaces of posterior ribs by dilated and tortuous intercostal arteries (Fig. 47.7). Rib notching may be unilateral if one subclavian artery is stenotic or arises distal to the coarctation.

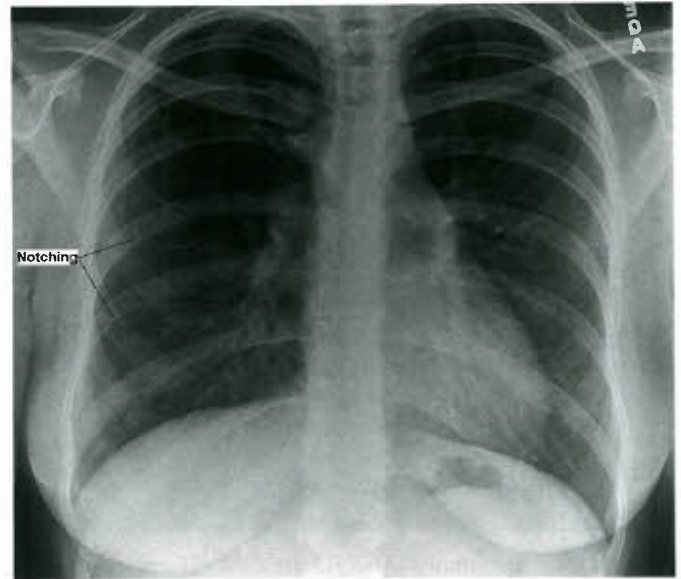


Figure 47.7 Chest radiograph of a woman with unrepaired coarctation demonstrating rib notching from dilated and tortuous intercostal arteries.

Magnetic Resonance Imaging and CT Angiography

High-quality images of coarctation can be obtained by magnetic resonance imaging (MRI). MRI images in the sagittal and parasagittal projections can clearly define the location and severity of coarctation (Fig. 47.8), and the anatomy of the aortic arch. Information about the presence of a patent ductus arteriosus and the collateral arterial circulation also may be obtained. Three-dimensional surface rendering can provide exquisite anatomic detail in these patients (34). MRI studies are particularly suited to patients who require high-resolution

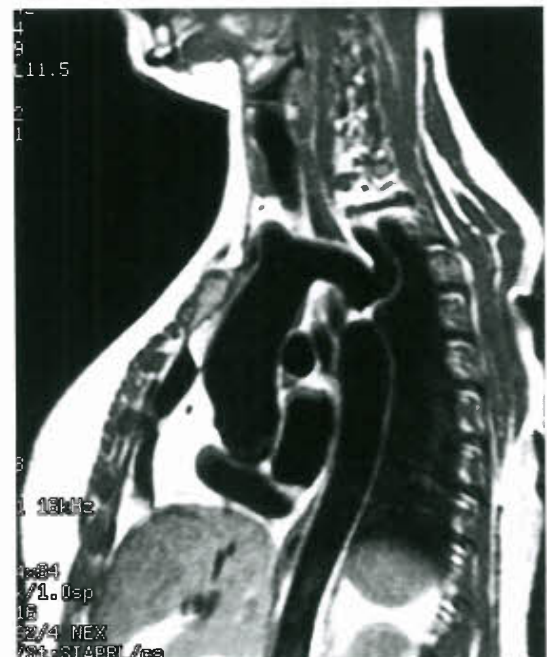


Figure 47.8 Magnetic resonance image in a sagittal projection demonstrating a discrete coarctation of the aorta just distal to the left subclavian artery. There is mild dilation of the descending aorta.

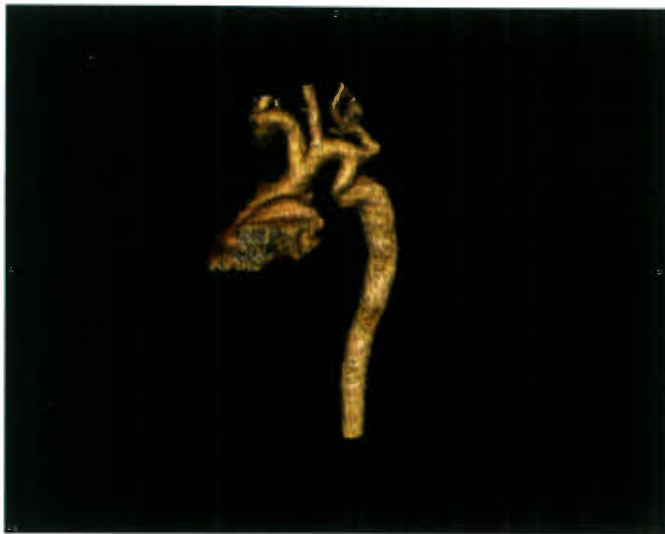


Figure 47.9 Three-dimensional reformatted CT angiogram in a left-lateral projection in a 19-month-old infant with a discrete coarctation and a tortuous, somewhat hypoplastic transverse arch and isthmus.

serial imaging, such as before and after surgical repair, angioplasty, or stenting (35). MRI studies can also provide an assessment of aortic flow, and can estimate pressure gradients (36). Multidetector CT angiography can also provide excellent anatomic diagnosis in patients with coarctation and aortic arch anomalies (Fig. 47.9). CT angiographic data are acquired very rapidly (typically in 4 to 5 seconds) as gating is not required as with MRI studies. Unlike MRI examinations, however, CT angiography does expose the patient to ionizing radiation.

Echocardiography

Two-dimensional echocardiography and Doppler studies provide an accurate, noninvasive assessment of coarctation anatomy and physiology in most patients. High-quality ultrasound images of coarctation can be obtained in infants but may be somewhat difficult to obtain in larger children and adolescents. From the suprasternal long-axis view, typical thoracic coarctation appears as a localized narrowing of the thoracic aorta just beyond the origin of the left subclavian artery (Fig. 47.10). The narrowing appears as a shelf of fibrous tissue protruding from the posterior aspect of the aorta and oriented toward the ductus arteriosus (the “posterior shelf”). Associated findings such as isthmus hypoplasia, poststenotic dilation, and diminished systolic pulsations in the descending aorta serve to confirm the presence of a significant coarctation. Color-flow Doppler assists in localizing the site of obstruction and is particularly helpful in cases where 2-D imaging is difficult or inconclusive.

Doppler echocardiography can assist in determining the hemodynamic severity of a coarctation. A continuous-wave Doppler study from the suprasternal window will detect high-flow velocity across the stenosis (Fig. 47.11). A peak instantaneous pressure gradient may be determined from the maximal flow velocity using the modified Bernoulli equation. The Doppler-flow display across the coarctation often demonstrates a pattern of diastolic runoff, particularly in patients with a severe stenosis or with a robust collateral circulation. The continuous wave Doppler flow profile across a coarctation is composed of two superimposed signals representing low-velocity flow in the proximal descending aorta (proximal to the coarctation) and higher-velocity flow across the coarctation itself. A corrected gradient is obtained by subtracting

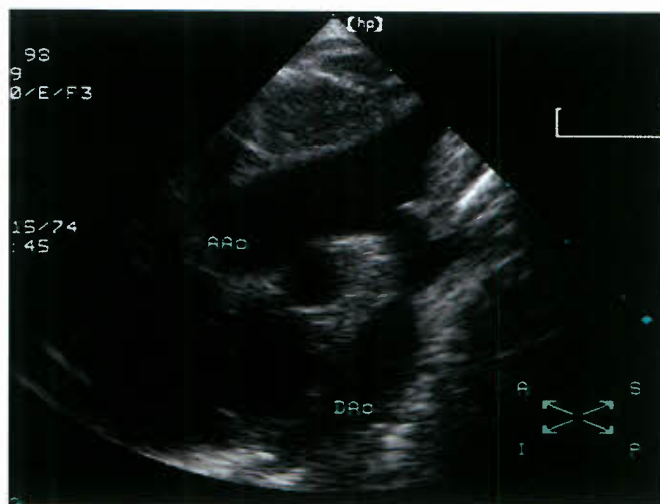


Figure 47.10 Two-dimensional echocardiogram obtained in the suprasternal long-axis view demonstrating a discrete coarctation of the aorta. Aao, ascending aorta; Dao, descending aorta.

the proximal gradient (V1) from the gradient at the coarctation site (V2).

Two-dimensional and Doppler echocardiography is particularly important in evaluating intracardiac lesions that may be associated with coarctation. High-quality echocardiographic studies yield sufficient anatomic and physiologic data to enable the clinician to make a comprehensive diagnosis without the need for further diagnostic imaging in most patients.

Cardiac Catheterization and Angiography

Cardiac catheterization can serve both diagnostic and therapeutic purposes in patients with a coarctation. Diagnostic cardiac catheterization is unnecessary if noninvasive evaluation clearly delineates the lesions that are present. If important clinical questions remain regarding the nature and severity of a coarctation or possible associated intracardiac lesions, a diagnostic cardiac catheterization may be performed. The objectives of a diagnostic cardiac catheterization in a patient with coarctation are to define the anatomy and severity of the coarctation, the nature of the arterial collateral circulation, the presence and severity of associated lesions, left ventricular function, and pulmonary artery pressure and resistance.

The hemodynamic severity of a coarctation often is assessed by the magnitude of the systolic pressure gradient. Coarctation causes an elevated systolic pressure and pulse pressure within the ascending aorta and a diminished systolic pressure and pulse pressure in the descending aorta (Fig. 47.6). In a child with an isolated coarctation and a normal cardiac output, a systolic gradient <20 mm Hg is often indicative of mild coarctation. However, pressure gradient alone may underestimate the hemodynamic importance of a coarctation. The pressure gradient may be diminished with left ventricular dysfunction and low cardiac output, by a large patent ductus arteriosus, by multiple left-sided obstructive lesions in series, or by a well-developed collateral circulation that decompresses the ascending aorta. Thus, the hemodynamic importance of a measured coarctation gradient must be assessed in the context of the patient's overall anatomy and hemodynamic status.

Angiography remains a gold standard for evaluating coarctation and aortic arch anatomy. The anatomy of the coarctation and collateral circulation generally is best imaged by an ascending aortogram filmed in the anteroposterior and straight lateral projections. In some patients, the anteroposterior camera is rotated 10 to 15 degrees left anterior oblique

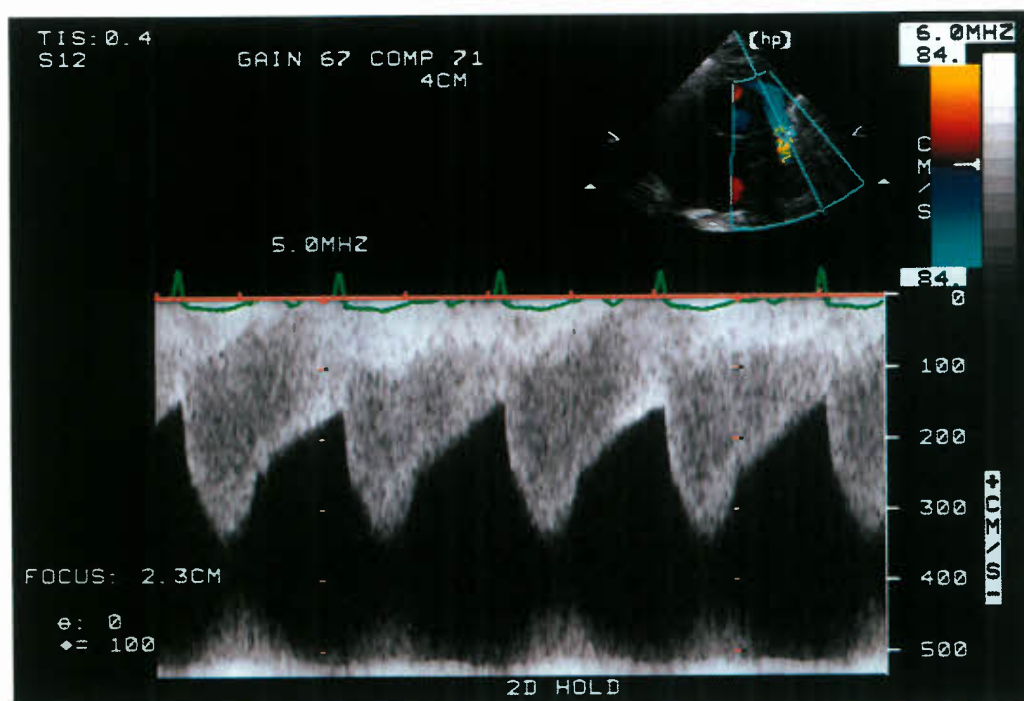


Figure 47.11 Typical continuous-wave Doppler display across a severe coarctation. The peak velocity is 3.4 m/s. Note the diastolic runoff pattern consistent with a pressure gradient throughout diastole.

(LAO) to unwrap the ascending from the descending aorta. If the ascending aorta is not catheterized, the coarctation anatomy may be visualized satisfactorily in some patients with a left ventricular angiogram alone.

TREATMENT

Untreated coarctation of the aorta has a poor natural history. In his classic 1970 study, Campbell reported natural history data obtained from necropsy and clinical records on 465 patients with coarctation (37). Only subjects who survived the first year of life were evaluated, thus excluding infants with critical coarctation and congestive heart failure. Nevertheless, Campbell's natural history data for untreated coarctation beyond infancy documented a mean age at death of only 34 years (median, 31 years); 75% of patients died by 46 years of age. The most common causes of death were congestive heart failure (26%), aortic rupture (21%), bacterial endocarditis (18%), and intracranial hemorrhage (12%). Given such a poor prognosis untreated, it is apparent that intervention is indicated in virtually all patients with coarctation of the aorta. The timing of therapy depends on the nature of the patient's presentation.

Presentation in Infancy

Coarctation presenting with heart failure in infancy requires immediate and aggressive treatment. Medical management consists of initially stabilizing the patient with inotropic support and diuretic therapy. A critically ill newborn also may benefit from prostaglandin E1 to promote ductal patency and improve perfusion of the descending aorta, renal, and mesenteric beds (38). Metabolic disturbances, such as acidosis, hypothermia, hypoglycemia, or anemia must be treated promptly. After a brief period of medical management to stabilize the child, definitive repair should be performed (39). In experienced centers, the mortality rate for surgical repair of isolated coarctation in infancy is extremely low (40–47).

The surgical risks are higher for infants with coarctation who have associated major intracardiac anomalies. Nevertheless, after a period of medical stabilization, early repair of the coarctation also is indicated in these children. The surgical mortality rate for these infants ranges from 2% to 10% and is highest for children with the most complex intracardiac defects (40–43,45). The need for intracardiac repair (or pulmonary artery banding) at the time of coarctation repair is not always clear. In some circumstances, coarctation repair alone is sufficient and actually may improve the pathophysiology of the associated lesion. For example, following repair of coarctation an infant with a ventricular septal defect may demonstrate a diminished left-to-right shunt and resolution of congestive heart failure. Subsequently, some will experience spontaneous diminution in size of the ventricular septal defect sufficient to avoid future intracardiac surgery. Modest hypoplasia of the aortic or mitral valves may improve in follow-up after surgical repair of the coarctation in the newborn period (48). Intracardiac repair at the time of coarctation repair is appropriate in infants with a large ventricular septal defect or with a more complex lesion such as D-transposition with ventricular septal defect or double-outlet right ventricle. A single-stage, anterior approach to complete repair in newborns with coarctation and intracardiac anomalies is an effective and relatively safe option in many centers (49,50).

Presentation in Childhood

Coarctation more commonly presents in childhood or adolescence as upper extremity hypertension and/or a heart murmur, but without overt symptoms. The timing of coarctation repair in this setting is relatively elective. Coarctation repair is commonly recommended at 1 to 3 years of age in asymptomatic children without severe upper-extremity hypertension. This practice is based on several considerations. First, the risk for late recurrence of coarctation appears to be increased when repair is performed on patients under 1 year of age (40–42,51–54). The influence of age at repair on restenosis is explained in part by the smaller diameter of

the surgical anastomosis when repair is performed in younger children (55). Second, even in the absence of residual stenosis, there is an increased risk for persistent hypertension and early atherosclerotic cardiovascular disease if coarctation repair is delayed into late childhood and adolescence (56). In a long-term follow-up study of 234 patients, the prevalence of residual hypertension was 6% in patients who underwent coarctation repair between 1 and 5 years of age compared with 30% to 50% in patients whose coarctation was repaired at an older age (57). An informative retrospective follow-up study (54) used multivariate analysis to assess influence of age at operation on composite outcomes of survival, residual hypertension, and recurrent stenosis. The study concluded that these outcomes are optimized if elective coarctation repair is performed at approximately 1.5 years of age.

Surgical Repair

Many surgical techniques have been used to repair aortic coarctation, and each has advantages and disadvantages. Surgical approaches to coarctation include resection and end-to-end anastomosis, subclavian flap aortoplasty, prosthetic patch aortoplasty, and bypass grafts between the ascending and descending aorta. Regardless of the technique, surgical coarctation repair generally is performed through a left lateral thoracotomy incision. If necessary, as when combined with repair of an intracardiac lesion, coarctation repair can be performed from an anterior approach. Regardless of the surgical technique used, most children with a discrete coarctation will have a residual resting systolic pressure gradient under 10 to 15 mm Hg immediately after repair.

The mortality rate for surgical coarctation repair varies depending on patient age and associated lesions. The surgical mortality for repair of isolated coarctation in infants and older children currently approaches 0% (45,46,58), rises to 2% to 10% for infants with an associated large ventricular septal defect, and is higher in the presence of more complex intracardiac lesions. Surgical morbidity includes postoperative paradoxical hypertension, spinal cord ischemia and paralysis, recurrent laryngeal or phrenic nerve injury, chylothorax, bleeding, and infection. Paradoxical hypertension (the postcoarctectomy syndrome) may occur during the first 2 to 5 days following coarctation repair, with systolic and diastolic pressures rising above pretreatment levels (59). In severe cases, mesenteric arteritis and bowel ischemia may develop. The mechanism is related to rebound activation of the sympathetic nervous system and the renin-angiotensin system with mesenteric arterial vasoconstriction. Postoperative paradoxical hypertension can be prevented with beta-blocker therapy (60) and by aggressive antihypertensive therapy during the immediate postoperative period. Spinal cord injury and subsequent paralysis may occur if aortic cross-clamping severely compromises perfusion to the descending aorta and spinal arteries. This rare complication appears to be limited to patients with a poor arterial collateral circulation. It is avoided by ensuring adequate descending aorta perfusion when the aorta is cross-clamped, limiting total cross-clamp time to under 30 minutes, minimizing the number of intercostal arteries sacrificed, avoiding hyperthermia, and using hypothermia if necessary (61). Left heart bypass may be necessary in some patients to maintain adequate descending aorta perfusion when the aorta is cross-clamped.

Reoperation for postoperative residual or recurrent coarctation is technically more difficult and carries a higher risk for morbidity and mortality than initial surgery for native disease (51,52). The surgical techniques used have included prosthetic or subclavian patch aortoplasty, bypass grafts from the ascending to descending aorta, and less commonly simple resection. Residual coarctation gradients and upper-extremity hypertension may persist postoperatively in a substantial

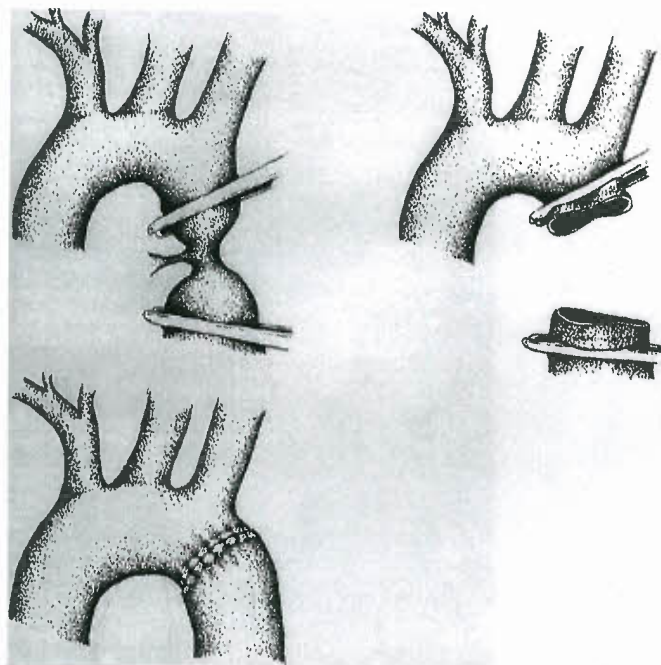


Figure 47.12 Coarctation resection and end-to-end anastomosis. The circumferential anastomosis is completed with interrupted sutures anteriorly.

portion of patients. The reported experience with reoperation, which is less satisfactory than initial surgery for native coarctation, is explained in part by patient selection. Patients requiring reoperation are older and more likely to have complex arch anatomy, such as long-segment coarctation or arch hypoplasia, compared with patients undergoing initial repair.

Surgical repair of coarctation of the aorta was first reported in 1945 by Crafoord and Nylin (62), who described the technique of resection and end-to-end anastomosis (Fig. 47.12). In most centers, this procedure remains the surgical treatment of choice for patients with a discrete coarctation. An extended end-to-end anastomosis using a broader longitudinal incision across the proximal aorta (Fig. 47.13) improves the effectiveness of this operation in infants with hypoplasia of the isthmus or transverse arch (63), and has decreased the risk of late restenosis (45,46,58). The advantages of resection include removal of the coarcted segment and adjacent areas of ductal tissue, avoidance of prosthetic materials, and sparing the left subclavian artery in most instances. Disadvantages of resection relate primarily to the presence of a circumferential suture line, which led to a high incidence of restenosis in early studies. The use of interrupted and absorbable sutures anteriorly and an extended anastomosis in patients with isthmus or arch hypoplasia have improved clinical outcomes after resection in more recent studies (45,46,49,58,63).

Prosthetic patch aortoplasty was the second surgical technique described for coarctation repair, by Vosschulte in 1961 (64). A longitudinal incision is made across the coarctation, if necessary extending onto the proximal left subclavian artery and the area is enlarged with a patch of Dacron or Gore-Tex (Fig. 47.14). The posterior shelf of the coarctation may or may not be resected. Compared with coarctation resection, patch aortoplasty has the advantages of requiring less extensive aortic mobilization, preserving intercostal arteries, and avoiding a circumferential suture line. Patch aortoplasty also can be used for some long-segment coarctations. The disadvantages of this technique include the use of prosthetic material and a relatively high incidence of late aortic aneurysm formation (34,65–67).

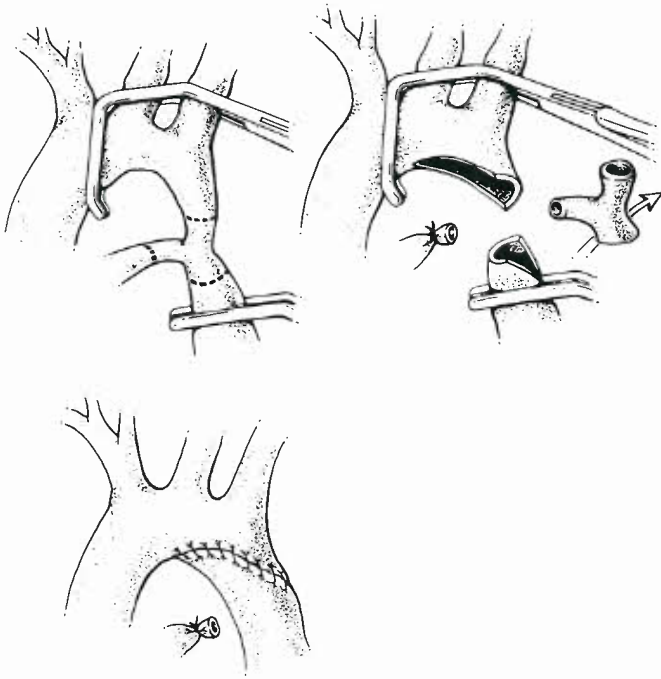


Figure 47.13 Resection with an extended end-to-end anastomosis. The anastomosis extends onto the transverse arch under the left common carotid.

The subclavian flap aortoplasty procedure was introduced in 1966 by Waldhausen and Nahrwold (68) in an attempt to improve on the high rates of restenosis originally reported following resection. The left subclavian artery is ligated and divided, and a longitudinal incision is extended through the proximal subclavian artery and beyond the coarctation. The proximal subclavian stump then is turned down onto the coarctation and used as a patch of autologous tissue (Fig. 47.15).

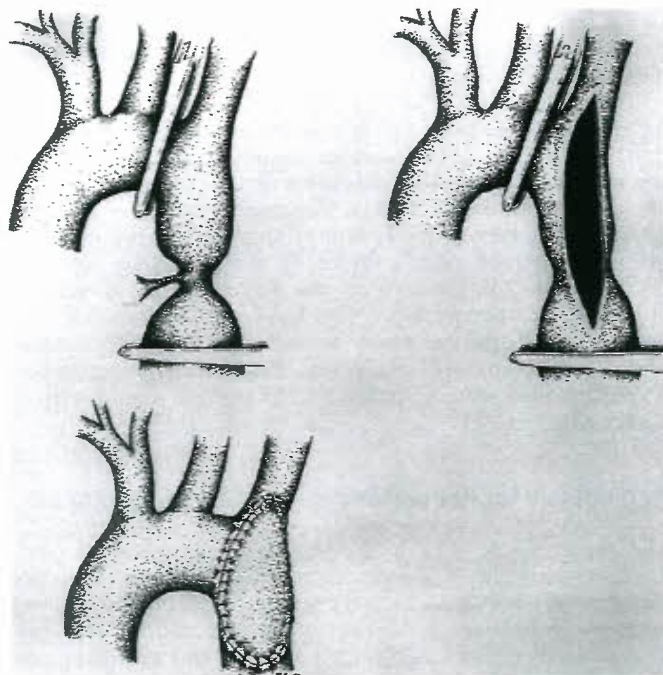


Figure 47.14 Prosthetic patch aortoplasty repair of coarctation.

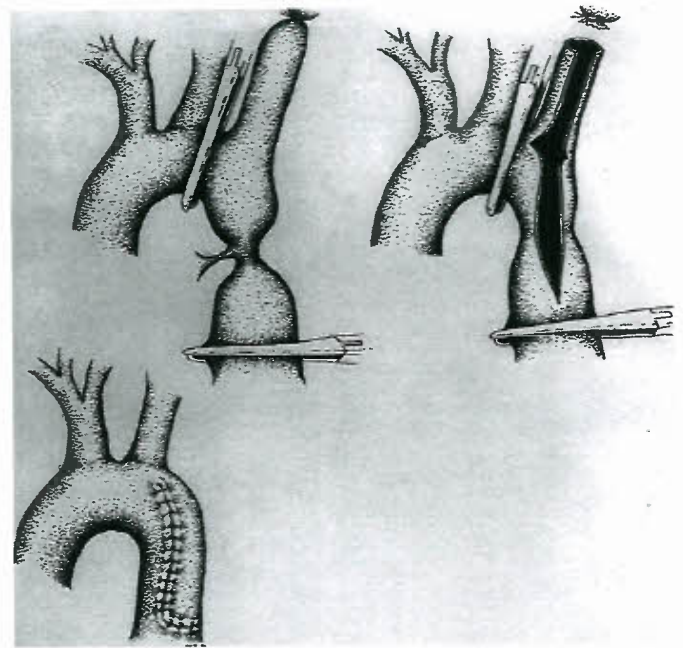


Figure 47.15 Left subclavian flap aortoplasty repair of coarctation.

The vertebral artery is ligated to avoid subclavian steal. The subclavian flap procedure has the advantages of requiring less extensive aortic mobilization, avoiding prosthetic materials, using living subclavian tissue as a patch with theoretical growth potential, and avoiding a circumferential anastomosis. It also can be used for some long-segment coarctations and coarctation associated with isthmus hypoplasia. An obvious disadvantage is that the procedure requires sacrifice of the left subclavian artery. Early studies suggested that the subclavian flap operation was the treatment of choice for infants with coarctation because of an apparent reduction in the incidence of late restenosis. More recent studies, however, failed to confirm this advantage (40,41,53). Therefore, because of the occasional untoward effects on the left upper extremity (69,70) many centers prefer resection if the anatomy is suitable.

Percutaneous Balloon Angioplasty and Stenting

Percutaneous balloon angioplasty is a less invasive alternative to surgical repair for patients with a discrete coarctation of the aorta. Balloon angioplasty has gained wide acceptance as effective therapy for a recurrent postoperative coarctation, but remains controversial as a primary treatment strategy for a native coarctation. The mixed reception for this less invasive procedure is best understood by considering the surgical alternatives. Surgical repair of an isolated native coarctation carries low risks and a high expectation of success. In contrast, reoperation for recurrent postoperative coarctation is technically more difficult and is associated with increased morbidity and mortality.

Balloon angioplasty has been used for coarctation since 1982, and a modest literature documents angioplasty safety and effectiveness in patients with a native coarctation (71–77) and with recurrent postoperative coarctation (78–84). The balloon dilation procedure typically is performed in a retrograde fashion from the femoral artery, although the antegrade transvenous approach may be used, and is particularly suitable in infants following the Norwood procedure (83).

The mechanism by which balloon angioplasty relieves coarctation stenosis has been elucidated in several postmortem

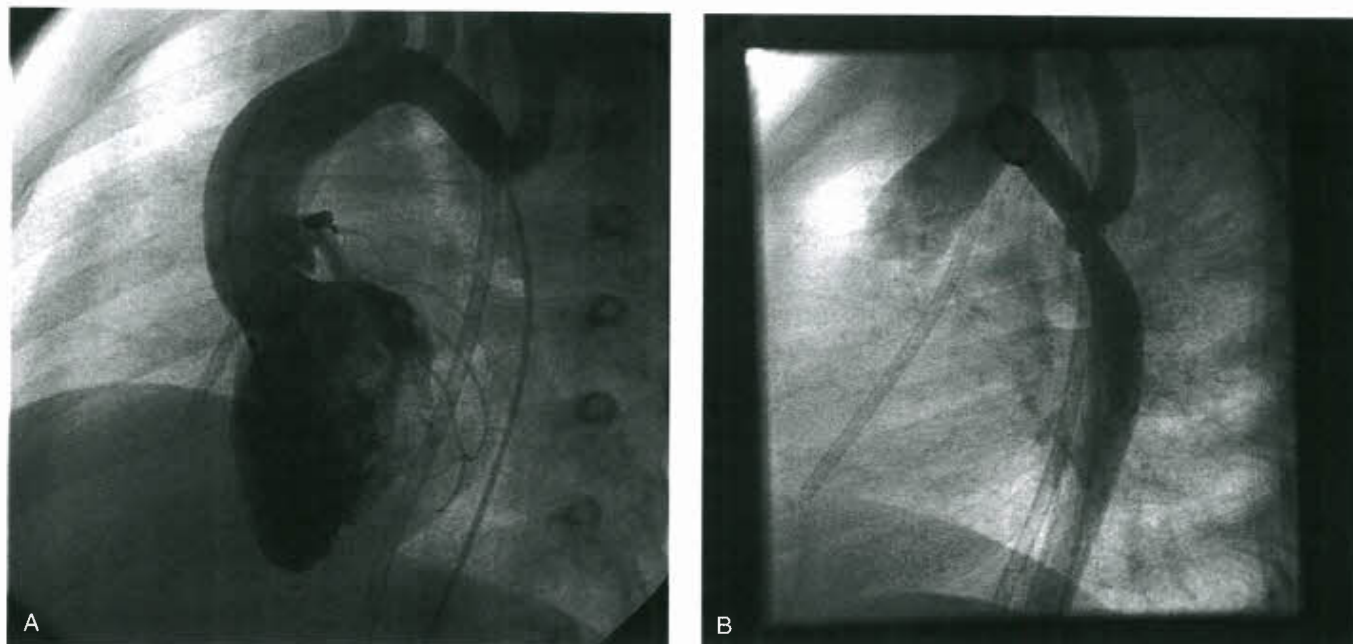


Figure 47.16 Angiograms in the lateral projection before (A) and immediately after (B) balloon angioplasty of a native coarctation in a 3-year-old girl. Prior to angioplasty (A) there is a severe discrete coarctation completely occluded by the catheter. Immediately after angioplasty (B), the aortogram documents improvement in the stenosis, with an intimal irregularity anteriorly. Two years later, CT angiography documented an excellent anatomic outcome without aneurysm. There was no residual pressure gradient in follow-up.

and experimental studies (85–88). Angioplasty enlarges the coarctation lumen by expanding the lesion diameter and producing linear intimal and medial tears at the coarctation site (and in the normal distal aorta as well). In most instances, the medial tears are shallow, but rarely some may extend to the adventitia. Histologic evaluation in animal models have shown vascular healing to have occurred by 8 weeks after angioplasty (88).

Angioplasty for Native Coarctation

The acute effectiveness of balloon angioplasty for discrete native (unoperated) coarctation has been demonstrated in numerous studies (Fig. 47.16). The early multicenter report from the Valvuloplasty and Angioplasty of Congenital Anomalies (VACA) Registry (71) described the procedure in 140 patients whose age ranged from 3 days to 29 years. Angioplasty acutely decreased the systolic gradient from 48 to 12 mm Hg, with an increase in the coarctation diameter from 3.9 to 8.8 mm. A residual gradient exceeding 20 mm Hg was reported in 14% of the patients. In a follow-up study of 59 children ≥ 2 years after native coarctation angioplasty, repeat cardiac catheterization found a residual systolic gradient of ≥ 20 mm Hg or more in 27% of patients (75); in the remaining patients, the mean residual systolic gradient was 6 mm Hg (median gradient 8 mm Hg). A more recent long-term follow-up study (up to 22 years) in 58 patients reported similar late effectiveness (77).

Angioplasty of native coarctation has not gained wide acceptance because of concerns related to residual or recurrent stenosis and to aneurysm formation at the dilation site. It is difficult to discern the difference between residual and recurrent stenosis in many reports. Published data suggest that the incidence of a residual gradient exceeding 20 mm Hg ranges from 8% to 27% (71,75,77). Recurrent stenosis after an initially successful angioplasty appears to be uncommon during intermediate-term

follow-up in children and adolescents, but is relatively common in infants younger than 6 months of age (73–76,89). The incidence of aneurysm formation at the dilation site varies widely in published reports, possibly reflecting varying definitions of an aneurysm. The larger follow-up studies suggest that the incidence of aneurysm formation is approximately 5% to 10% (75–77). An aneurysm was identified in three of 59 children (5.1%) in our angiographic follow-up study ≥ 2 years after angioplasty. Serial angiography showed no progression in aneurysm size in two of these children over a 2- and 6-year period (75). In Fletcher's series of 102 patients, an aneurysm was identified in only 2 patients (1.9%), but longer follow-up for possible late aneurysm development was advised (76).

A number of acute complications has been reported with balloon angioplasty of native coarctation of the aorta. Mortality is rare beyond the newborn period. In the VACA Registry, one death (a neonate) was reported in 140 cases, yielding a mortality rate of 0.7% (71). The most common acute complication has been femoral artery injury. This appears to be more common in infants under 12 months of age and has decreased in frequency with the development of smaller angioplasty catheters (90). Other less common complications have included femoral artery hemorrhage requiring transfusion and cerebrovascular accident. Paradoxical hypertension is uncommon following percutaneous balloon angioplasty of coarctation (91).

Angioplasty for Recurrent Postoperative Coarctation

The acute effects of balloon angioplasty for recurrent postoperative coarctation are similar to those reported for native coarctation. The VACA Registry reported data on 200 patients undergoing balloon angioplasty for recoarctation (79). The systolic gradient decreased acutely from 42 to 13 mm Hg, and the diameter of the recurrent coarctation increased from 5.2 to 8.9 mm. Residual pressure gradients exceeding 20 mm Hg

were present in 20% of the patients. Similar outcomes have been reported from several centers (78–84). In general, the type of prior surgical repair has not affected angioplasty outcomes.

Follow-up data from several centers have addressed the longer-term effectiveness of balloon angioplasty for recurrent coarctation (80–82,84). As with native coarctation, restenosis does occur after angioplasty of postoperative recoarctation. Yetman et al. (81) reported follow-up data of 3 to 144 months (median, 39 months) in 74 patients with a good early result of angioplasty. Nineteen (26%) patients had repeat angioplasty or surgery for recurrent stenosis. Hypoplasia of the transverse aortic arch was the best predictor of the need for later reintervention. The incidence of aneurysm formation after balloon dilation of recurrent coarctation appears to be similar to that reported after native coarctation angioplasty (81,82,84).

Acute complications of balloon angioplasty for recurrent postoperative coarctation are similar to those for native

coarctation, although the reported mortality rate has been somewhat higher. Five deaths occurred among the 200 patients with recoarctation reported by the VACA Registry, giving a mortality rate of 2.5% (79). One death was caused by aortic rupture, and one was related to a cerebrovascular accident. The remaining three deaths were believed to be related to the associated cardiac disease. Other complications include femoral artery thrombosis, rare paradoxical hypertension, and transient neurologic events.

Coarctation Stenting

Balloon-expandable stents provide an effective therapy for many patients with coarctation of the aorta (Fig. 47.17). A stent implanted concurrently with balloon angioplasty functions as an endovascular buttress to support the dilated

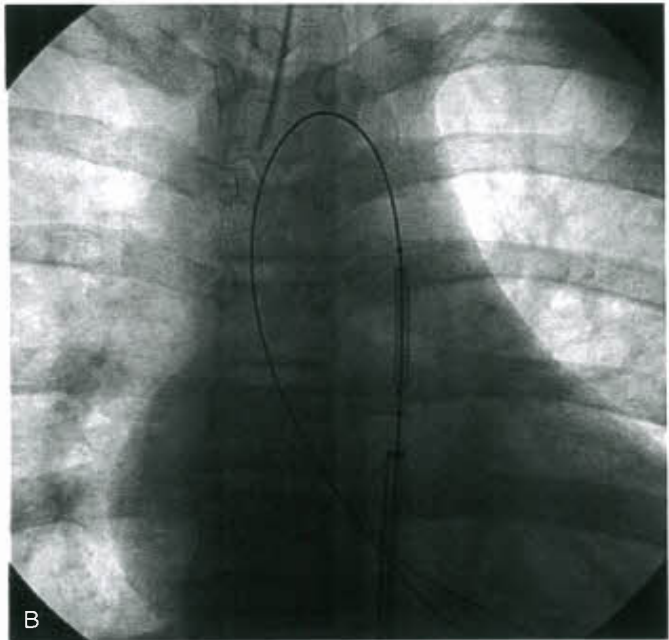
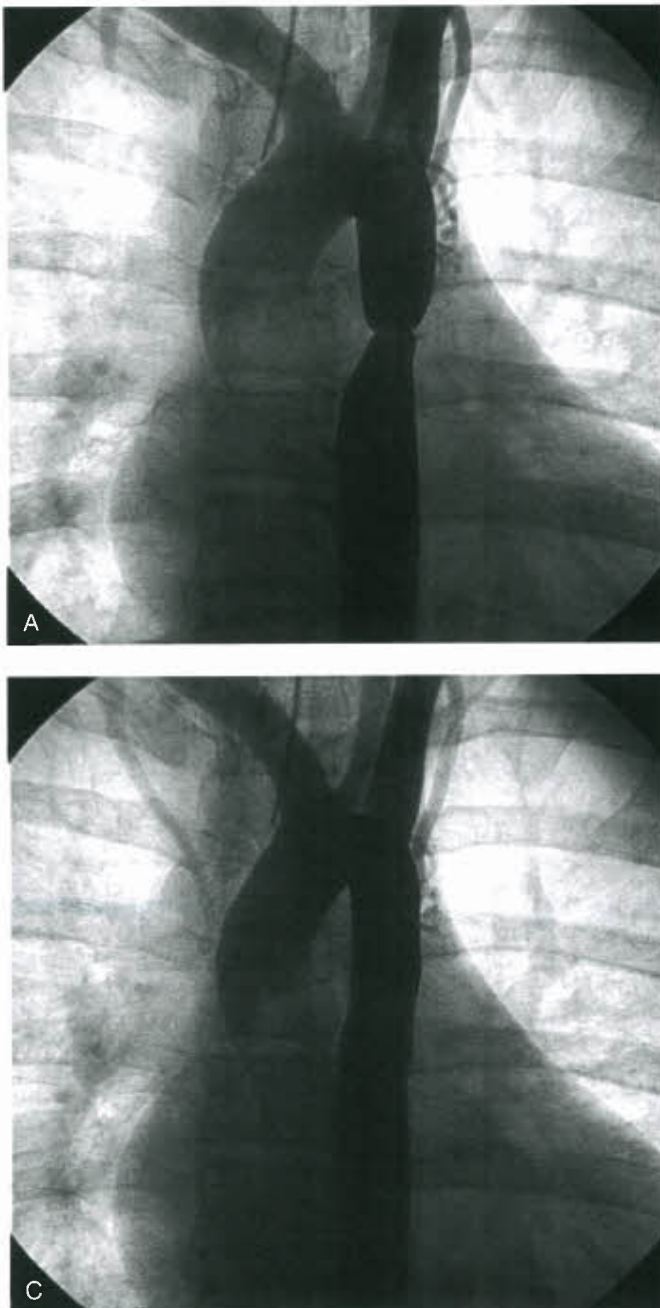


Figure 47.17 Angiographic images in a slight LAO projection before (A), during (B), and immediately after (C) coarctation stenting in a 15-year-old girl with a native coarctation. The systolic pressure gradient was reduced from 40 to 0 mm Hg immediately after the stent procedure.

aortic segment. Stents decrease coarctation restenosis related to vessel recoil and may also diminish the late incidence of aneurysm formation. Covered stents may provide important added safety for patients with a vulnerable aortic wall, as in Turner syndrome or older adult patients.

The safety and effectiveness of percutaneous stent therapy for native or recurrent coarctation have been documented in numerous clinical series (92–101). Stenting provides very effective relief of stenosis and generally decreases the resting systolic gradient to <5 mm Hg in patients with a discrete coarctation. Furthermore, stent therapy may be beneficial in some patients with transverse arch hypoplasia as well (102). Several studies with modest intermediate-term follow-up data suggest that restenosis is uncommon following coarctation stenting. Stents implanted in growing children, however, are likely to require redilation to a larger diameter when the children grow. For this reason, even in children it is important to implant stents with a diameter potential suitable for the adult aorta.

Late aneurysm formation at the coarctation site may occur after stenting, but seems to be less frequently encountered than after balloon angioplasty alone. The primary use of covered stents may decrease the aneurysm risk further, and may be particularly valuable in patients with a very small coarctation lumen (<3 mm) or with increased aortic wall fragility (e.g., genetic syndromes, advanced age) (103). Larger follow-up studies are necessary to more precisely quantify the risk of aneurysm formation in patients who have undergone coarctation stenting, with either bare-metal or covered stents.

PROGNOSIS

The prognosis for a normal life following successful repair of coarctation in childhood is excellent. Normal growth and development are to be expected, and only minimal restrictions should be placed on physical activity. In treated patients without a significant residual systolic gradient (<10 mm Hg at rest), with normal upper-extremity blood pressure at rest and with exercise, and without an aortic aneurysm or significant associated intracardiac lesions, participation in sports is generally permitted with the exception of activities with a high static (isometric) component (104).

Nevertheless, the long-term prognosis after coarctation treatment may be affected by a number of clinical and hemodynamic conditions (Table 47.1). Residual or recurrent coarctation may occur, particularly after repair in infancy, regardless of whether the primary treatment was surgery or balloon angioplasty. The term *residual coarctation* implies the presence of an aortic arch gradient immediately after repair. The causes include inadequate repair of the coarctation and/or hypoplasia of the isthmus or transverse aortic arch. There is evidence to suggest that the transverse aortic arch may grow in some children following coarctation repair in infancy (105). The term *recurrent coarctation* implies the development of restenosis after an initially successful repair. Recurrent coarctation most commonly occurs because of inadequate growth at the coarctation repair site, consistent with the observation that recurrent coarctation is uncommon if surgical repair is performed after a child is 2 years of age. More recent surgical experience suggests that the use of an extended end-to-end anastomosis in infants may substantially decrease the risk of late recurrent coarctation (45,46). Residual and recurrent coarctations after balloon angioplasty also occur more commonly when the procedure is performed in infancy. Recurrence of stenosis is likely to occur with somatic growth after coarctation stenting in childhood, and will commonly require stent redilation to a larger diameter.

TABLE 47.1

Clinical and Hemodynamic Conditions that May Affect Long-Term Prognosis after Repair of Coarctation

Residual or recurrent coarctation
Hypertension (rest and exercise)
Aortic aneurysm
Aortic dissection
Intracranial hemorrhage
Diminished left arm growth/subclavian steal
Endocarditis/endarteritis
Associated intracardiac lesions

The long-term prognosis following repair of coarctation may be adversely affected by systemic arterial hypertension and an increase in premature atherosclerotic cardiovascular events (56,106). Even in the absence of a residual coarctation gradient, patients may exhibit late systolic and diastolic hypertension. This is most common in patients whose coarctation repair is delayed beyond late childhood. The risk for late hypertension may be as high as 10% to 20% however, even if a coarctation is repaired in infancy (54,107). The etiology of late postoperative hypertension in patients without a residual coarctation gradient may relate to anatomic and functional changes in the arterial vasculature. Animal studies document abnormal intimal thickening and medial hypertrophy in the proximal aortic arch late following successful relief of experimental coarctation (108). Such morphologic changes would be expected to decrease arterial compliance and provide an anatomic basis for the functional abnormalities in vascular reactivity and baroreceptor function that have been reported following coarctation repair (28,30,31,109). Systolic hypertension after coarctation repair also may occur during dynamic exercise, even in patients without resting hypertension or a resting coarctation gradient (110). Although alterations of vascular physiology may play a role, exercise-induced upper-extremity hypertension often is associated with an increase in the coarctation pressure gradient during exercise. The increase in blood flow across a relatively nondistensible aortic repair site that occurs with dynamic leg exercise may be primarily responsible for exercise-induced elevations in coarctation gradient and upper-extremity systolic pressure following coarctation repair. Patients with exercise hypertension, but without a significant residual coarctation gradient at rest, may benefit from beta-blocker therapy (111).

An aortic aneurysm may develop at the site of surgical coarctation repair (Figs. 47.18 and 47.19). The incidence of postoperative aortic aneurysm is highest following prosthetic patch aortoplasty (65–67), although aneurysms have been reported following other surgical procedures as well. In a prospective study, the presence of an aortic aneurysm was documented in 24% of patients evaluated 1 to 19 years after patch aortoplasty repair of coarctation (65). Once present, such aneurysms may progress rapidly and may be responsible for aortic rupture and sudden death (112). Aortic aneurysms also occur following balloon angioplasty of coarctation and have been largely responsible for the reluctance of some cardiologists to recommend angioplasty for a native coarctation. The risk of aortic aneurysm following coarctation angioplasty

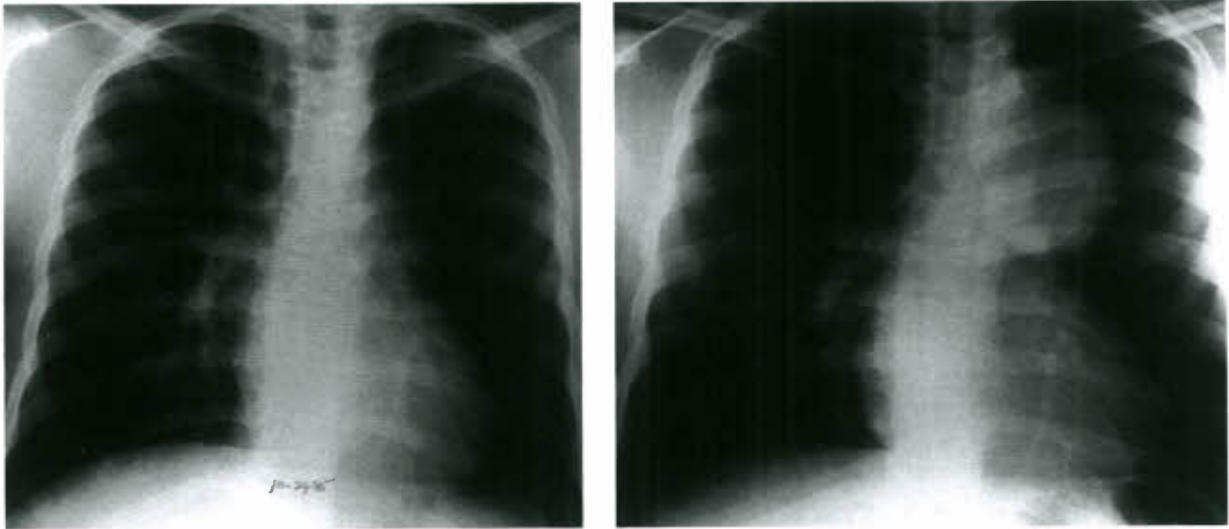


Figure 47.18 Chest radiograph 3 years (left panel) and 8 years (right panel) after prosthetic patch aortoplasty repair of coarctation, documenting progressive aneurysmal dilation at the repair site. (Reprinted from Mendelsohn AM, Crowley DC, Lindauer A, et al. Rapid progression of aortic aneurysms after patch aortoplasty repair of coarctation of the aorta. *J Am Coll Cardiol* 1992;20:381–385, with permission from Elsevier.)

varies widely in published reports, with the larger follow-up studies estimating its incidence to be approximately 5% to 10% (75–77). Late aneurysms may occur less commonly after coarctation stenting (Fig. 47.20), particularly if a covered stent

is employed primarily, but more follow-up data are necessary to precisely define this risk.

Other vascular abnormalities that affect long-term outcomes in some patients after coarctation repair include aortic dissection, intracranial hemorrhage, and diminished left arm growth or subclavian steal syndrome. Aortic dissection may occur with or without the presence of an aortic aneurysm at the coarctation repair site. Factors predisposing to dissection include cystic medial necrosis of the aortic wall, atherosclerosis, persistent arterial hypertension, and dilation of the ascending aorta, which is particularly common in patients with Turner syndrome. Intracranial hemorrhage may occur late following coarctation repair, with or without associated hypertension, and may be related to the presence of berry aneurysms in the circle of Willis. Cerebrovascular accidents have been an important cause of late morbidity in the larger studies of long-term coarctation outcomes (56,113). Procedures such as left subclavian flap aortoplasty that sacrifice the subclavian artery may be responsible for detrimental long-term effects. Late studies following subclavian flap aortoplasty documented diminished arterial blood supply to the left arm with a diminished reactive hyperemia response (69). These patients may experience arm claudication with exercise and diminished growth of the left arm (40,69,70). The subclavian steal syndrome may occur if the vertebral artery remains intact distally.

Bacterial endocarditis or endarteritis is responsible for important morbidity in some patients with coarctation of the aorta. Endocarditis may occur on a bicuspid aortic valve or other associated intracardiac lesions. Endarteritis typically occurs at or just distal to the site of coarctation repair in the area of turbulence and intimal thickening and has resulted in mycotic aneurysms in some patients.

Finally, the long-term prognosis after coarctation repair may be affected by the presence of associated intracardiac lesions such as aortic or mitral valve disease (106). Patients who required repair of associated intracardiac defects earlier in life (e.g., ventricular septal defect (VSD) closure) may have long-term issues related to a residual VSD, postoperative heart block, or progressive left ventricular outflow obstruction. Such patients require lifelong cardiology follow-up and surveillance for the late evolution of residual postoperative lesions and sequelae of therapy.

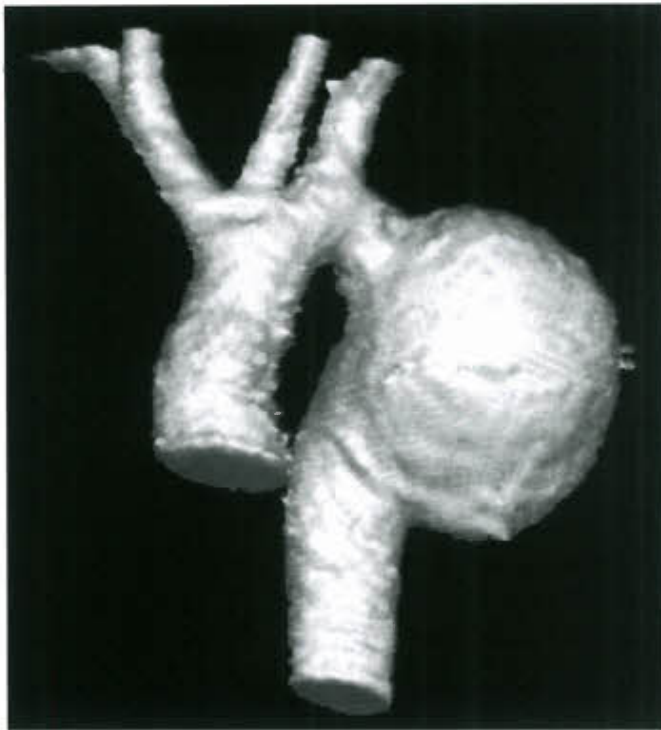


Figure 47.19 Large (65 × 76 mm) aortic aneurysm in a 28-year-old patient 16 years after prosthetic patch repair of coarctation. The anatomy of the arch and aneurysm are delineated by a 3-D surface rendered image reconstructed from a magnetic resonance angiography study. (Courtesy of W. James Parks, M.D., The Children's Heart Center, Emory University, Atlanta, GA.)

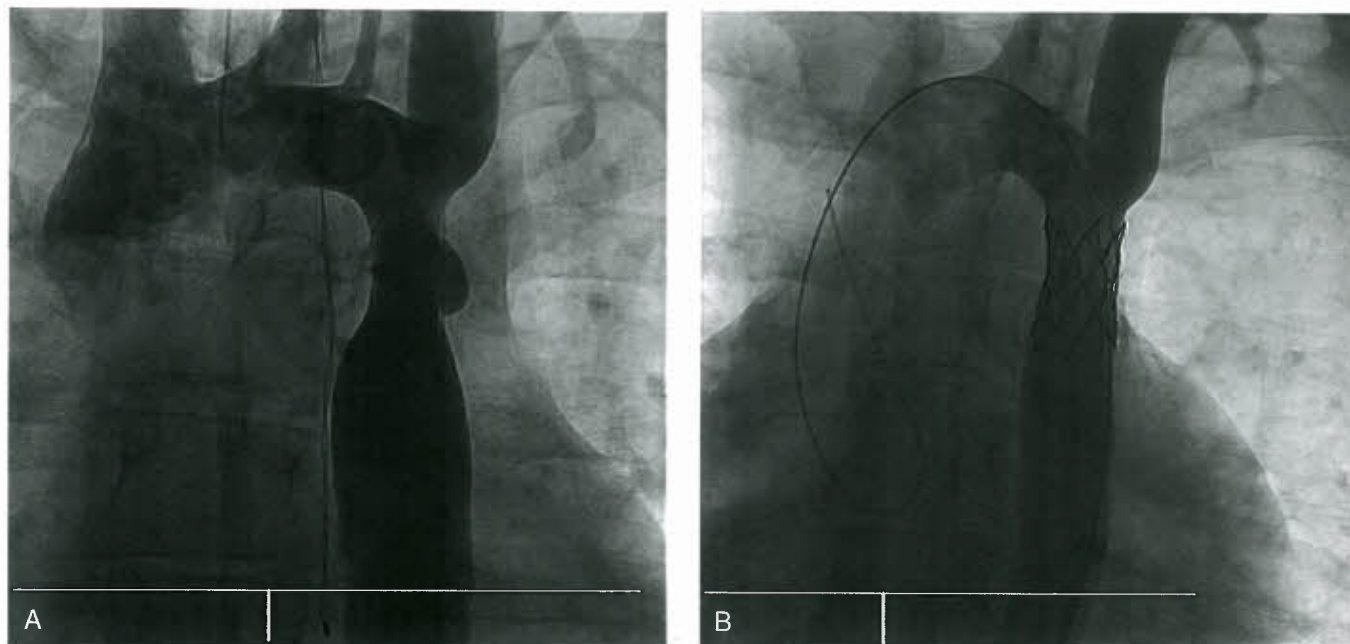


Figure 47.20 Moderate saccular aneurysm 8 months after bare-metal stenting of a severe native coarctation in a 16-year-old boy (A). After implantation of a covered stent (B), the aneurysm was completely excluded from the aortic lumen. There was no residual coarctation gradient.

REFERENCES

- Fyler DC, Buckley LP, Hellenbrand WE, et al. Report of the New England regional infant cardiac program. *Pediatrics* 1980;65:432–436.
- Campbell M, Polani PE. The aetiology of coarctation of the aorta. *Lancet* 1961;1:463–468.
- Loffredo CA, Chokkalingam A, Sill AM, et al. Prevalence of congenital cardiovascular malformations among relatives of infants with hypoplastic left heart, coarctation of the aorta, and d-transposition of the great arteries. *Am J Med Genet A* 2004;124:225–230.
- Cripe L, Andelfinger G, Martin LJ, et al. Bicuspid aortic valve is heritable. *J Am Coll Cardiol* 2004;44:138–143.
- McBride KL, Pignatelli R, Lewin M, et al. Inheritance analysis of congenital left ventricular outflow tract obstruction malformations: segregation, multiplex relative risk, and heritability. *Am J Med Genet A* 2005;134:180–186.
- McBride KL, Zender GA, Fitzgerald-Butt SM, et al. Linkage analysis of left ventricular outflow tract malformations (aortic valve stenosis, coarctation of the aorta, and hypoplastic left heart syndrome). *Eur J Hum Genet* 2009;17:811–819.
- Hinton RB, Martin LJ, Rame-Gowda S, et al. Hypoplastic left heart syndrome links to chromosomes 10q and 6q and is genetically related to bicuspid aortic valve. *J Am Coll Cardiol* 2009;53:1065–1071.
- McBride KL, Riley MF, Zender GA, et al. NOTCH1 mutations in individuals with left ventricular outflow tract malformations reduce ligand-induced signaling. *Hum Mol Genet* 2008;17:2886–2893.
- Miettinen OS, Reiner ML, Nadas AS. Seasonal incidence of coarctation of the aorta. *Br Heart J* 1970;32:103–107.
- Edwards JE, Christensen NA, Clagett OT, et al. Pathologic considerations in coarctation of the aorta. *Mayo Clin Proc* 1948;23:324–332.
- Ho SY, Anderson RH. Coarctation, tubular hypoplasia, and the ductus arteriosus: histological study of 35 specimens. *Br Heart J* 1979;41:268–274.
- Bharati S, Lev M. The surgical anatomy of the heart in tubular hypoplasia of the transverse aorta (preductal coarctation). *J Thorac Cardiovasc Surg* 1986;91:79–85.
- Isner JM, Donaldson RF, Fulton D, et al. Cystic medial necrosis in coarctation of the aorta: a potential factor contributing to adverse consequences observed after percutaneous balloon angioplasty of coarctation sites. *Circulation* 1987;75:689–695.
- Anderson RH, Lenox CC, Zuberbuhler JR. Morphology of ventricular septal defect associated with coarctation of aorta. *Br Heart J* 1983;50:176–181.
- Moene RJ, Gittenberger-de Groot AC, Oppenheimer-Dekker A, et al. Anatomic characteristics of ventricular septal defect associated with coarctation of the aorta. *Am J Cardiol* 1987;59:952–955.
- Rosenquist GC. Congenital mitral valve disease associated with coarctation of the aorta. *Circulation* 1974;49:985–989.
- Shone JD, Sellers RD, Anderson RC, et al. The development complex of “parachute mitral valve,” supraventricular ring of left atrium, subaortic stenosis and coarctation of the aorta. *Am J Cardiol* 1963;11:714–725.
- Greenwood RD, Rosenthal A, Parisi L, et al. Extracardiac abnormalities in infants with congenital heart disease. *Pediatrics* 1975;55:485–492.
- Kappetein AP, Gittenberger-de Groot AC, Zwinderman AH, et al. The neural crest as a possible pathogenetic factor in coarctation of the aorta and bicuspid aortic valve. *J Thorac Cardiovasc Surg* 1991;102:830–836.
- Barry A. The aortic arch derivatives in the human adult. *Anat Rec* 1951;111:221–238.
- Ho SY, Anderson RH. Coarctation, tubular hypoplasia and the ductus arteriosus. *Br Heart J* 1979;41:268–270.
- Rudolph AM, Heymann MA, Spitznas U. Hemodynamic considerations in the development of narrowing of the aorta. *Am J Cardiol* 1972;30:514–525.
- Hornberger LK, Sahn DJ, Kleinman CS, et al. Antenatal diagnosis of coarctation of the aorta: a multicenter experience. *J Am Coll Cardiol* 1994;23:417–423.
- Clark EB. Neck web and congenital heart defects: a pathogenic association in 45 X-O Turner syndrome? *Teratology* 1984;29:355–361.
- Graham TP, Lewis BW, Jarmakani MM, et al. Left heart volume and mass quantification in children with left ventricular pressure overload. *Circulation* 1970;41:203–212.
- Friedman WF. The intrinsic physiologic properties of the developing heart. In: Friedman WF, Lesch M, Sonnenblick EH, eds. *Neonatal heart disease*. New York, NY: Grune & Stratton, 1973:21–49.
- Meliones JN, Snider AR, Serwer GA, et al. Pulsed Doppler assessment of left ventricular diastolic filling in children with left ventricular outflow obstruction before and after balloon angioplasty. *Am J Cardiol* 1989;63:231–236.
- Gidding SS, Rocchini AP, Moorehead C, et al. Increased forearm vascular reactivity in patients with hypertension after repair of coarctation. *Circulation* 1985;71:495–499.
- deDivitiis M, Pilla C, Kattenhorn M, et al. Vascular dysfunction after repair of coarctation of the aorta: impact of early surgery. *Circulation* 2001;104:1165–1170.
- Trojnarska O, Mizia-Stec K, Gabriel M, et al. Parameters of arterial function and structure in adult patients after coarctation repair. *Heart Vessels* 2011;26:414–420.
- Beekman RH, Katz BP, Moorehead-Steffens C, et al. Altered baroreceptor function in children with systolic hypertension after coarctation repair. *Am J Cardiol* 1983;52:112–117.
- Strafford MA, Griffiths SP, Gersony WM. Coarctation of the aorta: a study in delayed detection. *Pediatrics* 1982;69:159–163.
- Ziegler RF. The genesis and importance of the electrocardiogram in coarctation of the aorta. *Circulation* 1954;9:371–375.
- Parks WJ, Mgo TD, Plauth WH, et al. Incidence of aneurysm formation after Dacron patch aortoplasty repair for coarctation of the aorta: long-term results and assessment utilizing magnetic resonance angiography with three-dimensional surface rendering. *J Am Coll Cardiol* 1995;26:266–271.
- Tsai SF, Trivedi M, Boettner B, et al. Usefulness of screening cardiovascular magnetic resonance imaging to detect aortic abnormalities after repair of coarctation of the aorta. *Am J Cardiol* 2011;107:297–301.

36. Nielsen JC, Powell AJ, Gauvreau K, et al. Magnetic resonance imaging predictors of coarctation severity. *Circulation* 2005;111:622–628.
37. Campbell M. Natural history of coarctation of the aorta. *Br Heart J* 1970;32:633–640.
38. Heymann MA, Berman W Jr, Rudolph AM, et al. Dilatation of the ductus arteriosus by prostaglandin E1 in aortic abnormalities. *Circulation* 1979;59:169–173.
39. Kilman JW, Williams TE Jr, Breza TS, et al. Reversal of infant mortality by early surgical correction of coarctation of the aorta. *Arch Surg* 1972;105:865–868.
40. van Son JA, Daniels O, Vincent JG, et al. Appraisal of resection and end-to-end anastomosis for repair of coarctation of the aorta in infancy: preference for resection. *Ann Thorac Surg* 1989;48:496–502.
41. Rubay JE, Sluysmans T, Alexandrescu V, et al. Surgical repair of coarctation of the aorta in infants under one year of age: long-term results in 146 patients comparing subclavian flap angioplasty and modified end-to-end anastomosis. *J Cardiovasc Surg (Torino)* 1992;33:216–222.
42. Merrill WH, Hoff SJ, Stewart JR, et al. Operative risk factors and durability of repair of coarctation of the aorta in the neonate. *Ann Thorac Surg* 1994;58:399–402.
43. Quaegebeur JM, Jonas RA, Weinberg AD, et al. Outcomes in seriously ill neonates with coarctation of the aorta: a multi-institutional study. *J Thorac Cardiovasc Surg* 1994;108:841–851.
44. Zehr KJ, Gillinov AM, Redmond JM, et al. Repair of coarctation of the aorta in neonates and infants: a thirty-year experience. *Ann Thorac Surg* 1995;59:33–41.
45. Wood AE, Javadpour H, Duff D, et al. Is extended arch aortoplasty the operation of choice for infant aortic coarctation? Results of 15 years' experience in 181 patients. *Ann Thorac Surg* 2004;77:1353–1357.
46. Wright GE, Nowak CA, Goldberg CS, et al. Extended resection and end-to-end anastomosis for aortic coarctation in infants: results of a tailored surgical approach. *Ann Thorac Surg* 2005;80:1453–1459.
47. Burch PT, Crowley CG, Holubkov R, et al. Coarctation repair in neonates and young infants: is small size or low weight still a risk factor? *J Thorac Cardiovasc Surg* 2009;138:547–552.
48. Puchalski MD, Williams RV, Hawkins JA, et al. Follow-up of aortic coarctation repair in neonates. *J Am Coll Cardiol* 2004;44:188–191.
49. Sandhu SK, Beekman RH, Mosca RS, et al. Single-stage repair of aortic arch obstruction and associated intracardiac defects in the neonate. *Am J Cardiol* 1995;75:370–373.
50. Kostelka M, Walther T, Geerdts I, et al. Primary repair for aortic arch obstruction associated with ventricular septal defect. *Ann Thorac Surg* 2004;78:1989–1993.
51. Beekman RH, Rocchini AP, Behrendt DM, et al. Reoperation for coarctation of the aorta. *Am J Cardiol* 1981;48:1108–1114.
52. Ibarra-Perez C, Castaneda AR, Varco RL, et al. Recoarctation of the aorta: nineteen year clinical experience. *Am J Cardiol* 1969;23:778–784.
53. Beekman RH, Rocchini AP, Behrendt DM, et al. Long-term outcome after repair of coarctation in infancy: subclavian angioplasty does not reduce the need for reoperation. *J Am Coll Cardiol* 1986;8:1406–1411.
54. Brouwer RM, Erasmus ME, Ebels T, et al. Influence of age on survival, late hypertension, and recoarctation in elective aortic coarctation repair. *J Thorac Cardiovasc Surg* 1994;108:525–531.
55. Moss AJ, Adams FH, O'Loughlin BJ, et al. The growth of the normal aorta and of the anastomotic site in infants following surgical resection of coarctation of the aorta. *Circulation* 1959;19:338–349.
56. Maron BJ, Humphries JO, Rowe RD, et al. Prognosis of surgically corrected coarctation of the aorta: a 20-year post-operative appraisal. *Circulation* 1973;47:119–126.
57. Libershon RR, Pennington DG, Jacobs ML, et al. Coarctation of the aorta: review of 234 patients and clarification of management problems. *Am J Cardiol* 1979;43:835–840.
58. Kaushal S, Backer CL, Patel JN, et al. Coarctation of the aorta: midterm outcomes of resection with extended end-to-end anastomosis. *Ann Thorac Surg* 2009;88:1932–1938.
59. Ho ECK, Moss AJ. The syndrome of mesenteric arteritis following surgical repair of aortic coarctation. *Pediatrics* 1972;49:40–46.
60. Gidding SS, Rocchini AP, Beekman RH, et al. Therapeutic effect of propranolol on paradoxical hypertension after repair of coarctation of the aorta. *N Engl J Med* 1985;312:1224–1228.
61. Brewer LA, Fosburg RG, Mulder GA, et al. Spinal cord complications following surgery for coarctation of the aorta. *J Thorac Cardiovasc Surg* 1979;64:368–372.
62. Crafoord C, Nylin G. Congenital coarctation of the aorta and its surgical treatment. *J Thorac Surg* 1945;14:347–352.
63. Van Heurn LW, Wong CM, Spiegelhalter DJ, et al. Surgical treatment of aortic coarctation in infants younger than three months: 1985 to 1990. Success of extended end-to-end arch aortoplasty. *J Thorac Cardiovasc Surg* 1994;107:74–85.
64. Vosschulte K. Surgical correction of coarctation of the aorta by an "isthmoplasty" operation. *Thorax* 1961;16:338–345.
65. Bromberg BI, Beekman RH, Rocchini AP, et al. Aortic aneurysm after patch aortoplasty repair of coarctation: a prospective analysis of prevalence, screening tests and risks. *J Am Coll Cardiol* 1989;14:734–741.
66. Del Nido P, Williams W, Wilson G, et al. Synthetic patch angioplasty for repair of coarctation of the aorta: experience with aneurysm formation. *Circulation* 1986;74:132–36.
67. Clarkson PM, Brandt PWT, Barratt-Boyes BG, et al. Prosthetic repair of coarctation of the aorta with particular reference to dacron onlay patch grafts and late aneurysm formation. *Am J Cardiol* 1985;56:342–346.
68. Waldhausen JA, Nahrwold DL. Repair of coarctation of the aorta with a subclavian flap. *J Thorac Cardiovasc Surg* 1966;51:532–533.
69. van Son JA, van Asten WN, van Lier HJ, et al. Detrimental sequelae on the hemodynamics of the upper left limb after subclavian flap angioplasty in infancy. *Circulation* 1990;81:996–1004.
70. Todd PJ, Dangerfield PH, Hamilton DI, et al. Late effects on the left upper limb of subclavian flap aortoplasty. *J Thorac Cardiovasc Surg* 1983;85:678–681.
71. Tynan M, Finley JR, Fontes V, et al. Balloon angioplasty for the treatment of native coarctation: results of valvuloplasty and angioplasty of congenital anomalies registry. *Am J Cardiol* 1990;65:790–792.
72. Lock JE, Bass JC, Amplatz K, et al. Balloon dilation angioplasty of aortic coarctations in infants and children. *Circulation* 1983;68:109–116.
73. Beekman RH, Rocchini AP, Dick M, et al. Percutaneous balloon angioplasty for native coarctation of the aorta. *J Am Coll Cardiol* 1987;10:1078–1084.
74. Morrow WR, Vick W, Nihill MR, et al. Balloon dilatation of unoperated coarctation of the aorta: short and intermediate term results. *J Am Coll Cardiol* 1988;11:133–138.
75. Mendelshon AM, Lloyd TR, Crowley DC, et al. Late follow-up of balloon angioplasty in children with a native coarctation of the aorta. *Am J Cardiol* 1994;74:696–700.
76. Fletcher SE, Nihill MR, Grifka RG, et al. Balloon angioplasty of native coarctation of the aorta: mid-term follow-up and prognostic factors. *J Am Coll Cardiol* 1995;25:730–734.
77. Fawzy ME, Fathala A, Osman A, et al. Twenty-two years of follow-up results of balloon angioplasty for discrete native coarctation of the aorta in adolescents and adults. *Am Heart J* 2008;156:910–917.
78. Saul JP, Keane JF, Fellows KE, et al. Balloon dilation angioplasty of postoperative aortic obstructions. *Am J Cardiol* 1987;59:943–948.
79. Hellenbrand WE, Allen HD, Golinko RJ, et al. Balloon angioplasty for aortic recoarctation: results of valvuloplasty and angioplasty of congenital anomalies registry. *Am J Cardiol* 1990;65:793–797.
80. Hijazi ZM, Fahey JT, Kleinman CS, et al. Balloon angioplasty for recurrent coarctation of the aorta. *Circulation* 1991;84:1150–1156.
81. Yetman AT, Nykanen D, McCrindle BW, et al. Balloon angioplasty of recurrent coarctation: a 12-year review. *J Am Coll Cardiol* 1997;30:811–816.
82. Siblini G, Rao PS, Nouri S, et al. Long-term follow-up results of balloon angioplasty of postoperative aortic recoarctation. *Am J Cardiol* 1998;81:61–67.
83. Zeltser I, Mentzer J, Gaynor JW, et al. Impact of re-coarctation following the Norwood operation on survival in the balloon angioplasty era. *J Am Coll Cardiol* 2005;45:1844–1848.
84. Reich O, Tax P, Bartakova H, et al. Long-term (up to 20 years) results of percutaneous balloon angioplasty of recurrent aortic coarctation without use of stents. *Eur Heart J* 2008;29:2042–2048.
85. Sos T, Sniderman KW, Retek-Sos B, et al. Percutaneous transluminal dilatation of coarctation of the thoracic aorta-postmortem. *Lancet* 1979;2:970–971.
86. Lock JE, Castaneda-Zuniga WR, Bass JL, et al. Balloon dilatation of excised aortic coarctations. *Radiology* 1982;143:689–691.
87. Ho SY, Somerville J, Yip WCL, et al. Transluminal balloon dilation of resected coarcted segments of thoracic aorta: histological study and clinical implications. *Int J Cardiol* 1988;19:99–105.
88. Lock JE, Niemi T, Burke BA, et al. Transcatheter angioplasty of experimental aortic coarctation. *Circulation* 1982;66:1280–1286.
89. Fiore AC, Fischer LK, Schwartz T, et al. Comparison of angioplasty and surgery for neonatal aortic coarctation. *Ann Thorac Surg* 2005;80:1659–1664.
90. Burrows PE, Benson LN, Williams WG, et al. Iliofemoral arterial complications of balloon angioplasty for systemic obstructions in infants and children. *Circulation* 1990;82:1697–1704.
91. Choy M, Rocchini AP, Beekman RH, et al. Paradoxical hypertension after repair of coarctation of the aorta in children: balloon angioplasty versus surgical repair. *Circulation* 1987;75:1186–1191.
92. Ebeid MR, Prieto LR, Latson LA. Use of balloon-expandable stents for coarctation of the aorta: initial results and intermediate-term follow-up. *J Am Coll Cardiol* 1997;30:1847–1852.
93. Suarez DeLezo J, Pan M, Romero M, et al. Immediate and follow-up findings after stent treatment for severe coarctation of the aorta. *Am J Cardiol* 1999;83:400–406.
94. Marshall AC, Perry SB, Keane JF, et al. Early results and medium-term follow-up of stent implantation for residual or recurrent aortic coarctation. *Am Heart J* 2000;139:1054–1060.
95. Hamdan MA, Maheshwari S, Fahey JT, et al. Endovascular stents for coarctation of the aorta: initial results and intermediate-term follow-up. *J Am Coll Cardiol* 2001;38:1518–1523.
96. Johnston TA, Grifka RG, Jones TK. Endovascular stents for treatment of coarctation of the aorta: acute results and follow-up experience. *Catheter Cardiovasc Interv* 2004;62:499–505.
97. Shah L, Hijazi Z, Sandhu S, et al. Use of endovascular stents for the treatment of coarctation of the aorta in children and adults: immediate and mid-term results. *J Invasive Cardiol* 2003;17:614–618.
98. Forbes TJ, Garekar S, Amin Z, et al. Procedural results and acute complications in stenting native and recurrent coarctation of the aorta in patients over 4 years of age: a multi-institutional study. *Catheter Cardiovasc Interv* 2007;70:276–285.

99. Forbes TJ, Moore P, Pedra CAC, et al. Intermediate follow-up following intravascular stenting for treatment of coarctation of the aorta. *Catheter Cardiovasc Interv* 2007;70:569–577.
100. Mohan UR, Danon S, Levi D, et al. Stent implantation for coarctation of the aorta in children <30 kg. *JACC Cardiovasc Interv* 2009;2:877–883.
101. Wheatley GH, Koullias GJ, Rodriguez-Lopez JA, et al. Is endovascular repair the new gold standard for primary adult coarctation? *Eur J Cardiothorac Surg* 2010;38:305–310.
102. Pihkala J, Pedra CA, Nykanen D, et al. Implantation of endovascular stents for hypoplasia of the transverse arch. *Cardiol Young* 2000;10:3–7.
103. Tzifa A, Ewert T, Brzezinska-Rajszy G, et al. Covered Cheatham-platinum stents for aortic coarctation. *J Am Coll Cardiol* 2006;47:1457–1463.
104. Graham TP, Driscoll DJ, Gersony WM, et al. 36th Bethesda Conference: eligibility recommendations for competitive athletes with cardiovascular abnormalities. Task Force 2: congenital heart disease. *J Am Coll Cardiol* 2005; 45:1326–1333.
105. Siewers RD, Ettehadgui J, Pahl E, et al. Coarctation and hypoplasia of the aortic arch: will the arch grow? *Ann Thorac Surg* 1991;52:608–613.
106. Toro-Salazar OH, Steinberger J, Thomas W, et al. Long-term follow-up of patients after coarctation of the aorta repair. *Am J Cardiol* 2002;89: 541–547.
107. O'Sullivan JJ, Derrick G, Darnell R. Prevalence of hypertension in children after early repair of coarctation of the aorta: a cohort study using casual and 24 hour blood pressure measurement. *Heart* 2002;88:163–166.
108. Leskinen M, Reinila A, Tarkka M, et al. Reversibility of hypertensive vascular changes after coarctation repair in dogs. *Pediatr Res* 1992;31: 297–299.
109. DeDivitiis M, Pilla C, Kattenhorn M, et al. Ambulatory blood pressure, left ventricular mass, and conduit artery function late after successful repair of coarctation of the aorta. *J Am Coll Cardiol* 2003;41: 2259–2265.
110. Freed MD, Rocchini AP, Rosenthal A, et al. Exercise-induced hypertension after surgical repair of coarctation of the aorta. *Am J Cardiol* 1979;43:253–258.
111. Kavey RE, Cotton JL, Blackman MS. Atenolol therapy for exercise-induced hypertension after aortic coarctation repair. *Am J Cardiol* 1990;66:1233–1236.
112. Mendelsohn AM, Crowley DC, Lindauer A, et al. Rapid progression of aortic aneurysms after patch aortoplasty repair of coarctation of the aorta. *J Am Coll Cardiol* 1992;20:381–385.
113. Siimon AB, Zlot AE. Coarctation of the aorta: longitudinal assessment of operated patients. *Circulation* 1974;50:456–464.

James S. Tweddell ■ George M. Hoffman ■ Nancy S. Ghanayem
Michele A. Frommelt ■ Kathleen A. Mussatto ■ Stuart Berger

EPIDEMIOLOGY AND ETIOLOGY

Hypoplastic left heart syndrome (HLHS) makes up 1.4% to 3.8% of congenital heart disease, an incidence of 0.016% to 0.036% of live births. Despite this low incidence, HLHS causes 23% of cardiac deaths during the first week of life and 15% of cardiac deaths within the first month of life (1–6). A male predominance has been reported for HLHS (55% to 67%) (1,2,7–9).

While no gene abnormality is specific to HLHS, there is strong evidence supporting a genetic etiology for HLHS. The recurrence risk in families with one affected child is 0.5% to 2%. Additionally, the recurrence risk for other forms of congenital heart disease in families with one affected child with HLHS is 2.2% to 13.5% (10–12). In addition, pedigree analyses have demonstrated a 12% prevalence of cardiac abnormalities involving the left ventricular outflow tract in first-degree relatives of patients with HLHS (13,14). Lewin et al. (15) studied 278 first-degree relatives of 113 patients with nonsyndromic left ventricular outflow obstruction and found that 4.6% had a bicuspid aortic valve; an additional 11.5% of relatives had anomalies of the aorta, aortic valve, left ventricle (LV), or mitral valve (MV).

Extracardiac anomalies and genetic syndromes have been recognized in patients with HLHS with a reported incidence of 15% to 30% (16–19). Identified heritable syndromes associated with HLHS include Kabuki syndrome, Noonan syndrome, Smith-Lemli-Opitz syndrome, Holt-Oram syndrome, Ellis-van Creveld syndrome, oral-digital-facial syndrome, and CHARGE syndrome (1,20–27). Additionally, several chromosomal abnormalities have been identified in patients with HLHS, including Turner syndrome, trisomy 13, trisomy 18, trisomy 21, duplication of short arm of chromosome 12, 2q-, a balanced 3:7 translocation, 4q-, 4p-, 7q-, 11q- (Jacobsen Syndrome), duplication of 16q, and 18p- (1,25,28). Mutations have been implicated in specific genes including GJA1 (Connexin Protein 43), NKX2-5, NOTCH1, and HAND1 (29–33). Linkage analyses have suggested additional loci on chromosomes: 2p23, 10q21, 16p12, 2p15, 10q22, and 6q23 (34–36). Future work in molecular genetics may allow determination of the cause of HLHS and will be assisted by population registry information, tissue banking, and improved gene sequencing technology.

Environmental factors have been implicated in the development of HLHS. The Baltimore-Washington Study identified a geographic cluster of HLHS in a region of Baltimore characterized by industrial land use and release of solvents, polychlorinated biphenyls, and dioxin into air (37). Environmental factors were also implicated in a study finding an increased incidence of HLHS in southeastern Wisconsin (38). A link between maternal group A beta-hemolytic streptococcal pharyngeal infection and HLHS has been suggested (39). Antibodies formed from Streptococcal pharyngitis cross the placenta

and are associated with injury to the developing left ventricular outflow tract of the fetus resulting in HLHS. A recent study found a seasonal occurrence to HLHS again implicating an infectious–environmental cause (40).

THE DEVELOPING FETUS: ECHOCARDIOGRAPHY AND INTERVENTION

Prior to the advent of fetal echocardiography, the embryologic cause of HLHS was not entirely clear. However, with advances in fetal cardiac imaging, it became evident that many forms of congenital heart disease evolve throughout gestation. In 1989, Allan et al. (41) observed the in utero evolution of HLHS in a fetus initially diagnosed with critical aortic stenosis. A similar case report was published by Danford and Cronican (42) in 1992. Since that time, several fetal cardiac centers have reported retrospective collaborative data that suggest that serial measurements of left heart growth and assessment of flow direction across the foramen ovale and distal aortic arch may identify fetuses at risk for severe left heart hypoplasia at term (42–45). It is now postulated that many cases of HLHS are dynamic and progressive throughout gestation, resulting from altered left ventricular outflow (aortic stenosis) or altered left ventricular inflow (MV stenosis/foramen ovale restriction/alterations of atrial septal anatomy) (46–48). The field of prenatal cardiac intervention is under way, and early successes with balloon dilation of the aortic valve led to investigations as to whether the development and incidence of HLHS at term can be altered (49).

Fetal Echocardiography

Recent advances in 2-D and Doppler echocardiography have made it feasible to diagnose all forms of congenital heart disease in the fetus. HLHS is one of the most common structural lesions diagnosed prenatally, as a screening obstetric ultrasound will preferentially identify lesions that dramatically alter the four-chamber view (50–52) (Fig. 48.1). The prenatal diagnosis of HLHS is easily made when a small, muscle-bound left ventricular chamber is identified. The challenge for the fetal echocardiographer today is to recognize the potential for the evolution of HLHS, especially since some of these patients may be candidates for prenatal intervention. Another challenge is to diagnose the severely restrictive or intact atrial septum in this patient group prior to birth, as these patients have a particularly dismal outcome and may also benefit from prenatal intervention.

The fetal LV is predominantly filled with oxygenated blood that returns from the placenta and traverses the foramen



FIGURE 48.1. Fetal echocardiogram demonstrating HLHS. Screening obstetric ultrasound will preferentially identify lesions that dramatically alter the four-chamber view. The left ventricular chamber size is small compared with the RV. The lining of the LV is echobright, indicative of endocardial fibroelastosis. LV, left ventricle; RA, right atrium; RV, right ventricle.

ovale (53). If blood flow across the foramen ovale is diminished or reversed, the combined cardiac output is redistributed to the right ventricle (RV) and pulmonary artery (PA), resulting in enlargement of the right heart structures and creating less impetus for normal growth of left heart structures, possibly evolving into HLHS. Perhaps the most well-recognized mechanism for decreased flow or reversal of flow through the foramen ovale in utero is the presence of severe aortic valve disease (41–45). With significant aortic valve stenosis, alterations in left ventricular compliance may occur, either secondary to the development of left ventricular hypertrophy or secondary to the development of left ventricular dilation and dysfunction. Endocardial fibroelastosis, a poorly understood phenomenon where the endocardial lining of the LV becomes fibrotic, may also be present. As the disease state progresses, with subsequent elevation in left atrial pressure, flow across the foramen ovale becomes bidirectional and eventually left to right, the result of which may be the cessation of left ventricular growth (54). In a classic study by Hornberger et al. (44), the prenatal and postnatal echocardiograms of 21 fetuses with left heart obstructive lesions were reviewed to identify possible prenatal indicators of postnatal disease severity. Prenatal indices that correlated with HLHS at birth included a smaller MV and ascending aorta in the midtrimester, as well as a decreased rate of growth for all left heart structures. Other prenatal features included reversal of flow across the foramen ovale and retrograde ductal supply of the distal aortic arch. In a more recent study, Makikallio et al. (55) reviewed the natural history of aortic stenosis in 43 fetuses initially referred prior to 30 weeks gestation. At the time of the initial examination, the LV:RV length ratio was $>0.8:1$, and aortic stenosis was the dominant lesion. The presence of moderate left ventricular dysfunction, retrograde transverse aortic arch flow, left-to-right atrial-level shunting, and a monophasic mitral inflow on the initial prenatal echocardiogram were found to be risk factors for the development of HLHS. Again, in this study there was decreased rate of growth of all left heart structures in those patients who developed HLHS. Based on these two series, it is now clear that the fetus with aortic stenosis is at risk for the development of HLHS. Serial echocardiographic follow-up is indicated in these fetuses, paying particular attention to growth of left heart structures and patterns of blood

flow across the foramen ovale and transverse aortic arch. Importantly, it now seems feasible to reliably select fetuses for prenatal intervention, using both anatomic and physiologic markers.

Although the operative survival for infants born with HLHS has improved significantly over time, the subgroup of patients with a highly restrictive or intact atrial septum continues to experience a higher mortality (56,57). These infants can be profoundly cyanotic at the time of delivery and are often unresponsive to medical intervention. Even with prompt resuscitation and adequate decompression of the atrial septum, there is ongoing morbidity and mortality, likely related to secondary anatomic changes in the lung. Some investigators have reported “arterialization” of the pulmonary veins and lymphatic dilation in this setting; others have postulated that there is associated PA hypoplasia. The ability to diagnose a restrictive atrial septal defect prior to birth would allow for more accurate prenatal counseling and planning immediate postnatal intervention. Theoretically, prenatal catheter intervention in this subgroup of patients may alter the secondary anatomic changes in the lung, possibly improving long-term outcome. For all of these reasons, routine evaluation of the atrial septum should be performed in all fetuses with HLHS. Direct assessment of foramen ovale size has not correlated well with the degree of left atrial hypertension at the time of birth, likely a reflection of the inability to clearly visualize the defect, which often lies more superiorly and posteriorly in the left atrium (LA) (58). Doppler interrogation of the pulmonary veins is technically much simpler, and the pattern of pulmonary venous flow in HLHS has correlated well with left atrial hemodynamics (58,59). The normal fetal pulmonary vein flow pattern consists of forward flow in systole and diastole, with cessation of flow or a small reversal wave with atrial systole. In a study by Taketazu et al. (58), a pattern of pulmonary vein flow with brief forward and reverse flow with minimal early ventricular diastolic flow was associated with the need for immediate respiratory support and emergent atrial decompression. Two of the three patients with this abnormal flow pattern died after neonatal heart transplantation, and the postmortem lung tissue analysis was notable for dilated lymphatic vessels, pulmonary vein arterialization, and abnormal PA musculature.

Fetal Intervention

It is important to remember that most fetuses with severe left ventricular outflow tract obstruction (LVOTO) will survive gestation. Therefore, fetal cardiac intervention in this setting does not serve as a lifesaving procedure but rather a procedure that may improve postnatal surgical options and outcomes. More specifically, it is hoped that successful intervention in the fetus with LVOTO will lead to a biventricular circulation at the time of birth. This possible benefit must be weighed against the risks of the procedure, which, even in the setting of technical success, may result in fetal death or extreme prematurity. Since the risk/benefit ratio of fetal cardiac intervention in the setting of severe LVOTO is still unknown, it is not surprising that these procedures are not universally accepted. Some centers have advocated fetal cardiac intervention only when it is felt to be a lifesaving procedure, such as in the setting of critical aortic stenosis with fetal hydrops.

In the year 2000, Kohl et al. (60) reported the world experience of fetal aortic balloon valvuloplasty. The small early clinical experience ($n = 12$) was quite poor, with only one “long-term” survivor. However, more encouraging data were recently reported by McElhinney et al. (61) from the Children’s Hospital of Boston and the Brigham and Women’s Hospital.

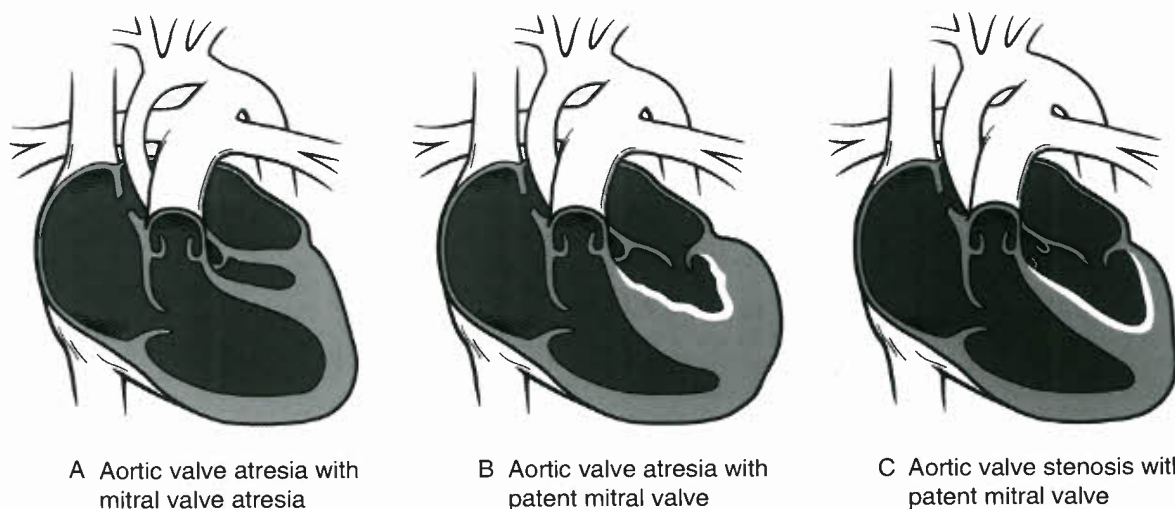


FIGURE 48.2. The spectrum of HLHS. **A:** Aortic atresia with mitral atresia is the most extreme form of HLHS. The LV is diminutive. The ascending aorta and arch are extremely hypoplastic, and flow is retrograde. Systemic output is ductal dependent. **B:** Aortic atresia with a patent MV. As in aortic atresia with mitral atresia, the ascending aorta and arch are hypoplastic and all systemic output is ductal dependent. There is inflow without outflow. As a result, the LV is hypertensive with hypertrophy and endocardial fibroelastosis. The left ventricular mass can be greater than normal and result in distortion of the inflow of the RV, resulting in tricuspid valve insufficiency. **C:** Aortic valve stenosis with a patent MV. The LV is hypoplastic, but antegrade flow through the aortic valve persists. The degree of ascending aortic and arch hypoplasia is less than that observed with aortic atresia. This end of the spectrum of HLHS blends smoothly into critical aortic stenosis, and decision making concerning suitability for two-ventricle repair can be challenging.

These data included 70 fetuses that underwent attempted aortic valvuloplasty for critical aortic stenosis with evolving HLHS between March 2000 and October 2008. There was a significant improvement in technical success (74%), and most procedures were performed with only percutaneous access (73%). Eight fetuses died related to the procedure (11% mortality). Although fetuses with a technically successful valvuloplasty had improved growth of the aortic valve and MV, intervention did not effectively promote left ventricular growth. Therefore, fetuses with a larger LV dimensions initially were more likely to sustain a biventricular circulation at the time of birth ($n = 15$). Based on these results, the authors were able to create a multivariable scoring system, excluding some fetuses that were not likely to respond to fetal intervention.

In utero therapy for HLHS with a severely restrictive or intact atrial septum has also been described. Successful decompression of the LA in utero may avoid severe hypoxemia at birth, and theoretically, may also reduce prenatal lung damage and improve otherwise-dismal outcomes (62–64). In a recent publication by Marshall et al. (65), technically successful atrial septoplasty was performed in 19 of 21 fetuses between October 2001 and November 2007, with two episodes of fetal death. The authors determined that creation of a larger defect was associated with better postnatal oxygenation; however, whether this confers a benefit to later survival is presently unknown.

ANATOMY

Various cardiac malformations characterized by variable degrees of underdevelopment of the left ventricular cavity are referred to as HLHS. Most broadly, HLHS includes any number of lesions with a dominant RV and systemic outflow obstruction that are not amenable to two-ventricle repair.

Underdevelopment of the Left Ventricle Outflow—Aorta Complex

Underdevelopment of the LV outflow—aorta complex, resulting in critical aortic valve stenosis or aortic valve atresia with an intact ventricular septum is the most recognized form of HLHS (66–68) (Fig. 48.2). A spectrum of abnormalities includes aortic valve atresia with mitral atresia, aortic valve atresia with a patent MV, and aortic stenosis with a patent MV. This final group with aortic stenosis and a patent MV blends smoothly into critical aortic stenosis. The general unifying etiologic explanation is that the growth and development of vascular structures are dependent to some degree on the relative quantity of blood flow during fetal development. As mentioned earlier, fetal echocardiographic observations have confirmed the progression from aortic stenosis to HLHS (41). In addition to these observations, supporting data for underdevelopment of the LV outflow—aortic complex as the inciting event are provided by the fact that with an intact ventricular septum, additional lesions, particularly MV hypoplasia, are always less severe than the degree of left ventricular outflow obstruction (69). The ascending aorta is hypoplastic; among patients undergoing surgery for HLHS, the mean aortic diameter was 3.3 ± 1.7 mm; 40% to 55% of patients had an ascending aorta of <2 mm (70,71). Blood flow in the arch is retrograde, and in aortic atresia, the ascending aorta serves only as a conduit for the retrograde flow of blood into the coronary arteries. A localized coarctation of the aorta is present in 80% of patients (9,72). Aortic stenosis with mitral stenosis makes up 23% to 26% of patients undergoing stage 1 palliation, whereas 36% to 46% have aortic atresia with mitral atresia and 20% to 29% have aortic atresia with a patent MV (73–75).

There are corresponding changes in the right side of the heart when there is left ventricular cavity hypoplasia. All right-sided cardiac structures are larger than normal including the right

atrium (RA), tricuspid valve, PA, and pulmonary valve. The RV is both enlarged and hypertrophied (8,9,66,68,72,76–78). The anatomy of the interventricular septum may be affected. The apex of the RV and apex of the hypoplastic LV remain in proximity and may be identified externally by the junction of the anterior descending coronary artery and the posterior descending coronary artery. The apical junction of the right and LV will not correspond to the apex of the ventricular mass, because the RV is folded around the hypoplastic LV (79). This may impact tricuspid valve anatomy and function of the RV (80,81).

Abnormalities of the tricuspid valve have been identified in up to 35% of patients with HLHS. In aortic atresia and a patent MV, the LV has inflow but not outflow; the result is significant hypertrophy of an LV that is larger than that with aortic and mitral atresia and in fact may have greater than normal mass (82). The larger ventricular mass may create distortion of the basilar inflow portion of the RV. The septal surface of the RV may appear to have deep apical sinuses or recesses, the result of the apex of the RV folding around the hypoplastic but hypertrophied LV. The subvalvar apparatus of the tricuspid valve may be more distorted than that found in aortic atresia with mitral atresia. The finding of tricuspid valve dysplasia is more common among patients with a patent MV, occurring in 50% in this subgroup (81,83). In addition to alterations of tricuspid valve function owing to left ventricular mass effect, other abnormalities of the tricuspid valve including identification of a bileaflet right atrioventricular valve are seen in 12% of patients whereas some degree of dysplasia of the tricuspid valve can be found in a third of patients. Volume overload of the single RV and resultant annular dilation may further contribute to the development of tricuspid insufficiency. An additional cause of tricuspid insufficiency may be right ventricular subendocardial ischemia occurring in the neonatal period either at the time of presentation or following stage 1 palliation. Evidence for this includes the observation of a bright appearance of the papillary muscles by echocardiography consistent with ischemia and elongated cords in association with the development of tricuspid insufficiency.

Patients with aortic atresia and a patent MV have been variably reported to be at increased risk for mortality after the Norwood procedure (84,85). Coronary artery abnormalities, specifically, fistulous connections between the epicardial coronaries and the LV, have been described in a subgroup of these patients (86). Endocardial fibroelastosis is frequently present and is thought to be the result of subendocardial ischemia as a consequence of suprasystemic left ventricular pressure during development (79,82,87,88). Within this subgroup, the potential for tricuspid valve insufficiency is increased and arrhythmias associated with endocardial fibroelastosis may also contribute to an increased mortality risk (89) (Fig. 48.3).

The least affected subgroup of HLHS is aortic stenosis with a patent MV. This form is thought to develop later during fetal development when the LV is more completely formed. This form blends smoothly into the spectrum of critical aortic stenosis. Decision making in patients with left ventricular outflow obstruction can be challenging. In the patient deemed to have an LV that is non-apex forming with a prohibitively hypoplastic MV, stage 1 palliation is generally chosen with a prognosis that may be favorable because the LV is able to contribute to cardiac output.

Forms of Hypoplastic Left Heart Syndrome with a Ventricular Septal Defect

There are various forms of HLHS that have in common a ventricular septal defect. This may include forms that otherwise resemble those described above except that they have a

ventricular septal defect that can be in any part of the septum. If these defects are small, the cause and development of HLHS may not be significantly different than in patients with HLHS and an intact septum. In this group, mitral atresia with a patent left ventricular outflow may be present and suggests that inflow obstruction may be the source of development of HLHS. Within this group are forms of double-outlet RV including double-outlet RV with mitral atresia without obstruction to aortic outflow and unbalanced atrioventricular septal defects. Although this latter group could arguably be placed outside HLHS, there are forms with undeniable hypoplasia of the LV.

Additional Anatomic Considerations

Abnormalities of systemic venous return are uncommon in the patient with HLHS. Persistent left superior vena cava (SVC) occurs in <5% (8,68). Abnormal pulmonary venous connection or drainage occurs in 5% of patients (90). Anomalous pulmonary venous connection may occur with an intact atrial septum or severely restrictive atrial septal defect. Frequently, there is a persistent levocardial vein that drains to the innominate vein (91). Rare cases of anomalous pulmonary venous connection directly to the RA also exist. Important coronary abnormalities are rare. Anomalous origin of either of the coronary arteries from the right PA has been described (92–95). Coronary–cameral fistulas have been observed in patients with aortic atresia and a patent MV. Additionally, patients with aortic atresia and a patent MV have been observed to have tortuous epicardial coronaries with increased medial thickness (96). Despite the origin of the coronary arteries from the small ascending aorta, the coronary ostia and proximal coronary artery calibers are normal (97).

Premature closure of the patent foramen ovale has been postulated as a cause of HLHS. Because the foramen ovale is the source of left ventricular preload in the fetus, one would expect that closure of the foramen ovale would starve the LV of preload and result in hypoplasia. Premature closure of the foramen ovale may also occur as a secondary event to LVOTO. As mentioned earlier, LVOTO will result in increased left atrial pressure, and increased left atrial pressure results in apposition of the fossa ovalis flap valve against the septum secundum. Premature closure or restriction of the foramen ovale might occur along with LVOTO and contribute to development of HLHS. Among patients with an intact ventricular septum, premature closure of the foramen ovale is associated with endocardial fibroelastosis and indicates that LVOTO with elevated left ventricular end-diastolic pressure and subendocardial ischemia was present (98). Among patients with premature foramenal closure and a ventricular septal defect, fibroelastosis is absent, indicating that premature closure was perhaps a primary event in the development of left ventricular hypoplasia.

PRESENTATION, DIAGNOSIS, AND ECHOCARDIOGRAPHIC IMAGING

Presentation

Today, many cases of HLHS are detected in the second trimester when a screening obstetric ultrasound shows an abnormal four-chamber view. Prenatal recognition of the disease allows timely parental counseling as well as optimal delivery planning. Delivery at a tertiary care facility is recommended, avoiding transport-related morbidities, and allows the mother to be in close proximity to her baby after birth (99). Most centers continue to advocate a vaginal delivery, although induction of labor may be deemed necessary if the mother lives a significant

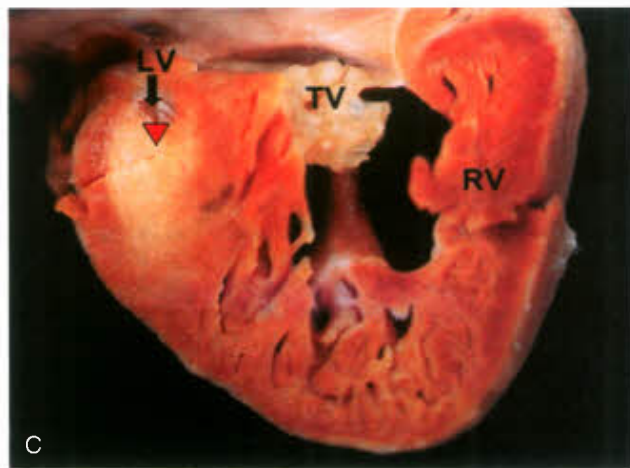
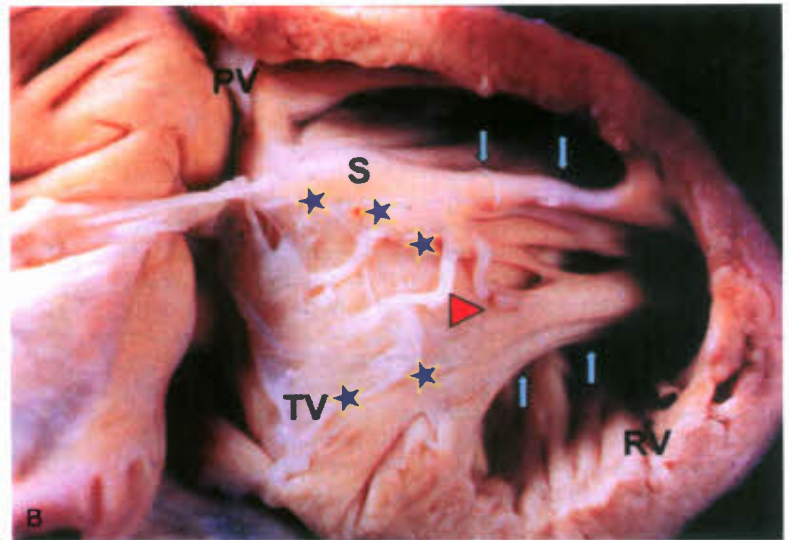
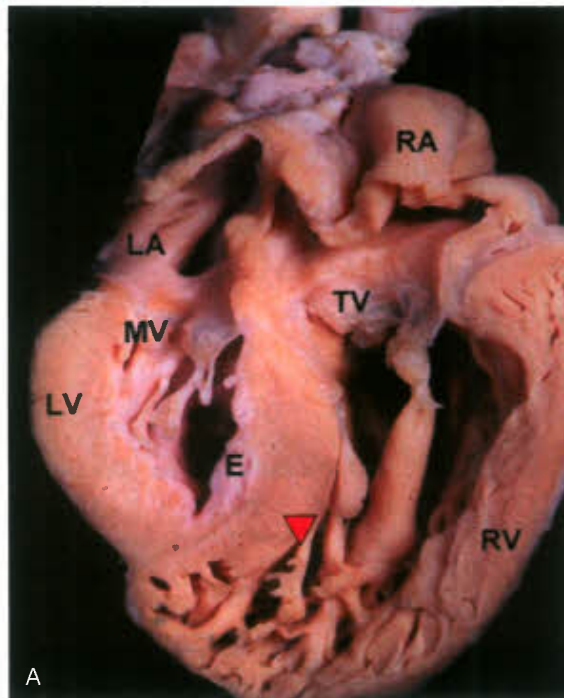


FIGURE 48.3. A: A view from the diaphragmatic surface of a heart with aortic valve atresia and a patent mitral valve (MV). The LV cavity is hypoplastic, but the LV is hypertrophied. Septal anatomy is distorted, and the *triangle* marks the apex of the interventricular septum. The hypertrophied but hypoplastic LV can distort the basilar septum and result in tricuspid valve insufficiency. B: The septal surface of a heart with aortic atresia and a patent MV. The *triangle* indicates the apex of the LV and the *stars* indicate the boundaries of the interventricular septum (S). The deep apical sinuses are the result of the remaining RV wrapping around the hypoplastic but hypertrophied LV. C: A view from the diaphragmatic surface of a heart with aortic and mitral atresia. The LV can be identified but is extremely hypoplastic. There is less potential for distortion of the anatomy of the interventricular septum and the subvalvar apparatus of the tricuspid valve. E, endocardium; LA, left atrium; PV, pulmonary valve; RA, right atrium; RV, right ventricle; TV, tricuspid valve. (Reprinted from Smith A, Pozzi M, and Anderson RH. *The Morphology of Hypoplasia of the Left Heart*. In: Anderson RH, Pozzi M, and Hutchinson S. *Hypoplastic Left Heart Syndrome*, 2005, with kind permission of Springer Science and Business Media.)

distance from the tertiary care facility. Following delivery, prostaglandins are initiated to maintain ductal patency, and an echocardiogram is performed to confirm the diagnosis. If severe atrial septal restriction is suspected on the prenatal ultrasound, interventional cardiology and/or cardiothoracic surgery should be immediately available.

If the infant has not been prenatally diagnosed with HLHS, timing of presentation is somewhat variable and dependent on the degree of atrial-level restriction as well as ductal patency. During late fetal development, pulmonary vascular resistance (PVR) is high and pulmonary blood flow is limited to <10% of ventricular output. At birth, PVR decreases abruptly as a result of mechanical distention of the lung, increased oxygen tension, and increased shear stress. Although the greatest fall in PVR occurs shortly after birth, a clinically important decline in PVR continues within days of birth (100–102). Abu-Harb et al. (103) reviewed the time of presentation of obstructive left heart malformations. About one-quarter of their infants with HLHS became symptomatic within 24 hours of age. However, most infants had a “normal” neonatal examination, with development of symptoms after 48 hours of age, often

after hospital discharge. When the atrial septum is restrictive, the resultant left atrial hypertension leads to pulmonary congestion, resulting in early onset of tachypnea and cyanosis. When the atrial septum is widely patent, neonates with HLHS may initially appear normal, with adequate oxygenation and systemic perfusion. These infants have a more delayed presentation, with symptoms developing as the ductus arteriosus undergoes gradual spontaneous closure. With ductal regression, there is hypoperfusion of the systemic circulation with an associated augmentation of pulmonary blood flow. These infants usually present in the first week of life with feeding difficulties and respiratory distress, with rapid progression to congestive heart failure and shock.

Diagnosis

Physical examination in the neonate with a severely restrictive atrial septum will be most notable for intense cyanosis with respiratory distress. In contrast, the infant with a nonrestrictive atrial defect may appear relatively pink. The infant with

ductal closure is often lethargic and has respiratory distress, cool extremities, and pallor. Auscultation is generally benign, especially in comparison with a sometimes dramatic clinical picture. The second heart sound is single and loud, reflecting the absence of the aortic valve component and the associated PA hypertension. A third heart sound may be heard, especially in the presence of ventricular dysfunction. Murmurs are uncommon, although a soft systolic ejection murmur may be generated from increased flow across the pulmonary valve. A louder S1-coincident murmur may be heard if there is significant tricuspid regurgitation. The upper- and lower-extremity pulses are palpable and symmetric early but are reduced later as ductal closure ensues. Hepatomegaly is common and is generally seen in infants with a delayed presentation.

Chest radiographs are generally nondiagnostic but typically reflect the degree of atrial-level restriction. In the infant with a severely restrictive atrial septum, the heart size may be relatively normal; however, there is significant pulmonary edema. The radiographic findings may be misinterpreted as lung disease, leading to a delay in diagnosis. In contrast, if the atrial septum is nonrestrictive, there is pulmonary overcirculation with cardiomegaly. The right atrial border may be prominent with absence of the ascending aortic shadow.

The electrocardiogram does reflect the underlying pathology; however, it is nondiagnostic. Right-axis deviation and right ventricular hypertrophy are common but not distinctly different from the normal electrocardiogram of the neonate. Tall, peaked P waves, indicative of right atrial enlargement, have been reported in 30% to 40% of patients (7,8).

With diagnostic 2-D echocardiography readily available, the need for cardiac catheterization in an infant with HLHS has dramatically decreased. Cardiac catheterization is generally used as an adjunct tool when trying to better identify pulmonary venous anomalies, or possibly, coronary anomalies. Also, in the setting of a severely restrictive atrial septum, catheter intervention may be lifesaving.

Echocardiography

The diagnosis of HLHS can be readily made by 2-D echocardiography, with additional important hemodynamic information provided by Doppler echocardiography (90,104–111). The intracardiac anatomy and physiology should be investigated using a standard echocardiographic approach and should include multiple imaging views (long axis, short axis, apical four chamber, subcostal coronal, subcostal sagittal, suprasternal notch) with repeated Doppler assessments.

Parasternal Long-Axis View

The diagnosis of HLHS is often suspected immediately from a parasternal long-axis view with identification of a small, muscle-bound left ventricular chamber that does not extend to the cardiac apex (Fig. 48.4). The endocardial surface of the LV is often echobright, indicating areas of endocardial fibroelastosis. The LA is usually small but may be dilated in patients with a restrictive atrial septal defect. The ascending aorta can be well visualized from the long-axis view and is frequently small (2 to 3 mm in diameter); the aortic valve may or may not be patent. The MV is often imperforate, but when patent, the leaflets are thickened, with short or even absent papillary muscle chordal attachments. A ventricular septal defect is rare in the presence of aortic atresia, but color Doppler interrogation of the ventricular septum may show ventriculocoronary arterial connections. Although the significance of these abnormal coronary connections in HLHS is unclear, coronary artery sinusoidal connections have had prognostic implications in other forms of congenital heart disease (112,113).

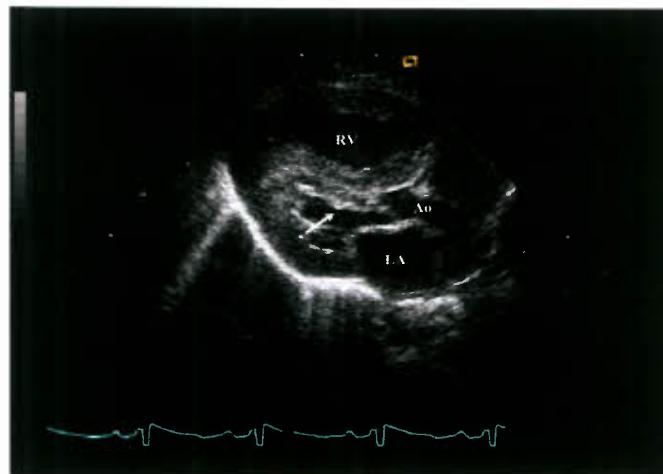


FIGURE 48.4. Parasternal long-axis view in a patient with HLHS. The left ventricular chamber is small and muscle bound. The endocardial surface of the LV is echobright, consistent with endocardial fibroelastosis (arrow). Ao, aorta; LA, left atrium; RV, right ventricle.

Several measurements are available from the parasternal long-axis view, which can be helpful when trying to differentiate critical aortic stenosis from HLHS. A left ventricular cross-sectional area $<1.5 \text{ cm}^2$ is found in most infants with HLHS, as well as a left ventricular end-diastolic inflow dimension $<25 \text{ mm}$ (measured from the hinge point of the posterior mitral leaflet to the apex) and a mitral annulus diameter of $\leq 6 \text{ mm}$ (104,105).

Parasternal Short-Axis View

The parasternal short-axis view again allows assessment of left ventricular size and function (Fig. 48.5A). The MV papillary muscles are well visualized from this window and should be carefully examined. At the base of the heart, aortic valve size and anatomy can be well visualized. Doppler interrogation of the coronary arteries is often best assessed here. Bidirectional coronary flow is consistent with left ventriculocoronary arterial connections. Last, the main PA, pulmonary valve, and branch pulmonary arteries are all well seen from the short-axis view. Scanning more superiorly, the patent ductus arteriosus can be visualized as it sweeps to the descending aorta (Fig. 48.5B).

Apical Four-Chamber View

The apical four-chamber view is often critical for definitively evaluating left ventricular size and function. If a large portion of the cardiac apex is occupied by the RV (Fig. 48.6), it is unlikely that the LV can support the systemic circulation. The four-chamber view also provides an excellent window to see the entire mitral apparatus, including the subvalvar and supravalar areas. MV anatomy and annulus size should be reassessed, especially in cases of borderline left ventricular size.

Right ventricular function and tricuspid valve anatomy and competency are best assessed from the four-chamber view. Right ventricular systolic function may be depressed, especially in those neonates with ductal closure and acidosis. Tricuspid valve abnormalities are common and can include a bileaflet valve, tricuspid valve dysplasia/prolapse, and abnormal papillary muscle arrangements (81).

Subcostal Views

Atrial septal anatomy is best imaged from the subcostal views. Large atrial septal aneurysms billowing into the RA are

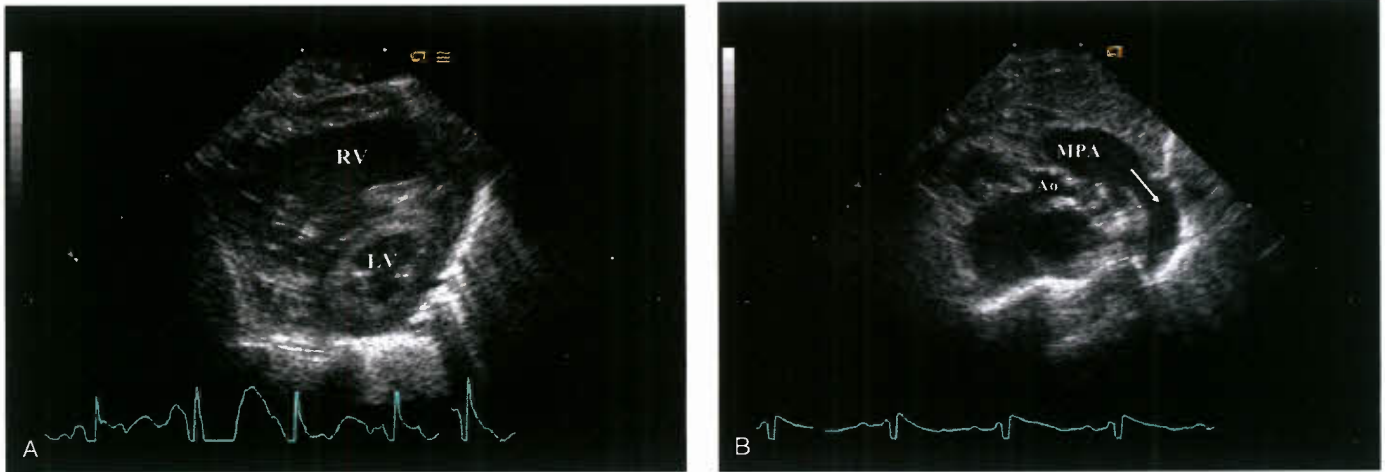


FIGURE 48.5. Parasternal short-axis views in a patient with HLHS. In (A) the right ventricle (RV) is enlarged with a smaller hypertrophied left ventricle (LV). Scanning more superiorly from a parasternal short-axis view (B), the larger main pulmonary artery (MPA) and patent ductus arteriosus (*arrow*) are seen connecting to the descending aorta. No brachiocephalic vessels are seen arising from the ductal arch, a key finding in differentiating the ductal arch from the true aortic arch. Ao aorta.

common (Fig. 48.7). Unusual attachments of septum primum can sometimes be seen, specifically anomalous attachment to the posterosuperior left atrial wall (Fig. 48.8). This anomalous attachment has been implicated in the pathogenesis of HLHS (48). If the atrial septal defect is small and restrictive, peak and mean Doppler gradients across the atrial septum should be obtained to estimate the degree of left atrial hypertension.

Pulmonary venous anatomy and drainage should also be interrogated from the subcostal window. It is important to identify connections of the pulmonary veins (anatomic attachment) as well as pulmonary venous drainage (the end point of pulmonary venous flow). The pulmonary veins may connect normally to the LA, but especially in cases of an intact atrial septum, there may be a levoatrial cardinal vein that originates directly from the LA and drains either all pulmonary veins (total) or some (partial) to a variable location. It is important to remember that this anomalous

venous structure can be stenotic, so the presence of the “decompressing” vein does not guarantee normal left atrial pressure (63). On the other hand, some or all of the pulmonary veins may not connect normally to the LA, but connect to a confluence behind the LA with anomalous drainage to a variable location. It is estimated that anomalous pulmonary venous anatomy and/or drainage occurs in about 5% to 10% of patients with HLHS.

Suprasternal Notch Views

The suprasternal notch provides an important window for evaluating aortic arch anatomy (Fig. 48.9). Although the ascending aorta can be imaged from many views, the transverse arch and descending thoracic aorta (DAo) are best seen from the suprasternal notch view. Coarctation of the aorta is common in patients with HLHS, and interruption of the aortic arch has also been reported. Doppler interrogation of the transverse arch should show retrograde systolic flow from the ductus; this finding indicates ductal-dependent systemic circulation and supports left ventricular inadequacy for biventricular repair (Fig. 48.10). The suprasternal notch views also provide images of the proximal pulmonary arteries and the ductus arteriosus. In the patient with a later presentation, the ductus may be restrictive; Doppler interrogation of the pressure gradient from PA to aorta should be quantified and follow-up studies performed when prostaglandin therapy is initiated. Pulmonary venous connection and drainage should be reassessed from this window. A persistent left SVC or levoatrial cardinal vein can be well imaged to the left of the descending aorta from the suprasternal notch view.

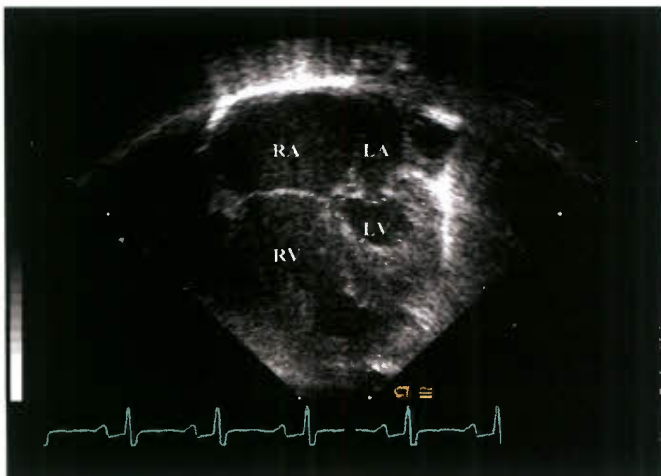


FIGURE 48.6. Apical four-chamber view in a patient with HLHS. The left atrium (LA) and left ventricle (LV) are much smaller than the right atrium (RA) and right ventricle (RV). The RV clearly occupies the cardiac apex.

PHYSIOLOGY, MONITORING, AND STABILIZATION

Parallel Circulation

The patient with HLHS faces similar physiologic challenges before, during, and after stage 1 palliation. The superimposition of inefficient parallel circulation, cyanosis, myocardial dysfunction, and autonomic and inflammatory

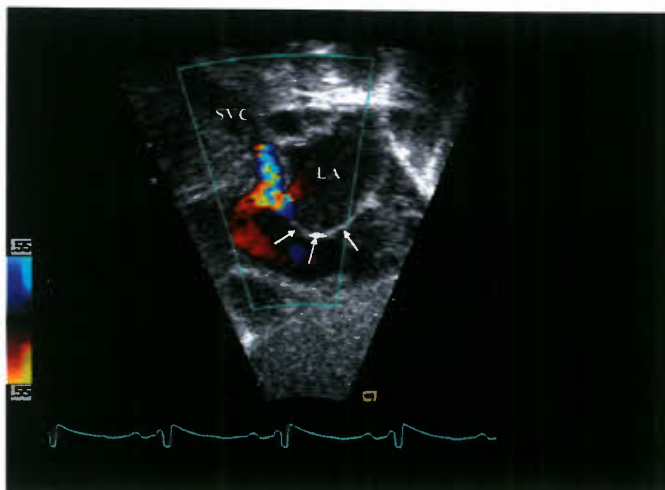


FIGURE 48.7. Subcostal sagittal view in a patient with HLHS. The atrial septum is aneurysmal (*arrows*), bowing into the RA. Color Doppler imaging identifies the superiorly positioned atrial shunt with the jet directed into the superior vena cava (SVC). Aliasing of the color Doppler flow signal across the atrial septum is consistent with a restrictive defect and can result in left atrial hypertension. LA, left atrium.

responses to stress and surgery result in high likelihood of critical impairment of oxygen delivery with subsequent organ dysfunction or death. Thus, facility with the principles of hemodynamics and oxygen supply/demand economy is a prerequisite for rational perioperative treatment of first-stage palliation patients.

Maintenance of adequate organ substrate delivery, oxygen, is necessary to reverse or prevent ischemic injury, which can result in multisystem organ dysfunction, prolonged morbidity, and mortality (114–120). Interventions targeting early treatment of inadequate whole-body or regional oxygen supply/demand relationships (shock) have improved outcome in critical illness; therefore detection of inadequate oxygen delivery is important for preventive or therapeutic interventions (114,115,121–126).

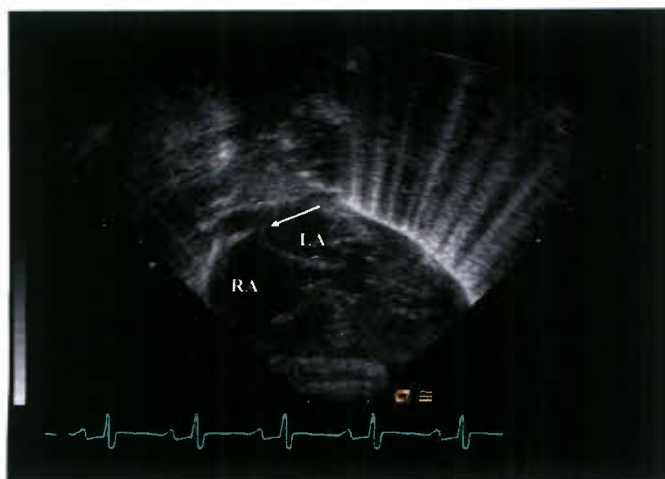


FIGURE 48.8. Subcostal coronal view in a patient with HLHS. The left atrium (LA) is small with leftward deviation of septum primum and anomalous attachment of the septum to the posterolateral left atrial wall (*arrow*). RA, right atrium.

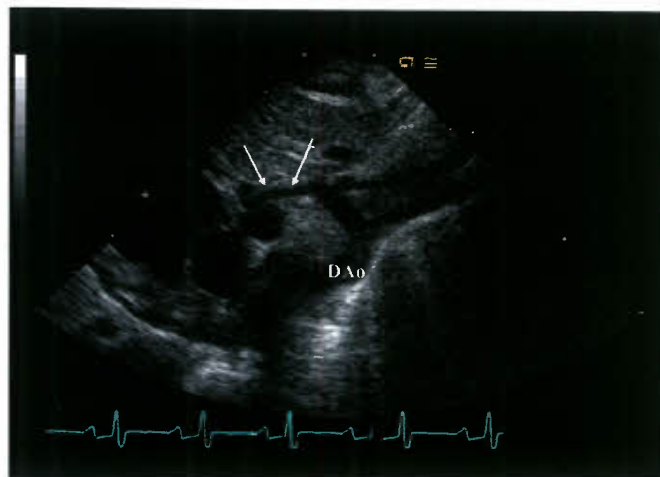


FIGURE 48.9. Suprasternal long-axis view from a patient with HLHS and aortic atresia. The ascending aorta (*arrows*) is markedly hypoplastic, measuring 2 mm, with a fair-sized transverse arch connecting to the descending thoracic aorta (DAo). Brachiocephalic vessels are seen arising from the transverse aorta, identifying this structure as the true aortic arch.

Cardiovascular Reflexes and Physiology of Shock

Efficient delivery of oxygen to meet metabolic demand occurs through regional and global circulatory controls. Global cardiac output is affected by preload, afterload, rate, rhythm, contractility, and the presence of aortopulmonary shunts. Regional resistance is determined by the interaction of neurohumoral factors related to inflammation and the sympathetic nervous system, and local factors related to autoregulation. The total systemic vascular resistance (SVR) is thus determined by the net effect of regional resistances. Oxygen delivery ($\dot{V}O_2$) is systemic cardiac output (Q_s) multiplied by arterial oxygen content (CaO_2), which is determined by the hemoglobin (Hb) concentration, oxygen saturation (SaO_2), and oxygen tension (PaO_2):

$$CaO_2 = 1.34 \times Hb \times SaO_2 + 0.003 \times PaO_2 \quad (1)$$

$$\dot{V}O_2 = CaO_2 \times Q_s \quad (2)$$

The sympathetic stress response as described with hypovolemic-septic shock (127–129) is activated in all shock states to redistribute blood flow to the brain and heart (130–132). The distribution of cardiac output can be significantly altered by stress responses, with the mesenteric and splanchnic circulations being at risk for silent ischemia during compensated shock (133–136). Circulatory reflexes to hemorrhage or hypotension will increase baroreflex gain to raise contractility, heart rate, and SVR, and decrease venous capacitance (137–140). These responses may be immediately protective in the face of hemorrhagic shock but often impair systemic flow in the face of myocardial dysfunction (141,142). These responses are also activated by cold stress, pain, and anxiety, and thus are not specific to hypovolemia (143–146). The vigor of the vascular component of the stress response may actually cause blood pressure to be elevated in the face of low cardiac output in the stressed neonate or child (147). The predominant profile of shock in pediatric patients is low cardiac output and very high SVR (148).

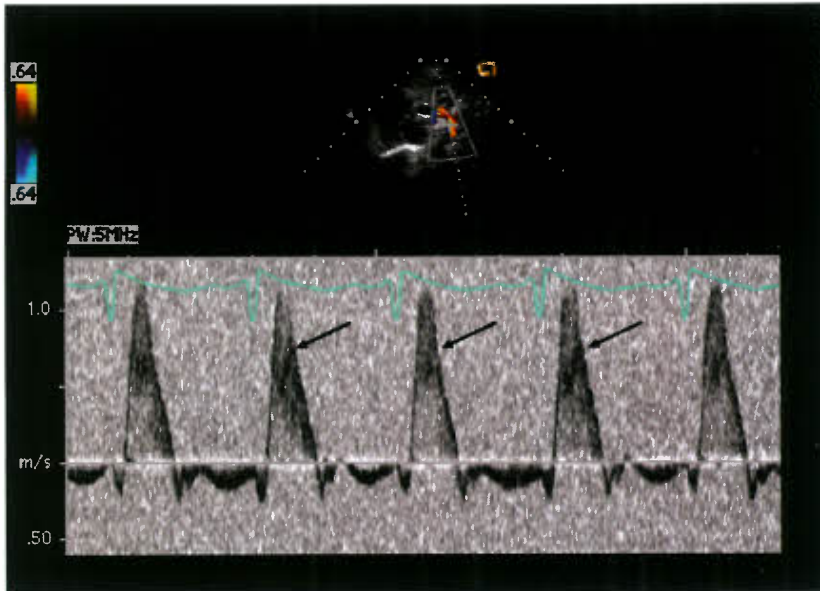


FIGURE 48.10. Pulsed Doppler examination from the suprasternal notch in a patient with HLHS. With the sample volume positioned in the transverse arch, retrograde systolic flow (arrows) from the patent ductus arteriosus into the aorta is identified, consistent with ductal-dependent systemic circulation.

The organs in the splanchnic circulation are the first to suffer ischemic injury because sympathetic outflow and innervation is rich in these regions (135,149–152) and because of the selective effects of angiotensin (153,154). Ischemic organ damage may occur even in the presence of normal global oxygen economy if regional vascular resistance is sufficiently elevated (133,134,155–157). There now exists compelling evidence that splanchnic/mesenteric ischemia is a frequent common pathway for multisystem organ dysfunction and death (158–161), and regional cellular oxygen deficit is underrecognized, underdiagnosed, and undertreated (162). Strategies targeting earlier detection and treatment of shock could improve outcome, with greater impact in populations with higher baseline mortality risk (163). The mortality risk in the neonate with HLHS, even with contemporary management, is high enough to justify the additional complexity of oxygen-delivery goal-directed approaches to prevention, detection, and management of shock states (164).

Oxygen Flux in Single-Ventricle Parallel Circulation

With univentricular parallel anatomy, both the pulmonary circulation and the systemic circulation are fed by arterial blood that is only partially saturated with oxygen. Because arterial saturation (SaO_2) is reduced by mixing, and because Q_s may be reduced by various factors, a reduction in $\dot{\text{D}}\text{O}_2$ is typically encountered in patients with HLHS, with a resulting higher risk of cellular hypoxia as a major physiologic vulnerability. Applying the Fick principle (equality of systemic oxygen consumption and pulmonary oxygen uptake) to the patient with HLHS yields the following relationships between oxygen consumption ($\dot{\text{V}}\text{O}_2$), pulmonary blood flow (Q_p), systemic blood flow (Q_s), SaO_2 , systemic venous saturation (SvO_2), and pulmonary venous saturation (SpvO_2), which allows estimation of the pulmonary-to-systemic flow ratio (Q_p/Q_s) in the parallel circulation:

$$\dot{\text{V}}\text{O}_2 = \text{Q}_s \times (\text{SaO}_2 - \text{SvO}_2) \quad (3)$$

$$\dot{\text{V}}\text{O}_2 = \text{Q}_p \times (\text{SpvO}_2 - \text{SaO}_2) \quad (4)$$

$$\frac{\text{Q}_p}{\text{Q}_s} = \frac{(\text{SaO}_2 - \text{SvO}_2)}{(\text{SpvO}_2 - \text{SaO}_2)} \quad (5)$$

Optimal systemic oxygen delivery in univentricular models occurs at the lowest total cardiac output when Q_p/Q_s is close to 1 (165). This economy occurs with the total ventricular output (Q_t) being twice the normal output of an in-series systemic ventricle, to yield normal values for both Q_s and Q_p . With a Q_p/Q_s of 1 and an arterial–venous saturation difference ($\text{SaO}_2 - \text{SvO}_2$) of 25%, oxygen uptake/consumption equilibrium will occur when the pulmonary capillary–arterial saturation difference ($\text{SpvO}_2 - \text{SaO}_2$) also equals 25%, resulting in an SaO_2 of 75% and an SvO_2 of 50%, assuming that pulmonary venous blood is fully saturated. If SaO_2 is >75%, a higher Q_p is necessary to maintain the same pulmonary O_2 uptake; conversely if Q_p falls, SaO_2 will also fall. If the SaO_2 is low, then a higher Q_s is necessary to maintain systemic O_2 uptake; if Q_s falls, then SaO_2 also falls. Changes in SaO_2 result in opposite effects on pulmonary and systemic oxygen economy. Conversely, since a tradeoff of Q_s and Q_p will exist for any Q_t , increases in SaO_2 that are not a result of increased Q_t will be offset by a reduction in Q_s . Referring to the first three examples in Table 48.1, moderately large changes in Q_p/Q_s with constant Q_t (assuming a hemoglobin of 15 g/dL, SpvO_2 of 100%, and indexed $\dot{\text{V}}\text{O}_2$ of 160 mL/m²/min) show a range of SaO_2 from 63% to 82% but a narrower range of SvO_2 for 44% to 50%. As a result, moderate alterations in Q_p/Q_s balance will have minimal effect on $\dot{\text{D}}\text{O}_2$; more effectively, alterable determinants of $\dot{\text{D}}\text{O}_2$ include hemoglobin and Q_t . Oxygen economy at higher or lower Q_p/Q_s and varying Q_t is illustrated in Table 48.1.

In single-ventricle parallel circulation, solution of the Fick equation shows that the SaO_2 depends on both systemic and pulmonary flow and saturation:

$$\text{SaO}_2 = \frac{(\text{Q}_p \times \text{SpvO}_2 + \text{Q}_s \times \text{SvO}_2)}{(\text{Q}_p + \text{Q}_s)} \quad (6)$$

Changes in Q_t , over a range of Q_p/Q_s , have a more profound effect on SvO_2 . Thus matching of $\dot{\text{D}}\text{O}_2$ to changes in $\dot{\text{V}}\text{O}_2$ are more effective via interventions in total cardiac output or hemoglobin concentration than by precise manipulation of Q_p/Q_s balance.

An important limitation in circulatory reserve resulting from this complex relationship is that increases in systemic oxygen consumption cannot be buffered by increased extraction (166). This limitation is best clarified by comparison of

TABLE 48.1 Effect of Varying Qp/Qs and Qt on Arteriovenous Saturations in Parallel Circulation

Qp/Qs	SvO ₂ (%)	Spv-aO ₂ (%)	Qp	Sa-vO ₂ (%)	Qs	Qt	SaO ₂ (%)
1.0	50	25	3.2	25	3.2	6.4	75
2.0	44	18	4.3	38	2.1	6.4	82
0.5	44	37	2.1	19	4.3	6.4	63
1.0	67	17	4.8	16	4.8	9.6	83
2.0	63	12	6.4	25	3.2	9.6	88
0.5	63	25	3.2	12	6.4	9.6	75
1.0	33	33	2.4	34	2.4	4.8	67
2.0	25	25	3.2	50	1.6	4.8	75
0.5	25	50	1.6	25	3.2	4.8	50

Assumptions: hemoglobin 15 g/dL, oxygen consumption 160 mL/m², pulmonary venous saturation of 100%.

the oxygen cascade diagram between in-series and parallel circulation (Fig. 48.11).

In a patient with *normal in-series circulation*, at constant cardiac output, increased VO₂ will reduce SvO₂, but pulmonary oxygen uptake will increase to match. In the critically ill patient, tissue oxygen utilization will usually continue until the SvO₂ falls to <50%; thus, a doubling of VO₂ can be met without an increase in cardiac output. Since normal lungs can fully oxygenate fully desaturated systemic venous blood, the resulting SaO₂ is unchanged, $\dot{D}O_2$ is maintained, and the increased VO₂ can be met by increased extraction alone. Similarly, cellular oxygen utilization can be maintained during a reduction in cardiac output and $\dot{D}O_2$ by increased extraction.

In a patient with *univentricular parallel circulation*, increased oxygen extraction (either because of increased VO₂ or decreased $\dot{D}O_2$) will reduce SvO₂ and SaO₂. The result is that conditions that increase oxygen extraction will also decrease oxygen delivery through a reduction in SaO₂. For any given Qp/Qs, the increased tissue oxygen demand can be met only by increased cardiac output. For any given fall in cardiac output, $\dot{D}O_2$ and SvO₂ will be disproportionately reduced, because SaO₂ will also fall. Thus, changes in oxygen supply and demand are interdependent and destabilizing in the patient with parallel univentricular physiology.

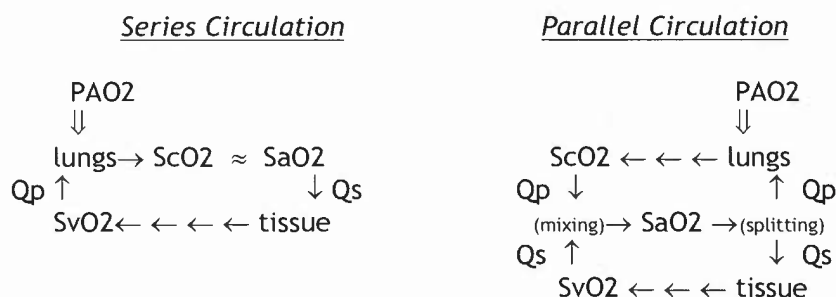
Monitoring the Parallel Circulation

The first successful approaches to monitoring and managing the patient with HLHS emphasized the central importance of SaO₂ in detecting and guiding treatment of unbalanced

pulmonary-to-systemic blood flow ratio and total cardiac output (167). Generalization of this approach was based on circulatory models that assumed either a constant arteriovenous oxygen difference (of typically 25%) or a constant mixed SvO₂ (of typically 50%). In either model, an SaO₂ of 75% would then result from mixing equal parts of systemic venous and (fully saturated) pulmonary venous blood; deviations of SaO₂ from 75% in these models would result from, and be diagnostic of, deviations of Qp/Qs from 1. These approaches also assumed adequate total cardiac output to meet oxygen delivery needs if Qp/Qs is optimized. Under these conditions, systemic oxygen delivery generally increases as SaO₂ approaches 75% to 80% and falls at higher saturation owing to increasing Qp/Qs imbalance. However, in the perioperative period, total cardiac output and metabolic demand may frequently be mismatched as a result of the inherent instability of parallel circulation as described above, and variability of Qp/Qs, Qt, and VO₂ (168–170). Inspection of Table 48.1 reveals that assertions about the Qp/Qs from a single measured SaO₂ value are unreliable unless either SvO₂, or VO₂ and Qt, are known. A target SaO₂ of 75% can result from a range of Qp/Qs and SvO₂ conditions, which may include inadequate systemic flow if Qt or VO₂ is variable. In a circulatory model that allows for variation in both total cardiac output and Qp/Qs, a wide range of tissue/venous saturation can result at any given SaO₂, shown graphically in Figure 48.12. The resulting domain of SvO₂ shows that severely impaired systemic oxygen delivery can occur with SaO₂ closely maintained in the target 75% to 80% range.

A report of increased stability with the use of inspired carbon dioxide (CO₂) (167) led to the wide adoption of manipulation of medical gases to control PVR and Qp/Qs. Theoretic

FIGURE 48.11. Oxygen flux in series and parallel circulations. In contrast to series circulation, in a parallel circulation, arterial blood derives from a mixture of systemic venous and pulmonary venous return and is divided into systemic and pulmonary flow according to relative resistances.



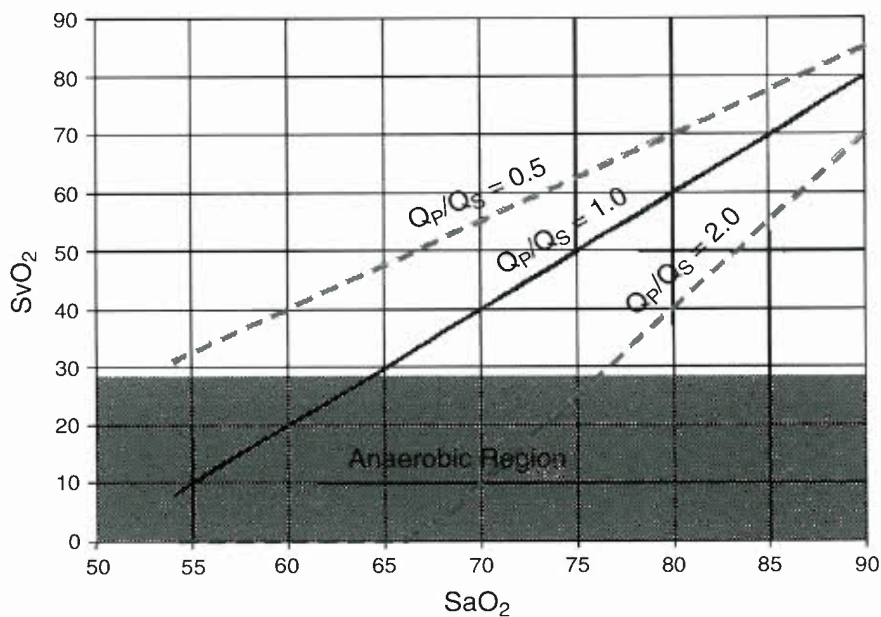


FIGURE 48.12. The range of SvO₂ at any given SaO₂ is shown in a model with variable total cardiac output and bounded by Qp/Qs as low as 0.5 and as high as two. For any SaO₂, a range of SvO₂ is possible. The slope of the SaO₂–SvO₂ relationship, as total cardiac output changes, is determined by the Qp/Qs ratio. (Reprinted from Hoffman GM and Stuth EA. Hypoplastic left heart syndrome. In: Lake CL, Booker PD, eds. *Pediatric Cardiac Anesthesia*. 4th ed. Philadelphia, PA: Lippincott Williams & Wilkins, 2005, with kind permission of Lippincott Williams & Wilkins.)

and experimental models showed that inspired CO₂ increased PVR, and moderately decreased SVR, and would increase systemic oxygen delivery (171,172). As part of this approach, the SaO₂ was used as a key indicator to detect pulmonary overcirculation, which would result in a higher SaO₂ as Qp/Qs rose. However, this would be true only if the systemic arteriovenous difference did not increase, which would occur only if the increase in Qp resulted from increased Qt at constant Qs. The primary concern over preventing a runaway spiral of increased Qp/Qs led to the use of low or even subatmospheric fraction of inspired oxygen (fiO₂) in further attempts to raise the PVR (173,174).

Preoperatively, these approaches may be partially effective in limiting pulmonary overcirculation, but only hypercapnia increases systemic oxygen delivery (175). In contrast, a synthetic shunt placed at the time of initial palliation imposes a large fixed resistor into the total pulmonary resistance, which is of similar magnitude to the SVR. This arrangement reduces the efficacy of PVR manipulations on hemodynamics (176,177). Reduction of fiO₂ may cause the resulting alveolar oxygen tension to be inadequate to fully oxygenate the pulmonary capillary blood, an effect that may be common at fiO₂ < 0.3 (178). Thus, reduction in SaO₂ by intentionally limiting fiO₂ may result solely from pulmonary capillary desaturation rather than reductions in Qp. This will reduce oxygen uptake across the lung, waste pulmonary blood flow, and reduce oxygen available for tissue utilization. Unless SpvO₂ is measured or fiO₂ is high enough to make pulmonary capillary desaturation unlikely, the calculated Qp/Qs at low fiO₂ may be falsely low because of SpvO₂ < 95%. Because of variability in both SpvO₂ and the arteriovenous saturation difference, the SaO₂ does not reliably characterize the parallel circulation.

The importance of both SVR and PVR in determining Qp/Qs was emphasized in modeling studies (176). In these studies, the Qp/Qs range could be restricted by placement of a resistive shunt, and the importance of shunt size was emphasized. These models also demonstrated that the combination of low total cardiac output and high Qp/Qs severely impaired systemic oxygen delivery. Even in the presence of a resistive shunt in the pulmonary circulation, control of elevated SVR was more effective than increases in PVR to optimize systemic oxygen delivery.

Without knowledge of SvO₂ or tissue oxygenation, the effect of any intervention on systemic oxygenation remains difficult to assess. Not surprisingly, perioperative management based primarily on optimization of SaO₂ is associated with an early mortality of >20%. With this approach, cardiovascular collapse and mortality typically result from an acute hemodynamic event that occurs unexpectedly in an apparently stable postoperative hemodynamic setting (73,179,180). Because sympathetic vasomotor tone and thus SVR increase as systemic flow falls, changes in Qp/Qs can occur rapidly, resulting in deterioration of systemic oxygen delivery in a self-reinforcing cycle. Precisely, because of the Qp/Qs tradeoff, these changes are usually not readily apparent with arterial pressure or oxygen saturation monitoring as demonstrated in Figure 48.13. This above analysis provides an explanation for the profound circulatory derangements that are possible despite having SaO₂ in the typical target range. These theoretical and actual limitations have led to the development of management strategies aided by SvO₂ measurement to more closely assess Qp/Qs, adequacy of oxygen delivery, and whole-body oxygen economy.

It is not possible to obtain a true mixed venous blood sample in the patient with HLHS, but approximate measures of the mixed venous oxyhemoglobin saturation can be obtained from blood withdrawn from the SVC. Placement of a catheter in the SVC primarily to allow sampling of quasi-mixed venous blood is more likely to be helpful in guiding perioperative management. Small (4 Fr) oximetric catheters placed in the SVC just prior to weaning from bypass in neonates undergoing Norwood-type repairs allow continuous readout of SVC saturation. Used as an approximation of SvO₂, monitoring SVC saturation allows timely hemodynamic intervention to avoid anaerobic metabolism, which has an apparent SVO₂ threshold near 30% in this population (181). The use of continuous SvO₂ has greatly reduced the perioperative occurrence of sudden unexpected circulatory collapse (73,179,182). However, this measure is available only rarely preoperatively, and for a limited time postoperatively.

Near-infrared spectroscopy (NIRS) monitoring of tissue oxygen status has been used as an adjunct to perioperative management. NIRS devices with a 4-cm source–detector distance can measure the average oxyhemoglobin saturation (rSO₂) in tissue about 2 to 3 cm below the skin, and has

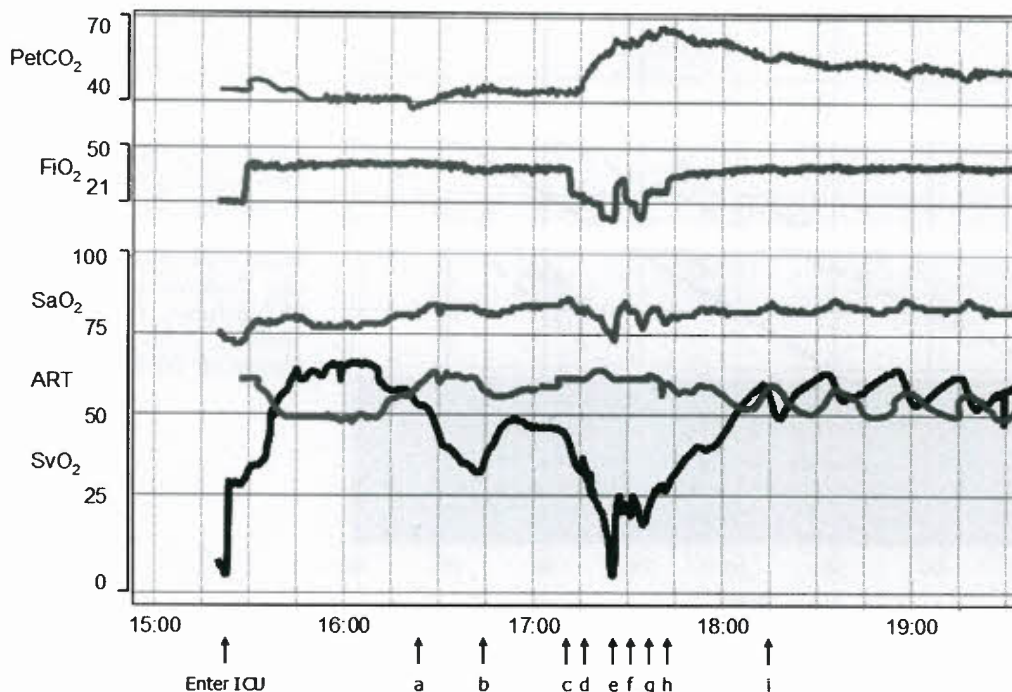


FIGURE 48.13. A Multichannel recording of early ICU course after Norwood procedure without phenoxybenzamine, showing severe deterioration in systemic oxygen delivery without significant changes in other conventionally monitored parameters. Continuously recorded data are from a single neonate arriving in the ICU after the Norwood procedure, performed without phenoxybenzamine. A life-threatening hemodynamic deterioration is clearly shown with SvO₂ monitoring despite SaO₂ in the 75% to 80% range. An initial deterioration in SvO₂ (arrow a) was partially corrected with additional analgesia (arrow b) but did not prevent a subsequent critical deterioration in systemic oxygen delivery (arrow e), which was effectively treated with a combination of additional analgesia/anesthesia and increased inotropic and vasodilator infusions. Conventional parameters (arterial blood pressure and SaO₂) show only subtle changes that provide neither an early warning of the critical situation nor feedback about the effectiveness of corrective measures. ART, mean arterial blood pressure; FiO₂, fraction of inspired oxygen; PetCO₂, end-tidal carbon dioxide; SaO₂, arterial saturation; SvO₂, systemic venous saturation. (Reprinted from Hoffman GM and Stuth EA. Hypoplastic left heart syndrome. In: Lake CL, Booker PD, eds. *Pediatric Cardiac Anesthesia*, 4th ed. 2005, with kind permission of Lippincott Williams & Wilkins.)

been used to monitor oxyhemoglobin saturation in a range of organs including brain, muscle, kidney, and gut (183,184). The probes are most commonly placed on the forehead to monitor cerebral oxygenation, and on the T10-L2 flank region to monitor somatic saturation, as an attempt to capture circulations under intense autoregulatory (cerebral) and autonomic (renal or splanchnic somatic) control. Combining NIRS rSO₂ from these two regional circulations in a linear model allows better approximation of SvO₂ and thus provides information about both regional and global oxygen economies as a noninvasive SvO₂ surrogate (185–188) (Fig. 48.14). Given the instability of oxygen supply/demand relationships, and the inadequacy of assessment based on arterial blood pressure and SaO₂ monitoring, improved outcome requires early detection and treatment of deficiencies in oxygen economy. Direct or surrogate measurement of SvO₂ permits continuous assessment of adequacy of systemic oxygen delivery in the most vulnerable postoperative period. Low total cardiac output and unbalanced Qp/Qs can be differentiated physiologically, interventions can be rationally based, and patient responses can be quantified and trended. We have found continuous SvO₂ monitoring to be the single most important factor in improving survival after stage 1 palliation (73), and our current approach relies on noninvasive pre- and postoperative detection of circulatory deterioration with NIRS (189–191).

Preoperative Preparation

Prostaglandin E₁

Maintaining ductal patency in a neonate with HLHS is vital in the preoperative management. Although ductal closure is rarely immediate, nearly all infants will have physiologic closure of the ductus arteriosus by the fourth day of life; 20% of infants will demonstrate functional ductal closure during the first day of life, and >80% of infants demonstrate ductal closure during the second day of life. For this reason, prostaglandin E₁ (PGE₁) therapy should be initiated immediately when HLHS is diagnosed or suspected (192–194). The patient's physiologic state often directs initial PGE₁ dosing. For patients who present in shock with suspected ductal closure or a restrictive duct, initial dosing will range from 0.05 to 0.1 µg/kg/min. Once ductal patency is ensured, the infusion rate can be decreased to an effective dose as low as 0.01 µg/kg/min (195).

Ductal patency with the lowest effective PGE₁ dose minimizes the most common dose-dependent side effects of PGE₁: hypotension prompting volume resuscitation and respiratory depression requiring mechanical support (195–197). Initiation of intravenous caffeine with a loading dose of 20 mg/kg followed by a maintenance dose of

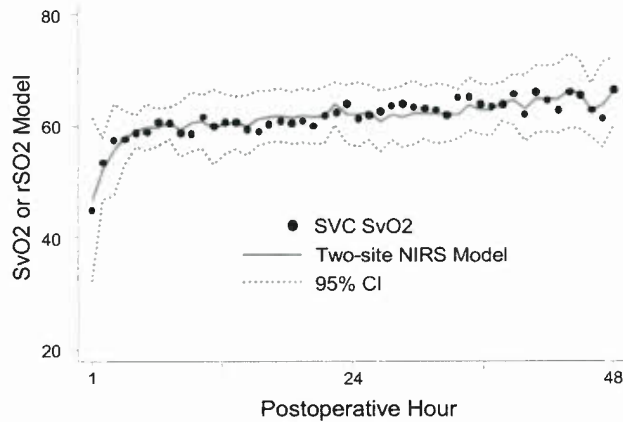


FIGURE 48.14. Actual SvO₂ and values predicted from two-site NIRS model. A neonate after the Norwood procedure performed with phenoxybenzamine has SVC SvO₂ monitoring and NIRS probes over frontal cerebral and T10-L2 somatic (renal) sites. A linear model of NIRS data closely tracks actual SvO₂ data. (Model SvO₂ = $0.45 \times rSO_2$ cerebral + $0.45 \times rSO_2$ somatic.) CI, confidence interval; rSO₂, regional oxygen saturation; SvO₂, systemic venous oxygen saturation. (Adapted from Hoffman GM, Stuth EA, Berens RJ, et al. Two-site near-infrared transcutaneous oximetry as a non-invasive indicator of mixed venous oxygen saturation in cardiac neonates. *Anesthesiology* 2003;97:A1393)

5 to 10 mg/kg/day has been effective in reducing the need for mechanical ventilation preoperatively. This approach is based on a study in neonates receiving low-dose PGE₁ who were simultaneously being treated with aminophylline or placebo. Patients who received aminophylline had a decreased incidence of apnea and did not require intubation when compared with the placebo group of whom 35% required intubation (198).

Respiratory Support and Inspired Gases

In the preoperative patient without anatomic limitation to pulmonary blood flow, mechanical ventilation and medical gas manipulation of pulmonary arteriolar resistance are sometimes necessary and beneficial. Controlled positive-pressure ventilation with care taken to avoid hyperventilation can limit pulmonary blood flow. Additionally, the use of positive end-expiratory pressure (PEEP) allows delivery of lung volumes that exceed functional residual capacity and subsequently results in compression of pulmonary vasculature with a resultant increase in PVR.

Medical gas management can be used to increase PVR and reduce Qp/Qs. Inspired CO₂ as a means to limit pulmonary blood flow and treat instability first became apparent in the early 1990s (167). Subsequent animal models have confirmed the effectiveness of inspired CO₂ on lowering the pH and raising PVR while successfully increasing systemic flow (171,172,199). Animal models have similarly demonstrated the effectiveness of subatmospheric FiO₂ in increasing PVR (172,199). Clinical experience supports the use of hypoxia as a means to attenuate an elevated Qp/Qs (173,200). Hypoxic gas mixtures are achieved through blending nitrogen and oxygen to achieve inspired subatmospheric FiO₂ of 0.14 to 0.20. The use of inspired gases in humans has been best studied in an acute model by Tabbutt et al. (175). Preoperative neonates with HLHS who were anesthetized and under neuromuscular blockade were ventilated with a hypoxic gas mixture (FiO₂ of 0.17) and with supplemental CO₂ (fICO₂ of 0.03). Although both strategies were successful in acutely

reducing SaO₂ and Qp/Qs, only hypercarbia improved systemic oxygen delivery (175). Furthermore, whereas hypercarbia improved cerebral oxygenation, hypoxia provided no benefit to cerebral saturation (201).

In general, excessive supplemental oxygen, a potent pulmonary vasodilator, is avoided in the preoperative management of HLHS, although patients with respiratory distress syndrome, pneumonia, atelectasis, or other primary lung pathology might benefit from the use of supplemental oxygen for severe hypoxia. Patients with restrictive atrial communication also necessitate supplemental oxygen administration. For these patients, controlled ventilation is instituted with supplemental oxygen, with titration based upon both arterial and regional or venous oxygen measures by NIRS, which allows the decoding of the complex interactions of FiO₂ and pCO₂ on pulmonary blood flow, systemic blood flow, and total oxygen delivery. In patients who have severely restrictive or absent atrial septal defect, supplemental oxygen and other medical therapies are ineffective in treating the severe arterial desaturation, prompting emergency intervention with balloon atrial septostomy, atrial septal balloon dilation and/or stent, surgical septectomy, or immediate stage 1 palliation.

Vasoactive Medications

The need for preoperative inotropic support is variable and directed by clinical presentation and echocardiographic features. More recently, we have used noninvasive but continuous monitoring with NIRS to facilitate a less-invasive preoperative stabilization strategy (189). Patients who present in cardiogenic shock most commonly benefit from inotropic support as do patients with significantly reduced right ventricular function. On whole, inotropic catecholamines have been shown to reduce or have little effect on Qp/Qs in an animal model (172), but dose escalation may result in an undesired increase in SVR that subsequently raises Qp/Qs. For those patients in whom Qp/Qs is elevated and systemic perfusion is compromised, inodilator therapy with milrinone, a phosphodiesterase inhibitor, might be warranted. Milrinone, however, also has been shown to reduce PVR and again carries the undesired risk of increasing Qp/Qs. Furthermore, milrinone could result in significant hypotension in patients already at risk for decreased perfusion secondary to aortopulmonary runoff. Strategic monitoring and thoughtful assessment of these patients will be directed at these concerns.

Other Adjunctive Therapies

The hypoxic patient with inefficient single-ventricle physiology benefits from increased oxygen carrying capacity. Increasing the hematocrit to 50% will benefit the patient with limited Qp or Qt. Other means to improve systemic perfusion include therapies that attenuate sympathetic vascular tone. Specifically, for the stressed neonate with increased SVR, low-dose morphine can be used to reduce agitation and work of breathing and to improve systemic oxygen balance (189). Parenteral nutrition is provided with volume administration that is consistent with gestational age, birth weight, and postnatal age. For the term infant who is >2,500 g, our recommendations for fluid requirements during the first day of life are 70 to 80 mL/kg/day with escalation to 100 mL/kg/day on day of life three and then, 120 to 140 mL/kg/day for infants 4 days of age and older. The preterm infant requires more fluid due to higher transdermal insensible losses at a lower weight. Diuretic therapy is reserved for those patients who demonstrate respiratory insufficiency from increased interstitial lung edema related to either pulmonary overcirculation or restrictive pulmonary venous return.

Any of the proposed preoperative management strategies can be used in isolation or combination to balance

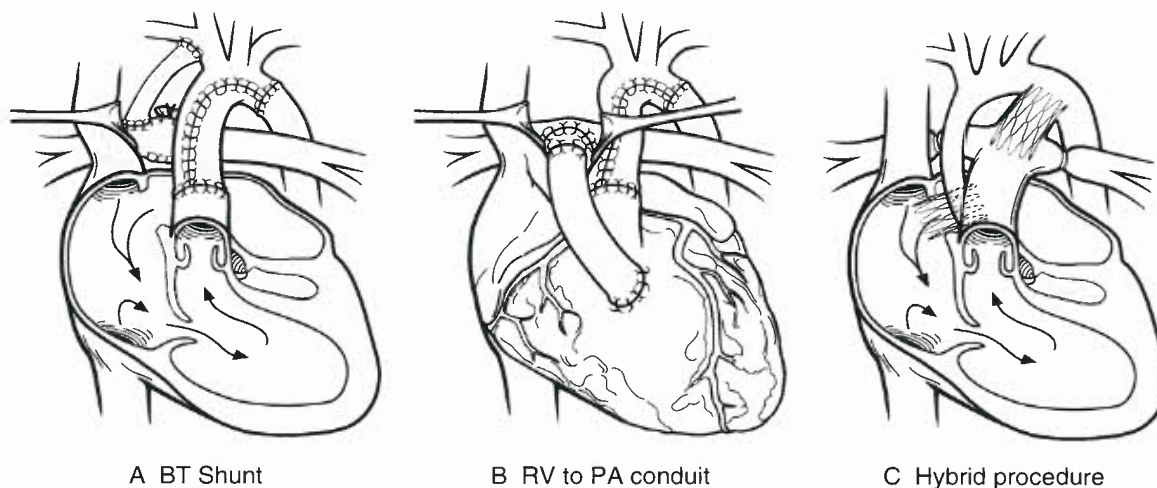


FIGURE 48.15. Stage 1 palliation of HLHS. **A:** Stage 1 palliation (Norwood procedure) using a modified BT shunt for provision of pulmonary blood flow. The shunt originates from the innominate artery and inserts into the central PA. **B:** Stage 1 palliation using an RV-to-PA conduit (Sano modification) for provision of pulmonary blood flow. A larger 5- or 6-mm graft is placed between the RV and the central PA. **C:** Stage 1 palliation using a hybrid approach. Pulmonary blood flow is restricted with branch PA bands, and the ductal patency is maintained by placement of a stent. A stent is placed to create a nonrestrictive atrial septal defect.

pulmonary-to-systemic flow, optimize systemic perfusion, and preserve organ function. However, each should be embarked on only with sufficient monitoring as they can pose potential risks to the neonate awaiting staged palliation for HLHS.

STAGED PALLIATION

With inadequate anatomic substrate for a two-ventricle repair, surgical approaches must address the relatively high and variable PVR in the neonate as well as the subsequent reduction in PVR that allows an eventual more stable and economical in-series circulation. Recognition of such physiologic necessities drove the development of numerous surgical approaches (202,203). Permutations of a staged surgical pathway that was successfully championed by Norwood et al. (204,205) are now widely used. The staged approach ultimately leads the patient on a pathway to a single-ventricle in-series circulation, usually culminating in a Fontan operation with the final result similar to patients with tricuspid atresia and hypoplastic right heart syndrome (206). Most commonly, stage 1 palliation consists of reconstruction of the aortic arch into the right ventricular outflow, separation of branch pulmonary arteries from the RV, and creation of a restrictive source of pulmonary blood flow from a systemic artery or directly from the single ventricle (205,207). Stage 2 palliation unloads the single ventricle by replacing the systemic-to-pulmonary shunt with a superior cavopulmonary anastomosis (208). The staged pathway is completed by modifications of a Fontan connection from the inferior vena cava (IVC) to the pulmonary arteries, with or without fenestration (205,209,210).

Stage 1 Palliation

Surgical Approaches

The goals of stage 1 palliation include relief of ductal-dependent systemic flow, provision of unrestricted coronary artery flow, creation of a nonrestrictive atrial septal defect

to prevent pulmonary venous hypertension, and provision of a reliable but restricted source of pulmonary blood flow (Fig. 48.15). Surgical strategies are varied, and the introduction of the hybrid procedure revisits early strategies of Litwin and Van Praagh to accomplish the goals of stage 1 palliation without the use of cardiopulmonary bypass (CPB) (211–214).

Stage 1 palliation using either a modified Blalock-Taussig (MBTT) shunt or RV-to-PA conduit (Sano modification) is accomplished using CPB, deep hypothermia, and altered perfusion—either circulatory arrest or regional perfusion. A connection is created between the smaller ascending aorta and the pulmonary root for provision of coronary blood flow. Restructuring of the heart's outflow via the pulmonary root is accomplished along with relief of coarctation and arch hypoplasia. Variations in surgical techniques include resection of ductal tissue or coarctectomy as opposed to patching of the region of ductal insertion. The aim of stage 1 palliation is to create a stable anatomy that permits growth and maturation of the pulmonary vasculature so that it can accommodate subsequent single-ventricle palliation. It is important that successful surgical strategies have a low incidence of recurrent or residual lesions because these are a source of interstage mortality and can limit suitability for single-ventricle palliation. Development of a restrictive atrial septal defect rarely complicates the interstage course (215). The observation that smaller ascending aortic size and presence of aortic atresia are risk factors for mortality is an indication that coronary insufficiency is a cause of death following stage 1 palliation, and strategies that target creation of a large ascending aorta-to-pulmonary root anastomosis are likely to result in improved outcome (216–219). Arch reconstruction strategies that include coarctectomy appear to have a lower incidence of late arch obstruction (70,216).

A modification of the systemic-to-pulmonary artery shunt developed by Blalock, Thomas, and Taussig has historically been the source of pulmonary blood flow following stage 1 palliation (220). Typically, this shunt originates from the innominate artery or the aorta. Both the diameter and length of this shunt are relevant to determining its flow-resistive characteristics (176). The resulting anatomy ideally provides

enough resistance to pulmonary blood flow to avoid destabilization from excessive pulmonary blood flow in the postoperative period. Physiologic limitations result from the inherent Qp/Qs mismatch of the parallel circulation and diastolic aortic runoff to the pulmonary circulation with risk of aortocoronary flow impairment (221,222). Additionally, competition between cerebral and pulmonary circulations for blood flow is possible if the shunt originates from the innominate artery (183). Furthermore, the systemic-to-pulmonary artery shunt is susceptible to occlusion from thrombosis or thromboembolism (215,223).

Recently, the right ventricle–pulmonary artery (RVPA) conduit as a source of pulmonary blood flow as part of the Norwood procedure was reintroduced (224,225). In this modification, pulmonary blood flow is supplied by conduit, generally a Gore-Tex tube graft, from the RV to the PA (224). A theoretical advantage of the RVPA shunt is the elimination of diastolic runoff and increased diastolic pressure with improved coronary perfusion pressure (226–233). Potential disadvantages include a negative effect on right ventricular function and ventricular arrhythmias due to the ventriculotomy, impaired growth of the pulmonary arteries, and the need for an earlier stage II procedure (230,234–236). Single-institution series comparing outcome of the Blalock-Thomas-Taussig shunt and RVPA conduit provided conflicting results (226–228,231,233,234,237–240). The Single-Ventricle Reconstruction Trial was a multi-institutional randomized trial of 549 patients comparing the MBTT shunt and the RVPA conduit. Among patients who had stage 1 palliation, transplantation-free survival 12 months after randomization was higher with the RVPA conduit than with the MBTT shunt (74% vs. 64%, $p = 0.01$) (Fig. 48.16). After 12 months, there was no survival advantage to the RVPA conduit, and the RVPA shunt group had more unintended interventions ($p = 0.003$) and complications ($p = 0.002$) (241).

Branch PA banding has been reported as a successful approach to reduce excessive pulmonary blood flow and permit a sufficient decrease in PVR to allow later stage 1 repair

or to reduce mortality while awaiting a donor heart (242). Use of this approach has also been reported in the rare neonate who cannot be stabilized by medical interventions because of excessive pulmonary blood flow (243). The hybrid approach uses surgical branch PA banding combined with transcatheter ductal stenting (211–213,244). Intervention to provide a reliable atrial septal communication is also necessary and may include a balloon septostomy and/or stent placement within the atrial septum (245). The result is anatomy that achieves the goals of stage 1 palliation without the need of CPB and deep hypothermia. The second-stage procedure combines aortic arch reconstruction and a superior cavopulmonary connection (191,212,213). Important shortcomings of hybrid palliation include the potential for retrograde arch obstruction that can result in cerebral and coronary ischemia (246,247). This risk is highest among patients with an atretic aortic valve, and inter-stage interventional catheterization procedures are commonly required. Branch PA banding either alone or in combination with ductal stenting may also be useful for the patient at increased risk for CPB-related complications such as a neonate with an intracranial hemorrhage or the premature, low-birth-weight newborn (248).

Anesthetic Management

Trauma and surgical stress induce a neurohumoral and cytokine response, the magnitude of which is associated with organ dysfunction and death (249). Anesthetic techniques that reduce the magnitude of biologic markers of stress are associated with decreased mortality (250). Because of the extent of surgical trauma and the use of profound hypothermia with or without circulatory arrest, anesthetic techniques that use high doses of synthetic opioids to reduce the stress response and preserve the limited neonatal cardiac reserve are rational and associated with improved outcome (146,251). Typically, profound analgesia and adequate blunting of the stress responses can be accomplished with 30 to 60 $\mu\text{g}/\text{kg}$ of fentanyl before CPB and a continuous fentanyl infusion of

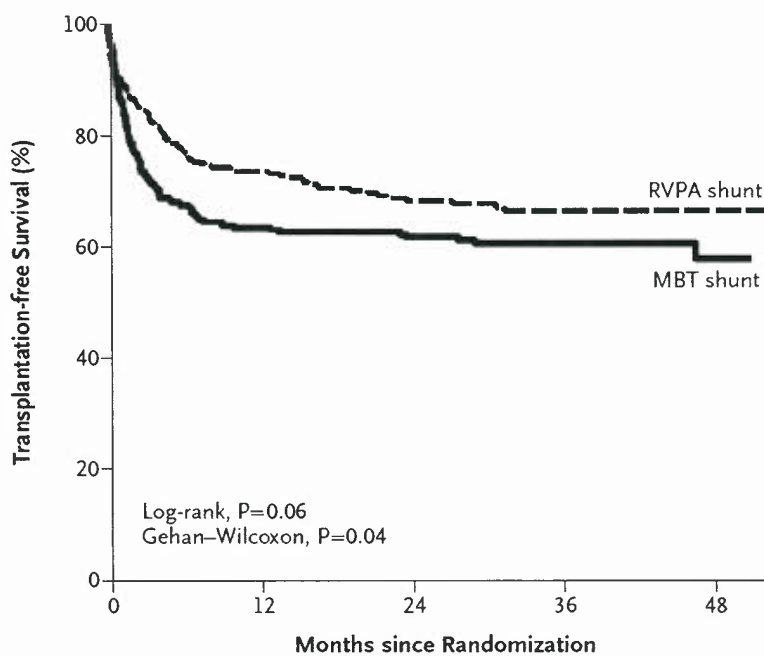


FIGURE 48.16. Kaplan-Meier curves for transplantation-free survival among all infants who underwent the Norwood procedure, according to the intention-to-treat analysis. Transplantation-free survival 12 months after randomization was higher with the RVPA shunt than with the MBTT shunt (74% vs. 64%, $p = 0.01$). MBTT, modified Blalock-Thomas-Taussig shunt; RVPA, RV-to-PA shunt. (From Ohye RG, Sleeper LA, Mahony L, et al. Pediatric Heart Network I. Comparison of shunt types in the Norwood procedure for single-ventricle lesions. *N Engl J Med* 2010;362:1980–1992. Copyright © 2010 Massachusetts Medical Society. Reprinted with permission from Massachusetts Medical Society.)

No. at Risk

RVPA shunt	274	202	139	76	15
MBT shunt	274	176	125	69	17

10 $\mu\text{g/kg/h}$ throughout the procedure and into the postoperative period (146,252). Low-dose volatile anesthetics (0.25 to 0.5 minimum alveolar concentration [MAC]) or benzodiazepines (lorazepam 100 to 200 $\mu\text{g/kg}$) for hypnosis and to further limit autonomic responses, particularly to CPB, are routinely used. Some patients may require dopamine at 2 to 5 $\mu\text{g/kg/min}$, or epinephrine or norepinephrine at 0.02 to 0.05 $\mu\text{g/kg/min}$ to counterbalance the reduction in sympathetic outflow resulting from profound unconsciousness, and such inotropic support will usually improve systemic flow to vital organs (253). Monitoring of regional circulation with NIRS is helpful to assess the complex circulatory changes that result from surgical and anesthetic effects in these patients, and can be applied noninvasively and continuously throughout the perioperative period.

Afterload Reduction

Anesthetic drugs alone cannot completely eliminate the stress response to profound hypothermia (146). Because increases in SVR as part of the stress response can impair systemic oxygen delivery, strategies to control Qp/Qs have been critical in the management of these infants. Medical gas management aimed at elevation of PVR with inspired CO_2 or hypoxic gas mixtures allows control of PVR independent of minute ventilation (167,173,177). Management based on modulating PVR guided by SaO_2 as an indicator of Qp/Qs does not eliminate early hemodynamic collapse, and autonomic influences on SVR remain active.

As an alternative approach to obtain Qp/Qs balance, pharmacologic interruption of systemic vasoconstrictor responses using α -adrenergic blockade was popularized by Poirier et al. (254). Such an approach has been shown to increase systemic oxygen delivery (179) and is associated with improved survival (179,180). The basic physiologic premise is that pharmacologic clamping of SVR in conjunction with clamping the total PVR with a resistive shunt will reduce the variability in systemic oxygen delivery through reduced variability in Qp/Qs. The importance of shunt size in limiting Qp/Qs extremes has been modeled, and smaller shunts make pulmonary overcirculation less likely (176). However, fourfold elevations in SVR are possible in the stressed neonate, making variable Qp/Qs unavoidable if the capacity for vasoconstriction is not blocked or at least reduced. Treatment with phenoxybenzamine, a long-acting irreversible α -adrenergic receptor blocker, improved systemic oxygen delivery as signaled by SvO_2 (178,255). The improved SvO_2 occurred during the early postoperative course, the time typically associated with critical reductions in systemic oxygen delivery (256,257). The relationship between blood pressure and SvO_2 was fundamentally altered in patients receiving phenoxybenzamine, suggesting that SVR was both lower and less variable (Figs. 48.17 and 48.18). With SVR effectively clamped by reducing autonomic influences, we found that phenoxybenzamine, compared to nitroprusside, largely eliminated the deterioration of systemic oxygen delivery at high SaO_2 and fundamentally changed the relationship between SaO_2 and SvO_2 in the postoperative parallel univentricular circulation, as depicted in Figure 48.19 (182). This has simplified management by reducing the extremes in Qp/Qs variability: the required total cardiac output to meet systemic oxygen requirements is less at Qp/Qs closer to one, and the cycle of increasing SVR resulting in falling oxygen delivery is interrupted. Our strategy had been to use 0.25 mg/kg phenoxybenzamine at the initiation of CPB, with a selective postoperative infusion of 0.25 mg/kg/day limited to infants who demonstrate reactive SVR despite fentanyl and benzodiazepine treatment, with benefits both from the specific pharmacologic effect of α blockade and from the prolonged duration of action,

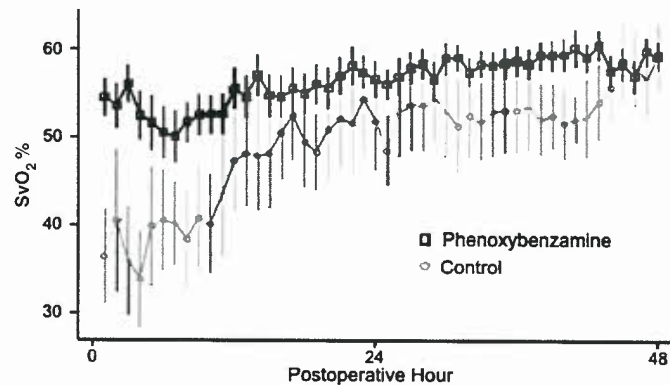


FIGURE 48.17. Effect of phenoxybenzamine on 48-hour SvO_2 trend. Mean and 95% confidence intervals of SvO_2 from neonates following the Norwood procedure with and without phenoxybenzamine. Phenoxybenzamine increases SvO_2 and reduces variability. SvO_2 , systemic venous saturation. (Adapted from Tweddell JS, Hoffman GM, Fedderly RT, et al. Phenoxybenzamine improves systemic oxygen delivery following the Norwood procedure. *Ann Thorac Surg* 1999;67:161–168.)

which committed the patient to a treatment strategy that both promotes and requires high systemic blood flow. Because an intravenous formulation of phenoxybenzamine is no longer commercially available, we have more recently substituted phentolamine 250 $\mu\text{g/kg}$ bolus on CPB with a continuous infusion at 1 to 2 $\mu\text{g/kg/min}$ continued through the first 24 to 48 postoperative hours. Both phentolamine and phenoxybenzamine have improved indices of systemic perfusion compared to nitrovasodilators (258–260), and this effect is likely related to the specific distribution of vascular resistance achieved via α -adrenergic blockade.

Management of Cardiopulmonary Bypass

High-flow CPB guided by SvO_2 provides the best organ perfusion and the least metabolic evidence of anaerobic metabolism. However, reconstruction of the aortic arch requires that blood flow be intermittently interrupted, and thus circulatory support for stage 1 palliation typically entails some degree of regional hypoperfusion. In addition to the usual invasive monitoring and venous oximetry on CPB, two-site NIRS has been identified as a useful adjunct to guide management of the determinants of oxygen delivery and consumption on CPB.

CPB strategies vary by institutional philosophy and patient-specific anatomy as well as the intended operation. Both cannula placement and perfusion strategy are interdependent factors. Most commonly, a single venous cannulation is used. Direct cannulation of the proximal PA trunk or ductus arteriosus permits high-flow bypass to commence with the intent of whole-body cooling to 18°C to 20°C prior to circulatory arrest, after which time the arterial cannula is repositioned in the neo-aortic trunk (207,261). Alternatively, the innominate artery can be cannulated either directly or via a synthetic graft that will later become the source of pulmonary blood flow. This approach permits continuous cerebral perfusion with enough access to the arch to permit reconstruction and also provides measurable descending aortic blood flow (183,184,261,262). By manipulation of pump flows, temperature, and pCO_2 , significant somatic blood flow may be maintained during regional perfusion via the innominate artery (183,184,263). Avoidance of somatic arrest and profound hypothermia has also been achieved with bifurcated aortic cannulation to the innominate and DAO (264).

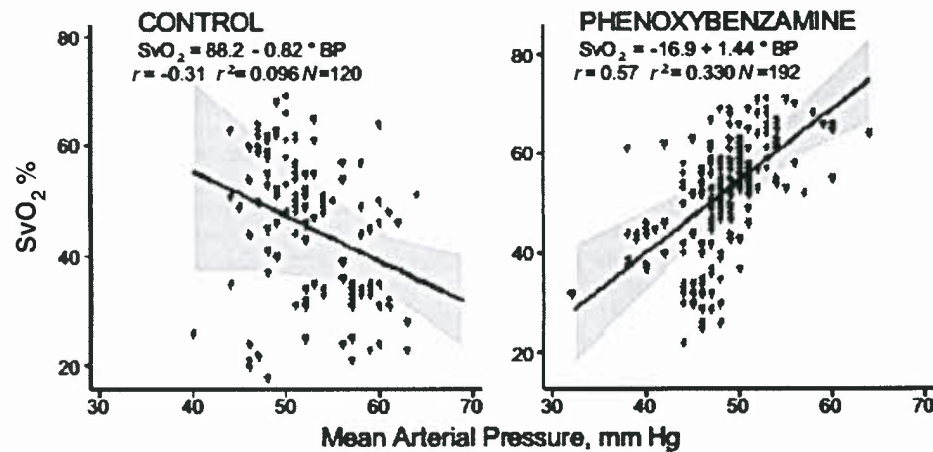


FIGURE 48.18. Effect of phenoxybenzamine on SvO_2 –blood pressure relationship. Real-time (hourly) values of SvO_2 and mean arterial blood pressure and linear fit equations from neonates after the Norwood operation. In neonates managed without phenoxybenzamine, blood pressure and systemic oxygen delivery are inversely related because blood pressure is determined mainly by SVR. In neonates who received phenoxybenzamine, blood pressure and oxygen delivery are positively related because blood pressure is determined mainly by cardiac output and SVR remains relatively constant. SvO_2 , systemic venous saturation. (Adapted from Tweddell JS, Hoffman GM, Fedderly RT, et al. Phenoxybenzamine improves systemic oxygen delivery following the Norwood procedure. *Ann Thorac Surg* 1999;67:161–168.)

Management of blood flow, hematocrit, temperature, and pCO_2 on CPB surrounding the time of circulatory arrest has been extensively investigated. Evidence suggests that cooling until jugular venous saturation is near 100%, at which time EEG silence occurs, maximally preserves cerebral oxygenation during subsequent ischemia. Neurologic outcomes

are presumably improved with longer cooling time, pH-stat management during cooling, higher hematocrit before and after deep hypothermic circulatory arrest (DHCA), and by providing more metabolic suppression from hypothermia with more oxygen delivery (265). Questions remain whether metabolic suppression from hypercapnia is additionally beneficial.

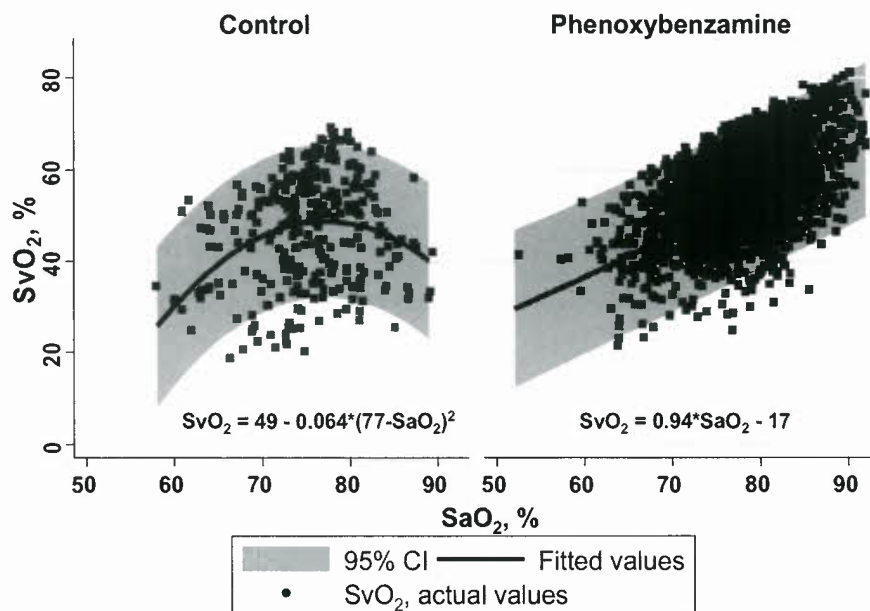


FIGURE 48.19. Effect of phenoxybenzamine on SaO_2 – SvO_2 relationship. Real-time (hourly) SaO_2 and SvO_2 values and best-fit polynomial equations in neonates after the Norwood procedure with and without phenoxybenzamine. The SaO_2 – SvO_2 pattern in control patients reveals variable Qp/Qs and a systemic-to-pulmonary flow tradeoff at high SaO_2 ; a critical peak of SvO_2 occurs at an average SaO_2 of 77%. In contrast, the SaO_2 – SvO_2 relationship follows the pattern of variable total output and relatively constant Qp/Qs with phenoxybenzamine treatment, with no evidence of systemic-to-pulmonary flow tradeoff. However, individual SvO_2 cannot be predicted from SaO_2 in either group. Qp , pulmonary blood flow; Qs , systemic blood flow; SaO_2 , oxygen saturation; SvO_2 , systemic venous saturation. (Adapted from Hoffman GM, Tweddell JS, Ghanayem NS, et al. Relationship between arterial and venous saturation following the Norwood procedure: sustained afterload reduction prevents hemodynamic deterioration at high arterial saturation. *J Thorac Cardiovasc Surg* 2004;127:738–745.)

The absolute safe time for DHCA in any individual patient remains unknown, although risk is clearly increased after 30 to 40 minutes at 18°C to 22°C (266). Neurologic injury, however, may occur despite all CPB parameters in the usual safe range. Anttila et al. (267) have shown that combinations of hematocrit, pCO₂, temperature, and flow rate could produce ischemic injury, which was consistently identified by a lower brain oxygen saturation by NIRS. Based on the premise that hypoxia is the major cause of cerebral injury in the perioperative period, it is hypothesized that strategies that provide continuous or near-continuous cerebral perfusion (268) may avoid the complications attributable to DHCA (269). A recent randomized prospective study of patients with single-ventricle anatomy undergoing arch reconstruction comparing DHCA to low-flow (10 mL/kg/min) continuous cerebral perfusion failed to identify a difference in neurodevelopmental outcome at 1 year of age (270). That study, although well designed from a structural viewpoint, unfortunately chose a flow rate for continuous cerebral perfusion below that which is required (40 to 60 mL/kg/min) to ensure adequate cerebral blood flow and oxygen delivery (271,272), and thus its findings cannot be generalized to answer the important question that it was designed to answer. A post-CPB period of increased risk of decreased cerebral perfusion has been identified (Fig. 48.20), and intraoperative strategies can influence postoperative cerebral hemodynamics in subtle but important ways (272). Because techniques are continuously evolving, and neurologic outcome assessment is best performed many years after neonatal surgery, a formal outcome study will not likely speak directly to current management.

During rewarming and reperfusion, oxygen consumption increases and may require adjustment of flow by physiologic parameters. Titration of hypnotic drugs may be necessary to limit both oxygen consumption and vascular responses. Ultrafiltration during rewarming should aim to raise the hematocrit to 40%. Uniform rewarming to a bladder temperature of 36°C is necessary to avoid thermoregulatory metabolic responses after separation from CPB, which will be imposed at the most critical point for oxygen delivery. Additional targets include an SVR of about 12 Wood units and anesthetic and inotropic support at a steady state. Before separation from CPB, milrinone (50 µg/kg load plus infusion of 0.5 µg/kg/min) is routinely used for inodilation (273). With pump flow of 3.2 L/m²/min, an organ perfusion pressure of 40 mm Hg (mean arterial pressure [MAP] – central venous pressure [CVP]) is targeted while the systemic-to-pulmonary artery shunt is still occluded. This translates into a systemic vascular resistance

index (SVRI) of 12 Wood units. Anesthetic depth is evaluated, but analgesic/hypnotic withdrawal is not used to raise SVR. Specifically, low-dose vapor or hypnotic infusion is maintained during rewarming, separation from CPB, and closure. If the SVR is low, as is typical with the use of phenoxybenzamine, norepinephrine is infused at 0.03 to 0.3 µg/kg/min. For additional inotropy, epinephrine in the 0.03 to 0.3 µg/kg/min range is titrated to systolic function and heart rate (169,257). If SVR is high, additional sedative/hypnotic, alpha-blockade, or, rarely, nitroprusside is administered. If phenoxybenzamine or phentolamine has been administered on CPB, then additional epinephrine often reduces SVR because of unopposed β-adrenergic activity in the face of α-adrenergic blockade.

Once the target SVR has been achieved and vasoactive infusions are constant, the lungs are reinflated and mechanical ventilation is resumed. Usual initial ventilator settings include a FiO₂ >0.5, inflating pressure of 25 to 28 cm H₂O, inspiratory time of 0.6 to 0.8 seconds, PEEP of 3 to 4 cm H₂O, and a rate of 10 to 20 breaths per minute to achieve normal alveolar ventilation without atelectasis. Prolonged ventilation without lung perfusion is avoided to reduce the likelihood of acute changes in PVR and lung injury (274–276). Shunt adequacy is evaluated with a test opening; a rise in end-tidal CO₂ to the 30-torr range and a drop in MAP of >10 mm Hg are suggestive of adequate shunt flow. An oximetric catheter may be placed in the SVC for post-CPB monitoring. Weaning from CPB is attempted over 30 to 45 seconds. The total cardiac output must double with shunt opening; preload must be carefully titrated to avoid ischemia and generally is optimal at an initial CVP of 10 to 12 mm Hg. Inotropic support may need further adjustment during this time. As pump flow decreases, the arterial and venous saturation falls. Generally, an organ perfusion pressure of 40 mm Hg is adequate. Real-time knowledge of Qp/Qs and direct or NIRS-surrogate SvO₂ drive physiologic adjustment of SVR and myocardial performance. SvO₂ or other measures of oxygen supply/demand become the primary hemodynamic target, with appropriate attention to coronary perfusion pressure and evidence of ischemia.

Successful separation from CPB is likely if arteriovenous saturation difference remains normal (20% to 30%) and SvO₂ remains above the anaerobic threshold of 30% to 35%. Modified ultrafiltration usually increases SvO₂ and apparent myocardial performance (277). A low SvO₂ (<40%) with high SaO₂ (>80%) indicates high Qp/Qs, and reduction in SVR is attempted. Increasing PaCO₂ may redistribute systemic blood flow to the brain but has little effect on Qp/Qs in the postoperative period in the presence of a relatively restrictive systemic

FIGURE 48.20. Changes in cerebral and somatic saturation during the Norwood procedure performed with continuous cerebral perfusion. Frontal cerebral and T10-L2 flank (renal-somatic) regional saturation (rSO₂) from continuous NIRS monitoring during the Norwood procedure. Cerebral oxygenation is well maintained during continuous regional cerebral perfusion (RCP) via the innominate artery, but somatic saturation falls. After weaning from cardiopulmonary bypass (CPB), the cerebral saturation falls, although somatic oxygenation is maintained. (Adapted from Hoffman GM, Stuth EA, Jaquiss RD, et al. Changes in cerebral and somatic oxygenation during stage 1 palliation of hypoplastic left heart syndrome using continuous regional cerebral perfusion. *J Thorac Cardiovasc Surg* 2004;127:223–233.)

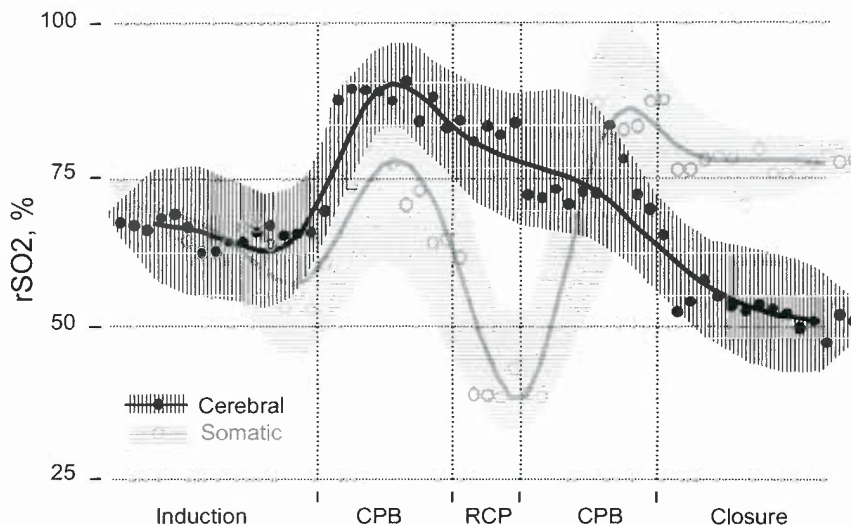


TABLE 48.2 Circulatory Management based on SvO₂ Interpretation

SaO ₂	SvO ₂	Qp/Qs	Suggested Intervention
80	60	1.0	None; slowly wean support
80	40	2.0	Sedation/analgesia, warmth, vasodilator
70	50	0.67	Resolve atelectasis, raise SVR
70	40	1.0	Raise cardiac output, raise hemoglobin, reduce VO ₂
75	25	2.0	Raise cardiac output, lower SVR
60	40	0.5	Resolve atelectasis, raise SVR, consider iNO, consider shunt augmentation
87	70	1.5	Wean support
87	40	3.6	Sedation/analgesia, vasodilation, consider shunt restriction

SaO₂, oxygen saturation; SvO₂, systemic venous saturation; Qp/Qs, pulmonary-to-systemic flow ratio; SVR, systemic vascular resistance; VO₂, oxygen consumption; iNO, nitric oxide.

to pulmonary shunt. Low SvO₂ and balanced Qp/Qs indicate inadequate total oxygen delivery. Increasing the inotropic state, preload optimization, increasing hemoglobin, and metabolic suppression can be used. High SVR must be addressed and may be present even if blood pressure is not high because of the accompanying reduction in systemic perfusion. Management based on SvO₂ or NIRS as a surrogate is shown in Table 48.2. Using cerebral (rSO₂C) and somatic (rSO₂R) NIRS approximations of regional venous saturation, the arteriovenous difference across brain and kidney, muscle, or gut can be continuously assessed and regional blood flow changes derived from application of the inverse Fick principle, allowing appropriate interventions directed at pulmonary, cerebral, and systemic blood flows specifically. Current targets include an SaO₂ >80%, SvO₂ >50%, cerebral arteriovenous difference of 20% to 30% and rSO₂C >50%, somatic arteriovenous difference of 10% to 20% and somatic rSO₂R >70%, CVP of 9 to 12 mm Hg, and MAP of 48 to 52 mm Hg (188,191,272,278).

After separation and completion of modified ultrafiltration, cannulae are removed and heparin reversal is achieved. Modification of Qp/Qs by PVR modulation is now less effective than manipulation of SVR because of the large fixed resistance imposed by the systemic-to-pulmonary artery interposition shunt and the potential lability in SVR. Lung management targets the usual goals of maintenance of functional residual capacity, avoidance of atelectasis, and fully saturated pulmonary capillary blood. In the presence of a restrictive shunt, adjustment of CO₂ will have more effect on the distribution of SVR than on total pulmonary resistance (176), and increasing the FiO₂ will usually increase oxygen delivery without adverse effect on Qp/Qs (177). Increases in SaO₂ are not deleterious in the presence of intense afterload reduction (182). Because changes in SVR, sympathetic outflow, and oxygen consumption with volatile anesthetic withdrawal can pose physiologic threat in these patients, transition to an intravenous hypnotic and analgesic strategy should occur before transfer to the ICU.

Mechanical Circulatory Support

Mechanical circulatory support should be initiated before global or regional hypoxia results in organ damage or death. The threshold for brain lactate production occurs with cerebral rSO₂ values around 40% (279,280), and the threshold for anaerobic metabolism appears to be at an SvO₂ around 30% in this patient population (181). If manipulation of

SVR, PVR, and inotropic state does not result in adequate systemic oxygen delivery, and if there is no issue with shunt size, patency, or other correctable anatomic limitations, then inotropic support should be aggressively escalated since individual dose-response effects are variable. Adequate oxygen delivery is the goal (257). Failure to achieve adequate organ oxygen delivery with sustainable inotropic support should prompt consideration of mechanical support. Elective mechanical support should be considered a defensible strategy and preferable over unplanned circulatory collapse and resuscitation (281). Treatment of the patient with single-ventricle physiology in the arrest and prearrest situation has recently been reviewed (282,283), with emphasis on SvO₂ and NIRS monitoring for assessment and continuous guidance about response to interventions.

Traditional venoarterial extracorporeal membrane oxygenator (ECMO) support must be used if there is any question about shunt patency or lung function, and rapid-response ECMO can effectively salvage some infants who have severe hypoxia and cardiogenic shock. Management of the systemic-to-pulmonary artery shunt on ECMO has evolved. Historically, the shunt was mechanically clipped during ECMO support (238). This strategy was used because of a desire to limit ECMO flow and concerns about excessive pulmonary blood flow hypothesized to result in pulmonary dysfunction while on support. The result of a clipped shunt strategy was development of pulmonary dysfunction, which has been postulated to be due to ischemia or more likely severe alveolar alkalosis that resulted from prolonged ventilation of underperfused lungs. Management with a patent shunt allows for gradual transition to pulmonary gas exchange while support flow is weaned (284). An alternative approach to mechanical support is to use the patient's lungs' total gas exchange, and a roller pump without oxygenator is interposed between atrial drainage and the aorta (285). This arrangement simplifies anticoagulation and requires maintenance of lung ultrastructure and function, which may be impaired by ECMO without pulmonary blood flow (276). Use of mechanical support to preserve end-organ function may improve outcomes (73,281,285). Problems with ECMO include bleeding, clotting, massive blood product requirements, lung "whiteout," acquired adult respiratory distress syndrome (ARDS) from ventilating an ischemic lung, and intracranial bleeding.

We prefer a technique that maintains shunt patency allowing continuous transition of circulatory work and gas

exchange between the patient and the machine. Critical attention to fluid and colloid administration with maintenance of CVP < 10 is necessary if pulmonary and myocardial function are to recover. Continued management of SVR may be necessary to maintain adequate organ perfusion pressure and regional blood flow. CO₂ is added to the inspired gas during ECMO to achieve an end-tidal CO₂ of 40 torr to avoid hypocapnic lung injury (275,276) and acute increases in PVR with lung reperfusion (274). This strategy allows progressive weaning of mechanical support as native myocardial function improves.

Postoperative Management

Unbalanced Qp/Qs, reduced total cardiac output, higher oxygen demand, and the potential for myocardial ischemia contribute to morbidity and mortality. Oxygen delivery is limited by myocardial edema with attendant diastolic dysfunction and the potential development of tamponade physiology (286–288). This physiologic vulnerability peaks in the first 6 to 12 hours postoperatively, and all monitoring appropriate for the operating room should be maintained throughout this period (122,257). Postoperative management should target adequate organ oxygenation including stabilization of oxygen consumption to reduce morbidity and mortality. Strategic improvements in oxygen delivery have paralleled improved survival (289) and neurologic outcomes (290) in our series. SvO₂ and NIRS data as primary markers of systemic oxygen delivery are used targeting SvO₂ > 50%, cerebral rSO₂ > 50%, and somatic rSO₂ > 60% to minimize organ dysfunction and the risk of secondary multisystem organ dysfunction (181,278,291). Evidence of anaerobic metabolism with SvO₂ approaching 30% has been demonstrated, and management strategies that target a SvO₂ of >50% have reduced mortality (73,181,292).

Delaying sternal closure until postoperative day 2 to 4 has reduced early hemodynamic compromise and the need for mechanical circulatory support (293). The development of moderate tamponade physiology is expected. Therefore, the procedure should be timed such that inotrope-recrutable stroke volume is available. An increase in inflammatory responses including elevated temperature setpoint is expected after sternal closure, with possible need for additional support.

An increase in oxygen consumption of about 30% can be expected with the transition to spontaneous ventilation. Pharmacologic support should be adjusted during this transition as appropriate. Excessive work of breathing owing to altered mechanics will quickly destabilize the circulation.

Interstage Management and the Timing of Stage 2 Palliation

After recovery from stage 1 palliation, acute care is transitioned to chronic therapies that allow preservation of organ function and somatic growth. As such, interstage management should include pharmacologic therapy targeted at optimizing the inefficient parallel circulation inherent to HLHS after stage 1 palliation, vigilant monitoring of physiologic variances as a means to identify destabilizing pathology, and ensuring adequate nutrition and somatic growth.

Prescribed Medical Therapy

Pharmacologic therapy between stages 1 and 2 palliation remains variable among institutions and potentially includes chronic afterload reduction, diuretics, and/or digoxin for support of the cardiovascular system, and anticoagulation. Chronic afterload reduction with an angiotensin-converting enzyme (ACE) inhibitor may be beneficial in patients who

have a pulmonary-to-systemic flow ratio (Qp/Qs) > 2 in the early postoperative period, greater than mild atrioventricular valve insufficiency, evidence of congestive heart failure, or noninvasive evidence of elevated SVR. If SVR is suboptimally controlled with ACE-inhibitor therapy, enteral or transdermal clonidine may be effective. Afterload reduction is titrated with caution to avoid worsening hypoxia from excessive lowering of the Qp/Qs ratio and diastolic hypotension that could result in impaired coronary flow. For patients with evidence of pulmonary overcirculation or heart failure, chronic diuretic therapy with furosemide is prescribed. Caution is taken to avoid intravascular volume depletion that might reduce total cardiac output as well as increase the risk of shunt thrombosis owing to hyperviscosity. Prophylactic antiplatelet therapy with aspirin 20 mg daily is uniformly administered to our patients unless there is evidence of atrial or venous clot, at which time subcutaneous low-molecular-weight heparin is prescribed with a therapeutic goal of 0.7 to 1.2 anti-Xa IU/mL. Finally, patients at our institution are expected to maintain SaO₂ >78% while awake and asleep, and if unable to do so, are placed on supplemental oxygen via nasal cannula. Any one of these prescribed therapies will likely require outpatient adjustments during the interstage period.

Risk Factors for Interstage Death

The limited circulatory reserve inherent in a volume-loaded single ventricle with parallel circulation and cyanosis places the infant with HLHS at risk for late morbidity and mortality. The incidence of sudden death in the interstage period has remained fairly constant at approximately 5% to 15% and does not seem to have been eliminated despite the introduction of perioperative surgical, medical, and monitoring strategies that have dramatically improved early inpatient survival (73,179,228,241,294–296).

Multiple risk factors and causes have been proposed for interstage death. Escalated risk of interstage mortality has been linked to anatomic diagnosis and residual or recurrent lesions. Specifically, the diagnosis of aortic atresia with a diminutive ascending aorta represents an anatomic subtype of HLHS presumably with the lowest physiologic reserve and has been associated with an increased risk of late death (219,254,297). The presence of a restrictive atrial communication, arch obstruction, obstructed shunt flow, PA distortion, atrioventricular valve insufficiency, and arrhythmias have also been associated with interstage mortality (215,217,228,232,295,296). Commonly acquired childhood gastrointestinal or respiratory diseases that result in hypovolemia and/or acute hypoxemia have also been implicated as causes for interstage death (71,217). After successful stage 1 palliation, any of the above-mentioned pathologic processes can lead to increased metabolic demands and an unfavorable oxygen supply/demand relationship, placing the infant with minimal myocardial reserve at even greater risk for mortality until progression to cavopulmonary anastomosis. Therefore, transitioning infants to home after stage 1 palliation warrants ongoing vigilance well beyond the initial early postoperative period and requires continued collaboration among caregivers, including parents.

Interstage Monitoring

To improve late outcomes, we developed an interstage monitoring program of SaO₂ and weight designed for home use as a means to identify modifiable risk factors that might fatally tax the inefficient circulation intrinsic to HLHS after stage 1 palliation (71). The monitoring program was based on the hypothesis that earlier recognition of decreased SaO₂ from baseline, poor weight gain, or weight loss might foretell the presence of

serious anatomic lesions or a developing intercurrent illness and subsequently allow for lifesaving intervention during the interstage period.

In infants with HLHS after stage 1 palliation, arterial desaturation from baseline might be indicative of anemia, respiratory illness, and myocardial dysfunction resulting from falling cardiac output, or limited pulmonary blood flow from shunt stenosis or outgrowth. Hypoxemia alone, however, might not occur early in an acute illness that results in elevation in SVR, with consequent reduced systemic flow and increased Qp/Qs. Specifically, dehydration that results in hypovolemic shock from increased fluid loss as seen with gastroenteritis or decreased intake might mimic such a clinical scenario and be reflected only by failure to have expected weight gain or even weight loss.

To detect acute hypoxemia, dehydration, or growth failure between stages 1 and 2 palliation, patients are discharged home with a digital infant scale and pulse oximeter as part of an interstage monitoring program, and parents obtain daily weights and oxygen saturations. Criteria for which parents are instructed to notify a member of the cardiac team are $\text{SaO}_2 < 75\%$ or $>90\%$, weight loss of 30 g, failure to gain 20 g of weight over 3 days, or enteral intake $<100 \text{ mL/kg/day}$. Breach of criteria prompts investigation to rule out an intercurrent illness or anatomic lesion as the cause of physiologic variance.

Initiation of interstage monitoring in September 2000 marked another milestone in the palliation of HLHS with improved interstage survival from 84% to 99% in a cohort of 139 patients who underwent stage 1 palliation with 95% early survival. Just over half of the monitored patients breached surveillance criteria with most patients presenting before 100 days of age. Worsening hypoxemia was the most common reason parents sought medical care. Shunt stenosis, outgrowth of the shunt, and innominate artery narrowing represented the cardiac diagnoses that led to interstage hypoxemia. Extracardiac causes of desaturation from baseline included viral illness, anemia, and dehydration. Isolated inappropriate weight change or generally poor weight gain occurred in a third of patients who breached surveillance criteria and was the result of recurrent arch obstruction, sepsis, poor oral intake necessitating gastrostomy tube placement, failure to adequately adjust gastrostomy tube feeds for weight gain, or progressive heart failure (233).

Nutritional Support and Somatic Growth

Adequate nutritional support and growth are important in the patient with univentricular circulation and planned surgical palliation. Specifically, preoperative hypoalbuminemia is associated with increased postoperative infection rates, longer hospital stays, and increased mortality (298). Poor interstage growth velocity and lower weight-for-age z-score at bidirectional cavopulmonary anastomosis predicts a more complex postoperative course and longer hospital stay (299,300). Studies to date report that 50% of infants with HLHS are malnourished in infancy with weight-for-age z-score <-2 or with an early infancy growth velocity $<20 \text{ g/day}$ (299–301). Etiology for growth failure in these patients is multifactorial and may include heart failure, extracardiac anomalies, genetic syndromes, gastrointestinal dysmotility, and/or malabsorption, any of which may contribute to inadequate enteral intake for energy utilization and growth.

Scrutiny of weight change during early infancy provided invaluable somatic growth data for this patient population. From >1,400 patient weight observations, a growth curve was generated for infants who survived the interstage period. Unlike the healthy infant who usually doubles the birth weight by 5 months of age, the patient with HLHS appears to have limited growth potential with a plateau phase of weight gain between 4 and 5 months of age (Fig. 48.21). Early growth velocity was generally $<20 \text{ g/day}$ whereas normal infant growth is 25 g/day . These initial data prompted a greater focus on ensuring adequate caloric intake prior to hospital discharge and increased attention to outpatient growth and nutrition. In an attempt to optimize adequate growth, infants are expected to take 110 to 130 kcal/kg/day with formula or breast milk fortified to 24 to 27 calories per ounce. Approximately, 25% of our patients have undergone open gastrostomy tube placement because of inability to consume adequate calories with oral feeding alone. Increased attentiveness to nutritional intake at our institution has resulted in improved somatic growth in monitored patients that nearly parallels normal infant growth with a growth velocity $>25 \text{ g/day}$ and an increase in weight for age z-score from -1.3 at hospital discharge after the Norwood procedure to -0.9 at stage 2 palliation.

Attentiveness to nutritional support also provided insight into optimal timing for stage 2 palliation. When comparing interstage monitored patients with those patients who were

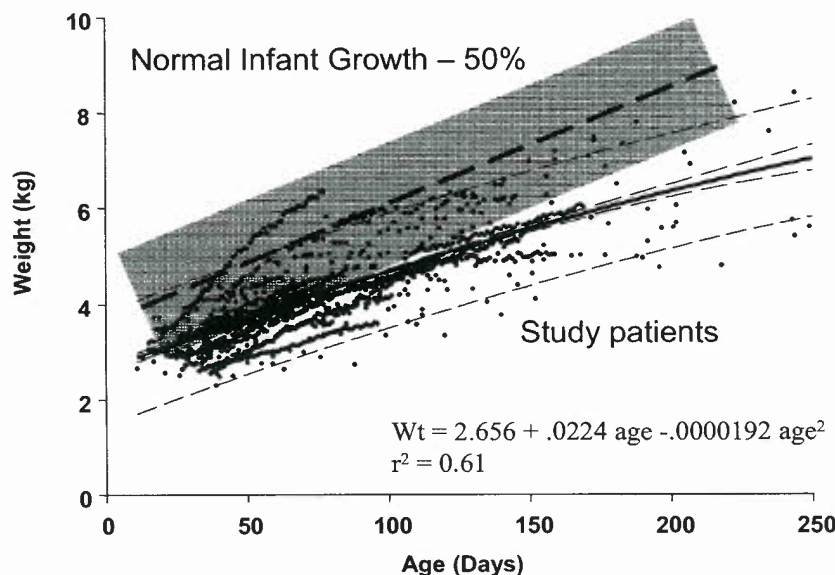
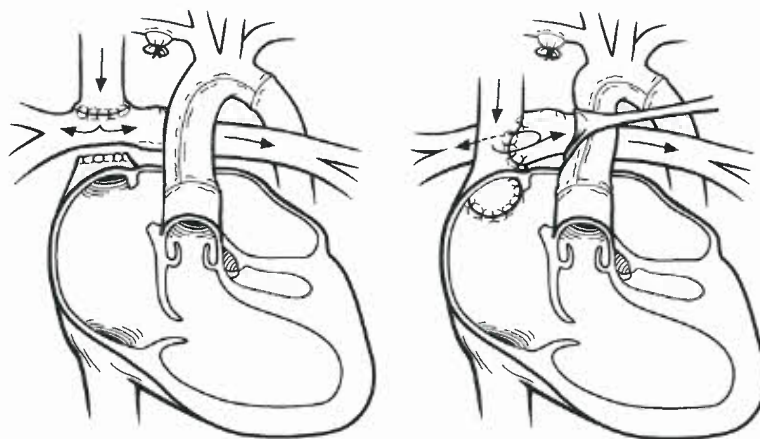


FIGURE 48.21. Interstage growth among survivors of the stage 1 palliation calculated using > 1,400 observations of weights. The regression line and 95% confidence intervals are indicated. Normal growth is depicted in the shaded area, with the dashed line representing 50% for age. The curve indicates the limited growth potential of the patient following the first stage of palliation. In this group of patients, growth into later infancy is limited, unlike a normal infant whose continued growth is expected. (Reproduced from Ghanayem NS, Tweddell JS, Hoffman GM, et al. Optimal timing of the second stage of palliation for hypoplastic left heart syndrome facilitated through home monitoring, and the results of early cavopulmonary anastomosis. *Cardiol Young* 2006;16:61–66, with permission.)

FIGURE 48.22. Connection of the SVC to the pulmonary arteries and takedown of previous systemic-to-PA shunts constitute the stage 2 procedure. Two surgical techniques are commonly used. **A:** The bidirectional Glenn shunt is a direct anastomosis of the SVC to the central PA. The principle advantage of the bidirectional Glenn shunt is the ease of construction; it can even be accomplished without the use of CPB in selected cases. **B:** In a hemi-Fontan procedure, the SVC is connected to the confluent pulmonary arteries without disconnecting it from the atrium; the atrial end of the SVC is closed with a patch. Although a more extensive operation than the bidirectional Glenn shunt, the hemi-Fontan allows for expeditious performance of a completion Fontan.



A Bidirectional Glenn

B Hemi-Fontan

not subjected to frequent monitoring of weight and saturation, monitored patients had similar weights to nonmonitored patients (5.5 ± 0.8 vs. 5.7 ± 1.3 kg) despite the younger age at stage 2 palliation in the monitored group (4.2 ± 1.4 vs. 5.6 ± 2.1 months, $p < 0.01$). This observation, along with the demonstrable flattening in growth velocity beyond 4 to 5 months of age call into question the benefit of arbitrarily delaying stage 2 palliation until after 6 months of age.

Stage 2: Superior Cavopulmonary Connection

Superior cavopulmonary anastomosis prior to completion Fontan improves ultimate survival and is associated with low operative and late mortality (219,302). In this operation, CPB is usually employed to allow anastomosis of the SVC to the proximal ipsilateral PA and takedown of prior shunts placed to provide pulmonary blood flow (Fig. 48.22). Anesthetic management usually includes a more balanced anesthetic technique that avoids prolonged postoperative ventilation, and approaches that include neuraxial opioids may have a favorable effect on early postoperative management (303). Progression to the cavopulmonary anastomosis reduces both wall stress and atrioventricular valve insufficiency through elimination of the volume load on the single systemic ventricle. It creates a more efficient in-series circulation and increases diastolic pressure with improved coronary artery perfusion (208,221,294). The delayed timing of stage 2 palliation to 6 months of age has been supported by previous reports that early cavopulmonary anastomosis has been associated with severe hypoxemia, prolonged pleural drainage, PA thrombosis, poor PA growth, early development of pulmonary arteriovenous malformations, and excess mortality (304–307). However, it seems logical that by simply shortening the period of risk linked to the inefficient parallel circulation after stage 1 palliation, interstage survival will be enhanced.

In a series of home-monitored patients, those who breached home-monitoring criteria proceeded to stage 2 palliation at a significantly younger age of 3.6 ± 1 months compared with 5.6 ± 2.1 months for those receiving conventional management ($p < 0.01$) (71). Despite the younger age at stage 2 palliation of the monitored patients, weights between groups were similar: 5.3 ± 0.9 versus 5.7 ± 1.3 kg ($p = ns$). The success of early cavopulmonary anastomosis in these patients deemed at greatest risk for interstage mortality has modified our overall practice in that stage 2 palliation is electively performed at 4 months of age or earlier if necessary.

The implications of early cavopulmonary anastomosis have been further reviewed by Jaquiss et al. (307,308). Patients who underwent cavopulmonary anastomosis at <4 months of age (mean 3.1 ± 1.4 months) were compared with their older counterparts (mean 5.5 ± 1.5 months). All patients survived with an actuarial survival of 96% at 1 year in both groups. The younger group, however, required prolonged mechanical ventilation, had a greater duration of pleural drainage, and had a longer hospital stay. Younger patients also had lower oxygen saturations postoperatively compared with the older group, but by hospital discharge, groups had similar oxygen saturations (307). Follow-up data on this cohort demonstrated no difference in late complications, preoperative hemodynamics at the time of Fontan palliation, or status of the patient after completion Fontan (308).

After the stage 2 operation, patients experienced improved activity and physiologic reserve, which lasted several years. However, increasing cyanosis following stage 2 palliation is predictable and is due to several factors including increased lower-body growth and oxygen consumption with concomitant increase in desaturated inferior vena caval blood return. Patients will also develop venovenous collaterals from the high-pressure SVC to veins ultimately draining to the IVC or atrium. Furthermore, patients are at risk for the development of arteriovenous malformations that result in intrapulmonary shunting of blood from PA to pulmonary vein without gas exchange. These are postulated to be the result of a lack of so-called hepatic factor, which prevents the shunt formation (309). Pulmonary arteriovenous malformations can be reversed by the completion Fontan operation, presumably by restoring hepatic factor to the pulmonary circulation.

Stage 3: Completion Fontan

For the patient with HLHS, the Fontan procedure is the last anticipated operation. The techniques and indications for surgery are not different from those for other single-ventricle patients, and indeed in many centers patients with HLHS make up the majority of patients undergoing the completion Fontan. For patients who have undergone a stage 2 procedure, either a bidirectional Glenn shunt or hemi-Fontan, the timing of completion Fontan is not critical; in general, the operation is performed between 18 months and 4 years of age, with anesthetic considerations similar to those for the stage 2 operation. The surgical goal is to route the blood from the IVC to the pulmonary arteries with as little energy loss as possible. Although interventional techniques to perform the completion Fontan using coated stents have been reported, much more commonly,

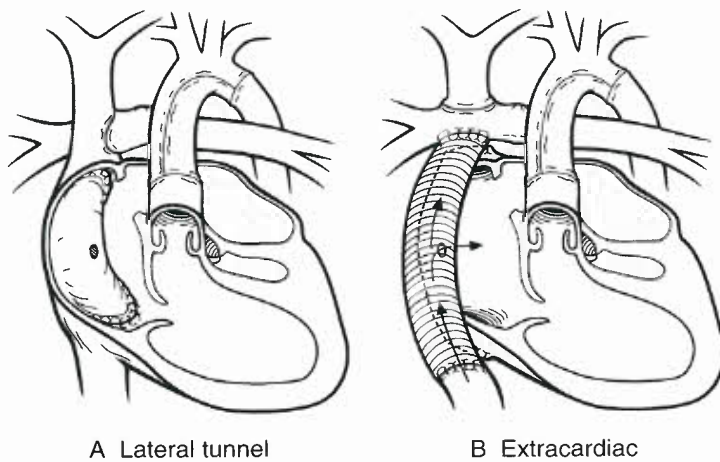


FIGURE 48.23. The completion Fontan operation can be accomplished in two ways. **A:** The lateral tunnel Fontan involves creating an intra-atrial baffle that connects the IVC to the pulmonary arteries. **B:** The extracardiac Fontan uses a tube graft to connect the IVC to the central PA. In both cases, all caval return with the exception of the coronary sinus is directed to the pulmonary arteries, simulating as closely as possible the normal circulatory pattern. To improve hemodynamics, especially in the early postoperative period, a fenestration is often placed between the baffle or conduit and the pulmonary venous atrium. This decreases CVP and increases preload to the single ventricle, albeit at the cost of some systemic desaturation.

this is performed in the operating room using one of two techniques; a lateral tunnel or extracardiac conduit (Fig. 48.23).

The lateral tunnel Fontan is commonly performed following the hemi-Fontan. As part of the hemi-Fontan, a dam is constructed between the pulmonary arteries and the RA. During the completion Fontan, this dam is removed and a section of prosthetic conduit is used to create a baffle to route the inferior caval blood return to the PA. The baffle is not circumferential, and a portion of the tunnel is made up of the patient's atrium, therefore maintaining, in theory, potential for growth. Additional advantages include a low level of power loss as determined by computational fluid dynamic studies (310). Although controversial, some studies suggest a higher incidence of sinus node dysfunction following the lateral tunnel Fontan (311–315). Another potential disadvantage of the lateral tunnel Fontan involves the presence of prosthetic material exposed to the pulmonary venous portion of the atrium with the potential for thrombus formation and systemic embolization.

The extracardiac Fontan is constructed by placing a prosthetic conduit between the IVC and the pulmonary arteries. The advantages include the ease of the operation and, although somewhat controversial, probably a lower incidence of sinus node dysfunction (311–315). In addition, no prosthetic material is placed in the pulmonary venous atrium, with potentially lower risk of thromboembolic complications. The principle disadvantage is the lack of growth potential. To this end, larger conduits, between 20 and 22 mm in diameter, are placed to accommodate growth. The larger and longer conduits may result in power loss, which, when combined with the potential for late revision for outgrowth, may impact the durability of the extracardiac Fontan.

The postoperative course of patients following the Fontan procedure for HLHS is not substantially different from that of other single-ventricle patients with equivalent function. Patients with HLHS more commonly have decreased systolic and altered diastolic function, and they are at increased risk for postoperative complications including decreased cardiac output with elevated CVP, pleural effusions, ascites, thrombosis, and arrhythmias. We routinely use a fenestration in the Fontan to permit right-to-left shunting, which decreases CVP and improves single-ventricle preload and cardiac output, at the expense of some degree of desaturation. The use of a fenestration has resulted in excellent survival and shorter hospital stay (206). Additional strategies that minimize postoperative hospital stay include routine use of the diuretics including spironolactone, an aldosterone antagonist, and furosemide. Supplemental oxygen is used as a pulmonary vasodilator, and afterload reduction is given to improve cardiac output and lower single-ventricle filling pressures (316).

Outcomes for Staged Palliation

Most mortality associated with the staged surgical approach occurs during and after stage 1 palliation, with recent cumulative early and interstage mortality in the 5% to 30% range (73,241,317,318). Improved outcome has been associated with early diagnosis, preoperative stabilization, early repair, systematic management approaches, and increased monitoring both in hospital and at home (71,73,294). The recent multi-institutional study comparing the modified Blalock-Thomas-Taussig shunt (MBTTS) to an RVPA conduit revealed that the early mortality was lower with the RVPA conduit approach; however, the variation in mortality across centers was a more significant factor than the type of shunt. The potential early advantage of the RVPA connection may result from a lower incidence of shunt thrombosis and associated mortality, with little improvement in systemic (233) or cerebral (235) hemodynamics.

Patient-related characteristics are increasingly recognized as risk factors for early and intermediate mortality after stage 1 palliation. Few studies have reported worsened outcomes in patients with prematurity, low birth weight, extracardiac anomalies, genetic syndromes, and/or additional cardiac anomalies. Patients with any of these characteristics have been designated as “high risk” for staged palliation due to early operative mortality rates of 30% to 50% compared to 10% to 15% operative mortality in patients without any of the aforementioned characteristics, the “standard-risk” cohort (75,319). We recently reported that intensive perioperative monitoring, early goal-directed treatment of shock, and greater resource utilization offset the vulnerability of “high-risk” patients resulting in comparable operative survival in “high-risk” and “standard-risk” patients, 87% versus 95%, respectively. In this series, ability to achieve stage 2 palliation or progression to transplant in lieu of stage 2 palliation was comparable between risk groups. Yet, “high-risk” patients had lower 1-year survival (78% vs. 93%) and survival to date (71% vs. 92%) compared to “standard-risk” patients (191). (see Fig. 48.24). Overall, for this cohort of 162 consecutive patients, operative survival was 91%, 1-year survival was 90%, and survival at last follow-up was 86%.

Cardiac Catheterization

Indications for cardiac catheterization in patients with HLHS may be either interventional in nature or may be elective studies performed prior to stage 2 palliation or prior to the Fontan connection.

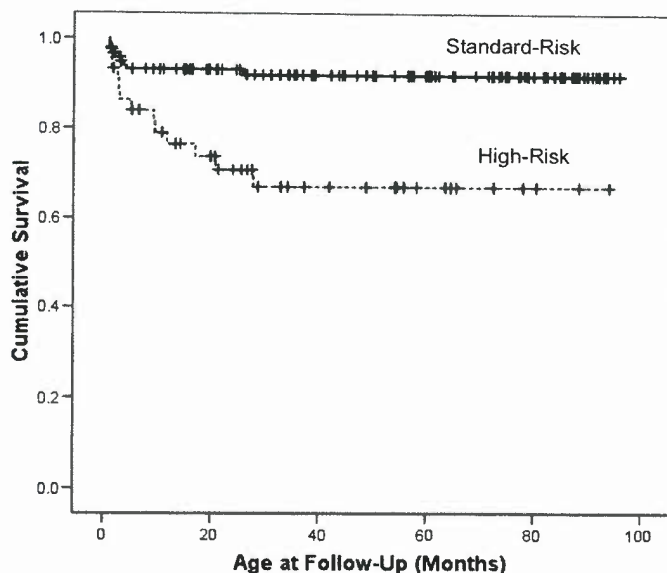


FIGURE 48.24. Actuarial survival following Norwood palliation for standard-risk and high-risk patients from September 2000 to September 2008. Operative survival and survival to cavopulmonary anastomosis are comparable between groups. One-year survival and survival to date are lower in high-risk patients compared to standard-risk patients ($p = 0.01$ and 0.001 , respectively). (Reprinted from Ghanayem NS, Hoffman GM, Mussatto KA, et al. Perioperative monitoring in high-risk infants after stage 1 palliation of univentricular congenital heart disease. *J Thorac Cardiovasc Surg* 2010;140:857–863, with permission from Elsevier.)

Ruiz et al. (320) and Gewillig et al. (321) have reported on the use of transcatheter stent placement within the ductus arteriosus in newborns with HLHS. This was performed in a group of patients that were listed for cardiac transplantation. This intervention allowed avoidance of long-term PGE1 therapy and its inherent complications including apnea, increased secretions, and chronic edema in patients who may wait weeks to months for a donor heart. Transcatheter ductal stenting is also performed as part of the hybrid procedure for HLHS. Transcatheter atrial septostomy is also employed in patients with HLHS and an intact or highly restrictive atrial septal defect. It is likely that this group of patients has irreversible changes in PVR that may not respond to intervention after birth. As a result, few centers are currently performing fetal intervention procedures including balloon atrial septostomy in select patients with HLHS. Interventional procedures after stage 1 palliation may be indicated prior to stage 2 palliation. Indications for interventional catheterization include excessive cyanosis as a result of stenosis of the systemic-to-pulmonary artery shunt, stenosis of the right ventricular-to-PA conduit, or recurrent arch obstruction.

Diagnostic catheterization is routinely performed prior to stage 2 palliation in most centers. Information obtained includes measurement of PA pressure, pulmonary capillary wedge pressure, right ventricular systolic and diastolic pressure, and pressure in the ascending and descending aorta. In addition, the PA anatomy, the adequacy of the atrial septal defect, neo-aortic arch obstruction, atrioventricular valve function, right ventricular function, and SVC anatomy are assessed. Some studies suggest that in select patients in whom clinical or anatomic concerns are absent by history, physical exam, and echocardiography, cardiac catheterization may not be necessary prior to stage 2 palliation.

Finally, interventional cardiac catheterization may be necessary after stage 2 palliation. Indications may include excessive hypoxemia after stage 2 palliation with the requirement for catheter occlusion of a venovenous collateral or less commonly, intervention for either a stenotic cavopulmonary connection or branch PA. Catheter intervention for aortic arch narrowing may also be occasionally necessary after stage 2 palliation (217,302).

Catheterization is routinely performed prior to the completion Fontan operation at some centers. At this study, determination of PA pressure, pulmonary capillary wedge pressure, and ventricular end-diastolic pressure is performed. In addition PA anatomy, neo-aortic arch anatomy, and the presence of venovenous or aortopulmonary collaterals are assessed. Some centers use cardiac MRI and less frequently 3-D CT scanning to determine the cardiovascular anatomy in select patients and do not routinely perform a catheterization study prior to completion Fontan operation (322). Cardiac catheterization following the Fontan operation may be necessary if there are anatomic or physiologic concerns not easily elucidated by noninvasive imaging techniques. Some centers routinely perform cardiac catheterization 6 to 12 months after the Fontan procedure with consideration for fenestration closure following hemodynamic assessment.

Finally, completion Fontan operation itself has been performed via catheter intervention (323). For patients with planned Fontan completion via interventional catheterization, a modification of the hemi-Fontan procedure is performed and includes a restrictive band that is placed at the superior venacava–right atrial junction. A transseptal needle perforation is undertaken through the banded SVC–right atrial junction with the subsequent placement of a covered stent from the IVC to the PA. In a report of five patients who underwent the Fontan operation with this technique, all returned home in 24 hours; however, several patients required subsequent intervention for baffle leak (213).

Late Fontan Concerns

Staged palliation for single-ventricle physiology has undergone a series of surgical revisions that have reduced early postoperative Fontan mortality from 20% to <2% (324,325). In late follow-up studies, 11% of Fontan survivors were found to have clinically significant morbidity including atrial dysrhythmias, protein-losing enteropathy (PLE), liver dysfunction, congestive heart failure, progressive ventricular dysfunction, or stroke at a median age of 8 years (range 1 to 25 years). Despite the significant morbidities associated with the Fontan operation, overall late mortality (range 4 months to 18 years) continues to decrease from 25% in the early experience to 5% in the recent era (325,326). Although long-term outcome data are sparse for isolated HLHS, when compared to other single-ventricle lesions with Fontan circulation, late mortality is comparable regardless of ventricle morphology (206,327).

Over the recent decades, indications for successful Fontan have been modified from the initial “Ten Commandments” described by Choussat and Fontan. From this list, specific physiologic risk factors for a failing Fontan prevail and relate to ventricular performance, atrioventricular and aortic valve function, and pulmonary circulation (328). Small PA size, PVR >4 wood units, preoperative PA pressure >15 mm Hg, or the presence of venovenous collaterals constitute a high-risk group of patients (326,329). In addition, more complex anatomy that requires main PA to ascending aorta anastomoses or ventricular septal defect enlargement, both indicators of ventricular outflow obstruction, has been identified as a risk factor for late morbidity.

Ventricular Dysfunction

Volume unloading provided by staged palliation results in reduction in ventricular size and wall thickness that, in turn, increases contractility and ventricular performance. Ventricular dilation, however, may persist in some patients due to early volume overload, as well the presence of aortopulmonary collaterals that are common in patients with chronic cyanosis. Regardless of the early success with staged palliation, late ventricular dysfunction after the Fontan operation may ensue due to morphologic/structural features of the single right systemic ventricle, residual obstructive lesions, and/or atrioventricular valve insufficiency. The failing systemic ventricle after staged palliation can be attributed to systolic dysfunction, diastolic dysfunction, or both (329–332). Systolic dysfunction is characterized by reduced contractility and an ejection fraction of <50%. Diastolic dysfunction is more difficult to define, but is evident by increased ventricular end-diastolic pressure and the rate of ventricular relaxation (333,334). As a result, late ventricular dysfunction and subsequent failure of Fontan circulation become clinically evident with symptoms of lower functional class, exercise intolerance, dyspnea, fatigue, and syncope (335, 336).

Hypoxemia

Slight hypoxemia with SaO_2 in the low 90s is common after Fontan completion even when residual atrial-level shunts (fenestrations) are absent (321,328). This desaturation is thought to result from coronary sinus blood return to the pulmonary venous atrium, and/or ventilation/perfusion imbalances within the lung. Desaturation also commonly occurs in patients with residual anatomic shunts such as a persistent atrial-level shunt (fenestration) or acquired collateral circulation within the lung.

In a study by Friedman et al. in which the prevalence and risk factors for aortopulmonary collateral vessels were assessed, collateral vessels were present in over 1/3 of patients who underwent either a bidirectional Glenn or Fontan procedure, and was most prevalent in patients with a history of a Blalock-Thomas-Taussig shunt. Most collateral vessels originated from the internal mammary arteries and thyrocervical trunk with fewer vessels originating from the brachiocephalic vessels (337). Admittedly, aortopulmonary collaterals should not cause hypoxemia but can result in volume overloading of the single RV.

Venovenous collaterals that drain directly into the LA or pulmonary venous circulation can also serve as a source of arterial desaturation after Fontan palliation. The collateral circulation that forms after Fontan palliation plays no role in gas exchange, produces right-to-left intrapulmonary shunts, and might contribute to progressive ventricular dysfunction as a source of chronic volume overload (338). Hence, the impact of intrapulmonary collateral circulation on oxygen saturation is variable but often most pronounced in the presence of progressive ventricular dysfunction.

Protein-Losing Enteropathy

PLE, a phenomenon of hypoalbuminemia through intestinal protein loss, occurs with an incidence of 3% to 15% in patients with Fontan circulation and has a reported mortality of 30% at 2 years and 50% at 5 years after diagnosis (339–341). Onset of PLE can be as early as 1 month to nearly two decades after Fontan palliation but occurs most commonly two to three years following the Fontan procedure (342).

The pathogenesis of PLE remains elusive despite increased understanding of univentricular physiology. Chronically elevated systemic venous/right atrial pressures with subsequent increased IVC and portal vein pressures have been implicated

as the primary cause of PLE. This elevation in abdominal venous pressures presumably leads to intestinal congestion, lymphatic obstruction, and enteric protein loss (342). Diastolic dysfunction, as mentioned previously, that results in low cardiac output in the face of elevated venous pressures, or even with venous pressures considered normal for Fontan physiology (<15 mm Hg), predisposes the patient to mesenteric ischemia and subsequent intestinal mucosal injury leading to the onset of enteric protein losses (328,342). Finally, inflammation due to infection or unexplained etiologies can result in epithelial membrane injury that may result in PLE despite the absence of hemodynamic derangements (343–346).

In a large retrospective multicenter study which included >3,000 patients with Fontan circulation in whom the incidence of PLE was 3.7%, ventricular anatomy other than dominant LV and an elevated preoperative ventricular end-diastolic pressure were risk factors for the development of PLE (342). Other large single-center studies have confirmed these findings, but also identified heterotaxy, polysplenia, anomalies of systemic venous drainage, increased pulmonary arteriolar resistance, and longer CPB time at Fontan palliation as risk factors for the development of PLE (328,339,340).

It has been agreed that PLE is poorly understood in its etiology and that it may occur from weeks to years after the Fontan operation. Rychik and Spray (341) suggested that an increase in mesenteric artery resistance after the Fontan operation, with a concomitant decrease in mesenteric artery blood flow, was associated with PLE. The clinical manifestations of PLE vary widely and the multiple potential therapies include diuretic use including aldactone and chlorothiazide, supplemental protein administration, attempts at minimizing intestinal protein loss with steroids and heparin, and altering the cardiovascular physiology with fenestration creation. If the above therapies prove unsuccessful, cardiac transplantation can be offered.

Thacker et al. (347) recently reported on the use of budesonide, a steroid with a high enteric anti-inflammatory effect, in the management of PLE after the Fontan operation. They suggested that budesonide resulted in an improvement of serum albumin within 6 months and that low-dose therapy must be continued in order to result in a sustained effect.

Finally, Bernstein et al. (348), in a retrospective multi-institutional review reported the results of cardiac transplantation in the therapy of failing Fontan patients, many of whom had PLE. Although the survival for this group of patients was slightly less (1 year 76%, 3 years 70%, 5 years 68%) than those patients with congenital heart disease, but without a Fontan, and those patients without congenital heart disease, the long-term results were encouraging and all surviving patients who had PLE had eventual resolution of PLE. Specifically, PLE was present in 34 of the 97 Fontan patients in this study and complete resolution of PLE was noted in all who survived >30 days after transplantation.

Thromboembolism

Patients with Fontan circulation have a lifelong risk of thromboembolic complications, particularly stroke and pulmonary embolism. In a large series by Coon, the reported prevalence of thrombus formation as detected by transthoracic echocardiography was 8.8% with the majority of thrombi detected within the first year of Fontan palliation (mean age 2.3 months, range 1 day to 163 months) (349). In smaller series, the diagnosis of thrombus formation was more common with transesophageal echo with a reported prevalence of 17% to 30% (350). The high rate of thrombus formation is postulated to be predominately secondary to venous stasis and impaired cardiac output that is inherent to single-ventricle circulation. No difference has been observed in patients who received a lateral

tunnel or atriopulmonary Fontan (349). Several studies report the presence of arrhythmias at the time of thrombus detection (349–352). Finally, liver dysfunction and coagulation factor deficiency, particularly protein C deficiency, have been identified in patients thought to have good outcomes after the Fontan operation; however, they appear to be time-related phenomena that resolve over time (353,354). The optimal anticoagulation regimen for the patient after the Fontan operation is still unclear and is the subject of current ongoing investigation.

Arrhythmias

Late atrial arrhythmias have a reported incidence of 10% to 5% in patients with Fontan physiology (326,328,334,335,355). Sinus node dysfunction, the presence of atrial suture lines, and increased atrial pressure have all been implicated in the etiology of late arrhythmias. In recent years, the surgical approach for the Fontan has been modified from the lateral tunnel to the extracardiac Fontan with the goal of reducing the incidence of atrial arrhythmias. The extracardiac Fontan has theoretic advantages in achieving this objective as this approach minimizes atrial suture lines and lessens the atrial hypertension that is expected with the lateral tunnel Fontan. Several series have reported this outcome with a decreased incidence of atrial tachyarrhythmias or pacemaker insertion for sinus node dysfunction in patients who underwent the extracardiac Fontan when compared to those patients subjected to the lateral tunnel Fontan (312,356,357). Conversely, Cohen reported no early benefit with either approach early after the Fontan operation (314).

Cardiac Transplantation

Primary Transplantation

In the past, some centers have chosen cardiac transplantation as the preferred primary therapeutic approach to HLHS (358–369). Bailey has reported the results of neonatal transplantation for HLHS. Between 1985 and 1996, 176 infants with HLHS were listed for cardiac transplantation. Nineteen percent of this group died prior to the identification of a donor heart. One-hundred and forty-two patients underwent transplantation between 1.5 hours and 6 months of life (median 29 days). Actuarial survival of patients who underwent transplant at 1 month, 1, 5, and 7 years was 91%, 84%, 76%, and 70%, respectively. This actuarial survival did not take into account the group of patients that died prior to an available donor heart. Intermediate-term follow-up of this group of patients has shown good growth and development (360). Evidence of neurodevelopmental delay has been noted in 11%, with normal psychomotor development in 91% and a normal developmental index in 96% (360,370).

Donor availability continues to be a limiting factor to primary transplantation with the donor shortage resulting in 25% to 30% mortality while on the waiting list. Alternative strategies to reduce pretransplant mortality include ABO incompatible neonatal transplantation. West has demonstrated promising results in patients who underwent ABO-incompatible transplantation with a concomitant decrease in mortality in those patients awaiting primary transplantation (371,372).

Transplant for Failed Palliation

Cardiac transplantation has been used at most centers for patients with HLHS who have failed or are poor candidates for staged palliation. Indications include severe, symptomatic right ventricular dysfunction and/or tricuspid valve regurgitation at any stage of repair. In addition, cardiac transplantation should be considered for the patient with severe, intractable PLE that is refractory to the usual therapeutic maneuvers,

occasionally seen after the completion Fontan operation. Transplantation required in the course of staged palliation may be complicated by immunologic sensitization as a result of previous surgical interventions and the inherent need for blood transfusion. In the past, this sensitization required prospective cross-matching of the donor and recipient in order to find a suitable donor. Currently, the availability and use of the virtual cross-matching technique (373) has eliminated the need for prospective cross-matching. This technique (374) can lead to shorter wait times and better outcomes as a listing strategy for the group of sensitized patients. In addition, although the sensitized group of patients may have a higher risk of antibody-mediated rejection after transplantation, this also can be monitored carefully post-transplantation by vigilant surveillance for the potential development of donor-directed antibodies and by the rapid and early intervention for antibody-mediated rejection if necessary.

Several centers have reported their results for heart transplantation in patients with previous Fontan operations. Gamba reviewed results from 1990 to 2002 in 14 patients who underwent heart transplantation after a previous Fontan operation. The mean age at the time of Fontan was 7.3 ± 2.8 years with the mean age at transplantation of 17.2 ± 6.3 years. The indication for transplantation was PLE in 7 patients, arrhythmia with ventricular dysfunction in five patients, and heart failure in two patients. Late survival was reported in 10 patients at a mean follow-up of 64 ± 42 months with patients in New York Heart Association class I category (375).

Michielon evaluated the incremental risk factors for early mortality after heart transplantation. Between 1988 and 2002, 25 patients underwent heart transplantation 15 of whom had a functional RV and 10 of whom had a functional LV. Twenty-two patients (88%) had received a previous completion Fontan operation. Transition to heart transplantation occurred from a shunt in 10 patients, a bidirectional cavopulmonary anastomosis in nine patients, and after Fontan failure in six patients. Overall 30-day survival was 68% with no additional mortality up to 14.1 years. Heart transplantation following bidirectional cavopulmonary anastomosis exhibited 100% long-term survival as opposed to 68% after systemic-to-PA shunt and 33% following the failing Fontan circulation. Michielon concluded that heart transplantation for patients with single-ventricle physiology is associated with substantial early mortality while the bidirectional cavopulmonary anastomosis provides the best transition to heart transplantation (376).

Bernstein's review of the outcomes of cardiac transplantation was noted earlier in the discussion of PLE (348). In this study, it should be noted that risk factors for death while waiting for cardiac transplantation included a young age, status 1 listing, shorter interval since the Fontan operation, and the need for mechanical ventilation.

Neurodevelopmental Outcomes and Quality of Life

Relative to other forms of congenital heart disease, the diagnosis of HLHS may impose one of the highest risks of neurodevelopmental and behavioral abnormalities for survivors. Neurologic outcomes are influenced by patient-related factors as well as preoperative, perioperative, and long-term risk factors. The collective effect of the multiple risks faced by children with HLHS results in a complex, multifaceted impact on development (377).

There are several factors that may impact neurodevelopment that are not readily modifiable such as congenital brain anomalies or abnormal fetal brain development (16,378–381); genetic syndromes, polymorphisms, and other comorbid conditions (25,382–384); prenatal versus postnatal diagnosis (385); and socioeconomic status or parental intelligence

(270,386,387). These must be taken into consideration when counseling parents or investigating the causes of an identified delay.

Recently implemented strategic approaches to care for infants and children with HLHS including improvements in hemodynamic stability before, during, and after surgery (175,177,183,290,388,389), perioperative neuroprotection (189,269,390), reduction of seizures and embolic events (391,392), and the effects of CPB (393,394) are anticipated to result in a reduction of cumulative neurologic risk. Treatment modalities for HLHS have evolved dramatically in a relatively short period of time making it difficult to generalize conclusions from historical cohorts to current patients. It is hoped that today's vastly improved understanding of the physiology of HLHS, optimal treatment choices, and reduction of the overall profile of risk for these patients will result in improved long-term neurodevelopmental outcomes for infants with HLHS born today.

Early studies of neurodevelopmental outcomes in children with HLHS demonstrated major delays in multiple areas of functioning and raised awareness of the importance of long-term monitoring in this population (395,396). More recently, research has demonstrated that children with HLHS often demonstrate overall IQ within the low range of normal but that they manifest important delays in visual-motor integration, executive functioning, and motor development as well as a higher than expected incidence of behavioral abnormalities, particularly attention deficits (382,387,397–401). IQ alone does not fully represent the spectrum of outcomes in this patient group, increasing the importance of comprehensive neuropsychological and behavioral follow-up. Routine developmental screening, beginning at 6 months of age in infants with complex heart disease has been shown to be useful in identifying patients who would benefit from early intervention therapy to reduce delays (402).

A range of outcomes for children with HLHS has been reported in the literature. The majority of parents (79%) of 115 school-aged children with HLHS rated their child's health as good to excellent (397). Eighty-eight percent reported minimal activity limitations and 84% rated school performance as average or above-average. Despite these encouraging parental perceptions, one-third of these children were receiving special education services. In the 28 children who underwent standardized developmental testing, the median full scale IQ was 86 with 18% of subjects demonstrating mental retardation ($IQ < 70$). The subjects in this study were all born prior to 1992 with a mean age of 9 ± 2.1 years at the time of study completion.

In 51 patients with Fontan physiology who underwent testing at a mean age of 4.8 ± 0.4 years, neurodevelopmental and behavioral outcomes were found to be within the normal range. However, children with HLHS demonstrated lower scores for overall, verbal and performance IQ than non-HLHS patients (93.8, 98.9, and 89.7 vs. 107, 110, and 101.9, respectively) (387). Scores for adaptive behavior and behavior problems did not differ between HLHS and non-HLHS subgroups. Very similar neurodevelopmental outcomes were reported for 26 children with HLHS who were treated with cardiac transplantation between 1993 and 1998 and tested at age 1.9 to 6.6 years (370). In this study, subjects had a median overall IQ of 89. Longer waiting time prior to transplantation was found to have a negative effect on later neurocognitive outcomes. These findings were subsequently confirmed in a multicenter study (401). Surgical approach, staged palliation versus transplantation, was not associated with any measure of developmental outcome in a group of 47 school-aged children representing four institutions. For the entire cohort, mean full-scale IQ was 86 ± 14 . Lower full-scale IQ, verbal, and math performance were associated with longer hospital stay at the

time of initial surgery. Wernovsky and Newburger (403) postulated that these similar findings, despite dramatically different treatment strategies, are evidence of the important impact of genetic factors, congenital brain abnormalities and insults incurred during the pre- and perioperative period. These risks are present despite the treatment method chosen.

In the Pediatric Heart Network cross-sectional study of 537 Fontan survivors at 6 to 18 years of age, parents reported problems with attention in 46%, learning in 43%, development in 24%, and behavior in 23% (398) demonstrating the wide spectrum of neurologic impact of complex heart disease. Operative factors have been the most widely studied and most significantly modified factors in an attempt to minimize intraoperative neurologic injury. However, operative factors typically only account for a small portion of the variance in outcomes (241,393,394,404,405). In a recent cohort of 88 patients with HLHS evaluated at 1 year of age, mental and psychomotor development was significantly lower than norms (382). The median Mental Development Index (MDI) was 90 with 11% of patients scoring greater than two standard deviations below the population mean (<70). The median Psychomotor Development Index (PDI) was 73 and 48% of the sample had scores of <70 . Motor delays are significantly more common than mental delays in all samples of infants with HLHS. Genetic abnormalities, lower gestational age, and the need for preoperative intubation were significant predictors of 1-year outcomes whereas operative variables, including duration of DHCA, were not.

Similarly, children undergoing surgery with DHCA versus continuous cerebral perfusion did not demonstrate differences in developmental outcomes at 1 year of age in a single institution randomized trial of perfusion techniques (270). In this cohort, the mean MDI was 92 and mean PDI was 77; however, as previously noted, the continuous cerebral perfusion flow rate in this trial was not likely high enough to meet brain metabolic demands. Children between 4 and 5 years of age with HLHS had significantly lower scores for cognition, fine motor skills, executive function, and math skills than children with transposition of the great arteries, tetralogy of Fallot, or ventricular septal defect. However, the mean scores for each domain were within normal limits for all groups (406). Perioperative risk has also been explored. A significant relationship between SVC SvO₂ in the first 48 hours following the Norwood procedure and developmental and behavioral outcomes in children with HLHS assessed at 4.5 years of age has been demonstrated (290). Postoperative SvO₂ values $<40\%$ were independently associated with poorer developmental outcomes. In a multivariable model, SvO₂, circulatory arrest time, CO₂ tension, and mean arterial blood pressure accounted for 79% of the variation in the developmental outcomes assessed; thus avoidance of conditions contributing to early cerebral hypoxia were associated with improved neurodevelopmental outcome (see Fig. 48.25).

These studies have evaluated children at multiple different ages and stages of repair. Generalization to today's child undergoing care for HLHS is difficult; however, these preliminary data emphasize the need for comprehensive follow-up and evaluation of developmental progress for these subjects. Further multicenter research involving thorough longitudinal assessment of children with HLHS is needed to understand neurodevelopmental risks and to optimize outcomes for these children. Several important studies including those of the Pediatric Heart Network, the Congenital Heart Surgeons Society, the Pediatric Heart Transplant Study Group, and individual investigators are carefully examining outcomes for the modern cohort of children with HLHS. Their findings will serve as a guide for future care and provide important information for counseling children, families, educators, and other health care practitioners.

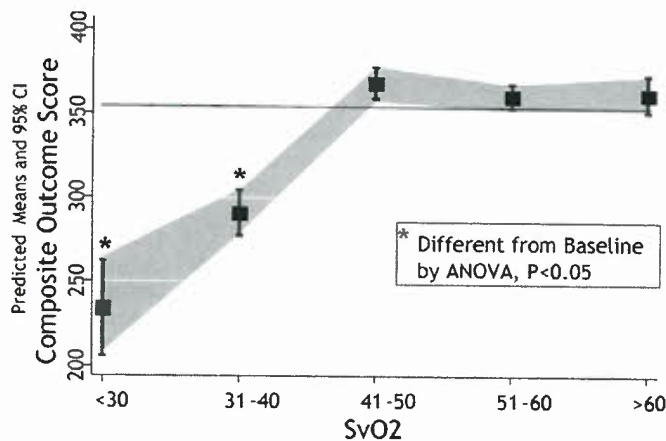


FIGURE 48.25. Neurodevelopmental outcome, as a composite of scores from four tests at 4 years of age, as a function of SVC SvO₂ in the 48 hours following the Norwood procedure. Reduced performance in this cohort was associated with SvO₂ <40%. ANOVA, analysis of variance; CI, confidence intervals; SvO₂ systemic venous oxygen saturation. (Reprinted from Hoffman GM, Mussatto KA, Brosig CS, et al. Systemic venous oxygen saturation after the Norwood procedure and childhood neurodevelopmental outcome. *J Thorac Cardiovasc Surg* 2005;130:1094–1100, with permission from Elsevier.)

The intensive focus on improving outcomes for children with HLHS has allowed us to begin to look beyond survival at the long-term psychosocial implications of this complex congenital heart disease. In 2010, a survey of 749 pediatric cardiologists and surgeons found that 99.7% discussed staged palliative surgery, 67% discussed cardiac transplantation and 62% discussed comfort care without surgery. Only 15% reported offering all of these options to families (407). The lack of long-term outcome data on quality of life (QOL) for survivors with HLHS is one of the major reasons for the continued debate about the applicability of a “no treatment” option and a variety of approaches to treatment decision making (407–410). While there is much yet to be learned, there is increasing awareness about QOL, functional outcomes, and impact on the family in children living with HLHS.

Children and families living with HLHS experience both physical and psychosocial challenges including uncertainty about long-term prognosis, chronic medication use, persistent symptoms, the prospect of developmental delay, and the need for repeated interventions. It would be inappropriate to propose that the combination of these factors has no impact on QOL. However, it is equally wrong to assume that bad outcomes are inevitable. QOL is a highly subjective, multidimensional concept that includes not only the impact of disease but also personal perceptions, expectations, satisfaction, and other factors (411,412). Although cultural differences in approaches to care for HLHS exist (413), health care professionals universally hope that patients realize “quality” of life versus “quantity” alone. The definition of quality, however, can be provided only by the children and families living the experience. It has been demonstrated repeatedly in congenital heart disease and other pediatric chronic illnesses that severity of illness is not a reliable predictor of QOL (414–417). It cannot be assumed that children with HLHS will experience a poor QOL.

Access to large cohorts of survivors of HLHS has been limited; therefore, few studies have examined psychosocial outcomes in this population exclusively. However, several studies have addressed these outcomes in groups representing

survivors of a variety of forms of single-ventricle heart disease. In studies by Casey et al. (418,419) of 26 children with various forms of single-ventricle lesions, it was found that 80% of parents underestimated the exercise tolerance of their children. Parents reported that their children had more social problems and decreased activities, and were more withdrawn than healthy children. Teachers also reported children with single-ventricle heart disease to be more withdrawn in the classroom setting. Sixty-five percent of these children attended school full-time, and 27% attended half-time or more. School adjustment in the children was found to be significantly related to both family strain and exercise tolerance. The impact of the child’s chronic condition on the family appeared to be a more important predictor of behavioral adjustment than the symptoms the children experienced. In another study, adults with single-ventricle heart disease ranging in age from 17 to 49 years reported QOL that was similar to healthy controls. Younger patients in the sample reported better overall QOL (420).

In a cross-sectional evaluation of the impact of HLHS in children at various stages of surgical palliation operated in the 1990s, QOL was rated as normal after stage 1 surgery; however, the lowest QOL reports were in children following stage 2 palliation (421). QOL was not related to the degree of developmental delay identified. However, longer circulatory arrest times were found to have a negative impact on QOL indicators. The authors speculated that differences in parental expectations during early childhood may account for these different responses. Parents reported lower self-esteem, more psychosomatic symptoms, and lower peer acceptance in a small cohort of 18 children with HLHS born between 1993 and 2005 and assessed at 2.7 to 10.6 years of age compared to age and gender-matched healthy children (422). There was also a higher rate of separation and divorces in the families of children with HLHS.

The Pediatric Heart Network reported outcomes of a cross-sectional study of 537 children with Fontan physiology in which QOL, heart rhythm, exercise tolerance, and data on other physical morbidities were collected (398,423,424). It was theorized that QOL may provide a proxy indicator of physical function. The study identified scores for quality of physical health that were approximately one standard deviation below normal and scores for psychosocial health that were one-half standard deviation lower than normative values for the Child Health Questionnaire. In the majority of health status domains, parents reported worse physical and psychosocial function than children reported for themselves (425). QOL in these Fontan survivors was less than that of healthy children; however, perceptions of QOL were influenced by multiple factors including socioeconomic status and the presence of other comorbid conditions, not only those related to cardiac outcomes. These findings once again emphasize the inherent disconnect between physiologic variables and subjective variables such as QOL.

For the first time in history, large cohorts of children with HLHS are developing into adolescents and young adults. This generation of children has benefited from numerous strategies to optimize neuroprotection and to support healthy psychosocial development. Further prospective, longitudinal research on neurodevelopmental and QOL outcomes, and their determinants, is needed to understand the impact of this disease. Strategies to help adolescents and young adults with HLHS achieve their full potential should be incorporated into our routine clinical surveillance and care. In December 2010, an interview with a 25-year-old survivor of HLHS aired on National Public Radio (426). Despite some physical limitations, the interviewer commented, “She seems to thrive within the context of her life.” This should be our goal for every patient with HLHS.

SUMMARY

The ventricle is a remarkably preserved structure throughout vertebrate evolution and is the workhorse of the circulation. The fundamental problem of an inadequate power supply remains the primary problem for those caring for the newborn with HLHS and persists throughout life. Although the early and intermediate outcomes in terms of survival have improved over the last decade, considerable challenges remain including options for the failing circulation, optimizing long-term neurodevelopmental outcome, and justifying allocation of increasingly scarce health care resources to a complex group of patients. Ongoing research provides hope for the future. Short-term goals include identification of the causes of HLHS to decrease the incidence, improvements in fetal intervention to improve the outcome for those born with HLHS, and improved medical, mechanical, and transplant strategies for treatment of the failing circulation to improve survival and QOL of affected individuals.

ACKNOWLEDGMENTS

The authors wish to thank Mara Koffarnus for her tireless and invaluable assistance in preparing this chapter.

REFERENCES

- Morris CD, Outcalt J, Menashe VD. Hypoplastic left heart syndrome: natural history in a geographically defined population. *Pediatrics* 1990;85:977–1000.
- Samanek M, Slavik Z, Zborilova B, et al. Prevalence, treatment, and outcome of heart disease in live-born children: a prospective analysis of 91,823 live-born children. *Pediatr Cardiol* 1989;10:205–211.
- Brownell LG, Shokeir MH. Inheritance of hypoplastic left heart syndrome (HLHS): Further observations. *Clin Genet* 1976;9:245–249.
- Fyler D. Report of the new england regional infant cardiac program. *Pediatrics* 1980;65:375–461.
- Watson DG, Rowe RD. Aortic valve atresia report of 43 cases. *JAMA* 1962;179:14–18.
- Fyler DC. The determinants of five-year survival of infants with critical congenital heart disease. In: Engle MA, ed. *Pediatric cardiovascular disease, cardiovascular clinics*. Philadelphia, PA: F.A. Davis Co., 1981:393–405.
- Sinha SN, Rusnak SL, Sommers HM, et al. Hypoplastic left ventricle syndrome. analysis of thirty autopsy cases in infants with surgical considerations. *Am J Cardiol* 1968;21:166–173.
- Roberts WC. Aortic valve atresia: a new classification based on necropsy study of 73 cases. *Am J Cardiol* 1976;37:753–756.
- Hawkins JA, Doty DB. Aortic atresia: Morphologic characteristics affecting survival and operative palliation. *J Thorac Cardiovasc Surg* 1984;88:620–626.
- Holmes LB, Rose V, Child AH. Comment on hypoplastic left heart syndrome. In: *Clinical delineation of birth defects: part XVI Urinary system and others*. Baltimore, MD: Williams and Wilkins, 1972:228–230.
- Nora JJ, Nora AH. *Genetics and counseling in cardiovascular diseases*. Springfield, IL: Thomas, 1978:227.
- Boughman JA, Berg KA, Astemborski JA, et al. Familial risks of congenital heart defect assessed in a population-based epidemiologic study. *Am J Med Genet* 1987;26:839–849.
- Brenner JJ, Berg KA, Schneider DS, et al. Cardiac malformations in relatives of infants with hypoplastic left-heart syndrome. *Am J Dis Child* 1989;143:1492–1494.
- Hinton RB, Martin LJ, Tabangin ME, et al. Hypoplastic left heart syndrome is heritable. *J Am Coll Cardiol* 2007;50:1590–1595.
- Lewin MB, McBride KL, Pignatelli R, et al. Echocardiographic evaluation of asymptomatic parental and sibling cardiovascular anomalies associated with congenital left ventricular outflow tract lesions. *Pediatrics* 2004;114:691–696.
- Glauser TA. Congenital brain anomalies associated with hypoplastic left heart syndrome. *Pediatrics* 1990;85: 984–990.
- Glauser TA, Rorke LB, Weinberg PM, et al. Acquired neuropathologic lesions associated with the hypoplastic left heart syndrome. *Pediatrics* 1990;85:991–1000.
- Olson DM, Shewmon DA. Electroencephalographic abnormalities in infants with hypoplastic left heart syndrome. *Pediatr Neurol* 1989;5:93–98.
- Halliday HL, Moore R, O'Hara D. Plasma amino acids in interrupted aortic arch and the hypoplastic left heart syndrome. *Biol Neonate* 1987;51:198–203.
- Natowicz M, Kelley RI. Association of turner syndrome with hypoplastic left-heart syndrome. *Am J Dis Child* 1987;141:218–220.
- Bidor-Lopez P, Matisoff D, Talner NS, et al. Hypoplastic left heart in a patient with 45,X/46,XX/47,XXX mosaicism. *Am J Med Genet* 1978;2:341–343.
- Glauser TA, Zackai E, Weinberg P, et al. Holt-oram syndrome associated with hypoplastic left heart syndrome. *Clin Genet* 1989;36:69–72.
- Antonelli D, Antonelli J, Rosenfeld T. Noonan's syndrome associated with hypoplastic left heart. *Cardiology* 1990;77:62–65.
- Lacro RV, Jones KL, Benirschke K. Coarctation of the aorta in turner syndrome: a pathologic study of fetuses with nuchal cystic hygromas, hydrops fetalis and female genitalia. *Pediatrics* 1988;81:445–451.
- Natowicz M, Chatten J, Clancy R, et al. Genetic disorders and major extracardiac anomalies associated with the hypoplastic left heart syndrome. *Pediatrics* 1988;82:698–706.
- vanEgmond H, Orye E, Praet M, et al. Hypoplastic left heart syndrome and 45X karyotype. *Br Heart J* 1988;60:69–71.
- Kung GC, Chang PM, Sklansky MS, et al. Hypoplastic left heart syndrome in patients with Kabuki syndrome. *Pediatr Cardiol* 2010;31:138–141.
- Qazi QH, Kanchanapoomi R, Cooper R, et al. Dup(12p) and hypoplastic left heart. *Am J Med Genet* 1981;9:195–199.
- Dasgupta C, Martinez AM, Zuppan CW, et al. Identification of connexin43 (alpha1) gap junction gene mutations in patients with hypoplastic left heart syndrome by denaturing gradient gel electrophoresis (DGGE). *Mutat Res* 2001;479:173–186.
- Elliott DA, Kirk EP, Yeoh T, et al. Cardiac homeobox gene NKX2-5 mutations and congenital heart disease: Associations with atrial septal defect and hypoplastic left heart syndrome. *J Am Coll Cardiol* 2003;41:2072–2076.
- McElhinney DB, Geiger E, Blinder J, et al. NKX2.5 mutations in patients with congenital heart disease. *J Am Coll Cardiol* 2003;42:1650–1655.
- Garg V, Muth A, Ransom J, et al. Mutations in NOTCH1 cause aortic valve disease. *Nature* 2005;437:270–274.
- Reamon-Buettner SM, Ciribilli Y, et al. A loss-of-function mutation in the binding domain of HAND1 predicts hypoplasia of the human hearts. *Hum Mol Genet* 2008;17:1397–1405.
- McBride KL, Zender GA, Fitzgerald-Butt SM, et al. Linkage analysis of left ventricular outflow tract malformations (aortic valve stenosis, coarctation of the aorta, and hypoplastic left heart syndrome). *Eur J Hum Genet* 2009;17:811–819.
- Grossfeld P, Ye M, Harvey R. Hypoplastic left heart syndrome: new genetic insights. *J Am Coll Cardiol* 2009;53:1072–1074.
- Hinton RB, Martin LJ, Rame-Gowda S, et al. Hypoplastic left heart syndrome links to chromosomes 10q and 6q and is genetically related to bicuspid aortic valve. *J Am Coll Cardiol* 2009;53:1065–1071.
- Kuehl KS, Loffredo CA. A cluster of hypoplastic left heart malformation in Baltimore, Maryland. *Pediatr Cardiol* 2006;27:25–31.
- Cronk CE, Pelech AN, Malloy ME, et al. Excess birth prevalence of hypoplastic left heart syndrome in eastern Wisconsin for birth cohorts 1997–1999. *Birth Defects Res A Clin Mol Teratol* 2004;70:114–120.
- Eghtesady P. Hypoplastic left heart syndrome: rheumatic heart disease of the fetus? *Med Hypotheses* 2006;66:554–565.
- Eghtesady P, Brar A, Hall M. Seasonality of hypoplastic left heart syndrome in the united states: a 10-year time-series analysis. *J Thorac Cardiovasc Surg* 2011;141:432–438.
- Allan LD, Sharland G, Tynan MJ. The natural history of the hypoplastic left heart syndrome. *Int J Cardiol* 1989;25:341–343.
- Danford DA, Cronican P. Hypoplastic left heart syndrome: progression of left ventricular dilation and dysfunction to left ventricular hypoplasia in utero. *Am Heart J* 1992;123:1712–1713.
- Sharland GK, Chita SK, Fagg NL, et al. Left ventricular dysfunction in the fetus: relation to aortic valve anomalies and endocardial fibroelastosis. *Br Heart J* 1991;66:419–424.
- Hornberger LK, Sanders SP, Rein AJ, et al. Left heart obstructive lesions and left ventricular growth in the midtrimester fetus. A longitudinal study. *Circulation* 1995;92:1531–1538.
- McCaffrey FM, Sherman FS. Prenatal diagnosis of severe aortic stenosis. *Pediatr Cardiol* 1997;18:276–281.
- Nowlen TT, Ayres NA, Kearney DL, et al. Premature closure of the foramen ovale associated with aortic stenosis, left ventricular dilation with thrombus, and early mortality. *Am J Cardiol* 2000;85:1159–1161.
- Remmell-Dow DR, Bharati S, Davis JT. Hypoplasia of the eustachian valve and abnormal orientation of the limbus of the foramen ovale in hypoplastic left heart syndrome. *Am Heart J* 1995;130:148–152.
- Chin AJ, Weinberg PM, Barber G. Subcostal two-dimensional echocardiographic identification of anomalous attachment of septum primum in patients with left atrioventricular valve underdevelopment. *J Am Coll Cardiol* 1990;15:678–681.
- Tworzky W, Wilkins-Haug L, Jennings RW, et al. Balloon dilation of severe aortic stenosis in the fetus: potential for prevention of hypoplastic left heart syndrome: candidate selection, technique, and results of successful intervention. *Circulation* 2004;110:2125–2131.
- Gembruch U. Prenatal diagnosis of congenital heart disease. *Prenat Diagn* 1997;17:1283–1298.

51. Perolo A, Prandstraller D, Ghi T, et al. Diagnosis and management of fetal cardiac anomalies: 10 years of experience at a single institution. *Ultrasound Obstet Gynecol* 2001;18:615-618.
52. Montana E, Khoury MJ, Cragan JD, et al. Trends and outcomes after prenatal diagnosis of congenital cardiac malformations by fetal echocardiography in a well defined birth population, atlanta, georgia, 1990-1994. *J Am Coll Cardiol* 1996;28:1805-1809.
53. Atkins DL, Clark EB, Marvin WJ Jr. Foramen ovale/atrial septum area ratio: a marker of transatrial blood flow. *Circulation* 1982;66:281-283.
54. Berning RA, Silverman NH, Villegas M, et al. Reversed shunting across the ductus arteriosus or atrial septum in utero heralds severe congenital heart disease. *J Am Coll Cardiol* 1996;27:481-486.
55. Makikallio K, McElhinney D, Levine J, et al. Aortic Valve Stenosis and the Evolution of Hypoplastic Left Heart Syndrome: Patient Selection for Fetal Intervention. *Circulation* 2006; 113:1401-1405.
56. Rychik J, Rome JJ, Collins MH, et al. The hypoplastic left heart syndrome with intact atrial septum: atrial morphology, pulmonary vascular histopathology and outcome. *J Am Coll Cardiol* 1999;34:554-560.
57. Maeda K, Yamaki S, Kado H. Hypoplasia of the small pulmonary arteries in hypoplastic left heart syndrome with restrictive atrial septal defect. *Circulation* 2004;110:139-146.
58. Taketazu M, Barrea C, Smallhorn JF, et al. Intrauterine pulmonary venous flow and restrictive foramen ovale in fetal hypoplastic left heart syndrome. *J Am Coll Cardiol* 2004 19;43:1902-1907.
59. Better DJ, Apfel HD, Zidere V, et al. Pattern of pulmonary venous blood flow in the hypoplastic left heart syndrome in the fetus. *Heart* 1999;81:646-649.
60. Kohl T, Sharland G, Allan LD, et al. World experience of percutaneous ultrasound-guided balloon valvuloplasty in human fetuses with severe aortic valve obstruction. *Am J Cardiol* 2000;85:1230-1233.
61. McElhinney DB, Marshall AC, Wilkins-Haug LE, et al. Predictors of technical success and postnatal biventricular outcome after in utero aortic valvuloplasty for aortic stenosis with evolving hypoplastic left heart syndrome. *Circulation* [Internet] 2009;120:1482-1490.
62. Lock J. Changing the natural history of borderline and hypoplastic left hearts in the fetus. Institutional Symposium: children's Hospital Boston. Converting the borderline left heart to a biventricular circulation: fetal, perinatal and postnatal diagnosis and management. Fourth World Congress of Pediatric Cardiology and Cardiac Surgery, 2005.
63. Vlahos AP, Lock JE, McElhinney DB, et al. Hypoplastic left heart syndrome with intact or highly restrictive atrial septum: Outcome after neonatal transcatheter atrial septostomy. *Circulation* 2004;109:2326-2330.
64. Marshall AC, vanderVelde ME, Tworetzky W, et al. Creation of an atrial septal defect in utero for fetuses with hypoplastic left heart syndrome and intact or highly restrictive atrial septum. *Circulation* 2004;110:253-258.
65. Marshall AC, Levine J, Morash D, et al. Results of in utero atrial septoplasty in fetuses with hypoplastic left heart syndrome. *Prenat Diagn* [Internet] 2008;28:1023-1028.
66. Lev M. Pathologic anatomy and interrelationship of hypoplasia of the aortic tract complexes. *Lab Invest* 1952;1:61-70.
67. Noonan JA, Nadas AS. The hypoplastic left heart syndrome; an analysis of 101 cases. *Pediatr Clin North Am* 1958;5:1029-1056.
68. Bharati S, Lev M. The surgical anatomy of hypoplasia of aortic tract complex. *J Thorac Cardiovasc Surg* 1984;88:97-101.
69. Cook AC. The phenotype during human fetal development. In: Anderson RH, Pozzi M, Hutchinson S, eds. *Hypoplastic left heart syndrome*. London: Springer-Verlag, 2005:19-38.
70. Tweddell J. The Norwood procedure with an innominate artery-to-pulmonary artery shunt. *Operat Tech Thorac Cardiovasc Surg* 2005;10:123-140.
71. Ghanayem NS, Hoffman GM, Mussatto KA, et al. Home surveillance program prevents interstage mortality after the Norwood procedure. *J Thorac Cardiovasc Surg* 2003;126:1367-1377.
72. VonRueden TJ, Knight L, Moller JH, et al. Coarctation of the aorta associated with aortic valvular atresia. *Circulation* 1975;52:951-954.
73. Tweddell JS, Hoffman GM, Mussatto KA, et al. Improved survival of patients undergoing palliation of hypoplastic left heart syndrome: Lessons learned from 115 consecutive patients. *Circulation* 2002;106:82-89.
74. Mahle WT, Spray TL, Wernovsky G, et al. Survival after reconstructive surgery for hypoplastic left heart syndrome: a 15-year experience from a single institution. *Circulation* 2000;102:136-141.
75. Stasik CN, Goldberg CS, Bove EL, et al. Current outcomes and risk factors for the Norwood procedure. *J Thorac Cardiovasc Surg* 2006;131:412-417.
76. Eliot RS, Shone JD, Kanjuh VI, et al. Mitral atresia. A study of 32 cases. *Am Heart J* 1965;70:6-22.
77. Kanjuh V, Eliot RS, Edwards JE. Coexistent mitral and aortic valvular atresia: a pathologic study of 14 cases. *Am J Cardiol* 1965;15:611-621.
78. vanderHorst RL, Hastreiter AR, DuBrow IW, et al. Pathologic measurements in aortic atresia. *Am Heart J* 1983;106:1411-1415.
79. Smith A, Pozzi M, Anderson RH. The morphology of hypoplasia of the left heart. In: Anderson RH, Pozzi M, Hutchinson S, eds. *Hypoplastic left heart syndrome*. London: Springer-Verlag, 2005:1-18.
80. Barber G, Chin AJ, Murphy JD, et al. Hypoplastic left heart syndrome: lack of correlation between preoperative demographic and laboratory findings and survival following palliative surgery. *Pediatr Cardiol* 1989;10:129-134.
81. Stamm C, Anderson RH, Ho SY. The morphologically tricuspid valve in hypoplastic left heart syndrome. *Eur J Cardiothorac Surg* 1997;12:587-592.
82. VanPraagh R, Bartram U, Kiaffas M. Hypoplastic left heart syndrome: incidence, epidemiology, and ethics. In: Hennein HA, Bove EL, eds. *Hypoplastic Left Heart Syndrome*. Armonk, NY: Futura, 2002:13-19.
83. Ho SY, Stamm C. Tricuspid valve in hypoplastic left heart syndrome. *J Thorac Cardiovasc Surg* 2004;128:329-330.
84. Vida VL, Bacha EA, Larrazabal A, et al. Surgical outcome for patients with the mitral stenosis-aortic atresia variant of hypoplastic left heart syndrome. *J Thorac Cardiovasc Surg* 2008;135:339-346.
85. Glatz JA, Fedderly RT, Ghanayem NS, et al. Impact of mitral stenosis and aortic atresia on survival in hypoplastic left heart syndrome. *Ann Thorac Surg* 2008;85:2057-2062.
86. Polimenakos AC, Sarhanandam SK, Husayni TS, et al. Hypoplastic left heart syndrome and aortic atresia-mitral stenosis variant: role of myocardial protection strategy and impact of ventriculo-coronary connections after stage I palliation. *Pediatr Cardiol* 2011;32:929-939.
87. VanPraagh R, Bano-Rodrigo A, Smolinski A. Anatomic variations in congenital valvar, subvalvar, and supravalvar aortic stenosis: a study of 64 postmortem cases In: Takahashi M, Wells MJ, Lindesmith GG, eds. *Challenges in the Treatment of Congenital Cardiac Anomalies*. New York, NY: Futura, 1986:13-41.
88. McElhinney DB, Benson CB, Brown DW, et al. Cerebral blood flow characteristics and biometry in fetuses undergoing prenatal intervention for aortic stenosis with evolving hypoplastic left heart syndrome. *Ultrasound Med Biol* 2010;36:29-37.
89. Glatz JA, Fedderly RT, Ghanayem NS, Tweddell JS. Impact of mitral stenosis and aortic atresia on survival in hypoplastic left heart syndrome. *Ann Thorac Surg*. 2008;85:2057-62.
90. Selim MA, Chin AJ, Norwood WL. Patterns of anomalous pulmonary venous connection/drainage in hypoplastic left heart syndrome: diagnostic role of doppler color flow mapping and surgical implications. *J Am Coll Cardiol* 1992;19:135-141.
91. Bernstein HS, Moore P, Stanger P, et al. The levoatriocardinal vein: morphology and echocardiographic identification of the pulmonary-systemic connection. *J Am Coll Cardiol* 1995;26:995-1001.
92. Sarris GE, Drummond-Webb JJ, Ebeid MR, et al. Anomalous origin of left coronary from right pulmonary artery in hypoplastic left heart syndrome. *Ann Thorac Surg* 1997;64:836-838.
93. Malec E, Mroczek T, Pajak J, et al. Hypoplastic left heart syndrome with an anomalous origin of the left coronary artery. *Ann Thorac Surg* 2001;72:2129-2130.
94. Cleuziou J, Haas F, Schreiber C, et al. Hypoplastic left heart syndrome with anomalous origin of the right coronary artery. *Ann Thorac Surg* 2006;81:341-343.
95. Nosal' M, Omeje I, Poruban R. Hypoplastic left heart syndrome with anomalous origin of left coronary artery from the right pulmonary artery: successful surgical treatment in a neonate. *Eur J Cardiothorac Surg* 2005;28:497-498.
96. Baffa JM, Chen SL, Guttenberg ME, et al. Coronary artery abnormalities and right ventricular histology in hypoplastic left heart syndrome. *J Am Coll Cardiol* 1992;20:350-358.
97. Lloyd TR, Evans TC, Marvin WJJ. Morphologic determinants of coronary blood flow in the hypoplastic left heart syndrome. *Am Heart J* 1986;112:666-671.
98. Lev M, Arcilla R, Rimoldi HJ, et al. Premature narrowing or closure of the foramen ovale. *Am Heart J* 1963;65:638-647.
99. Cohen M, Frommelt M. Does fetal diagnosis make a difference? Clinics in Perinatology 2005;32: 877-890.
100. Haworth SG. Normal structural and functional adaptation to extrauterine life. *J Pediatr* 1981;98:915-918.
101. Haworth SG, Hall SM, Chew M, et al. Thinning of fetal pulmonary arterial wall and postnatal remodelling: ultrastructural studies on the respiratory unit arteries of the pig. *Virchows Arch A Pathol Anat Histopathol* 1987;411:161-171.
102. Michel RP, Gordon JB, Chu K. Development of the pulmonary vasculature in newborn lambs: structure-function relationships. *J Appl Physiol* 1991;70:1255-1264.
103. Abu-Harb M, Wyllie J, Hey E, et al. Presentation of obstructive left heart malformations in infancy. *Arch Dis Child Fetal Neonatal Ed* 1994;71:F179-F183.
104. Leung MP, McKay R, Smith A, et al. Critical aortic stenosis in early infancy. Anatomic and echocardiographic substrates of successful open valvotomy. *J Thorac Cardiovasc Surg* 1991;101:526-535.
105. Parsons MK, Moreau GA, Graham TP Jr, et al. Echocardiographic estimation of critical left ventricular size in infants with isolated aortic valve stenosis. *J Am Coll Cardiol* 1991;18:1049-1055.
106. Sahn DJ, Allen HD, Goldberg SJ, et al. Pediatric echocardiography: a review of its clinical utility. *J Pediatr* 1975;87:335-352.
107. Bash SE, Huhta JC, Vick GW III, et al. Hypoplastic left heart syndrome: is echocardiography accurate enough to guide surgical palliation? *J Am Coll Cardiol* 1986;7:610-616.
108. Bass JL, Berry JM, Einzig S. Flow in the aorta and patent ductus arteriosus in infants with aortic atresia or aortic stenosis: a pulsed doppler ultrasound study. *Circulation* 1986;74:315-322.
109. Helton JG, Aglira BA, Chin AJ, et al. Analysis of potential anatomic or physiologic determinants of outcome of palliative surgery for hypoplastic left heart syndrome. *Circulation* 1986;74:70-76.

110. Altmann K, Printz BF, Solowiejczyk DE, et al. Two-dimensional echocardiographic assessment of right ventricular function as a predictor of outcome in hypoplastic left heart syndrome. *Am J Cardiol* 2000;86:964-968.
111. Michelfelder EC, Vermilion RP, Ludomirsky A, et al. Comparison of simultaneous doppler- and catheter-derived right ventricular dp/dt in hypoplastic left heart syndrome. *Am J Cardiol* 1996;77:212-214.
112. Akagi T, Benson LN, Williams WG, et al. Ventriculo-coronary arterial connections in pulmonary atresia with intact ventricular septum, and their influences on ventricular performance and clinical course. *Am J Cardiol* 1993;72:586-590.
113. Gentles TL, Colan SD, Giglia TM, et al. Right ventricular decompression and left ventricular function in pulmonary atresia with intact ventricular septum. The influence of less extensive coronary anomalies. *Circulation* 1993;88:183-188.
114. Schlag G, Redl H, Hallstrom S. The cell in shock: the origin of multiple organ failure. *Resuscitation* 1991;21:137-180.
115. Shoemaker WC. Relation of oxygen transport patterns to the pathophysiology and therapy of shock states. *Intensive Care Med* 1987;13:230-243.
116. Rhodes A, Bennett ED. Early goal-directed therapy: an evidence-based review. *Crit Care Med* 2004;32:S448-S450.
117. Tantalean JA, Leon RJ, Santos AA, et al. Multiple organ dysfunction syndrome in children. *Pediatr Crit Care Med* 2003;4:181-185.
118. Proulx F, Gauthier M, Nadeau D, et al. Timing and predictors of death in pediatric patients with multiple organ system failure. *Crit Care Med* 1994;22:1025-1031.
119. Hatherill M, Waggie Z, Purves L, et al. Mortality and the nature of metabolic acidosis in children with shock. *Intensive Care Med* 2003;29:286-291.
120. Rivers EP, Ander DS, Powell D. Central venous oxygen saturation monitoring in the critically ill patient. *Curr Opin Crit Care* 2001;7:204-211.
121. Han YY, Carcillo JA, Dragotta MA, et al. Early reversal of pediatric-neonatal septic shock by community physicians is associated with improved outcome. *Pediatrics* 2003;112:793-799.
122. Rivers E, Nguyen B, Havstad S, et al. Early goal-directed therapy in the treatment of severe sepsis and septic shock. *N Engl J Med* 2001;345:1368-1377.
123. Alia I, Esteban A, Gordo F, et al. A randomized and controlled trial of the effect of treatment aimed at maximizing oxygen delivery in patients with severe sepsis or septic shock. *Chest* 1999;115:453-461.
124. Boyd O, Bennett ED. Enhancement of perioperative tissue perfusion as a therapeutic strategy for major surgery. *New Horiz* 1996;4:453-465.
125. Yu M, Burchell S, Hasaniya NW, et al. Relationship of mortality to increasing oxygen delivery in patients ≥ 50 years of age: a prospective, randomized trial. *Crit Care Med* 1998;26:1011-1019.
126. Tibby SM, Murdoch IA. Monitoring cardiac function in intensive care. *Arch Dis Child* 2003;88:46-52.
127. Shen FM, Guan YF, Xie HH, et al. Arterial baroreflex function determines the survival time in lipopolysaccharide-induced shock in rats. *Shock* 2004;21:556-560.
128. Izzo JL Jr, Taylor AA. The sympathetic nervous system and baroreflexes in hypertension and hypotension. *Curr Hypertens Rep* 1999;1:254-263.
129. Kimmerly DS, Shoemaker JK. Hypovolemia and neurovascular control during orthostatic stress. *Am J Physiol Heart Circ Physiol* 2002;282:H645-H655.
130. Haljamae H. The pathophysiology of shock. *Acta Anaesthesiol Scand Suppl* 1993;98:3-6.
131. Dyess DL, Powell RW, Swafford AN Jr, et al. Redistribution of organ blood flow after hemorrhage and resuscitation in full-term piglets. *J Pediatr Surg* 1994;29:1097-1102.
132. Dantzer DR. Monitoring tissue oxygenation. The search for the grail. *Chest* 1997;111:12-14.
133. Ceppa EP, Fuh KC, Bulkley GB. Mesenteric hemodynamic response to circulatory shock. *Curr Opin Crit Care* 2003;9:127-132.
134. Kvarstein G, Mitrachi P, Tonnessen TI. Detection of organ ischemia during hemorrhagic shock. *Acta Anaesthesiol Scand* 2003;47:675-686.
135. Reilly PM, Wilkins KB, Fuh KC, et al. The mesenteric hemodynamic response to circulatory shock: an overview. *Shock* 2001;15:329-343.
136. Tatevossian RG, Wo CC, Velmahos GC, et al. Transcutaneous oxygen and CO₂ as early warning of tissue hypoxia and hemodynamic shock in critically ill emergency patients. *Crit Care Med* 2000;28:2248-2253.
137. Convertino VA, Baumgartner N. Effects of hypovolemia on aortic baroreflex control of heart rate in humans. *Aviat Space Environ Med* 1997;68:838-843.
138. Wood CE, Tong H. Central nervous system regulation of reflex responses to hypotension during fetal life. *Am J Physiol* 1999;277:R1541-R1552.
139. Newton GE, Parker JD. Cardiac sympathetic responses to acute vasodilation. normal ventricular function versus congestive heart failure. *Circulation* 1996;94:3161-3167.
140. Pang CC. Autonomic control of the venous system in health and disease: effects of drugs. *Pharmacol Ther* 2001;90:179-230.
141. Modesti PA, Polidori G, Bertolozzi I, et al. Impairment of cardiopulmonary receptor sensitivity in the early phase of heart failure. *Heart* 2004;90:30-36.
142. Neumann T, Heusch G. Myocardial, skeletal muscle, and renal blood flow during exercise in conscious dogs with heart failure. *Am J Physiol* 1997;273:H2452-H2457.
143. Heistad DD, Abboud FM, Dickinson W. Richards lecture: circulatory adjustments to hypoxia. *Circulation* 1980;61:463-470.
144. Li SG, Randall DC, Brown DR. Roles of cardiac output and peripheral resistance in mediating blood pressure response to stress in rats. *Am J Physiol* 1998;274:R1065-R1069.
145. Yamazaki F, Sone R. Modulation of arterial baroreflex control of heart rate by skin cooling and heating in humans. *J Appl Physiol* 2000;88:393-400.
146. Anand KJ, Hickey PR. Halothane-morphine compared with high-dose sufentanil for anesthesia and postoperative analgesia in neonatal cardiac surgery. *N Engl J Med* 1992;326:1-9.
147. Pladys P, Wodey E, Betremieux P, et al. Effects of volume expansion on cardiac output in the preterm infant. *Acta Paediatr* 1997;86:1241-1245.
148. Parker MM, Hazelzet JA, Carcillo JA. Pediatric considerations. *Crit Care Med* 2004;32:S591-S594.
149. Ai K, Kotake Y, Satoh T, et al. Epidural anesthesia retards intestinal acidosis and reduces portal vein endotoxin concentrations during progressive hypoxia in rabbits. *Anesthesiology* 2001;94:263-269.
150. Bersten AD, Hersch M, Cheung H, et al. The effect of various sympathomimetics on the regional circulations in hyperdynamic sepsis. *Surgery* 1992;112:549-561.
151. Breslow MJ, Miller CF, Parker SD, et al. Effect of vasopressors on organ blood flow during endotoxin shock in pigs. *Am J Physiol* 1987;252:H291-H300.
152. Meakins JL, Marshall JC. The gut as the motor of multiple system organ failure. In: Marston A, Bulkley GB, eds. *Splanchnic Ischemia and Multiple Organ Failure*. London: Edward Arnold, 1989:339-348.
153. Aneman A, Pettersson A, Eisenhofer G, et al. Sympathetic and renin-angiotensin activation during graded hypovolemia in pigs: impact on mesenteric perfusion and duodenal mucosal function. *Shock* 1997;8:378-384.
154. Toung T, Reilly PM, Fuh KC, et al. Mesenteric vasoconstriction in response to hemorrhagic shock. *Shock* 2000;13:267-273.
155. Groeneveld AB, Kolkman JJ. Splanchnic tonometry: a review of physiology, methodology, and clinical applications. *J Crit Care* 1994;9:198-210.
156. DiGiantomasso D, May CN, Bellomo R. Vital organ blood flow during hyperdynamic sepsis. *Chest* 2003;124:1053-1059.
157. Peters J, Mack GW, Lister G. The importance of the peripheral circulation in critical illnesses. *Intensive Care Med* 2001;27:1446-1458.
158. Deitch EA, Morrison J, Berg R, et al. Effect of hemorrhagic shock on bacterial translocation, intestinal morphology, and intestinal permeability in conventional and antibiotic-decontaminated rats. *Crit Care Med* 1990;18:529-536.
159. Marshall JC, Nathens AB. The gut in critical illness: evidence from human studies. *Shock* 1996;6:S10-S16.
160. Hansen PR. In vitro studies on responses to pentoxifylline and aminophylline of rat mesenteric resistance vessels. *Eur J Pharmacol* 1994;261:105-110.
161. Fink MP, Kaups KL, Wang HL, et al. Maintenance of superior mesenteric arterial perfusion prevents increased intestinal mucosal permeability in endotoxic pigs. *Surgery* 1991;110:154-160.
162. Marshall JC. An intensivist's dilemma: support of the splanchnic circulation in critical illness. *Crit Care Med* 1998;26:1637-1638.
163. Hamilton MA, Cecconi M, Rhodes A. A systematic review and meta-analysis on the use of preemptive hemodynamic intervention to improve postoperative outcomes in moderate and high-risk surgical patients. *Anesth Analg* 2011;112:1392-1402.
164. Miller TE, Roche AM, Gan TJ. Poor adoption of hemodynamic optimization during major surgery: are we practicing substandard care? *Anesth Analg* 2011;112:1274-1276.
165. Barnea O, Austin EH, Richman B, et al. Balancing the circulation: theoretic optimization of pulmonary/systemic flow ratio in hypoplastic left heart syndrome. *J Am Coll Cardiol* 1994;24:1376-1381.
166. Barnea O, Santamore WP, Rossi A, et al. Estimation of oxygen delivery in newborns with a univentricular circulation [see comment]. *Circulation* 1998;98:1407-1413.
167. Jobs DR, Nicolson SC, Steven JM, et al. Carbon dioxide prevents pulmonary overcirculation in hypoplastic left heart syndrome. *Ann Thorac Surg* 1992;54:150-151.
168. Rossi AF, Sommer RJ, Lotvin A, et al. Usefulness of intermittent monitoring of mixed venous oxygen saturation after stage I palliation for hypoplastic left heart syndrome. *Am J Cardiol* 1994;73:1118-1123.
169. Riordan CJ, Locher JP Jr, Santamore WP, et al. Monitoring systemic venous oxygen saturations in the hypoplastic left heart syndrome. *Ann Thorac Surg* 1997;63:835-837.
170. Li J, Zhang G, Holtby H, et al. Inclusion of oxygen consumption improves the accuracy of arterial and venous oxygen saturation interpretation after the Norwood procedure. *J Thorac Cardiovasc Surg* 2006;131:1099-1107.
171. Mora GA, Pizarro C, Jacobs ML, et al. Experimental model of single ventricle. influence of carbon dioxide on pulmonary vascular dynamics. *Circulation* 1994;90:43-46.
172. Riordan CJ, Randsbeck F, Storey JH, et al. Effects of oxygen, positive end-expiratory pressure, and carbon dioxide on oxygen delivery in an animal model of the univentricular heart. *J Thorac Cardiovasc Surg* 1996;112:644-654.
173. Shime N, Hashimoto S, Hiramatsu N, et al. Hypoxic gas therapy using nitrogen in the preoperative management of neonates with hypoplastic left heart syndrome. *Pediatr Crit Care Med* 2000;1:38-41.

174. Keidan I, Mishaly D, Berkenstadt H, et al. Combining low inspired oxygen and carbon dioxide during mechanical ventilation for the Norwood procedure. *Paediatr Anaesth* 2003;13:58–62.
175. Tabbutt S, Ramamoorthy C, Montenegro LM, et al. Impact of inspired gas mixtures on preoperative infants with hypoplastic left heart syndrome during controlled ventilation. *Circulation* 2001;104:159–164.
176. Migliavacca F, Pennati G, Dubini G, et al. Modeling of the Norwood circulation: effects of shunt size, vascular resistances, and heart rate. *Am J Physiol Heart Circ Physiol* 2001;280:H2076–H2086.
177. Bradley SM, Atz AM, Simsic JM. Redefining the impact of oxygen and hyperventilation after the Norwood procedure. *J Thorac Cardiovasc Surg* 2004;127:473–480.
178. Taeed R, Schwartz SM, Pearl JM, et al. Unrecognized pulmonary venous desaturation early after Norwood palliation confounds Qp: Qs assessment and compromises oxygen delivery. *Circulation* 2001;103:2699–2704.
179. Tweddell JS, Hoffman GM, Fedderly RT, et al. Phenoxybenzamine improves systemic oxygen delivery after the Norwood procedure. *Ann Thorac Surg* 1999;67:167–168.
180. Wright GE, Crowley DC, Charpie JR, et al. High systemic vascular resistance and sudden cardiovascular collapse in recovering Norwood patients. *Ann Thorac Surg* 2004;77:48–52.
181. Hoffman GM, Ghanayem NS, Kampine JM, et al. Venous saturation and the anaerobic threshold in neonates after the Norwood procedure for hypoplastic left heart syndrome. *Ann Thorac Surg* 2000;70:1515–1520.
182. Hoffman GM, Tweddell JS, Ghanayem NS, et al. Alteration of the critical arteriovenous oxygen saturation relationship by sustained afterload reduction after the Norwood procedure. *J Thorac Cardiovasc Surg* 2004;127:738–745.
183. Hoffman GM, Stuth EA, Jaquiss RD, et al. Changes in cerebral and somatic oxygenation during stage 1 palliation of hypoplastic left heart syndrome using continuous regional cerebral perfusion. *J Thorac Cardiovasc Surg* 2004;127:223–233.
184. Pigula FA, Gandhi SK, Siewers RD, et al. Regional low-flow perfusion provides somatic circulatory support during neonatal aortic arch surgery. *Ann Thorac Surg* 2001;72:401–407.
185. Hoffman GM, Stuth EA, Berens RJ, et al. Two-site near-infrared transcutaneous oximetry as a non-invasive indicator of mixed venous oxygen saturation in cardiac neonates. *Anesthesiology* 2003;97:A1393.
186. Li J, Van Arsdell GS, Zhang G, et al. Assessment of the relationship between cerebral and splanchnic oxygen saturations measured by near-infrared spectroscopy and direct measurements of systemic haemodynamic variables and oxygen transport after the Norwood procedure. *Heart* 2006;92:1678–1685.
187. Kaufman J, Almodovar MC, Zuk J, et al. Correlation of abdominal site near-infrared spectroscopy with gastric tonometry in infants following surgery for congenital heart disease. *Pediatr Crit Care Med* 2008;9:62–68.
188. Ghanayem NS, Wernovsky G, Hoffman GM. Near-infrared spectroscopy as a hemodynamic monitor in critical illness. *Pediatr Crit Care Med* 2011;12:S27–S32.
189. Johnson BA, Hoffman GM, Tweddell JS, et al. Near-infrared spectroscopy in neonates before palliation of hypoplastic left heart syndrome. *Ann Thorac Surg* [Internet] 2009;87:571–577.
190. Tweddell JS, Ghanayem NS, Hoffman GM. Pro: NIRS is “standard of care” for postoperative management. *Semin Thorac Cardiovasc Surg Pediatr Card Surg Annu* 2010;13:44–50.
191. Ghanayem NS, Hoffman GM, Mussatto KA, et al. Perioperative monitoring in high-risk infants after stage 1 palliation of univentricular congenital heart disease. *J Thorac Cardiovasc Surg* 2010;140:857–863.
192. Lim MK, Hanretty K, Houston AB, et al. Intermittent ductal patency in healthy newborn infants: demonstration by colour doppler flow mapping. *Arch Dis Child* 1992;67:1217–1218.
193. Reller MD, Rice MJ, McDonald RW. Review of studies evaluating ductal patency in the premature infant. *J Pediatr* 1993;122:S59–S62.
194. Gentile R, Stevenson G, Dooley T, et al. Pulsed doppler echocardiographic determination of time of ductal closure in normal newborn infants. *J Pediatr* 1981;98:443–448.
195. Kramer HH, Sommer M, Rammos S, et al. Evaluation of low dose prostaglandin E1 treatment for ductus dependent congenital heart disease. *Eur J Pediatr* 1995;154:700–707.
196. Lewis AB, Freed MD, Heymann MA, et al. Side effects of therapy with prostaglandin E1 in infants with critical congenital heart disease. *Circulation* 1981;64:893–898.
197. Saxena A, Sharma M, Kothari SS, et al. Prostaglandin E1 in infants with congenital heart disease: indian experience. *Indian Pediatr* 1998;35:1063–1069.
198. Lim DS, Kulik TJ, Kim DW, et al. Aminophylline for the prevention of apnea during prostaglandin E1 infusion. *Pediatrics* 2003;112:e27–e29.
199. Reddy VM, Liddicoat JR, Fineman JR, et al. Fetal model of single ventricle physiology: Hemodynamic effects of oxygen, nitric oxide, carbon dioxide, and hypoxia in the early postnatal period. *J Thorac Cardiovasc Surg* 1996;112:437–449.
200. Day RW, Tani LY, Minich LL, et al. Congenital heart disease with ductal-dependent systemic perfusion: doppler ultrasonography flow velocities are altered by changes in the fraction of inspired oxygen. *J Heart Lung Transplant* 1995;14:718–725.
201. Ramamoorthy C, Tabbutt S, Kurth CD, et al. Effects of inspired hypoxic and hypercapnic gas mixtures on cerebral oxygen saturation in neonates with univentricular heart defects. *Anesthesiology* 2002;96:283–288.
202. Cayler GG, Smeloff EA, Miller GE Jr. Surgical palliation of hypoplastic left side of the heart. *N Engl J Med* 1970;282:780–783.
203. Doty DB, Marvin WJ Jr, Schieken RM, et al. Hypoplastic left heart syndrome: successful palliation with a new operation. *J Thorac Cardiovasc Surg* 1980;80:148–152.
204. Norwood WI, Kirklin JK, Sanders SP. Hypoplastic left heart syndrome: experience with palliative surgery. *Am J Cardiol* 1980;45:87–91.
205. Norwood WI, Lang P, Hansen DD. Physiologic repair of aortic atresia-hypoplastic left heart syndrome. *N Engl J Med* 1983;308:23–26.
206. Gaynor JW, Bridges ND, Cohen MI, et al. Predictors of outcome after the fontan operation: is hypoplastic left heart syndrome still a risk factor? *J Thorac Cardiovasc Surg* 2002;123:237–245.
207. Pigott JD, Murphy JD, Barber G, et al. Palliative reconstructive surgery for hypoplastic left heart syndrome. *Ann Thorac Surg* 1988;45:122–128.
208. Jacobs ML, Rychik J, Rome JJ, et al. Early reduction of the volume work of the single ventricle: the hemi-fontan operation. *Ann Thorac Surg* 1996;62:456–461.
209. Azakie A, McCrindle BW, Benson LN, et al. Total cavopulmonary connections in children with a previous Norwood procedure. *Ann Thorac Surg* 2001;71:1541–1546.
210. Tweddell JS, Nersesian M, Mussatto KA, et al. Fontan palliation in the modern era: factors impacting mortality and morbidity. *Ann Thorac Surg* [Internet] 2009;88:1291–1299. Available from: <http://ovidsp.ovid.com/ovidweb.cgi?T=JS&NEWS=N&PAGE=fulltext&AN=197668248&D=medl>
211. Bacha EA, Daves S, Hardin J, et al. Single-ventricle palliation for high-risk neonates: the emergence of an alternative hybrid stage I strategy. *J Thorac Cardiovasc Surg* 2006;131:163–171.
212. Akintuerk H, Michel-Behnke I, Valeske K, et al. Stenting of the arterial duct and banding of the pulmonary arteries: basis for combined norwood stage I and II repair in hypoplastic left heart. *Circulation* 2002;105:1099–1103.
213. Galantowicz M, Cheatham JP. Lessons learned from the development of a new hybrid strategy for the management of hypoplastic left heart syndrome. *Pediatr Cardiol* 2005;26:190–199.
214. Litwin SB, VanPraagh R, Bernhard WF. A palliative operation for certain infants with aortic arch interruption. *Ann Thorac Surg* 1972;14:369–375.
215. Jonas RA. Intermediate procedures after first-stage norwood operation facilitate subsequent repair. *Ann Thorac Surg* 1991;52:696–700.
216. Burkhardt HM, Ashburn DA, Konstantinov IE, et al. Interdigitating arch reconstruction eliminates recurrent coarctation after the Norwood procedure. *J Thorac Cardiovasc Surg* 2005;130:61–65.
217. Bartram U, Grunenfeller J, VanPraagh R. Causes of death after the modified Norwood procedure: a study of 122 postmortem cases. *Ann Thorac Surg* 1997;64:1795–1802.
218. Mahle WT, Spray TL, Gaynor JW, et al. Unexpected death after reconstructive surgery for hypoplastic left heart syndrome. *Ann Thorac Surg* 2001;71:61–65.
219. Forbess JM, Cook N, Roth SJ, et al. Ten-year institutional experience with palliative surgery for hypoplastic left heart syndrome. Risk factors related to stage I mortality. *Circulation* 1995;92:262–266.
220. de Leval MR, McKay R, Jones M, et al. Modified blalock-taussig shunt. Use of subclavian artery orifice as flow regulator in prosthetic systemic-pulmonary artery shunts. *J Thorac Cardiovasc Surg* 1981;81:112–119.
221. Fogel MA, Rychik J, Vetter J, et al. Effect of volume unloading surgery on coronary flow dynamics in patients with aortic atresia. *J Thorac Cardiovasc Surg* 1997;113:718–726.
222. Donnelly JP, Raffel DM, Shulkin BL, et al. Resting coronary flow and coronary flow reserve in human infants after repair or palliation of congenital heart defects as measured by positron emission tomography. *J Thorac Cardiovasc Surg* 1998;115:103–110.
223. Thourani V, Kirshbom P, Kanter K, et al. Venoarterial extracorporeal membrane oxygenation (VA-ECMO) in pediatric cardiac support. *Ann Thorac Surg* 2006;82:138–145.
224. Sano S, Ishino K, Kawada M, et al. Right ventricle-pulmonary artery shunt in first-stage palliation of hypoplastic left heart syndrome. *J Thorac Cardiovasc Surg* 2003;126:504–509.
225. Norwood WI, Lang P, Casteneda AR, et al. Experience with operations for hypoplastic left heart syndrome. *J Thorac Cardiovasc Surg* 1981;82:511–519.
226. Mair R, Tulzer G, Sames E, et al. Right ventricular to pulmonary artery conduit instead of modified Blalock-Taussig shunt improves postoperative hemodynamics in newborns after the Norwood operation. *J Thorac Cardiovasc Surg* 2003;126:1378–1384.
227. Pizarro C, Malec E, Maher KO, et al. Right ventricle to pulmonary artery conduit improves outcome after stage I Norwood for hypoplastic left heart syndrome. *Circulation* 2003;108:155–160.
228. Sano S, Ishino K, Kado H, et al. Outcome of right ventricle-to-pulmonary artery shunt in first-stage palliation of hypoplastic left heart syndrome: a multi-institutional study. *Ann Thorac Surg* 2004;78:1951–1958.
229. Ohye RG, Ludomirsky A, Devaney EJ, et al. Comparison of right ventricle to pulmonary artery conduit and modified blalock-taussig shunt hemodynamics after the Norwood operation. *Ann Thorac Surg* 2004;1090–1093.
230. Lai L, Laussen PC, Cua CL, et al. Outcomes after bidirectional glenn operation: blalock-Taussig shunt versus right ventricle-to-pulmonary artery conduit. *Ann Thorac Surg* [Internet] 2007;83:1768–1773.

231. Mahle WT, Cuadrado AR, Tam VK. Early experience with a modified Norwood procedure using right ventricle to pulmonary artery conduit. *Ann Thorac Surg* 2003;76:1084–1088.
232. Pizarro C, Mroczek T, Malec E, et al. Right ventricle to pulmonary artery conduit reduces interim mortality after stage 1 Norwood for hypoplastic left heart syndrome. *Ann Thorac Surg* 2004;78:1959–1963.
233. Ghanayem NS, Tweddell JS, Hoffman GM, et al. Optimal timing of the second stage of palliation for hypoplastic left heart syndrome facilitated through home monitoring, and the results of early cavopulmonary anastomosis. *Card Young* 2006; 16 Suppl 1:61–6.
234. Cua CL, Thiagarajan RR, Gauvreau K, et al. Early postoperative outcomes in a series of infants with hypoplastic left heart syndrome undergoing stage I palliation operation with either modified Blalock-Taussig shunt or right ventricle to pulmonary artery conduit. *Pediatr Crit Care Med* 2006;7:238–244.
235. Kussman BD, Gauvreau K, DiNardo JA, et al. Cerebral perfusion and oxygenation after the Norwood procedure: comparison of right ventricle-pulmonary artery conduit with modified Blalock-Taussig shunt. *J Thorac Cardiovasc Surg* 2007;133:648–655.
236. Alsoufi B, Bennetts J, Verma S, et al. New developments in the treatment of hypoplastic left heart syndrome. *Pediatrics* 2007;119:109–117.
237. Malec E, Januszewska K, Kolcz J, et al. Right ventricle-to-pulmonary artery shunt versus modified Blalock-Taussig shunt in the Norwood procedure for hypoplastic left heart syndrome—influence on early and late haemodynamic status. *Eur J Cardiothorac Surg* 2003;23:728–733.
238. Pizarro C, Davis DA, Healy RM, et al. Is there a role for extracorporeal life support after stage I norwood? *Eur J Cardiothorac Surg* 2001;19:294–301.
239. Tabbutt S, Dominguez TE, Ravishanker C, et al. Outcomes after the stage I reconstruction comparing the right ventricular to pulmonary artery conduit with the modified Blalock Taussig shunt. *Ann Thorac Surg* 2005;80:1582–1590.
240. Azakie A, Martinez D, Sapru A, et al. Impact of right ventricle to pulmonary artery conduit on outcome of the modified Norwood procedure. *Ann Thorac Surg* 2004;77:1727–1733.
241. Ohye RG, Sleeper LA, Mahony L, et al. Pediatric Heart Network I. Comparison of shunt types in the Norwood procedure for single-ventricle lesions. *N Engl J Med* 2010;362:1980–1992.
242. Mitchell MB, Campbell DN, Boucek MM, et al. Mechanical limitation of pulmonary blood flow facilitates heart transplantation in older infants with hypoplastic left heart syndrome. *Eur J Cardiothorac Surg* 2003;23:735–742.
243. Pizarro C, Norwood WI. Pulmonary artery banding before Norwood procedure. *Ann Thorac Surg* 2003;75:1008–1010.
244. Galantowicz M, Cheatham JP, Phillips A, et al. Hybrid approach for hypoplastic left heart syndrome: intermediate results after the learning curve. *Ann Thorac Surg* 2008;85:2070–2071.
245. Holzer RJ, Wood A, Chisolm JL, et al. Atrial septal interventions in patients with hypoplastic left heart syndrome. *Catheter Cardiovasc Interv* 2008;72:696–704.
246. Stoica SC, Philips AB, Egan M, et al. The retrograde aortic arch in the hybrid approach to hypoplastic left heart syndrome. *Ann Thorac Surg* 2009;88:1939–1946.
247. Egan MJ, Hill SL, Boettner BL, et al. Predictors of retrograde aortic arch obstruction after hybrid palliation of hypoplastic left heart syndrome. *Pediatr Cardiol* 2011;32:67–75.
248. Cua CL, Galantowicz ME, Turner DR, et al. Palliation via hybrid procedure of a 1.4-kg patient with a hypoplastic left heart. *Congenit Heart Dis* 2007;2:191–193.
249. Anand KJ, Aynsley-Green A. Measuring the severity of surgical stress in newborn infants. *J Pediatr Surg* 1988;23:297–305.
250. Anand KJ, Sippell WG, Aynsley-Green A. Randomised trial of fentanyl anaesthesia in preterm babies undergoing surgery: effects on the stress response. *Lancet* 1987;1:62–66.
251. Hickey PR, Hansen DD. High-dose fentanyl reduces intraoperative ventricular fibrillation in neonates with hypoplastic left heart syndrome. *J Clin Anesth* 1991;3:295–300.
252. Duncan HP, Cloote A, Weir PM, et al. Reducing stress responses in the pre-bypass phase of open heart surgery in infants and young children: a comparison of different fentanyl doses. *Br J Anaesth* 2000;84:556–564.
253. Riordan CJ, Randsbaek F, Storey JH, et al. Inotropes in the hypoplastic left heart syndrome: effects in an animal model. *Ann Thorac Surg* 1996;62:83–90.
254. Poirier NC, Drummond-Webb JJ, Hisamochi K, et al. Modified Norwood procedure with a high-flow cardiopulmonary bypass strategy results in low mortality without late arch obstruction. *J Thorac Cardiovasc Surg* 2000;120:875–884.
255. Tweddell JS, Berger S, Frommelt PC, et al. Aprotinin improves outcome of single-ventricle palliation. *Ann Thorac Surg* 1996;62:1329–1335.
256. Wernovsky G, Wypij D, Jonas RA, et al. Postoperative course and hemodynamic profile after the arterial switch operation in neonates and infants. A comparison of low-flow cardiopulmonary bypass and circulatory arrest. *Circulation* 1995;92:2226–2235.
257. Tweddell JS, Hoffman GM. Postoperative management in patients with complex congenital heart disease. *Semin Thorac Cardiovasc Surg Pediatr Card Surg Annu* 2002;5:187–205.
258. Köner O, Tekin S, Köner A, et al. Effects of phentolamine on tissue perfusion in pediatric cardiac surgery. *J Cardiothorac Vasc Anesth* 1999;13:191–197.
259. Motta P, Mossad E, Toscana D, et al. Comparison of phenoxybenzamine to sodium nitroprusside in infants undergoing surgery. *J Cardiothorac Vasc Anesth* 2005;19:54–59.
260. Mossad E, Motta P, Sehmbeiy K, et al. The hemodynamic effects of phenoxybenzamine in neonates, infants, and children. *J Clin Anesth* 2008;20:94–98.
261. Fraser CD Jr, Mee RB. Modified Norwood procedure for hypoplastic left heart syndrome. *Ann Thorac Surg* 1995;60:S546–S549.
262. Pigula FA. Arch reconstruction without circulatory arrest: scientific basis for continued use and application to patients with arch anomalies. *Semin Thorac Cardiovasc Surg Pediatr Card Surg Annu* 2002;5:104–115.
263. Hoffman GM, Ghanayem NS, Musa N, Mussatto KA, Berens RJ. Differential Effects of Carbon Dioxide Tension on Cerebral and Somatic Oxygenation Assessed by Near Infrared Spectroscopy in Postoperative Neonates. *Anesthesiology*. 2005; 103:[A1374].
264. Imoto Y, Kado H, Shiokawa Y, et al. Experience with the Norwood procedure without circulatory arrest. *J Thorac Cardiovasc Surg* 2001;122:879–882.
265. duPlessis AJ, Jonas RA, Wypij D, et al. Perioperative effects of alpha-stat versus pH-stat strategies for deep hypothermic cardiopulmonary bypass in infants. *J Thorac Cardiovasc Surg* 1997;114:1000–1001.
266. Wypij D, Newburger JW, Rappaport LA, et al. The effect of duration of deep hypothermic circulatory arrest in infant heart surgery on late neurodevelopment: the boston circulatory arrest trial [see comment]. *J Thorac Cardiovasc Surg* 2003;126:1397–1403.
267. Antila V, Hagino I, Zurakowski D, et al. Specific bypass conditions determine safe minimum flow rate. *Ann Thorac Surg* 2005;80:1460–1467.
268. Lim C, Kim WH, Kim SC, et al. Aortic arch reconstruction using regional perfusion without circulatory arrest. *Eur J Cardiothorac Surg* 2003;23:149–155.
269. Hoffman GM. Detection and prevention of neurologic injury in the intensive care unit. *Cardiol Young* 2005;15:149–153.
270. Goldberg CS, Bove EL, Devaney EJ, et al. A randomized clinical trial of regional cerebral perfusion versus deep hypothermic circulatory arrest: outcomes for infants with functional single ventricle. *J Thorac Cardiovasc Surg* 2007;133:880–887.
271. Pastuszko P, Liu H, Mendoza-Paredes A, et al. Brain oxygen and metabolism is dependent on the rate of low-flow cardiopulmonary bypass following circulatory arrest in newborn piglets. *Eur J Cardiothorac Surg* 2007;31:899–905.
272. Hoffman GM, Ghanayem NS. Perioperative neuromonitoring in pediatric cardiac surgery: techniques and targets. *Prog Pediatr Cardiol* 2010;29:123–130.
273. Hoffman TM, Wernovsky G, Atz AM, et al. Efficacy and safety of milrinone in preventing low cardiac output syndrome in infants and children after corrective surgery for congenital heart disease. *Circulation* 2003;107:996–1002.
274. Gordon JB, Rehorst-Paea LA, Hoffman GM, et al. Pulmonary vascular responses during acute and sustained respiratory alkalosis or acidosis in intact newborn piglets. *Pediatr Res* 1999;46:735–741.
275. Reynolds AM, Zadow SP, Scicchitano R, et al. Airway hypoxemia increases microvascular leakage in the guinea pig trachea. *Am Rev Respir Dis* 1992;145:80–84.
276. Laffey JG, Engelberts D, Duggan M, et al. Carbon dioxide attenuates pulmonary impairment resulting from hyperventilation. *Crit Care Med* 2003;31:2634–2640.
277. Gaynor JW. Use of modified ultrafiltration after repair of congenital heart defects. *Semin Thorac Cardiovasc Surg Pediatr Card Surg Annu* 1998;1:81–90.
278. Hoffman GM, Ghanayem NS, Tweddell JS. Noninvasive assessment of cardiac output. *Semin Thorac Cardiovasc Surg Pediatr Card Surg Annu* 2005:12–21.
279. Levy WJ, Levin S, Chance B. Near-infrared measurement of cerebral oxygenation. Correlation with electroencephalographic ischemia during ventricular fibrillation. *Anesthesiology* 1995;83:738–746.
280. Kurth CD, Levy WJ, McCann J. Near-infrared spectroscopy cerebral oxygen saturation thresholds for hypoxia-ischemia in piglets. *J Cereb Blood Flow Metab* 2002;22:335–341.
281. Tweddell JS. Extracorporeal membrane oxygenation for pediatric cardiac failure: limitations and future directions. *Crit Care Med* 2004;32:1091–1092.
282. Tibby S, Hoffman GM. Resuscitation of the patient with single ventricle. Peds-059b. Worksheet for Evidence-Based Review of Science for Emergency Cardiac Care. International Liaison Committee on Resuscitation. 2010.
283. Kleinman ME, de Caen AR, Chameides L, et al. Part 10: Pediatric basic and advanced life support. *Circulation* 2010;122:S466–S515.
284. Jagers JJ, Forbess JM, Shah AS, et al. Extracorporeal membrane oxygenation for infant postcardiotomy support: significance of shunt management. *Ann Thorac Surg* 2000;69:1476–1483.
285. Ungerleider RM, Shen I, Yeh T, et al. Routine mechanical ventricular assist following the Norwood procedure-improved neurologic outcome and excellent hospital survival. *Ann Thorac Surg* 2004;77:18–22.

286. Austin EH. Postoperative management after the Norwood procedure. *Semin Thorac Cardiovasc Surg Pediatr Card Surg Annu* 1998;1:109-122.
287. Tweddell JS, Hoffman GM, Fedderly RT, et al. Patients at risk for low systemic oxygen delivery after the Norwood procedure. *Ann Thorac Surg* 2000;69:1893-1899.
288. Charpie JR, Dekeon MK, Goldberg CS, et al. Postoperative hemodynamics after Norwood palliation for hypoplastic left heart syndrome. *Am J Cardiol* 2001;87:198-202.
289. Tweddell JS, Hoffman GM, Ghanayem NS, et al. Evaluation of strategies to improve systemic oxygen delivery following stage 1 palliation for hypoplastic left heart syndrome. *Circulation* 2005;112:U423.
290. Hoffman GM, Mussatto KA, Brosig CL, et al. Systemic venous oxygen saturation after the Norwood procedure and childhood neurodevelopmental outcome. *J Thorac Cardiovasc Surg* 2005;130:1094-1100.
291. Hoffman GM, Ghanayem NS, Mussatto KA, et al. Perioperative Perfusion assessed by Somatic NIRS predicts postoperative renal dysfunction. Paper presented at the ASA annual meeting, 2005.
292. Tweddell JS, Ghanayem NS, Mussatto KA, et al. Mixed venous oxygen saturation monitoring after stage 1 palliation for hypoplastic left heart syndrome. *Ann Thorac Surg* [Internet] 2007;84:1301-1310.
293. Tabbutt S, Duncan BW, McLaughlin D, et al. Delayed sternal closure after cardiac operations in a pediatric population. *J Thorac Cardiovasc Surg* 1997;113:886-893.
294. Azakie A, Merklinger SL, McCrindle BW, et al. Evolving strategies and improving outcomes of the modified Norwood procedure: a 10-year single-institution experience. *Ann Thorac Surg* 2001;72:1349-1353.
295. Simsic JM, Bradley SM, Stroud MR, et al. Risk factors for interstage death after the Norwood procedure. *Pediatr Cardiol* 2005;26:400-403.
296. Hehir DA, Dominguez TE, Ballweg JA, et al. Risk factors for interstage death after stage 1 reconstruction of hypoplastic left heart syndrome and variants. *J Thorac Cardiovasc Surg* [Internet] 2008;136:94. Available from: <https://login.proxy.lib.mcu.edu/login?url=http://ovidsp.ovid.com/ovidweb.cgi?T=JS&CSC=Y&NEWS=N&PAGE=fulltext&D=medl&AN=18603060>
297. Jonas RA, Hansen DD, Cook N, et al. Anatomic subtype and survival after reconstructive operation for hypoplastic left heart syndrome. *J Thorac Cardiovasc Surg* 1994;107:1121-1128.
298. Leite HP, Fisberg M, de Carvalho WB, et al. Serum albumin and clinical outcome in pediatric cardiac surgery. *Nutrition* 2005;21:553-558.
299. Anderson JB, Beekman RH III, Border WL, et al. Lower weight-for-age z score adversely affects hospital length of stay after the bidirectional Glenn procedure in 100 infants with a single ventricle. *J Thorac Cardiovasc Surg* [Internet] 2009;138:397-404. Available from: <https://login.proxy.lib.mcu.edu/login?url=http://ovidsp.ovid.com/ovidweb.cgi?T=JS&CSC=Y&NEWS=N&PAGE=fulltext&D=medl&AN=19619784>
300. Kelleher DK, Laussen P, Teixeira-Pinto A, et al. Growth and correlates of nutritional status among infants with hypoplastic left heart syndrome (HLHS) after stage 1 Norwood procedure. *Nutrition* 2006;22:237-244.
301. Vogt KN, Manliot C, Van Arsdell G, et al. Somatic growth in children with single ventricle physiology impact of physiologic state. *J Am Coll Cardiol* [Internet] 2007;50:1876-1883. Available from: <https://login.proxy.lib.mcu.edu/login?url=http://ovidsp.ovid.com/ovidweb.cgi?T=JS&CSC=Y&NEWS=N&PAGE=fulltext&D=medl&AN=17980255>
302. Norwood WI, Jacobs ML. Fontan's procedure in two stages. *Am J Surg* 1993;166:548-551.
303. Stuth EAE, Berens RJ, Staudt SR, et al. The effect of caudal vs intravenous morphine on early extubation and postoperative analgesic requirements for stage 2 and 3 single-ventricle palliation: a double blind randomized trial. *Pediatr Anaesth* 2011;21:441-453.
304. Chang AC, Hanley FL, Wernovsky G, et al. Early bidirectional cavopulmonary shunt in young infants. Postoperative course and early results. *Circulation* 1993;88:149-158.
305. Reddy VM, McElhinney DB, Moore P, et al. Outcomes after bidirectional cavopulmonary shunt in infants less than 6 months old. *J Am Coll Cardiol* 1997;29:1365-1370.
306. Bradley SM, Mosca RS, Hennein HA, et al. Bidirectional superior cavopulmonary connection in young infants. *Circulation* 1996;94:5-11.
307. Jaquiss RD, Ghanayem NS, Hoffman GM, et al. Early cavopulmonary anastomosis in very young infants after the Norwood procedure: impact on oxygenation, resource utilization, and mortality. *J Thorac Cardiovasc Surg* 2004;127:982-989.
308. Jaquiss RD, Siehr SL, Ghanayem NS, et al. Early cavopulmonary anastomosis after Norwood procedure results in excellent Fontan outcome. *Ann Thorac Surg* [Internet] 2006;82:1260-1265.
309. Knight WB, Mee RB. A cure for pulmonary arteriovenous fistulas? *Ann Thorac Surg* 1995;59:999-1001.
310. Bove EL, deLeval MR, Migliavacca F, et al. Computational fluid dynamics in the evaluation of hemodynamic performance of cavopulmonary connections after the Norwood procedure for hypoplastic left heart syndrome. *J Thorac Cardiovasc Surg* 2003;126:1040-1047.
311. Nurnberg J, Ovroutski S, Alexi-Meskishvili V, et al. New onset arrhythmias after the extracardiac conduit fontan operation compared with the intraatrial lateral tunnel procedure: early and midterm results. *Ann Thorac Surg* 2004;78:1979-1988.
312. Azakie A, McCrindle BW, VanArsdell G, et al. Extracardiac conduit versus lateral tunnel cavopulmonary connections at a single institution: impact on outcomes. *J Thorac Cardiovasc Surg* 2001;122:1219-1228.
313. Bae E, Lee J, Noh C, et al. Sinus node dysfunction after Fontan modifications-influence of surgical method. *Int J Cardiol* 2003;88:285-291.
314. Cohen MI, Bridges ND, Gaynor JW, et al. Modifications to the cavopulmonary anastomosis do not eliminate early sinus node dysfunction. *J Thorac Cardiovasc Surg* 2000;120:891-900.
315. Kumar SP, Rubinstein CS, Simsic JM, et al. Lateral tunnel versus extracardiac conduit Fontan procedure: a concurrent comparison. *Ann Thorac Surg* 2003;76:1389-1396.
316. Cava J, Bevanic S, Steltzer M, et al. A medical strategy to reduce persistent chest tube drainage after the Fontan operation. *Am J Cardiol* 2005;96:130-133.
317. Brown JW, Ruzmetov M, Rodefeld MD, et al. Staged reconstruction for hypoplastic left heart syndrome: a single institution experience [abstract]. *J Surg Res* 2003;114:278.
318. Jacobs ML, Blackstone EH, Bailey LL. Intermediate survival in neonates with aortic atresia: a multi-institutional study. The congenital heart surgeons society. *J Thorac Cardiovasc Surg* 1998;116:417-431.
319. Gaynor JW, Mahle WT, Cohen MI, et al. Risk factors for mortality after the Norwood procedure. *Eur J Cardiothorac Surg* 2002;22:82-89.
320. Ruiz CE, Gamra H, Zhang HP, Garcia et al. Brief report: stenting of the ductus arteriosus as a bridge to cardiac transplantation in infants with the hypoplastic left-heart syndrome. *N Engl J Med* 1993;328:1605-1608.
321. Gewillig M, Boshoff DE, Dens J, et al. Stenting the neonatal arterial duct in duct-dependent pulmonary circulation: new techniques, better results. *J Am Coll Cardiol* 2004;43:107-112.
322. Prakash A, Khan MA, Hardy R, et al. A new diagnostic algorithm for assessment of patients with single ventricle before a Fontan operation. *J Thorac Cardiovasc Surg* [Internet] 2009;138:917-923.
323. Galantowicz M, Cheatham JP. Fontan completion without surgery. *Semin Thorac Cardiovasc Surg Pediatr Card Surg Annu* 2004;7:48-55.
324. Hennein HA. The Fontan operation for hypoplastic left heart syndrome In: Hennein HA, Bove EL, eds. *Hypoplastic Left Heart Syndrome*. Armonk, NY: Futura, 2002:155-178.
325. Mair DD, Puga FJ, Danielson GK. The Fontan procedure for tricuspid atresia: early and late results of a 25-year experience with 216 patients. *J Am Coll Cardiol* 2001;37:933-939.
326. Burkhardt H, Dearani J, Mair D, et al. The modified Fontan procedure: early and late results in 132 adult patients. *J Thorac Cardiovasc Surg* 2003;125:1252-1258.
327. Farrell PE Jr, Chang AC, Murdison KA, et al. Outcome and assessment after the modified Fontan procedure for hypoplastic left heart syndrome. *Circulation* 1992;85:116-122.
328. Driscoll D, Offord K, Feldt R, et al. Five- to fifteen-year follow-up after Fontan operation. *Circulation* 1992;85:469-496.
329. Mahle WT, Coon PD, Wernovsky G, et al. Quantitative echocardiographic assessment of the performance of the functionally single right ventricle after the Fontan operation. *Cardiol Young* 2001;11:399-406.
330. Cheung YF, Penny DJ, Redington AN. Serial assessment of left ventricular diastolic function after Fontan procedure. *Heart* 2000;83:420-424.
331. Marino BS. Outcomes after the Fontan procedure. *Curr Opin Pediatr* 2002;14:620-626.
332. Senzaki H, Masutani S, Kobayashi J, et al. Ventricular afterload and ventricular work in Fontan circulation: comparison with normal two-ventricle circulation and single-ventricle circulation with Blalock-Taussig shunts. *Circulation* 2002;105:2885-2892.
333. Border W, Syed A, Michelfelder E, et al. Impaired systemic ventricular relaxation affects postoperative short-term outcome in Fontan patients. *J Thorac Cardiovasc Surg* 2003;126:1760-1764.
334. Mair DD, Puga FJ, Danielson GK. Late functional status of survivors of the Fontan procedure performed during the 1970s. *Circulation* 1992;86:106-109.
335. Gentles T, Gauvreau K, Mayer J, et al. Functional outcome after the Fontan operation: Factors influencing late morbidity. *J Thorac Cardiovasc Surg* 1997;114:392-403.
336. Fredriksen PM, Therrien J, Veldtman G, et al. Lung function and aerobic capacity in adult patients following modified Fontan procedure. *Heart* 2001;85:295-299.
337. Triedman JK, Bridges ND, Mayer JE Jr, et al. Prevalence and risk factors for aortopulmonary collateral vessels after Fontan and bidirectional Glenn procedures. *J Am Coll Cardiol* 1993;22:207-215.
338. deLeval MR. The Fontan circulation: What have we learned? What to expect? *Pediatr Cardiol* 1998;19:316-320.
339. Feldt RH, Driscoll DJ, Offord KP, et al. Protein-losing enteropathy after the Fontan operation. *J Thorac Cardiovasc Surg* 1996;112:672-680.
340. Powell AJ, Gauvreau K, Jenkins KJ, et al. Perioperative risk factors for development of protein-losing enteropathy following a Fontan procedure. *Am J Cardiol* 2001;88:1206-1209.
341. Rychik J, Spray TL. Strategies to treat protein-losing enteropathy. *Semin Thorac Cardiovasc Surg Pediatr Card Surg Annu* 2002;5:3-11.
342. Mertens L, Hagler DJ, Sauer U, et al. Protein-losing enteropathy after the Fontan operation: an international multicenter study. PLE study group. *J Thorac Cardiovasc Surg* 1998;115:1063-1073.
343. Lenz D, Hamsch J, Schneider P, et al. Protein-losing enteropathy in patients with Fontan circulation: is it triggered by infection? *Crit Care* 2003;7:185-190.

344. Sorensen GK, Ramamoorthy C, Lynn AM, et al. Hemodynamic effects of amrinone in children after Fontan surgery. *Anesth Analg* 1996;82:241-246.
345. Therrien J, Webb GD, Gatzoulis MA. Reversal of protein losing enteropathy with prednisone in adults with modified Fontan operations: long term palliation or bridge to cardiac transplantation? *Heart* 1999;82:241-243.
346. Zellers TM, Brown K. Protein-losing enteropathy after the modified Fontan operation: oral prednisone treatment with biopsy and laboratory proved improvement. *Pediatr Cardiol* 1996;17:115-117.
347. Thacker D, Patel A, Dodds K, et al. Use of oral budesonide in the management of protein-losing enteropathy after the Fontan operation. *Ann Thorac Surg* [Internet] 2010;89:837-842.
348. Bernstein D, Naftel D, Chin C, et al.; Pediatric Heart Transplant Study. Outcome of listing for cardiac transplantation for failed Fontan: a multi-institutional study. *Circulation* [Internet] 2006;114:273-280.
349. Coon PD, Rychik J, Novello RT, et al. Thrombus formation after the Fontan operation. *Ann Thorac Surg* 2001;71:1990-1994.
350. Monagle P, Karl TR. Thromboembolic problems after the Fontan operation. *Semin Thorac Cardiovasc Surg Pediatr Card Surg Annu* 2002;5:36-47.
351. Rosenthal DN, Friedman AH, Kleinman CS, et al. Thromboembolic complications after Fontan operations. *Circulation* 1995;92:287-293.
352. Day RW, Boyer RS, Tait VF, et al. Factors associated with stroke following the Fontan procedure. *Pediatr Cardiol* 1995;16:270-275.
353. Cromme-Dijkhuis AH, Hess J, Hahlen K, et al. Specific sequelae after Fontan operation at mid- and long-term follow-up: arrhythmia, liver dysfunction, and coagulation disorders. *J Thorac Cardiovasc Surg* 1993;106:1126-1132.
354. Jahangiri M, Shore D, Kakkar V, et al. Coagulation factor abnormalities after the Fontan procedure and its modifications. *J Thorac Cardiovasc Surg* 1997;113:989-993.
355. Deal BJ, Mavroudis C, Backer CL, et al. Diagnosis and management of late atrial arrhythmias following Fontan surgery. In: Hennein HA, Bove EL, eds. *Hypoplastic Left Heart Syndrome*. Armonk, NY: Futura Publishing, 2002:253-263.
356. Amodeo A, Galletti L, Marianeschi S, et al. Extracardiac Fontan operation for complex cardiac anomalies: seven years' experience. *J Thorac Cardiovasc Surg* 1997;114:1020-1030.
357. Ovroutsaki S, Dahnert I, Alexi-Meskishvili V, et al. Preliminary analysis of arrhythmias after the Fontan operation with extracardiac conduit compared with intra-atrial lateral tunnel. *Thorac Cardiovasc Surg* 2001;49:334-337.
358. Canter CE, Moorehead S, Huddleston CB, et al. Restrictive atrial septal communication as a determinant of outcome of cardiac transplantation for hypoplastic left heart syndrome. *Circulation* 1993;88:456-460.
359. Turrentine MW, Kesler KA, Caldwell R, et al. Cardiac transplantation in infants and children. *Ann Thorac Surg* 1994;57:546-553.
360. Bailey LL, Gundry SR, Razzouk AJ, et al. Bless the babies: one hundred fifteen late survivors of heart transplantation during the first year of life. *J Thorac Cardiovasc Surg* 1993;105:805-814.
361. Backer CL, Zales VR, Harrison HL, et al. Intermediate term results of infant orthotopic cardiac transplantation from two centers. *J Thorac Cardiovasc Surg* 1991;101:826-832.
362. Merrill WH, Frist WH, Stewart JR, et al. Heart transplantation in children. *Ann Surg* 1991;213:393-398.
363. Hehrlein FW, Netz H, Moosdorf R, et al. Pediatric heart transplantation for congenital heart disease and cardiomyopathy. *Ann Thorac Surg* 1991;52:112-117.
364. Pennington DG, Noedel N, McBride LR, et al. Heart transplantation in children: an international survey. *Ann Thorac Surg* 1991;52:710-715.
365. Backer CL, Idriss FS, Zales VR, et al. Cardiac transplantation for hypoplastic left heart syndrome: a modified technique. *Ann Thorac Surg* 1990;50:894-898.
366. Zuberbuhler JR, Fricker FJ, Griffith BP. Cardiac transplantation in children. *Cardiol Clin* 1989;7:411-418.
367. Mavroudis C, Harrison H, Klein JB, et al. Infant orthotopic cardiac transplantation. *J Thorac Cardiovasc Surg* 1988;96:912-924.
368. Razzouk AJ, Chinnock RE, Gundry SR, et al. Transplantation as a primary treatment for hypoplastic left heart syndrome: intermediate-term results. *Ann Thorac Surg* 1996;62:1-7.
369. Stuart AG, Wren C, Sharples PM, et al. Hypoplastic left heart syndrome: more potential transplant recipients than suitable donors. *Lancet* 1991;337:957-959.
370. Ikle L, Hale K, Fashaw L, et al. Developmental outcome of patients with hypoplastic left heart syndrome treated with heart transplantation. *J Pediatr* 2003;142:20-25.
371. West LJ, Pollock-Barziv SM, Dipchand AI, et al. ABO-incompatible heart transplantation in infants. *N Engl J Med* 2001;344:793-800.
372. West LJ, Pollock-Barziv SM, Lee KJ, et al. Graft accommodation in infant recipients of ABO-incompatible heart transplants: donor ABH antigen expression in graft biopsies. *J Heart Lung Transplant* 2001;20:222.
373. Zangwill S, Ellis T, Stendahl G, et al. Practical application of the virtual crossmatch. *Pediatr Transplant* 2007;11:650-654.
374. Zangwill SD, Ellis TM, Zlotocha J, et al. The virtual crossmatch? A screening tool for sensitized pediatric heart transplant recipients. *Pediatr Transplant* 2006;10:38-41.
375. Gamba A, Merlo M, Fiocchi R, et al. Heart transplantation in patients with previous Fontan operations. *J Thorac Cardiovasc Surg* 2004;127:555-562.
376. Michielon G, Parisi F, DiCarlo D, et al. Orthotopic heart transplantation for failing single ventricle physiology. *Eur J Cardiothorac Surg* 2003;24:502-510.
377. Wernovsky G. Current insights regarding neurological and developmental abnormalities in children and young adults with complex congenital cardiac disease. *Cardiol Young* 2006;16:92-104.
378. Licht DJ, Shera DM, Clancy RR, et al. Brain maturation is delayed in infants with complex congenital heart defects. *J Thorac Cardiovasc Surg* 2009;137:529-536.
379. Andropoulos DB, Hunter JV, Nelson DP, et al. Brain immaturity is associated with brain injury before and after neonatal cardiac surgery with high-flow bypass and cerebral oxygenation monitoring. *J Thorac Cardiovasc Surg* 2010;139:543-556.
380. Limperopoulos C, Tworetzky W, McElhinney DB, et al. Brain volume and metabolism in fetuses with congenital heart disease: evaluation with quantitative magnetic resonance imaging and spectroscopy. *Circulation* 2010;121:26-33.
381. Shillingford AJ, Ittenbach RF, Marino BS, et al. Aortic morphometry and microcephaly in hypoplastic left heart syndrome. *Cardiol Young* 2007;17:189-195.
382. Tabbutt S, Nord AS, Jarvik GP, et al. Neurodevelopmental outcomes after staged palliation for hypoplastic left heart syndrome. *Pediatrics* 2008;121:476-483.
383. Gaynor JW, Gerdes M, Zackai EH, et al. Apolipoprotein E genotype and neurodevelopmental sequelae of infant cardiac surgery. *J Thorac Cardiovasc Surg* 2003;126:1736-1745.
384. Gaynor JW, Wernovsky G, Jarvik GP, et al. Patient characteristics are important determinants of neurodevelopmental outcome at one year of age after neonatal and infant cardiac surgery. *J Thorac Cardiovasc Surg* 2007;133:1344-1353.
385. Mahle WT, Clancy RR, McGaurn SP, et al. Impact of prenatal diagnosis on survival and early neurologic morbidity in neonates with the hypoplastic left heart syndrome. *Pediatrics* 2001;107:1277-1282.
386. Wernovsky G, Stiles KM, Gauvreau K, et al. Cognitive development after the fontan operation. *Circulation* 2000;102:883-889.
387. Goldberg CS, Schwartz EM, Brunberg JA, et al. Neurodevelopmental outcome of patients after the Fontan operation: a comparison between children with hypoplastic left heart syndrome and other functional single ventricle lesions [see comment]. *J Pediatr* 2000;137:646-652.
388. Hoffman GM, Mussatto KA, Brosig CL, et al. Cerebral oxygenation and neurodevelopmental outcome in hypoplastic left heart syndrome. *Anesthesiology* 2008;109:A7.
389. Bradley SM, Simsic JM, Atz AM. Hemodynamic effects of inspired carbon dioxide after the Norwood procedure. *Ann Thorac Surg* 2001;72:2088-2093.
390. Bradley SM, Atz AM. Postoperative management: the role of mixed venous oxygen saturation monitoring. *Semin Thorac Cardiovasc Surg Pediatr Card Surg Annu* 2005:22-27.
391. Mahle WT, Wernovsky G. Neurodevelopmental outcomes in hypoplastic left heart syndrome. *Semin Thorac Cardiovasc Surg Pediatr Card Surg Annu* 2004;7:39-47.
392. Gaynor JW, Jarvik GP, Bernbaum J, et al. The relationship of postoperative electrographic seizures to neurodevelopmental outcome at 1 year of age after neonatal and infant cardiac surgery. *J Thorac Cardiovasc Surg* 2006;131:181-189.
393. Jonas RA, Wypij D, Roth SJ, et al. The influence of hemodilution on outcome after hypothermic cardiopulmonary bypass: results of a randomized trial in infants. *J Thorac Cardiovasc Surg* 2003;126:1765-1774.
394. Ohye RG, Goldberg CS, Donohue J, et al. The quest to optimize neurodevelopmental outcomes in neonatal arch reconstruction: the perfusion techniques we use and why we believe in them. *J Thorac Cardiovasc Surg* 2009;137:803-806.
395. Rogers BT, Msall ME, Buck GM, et al. Neurodevelopmental outcome of infants with hypoplastic left heart syndrome. *J Pediatr* 1995;126:496-498.
396. Kern JH, Hinton VJ, Nereo NE, et al. Early developmental outcome after the Norwood procedure for hypoplastic left heart syndrome. *Pediatrics* 1998;102:1148-1152.
397. Mahle WT, Clancy RR, Moss EM, et al. Neurodevelopmental outcome and lifestyle assessment in school-aged and adolescent children with hypoplastic left heart syndrome. *Pediatrics* 2000;105:1082-1089.
398. McCrindle BW, Williams RV, Mitchell PD, et al. Pediatric Heart Network Investigators. Relationship of patient and medical characteristics to health status in children and adolescents after the Fontan procedure. *Circulation* 2006;113:1123-1129.
399. Brosig CL, Mussatto KA, Kuhn EM, et al. Neurodevelopmental outcome in preschool survivors of complex congenital heart disease: Implications for clinical practice. *J Pediatr Health Care* 2007;21:3-12.
400. Brosig CL, Mussatto KA, Kuhn EM, et al. Psychosocial outcomes for preschool children and families after surgery for complex congenital heart disease. *Pediatr Cardiol* 2007;28:255-262.
401. Mahle WT, Visconti KJ, Freier MC, et al. Relationship of surgical approach to neurodevelopmental outcomes in hypoplastic left heart syndrome. *Pediatrics* 2006;117:e90-e97.

402. Soto CB, Olude O, Hoffmann RG, et al. Implementation of a routine developmental follow-up program for children with congenital heart disease: early results. *Congenit Heart Dis* 2011;6:451-460.
403. Wernovsky G, Newburger J. Neurologic and developmental morbidity in children with complex congenital heart disease [see comment]. *J Pediatr* 2003;142:6-8.
404. Bellinger DC, Wypij D, duPlessis AJ, et al. Developmental and neurologic effects of alpha-stat versus pH-stat strategies for deep hypothermic cardiopulmonary bypass in infants. *J Thorac Cardiovasc Surg* 2001;121:374-383.
405. Fuller S, Rajagopalan R, Jarvik GP, et al. Maxwell Chamberlain memorial paper for congenital heart surgery. Deep hypothermic circulatory arrest does not impair neurodevelopmental outcome in school-age children after infant cardiac surgery. *Ann Thorac Surg* 2010;90:1985-1994.
406. Gaynor JW, Gerdes M, Nord AS, et al. Is cardiac diagnosis a predictor of neurodevelopmental outcome after cardiac surgery in infancy? *J Thorac Cardiovasc Surg* 2010;140:1230-1237.
407. Prsa M, Holly CD, Carnevale FA, et al. Attitudes and practices of cardiologists and surgeons who manage HLHS. *Pediatrics* 2010;125:e625-e630.
408. Kon AA, Ackerson L, Lo B. Choices physicians would make if they were the parents of a child with hypoplastic left heart syndrome. *Am J Cardiol* 2003;91:1506-1509.
409. Kon AA. Healthcare providers must offer palliative treatment to parents of neonates with hypoplastic left heart syndrome. *Arch Pediatr Adolesc Med* 2008;162:844-848.
410. Wernovsky G. The paradigm shift toward surgical intervention for neonates with hypoplastic left heart syndrome. *Arch Pediatr Adolesc Med* 2008;162:849-854.
411. Bredow T. Health-related quality of life. In: *Middle Range Theories: Application to Nursing Research*. Philadelphia, PA: Lippincott Williams & Wilkins, 2004:274-287.
412. Drotar D. Health status and quality of life. In: Naar-King S, Ellis DA, Frey MA, eds. *Assessing Children's Well-being: A Handbook of Measures*. Mahwah, NJ: Lawrence Erlbaum Associates, 2004:1-4.
413. Elliott MJ. A European perspective on the management of hypoplastic left heart syndrome. *Cardiol Young* 2004;14:41-46.
414. Uzark K, Jones K, Slusher J, et al. Quality of life in children with heart disease as perceived by children and parents. *Pediatrics* [Internet] 2008;121:e1060-e1067. Available from: <https://login.proxy.lib.mcw.edu/login?url=http://ovidsp.ovid.com/ovidweb.cgi?T=JS&CSC=Y&NEWS=N&PAGE=fulltext&D=medl&AN=18450848>
415. Varni JW, Seid M, Rode CA. The PedsQL: measurement model for the pediatric quality of life inventory. *Med Care* 1999;37:126-139.
416. Rose M, Kohler K, Kohler F, et al. Determinants of the quality of life of patients with congenital heart disease. *Qual Life Res* 2005;14:35-43.
417. Moons P, VanDeyk K, DeGeest S, et al. Is the severity of congenital heart disease associated with the quality of life and perceived health of adult patients? *Heart* 2005;91:1193-1198.
418. Casey FA, Craig BG, Mulholland HC. Quality of life in surgically palliated complex congenital heart disease. *Arch Dis Child* [Internet] 1994;70:382-386. Available from: <https://login.proxy.lib.mcw.edu/login?url=http://ovidsp.ovid.com/ovidweb.cgi?T=JS&CSC=Y&NEWS=N&PAGE=fulltext&D=med3&AN=7517133>
419. Casey FA, Sykes DH, Craig BG, et al. Behavioral adjustment of children with surgically palliated complex congenital heart disease. *J Pediatr Psychol* 1996;21:335-352.
420. Saliba Z, Butera G, Bonnet D, et al. Quality of life and perceived health status in surviving adults with univentricular heart [see comment]. *Heart* 2001;86:69-73.
421. Williams DL, Gelijns AC, Moskowitz AJ, et al. Hypoplastic left heart syndrome: valuing the survival. *J Thorac Cardiovasc Surg* 2000;119:720-731.
422. Mellander M, Berntsson L, Nilsson B. Quality of life in children with hypoplastic left heart syndrome. *Acta Paediatr* 2007;96:53-57.
423. McCrindle BW, Williams RV, Mital S, et al. Physical activity levels in children and adolescents are reduced after the Fontan procedure, independent of exercise capacity, and are associated with lower perceived general health. *Arch Dis Child* 2007;92:509-514.
424. Lambert LM, Minich LL, Newburger JW, et al. Pediatric Heart Network I. Parent- versus child-reported functional health status after the Fontan procedure. *Pediatrics* 2009;124:e942-e949.
425. As Newborn Heart Surgery Improves, Survivors Thrive: NPR [Internet]. [Cited 5/26/2011].

Gil Wernovsky

Transposition of the great arteries (TGA) is a lethal and relatively frequent malformation, accounting for 5% to 7% of all congenital cardiac malformations. Without treatment, about 30% of these infants die in the first week of life, 50% within the first month, 70% within 6 months, and 90% within the first year (Fig. 49.1). Today, aggressive medical and surgical interventions in the neonate can provide >90% early and midterm survival and, for many patients, the prospect of a vigorous adolescent and adult life.

The incidence is reported to range from 20.1 to 30.5/100,000 live births with a strong (60% to 70%) male preponderance. Although earlier epidemiologic and genetic surveys suggested some other associations, for example, increased prevalence in infants of diabetic mothers or prenatal exposure to sex-hormone therapy, these have not been confirmed. Extracardiac anomalies are less frequent in infants with TGA (<10%) compared with other forms of congenital heart disease, such as truncus arteriosus (48%), ventricular septal defect (VSD) (34%), or tetralogy of Fallot (31%).

ANATOMY AND PATHOLOGY

Nomenclature

Anatomists, surgeons, and cardiologists have chosen a variety of terms to describe the basic anatomic abnormality in transposition: the aorta arising from a morphologically right ventricle and the pulmonary artery arising from a morphologically left ventricle (Fig. 49.2). The great arteries may be related normally or abnormally to each other, to the ventricles, to the ventricular septum, and to the atrioventricular (AV) valves. Normally and abnormally related great arteries customarily are designated in terms of their ventriculoarterial connections or alignments, that is, normal, transposed, double-outlet right or left ventricle, and anatomically corrected malposition.

The common clinical type, that is, with situs solitus of the atria, concordant AV (right atrium to right ventricle and left atrium to left ventricle), and discordant ventriculoarterial alignments, is widely termed complete TGA. The modifying term complete by present classification and nomenclature is redundant; however, it has, by common usage, come to indicate that the transposed great arteries are physiologically uncorrected, that is, that systemic venous blood flows predominantly to the aorta and pulmonary venous blood to the pulmonary artery. In this usage, the term complete is contrasted to the term corrected, as in corrected TGA (i.e., physiologically corrected), in

which systemic venous blood flows to the pulmonary artery and pulmonary venous blood to the aorta. It should be recognized, however, that both the physiologically uncorrected and physiologically corrected transposition hearts are morphologically complete transpositions; that is, both great arteries are completely (or predominantly) misplaced across the ventricular septum and arise from morphologically inappropriate ventricles and thus have discordant ventriculoarterial connections.

Using the segmental (atria, ventricles, arteries) approach and the situs-independent dextro-(D) and levo-(L) denotations favored by Van Praagh, the clinical material in this chapter concerns almost exclusively TGA {S,D,D}, that is, TGA with situs solitus (S) of the atria and viscera, usual (D) looping of the ventricles, and an anterior and rightward (D) aorta. If the transposed aorta at the valve annulus level is positioned to the left of the transposed pulmonary artery, the malformation may be denoted as TGA {S,D,L}. A rare type of transposition has been described with the aorta posteriorly positioned but nevertheless aligned with and connected to the anterior morphologically right ventricle. An additional modifying term, simple, has been used by some morphologists to exclude hearts with transposition that have additional associated malformations such as AV valve atresia or straddling, common AV orifice, or single-ventricle hearts with small outlet chambers. This chapter is concerned primarily with the category of simple transposition and includes TGA with intact ventricular septum (IVS), VSD, patent ductus arteriosus (PDA), and left ventricular outflow tract obstruction (LVOTO), in all, a group comprising about 80% of patients with TGA. In addition, double-outlet right ventricle (DORV) with subpulmonary VSD (considered within the spectrum of Taussig-Bing anomaly) is also discussed here because it has some of the morphologic features, similar physiology, and all the surgical options that pertain to TGA with large subpulmonary VSD. It is important to note that many surgical and clinical reports use this same term, simple TGA, to designate the large important subgroup of TGA patients with IVS (or extremely small VSD) but without any other significant associated lesion (thus excluding TGA with large VSD, large PDA, and significant LVOTO).

Morphogenesis and Etiology

The detailed developmental aspects of abnormal ventriculoarterial relationships remain largely unknown; however, abnormal development, growth, and absorption of the distal infundibulum (conus) are considered by some major factors. Recent work with more modern genome-wide array testing

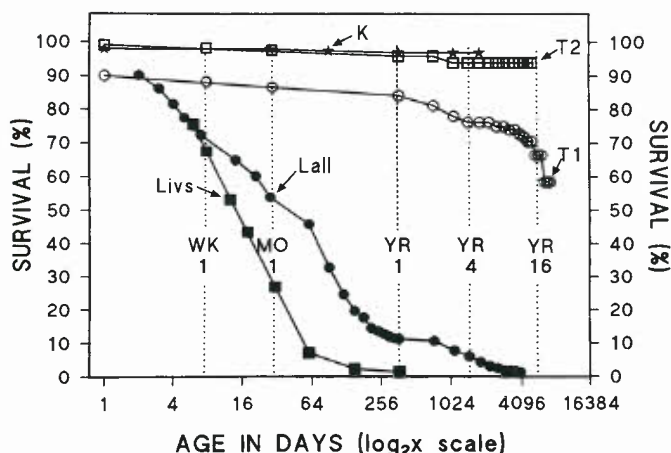


Figure 49.1. Survival of patients with TGA. Lall and Livs represent “natural history” survival data on 742 patients from 1957 through 1964 antedating both Mustard repair and BAS. (Data from Liebman J, Cullum L, Belloc NB. Natural history of transposition of the great arteries: anatomy and birth and death characteristics. *Circulation* 1969;40:237–262.) Lall represents all TGA subtypes, and Livs represents only patients with TGA/IVS. T1 represents 20-year actuarial survival of 106 infants with TGA/IVS following Mustard repair performed from 1963 through 1973; T2 represents 12-year actuarial survival of 223 children following Mustard repair performed from 1974 through 1985. (Data from Trusler GA, Castaneda AR, Rosenthal A, et al.; Congenital Heart Surgeons Society. Current results of management in transposition of the great arteries, with special emphasis on patients with associated ventricular septal defect. *J Am Coll Cardiol* 1987;10:1061–1071.) K represents risk-adjusted probability of survival after an arterial switch repair in a neonate with TGA/IVS or TGA/VSD as observed in a study conducted by the Congenital Heart Surgeons Society from 1985 through 1989 on 513 patients undergoing the arterial switch operation. (Data from Kirklin JW, Blackstone EH, Tchervenkov CI, et al.; Congenital Heart Surgeons Society. Clinical outcomes after the arterial switch operation for transposition: patient, support, procedural and institutional risk factors. *Circulation* 1992;86:1501–1515.) Risk-adjustment conditions included neonate operated on in an institution of proven competence (“low-risk” institutions, $n = 7$), “usual” TGA coronary artery pattern, single VSD, absence of coexisting noncardiac anomalies, and average birth weight.

shows early promise in detecting a genetic etiology in some, particularly mutations in the laterality genes in the spectrum of heterotaxy syndrome (1).

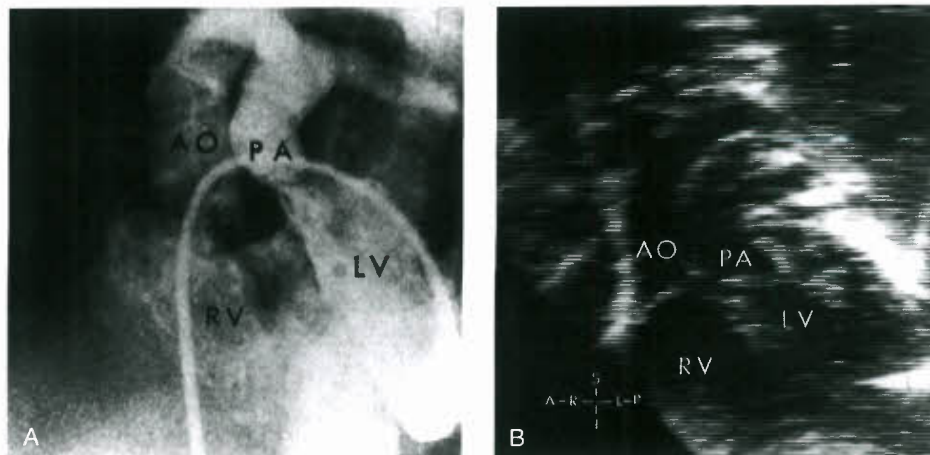
The normal conus is subpulmonary, left sided, and anterior, and it prevents fibrous continuity between the pulmonary and tricuspid valve rings. In TGA, the infundibulum is usually subaortic, right sided, and anterior, and it prevents fibrous continuity between the aortic and tricuspid valve rings (Fig. 49.3B). It has been noted in human embryos that normal movement of the pulmonary valve proceeds from posterior to anterior on the left side in the interval between 30 and 34 days of age and is related to normal development of the subpulmonary infundibulum. During this same interval, the aortic valve remains stationary, apparently because of the normal lack of development (or absorption) of the subaortic infundibulum. The morphogenesis of TGA can be hypothesized to result from the abnormal growth and development of the subaortic infundibulum and the absence of growth of the subpulmonary infundibulum. The aortic valve is protruded superiorly and anteriorly by the development of the subaortic infundibulum, placing it above the anterior right ventricle (Fig. 49.3). Failure of development of the subpulmonary infundibulum prevents the normal morphogenetic movement of the pulmonary valve from posterior to anterior and further results in abnormal pulmonary to mitral valve ring fibrous continuity. Pasquini et al. (2) demonstrated considerable variation in the conal anatomy of hearts with TGA.

Cardiac Segments

Usually, the atria are formed normally, with normal internal anatomy. Almost always, there is a patent foramen ovale and only rarely (5%) a true secundum atrial septal defect (ASD). Consistent with the normal atrial anatomy, the sinus and AV nodes are in their usual locations. Specialized tracts of conduction tissue between the nodes have not been conclusively demonstrated; however, surgical damage to the crista terminalis or superior rim of the fossa ovale may be important in the genesis of supraventricular dysrhythmias frequently noted after atrial inversion procedures.

The right ventricle is normally positioned and becomes progressively hypertrophied and enlarged in the uncorrected patient and in patients following Mustard or Senning repairs. The inflow and sinus portions are essentially normal in architecture, but the central fibrous body is abbreviated and the AV and membranous interventricular septa are smaller than normal. With IVS, the entire septum is usually a relatively straight structure and does

Figure 49.2. Complete TGA. A: Angiocardiogram (left anterior oblique view). B: Two-dimensional echocardiogram (subcostal view) showing discordant ventriculoarterial alignments. Right-sided (anterior) aorta (AO) connected to right-sided (anterior) morphologically right ventricle (RV) and left-sided (posterior) pulmonary artery (PA) connected to left-sided (posterior) morphologically left ventricle (LV).



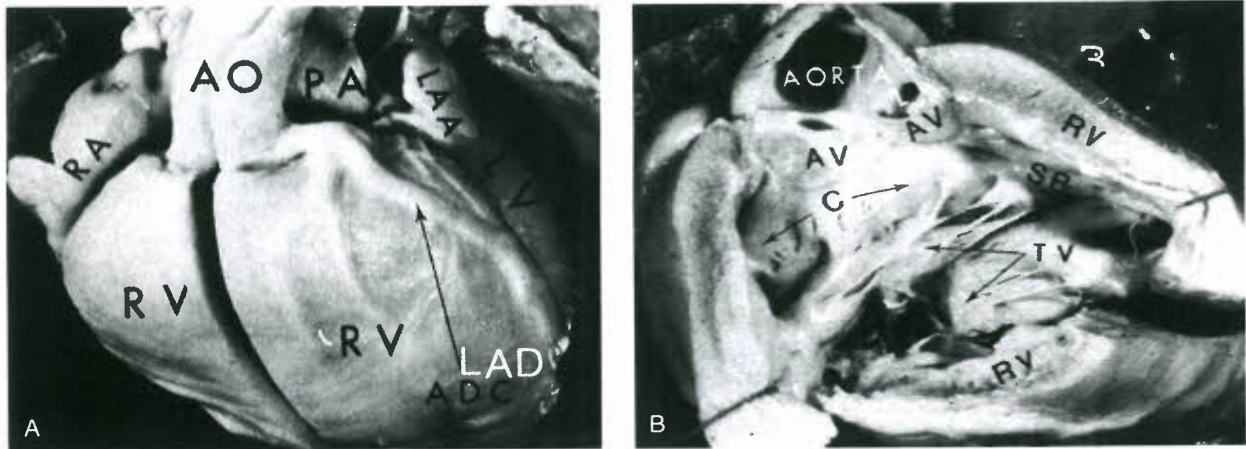


Figure 49.3. Morphology in typical TGA. **A:** Anterior view of right ventricle (RV): aorta (AO) arising anterior and to the right of pulmonary artery (PA) and left anterior descending coronary artery (LAD), which arises from the left posterior “facing” sinus of Valsalva. LAA, left atrial appendage; LV, left ventricle; RA, right atrium. **B:** Interior view of right ventricle with prominent subaortic conus (C). Arrows embracing C delineate prominent muscle bar composed of portions of right ventriculoinfundibular fold (parietal band), infundibular septum, and rightward extension of trabecular septomarginalis (septal band) musculature. AV, aortic valve; SB, septal band; TV, tricuspid valve.

not have the sigmoid curvature typical of the normal heart; consequently, the right ventricular outflow tract runs parallel to the left ventricular outflow tract (LVOT) (Fig. 49.2). Almost always, when the ventricular septum is intact, there is a subaortic conus separating the aortic valve from the tricuspid valve (Fig. 49.3B), whereas the pulmonary valve is in fibrous continuity with the mitral valve (Fig. 49.4A). The outlet (infundibular) septum joins normally with the ventricular septum between the limbs of the trabecula septomarginalis (septal band). The infundibulum projects directly superiorly to the aorta from the sinus portion of the ventricle rather than superiorly, anteriorly, and leftward to the pulmonary artery as in the normal heart.

In the left ventricle, there is usually pulmonary–mitral fibrous continuity comparable to the aortic–mitral continuity present in the normal heart (Figs. 49.4 and 49.5). Left ventricular posterior wall thickness and cavity shape are dependent on age and the presence of associated lesions (VSD, PDA, LVOTO), and are of major importance when considering arterial switch surgery.

The aortic position is the most obvious external abnormality that manifests in TGA. In most patients with situs solitus

and IVS, the aortic root is directly anterior or anterior and to the right of the pulmonary trunk in a slightly oblique relationship (Fig. 49.6). Less commonly, the aorta may be positioned anterior and to the left or, rarely, posterior and to the right of the pulmonary trunk.

Until recently, the extensive anatomic variability of the coronary arteries in hearts with TGA was of academic interest only. Shafer and Puddu described the multiple variations in the origin and epicardial course of the coronary arteries as early as 1966. This marked diversity has been confirmed in other pathologic and surgical series (3–5). In normally related great arteries, the fixed interrelationship between the aorta and pulmonary trunk minimizes the abnormalities of the origin and distribution of the coronary arteries. The variable interrelationship of the aorta and pulmonary trunk in TGA, however, as well as the variability in the size and orientation of the conal septum probably account for the greater variation in the origin and distribution of the epicardial coronary arteries in TGA. The coronary arteries appear to take the “shortest route” to a sinus in the aortic root. For example, when the aorta is more

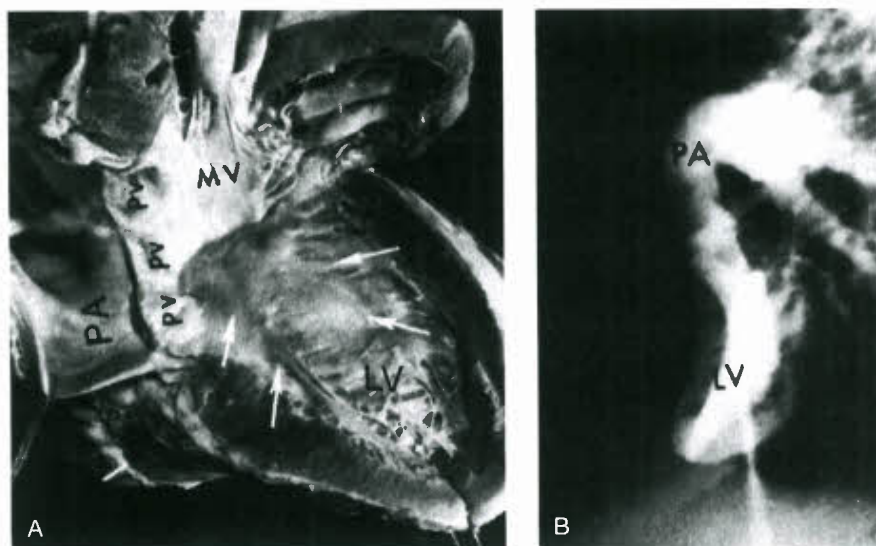


Figure 49.4. Septal bulge in TGA. **A:** Autopsy specimen from 2-year-old patient showing prominent convex bulging (arrows) of interventricular septum toward left ventricular (LV) cavity. Catheterization revealed a peak systolic left ventricular outflow tract pressure gradient of 58 mm Hg. Note mitral valve (MV) to pulmonary valve (PV) fibrous continuity and the absence of any discrete fibromuscular ridge at the septal impact site of the mitral valve. **B:** Superimposed systolic and diastolic angiographic frames from 4-year-old patient 2 years after intra-atrial repair illustrating abnormally prominent posterior septal bulging into the left ventricular cavity during systole. No localized fibromuscular ridge stenosis was visualized. Pressures were LV apex, 60/8; LV outflow, 24/8; and pulmonary artery (PA), 24/18 mm Hg.

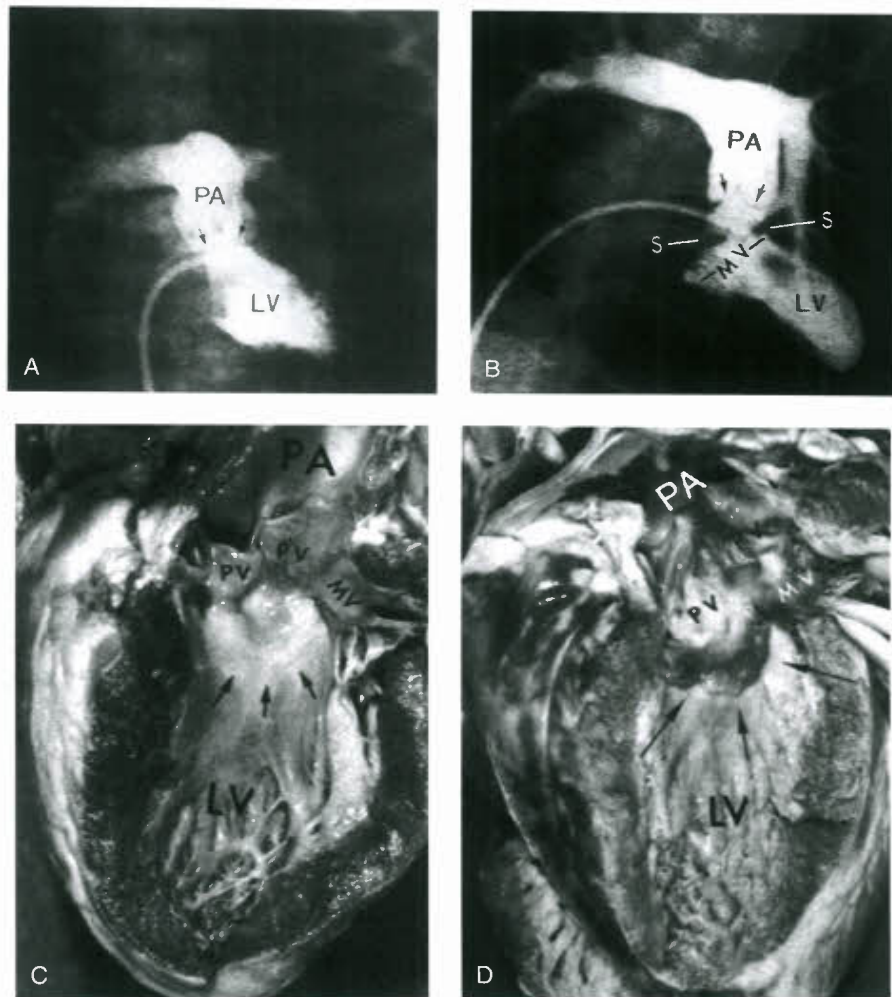


Figure 49.5. A,B: Left ventricular (LV) angiocardiograms (frontal view) in a patient with TGA/IVS illustrating development and progression of LVOTO. A: At 2 days of age, no angiographic evidence of LVOTO; pressures were right ventricle (RV), 70/7 mm Hg; LV, 35/5 mm Hg. B: Same patient at 4 months of age when selective LV angiogram demonstrated prominent subpulmonary fibromuscular ridge causing LVOTO; pressures were RV, 80/6 mm Hg; LV, 80/6 mm Hg; and pulmonary artery (PA), 14/10 mm Hg. MV, mitral valve; S, obstructive subpulmonary fibromuscular ridge. Arrows indicate pulmonary valve leaflets. C,D: Autopsy specimens illustrating LVOT with fibromuscular ridge pathology (arrows). Note the relationship of the mitral valve (MV) impact region to site of ridge. C: Pathologic specimen, early fibromuscular ridge in 2-month-old infant. D: Pathologic specimen, moderately severe fibromuscular ridge obstruction in 2-year-old patient with peak systolic pressure gradient of 64 mm Hg across LVOT. PV, pulmonary valve.

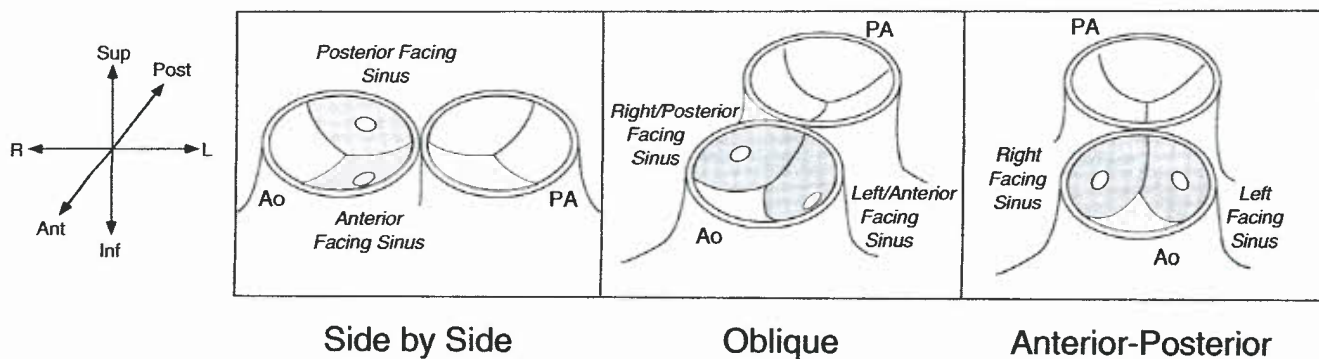


Figure 49.6. Nomenclature of the aortic sinuses that contain the coronary ostia, based on the interrelationship of the great arteries. Ant, anterior; Ao, aorta; Inf, inferior; PA, pulmonary artery; Post, posterior; Sup, superior. (Modified from Wernovsky G, Sanders SP. Coronary artery anatomy and transposition of the great arteries. *Coron Artery Dis* 1993;4:148–157, with permission.)

posterior (as in side-by-side great arteries), the circumflex coronary artery or even the entire left coronary artery system may arise from the posterior facing sinus, whereas the right coronary artery arises from the aorta anteriorly, a distribution similar to normally related great arteries.

The two aortic sinuses of Valsalva adjacent to the aorticopulmonary septum that “face” the pulmonary artery contain the ostia of the coronary arteries in more than 99% of cases; these are termed the septal or facing sinuses. When the great arteries are directly anterior–posterior, the facing sinuses are directed leftward and rightward. When the great arteries are directly side-by-side, the facing sinuses are directed anteriorly and posteriorly. When the aorta is anterior to and rightward of the pulmonary artery (the typical interrelationship), the facing sinuses are leftward/anterior and rightward/posterior (Fig. 49.6). Alternative classification systems label the septal or facing sinuses with arbitrary numbers (e.g., sinus 1 and sinus 2) (6) or letters (3), whereas others have suggested labeling the facing sinuses right or left, but as it relates to the surgeon’s hands rather than the patient’s anatomy (7). Although this labeling might be a helpful distinction during surgery, it is certainly not standard anatomic practice (the anatomically right ventricle is not considered to be the left ventricle when the surgeon is operating on it).

As in hearts with normally related great arteries, the three major coronary arteries are (a) the right coronary artery, defined as the coronary artery that passes in the right AV groove; (b) the circumflex coronary artery, defined as the coronary artery that passes in the left AV groove; and (c) the left anterior descending artery, the coronary artery that parallels the interventricular septum on the anterior surface of the heart. In addition, the proximal portion of each of the three major branches may pursue an intramural course, usually between the two great vessels. In these cases, the media of the aortic and coronary walls are attached without interposed adventitia. Thus, given the two sinuses of origin, three major branches, and the possibility of a proximal intramural course, nine major anatomic types can be defined and account for more than 95% of the coronary variability in TGA (Fig. 49.7).

In addition, multiple ostia may be present in a given sinus, the epicardial course may be unusual, or there may be complete absence of one of the branches (e.g., absent circumflex coronary artery). If one accounted for every possible variation, the nomenclature would become too cumbersome to be useful. Therefore, this chapter uses a previously described (5) classification scheme that characterizes in text form (rather than arbitrary symbols) the nine most common variations (Fig. 49.7). Table 49.1 summarizes the frequency distribution of the coronary patterns in a number of pathologic and surgical series.

The course of the sinus node artery, which typically arises as the first branch from the right coronary artery close to its aortic origin, may be of surgical importance. Damage to the sinus node artery has been implicated in the widespread prevalence of atrial arrhythmias and sinus node dysfunction seen after atrial level (Mustard or Senning) repair (8). Although the origin and proximal course of this artery may be variable, it eventually reaches the sinus node by the interatrial groove on the anterior surface of the heart, occasionally with an intramyocardial course in the anterosuperior rim of the fossa ovalis. Because it is partially embedded in the anterosuperior portion of the atrial septum, it can be damaged easily during balloon atrial septostomy (BAS), during surgical septectomy, or when this portion of the septum is widely excised, as in the Mustard or Senning atrial switch operation.

Coexisting Anomalies

Nearly half of the hearts with TGA have no other anomaly except a persistent patent foramen ovale or a PDA. In the other half, isolated LVOTO with IVS is uncommon, about

5%. VSD is common and present in about 40% to 45% (however, one-third of the defects are small and with little hemodynamic significance), and a combination of VSD and significant LVOTO occurs in about 10%. These coexisting anomalies, together with AV valve and valve tensor abnormalities and aortic obstructive lesions, constitute additional challenges for diagnosis and surgical therapy.

Ventricular Septal Defect

The VSD is the most frequent coexisting anomaly. It may be small, large, or (rarely) multiple and can be located anywhere in the septum. The approximate distribution of VSD location includes perimembranous (conovertricular, 33%), AV septal defect (inlet septum, 5%), muscular (27%), malalignment (30%), and conal septal hypoplasia type (5%) (9).

TYPES OF VENTRICULAR SEPTAL DEFECT

The typical membranous defect lies adjacent to the membranous septum and tricuspid annulus at the anterosseptal tricuspid valve commissure and is situated between the conal (outlet) septum above and the muscular ventricular septum below. Defects in this location may close spontaneously or become smaller with time.

Most muscular defects are in the midseptum, and others occur in the posterior inflow, apical, or high anterior septum; muscular defects are rarely multiple. Spontaneous decrease in size with eventual closure has been documented frequently, particularly with an initially small, slit-shaped muscular inlet or trabecular defect.

AV septal defect (inlet septum) types of VSDs may be associated with coexisting AV valve or conduction tissue anomalies. This type of defect provides the potential for the tricuspid valve/orifice to straddle the ventricular septum and sometimes is associated with a hypoplastic right ventricle.

Of particular surgical importance are the malalignment (outlet) septal defects (Fig. 49.8). Anterior (rightward) malalignment defects are associated with varying degrees of overriding of the pulmonary annulus onto the right ventricle. With increasing degrees of overriding, a series of anomalies are encountered that culminate, effectively, in DORV with subpulmonary defect in the morphologic spectrum of the Taussig-Bing anomaly (Fig. 49.9). The VSD is an anterior defect, often with a muscular posterior rim, but it sometimes extends posteriorly to the tricuspid annulus (perimembranous extension). The subaortic stenosis caused by the anterior malalignment of the infundibular septum is frequently associated with aortic arch hypoplasia, coarctation, or even complete interruption of the aortic arch. Posterior (leftward) malalignment is associated with varying degrees of LVOTO–subpulmonary stenosis, annular hypoplasia, or even pulmonary valvar atresia (see also LVOTO). An outlet septum deficiency type of defect, also termed doubly committed subarterial defect, is characterized by an absence of the muscular outlet septum so that the defect’s superior rim is the area of fibrous continuity between the aortic and pulmonary valve annuli.

Left Ventricular Outflow Tract Obstruction

Obstruction to pulmonary blood flow is possible at multiple levels in patients with TGA. In one large clinical–surgical series (10), some form of LVOTO was present in about 25% of 260 patients, 20% of the patients with IVS (but only 5% had important hemodynamic obstructions), and 30% of the patients with VSD. Gradients measured preoperatively across the LVOT by Doppler echocardiography or during cardiac catheterization may overestimate the degree of anatomic obstruction as a result of the greatly increased pulmonary blood flow in children with TGA, especially with an associated VSD.

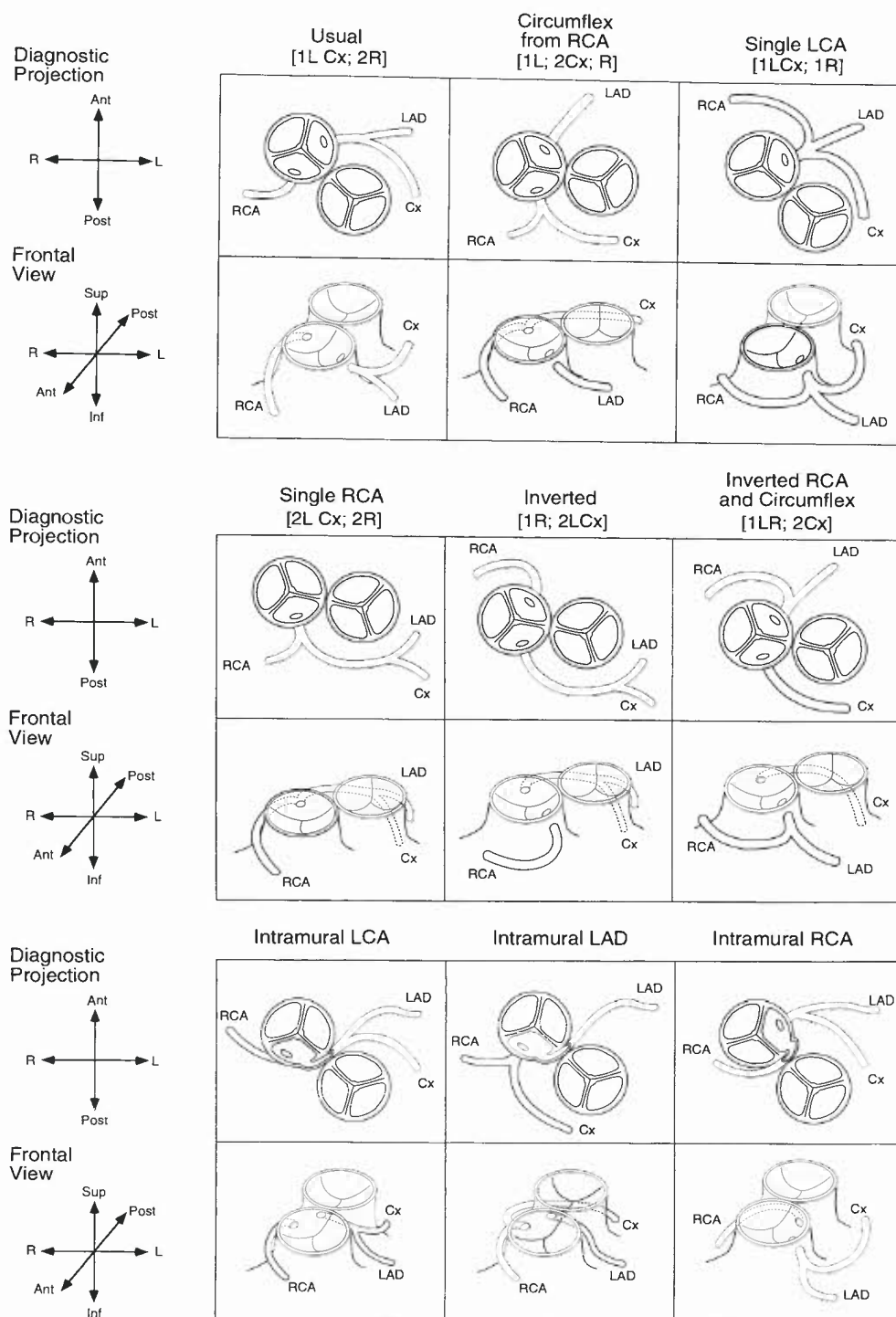


Figure 49.7. Coronary artery distribution in TGA. **Upper panels:** Diagnostic projection; diagram of the origin and proximal course as visualized by 2-D echocardiography and caudally angulated aortography (see text). **Lower panels:** Same coronary artery distribution as viewed anteriorly (“surgeon’s view,” frontal projection). Note that the circumflex coronary artery, or even the entire left coronary artery system, is more likely to pursue a retropulmonary course (*dashed lines*) when the great arteries are in a side-by-side relationship (*shown*). An intramural course (*shaded*) of the proximal coronary artery exists in fewer than 3% of cases but has been associated with higher risk for transfer during an arterial switch operation. Alternative terminology in *brackets* are shown as popularized by Quagebeur and Kirklin and the Congenital Heart Surgeons Society. Ant, anterior; Cx, circumflex coronary artery; Inf, inferior; LAD, left anterior descending coronary artery; Post, posterior; RCA, right coronary artery; Sup, superior. (Modified from Wernovsky G, Sanders SP. Coronary artery anatomy and transposition of the great arteries. *Coron Artery Dis* 1993;4:148–157, with permission.)

TABLE 49.1

Frequency Distribution of the Coronary Patterns in Transposition of the Great Arteries

Coronary Pattern	Cases (%)
Usual	66.9
Circumflex from RCA	16.1
Single RCA	3.9
Single LCA	1.7
Inverted	2.4
Inverted circumflex/RCA	4.2
Intramural LCA	2.1
Intramural LAD	0.1
Intramural RCA	1.0
Other	1.6

LAD, left anterior descending; LCA, left coronary artery; RCA, right coronary artery.

Modified from Wernovsky G, Sanders SP. Coronary artery anatomy and transposition of the great arteries. *Coronary Artery Dis* 1993;4:148–157; Hayes CJ, Gersony WM. Arrhythmias after the Mustard operation for transposition of the great arteries: a long-term study. *J Am Coll Cardiol* 1986;7:133–137. 143; Wetter J, Sinzobahamya N, Blaschczok HC, et al. Results of arterial switch operation for primary total correction of the Taussig-Bing anomaly. *Ann Thorac Surg* 2004;77:41–46; LacourGayet F, Serraf A, Galletti L, et al. Biventricular repair of conotruncal anomalies associated with aortic arch obstruction—103 patients. *Circulation* 1997;96:328–334.

In TGA/IVS, a dynamic type of obstruction is common, usually mild and not readily apparent on autopsy specimen without careful analysis. Angiography and echocardiography clearly demonstrate a dynamic leftward bulging of the basal muscular ventricular septum toward the lower-pressure left ventricle, which narrows the LVOT during systole (Fig. 49.4B) but opens widely during diastole. This systolic septal bulge reflects the reversal in TGA of the normal transseptal ventricular systolic pressure relationships. Dynamic obstruction is rare in the neonate with elevated pulmonary

artery resistance and left ventricular pressure or in the presence of a nonrestrictive ductus arteriosus because the left ventricle assumes systemic systolic pressure and geometry. Following atrial level repair, cardiac catheterization or Doppler echocardiography frequently demonstrates slight to moderate (10 to 40 mm Hg) systolic pressure differences across the subpulmonary outflow tract.

Fixed obstruction develops in some infants; it initially appears as a patch of endocardial thickening on the septal bulge but later can evolve into a sharp fibrous ridge or a discrete membrane, analogous to membranous subaortic stenosis, along the line of systolic mitral valve contact (Fig. 49.5). Less commonly, fixed subpulmonary obstruction is caused by a tunnel-like subpulmonary fibromuscular ridge that extends across the outflow tract and onto the base of the anterior mitral leaflet. Pulmonary valve stenosis and annular hypoplasia are rare in patients with TGA/IVS but, when present, are almost always associated with combined subvalvar obstructive lesions.

With TGA/VSD, LVOTO coexists in about 30% of patients, and the stenosis is usually more severe and complex than in TGA with IVS. The stenosis is most often subvalvar and may be a localized fibrous ring, a tunnel type of fibromuscular narrowing, or a muscular obstruction related to malposition of the outlet septum impinging into the anteromedial aspect of the subpulmonary outflow tract (Figs. 49.8A, 49.10, and 49.11). Other uncommon forms of subpulmonary stenosis result from (a) malattachment of the anterior mitral valve to the muscular outlet septum by anomalous fibrous or chordal tissue (which may be associated with varying degrees of left ventricular hypoplasia), (b) redundant tricuspid valve tissue (“pouch”) protruding through the VSD (Figs. 49.12 and 49.13), (c) subpulmonic membrane (Fig. 49.14), (d) aneurysm of the membranous septum, and (e) hypertrophy of the muscle of Moutaert.

Other Associated Anomalies

Prior to the extensive present-day use of prostaglandin E₁ therapy, a PDA was found in almost half the neonates at the initial cardiac catheterization for BAS. The ductus is usually functionally closed by 1 month of age (see sections on “Physiology and Treatment”).

Functionally important tricuspid valve anomalies were present in about 4% of surgical patients, but in autopsy series,

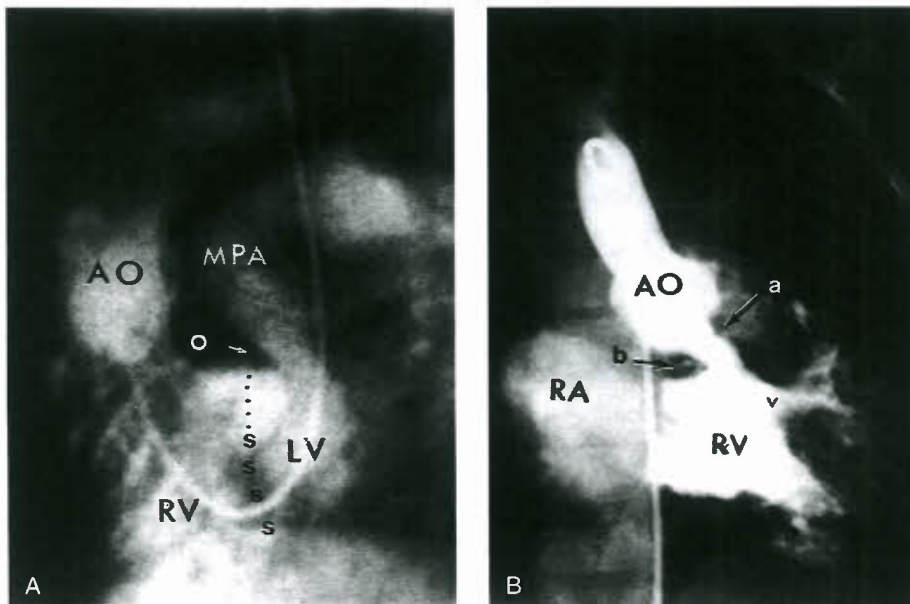


Figure 49.8. A: Angiocardiogram (oblique lateral view) in patient with TGA/VSD showing LVOTO due to leftward posterior malalignment of conal septum (o). Pressures were right ventricle (RV), 86/10 mm Hg; left ventricle (LV), 85/10 mm Hg; main pulmonary artery (MPA), 30/18 mm Hg. B: Right ventriculogram (frontal view) in 21-month-old with TGA/VSD showing unusually prominent obstructing subaortic outlet musculature (arrows); rightward anterior displacement (malalignment) of outlet (infundibular) septum (a); and prominent hypertrophy and anterior displacement of right ventriculoinfundibular fold (parietal band) (b). Pressures were RV, 105/6 mm Hg; AO 60/40 mm Hg; LV, 35/6 mm Hg; MPA, 26/6 mm Hg. The VSD (v) had become small and restrictive since early infancy. AO, aorta; RA, right atrium; s, interventricular septum.

Figure 49.9. Angiocardiograms (left anterior oblique views) illustrating spectrum of outflow tract morphology extending from DORV with subpulmonary VSD to TGA/VSD. **A:** DORV (Taussig-Bing type) with pulmonary trunk emerging completely or maximally from the right ventricle. Note the prominent muscular structure (o), variably termed outlet, conal, or infundibular septum, that separates the subpulmonary and subaortic outflow tract and the characteristic anterior malalignment of this outlet septum (o) relative to the rest of the ventricular septum (S). Note a second prominent subpulmonary muscle structure (x) separating the pulmonary (PV) and mitral (MV) valves. These two prominent muscle bundles are elements of the bilateral (subaortic and subpulmonary) conus present to varying degrees in these hearts. **B:** DORV with subpulmonary VSD with pulmonary trunk emerging more or less equally from both ventricles. **C:** DORV, subpulmonary VSD with pulmonary trunk emerging predominantly from left ventricle but lack of fibrous continuity between mitral and pulmonary valves. Note the prominent outlet septum (o) with malalignment relative to ventricular septum (S). **D:** TGA/VSD, outlet (o) and ventricular (S) septum are in alignment. Ao, aorta; AOV, aortic valve; LV, left ventricle; MPA, main pulmonary artery; MV, mitral valve; S, interventricular septum.

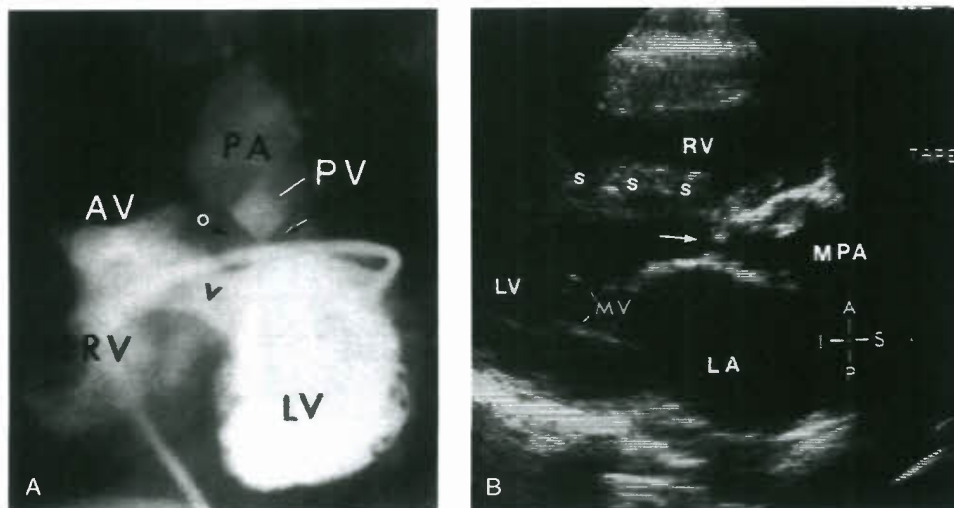
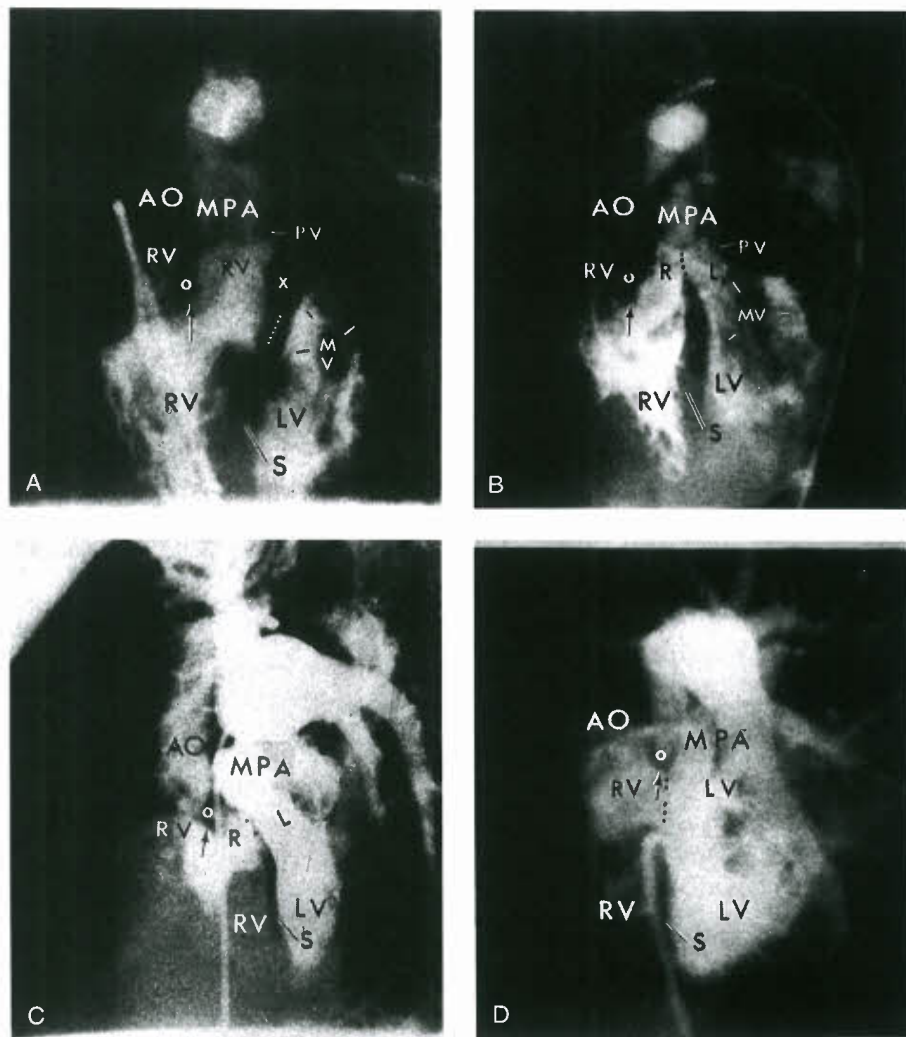


Figure 49.10. TGA/VSD and LVOTO. **A:** Left ventriculogram (left anterior oblique view) showing large VSD (v) with tunnel form of severe subpulmonary obstruction associated with some leftward posterior deviation of outlet septum (o). AV, aortic valve; LV, left ventricle; PV, pulmonary valve; RV, right ventricle; v, VSD. **B:** Two-dimensional echo (parasternal long axis view) in 2-year-old child with TGA, small VSD, and severe LVOTO. Note the subpulmonary circumferential stenosis and hypoplasia of pulmonary annulus (arrow). Aorta partially (25%) overrides the ventricular septum. At catheterization, pressures were RV, 85/12 mm Hg; LV, 85/8 mm Hg; and MPA, 37/25 mm Hg. Arterial switch was achieved with aortic translocation and biventricular outflow tract reconstruction. LA, left atrium; MPA, main pulmonary artery; MV, mitral valve; s, septum.

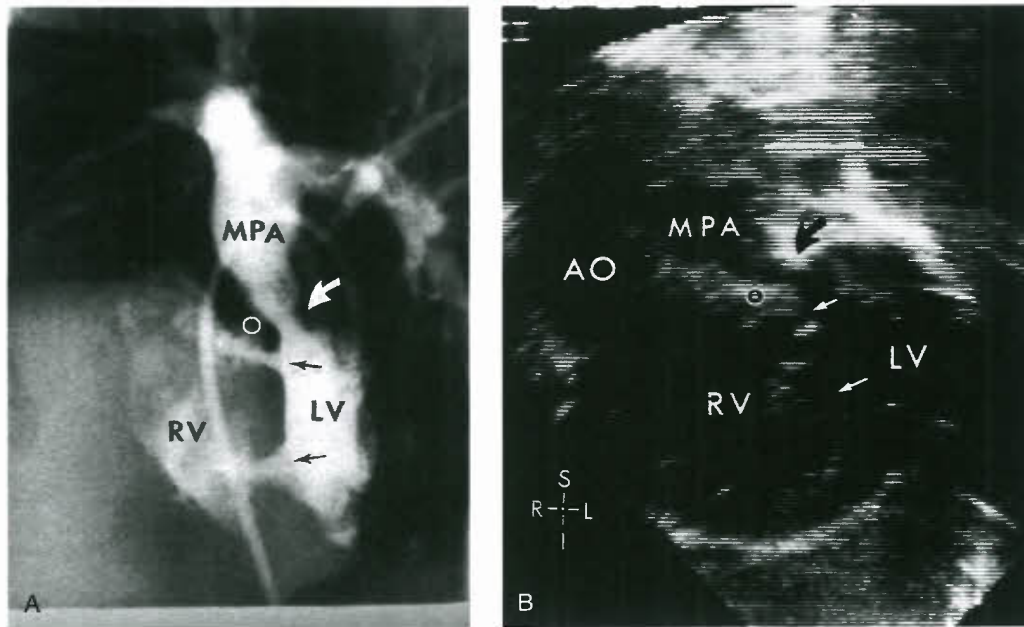


Figure 49.11. A: Left ventriculogram (hepatoclavicular projection). B: The companion 2-D echo (apical view) in a 4-month-old child with TGA, two muscular VSDs (*small straight arrows*) in apical and trabecular/outlet septum, and LVOTO caused by posterior-leftward malaligned outlet septum (o) and a subpulmonary fibromuscular “collar” (*large curved arrow*). At catheterization, pressures were RV 75/6 mm Hg; LV, 61/7 mm Hg; MPA, 20/12 mm Hg. AO, aorta; LV, left ventricle; MPA, main pulmonary artery; RV, right ventricle.

particularly with VSD, a considerably higher frequency (31%) was noted (11). In TGA with VSD, there may be anomalous chordal attachments to the edges of the perimembranous or outlet septum malalignment defects, and these may complicate surgical transatrial closure of the defect or construction of an intraventricular tunnel in the Rastelli operation. An unusual, infrequent, and surgically important (and remediable) type

of subpulmonary stenosis can be caused by a mass of redundant tricuspid septal valve tissue (tricuspid pouch) protruding through a VSD into the LVOT (Figs. 49.12 and 49.13). When the VSD is in the inlet septum, there may be annular overriding, tensor apparatus straddling, or both that, when extensive, may be associated with marked hypoplasia of the right ventricular sinus. Significant tricuspid valve incompetence is rare in the pre-operative heart, but it may be observed following atrial level repair (a) when severe right ventricular dysfunction can result in annular dilation and (b) in TGA with VSD when the VSD

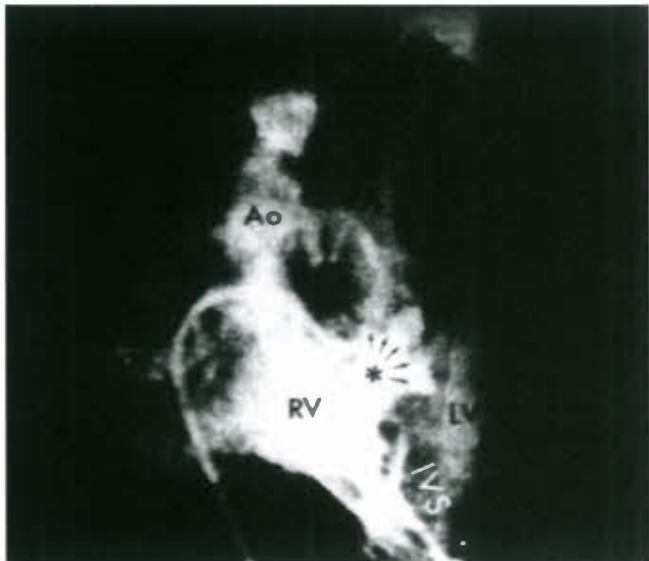


Figure 49.12. Right ventriculogram, four-chamber view, showing outpouching of tricuspid valve tissue (*asterisk*) through a VSD into the subpulmonary area, causing significant subpulmonary obstruction. At catheterization, pressures were LV, 60/9 mm Hg; LV outflow tract, 22/9 mm Hg; and PA, 22/10 mm Hg. Ao, aorta; IVS, interventricular septum; LV, left ventricle; PA, pulmonary artery; RV, right ventricle.



Figure 49.13. Two-dimensional echocardiogram, subcostal imaging position, in 18-month-old child with TGA/VSD and outpouching (*asterisk*) of accessory tricuspid valve leaflet tissue causing significant subpulmonary obstruction. Ao, aorta; IVS, interventricular septum; LV, left ventricle; PA, pulmonary artery; RV, right ventricle.

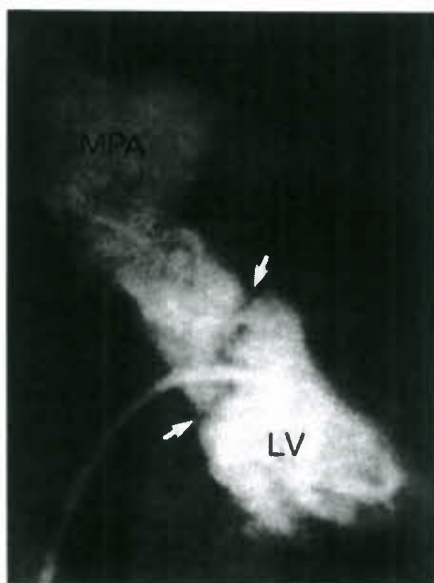


Figure 49.14. Transvenous left ventriculogram (long-axial oblique projection) in a 7-month-old with TGA/IVS. At catheterization, there was a 45 mm Hg peak systolic ejection gradient across the LVOT resulting from a thick subpulmonary membrane (arrows). At arterial switch surgery, the membrane was found to be adherent to the anterior leaflet of the mitral valve but was adequately removed without damage to the mitral apparatus. Note the mild poststenotic dilatation of the main pulmonary artery. LV, left ventricle; MPA, main pulmonary artery. (From Wernovsky G, Jonas RA, Colan SD, et al. Results of the arterial switch operation in patients with transposition of the great arteries and abnormalities of the mitral valve or left ventricular outflow tract. *J Am Coll Cardiol* 1990;16:1446–1454, with permission.)

is repaired through the tricuspid valve. Of interest, in TGA, the ratio of tricuspid to mitral annulus circumference is <1 in almost 50% of cases, whereas in normal hearts, this ratio is always >1 .

Structural anomalies of the mitral valve have been observed at autopsy in about 20% of hearts with TGA, particularly in the VSD group; however, functionally significant lesions were present in only about 4% (9). Cleft anterior mitral valve leaflet, anomalous papillary muscles and chordae, and redundant tissue tags have been described. The most significant abnormalities from a surgical standpoint are those in which the mitral valve and portions of its tensor apparatus straddle the VSD or in which the anterior mitral valve leaflet is abnormally tethered with anomalous septal attachments and causes LVOTO.

Coarctation of the aorta, arch hypoplasia, or rarely interrupted aortic arch coexist in about 5% of patients with complete TGA, occurring much more commonly in association anterior malalignment types of VSD, especially (20%) in patients with DORV with subpulmonary defect (Taussig-Bing anomaly). The obstruction may be the usual discrete “shelf” lesion, tubular hypoplasia of the distal aortic arch, or a combination. The outlet septum may be displaced anterior and rightward vis-à-vis the trabecular interventricular septum, and there may be additional anterior encroachment by a markedly hypertrophied right ventriculofundibular fold (parietal band), both resulting in subaortic narrowing (Fig. 49.8B). The frequent association of aortic arch malformations in TGA with systemic (right) ventricular outlet obstruction is consonant with observations on malformations with normally related great arteries that link the genesis of arch anomalies with intra-

cardiac systemic (left) ventricle obstructive factors. With TGA, VSD, and arch abnormalities, there may also be hypoplasia of the tricuspid annulus and the right ventricular sinus.

Leftward juxtaposition of atrial appendages is an anomaly sometimes associated with TGA in which the right atrial appendage passes immediately behind the transposed main pulmonary artery. It occurs in about 2% to 5% of patients and can be diagnosed readily by 2-D echocardiography, angiography, or direct inspection at surgery. This anomaly is often additionally associated with major cardiac pathology, including dextrocardia, VSD, bilateral infundibulum, right ventricular hypoplasia, and tricuspid stenosis or atresia.

PHYSIOLOGY

The dominant physiologic abnormalities in TGA are a deficiency of oxygen supply to the tissues and an excessive right and left ventricular workload. The systemic and pulmonary circulations function in parallel rather than in series as in the normal infant; hence, the greatest portion of the output of each ventricle is recirculated to that ventricle (Fig. 49.15A). Particularly in TGA with IVS, only a relatively small proportion of blood is exchanged by intercirculatory shunts between the two circulations to eventually reach the appropriate vascular bed. The systemic and pulmonary arterial oxygen saturations are thus dependent on one or more of the following anatomic paths for this exchange: intracardiac (patent foramen ovale, ASD, VSD) and extracardiac (PDA, bronchopulmonary collateral circulation).

Intercirculatory Mixing

The net volume of blood passing from the pulmonary circulation (left atrium, left ventricle, pulmonary arteries) to the systemic circulation (right atrium, right ventricle, aorta) represents the anatomic left-to-right shunt and is, in fact, the effective systemic blood flow (i.e., oxygenated pulmonary venous return perfusing the systemic capillary bed) (Fig. 49.15B). Conversely, the net volume of blood passing from the systemic circulation to the pulmonary circulation represents the anatomic right-to-left shunt and is, in fact, the effective pulmonary blood flow (systemic venous return perfusing the pulmonary capillary bed). The effective pulmonary blood flow, effective systemic blood flow, and net anatomic right-to-left and net anatomic left-to-right shunts are all equal to one another, and this volume is the intercirculatory mixing: the flow in TGA on which survival depends. The net volume exchanged between systemic and pulmonary circulations must be equal over a given short interval of time because any major differences will result in a depletion of the blood volume of one circulation at the expense of overloading the other. The volumes of anatomic right-to-left and left-to-right shunted blood (i.e., “effective blood flows”) that participate in functional gas exchange at the pulmonary and systemic capillary levels are relatively small compared with the large volumes of blood circulating (total systemic and pulmonary blood flow) or recirculating (physiologic left-to-right and right-to-left shunt flows) within each circulation. The physiologic left-to-right shunt represents the volume of the pulmonary venous blood recirculating through the lungs without having passed through the body, and the physiologic right-to-left shunt is the volume of systemic venous blood reentering the systemic circulation without having passed through the lungs.

The extent of intercirculatory mixing in TGA depends on the number, size, and position of the anatomic communications and on the total blood flow through the pulmonary

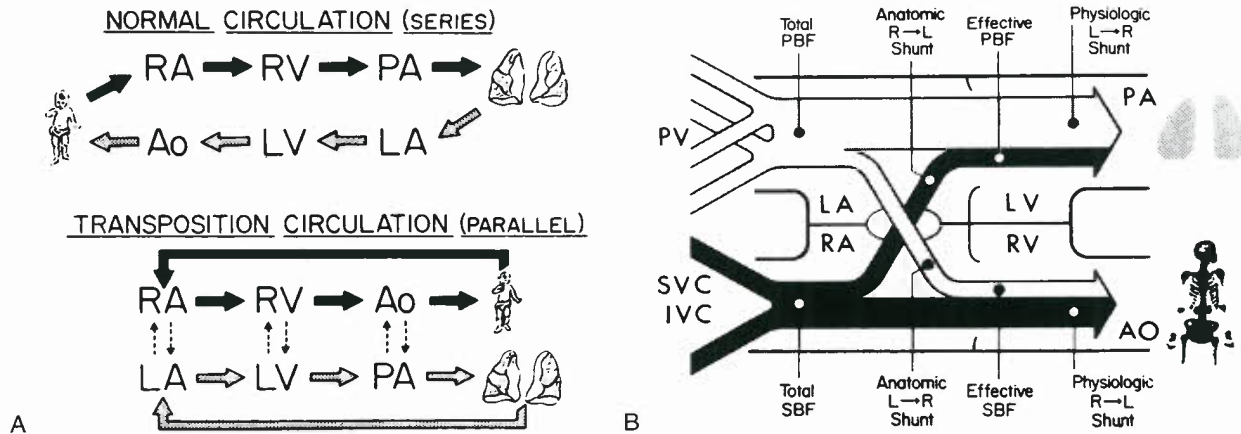


Figure 49.15. The circulation in TGA. **A:** Systemic and pulmonary circulation pathways; in series, with normally related great arteries; in parallel, with TGA. *Solid arrows*, relatively unoxygenated blood; *stippled arrows*, oxygenated blood; *dashed arrows*, intercirculatory shunts. **B:** Circulation schema demonstrating flows and shunts in infants with TGA/IVS. Note that the anatomic LR shunt constitutes the effective SBF and the anatomic RL shunt, the effective PBF (see text). AO, aorta; IVC, inferior vena cava; LA, left atrium; LV, left ventricle; LR, left-to-right; RA, right atrium; RV, right ventricle; PA, pulmonary artery; PBF, pulmonary blood flow; PV, pulmonary veins; SBF, systemic blood flow; SVC, superior vena cava.

circuit. In the neonate with an IVS and a closed or closing ductus arteriosus, severe hypoxemia secondary to inadequate mixing at the foramen ovale level is usually present. When the interatrial or interventricular shunting sites are of adequate size, the level of arterial oxygen saturation is influenced primarily by the pulmonary-to-systemic blood flow ratio, with a high pulmonary blood flow resulting in relatively high arterial oxygen saturation. If the pulmonary blood flow is decreased by subpulmonary or pulmonary stenosis or elevated pulmonary vascular resistance, the arterial oxygen saturation will be lowered, despite adequately sized anatomic shunting sites.

The physiologic mechanisms that precisely control the equalization of interchange between the two circulations remain speculative. The shunting patterns appear to be determined by local pressure gradients, which in turn are influenced by respiratory cycle phase, compliance of the cardiac chambers, heart rate and volume of blood flow, and the vascular resistance in each of the circulations. With TGA/IVS, the interatrial shunt is from right atrium to left atrium during ventricular diastole because left ventricular resistance to filling is less than right ventricular. Pulsed Doppler echocardiography confirmed that the shunt is from left atrium to right atrium in ventricular systole because the left atrium is less distensible than the right, and the net pressure in the left atrium is higher during ventricular systole. The pattern is affected by respiration, with the interatrial right-to-left (systemic-to-pulmonary) shunt increasing during inspiration when the systemic venous return increases and pulmonary venous return decreases. Flow patterns are less well documented in the presence of a large VSD. When the defect is large and nonrestrictive, peak systolic pressures in the ventricles are equal; during ventricular systole, some right ventricular output flows preferentially to the lower-resistance pulmonary circulation, with a concomitant increase in left atrial return. During ventricular diastole, the increased pulmonary venous return favors shunting of oxygenated blood to the right atrium and ventricle. The balances between right and left atrial and ventricular compliances and pulmonary and systemic vascular resistances are important operative factors. Other important hydraulic aspects are the location of the VSD, the influence of LVOTO, and other infrequent abnormalities, such as straddling of the right AV valve across

the VSD. Infants with a large VSD but without pulmonary stenosis or increased pulmonary vascular resistance may have torrential pulmonary blood flow with high left atrial pressure, marked left ventricular volume overload, and relatively high arterial oxygen saturation, until severe heart failure with pulmonary edema intervenes.

If a large PDA persists in the neonate with TGA and IVS, bidirectional shunting at this site can be demonstrated by angiography and Doppler; however, as the pulmonary vascular resistance falls, only systemic-to-pulmonary ductal shunting persists.

Bronchopulmonary Collateral Circulation

A significant role has been postulated for the bronchopulmonary collateral circulation in TGA (10). Bronchopulmonary anastomotic channels have been visualized by angiography in more than 30% of infants with TGA under 2 years of age, and balloon occlusion studies demonstrated that these bronchopulmonary anastomotic channels functionally and freely communicate with the pulmonary vascular bed proximal to the pulmonary capillary bed (Fig. 49.16A). In addition to representing a potential intercirculatory (systemic-to-pulmonary) mixing pathway, these bronchopulmonary communications may play a role in the accelerated and more widespread pulmonary vascular disease process observed in TGA patients. Rarely, persistence of a significant bronchopulmonary collateral circulation after surgical repair results in a large enough left-to-right shunt to warrant interventional catheter embolization therapy (Fig. 49.16B) (10).

Application of the Fick principle for calculating pulmonary and systemic blood flow in infants with TGA can have major sources of error. Oxygen consumption is not normal in the severely hypoxemic infant, and assumed values are unreliable. Systemic and pulmonary arteriovenous oxygen differences may be quite small; consequently, minor errors in oxygen saturation measurement introduce large errors in calculations of flow. Furthermore, the contribution to pulmonary blood flow from the bronchopulmonary collateral circulation enters the pulmonary vascular circuit distal to the usual catheter sampling sites. The true mixed pulmonary artery saturation

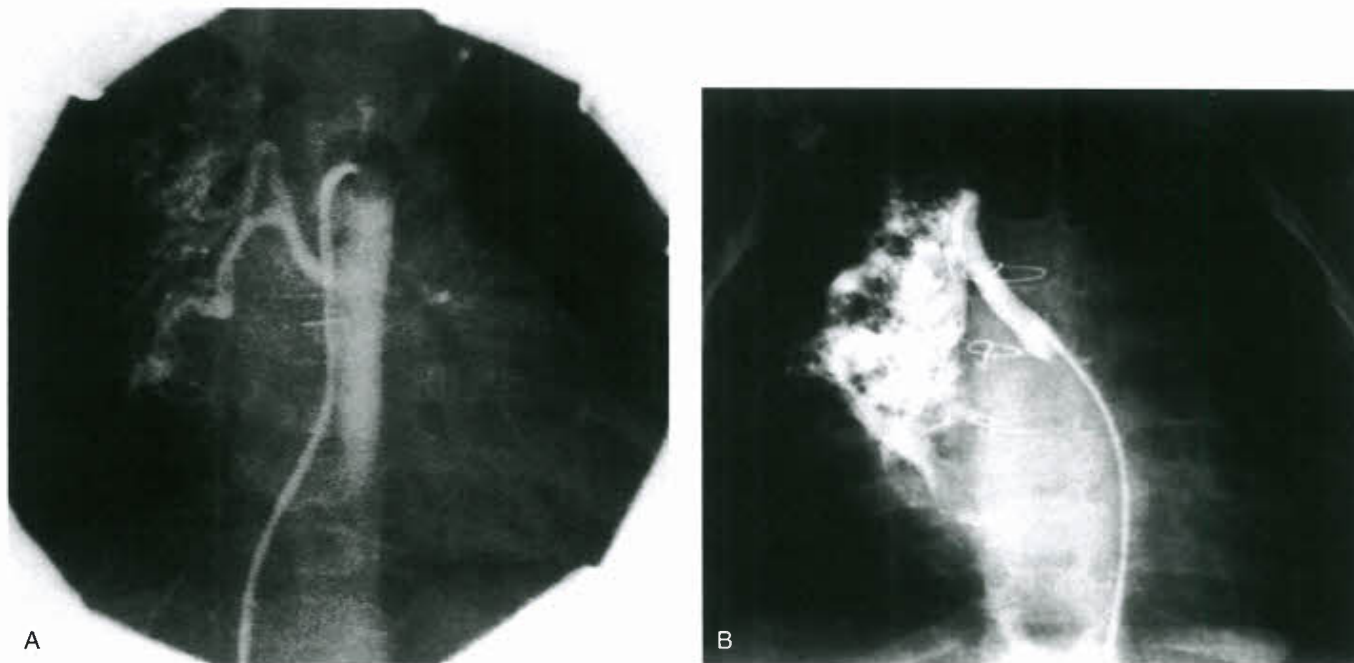


Figure 49.16. A: Preoperative transvenous descending aortogram in a neonate with TGA/IVS showing enlarged bronchial arteries (following the right main stem bronchus) to the right lung. B: Same patient 42 years after a primary arterial switch; a selective injection in the same bronchial artery shows a markedly enlarged vessel, with prompt visualization of the pulmonary veins and left atrium on levophase. At the postoperative catheterization, the left ventricular end-diastolic pressure was elevated at 18 mm Hg, and M-mode echocardiographic measurements of left ventricular end-diastolic dimension were increased, suggesting a significant volume overload. Following successful coil embolization, the left ventricular end-diastolic pressure fell to 7 mm Hg, and the echocardiographic indices normalized.

present at the precapillary level cannot be sampled; therefore, a falsely high pulmonary artery oxygen saturation and blood flow calculation will result. A modest bronchopulmonary contribution (20%) to the pulmonary precapillary blood flow can result in 30% overestimation of pulmonary blood flow; hence, calculated pulmonary vascular resistance always should be viewed as minimum values. Pulmonary blood flow in TGA is less when derived from angiographic stroke volume measurements compared with Fick measurements. With IVS, the pulmonary blood flow by angiography was within the range for normal infants in the first few weeks of life but averages approximately twice the normal flow in older infants and children, presumably because of the progressive changes in pulmonary vascular resistance and ventricular compliance that occur with age.

Determinants of the magnitude of pulmonary blood flow in TGA remain obscure. A major fall in pulmonary artery pressure and vascular resistance occurs during the first few days and weeks of life in TGA/IVS, and therefore, the early maturation of the pulmonary circulation has been considered similar to that of the normal infant. Left ventricular compliance progressively increases during this time, in association with decreasing left ventricular muscle mass. The outputs of the two ventricles are determined presumably by their respective preload, compliance, afterload, and contractility but must be autoregulated constantly by some remarkable mechanism to meet the special requirements of the unique transposition intercirculatory shunt; that is, that the net flow from the pulmonary to the systemic circuit equals the net flow from the systemic to the pulmonary circuit.

In the neonate with TGA/IVS who has been palliated by balloon septostomy or surgical atrial septectomy, the pulmonary blood flow pattern should resemble that in an

infant with normally related great arteries and isolated large secundum ASD; that is, as the pulmonary vascular resistance falls, the pulmonary ventricle circulates an increased blood volume at low pressure. In TGA, this increased level of pulmonary blood flow will result in improved intercirculatory mixing and systemic arterial oxygen saturation, assuming that an adequately sized and favorably placed anatomic opening was created (see also section on Fetal and Perinatal Physiology).

If the pulmonary blood flow decreases in a patient with TGA as a consequence of increasing LVOT stenosis or pulmonary vascular resistance, the intercirculatory mixing and systemic arterial oxygen saturation also will decrease. It is important to stress, however, that not all infants with progressive cyanosis with the combination of TGA and LVOTO are progressively more hypoxemic as a result of decreasing pulmonary blood flow. Progressive restriction of a catheterization or surgically created atrial communication can limit intercirculatory mixing and may cause progressive cyanosis. Cardiac catheterization is mandatory to assess the adequacy of pulmonary blood flow and the interatrial communication in these infants, especially if a palliative aortic-pulmonary shunt is being considered (see also section on Surgery).

There is a prevalent but clinically silent maldistribution pattern of pulmonary blood flow in TGA patients (12). Pulmonary angiograms, radionuclide lung perfusion images, and chest roentgenograms indicate that about half the patients with complete TGA have a significantly greater proportion of blood flow distributed to the right lung than normal (Fig. 49.17). The maldistribution is dependent on a common anatomic feature found in transposition, that is, abnormal rightward inclination of the main pulmonary artery, which results in a straight ejection direction from left ventricle to

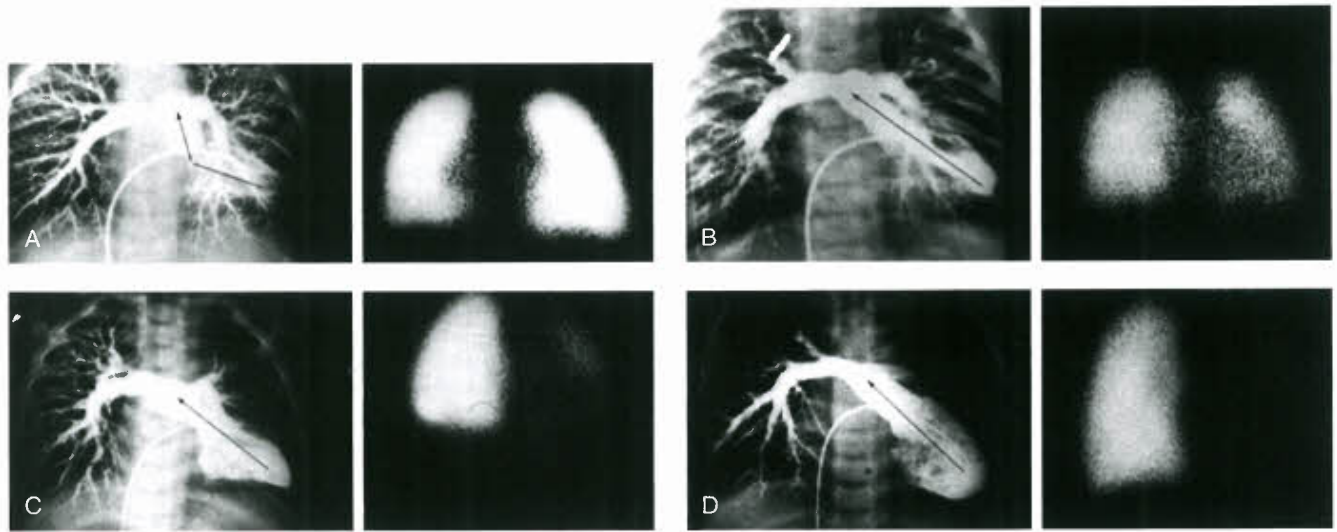


Figure 49.17. Abnormal distribution of pulmonary blood flow favoring the right lung in TGA observed prior to surgery. Pulmonary and radionuclide angiograms from four patients. **A:** Normal right–left distribution. **B:** Slight rightward distribution. **C:** Moderate rightward distribution. **D:** Marked preferential rightward distribution.

main pulmonary artery to right pulmonary artery. Under these morphologic circumstances, the momentum of blood flow in the main pulmonary artery carries the blood preferentially into the right pulmonary artery. The abnormally increased distribution of pulmonary blood flow to the right lung in TGA often is associated with some degree of hypoplasia of the left pulmonary arterial vessels and is further manifested in the occasional reports of unilateral, always left-sided, pulmonary vein stenosis or hypoplasia at catheterization or atrial switch surgery (13–15). It is unlikely that this phenomenon of pulmonary blood flow maldistribution has any significant effect on the clinical course of TGA. Further, these maldistribution patterns are not observed in patients who have neonatal arterial switch repair.

In the neonate with IVS, the systemic arterial PO_2 may be as low as 15 to 25 mm Hg at presentation, with resultant anaerobic glycolysis and severe metabolic acidemia. The newborn infant may not manifest acidemia in the first day or two of life, perhaps because of favorable blood tissue dissociation characteristics or tissue resistance factors. Inevitably, unless intracardiac mixing is improved by palliative or corrective intervention, severe hypoxemia results in advanced acidemia, hypoglycemia, hypothermia, and eventual death.

Arterial Blood Gases and Metabolic Responses

In TGA with poor intercirculatory mixing, the contrast between systemic arterial and pulmonary venous blood gases while the patient is breathing room air is striking. The pulmonary venous blood reflects chemoreceptor-stimulated hyperventilation; in room air, the PO_2 levels may be increased to as high as 110 mm Hg and the PCO_2 levels reduced to 15 to 25 mm Hg. In contrast, systemic arterial PO_2 levels are rarely higher than 35 mm Hg, and the PCO_2 is usually normal or only slightly elevated (<45 mm Hg) because of the limited anatomic left-to-right (effective systemic blood flow) shunt. Arterial blood gases obtained in both room air and 100% oxygen are helpful in discriminating cyanotic infants with TGA from those with lung disease. The response of systemic arterial PO_2 to 100% oxygen administration is related primarily to the extent of intercirculatory mixing rather than to the increase in pulmonary venous oxygen content derived

from dissolved oxygen. When systemic arterial PO_2 values are <30 mm Hg in room air and remain below 35 to 40 mm Hg during high-oxygen-content breathing, poor intracardiac mixing is present.

Fetal and Perinatal Physiology

Fetal Circulation

Both TGA physiology and anatomy appear compatible with normal fetal survival and relatively normal gestational development. The course of fetal circulation is modified because the right side of the heart ejects blood directly into the ascending aorta, in contrast to the sequence in the normal fetus, where the right ventricle ejects essentially into the descending aorta via the PDA. In the fetus with TGA, the superior vena caval blood is directed through the tricuspid valve to the right ventricle and ascending aorta and provides blood of slightly lower glucose concentration and PO_2 to the coronary and cerebral circulations than in the normal fetus. The blood entering both the pulmonary circulation and the descending aorta is derived mainly from the glucose- and oxygen-rich placental return that has shunted across the patent foramen ovale and may be expected to have a glucose concentration and PO_2 somewhat higher than that found in normal fetuses.

The clinical effects of these abnormalities of fetal flow remain to be precisely defined. In one pathology study, infants with TGA had cardiac and central nervous system structures similar in size and weight to control values; however, increased numbers (270% of control) and size (220% of control) of pancreatic islet cells, as well as a significantly increased weight of the adrenal cortex (116% of control), were found in infants with TGA (16). These findings in the pancreas and adrenal cortex are similar to those seen in infants of diabetic mothers and support the contention that the higher-than-usual glucose concentration in the descending aorta during fetal development may play a role.

It is increasingly recognized that the transposed fetal circulation results in lower substrate delivery to the rapidly developing brain, particularly in the second half of pregnancy (17–19). This may account for, in part, the higher-than-expected incidence of microcephaly, white matter injury, and immaturity of the brain seen on MRI scans of neonates with TGA (20–22).

Transitional Circulation

After birth, the pulmonary vascular resistance falls with expansion of the lungs and pulmonary blood flow and left atrial pressures increase in accordance with the more or less normal neonatal transitional physiology. The systemic vascular resistance increases because of removal of the low-resistance placental circulation. In the normal neonate, the right atrial pressure falls as the right side of the heart faces the rapidly decreasing pulmonary vascular resistance and the interatrial pressure difference favors closure of the septum primum flap over the foramen ovale. With TGA, however, the right atrial pressures are increased, and the similarity of atrial pressures tends to keep the foramen ovale open (incompetent valve), with resulting bidirectional shunting (see section on Intercirculatory Shunting).

In TGA with IVS, the ductus arteriosus is often widely patent after birth. Early after birth, when pulmonary vascular resistance is still high, there is bidirectional ductal flow: in systole, left ventricle–pulmonary artery–ductus–descending aorta; and in diastole, aorta–ductus–pulmonary artery. With continued fall in pulmonary vascular resistance, the shunt at the PDA is primarily from aorta to pulmonary artery (effective pulmonary blood flow), with an equal amount of blood passing from the pulmonary circuit to systemic circuit at the atrial level (effective systemic blood flow). Rarely, there is a delayed fall in pulmonary vascular resistance that results in persistent pulmonary hypertension, little ductal shunting, and limited intercirculatory mixing. Urgent balloon septostomy or even surgical septectomy may not improve the severe hypoxemia, and these neonates may need urgent support with early repair, extracorporeal membrane oxygenation, or both. Finally, severe hypoxemia in some neonates may be due to an intact or virtually intact atrial septum. Despite a widely PDA, there is poor intercirculatory mixing at this site alone; the primarily aorta–pulmonary artery shunting cannot be “balanced” by an equal volume of shunting from left atrium to right atrium. These neonates are typically severely hypoxemic and acidotic shortly after birth, may have severe pulmonary edema and hemorrhage, and may not survive if septostomy or arterial switch repair cannot be accomplished in a timely fashion. The *only* way to provide oxygenated blood to the coronary arteries and brain is via a shunt from left atrium to right atrium (and then to the right ventricle and aorta). Thus, the neonate with an intact (or virtually intact) atrial septum cannot survive with an open ductus arteriosus alone; an emergency BAS is necessary (see section on “Treatment”).

During the brief perinatal transitional interval, there may be enough intercirculatory mixing to limit cyanosis and avoid severe hypoxemia; however, in most such infants, the ductus soon constricts with resulting increased hypoxemia. At this time, when oxygen delivery to the tissues is seriously compromised, the newborn's oxygen consumption is rapidly increasing because of increased body metabolism, the need to maintain body temperature, and β -adrenergic receptor stimulation. These factors further decrease mixed venous—and hence arterial—oxygen saturation because most of the circulating systemic blood flow is the recirculated systemic venous return. An additional negative factor during this critical neonatal period is the presence of a high proportion of fetal hemoglobin, which limits oxygen extraction by the tissues because of its high affinity for oxygen. Finally, there are serious metabolic consequences to severe arterial hypoxemia, including increased anaerobic metabolism, excessive lactate production, depletion of glycogen stores, and metabolic acidosis with the eventual catastrophic outcome of generalized impaired cellular function. The importance of the ductus arteriosus in maintaining and increasing intercirculatory

mixing in the early postnatal period explains the value of infusion of prostaglandin E_1 , particularly in infants with TGA/IVS, but only when there is also an atrial communication to allow pulmonary venous return to reach the ascending aorta.

Pulmonary Vascular Disease

The early development and widespread presence of pulmonary vascular obstruction in patients with TGA have been widely documented by autopsy findings, biopsy studies, and hemodynamic data (23–27). Compared with most other forms of congenital heart disease with increased pulmonary blood flow, TGA has an apparent accelerated rate of development and an increased frequency of this complication. Histologic evidence for advanced pulmonary vascular disease grade 3 or greater using Heath–Edwards (H–E) classification is almost the rule in infants over 1 year of age with large VSD and pulmonary artery pressures at or near systemic level. In one study by Newfeld et al. (23), 25 of 28 children older than 1 year with persistent large VSD had grade 4 H–E histologic changes present (Fig. 49.18). Significant subpulmonary or pulmonary stenosis (i.e., peak systolic pulmonary artery pressure <50% of peak systolic left ventricular pressure) usually prevents the early occurrence of advanced pulmonary vascular disease in patients with large VSD and increased pulmonary blood flow. Even in infants and children with TGA/IVS, extensive abnormal histologic changes have been noted, although the process seems somewhat slower and much less prevalent than with large VSD. Microthrombi, in addition to the classical vascular pathology, were identified in the pulmonary vessels of 23% of the lung specimens, and these may represent an etiologic factor. The persistence of a large PDA in infants with IVS has been implicated as a cause for increased pulmonary vascular disease as has prolonged hypoxemia or polycythemia.

A summary of four comprehensive histologic studies (27) indicated that patients with TGA and large VSD have pulmonary vascular changes grade 3 or greater occurring in 20% before 2 months of age, 25% from 3 to 12 months, and 78% after 12 months of age. The comparable findings for TGA patients with IVS were 1% before 2 months, 17% from 3 to 12 months, and 34% after 12 months of age.

Rarely, the occurrence, or more likely progression, of pulmonary vascular obstruction has been noted even after successful atrial correction in infants with preoperative documentation of minimal pulmonary hypertension preoperatively (23–28). The pathogenesis of the more accelerated and widespread pulmonary vascular disease in TGA is undoubtedly multifactorial. Although the pulmonary vascular bed may be functionally normal at birth, histologic studies indicate that shortly thereafter an accelerated pathologic process occurs. Pulmonary vascular morphometry in a number of congenital cardiac malformations has shown that, in addition to the marked increases in pulmonary vascular muscularity and intimal hyperplasia with vessel obstruction, there is a reduction in the number of intra-acinar pulmonary arteries in patients with elevated pulmonary vascular resistance. Intense systemic hypoxemia is commonly present, and local pulmonary hypoxemia can result from increased bronchial arterial vessels and bronchopulmonary anastomoses carrying hypoxemic systemic blood to the precapillary pulmonary arterioles. Thus, increased pulmonary vascular flow, pressure, and vasoconstrictive factors, possibly in association with abnormal platelet and red cell factors, can result in increased pulmonary vessel shear stress, endothelial damage, microthrombi, and the early induction and rapid progression of vascular disease. These findings suggest that the pulmonary vascular state

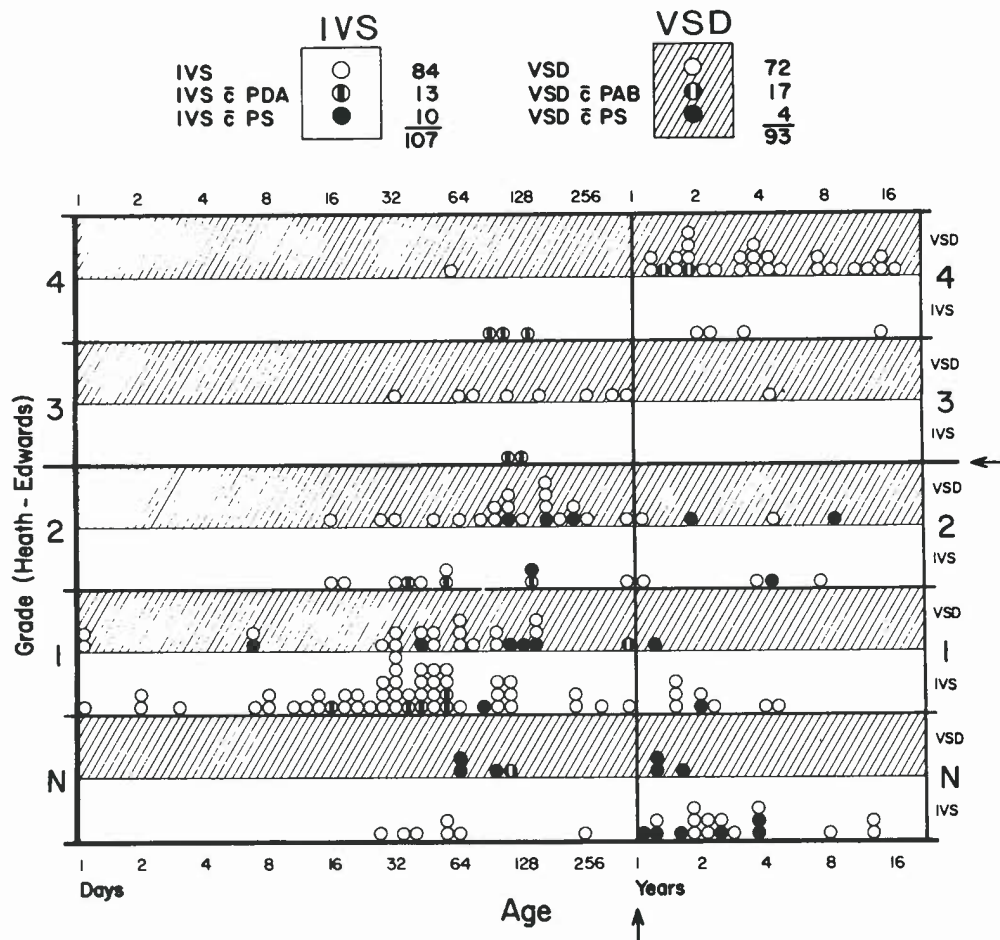


Figure 49.18. Pulmonary vascular disease in patients with TGA. Histologic analysis according to Heath–Edwards classification of lung specimens from 200 patients: 107 with IVS or small VSD and 93 with large VSD. Age, plotted with log 2 scale progression in days and years; *vertical arrow* indicates 1 year of age; *horizontal arrow* indicates separation between grades 1 to 2 pathology and grades 3 to 4 pathology. Grade 3, occlusive intimal fibrosis and grade 4, plexiform lesions and vascular dilatation, represent advanced pulmonary vascular disease. N, normal vascular histology; PDA, patent ductus arteriosus; PAB, pulmonary artery banding; PS, pulmonary stenosis. (From Newfeld EA, Paul MH, Muster AJ, et al. Pulmonary vascular disease in complete transposition of the great arteries: a study of 200 patients. *Am J Cardiol* 1974;34:75–82; Newfeld EA, Paul MH, Muster AJ, et al. Pulmonary vascular disease in transposition of the great vessels and intact ventricular septum. *Circulation* 1979;59:525–530, with permission.)

may influence the rate of destruction of platelets and platelet aggregate formation in the lung and perhaps contribute to the rapid progression of pulmonary vascular disease. The implications of these findings are clear in regard to the timing of surgery to minimize initiation or progression in pulmonary vascular obstructive disease processes. In the current era of wide success with arterial switch repair within the first few weeks of life, progressive pulmonary vascular obstructive disease will likely become infrequent, just as has occurred with early repair in patients with large VSD and normally related great arteries.

The quantitative assessment of pulmonary vascular resistance at catheterization in TGA can be beset with problems. It may not be possible to enter the pulmonary artery for pressure measurements. Application of the Fick principle tends to overestimate pulmonary blood flow and hence underestimate pulmonary vascular resistance (see also section on “Intercirculatory Mixing”). A limited comparison of Fick-estimated pulmonary vascular resistance with histologic grading suggested that patients with advanced

pathology (grade 4, H–E) usually have pulmonary vascular resistance >7 to 8 U and mean pulmonary artery pressures >55 mm Hg (23).

CLINICAL MANIFESTATIONS

In the past, the conventional diagnostic sequence for an infant with suspected TGA was physical examination, electrocardiogram (ECG), and chest roentgenogram, followed by cardiac catheterization, angiography, and usually concurrent palliative BAS. Presently, 2-D and Doppler echocardiography can provide sufficiently detailed information for the cardiac surgical team to proceed directly with an arterial switch operation in the appropriate neonate. If necessary, BAS can be performed and assessed under 2-D echocardiographic visualization. Nevertheless, an understanding and integration of the following clinical components of diagnosis are useful for the comprehensive management of infants with this malformation.

TABLE 49.2

Transposition of the Great Arteries: Physiologic–Clinical Classification

I	TGA (IVS or small VSD) with increased PBF and small ICS ^a
II	TGA (VSD large) with increased PBF and large ICS
III	TGA (VSD and LVOTO), with restricted PBF
IV	TGA (VSD and PVOD), with restricted PBF

^aA subgroup with large PDA has similar characteristics to group II.

IVS, intact ventricular septum; VSD, ventricular septal defect; PBF, pulmonary blood flow; ICS, intercirculatory shunting; PVOD, pulmonary vascular obstructive disease; LVOTO, left ventricular outflow tract obstruction.

Cyanosis, hypoxemic deterioration, or heart failure with early death summarizes the usual clinical course in the untreated infant with complete TGA. The clinical manifestations and course are influenced predominantly by the extent of intercirculatory mixing, which, in turn, depends on several anatomic and functional factors that can be integrated into a useful clinical classification (Table 49.2).

Transposition of the Great Arteries (IVS or Small VSD) with Increased Pulmonary Blood Flow and Small Intercirculatory Shunt

Prominent hypoxemia (“cyanosis”) is an early and almost universal finding in the neonate with TGA who has inadequate intercirculatory mixing (group I). The cyanosis may be initially mild (see section on “Fetal and Perinatal Physiology”) but is rapidly progressive. In neonates diagnosed after birth, cyanosis was recognized by the nursery staff or physician within the first hour of life in 56% and during the first day of life in 92% of neonates with TGA and IVS (29). Early diagnosis and prompt therapy for the neonate with TGA/IVS are critical. Undue emphasis has been placed in the past on diagnostic features, such as significant systolic murmur, heart failure, cardiomegaly, and cardiopulmonary distress. For this subgroup, it must be recognized that beyond cyanosis, the clinical examination is often unrewarding with regard to useful diagnostic physical findings. Even the chest roentgenogram and ECG may be normal in appearance in the immediate newborn period. In the current era, prompt echocardiographic examination is clearly indicated for any cyanotic neonate with suspected congenital heart malformation.

Reverse differential cyanosis, that is, cyanosis of the upper body greater than that of the lower body, is rare and always indicates the presence of TGA with a PDA and pulmonary artery to aortic shunting. In the neonate with TGA and an IVS and uncomplicated large PDA, this pattern may be transiently observed, particularly if pulmonary vascular resistance remains high. Importantly, reverse differential cyanosis suggests a more complex TGA malformation including an aortic arch anomaly, such as coarctation of the aorta or interruption of the aortic arch, or TGA with suprasystemic pulmonary vascular resistance.

On physical examination, the neonate, if seen early, will appear healthy and well developed except for cyanosis. With time, one of two clinical pictures emerges: either hypoxemia (TGA with intact or virtually IVS) or heart failure (TGA with large VSD). Early systolic ejection sounds are rare; the first heart sound is normal or loud. No systolic murmur is heard in most neonates, and those heard are typically soft, grade 2/6 or less. These systolic murmurs are ejection in quality, maximum at the middle and upper left sternal border, and probably represent a functional LVOT murmur related to increased blood flow velocity or a closing PDA.

A large, persistent PDA can modify the clinical findings in the neonate with TGA/IVS because a large intercirculatory shunt may be present. Characteristically, these infants present quite early with prominent tachypnea and relatively slight cyanosis. Importantly, the classic signs indicative of a large PDA, such as continuous murmur, bounding pulses, and a prominent middiastolic rumble, are present in fewer than half of this group. The risk for necrotizing enterocolitis may be increased in neonates with TGA and a large PDA. In these infants, the mesenteric circulation may be at risk because of (a) retrograde diastolic flow in the descending aorta producing a “steal” phenomenon, (b) decreased oxygen delivery, and (c) cardiac catheterization/angiography and umbilical artery catheterization in some cases.

Transposition of the Great Arteries (Large VSD) with Increased Pulmonary Blood Flow and Large Intercirculatory Shunt

The neonate with a large VSD may not manifest any signs or symptoms of heart disease initially, although mild cyanosis, most evident during crying, may be noted in the nursery. Characteristically signs of congestive heart failure develop within 2 to 6 weeks. Tachypnea and tachycardia become prominent; cyanosis, although evident with stress and crying, may remain quite mild and be overlooked. Heart murmurs also may be minimal initially, but a prominent grade 3 to 4/6 pansystolic murmur, third heart sound with middiastolic rumble, gallop rhythm, and narrowly split second heart sound with loud pulmonary component eventually emerge in these infants.

Transposition of the Great Arteries (VSD and LVOTO) with Restricted Pulmonary Blood Flow

Neonates with TGA, VSD, and severe pulmonary stenosis or atresia have diminished pulmonary blood flow. They represent a relatively small proportion (5% to 8%) of the neonatal TGA population. Clinical findings are similar to those in the infant with tetralogy of Fallot with severe pulmonary stenosis or atresia, and the cyanosis is extreme from birth.

Transposition of the Great Arteries (VSD and Pulmonary Vascular Obstructive Disease) with Restricted Pulmonary Blood Flow

Pulmonary vascular obstructive disease is not present in the newborn with TGA. Progressively advancing pulmonary vascular disease may not be evident early from physical findings. A secondary increase in cyanosis with increasing hematocrit in infants who have had successful palliative procedures always should raise the suspicion of a decrease in pulmonary blood flow caused by progression either in pulmonary vascular disease or in LVOT stenosis. With advanced pulmonary vascular obstructive disease, an early systolic ejection sound is commonly heard. There may be no murmurs present or only a faint short ejection systolic murmur. Eventually, in later childhood or adolescence, a high-pitched, blowing early decrescendo diastolic murmur of pulmonary insufficiency and a blowing apical murmur of mitral insufficiency result from gross dilation of the left heart.

Central Nervous System

Associated anatomic abnormalities of the central nervous system are rare in children with TGA, although head circumference is slightly less than normal (20). Spontaneous

cerebrovascular accidents, particularly in infants younger than 2 years of age, were an infrequent but tragic complication in the past for the inadequately palliated or uncorrected infant. The recent decrease in frequency undoubtedly is related to programs achieving more satisfactory early palliation or correction. The most common presentation is the sudden onset of hemiparesis. Hypochromic, microcytic anemia in conjunction with severe hypoxemia has been implicated as a mechanism for cerebrovascular accidents in the neonate and young infant. In the older child, polycythemia and the increased blood viscosity secondary to long-standing, severe hypoxemia have been regarded as the etiologic factors.

Brain abscesses have been infrequent: when they occur, they are almost always in a surgically uncorrected patient over 2 years of age, in contrast to cerebrovascular accidents, which occur most commonly in infants younger than 2 years of age. Symptoms such as persistent headache or, less frequently, slowly developing neurologic abnormalities distinguish this complication from acute cerebrovascular accident.

Psychologic testing has shown that preschool-aged children who had prolonged uncorrected cyanotic heart disease in infancy have slightly lower intelligence quotient scores and tend to perform poorer with perceptual motor tasks than children with asymptomatic acyanotic heart disease. Early atrial corrective surgery has been demonstrated to have beneficial effects on weight and linear growth; however, the long-term effects of intense, prolonged early cyanosis are not yet fully evaluated. Although the benefits of early detection (30) and correction (31) are likely to minimize secondary end-organ damage, more recent data suggest that the Full Scale IQ scores for these children, as a group, may be lower than the normal population, and there is a higher-than-expected incidence of learning disabilities, speech and language problems, and motor delays (32–36).

Electrocardiographic Features

The usual ECG findings are right-axis deviation with right or combined ventricular hypertrophy; the findings, however, vary considerably, depending on age and anatomic and physiologic factors. The ECG in the first days of life is typically normal for age. Within weeks, however, abnormal right ventricular hypertrophy appears in most infants with IVS or small VSD. Initially, this may be identified solely by the persistence, beyond 3 to 5 days of age, of a positive T wave in the right precordial leads. Right-axis deviation predominates when the septum is intact; in contrast, one-third of infants with large VSD have

normal QRS axis for age. Left-axis deviation occurs rarely in TGA/IVS but is typical in TGA with AV septal defect types of VSD, with or without straddling tricuspid valve or right ventricular hypoplasia.

Combined ventricular hypertrophy is present in about 60% to 80% of patients with large VSD. These ECG patterns are modified by LVOT stenosis or increased pulmonary vascular resistance. A Q wave in V6 is usually present (70%) in TGA with large VSD but is infrequent (15%) when the ventricular septum is intact (37). Isolated left ventricular hypertrophy is rarely encountered and suggests TGA with VSD, straddling of the tricuspid valve, and associated hypoplasia of the right ventricle.

Dysrhythmias are rarely noted in the newborn period, but short periods of bradycardia and junctional rhythm may be seen in 24-hour ambulatory ECG recordings. Atrial flutter may be seen during and after BAS.

Radiologic Features

Roentgenographic findings may provide diagnostic assistance (Fig. 49.19); however, in the neonate particularly, the findings may be normal. In the neonate with TGA/IVS, the diagnostic triad includes (a) oval or egg-shaped cardiac silhouette with narrow superior mediastinum, (b) mild cardiomegaly, and (c) increased pulmonary vascular markings.

Transposition of the Great Arteries with Intact Ventricular Septum

In the first few days and weeks of life, the chest roentgenogram may appear normal. The heart is usually slightly enlarged, but one-third of the neonates have no cardiac enlargement. Pulmonary vascular markings are considered normal in from one-third to one-half the neonates seen, and the typical oval-shaped silhouette is not present in one-third to one-half of these infants. The vascular pedicle or superior mediastinal silhouette is narrow because of the usual anteroposterior relationships of the great arteries and the hypoplasia of thymus tissue associated with cyanosis and stress. Right aortic arch is relatively uncommon: 4% in patients with TGA/IVS and 11% in patients with TGA/VSD (38,39).

After the first few weeks of life, cardiac enlargement may become evident, and the pulmonary vascular markings appear increased in almost every infant with TGA without LVOTO. In some neonates, however, even following adequate BAS, the pulmonary vascular markings do not appear increased initially,

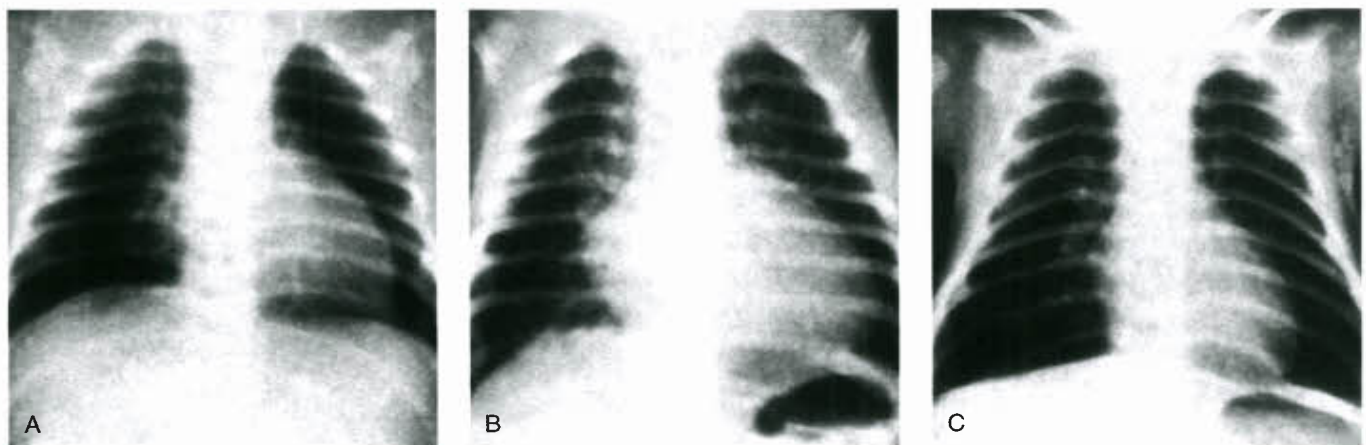


Figure 49.19. Frontal chest roentgenograms in three neonates with TGA/IVS and no significant PDA at 1 day of age. Note variations in cardiac size, shape, and pulmonary vasculature.

and these infants often have persistent low systemic arterial oxygen saturation. Such observations support the hypothesis that functionally the pulmonary vascular bed may remain relatively vasoconstricted, and the resultant inadequate increase in pulmonary blood flow minimizes the functional effectiveness of an adequate BAS. In the past, when surgical repair usually was delayed for months following BAS, clinical deterioration sometimes occurred and was characterized by increasing cyanosis with progressive diminution in pulmonary vascularity secondary to progressive dynamic LVOTO. Recognition and assessment by echocardiography are important for this subset of infants.

Transposition of the Great Arteries/Large Ventricular Septal Defect

The pulmonary vascular markings in infancy appear particularly prominent when a large VSD is present with low pulmonary vascular resistance, and the cardiac silhouette is usually considerably larger than seen in TGA/IVS. If advanced pulmonary vascular obstruction is present (in older infants and children), the hilar vessels are enlarged, but the peripheral pulmonary vessels appear small and constricted; the left cardiac border is often grossly distorted by a dilated pulmonary artery trunk. Pulmonary vascular markings remain increased in the face of moderate LVOT stenosis, and only severe obstruction or atresia is associated with diminished pulmonary vascular markings.

Echocardiographic Features

In the current era, echocardiography has become the diagnostic method of choice in the patient with TGA (Fig. 49.20). Subcostal imaging provides a flexible acoustic window that allows wide angulation and rotation of the transducer beam to optimize simultaneous visualization of the great arteries (ascending aorta and main pulmonary artery with its primary branches) and their respective ventricular connections. Additional imaging from the apex (four-chamber view) is useful in establishing the identity of the posterior vessel as the pulmonary artery from its branching morphology. Suprasternal and high parasternal views enable the aorta to be traced arising from the right ventricle to the arch and its branches. Spatial orientation of the great arteries and the origin and proximal segments of the coronary arteries can be viewed on parasternal and short-axis scans at the base of the heart. Echocardiography can diagnose most of the important associated anomalies with a high degree of accuracy, including size, number, and location of VSDs; anatomic type of LVOTOs; form and function of tricuspid and mitral valve anomalies; and outlet septum malalignment defects. Imaging can be used to guide catheter placement and movements during BAS (Fig. 49.21) and to assess the anatomic adequacy of the septostomy.

In the current era, echocardiography has assumed the primary role in determining the candidacy of a neonate with simple TGA for arterial switch, even to the extent of replacing cardiac catheterization in many centers. Routine obstetric fetal echocardiography may lead only to the prenatal diagnosis of TGA in those patient subgroups who have associated large VSD, common AV septal defect, or severe outflow tract obstruction where the usual four-chamber screening examination reveals the presence of a serious malformation and leads to a more extensive (cardiac-expert) examination of the great vessel origins. Conversely, for TGA with IVS, an obstetric screening examination frequently does not readily identify the malformation and presently may not influence clinical management or referral programs. The diagnosis of TGA (even with IVS) can readily be made, however, by specialized fetal echocardiography. Perhaps the greatest advantage of prenatal

diagnosis is the ability to deliver the infant in an obstetric facility with the expectation of cardiac disease, institution of PGE₁ therapy, and prompt transfer to a specialized cardiac facility before clinical deterioration may take place.

Cardiac Catheterization

Cardiac catheterization with BAS in some centers continues to assume an emergency priority, particularly for the neonate with poor intercirculatory mixing. In any event, successful management includes prompt initiation of any indicated supportive medical therapy, such as airway protection, oxygen, acid-base correction, PGE₁ infusion, antibiotics, and, in some patients with large intercirculatory shunts, inotropic support and diuretics. Increasingly, catheterization with BAS is not routinely undertaken in many centers where the neonate with TGA often proceeds directly to primary arterial switch correction during the first few days of life. A complete echocardiographic diagnosis (and possible simultaneous balloon septostomy) with interim supportive PGE₁ infusion may be all that is necessary prior to surgery. Some centers will not perform septostomy at all unless there is echocardiographic evidence of a restrictive foramen ovale or absence of a significant rise in arterial PO₂ on initiating prostaglandin infusion.

Cardiac catheterization, angiography, BAS, and meaningful physiologic information can be obtained safely only if optimum techniques are expertly and judiciously employed using percutaneous femoral vein entry, umbilical vein catheterization, or (rarely) direct femoral vein cutdown. In the unstable neonate with poor mixing, it is advisable to proceed with therapeutic BAS promptly before attempting more extensive hemodynamic and angiographic investigations.

Cardiac catheterization remains an important adjunct in the diagnostic evaluation of infants with echocardiographic diagnoses of more complex forms of TGA. Additional observations on the following items are important in planning appropriate palliative or corrective surgery: pulmonary artery pressure; pulmonary blood flow (and vascular resistance); coronary artery anatomy; morphologic details of pulmonary or subpulmonary obstruction; VSD number, site, and size; great-vessel alignments in relation to the VSD and outlet septum; and type and severity of aortic arch abnormalities. In such cases, when surgical palliation (e.g., pulmonary artery banding, septectomy) is planned or repair is electively delayed, BAS should be strongly considered, even in patients with large VSD, to improve interatrial left-to-right shunting (effective systemic blood flow) to decrease left atrial pressures.

Entrance into the pulmonary artery in the neonate is usually difficult, time-consuming, and occasionally traumatic. Aside from the value of these measurements for later comparisons, such measurements are usually not essential for management in the neonate or infant as the peak systolic pulmonary arterial and left ventricular pressures are usually equal in neonates, except when there is significant subpulmonary stenosis or pulmonary atresia, both of which can be easily recognized by echocardiography or angiography.

A deflated balloon-tipped catheter can be directed across the interatrial communication to the left atrium, where the balloon is inflated. The catheter usually advances rapidly to the left ventricle, either to form a curve with the tip directed to the outflow tract or to become wedged in the apex. If the latter occurs, the catheter tip is best withdrawn to the mitral level and then advanced and withdrawn slowly with lesser degrees of balloon inflation until the catheter tip is carried into the LVOT, where it then can be advanced rapidly into the pulmonary artery. Tip-deflecting wires are extremely helpful in directing the balloon toward the LVOT; the catheter then may

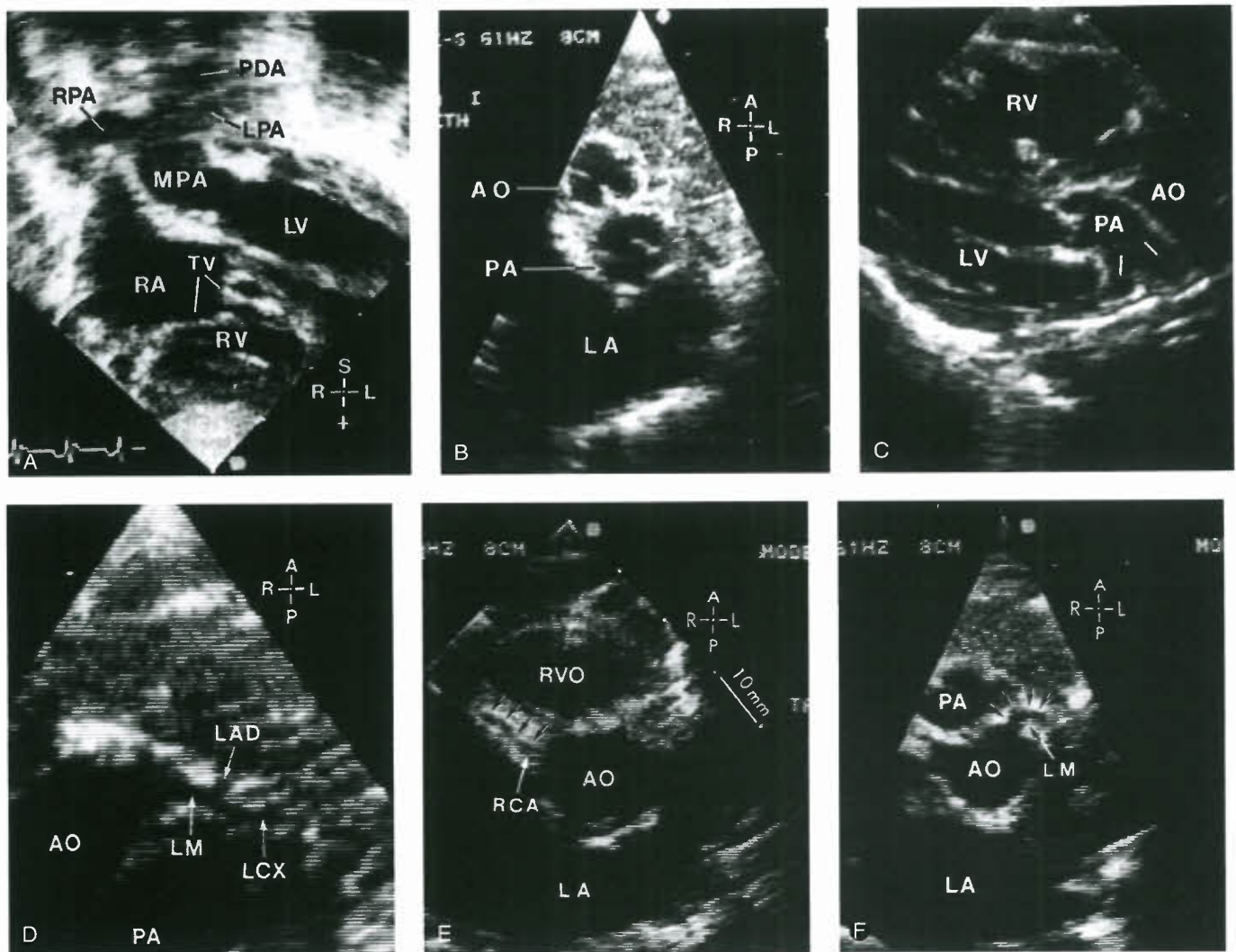


Figure 49.20. Two-dimensional echocardiographic images in 1-day-old with TGA/IVS. **A:** Subcostal view demonstrates left ventricle (LV) and unobstructed LVOT aligned (connected) with normal pulmonary (potential neo-aortic) valve, main (MPA), right (RPA), and left (LPA) pulmonary arteries. A large PDA is seen (on prostaglandin E1 infusion). **B:** Parasternal short-axis view demonstrates slightly oblique interrelationship of the great arteries consistent with TGA [S,D,D] (AO). LA, left atrium; PA, pulmonary artery. **C:** Parasternal long-axis view confirms discordant ventriculoarterial connection: the pulmonary trunk by its abrupt posterior turn shortly distal to the pulmonary valve, and (in other planes of this echo view) the aorta by the origin of the brachiocephalic artery. **D:** Origin and proximal branches of the left coronary artery in the usual coronary artery anatomy for TGA (see also Fig. 49.7). Note origin of left main coronary (LM) from left/posterior facing sinus and its bifurcation into proximal left circumflex (LCX) and anterior descending (LAD) branches. The right coronary artery, in another echo plane, arises from the posterior right aortic sinus. **E,F:** Echocardiographic images obtained at postoperative examination 1 year after surgery (arterial switch at 13 days of age) shows moderate dilation of the neo-aortic root. Right (RCA) and left main (LM) coronary arteries show no stenosis or obstructive kinking in the proximal segments. RVO, right ventricular outflow.

be “peeled off” the deflecting wire and advanced into the pulmonary artery.

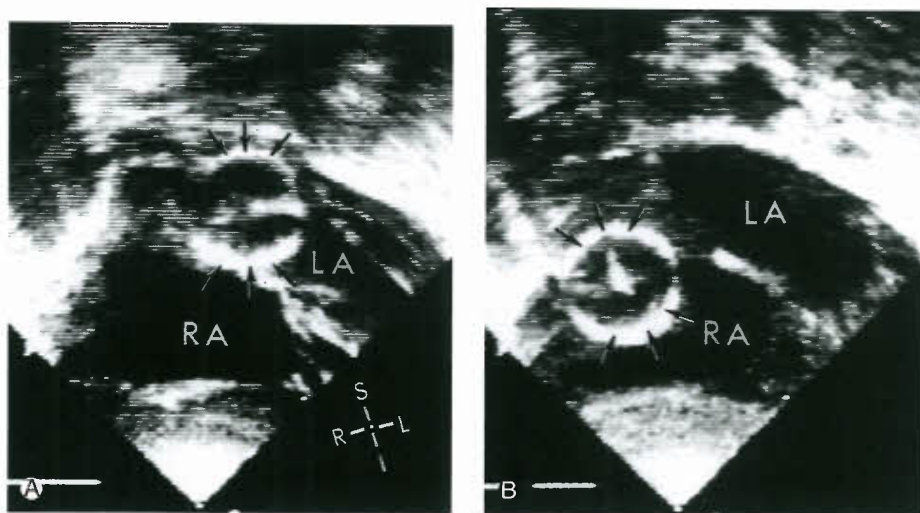
In patients with significant inlet or outlet VSDs, it may be possible to manipulate the catheter directly from the right ventricle through the VSD into the pulmonary artery, although this may induce heart block. If the pulmonary artery is not entered, pulmonary-vein wedge pressures should be obtained; if they are normal, it is unlikely that the pulmonary artery pressure is elevated. Catheterization findings are consistent with the detailed discussions under the section on Physiology and with the classification schema (Table 49.2).

In the newborn with TGA/IVS and markedly inadequate intercirculatory mixing (group I), the oxygen saturation in the

vena cava may be as low as 20%, although usually it is about 40%. There is usually only a small increase of 5% to 10% in the right atrium and right ventricle; the systemic arterial saturation is quite similar to that in the right ventricle. Pulmonary venous saturation is generally normal, and there may be a 4% to 8% decrease in the left atrium or left ventricle. A marked combined respiratory and metabolic acidosis, along with severe hypoxemia, is a hallmark of TGA/IVS with poor mixing.

In the infant with a large intercirculatory communication (group II, TGA/VSD), the vena caval saturations are modestly reduced, and there is usually an increase in oxygen saturation at the atrial level of 5% to 10% as a result of interatrial

Figure 49.21. BAS performed in newborn with 2-D echo imaging to guide catheter placement and septostomy balloon withdrawal from (A) left atrium (LA) to (B) right atrium (RA). Arrows delineate balloon.



shunting. A large increase in oxygen saturation is observed in the right ventricle, to levels of 70% to 85%, and similar levels are noted in the aorta. The pulmonary venous oxygen saturation rarely may be reduced because of left atrial hypertension and pulmonary edema. Similar oxygen saturations are noted in the left atrium and left ventricle, but the pulmonary artery saturation may be somewhat lower than that in the left ventricle due to some preferential pulmonary artery streaming from the interventricular right-to-left shunt. The distinguishing feature of “transposition physiology” is that the oxygen saturation in the pulmonary artery is always higher than in the aorta; however, with extensive intracardiac mixing, the saturations may be quite similar. In the absence of an adequate atrial communication, left atrial pressures may be quite elevated, up to 20 mm Hg or more, with quite prominent V waves. With a large VSD, the left and right ventricular systolic and end-diastolic pressures and pulmonary and aortic systolic pressures may be essentially identical; the pulmonary arterial end-diastolic and mean pressures, however, are commonly lower than the systemic levels, reflecting the lower pulmonary vascular resistance.

When there is LVOT stenosis associated with a large VSD (group III), the findings depend on the severity of the pulmonary outflow tract obstruction. When the obstruction is severe, along with a small or closed ductus arteriosus, the systemic arterial oxygen saturation may be quite low (30% to 50%), and the clinical findings are similar to those in tetralogy of Fallot with severe pulmonary stenosis or atresia.

Angiocardiography

When indicated, selective cardiac chamber and great vessel angiographic injections should be performed to identify or confirm the echocardiographic diagnoses and associated cardiac defects. In the current era, echocardiography provides superior imaging of many of these abnormalities, particularly those associated with the AV and semilunar valve structures and the ostia and proximal course of the coronary arteries.

In the lateral angiogram in TGA/IVS, the aorta usually forms a wide open arch with the ascending portion proceeding far ventrally. The aortic valve cusp level is higher (fourth to fifth thoracic vertebral level) than in the normal heart (seventh thoracic vertebral level) and reflects the well-developed subaortic conus characteristic of TGA. Deviation occurs particularly when a large VSD with atypical conal morphology (bilateral conus or deficient conus) is present or with

the rare form of posterior transposition. The ascending aorta is typically anterior and to the right of the pulmonary artery in an oblique relationship; the large main pulmonary artery arises slightly to the left and definitely posterior to the aorta.

Variations and some ambiguity may arise when angiographically the transposed aortic valve appears to lie directly anterior to the transposed pulmonary valve and more particularly when the transposed aortic valve lies anterior and slightly to the left of the transposed pulmonary valve (6% to 14%). The physiologic findings in the latter instance again are those of physiologically uncorrected TGA, but the segmental findings are TGA {S,D,L}, AV-concordant connection, that is, situs solitus of viscera and atria (S), ventricular D-loop (D), and an apparent L-position of the semilunar valves (L) (Fig. 49.22A–D). This configuration is to be differentiated, particularly in the anteroposterior angiographic view, from the usual physiologically corrected TGA, {S,L,L} TGA AV discordant connection (Fig. 49.22E–H).

Identification and localization of the conal musculature and semilunar–AV valve relationships can be helpful in analyzing the more complex variations. The tricuspid valve is best visualized by using selective right ventricular injection in the frontal or right anterior oblique views by noting intra-atrial bulging of the leaflets during ventricular systole and during diastole by the negative silhouette of the orifice as nonopacified blood enters the ventricle. Continuity of the anterior leaflet of the mitral valve with the pulmonary valve is best visualized in the four-chamber long-axial or left anterior oblique views in diastole when the anterior leaflet is noted to form the posterior wall of the LVOT. In the frontal view, the line of attachment of the posterior mitral valve leaflets can best be seen in diastole. Straddling or overriding tricuspid valve with VSD must be suspected whenever hypoplasia of the right ventricle is observed. Levoposition (“juxtaposition”) of the right atrial appendage frequently accompanies this constellation of anatomic findings.

The number, site, and size of VSD(s) can be well visualized by angiography, particularly when an appropriate long axial or hepatoclavicular four-chamber oblique (rather than lateral) view is used (Figs. 49.9, 49.10A, and 49.11A). In many instances, the VSD represents an additional but uncomplicated anatomic component of the surgical repair. When there are various types of atypical conus associated with malalignment or straddling AV orifices, valve leaflets, or their attachments, however, foreknowledge of the precise size and location of the VSD and its relationship to the semilunar and AV valves is

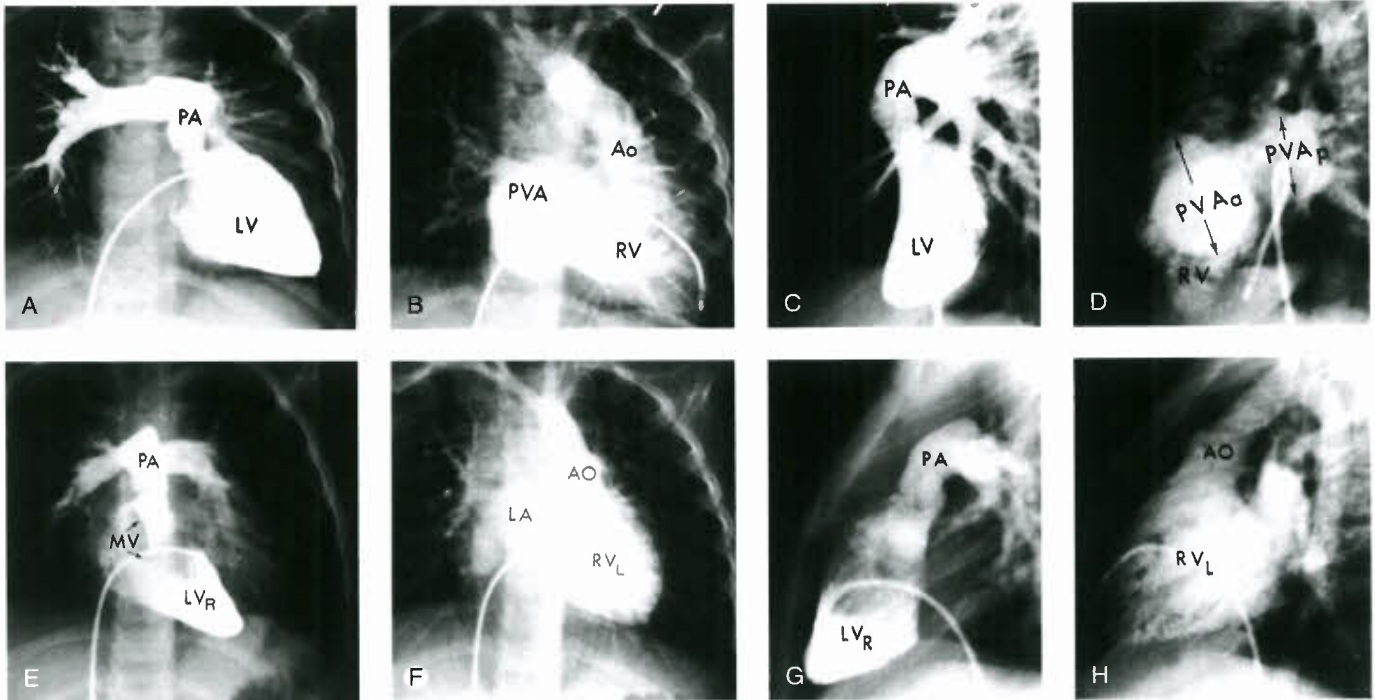


Figure 49.22. Angiograms (A–D) illustrating variant leftward position of aortic valve in 4-year-old with TGA {S,D,L} following intra-atrial (Mustard) repair. **A:** Frontal view, selective transvenous injection into left-sided morphologically left ventricle (LV). **B:** Frontal view, after pulmonary circulation and opacification of new pulmonary venous atrium (PVA), right-sided, morphologically right ventricle (RV) and left-malpositioned aortic (Ao) valve. **C:** Lateral view of (A). **D:** Lateral view of (B). PVAa, anterior segment; PVAp, posterior segment of pulmonary venous atrium. Angiograms (E–H) illustrating leftward position of aortic valve in 4-year-old with TGA {S,L,L}. **E:** Frontal view, selective injection into right-sided morphologically left ventricle (LV). **F:** Frontal view, after pulmonary circulation and opacification of left atrium (LA) and left-sided morphologically right ventricle (RV) and left positioned aortic (AO) valve. **G:** Lateral view of (E). **H:** Lateral view of (F).

mandatory. The four-chamber hepatoclavicular projection is particularly useful for profiling the posterior inlet component of the ventricular septum. Long axial oblique views are useful for demonstrating the various outlet septum malalignment abnormalities, including the VSD and right and left ventricular outlet obstructions.

The various forms of LVOT stenosis can be best discriminated angiographically by long axial left ventricular views. Small peak systolic pressure differences (<20 mm Hg) between left ventricle and main pulmonary artery have been attributed to a “functional” stenosis of the pulmonary valve and outflow tract, similar to that observed in patients with secundum ASD with high pulmonary blood flow. In TGA/IVS, however, such systolic pressure differences also may be associated with a recognizable systolic septal bulge abnormality. Minor degrees of abnormal protrusion of the upper muscular ventricular septum into the LVOT in systole are subtle but can be appreciated angiographically in the lateral and left anterior oblique views. Occasionally, the entire ventricular septum encroaches convexly and posteriorly during systole, and the left ventricle appears small and flattened (“pancaked”) (Fig. 49.4).

A more obvious angiographic subpulmonary ridge-like obstruction is associated with somewhat larger LVOT pressure differences and reflects a subvalvar fibrous muscular ridge obstruction, often with an underlying abnormal septal bulge. This fibromuscular ridge is probably a systolic impact lesion and angiographically appears as a prominent irregular curvilinear radiolucent line during systole in the region of the mitral valve. The ridge is often most prominent medially and may demarcate sharply a small subpulmonary vestibule (Fig. 49.5B,D). Isolated pulmonary valve stenosis is infrequent

as a major lesion, but thickened valve cusps may be observed. The fibromuscular tunnel-type stenosis can best be recognized in the left long-axial oblique view as an extensive, narrow, fixed restrictive passage extending from above the VSD for some length toward the pulmonary valve. This form is commonly associated with a VSD with a posterior malalignment of the conal septum, with crowding of the LVOT (Figs. 49.8A and 49.10A). Subpulmonary obstruction resulting from aneurysm of the membranous ventricular septum or redundant tricuspid valve tissue displaced into the LVOT may be recognized by careful angiographic assessment (Fig. 49.12A). Persistent subpulmonary obstruction also can be caused by anomalous septal attachments of straddling mitral valve tissue.

Malalignment defects of the ventricular outlet septum also may be associated with anterior–rightward septal deviation, which causes distinct anatomic, but less frequently hemodynamic, right ventricular outflow tract obstruction (Fig. 49.8B); with this abnormality, distal systemic circulation malformations such as coarctation or interruption of the aorta should be anticipated and investigated by angiography and echocardiography.

Although the coronary artery anatomy sometimes may be outlined from a right ventriculogram, better visualization is achieved by selective transvenous coronary angiography or antegrade aortic root angiography with distal balloon occlusion of the ascending aorta. Using this technique, a balloon angiographic catheter (with injection holes proximal to the balloon), introduced transvenously, is positioned in the ascending aorta proximal to the brachiocephalic arteries so that the side holes are approximately 1 cm above the aortic valve. The balloon is inflated with carbon dioxide and

stabilized in the ascending aorta. During cineangiography, between 0.5 and 1.0 mL/kg of contrast medium are injected over approximately 1 second, and the balloon is deflated immediately after the injection. Inflation of the balloon during injection allows contrast medium to be preferentially directed toward the aortic root and coronary ostia.

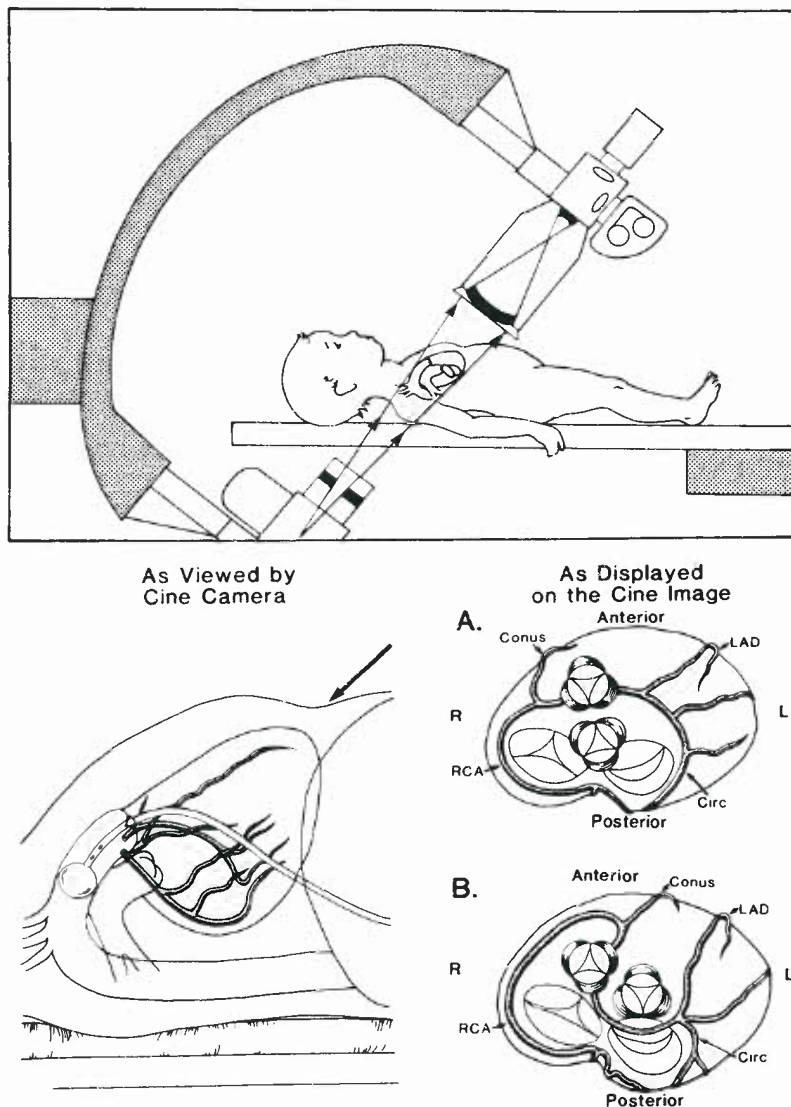
Mandell et al. (40) combined balloon occlusion aortography with extreme caudal angulation of the anterior-posterior camera, producing the so-called laid-back aortogram (Figs. 49.23 and 49.24). This is perhaps the most anatomically precise angiographic technique for the preoperative assessment of the coronary arteries in TGA because it provides visualization of both the proximal ostia and distal distribution of the coronary arteries in the same plane of view (see section on "Morphology").

Balloon Atrial Septostomy

In the newborn <48 to 72 hours of age, the umbilical vein has been used successfully for BAS as well as diagnostic catheterization. More commonly, percutaneous needle and catheter sheath placement is used to gain access to the femoral vein. Successful, adequately sized rupture of the septum primum flap to enlarge the interatrial opening is dependent on both structural-design elements of the balloon catheter and procedural techniques.

The catheter should be advanced across the foramen ovale into the left atrium or a pulmonary vein and the position of the tip established with certainty in the left atrium prior to proceeding. Location of the catheter tip is established most readily by echocardiography or by using fluoroscopy to visually confirm the posterior position of the tip in the lateral or left anterior oblique view or entry of the catheter into a pulmonary vein. Once the position is verified, the balloon is inflated with diluted angiographic contrast medium to at least 12- to 15-mm diameter and then rapidly withdrawn across the atrial septum with an abrupt, short tug, "like a backhand in squash" (Keane JF, *personal communication*). The balloon and interatrial septum are displaced toward the inferior vena cava, and the septum primum flap of the fossa ovalis is ruptured as the balloon is carried in a single movement from the left atrium to the right atrial-inferior vena caval junction. The catheter should be advanced immediately and the balloon pushed cephalad out of the inferior vena caval orifice into the right atrium toward the superior vena cava to verify crossing the septum and to avoid obstruction to inferior vena caval return while the balloon is being deflated. This same procedure should be repeated several times with increasing balloon volumes, so that withdrawal of the balloon, inflated tensely to a diameter of at least 15 mm, is achieved without much resistance being perceived at the atrial septum level. Slow or gentle withdrawal of the balloon from the left-to-right atrium is considered by some to

Figure 49.23. Upper panel: Position of frontal C-arm with extreme caudal angulation of the tube. The lateral tube, necessary for balloon positioning, is not shown. Lower left panel: View of heart and balloon position as "seen" by lateral image intensifier. Solid arrow in right upper corner shows "viewpoint" of frontal camera when it assumes its caudal angulation. Lower right panel: Caudal view of heart and coronary arteries as displayed by frontal cine camera. An example of coronary course in anterior-posterior (A) and side-by-side (B) great arteries is shown. Circ, circumflex coronary artery; LAD, left anterior descending artery; RCA, right coronary artery. (From Mandell VS, Lock JE, Mayer JE Jr, et al. The "laid-back" aortogram: an improved angiographic view for demonstration of coronary arteries in transposition of the great arteries. *Am J Cardiol* 1990;65:1379-1383, with permission.)



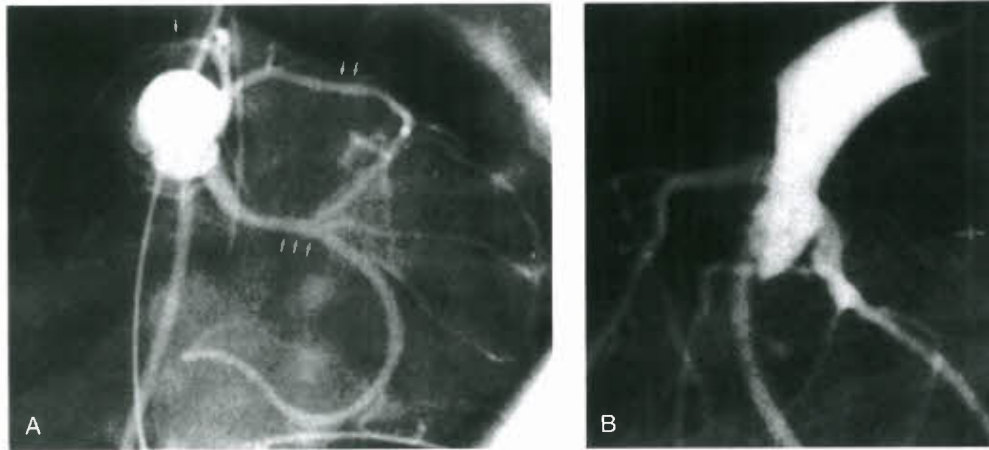


Figure 49.24. A: Caudal view in a patient whose great arteries are side by side with inverted right and circumflex coronary arteries (see Fig. 49.7). From the anterior-facing sinus, a coronary artery originates and gives rise to the left anterior descending artery (*double arrow*), which crosses anterior to the pulmonary artery and a small right coronary artery (*single arrow*). From the posterior facing sinus arises a dominant circumflex artery (*triple arrow*), which courses behind the pulmonary artery and supplies the lateral, posterior, and inferior walls of the left ventricle. B: Lateral view of the same showing ideal balloon position and occlusion of the aorta at time of injection. (From Mandell VS, Lock JE, Mayer JE Jr, et al. The “laid-back” aortogram: an improved angiographic view for demonstration of coronary arteries in transposition of the great arteries. *Am J Cardiol* 1990;65:1379–1383, with permission.)

be counterproductive because it causes stretching rather than tearing of the septum primum flap with temporary functional rather than permanent anatomic enlargement of the foramen ovale defect.

Cardiac complications of the procedure are uncommon when the aforementioned precautions are observed, but the operator must be knowledgeable and skilled to avoid atrial wall, pulmonary vein, or inferior vena caval perforation or tears or AV valve damage. Other injuries that have been reported include damage to the inferior vena cava, which probably can be minimized by using an adequately inflated balloon so that it is not pulled deep into the inferior vena cava. Patients may develop complete heart block, although it is typically self-limited and rarely requires long-term pacing. Intracardiac rupture of the balloon occurs infrequently, but it is important to avoid introducing air bubbles during inflation with the contrast medium to prevent air embolization. Rubber fragmentation and embolization from a ruptured balloon have been virtually abolished by new materials and fabrication techniques. A recent report raised the important question of CNS complications such as stroke or ischemia identified in critically ill patients with TGA undergoing urgent septostomy (41). In this retrospective review, it was difficult to separate out the CNS effects of the profound hypoxemia leading to the need for urgent intervention, from the CNS effects of the intervention itself. Nonetheless, potential CNS complications should factor in the decision to perform septostomy, especially in nonemergent situations (see below). Deflation failure of the balloon in the right atrium after septostomy, a rare complication in the past, has been obviated by the newer fabrication techniques. The inability to deflate the balloon using the syringe can be managed without surgery, however, by carefully inserting the sharpened, stiff end of a guidewire along the catheter shaft and rupturing the balloon.

If levoposition of the right atrial appendage (juxtaposition of atrial appendages) is present, the catheter tip, still in the right atrial appendage, may appear falsely to conform to conventional criteria for left atrial positioning. With this anomaly, the right atrial appendage is more posterior than normal and occupies the left upper heart border in the anteroposterior view. The operator should suspect levoposition of the right atrial

appendage if the catheter tip cannot be directed into a pulmonary vein or pass quite as much posteriorly as usual. Selective right atrial angiograms, or preferably a precatheterization echocardiographic examination, will verify the diagnosis.

In the neonate, satisfactory rupture of the septum primum flap covering the fossa ovalis is nearly always affected by proper BAS technique. In older infants, particularly those with TGA/VSD, a thickened interatrial flap may preclude successful balloon catheter septal rupture. If necessary, a catheter equipped with an extendable blade may be used to enlarge the interatrial communication prior to septostomy. Finally, in patients with a markedly thick atrial septum, a new defect (separate from the foramen ovale) can be created with a transseptal needle and dilated with an 8- to 15-mm-diameter balloon angioplasty catheter (static balloon septoplasty). A second hole is recommended because long-term dilation of the true foramen ovale has been unsuccessful in most cases (Lock JE, *personal communication*).

TREATMENT

Consideration of optimal treatment choices for the various subsets of patients with complete transposition must integrate the current information available on over 50 years' experience with atrial level repair and 30+ years of arterial level repair. Abundant early and midterm postoperative observations warrant cautiously optimistic support for the choice of an arterial switch repair for newborns with nearly all forms of TGA. This trend is reflected in data from a multi-institutional study showing an increase in arterial switch repair from 40% of the eligible TGA study population in 1985 to 80% in 1990.

Palliative Therapy

In the past, the keystone to improved survival and eventual corrective surgery has been the successful application of palliative procedures: BAS, surgical septectomy, partial venous correction, pulmonary artery banding, and systemic–pulmonary shunts.

Balloon Atrial Septostomy

Accumulated experience over the past four decades clearly has established the value of BAS for the initial management of the severely hypoxemic neonate with TGA: Survival for the first month of life improved from 20% before septostomy was introduced to as high as 95% afterward. Accordingly, BAS was performed in neonates as the first step in any management program for patients destined to have atrial repair procedures later in infancy. In the past two decades of the widespread adoption of an early arterial switch, coupled with the potential complications of “routine” septostomy (41), many centers have chosen to perform a BAS only in cases of profound hypoxemia, or in cases when corrective surgery must be delayed, and in routine cases, maintaining acceptable oxygenation with a PDA, a native septal communication, and PGE₁.

In the past, when atrial repair surgery was electively delayed, particularly beyond the first year of life, a significant interval of morbidity and mortality occurred from complications, including cerebrovascular accidents, progressive pulmonary vascular disease, myocardial failure, and intravascular thrombosis. A multi-institutional protocol followed up on neonates with simple TGA entering the study at <15 days of age (Fig. 49.25) (37). Among the 106 patients assigned to an atrial switch repair (median age at repair: Senning, 2.9 months; Mustard, 6.7 months), five deaths occurred before repair and were associated with hypoxia or heart failure. No deaths before repair occurred among 76 patients assigned in this study to an arterial switch repair protocol (median age at repair: 6 days).

Prostaglandin E1 (in Conjunction with Management Protocol for Early Neonatal Arterial Switch Repair with or without Balloon Atrial Septostomy)

BAS: CURRENT INDICATIONS, TIMING, AND ANALYSIS OF RISK/BENEFIT

It has become apparent that if arterial switch repair is to be performed early after birth, most cyanotic neonates with TGA/IVS benefit from interval prostaglandin-induced increased

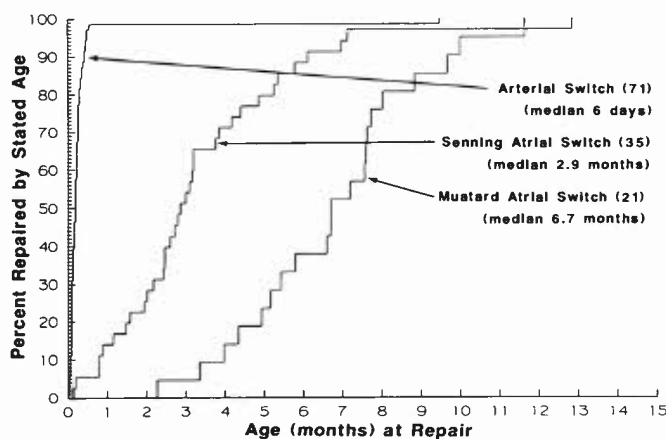


Figure 49.25. Cumulative frequency distribution of patient age at the time of planned-executed repairs according to the type of repair from a 20-institution cooperative protocol study (Congenital Heart Surgeons Society, 1985, 1986). No deaths occurred before repair of patients assigned to an arterial switch protocol (median age at surgery, 6 days), whereas 5% of patients assigned an atrial switch protocol died before repair. (From Castañeda AR, Trusler GA, Paul MH, et al. and the Congenital Heart Surgeons Society: the early results of treatment of simple transposition in the current era. *J Thorac Cardiovasc Surg* 1988;95:14–27, with permission.)

arterial oxygen saturation even without BAS. For these neonates, a prostaglandin infusion may be instituted as soon as feasible, including during transport to the cardiac surgical center, even before the diagnosis has been confirmed echocardiographically. Some neonates will not improve following the institution of PGE₁, suggesting inadequate mixing due to a restrictive foramen ovale. With an inadequate interatrial opening, the markedly increased pulmonary blood flow resulting from the prostaglandin infusion can lead to deleterious increased pulmonary congestion, and BAS (bedside echocardiography or cardiac catheterization–fluoroscopy) may be required on an urgent basis in this subgroup.

But for approximately 85% to 90% of neonates with TGA, an electively timed arterial switch operation (with or without concomitant procedures) is the surgical procedure of choice. Despite this general agreement among cardiologists and surgeons, there is surprisingly little consensus regarding the optimal timing of the procedure, and hence, the role of “routine” BAS and continuation of PGE₁ in these patients is very institution dependent. In a recent meta-analysis in 2012, BAS frequency was 22.4%, with reported rates ranging from 20% to 75% (42).

Excluding the subgroup with TGA and profound hypoxemia from poor intercirculatory mixing—in whom an emergent BAS is the mainstay of the initial stabilization—many babies are scheduled for surgery on a “semi-elective” basis if oxygen saturations are acceptable and the baby is without symptoms. On the one hand, there are potential benefits of waiting 4 to 7 days before an arterial switch operation such as to allow the baby to make an effective transition from the fetal to the neonatal circulation, allow pulmonary vascular resistance to fall, allow some improvement in kidney and liver function to occur, to begin enteral nutrition, to evaluate for any additional congenital anomalies, and to be sure the family understands the risks and benefits of the proposed surgery. While these are “potential” benefits for the baby and family, one must also be cognizant of the “risks” that accompany a delay in surgery, with or without BAS.

If surgery is not performed immediately after birth, the two most common strategies employed are to (i) maintain an intravenous infusion of PGE₁ (usually at low doses of 0.01 to 0.02 $\mu\text{g/kg/min}$ to avoid some of the side effects including apnea, fever, and hypotension) or (ii) perform a BAS and discontinue the PGE₁, accepting lower oxygen saturations with a small or closed ductus arteriosus, but with improved diastolic blood pressure and less symptoms of heart failure from the large ductus. In fact, even with strategy ii above, only the minority of patients actually remained off PGE₁ until surgery despite a “successful” BAS (43). This group was also unable to identify any patient- or procedure-related factors that predicted the ability to remain adequately oxygenated when not receiving PGE₁.

The decision-making process involves a complex interaction between the choice of day of surgery and whether the neonate should undergo a BAS with discontinuation of PGE₁ or should “just wait” while maintaining ductal patency on PGE₁. The cardiac risks of BAS are described above; however, there are conflicting data in the literature regarding the acute risk to the central nervous system from a BAS, with some single center reports and one large registry analysis suggesting that embolic brain injury is related to BAS, while other studies and a separate registry showed no increased risk stroke (41,42,44–48).

From a whole-body perspective, maintaining a widely PDA results in a higher systemic saturation of oxygen but in a “steal” of systemic cardiac output into the lungs. Although the oxygen saturation may be in the “acceptable” range, this left-to-right shunt may in fact result in worse tissue delivery of oxygen in some patients. The pulse pressure is typically wide,

and this diastolic runoff causes worse tissue oxygen saturation resulting in potential ischemia, specifically to the brain and gut.

There may be a “false sense of security” in the preoperative baby with TGA who has little to no symptoms and adequate oxygen saturation on an infusion of PGE₁. During the waiting period, the baby is at risk for “paradoxical embolus” from an peripheral IV catheter to the central nervous system due to the uncorrected circulation, and there are increasing data showing an increased risk of infection, medical errors, and increased cost associated with increased length of stay, which a delay in surgery will cause. However, most importantly, the “reassuring” peripheral oxygen saturation may be associated with paradoxically low oxygen delivery, particularly to the brain. Measurements of cerebral venous oxygen saturation have been invasively sampled during cardiac catheterization in children who were both cyanotic and acyanotic (49–51), and noninvasively in children with right-to-left shunt lesions. In all of these situations, direct measurements of cerebral venous oxygen saturation were significantly lower than would have been predicted from the arterial or “mixed venous” oxygen saturation alone, and the babies with the lowest delivery of oxygen to the brain were those with the combination of arterial hypoxemia and a runoff lesion, either a PDA or a systemic to pulmonary shunt—exactly the situation in the preoperative neonate with TGA and a PDA. Consistent with these observations, there are evolving data demonstrating *increased* central nervous system injury—particularly to the white matter—if an arterial switch operation is delayed even by days, particularly if accompanied by hypoxemia (45). In addition, recent follow-up neurodevelopmental outcome studies in infancy and beyond suggest that earlier elimination of hypoxemia may contribute to improved motor outcomes and brain growth in certain subgroups of patients (52).

Based on currently available information, at The Children’s Hospital of Philadelphia, we have adopted a neuroprotective strategy in TGA of an early arterial switch operation (2 to 3 days of age if possible), with BAS performed if there is an anticipated delay beyond this time frame, and/or oxygen saturations are <80% despite PGE₁. In neonates receiving a BAS, the PGE₁ is then discontinued and not restarted unless there are symptoms of respiratory compromise or consistent peripheral oxygen saturation of <70% (with a small or closed PDA). With this approach in the past 2 to 3 years, preliminary data suggest a significant reduction in the incidence of preoperatively identified white matter injury compared with historical controls, but further work is necessary to confirm these preliminary data and rule out confounding factors always inherent when utilizing historical controls.

In the author’s opinion, there is little benefit (and accumulating risk) in not repairing a newborn with TGA and typical transposition physiology—especially with an open ductus arteriosus. As soon as there is evidence of a fall in pulmonary vascular resistance (usually seen by Doppler at the ductus within 24 to 48 hours) and there are no noncardiac contraindications to surgery, the baby is scheduled for the next available surgical date.

At our institution and elsewhere, there is incomplete agreement on physiologic criteria for satisfactory post balloon septostomy improvement. Obviously, clinical stabilization and decreased hypoxemia must occur. Excluding poor technical performance, a number of anatomic and physiologic factors may be responsible for unsatisfactory improvement. The fossa ovalis may be relatively small, or the valve of the foramen ovale may be quite thick, particularly in older infants and those with a large VSD. Repeat BAS for complete TGA is rarely effective, and only in a few selective cases is catheter-blade atrial septostomy indicated. 2-D echocardiographic imaging of the interatrial septum, augmented with Doppler or color techniques, can readily establish the anatomic and physiologic results of

balloon septostomy. In general, adequately palliated neonates have an interatrial defect at least 5 to 6 mm in diameter resulting from the septostomy maneuver. Nevertheless, despite the presence of adequately sized anatomic communications, inadequate circulatory mixing and disappointing clinical improvement have been noted in some infants. It has been postulated that in such cases, a delayed decrease in the pulmonary vascular resistance, with consequent low pulmonary blood flow and left atrial volumes and pressures, at times may result in inadequate interatrial mixing (see also section on “Fetal and Perinatal Physiology”).

Surgical Creation of Atrial Septal Defect

The Blalock-Hanlon operation or one of its modifications was a widely applied palliative surgical procedure for TGA in the past, but it now assumes the position of a historical footnote. An interatrial septal defect is created by excising the posterior aspect of the interatrial septum in a relatively simple closed heart procedure that can be performed rapidly on even the smallest infant (Fig. 49.26). The Blalock-Hanlon operation (closed-heart) and atrial septectomy (open-heart) produced systemic arterial oxygen saturation levels modestly higher than BAS; mean systemic arterial oxygen saturation levels range as high as 79%, and these increases were well maintained for long periods. Although early in the experience operative, mortality rates approached 30%, later series reported mortality risks <3% to 5%. Postoperative atrial dysrhythmias were infrequent and usually transient. Palliative Blalock-Hanlon or atrial septectomy procedures are rarely performed in the present era as a result of the trend toward earlier atrial and neonatal arterial repairs.

Partial Venous Return Repair (Baffles)

Historically, in the 1950s, a partial physiologic repair was proposed and achieved by connecting the inferior vena cava to the left atrium with a homograft or synthetic conduit and concurrently detaching the right pulmonary veins and directly transferring them to the right atrium. This palliative operation then results in an obligate, effective shunt at the atrial level. Subsequently, some of these patients had a modified Mustard type of atrial repair to achieve complete physiologic correction.

Pulmonary Artery Banding

Transposition associated with large VSD without LVOT stenosis, if untreated, is complicated by two major problems: heart failure and pulmonary vascular disease. Surgical constriction of the pulmonary artery can provide effective palliation for both these complications in infants and, until the arterial repair era, was commonly performed in early infancy. Although early corrective surgery with arterial switch and VSD closure is currently the procedure of choice, pulmonary artery banding in the neonatal period may be indicated, when complex, multiple VSDs are present or there are coexisting medical conditions that cause a delay in surgery to later in infancy.

Operative mortality for banding in the newborn period historically should be in the range of 5% or less. The pulmonary artery in infants with TGA in general banded more loosely than in infants with normally related great arteries because TGA pathophysiology requires a somewhat higher pulmonary blood flow for optimum intercirculatory mixing. Hemodynamically important subaortic stenosis may develop following pulmonary artery banding, although the patient population who receive palliative pulmonary artery banding includes patients with anterior malalignment types of VSDs in whom subaortic obstruction is common and occasionally progressive.

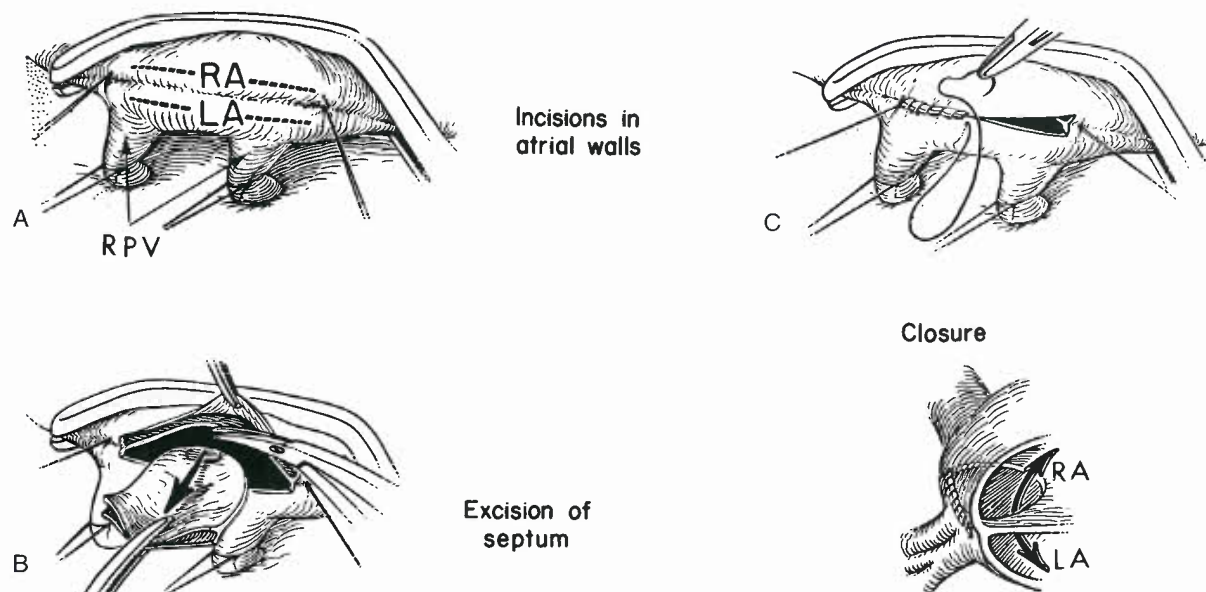


Figure 49.26. Blalock-Hanlon operation. A: Clamp placed across both atria (RA, LA) and right pulmonary veins (RPV) in the region of the interatrial sulcus. B: Excision of posterior portion of atrial septum. C: Closure of atrial incision with resultant surgically created ASD. (Modified from Cooley DA, Hallman GL. *Surgical Treatment of Congenital Heart Disease*. Philadelphia, PA: Lea & Febiger, 1966.)

Systemic-Pulmonary Anastomosis

Infants with TGA/VSD and severe LVOTO have been successfully palliated with systemic-pulmonary anastomosis. Statistics are limited but presently operative mortality with a Gore-Tex interposition shunt may be as low as 5%. The higher risk for developing pulmonary vascular obstructive disease in patients with TGA makes continuing reassessment of pulmonary vascular resistance imperative during follow-up.

CORRECTIVE SURGERY

Although medical management and interventional procedures play an important role in the initial care of the neonate with TGA, this anomaly remains a surgical disease; initial medical management is geared toward making the infant as good a candidate as possible for surgical correction. Numerous surgical options have been available to the infant with various variations of TGA (Table 49.3), although the arterial switch (\pm additional procedures as necessary) is currently the procedure of choice for most of these patients.

Surgery for TGA/IVS or TGA/VSD without Associated Outflow Tract Obstruction

Physiologic Correction (Atrial Switch)

Physiologic correction of TGA became a reality with the atrial switch procedures described by Senning (53) and by Mustard (54). In the Senning repair (Fig. 49.27), the atrial baffle is fashioned in situ using tissue from the right atrial wall and interatrial septum, whereas in the Mustard operation (Fig. 49.28), after resection of most of the atrial septum, the baffle is made from autologous pericardial tissue or (rarely) synthetic material. In terms of connections, the atrial switch repair imposes a discordant AV connection on the existing discordant AV connections; this “double-negative” results in a “normal” (i.e., series) circulation (Fig. 49.29).

The optimum timing for atrial switch repair has also become a historical footnote in the arterial switch era. In contrast to the arterial switch, atrial switch operations may be delayed for a few weeks to several months after birth (and BAS). The intervals between diagnosis, palliative BAS, and surgery may result in additional mortality and morbidity; in a current era multi-institutional report (55), 4% of uncorrected patients with simple TGA died by 30 days of age despite what was considered an adequate BAS. In the atrial switch era, the choice between the Senning and Mustard operations was controversial. Proponents of the Senning repair advanced that the operation was easier to perform, used minimal (if any) prosthetic material or nonviable tissue, had less compromised atrial volumes and compliances, and was followed with a lower frequency of systemic venous obstruction and “late” dysrhythmia. Others demonstrated that modifications to the Mustard procedure resulted in reduced early mortality, reduced systemic and pulmonary venous obstructions, and less dysrhythmia. Superiority of either surgical technique outside of individual experience has not been convincingly established.

Results and Sequelae of Physiologic Correction

Using cardiopulmonary bypass with profound hypothermia (with or without circulatory arrest), these operations were routinely applied to neonates and infants often with a remarkably low early operative mortality through the early 1990s (56). Combined data more broadly representative of current results suggest 10-year survival rates of 85% to 90% (56,57).

In patients with TGA/VSD, atrial repair may be more complicated, early and late postoperative mortality is higher, and postoperative complications are more frequent than for TGA/IVS. A literature review (9) concerned with 234 patients operated on mostly in the 1970 decade indicated an average early mortality of 23%; other reported hospital mortality rates ranged from 10% to 60%, and long-term survival rates remain disappointing, with 5-year survival estimates about 60% to 70%. The problems encountered with this subgroup most likely reflect the increased coexistence of adverse morphologic (associated anomalies) and physiologic (pulmonary hypertension and vascular disease) factors.

TABLE 49.3 Surgical Options Available to the Infant with Transposition of the Great Arteries

Anatomy	Surgical Options	Comments
TGA/IVS	Physiologic repair Senning or Mustard	Usually elective, neonatal–1 y
	Anatomic repair (primary) Arterial switch (Jatene)	Neonatal period, usually within 2 wk of age
TGA/IVS with “prolonged” low LV pressure	Physiologic repair Senning or Mustard	Usually elective, 1 mo–1 y
	Anatomic repair (delayed) Two-stage arterial switch	Long “preparation” period “Rapid two-stage switch”
TGA/VSD	Physiologic repair Senning or Mustard with VSD closure	Poor long-term results
	Anatomic repair Arterial switch with VSD closure	Usually neonatal repair; PAB occasionally (multiple VSDs)
	Interventricular baffle repair	Not all VSDs suitable
	Damus-Kaye-Stansel: VSD closure (LV→PA); proximal PA to Ao anastomosis; RV to distal PA conduit	Used when coronary translocation impossible aortic valve closure
TGA/VSD/PS	VSD closure (LV→Ao), RV to PA conduit (Rastelli)	Palliative systemic-to-pulmonary shunt frequently performed
		Conduit replacement frequently necessary
	VSD closure (LV→Ao), anterior translo- cation of PA with direct connection to RV–“REV” procedure (LeCompte)	Long-term pulmonary regurgitation
TGA/PVOD	Physiologic repair, palliative	Symptomatic improvement
	Anatomic repair, palliative	

Ao, aorta; IVS, interventricular septum; LV, left ventricle; PA, pulmonary artery; PAB, premature atrial beats; PS, pulmonary stenosis; PVOD, peripheral vascular occlusive disease; REV, Réparation à l'étage ventriculaire; RV, right ventricle; TGA, transposition of the great arteries; VSD, ventricular septal defect.

Persistent and frequently progressive functional cardiac abnormalities have long been recognized following physiologic repair and include (a) residual intra-atrial shunts, (b) caval and pulmonary venous obstructions, (c) right ventricular dysfunction, (d) tricuspid valve insufficiency, and (e) arrhythmia. More recent series of either the Mustard or Senning repairs report a significantly reduced incidence of baffle leaks or venous obstruction, but right ventricular dysfunction to some extent and dysrhythmias in particular remain important late concerns.

Residual intra-atrial baffle shunts occur most commonly at the superior right atrial-baffle suture line, may cause either systemic-to-pulmonary or pulmonary-to-systemic venous shunting, and are readily detected by color Doppler echocardiography. In the absence of major coexistent systemic venous obstruction, there is usually little or no arterial oxygen desaturation, and a net left-to-right shunt takes place. Although trivial leaks have been observed at late postoperative angiography in 10% to 20% of patients, significant leaks requiring reoperation have been uncommon (1% to 2%).

Systemic and pulmonary venous pathway obstructions are potentially serious complications. The neonate has been considered at greater risk for both types of venous obstruction because of the limited anatomic spaces involved. The causes of obstruction that have been implicated include (a) improper baffle geometry and suture line placement, (b) contraction of the pericardial or synthetic material baffle, and (c) scar tissue or adhesions involving the baffle and excised margins of the atrial septum.

Superior vena caval pathway obstruction appears postoperatively in about 5% to 10% of patients with a Mustard type repair (Fig. 49.30). Severe obstruction may present early after surgery with clinical signs of upper extremity plethora or chylothorax, and long-standing obstruction may lead to hydrocephalus. Even anatomically severe obstruction may remain asymptomatic, however, because of decompression of the superior vena cava by the azygous or hemiazygos system. Because obstruction can be present without signs or symptoms, a more appropriate frequency (about 17%, in Mustard series; about 14%, in Senning series) may be reflected by considering only patients who had late postoperative catheterization examination. The usual location of the obstruction is distal to the superior vena caval entrance, within the systemic venous atrium at the site of excision of the superior remnant of the atrial septum (Fig. 49.30). In addition to surgical revision, balloon catheter dilation, stent placement, and an innominate vein to left (physiologic right) atrial appendage shunt all have been used successfully to achieve temporary relief for both acute and chronic superior vena cava obstruction.

Inferior vena caval obstruction is a serious but infrequent (about 1%) complication of atrial switch repair. The low occurrence may reflect a technical modification (Figs. 49.31 and 49.32) that involves incising the free (atrial) wall of the coronary sinus, which enlarges the sinus opening into the systemic venous chamber and widens the area that serves as the inferior vena caval entrance to this chamber.

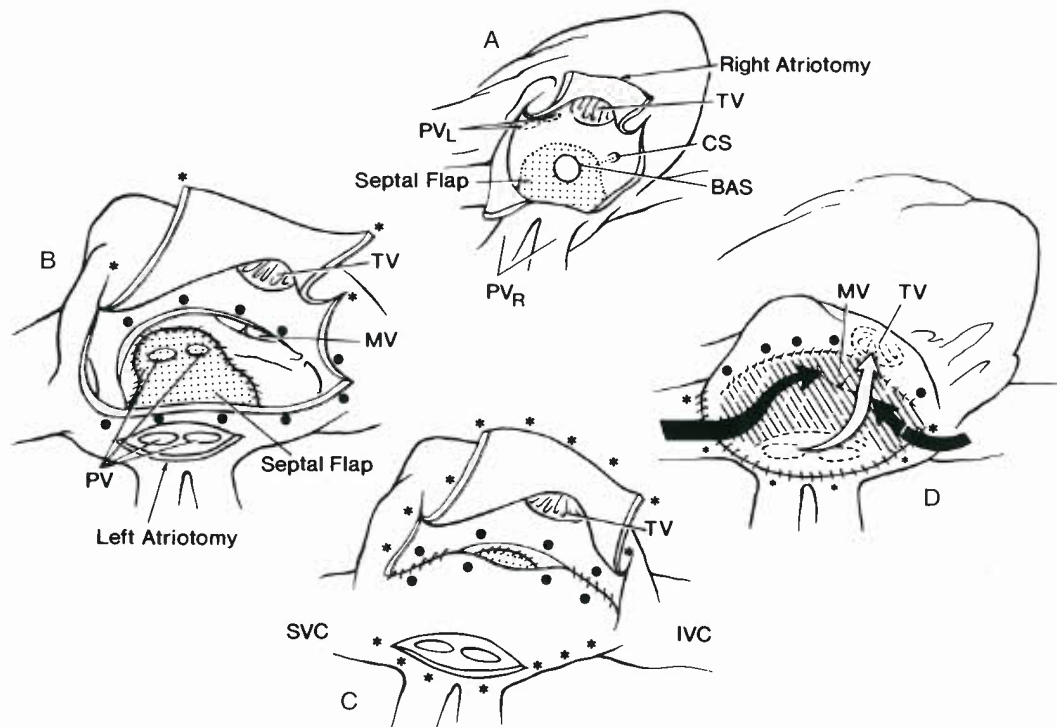


Figure 49.27. Atrial switch operation (Senning technique). Operation is performed using cardiopulmonary bypass with cold cardioplegic myocardial protection or during profound hypothermia with total circulatory arrest. **A:** A right atriotomy is made in front of and parallel to the caval veins and extended into the atrial appendage. This exposes the atrial septum (with its balloon septostomy defect). The atrial septum is now incised anteriorly, superiorly, and inferiorly to form a septal flap (shaded area) as large as possible, which remains fixed posteriorly between the caval entrances. The wall between the coronary sinus (CS) and the left atrium may be incised to provide a large posterior lip for the inferior septal flap suture line (see B) and direct coronary sinus return to the newly formed systemic venous return chamber. **B:** The systemic venous chamber and conduit to the mitral valve is formed posteriorly by the repositioned septal flap (shaded area), and the conduit then is completed anteriorly by suturing the posterior right atrial free wall flap (z z z) anteriorly to the anterior septal limb (z z z) as in (C). A left atriotomy is made as long as possible in the internal atrial groove (exposing the orifices of the right pulmonary veins). **C,D:** The pulmonary venous chamber and pathway to the tricuspid valve are completed with the suturing of the anterior right free wall atrial flap (asterisk) over the right pulmonary veins to the anterior lip of the left atriotomy (asterisk). **D:** Black arrows indicate systemic venous caval flow through the newly created atrial tissue conduit and systemic venous chamber (cross-hatched area) toward the mitral valve. White arrow indicates pulmonary venous flow path in pulmonary venous atrium passing behind, rightward, and anterior to the systemic venous chamber behind the tricuspid valve (TV). BAS, balloon atrial septostomy; IVC and SVC, inferior and superior vena cavae; MV, mitral valve; PV, PVL, and PVR pulmonary veins, left and right.

Pulmonary venous obstruction, which may be evident immediately after surgery or become prominent a few weeks or months later, is a less common but more lethal type of obstruction than the systemic venous type. A low frequency (about 2%) of pulmonary venous obstruction has been reported for both the Mustard and Senning types of atrial repair in two series representing the original surgical development teams. Prompt suspicion should be aroused by a postoperative chest roentgenogram with pulmonary venous congestion or unexplained arterial desaturation in the postoperative period. The diagnosis usually can be made by echocardiography. At cardiac catheterization or Doppler echocardiography, a significant mean pressure difference is obtained between the posterior and anterior segments (Fig. 49.31) of the new pulmonary venous atrium. Reoperation with atrial baffle revision should be considered for hemodynamically severe obstructive complications of the atrial switch repair.

Tricuspid valve regurgitation has been recognized postoperatively, but hemodynamically important tricuspid regurgitation (TR) is rare (1% to 2%) in most series concerned with

TGA/IVS. In contrast, moderate and severe TR is more prevalent (about 5% to 10%) in patients with TGA/VSD. Manipulation and damage to the tricuspid valve and its support apparatus, as well the occurrence of a right bundle-branch-block pattern during repair of the defect, are considered responsible for the TR. Surgery for important TR, including annuloplasty and prosthetic valve replacement, has been disappointing in the long term.

The depressed right ventricular function that has been reported in many studies is in sharp contrast to the normal daily activities and the absence of clinical symptoms in most postoperative children (58,59). Most intermediate (5- to 15-year) postoperative assessments report significantly abnormal resting and exercise responses for right ventricular ejection fraction (decreased) and abnormal resting measurements for right ventricular volumes (increased) in most patients (59,60). The progressive increase in right ventricular volume also may be due to increased flow from persistently enlarged bronchial arteries, producing a "silent" volume overload to the systemic ventricle (Fig. 49.16B).

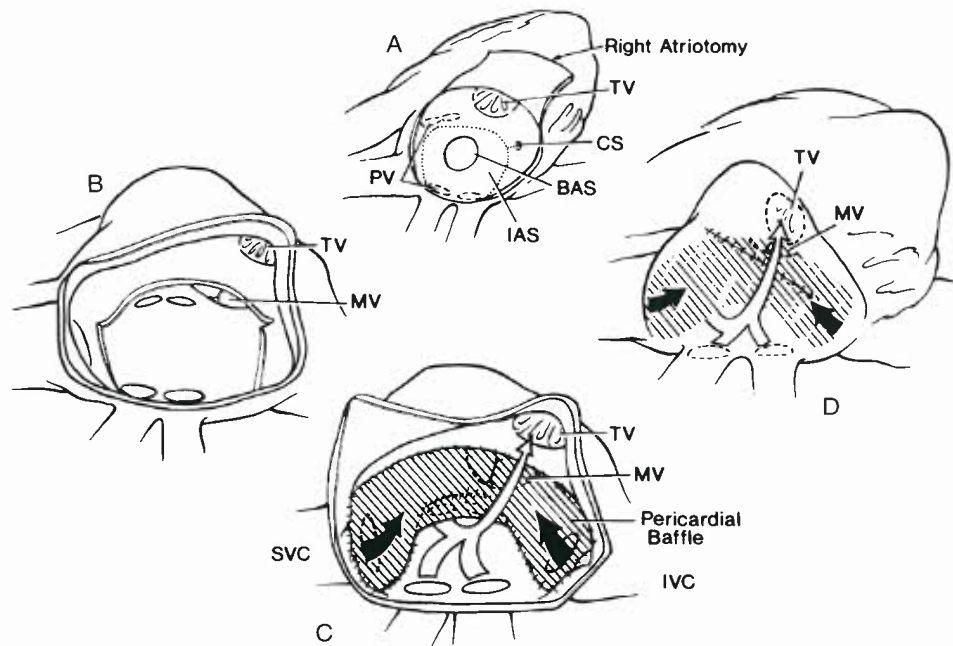


Figure 49.28. Atrial switch operation (Mustard technique). **A:** After establishing cardiopulmonary bypass or profoundly hypothermic total circulatory arrest, the right atrium is opened through an oblique atriotomy incision, exposing the interatrial septum (IAS) with its BAS defect. **B:** The atrial septal remnants are excised widely posteriorly, inferiorly, and superiorly but not anteriorly to preserve a small anterosuperior rim of atrial septal tissue between the superior vena cava and tricuspid valve (TV). In all atrial switch operative techniques, the area of the sinus node and the sinus node artery must be scrupulously avoided in an effort to minimize dysrhythmia complications. As often done in the Senning operation (Fig. 49.27), the free margin of coronary sinus (CS) may be divided downward for several millimeters, a maneuver that transfers the coronary sinus opening into the future systemic venous chamber and also widens the area that becomes the extension of the inferior vena cava into this chamber. **C:** An appropriate baffle material, usually pericardium (*cross-hatched area*) is sutured in place. Suturing starts across the floor of the left atrium along a line immediately to the left of the left pulmonary vein orifices. The suturing continues around the orifices of the superior and inferior vena cavae (SVC, IVC) and finally along the anterior atrial septum resection line to complete the baffle conduit. **D:** The oblique atriotomy is closed. *Black arrows* indicate systemic vena caval flow patch through the newly fashioned pericardial (or synthetic material) conduit and systemic venous chamber (*cross-hatched area*) toward the mitral valve (MV); *white arrow* indicates pulmonary venous flow path in pulmonary venous atrium passing behind, rightward, and anterior to the systemic venous chamber toward the tricuspid valve (TV). PV, pulmonary valve.

Formal exercise performance testing demonstrated decreased endurance indices in intermediate and late postoperative studies (61–65). Post-Mustard repair patients perform significantly less work and have lower peak heart rate and peak minute oxygen consumption than controls. They also manifest an abnormal increased ventilatory response to exercise. Exercise performance in this patient population is uniformly diminished, which appears to be a consequence of both decreased heart rate and stroke volume response.

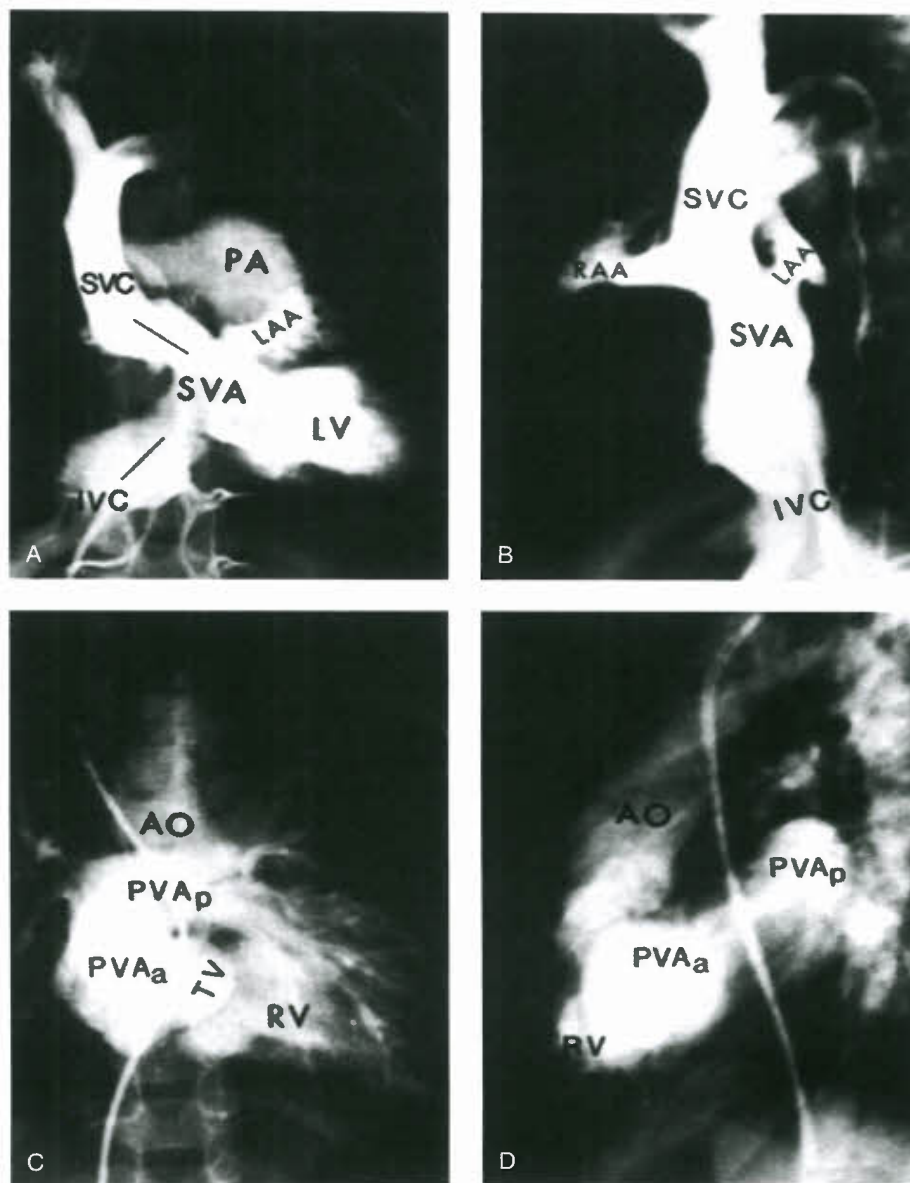
At least 10% of operative survivors have important depression of right ventricular function and about 90% are in New York Heart Association functional Class I. Severe, symptomatic right ventricular failure is an infrequent but major complication (66). It may be associated with progressive TR and is observed more often in the VSD repair subgroup. In severely symptomatic patients, heart transplantation has been used as a treatment option, as has “conversion” to anatomic correction (66–70) (see section on “Surgery for Right Ventricular Failure Following Physiologic Correction”).

Postnatally, the morphologic right ventricle may be incapable of functioning normally as a systemic ventricle, despite the fact that prenatally the right ventricle and tricuspid valve sustain systemic pressures as well as larger blood flow volumes than the left ventricle and mitral valve. The following

explanations for postnatal and postatrial repair subnormal right (systemic) ventricular function remain speculative:

1. Right ventricular myocardial fiber arrangements may not be optimum for systemic function, and there may be a mismatch between right ventricular coronary blood supply and systemic ventricular work demand. In this regard, the anatomic structure of the ventricular free walls is dissimilar; the left ventricular free wall is composed predominantly of stratum compactum (coronary-supplied myocardium), whereas the right ventricular free wall consists predominantly of stratum spongiosum (trabeculae carneae).
2. The right ventricle can achieve only suboptimal pumping function because the transposed ventricular pressure relationships force the ventricular septum to bulge posterior–leftward and to present a concave septal surface during contraction. Furthermore, the tricuspid valve is supported by relatively small papillary muscles in comparison to the mitral valve and this, in conjunction with the abnormal concave right ventricular septal surface, may result in TR.
3. The right ventricle is functionally diminished as a systemic ventricle compared with the left ventricle because it contains a hypokinetic segment (i.e., the infundibulum).

Figure 49.29. Angiocardiograms showing systemic and pulmonary venous atrial morphology following intra-atrial baffle repair (Mustard) operation. Frontal (A) and lateral (B) views of the systemic veins (superior [SVC] and inferior vena cava [IVC]), new systemic venous atrium (SVA), left ventricle (LV), and pulmonary artery (PA). Note the adequate conduit diameters and the absence of constriction in the superior and inferior limbs of the systemic venous atrium. LAA and RAA, left and right atrial appendages. Frontal (C) and lateral (D) views of the new pulmonary venous atrium (PVA). This chamber consists of a posterior segment (PVA_p) receiving the pulmonary veins and an anterior segment (PVA_a) that formerly was a portion of the original right atrium. The PVA_a empties via the tricuspid valve (TV) into the right ventricle (RV) and aorta (AO).



4. Prerepair hypoxemic coronary perfusion may cause sufficient myocardial fibrosis and functional damage to preclude normal systemic right ventricular function, but normal pulmonary right ventricular function usually returns after late second-stage arterial switch repair.

Speculations aside, the accumulating short-term and mid-term postarterial switch repair findings of normal left ventricular systemic function support the basic premise that the left ventricle and mitral valve are better suited for this function.

After atrial repair procedures, several other functional abnormalities persist as a consequence of the continuing anatomic transposition: abnormal function of the mitral valve-LVOT subunit (characterized by abnormal systolic movement and coarse diastolic flutter of the anterior mitral valve leaflet, systolic bulging of the basal segment of the ventricular septum into the outflow tract, and systolic pressure differences across the outflow tract) and abnormal distribution of pulmonary blood flow to the right lung and hypoplastic changes in the left pulmonary vascular bed. The infrequent late occurrence

of pulmonary vascular obstructive disease, new or progressive, has been observed postoperatively, even in patients with TGA/IVS.

Postoperative dysrhythmias after atrial switch procedures are commonly encountered during long-term follow-up studies. Indeed, the prevalence of atrial electrophysiologic disturbances in these patients constituted one of the major arguments for the arterial switch repair. The reported loss of sinus rhythm and the occurrence of dysrhythmias range widely, from 13% to 100% (8,56,57,71–74). This disparity primarily reflects differences in the definition of dysrhythmia, the type and extent of follow-up study (routine ECG, 24-hour ambulatory monitoring, exercise ECG monitoring, electrophysiologic testing), and, importantly, the interval since surgery. The pattern of progressive loss of normal sinus rhythm and increase in atrial rhythm disturbances over years is particularly well documented following the Mustard-type repair but also is widely observed after the Senning-type repair. There appears to be a gradual time-related decrease in normal sinus rhythm: In one series concerned with the Mustard repair of TGA (without

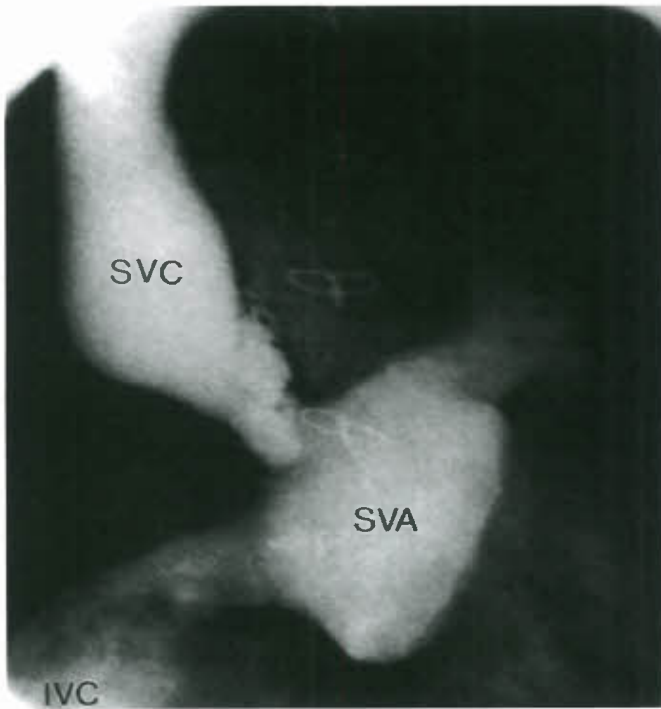


Figure 49.30. Frontal angiogram of systemic venous pathways following atrial repair. Note the dilated superior vena cava (SVC); a 5 mm Hg mean gradient was detected on catheter pullback. IVS, inferior vena cava; SVA, systemic venous atrium.

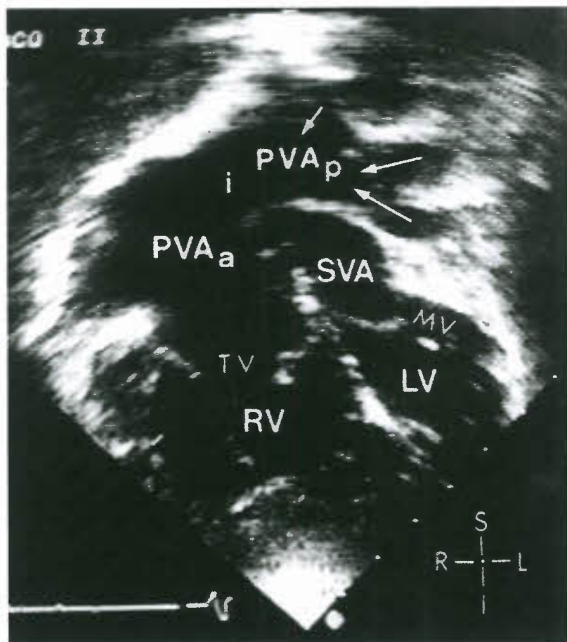


Figure 49.31. Two-dimensional echocardiogram (subcostal view) in 8-year-old with TGA/IVS with Mustard repair at 1 year of age. Note reconstructed pulmonary venous atrium (PVA) compartmentalized into posterior segment (PVA_p) with left pulmonary venous drainage and anterior segment (PVA_a) with tricuspid valve. Note wide unobstructed isthmus (i) between PVA_p and PVA_a, and pericardial baffle separating PVA from systemic venous atrium (SVA). TV, tricuspid valve.

significant VSD), the probability of being in sinus rhythm at 1 year was 72%, at 5 years 56%, at 10 years 50%, and at 13 years 43%.

The predominant dysrhythmias include marked sinus bradycardia, ectopic atrial rhythm, slow junctional rhythm, and supraventricular tachycardia, especially atrial flutter. AV conduction disturbances, surgical complete heart block, and premature ventricular beats have been noted as well (Table 49.4). The most prevalent basic mechanisms observed are sinus bradycardia and intermittent or fixed slow junctional rhythms. Not only is bradycardia present at rest, but peak heart rate response to exercise is blunted as well. Episodes of atrial tachycardia or atrial flutter are not infrequent, occurring in about 5% to 15% of long-term survivors. The terms bradycardia-tachycardia syndrome and sick-sinus syndrome have been applied descriptively when patients manifest periods of marked bradycardia, sinoatrial arrest, or block with AV junctional escape and slow junctional rhythms, as well as the episodes of tachycardia. Risk factors for these rhythm and conduction disturbances are not known to be different for the Mustard and Senning atrial switch procedures.

The origin of the various dysrhythmias may be intraoperative damage to the sinus node or sinus artery, interruption of intra-atrial conduction by damage to internodal pathways, or intraoperative damage to AV node conduction tissue. Histologic examination of the sinus node region revealed that the sinus node, sinus node artery, and paranodal tissues are frequently abnormal. Acute changes include suture compression, necrosis, or infarction of the sinus node itself with perinodal hemorrhage and edema; chronic changes include marked nodal and paranodal fibrosis. Although it is no longer contended that atrial conduction occurs through discrete, well-defined atrial intranodal tracts, the various extensive surgical incisions, and suture lines in atrial switch procedures result in marked delays in intra-atrial conduction throughout the atria. These local areas of conduction delay are significant in providing the substrate for the development of intra-atrial reentry types of tachycardia, and late postoperative electrophysiologic studies indicate a high frequency of inducible sustained atrial flutter. Despite changes in surgical technique, including special care to avoid direct surgical damage to the sinus node and its artery, and perhaps also efforts at preserving the anterior portion of the atrial septal limbus for intranodal conduction, a high frequency of late arrhythmia persists in essentially all atrial repair series.

Symptoms of palpitations, dizziness, or syncope may result during either tachycardia or bradycardia events; consequently, ECG documentation in symptomatic patients is critical. Patients with atrial tachycardia may be unaware of its occurrence if the ventricular rate is the result of 2:1 or 3:1 AV conduction. During exercise or excitement, however, 1:1 conduction may occur and result in abrupt onset of palpitations, dizziness, or syncope as a result of the rapid ventricular rate. Some patients may not experience an abrupt onset but rather may develop symptoms of tachycardia-induced heart failure over weeks or months.

Antiarrhythmic control in these patients may be quite difficult because bradycardia and tachycardia often occur concurrently, and pharmacologic therapy for the tachycardia may severely further depress pacemaker function and thus aggravate bradycardia. Permanent implanted pacing has been recommended by some in this situation, and also for isolated symptomatic bradycardia, including heart rates <30 beats per minute, Stokes-Adams episodes, and poor ventricular function with bradycardia, especially when associated with major ventricular ectopic activity. Although clearly indicated for the management of some patients, neither ant arrhythmic medication nor standard pacemaker implantation has been conclusively shown to affect the frequency of sudden death. The recent successful use of episodic transvenous and transesophageal

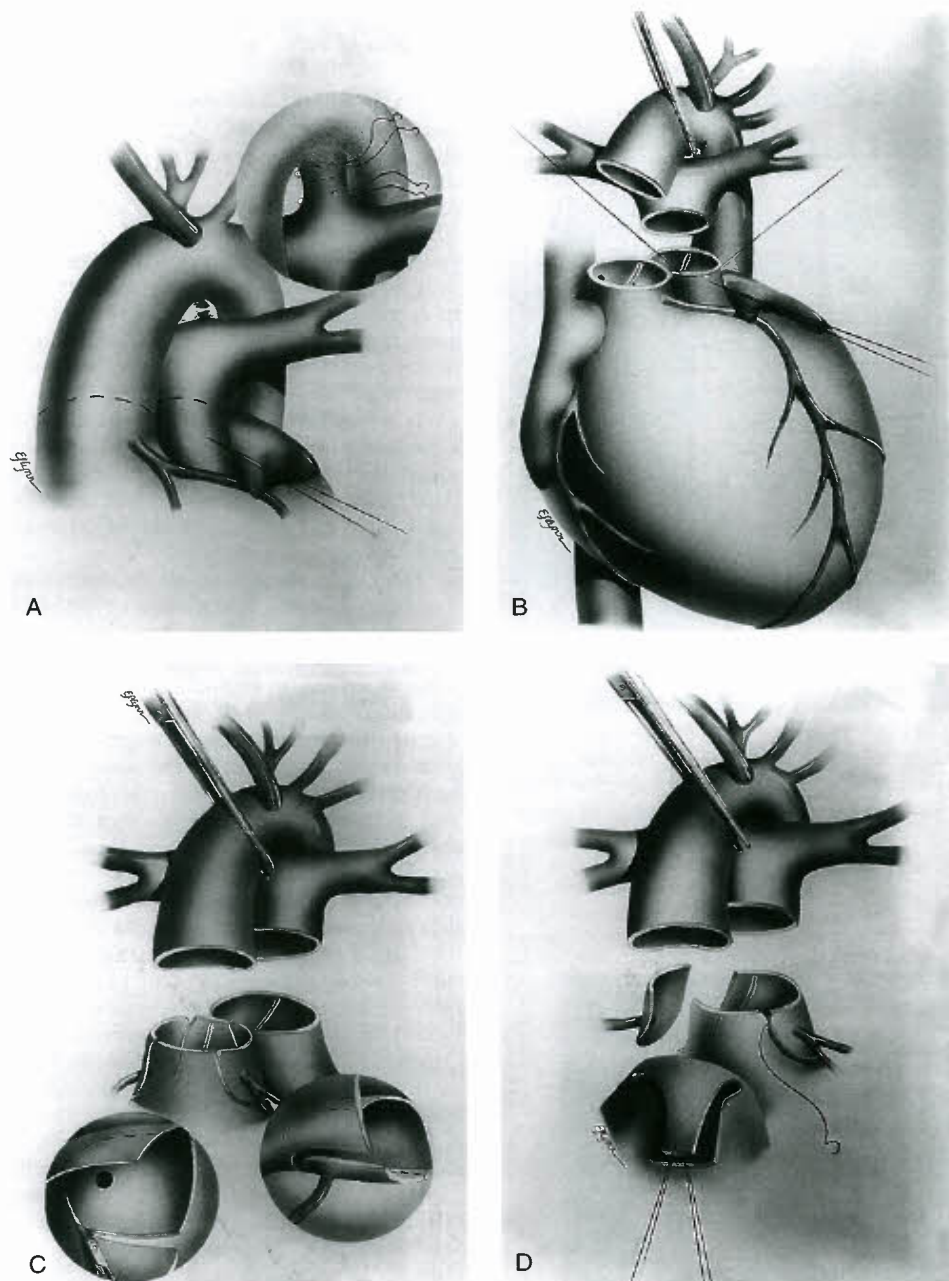


Figure 49.32. Surgical technique of the arterial switch operation. **A:** Aortic cannula is positioned distally in the ascending aorta, the ductus arteriosus is divided between suture ligatures, and the branch pulmonary arteries are dissected out to the hilum to provide adequate mobility for anterior translocation. The broken lines represent the levels of transection of the aorta and the main pulmonary artery. Marking sutures are placed in the anticipated sites of coronary transfer. **B:** Transection of the great arteries. The LVOT, neo-aortic valve, and coronary arteries are thoroughly inspected. **C:** The coronary arterial buttons are excised from the free edge of the aorta to the base of the sinus of Valsalva. **D:** The coronary buttons are anastomosed to V-shaped excisions made in the neo-aorta.

pacing for tachycardia cardioversion and the development of implantable devices for pacing-induced cardioversion offer the potential for both treating tachycardia and preventing bradycardia with backup demand pacing.

Late, sudden, unexplained death has been reported with a frequency of 2% to 10% (75,76). The presence of either sinus node dysfunction or rapid atrial dysrhythmias, alone or in combination (as is frequently observed), could result in sudden death. Although these rare events are possibly bradyarrhythmic in origin, the recent recognition of a higher-than-expected frequency of intramural coronary arteries in TGA (4,77) may play

a role as well. Many cases of late sudden death occur during exercise or increased activity, during which time bradyarrhythmias would be less likely; impaired coronary flow resulting from compression of the transmural segment of the (usually left) coronary artery may in fact be the precipitating cause.

“Anatomic Correction” (Arterial Switch)

Although the Mustard and Senning atrial switch procedures achieved widespread acceptance and success during the past four

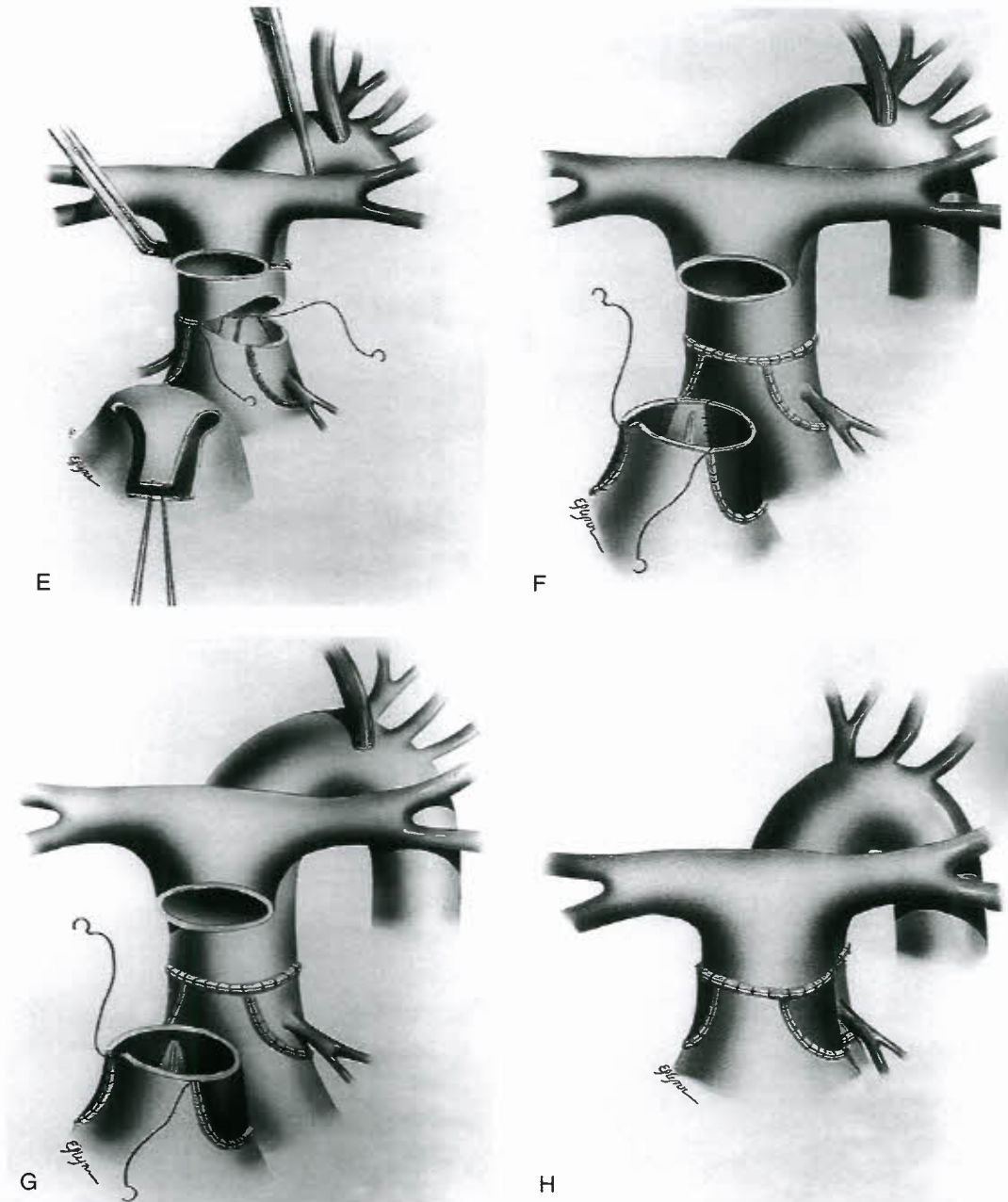


Figure 49.32. (Continued) E: The pulmonary artery is brought anterior to the aorta (LeCompte maneuver). Anastomosis of the proximal neo-aorta is shown. F: The coronary donor sites are filled with autologous pericardial patches. A single U-shaped patch (F) or two separate patches (G) may be used. H: Anastomosis of the proximal neopulmonary artery and the distal pulmonary artery. (Modified from Castañeda AR. Anatomic correction of transposition of the great arteries at the arterial level. In: Sabiston DC Jr, Spencer FC, eds. *Surgery of the Chest*. Philadelphia, PA: WB Saunders, 1990:1435–1446.)

decades, the search for an operation to return the great arteries to their normal ventricular connections continued. This search was stimulated primarily by the accumulating observations at mid- to late-term follow-up studies of (a) an increasing frequency of important dysrhythmic complications, including sudden, unexplained death; (b) the threat of late right ventricular dysfunction and major TR in a ventricle most likely unsuited for a lifetime of systemic function; and (c) dissatisfaction with the operative mortality and results in the subgroup of infants with TGA and large VSD. Starting in 1954, numerous innovative procedures to achieve an anatomic correction were described, but clinical success was not achieved until 1975 by Jatene et al. (78).

In the 35+ years since the introduction of the arterial switch operation by Jatene and colleagues in 1975, arterial level repair has replaced atrial level repair as the surgical procedure of choice for both simple and complex forms of TGA. Although frequently referred to as “anatomic” correction, in reality, there are important differences in the postoperative patient compared with the structurally normal heart. The anatomic pulmonary valve must serve in the systemic circulation lifelong, and there are accumulating data on progressive neo-aortic valve dysfunction and root dilation during the second and third decades of follow-up. In addition, as opposed to the normal heart, following the LeCompte maneuver both pulmonary arteries are ante-

TABLE 49.4 Electrophysiologic Consequences of Surgical Repair of Transposition of the Great Arteries

	Mustard ^a	Mustard ^b	ASO ^c	ASO ^d	ASO ^e
Surface ECG					
	64 patients	95 patients	269 patients	<20 patients	95 patients
Age at surgery	Mean, 1.4–1.7 y	Median 21 mo	Median 6 d	Mean 13 ± 26 d	
	Range, 2 mo–10.3 y	Range, 1 mo–11 y	1 d–7.8 y	1–120 d	
Follow-up time (mo)	5.8" 3.5 y	3 mo–13 y	Mean 2.1 y	Mean, 12.7–4 mo	Mean 26 mo
			Range, 1–8.6 y	Range, 7–25 mo	Range 3–90 mo
IVS	78%	80%	51%	43%	71%
VSD	22%	20%	49%	55%	29%
Sinus rhythm	51%	54%	96%	95%	
Ectopic atrial rhythm	7%		2%	5%	
Junctional rhythm	42%				
Paced			2%		
24-h ambulatory ECG					
Patients (n)	53	52	218	20	51
Sinus rhythm	42%	33%	97%	100%	98%
Junctional rhythm	50%	67%	1%	0%	0%
1E AVB			0%	5%	
2 E AVB		2%	0%	0%	2%
CHB			2% (all VSD)		2%
APB (rare-occ)			61%		29%
APB (freq)			15%		
SVT	13%		7%		
VPB (rare-occ)	38%		50%	25%	7.8%
VPB (freq)			12%		
Couplets/VT			0%		2%
Intracardiac electrophysiologic studies					
Patients (n)	64		158	20	
CSNRT 275 ms	14%		94%	70%	
A–H interval 100 ms			96%	100%	
H–V interval 50 ms			97%	100%	
Inducible SVT	51%			0%	
Inducible VT	0%			0%	

Rare to occasional VPBs are common in both groups.

^aModified from Vetter VL, Tanner CS, Horowitz LN. Electrophysiologic consequences of the Mustard repair of D-transposition of the great arteries. *J Am Coll Cardiol* 1987;10:1265–1273, with permission.

^bModified from Hayes CJ, Gersony WM. Arrhythmias after the Mustard operation for transposition of the great arteries: a long-term study. *J Am Coll Cardiol* 1986;7:133–137.

^cDate from Children's Hospital, Boston. Includes data from three separate reports (32,31,82).

^dModified from Vetter VL, Tanner CS. Electrophysiologic consequences of the arterial switch repair of D-transposition of the great arteries. *J Am Coll Cardiol* 1988;12:229–237.

^eModified from Martin RP, Radley-Smith R, Yacoub MH. Arrhythmias before and after anatomic correction of transposition of the great arteries. *J Am Coll Cardiol* 1987;10:200–204. Although follow-up data from arterial switch patients are necessarily shorter than that available from Mustard patients, note the markedly abnormal sinus node function and inducible SVT in patients after atrial-level repair. Rare to occasional VPBs are common in both groups.

A–H, atrio-His conduction interval; ASO, arterial switch operation; APB, atrial premature beat; AVB, atrioventricular block; CHB, complete heart block; CSNRT, corrected sinus node recovery time; ECG, electrocardiogram; Freq, frequent; H–V, His-ventricle conduction interval; IVS, intact ventricular septum; Occ, occasional; SVT, supraventricular tachycardia; TGA, transposition of the great arteries; VPB, ventricular premature beat; VSD, ventricular septal defect; VT, ventricular tachycardia.

rior to the ascending aorta; posterior tension can cause further distortion of the neo-aortic root and/or cause supra-valvar pulmonary stenosis. In patients without significant comorbidities or major coexisting cardiac defects (e.g., dextrocardia, aortic arch obstruction), surgical mortality can be expected to be <5%.

The anatomic challenges of arterial switching have been met by the application of novel surgical techniques. In brief (Fig. 49.32), the great arteries are transected in a manner that allows eventual reanastomosis of the distal aortic segment to the proximal pulmonary artery (neo-aortic root). Transfer of the coronary arteries to this pulmonary segment is facilitated by their excision from the aortic sinus with a cuff of adjacent aortic wall. The proximal aortic segment (neopulmonary root) may be connected to the distal pulmonary artery segment by an end-to-end anastomosis using LeCompte and associates' innovative maneuver, which passes the anterior aorta posterior to the bifurcation of the pulmonary artery (Fig. 49.33). Alternatively, the pulmonary artery connections can be established by using an interposed prosthetic tubular conduit or direct connection.

A critical physiologic challenge to anatomic repair concerns the functional adequacy of the left ventricle, which preoperatively faces the pulmonary circulation and postoperatively must instantly cope with the systemic workload. In the current era of increasing numbers of babies detected before or shortly after birth, an "unprepared" left ventricle is increasingly uncommon. Adequate left ventricular muscle mass for successful systemic function is usually present in early infancy in patients with TGA/IVS (see also section on "Surgery for TGA with Low Left Ventricular Pressure"), but may also be present in older patients with TGA and associated anatomic abnormalities that cause a continued increased afterload to the left ventricle (Fig. 49.34). These associated anomalies include (a) a nonrestrictive PDA, (b) surgically remediable or "dynamic" left ventricular outflow obstruction, (c) a delayed decrease in pulmonary vascular resistance and persistent pulmonary hypertension, or (d) a large, nonrestrictive VSD.

Indeed, the initial clinical success with surgical arterial switch and the first confirming reports approximately three

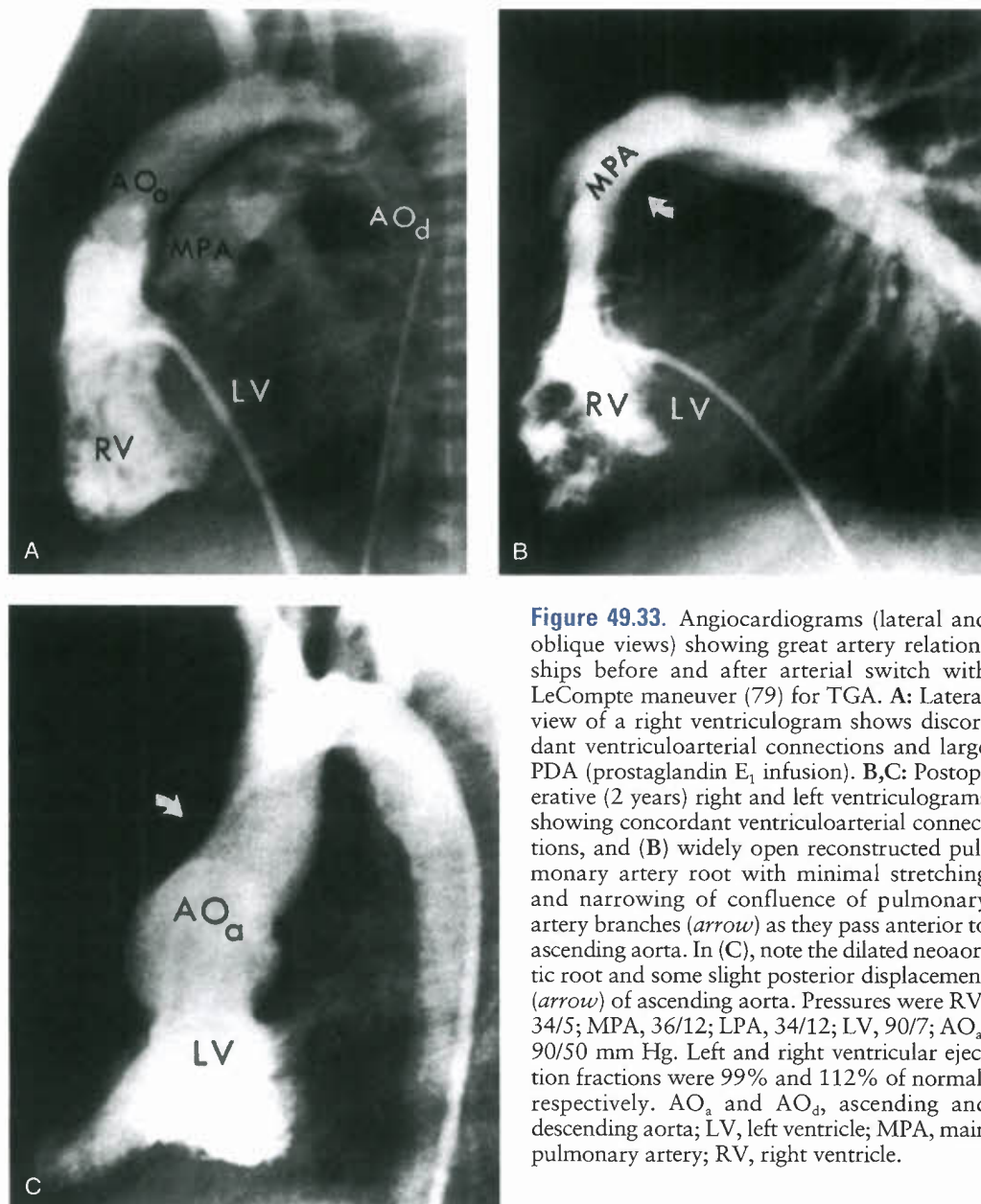


Figure 49.33. Angiocardiograms (lateral and oblique views) showing great artery relationships before and after arterial switch with LeCompte maneuver (79) for TGA. **A:** Lateral view of a right ventriculogram shows discordant ventriculoarterial connections and large PDA (prostaglandin E_1 infusion). **B,C:** Postoperative (2 years) right and left ventriculograms showing concordant ventriculoarterial connections, and (B) widely open reconstructed pulmonary artery root with minimal stretching and narrowing of confluence of pulmonary artery branches (arrow) as they pass anterior to ascending aorta. In (C), note the dilated neo-aortic root and some slight posterior displacement (arrow) of ascending aorta. Pressures were RV, 34/5; MPA, 36/12; LPA, 34/12; LV, 90/7; AO_a , 90/50 mm Hg. Left and right ventricular ejection fractions were 99% and 112% of normal, respectively. AO_a and AO_d , ascending and descending aorta; LV, left ventricle; MPA, main pulmonary artery; RV, right ventricle.

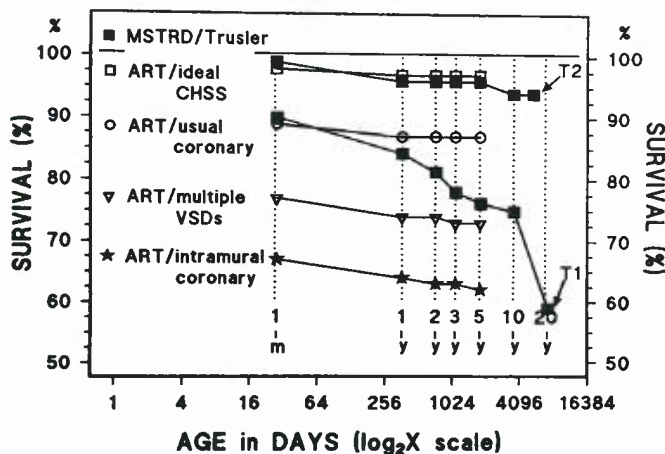


Figure 49.34. Percent survival (up to 5 years) after arterial switch repair for TGA/IVS and TGA/VSD. G, “ideal” risk-adjusted subgroup in an institution of proven competence; risk-adjusted with usual coronary arterial pattern; asterisk, risk-adjusted with multiple VSDs. c, risk-adjusted with intramural left coronary (with ostium in the posterior/leftward facing sinus). For comparison, note actuarial percent survival (up to 20 years) after Mustard operation performed; O, T1 in 1963 through 1973; O, T2 in 1974 through 1985. (Arterial switch repair data derived from Kirklin JW, Blackstone EH, Tchervenkov CI, et al.; Congenital Heart Surgeons Society. Clinical outcomes after the arterial switch operation for transposition: patient, support, procedural and institutional risk factors. *Circulation* 1992;86:1501–1515; Mustard repair data derived from Trusler GA, Williams WG, Duncan KF, et al. Results with the Mustard operation in simple transposition of the great arteries 1963–1985. *Ann Surg* 1987;206:251–260.)

decades ago concerned only infants with TGA/VSD without major pulmonary vascular disease. The use of arterial switch for patients with TGA/VSD as well as the Taussig-Bing anomaly is now widely regarded as the surgical procedure of choice, both with regard to operative mortality and intermediate-term results.

Definitive early (neonatal) one-stage arterial repair is presently preferable to early palliation with pulmonary artery banding and later arterial switch surgery. In an ongoing multi-institutional study (see later), older age at surgery was determined to be an incremental risk factor for death (55) and increasing neurologic morbidity was seen with older age at repair in the Boston Circulatory Arrest Study (35,36,79). In patients with TGA/large VSD who undergo palliative pulmonary artery banding, improper adjustment of the band may cause either persistent pulmonary hypertension with possible pulmonary vascular disease or unacceptable hypoxemia. Banding too close to the pulmonary valve may distort and damage the pulmonary (neo-aortic) valve and has been related to a higher frequency of neo-aortic valvar insufficiency than that observed after primary one-stage arterial repair.

The concept that the neonatal left ventricle in TGA/IVS would successfully sustain the systemic circulation after arterial switch repair, if accomplished in the first few weeks of life (or longer), has been validated. Although most early and midterm follow-up studies concerned with systemic ventricular function in the arterial repair patient have established the functional advantages of arterial over atrial switch repair (80,81), past experience with other complex surgical procedures urges caution about final pronouncements because the potential for later problems clearly exists (82).

Results and Sequelae of the Arterial Switch Operation

Early, risk-unadjusted mortality rates are <10% in most recent reports (31,83–87). Several anatomic, technical, and institutional risk factors for increased mortality have been reported. Anatomic variants that may impact operative mortality include (a) an intramural course of a coronary artery, (b) a retropulmonary course of the left coronary artery, (c) multiple VSDs, (d) coexisting abnormalities of the aortic arch, (e) straddling AV valves, and (f) prior pulmonary artery banding. It appears that with increased surgical experience these effects may be minimized. Longer duration of global myocardial ischemic (cross-clamp) and prolonged circulatory arrest times are risk factors for operative mortality and prolonged hospital length of stay, as is the number of procedures done at a given institution (55,88–90).

Early mortality usually is related to kinking or obstruction of the coronary arteries during transfer to the neo-aorta, an “unprepared” left ventricle, or hemorrhage from the multiple suture lines. Late mortality has been reported with an incidence of 1% to 2% (with a shorter follow-up duration than for physiologic correction), usually as a result of myocardial ischemia or pulmonary vascular obstructive disease or during reoperation for supraventricular obstruction.

Supraventricular pulmonary stenosis is widely recognized as the most frequent short-term complication of arterial level repair (91,31). The need for reintervention for supraventricular pulmonary stenosis ranges between 5% and 30%; most institutions report a decreasing incidence of this complication with increasing experience with the operation. Postoperative obstruction may occur at multiple levels following anatomic correction:

1. Diffuse hypoplasia of the main pulmonary artery may result from inadequate mobilization of the branch pulmonary arteries causing tension on the anastomosis. With somatic growth, there may be inadequate growth of the main pulmonary artery resulting in “flattening” of the reconstructed right ventricular outflow tract in the anterior–posterior direction (Fig. 49.35A,B).
2. Circumferential narrowing at the suture line may occur and cause a more discrete type of supraventricular narrowing (Fig. 49.35C,D).
3. Branch pulmonary artery stenosis (usually left) is more common in cases of more side-by-side great arteries when the LeCompte maneuver is used. In these cases, the left pulmonary artery may “bowstring” over the reconstructed neo-aorta, causing significant hypoplasia of the left pulmonary artery (Fig. 49.35E,F).
4. Finally, multiple levels of obstruction may occur in combination.

Treatment for supraventricular pulmonary stenosis includes both reoperation and balloon angioplasty and is generally indicated when right ventricular pressure approaches or exceeds systemic levels. Surgical relief of supraventricular pulmonary stenosis usually requires patch angioplasty; the patch may need to extend through the neopulmonary annulus into the infundibulum. In these cases, it is critical that the course of the right coronary artery is properly identified preoperatively because the right coronary may be difficult to identify during surgery due to dense adhesions. If the right coronary artery has an anterior course to reach the right AV groove (“inverted” right or single left coronary pattern) (see also the section on Morphology), transannular patching is contraindicated and a conduit may be necessary. Balloon angioplasty has only rarely been successful. The discrete branch pulmonary artery stenoses or circumferential stenoses in the main pulmonary artery (Fig. 49.35D) are the types most likely to be successfully relieved with balloon angioplasty.

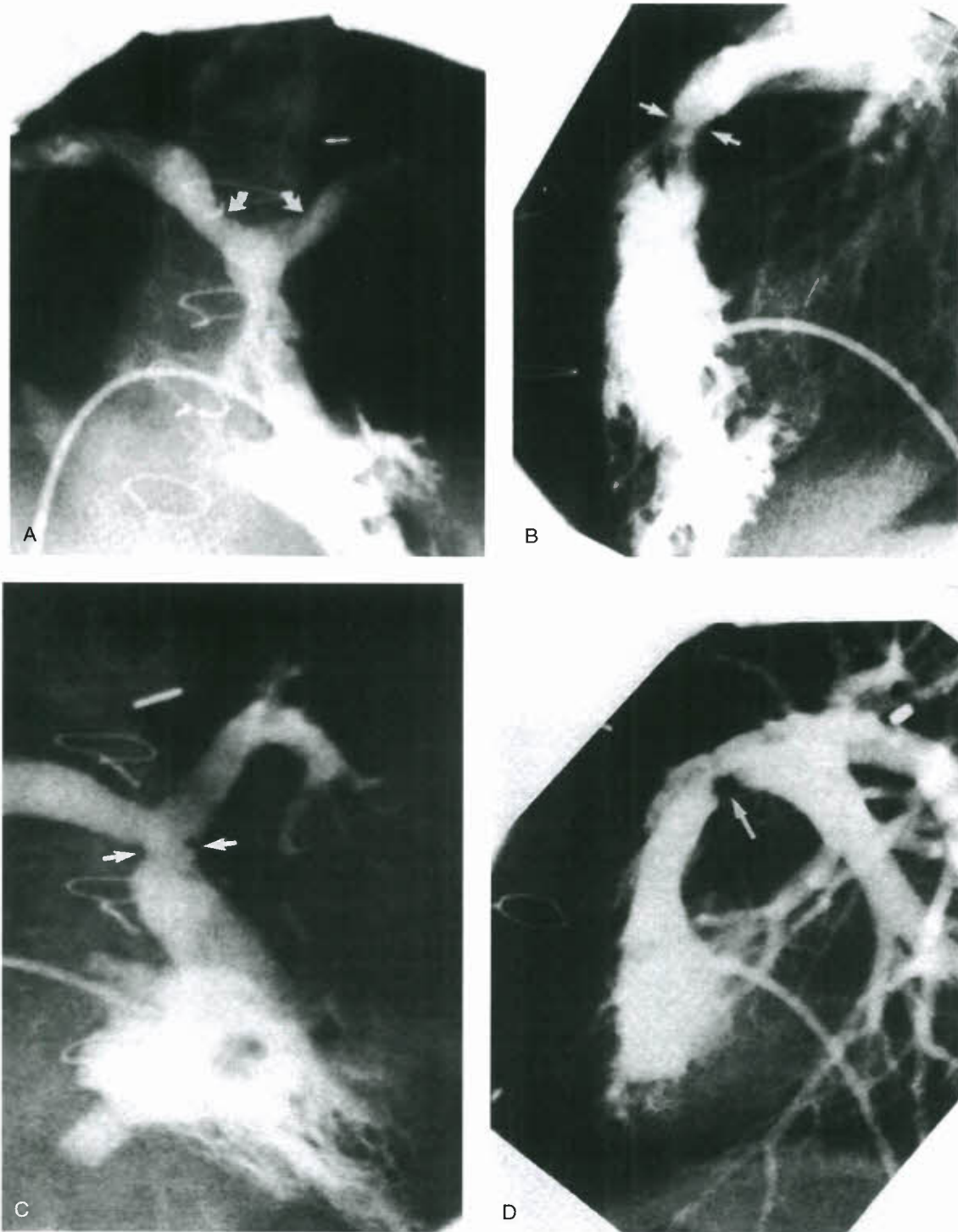


Figure 49.35. Anteroposterior (A) and lateral (B) angiographic frames of a patient with severe supravulvar pulmonary stenosis causing systemic right ventricular pressure. Note anterior–posterior narrowing (*straight arrows*) and moderate peripheral narrowing (*curved arrows*). This type of narrowing is due to tension on the pulmonary anastomosis caused by inadequate dissection of the branch pulmonary arteries. Anteroposterior (C) and lateral (D) angiographic frames of a patient with supravulvar pulmonary stenosis due to circumferential narrowing at the anastomosis (*arrows*). Right ventricular pressure was 110% systemic. Anteroposterior (*continued*)

Supravulvar aortic stenosis (see Fig. 49.35F) is significantly less common than supravulvar pulmonary stenosis. Peak systolic ejection gradients across the aortic anastomosis of >20 mm Hg are extremely uncommon, being present in fewer than 5% of patients, with reoperation necessary in <2% of patients. After the LeCompte maneuver, the anterior

aspect of the ascending aorta often manifests some posterior displacement caused by the stretched anterior-placed pulmonary trunk and bifurcation (Figs. 49.35F and 49.36). A rarely experienced pathologic expression of this posterior displacement, obstructive kinking of the proximal transverse aortic arch (Fig. 49.36), has been reported after the arterial

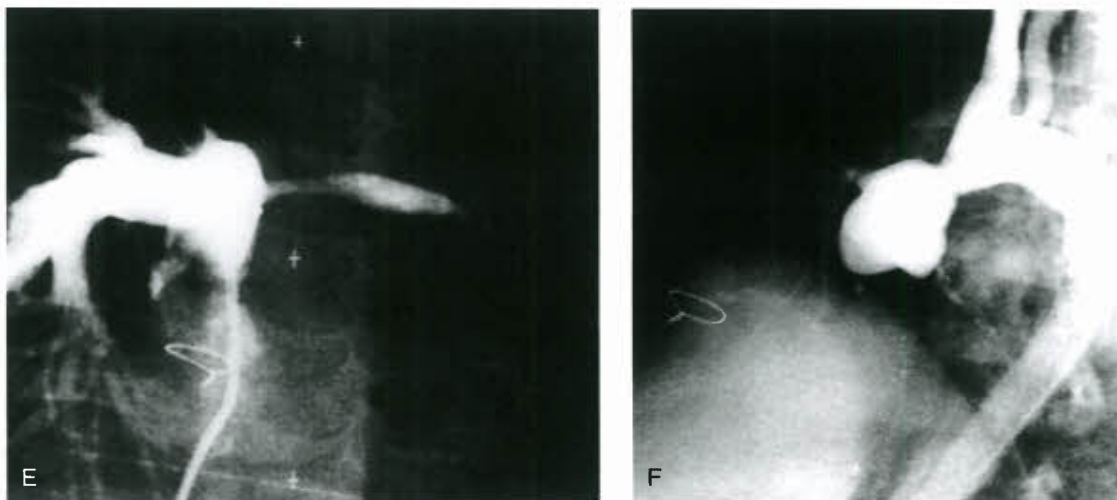


Figure 49.35. (Continued) (E) angiogram in the main pulmonary artery showing severe stenosis and hypoplasia of the left pulmonary artery. This patient had TGA/IVS with side-by-side great arteries; following the LeCompte maneuver, the left pulmonary artery draped over the aortic anastomosis causing, in addition, moderate supravalvular aortic stenosis (F) (with a peak systolic ejection gradient from left ventricle to aorta of 30 mm Hg). A lung perfusion scan demonstrated that 95% of the pulmonary blood flow entered the right lung. Following balloon angioplasty, the diameter of the left pulmonary artery increased by 200%, and the left lung flow increased to 22% by follow-up lung scan. (Parts A–D from Wernovsky G, Hougen TJ, Walsh EP, et al. Midterm results after the arterial switch operation for transposition of the great arteries with intact ventricular septum: clinical, hemodynamic, echocardiographic and electrophysiologic data. *Circulation* 1988;77:1333–1344, with permission.)

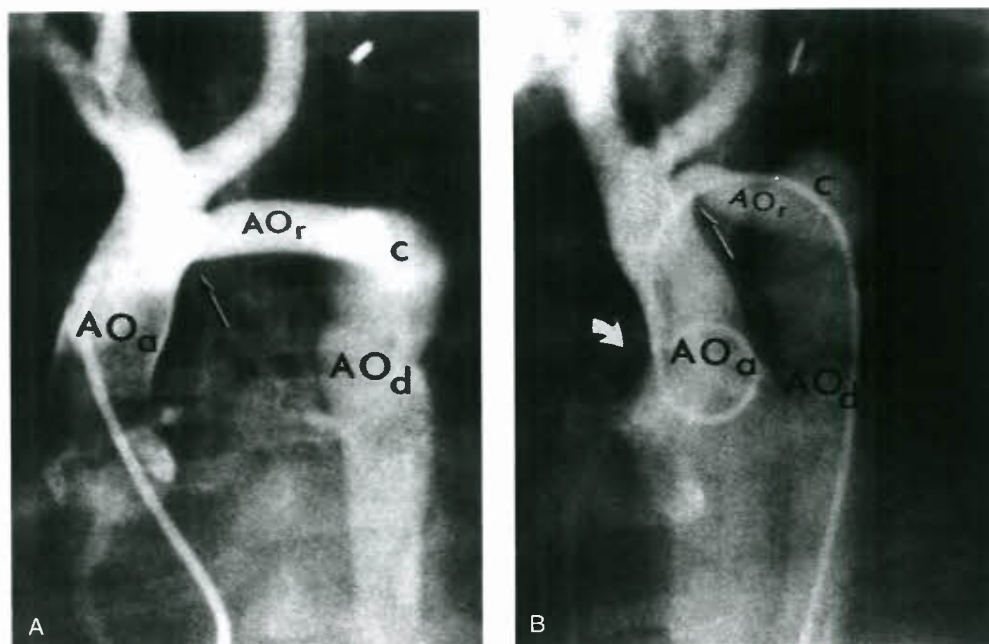


Figure 49.36. Aortograms in a patient with DORV, anterior malalignment subpulmonary VSD (with previous coarctation repair) illustrating new obstructive kinking in the proximal aortic arch following to arterial switch with LeCompte maneuver. **A:** At 10 months of age before arterial switch, note the well-repaired distal arch (c); only a 5-mm Hg gradient was registered across the moderately hypoplastic transverse aortic arch (AO_t). **B:** At 2 years of age, 1 year after the arterial switch, note that the anterior positioning of the pulmonary artery trunk (white curved arrow) has caused posterior displacement, kinking, and acute angulation (black arrow) where the transverse aortic arch joins the ascending aorta (AO_a). A 30-mm Hg systolic gradient was present. AO_d.

switch using the LeCompte maneuver. This significant “neocoarctation” has only been reported in patients with TGA associated with a prior coarctation repair (with associated tubular hypoplasia of the transverse arch) and may reflect either inherent anatomic abnormalities of the arch or inadequate surgical technique rather than the LeCompte maneuver per se.

The status of the neo-aortic (anatomic pulmonary) root and valve remains a subject of long-term concern (82). At the time of neonatal correction, the native pulmonary root is frequently larger than the ascending aorta, especially in TGA/VSD. Despite the “tailoring” that is frequently necessary to accommodate this size “mismatch,” the aortic anastomosis is not under much tension, and adequate circumferential growth of the suture line, commensurate with somatic growth, is characteristic (31). Multiple follow-up studies have described an enlarged neo-aortic root (Fig. 49.37) and annulus (Fig. 49.38) following both neonatal and two-stage anatomic correction (92–95).

The “Achilles’ Heel” of the Arterial Switch Operation: The Neo-aortic Root, Valve, and Translocated Coronary Arteries

Now that there are increasing numbers of patients with TGA surviving into their fourth decade of life following the arterial switch operation where they are at increasing risk for atherosclerosis, hypertension, obesity, diabetes, etc., there is growing concern about the long-term (“life-long”) fate of the anatomic pulmonary (“neo-aortic”) valve in the systemic circulation and the function and long-term health of coronary arteries that underwent removal and translocation in the first few weeks of life. There remain many unknowns: does the

heart eventually reinnervate decades after the great vessels are transected, “switched,” and reanastomosed? Can an arterial switch survivor feel angina if he or she has ischemia?; Will there be accelerated coronary disease—or “different” coronary disease—in this population? and What is decades-long likelihood that the anatomic pulmonary valve will remain competent?

First and foremost, increasingly prevalent in the literature are reports of inappropriately progressive dilation of the neo-aortic root following anatomic correction. There appears to be enlargement out of proportion to somatic growth in most reports (92,94–96). The data from Marino et al. (92) suggests that neo-aortic root dilation is progressive, and finding not replicated with the report from Schwartz et al. (94). Of some concern is the earlier appearance of significant root dilation in one recent report from Boston (94). In one of the initial reports of neo-aortic root dilation (97), in 50 patients with serial echocardiographic measurements, there was (a) normal growth of the anastomosis, (b) stable growth of the dilated neo-aortic annulus, but (c) progressive dilation of the neo-aortic root (Figs. 49.37 and 49.38). This phenomenon is more likely to occur in patients with TGA/VSD, in whom the native pulmonary root is significantly larger than that seen in TGA/IVS. The etiology and long-term effects of progressive dilation of the neo-aortic root are unknown. Removal of the sinuses of valsalva with reimplantation of the coronary “buttons” and the supra-avalvular suture line may be causative factors of this progressive dilation.

There is a surprisingly high incidence of neo-aortic regurgitation following the arterial switch operation; however, in the overwhelming majority of cases, the degree of regurgitation is trivial to mild (92–95,98,99). There have been rare reports of more significant regurgitation, including isolated reports of

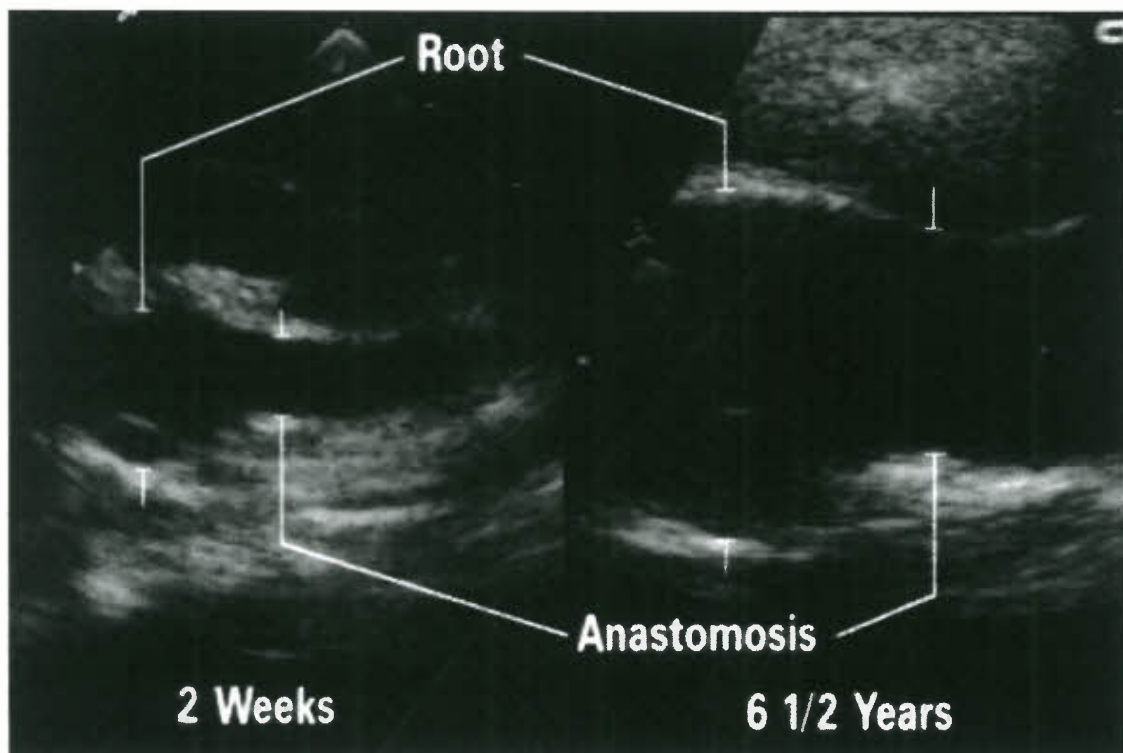


Figure 49.37. Echocardiographic images of the neo-aortic root and the aortic anastomosis at 2 weeks (left) and 6 1/2 years (right) after arterial switch. Note that the anastomosis is well seen at 2 weeks but is indistinguishable from the rest of the ascending aorta at 6 1/2 years. (From Hourihan M, Colan SD, Wernovsky G, et al. Growth of the aortic anastomosis, annulus and root after the arterial switch procedure performed in infancy. *Circulation* 1993;88:615–620, with permission.)

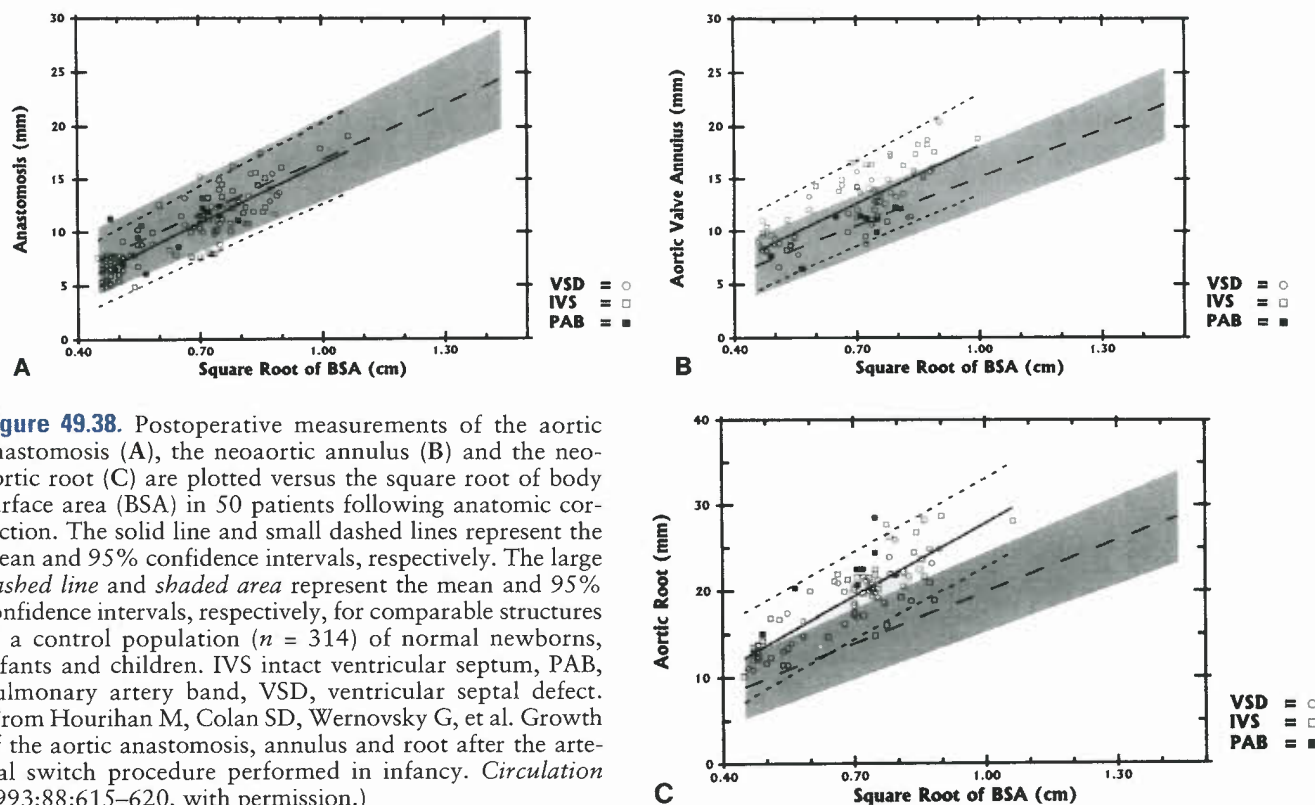


Figure 49.38. Postoperative measurements of the aortic anastomosis (A), the neo-aortic annulus (B) and the neo-aortic root (C) are plotted versus the square root of body surface area (BSA) in 50 patients following anatomic correction. The solid line and small dashed lines represent the mean and 95% confidence intervals, respectively. The large dashed line and shaded area represent the mean and 95% confidence intervals, respectively, for comparable structures in a control population ($n = 314$) of normal newborns, infants and children. IVS intact ventricular septum, PAB, pulmonary artery band, VSD, ventricular septal defect. (From Hourihan M, Colan SD, Wernovsky G, et al. Growth of the aortic anastomosis, annulus and root after the arterial switch procedure performed in infancy. *Circulation* 1993;88:615–620, with permission.)

aortic valve replacement (96). There is a higher incidence of neo-aortic root dilation and regurgitation following two-stage repair compared with primary repair. The highly variable incidence of neo-aortic regurgitation (from 0% to 50%) is most likely related to the methodology of investigation by which it is sought rather than due to technical modifications of the operation. Angiographic and auscultatory neo-aortic regurgitation is significantly less common than that reported in studies using color Doppler.

This high prevalence of neo-aortic regurgitation raises the important question of the adequacy of the anatomic pulmonary valve, normally with thin leaflets and little collagen and elastic tissue when present in the low-pressure pulmonary circulation to support the high-pressure systemic circulation over a patient's lifetime (97). Although trivial (color Doppler) regurgitation of a semilunar valve may be a normal finding, large studies using color Doppler in patients with normal hearts detect a high incidence of trivial to mild anatomic pulmonary valve regurgitation, but no aortic regurgitation is rarely detected using the same methodology. Before final pronouncements are made on the superiority of anatomic correction, long-term follow-up of the functioning of the neo-aortic valve and root must be obtained.

The long-term patency and growth of the coronary arteries are crucial for the arterial switch operation to be considered the procedure of choice for the surgical management of TGA. Patients with occlusion of the coronary arteries following anatomic correction may present with a spectrum of symptoms from cardiogenic shock to no symptoms at all (100–104). Intraoperative kinking or occlusion of a coronary artery usually results in acute ischemia and ventricular dysfunction, with inability to separate the patient from cardiopulmonary bypass. This problem must be suspected if the hemodynamics are poor, especially in association with arrhythmias or ECG changes, and may be confirmed with intraoperative echocardiography. The coronary anastomo-

ses should be inspected and revised if necessary; an internal mammary artery bypass may be necessary in extreme circumstances. Subacute kinking or occlusion may result in a chronic low-output state immediately after surgery. Although patients in this chronic low-output state eventually may leave the hospital, they are at risk for acute circulatory collapse weeks to months after the arterial switch operation. Late postoperative myocardial infarction and death have been reported in 1% to 2% of hospital survivors following the arterial switch. However, in one recent series, 13.5% underwent coronary revascularization at an average of 8 ± 4.3 years after surgery (105), and there are growing numbers or reports of coronary interventions in the second and third decades of life (106–109).

Although growth of the coronary anastomosis and continued patency are present in most patients at follow-up, asymptomatic occlusion of one of the coronary arteries may occur in as many as 1% to 2% of hospital survivors (103). Presumably, this type of occlusion takes place gradually, allowing adequate collateralization from the contralateral coronary system (Fig. 49.39). Myocardial perfusion studies following the arterial switch operation have shown a surprisingly high incidence of perfusion defects, the clinical significance of which are uncertain to date (110–113). Formal exercise testing has shown no evidence of ischemic changes in this group of patients (112,114).

Systemic (left) ventricular function has been preserved at early and midterm follow-up studies (80,115). Echocardiographic assessments in neonates and older infants indicate excellent preservation of both regional and global function, which suggests that permanent ischemic injury is uncommon. In the neonate, immediate post-repair left ventricular function has been noted to be impaired for the first few days after surgery, but subsequent predischarge assessments show almost uniformly normal systolic function, as do angiographic studies during follow-up. Left ventricular

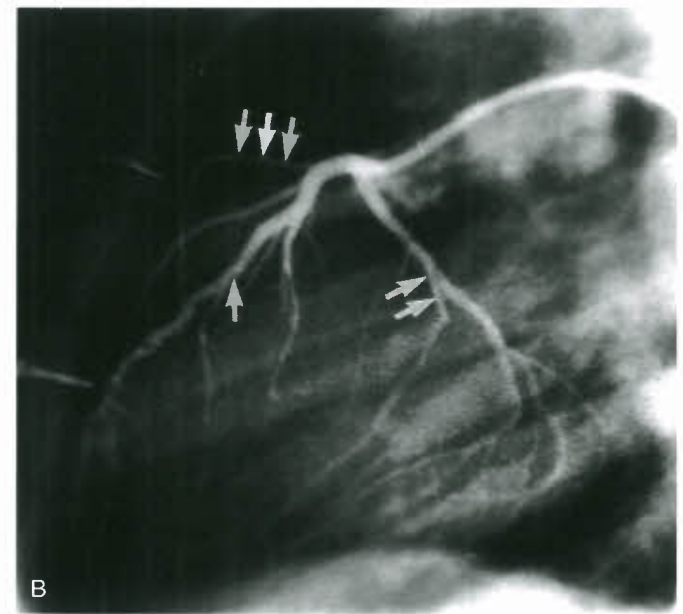
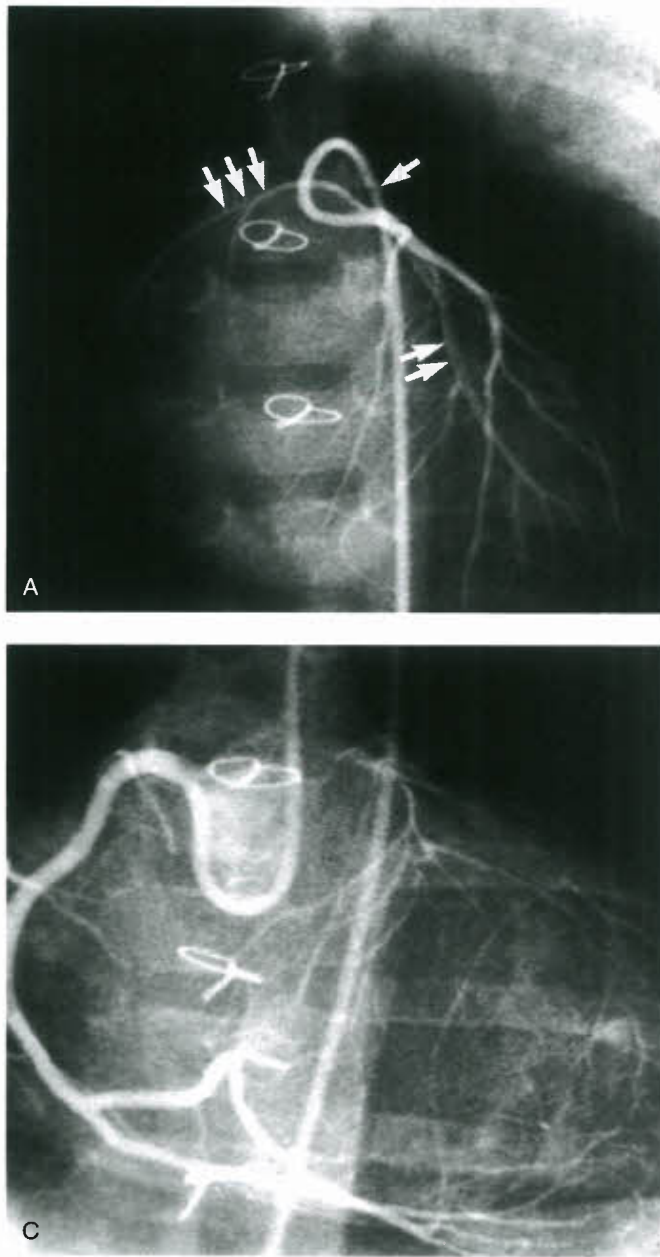


Figure 49.39. Anterior (A) and lateral (B) projections of a selective injection in the left coronary system in a 2 ½-year-old child following neonatal anatomic correction. The coronary pattern was the “usual” variety for transposition; the left anterior descending (*single arrow*) and circumflex (*double arrows*) are well seen without distal stenoses. A prominent anterior right ventricular branch (*triple arrows*) is present. Selective right coronary injection (C) in an asymptomatic 15-month-old (also with “usual” coronary arteries for TGA) following neonatal anatomic correction. The proximal left coronary artery is completely occluded with collateralization from a markedly enlarged right coronary system. This child had a normal ECG; echocardiographic measurements of regional wall motion and left ventricular function (at rest) were normal, and cardiac index (3.4 L/min/m²) and left ventricular end-diastolic pressure (8 mm Hg) were normal at catheterization. (A and B courtesy of Dr. Henry Wiles, C courtesy of Dr. Daniel Diana.)

shape has been described as more globular following anatomic repair, end-diastolic volumes have been normal to only slightly enlarged, and ejection fraction and contractility have been normal. Follow-up of left ventricular function, particularly in patients following two-stage arterial repair, has shown some to have abnormal ventricular function, and end-diastolic and end-systolic volumes were slightly elevated (80).

Perhaps the most striking midterm advantage of anatomic correction over physiologic correction has been the low incidence of postoperative dysrhythmias (Table 49.4). Sinus rhythm has been present postoperatively with rare exceptions. Intracardiac electrophysiologic studies confirm normal sinus node function and normal AV conduction, with no evidence of ischemia-related ventricular ectopy on 24-hour ambulatory ECG monitoring (81,116).

In both surgical groups, there is a growing recognition of neurodevelopmental, social, and behavioral sequelae that may significantly impact on health-related quality of life

(117–119). Reports are mixed in this area, with some favoring the outcomes in the arterial switch patients, possibly related to improved cardiovascular health (65), while others suggest a similar patient-reported quality of life with either surgical technique that is similar to that in the general population (120). It has been shown that patients following the arterial switch operation get less physical exercise than the general US population, and have similar risk profiles to the rest of the United States for obesity, with one-third being either obese or at risk for obesity. In the most recent publication from the Boston Circulatory Arrest Study, patients at age 16 were four times more likely to be taking psychotropic medications compared to cardiovascular medications, and approximately two-thirds of that cohort received behavioral therapies and/or additional help at school. One-third had brain abnormalities detected on MRI (121). Multiple investigations confirm a higher-than-expected rate of attention deficit hyperactivity disorder, deficits in social cognition, theory of mind, and executive function (79,122).

TABLE 49.5 Postoperative Sequelae after the Mustard and Senning Operations

Postoperative Sequelae	Incidence (%)
■ Right ventricular failure	15
■ Moderate–severe TR	20
■ Bradyarrhythmias requiring pacing	20
■ Tachyarrhythmias requiring treatment	15
■ Subpulmonary obstruction	10
■ Reduced exercise capacity	>75
■ Pulmonary hypertension	10
■ Sudden death	1 (per year)

Nonelectrophysiologic consequences of the atrial level repairs are shown in Table 49.5 and for the arterial switch operation in Table 49.6.

Surgery for Transposition of the Great Arteries with Low Left Ventricular Pressure

Some circumstances may arise that will cause postponement of surgery beyond the safe period for an arterial switch. A neonate may be seriously ill with necrotizing enterocolitis, renal failure, or hemorrhage or may be premature or have low birth weight. A neonate may be geographically distant from a center offering the arterial switch operation; and, occasionally, a patient with TGA/VSD awaiting elective repair may have spontaneous partial or complete closure of the VSD resulting in an inadequate left ventricular mass. Surgical options for these patients include (a) primary atrial correction (see preceding) or (b) two-stage anatomic correction.

TABLE 49.6 Postoperative Sequelae Following the Arterial Switch Operation

Postoperative Sequelae	Incidence (%)
■ Supravalvar pulmonary stenosis ^a	~10
■ Supravalvar aortic stenosis ^a	<5
■ Neo-aortic root dilation	Essentially 100 ^b
■ Neo-aortic regurgitation	~50 ^b
■ Significant arrhythmia	<10
■ Asymptomatic coronary occlusion	2–3
■ Pulmonary hypertension	Rare
■ Hypertrophied bronchial collaterals ^a	<5
■ Abnormal coronary flow reserve	Unknown
■ Reduced exercise capacity	>75
■ Sudden death	Rare ^b

^aRequiring intervention.

^bIncreases with increasing duration of follow-up.

Pulmonary artery banding has been used to increase left ventricular afterload and stimulate hypertrophy. Indeed, the first successful anatomic repairs in patients with TGA/IVS consisted of placement of a pulmonary artery band, with or without a simultaneous systemic–pulmonary shunt, with an interval period of months before band removal and anatomic correction. Pulmonary artery banding can produce adequate muscle retraining within days (123), so that the preparatory procedure and the arterial switch operation can be done during the same hospitalization (rapid two-stage arterial switch) (124–127).

When this technique is used, left ventricular function may be extremely impaired following banding; therefore, a systemic–pulmonary artery shunt is frequently placed to ensure adequate pulmonary blood flow. The interval period between banding and correction is frequently characterized by a low output syndrome, most likely resulting from a combination of acute (fixed) right ventricular volume overload from the shunt and acute (transient) left ventricular dysfunction from the pulmonary artery band. Clinical improvement coincides with improvement in left ventricular function such that anatomic correction can be performed within 7 to 10 days in most cases.

Left Ventricular Preparation

There is little information as to just how late primary anatomic correction can be successfully performed. The normal postnatal decrease in pulmonary vascular resistance results in a rapid fall in left ventricular afterload following closure of the ductus arteriosus. With time, this leads to an inadequate left ventricular muscle mass to sustain systemic pressure immediately following the arterial switch operation. Although absolute guidelines are difficult to make, identifying a “prepared” left ventricle may be easier than defining an “unprepared” one; a left ventricle that can generate a normal (or near normal) systolic pressure for age and with normal posterior wall thickness/muscle mass will most likely be able to perform at systemic pressure following anatomic correction.

It is much more difficult to state when a left ventricle has become unprepared (128,129). In some cases, direct pressure measurements in the left ventricle or the ratio of left-to-right ventricular pressure may not be predictive of the capability of the left ventricle to perform systemic work. For example, in a neonate with immediate closure of the ductus and a prompt fall in pulmonary vascular resistance, the left ventricular systolic pressure can fall to less than half the systemic levels (or 25 to 30 mm Hg) as soon as 4 or 5 days after birth. This does not mean that the left ventricle is incapable of producing systemic work if the arterial switch is done at that time, but if left at low pressure for an additional period of time (perhaps beyond 2 to 3 months), this left ventricle would most likely be unable to support systemic work. Also, age alone does not necessarily dictate whether a left ventricle is unprepared, even in patients with TGA/IVS. A 6-week-old patient whose ductus has only recently closed will more likely have a prepared left ventricle than a 6-week-old patient whose ductus closed directly after birth. Finally, identifying the rate and degree of fall of pulmonary vascular resistance is difficult or impossible to do, especially if the patient presents for surgery in the 1- to 3-month age range.

Thus, it is frequently a difficult clinical decision as to when a patient's left ventricle is unprepared. Empiric criteria to determine adequate left ventricular preparation may include (a) an absolute left ventricular systolic pressure that is appropriate for age, (b) a left ventricular pressure at cardiac catheterization that is at or above 70% systemic levels (left-to-right ventricular ratio >0.7), or (c) left ventricular muscle mass that is within the normal range for body surface area.

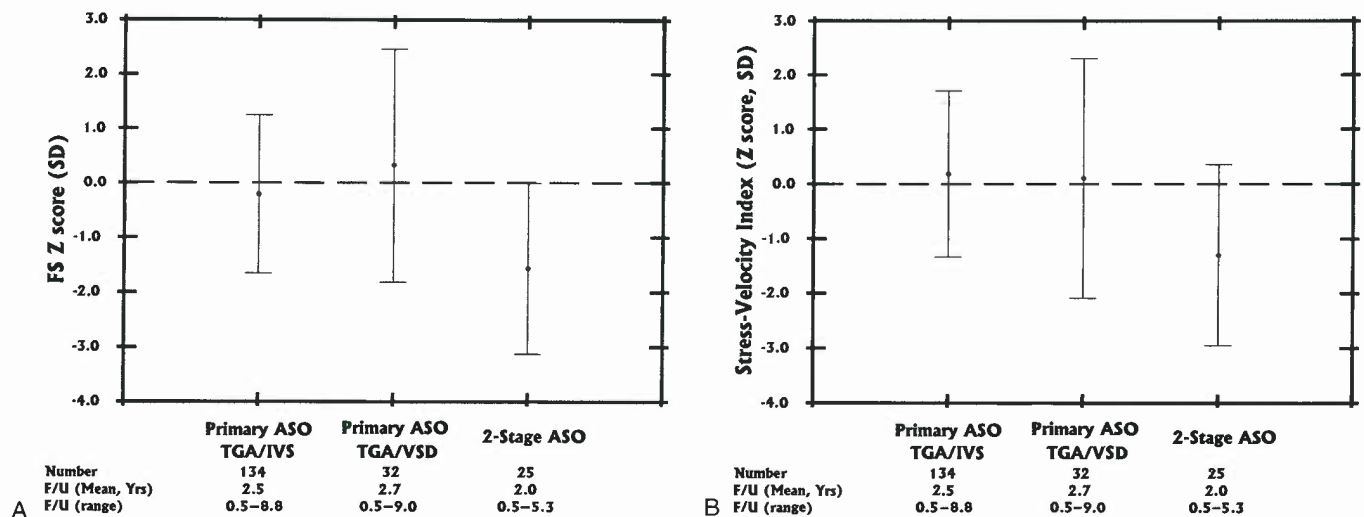


Figure 49.40. Indices of late left ventricular function after primary arterial switch in 134 patients with TGA/IVS, 32 with TGA/VSD and 25 following a rapid two-stage arterial switch. Fractional shortening (A) and (B) myocardial contractility (the relationship of end-systolic stress to the rate-corrected velocity of fiber shortening is a load independent index of contractility) are expressed as the Z-score \pm 2 SD from the mean. Function appears better preserved following a primary repair compared with the two-stage approach. ASO, arterial switch operation; FS, fractional shortening; F/U, follow-up. (Data modified from Boutin C, Jonas RA, Sanders SP, et al. Rapid two-stage arterial switch operation: acquisition of left ventricular mass following pulmonary artery banding in infants with transposition of the great arteries. *Circulation* 1994;90:1304–1309.)

Although pulmonary artery banding remains the standard surgical method to “retrain” the left ventricle, other innovative approaches have included a percutaneously adjustable band (130), partial balloon occlusion of the main pulmonary artery with a percutaneously placed balloon-tipped catheter, systemic–pulmonary artery shunting alone, and a primary arterial switch with left ventricular assist in the perioperative period (128,129,131).

Following the preparatory procedure, usually performed through a midline sternotomy, anatomic correction is performed in a standard fashion based on the patient’s anatomy, with removal of the pulmonary artery band and takedown of the shunt (if present). Mortality following pulmonary artery banding may be as high as 10%, although the early postoperative course following the arterial switch seems comparable to that of primary repair.

Several follow-up studies have shown less-well preserved ventricular function in patients who undergo two-stage anatomic correction compared with those who undergo primary anatomic correction (Fig. 49.40) (80,124,132). Also, follow-up studies revealed a higher incidence of neo-aortic regurgitation and root dilation following two-stage repair.

Anatomic Correction without Coronary Translocation

In 1975, Damus, Kaye, and Stansel—in independent reports—proposed an arterial level repair without coronary translocation. The so-called Damus-Kaye-Stansel technique is now generally reserved for children with TGA and coronary artery patterns not suitable for transfer or for patients with DORV (Taussig-Bing type) with severe subaortic stenosis. The main pulmonary artery is transected and anastomosed in an end-to-side fashion to the ascending aorta. The coronary arteries are perfused in a retrograde fashion. The native aortic valve may be left intact. A VSD (if present) is closed to direct left ventricular blood to the native pulmonary (neo-aortic) valve. Finally, a right ventricular–pulmonary artery conduit is placed to establish a normal series circulation.

Long-term follow-up studies of the Damus-Kaye-Stansel operation are limited. Anecdotal experience suggests that the native aortic valve regurgitation is common in this group of patients, perhaps because of the lack of antegrade flow across the valve combined with the continued retrograde pressure load. This type of regurgitation has the physiologic sequelae of a wide pulse pressure and increased volume load on the systemic ventricle and results in a left-to-right shunt and pulmonary overcirculation; however, closure of the native aortic valve or subaortic region at surgery prevents decompression of a suprasystemic right ventricle in patients with conduit obstruction or in patients with elevated pulmonary vascular resistance. Thus, routine closure of the native aortic valve at the time of the Damus-Kaye-Stansel operation remains somewhat controversial.

In older infants and children with TGA/large VSD, anatomic repair sometimes can be achieved by using an intraventricular patch-tunnel technique that establishes a normal ventriculoarterial connection. Functionally, such patients with large VSD have maintained a hypertrophied left ventricle capable of assuming systemic afterload; many have had palliative pulmonary artery banding early in infancy. To construct a relatively straight tunnel that does not obstruct the pulmonary outflow tract, it is usually necessary to resect portions of the outlet (infundibular) septum and enlarge the VSD by resecting a portion of the interventricular septum that is anterior to the VSD. These segments of the septum do not carry the AV conduction axis, and the septal resection can make some defects subarterial in position even if they do not originally have this necessary condition for the intraventricular repair. Anatomically, the feasibility of intraventricular repair depends on the relationship of the VSD to the great arteries, the distances between the tricuspid valve and the semilunar valves, and the nature of the AV valve leaflets, particularly their chordae tendineae attachments. This operation is essentially the same as the intraventricular repair that is applicable to some patients of the subgroup of DORV characterized by the pulmonary trunk overriding an anterosuperior VSD (Taussig-Bing malformation).

Several other innovative techniques have been described for anatomic correction without coronary translocation, including creation of aortopulmonary tunnel (Aubert procedure) or baffling the left ventricular outflow to the non-translocated coronary ostia with a patch of native aorta or pericardium. Finally, the entire aortic root may be translocated to the left ventricle with biventricular outflow tract reconstruction.

Surgery for Transposition of the Great Arteries with Associated LVOTO

Direct surgical relief of severe LVOTO may be difficult and depends primarily on the anatomic type and severity of obstruction, which usually is directly related to the state of the interventricular septum and its alignment with the infundibular septum. In the older, palliated (septostomy or septectomy) infant with TGA/IVS, there is often a mild or moderate dynamic LVOTO, but this is clinically unimportant. Furthermore, the obstruction has only rarely been noted to progress during late follow-up after atrial switch repair. Predictably, this form of systolic dynamic LVOTO is reduced or eliminated in older infants with TGA/IVS following pulmonary artery banding as a left ventricular preparative procedure for secondary arterial switch repair.

Transpulmonary or transmitral resection has been performed for severe fixed obstruction caused by a short, discrete fibromuscular subvalvar shelf in patients with TGA/IVS. Because access is often limited and extensive resection may carry excessive risk of conduction abnormalities, residual pressure gradients have been common. If the obstruction is severe, with left ventricular systolic pressures at systemic (or suprasystemic) levels, and the pathology is not amenable to direct relief, an atrial switch operation with placement of a left ventricular-pulmonary artery valved conduit has been successfully used.

In the neonate or young infant with TGA/large VSD, some moderate LVOTO can function to prevent heart failure and limit early and rapidly progressing pulmonary vascular disease. As long as intercirculatory mixing and systemic arterial oxygen saturation are satisfactory and the peak systolic pulmonary artery pressure is low, intracardiac surgery can be safely delayed with careful follow-up regarding the pulmonary artery.

In the infant with TGA/large VSD and severe left ventricular outflow obstruction, there may be markedly restricted pulmonary blood flow and severe hypoxemia. In some neonates, a palliative systemic-to-pulmonary arterial shunt (Gore-Tex interposition shunt or classic Blalock-Thomas-Taussig shunt) may be performed, with intracardiac correction carried out at a later age. Alternatively, corrective surgery can be performed in early infancy.

One such procedure, the Rastelli operation (133), is a combination of intraventricular repair and placement of an extracardiac right ventricular to pulmonary artery conduit. The Rastelli repair has been considered the most appropriate operation for TGA with large VSD and extensive LVOTO because it achieves complete bypass of the LVOTO and an anatomic correction of the transposition pathology. In this operation (Fig. 49.41), the proximal main pulmonary artery is functionally divided either by pledgetted mattress suture closure of the subvalvar obstruction or by oversewing a stenotic pulmonary valve orifice (Fig. 49.42). The left ventricular output is directed to the aorta by placement of an intraventricular patch-tunnel technique. Finally, the right ventricle is connected to the proximal main pulmonary artery by means of a valved extracardiac conduit. The VSD must be of adequate size to permit unobstructed outflow from the left ventricle, and enlargement of

the defect by anterior excision of septal muscle may be necessary. Intracardiac repair with the Rastelli operation until recently has had an operative mortality of 20% to 30%, but more recently, operative survival of about 95% and midterm survival of about 90% are reported with good results, particularly in children older than 1 to 2 years of age.

Complications can result from unfavorable anatomic variants, such as a restrictive VSD or anomalous tricuspid valve connections to the infundibular septum that prevent baffling the left ventricle to the anterior aorta. As with other such complex repairs, residual VSD, late unexpected death, and myocardial dysfunction have been reported. As with all extracardiac conduiting operative techniques, there is concern about the functional longevity of the valved conduits. Improved results are noticeable with fresh or cryopreserved homograft-valved conduits compared with the previously used Dacron heterograft structures.

An interesting alternative corrective technique, termed REV (*Réparation à l'étage ventriculaire*) by LeCompte, has been used recently for patients with TGA and LVOTO. The REV procedure appears to have some advantages over the Rastelli operation: application in younger patients and avoidance of prosthetic extracardiac conduit and avoidance of intracardiac tunnel obstruction. This operation involves performing a high, anterior right ventricular incision and a radical excision of the outlet septum to create an unobstructed anterior right ventricular cavity; establishing a short and direct intraventricular tunnel from the LV to the aorta; closure of the pulmonary artery orifice; and reimplantation of the transected (and usually anteriorly translocated) pulmonary artery directly onto the right ventricular outflow cavity without a prosthetic conduit (134). A comparative study of the traditional Rastelli operation with the newer REV approach suggested that the REV allows complete repair earlier in infancy, is feasible in patients with anatomic contraindications to the Rastelli operation, and may reduce the need for reoperation and the prevalence of residual pulmonary outflow tract obstruction; (135) however, the life-long implications of pulmonary regurgitation following this newer operative approach require continued investigation.

Finally, posterior translocation of the aortic root and coronary arteries can be performed, with enlargement of the LVOT, with conduit placement from the right ventricle to the pulmonary arteries anteriorly, as originally described by Nikaidoh (136,137).

Controversy exists regarding the optimal initial management of the neonate or infant with severe hypoxemia and TGA/VSD with significant LVOTO. Arguments can be made that a Rastelli procedure should be performed in early infancy rather than a palliative systemic-to-pulmonary artery shunt. Although in an infant the Rastelli procedure still must be considered a palliative operation—a second operation for conduit replacement is inevitable—an early Rastelli repair results in a normal series circulation, avoidance of prolonged hypoxemia, and, presumably, a better long-term hemodynamic and neurologic outcome. Conduit replacement generally can be performed at low risk and with good results; therefore, many centers with expertise in neonatal and infant surgery have moved toward performing infant Rastelli repairs as the procedure of choice for the hypoxemic neonate or infant with TGA/VSD and LVOTO.

The arterial switch operation has been applied successfully in patients with TGA and certain types of LVOTO (138,139). Mild pulmonary valve abnormalities, dynamic or surgically remediable subpulmonary obstruction (e.g., AV valve tissue, a hypertrophied muscle of Moutaert, or a discrete membrane), or abnormal mitral valve attachments do not preclude application of the arterial switch operation in certain patients. Gradients measured preoperatively across the LVOT must be interpreted cautiously because there is frequently increased pulmonary blood flow in these patients. Left ventricular outflow gradients are typically significantly less after the arterial switch operation,

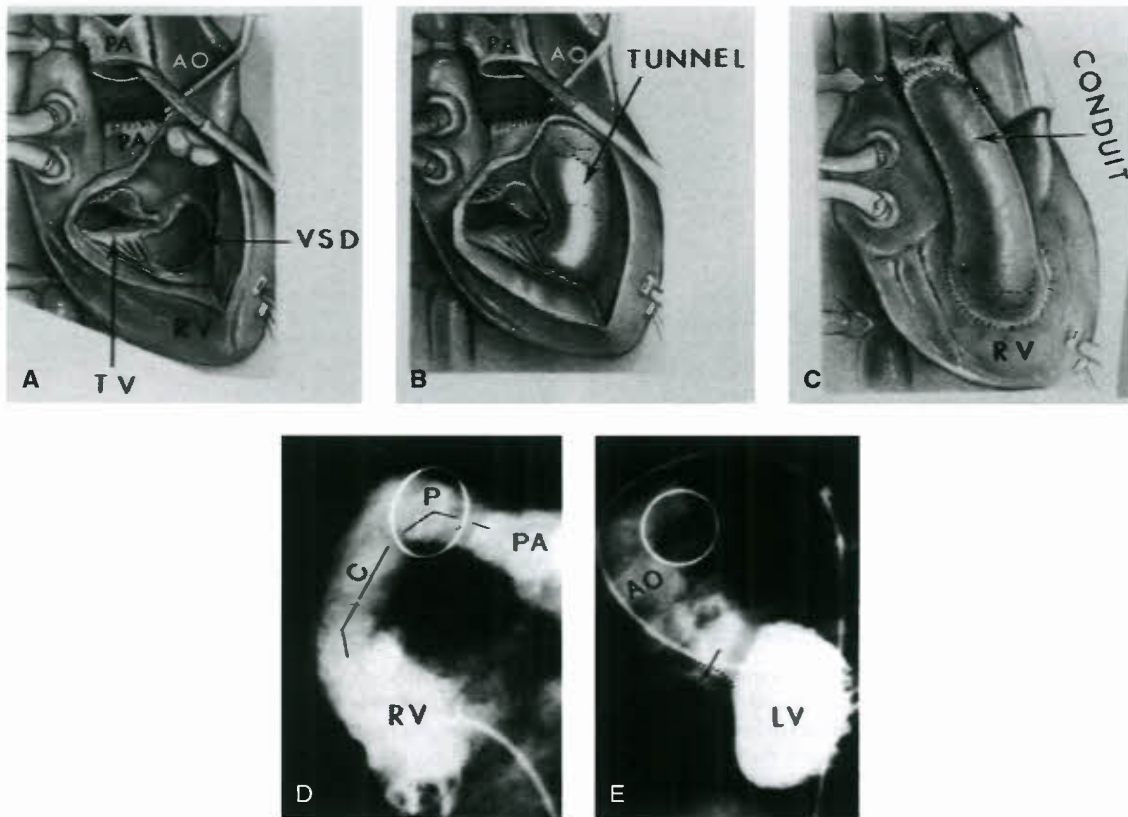


Figure 49.41. Rastelli operation for TGA/VSD and significant LVOTO. A–C: Details of surgical procedure. (Modified from Rastelli GC, McGoon DC, Wallace RB. Anatomic correction of transposition of the great arteries with ventricular septal defect and subpulmonary stenosis. *J Thorac Cardiovasc Surg* 1969;58:545–552.) A: Interior of right ventricle (RV) demonstrating relationship of VSD, tricuspid valve (TV), and aortic valve. B: Left ventricle is connected to aorta (AO) by tunnel patch extending between VSD and aorta. C: Completed repair with RV connected to the distal end of pulmonary artery (PA) by valved prosthetic conduit or (currently) homograft. D,E: Lateral angiograms with selective left ventricle (LV) and RV injections after Rastelli operation in 5-year-old. In (E), note the small (left-to-right) leak across tunnel patch (arrow), and (D) porcine (P) valved conduit (C) between RV and PA.

even if no surgical procedure is performed on the LVOT, as the blood flow across this region is reduced to normal (139).

Surgery for Transposition of the Great Arteries with Associated Right Ventricular Outflow Tract Obstruction

A spectrum of hearts exists from TGA with large subpulmonary VSD to {S,D,D} DORV (Taussig-Bing anomaly). These defects typically are characterized by varying degrees of anterior malalignment of the infundibular septum, subaortic narrowing/stenosis, aortic annular hypoplasia, a small hypoplastic arch, and coarctation or interruption of the distal aorta. If a coarctation is present (see also the section on Associated Anomalies), a VSD almost invariably coexists. Although more severe degrees of right-sided hypoplasia typically are associated with hypoplasia of the tricuspid valve and right ventricle and, not infrequently, left juxtaposition of the right atrial appendage, numerous treatment options are available for the subgroup of patients with an adequate-sized right heart.

In cases with only discrete coarctation, the coarctation can be repaired by a left thoracotomy with or without associated pulmonary artery banding. As pulmonary artery banding has been associated with progressive dilation of the neo-aortic root and propensity for neo-aortic regurgitation, many centers now limit pulmonary artery banding in these situations to cases with coarctation and multiple VSD. When pulmonary artery

banding is not performed, the arterial switch operation can be performed shortly after the child recovers from the coarctation repair. BAS should be performed prior to this repair so that following ligation of the ductus arteriosus (which is typically kept patent with a prostaglandin infusion), adequate mixing and arterial oxygen saturation may take place.

In cases of more significant proximal arch hypoplasia in association with coarctation or interruption, the entire corrective surgical procedure can be accomplished from the midline (140–142). This procedure involves arch reconstruction in a similar fashion to Norwood's reconstructive procedure for hypoplastic left heart syndrome, LeCompte maneuver to bring the (usually much larger) pulmonary arteries anterior to the reconstructed aorta, and an arterial switch operation with VSD closure.

Coronary artery patterns are more frequently unusual in these patients, and typically the anterior facing sinus gives rise to the right coronary artery and the left anterior descending, and the posterior sinus of Valsalva gives rise to the circumflex. The anterior course of the right coronary artery may complicate the repair; because an anterior malalignment VSD with subaortic narrowing frequently coexists in these patients, the coronary artery course may prevent or limit the size of the ventriculotomy necessary to relieve subaortic stenosis or to expose and close the VSD. A right ventricular–pulmonary artery conduit may be necessary in cases of severe subaortic obstruction or aortic (neopulmonary) annular hypoplasia. Care must be taken to avoid compression of the coronary arteries by the extracardiac conduit.

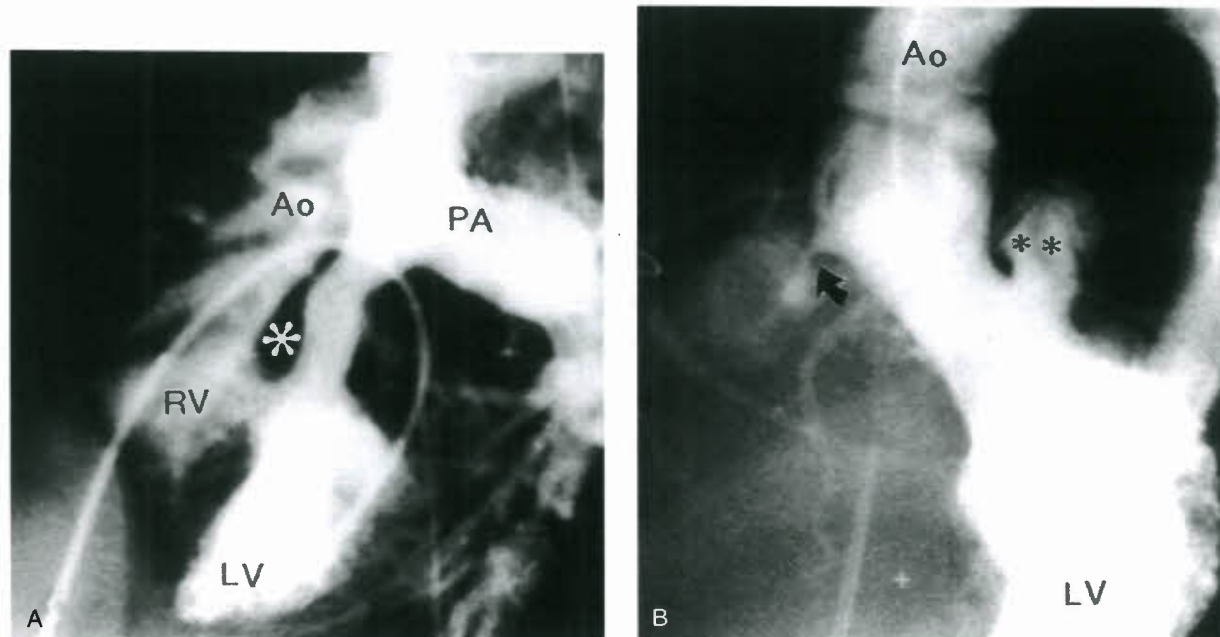


Figure 49.42. Preoperative (A) and postoperative (B) left ventriculograms in the same patient with TGA/VSD/left ventricular (LV) outflow tract obstruction. A: A transvenous (across the atrial septum) injection at 3 days of age. Posteriorly deviated conal septum (below a mildly hypoplastic pulmonary annulus) resulting in a malalignment type of VSD (*asterisk*). The branch pulmonary arteries (PA) are good sized. B: Retrograde left ventriculogram taken 4 years after the infant's repair (with an aortic homograft to establish right ventricular [RV] to PA continuity, not shown). The tunnel from LV to aorta (AO) is unobstructed. The blind-ending stump of main pulmonary artery fills with contrast (*double asterisk*). A tiny residual VSD is demonstrated (*arrow*).

Whereas single-stage corrective procedures for TGA/VSD/arch hypoplasia carry a significant mortality risk, alternative palliative surgical procedures have been less than satisfactory. Indeed, perhaps the worst results for atrial switch surgery are in patients with TGA, VSD, and associated arch hypoplasia. Palliative operations are particularly suboptimal in this subgroup of patients; therefore, an arterial switch operation/arch reconstructive surgery, albeit at high risk, is generally recommended for these patients.

Surgery for Right Ventricular Failure Following Physiologic Correction

With the growing recognition of progressive systemic (right) ventricular failure following physiologic correction (see preceding), with or without associated tricuspid insufficiency, numerous surgical procedures have been used in advanced, symptomatic patients. These include tricuspid valvuloplasty/replacement, cardiac transplantation, or anatomic correction.

Tricuspid valve surgery has been of limited success; this operation carries high mortality and morbidity rates and is frequently only a temporizing measure. Cardiac transplantation has been used in cases of significant, symptomatic ventricular (especially biventricular) dysfunction; indeed, TGA is the single most common anatomic diagnosis for patients with congenital heart disease listed in most cardiac transplantation registries. The life-long need for immunosuppressive therapy, the limited supply of donor organs, and the current mortality and morbidity risks make this radical therapy reserved for only the most symptomatic of patients.

A creative alternative approach of "retraining" and using the left ventricle (anatomic repair) together with takedown of the atrial repair was advocated by Mee et al. (143,144) and since then has been performed at other centers (145–147). Anatomic correction can be performed either by a standard arterial

switch operation with coronary translocation (see preceding) or, alternatively, transection of the main pulmonary artery with an end-to-side anastomosis and right ventricular-to-pulmonary artery conduit placement (Damus-Kaye-Stansel operation, see preceding). Both anatomic corrective procedures have their disadvantages. The arterial switch operation may be technically more difficult in the older patient with a prior physiologic correction because frequently dense adhesions are present that may restrict anterior mobilization of the branch pulmonary arteries and limit precise identification and adequate mobilization of the coronary arteries. A Damus-Kaye-Stansel operation may be technically easier to perform, but it requires the use of a prosthetic conduit from the right ventricle to pulmonary arteries.

Issues of left ventricular preparedness are defined even more poorly in this group of patients than in the unrepaired, cyanotic neonatal and infant subgroup (see also section on "Surgery for TGA with Low Left Ventricular Pressure"). The ability for the older child or adolescent's heart to hypertrophy following a pulmonary artery band, the rapidity with which this hypertrophy occurs, and the interval period necessary for adequate preparation are not yet established. Some patients may have a prepared left ventricle as a result of (a) coexisting subpulmonary stenosis or (b) pulmonary venous obstruction (leading to pulmonary artery and left ventricular hypertension). In the face of systemic or near systemic left ventricular pressure, anatomic correction with Senning or Mustard takedown can be performed as a single operation. In most cases, however, pulmonary artery banding is necessary to prepare the left ventricle.

Results of this approach are limited to a few series. Operative mortality is high (as high as 20% to 30%) (70) when considering both the preparatory and corrective procedures. Although follow-up studies have shown improvement in symptoms and systemic (now left) ventricular function, there has been a disappointingly high incidence of neo-aortic regurgitation in this group

of patients (148). Some have speculated that the pulmonary valve, if subjected to low pressure for many years, may be susceptible to neo-aortic regurgitation following anatomic correction. Thus, not only is the left ventricle unprepared; the pulmonary valve may be unprepared as well. Nonetheless, this innovative surgical approach continues to be used with modest success in patients with symptomatic right ventricular failure following physiologic correction. Longer follow-up certainly will be necessary to assess the long-term merits of this rather aggressive surgical approach.

Surgery for TGA/VSD and Pulmonary Vascular Obstructive Disease

Elevated pulmonary vascular resistance markedly increases the risk of surgery with closure of the VSD. Advanced pulmonary vascular disease characterized by calculated pulmonary vascular resistances >10 U or grade 4 (H–E) histologic changes is considered a contraindication to closure of the VSD. Extensive grade 4 (H–E) pathology has been observed even in patients with lower pulmonary vascular resistance levels of 6 to 8 U. Despite the advanced pulmonary vascular changes, the pulmonary artery oxygen saturation is higher than the aortic saturation in most patients. Palliative switch (either atrial or arterial) allows more effective pulmonary and systemic flows and a significantly improved systemic arterial oxygen saturation.

Palliative atrial switch repairs (without closure of the VSD) have been accomplished with low surgical risk and substantial hemodynamic and clinical benefit. In one series (149) concerned with 41 palliative Mustard procedures, operative mortality was 7%, late mortality was 5%, and actuarial survival was 92% at 7 years. After palliative atrial switch repair, the effective systemic blood flow is markedly increased. Mean systemic arterial oxygen saturations were increased in two series from preoperative levels of 68% to 74% to postoperative levels of 87% to 90%. This procedure should be reserved for patients in whom peripheral desaturation is a major cause of symptomatology because there is no favorable postoperative change in the pulmonary artery pressures or calculated pulmonary vascular resistances. The concept of the palliative Mustard operation also has been applied successfully to patients with pulmonary vascular disease with IVS by creating concurrently a VSD in the apical segment of the muscular septum: In one child, there was an increase of systemic arterial oxygen saturation from 46% preoperatively to 93% postoperatively. Fortunately, the inevitability of advanced pulmonary vascular disease, previously so tragically prevalent in older infants and children with TGA/large VSD, has been markedly reduced during the past two decades.

ACKNOWLEDGMENT

The author thanks Milton H. Paul, M.D., whose pioneering work in the diagnosis and management of TGA forms the basis for much of the data in this chapter.

REFERENCES

- De Luca A, Sarkozy A, Ferese R, et al. Familial transposition of the great arteries caused by multiple mutations in laterality genes. *Heart* 2010;96:673–677.
- Pasquini L, Sanders SP, Parness IA, et al. Conal anatomy in 119 patients with d-loop transposition of the great arteries and ventricular septal defect: an echocardiographic and pathologic study. *J Am Coll Cardiol* 1993;21:1712–1721.
- Gittenberger-de Groot AC, Sauer U, Oppenheimer-Dekker A, et al. Coronary arterial anatomy in transposition of the great arteries: a morphologic study. *Pediatr Cardiol* 1983;4:15–24.
- Mayer JE Jr, Sanders SP, Jonas RA, et al. Coronary artery pattern and outcome of arterial switch operation for transposition of the great arteries. *Circulation* 1990;82:139–145.
- Wernovsky G, Sanders SP. Coronary-artery anatomy and transposition of the great arteries. *Coron Artery Dis* 1993;4:148–157.
- Quaegebeur JM. Coronary arterial anatomy in transposition of the great arteries: an anatomical and clinical study (Thesis). *The Arterial Switch Operation: Rationale, Results, Perspectives*. Leiden: Rosengaard-Deerlijk, 1986: 43–71.
- Anderson RH. Description of the origins and epicardial course of the coronary arteries in complete transposition. *Cardiol Young* 1991;1:11–12.
- Hayes CJ, Gersony WM. Arrhythmias after the Mustard operation for transposition of the great arteries: a long-term study. *J Am Coll Cardiol* 1986;7:133–137.
- Kirklin JW, Barratt-Boyes BG. Complete transposition of the great arteries. In: Kirklin JW, Barratt-Boyes BG, eds. *Cardiac Surgery*. New York, NY: Churchill Livingstone, 1993:1383–1467.
- Wernovsky G, Bridges ND, Mandell VS, et al. Enlarged bronchial arteries after early repair of transposition of the great arteries. *J Am Coll Cardiol* 1993;21:465–470., et al. Abnormalities of the tricuspid valve in complete transposition of the great arteries with ventricular septal defect. *J Thorac Cardiovasc Surg* 1982;83:569–576.
- Huhta JC, Edwards WD, Danielson GK et al. Abnormalities of the tricuspid valve in complete transposition of the great arteries with ventricular septal defect. *J Thorac Cardiovasc Surg*. 1982;83:569–576.
- Vidne BA, Duszynski D, Subramanian S. Pulmonary blood-flow distribution in transposition of great arteries. *Am J Cardiol* 1976;38:62–66.
- Ussia GP, Marasini M, Zannini L, et al. Acquired pulmonary vein obstruction after open-heart surgery. *Eur J Cardiothorac Surg* 2002;22: 465–467.
- Pappas G. Left pulmonary vein stenosis associated with transposition of the great arteries. *Ann Thorac Surg* 1986;41:208–209.
- Vogel M, Ash J, Rowe RD, et al. Congenital unilateral pulmonary vein stenosis complicating transposition of the great arteries. *Am J Cardiol* 1984;54:166–171.
- Naeye RL. Transposition of the great arteries and prenatal growth. *Arch Pathol* 1966;82:412–418.
- Clouchoux C, Cuizard N, Evans AC, et al. Normative fetal brain growth by quantitative in vivo magnetic resonance imaging. *Am J Obstet Gynecol* 2012;206:e1–e8.
- Limperopoulos C, Tworetzky W, McElhinney DB, et al. Brain volume and metabolism in fetuses with congenital heart disease: evaluation with quantitative magnetic resonance imaging and spectroscopy. *Circulation* 2010;121:26–33.
- Turah S, Turan O, Hussein M, et al. Patterns of compromised fetal brain growth in congenital heart disease (CHD). *Am J Obstet Gynecol* 2012;206:S176–S177.
- Manzar S, Nair AK, Pai MG, et al. Head size at birth in neonates with transposition of great arteries and hypoplastic left heart syndrome. *Saudi Med J* 2005;26:4453–4456.
- Licht DJ, Shera DM, Clancy RR, et al. Brain maturation is delayed in infants with complex congenital heart defects. *J Thorac Cardiovasc Surg* 2009;137:529–537.
- Watanabe K, Matsui M, Matsuzawa J, et al. Impaired neuroanatomic development in infants with congenital heart disease. *J Thorac Cardiovasc Surg* 2009;137:146–153.
- Newfeld EA, Paul MH, Muster AJ, et al. Pulmonary vascular disease in complete transposition of the great arteries: a study of 200 patients. *Am J Cardiol* 1974;34:75–82.
- Newfeld EA, Paul MH, Muster AJ, et al. Pulmonary vascular disease in transposition of the great vessels and intact ventricular septum. *Circulation* 1979;59:525–530.
- Beitzke A, Justich E, Suppan C. Systemic arterial collateral vessels as a cause of pulmonary-hypertension in an infant with transposition of the great arteries. *Herz* 1983;8:55–62.
- Yamaki S, Horiuchi T. Quantitative-analysis of post-operative changes in the pulmonary vasculature of patients with complete transposition of the great arteries and pulmonary-hypertension. *Am J Cardiol* 1979;44:284–289.
- Clarkson PM, Neutze JM, Wardill JC, et al. The pulmonary vascular bed in patients with complete transposition of the great arteries. *Circulation* 1976;53:539–543.
- Rosengart R, Fishbein M, Emmanolides GC. Progressive pulmonary vascular disease after surgical correction (Mustard Procedure) of transposition of great arteries with intact ventricular septum. *Am J Cardiol* 1975;35: 107–111.
- Levin DL, Paul MH, Muster AJ, et al. d-Transposition of the great vessels in the neonate: a clinical diagnosis. *Arch Intern Med* 1977;137:1421–1425.
- Bonnet D, Coltri A, Butera G, et al. Detection of transposition of the great arteries in fetuses reduces neonatal morbidity and mortality. *Circulation* 1999;99:916–918.
- Wernovsky G, Mayer JE, Jonas RA, et al. Factors influencing early and late outcome of the arterial switch operation for transposition of the great arteries. *J Thorac Cardiovasc Surg* 2000;109:289–302.

32. Freed DH, Robertson CMT, Sauve RS, et al. Intermediate-term outcomes of the arterial switch operation for transposition of great arteries in neonates: alive but well? *J Thorac Cardiovasc Surg* 2006;132:U845-U863.
33. Majnemer A, Limperopoulos C, Shevell M, et al. Long-term neuromotor outcome at school entry of infants with congenital heart defects requiring open-heart surgery. *J Pediatr* 2006;148:72-77.
34. Limperopoulos C, Majnemer A, Shevell M, et al. Predictors of developmental disabilities after open heart surgery in young children with congenital heart defects. *J Pediatr* 2002;141:51-58.
35. Dunbar-Masterson C, Wypij D, Bellinger DC, et al. General health status of children with D-transposition of the great arteries after the arterial switch operation. *Circulation* 2001;104:1138-1142.
36. Bellinger DC, Rappaport LA, Wypij D, et al. Patterns of developmental dysfunction after surgery during infancy to correct transposition of the great arteries. *J Dev Behav Pediatr* 1997;18:75-83.
37. Castañeda AR, Trusler GA, Paul MH, et al. The early results of treatment of simple transposition in the current era. *J Thorac Cardiovasc Surg* 1988;95:14-27.
38. Glew D, Hartnell GG. The right aortic-arch revisited. *Clin Radiol* 1991;43:305-307.
39. Mathew R, Rosenthal A, Fellows K. Significance of right aortic-arch in D-transposition of great arteries. *Am Heart J* 1974;87:314-317.
40. Mandell VS, Lock JE, Mayer JE Jr, et al. The "laid-back" aortogram: an improved angiographic view for demonstration of coronary arteries in transposition of the great arteries. *Am J Cardiol* 1990;65:1379-1383.
41. McQuillen PS, Hamrick SEG, Perez MJ, et al. Balloon atrial septostomy is associated with preoperative stroke in neonates with transposition of the great arteries. *Circulation* 2006;113:280-285.
42. Polito A, Ricci Z, Fragasso T, et al. Balloon atrial septostomy and preoperative brain injury in neonates with transposition of the great arteries: a systematic review and a meta-analysis. *Cardiol Young* 2012;22:1-7.
43. Oxenius A, Hug M, Dodge-Khatami A, et al. Do predictors exist for a successful withdrawal of preoperative prostaglandin E(1) from neonates with d-transposition of the great arteries and intact ventricular septum? *Pediatr Cardiol* 2010;31:1198-1202.
44. Beca J, Gunn J, Coleman L, et al. Pre-operative brain injury in newborn infants with transposition of the great arteries occurs at rates similar to other complex congenital heart disease and is not related to balloon atrial septostomy. *J Am Coll Cardiol* 2009;53:1807-1811.
45. Petit CJ, Rome JJ, Wernovsky G, et al. Preoperative brain injury in transposition of the great arteries is associated with oxygenation and time to surgery, not balloon atrial septostomy. *Circulation* 2009;119:709-716.
46. Applegate SE, Lim DS. Incidence of stroke in patients with d-transposition of the great arteries that undergo balloon atrial septostomy in the University Healthsystem Consortium Clinical Data Base/Resource Manager. *Catheter Cardiovasc Interv* 2010;76:129-131.
47. Mukherjee D, Lindsay M, Zhang Y, et al. Analysis of 8681 neonates with transposition of the great arteries: outcomes with and without Rashkind balloon atrial septostomy. *Cardiol Young* 2010;20:373-380.
48. Hiremath G, Natarajan G, Math D, et al. Impact of balloon atrial septostomy in neonates with transposition of the great arteries. *J perinatol* 2011;31:494-499.
49. Kurth CD, Steven JL, Montenegro LM, et al. Cerebral oxygen saturation before congenital heart surgery. *Ann Thorac Surg* 2001;72:187-192.
50. Fenton KN, Lessman K, Glogowski K, et al. Cerebral oxygen saturation does not normalize until after Stage 2 single ventricle palliation. *Ann Thorac Surg* 2007;83:1431-1436.
51. Redlin M, Koster A, Huebler M, et al. Regional differences in tissue oxygenation during cardiopulmonary bypass for correction of congenital heart disease in neonates and small infants: relevance of near-infrared spectroscopy. *J Thorac Cardiovasc Surg* 2008;136:962-967.
52. Ibuki K, Watanabe K, Yoshimura N, et al. The improvement of hypoxia correlates with neuroanatomic and developmental outcomes: comparison of midterm outcomes in infants with transposition of the great arteries or single-ventricle physiology. *J Thorac Cardiovasc Surg* 2012;143:1077-1085. Epub 2011 Oct 2.
53. Senning A. Surgical correction of transposition of the great vessels. *Surgery* 1959;45:966-980.
54. Mustard WT. Successful two-stage correction of transposition of the great vessels. *Surgery* 1964;55:469-472.
55. Kirklin JW, Blackstone EH, Tchervenkov CI, et al. Clinical outcomes after the arterial switch operation for transposition: patient, support, procedural and institutional risk factors. *Circulation* 1992;86:1501-1515.
56. Williams WG, Trusler GA, Kirklin JW, et al. Early and late results of a protocol for simple transposition leading to an arterial switch (Mustard) repair. *J Thorac Cardiovasc Surg* 1988;95:717-726.
57. Kirjavainen M, Happonen J, Louhimo I. Late results of senning operation. *J Thorac Cardiovasc Surg* 1999;117:488-495.
58. Moons P, De Bleser L, Budts W, et al. Health status, functional abilities, and quality of life after the Mustard or Senning operation. *Ann Thorac Surg* 2004;77:1359-1365.
59. Fritsch J, Winter UJ, Kaemmerer H, et al. Cardiopulmonary exercise capacity in patients with congenital heart-disease. *Z Kardiol* 1994;83:131-139.
60. Musewe NN, Reisman J, Benson LN, et al. Cardiopulmonary adaptation at rest and during exercise 10 years after Mustard atrial repair for transposition of the great-arteries. *Circulation* 1988;77:1055-1061.
61. Reybrouck T, Mertens L, Brown S, et al. Long-term assessment and serial evaluation of cardiorespiratory exercise performance and cardiac function in patients with atrial switch operation for complete transposition. *Cardiol Young* 2001;11:17-24.
62. Paul MH, Wessel HU. Exercise studies in patients with transposition of the great arteries after atrial repair operations (Mustard/Senning): a review. *Pediatr Cardiol* 1999;20:49-55.
63. Meijboom F, Szatmari A, Deckers JW, et al. Long-term follow-up (10 to 17 years) after Mustard repair for transposition of the great arteries. *J Thorac Cardiovasc Surg* 1996;111:1158-1168.
64. Sterrett LE, Ebenroth ES, Montgomery GS, et al. Pulmonary limitation to exercise after repair of D-transposition of the great vessels: atrial baffle versus arterial switch. *Pediatr Cardiol* 2011;32:910-916.
65. Müller J, Hess J, Hörer J, et al. Persistent superior exercise performance and quality of life long-term after arterial switch operation compared to that after atrial redirection. *Int J Cardiol* 2011 [epub ahead of print].
66. Roos-Hesselink JW, Meijboom FJ, Spitaels SEC, et al. Decline in ventricular function and clinical condition after mustard repair for transposition of the great arteries (a prospective study of 22-29 years). *Eur Heart J* 2004;25:1264-1270.
67. Benzaquen BS, Webb GD, Colman JM, et al. Arterial switch operation after mustard procedures in adult patients with transposition of the great arteries: is it time to revise our strategy? *Am Heart J* 2004;147:C1-C5.
68. Daebritz SH, Tiete AR, Sachweh JS, et al. Systemic right ventricular failure after atrial switch operation: midterm results of conversion into an arterial switch. *Ann Thorac Surg* 2001;71:1255-1259.
69. Mavroudis C, Backer CL. Arterial switch after failed atrial baffle procedures for transposition of the great arteries. *Ann Thorac Surg* 2000;69:851-857.
70. Cochrane AD, Karl TR, Mee RBB, et al. Staged conversion to arterial switch for late failure of the systemic right ventricle. *Ann Thorac Surg* 1993;56:854-862.
71. Khairy P, Landzberg MJ, Lambert J, et al. Long-term outcomes after the atrial switch for surgical correction of transposition: a meta-analysis comparing the Mustard and Senning procedures. *Cardiol Young* 2004;14:284-292.
72. Moons P, Gewillig M, Sluysmans T, et al. Long term outcome up to 30 years after the Mustard or Senning operation: a nationwide multicentre study in Belgium. *Heart* 2004;90:307-313.
73. Puley G, Siu S, Connelly M, et al. Arrhythmia and survival in patients >18 years of age after the mustard procedure for transposition of the great arteries. *Am J Cardiol* 1999;83:1080-1084.
74. Roubertie F, Thambo JB, Bretonneau A, et al. Late outcome of 132 Senning procedures after 20 years of follow-up. *Ann thorac Surg* 2011;92:2206-2013.
75. Schwertmann M, Salehian O, Harris L, et al. Ventricular arrhythmias and sudden death in adults after a Mustard operation for transposition of the great arteries. *Eur Heart J* 2009;30:1873-1879.
76. Kammeraad JA, van Deuren CH, Sreeram N, et al. Predictors of sudden cardiac death after Mustard or Senning repair for transposition of the great arteries. *J Am Coll Cardiol* 2004;44:1095-1102.
77. Pasquini L, Sanders SP, Parness IA, et al. Coronary echocardiography in 406 patients with d-loop transposition of the great arteries. *J Am Coll Cardiol* 1994;24:763-768.
78. Jatene AD, Fontes VF, Paulista PP, et al. Anatomic correction of transposition of the great vessels. *J Thorac Cardiovasc Surg* 1976;72:364-370.
79. Bellinger DC, Wypij D, Rivkin MJ, et al. Adolescents with d-transposition of the great arteries corrected with the arterial switch procedure: neuropsychological assessment and structural brain imaging. *Circulation* 2011;124:1361-1369.
80. Colan SD, Boutin C, Castaneda AR, et al. Status of the left ventricle after arterial switch operation for transposition of the great arteries: hemodynamic and echocardiographic evaluation. *J Thorac Cardiovasc Surg* 1995;109:311-321.
81. Hayashi G, Kurosaki K, Echigo S, et al. Prevalence of arrhythmias and their risk factors mid- and long-term after the arterial switch operation. *Pediatr Cardiol* 2006;27:689-694.
82. Cohen MS, Wernovsky G. Is the arterial switch operation as good over the long term as we thought it would be? *Cardiol Young* 2006;16:117-124.
83. Sarris GE, Chatzis AC, Giannopoulos NM, et al. The arterial switch operation in Europe for transposition of the great arteries: a multi-institutional study from the European Congenital Heart Surgeons Association. *J Thorac Cardiovasc Surg* 2006;132:633-639.
84. Brown JW, Park HJ, Turrentine MW. Arterial switch operation: factors impacting survival in the current era. *Ann Thorac Surg* 2001;71:1978-1984.
85. Rudra HS, Mavroudis C, Backer CL, et al. The arterial switch operation: 25-year experience with 258 patients. *Ann Thorac Surg* 2011;92:1742-1746.
86. Wong SH, Finucane K, Kerr AR, et al. Cardiac outcome up to 15 years after the arterial switch operation. *Heart Lung Circ* 2008;17:48-53.
87. Lalezari S, Bruggemans EF, Blom NA, et al. Thirty-year experience with the arterial switch operation. *Ann Thorac Surg* 2011;92:973-979.
88. Hraska V, Podnar T, Kunovsky P, et al. Is a learning curve for arterial switch operation in small countries still acceptable? Model for cooperation in Europe. *Eur J Cardiothorac Surg* 2003;24:352-357.
89. Dagan O, Birk E, Katz Y, et al. Relationship between caseload and morbidity and mortality in pediatric cardiac surgery—a four year experience. *Isr Med Assoc J* 2003;5:471-474.

90. Scott WA, Fixler DE. Effect of center volume on outcome of ventricular septal defect closure and arterial switch operation. *Am J Cardiol* 2001;88:1259-1263.
91. Losay J, Touchot A, Serraf A, et al. Late outcome after arterial switch operation for transposition of the great arteries. *Circulation* 2001;104:1121-1126.
92. Marino BS, Wernovsky G, McElhinney DB, et al. Neo-aortic valvar function after the arterial switch. *Cardiol Young* 2006;16:481-489.
93. Losay J, Touchot A, Capderou A, et al. Aortic valve regurgitation after arterial switch operation for transposition of the great arteries - Incidence, risk factors, and outcome. *J Am Coll Cardiol* 2006;47:2057-2062.
94. Schwartz ML, Gauvreau K, del Nido P, et al. Long-term predictors of aortic root dilation and aortic regurgitation after arterial switch operation. *Circulation* 2004;110:1128-1132.
95. McMahon CJ, Ravekes WJ, Smith EOB, et al. Risk factors for neo-aortic root enlargement and aortic regurgitation following arterial switch operation. *Pediatr Cardiol* 2004;25:329-335.
96. Vandekerckhove KD, Blom NA, Lalezari S, et al. Long-term follow-up of arterial switch operation with an emphasis on function and dimensions of left ventricle and aorta. *Eur J Cardiothorac Surg* 2009;35:582-587.
97. Hourihan M, Colan SD, Wernovsky G, et al. Growth of the aortic anastomosis, annulus, and root after the arterial switch procedure performed in infancy. *Circulation* 1993;88:615-620.
98. Formigari R, Toscano A, Giardini A, et al. Prevalence and predictors of neo-aortic regurgitation after arterial switch operation for transposition of the great arteries. *J Thorac Cardiovasc Surg* 2003;126:1753-1759.
99. Daebritz SH, Nollert G, Sachweh JS, et al. Anatomical risk factors for mortality and cardiac morbidity after arterial switch operation. *Ann Thorac Surg* 2000;69:1880-1886.
100. Ou P, Mousseaux E, Azarine A, et al. Detection of coronary complications after the arterial switch operation for transposition of the great arteries: first experience with multislice computed tomography in children. *J Thorac Cardiovasc Surg* 2006;131:639-643.
101. Gagliardi MG, Adorisio R, Crea F, et al. Abnormal vasomotor function of the epicardial coronary arteries in children five to eight years after arterial switch operation - an angiographic and intracoronary Doppler flow wire study. *J Am Coll Cardiol* 2005;46:1565-1572.
102. Pedra SRFF, Pedra CAC, Abizaid AA, et al. Intracoronary ultrasound assessment late after the arterial switch operation for transposition of the great arteries. *J Am Coll Cardiol* 2005;45:2061-2068.
103. Tanel RE, Wernovsky G, Landzberg ML, et al. Coronary artery abnormalities detected by cardiac catheterization after the arterial switch operation for transposition of the great arteries. *Am J Cardiol* 1995;76:153-157.
104. Tsuda E, Imakita M, Yagihara T, et al. Late death after arterial switch operation for transposition of the great arteries. *Am Heart J* 1992;124:1551-1557.
105. Choi BS, Kwon BS, Kim GB, et al. Long-term outcomes after an arterial switch operation for simple complete transposition of the great arteries. *Korean Circ J* 2010;40:23-31.
106. Oztunc F, Bariçscedil S, Adaletli I, et al. Coronary events and anatomy after arterial switch operation for transposition of the great arteries: detection by 16-row multislice computed tomography angiography in pediatric patients. *Cardiovasc Intervent Radiol* 2009;32:206-212.
107. Kampmann C, Kuroczynski W, Trübel H, et al. Late results after PTCA for coronary stenosis after the arterial switch procedure for transposition of the great arteries. *Ann Thorac Surg* 2005;80:1641-1646.
108. Angeli E, Formigari R, Pace Napoleone C, et al. Long-term coronary artery outcome after arterial switch operation for transposition of the great arteries. *Eur J Cardiothorac Surg* 2010;38:714-720.
109. El-Segaier M, Lundin A, Hochbergs P, et al. Late coronary complications after arterial switch operation and their treatment. *Catheter Cardiovasc Interv* 2010;76:1027-1032.
110. Hayes AM, Baker EJ, Kakadekar A, et al. Influence of anatomic correction for transposition of the great arteries on myocardial perfusion: radionuclide imaging with technetium-99 m 2-methoxy isobutyl isonitrile. *J Am Coll Cardiol* 1994;24:769-777.
111. Vogel M, Smallhorn JF, Trusler GA, et al. Echocardiographic analysis of regional left ventricular wall motion in children after the arterial switch operation for complete transposition of the great arteries. *J Am Coll Cardiol* 1990;15:1417-1423. [Abstract]
112. Weindling SN, Wernovsky G, Colan SD, et al. Myocardial perfusion, function and exercise tolerance after the arterial switch operation. *J Am Coll Cardiol* 1994;23:424-433.
113. Acar P, Maunoury C, Bonnet D, et al. Comparison of myocardial perfusion single-photon emission computed tomography with coronary artery angiography after arterial switch operation. *Am J Cardiol* 2001;87:1425-1427.
114. Mahle WT, McBride MG, Paridon SM. Exercise performance after the arterial switch operation for D-transposition of the great arteries. *Am J Cardiol* 2001;87:753-758.
115. Hui L, Chau AKT, Leung MP, et al. Assessment of left ventricular function long term after arterial switch operation for transposition of the great arteries by dobutamine stress echocardiography. *Heart* 2005;91:68-72.
116. Rhodes LA, Wernovsky G, Keane JF, et al. Arrhythmias and intracardiac conduction after the arterial switch operation. *J Thorac Cardiovasc Surg* 1995;109:303-310.
117. de Koning WB, van Osch-Gevers M, Ten Harkel AD, et al. Follow-up outcomes 10 years after arterial switch operation for transposition of the great arteries: comparison of cardiologic health status and health-related quality of life to those of the a normal reference population. *Eur J Pediatr* 2008;167:995-1004.
118. Mussatto K, Wernovsky G. Challenges facing the child, adolescent, and young adult after the arterial switch operation. *Cardiol Young* 2005;15:111-121.
119. Latal B, Helfricht S, Fischer JE, et al. Psychological adjustment and quality of life in children and adolescents following open-heart surgery for congenital heart disease: a systematic review. *BMC Pediatr* 2009;9:6-15.
120. Görler H, Ono M, Thies A, et al. Long-term morbidity and quality of life after surgical repair of transposition of the great arteries: atrial versus arterial switch operation. *Interact Cardiovasc Thorac Surg* 2011;12:569-574.
121. Pasquali SK, Marino BS, Powell DJ, et al. Following the arterial switch operation, obese children have risk factors for early cardiovascular disease. *Congenit Heart Dis* 2010;5:16-24.
122. Calderon J, Bonnet D, Courtin C, et al. Executive function and theory of mind in school-aged children after neonatal corrective cardiac surgery for transposition of the great arteries. *Dev Med Child Neurol* 2010;52:1139-1144.
123. Boutin C, Jonas RA, Sanders SP, et al. Rapid two-stage arterial switch operation: acquisition of left ventricular mass following pulmonary artery banding in infants with transposition of the great arteries. *Circulation* 1994;90:1304-1309.
124. Boutin C, Wernovsky G, Sanders SP, et al. Rapid two-stage arterial switch operation: evaluation of left ventricular systolic mechanics late after an acute pressure overload stimulus in infancy. *Circulation* 1994;90:1294-1303.
125. Jonas RA, Giglia TM, Sanders SP, et al. Rapid, two-stage arterial switch for transposition of the great arteries and intact ventricular septum beyond the neonatal period. *Circulation* 1989;80:203-208.
126. Wernovsky G, Giglia TM, Jonas RA, et al. Course in the intensive care unit following "preparatory" pulmonary artery banding and aortopulmonary shunt placement for transposition of the great arteries with low left ventricular pressure. *Circulation* 1992;86:133-139.
127. Iyer KS, Sharma R, Kumar K, et al. Serial echocardiography for decision-making in rapid 2-stage arterial switch operation. *Ann Thorac Surg* 1995;60:658-664.
128. Kang N, de Leval MR, Elliott M, et al. Extending the boundaries of the primary arterial switch operation in patients with transposition of the great arteries and intact ventricular septum. *Circulation* 2004;110:1123-1127.
129. Davis AM, Wilkinson JL, Karl TR, et al. Transposition of the great-arteries with intact ventricular septum - arterial switch repair in patients 21 days of age or older. *J Thorac Cardiovasc Surg* 1993;106:111-115.
130. Sekarski N, Hurni M, Mivelaz Y, et al. Arterial switch after left ventricular retraining for late transposition of the great arteries: experience with conventional versus adaptable pulmonary artery banding. *Circulation* 2006;114:546.
131. Naughton P, Mossad E. Retraining the left ventricle after arterial switch operation: emerging uses for the left ventricular assist device in pediatric cardiac surgery. *J Cardiothorac Vasc Anesth* 2000;14:454-456.
132. Kramer HH, Scheewe J, Fischer G, et al. Long term follow-up of left ventricular performance and size of the great arteries before and after one- and two-stage arterial switch operation of simple transposition. *Eur J Cardiothorac Surg* 2003;24:898.
133. Rastelli GC, McGoon DC, Wallace RB. Anatomic correction of transposition of the great arteries with ventricular septal defect and subpulmonary stenosis. *J Thorac Cardiovasc Surg* 1969;58:545-552.
134. Lecompte Y, Zannini L, Hazan E, et al. Anatomic correction of transposition of the great-arteries - new technique without use of a prosthetic conduit. *J Thorac Cardiovasc Surg* 1981;82:629-631.
135. Vouhe PR, Tamisier D, Leca F, et al. Transposition of the great-arteries, ventricular septal-defect, and pulmonary outflow tract obstruction - Rastelli Or Lecompte Procedure. *J Thorac Cardiovasc Surg* 1992;103:428-436.
136. Morell VO, Jacobs JP, Quintessenza JA. Aortic translocation in the management of transposition of the great arteries with ventricular septal defect and pulmonary stenosis: results and follow-up. *Ann Thorac Surg* 2005;79:2089-2093.
137. Nikaidoh H. Aortic translocation and biventricular outflow tract reconstruction. *J Thorac Cardiovasc Surg* 1984;88:365-372.
138. Sharma R, Choudhary SK, Bhan A, et al. Late outcome after arterial switch operation for complete transposition of great arteries with left ventricular outflow tract obstruction. *Ann Thorac Surg* 2002;74:1986-1991.
139. Wernovsky G, Jonas RA, Colan SD, et al. Results of the arterial switch operation in patients with transposition of the great arteries and abnormalities of the mitral valve or left ventricular outflow tract. *J Am Coll Cardiol* 1990;16:1446-1454.
140. Dibardino DJ, Allison AE, Vaughn WK, et al. Current expectations for newborns undergoing the arterial switch operation. *Ann Surg* 2004;239:588-596.
141. Wetter J, Sinzobahamvya N, Blaszczyk HC, et al. Results of arterial switch operation for primary total correction of the Taussig-Bing anomaly. *Ann Thorac Surg* 2004;77:41-46.

142. LacourGayet F, Serraf A, Galletti L, et al. Biventricular repair of conotruncal anomalies associated with aortic arch obstruction—103 patients. *Circulation* 1997;96:328–334.
143. Mee RBB. Severe right ventricular failure after Mustard or Senning operation: two-stage repair—pulmonary artery banding and switch. *J Thorac Cardiovasc Surg* 1986;92:385–390.
144. Duncan BW, Mee RBB, Mesia CI, et al. Results of the double switch operation for congenitally corrected transposition of the great arteries. *Eur J Cardiothorac Surg* 2003;24:11–19.
145. Bautista-Hernandez V, Marx GR, Gauvreau K, et al. Determinants of left ventricular dysfunction after anatomic repair of congenitally corrected transposition of the great arteries. *Ann Thorac Surg* 2006;82:2059–2066.
146. Koh M, Yagihara T, Uemura H, et al. Intermediate results of the double-switch operations for atrioventricular discordance. *Ann Thorac Surg* 2006;81:671–677.
147. Ilbawi MN, Ocampo CB, Allen BS, et al. Intermediate results of the anatomic repair for congenitally corrected transposition. *Ann Thorac Surg* 2002;73:594–599.
148. Chang AC, Wernovsky G, Wessel DL, et al. Surgical management of late right ventricular failure after Mustard or Senning repair. *Circulation* 1992;86:140–149.
149. Dhasmana JP, Stark J, DeLeval M, et al. Long-term results of the “palliative” Mustard operation. *J Am Coll Cardiol* 1985;6:1138–1141.

Congenitally Corrected Transposition of the Great Arteries (Atrioventricular and Ventriculoarterial Discordance)

Joseph Atallah ■ Jennifer M. Rutledge ■ John D. Dyck

The language of corrected transposition can be difficult. Isolated ventricular inversion, double discordance, physiologically corrected transposition, and L-transposition are all terms that have been applied to congenitally corrected transposition of the great arteries (ccTGA). For the patient with ccTGA, situs solitus, and normal atrial arrangement, the systemic venous return joins the morphologic right atrium. This atrium is connected by a mitral valve with the morphologic left ventricle, which in turn supports a discordantly connected, transposed pulmonary artery (PA) (Fig. 50.1). The left atrium, receiving the pulmonary veins, connects through a tricuspid valve (TV) with the morphologic right ventricle (RV), which in turn supports a transposed aorta (Fig. 50.1). These atrioventricular (AV) and ventriculoarterial (VA) connections do occur in the setting of situs inversus. Patients with other abnormalities of situs and other AV connections are properly excluded from discussion here (1,2).

In ccTGA, the effects of ventricular inversion are potentially physiologically corrected by the associated TGA. That is, the path of venous blood returning to the heart leads to the PA and the path of pulmonary venous return leads to the aorta. However, even in the patient with no associated abnormalities, it is increasingly apparent that natural history and hemodynamics will be far from normal (3).

PREVALENCE, ETIOLOGY, AND MORPHOGENESIS

Corrected transposition is an uncommon lesion. Data from several sources would suggest a prevalence of 0.03 per 1,000 live births accounting for approximately 0.05% of congenital heart malformations (4–6). The majority of these patients will have situs solitus, and about 5% will have situs inversus (7).

Population-based studies continue to support the possible importance of environmental factors in the etiology of this condition (8). Still, the familial occurrence and molecular biology investigations suggest the importance of the genetic influence (9,10). It would seem wise therefore to continue to counsel a multifactorial etiology with a recurrence risk in first-degree relatives of approximately 2% (11).

Morphogenetically, the primitive cardiac tube, anchored at one end by the sinus venosus and at the other end by the truncus arteriosus, loops to the left (L-looped) and not to the right (D-looped) as in the normal heart (12). This abnormal cardiac looping brings the morphologic left ventricle to the right and the morphologic RV to the left. The origins of abnormal cardiac looping continue to be an area of active investigation (13,14). Most frequently, such abnormal looping of the ventricles is associated with a transposed VA connection.

MORPHOLOGY

Despite the relative rarity of corrected transposition, important studies and descriptions of the basic morphology have been published for some years (15–18). Advances in the surgical management of corrected transposition have occasioned reassessments of the pertinent anatomy (19,20).

As noted, some 5% of patients with corrected transposition will have situs inversus (7). Furthermore, approximately 25% of patients will demonstrate either dextrocardia or mesocardia (17). The ventricular topology (relative orientation of the ventricles) in corrected transposition places the RV to the left of the morphologic left ventricle. As a result of the abnormal looping, the ventricles conform to a left hand pattern (21). That is, if one places the palm of the hand against the right ventricular surface of the interventricular septum, the thumb in the inlet and the fingers in the outlet, it is necessary to use the left hand in ccTGA in contradistinction to the right hand in the normally D-looped ventricles. Further twisting can result in a more superior to inferior relationship of the RV to the left ventricle (22). The interventricular septum tends to a more sagittal or horizontal position resulting in one of the central features of AV discordance, that of malalignment of the atrial and ventricular septum. The atrial septum and ventricular septum meet at the crux of the heart. However, as the atrial septum continues anterior and to the right, it will deviate to a variable degree from the ventricular septum creating a variable gap that in extreme cases will go back as far as the crux (16). This concept of malalignment of the atrial septum and the ventricular septum has implications for the size and extent of the ventricular septal defect (VSD), the ventricular outflows, and the conduction system (23).

The AV valve on the right side has the features of a mitral valve with two papillary muscles and no insertion onto the interventricular septum. Penny et al. (24) have pointed out that 10% of mitral valves in this setting will demonstrate significant echocardiographic abnormalities. On the left, the AV valve has features of a TV. This valve frequently is abnormal with anterior positioning bringing the septal leaflet into the “gap” created by the septal malalignment at the membranous septum. This leaflet may thus form one wall of the left ventricular outflow tract (16).

Most frequently, AV discordance is associated with transposition of the great arteries (TGA) and a leftward anterior position of the aortic valve relative to the pulmonary valve, though this is not absolute (21). Freedom et al. (25) have shown that leftward anterior positioning of the aorta also may occur in the setting of complete transposition, double-outlet RV, anatomically corrected malposition, crossed AV connections, supero-inferior ventricles, and univentricular connections (26). The left ventricular outflow tract is deeply wedged between the left

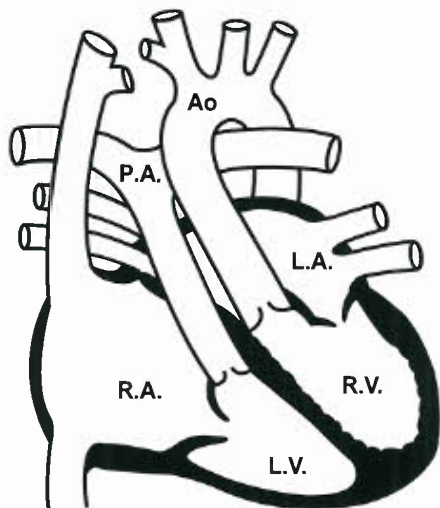


Figure 50.1. Diagram of congenitally corrected transposition of the great arteries demonstrating atrioventricular and ventriculoarterial discordance. Ao, aorta; LA, left atrium; LV, left ventricle; PA, pulmonary artery; RA, right atrium; RV, right ventricle.

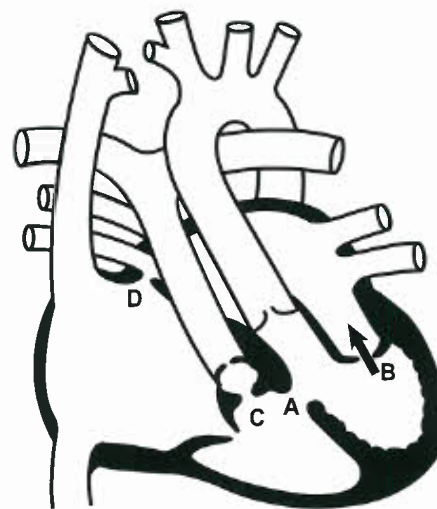


Figure 50.2. Associated anomalies in congenitally corrected transposition of the great arteries. (A) Ventricular septal defect (VSD); (B) Ebstein anomaly of the tricuspid valve; (C) multiple-level left ventricular outflow obstruction; (D) atrial septal defect (ASD).

and right AV valves and is therefore more readily subject to obstruction. The pulmonary valve is most often in fibrous continuity with the mitral valve.

The leftward anterior aorta is supported by a muscular infundibulum and is not in fibrous continuity with either AV valve. Obstructive lesions of the right ventricular outflow tract and aorta perhaps have been underemphasized. Several reports suggest the higher frequency of this problem in association with severe left AV valve regurgitation. Systemic outflow obstruction may take the form of functional and/or true aortic valve atresia as well as obstructive anomalies of the aortic arch (27–29).

ASSOCIATED LESIONS

Patients with congenitally corrected transposition and no associated abnormalities are in fact the exception, with associated anomalies occurring in well over 90% (30). The most frequent abnormalities include VSD, left ventricular outflow tract obstruction, and anomalies of the left-sided TV (Fig. 50.2).

VENTRICULAR SEPTAL DEFECT

VSDs occur in approximately 80% of hearts with corrected transposition (18). The defects are most often perimembranous and a consequence of the atrial and septal malalignment (16). This positioning will put them in a subpulmonary position and in approximation to the septal leaflet of the left-sided TV. The defects are often large with anterior extension and therefore suitable for intraventricular tunneling. Other defects such as the subarterial or muscular defect do occur but are unusual.

PULMONARY OUTFLOW OBSTRUCTION

Obstruction to the outflow tract of the morphologic left ventricle is identified in 30% to 50% of patients with ccTGA and atrial situs solitus. Such pulmonary outflow tract obstruction rarely occurs in isolation at the valve or infundibular level, but usually

is associated with a large VSD. In about one-third of patients with a VSD and pulmonary outflow tract obstruction, abnormalities of the morphologic TV are observed as well. The left ventricular outflow tract obstruction may be muscular, reflecting wedging of the subpulmonary outflow tract between the infundibular septum and the ventricular free wall, with contributions from the right-sided ventriculoinfundibular fold. Fibrous tissue derived from the membranous septum may participate in left ventricular outflow tract obstruction. Tissue tags derived from the tricuspid or mitral valve or stenosis of the pulmonary valve itself also may obstruct flow into the pulmonary trunk. Such tissue tags are likely the most common obstructive lesion (31).

LESIONS OF THE MORPHOLOGIC TRICUSPID VALVE

Abnormalities of the morphologic TV are intrinsic to hearts exhibiting ccTGA. Although at autopsy about 90% of hearts exhibit some abnormality of the morphologic TV, a clinically apparent functional disturbance during life is considerably less often manifest. The most common and important underlying pathology is dysplasia of the valve, with or without displacement of the septal or posterior leaflets of the TV. Anderson et al. (32) has described the features associated with “Ebstein” anomaly of the left-sided TV and has suggested along with others that these valves in general may represent a poor substrate for repair. Both the morphologic TV and on occasion the mitral valve can be seen to straddle the ventricular septum. It is of course very important to recognize this anomaly preoperatively (33).

CORONARY ARTERY ANATOMY

Changing approaches to the surgical management of corrected transposition, including the so-called double switch procedure, have refocused attention on the coronary artery anatomy. In general, the coronary arteries originate from the posterior-facing sinuses of the aortic valve. In patients with atrial situs solitus and ccTGA, the coronary arteries show a mirror-image

distribution. The right-sided coronary artery has the epicardial distribution of a morphologic left coronary artery. The main right-sided coronary artery bifurcates into circumflex and anterior descending branches, whereas the left-sided coronary artery runs in the left AV groove and gives rise to infundibular and marginal branches.

Several investigators have demonstrated a variable pattern of coronary artery anomalies. In an angiographic study of 13 children, investigators reported a prevalent pattern of ‘coronary artery–ventricular concordance’ (34). In a 14-specimen study, McKay et al. (35) observed the persistent origin of the sinus node artery from the circumflex artery and speculated on its course along the medial side of the right atrial wall. They commented on the potential surgical risk of damaging the artery during an atrial baffle procedure or atriotomy repair. In that same report, a correlation between commissural malalignment and eccentric coronary ostia was observed. Ismat et al. (36) analyzed 20 specimens and found 7 with eccentric ostia. Rare cases of an isolated origin of the sinus node artery from a coronary sinus have also been reported (37). The largest pathologic study (46 specimens) was undertaken by Uemura and colleagues. They reported a 76% incidence of a relatively “normal” pattern with the right and left coronaries originating from the left and right facing sinuses, respectively. Anomalies were found in 11 specimens. Single coronary artery was the most common in four, with two originating from the right and two from the left facing sinuses. A main coronary branch coursing anterior to the pulmonary trunk was found in 96% of the specimens, and a large coronary branch crossing the right ventricular outflow tract was found in 61% of the specimens. The latter finding is of most importance when considering a ventricular to PA conduit. Chiu et al. (38) described a segmental approach to the coronary anatomy. From their study of 62 patients, they concluded: (a) the proximal coronary pattern at the aortic sinus depends on the aortopulmonary rotation, (b) the peripheral coronary pattern depends on the atrial situs and apical position or the so-called apicocaval ipsilaterality, as well as the ventricular looping (38). A good understanding of the type and degree of variability of the coronary anatomy in patients with congenitally corrected transposition is crucial in the era of “double switch” surgical approaches to these patients.

SPECIALIZED CONDUCTION TISSUES

The conduction system in patients with ccTGA is abnormal and potentially unstable. The extensive works done by Anderson, Becker, Losekoot, and others, have elucidated the presence of normal and abnormal conduction tissue (17,39–42). The sinoatrial (SA) node lies in its normal position in relation to the atrial situs. The AV conduction tissue, on the other hand, is abnormal. The classic description is that of two AV nodes. A normal posterior AV node located at the apex of the triangle of Koch but with no AV bundle, and an abnormal right anterior AV node giving rise to the penetrating AV bundle. The latter is located anterosuperiorly in the area lateral to the pulmonary–mitral valve continuity, underneath the opening of the right atrial appendage. Its AV bundle has a superficial course along the anterior aspect of the subpulmonary outflow tract and superior left ventricular wall. The bundle then courses onto the upper interventricular septum from which it descends and branches. If a VSD is present, the anterior AV bundle courses along its anterosuperior margin.

The conduction tissue abnormality is not universal to all patients with ccTGA. The reason why certain patients had a normal AV node and AV bundle may have been elucidated by Hosseinpour et al. (23). They hypothesized that the development of an AV bundle from the normal posterior AV node to the summit of the interventricular septum

is anatomically hindered by the atrial and ventricular septal malalignment. The degree of malalignment is related to the size of the left ventricular outflow tract and the pulmonary trunk. They showed that patients with congenitally corrected transposition and a normal conduction system were frequently characterized by the presence of pulmonary atresia or significant pulmonary stenosis. These anatomical variants resulted in a lesser degree of atrial and ventricular septal malalignment. Therefore, a correlation is made between the size of the LV outflow tract, the degree of septal malalignment, and the presence of normal AV conduction tissue. It is thought that the normal conduction tissue is “in addition to” rather than “instead of” the abnormal anterior conduction system. In patients with both conduction systems straddling the anterosuperior and inferoposterior margins of a VSD, there can exist a sling-like bundle located over the anterior margin of the VSD and connecting both AV bundles, as described by Monckeberg (42).

CLINICAL FEATURES

The clinical features of patients with ccTGA have been well documented (43,44). Patients with isolated ccTGA should be asymptomatic in childhood, though there is a high incidence of clinical problems in adults (30). In childhood, the timing and severity of symptoms, in general, reflects the associated lesions. Infants with ccTGA may come to attention because of bradycardia, (with or without heart failure) reflecting high-degree AV block, tachyarrhythmia, cyanosis reflecting inadequate pulmonary blood flow, and/or congestive heart failure. Congestive heart failure may reflect a cardiac arrhythmia, but more likely indicates a large VSD, dysplasia or displacement of the left-sided morphologic TV with regurgitation, obstructive anomalies of the aortic arch, or a combination of these anomalies.

The older child may be referred to a pediatric cardiologist for evaluation of a loud second heart sound (and thus the clinical suspicion of PA hypertension), but this is most uncommon in the neonate. The physical examination only occasionally raises the possibility of AV and VA discordance. Clearly, the presence of clinical features suggestive of “mitral regurgitation” in a neonate should prompt consideration of ccTGA and an abnormal systemic AV valve.

In some neonates with ccTGA, regurgitation of the systemic AV valve may be massive, and such patients may have such profound cardiomegaly that they are considered clinically to have classical Ebstein anomaly of the TV (with concordant AV and VA connections). Organic or functional aortic atresia has been described in these patients, and common to them all is a terribly disorganized and deficient morphologic TV and an extremely thinned morphologic RV.

ELECTROCARDIOGRAPHIC FEATURES

In the patient with normal atrial situs and discordant AV and VA connections who is free of significant associated intracardiac malformations, the direction of the frontal P-wave axis is normal and, therefore, positive in leads I, II, III, and aVF, but negative in aVR. Clearly, the position of the heart within the thorax does not influence the P-wave vector or axis.

The electrical activation of the ventricles in the normal heart begins in the interventricular septum and is directed from left to right and in a slightly anterior direction as well. This initial activation is responsible for the normal pattern of Q waves in the precordial leads: a qR pattern in V₆ and an Rs in V₁. The absence of Q waves in the left precordial leads is seldom observed in normal children, but 25% of normal neonates may not demonstrate a Q wave in V₆.

In corrected TGA, the interventricular septum has a more or less sagittal disposition and is oriented from left posterior to right anterior. With ventricular inversion, both its surfaces and ventricular bundle branches are inverted, and thus the sequence of initial activation is oriented from right to left and usually in a more superior and anterior direction. This results in a reversal of the normal Q wave pattern in the precordial leads: Q waves are present in the right precordial leads but are absent in the left precordial leads. This pattern of reversal is appreciated less commonly when the heart is right-sided or when there are confounding associated lesions producing pressure or volume overload (15).

If one were to catalogue the electrocardiographic change identified in patients with corrected transposition, they would include reversal of Q wave disposition in the precordial leads with QS complexes in the right precordial leads, large Q waves in leads III and aVF, and left axis deviation.

With the precarious nature of the conduction system, as previously noted, the occurrence of congenital and postsurgical complete AV block is significant. Complete AV block is present in about 4% of patients at birth and the overall lifetime incidence is 20% to 30% (45). The most important feature is the increasing prevalence of complete heart block in the corrected transposition population during follow-up, with an estimated rate of 2% per year after diagnosis (45,46). Despite the development of surgical techniques to reduce the incidence of complete heart block at surgery, this problem continues to be significant and progressive (47). It is imperative for this reason alone that all patients with corrected transposition have long-term follow-up.

RADIOGRAPHIC FEATURES

Although the chest radiograph is thought to provide useful information in the diagnosis and evaluation of the patient with ccTGA, these observations are probably more germane to the older infant or child than to the neonate with this disorder. The chest radiograph of the patient with levocardia, atrial situs solitus, and ccTGA may reflect the abnormal ventriculoarterial junction. The most common spatial relationship of the great arteries in corrected TGA is a side-by-side or oblique one, with the aorta to the left. This is manifest in the plain chest radiograph in the frontal projection as a deformity of the left upper mediastinal border characterized by a convex prominence at its middle and upper portions with a mild convexity in the anticipated position of the pulmonary trunk (Fig. 50.3). This shadow represents the levopositioned ascending aorta, which originates from the left-sided morphologic RV. A levopositioned aorta is not diagnostic of discordant AV and VA connections.

ECHOCARDIOGRAPHY

The examination of the patient with complex AV and VA connections should begin with the definition of situs, which can be achieved adequately by cross-sectional ultrasound examination of the great vessels in the abdomen. In the patient with situs inversus, the aorta lies on the right of the spine, with the inferior vena cava (IVC) on the left and the morphologic right atrium on the left. This is important since 5% of cases of corrected transposition will occur in the setting of situs inversus. Patients with situs ambiguous will demonstrate either interruption of the IVC, or the aorta and IVC on the same side of the spine. By definition, these patients cannot demonstrate true ccTGA, but nevertheless, this may be important in the

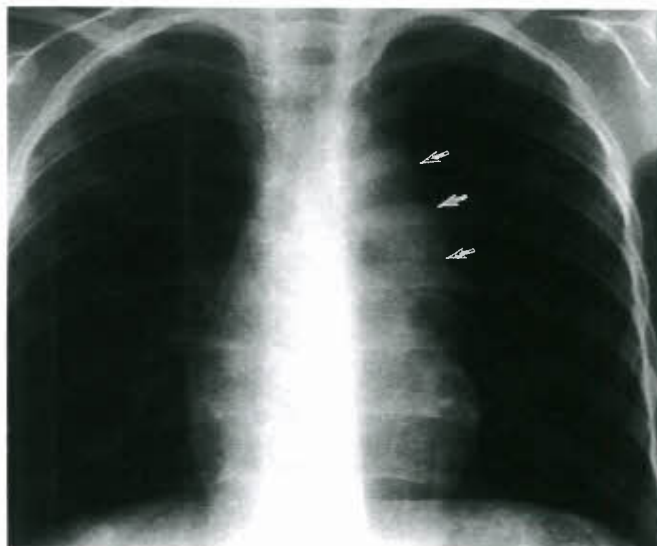


Figure 50.3. Chest radiography in congenitally corrected transposition of the great arteries. No intracardiac abnormalities. Note levopositioned aorta (arrows).

differential diagnosis. In some patients, despite an ambiguous atrial situs, the atria may be relatively well lateralized.

By moving up from the cross-sectional (horizontal) view of the abdominal vessels to the subcostal view of the heart, cardiac position can be determined accurately. This is crucial as 25% of patients with ccTGA will demonstrate either dextrocardia or mesocardia. In addition, this approach should make clear other abnormalities of the spatial relationships of the chambers, such as crisscross AV connections and superoinferior ventricles.

The subcostal views are important in the identification of a case of ccTGA because they allow imaging of all chambers and vessels. From this position, the first clue to the presence of AV discordance may be the significant malalignment between the atrial and ventricular septa that occurs in this condition (Fig. 50.4).

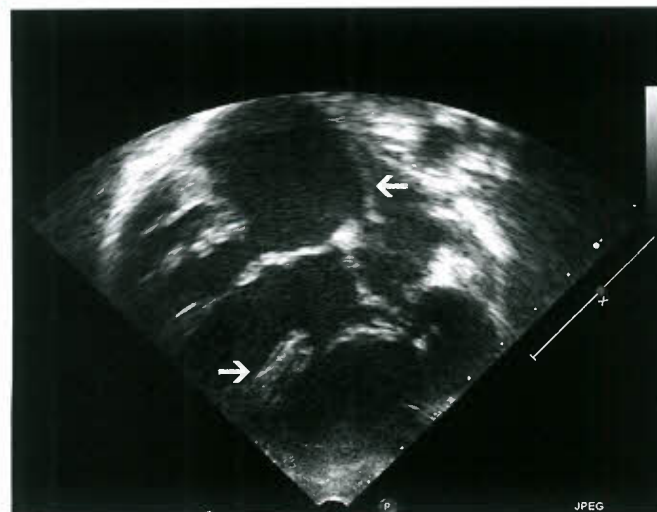


Figure 50.4. Subcostal four-chamber view of congenitally corrected transposition of the great arteries with dextroposition, demonstrating malalignment of atrial septum and ventricular septum (arrows) with inlet ventricular septal defect.

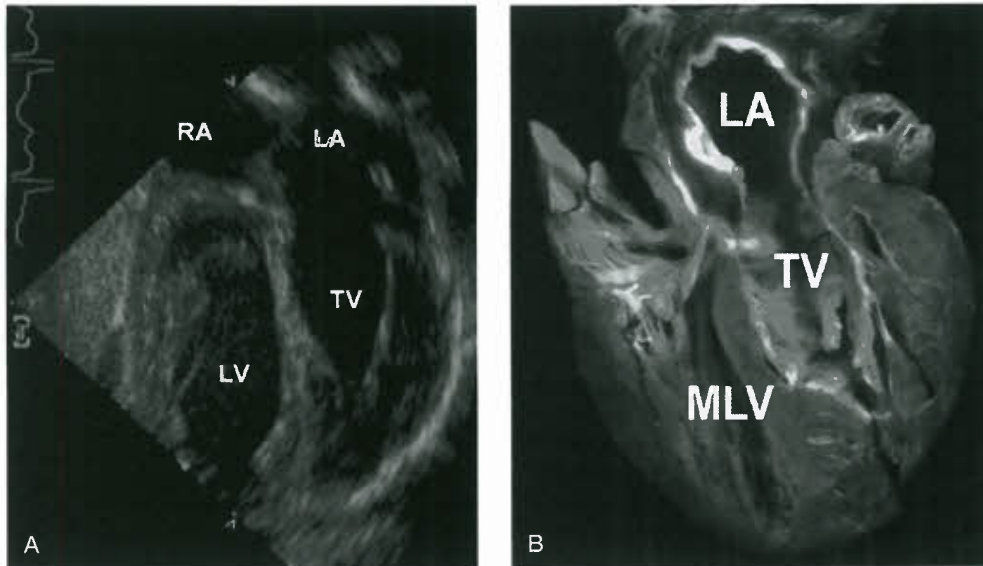


Figure 50.5. Four-chamber view (A) and pathologic specimen (B) demonstrating morphologic features of congenitally corrected transposition of the great arteries. (LA, left atrium; LV, left ventricle; MLV, morphologic left ventricle; RA, right atrium; TV, tricuspid valve.)

In all cases, the sonographer should look for features that define the morphologic right versus the morphologic left ventricle. These features include the apical displacement of the AV valve of the RV relative to the left (exaggerated in the presence of an Ebstein-like malformation and absent in the presence of an AV septal defect or a large perimembranous inlet VSD), a trileaflet (tricuspid) versus a bileaflet (mitral) AV valve, septal attachments of the AV valve of the RV (TV), the presence of a moderator band in the RV, an irregular mural endocardial surface of the RV relative to the smooth endocardial surface of the left ventricle, and a round or triangular shape to the right ventricular cavity versus an elongated or ellipsoidal shape to the left ventricular cavity. The subcostal four-chamber view is important in obtaining information about these features (Fig. 50.5).

The long-axis views from the chest tend to be more vertically oriented than in the normal heart, and the two great arteries are seen to arise in parallel, confirming the presence of TGA. As the ventricular septum is often horizontally oriented in ccTGA, the long-axis views can be confusing, particularly in the presence of a large perimembranous inlet VSD. In this case, the pulmonary valve can be seen related to either AV valve, creating some confusion with respect to VA connection. Nevertheless, the long-axis views are particularly important in establishing the mechanisms of possible outflow tract obstruction to either the aorta or PA (Fig. 50.6).

Short-axis views from the chest, on the other hand, prove extremely useful. At the level of the aortic and pulmonary valves, the aorta with its coronary arteries usually is demonstrated in an L-position (leftward and anterior) relative to the bifurcating PA (Fig. 50.7). This relationship of the great arteries, although typical, is not absolute. Short-axis sweeps will confirm the VA connection to be discordant, as suspected from the subcostal views, and will demonstrate the orientation of the ventricular septum as well as the AV valve leaflet anatomy and papillary muscle distribution.

By tilting the transducer upward from the four-chamber view, one can demonstrate how the pulmonary outflow tract from the right-sided left ventricle is deeply wedged between the two AV valves. Indeed, the pulmonary outflow tract is even more deeply wedged than the aorta in normal hearts and subject to obstruction from more than one source.

The apical four-chamber views are especially useful for reviewing the AV valve anatomy with particular reference to Ebstein malformation of the left AV (tricuspid) valve.

Color-flow Doppler is used to quantitate AV valve regurgitation. This view also clearly shows the usual perimembranous inlet VSD.

A high left parasternal view oriented in the sagittal plane, similar to the so-called ductal cut position, not only will demonstrate the ductus arteriosus but, because of its usual leftward and anterior position, will also open up the entire aortic arch. The suprasternal views, in fact, often demonstrate the aorta less well. Demonstration of the branching pattern of the aorta is important because a right aortic arch is more common than previously believed (18%).

Atrial defects are seen in about 12% of cases and are most usually of the secundum type. Echocardiographically, the atrial septum, as in the normal heart, is best imaged from subcostal and foreshortened four-chamber views with color-flow Doppler, confirming the usual left-to-right atrial shunt. Alternatively, ccTGA is occasionally associated with an AV septal defect. Such an occurrence may complicate the

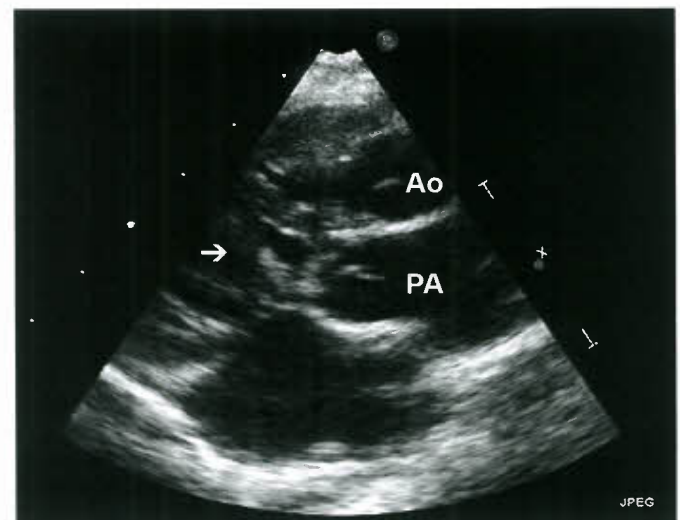


Figure 50.6. Long-axis view in congenitally corrected transposition of the great arteries. Note posterior pulmonary artery (PA). Subpulmonary stenosis with accessory atrioventricular tissue from both right and left atrioventricular valves. (Ao, aorta.)



Figure 50.7. Parasternal short-axis view of anterior levopositioned aorta with posterior pulmonary artery bifurcation. (Ao, aorta; PA, pulmonary artery.)

diagnosis of AV discordance, as described already, but accurate echocardiographic identification is certainly possible.

The left AV valve can display a wide range of structural abnormalities. Perhaps the most common is a variable degree of dysplasia with less displacement than seen in the usual form of Ebstein anomaly of the TV in the patient with concordant connections. These features are best demonstrated echocardiographically from the four-chamber (Fig. 50.8) and modified short-axis views. As the usual functional problem is valvular regurgitation, this will be readily evaluated with color-flow Doppler. Stenosis of the valve in this situation is unusual; nevertheless, inflow velocities should be evaluated. Significant “Ebstein-like” malformation of the left AV valve may be associated with right ventricular hypoplasia and occasional subaortic obstruction. These possible associations should be sought. Other anomalies may affect the left AV valve, including a supra-valvar stenosing ring and varying degrees of AV valve override and straddle. As the usual VSD in ccTGA is perimembranous inlet, posterior straddling of the left AV valve is significantly more common than straddling of the right AV valve, which requires an anterior VSD. There is little doubt that echocardiography is the method of choice for

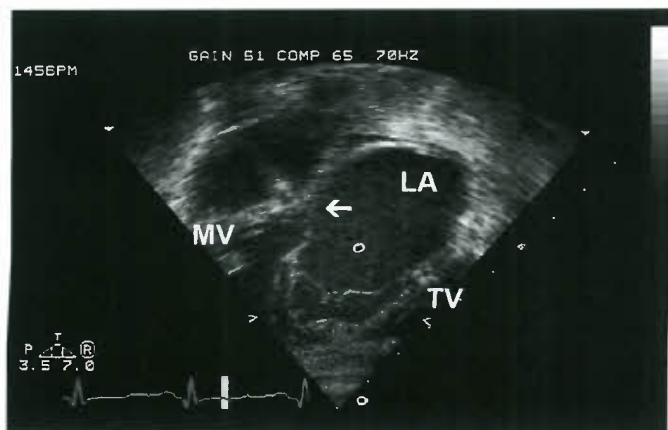


Figure 50.8. Apical four-chamber view in congenitally corrected transposition of the great arteries. Dilated LA from tricuspid regurgitation and Ebstein-like displacement of septal leaflet. The arrow indicates the level of the tricuspid annulus. (LA, left atrium; MV, mitral valve; TV, tricuspid valve.)

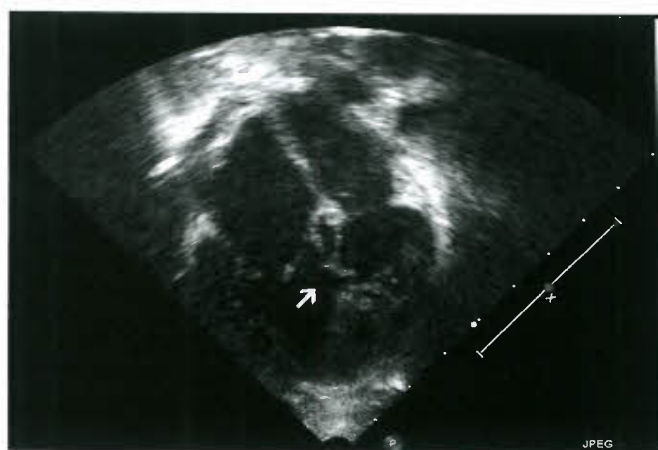


Figure 50.9. Apical four-chamber view in congenitally corrected transposition of the great arteries demonstrating herniation of the tricuspid valve septal leaflet (TV) into the ventricular septal defect. Arrow indicates septal leaflet of TV.

establishing the presence or absence of straddling of the AV valve. The parasternal short-axis and four-chamber views are particularly useful in this regard. Again, the presence of AV valve straddle should be a clue to the possibility of ventricular hypoplasia.

Abnormalities of the right AV valve usually are not described among the common anomalies associated with ccTGA. A necropsy series however, suggested that up to 55% of cases demonstrated a wide variety of abnormalities of the left AV valve. Parachute deformity of the right-sided mitral valve has been described (48). The subcostal four-chamber view generally demonstrates the right AV valve to best advantage.

A VSD will be seen in approximately 80% of patients with ccTGA. Most frequently, these defects can be described as perimembranous with inlet or posterior extension. Such defects, by the nature of their posterior extension, are predisposed to demonstrate partial occlusion by the apically displaced septal leaflet of the TV (Fig. 50.9) and also are positioned to allow straddling of the TV. Such anatomy is best demonstrated in parasternal short-axis views and apical or subcostal four-chamber views. Outlet defects and muscular defects are seen less commonly. The ventricular apex is often not well seen from the subcostal position; therefore, apical muscular VSDs are best sought in the apical four-chamber view.

The unique anatomy of the left ventricular outflow tract to the PA is best demonstrated from the subcostal position by directing the transducer anteriorly from the four-chamber view. Pulsed or continuous-wave Doppler assessment of the outflow tract also is best undertaken from this position, as flow will be most parallel to the Doppler line of interrogation. As stated, the pulmonary outflow tract is wedged deeply between the right and left AV valves. Obstruction can result from one or more possible mechanisms: abnormality of the valve itself; prominent right-sided, muscular, ventriculofundibular fold with the muscular infundibular septum causing subpulmonary obstruction; and accessory tissue from either the right or left AV valve or aneurysmal tissue about the inlet VSD causing obstruction of the left ventricular outflow tract (Fig. 50.10).

Abnormalities of the right ventricular outflow tract to the aorta are somewhat unusual but have a number of interesting aspects. Obstruction or severe regurgitation of the left AV valve commonly is associated with outflow tract obstruction. In fact, in the setting of severe left AV valve regurgitation, one must be certain that the aortic obstruction is not simply functional. The aortic annulus is separated from the body of

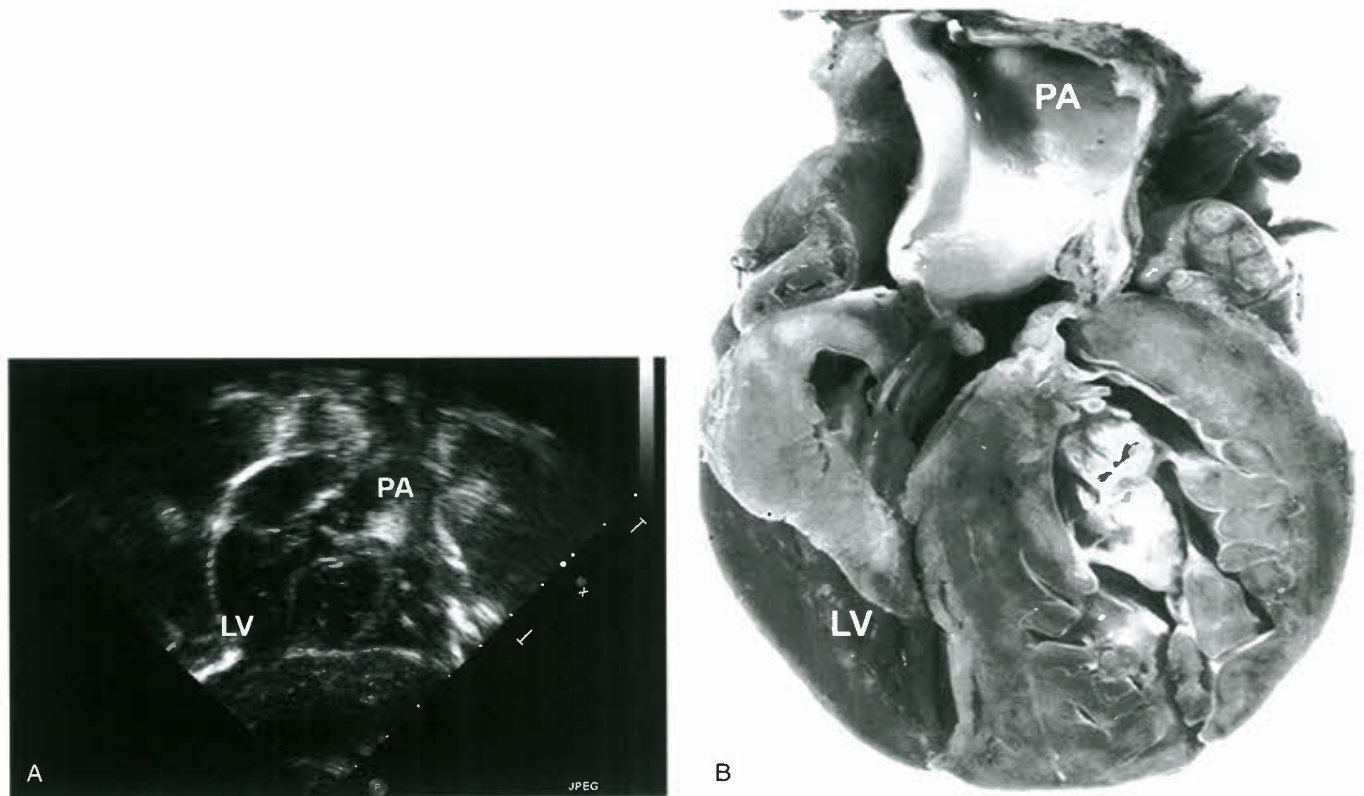


Figure 50.10. A: Subcostal view in patient with congenitally corrected transposition of the great arteries and subpulmonary obstruction. Accessory tissue is seen from both left and right atrioventricular valves. B: Pathologic specimen cut in same plane as echocardiogram. (LV, left ventricle; PA, pulmonary artery.)

the ventricle by a complete muscular infundibulum; therefore, muscular outflow tract obstruction may seem dynamic. In addition, obstruction may be due to subaortic membrane, valvar stenosis, and accessory AV valve tissue (49). The subaortic area is best imaged in the left parasternal or occasionally a subcostal position.

As with subaortic obstruction, coarctation of the aorta often is associated with severe left AV valve regurgitation, VSD, or hypoplasia of the RV. The diagnosis can be made from the high left parasternal position.

With an anteriorly positioned aorta, imaging of the coronary arteries is excellent (Fig. 50.11). Seventy-six percent of patients will have a coronary distribution concordant with the ventricular anatomy; however, single coronary artery anomalies and others occur.

The fetus with congenitally corrected transposition could come to the attention of the fetal sonographer for several reasons, including family history, detection of cardiac abnormality on prior obstetrical ultrasound examination, and hydrops fetalis. Hydrops fetalis in congenitally corrected transposition may result from severe left AV valve regurgitation or complete AV block with bradycardia. The cardiac anatomy and cardiac rhythm are demonstrated readily by fetal echocardiography. The occurrence of AV block leading to the detection of congenitally corrected transposition in utero is unusual. The fetus with severe AV valve regurgitation and ccTGA has a very guarded prognosis and may undergo spontaneous abortion. A study of 34 fetuses documents the most valuable features of the ultrasound diagnosis of corrected transposition in the fetus (50).

Transesophageal echocardiography appears to be well suited to the examination of the patient with congenitally corrected transposition. It provides a reliable window in the older patient

who has had prior surgery and has a limited transthoracic window. Furthermore, the transesophageal echocardiography window is ideal for examination of those structures critical to the patient with this disorder, including the atrial septum, left and right AV valves, and the inlet ventricular septum. Several studies have documented the advantages and disadvantages of transesophageal echocardiography (51,52).



Figure 50.11. Cross-sectional view of levopositioned aorta demonstrating a coronary artery (arrow). PA, pulmonary artery.



Figure 50.12. Three-dimensional view of tricuspid valve in congenitally corrected transposition of the great arteries demonstrating dysplasia of septal leaflet. (ant, anterior leaflet; post, posterior leaflet; sept, septal leaflet.)

Three-dimensional echocardiography is increasingly used in the setting of ccTGA (53,54). We use this modality to assess the left AV and have found it useful (Fig. 50.12). Establishing the nature of left ventricular outflow tract obstruction and the relationship of the VSD to the aorta are other areas where we have found three-dimensional echo to be of great value.

MAGNETIC RESONANCE IMAGING

Magnetic resonance imaging (MRI) allows both anatomic and physiologic diagnostic information, particularly for the assessment of the systemic RV. We have found MRI particularly useful in the assessment of patients prior to contemplated anatomic repair (Figs. 50.13 and 50.14). Studies to date have

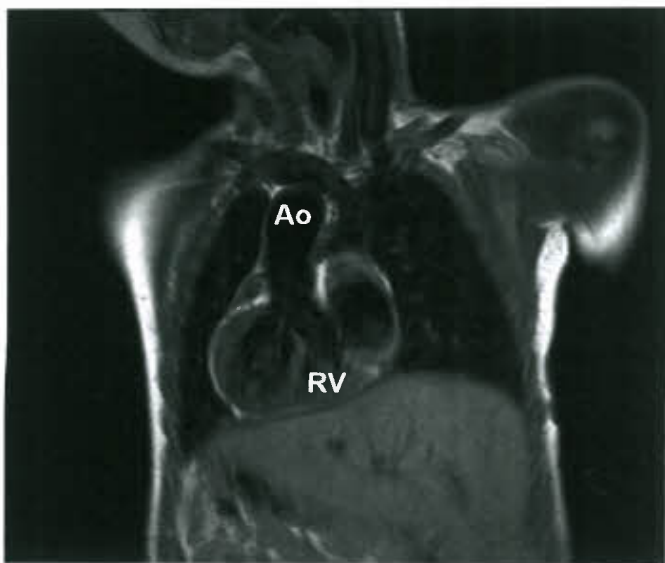


Figure 50.13. Frontal cut of T1-weighted MRI in congenitally corrected transposition of the great arteries with dextroposition, ventricular septal defect, and pulmonary atresia. (Ao, aorta; RV, right ventricle.)

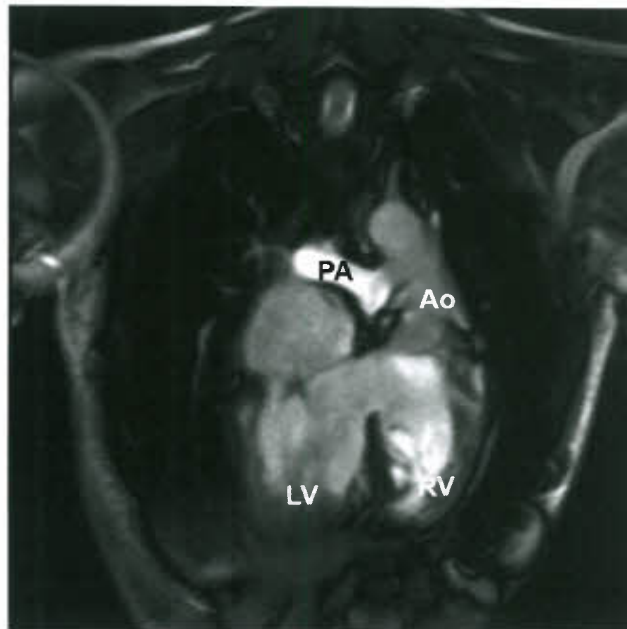


Figure 50.14. Frontal cut of T2-weighted MRI, in congenitally corrected transposition of the great arteries with mesocardia, ventricular septal defect, and pulmonary atresia. (Ao, aorta; LV, left ventricle; PA, pulmonary artery; RV, right ventricle.)

shown good correlation with other modalities in terms of functional evaluation and have confirmed the concerns regarding systemic right ventricular function (55–59). In addition, MRI proves to be useful and reliable in patients with PA banding for LV retraining. It allows accurate assessment of the LV mass/LV volume ratio, used as one of the determinants of adequate LV retraining for proceeding with the double switch operation.

CARDIAC CATHETERIZATION

Anatomic and functional detail provided by 2-D and 3-D echocardiography and MRI have reduced the need for routine preoperative catheterization in the majority of patients with ccTGA. In the recent past, diagnostic right and left-sided heart catheterization was performed prior to intracardiac repair, focusing on imaging the PA and coronary anatomy (60,61). Diagnostic catheterization remains important in the preoperative assessment of patients in whom pulmonary vascular resistance may be elevated (long-standing VSD shunt, severe left-sided AV valve regurgitation) along with the response to pulmonary vasodilators, in patients with suspected aortopulmonary collaterals or unexplained cyanosis, and less commonly in those with abnormal coronary artery anatomy that is not well-defined with noninvasive imaging. The adult with unrepaired ccTGA may still benefit from preoperative catheterization, especially in the setting of arrhythmias, ventricular dysfunction, long-standing intracardiac shunting, or unexplained cyanosis (62). Cardiac catheterization remains a part of the assessment of left ventricular hemodynamics in patients undergoing left ventricular retraining prior to anatomic repair (63).

Since ccTGA of the great vessels may occur with cardiac malposition, noting the catheter course in the abdomen to identify the course of the IVC or aorta aids in the diagnosis of the underlying situs and malposition. Observations about the course of the catheter may be important in recognizing the abnormal position of the great arteries in relation to the ventricles as well. Using anteroposterior and lateral fluoroscopy,

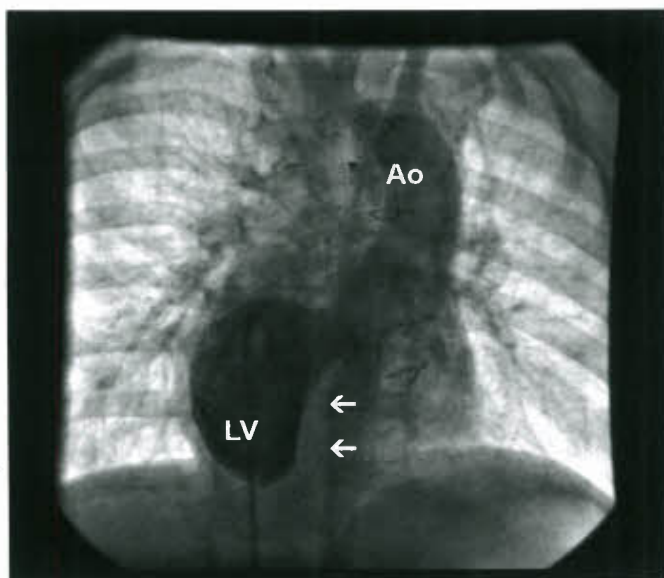


Figure 50.15. Angiogram, A-P projection with contrast injection in left ventricle in congenitally corrected transposition of the great arteries with pulmonary atresia and ventricular septal defect (arrows). Note vertical position of ventricular septum (Ao, aorta; LV, left ventricle.)

their course can be determined. In patients with situs solitus and levocardia, the PA lies medially and posteriorly, with the venous catheter following a course close to the spine. The aorta lies anteriorly and along the left cardiac border.

Because of the anterior position of the AV node and the intrinsically fragile conduction system, patients with ccTGA are at higher risk of developing heart block during catheter manipulation, especially, but not invariably, when attempting access into the PA. Thus, it is always important to have available a system for emergent transvenous pacing during the procedure itself.

ANGIOCARDIOGRAPHY

Angiocardiography today is not performed without prior echocardiographic or MRI imaging. These modes of imaging should establish the diagnosis and also should indicate the relative topography of the ventricular septum. In most patients with ccTGA, the ventricular mass is aligned about a septum that is much more sagittal than in the normal heart (Fig. 50.15). A horizontal ventricular septum also is well described in patients with AV discordance. These observations of the disposition of the ventricular septum are important to the determination of the axial projection for angiocardiography.

Assuming the usual position of the ventricular septum, a frontal and lateral left ventriculogram, perhaps with 20 to 25 degrees of right anterior oblique (RAO), should profile the ventricular septum, the left ventricular outflow tract, and the mitral inflow (Fig. 50.16). A similar projection can be used for the injection in the morphologic RV. Obviously, if there are defects in other portions of the ventricular septum, the axial projections will have to be modified and expanded. The character of the subpulmonary obstruction is best imaged by selective injection of contrast into the morphologic left ventricle. In the setting of VSD, adding 20 to 25 of RAO will demonstrate to advantage both the VSD and the left ventricular outflow tract obstruction. The functional status of the left AV valve is perhaps best assessed by echocardiography and color Doppler, but right

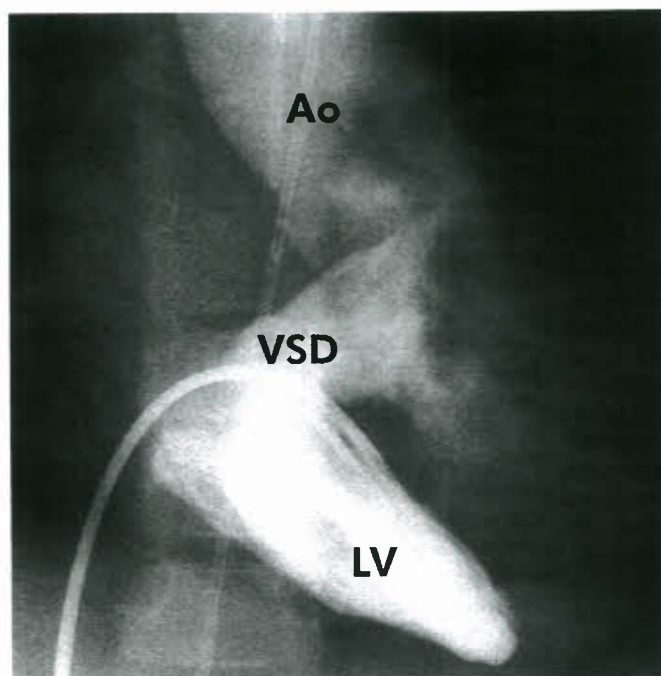


Figure 50.16. A single-outlet aorta (Ao) in a patient with atrioventricular discordance. This left ventriculogram (LV) demonstrates a large ventricular septal defect (VSD).

ventricular angiography will also add information (Fig. 50.17). The character of subaortic stenosis, admittedly uncommon, may best be demonstrated by right ventricular angiography. Varying degrees of obliquity may be required to profile the small left ventricle or the VA connection of double-outlet RV.

The pulmonary arteries and their bifurcation are best imaged by a selective injection of contrast into the pulmonary

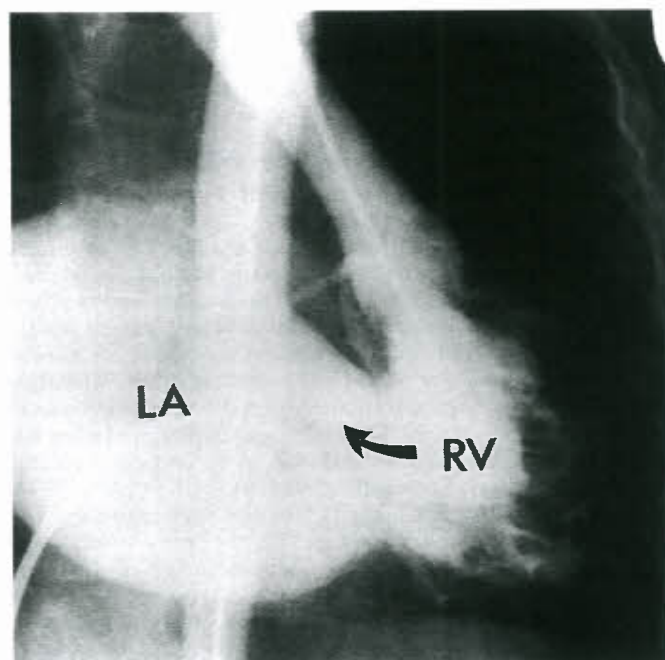


Figure 50.17. Severe systemic atrioventricular valve regurgitation (arrow) demonstrated by injection of contrast into the morphologic right ventricle (RV). The left atrium (LA) is severely enlarged.

arteries with craniocaudal angulation. A degree of right or left anterior obliquity will focus on the right or left PA, respectively.

The aorta and the coronary arteries can be profiled by aortography, filmed in the frontal and lateral projections. The coronary arteries originate from the posterior-facing sinuses, and selective coronary angiography may be necessary to obtain adequate demonstration of the anatomy.

NATURAL HISTORY AND MANAGEMENT

ccTGA is a complex and unusual form of congenital heart disease. As such, it takes time to accumulate experience, and then meaningfully study the natural history, surgical outcomes, and results of changes in surgical management.

The underlying problem with AV and VA discordance may be the issue of the RV as the systemic ventricle. There is however, a very high frequency of associated lesions, which, in their turn, tend to have quite different pathophysiologic effects on systemic right ventricular function. VSDs are volume loading. Pulmonary outflow obstruction will alter pulmonary blood flow, volume loading, and right ventricle–left ventricle interaction. Tricuspid regurgitation will both volume load the ventricle and reduce its afterload. The complex interactions of these anatomic and physiologic variables complicate outcome analysis.

MEDICAL MANAGEMENT

The neonate with ductal-dependent pulmonary blood flow requires immediate institution of intravenous prostaglandin to maintain patency of the arterial duct until such time that a stable source of blood supply to the lungs can be surgically constructed. Similar management is required for the infant who has severe coarctation of the aorta or interruption of the aortic arch. The medical management of the associated lesions thereafter dominates early medical management. Later, the medical management is likely to focus on systemic AV valve regurgitation and heart failure. The appropriate use of diuretics along with afterload reduction and beta-blockade may be required.

PACING

A significant proportion of patients will develop spontaneous or postoperative complete heart block. AV block frequently occurs in the setting of associated cardiac anomalies or results in significant bradycardia, necessitating permanent pacing. Depending on the patient's size, venous anatomy, residual intracardiac lesions, and type of surgical repair, pacing can be endocardial via a transvenous approach, epicardial, or a combination of the two. For heart block, selective site RV apical or LV apical pacing is preferred after physiologic repair or anatomic repair, respectively. The latter also is preferred after PA banding. The indication for and role of biventricular pacing and cardiac resynchronization therapy (CRT) in ccTGA patients with significant heart failure and ventricular dyssynchrony has been explored (64). In fact, the first reported case of CRT pacing in congenital heart disease involved a patient with ccTGA (65). The placement of a transvenous CRT system is challenging due to the unusual coronary sinus and great cardiac vein anatomy (66). The latter would allow CRT of the systemic morphologic RV. In patients with an anatomical repair (described below), the coronary sinus is not transvenously accessible and a hybrid or epicardial approach is required for CRT of the morphologic left ventricle. Data on the outcome of CRT in ccTGA patients remain limited (67–69).

UNOPERATED NATURAL HISTORY

Early natural history is impacted significantly by the severity of associated lesions and surgical management. Although there have been repeated case reports of long-term survival with ccTGA, this is probably unusual (70,71). A few investigators who have tried to separate natural history from associated lesions and surgical outcomes suggest a different set of probabilities. Beauchesne et al. (72) followed 44 unoperated patients for up to 144 months and found that the majority (59%) had grade 3 or greater systemic AV valve regurgitation and that many of these demonstrated significant systemic RV dysfunction and were symptomatic. Presbitero et al. (30) have followed 18 patients, again pointing to systemic AV valve regurgitation and ventricular dysfunction as major concerns. In a large multi-institutional study, Graham et al. (73) found that while patients without associated lesions had a lower occurrence rate of heart failure and systemic ventricular dysfunction than those with associated lesions at a given age, these problems tended to increase in frequency with advancing age in both groups.

CONVENTIONAL SURGERY AND OUTCOMES

Conventional surgery for ccTGA includes several options based largely on the underlying associated lesions and their hemodynamic effects. PA banding or systemic to PA shunting has been used for palliation of increased or decreased pulmonary blood flow, respectively. VSD closure may be undertaken as a primary procedure or following debanding. Techniques for reducing the surgical complication of heart block following defect closure have been described (47). Left ventricle to PA outflow tract obstruction may be locally resected or managed with placement of a left ventricle to PA conduit. TV regurgitation has been managed with repair or replacement. However, valve dysplasia which frequently is severe, along with surgical series showing recurrent or progressive regurgitation after repair, suggest that valve replacement is the preferred option when possible. When complicated by significant AV valve straddle or ventricular hypoplasia, management leading to “Fontan” type palliation has been successful. Finally, for the patient with poor ventricular function, with severe tricuspid regurgitation, or with aortic atresia, cardiac transplantation may be the most successful approach.

Many series assessing the long-term outcomes of conventional surgical approaches and factors thought to determine outcome have been reported (74–81). Immediate surgical results clearly have improved, and surgical risk is likely to be 3% to 10%. Hraska (77) reported 5-year survival rates at 75% and 10 year at 68%. These results would appear to be remarkably similar to those reported by the other groups. Reoperations for conduit replacement and systemic AV valve repair/replacement are frequent and may approach 40% over 10 years. Risk factor analyses for a poor outcome repeatedly identify “Ebstein” malformation of the TV, the degree of tricuspid insufficiency, systemic right ventricular dysfunction, and complete heart block as important.

RIGHT VENTRICULAR DYSFUNCTION AND TRICUSPID REGURGITATION

Ventricular dysfunction and AV valve regurgitation are, of course, linked through the pathophysiologies of volume loading, ventricular and annular dilation and distortion, and right ventricular–left ventricular interaction. In the setting of corrected transposition, this is complicated by the frequency of congenital dysplasia of the TV and the impact of the other associated lesions.

The RV as the systemic ventricle relative to the left ventricle may be disadvantaged because of poor geometry, a lower ejection fraction, and lower coronary flow reserve (82,83). In the setting of simple transposition after atrial switch repair, studies of RV function give evidence of ongoing right ventricular dysfunction (84,85). Overall, however, right ventricular function may be preserved for many years. Studies in corrected transposition patients are limited, but tend to confirm the impression of systemic right ventricular dysfunction (82,86). Investigators of several series have reported a tendency toward worsening of systemic right ventricular function after conventional biventricular repair (78,87). The potential causes of this observation may be multiple, including complex alterations in right ventricular–left ventricular interaction, and the effects of surgical intervention itself.

While intimately connected to the issue of systemic right ventricular dysfunction, several studies have drawn specific attention to the importance of TV regurgitation. Prieto et al. (88) in a study of 40 patients with corrected transposition concluded that tricuspid insufficiency was the single most important factor associated with poor outcome and that the occurrence of systemic right ventricular dysfunction almost always was linked to long-standing tricuspid regurgitation. Acar (89) concluded that TV function depended upon the loading condition of both ventricles and upon septal geometry. Nevertheless, the cause of death after TV replacement most frequently is progressive systemic ventricular dysfunction (90).

The relationship between systemic right ventricular function and tricuspid regurgitation was most recently evaluated by the group from the Mayo Clinic. Mongeon et al. (91) hypothesized that patients with preserved ventricular function at the time of TV replacement would maintain preserved ventricular function long term. In a retrospective analysis of 46 patients, preoperative systemic ventricular ejection fraction as assessed by echocardiography was an independent predictor of ventricular function at ≥ 1 year after operation. This study is the first to suggest that surgery for TV regurgitation should be considered while systemic right ventricular function is preserved and may halt the deterioration of ventricular function long term in the majority of patients.

Several studies have focused on the impact of PA banding on systemic right ventricular function and AV valve regurgitation. In a series where banding was used for left ventricular conditioning prior to arterial switching, it has been suggested that PA banding may improve systemic ventricular function and AV valve regurgitation through a mechanism involving septal shift (92). In another series, Winlaw et al. (93) did not

find significant improvements in AV valve regurgitation but did find clinical improvement. Success at achieving biventricular repair was associated with the age at which banding was undertaken, with younger patients benefiting most. In the report by Jahangiri et al. (94), PA banding likely more often improved tricuspid regurgitation primarily by altering pulmonary blood flow and thereby altering loading conditions for the systemic RV. Neonatal PA banding has also been reported with similar results (95).

Patients with low left ventricular (subpulmonary) pressures and a deconditioned left ventricle require “retraining” prior to a double switch procedure. A strategy of progressive PA banding is performed to increase the pressure load on the left ventricle and promote left ventricular hypertrophy. The adequacy of banding can be assessed intraoperatively with echocardiography or with the use of conductance catheters to assess pressure–volume relationships, or with postoperative echocardiography, MRI, or cardiac catheterization. Suggested requirements for proceeding to double switch operation include LV pressure $\geq 70\%$ to 80% systemic, LV mass/LV volume ratio >1.5 , normal LV wall thickness for a systemic LV, and normal LV function after PA banding.

OUTCOMES OF THE “DOUBLE SWITCH” OR ANATOMIC REPAIR FOR ccTGA

The relatively poor outcomes associated with conventional surgery combined with considerations of the potential for progressive right ventricular dysfunction and tricuspid regurgitation has led to an exploration of alternative surgical approaches to the patient with ccTGA. Ilbawi et al. (96) first reported the anatomic repair of corrected transposition as opposed to the standard physiologic repair. The approach combined atrial switching (Mustard or Senning procedures) with intraventricular rerouting of the VSD, such that the anatomic left ventricle would carry on the role of the systemic ventricle and the anatomic RV would become the subpulmonary ventricle after a RV to PA conduit (Fig. 50.18). They subsequently reported their series of anatomic repairs (97). The pathologic anatomy of corrected transposition that could potentially preclude such an approach has been reviewed (19,20). Relative or absolute contraindications to the “double switch” might include a restrictive VSD, specific coronary artery anatomy, ventricular hypoplasia by more than 50%, AV valve straddle and anomalies of the mitral valve. Imai (98) was the first to

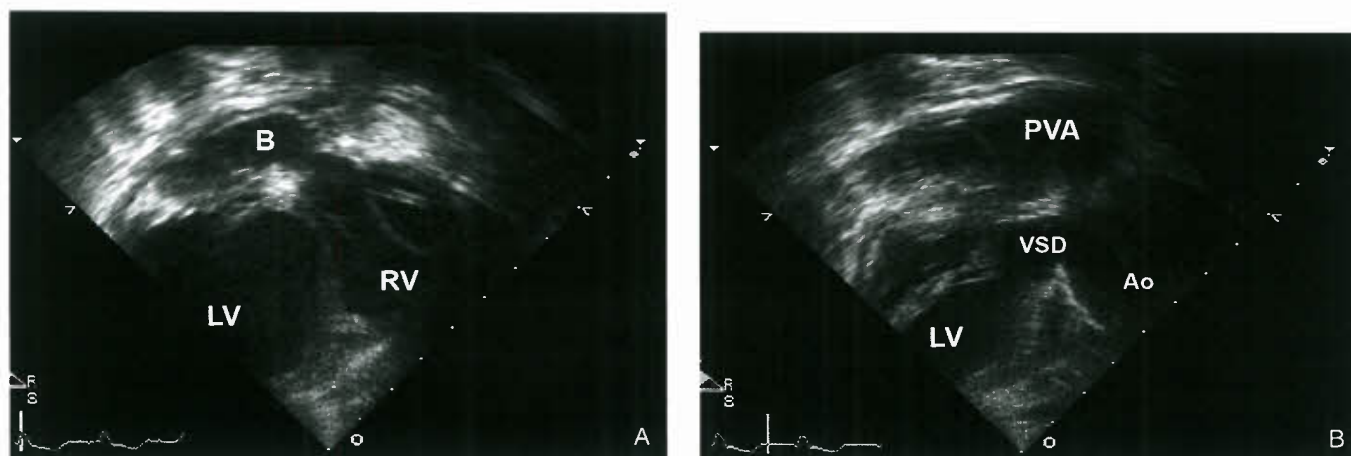


Figure 50.18. A,B: Congenitally corrected transposition of the great arteries following double-switch repair. A: Inferior limb of atrial baffle to the right ventricle. (B, baffle; LV, left ventricle; RV, right ventricle.) B: Ventricular septal defect (VSD) tunneling left ventricle to aorta. (Ao, aorta; PVA, pulmonary venous atrium.)

report a true “double switch” procedure involving both an atrial level switch and a full arterial level switch with coronary artery transfer (100). Subsequently, there has been a significant number of reports of anatomic repairs involving both ventricular level rerouting and/or arterial switching with some series large enough to address risk analysis (99–104). Complications of these often lengthy procedures can be expected to include those of the atrial switch (sinus node dysfunction, supraventricular dysrhythmias, baffle obstructions, and baffle leaks), the ventricular switch (subaortic obstruction, aortic regurgitation, conduit obstruction, or regurgitation), and/or the arterial switch (coronary artery obstructions, aortic valve incompetence, pulmonary arterial obstruction).

Left ventricular dysfunction following the anatomic repair operation may be relatively common. Quinn et al. (105) reported the outcome of 44 patients following double switch in which LV retraining was required in 11. By multivariate analysis, the completion of LV retraining predicted death/transplantation, the development of moderate-to-severe LV dysfunction, or both. Moderate to severe LV dysfunction was seen in 6/11 patients with prior retraining compared to 6/33 patients without retraining. Similarly, the Boston group has reported on the determinants of late LV dysfunction following anatomic repair (106).

The quality of life of patients after the anatomic repair compared to patients with nonanatomic repair and a systemic RV has recently been reported. Initial data showed comparable results, with lower school performance in the anatomic repair group (107).

In summary, when addressing the complex patient with ccTGA, the surgeon will need to choose between the risks and benefits of physiologic, anatomic, and on occasion, single ventricle type repairs.

CONCLUSION

Corrected TGA is an unusual congenital heart defect characterized by AV and VA discordance. The etiology, morphogenesis, and morphology are complex and fascinating to consider. The clinical picture is dominated by the pathophysiology of associated cardiac anomalies. Long-term follow-up of conventional surgical approaches is disappointing and has led to novel surgical approaches aimed at restoring normal AV and VA connections. Early results may be promising, but final assessment of the evidence requires further long-term follow-up.

ACKNOWLEDGMENTS

The authors would like to acknowledge the contribution of figures related to 3-D echo by Dr. Jeffrey Smallhorn and figures related to MRI by Dr. Michelle Noga. We would also like to acknowledge Dr. Robert Freedom's prior contributions to this work.

REFERENCES

- De La Cruz MV, Anselmi G, Cisneros F, et al. An embryologic explanation for the corrected transposition of the great vessels: additional description of the main anatomic features of this malformation and its varieties. *Am Heart J* 1959;57:104–117.
- Van Praagh R. What is congenitally corrected transposition? *N Engl J Med* 1970;282:1097–1098.
- Presbitero P, Somerville J, Rabajoli F, et al. Corrected transposition of the great arteries without associated defects in adult patients: clinical profile and follow up. *Br Heart J* 1995;74:57–59.
- Ferencz C, Rubin JD, McCarter RJ, et al. Congenital heart disease: prevalence at livebirth. The Baltimore-Washington infant study. *Am J Epidemiol* 1985;121:31–36.
- Fyler DC. Report of the New England Regional Infant Cardiac Program. *Pediatrics* 1980;65:376–461.
- Samanek M, Voriskova M. Congenital heart disease among 815,569 children born between 1980 and their 15-year survival: a prospective Bohemia survival study. *Pediatr Cardiol* 1999;20:411–417.
- Witham AC. Double outlet right ventricle; a partial transposition complex. *Am Heart J* 1957;53:928–939.
- Kuehl KS, Loffredo CA. Population-based study of l-transposition of the great arteries: possible associations with environmental factors. *Birth Defects Res A Clin Mol Teratol* 2003;67:162–167.
- Piacentini G, Digilio MC, Capolino R, et al. Familial recurrence of heart defects in subjects with congenitally corrected transposition of the great arteries. *Am J Med Genet* 2005;137:176–180.
- McElhinney DB, Geiger E, Blinder J, et al. NKX2.5 mutations in patients with congenital heart disease. *J Am Coll Cardiol* 2003;42:1650–1655.
- Becker TA, Van Amber R, Moller JH, et al. Occurrence of cardiac malformations in relatives of children with transposition of the great arteries. *Am J Med Genet* 1996;66:28–32.
- Steding G, Seidl W. Contribution to the development of the heart, part II: morphogenesis of congenital heart diseases. *Thorac Cardiovasc Surg* 1981;29:1–16.
- Verzi MP, McCulley DJ, De Val S, et al. The right ventricle, outflow tract, and ventricular septum comprise a restricted expression domain within the secondary/anterior heart field. *Dev Biol* 2005;287:134–145.
- Linask KK, Han M, Cai DH, et al. Cardiac morphogenesis: matrix metalloproteinase coordination of cellular mechanisms underlying heart tube formation and directionality of looping. *Dev Dyn* 2005;233:739–753.
- Anderson R, Lillehei C, Lester R. Corrected transposition of the great vessels of the heart. *Pediatrics* 1957;20:626–646.
- Becker A, Anderson R. Conditions with discordant atrioventricular connections-anatomy and conducting tissues. In: Anderson RH, Macartney FJ, Shinebourne EA, eds. *Pediatric Cardiology*. Churchill Livingstone: Edinburgh, 1978:184–197.
- Losekoot TG, Becker AE. Discordant atrioventricular connexion and congenitally corrected transposition. In: Anderson RH, Macartney FJ, Shinebourne EA, Tynan M, eds. *Pediatric Cardiology*. Churchill Livingstone: Edinburgh, 1987:867–888.
- Allwork SP, Bentall HH, Becker AE, et al. Congenitally corrected transposition of the great arteries: morphologic study of 32 cases. *Am J Cardiol* 1976;38:910–923.
- Van Praagh R, Papagiannis J, Grunenfelder J, et al. Pathologic anatomy of corrected transposition of the great arteries: medical and surgical implications. *Am Heart J* 1998;135:772–785.
- Alva C, Horowitz S, Ho S, et al. The feasibility of complete anatomical correction in the setting of discordant atrioventricular connections. *Heart* 1999;81:539–545.
- Van Praagh R. Diagnosis of complex congenital heart disease: morphologic-anatomic method and terminology. *Cardiovasc Intervent Radiol* 1984;7:115–120.
- Franco-Vazquez JS, Perez-Trevino C, Gaxiola A. Corrected transposition of the great arteries with extreme counter-clockwise torsion of the heart. *Acta Cardiol* 1973;28:636–643.
- Hosseinpour AR, McCarthy KP, Griselli M, et al. Congenitally corrected transposition: size of the pulmonary trunk and septal malalignment. *Ann Thorac Surg* 2004;77:2163–2166.
- Penny DJ, Somerville J, Redington AN. Echocardiographic demonstration of important abnormalities of the mitral valve in congenitally corrected transposition. *Br Heart J* 1992;68:498–500.
- Freedom RM, Harrington DP, White RI, Jr. The differential diagnosis of levo-transposed or malposed aorta. An angiocardiographic study. *Circulation* 1974;50:1040–1046.
- Otero Coto E, Quero Himenez M, Cabrera A, et al. Aortic levopositions without ventricular inversion. *Eur J Cardiol* 1978;8:523–541.
- Craig BG, Smallhorn JF, Rowe RD, et al. Severe obstruction to systemic blood flow in congenitally corrected transposition (discordant atrioventricular and ventriculo-arterial connexions): an analysis of 14 patients. *Int J Cardiol* 1986;11:209–217.
- Marino B, Sanders SP, Parness IA, et al. Obstruction of right ventricular inflow and outflow in corrected transposition of the great arteries (S,L,L): two-dimensional echocardiographic diagnosis. *J Am Coll Cardiol* 1986;8:407–411.
- Deanfield J, Anderson R, Macartney F. Aortic atresia with “corrected transposition of the great arteries” (atrioventricular and ventriculoarterial discordance). *Br Heart J* 1981;46:683–686.
- Presbitero P, Somerville J, Rabajoli F, et al. Corrected transposition of the great arteries without associated defects in adult patients: clinical profile and followup. *Br Heart J* 1995;74:57–59.
- Anderson RH, Becker AE, Gerlis LM. The pulmonary outflow tract in classically corrected transposition. *J Thorac Cardiovasc Surg* 1975;69:747–757.
- Anderson KR, Danielson GK, McGoon DW, et al. Ebstein's anomaly of the left-sided tricuspid valve: pathological anatomy of the valvular malformation. *Circulation* 1978;58:87–91.

33. Becker AE, Ho SY, Caruso G, et al. Straddling right atrioventricular valves in atrioventricular discordance. *Circulation* 1980;61:1133–1141.
34. Dabizzi RP, Barletta GA, Caprioli G, et al. Coronary artery anatomy in corrected transposition of the great arteries. *J Am Coll Cardiol* 1998;12:486–491.
35. McKay R, Anderson RH, Smith A. The coronary arteries in hearts with discordant atrioventricular connections. *J Thorac Cardiovasc Surg* 1996;111:988–997.
36. Ismat FA, Baldwin HS, Karl TR, et al. Coronary anatomy in congenitally corrected transposition of the great arteries. *Int J Cardiol* 2002;86:207–216.
37. Uemara H, Ho SY, Anderson RH, et al. Surgical anatomy of the coronary circulation in hearts with discordant atrioventricular connections. *Eur J Cardiothorac Surg* 1996;10:194–200.
38. Chiu IS, Wu SJ, Chen SJ, et al. Sequential diagnosis of coronary arterial anatomy in congenitally corrected transposition of the great arteries. *Ann Thorac Surg* 2003;75:422–429.
39. Anderson RH, Arnold R, Wilkinson JL. The conducting system in congenitally corrected transposition. *Lancet* 1973;1:1286–1288.
40. Anderson RH, Becker AE, Arnold R, et al. The conducting tissues in congenitally corrected transposition. *Circulation* 1974;50:911–923.
41. Becker AE, Anderson RH. The atrioventricular conduction tissues in congenitally corrected transposition. *Embryology and Teratology of the Heart and the Great Arteries*. Leiden: Leiden University Press, 1978:29–42.
42. Monckeberg JG. Zur Entwicklungsgeschichte des atrioventricular-systems. *Verhandl d Deutsche path Gesellsch* 1913;16:228–249.
43. Bjarke BB, Kidd BS. Congenitally corrected transposition of the great arteries. A clinical study of 101 cases. *Acta Paediatr Scand* 1976;65:153–160.
44. Friedberg DZ, Nadas AS. Clinical profile of patients with congenital corrected transposition of the great arteries. A study of 60 cases. *N Engl J Med* 1970;282:1053–1059.
45. Huhta JC, Maloney JD, Ritter DG, et al. Complete atrioventricular block in patients with atrioventricular discordance. *Circulation* 1983;67:1374–1377.
46. Daliento L, Corrado D, Buja G, et al. Rhythm and conduction disturbances in isolated, congenitally corrected transposition of the great arteries. *Am J Cardiol* 1986;58:314–318.
47. de Leval MR, Bastos P, Stark J, et al. Surgical technique to reduce the risks of heart block following closure of ventricular septal defect in atrioventricular discordance. *J Thorac Cardiovasc Surg* 1979;78:515–526.
48. Gerlis LM, Wilson N, Dickinson DF. Abnormalities of the mitral valve in congenitally corrected transposition (discordant atrioventricular and ventriculoarterial connections). *Br Heart J* 1986;55:475–479.
49. Miche E, Manneback H, Boyunovic N, et al. Right ventricular outflow obstruction due to accessory tricuspid valve tissue in corrected transposition of the great arteries with ventricular septal defect. *Z Kardiol* 1991;80:468–470.
50. Sharland G, Tingay R, Jones A, et al. Atrioventricular and ventriculoarterial discordance (congenitally corrected transposition of the great arteries): echocardiographic features, associations, and outcome in 34 fetuses. *Heart* 2005;91:1453–1458.
51. Sreeram N, Stumper OFW, Kaulitz R, et al. Comparative value of transthoracic and transesophageal echocardiography in the assessment of congenital abnormalities of the atrioventricular junction. *J Am Coll Cardiol* 1990;16:1205–1214.
52. Caso P, Acione L, Lange A, et al. Diagnostic value of transesophageal echocardiography in the assessment of congenitally corrected transposition of the great arteries in adult patients. *Am Heart J* 1998;135:43–50.
53. Ahmed S, Nekkanti R, Nanda NC, et al. Three-dimensional transesophageal echocardiographic demonstration of intraatrial baffle obstruction. *Echocardiography*. 2003;20:683–686.
54. Bartel T, Muller S. Corrected transposition of the great arteries: dynamic three-dimensional echocardiography and volumetry. A new diagnostic tool in intensive care management. *Jpn Heart J* 1995;36:819–824.
55. Scardi S, Pagnan L, Perkan A. Magnetic resonance assessment of an adult patient with congenitally corrected transposition of the great arteries. *Ital Heart J* 2005;6:939–940.
56. van der Zedde J, Oosterhof T, Tulevski II, et al. Comparison of segmental and global systemic ventricular function at rest and during dobutamine stress between patients with transposition and congenitally corrected transposition. *Cardiol Young* 2005;15:148–153.
57. Tulevski II, Zijta FM, Smeijers AS, et al. Regional and global right ventricular dysfunction in asymptomatic or minimally symptomatic patients with congenitally corrected transposition. *Cardiol Young* 2004;14:168–173.
58. Salehian O, Schwerzmann M, Merchant N, et al. Assessment of systemic right ventricular function in patients with transposition of the great arteries using the myocardial performance index: comparison with cardiac magnetic resonance imaging. *Circulation* 2004;110:3229–3233.
59. Dodge-Khatami A, Tulevski II, Bennink GB, et al. Comparable systemic ventricular function in healthy adults and patients with unoperated congenitally corrected transposition using MRI dobutamine stress testing. *Ann Thorac Surg* 2002;73:1759–1764.
60. Freedom RM, Benson LN. Congenitally corrected transposition of the great arteries. In: Freedom RM, Benson LN, Smallhorn JF, eds. *Neonatal Heart Disease*. New York, NY: Springer-Verlag, 1992:523–542.
61. Freedom R, Yoo S, Williams W. Ch 26a conditions with double discordance. In: Freedom R, et al., eds. *The Natural and Modified History of Congenital Heart Disease*. Elmsford, New York: Blackwell Publishing, 2004:356–366.
62. Warnes CA, Williams RG, Bashore TM, et al. ACC/AHA 2008 Guidelines for the management of adults with congenital heart disease: executive summary: a report of the American College of Cardiology/American Heart Association Task Force on Practice Guidelines. *Circulation* 2008;118:2395–2451.
63. Winlaw DS, McGuirk SP, Baler C, et al. Intention-to-treat analysis of pulmonary artery banding in conditions with a morphological right ventricle in the systemic circulation with a view to anatomic biventricular repair. *Circulation* 2005;111:405–411.
64. Diller GP, Okonko D, Uebing A, et al. Cardiac resynchronization therapy for adult congenital heart disease patients with a systemic right ventricle: analysis of feasibility and review of early experience. *Europace* 2006;8:267–272.
65. Rodriguez-Cruz E, Karpawich PP, Lieberman RA, et al. Biventricular pacing as dilated cardiomyopathy associated with congenital heart disease. *Pacing Clin Electrophysiol* 2001;24:235–237.
66. Bottega NA, Kapa S, Edwards WD, et al. The cardiac veins in congenitally corrected transposition of the great arteries: delivery options for cardiac devices. *Heart Rhythm* 2009;6:1450–1456.
67. Jauvert G, Rousseau-Paziaud J, Villain E, et al. Effects of cardiac resynchronization therapy on echocardiographic indices, functional capacity, and clinical outcomes of patients with a systemic right ventricle. *Europace* 2009;11:184–190.
68. Kiesewetter C, Michael K, Morgan J, et al. Left ventricular dysfunction after cardiac resynchronization therapy in congenital heart disease patients with a failing systemic right ventricle. *Pacing Clin Electrophysiol* 2008;31:159–162.
69. Cecchin F, Frangini PA, Brown DW, et al. Cardiac resynchronization therapy (and multisite pacing) in pediatrics and congenital heart disease: five years experience in a single institution. *J Cardiovasc Electrophysiol* 2009;20:58–65.
70. Ikeda U, Furuse M, Suzuki O, et al. Long-term survival in aged patients with corrected transposition of the great arteries. *Chest* 1992;101:1382–1385.
71. Roffi M, de Marchi SF, Seiler C. Congenitally corrected transposition of the great arteries in an 80 year old woman. *Heart* 1998;79:622–623.
72. Beauchesne LM, Warnes CA, Connolly HM, et al. Outcome of the unoperated adult who presents with congenitally corrected transposition of the great arteries. *J Am Coll Cardiol* 2002;40:285–290.
73. Graham TP Jr, Bernard YD, Mellen BG, et al. Long-term outcome in congenitally corrected transposition of the great arteries: a multi-institutional study. *J Am Coll Cardiol* 2000;36:255–261.
74. Lundstrom U, Bull C, Wyse RK, et al. The natural and “unnatural” history of congenitally corrected transposition. *Am J Cardiol* 1990;65:1222–1229.
75. Huhta JC, Danielson GK, Ritter DG, et al. Survival in atrioventricular discordance. *Pediatr Cardiol* 1985;6:57–60.
76. Biliciler-Denktaş G, Feldt RH, Connolly HM, et al. Early and late results of operations for defects associated with corrected transposition and other anomalies with atrioventricular discordance in a pediatric population. *J Thorac Cardiovasc Surg* 2001;122:234–241.
77. Hraska V, Duncan BW, Mayer JE Jr, et al. Long-term outcome of surgically treated patients with corrected transposition of the great arteries. *J Thorac Cardiovasc Surg* 2005;129:182–191.
78. Rutledge JM, Nihill MR, Fraser CD, et al. Outcome of 121 patients with congenitally corrected transposition of the great arteries. *Pediatr Cardiol* 2002;23:137–145.
79. McGrath LB, Kirklin JW, Blackstone EH, et al. Death and other events after cardiac repair in discordant atrioventricular connection. *J Thorac Cardiovasc Surg* 1985;90:711–728.
80. Yeh T Jr, Connolly MS, Coles JG, et al. Atrioventricular discordance: results of repair in 127 patients. *J Thorac Cardiovasc Surg* 1999;117:1190–1203.
81. Voskuil M, Hazekamp MG, Kroft LJ, et al. Postsurgical course of patients with congenitally corrected transposition of the great arteries. *Am J Cardiol* 1999;83:558–562.
82. Hornung TS, Bernard EJ, Celermajer DS, et al. Right ventricular dysfunction in congenitally corrected transposition of the great arteries. *Am J Cardiol* 1999;84(9):1116–1119, A10.
83. Hornung TS, Bernard EJ, Jaeggi ET, et al. Myocardial perfusion defects and associated systemic ventricular dysfunction in congenitally corrected transposition of the great arteries. *Heart* 1998;80:322–326.
84. Tops LF, Roest AA, Lamb HJ, et al. Intraatrial repair of transposition of the great arteries: use of MR imaging after exercise to evaluate regional systemic right ventricular function. *Radiology* 2005;237:861–867.
85. Norozi K, Buchhorn R, Alpers V, et al. Relation of systemic ventricular function quantified by myocardial performance index (Tei) to cardiopulmonary exercise capacity in adults after Mustard procedure for transposition of the great arteries. *Am J Cardiol* 2005;96:1721–1725.
86. Connolly MS, Liu PP, Williams WG, et al. Congenitally corrected transposition of the great arteries in the adult: functional status and complications. *J Am Coll Cardiol* 1996;27:1238–1243.
87. Sano T, Riesenfeld T, Karl TR, et al. Intermediate-term outcome after intra-cardiac repair of associated cardiac defects in patients with atrioventricular and ventriculoarterial discordance. *Circulation* 1995;92:II272–II278.

88. Prieto LR, Hordof AJ, Secic M, et al. Progressive tricuspid valve disease in patients with congenitally corrected transposition of the great arteries. *Circulation* 1998;98:997-1005.
89. Acar P, Sidi D, Bonnet D, et al. Maintaining tricuspid valve competence in double discordance: a challenge for the paediatric cardiologist. *Heart* 1998;80:479-483.
90. van Son JA, Danielson GK, Huhta JC, et al. Late results of systemic atrioventricular valve replacement in corrected transposition. *J Thorac Cardiovasc Surg* 1995;109:642-652; discussion 652-653.
91. Mongeon FP, Connolly HM, Dearani JA, et al. Congenitally corrected transposition of the great arteries: ventricular function at the time of systemic atrioventricular valve replacement predicts long-term ventricular function. *J Am Coll Cardiol* 2011;57:2008-2017.
92. Poirier NC, Mee RB. Left ventricular reconditioning and anatomical correction for systemic right ventricular dysfunction. *Semin Thorac Cardiovasc Surg Pediatr Card Surg Annu* 2000;3:198-215.
93. Winlaw DS, McGuirk SP, Balmer C, et al. Intention-to-treat analysis of pulmonary artery banding in conditions with a morphological right ventricle in the systemic circulation with a view to anatomic biventricular repair. *Circulation* 2005;111:405-411.
94. Jahangiri M, Redington AN, Elliott MJ, et al. A case for anatomic correction in atrioventricular discordance? Effects of surgery on tricuspid valve function. *J Thorac Cardiovasc Surg* 2001;121:1040-1045.
95. Metton O, Gaudin R, Ou P, et al. Early prophylactic pulmonary artery banding in isolated congenitally corrected transposition of the great arteries. *Eur J Cardiothorac Surg* 2010;38:728-734.
96. Ilbawi MN, DeLeon SY, Backer CL, et al. An alternative approach to the surgical management of physiologically corrected transposition with ventricular septal defect and pulmonary stenosis or atresia. *J Thorac Cardiovasc Surg* 1990;100:410-415.
97. Ilbawi MN, Ocampo CB, Allen BS, et al. Intermediate results of the anatomic repair for congenitally corrected transposition. *Ann Thorac Surg* 2002;73(2):594-599; discussion 599-600.
98. Imai Y. Double-switch operation for congenitally corrected transposition. *Adv Card Surg* 1997;9:65-86.
99. Langley SM, Winlaw DS, Stumper O, et al. Midterm results after restoration of the morphologically left ventricle to the systemic circulation in patients with congenitally corrected transposition of the great arteries. *J Thorac Cardiovasc Surg* 2003;125:1229-1241.
100. Jacobs ML, Buckley MJ, Liberthson RL. Combined Rastelli and atrial switch procedure: a 10-year follow up. *Ann Thorac Surg* 1999;68:570-571.
101. Imamura M, Drummond-Webb JJ, Murphy DJ Jr, et al. Results of the double switch operation in the current era. *Ann Thorac Surg* 2000;70:100-105.
102. Shin'oka T, Kurosawa H, Imai Y, et al. Outcomes of definitive surgical repair for congenitally corrected transposition of the great arteries or double outlet right ventricle with discordant atrioventricular connections: risk analyses in 189 patients. *J Thorac Cardiovasc Surg* 2007;133:1318-1328, 1328 e1311-1314.
103. Sharma R, Talwar S, Marwah A, et al. Anatomic repair for congenitally corrected transposition of the great arteries. *J Thorac Cardiovasc Surg* 2009;137:404-412 e404.
104. Malhotra SP, Reddy VM, Qiu M, et al. The hemi-mustard/bidirectional Glenn atrial switch procedure in the double-switch operation for congenitally corrected transposition of the great arteries: rationale and midterm results. *J Thorac Cardiovasc Surg* 2011;141:162-170.
105. Quinn DW, McGuirk SP, Metha C, et al. The morphologic left ventricle that requires training by means of pulmonary artery banding before the double-switch procedure for congenitally corrected transposition of the great arteries is at risk of late dysfunction. *J Thorac Cardiovasc Surg* 2008;135:1137-1144.
106. Bautista-Hernandez V, Marx GR, Gauvreau K, et al. Determinants of left ventricular dysfunction after anatomic repair of congenitally corrected transposition of the great arteries. *Ann Thorac Surg* 2006;82:2059-2065; discussion 2065-2056.
107. Gaies MG, Watnick CS, Gurney JG, et al. Health-related quality of life in patients with congenitally corrected transposition of the great arteries. *J Thorac Cardiovasc Surg* 2011;142:136-141.

Double Outlet Right Ventricle

Gail E. Wright ■ Katsuhide Maeda ■ Norman H. Silverman
Frank L. Hanley ■ Stephen J. Roth

DEFINITION

Double outlet right ventricle (DORV) is a type of ventriculoarterial connection in which both great arteries arise 50% or more from the right ventricle (RV). This chapter focuses on DORV with concordant atrioventricular (AV) connection with two ventricles. DORV may occur in univentricular hearts, particularly in the constellation of heterotaxy syndrome, and with AV discordance.

Although there were reports of hearts with DORV anatomy as early as 1893, the term double outlet right ventricle came into use in 1957 at the time of the first surgical repair of a patient with this lesion at the Mayo Clinic (1,2). Prior descriptions, including the original report in 1949 of what is now known as Taussig-Bing heart, included DORV variants as a form of partial transposition of the great arteries (3–5). There has been much debate about this terminology. For the purposes of this chapter, DORV is considered within the spectrum of conotruncal defects, with some forms exhibiting transposition physiology in which the pulmonary arterial oxygen saturation is higher than the aortic oxygen saturation. However, DORV and transposition are considered distinct anatomically, because discordant ventriculoarterial connections are core to the anatomic definition of transposition. In 1961, Neufeld et al. (6–8) developed a classification of DORV with and without pulmonic stenosis (PS). Subsequently in 1972, Lev et al. (9) categorized many types of DORV. Shortly thereafter, Sridaromont et al. (10,11) reported on hemodynamic and angiocardiographic correlations of anatomic variants. DORV nomenclature was reviewed more recently in the Congenital Heart Surgery Nomenclature and Database Project (12,13).

INCIDENCE

DORV accounts for fewer than 1% of all congenital heart defects. Its incidence is approximately 0.06 cases per 1,000 live births (14). There is no known racial or gender predilection, and no associated genetic defect has been identified.

MORPHOLOGY

DORV falls within the morphologic spectrum of conotruncal defects. As with much of congenital heart disease, the physiology

and treatment of these defects derive from the embryology and morphology.

With the exception of truncus arteriosus, which occurs due to failure of septation, other conotruncal defects are essentially rotational defects. The development of the conal septum drives that rotation. The variability among the individual lesions is best understood in terms of the spectrum of development of the conal septum, which determines the relative position of the two semilunar valves to the ventricles. The more conal muscle present beneath a semilunar valve, the more that valve is pushed superiorly and anteriorly, and the more likely it is that the associated great artery will align with the RV (15,16).

In the normal heart, the pulmonary valve sits up on the conus, a circular tube of muscle, and is positioned anteriorly and superiorly (17). In contrast, the aortic, mitral, and tricuspid valves are all attached to the central fibrous body of the heart. The conal muscle beneath the aortic valve largely resorbs, leaving the aorta positioned inferiorly and posteriorly (Fig. 51.1).

In conotruncal defects, there is a spectrum between hearts in which no conus exists beneath the aorta, as seen in tetralogy of Fallot, and hearts in which no conus exists under the pulmonary valve, as with transposition of the great arteries (Fig. 51.1). At each end of this spectrum, it is “all or nothing” in terms of the conus. DORV falls in the middle of the spectrum, with forms that have variable amounts of conus under each semilunar valve scattered across the continuum (18).

One common form of DORV is anatomically and physiologically similar to tetralogy of Fallot (19). There is a nearly normal length of conus beneath the pulmonary valve and minimal conus beneath the aortic valve. Consequently, there is no aorto-mitral continuity, and the pulmonary valve is anterior and superior. At the other end of the spectrum, another DORV variant has conus mostly under the aortic valve but has a small amount of conus under the pulmonary valve, resulting in the loss of pulmonary-mitral continuity. This form is morphologically and physiologically similar to transposition of the great arteries. In the middle is a type that has equal bilateral conus, such that the great arteries are side by side, with neither vessel tucked in posteriorly. Between the “tetralogy type” and the “transposition type,” there are many “shades of gray”—that is, DORV variants that have neither aorto-mitral nor pulmonary-mitral continuity and have variable distribution of conal septum (Fig. 51.1). These variations are more ambiguous both anatomically and physiologically and should be approached with an individualized management plan.

Common nomenclature for the types of DORV—for example, DORV with subaortic ventricular septal defect (VSD), DORV

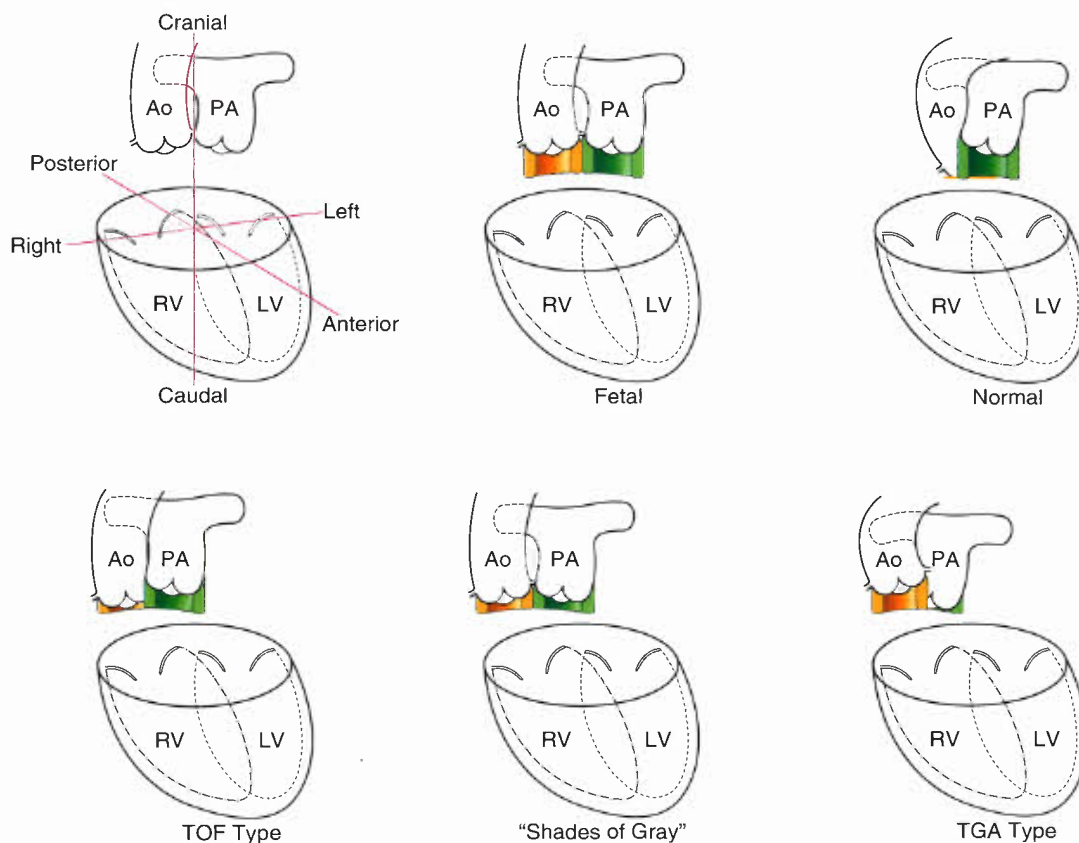


Figure 51.1. Development of the conal septum in the fetus, in the normal heart, and in different types of DORV. In the fetus, there is a circular tube of muscle, the conus, beneath each great artery. The distribution of conal muscle is equal beneath the aorta and the pulmonary artery.

In the normal heart, the pulmonary valve sits up on the conus, and is positioned anteriorly and superiorly. The conal muscle beneath the aortic valve largely resorbs, leaving the aorta positioned inferiorly and posteriorly.

In DORV variants, the spectrum of distribution of conal muscle beneath each great artery determines the relative position of the two semilunar valves to the ventricles. The more conal muscle present beneath a semilunar valve, the more that valve is pushed superiorly and anteriorly.

“Tetralogy type”: One end of the spectrum—nearly normal length of conus beneath the pulmonary valve and minimal conus beneath the aortic valve. Pulmonary valve is anterior and superior. No aorto-mitral continuity.

“Shades of gray”: Between the “tetralogy type” and the “transposition type,” there are many “shades of gray”—variants with bilateral conus that have neither aorto-mitral nor pulmonary-mitral continuity and have variable distribution of conal septum. Neither of the great vessels is tucked in posteriorly.

“Transposition type”: At the other end of the spectrum—large amount of conus under the aortic valve with relatively little under the pulmonary valve. Aorta is pushed anteriorly and superiorly, resulting in rightward positioning of the aorta relative to the pulmonary artery. No pulmonary-mitral continuity.

NOTE: Although 2-D diagrams and images demonstrate the conus as a “tear drop,” it is important to note that in three dimensions, it is a circular tube of muscle.

Yellow, subaortic conus; Green, subpulmonary conus; Ao, aorta; PA, pulmonary artery; RV, right ventricle; LV, left ventricle; TGA, transposition of the great arteries; TOF, tetralogy of Fallot.

with subpulmonic VSD, and DORV with doubly-committed VSD—gives the impression that VSD position creates the difference, and that the relationship of the great arteries does not change (9,11). In fact, however, across the spectrum of DORV, it is the rotation of the great arteries, driven by conal development, that changes, not the position of the VSD. The VSD is constant; it is almost always a typical conoventricular VSD located in the perimembranous area and extending into the trabecular ventricular septum, with the upper part of the defect bordered by the lower edge of the conus. Emphasis on the influence of infundibular development unifies the conceptual approach to the spectrum of defects that constitute DORV. Due to the degree of morphologic variability, the description of an individual patient's heart with DORV must

include the associated relationship of the great vessels and the VSD to be most meaningful.

PS is by far the most common lesion associated with DORV. It occurs in approximately 50% of patients and may be valvar or subvalvar. Secundum atrial septal defects are seen in 25% of all types, whereas primum defects are seen in the 8% of DORV patients with AV canal defects. Multiple other associated lesions have been reported at low rates: patent ductus arteriosus, right aortic arch, subaortic stenosis, additional muscular VSDs, left superior vena cava (SVC) to the coronary sinus or left atrium, intact ventricular septum, and mitral valve anomalies including mitral atresia (9,10,20–22). Coronary artery anomalies occur in about 10% of patients—the most common being the anomalous

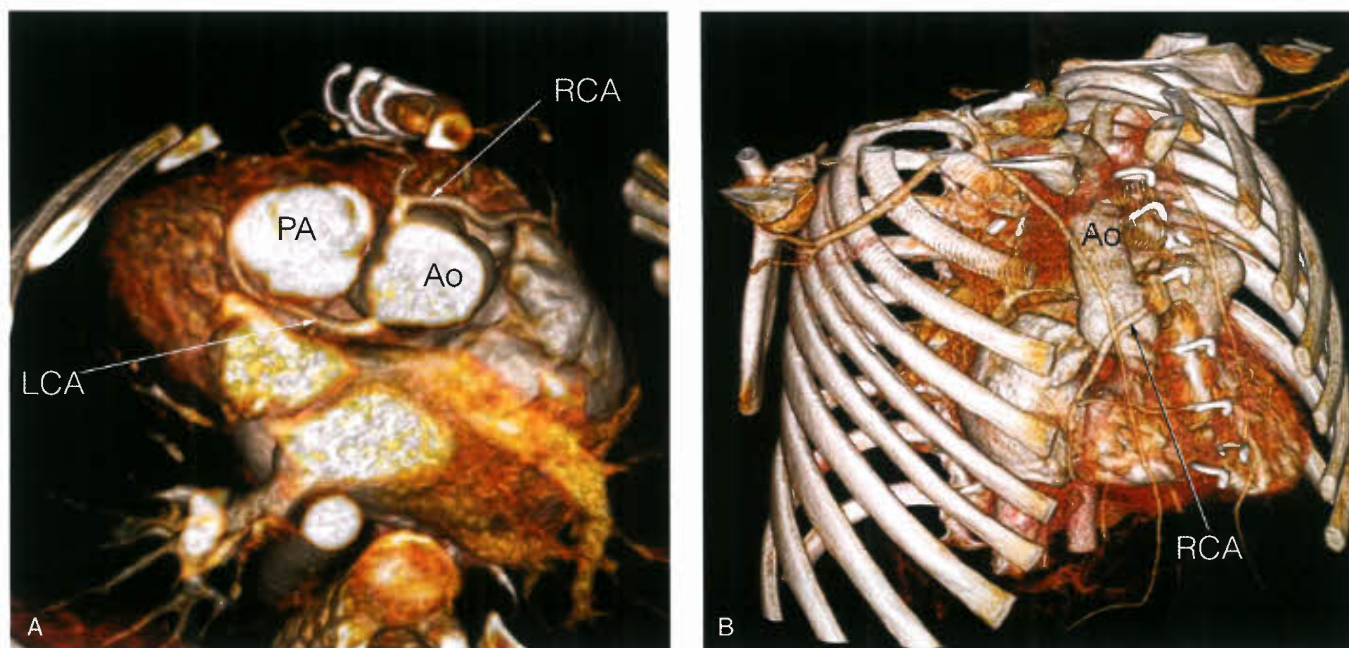


Figure 51.2. Coronary artery anomalies are of particular importance, because they may alter considerations for surgical repair due to their effect on feasibility of conduit placement or coronary transfer. CT angiograms demonstrate anomalous coronary origins and the relationship of the coronaries to the sternum well. **A:** CT angiogram, 3-D reconstruction: The right coronary artery (RCA) arises anteriorly and passes just under the sternum. LCA, left coronary artery; PA, pulmonary artery; Ao, aorta. **B:** CT angiogram, 3-D reconstruction: In a different patient, the RCA arises anomalously and crosses anterior to the aorta. Ao, aorta; RCA, right coronary artery.

origin of the anterior descending coronary artery from the right coronary artery. However, coronary artery anomalies are of particular importance, because they may alter considerations for surgical repair due to their effect on feasibility of conduit placement or coronary transfer (23) (Fig. 51.2). Likewise, associated aortic arch coarctation, hypoplasia, or interruption—also found in about 10% of patients—significantly increases the complexity of surgical repair when present (24,25).

CLINICAL FEATURES—COMMON VARIANTS

The clinical features and pathophysiology of DORV are determined by the morphologic variant (22). Even within the same subtype, there can be substantial variability in the clinical presentation. Historically, cardiac catheterization with angiography and hemodynamic assessment were used routinely for diagnostic evaluation. Currently, however, transthoracic echocardiography can identify all of the essential anatomic features in most cases, and the echocardiogram along with bedside pulse oximetry provides definitive diagnosis of the pathophysiology noninvasively (26). For patients with complex aortic arch anatomy, angiography may also be needed (27,28). Magnetic resonance imaging (MRI) is helpful to further define the relationship between the VSD and the semilunar valves in cases in which it is not clear which way to baffle the VSD during reparative surgery (29–32). In a minority of patients, for example those for whom the technical feasibility of a two-ventricle repair is debatable, cardiac catheterization is used to define pulmonary vascular resistance to determine suitability for a Fontan operation. Hemodynamic assessment via cardiac catheterization may also be necessary for another small subset of patients in whom the effects of streaming are variable and less apparent (10).

“TETRALOGY TYPE”

The most common variant is the “tetralogy of Fallot type,” with most of the conus under the pulmonary valve and minimal conal septum under the aorta (Fig. 51.1). This variant, also known as “DORV with subaortic VSD with PS,” is seen in approximately 40% of cases (9,11). The pulmonary valve is positioned anteriorly and superiorly, and the aorta overrides the interventricular septum. Blood from the left ventricle (LV) passes through the VSD to the aorta. The cardiovascular pathophysiology is determined predominantly by the degree of PS, which generally increases over time in early infancy. Typically there is progressive, dynamic obstruction to pulmonary blood flow at the subvalvar level, leading to oxygen saturations between 80% and 90% at baseline, with further desaturation during agitation. There is the potential for hypercyanotic spells as in tetralogy of Fallot. The cardiovascular exam is notable for a long, harsh systolic ejection murmur, loudest at the left upper sternal border and caused by the subvalvar PS. Since the VSD is not pressure restrictive, there is no additional VSD murmur. Infants with this anatomy may present as cyanotic neonates if there is severe PS, but more often the lesion is detected due to an evaluation performed because of a murmur. Cyanosis may not be present for several weeks, but after that time, it gradually worsens. The chest radiograph demonstrates normal to mildly diminished pulmonary vascular markings. The electrocardiogram is notable for right axis deviation and a right ventricular hypertrophy pattern, with rR', qR, or rsR' pattern; these findings are not, however, sufficiently specific to be diagnostic. Echocardiography can clearly define the essential anatomic features (Fig. 51.3A,B). In the parasternal long axis view, the absence of mitral–aortic continuity is shown as well as the presence of a large VSD. Subcostal views highlight the narrow subpulmonic tunnel. The apical four-chamber view demonstrates the

degree of aortic override over the crest of the interventricular septum along with two dimensions of the pathway for closure of the VSD to the aorta. Attention must be given to the chordal attachments of each AV valve and their relationships to the VSD. The diagnosis may be made with fetal echocardiography; accurate assessment of the relationships of the great vessels and the VSD are possible prenatally with enough precision to guide surgical planning in most cases with tetralogy features (33–35).

Surgery is indicated to relieve the obstruction to pulmonary blood flow and to septate the circulations. For this type of DORV, surgical outcomes are excellent in both neonates and older infants. Surgical repair as a neonate is indicated when there is severe limitation to pulmonary blood flow. In most patients, however, surgery is performed electively between 2 and 4 months of age before the infant becomes excessively cyanotic or develops hypercyanotic spells.

“TRANSPOSITION TYPE”

The second most common variant is the “transposition type” of DORV, with a large amount of conal tissue beneath the aorta and relatively little beneath the pulmonary artery (Fig. 51.1). Other designations for this variant, noted in approximately 20% of cases, include “Taussig-Bing anomaly” or “DORV with subpulmonic VSD” (9,11,36–38). In this type, the aorta is pushed anteriorly and superiorly, resulting in rightward positioning of the aorta relative to the pulmonary artery. There is no pulmonary–mitral continuity. The pathophysiology is determined by streaming of blood such that most of the highly oxygenated blood from the LV passes through the VSD into the pulmonary artery, whereas most of the deoxygenated blood from the RV flows directly into the aorta. Thus, there is transposition physiology with a pulmonary arterial oxygen saturation that is higher than the aortic oxygen saturation.

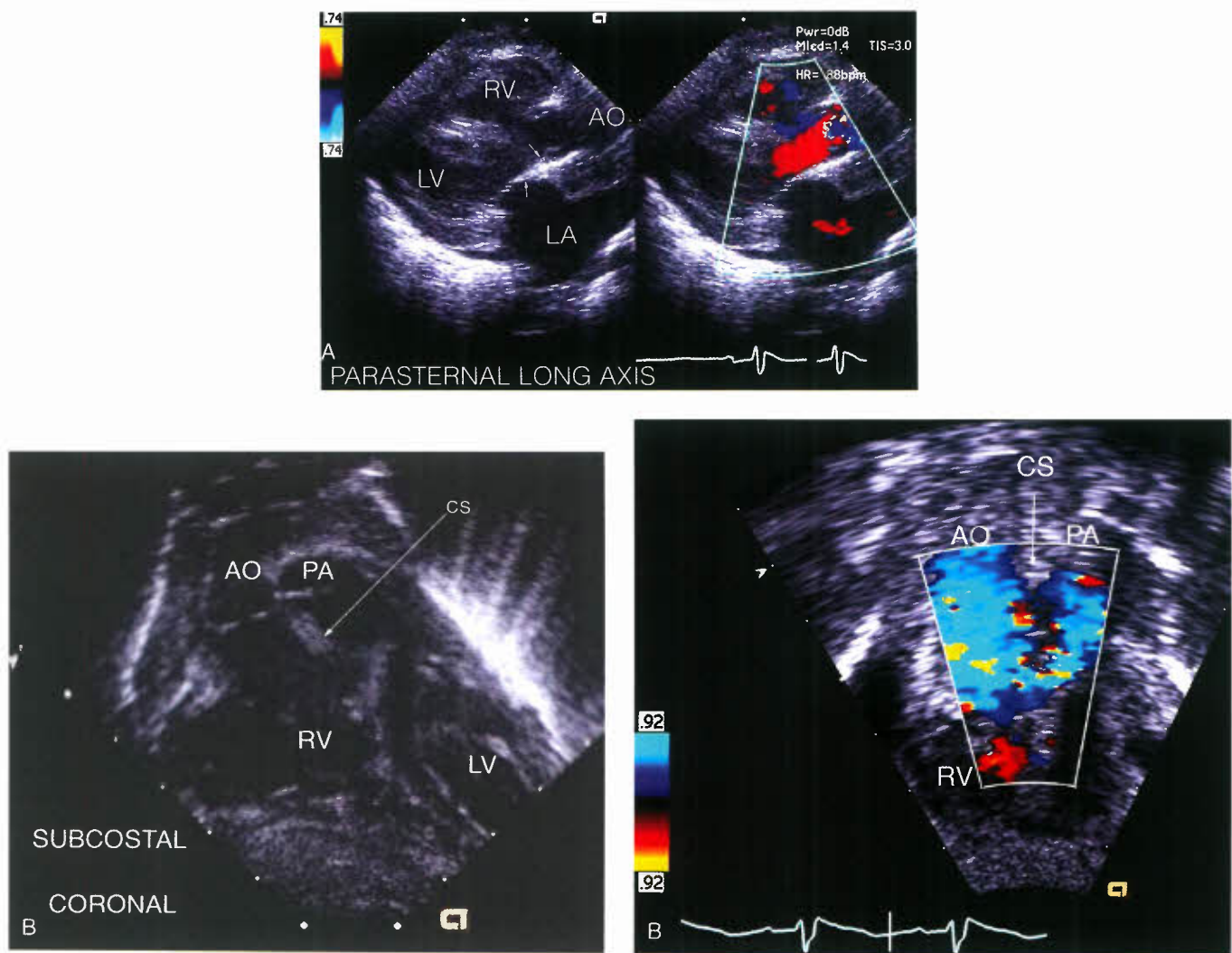


Figure 51.3. Echocardiographic views, CT angiogram image, and pathologic specimen of anatomy in “Tetralogy type.” **A:** Echocardiogram, parasternal long axis view: (**Left panel**) Note lack of mitral–aortic continuity due to conal septum beneath the aortic valve (*arrows* mark the conal septum). (**Right panel**, same image with addition of color flow mapping) There is no flow disturbance through the ventricular septal defect, which is large and not pressure-restrictive. RV, right ventricle; LV, left ventricle; LA, left atrium; AO, aorta. **B:** Echocardiogram, subcostal coronal view: (**Left panel**) This image demonstrates both great arteries arising from the RV, with conal septum separating the aorta and the pulmonary artery. (**Right panel**, same image with addition of color-flow mapping) Color-flow mapping demonstrates mild obstruction in the subvalvar area beneath the pulmonary valve due to conal muscle. RV, right ventricle; LV, left ventricle; PA, pulmonary artery; AO, aorta; CS, conal septum.

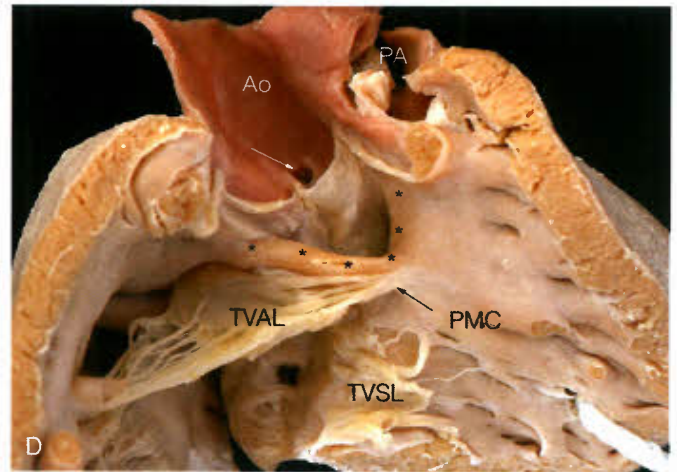
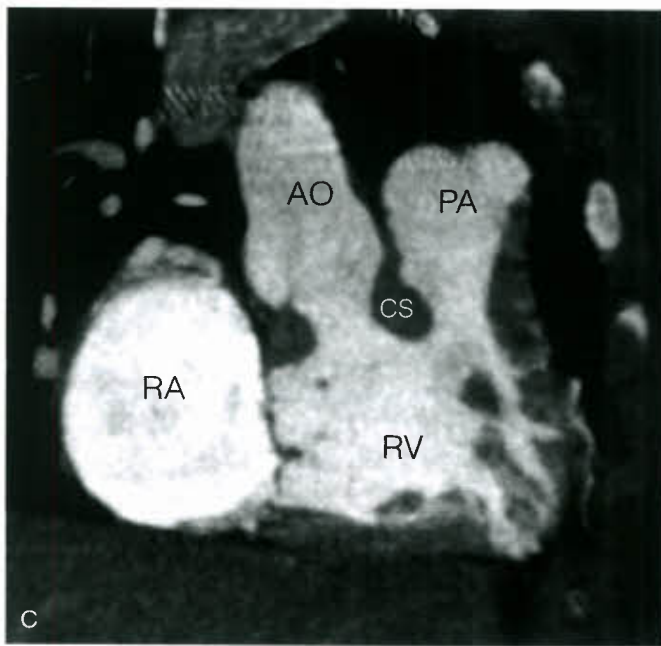


Figure 51.3. (Continued) C: Computed tomography angiogram, oblique image: Similar to the echo subcostal view in 3B, CT angiography demonstrates both great arteries arising from the RV, with conal septum separating the aorta and the pulmonary artery. RA, right atrium; AO, aorta; PA, pulmonary artery; CS, conal septum; RV, right ventricle. (Courtesy of Frandics Chan, M.D., Ph.D., Stanford University) D: Pathologic specimen: The VSD is bounded by the underside of the aortic valve and cradled in the arms of the septomarginal trabeculations. The pulmonary artery is walled off by infundibular muscle. **, = borders of the VSD, white arrow = coronary artery orifice, black arrow = PMC, papillary muscle of the conus, Ao, aorta; PA, pulmonary artery; TVAL, tricuspid valve anterior leaflet; TVSL, tricuspid valve septal leaflet. (Courtesy of Diane Spicer, B.S., University of Florida.)

These patients present as cyanotic neonates, with the degree of arterial hypoxemia determined by the degree of streaming and the presence and size of the interatrial connection and ductus arteriosus. The chest radiograph demonstrates a normal-sized cardiac silhouette and mildly increased pulmonary vascular markings. Echocardiography usually provides comprehensive anatomic definition with this type as well (Fig. 51.4). In particular, subcostal views can demonstrate the precise relationship of the great vessels and the length and extent of the subaortic conus. When there is significant subaortic narrowing, there is associated aortic arch hypoplasia, which must be imaged from the suprasternal notch views. There must be a high index of suspicion for arch hypoplasia or interruption in neonates with severe subaortic narrowing (Fig. 51.5). Angiography, either via computed tomography or via cardiac catheterization, may be required when the arch anatomy cannot be fully visualized by echocardiography, especially in the face of a patent ductus arteriosus (Fig. 51.6).

Surgery is indicated to improve systemic oxygenation and is performed in the neonatal period. Surgical repair also establishes continuity between the LV and the aorta. When there is severe hypoxemia with a small interatrial communication, balloon atrial septostomy improves atrial mixing sufficiently to allow for non-emergent surgical repair in the first weeks of life, as is often true for newborns with d-transposition of the great arteries and intact ventricular septum.

"VSD TYPE"

The third common variant is the "VSD type" of DORV, which is also known as "DORV with subaortic VSD without PS." This variant is seen in approximately 15% of patients (9,11). In this type, there is slightly more conal tissue beneath the pulmonary

valve than the aortic valve such that the pulmonary valve is still anterior, but sufficient conus is beneath the aorta so that the aorta is rotated rightward (Fig. 51.1). Because there is bilateral conus, there is loss of mitral-aortic continuity; however, the subaortic conus is not as large as in the "transposition type," and the subpulmonary conus is not as large as in the "tetralogy type." The pathophysiology is that of a large VSD with significant left-to-right shunting and pulmonary overcirculation. As for the other two common variants, echocardiography can typically define the essential features of the intracardiac anatomy. Infants typically present with signs of congestive heart failure as the pulmonary vascular resistance falls between 4 and 8 weeks of age. Failure to thrive gradually ensues, as is seen in other lesions with excessive pulmonary blood flow.

Surgery is indicated to eliminate the left-to-right shunt with associated high pulmonary blood flow and volume load on the left heart. The timing of surgery is elective. However, surgical outcomes for this variant are excellent in early infancy, and medical management with diuretics and nutritional supplementation is only temporizing, so there is no benefit in deferring surgery once symptoms of pulmonary overcirculation arise.

CLINICAL FEATURES OF LESS COMMON VARIANTS

DORV encompasses a broad range of variation in the spectrum of conotruncal development. In all forms there is bilateral conus, but the distribution of the amount of conus beneath each semilunar valve is different (Fig. 51.1). Consequently, there are many "shades of gray" subtypes. In these, the distribution of conal tissue is closer to 50:50 beneath each semilunar valve.

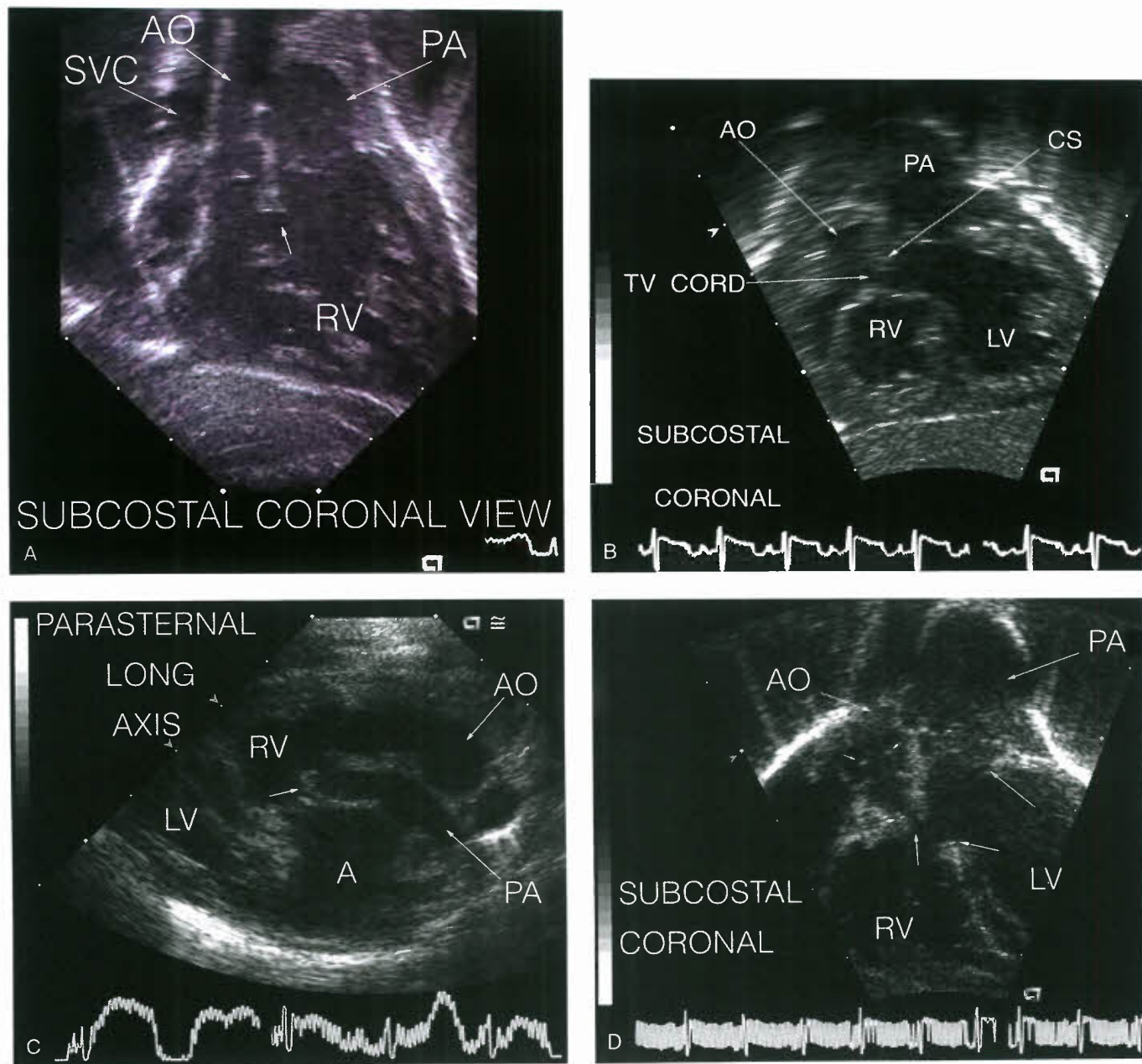


Figure 51.4. Echocardiographic views of anatomy in “transposition type.” **A:** Subcostal coronal view: Aorta and pulmonary artery both arise from the RV and are side-by-side in the same plane with the aorta rightward. Relatively large subaortic conus (*small arrow*) separates the aorta and pulmonary artery. Aortic valve and ascending aorta are hypoplastic. SVC, superior vena cava; AO, aorta; PA, pulmonary artery; RV, right ventricle. **B:** Subcostal coronal view: Aorta and pulmonary artery both arise from the RV with the aorta rightward and slightly anterior. Large subaortic conus separates the aorta and pulmonary artery with narrowing of the egress from the LV due to the conal septum and tricuspid valve cordal attachments. RV, right ventricle; LV, left ventricle; PA, pulmonary artery; AO, aorta; CS, conal septum; TV cord, tricuspid valve cordal attachment. **C:** Parasternal long axis view: Aorta and pulmonary artery both arise from the RV with the aorta rightward and anterior. There is tissue beneath the pulmonary valve (*small arrow*); due to this subvalvar obstruction, the pulmonary artery is relatively small compared to the aorta. RV, right ventricle; LV, left ventricle; AO, aorta; PA, Pulmonary artery; A, atrium. **D:** Subcostal coronal view: Aorta and pulmonary artery both arise from the RV, side-by-side, in the same plane with the aorta rightward. Aortic valve leaflet tips marked with small arrows. Note subaortic obstruction due to large subaortic conus (*vertical arrow*). Due to the subaortic obstruction, the aortic valve and ascending aorta are relatively hypoplastic. VSD demarcated by arrows at the crest of the interventricular septum and at the small rim of conal septum beneath the pulmonary valve. RV, right ventricle; LV, left ventricle; AO, aortic valve; PA, pulmonary artery.

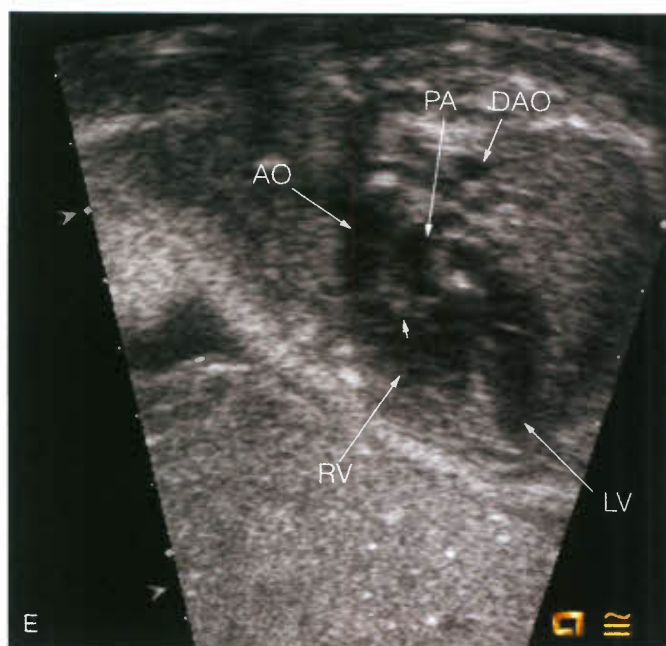


Figure 51.4. (Continued) E: Fetal echocardiogram in Taussig-Bing heart: Aorta and pulmonary artery both arise from RV, side-by-side with the aorta rightward. Small arrow marks conal septum. RV, right ventricle; LV, left ventricle; AO, aorta; PA, pulmonary artery; DAO, descending aorta.

In these variants, because the anatomy is more ambiguous, the diagnostic evaluation should be as comprehensive as possible, and serial assessments over time using complementary imaging modalities may be needed to plan the optimal approach and timing of surgical repair. Often even with a comprehensive preoperative diagnostic evaluation, the ultimate decision making will depend on intraoperative inspection of the anatomy and potential approaches to VSD closure by the surgeon.

Discussion of all of the possible morphologic combinations of DORV is invigorating to the experienced cardiologist and surgeon because of the uniqueness of each patient; however, it may be cumbersome for those gaining mastery of the lesion. One of the less common variants, DORV with noncommitted VSD, warrants specific attention because it presents difficult management decisions, and as such constitutes a high-risk subgroup. Additionally, patients with this variant, who in the past either were marginally palliated in infancy or were deemed inoperable, are now resurfacing as adolescents and young adults for consideration for technically challenging operations.

DORV WITH “NONCOMMITTED VSD”

DORV with a “noncommitted VSD” occurs in slightly <10% of cases (9,11). In this subtype, there is a significant amount of conus beneath each great vessel such that neither vessel is truly posterior, and the interventricular connection is not directly related to either great vessel. Since both great arteries are rotated somewhat superiorly, the typically positioned VSD opens primarily into the body of the RV. Alternatively, there may be a muscular VSD connecting to the inlet or apical part of the RV. The pathophysiology of these variants is complete admixture. There may be little or no obstruction to flow to the pulmonary or systemic circulations, or there may be some degree of subvalvar and valvar pulmonic stenosis resulting

either in balanced circulations or inadequate pulmonary blood flow. Complete repair in early infancy is seldom technically feasible. No operation may be necessary early in life, but if PS causing hypoxemia is present, a palliative aortopulmonary shunt may be required to increase the systemic oxygen level.

As with other forms of DORV, echocardiography is used to define the relationships of the great vessels, the relative position of the VSD to the great vessels, the anatomy of the subvalvar regions and the semilunar valves, and the adequacy of both ventricles (Fig. 51.7). Particular attention must be paid to the attachments of the AV valves, especially the tricuspid valve leaflets, which may be interposed between the VSD and the great arteries in a way that may impact VSD closure. Echocardiography, angiography, and MRI are complementary in defining a potential surgical pathway for VSD closure. MRI in particular allows for 3-D imaging of the potential pathway from LV to aorta and also may provide superior imaging in older patients whose body habitus precludes excellent transthoracic echocardiographic imaging. Cardiac catheterization provides definition of the size and shape of the VSD and its relationship to the great vessels, and it allows assessment of the pulmonary vascular resistance. Catheterization is advisable when it remains debatable whether the VSD can be closed to direct flow to either great vessel; for these patients, a Fontan operation is typically the fallback option intraoperatively.

Because these repairs are technically complex, and because the VSD patch may encroach upon the RV cavity, repair of this subtype is generally deferred until the patient is at least several years of age. Young adult patients presenting for evaluation without detailed information about their prior care warrant special attention. Because serial data or multiple prior echocardiograms for comparison of the anatomy are often not available, obtaining multiple complementary imaging studies is critical. Although intraoperative inspection of the anatomy is always necessary, obtaining comprehensive anatomic detail preoperatively minimizes the additional time on cardiopulmonary bypass required to determine the optimal operation. This is an important consideration since the bypass times for these patients are typically prolonged due to the technical complexity.

OTHER LESS COMMON VARIANTS

DORV with “doubly committed VSD” occurs in approximately 10% of cases (9,11). In this variant, only fibrous as opposed to muscular conal septum separates the leaflets of the pulmonary and aortic valves (Fig. 51.8). Both great vessels override the crest of the ventricular septum. The VSD is in the typical position, cradled between the limbs of the septomarginal trabeculation. The pathophysiology is predominantly left-to-right shunting with pulmonary overcirculation. Surgical VSD closure directs flow from the LV to the posterior and rightward aorta.

DORV occurs with mitral atresia and with AV canal defects in the constellation of heterotaxy syndrome. DORV is also noted with AV discordance.

HISTORY OF SURGICAL REPAIR OF DOUBLE OUTLET RIGHT VENTRICLE

The first successful correction of DORV was performed by Kirklin and associates in 1957 and subsequently by Barratt-Boyes and associates in 1958 (39, 40). Although these first repairs were for “VSD type” DORV, since that time, a large number of surgical reports have appeared including “tetralogy

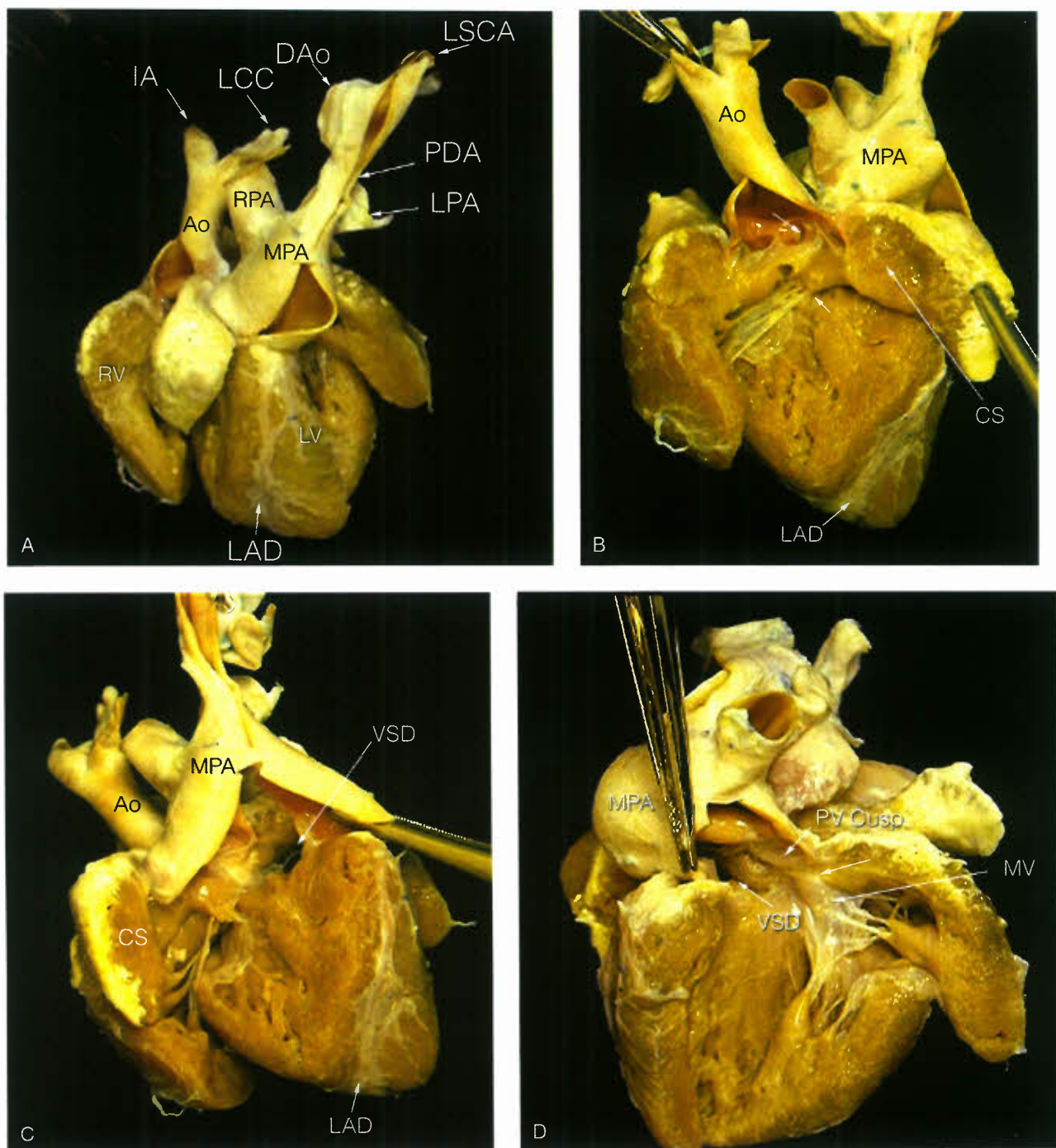


Figure 51.5. Series of views of a pathologic specimen demonstrating Taussig-Bing anomaly with interrupted aortic arch. These images are all from the same specimen, which has been opened from different perspectives in each view to demonstrate different anatomic elements optimally. **A:** The specimen was dissected into the RV. The delimiting coronary artery, the LAD, is shown. Both the aorta and the pulmonary artery arise from the RV. The aorta is smaller and rightward. The innominate artery and left common carotid arise from the ascending aorta. The ductus arteriosus arises from the pulmonary artery. The ductus arteriosus supplies the descending aorta and the left subclavian artery. RV, right ventricle; LV, left ventricle; LAD, left anterior descending coronary artery; MPA, main pulmonary artery; LPA, left pulmonary artery; RPA, right pulmonary artery; Ao, aorta; PDA, patent ductus arteriosus; IA, innominate artery; LCC, left common carotid artery; DAo, descending aorta; LSCA, left subclavian artery. **B:** In this view of the same specimen, the large circular tube of conal septum (CS) has been cut through to show the aorta, the coronary artery (*small arrow*), and the papillary muscle of the conus (*small arrow*). Ao, aorta; MPA, main pulmonary artery; LAD, left anterior descending coronary artery. **C:** The conal septum has been moved toward the RV. In this view, note the VSD just inferior to the pulmonary artery. The papillary muscle of the conus can be seen attached to the malaligned conal septum. LAD, left anterior descending coronary artery; MPA, main pulmonary artery; Ao, aorta; CS, conal septum; VSD, ventricular septal defect. **D:** Left ventricular view demonstrates that the only egress from the left ventricle is through the VSD, which is immediately inferior to the pulmonary artery. Note proximity of the VSD to the cusps of the pulmonary valve (*small arrows*) as well as the fibrous continuity between the anterior leaflet of the mitral valve and the pulmonary valve cusps. MPA, main pulmonary artery; VSD, ventricular septal defect; MV, mitral valve; PV Cusp, cusp of pulmonary valve.

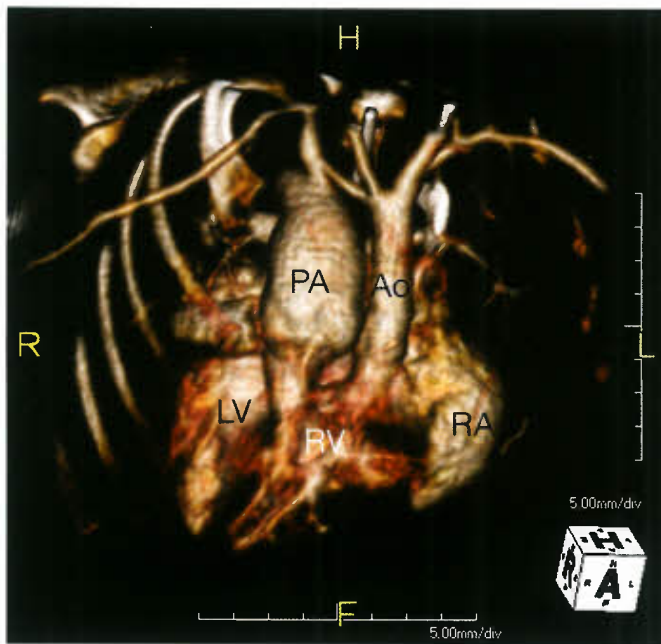


Figure 51.6. For patients with complex aortic arch anatomy, angiography may further define associated aortic arch coarctation, hypoplasia, or interruption. CT angiogram: Hypoplastic ascending aorta nearly side by side and leftward of the pulmonary artery with associated aortic arch hypoplasia. PA, Pulmonary artery; Ao, Aorta; LV, Left ventricle; RV, Right ventricle; RA, right atrium; H, Head; R, Right; F, Front; L, Left

type,” “transposition type,” and “noncommitted type” by multiple surgical teams (41–45). Because of the complexity of the lesion and associated anomalies, various surgical procedures have been described over time. Due to the variety of procedures described, surgical planning must be applied to individual patients based on their specific cardiac anatomy.

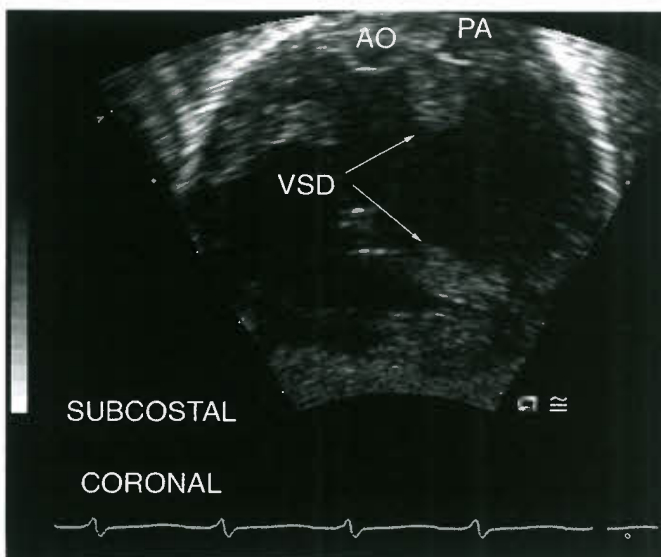


Figure 51.7. Echocardiogram of DORV with noncommitted VSD. Subcostal coronal view demonstrates the VSD (arrows mark the crest of the interventricular septum and the tip of the conal septum), which is remote from both great arteries due to bilateral conus. VSD, ventricular septal defect; AO, aorta; PA, pulmonary artery.

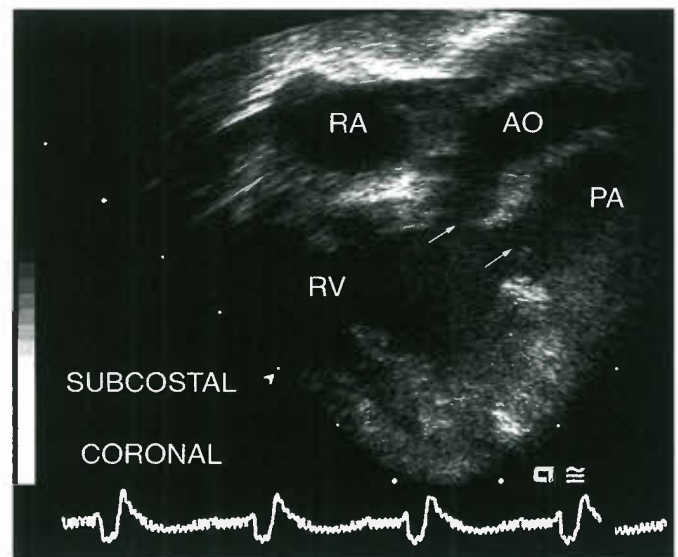


Figure 51.8. Echocardiogram of DORV with doubly committed VSD. Subcostal coronal view demonstrates VSD in continuity with both great arteries (arrows demonstrate egress to both aorta and pulmonary artery). RV, right ventricle; AO, aorta; PA, pulmonary artery; RA, right atrium.

ESSENTIAL DETERMINANTS OF SURGICAL CORRECTION AND TIMING OF THE OPERATION

It is not an exaggeration to state that surgical decision making for DORV is the most complicated in congenital heart surgery. Surgical decisions depend not only on specific anatomic features, but also on the patient’s age, body size, and clinical condition and the surgeon’s skill. Because each patient may be sufficiently unique to require an individual approach, repeated imaging with transthoracic or transesophageal echocardiography, angiography, computed tomography, or MRI may be required to obtain a precise anatomic roadmap. The relatively poor outcomes in the early years of surgery for DORV were due in part to the lack of precise anatomic definition and recognition of associated lesions.

Several anatomic features must be identified and defined well to allow for optimal surgical decision making (Table 51.1). The exact position, size, and number of VSDs are crucial to decide the type of repair. In addition, the relationship of the

TABLE 51.1

Essential Anatomic Determinants of Method of Surgical Repair of DORV

The position, size, and number of VSD(s) and its relationship to the conduction system
The distance between the tricuspid valve and the pulmonary valve
Straddling or overriding of the AV valve
Relationship of the great arteries
Presence of pulmonary (right ventricular outflow tract) stenosis
Presence of aortic (left ventricular outflow tract) stenosis
Coronary artery anatomy

TABLE 51.2 Usual Timing of Surgery for DORV

"VSD type": one-stage complete repair as a neonate or young infant because of pulmonary overcirculation
"Transposition type": one-stage complete repair as a neonate before the LV becomes unprepared
"Tetralogy type": one-stage repair within a few months of birth, or two stages with an initial palliative shunt followed by complete repair ≥ 6 mo of age
"Noncommitted type": complete biventricular repair is usually deferred beyond 6 mo of age because of the complexity of the baffle. Initial palliation with either an aortopulmonary shunt or pulmonary artery band may be needed.

conduction system to the VSD is important, because some VSDs must be enlarged to create a sufficient pathway for intracardiac baffling. The distance between the tricuspid valve and the pulmonary valve should be large enough to employ a LV-to-aorta baffle repair. If papillary muscle tissue is located in the pathway from the LV to aorta, relocation of the papillary muscle or valve replacement may need to be considered. An example of this situation would be straddling or severe overriding of the AV valve (46). If an adequate pathway cannot be achieved, a Fontan operation is required. In the current era, coronary artery anomalies are less challenging technically. However, the exact course of the coronary arteries is relevant to plan for coronary transfer and/or right ventriculotomy, if required.

The timing of the surgical intervention depends on the type of DORV and the specifics of the procedure (Table 51.2). In general, patients with "VSD type" DORV develop clinical signs of pulmonary overcirculation as young infants from an unrestricted VSD and usually require intracardiac repair. Patients with "transposition type" DORV develop progressive cyanosis and should undergo surgical repair as neonates while the LV remains prepared for systemic afterload. Patients with "tetralogy type" DORV show signs of cyanosis and require surgery in the first several months of life. However, because of the complexity of the intracardiac baffle and right ventricular outflow reconstruction, some surgeons opt for initial palliation with a systemic-to-pulmonary artery shunt and defer corrective surgery beyond 6 months of age. Patients with "noncommitted type" DORV often require complex intracardiac baffling. Because of the complexity of intracardiac repair, many surgeons prefer to defer corrective surgery and initially palliate those infants and young children who become symptomatic in the first 1 to 2 years of life. Lastly, for those whose anatomy precludes complex repair and a Fontan operation is the final palliation, an aortopulmonary shunt or pulmonary artery band is often selected as the initial technique to control pulmonary blood flow.

TYPES OF SURGERY AND SURGICAL STRATEGY

Historically, beginning with simple VSD closure in "VSD type" DORV, various surgeries have been proposed for the multiple forms of DORV (Table 51.3). These range from simple VSD closure to arterial switch to the highly complicated types of surgery such as aortic translocation (47). Some techniques are no longer employed because of poor outcomes, and others are not preferred because of the complexity of the procedure. In order to appreciate the strategic approach to surgical

TABLE 51.3 Possible Surgical Procedures for DORV

Palliation (banding or systemic-to-pulmonary shunt)
LV-to-aorta baffle closure (intracardiac rerouting)
Simple VSD closure (subaortic VSD type)
Patrick-McGoon
Kawashima (for original Taussig-Bing anomaly)
Intraventricular repair with RVOT reconstruction
Rastelli
REV (Lecompte)
Switch operation
Arterial switch operation (Jatene)
Atrial switch operation (Senning, Mustard)
Switch with RVOT reconstruction
Switch + Rastelli (or REV)
Aortic translocation (Nikaidoh, double root, truncal switch)
Single ventricle approach
Bidirectional Glenn shunt
Fontan operation
Biventricular repair with DKS
Yasui procedure

VSD, ventricular septal defect; RVOT, right ventricular outflow tract; DKS, Damus-Kaye-Stansel.

management of DORV, the following principles should be applied: (a) biventricular repair is performed if it is feasible, and (b) an adequate left ventricular outflow tract must be created, even if it compromises the right ventricular outflow (the right ventricular outflow tract can be reconstructed by infundibulectomy, valvotomy, gusset or conduit). The primary reason multiple surgical approaches have been proposed is that the left ventricular outflow tract must be created without obstruction in multiple anatomic variants. In addition, many variations have been proposed for surgical right ventricular outflow tract reconstruction.

In thinking of the surgical strategy for DORV, it is important to understand the patient's cardiovascular physiology. The surgical correction should also be a physiologic correction. For "VSD type" DORV, the purpose of the surgery physiologically is to eliminate the left-to-right shunt. This can be achieved by closing the VSD. In "transposition type" DORV, the ventricular outflows must be switched to achieve normal two-ventricle physiology. In "tetralogy type" DORV, routing blood from the LV to the aorta with enlargement of right ventricular outflow tract is required. After determining each patient's physiology, the anatomic features are identified to determine which surgical procedure is feasible (Figs. 51.9 and 51.10).

First, the sizes of the ventricles and AV valves should be measured. If the sizes of the ventricles and AV valves are adequate, a biventricular repair is planned. If the tricuspid valve or RV is small, a "one and one-half ventricle" repair can be selected. In this approach, the systemic and pulmonary circulations are fully separated, but the RV only pumps systemic venous blood from the inferior vena cava (IVC) to the lungs; blood from the SVC enters the lungs by a cavopulmonary anastomosis (typically a bidirectional Glenn shunt). Therefore,

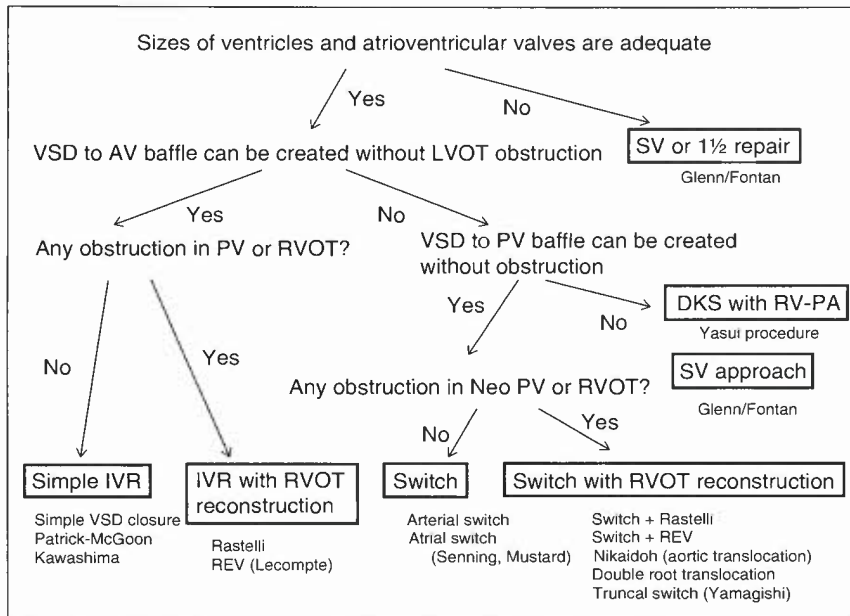


Figure 51.9. Anatomical approach to the repair of the various anatomic subtypes of DORV. SV, single ventricle; PV, pulmonary valve; RVOT, right ventricular outflow tract; VSD, ventricular septal defects; DKS, Damus-Kaye-Stansel; RV-PA, right ventricle to pulmonary artery; IVR, intraventricular repair.

the RV is only required to pump IVC blood, since blood from the SVC is diverted directly into the pulmonary arteries.

Second, a determination must be made about whether a LV-to-aortic baffle can be created without creating any LV outflow tract obstruction. For this purpose, the distance between the tricuspid valve and pulmonary valve should be greater than normal. Some VSDs need to be enlarged, if possible, or the outlet septum should be resected. Some papillary muscles may need to be reattached. Most “VSD type” DORV patients can be repaired by simple patch closure of the VSD. In some cases of “transposition type,” this type of repair is also technically feasible and can be successful. Other approaches to “transposition type” DORV include the Patrick-McGoan procedure (if great vessel relationships are anterior-posterior or I-position with a large VSD) or a Kawashima procedure (Taussig-Bing anatomy with a large distance between the tricuspid valve and pulmonary valve) (41,42). Currently, however, because of the complexity of the intracardiac baffling techniques, an arterial switch operation is preferred, if possible (48,49). If right ventricular outflow reconstruction is required due to stenosis, a Rastelli procedure (right ventricle-to-pulmonary artery conduit) or REV procedure (Lecompte) is chosen (50,51).

Third, when a left ventricle-to-aortic baffle cannot be created, but a left ventricle-to-pulmonary valve pathway can be constructed without any stenosis, an arterial switch operation can be performed. In the past, an atrial switch operation with an intraventricular tunnel repair was used. However, this strategy has produced poor results in general, including hospital mortality rates as high as 30% to 40% (52,53). For this reason it is no longer employed. If there is any stenosis in the right ventricle-to-pulmonary artery route, a Rastelli conduit or REV procedure is added to the arterial switch. For this group of patients, and as an alternative to the arterial switch with right ventricular outflow tract reconstruction, more complicated approaches such as the Nikaidoh procedure (aortic translocation), double root translocation, or truncal switch operation were described (47,54,55).

If neither a LV-to-aortic valve nor a pulmonary valve pathway can be created without obstruction, a Damus-Kaye-Stansel (DKS) anastomosis with right ventricle-to-pulmonary artery conduit (Yasui procedure) for biventricular repair can be performed (56). Otherwise, conversion to a Fontan pathway is chosen. In some patients in whom straddling of the right or left AV valve complicates the anatomy of the VSD,

septation may not be possible without replacement of the straddling valve. Alternatively, if the pulmonary pressure and resistance are low, definitive palliation can be achieved in a stepwise fashion by an initial bidirectional Glenn shunt followed by a Fontan operation.

SURGICAL OUTCOMES

Mortality for repair of DORV depends on the anatomic variant and presence of any associated anomalies. Overall, early mortality for repair of DORV has been reported to range from 2% to 9%, and 15-year overall survival ranges from 56% to 90% in most recent large series (57–61).

In 1997, Kleinert et al. reported 193 DORV patients operated at Royal Children's Hospital in Melbourne from 1978 to 1993 (24). They divided patients into two groups. Patients in group 1 had AV concordance, a single VSD, balanced ventricle size, no straddling AV valve tissue, and no major pulmonary artery anomaly. Patients in group 2 were complex; they had multiple VSDs, straddling AV valve tissue, and ventricular hypoplasia. Of the 193 patients, 148 had a biventricular repair. Early mortality in group 1 was 3.6% versus 22% in group 2. Risk factors for mortality were multiple VSDs, operation before 1985, and aortic arch obstruction.

In 1999, Masuda et al. reported a series of 27 DORV patients with subpulmonary VSD (62). There was one operative death (3.7%) and three late deaths. The actuarial survival rate was 83% at 9 years. In 2001, Brown et al. reviewed 124 DORV patients from 1980 to 2000 (57). In this series, the early mortality was 4.8%; survival at 15 years was 95.8% for non-complex patients, 89.7% for subpulmonary VSD patients, and 89.5% for patients with straddling AV valve or hypoplastic ventricle.

In 2001, Takeuchi et al. reported the experience of patients with DORV and a subpulmonary VSD at Children's Hospital, Boston, from 1992 to 1999 (58). Of 34 total patients, 20 patients underwent an arterial switch operation and 12 underwent a bidirectional Glenn procedure followed by a modified Fontan. There were no deaths in the Glenn/Fontan group. Four patients in the arterial switch operation group died within 33 days of surgery. Actual survival at 5 years for the entire group was 87%.

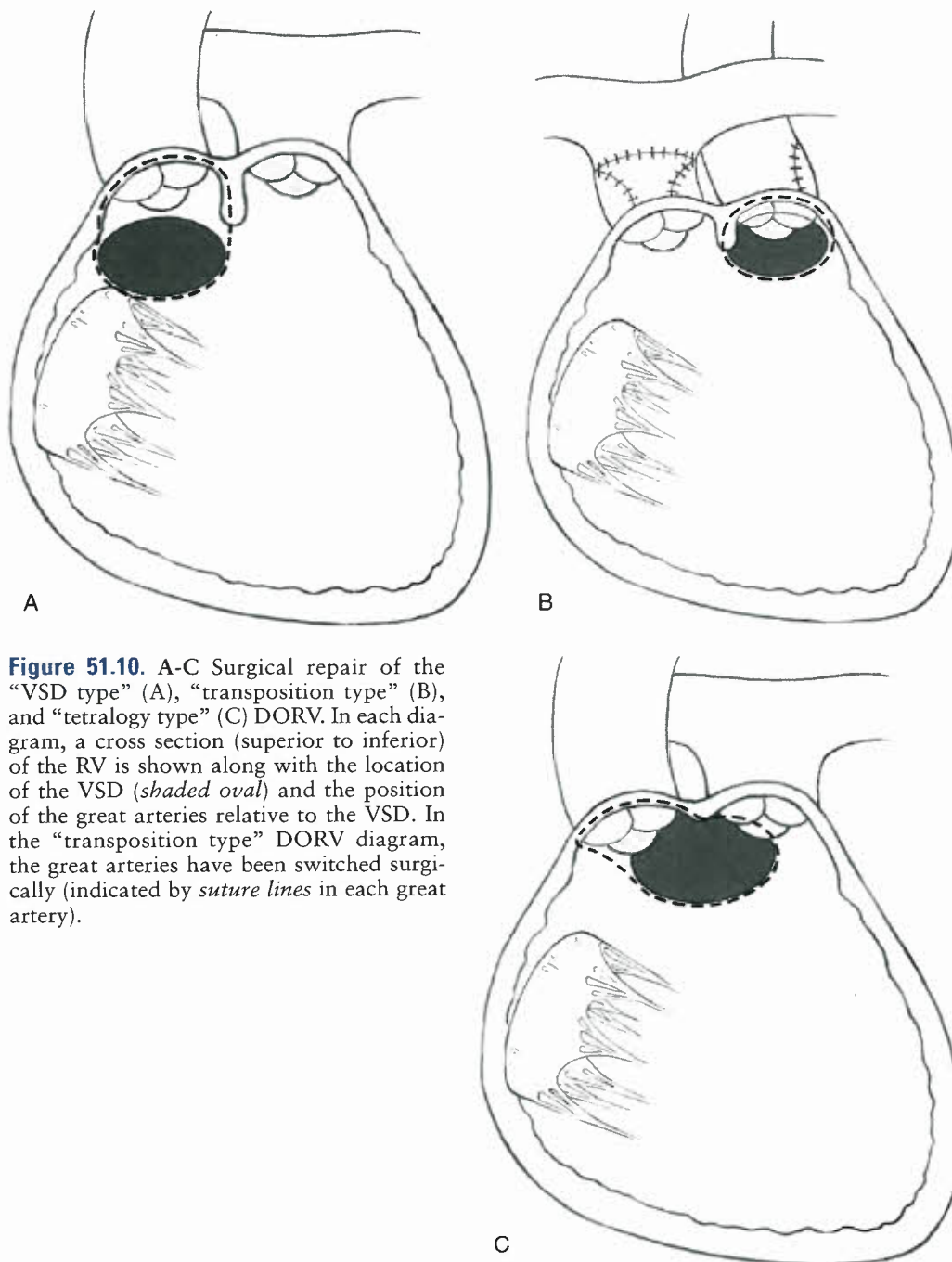


Figure 51.10. A-C Surgical repair of the “VSD type” (A), “transposition type” (B), and “tetralogy type” (C) DORV. In each diagram, a cross section (superior to inferior) of the RV is shown along with the location of the VSD (*shaded oval*) and the position of the great arteries relative to the VSD. In the “transposition type” DORV diagram, the great arteries have been switched surgically (indicated by *suture lines* in each great artery).

In 2002, Lacour-Gayet et al. reported 10 patients with DORV with noncommitted VSD repaired by intracardiac rerouting to the pulmonary artery and arterial switch (63). At a mean follow-up of 20 months, there was one non-cardiac death, and all nine survivors had normal sinus rhythm and subaortic gradients <15 mm Hg.

In 2007, Bradley et al. published a review of 393 children with DORV at the Hospital for Sick Children in Toronto (64). These patients were classified as follows: subaortic VSD with or without pulmonary stenosis in 47%, subpulmonic VSD in 23%, noncommitted VSD in 26%, and doubly committed VSD in 4%. Biventricular repair was performed in 55% at a median age of 10 months, and a Fontan operation was performed in 23% at a median age of 3.7 years. Overall survival was 56% at 15 years. Interestingly, for complex DORV,

a Rastelli-type repair increased the early reintervention risk ($p = 0.04$) and late post-repair mortality ($p = 0.02$), whereas the arterial switch operation increased early post-repair mortality ($p = 0.02$) but improved late post-repair survival. They concluded that extending biventricular repair to borderline anatomic candidates who had hypoplastic left-sided structures or a non-subaortic VSD is a questionable strategy.

REINTERVENTION AND REOPERATION

In patients with simpler forms of DORV such as “VSD type” or “tetralogy type,” freedom from reoperation is excellent and comparable to the outcomes of patients with simple VSD and

tetralogy of Fallot (57,64,65). However, patients who undergo a Rastelli-type repair require one or more right-ventricle-to-pulmonary artery conduit replacements.

Patients with a complex intracardiac baffle are at substantial risk of left ventricular outflow tract obstruction. The risk of reoperation has been reported to vary from 5% to 50%, and this risk is particularly high in those with a subpulmonary VSD (66).

The survival of patients with “transposition type” DORV is now comparable to the outcomes of those with uncomplicated d-transposition of the great arteries (67). However, neo-aortic valve regurgitation in these patients is more common than in uncomplicated d-transposition of the great arteries, implying that they may need future aortic valve repair or replacement (67).

MANAGEMENT OF THE ADULT WITH DORV

The surgical treatment of DORV is so varied that the appropriate follow-up depends on multiple factors including the patient's condition, type of repair, and residual lesion(s), if any. The American College of Cardiology/American Heart Association (ACC/AHA) and Canadian Cardiovascular Society have published consensus guidelines for the management of adults with VSD, d-transposition of the great arteries, tetralogy of Fallot, and single ventricle with a Fontan operation individually, and these types of DORV patients should be managed according to the appropriate diagnosis-specific guidelines (68,69). All patients with DORV, whether they have undergone surgery or not, can benefit from regular follow-up with a cardiologist who has expertise and experience in the management of adults with congenital heart disease. Exercise intolerance and decline in functional status are important changes that should alert the cardiologist to the possibility of either a residual lesion or reduction in ventricular function. Patients with DORV, whether operated on or not, are at risk of both atrial and ventricular arrhythmias. Arrhythmia in these patients is typically caused by progressive, abnormal hemodynamics leading to chamber dilatation and/or hypertrophy with resultant ventricular dysfunction. Right bundle branch block and QRS prolongation after repair are common and may suggest an increased risk of sustained ventricular tachycardia and sudden cardiac death (70). These and other complications associated with DORV in adults are listed in Table 51.4.

Successful pregnancy and delivery after biventricular repair of DORV have been reported (71). When complications occur,

they are primarily non-cardiac, and the cardiac complications are less common and typically minor in comparison. However, infertility and menstrual cycle disorders appear to be more prevalent. Because of the lack of large studies with follow-up data on DORV patients, it seems reasonable to monitor pregnancy closely in “tetralogy type” patients with a subaortic VSD who underwent intracardiac biventricular repair. Generally, patients with a biventricular repair should have a low pregnancy risk, assuming good biventricular function, normal oxygen saturations, and absence of significant residual lesions causing hemodynamic effects (72,73). For patients with a Fontan palliation, successful pregnancy and delivery after a Fontan procedure for DORV have been reported (74).

Patients following DORV repair do not require routine endocarditis prophylaxis except in the following situations: prosthetic cardiac valve or device, previous endocarditis, for the first 6 months after intervention, and residual defect(s) at the site or adjacent to the site of a prosthetic patch or device (75).

ACKNOWLEDGMENTS

The authors wish to acknowledge assistance with CT images from Frandics Chan, M.D., Ph.D., Department of Radiology, Stanford University School of Medicine, pathologic specimen images from Diane Spicer, B.S., Congenital Heart Institute of Florida, University of Florida, and drawings of surgical repair techniques by Butch Colyear, B.A., M.A., Butch Colyear Design & Illustration.

REFERENCES

1. Birmingham A. Extreme anomaly of the heart and great vessels. *J Anat Physiol* 1892;27:139–150.
2. Witham AC. Double outlet right ventricle; a partial transposition complex. *Am Heart J* 1957;53:928–939.
3. Taussig HB, Bing RJ. Complete transposition of the aorta and a levoposition of the pulmonary artery; clinical, physiological, and pathological findings. *Am Heart J* 1949;37:551–559.
4. Van Praagh R. What is the taussig-bing malformation? *Circulation* 1968;38:445–449.
5. Van Mierop LHS, Wiglesworth FW. Pathogenesis of transposition complexes: II. Anomalies due to faulty transfer of the posterior great artery. *Am J Cardiol* 1963;12:226–232.
6. Neufeld HN, Dushane JW, Wood EH, et al. Origin of both great vessels from the right ventricle. I. Without pulmonary stenosis. *Circulation* 1961;23:399–412.
7. Neufeld HN, Dushane JW, Edwards JE. Origin of both great vessels from the right ventricle. II. With pulmonary stenosis. *Circulation* 1961;23:603–612.
8. Neufeld HN, Lucas RV Jr, Lester RG, et al. Origin of both great vessels from the right ventricle without pulmonary stenosis. *Br Heart J* 1962;24:393–408.
9. Lev M, Bharati S, Meng CC, et al. A concept of double-outlet right ventricle. *J Thorac Cardiovasc Surg* 1972;64:271–281.
10. Sridaromont S, Feldt RH, Ritter DG, et al. Double outlet right ventricle: hemodynamic and anatomic correlations. *Am J Cardiol* 1976;38:85–94.
11. Sridaromont S, Ritter DG, Feldt RH, et al. Double-outlet right ventricle. Anatomic and angiocardigraphic correlations. *Mayo Clin Proc*. 1978;53:555–577.
12. Walters HL III, Mavroudis C, Tchervenkov CI, et al. Congenital heart surgery nomenclature and database project: double outlet right ventricle. *Ann Thorac Surg* 2000;69:S249–S263.
13. Ueda M, Becker AE. Classification of hearts with overriding aortic and pulmonary valves. *Int J Cardiol* 1985;9:357–369.
14. Ferencz C, Rubin JD, McCarter RJ, et al. Congenital heart disease: prevalence at livebirth. The baltimore-washington infant study. *Am J Epidemiol* 1985;121:31–36.
15. Goor DA, Edwards JE. The spectrum of transposition of the great arteries: with specific reference to developmental anatomy of the conus. *Circulation* 1973;48:406–415.
16. Angelini P, Leachman RD. The spectrum of double outlet right ventricle: an embryologic interpretation. *Cardiovasc Dis* 1976;3:127–149.
17. Van Praagh R, Van Praagh S. Isolated ventricular inversion. A consideration of the morphogenesis, definition and diagnosis of nontransposed and transposed great arteries. *Am J Cardiol* 1966;17:395–406.

TABLE 51.4

Complications Associated with DORV in Adults

LV outflow tract obstruction
RV outflow tract obstruction and pulmonary regurgitation
Failure of the right ventricle-to-pulmonary artery conduit (stenosis or regurgitation)
Aortic valve regurgitation (following arterial switch operation)
Coronary artery stenosis (following coronary transfer)
Right ventricle failure
Arrhythmia (atrial or ventricular) and sudden death
Endocarditis
Thromboembolic event

18. Howell CE, Ho SY, Anderson RH, et al. Fibrous skeleton and ventricular outflow tracts in double-outlet right ventricle. *Ann Thorac Surg* 1991;51:394-400.
19. Edwards WD. Double-outlet right ventricle and tetralogy of fallot. Two distinct but not mutually exclusive entities. *J Thorac Cardiovasc Surg* 1981;82:418-422.
20. MacMahon HE, Lipa M. Double-outlet right ventricle with intact interventricular septum. *Circulation* 1964;30:745-748.
21. Bharati S, Lev M. The conduction system in double outlet right ventricle with subpulmonic ventricular septal defect and related hearts (the taussig-bing group). *Circulation* 1976;54:459-467.
22. Sondheimer HM, Freedom RM, Olley PM. Double outlet right ventricle: clinical spectrum and prognosis. *Am J Cardiol* 1977;39:709-714.
23. Wilcox BR, Ho SY, Macartney FJ, et al. Surgical anatomy of double-outlet right ventricle with situs solitus and atrioventricular concordance. *J Thorac Cardiovasc Surg* 1981;82:405-417.
24. Kleinert S, Sano T, Weintraub RG, et al. Anatomic features and surgical strategies in double-outlet right ventricle. *Circulation* 1997;96:1233-1239.
25. Serraf A, Lacour-Gayet F, Houyel L, et al. Subaortic obstruction in double outlet right ventricles. Surgical considerations for anatomic repair. *Circulation* 1993;88:II177-II182.
26. Macartney FJ, Rigby ML, Anderson RH, et al. Double outlet right ventricle. Cross sectional echocardiographic findings, their anatomical explanation, and surgical relevance. *Br Heart J* 1984;52:164-177.
27. Dogan OF, Karcaaltincaba M, Yorgancioglu C, et al. Demonstration of coronary arteries and major cardiac vascular structures in congenital heart disease by cardiac multidetector computed tomography angiography. *Heart Surg Forum* 2007;10:E90-E94.
28. Hallermann FJ, Kincaid OW, Ritter DG, et al. Angiocardigraphic and anatomical findings in origin of both great arteries from the right ventricle. *Am J Roentgenol Radium Ther Nucl Med* 1970;109:51-66.
29. Frank L, Dillman JR, Parish V, et al. Cardiovascular mr imaging of conotruncal anomalies. *Radiographics* 2010;30:1069-1094.
30. Yoo SJ, Lim TH, Park IS, et al. Mr anatomy of ventricular septal defect in double-outlet right ventricle with situs solitus and atrioventricular concordance. *Radiology* 1991;181:501-505.
31. Niezen RA, Beekman RP, Helbing WA, et al. Double outlet right ventricle assessed with magnetic resonance imaging. *Int J Card Imaging* 1999;15:323-329.
32. Beekman RP, Roest AA, Helbing WA, et al. Spin echo MRI in the evaluation of hearts with a double outlet right ventricle: usefulness and limitations. *Magn Reson Imaging* 2000;18:245-253.
33. Gelehrter S, Owens ST, Russell MW, et al. Accuracy of the fetal echocardiogram in double-outlet right ventricle. *Congenit Heart Dis* 2007;2:32-37.
34. Galindo A, Mendoza A, Arbues J, et al. Conotruncal anomalies in fetal life: accuracy of diagnosis, associated defects and outcome. *Eur J Obstet Gynecol Reprod Biol* 2009;146:55-60.
35. Tometzki AJ, Suda K, Kohl T, et al. Accuracy of prenatal echocardiographic diagnosis and prognosis of fetuses with conotruncal anomalies. *J Am Coll Cardiol* 1999;33:1696-1701.
36. Chiechi MA. Incomplete transposition of the great vessels with biventricular origin of the pulmonary artery (taussig-bing complex); report of four cases and review of the literature. *Am J Med* 1957;22:234-251.
37. Lev M, Rimoldi HJ, Eckner FA, et al. The taussig-bing heart. Qualitative and quantitative anatomy. *Arch Pathol* 1966;81:24-35.
38. Hightower BM, Barcia A, Bargerion LM, et al. Double-outlet right ventricle with transposed great arteries and subpulmonary ventricular septal defect. The taussig-bing malformation. *Circulation* 1969;39:1207-1213.
39. Kirklin JW, Harp RA, McGoon DC. Surgical treatment of origin of both vessels from right ventricle, including cases of pulmonary stenosis. *J Thorac Cardiovasc Surg* 1964;48:1026-1036.
40. Barratt-Boyes BG, Lowe JB, Watt WJ, et al. Initial experiences with extracorporeal circulation in intracardiac surgery. *Br Med J* 1960;2:1826-1831.
41. Kawashima Y, Fujita T, Miyamoto T, et al. Intraventricular rerouting of blood for the correction of taussig-bing malformation. *J Thorac Cardiovasc Surg* 1971;62:825-829.
42. Patrick DL, McGoon DC. An operation for double-outlet right ventricle with transposition of the great arteries. *J Cardiovasc Surg (Torino)* 1968;9:537-542.
43. Pacifico AD, Kirklin JK, Colvin EV, et al. Intraventricular tunnel repair for taussig-bing heart and related cardiac anomalies. *Circulation* 1986;74:153-160.
44. Sakata R, Lecompte Y, Batisse A, et al. Anatomic repair of anomalies of ventriculoarterial connection associated with ventricular septal defect. I. Criteria of surgical decision. *J Thorac Cardiovasc Surg* 1988;95:90-95.
45. Kirklin JK, Castaneda AR. Surgical correction of double-outlet right ventricle with noncommitted ventricular septal defect. *J Thorac Cardiovasc Surg* 1977;73:399-403.
46. Serraf A, Nakamura T, Lacour-Gayet F, et al. Surgical approaches for double-outlet right ventricle or transposition of the great arteries associated with straddling atrioventricular valves. *J Thorac Cardiovasc Surg* 1996;111:527-535.
47. Nikaidoh H. Aortic translocation and biventricular outflow tract reconstruction. A new surgical repair for transposition of the great arteries associated with ventricular septal defect and pulmonary stenosis. *J Thorac Cardiovasc Surg* 1984;88:365-372.
48. Yacoub MH, Radley-Smith R. Anatomic correction of the taussig-bing anomaly. *J Thorac Cardiovasc Surg* 1984;88:380-388.
49. Serraf A, Bruniaux J, Lacour-Gayet F, et al. Anatomic correction of transposition of the great arteries with ventricular septal defect. Experience with 118 cases. *J Thorac Cardiovasc Surg* 1991;102:140-147.
50. Lecompte Y, Neveux JY, Leca F, et al. Reconstruction of the pulmonary outflow tract without prosthetic conduit. *J Thorac Cardiovasc Surg* 1982;84:727-733.
51. Vouhe PR, Tamisier D, Leca F, et al. Transposition of the great arteries, ventricular septal defect, and pulmonary outflow tract obstruction. Rastelli or lecompte procedure? *J Thorac Cardiovasc Surg* 1992;103:428-436.
52. Piccoli G, Pacifico AD, Kirklin JW, et al. Changing results and concepts in the surgical treatment of double-outlet right ventricle: analysis of 137 operations in 126 patients. *Am J Cardiol* 1983;52:549-554.
53. Kirklin JW, Pacifico AD, Blackstone EH, et al. Current risks and protocols for operations for double-outlet right ventricle. Derivation from an 18 year experience. *J Thorac Cardiovasc Surg* 1986;92:913-930.
54. Hu S, Xie Y, Li S, et al. Double-root translocation for double-outlet right ventricle with noncommitted ventricular septal defect or double-outlet right ventricle with subpulmonary ventricular septal defect associated with pulmonary stenosis: an optimized solution. *Ann Thorac Surg* 2010;89:1360-1365.
55. Yamagishi M, Shuntoh K, Matsushita T, et al. Half-turned truncal switch operation for complete transposition of the great arteries with ventricular septal defect and pulmonary stenosis. *J Thorac Cardiovasc Surg* 2003;125:966-968.
56. Yasui H, Kado H, Nakano E, et al. Primary repair of interrupted aortic arch and severe aortic stenosis in neonates. *J Thorac Cardiovasc Surg* 1987;93:539-545.
57. Brown JW, Ruzmetov M, Okada Y, et al. Surgical results in patients with double outlet right ventricle: a 20-year experience. *Ann Thorac Surg* 2001;72:1630-1635.
58. Takeuchi K, McGowan FX, Jr, Moran AM, et al. Surgical outcome of double-outlet right ventricle with subpulmonary vsd. *Ann Thorac Surg* 2001;71:49-52; discussion 52-43.
59. Belli E, Serraf A, Lacour-Gayet F, et al. Biventricular repair for double-outlet right ventricle. Results and long-term follow-up. *Circulation* 1998;98:II360-II365; discussion II365-II367.
60. Artrip JH, Sauer H, Campbell DN, et al. Biventricular repair in double outlet right ventricle: surgical results based on the sts-eacts international nomenclature classification. *Eur J Cardiothorac Surg* 2006;29:545-550.
61. Lacour-Gayet F. Intracardiac repair of double outlet right ventricle. *Semin Thorac Cardiovasc Surg Pediatr Card Surg Annu* 2008:39-43.
62. Masuda M, Kado H, Shiokawa Y, et al. Clinical results of arterial switch operation for double-outlet right ventricle with subpulmonary vsd. *Eur J Cardiothorac Surg* 1999;15:283-288.
63. Lacour-Gayet F, Haun C, Ntalakoura K, et al. Biventricular repair of double outlet right ventricle with non-committed ventricular septal defect (vsd) by vsd rerouting to the pulmonary artery and arterial switch. *Eur J Cardiothorac Surg* 2002;21:1042-1048.
64. Bradley TJ, Karamlou T, Kulik A, et al. Determinants of repair type, reintervention, and mortality in 393 children with double-outlet right ventricle. *J Thorac Cardiovasc Surg* 2007;134:967-973 e966.
65. Vogt PR, Carrel T, Pasic M, et al. Early and late results after correction for double-outlet right ventricle: uni- and multivariate analysis of risk factors. *Eur J Cardiothorac Surg* 1994;8:301-307.
66. Rubay J, Lecompte Y, Batisse A, et al. Anatomic repair of anomalies of ventriculo-arterial connection (rev). Results of a new technique in cases associated with pulmonary outflow tract obstruction. *Eur J Cardiothorac Surg* 1988;2:305-311.
67. Haas F, Wotke M, Poppert H, et al. Long-term survival and functional follow-up in patients after the arterial switch operation. *Ann Thorac Surg* 1999;68:1692-1697.
68. Warnes CA, Williams RG, Bashore TM, et al. ACC/AHA 2008 Guidelines for the Management of Adults with Congenital Heart Disease: a report of the American College of Cardiology/American Heart Association Task Force on Practice Guidelines (Writing Committee to Develop Guidelines on the Management of Adults with Congenital Heart Disease). Developed in collaboration with the American Society of Echocardiography, Heart Rhythm Society, International Society for Adult Congenital Heart Disease, Society for Cardiovascular Angiography and Interventions, and Society of Thoracic Surgeons. *J Am Coll Cardiol* 2008;52:e1-e121.
69. Howlett JG, McKelvie RS, Arnold JM, et al. Canadian Cardiovascular Society Consensus Conference Guidelines on Heart Failure, update 2009: diagnosis and management of right-sided heart failure, myocarditis, device therapy and recent important clinical trials. *Can J Cardiol* 2009;25:85-105.
70. Houyel L, Vaksman G, Fournier A, et al. Ventricular arrhythmias after correction of ventricular septal defects: importance of surgical approach. *J Am Coll Cardiol* 1990;16:1224-1228.
71. Drenthen W, Pieper PG, van der Tuuk K, et al. Fertility, pregnancy and delivery in women after biventricular repair for double outlet right ventricle. *Cardiology* 2008;109:105-109.
72. Bashore TM. Adult congenital heart disease: right ventricular outflow tract lesions. *Circulation* 2007;115:1933-1947.
73. Meijer JM, Pieper PG, Drenthen W, et al. Pregnancy, fertility, and recurrence risk in corrected tetralogy of fallot. *Heart* 2005;91:801-805.
74. Ito M, Takagi N, Sugimoto S, et al. Pregnancy after undergoing the fontan procedure for a double outlet right ventricle: report of a case. *Surg Today* 2002;32:63-65.
75. Gatzoulis MA, Webb GD, Daubeney PEF. *Diagnosis and Management of Adult Congenital Heart Disease*. Philadelphia, PA: Elsevier Saunders; 2011.

Michael G. Earing ■ Donald J. Hagler ■ William D. Edwards

NOMENCLATURE

Considerable controversy exists regarding the definition, classification, and nomenclature for various forms of complex congenital heart disease. As a result, the potential exists for confusion and misunderstanding both between and within institutions. This is especially true for the nomenclature of hearts with a large dominant ventricle and a small rudimentary ventricle. Terms that have been used to describe this group of hearts include single ventricle, univentricular heart, common ventricle and, more recently, single functional ventricle.

Van Praagh et al. (1) have emphasized that it is inaccurate to label hearts in this category as “single ventricle,” given that there are always two ventricular chambers present in mammalian hearts. In the late 1970s and early 1980s, Anderson et al. (2,3) attempted to clarify the classification of these hearts by introducing a new definition for what constitutes a ventricle. This definition was based on several important observations. First, normal ventricles possess an inlet, trabecular, and outlet portion. The inlet portion extends from the atrioventricular (AV) annulus to the insertions of the papillary muscles and does not require a perforate AV valve annulus. The trabecular portion exists between the inlet and outlet portions and includes the ventricular apex. Finally, the outlet portion of the ventricle includes the nontrabeculated region beneath a semilunar valve. The second observation that Anderson et al. based their definition on was that in the normal heart the inlet and outlet portions of the morphologic left ventricle (LV) are in fibrous continuity. But, in a morphologic right ventricle, the inlet and outlet portions are separated from one another by the crista supraventricularis. Their final observation that they based their definition of a ventricle on was that in the normal heart, each trabecular zone receives its own inlet. Based on these observations, Anderson et al. proposed that a chamber must have 50% or more of an inlet portion to be classified as a ventricle and need not have an outlet portion. Chambers receiving <50% of an inlet were defined as rudimentary chambers. Rudimentary chambers consisting of an outlet portion were classified further as an “outlet chamber.” Those possessing only a trabecular zone were called “trabecular pouches.” Based on these rules, Anderson et al. used the term univentricular heart of left ventricular type to describe hearts in which the dominant chamber was morphologically a LV and the rudimentary chamber had characteristics of the trabecular portion of a right ventricle. They used the term univentricular heart of the right ventricular type to describe hearts in which the dominant chamber was morphologically a right ventricle and the rudimentary chamber had the characteristics of the trabecular portion of a LV.

While their definitions have been accepted by many, other investigators believed these definitions were confusing, arguing that using the term “univentricular heart” is misleading because all hearts have two ventricular chambers. As result, in the late 1970s and early 1980s, many other authors continued

to describe these hearts based upon their abnormal AV connection, and preferred terms such as double inlet LV and tricuspid atresia. In 1984, in response to arguments against their definition of a ventricle, Anderson et al. (2) introduced the term “univentricular AV connection” to describe hearts in which both inlets (whether patent or not) were committed primarily to one dominant ventricle. In this system, the emphasis is on the use of the sequential segmental approach to define the dominant ventricular morphology present, the position and morphology of the rudimentary ventricle, the type of AV connection, and, finally, the position of the semilunar valves.

As discussed in some detail by Edwards and Maleszewski in Chapter 2, there are six possible AV connections. Two are biventricular (concordance and discordance), one is ambiguous (in cases of atrial isomerism), and three are univentricular (double inlet, single inlet, and common inlet). We prefer the definition of a ventricle as an endocardial-lined chamber within the ventricular mass, regardless of the ventricular components that are present or absent. The term “single functional ventricle” encompasses hearts with a small nonfunctional ventricle and includes hearts with univentricular AV connections, as well as those with an atretic semilunar valve and an intact ventricular septum (the hypoplastic left and right heart syndromes). Patients with any type of single functional ventricle are amenable to a modified Fontan type of surgical repair.

Throughout the remainder of this chapter we will use the sequential segmental approach to discuss conditions resulting in a univentricular AV connection (aortic or pulmonary atresia with an intact septum are discussed in two Chapters 41 and 48). For each condition, we will describe the dominant ventricular morphology as left or right, the type of AV connection, the position and morphology of the hypoplastic ventricle, and the spatial relationship of the great arteries. We will use the term “single functional ventricle” to help avoid any conceptual confusion that terms like “univentricular heart” and “single ventricle” might cause.

PATHOLOGIC ANATOMY

Ventricular Morphology

The most common form of univentricular AV connection is a double inlet LV with a hypoplastic right ventricle (1). In this anomaly, the rudimentary right ventricle is located anterior and superior to the dominant left ventricular chamber and most commonly connects to the ascending aorta (ventriculoarterial discordance). If the hypoplastic right ventricle lies along the right shoulder of the heart, the sidedness of the dominant LV will be normal, and if it is found on the left shoulder of the heart, then the left ventricular sidedness will be the mirror image (ventricular inversion or L-loop ventricles). In the dominant chamber, direct continuity between one or both AV valves and the semilunar valve establishes its morphology as

left ventricular. In short axis, the plane of the ventricular septum will be angled rather than perpendicular to the diaphragmatic ventricular wall and it will be displaced superiorly.

Double inlet right ventricle is an exceedingly rare anomaly. In this condition, the hypoplastic left ventricular chamber will be located along the inferior (diaphragmatic) aspect of the heart, usually to the right or left of midline. Only rarely will the hypoplastic chamber give rise to a great artery. Consequently, the ventriculoarterial connections are almost always right ventricular and may be double outlet, common outlet (truncus arteriosus), or single outlet (with pulmonary or aortic atresia). Demonstration of separation of the AV valves from the semilunar valves by a collar of myocardium (the conus, infundibulum, or outflow tract) will establish the morphology of the dominant chamber as right ventricular.

Rarely, the morphology of neither the dominant chamber nor the hypoplastic chamber can be determined with certainty. Such cases are typically categorized as single functional ventricle of undifferentiated or indeterminate type.

Atrioventricular Connections

A double inlet AV connection is almost always associated with a dominant morphologic LV. In this situation, both atria connect to the dominant ventricle by two distinct AV valves, which are usually mirror-image morphologic mitral valves, thus fulfilling the embryologic concept that AV valve morphology always corresponds to the morphology of the ventricle to which they connect (Fig. 52.1). When one of the valves straddles into the hypoplastic right ventricle, it will have a hybrid mitral–tricuspid morphology. In such hearts, the AV valves should be labeled as “right” and “left” rather than ambiguously as “mitral” and “mitral.”

In contrast, in hearts with a common inlet AV connection, the dominant ventricle is almost always of right ventricular morphology. It should be noted that common inlet right ventricle occurs much less frequently than double inlet LV (12% vs. 88%) (4).

The third form of univentricular AV connection is a single inlet ventricle, which includes tricuspid atresia and mitral atresia (discussed in detail in Chapters 38 and 48). These are characterized either by an imperforate valve orifice with a fibrous plug or by absence of the AV connection such that the corresponding atrium and ventricle are completely separated from one another (Fig. 52.2 and 52.3).

Annular, rather than cordal, features are used to determine AV connections. Overriding refers to partial commitment of an AV valve annulus to the contralateral ventricular chamber and results from malalignment of the atrial and ventricular septa.

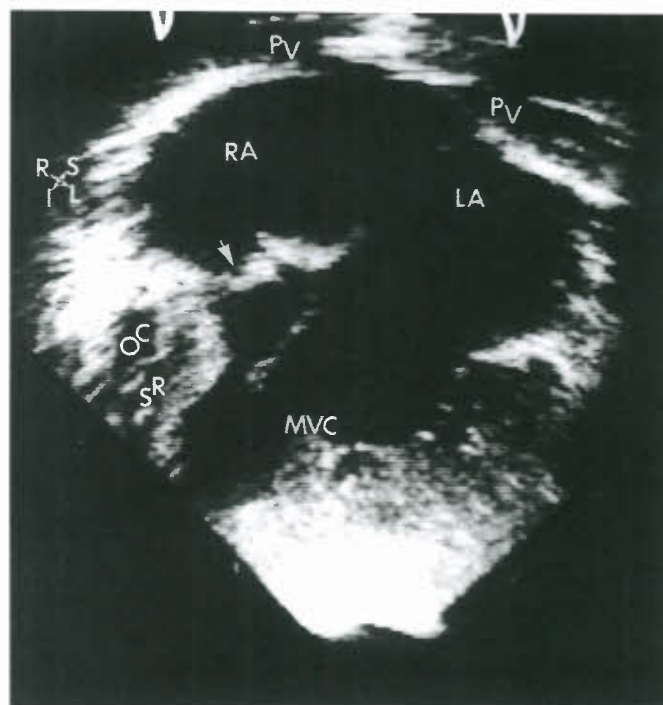


Figure 52.2. Double inlet with single AV valve. Echocardiogram demonstrating an apical four-chamber view. There is DILV with atresia of the right AV valve. Note that the atretic right AV valve plate (arrow) is directed to the main ventricular chamber (MVC) of left ventricular morphology with malalignment of the atrial and ventricular septa. I, inferior; L, left; LA, left atrium; OC, outlet chamber of right ventricular morphology; PV, pulmonary vein; R, right; RA, right atrium; S, superior; SR, ventricular septal remnant. (From Seward JB, Tajik AJ, Hagler DJ, et al. *Two-dimensional echocardiographic Atlas*. Vol. 1. *Congenital Heart Disease*. New York, NY: Springer-Verlag, 1987:250, with permission.)

It can influence the determination of an AV connection. The percentage of annular commitment to a ventricular chamber relative to the position of the ventricular septum determines the AV connection to a ventricular chamber. In the setting of an overriding AV valve, an atrium is considered to connect to the ventricle into which 50% of its valve empties. Thus, an annular commitment of 50% or more to a ventricular

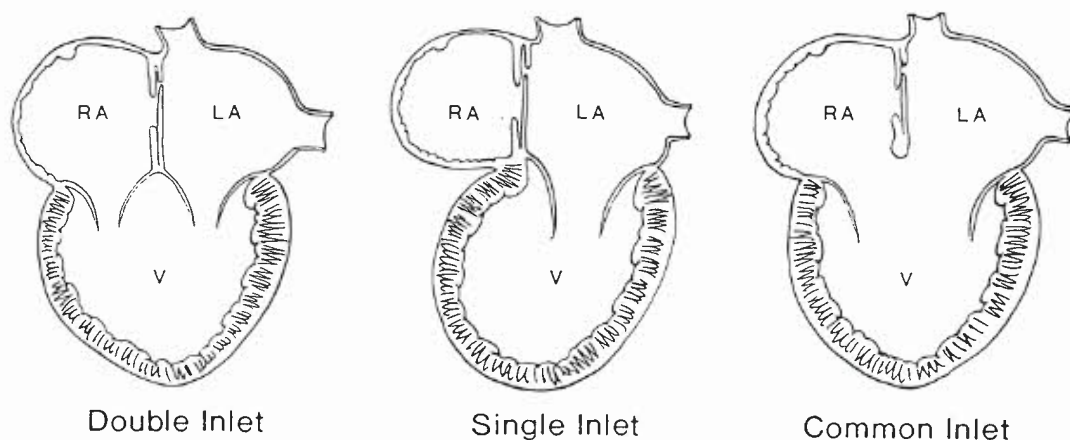


Figure 52.1. Univentricular AV connection. Schematic illustrating three basic types of univentricular connection: double inlet, single inlet, and common inlet. LA, left atrium; RA, right atrium; V, ventricle.

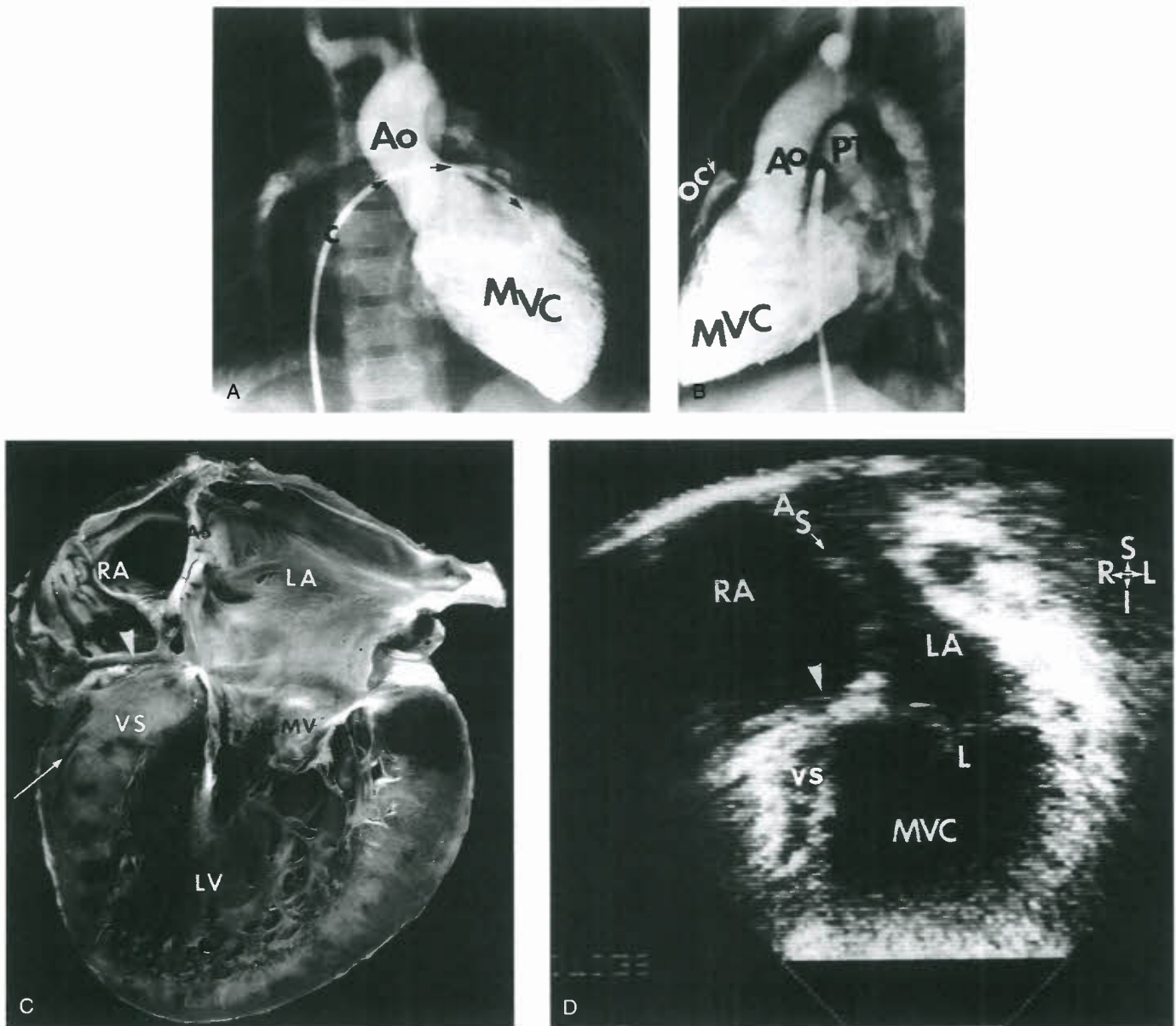


Figure 52.3. Angiographic, pathologic, and echocardiographic correlation in single-inlet LV. **A,B:** Anteroposterior and lateral views of a selective injection into the LV or main ventricular chamber (MVC) with absent right AV valve or tricuspid atresia. A hypoplastic right ventricular outlet chamber (OC) is observed anteriorly and supplies the pulmonary artery (PT). The great arteries are normally related, with the aorta (Ao) originating from the LV. **C,** catheter. **C,D:** Pathologic and echocardiographic comparison of findings observed in absent right AV valve. The specimen is cut similarly to the echocardiographic four-chamber view. The *small arrow* points to a tiny slit-like remnant of right ventricle. The main ventricular chamber (MVC) is the morphologic LV. The *arrowhead* points to the junction of the atrial and ventricular septa (VS), which are aligned. Only the left AV (mitral) valve (L) is committed to the LV. The right atrium (RA) is enlarged, and the atrial septum (AS) bulges into the left atrium (LA). MV, mitral valve.

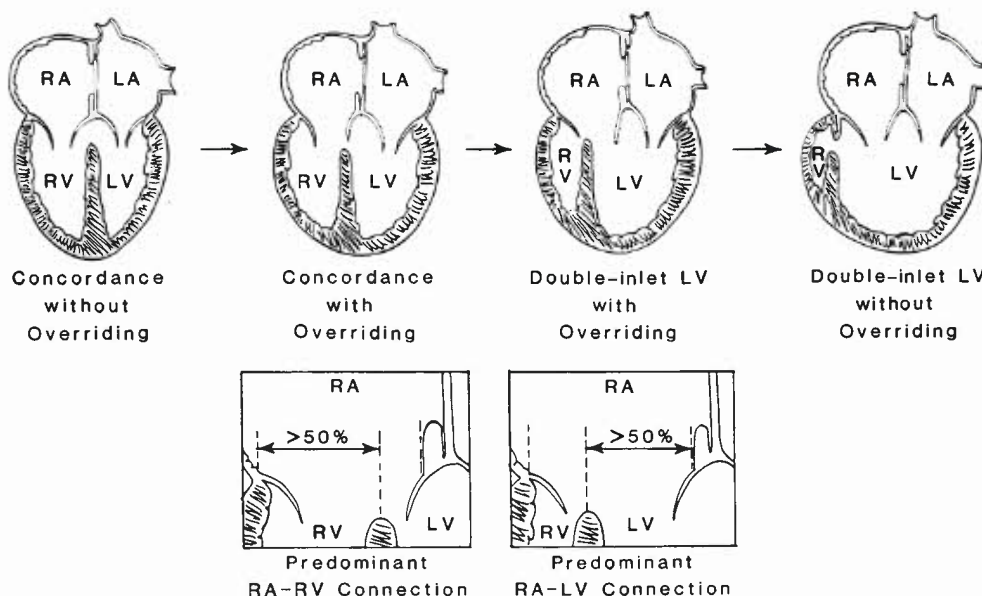
chamber establishes the valve connection to that ventricular chamber (Fig. 52.4). If 75% or more of the annulus of a common AV valve empties into one ventricular chamber, then a common inlet ventricle pertains.

In contrast to annular overriding, straddling is a feature of the tendinous cords and papillary muscles and results from their insertions into the contralateral ventricle through a ventricular septal defect (VSD). In double inlet LV, an AV valve may straddle into the hypoplastic right ventricular chamber. The valve that straddles is almost always on the same side as the hypoplastic

outlet chamber. Thus, with a right-sided hypoplastic right ventricle, it is the right AV valve that may straddle. Figure 52.5 schematically depicts the progressive changes in AV connections that occur, linking double inlet connection to overriding connections to normal concordant connection. This may occur with either D-loop or L-loop ventricles. Straddling AV valves are often large and redundant and can develop appreciable regurgitation.

Occasionally, stenosis of an AV valve may be encountered. In a study by Shiraishi and Silverman (4), 30% of patients with a double inlet ventricle had at least mild stenosis of an AV

Figure 52.4. AV commitment. Schematic illustration of the determination of AV connection based on the 50% rule. Note the associated effect of increasing atrial and ventricular septal malalignment produced by increasing annular override. When the right AV annulus overrides >50%, there is a predominant right atrium (RA) to the LV connection. LA, left atrium, RV, right ventricle.



valve, most commonly the left-sided valve. Parachute mitral valve can also occur (Fig. 52.6).

Ventricular Arterial Connections

In univentricular heart, any ventriculoarterial connection can occur, including concordant connection (i.e., aorta arising

from morphologic LV), discordant connections (i.e., aorta arising off rudimentary outlet chamber with right ventricular morphology), double outlet from the dominant ventricular mass or from the hypoplastic rudimentary outlet chamber, and single outlet from the dominant ventricular mass. Similar to the normal two-ventricle heart, the ventriculoarterial relationship is defined by the ventricle from which most (>50%) of an overriding semilunar valve originates.

Figure 52.5. Embryology. A: The series of anomalies that link the different types of double-inlet ventricles with the normal heart when there has been right-hand (d) embryonic ventricular looping. B: The comparable series of double-inlet ventricles when there has been left-hand (l) embryonic ventricular looping. L, left; R, right; LV, left ventricle; RV, right ventricle. Double inlet with single AV valve. Echocardiogram demonstrating an apical four-chamber view. There is DILV with atresia of the right AV valve. Note that the atretic right AV valve plate (arrow) is directed to the main ventricular chamber (MVC) of left ventricular morphology with malalignment of the atrial and ventricular septa. I, inferior; L, left; LA, left atrium; OC, outlet chamber of right ventricular morphology; PV, pulmonary vein; R, right; RA, right atrium; S, superior; SR, ventricular septal remnant. (From Seward JB, Tajik AJ, Hagler DJ, et al. Two-Dimensional Echocardiographic Atlas. *Congenital Heart Disease*. Vol. 1. New York: Springer-Verlag, 1987:250, with permission.)

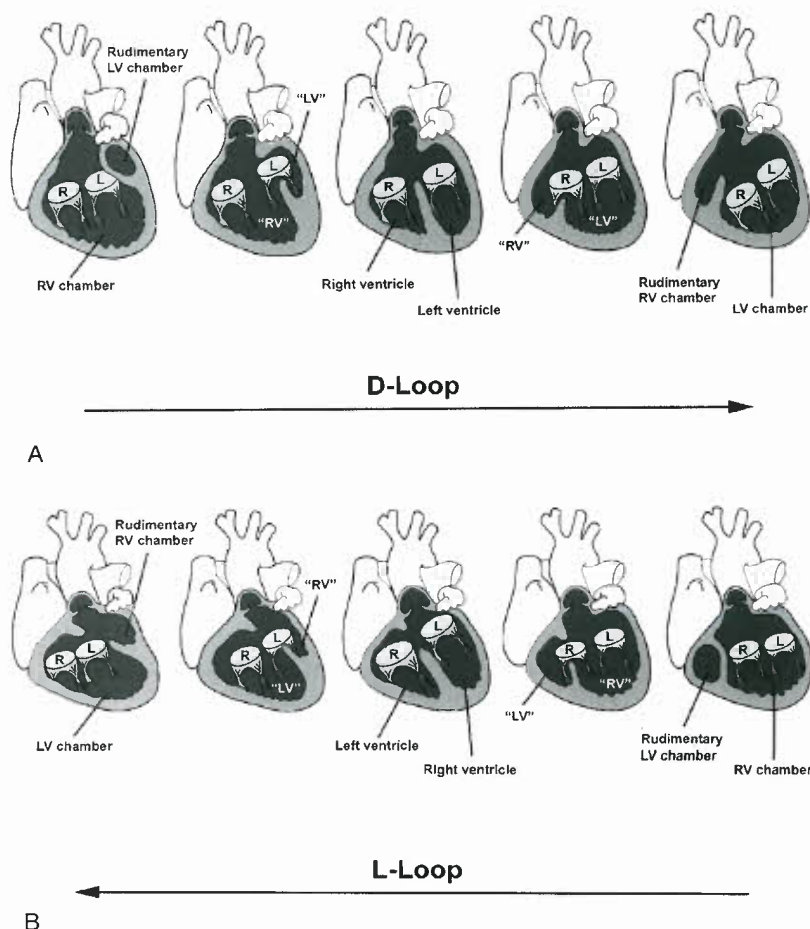




Figure 52.6. AV valve abnormalities. Echocardiogram demonstrating double-inlet right ventricle (RV) with severe stenosis of the left AV valve. There is a parachute-like deformity of the left AV valve with all the valve chordae committed to a single papillary muscle (P). The leaflets are also severely thickened (arrows). The left atrium (LA) is severely enlarged, consistent with severe left AV valve obstruction. A hypoplastic left ventricle (LV) is located posterior and to the left. I, inferior; R, right; S, superior; VS, ventricular septum.

Although many types of ventriculoarterial connections can occur in the setting of the univentricular heart, certain combinations are more common than others. In the setting of univentricular heart of left ventricular morphology, the majority of patients will have discordant ventriculoarterial connections, with the aorta arising from the rudimentary outlet chamber of right ventricular morphology, and the pulmonary artery arising from the dominant ventricular mass of left ventricular morphology. In the series by Shiraishi and Silverman (4), 86% of patients with univentricular LVs with a double inlet AV connection had transposition of the great arteries (4). Similar to the series published by Van Praagh et al. (1), the majority of patients in their series who had transposition of the great arteries also had L-looped ventricles (occurring in 63% of the patients). In this form, the aorta arises from the rudimentary outlet chamber of right ventricle morphology that is anterior, and leftward of the AV valves. The pulmonary artery arises from the morphologic LV. For the rest of the patients in their series, 23% were found to have transposition of the great arteries of the D-loop variety (i.e., aorta arising from outlet chamber of right ventricle morphology that sits anterior and rightward) and 14% of the patients had normally related great vessels (Holmes heart). Other common combinations described in the literature include the pattern seen with univentricular heart of right ventricular morphology. In this situation, the ventriculoarterial connection usually is double outlet from the dominant ventricular mass or is a single outlet with pulmonary atresia. In the univentricular heart of indeterminate morphology, there often is no outlet chamber and as result, there can only be a double outlet or a single outlet.

Pulmonary outflow tract obstruction frequently occurs with a univentricular heart. This can occur with either concordant

or discordant ventricular–arterial connections. When subpulmonary obstruction occurs, it typically is present within the ventricle of left ventricular morphology and is due to posterior deviation of the infundibular septum. Other causes of pulmonary outflow tract obstruction include anomalous attachments of the right AV valve or herniation of valvular tissue into the pulmonary outflow tract. In rare cases, there can be severe stenosis at the level of the pulmonary valve due to malformed leaflets or annulus hypoplasia.

Interventricular Communications

The connection between the dominant ventricular mass and the rudimentary hypoplastic outlet chamber has been referred to by several terms in the literature, including VSD, the bulboventricular foramen, and the outlet foramen. In double inlet LV, the defect will be in the muscular portion of the trabecular septum in most cases, separated from the semilunar valves and completely surrounded by muscle. However, when there is hypoplasia of the infundibulum, the defect may extend into the outlet septum to sit immediately underneath the semilunar valve (subaortic VSD). The outlet foramen often can be restrictive, occurring in 47% of cases in the series published by Bevilacqua et al. (5). The defect can be restrictive or unrestrictive at birth but often will become restrictive over time. In the series by Bevilacqua et al. (5), patients with double-inlet left ventricle (DILV) and transposed great arteries and pulmonary stenosis, the outlet foramen rarely was restrictive. However, when transposition of the great arteries was present without pulmonary stenosis, a restrictive outlet foramen was significantly more common.

COMMON FORMS OF SINGLE VENTRICLE

Double Inlet Left Ventricle

DILV is the most common form of single ventricle described in all series and represents the classically described form of single ventricle. It represents 78% of the cases reviewed by Van Praagh et al. (1). The Van Praagh classification also distinguished four subgroups of DILV based on the great artery relationships: I, normally related great arteries; II, right-anterior aorta; III, left-anterior aorta; and IV, left-posterior aorta (inverted). By combining the criteria distinguishing the types of DILV, three clinically observed forms occur (A-I, A-II, and A-III). In each of these clinical forms, other common associations include subaortic obstruction, pulmonary outflow tract obstruction, and conduction abnormalities (6).

Subaortic obstruction usually occurs with ventricular–great artery (VA) discordance and is located primarily at the VSD (bulboventricular foramen type). It also can be secondary to severe ventricular hypertrophy of muscle bundles within the hypoplastic right ventricle (Fig. 52.7). Subaortic obstruction occurs more often in patients with associated right AV valve atresia and in patients who have had previous pulmonary artery banding procedures. Pulmonary artery banding can set the stage for progressive ventricular hypertrophy and obstruction in patients who have naturally occurring mild restriction at the VSD. These patients often present in infancy with associated coarctation of the aorta.

Pulmonary outflow tract obstruction frequently occurs in DILV and may occur with either concordant or discordant VA connections. When subpulmonary obstruction occurs within the left ventricular chamber, it most frequently is due to posterior deviation of the infundibular septum. Alternatively, it may be due to anomalous attachments of the right AV valve or herniation of valvular tissue into the pulmonary outflow tract.

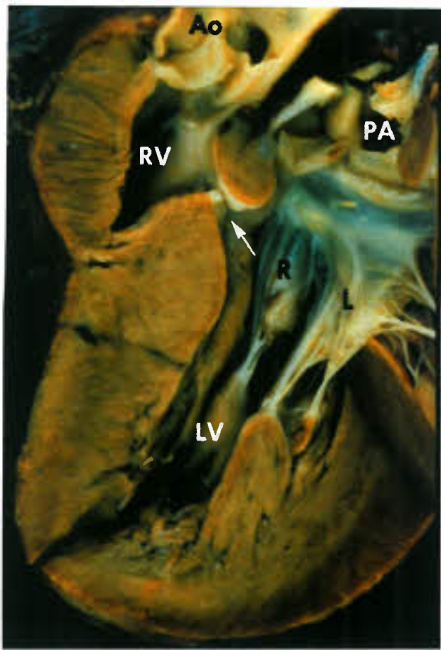


Figure 52.7. Subaortic obstruction. Pathologic specimen demonstrating the anatomic substrate of subaortic stenosis in double-inlet left ventricle (LV). There is severe stenosis of the VSD, or the embryologic bulboventricular foramen (arrow), communicating to the hypoplastic subaortic right ventricle (RV). There is secondary endocardial fibrosis at the site of obstruction. There is severe hypertrophy of the ventricular septum and the free walls of both RV and LV. A pulmonary artery (PA) band was present previously and has been removed. Ao, aorta; R, right atrioventricular valve; L, left atrioventricular valve.

Severe pulmonary valve stenosis and annular hypoplasia can occur. The valve is often bicuspid and thickened.

Conduction abnormalities similar to those described with AV and VA discordance (corrected transposition of the great arteries) can be present. When the AV connection is double inlet, the connecting AV node always is located anterolaterally at the acute margin of the right AV valve orifice (7,8). It subsequently perforates the annulus of the right AV valve to enter the main left ventricular chamber (Fig. 52.8). The nonbranching bundle courses along the right-sided rim of the VSD (outlet foramen) to reach the trabecular septum. The subsequent course of the bundle depends on the location of the rudimentary right ventricular chamber relative to the main ventricular chamber (MVC). If the hypoplastic right ventricle is right-sided, the right margin of the VSD is adjacent to the anterolateral node, and the nonbranching bundle passes

down directly onto the right rim of the VSD. The nonbranching bundle then descends toward the crest of the trabecular septum along the left ventricular aspect of the ventricular septum and branches beneath the septal crest. When the hypoplastic right ventricle is left-sided, the right rim of the VSD, which is now also the anterior margin of the defect, is separated from the anterolateral node by the posterior great artery. The nonbranching bundle therefore must run a more extensive course anterior to the posterior semilunar valve annulus to reach the trabecular septum (Fig. 52.8). In all instances, it is located on the left ventricular aspect of the trabecular septum and descends down the right rim of the ventricular septum, branching below the septal crest. Although the nonbranching bundle always maintains the same relationship to the right rim of the VSD, it appears to be in a different location with right- or left-sided hypoplastic right ventricle when viewed from the hypoplastic right ventricle. If the hypoplastic right ventricle is left-sided, the conduction tissue appears to run above the ventricular defect when viewed from the MVC. If the hypoplastic right ventricular chamber is right-sided, the conduction bundle appears to run beneath the VSD when viewed from the MVC.

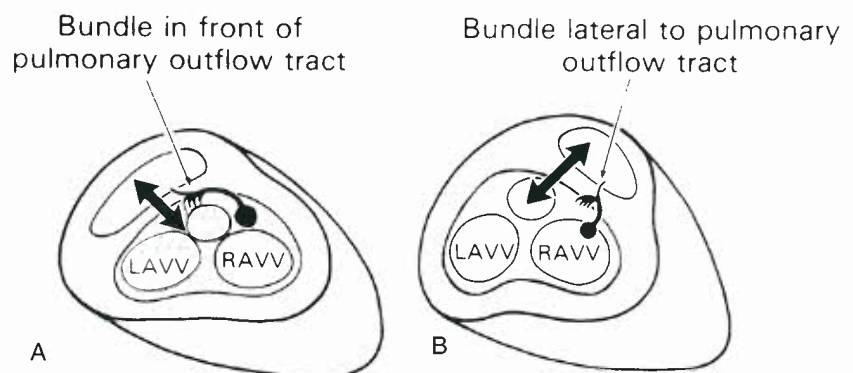
DILV with Normally Related Great Arteries (A-I Single Ventricle, "Holmes Heart")

This form of DILV remains relatively rare, observed in only 15% of the Van Praagh series (7) (Fig. 52.9). Embryologically, the VSD providing communication between the main left ventricular chamber and the hypoplastic right ventricle represents the primitive bulboventricular foramen. Frequently, the VSD creates significant subpulmonary obstruction, resulting in a somewhat balanced circulation with some hypoxia and low pulmonary artery pressure.

DILV with Right-Sided Hypoplastic Subaortic Right Ventricle (A-II Single Ventricle)

DILV with right-sided hypoplastic subaortic right ventricle shares many anatomic features with a similar anomaly consisting of complete transposition of the great arteries with severe override and straddling of the right AV valve into the morphologic LV and associated hypoplasia of the morphologic right ventricle (Fig. 52.10). It was observed in 25% of the cases of single ventricle reviewed by Van Praagh et al. (9). The embryologic development of various types of DILV representing the extreme forms of AV valve straddling (Fig. 52.5) easily supports the common features shared by these defects. In some cases, the AV valve morphology also may follow this schema, with the left-sided AV valve having morphologic features of a mitral valve and the right AV valve features of a tricuspid valve. With VA discordance, the aorta also typically is right-anterior in location. Subaortic and pulmonary stenosis may occur. The conduction tissue enters the trabecular septum

Figure 52.8. Conduction tissue. Schematic illustration of the course of the nonbranching bundle of the conduction tissue along the right rim of the VSD in DILV. **A:** The findings in DILV with a left-anterior subaortic right ventricle. **B:** The conduction tissue in DILV with a right-anterior subaortic right ventricle. LAVV, left atrioventricular valve; RAVV, right atrioventricular valve. (From Davies MJ, Anderson RH, Becker AE. Atrioventricular conduction tissues in congenital heart disease. In: Davies MJ, Anderson RH, Becker AE, eds. *The Conduction System of the Heart*. London: Butterworths, 1983:137.)



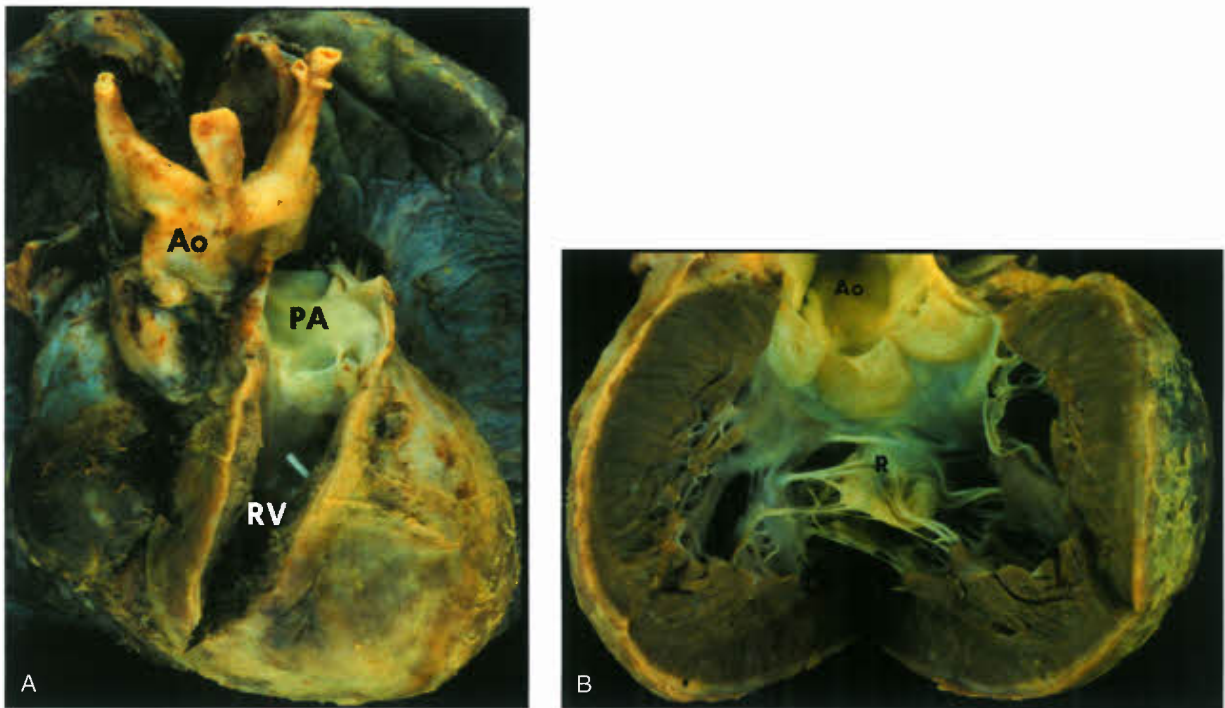


Figure 52.9. Holmes heart. Pathologic specimen illustrating DILV with VA concordance and normally related great arteries. **A:** An external view demonstrating the opened hypoplastic right ventricle (RV), which gives off the pulmonary artery (PA). The aorta (Ao) is right posterior. **B:** Opened view of the LV, which receives both the right (R) and left (L) atrioventricular valves. The aorta originates entirely from the LV.

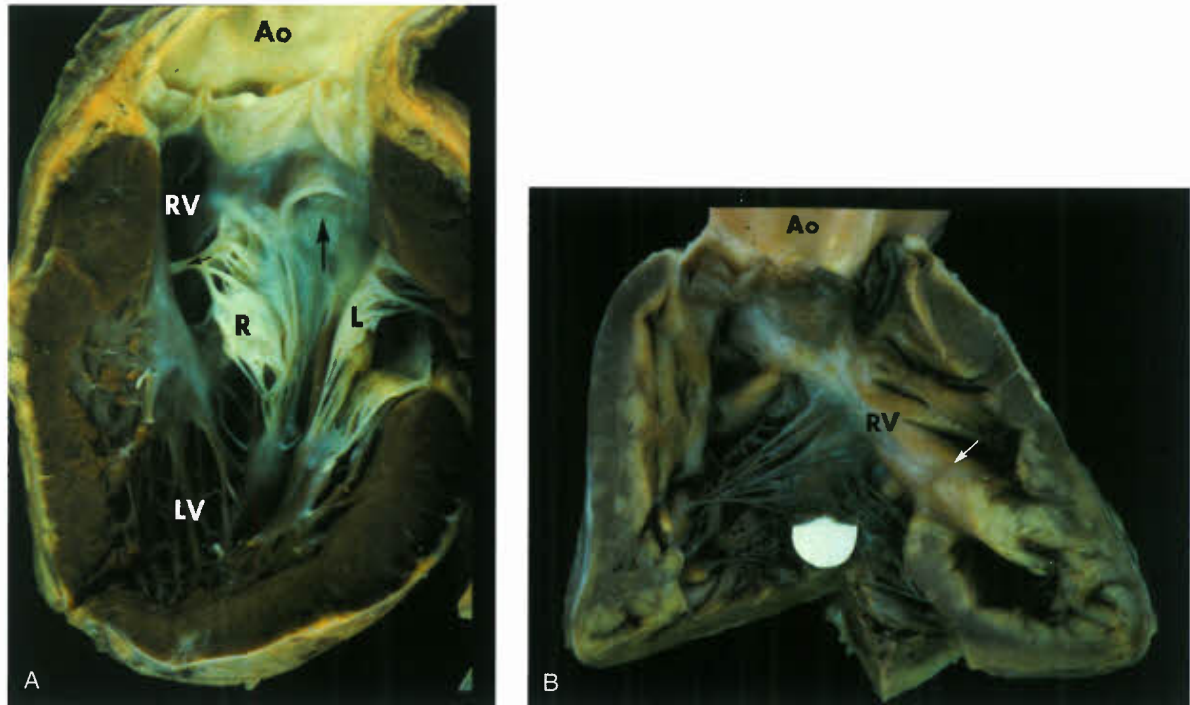


Figure 52.10. Ventricular myocardial morphology. **A:** Pathologic specimen demonstrating the typical left ventricular wall and fine myocardial trabeculations in the left ventricular (LV) chamber of DILV. There is also straddling (*small arrow*) of the right AV valve (R) into the hypoplastic right ventricle (RV). The *large arrow* indicates the stenotic pulmonary outflow tract. Subpulmonary stenosis is present because of posterior deviation of the conus septum the aorta [Ao] overrides the ventricular septum producing a tunnel-like fibromuscular stenosis. **B:** Pathologic specimen demonstrating typical right ventricular myocardial pattern of an irregular coarse ventricular wall with thick heavy trabeculations in the main chamber of common-inlet RV. The *white probe* enters the ventricle through a common atrioventricular valve. L, left atrioventricular valve.

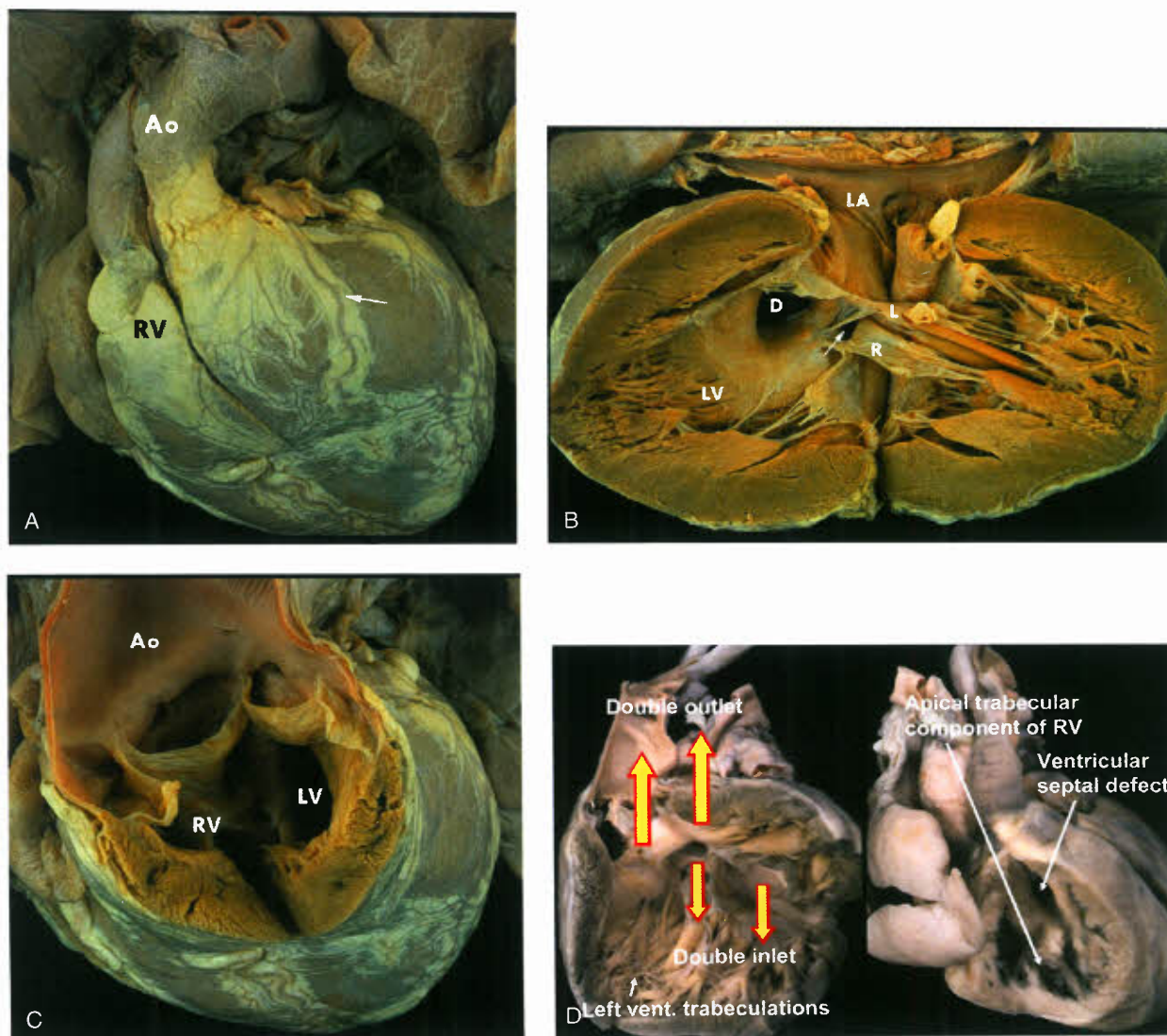


Figure 52.11. Pathologic specimen of the most common form of DILV with left-sided hypoplastic subaortic right ventricle (RV) and left-anterior aorta (Ao) (A-III single ventricle). There is situs solitus of the atria and both right (R) and left (L) AV valves are entirely committed to the LV with no AV valve straddling. The VSD is well observed in the short-axis cut demonstrated in C. LA, left atrium; PA, pulmonary artery; RA, right atrium.

from an anterolateral node (7). The nonbranching bundle courses along the rightward rim of the VSD and subsequently distributes over the crest of the ventricular septum. Cook and Anderson reported an example of DILV with double-outlet LV and a small right-sided morphologic right ventricle which lacked both inlet and outlet components.

DILV with Left-Sided Subaortic Hypoplastic Right Ventricle (A-III Single Ventricle)

DILV with left-sided subaortic hypoplastic right ventricle is the most common type of univentricular connection observed in most reviews (9,10). It was encountered in 38% of the series review by Van Praagh et al. (9) In this early series, most examples of this defect were thought to represent examples of ventricular l-looping with the morphologic LV to the right and therefore with the morphologic mitral valve to the right of the morphologic tricuspid valve. Developmentally, one could speculate that this form of DILV shares anatomic features similar to AV and VA discordance (corrected transposition of the great arteries) but that severe overriding and straddling of the

left-sided tricuspid valve ultimately resulted in predominant commitment of the left AV valve to the morphologic LV and DILV (Fig. 52.11). Thus, varying degrees of residual straddling of the left AV valve into the morphologic right ventricle would not be an unusual finding in this form of DILV. This seems a plausible and rational developmental explanation; however, in many instances of DILV, the AV valve anatomy is not sufficiently distinct to allow accurate differentiation of morphologic mitral or tricuspid valves. There also is significant variation in the size of the morphologic right ventricular cavity. It may be extremely hypoplastic—a tiny slit-like chamber—or can be 75% or 80% of the size of a normal right ventricular chamber, particularly when the left AV valve straddles into the right ventricle.

A variety of associated AV valve, semilunar valve, and outflow tract anomalies may occur. Subaortic obstruction is an important associated lesion that must be assessed when considering a modified Fontan procedure. Significant ventricular hypertrophy substantially increases operative risk for Fontan operation because of associated ventricular diastolic filling abnormalities and elevated left ventricular end-diastolic pressure.

The conduction tissue abnormalities are similar to those described for AV and VA discordance (7). The AV node is anterolateral, and the nonbranching bundle courses into the ventricle anterior to the pulmonary outflow tract, subsequently coursing superiorly along the right (anterior) rim of the VSD. An ECG feature typically described for DILV is abnormal initial septal depolarization with the initial horizontal plane QRS vector directed leftward and anteriorly rather than rightward. There is an absence of a precordial Q wave. This abnormal septal depolarization is secondary to the abnormal course of the conduction system as previously described and in patients with AV and VA discordance.

Double-Inlet Right Ventricle

Double-inlet right ventricle was found in only two patients, or 5%, of the series reviewed by Van Praagh et al. (1,9). These investigators described it as an absence of the left ventricular sinus. There was a virtual absence of the LV, however. The ventricular myocardium had coarse, straight trabeculations consistent with right ventricular morphology. However, investigators in more recent reviews (6) noted the presence of a hypoplastic rudimentary left ventricular chamber that usually can be recognized by careful angiographic or echocardiographic analysis. Both AV valves either have >75% of the total AV valve orifices or complete connection to the morphologic right ventricle. The hypoplastic LV usually is located posteriorly and slightly to the left of the morphologic right ventricle. This ventricular relationship is consistent with an embryologic D-ventricular loop. Less often, the ventricular relationships are inverted, with the hypoplastic LV anterior and to the right, consistent with an L-ventricular loop. There is considerable variability in the size of the hypoplastic left ventricular chamber, but most often it is very hypoplastic. The VA connections may be concordant or discordant, but double-outlet right ventricle is usually present. Frequently, pulmonary stenosis or atresia is present with infundibular and pulmonary annular hypoplasia. If there is significant straddling of the AV valve, the LV may be large.

The path of the conduction tissue is related to the location of the hypoplastic LV and is normal when the hypoplastic LV is leftward and posterior (7). With the ventricular relationships inverted, the pattern is typical of that observed with AV and VA discordance (congenitally corrected transposition of the great arteries). Essed et al. (11) reported a sling of conduction tissue between a regularly positioned posterior node and a typical anterolateral node in AV and VA discordance.

Double-Inlet Ventricle of Mixed Morphology

Double-inlet ventricle of mixed morphology is a rare form of univentricular connection and occurred in only 5% of the series reported by Van Praagh et al. (1,9). Also called a common ventricle, it was designated by Van Praagh as the C type of single ventricle with absence of the ventricular septum or undivided ventricles with a rudimentary septum. A small apical ridge of ventricular septum may often separate the right and left ventricular zones of the heart. Relationships of the ventricular zones are usually consistent with normal ventricular locations or D-ventricular looping. Often, the great arteries are normally related; however, malposition with right- or left anterior aorta may occur. Subvalvular and valvular pulmonary stenosis may be present.

The conduction system has been described as normal, with a regular posterior position for the AV node (7). In some, there may be dual AV nodes with a sling of conduction tissue connecting the two. The nonbranching bundle appears to descend into the remnant of ventricular septum that separates the right and left ventricular zones.

Double-Inlet Ventricle with Indeterminate or Undifferentiated Morphology

This often is considered a primitive form of univentricular AV connection without a rudimentary chamber. It shares many of the pathologic features of both double-inlet right ventricle and double-inlet of mixed morphology (Fig. 52.12). This type

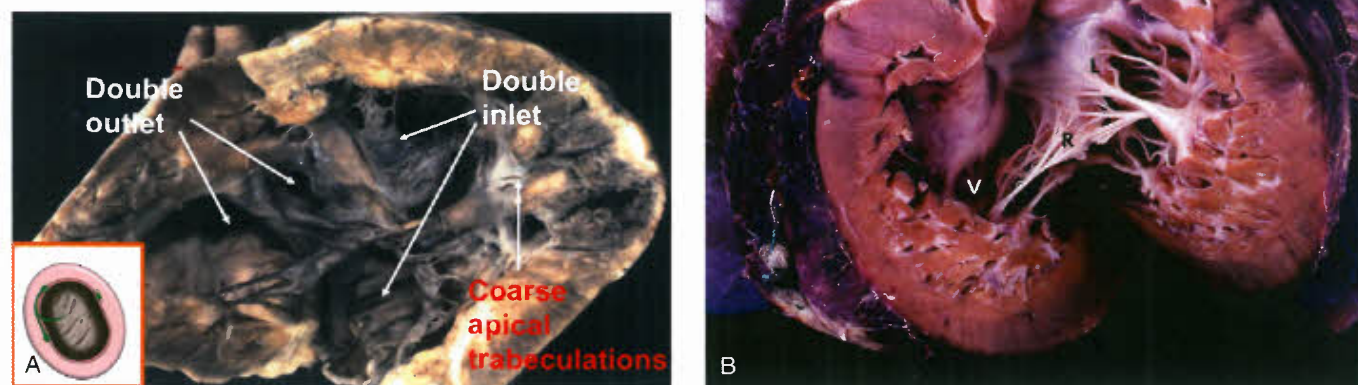


Figure 52.12. Double-inlet ventricle (mixed and indeterminate). The pathologic descriptions of these forms of double-inlet ventricle often share similar features. **A:** Pathologic features of mixed or indeterminate ventricular morphology with coarse trabeculated myocardium on the right and smooth-walled myocardium on the left. **B:** Pathologic specimen demonstrating double-inlet ventricle (V) of indeterminate morphology. Some features of this specimen suggest DILV but with left ventricular noncompaction. The right (R) and left (L) AV valve chordae interdigitate into the same papillary muscles within the same ventricle. Only the aorta (Ao) originated from the ventricular chamber.

of double-inlet ventricle often is diagnosed when no clear-cut differentiation or distinction of ventricular myocardium can be determined. AV valve abnormalities can include valvular stenosis or hypoplasia. Large, malformed AV valves often are regurgitant. The great arteries may be normally related. However, most commonly, the aorta is located anteriorly and to the right or left of the pulmonary artery. Pulmonary stenosis with subvalvular and valvular stenosis or pulmonary atresia may be present.

Location of the conduction system varies, with anterolateral and normally positioned posterior nodes described (7). The nonbranching bundle either penetrates directly into the right lateral wall of the ventricular chamber or descends through a large trabeculation toward the ventricular apex.

Single-Inlet Ventricle

This can include all forms of univentricular AV connection resulting from atresia or absence of either the right or left AV valve. The single-inlet connection may be to either a morphologic right ventricle with mitral valve atresia or a morphologic LV with tricuspid valve atresia. AV concordance is common, but the AV connection can be discordant. Either ventricle can be hypoplastic. Figure 52.3 illustrates a pathologic, angiographic, and echocardiographic correlation of single-inlet LV with right AV valve (tricuspid) atresia. VA concordance or discordance occurs with a range of great artery relationships from normal

to transposition with a right or left anterior aorta. Subvalvular and valvular pulmonary stenosis can occur with concordant or discordant VA connections. Subaortic obstruction may occur predominantly with discordant VA connections.

When there is AV concordance with absent right AV connection or classic tricuspid atresia, the conduction system is similar to that seen in isolated VSD (12). As viewed from the hypoplastic right ventricle, the nonbranching bundle is located on the left ventricular aspect of the right rim of the VSD, unrelated to the septal crest. With AV discordance, the regular posterior node cannot make contact with the ventricular myocardium. Instead, the anterior AV node is the connecting node, and the nonbranching bundle encircles the anterior aspect of the pulmonary valve to reach the right rim of the VSD where the bundle branches. With single-inlet right ventricle, the nonbranching bundle on the ventricular septum makes contact with the normally located posterior AV node. In some cases, the conduction tissues may descend through a large, free-running trabeculation to the ventricular apex.

Common-Inlet Ventricle

Common-inlet ventricle is a unique form of univentricular AV connection that is characterized by communication of both atria to a single-ventricular chamber by a common AV valve. It is a form of AV septal defect. Frequently, this is associated with situs ambiguus, particularly asplenia (Fig. 52.13). In the

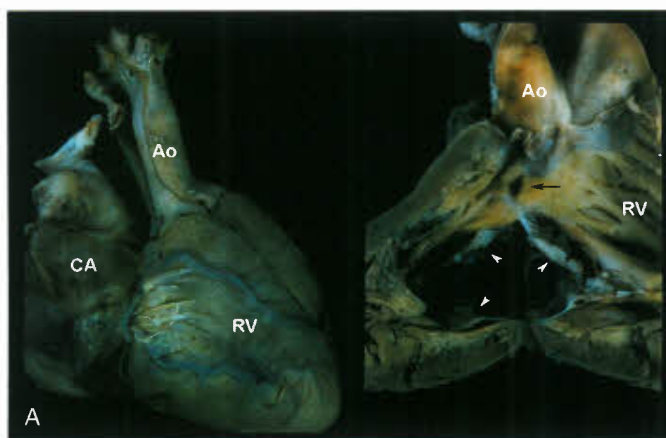
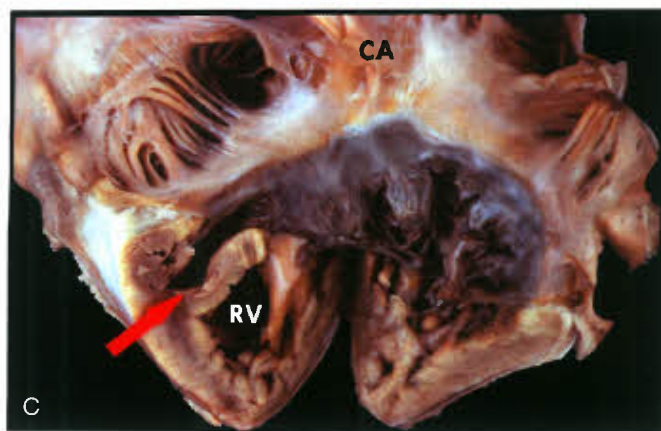
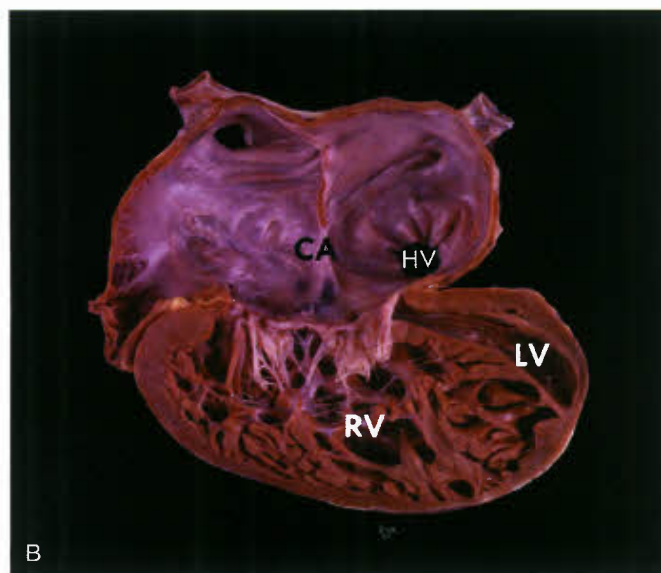


Figure 52.13. Common-inlet AV connections. **A:** Pathologic specimens illustrating features of common atrium and common-inlet right ventricle (RV). **A,** 2-day-old infant with situs ambiguus, levocardia, and asplenia (right isomerism). There is a common atrium (CA) and common-inlet RV. With the opened view of the RV, the white arrows outline the common inlet. The atretic pulmonary outflow tract (*black arrow*) is to the right and slightly posterior to the aorta (Ao). There is no evidence of a LV. **B:** Common-inlet RV in a 14-year-old with levocardia and polysplenia (left isomerism). The hepatic veins (HV) entered the floor of the left side of the common atrium (CA) while the pulmonary veins entered the ipsilateral side of the atrium. A tiny slit-like left ventricle (LV) does not receive inflow from the common AV valve. **C:** Common-inlet RV in a 7-year-old patient with right isomerism. The common AV valve is nearly entirely committed to the large morphologic RV. There is an L ventricular loop with a small right-sided morphologic LV (probe), which receives a few cords of the AV valve.



common-ventricle series of Van Praagh et al. (1,9), about 33% had a common AV inlet, with 40% of these having asplenia. As with unbalanced AV septal defects, the main or larger ventricular chamber, depending on the predominant commitment of the common AV valve, may be a morphologic LV (type A Van Praagh), a morphologic right ventricle (type B), or a ventricle with undifferentiated myocardium (type D). There often is double-outlet right ventricle or VA discordance with a right or left anterior aorta, but normally related great arteries also have been reported. Stenosis or atresia of the pulmonary valve is frequent. In hearts with MVC of left ventricular type, the right ventricular portion of the common AV valve may be stenotic or partially atretic, resulting in predominant commitment of the common AV valve to the morphologic LV. Similarly, stenosis or atresia of the left component of the common AV valve may occur with a predominant right AV component and morphologic right ventricle. Because of the common drainage of both atria through a common AV orifice, the stenotic or atretic portion of the AV valve does not seem to disqualify such cases from the category of common AV connection. The disposition of the AV conduction tissue seems determined primarily by the anatomic relationships observed in AV septal defects. Often, both posterior and anterolateral node structures give rise to the penetrating bundles and a sling of conduction tissue. With indeterminate or morphologic right ventricular morphology, the penetrating bundles are described as descending along the posterolateral aspect of the MVC. Some hearts with 1-loop ventricular relationships have been described as having predominant or single anterolateral node with the penetrating bundle having a relationship to the ventricular septum typical of that observed with corrected transposition of the great arteries.

Clinical Features

The clinical features of univentricular AV connection are determined primarily by the presence or absence of pulmonary outflow obstruction. Patients without obstruction to pulmonary blood flow will demonstrate signs and symptoms typical of other large, left-to-right shunting VSDs. Severe congestive heart failure with tachypnea, tachycardia, diaphoresis, hepatomegaly, and failure to thrive may manifest within the first 3 months of life. Symptoms of congestive heart failure earlier in the neonatal period will more often be secondary to associated lesions such as AV valve abnormalities, aortic outflow obstruction, and coarctation of the aorta. Because of increased pulmonary blood flow, cyanosis may not be evident. Some patients with DILV and subaortic right ventricle to the left (inverted) have “favorable streaming,” with systemic venous blood preferentially directed into the pulmonary artery and pulmonary venous return directed to the aorta. Similarly, patients with right-sided subaortic right ventricle and various degrees of straddling right AV valve may have “unfavorable” streaming with transposition-like blood flow patterns resulting in significant systemic hypoxemia and cyanosis. A soft systolic ejection murmur secondary to flow-related relative pulmonary outflow obstruction or flow through the VSD to the hypoplastic right ventricle may be heard. Because of the presence of large pulmonary blood flow, a diastolic AV valve inflow murmur may be present. Pulmonary congestion and pneumonia can be the presenting findings.

If moderate pulmonary outflow obstruction or atresia is present, hypoxemia and cyanosis may be observed during the neonatal period. A systolic thrill may be present with pulmonary or subaortic outflow obstruction. A systolic ejection murmur and single second heart sound may be heard. The pulmonary valve closure sound may be audible and have mild degrees of pulmonary obstruction. No murmur may be

audible, or a soft continuous murmur may be evident secondary to a patent ductus arteriosus or a systemic pulmonary collateral artery with pulmonary atresia. In older patients with long-standing pulmonary hypertension, severe pulmonary vascular obstructive disease may be present by 2 years of age, resulting in progressive reduction in pulmonary blood flow and cyanosis. The second heart sound may be single and accentuated. A diastolic murmur of pulmonary valve regurgitation may be present.

Echocardiographic Features

Diagnostic features of univentricular AV connection are best detailed from the apical view delineating the crux of the heart, as in the apical four-chamber view, demonstrating the AV connection and the status and commitment of the AV valves (13–15). Figure 52.14 demonstrates the echocardiographic apical view in the basic type of univentricular connection, including double-inlet ventricle, single-inlet ventricle, and common-inlet ventricle. Additionally, parasternal short-axis scans and subcostal four-chamber views are particularly important for detailing the location of papillary muscle and chordal attachments within the ventricular chambers, the location of hypoplastic outlet or rudimentary chambers, the status of the AV valve leaflets and orifice sizes to assess for valvular stenosis, and for illustrating the location, commitment, and relationships of the great arteries. Figure 52.15 illustrates progressive short-axis scans in a patient with DILV with hypoplastic subaortic right ventricle anterior and to the left. At the apex (Fig. 52.15A), a large MVC of left ventricular morphology is observed posteriorly. As the scan progresses to the base, both AV valves are committed nearly entirely to the LV, and a single chordae of the left AV valve attaches near the VSD in the hypoplastic right ventricular outlet chamber. At the base of the heart (Fig. 52.15D), the aorta is anterior and to the left. There is evidence of severe pulmonary valve stenosis with a thickened bicuspid pulmonary valve. Short-axis scans demonstrate the ventricular chamber dimensions and wall thickness and provide a visual estimate of global ventricular contractility. Figure 52.16 illustrates parasternal short- and long-axis scans in a patient with DILV and hypoplastic subaortic right ventricle. Both the short- and long-axis scans allow estimation of the size of the VSD, which is relatively obstructive. There also is hypertrophy of the ventricular septum, producing additional right ventricular outflow obstruction. A tight pulmonary artery band that produces severe main pulmonary artery obstruction is seen. Subaortic obstruction has been observed frequently in patients with DILV following pulmonary artery banding and Fontan operation (16). It remains uncertain whether pulmonary artery banding simply provokes progressive ventricular hypertrophy in a patient with an underlying substrate of mild subaortic obstruction or whether the development of subaortic obstruction occurs *de novo* in a patient with no previous evidence of aortic obstruction.

Continuous-wave Doppler interrogation of the ascending aorta from a high left parasternal location (near the second intercostal space in the midclavicular line) provides an estimate of the subaortic obstruction by determining the mean subaortic gradient by planimetry of the ascending aortic velocity tracing to obtain a mean velocity and applying the Bernoulli equation ($\text{pressure gradient} = 4V^2$). A mean gradient estimate of the subaortic obstruction is used because the maximum instantaneous gradient overestimates the catheter-measured peak-to-peak systolic gradient (17). If significant subaortic obstruction is observed, there may be concomitant hypoplasia of the aortic annulus and ascending aorta with associated coarctation of the aorta. Adequate parasternal and suprasternal notch imaging must be obtained to assess the

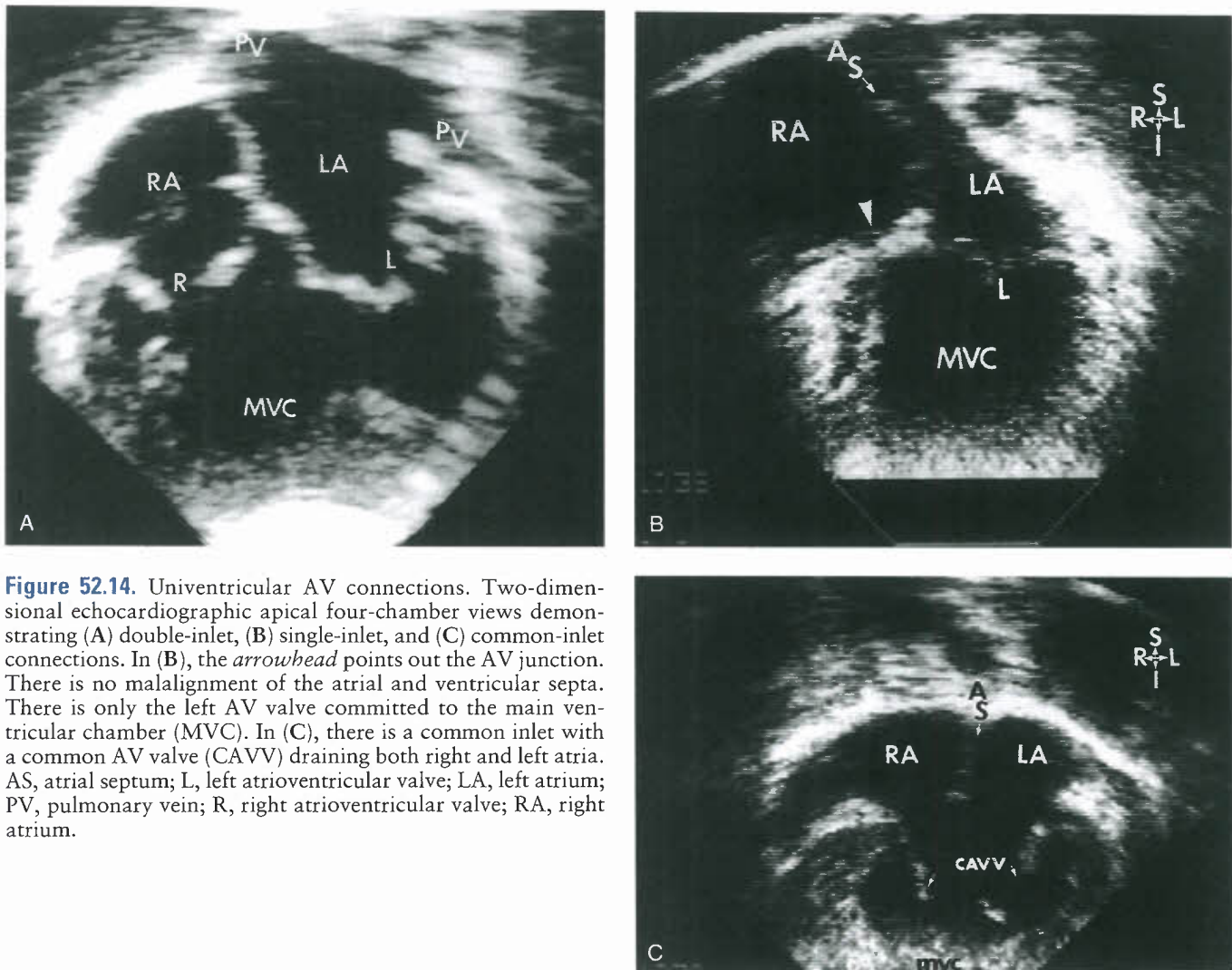


Figure 52.14. Univentricular AV connections. Two-dimensional echocardiographic apical four-chamber views demonstrating (A) double-inlet, (B) single-inlet, and (C) common-inlet connections. In (B), the arrowhead points out the AV junction. There is no malalignment of the atrial and ventricular septa. There is only the left AV valve committed to the main ventricular chamber (MVC). In (C), there is a common inlet with a common AV valve (CAVV) draining both right and left atria. AS, atrial septum; L, left atrioventricular valve; LA, left atrium; PV, pulmonary vein; R, right atrioventricular valve; RA, right atrium.

status of the aorta and aortic arch. Figure 52.17 illustrates parasternal short-axis scans of two examples of double-inlet right ventricle with posterior rudimentary left ventricular chambers. Ventricular morphology can be assessed from similar parasternal short-axis scans, demonstrating the AV valve leaflet configuration (trileaflet vs. bileaflet) and the papillary muscle arrangement (multiple vs. double). Ventricular myocardial morphology suggested by a coarse trabecular ventricular wall pattern or smooth wall appearance is illustrated with short-axis scans of Figure 52.18, demonstrating double-inlet ventricle of mixed morphology. The anatomy is suggestive of the type C common ventricle of Van Praagh et al. (1,9) or an undivided ventricle with right ventricular morphology on the right and left ventricular morphology on the left.

Apical and subcostal four-chamber views should be used to demonstrate AV valvular abnormalities, including atresia or stenosis, and annular override or valvular straddling. Figure 52.19 illustrates an apical view in a patient with DILV and overriding and straddling right AV valve. There is >50% commitment of the right AV valve into the LV, establishing the diagnosis of DILV; however, the right AV valve also has some commitment and chordal attachment into the morphologic right ventricle. This observation is similar to the schematic drawings proposing the embryologic development of double-inlet ventricle from a progressively increasing degree of

AV valve override. The apical four-chamber view of Figure 52.2 illustrates an example of DILV with right AV valve atresia. The AV septum is shifted to the left, resulting in primary commitment of the atretic plate of the right AV valve into the morphologic LV and establishing the diagnosis of DILV. A small subpulmonary right ventricular outlet chamber is observed on the right. The apical view allows assessment of the planes of the atrial and ventricular septa, determining the degree of atrial commitment to a ventricular chamber. When combined with Doppler echocardiography and color-flow imaging, an estimate of severity of AV valve stenosis or regurgitation can be made. Subcostal views may be used to illustrate the status of the AV connection (double, single, common) and to obtain parasagittal or long-axis views to demonstrate the aortic and pulmonary outflow tracts. The four-chamber view illustrated in Figure 52.6 demonstrates an example of double-inlet right ventricle with severe stenosis of the left AV valve. There is marked thickening of the valve leaflets with short, thickened chordae to a papillary muscle in the right ventricle. The left atrium is enlarged, consistent with left AV valve obstruction. A hypoplastic, rudimentary left ventricular chamber also is observed to the left of the large right ventricle. Figure 52.20 illustrates a pathologic specimen and an echocardiographic subcostal view demonstrating single-inlet right ventricle with left AV valve atresia. Atretic valve tissue forms a dense plate at

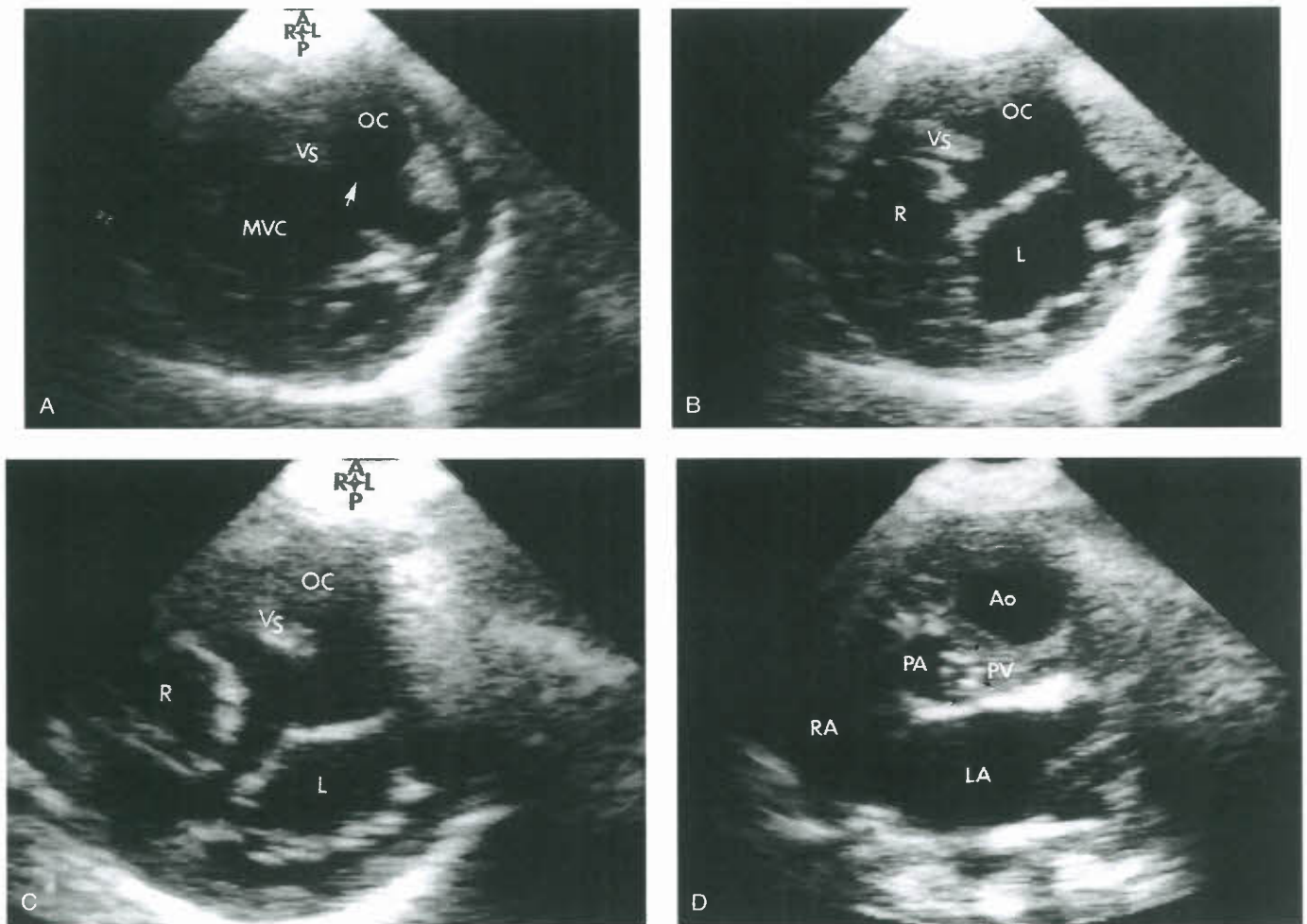


Figure 52.15. Progressive parasternal short-axis scans from apex (A) to base (D) in a patient with DILV with left-anterior subaortic right ventricle. There is a large VSD (white arrow) from the main ventricular chamber (MVC) of the left ventricular morphology into the hypoplastic outlet chamber (OC) of right ventricular morphology. The left (L) AV valve straddles into the right ventricular chamber through the VSD. There is pulmonary valve (PV) stenosis with thickened leaflets (black arrows). Ao, aorta; LA, left atrium; PA, pulmonary artery; R, right atrioventricular valve; RA, right atrium; VS, ventricular septum.

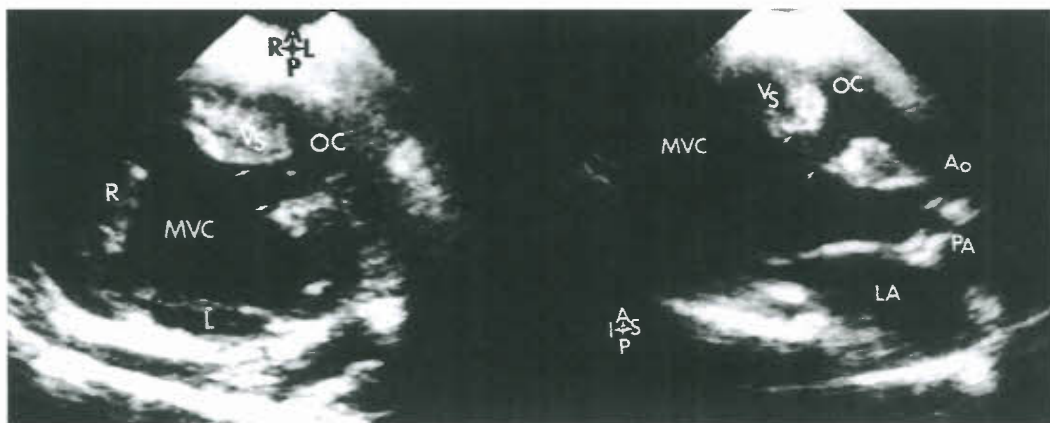


Figure 52.16. Parasternal short-axis (left panel) and long-axis (right panel) scans in a patient with DILV with previously placed pulmonary artery (PA) band. The VSD (arrows) is a moderately restrictive communication between the main ventricular chamber (MVC) and the outlet chamber (OC) of right ventricular morphology. In addition, the ventricular septum (VS) is moderately hypertrophied. Ao, aorta; L, left atrioventricular valve; LA, left atrium; R, right atrioventricular valve; RA, right atrium; VS, ventricular septum. (From Seward JB, Tajik AJ, Hagler DJ, et al. Two-dimensional echocardiographic Atlas. *Congenital Heart Disease*. Vol. 1. New York: Springer-Verlag, 1987:240, with permission.)

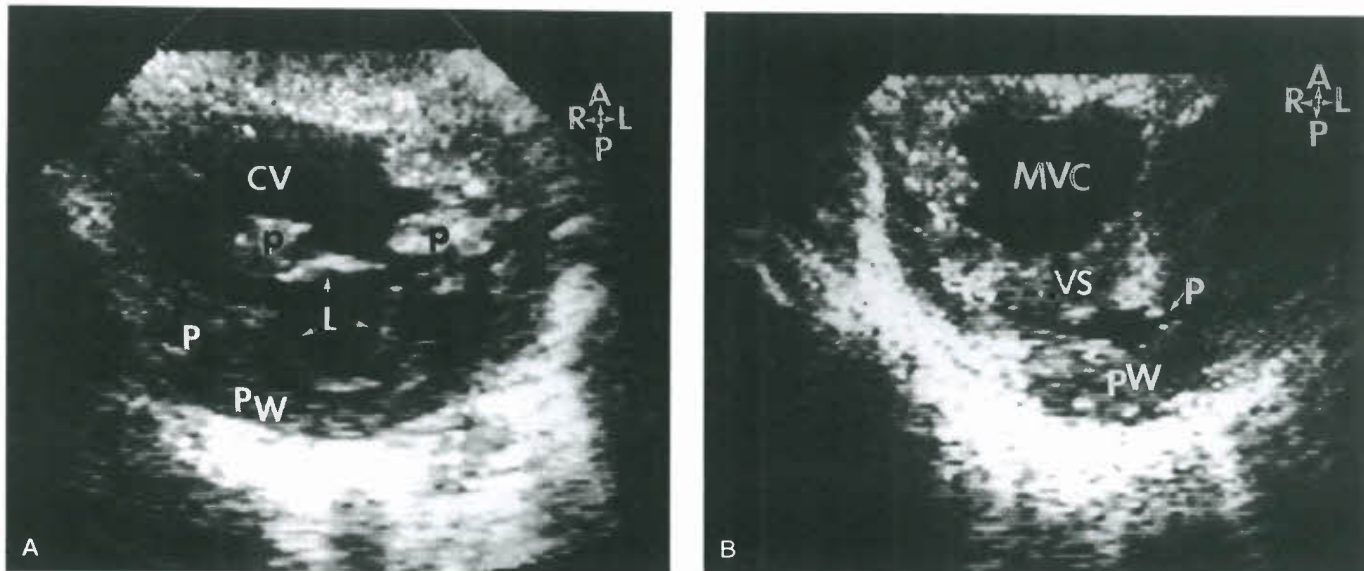


Figure 52.17. Parasternal short-axis scans demonstrating two examples of double-inlet right ventricle with a posterior hypoplastic LV. A: Hypoplastic LV (white P) posterior and to the right. B: Hypoplastic LV (P) posterior and to the left. The right-sided hypoplastic LV suggests that L-ventricular looping occurred, and the LV suggests a D-ventricular loop. In both cases, the AV valves were entirely committed to the main ventricular chamber (CV and MVC). L, left atrioventricular valve; black p, papillary muscle; PW, posterior wall; VS, ventricular septum.

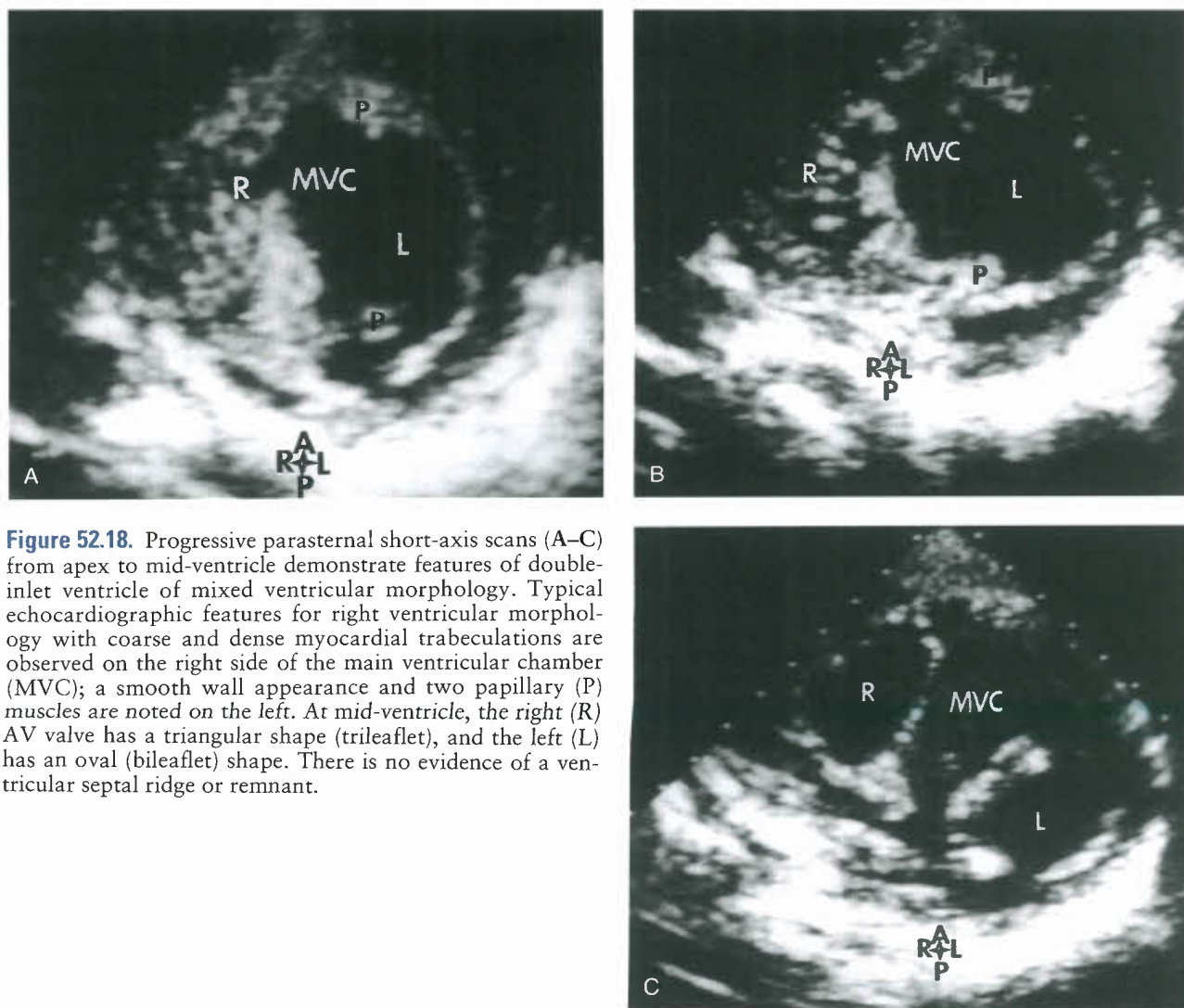


Figure 52.18. Progressive parasternal short-axis scans (A–C) from apex to mid-ventricle demonstrate features of double-inlet ventricle of mixed ventricular morphology. Typical echocardiographic features for right ventricular morphology with coarse and dense myocardial trabeculations are observed on the right side of the main ventricular chamber (MVC); a smooth wall appearance and two papillary (P) muscles are noted on the left. At mid-ventricle, the right (R) AV valve has a triangular shape (trileaflet), and the left (L) has an oval (bileaflet) shape. There is no evidence of a ventricular septal ridge or remnant.

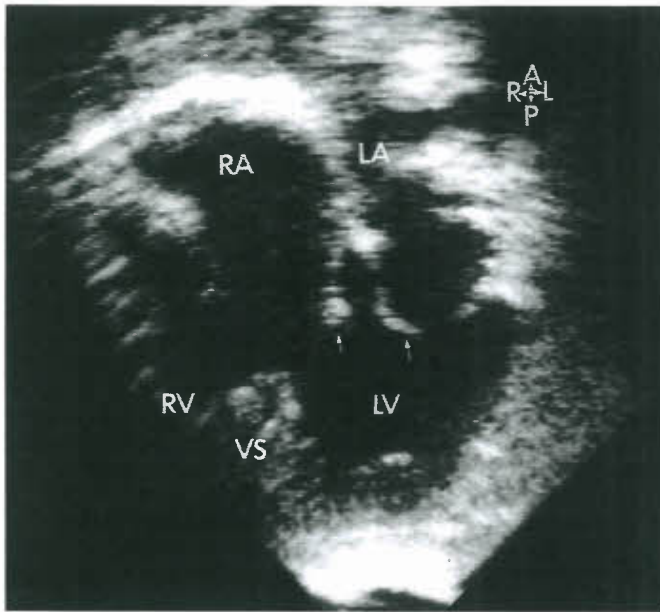


Figure 52.19. Apical four-chamber view demonstrating double-inlet LV with straddling right AV valve. More than 50% of the right AV valve annulus is committed to the left-sided morphologic LV. Arrows point to abutting leaflet of the right and left AV valves. LA, left atrium; RA, right atrium; RV, right ventricle; VS, ventricular septum.

the expected site of the mitral valve. A hypoplastic rudimentary LV is observed inferior to the atretic valve tissue. Both great arteries arise from the morphologic right ventricle.

Radiographic Features

Several typical radiographic findings may be observed in patients with double inlet with hypoplastic subaortic right ventricle located anteriorly and to the left (18). As in AV and VA discordance (corrected transposition), the posteroanterior chest film demonstrates a prominent upper left-sided heart border consisting of the right ventricular infundibulum, the aortic root, and the ascending aorta (Fig. 52.21). The main pulmonary artery and the right pulmonary artery may be dilated and can produce a prominent upper right-sided heart border and right pulmonary hilum described as a waterfall right hilum.

In cases with a moderate degree of pulmonary stenosis, the pulmonary vascularity may appear normal or slightly decreased. The heart size may be normal or only mildly enlarged. With pulmonary atresia, the pulmonary vascularity may be reduced or asymmetric as a result of systemic-to-pulmonary artery shunting.

Magnetic resonance imaging (MRI) is extremely valuable for demonstration of extracardiac abnormalities of systemic and pulmonary venous connections and aortic arch and central and proximal pulmonary artery branch abnormalities. When used in combination with coronal images, MRI has been an effective means of establishing segmental descriptions of congenital cardiovascular anomalies, including viscerotransposition and types of AV and VA connections. ECG-gated transverse images should provide an excellent means of accurate assessment of ventricular mass, similar to techniques described for cine computed tomography (CT) studies. Recognition of the impact of increased ventricular mass on surgical mortality and morbidity has been described in several studies that investigated the development of subaortic stenosis in patients with

double-inlet ventricle both before and after surgical repair by the modified Fontan procedure (16,19). Recent studies demonstrated that MRI provides an excellent noninvasive method for preoperative assessment of ventricular mass, volume, and function for the irregularly shaped ventricular chambers observed in the various types of univentricular AV connection.

Cardiac Catheterization and Angiography

The goals of cardiac catheterization should include a demonstration of (a) the location and integrity of systemic and pulmonary venous connections, including the presence and adequacy of atrial communications; (b) the status and function of AV and VA connections and valves; (c) basic ventricular morphology and function, including chamber dimensions, hypertrophy, and systolic and diastolic function; (d) the size, integrity, distribution, and arteriolar resistance of the pulmonary vascular bed; and (e) the location and integrity of the aorta and aortic arch to exclude coarctation and to assess presence of systemic-pulmonary arterial collaterals or shunts.

Venous Connections

An assessment of the systemic venous connections should include demonstration of hepatic and inferior vena caval connections either by echocardiography or angiography. Also, angiographic demonstration of the innominate vein should establish its drainage through the right superior vena cava and exclude the presence of a persistent left superior vena cava. If a left superior vena cava is present, its size and connection either to the right or left atrium should be determined. If surgical ligation of a persistent left superior vena cava is considered, balloon occlusion of each superior vena cava with an end-hole balloon-tipped catheter should be used to determine the rise in venous pressure distal to the balloon. An increase in superior vena caval pressure to >20 mm Hg suggests inadequate collateral venous communications to allow safe ligation of the superior vena cava. The presence and integrity of pulmonary venous connections should be determined either by direct catheter measurement of pulmonary venous pressure and pulmonary venous angiography or by pulmonary arterial angiography and pulmonary venous wedge pressure measurement. Anomalous pulmonary venous connections and pulmonary venous stenoses should be excluded. If a single-inlet or an atretic AV connection is present, the presence and adequacy of an interatrial communication should be assessed by echocardiography and Doppler color-flow imaging and by direct catheter measurement of the interatrial pressure gradient. If obstructed systemic or pulmonary venous drainage is determined, atrial septostomy should be performed.

Atrioventricular and Ventricular-Great Artery Connections

Two-dimensional (2-D) echocardiography provides excellent demonstration of the status of the AV connections; however, cineangiography also provides clear demonstration of AV valve commitment, annulus size, and leaflet abnormalities as well as reliable assessment of the presence and severity of valvular regurgitation. Severe AV valvular regurgitation results in ventricular volume overload and elevated filling pressures. Preoperative recognition of these abnormal hemodynamic states is mandatory for accurate assessment of the potential benefits, morbidity, and mortality of the modified Fontan procedure compared with staged palliative procedures (19,20). An initial ventriculogram using standard anteroposterior (AP) and lateral projections provides excellent demonstration of the AV valves and function. As with echocardiography, better demonstration of AV valve commitment and annulus size is obtained from a four-chamber view. The standard AP and lateral views

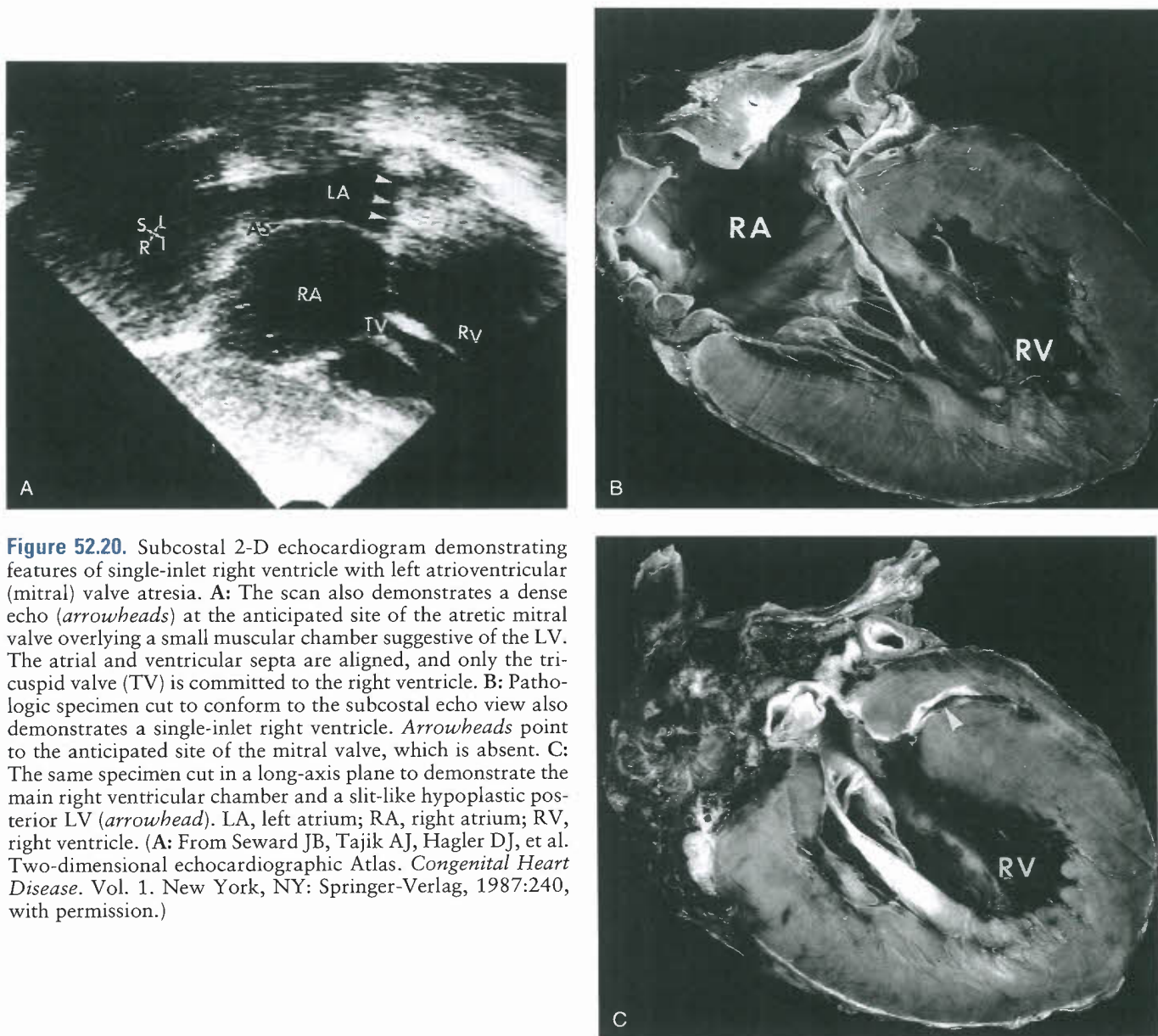


Figure 52.20. Subcostal 2-D echocardiogram demonstrating features of single-inlet right ventricle with left atrioventricular (mitral) valve atresia. **A:** The scan also demonstrates a dense echo (*arrowheads*) at the anticipated site of the atretic mitral valve overlying a small muscular chamber suggestive of the LV. The atrial and ventricular septa are aligned, and only the tricuspid valve (TV) is committed to the right ventricle. **B:** Pathologic specimen cut to conform to the subcostal echo view also demonstrates a single-inlet right ventricle. *Arrowheads* point to the anticipated site of the mitral valve, which is absent. **C:** The same specimen cut in a long-axis plane to demonstrate the main right ventricular chamber and a slit-like hypoplastic posterior LV (*arrowhead*). LA, left atrium; RA, right atrium; RV, right ventricle. (A: From Seward JB, Tajik AJ, Hagler DJ, et al. Two-dimensional echocardiographic Atlas. *Congenital Heart Disease*. Vol. 1. New York, NY: Springer-Verlag, 1987:240, with permission.)

of the ventriculogram generally provide an excellent demonstration of the VA connections and great artery relationships. Figure 52.22 demonstrates AP and lateral views in three types of DILV with anterior hypoplastic right ventricular outlet chamber. These views demonstrate examples of VA concordance, VA discordance, and double-outlet chamber connections. In most cases of DILV, the AP view provides clear demonstration of the size and adequacy of the VSD and the presence of subaortic obstruction at the VSD or within the hypoplastic right ventricle (Fig. 52.23). With angiographic or echocardiographic evidence of subaortic obstruction or a restrictive VSD, careful catheter measurement of aortic and ventricular pressures should be obtained to assess the presence and severity of subaortic obstruction. Simultaneous pressure recordings from the LV and aorta provide accurate measurements of the subaortic gradient. Isoproterenol infusion with simultaneous catheter measurement of left ventricular and aortic pressures also has been recommended to unmask mild or potential subaortic obstruction in the absence of a resting significant pressure gradient (16,21). Resting subaortic pressure gradients of

40 mm Hg or greater have been associated with high operative mortality for the modified Fontan procedure (19). Aortic valve regurgitation usually is demonstrated by 2-D Doppler color-flow imaging; however, in the presence of severe regurgitation, aortic root angiography is necessary to assess the severity of valvular regurgitation prior to aortic valve replacement.

Ventricular Morphology and Function

The basic intracardiac anatomy and ventricular morphology usually can be determined using standard AP and lateral projections by selective injection into the MVC. Figure 52.23 illustrates AP and lateral views of three types of double-inlet ventricle. Double-inlet ventricles of left, right, and indeterminate morphology are demonstrated. Rudimentary hypoplastic right and left ventricular chambers also can be recognized in the same views. Some investigators prefer axial cineangiography to demonstrate the ventricular anatomy. An AP projection of double-inlet ventricle with mixed morphology is demonstrated in Figure 52.24. In this example, the morphologic right

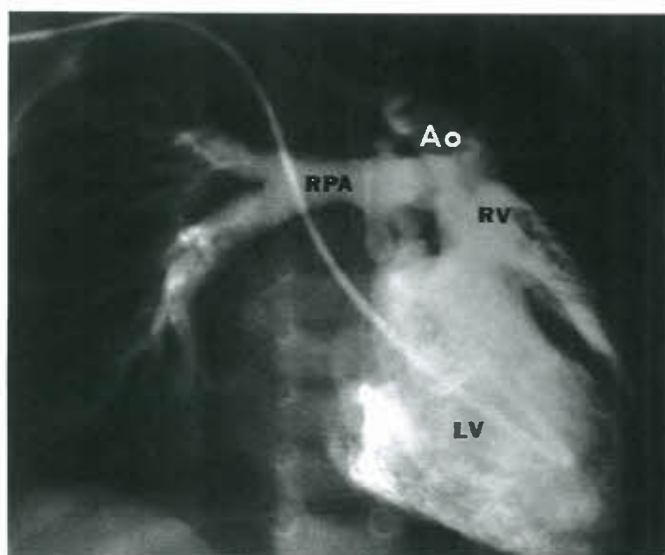


Figure 52.21. Anteroposterior left ventricular angiogram demonstrating the cardiac structures making up typical cardiac shape or contour observed in DILV with left-anterior aorta. Arrows point out the descending right lower lobe pulmonary artery described as producing a waterfall right hilum appearance. Ao, aorta; LV, left ventricle; RPA, right pulmonary artery; RV, right ventricle.

ventricle is located on the left, and there is a double-outlet right ventricle. Despite the irregular ventricular shape, estimates of ventricular ejection fraction obtained from ventricular volume calculations provide a global assessment of systolic ventricular function. Both 2-D and 3-D echocardiography can provide reliable assessments of ventricular volume, mass, and systolic function. Recent comparisons of 3-D echocardiography and MRI images in univentricular AV connection demonstrated similar results.

Ventricular diastolic function may be assessed by 2-D and Doppler echocardiography by assessing pulmonary venous and AV inflow patterns. Findings associated with restrictive disease and ventricular hypertrophy have been described. Further assessment in the cardiac catheterization laboratory can be achieved by measuring ventricular end-diastolic volume, ventricular mass, and estimates of ventricular mass to end-diastolic volume ratio, with concomitant measurement of atrial filling pressures and ventricular end-diastolic pressures. Mean atrial pressures and ventricular end-diastolic pressures exceeding 14 mm Hg may reflect ventricular volume load states, decreased ventricular compliance, or intermediate combinations of both hemodynamic conditions. Elevated filling pressures obligatorily result in elevated mean pulmonary artery pressures, but pulmonary arteriolar vascular resistance determinations also depend on pulmonary flow volume. Several groups demonstrated successful Fontan repairs in patients who did not meet the selection criteria originally proposed by Choussat et al. (22).

Pulmonary Circulation

Adequate pulmonary artery size and distribution have been considered critical components in planning palliative surgical procedures as well as in predicting successful definitive surgical repair, such as modified Fontan procedure. Adequate demonstration of the pulmonary arterial system to delineate the central pulmonary artery size and to exclude distortion or stenoses of the central pulmonary arteries and the distal

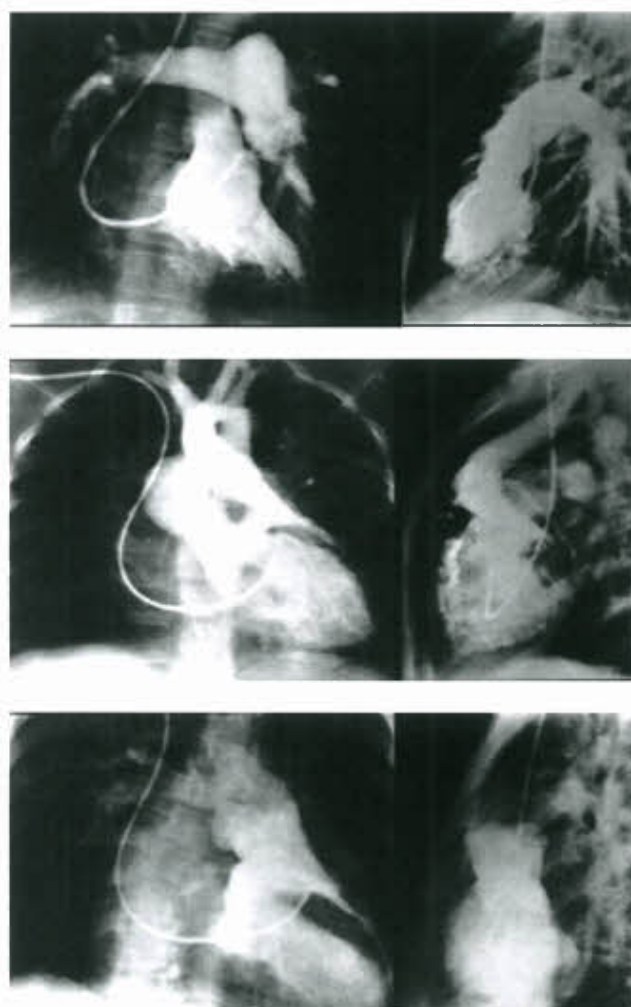


Figure 52.22. Anteroposterior and lateral views of selective left ventricular angiography in DILV demonstrating three types of great artery relationships. **Top panel (A-I)** illustrates ventricular-great artery (VA) concordance with normally related great arteries. **Middle panel (A-III)** illustrates VA discordance with left-anterior aorta. In addition, an aortic arch anomaly with coarctation is present. The subaortic area and the VSD are mildly stenotic. After a Fontan operation, the subaortic stenosis increased requiring further intervention. **Bottom panel (DORV)** illustrates a double-outlet "outlet chamber," or double-outlet right ventricle.

pulmonary arterial distribution remains a critical component of a complete preoperative assessment. This requires special efforts to obtain selective pulmonary artery injections in AP and lateral projections and, if necessary, using cranially angulated right and left oblique views to delineate the central and distal pulmonary arteries. Nakata et al. (12) proposed a method for quantitative standardization of pulmonary artery cross-sectional areas. They determined a normal pulmonary artery area index of $330 \text{ mm}^2/\text{m}^2$. Girod et al. (23), however, observed Fontan survivors with pulmonary artery cross-sectional areas as low as $188 \text{ mm}^2/\text{m}^2$. Previously placed surgical systemic-to-pulmonary artery shunts and Glenn-type cavopulmonary artery shunts must be demonstrated angiographically to exclude pulmonary artery distortion or stenosis.

Pulmonary arteriovenous fistulae are a recognized complication of the standard Glenn shunt to the right pulmonary artery. Angiographic study of Glenn shunts should be routinely obtained to detect the presence of venous collaterals,

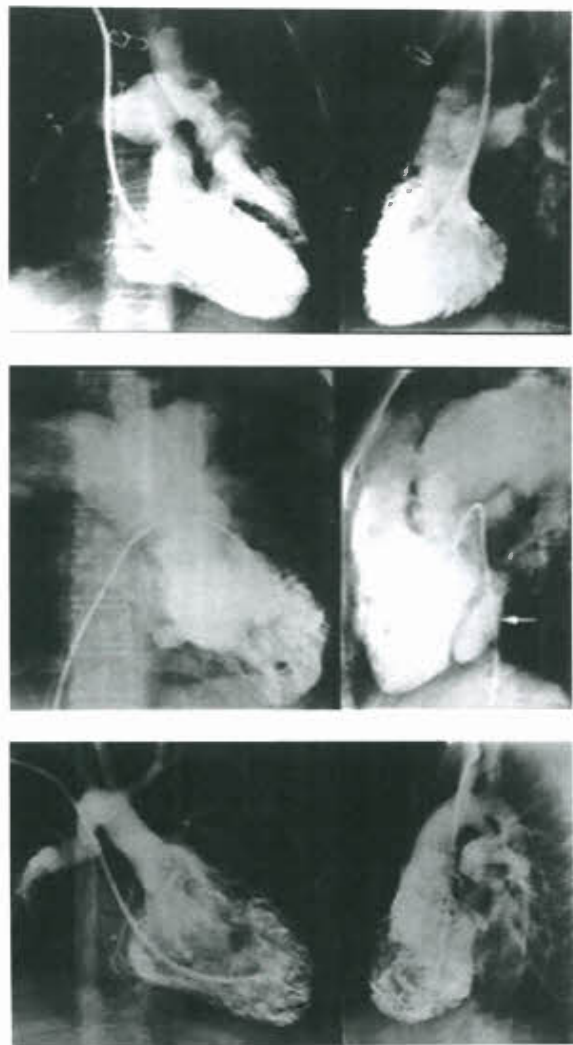


Figure 52.23. Anteroposterior and lateral views of selective ventricular injections in three morphologic types of DILV. (Top panel) illustrates typical features of DILV. Note the pulmonary band and anatomic evidence of subaortic stenosis at the VSD. (Middle panel) demonstrates an example of double-inlet right ventricle with double-outlet right ventricle and an anterior aorta. A hypoplastic rudimentary LV is noted posteriorly (*arrow*). (Bottom panel) demonstrates double-inlet indeterminate ventricle with pulmonary atresia. The ventricle is coarsely trabeculated and irregular, but no hypoplastic LV could be identified.

pulmonary artery stenoses, and pulmonary arteriovenous fistulae. However, contrast echocardiography demonstrating contrast effect appearing within the right pulmonary veins remains a most sensitive method for detection of fistulae. Demonstration of a lower right pulmonary venous blood oxygen saturation compared with the oxygen saturation of the left pulmonary venous blood also may suggest the presence of right pulmonary arteriovenous fistulae.

Systemic Circulation

Aortic arch anatomy should be adequately demonstrated by ventricular angiography or by selective injections to delineate the location of the aortic arch, to obtain the status of the brachiocephalic branches, and to exclude significant coarctation of the aorta. The progressive ventricular hypertrophy and decreased ventricular compliance secondary to the systemic

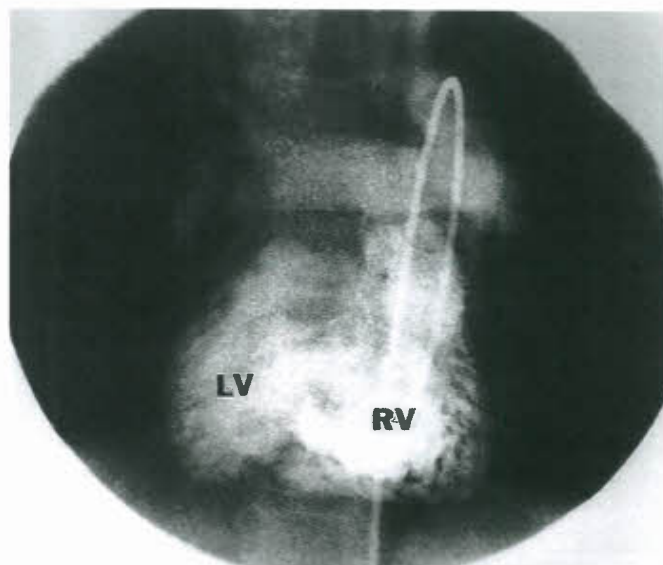


Figure 52.24. Anteroposterior view of selective ventricular injection in patient with situs solitus, mesocardia, double-inlet ventricle of mixed myocardial morphology. The aorta is anterior and slightly to the left of the pulmonary artery. Angiographically, the ventricle is divided into a smooth-walled left ventricular (LV) zone on the patient's right and a trabecular right ventricular (RV) zone on the left, consistent with embryologic L-ventricular looping. Both great arteries originate from the right ventricular zone. The patient underwent a modified Fontan procedure.

hypertension and increased afterload associated with significant coarctation of the aorta are hemodynamic conditions that are poorly tolerated following modified Fontan operation. Preoperative assessment should include angiographic or catheter pressure measurements to exclude this associated lesion. Also, patency of surgically placed systemic pulmonary shunts, persistent ductus arteriosus, or systemic pulmonary collateral vessels should be determined preoperatively with aortic or selective arterial angiography.

Treatment

Rarely, unoperated patients with perfectly balanced circulation may survive into the sixth decade (24). Palliative surgical procedures are important to protect the integrity of both the pulmonary vascular bed and the myocardium. Pulmonary artery banding has been recommended for patients with univentricular AV connection without pulmonary stenosis. Uncontrollable congestive heart failure, excessive pulmonary blood flow, and severe pulmonary hypertension should prompt pulmonary artery banding in early infancy (i.e., younger than 6 months of age) to prevent the development of pulmonary vascular obstructive disease. When performed, pulmonary artery banding should be monitored carefully to determine that reduction of the pulmonary blood flow reduces the pulmonary pressure to normal levels. Even mild elevations of pulmonary vascular resistance (3 U/m^2) will preclude successful Fontan operation. However, several reports have recognized that some patients with univentricular AV connections subjected to pulmonary artery banding will develop subaortic stenosis (24). One must be cognizant of the potential for development of subaortic stenosis and its consequences. Patients with subaortic stenosis, but without pulmonary stenosis, may require alternative methods to protect the pulmonary vasculature. One option is

to interrupt the pulmonary outflow tract and place a systemic-to-pulmonary artery shunt large enough to provide adequate pulmonary blood flow. If significant subaortic stenosis already is present, an aortopulmonary window together with a distal pulmonary artery band has been recommended.

Progressive cyanosis and secondary erythrocytosis in patients with naturally occurring pulmonary stenosis may require a systemic-to-pulmonary artery shunt. The modified Blalock–Thomas–Taussig (BTT) shunt uses a Gore-Tex graft from the subclavian artery to the pulmonary artery. It is preferred because it does not require ligation of the subclavian artery and the length of graft is not limited. Beyond the first 4 to 6 months of life, the bidirectional cavopulmonary connection (bidirectional Glenn shunt) is an effective means of providing long-term palliation for patients with univentricular connection. The bidirectional cavopulmonary shunt includes anastomosis of the cardiac end of the superior vena cava to the right pulmonary artery but leaves the pulmonary arteries confluent. The bidirectional Glenn shunt provides effective pulmonary blood flow by directing desaturated blood directly into the pulmonary circuit. It does not increase the ventricular volume load as does a systemic-to-pulmonary shunt.

Previously, the classic Glenn shunt was the preferred technique, consisting of anastomosing the superior vena cava to the right pulmonary artery resulting in nonconfluent pulmonary arteries. Several serious complications and disadvantages however became increasingly recognized and as result, the classic Glenn is no longer done routinely (25). The most significant complication was the development of pulmonary arteriovenous fistulae. They develop around 5 years after placement of the Glenn shunt. Other significant disadvantages include loss of confluence between right and left pulmonary arteries, distortion or stenosis of the superior vena cava or the right pulmonary artery, right pulmonary artery thrombosis, abnormal right pulmonary blood flow distribution, and failure of the right pulmonary artery to develop normally.

Although the bidirectional cavopulmonary shunt produces excellent palliation in the first 2 to 3 years of life, progressive cyanosis and secondary erythrocytosis usually prompt further palliative efforts to improve pulmonary flow. If the pulmonary arteries remain hypoplastic, an additional systemic-to-pulmonary shunt may provide greater pulmonary blood flow for relief of cyanosis and promote growth of the pulmonary vascular bed. In general, the bidirectional cavopulmonary shunt alone does not provide sufficient pulmonary blood flow to palliate adequately patients with univentricular AV connection to childhood.

Three options for more definitive surgical correction of patients with univentricular AV connection are ventricular septation, modified Fontan operation, and cardiac transplantation (19–26). In 1956, Kirklin performed a septation operation in a 12-year-old patient who had a single ventricle with a small ridge of apical ventricular septum. Based on this and similar early successes, the initial efforts at surgical correction of univentricular AV connection were directed toward ventricular septation or placement of a prosthetic patch to separate the MVC into right and left components, basically in a plane between the two AV valves. The earliest report by McGoon et al. (27) described the most successful early septation results in patients with DILV and left-anterior subaortic right ventricle (A-III single ventricle). However, early mortality rates were high, approximately 38% to 40%, and subsequent reports noted similar results (27,28). A progressive late mortality rate secondary to ventricular failure, progressive AV valve regurgitation, residual left-to-right shunts, conduit failure, and complete heart block prompted abandonment of this method of surgical correction for univentricular AV connection.

The modified Fontan procedure with direct atriopulmonary connection and a lateral right atrial tunnel to produce a

bicaval bidirectional or “total” cavopulmonary anastomosis have become common methods for a more definitive surgical “correction” or palliation for patients with univentricular AV connection. Also, the bidirectional caval pulmonary anastomosis and an added external or internal conduit from the inferior vena cava to the right pulmonary artery are optional methods for surgical repair. Although initial surgical reports from 1973 to 1980 suggested that the mortality for modified Fontan procedure was somewhat higher for patients with single ventricle (21%) than for patients with classic tricuspid atresia (17%) (26), current results (1988 to 1992) indicate substantial improvement with the same early mortality rate of about 4% for both tricuspid atresia and DILV (29). Even the more complex forms with common-inlet AV connection and situs ambiguus have early mortality rates of approximately 11% when stronger screening efforts are used to provide better patient selection, as described in the catheterization section. Earlier operation, that is, when the patient is between 2 and 3 years of age, is now recommended to avoid complications related to long-term ventricular volume overload, hypoxia, cyanosis, AV valve regurgitation, pulmonary artery distortion, and pulmonary hypertension. Surgical techniques have improved to provide more efficient and direct flow from the caeae into the pulmonary arteries by lateral tunnels or external conduits and direct anastomoses described as bicaval, bidirectional, or total cavopulmonary connections. Such direct connections seem to provide more efficient and directed flow to the pulmonary artery and avoid dilated atrial chambers that appear to promote blood stasis and pooling with potential for thromboses and atrial arrhythmias. The use of a lateral tunnel, intra-atrial, or extracardiac conduits in univentricular connection also provides greater flexibility for management of patients with common and single-inlet connections and avoids the necessity for AV valve patch closure in double-inlet connections. Some reports suggesting extremely poor results and high mortality rates in earlier series (1973 to 1983) typically included older and more debilitated patients prior to attempted repair and did not reflect recent improvements in medical and surgical management currently available (29).

Current data from the long-term evaluation of postoperative univentricular AV connection patients continue to demonstrate generally satisfactory results in most patients after the modified Fontan procedure (29,30). Most surviving patients report a subjective improvement in their quality of life and exercise tolerance compared with their preoperative conditions. A number of reports reviewed some of the hemodynamic abnormalities, rhythm disturbances, and protein-losing enteropathy that have been recognized in late survivors following modified Fontan procedure. Mechanical causes for a poor clinical result and high right atrial pressure include obstruction of caval or atriopulmonary connections, pulmonary artery distortion or hypoplasia, pulmonary vascular obstructive disease, pulmonary venous obstruction, poor ventricular function, significant AV or semilunar valve regurgitation, and residual left-to-right shunts. Elevated right atrial pressures also result in right atrial distension and stretching of the right atrial wall. Significant arrhythmias have been reported following modified Fontan procedure and are primarily supraventricular in origin. They have included atrial flutter, primary atrial tachycardia, atrial fibrillation, and accelerated junctional tachycardia. Medical management and antitachycardia pacing devices have been used successfully to control these rhythm disturbances.

Orthotopic cardiac transplantation also has been used successfully in chronically debilitated patients who have a variety of congenital cardiac defects, including univentricular AV connection. Usually, patients with severe ventricular dysfunction following modified Fontan procedure have experienced progressive physical deterioration and have required cardiac transplantation for survival. Although the early surgical results for

these patients have been encouraging, the long-term morbidity and mortality rates for cardiac transplantation have not warranted consideration of cardiac transplantation as the first or primary option for surgical management of patients with univentricular AV connection. In spite of the apparent benefits, 40 years of experience with the Fontan procedure have gradually revealed the shortfalls of such a circulatory arrangement. Sequelae related to the underlying congenital anomaly or to the altered physiology of passive, nonpulsatile flow through the pulmonary arterial bed commonly contribute to an increasing incidence of failure of the Fontan circulation over time (31). Morbidities include rhythm disturbances, thromboembolic events, protein-losing enteropathy, systemic ventricular dysfunction, and heart failure (31–33). Extracardiac late complications also appear to be common. These late extracardiac complications include restrictive lung disease, renal dysfunction, and liver dysfunction (34–36). Liver abnormalities include clotting cascade, cirrhosis, and hepatocellular carcinoma (36). The clinical significance of these findings, however, remains poorly understood (36).

We, therefore, currently recommend palliative support, including selected pulmonary artery banding and systemic-to-pulmonary shunts in univentricular AV connection patients during the first 6 months of life. If significant subaortic obstruction is present, an aortopulmonary window and an endoluminal banding operation should be performed early to prevent ventricular hypertrophy and to protect the pulmonary vasculature. After 6 months of age, a bidirectional cavopulmonary shunt could be considered to increase pulmonary blood flow and to reduce ventricular volume loading. This, in conjunction with additional pulmonary flow through the native pulmonary outflow tract or a small systemic-to-pulmonary shunt, should provide adequate pulmonary blood flow to reduce cyanosis and promote growth of the pulmonary arteries without substantial ventricular volume overload. If this provides adequate palliation, a complete modified Fontan procedure could be considered when the patient is between 2 and 3 years of age.

REFERENCES

- Van Praagh R, Van Praagh S, Vlad P, et al. Diagnosis of the anatomic types of single or common ventricle. *Am J Cardiol* 1965;15:345–366.
- Anderson RH, et al. The univentricular atrioventricular connection: getting to the root of a thorny problem. *Am J Cardiol* 1984;54:822.
- Anderson RH, et al. Problems in the nomenclature of the univentricular heart. *Herz* 1979;4:184.
- Shiraishi H, Silverman NH. Echocardiographic spectrum of double inlet ventricle: evaluation of the interventricular communication. *J Am Coll Cardiol* 1990;15:1401.
- Bevilacqua M, et al. Double inlet single ventricle: echocardiographic anatomy with emphasis on morphology of the atrioventricular valves and ventricular septal defect. *J Am Coll Cardiol* 1991;18:559.
- Elliott LP, Anderson RH, Barger LM Jr, et al. Single ventricle or univentricular heart. In: Adams FH, Emmanouilides GC, Riemenschnieder TA, eds. *Moss' Heart Disease in Infants, Children and Adolescents*. 4th ed. Baltimore, MD: Williams & Wilkins, 1989:485.
- Cook AC, Anderson RH. The functionally univentricular circulation: anatomic substrates as related to function. *Cardiol Young* 2005;15:7–16.
- Davies MJ, Anderson RH, Becker AE. Atrioventricular conduction tissues in congenital heart disease. In: Davies MJ, Anderson RH, Becker AE, eds. *The Conduction System of the Heart*. Stoneham, MA: Butterworth-Heinemann, 1983:135–153.
- Van Praagh R, Ongley PA, Swan HJC. Anatomic types of single or common ventricle in man: morphologic and geometric aspects of sixty necropsied cases. *Am J Cardiol* 1964;13:367–386.
- Lev M, Liberthson RR, Kirkpatrick JR, et al. Single (primitive) ventricle. *Circulation* 1969;39:577–591.
- Essed CE, Ho SY, Shinebourne EA, et al. Further observations on conduction tissues in univentricular hearts: surgical implications. *Eur Heart J* 1981;2:87–96.
- Nakata S, Yasuharu I, Yoshinori T, et al. A new method for the quantitative standardization of cross-sectional areas of the pulmonary arteries in congenital heart disease with decreased pulmonary blood flow. *J Thorac Cardiovasc Surg* 1984;88:610–619.
- Ritter DG, Seward JB, Moodie D, et al. Univentricular heart (common ventricle) preoperative diagnosis: hemodynamic, angiographic and echocardiographic features. *Herz* 1979;4:198–205.
- Huhta JC, Seward JB, Tajik AJ, et al. Two-dimensional echocardiographic spectrum of univentricular atrioventricular connection. *J Am Coll Cardiol* 1985;5:149–157.
- Seward JB, Tajik AJ, Hagler DJ, et al. Internal cardiac crux: two-dimensional echocardiography of normal and congenitally abnormal hearts. *Ultrasound Med Biol* 1984;10:735–745.
- Razzouk AJ, Freedom RM, Cohen AJ, et al. The recognition, identification of morphologic substrate, and treatment of subaortic stenosis after a Fontan operation. *J Thorac Cardiovasc Surg* 1992;104:938–944.
- Currie PJ, Hagler DJ, Seward JB, et al. Instantaneous pressure gradient: a simultaneous Doppler and dual catheter correlative study. *J Am Coll Cardiol* 1986;7:873–879.
- Tonkin IL, Kelley MJ, Bream PR, et al. The frontal chest film as method of suspecting transposition complexes. *Circulation* 1976;53:1016–1025.
- Oleary PW, Driscoll DD, Connor AR, et al. Subaortic obstruction in hearts with a univentricular connection to a dominant left ventricle and an anterior subaortic outlet chamber: results of a staged approach. *J Thorac Cardiovasc Surg* 1992;104:1231–1237.
- Barber G, Hagler DJ, Edwards WD, et al. Surgical repair of univentricular heart (double inlet left ventricle) with obstructed anterior subaortic outlet chamber. *J Am Coll Cardiol* 1984;4:771–778.
- Freedom RM, Sondheimer H, Dische R, et al. Development of "subaortic stenosis" after pulmonary arterial banding for common ventricle. *Am J Cardiol* 1977;39:78–83.
- Choussat A, Fontan F, Besse P, et al. Selection criteria for Fontan procedure. In: Anderson FH, Shinebourne EA, eds. *Pediatric Cardiology*. White Plains, NY: Churchill Livingstone, 1978:559–566.
- Girod DA, Rice MJ, Mair DD, et al. Relationship of pulmonary artery size to mortality in patients undergoing the Fontan operation. *Circulation* 1985;72:II93–II95.
- Freedom RM, Benson LN, Smallhorn JF, et al. Subaortic stenosis, the univentricular heart, and banding of the pulmonary artery: an analysis of the courses of 43 patients with univentricular heart palliated by pulmonary artery banding. *Circulation* 1986;73:758–764.
- McFaul RC, Tajik AJ, Mair DD, et al. Development of pulmonary arteriovenous shunt after superior vena cava–right pulmonary artery (Glenn) anastomosis: report of four cases. *Circulation* 1977;55:212–216.
- Fontan F, Baudet E. Surgical repair of tricuspid atresia. *Thorax* 1971;26:240–248.
- McGoon DC, Danielson GK, Ritter DG, et al. Correction of the univentricular heart having two atrioventricular valves. *J Thorac Cardiovasc Surg* 1977;74:218–226.
- Feldt RH, Mair DD, Danielson GK, et al. Current status of the septation procedure for univentricular heart. *J Thorac Cardiovasc Surg* 1981;82:93–97.
- Cetta F, Feldt R, O'Leary TW, et al. Improved early morbidity and mortality after Fontan operation: the Mayo clinic experience, 1987–1992. *J Am Coll Cardiol* 1996;28:480–486.
- Earing MG, Cetta F, Driscoll DJ, et al. Long-term results of the Fontan operation for double-inlet left ventricle. *Am J Cardiol* 2005;96:291–298.
- Khairy P, Fernandes SM, Mayer JE, et al. Long-term survival, modes of death, and predictors of mortality in patients with Fontan surgery. *Circulation* 2008;117:85–92.
- Bartz PJ, Driscoll DJ, Dearani JA, et al. Early and late results of the modified Fontan operation for heterotaxy syndrome. *J Am Coll Cardiol* 2006;48:2301–2305.
- Ghai A, Harris L, Harrison DA, et al. Outcomes of late atrial tachyarrhythmias in adults after the Fontan operation. *J Am Coll Cardiol* 2001;37:585–592.
- Varma C, Warr MR, Hendler AL, et al. Prevalence of silent pulmonary emboli in adults after the Fontan operation. *J Am Coll Cardiol* 2003;41:2252–2258.
- Fredriksen PM, Therrien J, Veldtman G, et al. Lung function and aerobic capacity in adult patients following modified Fontan procedure. *Heart* 2001;85:295–299.
- Wu FM, Chinweike U, Odze RD, et al. Liver disease in the patient with Fontan circulation. *Congenit Heart Dis* 2011;6:190–201.

Cardiac Malpositions and Abnormalities of Atrial and Visceral Situs

Patrick W. O'Leary ■ Donald J. Hagler

Cardiac malposition describes an abnormal or anomalous location of the heart. Our discussion of cardiac malposition includes abnormalities of overall cardiac position (dextrocardia, mesocardia, levocardia [isolated]), as well as pericardial defects, and the complex anomaly of ectopia cordis (1,2). Cardiac malpositions often are integral components of complex cardiac anomalies involving abnormal visceral and atrial situs (sidedness). Due to the complex nature of these groups of anomalies, pathologists and clinicians have pursued a logical, systematic, and consistent method of analysis typically described as a segmental approach to the diagnosis of congenital heart disease. This approach begins with a description of the asymmetrically arranged organ systems of the abdomen and thorax (determination of situs), proceeds to define the cardiac position and orientation within the chest, and concludes with a detailed description of the venous, cardiac, and arterial segmental anatomy, as well as the spatial relationships of the segment components and the connections of adjacent segments to one another (see Chapter 2).

DEFINITIONS

Understanding of the often complex malformations associated with abnormal cardiac position is facilitated by a clear definition of the terminology used to describe them.

The classification of overall cardiac position is determined by the cardiac base–apex axis as illustrated in Figure 53.1. **Dextrocardia** has been defined classically and most consistently as the location of the heart in the right hemithorax with the apex pointing (base–apex axis) to the right. Dextrocardia may occur with atrial situs solitus, situs inversus, or situs ambiguus. When it occurs with situs solitus, it also has been called isolated dextrocardia. Although the normal heart can be “shifted” into the right chest by a variety of extracardiac processes (diaphragmatic hernia, tumors, or tension pneumothorax), these situations, in which the cardiac base–apex axis is still oriented to the left, are better described as “dextroposition,” rather than dextrocardia.

Mesocardia is the location of the heart with the cardiac base–apex axis directed inferiorly in the midline of the thorax (neither to the right nor left). The ventricular apices are equally directed to both right and left side of the sternum. This anatomic description of cardiac malposition often is ignored as being infrequent and atypical. However, many cases accepted as having dextrocardia may be described more accurately as mesocardia, because of a midline cardiac position. Most cases of mesocardia have been described with situs solitus. However, mesocardia also has been described with situs inversus and situs ambiguus.

Levocardia as a cardiac malposition only is considered as isolated levocardia, occurring in conjunction with situs inversus and situs ambiguus. Thus, despite an abnormal atrial and

visceral situs, the heart is in its normal location in the left hemithorax with the apex (base–apex axis) pointing to the left.

Situs (or sidedness) is a term used to describe the spatial relation of an asymmetrically arranged organ system (or group of related organs). For our discussion, the situs of the abdominal organs (stomach, liver, bowel, and spleen) and the atria would receive the most attention. **Situs solitus** describes the normal site or position of the viscera or atria. Typically, both must be independently considered and described for a precise segmental approach. **Situs inversus** describes an inversion or right/left reversal of visceral or atrial site or position, i.e., a mirror image of the normal situation. In cases of atrial situs inversus, the right atrium will lie to the left and the anatomic left atrium to the right. Abdominal situs inversus consists of a right-sided stomach and spleen, and a left-sided liver. **Situs ambiguus** describes an uncertain or indeterminate visceral or atrial position because of symmetric or indeterminate anatomy bilaterally. Frequently, patients with abdominal situs ambiguus will have a liver that is “bilateral” and in a midline position, and absence of the spleen (asplenia) is common. Figure 53.2 schematically illustrates the three types of visceral–atrial situs.

Heterotaxia is the term used to describe an anomalous position of the viscera. In humans, anatomic left–right asymmetry is established during embryogenesis. Variations from the normal situs solitus result in heterotaxy, expressed as either randomization (situs ambiguus) or complete reversal of visceral position as in situs inversus. In 1993, Casey et al. (1,2) localized a genetic defect in familial heterotaxy. They found an X-linked recessive trait associated with the inability of the developing embryo to establish normal left–right asymmetry. They later localized this deletion to X q26.2. They further reported that familial heterotaxy occurs with autosomal dominant, recessive, and X-linked inheritance. Kato et al. (3) and Peeters et al. (4) have reported *de novo* balanced translocations involving chromosome band 6q21 in a patient with heterotaxy and left isomerism. Genes implicated in human heterotaxy include *Zic3*, *LeftyA*, *Cryptic*, and *Acvr2B* (5). Both situs ambiguus and situs inversus can appear in some families with heterotaxy.

SEGMENTAL DIAGNOSIS

A segmental approach implies a systematic and therefore sequential review of all structures involved by the congenital anomalies. This sequence would determine the pathologic status of the viscera, the atria, the atrioventricular (AV) connection(s), the ventricles, the ventriculoarterial (VA) connection(s), and the great arteries.

Pathologists have emphasized cardiac segments as the anatomic and developmental components of all human hearts. Van Praagh included ten cardiac segments from an embryologic standpoint: the sinus venosus, the primitive atrium, the common pulmonary vein, the AV canal, the primitive ventricle

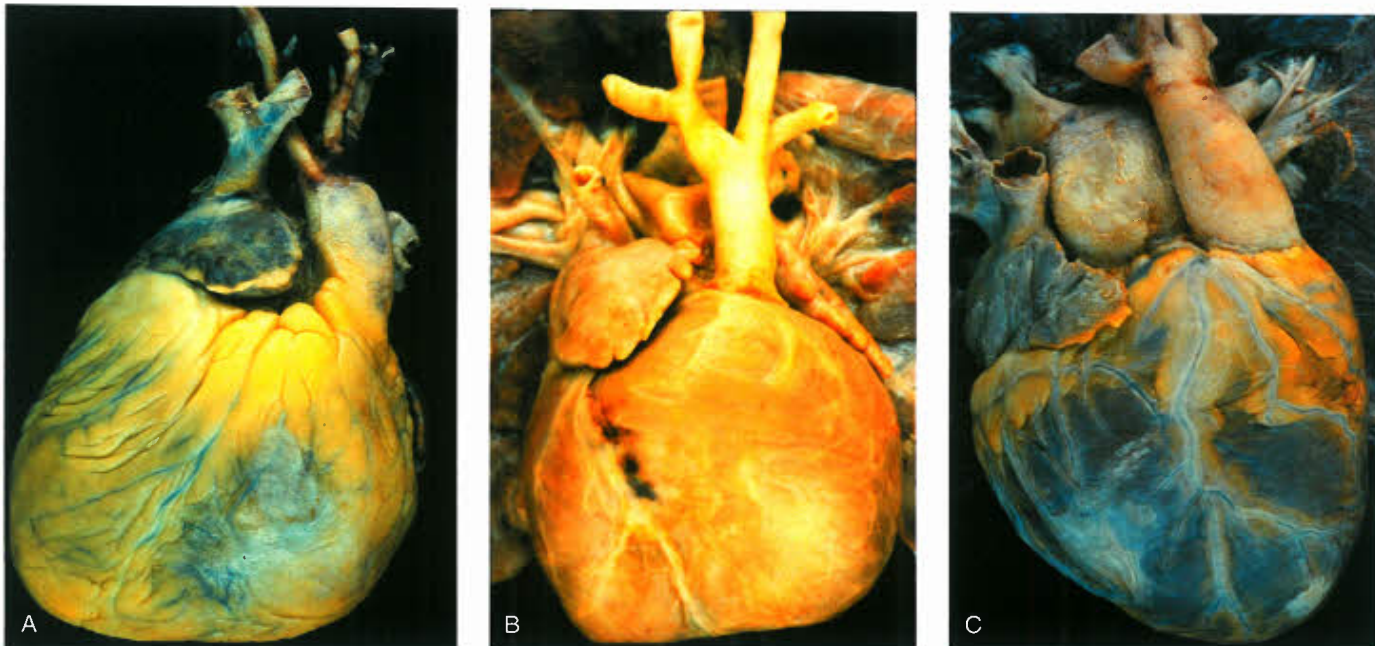


Figure 53.1. Cardiac positions. Pathologic specimens of anatomically corrected TGA. **A:** Dextrocardia. **B:** Mesocardia. **C:** Levocardia. The base–apex axis of the heart defines the type of cardiac malposition. Note that with mesocardia there are two relatively well-defined apices of the heart defined by each ventricle but with the major axis of the heart directed in the midline.

(proampulla), the proximal bulbus cordis (meta-ampulla), the infundibulum (conus), the truncus arteriosus, the aortic sac, and the arterial arches (6). However, from a practical clinical approach, some embryologic segments have little relevance or application for anatomic or pathologic examination.

Therefore, a more practical clinical and pathologic segmental analysis begins with definition of major organ positions (visceral situs, atrial situs, and cardiac position/orientation), followed by a detailed description of four segments and the three connections between them. The seven components of this sequential system are (a) the venous segment (systemic and pulmonary veins, plus the coronary sinus), (b) the venoatrial connections, (c) the atria and the atrial septum, (d) the AV connection(s), (e) the ventricles and the ventricular septum, (f) the ventriculoarterial (VA) connection(s), and (g) the great arteries (aorta, pulmonary arteries, coronary arteries, and ductus arteriosus). Table 53.1 illustrates a basic strategy for segmental diagnosis including many criteria and anatomic features that must be determined for accurate diagnosis. This approach should be applied regardless of the method of examination being used (clinical imaging or pathologic examination).

VISCERAL AND ATRIAL SITUS ABNORMALITIES

As illustrated in Table 53.1, the evaluation begins with definition of visceral and atrial situs. Visceral (abdominal) situs is determined by the positions of the liver and stomach (Fig. 53.1). The pancreas and spleen generally are located on the same side of the vertebral column as the stomach. Atrial and visceral situs generally are considered together because they are concordant in most cases (the atrial and visceral situs are the same). However, exceptions occur, and venous connections and visceral situs may not necessarily agree with the apparent atrial situs. These features can be particularly variable in situs ambiguus. Situs ambiguus may be best defined as an uncertain or indeterminate situs (organ positions do not fit into any

standard category). However, in many cases, the right and left components appear very similar to each other, and have been described as mirror images. Such cases also have been referred to as “isomeric” or as having *bilateral* right or left sidedness.

In visceral situs ambiguus with right isomerism (bilateral right sidedness), the spleen is usually absent (asplenia) and the liver is centrally located, symmetrically straddling the midline. In this situation, two mirror-image morphologic right hepatic lobes are present. In contrast to the normal arrangement, the inferior vena cava (IVC) and abdominal aorta will be found on the same side of the vertebral column. In addition, these patients almost always will have malrotations of the bowel.

Situs ambiguus with polysplenia has been described as bilateral left-sidedness or left isomerism (5–12). However, the degree of right/left symmetry is less pronounced in cases of polysplenia than in those with asplenia and bilateral right sidedness. In fact, the most common arrangement of the abdominal viscera in polysplenic patients is more consistent with situs inversus. As a teaching tool, the concept of isomerism (mirror image sidedness) is an attempt to simplify (group) the typical features of complex anomalies in which multiple abnormalities tend to occur together as a syndrome. Thus, the asplenia syndrome (Ivemark syndrome) appears as a pathologic grouping of features emphasizing right sidedness, such as bilateral right bronchi and bilateral right (trilobed) lungs, bilateral right atria, and a symmetrical liver. Ivemark described the implications of asplenia on the pathogenesis of conotruncal anomalies in 1955. Van Mierop et al. (12) pointed out that the asplenia syndrome is associated with pulmonary stenosis or atresia, whereas in polysplenia syndrome, presence of single ventricle physiology and obstruction to pulmonary arterial blood flow are less common. In contrast, interruption of the IVC with azygous continuation of the inferior venous system and anomalous, bilateral pulmonary venous connection of each lung to the ipsilateral atrium are common in polysplenia, but rare in asplenia.

Although splenic anomalies often are associated with complex congenital heart disease and with abnormalities of

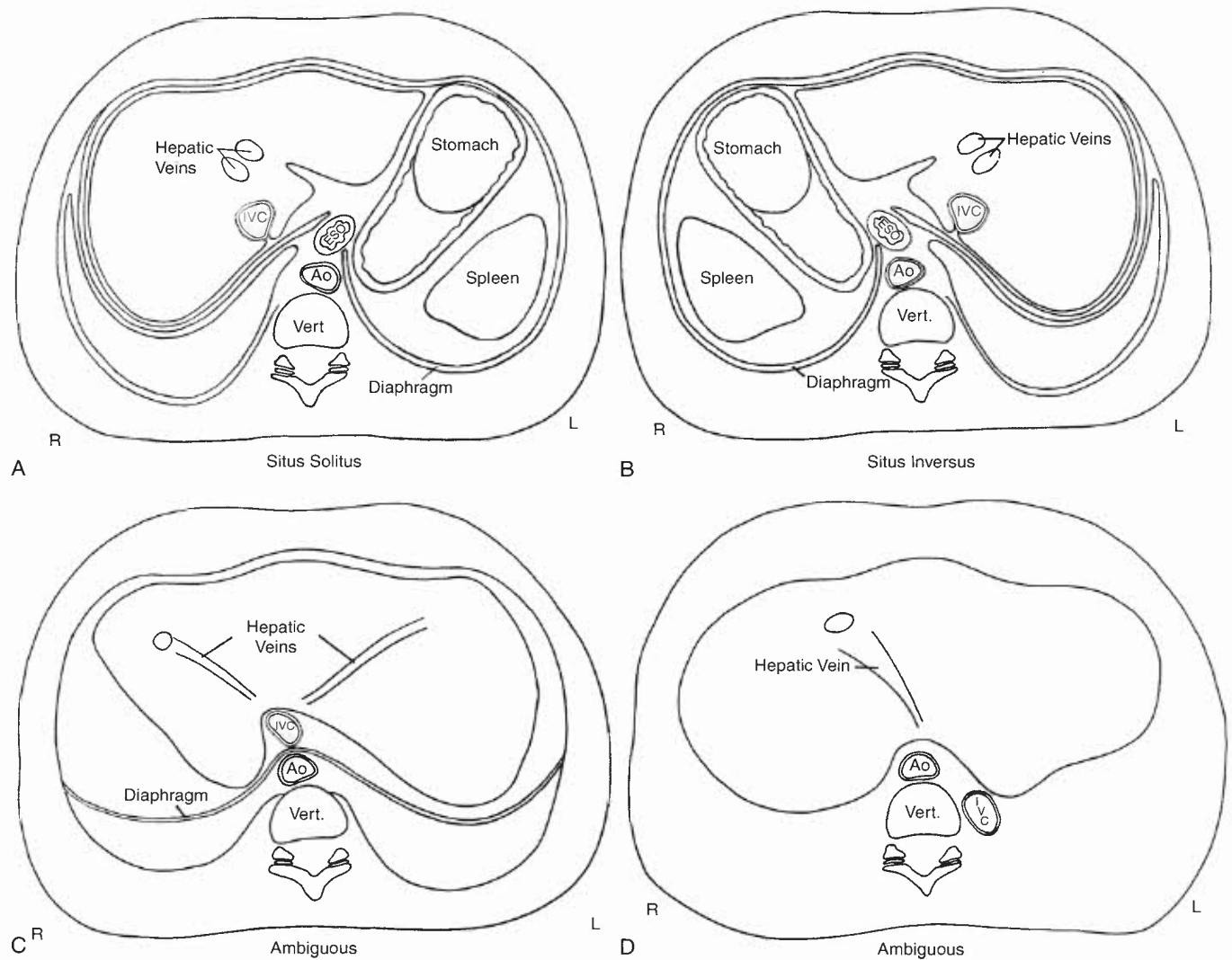


Figure 53.2. Cross-sectional drawings of the abdomen illustrating visceral anatomy similar to that observed echocardiographically during a short-axis scan of the abdomen from a costal position. They demonstrate the three basic types of visceral atrial situs: situs solitus (A), situs inversus (B), and situs ambiguus (C,D). The cross-sectional relationships of the visceral structures are easily defined relative to fixed structures such as the vertebral body (Vert) and the diaphragm. The diaphragm limits the abdominal cavity so that posterior structures such as the aorta (Ao) and the azygous continuation of the IVC are retroperitoneal structures, as demonstrated in (D). Separate hepatic venous connections may be present in situs ambiguus, as evident in (C). (ESO, esophagus.)

visceral situs, they are not the cause. Embryologically, the spleen, in contrast to the other thoracoabdominal viscera, does not initially develop as a midline structure. Rather, the splenic anlage is left-sided from its inception. As a result, in the case of bilateral right-sided symmetry, the spleen would not be expected to develop—hence the association of right isomerism with asplenia. In contrast, left isomerism frequently is associated with polysplenia, although multiple spleens are usually found on only one side of the vertebral column (along the dorsal aspect of the stomach).

Clinically, the identification of the morphologic right atrium is important for establishing atrial situs. This is due to the fact that much of the anatomic left atrium is derived from the embryonic common pulmonary vein. As a result, its walls are relatively smooth and lack distinctive features for identification by clinical imaging modalities. In contrast, the anatomic right atrium is derived from the primitive atrium and has several muscular structures that make it more recognizable. Its most reliable anatomic hallmark is the relatively thick superior

limbus of the fossa ovalis, which can be observed by direct inspection at operation, at autopsy, or by tomographic imaging techniques (echocardiographic, CT, or cardiac MR scanning). In cases in which the atrial septum is absent, distorted, or cannot be visualized, atrial morphology may be inferred by inspection of the free atrial wall. A morphologic right atrium contains a large pyramidal appendage, a crista terminalis, and pectinate muscles (13). Angiographically, identification of the morphologically right atrium usually is inferred based upon the presence of large, wide-based, triangular atrial appendage, because the limbus and pectinate architecture cannot be visualized with this type of projection imaging. In situs ambiguus and other complex cases, the atrial septum essentially can be absent, resulting in a common atrium. In these cases, assignment of atrial “identity” can be challenging. The presence of pectinate muscles and the crista is helpful in anatomic specimens. However, when imaging a patient, the connection of the coronary sinus and/or the suprahepatic segment of the IVC can provide a reasonable marker identifying the position of

TABLE 53.1

Segmental Approach to Evaluation of Complex Congenital Heart Disease

Visceral, atrial situs and cardiac position/orientation
The venous segment
Systemic: superior and inferior caval position, number, and connections
Hepatic veins
Coronary sinus
Pulmonary venous connections
The AV connections (morphology/function)
Valve "number," morphology, and commitment (AV malalignment—overriding, crisscross)
Insertion of valvar supports (chordal attachments; septal versus intracavitary, straddling, ...)
Leaflet anomalies (thickening, clefts, fenestrations, ...)
Papillary muscles (position, number, abnormality—parachute)
Valvar function (stenosis, regurgitation)
Functional status (regurgitation, stenosis)
The ventricular segment
Ventricular morphology
- Relative AV valve septal insertion/hinge point (more basal—LV, more apical—RV)
- Papillary muscle anatomy (large, discrete, midcavitary—LV, irregular, small and multiple—RV)
- Endocardial appearance (smooth with small trabeculae—LV, multiple, coarse trabeculae with a moderator band—RV)
Ventricular positions (relative to the other ventricle, to any VSD, and to the great arteries)
Ventricular free walls (hypertrophied, thin, dyskinetic, ...)
Ventricular septum (intact, defect(s), malalignment, ...)
AV valve chordal attachments (relative to the outlets, or any VSD)
Functional assessment (systolic contractility, diastolic relaxation)
The ventricular–arterial connection(s)
Number, patency vs. atresia, and appropriateness (concordant/discordant) of connections
Relative position of the semilunar valves to
- any VSD (override, remote, ...)
- any other outlet valve (normal, side-by-side, right anterior aorta, left anterior aorta)
Functional assessment (stenosis, regurgitation)
The great arteries (aorta, pulmonary arteries, coronary arteries, and the ductus)
Identification of the presence (absence/atresia) and size of each vessel
Identification of relative spatial relationships between vessels
Definition of the extracardiac course and branching patterns
Aortic arch location (right, left) and the brachiocephalic branching pattern
Arch anomalies (hypoplasia, coarctation, patent ductus arteriosus)

AV, atrioventricular; VSD, ventricular septal defect

the morphologic right atrium (14,15). Anatomic determinants of the other cardiac segments also have been described and are summarized in Table 53.2.

One can encounter cases of truly bilateral right atria (or right atrial isomerism). In these patients the appearance of both atrial appendages and the atrial free walls will have the characteristics of a right atrium (Fig. 53.3). Even more rarely, in polysplenia syndrome with left atrial isomerism, both atrial appendages and free walls typically resemble a left atrial appendage. The left atrial appendage usually has a narrow base

and a tubular, hooked shape (13) (Fig. 53.2) (16). However, the atrial appendage shape often is quite variable and may be described best in some instances as simply abnormal. In most cases with asplenia or polysplenia, the atrial anatomy is poorly defined, with a large common atrium, a thin rudimentary remnant of atrial septum, anomalies of systemic and pulmonary venous connections, and abnormal but similarly shaped bilateral appendages. Van Praagh et al. (14) have argued that the concept of bilateral or two right atria and bilateral or two left atria is anatomically unrealistic. These researchers and also

TABLE 53.2 Anatomic Features of Cardiac Segments

Right Atrium	Left Atrium
Thick, superior limbus of fossa ovalis	Thin valve of the fossa ovalis
Large pyramidal appendage	Ostium secundum
Crista terminalis	Small finger-like appendage
Pectinate muscles	No crista terminalis
Receives suprahepatic IVC, coronary sinus	No pectinate muscles
Tricuspid valve	Mitral valve
Septal chordal attachments	No septal chordal attachments
Apical septal annular attachment/hinge	Basal septal annular attachment/hinge
Triangular orifice (midleaflet)	Elliptical orifice (midleaflet)
Three leaflet AV valve	Two leaflet AV valve
Multiple, small papillary muscles	Two large papillary muscles
Empties into RV	Empties into LV
Right ventricle	Left ventricle
Large apical trabeculations	Small apical trabeculations
Coarse septal surface	Smooth upper surface
Moderator, septal and parietal bands	No moderator, septal or parietal band
Receives tricuspid valve	Receives mitral valve
Tricuspid–pulmonary discontinuity - muscular outflow tract (infundibulum)	Usually mitral–aortic continuity
Crescentic in cross section	Circular in cross section
Pulmonary valve	Aortic valve
Empties into pulmonary trunk	Empties into ascending aorta

IVC, inferior vena cava; SVC, superior vena cava.

De la Cruz and Nadal-Ginard (15) emphasized the importance of the suprahepatic segment of the IVC as a reliable marker for the morphologic right atrium, because embryologically, the sinus venosus is incorporated into the right atrium, and IVC-to-right atrium concordance is diagnostically accurate, even when there is viscerotransposition. With incorporation of the sinus venosus, the coronary sinus also can be recognized as a reliable marker for the morphologic right atrium. The morphologic right atrium, then, can be determined by a normally formed coronary sinus, a larger and more anterior appendage, and connection of the suprahepatic portion of the IVC. This approach allows clinical assignment of atrial situs in most cases, although the most important clinical issues are often related to the position and spatial arrangement of the venoatrial connections rather than the morphologic identities of the atria themselves.

Pulmonary situs is determined by the sidedness of the morphologic right and left lungs. Clinically, this is defined by the relationship of the pulmonary arteries to their adjacent bronchi, and not by the number of lobes in each lung. In a morphologic right lung, the pulmonary artery travels anterior to the upper lobe and intermediate bronchi. In contrast, a morphologic left lung is characterized by a pulmonary artery that courses over the main bronchus and posterior to the upper lobe bronchus. The distance from the carina to the origin of the upper lobe bronchus is 1.5 to 2 times greater for the morphologic left lung than for the right lung (17). These relative distances may be used clinically to infer pulmonary situs. The

simplest method is by examination of the air bronchograms on a plain chest x-ray. This ratio applies regardless of the sidedness of the aortic arch (i.e., regardless of the bronchus over which the aorta travels) (Fig. 53.4). In the setting of pulmonary isomerism (both lungs having the same morphology), however, the ratio approaches unity, because the lengths of the two main bronchi are similar. In these cases, bilateral trilobed (right) lungs should suggest the diagnosis of situs ambiguus with the asplenia syndrome (right isomerism), and bilateral bilobed (left) lungs the polysplenia syndrome (left isomerism). However, lung isomerism does not exist in all cases of cardiac isomerism and pulmonary isomerism can occur in patients without features of cardiac heterotaxia.

The cardiac and vascular segments are evaluated not only according to morphology but also in terms of spatial orientation. For example, atria and ventricles should be described both by their morphology and right or left sidedness. In general, the position and orientation of the ventricular septum is used to describe the location of the ventricular chambers. In hearts with levocardia with normally positioned ventricles, the right ventricle (RV) is to the right and anterior, while the left ventricle (LV) is left and posterior. In contrast, in situs inversus totalis the usual ventricular arrangement is the LV—right posterior and the RV—left anterior. Mesocardia is characterized by a vertical midline septum with side-by-side ventricles. Rarely, the ventricular septum is horizontal rather than vertical and results in superior-inferior (over-and-under or “upstairs-downstairs”) ventricles.

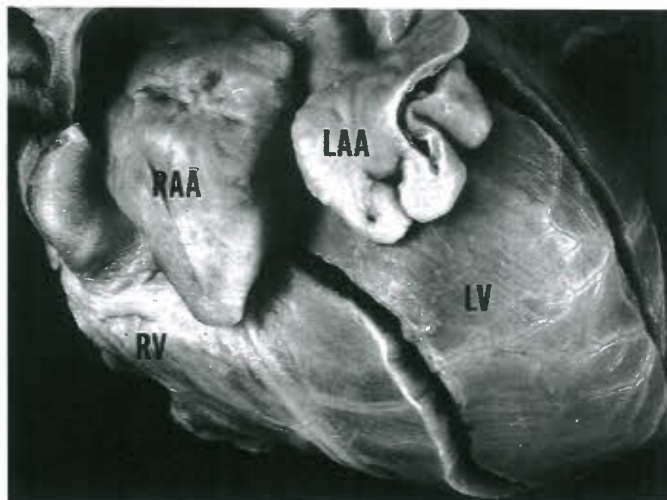


Figure 53.3. Atrial appendage anatomy. Pathologic specimen illustrating the anatomic features of the morphologic right and left atrial appendages with left-juxtaposed atrial appendages. The right atrial appendage (RAA) has a large pyramidal shape with a broad base, whereas the left atrial appendage (LAA) has a narrow base and a tubular, hooked, or irregular shape. (LV, left ventricle; RV, right ventricle.) (Provided by Dr. William D. Edwards.)

The position of the aorta is described relative to the pulmonary trunk. Normal hearts are characterized by a right posterior aorta. After the morphology and position of the cardiac segments are determined, the manner in which they connect to one another is evaluated. The three forms of connections to be investigated are venoatrial, AV, and VA.

The difficulties encountered in the accurate definition of atrial situs based on atrial anatomy alone emphasize the importance of accurate determination of systemic and pulmonary venous connections, as described in Tables 53.1 and 53.2. Regardless of the designation of a right or left atrium or the shape of the atrial appendages, the localization of the superior

vena cava (SVC), IVC, hepatic veins, coronary sinus, and pulmonary venous connections should be determined individually and recognized as unilateral or bilateral. This determination is particularly important for surgical management and should be a routine part of any imaging study.

ATRIOVENTRICULAR CONNECTIONS AND ATRIOVENTRICULAR VALVE MORPHOLOGY

The AV connection defines which atrium is connected or aligned with which ventricle. The normal AV connection, or right atrium-to-RV connection, defines a concordant AV connection, whereas a discordant connection is the abnormal connection of the right atrium to the morphologically LV. The term ventricular inversion also has been used to describe a discordant AV connection, but this terminology does not convey the central nature of the connection to these malformations. Discordant AV connections develop during the embryonic process of cardiac looping. The normal looping process begins with the embryonic heart tube bending and growing anteriorly and to the right, allowing the right horn of the sinus venosus to associate with the precursor of the RV. This has been described as a d-ventricular loop and results in AV concordance. In contrast, it is inferred that AV discordance develops due to a defect in cardiac looping, with the heart tube bending anterior and to the left (l-loop). A simplified form of the ventricular loop rule as proposed by De la Cruz et al. (18) and illustrated by Van Praagh et al. (8) is demonstrated in Figure 53.5, which presents four clinical conditions associated with d- or l-ventricular looping. Although originally proposed as an embryologic hypothesis to explain ventricular inversion, there has been mouse embryo documentation that both ventricular d- and l-loops do occur (19). Although this study demonstrated the occurrence of l-loops in mouse embryos with situs inversus, it did not document the occurrence of l-looping as the cause of AV discordance.

The concept of d- and l-ventricular looping has been developed further and defined anatomically in terms of chirality

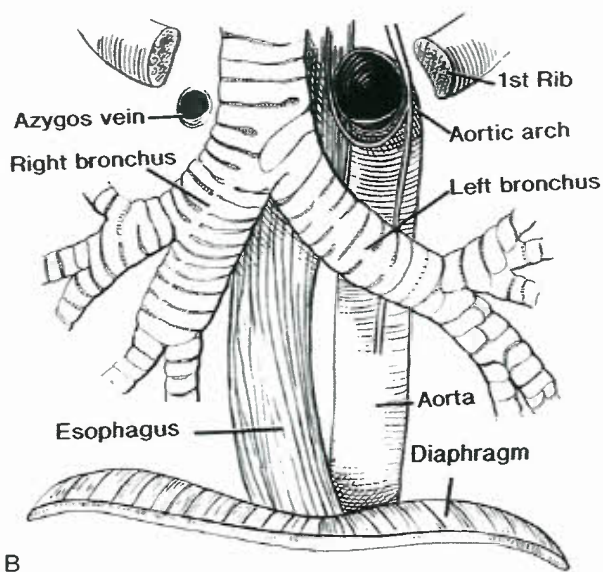


Figure 53.4. Normal bronchial anatomy. Pathologic specimen (A) and drawing (B) illustrate normal tracheobronchial branching pattern as observed from anterior. The left bronchus and lung are on the right side of each image. Note that the length of the left bronchus from the carina to its first branch is normally 1.5 to 2 times as long as the length of the right bronchus from the carina to its first branch. This anatomic feature allows prediction of the pulmonary visceral situs based on measurements of the bronchial length. (Provided by Dr. William D. Edwards.)

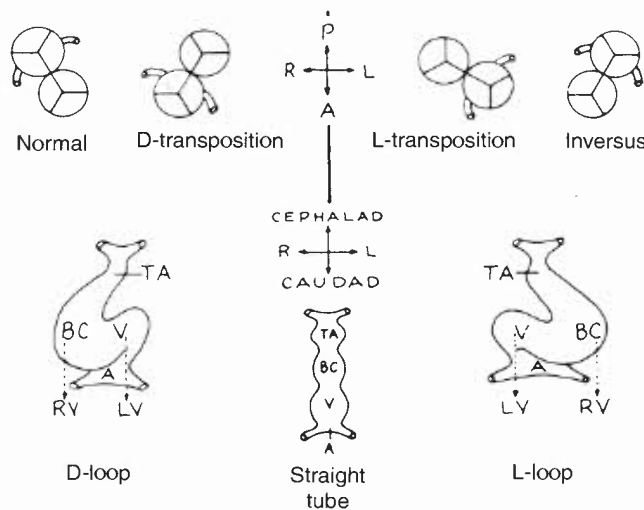


Figure 53.5. Cardiac loop formation as observed embryologically with the loop rule for ventricular localization as proposed by De la Cruz et al. (17) as an explanation for corrected transposition of the great arteries. d-Ventricular looping would result in normal ventricular situs, with the morphologic right ventricle to the right and anterior and the morphologic left ventricle to the left and posterior. l-Ventricular looping would result in inverted ventricular situs. (A, anterior; P, posterior; R, right; L, left; V, ventricle; RV, right vent; LV, left vent; BC, bulb cardis; TA, truncus arteriosus.) (From Van Praagh R. Malpositions of the heart. In: Moss AJ, Adams FH. *Heart Disease in Infants, Children, and Adolescents*. 1st ed. Baltimore, MD: Williams & Wilkins, 1968:604, with permission.)

(20,21) to explain other more-complex abnormalities of ventricular situs (criss-cross relations, as discussed below). The concept of chirality has been used to easily predict the ventricular “loop” that led to a particular malformation based on a right- or left-handed orientation as illustrated in Figure 53.6. The type of AV connection is associated with intrinsic variations of AV conduction tissue pathways.

The concepts of AV concordance or discordance usually will adequately define the type of AV connection in biventricular situations. Other more complex malformations can be described based on their presence (or absence), number, and their relationship(s) to the ventricular inlet(s). These abnormal categories of AV connection, whether concordant or discordant, include absent (atretic), overriding, and crisscross and are more fully described in a separate chapter detailing univentricular AV connection. When both atria connect with only one ventricular chamber, a univentricular AV connection applies. The same discussion reviewed the classification of single-, double-, and common-inlet ventricles.

Crisscross AV connection results due to a rotational abnormality of the ventricles (22). The ventricles often have a superoinferior ventricular relationship that appears to result primarily from an abnormally rightward or leftward rotation of the ventricular mass, and crossed AV connections. The right-sided AV inlet relates to the ventricular chamber that forms the left apex, while the left connection is associated with the right (and usually superior) ventricle. These complex abnormalities frequently are associated with large ventricular septal defects (VSDs), allowing overriding AV connections. These frequently are associated with straddling AV valve chordae and/or malaligned AV connections. Straddling is a feature of the tensor apparatus (chordae tendineae and papillary muscles) of an AV valve and indicates anomalous insertion into the contralateral ventricle, either along its septum or its free wall. The severity

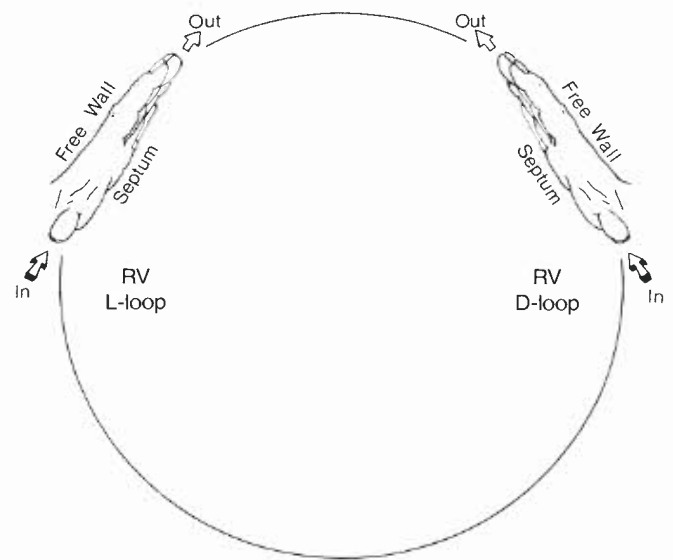


Figure 53.6. The use of chirality to describe what is a d-loop and what is an l-loop. The morphologic right ventricle (RV) of d-looped ventricles is right handed. The RV of l-looped ventricles is left handed. The d-loop RV in situs solitus and the l-loop RV in situs inversus totalis are stereoisomers, or spatial mirror images, just as are the right and left hands. Hence, it is possible to diagnose the type of ventricular loop (d or l) no matter what the spatial relationships of the ventricles may be. Whichever hand fits within the morphologically RV such that the palmar surface is toward the septum and the thumb in the inlet and the fingers in the outlet defines the ventricular loop.

of AV valve straddling has been categorized as type A, B, or C, depending on the position of the abnormal straddling chordae.

The simplest form of chordal straddling, type A, occurs when the abnormal chordae are attached to the upper portion (crest) of the ventricular septum (within 1 cm of the VSD), but on the side opposite from the position of the originating AV valve. In cases of Type B straddling, the anomalous chordal attachment is still found on the contralateral septal surface, but more than 1 cm removed from the edge of the VSD. Valves with type C straddling have abnormal chordal attachments that are supported by papillary muscles within the contralateral ventricular cavity or arising from the opposite ventricular free wall.

VENTRICULAR SITUS AND MORPHOLOGY

Complete assessment of this segment includes an assessment of the cardiac base–apex axis to describe the three basic possibilities of levocardia, dextrocardia, or mesocardia as detailed previously. In addition, an evaluation of this segment should incorporate descriptions of the ventricular locations, relationships, function, and morphology, as well the anatomy of the ventricular septum and any defects in it. These details have been covered elsewhere and need not be repeated here.

GREAT ARTERY RELATIONS

The great arterial connections, the spatial relationships between the arteries and their subsequent distribution/branching patterns, must be determined as described in Table 53.1. Eight basic types of great artery relationship are possible based

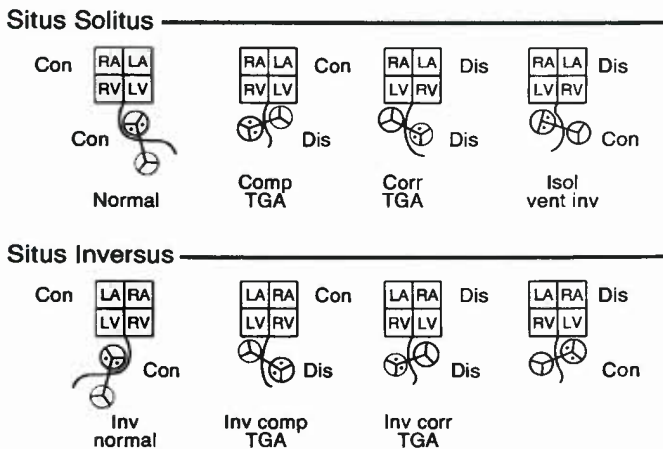


Figure 53.7. Four basic combinations of atrioventricular and ventricle–great artery relationships schematically displayed for atrial visceral situs solitus and situs inversus. Although these basic combinations do not include all possible variations in ventricular and great artery spatial relationships, the important aspects of atrioventricular and ventricle–great artery connections are demonstrated, allowing an understanding of the possible hemodynamic variables and the surgical manipulation required for correction. (Comp TGA, complete transposition of the great arteries; Con, concordant; Corr TGA, congenitally corrected transposition of the great arteries; Dis, discordant; Isol vent inv, isolated ventricular inversion; Inv, inverted; LA, left atrium; LV, left ventricle; RA, right atrium; RV, right ventricle.)

on the aortic and pulmonary valve positions at the level of the semilunar valves. They can be best described by the aortic location as follows:

1. Right posterior aorta (normally related)
2. Right lateral aorta (side by side)
3. Right anterior aorta (d-malposed)
4. Directly anterior aorta
5. Left anterior aorta (l-malposed)
6. Left lateral aorta (left side by side)
7. Left posterior aorta (inverted normal)
8. Directly posterior aorta

This type of segmental approach to complex cardiovascular malformations allows prediction of all possible cardiac conditions that could be encountered. Its flexibility depends upon the sequential addition of each cardiac segment and its relevant connections, accounting for all possible combinations of atrial, ventricular, and great arterial anomalies. Figure 53.7 schematically illustrates four typical clinical examples of segmental variations occurring in both atrial situs solitus and situs inversus. The remainder of this chapter is devoted to descriptions of these complex malformations and the other defects associated with them as they are encountered clinically.

DEXTROCARDIA

Dextrocardia with Atrial Situs Solitus

Isolated Dextrocardia with Atrioventricular Concordance and Normally Related Great Arteries

Isolated dextrocardia with AV concordance and normally related great arteries represents a true form of dextrocardia with the cardiac base–apex axis oriented inferiorly and to the right. It has been described using several names, including

pivotal dextrocardia and dextroversion. All the above descriptions try to convey the concept that the heart in this condition appears externally normal, but the apex is rotated toward the right hemithorax. Figure 53.8 illustrates pathologic features of this form of dextrocardia. The heart appears to have twisted to the right. The base–apex axis of the heart is actually directed to the right, and the ventricular and great artery relationships are normal. There were no gross intracardiac defects. In a series reported by Van Praagh et al. (8), 17 of 23 patients had multiple congenital extracardiac anomalies and 17 of 24 cases had congenital heart defects, including VSD, left SVC to the coronary sinus, coarctation of the aorta, secundum atrial septal defect (ASD), anomalous pulmonary venous connections, and complete AV septal defect.

The clinical presentation of patients with this form of dextrocardia depends upon any other lesions that may be present, such as VSD, coarctation, and AV septal defect, rather than upon the malposition itself. The geometric distortion of isolated dextrocardia compounds the clinical differential diagnosis and surgical management. Radiographic findings include the finding of dextrocardia with the heart positioned in the right chest. Volume overload lesions have radiographic evidence of pulmonary hyperperfusion. Bronchial branching patterns are normal. Visceral situs solitus is recognized by the left-sided stomach bubble and right-sided liver. Electrocardiographic findings can be typical for isolated dextrocardia. Atrial activation is normal, and the P-wave frontal plane axis is 70 to 80 degrees. Due to the shift of the ventricular mass toward the right, the frontal plane QRS axis shows a rightward shift or right-axis deviation. The most striking feature is a translocation or shift of the typical horizontal loop R-wave progression into the right chest. Therefore, as typical left precordial leads are observed, a gradual and progressive reduction in the QRS R-wave voltage is observed. It is therefore necessary to obtain additional complete right precordial leads (V3R to V6R) to correctly record the more typical QRS pattern and R-wave progression that is normally expected from the left chest. Other voltage abnormalities would depend on associated congenital cardiac anomalies.

Isolated Dextrocardia with Atrial Situs Solitus, Atrioventricular and Ventriculoarterial Discordance, and Left Anterior Aorta (Corrected Transposition of the Great Arteries with Isolated Dextrocardia)

Isolated dextrocardia with atrial situs solitus, AV and VA discordance, and left anterior aorta is a spatially complex form of congenitally corrected transposition of the great arteries (TGA). Congenitally corrected TGA is the most common complex cardiac malformation associated with dextrocardia and normal atrial situs. Although these hearts meet all the criteria for dextrocardia, the cardiac position is often close to the midline with only a slight rightward dominance, mimicking mesocardia (Figs. 53.9 and 53.10). There is a high incidence of additional cardiac anomalies observed with this form of isolated dextrocardia, including VSD and pulmonary stenosis. A similar group of anomalies associated with double-outlet RV (instead of TGA) has been well documented. Isolated dextrocardia with atrial situs solitus is also frequently seen in double-inlet LV with hypoplastic subaortic RV. Pulmonary atresia, complete AV septal defect, mitral atresia (right AV valve), tricuspid regurgitation (left AV valve) with Ebstein anomaly–like malformation, and anomalous systemic and pulmonary venous connections (especially with a persistent left SVC to the right atrium or directly to the left atrium with an unroofed coronary sinus) have also been reported (6,8,9).

Radiographic and electrocardiographic findings in this form of isolated dextrocardia are similar to those observed in dextrocardia with normally related great arteries.

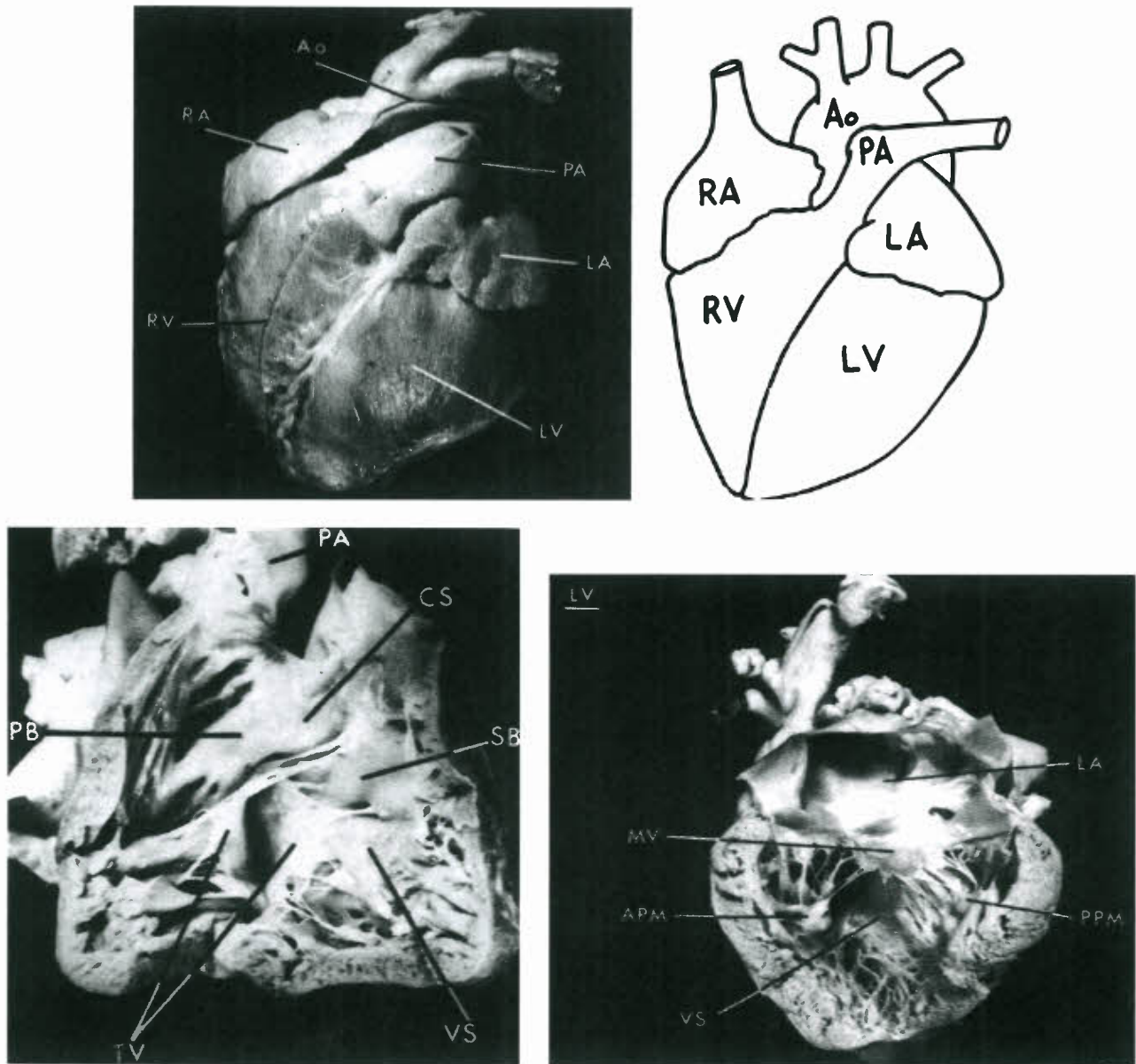


Figure 53.8. Upper left: Situs solitus, dextrocardia with normally related great arteries. The schematic drawing at (upper right) depicts normal atrioventricular and ventricle–great artery relationships. The pathologic specimen illustrates normal internal morphologic characteristics of both ventricles. (Ao, aorta; APM, anterolateral papillary muscle; CS, crista supraventricularis; LA, left atrium; LV, left ventricle; MV, mitral valve; PA, pulmonary artery; PB, parietal bond; PPM, posteromedial papillary muscle; RA, right atrium; RV, right ventricle; SB, septal band; TV, tricuspid valve; VS, ventricular septum.) (From Van Praagh R, Van Praagh S, Vlad P, et al. Anatomic types of congenital dextrocardia: diagnostic and embryologic implications. *Am J Cardiol* 1964;13:510–531, with permission.)

The ECG shows normal P-wave axis and right QRS axis deviation. However, the initial qR wave of the QRS complex is abnormally directed to the left, consistent with abnormal septal depolarization associated with AV discordance.

Dextrocardia with Situs Inversus

Dextrocardia with Situs Inversus, AV and VA Concordance, and Inverted Great Arteries (Left Posterior Aorta)

Although the atria, ventricles, and great arteries are all inverted from their normal location and spatial relationships, in this form of dextrocardia, there is persistence of

normal AV and VA connections. This form of dextrocardia was not reported with high frequency in pathologic series, perhaps because of normal physiology often associated with it. However, in life it may be one of the more common forms of dextrocardia. In the review of Van Praagh et al. (21), it occurred in only 7 of 24 cases with situs inversus, and all but 2 cases had associated cardiac anomalies. Ventricular septal defect, tetralogy of Fallot, pulmonary atresia, complete AV septal defect, and secundum ASD were observed in this group. The radiographic findings are consistent with visceral situs inversus and dextrocardia. The electrocardiographic findings in this form of dextrocardia include atrial and ventricular voltage changes that are inverted from normal.

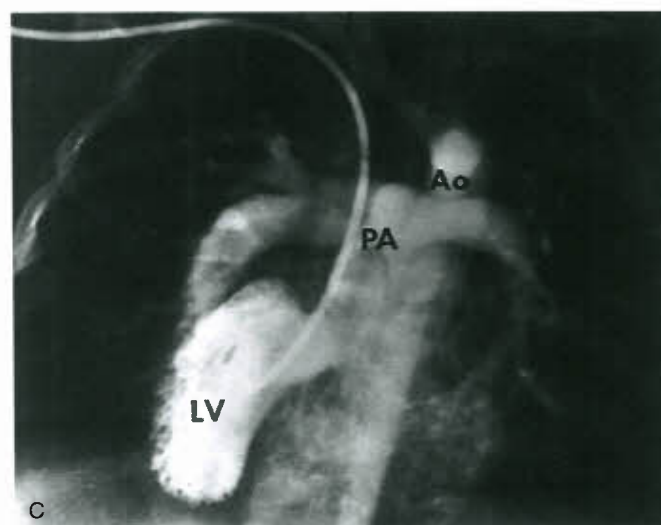
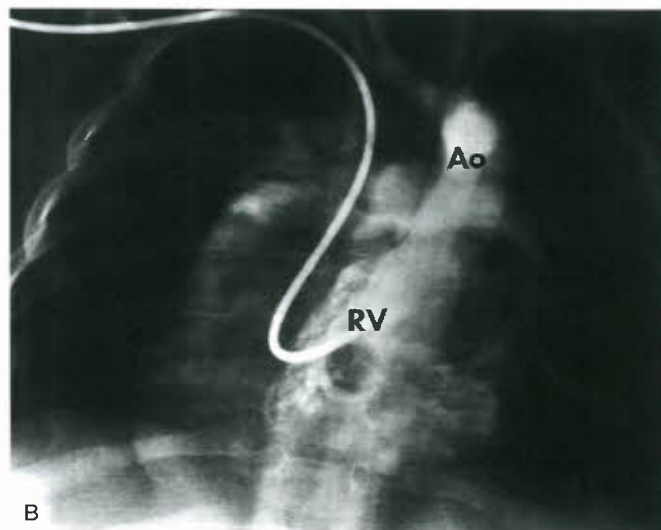


Figure 53.9. Isolated dextrocardia. **A:** Posteroanterior chest radiograph demonstrating cardiac malposition consistent with dextrocardia, with the base–apex axis oriented to the right; however, the heart is just slightly to the right of a midline location, illustrating an intermediate position between mesocardia and dextrocardia. **B,C:** Angiocardiograms demonstrating dextrocardia with atrioventricular and ventriculoarterial discordance. They also show a large ventricular septal defect and some degree of pulmonary arterial overriding. (Ao, aorta; LV, left ventricle; PA, pulmonary artery.)

The P-wave axis is directed to the right and inferiorly because of atrial inversion. Other voltage abnormalities depend on the associated cardiac lesions.

Dextrocardia with Situs Inversus, Atrioventricular Concordance, and Ventriculoatrial Discordance with Left Anterior Aorta

Dextrocardia with situs inversus, AV concordance, and VA discordance with left anterior aorta represents an “inverted” form of complete TGA (Fig. 53.11) and is one of the most common reported forms of dextrocardia with situs inversus, occurring in seven of 24 patients in the Van Praagh et al. (21) series. The hemodynamics and physiology are identical to complete TGA with levocardia. The electrocardiogram shows an inverted P-wave axis because of the atrial inversion; however, there may be more evidence of associated right and left ventricular hypertrophy because of transposition physiology.

Dextrocardia with Situs Inversus and Atrioventricular and Ventriculoatrial Discordance, with Right Anterior Aorta

Dextrocardia with situs inversus and AV and VA discordance, with right anterior aorta, is an inverted form of congenitally corrected TGA. It is rare, occurring in only 3 of 136 cases of

dextrocardia (21) (Fig. 53.12). Although the segmental cardiac connections would, theoretically, be physiologically correct in these hearts, there was a high frequency of significant additional associated anomalies, resulting in profound hemodynamic impairments. In the example demonstrated, there is a VSD and subpulmonary stenosis. Also, there is significant cardiac rotation to the right, so that the aorta is actually in a right posterior position relative to the pulmonary valve and main pulmonary artery.

Dextrocardia with Situs Inversus, Atrioventricular Discordance, and Ventriculoatrial Concordance with Inverted Normally Related Great Arteries (Left Posterior Aorta)

Dextrocardia with situs inversus, AV discordance, and VA concordance with inverted normally related great arteries (left posterior aorta) has been described as being similar to isolated ventricular inversion, and shares hemodynamics comparable to those of complete TGA. This is also an extremely rare form of dextrocardia, with only two cases reported in the Van Praagh et al. (21) review. One of these patients had multiple additional cardiac abnormalities, including common atrium, common AV valve, and severe right ventricular hypoplasia.

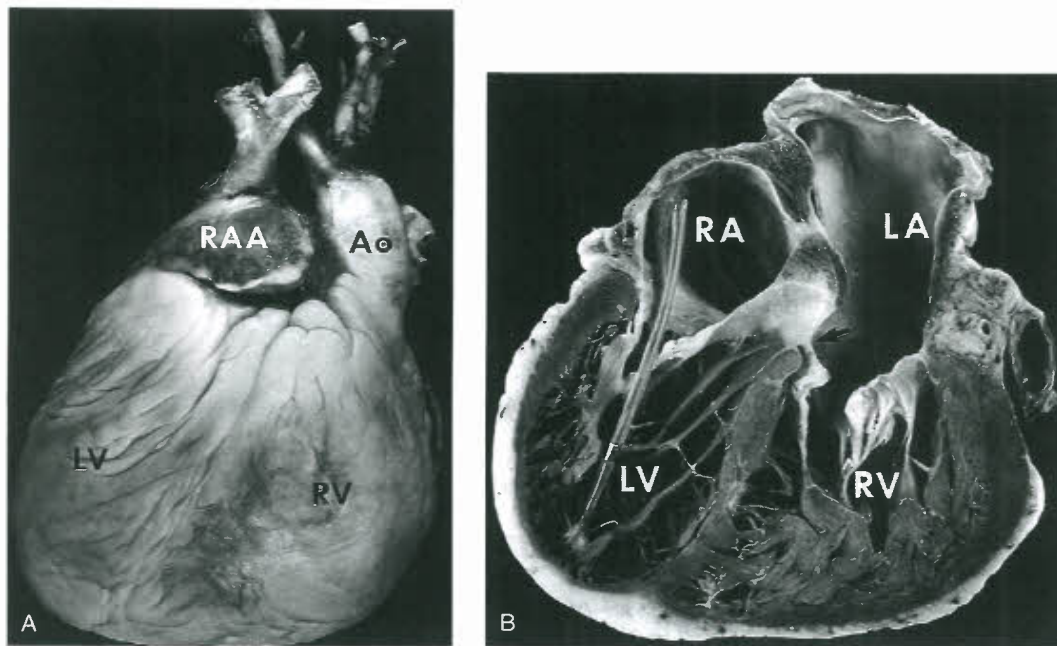


Figure 53.10. Isolated dextrocardia. Pathologic specimen illustrating the most common form of dextrocardia associated with atrial and visceral situs solitus. There is atrioventricular (AV) and ventriculoarterial discordance. Note the great artery orientation with the left anterior aorta (Ao). The resulting hemodynamics are consistent with the physiology of congenitally corrected transposition of the great arteries. **A:** External view of the heart. **B:** A four-chamber cut demonstrating the pathologic features of AV discordance. The left atrium (LA) connects to the morphologic right ventricle (RV) on the left. The *arrow* points out one identifying feature of the morphologic RV, the typical tricuspid valve attachment to the ventricular septum at a point inferior to the mitral valve attachment. (LV, morphologic left ventricle; RA, right atrium; RAA, right atrial appendage.) (Provided by Dr. William D. Edwards.)

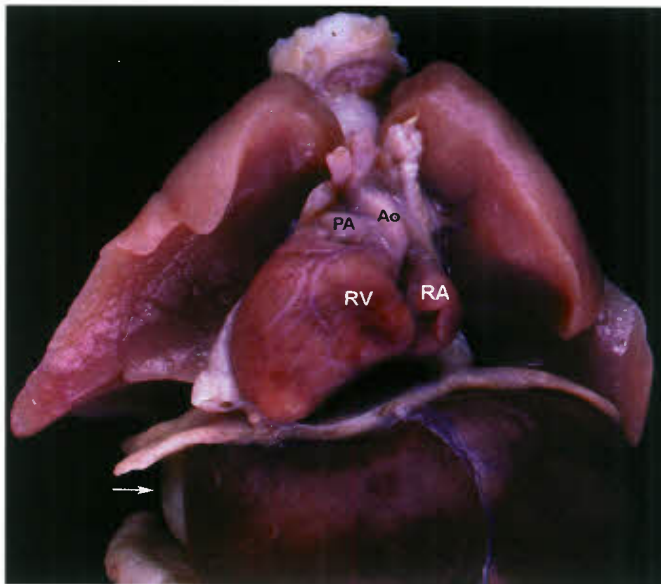


Figure 53.11. Pathologic specimen demonstrating situs inversus, dextrocardia with AV concordance, VA discordance, and left anterior aorta in a 26-week-gestation stillborn fetus. It represents an inverted form of complete transposition of the great arteries. A prominent morphologic right (systemic venous) atrial appendage (RA) and the ascending aorta (Ao) are noted on the left of the fetus. The *arrow* points to the stomach on the right side of the fetus. (PA, main pulmonary artery; RV, right ventricle.) (Provided by Dr. William D. Edwards.)

The eight forms of dextrocardia described above are identical to the eight possible theoretical variations of possible AV and VA connections previously outlined in Figure 53.7.

SITUS AMBIGUUS

Situs ambiguus could be present in association with right atrial (asplenia) or left atrial (polysplenia) isomerism. Dextrocardia with situs ambiguus was the most common form of dextrocardia in the Van Praagh et al. (21) review, occurring in 46 of 136 cases; 27 patients had asplenia and 18 had polysplenia. In the pathologic series reported by Lev et al. (9), 12 of 41 cases were “undetermined” or “presumptive” forms of dextrocardia with some features typical of situs ambiguus. Eight of these patients had asplenia.

ASPLENIA

Three of the six examples of dextrocardia with situs ambiguus and asplenia originally reviewed by Van Praagh and Vlad (6) demonstrated features of common atrium, common AV valve, common-inlet ventricle of right ventricular type, hypoplastic LV, and VA discordance or double-outlet RV with pulmonary atresia or severe stenosis. All had normally related ventricles with the RV to the right (d-ventricular loop) and a right anterior aorta. The remaining three were similar with the exception of the ventricular arrangement. They had the RV positioned to the left of the LV remnant (l-ventricular loop, ventricular inversion)

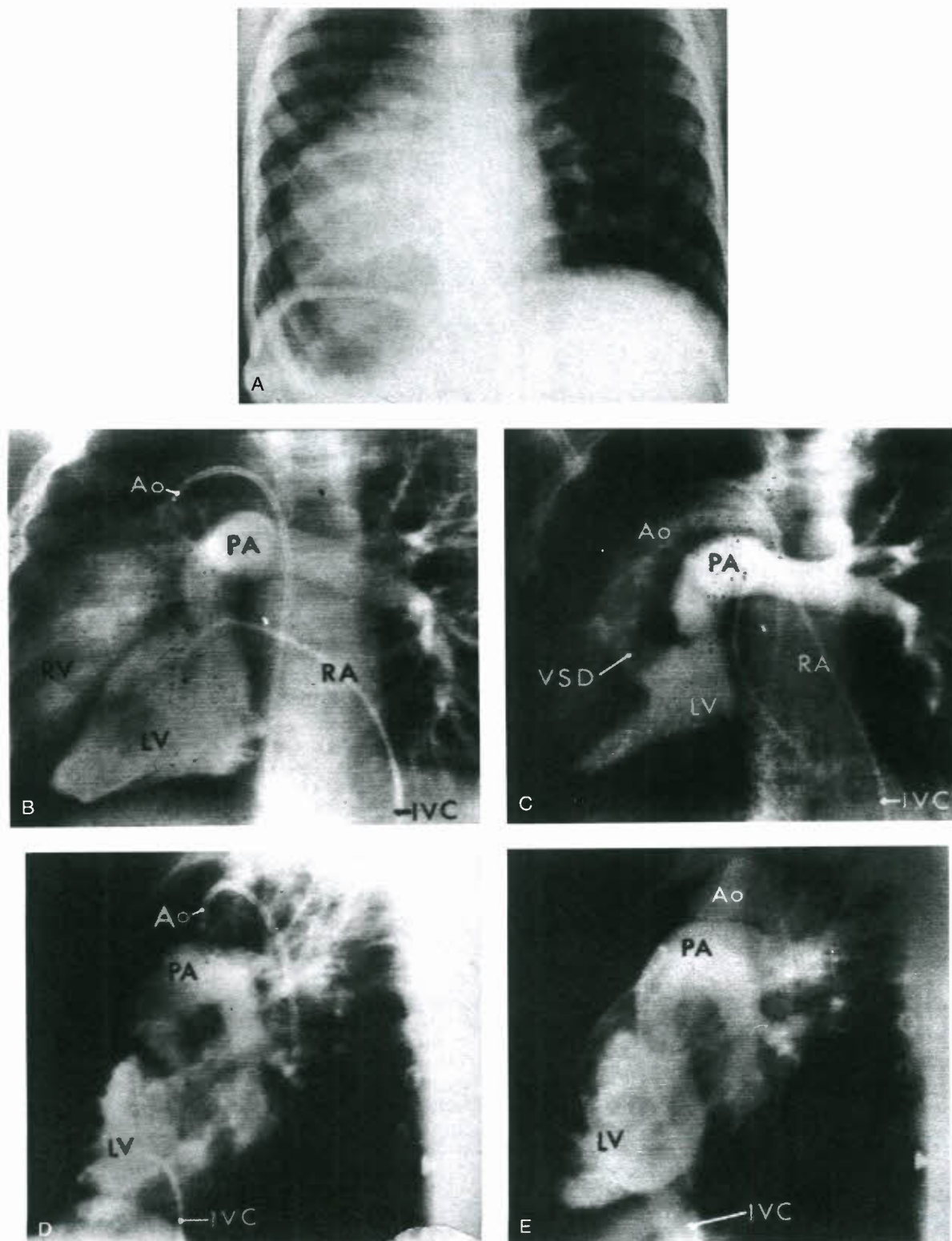


Figure 53.12. Dextrocardia with situs inversus and atrioventricular and ventriculoarterial discordance (congenitally corrected transposition). **A:** The posteroanterior chest radiograph demonstrates dextrocardia with a right-sided stomach bubble consistent with situs inversus and dextrocardia. The angiocardiograms (**B–E**) demonstrate a catheter in a left-sided inferior vena cava (IVC) joining a left-sided systemic venous atrium (RA), which connects with a morphologic left ventricle (LV) and a left-sided pulmonary artery (PA). Note that the ascending aorta (Ao) is right posterior in relation to the pulmonary valve because of marked cardiac rotation to the right. (VSD, ventricular septal defect.) (From Van Praagh R, Van Praagh S, Vlad P, et al. Diagnosis of anatomic types of dextrocardia. *Am J Cardiol* 1965;15:234–243, with permission.)

and left anterior aorta (Fig. 53.13). As is typical with asplenia, all had multiple anomalies of systemic and pulmonary venous connections. Bilateral superior venae cavae with direct connections to the atria, bilateral pulmonary venous connections (direct right and left pulmonary venous connections to the ipsilateral atrium), anomalous supracardiac pulmonary venous connections, absent coronary sinus, bilateral hepatic venous connections to the ipsilateral atrium, and azygous or hemiazygous continuation of the IVC to the SVC are all typical venous anomalies in situs ambiguus. This constellation of anatomic features is characteristic of situs ambiguus and right isomerism, regardless of the cardiac position (levocardia, mesocardia, or dextrocardia). Eleven patients with dextrocardia and asplenia were observed in the series reported by Stanger et al. (11). All had AV septal defects, and seven of these had ventricular inversion (l-loop) and VA discordance with an anterior left aorta. Two had noninverted ventricles (d-loop) and VA discordance with anterior right aorta, and two had single LVs with an anterior left aorta. Although these were the most common types of anomalies reported, several other variations have been reported. Most patients have some AV valve abnormality, such as common AV inlet, but right or left AV valve atresia is also recognized. Many have an unbalanced form of VSD, most often with left ventricular hypoplasia, but they may have tricuspid valve atresia and right ventricular hypoplasia. Some may have a single ventricle of uncertain or indeterminate morphology with a common AV inlet. As previously noted, most patients with asplenia have pulmonary stenosis or atresia. Aortic atresia is a rare finding in asplenia.

POLYSPLENIA

The features classically included with the polysplenia syndrome and dextrocardia are similar to those just described with asplenia, including common-inlet ventricle of right ventricular morphology and double-outlet RV. However, some outstanding differences are noteworthy, including a lower incidence of associated pulmonary stenosis and a more frequent occurrence of bilateral pulmonary venous connections to the ipsilateral atrium. In addition, patients with polysplenia have had

a much wider variation in the cardiac anomalies described, in many cases having features more typically observed with situs inversus totalis. In the review by Van Praagh et al. (21), the most common form of congenital heart disease associated with the polysplenia syndrome was dextrocardia, atrial situs ambiguus, ventricular inversion, and VA concordance with left posterior aorta. The next most frequent complex observed was dextrocardia, situs ambiguus, ventricular inversion, and VA discordance with left anterior aorta. In the Stanger et al. (11) series, nine patients had dextrocardia and four had AV discordance with VA concordance (ventricular inversion) or double-outlet RV. This review also suggested that situs inversus and polysplenia with dextrocardia may be interrelated etiologically and embryologically. They noted that the associated cardiovascular malformations found in the polysplenia syndrome were similar to, but often less severe than, those found in the asplenia syndrome. For example, only complete common AV septal defects were found in the asplenia syndrome, but partial AV septal defects also were observed in the polysplenia syndrome. Pulmonary outflow tract obstruction (stenosis or atresia) occurred in 5 of 18 patients with polysplenia, whereas pulmonary outflow tract obstruction was present with asplenia in 16 of 18. Features characteristic of the polysplenia syndrome, such as interruption of the IVC with azygous continuation to the SVC and ipsilateral pulmonary veins, also were noted.

LEVOCARDIA (ISOLATED LEVOCARDIA)

When the heart is in a normal position and has a normal base-apex cardiac axis, isolated levocardia implies that either atrial situs inversus or atrial situs ambiguus is present. In the autopsy series reported by Van Praagh et al. (8) and by Stanger et al. (11), atrial situs inversus with levocardia was unusual and occurred in only 3% to 14% of the cases described with isolated levocardia. Most of these had AV discordance and either VA discordance or double-outlet RV with anterior right aorta, resembling malpositioned forms of corrected TGA.

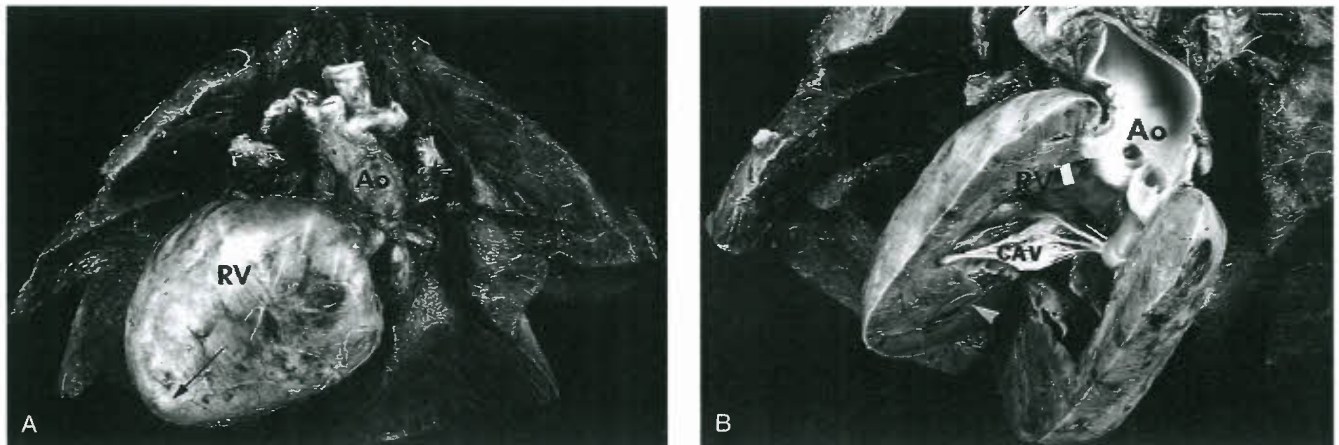


Figure 53.13. Pathologic specimen demonstrating anatomic features observed with situs ambiguus, dextrocardia with asplenia. **A:** Frontal view demonstrating the heart and lungs. The cardiac base-apex axis (arrow) points to the right, consistent with dextrocardia. The lungs are trilobed bilaterally. The aorta (Ao) is left anterior with a right aortic arch. **B:** An open view of the morphologic right ventricle (RV). There was a common-inlet (CAV) RV with double-outlet RV and severe pulmonary stenosis. A white probe is inserted into the stenotic pulmonary outflow tract. The white arrowhead indicates a hypoplastic rudimentary morphologic left ventricle to the right and posterior. The ventricular relationships are consistent with ventricular inversion or l-ventricular looping. (Provided by Dr. William D. Edwards.)

MESOCARDIA

As defined previously, mesocardia is present when the heart is in a midline position and the cardiac base–apex axis is oriented directly inferiorly (neither to the right nor left). Autopsy series (6,8,9,23) have consistently included a very low incidence of mesocardia. The series by Stanger et al. (11) included only patients with asplenia (situs ambiguous). However, the series by Lev et al. (23) included 17 cases with situs solitus, inversus, and ambiguous. Most of these had situs solitus and were either normal hearts or examples of VA discordance with and without AV discordance (complete or congenitally corrected TGA). Lev et al. (23) defined mesocardia as that condition in which the longitudinal axis of the heart lies in the midsagittal plane with the heart possessing no distinct apex. The low incidence of mesocardia in these reports may reflect a tendency to have included such cases in the groups with dextrocardia or isolated levocardia. As a group, the hemodynamic and clinical findings in mesocardia are also similar to those previously described with dextrocardia. Figure 53.1 (panel B) illustrates pathologic findings in a patient with situs solitus and mesocardia, as well as AV and VA discordance.

ECHOCARDIOGRAPHIC FEATURES OF CARDIAC MALPOSITION

Two-dimensional and Doppler echocardiography have become the cornerstone of the initial diagnostic evaluation of patients with all forms of congenital heart disease and provide essential

anatomic data in patients with cardiac malpositions. Transthoracic echocardiography is a convenient and noninvasive technique that can provide most of the clinically relevant information concerning the cardiovascular anatomy and physiology, especially in young patients. In situations where a transthoracic examination is inadequate (i.e., patients with poor transthoracic images, large body size, or postoperative bandaging, etc.) or impossible (during an operation), transesophageal echocardiography can be used to obtain additional echocardiographic information.

Segmental Approach

The echocardiographic approach to patients with cardiac malpositions should follow the sequential segmental analysis that was outlined earlier in this chapter and in many other reports (24–26). The following section and its echocardiographic images of normal and malpositioned hearts are included to illustrate the tomographic anatomy associated with these malformations and to assist the reader in correlating the echocardiographic findings with the previously presented anatomic and angiographic examples of these complex hearts.

Visceral Situs

Images of the liver, hepatic veins, IVC, stomach, spleen, and abdominal aorta are obtained from the subcostal transducer position. The normal position of these organs and vessels is demonstrated in Figure 53.14. Visceral situs inversus is characterized by a left-sided liver and IVC in association with a right-sided stomach, spleen, and abdominal aorta (Fig. 53.15).

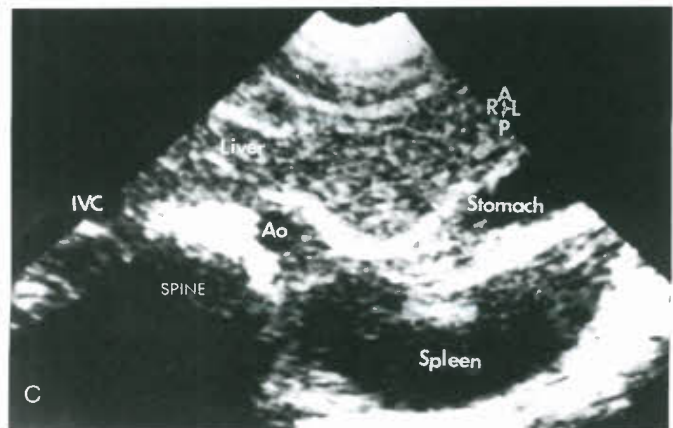
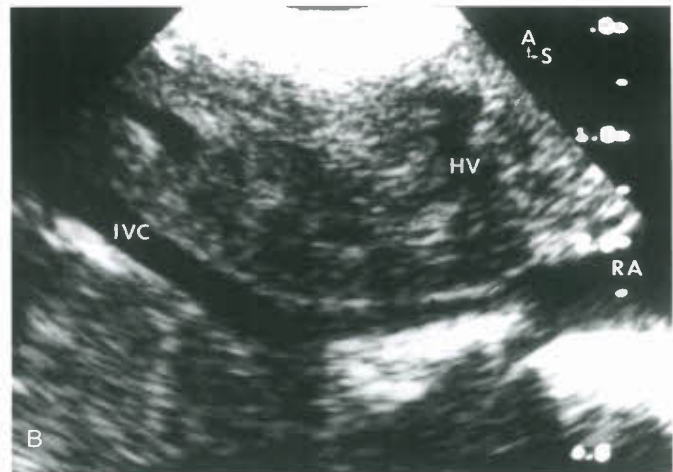
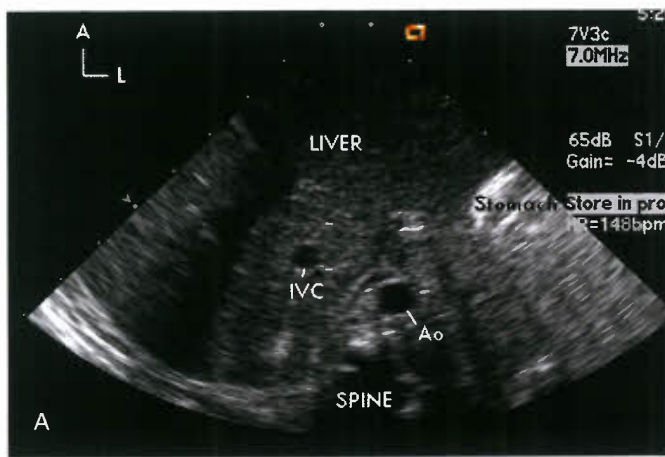


Figure 53.14. Atrial and visceral situs solitus. **A:** The subcostal short-axis scan of the abdomen demonstrates an initial right-to-left orientation for visceral situs determination. The spine is readily recognized as a posterior midline structure. The liver mass is noted predominately in the right side of the abdomen. The intrahepatic portion of the inferior vena cava (IVC) is observed on the right and the abdominal aorta (Ao) on the left. The stomach is noted on the left as a bright echo. **B:** A long-axis view of the IVC illustrates the connection of the IVC to the right atrium (RA) consistent with situs solitus. The hepatic vein (HV) is also noted draining to the IVC–RA junction. **C:** With the transducer oriented to the left of the abdomen, the stomach and spleen are identified.

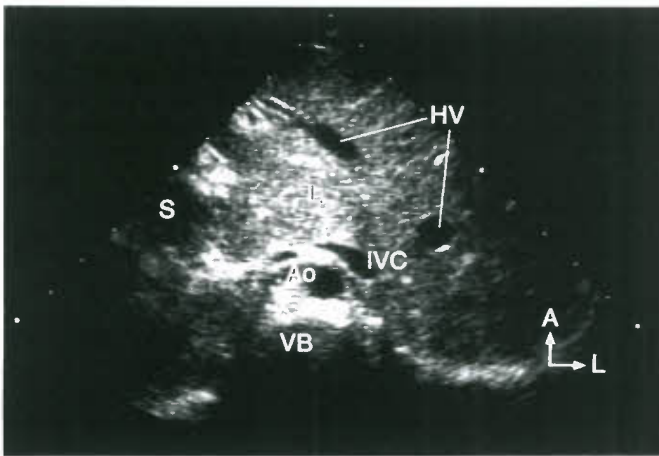


Figure 53.15. Atrial and visceral situs inversus. Subcostal short-axis scan of the abdomen provides right-to-left spatial orientation. The liver (L), inferior vena cava (IVC), and hepatic veins (HVs) are on the patient's left, and the stomach (S) is seen on the patient's right. The descending abdominal aorta (Ao) is directly anterior to the vertebral body (VB).

As previously described, situs ambiguus has been used to describe a wide spectrum of anomalies, including the visceral abnormalities present in the asplenia and polysplenia syndromes (Fig. 53.16). The visceral situs is considered

“ambiguous,” because it does not conform to the classical patterns of situs solitus or inversus. Nearly all possible combinations of abdominal organ and great vessel location have been reported (17,21). The term visceral situs ambiguus does not mean that the positions of the abdominal organs cannot be determined. Their positions and venous connections can and must be accurately defined before corrective surgical procedures can be performed.

The obvious echocardiographic finding in patients with asplenia is the *absence* of or the inability to demonstrate the presence of a spleen. The spleen, when present, is always located posterolateral to the stomach (7,11,17,27). Routine transthoracic echocardiography can easily determine splenic status by locating the stomach and interrogating the area posterior and lateral to the stomach (Fig. 53.14). The splenic tissue may have a denser echocardiographic appearance than the liver and its comma-shaped curvilinear splenic vein may be identifiable. In patients with asplenia, no splenic tissue can be identified in this position; however, both flank areas must be carefully examined. When this echocardiographic finding is associated with the presence of Howell–Jolly bodies on the peripheral blood smear, the diagnosis of asplenia can be made with 100% confidence. Patients with asplenia usually will have a midline liver (a large central liver mass equally committed to both the right and left upper quadrants of the abdomen) (Fig. 53.16). The liver will frequently have two lobes that are relatively equal in size and resemble morphologic right lobes. Occasionally, some of the hepatic veins will connect directly to the atrium instead of draining to the IVC. The positions of the stomach, IVC, and

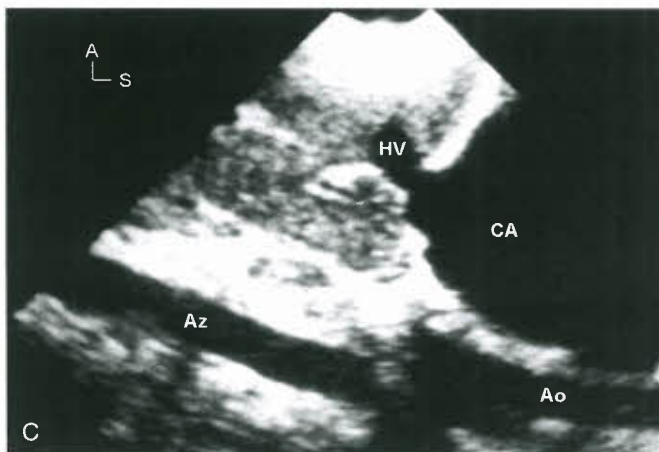
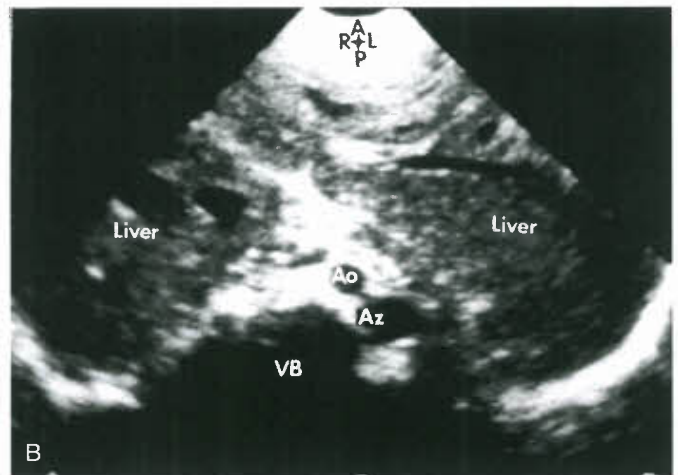
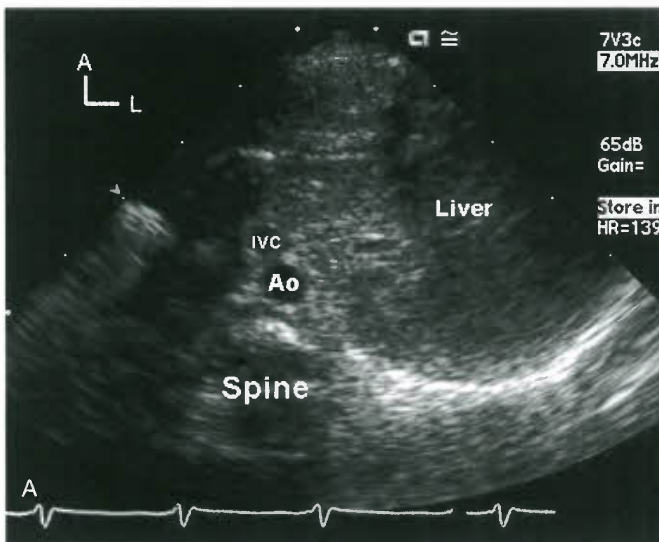


Figure 53.16. Visceral situs ambiguus: A: Asplenia: subcostal short-axis horizontal-plane image of the upper abdomen in a patient with situs ambiguus and asplenia. Note the large midline liver mass occupying both (especially the left) quadrants of the abdomen. The stomach was on the right side of the abdomen. The inferior vena cava (IVC) and aorta (Ao) both occupy a position directly anterior to the spine with the Ao posterior to the IVC. B: Polysplenia: subcostal short-axis horizontal-plane image of the abdomen in a patient with situs ambiguus and polysplenia. The liver is large and midline. The aorta (Ao) and an azygous (Az) continuation of the IVC are noted on the left side of the spine (VB). The azygous continuation is located posteriorly in the retroperitoneal space. C: Long-axis image in the same patient demonstrating the aorta and the azygous vein. Note that a hepatic vein (HV) enters directly into the common atrium (CA).



Figure 53.17. Polysplenia. Long-axis image from the left flank demonstrating two equal-sized spleens adjacent to the liver and superior to the left kidney. This finding is consistent with the diagnosis of situs ambiguous, with left isomerism.

aorta are more variable than that of the liver, and they must be individually described. Characteristically, the IVC and aorta are both located on the right side of the vertebral column in a parallel anteroposterior orientation (Figs. 53.2 and 53.16).

Patients with polysplenia will have multiple, separate spleens positioned posterior to the stomach (Fig. 53.17). As with asplenia, multiple or multilobulated spleens can be readily detected by echocardiography (27). Other visceral features of the polysplenia syndrome may include interruption of the IVC with azygous continuation and a midline location of abdominal aorta. With interruption of the suprahepatic portion of the IVC, the hepatic veins will connect directly to the atrium. Occasionally, there may be two or more separate hepatic vein connections to the right or left sides of the atrium. The location of the liver and stomach are variable, but most commonly in polysplenia syndrome with cardiac malposition, they are inverted, with the stomach and multiple spleens located on the right side of the abdomen.

Venous Connections

Venous abnormalities are common when cardiac malpositions are present. These abnormalities include, but are not limited to, bilateral superior vena cavae connecting directly to the ipsilateral atrium (absent coronary sinus), interruption of the IVC with azygous or hemiazygous continuation to the ipsilateral SVC, and various anomalous pulmonary venous connections as described earlier in this chapter. Direct pulmonary venous connections to the ipsilateral atrium, as well as complete or partial connections to the right or left SVC can be defined echocardiographically (26,28), especially during the newborn and neonatal period. If transthoracic images are inconclusive, a complete transesophageal study can be helpful to define these abnormal pulmonary venous connections.

Atrial Situs

Once visceral situs and the venous structures and connections have been defined, atrial situs should be determined. These two portions of the exam, however, are intimately related.

Each major venous connection (SVC, IVC, hepatic veins, and each pulmonary vein) to the heart must be identified. Specific attention should be paid to the coronary sinus, when present, as its connection represents a marker for the morphologic right atrium. Additionally, dilation of the coronary sinus may signal an anomalous venous connection, and, unroofing of the coronary sinus should be ruled out, which if undetected could lead to residual atrial shunting after repair.

Although venous connections can assist in determining atrial situs, it is the relationship between septum primum and septum secundum that is the most reliable determinant of atrial situs (7). The thick remnant of septum secundum is best seen by echocardiography as the superior limbus of the fossa ovalis (Fig. 53.18). This limbus will be associated with the morphologic *right atrium*. The thin remnant of septum primum, best seen by echocardiography as the valve of the fossa ovalis, will be associated with the morphologic *left atrium*. Unfortunately, these structures are not always present in patients with congenital heart disease. When the remnants of these septa are absent, other markers for atrial situs must be used. Van Praagh et al. (21) suggest that the connection of the suprahepatic IVC be used as the next most reliable marker. In their experience, the suprahepatic IVC always connects to the morphologic right atrium. The morphology of the atrial appendages also has been used to determine atrial situs (13). Classically, the appendage associated with a morphologic right atrium (Fig. 53.19) is described as a broad, somewhat triangular structure, whereas the left atrial appendage is more of a finger-like, narrow projection. Figure 53.20 demonstrates the echocardiographic features of left-juxtaposed atrial appendages in a patient with double-outlet RV. In this short-axis view, both atrial appendages are well visualized and demonstrate the typical anatomic features described above for the atrial appendages. The connections of the SVC and pulmonary veins are not reliable predictors of atrial situs.

Atrioventricular Connection

The routine evaluation of the AV connection has been described earlier in this chapter. In the presence of cardiac malposition, the echocardiographic evaluation includes an extensive assessment of the AV connection using the segmental approach. Few generalizations are valid with respect to the complex AV connections found in malpositioned hearts, and each type of connection is best considered as unique to the patient being examined. Right and left parasternal short-axis, as well as apical and subcostal four-chamber views, generally, are best used for assessment of the AV connections. As described in Table 53.1, abnormalities of both AV commitment and valve abnormalities must be defined. Echocardiographic examples of three types of abnormal AV connection often observed in cardiac malposition (single-, double-, and common-inlet connections) were discussed in the previous chapter dealing with univentricular AV connections. Figure 53.21 demonstrates an example of dextrocardia with severe overriding and straddling (type C) of the tricuspid valve with AV concordance, illustrating one of the variations on the basic themes that may exist in these complex patients.

Cardiac Base–Apex Axis

Previously, we have defined cardiac malpositions including dextrocardia, mesocardia, and levocardia based on the orientation of the cardiac apex or the cardiac base–apex axis. Not only can the position of the heart in the chest be defined, but also its base–apex axis can be accurately defined echocardiographically. The subcostal transducer position is most useful for making these assessments. The center of the scan plane is positioned at the upper abdominal midline, and coronal images of the heart are obtained. Thus, the position of the

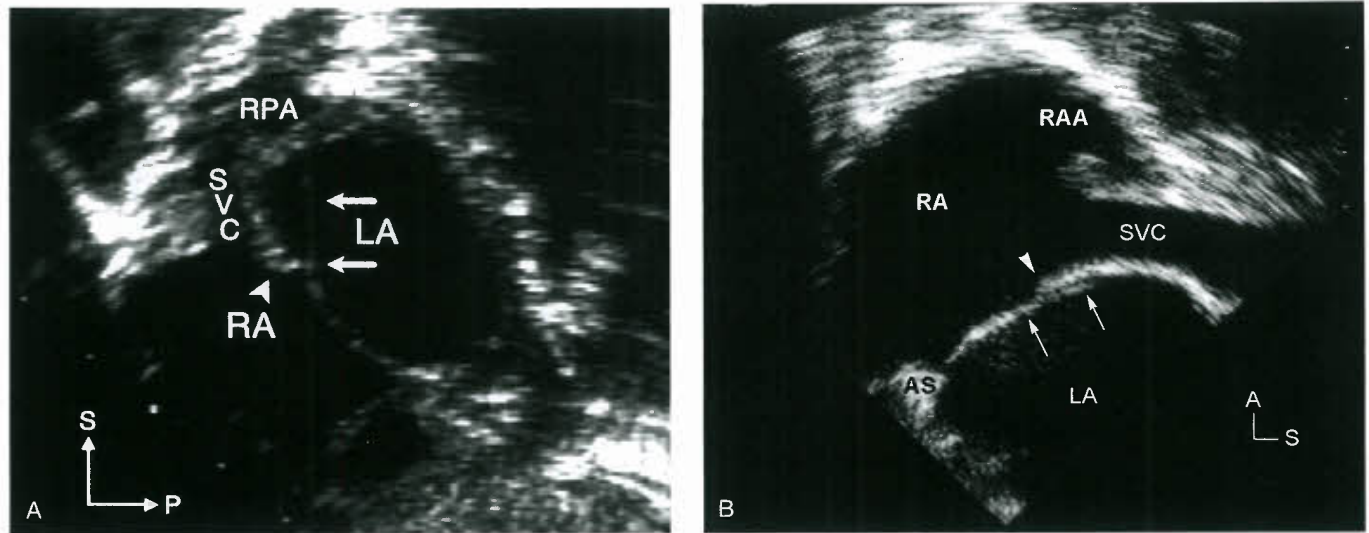


Figure 53.18. Atrial situs. **A:** Subcostal parasagittal view demonstrating the right and left atria in a newborn. The right atrial aspect, the limbus of the fossa ovalis (septum secundum) is identifiable (*arrowhead*), and on the left atrial side, the valve of the fossa ovalis (septum primum) is evident (*arrows*). **B:** Long-axis transesophageal scan of the atrial septum (AS) demonstrating similar anatomic landmarks to define atrial situs. Again the *arrowhead* points to the limbus of the fossa ovalis of the morphologic right atrium (RA). The *arrows* point to septum primum on the left. Note that the right atrial appendage (RAA) is observed anterior and adjacent to the superior vena cava (SVC). The RAA has a broad base and pyramidal shape. (A, anterior; LA, left atrium; P, posterior; RPA, right pulmonary artery; S, superior.)

heart within the thorax can be defined easily. When most of the heart is located to the left of the midline, the heart is then said to have levoposition. When most of the cardiac mass is to the right or evenly spread across the midline, there is dextroposition or mesoposition, respectively. The second component of cardiac position is more anatomically descriptive and involves the cardiac base–apex axis. When the cardiac axis is oriented to the left, levocardia is present (Fig. 53.1). When this axis is oriented to the right or directly inferior, there is dextrocardia or mesocardia, respectively (Fig. 53.1).

As previously described, isolated levocardia and isolated dextrocardia can be associated with various complex congenital anomalies. These diagnoses imply the presence of discordance between atrial situs, and the plane of the atrial septum will be distorted and it will not be found in a plane parallel to the cardiac base–apex axis and ventricular septum. Rather, the bulk of the atrial septum in hearts with isolated dextro- or levocardia will be perpendicular to that plane (Fig. 53.22). As a result of the discordance between the atrial situs and the base–apex orientation, the atrial septum assumes a curved shape that is characteristic of this abnormality.

Ventricles, Ventriculoarterial Connection, and Great Arteries

Ventricular anatomy, ventricular–great artery connection, and the great arteries themselves can be described according to the standard techniques described in earlier echocardiographic reports (25,26). Abnormalities of VA connections and great artery relationships are common in cardiac malpositions. Positioning of echocardiographic scans must be modified from the standard right or left parasternal and subcostal positions to adequately delineate VA connections and great artery relationships in these complex hearts. Parasternal long and short-axis scans are particularly helpful in determining concordant, discordant, or double-outlet connections as described in previous chapters devoted to these specific entities. Figure 53.20B illustrates a parasternal long-axis scan in a patient with

double-outlet RV. The pulmonary artery is demonstrated coursing posteriorly and is primarily committed to the anterior RV. The accompanying short-axis scan illustrates the great artery relationship with left anterior aorta. Additionally, suprasternal scans should be obtained to assess the proximal pulmonary and aortic arch anatomy. The aortic arch should be determined as right or left sided and the brachiocephalic branching pattern defined.

TREATMENT

Treatment of the wide variety of congenital cardiac malformations observed in cardiac malpositions, obviously, must depend on the specific lesion. Surgical correction should be achieved as frequently as possible using a standard two-ventricular-type repair such as an arterial switch procedure (Jatene, Kaye-Damus-Stansel, or Aubert procedure), or with VSD closure connecting the systemic ventricle to the aorta, transection of the pulmonary artery, and establishment of pulmonary ventricle-to-pulmonary artery continuity with an extracardiac conduit.

More complex malformations associated with situs ambiguus, such as common atrium with common-inlet single ventricle or unbalanced ventricles, and complex malformations associated with crisscross AV relations and severe AV valve straddling have fewer options for successful biventricular surgical correction. Most can only be directed toward a single ventricle pathway with systemic–pulmonary artery shunts, Glenn-type shunts, bidirectional cavopulmonary shunts, and finally the modified Fontan procedure.

All such procedures have had moderately increased mortality risks when applied to patients with the more-complex lesions observed in situs ambiguus. When anomalies of systemic and pulmonary venous connection are present, special efforts must also be directed toward surgical establishment of appropriate venous connections or relief of venous stenoses

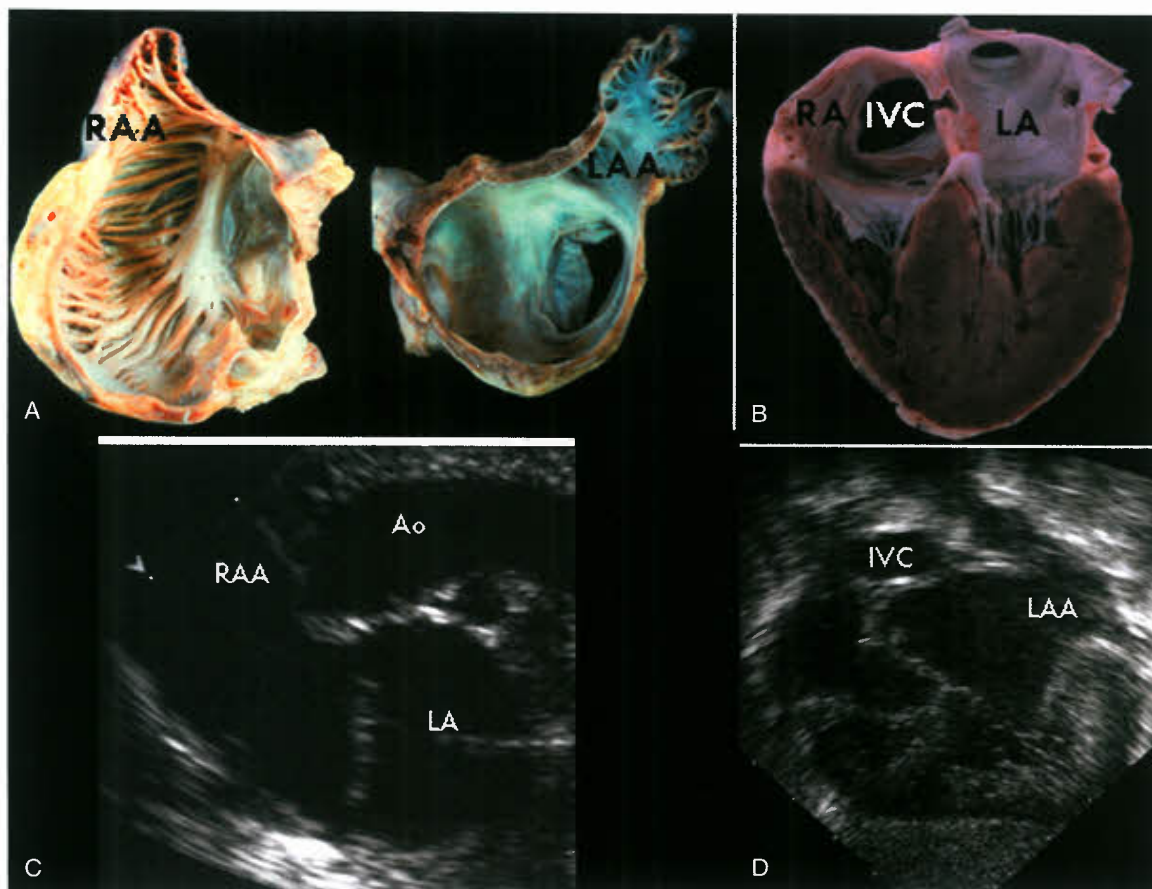


Figure 53.19. Atrial situs. Composite images showing pathologic and echocardiographic correlates of atrial morphologic features. **A:** Typical anatomic features of right and left atrial appendages (RAA and LAA). **B:** A right parasternal image illustrating the right atrial appendage (RAA), which is broad based and pyramidal. **C:** A specimen showing the inferior vena cava (IVC) draining to the right atrium (RA). **D:** Similarly, a subcostal echocardiogram illustrating the IVC connection to the right atrium and the small finger-like left atrial appendage (LAA) of the left atrium (LA). Ao, aorta.

that may be present. Unfortunately, because of their complex anatomic and situs abnormalities, such patients present significant challenges for cardiac transplantation when this is considered the only possible or one of the best options for surgical management. Medical management of these complex malformations offers little hope for long-term survival because of known complications of progressive hypoxia and polycythemia, progressive ventricular fibrosis, and ventricular failure, stroke, and brain abscess associated with such lesions (5,11,21).

Waldman et al. (29) showed a greatly increased frequency of fulminating and fatal septicemia produced by encapsulated bacteria in patients with the asplenia syndrome compared with appropriate controls. It generally is recommended that some form of antibiotic prophylaxis be given for congenitally asplenic patients. *Klebsiella* and *Escherichia coli* are the principle pathogens in patients younger than 6 months of age, whereas *Streptococcus pneumoniae* (pneumococcus) and *Haemophilus influenzae* predominate after 6 months. The report of the Committee on Infectious Diseases of the American Academy of Pediatrics recommends using continuous antibiotic prophylaxis in infants, children, and adults with the asplenia syndrome. For antimicrobial prophylaxis, oral penicillin V (125 mg, twice a day, for children younger than 5 years of age and 250 mg, twice a day, for children 5 years of age and older) is recommended. Some experts

recommend amoxicillin (20 mg/kg/day) (30). *H. influenzae* vaccine (Hib Vax), and hepatitis B vaccine should be given as routinely recommended in infancy. Pneumococcal conjugate vaccine is recommended for routine administration as a four-dose series for all children 23 months and younger (PCV7), and a dose of PS23 is recommended to be given at 24 months and an additional dose 3 to 5 years after the first dose. Quadrivalent meningococcal vaccine is recommended for optimal effect at 2 years of age or older. Routine use of yearly influenza vaccine is also recommended.

CONGENITAL PERICARDIAL DEFECTS

Congenital pericardial defects include a wide range of defects varying from minor partial defects to total absence of the pericardium (31).

Van Praagh et al. (21) noted the first report of congenital pericardial defects by Columbus in 1559. Although an uncommon lesion, congenital pericardial defects are difficult to diagnose clinically and often are first recognized at autopsy. Pericardial defects represent defective formation of the pleuropericardial membrane or, if diaphragmatic, defective formation of the septum transversum (32). Most investigators (31) reported left-sided congenital pericardial defects

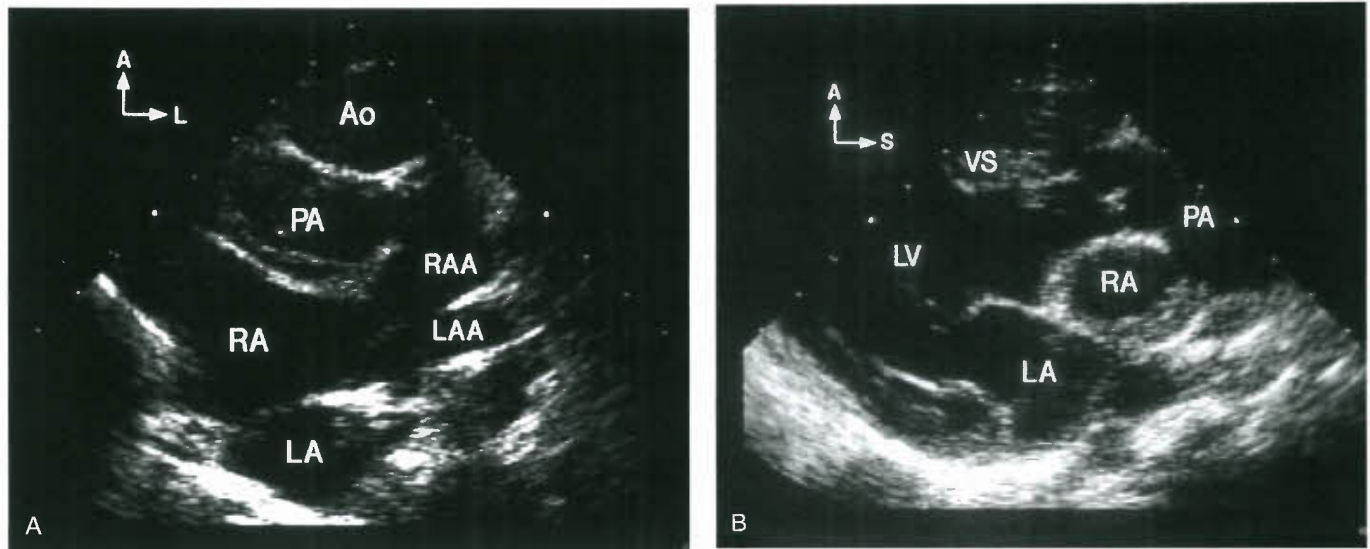


Figure 53.20. Left-juxtaposed atrial appendages in double-outlet right ventricle (RV). **A:** High left parasternal short-axis scan demonstrating left-juxtaposed atrial appendages in a patient with double-outlet right ventricle. Note the wide base and more bulbous appearance of the right atrial appendage (RAA) located more anteriorly and superiorly. The left atrial appendage (LAA) has a narrow base and finger-like projection. **B:** Parasternal long-axis scan of the same patient demonstrating the pulmonary artery (PA) coursing posteriorly and primarily originating from the anterior RV. Because the right atrium (RA) courses behind the PA in left-juxtaposed atrial appendages, it also separates the pulmonary artery from the mitral valve. A, anterior; Ao, aorta; L, left; LA, left atrium; S, superior; VS, ventricular septum.

as the most common, and the classification by Ellis et al. (33) demonstrated the complete left-sided defect as by far the most common form, representing 56% of their cases. Right-sided, diaphragmatic, and total absence of the pericardium are rare. Approximately one-third of patients with total absence of the

pericardium have associated pulmonary lesions such as bronchogenic cyst or sequestration and congenital heart lesions such as tetralogy of Fallot.

Manifestations

Associated anomalies may dominate the clinical presentation if the pericardial defect is associated with other congenital anomalies such as diaphragmatic hernia or congenital heart disease. Many patients with isolated pericardial defect are asymptomatic. Symptoms, when present, are nonspecific, consisting of vague left chest discomfort, recurrent pulmonary infection, palpitations, and occasionally dizziness and syncope. Partial left-sided pericardial defects may be associated with herniation of the ventricles through the patent pleurop-pericardial foramen, resulting in strangulation of the ventricles and leading to death. Herniation and strangulation of the left atrial appendage also can occur. Obstruction of the SVC can be associated with a right-sided pericardial defect secondary to herniation of the right lung into the pericardial space. Chest pain and the radiographic appearance of cardiomegaly may occur with diaphragmatic pericardial defect, because the associated diaphragmatic defect allows herniation of the greater omentum into the pericardial space.

Diagnosis

Physical examination may yield few abnormal signs. A crescendo-decrescendo systolic murmur at the left sternal border has been attributed to turbulent blood flow with an unusually mobile heart. The apical impulse may be hyperactive and displaced to the left.

The chest radiograph often provides the first clues to the diagnosis. In those with a complete left pericardial defect, the cardiac silhouette is displaced to the left and the left heart border has unusually prominent bulges at the aortic knob, the pulmonary artery, and the LV. There may be insertion of a

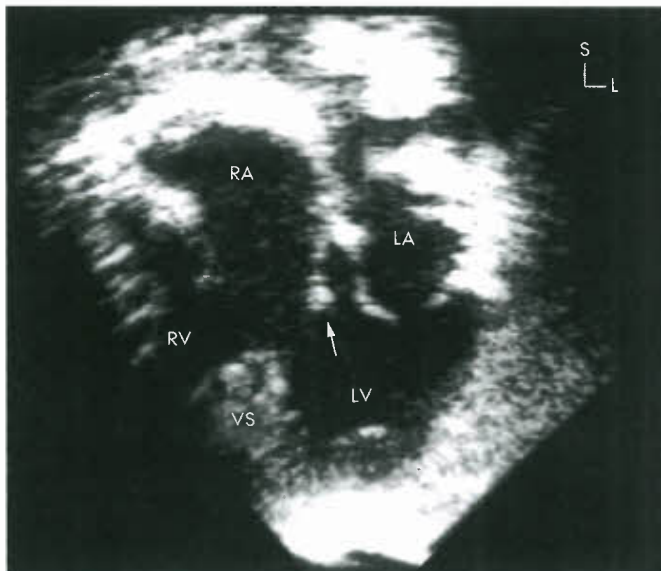


Figure 53.21. Atrioventricular override and straddling. Apical four-chamber view in a patient with isolated dextrocardia and severe (type C) straddling of the tricuspid valve in situs solitus, atrioventricular concordance, and dextrocardia. The arrow points to the septal tricuspid leaflet crossing into the left ventricle (LV) with a chordal attachment near the apex. The tricuspid annulus also overrides the ventricular septum (VS) and is partially committed to the LV. L, left; LA, left atrium; RA, right atrium; RV, right ventricle; S, superior.

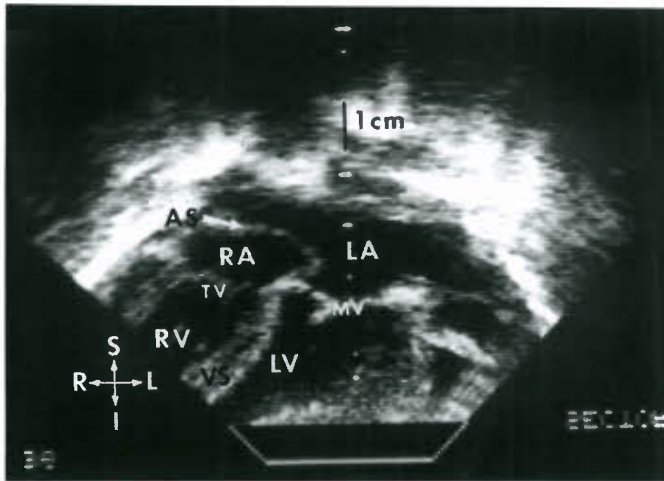


Figure 53.22. Two-dimensional echocardiographic demonstration of isolated dextrocardia. The subcostal four-chamber view illustrates features similar to those noted in the pathologic specimen of Figure 53.10. There is atrioventricular concordance, with a lower attachment of the right atrioventricular valve along the ventricular septum (VS) consistent with the tricuspid valve (TV). Because of the orientation of the ventricular mass, the atrial septum (AS) assumes a curvilinear shape (white arrow) extending from the right pulmonary veins (PV) to the crest of the VS. (I, inferior; L, left; LA, left atrium; LV, left ventricle; MV, mitral valve; R, right; RA, right atrium; RV, right ventricle; S, superior.)

small portion of the lung between the aorta and the main pulmonary artery or between the left portion of the diaphragm and the inferior border of the heart. A partial left pericardial defect may result in herniation of the left atrial appendage, and there may be prominence of the pulmonary artery segment or the atrial appendage or both. Computed tomography of the chest or magnetic resonance imaging now permit better visualization of absence of the pericardium.

Treatment

Complete absence of the pericardium is usually asymptomatic and is not treated. Only partial forms of pericardial defect (left sided, right sided, or diaphragmatic) require surgical treatment. Surgical treatment of partial pericardial defect has been of two types: enlargement, to avoid the risk of strangulation or closure, usually with a flap of mediastinal pleura. The latter is considered preferable. A defect of the diaphragmatic pericardium requires reduction of the abdominal contents into the abdomen and repair of the diaphragmatic defect.

ECTOPIA CORDIS

Ectopia cordis represents a form of pericardial defect but is further complicated by a partial or complete displacement of the heart outside the thorax. The term ectopia implies an abnormal displacement away from the expected position. A strict interpretation of this term would include any cardiac malposition, such as simple dextrocardia. However, the classic definition of ectopia cordis has represented this entity as a congenital displacement of the heart to a position outside of the thoracic cavity. Kanagasuntheram and Verzin (34) suggested a classification including five types: cervical, thoracocervical,

thoracic, thoracoabdominal, and abdominal. Van Praagh et al. (21) classified ectopia cordis as represented by four types—cervical, thoracic, thoracoabdominal, and abdominal—but suggested that for practical purposes, only two types, thoracic and thoracoabdominal, are clearly represented clinically. Tetralogy of Fallot has been reported in association with the thoracoabdominal form of ectopia cordis.

Cervical forms of ectopia usually are observed with the sternum intact. This form is thought to be rare and may simply represent retention of the heart in its embryonic position in the neck. In the review by Leca et al. (35), they noted 18 cases of cervical ectopia (8.5%), but included some cases with a partial sternal defect.

However, thoracocervical forms of ectopia cordis, with the heart partially in the cervical region and a defect in the superior end of the sternum appear to represent a distinct type of complete ectopia cordis. This form was not included in their review (35) (Fig. 53.23). In this abnormality, the heart is completely outside the thoracic cavity, and there is a complete absence of parietal pericardium and a cephalic orientation of the cardiac apex. No omphalocele or abdominal diastasis was present.

The thoracic type is the classic form of ectopia cordis (21), which is characterized by the following: a sternal cleft allowing protrusion of the heart outside the chest cavity, complete absence of the parietal pericardium, cephalic orientation of the cardiac apex, epigastric omphalocele or diastasis recti, and a small thoracic cavity (Fig. 53.24). The thoracic type occurred in 80 cases (37%) in the review by Leca et al. (35). A small thoracic cavity appears to be a significant etiologic agent as well as having significant implications for successful surgical correction of this defect. Congenital heart disease, most commonly tetralogy of Fallot, but also ventricular hypoplasia, TGA, and double-outlet RV, may be present. Van Praagh et al. (21) also hypothesized that the ruptured amnion syndrome associated with some cases of thoracic ectopia cordis results in oligohydramnios and leads to excessive



Figure 53.23. Thoracocervical ectopia cordis in a 20-week-gestation fetus. There is a defect in the superior portion of the sternum. There is cephalic orientation of the cardiac apex and complete absence of the parietal pericardium. However, there is no omphalocele, and no abdominal visceral anomalies were present. Double-outlet right ventricle and left ventricular hypoplasia were found. Extracardiac defects were also present as evidenced by the bilateral cleft lip and palate. Chromosome analysis was normal. (Provided by Dr. William D. Edwards.)



Figure 53.24. Thoracic ectopia cordis in a newborn infant. There is a sternal defect with complete ectopia cordis. There is cephalic orientation of the cardiac apex and complete absence of the parietal pericardium. There is also a typical epigastric omphalocele. (From Bryon F. Ectopia cordis: report of a case with attempted operative correction. *J Thorac Surg* 1948;17:717, with permission.)

compression of the heart during cardiogenesis, resulting in anterior extrusion of the heart from the chest cavity. Despite this apparent mechanical explanation, chromosomal abnormalities and multiple extracardiac malformations also have been associated with complete thoracic ectopia cordis. Pro-lapse of the forebrain, meningocele, cleft lip, and palate deformities predominated. A defect in the primitive mesenchyme of the body wall also has been proposed as an explanation for ectopia cordis.

Thoracoabdominal ectopia cordis appears to represent a partial form of ectopia cordis. It typically includes the following: partial absence or a cleft of the lower sternum, a crescentic midline anterior diaphragmatic defect, a defect of the diaphragmatic parietal pericardium resulting in a free pericardioperitoneal communication, an omphalocele-like ventral abdominal defect or diastasis recti with partial displacement of the ventricular portion of the heart through the diaphragmatic defect into the epigastrium, and intracardiac congenital heart disease. It has been reported in approximately 37% of cases with ectopia cordis (21). Many different types of congenital heart disease have been reported with thoracoabdominal ectopia cordis including tetralogy of Fallot, double-outlet RV, VSD, ASD, tricuspid atresia, Ebstein anomaly, common atrium, common AV septal defect, anomalous pulmonary venous connections, single-ventricle pulmonary stenosis/atresia, aortic stenosis, coarctation of the aorta, TGA, and diverticulum of the LV or both ventricles. Toyama (36) also reported that at least five cases have had no congenital cardiac malformations.

The abdominal form of ectopia cordis has been extremely rare in some reviews and appears to represent a diaphragmatic defect with continued migration of the heart into the abdominal cavity. In some cases, the patients were apparently healthy, had no other cardiac disease, and died as adults. In the review of Leca et al. (35), 24 cases (11%) were reported to be the abdominal type.

Treatment

Saxena (37) reported the first successful surgical repair of thoracic ectopia cordis. Scott (38) reported the first successful surgical repair of thoracoabdominal ectopia cordis in 1950 by Brock. Repair in this case included repair of the diaphragmatic defect and of the epigastric hernia.

However, most surgical reports have demonstrated poor results for repair of this defect. Nevertheless, due to the complex nature of these malformations and the risk of infection, most have advocated immediate surgery to correct their congenital heart disease and the anterior chest wall defect. Most advocate some form of prosthetic reconstruction of the chest wall and covering the heart with skin. Dobel et al. (39) advised a staged approach with enlargement of the posterior pericardial space by dividing posterior pericardial attachments to the rib margins. Van Praagh et al. (21) advocated avoidance of sepsis, compression, and kinking of the heart. Thus, it was recommended that the cephalic orientation of the ventricular apex not be corrected or altered.

REFERENCES

- Casey B, Devoto M, Jones K, et al. Mapping a gene for familial situs abnormalities to human chromosome Xq24-q27.1. *Nat Genet* 1993;5:403-407.
- Kosaki K, Casey B. Genetics of human left-right axis malformations. *Semin Cell Dev Biol* 1998;9:89-99.
- Kato R, Yamada Y, Niikawa N. De Novo balanced translocation (6:18) q21;q21.3 or q22 in a patient with heterotaxia. *Am J Med Genet* 1996;66:184-186.
- Peeters H, Debeer P, Groenen P, et al. Recurrent involvement of chromosome region 6q21 in heterotaxy. *Am J Med Genet* 2001;103:44-47.
- Freedom R, Jaeggi E, Lim J, et al. Hearts with isomerism of the right atrial appendages—one of the worst forms of disease in 2005. *Cardiol Young* 2005;15:554-567.
- Van Praagh R, Vlad P. Dextrocardia, mesocardia and levocardia: the segmental approach to diagnosis in congenital heart disease In: Keith J, Rowe R, Vlad P, eds. *Heart Disease in Infancy and Childhood*. 3rd ed. New York, NY: Macmillan, 1978:638.
- Edwards W. Preoperative pathology of congenital heart disease In: Schoen F, ed. *Interventional and Surgical Cardiovascular Pathology: Clinical Correlations and Basic Principles*. Philadelphia, PA: WB Saunders, 1989:281.
- Van Praagh R, Van Praagh S, Vlad P, et al. Diagnosis of anatomic types of dextrocardia. *Am J Cardiol* 1965;15:234-243.
- Lev M, Liberthson R, Eckner F, et al. Pathologic anatomy of dextrocardia and its clinical implications. *Circulation* 1968;37:979-999.
- Van Mierop L, Patterson P, Reynolds R. Two cases of congenital asplenia with isomerism of the cardiac atria and the sinoatrial nodes. *Am J Cardiol* 1964;13:407.
- Stanger P, Rudolph A, Edwards J. Cardiac malpositions. An overview based on study of sixty-five necropsy specimens. *Circulation* 1977;56:159-172.
- Van Mierop L, Gessner I, Schiebler G. Asplenia and polysplenia syndrome. *Birth Defects* 1972;8:74.
- Becker A, Anderson R. Isomerism of the atrial appendages: goodbye to asplenia and all that. In: Clark E, Takao A, eds. *Developmental Cardiology: Morphogenesis and Function*. Mt Kisco, NY: Futura Publishing, 1990:659.
- Van Praagh S, Kreutzer J, Alday L, et al. Systemic and pulmonary venous connections in visceral heterotaxy, with emphasis on the diagnosis of the atrial situs: a study of 109 postmortem cases. In: Clark E, Takao A, eds. *Developmental Cardiology: Morphogenesis and Function*. Mt Kisco, NY: Futura Publishing, 1990:671.
- De la Cruz M, Nadal-Ginard B. Rules for the diagnosis of visceral situs, truncconal morphologies, and ventricular inversions. *Am Heart J* 1972;84:19-32.
- Chatrath R, O'Leary P, Edwards W. Left atrial isomerism: clinicopathologic findings in a 14-year-old boy. *Clin Anat* 2003;16:331-334.
- Edwards W. Applied anatomy of the heart. In: Brandenburg R, Fuster V, Giuliani E, eds. *Cardiology: Fundamentals and Practice*. Chicago, IL: Year Book Medical, 1987:47.
- De la Cruz M, Anselmi G, Cisneros F, et al. An embryologic explanation for the corrected transposition of the great vessels: additional description of the main anatomic features of this malformation and its varieties. *Am Heart J* 1959;57:104-107.
- Layton W, Manasek F. Cardiac looping in early iv/iv mouse embryos. In: Van Praagh R, Takao A, eds. *Etiology and Morphogenesis of Congenital Heart Disease*. Mt. Kisco, NY: Future Publishing, 1980:109.

20. Cook A, Anderson R. The functionally univentricular circulation. *Cardiol Young* 2005;15:7-16.
21. Van Praagh R, Weinberg P, Smith S, et al. Malpositions of the heart. In: Adams F, Emmanouilides G, Riemenschneider T, eds. *Heart Disease in Infants, Children, and Adolescents*. 4th ed. Baltimore, MD: Williams & Wilkins, 1989:530.
22. Anderson K, Lie J, Sieg K, et al. A criss-cross heart: Detailed anatomic description and discussion of morphogenesis. *Mayo Clin Proc* 1977;52:569-575.
23. Lev M, Liberthson R, Golden J, et al. The pathologic anatomy of mesocardia. *Am J Cardiol* 1971;28:428-435.
24. Van Praagh R. The segmental approach to diagnosis in congenital heart disease. *Birth Defects* 1972;8:4-23.
25. Huhta J, Hagler D, Seward J, et al. Two-dimensional echocardiographic assessment of dextrocardia: a segmental approach. *Am J Cardiol* 1982;50:1351-1360.
26. Gillis E, Springer R, O'Leary P. Practical issues related to the examination, anatomic image orientation, and segmental cardiovascular analysis. In: Eidem B, Cetta F, O'Leary P, eds. *Echocardiography in Pediatric and Adult Congenital Heart Disease*. Philadelphia, PA: Wolters Kluwer Health/Lippincott Williams & Wilkins, 2010:10-28.
27. O'Leary P, Seward J, Hagler D, et al. Splenic anatomy: echocardiographic demonstration in complex congenital heart disease. *Am J Cardiol* 1991;68:1536-1538.
28. Cetta F, Ammash N. Anomalies of the pulmonary and systemic venous connections. In: Eidem B, Cetta F, O'Leary P, eds. *Echocardiography in Pediatric and Adult Congenital Heart Disease*. Philadelphia, PA: Wolters Kluwer Health/Lippincott Williams & Wilkins, 2010:70-86.
29. Waldman J, Rosenthal A, Smith A, et al. Sepsis in congenital asplenia. *J Pediatr* 1977;90:555-559.
30. Red Book: 2003. Report of the Committee on Infectious Disease, 26th ed. Elk Grove Village, IL: American Academy of Pediatrics, 2003.
31. Southworth H, Stevenson C. Congenital defects of the pericardium. *Arch Intern Med* 1938;61:223-240.
32. Cantrell J, Haller J, Ravitch M. A syndrome of congenital defects involving the abdominal wall, sternum, diaphragm, pericardium, and heart. *Surg Gynecol Obstet* 1958;107:602.
33. Ellis K, Leeds N, Himmelstein A. Congenital deficiencies in the parietal pericardium: a review with 2 new cases including successful diagnosis by plain roentgenography. *Am J Roentgenol Radium Ther Nucl Med* 1959;182:125.
34. Kanagasuntheram R, Verzin J. Ectopia cordis in man. *Thorax* 1962;17:159-167.
35. Leca R, Thibert M, Khoury W, et al. Extrathoracic heart (ectopia cordis): report of two cases and review of the literature. *Int J Cardiol* 1989;22:221-228.
36. Toyama W. Combined congenital defects of the anterior abdominal wall, sternum, diaphragm, pericardium, and heart: a case report and review of the syndrome. *Pediatrics* 1972;50:778.
37. Saxena N. *Pediatr News* 1975;9:1.
38. Scott G. Ectopia cordis: report of a case successfully treated by operation. *Guy's Hosp Rep* 1955;104:55.
39. Dobel A, Williams H, Long R. Staged repair of ectopia cordis. *J Pediatr Surg* 1982;17:353.

SECTION

VII

Diseases of the Endocardium, Myocardium, and Pericardium

CHAPTER

54

Hypertrophic Cardiomyopathy

Barry J. Maron

Cardiomyopathies, or primary diseases of the myocardium, are not uncommon in infants and children. Although these conditions have been the subject of intensive investigation, our understanding of this diverse group of diseases is constantly evolving with regard to clinical identification, genetics, natural history, and therapy. A contemporary diagnostic classification of cardiomyopathies, including those occurring in young patients, has been proposed through the American Heart Association (AHA) (1).

Hypertrophic cardiomyopathy (HCM) is a genetic cardiac disease with heterogeneous clinical expression, unique pathophysiology, and a diverse natural history caused by >1,400 distinct disease-causing mutations in 11 or more genes encoding proteins of the cardiac sarcomere (1–21). HCM may be diagnosed and cause disability and death at virtually any age, including early childhood and infancy, and notably is the most common cause of sudden death (SD) in young people, including competitive athletes (2–4). Since its modern description almost 50 years ago (8), our understanding of the complexity of HCM has increased dramatically. On the other hand, perhaps no other childhood cardiovascular disease continues to present the challenges and controversies with respect to diagnosis, clinical course, and management as does HCM.

DEFINITION AND NOMENCLATURE

HCM is characterized by a thickened but nondilated left ventricle (LV) in the absence of another cardiac or systemic disease capable of producing the magnitude of hypertrophy

evident (e.g., aortic valve stenosis, systemic hypertension, or some physiologic expressions of athlete's heart) (1–7,22).

In 1958, Donald Teare (8), the coroner of London, published the first modern pathologic report of this disease, in which he described SD in eight young people due to asymmetrical hypertrophy of the ventricular septum (VS). Subsequent investigations led to a dramatic evolution in our perceptions of the HCM clinical spectrum. In the process, the disease acquired a confusing array of names, all presumably describing the same clinical entity. Most of these terms used to describe HCM emphasized LV outflow obstruction. Thus, the names "idiopathic hypertrophic subaortic stenosis," "hypertrophic obstructive cardiomyopathy," and "muscular subaortic stenosis" (as well as their abbreviations: IHSS, HOCM, and MSS) became widely used. However, about one-third of patients with HCM have either no or only mild obstruction to LV outflow at rest or with exercise (2,3,23). Hence, the preferred name for this condition has become *hypertrophic cardiomyopathy* (with or without obstruction). However, it is potentially confusing to apply this term to describe systemic, metabolic, or multiorgan syndromes associated with increased LV wall thickness (21).

PREVALENCE

Several epidemiologic studies are now available showing that HCM is the most common of the genetic heart diseases occurring in at least 1:500 of the general population (2,24,25). This overall prevalence is disproportionate to the numerical recognition of HCM in clinical cardiology practice (26),

particularly pediatric cardiology. HCM is a global disease now reported from >50 countries (27), with the most intense interest and reporting of cases from North America, Western Europe, Africa, and Asia (Japan and China).

MORPHOLOGY

Left Ventricular Hypertrophy

Multiple echocardiographic studies have defined the gross morphologic features of HCM, particularly its pronounced diversity and myriad patterns of LV hypertrophy (LVH) (2,3,6,7,9–18,28–30) (Figs. 54.1–54.4). Indeed, in HCM, there is no single or classic morphologic form, and virtually all possible patterns of LVH have been observed. Even closely related relatives with the same genetic substrate usually have dissimilar patterns of LVH with the exception of identical twins in whom the hearts appear identical. Although a truly symmetric (concentric) pattern of LVH may occur occasionally (6) (Fig. 54.2), the distribution of wall thickening in HCM is characteristically asymmetric, in which ≥ 1 segment of the wall shows greater hypertrophy than other areas (6,7,28–30). Frequently, the pattern of hypertrophy is particularly heterogeneous, with contiguous segments of the LV wall differing greatly in thickness (7).

Clinical diagnosis of HCM is usually made with 2-D echocardiography (6) or cardiovascular magnetic resonance (CMR) imaging (7). CMR may be advantageous by visualizing areas of segmental hypertrophy, specifically in the anterolateral free wall and LV apex, not always reliably identifiable with echocardiography (Fig. 54.3) (7,28,29).

Hypertrophy may be diffuse and involve substantial portions of VS and LV free wall, including the most substantial hypertrophy observed in any cardiac disease, with wall thicknesses ranging up to 5 to 6 cm (6,7,12,29), and often three to five times normal (Figs. 54.1–54.4). However, notably, in about one-third of HCM patients, LVH is relatively mild (13) and confined to limited areas of the LV wall, that is, usually basal anterior septum, but less frequently the apex, posterior portion of septum, and anterolateral or posterior free wall (6,7,28–30) (Figs. 54.1–54.3).

Segmental wall thickening confined to the LV apex (Fig. 54.2), a form of HCM more commonly reported from Japan, is associated with a “spade” deformity of the distal LV and striking T-wave inversion and increased R-wave voltages in the lateral precordial leads on ECG (15–17,31). However, it should be underscored that asymmetric patterns of LVH are not unique to HCM and may also be observed in systemic hypertension and in children and adults associated with other congenital or acquired heart diseases, including those with pulmonary arterial hypertension (1). Notably, based on genotype–phenotype studies in HCM families, genetically affected relatives may nevertheless have normal LV wall thicknesses (a subgroup referred to as genotype positive/phenotype negative) (32). Therefore, any absolute LV wall thickness is compatible with HCM.

Serial echocardiographic investigations have shown that LVH in HCM is not usually present at birth, but commonly develops in a dynamic fashion after a period of prolonged latency (33–36). Typically, the HCM phenotype (i.e., LVH) is not complete until adulthood, and during adolescence when body growth accelerates, genetically affected patients often show striking spontaneous increases in wall thickness (i.e., by an average of 100%) and more extensive distribution of hypertrophy (33) (Fig. 54.4). These dynamically evolving changes in LVH occurring during adolescence appear to be part of the genetically predetermined morphologic expression of HCM and are not per se associated with development or progression of symptoms or cardiac events. Mitral valve

systolic anterior motion (SAM) and outflow obstruction may also develop in childhood, during the period of progressive LVH, and in the presence of a developmentally small outflow tract (35). Of note, in genetically affected children, 12-lead ECG abnormalities may be the initial clinical manifestation of the disease, even preceding appearance of LVH on 2-D echocardiogram or CMR (34,36) (Fig. 54.4).

Mitral Valve

Structural abnormalities of the mitral valve, characteristic of many patients with LV outflow obstruction, may also be regarded as primary features of HCM (37,38). The majority of patients studied at necropsy (37) or by CMR (38) show important alterations in mitral valve size and shape. These primary abnormalities include increased overall mitral leaflet area (up to twice normal) owing largely to elongation of the leaflets (37) and, with considerable diversity, an increased size of both anterior and posterior leaflets.

Secondary thickening of the anterior mitral leaflet may result from frequent contact with the VS, associated with localized endocardial thickening of the septum in the LV outflow tract adjacent to the anterior leaflet. Endocardial plaques on ventricular septum occur most commonly in the presence of LV outflow obstruction (due to mitral valve–septal systolic contact), but may also develop in nonobstructive HCM due to diastolic mitral valve–septal contact.

Histopathology

Cardiac muscle cells (myocytes) in VS and LV free wall have increased transverse diameter as well as bizarre shapes, often maintaining intercellular connections with several adjacent cells (39–43). Of note, many of these myocytes do not show normal parallel alignment, but are arranged in a chaotic, disorganized fashion at oblique and perpendicular angles to each other (Fig. 54.3); myofibrils within cardiac muscle cells may also show disarray. Areas of disorganized cardiac muscle cells are found in about 95% of patients dying of HCM and usually occupy substantial portions of LV myocardium, that is, about 33% of septum and 25% of free wall (39,43). Disorganized myocytes are not confined to markedly thickened segments of the wall but can also be present in nonhypertrophied areas of the LV, and with little relationship evident between the magnitude of wall thickening and extent of disarray (41). The finding of marked cellular disorganization in a few symptomatic infants with HCM suggests that this histologic abnormality can be present from birth (42).

It is likely that disorganized cells dispersed in the LV wall impair transmission of normal electrophysiologic impulses and predispose to disordered patterns and increased dispersion of electrical depolarization and repolarization. Therefore, this chaotic architecture may well serve as an electrically unstable arrhythmogenic substrate and the nidus for potentially lethal ventricular tachyarrhythmias and SD in HCM or as a determinant of LV diastolic or systolic dysfunction.

Abnormalities of intramural coronary arteries (i.e., “small vessel disease”) are present in about 80% of patients studied at necropsy, most commonly in VS (44,45) (Fig. 54.3). These vessels are characterized by thickening of the arterial wall with increased intimal or medial components and apparent narrowing of the lumen. The abnormal arterioles may be responsible for silent myocardial ischemia and are most frequently observed within or in close proximity to areas of replacement fibrosis. HCM patients show variable severity and distribution of such fibrous tissue formation within LV myocardium, including patchy replacement fibrosis and grossly visible scars

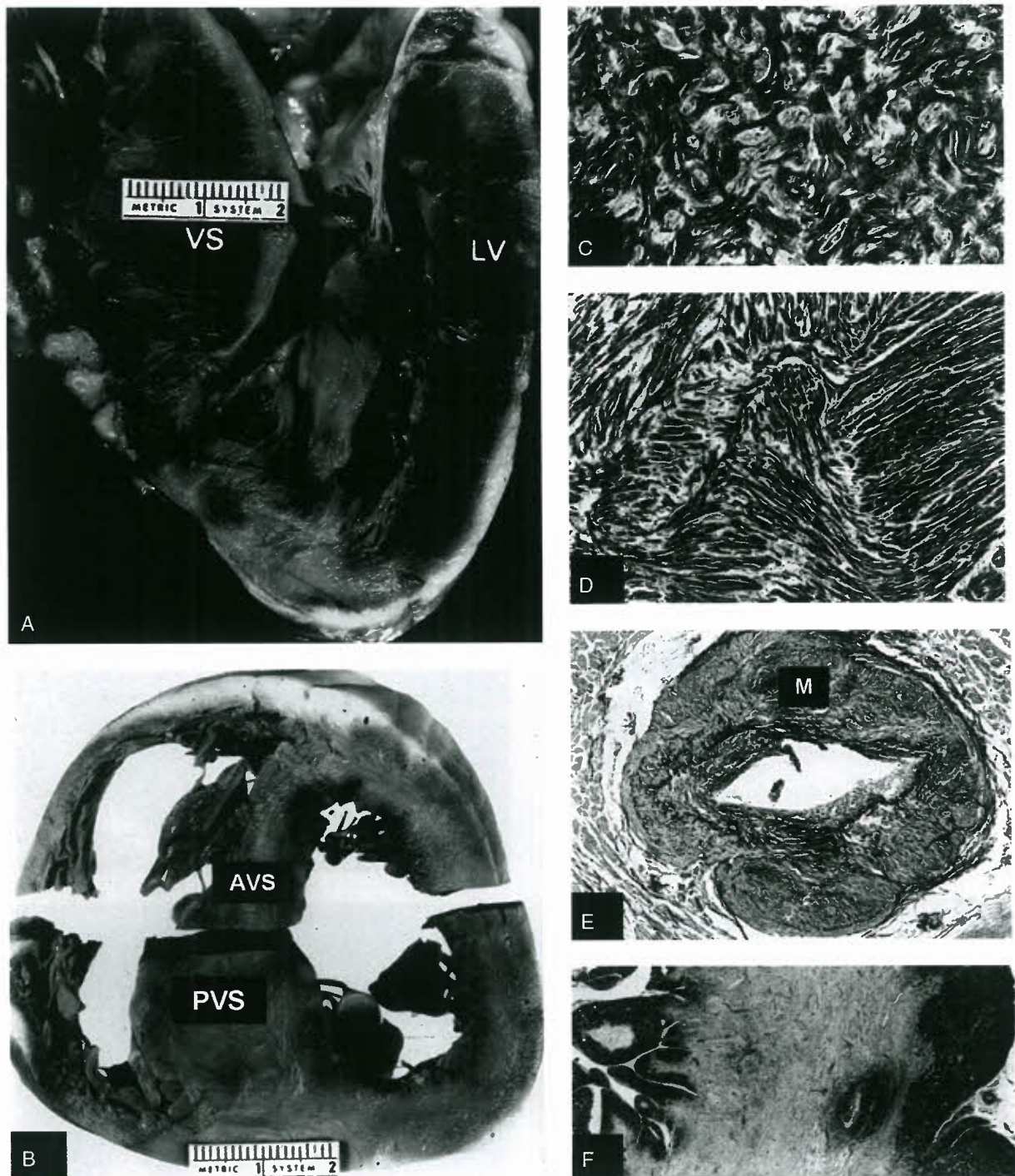


FIGURE 54.1. Morphologic components of the underlying disease process in HCM. **A:** A gross heart specimen sectioned in a cross-sectional plane similar to that of the echocardiographic (parasternal) long axis showing a common pattern of asymmetric LVH with wall thickening confined primarily to the AVS, which bulges prominently into the left ventricular outflow tract. LV denotes left ventricular free wall. **B:** A heart specimen in the transverse cross-sectional plane with a different pattern of hypertrophy; here, marked LV wall thickening is also asymmetric but predominantly in the PVS, whereas the AVS is only minimally thickened. **C,D:** Histology characteristic of the LV in HCM. **C:** The septal myocardium shows a markedly disordered architecture with adjacent hypertrophied cardiac muscle cells arranged at perpendicular and oblique angles. **D:** Bundles of hypertrophied cells show a disorganized, interwoven arrangement. **E:** An intramural coronary artery with an apparently narrowed lumen and thickened wall owing primarily to medial (M) hypertrophy. **F:** Extensive scarring of ventricular septum that is transmural in distribution, characteristic of the end-stage phase. LV, left ventricle; AVS, anterior ventricular septum; PVS, posterior ventricular septum; VS, ventricular septum. (From Maron BJ, Bonow RO, Cannon RO, et al. Hypertrophic cardiomyopathy. Interrelations of clinical manifestations, pathophysiology, and therapy. *N Engl J Med* 1987;316:780, with permission of Massachusetts Medical Society.)

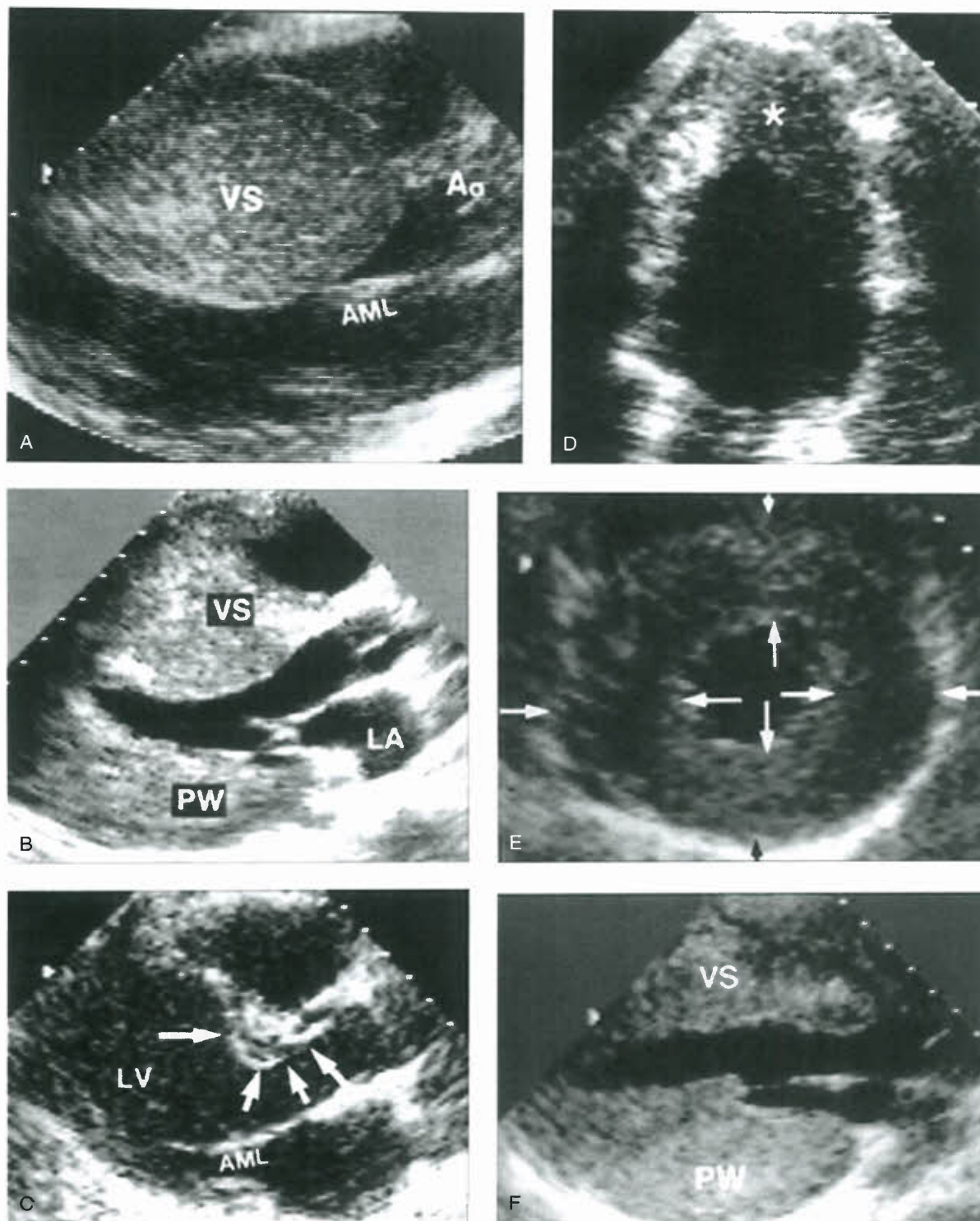


FIGURE 54.2. Patterns of LVH in HCM. Heterogeneous distribution and extent of LV wall thickening by echocardiography. **A:** Massive asymmetrical hypertrophy of VS with thickness >50 mm. **B:** Septal hypertrophy with distal portion considerably thicker than proximal region. **C:** Hypertrophy confined to proximal septum just below aortic valve (arrows); **D:** Hypertrophy localized to LV apex (asterisk)—that is, “apical HCM”; **E:** Relatively mild hypertrophy in symmetrical pattern showing similar or identical thicknesses within each segment (paired arrows); **F:** Inverted pattern with posterior free wall (PW) thicker (40 mm) than anterior VS. Calibration marks = 1 cm. Ao, aorta; AML, anterior mitral leaflet; LA, left atrium. (Reproduced from, Maron MS, Maron BJ, Harrigan C, et al. Hypertrophic cardiomyopathy phenotype revisited after 50 years with cardiovascular magnetic resonance. *J Am Coll Cardiol* 2009;54:220–228, with permission of Elsevier).

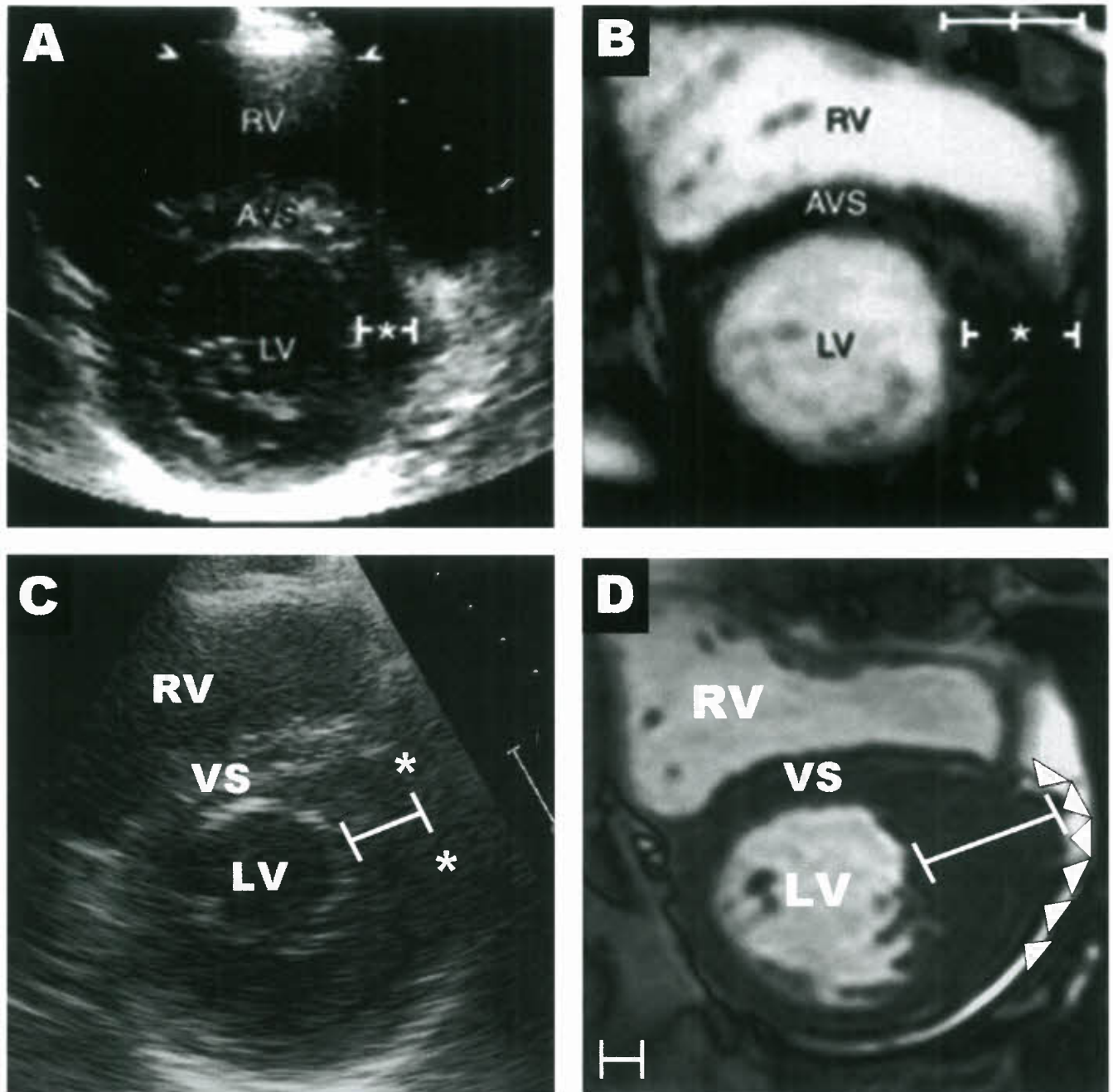


FIGURE 54.3. CMR identification of segmental LV wall thickening in HCM. Diagnosis. Two-dimensional echocardiogram (A) and comparative CMR (B) images acquired in short-axis plane at end-diastole at the same level from 13-year-old asymptomatic identical twin. A: Echocardiogram shows normal anterolateral free wall thickness (asterisks). B: CMR shows segmental area of hypertrophy confined to anterolateral LV free wall (20 mm) and small portion of contiguous anterior septum. Calibration marks are 1 cm apart. (Reproduced from Maron MS, Maron BJ, Harrigan C, et al. Hypertrophic cardiomyopathy phenotype revisited after 50 years with cardiovascular magnetic resonance. *J Am Coll Cardiol* 2009;54:220–228, with permission of AHA). Echocardiogram (C) and comparative CMR (D) from 46-year-old man with HCM. C: Echocardiographic short-axis shows anterolateral free wall thickness of 18 mm. D: CMR shows focal area of massive LVH (wall thickness, 35 mm) in the same region of LV, significantly underestimated by 2-D echocardiography. CMR finding defined high-risk status, prompting altered management strategy with an ICD recommendation for primary prevention of SD. Calibration markers are 1 cm apart. RV, right ventricle. (Reproduced from, Maron MS, Maron BJ, Harrigan C, et al. Hypertrophic cardiomyopathy phenotype revisited after 50 years with cardiovascular magnetic resonance. *J Am Coll Cardiol* 2009;54:220–228, with permission of Elsevier).

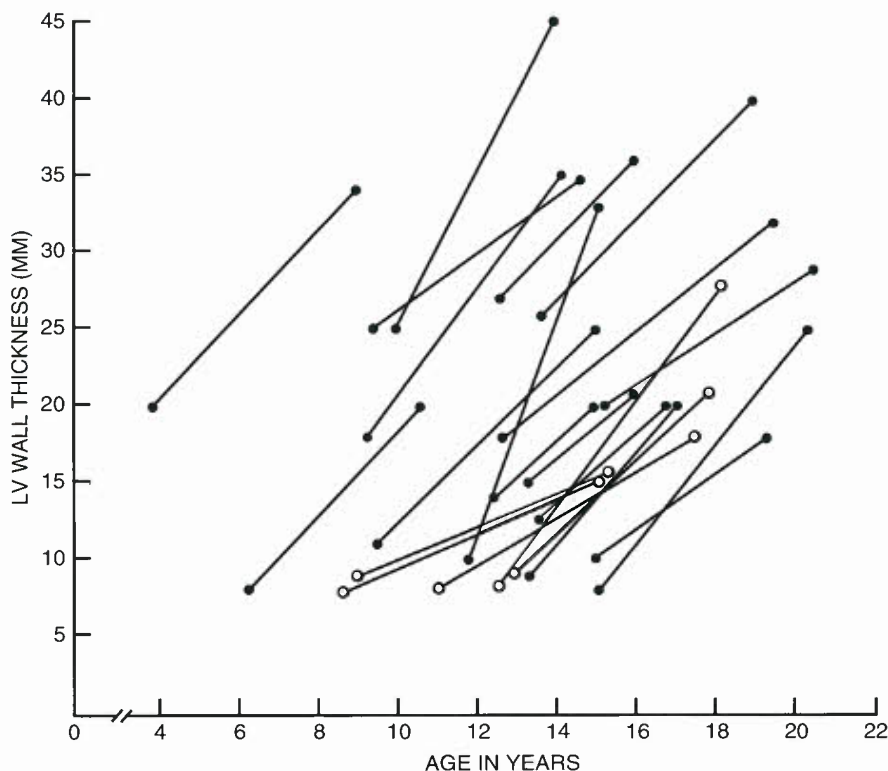


FIGURE 54.4. LV remodeling with development or progression of HCM phenotype. **Left:** Childhood/adolescence. Increased echocardiographic LV wall thickness in patients with familial HCM, unassociated with changes in clinical course. Open symbols denote those without initial evidence of hypertrophy in any LV segment. (Reproduced from Maron BJ, Spirito P, Wesley Y, et al. Development and progression of left ventricular hypertrophy in children with hypertrophic cardiomyopathy. *N Engl J Med* 1986;315:610–614, with permission of Massachusetts Medical Society). **Right:** Adulthood. Woman with myosin-binding protein C mutation shown at age 30 years with normal LV thickness (≤ 12 mm) in all segments of the wall (Top); 6 years later, at age 36, wall thickness has increased to 20 mm in both anterior ventricular septum and posterior septum, as well as anterolateral free wall. Bottom: LV wall thickness eventually increased to >30 mm, and the patient was prophylactically implanted with a defibrillator for primary prevention of SD. Calibration marks are 10 mm apart. VS, ventricular septum. (Reproduced from Maron BJ, Niimura H, Casey SA, et al. Development of left ventricular hypertrophy in adults with hypertrophic cardiomyopathy caused by cardiac myosin-binding protein C mutations. *J Am Coll Cardiol* 2001;38:315–321, with permission of Elsevier).

that may be extensive or even transmural, representing a repair process following myocyte death (44–49) (Fig. 54.3). This myocardial fibrosis, long recognized at autopsy (48), can now be identified in vivo with contrast CMR (50). In addition, the interstitial (matrix) collagen compartment, constituting the structural framework of LV is substantially increased in size; its components (perimysial coils, pericellular weaves and struts) are increased in number, appear morphologically abnormal, and often show disorganized arrangement (49).

Taken together, these findings suggest a form of small-vessel disease that may be responsible for silent myocardial ischemia, necrosis, and ultimately replacement fibrosis in HCM (51–55). Areas of myocardial fibrosis and scar can be responsible for LV systolic dysfunction (i.e., end-stage HCM) (56) and/or represent a substrate for clinically important ventricular tachyarrhythmias (57,58).

PATHOPHYSIOLOGY

Left Ventricular Outflow Obstruction

The presence of LV outflow tract obstruction under basal conditions (gradient ≥ 30 mm Hg) over many years is a

determinant of progressive heart failure symptoms and cardiovascular death in HCM (59) (Fig. 54.5). The relationship of obstruction specifically to sudden cardiac death is much weaker, encumbered by particularly low positive-predictive value (59). Obstruction in HCM represents true mechanical impedance to LV outflow, producing markedly increased intraventricular pressures, which can be detrimental to LV function by increasing myocardial wall stress and oxygen demand.

Dynamic subaortic obstruction in HCM is usually produced by the mitral valve, causing contact between the mitral valve and VS (SAM). Characteristic of young patients with this disease is an abrupt anterior motion in which the elongated mitral valve leaflets move toward (or contact) the VS in early systole (with a 90-degree sharp-angled bend). Magnitude of the outflow gradient is directly related to duration of mitral-septal contact with prolonged contact throughout midsystole indicative of marked obstruction. Estimation of the magnitude of outflow obstruction is made conventionally with continuous wave Doppler (60), which obviates the need for diagnostic cardiac catheterization.

SAM and subaortic obstruction are determined by several geometric factors including the size of the outflow tract, distribution of LVH, and length of the mitral leaflets (37,61,62) as well as the ejection velocity. SAM appears to occur either by virtue of the high-velocity jet streaming through a narrowed outflow tract

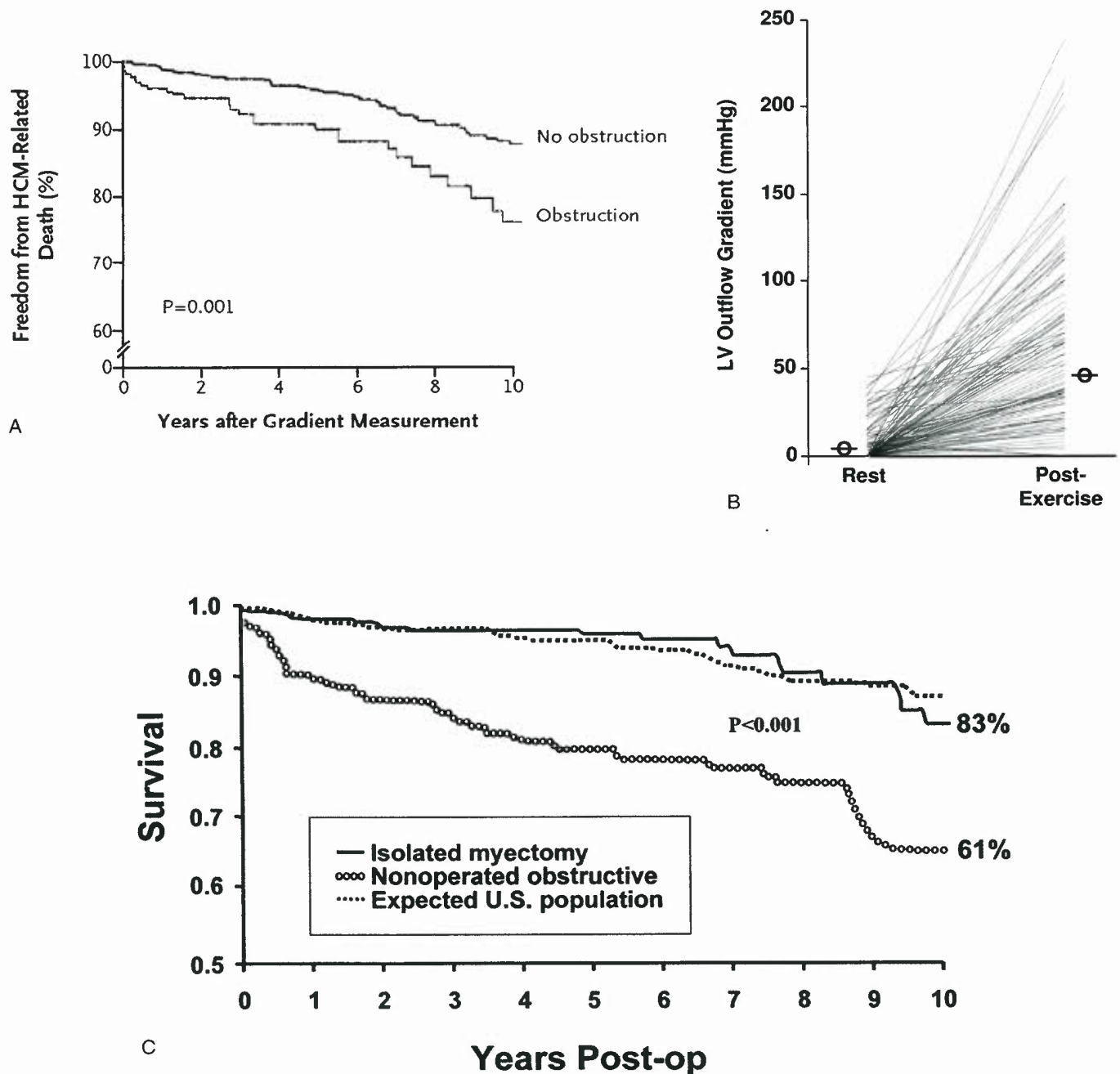


FIGURE 54.5. Left ventricular outflow tract obstruction. **A:** Probability of severe progressive heart failure (NYHA classes III or IV), heart failure death, or stroke in patients with LV outflow obstruction exceeds that in patients without obstruction (relative risk, 4.4; $p < 0.001$). (Reproduced from Maron MS, Olivotto I, Betocchi S, et al. Effect of left ventricular outflow tract obstruction on clinical outcome in hypertrophic cardiomyopathy. *N Engl J Med* 2003;348:295–303, with permission of Massachusetts Medical Society). **B:** Changes in LV outflow tract gradient from resting (basal) conditions to immediately after termination of treadmill exercise. Each patient is depicted by a line connecting the two gradient measurements. θ indicates the mean. (Reproduced from Maron MS, Olivotto I, Zenovich AG, et al. Hypertrophic cardiomyopathy is predominantly a disease of left ventricular outflow tract obstruction. *Circulation* 2006;114:2232–2239, with permission of AHA.) **C:** Following myectomy with relief of LV outflow obstruction, survival free from all-cause mortality compared with age- and gender-matched U.S. population and also nonoperated patients with obstruction ($p < 0.001$). (Reproduced from Ommen SR, Maron BJ, Olivotto I, et al. Long-term effects of surgical septal myectomy on survival in patients with obstructive hypertrophic cardiomyopathy. *J Am Coll Cardiol* 2005;46:470–476, with permission of Elsevier.)

and pulling the mitral leaflets toward the septum (i.e., Venturi effect) or probably more likely due to drag (the hydrodynamic pushing force of flow) on the leaflets (63). The posteriorly directed mitral regurgitation jet, as a consequence of SAM, is usually only mild to moderate; severe mitral regurgitation in an HCM patient should raise the possibility of an intrinsic mitral valve abnormality such as myxomatous degeneration (64).

The subaortic gradient (and systolic ejection heart murmur) in HCM is characteristically dynamic (65) and may show considerable spontaneous variability, that is, reduced or abolished by interventions that decrease myocardial contractility (e.g., β -adrenergic receptor blocking drugs) or increase ventricular volume or arterial pressure (e.g., squatting, isometric hand-grip, or phenylephrine administration). Alternatively, the outflow gradient and murmur can be augmented by circumstances that decrease arterial pressure or ventricular volume (e.g., the Valsalva maneuver or administration of nitroglycerin) or that increase contractility, such as premature ventricular contraction, standing, amyl nitrite inhalation, administration of isoproterenol, or exercise (2–4,65). Daily activities such as consuming a heavy meal may also transiently magnify the subaortic gradient (2,3). A large proportion of HCM patients without SAM or gradients at rest may nevertheless generate outflow obstruction with physiologic exercise. Indeed, fully 70% of an HCM cohort may have the propensity to develop obstruction (gradient ≥ 30 mm Hg) either at rest or with exercise (Fig. 54.5) (23).

In infants and young children with HCM, obstruction to right ventricular outflow is not uncommon, usually occurring in association with subaortic obstruction. Subpulmonic gradients represent a form of fixed obstruction due to exaggerated hypertrophy of right ventricular musculature that projects into the relatively small outflow tract (i.e., crista supraventricularis muscle, papillary muscles, moderator band, or trabeculae) (66). The infrequency of subpulmonic obstruction in adult HCM patients suggests that these gradients probably disappear with body growth and cardiac remodeling.

Myocardial Ischemia

Regional myocardial ischemia (in the absence of atherosclerotic coronary artery disease) occurs commonly in HCM (51–54,67), as demonstrated by atrial pacing, reversible exercise-induced myocardial perfusion defects, dipyridamole stress ECG, necrosis, and replacement fibrosis observed at autopsy or by CMR imaging (as delayed enhancement), or abnormalities recognized by position emission tomography (PET) (54,67). Potential mechanisms by which myocardial ischemia may occur in HCM include inadequate capillary density compared with greatly increased LV muscle mass, or alternatively, small vessel disease with narrowed intramural coronary arteries (44,45). It is difficult to clinically measure and quantitate the extent or location of myocardial ischemia in HCM patients, or consistently derive relevant correlations or prognostic information from these observations, although observations with PET suggest ischemia is a determinant of progressive heart failure in HCM (67).

Diastolic Dysfunction

Abnormalities of LV relaxation and filling have been identified by a variety of echocardiographic-Doppler methods in a majority of patients with HCM and presumably contribute to (or are responsible for) symptoms of fatigue, exertional dyspnea, and angina pectoris (2,3,5,68–74). The rapid filling phase of diastole is significantly prolonged and associated with decreased rate and volume compared with normal. Consequently, there is usually a compensatory increase in the

contribution of atrial systole to overall LV filling. Conversely, diastolic dysfunction may be present in the absence of both symptoms and outflow obstruction and unrelated to the severity or distribution of ventricular hypertrophy (70). Reduced ventricular distensibility probably results largely from those factors, which determine the passive elastic properties of the LV chamber, such as severity of hypertrophy, replacement and interstitial myocardial fibrosis, and cardiac muscle cell disorganization.

GENETICS

The capability of achieving an unequivocal diagnosis of HCM with DNA-based laboratory methods has led to enhanced recognition of HCM and consequently to a more complete definition of its broad clinical spectrum, as well as providing practical insights into appropriate genetic counseling (1–3,19,20,75–79).

HCM is a Mendelian trait with an autosomal dominant pattern of inheritance (1,19,20,75,80,81). Molecular studies with clinical genotype–phenotype correlations, conducted intensively over more than a decade, have provided important insights into the genetics of HCM, as well as access to definitive laboratory-based diagnosis by virtue of detecting pathogenic mutations, even in the absence of obvious clinical evidence of the disease. This substantial investigative effort has demonstrated convincingly that HCM is caused by dominant mutations in 11 or more genes encoding thick and thin contractile myofilament protein components of the sarcomere and the adjacent Z-disc. Several additional mutations have also been identified but are associated with less definitive evidence to support their pathogenicity. About 70% of the HCM mutations are reported in the two most common genes, β -myosin heavy chain and myosin-binding protein C, while troponin T and several other genes account for much smaller proportions. Underscoring the vast genetic heterogeneity of HCM, over the last 20 years >1,400 individual mutations (mostly missense, but also insertions, deletions, splice, and truncated mutations) have been identified among these genes, with about two-thirds unique to individual families when first identified (i.e., “private”).

The vast majority of patients who inherit a disease-causing mutation will demonstrate structural evidence of HCM (i.e., LVH) by early adulthood, appearing typically during periods of accelerated adolescent growth and usually completed when physical maturity is achieved (age 17 to 18 years), but generally unassociated with symptom onset or disease progression (33). However, variable and age-related penetrance can occasionally result in delayed expression of the phenotype into the third decade of life, or potentially even later (77).

Development of rapid, automated DNA sequencing now provides the opportunity for comprehensive genetic testing panels, which permit identification of HCM mutations and definitive molecular diagnosis as part of routine clinical practice (19,77–79,80,81). However, disease-causing mutations can be identified definitively in only about one third of those probands studied, underscoring that all genes that cause HCM are not known. Therefore, the precise mutation responsible for HCM remains uncertain in a significant proportion of patients. In addition, not uncommonly, DNA-based testing may identify novel DNA sequence variants for which true pathogenicity is unresolved (“variants of uncertain significance”) (80,81).

Despite these limitations, the most important role of DNA molecular testing is to identify HCM family members at risk for developing disease who do not have LV hypertrophy. If a disease-causing mutation can be identified in a phenotypically expressed relative with HCM, the genetic status

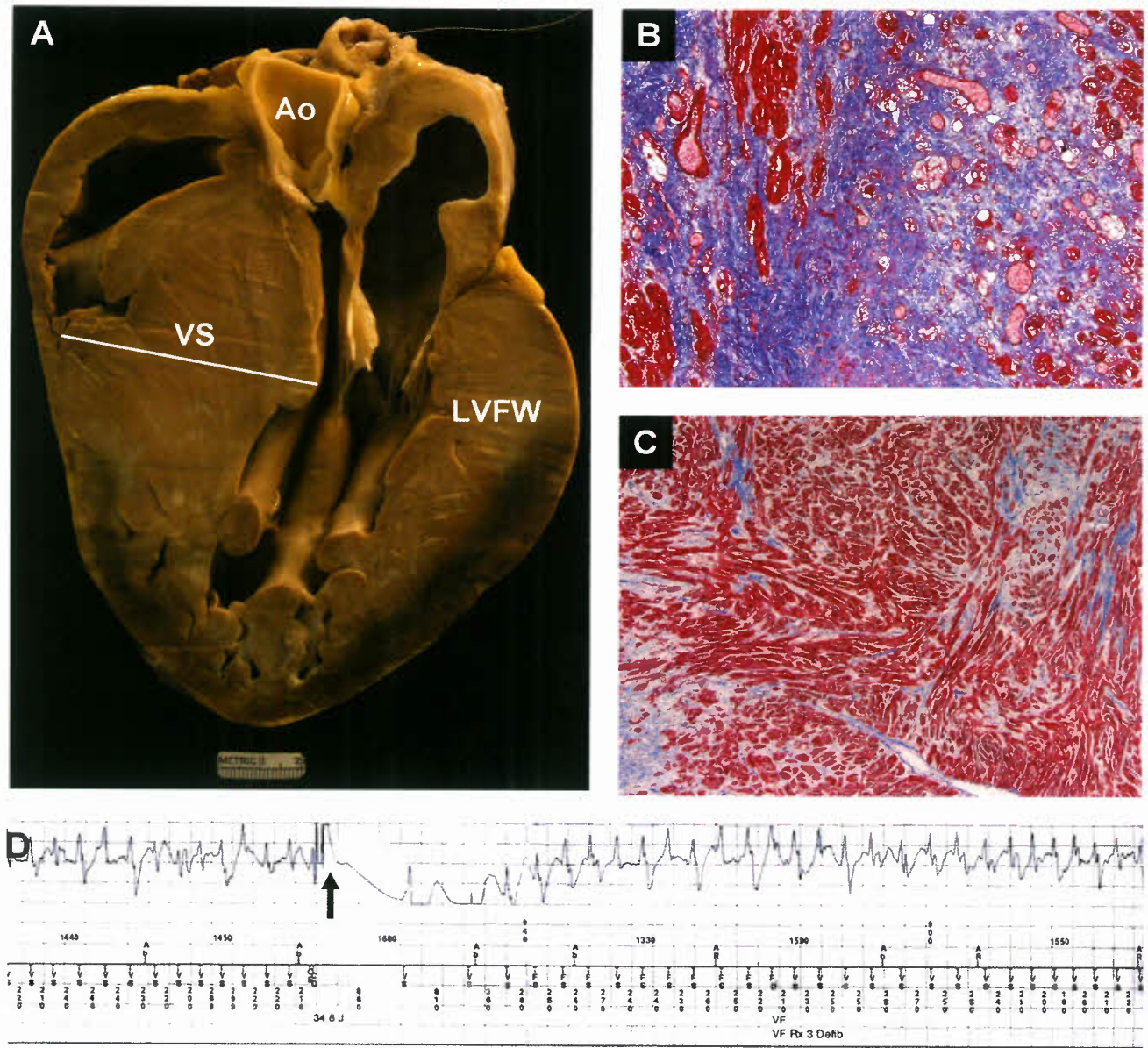


FIGURE 54.6. LAMP2 cardiomyopathy. **A:** From 14-year-old boy with SD and septal thickness of 65 mm (heart weight 1,425 g); **B:** Clusters of myocytes with vacuolated sarcoplasm (stained red) embedded in area of scar (stained blue; Masson trichrome). **C:** Disorganized arrangement of myocytes most typical of sarcomeric HCM. **D:** Intracardiac electrogram. ICD elicited five defibrillation shocks that failed to interrupt VF (280 beats/min). (Reproduced from Maron BJ, Roberts WC, Arad M, et al. Clinical outcome and phenotypic expression in LAMP2 cardiomyopathy. *JAMA* 2009;301:1253–1259, with permission of American Medical Association.)

of other members of the family can be determined definitively. In addition, genetic testing has the potential to clarify diagnosis in patients for whom the pattern of LVH mimics HCM, for example, metabolic storage disease phenocopies: PRKAG2 (regulatory subunit of adenosine monophosphate-activated protein kinase); Fabry disease (alpha-galactosidase deficiency), and LAMP2 (Danon disease; lysosome-associated membrane protein-2) (82,83) (Fig. 54.6). Genetic diagnosis of Fabry disease is highly advantageous, given the availability of enzyme replacement therapy (84). LAMP2 cardiomyopathy is associated with severe and lethal natural history with survival uncommon over 25 years of age (and implantable defibrillators [ICDs] are unreliable), requiring early recognition by genetic testing to permit timely consideration for prophylactic heart transplant (83) (Fig. 54.6).

However, after two decades of the molecular era and many genotype–phenotype correlation studies, the overall relationship between single sarcomere mutations and prognosis or clinical outcome in HCM has proved unreliable, due largely to genetic heterogeneity, disputing earlier notions that specific mutations would have prognostic relevance (i.e., “malignant” or “benign” mutations) (80,81,85). Therefore, despite considerable initial optimism and perhaps the unrealistic expectation that the discipline of molecular biology would create a new paradigm for predicting prognosis and directing management in HCM, this aspiration has been largely unrealized. Nevertheless, preliminary data suggest that double or compound sarcomere mutations (present in about 5% of HCM patients) may be associated with greater disease severity and adverse events (86).

It is presently unknown what proportion of mutation carriers (gene positive–phenotype negative family members without hypertrophy) will ultimately develop LVH, but the risk for SD (or disease progression) in this subset appears particularly low (32). At present, clinical decisions regarding disqualification from competitive sports or occasionally consideration for prophylactic ICDs (74) in such individual are unavoidably made on a case-by-case basis (32). This emerging patient subset will require much longer periods of follow-up before reliable guidelines regarding management can be formulated.

CLINICAL SCREENING STRATEGIES IN FAMILIES

In clinical practice, prospective screening of HCM family members to ascertain affected or unaffected disease status usually takes place independent of genetic testing and is performed primarily with 2-D echocardiography, CMR, and ECG, as well as history-taking and physical examination (20).

The traditional recommended strategy for screening relatives in most HCM families calls for such evaluations on a 12- to 18-month basis, usually beginning at least by age 12 (20). If these studies do not show evidence of LVH by the time full growth is achieved (at the age of about 18 to 21 years), it had been customary practice to conclude that a HCM-mutant gene is probably absent and reassure family members accordingly that further echocardiographic testing would be unnecessary. However, recognition of the possibility that later-onset morphologic conversions to the HCM phenotype may occur in young and middle-aged adults (and even older individuals) has potentially created new practice strategies for screening families and genetic counseling in this disease (2,20,77) (Table 54.1). Therefore, it is no longer possible to routinely hold to the traditional tenet that a normal echocardiogram (and ECG) obtained at maturity itself defines a genetically unaffected

family member. It is now probably prudent to extend the time period into adulthood for clinical surveillance of phenotype-negative relatives at about 5-year intervals with serial 2-D echocardiography or CMR, and ECG (20).

While this recommendation (triggered by the recognized potential for adult-onset hypertrophy) is probably unavoidable in current clinical practice, there are nevertheless potentially negative implications for this strategy. By extending almost indefinitely the period of morphologic (i.e., echocardiographic) surveillance and implied indecision regarding the diagnosis of HCM in family members, there is the potential risk of eliciting the psychological perception and stigma of cardiac disease in young, healthy individuals, the vast majority of whom are not in fact affected by a mutant gene. If the causative HCM gene is identified in a family member, molecular testing can be definitive by excluding affected status and thereby eliminating the need for serial clinical studies and prolonged surveillance.

CLINICAL FEATURES

Physical Examination

The classic findings on physical examination in patients with HCM are variable and related in large measure to hemodynamic state (65). For example, in patients with obstruction to outflow, a double or triple LV apical impulse may be palpable. These impulses probably reflect the usual outward systolic thrust due to ventricular contraction, a presystolic thrust of accentuated atrial contraction, and occasionally the expansion of early diastolic filling. In addition, patients with obstruction have a medium-pitch systolic ejection murmur that varies in intensity with respect to the magnitude of the subaortic gradient. Patients with loud systolic murmurs along the lower left sternal border and at the apex of at least grade 3/6 in intensity will probably have a peak systolic gradient >50 mm Hg. In some patients, the murmur may sound holosystolic at the apex and mimic mitral regurgitation. In the presence of outflow obstruction, the arterial pulses are unusually sharp and rapid rising with a distinct Bisferiens contour. External carotid pulse recordings demonstrate a bifid pulse contour, shortened upstroke time, and increased systolic ejection period. Indeed, infants and young children with HCM are most commonly identified because of a heart murmur or vigorous precordial thrust, with a diagnosis subsequently confirmed by imaging (87–92).

In contrast, physical findings in HCM patients without outflow obstruction may be subtle and not suggestive of underlying heart disease. The systolic murmur is characteristically soft or absent, although the LV apical impulse may nevertheless be forceful. In some patients, a murmur representing dynamic outflow obstruction may be provoked by standing, or with the Valsalva maneuver.

Symptoms

The onset of heart-failure symptoms often occurs in early adulthood, between 20 and 40 years of age, although symptoms can become evident at any age, from young children to the elderly (2). Nevertheless, it is uncommon for children or adolescents to experience marked progressive functional disability equivalent to New York Heart Association (NYHA) class III. In most patients, the predominant complaint is exertional limitation due to heart failure-related symptoms such as dyspnea and/or fatigue and also occasionally orthopnea or paroxysmal nocturnal dyspnea (very uncommon in children),

TABLE 54.1
Proposed Clinical Family Screening Strategies with Echocardiography or CMR (and 12-lead ECG) for Detection of HCM with LVH

Age ≤12 y
Optional unless
Malignant family history of premature death from HCM, or other adverse complications
Competitive athlete in an intense training program
Onset of symptoms
Other clinical suspicion or early LVH
Age 12 to 18–21 y*
Every 12–18 months
Age ≥ 21 years
At onset of symptoms or possibly every 5 years. More frequent intervals are appropriate in families with a malignant clinical course or late-onset HCM

*Age range takes into consideration individual variability in achieving physical maturity and in some patients may justify screening at an earlier age. Initial evaluation should occur no later than early pubescence.

which may be accompanied by chest discomfort that is either typical or atypical of angina. The etiology of chest pain in HCM is not completely understood, but may be a manifestation of myocardial ischemia due to microvascular structural abnormalities (44,54). Severity and character of these symptoms may be similar in patients with or without obstruction to LV outflow. Episodes of impaired consciousness (syncope/presyncope/near syncope) are common and may raise consideration of SD risk.

Electrocardiogram

The 12-lead ECG is abnormal in about 90% to 95% of HCM probands identified as part of hospital-based populations and shows a wide variety of abnormal patterns, some of which may be bizarre in appearance (31,93–95). Normal ECGs are much more common in asymptomatic family members recognized during pedigree screening (up to 25%). Most common ECG abnormalities are increased voltages suggestive of LVH, ST-T changes including marked T-wave inversion in the lateral precordial leads, left atrial enlargement, deep and narrow Q waves, and diminished R waves in the lateral precordial leads.

However, no particular ECG pattern is characteristic of HCM or predictive of future events (94), although normal ECGs appear to be most commonly associated with benign clinical course (95). Increased voltages (tall R or deep S waves) show only a weak correlation with magnitude of LVH by echocardiography and do not discriminate the presence or absence of outflow obstruction at rest (94). Paradoxically, infants with HCM often show a pattern of right ventricular hypertrophy, which only in some cases may reflect obstruction to right ventricular outflow (66,87).

HCM AND ATHLETE'S HEART

Long-term athletic training can produce increases in LV diastolic cavity dimension, wall thickness, and calculated mass that constitute a syndrome commonly known as “athlete’s heart” (22,96–98). Such absolute increases in LV wall thickness are usually modest, but may be more substantial in some athletes, particularly those participating in the rowing and cycling sports (97). In this way, a diagnostic dilemma in distinguishing the clinically benign physiologic hypertrophy of the athlete’s heart from HCM (with relatively mild LVH) may arise (22,96). Several clinical parameters have been suggested to aid this differential diagnosis (Fig. 54.7). Some useful criteria that support the diagnosis of HCM in trained athletes who fall into the “gray zone” of overlap between the two conditions with maximum LV wall thickness of 13 to 15 mm include (22,96) demonstration of a HCM disease-causing mutation with genetic testing, documentation of HCM in a relative, an abnormal transmitral Doppler waveform consistent with altered LV relaxation and filling, or LV end-diastolic cavity dimension <45 mm. Parameters favoring athlete’s heart include regression of LV wall thickness following a brief (4 to 8 weeks) period of deconditioning and LV end-diastolic cavity dimension >55 mm.

PREPARTICIPATION SCREENING FOR HCM IN ATHLETIC POPULATIONS

Detection of preexisting cardiovascular abnormalities such as HCM, with the potential for SD or significant morbidity associated with intense physical training and competition, is

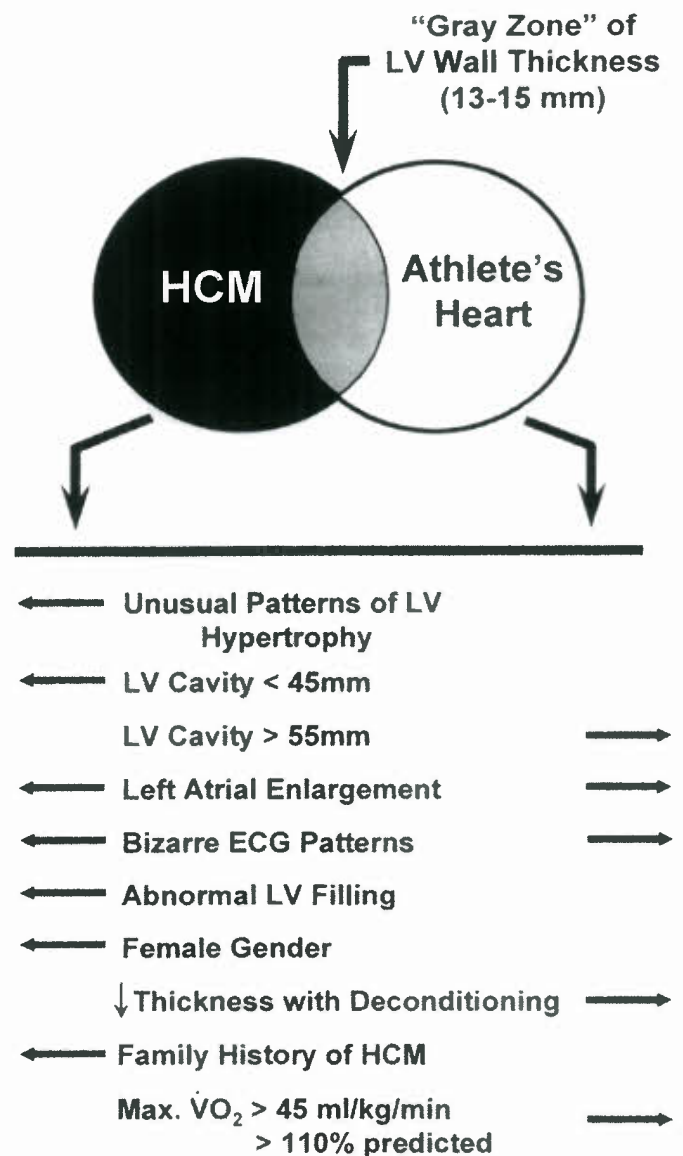


FIGURE 54.7. Differential diagnosis of HCM versus physiologic athlete’s heart. Clinical criteria used to distinguish non-obstructive HCM from athlete’s heart when maximal LV wall thickness is within the shaded gray area of overlap, consistent with both diagnoses. ↓, decreased. (Adapted from, Maron BJ, Pelliccia A. The heart of trained athletes: cardiac remodeling and the risks of sports, including sudden death. *Circulation* 2006;114:1633–1644, reproduced with permission of AHA.)

a major objective of preparticipation screening of high school and college-aged sports participants (99–101). In the United States, customary screening practice dictates that a personal and family history be obtained and a physical examination performed. However, although HCM can be identified by this process, in some cases, the disease remains unsuspected, given that many affected individuals do not have a diagnostic heart murmur or historical clues (e.g., syncope or family history of HCM). It has been suggested that identification of HCM by screening would theoretically be enhanced by routinely incorporating noninvasive testing with the 12-lead ECG (or echocardiography) (102). However, cost-effectiveness and a number of resource and practical obstacles make routine application of such tests impractical as part of a theoretical mandated and nationally administered (and federally funded)

mass screening program of U.S. athletes (99). Frequency of borderline and false-positive (or false-negative) test results, and the uncertainty and anxiety that accompanies such circumstances, represent additional limitations to high school screening programs with routine ECGs (99).

CLINICAL COURSE

Overall Patient Population

Predicting the clinical course and outcome for individual young patients with HCM continues to be difficult because of the marked variability and heterogeneity in disease expression. For patients first identified in the pediatric age group, accurate predictions regarding natural history and prognosis are particularly daunting given the particularly long period (>50 years) of potential risk that lies ahead. Annual HCM mortality rates have previously been reported at 3% to 6%, with the highest rate in children (103,104). However, these are now outdated estimates derived largely from HCM cohorts at major HCM referral centers, incorporating substantial patient selection bias skewed toward high-risk patients (105). Therefore, highly selective referral patterns have previously overestimated and mischaracterized the risk for premature death in the overall HCM population. Over the more recent 15 years, in unselected community-based patient populations less contaminated by tertiary center referral basis (and therefore more representative of the true disease state), more realistic mortality rates for HCM of about 1% per year have been reported, although somewhat higher in children (i.e., 2% per year) (2,3,106–109).

The clinical dilemma encountered in pediatric cardiology practice with respect to HCM is unique, given the youth of the patients and the difficulties encountered in predicting outcome for such a heterogeneous disease over long periods. This is compounded by the fact that most children who die suddenly have previously been asymptomatic (or only mildly symptomatic), and such catastrophes are often the first clinical manifestation of the disease (2,3). On the other hand, it is inappropriate to regard all patients identified with HCM in infancy and childhood as having an ominous prognosis simply by virtue of diagnosis early in life, particularly since most such clinical identifications are made under fortuitous circumstances.

Thus, HCM should be viewed as a complex disorder capable of producing important clinical consequences and premature death in some patients, whereas many other patients may live their natural lives (even achieve statistical life expectancy) with little or no disability and do not require aggressive therapeutic interventions. These observations emphasize the importance of providing many HCM patients (including many children) with reassurance regarding their prognosis, but also with prudent caution and long-term regular surveillance, for what is also an unpredictable disease.

Infants

Experience with assessing the clinical course and prognosis of patients with HCM identified in the first 2 years of life has been limited. Relatively few patients considered to have HCM are reported so early in life (87–92), and a large proportion of such infants with LVH do not have true familial HCM caused by mutations in genes encoding sarcomere proteins (1). Such HCM phenocopies include Noonan syndrome, glycogen storage disease, or a transient and nonfamilial cardiomyopathy in infants of insulin-dependent diabetic mothers with generalized organomegaly (1).

Other diseases in this category are primary mitochondrial myopathies caused by mutations encoding mitochondrial DNA (e.g., Kearns-Sayre syndrome) or mitochondrial proteins associated with adenosine triphosphate (ATP) electron transport chain enzyme defects (1). Also included in these considerations are metabolic myopathies representing ATP production and utilization defects involving abnormalities of fatty acid oxidation (acyl CoA dehydrogenase deficiencies) and carnitine deficiency, as well as infiltrative myopathies such as Hunter and Hurler diseases (1).

HCM is a particularly uncommon cause of SD during infancy and is not a cause of the sudden infant death syndrome (110). Nevertheless, the onset of symptoms and heart failure in infancy or early childhood appears to be an unfavorable prognostic sign indicative of early disease progression (87,89,103) with high mortality in the ensuing months or years from heart failure, despite aggressive surgical and/or medical therapy. Reports of spontaneous regression of LVH and resolution of heart failure within the first few months of life appear to be virtually confined to infants of diabetic mothers.

Children

Prognostic assessment of children with HCM is also limited by the low frequency with which such patients are identified in standard pediatric practice, and the relatively brief period of their life time they are followed. Most HCM patients recognized as children and adolescents are asymptomatic, and it is uncommon for severe functional disability, such as with NYHA class III, to appear at this time in life. Nevertheless, HCM-related mortality has consistently been reported to be highest in HCM patients identified as children or adolescents, with most of these deaths occurring suddenly and unexpectedly (89,92,109,111–114).

Noonan syndrome, an autosomal dominant cardiofacial condition, can mimic sarcomeric HCM. In about 50% of cases, Noonan syndrome is familial with an autosomal dominant transmission, caused by mutations in PTPN11, a gene encoding the nonreceptor protein tyrosine phosphatase SHP-2 genes (1). Noonan syndrome deserves special emphasis here because of the frequency with which LVH occurs (about 25% of such patients). There is also frequent association with other congenital heart malformations, the most common of which is dysplastic pulmonary valve stenosis and atrial septal defect. Cardiomyopathies characterized by LV wall thickening have also occasionally been reported in young children with other systemic diseases: neuroectodermal anomalies, pheochromocytoma, tuberous sclerosis, neurofibromatosis, lentiginosis, Friedreich ataxia, Turner syndrome, and hyperthyroidism (1). It is more likely that such infrequent associations represent only the sporadic association of two rare diseases rather than constituting an etiologic relationship.

SUDDEN CARDIAC DEATH AND RISK STRATIFICATION

SD may occur in HCM at a wide range of ages, but most commonly during adolescence and young adulthood (usually 12 to 35 years of age) and rarely before 10 years (2–4,57,103,109,111–115) (Fig. 54.8). Indeed, HCM is the most common cause of SD in the young. Although most patients die while sedentary or during normal or modest physical exertion, an important proportion die suddenly during or just after vigorous activity. HCM is also the most common cause of sudden cardiac death in young competitive athletes (2,3,111,116) (Fig. 54.8). This latter observation is the basis for the standard recommendation

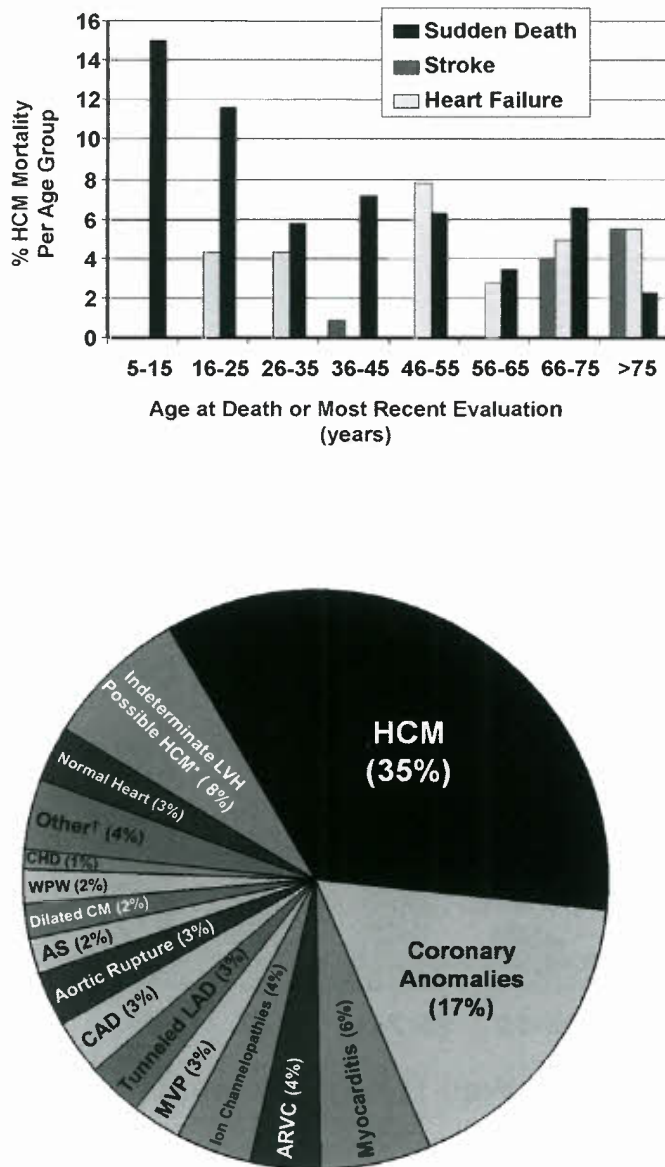


FIGURE 54.8. Clinical profile of SD. Top: SD is most common in children and young adults before about 25 years of age, while heart failure and stroke generally occur later in life. (Reproduced from Maron BJ, Olivetto I, Spirito P, et al. Epidemiology of hypertrophic cardiomyopathy-related death. Revisited in a large non-referral-based patient population. *Circulation* 2000;102:858–864, with permission of AHA.) Bottom: HCM is the single most common cause of SD in young competitive athletes in United States. ARVC, arrhythmogenic right ventricular cardiomyopathy; AS, aortic valve stenosis; CAD, coronary artery disease; CHD, congenital heart disease; CM, cardiomyopathy; LAD, left anterior descending; MVP, mitral valve prolapse; WPW, Wolff-Parkinson-White. †Regarded as possible (but not definitive) evidence for HCM at autopsy with mildly increased LV wall thicknesses (18 ± 4 mm) and heart weight (447 ± 76 g). ‡Includes most commonly Kawasaki disease, sickle cell trait, and sarcoidosis. (Reproduced from Maron BJ, Doerer JJ, Haas TS, et al. Sudden deaths in young competitive athletes: analysis of 1866 deaths in the United States, 1980–2006. *Circulation* 2009;119:1085–1092, with permission of AHA.)

to disqualify young patients with HCM from intense competitive sports to reduce their risk for SD under the guidelines of the 36th Bethesda Conference (117).

At present, the greatest risk for SD in children with HCM appears to be associated with one or more of the following clinical risk markers (Fig. 54.9) (118): (a) prior cardiac arrest or sustained ventricular tachycardia (VT) for secondary prevention. For primary prevention: (b) family history of one or more premature HCM-related deaths, particularly if sudden and multiple; (c) unexplained syncope; and (d) massive degrees of LVH (maximum wall thickness ≥ 30 mm, a cutoff independent of age or body size) (Fig. 54.9) and most relevant to young patients. Other risk factors, more applicable to adults with HCM, are multiple, repetitive (or prolonged) nonsustained VT on serial Holter monitoring and hypotensive or attenuated blood pressure response to exercise.

Of note, although the presence of a subaortic gradient (≥ 30 mm Hg at rest) is a strong determinant of progressive heart failure and cardiovascular death (Fig. 54.5) (59), it is a much weaker marker specifically for sudden cardiac death, and consequently obstruction has insufficient power to be regarded as a sole or primary factor to justify primary prevention intervention with an ICD (57). However, due to the substantial genetic heterogeneity in HCM, it is now evident that the prediction of clinical course and SD risk based on knowledge of the disease-causing mutation is unreliable for the management of individual patients (80,81).

Also, the relationship between SD risk and intramuscular course of a segment of the proximal left anterior descending coronary artery (i.e., myocardial bridging; tunneled coronary arteries) in children is not established (119). Electrophysiologic testing with programmed ventricular stimulation has been abandoned as a workable strategy to risk stratify young HCM patients (2,3).

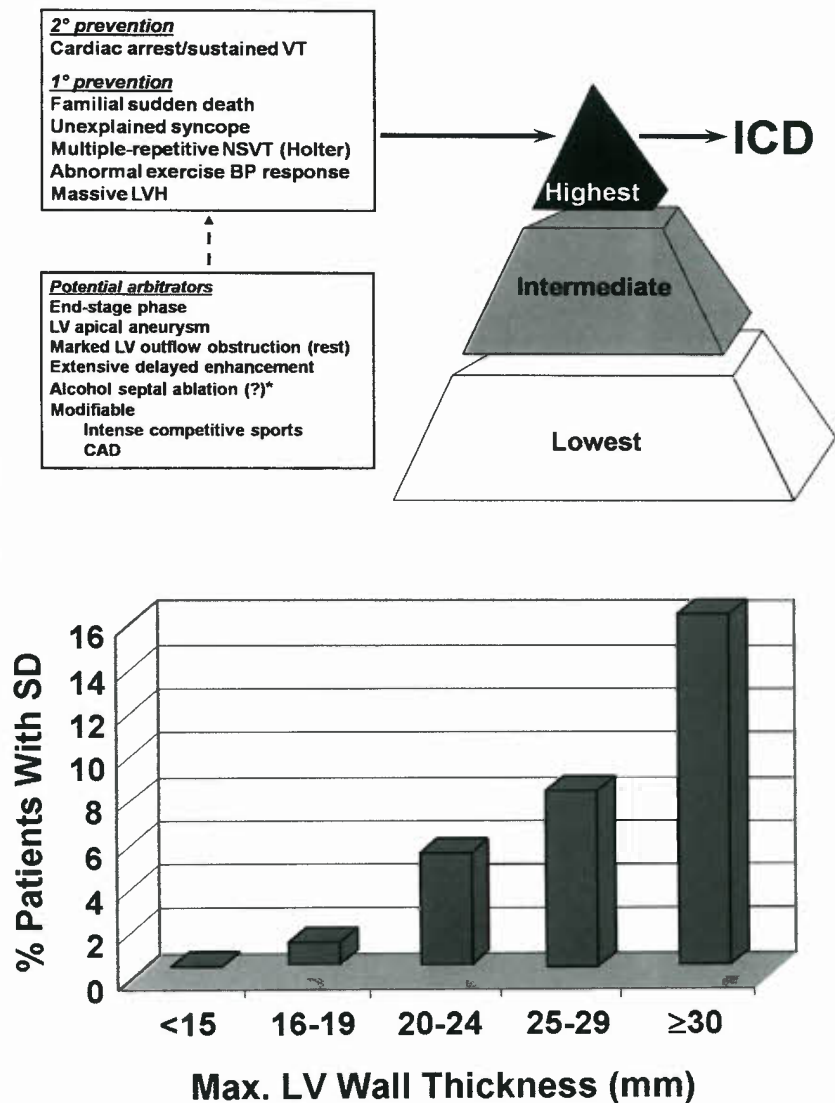
MANAGEMENT

Medical

Response of heart failure symptoms to medical treatment is highly variable, and therapy must often be empirically tailored to the individual requirements of patients (2–5). Figure 54.10 presents a current management algorithm. Since the mid-1960s, various β -adrenergic receptor blocking drugs have been used extensively to relieve and control heart failure symptoms in HCM patients with either the obstructive or nonobstructive forms (2). Long-acting preparations of propranolol, atenolol, metoprolol, or nadolol are now most commonly used. β -blockers may improve symptoms by slowing heart rate and reducing force of LV contraction, thus augmenting ventricular filling and relaxation and decreasing myocardial oxygen consumption. In addition, β -blockers inhibit sympathetic stimulation of the heart and may reduce the outflow gradient under conditions of exercise and augmented sympathetic stimulation.

Most experience with verapamil has been in adult HCM patients (daily dose ≤ 480 mg; 5 mg/kg/day) (120), although some children have also achieved symptomatic benefit from this drug (73,121). Short- and long-term studies have reported oral verapamil to improve cardiac symptoms and exercise capacity, largely in nonobstructive patients, due to a beneficial effect on LV relaxation and filling (72,73). Patients with elevated pulmonary venous pressures, particularly when associated with marked outflow obstruction, may be at increased risk for pulmonary edema or SD while taking verapamil. When patients fail to experience symptom control from β -blockers and verapamil (administered separately), empiric trials with

FIGURE 54.9. SD risk stratification. **Top:** Risk pyramid currently used to identify the most likely high-risk candidates for prevention of SD with ICDs. Depending on the age of the patient, certain markers of risk may be less relevant, for example, NSVT less than age 18 years. BP, blood pressure; LVH, left ventricular hypertrophy; NSVT, nonsustained ventricular tachycardia. **Bottom:** Relation between magnitude of LVH (maximum [max] wall thickness by echocardiography) and SD risk in an unselected HCM cohort. Mild hypertrophy conveys generally lower risk and extreme hypertrophy (wall thickness ≥ 30 mm) the highest risk. CAD, coronary artery disease. (Reproduced from Spirito P, Bellone P, Harris KM, et al. Magnitude of left ventricular hypertrophy predicts the risk of sudden death in hypertrophic cardiomyopathy. *N Engl J Med* 2000;342:1778–1785, with permission of Massachusetts Medical Society.) *Sustained ventricular tachyarrhythmias have been reported in a significant minority of patients short term following the alcohol septal ablation procedure (118).



disopyramide in combination with a β -blocker (122) have been reported to reduce outflow gradient and symptoms. Data on the use of this drug in HCM have to date been largely limited in adults. Diuretic agents may also be administered judiciously, either alone or in conjunction with either β -blockers or verapamil, to reduce pulmonary congestion and improve symptoms. These beneficial actions likely result from a reduction in LV filling pressures.

Patients with HCM may manifest evidence of heart failure in either of two clinical profiles, which largely require different therapeutic strategies (2–5). The usual circumstance occurs in children or adults who experience exertional dyspnea indicative of elevated pulmonary venous pressures, associated with intact or hyperdynamic systolic function. Medical treatment is generally with the aforementioned β -blockers or calcium antagonist drugs, although either medication can be administered first. There is no evidence that taking β -blockers and verapamil together is more advantageous than either drug alone. Furthermore, this combination may lower heart rate and/or blood pressure excessively.

Alternatively, about 3% of HCM patients will manifest the end stage of HCM with systolic dysfunction (ejection fraction < 50%) in which progressive heart failure is often associated with LV remodeling, including wall thinning, and cavity

dilation (56). The therapeutic approach to these patients is similar to that of congestive heart failure in other cardiac diseases, including administration of β -blockers, angiotensin-converting enzyme inhibitors, angiotensin-receptor blockers, and diuretics, as well as selectively digoxin, spironolactone, and warfarin.

Bacterial endocarditis appears to be virtually confined to patients with the obstructive form of HCM, with a prevalence of <1% (123). Vegetations most commonly involve the anterior mitral leaflet or septal endocardium at the site of mitral valve–septal contact and less commonly the aortic valve. Therefore, this investigator believes that children with obstructive HCM should receive standard antibiotic prophylaxis prior to dental procedures, despite the recent revised AHA recommendations (124).

Prevention of Sudden Death

In selected patients with evidence of high risk for SD, treatment for the prevention of SD with an ICD is recommended as the only treatment known to extend life in HCM (57). The strategy of long-term prophylactic treatment with amiodarone (125) is obsolete and has been abandoned, and is particularly

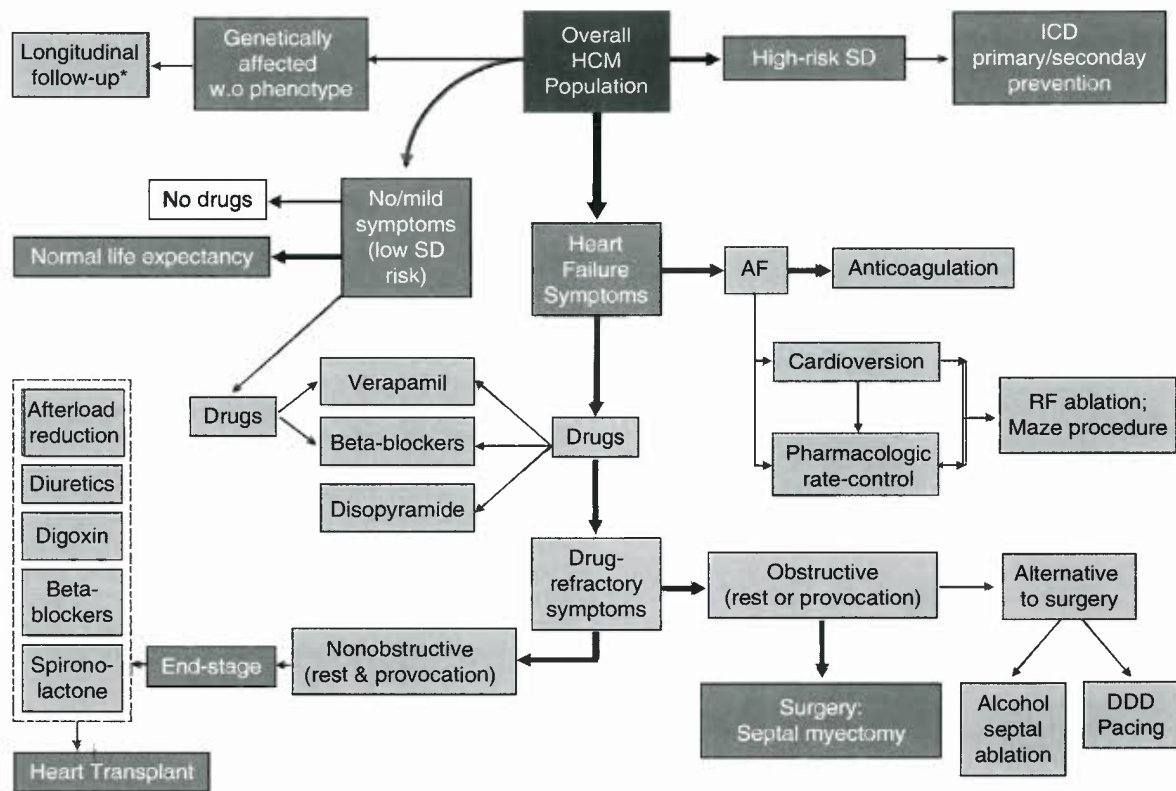


FIGURE 54.10. Management strategies for patient subgroups within the broad HCM clinical spectrum. Notably, atrial fibrillation (AF) is distinctly uncommon in the pediatric age group. *Generally no specific treatment or intervention indicated. AF, atrial fibrillation; DDD, dual chamber; ICD, implanted cardioverter-defibrillator; RF, radiofrequency; SD, sudden death.

unrealistic for children given the likelihood of side effects over the long period of risk, as well as the lack of data substantiating the effectiveness of amiodarone in protecting young HCM patients against SD.

The ICD is proven to be effective in high-risk HCM patients by reliably sensing ventricular tachycardia/fibrillation (VT/VF) and restoring sinus rhythm by delivering appropriate defibrillation shocks or antitachycardia pacing (Fig. 54.11) (57,126). The ICD may be lifesaving in young patients, both in the context of secondary prevention after a cardiac arrest (11% per year) or for primary (prophylactic) prevention owing to high-risk status based on the presence of one or more risk factors (4% per year) (57) (Fig. 54.11). Appropriate intervention rates for primary prevention are even higher in young patients, that is, 7%/year when implanted ≤ 20 years of age and 11% per year when implanted ≤ 15 years old, consistent with the known age predilection for HCM-related SD.

Of the single risk factors that triggered the ICD option, unexplained syncope was most commonly associated with appropriate ICD interventions (massive LV hypertrophy in children). Notably, long time periods may elapse between the decision to implant an ICD and when the device is required to issue an appropriate defibrillation shock to terminate VT/VF (Fig. 54.11). The ICD has altered the natural history of HCM for many young patients, and in fact, is the only therapeutic intervention that prolongs life in this disease.

While this consideration for prophylactic ICDs is particularly relevant to young patients who may anticipate extended periods of risk over many decades, the strategy of implanting

young patients with lifelong devices (and perhaps the inevitable possibility of device complications) requires some adjustment in management philosophy within the practicing pediatric cardiology community. Device complications are an important consideration but, nevertheless, the risk for SD in HCM has a predilection for patients in the pediatric age group (particularly adolescents) (2,3,57,126,127). Therefore, to ultimately impede occurrence of SD due to HCM, more of the availability of a definitive intervention such as the ICD probably will be necessary.

Surgical

Based on substantial data accumulated over >40 years, operation for HCM (surgical septal myectomy) is the primary treatment for most patients with severe drug-refractory symptoms resulting in functional disability and associated with mechanical obstruction to LV outflow under basal conditions or with physiologic exercise (gradient ≥ 50 mm Hg) (2–5,128–132). The traditional operative procedure has been the transaortic septal myectomy (Morrow procedure) in which a portion of muscle is resected from the basal septum (usually about 2 to 5 g). At some centers, the myectomy is extended much more distally in the septum (extended myectomy) (129). Results achieved at several institutions with this operation over the past 45 years have been excellent, with the vast majority of patients afforded substantial symptomatic and hemodynamic benefit (2–5,128–132). Operative mortality has steadily

decreased and is now <1% at the most experienced centers. A Mayo Clinic operative series of children with HCM reported zero operative mortality over a 20-year period (131).

More than 90% of patients who undergo myectomy experience abolition or substantial reduction in the outflow gradient under basal conditions (owing to reduction of SAM), but without important compromise in global LV function.

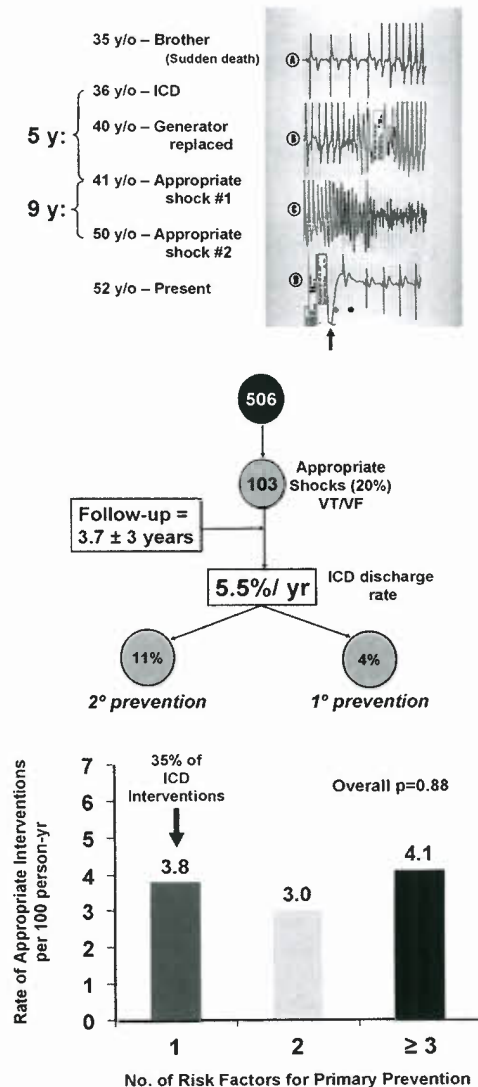


FIGURE 54.11. Prevention of SD. **Top:** Primary prevention. Intracardiac electrogram obtained at 1:20 AM with patient asleep, 5 years after implant. Patient received prophylactic ICD based on family history of SD and extreme ventricular septal thickness. **A:** Ventricular tachycardia (VT) begins abruptly, apparently unprovoked, at 200 beats/minute. **B:** Defibrillator senses VT and charges. **C:** VT deteriorates into VF. **D:** Defibrillator issues 20-J shock (arrow) immediately restoring sinus rhythm. A virtually identical sequence occurred 9 years later, also during sleep; Patient is now 53 years old and asymptomatic. (Reproduced from Maron BJ, Shen WK, Link MS, et al. Efficacy of implantable cardioverter-defibrillators for the prevention of sudden death in patients with hypertrophic cardiomyopathy. *N Engl J Med* 2000;342:365–373, with permission of Massachusetts Medical Society.) **Center:** Flow diagram summarizing ICD-related outcome in 506 high-risk HCM patients from international, multicenter ICD registry (57,126). **Bottom:** ICD intervention rates in patients implanted prophylactically for only one risk factor. ICD, implanted cardioverter-defibrillator; LVH, left ventricular hypertrophy; NSVT, nonsustained ventricular tachycardia.

Long-term follow-up studies from surgical centers have demonstrated that basal outflow obstruction does not recur and heart failure is largely reversed by surgical septal myectomy, with symptoms relieved long term in about 90% of patients (132). Of particular note, recent data from the Mayo Clinic myectomy cohort show that operated patients achieve the same longevity as the general population and demonstrate significantly better survival than nonoperated patients with outflow obstruction (129).

Occasionally, patients develop outflow obstruction from a mechanism other than SAM. For example, anomalous papillary muscle insertion directly into the anterior mitral leaflet (without the interposition of chordae tendinae) produces muscular midventricular obstruction (133,134). This congenital anomaly of the mitral apparatus should be considered prior to intervention since targeted surgical strategy requires distally extended myectomy to relieve obstruction (134).

The technique of alcohol septal ablation has been introduced to reduce outflow gradient in selected symptomatic adult HCM patients as an alternative to surgery (128,135). This method involves introduction of about 2 ml of 95% alcohol into the first major septal perforator to produce a transmural myocardial infarction. This procedure should not be performed (or even considered) in young HCM patients, given their long period of potential longevity and the distinct possibility that the healed scar may enhance the pre-existent arrhythmogenic LV substrate and ultimately increase the risk of SD (128).

REFERENCES

- Maron BJ, Towbin JA, Thiene G, et al. Contemporary definitions and classification of the cardiomyopathies: an American Heart Association Scientific Statement from the Council on Clinical Cardiology, Heart Failure and Transplantation Committee; Quality of Care and Outcomes Research and Functional Genomics and Translational Biology Interdisciplinary Working Groups; and Council on Epidemiology and Prevention. *Circulation* 2006;113:1807–1816.
- Maron BJ, McKenna WJ, Danielson GK, et al. American College of Cardiology/European Society of Cardiology Clinical Expert Consensus Document on Hypertrophic Cardiomyopathy. A report of the American College of Cardiology Task Force on Clinical Expert Consensus Documents and the European Society of Cardiology Committee for Practice Guidelines Committee to Develop an Expert Consensus Document on Hypertrophic Cardiomyopathy. *J Am Coll Cardiol* 2003;42:1687–1713.
- Maron BJ. Hypertrophic cardiomyopathy: A systematic review. *JAMA* 2002;287:1308–1320.
- Spirito P, Seidman CE, McKenna WJ, et al. The management of hypertrophic cardiomyopathy. *N Engl J Med* 1997;336:775–785.
- Wigle ED, Rakowski H, Kimball BP, et al. Hypertrophic cardiomyopathy. Clinical spectrum and treatment. *Circulation* 1995;92:1680–1692.
- Klues HG, Schiffrs A, Maron BJ. Phenotypic spectrum and patterns of left ventricular hypertrophy in hypertrophic cardiomyopathy: Morphologic observations and significance as assessed by two-dimensional echocardiography in 600 patients. *J Am Coll Cardiol* 1995;26:1699–1708.
- Maron MS, Maron BJ, Harrigan C, et al. Hypertrophic cardiomyopathy phenotype revisited after 50 years with cardiovascular magnetic resonance. *J Am Coll Cardiol* 2009;54:220–228.
- Teare D. Asymmetrical hypertrophy of the heart in young adults. *Br Heart J* 1958;20:1–8.
- Lewis JF, Maron BJ. Hypertrophic cardiomyopathy characterized by marked hypertrophy of the posterior left ventricular free wall: Significance and clinical implications. *J Am Coll Cardiol* 1991;18:421–428.
- Ciró E, Nichols PF, Maron BJ. Heterogeneous morphologic expression of genetically transmitted hypertrophic cardiomyopathy: two-dimensional echocardiographic analysis. *Circulation* 1983;67:1227–1233.
- Maron BJ, Casey SA, Almquist AK. Hypertrophic cardiomyopathy in monozygotic twins. *Circulation* 2002;105:2229.
- Louie EK, Maron BJ. Hypertrophic cardiomyopathy with extreme increase in left ventricular wall thickness: Functional and morphologic features and clinical significance. *J Am Coll Cardiol* 1986;8:57–65.
- Spirito P, Maron BJ, Bonow RO, et al. Severe functional limitation in patients with hypertrophic cardiomyopathy and only mild localized left ventricular hypertrophy. *J Am Coll Cardiol* 1986;8:537–544.
- Spirito P, Lakatos E, Maron BJ. Degree of left ventricular hypertrophy in chronic atrial fibrillation in hypertrophic cardiomyopathy. *Am J Cardiol* 1992;69:1217–1222.
- Yamaguchi H, Ishimura T, Nishiyama S, et al. Hypertrophic nonobstructive cardiomyopathy with giant negative T waves (apical hypertrophy): Ventriculographic and echocardiographic features in 30 patients. *Am J Cardiol* 1979;44:401–412.
- Louie EK, Maron BJ. Apical hypertrophic cardiomyopathy: clinical and two-dimensional echocardiographic assessment. *Ann Intern Med* 1987;106:663–670.

17. Webb JG, Sasson Z, Rakowski H, et al. Apical hypertrophic cardiomyopathy: clinical follow-up and diagnostic correlates. *J Am Coll Cardiol* 1990;15:83-90.
18. Maron MS, Finley JJ, Bos JM, et al. Prevalence, clinical significance, and natural history of left ventricular apical aneurysms in hypertrophic cardiomyopathy. *Circulation* 2008;118:1541-1549.
19. Wang L, Seidman JG, Seidman CE. Narrative review: harnessing molecular genetics for the diagnosis and management of hypertrophic cardiomyopathy. *Ann Intern Med* 2010;152:513-520.
20. Maron BJ, Seidman JG, Seidman CE. Proposal for contemporary screening strategies in families with hypertrophic cardiomyopathy. *J Am Coll Cardiol* 2004;44:2125-2132.
21. Maron BJ, Seidman CE, Ackerman MJ, et al. How should hypertrophic cardiomyopathy be classified?: what's in a name? Dilemmas in nomenclature characterizing hypertrophic cardiomyopathy and left ventricular hypertrophy. *Circ Cardiovasc Genet* 2009;2:81-85.
22. Maron BJ, Pelliccia A. The heart of trained athletes: cardiac remodeling and the risks of sports, including sudden death. *Circulation* 2006;114:1633-1644.
23. Maron MS, Olivetto I, Zenovich AG, et al. Hypertrophic cardiomyopathy is predominantly a disease of left ventricular outflow tract obstruction. *Circulation* 2006;114:2232-2239.
24. Maron BJ, Gardin JM, Flack JM, et al. Assessment of the prevalence of hypertrophic cardiomyopathy in a general population of young adults: echocardiographic analysis of 4111 subjects in the CARDIA Study. *Circulation* 1995;92:785-789.
25. Zou Y, Song L, Want Z, et al. Prevalence of idiopathic hypertrophic cardiomyopathy in China: a population-based echocardiographic analysis of 8080 adults. *Am J Med* 2004;116:14-18.
26. Maron BJ, Peterson EE, Maron MS, et al. Prevalence of hypertrophic cardiomyopathy in an outpatient population referred for echocardiographic study. *Am J Cardiol* 1994;73:577-580.
27. Maron BJ. Hypertrophic cardiomyopathy: an important global disease [editorial]. *Am J Med* 2004;116:63-65.
28. Maron MS, Lesser JR, Maron BJ. Management implications of massive left ventricular hypertrophy in hypertrophic cardiomyopathy significantly underestimated by echocardiography but identified by cardiovascular magnetic resonance. *Am J Cardiol* 2010;105:1842-1843.
29. Moon JC, Fisher NG, McKenna WJ, et al. Detection of apical hypertrophic cardiomyopathy by cardiovascular magnetic resonance in patients with non-diagnostic echocardiography. *Heart* 2004;90:645-649.
30. Rickers C, Wilke NM, Jerosch-Herold M, et al. Utility of cardiac magnetic resonance imaging in the diagnosis of hypertrophic cardiomyopathy. *Circulation* 2005;112:855-861.
31. Alfonso F, Nihoyannopoulos P, Stewart J, et al. Clinical significance of giant negative T waves in hypertrophic cardiomyopathy. *J Am Coll Cardiol* 1990;15:965-971.
32. Maron BJ, Yeates L, Semsarian C. Clinical challenges of genotype positive (+)-phenotype negative (-) family members in hypertrophic cardiomyopathy. *Am J Cardiol* 2011;107:604-608.
33. Maron BJ, Spirito P, Wesley Y, et al. Development and progression of left ventricular hypertrophy in children with hypertrophic cardiomyopathy. *N Engl J Med* 1986;315:610-614.
34. Panza JA, Maron BJ. Relation of electrocardiographic abnormalities to evolving left ventricular hypertrophy in hypertrophic cardiomyopathy. *Am J Cardiol* 1989;63:1258-1265.
35. Panza JA, Maris TJ, Maron BJ. Development and determinants of dynamic obstruction to left ventricular outflow in young patients with hypertrophic cardiomyopathy. *Circulation* 1992;85:1398-1405.
36. Gregor P, Widimsky P, Cervenka V, et al. Electrocardiographic changes can precede the development of myocardial hypertrophy in the setting of hypertrophic cardiomyopathy. *Int J Cardiol* 1989;23:335-341.
37. Klues HG, Maron BJ, Dollar AL, et al. Diversity of structural mitral valve alterations in hypertrophic cardiomyopathy. *Circulation* 1992;85:1651-1660.
38. Maron MS, Olivetto I, Harrigan C, et al. Mitral valve abnormalities identified by cardiovascular magnetic resonance represents a primary phenotypic expression of hypertrophic cardiomyopathy. *Circulation* 2011;124:40-47.
39. Maron BJ, Roberts WC. Quantitative analysis of cardiac muscle cell disorganization in the ventricular septum of patients with hypertrophic cardiomyopathy. *Circulation* 1979;59:689-706.
40. St. John Sutton MG, Lie JT, Anderson KR, et al. Histopathological specificity of hypertrophic obstructive cardiomyopathy. *Br Heart J* 1980;44:433-443.
41. Maron BJ, Wolfson JK, Roberts WC. Relation between extent of cardiac muscle cell disorganization and left ventricular wall thickness in hypertrophic cardiomyopathy. *Am J Cardiol* 1992;70:785-790.
42. Maron BJ, Sato N, Roberts WC, et al. Quantitative analysis of cardiac muscle cell disorganization in the ventricular septum. Comparison of fetuses and infants with and without congenital heart disease and patients with hypertrophic cardiomyopathy. *Circulation* 1979;60:685-696.
43. Maron BJ, Anan TJ, Roberts WC. Quantitative analysis of the distribution of cardiac muscle cell disorganization in the left ventricular wall of patients with hypertrophic cardiomyopathy. *Circulation* 1991;63:882-894.
44. Maron BJ, Wolfson JK, Epstein SE, et al. Intramural ("small vessel") coronary artery disease in hypertrophic cardiomyopathy. *J Am Coll Cardiol* 1986;8:545-557.
45. Tanaka M, Fujiwara H, Onodera T, et al. Quantitative analysis of narrowings of intramyocardial small arteries in normal hearts, hypertensive hearts, and hearts with hypertrophic cardiomyopathy. *Circulation* 1987;75:1130-1139.
46. Factor SM, Butany J, Sole MJ, et al. Pathologic fibrosis and matrix connective tissue in the subaortic myocardium of patients with hypertrophic cardiomyopathy. *J Am Coll Cardiol* 1991;17:1343-1351.
47. Tanaka M, Fujiwara H, Onodera T, et al. Quantitative analysis of myocardial fibrosis in normals, hypertensive hearts, and hypertrophic cardiomyopathy. *Br Heart J* 1986;55:575-581.
48. Maron BJ, Epstein SE, Roberts WC. Hypertrophic cardiomyopathy and transmural myocardial infarction without significant atherosclerosis of the extramural coronary arteries. *Am J Cardiol* 1979;43:1086-1102.
49. Shirani J, Pick R, Roberts WC, et al. Morphology and significance of the left ventricular collagen network in young patients with hypertrophic cardiomyopathy and sudden cardiac death. *J Am Coll Cardiol* 2000;35:36-44.
50. Maron MS, Appelbaum E, Harrigan CJ, et al. Clinical profile and significance of delayed enhancement in hypertrophic cardiomyopathy. *Circ Heart Fail* 2008;1:184-191.
51. Cannon RO, Rosing DR, Maron BJ, et al. Myocardial ischemia in hypertrophic cardiomyopathy: Contribution of inadequate vasodilator reserve and elevated left ventricular filling pressures. *Circulation* 1985;71:234-243.
52. Basso C, Thiene G, Corrado D, et al. Hypertrophic cardiomyopathy and sudden death in the young: pathologic evidence of myocardial ischemia. *Hum Pathol* 2000;31:988-998.
53. O'Gara PT, Bonow RO, Maron BJ, et al. Myocardial perfusion abnormalities in patients with hypertrophic cardiomyopathy: Assessment with thallium-201 emission computed tomography. *Circulation* 1987;76:1214-1223.
54. Maron MS, Olivetto I, Maron BJ, et al. The case for myocardial ischemia in hypertrophic cardiomyopathy. *J Am Coll Cardiol* 2009;54:866-875.
55. Roberts CS, Roberts WC. Morphologic features. In: Zipes DP, Rowlands DJ, eds. *Progress in Cardiology* 2/2. Malvern, PA: Lea & Febiger, 1989:3-22.
56. Harris KM, Spirito P, Maron MS, et al. Prevalence, clinical profile and significance of left ventricular remodeling in the end-stage phase of hypertrophic cardiomyopathy. *Circulation* 2006;114:216-225.
57. Maron BJ, Shen WK, Link MS, et al. Efficacy of implantable cardioverter-defibrillators for the prevention of sudden death in patients with hypertrophic cardiomyopathy. *N Engl J Med* 2000;342:365-373.
58. Adabag AS, Casey SA, Kuskowski MA, et al. Spectrum and prognostic significance of arrhythmias on ambulatory Holter electrocardiogram in hypertrophic cardiomyopathy. *J Am Coll Cardiol* 2005;45:697-704.
59. Maron MS, Olivetto I, Betocchi S, et al. Effect of left ventricular outflow tract obstruction on clinical outcome in hypertrophic cardiomyopathy. *N Engl J Med* 2003;348:295-303.
60. Panza JA, Petrone RK, Fananapazir L, et al. Utility of continuous wave Doppler in noninvasive assessment of the left ventricular outflow tract pressure gradient in patients with hypertrophic cardiomyopathy. *J Am Coll Cardiol* 1992;19:91-99.
61. Spirito P, Maron BJ. Significance of left ventricular outflow tract cross-sectional area in hypertrophic cardiomyopathy: A two-dimensional echocardiographic assessment. *Circulation* 1983;67:1100-1108.
62. Klues HG, Roberts WC, Maron BJ. Morphologic determinants of echocardiographic patterns of mitral valve systolic anterior motion in obstructive hypertrophic cardiomyopathy. *Circulation* 1993;87:1570-1579.
63. Sherrid MV, Chu CK, Delia E, et al. An echocardiographic study of the fluid mechanics of obstruction in hypertrophic cardiomyopathy. *J Am Coll Cardiol* 1993;22:816-825.
64. Petrone RK, Klues HG, Panza JA, et al. Coexistence of mitral valve prolapse in a consecutive group of 528 patients with hypertrophic cardiomyopathy assessed with echocardiography. *J Am Coll Cardiol* 1992;20:55-61.
65. Braunwald E, Lambrew CT, Rockoff SD, et al. Idiopathic hypertrophic subaortic stenosis. I. A description of the disease based upon an analysis of 64 patients. *Circulation* 1964;30:3-119.
66. Maron BJ, McIntosh CL, Klues HG, et al. Morphologic basis for obstruction to right ventricular outflow in hypertrophic cardiomyopathy. *Am J Cardiol* 1993;71:1089-1094.
67. Cecchi F, Olivetto I, Gistri R, et al. Coronary microvascular dysfunction and prognosis in hypertrophic cardiomyopathy. *N Engl J Med* 2003;349:1027-1035.
68. Maron BJ, Spirito P, Green KJ, et al. Noninvasive assessment of left ventricular diastolic function by pulsed Doppler echocardiography in patients with hypertrophic cardiomyopathy. *J Am Coll Cardiol* 1987;10:733-742.
69. Nihoyannopoulos P, Karatasakis G, Frenneaux M, et al. Diastolic function in hypertrophic cardiomyopathy: relation to exercise capacity. *J Am Coll Cardiol* 1992;19:536-540.
70. Spirito P, Maron BJ. Relation between extent of left ventricular hypertrophy and diastolic filling abnormalities in hypertrophic cardiomyopathy. *J Am Coll Cardiol* 1990;15:808-813.
71. Briguori C, Betocchi S, Romano M, et al. Exercise capacity in hypertrophic cardiomyopathy depends on left ventricular diastolic function. *Am J Cardiol* 1999;84:309-315.
72. Bonow RO, Frederick TM, Bacharach SL, et al. Atrial systole and left ventricular filling in patients with hypertrophic cardiomyopathy: Effect of verapamil. *Am J Cardiol* 1983;51:1386-1391.
73. Shaffer EM, Rocchini AP, Spicer RL, et al. Effects of verapamil on left ventricular diastolic filling in children with hypertrophic cardiomyopathy. *Am J Cardiol* 1988;61:413-417.
74. Maron BJ, Spirito P, Green KJ, et al. Noninvasive assessment of left ventricular diastolic function by pulsed Doppler echocardiography in patients with hypertrophic cardiomyopathy. *J Am Coll Cardiol* 1987;10:733-742.
75. Seidman JG, Seidman CE. The genetic basis for cardiomyopathy: From mutation identification to mechanistic paradigms. *Cell* 2001;104:557-567.

76. Arad M, Penas-Lado M, Monserrat L, et al. Gene mutations in apical hypertrophic cardiomyopathy. *Circulation* 2005;112:2805-2811.
77. Maron BJ, Niiimura H, Casey SA, et al. Development of left ventricular hypertrophy in adults with hypertrophic cardiomyopathy caused by cardiac myosin-binding protein C mutations. *J Am Coll Cardiol* 2001;38:315-321.
78. Richards P, Charron P, Carrier L, et al. Hypertrophic cardiomyopathy. Distribution of disease genes, spectrum of mutations, and implications for a molecular diagnosis strategy. *Circulation* 2003;107:2227.
79. Niiimura H, Bachinski LL, Sangwatanaroj S, et al. Mutations in the gene for human cardiac myosin-binding protein C and late-onset familial hypertrophic cardiomyopathy. *N Engl J Med* 1998;338:1248-1257.
80. Ho CY. Genetics and clinical destiny: improving care in hypertrophic cardiomyopathy. *Circulation* 2010;122:2430-2440.
81. Landstrom AP, Ackerman MJ. Mutation type is not clinically useful in predicting prognosis in hypertrophic cardiomyopathy. *Circulation* 2010;122:2441-2449.
82. Arad M, Maron BJ, Gorham JM, et al. Glycogen storage diseases presenting as hypertrophic cardiomyopathy. *N Engl J Med* 2005;352:362-372.
83. Maron BJ, Roberts WC, Arad M, et al. Clinical outcome and phenotypic expression in LAMP2 cardiomyopathy. *JAMA* 2009;301:1253-1259.
84. Weidemann F, Niemann M, Breunig F, et al. Long-term effects of enzyme replacement therapy on Fabry cardiomyopathy: evidence for a better outcome with early treatment. *Circulation* 2009;119:524-529.
85. Watkins H, Rosenzweig A, Hwang D-S, et al. Characteristics and prognostic implications of myosin missense mutations in familial hypertrophic cardiomyopathy. *N Engl J Med* 1992;326:1108-1114.
86. Kelly M, Semsarian C. Multiple mutations in genetic cardiovascular disease: a marker of disease severity? *Circ Cardiovasc Genet* 2009;2:182-190.
87. Maron BJ, Tajik AJ, Ruttenberg HD, et al. Hypertrophic cardiomyopathy in infants: clinical features and natural history. *Circulation* 1982;65:7-17.
88. Comparato C, Pipitone S, Sperandio V, et al. Clinical profile and prognosis of hypertrophic cardiomyopathy when first diagnosed in infancy as opposed to childhood. *Cardiolog Young* 1997;7:410-416.
89. Towbin JA. Pediatric myocardial disease. *Pediatr Clin North Am* 1999;46:289-312.
90. Suda K, Kohl T, Kovalchin JP, et al. Echocardiographic predictors of poor outcome in infants with hypertrophic cardiomyopathy. *Am J Cardiol* 1997;80:595-600.
91. Skinner JR, Manzoar A, Hayes AM, et al. A regional study of presentation and outcome of hypertrophic cardiomyopathy in infants. *Heart* 1997;77:229-233.
92. Maron BJ. Hypertrophic cardiomyopathy in childhood. *Pediatr Clin North Am* 2004;51:1305-1346.
93. Maron BJ, Wolfson JK, Ciró E, et al. Relation of electrocardiographic abnormalities and patterns of left ventricular hypertrophy identified by two-dimensional echocardiography in patients with hypertrophic cardiomyopathy. *Am J Cardiol* 1983;51:189-194.
94. Montgomery JV, Harris KM, Casey SA, et al. Relation of electrocardiographic patterns to phenotypic expression and clinical outcome in hypertrophic cardiomyopathy. *Am J Cardiol* 2005;96:270-275.
95. McLeod CJ, Ackerman MJ, Nishimura RA, et al. Outcome of patients with hypertrophic cardiomyopathy and a normal electrocardiogram. *J Am Coll Cardiol* 2009;54:229-233.
96. Maron BJ, Pelliccia A, Spirito P. Cardiac disease in young trained athletes: insights into methods for distinguishing athlete's heart from structural heart disease with particular emphasis on hypertrophic cardiomyopathy. *Circulation* 1995;91:1596-1601.
97. Pelliccia A, Maron BJ, Spataro A, et al. The upper limit of physiologic cardiac hypertrophy in highly trained elite athletes. *N Engl J Med* 1991;324:295-301.
98. Pelliccia A, Kinoshita N, Pisicchio C, et al. Long-time clinical consequences of intense, uninterrupted endurance training in Olympic athletes. *J Am Coll Cardiol* 2010;55:1619-1625.
99. Maron BJ, Thompson PD, Ackerman MJ, et al. Recommendations and considerations related to preparticipation screening for cardiovascular abnormalities in competitive athletes: Update 2007. A Scientific Statement from the American Heart Association, Nutrition, Physical Activity, and Metabolism Council. *Circulation* 2007;115:1643-1645.
100. Corrado D, Basso C, Schiavon M, et al. Determinants for clinical diagnosis of hypertrophic cardiomyopathy. *Am J Cardiol* 2006;98:1507-1511.
101. Glover DW, Glover BW, Maron BJ. Evolution in the process of screening United States high school student athletes for cardiovascular disease. *Am J Cardiol* 2007;100:1709-1712.
102. Corrado D, Basso C, Pavei A, et al. Trends in sudden cardiovascular death in young competitive athletes after implementation of a preparticipation screening program. *JAMA* 2006;296:1593-1601.
103. Maron BJ, Henry WL, Clark CE, et al. Asymmetric septal hypertrophy in childhood. *Circulation* 1976;53:9-19.
104. McKenna WJ, Franklin RCG, Nihoyannopoulos P, et al. Arrhythmia and prognosis in infants, children and adolescents with hypertrophic cardiomyopathy. *J Am Coll Cardiol* 1988;11:147-153.
105. Maron BJ, Spirito P. Impact of patient selection biases on the perception of hypertrophic cardiomyopathy and its natural history. *Am J Cardiol* 1993;72:970-972.
106. Cecchi F, Olivetto I, Monterecci A, et al. Hypertrophic cardiomyopathy in Tuscany: clinical course and outcome in an unselected regional population. *J Am Coll Cardiol* 1995;26:1529-1536.
107. Spirito P, Chiarella F, Carratino L, et al. Clinical course and prognosis of hypertrophic cardiomyopathy in an outpatient population. *N Engl J Med* 1989;320:749-755.
108. Cannan CR, Reeder GS, Bailey KR, et al. Natural history of hypertrophic cardiomyopathy: a population-based study, 1976 through 1990. *Circulation* 1995;92:2488-2495.
109. Maron BJ, Casey SA, Poliac LC, et al. Clinical course of hypertrophic cardiomyopathy in a regional United States cohort. *JAMA* 1999;281:650-655.
110. Maron BJ, Fisher RS. Sudden infant death syndrome: cardiac pathologic observations in infants with SIDS. *Am Heart J* 1977;93:762-766.
111. Maron BJ. Sudden death in young athletes. *N Engl J Med* 2003;349:1064-1075.
112. Maki S, Ikeda H, Muro A, et al. Predictors of sudden cardiac death in hypertrophic cardiomyopathy. *Am J Cardiol* 1998;82:774-778.
113. Spirito P, Bellone P, Harris KM, et al. Magnitude of left ventricular hypertrophy predicts the risk of sudden death in hypertrophic cardiomyopathy. *N Engl J Med* 2000;342:1778-1785.
114. Maron BJ, Piccininno M, Casey SA, et al. Relation of extreme left ventricular hypertrophy to age in hypertrophic cardiomyopathy. *Am J Cardiol* 2003;91:626-628.
115. Bos JM, Maron BJ, Ackerman MJ, et al. Role of family history of sudden death in risk stratification and prevention of sudden death with implantable defibrillators in hypertrophic cardiomyopathy. *Am J Cardiol* 2010;106:1481-1486.
116. Maron BJ, Doerer JJ, Haas TS, et al. Sudden deaths in young competitive athletes: analysis of 1866 deaths in the United States, 1980-2006. *Circulation* 2009;119:1085-1092.
117. Maron BJ, Zipes DP. 36th Bethesda Conference: eligibility Recommendations for Competitive Athletes with Cardiovascular Abnormalities. *J Am Coll Cardiol* 2005;45:1312-1375.
118. Maron BJ. Contemporary insights and strategies for risk stratification and prevention of sudden death in hypertrophic cardiomyopathy. *Circulation* 2010;121:445-456.
119. Basso C, Thiene G, Mackey-Bojack S, et al. Myocardial bridging, a frequent component of the hypertrophic cardiomyopathy phenotype, lacks systematic association with sudden cardiac death. *Eur Heart J* 2009;30:1627-1634.
120. Rosing DR, Condit JR, Maron BJ, et al. Verapamil therapy: a new approach to the pharmacologic treatment of hypertrophic cardiomyopathy. III: Effects of long-term administration. *Am J Cardiol* 1981;48:545-553.
121. Spicer RL, Rocchini AP, Crowley DC, et al. Chronic verapamil therapy in pediatric and young adult patients with hypertrophic cardiomyopathy. *Am J Cardiol* 1984;53:1614-1619.
122. Sherrid MV, Barac I, McKenna WJ, et al. Multicenter study of the efficacy and safety of disopyramide in obstructive hypertrophic cardiomyopathy. *J Am Coll Cardiol* 2005;45:1251-1258.
123. Spirito P, Rapezzi C, Bellone P, et al. Infective endocarditis in hypertrophic cardiomyopathy. Prevalence, incidence and indications for antibiotic prophylaxis. *Circulation* 1999;99:2132-2137.
124. Wilson W, Taubert KA, Gewitz M, et al. Prevention of infective endocarditis: guidelines from the American Heart Association: a guideline from the American Heart Association Rheumatic Fever, Endocarditis, and Kawasaki Disease Committee, Council on Cardiovascular Disease in the Young, and the Council on Clinical Cardiology, Council on Cardiovascular Surgery and Anesthesia, and the Quality of Care and Outcomes Research Interdisciplinary Working Group. *Circulation* 2007;116:1736-1754.
125. McKenna WJ, Oakley CM, Krikler DM, et al. Improved survival with amiodarone in patients with hypertrophic cardiomyopathy and ventricular tachycardia. *Br Heart J* 1985;53:412-416.
126. Maron BJ, Spirito P. Implantable defibrillators and prevention of sudden death in hypertrophic cardiomyopathy. *J Cardiovasc Electrophysiol* 2008;19:1118-1126.
127. Maron BJ, Olivetto I, Spirito P, et al. Epidemiology of hypertrophic cardiomyopathy-related death. Revisited in a large non-referral-based patient population. *Circulation* 2000;102:858-864.
128. Maron BJ. Surgery for hypertrophic obstructive cardiomyopathy: alive and quite well. *Circulation* 2005;111:2016-2018.
129. Ommen SR, Maron BJ, Olivetto I, et al. Long-term effects of surgical septal myectomy on survival in patients with obstructive hypertrophic cardiomyopathy. *J Am Coll Cardiol* 2005;46:470-476.
130. Maron BJ, Dearani JA, Ommen SR, et al. The case for surgery in obstructive hypertrophic cardiomyopathy. *J Am Coll Cardiol* 2004;44:2044-2053.
131. Theodoro DA, Danielson GK, Feldt RH, et al. Hypertrophic obstructive cardiomyopathy in pediatric patients: Results of surgical treatment. *J Thorac Cardiovasc Surg* 1996;112:1589-1599.
132. Woo A, Williams WG, Choi R, et al. Clinical and echocardiographic determinants of long-term survival following surgical myectomy in obstructive hypertrophic cardiomyopathy. *Circulation* 2005;111:2033-2041.
133. Klues HG, Roberts WC, Maron BJ. Anomalous insertion of papillary muscle directly into anterior mitral leaflet in hypertrophic cardiomyopathy: Significance in producing left ventricular outflow obstruction. *Circulation* 1991;84:1188-1197.
134. Maron BJ, Nishimura RA, Danielson GK. Pitfalls in clinical recognition and a novel operative approach for hypertrophic cardiomyopathy with severe outflow obstruction due to anomalous papillary muscle. *Circulation* 1998;98:2505-2508.
135. Sorajja P, Valeti U, Nishimura RA, et al. Outcome of alcohol septal ablation for obstructive hypertrophic cardiomyopathy. *Circulation* 2008;118:131-139.

Timothy M. Olson ■ David P. Chan

ETIOLOGY AND PATHOGENESIS

Cardiac dilation and decreased systolic function, the uniform diagnostic features of dilated cardiomyopathy (DCM), fail to reflect the many causes of DCM (Table 55.1). Infectious, metabolic, ischemic, toxic, and hereditary factors have been implicated in the disease pathogenesis (1–5). DCM, with a prevalence of 36.5 per 100,000 population (1), is thus a final common pathway for diverse disease processes that lead to heart failure. When an infant or child presents with echocardiographically confirmed DCM, knowledge of the broad differential diagnosis and additional testing may uncover a reversible cause for myopathic heart failure and/or aid in establishing prognosis (6,7). However, the primary cause of DCM is unknown in 66% of children (7) and 50% of adults (8). The preclinical cascade of molecular and cellular events leading to heart failure thus remains poorly understood. Most patients with idiopathic DCM have clinically silent disease in childhood, developing symptoms only in middle age (mean age at diagnosis 45 ± 17 years) (9). The delayed onset of clinically apparent disease suggests a subtle congenital defect in myocardial function inciting a gradual degenerative process that progresses over several decades.

Sensitive preclinical markers of DCM unfortunately are lacking, and family history may be the only clue prompting echocardiographic screening and presymptomatic diagnosis in hereditary forms of DCM. Despite an insidious onset, advanced myocardial disease with substantial maladaptive ventricular remodeling often is present in both adults and children with symptomatic DCM. As a result, DCM is the indication for cardiac transplantation in 31% of infants and 64% of older children (10). Late diagnosis is confounded further by limited evidence-based guidelines for the treatment of cardiomyopathic heart failure in children (11). Indeed, conventional medical therapies with established efficacy in adults appear to have a limited impact on pediatric outcomes (12,13). Consequently, only 46% of children with DCM are alive and free from cardiac transplantation at 10 years of follow-up (7). The prognosis in individual patients, nevertheless, often is unpredictable ranging from intractable heart failure to occasional spontaneous recovery (1,14). Improved treatment and prevention of DCM will require identification of preclinical markers, new insights into disease mechanisms and risk classification, and optimal therapies that specifically alter pathologic molecular and cellular processes prior to the development of end-stage myocardial disease.

Cardiac Dilation

Cardiac performance is determined by preload, afterload, contractility, and heart rate. In the normal heart, dilation, like hypertrophy, may represent an appropriate response to

(patho)physiologic demands. According to the Frank-Starling Law, increased preload results in enhanced cardiac output. For example, increased left ventricular end-diastolic volume may be an adaptation to inadequate systemic oxygen delivery (chronic anemia) or contractile dysfunction (acute hypoxic-ischemic insult). In idiopathic DCM, by contrast, dilation initially or eventually becomes maladaptive. The cardiothoracic ratio on chest radiography is predictive of mortality in patients with DCM (1). Moreover, clinical studies of familial DCM indicate that left ventricular dilation is present in 9% to 20% of asymptomatic relatives and serves as a marker for later progression to DCM (9,15,16). It is unknown whether dilation initially is an adaptive response to myocellular dysfunction or a primary, pathologic process of ventricular remodeling. In either case, unless wall thickness increases, dilation leads to increased wall stress (Laplace law) and mismatch of myocardial oxygen supply and demand. In fact, decreased posterior wall thickness in DCM is associated with a worse prognosis (1).

Myocellular Hypertrophy and Death

In acquired forms of heart failure due to ischemia or increased afterload, cardiac hypertrophy is an adaptive response that preserves myocardial performance. Although myocardial mass is increased in DCM because of a severalfold increase in interstitial collagen content (17), left ventricular posterior wall thickness is normal or decreased (2). On microscopic examination, compensatory hypertrophy of viable myocytes is present in human DCM and in animal models of DCM (18,19). However, cumulative loss of myofibrils and cardiac myocytes, lacking sufficient capacity to regenerate (20), occurs concomitantly. Consequently, ongoing myocyte death coupled with progressive chamber dilation contributes to lack of compensatory increase in wall thickness. Myocyte loss in chronic DCM occurs by two general processes—apoptosis, programmed cellular self-destruction (21), and subclinical necrosis, detected by release of cardiac enzymes into the blood stream (22). Quantitative morphometric studies of pathologic heart specimens confirm that cardiac myocyte death is a major pathologic process in DCM (23) and correlates with worse prognosis (2).

Extracellular Matrix Remodeling

Cardiac myocytes play an indispensable role in the heart, yet they constitute only one-third of total myocardial cells (24). Fibroblasts, vascular smooth muscle, and endothelial cells make up the remainder of cells and, unlike cardiac myocytes, retain the capacity to rapidly proliferate. The extracellular matrix is composed of connective tissue proteins such as collagen, fibronectin, and laminin (25). These proteins form a scaffold that maintains cardiac architecture

TABLE 55.1 Causes of Dilated Cardiomyopathy

Acute and chronic myocarditis
Autoimmune disease
Chronic tachycardia
Drugs—alcohol, sympathomimetics, anthracyclines
End-stage hypertrophic cardiomyopathy
Endocrine—growth hormone deficiency, thyroid disease, hypocalcemia, diabetes mellitus, pheochromocytoma
Hereditary—autosomal dominant, autosomal recessive, X-linked, mitochondrial
Inborn errors of metabolism
Infiltrative—glycogen storage disorders, hemochromatosis, amyloidosis
Ischemic—atherosclerosis, Kawasaki disease, anomalous origin of left coronary artery
Muscular dystrophies
Nutritional deficiency—selenium, carnitine, thiamine
Peripartum
Structural heart disease
Systemic hypertension
Toxins—cobalt, lead

and myocyte alignment, and transmits mechanical force generated by cardiac myocytes (17). Ventricular remodeling is a pathologic process of the failing heart, whereby cardiac fibroblasts proliferate, mechanically stable cross-linked collagen is degraded by metalloproteinases, and an excess of poorly cross-linked collagen is deposited into the interstitium (17). In DCM, this remodeling process contributes to both increased myocardial mass, owing to interstitial fibrosis, and ventricular dilation and wall thinning, owing to slippage of aligned myocytes (24). Contemporary medications to treat heart failure, such as angiotensin-converting enzyme (ACE) inhibitors and beta-receptor blockers, may exert their beneficial effects by retarding or reversing maladaptive ventricular remodeling (26).

Familial Dilated Cardiomyopathy

Prior to 1992, the importance of hereditary factors in the pathogenesis of idiopathic DCM was not fully recognized. A focused family history identified a hereditary form of DCM in only 6% to 8% of cases (9). Moreover, when familial and nonfamilial cases of idiopathic DCM were compared, no differences in baseline clinical, serologic, histopathologic characteristics, or long-term outcome were observed to help distinguish familial cases (9,27,28). The concept of DCM as a genetic disorder received major impetus from a 1992 study in which first-degree relatives of index patients were screened by echocardiography (9). DCM was identified in presymptomatic members of several families, accounting for a 20% frequency of familial disease in this patient cohort. A similarly designed study identified familial disease in 25% of cases (29). In both studies, the average age at diagnosis in probands and their relatives was in the fourth to fifth decade, yet children in their first decade of life also were diagnosed with either symptomatic or clinically silent DCM. In children presenting with idiopathic

DCM, recent epidemiologic studies show an 8% to 19% frequency of familial disease despite lack of systematically applied family screening (4,5). If less stringent criteria, such as isolated left ventricular enlargement or sudden unexplained death, are used to diagnosis DCM in relatives, the frequency of familial DCM may be as high as 35% to 48% (15,30).

Familial DCM most commonly is inherited as an autosomal dominant trait, conferring a 50% risk of DCM for children of an individual with DCM (31). Less commonly, DCM is an X-linked disorder in males who have inherited a mutation from their mothers who exhibit only mild or no cardiac disease (32,33). Autosomal recessive and maternally inherited forms of DCM, as in disorders of cardiac energy metabolism (34), are relatively rare and frequently are associated with neuromuscular disease or metabolic derangements. Only one instance of autosomal recessive inheritance of nonsyndromic DCM has been reported (35).

Penetrance and Expression

Traits such as subtle skeletal myopathy, cardiac conduction system disease, and atrial arrhythmia segregate with DCM in certain families with autosomal dominant or X-linked disease (30,36–38). These phenotypic subtypes may suggest specific gene defects and predict progression of DCM (39). Most reports of familial DCM as an isolated disorder or as part of a syndrome, however, have shown age-dependent penetrance and variable expression of disease among members of the same family. Some carriers of a gene mutation may not have DCM or may have an intermediate cardiomyopathy phenotype, such as isolated left ventricular enlargement or conduction system disease. Consequently, interpretation of a normal or nondiagnostic screening echocardiogram and electrocardiogram in a child or adolescent at risk for familial DCM should take into account disease penetrance as low as 5% to 20% in this age group (40). Conversely, when a child presents in congestive heart failure, familial DCM may not be suspected because of variable expression, for example, a parent with a milder form of DCM who is asymptomatic (41,42). Collectively, family-based studies of DCM provide the rationale for clinical screening by echocardiography and electrocardiography in first-degree relatives, regardless of family history or age of the index case (9,15,16,31). Early diagnosis and treatment of asymptomatic DCM may prevent or attenuate heart failure (26). Moreover, in individuals with a recognized genetic predisposition to DCM, close surveillance and modification of acquired traditional risk factors can be implemented to reduce the overall risk burden for heart failure.

Dilated Cardiomyopathy Genes

Dramatic technologic advances in DNA and genomic analysis have evolved over the last half-century, beginning with Watson and Crick's discovery of the double helical structure of DNA and culminating in the decoding of the entire human genome through the Human Genome Project. These advances, together with the emerging recognition of DCM as a familial disorder (9), have culminated in discovery of mutations in 37 genes that cause or confer susceptibility to DCM (43–45) (Table 55.2). While a majority have been identified by hypothesis-based candidate gene approaches, unanticipated DCM genes have been revealed by genomic mapping in multigenerational families (32,37,38,48,50,57,66) or microarray-based “molecular karyotyping” (67). In a less restrictive classification scheme, which includes DCM associated with primary skeletal myopathies, multisystem

TABLE 55.2 Dilated Cardiomyopathy Genes

Locus	Gene Symbol, Protein	Protein Class	Cellular Defect (Fig. 55.1)	Variably Associated Phenotypes	Allelic Disorders	Primary References
1p31.1	<i>NEXN</i> , nexilin	Z-disc	A	None	HCM	46
1q21.2–q21.3	<i>LMNA</i> , lamin A/C	Nuclear membrane	C	Conduction defects, atrial arrhythmia, myopathy, CK	Six distinct disorders ^a	37
1q31–q42	<i>PSEN2</i> , presenilin 2	Gamma-secretase complex	G	None	Alzheimer disease	47
1q32	<i>TNNT2</i> , cardiac troponin T2	Thin filament of sarcomere	B	None	HCM, RCM, LVNC	48
1q42–q43	<i>ACTN2</i> , actinin, alpha 2	Z-disc, intercalated disc	A	None	None	49
2q31	<i>TTN</i> , titin	Sarcomeric cytoskeleton	A	None	HCM, primary skeletal myopathy	50
2q35	<i>DES</i> , desmin	Extrasarcomeric cytoskeleton	A	None	Primary skeletal myopathy, RCM	51
3p21	<i>SCN5A</i> , sodium channel, voltage-gated, type V, alpha	Voltage-gated ion channel	E	Conduction defects, atrial arrhythmia	Primary arrhythmia syndromes ^b	38
3p21.3–p14.3	<i>TNNC1</i> , troponin C, slow	Thin filament of sarcomere	B	None	HCM	52
4q35	<i>PDLIM3</i> , PDZ and LIM domain 3	Z-disc	A	None	None	53
5q33–q34	<i>SGCD</i> , delta sarcoglycan	Membrane-associated cytoskeleton	A	None	Primary skeletal myopathy	54
6q21	<i>LAMA4</i> , laminin, alpha 4	Extracellular matrix	F	None	None	55
6q22.1	<i>PLN</i> , phospholamban	Sarcoplasmic reticulum	E	None	HCM	56
6q23	<i>EYA4</i> , eyes absent homolog 4	Transcription coactivator	D	Sensorineural hearing loss	Sensorineural hearing loss	57
6q25	<i>SYNE1</i> , spectrin repeat containing, nuclear envelope 1	Nuclear membrane	C	None	Spinocerebellar ataxia, primary skeletal myopathy	58
7q31–q35	<i>CHRM2</i> , cholinergic receptor, muscarinic 2	G-protein-coupled receptor	E	Ventricular arrhythmia	None	59
10p12	<i>NEBL</i> , nebulin	Sarcomeric cytoskeleton	A	None	None	60
10q21.3	<i>MYPN</i> , myopalladin	Z-disc	A	None	None	61
10q22.1–q23	<i>VCL</i> , vinculin	Intercalated disc	A	None	HCM	62
10q22.3–q23.2	<i>LDB3</i> , LIM domain binding 3 (ZASP)	Z-disc	A	LV noncompaction	LVNC	63
10q23.31	<i>ANKRD1</i> , ankyrin repeat domain 1 (cardiac muscle)	Transcription corepressor	D	None	HCM	64,65
10q25.2	<i>RBM20</i> , RNA-binding protein motif protein 20	Spliceosome	D	None	None	66
10q25.2–q26.2	<i>BAG3</i> , BCL2-associated athanogene 3	Co-chaperone of heat shock proteins	G	None	Primary skeletal myopathy with HCM or RCM	67
11p15.4	<i>ILK</i> , integrin-linked kinase	Extracellular matrix	F	None	None	55

(Continued)

TABLE 55.2 Dilated Cardiomyopathy Genes (Continued)

Locus	Gene Symbol, Protein	Protein Class	Cellular Defect (Fig. 55.1)	Variably Associated Phenotypes	Allelic Disorders	Primary References
11p15.1	<i>CSRP3</i> , cardiac LIM protein (MLP)	Z-disc	A	None	HCM	68
11p11.2	<i>MYBPC3</i> , myosin-binding protein C, cardiac	Sarcomeric cytoskeleton	B	None	HCM	69
11q22.3–q23.1	<i>CRYAB</i> , crystallin, alpha B	Chaperone protein	G	None	Cataract, primary skeletal myopathy	70
12p12.1	<i>ABCC9</i> , sulfonylurea receptor 2A	ATP-sensitive ion channel	H	Ventricular arrhythmia	None	71
12q22	<i>TMPO</i> , thymopoietin	Nuclear membrane	C	None	None	72
14q12	<i>MYH7</i> , cardiac beta myosin heavy chain	Thick filament of sarcomere	B	None	HCM, RCM, LVNC	48
14q12	<i>MYH6</i> , cardiac alpha myosin heavy chain	Thick filament of sarcomere	B	None	HCM	73
14q24.3	<i>PSEN1</i> , presenilin 1	Gamma-secretase complex	G	None	Alzheimer disease	47
15q11–q14	<i>ACTC1</i> , cardiac actin	Thin filament of sarcomere	B	None	HCM, RCM, LVNC	41
15q22.1	<i>TPM1</i> , alpha-tropomyosin 1	Thin filament of sarcomere	B	None	HCM	42
17q12	<i>TCAP</i> , titin-cap (telethonin)	Z-disc	A	None	HCM, primary skeletal myopathy	74
19q13.4	<i>TNNI3</i> , troponin I, cardiac	Thin filament of sarcomere	B	None	HCM, RCM	35,75
Xp21.2	<i>DMD</i> , dystrophin	Membrane-associated cytoskeleton	A	Subclinical myopathy, CK	Primary skeletal myopathy	32,33

Genes for which DCM is only associated with primary skeletal myopathies, multisystem syndromes, or metabolic disorders are excluded.

*Charcot-Marie-Tooth disease, Emery-Dreifuss muscular dystrophy, familial partial lipodystrophy, Hutchinson-Gilford progeria syndrome, limb girdle muscular dystrophy, LVNC.

*Brugada syndrome, heart block, long QT syndrome 3, sick sinus syndrome, ventricular fibrillation, atrial fibrillation.

HCM, hypertrophic cardiomyopathy; CK, creatine kinase; LVNC, left ventricular noncompaction; ATP, adenosine triphosphate; RCM, restrictive cardiomyopathy.

syndromes, or metabolic disorders, an even larger number of genes have been identified (44). Mutations in known genes are estimated to account for only a third of cases (43), however, prompting continued research efforts to discover novel DCM genes. No common gene (genetic heterogeneity) or mutation (allelic heterogeneity) for DCM has emerged. However, targeted genetic testing of *LMNA* (encoding lamin A/C, a nuclear membrane protein) and *SCN5A* (encoding the cardiac sodium channel) may be justified in the subset of patients with DCM associated with atrial arrhythmia and conduction system disease (37,38). In addition, early-onset, clinically aggressive DCM has been reproducibly associated (albeit not invariably) with mutations in *TNNT2* (encoding cardiac troponin T) and *RBM20* (encoding RNA binding motif protein 20), and recurring mutations/mutation hot-spots have been identified in these genes (43,66). To address the challenge of marked genetic and allelic heterogeneity in DCM, chip-based resequencing arrays have been developed to facilitate efficient clinical genetic testing of many of the established DCM genes (76).

Knowledge of the molecular underpinnings of DCM continues to evolve with the identification of mutant genes that serve diverse functions within the heart, implicating perturbation of distinct biologic pathways in myopathic heart failure (see Table 55.2; Fig. 55.1). In a broad classification scheme, eight types of heritable myocellular defects have been linked to DCM: (a) disruption of cytoskeletal structure/integrity ($n = 13$); (b) altered contractile force transmission or generation ($n = 8$); (c) defective nuclear structure ($n = 3$); (d) altered gene transcription or translation ($n = 3$); (e) dysregulation of ion flux ($n = 3$); (f) disruption of extracellular matrix structure/integrity ($n = 2$); (g) impaired protein-protein interactions ($n = 4$); and (h) deficit in stress adaptation ($n = 1$). The emerging technology of next generation sequencing, enabling comprehensive mutation scanning of all genes, provides an unprecedented opportunity to complement traditional disease gene discovery strategies (77). Ongoing discovery of novel DCM genes, together with biochemical, cellular, and animal studies of DCM-associated mutant proteins, will continue to advance our understanding of the pathobiology of myopathic heart failure.

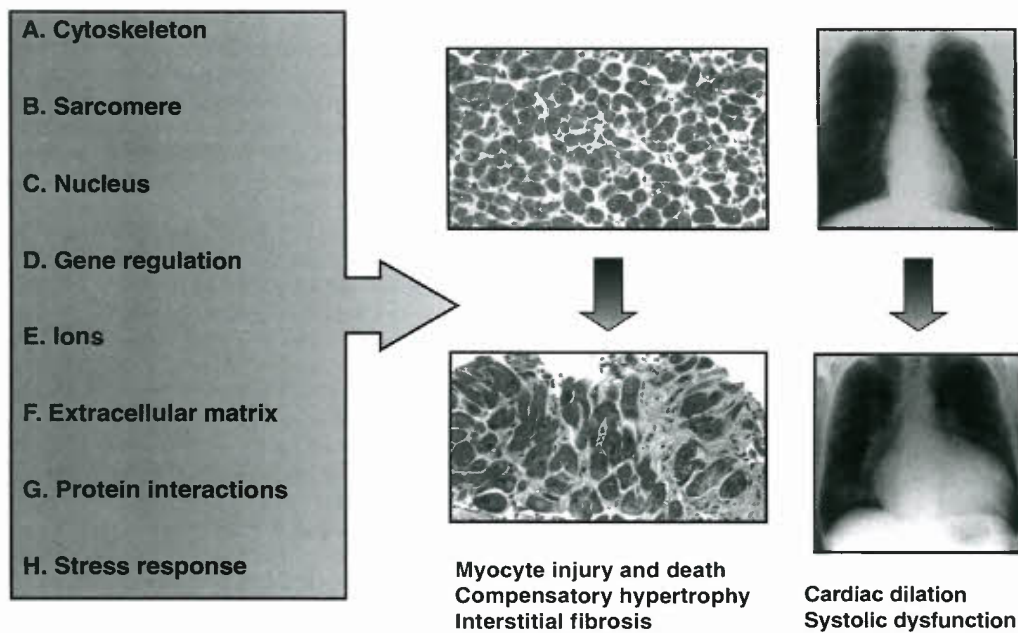


Figure 55.1. Defects in proteins governing diverse myocellular processes lead to cardiac remodeling and the phenotype of dilated cardiomyopathy. (Modified from Olson TM. Monogenic dilated cardiomyopathy. In: Walsh RA, ed. *Molecular Mechanisms of Cardiac Hypertrophy and Failure*. London: Taylor & Francis, 2005:525–540.)

Clinical Heterogeneity

Clinical and genetic overlap of familial DCM with other cardiac and noncardiac disorders is an established paradigm (Fig. 55.2). For example, mutations in the same gene can lead to muscular dystrophies with variable cardiac involvement or to DCM with subclinical skeletal muscle involvement, evident only by elevated serum muscle creatine kinase (32,33). Similarly, heritable defects in certain contractile and other proteins can cause dilated, hypertrophic, restrictive, or left ventricular noncompaction cardiomyopathy. The divergence of cardiac remodeling pathways into either dilated congestive heart

failure or pathologic cardiac hypertrophy can be attributable partially to mutation-specific effects. For instance, mapping of *cardiac actin* mutations in an atomic model of the actin-myosin complex indicated that hypertrophic cardiomyopathy-associated mutations were in myosin-binding domains critical for contractile force generation (41,78). In contrast, DCM-associated mutations were in anchoring domains that transmit contractile force from the thin filament to other myocellular proteins. The modifying effects of other genes also are important in cardiac remodeling pathways. This is exemplified by an animal model of genetic cardiomyopathy in which development of either dilated or hypertrophic cardiomyopathy

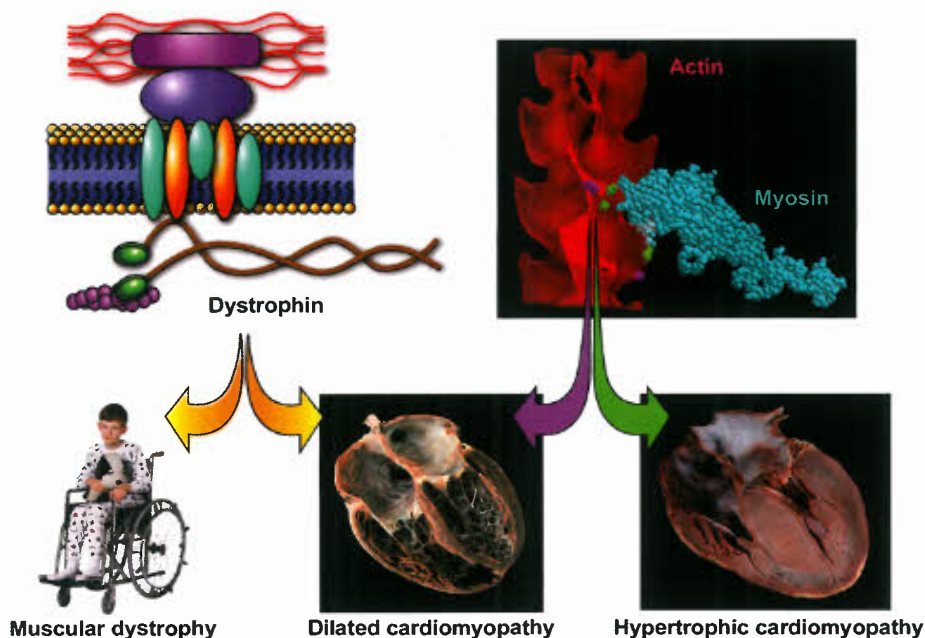


Figure 55.2. Heritable defects in dystrophin cause muscular dystrophy and/or dilated cardiomyopathy. Similarly, amino acid substitutions in cardiac actin cause either dilated cardiomyopathy (purple residues) or hypertrophic cardiomyopathy (green residues). (From Olson TM. Monogenic dilated cardiomyopathy. In: Walsh RA, ed. *Molecular Mechanisms of Cardiac Hypertrophy and Failure*. London: Taylor & Francis, 2005:525–540, with permission.)

depends on genetic background (79). This concept was established further by identification of similar or identical cardiac sodium channel mutations in humans that cause either isolated rhythm disorders or a syndrome of DCM, conduction disease, and atrial fibrillation (38).

CLINICAL FEATURES AND TREATMENT

History

Patients with DCM usually develop symptoms correlating with the degree of myocardial dysfunction. The onset of symptoms often is gradual unless it is due to acute viral myocarditis. Shortness of breath and exercise intolerance are the most common symptoms in the older child and are related to low cardiac output and pulmonary venous congestion. In severe cases, fulminant pulmonary edema may occur. In younger children, especially infants, the symptoms are often vague. They present with tachypnea, dyspnea, irritability, and poor feeding. Additional symptoms related to recent viral infections, signs of rheumatic fever, and Kawasaki disease may coexist in patients who develop a cardiomyopathy secondary to these inflammatory diseases. A history of dry skin and peripheral edema may indicate hypothyroidism.

A careful family history is critical to identify hereditary forms of DCM. Also, one must identify previous exposure to cardiac toxins, especially previous chemotherapeutic agents. Trypanosomiasis and Lyme disease should be suspected if recent travel into endemic areas has occurred. A history of cardiac surgical procedures and tachyarrhythmias should be determined.

Physical Examination

A child who has heart failure may be anxious, diaphoretic, tachycardic, and tachypneic. Grunting may result from efforts to minimize alveolar collapse secondary to pulmonary edema. Often, accessory muscles are recruited for increased respiratory effort. The older child often may have orthopnea. Wheezing is common. Of note, these patients will rarely respond to beta-receptor agonist aerosol treatments. Indeed, use of these agents may be detrimental owing to their possible arrhythmogenic potential.

The patient may be febrile because of an acute infectious illness that may be exacerbating symptoms that otherwise would be subtle. The patient's blood pressure can be low because of inadequate cardiac output. Invariably, the heart rate is elevated. If the tachycardia exceeds the maximum heart rate for age, supraventricular tachycardia or ventricular tachycardia should be considered. The oxygen saturation level often is within normal limits except in severe cases when pulmonary edema has affected normal gas exchange.

Palpation of the precordium usually demonstrates an apical impulse displaced downward and laterally. A right ventricular lift may be present as a result of elevated pulmonary artery pressure. The first heart sound often is normal, whereas the pulmonic component of the second heart sound may be increased. An S3–S4 gallop rhythm is often audible. However, the absence of a gallop rhythm may occur in a patient who is *in extremis* owing to severe congestive heart failure. If the heart sounds are distant, it is imperative to exclude pericardial effusion. Jugular venous distention may be present but is difficult to appreciate in young infants.

A murmur of mitral regurgitation is common. This murmur is coincident with the first heart sound and best heard at the apex and the left lower sternal border. It can be accentuated by having the patient lean forward while in the sitting position or lie in the left lateral position. With improved ventricular function in response to therapy, the murmur may become more prominent, and S3 and S4 may be heard.

A distended abdomen is common. The liver span is increased with descent of the liver edge. Occasionally there may be ascites. Pretibial edema can be present in older patients. The extremities may be cool and poorly perfused because of vasoconstriction. Capillary refill time can be increased.

Electrocardiogram

There usually is sinus tachycardia. The presence of incessant supraventricular or ventricular tachycardia should be treated aggressively because these rhythms are poorly tolerated in patients with DCM. Indeed, these tachyarrhythmias may be the cause of the cardiomyopathy. Left ventricular hypertrophy often is present and manifest by increased left precordial voltages (Fig. 55.3). Nonspecific ST-segment and T-wave abnormalities often are present. The presence of deep Q waves in leads I and aVL should suggest anomalous origin of the left coronary artery from the pulmonary artery.

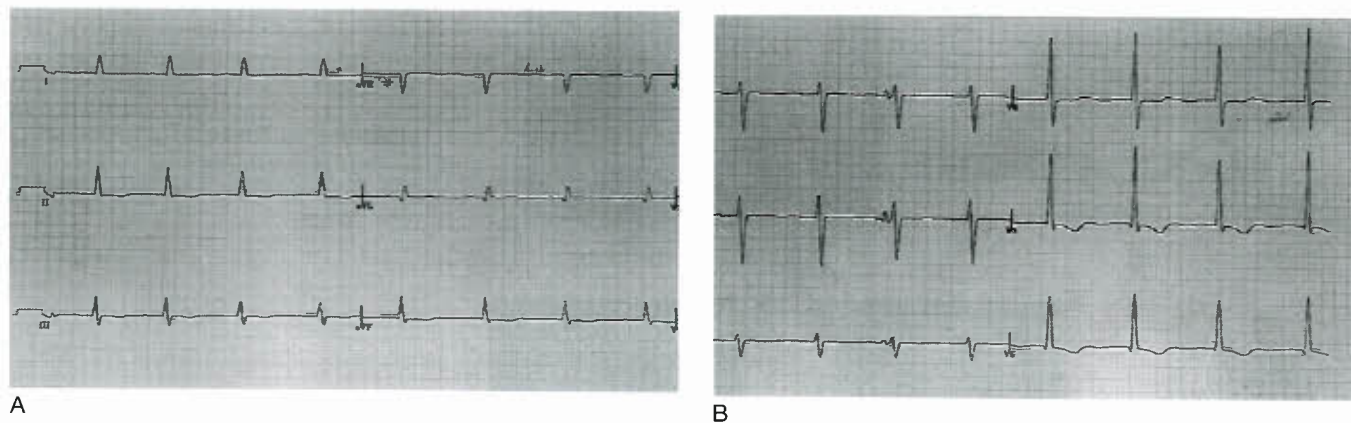


Figure 55.3. (A,B) correspond to limb leads and precordial leads, respectively. Twelve-lead electrocardiogram of a 14-year-old boy with severe dilated cardiomyopathy. Note the voltages are at one-quarter standard and the recording speed is 50 mm/s. There is severe left ventricular hypertrophy. There are also T-wave and ST-segment changes. An ectopic atrial beat is seen in leads V1, V2, and V3R.

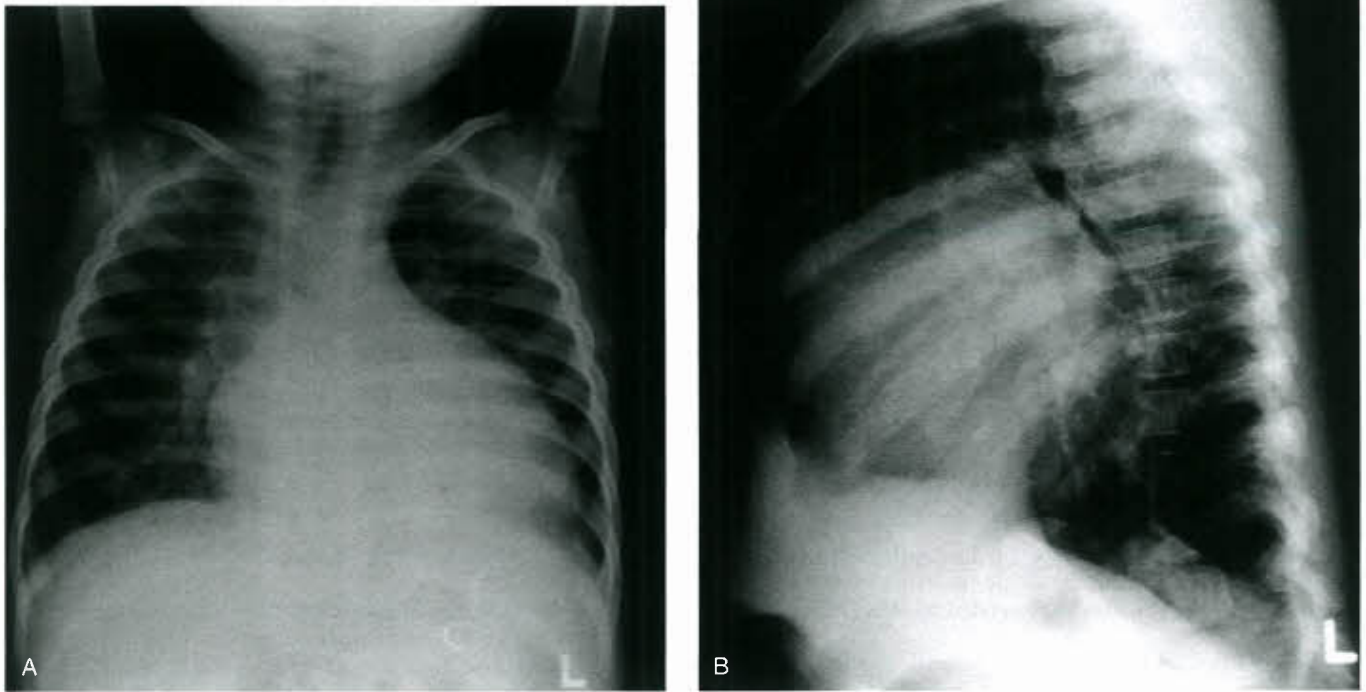


Figure 55.4. Posteroanterior (A) and lateral (B) chest roentgenograms of the same patient shown in Figure 55.3, demonstrating marked cardiomegaly, elevated left mainstem bronchus from left atrial enlargement, and pulmonary congestion.

Thoracic Roentgenography

The cardiothymic silhouette is enlarged mainly because of left atrial and ventricular dilation (Fig. 55.4). Left atrial enlargement may cause elevation of the left main stem bronchus. Pulmonary venous congestion and pulmonary edema often are evident. The pattern of the increased pulmonary vascular markings is reticular. Pleural effusion may be present, demonstrated by loss of the sharp posterior and lateral pleural angles. Lateral decubitus films better define the location and extent of any fluid collection.

Doppler Echocardiography

Echocardiography is an excellent noninvasive method for detecting DCM. The cardiac chambers, especially the left atrium and ventricle, are enlarged (Fig. 55.5). End-diastolic and end-systolic volumes are increased when indexed to body surface area. Systolic function is decreased and can be assessed by shortening fraction and ejection fraction. Segmental dyskinesia may suggest an ischemic cause for the cardiomyopathy. During diastole, nonapposition of the mitral valve to the interventricular septum can be measured as E-point septal separation. This displacement is most notable on M-mode echocardiography and reflects left ventricular enlargement. In severe cases, spontaneous echogenic signals result from slowly moving red blood cells and may predict an increased risk of spontaneous thrombosis. Occasionally, fibroelastosis may be demonstrated by an echo-bright appearance to the endocardium. Care should be taken to

document the origin of the coronary arteries, especially the left. The presence of diastolic flow in the main pulmonary artery toward the transducer may indicate the presence of anomalous pulmonary artery origin of the left coronary artery. Additional coronary artery abnormalities such as aneurysms or ectasia also should be identified. With DCM, the vena cavae and hepatic veins may be dilated. Pericardial and pleural effusion may be evident.

Mitral regurgitation is well demonstrated by color-flow Doppler imaging (Fig. 55.6). If tricuspid regurgitation is present, Doppler interrogation can estimate the right ventricular systolic pressure, and in the absence of right ventricular outflow obstruction, pulmonary arterial systolic pressure. Doppler interrogation of the ascending aorta may demonstrate decreased forward flow, and diastolic flow reversal may occur in the descending aorta.

Cardiac Catheterization

Indications for cardiac catheterization include documentation of coronary artery anatomy and endomyocardial biopsy. The presence of left ventricular thrombus is a relative contraindication for cardiac catheterization. Meticulous monitoring should be performed at all times. Catheter manipulation can result in arrhythmias, and the laboratory should be equipped to handle any emergencies.

A carefully planned hemodynamic study should include pressure measurements in the aorta, left ventricle, pulmonary capillary wedge position, and pulmonary artery. Cardiac output calculated by the Fick method or thermodilution

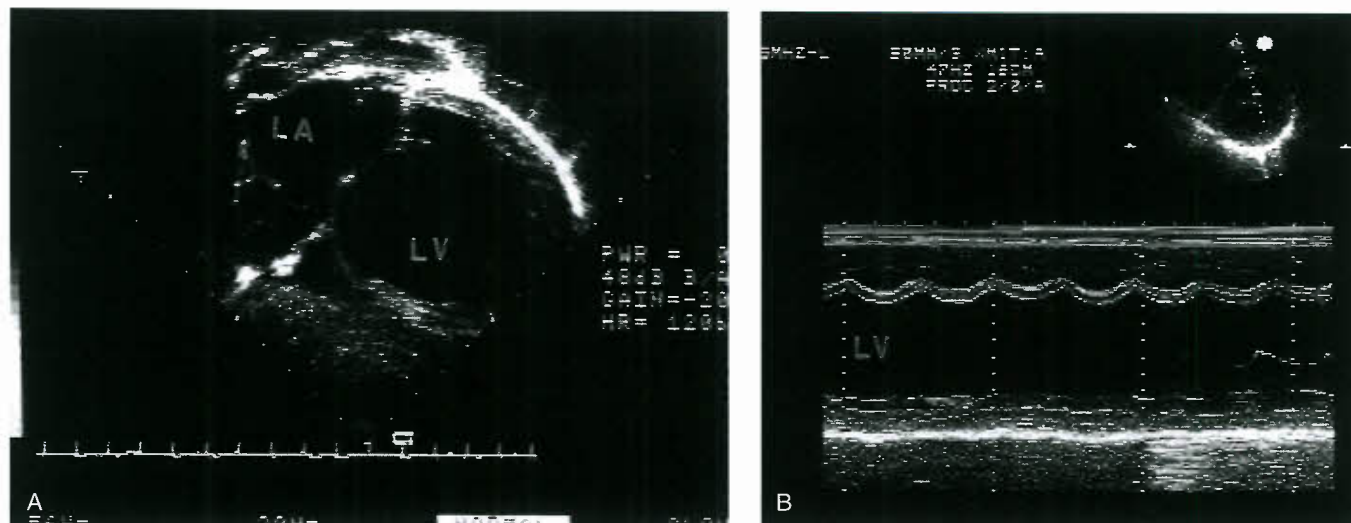


Figure 55.5. A: Two-dimensional echocardiographic findings of a patient with dilated cardiomyopathy. Note the severely dilated left atrium and ventricle. B: M-mode findings of another child with congestive cardiomyopathy. Note the large chamber dimensions and the depressed systolic wall motion. LA, left atrium; LV, left ventricle.

often will demonstrate a low cardiac index. Angiography should include an ascending aortic injection. Selective coronary angiography sometimes is needed to clearly define these vessels.

Endomyocardial biopsy may be helpful in determining the cause of the myopathy. Because of frequent nonuniformity of myocardial involvement, there can be false-negative results. Standard techniques using either the femoral or internal jugular vein approaches may be chosen depending on the experience of the operator. How the specimen is going to be used should be well defined prior to the biopsy so that unnecessary sampling can be avoided. After the biopsy is performed, a pericardial effusion from perforation of the thinned myocardium can be excluded by echocardiography.



Figure 55.6. Two-dimensional echocardiographic image with color-flow Doppler demonstrating severe mitral regurgitation seen in a case of severe dilated cardiomyopathy. (From Armstrong WF, Ryan T. *Feigenbaum's Echocardiography*, 7th ed. Philadelphia, PA: Lippincott Williams & Wilkins, 2010:519, with permission.)

Treatment

Please refer to other chapters on Chronic Congestive Heart Failure (Chapter 73) and Cardiac Intensive Care (Chapter 20) for comprehensive discussions of management of chronic heart failure and acute decompensated heart failure in children. This section provides a framework for treatment options, with specific issues unique to DCM, where necessary.

The clinical picture of a patient with symptomatic DCM usually consists of low cardiac output, fluid retention, and increased peripheral vasoconstriction owing to neurohumoral activation to maintain adequate perfusion pressure. The goals of medical therapy, therefore, are to address each of these issues. Additionally, if a metabolic abnormality is present, appropriate treatment should be started without delay. Recent practice guidelines for the management of heart failure in children have been reported. These recommendations largely represent expert consensus opinion in the absence of randomized clinical trials (80). Nonetheless, this document is the most contemporary consensus resource providing guidelines for care of heart failure in children.

Combined Inotropic and Vasodilator Support

The phosphodiesterase inhibitors milrinone and amrinone increase stroke work and cardiac output. Both systemic and pulmonary vascular resistances are decreased, and these drugs evoke unique lusitropic properties affecting relaxation and ventricular compliance. Because of untoward side effects, amrinone is no longer used. Milrinone, a bipyridine compound and derivative of amrinone, is the primary agent of choice. This drug is thought to promote increase in intracellular calcium concentration by inhibition of phosphodiesterase III. In studies done in adults, potential side effects included thrombocytopenia, hypotension, and arrhythmias. In children, the efficacy of milrinone is supported by the prevention of low cardiac output syndrome after biventricular repair (PRIMACORP multicenter trial). However, there have been no longitudinal studies in pediatric patients with cardiomyopathy and decompensated heart failure. In the PRIMACORP trial, milrinone did not have the same incidence of side effects that were reported in adults (81,82). Many clinicians use

milrinone for decompensated heart failure, often in combination with catecholamines such as dobutamine or dopamine. Synergistically, these medications may augment cardiac output via different mechanisms and may prove beneficial in lowering pulmonary vascular resistance. The half-life of milrinone varies depending on the age of the patient but generally is between 1 and 4 hours. The dose should be adjusted if there is renal impairment.

Levosimendan is a calcium-sensitizing agent that has been evaluated in adults with acute decompensated heart failure and in patients with chronic heart failure (83–86). This agent binds to troponin-C in cardiac myocytes and improves cardiac contractility. It also opens adenosine triphosphate (ATP)-sensitive potassium channels causing peripheral arterial and venous dilation. There is no increase in myocardial oxygen consumption or arrhythmias. Although initial experience with levosimendan was encouraging in both adults and children (87), results from a large prospective randomized trial failed to show any benefit of levosimendan over dobutamine in 180-day mortality or any other secondary outcomes (88).

Catecholamines

Sympathomimetic agents, such as dopamine, dobutamine, isoproterenol, and epinephrine, stimulate adrenergic receptors directly and/or indirectly. The average half-life of these medications is 2 to 7 minutes, and steady-state concentrations are reached in 10 to 15 minutes. Many patients are treated with beta-blockers such as carvedilol. One must be careful when administering catecholamines to patients receiving beta-blocking drugs because the alpha-adrenergic effects of the catecholamines may predominate in the presence of beta-blockade. Many clinicians consider phosphodiesterase inhibitors to be the treatment of choice for patients who are taking beta-blocker drugs. Milrinone retains its full hemodynamic effects in the presence of beta-blocker therapy.

Digoxin

Digoxin, a cardiac glycoside, is the primary long-term medication used to improve ventricular contraction. It blocks the $\text{Na}^+\text{-K}^+$ ATPase pump, resulting in increased intracellular calcium concentrations. Its effectiveness as an inotropic agent has been questioned, but it continues to be used widely. An additional potential benefit of digoxin may be its central nervous system effects that lessen sympathetic tone. This may decrease heart rate, allowing more efficient ventricular filling.

Digoxin should be used with caution in acutely ill children. In this group of patients who may have decreased renal function, drug toxicity can occur owing to decreased renal excretion of the medication. Additionally, some clinicians believe that the use of digoxin in patients with an inflamed myocardium may promote ventricular arrhythmias. Careful attention to normalize electrolytes, especially potassium, will help to minimize the potential for digoxin toxicity. There is evidence that lower serum concentrations of digoxin in adults may be safer and possibly more beneficial than higher serum concentrations (89,90). Use of digoxin has been controversial in many clinical situations in pediatric cardiology. Extrapolated from adult trials, digoxin is not recommended for pediatric patients who have asymptomatic left ventricular dysfunction, yet digoxin, in low doses, is recommended for those patients who are symptomatic (80).

Diuretics

Furosemide is the agent of choice in most patients with fluid overload. Its primary mode of action is to block electrolyte reab-

sorption at the loop of Henle. Thus, monitoring the electrolyte status is imperative. Hypokalemia can be avoided by using KCl supplementation or by the addition of spironolactone. Spironolactone, a weak diuretic, can help maintain potassium homeostasis by countering the actions of aldosterone. In adults, spironolactone was shown to improve survival (Randomized Aldactone Evaluation Study). This study was terminated early because patients had improved survival, reduction in hospitalizations, and improved New York Heart Association class (91). A similar survival benefit was found in the study of the newer aldosterone antagonist, eplerenone, in adults with heart failure (92). The potential mechanisms of this benefit are complex, and may be at least partially related to an attenuation of aldosterone-induced myocardial fibrosis or catecholamine release (93).

Other potent diuretics include ethacrynic acid and bumetanide. These drugs also act at the loop of Henle. The effects may be synergistic with other diuretics. As with furosemide, electrolyte imbalance can occur with aggressive diuresis. Excessive diuresis may reduce preload and lead to diminished cardiac output. Thiazides should be considered as additive therapy for those patients who become resistant to loop diuretics, or who require additional diuresis. A recent study failed to show any benefit of continuous infusion of diuretics over high-dose intermittent infusion of diuretics in adults with acute decompensated heart failure (94).

Vasodilator Agents

Nitroprusside and hydralazine effectively dilate peripheral vessels and decrease afterload, increase cardiac output, and decrease filling pressures. The action of both agents is relaxation of smooth muscle cells in the muscular layer of arterioles. Prolonged nitroprusside use can result in cyanide accumulation, a metabolic by-product of the drug. A possible side effect of hydralazine is a lupus-like reaction.

Effective orally administered afterload-reducing agents include ACE inhibitors. Captopril and enalapril are used most commonly in children. Other commonly used agents are monoproil, lisinopril, and quinapril. The choice depends on cost and dosage convenience. The actions of ACE inhibitors include decreased synthesis of angiotensin II, a potent vasoconstrictor, and decreased breakdown of bradykinins, which are potent vasodilators. Additional effects of these medications include sparing urinary potassium loss by inhibiting aldosterone secretion.

The use of ACE inhibitors has gained wide acceptance for treating children with DCM. This has been supported by large multicenter studies in adults that demonstrated improved survival in patients with chronic congestive heart failure treated with enalapril. Angiotensin receptor blockers have been studied in adult patients, but there are no data in pediatric patients with heart failure. Studies in adults have not shown significant differences between ACE inhibitors and angiotensin receptor blockers in either efficacy or safety. Angiotensin receptor blockers do not cause bradykinin accumulation and thus do not cause cough as a side effect as occurs with ACE inhibitors (80). In patients of African ancestry with DCM and heart failure, one may want to consider the use of isosorbide dinitrate and hydralazine (95).

Beta-Blocking Agents

Clinical trials have suggested that carvedilol, a drug that has both beta-receptor-blocking and vasodilating actions, improved the left ventricular performance and clinical status of adult patients with heart failure (96–100).

Both metoprolol and carvedilol use has been reported in children. Many of these early studies showed a beneficial effect in a subset of patients (101–104). However, in the prospective, randomized, multicenter trial of carvedilol in children with heart

failure, carvedilol failed to show a benefit over placebo (added to background therapy) on a composite endpoint of clinical heart failure outcomes in children with symptomatic heart failure (11). In a prespecified analysis, the response to carvedilol may be dependent on ventricular morphology, in that there was a significant difference in the degree of improvement in those whose systemic ventricle was a left ventricle compared with those whose systemic ventricle was a right or single ventricle.

Other Therapeutic Options

Antiplatelet and antithrombotic agents may have a role in the treatment of DCM. The propensity for thrombus formation in patients with large cardiac chambers and blood stasis may prompt the use of antiplatelet or antithrombotic agents such as aspirin, low molecular weight heparin, or warfarin. Certainly, if thrombi are detected, they should be treated aggressively with heparin and then with warfarin.

Bed rest may be helpful for the acutely ill child. Salt and free water intake may need to be restricted. Careful attention to daily weights is an effective gauge of diuretic therapy and the degree of fluid retention.

If carnitine deficiency is the cause of the cardiomyopathy, carnitine supplementation must be started without delay. Confirmatory diagnostic testing from urine and plasma sampling can still be performed with concurrent treatment of the presumed deficiency.

Antiarrhythmic drugs and/or radiofrequency ablation are used when the diagnosis of tachycardia-induced cardiomyopathy is established. The therapy of choice depends on the cause of the tachyarrhythmia. Many effective antiarrhythmics, such as procainamide, may have negative inotropic effects and should be used with caution in this group of patients. Ultimately, these patients should be considered for ablative therapy as a potential cure.

Cardiac Resynchronization Therapy

Resynchronization therapy in adult patients with a left bundle branch block (QRS duration ≥ 130 ms) and decreased ventricular function (ejection fraction $\leq 35\%$) has proven to be efficacious in improving symptoms and decreasing hospitalization rates (105,106). A few experiences with this therapy in pediatric patients, including those with congenital heart disease, have been published (107–109). Further studies are necessary before the usefulness of this type of treatment for children is known.

ICD Implantation

Implantation of a defibrillator for secondary prevention due to previous arrhythmic event is a fairly well-accepted practice (110). In contrast, primary prevention among children is not well established. Reports of ICD use in children with DCM are extremely limited. Extrapolation of indicators from large multicenter studies with adults should be done with caution as the heterogeneity of etiologies is quite different between the two age groups.

The obvious indication for ICD implantation is to prevent sudden cardiac death. A large single center study has reported only a 1% incidence of sudden death (111,112). This would suggest primary prevention in this cohort is usually not indicated. To further the difficulty in offering guidelines for primary prevention, the single case of sudden cardiac death did not have a history of sustained arrhythmias.

Cardiac Transplantation

For a more complete discussion of heart transplantation, see Chapter 65. Transplantation should be considered if short-term survival is unlikely or for severe symptoms unresponsive

to conventional therapy. Griffin et al. (113) identified age at presentation, presence of arrhythmias, and heart size as useful determinants of timing for cardiac transplantation. Lewis and Chabot (114) suggested that left ventricular end-diastolic pressure >25 mm Hg is a predictor of poor outcome and therefore an indication for earlier transplantation. In a multivariate analysis, investigators concluded that although pediatric patients with DCM may have one of many outcomes, recovery is the most frequent. The greatest risk of death or transplantation was associated with age younger than 1 year or older than 12 years, and female sex. With transplantation, 1- and 5-year actuarial survival for pediatric patients with DCM was 90% and 83%, respectively (115).

Natural History of Dilated Cardiomyopathy

The natural history of DCM in children is difficult to predict owing to the heterogeneous diseases that can result in cardiomyopathy. If the cause for the cardiomyopathy is identified and is treatable, such as carnitine deficiency, one should expect a high survival rate. Children with idiopathic DCM constitute the cohort of most studies that attempt to identify predictors of poor outcome. The actuarial survival rate in this group of patients is 63% to 90% at 1 year and 20% to 80% at 5 years (7,113–116). The cause of death usually involves ventricular arrhythmias and progressive intractable ventricular failure or, more rarely, complications of heart transplantation. Among the survivors, about half demonstrate an improvement in cardiac function. Taliercio et al. (119) reported that a history of viral symptoms within 3 months of presentation was associated with improved survival.

The presence of arrhythmias is not uniformly predictive of poor outcome. Indeed, patients may succumb at the time of their initial documented arrhythmia. However, patients with treatable arrhythmias, supraventricular or ventricular, had a higher survival rate when the arrhythmia was adequately controlled (114,118).

Intracardiac thrombi were identified in 16% to 23% of patients by thorough 2-D echocardiograms (119). In a study of autopsy specimens, 43% had thrombi (117). Although thrombus is not a predictor of survival, it does point to the importance of anticoagulation therapy and the potential morbidity in this group of patients.

Other suggested predictors of outcome include cardiothoracic ratio on chest roentgenograms, electrocardiogram abnormalities such as ST-T wave changes, left ventricular hypertrophy, left atrial enlargement, right atrial enlargement, and right ventricular hypertrophy. Unfortunately, none of these factors is a dependable predictor of survival.

REFERENCES

- Manolio TA, Baughman KL, Rodeheffer R, et al. Prevalence and etiology of idiopathic dilated cardiomyopathy (summary of a National Heart, Lung, and Blood Institute workshop). *Am J Cardiol* 1992;69:1458–1466.
- Dec GW, Fuster V. Idiopathic dilated cardiomyopathy. *N Engl J Med* 1994;331:1564–1575.
- Schwartz ML, Cox GF, Lin AE, et al. Clinical approach to genetic cardiomyopathy in children. *Circulation* 1996;94:2021–2038.
- Lipshultz SE, Sleeper LA, Towbin JA, et al. The incidence of pediatric cardiomyopathy in two regions of the United States. *N Engl J Med* 2003;348:1647–1655.
- Nugent AW, Daubeney PEF, Chondros P, et al. The epidemiology of childhood cardiomyopathy in Australia. *N Engl J Med* 2003;348:1639–1646.
- Foerster SR, Canter CE, Cinar A, et al. Ventricular remodeling and survival are more favorable for myocarditis than for idiopathic dilated cardiomyopathy in childhood: an outcomes study from the Pediatric Cardiomyopathy Registry. *Circ Heart Fail* 2010;3:689–697.
- Towbin JA, Lowe AM, Colan SD, et al. Incidence, causes, and outcomes of dilated cardiomyopathy in children. *JAMA* 2006;296:1867–1876.

8. Felker GM, Thompson RE, Hare JM, et al. Underlying causes and long-term survival in patients with initially unexplained cardiomyopathy. *N Engl J Med* 2000;342:1077–1084.
9. Michels VV, Moll PP, Miller FA, et al. The frequency of familial dilated cardiomyopathy in a series of patients with idiopathic dilated cardiomyopathy. *N Engl J Med* 1992;326:77–82.
10. Kirk R, Edwards LB, Kucheryavaya AY, et al. The Registry of the International Society for Heart and Lung Transplantation: thirteenth official pediatric heart transplantation report—2010. *J Heart Lung Transplant* 2010;29:1129–1141.
11. Shaddy RE, Boucek MM, Hsu DT, et al. Carvedilol for children and adolescents with heart failure: a randomized controlled trial. *JAMA* 2007;298:1171–1179.
12. Strauss A, Lock JE. Pediatric cardiomyopathy—a long way to go. *N Engl J Med* 2003;348:1703–1705.
13. Canter CE. Treating pediatric DCM—great expectations unfulfilled. *Nat Rev Cardiol* 2010;7:420–422.
14. Arola A, Tuominen J, Ruuskanen O, et al. Idiopathic dilated cardiomyopathy in children: prognostic indicators and outcome. *Pediatrics* 1998;101:369–376.
15. Baig MK, Goldman JH, Caforio ALP, et al. Familial dilated cardiomyopathy: cardiac abnormalities are common in asymptomatic relatives and may represent early disease. *J Am Coll Cardiol* 1998;31:195–201.
16. Michels VV, Olson TM, Miller FA, et al. Frequency of development of idiopathic dilated cardiomyopathy among relatives of patients with idiopathic dilated cardiomyopathy. *Am J Cardiol* 2003;91:1389–1392.
17. Gunja-Smith Z, Morales AR, Romanelli R, et al. Remodeling of human myocardial collagen in idiopathic dilated cardiomyopathy. Role of metalloproteinases and pyridinoline cross-links. *Am J Pathol* 1996;148:1639–1648.
18. Schaper J, Froede R, Hein ST, et al. Impairment of the myocardial ultrastructure and changes of the cytoskeleton in dilated cardiomyopathy. *Circulation* 1991;83:504–514.
19. Kajstura J, Zhang X, Liu Y, et al. The cellular basis of pacing-induced dilated cardiomyopathy. Myocyte cell loss and myocyte cellular reactive hypertrophy. *Circulation* 1995;92:2306–2317.
20. Bergmann O, Bhardwaj RD, Bernard S, et al. Evidence for cardiomyocyte renewal in humans. *Science* 2009;324:98–102.
21. Davies MJ. Apoptosis in cardiovascular disease. *Heart* 1997;77:498–501.
22. Missov E, Calzolari C, Pau B. Circulating cardiac troponin I in severe congestive heart failure. *Circulation* 1997;96:2953–2958.
23. Beltrami CA, Della-Mea V, Finato N, et al. Computer-assisted morphometric analysis of the heart. *Anal Quant Cytol Histol* 1996;18:129–136.
24. Weber KT, Brilla CG, Janicki JS. Myocardial remodeling and pathologic hypertrophy. *Hosp Pract* 1991;26:73–80.
25. Schaper J, Hein S. The structural correlate of reduced cardiac function in human dilated cardiomyopathy. *Heart Failure* 1993;9:95–111.
26. Eichhorn EJ, Bristow MR. Medical therapy can improve the biological properties of the chronically failing heart. A new era in the treatment of heart failure. *Circulation* 1996;94:2285–2296.
27. Michels VV. Genetics of idiopathic dilated cardiomyopathy. *Heart Failure* 1993;9:87–94.
28. Michels VV, Driscoll DJ, Miller FA, et al. Progression of familial and non-familial dilated cardiomyopathy: long term follow up. *Heart* 2003;89:757–761.
29. Keeling PJ, Gang Y, Smith G, et al. Familial dilated cardiomyopathy in the United Kingdom. *Br Heart J* 1995;73:417–421.
30. Grunig E, Tasman JA, Kucherer H, et al. Frequency and phenotypes of familial dilated cardiomyopathy. *J Am Coll Cardiol* 1998;31:186–194.
31. Hershberger RE, Siegfried JD. Update 2011: clinical and genetic issues in familial dilated cardiomyopathy. *J Am Coll Cardiol* 2011;57:1641–1649.
32. Towbin JA, Hejtmanic JF, Brink P, et al. X-linked dilated cardiomyopathy: molecular genetic evidence of linkage to the Duchenne muscular dystrophy (dystrophin) gene at the Xp21 locus. *Circulation* 1993;87:1854–1865.
33. Muntoni F, Cau M, Ganau A, et al. Deletion of the dystrophin muscle-promoter region associated with x-linked dilated cardiomyopathy. *N Engl J Med* 1993;329:921–925.
34. Hanna BD. Metabolic causes of pediatric heart failure. In: Shaddy RE, Wernovsky G, eds. *Pediatric Heart Failure*. Boca Raton, FL: Taylor & Francis, 2005:241–272.
35. Murphy RT, Mogensen J, Shaw A, et al. Novel mutation in cardiac troponin I in recessive idiopathic dilated cardiomyopathy. *Lancet* 2004;363:371–372.
36. Mestroni L, Rocco C, Gergori D, et al. Familial dilated cardiomyopathy: evidence for genetic and phenotypic heterogeneity. *J Am Coll Cardiol* 1999;34:181–190.
37. Fatkin D, MacRae C, Sasaki T, et al. Missense mutations in the rod domain of the lamin A/C gene as causes of dilated cardiomyopathy and conduction-system disease. *N Engl J Med* 1999;341:1715–1724.
38. Olson TM, Michels VV, Ballew JD, et al. Sodium channel mutations and susceptibility to heart failure and atrial fibrillation. *JAMA* 2005;293:447–454.
39. Taylor MR, Fain PR, Sinagra G, et al. Natural history of dilated cardiomyopathy due to lamin A/C gene mutations. *J Am Coll Cardiol* 2003;41:771–780.
40. Mestroni L, Krajcinovic M, Severini GM, et al. Familial dilated cardiomyopathy. *Br Heart J* 1994;72:S35–S41.
41. Olson TM, Michels VV, Thibodeau SN, et al. Actin mutations in dilated cardiomyopathy, a heritable form of heart failure. *Science* 1998;280:750–752.
42. Olson TM, Kishimoto NY, Whitby FG, et al. Mutations that alter the surface charge of alpha-tropomyosin are associated with dilated cardiomyopathy. *J Mol Cell Cardiol* 2001;33:723–732.
43. Hershberger RE, Morales A, Siegfried JD. Clinical and genetic issues in dilated cardiomyopathy: a review for genetics professionals. *Genet Med* 2010;12:655–667.
44. Menon SC, Olson TM, Michels VV. Genetics of familial dilated cardiomyopathy. *Prog Pediatr Cardiol* 2008;25:57–67.
45. Olson TM. Genetics of pediatric heart failure. In: Shaddy RE, Wernovsky G, eds. *Pediatric Heart Failure*. Boca Raton, FL: Taylor & Francis, 2005:137–170.
46. Hassel D, Dahme T, Erdmann J, et al. Nexilin mutations destabilize cardiac Z-disks and lead to dilated cardiomyopathy. *Nat Med* 2009;15:1281–1288.
47. Li D, Parks SB, Kushner JD, et al. Mutations of presenilin genes in dilated cardiomyopathy and heart failure. *Am J Hum Genet* 2006;79:1030–1039.
48. Kamisago M, Sharma SD, DePalma SR, et al. Mutations in sarcomere protein genes as a cause of dilated cardiomyopathy. *N Engl J Med* 2000;343:1688–1696.
49. Mohapatra B, Jimenez S, Lin JH, et al. Mutations in the muscle LIM protein and alpha-actinin-2 genes in dilated cardiomyopathy and endocardial fibroelastosis. *Mol Genet Metab* 2003;80:207–215.
50. Gerull B, Gramlich M, Atherton J, et al. Mutations of TTN, encoding the giant muscle filament titin, cause familial dilated cardiomyopathy. *Nat Genet* 2002;30:201–204.
51. Li D, Tapscott T, Gonzalez O, et al. Desmin mutation responsible for idiopathic dilated cardiomyopathy. *Circulation* 1999;100:461–464.
52. Mogensen J, Murphy RT, Shaw T, et al. Severe disease expression of cardiac troponin C and T mutations in patients with idiopathic dilated cardiomyopathy. *J Am Coll Cardiol* 2004;44:2033–2040.
53. Arola AM, Sanchez X, Murphy RT, et al. Mutations in PDLIM3 and MYOZ1 encoding myocyte Z line proteins are infrequently found in idiopathic dilated cardiomyopathy. *Mol Genet Metab* 2007;90:435–440.
54. Tsubata S, Bowles KR, Vatta M, et al. Mutations in the human β -sarcoglycan gene in familial and sporadic dilated cardiomyopathy. *J Clin Invest* 2000;106:655–662.
55. Knoll R, Postel R, Wang J, et al. Laminin-alpha4 and integrin-linked kinase mutations cause human cardiomyopathy via simultaneous defects in cardiomyocytes and endothelial cells. *Circulation* 2007;116:515–525.
56. Schmitt JP, Kamisago M, Asahi M, et al. Dilated cardiomyopathy and heart failure caused by a mutation in phospholamban. *Science* 2003;299:1410–1413.
57. Schonberger J, Wang L, Shin JT, et al. Mutation in the transcriptional coactivator EYA4 causes dilated cardiomyopathy and sensorineural hearing loss. *Nat Genet* 2005;37:418–422.
58. Puckelwartz MJ, Kessler EJ, Kim G, et al. Nesprin-1 mutations in human and murine cardiomyopathy. *J Mol Cell Cardiol* 2010;48:600–608.
59. Zhang L, Hu A, Yuan H, et al. A missense mutation in the CHRM2 gene is associated with familial dilated cardiomyopathy. *Circ Res* 2008;102:1426–1432.
60. Purevjav E, Varela J, Morgado M, et al. Nebulette mutations are associated with dilated cardiomyopathy and endocardial fibroelastosis. *J Am Coll Cardiol* 2010;56:1493–1502.
61. Duboscq-Bidor L, Xu P, Charron P, et al. Mutations in the Z-band protein myopalladin gene and idiopathic dilated cardiomyopathy. *Cardiovasc Res* 2008;77:118–125.
62. Olson TM, Illenberger S, Kishimoto NY, et al. Metavinculin mutations alter actin interaction in dilated cardiomyopathy. *Circulation* 2002;105:431–437.
63. Vatta M, Mohapatra B, Jimenez S, et al. Mutations in Cypher/ZASP in patients with dilated cardiomyopathy and left ventricular non-compaction. *J Am Coll Cardiol* 2003;42:2014–2027.
64. Moulik M, Vatta M, Witt SH, et al. ANKRD1, the gene encoding cardiac ankyrin repeat protein, is a novel dilated cardiomyopathy gene. *J Am Coll Cardiol* 2009;54:325–333.
65. Duboscq-Bidor L, Charron P, Ruppert V, et al. Mutations in the ANKRD1 gene encoding CARP are responsible for human dilated cardiomyopathy. *Eur Heart J* 2009;30:2128–2136.
66. Brauch KM, Karst ML, Herron KJ, et al. Mutations in ribonucleic acid binding protein gene cause familial dilated cardiomyopathy. *J Am Coll Cardiol* 2009;54:930–941.
67. Norton N, Li D, Rieder MJ, et al. Genome-wide studies of copy number variation and exome sequencing identify rare variants in BAG3 as a cause of dilated cardiomyopathy. *Am J Hum Genet* 2011;88:273–282.
68. Knoll R, Hoshijima M, Hoffman HM, et al. The cardiac mechanical stretch sensor machinery involves a Z disc complex that is defective in a subset of human dilated cardiomyopathy. *Cell* 2002;111:943–955.
69. Daehmlow S, Erdmann J, Kneupp T, et al. Novel mutations in sarcomeric protein genes in dilated cardiomyopathy. *Biochem Biophys Res Commun* 2002;298:116–120.
70. Inagaki N, Hayashi T, Arimura T, et al. Alpha B-crystallin mutation in dilated cardiomyopathy. *Biochem Biophys Res Commun* 2006;342:379–386.

71. Bienengraeber M, Olson TM, Selivanov VA, et al. ABCC9 mutations identified in human dilated cardiomyopathy disrupt catalytic KATP channel gating. *Nat Genet* 2004;36:382–387.
72. Taylor MR, Slavov D, Gajewski A, et al. Thymopoietin (lamina-associated polypeptide 2) gene mutation associated with dilated cardiomyopathy. *Hum Mutat* 2005;26:566–574.
73. Carniel E, Taylor MR, Sinagra G, et al. Alpha-myosin heavy chain: a sarcomeric gene associated with dilated and hypertrophic phenotypes of cardiomyopathy. *Circulation* 2005;112:54–59.
74. Hayashi T, Arimura T, Itoh-Satoh M, et al. Tcap gene mutations in hypertrophic cardiomyopathy and dilated cardiomyopathy. *J Am Coll Cardiol* 2004;44:2192–2201.
75. Carballo S, Robinson P, Orway R, et al. Identification and functional characterization of cardiac troponin I as a novel disease gene in autosomal dominant dilated cardiomyopathy. *Circ Res* 2009;105:375–382.
76. Zimmerman RS, Cox S, Lakdawala NK, et al. A novel custom resequencing array for dilated cardiomyopathy. *Genet Med* 2010;12:268–278.
77. Ng SB, Nickerson DA, Bamshad MJ, et al. Massively parallel sequencing and rare disease. *Hum Mol Genet* 2010;19:R119–R124.
78. Olson TM, Doan TP, Kishimoto NY, et al. Inherited and de novo mutations in cardiac actin cause hypertrophic cardiomyopathy. *J Mol Cell Cardiol* 2000;32:1687–1694.
79. Sakamoto A, Ono K, Abe M, et al. Both hypertrophic and dilated cardiomyopathies are caused by mutation of the same gene, delta-sarcoglycan, in hamster: an animal model of disrupted dystrophin-associated glycoprotein complex. *Proc Natl Acad Sci U S A* 1997;94:13873–13878.
80. Rosenthal D, Chrisant MRK, Edens E, et al. International Society for Heart and Lung Transplantation: practice guidelines for management of heart failure in children. *J Heart Lung Transplant* 2004;23:1313–1333.
81. Hoffman TM, Wernovsky G, Atz AM, et al. Trial designs: prophylactic intravenous use of milrinone after cardiac operation in pediatrics (PRIMA-CORP study). *Am Heart J* 2002;143:15–21.
82. Hoffman TM, Wernovsky G, Atz AM, et al. The efficacy and safety of milrinone in preventing low cardiac output syndrome in infants and children after corrective surgery for congenital heart disease. *Circulation* 2003;107:996–1002.
83. Follath F, Cleland JG, Just H, et al. Efficacy and safety of intravenous levosimendan compared with dobutamine in severe low-output heart failure (the LIDO study): a randomized double-blind trial. *Lancet* 2002;260:196–202.
84. Turanlahti M, Boldt T, Palkama T, et al. Pharmacokinetics of levosimendan in pediatric patients evaluated for cardiac surgery. *Pediatr Crit Care Med* 2004;5:457–462.
85. Parissis JT, Filippatos G, Farmakis D, et al. Levosimendan for the treatment of acute heart failure syndromes. *Expert Opin Pharmacother* 2005;6:2741–2751.
86. Earl GL, Fitzpatrick JT. Levosimendan: a novel inotropic agent for treatment of acute, decompensated heart failure. *Ann Pharmacother* 2005;39:1888–1896.
87. Namachivayam P, et al. Early experience with levosimendan in children with ventricular dysfunction. *Pediatr Crit Care Med* 2006;7:445–448.
88. Mebazza A, et al. Levosimendan vs dobutamine for patients with acute decompensated heart failure: the SURVIVE Randomized Trial. *JAMA* 2007;297:1883–1891.
89. Rathore SS, Curtis JP, Wang Y, et al. Association of serum digoxin concentration and outcomes in patients with heart failure. *JAMA* 2003;289:871–878.
90. Adams KF, Jr, Patterson JH, Gattis WA, et al. Relationship of serum digoxin concentration to mortality and morbidity in women in the digitalis investigation group trial: a retrospective analysis. *J Am Coll Cardiol* 2005;46:497–504.
91. Pitt B, Zannad F, Remme WJ, et al. The effect of spironolactone on morbidity and mortality in patients with severe heart failure. *N Engl J Med* 1999;341:709–717.
92. Pitt B, Remme W, Zannad F, et al. Eplerenone, a selective aldosterone blocker, in patients with left ventricular dysfunction after myocardial infarction. *N Engl J Med* 2003;348:1309–1321.
93. Ezekowitz JA, McAlister FA. Aldosterone blockade and left ventricular dysfunction: a systematic review of randomized clinical trials. *Eur Heart J* 2009;30:469–477.
94. Felker GM, Lee KL, Bull DA, et al. Diuretic strategies in patients with acute decompensated heart failure. *N Engl J Med* 2011;364:797–805.
95. Taylor AL, et al. Combination of isosorbide dinitrate and hydralazine in blacks with heart failure. *N Engl J Med* 2004;351:2049–2057.
96. Bristow MR, Gilbert EM, Abraham WT, et al. Carvedilol produces dose-related improvements in left ventricular function and survival in subjects with chronic heart failure. *Circulation* 1996;94:2807–2816.
97. Packer M, Bristow MR, Cohn JN, et al. The effect of carvedilol on morbidity and mortality in patients with chronic heart failure. *N Engl J Med* 1996;334:1349–1355.
98. CIBIS II Investigators. The Cardiac Insufficiency Bisoprolol study (CIBIS - II). *Lancet* 1999;353:9–13.
99. Hjalmarson A, Goldstein S, Fagerberg B, et al. Effect of metoprolol CR/XL in chronic heart failure: metoprolol CR/XL randomized intervention trial in congestive heart failure. *Lancet* 1999;353:2001–2007.
100. Packer M, Fowler MB, Roecker EB, et al. Effect of carvedilol on the morbidity of patients with severe chronic heart failure: results of the Carvedilol Prospective Randomized Cumulative Survival (COPERNICUS) study. *Circulation* 2002;106:2194–2199.
101. Shaddy RE, Olsen SL, Bristow MR, et al. Efficacy and safety of metoprolol in the treatment of doxorubicin-induced cardiomyopathy in pediatric patients. *Am Heart J* 1995;129:197–199.
102. Shaddy RE. Beta-blocker therapy in young children with congestive heart failure under consideration for heart transplantation. *Am Heart J* 1998;136:19–21.
103. Shaddy RE, Tani LY, Gidding SS, et al. Beta-blocker treatment of dilated cardiomyopathy with congestive heart failure in children: a multi-institutional experience. *J Heart Lung Transplant* 1999;18:269–274.
104. Bruns LA, Crisant MK, Lamour JM, et al. Carvedilol as therapy in pediatric heart failure: an initial multicenter experience. *J Pediatr* 2001;138:505–511.
105. Kass DA. Cardiac resynchronization therapy. *J Cardiovasc Electrophysiol* 2005;16:S35–S41.
106. Al-Khatib SM, Sanders GD, Mark DB, et al. Implantable cardioverter defibrillators and cardiac resynchronization therapy in patients with left ventricular dysfunction: randomized trial evidence through 2004. *Am Heart J* 2005;149:1020–1034.
107. Dubin AM, Janousek J, Rhee E, et al. Resynchronization therapy in pediatric and congenital heart disease patients: An international multicenter study. *J Am Coll Cardiol* 2005;46:2277–2283.
108. Greene EA, Berul CI, et al. Pacing treatment for dilated cardiomyopathy: optimization of resynchronization pacing in pediatrics. *Curr Opin Cardiol* 2010;25:95–101.
109. Cecchin F, Frangini PA, Brown DW, et al. Cardiac resynchronization therapy (and multisite pacing) in pediatrics and congenital heart disease: five years experience in a single institution. *J Cardiovasc Electrophysiol* 2009;20:58–65.
110. Silka MJ, Kron J, Dunnigan A, et al. Sudden cardiac death and the use of implantable cardioverter-defibrillators in pediatric patients. The Pediatric Electrophysiology Society. *Circulation* 1993;87:800–807.
111. Rhee EK, Canter CE, Basile S, et al. Sudden death prior to pediatric heart transplantation: would implantable defibrillators improve outcome? *J Heart Lung Transplant* 2007;26:447–452.
112. Dimas VV, Denfield SW, Friedman RA, et al. Frequency of cardiac death in children with idiopathic dilated cardiomyopathy. *Am J Cardiol* 2009;104:1574–1577.
113. Griffin ML, Hernandez A, Martin TC, et al. Dilated cardiomyopathy in infants and children. *J Am Coll Cardiol* 1988;11:139–144.
114. Lewis AB, Chabot M. Outcome of infants and children with dilated cardiomyopathy. *Am J Cardiol* 1991;68:365–369.
115. Tsirka AE, Trinkaus K, Chen SC, et al. Improved outcomes of pediatric dilated cardiomyopathy with utilization of heart transplantation. *J Am Coll Cardiol* 2004;44:391–397.
116. Chen SC, Nouri S, Balfour I, et al. Clinical profile of congestive cardiomyopathy in children. *J Am Coll Cardiol* 1990;15:189–193.
117. Akagi T, Benson LN, Lightfoot NE, et al. Natural history of dilated cardiomyopathy in children. *Am Heart J* 1991;121:1502–1506.
118. Friedman RA, Moak JP, Garson A. Clinical course of idiopathic dilated cardiomyopathy in children. *J Am Coll Cardiol* 1991;18:152–156.
119. Taliercio CO, Seward JB, Driscoll DJ, et al. Idiopathic dilated cardiomyopathy in the young: clinical profile and natural history. *J Am Coll Cardiol* 1985;6:1126–1131.

Jeffrey A. Towbin ■ Angela Lorts ■ John Lynn Jefferies

Myocarditis is an inflammatory disease of the myocardium with necrosis and/or degeneration of adjacent myocytes not typical of the ischemic damage associated with coronary artery disease (1). This definition does not take into account the underlying causative mechanism of disease.

ETIOLOGY

Many cases of myocarditis remain unrecognized because they may have a nonspecific or benign presentation leaving the true incidence of myocarditis unknown. However, in those children presenting with dilated cardiomyopathy (DCM), myocarditis (46%) is the most frequent *known* cause for this newly diagnosed myocardial disease (2). Cases that are definitively diagnosed as myocarditis in developed countries are most commonly a result of a viral infection diagnosed by the molecular biologic amplification method called polymerase chain reaction (PCR) from an endomyocardial biopsy (EMB) (3–6). The true incidence of viral-induced myocardial inflammation is difficult to predict since children with new-onset DCM are infrequently biopsied due to the small but measurable risk of myocardial perforation or the development of untoward hemodynamic or arrhythmic events during the catheterization and biopsy. However, using data from both pediatric and adult centers, it has been shown that the most common virus detected, in those patients who have had a biopsy, has shifted with each decade. In the 1970s and 1980s, coxsackievirus was the most common viral etiology in both adult and pediatric patients, but in the 1990s and early 2000s, the most common viral causes included adenovirus (especially serotypes 2 and 5) (7,8) and enterovirus (coxsackieviruses A and B, echovirus, and poliovirus), particularly coxsackievirus B (CVB) (9,10) (Table 56.1). Most recently, parvovirus B19 (PVB19) has become the most commonly identified virus in patients with myocarditis (11–17). Many reports have shown a strong association between inflammation, coronary artery inflammation and insufficiency, and resulting systolic dysfunction with PVB19 infection, but interestingly, approximately 50% of adult patients with isolated diastolic dysfunction were also found to be PCR positive for a viral genome, most commonly PVB19 (17).

Although there is an era effect, many other viral causes of myocarditis (18) have been described, including influenza A (19), influenza H1N1 (20,21), cytomegalovirus (CMV) (22), herpes simplex type 2 (HSV) (23), hepatitis C virus (24,25), rubella (26), varicella (27), mumps (28), Epstein-Barr virus (EBV) (29), human immunodeficiency virus (HIV) (30), human herpesvirus (HHV6) (31), respiratory syncytial virus (32), among others. Other nonviral causes include other infectious agents such as rickettsiae, bacteria, protozoa, and other parasites, fungi, and yeasts (Table 56.2) (33–44); various drugs, including antimicrobial medications (45); hypersensitivity,

autoimmune, or collagen-vascular diseases (46–48) such as systemic lupus erythematosus, mixed connective tissue disease, rheumatic fever, rheumatoid arthritis, and scleroderma; toxic reactions to infectious agents (49) (e.g., mumps or diphtheria); or other disorders such as Kawasaki disease and sarcoidosis (Table 56.3) (50,51).

EPIDEMIOLOGY

Myocarditis is an underdiagnosed entity, but estimates of the incidence can be made via review of autopsy results. In the large multicenter Myocarditis Treatment trial, there was a reported incidence of myocarditis in 9% of adult patients (52). A review of all autopsies in children ($n = 1,516$) at a single center over a 10-year period demonstrated that only 1.8% of postmortem exams were consistent with myocarditis. Of the positive cases, 57% had presented with sudden cardiac death (6). Viral myocarditis is a major cause of unexpected death in persons <40 years of age and may progress to DCM, which is a major health concern worldwide (53,54).

Usually sporadic, viral myocarditis can also occur as an epidemic, correlating with viral outbreaks (55). In children and adults, outbreaks usually occur in a seasonal distribution.

In pediatrics, the prevalence of virus-associated myocarditis is highest in the neonatal period, and the most common etiology in this age group was previously CVB, but PVB19 has been important this past decade as well. In the case of CVB, the neonatal infection can be secondary to intrauterine exposure or postnatal spread of coxsackievirus via the fecal/oral or airborne route. Other important viral causes, such as PVB19, adenovirus, and influenza A, are transmitted through the air.

CLINICAL MANIFESTATIONS

Presentation depends on the age of the child (4,18,56). Nonspecific flu-like illness or episodes of gastroenteritis may precede symptoms of congestive heart failure.

Newborns and Infants

Newborns or infants present with poor appetite, vomiting, fever, irritability or listlessness, pallor, and diaphoresis. Sudden death may occur in this subgroup of children (57). On physical examination, pallor, in addition to classic signs of congestive heart failure, such as hepatomegaly, tachypnea, tachycardia, and occasionally a gallop, is commonly noted. It is important to keep in mind that the younger the child, the more likely it is that intrauterine myocarditis is now expressed as a chronic disease (18,49).

TABLE 56.1 Viral Causes of Myocarditis

Enterovirus	Varicella
Coxsackie A	Mumps
Coxsackie B	Measles
Echovirus	Rabies
Poliovirus	Hepatitis B, C
Adenovirus	Rubella
Parvovirus B19	Rubeola
Cytomegalovirus	Respiratory syncytial virus
Herpesvirus	Human immunodeficiency virus
Influenza A and H1N1	Epstein-Barr virus
Human herpesvirus 6	

Children and Adolescents

Older children and adolescents commonly have a recent history of viral disease 10 to 14 days prior to presentation. Initial symptoms include lethargy, low-grade fever, and pallor; the child usually has decreased appetite and associated vomiting with complaints of episodic abdominal pain. Diaphoresis, palpitations, rashes, exercise intolerance, and general malaise are common signs and symptoms. Later in the course of illness, respiratory symptoms become predominant; syncope or sudden death may occur owing to cardiac collapse. Physical examination findings are consistent with congestive heart failure (8), as

described above. Unlike in newborns, jugular venous distention and pulmonary rales may be observed, and resting tachycardia may be prominent. Occasional ectopy and arrhythmias including atrial fibrillation, supraventricular tachycardia, ventricular tachycardia, and atrioventricular block may occur (56) (Fig. 56.1).

DIAGNOSTIC TESTS

The diagnosis of myocarditis is often difficult to establish but should be suspected in any infant or child who presents with unexplained congestive heart failure or ventricular tachycardia. Each patient must be approached individually recognizing the availability of modalities at the managing institution with the diagnostic evaluation including the following tests.

Chest Radiography

Chest radiography is routinely performed in the evaluation of patients with clinical suspicion of myocarditis. Cardiomegaly is often present with well-described prominent vascular markings of pulmonary edema consistent with left-sided heart failure (Fig. 56.2). There may also be evidence of right ventricular dilation with loss of the retrosternal space on a lateral view if there is biventricular involvement or severe left ventricular disease. Patients with chronic myocarditis may have evidence of left atrial dilation that can result in widening of the carinal angle which is typically <75 degrees. However, a normal radiograph may be seen if the patient presents early in the course.

Electrocardiography

Sinus tachycardia with or without low-voltage QRS complexes and/or inverted T waves is classically described (Fig. 56.3A).

TABLE 56.2 Nonviral Causes of Myocarditis

Rickettsial	Protozoal	Fungi and Yeasts
<i>Rickettsia rickettsii</i>	<i>Trypanosoma cruzi</i>	Actinomycosis
<i>Rickettsia tsutsugamushi</i>	Toxoplasmosis	Coccidioidomycosis
	Amebiasis	Histoplasmosis
		<i>Candida</i>
Bacterial	Other Parasites	
Meningococcus	<i>Toxocara canis</i>	
<i>Klebsiella</i>	Schistosomiasis	
<i>Leptospira</i>	Heterophyiasis	
Mycoplasma	Cysticercosis	
<i>Salmonella</i>	<i>Echinococcus</i>	
Clostridia	Visceral larva migrans	
Tuberculosis	Trichinosis	
<i>Brucella</i>		
<i>Legionella pneumophila</i>		
Streptococcus		
Smallpox		

TABLE 56.3 Causes of Myocarditis: Noninfectious Etiologic Agents

Toxic	Hypersensitivity/Autoimmune
Scorpion	Rheumatoid arthritis
Diphtheria	Rheumatic fever
	Ulcerative colitis
	Systemic lupus erythematosus
	Mixed connective tissue disease
	Scleroderma
	Whipple disease
Drugs	Other
Sulfonamides	Sarcoidosis
Phenylbutazone	Kawasaki disease
Cyclophosphamide	Cornstarch
Neomercazole	
Acetazolamide	
Amphotericin B	
Indomethacin	
Tetracycline	
Isoniazid	
Methyldopa	
Phenytoin	
Penicillin	

A pattern of myocardial injury or infarction may be seen with changes in ST segments (Fig. 56.3B). These changes may be diffuse or in a defined coronary distribution pattern. With sufficient time and myocardial damage, Q waves may also be seen and are commonly wide and notched. Pericarditis may also accompany the clinical picture with resultant diffuse ST segment elevation. Ventricular arrhythmias including ventricular tachycardia (Fig. 56.3C) and fibrillation, supraventricular tachycardias and atrial fibrillation, or conduction system disease including atrioventricular block (Fig. 56.3D) may occur in some patients and may even be the presenting complaint (58).

Echocardiography

Echocardiography is widely used in the assessment of suspected myocarditis because it is readily available at most institutions. Assessment of chamber size, ventricular thickness, and systolic function has been classically pursued as part of the evaluation as well as evaluation for pericardial effusion (PE). This includes described views with the use of Z-scores based on normal calculations for body surface area. In addition, assessment for segmental wall motion abnormalities is advocated as there may be regional dysfunction in the setting of a normal shortening fraction (SF) and/or ejection fraction (EF). Newer echocardiographic modalities have greatly enhanced the ability to assess diastolic function and should be pursued when possible. A dilated and dysfunctional left ventricle consistent with DCM is often seen on two-dimensional (Fig. 56.4A,B) and M-mode echocardiography (Fig. 56.4C) (59). Segmental wall motion abnormalities are relatively common, but global hypokinesis is predominant. PE frequently occurs. Doppler and color Doppler commonly demonstrate mitral regurgitation (Fig. 56.4A). Dilation of other chambers also may be seen. Newer strategies that assess regional myocardial deformation such as strain and strain rate imaging may offer opportunities to detect myocardial inflammation prior to overt changes in regional or global systolic function (60).

Serologic Testing

Serologic markers are increasingly used to identify ongoing myocardial damage and may offer insight into future prognosis. However, there are no current serologic biomarkers that clearly differentiate myocarditis from other causes of acute myocardial dysfunction such as ischemia. Traditional markers of myocardial cell lysis such as creatine kinase (CK), creatine kinase myocardial band (CKMB), and troponin may be elevated in acute myocarditis and are readily available at the majority of hospitals. The identification of elevated troponin I levels may assist in the identification of pediatric patients with myocarditis but may not be as helpful in predicting outcomes as in the adult with myocardial infarction. (61,62) In actuality, troponin measurements may only be elevated in 35% to 45% of biopsy-proven myocarditis cases. (63) There are increasing reports describing the utility of B-type natriuretic peptide (BNP) in children. Mlczech et al. (64) recently reported serial measurement of NT-pro BNP in children with acute myocarditis and found them to be elevated at time of presentation and that they decreased over the following year with appropriate medical therapy. In addition, nontraditional cardiac biomarkers to assess end-organ function may be of benefit to assist in evaluation for perfusion as well as aiding in the decision to pursue mechanical support (65).

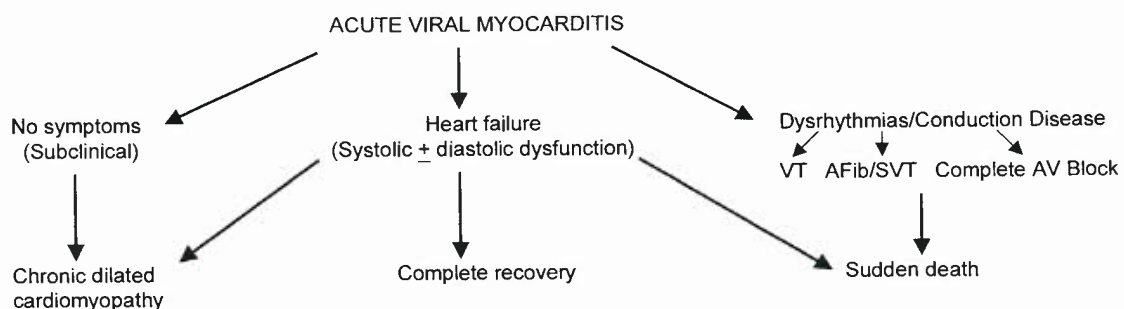


Figure 56.1. Clinical presentation of myocarditis. AFib, atrial fibrillation; AV, atrioventricular; SVT, supraventricular tachycardia; VT, ventricular tachycardia.

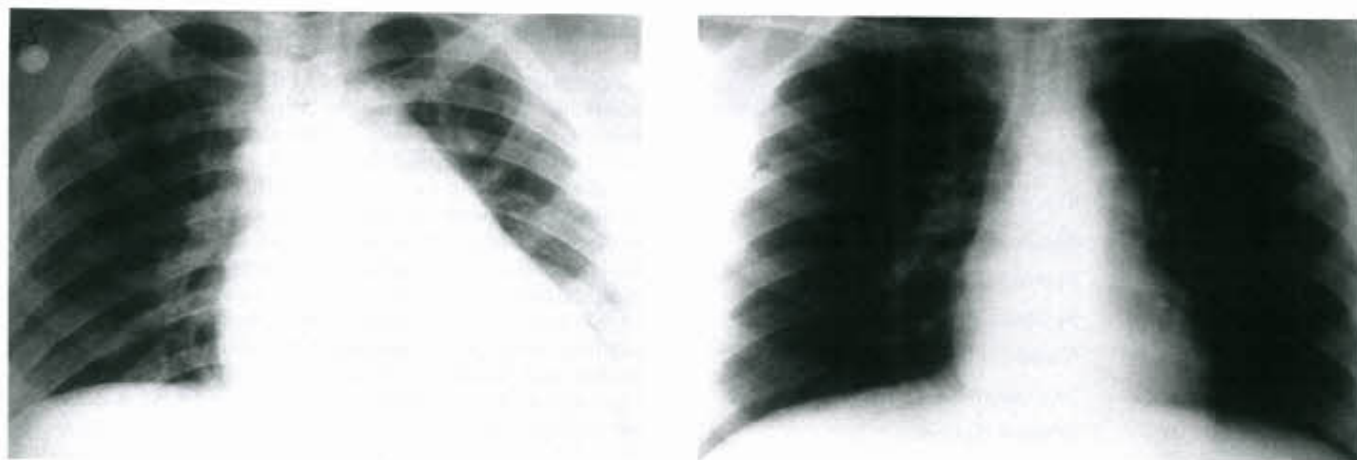


Figure 56.2. Chest radiograph in a child with acute myocarditis. **Left:** Initial radiograph demonstrating cardiomegaly and increased pulmonary vascular markings consistent with pulmonary edema. **Right:** Radiograph obtained 6 months after initial presentation demonstrates normalization of heart size and lung markings.

Magnetic Resonance Imaging

Advanced imaging techniques have greatly enhanced the opportunities to characterize myocardial inflammation in patients with myocarditis as well as predict all-cause and cardiac mortality. Cardiovascular magnetic resonance (CMR) imaging offers a noninvasive strategy that reports reproducible volumetric and functional data as well as localizing areas of myocardial inflammation and edema. Specific techniques for myocardial characterization have been developed including T2-weighted imaging to localize myocardial edema and T1-weighted contrast enhanced fast spin echo images for hyperemic responses. Furthermore, with the use of gadolinium, late gadolinium enhancement (LGE) can be obtained on technically feasible patients, which will localize areas of irreversible myocardial injury (necrosis and fibrosis) (66). A recent report described 203 consecutive adult patients with biopsy-proven myocarditis who also underwent CMR on presentation as well as during clinical follow-up. The presence of LGE resulted in hazard ratios of 8.4 and 12.8 for all-cause mortality and cardiac mortality, respectively. This was a more robust predictor than the typical echocardiographic markers typically assessed including left ventricular EF and LV end-diastolic volume. Furthermore, no subject without presence of LGE was found to have sudden cardiac death (67). CMR offers a unique modality to follow patients with myocarditis longitudinally assessing for reversible/irreversible myocardial injury, myocardial viability, favorable remodeling, and scar burden (68). All of these findings may have impact on clinical decision making including response to therapy and need for advanced interventions such as implantable cardioverter defibrillators as well as need for cardiac transplantation.

Endomyocardial Biopsy

The gold standard for identification of the underlying cause of acute and chronic myocarditis remains the analyses performed on tissue obtained by EMB. These tests include routine histologic examination as well as targeted immunohistochemical analysis. In addition, we perform viral PCR analysis on all EMB samples, given the inherent limitations of the existing Dallas criteria used for diagnosis (69). Cardiac catheterization typically demonstrates low cardiac output and elevated ventricular end-diastolic pressures in patients with significant myocardial involvement. EMB (Fig. 56.5) from

the right ventricle is evaluated for inflammation (Fig. 56.6). The inflammatory infiltrate is usually patchy and scattered in the ventricular myocardium. A mononuclear cell infiltrate is diagnostic of myocarditis, although this does not delineate cause. EMB is diagnostically sensitive in 3% to 63% of cases (70–73). Because of the reported insensitivity of biopsy, Chow et al. (72) and Hauck et al. (73) reported that to identify 80% of cases, 17 or more specimens must be obtained. Because there is risk associated with EMB, particularly in young children or those with thinning of the ventricular wall and/or active inflammation, many centers have abandoned this procedure. However, in experienced centers, the risk associated with EMB is quite low in children of all age groups (74). It should be noted that foci of inflammation may be seen in all forms of cardiomyopathy, irrespective of etiology, due to the disruption of cardiomyocytes as part of the pathophysiology and cellular biology of the disease. These are not cases of myocarditis in the usual sense.

The Dallas Criteria

The Dallas Criteria define myocarditis as “a process characterized by an inflammatory infiltrate of the myocardium with necrosis and/or degeneration of adjacent myocytes not typical of ischemic damage” owing to coronary artery or other disease (75). At the time of initial EMB, a specimen may be classified as active myocarditis, borderline myocarditis, or no myocarditis, depending on whether an inflammatory infiltrate occurs in association with myocyte degeneration or necrosis (active), too sparse an infiltrate, or no myocyte degeneration (borderline) (75). Repeat EMB may be appropriate in cases where strong suspicion of myocarditis exists clinically; on repeat EMB, histology may be classified as ongoing myocarditis, resolving myocarditis, or resolved myocarditis. However, increasing evidence has led to more extensive studies on EMB samples including histopathology, immunohistochemistry, viral PCR, and cardiac antibody testing to better make the diagnosis of myocarditis.

Viral Studies

A positive viral culture from the myocardium has been considered the diagnostic standard in the past. Viral culture of peripheral specimens, such as blood, stool, or urine, is commonly

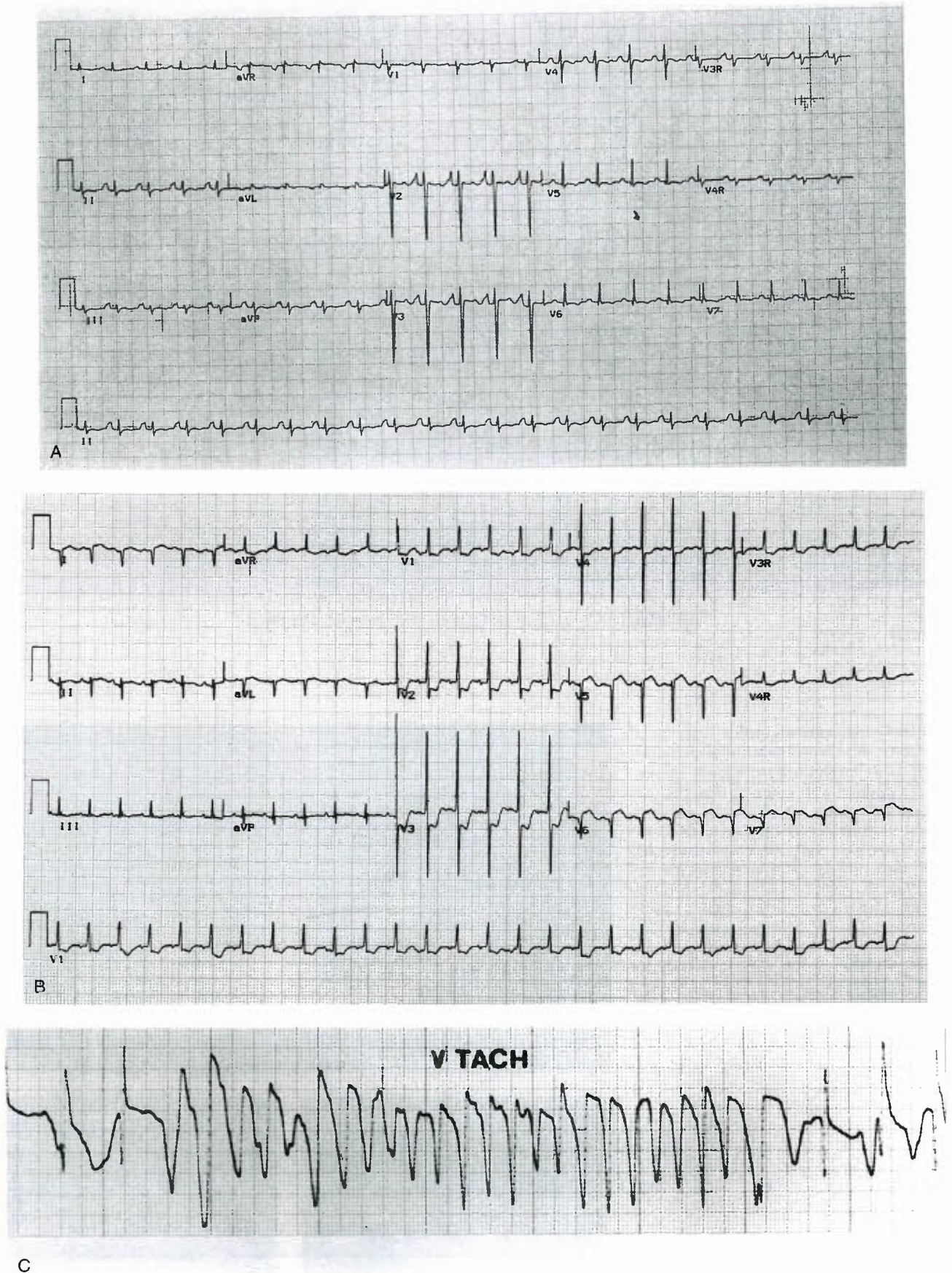


Figure 56.3. Electrocardiogram in a case of myocarditis. A: Sinus tachycardia and low-voltage QRS complexes with inverted T waves. B: Pattern of myocardial infarction with wide Q waves in leads I and aVL, and ST-segment changes consistent with ischemia noted throughout. C: Ventricular tachycardia. (*Continued*)

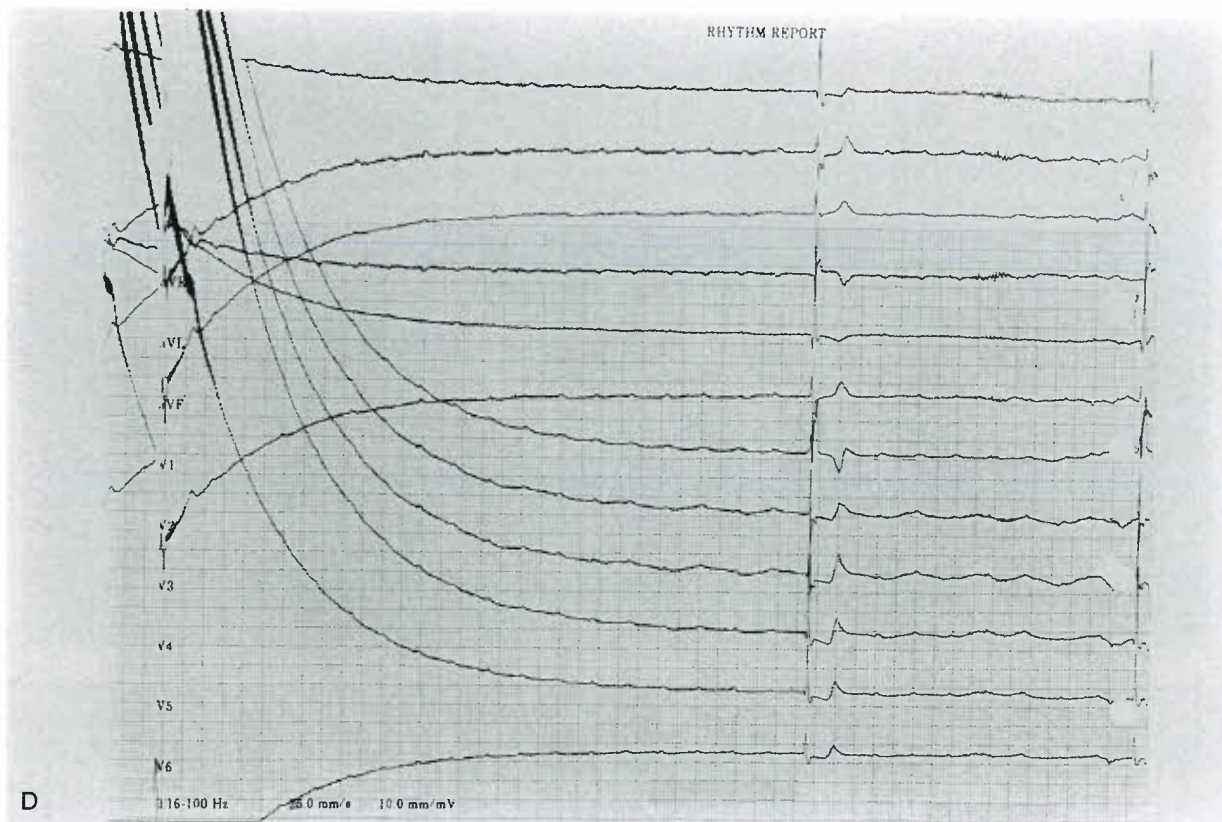
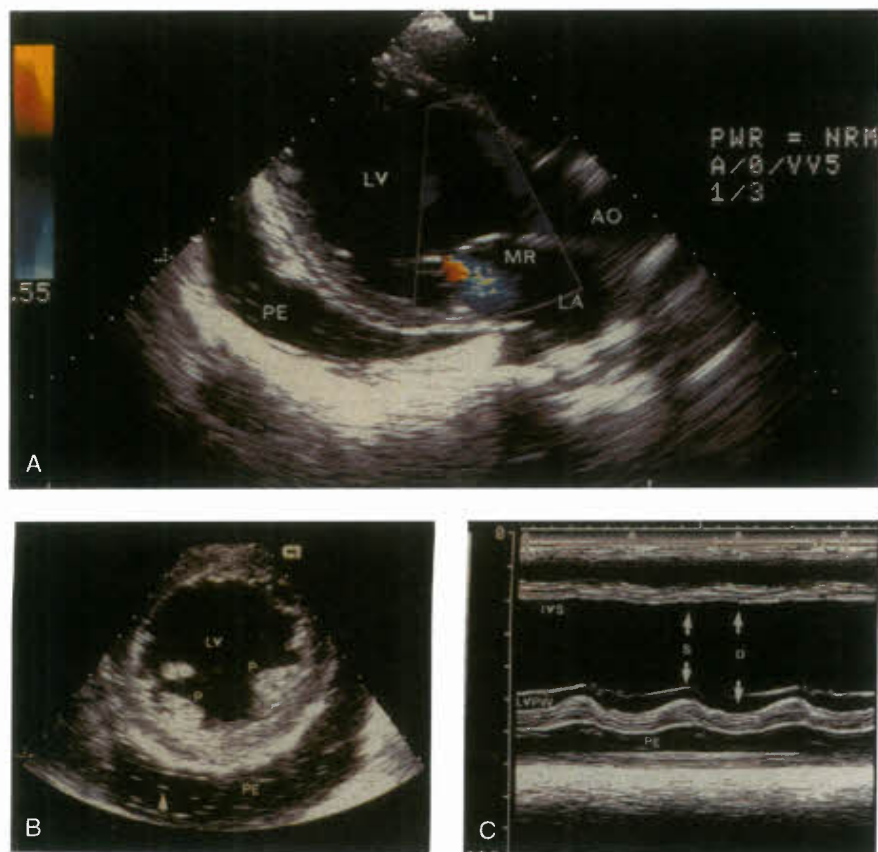


Figure 56.3. (Continued) D: Complete atrioventricular block.

Figure 56.4. Echocardiographic features of myocarditis. **A:** Two-dimensional parasternal long-axis view demonstrating left ventricular (LV) dilation and a pericardial effusion (PE). Color Doppler interrogation provides evidence of mitral regurgitation. **B:** Parasternal short-axis view demonstrating LV dilation and normal papillary muscles (P). **C:** M mode demonstrating systolic dysfunction with flattened interventricular septal (IVS) motion, fair LV posterior wall (LVPW) excursion, LV dilation with increased LV end-diastolic dimension (D), and reduced systolic function (S) and PE. Ao, aorta; LA, left atrium; MR, mitral regurgitation.



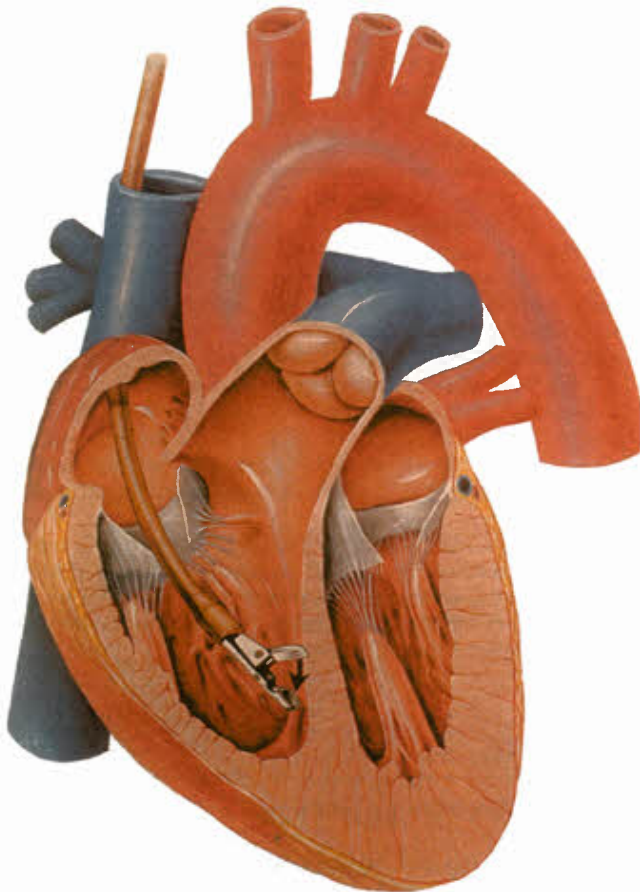


Figure 56.5. Endomyocardial biopsy technique. The biptome is advanced via the superior vena cava into the right atrium, across the tricuspid valve into the right ventricle, and finally situated against the interventricular septum, where the biopsy is performed. The biptome also can be advanced via the inferior vena cava with similar results. (Reprinted from Towbin JA. Molecular genetic aspects of cardiomyopathy. *Biochem Med Metab Biol* 1993;49:285–320, with permission from Elsevier.)

performed but is unreliable in identifying the causative infection. A fourfold increase in antibody titer correlates with infection (76). However, these studies are nonspecific because prior infection with the causative virus is commonplace. PCR

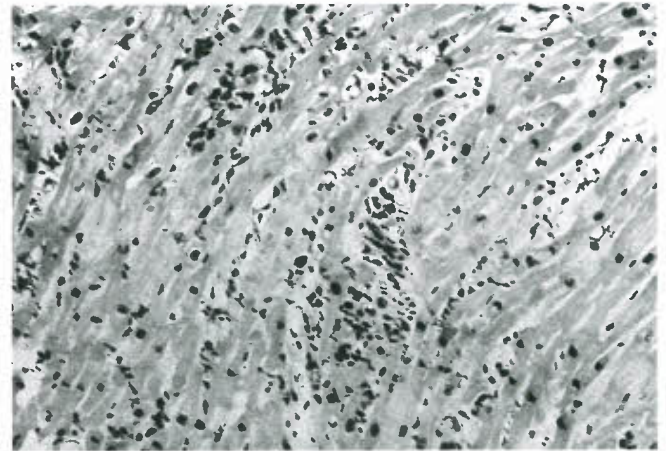


Figure 56.6. Endomyocardial biopsy histology demonstrates lymphocytic infiltrates, myocardial edema, and necrosis.

(5) amplifies viral sequences from cardiac tissue samples, is extremely sensitive, and is typically specific.

Molecular Diagnostics

First reported in 1986, in situ hybridization was performed on myocardial tissue using probes for coxsackievirus (65,66) (Fig. 56.7). This technique is difficult to use in a hospital setting and, for this reason, lost favor and has never gained widespread use. The PCR amplification process, which identifies specific portions of a viral genome, is quite sensitive and specific (5,7) (Fig. 56.8). Around 20% to 50% of cases were initially reported to identify enterovirus PCR-positive results although no other viral genome was analyzed in these early cases (77–79). PCR also has been used to screen for other viral genomes within cardiac tissue specimens. We showed that adenovirus (Fig. 56.9) is identified as commonly as enterovirus in heart tissue specimens of patients with myocarditis or DCM in the 1990s and through 2003 (Table 56.4) (18). Additional viral genomes identified using PCR include CMV, parvovirus, respiratory syncytial virus, EBV, HSV, and influenza A virus. (18,80,81) Mumps virus (Fig. 56.10) is responsible for endocardial fibroelastosis (EFE), a previously important cause of heart failure in children that has decreased significantly over the past three decades (49). Since 2000, other viruses have been increasingly reported as causative

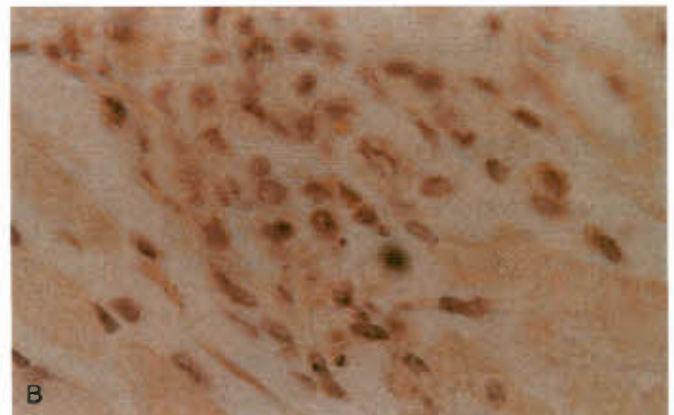
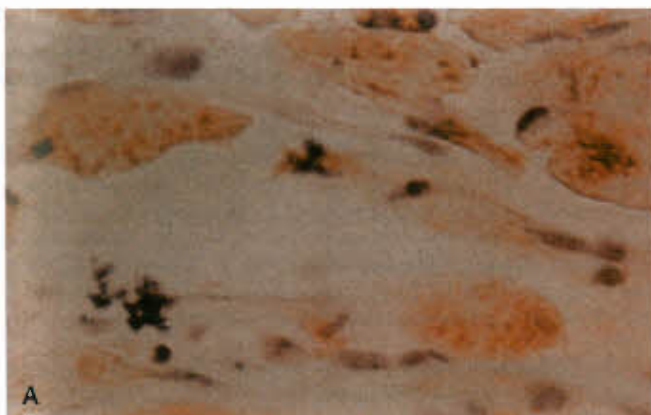


Figure 56.7. In situ hybridization using coxsackievirus B3 probe. A: Note the brown-stained coxsackievirus in the infected myocytes. B: Negative control. (Reprinted from Bowles NE, Richardson PJ, Olsen EGJ, et al. Detection of coxsackie-B virus specific RNA sequences in myocardial biopsy samples from patients with myocarditis and dilated cardiomyopathy. *The Lancet* 1986;327:1120–1123, with permission from Elsevier.)

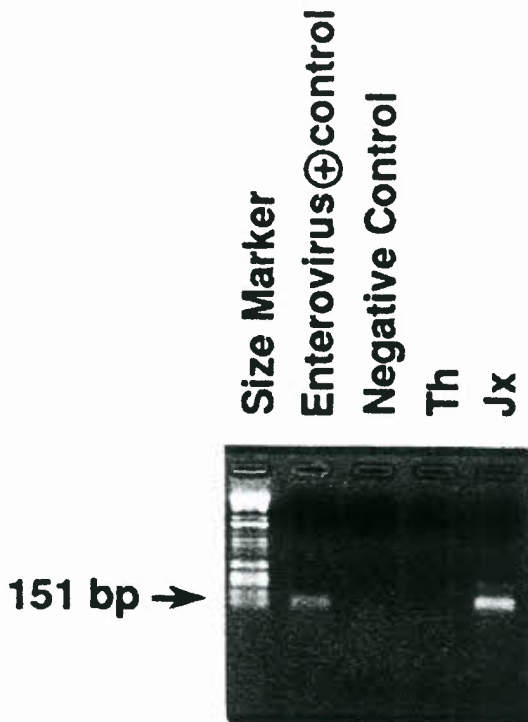


Figure 56.8. PCR for enterovirus. Note the 151-bp band on this agarose gel in the enterovirus-positive (+) control and patient (Jx) lanes. The negative control is devoid of any band, excluding contamination. Another patient (Th) is negative for enterovirus.

of myocarditis including PVB19 (82). HHV6 is becoming increasingly recognized as a cause of viral myocarditis worldwide (31).

PCR analysis may identify viral genome in peripheral blood of patients with myocarditis in about one-third of cases, but the viral genome has been shown to be able to be identified in tracheal aspirates of intubated children with myocarditis, potentially reducing the need for EMB (83).

DIFFERENTIAL DIAGNOSIS

Any cause of acute circulatory failure may mimic myocarditis. Table 56.5 lists the differential diagnosis of congestive heart failure based on the age range of the child.

PATHOPHYSIOLOGY

Viral infection triggers interstitial inflammation and myocardial injury, resulting in cardiac enlargement and an increase in ventricular end-diastolic volume (84) (Fig. 56.11). Normally, this increase in volume results in an increased force of contraction, improved EF, and improved cardiac output as described by the Starling mechanism. In myocarditis, the myocardium is unable to respond to these stimuli, resulting in a reduction in stroke volume. Figure 56.11 identifies the following domino effect of the various changes that occur and result in the pathophysiologic response in patients with myocarditis.

1. Interactions with the sympathetic nervous system may preserve vital systemic blood flow via vasoconstriction, but this will increase afterload on the failing myocardium. This sympathetic nervous system input results in a preserved blood pressure (initially), tachycardia, and diaphoresis.
2. Congestive heart failure ensues with disease progression. The progressive increase in ventricular end-diastolic volume and pressure results in increased left atrial pressure, which is transmitted into the pulmonary venous system. This causes increasing hydrostatic forces, which overcome the colloid osmotic pressure that normally prevents transudation of fluid across the capillary membranes. This results in pulmonary edema.
3. Concomitantly, all cardiac chambers dilate, particularly the left ventricle. This dilation, in addition to causing poor ventricular function, creates worsening pulmonary edema and worsening cardiac function. The ventricular dilation also results in stretching of the mitral annulus and resultant mitral regurgitation, further increasing left atrial volume and pressure.
4. During the healing stages of myocarditis, fibroblasts replace normal myofibers and result in scar formation. Reduced elasticity and ventricular performance can result in persistent heart failure. In addition, ventricular arrhythmias commonly accompany fibrosis.

PATHOLOGY

Gross and Microscopic Findings

Pathologic findings are nonspecific, with similar gross and microscopic changes noted irrespective of the causative agent (4). The heart weight is increased, and all four chambers are affected. The muscle is flabby and pale, with petechial hemorrhages often seen on the epicardial surfaces. A PE also may be seen relating to the often combined finding of pericarditis (in other words, myopericarditis). The ventricular wall is frequently thin, although hypertrophy may be found as well. The valves and endocardium are usually not involved.

In cases of chronic myocarditis, the valves may be glistering white, consistent with EFE, suggesting the result of long-standing inflammation in patients or even an in utero viral myocarditis in newborns with findings of heart failure (85). In North America, newborn EFE has become quite rare. Among children with myocarditis compared with those who had EFE in a prior era, those with myocarditis typically had symptoms for <2 weeks, whereas those with EFE had symptoms for >4 months. Mumps and CVB3 have been identified in the myocardium of infants with EFE, consistent with this being a viral-induced disorder in the past, and its disappearance consistent with the disappearance of these inciting viruses (49).

Mural thrombi can occur in the left ventricle, and small emboli are often found in the coronary and cerebral vessels (86). Coronary emboli, although rare, may produce areas of ischemia or injury with resultant production of the cardiac arrhythmias that sometimes occur during the acute disease. Coronary insufficiency appears to be a common occurrence in children with PVB19 myocarditis as PVB19 infects the endothelium, including coronary endothelium, and not myocytes.

An interstitial collection of mononuclear cells, including lymphocytes, plasma cells, and eosinophils (Fig. 56.6) is typical of early myocarditis (9). Polymorphonuclear cells are rare, as are viral particles. Extensive necrosis of the myocardium, with loss of cross-striation in the muscle fibers and edema, is seen

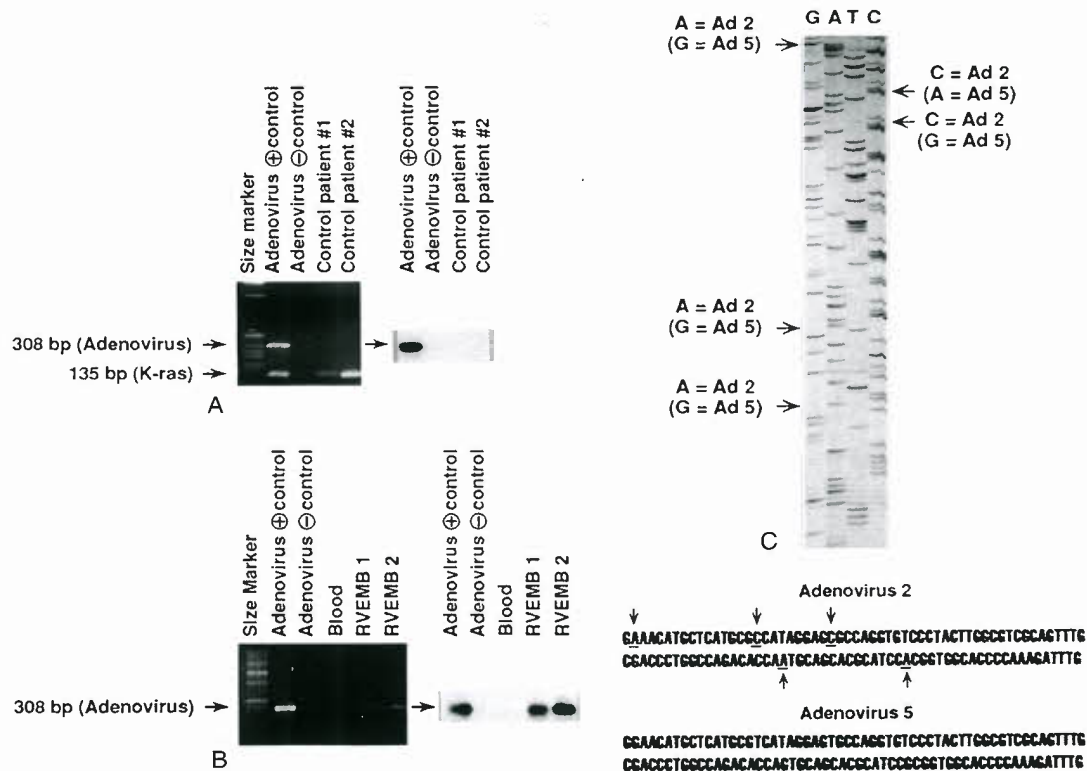


Figure 56.9. PCR for adenovirus. **A:** Control analysis. The *left panel* shows an agarose gel with a 308-bp PCR-positive band in the adenovirus-positive control only. In the adenovirus-positive lane and in control patients 1 and 2, K-ras, a constitutive product of all cells that is used to show extracted nucleic acid, is positive in each. The *right panel* identifies a Southern blot of the left panel with a radioactive probe specific for adenovirus. **B:** The *left panel* shows a PCR-positive 308-bp band in the two right ventricular endomyocardial biopsy (RVEMB) samples and negative in the lane of blood. The *right panel* again shows adenoviral specificity. **C:** DNA sequencing of RVEMB1 is consistent with type 2 adenovirus in the patient, which is compared with the sequence of the type 5 positive control. A, adenine; C, cytosine; G, guanosine; T, thymidine.

in severe infections, especially with coxsackievirus. Perivascular accumulation of lymphocytes and plasma cells has been described with CVB myocarditis but is usually a minor finding. This is a much more prominent finding in disease caused by rickettsiae, varicella, trypanosomes, or other parasites, and in reactions to sulfonamides (87). In cases of adenoviral myocarditis, mild to moderate inflammation with moderate to severe fibrosis was common, while coronary insufficiency is common with PVB19.

Diphtheria myocarditis is frequently complicated by arrhythmias and complete atrioventricular block (88). Diphtheria exotoxin attaches to conduction tissue and interferes with protein synthesis by inhibiting a translocating enzyme in the delivery of amino acids (88). Triglyceride accumulates, producing fatty changes of the myofibers.

Bacterial myocarditis produces microabscesses and patchy focal suppurative changes. A combined perimyocarditis is also frequently encountered. Parasitic myocarditis caused by trichinella has a focal infiltrate with lymphocytes and eosinophils, but larvae are usually not identified (37).

A severe myocarditis caused by *Trypanosoma cruzi* results in Chagas disease, which can have both acute and chronic cardiac sequelae (89,90). Rare in North America, Chagas disease is endemic in South America, affecting ≤50% of the population. Microscopic examination shows the organism as well as neutrophils, lymphocytes, macrophages, and eosinophils.

Sudden death in infancy may result from myocardial inflammation. James described a resorptive, degenerative process in the His bundle and left margin of the atrioventricular node with the absence of inflammatory cells in cases of infants who died in northern Ireland (91).

Giant cell myocarditis (GCM) is a rare, virulent form of myocarditis and is thought to have an autoimmune basis that is histologically defined by the presence of multinucleated giant cells, a lymphocytic inflammatory infiltrate, and myocyte necrosis. It usually occurs in children and young adults and reportedly has a high risk of death unless cardiac transplantation is performed. GCM has been considered to have an underlying autoimmune basis due to its association with other autoimmune disorders, thymoma, and drug hypersensitivity, and is associated with immune-mediated disease in other organs. GCM occurs with tuberculosis, syphilis, rheumatoid arthritis, rheumatic heart disease, sarcoidosis, and fungal or parasitic infections (51,92–94). Giant cells also occur in idiopathic (Fiedler) myocarditis. There are two types of giant cells: cells originating from the myocardium and cells derived from interstitial histiocytes.

Immunology

The immunopathogenesis of CVB and encephalomyocarditis has been studied in mice. CMV, HIV, and adenovirus models also have been described (95–100).

TABLE 56.4 Myocarditis Etiologic Agents in Children by PCR Analysis

Diagnosis	No. of Samples	No. of PCR + Samples	No. of PCR Amplimer
Myocarditis	624	239 (38%)	Adenovirus 142 (23%) Enterovirus 85 (14%) CMV 18 (3%) Parvovirus 6 (<1%) Influenza A 5 (<1%) HSV 5 (<1%) EBV 3 (<1%) RSV 1 (<1%)
DCM	149	30 (20%)	Adenovirus 18 (12%) Enterovirus 12 (8%)
Controls	215	3 (1.4%)	Enterovirus 1 (<1%) CMV 2 (<1%)

CMV, cytomegalovirus; DCM, dilated cardiomyopathy; EBV, Epstein-Barr virus; HSV, herpes simplex virus; PCR, polymerase chain reaction; RSV, respiratory syncytial virus.

Twenty-four to seventy-two hours after infection with CVB, a viremia exists, with maximum growth in the tissues at 72 to 96 hours (9). Shortly thereafter, virus titers decline; essentially no organisms can be found by 7 to 10 days after inoculation. As virus titers decline, antibody concentrations increase, implying that antibody has an active role in viral clearance. Macrophages appear 5 to 10 days after infection in the CVB model of myocarditis (9).

Risk factors for severe myocarditis include age, mouse strain, viral variant, exercise, and sex (9). Pathogenetic mechanisms

include direct viral myofiber destruction and T-lymphocyte cytotoxicity (97–99,101). Animals with absent or blocked T-cell function have less myocardial injury.

The natural killer (NK) cell is important in the pathogenesis of myocarditis. Animals that are depleted of their NK cells prior to infection with coxsackievirus develop a more severe myocarditis (84). NK cells are activated by interferon, which is an indirect modulator of myocardial injury. Murine skin fibroblasts serve as target cells for CVB-sensitized cytotoxic T cells. The NK cells specifically limit the nonenveloped virus infection by killing the virally infected cells. Male mice are less efficient in activating NK cells. Presumably, the more efficiently viral clearance occurs, the less virally induced neoantigen production occurs, reducing recognition by cytotoxic T lymphocytes.

T cells can affect injury by accumulation of activated macrophages, production of antibody and antibody-dependent cell-mediated cytotoxicity, direct lysis by antibody and complement, and direct action of cytotoxic T cells (102). In the BALB/c mouse, the greatest susceptibility was between 16 and 18 weeks, with males having a more rapid and severe course of myocarditis than that seen in females. Estradiol decreased severity, and testosterone increased the cytolytic activity in males. Either a preferential stimulation of T helper cells or an inadequate stimulation of T-cytolytic/suppressor cells could explain why antibody responses to various antigens may frequently be enhanced and cellular immune responses depressed in females.

Host genetic composition affects not only the severity of disease but also pathogenic mechanisms (100,101,103,104). The BALB/c mouse developed myocarditis in response to cytolytic T cells. Two distinct cytolytic T-cell populations are formed in the BALB/c mouse: one recognizing virus-infected cells and producing direct myocytolysis, and another that destroys uninfected myocytes and is believed to be an autoreactive lymphocyte. Complement depletion increased the amount of inflammation in this species, and no reactive immunoglobulin G antibody was found in the myocytes. In the DBA/2 mouse, it was the T helper cells that indirectly mediated the course of disease, and complement depletion reduced inflammation in this species. Cytolytic T cells were found to be produced but apparently were not pathogenic; immunoglobulin G antibody was found in the myocytes.

In humans, antibody-mediated cytotoxicity was found among 30% of patients with suspected myocarditis, as well as in 18 of 19 patients with proven viral infections owing to CVB,



Figure 56.10. Mumps virus PCR in endocardial fibroelastosis.

TABLE 56.5 Differential Diagnosis of Myocarditis by Age

Newborn and Infant	Child
Sepsis	Idiopathic dilated cardiomyopathy
Hypoxia	X-linked dilated cardiomyopathy
Hypoglycemia	Autosomal dominant dilated cardiomyopathy
Hypocalcemia	Anomalous left coronary artery from the pulmonary artery
Structural heart disease	Endocardial fibroelastosis
Idiopathic dilated cardiomyopathy	Chronic tachyarrhythmia
	Pericarditis
Anomalous left coronary artery from the pulmonary artery	
Cerebral arteriovenous malformation	

influenza A, or mumps virus (95). A muscle-specific antimyolemmal antibody was found in these patients and correlated with the degree of in vitro–induced cytolysis of rat cardiocytes. Bowles et al. (105,106) used complementary DNA (to CVB2 RNA) cloning techniques and developed a CVB-specific complementary DNA hybridization probe that detected virus nucleic acid sequences in patients diagnosed as having active or healed myocarditis or DCM. As controls, they used patients with unrelated disorders and found no virus-specific sequences in those patients (105). This suggested that viral particles persist in patients with congestive cardiomyopathy or healing myocarditis, even though viral culture is almost always negative. The findings imply a continual viral replication in cells, which may conceal the antigenicity by an immunologic process that prevents correct posttranslational processing of capsid proteins. Hori et al. (107) found adult patients with myocarditis to have been exposed to a greater number of CVB1 to CVB6, as

demonstrated by the number of positive and negative responses to neutralizing antibodies of those viruses. They believed that immunization against several types of CVB was essential in the development of myocarditis. Although they postulated this cross-immunization theory, a few cases of myocarditis in their patients involved exposure to only one type of CVB, shedding doubt on the validity of their theories.

Defective cell-mediated immunity occurs in patients with myocarditis and DCM when compared with healthy controls. Pathogenesis of adenoviral myocarditis differs from CVB (108,109). The inflammatory infiltrate is substantially less in adenoviral infection (110). The number of CD2, CD3, and CD45RO lymphocytes seen in the adenovirus-infected patients was reduced compared with those patients who had myocarditis not owing to adenovirus (110). The adenoviruses have a number of strategies for modulating the immune response, which could impact the number of activated lymphocytes in

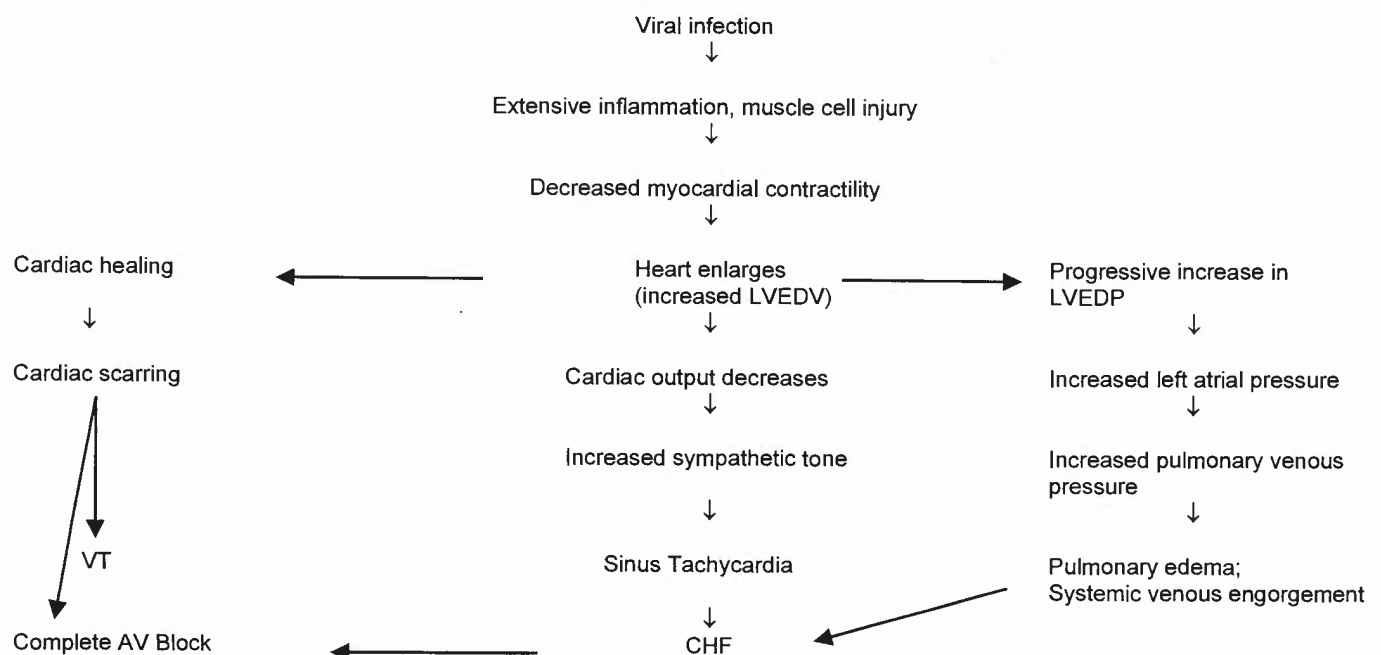


Figure 56.11. Pathophysiology of myocarditis. AV, atrioventricular; CHF, congestive heart failure; LVEDP, left ventricular end-diastolic pressure; LVEDV, left ventricular end-diastolic velocity; VT, ventricular tachycardia.

the adenovirus-infected myocardium (99). Several adenovirus-encoded proteins can interact with host immune components, including proteins encoded by the E3 region, which can protect cells from tumor necrosis factor (TNF)-mediated lysis, as well as downregulation of major histocompatibility complex class I antigen expression. The E1A proteins are capable of promoting the induction of apoptosis (111) and inhibiting interleukin-6 (IL-6) expression, as well as interfering with IL-6 signal transduction pathways. These functions of E1A may be pertinent to the development of the myocardial pathology seen in DCM. First, IL-6 promotes lymphocyte activation, which is reduced in adenovirus-infected patients. In addition, it has been shown that apoptotic cells occur in the myocardium of patients with DCM. Taken together, these events are likely to result in DCM.

Autoimmunity

Persistent viral infection of the myocardium is linked to the induction of autoantibodies against the adenine nucleotide translocator (ANT) and myosin (112,113). ANT shuttles energy from the mitochondria to the cells, whereas myosin is a contractile protein (Fig. 56.12).

Anti-ANT antibodies correlate with cardiac dysfunction (112). An increase in the ANT1 isoform was detected in patients together with a concomitant decrease in ANT2. Furthermore, in patients with enterovirus infection, this was more pronounced than in patients in whom no enterovirus was detected. In animal models of CVB3 infection, nucleotide transport is inhibited. ANT1 transgenic mutant mice have a cardiomyopathic phenotype, supporting the concept that it is important in cardiac function (114).

Novel autoantigens also have been identified in patients with myocarditis (115–117). These include dihydrolipoamide dehydrogenase and sarcomere-specific CK. It is not clear, however, if these autoantigens are important pathogenetically. As yet, autoantibodies associated with persistent adenovirus infection of the myocardium have not been described.

Role of Cytokines in Myocarditis and Dilated Cardiomyopathy

Over the past several years, there has been considerable interest in the role of cytokines in the pathogenesis of myocarditis and DCM (103,118). Recent animal studies suggest that a relationship may

exist between subclinical viral infection and later development of DCM. This process is presumed to occur by an autoimmune-like mechanism triggered by the initial viral insult. Several murine models have been studied that suggest that cytokine-mediated modulation of the immune response to viral infection may lead to induction of chronic autoimmune myocarditis (118–124). Cytokines contribute to regulation of antibody production and maintenance of self-tolerance. Susceptible murine strains, when infected with CVB3, develop myocyte necrosis and an acute inflammatory response. After the initial viral infection, resolution of inflammation eventually occurs. In other strains, however, a second autoimmune phase of myocarditis appears later, with findings of diffuse mononuclear cell infiltrates within the heart. These mononuclear cells are a significant source of the cytokines IL-1 and TNF- α , and they release large amounts of TNF- α and IL-1 β by human monocytes when exposed to CVB3 (119). Both of these cytokines are known to participate in leukocyte activation, which may be beneficial in promoting a specific lymphocyte response to viral infection. However, these cytokines also may promote cardiac fibroblast activity. Therefore, it has been speculated that local secretion of cytokines in the myocardium perpetuates the inflammatory process, which secondarily leads to the fibrosis associated with DCM and resultant deterioration of cardiac function.

IL-1 and TNF- α are potential inhibitors of cardiac myocyte β -adrenergic responsiveness, and further studies have shown IL-1 and TNF- α to be the macrophage factors mediating this effect (118). TNF- α levels are elevated in patients with chronic heart disease, myocarditis, or DCM. TNF- α is able to potentiate the immune response and induce apoptosis in cells, integral to the pathogenesis of myocarditis. Other inflammatory mediators, including IL-1 and granulocyte colony-stimulating factor, are also elevated in myocarditis patients. Inflammatory cytokines may cause a direct negative inotropic response.

The role of cytokine activity relative to the pathogenesis of viral myocarditis or subsequent development of chronic autoimmune myocarditis is under investigation. Mice that are genetically resistant to postinfection autoimmune myocarditis develop severe disease when infected with CVB3 in addition to therapy with lipopolysaccharide, TNF- α , or IL-1 (121). CVB3 infection of cardiac tissue likely promotes local production of cytokines by activated monocytes as a response to viral infection. Anti-TNF- α blocks or reduces the severity of myocarditis. Thus, local TNF- α expression is sufficient to cause cardiac pathology and dysfunction and support its role in human disease.

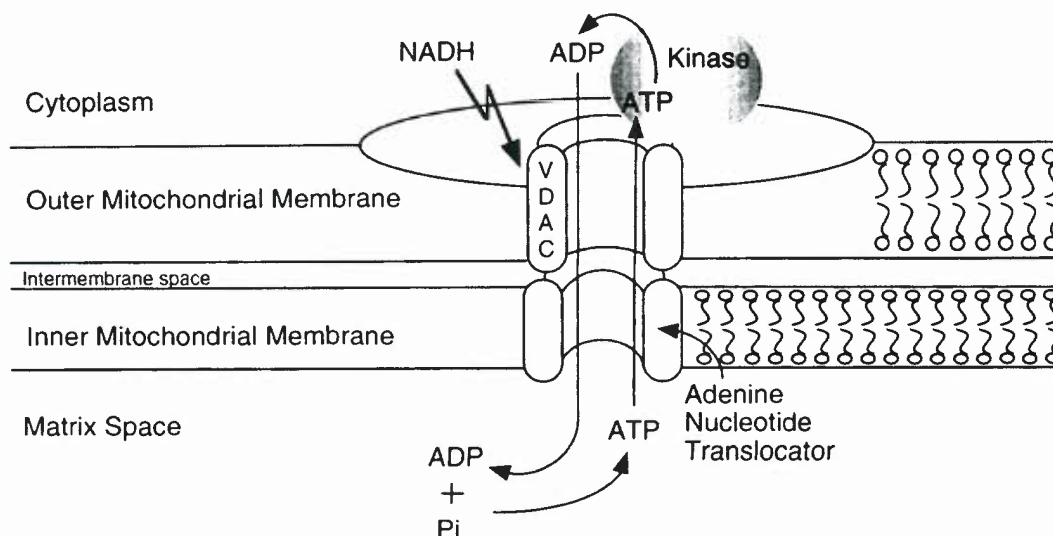


Figure 56.12. ANT and its role in energy utilization.

IL-2 limits myocardial damage when administered in the acute viremic stage by enhancing NK cell activity (122,123). In contrast, IL-2 exacerbated the course and severity of the disease when given in the subacute, nonviremic stage by increasing the number of infiltrating T cells. IL-12 protects mice from encephalomyocarditis virus-induced myocarditis (124). IL-12 augments cytotoxic activity and induces Th1-specific immune responses.

Cytokines may act through inducible nitric oxide synthase (iNOS) (124). In a cardiac myosin-induced myocarditis model, NOS expression is induced in both macrophages and cardiomyocytes. However, nitric oxide synthesis did not appear to be essential for the development of pathology because myocarditis developed in mice lacking interferon regulatory transcription factor (IRF)-1, a transcription factor that controls iNOS expression. Despite the failure to synthesize NOS in the myocardium, the prevalence and severity of disease in IRF-1-deficient animals were similar to results observed in control animals. In addition, no difference was detected in animals lacking the IRF-2 gene, a negative regulator of IRF-1-induced transcription.

In the rat model, nitric oxide expression is critical to the pathology of autoimmune myocarditis (124). Rats that were treated with aminoguanidine, an inhibitor of iNOS, had only focal mononuclear infiltration and reduced numbers of cardiomyocytes positive for iNOS, by comparison with untreated animals that had considerable inflammatory infiltration and myocyte damage. In addition, serum levels of CK were significantly reduced in the treated animals, indicating reduced muscle damage. In a separate study of autoimmune myocarditis in the rat, IL-2 levels appeared early, whereas IL-3, TNF- α , and iNOS were present later, during the period of peak inflammation. IL-10 was detected only after inflammation began to subside and persisted during recovery. These data support the notion that changes in the Th1 and Th2 responses are important for controlling outcome, as previously suggested for CVB3-induced myocarditis.

It is difficult to extrapolate the information obtained in animal models of myocarditis to human disease. Further studies to clarify the role of cytokines and nitric oxide in the pathogenesis of myocarditis in humans are warranted, as is consideration of the potential efficacy of drugs to inhibit cytokine or iNOS expression. We need to know if virus persistence combined with ongoing IL-6, IL-8, and TNF- α expression, in the absence of IL-10, leads to the progression from myocarditis to DCM.

Role of Cell Adhesion Molecules in Myocarditis and Dilated Cardiomyopathy

Cell adhesion molecules (CAMs) also may play a role in the pathogenesis of myocarditis (108). One molecule that is well

known to play a major role in cell-cell adhesion, particularly leukocyte adherence and transendothelial migration, is intercellular adhesion molecule 1 (ICAM-1). ICAM-1 is a member of the immunoglobulin supergene family of CAMs and is a single-chain glycoprotein of 80 to 115 kDa with an extracellular domain made up of five immunoglobulin-like repeats. ICAM-1 is predominantly expressed on endothelial cells, but also on fibroblasts, epithelial cells, mucosal cells, lymphocytes, monocytes, and cardiac myocytes after inflammatory injury. Expression of ICAM-1 on endothelial cells is upregulated by cytokines such as IL-1 and TNF- α . A well-established binding ligand of ICAM-1 is lymphocyte function-associated antigen 1 (LFA-1), a molecule that is part of the β 2 integrin family and consists of a 180-kDa α subunit (CD11a) and a 95-kDa β subunit (CD18). LFA-1 is expressed on virtually all leukocytes, including monocytes. The adhesive interaction between LFA-1 and ICAM-1 mediates adhesion-dependent helper T cell, cytotoxic T cell, and NK cell functions. Antibody to LFA-1 blocks inflammatory response in animal models of myocarditis.

Apoptosis

Apoptosis, or programmed cell death, has an important role in embryogenesis, tissue homeostasis, and regulation of immunologic responses, among normal physiologic processes, and is associated with the growth and regression of tumors (108). Cells undergoing apoptosis exhibit characteristic morphologic and biochemical features, including chromatin aggregation, nuclear and cytoplasmic aggregation, and formation of apoptotic bodies resulting from the partition of the cytoplasm and nucleus into membrane-bound vesicles. These apoptotic bodies are rapidly phagocytosed by adjacent macrophages or epithelial cells, without resulting in an inflammatory response. Apoptotic cells are detectable by terminal transferase labeling (terminal deoxynucleotide transferase-mediated biotin-deoxyuridine triphosphate nick end labeling [TUNEL]) in myocardial tissue samples from patients with DCM. It has been shown that up to 0.1% of cells stained positive by this technique.

Several viruses have been implicated in the induction of apoptosis, including HIV, EBV, and adenovirus. Apoptotic cells are detected in adenovirus-associated myocarditis and DCM (Fig. 56.13). Within such areas, $\leq 1\%$ of cells may stain positive, including myocytes, infiltrating inflammatory cells, and endothelial cells. In the tissue sections from control patients, either unstained cells or sporadically stained cells (one or two per section) may be detected. These data suggest a relationship between infection of the myocardium by adenovirus and the onset of apoptosis, which could result in pathologic processes

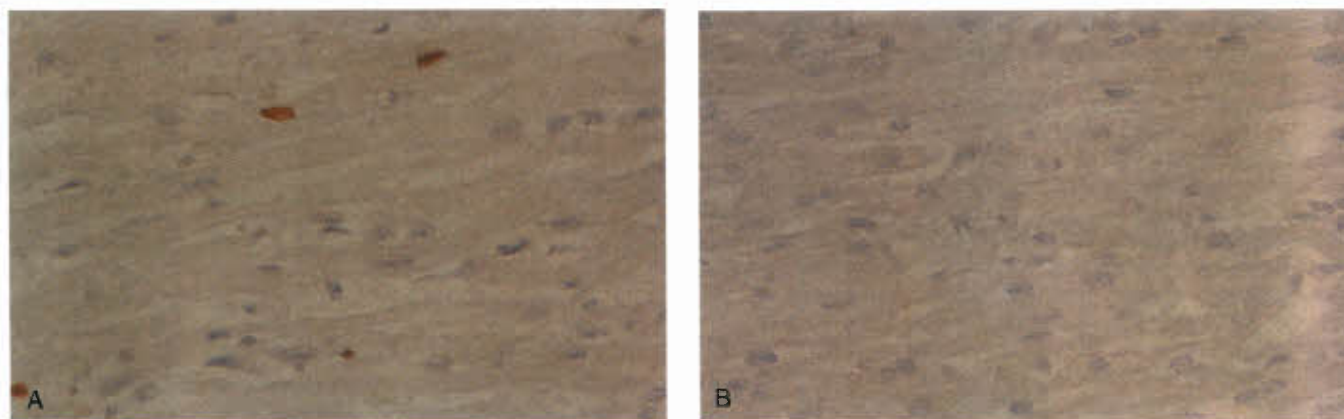


Figure 56.13. A: TUNEL (see text) staining of endomyocardium demonstrates apoptotic bodies (red inclusions). B: Negative control.

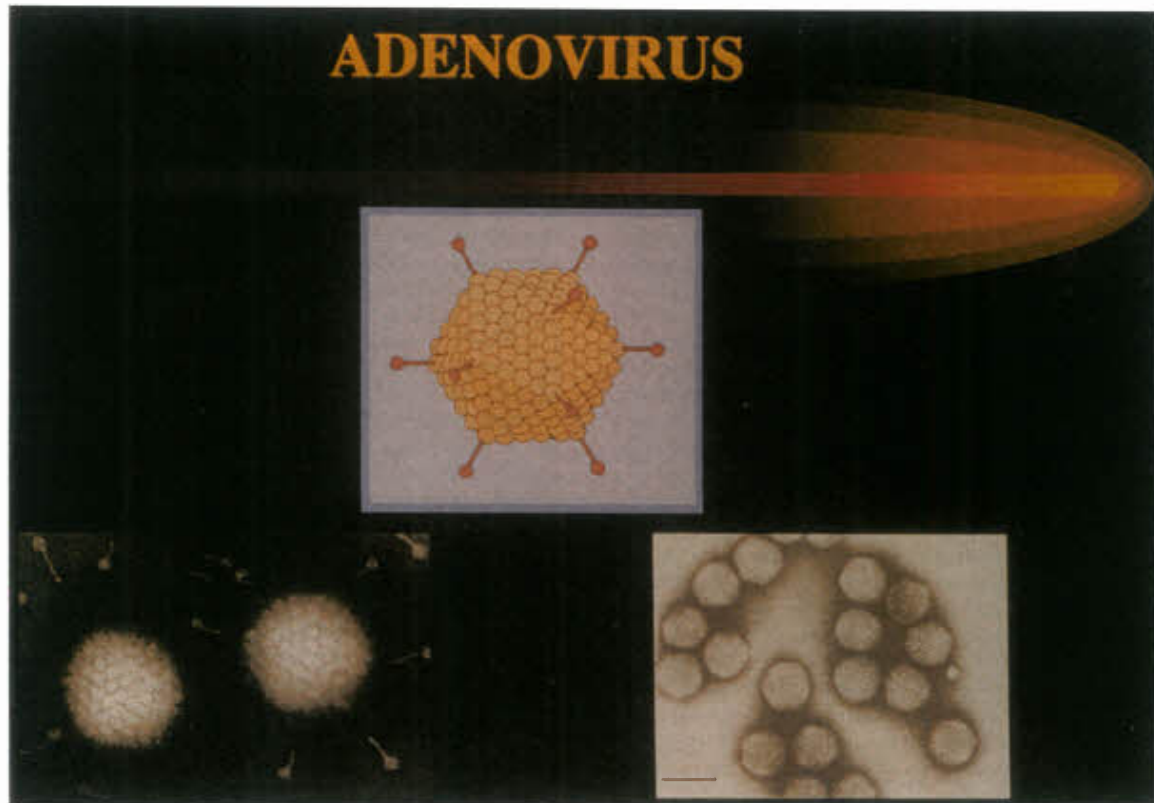


Figure 56.14. Illustrated adenovirus structure (top), with electron micrographs below. Note the hexagonal shape and its projections.

associated with myocarditis and DCM. Furthermore, a number of inflammatory cells may be seen to be undergoing apoptosis. Although this could reflect the natural defense mechanism of the host against the virus, it also raises the possibility of virus-induced apoptosis as a mechanism of immune system avoidance. In tumors, infiltrating immune cells are destroyed by the induction of apoptosis through the expression of Fas ligand on the tumor cell that binds Fas on the lymphocyte.

Two of the genes of adenovirus (Fig. 56.14), E1A and E1B, regulate apoptosis via a p53-dependent pathway (109). The expression of E1A in cells results in the induction of apoptosis, but the coexpression of E1B (or the bcl-2 proto-oncogene) suppresses this effect and results in cell transformation. E1B encodes 19- and 55-kDa proteins, either of which can suppress apoptosis. The 55-kDa protein of E1B binds to, and inhibits, p53, but the mechanism of suppression by the 19-kDa protein is unknown.

As previously noted, most models of experimental myocarditis have used CVB3 variants. It has been known for a number of years, however, that different variants induce different pathologic mechanisms and that different strains of mice are affected differently. Infection of BALB/c, MRL^{+/+}, or DBA/2 mice with a cardiotropic variant of CVB3 resulted in similar levels of inflammation, but only in DBA/2 mice was antiheart immunoglobulin G generated (84). Few CD8⁺ T cells infiltrated the myocardium of MRL^{+/+} and DBA/2 mice, but in BALB/c mice, they are the major component of the T-cell response. The detection of apoptotic cells using TUNEL staining revealed no apoptotic cells in DBA/2 myocardium, inflammatory cells undergoing apoptosis in MRL^{+/+} mice, and myocyte and inflammatory cell apoptosis in BALB/c mice (92). In BALB/c mice with myocarditis, there was a decrease in ventricular contractility, indicative of cardiomyopathy, whereas in DBA/2 mice, there was no change in contractility.

LONG-TERM SEQUELAE

Many cases of myocarditis survive the critical phase of illness. It is increasingly recognized that myocardial dysfunction and evidence of heart failure can present at some point during their lifetimes (70,125–127). It remains unclear what the underlying cause of these long-term sequelae could be, but viral persistence and autoimmunity have been widely speculated. Enteroviral protease 2A directly cleaves the cytoskeletal protein dystrophin, resulting in dysfunction of this protein (Fig. 56.15) (128). Because mutations in dystrophin are known to cause an inherited form of DCM (as well as the DCM associated with the neuromuscular diseases, Duchenne muscular dystrophy, and Becker muscular dystrophy), it is likely that this is, to a large extent, responsible for the chronic DCM seen in enteroviral myocarditis (129,130). Other viruses, such as adenoviruses, also have enzymes that cleave membrane structural proteins or result in activation or inactivation of transcription factors, cytokines, or adhesion molecules to cause chronic DCM (131,132). Andreoletti et al. (133) reported presence of enteroviral infection, specifically CVB, in association with the pathogenesis of acute myocardial infarction secondary to a disruption in the dystrophin–glycoprotein complex. Therefore, it appears that a complex interaction between the viral genome and the heart occurs and results in the short- and long-term outcome of affected patients.

As in mice, myocarditis in humans may have a genetic basis (134). Support for this includes the frequent finding of myocardial lymphocytic infiltrate in patients with familial and sporadic DCM, as well as the few reports of families in which two or more individuals have been diagnosed with myocarditis on EMB. The findings of a common receptor for the four most common viral causes of myocarditis (CVB3 and CVB4 and

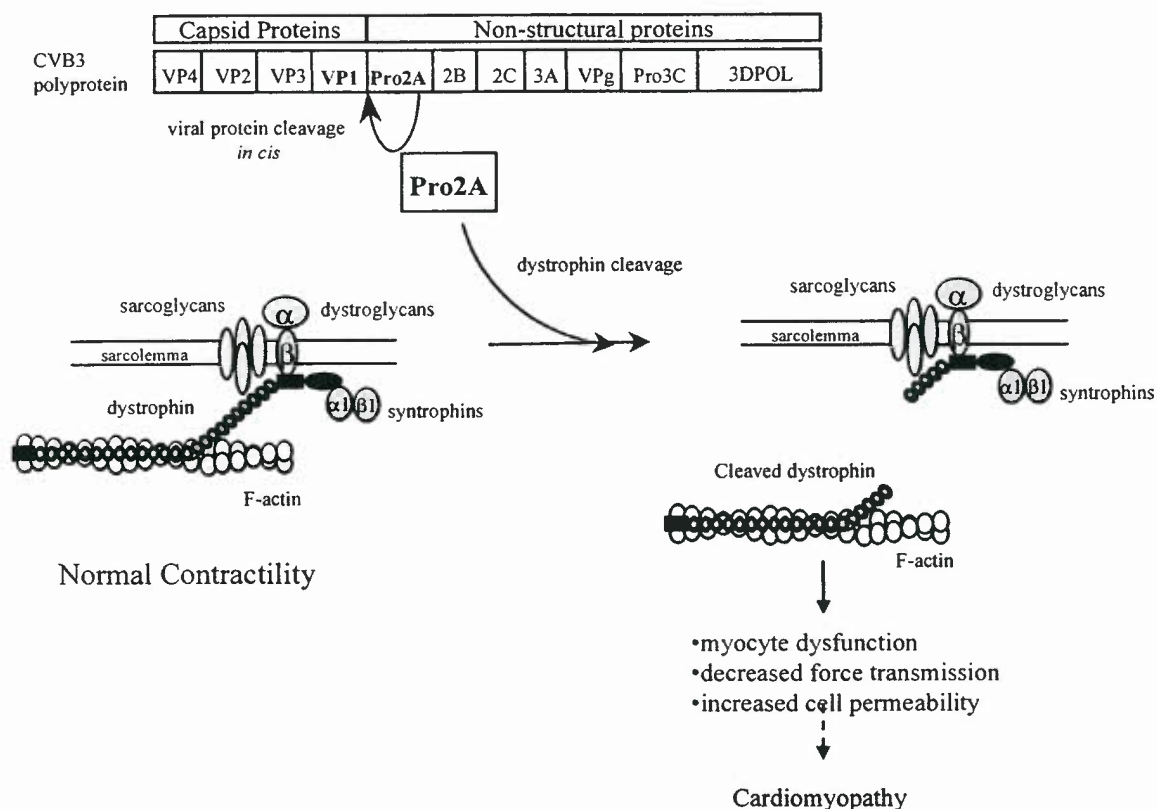


Figure 56.15. Dystrophin cleavage by enteroviral protease 2A (Pro2A). (Reprinted from Badorff C, Lee G-H, Lamphear BJ, et al. Enteroviral protease 2A cleaves dystrophin: evidence of cytoskeletal disruption in an acquired cardiomyopathy. *Nat Med* 1999;5:320–326, with permission from Macmillan Publishers Ltd.)

adenoviruses 2 and 5), the human coxsackievirus, and adenovirus receptor (CAR) (Fig. 56.16) (135,136), which if mutated could result in responsible host differences leading to myocarditis (137,138), support the concept of a genetic link to virally induced inflammatory heart disease. CAR is a tight junction protein of the intercalated disk and has been linked with the innate immune response in CVB myocarditis (139). Recent mouse studies have shown that CAR upregulation results in myocardial inflammation that is histologically similar to that of early viral myocarditis (140). Newer approaches to genetic

study, including genome-wide association studies, may lead to an enhanced understanding of genetic predispositions for acquiring viral myocarditis.

SUPPORT FOR VIRAL CAUSE-AND-EFFECT RELATIONSHIP WITH MYOCARDITIS

Despite the increasingly common association of viral genome within the myocardium in patients with myocarditis, limited definitive data exist that prove that the virus causes ventricular disturbance directly leading to the clinical phenotype. Many physicians and scientists hold onto the concept that myocarditis is a primary inflammatory disorder, but definitive data are limited to support that hypothesis. Further limiting our understanding of myocarditis and the role of viruses is the low percentage of EMBs performed and the even fewer attempts at performing PCR on the myocardium.

An excellent human model exists, however, that we have studied extensively that offers insight into the acute and chronic effects of cardiotropic viruses. Cardiac transplant recipients undergo routine surveillance EMBs for rejection and, in all cases, histopathology is performed. In our institution, all such subjects also undergo myocardial PCR analysis with screening of adenovirus, enterovirus including coxsackievirus, PVB19, CMV, influenza, HCV, and EBV. We have shown that identification of viral genome in these samples correlated with outcome, with a 96% 5-year survival in subjects not having PCR-positive studies any time during the 5-year follow-up, whereas those with a single PCR-positive result (or more) have a 5-year survival of 67% (Fig. 56.17) (141).

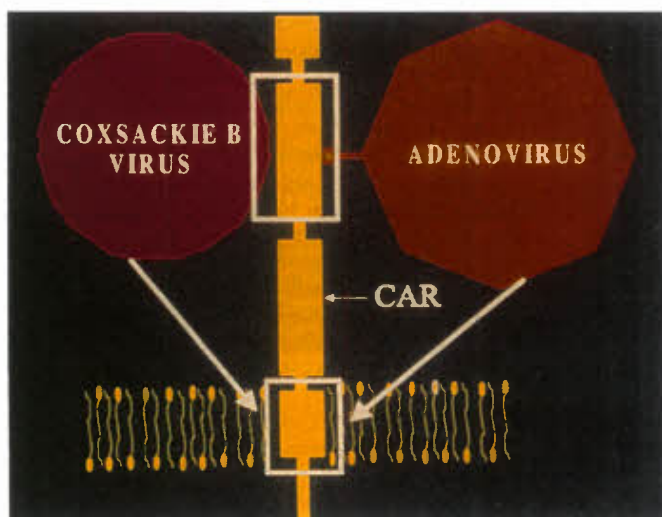


Figure 56.16. Illustrated human CAR.

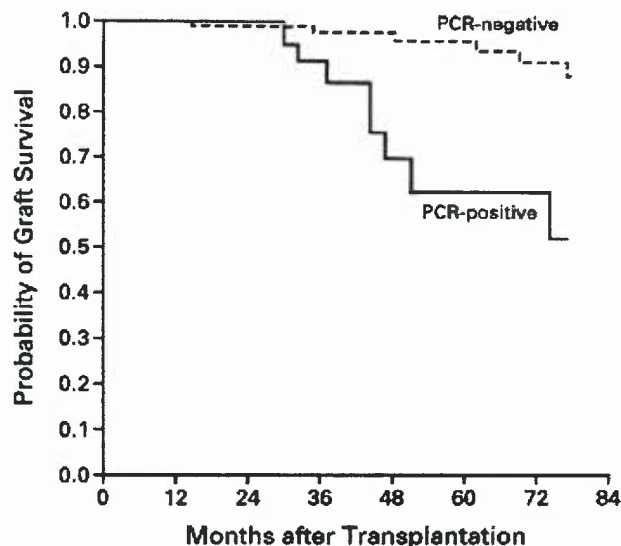


Figure 56.17. Kaplan-Meier survival curve of adenovirus-positive versus adenovirus-negative PCR from endomyocardial biopsies of cardiac transplant recipients (Reprinted from Shirali GS, Ni J, Chinnock RE, et al. Association of viral genome with graft loss in children after cardiac transplantation. *N Engl J Med* 2001;344:1498–1503, with permission from the Massachusetts Medical Society.)

Interestingly, survival does not closely correlate with the level of inflammatory infiltrate seen on histopathology. This appears, at least in part, to do with the specific viruses identified in the myocardium. Adenovirus tends to cause a lower level of inflammatory infiltrate than enteroviruses or PVB19 (141). We have reported that cardiotropic viruses continue to be a significant cause of pediatric heart transplant dysfunction and that this disease is shifting with respect to the viruses involved, specifically an endemic shift to PVB19 in the current era (16). Furthermore, we recently reported that viral endomyocardial infection is an independent predictor of graft loss in pediatric heart transplant patients that appears to be mediated by premature development of transplant coronary artery disease (TCAD) (82). Interestingly, patients who were treated with IVIG and were PCR-positive on EMB had a delayed time in the development of TCAD suggesting a possible treatment strategy. Similar findings have been found in lung transplant recipients (Fig. 56.18) (142).

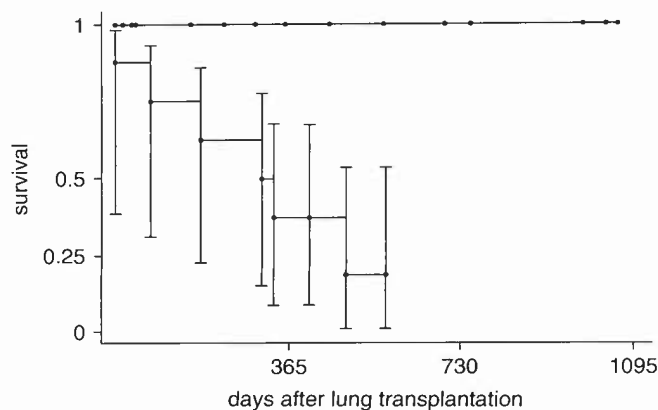


Figure 56.18. Kaplan-Meier survival curve of adenovirus-positive versus adenovirus-negative PCR from biopsies of lung transplant recipients. (Reprinted from Bridges ND, Spray TL, Collins MH, et al. Adenovirus infection in the lung results in graft failure after lung transplantation. *J Thorac Cardiovasc Surg* 1998;116:617–623, with permission from Elsevier.)

TREATMENT

The care for patients with suspected or proven myocarditis must be individualized given the wide range of presenting symptoms that may vary from being relatively asymptomatic to cardiogenic shock. Continual reassessment of patients with myocarditis is recommended as their clinical picture can change dramatically in a very short period of time. Many patients present with relatively mild disease, with minimal or no respiratory compromise and only mild signs and/or symptoms of congestive heart failure. These patients require close hemodynamic and electrocardiographic monitoring to assess whether the disease will progress to worsening heart failure and the need for more intensive medical care. Murine models of myocarditis suggest that exercise may result in increased viral replication as well as myocardial inflammation and necrosis (143). Thus, it appears prudent to place patients under this restriction at the time of diagnosis. Normal arterial blood oxygen levels should be maintained for any patient with compromised hemodynamics resulting in hypoxemia.

Although no specific therapy aimed at reversing myocardial injury is currently widely recommended, maintenance of cardiac output at levels that supply adequate tissue perfusion and prevent metabolic disturbances and end-organ dysfunction is critical to good outcome.

Medical Management

The appropriate medical management of patients with myocarditis is dependent on their clinical presentation. Patients presenting with mild symptoms of congestive heart failure and preserved cardiac output should be continually evaluated as they may progress to a more decompensated state. Diuretics may be used judiciously to treat symptoms of shortness of breath or peripheral edema. There are convincing data that long-term oral therapies may be of benefit. Angiotensin-converting enzyme inhibitors (ACEi) or angiotensin receptor blockers (ARBs) should be considered in patients with evidence of depressed left ventricular systolic function and/or dilation of the left ventricle to assist in favorable remodeling (144). Captopril has been shown to reduce inflammatory infiltrates and calcification and the ARB candesartan has been shown to enhance survival and decrease inflammatory mediators in murine models of myocarditis (145,146). There are increasing data that support the use of nonselective beta blockade in patients with myocarditis. Murine models treated with beta blockade have decreased inflammation (147). Human studies clearly report the lack of beta blocker use as an independent predictor of poor prognosis (148). Therapy with aldosterone antagonists such as aldosterone or eplerenone may be considered in patients with evidence of fibrosis but they must be monitored closely for hyperkalemia if receiving concomitant ACEi or ARB therapy. Additional possible therapeutic strategies for heart failure may be found elsewhere (144). Patients with evidence of decompensated heart failure may be best managed in an intensive care setting. Significant volume overload should be treated with diuretic therapy accompanied by avoidance of significant electrolyte disturbances as this may provoke arrhythmias. Patients who show signs of poor perfusion and low cardiac output should all be managed in an intensive care setting with careful selection of inotropic agents. A more extensive management approach to patients with decompensated heart failure may be found elsewhere in this text as well in current evidence-based guideline statements (144,149).

Arrhythmias should be treated appropriately and aggressively (56). Supraventricular and ventricular tachyarrhythmias

may be seen and should be treated quickly. Ventricular arrhythmias in the setting of systolic dysfunction may require intravenous amiodarone. Despite aggressive treatment of these arrhythmias, rapid deterioration to ventricular fibrillation, especially in the very young, may occur and should be treated immediately by direct-current cardioversion. Refractory ventricular tachycardia/fibrillation may suggest the need for mechanical circulatory support (MCS). Acute or chronic conduction system disease, including complete heart block, may be seen and should be treated with temporary or permanent pacing based on the clinical scenario.

Chronic arrhythmias may persist long after the acute disease has passed, especially in the setting of myocardial fibrosis. Thus, children who recover from myocarditis, regardless of cause, should be followed indefinitely with appropriate arrhythmia surveillance. Our practice has been to perform ambulatory Holter monitoring annually at a minimum with more frequent assessment or alternative strategies such as event recorders in patients with symptoms or concerns for ongoing arrhythmia. Antibiotic agents should not be given unless a bacterial infection is suspected and appropriate cultures are obtained prior to initiating therapy.

The use of immunosuppressive and immunomodulatory agents in suspected cases or proven cases of viral myocarditis remains controversial. The routine use of immunosuppressive agents for adults with myocarditis in the United States is not recommended based on results from the Myocarditis Treatment Trial. The Myocarditis Treatment Trial analyzed the use of immunosuppressive and steroid therapy (52). Although the study was performed in adult patients, the results are potentially applicable to children. There was no difference among patients treated with azathioprine and prednisone, cyclosporine and prednisone, and conventional therapy. Immunosuppressive therapy was not beneficial in most patients with histologically confirmed myocarditis. However, there may be selected populations with chronic myocarditis that benefit from immunosuppression. Frustaci et al. have reported favorable responses in adult patients with active myocarditis, chronic heart failure, absence of viral genome in the myocardium, and positive cardiac autoantibodies when treated with azathioprine and prednisone (150). One pediatric study suggested that immunosuppression may actually result in an improvement in patients who have evidence of viral myocarditis (151). Further pediatric investigation will be required to better define this strategy.

Another important therapeutic option is the use of intravenous γ -globulin (IVIG) in children with myocarditis. This option is based on the early results of Drucker et al. (152), who investigated the use of this agent in 21 of 46 children with myocarditis. Patients who received IVIG had better left ventricular function at follow-up. However, there was no clear survival benefit. Murine data also support the use of IVIG in viral myocarditis (153). The results of the Intervention for Myocarditis and Acute Cardiomyopathy (IMAC-1) trial evaluating the use of IVIG in adults with recent myocarditis or DCM < 6 months in duration showed no benefit when compared to placebo (154). However, our recent data in the pediatric transplant population suggest there may be a role for IVIG and viral myocarditis, especially in PVB19-positive patients (82).

The use of interferon has also been proposed as a potential treatment option. Kuhl et al. reported efficacy of interferon- β treatment in myocarditis with viral clearance and prevention of progressive deterioration of left ventricular function (155). In this phase-II study, 22 consecutive patients with chronic left ventricular dysfunction and PCR-proven enteroviral or adenoviral infection were injected subcutaneously with interferon- β three times weekly for approximately 6 months, with all 22 patients demonstrating viral clearance, reduced

left ventricular dilation, and improved systolic function. D'Alto et al. (156) reported similar success with interferon- α in patients with enterovirus-induced myocarditis. No reports exist regarding interferon therapy for adenovirus.

The prognosis of acute myocarditis in newborns has been poor over the years (157–159). A 75% mortality rate was observed in 25 infants with suspected CVB myocarditis (157). Most deaths occurred in the first week of the illness. The six infants who survived had no apparent sequelae, although long-term follow-up was not reported. It is likely that other viral causes of myocarditis such as adenovirus have similar poor outcomes as infants. Older infants and children have a better prognosis, with a mortality rate between 10% and 25% in clinically recognizable cases. Has-treiter reported complete recovery in 50% of their patients (158). Twenty-five percent of the patients continued to have an abnormal electrocardiogram or chest radiograph even though they were clinically asymptomatic. Abnormalities in the resting electrocardiogram may not be seen, but may be brought out with exercise. Adult patients who recover may be asymptomatic at rest or with light exertion but may demonstrate a reduced working capacity with exercise stress testing. We suggest continued surveillance of children and adults as long-term sequelae are becoming increasingly recognized with the use of more sophisticated imaging modalities such as cardiac MRI.

Advanced Therapies Including Mechanical Support

Patients with fulminant myocarditis may progress to need for advanced therapies including MCS. Extracorporeal membrane oxygenation (ECMO) is a widely used tool for patients who have cardiorespiratory compromise as an acute support strategy (160,161). Teele et al. (65) recently reported a single-center cohort of pediatric patients with acute fulminant myocarditis and the use of ECMO as a rescue strategy in patients with end-organ dysfunction or arrhythmias with a transplant-free survival rate of 80%. With the development of newer and miniaturized devices, alternative options are now available for both short- and long-term support (162). We recently published our single-center data on the effectiveness of MCS in pediatric patients with acute fulminant and persistent myocarditis, which is the largest report of its kind in children (163). In our cohort, 16 patients were treated for myocarditis with conventional therapies plus ECMO, ventricular assist device (VAD), or both. Of these, 75% survived with seven recovering ventricular function with device removal and five went on to uncomplicated cardiac transplant. Patients without inflammation or evidence of viral infection on EMB were significantly more likely to recover. VADs are used successfully in adults with good outcome (164). Their use will increase in the pediatric population given the increasing availability of devices and the potential need for sustained support in select patients. Furthermore, these devices allow time for myocardial recovery and favorable remodeling of key proteins that may be damaged in viral myocarditis (165).

Vaccination

Vaccination has been used successfully to prevent diseases. The efficacy of the polio vaccine has led to the suggestion that a broadly specific enteroviral vaccine, or at least a CVB-specific vaccine, could be beneficial for reducing the incidence of myocarditis or DCM. Development of CVB3 vaccine has afforded protection in mice but no human studies have been conducted (166).

The possibility of success in this regard is supported by the study of EFE. This form of DCM was the most common form

identified in children until the late 1960s, with an incidence of 1 in 5,000 live births in the United States. Since that time, the incidence has declined significantly. Mumps virus genomic RNA sequences were found in 90% of myocardial samples from EFE patients analyzed (49) (Fig. 56.10). Thus, EFE may have resulted from persistent in utero mumps infection of the myocardium. The mumps virus vaccine has all but eliminated this form of DCM. Although a CVB-specific vaccine may reduce the incidence of myocarditis, other viruses, particularly adenovirus, are potential etiologic agents.

REFERENCES

1. Jefferies JL, Towbin JA. Dilated cardiomyopathy. *Lancet* 2010;375:752-762.
2. Towbin JA, et al. Incidence, causes, and outcomes of dilated cardiomyopathy in children. *JAMA* 2006;296:1867-1876.
3. Berkovich S, Rodriguez-Torres R, Lin JS. Virologic studies in children with acute myocarditis. *Am J Dis Child* 1968;115:207-212.
4. Dec GW Jr, et al. Active myocarditis in the spectrum of acute dilated cardiomyopathies. Clinical features, histologic correlates, and clinical outcome. *N Engl J Med* 1985;312:885-890.
5. Bowles NE, Bowles KR, Towbin JA. Viral genomic detection and outcome in myocarditis. *Heart Fail Clin* 2005;1:407-417.
6. Weber MA, et al. Clinicopathological features of paediatric deaths due to myocarditis: an autopsy series. *Arch Dis Child* 2008;93:594-598.
7. Martin AB, et al. Acute myocarditis. Rapid diagnosis by PCR in children. *Circulation* 1994;90:330-339.
8. Bowles NE, Towbin JA. Molecular aspects of myocarditis. *Curr Opin Cardiol* 1998;13:179-184.
9. Woodruff JF. Viral myocarditis. A review. *Am J Pathol* 1980;101:425-484.
10. Hirschman SZ, Hammer GS. Coxsackie virus myopericarditis. A microbiological and clinical review. *Am J Cardiol* 1974;34:224-232.
11. Schowengerdt KO, et al. Association of parvovirus B19 genome in children with myocarditis and cardiac allograft rejection: diagnosis using the polymerase chain reaction. *Circulation* 1997;96:3549-3554.
12. Francalanci P, et al. Cardiotropic viruses in the myocardium of children with end-stage heart disease. *J Heart Lung Transplant* 2004;23:1046-1052.
13. Maisch B, et al. Human viral cardiomyopathy. *Front Biosci* 2003;8:s39-s67.
14. Wang X, et al. Prevalence of human parvovirus B19 DNA in cardiac tissues of patients with congenital heart diseases indicated by nested PCR and in situ hybridization. *J Clin Virol* 2004;31:20-24.
15. Pankuweit S, et al. Parvovirus B19 genome in endomyocardial biopsy specimen. *Circulation* 2004;109:e179.
16. Breinholt JP, et al. Viral epidemiologic shift in inflammatory heart disease: the increasing involvement of parvovirus B19 in the myocardium of pediatric cardiac transplant patients. *J Heart Lung Transplant* 2010;29:739-746.
17. Tschöpe C, et al. High prevalence of cardiac parvovirus B19 infection in patients with isolated left ventricular diastolic dysfunction. *Circulation* 2005;111:879-886.
18. Bowles NE, et al. Detection of viruses in myocardial tissues by polymerase chain reaction. Evidence of adenovirus as a common cause of myocarditis in children and adults. *J Am Coll Cardiol* 2003;42:466-472.
19. Proby CM, et al. Acute myopericarditis in influenza A infection. *Q J Med* 1986;60:887-892.
20. Khouzam RN, et al. Fulminant myocarditis associated with novel H1N1 influenza A. *Heart Lung* 2011;40:566-568.
21. Khambekar SK, Harden S, Corbett S. Influenza A (H1N1) and myocarditis. *Heart* 2011;97:1630.
22. Schonian U, et al. Cytomegalovirus-associated heart muscle disease. *Eur Heart J* 1995;16:46-49.
23. Lowry PJ, Thompson RA, Littler WA. Humoral immunity in cardiomyopathy. *Br Heart J* 1983;50:390-394.
24. Matsumori A. Hepatitis C virus infection and cardiomyopathies. *Circ Res* 2005;96:144-147.
25. Okabe M, et al. Chronic variant of myocarditis associated with hepatitis C virus infection. *Circulation* 1997;96:22-24.
26. Ainger LE, Lawyer NG, Fitch CW. Neonatal rubella myocarditis. *Br Heart J* 1966;28:691-697.
27. Lorber A, et al. The scale of myocardial involvement in varicella myocarditis. *Int J Cardiol* 1988;20:257-262.
28. Chaudary S, Jaski BE. Fulminant mumps myocarditis. *Ann Intern Med* 1989;110:569-570.
29. Frishman W, et al. Infectious mononucleosis and fatal myocarditis. *Chest* 1977;72:535-538.
30. Barbaro G, et al. Incidence of dilated cardiomyopathy and detection of HIV in myocardial cells of HIV-positive patients. Gruppo Italiano per lo Studio Cardiocologico dei Pazienti Affetti da AIDS. *N Engl J Med* 1998;339:1093-1099.
31. Mahrholdt H, et al. Presentation, patterns of myocardial damage, and clinical course of viral myocarditis. *Circulation* 2006;114:1581-1590.
32. Puchkov GE, Min'kovich BM. Respiratory syncytial infection in a child complicated by interstitial myocarditis with fatal outcome. *Arkh Patol* 1972;34:70-73.
33. Vargo TA, et al. Myocarditis due to visceral larva migrans. *J Pediatr* 1977;90:322-323.
34. Poltera AA, Cox JN, Owor R. Pancarditis affecting the conducting system and all valves in human African trypanosomiasis. *Br Heart J* 1976;38:827-837.
35. Marsden PD. South American trypanosomiasis (Chagas' disease). *Int Rev Trop Med* 1971;4:97-121.
36. Leak D, Meghji M. Toxoplasmic infection in cardiac disease. *Am J Cardiol* 1979;43:841-849.
37. Bessoudo R, Marrie TJ, Smith ER. Cardiac involvement in trichinosis. *Chest* 1981;79:698-699.
38. Karjalainen J. Streptococcal tonsillitis and acute nonrheumatic myopericarditis. *Chest* 1989;95:359-363.
39. Brasier AR, et al. Myopericarditis as an initial presentation of meningococemia. Unusual manifestation of infection with serotype W135. *Am J Med* 1987;82:641-644.
40. Gross D, Willens H, Zeldis SM. Myocarditis in legionnaires' disease. *Chest* 1981;79:232-234.
41. Lewes D, Rainford DJ, Lane WF. Symptomless myocarditis and myalgia in viral and Mycoplasma pneumoniae infections. *Br Heart J* 1974;36:924-932.
42. Marin-Garcia J, Barrett FF. Myocardial function in Rocky Mountain spotted fever: echocardiographic assessment. *Am J Cardiol* 1983;51:341-343.
43. McAlister HF, et al. Lyme carditis: an important cause of reversible heart block. *Ann Intern Med* 1989;110:339-345.
44. Afzal A, et al. Myocarditis and pericarditis with tamponade associated with disseminated tuberculosis. *Can J Cardiol* 2000;16:519-521.
45. Butany J, Ahn E, Luk A. Drug-related cardiac pathology. *J Clin Pathol* 2009;62:1074-1084.
46. Ferrans VJ, Rodriguez ER. Cardiovascular lesions in collagen-vascular diseases. *Heart Vessels Suppl* 1985;1:256-261.
47. Lash AD, Wittman AL, Quismorio FP Jr. Myocarditis in mixed connective tissue disease: clinical and pathologic study of three cases and review of the literature. *Semin Arthritis Rheum* 1986;15:288-296.
48. Kerr LD, Spiera H. Myocarditis as a complication in scleroderma patients with myositis. *Clin Cardiol* 1993;16:895-899.
49. Ni J, et al. Viral infection of the myocardium in endocardial fibroelastosis. Molecular evidence for the role of mumps virus as an etiologic agent. *Circulation* 1997;95:133-139.
50. Yamamoto LG. Kawasaki disease. *Pediatr Emerg Care* 2003;19:422-424.
51. Okura Y, et al. A clinical and histopathologic comparison of cardiac sarcoidosis and idiopathic giant cell myocarditis. *J Am Coll Cardiol* 2003;41:322-329.
52. Mason JW, et al. A clinical trial of immunosuppressive therapy for myocarditis. The Myocarditis Treatment Trial Investigators. *N Engl J Med* 1995;333:269-275.
53. Drory Y, et al. Sudden unexpected death in persons less than 40 years of age. *Am J Cardiol* 1991;68:1388-1392.
54. Kawai C. From myocarditis to cardiomyopathy: mechanisms of inflammation and cell death: learning from the past for the future. *Circulation* 1999;99:1091-1100.
55. Kuhl U, Schultheiss HP. Myocarditis in children. *Heart Fail Clin* 2010;6:483-496, viii-ix.
56. Friedman RA, et al. Persistence of ventricular arrhythmia after resolution of occult myocarditis in children and young adults. *J Am Coll Cardiol* 1994;24:780-783.
57. Shimizu C, et al. Molecular identification of viruses in sudden infant death associated with myocarditis and pericarditis. *Pediatr Infect Dis J* 1995;14:584-588.
58. Ichikawa R, et al. The follow-up evaluation of electrocardiogram and arrhythmias in children with fulminant myocarditis. *Circ J* 2011;75:932-938.
59. Felker GM, et al. Echocardiographic findings in fulminant and acute myocarditis. *J Am Coll Cardiol* 2000;36:227-232.
60. Di Bella G, et al. Myocardial deformation in acute myocarditis with normal left ventricular wall motion—a cardiac magnetic resonance and 2-dimensional strain echocardiographic study. *Circ J* 2010;74:1205-1213.
61. Brown JL, Hirsh DA, Mahle WT. Use of troponin as a screen for chest pain in the pediatric emergency department. *Pediatr Cardiol* 2012;33:337-342.
62. Kobayashi D, et al. Myopericarditis in children: elevated troponin I level does not predict outcome. *Pediatr Cardiol* 2012; Feb 10. [Epub ahead of print].
63. Lauer B, et al. Cardiac troponin T in patients with clinically suspected myocarditis. *J Am Coll Cardiol* 1997;30:1354-1359.
64. Mlczoch E, et al. NT-pro BNP in acute childhood myocarditis. *J Pediatr* 2012;160:178-179.
65. Teele SA, et al. Management and outcomes in pediatric patients presenting with acute fulminant myocarditis. *J Pediatr* 2011;158:638 e1-643 e1.
66. Friedrich MG, et al. Cardiovascular magnetic resonance in myocarditis: a JACC White Paper. *J Am Coll Cardiol* 2009;53:1475-1487.
67. Grun S, et al. Long-term follow-up of biopsy-proven viral myocarditis: predictors of mortality and incomplete recovery. *J Am Coll Cardiol* 2012;59:1604-1615.

68. Zagrosek A, et al. Cardiac magnetic resonance monitors reversible and irreversible myocardial injury in myocarditis. *JACC Cardiovasc Imaging* 2009;2:131–138.
69. Baughman KL. Diagnosis of myocarditis: death of Dallas criteria. *Circulation* 2006;113:593–595.
70. Grogan M, et al. Long-term outcome of patients with biopsy-proved myocarditis: comparison with idiopathic dilated cardiomyopathy. *J Am Coll Cardiol* 1995;26:80–84.
71. Mason JW. Distinct forms of myocarditis. *Circulation* 1991;83:1110–1111.
72. Chow LH, et al. Insensitivity of right ventricular endomyocardial biopsy in the diagnosis of myocarditis. *J Am Coll Cardiol* 1989;14:915–920.
73. Hauck AJ, Kearney DL, Edwards WD. Evaluation of postmortem endomyocardial biopsy specimens from 38 patients with lymphocytic myocarditis: implications for role of sampling error. *Mayo Clin Proc* 1989;64:1235–1245.
74. Holzmann M, et al. Complication rate of right ventricular endomyocardial biopsy via the femoral approach: a retrospective and prospective study analyzing 3048 diagnostic procedures over an 11-year period. *Circulation* 2008;118:1722–1728.
75. Aretz HT. Myocarditis: the Dallas criteria. *Hum Pathol* 1987;18:619–624.
76. Piedra PA, et al. Incidence and prevalence of neutralizing antibodies to the common adenoviruses in children with cystic fibrosis: implication for gene therapy with adenovirus vectors. *Pediatrics* 1998;101:1013–1019.
77. Archard LC, et al. Characterization of Coxsackie B virus RNA in myocardium from patients with dilated cardiomyopathy by nucleotide sequencing of reverse transcription-nested polymerase chain reaction products. *Hum Pathol* 1998;29:578–584.
78. Jin O, et al. Detection of enterovirus RNA in myocardial biopsies from patients with myocarditis and cardiomyopathy using gene amplification by polymerase chain reaction. *Circulation* 1990;82:8–16.
79. Weiss LM, et al. Detection of enteroviral RNA in idiopathic dilated cardiomyopathy and other human cardiac tissues. *J Clin Invest* 1992;90:156–159.
80. Donoso Mantke O, et al. High prevalence of cardiotropic viruses in myocardial tissue from explanted hearts of heart transplant recipients and heart donors: a 3-year retrospective study from a German patients' pool. *J Heart Lung Transplant* 2005;24:1632–1638.
81. Klingel K, et al. Molecular pathology of inflammatory cardiomyopathy. *Med Microbiol Immunol* 2004;193:101–107.
82. Moulik M, et al. Viral endomyocardial infection is an independent predictor and potentially treatable risk factor for graft loss and coronary vasculopathy in pediatric cardiac transplant recipients. *J Am Coll Cardiol* 2010;56:582–592.
83. Akhtar N, et al. Tracheal aspirate as a substrate for polymerase chain reaction detection of viral genome in childhood pneumonia and myocarditis. *Circulation* 1999;99:2011–2018.
84. Sole MJ, Liu P. Viral myocarditis: a paradigm for understanding the pathogenesis and treatment of dilated cardiomyopathy. *J Am Coll Cardiol* 1993;22:99A–105A.
85. Hutchins GM, Vie SA. The progression of interstitial myocarditis to idiopathic endocardial fibroelastosis. *Am J Pathol* 1972;66:483–496.
86. Saphir O, Field M. Complications of myocarditis in children. *J Pediatr* 1954;45:457–463.
87. Cooper LT Jr. Myocarditis. *N Engl J Med* 2009;360:1526–1538.
88. Burch GE, et al. Diphtheritic myocarditis. A histochemical and electron microscopic study. *Am J Cardiol* 1968;21:261–268.
89. Hidron AI, et al. Chagas cardiomyopathy in the context of the chronic disease transition. *PLoS Negl Trop Dis* 2010;4:e688.
90. Marin-Neto JA, et al. Pathogenesis of chronic Chagas heart disease. *Circulation* 2007;115:1109–1123.
91. James TN. Sudden death in babies: new observations in the heart. *Am J Cardiol* 1968;22:479–506.
92. Davidoff R, et al. Giant cell versus lymphocytic myocarditis. A comparison of their clinical features and long-term outcomes. *Circulation* 1991;83:953–961.
93. Rosenstein ED, Zucker MJ, Kramer N. Giant cell myocarditis: most fatal of autoimmune diseases. *Semin Arthritis Rheum* 2000;30:1–16.
94. Stoica SC, et al. Ventricular assist surprise: giant cell myocarditis or sarcoidosis? *J Thorac Cardiovasc Surg* 2003;126:2072–2074.
95. Maisch B, et al. Diagnostic relevance of humoral and cell-mediated immune reactions in patients with acute viral myocarditis. *Clin Exp Immunol* 1982;48:533–545.
96. Langley RJ, Prince GA, Ginsberg HS. HIV type-1 infection of the cotton rat (*Sigmodon fulviventer* and *S. hispidus*). *Proc Natl Acad Sci U S A* 1998;95:14355–14360.
97. Henke A, et al. The role of CD8+ T lymphocytes in coxsackievirus B3-induced myocarditis. *J Virol* 1995;69:6720–6728.
98. Godeny EK, Gauntt CJ. Murine natural killer cells limit coxsackievirus B3 replication. *J Immunol* 1987;139:913–918.
99. Hayder H, Mullbacher A. Molecular basis of immune evasion strategies by adenoviruses. *Immunol Cell Biol* 1996;74:504–512.
100. Brownstein DG. Comparative genetics of resistance to viruses. *Am J Hum Genet* 1998;62:211–214.
101. Knowlton KU, et al. A mutation in the puff region of VP2 attenuates the myocarditic phenotype of an infectious cDNA of the Woodruff variant of coxsackievirus B3. *J Virol* 1996;70:7811–7818.
102. Wong CY, Woodruff JJ, Woodruff JF. Generation of cytotoxic T lymphocytes during coxsackievirus tb-3 infection. II. Characterization of effector cells and demonstration cytotoxicity against viral-infected myofibers. *J Immunol* 1977;118:1165–1169.
103. Matsumori A. Molecular and immune mechanisms in the pathogenesis of cardiomyopathy—role of viruses, cytokines, and nitric oxide. *Jpn Circ J* 1997;61:275–291.
104. Lee C, et al. Genomic regions of coxsackievirus B3 associated with cardiomyopathy. *J Med Virol* 1997;52:341–347.
105. Bowles NE, et al. Detection of Coxsackie-B-virus-specific RNA sequences in myocardial biopsy samples from patients with myocarditis and dilated cardiomyopathy. *Lancet* 1986;1:1120–1123.
106. Bowles NE, et al. End-stage dilated cardiomyopathy. Persistence of enterovirus RNA in myocardium at cardiac transplantation and lack of immune response. *Circulation* 1989;80:1128–1136.
107. Hori H, et al. The role of cell mediated immunity in coxsackie B viral myocarditis. *Jpn Circ J* 1981;45:1409–1414.
108. Strand S, et al. Lymphocyte apoptosis induced by CD95 (APO-1/Fas) ligand-expressing tumor cells—a mechanism of immune evasion? *Nat Med* 1996;2:1361–1366.
109. Huber SA. Coxsackievirus-induced myocarditis is dependent on distinct immunopathogenic responses in different strains of mice. *Lab Invest* 1997;76:691–701.
110. Pauschinger M, et al. Detection of adenoviral genome in the myocardium of adult patients with idiopathic left ventricular dysfunction. *Circulation* 1999;99:1348–1354.
111. Narula J, et al. Apoptosis in myocytes in end-stage heart failure. *N Engl J Med* 1996;335:1182–1189.
112. Schultheiss HP, Schulze K, Dörner A. Significance of the adenine nucleotide translocator in the pathogenesis of viral heart disease. *Mol Cell Biochem* 1996;163–164:319–327.
113. Pankuweit S, et al. Autoantibodies in sera of patients with myocarditis: characterization of the corresponding proteins by isoelectric focusing and N-terminal sequence analysis. *J Mol Cell Cardiol* 1997;29:77–84.
114. Graham BH, et al. A mouse model for mitochondrial myopathy and cardiomyopathy resulting from a deficiency in the heart/muscle isoform of the adenine nucleotide translocator. *Nat Genet* 1997;16:226–234.
115. Baba A, Yoshikawa T, Ogawa S. Autoantibodies produced against sarcolemmal Na-K-ATPase: possible upstream targets of arrhythmias and sudden death in patients with dilated cardiomyopathy. *J Am Coll Cardiol* 2002;40:1153–1159.
116. Caforio AL, et al. Novel organ-specific circulating cardiac autoantibodies in dilated cardiomyopathy. *J Am Coll Cardiol* 1990;15:1527–1534.
117. Caforio AL, et al. Circulating cardiac-specific autoantibodies as markers of autoimmunity in clinical and biopsy-proven myocarditis. The Myocarditis Treatment Trial Investigators. *Eur Heart J* 1997;18:270–275.
118. Matsumori A, et al. Increased circulating cytokines in patients with myocarditis and cardiomyopathy. *Br Heart J* 1994;72:561–566.
119. Kubota T, et al. Cardiac-specific overexpression of tumor necrosis factor- α causes lethal myocarditis in transgenic mice. *J Card Fail* 1997;3:117–124.
120. Kroemer G, Martinez C. Cytokines and autoimmune disease. *Clin Immunol Immunopathol* 1991;61:275–295.
121. Yamada T, Matsumori A, Sasayama S. Therapeutic effect of anti-tumor necrosis factor- α antibody on the murine model of viral myocarditis induced by encephalomyocarditis virus. *Circulation* 1994;89:846–851.
122. Kishimoto C, et al. Cytokine and murine coxsackievirus B3 myocarditis. Interleukin-2 suppressed myocarditis in the acute stage but enhanced the condition in the subsequent stage. *Circulation* 1994;89:2836–2842.
123. Shioi T, et al. Protective role of interleukin-12 in viral myocarditis. *J Mol Cell Cardiol* 1997;29:2327–2334.
124. Okura Y, et al. Characterization of cytokine and iNOS mRNA expression *in situ* during the course of experimental autoimmune myocarditis in rats. *J Mol Cell Cardiol* 1997;29:491–502.
125. McCarthy RE III, et al. Long-term outcome of fulminant myocarditis as compared with acute (nonfulminant) myocarditis. *N Engl J Med* 2000;342:690–695.
126. Felker GM, et al. Myocarditis and long-term survival in peripartum cardiomyopathy. *Am Heart J* 2000;140:785–791.
127. Baboonian C, Treasure T. Meta-analysis of the association of enteroviruses with human heart disease. *Heart* 1997;78:539–543.
128. Badorff C, et al. Enteroviral protease 2A cleaves dystrophin: evidence of cytoskeletal disruption in an acquired cardiomyopathy. *Nat Med* 1999;5:320–326.
129. Towbin JA. The role of cytoskeletal proteins in cardiomyopathies. *Curr Opin Cell Biol* 1998;10:131–139.
130. Towbin JA, Bowles NE. The failing heart. *Nature* 2002;415:227–233.
131. Grumbach IM, et al. Adenoviruses and enteroviruses as pathogens in myocarditis and dilated cardiomyopathy. *Acta Cardiol* 1999;54:83–88.
132. Calabrese F, Thiene G. Myocarditis and inflammatory cardiomyopathy: microbiological and molecular biological aspects. *Cardiovasc Res* 2003;60:11–25.
133. Andreoletti L, et al. Active Coxsackieviral B infection is associated with disruption of dystrophin in endomyocardial tissue of patients who died suddenly of acute myocardial infarction. *J Am Coll Cardiol* 2007;50:2207–2214.

134. O'Connell JB, et al. Clinical and pathologic findings of myocarditis in two families with dilated cardiomyopathy. *Am Heart J* 1984;107:127-135.
135. Bergelson JM, et al. Isolation of a common receptor for Coxsackie B viruses and adenoviruses 2 and 5. *Science* 1997;275:1320-1323.
136. Tomko RP, Xu R, Philipson L. HCAR and MCAR: the human and mouse cellular receptors for subgroup C adenoviruses and group B coxsackieviruses. *Proc Natl Acad Sci U S A* 1997;94:3352-3356.
137. Poller W, et al. Highly variable expression of virus receptors in the human cardiovascular system. Implications for cardiotropic viral infections and gene therapy. *Z Kardiol* 2002;91:978-991.
138. Bowles NE, et al. Analysis of the coxsackievirus B-adenovirus receptor gene in patients with myocarditis or dilated cardiomyopathy. *Mol Genet Metab* 2002;77:257-259.
139. Fischer R, et al. CAR-diology—a virus receptor in the healthy and diseased heart. *J Mol Med (Berl)* 2009;87:879-884.
140. Yuen S, et al. The coxsackie-adenovirus receptor induces an inflammatory cardiomyopathy independent of viral infection. *J Mol Cell Cardiol* 2011;50:826-840.
141. Shiral GS, et al. Association of viral genome with graft loss in children after cardiac transplantation. *N Engl J Med* 2001;344:1498-1503.
142. Bridges ND, et al. Adenovirus infection in the lung results in graft failure after lung transplantation. *J Thorac Cardiovasc Surg* 1998;116:617-623.
143. Kiel RJ, et al. Coxsackievirus B3 myocarditis in C3H/HeJ mice: description of an inbred model and the effect of exercise on virulence. *Eur J Epidemiol* 1989;5:348-350.
144. Jessup M, et al. 2009 focused update: ACCF/AHA Guidelines for the Diagnosis and Management of Heart Failure in Adults: a report of the American College of Cardiology Foundation/American Heart Association Task Force on Practice Guidelines: developed in collaboration with the International Society for Heart and Lung Transplantation. *Circulation* 2009;119:1977-2016.
145. Rezkalla S, et al. Effect of delayed captopril therapy on left ventricular mass and myonecrosis during acute coxsackievirus murine myocarditis. *Am Heart J* 1990;120:1377-1381.
146. Shijie Z, et al. Mao-to prolongs the survival of and reduces TNF-alpha expression in mice with viral myocarditis. *Evid Based Complement Alternat Med* 2010;7:341-349.
147. Pauschinger M, et al. Carvedilol improves left ventricular function in murine coxsackievirus-induced acute myocarditis association with reduced myocardial interleukin-1beta and MMP-8 expression and a modulated immune response. *Eur J Heart Fail* 2005;7:444-452.
148. Kindermann I, et al. Predictors of outcome in patients with suspected myocarditis. *Circulation* 2008;118:639-648.
149. Swedberg K, et al. Guidelines for the diagnosis and treatment of chronic heart failure: executive summary (update 2005): The Task Force for the Diagnosis and Treatment of Chronic Heart Failure of the European Society of Cardiology. *Eur Heart J* 2005;26:1115-1140.
150. Frustaci A, et al. Immunosuppressive therapy for active lymphocytic myocarditis: virological and immunologic profile of responders versus nonresponders. *Circulation* 2003;107:857-863.
151. Camargo PR, et al. Favorable effects of immunosuppressive therapy in children with dilated cardiomyopathy and active myocarditis. *Pediatr Cardiol* 1995;16:61-68.
152. Drucker NA, et al. Gamma-globulin treatment of acute myocarditis in the pediatric population. *Circulation* 1994;89:252-257.
153. Takada H, Kishimoto C, Hiraoka Y. Therapy with immunoglobulin suppresses myocarditis in a murine coxsackievirus B3 model. Antiviral and anti-inflammatory effects. *Circulation* 1995;92:1604-1611.
154. McNamara DM, et al. Controlled trial of intravenous immune globulin in recent-onset dilated cardiomyopathy. *Circulation* 2001;103:2254-2259.
155. Kuhl U, et al. Interferon-beta treatment eliminates cardiotropic viruses and improves left ventricular function in patients with myocardial persistence of viral genomes and left ventricular dysfunction. *Circulation* 2003;107:2793-2798.
156. Daliento L, et al. Successful treatment of enterovirus-induced myocarditis with interferon-alpha. *J Heart Lung Transplant* 2003;22:214-217.
157. Bengtsson E, Lamberger B. Five-year follow-up study of cases suggestive of acute myocarditis. *Am Heart J* 1966;72:751-763.
158. Hastreiter AR, Miller RA. Diagnosis and treatment of myocarditis and other myocardial diseases. *Adv Cardiol Pulm Dis* 1964;22:250-258.
159. English RF, et al. Outcomes for children with acute myocarditis. *Cardiol Young* 2004;14:488-493.
160. Duncan BW, et al. Mechanical circulatory support for the treatment of children with acute fulminant myocarditis. *J Thorac Cardiovasc Surg* 2001;122:440-448.
161. Rajagopal SK, et al. Extracorporeal membrane oxygenation for the support of infants, children, and young adults with acute myocarditis: a review of the Extracorporeal Life Support Organization registry. *Crit Care Med* 2010;38:382-387.
162. Jefferies JL, Price JF, Morales DL. Mechanical support in childhood heart failure. *Heart Fail Clin* 2010;6:559-573, x.
163. Wilmot I, et al. Effectiveness of mechanical circulatory support in children with acute fulminant and persistent myocarditis. *J Card Fail* 2011;17:487-494.
164. Topkara VK, et al. Ventricular assist device use for the treatment of acute viral myocarditis. *J Thorac Cardiovasc Surg* 2006;131:1190-1191.
165. Vatta M, et al. Molecular remodelling of dystrophin in patients with end-stage cardiomyopathies and reversal in patients on assistance-device therapy. *Lancet* 2002;359:936-941.
166. Zhang L, et al. Vaccination with coxsackievirus B3 virus-like particles elicits humoral immune response and protects mice against myocarditis. *Vaccine* 2012;30:2301-2308. [Epub 2012 Jan 31.]

Susan W. Denfield

Cardiomyopathies are defined as diseases of the myocardium associated with cardiac dysfunction (1). Per the World Health Organization (WHO), restrictive cardiomyopathy (RCM) is characterized by restrictive filling and reduced diastolic volume of either or both ventricles with normal or near-normal systolic function and wall thicknesses. Increased interstitial fibrosis may be present. It may be idiopathic or associated with another disease.

“Contemporary Definitions and Classification of the Cardiomyopathies” have been proposed by a consensus panel organized by the American Heart Association (AHA) to draw attention to the rapid advancement of molecular genetics in cardiology (2). The AHA consensus statement defined primary RCM as a rare form of heart disease characterized by “normal or decreased volume of both ventricles associated with biatrial enlargement, normal left ventricular wall thickness and atrioventricular valves, impaired ventricular filling with restrictive physiology, and normal (or near normal) systolic function” (2). At that time, the panel placed RCM in a “mixed” cardiomyopathy category because the causes of the diseases resulting in RCM were believed to be predominantly nongenetic.

This chapter reviews the epidemiology, etiologies including known genes and associated syndromes, pathology, pathophysiology, clinical presentation, diagnostic evaluation, differential diagnosis, outcome, and management of pediatric patients with RCM.

EPIDEMIOLOGY

Of the four types of cardiomyopathy categorized by the WHO, dilated, hypertrophic, restrictive, and arrhythmogenic right ventricular cardiomyopathy, restrictive cardiomyopathy is the least common (1). In children, RCM accounts for 2.5% to 5% of the diagnosed cardiomyopathies (3–7). In the Australian-based study by Nugent et al., RCM accounted for 2.5% of the cardiomyopathies diagnosed in children <10 years of age (6). This is similar to the two-region United States–based study by Lipshultz et al., who reported that RCM or other specified types (not dilated or hypertrophic) accounted for 3% of the cardiomyopathies in children <18 years of age (7). Three different single institution studies reported 5%, which may have been due to referral bias (3–5).

Overall, the incidence of cardiomyopathies is higher in children <1 year of age when all types of cardiomyopathy are considered (6,7). RCM may be an exception. In the Nugent et al. study, the incidence of all types of cardiomyopathy except restrictive declined rapidly after infancy to their maximum study age of 10 years (6). In the studies of RCM in children, the average age at the time of diagnosis was 6 years with median of 5 years and a range from 0.1 to 19 years (3–5,8–33). Only two of the patients were 19 at the time of diagnosis with the remainder <18 years old. At the time of diagnosis, 8% were

1 year of age or younger, with 12% between the ages of 12 and 19 years. Whether this apparent difference in usual age of onset is due to case ascertainment or true differences in the disease onset is unknown.

Gender differences have also been reported in cardiomyopathies. Beyond infancy, boys had a higher incidence of cardiomyopathy than girls in the study by Lipshultz et al. (7). Only hypertrophic and unspecified cardiomyopathies occurred with higher frequency in boys in the Nugent et al. study, with RCM occurring with equal frequency in boys and girls (6). Of the 205 subjects with RCM in whom gender was reported, 54% were female (3–37).

Sporadic and familial cases of RCM are reported. Approximately 30% of patients, in whom family history was reported, had a positive family history (3–37).

GENETICS

Mutations in at least 10 genes have been associated with the RCM phenotype and include sarcomeric and nonsarcomeric gene defects (Table 57-1) (38–51).

Sarcomeric Protein Gene Defects

Troponin I mutations have been identified in patients with RCM and hypertrophic cardiomyopathy (HCM) (39). Both the RCM phenotype and the HCM phenotype can be expressed in the same family. This indicates that idiopathic RCM can be part of the clinical expression of sarcomeric contractile protein disease. The diversity of the phenotypic expression of troponin mutations in families suggests that additional genetic or environmental factors or both play a role in disease expression. *De novo* mutations and autosomal dominant transmission have been documented in RCM patients and their families (39).

Kaski et al. (44) reported a small series of pediatric patients with RCM; 4 of the 12 patients had a positive family history of cardiomyopathy, but the phenotypes varied and included restrictive, dilated, and left ventricular noncompaction forms. Gene mutations were found in troponin I (TNNI3), troponin T (TNNT2), and alpha cardiac actin. Peddy et al. reported an infant who presented with malignant arrhythmias and RCM and had a *de novo* mutation of cardiac troponin T (45).

Ware et al. (46) described a mutation in a beta-myosin heavy chain gene in an infant with RCM. Mutations in the beta-myosin heavy chain account for approximately 40% of mutations found in HCM in adults (47). The overlapping genotypic–phenotypic correlations are also evident in a report by Olson et al. (48). The proband was a child with a myosin light-chain mutation resulting in a cardiomyopathy with midcavitary hypertrophy and restrictive physiology that was inherited in an autosomal recessive pattern. His two older brothers had cardiomyopathy with dilated atria, both

TABLE 57.1 Gene Mutations Reported in Association with RCM

Sarcomeric Mutations	Nonsarcomeric Mutations
Troponin I	Desmin
Troponin T	RSK2 (Coffin-Lowry syndrome)
Alpha cardiac actin	Lamin A/C (Emery-Dreifuss)
Myosin-binding protein C	Transthyretin (amyloidosis)
Beta-myosin heavy chain	
Myosin light chain	

of whom died related to thrombotic complications. Clinically unaffected family members were either heterozygotes or lacked the mutant allele. Additional gene mutations are likely to be found with ongoing genetic studies.

Nonsarcomeric Protein Gene Defects

Desmin and RSK2 mutations have been reported in children with RCM, while lamin A/C and transthyretin mutations have been reported to cause an RCM phenotype in adults. A Danish kindred has been documented in whom children have been identified as carriers of the familial transthyretin methionine 111 mutation, but none of the kindred has manifested amyloid-associated RCM in childhood (49), although adults in the family have developed RCM. The transthyretin Ile 122 mutation resulting in RCM with amyloidosis has only been reported to manifest RCM in adulthood, as well (40).

Desmin is a myofibrillar protein that is the chief intermediate filament of skeletal and cardiac muscle (41). It maintains the structural and functional integrity of the myofibrils and functions as a cytoskeletal protein linking Z bands to the plasma membrane. Mutations in the desmin gene may cause RCM with or without skeletal myopathy and with or without conduction system disease (41,42,50,51). The inheritance pattern is usually autosomal dominant. Sporadic mutations have also been identified (41).

Coffin-Lowry syndrome is an X-linked disorder caused by mutations in the RSK2 gene on chromosome Xp22.2 (43). It is characterized by developmental delays, short stature, facial dysmorphism, and progressive skeletal deformities. Cardiac anomalies are reported in approximately 14% of affected males with cardiomyopathy being one of the rare but reported cardiac abnormalities, including one patient with a restrictive phenotype (33).

Emery-Dreifuss muscular dystrophy was first described as an X-linked disorder caused by mutations in the gene encoding for emerin on chromosome Xq28 (38). However, it can also be an autosomal disorder caused by mutations in the gene encoding for lamin A and lamin C (LMNA) on chromosome 1q21.2–q21.3 (38). Both variants of the disease can cause cardiac abnormalities including dilated cardiomyopathy, atrial and ventricular arrhythmias, conduction abnormalities, and sudden death. Sanna et al. (38) reported on the cardiac features of Emery-Dreifuss caused by lamin A/C gene mutations, including one adult patient with a restrictive phenotype. The RCM phenotype has not been reported in children with Emery-Dreifuss to date.

Alstrom syndrome is characterized by cone-rod dystrophy resulting in progressive visual impairment, photophobia

and nystagmus, obesity, progressive sensorineural hearing impairment, dilated or RCM, insulin resistance, and multiple organ failure (52). ALMS1 is the only gene currently known to be associated with the syndrome and is estimated to be detected in 25% to 40% of individuals.

Mulibrey nanism is an autosomal recessive disease caused by mutations in the TRIM37 gene on chromosome 17q22–q23 encoding the peroxisomal TRIM37 protein of unknown function (53). Congestive heart failure and pericardial constriction were diagnosed during infancy in 12% and 6% of the patients, respectively, in a report by Karlberg et al. (53). Characteristic craniofacial features included scaphocephaly, facial triangularity, high and broad forehead, and low nasal bridge in more than 90% of the patients. Other findings included a peculiar high-pitched voice (96%), yellowish dots in ocular fundi (79%), cutaneous naevi flammei (65%), hepatomegaly (45%), and fibrous dysplasia of long bones (25%). Mild muscular hypotonicity (68%) was the only neurologic abnormality. Although more typically associated with constrictive pericarditis (CP), a mixed constrictive–restrictive phenotype has been described as not all patients have improved with pericardiectomy, and myocardial hypertrophy and fibrosis have been reported (54,55).

ETIOLOGIES

RCM has multiple causes and may result from myocardial diseases including noninfiltrative or infiltrative processes, storage diseases, endomyocardial diseases, myocarditis, and following cardiac transplantation (56) (Table 57.2). The pathology and histology vary with the underlying disease process. The most common etiology of RCM worldwide is secondary to endomyocardial fibrosis (EMF). EMF is estimated to affect 10 million people worldwide, occurring most often in children and adolescents (57,58). In adults outside the tropics, amyloidosis is the most common cause of RCM (59). One case of cardiac amyloidosis has been reported in a pediatric patient (5). In the pediatric population, outside the tropics, idiopathic RCM is probably the most common cause of RCM based on reported cases in the literature (3–37).

Endomyocardial Disease

EMF was first described by Davies in 1948 (60). It occurs most frequently in tropical and subtropical Africa, particularly Uganda and Nigeria. However, it is also found in tropical and subtropical regions throughout the world. It is occasionally seen in temperate climates, usually in individuals who previously lived in tropical areas. The etiology or etiologies remain unknown. Hypereosinophilia, likely related to parasitic infections, has occurred in some patients. However, there does not appear to be an increased prevalence of parasitic infections in patients with EMF. Autoimmunity, genetic, dietary, and environmental chemical factors have all been implicated in the development of EMF (58).

The disease occurs most often in children to young adults (57,58,61). Familial occurrence, and in some countries a high incidence in some ethnic groups, suggests a possible genetic predisposition (57,58). In a rural area of Mozambique, the overall prevalence of EMF was 20% in the population, but increased to 28% when two family members were affected and 39% when three or more family members were affected (57).

The disease is most commonly biventricular, followed by pure left ventricular involvement approximately 40% of the time and purely right ventricular in 10% (62). The symptom

TABLE 57.2 Causes of Restrictive Cardiomyopathies in Children and/or Adults

Myocardial	Endomyocardial
Idiopathic	Endomyocardial fibrosis
Familial/genetic	Hypereosinophilic syndrome (Löffler endocarditis)
Scleroderma	Endocardial fibroelastosis
Myocarditis	Carcinoid
Cardiac transplant	Metastatic cancers
Pseudoxanthoma elasticum	Radiation
Diabetic cardiomyopathy	Drugs—anthracyclines
Amyloidosis	Serotonin
Sarcoidosis	Methysergide
Gaucher disease	Ergotamine
Hurler disease	Mercurials
Fatty infiltration	Busulfan
Hemochromatosis	
Fabry disease	
Glycogen storage diseases	
Cystinosis (possibly)	
Emery-Dreifuss	
Coffin-Lowry syndrome	

complex varies with the site or sites of involvement. Symptoms from pulmonary venous congestion result from left-sided disease, while right-sided disease results in signs and symptoms from systemic venous congestion. Involvement of the mitral or tricuspid valve apparatus can result in significant valvular regurgitation. Medical and surgical therapy is palliative.

The histology of EMF is characterized by endocardial fibrosis of variable thickness. Histologic changes occur in predominantly three areas: the left ventricular apex, the mitral valve apparatus, and the right ventricular apex that may extend to the supporting structures of the tricuspid valve. In severe cases, the process may extend to the outflow tracts. Small patches of fibroelastosis may occur in the outflow tracts, but the elastin component is thought to be secondary and not a primary part of the process. Cellular infiltrates are not prominent. Eosinophilia is not typically a prominent feature in contrast to Löffler endocarditis.

Hypereosinophilic Syndrome/Löffler Endocarditis

Löffler endocarditis or the hypereosinophilic syndrome (HES) is similar to EMF in many respects. There is continued debate whether they are variants of the same disease. Although there are pathologic and clinical similarities, there are important contrasts. HES is typically seen in temperate climates. It is more common in adult males. Hypereosinophilia is present. HES includes persistent eosinophilia with 1,500 eosinophils/mm³ for at least 6 months or until death with evidence of organ involvement. Usually, in HES, various organs besides the heart are involved and may include the lungs, bone marrow, and brain (63). The cause of the eosinophilia is usually unknown,

but may be leukemic or secondary to parasitic, allergic, granulomatous, hypersensitivity, or neoplastic disorders (64).

Cardiac histologic findings include variable degrees of eosinophilic myocarditis (not characteristically seen in EMF), inflammatory reaction in the small intramural coronary vessels with thrombosis and fibrinoid change, and endocardial mural thrombosis and fibrotic thickening (62).

The clinical picture may include weight loss, fever, cough, rash, and heart failure. Systemic embolism is frequent. Death is usually secondary to the cardiac manifestations of the disease. Therapy for the hypereosinophilia may include corticosteroids, hydroxyurea, or vincristine, but this area of therapy is usually not directed by a cardiologist. Cardiac therapy has included digoxin, diuretics, afterload reduction, and anticoagulation. Surgical approaches have included mitral and/or tricuspid valve repair or replacement and excision of fibrotic endocardium and may be useful for symptom palliation of intractable heart failure. However, pediatric case reports and case series of HES and EMF patients report a relatively high reoperation rate secondary to dysfunction of the mechanical or bioprosthetic valves with recurrent thrombosis, fibrosis, or tearing despite anticoagulation (65,66). Significant cardiac symptoms may persist (class II to IV) (66).

Infiltrative and Storage Diseases

Several metabolic disorders with specific enzyme deficiencies can result in RCM, including lysosomal disorders such as Hurler syndrome, Gaucher disease, and Fabry disease and glycogen storage diseases that can be lysosomal disorders or result from cytoplasmic enzyme deficiencies.

Hemochromatosis may be a primary or secondary disease resulting from iron overload with subsequent dysfunction of multiple organs including the heart. Either RCM or more commonly dilated cardiomyopathy may result from hemochromatosis.

Nephropathic cystinosis is an autosomal recessive disease that leads to multiorgan failure from intracellular accumulation of cystine (67). Dixit and Greifer reported one patient followed from infancy who developed a cardiomyopathy with restrictive features in adulthood and had extremely high cystine levels in the myocardium. Owing to the patient's history of renal failure, renal transplantation, and hypertension, the exact etiology of the restrictive physiology is uncertain.

Sarcoidosis is a noncaseating granulomatous disorder that is more common in adults than in children. The granulomatous inflammatory process can affect the heart and result in RCM. Systolic dysfunction, pericarditis, conduction system disease, and sudden death may also occur. Although a common cause of RCM in adults, amyloidosis as a cause for RCM in pediatrics has been reported in only one case (5).

Drugs and Therapeutic Agents

Anthracyclines, serotonin, methysergide, ergotamine, mercurial agents, busulfan, and chloroquine have been reported to cause RCM (68–72). Mediastinal radiation has also resulted in RCM (73).

Idiopathic

Outside the tropics, the idiopathic form of RCM is probably the most common form in children. Although the family history is positive in only approximately 30% of this population, a genetic basis or predisposition for the development of the disease is likely.

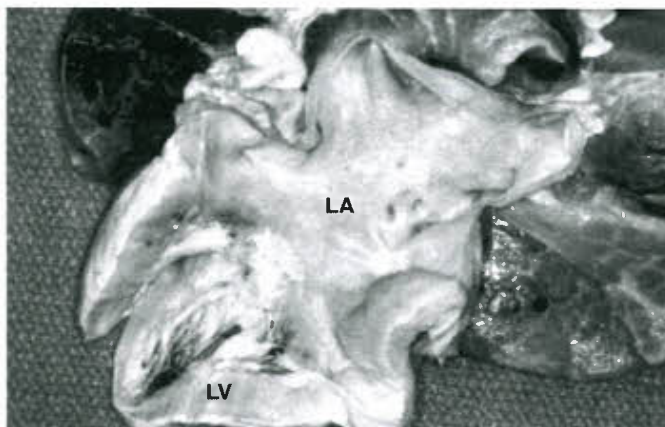


Figure 57.1. The left atrium (LA) is massively dilated, dwarfing the size of the left ventricle (LV) in this autopsy specimen from a patient with restrictive cardiomyopathy.

PATHOLOGY

Figure 57.1 demonstrates the typical appearance of a heart from a patient with idiopathic RCM. The left atrium dwarfs the left ventricle. The left ventricular cavity size is normal with no appreciable left ventricular hypertrophy. In the vast majority of cases, the hearts are otherwise structurally normal, although there have been rare reports of patients who also have atrial septal defects or small hemodynamically insignificant ventricular septal defects (11,30). The histology in idiopathic RCM is nonspecific revealing varying degrees of fibrosis and myocyte hypertrophy (3,34,37). The histology may vary with the underlying disease process.

PATHOPHYSIOLOGY

Diastolic function is primarily affected by ventricular compliance/stiffness and relaxation. In the normal heart, the phase of rapid or early filling occurs as the left ventricular pressure drops below that in the left atrium, just after the mitral valve opens, and accounts for most of the ventricular filling (74,75). The duration of the next phase, called diastasis, is variable and heart rate dependent, permitting <5% of filling. The last phase of diastole is atrial systole and accounts for approximately 15% of normal ventricular filling. In the classic description of RCM, ventricular filling is completed in early diastole with little or no filling in late diastole. In this model, restrictive physiology results from increased myocardial stiffness with decreased compliance, causing a marked ventricular pressure rise with small changes in volume.

The earliest phase of clinical diastole is isovolumic relaxation which is an active energy-requiring process for the uptake of calcium ions into the sarcoplasmic reticulum. Ischemia and hypertrophy can both result in abnormal relaxation owing to changes in calcium uptake. Gewillig et al. reported on six children with RCM who by catheterization and echocardiography had parameters suggesting delayed relaxation as well as restrictive filling as the mechanisms for the RCM. In their patients, early filling contributed approximately 56%, middiastolic filling 28%, and atrial filling 16% to total ventricular filling. They suggested that the restrictive hemodynamics were caused by dysfunction and delay of active relaxation of the ventricle rather than increased intrinsic stiffness of the ventricular wall (12).

It is likely that, as diastolic diseases become better understood, RCM is likely to result from abnormal stiffness or

abnormal relaxation or both depending on the underlying cause of the disease and disease progression.

CLINICAL PRESENTATION

In children, heart failure signs and symptoms from RCM are often confused with other diseases. Common presenting symptoms often appear to be pulmonary related. Children with RCM frequently have dyspnea on exertion and older children may complain of exercise intolerance. A history of "recurrent lower respiratory tract infections" or "asthma" is common. Referral to a cardiologist eventually occurs when cardiomegaly is noted on chest x-ray.

Additional common reasons for referral are abnormal physical exam findings. Patients who have ascites, hepatomegaly, and edema are frequently referred to a gastroenterologist first. Referral to the cardiologist occurs when additional cardiac signs or symptoms occur, a chest x-ray is noted to be abnormal, or no specific gastrointestinal etiology is found for the edema and hepatomegaly. Earlier referral to a cardiologist occurs when the presenting sign is an abnormal heart sound, such as murmur, gallop, or loud P2.

Syncope accounts for approximately 10% of the presenting complaints. Syncope in this patient population may be related to ischemia, arrhythmias, or thromboembolism (11,12). Ischemia and/or arrhythmias may be the most common causes of syncope and sudden death in this patient population (7,37). In one case, no definitive mechanism for syncopal episodes was found, an arrhythmia was ruled out, and there were no ischemic changes on treadmill testing (4).

Two children had sudden cardiac death as their presentation at ages 6 and 16 years, presumably secondary to familial RCM as there were 13 other affected family members in five generations (14).

A positive family history was an infrequent reason for referral in the published reports.

Physical Examination

Common findings include a gallop rhythm and a loud P2. Hepatomegaly, ascites, and edema are also commonly found.

DIAGNOSTIC STUDIES

Electrocardiograms

The electrocardiogram is extremely useful in screening for RCM. Approximately 98% are abnormal (3–12,14–27,30,32,37). Figure 57.2 is a representative example. The most common abnormalities are right and/or left atrial enlargement; however, ST segment depression and ST-T wave abnormalities are frequently present. Right and/or left ventricular hypertrophy can also be seen as well as conduction abnormalities.

Holter

Holter evaluations can also be useful, not only for rhythm evaluation but also for ST segment analysis. Rivenes et al. (11) reported Holter results in 12 patients, 8 of whom had ischemic changes with ST segment depression from 3 to 12.7 mm, most evident at higher heart rates. In one patient, the development of ventricular tachycardia was preceded by chest

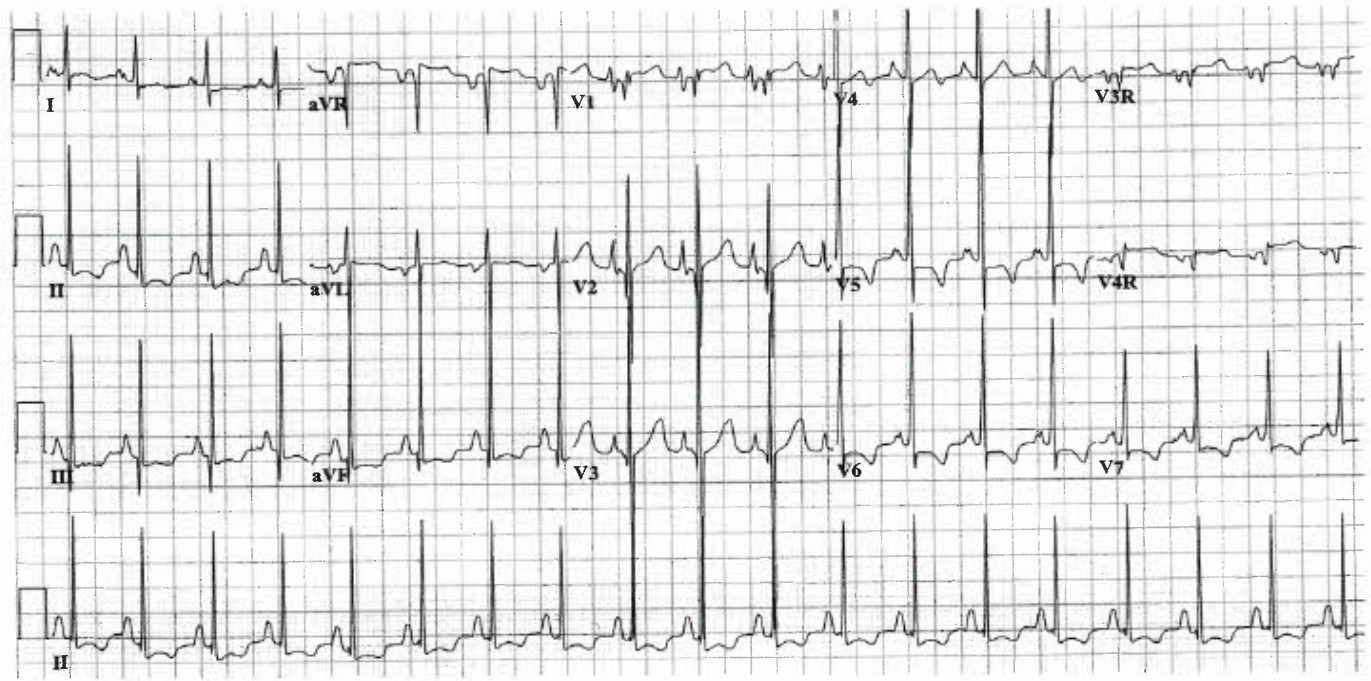


Figure 57.2. ECG from a 2-year-old with restrictive cardiomyopathy demonstrating sinus rhythm with biatrial enlargement, qR pattern in the right chest leads, and ST segment depression and T wave inversion in the inferolateral and lateral chest leads.

pain and ST—segment depression of 8.2 mm. The patient had been hospitalized at the time due to recurrent chest pain. Case reports have also demonstrated ischemic or infarct patterns on ECG and autopsy, and in some children, chest pain related to the ischemia was identified, suggesting this is an important cause of morbidity and mortality in this patient population (8,11,17,18). Hayashi et al. (37) did not find coronary abnormalities by catheterization in their RCM patients with ST segment depression, nor did they find perfusion defects on exercise testing in the majority of their patients leading them to conclude that arrhythmia is a more common cause of sudden death than ischemia-mediated events. However, the most likely cause of ischemia in this patient population would be relatively diffuse hypoperfusion of the subendocardial myocardium due to the high diastolic filling pressures impairing coronary perfusion, and not coronary abnormalities *per se*. This type of hypoperfusion, if diffuse, would also be harder to detect by exercise myocardial perfusion studies. Cardiac MRI with delayed enhancement might be a better tool to further investigate this mechanism.

Of the pediatric studies reporting arrhythmias, approximately 15% of the patients had arrhythmias and/or conduction disturbances (3,4,9–11,21,25,27,30,34,37). Atrial flutter was the most commonly reported arrhythmia. High-grade second-degree and third-degree heart block were the next most commonly reported rhythm disturbances. Atrial fibrillation and atrial tachycardias, Wolff-Parkinson-White syndrome with supraventricular tachycardia, symptomatic sinus bradycardia requiring pacing, and ventricular tachycardia and torsade were also reported.

Chest Radiographs

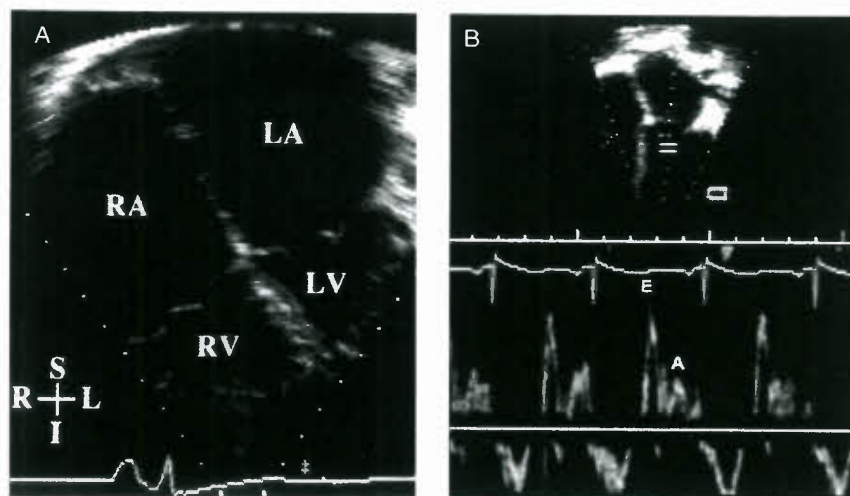
The chest x-ray appears to be a useful screening test, as it is abnormal in approximately 90% of cases (3–12,14–24,30,37). Cardiomegaly and pulmonary venous congestion are the most common abnormalities.

Echocardiography

The echocardiogram is usually diagnostic (Fig. 57.3). On 2-D imaging, classic cases demonstrate markedly dilated atria, often dwarfing the size of the ventricles. Typically, there is normal or nearly normal left ventricular systolic function and absence of significant hypertrophy or dilation. However, based on studies reporting systolic functional parameters, as many as 30% may present with or develop a depressed shortening or ejection fraction (3,10,12,30). Reported shortening fractions have been as low as the low 20s with ejection fractions as low as the upper 30s. In addition, as many as 40% have or develop mild, and sometimes progressive, left ventricular hypertrophy (3,4,10,12,30). Variable patterns of hypertrophy have been reported including concentric, “mid septal bulge,” apical hypertrophy, and “atypical hypertrophy.” It is possible that the subset of patients with hypertrophy may have a troponin I mutation. The “mixed restrictive/hypertrophic phenotype” can result in a confusing clinical picture in terms of diagnosis, RCM versus HCM, and optimal therapeutic approaches. During 2-D imaging, thrombi should be specifically sought. Thrombotic and embolic events have been described in approximately 20% of pediatric patients with idiopathic RCM reported in nine studies (3,4,9,10,12,26,30,76,77). In HES and EMF, there may be obliteration of the apex by thrombus. In HES and EMF, the atrioventricular valve apparatus are frequently involved in the pathologic process with thickening of valve leaflets and decreased excursion, particularly of the mitral valve. In idiopathic RCM, the valves are typically normal in appearance. Pericardial thickening on 2-D evaluation would suggest CP and not RCM.

Doppler patterns of diastolic dysfunction have been well characterized in adults and pediatric data have also been reported (78,79). Although many studies have characterized Doppler findings in adults with RCM, only a few pediatric studies have described Doppler findings in children with RCM

Figure 57.3. Echocardiogram from a child with RCM. Panel A demonstrates severe biatrial enlargement, dwarfing the size of the ventricles. Panel B demonstrates mitral inflow with an increased E to A ratio and a shortened deceleration time. RA, right atrium; LA, left atrium; RV, right ventricle; LV, left ventricle.



(9,10,12,27). Some of the children in some of these studies did not have complete Doppler data as all the pediatric studies have been retrospective. In the patients described, the findings consistent with restrictive filling and increased left ventricular end diastolic pressure included elevated E/A ratios, short mitral deceleration times, increased pulmonary vein atrial reversal velocity and duration, and pulmonary vein atrial reversal duration greater than mitral A duration (9,10,27). Restrictive hemodynamics are typically thought to be caused by increased ventricular wall stiffness; however, idiopathic RCM may also result from disorders of delayed active relaxation. The Gewillig et al. (12) study described six children with idiopathic RCM whose Doppler profiles were consistent with restrictive filling with elevated E/A ratios and shortened deceleration times, but who also had parameters suggesting dysfunction and delay of active relaxation of the ventricle. In their patients, mitral inflow patterns revealed a prominent mitral L wave with middiastolic filling accounting for approximately 28% of total ventricular filling. The left ventricular pressure curve showed a small but steady decline during middiastolic filling on cardiac catheterization, implying that the driving force for filling was “ventricular suction” and not increased left atrial pressure. Friedberg and Silverman have reported on the systolic (S) to diastolic (D) duration ratio in children with heart failure secondary to RCM (80). Children with RCM had

an elevated S/D ratio compared to controls due to a prolongation of systole with shortened diastole. This was not specific to heart failure in RCM, however, as they found similar results in children with dilated cardiomyopathy.

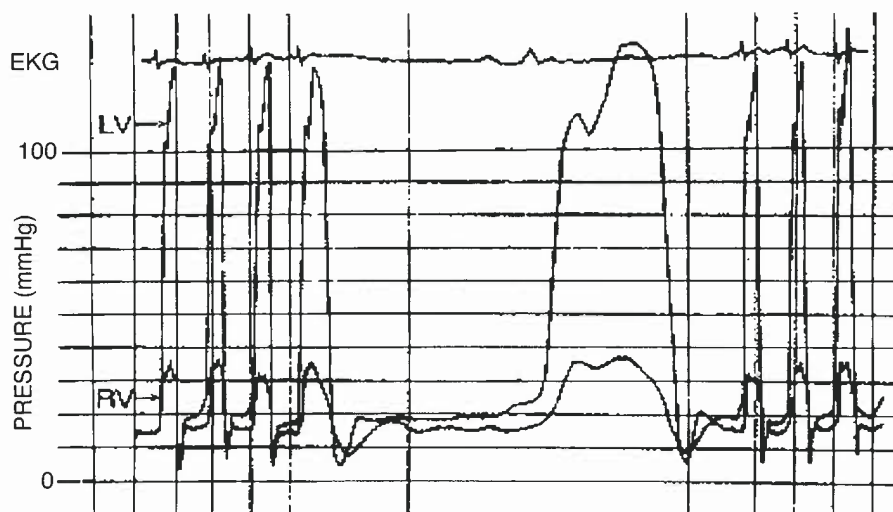
In adults, Doppler tissue imaging has been used to help differentiate between RCM and CP (81,82). A mitral E' of ≥ 8 cm/s was highly sensitive and specific for differentiating CP from RCM (82). This cutoff point needs further evaluation in children.

Cardiac Catheterization and Endomyocardial Biopsy

Cardiac catheterization is an important part of the evaluation in patients with RCM and should be performed at the time of diagnosis. Catheterization can help differentiate between RCM and CP, although virtually all hemodynamic features can overlap (83).

Both diseases typically have an early diastolic dip and subsequent plateau pattern, also called the square root sign (Fig. 57.4) (62,83). In “classic” RCM, the left ventricular end diastolic pressure, left atrial pressure, and pulmonary capillary wedge pressure are markedly elevated and at least 4 to 5 mm Hg (preferably 10 mm Hg) greater than the right atrial pressure and right ventricular end diastolic pressure. In cases

Figure 57.4. Pressure tracing during cardiac catheterization in a patient with restrictive cardiomyopathy (RCM) demonstrating the dip and plateau or square root sign that may be seen in either RCM or constrictive pericarditis. LV, left ventricle; RV, right ventricle.



in which the pressures are essentially equal, volume loading may bring out the differences in pressure between the right and left sides.

Pulmonary hypertension is frequently present at the time of initial catheterization in addition to elevated left and/or right ventricular end diastolic pressures (3,10,27,29–31,34–36). The initial pulmonary vascular resistance index (PVRI) may be normal to as high as 24 U m^2 (3,10,27,29–31,34–36). In studies providing follow-up data 0.3 to 8 years after presentation, the PVRI ranged from normal to 30 U m^2 (3,30,31). The pulmonary vasculature frequently remains reactive, however (31,35,36). The Kinberling study suggested the best response was to nitric oxide (31). However, in the study by Weller et al. (30), 40% were precluded from orthotopic heart transplant due to an elevated and nonreactive pulmonary vascular resistance at the time they were evaluated for cardiac transplantation. None of the studies predicted when or in whom fixed pulmonary vascular resistance would develop.

Endomyocardial biopsies generally are nondiagnostic, showing varying degrees of fibrosis and hypertrophy (3,34,37). Increased numbers of mitochondria are seen in some patients as is an increase in glycogen (3,5,10). One case of cardiac amyloidosis in a pediatric patient has been reported, but endomyocardial biopsy is rarely diagnostic of a specific etiology (3,5,10,12,34,37). Desmin myopathy has been seen in skeletal muscle biopsy and cardiac tissue, leading to an etiologic diagnosis (26,41). This can signify impending skeletal myopathy and/or conduction system disease and should be evaluated for in any biopsy tissue obtained. However, finding a specific etiology by endomyocardial biopsy is uncommon, and the procedure is not risk free in these tenuous patients (3,19,34).

DIFFERENTIAL DIAGNOSIS

CP is the disease process that is most commonly confused with RCM. The clinical presentation of patients with RCM and CP can be very similar as can results of tests used to differentiate between the two. Table 57.3 summarizes the findings of typical test results for the two disease processes; however, considerable overlap may occur. In most cases, noninvasive studies and hemodynamic catheterization without an endomyocardial biopsy can distinguish between RCM and CP. However, in limited cases, endomyocardial biopsy may be necessary to help distinguish CP from RCM. The findings in CP are nonspecific. The absence of myopathic findings lends support to the diagnosis of CP, while the presence of myopathic changes suggests RCM, but infrequently identifies a specific diagnosis in RCM (3,10,12,34,37). Children with RCM or CP are hemodynamically fragile. Case series and reports in children with RCM have reported deterioration and death during or shortly after catheterization and biopsy (4,19,34). Therefore, careful consideration of the risk–benefit ratio of the information that is likely to be obtained by the biopsy should be undertaken prior to catheterization. Rarely, exploratory thoracotomy is necessary to differentiate CP from RCM, as there continue to be cases in which the hemodynamic profile has so much overlap that thoracotomy is necessary for diagnosis. Henein et al. (84) have suggested that, in those cases in which pericardial disease is found, the term restrictive pericarditis should be applied. Wang et al. (85) reported a case of a child with mixed CP and RCM features. Features consistent with CP included pericardial calcification and a lateral mitral annular tissue Doppler

TABLE 57.3 Restrictive Cardiomyopathy Versus Constrictive Pericarditis

	RCM	CP
ECG finding		
Atrial enlargement	Nearly universal	May be present
LVH and/or RVH	Common	Usually absent
Low-voltage QRS	Unusual	Common
ST-T wave abnormality	Common	Common
Chest x-ray		
Calcification	Absent	≤21%
Echocardiogram		
Pericardial thickening	Absent	May be thickened
Atrial dilation	Marked	May be enlarged
Wall thicknesses	Normal to mild hypertrophy	Usually normal
Systolic function	Normal to depressed	Normal
Septal bounce	Absent	Usually present
Doppler		
Respiratory flow changes	Occasional	Usually marked
Gated MRI/CT		
	Normal pericardium	Usually thickened
Cardiac catheterization		
	PWP and LVEDP may exceed RAP and RVEDP by >4 mm Hg. RVSP often >50 mm Hg	RAP = PWP, RVEDP = LVEDP usually within 4 mm Hg RVSP usually <50 mm Hg
RV endomyocardial biopsy		
	Usually abnormal (frequently nonspecific)	Usually normal
Thoracotomy		
	Normal pericardium	Usually abnormal pericardium

CP, Constrictive pericarditis; LVH, left ventricular hypertrophy; RVH, right ventricular hypertrophy; PWP, pulmonary wedge pressure; LVEDP, left ventricular end diastolic pressure; RAP, right atrial pressure; RVEDP, right ventricular end diastolic pressure; RVSP, right ventricular systolic pressure; RV, right ventricular.

velocity of 18 cm/s; however, endomyocardial biopsy showed myocyte hypertrophy and fibrosis, thought to be more consistent with a cardiomyopathic process. Pericardiectomy resulted in symptomatic improvement despite the myopathic features on endomyocardial biopsy even though the calcified pericardium could not be completely resected. If CP is identified, pericardiectomy may be curative and is the treatment of choice. However, in patients with RCM, exploratory thoracotomy is not a benign procedure, has no therapeutic benefit, and may result in death (30). Therefore, every effort should be made to establish the diagnosis of RCM without exploratory thoracotomy.

Brain natriuretic peptide (BNP) has been used to help differentiate CP from RCM in adults (86,87). In a small case series of adults by Leya et al. (87), all patients with CP had BNPs that were <200 pg/mL and were statistically significantly less than those with RCM. The lowest BNP in the RCM group was 639 pg/mL. Subsequent studies in adults have found statistically significant differences in BNP levels between those with CP and those with RCM, but significantly more overlap was seen in the BNPs between groups, particularly if the CP was secondary to prior cardiac surgery or radiation therapy rather than a primary CP, making the BNP less definitive for differentiating between CP and RCM (86,87).

Cardiomyopathies may be difficult to classify as overlapping phenotypes occur (3,10,12,30). Because some children with RCM may have some degree of left ventricular hypertrophy (3,4,10,12,30), confusion may arise as to whether the patient has RCM versus HCM, that is, the "mixed restrictive/hypertrophic phenotype." Other patients with HCM may have very dilated atria with restrictive physiology. Since a variety of phenotypes can be seen in the same family with the same gene defect, it is not surprising that phenotypes sometimes overlap. This is of more than semantic importance as children with HCM with restrictive physiology have a better prognosis than children with "pure" RCM, but not as good a prognosis as those with "pure" HCM (88). In addition, the Maskatia et al. study suggests that children with HCM and restrictive physiology have a long-term survival that is equivalent to average post-heart transplant survival in children. Therefore, listing in a number of these patients may be delayed longer than listing for "pure" RCM (89). There is also evidence of phenotypic overlap between RCM and noncompaction cardiomyopathy (90–92). Patients with dilated cardiomyopathy can also develop restrictive physiology (29).

OUTCOME

The prognosis in children with RCM is poor (3–5,8,9,11,12,29,34,37). Approximately half of the children die or have transplantation within 2 to 3 years of diagnosis. The prognosis in RCM appears to be significantly worse than in patients with HCM or dilated cardiomyopathy in whom the 2-year mortality rates are reported to be 12.7% and 13.6%, respectively (7). In RCM, heart failure–related deaths are the most common. Sudden cardiac death has also been reported to be a common cause of death in children with RCM (11,37). In the study by Rivenes et al. (11), sudden cardiac death occurred in 28% of children with an annual mortality rate of 7%. This is comparable to a 31% incidence of sudden death in children with HCM reported by Maron et al. (93). Sudden death occurred in 14% of the patients reported by Russo and Webber (34) and in 33% in the Hayashi study (37).

Factors associated with poor prognosis have not been consistent between studies. Some studies suggest an increased risk for death from heart failure in the presence of cardiomegaly and pulmonary venous congestion on chest x-ray, age younger

than 5 years, thromboembolism, and elevated PVRI (9,10,30). However, Russo and Webber did not find age or presence or absence of heart failure symptoms at presentation to be prognostic (34). They found that higher end diastolic pressures and larger left atrial:aortic ratios correlated negatively with survival. Children with heart failure are also at risk from ischemic complications as well (11). When comparing survival with RCM versus survival after transplant, it is evident that transplant results in longer survival in the majority of cases (30).

MANAGEMENT

There was no consistent approach to therapy in the studies reviewed. Various medications were given in various combinations including diuretics, digoxin, afterload reducing agents, calcium channel blockers, and beta-blockers. Due to the small number of patients in each study and the lack of uniformity of treatment within studies, the benefits or risks of these therapies could not be determined. Bengur et al. (94) reported that captopril lowered the aortic pressure by 24% without an increase in cardiac output, when administered during cardiac catheterization to four pediatric patients with RCM. They suggested that captopril should not be used in patients with RCM. However, in the studies that reported the use of ACE inhibitors, acute decompensation was not reported, nor was therapeutic or symptomatic benefit reported (3,4,10,27,30,31,37). Modulation of neurohumoral activation by ACE inhibitors may affect fibroblast activity, interstitial fibrosis, intracellular calcium handling, and myocardial stiffness. In adults with diastolic heart failure, the use of ACE inhibitors has been suggested, but data are limited in adults as well (95). The risks and benefits of ACE inhibitors in pediatric RCM remain to be determined.

In adults with diastolic dysfunction, tachycardia is poorly tolerated; therefore, beta-blockers or some calcium channel blockers have been suggested as part of the treatment regimen (95). In the pediatric article by Rivenes et al. (11), beta-blocker therapy was suggested to blunt rapid heart rates in their patient population in whom significant ST segment depression was noted at higher heart rates. Subsequently, three children <5 years old were reported who were begun on propranolol ($n = 2$) or metoprolol ($n = 1$) and who did not tolerate beta-blocker therapy (96). In the first patient, episodes of pallor, weakness, and listlessness occurred. The patient was on telemetry and no arrhythmias were documented, nor were neurologic sequelae seen. The episodes stopped when propranolol was discontinued. The second patient developed staring spells and profound diaphoresis. One episode occurred while the patient was in the hospital; it was terminated with the administration of a high dextrose infusion (D50) before a blood glucose was obtained. The propranolol was discontinued and the episodes stopped. The patient who received metoprolol became irritable and restless after 2 to 3 days on the medication with some improvement initially after stopping the drug. Further studies are needed to determine the role of beta-blocker therapy in this disease.

At present, medical therapy remains supportive and should be started with the patient hospitalized due to the fragile nature of these patients. Diuretics are useful in patients with signs and symptoms of systemic or pulmonary venous congestion. Overdiuresis should be avoided because these patients are sensitive to alterations in preload. Due to the 20% incidence of thromboembolic events, antiplatelet therapy or anticoagulants should be administered.

Since current medical therapy appears to be ineffective, the development of pulmonary hypertension is common and mortality is high, cardiac transplantation is the definitive

therapy. Outcomes in children transplanted for RCM are comparable to children transplanted for other forms of heart disease (31,35,36,97). Although some untransplanted patients may remain relatively well for over 10 years (34), this is an unpredictable minority. Most patients should be evaluated and listed for transplantation "early"; however, the definition of "early" remains controversial (11,34–35,97). Patients should undergo cardiac catheterization at the time of diagnosis with testing for pulmonary vasoreactivity if the PVRI is >6 U·m² or the transpulmonary gradient is >14 to 15 mm Hg. In many patients, the resistance can be lowered, and successful orthotopic transplants have been performed in children whose PVRI was above 9 U·m², as long as they demonstrated pulmonary vascular bed reactivity (35,36). Some children may benefit from continuous infusion of prostacyclin while awaiting determination of the best transplant strategy, that is, orthotopic versus heterotopic versus heart–lung (35). Orthotopic heart transplant is the preferred transplant since survival is better than heart–lung transplant and more feasible than heterotopic transplant in small children, although heterotopic heart transplantation has been performed in small children with RCM (35,98). When pulmonary vasodilator therapies are used, careful monitoring for the development of pulmonary edema is necessary as the left atrial pressure may rise, negating the benefit of the fall in pulmonary artery pressures. It is preferable to list patients before these treatment strategies are necessary. If patients are not listed at the time of diagnosis, then close follow-up with regular reassessment of the pulmonary artery pressure and resistance is necessary.

Dipchand et al. (99) reported that children with RCM were less likely to be listed as status 1, ventilated, or to be receiving inotropes, and had fewer arrhythmias at listing than their counterparts with dilated cardiomyopathy. However, their likelihood of death while waiting was similar, suggesting that these lower status patients were as vulnerable as the higher status children with dilated cardiomyopathy (99). Zangwill et al. (97) reviewed the outcomes of 145 children with RCM listed for heart transplantation, 44% of whom were listed UNOS status 1. They found that children requiring mechanical support and infants had a significantly higher risk of death while waiting than other children listed with RCM. These studies underscore the importance of not waiting "too long" to list these patients.

While listed for transplantation, patients should have periodic Holter monitoring performed, and as symptoms dictate, to evaluate for signs of ischemia, ventricular arrhythmias, or developing conduction disturbances. Implantable defibrillators should be considered for patients with evidence of ischemia and ventricular arrhythmias. Strenuous physical activity should be avoided.

Since the only definitive therapy for RCM, at the present time, is cardiac transplantation, better medical therapies are needed for the treatment of RCM. Improved methods of risk stratification are needed for RCM patients to identify those at greatest risk for thromboembolism, rapid progression of elevated pulmonary vascular resistance, and sudden death.

REFERENCES

- Richardson P, McKenna W, Bristow M, et al. Report of the 1995 World Health Organization/International Society and Federation of Cardiology Task Force on the Definition and Classification of Cardiomyopathies. *Circulation* 1996;93:841–842.
- Maron BJ, Towbin JA, Thiene G, et al. Contemporary definitions and classification of the cardiomyopathies: an American Heart Association scientific statement. *Circulation* 2006;113:1807–1816.
- Denfield SW, Rosenthal G, Gajarski RJ, et al. Restrictive cardiomyopathies in childhood etiologies and natural history. *Tex Heart Inst J* 1997;24:38–44.
- Lewis AB. Clinical profile and outcome of restrictive cardiomyopathy in children. *Am Heart J* 1992;123:1589–1593.
- Malčić I, Jelušić M, Kneiwald H, et al. Epidemiology of cardiomyopathies in children and adolescents: a retrospective study over the last 10 years. *Cardiol Young* 2002;12:253–259.
- Nugent AW, Daubeney PEF, Chondros P, et al. The epidemiology of childhood cardiomyopathy in Australia. *N Engl J Med* 2003;348:1639–1646.
- Lipshultz SE, Sleeper CA, Towbin JA, et al. The incidence of pediatric cardiomyopathy in two regions of the United States. *N Engl J Med* 2003;348:1647–1655.
- Harris LC, Rodin AE, Nghiem QX. Idiopathic, nonobstructive cardiomyopathy in children. *Am J Cardiol* 1968;21:153–165.
- Cetta F, O'Leary PW, Seward JB, et al. Idiopathic restrictive cardiomyopathy in childhood: diagnostic features and clinical course. *Mayo Clin Proc* 1995;70:634–640.
- Chen S, Balfour IC, Jureidini S. Clinical spectrum of restrictive cardiomyopathy in children. *J Heart Lung Transplant* 2001;20:90–92.
- Rivenes SM, Kearney DL, Smith EO, et al. Sudden death and cardiovascular collapse in children with restrictive cardiomyopathy. *Circulation* 2000;102:876–882.
- Gewillig M, Mertens L, Moerman P, et al. Idiopathic restrictive cardiomyopathy in childhood. A diastolic disorder characterized by delayed relaxation. *Eur Heart J* 1996;17:1413–1420.
- Mehta AV, Ferrer PL, Pickoff AS, et al. M-mode echocardiographic findings in children with idiopathic restrictive cardiomyopathy. *Pediatr Cardiol* 1984;5:273–280.
- Fitzpatrick AP, Shapiro LM, Rickards AF, et al. Familial restrictive cardiomyopathy with atrioventricular block and skeletal myopathy. *Br Heart J* 1990;63:114–118.
- Toussaint M, Planche C, Villain E, et al. Restrictive cardiomyopathy in children. Ultrastructural findings. *Virchows Arch A* 1987;412:27–29.
- Sapire DW, Casta A, Swischuk LE, et al. Massive dilatation of the atria and coronary sinus in a child with restrictive cardiomyopathy and persistence of the left superior vena cava. *Cathet Cardiovasc Diagn* 1983;9:47–53.
- Erath GH, Graham TP, Smith CW, et al. Restrictive cardiomyopathy in an infant with massive biatrial enlargement and normal ventricular size and pump function. *Cathet Cardiovasc Diagn* 1978;4:289–296.
- Ishijima M, Kawai S, Okada R, et al. An autopsy case of cardiomyopathy with restrictive physiology in a child. *Heart Vessels* 1990;70:70–73.
- Maki T, Niimura I, Nishikawa T, et al. An atypical case of cardiomyopathy in a child: Hypertrophic or restrictive. *Heart Vessels* 1990;84–87.
- Schieber RA, Lurie PR, Neustein HB. Restrictive cardiomyopathy with pseudotumor formation of the left ventricle. *Ped Cardiol* 1982;3:153–159.
- Miyazaki A, Ichida F, Suzuki Y, et al. Long-term follow-up of a child with idiopathic restrictive cardiomyopathy. *Heart Vessels* 1990;74–76.
- Nishikawa T, Tanaka Y, Sasaki Y, et al. A case of pediatric cardiomyopathy with severely restrictive physiology. *Heart Vessels* 1992;7:206–210.
- Aroney C, Bett N, Radford D. Familial restrictive cardiomyopathy. *Aust NZ J Med* 1988;18:877–878.
- Izumi T, Masani F, Mitsuma S, et al. Juvenile cases of restrictive cardiomyopathy without eosinophilia. *Heart Vessels* 1990;77–79.
- Rapezzi C, Ortolani P, Binetti G, et al. Idiopathic restrictive cardiomyopathy in the young: report of two cases. *Int J Cardiol* 1990;29:121–126.
- Bertini E, Bosman C, Bevilacqua M, et al. Cardiomyopathy and multi-core myopathy with accumulation of intermediate filaments. *Eur J Pediatr* 1990;149:856–858.
- Neudorf U, Bolte A, Lang D, et al. Diagnostic findings and outcome in children with primary restrictive cardiomyopathy. *Cardiol Young* 1996;6:44–47.
- Angelini A, Calzolari V, Thiene G, et al. Morphologic spectrum of primary restrictive cardiomyopathy. *Am J Cardiol* 1997;80:1046–1050.
- Hughes ML, Kleinert S, Keogh A, et al. Pulmonary vascular resistance and reactivity in children with end-stage cardiomyopathy. *J Heart Lung Transplant* 2000;19:701–794.
- Weller RJ, Weintraub R, Addonizio LJ, et al. Outcome of idiopathic restrictive cardiomyopathy in children. *Am J Cardiol* 2002;90:501–506.
- Kimberling MT, Balzer DT, Hirsch R, et al. Cardiac transplantation for pediatric restrictive cardiomyopathy: presentation, evaluation and short term outcome. *J Heart Lung Transplant* 2002;21:455–459.
- Schwartz ML, Colan SD. Familial restrictive cardiomyopathy with skeletal abnormalities. *Am J Cardiol* 2003;92:636–639.
- Facher JJ, Regier EJ, Jacobs GH, et al. Cardiomyopathy in the Coffin-Lowry Syndrome. *Am J Med Genet Part A* 2004;128A:176–178.
- Russo LM, Webber SA. Idiopathic restrictive cardiomyopathy in children. *Heart* 2005;91:1199–1202.
- Fenton MJ, Chubb H, McMahon, et al. Heart and heart lung transplantation for idiopathic restrictive cardiomyopathy in children. *Heart* 2005;91:185–189.
- Bogard AJ, Mital S, Schwarzenberger JC, et al. Twenty-year experience with heart transplantation infants and children with restrictive cardiomyopathy: 1986–2006. *Am J Transplant* 2008;8:201–207.
- Hayashi T, Tsuda E, Kurosaki K, et al. Electrocardiographic and clinical characteristics of idiopathic restrictive cardiomyopathy in children. *Circ J* 2007;71:1534–1539.
- Sanna T, Dello Russo A, Toniolo D, et al. Cardiac features of Emery-Dreifuss muscular dystrophy caused by lamin A/C gene mutations. *Eur Heart J* 2003;24:2227–2236.

39. Mogensen J, Kubo T, Duque M, et al. Idiopathic restrictive cardiomyopathy is part of the clinical expression of cardiac troponin I mutations. *J Clin Invest* 2003;111:209–216.
40. Jacobson R, Ittmann M, Buxbaum JN, et al. Transthyretin Ile 122 and cardiac amyloidosis in African-Americans: 2 case reports. *Tex Heart Inst J* 1997;24:45–52.
41. Dalakas MC, Park K-Y, Semino-Mora C, et al. Desmin myopathy, a skeletal myopathy with cardiomyopathy caused by mutations in the desmin gene. *N Engl J Med* 2000;342:770–780.
42. Goldfarb LG, Park K-Y, CerveneKova L, et al. Missense mutations in desmin associated with familial cardiac and skeletal myopathy. *Nat Genet* 1998;19:402–403.
43. Delaunoy J, Abidi F, Zeniou M, et al. Mutations in the x-linked RSK 2 gene (RPS6KA3) in patients with Coffin-Lowry Syndrome. *Hum Mutat* 2001;17:103–116.
44. Kaski JP, Syrris P, Burch M, et al. Idiopathic restrictive cardiomyopathy in children is caused by gene mutations in cardiac sarcomere protein genes. *Heart* 2008;94:1478–1484.
45. Peddy SB, Vricella LA, Crosson JE, et al. Infantile restrictive cardiomyopathy resulting from a mutation in the cardiac troponin T gene. *Pediatrics* 2006;117:1830–1833.
46. Ware SM, Quinn ME, Ballard ET, et al. Pediatric restrictive cardiomyopathy associated with a mutation in beta-myosin heavy chain. *Clin Genet* 2008;73:165–170.
47. Richard P, Charron P, Carrier L, et al. Hypertrophic cardiomyopathy: distribution of disease genes, spectrum of mutations, and implications for molecular diagnosis strategy. *Circulation* 2003;107:2227–2232.
48. Olson TM, Karst ML, Whitby FG, et al. Myosin light chain mutation causes autosomal recessive cardiomyopathy with mid-cavitary hypertrophy and restrictive physiology. *Circulation* 2002;105:2337–2340.
49. Svendsen IH, Steensgaard-Hansen F, Nordvag BY. A clinical and echocardiographic characterization of a Danish kindred with familial amyloid transthyretin methionine 111 linked cardiomyopathy. *Eur Heart J* 1998;5:782–789.
50. Arbustini E, Pasotti M, Pilotto A, et al. Desmin accumulation restrictive cardiomyopathy and atrioventricular block associated with desmin gene defects. *Eur J Heart Fail* 2006;8:477–483.
51. Zhang J, Kumar A, Stalker HJ, et al. Clinical and molecular studies of a large family with desmin-associated restrictive cardiomyopathy. *Clin Genet* 2001;59:248–256.
52. Marshall JD, Paisley RB, Carey C, et al. Alstrom syndrome. In: Pagan RA, Bird TD, Dolan CR, et al., eds. *GeneReviews [Internet]*. Seattle (WA): University of Washington, Seattle; 1993–2003 Feb07 [updated 2010 Jun 08].
53. Karlberg N, Jalanko H, Perheentupa J, et al. Mulibrey nanism; clinical features and diagnostic criteria. *J Med Genet* 2004;41:92–98.
54. Erola A, Pihkala JJ, Karlberg N, et al. Cardiac dysfunction in children with Mulibrey nanism. *Pediatr Cardiol* 2007;28:155–162.
55. Lipsanen-Nyman M, Perheentupa J, Rapola J, et al. Mulibrey heart disease: clinical manifestation, long-term course and results of pericardiectomy in a series of 49 patients born before 1985. *Circulation* 2003;107:2810–2815.
56. Pahl E, Miller SA, Griffith BP, et al. Occult restrictive hemodynamics after pediatric heart transplantation. *J Heart Lung Transplant* 1995;14:1109–1115.
57. Mocumbi AO, Ferreira MB, Sidi D, et al. A population study of endomyocardial fibrosis in a rural area of Mozambique. *N Engl J Med* 2008;359:43–49.
58. Mocumbi AO, Yacoub S, Yacoub MH. Neglected tropical cardiomyopathies: II. *Heart* 2008;94:384–390.
59. Kushwaha SS, Fallon JT, Fuster V. Restrictive cardiomyopathy. *N Engl J Med* 1997;336:267–276.
60. Davies JNP. Endocardial fibrosis in Africans. *East Afr Med J* 1948;25:10.
61. Johnson RA, Palacios I. Nondilated cardiomyopathies. *Adv Intern Med* 1984;30:243–274.
62. Wynne J, Braunwald E. The cardiomyopathies and myocarditis. In: Braunwald E, Zipes DP, Libby P, eds. *Heart Disease a Textbook of Cardiovascular Medicine*. 6th ed. Philadelphia, PA: W.B. Saunders Company, 2001: 1774–1782.
63. Weller PF, Bubley GJ. The idiopathic hyper eosinophilia syndrome. *Blood* 1994;83:2759–2779.
64. Felice PV, Sawicki J, Anto J. Endomyocardial disease and eosinophilia. *Angiology* 1993;44:869.
65. Radford DJ, Garlick RB, Pohlner PG. Multiple valvar replacements for hyper eosinophilia syndrome. *Cardiol Young* 2002;12:67–70.
66. Santos CL, Moraes CR, Santos FL, et al. Endomyocardial fibrosis in children. *Cardiol Young* 2001;11:205–209.
67. Dixit MP, Greifer I. Nephropathic cystinosis associated with cardiomyopathy: a 27-year clinical follow-up. *BMC Nephrol* 2002;3:8–16.
68. Mortensen SA, Olsen HS, Baandrup U. Chronic anthracycline cardiotoxicity: haemodynamic and histopathological manifestations suggesting a restrictive endomyocardial disease. *Br Heart J* 1986;55:274–282.
69. Bu'Lock FA, Mott MG, Oakhill A, et al. Left ventricular diastolic function after anthracycline chemotherapy in childhood: relation with systolic function, symptoms and pathophysiology. *Br Heart J* 1995;73:340–350.
70. Mason JW, Billingham ME, Friedman JP. Methysergide-induced heart disease: a case of multivalvular and myocardial fibrosis. *Circulation* 1977;56:889–890.
71. Billingham ME. Pharmacotoxic myocardial disease: an endomyocardial study. *Heart Vessels* 1985;278–282.
72. Pieroni M, Smaldone C, Camporeale A, et al. Chloroquine-induced transition from dilated to restrictive cardiomyopathy. *J Am Coll Cardiol* 2011;57:515.
73. Gottdiener JS, Katin MJ, Borer JS, et al. Late cardiac effects of therapeutic mediastinal irradiation: assessment by echocardiography and radionuclide angiography. *N Engl J Med* 1983;308:569–572.
74. Opie LH. Normal and abnormal cardiac function. In: Braunwald E, Zipes DP, Libby P, eds. *Heart Disease a Textbook of Cardiovascular Medicine*. 6th ed. Philadelphia, PA: W.B. Saunders Company, 2001:463–464.
75. Child JS, Perloff JK. The restrictive cardiomyopathies. *Cardiol Clin* 1988;6:289–316.
76. Turhan H, Ocal A, Erby AL, et al. Free-floating left atrial ball thrombus developed in an 11-year old child with restrictive cardiomyopathy during sinus rhythm: manifested as a major embolic event. *Int J Cardiol* 2005;103:111–113.
77. Al-Ammouri IA. Massive intra-atrial thrombosis in an 11 year-old child with restrictive cardiomyopathy. *Pediatr Cardiol* 2010;31:735–736.
78. Quiñones MA. Assessment of diastolic function. *Prog Cardiovasc Dis* 2005;47:340–355.
79. O'Leary PW, Durongpisitkul K, Cordes TM, et al. Diastolic ventricular function in children: a Doppler echocardiographic study establishing normal values and predictors of increased ventricular end-diastolic pressure. *Mayo Clin Proc* 1998;73:616–628.
80. Friedberg MK, Silverman NH. The systolic to diastolic duration ratio in children with heart failure secondary to restrictive cardiomyopathy. *J Am Soc Echocardiogr* 2006;19:1326–1331.
81. Palka P, Lange A, Donnelly JE, et al. Differentiation between restrictive cardiomyopathy and constrictive pericarditis by early diastolic Doppler myocardial velocity gradient at the posterior wall. *Circulation* 2000;102:655–662.
82. Rajagopalan N, Garcia MJ, Rodriguez L, et al. Comparison of new Doppler echocardiographic methods to differentiate constrictive pericardial heart disease and restrictive cardiomyopathy. *Am J Cardiol* 2001;87:86–94.
83. Schoenfeld MH. The differentiation of restrictive cardiomyopathy from constrictive pericarditis. *Cardiol Clin* 1990;8:663–671.
84. Henein MY, Rakhit RD, Sheppard MN, et al. Restrictive pericarditis. *Heart* 1999;82:389–392.
85. Wang A, Vincent RN, Johnson G, et al. Mixed constrictive pericarditis and restrictive cardiomyopathy in a child: treatment guided by tissue Doppler imaging. *Congenit Heart Dis* 2006;1:35–39.
86. Sengupta PP, Krishnamoorthy VK, Abhayaratna WP, et al. Comparison of usefulness of tissue Doppler imaging versus brain natriuretic peptide for differentiation of constrictive pericardial disease from restrictive cardiomyopathy. *Am J Cardiol* 2008;102:876–882.
87. Leya FS, Arab D, Joyal D, et al. The efficacy of brain natriuretic peptide levels in differentiating constrictive pericarditis from restrictive cardiomyopathy. *J Am Coll Cardiol* 2005;45:1900–1902.
88. Webber S, Lipshultz SE, Sleeper LA, et al. Phenotypic heterogeneity and outcomes of restrictive cardiomyopathy in childhood – a report from the NHLBI Pediatric Cardiomyopathy Registry. *Circulation* 2008;118: S1055.
89. Maskatia SA, Decker JA, Spinner JA, et al. Restrictive physiology is a major predictor of poor outcomes in children with hypertrophic cardiomyopathy. *J Am Coll Cardiol* 2011;57:A132.
90. Hook S, Ratliff NB, Rosenkranz E, et al. Isolated noncompaction of the ventricular myocardium. *Pediatr Cardiol* 1996;17:43–45.
91. Ozkutlu S, Hascelik S, Yalnizoglu D, et al. Familial isolated non-compaction of myocardium presenting as restrictive cardiomyopathy. *Pediatr Int* 2007;49:536–539.
92. Biagini E, Ragni L, Ferlito M, et al. Different types of cardiomyopathy associated with isolated ventricular noncompaction. *Am J Cardiol* 2006;98:821–824.
93. Maron BJ, Henry WL, Clark CE, et al. Asymmetric septal hypertrophy in childhood. *Circulation* 1976;53:9–19.
94. Bengur AR, Beekman RH, Rocchini AP, et al. Acute hemodynamic effects of Captopril in children with a congestive or restrictive cardiomyopathy. *Circulation* 1991;83:523–527.
95. Zile MR, Brutsaert DL. New concepts in diastolic dysfunction and diastolic heart failure: part II. *Circulation* 2002;105:1503–1508.
96. Denfield SW. Sudden death in children with restrictive cardiomyopathy. *CEPR* 2002;6:163–167.
97. Zangwill SD, Naftel D, L'Ecuyer, et al. Outcomes of children with restrictive cardiomyopathy listed for heart transplantation: a multi-institutional study. *J Heart Lung Transplant* 2009;28:1335–1340.
98. Al-Khaldi A, Reitz BA, Zhu H, et al. Heterotopic heart transplant with postoperative sildenafil use for the treatment of restrictive cardiomyopathy. *Ann Thorac Surg* 2006;81:1505–1507.
99. Dipchand AI, Naftel DC, Feingold B, et al. Outcomes of children with cardiomyopathy listed for heart transplant: a multi-institutional study. *J Heart Lung Transplant* 2009;28:1321–1321.

Hugh D. Allen ■ Jerry R. Mendell ■ Kevin M. Flanigan ■ Timothy M. Hoffman

Muscular dystrophy (MD) is associated with cardiomyopathy (CM) (sometimes dilated), conduction disturbances, or both. Depending on the type of dystrophy, and possibly the location of the gene abnormality, expression can be variable. With the advent of genetic testing, these diseases are being studied much more systematically and vigorously. The result is that more specific information about each type and subtype has been gained. These newer understandings about the diseases and their nuances will ultimately lead to improved diagnosis and likely different classifications and therapeutic approaches.

MUSCULAR DYSTROPHIES WITH CLINICAL CARDIAC DISEASE

Myotonic muscular dystrophy is the most common form of MD (inclusive of both adults and children). On the basis of new molecular insights, at least two variants must be considered (1,2). The classic disorder is referred to as dystrophic myotonia type 1 (DM1). It is associated with a CTG repeat in the 3' untranslated region of dystrophica myotonica-protein kinase gene. Repeat size instability leads to anticipation in disease onset from one generation to the next, and the children of mothers with DM1 can have congenital dystrophica myotonia, a severe grave form of the disease in which the CTG repeat is far more expanded. In these infants, the cardiac manifestations are considerably more severe (dilated cardiomyopathy (DCM), cardiac rhythm disturbances, and sudden death). A second variant of myotonic dystrophy, characterized only in the last few years, is referred to as DM2. Several notable differences from the classic disorder start with the molecular defect characterized by a CCTG expansion in intron 1 of the finger protein 9 (ZNF9) gene. The cardiac manifestations also include conduction system disease as in DM1. The congenital form of the disease is not seen in DM2.

Dystrophin deficiency causes the second largest group of dystrophies with cardiac involvement (and the most common in childhood). The severity of the skeletal muscle disease correlates with the quality and quantity of dystrophin, the product of the X-linked *DMD* gene. *Duchenne muscular dystrophy* (DMD) is the most severe variant, and is typically associated with <5% of normal levels of dystrophin in skeletal muscle. *Becker muscular dystrophy* (BMD) is a milder form of dystrophinopathy, in which greater amounts of dystrophin protein are present in the muscle. These differences in dystrophin expression are due to differing *DMD* mutations that either truncate protein expression or allow expression of protein of diminished size or amount.

Another unique disorder with prominent cardiac manifestations is *Emery-Dreifuss muscular dystrophy* (EDMD).

EDMD refers to a syndrome caused by more than one gene defect. The classic disease, X-linked EDMD (XL-EDMD), is marked by striking contractures (particularly at the elbow) and in most cases is caused by a mutation of the *STA* gene that encodes emerin, a protein of the inner nuclear membrane. Recently, another X-linked gene *FHL1* has been demonstrated to be the cause of about 10% of XL-EDMD (3). Mutations in the *LMNA* gene are responsible for autosomal forms of EDMD, which occur most commonly as autosomal dominant (AD) and occasionally as autosomal recessive (AR) traits. Both are almost identical in signs and symptoms to the X-linked form. The *LMNA* gene encodes alternatively spliced isoforms of type A lamins, lamin A and lamin C (4). Lamins are found on the inner nuclear membrane where they interact directly with other proteins including emerin, seeming to account for the overlapping clinical picture. Perhaps adding to the confusion is a DCM occurring in the absence of MD also associated with LMNA mutations. On the other end of the spectrum, adding further complexity to the LMNA phenotypes, is a generalized form of weakness affecting pelvic and shoulder muscles referred to as limb-girdle muscular dystrophy 1B (LGMD1B). It is distinct clinically from EDMD because of lack of extremity contractures. Of particular relevance, LMNA mutations causing LGMD1B, EDMD, and DCM all carry a risk of atrial arrhythmia, CM with heart failure, and sudden death (probably owing to tachyarrhythmias (5).

The limb-girdle muscular dystrophies (LGMDs) are a clinically and genetically heterogeneous group of disorders. LGMDs include both AD (LGMD1) and AR (LGMD2) forms. Based on linkage analysis, letters of the alphabet have been sequentially assigned to these disorders depending on the order in which linkage was established. Thus far identified and classified are six types of LGMD1A to 1E and fourteen subtypes of LGMD2A to 2N (6). Patients usually have pelvic girdle weakness with varying degrees of shoulder girdle muscle weakness. Mild contractures are seen with LGMDs but are never the predominant clinical feature as seen in EDMDs. The LGMD phenotypes with CM are described later.

A comment about the term *X-linked cardiomyopathies* is necessary here for clarification. This is a clinical term that did have value in the premolecular genetic era, but, with our current degree of understanding regarding specific gene defects, it is best to consider the major X-linked cardiomyopathies separately. Four separate genetic disorders with cardiac and skeletal myopathies are found on the X chromosome. DMD and BMD already have been discussed. These disorders, caused by the same gene mutation with varying degrees of dystrophin deficiency, are linked to the short arm of the X chromosome at Xp21. The other major CM on the X chromosome, EDMD (7), with a mutation in the *STA* gene, is linked to the long arm of the X chromosome at Xq28. A third CM on the X chromosome

is Danon disease (8), also known as X-linked vacuolar CM and myopathy, which is caused by a mutation in the gene encoding lysosome-associated membrane protein-2 (*LAMP2*) at Xq24. This form of dystrophy can have hypertrophic CM. The final disorder of this group is Barth syndrome (9). It is perhaps the most novel of these X-linked disorders. It is a mitochondrial disease caused by a mutation of the tafazzin gene associated with decreased amounts and altered structure of cardiolipin, the main phospholipid of the inner mitochondrial membrane. The gene maps to the long arm of the X chromosome at Xq28. Patients have variable clinical findings, often including heart failure, CM, neutropenia, and growth retardation.

ASSESSMENT TOOLS

Electrocardiography

Since many of the dystrophies affect cardiac conduction, the electrocardiogram (ECG) offers important information regarding abnormalities of rhythm, rate, axis, and pattern change(s). Specific abnormalities are discussed below with respect to findings in particular lesions.

Holter Monitoring

Twenty-four-hour electrocardiography gives insight into arrhythmias and disorders of conduction seen in patients who are often asymptomatic. It also allows measurement of heart rate variability in patients with disordered automaticity.

Echo Doppler Studies

Somatic deformities associated with various forms of dystrophy may include chest wall deformities and kyphoscoliosis that distort the relationship of lungs and heart, creating challenges for ultrasound evaluation. It is important to record and measure the left ventricular dimensions in diastole and systole, areas of dyskinesis and akinesis, anterior mitral valve leaflet E-point septal separation (EPSS), shortening fraction (SF), ejection fraction (EF), and rates of wall contraction and relaxation. Planimetry of 2-D images allows fairly accurate predictions of left ventricular volumes and EF. More recently, the sphericity index, derived from comparing the long-axis left ventricular dimensions in diastole and systole with the chord from the mitral annulus to the apex in diastole and systole, has been used to quantify the myopathy. The value should be <0.66 . If it approaches 1.0, it indicates that the chamber is rounded instead of elliptical (remodeled), and a dilated myopathy is likely (10).

Friedberg and Silverman (11) have defined criteria for DCM that include prolonged systolic duration and shortened diastolic duration. Doppler mitral and tricuspid regurgitation jet durations were used to measure systole. Diastole was measured as the time from cessation of the regurgitation jet to the onset of the next atrioventricular (AV) valve regurgitant jet. A ratio of systolic time/diastolic time was derived and corrected in relation to heart rate. The tricuspid systolic interval/RR interval in normal subjects was 0.41 ± 0.07 (mitral, 0.42 ± 0.08), and the systolic/diastolic ratio in normal subjects was 0.77 ± 0.24 . There are few studies in MD that have used this method, but it holds promise as another useful measurement. See Chapter 9 for a detailed description of functional testing by echo and Doppler techniques.

Doppler analysis is used to demonstrate mitral and aortic valve regurgitation. Quantification of tricuspid regurgitation

allows prediction of systolic right ventricle and pulmonary artery pressures. Evaluation of pulmonary regurgitation allows estimation of pulmonary arterial diastolic pressures. It also is possible to estimate cardiac output by planimetry of the pulsed Doppler aortic waveforms with respect to space and time. Newer studies, especially in adult patients, and a few in the pediatric population, have used Doppler tissue analysis to evaluate wall contractile function and diastolic function. These approaches are beginning to have usefulness for evaluation of CM in the MD population.

Because many of these patients cannot exercise physically, dobutamine stress echo studies may provide information regarding myocardial performance, especially in patients with borderline normal resting studies. These studies should be performed carefully, recognizing that atrial and ventricular tachyarrhythmias could occur during such stress testing.

Other Imaging Methods

Other tools can be used to measure left ventricular volumes and derivation of EFs when patients cannot have adequate echo studies; these include magnetic resonance imaging (MRI), computerized tomography imaging, radionuclide imaging, and positron emission testing. Each has advantages and disadvantages, including cost, accessibility, and limitations, for example, the presence of metal rods in patients with previous scoliosis surgery may interfere with MRI analysis. There may be variability in the information that can be derived from these other imaging methods depending on the availability of the most recent equipment and the sophistication of the software used for analysis.

MUSCULAR DYSTROPHIES WITH CARDIAC INVOLVEMENT

Dystrophinopathies

DMD and BMD are related disorders (12–14), differing in severity because of the amount or quality of the expressed dystrophin protein. In nearly all cases, DMD patients express $<5\%$ dystrophin in skeletal muscle biopsies, an amount insufficient to maintain ambulation much beyond age 12. In contrast, in BMD, the gene mutation permits varying degrees of dystrophin expression that can be quantified on skeletal muscle biopsy. In most cases, both the quantity and the size of dystrophin are reduced. The amount of dystrophin expressed also can be determined by cardiac biopsy, but this is not a common or practical approach. It is important to understand that BMD covers a very broad spectrum of disability from mild to severe depending on the specific gene mutation. It also is important to note that skeletal and cardiac muscle may exhibit paradoxical clinical responses. In DMD with severe skeletal muscle loss early in the course of the disease related to almost complete dystrophin deficiency, patients lose ambulation between 10 and 12 years of age and have a sedentary wheelchair-dependent lifestyle. In this environment, there may be very little stress on the heart on a day-to-day basis. This probably accounts for the uncommon presence of symptoms and signs of clinical heart failure, which often do not manifest without a catastrophic event, such as a life-threatening pulmonary infection. In contrast, the patient with BMD who has CM will have more skeletal muscle and preserved ambulation that create more cardiac demands, leading to symptoms of heart failure that mandate treatment.

DYSTROPHINOPATHIES: DUCHENNE MUSCULAR DYSTROPHY

Boys with DMD have few problems in the neonatal period. Some have delayed onset in walking independently. They sometimes crawl later than average. The disease usually is not recognized until about 3 years of age because the affected boys run and jump poorly and cannot keep up with other children in normal play activity. If there is a known family history, for example, siblings with DMD, a new male infant may be recognized as having DMD with CK and genetic confirmation. Through such recognition, the Muscular Dystrophy Association is sponsoring a multicenter trial of early diagnosis and natural history in infants. By school age, the difference in muscular function becomes very apparent. Stair climbing usually requires a handrail. They usually climb stairs one step at a time rather than alternating from step to step. Falling becomes an increasing problem. Facial injuries can result from forward falls because the arms are too weak to brace against the fall. To get up from the floor, boys roll to a prone position, spread their legs for balance, first lift their buttocks and then “walk” their hands up their legs (Gower sign). By age 6 to 7 years, most boys assume a waddling gait with a lordotic posture. Walking becomes increasingly difficult about age 10, and without intervention, most of these patients will become wheelchair dependent by about age 12. For the DMD population at large, the IQ is reduced by approximately one standard deviation (SD) from the normal population. Cognitive difficulties affect verbal and memory skills selectively.

On physical examination, certain features are easily recognized and include the following: enlarged (hypertrophied, not “pseudohypertrophied”) calf muscles that feel rubbery on palpation; weak neck muscles that cannot raise the head from supine, especially if the neck is first hyperextended; and weakness of proximal muscles of varying degrees, always worse than distal muscle. Late in the course, all muscle function is impaired except for minimal hand movement. Diaphragm and intercostal muscles are compromised, leading to poor cough, aspiration, and predisposition to pneumonia. A typical scenario is an episode of pneumonia that increases cardiac demands leading to heart failure. Some patients may have a tachyarrhythmia at any time prior to this. Death has historically occurred sometime in the early twenties, although aggressive and early use of nocturnal ventilatory support may have created a significant impact in extending life expectancy (15).

Cardiac Pathology

Cardiac involvement is universal. There is epimyocardial muscle replacement with fat and fibrosis beginning in the left ventricular posterior wall behind the posterior mitral annulus. Histologic studies show that the fibrosis begins at the epicardium and progresses toward the endocardium (16). The myocardial scarring progresses apically and ultimately invades the septum (17). The right ventricle and the atria seldom are involved. The fibrosis leads to dysfunction and occasional dilation, especially with severe dysfunction, with initial thinning and even outpouching of the left ventricular posterior wall behind the mitral area to a severe generalized CM. It is possible that the left ventricle cannot dilate if the wall is severely fibrotic, creating a restrictive myopathy. If dilation is present, the patient can develop mitral regurgitation and occasionally, aortic regurgitation. With left ventricular failure, there can be secondary pulmonary hypertension and right ventricular failure associated with pulmonary and tricuspid regurgitation. Fibrosis and fatty infiltration also can involve the conduction system, including the sinoatrial (SA) node and AV node (18,19).

Cardiac History and Physical Examination

The patient has very few cardiac complaints, mainly because of physical inactivity. Even those with severe CM have few symptoms, other than shortness of breath, which can also be due to respiratory compromise from their weak chest and diaphragmatic musculature. Some will have postural nocturnal dyspnea. Others may detect palpitations if they have ventricular or atrial arrhythmias.

It is important to realize that patients with DMD and BMD can have severe complications from anesthesia, including cardiac arrest. Most complications seem to be related to use of succinylcholine, a muscular relaxant that may trigger hyperkalemia (20). Others have been attributed to use of volatile anesthetic agents. Patients also can have a reaction similar to malignant hyperthermia (20), develop rhabdomyolysis, and have masseter muscle spasm. It is apparent that anesthesia must be approached with caution in patients who have dystrophinopathies (20,21).

The cardiac examination is seldom abnormal, even in the presence of CM. Occasionally, third or fourth heart sounds may be present. According to Perloff et al. (22), a pulmonary outflow murmur is present in most patients, but that has not been our experience. Some will have a click and murmur of mitral valve prolapse; we have heard this in patients with severe chest wall deformities secondary to scoliosis. There may be neck vein distention, peripheral edema, or sacral edema. The overall examination is often distorted by chest wall deformities, especially in older patients who have scoliosis.

Electrocardiographic Features

Historically, we have been taught that the characteristic ECG in Duchenne shows a shortened PR interval, deep Q waves in leads I, aVL, V5, and V6, and occasionally in leads II, III, and aVF. There is often a tall right precordial R wave and an increased R/S ratio (19,23) (Fig. 58.1). Some have reported QT prolongation (24,25) and QT dispersion abnormalities (26).

A recent prospective study of 115 boys with DMD (40 with CM) confirmed that the most commonly seen findings were (a) short PR interval (43%), (b) Right Ventricular Hypertrophy (RVH) (37%), (c) prominent Q waves in leads V5 (34%) and V6 (33%), (d) Q waves in the inferior lateral leads in only 9, and (e) Q waves in leads I, aVL, V5 and V6 in only 3. None had prolonged QTc intervals, Two had ST-T depression (1 with CM) and 38 had flat/biphasic ST segments (15 with CM). The EKG did not discriminate the CM subgroup from the DMD boys who had EF > 55% (27).

An unpublished recent serial analysis of 154 DMD boys (91 with CM) studied prospectively over a 9.4-year period with a total of 805 EKGs (367 in CM group) showed no correlation of RVH amplitude with echocardiographic LVID, EPSS, SF, or EF. Thus RVH does not correlate with CM (Thrush PT, Allen HD, *unpublished data*).

Another recent retrospective study of 150 MD patients, including 86 DMD boys (51 with CM defined as EF < 55% or LVIDd > 2SD = 59%) showed that abnormalities (mainly repolarization artifacts, ST-T changes, RVH, or BVH) correlated well with a general MD population who had CM defined as left ventricular internal dimension at diastole (LVIDd) > 2 SD or EF < 55%. The DMD population was not separated in the retrospective paper's data analysis but abnormalities were seen in only 63/213 (29.5%) of the DMD EKGs that were analyzed. There was no mention of shortened PR interval or correlation with CM in the DMD subpopulation (28).

Holter analysis has shown that automaticity is also affected whereby there is a resting sinus tachycardia, loss of circadian rhythm, and reduced heart rate variability in many patients

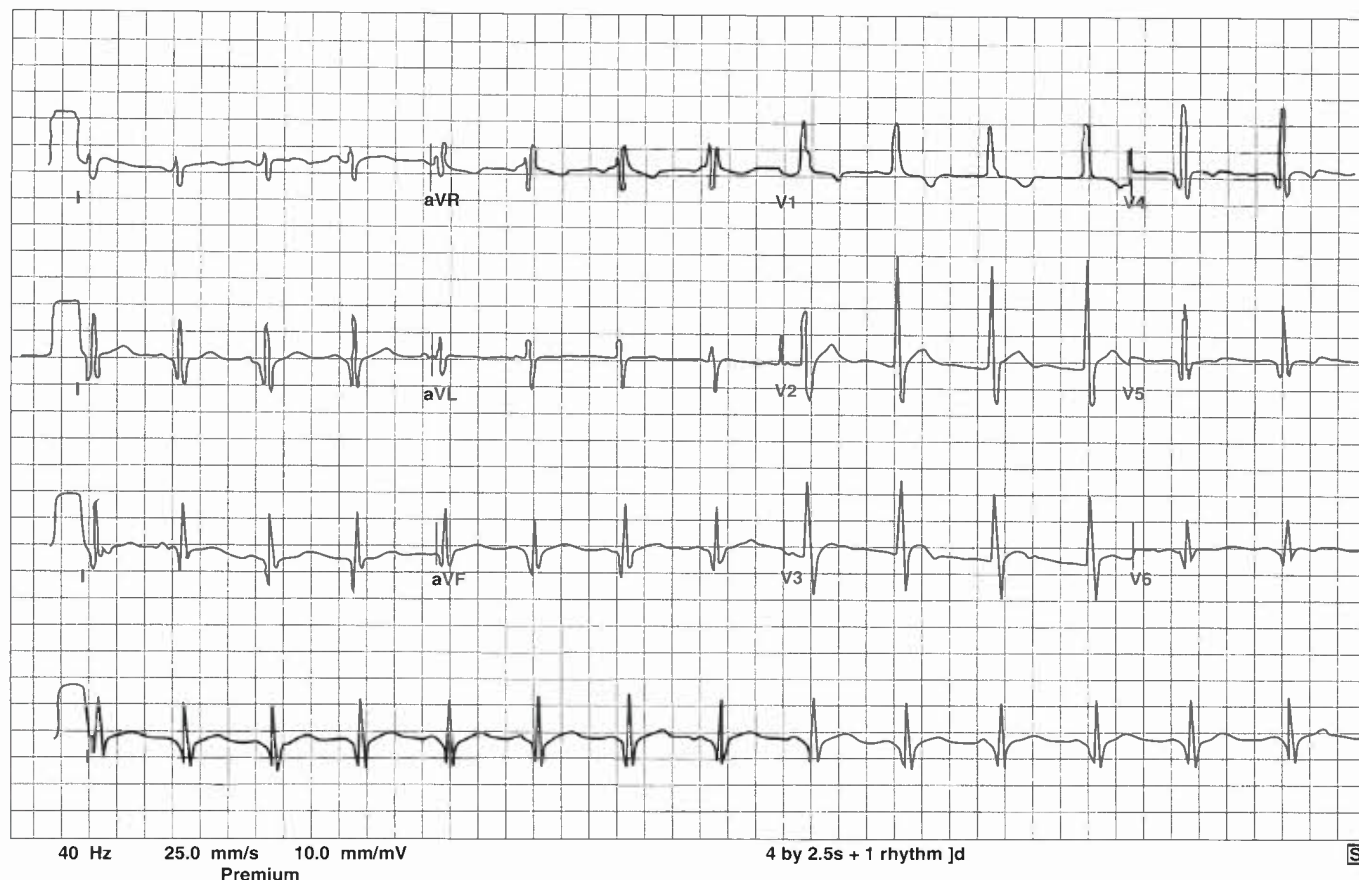


FIGURE 58.1. ECG from a 20-year-old patient with DMD. Note the shortened PR interval; Q waves in II, III, aVF, V5, and V6; intraventricular conduction delay; and RVH. The QTc was 430 ms.

with DMD (29–33). There are frequent arrhythmias in older patients including ectopic atrial tachycardia, atrial fibrillation, transient second- and third-degree AV block, and more ominous ventricular tachycardias (Thrush PT, Allen HD, unpublished data) (29). One publication showed that there was a predictive ECG pattern in terminal DMD consisting of $RV1 < 0.6$ mV, $RV5 < 1.1$ mV, and $RV6 < 1.0$ mV; abnormal T waves in II, III, aVF, V5, and V6; conduction disturbances; ventricular premature contractions (VPCs); and sinus tachycardia (34). The presence of multiform VPCs and ventricular tachycardia on Holter monitoring portends possible sudden death due to ventricular fibrillation (35–37).

Doppler Echocardiogram and Other Imaging Studies

The echocardiographic findings in boys with Duchenne correlate with the autopsy findings of posterior epicardial thinning leading to ultimate DCM. The first descriptions were by Goldberg et al. (37), who showed thinner left ventricular posterior walls, especially behind the posterior mitral valve leaflet, diastolic dysfunction, contraction abnormalities that progressed inferiorly, and temporally progressive wall thinning in these patients during serial studies (37–40). Other serial studies showed progressive deterioration toward left ventricular dilation and dysfunction by evaluation of left ventricular diameter changes (25) (Fig. 58.2), systolic time interval changes (38–40), and development of mitral valve prolapse (35).

Findings of CM do not necessarily parallel the progressive skeletal muscle changes (41,42). Increasing left ventricular

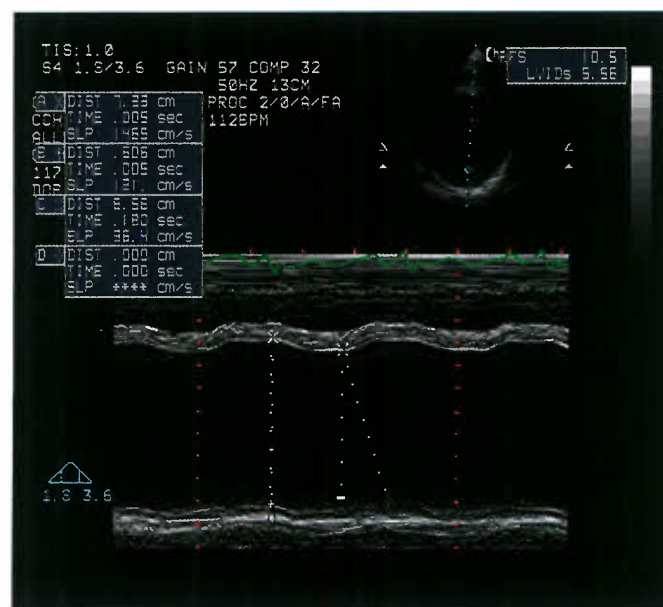


FIGURE 58.2. M-Mode tracing from a 24-year-old patient with advanced DMD. His e-point septal separation was nearly 2 cm (normal is < 5 mm).

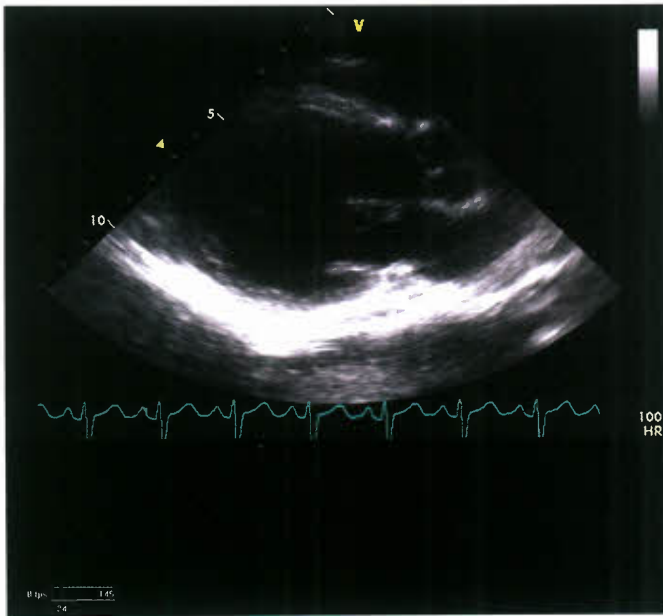


FIGURE 58.3. Two-dimensional long-axis echo from patient in Figure 61.2. Note the dilation of the left ventricle at 4.6 Z score (SDs). His EF on afterload reduction and beta-blocker treatment is 39%, and SF is 19%. The sphericity index is 0.8 (normal is <0.66). He has posterior wall thinning, and that area is nearly akinetic.

diastolic and ultimately systolic volumes, decreasing shortening and EFs, and increasing sphericity indices (10,43) (Fig. 58.3) indicate worsening CM (43–45). Tissue Doppler echocardiography studies have shown decreased systolic contraction and diastolic relaxation rates in patients with DMD, even when they had otherwise normal echocardiographic findings (44,45). Further studies using this technology are necessary to confirm these findings, but it appears to be promising for assessment of these populations.

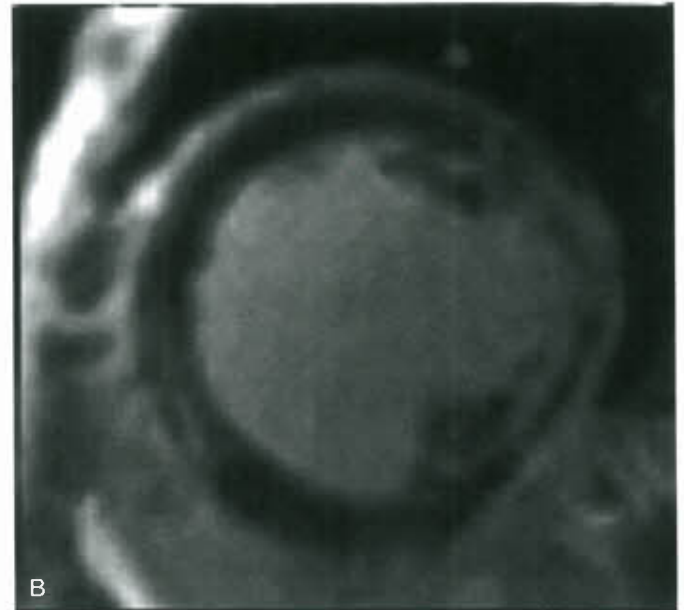


FIGURE 58.4. MRI from same patient as in Figures 59.2 and 59.3 (Courtesy of Stephen Cook, MD.). **A:** Note that fibrosis (white appearance) posterior to the mitral papillaries has nearly completely replaced muscle. **B:** Fibrosis extends through the myocardium. Functional information was similar to the echo results.

One study using equilibrium radionuclide angiography in 9- to 18-year-old patients with DMD showed normal resting EFs (>50%) in 79% of the patients and normal right ventricular EFs (>45%) in 95%. However, when they used dobutamine perfusion, there were marked age-related decreases in both left and right ventricular EFs (46). Another 5-year follow-up serial radioisotope study showed resting changes in the septum that portended a fatal outcome (47).

MRI and angiography hold great promise for detection of scarring and fibrosis within the muscle (48–50) (Fig. 58.4) and quantification of left ventricular function by using circumferential strain analysis (48,51,52) (see chapter 10). The presence of non-steel-containing Harrington rods is not a contraindication for MRI evaluation. These studies have shown that fibrosis and abnormal circumferential strain are noted long before EF abnormalities are seen on echo. This raises the question of “what/when is CM in DMD?” Perhaps CM is always present in DMD regardless of age (Canter CE, *personal communication*, St. Louis Children’s Hospital, 2011).

Neuroendocrine Abnormalities

Plasma α -atrial natriuretic peptide (α -ANP) and brain natriuretic peptide (BNP) levels are elevated in adults with congestive heart failure. A few studies of patients with DMD have shown these to be elevated in patients with echocardiographic evidence of left ventricular dysfunction (EF \leq 15%) or end-stage cardiorespiratory failure (53,54). More studies are necessary to clarify the meaning of these findings, but ANP and BNP levels seem to be a promising method of evaluating these patients and assessing the patient’s response to treatment (see Chapter 73).

Therapy

The approaches to treatment include symptomatic, preventive, and curative. Most emphasis had been on treating symptoms, but they are seldom present in DMD boys. In the past, the empiric standard treatment was use of digitalis and diuretics. Digitalis has fallen out of favor with many cardiologists who treat DMD because of its proarrhythmic potential.

A recent consensus statement recommends doing echo exams after the age of 6 years and repeating them at least every 2 years thereafter until 10 years of age, then annually. "Use of standard heart failure interventions with deterioration of function"—"even if asymptomatic"—was also recommended (55).

More recently, afterload reduction with angiotensin-converting enzyme inhibitors (ACE inhibitors) has been used with some success (42). Some (42,46,47,56) have advocated using ACE inhibition for patients with EF <55%, left ventricular dilation (>2 Z scores/body surface area [bsa]), sphericity index (>0.66), and/or an abnormal tissue Doppler myocardial performance index (<0.35). They (42) reported that ACE inhibition (and sometimes additional beta-blocker treatment if the echocardiographic indices of remodeling did not improve after 3 months) resulted in stabilization in 2 of 29 boys, improvement in 8 of 29, and normalization in 19 of 29 (16 Duchenne, 3 Becker). Others have evaluated a similar population with EF <55% who were treated with ACE inhibition with varied results (56). Some controversy exists as is evident from a letter to the editor (57) responding to this study with many important questions about the true effect of the drug, selection bias, and variable expressions of the disease.

Viollet, Thrush et al. (58) evaluated the natural history and responses to treatment in a prospective study of 65 boys with DMD and CM. Natural history information was available on 24 patients before onset of CM. The expected downward trend was noted with mean EF decreasing from $53\% \pm 8.5\%$ to $44.3\% \pm 8.3\%$ over a mean 40-month period, ranging from 6 to 50 months. By Kaplan-Meier analysis, the mean age of onset of CM was 14.1 years, similar to that seen in other studies. The range in age of onset of CM was 7 to 27.3 years. ACE inhibitor (lisinopril) was initiated when the EF <55%. Beta-blocker therapy (metoprolol) was used to treat disordered automaticity (average 24-hour heart rate >100 bpm). The CM population separated into two groups, those receiving ACE inhibitor only (mean age 14.1 years), and those receiving ACE inhibitor plus β -blocker (mean age 16.1 years). The responses to treatment were similar ($p = 0.947$) between the two groups, with the ACE inhibitor group improving from mean EF 48% to 54% ($p < 0.0001$) and the ACE inhibitor + β -blocker group from mean EF 45% to 50% ($p < 0.001$).

ACE blocker (ARB) therapy has also been advocated with the argument that they are less prone to complications of cough and by inhibition of the TGF- β signaling and is associated with skeletal and cardiac muscle regeneration in the MDX mouse model of DMD and Marfan (59, 60). An muscular dystrophy association (MDA)-sponsored multicenter study prospectively evaluating ACE inhibitor versus ARB including skeletal muscle evaluations is presently under way to see if one treatment has advantages over the other.

Other investigators (61,62) used neuroendocrine parameters along with echocardiographic evaluation of left ventricular function to determine whether or not to treat. They defined left ventricular failure on the basis of an EF of <40%, fractional shortening of <20%, and left ventricular dimension >2 SD. Elevation of ANP and BNP correlated with echo findings, and many of the patients were symptomatic. After treatment with ACE inhibitor and beta-blocker, neuroendocrine levels normalized and echo parameters improved. Improvement was temporary for some of the patients who worsened after normalizing. Increasing neuroendocrine levels portended impending death. Clearly, ongoing prospective studies of whom to treat, which parameters should be used to indicate the need for treatment, serial assessment, and clear measurements of outcomes are necessary.

Ventricular tachyarrhythmias are ominous and warrant treatment with an appropriate agent. Often, a beta-blocker is the first drug used, followed by class III agents such as sotalol

or flecainide. An automatic implantable cardioverter defibrillator may be considered for this problem, as well as in patients with EFs <15%, similar to the approach used in adult patients with congestive heart failure.

Preventive treatment is a debatable topic. The usual adult patient with congestive failure is treated once the EF is <50%. What number should be applied to the Duchenne patient to imply the correct time to use an ACE inhibitor? Will it make any difference? The work of Jefferies et al. (42), Towbin et al. (45) implies that it might be beneficial. Again, serial controlled double-blind studies are necessary to answer these questions.

The timing of initiation of heart failure care is debatable and often is accomplished when there are obvious signs or symptoms of decreased cardiac function. However, a recent study in a mouse model of DMD noted a protective effect of early initiation of an aldosterone antagonist (Aldactone) in combination with an ACE inhibitor (lisinopril) on both skeletal and cardiac muscle (63). The mechanism is thought to be related to the antifibrotic effects of this class of medications in combination. Cardiac and skeletal muscle function evaluated *ex vivo* remained at 80% of normal with this therapeutic regimen whereas those mice not treated had a decline to 40% of normal (63).

Some have noted that eplerenone, another aldosterone antagonist that does not have the gynecomastia effects that are seen in teen boys taking Aldactone may be a valid substitute. An adult trial in patients with congestive heart failure showed reduced risk of death and fewer hospitalizations in the cohort studied (64). Additionally, the drug has been used safely in a pediatric population with systemic hypertension (65). A multicenter MDA-sponsored "prophylactic" trial will be under way in the near future to assess the effects of this drug on cardiac fibrosis and abnormal systolic strain evaluated by serial MRI in a DMD population.

As therapy initiation is debated, detection of early cardiac changes is also being evaluated further. Echocardiographic and cardiac MRI advancements have led to earlier detection of functional changes of the myocardium in many disease states. A recent study in those with DMD evaluated left ventricular myocardial peak circumferential strain via advanced cardiac MRI techniques and found that in patients with a normal EF, the peak circumferential strain was decreased and echo EF showed abnormality at a mean age of 15.8 years (49,50). Patients <10 years of age exhibited abnormal strain, and older boys had a further decline in strain analysis. It is thus hypothesized that using tissue Doppler and strain analysis on patients with DMD even with a normal EF may lead to early detection of myocardial changes (49). This study did not follow patients longitudinally, and therefore, no strong conclusions can be made as to the natural history of cardiac changes in those with DMD and to the applicability of a management scheme of early detection and therapeutic intervention.

In selected patients with end-stage heart failure where usual medical therapies have been optimized and symptoms persist, outpatient inotropic support has been reported (66). The use of milrinone at home is not without potential adverse events, and a detailed discussion with the family in regard to the role and risks of this therapy must be done prior to initiation. Inherent risks exist with long-term access including infection; however, inotropic support is associated with a multitude of potential side effects, yet potential exacerbation of arrhythmias is paramount. Nonetheless, inotropic support may allow for more time at home or school and may provide symptomatic relief (66).

Clinical trials have been done sporadically in this patient population to assess novel therapies. Recently, idebenone, a

benzoquinone with antioxidant properties, which improves respiratory chain function and cellular energy production, was evaluated in a double-blind, placebo-controlled trial in 21 patients with DMD ranging in age from 8 to 16 years (67). Idebenone was found to be safe and well tolerated and its use was associated with a trend toward an increase in strain of the left ventricular inferolateral wall. Additionally, from a respiratory standpoint, there was a significant increase in peak expiratory flow. It is felt that this drug may be suited for those with DMD due to its facilitation of electron flux along the mitochondrial respiratory chain and the reduction of oxidative stress (67). A larger trial is ongoing. Other current trials that are enrolling subjects include an evaluation of the effect of sildenafil on cardiac remodeling as well as another one studying carvedilol in a preventive fashion in those with DMD.

Duboc et al. (68), in a multicenter trial of an ACE inhibitor, perindopril, did a prospective double-blinded trial where 57 boys with DMD and normal EF (>55%) by radioisotope evaluation were in a 3-year evaluation where they received either ACE inhibitor or placebo, followed by 24 more months, when all received ACE inhibitor. Left ventricular ejection fraction was checked at baseline, 3 years, and 5 years. Although there was no significant difference between the treatment groups at 3 years or 5 years ($p = \text{ns}$), individually, one patient in the treatment group versus eight in the placebo group had EF<45% at the end of the trial ($p = 0.02$). A 10-year follow-up study (69) of members of the study groups showed that 26/28 patients in the treated group were alive versus 19/29 in the placebo group. Kaplan-Meier survival was significantly lower in the placebo group ($p = 0.13$). From this, he concluded that early (9.5 years of age) treatment with ACE inhibitor was associated with lower mortality. Although the causes of deaths were not detailed, the study is provocative and has resulted in many centers adopting a “prophylactic” approach by treating all boys with DMD, as Duboc suggests, with an ACE inhibitor after 9.5 years of age.

The obvious hope is that a cure for this genetic disease is on the horizon. A wide range of prospects exists, which include growth-modulating agents that increase muscle regeneration and delay fibrosis, antisense oligonucleotides (2'-O-methyl phosphorothioate backbone or morpholinos) with the capacity to skip exons and agents designed to suppress or stop codon mutations, gene-therapy approaches including strategies to replace or repair genes or use surrogate genes to replace defective ones, and stem cell therapy, especially using mesangioblasts. What effect will any of these approaches have on the myocardium? Future studies should help answer this question. If these treatments do not improve the myocardium, it is incumbent upon the pediatric cardiology community to evaluate and employ the most effective cardiac therapies possible so that the hopes for skeletal muscle improvements are not encumbered by congestive heart failure.

Another question is whether we should reevaluate our therapeutic attitudes toward this population in light of improved pulmonary care, greater longevity, and possible improvements in skeletal muscle from gene therapy or exon-skipping treatments. If severe heart failure happens at a young age, what is the role of synchronization pacing, ICDs, or destination treatment, either mechanical (see Chapter 21) or transplant (see Chapter 65)?

The Duchenne Carrier

Few investigators have evaluated DNA-proven Duchenne and Becker female carriers (mothers and sisters). Earlier evaluations showed ECG abnormalities (70,71). Hoogerwaard et al. (72) studied 129 female Duchenne ($n = 85$) and Becker

($n = 44$) carriers and found that 47% had ECG changes (50% Duchenne, 40.9% Becker) similar to those seen in the dystrophinopathy patients. DCM detected by echo was present in seven Duchenne carriers (one was symptomatic) and in none of the Becker carriers. Subtle echocardiographic findings were present in 36% of the entire group (38% Duchenne, 34% Becker). Only 38% had normal echoes and ECGs. A more recent study (73) showed that DMD carriers (heterozygotic mothers) had mildly lower EF at rest versus controls (EF 55% vs. 62%) and after exercise, mean EF fell to 53% versus 73% in controls. Twenty-one of the twenty-four had one or more of abnormal resting EF, EF response to exercise or exercise-induced LV wall abnormality. These studies imply the need for evaluation of proven female carriers, even if they are asymptomatic.

DYSTROPHINOPATHIES: BECKER MUSCULAR DYSTROPHY

By strict criteria, patients with BMD remain ambulatory until 15 years of age and older. This is an arbitrary cutoff between DMD and BMD because the disorders represent a continuous spectrum related to the quantity and quality of dystrophin. In most cases, dystrophin is reduced in amount and size (74,75). In addition, the clinical disease varies from very mild to very severe, meaning that patients may lose ambulation shortly after age 15 years or remain ambulatory for many decades (62). Serum creatine kinase (CK) levels are very high, falling into the same range as the patients with DMD (usually >20 to 75 times normal). Again, the cardiac manifestations do not necessarily correlate with skeletal muscle progression and can be present sooner or later than the skeletal problems (75,76).

The ECG findings in patients with BMD are similar to those in patients with DMD with prominent Q waves in I, aVL, and V6, or in II, III, and aVF; tall R waves in V1; and increased QT dispersion (70). They can have supraventricular arrhythmias including atrial fibrillation/flutter and can have ventricular arrhythmias, especially toward end-stage myocardial dysfunction (77,78–80). They can also have ST changes and prolonged QTc intervals but do not have the problems with automaticity that patients with DMD show (31,32).

Their cardiac involvement is that of a DCM, sometimes starting with right ventricular dilation (80,81) and progressing to a generalized DCM. The presence of cardiac involvement with BMD is associated with exon 49 deletion and in most with exon 48 deletion according to a study by Melacini et al. (80), although other studies have not confirmed this observation, including a later study from the same group (82,83). Additionally, a recent MRI study showed many of the same findings seen in DMD, including fibrosis and was more discreet in detecting abnormalities of EF than echo (84).

A much more extensive analysis of genotype–phenotype correlation in BMD patients addressed age of CM onset and the protein domain deleted, showing that early-onset CM was associated with mutations in the amino-terminal domain; in contrast, deletions removing portions of the rod domain along with the hinge 3 domain have a later onset, likely due to preservation of the spectrin-repeat structure of the protein (85).

One study of 13 patients with BMD with cardiac involvement (78) showed that only one was wheelchair dependent. Since skeletal muscle is better preserved in BMD than in DMD, cardiac transplantation is a therapeutic option that can be lifesaving for patients with BMD assuming that they

have first had a careful trial of medical therapy, including use of afterload-reducing agents and, in some, implantable cardiac defibrillators (86–88). Use of mechanical support devices while awaiting transplant is desirable if necessary (see Chapter 21).

Multidisciplinary care of patients with DMD and BMD may enhance quality of life and life expectancy. In addition to neurologic and cardiac sequelae, respiratory failure from muscle weakness is a prominent issue with these patients. Some data advocate early intervention with noninvasive positive-pressure ventilation at the first signs of nocturnal hypoventilation. Positive-pressure ventilation physiologically reduces left ventricular afterload and is used for symptomatic respiratory relief of congestive heart failure in adults and adolescents. Noninvasive positive-pressure ventilation, even for periods of time acutely, may induce favorable hemodynamic effects on the left ventricle. However, theoretically, this intervention may elicit long-term improved hemodynamics (89).

DYSTROPHINOPATHIES: X-LINKED CARDIOMYOPATHY

Boys with this abnormality of the dystrophin gene complain of muscle fatigue, pain, and cramping with exercise but do not manifest the weakness seen in patients with BMD and DMD (90). Towbin et al. (91) analyzed one family and found a missense mutation at exon 9 of the dystrophin gene. They can have calf hypertrophy and have elevated serum CK levels (81). Some have no skeletal muscle dystrophin abnormality but have abnormalities of the cardiac dystrophin (14,91–93). Other studies have shown a mild decrease in skeletal muscle dystrophin with normal distribution, but no dystrophin was found in heart muscle (94). By the late teen years to early adulthood, they can develop a congestive CM that usually progresses to death within 2 years of the onset of the myopathy diagnosis. They also can have arrhythmias and AV block with much greater frequency than that seen in patients with either DMD or BMD. Of note, female carriers can show heart failure that is slowly progressive and often fatal (95).

MYOTONIC MUSCULAR DYSTROPHY

Myotonic MD, with its two adult forms (see above), DM1 and DM2, is inherited as an AD disorder representing the most common form of MD in adults (96). Patients may complain of sleep disturbances and gastrointestinal problems, both constipation and diarrhea, before developing muscle weakness. Progressive facial muscle, temporalis, sternocleidomastoid, and limb weaknesses develop along with cataracts (77). The weakness is unique among the common muscular dystrophies, affecting distal equal to or greater than proximal muscles. Patients also can have frontal baldness, diabetes, and frequently, infertility (97). When Steinert (98) described the disease, he noted that patients often had a slow pulse rate. Few adult patients have DCM, and pathology studies seldom show myocardial involvement (99). Conduction problems are common. They include bradycardia, prolonged PR interval, AV block, prolonged QRS and QT intervals, *torsades de pointes*, ventricular tachycardia and fibrillation, and atrial fibrillation/flutter with slow ventricular response owing to impaired AV conduction (93,100–102). These findings worsen with time and will be found in 75% of patients

with myotonic dystrophy (13,96,100,103). Cardiac syncope and sudden death have been reported, indicating that these patients would have benefited from pacemaker implantation (96). A recent study using MRI found that patients with fatty infiltration of the right ventricle correlated with the presence of inducible ventricular tachyarrhythmias in patients with myotonic dystrophy (101).

Affected children of mothers with DM1 show earlier and more aggressive expression of the abnormalities than seen in their mothers and in previous generations (anticipation phenomenon). Additionally, they often will present in infancy with an aggressive form of DCM (13,100–102).

EMERY-DREIFUSS MUSCULAR DYSTROPHY

In 1966, Emery and Dreifuss (7,104) described an X-linked MD that had unique clinical features including elbow, Achilles tendon, and posterior cervical muscle contractures that appear before muscular humeroperoneal weakness, including progressive biceps, triceps, anterior tibial, and peroneal muscle wasting with later pectoral, knee, and hip extensor weakness and ultimate development of complete heart block. In addition to the original X-linked form, another X-linked form is due to mutations in the *FHL1* gene, and autosomal forms of Emery-Dreifuss disease have been found to be dominant and recessive lamin A/C (*LMNA*) gene abnormality (5,105–111). (See introductory comments).

The progressive fibrous and fatty depositions mainly involve the atria, ultimately causing mechanical and electrical atrial paralysis. Patients can have prolonged PR interval, atrial fibrillation/flutter, bradyarrhythmia and tachyarrhythmia, stroke from atrial emboli, and death. Some patients will have late ventricular dilation, severe congestive failure, and arrhythmias. Pacemaker implantation can be lifesaving, but late deaths have happened even in patients who have pacemakers (7,105–115). Cardiac transplantation is sometimes lifesaving.

FACIOSCAPULOHUMERAL MUSCULAR DYSTROPHY

This disorder represents one of the most common forms of MD. It is inherited as an AD disorder that maps to chromosome 4q35, and is associated with an integral deletion in the number of a 3.3 kilobase (kb) repeat element, the D4Z4 repeat. This feature has for years allowed reliable diagnostic testing, but only recently has a unifying model of pathogenesis been proposed in which the deleted repeat results in a structural change at the D4Z4 locus, allowing the expression of the polyadenylated transcripts of the *DUX4* gene (116). *DUX4* encodes a transcription factor, and there is significant effort under way to understand the downstream targets that presumably play a central role in disease pathogenesis.

Clinically, patients have weakness involving face, scapular stabilizer muscles, and distal lower-extremity muscles. Progressive weakness involves both distal and hip-girdle muscles. The distribution of weakness is typically asymmetric. The disease is variable in severity with about 20% of patients being wheelchair dependent sometime in the course of the illness. Cardiac involvement has been reported in genetically confirmed facioscapulohumeral MD, but it is extremely rare, consisting of atrial and ventricular conduction defects (115).

LIMB-GIRDLE MUSCULAR DYSTROPHIES

LGMDs represent a group of disorders that share, as a common feature, weakness of the shoulder and pelvic girdles with onset around the second decade of life, and progression to significant disability over 20 to 30 years. Several genetic causes exist. So far described are six (LGMD1A to E) AD and fourteen (LGMD2A to N) AR types. A subset of recessive forms is caused by sarcoglycan deficiency (four isoforms include alpha [LGMD2D], beta [LGMD2E], gamma [LGMD2F], and delta [LGMD2]). Nonspecific CM and DCM rarely have been reported to occur in association with sarcoglycan deficiencies (seen in Amish families in Indiana) (77,116–119). Among the common forms of LGMD, only in LGMD2I (due to mutations in the *FKRP* gene, encoding fukutin-related protein) is CM frequently seen; altered EF may be detected in up to 60% of patients (120), and a case presenting with isolated DCM has been reported (120). Some patients with LGMD1B have had progressive AV conduction disturbances requiring pacemaker placement (121, 122).

REFERENCES

- Schara U, Schosser BGH. Myotonic dystrophies type 1 & 2: a summary on current aspects. *Semin Pediatr Neurol* 2006;13:71–79.
- Machuca-Tzili L, Brook D, Hilton-Jones D. Clinical and molecular aspects of the myotonic dystrophies: a review. *Muscle Nerve* 2005;32:1–18.
- Guenneau L, Bertrand AT, Jais JP, et al. Mutations of the *FHL1* gene cause Emery-Dreifuss muscular dystrophy. *Am J Hum Genet* 2009;85:338–353.
- Rankin J, Ellard S. The laminopathies: a clinical review. *Clin Genet* 2006;70:261–274.
- van Berlo JH, de Voigt WG, van der Kooij AJ, et al. Meta-analysis of clinical characteristics of 299 carriers of LMNA gene mutations: do lamin A/C mutations portend a high risk of sudden death? *J Mol Med* 2005;83:79–83.
- Moore SA, Shilling CJ, Westra S, et al. Limb-girdle muscular dystrophy in the United States. *J Neuropathol Exp Neurol* 2006;65:995–1003.
- Emery AE. Emery-Dreifuss syndrome. *J Med Genet* 1989;26:637–641.
- Bertini E, Donati MA, Broda P, et al. Phenotypic heterogeneity in two unrelated Danon patients associated with the same LAMP-2 gene mutation. *Neuropediatrics* 2005;36:309–313.
- Spencer CT, Bryant RM, Day J, et al. Cardiac and clinical phenotype in Barth syndrome. *Pediatrics* 2006;118:337–346.
- Tani LY, Minich LL, Williams RV, et al. Ventricular remodeling in children with left ventricular dysfunction secondary to various cardiomyopathies. *Am J Cardiol* 2005;96:1157–1161.
- Friedberg MK, Silverman NH. Cardiac ventricular diastolic and systolic dysfunction in children with heart failure secondary to idiopathic dilated cardiomyopathy. *Am J Cardiol* 2006;97:101–105.
- Kelly DP, Strauss AW. Inherited cardiomyopathies. *N Engl J Med* 1994;330:930–932.
- Marian AJ, Roberts R. Molecular genetics of cardiomyopathies. *Herz* 1993;18:230–237.
- Towbin JA. The role of cytoskeletal proteins in cardiomyopathies. *Curr Opin Cell Biol* 1998;10:131–139.
- Eagle M, Baudouin SV, Chandler C, et al. Survival in Duchenne muscular dystrophy: improvements in life expectancy since 1967 and the impact of home nocturnal ventilation. *Neuromuscul Disord* 2002;12:926–929.
- Frankel KA, Rosser RJ. The pathology of the heart in progressive muscular dystrophy: epimycocardial fibrosis. *Hum Pathol* 1976;7:375–386.
- Moriuchi T, Kagawa N, Mukoyama M, et al. Autopsy analyses of the muscular dystrophies. *Tokushima J Exp Med* 1993;40:83–93.
- James TN. Observations of the cardiovascular involvement, including the cardiac conduction system, in progressive muscular dystrophy. *Am Heart J* 1962;63:48–56.
- Perloff JK, Roberts WC, deLeon AC Jr. The distinctive electrocardiogram of Duchenne's progressive muscular dystrophy. An electrocardiographic-pathologic correlative study. *Am J Med* 1967;42:179–188.
- Breucking E, Reimnitz P, Schara U, et al. Anesthetic complications. The incidents of severe anesthetic complications in patients and families with progressive muscular dystrophy of the Duchenne and Becker types [in German]. *Anaesthesist* 2000;49:187–195.
- American Academy of Pediatrics Section on Cardiology and Cardiac Surgery. Cardiovascular health supervision for individuals affected by Duchenne or Becker muscular dystrophy. *Pediatrics* 2005;116:1569–1573.
- Perloff JK, de Leon AC Jr, O'Doherty D. The cardiomyopathy of progressive muscular dystrophy. *Circulation* 1966;33:625.
- Perloff JK. Cardiac rhythm and conduction in Duchenne's muscular dystrophy: a prospective study of 20 patients. *J Am Coll Cardiol* 1984;3:1263–1268.
- Bhattacharyya KB, Basu N, Ray TN, et al. Profile of electrocardiographic changes in Duchenne muscular dystrophy. *J Indian Med Assoc* 1997;95:40–42.
- Nigro G, Comi LI, Politano L, et al. The incidence and evolution of cardiomyopathy in Duchenne muscular dystrophy. *Int J Cardiol* 1990;26:271–277.
- Yotsukura M, Yamamoto A, Kajiura T, et al. QT dispersion in patients with Duchenne-type progressive muscular dystrophy. *Am Heart J* 1999;137:672–677.
- Thrush PJ, Allen HD, Viollet L, et al. Re-examination of the electrocardiogram in boys with Duchenne muscular dystrophy and correlation with its dilated cardiomyopathy. *Am J Cardiol* 2009;103:262–265.
- Shah AM, Jefferies JL, Rossano JW, et al. Electrocardiographic abnormalities and arrhythmias are strongly associated with the development of cardiomyopathy in muscular dystrophy. *Heart Rhythm* 2010;7:1484–1488.
- Ishikawa K. Cardiac involvement in progressive muscular dystrophy of the Duchenne type. *Jpn Heart J* 1997;38:163–180.
- Lanza GA, Delio Russo A, Giglio V, et al. Impairment of cardiac autonomic function in patients with Duchenne muscular dystrophy: relationship to myocardial and respiratory function. *Am Heart J* 2001;141:808–812.
- Kirschmann C, Kececioglu D, Korinthenberg R, et al. Echocardiographic and electrocardiographic findings of cardiomyopathy in Duchenne and Becker-Kiener muscular dystrophies. *Pediatr Cardiol* 2005;26:66–72.
- Vita G, DiLeo R, DeGregorio C, et al. Cardiovascular autonomic control in Becker muscular dystrophy. *J Neurol Sci* 2001;186:45–49.
- Akita H, Matsuoka S, Kuroda Y. Predictive electrocardiographic score for evaluating prognosis in patients with Duchenne's muscular dystrophy. *Tokushima J Exp Med* 1993;40:55–60.
- D'Orsogna L, O'Shea JP, Miller G. Cardiomyopathy of Duchenne muscular dystrophy. *Pediatr Cardiol* 1988;9:205–213.
- Chenard AA, Becane HM, Tertrain F, et al. Ventricular arrhythmia in Duchenne muscular dystrophy: prevalence, significance and prognosis. *Neuromuscul Disord* 1993;3:201–206.
- Corrado G, Lissani A, Beretta S, et al. Prognostic value of electrocardiograms, ventricular late potentials, ventricular arrhythmias, and left ventricular systolic dysfunction in patients with Duchenne muscular dystrophy. *Am J Cardiol* 2002;89:838–841.
- Goldberg SJ, Feldman L, Reinecke C, et al. Echocardiographic determination of contraction and relaxation measurements of the left ventricular wall in normal subjects and patients with muscular dystrophy. *Circulation* 1980;62:1061–1069.
- Hunsaker RH, Fulkerson PK, Barry FJ, et al. Cardiac function in Duchenne's muscular dystrophy. Results of a 10-year follow-up study and noninvasive tests. *Am J Med* 1982;73:235–238.
- Goldberg SJ, Stern LZ, Feldman L, et al. Serial two-dimensional echocardiography in Duchenne muscular dystrophy. *Neurology* 1982;32:1101–1105.
- Goldberg SJ, Stern LZ, Feldman L, et al. Serial left ventricular wall measurements in Duchenne's muscular dystrophy. *J Am Coll Cardiol* 1983;2:36–142.
- Zhu X, Wheeler MT, Hadhazy M, et al. Cardiomyopathy is independent of skeletal muscle disease in muscular dystrophy. *FASEB J* 2002;16:1096–1098.
- Jefferies JL, Eidem BW, Belmont JW, et al. Genetic predictors and remodeling of dilated cardiomyopathy in muscular dystrophy. *Circulation* 2005;112:2799–2804.
- Sasaki K, Sakata K, Kachi E, et al. Sequential changes in cardiac structure and function in patients with Duchenne type muscular dystrophy: a two-dimensional echocardiographic study. *Am Heart J* 1998;135:937–944.
- Mori K, Edagawa T, Inoue M, et al. Peak negative myocardial velocity gradient and wall-thickening velocity during early diastole are noninvasive parameters of left ventricular diastolic function in patients with Duchenne's progressive muscular dystrophy. *J Am Soc Echocardiogr* 2004;17:322–329.
- Mori K, Hayabuchi Y, Inoue M, et al. Myocardial strain imaging for early detection of cardiac involvement in patients with Duchenne's progressive muscular dystrophy. *Echocardiography* 2007;6:598–608.
- Bosser G, Lucron H, Lethor JP, et al. Evidence of early impairments in both right and left ventricular inotropic reserves in children with Duchenne's muscular dystrophy. *Am J Cardiol* 2004;93:724–727.
- Naruse H, Miyagi J, Arai T, et al. The relationship between clinical stage, prognosis and myocardial damage in patients with Duchenne-type muscular dystrophy: five-year follow-up study. *Ann Nucl Med* 2004;18:203–208.
- Bilchick KC, Salerno M, Plitt D, et al. Prevalence and distribution of regional scar in dysfunctional myocardial segments in Duchenne muscular dystrophy. *J Cardiovasc Magn Reson* 2011;13:20.
- Hor KN, Wanasapura J, Markham LW, et al. Circumferential Strain Analysis Identifies Strata of Cardiomyopathy in duchenne Muscular dystrophy. A Cardiac Magnetic Resonance Tagging Study. *J Am Coll Cardiol* 2009;53:1204–1210.
- Puchalski MD, Williams RV, Askovich B, et al. Late gadolinium enhancement: precursor to cardiomyopathy in Duchenne muscular dystrophy? *Int J Cardiovasc Imaging* 2009;25:57–63.
- Ashford MW Jr, Liu W, Lin SJ, et al. Occult Cardiac Contractile Dysfunction in Dystrophin-Deficient Children Revealed by Cardiac Magnetic Resonance Strain Imaging. *Circulation* 2005;112:2462–2467.
- Hagenbuch SC, Gottliebson WM, Wanasapura J, et al. Detection of progressive cardiac dysfunction by serial evaluation of circumferential strain in patients with Duchenne muscular dystrophy. *Am J Cardiol* 2010;105:1451–1455.
- Yanagisawa A, Yokota N, Miyagawa M, et al. Plasma levels of atrial natriuretic peptide in patients with Duchenne's progressive muscular dystrophy. *Am Heart J* 1990;120:1154–1158.
- Mori K, Manabe T, Nii M, et al. Plasma levels of natriuretic peptide and echocardiographic parameters in patients with Duchenne's progressive muscular dystrophy. *Pediatr Cardiol* 2002;23:160–166.
- Bushby K, Finkel R, Birnkrant DJ, et al. Diagnosis and management of Duchenne muscular dystrophy, part 1: diagnosis, and pharmacological and psychosocial management. *Lancet Neurol* 2010;9:77–93. [Published online November 30, 2009 DOI:10.1016/S1474-S4422 (09)70271-6.]

56. Duboc D, Meune C, Lerebours G, et al. Effect of perindopril on the onset and progression of left ventricular dysfunction in Duchenne muscular dystrophy. *J Am Coll Cardiol* 2005;45:855–857.
57. Stöllberger C, Finsterer J. Can perindopril delay the onset of heart failure in Duchenne muscular dystrophy? *J Am Coll Cardiol* 2005;46:1781.
58. Viollet L, Thrush PT, Flanagan KM, et al. Natural history of cardiomyopathy in Duchenne muscular dystrophy and the effects of angiotensin-converting enzyme inhibitor and/or β -blocker. *Am J Cardiol* (in press) July, 2012.
59. Cohn RD, van Erp C, Habashi JP, et al. Angiotensin II type 1 receptor blockade attenuates TGF- β -induced failure of muscle regeneration in multiple myopathic states. *Nat Med* 2007;13:204–210. (Erratum in: *Nat Med* 2007;13:511)
60. Brooke BS, Habashi JP, Judge DP, et al. Angiotensin II blockade and aortic-root dilation in Marfan's syndrome. *N Engl J Med* 2008;358:2787–2795.
61. Ishikawa Y, Bach JR, Minami R. Cardioprotection for Duchenne's muscular dystrophy. *Am Heart J* 1999;137:895–902.
62. Finsterer J. Cardiopulmonary support in Duchenne muscular dystrophy. *Lung* 2006;184:205–215.
63. Rafael-Fortney JA, Chimanji NS, Schill KE, et al. Early treatment with lisinopril and spironolactone preserves cardiac and skeletal muscle in Duchenne Muscular Dystrophy mice. *Circulation* 2011;124:582–588.
64. Zannad F, McMurray JJV, Krum H, et al. Eplerenone in Patients with Systolic Heart Failure and Mild Symptoms. *N Engl J Med* 2011;364:11–21.
65. Li JS, Flynn JT, Portman R, et al. The Efficacy and Safety of the Novel Aldosterone Antagonist Eplerenone in Children with Hypertension: a Randomized, Double-Blind, Dose-Response Study. *J Pediatr* 2010;157:282–287.
66. Cripe LH, Barber BJ, Spicer RL, et al. Outpatient continuous inotrope infusion as an adjunct to heart failure therapy in Duchenne muscular dystrophy. *Neuromuscul Disord* 2006;16:745–748.
67. Buyse GM, Goemans N, van den Hauwe M, et al. Idebenone as a novel, therapeutic approach for Duchenne muscular dystrophy: results from a 12 month, double-blind, randomized placebo-controlled trial. *Neuromuscul Disord* 2011;21:396–405.
68. Duboc D, Meune C, Lerebours G, et al. Effect of perindopril on the onset and progression of left ventricular dysfunction in Duchenne muscular dystrophy. *J Am Coll Cardiol* 2005;45:855–857.
69. Duboc D, Meune C, Pierre B, et al. Perindopril preventive treatment on mortality in Duchenne muscular dystrophy: 10 years' follow-up. *Am Heart J* 2007;154:596–602.
70. Emery AEH. Abnormalities of the electrocardiogram in female carriers of Duchenne muscular dystrophy. *Br Med J* 1969;2:418–420.
71. Lane RJM, Gardner-Medwin D, Roses AD. Electrocardiographic abnormalities in carriers of Duchenne muscular dystrophy. *Neurology* 1980;30:497–501.
72. Hoogerwaard EM, van der Wouwe PA, Wilde AA, et al. Cardiac involvement in carriers of Duchenne and Becker muscular dystrophy. *Neuromuscul Disord* 1999;9:347–351.
73. Weiss RM, Kerber RE, Jones JK, et al. Exercise-induced left ventricular systolic dysfunction in women heterozygous for dystrophinopathy. *J Am Soc Echocardiogr* 2010;23:848–853.
74. Hoffman EP, Fischbeck KH, Brown RH, et al. Characterization of dystrophin in muscle-biopsy specimens from patients with Duchenne's or Becker's muscular dystrophy. *N Engl J Med* 1988;318:1363–1368.
75. Maeda M, Nakao S, Hiyazato H, et al. Cardiac dystrophin abnormalities in Becker muscular dystrophy assessed by endomyocardial biopsy. *Am Heart J* 1995;129:702–707.
76. Sachdev B, Elliott PM, McKenna WJ. Cardiovascular complications of neuromuscular disorders. *Curr Treat Options Cardiovasc Med* 2002;4:171–179.
77. Nigro G, Comi LI, Politano L, et al. Evaluation of the cardiomyopathy in Becker muscular dystrophy. *Muscle Nerve* 1995;18:283–291.
78. de Visser M, de Voogt WG, la Riviere GV. The heart in Becker muscular dystrophy, facioscapulohumeral dystrophy and Bethlem myopathy. *Muscle Nerve* 1992;15:591–596.
79. Hoogerwaard EM, deVoogt WG, Wilde AAM, et al. Evolution of cardiac abnormalities in Becker muscular dystrophy over a 13-year period. *J Neurol* 1997;244:657–663.
80. Melacini P, Fanin M, Danieli GA, et al. Cardiac involvement in Becker muscular dystrophy. *J Am Coll Cardiol* 1993;22:1927–1934.
81. Angelini C, Fanin M, Freda MP, et al. Prognostic factors in mild dystrophinopathies. *J Neurol Sci* 1996;142:70–78.
82. Melacini P, Fanin M, Danieli GA, et al. Myocardial involvement is very frequent among patients affected with subclinical Becker's muscular dystrophy. *Circulation* 1996;94:3168–3175.
83. Saito M, Kawai H, Aitaki M, et al. Cardiac dysfunction with Becker muscular dystrophy. *Am Heart J* 1996;132:642–647.
84. Yilmaz A, Gdynia H-J, Baccouche H, et al. Cardiac involvement in patients with Becker muscular dystrophy: new diagnostic and pathophysiological insights by a CMR approach. *J Cardiovasc Magn Reson* 2008;10:50.
85. Kaspar RW, Allen HD, Ray WC, et al. Analysis of dystrophin deletion mutations predicts age of cardiomyopathy onset in becker muscular dystrophy. *Circ Cardiovasc Genet* 2009;2:544–551.
86. Doing AH, Renlund DG, Smith RA. Becker muscular dystrophy-related cardiomyopathy: a favorable response to medical therapy. *J Heart Lung Transplant* 2002;21:496–498.
87. Casazza F, Brambilla G, Salvato A, et al. Cardiac transplantation in Becker muscular dystrophy. *J Neurol* 1988;235:496–498.
88. Stöllberger C, Finsterer J. Left ventricular synchronization by biventricular pacing in Becker muscular dystrophy as assessed by tissue Doppler imaging. *Heart Lung* 2005;34:317–320.
89. Finsterer J, Stöllberger C. The heart in human dystrophinopathies. *Cardiology* 2003;99:1–19.
90. Angelini C, Fanin M, Gegeraro E, et al. Clinical-molecular correlation in 104 mild X-linked muscular dystrophy patients: characterization of sub-clinical phenotypes. *Neuromuscul Disord* 1994;4:349–358.
91. Towbin JA, Hejmancik JF, Brink P, et al. X-linked dilated cardiomyopathy. Molecular genetic evidence of linkage to the Duchenne muscular dystrophy (dystrophin) gene at the XP21 locus. *Circulation* 1993;87:1854–1865.
92. Ortiz-Lopez R, Li H, Su J, et al. Evidence for a dystrophin missense mutation as a cause of X-linked dilated cardiomyopathy. *Circulation* 1997;95:2434–2440.
93. Muntoni F, Cau M, Ganau A, et al. Brief report: deletion of the dystrophin muscle-promoter region associated with X-linked dilated cardiomyopathy. *N Engl J Med* 1993;329:921–925.
94. Milasin J, Muntoni F, Severini GM, et al. A point mutation in the 5' splice site of the dystrophin gene first intron responsible for X-linked dilated cardiomyopathy. *Hum Mol Genet* 1996;5:73–79.
95. Cox GF, Kunkel LM. Dystrophies and heart disease. *Curr Opin Cardiol* 1997;12:329–343.
96. Sabovic M, Medica I, Logar N, et al. Relation of CTG expansion and clinical variables to electrocardiogram conduction abnormalities and sudden death in patients with myotonic dystrophy. *Neuromuscul Disord* 2003;13:822–826.
97. Finsterer J, Stöllberger C. Cardiac involvement in primary myopathies. *Cardiology* 2000;94:1–11.
98. Steinert H. Über das klinische und anatomische bild des muskelschwundes der myotoniker. *Deutsche Ztschr f Neuemb* 1909;37:38–104.
99. Badano L, Autore C, Fragola PV, et al. Left ventricular myocardial function in myotonic dystrophy. *Am J Cardiol* 1993;71:987–991.
100. Perloff JK, Stevenson WG, Roberts NK, et al. Cardiac involvement in myotonic muscular dystrophy (Steinert's disease): a prospective study of 25 patients. *Am J Cardiol* 1984;54:1074–1081.
101. Finsterer J, Stöllberger C, Blazek G, et al. Cardiac involvement in myotonic dystrophy, Becker muscular dystrophy and mitochondrial myopathy: a five-year follow-up. *Can J Cardiol* 2001;17:1061–1069.
102. Vignaux O, Lazarus A, Varin J, et al. Right ventricular MR abnormalities in myotonic dystrophy and relationship with intracardiac electrophysiologic test findings: initial results. *Radiology* 2002;224:231–235.
103. Colleran JA, Hawley RJ, Pinnow EE, et al. Value of the electrocardiogram in determining cardiac events and mortality in myotonic dystrophy. *Am J Cardiol* 1997;80:1494–1497.
104. Emery AEH, Dreifuss FE. Unusual type of benign X-linked muscular dystrophy. *J Neurol Neurosurg Psychiatr* 1966;29:338–342.
105. Buckley AE, Dean J, Mahy IR. Cardiac involvement in Emery Dreifuss muscular dystrophy: a case series. *Heart* 1999;82:105–108.
106. Tsuchiya Y, Arahata K. Emery-Dreifuss syndrome. *Curr Opin Neurol* 1997;10:421–425.
107. Boriani G, Gallina M, Merlini L, et al. Clinical relevance of atrial fibrillation/flutter, stroke, pacemaker implant, and heart failure in Emery-Dreifuss muscular dystrophy: a long-term longitudinal study. *Stroke* 2003;34:901–908.
108. Bonne G, Mercuri E, Muchir A, et al. Clinical and molecular genetic spectrum of autosomal dominant Emery-Dreifuss muscular dystrophy due to mutations of the lamin A/C gene. *Ann Neurol* 2000;48:170–180.
109. Jakobs PM, Hanson EL, Crispell KA, et al. Novel lamin A/C mutations in two families with dilated cardiomyopathy and conduction system disease. *J Card Fail* 2001;7:249–256.
110. Becane HM, Bonne G, Varnous S, et al. High incidence of sudden death with conduction system and myocardial disease due to lamins A and C gene mutation. *Pacing Clin Electrophysiol* 2000;23:1661–1666.
111. Sanna T, Dello Russo A, Toniolo D, et al. Cardiac features of Emery-Dreifuss muscular dystrophy caused by lamin A/C gene mutations. *Eur Heart J* 2003;24:2227–2236.
112. Bialer MG, McDaniel NL, Kelly TE. Progression of cardiac disease in Emery-Dreifuss muscular dystrophy. *Clin Cardiol* 1991;14:411–416.
113. Yoshioka M, Saida K, Itagaki Y, et al. Follow up study of cardiac involvement in Emery-Dreifuss muscular dystrophy. *Arch Dis Child* 1989;64:713–715.
114. Stevenson WG, Perloff JK, Weiss JN, et al. Facioscapulohumeral muscular dystrophy: evidence for selective, genetic electrophysiologic cardiac involvement. *J Am Coll Cardiol* 1999;15:292–299.
115. Laforet P, de Toma C, Eymard B, et al. Cardiac involvement in genetically confirmed facioscapulohumeral muscular dystrophy. *Neurology* 1998;51:1454–1456.
116. Lemmers RJ, van der Vliet PJ, Klooster R, et al. A unifying genetic model for facioscapulohumeral muscular dystrophy. *Science* 2010;329:1650–1653.
117. Beckmann JS, Bushby K. Advances in the molecular genetics of the limb-girdle type of autosomal recessive progressive muscular dystrophy. *Curr Opin Neurol* 1996;9:389–393.
118. Melacini P, Fanin M, Duggan DJ, et al. Heart involvement in muscular dystrophies due to sarcoglycan gene mutations. *Muscle Nerve* 1999;22:473–479.
119. Duggan DJ, Gorospe JR, Fanin M, et al. Mutations in the sarcoglycan genes in patients with myopathy. *N Engl J Med* 1997;336:618–624.
120. Wahbi K, Meune C, Hamouda el H, et al. Cardiac assessment of limb-girdle muscular dystrophy 2I patients: an echography, Holter ECG and magnetic resonance imaging study. *Neuromuscul Disord* 2008;18:650–655.
121. D'Amico A, Petrini S, Parisi F, et al. Heart transplantation in a child with LGMD2I presenting as isolated dilated cardiomyopathy. *Neuromuscul Disord* 2008;18:153–155.
122. van der Kooij AJ, de Voogt WG, Barth PG, et al. The heart in limb girdle muscular dystrophy. *Heart* 1998;79:73–77.

Kawasaki Disease (Mucocutaneous Lymph Node Syndrome)

Sarah D. De Ferranti ■ Jane W. Newburger

Kawasaki disease (KD), first described in Japan in 1967 by Kawasaki, is now encountered worldwide (1,2). The first US cases were reported from Hawaii in 1976 by Melish et al. (3). Despite intensive research, the cause of KD remains unknown. The principal symptoms and associated features of the acute phase of the syndrome are shown in Tables 59.1 and 59.2. Although the cardiovascular manifestations of KD were not appreciated originally, by the mid-1970s, researchers reported that about 2% of affected children died suddenly in the subacute or convalescent stage of this illness due to myocardial infarction caused by acute thrombosis within coronary artery aneurysms or rarely from aneurysm rupture. Despite recent increases in incidence, current estimates of mortality in the United States are lower (0% to 0.17%) than originally reported (2), likely due to a combination of improvements in treatment and ascertainment of milder cases.

EPIDEMIOLOGIC FEATURES

While rare, KD is an important cause of acquired cardiovascular disease in the young that appears to be increasing in incidence. In Japan, nationwide biennial active surveillance shows the incidence of KD in children under 5 years of age has gradually increased from 74 per 100,000 in 1987 to 140 per 100,000 in 2000, and to 219 in 2008 (4,5). In children younger than 5 years of age, US estimates based on 2006 hospital discharge data suggest the annual incidence is 20 per 100,000 children (6). The typical KD patient is more likely to be male (ratio of males to females 1.5:1) and < 5 years of age (80%). In US children under 5 years of age, the prevalence of KD is the highest in Asians and Pacific Islanders (32.5 per 100,000), intermediate in non-Hispanic Blacks (16.9 per 100,000) and Hispanics (11.1 per 100,000), and lowest in Whites (9.1 per 100,000) (6,7).

Coronary aneurysms are the most important complication of KD. Young infants have the highest rate of coronary artery aneurysm formation and often present with incomplete clinical criteria. Children older than age 8 years also have a higher rate of coronary involvement (8–10). The rates of coronary artery aneurysm according to race/ethnicity have been estimated using administrative data; rates were highest in Hispanics (5.9%), followed by white non-Hispanics (3.4%), with blacks having lower rates (1.8%) (11). The study design did not allow the authors to determine whether differences in rates of aneurysms among racial/ethnic groups were related to late or inadequate treatment versus higher relative risk.

Children who have had KD once are at increased risk for a second episode. In Japan, the recurrence rate of KD is approximately 3%, and the proportion of cases with a positive family history is approximately 1% (12,13). Siblings have a relative risk that is 10-fold of the normal Japanese population; half

develop KD within 10 days of the first case (14). The risk of occurrence in twins may be as much as 100-fold higher than in the general population (14,15). These data, together with the occurrence of KD in the children of parents who themselves were affected, support the role of genetic factors in susceptibility to KD (12,14–16). Of note, in the United States, the familial incidence of KD appears to be much lower than in Japan.

ETIOLOGY AND PATHOGENESIS

An etiologic agent for KD has not been identified, despite extensive research into infectious, immunologic, and genetic causes. An infectious trigger is suggested by the epidemiologic characteristics of this syndrome, especially its tendency to target young children, time/place clustering, a predilection for winter and spring months, and epidemic cycles every 3 years (observed most clearly during the 1970s and 1980s). Indeed, various infectious agents have been proposed including rickettsia (17), propionibacterium (18), streptococci or their products (19), house dust mite antigen (20), and retrovirus (21). However, causality by these agents has not been independently confirmed. The clinical features of KD are similar to those of toxin-related diseases, such as scarlet fever or toxic shock syndrome, and to adenovirus. Furthermore, other processes can mimic the presentation of KD, such as drug reactions (Table 59.3). Exposure to recently shampooed carpets has been linked with KD in case-control studies, but additional studies contradict the association (22,23).

Immunologic causes of KD are another line of etiologic investigation. Vasculitides involve excessive or abnormal immune responses, and many hypothesize that, in KD, an infectious episode sparks a detrimental immune response in a host who is genetically or otherwise vulnerable. The suspicion of an immunoregulatory abnormality is supported by the activation of monocytes, macrophages, CD4+ T-helper cells, and B lymphocytes during the acute phase of illness (24). There is increased production of immunoglobulins, including circulating antiendothelial antibodies (25). In particular, IgA seems to be implicated; IgA plasma cells were found in the vascular wall and an oligoclonal proliferation of IgA was seen in several fatal KD cases (26). In addition to circulating immunoglobulins, cytokines are up-regulated, including interleukin (IL)-1, IL-2, IL-6, and tumor necrosis factor α (TNF- α) (24). Proinflammatory cytokines appear to render the vascular endothelium susceptible to lysis by antibodies (27). An example of this is the inflammatory mediator S100A12, which is involved in binding of advanced glycation end products (RAGE). Some studies report high RAGE levels that persist in patients who do not respond to intravenous immunoglobulin (IVIG) (28,29). Activated vascular endothelium expresses inflammatory antigens such as intercellular adhesion molecules.

TABLE 59.1 Principal Symptoms in Kawasaki Disease

Fever of at least 5 days' duration
Presence of at least four ^a of the following principal features:
Changes in the extremities, including erythema and/or indurative edema and later (2nd week of illness) membranous desquamation starting in the subungual regions
Polymorphous exanthema (but not including bullous or vesicular lesions)
Bilateral nonexudative conjunctival injection
Changes in lips and oral cavity (but not including discrete oral lesions)
Cervical lymphadenopathy, usually unilateral and large (≥ 1.5 cm)
Exclusion of other diseases with similar findings

^aPatients with fever and fewer than four principal clinical features can be diagnosed as having Kawasaki disease when coronary artery disease is detected by 2-D echocardiography or coronary angiography.

From Newburger JW, Takahashi M, Gerber MA, et al. Diagnosis, treatment, and long-term management of Kawasaki disease: A statement for health professionals from the Committee on Rheumatic Fever, Endocarditis, and Kawasaki Disease, Council on Cardiovascular Disease in the Young, American Heart Association. *Circulation* 2004;110:2747–2771, with permission.

Various mitogenic factors such as vascular endothelial growth factor and platelet-derived growth factors are expressed during acute and subacute phases. There is an extensive literature on markers of inflammation in KD, which generally rise more dramatically in patients with persistent fever or aneurysms. However, to date, there is no “diagnostic signature” of

TABLE 59.2 Features Associated with Kawasaki Disease

Clinical findings
Myocarditis
Pericarditis
Aseptic meningitis
Diarrhea
Gallbladder hydrops
Obstructive jaundice
Uveitis
Urethritis
Laboratory findings
Elevated acute phase reactants: CRP, sedimentation rate, α -1 antitrypsin
Thrombocytosis (usually in the 2nd and 3rd weeks of illness)
Sterile pyuria and proteinuria
Elevation of liver enzymes
Decreased serum protein and albumin
Anemia (normochromic, normocytic, and self-limited)
Negative or low antistreptolysin O titer

TABLE 59.3 Diseases and Disorders with Clinical Findings Similar to Kawasaki Disease

Viral infections (e.g., measles, adenovirus, enterovirus, Epstein-Barr virus)
Scarlet fever
Staphylococcal scalded skin syndrome
Toxic shock syndrome
Bacterial cervical lymphadenitis
Drug hypersensitivity reactions
Stevens-Johnson syndrome
Juvenile rheumatoid arthritis
Rocky Mountain spotted fever
Leptospirosis
Mercury hypersensitivity reaction (acrodynia)

From Newburger JW, Takahashi M, Gerber MA, et al. Diagnosis, treatment, and long-term management of Kawasaki disease: A statement for health professionals from the Committee on Rheumatic Fever, Endocarditis, and Kawasaki Disease, Council on Cardiovascular Disease in the Young, American Heart Association. *Circulation* 2004;110:2747–2771, with permission.

inflammatory markers that permits the reliable distinction of KD from other inflammatory processes.

If the pathophysiology of KD involves inciting infectious agent(s) that spark an abnormal immune response, the species responsible remain unclear. Various strains of *Staphylococcus* and *Streptococcus* have been proposed as the inciting immune perturbation, with toxins acting as superantigens recruiting T lymphocytes bearing V β 2 and V β 8 receptors (30). However, this hypothesis remains unconfirmed; in a prospective, multicenter study, the prevalence of toxin-producing strains was similar in patients with KD and febrile controls (31). Rowley et al. (26) identified immunoglobulin (Ig) A-secreting plasma cells within cardiovascular tissues from a number of patients who died from KD, suggesting that an unknown pathogen might have gained entry through the respiratory or gastrointestinal tract. The same investigators demonstrated immunohistochemical evidence of antigens within the respiratory epithelium and macrophages that react with synthetic IgA antibodies genetically engineered from these plasma cells (32).

A genetic predisposition of the host appears to be important in the pathogenesis of KD. This hypothesis is supported by the racial/ethnic differences in incidence (Asian and Pacific Islanders being more frequently affected) and the increased susceptibility of family members to KD (33). An increasing literature has explored the association of gene polymorphisms to susceptibility to KD or to development of aneurysms in those with KD (16,34–43), and studies are ongoing to examine this question. For example, patients with KD are more likely to have certain polymorphisms of the angiotensin-1 converting enzyme, the chemokine receptor CCR5 and ligand CCL3L1 (44), the butyrophilin-like 2 gene involved in T-cell stimulation (45), and inositol 1,4,5-trisphosphate 3-kinase C (ITPKC) SNP, the presence of which allows the T-cell response to be greater than the wild-type allele (46). A genome-wide association study implicated ATP-binding cassette, subfamily C (47), although this has not been confirmed elsewhere. Polymorphisms of endothelial growth factor and growth factor receptor and matrix metalloproteinase are associated with a greater

likelihood of coronary aneurysm formation in patients who have KD (40,48).

PATHOLOGY

Our understanding of the stages of cardiovascular pathology is based on the analysis of available postmortem specimens by Fujiwara and Hamashima (49) (Table 59.4). The initial 10 days of illness is characterized by a generalized microvasculitis. Clinical evidence of myocarditis may be present in the acute phase, and can persist into the first 3 to 4 weeks; right ventricular biopsies show mononuclear cell infiltration and edema within the myocardium and conduction system and late myocyte hypertrophy and fibrosis (50,51). Valvulitis may affect the mitral and aortic valves (52). Inflammation persists in the walls of medium and large arteries as a panarteritis, with particular predilection for the coronary arteries, and is characterized by edema, mononuclear cell infiltration, and progressive fibrosis with disruptions in the internal elastic lamina. Such destructive changes lead to aneurysm formation and are most common in the proximal segments and branching points of the coronary arteries, suggesting a role for hemodynamic stress in development of aneurysms (53). Aneurysms may be fusiform, saccular, cylindrical, or segmented (resembling beads on a string) (54,55). Noncoronary arteries, such as

iliac, femoral, axillary, and renal, are less frequently involved, and only in patients with coronary aneurysms. Involvement of intracranial arteries or intraparenchymal vessels within abdominal organs is extremely rare.

MANIFESTATIONS

Clinical Features: Systemic

The acute phase of KD often is preceded by prodromal upper respiratory or gastrointestinal symptoms (56). The beginning of KD is marked by an abrupt onset of high fever, accompanied by skin rash, conjunctival injection, reddening and fissuring of lips, erythema of the buccal mucosa, strawberry tongue, nonsuppurative cervical lymphadenitis, and erythema and edema of the hands and feet (1). The skin rash may take different forms, but bullae and vesicles are rare. The rash frequently begins in the diaper area and spreads to the torso and extremities. It may be evanescent, especially in young infants (see Table 59.1). Erythema and edema of the hands and feet may be accompanied by fusiform swelling of the proximal interphalangeal joints of the hands. Patients may refuse to move their hands or bear weight on their feet. Occasionally, they may show transient Raynaud phenomenon. The most dramatic extremity symptom is gangrene of fingers and toes, which occurs rarely in very young infants, mostly of non-Asian background (57). Clinical and spinal fluid findings of aseptic meningitis may be present in the acute phase.

This acute phase is followed by a subacute phase, which occurs from the 2nd to the 4th week of illness. During this time, most patients show desquamation starting in the subungual regions and spreading to the palms and soles. In addition to the principal symptoms, there may be hepatomegaly, hydrops of the gallbladder (58), transient jaundice, and abnormal liver function tests. Some patients develop transient diarrhea and abdominal discomfort. In some patients, arthralgia or arthritis appears late in the acute or subacute phase and very rarely may last up to 4 months (3). In the genitourinary system, the patient may show signs of urethritis and phimosis (in uncircumcised males) sometimes accompanied by dysuria and sterile pyuria. Orchitis may occur in boys. Transient and isolated peripheral nerve impairment such as facial palsy, phrenic nerve paralysis, or sensorineural hearing loss has also been described (59,60). Associated clinical and laboratory findings are summarized in Table 59.2.

If the patient remains untreated or is treated with aspirin only, the febrile course usually lasts from 1 to 3 weeks. The patient may show transient anemia and leukocytosis with increased numbers of neutrophils and bands. The platelet count increases in the 2nd and 3rd weeks of illness. Thrombocytosis and elevated sedimentation rate or C-reactive protein (CRP) will gradually subside by the 6th to 8th week of illness.

In Japan, KD recurs in 3% of the patients who have recovered completely from the original episode, although recurrent cases are less common in the United States. Children who have recurrent disease appear to be at increased risk of coronary complications (13). Recurrence of KD must be distinguished from so-called recrudescence, which is a variation within the acute phase of illness characterized by temporary remission of fever and other symptoms followed by relapsing fever. In the current era, recrudescence most commonly occurs after an initial response to IVIG therapy. Children with recrudescence fever, similar to those with recurrent disease, are at higher risk of coronary artery complications. It is important to instruct the family to monitor the patient's temperature daily after hospital discharge until the patient has been afebrile for a week, so that IVIG retreatment can be instituted if fever recurs.

TABLE 59.4

Stages of Cardiovascular Pathology in Kawasaki Disease

Stage 1 (0–9 d)

Microvascular angiitis

Acute endoarteritis and perivasculitis of major coronary arteries

Pericarditis, valvulitis, and endocarditis

Myocarditis including atrioventricular conduction system

Causes of death: heart failure and dysrhythmia

Stage 2 (12–25 d)

Panvasculitis of major coronary arteries with aneurysms and thrombus formation

Intimal proliferation of coronary arteries

Myocarditis, endocarditis, and pericarditis

Causes of death: same as in stage 1; also myocardial infarction, aneurysm rupture

Stage 3 (28–31 d)

Granulation of coronary arteries

Marked intimal thickening

Disappearance of microvascular angiitis

Cause of death: myocardial infarction

Stage 4 (40 d to 4 y)

Scarring, stenosis, calcification, and recanalization of major coronary arteries

Fibrosis of myocardium and endocardium

Cause of death: myocardial infarction

Summarized from Fujiwara H, Hamashima Y. Pathology of the heart in Kawasaki disease. *Pediatrics* 1978;61:100, with permission.

DIAGNOSIS AND DIFFERENTIAL DIAGNOSIS

The 2004 American Heart Association (AHA) epidemiologic case definition of KD requires the presence of ≥ 4 days of fever and at least four of the five principal clinical features, including bilateral nonexudative conjunctivitis, erythema of the lips and oral mucosa, changes in the extremities, rash, and cervical lymphadenopathy (see Table 59.1) (61). When coronary artery disease is documented, the diagnosis of KD can be made with fewer than four principal features. All clinical features are rarely present at the same time, so the diagnosis requires sequential evaluation of the patient with detailed day-by-day history of the present illness.

No specific diagnostic test exists for KD, and many illnesses mimic KD (see Table 59.3: viral or rickettsial exanthems [measles, Epstein-Barr virus infection, and Rocky Mountain spotted fever], scarlet fever, leptospirosis, toxic shock syndrome, juvenile rheumatoid arthritis, Stevens-Johnson syndrome, reaction to drugs, and hypersensitivity to mercury) (62). Careful history, physical examination, and appropriate laboratory tests are necessary to exclude these conditions. At least moderate elevation of acute phase reactants, that is, the erythrocyte sedimentation rate (ESR) or CRP, is almost universal at the time of presentation. Both ESR and CRP should be measured because these test values may be discrepant at presentation (63). Elevations of liver function tests, including plasma gamma-glutamyl transpeptidase, transaminases, and bilirubin, are also common (62,64). Albumin synthesis declines in the acute phase, and hypoalbuminemia is common. Urinalysis shows so-called sterile pyuria, with white cells (often in the range of 10 to 50/high-power field [HPF]) noted on microscopic evaluation but not by dipstick. Lumbar puncture may show findings compatible with aseptic meningitis, with a predominance of mononuclear cells, but with normal glucose and protein levels (65). The degree of elevation of serum cardiac troponins in acute KD is controversial (66–68).

Although most cases fulfill the principal diagnostic criteria listed in Table 59.1, about 15% of cases have incomplete clinical presentations with coronary artery complications (69). In any child with unexplained fever lasting >5 to 7 days with some of the above-mentioned laboratory findings, the diagnosis of incomplete KD should be considered and echocardiography should be obtained (see section below and Fig. 59.3). Very young infants are especially likely to present with incomplete KD; indeed, some have fever as their only manifestation. For this reason, echocardiography should be performed on any infant younger than age 6 months with fever duration of ≥ 7 days, elevation of CRP and/or ESR, and no other explanation for the febrile illness.

ALGORITHM FOR CLINICAL EVALUATION AND TREATMENT OF CHILDREN WITH SUSPECTED KAWASAKI DISEASE

When the epidemiologic case definition for KD was first constructed by a committee of the Japanese Ministry of Health in 1970, the association of coronary artery sequelae with KD was not appreciated (70). Indeed, at that time, neither an effective treatment nor a noninvasive method of assessing coronary artery abnormalities was available. The original case definition was designed to be highly specific (i.e., to yield a low false-positive rate), but its sensitivity was limited and did not include echocardiographic data as part of the diagnostic criteria. Because coronary artery aneurysms are now well recognized to occur not only in children with typical KD but also in children with incomplete features of KD, and because IVIG therapy

must be given within the time frame of 7 to 10 days to be most effective in preventing coronary artery aneurysms, an algorithm for evaluation and treatment of the child with suspected KD was developed by members of the American Heart Association Committee on Rheumatic Fever, Endocarditis, and Kawasaki Disease that incorporates echo findings and laboratory tests (Fig. 59.1) (61). This algorithm as originally published was not evidence based, but rather reflected the consensus of experts. Salient features of patients with incomplete KD include laboratory tests indicating inflammation (e.g., elevated ESR, CRP, and white blood cell count), evidence of anemia, elevated alanine aminotransferase (ALT) and low albumin, and sterile pyuria. Ectasia and/or lack of tapering of the coronary arteries, left ventricular dysfunction, and, definitively, aneurysms support the diagnosis of KD in the incomplete presentation. The performance of the 2004 AHA recommendations for treatment of suspected or definite KD has been evaluated retrospectively in patients with definite coronary artery aneurysms. Of those with aneurysms, 97% would have received IVIG therapy with application of the classic criteria together with the algorithm for suspected incomplete KD (71).

Clinical Features: Cardiovascular

During the acute phase, patients may manifest signs of myocarditis, such as sinus tachycardia out of proportion to the fever, gallop rhythm, and sometimes muffled heart tones. These findings are generally self-limited and improve with IVIG treatment, although overt heart failure may occur occasionally. A pericardial effusion by echocardiography is not uncommon, but the effusions generally measure <1 mm (72); pericardial tamponade is very rare (73). Systolic murmurs are often heard owing to increased cardiac output and anemia, and approximately one-quarter of patients have mitral insufficiency (72). Rarely, children may present in low cardiac output shock.

Echocardiography may show mild diffuse coronary artery dilation and enhanced perivascular brightness in 30% to 50% of patients during the acute phase of KD. Without IVIG treatment, these lesions may become aneurysmal 1 to 3 weeks from onset of illness (average 10 days) (Fig. 59.2). The reported rates of aneurysm vary based on the definition of an aneurysm used. The Japanese National Kawasaki Disease surveillance data estimates the incidence of coronary aneurysms to be between 10.0% and 17.9%, with reported rates increasing as coronary dimensions are indexed to body surface area (BSA) (74). Information from the Pediatric Health Information System, an administrative database of free-standing children's hospitals, indicates lower rates of aneurysms at 1.8% to 5.9% (11). Coronary artery aneurysms tend to develop most frequently in the proximal segments of the left anterior descending and the right coronary artery (RCA), and less commonly in the left main coronary artery. The left circumflex branch is least often involved. An aneurysm in the distal arterial segment is usually but not always accompanied by an aneurysm in the proximal segment of the same artery. Aneurysms with internal diameters >8 mm or a z-score of ≥ 10 (so-called giant aneurysms) present disproportionately higher risks of myocardial infarction as compared with aneurysms of smaller dimensions (75,76). Several risk scores have been formulated to predict the development of coronary artery aneurysms based on clinical and laboratory data at presentation (77–81). Independent predictors include protracted fever, presumably reflecting worse vasculitis, anemia, elevated white blood count, low albumin, elevated CRP, male gender, and age younger than 1 year or older than 9 years. Younger age in particular seems to be an important predictor for worse presentation.

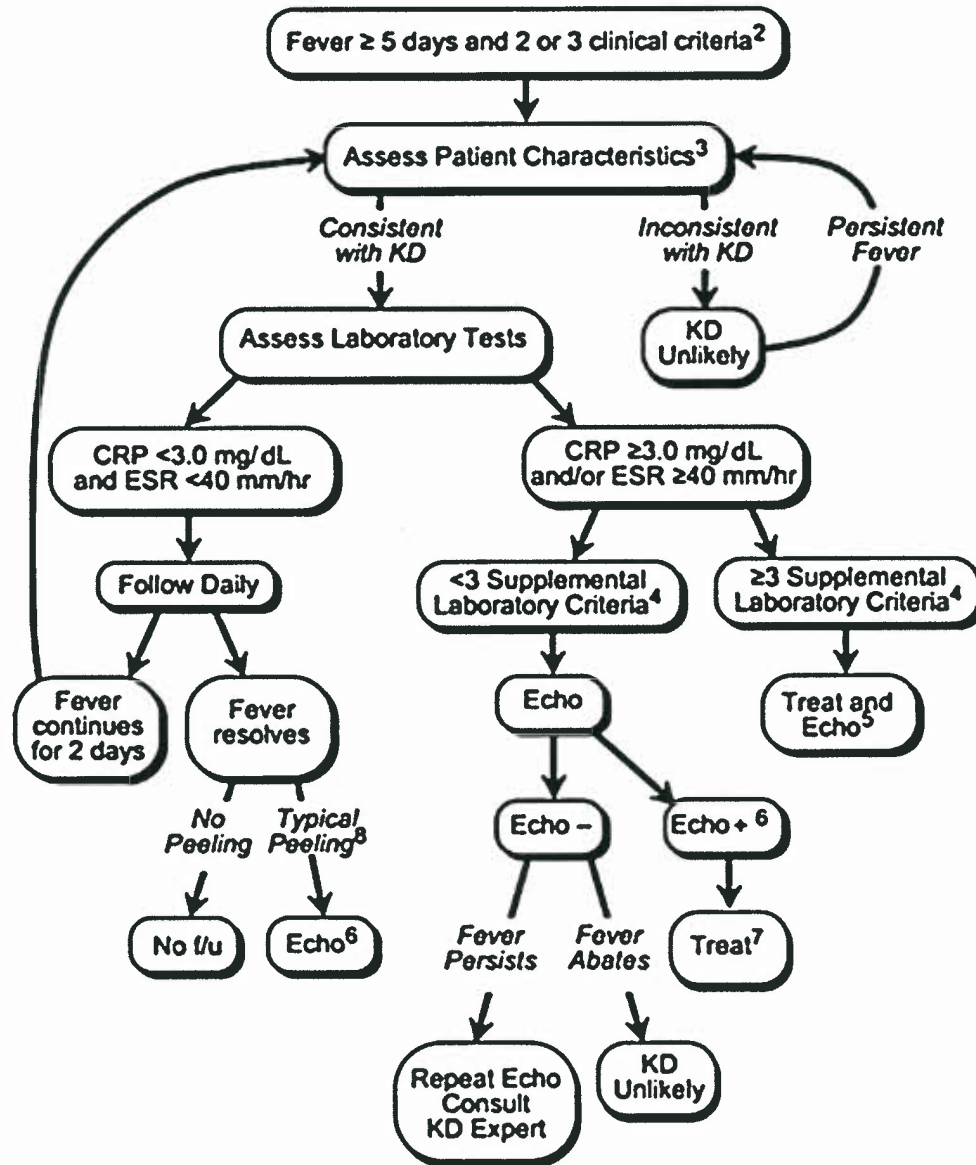
Evaluation of Suspected Incomplete Kawasaki Disease (KD)¹

Figure 59.1. This algorithm is a guide to evaluation of patients with suspected incomplete Kawasaki disease (KD). (1) In the absence of gold standard for diagnosis, this algorithm cannot be evidence based, but rather, represents the informed opinion of the expert committee. Consultation with an expert should be sought any time assistance is needed. (2) Infants ≤ 6 months old on day ≥ 7 of fever without other explanation should undergo laboratory testing, and if evidence of systemic inflammation is found, an echocardiogram should be obtained, even if the infants do not fulfill clinical criteria for KD. (3) Patient characteristics suggesting KD are listed in Table 59.2. Characteristics suggesting disease other than KD include exudative conjunctivitis, exudative pharyngitis, discrete intraoral lesions, bullous or vesicular rash, or generalized adenopathy. For these patients, one should consider alternative diagnoses (see Diagnosis and Differential Diagnosis, Table 59.3). (4) Supplemental laboratory criteria include albumin <3 g/dL, anemia for age, elevation of alanine aminotransferase, platelets after 7 days $>450,000/\text{mm}^3$, white blood cell count $\geq 15,000/\text{mm}^3$, and urine ≥ 10 white blood cells/HPF. (5) These patients can be treated before performing echocardiography. (6) Echocardiography is considered positive for purposes of this algorithm if any of three conditions are met: z-score of left anterior descending coronary artery (LAD) or RCA ≥ 2.5 , coronary arteries meet Japanese Ministry of Health criteria for aneurysms, or more than 3 other suggestive features exist including perivascular brightness, lack of tapering, decreased LV function, mitral regurgitation, pericardial effusion, or z-scores in LAD or RCA of 2 to 2.5. (7) If the echocardiogram is positive, treatment should be given to children within 10 days of fever onset and those beyond day 10 with clinical and laboratory signs (CRP, ESR) of ongoing inflammation. (8) Typical peeling begins under nail bed of fingers and then toes. CRP, C-reactive protein; ESR, erythrocyte sedimentation rate; f/u, follow-up. (From Newburger JW, Takahashi M, Gerber MA, et al. Diagnosis, treatment, and long-term management of Kawasaki disease: a statement for health professionals from the Committee on Rheumatic Fever, Endocarditis and Kawasaki Disease, Council on Cardiovascular Disease in the Young, American Heart Association. *Circulation* 2004;110:2747–2771, with permission.)

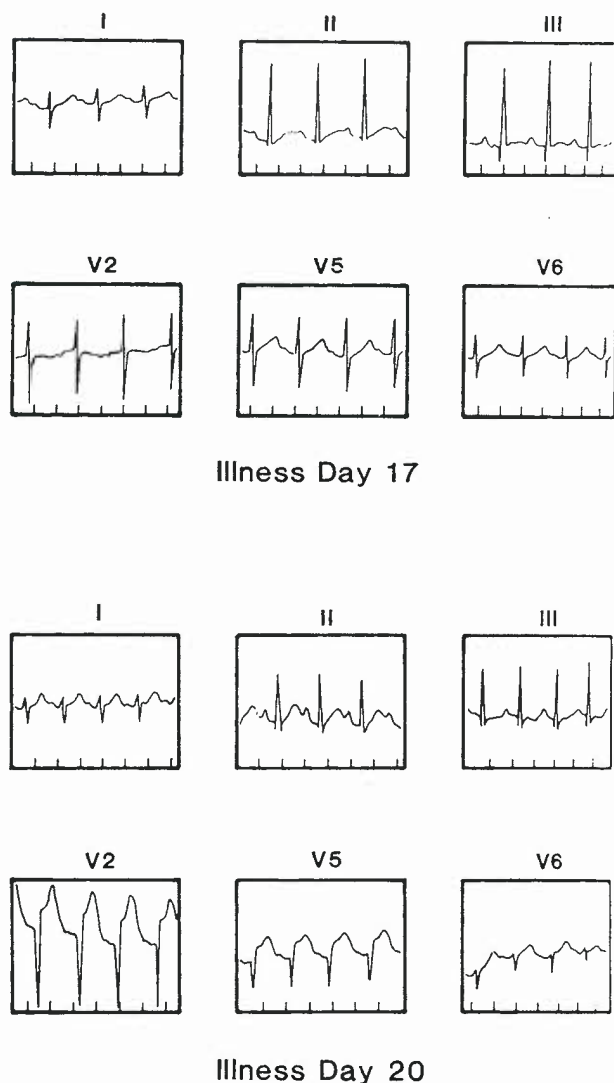


Figure 59.2. Representative electrocardiogram leads in a 4-month-old girl with Kawasaki disease recorded on illness days 17 and 20. The latter tracings show marked decrease in R-wave voltage (V2–V5), indicative of acute anterior wall infarction, which was proven at autopsy.

Myocardial infarctions present differently in childhood compared to adults, with the most common symptoms being shock, chest pain, vomiting, inconsolable crying, and abdominal pain; the authors are aware of one case of referred left otalgia as a presentation of myocardial ischemia in a toddler with KD. Chest pain is reported much less frequently in children younger than 4 years of age. Approximately one-third of the patients are asymptomatic at the time of infarction, which often occurs at rest or during sleep, and infrequently during exertion (82). Fatality associated with the first episode of myocardial infarction has been reported to be 22%, with a progressively worsening mortality rates with subsequent attacks. Giant aneurysms are associated with higher rates of mortality. Fortunately, survival rates at 10, 20, and 30 years after the onset of KD are good, reported at 95%, 88%, and 88%, respectively (83). Rarely, aneurysms may rupture and cause sudden death. In general, late consequences of KD are isolated to cardiovascular disease and occur only in patients who had coronary disease at presentation. Preexisting obstructions in two or more major coronary arteries or in the left main coronary artery are associated with increased mortality.

Electrocardiographic Features

During the acute phase of KD, the electrocardiogram (ECG) may show sinus tachycardia, prolongation of PR and corrected QT intervals, decreased QRS voltage, and T-wave flattening. The presence of large aneurysms may lead to acute myocardial infarction manifested as ST-segment elevation and inversion of T waves (Fig. 59.2). Thrombosis of an RCA aneurysm may produce a silent posterior wall infarction manifested as abnormally deep Q waves in leads II, III, and aVF. One report of invasive electrophysiology studies in patients with KD-related coronary disease demonstrated a high rate of a variety of conduction abnormalities and arrhythmias, including dual AV node and atrial fibrillation; the clinical implications of these findings outside the catheterization lab are unclear (84).

Radiologic Features

The chest radiograph is usually unremarkable, although transient cardiomegaly is seen in 20% of cases during the acute phase. Rarely, the chest x-ray may show localized pulmonary infiltration or pleural effusion. Patients whose coronary aneurysms persist ≥ 1 year after the onset of the disease may show a thin, eggshell-like calcification outlining the aneurysms.

Echocardiographic Features

Echocardiography is essential in the evaluation and management of KD. It is invaluable for detecting coronary artery aneurysms during the acute stage and should be performed at diagnosis to establish a baseline and in some cases to aid in diagnosis (Fig. 59.1). Findings of perivascular brightness, mild coronary artery ectasia, and lack of tapering of the coronary arteries are relatively common in the acute stage of KD, affecting as many as a third of patients (85). Decreased left ventricular contractility (20% of acute KD), diastolic dysfunction, mild valvular regurgitation (most commonly, mitral regurgitation in 25% of acute KD), and minor pericardial effusion also may be seen on echocardiography in acute KD (72,86). Myocardial dysfunction is associated with a greater risk of coronary artery dilation (72). Aortic regurgitation occurs rarely during the chronic phase (52). Echocardiography is usually repeated at 2 and 6 weeks after the onset of illness to see the extent of coronary involvement and to guide therapy. Echocardiograms may be done more frequently in patients who have a more complicated clinical course to help guide treatment. For patients with giant aneurysms, we perform echocardiograms twice weekly early in the illness, then weekly through the first 45 days of illness, monthly until the 3rd month, and then every 3 months for the first year to assess for thrombosis. For long-term cardiac follow-up, echocardiography is useful for evaluating global left ventricular function, regional wall motion characteristics, and competency of mitral and aortic valves. Proximal segments of the right and left coronary arteries may be visualized in nearly all patients. Visualization of distal coronary artery segments may be technically demanding, necessitating patient sedation, use of special views (87), and careful optimization of machine settings.

Capannari et al. (88) have shown that cross-sectional echocardiography has excellent sensitivity and acceptable specificity for detection of coronary aneurysms, as compared with coronary angiography. Standards published by the Japan Kawasaki Disease Research Committee use an empiric definition of abnormality (89). By these standards, a coronary artery is classified as abnormal if (a) the internal diameter is >3 mm in children younger than 5 years of age; (b) the internal diameter is >4 mm in children ≥ 5 years of age; (c) if the internal diameter of a segment measures 1.5 times that of an adjacent

segment; or (d) if the coronary artery lumen is clearly irregular. Nakano et al. (75) first noted that angiographically measured right and left coronary artery diameters correlated with BSA. In children with a BSA of $<0.5 \text{ m}^2$, coronary arteries measured $\leq 2.5 \text{ mm}$. In children with a BSA of 0.5 to 1 m^2 , coronary diameters were 2.5 to 3 mm in most cases. In children with a BSA $>1 \text{ m}^2$, coronary diameters were $\geq 3 \text{ mm}$. Published normative coronary artery dimensions by echocardiography encompass such a wide range of values that there is a significant overlap between normal and abnormal arteries (90–92). Using echocardiographic coronary artery measurements, de Zorzi et al. (91) reported that the BSA-adjusted internal diameters of coronary arteries of KD patients were significantly larger than a normal comparison group and that 27% of the patients classified as having normal coronary arteries by the Japanese Research Committee criteria would have had enlargement of at least one coronary by their new criteria, that is, $z\text{-score} \geq 2.5$ (Fig. 59.3). Therefore, an alternate aneurysm classification schema considers the size of the coronary in relation to the size of the patient (61). When $z\text{-scores}$ are used, the following cut-points have been proposed: a small aneurysm has $z\text{-score} \geq 2.5$ to <5.0 , a large aneurysm has a $z\text{-score} \geq 5.0$ to <10.0 , and a giant aneurysm has $z\text{-score} \geq 10.0$ (92).

Stress Testing

Cardiac stress testing for reversible ischemia should be performed in children with coronary aneurysms. Virtually all types of stress tests performed in adults with ischemic heart disease have been applied to the pediatric population. These include nuclear perfusion scans with exercise (93,94), exercise echocardiography (94), stress echocardiography using pharmacologic agents, such as dobutamine (95,96), dipyridamole, or adenosine (97), magnetic resonance stress imaging, with quantification of regional perfusion (98), and stress myocardial contrast echocardiography (99–101). The combination of resting and stress myocardial perfusion imaging using thallium 201 or a technetium-99m-based compound has high sensitivity but moderate to low specificity in detecting coronary artery obstruction (102). Nevertheless, the technique is useful in longitudinal follow-up of patients with known coronary pathology.

The predictive value of stress tests for coronary artery disease requiring intervention is a function of the probability of significant disease in the population tested (Bayes theorem). For example, false-positive tests are more likely in patients with a low prior probability of coronary disease. Used appropriately, the results of stress testing may guide the decision to refer a patient for invasive evaluation (i.e., cardiac catheterization) as well as for catheter or surgical intervention. The choice of stress modality should be guided by institutional expertise with particular techniques and by the age of the child (e.g., pharmacologic stress should be used in young children in whom traditional exercise protocols are not feasible). In the older child, exercise stress testing best simulates everyday life exposure and should be accompanied by some imaging technique to enhance sensitivity to detect ischemia. Post-exercise ECHO imaging has been trialed as a methodology for assessing for ischemia. Single-photon emission computed tomography (SPECT) perfusion imaging has also been used to demonstrate myocardial perfusion, particularly in experienced hands, and demonstrates differential response to the cold pressor test (103). There is no role for stress testing in children with KD who never had coronary artery abnormalities.

Cardiac Catheterization and Angiography

Cardiac catheterization and angiography may be helpful for determining prognosis and therapeutic strategy in children

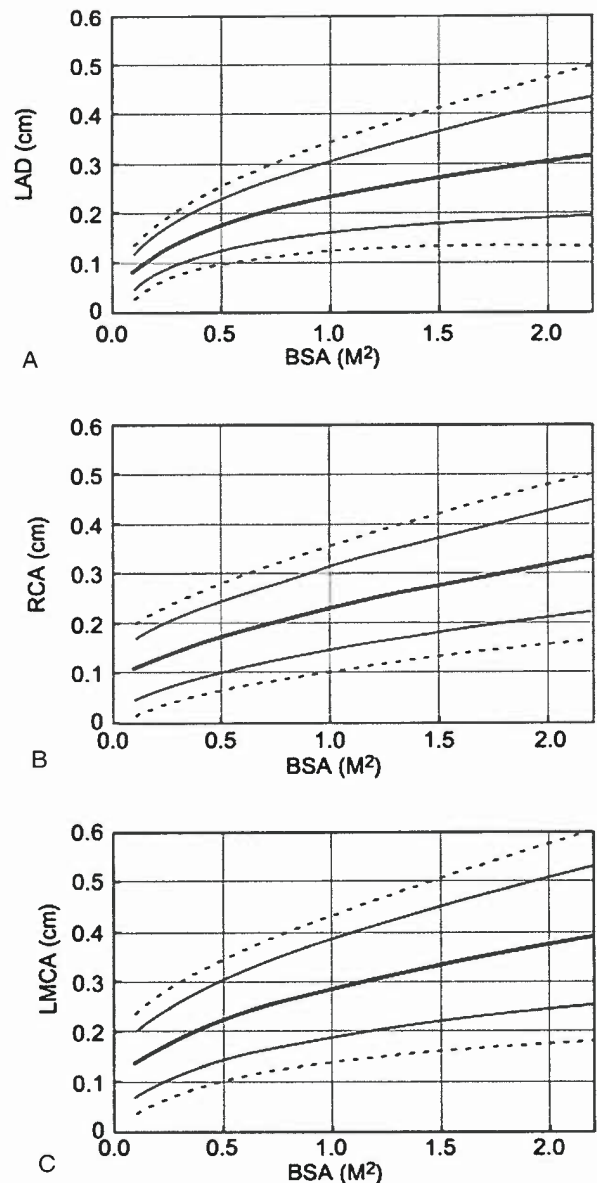


Figure 59.3. Mean and prediction limits for 2 and 3 SDs for size of (A) LAD, (B) proximal RCA, and (C) LMCA according to body surface area for children <18 years old. LMCA $z\text{-scores}$ should not be based on dimension at orifice and immediate vicinity; enlargement of LMCA secondary to Kawasaki disease usually is associated with ectasia of LAD, LCX, or both. BSA, body surface area; LAD, left anterior descending coronary artery; LMCA, left main coronary artery; RCA, right coronary artery. (From Newburger JW, Takahashi M, Gerber MA, et al. Diagnosis, treatment, and long-term management of Kawasaki disease: a statement for health professionals from the Committee on Rheumatic Fever, Endocarditis and Kawasaki Disease, Council on Cardiovascular Disease in the Young, American Heart Association. *Circulation* 2004;110:2747–2771, with permission.)

with echocardiographic evidence of large or multiple coronary artery aneurysms or with clinical, ECG, or stress test evidence of myocardial ischemia. Traditionally, catheterization has been an important adjunct in the long-term follow-up of patients with known coronary obstruction. However, newer methods of coronary artery visualization and a greater focus on functional testing are diminishing the frequency with which

invasive testing is required. There is little incremental value in angiography if echocardiography clearly shows a small solitary aneurysm in continuity with normal proximal and distal segments in an asymptomatic patient. Elective catheterizations are not recommended in the acute phase, in part due to lack of additional information gained, and because of the higher risk of arterial complications seen in acute KD (104). However, emergent catheterization may be necessary for therapeutic decision-making in cases where coronary artery thrombosis is suspected. Left ventricular end-diastolic pressure may be elevated in the presence of acute infarction or severe chronic ischemia.

If catheterization is necessary, the safety and efficacy of selective coronary arteriography in infants and children have been established. Selective coronary arteriography is advantageous over aortic root injection because aneurysms, obstructions, and collateral arteries can be precisely delineated. Such information may be helpful for planning treatment and post-treatment evaluation for coronary bypass surgery or thrombolytic therapy. More recently, interventional catheterizations are being applied to KD patients (see Treatment section below). Our current practice is to perform cardiac catheterization for angiography at 1 year after the onset of illness in patients with complex or large coronary aneurysms who cannot be imaged in other ways, who have symptoms of ischemia, or in whom findings would guide therapeutic decisions. Because peripheral artery aneurysms may occur, particularly in children with giant aneurysms, angiograms of peripheral arteries, including the subclavian arteries, internal mammary arteries, and iliac/femoral vessels should be performed in children undergoing radiographic coronary angiography.

Magnetic Resonance Imaging, Magnetic Resonance Angiography, and Computed Tomography

Magnetic resonance imaging (MRI) and computed tomography (CT) imaging modalities for diagnosing coronary artery lesions in KD are increasingly used as alternatives to traditional invasive angiography, particularly for assessment of coronary stenosis late in the clinical course. MRI has been shown to accurately image proximal segments of coronary arteries, including aneurysms, but not stenotic segments (105,106). During the acute phase, MRI may show marked enhancement of coronary vascular wall, probably reflecting vasculitis (107). A major drawback of the earlier generation of MRI was need for a prolonged voluntary breath-hold, making the examination of younger children difficult. However, more recent models have the capability to track and correct for the patient's respiratory movement. MRI can also incorporate functional testing using dobutamine or adenosine stress testing. Multidetector CT successfully identifies not only coronary artery aneurysms but also stenotic segments with sensitivity close to 90% (108,109), with one study showing that CT was in complete concordance with conventional angiography, while MRI failed to identify 7% of aneurysms and missed one stenosis (110). However, unlike MRI/magnetic resonance angiography (MRA), CT has the drawback of exposure to ionizing radiation—generally less than conventional cineangiography, but still a concern in the pediatric patient who might need serial coronary imaging.

Long-Term Cardiovascular Effects

Patients who have never had coronary artery aneurysms appear to have a good prognosis, with a standardized mortality ratio in Japan that is indistinguishable from the general population (5). Follow-up over 10 to 21 years of Japanese patients with KD,

including catheterization at 1 year, did not demonstrate any cardiac abnormalities among those whose coronary arteries had been normal earlier (111). However, lingering concern about late morbidity and subclinical abnormalities has prompted studies to examine preclinical vascular dysfunction in systemic arteries in KD patients who never were noted to have coronary artery abnormalities. Some studies reported abnormalities in noninvasive vascular testing, including brachial artery reactivity testing (112) and pulse wave velocity (113–115), while other studies do not confirm these results (116,117). Children who have recovered from KD may develop dyslipidemia in the form of mild to moderately low high-density lipoprotein that resolves gradually over years (118). Patients who have never had coronary abnormalities should be counseled on modifiable risk factors for future atherosclerotic cardiovascular disease.

Children who develop small- to medium-sized coronary artery aneurysms also tend to have good prognosis, at least through childhood, because their coronary arteries usually undergo regression to normal lumen diameter. Among coronary arterial segments with aneurysms, approximately half will regress to normal internal lumen diameter within 1 to 2 years (54,55,111). Figure 59.4 shows an example of dramatic regression of a complex aneurysm over a relatively short time. Factors favoring aneurysm regression include age of onset >1 year, female sex, fusiform shape of the aneurysm, and aneurysm diameter <8 mm. Regression appears to occur by neointimal thickening due to migration, transformation, and proliferation of smooth muscle cells derived from the tunica media (54) and replacement of the inflammation with fibroblasts and extracellular matrix. However, vessels with regressed aneurysms, even with normal appearing lumens, may have an abnormally thick intima-medial layer as seen by coronary intravascular ultrasonography (119), with thicker intima in vessels that had greater initial diameters (120). In addition, these vessels have a reduced capacity for vasodilation when challenged by infusion of nitrates (non-endothelium-dependent vasodilators) and may undergo paradoxical vasoconstriction in response to acetylcholine (an endothelium-dependent vasodilator) (121–123). Carotid ultrasound of individuals who had KD and coronary aneurysms showed thickened intimal-medial thickness (IMT), a sign of atherosclerosis, many years after the episode of KD (124). Other data showed greater arterial stiffness in KD patients 10 years after disease (125). A postmortem histologic study in children who died years later due to unrelated causes showed extensive intimal thickening in coronary artery segments (53). Thus, the coronary aneurysm that has regressed is not a normal coronary artery, even if the lumen size is normal angiographically.

Large or complex aneurysms are less likely to undergo regression and place patients at risk for ischemic heart disease. A history of KD in childhood may first be diagnosed when young adults present with angina or myocardial infarction and are found to have large coronary artery aneurysms (126,127). CRP levels are higher in patients with persistent coronary aneurysms compared to KD patients without aneurysms or normal controls (114,115).

Children who develop coronary aneurysms are at risk for increased mortality, with the highest hazard occurring secondary to coronary artery thrombosis in the period between 15 and 45 days after onset of KD (82). In the acute phase of illness, coronary thrombosis is promoted by increased number and activity of platelets, activated procoagulant endothelium, stagnation of blood flow within aneurysm, and abnormal vascular wall shear stress at the entrance of aneurysm. Later onset myocardial ischemia or infarction is more likely due to acute thrombosis at the site of progressive coronary artery stenosis due to myointimal proliferation; in severe cases, myocardial infarction or ischemic cardiomyopathy may result. According to a nationwide hospital survey in Japan, 73% of myocardial infarctions occurred during the first year after illness onset

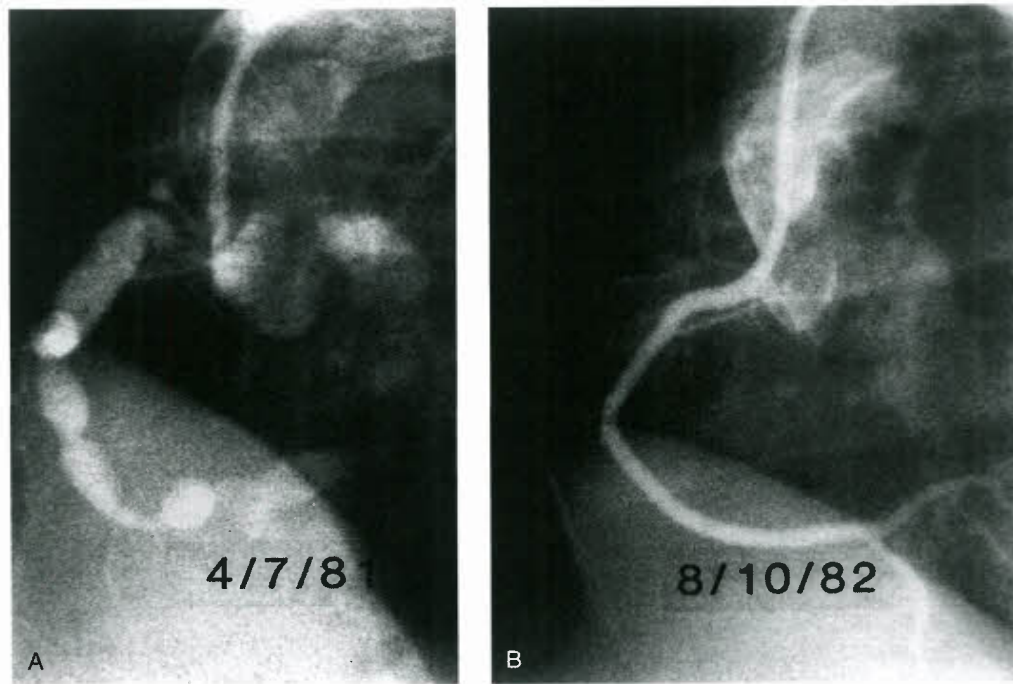


Figure 59.4. Serial right coronary arteriograms in a boy who developed Kawasaki disease at 3 months of age. **A:** Right coronary arteriogram performed 3 months after the onset shows an extensive segmented aneurysm involving the entire right coronary artery. **B:** Follow-up study obtained 16 months later shows near-complete regression of the aneurysm. (From Takahashi M, Mason W, Lewis AB. Regression of coronary aneurysms in patients with Kawasaki syndrome. *Circulation* 1987;75:387–394, with permission.)

(82). However, fatal infarctions can occur many years and even decades after illness onset. Fortunately, spontaneous myocardial revascularization through formation of collateral arteries and recanalization is common (Fig. 59.5). Large aneurysms in the RCA are more likely than those in the left coronary artery

system to undergo thrombosis followed by recanalization in the form of braided small vessels, creating a unique pathologic phenomenon referred to as *arteriae in arteria* (arteries within an artery). However, aneurysms in either system may develop progressive focal stenosis (53).

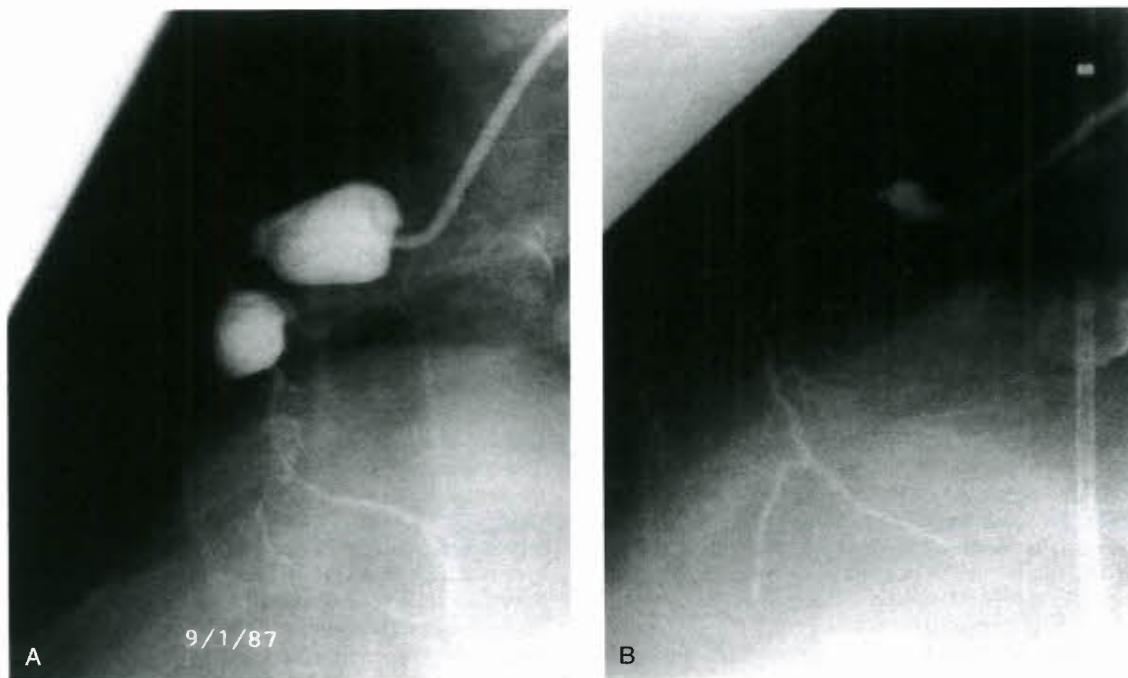


Figure 59.5. Serial right coronary angiograms in a girl who developed Kawasaki disease at 2 months of age. **A:** Right coronary arteriogram obtained 8 months after the onset shows two large saccular aneurysms. **B:** Follow-up right coronary arteriogram 3.5 years later shows thrombotic obstruction of both aneurysms. The distal right coronary artery is opacified via tortuous recanalized arteries.

Children with a history of KD coronary aneurysms, whether regressed or persistent, are considered to be “at risk” for early atherosclerosis by the AHA (128). AHA pharmacologic treatment thresholds for cardiovascular risk factors such as hypertension or hyperlipidemia are lower in KD patients with aneurysms compared to the general population (128). These guidelines are based on expert consensus, because rigorous trial data remain unavailable at present but data from preclinical testing noted above and one small interventional trial of statins in KD patients support these recommendations. Fluvastatin use improved a variety of noninvasive indicators of vascular dysfunction in a small series of children with significant KD coronary aneurysms (129).

TREATMENT: ACUTE PHASE

Intravenous Immunoglobulin

The standard of care for treatment of acute KD is high-dose IVIG together with aspirin. High-dose IVIG has been shown in many clinical trials to reduce the incidence of coronary aneurysms from 25% to 30% to <5% when administered ≤ 7 to 10 days of the disease onset (130). Meta-analysis shows a dose-response effect for IVIG, with low doses being relatively ineffective while a high dose of 2 g/kg as a single infusion is the most effective, of the doses trialed (131). Because patients with KD often have diminished left ventricular contractility, IVIG is administered slowly, over 8 to 12 hours to minimize the chance of hypersensitivity or hyperpyrexia reaction and to prevent solute overloading. A 5% solution of IVIG has osmolality equivalent to normal saline.

Treatment with IVIG should be administered to all children with KD within the first 10 days of illness, and ideally in the first 7 days (Table 59.5). IVIG should also be administered to those beyond illness day 10 in whom fever persists or who have coronary artery abnormalities together with persistent clinical and laboratory evidence of inflammation. Persistent fever after IVIG treatment is related to a higher risk of coronary aneurysms and therefore, although randomized trials are lacking, most experts believe that children who are febrile without other explanation more than 36 hours after completion of the first IVIG infusion should be retreated with IVIG, 2 g/kg, as a single infusion. A retrospective review of risk factors for aneurysms among KD patients treated with an additional dose of IVIG showed that the number of days of fever before initiation of IVIG retreatment was an independent predictor of coronary aneurysms (132), with treatment within 10 days leading to a significant reduction in coronary aneurysms (fivefold). The exact mechanism of immunoglobulin action in this setting remains unknown.

Adverse effects of IVIG include anaphylaxis, hypotension, rigors, headache, and hemolytic anemia. Many physicians prescribe IV diphenhydramine, 1 mg/kg, to a maximum of 50 mg, prior to IVIG infusion, to reduce the likelihood of allergic reactions. Measles and varicella immunizations should not be given for 11 months after IVIG treatment because of a risk of inadequate immunoresponse, unless the risk of exposure is considered to be high. If these vaccines are given earlier, the serologic response should be assessed, and, if inadequate, the child should be reimmunized at least 11 months after IVIG administration.

For children who defervesce with a second IVIG infusion, but in whom fever recurs, alternate therapies must be considered (see below, Other Anti-inflammatory Therapies). Retrospective data suggest persistent fever despite IVIG therapy is higher in males and in those who have lower albumin, higher AST levels, and CRP ≥ 8 mg/dL after IVIG infusion (133,134).

TABLE 59.5 Treatment of Kawasaki Disease During the Acute Phase

Initial anti-inflammatory treatment: intravenous immunoglobulin (IVIG) plus high-dose aspirin

IVIG dosage: 2 g/kg as single infusion over 8–12 h

Aspirin dosage: 80–100 mg/kg/d orally in four divided doses given every 6 h until the patient is afebrile for 48 h

In case of persistent or recrudescence fever:

Repeat dose of IVIG 2 g/kg as single infusion; consider IV methylprednisolone 30 mg/kg once a day; may be repeated as necessary up to a total of three doses

Subsequent antiplatelet treatment:

Aspirin 3–5 mg/kg orally once daily

Duration of treatment: 6–8 wk from onset or until sedimentation rate and platelet count return to normal; aspirin is discontinued at this point, if no coronary artery abnormalities are observed on echocardiogram

Continued indefinitely if coronary abnormalities are observed

If large aneurysms are noted with or without thrombus:

Start IV heparin or subcutaneous low-molecular-weight heparin

Start warfarin and titrate dose (target INR 2–2.5); continue low-dose aspirin at the same time

Following IVIG administration, immunization of the patient with live virus vaccine such as measles, mumps, and rubella (MMR) should be delayed by 11 mo or until the antibody titer has returned to a very low level

Several algorithms have been proposed to predict resistance to IVIG (135); however, the sensitivity of these algorithms in North American populations is currently too low to make the scores clinically useful (133).

Aspirin and Other Antithrombotic Therapies

Aspirin is used in high dose (80 to 100 mg/kg/d, divided into four daily doses) early in the disease for its anti-inflammatory and antipyretic effects (136). It should be noted that aspirin does not influence the incidence of coronary artery aneurysms (131). Its safety and efficacy relative to other antipyretic or anti-inflammatory agents in the acute phase of the disease have not been tested prospectively, and retrospective data suggest that high-dose aspirin use may not have advantages over other agents (131). However, ibuprofen has been shown to antagonize the irreversible platelet inhibition induced by aspirin (137). Thus, short-term use of high-dose aspirin for its anti-inflammatory, analgesic, and antipyretic effects remains a reasonable therapeutic strategy. Blood salicylate level and liver function tests should be checked if the patient remains on high-dose aspirin for >3 days to avoid salicylate intoxication, although gastrointestinal absorption of aspirin is generally decreased during the acute phase. After fever has resolved for ≥ 48 hours, the aspirin dose is lowered to 3 to 5 mg/kg/d for its antiplatelet effects. Low-dose aspirin is administered for approximately 6 weeks and then discontinued in patients without coronary artery aneurysms.

In children with small coronary aneurysms, low-dose aspirin is generally sufficient as monotherapy to prevent thrombosis. Aneurysms that are moderate or large, with maximal internal diameter 5 to 7 mm or z -score 7 to 9, are often treated with dual antiplatelet therapy, for example, low-dose aspirin and clopidogrel; without clinical trial evidence to support this approach, care is individualized. For high-risk coronary lesions, including giant aneurysms (≥ 8 mm or z -score ≥ 10), warfarin is often used. The use of warfarin in this context is associated with a lower rate of myocardial infarction compared to aspirin (138). Low-molecular-weight heparin is usually substituted for warfarin in infants to lessen the number of blood draws necessary for monitoring; outcomes seem to be at least as good, or possibly better with low-molecular-weight heparin (139).

Reye syndrome has been reported in children with KD taking high-dose aspirin (140). Although Reye syndrome has not been associated with use of low-dose aspirin, an annual influenza vaccine is recommended for all children on chronic aspirin therapy. When a child on chronic aspirin therapy develops a flu-like illness, aspirin should be withheld transiently and, if necessary, another antiplatelet medication (e.g., dipyridamole or clopidogrel) should be substituted until resolution of the illness.

Supportive Care

Intravenous fluid is often necessary because of poor oral intake and increased insensible losses. The patient should be kept comfortable in a quiet semidark room because of photophobia and irritability. Topical skin and mouth care should be provided to relieve itching and soreness in the lips and oral mucosa. As above, the use of ibuprofen is not advised in patients with coronary aneurysms, due to some evidence demonstrating an inhibition of the antiplatelet effects of aspirin in the acute phase of KD (141).

Other Anti-Inflammatory Therapies

If two courses of IVIG are not sufficient, other anti-inflammatory therapies may be considered. Corticosteroids have been administered to children with KD both as primary therapy and as rescue therapy (142), with mixed support. One early trial in Japan assessing primary therapy suggested that steroids increased the incidence of coronary artery aneurysms. Several subsequent studies have suggested that primary steroid therapy may shorten the length of fever and diminish the inflammatory response. Because the data on IVIG efficacy are so clear, steroids are no longer considered reasonable monotherapy. However, steroids have been evaluated in a number of retrospective studies and case series as rescue therapy to patients with IVIG-resistant KD, with conflicting results. Steroid therapy alternately improves fever and the inflammatory response (142–144), or prolongs fever and lowers rates of aneurysm regression (145). The influence of primary pulse steroid therapy given together with high-dose IVIG and aspirin on coronary artery outcome was investigated in a multicenter double-blind placebo-controlled randomized trial (146). Although inclusion of steroids in the primary therapy tended to result in more rapid recovery of ESR and CRP and shorter initial hospital stay, there was no difference in coronary outcome. Based on currently available literature, treatment with intravenous methylprednisolone 30 mg/kg (142) should be reserved for children who have persistent or recrudescence fever despite at least two courses of IVIG, 2 g/kg.

In addition to steroids, other anti-inflammatory therapies have been considered for recalcitrant cases of KD. Options include a third IVIG infusion, abciximab in patients with

persistent aneurysms, infliximab, and agents borrowed from rheumatologic treatments (147). Abciximab is a chimeric human-murine monoclonal antibody to platelet glycoprotein IIb/IIIa receptor. It has been used as therapy for enlarging coronary artery aneurysms in the acute phase of KD, and also to treat clots in patients with KD, late or early. Compared with historical controls in a single-center experience, patients with coronary aneurysms who received abciximab in the acute or subacute phase of KD showed greater regression in maximal aneurysm diameter (148), and at late follow-up of 3 to 5 years (149). The exact mechanism of this possible effect on aneurysm regression is unknown, but it may involve promotion of vascular remodeling through secondary anti-inflammatory effects.

Methotrexate has also been used in recalcitrant KD, with good retrospective data showing faster resolution of fever and lower CRP. No difference in the coronary artery status was demonstrated (150).

Because TNF- α levels are elevated in children with KD, investigation into therapies directed against TNF- α is the subject of considerable interest. High-dose pentoxifylline, when administered together with standard therapy, was associated with a lower prevalence of coronary aneurysms than standard therapy alone (151). Infliximab is a chimeric monoclonal antibody to TNF- α that may reduce circulating cytokines. Its use in KD has also been reported (152,153); a retrospective review of infliximab versus IVIG as a treatment for recurrent fever in children treated once with IVIG showed a shorter duration of fever compared to second IVIG dosing. No differences were seen in coronary artery dimensions; however, the study was not sufficiently powered to examine this question definitively (154). Etanercept is a TNF- α receptor blocker used in juvenile rheumatoid arthritis when methotrexate is insufficient (155). A small Phase I open-label study suggested etanercept appeared to be generally safe as an additional therapy in patients who receive IVIG and high-dose aspirin (156). In this study, one patient with meningococemia was notably mistakenly diagnosed as KD, serving as a warning to clinicians that powerful immunosuppressant therapies should be used only in patients with indisputable diagnoses of KD. Double-blind randomized controlled trials of primary therapy with etanercept and infliximab each are ongoing (157,158).

Finally, plasma exchange has been reported to lower the incidence of coronary artery aneurysms in uncontrolled studies (159–161). Because of the technical complexity of this therapy, it should be used only when other methods have failed. Rarely, cytotoxic agents have been used to treat patients with refractory acute KD (162,163), but the risks of such therapies exceed their benefits for the vast majority of patients.

TREATMENT: CHRONIC PHASE

Coronary Risk Stratification

Long-term management of patients with KD and coronary aneurysms should be tailored to each patient's estimated risk level for ischemic heart disease. Despite the lack of actuarial data in KD, attempts have been made to stratify patients' coronary risks based on echocardiographic or angiographic findings. Such an empiric risk stratification published by a committee of the AHA (61) may serve as an interim guide in patient management issues such as antiplatelet or anticoagulant therapy, restriction of physical activities, frequency of cardiac evaluation, and types of diagnostic tests, including coronary angiography (Table 59.6). A patient's overall risk may decrease or increase over time depending on whether the coronary artery aneurysm(s) undergo regression or develop an obstructive lesion.

TABLE 59.6 Coronary Risk Stratification

Risk Level	Pharmacologic Therapy	Physical Activity	Follow-up and Diagnostic Testing	Invasive Testing
I (no coronary artery changes at any stage of illness)	None beyond first 6–8 wk	No restrictions beyond first 6–8 wk	Cardiovascular risk assessment, counseling at 5-y intervals	None recommended
II (transient coronary artery ectasia disappears within first 6–8 wk)	None beyond first 6–8 wk	No restrictions beyond first 6–8 wk	Cardiovascular risk assessment, counseling at 3- to 5-y intervals	None recommended
III (1 small–medium coronary artery aneurysm/major coronary artery)	Low-dose aspirin (3–5 mg/kg aspirin/d), at least until aneurysm regression documented	For patients <11 y old, no restriction beyond first 6–8 wk; patients 11–20 y old, physical activity guided by biennial stress test, evaluation of myocardial perfusion scan; contact or high-impact sports discouraged for patients taking antiplatelet agents	Annual cardiology follow-up with echocardiogram + ECG, combined with cardiovascular risk assessment, counseling; biennial stress test/evaluation of myocardial perfusion scan	Angiography, if noninvasive test suggests ischemia
IV (≥ 1 large or giant coronary artery aneurysm, or multiple or complex aneurysms in same coronary artery, without obstruction)	Long-term antiplatelet therapy and warfarin (target INR 2.0–2.5) or low-molecular-weight heparin (target: anti-factor Xa level 0.5–1.0 U/mL) should be combined in giant aneurysms	Contact or high-impact sports should be avoided because of risk of bleeding; other physical activity recommendations guided by stress test/evaluation of myocardial perfusion scan outcome	Biannual follow-up with echocardiogram + ECG; annual stress test/evaluation of myocardial perfusion scan	First angiography at 6–12 mo or sooner if clinically indicated; repeated angiography if noninvasive test, clinical, or laboratory findings suggest ischemia; elective repeat angiography under some circumstances (see text)
V (coronary artery obstruction)	Long-term low-dose aspirin; warfarin or low-molecular-weight heparin if giant aneurysm persists; consider use of β -blockers to reduce myocardial O ₂ consumption	Contact or high-impact sports should be avoided because of risk of bleeding; other physical activity recommendations guided by stress test/myocardial perfusion scan outcome	Biannual follow-up with echocardiogram and ECG; annual stress test/evaluation of myocardial perfusion scan	Angiography recommended to address therapeutic options

From Newburger JW, Takahashi M, Gerber MA, et al. Diagnosis, treatment, and long-term management of Kawasaki disease: a statement for health professionals from the Committee on Rheumatic Fever, Endocarditis, and Kawasaki Disease, Council on Cardiovascular Disease in the Young, American Heart Association. *Circulation* 2004;110:2747–2771, with permission.

Anticoagulation for Giant Aneurysms

Giant aneurysms are particularly susceptible to thrombotic occlusion, with the overall probability of either complete thrombotic occlusion, severe stenosis requiring surgery, or death caused by myocardial infarction estimated to be about 7.5% per year for KD patients with giant aneurysms treated with aspirin therapy alone. A retrospective chart review showed the use of warfarin likely improved event-free survival without risk of significant bleeding episodes (Fig. 59.6). (138). We recommend patients with giant aneurysms be anticoagulated with either warfarin to an international normalized ratio (INR) range of 2 to 2.5 or low-molecular-weight heparin, in combination with low-dose aspirin.

Management of Coronary Thrombosis

In the event of myocardial infarction secondary to acute coronary artery thrombosis substantiated by ECG findings and elevated troponin T or I, the treatment of choice is catheterization to restore coronary perfusion. If sufficient expertise in interventional catheterization is not immediately available, or the patient is too small to undergo transcatheter restoration of coronary blood flow, thrombolytic therapy should be administered with alteplase, a recombinant tissue plasminogen activator, at 0.5 mg/kg/h intravenously for 6 hours, low-dose aspirin 3 to 5 mg/kg, and therapeutic heparin infusion to achieve a PTT of 50 to 70 seconds (164). Even in the absence of clinical infarction, acute development of a large thrombus within the aneurysm lumen is an indication for thrombolysis. After 6 hours, treatment should be continued based on reassessment of the thrombus and clinical picture. Blood fibrinogen level, activated partial thromboplastin time, and fibrin degradation products must be monitored. Patients with a particularly large thrombus burden may be appropriate for intravenous alteplase given at half dose (0.25 mg/kg/h), together with abciximab (platelet glycoprotein IIb/IIIa inhibitor), as an initial bolus of 0.25 mg/kg bolus over 30 minutes, followed by an infusion of 0.125 μ g/kg/min for 12 hours. Abciximab may be given together with low-dose heparin (10 U/kg/h) to prevent clot extension in acute KD to treat mural thrombus. The

progress of therapy with thrombolytic agents or abciximab should be followed by serial echocardiography or, if needed, coronary arteriography, and all decisions need to be made the context of the specific clinical circumstances.

Surgical and Transcatheter Revascularization

Because evidence-based data in KD patients are limited, recommendations for surgical and percutaneous revascularization in patients with KD coronary artery aneurysms are based upon expert consensus, retrospective series, and adult atherosclerotic coronary artery disease experience. Indeed, coronary revascularization in KD patients is too rare to be studied with adequate power in randomized trials. In principle, coronary bypass surgery or transcatheter revascularization should be performed with the goal of relieving symptoms of angina and reducing the risk of myocardial infarction or sudden death. For the most part, such procedures should be performed in patients with coronary artery sequelae of KD who have angina and/or a risk of subsequent myocardial infarction after stress testing has revealed reversible ischemia (165–167). Decisions about revascularization should always be made in concert with experts in adult interventional cardiology and cardiovascular surgery.

Japanese guidelines suggest surgical revascularization for those patients who have high-grade obstructions in at least two major coronary arteries or in the left main coronary artery because of the high risk of fatal or incapacitating myocardial infarction (168). These guidelines also suggest that patients with high-grade stenosis in the left anterior descending artery should undergo surgery. However, indications for surgery must be considered on a case-by-case basis. Of note, as is the case in adults with atherosclerotic coronary disease, lesions with competitive flow through collaterals are more likely to have graft stenosis or development of a “string sign” and are less likely to benefit from coronary artery bypass grafting (CABG) (169). Indeed, in a recent Japanese series, patients whose interventions were performed in the absence of ischemic findings had higher rates of reinterventions (169).

Fortunately, mortality and morbidity rates after CABG are low, and complications of CABG can often be managed with percutaneous intervention. Late patient survival rates after the CABG procedure have been reported to be 95% at 25 years, with event-free survival rates of approximately 60% (170). In the single-center experience of Kitamura et al. (165,170), the use of internal thoracic arteries resulted in nearly 100% 1-year graft patency and documented the growth of the graft over time, in keeping with the somatic growth. In contrast, saphenous vein grafts had only a 50% 1-year patency rate. The patient's age also influenced graft patency rate with children over 12 years having higher graft patency than those under age 12 years (95% and 91% vs. 93% and 63%, respectively).

Percutaneous intervention is increasingly used as a substitute for CABG. Indications for angioplasty in adults with atherosclerotic coronary artery disease should be considered in the management of patients with KD. In addition, the Japanese Ministry of Health has published indications for percutaneous intervention that include (a) ischemic symptoms, (b) stress testing revealing reversible ischemia, and (c) 75% stenosis of the LAD. These guidelines recommend surgical revascularization when there is significant left ventricular dysfunction, or long-segment, complex, or ostial lesions, provided that there is viable myocardium distal to the obstruction (168). Early reports suggested that percutaneous revascularization had success rates equivalent to surgical methods but was associated with the need for more reinterventions (171,172). A recent multicenter survey in Japan noted that patients treated by percutaneous intervention, compared to

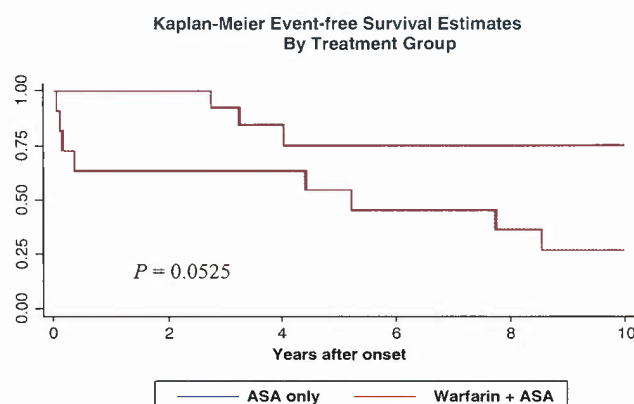


Figure 59.6. Kaplan–Meier event-free survival estimates of two groups of patients with giant coronary artery aneurysms: one group (historical control; $n = 11$) treated with aspirin only (shown in blue) and the other group ($n = 18$) treated with warfarin and aspirin (shown in red). The warfarin group appears to have longer survival to composite end points of total thrombotic occlusion, severe coronary artery stenosis requiring surgical intervention, or death owing to myocardial infarction. ASA, acetylsalicylic acid (aspirin).

CABG procedure, had similar mortality and rates of acute myocardial infarction, but were more likely to require repeat revascularization (169,173). Long-term outcomes of KD patients after myocardial infarction are related to post-infarct left ventricular ejection fraction, and ventricular arrhythmia rates are significant in those with decreased ejection fraction (172). Finally, cardiac transplantation is an option for some patients with ischemic cardiomyopathy not amenable to percutaneous or surgical revascularization.

REFERENCES

- Kawasaki T, Kosaki F, Okawa S, et al. A new infantile acute febrile mucocutaneous lymph node syndrome (MLNS) prevailing in Japan. *Pediatrics* 1974;54:271-276.
- Newburger JW, Takahashi M, Gerber MA, et al. Diagnosis, treatment, and long-term management of Kawasaki disease: a statement for health professionals from the Committee on Rheumatic Fever, Endocarditis and Kawasaki Disease, Council on Cardiovascular Disease in the Young, American Heart Association. *Circulation* 2004;110:2747-2771.
- Melish ME, Hicks RM, Larson EJ. Mucocutaneous lymph node syndrome in the United States. *Am J Dis Child* 1976;130:599-607.
- Burns JC, Cayan DR, Tong G, et al. Seasonality and temporal clustering of Kawasaki syndrome. *Epidemiology* 2005;16:220-225.
- Nakamura Y, Yashiro M, Uehara R, et al. Epidemiologic features of Kawasaki disease in Japan: results of the 2007-2008 nationwide survey. *J Epidemiol* 2010;20:302-307.
- Holman RC, Belay ED, Christensen KY, et al. Hospitalizations for Kawasaki syndrome among children in the United States, 1997-2007. *Pediatr Infect Dis J* 2010;29:483-488.
- Holman RC, Curns AT, Belay ED, et al. Kawasaki syndrome hospitalizations in the United States, 1997 and 2000. *Pediatrics* 2003;112:495-501.
- Stockheim JA, Innocentini N, Shulman ST. Kawasaki disease in older children and adolescents. *J Pediatr* 2000;137:250-252.
- Momenah T, Sanatani S, Potts J, et al. Kawasaki disease in the older child. *Pediatrics* 1998;102:e7.
- Muta H, Ishii M, Sakaue T, et al. Older age is a risk factor for the development of cardiovascular sequelae in Kawasaki disease. *Pediatrics* 2004;114:751-754.
- Son MB, Gauvreau K, Ma L, et al. Treatment of Kawasaki disease: analysis of 27 US pediatric hospitals from 2001 to 2006. *Pediatrics* 2009;124:1-8.
- Yanagawa H, Nakamura Y, Yashiro M, et al. Results of the nationwide epidemiologic survey of Kawasaki disease in 1995 and 1996 in Japan. *Pediatrics* 1998;102:E65.
- Hirata S, Nakamura Y, Yanagawa H. Incidence rate of recurrent Kawasaki disease and related risk factors: from the results of nationwide surveys of Kawasaki disease in Japan. *Acta Paediatr* 2001;90:40-44.
- Fujita Y, Nakamura Y, Sakata K, et al. Kawasaki disease in families. *Pediatrics* 1989;84:666-669.
- Harada F, Sada M, Kamiya T, et al. Genetic analysis of Kawasaki syndrome. *Am J Hum Genet* 1986;39:537-539.
- Quasney MW, Bronstein DE, Cantor RM, et al. Increased frequency of alleles associated with elevated tumor necrosis factor- α levels in children with Kawasaki disease. *Pediatr Res* 2001;49:686-690.
- Hamashima Y, Kishi K, Tasaka K. Rickettsia-like bodies in infantile acute febrile mucocutaneous lymph-node syndrome. *Lancet* 1973;2:42.
- Kato H, Fujimoto T, Inoue O, et al. Etiological investigation of Propionibacterium acnes variant isolated from children with Kawasaki disease. *Nippon Rinsho* 1983;41:2029-2039.
- Kotani S. Evaluation of evidence related to streptococci in the etiology of Kawasaki disease. *Prog Clin Biol Res* 1987;250:101-111.
- Furusko K, Ohba T, Soeda T, et al. Possible role for mite antigen in Kawasaki disease. *Lancet* 1981;2:194-195.
- Burns JC, Geha RS, Schneeberger EE, et al. Polymerase activity in lymphocyte culture supernatants from patients with Kawasaki disease. *Nature* 1986;323:814-816.
- Patriarca PA, Rogers MF, Morens DM, et al. Kawasaki syndrome: association with the application of rug shampoo. *Lancet* 1982;2:578-580.
- Daniels SR, Specker B. Association of rug shampooing and Kawasaki disease. *J Pediatr* 1991;118:485-488.
- Barron K, DeCunto C, Montalvo J, et al. Abnormalities of immunoregulation in Kawasaki syndrome. *J Rheumatol* 1988;15:1243-1249.
- Mason WH, Jordan SC, Sakai R, et al. Circulating immune complexes in Kawasaki syndrome. *Pediatr Infect Dis* 1985;4:48-51.
- Rowley AH, Eckerley CA, Jack HM, et al. IgA plasma cells in vascular tissue of patients with Kawasaki syndrome. *J Immunol* 1997;159:5946-5955.
- Leung DY, Geha RS, Newburger JW, et al. Two monokines, interleukin 1 and tumor necrosis factor, render cultured vascular endothelial cells susceptible to lysis by antibodies circulating during Kawasaki syndrome. *J Exp Med* 1986;164:1958-1972.
- Foell D, Ichida F, Vogl T, et al. S100A12 (EN-RAGE) in monitoring Kawasaki disease. *Lancet* 2003;361:1270-1272.
- Ye F, Foell D, Hirono KI, et al. Neutrophil-derived S100A12 is profoundly upregulated in the early stage of acute Kawasaki disease. *Am J Cardiol* 2004;94:840-844.
- Abe J, Kotzin BL, Jujo K, et al. Selective expansion of T cells expressing T-cell receptor variable regions V beta 2 and V beta 8 in Kawasaki disease. *Proc Natl Acad Sci U S A* 1992;89:4066-4070.
- Leung DY, Meissner HC, Shulman ST, et al. Prevalence of superantigen-secreting bacteria in patients with Kawasaki disease. *J Pediatr* 2002;140:742-746.
- Rowley AH, Baker SC, Shulman ST, et al. Detection of antigen in bronchial epithelium and macrophages in acute Kawasaki disease by use of synthetic antibody. *J Infect Dis* 2004;190:856-865.
- Uehara R, Yashiro M, Nakamura Y, et al. Parents with a history of Kawasaki disease whose child also had the same disease. *Pediatr Int* 2011;53:511-514.
- Jibiki T, Terai M, Kohno Y. High concentrations of interleukin-8 and monocyte chemoattractant protein-1 in urine of patients with acute Kawasaki disease. *Eur J Pediatr* 2004;163:749-750.
- Nishimura S, Zaito M, Hara M, et al. A polymorphism in the promoter of the CD14 gene (CD14/-159) is associated with the development of coronary artery lesions in patients with Kawasaki disease. *J Pediatr* 2003;143:357-362.
- Chien YH, Chang KW, Yang YH, et al. Association between levels of TNF-alpha and TNF-alpha promoter -308 A/A polymorphism in children with Kawasaki disease. *J Formos Med Assoc* 2003;102:147-150.
- Khajoe V, Kariyazono H, Ohno T, et al. Inducible and endothelial constitutive nitric oxide synthase gene polymorphisms in Kawasaki disease. *Pediatr Int* 2003;45:130-134.
- Ouchi K, Suzuki Y, Shirakawa T, et al. Polymorphism of SLC11A1 (formerly NRAMP1) gene confers susceptibility to Kawasaki disease. *J Infect Dis* 2003;187:326-329.
- Tomasdottir H, Hjartarson H, Ricksten A, et al. Tumor necrosis factor gene polymorphism is associated with enhanced systemic inflammatory response and increased cardiopulmonary morbidity after cardiac surgery. *Anesth Analg* 2003;97:944-949.
- Kariyazono H, Ohno T, Khajoe V, et al. Association of vascular endothelial growth factor (VEGF) and VEGF receptor gene polymorphisms with coronary artery lesions of Kawasaki disease. *Pediatr Res* 2004;56:953-959.
- Fukazawa R, Sonobe T, Hamamoto K, et al. Possible synergic effect of angiotensin-I converting enzyme gene insertion/deletion polymorphism and angiotensin-II type-1 receptor 1166A/C gene polymorphism on ischemic heart disease in patients with Kawasaki disease. *Pediatr Res* 2004;56:597-601.
- Yang J, Li CR, Li YB, et al. Correlation between mannose-binding lectin gene codon 54 polymorphism and susceptibility of Kawasaki disease. *Zhonghua Er Ke Za Zhi* 2004;42:176-179.
- Onouchi Y, Onoue S, Tamari M, et al. CD40 ligand gene and Kawasaki disease. *Eur J Hum Genet* 2004;12:1062-1068.
- Burns JC, Shimizu C, Gonzalez E, et al. Genetic variations in the receptor-ligand pair CCR5 and CCL3L1 are important determinants of susceptibility to Kawasaki disease. *J Infect Dis* 2005;192:344-349.
- Hsueh KC, Lin YJ, Chang JS, et al. BTNL2 gene polymorphisms may be associated with susceptibility to Kawasaki disease and formation of coronary artery lesions in Taiwanese children. *Eur J Pediatr* 2010;169:713-719.
- Onouchi Y, Gunji T, Burns JC, et al. ITPKC functional polymorphism associated with Kawasaki disease susceptibility and formation of coronary artery aneurysms. *Nat Genet* 2008;40:35-42.
- Khor CC, Davila S, Shimizu C, et al. Genome-wide linkage and association mapping identify susceptibility alleles in ABCA4 for Kawasaki disease. *J Med Genet* 2011;48:467-472.
- Shimizu C, Matsubara T, Onouchi Y, et al. Matrix metalloproteinase haplotypes associated with coronary artery aneurysm formation in patients with Kawasaki disease. *J Hum Genet* 2010;55:779-784.
- Fujiwara H, Hamashima Y. Pathology of the heart in Kawasaki disease. *Pediatrics* 1978;61:100-107.
- Yutani C, Okano K, Kamiya T, et al. Histopathological study on right endomyocardial biopsy of Kawasaki disease. *Br Heart J* 1980;43:589-592.
- Yutani C, Go S, Kamiya T, et al. Cardiac biopsy of Kawasaki disease. *Arch Pathol Lab Med* 1981;105:470-473.
- Gidding SS, Shulman ST, Ilbawi M, et al. Mucocutaneous lymph node syndrome (Kawasaki disease): delayed aortic and mitral insufficiency secondary to active valvulitis. *J Am Coll Cardiol* 1986;7:894-897.
- Naoe S, Takahashi K, Masuda H, et al. Coronary findings post Kawasaki disease in children who died of other causes. *Prog Clin Biol Res* 1987;250:341-346.
- Kato H, Ichinose E, Yoshioka F, et al. Fate of coronary aneurysms in Kawasaki disease: serial coronary angiography and long-term follow-up study. *Am J Cardiol* 1982;49:1758-1766.
- Takahashi M, Mason W, Lewis AB. Regression of coronary aneurysms in patients with Kawasaki syndrome. *Circulation* 1987;75:387-394.
- Baker AL, Lu M, Minich LL, et al. Associated symptoms in the ten days before diagnosis of Kawasaki disease. *J Pediatr* 2009;154:592-595.
- Tomita S, Chung K, Mas M, et al. Peripheral gangrene associated with Kawasaki disease. *Clin Infect Dis* 1992;14:121-126.
- Suddleson EA, Reid B, Woolley MM, et al. Hydrops of the gallbladder associated with Kawasaki syndrome. *J Pediatr Surg* 1987;22:956-959.

59. Gallagher PG. Facial nerve paralysis and Kawasaki disease. *Rev Infect Dis* 1990;12:403-405.
60. Sundel RP, Newburger JW, McGill T, et al. Sensorineural hearing loss associated with Kawasaki disease. *J Pediatr* 1990;117:371-377.
61. Newburger JW, Takahashi M, Gerber MA, et al. Diagnosis, treatment, and long-term management of Kawasaki disease: a statement for health professionals from the Committee on Rheumatic Fever, Endocarditis, and Kawasaki Disease, Council on Cardiovascular Disease in the Young, American Heart Association. *Pediatrics* 2004;114:1708-1733.
62. Burns JC, Mason WH, Glode MP, et al. Clinical and epidemiologic characteristics of patients referred for evaluation of possible Kawasaki disease. United States Multicenter Kawasaki Disease Study Group. *J Pediatr* 1991;118:680-686.
63. Anderson MS, Burns J, Treadwell TA, et al. Erythrocyte sedimentation rate and C-reactive protein discrepancy and high prevalence of coronary artery abnormalities in Kawasaki disease. *Pediatr Infect Dis J* 2001;20:698-702.
64. Ting EC, Capparelli EV, Billman GF, et al. Elevated gamma-glutamyltransferase concentrations in patients with acute Kawasaki disease. *Pediatr Infect Dis J* 1998;17:431-432.
65. Dengler LD, Capparelli EV, Bastian JF, et al. Cerebrospinal fluid profile in patients with acute Kawasaki disease. *Pediatr Infect Dis J* 1998;17:478-481.
66. Kim M, Kim K. Changes in cardiac troponin I in Kawasaki disease before and after treatment with intravenous gammaglobulin. *Jpn Circ J* 1998;62:479-482.
67. Kim M, Kim K. Elevation of cardiac troponin I in the acute stage of Kawasaki disease. *Pediatr Cardiol* 1999;20:184-188.
68. Checchia PA, Borensztajn J, Shulman ST. Circulating cardiac troponin I levels in Kawasaki disease. *Pediatr Cardiol* 2001;22:102-106.
69. Rowley AH, Gonzalez-Crussi F, Gidding SS, et al. Incomplete Kawasaki disease with coronary artery involvement. *J Pediatr* 1987;110:409-413.
70. Kushner HI, Turner CL, Bastian JF, et al. The narratives of Kawasaki disease. *Bull Hist Med* 2004;78:410-439.
71. Yellen ES, Gauvreau K, Takahashi M, et al. Performance of 2004 American Heart Association recommendations for treatment of Kawasaki disease. *Pediatrics* 2010;125:e234-e241.
72. Printz BF, Sleeper LA, Newburger JW, et al. Noncoronary cardiac abnormalities are associated with coronary artery dilation and with laboratory inflammatory markers in acute Kawasaki disease. *J Am Coll Cardiol* 2011;57:86-92.
73. Ozdogu H, Boga C. Fatal cardiac tamponade in a patient with Kawasaki disease. *Heart Lung* 2005;34:257-259.
74. Belay ED, Maddox RA, Holman RC, et al. Kawasaki syndrome and risk factors for coronary artery abnormalities: United States, 1994-2003. *Pediatr Infect Dis J* 2006;25:245-249.
75. Nakano H, Ueda K, Saito A, et al. Repeated quantitative angiograms in coronary arterial aneurysm in Kawasaki disease. *Am J Cardiol* 1985;56:846-851.
76. Tataru K, Kusakawa S. Long-term prognosis of giant coronary aneurysm in Kawasaki disease: an angiographic study. *J Pediatr* 1987;111:705-710.
77. Koren G, Lavi S, Rose V, et al. Kawasaki disease: review of risk factors for coronary aneurysms. *J Pediatr* 1986;108:388-392.
78. Ichida F, Fatica NS, Engle MA, et al. Coronary artery involvement in Kawasaki syndrome in Manhattan, New York: risk factors and role of aspirin. *Pediatrics* 1987;80:828-835.
79. Daniels SR, Specker B, Capannari TE, et al. Correlates of coronary artery aneurysm formation in patients with Kawasaki disease. *Am J Dis Child* 1987;141:205-207.
80. Harada K. Intravenous gamma-globulin treatment in Kawasaki disease. *Acta Paediatr Jpn* 1991;33:805-810.
81. Beiser AS, Takahashi M, Baker AL, et al. A predictive instrument for coronary artery aneurysms in Kawasaki disease. US Multicenter Kawasaki Disease Study Group. *Am J Cardiol* 1998;81:1116-1120.
82. Kato H, Ichinose E, Kawasaki T. Myocardial infarction in Kawasaki disease: clinical analyses in 195 cases. *J Pediatr* 1986;108:923-927.
83. Suda K, Iemura M, Nishiono H, et al. Long-term prognosis of patients with Kawasaki disease complicated by giant coronary aneurysms: a single-institution experience. *Circulation* 2011;123:1836-1842.
84. Sumitomo N, Karasawa K, Taniguchi K, et al. Association of sinus node dysfunction, atrioventricular node conduction abnormality and ventricular arrhythmia in patients with Kawasaki disease and coronary involvement. *Circ J* 2008;72:274-280.
85. Baer AZ, Rubin LG, Shapiro CA, et al. Prevalence of coronary artery lesions on the initial echocardiogram in Kawasaki syndrome. *Arch Pediatr Adolesc Med* 2006;160:686-690.
86. Selamet Tierney ES, Newburger JW, Graham D, et al. Diastolic function in children with Kawasaki Disease. *Int J Cardiol* 2011;148:309-312.
87. Satomi G, Nakamura K, Narai S, et al. Systematic visualization of coronary arteries by two-dimensional echocardiography in children and infants: evaluation in Kawasaki's disease and coronary arteriovenous fistulas. *Am Heart J* 1984;107:497-505.
88. Capannari TE, Daniels SR, Meyer RA, et al. Sensitivity, specificity and predictive value of two-dimensional echocardiography in detecting coronary artery aneurysms in patients with Kawasaki disease. *J Am Coll Cardiol* 1986;7:355-360.
89. Research Committee on Kawasaki Disease. Report of Subcommittee on Standardization of Diagnostic Criteria and Reporting of Coronary Artery Lesions in Kawasaki Disease. 1984. Tokyo, Ministry of Health and Welfare.
90. Arjunan K, Daniels SR, Meyer RA, et al. Coronary artery caliber in normal children and patients with Kawasaki disease but without aneurysms: an echocardiographic and angiographic study. *J Am Coll Cardiol* 1986;8:1119-1124.
91. de Zorzi A, Colan SD, Gauvreau K, et al. Coronary artery dimensions may be misclassified as normal in Kawasaki disease. *J Pediatr* 1998;133:254-258.
92. Manlihot C, Millar K, Golding F, et al. Improved classification of coronary artery abnormalities based only on coronary artery z-scores after Kawasaki disease. *Pediatr Cardiol* 2010;31:242-249.
93. Kondo C, Hiroe M, Nakanishi T, et al. Detection of coronary artery stenosis in children with Kawasaki disease. Usefulness of pharmacologic stress 201Tl myocardial tomography. *Circulation* 1989;80:615-624.
94. Jan SL, Hwang B, Fu YC, et al. Comparison of 201Tl SPET and treadmill exercise testing in patients with Kawasaki disease. *Nucl Med Commun* 2000;21:431-435.
95. Noto N, Ayusawa M, Karasawa K, et al. Dobutamine stress echocardiography for detection of coronary artery stenosis in children with Kawasaki disease. *J Am Coll Cardiol* 1996;27:1251-1256.
96. Kimball TR, Witt SA, Daniels SR. Dobutamine stress echocardiography in the assessment of suspected myocardial ischemia in children and young adults. *Am J Cardiol* 1997;79:380-384.
97. Bezold LI, Lewin MB, Vick GW III, et al. Update on new technologies in pediatric echocardiography. *Tex Heart Inst J* 1997;24:278-286.
98. Muhling O, Jerosch-Herold M, Nabauer M, et al. Assessment of ischemic heart disease using magnetic resonance first-pass perfusion imaging. *Herz* 2003;28:82-89.
99. Kaul S, Ito H. Microvasculature in acute myocardial ischemia: part I: evolving concepts in pathophysiology, diagnosis, and treatment. *Circulation* 2004;109:146-149.
100. Zilberman MV, Witt SA, Kimball TR. Is there a role for intravenous transpulmonary contrast imaging in pediatric stress echocardiography? *J Am Soc Echocardiogr* 2003;16:9-14.
101. Ishii M, Himeno W, Sawa M, et al. Assessment of the ability of myocardial contrast echocardiography with harmonic power Doppler imaging to identify perfusion abnormalities in patients with Kawasaki disease at rest and during dipyridamole stress. *Pediatr Cardiol* 2002;23:192-199.
102. Fukazawa M, Fukushige J, Takeuchi T, et al. Discordance between thallium-201 scintigraphy and coronary angiography in patients with Kawasaki disease: myocardial ischemia with normal coronary angiogram. *Pediatr Cardiol* 1993;14:67-74.
103. Cicala S, Pellegrino T, Storto G, et al. Noninvasive quantification of coronary endothelial function by SPECT imaging in children with a history of Kawasaki disease. *Eur J Nucl Med Mol Imaging* 2010;37:2249-2255.
104. Gurofsky RC, Sabharwal T, Manlihot C, et al. Arterial complications associated with cardiac catheterization in pediatric patients with a previous history of Kawasaki disease. *Catheter Cardiovasc Interv* 2009;73:809-813.
105. Greil GF, Stuber M, Botnar RM, et al. Coronary magnetic resonance angiography in adolescents and young adults with Kawasaki disease. *Circulation* 2002;105:908-911.
106. Mavrogeni S, Papadopoulos G, Douskou M, et al. Magnetic resonance angiography is equivalent to X-ray coronary angiography for the evaluation of coronary arteries in Kawasaki disease. *J Am Coll Cardiol* 2004;43:649-652.
107. McMahon CJ, Su JT, Taylor MD, et al. Images in cardiovascular medicine. Detection of active coronary arterial vasculitis using magnetic resonance imaging in Kawasaki disease. *Circulation* 2005;112:e315-e316.
108. Peng Y, Zeng J, Du Z, et al. Usefulness of 64-slice MDCT for follow-up of young children with coronary artery aneurysm due to Kawasaki disease: initial experience. *Eur J Radiol* 2009;69:500-509.
109. Kanamaru H, Sato Y, Takayama T, et al. Assessment of coronary artery abnormalities by multislice spiral computed tomography in adolescents and young adults with Kawasaki disease. *Am J Cardiol* 2005;95:522-525.
110. Arnold R, Ley S, Ley-Zaporozhan J, et al. Visualization of coronary arteries in patients after childhood Kawasaki syndrome: value of multidetector CT and MR imaging in comparison to conventional coronary catheterization. *Pediatr Radiol* 2007;37:998-1006.
111. Kato H, Sugimura T, Akagi T, et al. Long-term consequences of Kawasaki disease. A 10- to 21-year follow-up study of 594 patients. *Circulation* 1996;94:1379-1385.
112. Dhillon R, Clarkson P, Donald AE, et al. Endothelial dysfunction late after Kawasaki disease. *Circulation* 1996;94:2103-2106.
113. Lee SJ, Ahn HM, You JH, et al. Carotid intima-media thickness and pulse wave velocity after recovery from Kawasaki disease. *Korean Circ J* 2009;39:264-269.
114. Cheung YF, Yung TC, Tam SC, et al. Novel and traditional cardiovascular risk factors in children after Kawasaki disease: implications for premature atherosclerosis. *J Am Coll Cardiol* 2004;43:120-124.
115. Ooyanagi R, Fuse S, Tomita H, et al. Pulse wave velocity and ankle brachial index in patients with Kawasaki disease. *Pediatr Int* 2004;46:398-402.
116. McCrindle BW, McIntyre S, Kim C, et al. Are patients after Kawasaki disease at increased risk for accelerated atherosclerosis? *J Pediatr* 2007;151:244-248.
117. Gupta-Malhotra M, Gruber D, Abraham SS, et al. Atherosclerosis in survivors of Kawasaki disease. *J Pediatr* 2009;155:572-577.
118. Newburger JW, Burns JC, Beiser AS, et al. Altered lipid profile after Kawasaki syndrome. *Circulation* 1991;84:625-631.

119. Sugimura T, Kato H, Inoue O, et al. Intravascular ultrasound of coronary arteries in children. Assessment of the wall morphology and the lumen after Kawasaki disease. *Circulation* 1994;89:258-265.
120. Tsuda E, Kamiya T, Kimura K, et al. Coronary artery dilatation exceeding 4.0 mm during acute Kawasaki disease predicts a high probability of subsequent late intima-medial thickening. *Pediatr Cardiol* 2002;23:9-14.
121. Suzuki A, Yamagishi M, Kimura K, et al. Functional behavior and morphology of the coronary artery wall in patients with Kawasaki disease assessed by intravascular ultrasound. *J Am Coll Cardiol* 1996;27:291-296.
122. Yamakawa R, Ishii M, Sugimura T, et al. Coronary endothelial dysfunction after Kawasaki disease: evaluation by intracoronary injection of acetylcholine. *J Am Coll Cardiol* 1998;31:1074-1080.
123. Mitani Y, Okuda Y, Shimpo H, et al. Impaired endothelial function in epicardial coronary arteries after Kawasaki disease. *Circulation* 1997;96:454-461.
124. Noto N, Okada T, Yamasage M, et al. Noninvasive assessment of the early progression of atherosclerosis in adolescents with Kawasaki disease and coronary artery lesions. *Pediatrics* 2001;107:1095-1099.
125. Iemura M, Ishii M, Sugimura T, et al. Long term consequences of regressed coronary aneurysms after Kawasaki disease: vascular wall morphology and function. *Heart* 2000;83:307-311.
126. Kato H, Inoue O, Kawasaki T, et al. Adult coronary artery disease probably due to childhood Kawasaki disease. *Lancet* 1992;340:1127-1129.
127. Burns JC, Shike H, Gordon JB, et al. Sequelae of Kawasaki disease in adolescents and young adults. *J Am Coll Cardiol* 1996;28:253-257.
128. Kavey RE, Allada V, Daniels SR, et al. Cardiovascular risk reduction in high-risk pediatric patients: a scientific statement from the American Heart Association Expert Panel on Population and Prevention Science; the Councils on Cardiovascular Disease in the Young, Epidemiology and Prevention, Nutrition, Physical Activity and Metabolism, High Blood Pressure Research, Cardiovascular Nursing, and the Kidney in Heart Disease; and the Interdisciplinary Working Group on Quality of Care and Outcomes Research: endorsed by the American Academy of Pediatrics. *Circulation* 2006;114:2710-2738.
129. Hamaoka A, Hamaoka K, Yahata T, et al. Effects of HMG-CoA reductase inhibitors on continuous post-inflammatory vascular remodeling late after Kawasaki disease. *J Cardiol* 2010;56:245-253.
130. Newburger JW, Takahashi M, Beiser AS, et al. A single intravenous infusion of gamma globulin as compared with four infusions in the treatment of acute Kawasaki syndrome. *N Engl J Med* 1991;324:1633-1639.
131. Terai M, Shulman ST. Prevalence of coronary artery abnormalities in Kawasaki disease is highly dependent on gamma globulin dose but independent of salicylate dose. *J Pediatr* 1997;131:888-893.
132. Miura M, Ohki H, Tsuchihashi T, et al. Coronary risk factors in Kawasaki disease treated with additional gammaglobulin. *Arch Dis Child* 2004;89:776-780.
133. Sleeper LA, Minich LL, McCrindle BM, et al. Evaluation of Kawasaki disease risk-scoring systems for intravenous immunoglobulin resistance. *J Pediatr* 2011;158:831-835.
134. Iwashima S, Kimura M, Ishikawa T, et al. Importance of C-reactive protein level in predicting non-response to additional intravenous immunoglobulin treatment in children with Kawasaki disease: a retrospective study. *Clin Drug Investig* 2011;31:191-199.
135. Seki M, Kobayashi T, Kobayashi T, et al. External validation of a risk score to predict intravenous immunoglobulin resistance in patients with Kawasaki disease. *Pediatr Infect Dis J* 2011;30:145-147.
136. Hsieh KS, Weng KP, Lin CC, et al. Treatment of acute Kawasaki disease: aspirin's role in the febrile stage revisited. *Pediatrics* 2004;114:e689-e693.
137. Catella-Lawson F, Reilly MP, Kapoor SC, et al. Cyclooxygenase inhibitors and the antiplatelet effects of aspirin. *N Engl J Med* 2001;345:1809-1817.
138. Sugahara Y, Ishii M, Muta H, et al. Warfarin therapy for giant aneurysm prevents myocardial infarction in Kawasaki disease. *Pediatr Cardiol* 2008;29:398-401.
139. Manlhiot C, Brandao LR, Somji Z, et al. Long-term anticoagulation in Kawasaki disease: Initial use of low molecular weight heparin is a viable option for patients with severe coronary artery abnormalities. *Pediatr Cardiol* 2010;31:834-842.
140. Takahashi M, Mason W, Thomas D, et al. Reye syndrome following Kawasaki syndrome confirmed by histopathology. In: Kato H, ed. *Kawasaki Disease. Proceedings of the 5th International Kawasaki Disease Symposium*. Amsterdam, The Netherlands: Elsevier Science, 1995: 436-444.
141. Sohn S, Kwon K. Accelerated thrombotic occlusion of a medium-sized coronary aneurysm in Kawasaki disease by the inhibitory effect of ibuprofen on aspirin. *Pediatr Cardiol* 2008;29:153-156.
142. Wright DA, Newburger JW, Baker A, et al. Treatment of immune globulin-resistant Kawasaki disease with pulsed doses of corticosteroids. *J Pediatr* 1996;128:146-149.
143. Adachi S, Sakaguchi H, Kuwahara T, et al. High regression rate of coronary aneurysms developed in patients with immune globulin-resistant Kawasaki disease treated with steroid pulse therapy. *Tohoku J Exp Med* 2010;220:285-290.
144. Durongpisitkul K, Soongswang J, Laohaprasitporn D, et al. Immuno-globulin failure and retreatment in Kawasaki disease. *Pediatr Cardiol* 2003;24:145-148.
145. Millar K, Manlhiot C, Yeung RS, et al. Corticosteroid administration for patients with coronary artery aneurysms after Kawasaki disease may be associated with impaired regression. *Int J Cardiol* 2012;154:9-13.
146. Newburger JW, Sleeper LA, McCrindle BW, et al. Randomized trial of pulsed corticosteroid therapy for primary treatment of Kawasaki disease. *N Engl J Med* 2007;356:663-675.
147. Shin JI, Lee JS, Choi JY, et al. Refractory Kawasaki disease: infliximab or methotrexate therapy? *Indian J Pediatr* 2009;76:1184.
148. Williams RV, Wilke VM, Tani LY, et al. Does Abciximab enhance regression of coronary aneurysms resulting from Kawasaki disease? *Pediatrics* 2002;109:E4.
149. McCandless RT, Minich LL, Tani LY, et al. Does abciximab promote coronary artery remodeling in patients with Kawasaki disease? *Am J Cardiol* 2010;105:1625-1628.
150. Lee TJ, Kim KH, Chun JK, et al. Low-dose methotrexate therapy for intravenous immunoglobulin-resistant Kawasaki disease. *Yonsei Med J* 2008;49:714-718.
151. Furukawa S, Matsubara T, Umezawa Y, et al. Pentoxifylline and intravenous gamma globulin combination therapy for acute Kawasaki disease. *Eur J Pediatr* 1994;153:663-667.
152. Oishi T, Fujieda M, Shiraishi T, et al. Infliximab treatment for refractory Kawasaki disease with coronary artery aneurysm. *Circ J* 2008;72:850-852.
153. Weiss JE, Eberhard BA, Chowdhury D, et al. Infliximab as a novel therapy for refractory Kawasaki disease. *J Rheumatol* 2004;31:808-810.
154. Burns JC, Best BM, Mejias A, et al. Infliximab treatment of intravenous immunoglobulin-resistant Kawasaki disease. *J Pediatr* 2008;153:833-838.
155. Culy CR, Keating GM. Etanercept: an updated review of its use in rheumatoid arthritis, psoriatic arthritis and juvenile rheumatoid arthritis. *Drugs* 2002;62:2493-2537.
156. Choueiri NF, Olson AK, Shen DD, et al. Prospective open-label trial of etanercept as adjunctive therapy for Kawasaki disease. *J Pediatr* 2010;157:960-966.
157. Portman MA, Olson A, Soriano B, et al. Etanercept as adjunctive treatment for acute Kawasaki disease: study design and rationale. *Am Heart J* 2011;161:494-499.
158. Blaisdell LL, Hayman JA, Moran AM. Infliximab treatment for pediatric refractory Kawasaki disease. *Pediatr Cardiol* 2011;32:1023-1027.
159. Imagawa T, Mori M, Miyamae T, et al. Plasma exchange for refractory Kawasaki disease. *Eur J Pediatr* 2004;163:263-264.
160. Takagi N, Kihara M, Yamaguchi S, et al. Plasma exchange in Kawasaki disease. *Lancet* 1995;346:1307.
161. Villain E, Kachaner J, Sidi D, et al. Trial of prevention of coronary aneurysm in Kawasaki's disease using plasma exchange or infusion of immunoglobulins. *Arch Fr Pediatr* 1987;44:79-83.
162. Wallace CA, French JW, Kahn SJ, et al. Initial intravenous gammaglobulin treatment failure in Kawasaki disease. *Pediatrics* 2000;105:E78.
163. Kuijpers TW, Biezeveld M, Achterhuis A, et al. Longstanding obliterative panarteritis in Kawasaki disease: lack of cyclosporin A effect. *Pediatrics* 2003;112:986-992.
164. Sonobe T, Kataoka T, Tsuchiya K, et al. Intravenous thrombolysis using recombinant tissue plasminogen activator for intra-aneurysmal thrombi in Kawasaki disease. In: Takahashi M, Taubert K, eds. *Proceedings of the 4th International Symposium on Kawasaki Disease*. Dallas, TX: American Heart Association, 1993:363-366.
165. Tsuda E, Kitamura S. National survey of coronary artery bypass grafting for coronary stenosis caused by Kawasaki disease in Japan. *Circulation* 2004;110:II61-II66.
166. Tsuda E, Kitamura S, Kimura K, et al. Long-term patency of internal thoracic artery grafts for coronary artery stenosis due to Kawasaki disease: comparison of early with recent results in small children. *Am Heart J* 2007;153:995-1000.
167. Akagi T. Interventions in Kawasaki disease. *Pediatr Cardiol* 2005;26:206-212.
168. Ishii M, Ueno T, Akagi T, et al. Guidelines for catheter intervention in coronary artery lesion in Kawasaki disease. *Pediatr Int* 2001;43:558-562.
169. Muta H, Ishii M. Percutaneous coronary intervention versus coronary artery bypass grafting for stenotic lesions after Kawasaki disease. *J Pediatr* 2010;157:120-126.
170. Kitamura S, Tsuda E, Kobayashi J, et al. Twenty-five-year outcome of pediatric coronary artery bypass surgery for Kawasaki disease. *Circulation* 2009;120:60-68.
171. Ishii M, Ueno T, Ikeda H, et al. Sequential follow-up results of catheter intervention for coronary artery lesions after Kawasaki disease: quantitative coronary artery angiography and intravascular ultrasound imaging study. *Circulation* 2002;105:3004-3010.
172. Tsuda E, Hirata T, Matsuo O, et al. The 30-year outcome for patients after myocardial infarction due to coronary artery lesions caused by Kawasaki disease. *Pediatr Cardiol* 2011;32:176-182.
173. Newburger JW, Fulton DR. Coronary revascularization in patients with Kawasaki disease. *J Pediatr* 2010;157:8-10.

Rheumatic Fever and Rheumatic Heart Disease

Lloyd Y. Tani

Acute rheumatic fever (RF) occurs as a result of a complex interaction between group A streptococcus (GAS), a susceptible host, and the environment. An abnormal immune response to GAS infection leads to an acute inflammatory illness that most commonly affects the joints, brain, heart, and/or skin. Although the other manifestations are self-limiting and resolve without sequelae, carditis may result in chronic rheumatic heart disease (RHD) with associated significant morbidity and mortality. The degree of cardiac involvement is quite variable, ranging from mild, asymptomatic valvulitis to severe carditis with significant acute mitral and/or aortic regurgitation resulting in heart failure. The acute rheumatic cardiac involvement may resolve or persist and evolve into chronic rheumatic valvular disease, with cardiac symptoms developing years after the initial episode.

EPIDEMIOLOGY

Scope of the Problem

RF continues to be a major public health problem in developing countries, where it is the most common cause of acquired cardiac disease in children and young adults (1–7). Worldwide, it is estimated that at least 470,000 cases of RF occur annually in patients of all ages, with approximately 340,000 cases occurring in children 5 to 14 years of age. The majority of cases occur in developing countries and in indigenous populations, where the reported incidence is as high as 200 to 300 per 100,000 (4–6,8). Because of the difficulty in obtaining data in these regions and populations, it is possible that the true incidence in some areas is even higher; community-based surveillance suggests that the true incidence in some settings may be as high as 500/100,000 (9,10). In these regions, the current situation is similar to that experienced by developed countries in the early part of the 20th century.

In sharp contrast, there has been a significant decline in the incidence of RF and RHD over the last 50 years in most developed countries of the world (Fig. 60.1). The initial decline, which began prior to the initiation of penicillin, was at least partly due to improved socioeconomic conditions. With the subsequent initiation of penicillin, there was further acceleration in the rate of decline of RF (11,12). Changes in streptococcal strains and decreased virulence may have also contributed to the decline in RF seen in these countries (13). These changes have resulted in a marked decline in the mortality due to acute rheumatic carditis from 8% to 30% to nearly zero (11,12). In fact, the decrease in the incidence of RF in developed countries was so dramatic that the disease was thought to have “virtually disappeared” by the early 1980s (12).

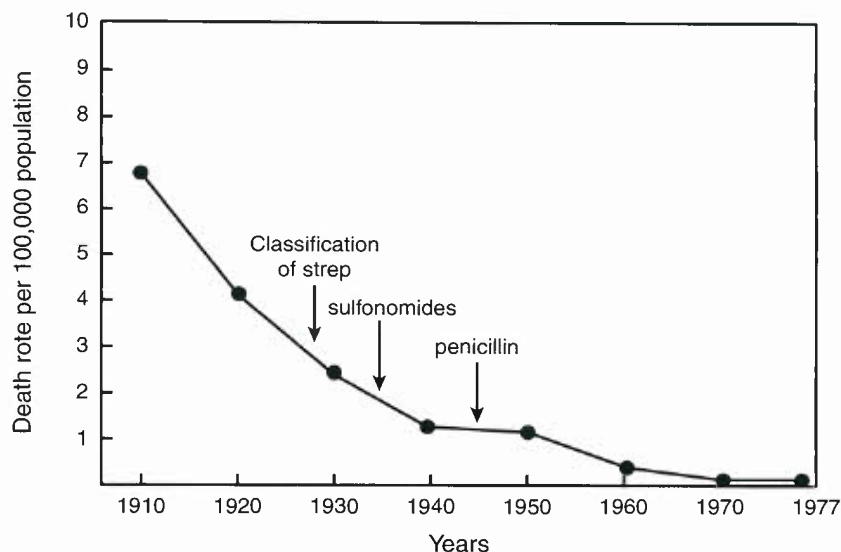
In the mid-1980s, several sites in the United States reported focal outbreaks or resurgences of RF activity (14–19), and by 1988, a survey of pediatric cardiologists revealed a 5 to

12 times increased incidence of RF in 24 states (20). Unique features of this resurgence included the following: (a) many cases came from suburban/rural neighborhoods; (b) the majority of patients were Caucasian and from middle-class families with medical insurance and ready access to medical care; (c) there was no clear-cut evidence of crowding; and (d) a preceding sore throat prompting the patient and family to seek medical attention was relatively uncommon. Although the reason(s) for these resurgences is unclear, the appearance of certain strains of GAS (in particular heavily encapsulated or mucoid strains) in the community coincident with the reported resurgence in Utah supports the concept of “rheumatogenicity” (21). Despite these resurgences, the incidence of RF in developed countries is much lower than in developing countries, and has been estimated at 0.5 to 3 per 100,000 population (7,12,22,23).

The prevalence of RHD parallels the reported incidences of RF. Both RF and RHD continue essentially unabated in many developing countries of the world, where RHD remains an important and significant cause of morbidity and mortality (Fig. 60.2). Worldwide, it is estimated that 15 to 20 million people have RHD (7), of whom about 2.4 million are children between the ages of 5 and 14 years (8). Given the current estimates of RF incidence and the proportion of patients who develop RHD, it is estimated that at least 282,000 people develop RHD each year (8). The prevalence of RHD varies greatly between countries, ranging from <0.5/1,000 in developed countries of the world (8) to 78/1,000 in Samoa (24), and increases with age, peaking in young adults aged 25 to 34 years (10). The older prevalence data based on clinically detected RHD may significantly underestimate the true disease burden. Recent studies using echocardiography reported prevalences on the order of 10-fold greater than that detected clinically, suggesting that approximately 90% of RHD cases are subclinical (25).

Compared to cases occurring in industrialized countries, the initial episode of RF in developing countries occurs at a younger age, and often goes unnoticed. In these settings, it has been estimated that as many as 50% or more of patients are unaware of their disease and as many as 70% do not receive secondary prophylaxis (6). Compared to the natural history in developed countries, chronic RHD in developing countries occurs earlier, evolves more rapidly, is of greater severity, and more commonly leads to heart failure with its associated morbidity and mortality (2,26–31). Once significant RHD has developed, the methods for providing care to such patients are also limited in many of these developing countries. In 1994, it was estimated that at least 3 million people with RHD required repeated hospitalization for heart failure (6). In developing countries, 12% to 65% of all cardiac admissions are for RHD, with an average length of stay of 3 to 4 weeks, resulting in absence from work and reduced productivity (2,32). In 2001, an estimated 6.6 million disability-adjusted life years were lost to RHD. The mortality rate from RHD has been

Figure 60.1. Crude death rates from RF, United States, 1910 to 1977. (From Gordis L. The virtual disappearance of rheumatic fever in the United States: Lessons in the rise and fall of disease. T. Duckett Jones memorial lecture. *Circulation* 1985;72:1155–1162, with permission.)



estimated to range from 0.9 to 8.0 per 100,000 population (6,7,33,34). Based on conservative estimates, a minimum of 1.5% of patients with RHD die each year in developing countries where secondary prophylaxis is uncommonly given and medical and surgical treatments are often unavailable. Worldwide, it has been estimated that 233,000 to 492,000 deaths per year occur due to RHD, with 95% of the mortality occurring in developing countries (8). Further, patients with RHD are at increased risk for endocarditis and stroke, and complications associated with additional morbidity and mortality (8,31). In contrast, an analysis of more than 2.5 million hospital discharges in 2000 from 2,784 institutions in 27 states in the United States reported only 503 hospitalizations for RF among children <21 years (35).

Environment

Despite the epidemiologic link between GAS pharyngitis and RF, other factors clearly influence the incidence of RF. Current data suggest that the incidence of GAS pharyngitis has remained more or less stable in most countries, and that there has been no change in host resistance to the GAS organism. Therefore, the marked differences in the incidence of RF and prevalence of RHD in developing versus developed countries are likely due to other factors. The importance of environmental and socioeconomic factors in the epidemiology and pathogenesis of RF has been recognized for decades. In developing countries, overcrowding, poverty, poor nutrition, poor hygiene, and poor access to health care are common and



Figure 60.2. Prevalence of RHD in children aged 5 to 14 years. (Reprinted from Carapetis JR, Steer AC, Mulholland EK, et al. The global burden of group A streptococcal diseases. *Lancet Infect Disease* 2005;5:685–694, with permission from Elsevier.)

contribute to rapid spread (respiratory droplets) and increased virulence of GAS (36,37). In particular, overcrowding appears to be a major factor contributing to the high incidence of RF in many parts of the world. With poor access to health care, GAS pharyngitis is less likely to be diagnosed and treated, precluding effective primary prevention of RF. In addition, because cases of RF are more likely to go unnoticed, secondary prophylaxis is not implemented and RF recurrences are common.

The seasonal variation of RF in the temperate climates parallels that of GAS pharyngitis. Both GAS pharyngitis and RF are more common during the winter and spring in temperate climates, but there is no consistent seasonal pattern in the tropics. Geographically, RF occurs in all latitudes and altitudes (36).

Host

Children between the ages of 5 and 15 years are most commonly affected. RF is uncommon before age 5 years, almost never occurs before 2 years of age, and is uncommon beyond the age of 35 years (4). Children with RF before age 5 years commonly present with arthritis and rarely present with chorea; when present, cardiac involvement is more severe than in older children and persistent RHD is common (38,39). Adults with a primary episode of RF are much more likely to have joint manifestations than cardiac involvement (40). Recurrences are most frequent during adolescence and early adulthood. With the exception that chorea is more common in girls, there is no definite gender predisposition (41–44).

There is evidence supporting the importance of a host predisposition to developing RF. First, only a small minority of patients with streptococcal pharyngitis develops RF, even during streptococcal epidemics (~3%). Second, the incidence of recurrent RF in patients with a previous history of RF with cardiac involvement is as high as 50% following GAS pharyngitis (45–47). Third, studies indicate a familial predilection (48,49) and a higher concordance rate between identical twins than in fraternal twins (18.7% vs. 2.5%) (50,51). Higher rates of RF and RHD have also been reported in certain ethnic groups, specifically Maoris and Pacific Islanders in New Zealand, Samoans in Samoa and Hawaii, and Aboriginal people in Australia (50,52–54). (See section on “Susceptible Host” in the “Pathogenesis” section below.)

Streptococcal Infection

Most children have at least one episode of pharyngitis per year, approximately 10% to 30% of which are due to GAS, the most common bacterial cause of pharyngitis (55,56). Streptococcal pharyngitis occurs most commonly in children aged 5 to 15 years, and is uncommon before age of 2 years. Although GAS may be present in the pharynx with either true infection and pharyngitis or a carrier state, only true infection results in an immune response and risk for the development of RF (57). The prevalence of GAS carrier state varies considerably (5% to 30%), depending on the population and series (58,59). Approximately 0.3% (during nonepidemic) to 3.0% to 5.0% (during streptococcal epidemics) of individuals who have not had RF will develop the illness following an untreated symptomatic or asymptomatic streptococcal pharyngitis. Older studies reported a relationship between the clinical severity of the pharyngitis and likelihood of developing RF, but recent reports emphasize that RF occurs following very mild or asymptomatic pharyngitis in up to two-thirds of cases (14,60).

The strain and virulence of the streptococcal organism influence the likelihood of development of RF. In the 1930s, GAS strains that reactivated RF were noted to be different from strains that did not (61). Other investigators subsequently

found that some strains were associated with pharyngitis, while other strains were associated with skin infections (62). Further, certain GAS strains have been associated with RF, while others have been associated with poststreptococcal glomerulonephritis (63). Based on epidemiologic data, certain GAS strains are more likely to lead to RF (“rheumatogenic”) than others (“nonrheumatogenic”) (41,62,64). The M protein is thought to be a major virulence factor because it affects the ability of host cells to undergo phagocytosis. Of the greater than 130 M types, M types 1, 3, 5, 6, 14, 18, 19, 24, 27, and 29 have been associated with outbreaks of RF, while M types 2, 4, 12, 22, and 28 rarely lead to RF (7,13,65,66). Further evidence of the importance of the M protein came from the discovery that epitopes of the M protein molecule cross-react antigenically with human heart and brain tissue. Recent reports have also emphasized the association between the appearance of heavily encapsulated (“mucoid”) strains in a community and an increase in the number of RF cases (21,67–71). Finally, there is evidence that the decrease in the incidence of RF in developed countries is in part due to a change in GAS strains (altered expression of M protein) and a decrease in the incidence of GAS pharyngitis caused by rheumatogenic strains (13).

Despite the evidence for GAS pharyngitis but not impetigo as the initiating event leading to RF, there is some recent epidemiologic evidence to suggest that skin strains may play a role in some populations. In the Aboriginal population of Australia where RF is endemic, GAS impetigo is common but GAS pharyngitis is uncommon. Although direct causation, immune priming, and movement of strains from the skin to the pharynx have been postulated, the precise role of GAS skin infections in the pathogenesis of RF remains to be elucidated (72–74).

PATHOGENESIS

Organism

RF occurs as a result of a complex interaction between the GAS organism, host, and environment. Although the relationship to a preceding streptococcal pharyngitis is established and well accepted, the pathogenesis of RF is still not completely understood. Initially thought to occur as a result of direct injury by the GAS or its toxins, the organism has not been isolated from the organ systems of affected individuals. Current evidence strongly suggests that RF occurs as a delayed autoimmune response to pharyngitis caused by a rheumatogenic strain of GAS in a susceptible individual. Streptococcal antigenic components mimic normal human tissue antigens, leading to abnormal autoimmune humoral and cellular responses (molecular mimicry). Several lines of evidence lead to and support the concept of RF occurring after GAS pharyngitis: (a) documented relationship between GAS pharyngitis epidemics and RF (11,36), (b) immunologic evidence of a preceding streptococcal infection via elevated/rising antibody titers (75), (c) adequate treatment of GAS pharyngitis preventing the RF (76,77), (d) antibiotic prophylaxis preventing RF recurrences (78–80), and (e) mass prophylaxis with penicillin-terminated RF epidemics in military and civilian populations (81–83).

Susceptible Host

Most of the clinical manifestations of RF occur approximately 10 days to 5 weeks (average 18 days) following GAS pharyngitis in a susceptible host (84). A number of sources support the importance of host susceptibility in the pathogenesis of RF (see “Epidemiology” section above), and studies suggest that the abnormal immune response to GAS infection is genetically

controlled. The major contributors to the autoimmune reaction in RF/RHD are the major histocompatibility complex HLA class II alleles (DR, DQ) located on human chromosome 6. Several HLA class II alleles have been associated with a greater likelihood of development of RF/RHD in different countries. Expressed on the surface of cells that present antigens, these HLA molecules are thought to participate in the development of both the humoral and cell-mediated responses to certain streptococcal antigens. It is thought that HLA molecules might be involved with inappropriate activation of T cells that have the ability to cross-react with streptococcal and self-antigens that have some similarities (molecular mimicry) (85–90).

Several studies have shown a difference in the expression of a specific B-cell alloantigen detected by monoclonal antibody (D8/17) between patients with RF/RHD and control patients. In most of these studies, D8/17 is expressed in >85% of RF patients, but <15% of controls. Furthermore, D8/17 expression has also been found to be higher in first-degree relatives of RF patients than in controls. A few studies have failed to confirm this association, possibly related to population differences. At present, the role of B-cell expression of this alloantigen in the immune response to GAS remains unclear, and there is no correlation between expression and clinical outcome (91–94). Clearly, this is an area that requires more study.

Other components of the immune response are being evaluated. There is some evidence for polymorphisms in the gene for tumor necrosis factor alpha (TNF- α) and RHD. Among individuals who have had RF, there is some evidence for genetic differences between those who develop rheumatic valvular disease and those who have had RF without associated RHD (e.g., angiotensin-converting enzyme polymorphisms) (95–97).

Immunopathogenesis

Although our understanding of the pathogenesis of RF and RHD is incomplete, the importance of the host immune response to a preceding GAS infection is clear. Current evidence supports the following:

- GAS pharyngitis in a genetically susceptible host leads to breakdown products and streptococcal antigens that are cross-reactive with heart proteins (molecular mimicry) (98,99).
- The immune response that occurs in response to the infection leads to cross-reactive antibodies and cytokine production (100,101).
- The antibodies bind to the endothelial valve surface resulting in injury, cellular infiltration of inflammatory cells, and upregulation of vascular cell adhesion molecule 1 (VCAM-1), which aids in the recruitment and infiltration of T cells and macrophages, leading to further inflammation and damage (102).
- Endothelial injury exposes subendothelial structures and proteins including vimentin (found in cardiac fibroblasts) and laminin (extracellular matrix protein present in the basement membrane of valves and around endothelium).
- Inflammation leads to neovascularization, allowing further recruitment of T cells, leading to granulomatous inflammation and many of the changes seen with chronic RHD.
- Cellular infiltration contributes to the formation of Aschoff bodies.
- Activated B lymphocytes and macrophages from Aschoff bodies express large amounts of HLA class II molecules on their surfaces and may play an important role in antigen presentation to T cells that have been recognized as important effectors of chronic rheumatic valvular disease (89).
- Infiltrating T cells are cross-reactive with streptococcal M protein and cardiac myosin and laminin (molecular mimicry); CD4+ T cells have been recognized as major effectors of this process leading to chronic RHD (103–106).

- Inflammatory cytokines (increased amounts of TNF- α and interferon gamma along with decreased amounts of interleukin-4) appear to be important in persistence and progression of rheumatic valvular lesions in a susceptible host.
- Through a process called epitope spreading, T cells may respond to other cardiac alpha-helical proteins, including tropomyosin and vimentin (89,90,107–109) (Fig. 60.3).

Natural History

The prognosis and natural history of rheumatic carditis and RHD are strongly influenced by both the severity of the initial carditis and RF recurrences (110–114). Mild carditis without recurrences is much more likely to show resolution than severe initial carditis and/or cases with recurrent episodes of RF. Only 30% to 40% of patients with acute mitral regurgitation have a persistent murmur at follow-up, with most of the clinical improvement occurring in the first 6 months after the acute illness. Patients with more severe carditis (heart failure and/or cardiomegaly) are more likely to have persistent RHD, and aortic regurgitation is less likely to disappear than mitral regurgitation (115–117). The proportion of patients with RF who develop chronic RHD has decreased from 60% to 90% during the prepenicillin era to 35% to 65% (110–112,118,119). Age and gender also influence prognosis, as acute rheumatic cardiac involvement resolves more frequently in boys (111,112), and children presenting with RF before age 5 years have more severe cardiac involvement and more commonly have persistent chronic RHD (38,39).

PATHOLOGY

The pathologic changes that occur with RF are characterized by inflammation of connective tissue in the heart, joints, and subcutaneous tissues. The pathologic changes in rheumatic carditis are primarily perivascular and interstitial, without evidence of myocyte necrosis. Two phases have been described. The “exudative” phase occurs in the first 2 to 3 weeks after disease onset and is characterized by interstitial edema, cellular infiltration (T cells, B cells, and macrophages), fragmentation of collagen, and scattered deposition of fibrinoid (eosinophilic granular material). During the second “proliferative” or “granulomatous” phase, which lasts for months to years (120), the Aschoff nodule, considered pathognomonic for, and the morphologic hallmark of, RHD may be found in the endocardium, subendocardium, or myocardial interstitium (121). The Aschoff nodule is a perivascular aggregation characterized by a central area of fibrinoid change (altered collagen) surrounded by or infiltrated by large multinucleated (“owl eye”) cells. These Aschoff bodies, which are not seen in the hearts of patients dying within the first week after onset of RF, may be seen years after initial illness and do not correlate with disease activity (120,122). Cells in Aschoff bodies located underneath activated valvular endothelium appear to play an important role in antigen presentation to infiltrating T cells, which have been recognized as critical in the evolution of chronic RHD (89) (see “Immunopathogenesis” above).

Pericarditis

Grossly, the pericardial surface may have a white, fibrinous, stringy to shaggy exudate; all cases show lymphocytic and mononuclear infiltration of the pericardium. Aschoff nodules may be present in pericardium. Pericarditis heals with no significant adhesions, and constrictive pericarditis rarely occurs.

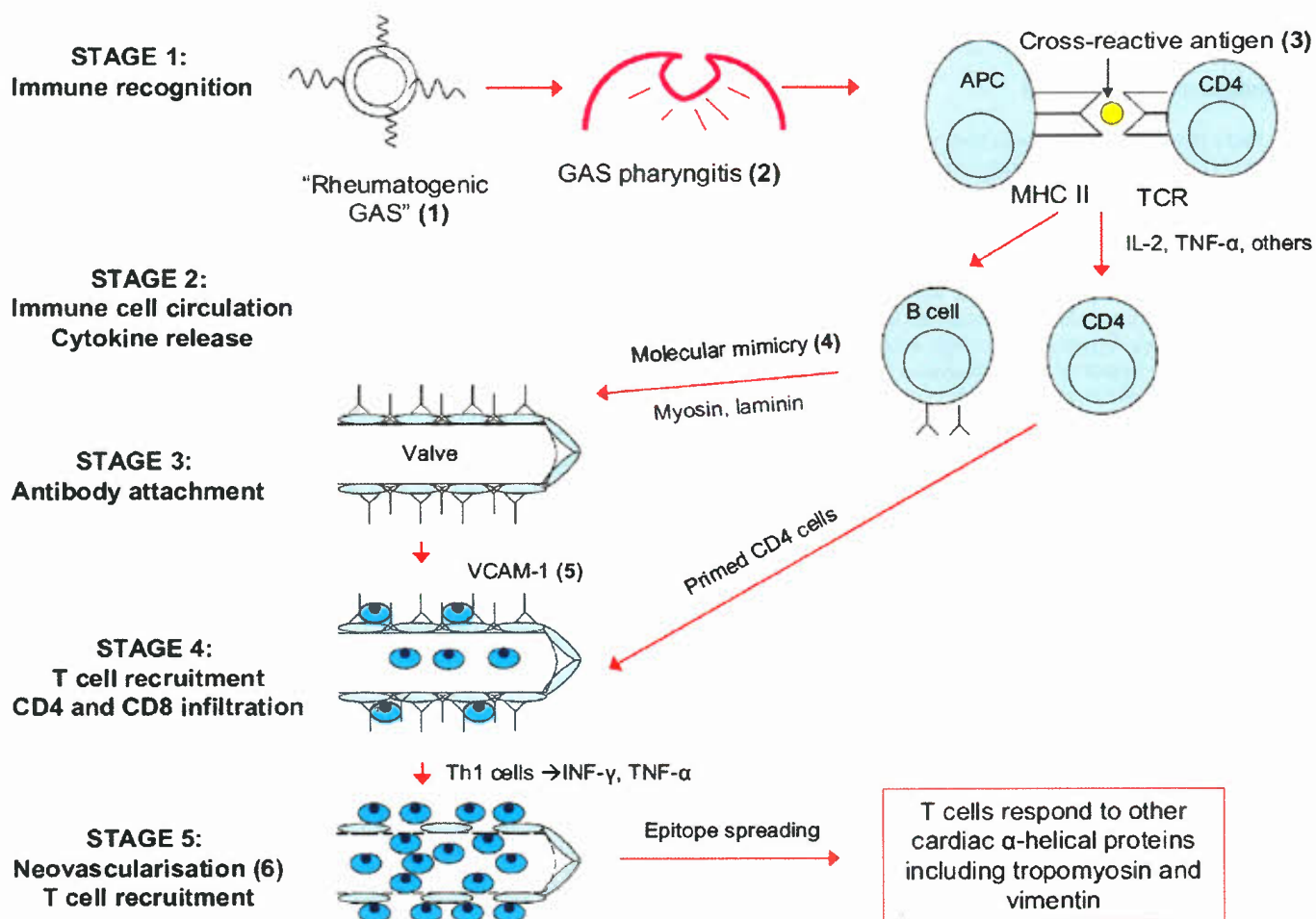


Figure 60.3. Immunopathogenesis of RF and RHD. (1) and (2) Rheumatogenic group A streptococcal (GAS) pharyngitis. (3) Cross-reactive antigen on GAS. (4) Molecular mimicry between GAS antigens and human host tissue is believed to be the basis of pathogen–host cross-reactivity, best documented with α -helical cardiac proteins such as myosin, laminin, and vimentin. (5) Vascular cell adhesion molecule 1 (VCAM-1) is upregulated at the valve and aids in recruitment and infiltration of T cells. (6) Inflammation leads to neovascularization, which allows further recruitment of T cells, leading to granulomatous inflammation and the establishment of chronic RHD. (Adapted from Steer AC and Carapetis JR. Acute Rheumatic Fever and Rheumatic Heart Disease in Indigenous Populations. *Pediatr Clin N Am* 2009;56:1401–1419, with permission from Elsevier.)

Myocarditis

The ventricles and atria are often enlarged in RHD. Histologically, the myocardium may be edematous and show non-specific inflammation. However, different from other forms of myocarditis, there is usually no evidence of cell damage. Inflammatory foci consist of lymphocytes, macrophages, and other inflammatory cells. Aschoff bodies may also be seen in locations of the myocardial interstitium. Despite frequent first-degree atrioventricular (AV) block on the ECG, the conduction system shows few pathologic changes (123,124).

Endocarditis

Endocardial inflammatory changes are responsible for the valvulitis and are therefore the most clinically significant. Small, 1 to 2 mm, friable, fibrinous, verrucous vegetations may occur on the atrial surface of the mitral valve or on the ventricular side of the aortic valve at sites of valve closure (125). Associated underlying inflammation consists of histiocytes and lymphocytes.

The mitral valve leaflets may be edematous and vascularized. With time, granulation tissue may occur, with

thickening and eventually fibrosis of the valve. Similarly, chordal inflammation may be followed by granulation tissue, fibrosis, and eventually chordal fusion. These changes may result in the mitral stenosis and regurgitation seen with chronic RHD.

Macroscopically, acute rheumatic mitral valvulitis results in chordal elongation (or even rupture) with prolapse of the anterior leaflet of the mitral valve, annular dilation, altered leaflet coaptation, and mitral regurgitation (126,127). This altered coaptation most commonly results in a posterolaterally directed jet of mitral regurgitation, directed toward an area of fibrotic thickening of the posterior left atrial wall called "McCallum's patch." Aortic valve prolapse has been proposed as one of the mechanisms contributing to acute rheumatic aortic regurgitation (128).

Vasculitis

Generalized vasculitis, in particular involving the coronary arteries and the aorta, has been described (129). It resembles changes of hypersensitivity angiitis, but rarely results in tissue damage or clinical manifestations.

CLINICAL MANIFESTATIONS

Diagnosis and Evaluation

Since there is no pathognomonic test, the diagnosis of an initial episode of RF is made using the modified Jones or other diagnostic criteria. First proposed by T. Duckett Jones (130) in 1944, these criteria have undergone four revisions or modifications, the last in 1992 (131–135). Revisions and modifications have increased the specificity but decreased the sensitivity of the criteria to avoid overdiagnosis. Although this makes sense in developed countries where RF is now relatively uncommon, strict adherence to the Updated Jones Criteria in settings where RF continues to be common may result in underdiagnosis (136–138). The latest Updated Jones Criteria (Table 60.1) are intended to be used to establish the initial attack of acute RF. The diagnosis of RF requires two major or one major and two minor Jones criteria along with evidence of a preceding streptococcal infection. The major criteria are polyarthritides, carditis, chorea, a characteristic rash called erythema marginatum, and subcutaneous nodules. The frequency of major manifestations from several published series of RF cases is shown in Table 60.2. The minor criteria are fever, arthralgia, elevated acute phase reactants, and a prolonged PR interval on the electrocardiogram. Table 60.3 lists suggested testing for patients with suspected RF. Evidence of a preceding GAS infection is discussed below in the section on *Laboratory*

Testing. The latest Update allows the diagnosis of RF to be made without fulfilling the above criteria in three circumstances: (a) patients who present with isolated chorea, (b) patients who present with indolent or insidious onset carditis (detected months to years after the acute illness), or (c) patients with a prior history of RF/RHD (133). While the Jones criteria may be used to diagnose a recurrent episode of RF in patients without RHD, diagnosing a recurrence may be difficult in the patient with existing RHD. In such cases, it is often difficult to differentiate acute carditis from progression and evolution of existing RHD. Such a distinction is important for at least two reasons: (a) cardiac changes related to an acute recurrence are likely to evolve over a shorter time period than chronic RHD and (b) some believe that steroids may be beneficial and even lifesaving in patients with severe, active carditis. On the other hand, steroids are of no therapeutic value in patients with chronic rheumatic valvular disease, and might delay more appropriate treatment. To address the diagnostic difficulty of this important group of patients, the World Health Organization has published guidelines for the diagnosis of recurrences: (a) a recurrent attack of RF in a patient without RHD requires fulfillment of the Jones criteria (two major or one major with two minor criteria, plus evidence of a preceding streptococcal infection) and (b) a recurrent attack of RF in a patient with underlying RHD requires two minor criteria and evidence of a preceding streptococcal infection (7) (Table 60.1).

TABLE 60.1 Diagnostic Criteria for Rheumatic Fever

Major Criteria	Minor Criteria
Carditis	Fever
Chorea	Arthralgia
Polyarthritides	Elevated acute-phase reactants
Erythema marginatum	Erythrocyte sedimentation rate
Subcutaneous nodules	C-reactive protein
	Prolonged PR interval (ECG)
Supporting evidence of antecedent group A streptococcal pharyngeal infection	
Positive throat culture or rapid streptococcal test	
Elevated or rising streptococcal antibody titer	
Criteria for diagnosis of:	
Primary episode of RF	Two major <i>or</i> one major plus two minor <i>plus</i> evidence of preceding streptococcal infection
RF recurrence in a patient	Two major <i>or</i> one major plus two minor <i>plus</i> evidence of preceding streptococcal infection
RF recurrence in a patient with RHD	Two minor <i>plus</i> evidence of preceding streptococcal infection
Special considerations	
Chorea or indolent/insidious onset carditis	No other criteria or evidence of preceding streptococcal infection needed
Modifications of diagnostic criteria (especially applicable where RF or RHD continues to be common)	- In order to improve sensitivity of criteria where there is concern for underdiagnosis
- Monoarthritides or polyarthralgia as a major criterion	- Especially when patient has received anti-inflammatory treatment
- Subclinical carditis as a major criterion	- Criteria for differentiating physiologic from pathologic valvular regurgitation

RF, rheumatic fever; RHD, rheumatic heart disease.

Based on references: Rheumatic fever and rheumatic heart disease. *World Health Organ Tech Rep Ser* 2004;923:1–122; Carapetis JR, Brown A, Wilson NJ, et al. An Australian guideline for rheumatic fever and rheumatic heart disease: an abridged outline. *Med J Aust* 2007;186:581–586; Atatoa-Carr P, Lennon D, Wilson N. Rheumatic fever diagnosis, management, and secondary prevention: a New Zealand guideline. *N Z Med J* 2008;121:59–69; Guidelines for the diagnosis of rheumatic fever. Jones Criteria, 1992 update. Special Writing Group of the Committee on Rheumatic Fever, Endocarditis, and Kawasaki Disease of the Council on Cardiovascular Disease in the Young of the American Heart Association. *JAMA* 1992;268:2069–2073. Ref. (139).

TABLE 60.2 Major Manifestations of Rheumatic Fever

Series (reference)	Location	Years	No. of RF cases	Carditis (%)	Arthritis (%)	Chorea (%)	Erythema Marginatum (%)	SQ Nodules (%)	Carditis with CHF (%)	Recurrences Included in Series (%)
Bland et al. (110)	Boston	1921–1931	1,000	65	41	52	7.1 (rash)	8.8	32	NS
Feinstein and Spagnuola (44)	New York	1958–1960	275	42	76	4	4	1.1	14	No
Giannoulia-Karantana et al. (140)	Greece	1980–1997	66	70	68	4.5	1.5	0	15	No
Sanyal et al. (141)	N. India	1967–1971	102	33	67	21	2	2	35	No
Ravisha et al. (142)	India	1971–2001	250	42	68	19	1.6	1.2	12	No
Veasy et al. (60)	Utah	1985–1992	274	68	36	37	4	2.6	19	10
Bitar et al. (143)	Lebanon	1980–1995	91	93	38	2	4.4	1	44	45
Arora et al. (144)	New Delhi	1968–1977	450	42	30	3	0.2	6	NS	NS
Chagani and Aziz (145)	Pakistan	1991–1994	57	61	61	16	3.5	7	5	No
Chockalingam et al. (146)	India	1992–2002	163	67	72	8	0	6.1	50	NS
Griffiths and Gersony (147)	New York	1969–1988	115	51	69	4.3	1.7	0	29	10
Khriesat et al. (148)	Jordan	1999–2002	50	48	88	6	0	0	4	NS
Carapetis and Currie (136)	Australia	1976–1996	555	55	55	28	0.5	0.5	20	39
Steer et al. (149)	Fiji	2005–2007	33	79	52	15	3	0	12	39
Cann et al. (150)	Australia (North Queensland)	1997–2007	98	47	38	16	1	1	NS	32

RF, rheumatic fever; SQ, subcutaneous; CHF, congestive heart failure; NS, not stated.

TABLE 60.3 Testing for Patients with Suspected Rheumatic Fever

- White blood cell count, erythrocyte sedimentation rate, C-reactive protein
- Electrocardiogram
- Chest radiograph (if clinical carditis)
- Echocardiogram
- Throat culture
- Antistreptococcal serology
- Consider blood culture

Modifications of the Jones diagnostic criteria have been published in parts of the world where the incidence of RF and prevalence of RHD remain high (Australia and New Zealand) (151,152). These modifications include (a) accepting monoarthritis or polyarthralgia as a major criterion, especially in cases where the patient has received anti-inflammatory treatment; (b) accepting echocardiographic detection of cardiac involvement (carditis) as a major diagnostic criterion, even in the absence of clinical carditis (see discussion of role of echocardiography below); (c) allowing for diagnosis of recurrent RF based on minor manifestations, especially in patients with RHD. The intent of these modifications is to improve the sensitivity of the diagnostic criteria in populations where RF and RHD are common and there is greater concern for underdiagnosis with its associated consequences. These modifications are presented in Table 60.1.

Arthritis

The latency period between GAS infection and most manifestations of RF ranges from 10 days to 5 weeks (latency between GAS infection and chorea is 1 to 6 months) (84). Of the major Jones criteria, migratory polyarthritis is most common, affecting 40% to 70% of cases (Table 60.2). The arthritis of RF classically migrates from large joint to large joint, and most commonly affects the knees, ankles, elbows, and wrists. Importantly, the presentation and evolution of the joint manifestations may be affected by administration of anti-inflammatory medications (aspirin or other nonsteroidal anti-inflammatory agents). It is noteworthy that in some parts of the world, monoarticular arthritis is a common mode of presentation (136,153). The joints affected with RF are red, swollen, and extremely tender, often with pain out of proportion to the objective findings. In some cases, the joints may be involved sequentially and simultaneously rather than in a migratory pattern, with a new joint becoming involved while a different joint is at a different phase of inflammation and resolution. Even untreated, the arthritis of RF usually resolves within 3 to 4 weeks and is not associated with residual abnormalities. Although carditis and arthritis commonly occur together, the severity of the joint and heart involvement tend to be inversely related (112). The reasons for this inverse relationship are unclear; some have speculated that joint involvement leads to earlier medical attention and initiation of anti-inflammatory treatment, thus preventing more severe cardiac involvement. Because of the different latency periods between the preceding streptococcal pharyngitis and the onset of symptoms, polyarthritis and chorea uncommonly occur simultaneously (154). The arthritis of RF typically responds to aspirin within 48 to 72 hours. In

fact, lack of clinical response and improvement within 2 to 3 days should prompt consideration of alternative diagnoses (155). It is worth noting that a small subset of patients relapses once or twice after a 6-week course of antirheumatic therapy (156,157). Unfortunately, although arthritis is the most common major manifestation of RF, it is also the least specific, and is therefore the *most common feature associated with misdiagnosis*. The Jones criteria often fail to exclude other causes of febrile polyarthritis (42), and an alternative diagnosis may be made only as more chronic findings develop (i.e., collagen vascular disease). The differential diagnosis for polyarthritis and fever is presented in Table 60.4 (158).

TABLE 60.4 Causes of Polyarthritis and Fever

Diagnoses	Confirmatory Study
Infectious arthritis	
Bacterial infections	
Septic arthritis	Synovial fluid and blood culture
Bacterial endocarditis	Blood culture
Lyme disease	Serologic studies
Mycobacterial and fungal arthritis	Culture or biopsy
Viral arthritis	Serologic studies
Postinfectious or reactive arthritis	
Enteric infection	Culture or serologic studies
Urogenital infection (Reiter syndrome)	Culture
Rheumatic fever	Clinical findings
Inflammatory bowel disease	Clinical findings
Rheumatoid arthritis and Still disease	Clinical findings
Systemic rheumatic illnesses	
Systemic vasculitis	Biopsy or angiography
Systemic lupus erythematosus	Serologic studies
Crystal-induced arthritis	
Gout and pseudogout	Polarizing microscopy of synovial fluid or tophus
Other diseases	
Familial Mediterranean fever	Clinical findings
Cancers	Biopsy
Sarcoidosis	Biopsy
Mucocutaneous disorders	Biopsy or clinical findings
Dermatomyositis	
Behçet disease	
Henoch-Schönlein purpura	
Kawasaki disease	
Erythema nodosum	
Erythema multiforme	
Pyoderma gangrenosum	
Pustular psoriasis	

From Pinals RS. Polyarthritis and fever. *N Engl J Med* 1994;330: 769–774. Copyright © 1994 Massachusetts Medical Society. Reprinted with permission from Massachusetts Medical Society.

Some patients develop arthritis after a streptococcal pharyngitis that differs from that typically associated with acute RF. This entity, termed *poststreptococcal reactive arthritis*, typically occurs after a shorter latent period (7 to 10 days), tends to be nonmigratory and more persistent, involves small joints or axial skeleton in some cases, and does not respond as dramatically to anti-inflammatory medications as does the typical arthritis of RF (159,160). The important implication of diagnosing poststreptococcal reactive arthritis as opposed to RF is the risk for subsequent valvular heart disease and need for antistreptococcal prophylaxis. Of particular importance is the fact that some patients thought to have poststreptococcal reactive arthritis have shown evidence of cardiac involvement (159–162). Conversely, a recent study showed no increased risk of valvular heart disease in a series of adults with poststreptococcal reactive arthritis (163). Given the uncertainty with respect to the risk of valvular heart disease for children with poststreptococcal reactive arthritis, some experts recommend that such patients receive secondary prophylaxis for up to a year after onset, but this is clearly an area of debate requiring further study. If valvular heart disease is detected, such patients should be considered as having had RF and should be treated accordingly (including secondary prophylaxis) (160,161,163–166).

Chorea

First described in the late 17th century, the association of chorea and rheumatism was not recognized until the 19th century. It is now known that the clinical manifestations of Sydenham chorea occur due to neuropathologic changes and inflammation in the basal ganglia, cerebral cortex, and the cerebellum (42,167).

Sydenham chorea occurs in approximately 10% to 30% of cases of RF (Table 60.2). The gender distribution is equal in younger children, but after age 10 years, females are more often affected, and chorea is uncommon in postpubertal males (42). Involuntary, purposeless movements, muscular incoordination and/or weakness, and emotional lability (42,43,168,169) characterize Sydenham chorea. Movements are abrupt and erratic, commonly affecting muscles of the face and extremities. Findings may include “fidgetiness,” facial grimaces, tongue movements described as resembling a “bag of worms,” halting and explosive speech, pronation of the hands when arms are extended above the head (“pronator sign”), irregular contractions of the hands when asked to squeeze an object (“milkmaid’s grip”), hyperextension of the fingers when hands are extended forward with eyes closed, (“spooning”), and clumsiness. Patients often come to attention based on deterioration in school performance, and neurobehavioral symptoms seen along with the chorea including irritability, poor attention span, lack of cooperation, and obsessive-compulsive symptoms are not uncommon. Sensory deficits do not occur. The neurologic manifestations are usually bilateral, but may be unilateral (hemichorea). The neurologic symptoms tend to decrease with rest and sedation and increase with effort or excitement. The duration of chorea is variable, ranging from 1 to 2 weeks to 2 to 3 years. The median duration is about 15 weeks, and 75% show resolution of symptoms by 6 months (7,152,170). Recurrent episodes of chorea are not uncommon (171). The differential diagnosis of chorea is presented in Table 60.5 (172).

The latency period between the streptococcal pharyngitis and the onset of chorea is longer than for arthritis or carditis, ranging from 1 to 6 months (42,173,174). As previously stated, because of this longer latency period, arthritis and chorea uncommonly occur simultaneously. Also related to the longer latency period for patients presenting with chorea,

acute phase reactants are often normal and antistreptococcal antibodies may not be elevated. When carditis and chorea are found in the same patient, it is often the chorea that prompts medical attention, at which time rheumatic cardiac involvement is detected. Although the combination of chorea and carditis is common, occurring in 47% of patients with RF in a recent series (60), the cardiac involvement tends to be relatively mild and heart failure is uncommon (44). However, rheumatic cardiac involvement in these patients may evolve and progress over time, with some patients presenting with chronic RHD years after the RF illness. Even patients with “pure” chorea are at risk, however, as 20% to 44% of such patients go on to develop chronic RHD that may eventually result in heart failure (110,154,168,175).

Neuroimaging (MRI or CT) abnormalities have been reported in some patients with Sydenham chorea (176). However, reported findings have been variable, and many patients have had normal imaging studies. Thus, neuroimaging should be reserved for atypical cases to exclude other causes of chorea. Similarly, although abnormalities have been described (177), EEG testing should be reserved for atypical cases.

In 1998, Swedo and colleagues proposed that, in some patients, childhood obsessive-compulsive symptoms and tics occur as a result of an autoimmune response to a preceding streptococcal infection, terming the entity PANDAS (pediatric autoimmune neuropsychiatric disorders associated with streptococcal infections) (178,179). Because the proposed mechanism of autoimmunity related to cross-reactivity between streptococcal antigens and brain tissue is similar to the mechanism invoked for Sydenham chorea, it has been suggested that secondary prophylaxis might prevent recurrent neurologic symptoms (180,181). In some patients, it can be difficult to differentiate choreiform movements from tics (168,172). Differentiating PANDAS from Sydenham chorea is important since the treatments and prognoses are different, in particular related to the risk of chronic RHD. Patients with PANDAS may respond to plasmapheresis or intravenous gamma globulin (182). Other manifestations of RF (including carditis and RHD) have not been reported in patients with PANDAS (179). At present, there continues to be considerable debate regarding the association of streptococcal infection and neuropsychiatric disorders (PANDAS), and some consider the entity as a yet-unproven hypothesis (165,183,184).

Carditis

The manifestation of RF associated with long-term morbidity and mortality is carditis, which occurs in 30% to 70% of cases (Table 60.2). Rheumatic carditis remains the most common cause of acquired heart disease in children and young adolescents in developing countries. Despite traditionally being described as a pancarditis, the dominant and most important abnormality with acute rheumatic cardiac involvement is the *valvulitis*, specifically mitral and/or aortic regurgitation. The clinical presentation may be quite variable, ranging from the asymptomatic patient with a characteristic heart murmur to the critically ill patient presenting in heart failure. Severe carditis and heart failure occur in 13% to 64% of RF cases and represent 15% to 50% of patients with carditis (Table 60.2) (60,110,112,136,140–148). Some of the variability is likely related to the fact that some patients present only after more than one episode of RF and carditis, a scenario much more likely to be associated with significant valvular disease and heart failure. Approximately 80% of patients who develop carditis do so within the first 2 weeks of the RF illness; if no cardiac involvement is detected in the first 2 weeks, the likelihood of subsequent cardiac involvement during the acute phase is low (185). The severity of carditis and valvular regurgitation

TABLE 60.5 Differential Diagnoses of Chorea

Category	Diagnoses and Causes
Drug-related	Anticonvulsants (phenytoin, carbamazepine) Anticholinergics CNS stimulants (amphetamines) Dopamine agonists (Levodopa) Oral contraceptives
Genetic/Hereditary	Huntington disease Wilson disease Lesch-Nyhan syndrome Benign familial chorea Ataxia telangiectasia Neuroacanthocytosis Familial paroxysmal choreoathetosis Hallervorden-Spatz Disease
Endocrine/Metabolic	Hyperthyroidism Hypoparathyroidism Chorea gravidarum (pregnancy) Hypoglycemia, hyperglycemia, hypocalcemia, hypomagnesemia
Immunologic	Systemic lupus erythematosus Antiphospholipid antibody syndrome
Infectious	Viral encephalitis AIDS related Lyme disease Bacterial endocarditis
Vascular	Arteriovenous malformation Cerebrovascular accident (stroke) Cerebral hemorrhage

often decreases as the inflammation subsides. If the cardiac involvement is mild, patients may show complete resolution of cardiac findings, but patients with moderate-to-severe carditis are more likely to experience persistent and/or evolving RHD (110,112).

Mitral regurgitation, the dominant cardiac abnormality in patients with RF, occurs in approximately 95% of cases with *acute* rheumatic carditis. Both echocardiographic and surgical observations have demonstrated the mechanism of this mitral regurgitation to be a combination of annular dilatation and chordal elongation that results in abnormal coaptation, and in some cases, prolapse of the tip of the anterior mitral leaflet (Figs. 60.4 and 60.5) (186–188). Rarely, the mitral valve chordae rupture, resulting in a flail mitral leaflet and severe mitral regurgitation (168,189–191) (Fig. 60.5).

Most patients with acute mild mitral regurgitation are asymptomatic. With acute moderate-to-severe mitral regurgitation, the left ventricular myocardium may be unable to handle the significant volume overload and left heart filling pressures rise, leading to pulmonary venous congestion and pulmonary edema. Such patients usually present with features of left heart failure, including dyspnea, orthopnea, paroxysmal nocturnal dyspnea, cough, and even hemoptysis. Secondary pulmonary hypertension may develop, resulting in right ventricular dysfunction, tricuspid regurgitation, and right heart failure. Children younger than age 5 years with RF and carditis



Figure 60.4. Acute rheumatic carditis. Two-dimensional echocardiographic parasternal long-axis image showing prolapse of the tip of the anterior leaflet, resulting in a regurgitant orifice (arrow) and left heart dilation. Note also the small pericardial effusion. LA, left atrium; LV, left ventricle.

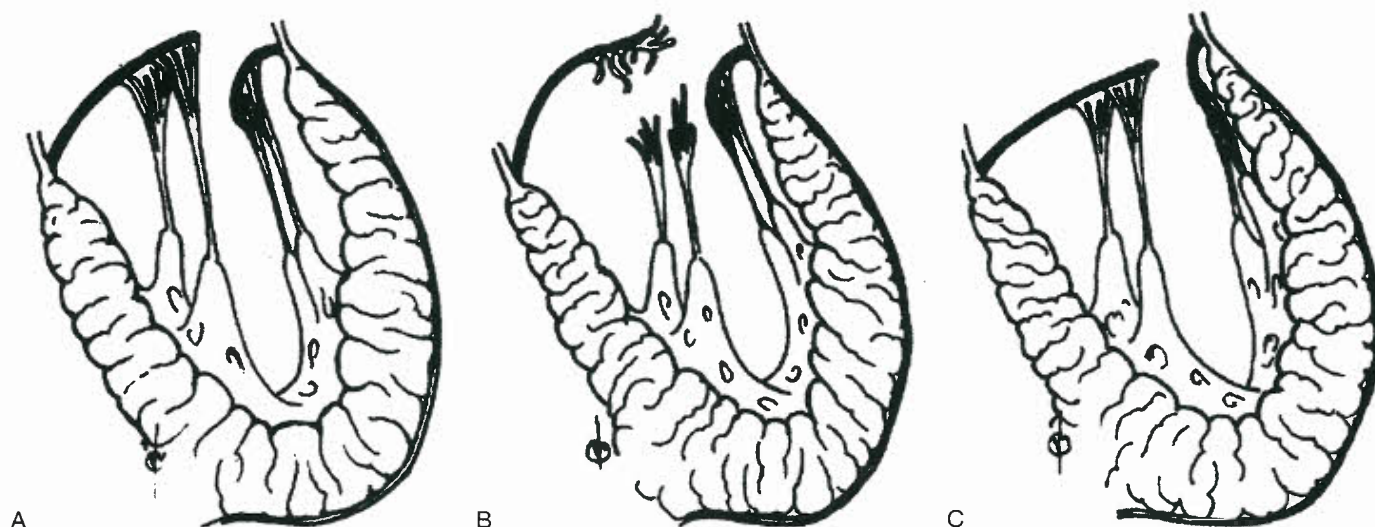


Figure 60.5. Mechanisms of anterior mitral leaflet prolapse in RHD. A: Prolapse owing to chordal elongation to anterior leaflet. B: Prolapse (flail leaflet) owing to ruptured primary chordae. C: Leaflet pseudoprolapse owing to immobile posterior leaflet, while the anterior leaflet remains at the annular plane in systole. (From Kalangos A, Beghetti M, Vala D, et al. Anterior mitral leaflet prolapse as a primary cause of pure rheumatic mitral insufficiency. *Ann Thorac Surg* 2000;69:755–761, with permission from Elsevier.)

may present more insidiously with fever, decreased appetite, lethargy, fatigue, and vague pains. Because of these subtle and nonspecific symptoms, the diagnosis may be delayed, and presentation with heart failure is more common than in older children (38,39). On physical examination, tachycardia is often one of the earliest signs of carditis. Significant mitral regurgitation may result in increased precordial activity, tachypnea, and increased work of breathing. A high-pitched, regurgitant, holosystolic murmur of mitral regurgitation is heard best at the apex, usually radiating into the left axilla. This murmur is best heard at end-expiration with the patient in the left lateral decubitus position. It is noteworthy that acute, severe mitral regurgitation may be present despite a fairly soft systolic murmur (192). Although mitral stenosis does not occur with the initial episode of acute RF and carditis, a low-pitched mid-diastolic apical murmur may be heard in the setting of significant mitral regurgitation due to increased diastolic flow across the mitral valve (Carey Coombs murmur) (193). Contrary to some reports (133), this murmur is never heard in isolation.

Aortic regurgitation occurs in approximately 20% to 25% of patients with acute rheumatic carditis, usually in combination with mitral regurgitation. Isolated aortic regurgitation occurs in approximately 5% of patients with acute rheumatic carditis (60,144). Leaflet prolapse has been reported to be one of the mechanisms of this acute valvular dysfunction (128,188). Patients with *acute* mild aortic regurgitation are usually asymptomatic. Moderate-to-severe acute aortic regurgitation is less well tolerated, and may result in heart failure. The large regurgitant volume imposed on a left ventricle that has not had time to compensate for the significant volume load results in decreased forward stroke volume in conjunction with significant elevation of ventricular end-diastolic pressure, leading to a combination of low cardiac output and pulmonary edema (194). Patients with acute severe aortic regurgitation are tachycardic and tachypneic. Unlike the clinical examination found with significant chronic aortic regurgitation, the pulse pressure is often narrow and the pulses are not increased or bounding. Precordial activity is often increased, but the apical impulse may not be significantly displaced. On auscultation, the decrescendo diastolic murmur is softer, lower-pitched, and shorter than the murmur heard with chronic regurgitation, and thus, this

murmur can be easily missed, especially with the tachycardia commonly present during the acute phase of the illness. A short systolic ejection murmur may be heard over the left ventricular outflow tract due to increased flow. A low-pitched mid-to-late diastolic rumbling murmur with presystolic accentuation may be heard at the apex, even with a nonstenotic mitral valve. If present, this “Austin Flint” murmur is softer and shorter in the setting of acute as compared to chronic severe aortic regurgitation. Acute rheumatic aortic regurgitation is less likely than mitral regurgitation to disappear with resolution of the acute inflammatory stage of the illness (110,112,115).

Pericarditis occurs in approximately 4% to 11% of patients with acute rheumatic carditis (60,143–145). When it occurs, it is invariably associated with significant left-sided valvular disease. In the absence of significant mitral and/or aortic regurgitation, pericarditis is unlikely related to RF, and other etiologies should be considered. Clinically, patients may have the typical positional chest and shoulder pain seen with pericarditis. On auscultation, a friction rub may obscure the murmur(s) of valvular regurgitation. In other cases, the friction rub may be evanescent and intermittent. Echocardiography allows detection and semiquantitation of pericardial effusions and evaluation of valvular function. Unlike pericarditis associated with other etiologies, pericardial tamponade (190) and constrictive pericarditis (195) rarely occur.

Although acute RHD has long been considered a pancarditis (173,196), the clinically important abnormalities are related to valvular pathology and regurgitation rather than myocarditis and myocardial dysfunction (197). Biopsy and autopsy pathologic specimens show evidence of myocardial involvement (including the characteristic Aschoff bodies), but unlike other types of myocarditis, myocyte necrosis associated with lymphocytic infiltration does not occur (198) and troponin I levels are not elevated (199,200). Further, although there may be evidence of subtle abnormalities of contractility (201), several studies have shown that left ventricular ejection phase indices (shortening and ejection fraction) are normal in these patients (197,202,203). Thus, it is important to emphasize that *heart failure does not occur in acute or chronic RHD in the absence of significant valvular regurgitation* (26,187,197,204).

Erythema Marginatum

The rash of erythema marginatum is a relatively uncommon finding, occurring in <5% of patients with RF (Table 60.2) (60,205,206). The rash appears as a bright pink macule or papule that spreads with serpiginous borders and central clearing. The lesions are painless, not pruritic, blanch on pressure, and are usually macular rather than papular. Most commonly seen on the trunk or proximal extremities, the rash is evanescent and the lesions may change in appearance rapidly. A hot bath or shower may bring out or accentuate the rash. Because of its evanescent nature and lack of associated symptoms, it may be easily missed. Although typically seen early in the course of RF, persistence or recurrence for months or even years has been described. Erythema marginatum is usually associated with carditis, and almost never occurs as the sole major Jones criterion (42,206,207).

Subcutaneous Nodules

Subcutaneous nodules are relatively uncommon in RF, reported in 0 to 10% of cases (Table 60.2). They are not pathognomonic of RF, and may occur with systemic lupus or rheumatoid arthritis. The nodules are 0.5 to 2.0 cm in diameter, round, firm, freely movable, nontender, and with no evidence of inflammation. They tend to occur in crops over extensor surfaces of joints or bony prominences of the elbows, wrists, knees, ankles, scalp, and spinous processes of the back. These nodules persist for a few days to as long as 1 to 2 weeks and are not evanescent. However, because they may be small and are not associated with symptoms, they may be easily missed. Similar to erythema marginatum, subcutaneous nodules are almost always associated with carditis and rarely occur as the sole major Jones manifestation (42,207,208).

Minor Criteria and Other Clinical Manifestations

The minor Jones manifestations are less specific than the major criteria and include fever, arthralgia, elevated acute phase reactants, and first-degree AV block (prolonged PR interval) on ECG (Table 60.1). Fever occurs at the onset of the RF illness in most cases, with temperatures usually ranging from 101°F to 104°F. Some patients have a history of fever, but are afebrile at the time of initial clinical evaluation. In particular, patients presenting with chorea are usually afebrile. Arthralgia, which is joint pain without objective findings, usually involves the large joints. The pain may be variable, ranging from mild to very severe, and may be migratory in nature. Arthralgia cannot be used as a minor criterion when polyarthritis is used as a major diagnostic criterion. Laboratory and ECG abnormalities are discussed in the following two sections.

Clinical manifestations seen in patients with RF not included in the Updated Jones Criteria include epistaxis and abdominal pain (typically epigastric or periumbilical), which occur in about 5% of cases, and may occur hours to days before any of the major manifestations (44). Both were minor manifestations in the original Jones criteria (130), but were removed because of lack of specificity. Other nonspecific features include anorexia, malaise, anemia, and a family history of RF or RHD.

Laboratory Testing

There is no definitive diagnostic test for RF. Suggested testing for patients with suspected RF are listed in Table 60.3. With few exceptions (chorea or insidious onset carditis), in addition to the major and/or minor Jones criteria, diagnosis of acute RF requires evidence of a preceding GAS infection. Although

a positive throat culture or rapid antigen test is accepted as such evidence, the rate of recovery of GAS from the pharynx of patient with RF is low. Moreover, some patients may have a positive culture or test due to a carrier state rather than true infection. Thus, elevated or rising antibody titers are more reliable evidence of a preceding GAS infection. The titers most commonly measured are antistreptolysin O (ASO) and antideoxyribonuclease B (anti-DNase b). When a single antibody is measured, 80% to 85% of patients with RF will have an elevated titer. When two titers are measured, well over 90% of patients with RF will have elevation of at least one titer (209,210). The ASO titer is often measured first; if it is not elevated, the anti-DNase b may be measured. ASO titers rise approximately 1 week and peak 3 to 6 weeks following infection. Anti-DNase b titer rises 1 to 2 weeks and peaks 6 to 8 weeks following infection (165). It should be emphasized that antistreptococcal antibody titers must be interpreted in the setting of clinical manifestations; elevated and/or rising titers only provide evidence of a preceding streptococcal infection, not RF.

Elevated acute phase reactants such as C-reactive protein and erythrocyte sedimentation rate are minor Jones criteria (133), and are invariably seen in patients with RF and arthritis and/or acute carditis. Thus, measurement of acute phase reactants is useful in differentiating acute carditis from indolent RHD (presenting after acute inflammation has resolved) and may guide treatment with anti-inflammatory agents (211). The degree of inflammation at presentation is of prognostic importance since acute carditis is more likely than chronic RHD to resolve over time. As previously stated, patients with chorea often show no elevation of acute phase reactants.

Electrocardiography

Patients with suspected RF should have an ECG since conduction abnormalities are not uncommon. Although first-degree AV block is a minor Jones criterion, it should be noted that a prolonged PR interval occurs in up to one-third of patients who have GAS infections, regardless of whether they develop RF (207). Though useful as a minor Jones criterion in support of the diagnosis of RF, first-degree AV block is not associated with either the severity of the initial cardiac involvement or a greater likelihood of developing chronic RHD (112,208). Less commonly, the ECG may reveal more advanced AV block or other abnormalities (212–214).

Echocardiography

Two-dimensional and Doppler echocardiography is central to the diagnosis and management of valvular disease and should be performed in all patients with acute or chronic RHD. Echocardiography is valuable for evaluating the mechanism and severity of valvular regurgitation and/or stenosis, leaflet and chordal morphology, annular size, chamber sizes and function, pericardial effusion, and pulmonary artery pressures (128,194,202,215,216). Echocardiography is also valuable in differentiating RHD from other entities such as innocent murmurs, congenital heart disease, or myocarditis, and thus helps avoid overdiagnosis of RF in up to 20% of cases (217–219). The mitral valve often appears normal on 2-D echocardiographic imaging of patients with mild acute rheumatic mitral regurgitation. Others have described focal nodular thickening of valve leaflets (thought to represent the verrucae seen at autopsy of patients who died with acute carditis) that disappears on follow-up (202). In cases severe enough to result in heart failure, chordal elongation and annular dilation may be seen, often resulting in anterior leaflet prolapse (Figs. 60.4 and 60.5) (186,197). The mitral valve prolapse seen in RF patients

differs from the redundant, myxomatous mitral valve and prolapse seen with Barlow syndrome. In rheumatic carditis, only the coapting portion of the anterior leaflet prolapses, and there is no billowing of the medial portion or body of the leaflet (220). This results in abnormal leaflet coaptation, a regurgitant orifice, and a jet of mitral regurgitation that is typically posterolaterally directed (221,222). Rarely, chordal rupture results in a flail leaflet and severe mitral incompetence (Fig. 60.5) (189–191,223,224). In the setting of acute rheumatic aortic regurgitation, the aortic valve may appear normal or show mild prolapse by 2-D echocardiographic imaging. The severity of mitral and/or aortic regurgitation should be evaluated using a combination of methods (216).

Echocardiography may detect mitral and/or aortic regurgitation in patients with RF who have no evidence of clinical carditis on physical examination (no murmur). Although a single report did not find evidence of cardiac involvement in the absence of clinical findings (202), there are now several reports of such subclinical or “silent” cardiac involvement in patients with either isolated polyarthritis or “pure” chorea at the time of presentation (219,222,225,226). The fact that some patients with RF have such subclinical evidence of cardiac involvement is not surprising. It is well known that the severity of cardiac involvement ranges from very mild to severe. Even in the “golden era” of clinical auscultation of the 1950s, some patients with no clinical carditis at presentation with RF (no murmur) were found to have RHD on follow-up (110,112). In the current era with diminished auscultatory skills (227), this is likely to be an even more frequent occurrence. Further support for the existence of subclinical echocardiographic evidence of cardiac involvement comes from the fact that some series have described a subset of patients with initially “silent” subclinical evidence of carditis who subsequently developed murmurs of mitral and/or aortic regurgitation (226,228). Indirect evidence in support of “silent” subclinical carditis comes from natural history studies. Many adults who present with chronic RHD cannot recall having a previous RF-like illness, suggesting very mild or subclinical cardiac involvement with acute RF illness (229). As many as 20% to 44%

of patients with “pure” chorea have been reported to develop chronic RHD (154,168,175,229). Despite evidence in support of these findings, there has appropriately been concern over creating “iatrogenic” disease since a significant percentage of normal individuals have very small amounts of “physiologic,” Doppler-detected valvular regurgitation (mostly tricuspid, pulmonary, and mitral), especially with advances in ultrasound technology. To avoid labeling such normal findings as abnormal, strict criteria should be used to differentiate pathologic mitral and aortic regurgitation from the Doppler signals seen in normal individuals. The World Health Organization recommends the following criteria to differentiate pathologic from physiologic mitral and aortic regurgitation: (a) color jet >1 cm in length, (b) color jet evident in at least two imaging planes, (c) color jet mosaic with peak velocity >2.5 m/s, and (d) Doppler signal holosystolic for mitral regurgitation and holodiastolic for aortic regurgitation (Fig. 60.6) (7). Although echocardiography may not be available in some of the developing countries where RF is most common (230), the World Health Organization recognizes its usefulness and recommends that echocardiography be performed in the evaluation of patients with RF if facilities are available. Furthermore, the World Health Organization recommends that silent but significant mitral and/or aortic regurgitation be considered *probable* RHD and that such patients be given secondary prophylaxis and followed long-term for evolution of heart disease (7). Echocardiography should also be performed in the evaluation and follow-up of patients with established chronic RHD. The role of echocardiography in *screening* for RHD is discussed below in the section on *Secondary Prophylaxis*.

Cardiac Catheterization

Catheterization and angiography are rarely necessary for the management of patients with acute rheumatic valvular disease, including those who ultimately require surgery. Endomyocardial biopsy does not add to the diagnosis or management (198). Catheterization should be reserved for those in whom

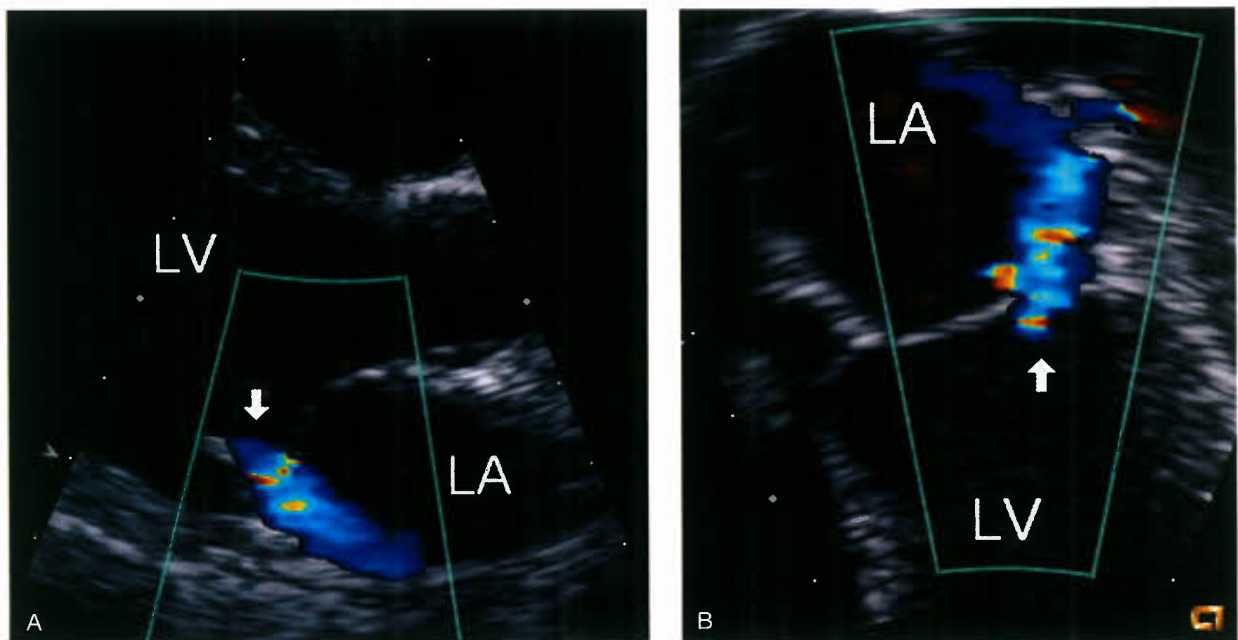


Figure 60.6. Silent rheumatic mitral regurgitation. Two-dimensional echocardiographic parasternal long-axis (A) and apical four-chamber (B) images showing a posterolaterally directed jet of mitral regurgitation extending into the left atrium well beyond the mitral valve leaflets.

symptoms, clinical findings, and noninvasive imaging are discrepant, when measurement of pulmonary artery pressure and pulmonary vascular resistance is important in decision-making, and when balloon valvuloplasty for mitral stenosis is being contemplated (231). In adults with RHD, catheterization and angiography may be indicated to evaluate the coronary vascular bed prior to surgical intervention for valvular RHD (194).

Other Cardiac Imaging

The chest radiograph may be valuable in assessing patients with acute or chronic RHD to evaluate cardiac size, configuration, and pulmonary venous markings. The cardiac silhouette may be enlarged due to valvular regurgitation and chamber enlargement and/or due to an associated pericardial effusion.

Although studies have shown white blood cell scanning (232) and antimyosin scintigraphy (233) to detect cardiac involvement in some patients with RF, there are insufficient data to support their routine use in the evaluation of patients with RF.

CHRONIC RHEUMATIC HEART DISEASE

Mitral Regurgitation

Chronic mitral regurgitation is the most common form of RHD in children and young adults (111,113,117), while mitral stenosis is increasingly common in patients in the fourth to sixth decades of life (85). In contrast to the chordal elongation and annular dilation that occur with acute rheumatic mitral valvulitis and regurgitation, leaflet shortening, rigidity, deformation, and retraction, often associated with chordal fusion and shortening, result in abnormal leaflet coaptation and chronic rheumatic mitral regurgitation. In addition, left ventricular dilation may alter the position and orientation of the mitral valve papillary muscles, further impairing leaflet coaptation and resulting in a larger regurgitant orifice and regurgitant volume (234). Chronic mitral regurgitation results in compensatory dilation of the left ventricle, allowing for an increased total stroke volume that maintains forward flow. The combination of compensatory dilation of the left ventricle and the left atrium initially prevents a rise in left ventricular filling, left atrial, and pulmonary venous pressures. Although patients may remain asymptomatic for years with this compensation, the mitral regurgitation may progress over time (235). Severe chronic mitral regurgitation may eventually result in ventricular dysfunction with decreased ejection fraction, elevated end-systolic volume, and elevated left heart filling pressures. Symptoms, most commonly exertional dyspnea or decreased exercise tolerance, may develop prior to, or with the onset of, ventricular dysfunction (194,236,237).

In the setting of chronic mitral regurgitation, precordial activity is increased and the apical impulse is displaced because of ventricular dilation. The first heart sound is often softer than normal, and the second heart sound may be widely split due to shortened left ventricular ejection and earlier aortic valve closure. If there is associated pulmonary hypertension, the pulmonary component of the second heart sound (P2) may be increased. A regurgitant systolic murmur is best heard at the apex; more subtle mitral regurgitant murmurs may be heard at end-expiration with the patient in the left lateral decubitus position. When the regurgitant jet is posterolaterally directed, the murmur radiates to the left axilla. Medially directed jets may result in radiation of the murmur toward the base of the heart. For chronic mitral regurgitation, the intensity of the murmur correlates with the severity of regurgitation. When

the regurgitant volume is significant, an apical diastolic flow rumble may be heard in the absence of mitral stenosis.

The chest radiograph is usually normal in patients with mild mitral regurgitation. With moderate-to-severe mitral regurgitation, left atrial and left ventricular enlargement occur, resulting in a straight left heart border and cardiomegaly. Elevation of the left mainstem bronchus may be evident. Pulmonary venous congestion and interstitial edema may be evident with severe, decompensated mitral regurgitation and heart failure.

The ECG in patients with chronic RHD is most important for demonstrating the rhythm. The ECG is normal in patients with mild mitral regurgitation but may show left atrial enlargement and/or left ventricular hypertrophy in patients with moderate-to-severe mitral valve incompetence. ECG changes do not correlate with the severity of the mitral regurgitation. Right ventricular hypertrophy may be evident in cases with secondary pulmonary hypertension. Atrial fibrillation is rare in children, but may be seen in adults with chronic rheumatic mitral valve disease.

On echocardiography, the mitral valve leaflets are thickened and often echogenic with variably decreased mobility. Leaflet excursion may be decreased during both diastole and systole. Abnormal leaflet coaptation results in a regurgitant orifice. In some cases, the anterior leaflet tip prolapse seen with acute carditis persists as chronic rheumatic mitral regurgitation. In other cases, the combination of a retracted, relatively immobile posterior (mural) leaflet with a more mobile anterior leaflet can give the impression of anterior prolapse even though the free edge of the anterior leaflet remains in the annular plane during systole. Such a combination, termed "pseudoprolapse," also results in poor leaflet coaptation and significant regurgitation (Fig. 60.5) (191).

Aortic Regurgitation

Chronic rheumatic aortic regurgitation occurs due to leaflet thickening, fibrosis, and leaflet contracture, resulting in abnormal leaflet coaptation and a regurgitant orifice. This regurgitation leads to both volume and pressure overload of the left ventricle (194). During a compensatory phase, ventricular dilation occurs to maintain forward stroke volume and cardiac output, and ejection fraction remains normal. Similar to patients with chronic mitral regurgitation, patients with chronic severe aortic regurgitation may remain asymptomatic for years (194,238). Over time, decompensation may occur, resulting in decreased left ventricular function and/or symptoms, most commonly dyspnea on exertion or decreased exercise tolerance.

On examination, significant chronic aortic regurgitation results in a wide pulse pressure (elevated systolic and low diastolic pressures) and bounding pulses. Precordial activity is increased, and the apical impulse is displaced laterally due to the dilated left ventricle. The typical diastolic murmur of aortic regurgitation is relatively high-pitched, decrescendo, and heard best along the left sternal border with the patient leaning forward at end-expiration. The duration of the murmur rather than the intensity correlates with the severity of regurgitation. A short systolic ejection murmur may be heard at the mid-left or upper right sternal border from increased flow across the left ventricular outflow tract or associated aortic valve stenosis. In patients with moderate-to-severe aortic regurgitation, a low-pitched mid-to-late diastolic rumbling murmur may be audible at the apex in the absence of organic mitral stenosis ("Austin Flint" murmur).

The chest radiograph is usually normal in mild aortic regurgitation and shows progressive cardiomegaly with increasing severity of aortic valve incompetence. With significant aortic regurgitation, a dilated ascending aorta may be evident.

The ECG is usually normal in cases with mild aortic regurgitation, but may show left ventricular hypertrophy with moderate-to-severe aortic valve incompetence.

On echocardiography, the aortic valve leaflets may show thickening, retraction, and variable commissural fusion. The severity of the aortic regurgitation should be assessed (216) along with documentation of associated lesions, in particular mitral valve stenosis or regurgitation. Left ventricular size and function should be assessed in all patients with aortic regurgitation.

Mitral Stenosis

RF resulting in chronic RHD is the most common cause of mitral stenosis. Mitral stenosis does not occur with acute initial carditis. In industrialized countries, the interval between the occurrence of RF and the onset of symptoms from mitral stenosis is usually 15 to 40 years, resulting in presentation in the third to fifth decades of life (85). In contrast, symptomatic rheumatic mitral stenosis may occur as early as the second decade of life in children from developing countries of the world (27,29,33). While both greater severity of cardiac involvement with the initial illness and multiple recurrences of RF likely contribute to the development of this more aggressive form of chronic RHD, it is also possible that the disease process itself is different in developing countries of the world (27). Mitral stenosis may occur as the dominant lesion, with insignificant amounts of associated regurgitation ("pure" mitral stenosis), or in combination with significant mitral regurgitation (239). Women are more likely than men to develop rheumatic mitral stenosis (66,111).

A combination of leaflet thickening, fusion of commissures, cusps and chordae, and chordal shortening result in a funnel-shaped, stenotic mitral valve orifice. Over time, the valve may calcify, further impairing leaflet mobility. The process is usually continuous and slowly progressive (at least in industrialized countries), eventually resulting in left ventricular inflow obstruction and a diastolic gradient between the left atrium and ventricle. Patients with mild stenosis are usually minimally symptomatic. With increasing stenosis, however, left atrial and pulmonary venous pressures rise, leading to pulmonary venous congestion and, eventually, pulmonary hypertension. Many patients accommodate their lifestyle to the gradual development of symptoms and are unaware of their significant functional limitations. The most common early symptoms are due to decreased cardiac output and include fatigue and decreased exercise tolerance. Dyspnea on exertion, cough, wheezing, shortness of breath, orthopnea, and paroxysmal nocturnal dyspnea may develop as the patient's condition worsens and pulmonary edema develops. Although uncommon in children, atrial fibrillation may result in atrial thrombi and systemic embolization. With severe mitral inflow obstruction and pulmonary hypertension, hemoptysis and signs of right heart failure, including edema and abdominal distension, may be evident.

On examination, findings depend on the severity of the stenosis and associated lesions. Precordial activity may be abnormal with a tapping, palpable first heart sound, but the apical impulse is not usually displaced unless there is associated mitral and/or aortic regurgitation. Prominent a-waves may be visible in the jugular venous pulsations. On auscultation, the characteristic findings of mitral stenosis are an increased S1, an early diastolic opening snap, and a low-pitched, rumbling diastolic murmur best heard at the apex with the patient in a left lateral decubitus position. The duration rather than the intensity of the murmur correlates with the severity of obstruction. In addition, the interval between S1 and the opening snap decreases with increased stenosis (elevated left atrial pressure

results in earlier opening snap). For patients in sinus rhythm, late diastolic or presystolic accentuation of the murmur may be audible due to the increased gradient associated with atrial contraction. With severe stenosis and a rigid, calcified mitral valve, the opening snap and S1 may be inaudible. When secondary pulmonary hypertension occurs, P2 increases, and a right ventricular impulse or lift may be noted. Tricuspid regurgitation due to a combination of rheumatic tricuspid valve involvement and pulmonary hypertension may become clinically evident with a regurgitant systolic murmur at the lower left sternal border, a pulsatile liver, and abnormal jugular venous pulsations.

Typically normal in patients with mild mitral stenosis, the chest radiograph may show left atrial enlargement in patients with more significant mitral valve obstruction. The left ventricle is not enlarged unless there is associated mitral or aortic regurgitation. The pulmonary artery and right ventricle may enlarge when there is associated pulmonary hypertension.

The ECG is most important for determining the rhythm, since atrial fibrillation is an important complication of significant mitral stenosis. The ECG is normal if the mitral stenosis is mild, but may show left atrial enlargement with significant stenosis. Right axis deviation or right ventricular hypertrophy may be evident if there is secondary pulmonary hypertension. It is notable that ECG findings do not correlate with the severity of the mitral stenosis.

On echocardiography, patients with rheumatic mitral stenosis have valvar and subvalvar changes including thickened echo-dense leaflets, commissural fusion, abnormal diastolic leaflet excursion (doming), and calcification; fusion, shortening, fibrosis, and calcification of the mitral valve chordae. Mitral regurgitation and stenosis may coexist in such patients. The leaflets begin to open in diastole, and although the body of the leaflets may continue to move, commissural fusion limits the excursion of the leaflet tips resulting in the characteristic "bent-knee" or "hockey-stick" appearance of the anterior leaflet typical of rheumatic mitral stenosis (Fig. 60.7). The posterior leaflet may show very limited excursion and appear "frozen." Over time, the valve may calcify, first at the leaflet tips and later extending toward the annulus. With increased thickness and calcification, the leaflets become less pliable and motion is further restricted. Although the left atrium is dilated with significant stenosis, the left ventricle is normal in size unless there is concomitant mitral and/or aortic regurgitation. The severity of the mitral stenosis may be assessed from Doppler peak and mean gradients, planimetry of the valve opening, pressure half-time, or proximal Doppler flow convergence (240). Leaflet mobility, thickening, calcification, and subvalvular thickening have been shown to be useful echocardiographic features for identifying patients who are good candidates for balloon valvotomy of mitral stenosis (241–243). When possible, pulmonary artery pressures should be estimated from the tricuspid and pulmonary regurgitation velocities since pulmonary hypertension may occur with more severe degrees of mitral stenosis. Both right and left ventricular function should be assessed in all patients with mitral stenosis. When available, 3-D echocardiography allows assessment of both valve area and candidacy for balloon valvotomy (244).

Exercise or other forms of stress testing may be of value in evaluating patients with equivocal symptoms or in whom the symptoms are greater than would be expected based on the resting echocardiogram. In some patients, the transmitral gradient and pulmonary artery pressure rise significantly with exercise. Asymptomatic patients with significant mitral stenosis who show poor exercise capacity or a significant rise in estimated pulmonary artery systolic pressure (>60 mm Hg) with stress testing should be considered for transcatheter or surgical intervention (245).

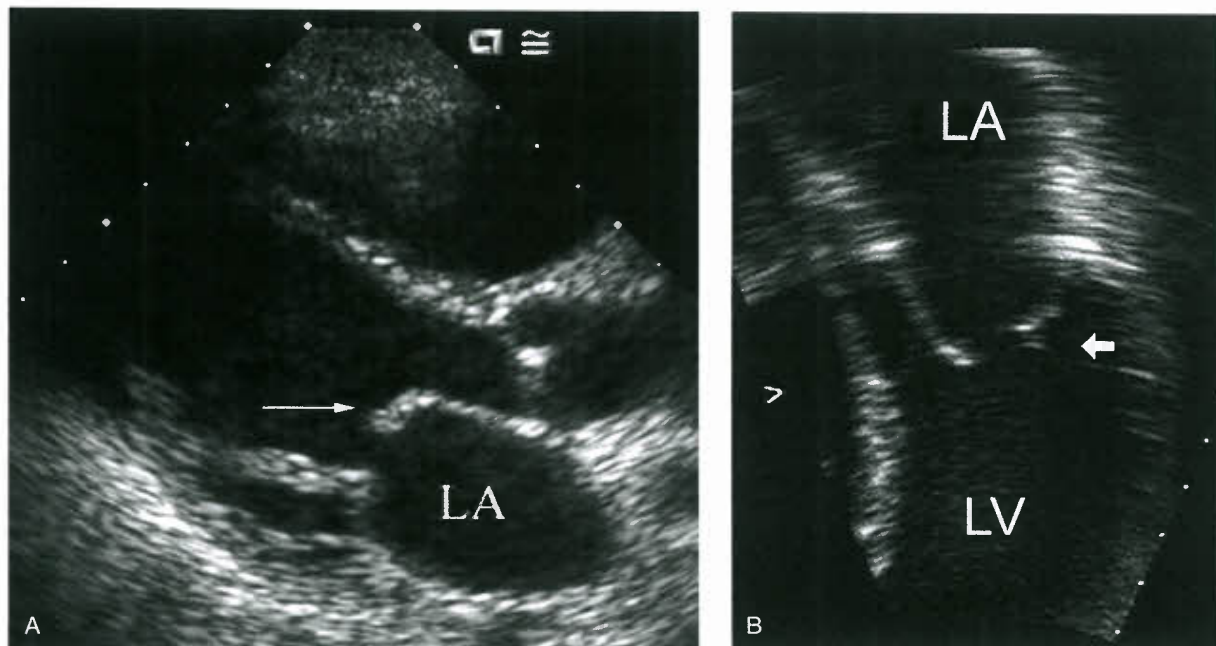


Figure 60.7. Chronic rheumatic mitral stenosis. A: Two-dimensional echocardiographic parasternal long-axis image demonstrating bent-knee or hockey-stick configuration to thickened anterior mitral valve leaflet (arrow). B: Apical four-chamber image showing thickened, echogenic leaflets and restricted diastolic opening (arrow); LA, left atrium; LV, left ventricle.

Aortic Stenosis

Like mitral stenosis, aortic valve stenosis is a form of chronic rather than acute RHD and occurs 20 to 40 years after the acute illness as adhesions, leaflet thickening, fibrosis, commissural fusion, and calcific nodules may develop over time. These changes lead to decreased leaflet mobility, decreased aortic orifice size, and obstruction to flow. Rheumatic aortic stenosis and regurgitation often occur concurrently, usually along with rheumatic mitral valve disease. The increase in stenosis is gradual, allowing for ventricular compensation and the absence of symptoms. With time, compensation fails and symptoms develop (including angina, syncope, dyspnea on exertion and heart failure), most often in the fifth to sixth decades of life (246).

With severe stenosis, the arterial pulse may be decreased, with a slow rate of rise. Conversely, if there is associated aortic regurgitation, the pulses may be increased. Similar to congenital aortic valve stenosis, a thrill may be palpable at the upper right sternal border or in the suprasternal notch. A systolic ejection murmur is heard best at the upper right sternal border, but in contrast to congenital aortic valve disease, an ejection click is uncommon with rheumatic aortic valve stenosis. A decrescendo diastolic murmur may be audible if there is associated aortic regurgitation.

On echocardiography, 2-D imaging often demonstrates thickened leaflets with variable degrees of commissural fusion and leaflet retraction, responsible for the variable degrees and combinations of aortic regurgitation and stenosis. Doming of the leaflets, increased echogenicity from calcification, and restricted motion develop as the stenosis progresses. The severity of aortic stenosis can be evaluated by measuring peak instantaneous and mean Doppler gradients or aortic valve area using the continuity equation. Left ventricular dimensions, volumes, wall thicknesses, mass, and function should be measured as they importantly contribute to clinical management decisions. The mitral valve should be carefully evaluated

in all patients with chronic rheumatic aortic valve disease since coexistent mitral valve involvement is common.

Right Heart Involvement

In patients with chronic RHD, tricuspid and/or pulmonary valve involvement may be functional (related to the pulmonary hypertension that may occur with significant left heart disease) or organic (chronic rheumatic changes) (247). The tricuspid valve is affected more often than the pulmonary valve by the rheumatic process, but clinically significant involvement of either valve is uncommon. Rheumatic tricuspid valve disease (stenosis and/or regurgitation) virtually always occurs with significant mitral or aortic valve disease. Although histologic evidence of rheumatic tricuspid valve involvement may be detectable in up to 15% to 40% of patients with RHD (247–250), significant tricuspid valve disease is detectable by echocardiography in only 7% to 9% (247,251) and is clinically apparent in 3% to 5% of patients with RHD (250,252). Rheumatic tricuspid stenosis results from a combination of leaflet thickening, fusion of commissures and chordae, and chordal contraction and shortening that limits diastolic leaflet motion and creates a stenotic orifice. Leaflet contraction and annular dilation may affect leaflet coaptation and result in tricuspid regurgitation.

In some cases, it may be difficult to determine whether a patient's symptoms (fatigue, exercise intolerance, peripheral edema) are from tricuspid stenosis or mitral stenosis. Features typical of tricuspid stenosis include prominent jugular venous a-wave pulsations, an opening snap, and a low-pitched diastolic rumbling murmur at the lower left or right sternal border as opposed to the apex where mitral stenosis is characteristically heard (253). Right heart failure with peripheral edema, hepatomegaly, right upper quadrant tenderness, and ascites may be evident in advanced disease.

On echocardiography, patients with tricuspid regurgitation may have right ventricular enlargement and/or hypertrophy,

right atrial enlargement, and tricuspid annular dilation. Similar to the rheumatic stenotic mitral valve, thickened leaflets with doming and decreased motion are characteristic findings in rheumatic tricuspid stenosis (254,255). Doppler allows estimation of the severity of both the tricuspid regurgitation (216,256,257) and stenosis (254).

Although uncommonly involved in either acute or chronic RHD, the pulmonary valve may show evidence of rheumatic involvement after the Ross procedure (pulmonary autograft replacement of the aortic valve) (258), leading to significant neo-aortic regurgitation and, in some cases, the need for subsequent aortic valve replacement (259,260).

TREATMENT

The medical management of acute rheumatic carditis has not changed substantially since the mid-1950s. Treatment remains largely supportive and directed at preventing recurrences, complications, and deciding on the optimal time for intervention for chronic valvular disease. Although anti-inflammatory treatment is widely accepted as an integral part of the treatment regimen of acute RF and provides symptomatic relief, there is little evidence that such treatment alters the natural history of RHD (33,111,261). Although quite variable, the duration of an untreated case of RF is approximately 3 months, with the course for patients with carditis varying from that of complete recovery with no sequelae to intractable heart failure requiring surgical intervention. The various forms of treatment of acute rheumatic carditis and chronic RHD are summarized in Tables 60.6 and 60.7.

TABLE 60.6 Treatment of Acute Carditis

- General management
 - Restricted activity: some recommend bed/chair rest for approximately 4–6 wk for carditis
 - Primary prophylaxis (see Table 60.8)
 - Initiate secondary prophylaxis (see Table 60.9)
- Anti-inflammatory therapy (see text for discussion)
 - Mild-to-moderate carditis
 - Aspirin: 80–100 mg/kg/d in four divided doses for children (target salicylate levels 20–30 mg/dL)
 - Aspirin: 4–8 g/d in adolescents and adults (target salicylate levels 20–30 mg/dL)
- Severe carditis
 - Initial steroids (prednisone 2 mg/kg/d) for approximately 2 wk, then taper
 - Begin aspirin approximately 1 wk prior to stopping steroids to prevent rebound
 - Follow acute phase reactants (erythrocyte sedimentation rate, C-reactive protein)
- Other treatment depends on severity of involvement and symptoms
 - Moderate-to-severe carditis: consider salt and fluid restriction, diuretics, afterload reduction as temporizing measures
 - Intractable heart failure: surgery

TABLE 60.7 Treatment of Chronic Rheumatic Heart Disease

- General medical management
 - Serial evaluation
 - Recognition of progression, symptoms
 - Echocardiography: valvular function, chamber sizes, ventricular function, pulmonary pressures
 - Education: early recognition of symptoms, prevent complications
 - Secondary prophylaxis
 - Infective endocarditis prophylaxis when indicated (see text)
 - Activity restrictions based on severity of valvular disease
- Mitral regurgitation (MR) (severe)
 - Specific medical management: none; no defined role for afterload reduction
 - Indications for surgery: symptoms, LV dysfunction, marked ventricular enlargement, new-onset atrial fibrillation, pulmonary hypertension (possible intervention for severe MR in asymptomatic patients with preserved LV function if valve repair likely in a center with expertise)
- Aortic regurgitation (severe)
 - Specific medical management: vasodilator therapy for patients with symptoms or LV dysfunction who are poor surgical candidates (cardiac or noncardiac reasons); vasodilator therapy may also be used for short term to improve hemodynamics prior to aortic valve surgery
 - Indications for surgery: symptoms, ventricular dysfunction, marked LV enlargement, and for patients undergoing other cardiac surgery (coronary, other valves, etc.)
- Mitral stenosis
 - Specific medical management: anticoagulation is recommended for (1) history of thromboembolic event, (2) atrial fibrillation, and (3) left atrial thrombus; possible role for rate control in selected cases
 - Indications for mechanical intervention (catheter-based or surgical): symptoms, pulmonary hypertension
 - Percutaneous balloon valvotomy: best results for those with echocardiographic evidence of noncalcified and pliable leaflets, without severe thickening or subvalvular pathology
 - Surgery (repair if possible; valve replacement) in patients not candidates for percutaneous intervention (expertise not available, left atrial thrombus, significant associated mitral regurgitation, unfavorable mitral valve morphology)
- Aortic stenosis (severe)
 - Specific medical management: none
 - Percutaneous treatment (catheter-based balloon valvotomy or transapical or transcatheter aortic valve implantation) is reserved for those who are poor surgical candidates
 - Indications for surgery: symptoms, LV dysfunction, and patients undergoing other cardiac surgery

Traditionally, many patients with RF have been hospitalized for evaluation, diagnosis, and initiation of appropriate treatment. In our experience, the majority of patients can be both evaluated and managed as outpatients.

Medical Management of Acute RF

In addition to a careful history and physical examination, patients with suspected RF should have a throat culture performed, lab tests including ASO and/or anti-DNase b titers, a white blood cell count, and acute phase reactants (erythrocyte sedimentation rate and C-reactive protein), an ECG, and an echocardiogram (if possible) (Table 60.3). Admission to the hospital should be considered, but some patients can be managed as outpatients with close follow-up.

Management of acute rheumatic carditis should include antibiotic treatment to eradicate pharyngeal streptococci, bed rest (262,263), and anti-inflammatory treatment (Table 60.5) (66,173,264–269). Although there is no evidence that it alters the course of RF, antibiotic therapy is recommended even if the throat culture is negative. In the 1940s, RF patients who were allowed to ambulate had a longer duration and greater severity of carditis (larger heart size on CXR) and more frequent reactivations than those placed at bed rest. Some restriction of activity during the acute phase is warranted, but the prolonged strict bed rest practiced in the 1940s and 1950s is probably unnecessary (269). Some experts recommend bed/chair rest for 4 to 6 weeks for patients with carditis, depending on the severity. Although of unproven benefit, many recommend anti-inflammatory treatment with either aspirin or steroids for patients with rheumatic carditis since a subset of patients with significant acute rheumatic mitral and/or aortic regurgitation improves as the acute inflammation subsides (270). There is no clear-cut evidence that steroids are superior to aspirin in affecting long-term outcome (271). However, compared to aspirin, steroids do result in a more prompt resolution of inflammation (272,273), fewer new murmurs (274), and more rapid disappearance of existing murmurs (275). Many experts recommend aspirin at a dose of 80 to 100 mg/kg/d (doses as high as 4 to 6 g/d for adults) for mild-to-moderate carditis. Salicylate levels should be checked, aiming for serum concentrations of 20 to 30 mg/dL. For patients with moderate-to-severe carditis and heart failure, many recommend steroids (prednisone 2 mg/kg/d or equivalent) for approximately 2 weeks, followed by tapering doses (reduce by 20% to 25% each week). Salicylates are started about a week prior to discontinuing steroids to prevent rebound. The optimal duration of anti-inflammatory treatment with salicylates and/or steroids is unknown; some recommend treatment for 4 to 6 weeks, while others recommend treatment until there is laboratory evidence of resolution of the acute inflammatory process (i.e., normalization of erythrocyte sedimentation rate and/or C-reactive protein). Although laboratory and clinical rebound may be seen following discontinuation of anti-inflammatory therapy, this usually resolves spontaneously without the need for reinstitution of therapy (7,156,266). While some patients with heart failure improve, it should be emphasized that for patients with severe valvular regurgitation and heart failure unresponsive to medical therapy, surgical restoration of valvular competence (repair or replacement) may be life saving (26). Neither intravenous gamma globulin (276) nor pentoxifylline (277) has been found to be of benefit.

As previously stated, the arthritis of RF is typically very responsive to aspirin within 48 to 72 hours. Nonsteroidal anti-inflammatory agents have been reported as an effective alternative to aspirin for patients with polyarthritis, but have not been evaluated for the treatment of carditis (278,279).

The duration of anti-inflammatory treatment for rheumatic arthritis can usually be guided by symptoms and response to therapy.

Most patients with chorea can be managed without pharmacologic treatment. In cases with severe symptoms, reported treatments include phenobarbital, haloperidol, valproic acid, corticosteroids, plasma exchange, and intravenous immune globulin (280–284).

Medical Management of Acute Rheumatic Carditis and Heart Failure

As stated above, many clinicians experienced in the management of RF and acute carditis recommend steroids for patients with acute heart failure (see section above). Although some of the older literature suggests a role for digoxin (50,266,285), this may have been due to the belief that myocardial dysfunction played an important role in rheumatic carditis. It should be emphasized that the primary hemodynamic abnormality is valvular incompetence rather than myocardial dysfunction. Diuretics and afterload reduction may be valuable as temporizing measures in patients with significant regurgitation and symptoms. However, in cases with intractable heart failure, surgical restoration of valvular competency (repair or replacement) may be life saving (191,286). In particular, patients with a flail mitral valve after chordal rupture do not respond to medical management and require surgery (189,223) (Table 60.6).

Medical Management of Chronic RHD

Guidelines for the management of chronic RHD are given in Table 60.7. In the absence of data on the natural history and impact of treatment on chronic valvular disease in children, many practitioners extrapolate from the adult literature and guidelines (194). Asymptomatic patients with rheumatic valvular disease can often be followed conservatively as most remain stable for years. In the absence of symptoms, medical management should include serial evaluation to detect interval change and/or the onset of symptoms, prevent complications (i.e., recurrent RF, endocarditis, or embolic events), and detect changes in valvular function, chamber sizes, and ventricular function. Anticoagulation with warfarin is recommended for patients with mitral stenosis who have a history of a prior embolic event and for those who have atrial fibrillation (194).

The role of afterload reduction in the management of asymptomatic patients with chronic severe mitral regurgitation and preserved left ventricular function remains unclear. Although some studies have demonstrated improvement in hemodynamic variables (287–289), other studies have suggested that vasodilators might result in hemodynamic worsening (290,291). At present, there are no long-term studies showing afterload reduction in this setting to delay the onset of symptoms or ventricular dysfunction or improve outcome. Thus, use of afterload reduction in the management of asymptomatic patients with chronic mitral regurgitation who have preserved left ventricular function is not recommended (194,292,293). Once symptoms develop, medical management of mitral or aortic regurgitation has little role except as a temporizing measure, and surgical intervention is indicated (194).

There is conflicting evidence regarding the role of afterload reduction for the management of asymptomatic adults with chronic, severe aortic regurgitation and preserved left ventricular function. One study comparing long-acting nifedipine with digoxin in a prospective randomized trial found that fewer patients in the nifedipine group underwent aortic valve replacement (symptoms or LV dysfunction) (294).

A subsequent study comparing placebo, long-acting nifedipine, and enalapril found no difference in the treatment groups with respect to development of symptoms or LV dysfunction (295). Accordingly, the current American College of Cardiology/American Heart Association Guidelines for the Management of Patients With Valvular Heart Disease do not recommend vasodilator therapy for long-term management of asymptomatic patients with severe aortic regurgitation who have normal ventricular systolic function (194,294–296).

Unfortunately, there are even less data to guide management of patients with combined mitral and aortic regurgitation. Although symptoms are an indication for surgical intervention, there is evidence suggesting that by the time such patients are symptomatic, the likelihood that left and right ventricular functions are compromised is greater than in similar patients with isolated mitral or aortic regurgitation. Since right ventricular function is a valuable predictor of postoperative mortality in patients with combined left-sided valvular regurgitation, detection of decreased right (or left) ventricular function should prompt referral for surgical intervention (297).

Recently, investigators have reported possible benefit from the use of statins on progression of chronic RHD. Retrospective studies have suggested that statins may slow the progression of both rheumatic mitral and aortic stenosis. The mechanism remains unclear; the anti-inflammatory properties of statins may play a role. Results from prospective trials in adults with valvar aortic stenosis have yielded conflicting results. Thus, although the possibility of medical therapy that can change the natural history of RHD (separate from preventing RF recurrences) is intriguing with important potential, the role of statins in the management of chronic RHD remains undefined (298–302).

Heart Failure in Chronic RHD

Guidelines for the management of patients with RHD and heart failure are given in Table 60.7. There is no role for long-term medical management of patients with *symptomatic* chronic mitral and/or aortic regurgitation. Unless surgery is contraindicated for other reasons, such patients should be referred for surgery (194,292).

Patients with rheumatic *mitral stenosis* and mild symptoms such as dyspnea on exertion related to higher heart rates may benefit from negative chronotropic agents, such as beta-blockers or calcium channel blockers. Judicious use of diuretics and/or sodium restriction may be valuable in cases with pulmonary venous congestion (194). With significant stenosis and symptoms, both percutaneous balloon valvuloplasty (303,304) and surgical intervention have been effective (305). An echocardiographically determined mitral valve morphology score combining assessment of leaflet mobility, subvalvular thickening, leaflet thickening, and leaflet calcification has been found to be a predictor of outcome after balloon valvuloplasty for mitral stenosis (241,243,306). Symptomatic patients who are not candidates for percutaneous balloon valvuloplasty should be referred for surgery.

There is no effective medical therapy for symptomatic rheumatic *aortic valve stenosis*. Unlike congenital aortic valve stenosis in children, balloon valvuloplasty is not effective and has a limited role in the treatment of symptomatic calcific aortic valve stenosis (307,308); it should be reserved for patients who are unacceptable surgical candidates (194).

Similarly, medical management of symptomatic rheumatic *tricuspid valve disease* is unlikely to be successful. Diuretics may be useful as a temporizing measure in symptomatic patients, but optimal treatment is surgical commissurotomy, usually at the time of concomitant mitral valve surgery (309).

SURGICAL AND CATHETER-BASED TREATMENT

(See Tables 60.6 and 60.7). Acute Carditis

Some patients with significant acute mitral or aortic regurgitation improve with time as the inflammation subsides, while others have intractable or progressive heart failure that is unresponsive to medical therapy. *Surgical intervention with valvuloplasty or valve replacement during the acute illness can be life-saving because valvular regurgitation rather than myocardial dysfunction is the underlying problem*, and restoration of valvular competence results in significant clinical improvement (197). Despite earlier reports of higher reoperation rates and surgical mortality for repair performed during the acute period (310,311), more recent investigators have shown no relationship to rheumatic activity, with mortality rates <5% (197,264,311,312). Because the dominant abnormalities underlying acute rheumatic mitral regurgitation are annular dilation and chordal elongation resulting in poor leaflet coaptation, surgical annuloplasty and/or chordal shortening have been performed with good results (186,197).

Chronic RHD

Rheumatic valvular disease is often progressive, resulting in a chronic hemodynamic burden that may require surgical intervention (211). Determining the optimal time for surgical intervention in children with chronic RHD is often difficult. The presence of significant symptoms is a logical and accepted indication, but the optimal timing of intervention for asymptomatic children is unclear. With little data to guide the timing of intervention for rheumatic valvular disease in children, many extrapolate from the guidelines for intervention in adults with valvular heart disease (194,243).

The primary indications for surgical intervention for adults with chronic severe *mitral regurgitation* are symptoms and/or left ventricular dysfunction. Additional indications include marked ventricular enlargement, atrial fibrillation, and pulmonary hypertension (194,237). Recently, some have advocated surgery in asymptomatic patients with severe mitral regurgitation and preserved ventricular function if valve repair rather than replacement is likely and can be performed with low morbidity and mortality (313). An effective regurgitant orifice area >40 mm² (314) or elevation of B-type natriuretic peptide (315) should also warrant careful evaluation and consideration, although when to refer such patients for surgical intervention remains controversial (316). The rheumatic mitral valve can be repaired using techniques including commissuroplasty, debridement, or thinning of the anterior leaflet, often in conjunction with a mitral annuloplasty (317–321). In some cases, the mitral valve cannot be repaired and must be replaced with a prosthetic valve (143,322).

Indications for surgical intervention for chronic *aortic regurgitation* are similar to those for mitral regurgitation and include symptoms, ventricular dysfunction, and marked ventricular enlargement (194). When surgery is indicated, the valve may be repaired or replaced. Historically, most aortic valves warranting intervention have been replaced, but there is increasing experience with valve repair techniques including commissuroplasty, leaflet shortening, and aortic cusp extension (286,310,323,324). Similar to the case with mitral valves, some valves are not amenable to repair and must be replaced. Although pulmonary autograft replacement of the aortic valve (Ross procedure) has been performed on some patients with rheumatic aortic valve disease, the autograft has been shown to be susceptible to rheumatic involvement with an increased risk of valve failure and reoperation (258,325,326).

Indications for intervention for chronic rheumatic *mitral stenosis* include symptoms and/or pulmonary hypertension (194,327). Although open mitral commissurotomy and mitral valve replacement were the surgical procedures of choice in the 1960s and 1970s, percutaneous balloon valvotomy has evolved as an accepted alternative to surgery in selected patients. Immediate results are similar to those of surgical commissurotomy, with success rates of >80% to 95%, doubling of valve area, and a 50% to 60% reduction in transmitral gradient. In addition to being operator dependent, results from percutaneous valvotomy are strongly influenced by patient factors and the morphology of the mitral valve. Patients whose mitral valves are noncalcified with mobile leaflets, without severe leaflet thickening or subvalvular pathology are the best candidates for percutaneous valvotomy, with the highest likelihood of immediate and sustained improvement with a low complication rate (240,241,327). Relative contraindications to percutaneous intervention for mitral stenosis include the presence of a left atrial thrombus and significant mitral regurgitation. When surgery is indicated for rheumatic mitral stenosis, open commissurotomy rather than valve replacement should be performed when possible. Results are similar to those reported for percutaneous valvotomy. When the valve is not amenable to repair, mitral valve replacement is performed with an operative risk of less than 5% in the absence of pulmonary hypertension or other comorbidities (194,328). For mitral stenosis patients who are judged to be good candidates for percutaneous balloon valvotomy, many cardiologists will schedule intervention somewhat earlier in the course than for surgical intervention. Conversely, if mitral valve replacement appears more likely than repair, stricter indications are used, and patients are often sent to surgery later in the course of the mitral valve disease (194,240).

As opposed to patients with congenital aortic valve stenosis in whom intervention is often guided by pressure gradient, indications for intervention for rheumatic *aortic stenosis* are symptoms (angina, syncope, and heart failure), left ventricular dysfunction, or an abnormal response to exercise (symptoms, hypotension, ventricular arrhythmias, impaired exercise tolerance, and new ST segment depression) (194). Also different from congenital aortic valve stenosis is the limited role for percutaneous balloon valvotomy in treating rheumatic aortic valve stenosis; studies have shown a less than optimal improvement in valve area associated with a significant complication rate in this setting (194). Thus, patients meeting indications for intervention should undergo aortic valve

replacement (see aortic regurgitation section for discussion of Ross procedure in this setting).

The surgical approach to rheumatic *tricuspid valve disease* is based on the underlying abnormality. A tricuspid annuloplasty may be performed for tricuspid regurgitation due to annular dilation. Tricuspid commissurotomy is the preferred approach to rheumatic tricuspid stenosis (247,249,252,309).

PREVENTION AND PROPHYLAXIS

Efforts to decrease the incidence of RF and the prevalence and severity of RHD and to prevent complications are focused on a combination of primary prophylaxis, secondary prophylaxis, improving living conditions and developing a vaccine (primordial prophylaxis), and medical management including endocarditis prophylaxis (Fig. 60.8).

Primary Prophylaxis

It is well established that appropriate treatment of streptococcal pharyngitis markedly decreases the risk of developing RF if started within 9 days after the onset of symptoms (11,23,165,329,330). Unfortunately, for as many as one-third to two-thirds of patients, the GAS pharyngitis is subclinical (60), precluding effective primary prevention. Even with a negative throat culture, all patients diagnosed with acute RF should be treated to eradicate GAS from the pharynx and prevent repetitive antigenic stimulation (165). A single intramuscular injection of benzathine penicillin is the most effective treatment, but oral penicillin is an alternative, requiring compliance with the full 10-day treatment course (Table 60.8). Penicillin-allergic patients should receive a narrow-spectrum cephalosporin, clindamycin, clarithromycin, or azithromycin, although some patients allergic to penicillin may also be allergic to cephalosporins (331). Penicillin-resistant strains of GAS have not been reported (266), and follow-up cultures are not necessary. Although some have suggested other antibiotics for the treatment of GAS pharyngitis (126), penicillin remains the treatment of choice for GAS pharyngitis. The American Heart Association, Infectious Disease Society of American, the American College of Physicians-American Society of Internal Medicine, American Academy of Family Physicians, and the U.S. Center for Disease Control

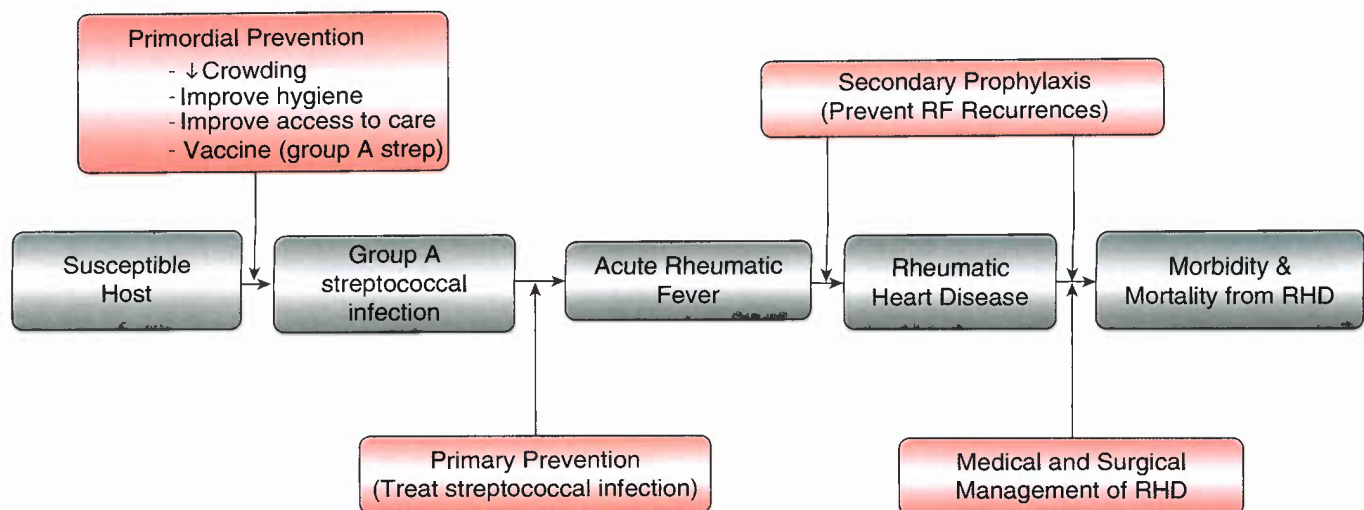


Figure 60.8. Prevention (and management) of acute RF and RHD. RF, rheumatic fever; RHD, rheumatic heart disease.

TABLE 60.8 Treatment of Streptococcal Pharyngitis (Primary Prophylaxis)

Benzathine penicillin G
600,000 U intramuscularly once for patients ≤ 27 kg
1.2 million U intramuscularly once for patients > 27 kg
or
Phenoxymethylpenicillin (penicillin V)
250 mg orally BID or TID for 10 d for patients ≤ 27 kg
500 mg orally BID or TID for 10 d for patients > 27 kg
or
Amoxicillin 50 mg/kg orally once daily for 10 d (max 1 g/dose)
Penicillin-allergic patients
Cephalosporin (narrow-spectrum): dosage regimen depends on agent, ^a oral for 10 d
Clindamycin: 20 mg/kg/d orally divided in three doses for 10 d (max 1.8 g/d)
Azithromycin: 12 mg/kg orally once daily for 10 d (max 500 mg)
Clarithromycin: 15 mg/kg/d orally divided in two doses for 10 d (max 250 mg per dose)

^aUp to 10% of penicillin-allergic individuals are also allergic to cephalosporins. From Gerber MA, Baltimore RS, Eaton CB, et al. Prevention of rheumatic fever and diagnosis and treatment of acute streptococcal pharyngitis: a scientific statement from the American Heart Association Rheumatic Fever, Endocarditis, and Kawasaki Disease Committee of the Council on Cardiovascular Disease in the Young, the Interdisciplinary Council on Functional Genomics and Translational Biology, and the Interdisciplinary Council on Quality of Care and Outcomes Research; endorsed by the American Academy of Pediatrics. *Circulation* 2009;119:1541–1551.

all recommend that GAS pharyngitis be treated for 10 days with oral penicillin or with long-acting benzathine penicillin (55,165,332). Although primary prophylaxis is both recommended and effective for individual patients, it remains unclear and controversial whether it is effective in decreasing the overall incidence of RF (109,333–336). Administration of antibiotics during an episode of RF does not alter the course or severity of cardiac involvement (115). No studies have shown tonsillectomy to be effective in reducing the incidence of RF.

Secondary Prophylaxis

In the absence of specific and effective treatment for RF, preventing RF recurrences is the most effective means of decreasing the likelihood and severity of long-term chronic RHD (7). All patients who have had RF, especially those with cardiac involvement, are at risk for recurrences. Some studies report this risk to be as high as 40% to 60% for patients with cardiac involvement (47,264,337). The risk of recurrence is greatest in the first few years following an episode of RF, and then decreases with time. The pattern of clinical involvement with such recurrences is often mimetic, following the pattern of the initial episode. Thus, patients who have carditis with their first episode of RF are likely to have cardiac involvement with recurrences. The recurrences often result in more severe rheumatic valvular dysfunction and a greater likelihood of significant chronic RHD (44,338). Unfortunately, the mimetic clinical pattern with recurrences is not absolute, and a minority (6% to 14%) of patients develops clinical carditis and subsequent RHD only after a recurrence (114,338,339).

TABLE 60.9 Secondary Prophylaxis After RF

Benzathine penicillin G
600,000 U intramuscularly every 3–4 wk for patients ≤ 27 kg (60 lb)
1.2 million U intramuscularly every 3–4 wk for patients > 27 kg (60 lb)
or
Phenoxymethylpenicillin (penicillin V)
250 mg orally twice daily
or
Sulfadiazine
0.5 g orally once daily for patients ≤ 27 kg
1 g orally once daily for patients > 27 kg
Penicillin- and sulfa-allergic patients
Macrolide or azalide (dose depends on agent and patient size)

Category	Duration
RF with carditis and residual RHD (clinical or echocardiographic)	10 y since last episode or until age 40 y ^a ; possibly lifelong
RF with carditis, but no residual RHD	10 y or until age 21 y ^a
RF without carditis	5 y or until age 21 y ^a

^aWhichever is longer.

From Gerber MA, Baltimore RS, Eaton CB, et al. Prevention of rheumatic fever and diagnosis and treatment of acute streptococcal pharyngitis: a scientific statement from the American Heart Association Rheumatic Fever, Endocarditis, and Kawasaki Disease Committee of the Council on Cardiovascular Disease in the Young, the Interdisciplinary Council on Functional Genomics and Translational Biology, and the Interdisciplinary Council on Quality of Care and Outcomes Research; endorsed by the American Academy of Pediatrics. *Circulation* 2009;119:1541–1551.

Thus, all patients who have had RF should receive secondary prophylaxis to prevent recurrences (Table 60.9). Intramuscular administration of benzathine penicillin (1.2 million units) is the most effective secondary prophylaxis regimen. In many areas, this injection is administered every 4 weeks. However, there is pharmacokinetic evidence that penicillin levels fall between 21 and 28 days after administration in a significant proportion of patients (340). Thus, in areas where RF is endemic and/or in cases with a documented RF recurrence on every 4-week prophylaxis, every 3-week administration of intramuscular penicillin may be preferable (Indian Academy of Pediatrics recommends every 2 weeks for some patients) (341,342). Oral penicillin is a reasonable alternative, especially in parts of the world where RF is less common and in low-risk cases (165,331). Sulfadiazine is recommended for patients allergic to penicillin. Recent reports emphasize the importance of noncompliance in the evolution of heart disease and precipitation of congestive heart failure in an at-risk population (343).

The recommended duration of secondary prophylaxis is influenced by the presence of acute and chronic cardiac involvement and by the time since the last episode of RF (Table 60.9) (165). Since patients who have had carditis are at higher risk for cardiac involvement with recurrences, the recommended duration of secondary prophylaxis is longer for this group of patients. In selected low-risk patients (e.g., no carditis or RHD) more than 5 years out from the RF illness,

discontinuation of prophylaxis earlier than suggested in the guidelines of Table 60.9 may be justified (344). Some recommend that patients with persistent RHD receive secondary prophylaxis indefinitely (165,267), while others have suggested that prophylaxis is unnecessary beyond age mid-20s (286). Patients should continue to receive secondary prophylaxis even after valve replacement since recurrence may result in damage to other cardiac valves (345). Allergic (3%) and anaphylactic (0.2%) reactions to monthly benzathine penicillin infections are uncommon and are unrelated to the duration of prophylaxis (7).

Unfortunately, many patients with RHD do not receive secondary prophylaxis, for at least two reasons. First, in order for secondary prophylaxis to be effective in reducing the prevalence and evolution of chronic RHD, patients who would benefit from such a prophylaxis program must be identified. Many patients with RHD do not recall having had prior RF and are unaware of their heart disease until they either develop symptoms or have their valvular abnormality detected incidentally. The World Health Organization recommends school-based screening to identify such patients, but the optimal method for screening remains to be established. Two reports of school-based screening using echocardiography performed in Mozambique and Cambodia found the prevalence of RHD detected using echocardiography to be 10 to 13 times greater than using clinical auscultation alone (346). Thus, 90% of RHD cases were only detected by echocardiography. A similar study performed in Tonga yielded a similar prevalence of RHD using echocardiography (347). There continues to be debate regarding the diagnosis of subclinical RHD. It is well known that many patients who present with RHD cannot recall having prior RF and that a significant proportion of patients with “pure” chorea (no clinical carditis) go on to develop chronic RHD (suggesting very mild or subclinical cardiac involvement). On the other hand, small amounts of valvular regurgitation can be seen in normals (“physiologic”) so that differentiation between mild pathologic and physiologic regurgitation can be difficult, leading to the potential for overdiagnosis. To address this difficulty, criteria have been evaluated and proposed that help distinguish physiologic from pathologic Doppler regurgitation (7,219,222,225,226). In addition, some have proposed that both 2-D morphologic changes and Doppler evidence of valvular regurgitation be required for the diagnosis of subclinical RHD (25). However, this requirement risks underdiagnosis as many patients with mild RHD show clearly pathologic valvular regurgitation with minimal morphologic changes.

Second, once patients who would benefit from secondary prophylaxis have been identified, compliance must be optimized. Both the World Health Organization and World Health Federation recommend register-based control programs to promote education, training, and early recognition of RF and RHD and to optimize and coordinate the delivery of secondary prophylaxis in populations with a high prevalence of RHD. Although establishing and sustaining such programs is challenging, especially in developing countries, the potential benefits of such programs are significant and form the basis of the joint global project on RF/RHD prevention and promotion (6,7,109).

Primordial Prevention

The fact that as many as one-third to two-thirds of cases of RF are preceded by a minimally symptomatic or asymptomatic GAS pharyngitis makes effective *primary prophylaxis* impossible in many cases. Poor access to health care in developing countries where the incidence of RF is high further decreases the likelihood of effective primary prophylaxis. If the initial episode of RF is not recognized, *secondary prophylaxis* (to

prevent recurrences) cannot be implemented. Even when the initial episode is diagnosed, poor compliance with long-term secondary prophylaxis may further limit effective prevention of RF recurrences that may lead to progressive RHD (6). While secondary prophylaxis is the most cost-effective approach to preventing RHD once a patient is known to have had RF/RHD, the most effective way to decrease the burden of RF and RHD in developing countries may be by reducing exposure to GAS, termed by some as “primordial prophylaxis.” Such primordial prevention can occur in at least two ways. Since improvement in socioeconomic conditions in industrialized countries has led to a significant decrease in the incidence of RF and the prevalence of RHD, it is not unreasonable to think that similar improvements in developing countries may result in similar benefit. There is also ongoing work to develop an effective GAS vaccine. Challenges in the development of such a vaccine include the fact that it must be multivalent (accounting for the numerous M types that may lead to RF), safe (cross-reactive antibody has the potential to produce significant unwanted side effects), and would be preferably mucosal (administered intranasal or orally rather than by injection) (7,109,348,349).

Endocarditis Prophylaxis

Endocarditis continues to be an important complication of RHD (8,350). The American Heart Association Guidelines for endocarditis prophylaxis were revised in 2007 such that prophylaxis is now recommended for patients undergoing dental procedures with cardiac conditions associated with the highest risk of adverse outcome from endocarditis. This includes patients with prosthetic cardiac valves or prosthetic material used for cardiac valve repair and those who have had previous endocarditis. Prophylaxis is no longer recommended for patients with other conditions (including many patients with RHD). Prophylaxis is recommended for “dental procedures that involve manipulation of gingival tissue or the periapical region of teeth or perforation of the oral mucosa,” but is no longer recommended for gastrointestinal or genitourinary procedures (351). The reader is referred to the Guideline statement for details regarding patient selection and antibiotic regimen. Since patients receiving chronic penicillin prophylaxis are likely to be colonized with amoxicillin-resistant organisms, clindamycin, clarithromycin, or azithromycin are recommended for indicated procedures (351,352).

SUMMARY

- RF and RHD continue to be major problems in developing countries, resulting in significant morbidity and mortality.
- Factors related to the streptococcal organism, the environment, and host susceptibility influence the likelihood of an individual developing RF.
- The pathogenesis of RF is likely related to an abnormal immune response to a preceding GAS infection; both humoral and cell-mediated immune responses contribute to the clinical manifestations, including acute carditis and chronic RHD.
- The most common clinical manifestations of RF are arthritis, carditis, and chorea; carditis and subsequent RHD are responsible for long-term morbidity and mortality.
- Diagnostic criteria should serve as guidelines to assist in the diagnosis of both initial and recurrent attacks of RF. In areas where RF and RHD continue to be common, modification of the diagnostic criteria (e.g., polyarthralgia, monoarthritis, and silent carditis as major criteria) may improve sensitivity and decrease underdiagnosis.

- Valvular dysfunction (rather than myocarditis or pericarditis) is the important abnormality in both acute rheumatic carditis and chronic RHD.
- Echocardiography should be performed (if available) on all patients with RF. It is useful in confirming and quantifying valvular regurgitation, in differentiating acute RHD from innocent murmurs or congenital heart disease, in the serial evaluation of patients with known RHD, and in identifying subclinical rheumatic cardiac involvement. The World Health Organization recommends that silent but significant mitral and/or aortic regurgitation be considered *probable* RHD, and that such patients be given secondary prophylaxis and followed long-term for evolution of heart disease. Guidelines from Australia and New Zealand recommend that subclinical rheumatic carditis be accepted as a major criterion in diagnosing RF.
- The most important factors influencing the likelihood and severity of chronic RHD are the severity of the initial carditis, and RF recurrences.
- Primary prophylaxis (treatment of GAS pharyngitis) is effective in preventing RF, but many cases go untreated (very mild symptoms or subclinical pharyngitis).
- Preventing recurrences of RF (secondary prophylaxis) is the most effective means of decreasing the likelihood and severity of long-term RHD.
- The most effective way to decrease the burden of RF and RHD in developing countries may be via improvement in living conditions (crowding, hygiene, access to care) and development of an effective vaccine against GAS ("primordial prophylaxis"); efforts are ongoing in these areas.
- Mechanical intervention techniques for RHD continue to improve. Percutaneous balloon valvotomy is effective in many patients with rheumatic mitral stenosis, and both mitral valve and aortic valve repair (as opposed to replacement) are being performed more commonly, with better outcomes.

REFERENCES

1. Steer AC, Carapetis JR, Nolan TM, et al. Systematic review of rheumatic heart disease prevalence in children in developing countries: the role of environmental factors. *J Paediatr Child Health* 2002;38:229–234.
2. Agarwal BL. Rheumatic heart disease unabated in developing countries. *Lancet* 1981;2:910–911.
3. Mendez GF, Cowie MR. The epidemiological features of heart failure in developing countries: a review of the literature. *Int J Cardiol* 2001;80:213–219.
4. Olivier C. Rheumatic fever—is it still a problem? *J Antimicrob Chemother* 2000;45:13–21.
5. Ibrahim A, Rahman AR. Rheumatic heart disease: how big is the problem? *Med J Malaysia* 1995;50:121–124.
6. Strategy for controlling rheumatic fever/rheumatic heart disease, with emphasis on primary prevention: memorandum from a joint WHO/ISFC meeting. *Bull World Health Organ* 1995;73:583–587.
7. Rheumatic fever and rheumatic heart disease. *World Health Organ Tech Rep Ser* 2004;923:1–122, back cover.
8. Carapetis JR, Steer AC, Mulholland EK, et al. The global burden of group A streptococcal diseases. *Lancet Infect Dis* 2005;5:685–694.
9. Carapetis JR, Currie BJ, Mathews JD. Cumulative incidence of rheumatic fever in an endemic region: a guide to the susceptibility of the population? *Epidemiol Infect* 2000;124:239–244.
10. Carapetis JR, McDonald M, Wilson NJ. Acute rheumatic fever. *Lancet* 2005;366:155–168.
11. Massell BF, Chute CG, Walker AM, et al. Penicillin and the marked decrease in morbidity and mortality from rheumatic fever in the United States. *N Engl J Med* 1988;318:280–286.
12. Gordis L. The virtual disappearance of rheumatic fever in the United States: lessons in the rise and fall of disease. T. Duckett Jones memorial lecture. *Circulation* 1985;72:1155–1162.
13. Shulman ST, Stollerman G, Beall B, et al. Temporal changes in streptococcal M protein types and the near-disappearance of acute rheumatic fever in the United States. *Clin Infect Dis* 2006;42:441–447.
14. Veasy LG, Wiedmeier SE, Orsmond GS, et al. Resurgence of acute rheumatic fever in the intermountain area of the United States. *New Engl J Med* 1987;316:421–427.
15. Hosier DM, Craenen JM, Teske DW, et al. Resurgence of acute rheumatic fever. *Am J Dis Children* 1987;141:730–733.
16. Congeni B, Rizzo C, Congeni J, et al. Outbreak of acute rheumatic fever in northeast Ohio. *J Pediatr* 1987;111:176–179.
17. Wald ER, Dashefsky B, Feidt C, et al. Acute rheumatic fever in western Pennsylvania and the tristate area. *Pediatrics* 1987;80:371–374.
18. Westlake RM, Graham TP, Edwards KM. An outbreak of acute rheumatic fever in Tennessee. *Pediatr Infect Dis J* 1990;9:97–100.
19. Leggiadro RJ, Birnbaum SE, Chase NA, et al. A resurgence of acute rheumatic fever in a mid-South children's hospital. *South Med J* 1990;83:1418–1420.
20. Kavey RE, Kaplan EL. Resurgence of acute rheumatic fever. *Pediatrics* 1989;84:585–586.
21. Veasy LG, Tani LY, Daly JA, et al. Temporal association of the appearance of mucoid strains of *Streptococcus pyogenes* with a continuing high incidence of rheumatic fever in Utah. *Pediatrics* 2004;113:e168–172.
22. Dajani A, Taubert K, Ferrieri P, et al. Treatment of acute streptococcal pharyngitis and prevention of rheumatic fever: a statement for health professionals. Committee on Rheumatic Fever, Endocarditis, and Kawasaki Disease of the Council on Cardiovascular Disease in the Young, the American Heart Association. *Pediatrics* 1995;96:758–764.
23. Gerber MA, Markowitz M. Management of streptococcal pharyngitis reconsidered. *Pediatr Infect Dis* 1985;4:518–526.
24. Steer AC, Adams J, Carlin J, et al. Rheumatic heart disease in school children in Samoa. *Arch Dis Child* 1999;81:372.
25. Marijon E, Celermajer DS, Taffler M, et al. Rheumatic heart disease screening by echocardiography: the inadequacy of World Health Organization criteria for optimizing the diagnosis of subclinical disease. *Circulation* 2009;120:663–668.
26. Barlow JB. Aspects of active rheumatic carditis. *Aust N Z J Med* 1992;22:592–600.
27. Marcus RH, Sareli P, Pocock WA, et al. The spectrum of severe rheumatic mitral valve disease in a developing country. Correlations among clinical presentation, surgical pathologic findings, and hemodynamic sequelae. [see comments.] *Ann Intern Med* 1994;120:177–183.
28. Carapetis JR, Currie BJ. Mortality due to acute rheumatic fever and rheumatic heart disease in the Northern Territory: a preventable cause of death in aboriginal people. *Aust N Z J Public Health* 1999;23:159–163.
29. Roy SB, Bhatia ML, Lazaro EJ, et al. Juvenile mitral stenosis in India. *Lancet* 1963;41:1193–1195.
30. Joshi MK, Kandath PW, Barve RJ, et al. Rheumatic fever. Clinical profile of 339 cases with long term follow up. *Indian Pediatr* 1983;20:849–853.
31. Oli K, Asmera J. Rheumatic heart disease in Ethiopia: could it be more malignant? *Ethiop Med J* 2004;42:1–8.
32. Soler-Soler J, Galve E. Worldwide perspective of valve disease. *Heart* 2000;83:721–725.
33. Rheumatic fever and rheumatic heart disease. Report of a WHO Study Group. *World Health Organ Tech Rep Ser* 1988;764:1–58.
34. Gibofsky A, Kerwar S, Zabriskie JB. Rheumatic fever. The relationships between host, microbe, and genetics. *Rheum Dis Clin North Am* 1998;24:237–259.
35. Miyake CY, Gauvreau K, Tani LY, et al. Characteristics of children discharged from hospitals in the United States in 2000 with the diagnosis of acute rheumatic fever. *Pediatrics* 2007;120:503–508.
36. Kumar RK, Rammohan R, Narula J, et al. Epidemiology of streptococcal pharyngitis, rheumatic fever, and rheumatic heart disease. In: Narula J, Virmani R, Reddy KS, et al., eds. *Rheumatic Fever*. Washington, DC: American Registry of Pathology, 1999:41–68.
37. Bisno AL. Group A streptococcal infections and acute rheumatic fever. *N Engl J Med* 1991;325:783–793.
38. Tani LY, Veasy LG, Minich LL, et al. Rheumatic fever in children younger than 5 years: is the presentation different? *Pediatrics* 2003;112:1065–1068.
39. Rosenthal A, Czoniczer G, Massell BF. Rheumatic fever under 3 years of age. A report of 10 cases. *Pediatrics* 1968;41:612–619.
40. McDonald EC, Weisman MH. Articular manifestations of rheumatic fever in adults. *Ann Intern Med* 1978;89:917–920.
41. Stollerman GH. Rheumatic fever. [see comments.] *Lancet* 1997;349:935–942.
42. Bisno AL. Noncardiac manifestations of rheumatic fever. In: Narula J, Virmani R, Reddy KS, et al., eds. *Rheumatic Fever*. Washington, DC: American Registry of Pathology, 1999:245–256.
43. Nausieda PA, Grossman BJ, Koller WC, et al. Sydenham chorea: an update. *Neurology* 1980;30:331–334.
44. Feinstein AR, Spagnuolo M. The clinical patterns of acute rheumatic fever: a reappraisal. *Medicine* 1962;41:279–305.
45. Feinstein AR, Spagnuolo M, Wood HF, et al. Rheumatic fever in children and adolescents. A long-term epidemiologic study of subsequent prophylaxis, streptococcal infections, and clinical sequelae. VI. Clinical features of streptococcal infections and rheumatic recurrences. *Ann Intern Med* 1964;60:68–86.
46. Rammelkamp CH. Epidemiology of streptococcal infections. *Harvey Lect* 1956;51:113–142.
47. Massell BF. Factors in the pathogenesis of rheumatic fever recurrences. *J Maine Med Assoc* 1962;53:88–93.
48. Wilson MG, Schweitzer MD, Rubshez R. The familial epidemiology of rheumatic fever. *J Pediatr* 1943;22:468–492.

49. Cheadle WB. The various manifestations of the rheumatic state as exemplified in childhood and early life. *Lancet* 1889;1:821-827.
50. DiSciascio G, Taranta A. Rheumatic fever in children. *Am Heart J* 1980;99:635-658.
51. Taranta A, Torosdag S, Metrakos JD, et al. Rheumatic fever in monozygotic and dizygotic twins. *Circulation* 1959;20:778.
52. Ayoub EM. The search for host determinants of susceptibility to rheumatic fever: the missing link. T. Duckett Jones Memorial Lecture. *Circulation* 1984;69:197-201.
53. Chun LT, Reddy V, Rhoads GG. Occurrence and prevention of rheumatic fever among ethnic groups of Hawaii. *Am J Dis Child* 1984;138:476-478.
54. Kurahara D, Tokuda A, Grandinetti A, et al. Ethnic differences in risk for pediatric rheumatic illness in a culturally diverse population. *J Rheumatol* 2002;29:379-383.
55. McIsaac WJ, Kellner JD, Aufricht P, et al. Empirical validation of guidelines for the management of pharyngitis in children and adults. *JAMA* 2004;291:1587-1595.
56. Giesecke KE, Roe MH, MacKenzie T, et al. Evaluating the American Academy of Pediatrics diagnostic standard for *Streptococcus pyogenes* pharyngitis: backup culture versus repeat rapid antigen testing. *Pediatrics* 2003;111:e666-670.
57. Kaplan EL, Huew BB. The sensitivity and specificity of an agglutination test for antibodies to streptococcal extracellular antigens: a quantitative analysis and comparison of the streptozyme test with the anti-streptolysin O and anti-deoxyribonuclease B tests. *J Pediatr* 1980;96:367-373.
58. Martin JM, Green M, Barbadora KA, et al. Group A streptococci among school-aged children: clinical characteristics and the carrier state. *Pediatrics* 2004;114:1212-1219.
59. Pichichero ME, Marsocci SM, Murphy ML, et al. Incidence of streptococcal carriers in private pediatric practice. *Arch Pediatr Adolesc Med* 1999;153:624-628.
60. Veasy LG, Tani LY, Hill HR. Persistence of acute rheumatic fever in the intermountain area of the United States. [see comments.]. *J Pediatr* 1994;124:9-16.
61. Coburn AF, Pauli RH. Studies of the immune response of the rheumatic subject and its relationship to activity of the rheumatic process. IV. Characteristics of strains of hemolytic streptococcus, effective and non-effective in initiating rheumatic activity. *J Clin Invest* 1935;14:755-762.
62. Bisno AL, Pearce IA, Stollerman GH. Streptococcal infections that fail to cause recurrences of rheumatic fever. *J Infect Dis* 1977;136:278-285.
63. Stollerman GH. Nephritogenic and rheumatogenic group A streptococci. *J Infect Dis* 1969;120:258-263.
64. Stollerman GH. The relative rheumatogenicity of strains of group A streptococci. *Mod Concepts of Cardiovasc Dis* 1975;44:35-40.
65. Cunningham MW. Pathogenesis of group A streptococcal infections. *Clin Microbiol Rev* 2000;13:470-511.
66. Stollerman GH. Rheumatic fever in the 21st century. *Clin Infect Dis* 2001;33:806-814.
67. Stollerman GH. Rheumatogenic streptococci and autoimmunity. *Clin Immunol Immunopathol* 1991;61:131-142.
68. Stollerman GH. Rheumatogenic group A streptococci and the return of rheumatic fever. *Adv Intern Med* 1990;35:1-25.
69. Johnson DR, Stevens DL, Kaplan EL. Epidemiologic analysis of group A streptococcal serotypes associated with severe systemic infections, rheumatic fever, or uncomplicated pharyngitis. *J Infect Dis* 1992;166:374-382.
70. Smoot JC, Korgenski EK, Daly JA, et al. Molecular analysis of group A Streptococcus type emm18 isolates temporally associated with acute rheumatic fever outbreaks in Salt Lake City, Utah. *J Clin Microbiol* 2002;40:1805-1810.
71. Miner LJ, Petheram SJ, Daly JA, et al. Molecular characterization of *Streptococcus pyogenes* isolates collected during periods of increased acute rheumatic fever activity in Utah. *Pediatr Infect Dis J* 2004;23:56-61.
72. Carapetis JR, Currie BJ. Group A streptococcus, pyoderma, and rheumatic fever. *Lancet* 1996;347:1271-1272.
73. McDonald MI, Towers RJ, Andrews RM, et al. Low rates of streptococcal pharyngitis and high rates of pyoderma in Australian aboriginal communities where acute rheumatic fever is hyperendemic. *Clin Infect Dis* 2006;43:683-689.
74. Kaplan EL, Bisno AL. Antecedent streptococcal infection in acute rheumatic fever. *Clin Infect Dis* 2006;43:690-692.
75. Stollerman GH, Lewis AJ, Schultz I, et al. Relationship of immune response to group A streptococci to the course of acute, chronic and recurrent rheumatic fever. *Am J Med* 1956;20:163-169.
76. Wannamaker LW, Rammelkamp CH Jr, Denny FW, et al. Prophylaxis of acute rheumatic fever by treatment of the preceding streptococcal infection with various amounts of depot penicillin. *Am J Med* 1951;10:673-695.
77. Denny FW, Wannamaker LW, Brink WR, et al. Prevention of rheumatic fever; treatment of the preceding streptococcal infection. *JAMA* 1950;143:151-153.
78. Massell BF. Management of rheumatic fever; therapy of the acute attack and prevention of recurrences. *Pediatr Clin North Am* 1958;5:1143-1159.
79. Massell BF, Dow JE, Jones TD. Orally administered penicillin in patient with rheumatic fever. *JAMA* 1948;138:1030-1036.
80. Thomas CB, France R. Preliminary report of prophylactic use of sulfanilamide in patients susceptible to rheumatic fever. *Bull Johns Hopkins Hosp* 1939;64:67-77.
81. Frank PF, Stollerman GH, Miller LF. Protection of a military population from rheumatic fever. Routine administration of Benzathine Penicillin G to healthy individuals. *JAMA* 1965;193:775-783.
82. Ottolini MG, Burnett MW. History of U.S. military contributions to the study of respiratory infections. *Mil Med*. 2005;170:66-70.
83. Acute rheumatic fever among Army trainees—Fort Leonard Wood, Missouri, 1987-1988. *MMWR Morb Mortal Wkly Rep* 1988;37:519-522.
84. Rammelkamp CH Jr, Stolzer BL. The latent period before the onset of acute rheumatic fever. *Yale J Biol Med* 1961;34:386-398.
85. Horstkotte D, Niehues R, Strauer BE. Pathomorphological aspects, aetiology and natural history of acquired mitral valve stenosis. *Eur Heart J* 1991;12:55-60.
86. Ayoub EM, Barrett DJ, Maclaren NK, et al. Association of class II human histocompatibility leukocyte antigens with rheumatic fever. *J Clin Invest* 1986;77:2019-2026.
87. Guede Y, Kotby A, El-DeMellawy M, et al. HLA class II associations with rheumatic heart disease are more evident and consistent among clinically homogeneous patients. *Circulation* 1999;99:2784-2790.
88. Gerbase-DeLima M, Scala LC, Temin J, et al. Rheumatic fever and the HLA complex. A cosegregation study. *Circulation* 1994;89:138-141.
89. Guilherme L, Cury P, Demarchi LM, et al. Rheumatic heart disease: pro-inflammatory cytokines play a role in the progression and maintenance of valvular lesions. *Am J Pathol* 2004;165:1583-1591.
90. Guilherme L, Kalil J. Rheumatic fever and rheumatic heart disease: cellular mechanisms leading autoimmune reactivity and disease. *J Clin Immunol* 2010;30:17-23.
91. Khanna AK, Buskirk DR, Williams RC Jr, et al. Presence of a non-HLA B cell antigen in rheumatic fever patients and their families as defined by a monoclonal antibody. *J Clin Invest* 1989;83:1710-1716.
92. Zabriskie JB, Lavenchy D, Williams RC Jr, et al. Rheumatic fever-associated B cell alloantigens as identified by monoclonal antibodies. *Arthritis Rheum* 1985;28:1047-1051.
93. Weisz JL, McMahon WM, Moore JC, et al. D8/17 and CD19 expression on lymphocytes of patients with acute rheumatic fever and Tourette's disorder. *Clin Diagn Lab Immunol* 2004;11:330-336.
94. Bryant PA, Robins-Browne R, Carapetis JR, et al. Some of the people, some of the time: susceptibility to acute rheumatic fever. *Circulation* 2009;119:742-753.
95. Hernandez-Pacheco G, Flores-Dominguez C, Rodriguez-Perez JM, et al. Tumor necrosis factor-alpha promoter polymorphisms in Mexican patients with rheumatic heart disease. *J Autoimmun* 2003;21:59-63.
96. Chou HT, Tsai CH, Tsai FJ. Association between angiotensin I-converting enzyme gene insertion/deletion polymorphism and risk of rheumatic heart disease. *Jpn Heart J* 2004;45:949-957.
97. Davutoglu V, Nacak M. Influence of angiotensin-converting enzyme gene insertion/deletion polymorphism on rheumatic valve involvement, valve severity and subsequent valve calcification. *J Heart Valve Dis* 2005;14:277-281.
98. Kaplan MH, Meyerserian M. An immunological cross-reaction between group-A streptococcal cells and human heart tissue. *Lancet* 1962;1:706-710.
99. Dale JB, Beachey EH. Epitopes of streptococcal M proteins shared with cardiac myosin. *J Exp Med* 1985;162:583-591.
100. Cunningham MW, McCormack JM, Talaber LR, et al. Human monoclonal antibodies reactive with antigens of the group A Streptococcus and human heart. *J Immunol* 1988;141:2760-2766.
101. Zabriskie JB, Hsu KC, Seegal BC. Heart-reactive antibody associated with rheumatic fever: characterization and diagnostic significance. *Clin Exp Immunol* 1970;7:147-159.
102. Roberts S, Kosanke S, Terrence Dunn S, et al. Pathogenic mechanisms in rheumatic carditis: focus on valvular endothelium. *J Infect Dis* 2001;183:507-511.
103. Ellis NM, Li Y, Hildebrand W, et al. T cell mimicry and epitope specificity of cross-reactive T cell clones from rheumatic heart disease. *J Immunol* 2005;175:5448-5456.
104. Guilherme L, Kalil J, Cunningham M. Molecular mimicry in the autoimmune pathogenesis of rheumatic heart disease. *Autoimmunity* 2006;39:31-39.
105. Carreno-Manjarrez R, Visvanathan K, Zabriskie JB. Immunogenic and genetic factors in rheumatic fever. *Curr Infect Dis Rep* 2000;2:302-307.
106. Cunningham MW. Molecular mimicry between group A streptococci and myosin in the pathogenesis of acute rheumatic fever. In: Narula J, Virmani R, Reddy KS, et al., eds. *Rheumatic Fever*. Washington, DC: American Registry of Pathology, 1999:135-165.
107. Guilherme L, Fae KC, Oshiro SE, et al. Rheumatic fever: how *S. pyogenes*-primed peripheral T cells trigger heart valve lesions. *Ann N Y Acad Sci* 2005;1051:132-140.
108. Fae KC, da Silva DD, Oshiro SE, et al. Mimicry in recognition of cardiac myosin peptides by heart-intralesional T cell clones from rheumatic heart disease. *J Immunol* 2006;176:5662-5670.
109. Steer AC, Carapetis JR. Prevention and treatment of rheumatic heart disease in the developing world. *Nat Rev Cardiol* 2009;6:689-698.
110. Bland EF, Jones TD. Rheumatic fever and rheumatic heart disease: a twenty year report on 1000 patients followed since childhood. *Circulation* 1951;4:836-843.

111. The natural history of rheumatic fever and rheumatic heart disease. Ten-year report of a cooperative clinical trial of ACTH, cortisone, and aspirin. *Circulation* 1965;32:457-476.
112. Feinstein AR, Stern EK, Spagnuolo M. The prognosis of acute rheumatic fever. *Am Heart J* 1964;68:817-834.
113. Sanyal S, Berry A, Duggal S, et al. Sequelae of the initial attack of acute rheumatic fever in children from North India. A prospective 5-year follow-up study. *Circulation* 1982;65:375-379.
114. Feinstein AR, Stern EK. Clinical effects of recurrent attacks of acute rheumatic fever: a prospective epidemiologic study of 105 episodes. *J Chronic Dis* 1967;20:13-27.
115. Tompkins DG, Boxerbaum B, Liebman J. Long-term prognosis of rheumatic fever patients receiving regular intramuscular benzathine penicillin. *Circulation* 1972;45:543-551.
116. Feinstein AR, Wood HF, Spagnuolo M, et al. Rheumatic fever in children and adolescents. A long-term epidemiologic study of subsequent prophylaxis, streptococcal infections, and clinical sequelae. VII. Cardiac changes and sequelae. *Ann Intern Med* 1964;60:87-123.
117. The Evolution of Rheumatic Heart Disease in Children. Five-year report of a cooperative clinical trial of ACTH, cortisone, and aspirin. *Circulation* 1960;22:503-515.
118. Majeed HA, Batnager S, Yousof AM, et al. Acute rheumatic fever and the evolution of rheumatic heart disease: a prospective 12 year follow-up report. *J Clin Epidemiol* 1992;45:871-875.
119. Thomas GT. Five-year follow-up on patients with rheumatic fever treated by bed rest, steroids, or salicylate. *Br Med J* 1961;5240:1635-1639.
120. Gross L, Ehrlich JC. Studies on the myocardial Aschoff body. II. Life cycle, sites of predilection and relation to clinical course of rheumatic fever. *Am J Pathol* 1934;10:489-503.
121. Saphir O. The Aschoff nodule. *Am J Clin Pathol* 1959;31:534-539.
122. Virmani R, Roberts W. Aschoff bodies in operatively excised atrial appendages and in papillary muscles. Frequency and clinical significance. *Circulation* 1977;55:559-563.
123. Gross L, Fried BM. Lesions in the auriculoventricular conduction system occurring in rheumatic fever. *Am J Pathol* 1936;12:31-43.
124. Virmani R, Farb A, Burke AP, et al. Pathology of acute rheumatic carditis. In: Narula J, Virmani R, Reddy KS, et al., eds. *Rheumatic Fever*. Washington, DC: American Registry of Pathology, 1999:217-234.
125. Gross L, Friedberg CK. Lesions of the cardiac valve rings in rheumatic fever. *Am J Pathol* 1935;12:469-493.
126. Camara EJ, Neubauer C, Camara GF, et al. Mechanisms of mitral valvar insufficiency in children and adolescents with severe rheumatic heart disease: an echocardiographic study with clinical and epidemiological correlations. *Cardiol Young* 2004;14:527-532.
127. Kamblock J, N'Guyen L, Pagis B, et al. Acute severe mitral regurgitation during first attacks of rheumatic fever: clinical spectrum, mechanisms and prognostic factors. *J Heart Valve Dis* 2005;14:440-446.
128. Tomaru T, Uchida Y, Mohri N, et al. Postinflammatory mitral and aortic valve prolapse: a clinical and pathological study. *Circulation* 1987;76:68-76.
129. Gross L, Kugel MA, Epstein EZ. Lesions of the coronary arteries and their branches in rheumatic fever. *Am J Pathol* 1935;11:253-279.
130. Jones TD. Diagnosis of rheumatic fever. *JAMA* 1944;126:481-484.
131. Anonymous. Jones criteria (revised) for guidance in the diagnosis of rheumatic fever. *Circulation* 1965;32:664-668.
132. Anonymous. Jones Criteria (revised) for guidance in the diagnosis of rheumatic fever. *Circulation*. 1984;69:204A-208A.
133. Anonymous. Guidelines for the diagnosis of rheumatic fever. Jones Criteria, 1992 update. Special Writing Group of the Committee on Rheumatic Fever, Endocarditis, and Kawasaki Disease of the Council on Cardiovascular Disease in the Young of the American Heart Association. [See comments.] [Erratum appears in *JAMA* 1993;269(4):476.] *JAMA* 1992;268:2069-2073.
134. Rutstein DD, Bauer, Dorfman A, et al. Jones Criteria (modified) for guidance in the diagnosis of rheumatic fever. *Mod Concepts Cardiovasc Dis* 1955;24:291-293.
135. Shiffman RN. Guideline maintenance and revision. 50 years of the Jones criteria for diagnosis of rheumatic fever. [See comments.] *Arch Pediatr Adolesc Med* 1995;149:727-732.
136. Carapetis JR, Currie BJ. Rheumatic fever in a high incidence population: the importance of monoarthritis and low grade fever. *Arch Dis Child* 2001;85:223-227.
137. Saxena A. Diagnosis of rheumatic fever: current status of Jones criteria and role of echocardiography. *Indian J Pediatr* 2000;67:S11-S14.
138. Ralph A, Jacups S, McGough K, et al. The challenge of acute rheumatic fever diagnosis in a high-incidence population: a prospective study and proposed guidelines for diagnosis in Australia's Northern Territory. *Heart Lung Circ* 2006;15:113-118.
139. Guidelines for the diagnosis of rheumatic fever. Jones Criteria, 1992 update. Special Writing Group of the Committee on Rheumatic Fever, Endocarditis, and Kawasaki Disease of the Council on Cardiovascular Disease in the Young of the American Heart Association. *JAMA* 1992;268:2069-2073.
140. Giannoulia-Karantana A, Anagnostopoulos G, Kostaridou S, et al. Childhood acute rheumatic fever in Greece: experience of the past 18 years. *Acta Paediatr* 2001;90:809-812.
141. Sanyal SK, Thapar MK, Ahmed SH, et al. The initial attack of acute rheumatic fever during childhood in North India; a prospective study of the clinical profile. *Circulation* 1974;49:7-12.
142. Ravisha MS, Tullu MS, Kamat JR. Rheumatic fever and rheumatic heart disease: clinical profile of 550 cases in India. *Arch Med Res* 2003;34:382-387.
143. Bitar FF, Hayek P, Obeid M, et al. Rheumatic fever in children: a 15-year experience in a developing country. *Pediatr Cardiol* 2000;21:119-122.
144. Arora R, Subramanyam G, Khalilullah M, et al. Clinical profile of rheumatic fever and rheumatic heart disease: a study of 2,500 cases. *Indian Heart J* 1981;33:264-269.
145. Chagani HS, Aziz K. Clinical profile of acute rheumatic fever in Pakistan. *Cardiol Young* 2003;13:28-35.
146. Chockalingam A, Gnanavelu G, Elangovan S, et al. Current profile of acute rheumatic fever and valvulitis in southern India. *J Heart Valve Dis* 2003;12:573-576.
147. Griffiths SP, Gersony WM. Acute rheumatic fever in New York City (1969 to 1988): a comparative study of two decades. *J Pediatr* 1990;116:882-887.
148. Khriesat I, Najada A, Al-Hakim F, et al. Acute rheumatic fever in Jordanian children. *East Mediterr Health J* 2003;9:981-987.
149. Steer AC, Kado J, Jenney AW, et al. Acute rheumatic fever and rheumatic heart disease in Fiji: prospective surveillance, 2005-2007. *Med J Aust* 2009;190:133-135.
150. Cann MP, Sive AA, Norton RE, et al. Clinical presentation of rheumatic fever in an endemic area. *Arch Dis Child* 1995;72:455-457.
151. Carapetis JR, Brown A, Wilson NJ, et al. An Australian guideline for rheumatic fever and rheumatic heart disease: an abridged outline. *Med J Aust* 2007;186:581-586.
152. Atatoa-Carr P, Lennon D, Wilson N. Rheumatic fever diagnosis, management, and secondary prevention: a New Zealand guideline. *N Z Med J* 2008;121:59-69.
153. Olgunturk R, Canter B, Tunaoglu FS, et al. Review of 609 patients with rheumatic fever in terms of revised and updated Jones criteria. *Int J Cardiol* 2006;112:91-98.
154. Carapetis JR, Currie BJ. Rheumatic chorea in Northern Australia: a clinical and epidemiological study. *Arch Dis Child* 1999;80:353-358.
155. Denny FW. T. Duckett Jones and rheumatic fever in 1986. T. Duckett Jones Memorial Lecture. *Circulation* 1987;76:963-970.
156. Feinstein AR, Spagnuolo M, Gill FA. The rebound phenomenon in acute rheumatic fever. I. Incidence and significance. *Yale J Biol Med* 1961;33:259-278.
157. Hilario MO, Terreri MT. Rheumatic fever and post-streptococcal arthritis. *Best Pract Res Clin Rheumatol* 2002;16:481-494.
158. Pinals RS. Polyarthritis and fever. *N Engl J Med* 1994;330:769-774.
159. Mackie SL, Keat A. Poststreptococcal reactive arthritis: what is it and how do we know? *Rheumatology (Oxford)* 2004;43:949-954.
160. Shulman ST, Ayoub EM. Poststreptococcal reactive arthritis. *Curr Opin Rheumatol*. 2002;14:562-565.
161. De Cunto CL, Giannini EH, Fink CW, et al. Prognosis of children with poststreptococcal reactive arthritis. *Pediatr Infect Dis J* 1988;7:683-686.
162. Ahmed S, Ayoub EM, Scornik JC, et al. Poststreptococcal reactive arthritis: clinical characteristics and association with HLA-DR alleles. *Arthritis Rheum* 1998;41:1096-1102.
163. van Bemmel JM, Delgado V, Holman ER, et al. No increased risk of valvular heart disease in adult poststreptococcal reactive arthritis. *Arthritis Rheum* 2009;60:987-993.
164. Ayoub EM, Majeed HA. Poststreptococcal reactive arthritis. *Curr Opin Rheumatol* 2000;12:306-310.
165. Gerber MA, Baltimore RS, Eaton CB, et al. Prevention of rheumatic fever and diagnosis and treatment of acute streptococcal pharyngitis: a scientific statement from the American Heart Association Rheumatic Fever, Endocarditis, and Kawasaki Disease Committee of the Council on Cardiovascular Disease in the Young, the Interdisciplinary Council on Functional Genomics and Translational Biology, and the Interdisciplinary Council on Quality of Care and Outcomes Research: endorsed by the American Academy of Pediatrics. *Circulation* 2009;119:1541-1551.
166. van der Helm-van Mil AH. Acute rheumatic fever and poststreptococcal reactive arthritis reconsidered. *Curr Opin Rheumatol* 22:437-442.
167. Buchanan DN. Pathologic changes in chorea. *Am J Dis Child* 1941;62:443-445.
168. Aron AM, Freeman JM, Carter S. The natural history of Sydenham's Chorea. Review of the literature and long-term evaluation with emphasis on cardiac sequelae. *Am J Med* 1965;38:83-95.
169. Goldenberg J, Ferraz MB, Fonseca AS, et al. Sydenham chorea: clinical and laboratory findings. Analysis of 187 cases. *Rev Paul Med* 1992;110:152-157.
170. Lessof MH, Bywaters EG. The duration of chorea. *Br Med J* 1956;1520-1523.
171. Berrios X, Quesney F, Morales A, et al. Are all recurrences of "pure" Sydenham chorea true recurrences of acute rheumatic fever? *J Pediatr* 1985;107:867-872.
172. Swedo SE. Sydenham's chorea. A model for childhood autoimmune neuropsychiatric disorders. *JAMA* 1994;272:1788-1791.
173. Burge DJ, DeHoratius RJ. Acute rheumatic fever. *Cardiovasc Clin* 1993;23:3-23.

174. Eshel G, Lahat E, Azizi E, et al. Chorea as a manifestation of rheumatic fever—a 30-year survey (1960–1990). *Eur J Pediatr* 1993;152:645–646.
175. Bland EF. Chorea as a manifestation of rheumatic fever: a long-term perspective. *Trans Am Clin Climatol Assoc* 1961;73:209–213.
176. Zomorodi A, Wald ER. Sydenham's chorea in western Pennsylvania. *Pediatrics* 2006;117:e675–e679.
177. Heye N, Jergas M, Hotzinger H, et al. Sydenham chorea: clinical, EEG, MRI and SPECT findings in the early stage of the disease. *J Neurol* 1993;240:121–123.
178. Swedo SE, Leonard HL, Schapiro MB, et al. Sydenham's chorea: physical and psychological symptoms of St Vitus dance. *Pediatrics* 1993;91:706–713.
179. Murphy TK, Goodman WK, Ayoub EM, et al. On defining Sydenham's chorea: where do we draw the line? *Biol Psychiatry* 2000;47:851–857.
180. Swedo SE, Leonard HL, Garvey M, et al. Pediatric autoimmune neuropsychiatric disorders associated with streptococcal infections: clinical description of the first 50 cases. *Am J Psychiatry* 1998;155:264–271.
181. Garvey MA, Giedd J, Swedo SE. PANDAS: the search for environmental triggers of pediatric neuropsychiatric disorders. Lessons from rheumatic fever. *J Child Neurol* 1998;13:413–423.
182. Perlmutter SJ, Leitman SF, Garvey MA, et al. Therapeutic plasma exchange and intravenous immunoglobulin for obsessive-compulsive disorder and tic disorders in childhood. *Lancet* 1999;354:1153–1158.
183. Kurlan R, Johnson D, Kaplan EL. Streptococcal infection and exacerbations of childhood tics and obsessive-compulsive symptoms: a prospective blinded cohort study. *Pediatrics* 2008;121:1188–1197.
184. Shulman ST. Pediatric autoimmune neuropsychiatric disorders associated with streptococci (PANDAS): update. *Curr Opin Pediatr* 2009;21:127–130.
185. Massell BF. The diagnosis and treatment of rheumatic fever and rheumatic carditis. *Med Clin North Am* 1958;42:1343–1360.
186. Marcus RH, Sareli P, Pocock WA, et al. Functional anatomy of severe mitral regurgitation in active rheumatic carditis. *Am J Cardiol* 1989;63:577–584.
187. Barlow JB, Marcus RH, Pocock WA, et al. Mechanisms and management of heart failure in active rheumatic carditis. *S Afr Med J* 1990;78:181–186.
188. Zhou LY, Lu K. Inflammatory valvular prolapse produced by acute rheumatic carditis: echocardiographic analysis of 66 cases of acute rheumatic carditis. *Int J Cardiol* 1997;58:175–178.
189. de Moor MM, Lachman PI, Human DG. Rupture of tendinous chords during acute rheumatic carditis in young children. *Int J Cardiol* 1986;12:353–357.
190. Oliveira DB, Dawkins KD, Kay PH, et al. Chordal rupture. I: aetiology and natural history. *Br Heart J* 1983;50:312–317.
191. Kalangos A, Beghetti M, Vala D, et al. Anterior mitral leaflet prolapse as a primary cause of pure rheumatic mitral insufficiency. *Ann Thorac Surg* 2000;69:755–761.
192. Sutton GC, Craige E. Clinical signs of severe acute mitral regurgitation. *Am J Cardiol* 1967;20:141–144.
193. Coombs CF. *Rheumatic Heart Disease*. New York: William Woods, 1924.
194. Bonow RO, Carabello B, de Leon AC Jr, et al. Guidelines for the management of patients with valvular heart disease: executive summary. A report of the American College of Cardiology/American Heart Association Task Force on Practice Guidelines (Committee on Management of Patients with Valvular Heart Disease). *Circulation* 1998;98:1949–1984.
195. Przybojewski JZ. Rheumatic constrictive pericarditis. A case report and review of the literature. *S Afr Med J* 1981;59:682–686.
196. Stollerman G. *Rheumatic Fever and Streptococcal Infection*. New York: Grune & Stratton, 1975:127–131.
197. Essop MR, Wisenbaugh T, Sareli P. Evidence against a myocardial factor as the cause of left ventricular dilation in active rheumatic carditis. *J Am Coll Cardiol* 1993;22:826–829.
198. Narula J, Chopra P, Talwar KK, et al. Does endomyocardial biopsy aid in the diagnosis of active rheumatic carditis? *Circulation* 1993;88:2198–2205.
199. Kamblock J, Payot L, Iung B, et al. Does rheumatic myocarditis really exist? Systematic study with echocardiography and cardiac troponin I blood levels. *Eur Heart J* 2003;24:855–862.
200. Williams RV, Minich LL, Shaddy RE, et al. Evidence for lack of myocardial injury in children with acute rheumatic carditis. *Cardiol Young* 2002;12:519–523.
201. Gentles TL, Colan SD, Wilson NJ, et al. Left ventricular mechanics during and after acute rheumatic fever: contractile dysfunction is closely related to valve regurgitation. *J Am Coll Cardiol* 2001;37:201–207.
202. Vasan RS, Shrivastava S, Vijayakumar M, et al. Echocardiographic evaluation of patients with acute rheumatic fever and rheumatic carditis. *Circulation* 1996;94:73–82.
203. Vardi P, Markiewicz W, Weiss Y, et al. Clinical-echocardiographic correlations in acute rheumatic fever. *Pediatrics* 1983;71:830–834.
204. Veasy LG. Time to take soundings in acute rheumatic fever. *Lancet* 2001;357:1994–1995.
205. al-Eissa YA. Acute rheumatic fever during childhood in Saudi Arabia. *Ann Trop Paediatr* 1991;11:225–231.
206. Burke JB. Erythema marginatum. *Arch Dis Child* 1955;30:359–365.
207. Feinstein AR. The natural histories of acute rheumatic fever. *Bull Rheum Dis* 1966;17:423–428.
208. Massell BF, Fyler DC, Roy SB. The clinical picture of rheumatic fever: diagnosis, immediate prognosis, course, and therapeutic implications. *Am J Cardiol* 1958;1:436–449.
209. Wannamaker LW, Ayoub EM. Antibody titers in acute rheumatic fever. *Circulation* 1960;21:598–614.
210. Ayoub EM, Wannamaker LW. Evaluation of the streptococcal deoxyribonuclease B and diphosphopyridine nucleotidase antibody tests in acute rheumatic fever and acute glomerulonephritis. *Pediatrics* 1962;29:527–538.
211. Spagnuolo M, Feinstein AR. Congestive heart failure and rheumatic activity in young patients with rheumatic heart disease. *Pediatrics* 1964;33:653–660.
212. Mirowski M, Rosenstein BJ, Markowitz M. A comparison of atrioventricular conduction in normal children and in patients with rheumatic fever, glomerulonephritis, and acute febrile illnesses. A quantitative study with determination of the P-R index. *Pediatrics* 1964;33:334–340.
213. Lenox CC, Zuberhuhler JR, Park SC, et al. Arrhythmias and Stokes-Adams attacks in acute rheumatic fever. *Pediatrics* 1978;61:599–603.
214. Zalzstein E, Maor R, Zucker N, et al. Advanced atrioventricular conduction block in acute rheumatic fever. *Cardiol Young* 2003;13:506–508.
215. Minich LL, Tani LY, Veasy LG. Role of echocardiography in the diagnosis and follow-up evaluation of rheumatic carditis. In: Narula J, Virmani R, Reddy KS, et al., eds. *Rheumatic Fever*. Washington, DC: American Registry of Pathology, 1999:307–318.
216. Zoghbi WA, Enriquez-Sarano M, Foster E, et al. Recommendations for evaluation of the severity of native valvular regurgitation with two-dimensional and Doppler echocardiography. *J Am Soc Echocardiogr* 2003;16:777–802.
217. Regmi PR, Pandey MR. Prevalence of rheumatic fever and rheumatic heart disease in school children of Kathmandu city. *Indian Heart J* 1997;49:518–520.
218. Grover A, Dhawan A, Iyengar SD, et al. Epidemiology of rheumatic fever and rheumatic heart disease in a rural community in northern India. *Bull World Health Organ* 1993;71:59–66.
219. Vijayalakshmi IB, Mithravinda J, Deva AN. The role of echocardiography in diagnosing carditis in the setting of acute rheumatic fever. *Cardiol Young* 2005;15:583–588.
220. Barlow JB. Idiopathic (degenerative) and rheumatic mitral valve prolapse: historical aspects and an overview. *J Heart Valve Dis* 1992;1:163–174.
221. Zucker N, Goldfarb BL, Zalzstein E, et al. A common color flow Doppler finding in the mitral regurgitation of acute rheumatic fever. *Echocardiography* 1991;8:627–631.
222. Minich LL, Tani LY, Pagotto LT, et al. Doppler echocardiography distinguishes between physiologic and pathologic “silent” mitral regurgitation in patients with rheumatic fever. *Clin Cardiol* 1997;20:924–926.
223. Hwang WS, Lam KL. Case reports. Rupture of chordae tendineae during acute rheumatic carditis. *Br Heart J* 1968;30:429–431.
224. Haizlip JA, Di Russo GB, Vernon DD, et al. Flail posterior leaflet of the mitral valve in acute rheumatic carditis. *Pediatr Cardiol* 2004;25:165–166.
225. Figueroa FE, Fernandez MS, Valdes P, et al. Prospective comparison of clinical and echocardiographic diagnosis of rheumatic carditis: long term follow up of patients with subclinical disease. [see comments.]. *Heart (British Cardiac Society)* 2001;85:407–410.
226. Abernethy M, Bass N, Sharpe N, et al. Doppler echocardiography and the early diagnosis of carditis in acute rheumatic fever. *Aust N Z J Med* 1994;24:530–535.
227. Mangione S. Cardiac auscultatory skills of physicians-in-training: a comparison of three English-speaking countries. *Am J Med* 2001;110:210–216.
228. Lanna CC, Tonelli E, Barros MV, et al. Subclinical rheumatic valvitis: a long-term follow-up. *Cardiol Young* 2003;13:431–438.
229. Vasan RS, Selvaraj N. Natural history of acute rheumatic fever. In: Narula J, Virmani R, Reddy KS, et al., eds. *Rheumatic Fever*. Washington, DC: American Registry of Pathology, 1999:347–358.
230. Vijaykumar M, Narula J, Reddy KS, et al. Incidence of rheumatic fever and prevalence of rheumatic heart disease in India. *Int J Cardiol* 1994;43:221–228.
231. Krishnamoorthy KM, Tharakan JA. Balloon mitral valvulotomy in children aged < or = 12 years. *J Heart Valve Dis* 2003;12:461–468.
232. Kao CH, Hsieh KS, Wang YL, et al. 99Tcm-HMPAO-labelled white blood cell scanning for the detection of carditis in the differentiation of rheumatic fever and inactive rheumatic heart disease in children. *Nucl Med Commun* 1992;13:478–481.
233. Narula J, Malhotra A, Yasuda T, et al. Usefulness of antimyosin antibody imaging for the detection of active rheumatic myocarditis. *Am J Cardiol* 1999;84:946–950, A947.
234. Otsuji Y, Handschumacher MD, Schwammenthal E, et al. Insights from three-dimensional echocardiography into the mechanism of functional mitral regurgitation: direct in vivo demonstration of altered leaflet tethering geometry. *Circulation* 1997;96:1999–2008.
235. Enriquez-Sarano M, Basmadjian AJ, Rossi A, et al. Progression of mitral regurgitation: a prospective Doppler echocardiographic study. *J Am Coll Cardiol* 1999;34:1137–1144.
236. Otto CM. Mitral regurgitation. In: Otto CM, ed. *Valvular Heart Disease*. Philadelphia, PA: Saunders, 2004:336–367.

237. Otto CM. Timing of surgery in mitral regurgitation. *Heart* 2003;89:100–105.
238. Greenberg BH. Congestive heart failure as a consequence of valvular heart disease. In: Hosenpud JD, Greenberg BH, eds. *Congestive Heart Failure: Pathophysiology, Diagnosis, and Comprehensive Approach to Management*. New York: Springer-Verlag, 1994:234–245.
239. Braunwald E. Valvular heart disease. In: Braunwald E, Zipes DP, Libby P, eds. *Heart Disease*. Philadelphia, PA: W.B. Saunders Company, 2001:1643–1722.
240. Carabello BA. Modern management of mitral stenosis. *Circulation* 2005;112:432–437.
241. Wilkins GT, Weyman AE, Abascal VM, et al. Percutaneous balloon dilatation of the mitral valve: an analysis of echocardiographic variables related to outcome and the mechanism of dilatation. *Br Heart J* 1988;60:299–308.
242. Reid CL, Chandraratna PA, Kawanishi DT, et al. Influence of mitral valve morphology on double-balloon catheter balloon valvuloplasty in patients with mitral stenosis. Analysis of factors predicting immediate and 3-month results. *Circulation* 1989;80:515–524.
243. Jung B, Cormier B, Ducimetiere P, et al. Immediate results of percutaneous mitral commissurotomy. A predictive model on a series of 1514 patients. *Circulation* 1996;94:2124–2130.
244. Zamorano J, Perez de Isla L, Sugeng L, et al. Non-invasive assessment of mitral valve area during percutaneous balloon mitral valvuloplasty: role of real-time 3D echocardiography. *Eur Heart J* 2004;25:2086–2091.
245. Rosca M, Lancellotti P, Magne J, et al. Stress testing in valvular heart disease: clinical benefit of echocardiographic imaging. *Expert Rev Cardiovasc Ther* 2011;9:81–92.
246. Kennedy KD, Nishimura RA, Holmes DR Jr, et al. Natural history of moderate aortic stenosis. *J Am Coll Cardiol* 1991;17:313–319.
247. Roguin A, Rinkevich D, Milo S, et al. Long-term follow-up of patients with severe rheumatic tricuspid stenosis. *Am Heart J* 1998;136:103–108.
248. Chopra P, Bhatia ML. Chronic rheumatic heart disease in India: a reappraisal of pathologic changes. *J Heart Valve Dis* 1992;1:92–101.
249. Duran CM. Tricuspid valve surgery revisited. *J Card Surg* 1994;9:242–247.
250. Kitchin A, Turner R. Diagnosis and treatment of tricuspid stenosis. *Br Heart J* 1964;26:354–379.
251. Goswami KC, Rao MB, Dev V, et al. Juvenile tricuspid stenosis and rheumatic tricuspid valve disease: an echocardiographic study. *Int J Cardiol* 1999;72:83–86.
252. Carpentier A, Deloche A, Hanania G, et al. Surgical management of acquired tricuspid valve disease. *J Thorac Cardiovasc Surg* 1974;67:53–65.
253. Wooley CF, Fontana ME, Kilman JW, et al. Tricuspid stenosis. Atrial systolic murmur, tricuspid opening snap, and right atrial pressure pulse. *Am J Med* 1985;78:375–384.
254. Guyer DE, Gillam LD, Foale RA, et al. Comparison of the echocardiographic and hemodynamic diagnosis of rheumatic tricuspid stenosis. *J Am Coll Cardiol* 1984;3:1135–1144.
255. Nanna M, Chandraratna PA, Reid C, et al. Value of two-dimensional echocardiography in detecting tricuspid stenosis. *Circulation* 1983;67:221–224.
256. Tribouilloy CM, Enriquez-Sarano M, Bailey KR, et al. Quantification of tricuspid regurgitation by measuring the width of the vena contracta with Doppler color flow imaging: a clinical study. *J Am Coll Cardiol* 2000;36:472–478.
257. Shapira Y, Porter A, Wurzel M, et al. Evaluation of tricuspid regurgitation severity: echocardiographic and clinical correlation. *J Am Soc Echocardiogr* 1998;11:652–659.
258. Choudhary SK, Mathur A, Sharma R, et al. Pulmonary autograft: should it be used in young patients with rheumatic disease? *J Thorac Cardiovasc Surg* 1999;118:483–490; discussion 490–481.
259. Pieters FA, Al-Halees Z, Hatle L, et al. Results of the Ross operation in rheumatic versus non-rheumatic aortic valve disease. *J Heart Valve Dis* 2000;9:38–44.
260. Pieters FA, al-Halees Z, Zwaan FE, et al. Autograft failure after the Ross operation in a rheumatic population: pre- and postoperative echocardiographic observations. *J Heart Valve Dis* 1996;5:404–408; discussion 408–409.
261. Czoniczer G, Amezcua F, Pelargonio S, et al. Therapy of severe rheumatic carditis. Comparison of adrenocortical steroids and aspirin. *Circulation* 1964;29:813–819.
262. Taran LM. The treatment of acute rheumatic fever and acute rheumatic heart disease. *Am J Med* 1947;2:285–295.
263. Bywaters EG, Thomas GT. Bed rest, salicylates, and steroid in rheumatic fever. *Br Med J* 1961;5240:1628–1634.
264. Chandrasekhar Y, Narula J. Rheumatic fever. In: Alpert JS, Dalen JE, Rahimtoola SH, eds. *Valvular Heart Disease*. Philadelphia, PA: Lippincott Williams & Wilkins, 2000:41–73.
265. Albert DA, Harel L. The treatment of rheumatic fever and rheumatic carditis. In: Narula J, Virmani R, Reddy KS, et al., eds. *Rheumatic Fever*. Washington, DC: American Registry of Pathology, 1999:359–370.
266. Thatai D, Turi ZG. Current guidelines for the treatment of patients with rheumatic fever. *Drugs* 1999;57:545–555.
267. da Silva NA, Pereira BA. Acute rheumatic fever. Still a challenge. *Rheum Dis Clin North Am* 1997;23:545–568.
268. Lennon D. Acute rheumatic fever in children: recognition and treatment. *Paediatr Drugs* 2004;6:363–373.
269. Lendrum BL, Simon AJ, Mack I. Relation of duration of bed rest in acute rheumatic fever to heart disease present 2 to 14 years later. *Pediatrics* 1959;24:389–394.
270. A COMPARISON of the effect of prednisone and acetylsalicylic acid on the incidence of residual rheumatic heart disease. Combined rheumatic fever study group. *N Engl J Med* 1960;262:895–902.
271. Albert DA, Harel L, Karrison T. The treatment of rheumatic carditis: a review and meta-analysis. *Medicine (Baltimore)* 1995;74:1–12.
272. TREATMENT of acute rheumatic fever in children a co-operative clinical trial of A.C.T.H., cortisone, and aspirin; a joint report by the Rheumatic Fever Working Party of the Medical Research Council of Great Britain and the Subcommittee of Principal Investigators of the American Council on Rheumatic Fever and Congenital Heart Disease, American Heart Association. *Br Med J* 1955;4913:555–574.
273. Saxena A. Treatment of rheumatic carditis. *Indian J Pediatr* 2002;69:513–516.
274. Rothman PE. Treatment of rheumatic carditis. A critical evaluation. *Clin Pediatr (Phila)* 1965;4:619–625.
275. Markowitz M, Kuttner G. Treatment of acute rheumatic fever. *Am J Dis Child* 1962;104:313–320.
276. Voss LM, Wilson NJ, Neutze JM, et al. Intravenous immunoglobulin in acute rheumatic fever: a randomized controlled trial. *Circulation* 2001;103:401–406.
277. Narin N, Karakucuk M, Narin F, et al. Is pentoxifylline therapy effective for the treatment of acute rheumatic carditis? A pilot study. *J Paediatr Child Health* 2003;39:214–218.
278. Hashkes PJ, Tauber T, Somekh E, et al. Naproxen as an alternative to aspirin for the treatment of arthritis of rheumatic fever: a randomized trial. *J Pediatr* 2003;143:399–401.
279. Uziel Y, Hashkes PJ, Kassem E, et al. The use of naproxen in the treatment of children with rheumatic fever. *J Pediatr* 2000;137:269–271.
280. Barash J, Margalit D, Matitau A. Corticosteroid treatment in patients with Sydenham's chorea. *Pediatr Neurol* 2005;32:205–207.
281. Araujo AP, Padua PA, Maia Filho HS. Management of rheumatic chorea: an observational study. *Arq Neuropsiquiatr* 2002;60:231–233.
282. Harel L, Zecharia A, Straussberg R, et al. Successful treatment of rheumatic chorea with carbamazepine. *Pediatr Neurol* 2000;23:147–151.
283. Tierney RC, Kaplan S. Treatment of Sydenham's chorea. *Am J Dis Child* 1965;109:408–412.
284. Garvey MA, Snider LA, Leitman SF, et al. Treatment of Sydenham's chorea with intravenous immunoglobulin, plasma exchange, or prednisone. *J Child Neurol* 2005;20:424–429.
285. Stollerman GH. Rheumatic fever. *AMA Arch Intern Med* 1956;98:211–220.
286. Kalangos A, Beghetti M, Baldovinos A, et al. Aortic valve repair by cusp extension with the use of fresh autologous pericardium in children with rheumatic aortic insufficiency. *J Thorac Cardiovasc Surg* 1999;118:225–236.
287. Gupta DK, Kapoor A, Garg N, et al. Beneficial effects of nifedipine versus enalapril in chronic rheumatic severe mitral regurgitation: six months follow up echocardiographic study. *J Heart Valve Dis* 2001;10:158–165.
288. Sampaio RO, Grinberg M, Leite JJ, et al. Effect of enalapril on left ventricular diameters and exercise capacity in asymptomatic or mildly symptomatic patients with regurgitation secondary to mitral valve prolapse or rheumatic heart disease. *Am J Cardiol* 2005;96:117–121.
289. Tunaoglu FS, Olgunturk R, Kula S, et al. Effective regurgitant orifice area of rheumatic mitral insufficiency: response to angiotensin converting enzyme inhibitor treatment. *Anadolu Kardiyol Derg* 2004;4:3–7.
290. Wisenbaugh T, Essop R, Rothlisberger C, et al. Effects of a single oral dose of captopril on left ventricular performance in severe mitral regurgitation. *Am J Cardiol* 1992;69:348–353.
291. Rothlisberger C, Sareli P, Wisenbaugh T. Comparison of single dose nifedipine and captopril for chronic severe mitral regurgitation. *Am J Cardiol* 1994;73:978–981.
292. Borer JS, Bonow RO. Contemporary approach to aortic and mitral regurgitation. *Circulation* 2003;108:2432–2438.
293. Jung B, Gohlke-Barwolf C, Tornos P, et al. Recommendations on the management of the asymptomatic patient with valvular heart disease. *Eur Heart J* 2002;23:1252–1266.
294. Scognamiglio R, Rahimtoola SH, Fasoli G, et al. Nifedipine in asymptomatic patients with severe aortic regurgitation and normal left ventricular function. *N Engl J Med* 1994;331:689–694.
295. Evangelista A, Tornos P, Sambola A, et al. Long-term vasodilator therapy in patients with severe aortic regurgitation. *N Engl J Med* 2005;353:1342–1349.
296. Bonow RO, Carabello BA, Chatterjee K, et al. 2008 focused update incorporated into the ACC/AHA 2006 guidelines for the management of patients with valvular heart disease: a report of the American College of Cardiology/American Heart Association Task Force on Practice Guidelines (Writing Committee to revise the 1998 guidelines for the management of patients with valvular heart disease). Endorsed by the Society of Cardiovascular Anesthesiologists, Society for Cardiovascular Angiography and Interventions, and Society of Thoracic Surgeons. *J Am Coll Cardiol* 2008;52:e1–e142.

297. Niles N, Borer JS, Kamen M, et al. Preoperative left and right ventricular performance in combined aortic and mitral regurgitation and comparison with isolated aortic or mitral regurgitation. *Am J Cardiol* 1990;65:1372-1378.
298. Antonini-Canterin F, Moura LM, Enache R, et al. Effect of hydroxymethylglutaryl coenzyme-a reductase inhibitors on the long-term progression of rheumatic mitral valve disease. *Circulation* 121:2130-2136.
299. Antonini-Canterin F, Leibal E, Enache R, et al. Hydroxymethylglutaryl coenzyme-a reductase inhibitors delay the progression of rheumatic aortic valve stenosis a long-term echocardiographic study. *J Am Coll Cardiol* 2009;53:1874-1879.
300. Cowell SJ, Newby DE, Prescott RJ, et al. A randomized trial of intensive lipid-lowering therapy in calcific aortic stenosis. *N Engl J Med* 2005;352:2389-2397.
301. Moura LM, Maganti K, Puthumana JJ, et al. New understanding about calcific aortic stenosis and opportunities for pharmacologic intervention. *Curr Opin Cardiol* 2007;22:572-577.
302. Rossebø AB, Pedersen TR, Boman K, et al. Intensive lipid lowering with simvastatin and ezetimibe in aortic stenosis. *N Engl J Med* 2008;359:1343-1356.
303. Shrivastava S, Dev V, Vasan RS, et al. Percutaneous balloon mitral valvuloplasty in juvenile rheumatic mitral stenosis. *Am J Cardiol* 1991;67:892-894.
304. Gamra H, Bertout F, Ben Hamda K, et al. Balloon mitral commissurotomy in juvenile rheumatic mitral stenosis: a ten-year clinical and echocardiographic actuarial results. *Eur Heart J* 2003;24:1349-1356.
305. Ben Farhat M, Ayari M, Maatouk F, et al. Percutaneous balloon versus surgical closed and open mitral commissurotomy: seven-year follow-up results of a randomized trial. *Circulation* 1998;97:245-250.
306. Abascal VM, Wilkins GT, Choong CY, et al. Echocardiographic evaluation of mitral valve structure and function in patients followed for at least 6 months after percutaneous balloon mitral valvuloplasty. *J Am Coll Cardiol* 1988;12:606-615.
307. Lieberman EB, Bashore TM, Hermiller JB, et al. Balloon aortic valvuloplasty in adults: failure of procedure to improve long-term survival. *J Am Coll Cardiol* 1995;26:1522-1528.
308. Otto CM, Mickel MC, Kennedy JW, et al. Three-year outcome after balloon aortic valvuloplasty. Insights into prognosis of valvular aortic stenosis. *Circulation* 1994;89:642-650.
309. Revuelta JM, Garcia-Rinaldi R, Duran CM. Tricuspid commissurotomy. *Ann Thorac Surg* 1985;39:489-491.
310. Duran CM, Gometza B, De Vol EB. Valve repair in rheumatic mitral disease. *Circulation* 1991;84:III125-III132.
311. Skoularigis J, Sinovich V, Joubert J, et al. Evaluation of the long-term results of mitral valve repair in 254 young patients with rheumatic mitral regurgitation. *Circulation* 1994;90:II167-II174.
312. Gometza B, al-Halees Z, Shahid M, et al. Surgery for rheumatic mitral regurgitation in patients below twenty years of age. An analysis of failures. *J Heart Valve Dis* 1996;5:294-301.
313. Enriquez-Sarano M. Timing of mitral valve surgery. *Heart* 2002;87:79-85.
314. Enriquez-Sarano M, Avierinos JF, Messika-Zeitoun D, et al. Quantitative determinants of the outcome of asymptomatic mitral regurgitation. *N Engl J Med* 2005;352:875-883.
315. Detaint D, Messika-Zeitoun D, Avierinos JF, et al. B-type natriuretic peptide in organic mitral regurgitation: determinants and impact on outcome. *Circulation* 2005;111:2391-2397.
316. Rosenhek R, Rader F, Kloor U, et al. Outcome of watchful waiting in asymptomatic severe mitral regurgitation. *Circulation* 2006;113:2238-2244.
317. Rumel WR, Vaughn CC, Guibone RA. Surgical reconstruction of the mitral valve. *Ann Thorac Surg* 1969;8:289-296.
318. Chauvaud S, Perier P, Touati G, et al. Long-term results of valve repair in children with acquired mitral valve incompetence. *Circulation* 1986;74:1104-1109.
319. Sulayman R, Mathew R, Thilenius OG, et al. Hemodynamics and annuloplasty in isolated mitral regurgitation in children. *Circulation* 1975;52:1144-1151.
320. Kitamura N, Uemura S, Kunitomo R, et al. A new technique for debridement in rheumatic valvular disease: the rasping procedure. *Ann Thorac Surg* 2000;69:121-125.
321. Talwar S, Rajesh MR, Subramanian A, et al. Mitral valve repair in children with rheumatic heart disease. *J Thorac Cardiovasc Surg* 2005;129:875-879.
322. John S, Ravikumar E, Jairaj PS, et al. Valve replacement in the young patient with rheumatic heart disease. Review of a twenty-year experience. *J Thorac Cardiovasc Surg* 1990;99:631-638.
323. Grinda JM, Latremouille C, Berrebi AJ, et al. Aortic cusp extension valvuloplasty for rheumatic aortic valve disease: midterm results. *Ann Thorac Surg* 2002;74:438-443.
324. Talwar S, Saikrishna C, Saxena A, et al. Aortic valve repair for rheumatic aortic valve disease. *Ann Thorac Surg* 2005;79:1921-1925.
325. al-Halees Z, Kumar N, Gallo R, et al. Pulmonary autograft for aortic valve replacement in rheumatic disease: a caveat. *Ann Thorac Surg* 1995;60:S172-S175; discussion S176.
326. Kumar AS, Talwar S, Saxena A, et al. Ross procedure in rheumatic aortic valve disease. *Eur J Cardiothorac Surg* 2005.
327. Bonow RO, Carabello BA, Chatterjee K, et al. 2008 Focused update incorporated into the ACC/AHA 2006 guidelines for the management of patients with valvular heart disease: a report of the American College of Cardiology/American Heart Association Task Force on Practice Guidelines (Writing Committee to Revise the 1998 Guidelines for the Management of Patients With Valvular Heart Disease): endorsed by the Society of Cardiovascular Anesthesiologists, Society for Cardiovascular Angiography and Interventions, and Society of Thoracic Surgeons. *Circulation* 2008;118:e523-e661.
328. Jamieson WR, Edwards FH, Schwartz M, et al. Risk stratification for cardiac valve replacement. National Cardiac Surgery Database. Database Committee of the Society of Thoracic Surgeons. *Ann Thorac Surg* 1999;67:943-951.
329. Denny FW, Wannamaker LW, Brink WR, et al. Landmark article May 13, 1950: Prevention of rheumatic fever: Treatment of the preceding streptococcal infection. By Floyd W. Denny, Lewis W. Wannamaker, William R. Brink, Charles H. Rammelkamp Jr. and Edward A. Custer. *JAMA* 1985;254:534-537.
330. Markowitz M. The decline of rheumatic fever: role of medical intervention. Lewis W. Wannamaker Memorial Lecture. *J Pediatr* 1985;106:545-550.
331. Pediatrics AAO. *Group A Streptococcal Infections*. Elk Grove Village, IL: American Academy of Pediatrics, 2003.
332. Shulman ST, Gerber MA. So what's wrong with penicillin for strep throat? *Pediatrics* 2004;113:1816-1819.
333. Robertson KA, Volmink JA, Mayosi BM. Antibiotics for the primary prevention of acute rheumatic fever: a meta-analysis. *BMC Cardiovasc Disord* 2005;5:11.
334. Lennon D, Kerdelidis M, Arroll B. Meta-analysis of trials of streptococcal throat treatment programs to prevent rheumatic fever. *Pediatr Infect Dis J* 2009;28:e259-264.
335. Lennon D, Stewart J, Farrell E, et al. School-based prevention of acute rheumatic fever: a group randomized trial in New Zealand. *Pediatr Infect Dis J* 2009;28:787-794.
336. Karthikeyan G, Mayosi BM. Is primary prevention of rheumatic fever the missing link in the control of rheumatic heart disease in Africa? *Circulation* 2009;120:709-713.
337. Spagnuolo M, Pasternack B, Taranta A. Risk of rheumatic-fever recurrences after streptococcal infections. Prospective study of clinical and social factors. *N Engl J Med* 1971;285:641-647.
338. Kuttner AG, Mayer FE. Carditis during second attacks of rheumatic fever. *N Engl J Med* 1963;268:1259-1261.
339. Chandrasekhar Y. Secondary prevention of rheumatic fever: theory, practice, and analysis of available studies. In: Narula J, Virmani R, Reddy KS, et al., eds. *Rheumatic Fever*. Washington, DC: American Registry of Pathology, 1999:399-442.
340. Kaplan EL, Berrios X, Speth J, et al. Pharmacokinetics of benzathine penicillin G: serum levels during the 28 days after intramuscular injection of 1,200,000 units. *J Pediatr* 1989;115:146-150.
341. Oran B, Tastekin A, Karaaslan S, et al. Prophylactic efficiency of 3-weekly benzathine penicillin G in rheumatic fever. *Indian J Pediatr* 2000;67:163-167.
342. Saxena A, Kumar RK, Gera RP, et al. Consensus guidelines on pediatric acute rheumatic fever and rheumatic heart disease. *Indian Pediatr* 2008;45:565-573.
343. Joshi PP, Mohanan CJ, Sengupta SP, et al. Factors precipitating congestive heart failure—role of patient non-compliance. *J Assoc Physicians India* 1999;47:294-295.
344. Majeed HA, Khuffash FA, Bhatnagar S, et al. Acute rheumatic polyarthritides. The duration of secondary prophylaxis. *Am J Dis Child* 1990;144:831-833.
345. Hodes RM. Recurrence of rheumatic fever after valve replacement. *Cardiology* 1989;76:465-468.
346. Marijon E, Ou P, Celermajer DS, et al. Prevalence of rheumatic heart disease detected by echocardiographic screening. *N Engl J Med* 2007;357:470-476.
347. Carapetis JR, Hardy M, Fakakovikaetau T, et al. Evaluation of a screening protocol using auscultation and portable echocardiography to detect asymptomatic rheumatic heart disease in Tongan schoolchildren. *Nat Clin Pract Cardiovasc Med* 2008;5:411-417.
348. Dale JB. Group A streptococcal vaccines. *Pediatr Ann* 1998;27:301-308.
349. Dale JB. Group A streptococcal vaccines. *Infect Dis Clin North Am* 1999;13:227-243, viii.
350. Deshpande J, Vaideeswar P, Amonkar G, et al. Rheumatic heart disease in the past decade: an autopsy analysis. *Indian Heart J* 2002;54:676-680.
351. Wilson W, Taubert KA, Gewitz M, et al. Prevention of infective endocarditis: guidelines from the American Heart Association: a guideline from the American Heart Association Rheumatic Fever, Endocarditis, and Kawasaki Disease Committee, Council on Cardiovascular Disease in the Young, and the Council on Clinical Cardiology, Council on Cardiovascular Surgery and Anesthesia, and the Quality of Care and Outcomes Research Interdisciplinary Working Group. *Circulation* 2007;116:1736-1754.
352. Dajani AS, Taubert KA, Wilson W, et al. Prevention of bacterial endocarditis. Recommendations by the American Heart Association. *JAMA* 1997;277:1794-1801.

Inflammatory Noninfectious Cardiovascular Diseases

Charles H. Spencer ■ Anjali Patwardhan ■ Sharon L. Roble

The chronic, multisystem rheumatic diseases of childhood affect many body organs, including the cardiovascular system. This chapter discusses the juvenile idiopathic arthritis (JIA), systemic lupus erythematosus (SLE), vasculitis syndromes, and other rheumatic diseases briefly and then focuses on their cardiac complications. The differential diagnosis of each cardiac complication is discussed as well.

JUVENILE IDIOPATHIC ARTHRITIS

JIA is an uncommon chronic arthritis disease in children. In the United States, close to 300,000 children have chronic arthritis diseases (1). The incidence of new cases ranges from 1 to 20 per 100,000 per year (2,3). The burden of JIA remains considerable despite the newest therapies, including biologics (3). Improvement in the outcome of JIA will require earlier diagnosis and aggressive early therapy as well as improvement in the therapy, understanding of the environmental triggers, and genetic predisposition.

Diagnosis

The diagnosis of JIA requires symptoms and the presence of arthritis on physical exam for at least 6 weeks. Other potential causes of arthritis must be considered and excluded. JIA has different subtypes that may evolve over the initial 6 months. Subtypes are differentiated by clinical features and the number of joints that become involved. Subtypes include systemic-onset JIA, oligoarticular JIA, rheumatoid factor (RF) negative polyarticular JIA, RF positive polyarticular JIA, psoriatic JIA, and enthesitis-related JIA (ERJIA) (Table 61.1).

Systemic-onset JIA is a systemic illness characterized by a triad of daily spiking fevers, an evanescent macular rash, and arthritis involving at least one joint. Some patients will have hepatosplenomegaly and lymphadenopathy. Oligoarticular JIA typically presents with arthritis in four or fewer joints affected and lack of systemic symptoms (4). RF negative polyarticular JIA typically affects five joints or more with a less symmetrical small and large joint arthritis than seen in the RF positive polyarticular JIA. RF positive polyarticular JIA closely resembles adult rheumatoid arthritis (RA). Psoriatic arthritis has its own personality with a very asymmetrical arthritis and a family history of psoriasis; the psoriatic rash may not be present at the onset of the arthritis. Enthesitis-related arthritis affects boys more often with the characteristic enthesitis, which involves inflammation of tendons and ligaments at points of insertion, as well as lower extremity arthritis. Each one of these JIA subtypes has its own very distinct clinical pattern (5).

Clinical Patterns for Diagnosis

Systemic-Onset Juvenile Idiopathic Arthritis

Systemic-onset JIA is an impressive systemic inflammatory disease that may have more in common with autoinflammatory diseases than the other subtypes of JIA (4). It may involve multiple target organs including the joints, skin, lymph nodes, liver, spleen, heart, and lungs. There is no distinct peak age of onset of systemic-onset JIA. The systemic presentation is often impressive with daily high spiking fevers associated with a pale, pink, evanescent small macular rash (Fig. 61.1), more on the trunk than the extremities. The rash is especially evident when the fever is at its peak. The child often suffers from terrible muscle and joint pains during the fever spike and is quite irritable. Arthritis may begin early in the course of the disease or may present later, sometimes up to several months after the onset of the disease. The arthritis usually follows a polyarticular pattern.

Laboratory testing reveals systemic inflammation with frequent leucocytosis, thrombocytosis, markedly elevated sedimentation rate, and a normocytic, normochromic anemia. The serum ferritin is often significantly elevated as well. Serologies including the antinuclear antibody (ANA) titer and the RF are negative. Though this presentation is classic for systemic-onset JIA, it is prudent to consider infections and malignancy in the differential diagnosis as there is not one diagnostic symptom, sign, or laboratory test for this subtype of JIA. The diagnosis is made by recognition of the clinical pattern of fever, rash, and arthritis with compatible laboratory testing and a negative infectious and malignancy evaluation, often including a bone marrow biopsy. The systemic features of systemic-onset JIA often remit with time and the course of these children follows a polyarthritis pattern.

Oligoarticular JIA

This subtype of JIA is seen most often in young girls with a peak of onset between 1 and 2 years of age. The children often develop one or several swollen large joints, usually one knee or both knees followed by ankles (Fig. 61.2). The arthritis typically begins in one joint and over the first 6 months, the child has only four or fewer joints involved. Despite the limited number of joints affected, the child can be disabled, for example, with difficulty walking, especially in the morning. The child may have major joint difficulties with pain, stiffness, and flexion contractures, but does not usually have systemic features such as fevers, rash, or hepatosplenomegaly. Uveitis is a major complication of this type of arthritis (Fig. 61.3). It is occasionally present at the time of diagnosis of the arthritis but more often develops over the next few years in a minority

TABLE 61.1 Multimodality Imaging for Diagnosis of Cardiac Sarcoidosis

Diagnostic Test	Feature	Sensitivity	Specificity
Electrocardiogram	Conduction disturbances, arrhythmias	Low	Low
Echocardiography	Abnormal wall motion, regional wall thinning/thickening, depressed ejection fraction, pericardial effusion	Low to moderate	Low
201 Thallium scintigraphy	Segmental perfusion defect	Moderate	Moderate
67 Gallium scintigraphy	Increased myocardial uptake	Low	High
18F FDG-PET	Increased myocardial uptake	High	Moderate to high
CMR	High intensity lesions, thinning of ventricular wall	Moderate to high	High

FDG-PET, fluorodeoxyglucose positron emission tomography; CMR, cardiac magnetic resonance
 From Kim JS, et al. Cardiac sarcoidosis. *Am Heart J* 2009;157:9–21.

of these oligoarticular children. The diagnosis of this subtype is made by the presence of typical joint involvement for at least 6 weeks. Laboratory tests are nonspecific. Synovial fluid analysis may reveal an inflammatory range of the white blood cell (WBC) count, a shift to the left in the WBC differential and normal synovial fluid glucose, protein, and cultures. The complete blood count (CBC) is usually normal and sedimentation rate may be elevated or normal. The ANA is often mildly elevated and RF negative.

A swollen joint of brief duration must be evaluated for a septic joint, osteomyelitis, trauma, hemarthrosis, and other acute processes. Most often these problems have been excluded by the time the diagnosis of oligoarticular JIA is considered. A minority of these oligoarticular JIA children will develop polyarthritis over time and are classified as extended oligoarticular JIA.

Rheumatoid Factor Negative Polyarticular JIA

This type of JIA occurs more in girls and begins both early in childhood and in older children and adolescents. These children develop arthritis in more than four joints in the first 6 months of the disease process. Small and large joints are affected as well as the cervical spine and the temporomandibular joint (TMJ) (Fig. 61.4). Disability can be profound.



Figure 61.1. The macular evanescent rash of systemic JIA on the thigh of a 12-year-old boy.

The number of joints affected may increase over time and the hips may eventually become involved. Systemic features such as fever, rash, serositis, and organomegaly are not typically present; however, uveitis may occur along with growth failure, fatigue, and malaise. Psoriatic disease as well as ankylosing spondylitis, reactive arthritis, inflammatory bowel disease, and other spondyloarthropathies must be excluded. Scleroderma and dermatomyositis may cause polyarthritis but have their own distinguishing skin and muscle features for diagnosis. Infections such as multiple-joint or bone septic processes, parvovirus disease, Lyme disease, and disseminated *Neisseria gonorrhoeae* may sometimes mimic polyarthritis due to JIA. Malignancies such as leukemia, lymphoma, and neuroblastoma may also mimic JIA.

Laboratory tests show mild, nonspecific abnormalities. Mild anemia of chronic disease may be present and occasionally the platelet count is elevated as an acute phase reactant. The sedimentation rate is often elevated. The ANA titer may be mildly elevated.

Rheumatoid Factor Positive Polyarticular JIA

Older children and adolescents may develop an arthritis disease involving joints or more with a positive RF (5). The RF should



Figure 61.2. A swollen, limited wrist of a 10-year-old girl with polyarticular RF negative JIA.



Figure 61.3. The swollen knees and ankles of a 13-year-old girl with severe RF negative JIA.

be positive on two or more occasions in tests done at least 3 months apart. This subtype is an overwhelmingly female disease and is very similar to adult RA. Small and large joints may be involved and, as in RF-polyarticular JIA, the cervical spine and TMJ are frequently affected. Rheumatoid nodules typical of adult RA are not uncommon, especially on the hands, feet, and elbows (Fig. 61.5). Uveitis may also occur. Systemic features such as fever and rash are rare although poor weight gain, fatigue, and malaise are common. The differential diagnosis is limited due to the utility of the positive RF, which, in lieu of any typical signs of other diseases, facilitates the diagnosis of polyarticular JIA. Although the specificity and sensitivity of the anti-cyclic citrullinated peptide antibody (anti-CCP) is not yet clear in children and adolescents, it holds promise for diagnosing RF positive JIA early in the disease course (6).



Figure 61.4. The facial rash of a 6-year-old boy with JDM; note the rash around his eyes and on his eyelids.



Figure 61.5. The necrotic ulcer on the fingertip of a 14-year-old boy with systemic scleroderma.

Psoriatic Arthritis

Children who have psoriatic arthritis often present a diagnostic challenge. The age ratio favors girls as in polyarticular JIA. The age of onset is bimodal in the early children years and later childhood and adolescence, again like many children with RF negative JIA. The psoriatic rash, which is frequently seen in adult psoriasis early in the course, may not be present at the time of onset of the arthritis in children. The joints are often involved in an asymmetrical, atypical pattern with a predilection for small joints. It is not unusual to have a swollen single peripheral joint such as a finger joint and several swollen toe joints present as well as one or two affected large joints, such as a knee, wrist, or ankle. Nail pitting is occasionally present as well as dactylitis. It is common to have a close relative with psoriasis though the significance of this history is seldom appreciated by the family members. Uveitis is a risk although not as much as seen in oligoarticular or polyarticular JIA. Lab testing may show mild anemia, elevated platelets, and sedimentation rate, and a positive ANA. A skin biopsy to confirm psoriasis may be useful (7).

Enthesitis-Related Arthritis

Children and adolescents can develop a spondyloarthropathy that is revealed over time to be due to ankylosing spondylitis, psoriatic arthritis, inflammatory bowel disease, reactive arthritis, or a seronegative enthesitis and arthritis syndrome. The exact diagnosis may not be evident at initial presentation. Children and adolescents often start with an enthesitis around a joint with inflammation causing swelling, tenderness, and pain at the insertion of a tendon, fascia, or ligament on bone. Lower extremity peripheral arthritis is often present or eventually develops. Back pain, back limitation, chest limitation, and radiographic evidence of sacroiliitis typical of ankylosing spondylitis in adults are seldom seen in the early stage of these diseases in the first two decades of life. Males predominate and age of onset is late childhood to adolescence. Acute uveitis may occur but is not common. Chronic uveitis as seen in other JIA subtypes is rare.

Laboratory testing is not typically helpful in making a diagnosis. Routine testing such as the CBC and sedimentation rate are often normal and the ANA titer is often negative. A positive human leukocyte antigen B27 (HLA-B27) is supportive of an enthesitis-related arthritis but not diagnostic. Radiographic

and MRI of sacroiliac joints are only occasionally abnormal early in the disease course.

Therefore, the diagnosis of the enthesitis-related arthritis is primarily a clinical one. Older childhood and adolescent males with enthesitis who develop lower extremity arthritis may be initially put under the JIA umbrella but are at risk for developing a chronic spondyloarthropathy that continues into adulthood and often require long-term follow-up.

JIA Cardiac Complications

Pericarditis

Pericarditis is the most frequent cardiac complication seen in JIA. The prevalence of pericarditis in JIA ranges from 3% to 9% and it is observed mostly in children with systemic-onset JIA. There is evidence that many clinically active systemic-onset JIA children have silent, clinically insignificant pericardial effusions (6–8).

Symptomatic pericarditis with a pericardial effusion occurs usually at times of systemic disease activity with some combination of fever, rash, and arthritis. These children usually develop acute substernal chest pain and difficulty while breathing, especially when lying flat. The child may complain of referred shoulder, back, or neck pain. They are most comfortable sitting up or leaning forward in bed. The children are tachycardic and may have a friction rub at the lower left sternal border on auscultation of the heart, especially if the pericardial effusion is small to moderate in severity. A chest radiograph shows cardiomegaly. The electrocardiogram shows a predictable series of ST and T wave changes, initially with ST segment elevation, then normalization of ST abnormalities, followed by T wave inversion, and finally a return to baseline ST-T waves. Other electrocardiographic findings include PR depression, which may be diffuse or localized to only a portion of the leads, low voltages, and electrical alternans with large effusions. An echocardiogram (Fig. 61.6) may demonstrate a pericardial effusion that confirms the diagnosis. Occasionally there may be minimal associated pericardial fluid, which does not meet echocardiographic criteria for a pathologic effusion. The diagnosis of pericarditis is made upon clinical grounds, especially if the JIA child has a pattern of pericarditis episodes (6–9).

Fortunately, cardiac tamponade is rare in children with JIA (10–12). The diagnosis of cardiac tamponade is a clinical diagnosis including elevated neck veins with loss of x and y

descents, pulsus paradoxus, tachycardia, and hypotension all of which indicate impaired cardiac output secondary to pericardial fluid impairing ventricular filling (see Chapter 62, Pericardial Diseases/Effusions). Emergent pericardiocentesis is indicated for cardiac tamponade and can be lifesaving.

Bernstein et al. (6) studied 55 patients with JIA and detected 20 patients with pericardial effusions by echocardiography. Sixteen of these twenty children had systemic JIA, four had polyarticular JIA, and none had oligoarticular JIA. Of the 20 patients with abnormal echocardiograms, 9 had an enlarged heart on chest radiograph, 8 had abnormal ECGs and a pericardial friction rub was detected in 4. In 11 of 20 patients with an abnormal echocardiogram, there was no other objective evidence of pericarditis by chest radiograph or electrocardiography.

Gedalia et al. (12) performed echocardiography on 116 children with JIA who were seen consecutively in a JIA clinic. Twenty-six of these children had a pericardial effusion detected, nearly all children with systemic onset JIA. Sixty-one children with systemic onset juvenile idiopathic arthritis (SOJIA) were included in the study. Twenty-one of the sixty-four (34%) had a pericardial effusion with five having large effusions, eight having moderate effusions, and eight having small effusions. All 13 of the children with large and moderate effusions had symptoms while none of the children with small effusions noted had any symptoms. As might be expected, only 1 of 37 children with polyarticular JIA and 3 of oligoarticular JIA children had an effusion. None of these four nonsystemic JIA children had any symptoms with their small effusions.

A more recent study by Alkady et al. (13) utilized newer technology to demonstrate left ventricular abnormalities. The study included 45 children with JIA without cardiac symptoms and 30 age-matched and sex-matched controls. M-mode, 2-D, and pulsed Doppler echocardiography was performed on 36 children with JIA and 30 controls. Tissue Doppler echocardiography (ECHO) was performed on 24 JIA patients to assess systolic and diastolic function of the left ventricle as well as controls. Children with JIA had higher systolic and diastolic blood pressures, resting heart rate, and left ventricular systolic size and volume. Compared to controls, the Doppler ECHO and the tissue Doppler analysis suggested that the JIA group had a lower peak filling capacity, higher peak atrial filling velocity, and prolonged diastolic E and A wave deceleration times and prolonged isovolumic relaxation time.

Myocarditis

Myocarditis is seen rarely in JIA and only in children with active systemic JIA. It can occur by itself or in association with pericarditis. It may result in heart failure and arrhythmias, which may be a fatal complication. Clinically, the child may present with signs of systemic JIA including fever, rash, and arthritis. Cardiac manifestations include tachycardia, hypotension, dyspnea secondary to pulmonary edema, abdominal distention secondary to ascites and poor cardiac output, lower extremity edema in older children and teenagers, cool extremities secondary to poor perfusion and low cardiac output, and feeding intolerance in infants. Diagnostic testing may demonstrate an enlarged heart on chest radiograph, various electrocardiographic changes from nonspecific ST-T wave changes to new bundle branch block or ST changes concerning ischemia (ST elevation or depression, T-wave inversions), and mild elevations in serum troponin levels. The diagnosis of myocarditis is confirmed by echocardiography showing depressed ventricular function, or MRI (Fig. 61.7) showing both depressed ventricular function and/or evidence of patchy mid-myocardial fibrosis on delayed-enhancement imaging.

Bernstein et al. found evidence of myocarditis in only 4 of 40 children while Miller and French (14) noted myocarditis in



Figure 61.6. Delayed enhancement MRI showing patchy mid-myocardial fibrosis in a patient with RA and myocarditis.



Figure 61.7. Echocardiogram from subcostal view showing moderate-sized posterior pericardial effusion in a patient with JIA.

3 of 246 patients. Svantesson et al. (15) noted symptomatic myocarditis in 4 of 320 children with JIA. In a review of the literature, Goldenberg et al. (10) found 4 of 172 children with JIA to have perimyocarditis and 2 to have myocarditis.

Endocarditis

Endocarditis is very rare in JIA and if present at onset requires exclusion of other diagnoses such as rheumatic fever or infectious causes. Aortic and mitral insufficiency have been reported in several patients with systemic onset JIA as well as in RF-positive JIA children years after the JIA diagnosis and tends to occur more in the most severe JIA patients (16–19).

Treatment

Children with JIA who are noted to have asymptomatic pericarditis may be observed and not treated. If treatment appears prudent, nonsteroidal anti-inflammatory drug therapy such as naproxen (15 mg/kg/day in two doses) or indomethacin (1 to 2 mg/kg/day in two doses) are preferable to corticosteroids. Symptomatic pericarditis secondary to JIA warrants corticosteroid therapy. Myocarditis and endocarditis due to JIA are more serious complications than pericarditis and require aggressive corticosteroid therapy.

Corticosteroid therapy should start with a 1- to 3-day course of intravenous methylprednisolone at a dose of 15 to 30 mg/kg/dose per day in a single dose. This aggressive therapy often relieves any pericarditis symptoms and the ECG and echocardiogram return to normal. Occasionally further corticosteroid therapy is needed such as high-dose prednisone at 1 to 2 mg/kg/day for a week with weaning of the drug over the next month depending on the child's response. If the child has systemic JIA, the other clinical features such as fever, rash, and arthritis may have to be considered in the treatment. Methotrexate, anakinra, tocilizumab, and other remissive therapies are often required to control the entire spectrum of clinical problems in systemic JIA children and should be considered when a cardiac complication has occurred. The treatment of myocarditis and endocarditis is similar to the treatment for more severe pericarditis; high-dose corticosteroid treatment with possible remissive therapy. In children with congestive heart failure, angiotensin receptor blockers such as lisinopril are used to improve left ventricular function and reduce ventricular remodeling. In severe ventricular dysfunction with evidence of significantly impaired cardiac output, patients may

require inotropic support with dobutamine, epinephrine, or milrinone. Arrhythmias are rare, but can be life threatening, and may require antiarrhythmic therapy or cardioversion. Rarely, mechanical devices such as intra-aortic balloon pumps or ventricular assist devices may be required to maintain cardiac output until ventricular function improves. In some cases of endocarditis, valve replacement surgery may be needed. The treatment of cardiac tamponade requires an emergency pericardiocentesis to restore adequate cardiac output.

SYSTEMIC LUPUS ERYTHEMATOSUS

SLE is the classic autoimmune rheumatic disease in adults and children. It causes severe constitutional symptoms and may affect multiple organ systems. It is uncommon in children but with its potential disease severity, must be considered in any child with multisystem disease and no obvious infectious or malignant cause.

The incidence of SLE in children and adolescents is low; one study by Malleson et al. (20) estimated an annual incidence rate of 0.36/100,000 in Canadian children. Patients with lupus comprise only 1% to 5% of the children seen in pediatric rheumatology clinics (21,22). Fifteen to seventeen percent of all patients with SLE have their onset in the first two decades of life and many more in the second decade than the first (21,22). Girls develop SLE more than boys. In one study, the onset of lupus in girls under 12 is three times more common than in boys and after 12 years, the girls outnumber the boys by 10:1 (23). SLE is seen in children worldwide. In the United States, SLE does seem to occur more in African-American, Hispanic-American, and Asian-American populations (23,24).

Clinical Patterns for Diagnosis

SLE is a great mimicker and may present in many ways. For example, it can start with arthritis, rash, serositis including pericarditis, nephritis and/or nephrosis, thrombocytopenia or other cytopenias, vasculitis, central nervous system problems such as seizures and psychosis, and other clinical presentations. Diagnosis requires a significantly positive ANA (>1:80) plus at least three of the other criteria of the American College of Rheumatology (ACR) SLE criteria (Table 61.1). Since SLE can have protean presentations, it must be considered in patients who have a systemic illness and no obvious infectious or malignant etiology.

The most common presentation of SLE is with constitutional symptoms and signs. The child may have malaise, fatigue, and fevers. The fevers are not usually high spiking fevers such as seen in systemic JIA but are more often low grade. Rashes such as the classic malar butterfly rash, a palatal rash or ulcerations, and/or vasculitic lesions on the palms and soles are common. Polyarthritis may be present and be indistinguishable from JIA. Other typical lupus signs are buccal ulcerations, hair thinning or alopecia, and Raynaud phenomenon. Less common early signs and symptoms might include chest pain due to pericarditis or pleuritis, hypertension, a photosensitive rash, abdominal pain, chorea, or a peripheral neuropathy. Diagnosis requires awareness both of the common and uncommon ways that SLE may present and knowledge of how to apply the ACR diagnostic criteria in a clinical situation.

Laboratory Testing

The elevated ANA titer test is the *sine qua non* of SLE. The sensitivity is close to 100%. Specificity, though, is a major issue in adults and children. False positives in the normal

population may be between 2% and 30% (25). Rheumatologists often receive consultations for SLE based solely on the presence of an elevated ANA titer. These patients usually do not have SLE as it takes much more than an elevated ANA titer to make the SLE diagnosis (Table 61.1). A positive ANA may be associated with other rheumatic diseases. In children, diseases such as oligoarticular and polyarticular JIA, juvenile dermatomyositis (JDM), mixed connective tissue disease (MCTD) and scleroderma may also have positive ANA titers. Elevated ANA titers may also be associated with viral infections (e.g., Epstein-Barr) as well as exposure to various drugs.

If the child has a positive ANA and has other possible features of SLE such as arthritis or rash, it is prudent to perform more testing. The first test to do is the anti-double stranded DNA (ds-DNA) titer. This test has a very high specificity for SLE, especially with high titers. Its sensitivity is considerably lower as many patients with SLE may have a negative ds-DNA titer at any particular time in the disease course, even at disease onset. It is important to be aware that a negative ds-DNA titer does not exclude a SLE diagnosis (26). A second serologic test to order is anti-Smith (anti-Sm) antibodies. This titer also has a very high specificity for SLE, but like the ds-DNA titer, has a low sensitivity of 10% to 30% (27). A positive antibody titer to the ribonuclear protein (RNP) may be found in 20% to 30% of SLE patients. With high titers, the anti-RNP antibody titer suggests the diagnosis of MCTD, in which the same child may have a mixed clinical picture of SLE, JIA, scleroderma, and myositis during the disease course (28). Antibodies to SS-A and SS-B antigens may also be found in patients with SLE but are more frequently associated with Sjögren syndrome (29–31). These antibodies are also associated with the neonatal lupus syndrome (32–34).

Serologies are essential to the diagnosis of SLE but other more basic testing is also required. The CBC may reveal a normocytic, normochromic anemia of chronic illness or a Coombs positive hemolytic anemia. Patients may also have leucopenia, thrombocytopenia, or lymphopenia. Elevated erythrocyte sedimentation rate, polyclonal hypergammaglobulinemia, and elevated α_2 -globulins are often seen (35). Complement levels C3, C4, and CH50 are frequently decreased but may be normal. Persistently low levels of complement suggest active SLE renal disease (36–38). A urinalysis should be done to check for proteinuria and hematuria, two indicators of active glomerulonephritis. The presence of elevated anti-DNA titers, low complements, and an abnormal urinalysis with proteinuria and/or hematuria confirms the presence of SLE renal disease (39,40). It is also prudent to order a chemistry panel of tests to assess liver and renal function.

A positive RF may be present at low titers in 10% to 30% of children with SLE but if a high titer is found, MCTD must be suspected rather than just SLE. In patients likely to have SLE, the antiphospholipid panel should be performed. This includes an activated partial thromboplastin time (aPTT) and prothrombin time (PT) as well as lupus anticoagulant and anticardiolipin antibodies including the anti-B2 glycoprotein-1.

The above evaluation includes a long list of expensive tests. Care should be taken to perform these tests in a step-wise fashion. The initial screen may include a CBC with a platelet count, sedimentation rate, chemistry panel, urinalysis, C3 and C4, ANA, and ds-DNA. If these tests and the clinical picture suggest a possibility of SLE, then the second group of tests such as anti-Sm, anti-RNP, anti-SS-A, anti-SS-B, lupus anticoagulant and anticardiolipin antibodies should be ordered.

Cardiac Disease in SLE

Cardiac involvement is common in SLE. All layers of the heart may be affected as well as the coronary and pulmonary arteries.

The causes of this cardiac involvement are multifactorial. The inflammatory process of SLE may involve all layers of the heart resulting in pericarditis or myocarditis. Thrombus formation related to both inflammation and the hypercoagulable state associated with SLE may lead to valvular involvement and noninfectious endocarditis. Treatment with corticosteroids and SLE dyslipoproteinemia may accelerate coronary atherosclerosis. Chronic hypertension or uremia may lead to myocardial dysfunction. Cardiac involvement may not be obvious and the clinician must keep a high level of awareness of potential cardiac complications.

Pericarditis

As in JIA, pericarditis is the most common cardiac presentation of SLE, occurring in 20% to 30% of lupus patients (41–43). The clinical presentation of pericarditis related to lupus is identical to any other patient presenting with acute pericarditis including substernal chest pain, difficulty lying flat, or pain with inspiration. The pain is often improved by sitting up and leaning forward. Clinical and diagnostic findings are similar to that seen in other cases of pericarditis including a friction rub, cardiomegaly on chest radiograph and pathologic electrocardiographic changes including ST-T wave changes, PR depression, low voltages and electrical alternans with large effusions. Echocardiogram documents at least some pericardial fluid in most cases. A mild pleural effusion often is seen with the pericardial effusion related to the systemic serositis seen in SLE. Pericardial fluid is often found in many asymptomatic children with active SLE consistent with a systemic serositis (44–46).

The initial presentation of a child with pericarditis of unknown etiology includes an evaluation for SLE. The clinician has to evaluate the child by use of the 11 ACR criteria (Table 61.1). At least four criteria must be present, especially an elevated ANA titer. However, the clinician must also consider other causes of pericarditis including acute rheumatic fever, systemic JIA, Kawasaki disease, MCTD, dermatomyositis, vasculitis diseases such as polyarteritis nodosa (PAN), Wegener granulomatosis, Takayasu arteritis, spondyloarthropathies such as ankylosing spondylitis, and inflammatory bowel disease. Nonrheumatic causes are more likely such as viral pericarditis, bacterial and mycobacterial pericarditis, idiopathic pericarditis, and pericarditis associated with tumors. Anterior chest wall pain in children may mimic the presentation of pericarditis to some extent. These problems include mild problems such as gastrointestinal reflux, costochondritis, and a pain augmentation syndrome. More serious problems such as pleuritis, pneumonia, pneumonitis, pulmonary embolus, myocardial ischemia or infarction, and pulmonary hypertension may present in any lupus patient and mimic symptoms of pericarditis.

Myocardial Involvement

Myocarditis is seen in 15% of children and adolescents with SLE (47). The first sign may be tachycardia even in the absence of fever. As ventricular function deteriorates, the patient may develop signs of volume overload such as poor appetite and ability to eat, abdominal distention/ascites, respiratory distress/pulmonary edema or signs of decreased cardiac output such as hypotension, poor perfusion, and narrowed pulse pressure. Arrhythmias may also develop and be life threatening. Myocarditis due to SLE from other causes of myocarditis is indistinguishable based solely on physical examination and requires further confirmatory testing.

Endocarditis

Libman-Sacks endocarditis (LSE) or noninfectious thrombotic endocarditis is due to SLE involvement of the heart valves



Figure 61.8. Transesophageal echocardiogram showing thickening of the mitral valve with small mobile structures consistent with Liebman-Sacks endocarditis in patient with SLE and transient ischemic attack (TIA).

(48–50). Small nodules accumulate on the supporting structures of the heart valves (Fig. 61.8). These nodules show fibrinoid necrosis and thrombotic material histologically. Involvement of the mitral valve is the most common. A heart murmur may or may not be easily heard. Lesions are typically small and may not result in significant valve destruction. The lesions may or may not be seen by transthoracic echocardiogram. When visualized, the lesions are typically tiny irregular vegetations of 2 to 4 mm in diameter that are seen on the valve itself or on the subvalvular apparatus. However, lesions may be atypical. Galve et al. (51) studied 74 patients with SLE prospectively and found 7 with classic Libman-Sachs lesions but also 8 with atypical lesions. These patients had no nodules but rather had thickening or stiffness of the aortic or mitral valves that led to regurgitation and rarely, stenosis (51). Transesophageal echocardiography is optimal for detection of SLE lesions and new tools such as the real-time 3-D echocardiography may help delineate these lesions further (<video callout>see video 61.1) (52,53). In a prospective study of 342 adults with SLE, LSE was detected by transthoracic echocardiogram (TTE) in 38 patients with 24/38 having mitral valve disease, all 24 with regurgitation, and 9 with stenosis in addition to regurgitation. One patient had mild tricuspid regurgitation (49). In 40 children with SLE, echocardiography noted mitral regurgitation in 4/30, tricuspid regurgitation in 3/40, aortic regurgitation in 2/40, and pulmonary valve involvement in 1/40 (54).

Patients with severe SLE endocarditis may present with congestive heart failure.

It is likely that antiphospholipid antibodies have a role in these endocardial lesions resulting in the layering of thrombotic material on the endocardial surface of the heart and valves.

Other cardiac involvement in patients with SLE includes early atherosclerosis, which may be due to chronic steroid use or primarily to an inflammatory process involving the coronary arteries. Gazarian et al. (55) did an extensive study of childhood SLE coronary artery involvement using echocardiography, thallium perfusion scans, and angiography in children with SLE thought to have normal hearts. Four children had myocardial perfusion scan abnormalities that could be reversed and one child had a fixed myocardial perfusion defect (55). Lipid abnormalities and antiphospholipid antibodies were found in a significant number of the study population. Studies in adults have supported the involvement of the

antiphospholipid antibodies in endocarditis and other cardiac lesions of adult SLE such as intracardiac thrombosis, myocardial disease including coronary artery involvement, microvascular thrombosis, and pulmonary hypertension (56,57). A recent systemic review of the research into the association of antiphospholipid antibodies with valvulopathy in SLE found that 15 of 20 studies demonstrated a positive association between these antibodies and valvular lesions and five studies did not (58).

Treatment of valvular disease in children with SLE will vary. In a child with acute endocarditis, corticosteroids are indicated although the effectiveness of corticosteroids for SLE valvular disease remains unclear. Milder cases may only require the long-term lupus therapy required for other organ systems. Close follow up for cardiac progression, particularly with worsening regurgitation, infective endocarditis, and thromboembolic complications (e.g., stroke) is essential. Valvular disease can also be treated with antiplatelet medication or anticoagulant therapy although there are no large studies looking at antiplatelet therapy versus anticoagulation therapy with warfarin and most data are from small case series or reports (59). Valve replacement may be needed for the most severe SLE endocarditis (60). Children with SLE who have antiphospholipid syndrome and endocarditis require aggressive anticoagulation therapy as well as corticosteroid therapy (61).

Endocarditis in children with SLE is a major concern. Subclinical involvement is common and it is likely that as our tools for detection improve, the degree of pathology found in these patients may increase. Long-term sequelae of this involvement are unknown. Routine echocardiography of children with active SLE appears appropriate, particularly if the patient has antiphospholipid antibodies.

Coronary Artery Involvement and Premature Atherosclerosis in SLE

Children and adolescents as well as adults with SLE may develop significant coronary artery disease with many potential etiologies. Systemic vasculitis or vasculopathy of SLE that affects skin, the gastrointestinal (GI) tract, the brain, and other organs may also target the coronary arteries. Myocardial infarctions have been reported in two young children and in a 17-year old adolescent with SLE (62–64). Giant and smaller diameter coronary aneurysms may develop due to arteritis (65). It is likely that antiphospholipid antibodies play a role in this pathology as well.

The third contributing factor may be premature atherosclerosis. There are several contributors to this increased risk including the high rate of dyslipidemia and hypertension as well as decreased flow-mediated dilation (66,67). Other risk factors reported to be present in adolescents with SLE include the uncontrolled inflammation of SLE, elevated triglycerides, apolipoprotein B, hemoglobin A1C, and insulin levels. Total prednisone dose and low-density lipoprotein cholesterol (LDL-C) levels correlate with the total cholesterol level and may also contribute to premature atherosclerosis (67).

The cardiovascular risk of children and adolescents with SLE is most likely multifactorial and the exact treatment and risk factor modification guidelines for the patients has not yet been well defined.

Conduction System Involvement

Occasionally older children and adolescents with SLE have been reported to develop conduction abnormalities and arrhythmias (68). These conduction problems tend to be mild. Yet AV block, intraventricular conduction problems, and sick sinus syndrome have been described in adults with SLE. Sinus tachycardia, atrial fibrillation, atrial ectopy, and long QT syndrome

have been noted (69). These heart abnormalities may present simply as dizziness or palpitations but also may lead to sudden death. The pathologic causes of these conduction abnormalities are unclear but some authors attribute the defects to the small vessel vasculitis, infiltration of the sinus or AV nodes, myocarditis, or local ischemic injury due to SLE (70).

Pulmonary Hypertension

Pulmonary hypertension (PAH) is unusual in SLE and, if it occurs, may be due to intrinsic lung disease, and not be due to a cardiac etiology (see Chapter 66). Xing et al. (71) reported that by echocardiography, 31 of 299 children age 7 to 18 years with rheumatic disease had pulmonary hypertension. Seventeen of these patients were from a group of 223 SLE children who were tested. These children often presented later in the disease course with shortness of breath or overt heart failure. Children with Raynaud phenomenon and antiphospholipid antibodies were more likely to have more severe pulmonary hypertension. Early detection may require early and routine use of echocardiography and pulmonary function testing with a diffusing capacity (DLCO) testing routine follow-up of children with SLE.

Neonatal lupus erythematosus (NLE) is a transient disease of newborns due to the passive transplacental transfer of maternal antibodies (anti-SS-A [anti-Rho] and anti-SS-B [anti-La]). The quantity of the antibodies, rather than the mere presence of these antibodies, appears to be crucial to NLE tissue damage (72). The newborns primarily present with a rash and congenital heart block (CHB) but may also develop hematologic, liver, kidney, and neurologic findings. Li et al. (73) reported 7 cases in 2011 and reviewed the 94 cases reported in China since 1980. Seventy-three of ninety-four cases had the skin rash, which was seen frequently around the eyes, which also involved other areas of skin. Twenty-three of the ninety-four children had cardiac abnormalities, thirteen with cardiac conduction problems (eight with atrioventricular block [AVB]), and five cases of right bundle branch block. Nine cases had structural defects including five with an atrial septal defect, two with ventricular septal defect, and two with enlarged atria. Forty-four of the ninety-four patients had hematologic changes including 28 with thrombocytopenia, 11 with leukopenia, and 34 with anemia. Thirty cases had hepatic or splenic issues; 28 with an enlarged liver or spleen, 24 with abnormal liver function tests, 6 with splenomegaly, and 4 with cholestasis.

These 94 children had numerous autoantibodies. Eighty-six of 94 had anti-SSA, 51 had anti-SSB, 16 anti-double-stranded DNA, 14 had anti U1-RNP, 13 anti-Sm, 6 anti-RNP, and 4 anti-rRNP.

Of the 94 mothers, 39 had no SLE signs or symptoms and no SLE diagnosis; 35 had definite SLE, 5 had discoid lupus, 3 had Sjögren syndrome, and 4 had miscellaneous autoimmune problems. Eight women developed SLE during their pregnancies. Twenty of the neonates were treated with corticosteroids and four with intravenous immunoglobulin (IVIG). Sixty-eight of the neonatal lupus children had follow-up up to 12 years with 58/68 totally normal at follow up, four still with cardiac abnormalities but improved (two with grade III AVB without pacemaker), and three died (73).

Another recent study of neonatal lupus by Wisuthsarewong et al. (74) reported 17 neonates with NLE who were seen over 15 years at one hospital in Thailand. Skin involvement was found in 70.6% with most having erythematosus patches (91.7%), some having subacute cutaneous LE (50%), 41.7% petechiae, 16.7% persistent cutis marmorata, and 8.3% discoid lesions. Nine cases had CHB and nine had cardiac structural abnormalities.

The heart disease of these neonates must be kept in perspective. Neonatal CHB is rare. But among pregnant women with

SLE, the incidence of neonates with CHB increases dramatically from 1/15,000 births to 1/37 births and if the mother with SLE has anti-SSA antibodies, to 1/13 births. Conversely, the risk of a mother with SLE and these anti-SSA antibodies giving birth to an infant with neonatal lupus is still quite low as 12/13 babies may be normal. If a mother with SLE has one child with neonatal lupus, her risk of having a second neonate with neonatal lupus is much higher at 17% to 49% (75,76).

Noncardiac neonatal lupus is often underappreciated. The incidence of the rash of this disease is variable, ranging from 15% to 70%. Most NLE rashes are photosensitive but some may not be as the rash can be present at birth or develop in non-sun-exposed areas. The rash occurs mostly around the infant's eyes but can be noted anywhere on the body. Liver and spleen involvement occurs without symptoms. Either organ may be mildly enlarged. The liver involvement (15% to 25%) may be reflected in elevated liver enzymes and cholestasis. The liver pathology is similar to neonatal giant cell hepatitis. Neutropenia and thrombocytopenia are the more common hematologic changes. Neurologic abnormalities described include nonspecific white matter changes, calcium deposits in the basal ganglia, hydrocephalus, and blood vessel changes (a vasculopathy). Stippling of the epiphyses may also be found (77).

Prevention of the cardiac damage in NLE is a major concern. Mevorach et al. (78) reviewed a recent report of 95 women who had anti-SSA/Ro antibodies during 98 pregnancies. They performed weekly Doppler echocardiograms and detected 10 fetuses that developed NLE, 3 with first-degree heart block, and 3 with complete heart block. It was difficult to detect the first-degree heart block in these fetuses using echocardiography. A second group studied 70 fetuses of 56 mothers using tissue velocity fetal kinetocardiography for measuring the fetal PR interval. They were able to detect six fetuses with first-degree heart block and treated those infants with fluorinated corticosteroids leading to normalization of atrioventricular (AV) conduction. The rapidity of progression from first-degree to third-degree or complete heart block in these NLE fetuses is cause for concern with development of permanent changes within 2 weeks of a normal sinus rhythm. Early detection with aggressive treatment with corticosteroids or IVIG may be critical (34).

Once born, the neonate with NLE should be evaluated for ongoing active myocarditis and the need for more corticosteroid therapy. Many of the children with complete heart block require pacemakers; however, some patients will resolve their heart block and not require pacemaker placement. The timing of pacemaker placement is critical as transvenous systems cannot be placed until the child is older. In infants requiring pacemaker placement, the procedure is more invasive requiring epicardial placement of the leads with the generator being placed in the abdominal wall. The mortality of these children is high, as much as 20%, due to congestive heart failure, supporting the need for early detection of heart involvement during pregnancy and aggressive treatment of the involved fetus. Any NLE child with cardiac involvement requires close cardiology follow-up to monitoring of ventricular function, for evidence of chronotropic competence, and for hemodynamic compromise related to the conduction disease.

Childhood Takayasu Arteritis (cTA)

Takayasu arteritis (TA) was first described by a Japanese ophthalmologist Dr. Takayasu in 1908 (79) as a pulseless disease. It is now known to be a chronic granulomatous arteritis that affects the large vessels such as the aorta and its major branches. It runs a relapsing and remitting course.

For diagnosis the patient must meet at least three of six American College of Rheumatology criteria for diagnosis. The six diagnostic criteria identified were:

1. Onset before 40 years of age;
2. Angiographic evidence of large arterial vessel disease;
3. A blood pressure differential between any of the limbs of more than 10 mm of Hg;
4. Bruits;
5. Decreased brachial artery pulses;
6. Claudication.

In a prospective validation in adults, this diagnostic scoring system was found to have a sensitivity of 90.5% and a specificity of 97.8% (80,81).

The recently proposed European League Against Rheumatism/Paediatric Rheumatology European Society (EULAR/PReS) European childhood TA criteria are stricter and make angiographic abnormalities in the large arteries as mandatory for the diagnosis. Apart from positive angiographic findings, it also requires one of the other four criteria (blood pressure differential, bruits, decreased brachial pulses, and claudication) for the diagnosis to be made. Apart from the six ACR criteria, these proposed criteria also include hypertension and raised acute phase reactants (82).

Epidemiology: The cTA experience mostly comes from the adult series with a few children as there are only a few published reports on juvenile onset TA. TA appears to be more common in Asian, African, and South American population than in Caucasians. It is mostly a disease of adults but can occur in young adults and children, even very young children. A few illustrative cases in very young children are worth mentioning:

1. A two-year-old child was diagnosed with cTA who presented with congestive cardiac failure and severe aortic stenosis (83).
2. A two-and-a-half-year-old boy was diagnosed with cTA who presented with severe aortic regurgitation and diffuse coronary artery involvement (84).
3. A three-year-old child who presented with severe brain and cardiac involvement and congestive cardiac failure was diagnosed with cTA (85).

In this chapter, TA with age of onset below 18 years is classified as cTA disease. The incidence in childhood is not known. There is a strong female predominance. The disease incidence varies in different geographical areas and the female-to-male ratio, clinical course, disease of onset, and organs involved also vary by geographic location. The cause for these geographical variations is not known (86). Japanese patients had more ascending aorta and coronary-cardiac involvement while Indian patients had more involvement of descending aorta and renal artery involvement. A role of gender in these variations was postulated in some Indian studies as the males were found to have significantly higher incidence of aortic arch and coronary disease while females had more of abdominal aorta and renal artery disease (86,87). Valentini et al. reported a mother and a child who were both diagnosed with TA. Based on the human leukocyte antigen (HLA) typing of the mother and daughter, they suggested a possible familial component and a possible association with type I diabetes mellitus (insulin-dependent diabetes mellitus [IDDM]) gene (88). Similar findings have been described by other researchers in familial occurrences of TA (89–91). On the other hand, Makino et al. (92) reported dissimilar HLA findings in the two siblings who were diagnosed with TA. An association between TA and the HLA Bw52 has been recognized in the patients from Japan and Mexico (93,94). Jeeva et al. in 2007 (95) reported a Pakistani family with five out of seven siblings between the ages of 12 to 19 years who developed TA. Based on their genetic studies and HLA typing, Jeeva et al. (95) speculated the possibility of autosomal recessive inheritance for that family.

Like adults, children with cTA present with very nonspecific initial symptoms that are mostly constitutional, such as



Figure 61.9. MRA of aorta in patient with TA. Note the irregularity of the aortic wall.

fever, arthralgia, headaches, palpitations, and abdominal pain (96). Compared to adults, Jales-Neto et al. (97) reported a worse prognosis in juvenile onset TA. In their series of 62 TA patients (17 juvenile onset and 45 adult onset), they suggested that juvenile onset TA more often had a specific type of renovascular involvement in which they were more likely to have aneurysms (Fig. 61.9). Their disease was more refractory to treatment as compared to their adult counterparts (97). In contrast, the cardiac involvement and cardiac prognosis between the two groups were similar (97).

Case series of TA: The largest, predominantly juvenile onset, TA series are reported from India, South Africa, Korea, and Belgium. The Indian series was a longitudinal 16-year follow-up of 106 patients with Takayasu disease. The mean age of onset was 27 years (± 9 years) with a 1:1.6 M:F ratio. The most common presentation was hypertension (77.4%); 12.3% patients had congestive cardiac failure. They were treated by antihypertensive drugs therapy (76.4%), antitubercular drugs (7.5%), steroids (15%), and cyclophosphamide in one patient. Four percent of patients had coronary angiography (98).

Sharma et al. (99) reported another Indian series of 83 patients with TA in 1992. The age range at diagnosis was between 5 to 53 years (mean 26.9 ± 9.7) with a similar male to female ratio. The clinical presentation and disease course was similar to the previous series of 106 patients. Muranjan et al. (100) reported 17 children with TA in the age range between 5 and 11 years (M:F = 1.1:1). In this series, the main presenting signs were hypertension (64.7%), congestive cardiac failure (47%), cardiomyopathy (41.1%), and cardiac valvular disease (35.2%).

Nineteen children with cTA were reported from Turkey (101) in 2008. The male to female ratio in this cohort was 1:2.8. The age range at diagnosis was between 8 and 17 years (mean 12.84 ± 2.69 years, median 13 years). The most common clinical finding was hypertension. Hong et al. (102) reported cTA in 70 Korean children. The male-to-female ratio was 1:4.4 and the youngest patient was a 3-year-old female. The most common manifestation was hypertension (93%) and

several of these children also had congestive cardiac failure. None was reported to have coronary artery involvement. Orea Tejada et al. (103) looked specifically at cardiac damage in 125 patients from a mixed age group cohort from Spain. In their series, cardiac damage was identified in a high percentage of patients (82.4%). The cardiac involvement included; precordial murmurs in 65%, cardiomegaly in 70%, congestive cardiac failure in 28%, angina in 13.6%, an abnormal electrocardiogram (EKG) in 60%, left ventricular hypertrophy in 40.8%, right ventricular hypertrophy in 8.8%, and conduction defects in 12%. Aortic regurgitation was diagnosed in 11.2% of patients and mitral valve regurgitation was diagnosed in 13.6% of cases due to left ventricular dilation. In their series, 4.8% patients died due to cardiac damage and congestive cardiac failure. Seguchi et al. (104) reported a 11-year old girl who had developed ostial stenosis of left coronary artery as the only manifestation of Takayasu arteritis. Emi et al. (105) reported both coronary ostial stenosis as a sole manifestation of TA. Also, left ventricular submitral aneurysms have been described in children with TA (105–107).

Coronary artery involvement in the mixed age cohort is reported to be present in 9% to 10% of the patients with TA (108–110). Matsubara et al. divided coronary artery lesions based on the pathologic findings into three categories; (i) involvement of the ostia and initial part of the coronary artery; (ii) coronary arteries with patchy and segmental disease as well as a more generally diffuse and wide spread coronary artery involvement; (iii) coronary aneurysms present (Fig. 61.10). They suggested that most of the lesions in TA belong in category one and are the result of extension of inflammation from the aortic root in the form of intimal proliferation and fibrosis of the media and adventitia in the coronary arteries (108,111). Category two lesions are due to coronary arteritis. These lesions have a predilection for the proximal part of coronary arteries though this involvement can be more generalized and diffuse in distribution. The third category with a coronary artery aneurysm was less common in their series (108). Due to these coronary lesions, TA should be suspected in differential diagnosis of a young Asian female with angina.

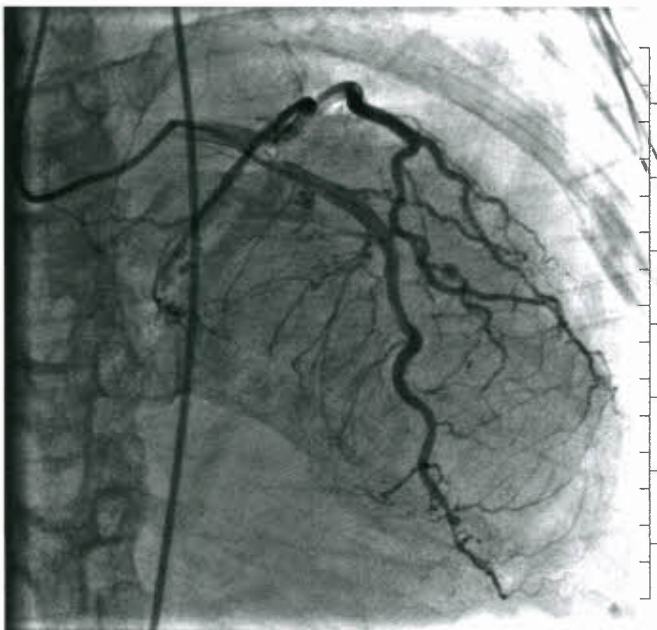


Figure 61.10. Coronary angiogram showing multiple small coronary artery saccular aneurysms in a patient with chest pain and vasculitis.

If required, surgical treatment should be performed when TA is in an inactive state. If an operation must be performed in active (histologically or clinically) TA, postoperative corticosteroids should always be given (112). Several procedures such as transaortic endarterectomy, coronary revascularization with vein grafts, and aortocoronary bypass surgery have been used successfully in patients who require surgery (113–115).

Pathology findings: Sharma et al. (116) described autopsy findings from 10 children with TA. In the series, cardiac involvement included left ventricular hypertrophy (nine), right ventricular hypertrophy (four), biventricular hypertrophy (three), myocarditis (two), and involvement of coronary artery (one). The authors concluded that the most common cause of mortality is severe hypertension and its effect on heart, kidneys, and brain. These problems appeared to be worsened by delay in diagnosis. In 12.5% of their autopsy findings from patients with TA, Rose et al. (117) reported the unusual autopsy findings of segments of narrowing and dilation of major epicardial coronary arteries with coronary aneurysm formation. In another autopsy series from India, Kinare et al. compared cardiac findings from pediatric patients ($n = 25$) and adults ($n = 35$). They reported that the heart was normal in autopsy in 20.5% of the adult patients, but the heart was normal in only 8.7% of pediatric patients. Renal and aortic stenosis was present in 91.3% of pediatric and 80.0% of adult patients. Congestive heart failure was more common in pediatric age group (68%) (118).

Associations

Several studies have reported association of many autoimmune diseases with TA, such as SLE (119–122), ankylosing spondylitis (92,123), JIA (124–126), anterior uveitis (127,128), sarcoidosis (129), seronegative spondyloarthropathy (130), Crohn disease (131), Wegener granulomatosis (132), Sweet syndrome (133,134), ulcerative colitis (135), and Wiskott-Aldrich syndrome (136). Interestingly, an association between rheumatic heart disease and TA has been found and a few reports comment on cardiac involvement due to both diseases at the same time (103).

Tuberculosis and TA

The Mantoux test was strongly positive in most patients from many series, especially those reported from India and South Africa. The tuberculin test and quantiferon gold was also significantly positive for their cohort in the patients reported from Europe. Yet the relationship with mycobacterium tuberculosis is still speculative. Some have suggested that TA patients show accelerated immune response to mycobacterium tuberculosis antigens, specifically its 65 kDa HSP (65 kDa heat shock protein). Several authors suggest a role of mycobacterium tuberculosis in the immunogenesis of TA (137–141).

Delay in Diagnosis

Common findings in all the published reports and series were that the time between the onset of symptoms and diagnosis was long (mostly in months and few in years). The delay may be due to several reasons including rarity of this diagnosis, absence of characteristic symptoms, incidence in the countries with less robust investigational facilities, and comorbidities with similar symptoms (142,143).

Clinical Manifestations of cTA

The most common manifestation in all series is hypertension. Other symptoms are secondary to congestive heart failure, ischemic symptoms due to aortic and coronary involvement, and renal artery involvement (144). Thomas et al. (110)

reported 86 children with TA in their series of 1,130 cases of Takayasu disease. Out of these 86 patients, 5% were treated for angina and myocardial infarction. Aortic valve involvement is usually associated with arterial involvement of other large vessels but can occur alone. Aortic root dilation causing valve regurgitation is common in cTA. It is also associated with coronary ostial involvement in 30% of cases and when accompanied with coronary artery disease can cause sudden death (145). It has been suggested that coronary angiography should be performed before operative treatment of aortic valve and early treatment of aortic disease could be lifesaving (146). The symptoms of myocardial ischemia or hypertension along with raised inflammatory markers in a young female should prompt for investigations for TA (147). Mitral valve involvement has also been reported in TA. Some other cardiac complications in cTA are aortic pseudoaneurysms (148), dissection of the aorta (149), and dilated cardiomyopathy (150).

Diagnostic Modalities

Routine labs for inflammatory markers and organ-specific investigations such as EKG and echocardiography are done first. Conventional angiography is considered the gold standard in TA and cTA. It generally agreed that only conventional angiography gives information on the lumen of the artery and may often be needed despite its invasiveness. Recently, less invasive investigations such as computed tomographic angiography (CTA) and gadolinium-enhanced 3-D magnetic resonance angiography (MRA) have been used more as they are increasingly useful in delineating the initial arterial wall changes such as arterial wall thickening (151–153).

Treatment

Corticosteroids, methotrexate, mycophenolate, azathioprine, total lymphoid irradiation (TLI), cyclophosphamide, and biologic therapies such as TNF- α blocking agents are treatment options. Mortality reduction with prednisone or methylprednisolone treatment has not been firmly established. Cyclophosphamide and mycophenolate are the most commonly used remittive agents. Sildenafil has been used in cTA to treat extremity ischemia (154).

Polyarteritis Nodosa

PAN was first described in 1866 by Kussmaul and Maier (155,156). PAN is an uncommon condition in pediatric age group. It is of two types, the cutaneous PAN and systemic PAN. This discussion focuses on the systemic PAN that can affect the heart. It is a peri nuclear antineutrophil cytoplasmic antibodies (p-ANCA) positive vasculitis of small and medium vessels and has predilection to involve bifurcations of blood vessel. The cause for this behavior is not clear but it is presumed to be related to turbulence-mediated injury initiating the inflammation at bifurcations. The vasculitis is typically patchy in nature and is characterized by endothelial proliferation, fibrinoid necrosis, microthrombi, and resulting ischemia damage to vessel and microaneurysm formation. Rupture or thrombosis of these microaneurysms can lead to organ ischemia and damage, intraperitoneal bleeds, and perirenal hematoma (157–160).

In systemic PAN, the most commonly involved organs are skin, joints, peripheral nerves, gut, scrotum, and kidneys, while lungs are usually spared (161). The cardiac, neurologic, and respiratory manifestations have been reported in children but are less frequent (158,162–167). In adults with PAN, the incidence of these involvements is up to 86% while in children it is between 0% and 85% reported in most published series (168,169). A familial Mediterranean Fever (FMF) gene has been found significantly more often in patients with PAN and vice versa (170–173), especially in the geographical areas

around Turkey and Israel. There has also been an association of PAN with hepatitis B infection (173,174). There is no evidence that children with these associations have a higher incidence of cardiac complications or involvement. Ozen et al. examined a cohort of 17 patients who had both PAN and FMF. They reported that when both conditions occurred, the PAN onset was at a younger age. When compared to patients with PAN alone, these children were less severely involved, including cardiac complications, had a better overall prognosis, and tended to respond better to steroid treatment. In contrast, the incidence of perirenal hematomas was higher in the PAN/FMF children compared to patients with only PAN. Several other workers have confirmed this finding (162,170,171,175–177). Cardiac involvement was not found in any of their cohorts of PAN/FMF patients. Though cardiac involvement is rare in PAN patients with FMF, there is not enough evidence to say that these genes together are protective for cardiac involvement.

Cardiac involvement in PAN is reported to be a bad prognostic factor (178–180). Gunwale et al. reported 15 cases of PAN with systemic involvement, between 4 and 14 years of age. The most common finding in their cohort was diminished left ventricular systolic function and atrioventricular valve regurgitation (mitral and tricuspid), even in asymptomatic patients. One patient had some pericardial thickening without effusion. The EKGs of these patients did not show any evidence of myocardial ischemia, infarction, or conduction defects (169).

Infantile polyarteritis nodosa is a systemic vasculitis that occurs below two years of age. Though multiple organs can be involved, it mainly affects the central nervous system and the heart. It shares some clinicopathologic features with Kawasaki disease (181,182). Some have questioned whether these two are the same disease. The diagnosis has usually been made postmortem because of the rarity of the disease and on occasion, the overwhelmingly acute presentation without an easy diagnosis. Munro et al. (183) described a fatal case of late onset enterocolitis in a 3-month-old infant who died after 3 weeks of enterocolitis onset. The postmortem findings were consistent with systemic arteritis including the coronary arteries and a probable diagnosis of Infantile PAN was made. Edwin et al. reported (184) two cases of pericardial hemorrhage in both a 9-month-old child and a 5-year-old child. Both died of cardiac tamponade with the diagnosis of PAN established on autopsy. The fact that the diagnosis of PAN in children may be established at autopsy has not changed over the years, especially when it presents in infants and when coronary arteries are involved (184–189). Surprisingly, PAN in these infants presented as an acute illness starting with symptoms of upper respiratory infection or gastroenteritis. Munro-Faure (190), examined 19 fatal cases of predominantly infantile coronary arteritis. Triggers such as Streptococcal infection, Coxsackie B virus, and exposure to antibiotics such as sulfa, were hypothesized as possible etiologic factors without any conclusive evidence.

MRI, CT, CTA, and Tc-99m dimercaptosuccinic acid (DMSA) renal scan have been used successfully as noninvasive methods to investigate arteritis and aneurysms of different organ systems (191,192). These methods have not been very useful in the past for investigating cardiac and coronary artery involvement. Kobayashi et al. (193) did recently report a more successful use of MRI of the heart to detect coronary artery ectasies and aneurysm. EKG and echocardiography are commonly performed but are less often revealing.

Lab findings include mild anemia and increased inflammatory markers (C-reactive protein [CRP], erythrocyte sedimentation rate [ESR], WBC, platelets and immunoglobulin). Myocardial enzymes such as the creatine kinase (CK) may increase indicating myocardial damage. ANCA are an important part of lab investigations in adults with PAN as opposed

to children with PAN who are mostly negative to this antibody (194). Other tests such as myeloperoxidase (MPO)-ANCA or proteinase 3 (PR3)-ANCA, are also negative in children and are not helpful in making the PAN diagnosis (194). The ANA is usually negative (195). The serum neopterin, factor VIII antigen and other markers of endothelial injury or repair may be elevated. Some have examined the use of endothelial microparticles (EMP) and platelet microparticles (PMP) as surrogate markers for endothelial injury (195–199).

Coronary angiography can delineate vessel aneurysms and ectasias. Other angiography may help with the definitive diagnosis of PAN. Brogan and Dillon (196) have suggested several nonaneurysmal features of visceral angiograms in PAN that are more commonly found than aneurysms and contribute to making the diagnosis. These signs are delayed emptying of small arteries, perfusion defects, and the presence of collateral arteries. Whether these nonaneurysmal findings could be useful increasing sensitivity of cardiac lesions is not known.

Biopsy and tissue sampling may be an option for diagnosis mostly when evaluating the visceral organs. Its utility in cardiac involvement has not been proven so far. Also the patchy and irregular distribution of PAN lesions and the risk of the procedure make it a less attractive diagnostic tool. The right combination of the clinical pattern, laboratory testing, and imaging are needed for the diagnosis of PAN with cardiac complications.

No randomized controlled trials are available to guide the therapy in PAN with cardiac disease. The information available is from experience-based published literature. High-dose corticosteroids still remain the mainstay of treatment especially in infantile PAN. Depending upon the severity of the disease, corticosteroids may be initiated by using initial boluses of methylprednisolone 15 to 30 mg/kg/dose (maximum of 1 gm.) for three to five consecutive days followed by oral prednisone/prednisolone at a dose of 1 to 2 mg/kg/day for 4 to 6 weeks. The dose can then be tapered over a variable period of time depending on the response (195,200–203). Others have used alternate day steroid therapy (195). The new strategies for treatment include using oral or intravenous cyclophosphamide (2 mg/kg/day or 500 to 1000 mg IV/M²) with steroids as induction therapy with dose corrections for renal or hepatic diseases as required. Cyclophosphamide IV is used on monthly basis for a period of 6 months for better compliance but it is claimed that oral regimen has better efficacy than IV bolus dose. After induction is achieved, several other agents can be used alone or in combination with steroids depending on the severity of disease and response to treatment for a further period of approximately one and a half years (202,204). These agents include azathioprine, methotrexate, and mycophenolate mofetil. There is no evidence that one agent is better than another for maintenance therapy. Intravenous immunoglobulin and plasma exchange has been used in emergency situations while waiting for other immunosuppressants to have an effect (205–209). A word of caution about use of IVIG as occasionally it can lead to ANCA positivity in otherwise ANCA negative patients (210). Anecdotal case reports of successful use of infliximab and rituximab in resistant cases have been recently published (211–215). Autologous stem cell transplant may be considered as an ultimate option keeping risk benefit in mind (216–219).

Hepatitis B-associated PAN cannot be treated by above regimens because of the possible flare up of the hepatitis virus and consequent liver damage. Intravenous immunoglobulin can still be used as rescue therapy and to facilitate immune complex removal. Steroids are used with antiviral therapy to induce remission under strict monitoring because these patients run a risk of acute fulminant hepatitis with liver failure. The steroid and antiviral therapies have been successfully used in combination with plasma exchange. After remission is achieved, only

antivirals are continued if needed and hepatitis B is allowed to undergo its seroconversion. There is evidence that patients who achieved seroconversion had a 0% relapse rate (174,220–223). Antiplatelet therapy with aspirin or clopidogrel is recommended in all cases as an adjuvant therapy (203).

Behçet Disease

In 1837, Dr. Huluci Behçets a Turkish dermatologist, first described the disease in three patients (224). Initially it was thought to be more prevalent near the old silk trading routes in the Middle East and in Central Asia and was called the Silk Road Disease. Behçet disease (BD) shows geographic and ethnic preferences as well as differences in disease course and outcomes (225,226). It is more common in Japan, Turkey, and Middle East compared to rest of the world (227). There is high frequency of familial cases especially in pediatric patients (228,229).

BD is a systemic vasculitis syndrome that affects all sizes of arteries as well as veins, both superficial and deep. It involves several organs such as central nervous system, gastrointestinal, skin, mucous membranes, eyes, and musculoskeletal system. Atzeni et al. (230) have reported cardiac involvement in 7% to 46% of adults with BD and 20% of those involved died due to their cardiac complications. Cardiac involvement in pediatric patients with BD is not common (227,229,231–233). Koné-Paut et al. (228) examined 86 pediatric BD retrospectively from Turkey, France, Iran, and Saudi Arabia in 1998. None of the patients in their cohort were found to have cardiac disease. Davatchi et al. (234) reported 0.6% cardiac involvement in their large cohort of 6,500 pediatric and adult patients with BD in Iran who were followed for as long as 35 years.

BD has been found to have association with HLA B51 (B51 is a split antigen of antigen B5) and HLA B27. It has been observed that patients who are positive for either or both genes have milder disease (235,236). On the other hand, Zouboulis et al. (232) found HLA-B5 gene positivity a marker of severe BD. Abdolhadi et al. (237) reported that HLA B27 positive patients with BD had a higher incidence of ankylosing spondylitis, chronic diarrhea, and type III or IV (WHO classification) glomerulonephritis, compared to HLA B27 negative patients. An association between FMF and BD has also been recognized (238–240). None of these associations has been reported to increase risk for cardiac complications in patients with BD.

There is no published literature on the incidence of cardiac complications in pediatric patients with BD. In BD adults, multiple cardiac complications can include; interatrial septum aneurysm, mitral valve prolapse, mitral regurgitation, aneurysmal dilatations of sinus of Valsalva and ascending aorta, coronary artery aneurysm, cardiac thrombus, myocarditis, and conduction disturbances (241). Most of these patients developed cardiac problems at an early adult age. It is not known whether their cardiac involvement started at an early age such as during adolescence. The average time between the oral ulceration and initial symptoms of BD to that of a second major manifestation has been estimated to be 8.8 years (242).

Anecdotal reports have described other cardiac problems such as endomyocardial fibrosis, noninfective endocarditis, aneurysms of the ascending aorta, intracardiac thrombus formation, coronary artery aneurysm, and pulmonary artery aneurysms (243–246). All of these patients responded to immunosuppressive therapy and recovered without residua. Coronary artery bypass and heart transplant in pediatric BD has also been reported (245,247). The posttransplant survival was only 1 year. Recurrence of the aneurysmal disease, hypercoagulable state, thrombosis, and the tendency for an exaggerated inflammatory response (pathergy) were major drawbacks reported with the procedure.

Zhuang et al. (248) reported myocardial infarction and aneurysm of the left ascending coronary artery in a 12-year-old boy in Turkey who responded well to urokinase, corticosteroids, colchicine, and aspirin.

Juvenile Dermatomyositis

The exact prevalence of cardiac complications in JDM is not known (249). Cardiac complications appear to be unusual in JDM. On the other hand, cardiac involvement may have been underinvestigated in children and that may in part be contributing to the reported low prevalence of cardiac complications in JDM. The most common cardiac finding is sinus tachycardia. Subtle conduction defects with the tachycardia are also reported. Karaca et al. (249) reported sinus bradycardia in a 11-year-old due to sinus node involvement in JDM who recovered after his myositis inflammation was treated without requiring any specific treatment for bradycardia. Severe conduction abnormalities are rare, for example, complete heart block resulting in congestive cardiac failure (250).

Sato et al. (251,252) identified anti-CADM-140 antibodies exclusively in 8 clinically amyopathic patients out of total 42 patients with JDM. Their data suggested that these amyopathic patients had significant and progressive interstitial lung disease and cardiac complications when compared to other JDM patients who did not have anti-CADM-140 antibodies (50% vs. 6%; $p = 0.008$).

Coronary artery disease has been reported. In some cases, this vasculitis appears to cause myocardial damage due to the combination of small vessel vasculitis of myocardial vessels, coronary artery involvement, and/or cytokine-induced myocarditis (250). Myocardial involvement is more commonly reported in adult dermatomyositis and in polymyositis (253–259). In adults, cardiac complications are the cause of death in 10%–20% of patients with adult dermatomyositis and polymyositis (250,260). Some have reported an association between heart complications and antisignal recognition particle myositis-specific autoantibodies in patients with JDM. A significant correlation was found between degree of myonecrosis as measured by muscle enzymes and the levels of antisignal recognition particle myositis-specific autoantibodies (261,262). Constantin et al. (263) compared cardiac complications among several other parameters between 66 adult dermatomyositis and 44 JDM patients using the Hungarian National Registry of patients with dermatomyositis. They did not find any evidence of cardiac involvement in JDM.

Schwartz et al. (264) performed a detailed cardiac examination including echocardiography, early diastolic transmitral flow/early diastolic tissue velocity (E/E') as a marker for diastolic dysfunction, 12-channel ECG and physical examination on 59 JDM patients and 59 age-matched and sex-matched controls. They reported that E/E' was elevated in 13 (22%) patients versus 0 controls ($p < 0.001$). In their series, 10 JDM patients presented with abnormal ECG as compared to only 4 in controls group ($p = 0.054$). It can be argued that if hypertension has a role in these cardiac findings, it may be in part due to corticosteroid therapy (265).

Scleroderma

Heine et al. (266) described cardiac involvement in scleroderma for the first time. In 1943, Weiss et al. (267) confirmed the findings of Heine and also identified cardiac fibrosis as the case of cardiac failure in systemic scleroderma patients. Systemic scleroderma with internal organ involvement is a rare disease in childhood and occurs less commonly than local scleroderma diseases such as linear scleroderma and morphea (268,269). The prognosis and mortality in juvenile onset systemic disease is, in general, better than adult onset disease

(270). Yet, in those children with severe or fatal scleroderma, disease progression and mortality may be more difficult to prevent (268,271–273).

The most common cause of death in these children is cardiopulmonary disease. The cardiac involvement in systemic scleroderma can be primarily due to the scleroderma disease process or secondary to severe lung involvement. Pulmonary involvement is the most common systemic organ affected by scleroderma (75% patients) and cardiac involvement alone is rare (1%) but a mixed picture of cardiopulmonary involvement is the most common cause of death in systemic scleroderma (272,274,275). Some reports have suggested that a few children with localized scleroderma have not only skin disease but may develop systemic, eye and central nervous system (CNS) involvement (275–277). These patients who evolve and develop extracutaneous disease appear to have a higher prevalence of antinuclear antibodies with a homogeneous pattern and a positive RF.

Quartier et al. (278) have described ischemic cardiac injuries and dilated cardiomyopathy in three children with systemic scleroderma. Of these three children, two died and one survived after cardiac transplant. The authors also believed that treatment with corticosteroids, methotrexate, and cyclosporin were effective on muscle, skin, and lung involvement but did not stop progression of esophageal or myocardial dysfunction (278). Most believe that patients who also had polymyositis with skeletal muscle involvement in addition to their scleroderma are more at risk for cardiac involvement and congestive cardiac failure (278–280). Some primary autoimmune myocardial inflammation is also considered as a small factor contributing to myocardial damage and fibrosis. The cardiac ischemic injuries are more common than that of cardiomyopathy.

Myocardial fibrosis is reported to be the most common autopsy finding in fatal cases of juvenile systemic sclerosis (279) and myocardial fibrosis is considered as a hallmark of cardiac involvement in systemic scleroderma. The myocardial fibrosis in scleroderma is histologically different from that due to atherosclerotic coronary artery disease. Fibrosis in scleroderma involves mainly the subendocardial layer of the heart that is spared in atherosclerosis and myocardial hemosiderin deposits that are found in atherosclerotic disease are absent in the myocardium of patients with systemic sclerosis. What this means from a therapeutic point of view is not yet clear (281–283,284–287).

Cardiac ischemic disease may result due to several causes such as restrictive pulmonary disease, coronary artery involvement, myocardial microvasculitis causing perfusion defects, impaired repair mechanism, and sclerosis. Raynaud phenomenon is very common in patients with scleroderma, and Raynaud equivalent vascular phenomenon in cardiac vessels and coronary arteries of these patients leads to repeated cardiac ischemia and myocardial fibrosis (288,289). Systemic vascular disease leading to systemic hypertension and renal crisis can also affect cardiac perfusion adversely and lead to left ventricular failure (280). Scleroderma may also present initially as pericardial disease or conduction abnormalities secondary to myocardial involvement.

The most common symptom due to myocardial involvement in juvenile scleroderma is dyspnea and reduced exercise tolerance. The symptoms of myocardial ischemic pain, angina, and right or left heart failure may develop depending on the mechanism and region of the myocardium that is affected.

The prevalence of the anti-Scl 70 antibody is rare in juvenile onset disease, with or without extracutaneous manifestations (276). The disease-specific autoantibody profile is not diagnostic and clinically useful in juvenile scleroderma. Serum anti-PM-Scl and anti-U1RNP antibodies are more frequently positive in juvenile onset disease while the anti-RNA polymerase III and anticentromere antibodies are more frequently positive in adult

onset disease (270). Apart from conventional studies such as lab tests, echocardiography, and EKG, other modalities, that is, thallium scintigraphy, single photon emission computed tomography (SPECT), and MRI have been utilized to estimate the prevalence of asymptomatic cardiac involvement. In adult series, the prevalence of cardiac disease was estimated to be around 69%. The prevalence of asymptomatic cardiac disease in children with systemic sclerosis is not known (289–294).

Unfortunately, there are not many investigative studies in the literature that provide more information on the cardiac risks and risk factor associations in juvenile onset systemic scleroderma. Endomyocardial biopsy is neither a risk-free procedure nor is it used very often in practice. The available information on cardiac involvement mostly comes from autopsy results that only represent the extreme end of the spectrum of the disease. It appears that while the cardiac involvement is not common in juvenile onset scleroderma, its presence suggests a poor prognosis. The prevalence of asymptomatic cardiac involvement in childhood systemic scleroderma is not known. It is in the best interest of the patient to investigate for cardiac involvement early with echocardiography or MRI and on a regular basis thereafter. Early and aggressive therapy with immunosuppressant medication, fibrinolytic medication, and supportive therapy may help to prevent cardiac disease and improve the outcome in patients with juvenile onset systemic scleroderma. It is also important to monitor children with local scleroderma for systemic disease.

Sarcoidosis

Bernstein et al. (295,296) described cardiac involvement for the first time in an autopsy of a sarcoidosis patient in 1929. Since

then, it is increasingly recognized that the incidence of cardiac sarcoidosis is far more common than previously thought. When it does occur, cardiac involvement in sarcoidosis is still often overlooked due to the lack of awareness of its possibility, its slow subclinical progression, and the absence of any robust and reliable diagnostic tool (297). Cardiac involvement in children and adults appears to be unusual in most areas of the world, but for unexplained reasons it is far higher in Japanese population than the rest of the world, affecting up to 50% to 78% of sarcoidosis patients. In Japanese patients, 85% of deaths with sarcoidosis are due to cardiac involvement (298–300).

Hoffmann et al. (301) studied 48 children in Denmark with pediatric sarcoidosis (ages <15 years). They reported that clinical features and presentations in their cohort were similar to that of adults but they found cardiac involvement to be more frequent in younger patients and adolescents than in adults (302–306). There are conflicting opinions regarding its prognostic significance. Several groups report that the significance of cardiac involvement from prognostic point of view is not known (195) while other groups believe it to be potentially fatal and a bad prognostic sign (296,298,307–309).

Most studies and reports are from the mixed age population of patients. Silverman et al. (310) reported autopsy findings in 84 sarcoidosis patients in 1978. These patients ranged from 18 to 80 years with a male to female ratio of 1:1.5. Of these patients, 27% were found to have cardiac granulomas. Of the patients who were found to have cardiac involvement, 35% did not have cardiac symptoms while there was a history of heart failure, arrhythmias, and/or conduction defects in 65%. Similar findings have been reported by others who note that the most common site for granulomas was the left ventricular

TABLE 61.2 Updated Guideline for Diagnosis of Cardiac Sarcoidosis by the Japanese Ministry of Health and Welfare in 2006	
Histologic diagnosis group	
Cardiac sarcoidosis is confirmed when endomyocardial biopsy specimens demonstrate noncaseating epithelioid cell granulomas with histologic or clinical diagnosis of extracardiac sarcoidosis.	
Clinical diagnosis group	
If endomyocardial biopsy specimens do not demonstrate noncaseating epithelioid cell granulomas, extracardiac sarcoidosis is diagnosed histologically or clinically if the disease satisfies the following conditions and more than one in six basic diagnostic criteria are present.	
1. Two or more of the four major criteria are satisfied.	
2. One in four of the major criteria and two or more of the five minor criteria are satisfied.	
Major criteria	
1. Advanced AVB.	
2. Basal thinning of the interventricular septum.	
3. Positive 67 gallium uptake in the heart.	
4. Depressed ejection fraction of the left ventricle (<50%).	
Minor criteria	
Abnormal ECG findings: ventricular arrhythmias (ventricular tachycardia, multifocal or frequent PVCs), CRBBB, axis deviation or abnormal Q-wave.	
Abnormal echocardiography: regional abnormal wall motion or morphologic abnormality (ventricular aneurysm, wall thickening).	
Nuclear medicine: perfusion defect detected by 201 thallium or 99 m technetium myocardial scintigraphy.	
Gadolinium-enhanced CMR imaging: delayed myocardial enhancement	
Endomyocardial biopsy: interstitial fibrosis or monocyte infiltration over moderate grade.	

CMR, cardiac magnetic resonance; CRBBB, complete right bundle branch block; ECG, electrocardiogram; PVC, premature ventricular contraction
From Tahara N, et al. Heterogeneous myocardial FDG uptake and the disease activity in cardiac sarcoidosis. *JACC Cardiovasc Imaging* 2010;3:1219–1228. Ref. 322.

free wall, followed by the interventricular septum, papillary muscles, right ventricular and atrial, and lastly, aortic arch (307,311,312). Sarcoidosis can affect the pericardium, myocardium, or endocardium with equal frequency (296,313).

These autopsy findings support recent clinical findings that the real incidence of clinical cardiac involvement in sarcoidosis may be between 5% and 50% (314). Cardiac disease is not necessarily always secondary to cor pulmonale or lung involvement as previously thought but isolated cardiac involvement can occur at any age and stage of the disease (296,314) in the absence of pulmonary and even any other systemic involvement. Sometimes cardiac involvement only got attention of physicians after the pulmonary disease resolved (315). Occasionally cardiac involvement may be the first presentation of the disease (306). The severity and duration of pulmonary disease cannot predict the presence and extent of cardiac involvement (316).

Diagnosis of the cardiac involvement may be problematic (Table 61.2). As an initial screening test, 12-lead EKG, especially the 24-hour Holter monitoring, and/or postexercise EKGs are very cost-effective tests. Echocardiography is recommended to diagnose the cardiac involvement in patients with sarcoidosis. Echocardiography may be useful if it demonstrates a classic basal interventricular septal thinning or localized ventricular aneurysmal dilation, usually without coronary artery disease. (317–319). Myocardial biopsies have a poor diagnostic yield (<20% to 30%) as the sarcoidosis disease involvement is patchy and most biopsies are performed on the right side of heart (311,312,320). Cardiac MRI with gadolinium enhancement and positron emission tomography (PET) scanning are also good investigational tools to diagnose and evaluate cardiac involvement (319,321). (See summary of testing in Table 61.1)

The most common symptoms due to cardiac involvement in sarcoidosis include cardiac arrhythmias and conduction defects. Sudden death has been reported. Less frequently, pericardial effusion, cardiac tamponade, and cardiac failure may be seen (195,317,323). These complications generally occur in patients with widespread myocardial involvement (311,324). Corticosteroids are the mainstay of the treatment for cardiac sarcoidosis but have not shown survival benefit in prospective trials (101,298). Other disease-modifying medications and immunosuppressants such as methotrexate, azathioprine, hydroxychloroquine, chloroquine, cyclophosphamide, cyclosporine A, thalidomide, pentoxifylline, and infliximab have been used with varying success (306,308,312,325–327). A combination of steroids and another immunosuppressant may be used to limit steroid side effects. In patients with disseminated myocardial involvement, the use of antiarrhythmic drugs and automated implantable cardiac defibrillator as bridge therapy while waiting for cardiac transplant has been advocated to prevent sudden death (312).

REFERENCES

- Helmick CG, Felson DT, Lawrence RC, et al. Estimates of the prevalence of arthritis and other rheumatic conditions in the United States: Part I. *Arthritis Rheum* 2008;58:15–25.
- Oen K. Comparative epidemiology of the rheumatic diseases in children. *Curr Opin Rheumatol* 2000;12:410–414.
- Moorthy LN, Peterson MG, Hassett A, et al. Burden of childhood-onset arthritis. *Pediatr Rheumatol Online J* 2010; 8:20–29.
- Jarvis JN, Jiang K, Petty HR, et al. Neutrophils: the forgotten cell in JIA disease pathogenesis. *Pediatr Rheumatol Online J* 2007;5:13–19.
- Low JM, Chauhan AK, Kietz DA, et al. Determination of anti-citrullinated peptide antibodies in the sera of patients with juvenile idiopathic arthritis. *J Rheumatol* 2004;31:1829–1833.
- Berstein B, Takahashi M, Hanson V. Cardiac involvement in juvenile rheumatoid arthritis. *J Pediatr* 1974;85:315–317.
- Tschachler E. Psoriasis: the epidermal component. *Clin Dermatol* 2007;25:589–595.
- Brewer E Jr. Juvenile rheumatoid arthritis-cardiac involvement. *Arthritis Rheum* 1977;20:231–236.
- Yancey CL, et al. Pericarditis and cardiac tamponade in juvenile rheumatoid arthritis. *Pediatrics* 1981;68:369–373.
- Goldenberg J, Pessoa AP, Roizenblatt S, et al. Cardiac tamponade in juvenile chronic arthritis: report of two cases and review of publications. *Ann Rheum Dis* 1990; 49:549–553.
- Rigante D, De Rosa G, Bertoni B, et al. Large pericardial effusion requiring pericardiocentesis as cardinal sign of macrophage activation syndrome in systemic onset-juvenile idiopathic arthritis. *Rheumatol Int* 2007;27:767–770.
- Gedalia A, Giannini EH, Brewer EJ, et al. Prevalence of pericardial effusion by echocardiography in juvenile rheumatoid arthritis. *J Rheumatol* 1993;20:206–207.
- Alkady EA, Helmy HA, Mohamed-Hussein AA. Assessment of cardiac and pulmonary function in children with juvenile idiopathic arthritis. *Rheumatol Int* 2012;32:39–46.
- Miller JJ III, French JW. Myocarditis in juvenile rheumatoid arthritis. *Am J Dis Child* 1977;131:205–209.
- Svantesson H, Bjorhem G, Elborgh R. Cardiac involvement in juvenile rheumatoid arthritis: a follow-up study. *Acta Paediatr Scand* 1983;72:345–350.
- Ozer S, et al. Mitral and aortic insufficiency in polyarticular juvenile rheumatoid arthritis. *Pediatr Cardiol* 1994;15:151–153.
- Chen YS, et al. A patient diagnosed with pauciarticular juvenile rheumatoid arthritis after a mechanical prosthetic valve replacement due to aortic regurgitation. *J Microbiol Immunol Infect* 2004;37:200–202.
- Stingl C, Moller JH, Binstadt BA. Cardiac operations for North American children with rheumatic diseases: 1985–2005. *Pediatr Cardiol* 2010;31:66–73.
- Svantesson H, Bjorkhem G, Elborgh R. Cardiac involvement in juvenile rheumatoid arthritis. A follow-up study. *Acta Paediatr* 1983;72:345–350.
- Malleson PN, Fung MY, Rosenberg AM. The incidence of pediatric rheumatic diseases: results from the Canadian Pediatric Rheumatology Association Disease Registry. *J Rheumatol* 1996;23:1981–1987.
- Cook CD, et al. Systemic lupus erythematosus. Description of 37 cases in children and a discussion of endocrine therapy in 32 of the cases. *Pediatrics* 1960;26:570–585.
- Harvey AM, et al. Systemic lupus erythematosus: review of the literature and clinical analysis of 138 cases. *Medicine (Baltimore)* 1954;33:291–437.
- King KK, et al. The clinical spectrum of systemic lupus erythematosus in childhood. *Arthritis Rheum* 1977;20:287–94.
- Cassidy JT, et al. Lupus nephritis and encephalopathy. Prognosis in 58 children. *Arthritis Rheum* 1977;20:315–322.
- Malleson PN, et al. Review for the generalist: The antinuclear antibody test in children—When to use it and what to do with a positive titer. *Pediatr Rheumatol Online J* 2010;8:27.
- Arkachaisri T, Lehman TJ. Systemic lupus erythematosus and related disorders of childhood. *Curr Opin Rheumatol* 1999;11:384–392.
- Barada FA Jr, et al. Antibodies to Sm in patients with systemic lupus erythematosus. Correlation of Sm antibody titers with disease activity and other laboratory parameters. *Arthritis Rheum* 1981;24:1236–1244.
- Sharp GC, et al. Mixed connective tissue disease—an apparently distinct rheumatic disease syndrome associated with a specific antibody to an extractable nuclear antigen (ENA). *Am J Med* 1972;52:148–159.
- Sánchez-Guerrero J, Lew RA, Fossel AH, et al. Utility of anti-Sm, anti-RNP, anti-Ro/SS-A, and anti-La/SS-B (extractable nuclear antigens) detected by enzyme-linked immunosorbent assay for the diagnosis of systemic lupus erythematosus. *Arthritis Rheum* 1996;39:1055–1061.
- Alspaugh M, Maddison P. Resolution of the identity of certain antigen-antibody systems in systemic lupus erythematosus and Sjogren's syndrome: an interlaboratory collaboration. *Arthritis Rheum* 1979;22:796–798.
- Harley JB, et al. Anti-Ro (SS-A) and anti-La (SS-B) in patients with Sjogren's syndrome. *Arthritis Rheum* 1986;29:196–206.
- Watson RM, et al. Neonatal lupus erythematosus. A clinical, serological and immunogenetic study with review of the literature. *Medicine (Baltimore)* 1984;63:362–378.
- Lockshin MD, et al. Neonatal lupus risk to newborns of mothers with systemic lupus erythematosus. *Arthritis Rheum* 1988;31:697–701.
- Buyon JP, Clancy RM, Friedman DM. Cardiac manifestations of neonatal lupus erythematosus: guidelines to management, integrating clues from the bench and bedside. *Nat Clin Pract Rheumatol* 2009;5:139–148.
- Egner W. The use of laboratory tests in the diagnosis of SLE. *J Clin Pathol* 2000;53:424–432.
- Hebert LA, Cosio FG, Neff JC. Diagnostic significance of hypocomplementemia. *Kidney Int* 1991;39:811–821.
- Yoshida H, Watanabe K. Clinical significance of the estimations of complement and immune complexes. *Rinsho Byori* 1989;37:1317–1323.
- Lewis EJ, Carpenter CB, Schur PH. Serum complement component levels in human glomerulonephritis. *Ann Intern Med* 1971;75:555–560.
- Garin EH, et al. The significance of serial measurements of serum complement C3 and C4 components and DNA binding capacity in patients with lupus nephritis. *Clin Nephrol* 1979;12:148–155.
- Lee HS, et al. Course of renal pathology in patients with systemic lupus erythematosus. *Am J Med* 1984;77:612–620.
- Hoffman IE, et al. Juvenile-onset systemic lupus erythematosus: different clinical and serological pattern than adult-onset systemic lupus erythematosus. *Ann Rheum Dis* 2009;68:412–415.

42. Carreno L, et al. Immunological and clinical differences between juvenile and adult onset of systemic lupus erythematosus. *Lupus* 1999;8:287-292.
43. Hanly JG, Fisk JD. Connective tissue diseases: Diagnosis of cognitive impairment in adult and pediatric SLE. *Nat Rev Rheumatol* 2011;7:564-565.
44. Bastos CJ, Queiroz AC, Martinelli R. Cardiac involvement in systemic lupus erythematosus: anatomic-pathological study. *Rev Assoc Med Bras* 1993;39:161-164.
45. Ansari A, Larson PH, Bates HD. Cardiovascular manifestations of systemic lupus erythematosus: current perspective. *Prog Cardiovasc Dis* 1985;27:421-434.
46. Cervera R, et al. Cardiac disease in systemic lupus erythematosus: prospective study of 70 patients. *Ann Rheum Dis* 1992;51:156-159.
47. Oshiro AC, et al. Anti-Ro/SS-A and anti-La/SS-B antibodies associated with cardiac involvement in childhood systemic lupus erythematosus. *Ann Rheum Dis* 1997;56:272-274.
48. Hohnik M, et al. Heart valve involvement (Libman-Sacks endocarditis) in the antiphospholipid syndrome. *Circulation* 1996;93:1579-1587.
49. Moyssakis I, et al. Libman-Sacks endocarditis in systemic lupus erythematosus: prevalence, associations, and evolution. *Am J Med* 2007;120:636-642.
50. Lee, JL, et al. Revisiting Libman-Sacks endocarditis: a historical review and update. *Clin Rev Allergy Immun* 2009;36:126-130.
51. Galve E, et al. Prevalence, morphologic types, and evolution of cardiac valvular disease in systemic lupus erythematosus. *N Engl J Med* 1988;319:817-823.
52. Roldan FJ, et al. Three-dimensional transesophageal echocardiography of the atrial septal defects. *Cardiovasc Ultrasound* 2008;6:38.
53. Plastiras SC, et al. Real-time three-dimensional echocardiography in evaluating Libman-Sacks vegetations. *Eur J Echocardiogr* 2010;11:184-185.
54. Al-Abbad AJ, et al. Echocardiography and pulmonary function testing in childhood onset systemic lupus erythematosus. *Lupus* 2001;10:32-37.
55. Gazarian M, et al. Assessment of myocardial perfusion and function in childhood systemic lupus erythematosus. *J Pediatr* 1998;132:109-116.
56. Kaplan SD, et al. Cardiac manifestations of the antiphospholipid syndrome. *Am Heart J* 1992;124:1331-1338.
57. Amigo MC. The Heart and APS. *Clin Rev Allergy Immun* 2007;32:178-183.
58. Mattos P, Santiago, MB. Association of antiphospholipid antibodies with valvulopathy in systemic lupus erythematosus: a systematic review. *Clin Rheumatol* 2011;30:165-171.
59. Fluture AS, Chaudhari S, Frishman WH. Valvular heart disease and systemic lupus erythematosus: therapeutic implications. *Heart Dis* 2003;5:349-353.
60. Bouma W, et al. Mitral valve surgery for mitral regurgitation caused by Libman-Sacks endocarditis: a report of four cases and a systematic review of the literature. *J Cardiothorac Surgery* 2010;5:13.
61. Gonzalez-Juanatey C, Gonzalez-Gay, M.A. Libman-sacks endocarditis and primary antiphospholipid syndrome. *J Heart Valve Dis* 2005;14:700-702.
62. Ishikawa S, et al. Myocardial infarct in a child with systemic lupus erythematosus. *Am J Dis Child* 1978;132:696-699.
63. Miller DJ, et al. Fatal myocardial infarction in an 8-year-old girl with systemic lupus erythematosus, Raynaud's phenomenon, and secondary antiphospholipid antibody syndrome. *J Rheumatol* 1995;22:768-773.
64. Meyringer R, et al. Acute coronary syndrome in a 17-year-old female with systemic lupus erythematosus. *Med Klin(Munich)* 2005;100:279-283.
65. Suzuki H, et al. Giant coronary aneurysm in a patient with systemic lupus erythematosus. *Intern Med* 2009;48:1407-1412.
66. Schanberg, LE, et al. Premature atherosclerosis in pediatric systemic lupus erythematosus: risk factors for increased carotid intima-media thickness in the atherosclerosis prevention in pediatric lupus erythematosus cohort. *Arthritis Rheum* 2009. 60:1496-1507.
67. Boros CA, et al. Early determinants of atherosclerosis in paediatric systemic lupus erythematosus. *Clin Exp Rheumatol* 2011;29:575-581.
68. Liautaud S, et al. Variable atrioventricular block in systemic lupus erythematosus. *Clin Rheumatol* 2005;24:162-165.
69. Teixeira RA, et al. Arrhythmias in systemic lupus erythematosus. *Rev Bras Rheumatol* 2010;50:81-89.
70. Seferovic PM, et al. Cardiac arrhythmias and conduction disturbances in autoimmune rheumatic diseases. *Rheumatology* 2006;45:39-42.
71. Xing Y, et al. Clinical analysis of pulmonary arterial hypertension secondary to connective tissue disease in children. *Zhonghua Er Ke Za Zhi* 2008;46:822-826.
72. Jaeggi E, et al. The importance of the level of maternal anti-Ro/SSA antibodies as a prognostic marker of the development of cardiac neonatal lupus erythematosus: a prospective study of 186 antibody-exposed fetuses and infants. *J Am Coll Cardiol* 2010;55:2778-2784.
73. Li L, et al. Neonatal lupus erythematosus: a report of 7 cases and review of 87 cases of China. *Zhonghua Er Ke Za Zhi* 2011;49:146-150.
74. Wisuthsarewong W, Soongswang J, Chantorn R. Neonatal lupus erythematosus: clinical character, investigation, and outcome. *Pediatr Dermatol* 2011;28:115-121.
75. Izmirly PM, et al. Cutaneous manifestations of neonatal lupus and risk of subsequent congenital heart block. *Arthritis Rheum* 2010;62:1153-1157.
76. Llanos C, et al. Recurrence rates of cardiac manifestations associated with neonatal lupus and maternal/fetal risk factors. *Arthritis Rheum* 2009;60:3091-3097.
77. Silverman E, Jaeggi E. Non-cardiac manifestations of neonatal lupus erythematosus. *Scand J Immunol* 2010;72:223-225.
78. Mevorach D, Elchalal U, Rein AJ. Prevention of complete heart block in children of mothers with anti-SSA/Ro and anti-SSB/La autoantibodies: detection and treatment of first-degree atrioventricular block. *Curr Opin Rheumatol* 2009;21:478-482.
79. Klinger H. Grenzformen der polyarteritis nodosa. *Frankf Z Pathol* 1931;42:455.
80. Bloch DA, et al. The American College of Rheumatology 1990 criteria for the classification of vasculitis. Patients and methods. *Arthritis Rheum* 1990;33:1068-1073.
81. Michel BA. Classification of vasculitis. *Curr Opin Rheumatol* 1992;4:3-8.
82. Ozen S, et al. EULAR/PRINTO/PRES criteria for Henoch-Schönlein purpura, childhood polyarteritis nodosa, childhood Wegener granulomatosis and childhood Takayasu arteritis: Ankara 2008. Part II: Final classification criteria. *Ann Rheum Dis* 2010;69:798-806.
83. Ladhani S, Tulloh R, Anderson D. Takayasu disease masquerading as interruption of the aortic arch in a 2-year-old child. *Cardiol Young* 2001;11:244-246.
84. Berman DP, Lewis AB, Kung GC. Case Report of a 2-year-old boy with Takayasu's arteritis: an atypical, severe presentation of a rare disease. *Pediatric Cardiol* 2010;31:1089-1092.
85. Araujo FD, et al. Takayasu's disease with severe heart and arterial involvement in a preschool-age child. *Arq Bras Cardiol* 2010;95:e101-e103.
86. Fraga A, Medina F. Takayasu's arteritis. *Curr Rheumatol Rep* 2002;4:30-38.
87. Moriaki R, et al. Clinical manifestations of Takayasu arteritis in India and Japan—new classification of angiographic findings. *Angiology* 1997;48:369-379.
88. Valentini F, Di Folci A. Takayasu's disease. A review of the literature. A study of a familial case of Takayasu's arteritis and the possible associations with type-1 diabetes mellitus. *Minerva Med*. 1989 Dec;80(12): 1351-1358.
89. Moriuchi J, et al. HLA-linked susceptibility gene of Takayasu Disease. *Hum Immunol* 1982;4:87-91.
90. Isohisa I, et al. Hereditary factors in Takayasu's disease. *Angiology* 1982;33:98-104.
91. Numano F, et al. Takayasu's disease in twin sisters. Possible genetic factors. *Circulation* 1978;58:173-177.
92. Makino N, Senda Y, Yamaguchi Y. Takayasu's disease in two brothers. Analysis of HLA types. *Heart* 1981;46:446-448.
93. Numano F, et al. HL-A antigens in Takayasu's disease. *Am Heart J* 1979;98:153-159.
94. Soto ME, et al. Comparison distribution of HLA-B alleles in Mexican patients with takayasu arteritis and tuberculosis. *Hum Immunol* 2007;68:449-453.
95. Jeeva I, et al. Atypical Takayasu arteritis: a family with five affected siblings. *Med Sci Monit* 2007;13:CS101-CS105.
96. Brunner J, et al. Takayasu arteritis in children and adolescents. *Rheumatology(Oxford)* 2010;49:1806-1814.
97. Jales-Neto LH, et al. Juvenile-onset Takayasu arteritis: peculiar vascular involvement and more refractory disease. *Scand J Rheumatol* 2010;39:506-510.
98. Jain S, et al. Current status of Takayasu arteritis in India. *Int J Cardiol* 1996;54:S111-S116.
99. Sharma BK, et al. Takayasu arteritis in India. *Heart Vessels* 1992;7:37-43.
100. Muranjan, MN, et al. Study of Takayasu's arteritis in children: clinical profile and management. *J Postgrad Med* 2000;46:3-8.
101. Cakar N, et al. Takayasu arteritis in children. *J Rheumatol* 2008;35:913-919.
102. Hong CY, et al. Takayasu arteritis in Korean children: Clinical report of seventy cases. *Heart Vessels* 1992;7:91-96.
103. Orea Tejada A, Sanchez Torres G, Kuri Alfaro J. Cardiac damage in Takayasu's arteritis. Study in 125 patients. *Arch Cardiol Mex* 1983;53:441-447.
104. Seguchi M, et al. Ostial stenosis of the left coronary artery as a sole clinical manifestation of Takayasu's arteritis: a possible cause of unexpected sudden death. *Heart Vessels* 1990;5:188-191.
105. Emi Y, et al. Isolated bilateral coronary ostial stenosis in Takayasu's arteritis. *Am Heart J* 1990. 119:962-964.
106. Baruteau AE, et al. Acquired left ventricular submitral aneurysms in the course of Takayasu arteritis in a child. *Congenit Heart Dis* 2012;7:76-79.
107. Rose, A.G, et al. Idiopathic annular submitral aneurysm associated with Takayasu's aortitis. A report of two cases. *Arch Pathol Lab Med* 1995;119:831-835.
108. Matsubara O, et al. Coronary artery lesions in Takayasu arteritis: pathological considerations. *Heart Vessels* 1992;7:26-31.
109. Inanami H, et al. Coronary ostial stenosis due to aortitis syndrome (Takayasu's arteritis) in a young female: report of a case. *J Cardiol* 1983. 13:761-768.
110. Thomas D, et al. Coronary involvement in Takayasu's disease. Apropos of 3 cases, of which 2 were surgically treated, and review of the literature. *Arch Mal Coeur Vaiss* 1984;77:386-396.
111. Cipriano PR, et al. Coronary arterial narrowing in Takayasu's aortitis. *Am J Cardiol* 1977;39:744-750.
112. Amano J, Suzuki A. Coronary artery involvement in Takayasu's arteritis. Collective review and guideline for surgical treatment. *J Thorac Cardiovasc Surg* 1991;102:554-560.
113. Makino N, et al. Coronary arterial involvement in Takayasu's disease. *Jpn Heart J* 1982;23:1007-1013.

114. Matsui K, et al. Coronary arterial involvement in Takayasu's arteritis-aortocoronary bypass in a patient. *Jpn J Surg* 1982;12:135-142.
115. Reddy E, Robbs JV. Surgical management of Takayasu's arteritis in children and adolescents. *Cardiovasc J Afr* 2007;18:393-396.
116. Sharma BK, Jain S, Radotra BD. An autopsy study of Takayasu arteritis in India. *Int J Cardiol* 1998;66:S85-S90.
117. Rose AG, Sinclair-Smith CC. Takayasu's arteritis. A study of 16 autopsy cases. *Arch Pathol Lab Medicine* 1980;104:231-237.
118. Kinare, SG. Cardiac lesions in non-specific aorto-arteritis. An autopsy study. *Indian Heart J* 1994;46:65-69.
119. Igarashi T, et al. Aortitis syndrome (Takayasu's arteritis) associated with systemic lupus erythematosus. *J Rheumatol* 1989;16:1579-1583.
120. Kameyama K, et al. Takayasu's aortitis with dissection in systemic lupus erythematosus. *Scand J Rheumatol* 1999;28:187-188.
121. Saxe PA, Altman RD. Takayasu's arteritis syndrome associated with systemic lupus erythematosus. *Semin Arthritis Rheum* 1992;21:295-305.
122. Nakashima A, et al. A case of aortitis syndrome (Takayasu's arteritis) associated with glomerulonephropathy mimicking lupus membranous glomerulonephropathy. *Nihon Jinzo Gakkai shi* 1988;30:233-238.
123. Cherin P, et al. The association of ankylosing spondylitis and Takayasu's disease. 3 new cases. *Rev Rhum Mal Osteoartic* 1990;57:33-37.
124. Hall S, Nelson AM. Takayasu's arteritis and juvenile rheumatoid arthritis. *J Rheumatol* 1986;13:431-433.
125. Ehrlich G. Takayasu's arteritis and Still's disease. *Arthritis Rheum* 1979;22:1422.
126. Rees AH. Pediatric autoimmune cardiovascular disease. *J Ky Med Assoc* 2000;98:289-295.
127. McDonald MA, Ojaimi E, Favilla I. Anterior uveitis in a child with Takayasu's arteritis. *Clin Experiment Ophthalmol* 2004;32:336-339.
128. Becker RW, et al. Takayasu's arteritis presenting as uveitis in a 5-year-old girl. *Ann Vasc Surg* 2005;19:258-262.
129. Schapiro JM, et al. Sarcoidosis as the initial manifestation of Takayasu's arteritis. *J Med* 1994; 25:121-128.
130. Magaro M, et al. Seronegative spondylarthritis associated with Takayasu's arteritis. *Ann Rheum Dis* 1988;47:595-597.
131. Van Elburg RM, et al. Vascular compromise prior to intestinal manifestations of Crohn's disease in a 14-year-old girl. *J Pediatr Gastroenterol Nutr* 1992;14:97-100.
132. Mejia-Hernandez C, Alvarez-Mendoza A, DeLeon-Bojorge B. Takayasu's arteritis coexisting with Wegener's granulomatosis in a teenager with renal insufficiency: case report. *Pediatr Dev Pathol* 1999;2:385-388.
133. Campos LM, et al. Takayasu's arteritis with aortic aneurysm associated with Sweet's syndrome in childhood. *Ann Rheum Dis* 2005;64:168-169.
134. Almeida LA, et al. Takayasu's Arteritis and Sweet's Syndrome - a rare combination. *Acta Reumatol Port* 2009;34:288-289.
135. Ikenaga, H, et al. Does a common pathophysiological basis exist in the association of ulcerative colitis and Takayasu's aortitis? Report of a case. *Postgrad Med J* 1989;65:761-764.
136. Lau YL, Wong SN, Lawton WM. Takayasu's arteritis associated with Wiskott-Aldrich syndrome. *J Paediatr Child Health* 1992;28:407-409.
137. Aggarwal A, et al. Takayasu's arteritis: role of Mycobacterium tuberculosis and its 65 kDa heat shock protein. *Int J Cardiol* 1996;55:49-55.
138. Hernandez-Pando, R, et al. Raised agalactosyl IgG and antimycobacterial humoral immunity in Takayasu's arteritis. *J Rheumatol* 1994;21: 1870-1876.
139. Hernandez Pando R, et al. Takayasu's arteritis. A seroimmunological test of its relationship to mycobacterial infection. *Arch Inst Cardiol Mex* 1994;64:331-337.
140. Qamra R, et al. The unusual chaperonins of Mycobacterium tuberculosis. *Tuberculosis* 2005;85:385-394.
141. Karopoulos C, et al. Antibody reactivity to mycobacterial 65 kDa heat shock protein: relevance to autoimmunity. *J Autoimmun* 1995;8:235-248.
142. Cybulska I. Takayasu's arteritis-course, diagnosis and long term results of treatment. *Pol Arch Med Wewn* 1994;91:451-460.
143. Ruige JB, et al. A 16-year survey of Takayasu's arteritis in a tertiary Belgian center. *Int Angiol* 2003;22:414-420.
144. Castellanos AZ, et al. Takayasu's arteritis. *An Pediatr* 2003;58:211-216.
145. Dubourg O, et al. Aortic insufficiency in Takayasu's disease. Apropos of 3 surgically treated cases and review of the literature. *Arch Mal Coeur Vaiss* 1984;77:998-1005.
146. Ohteki H, et al. Aortic valve replacement for Takayasu's arteritis. *J Thorac Cardiovasc Surg* 1992;104:482-486.
147. Fieldston E, Albert D, Finkel T. Hypertension and elevated ESR as diagnostic features of Takayasu arteritis in children. *J Clin Rheumatol* 2003;9:156-163.
148. Kim GB, Bae EJ, Lee W. Aortic pseudoaneurysms associated with Takayasu's arteritis in a 10-year old boy. *Cardiol Young* 2008;18:437-438.
149. Civilibal M, et al. Dissection of the abdominal aorta in a child with Takayasu's arteritis. *Acta Radiol* 2008;49:101-104.
150. Yadav MK, Leeneshwar H, Jai RP. Pulseless cardiomyopathy. *J Assoc Physicians India* 2006;54:814-816.
151. Kissin EY, Merkel PA. Diagnostic imaging in Takayasu arteritis. *Curr Opin Rheumatol* 2004;16:31-37.
152. Lin J, et al. Whole-body three-dimensional contrast-enhanced magnetic resonance (MR) angiography with parallel imaging techniques on a multi-channel MR system for the detection of various systemic arterial diseases. *Heart Vessels* 2006;21:395-398.
153. Jiang L, et al. Evaluation of Takayasu arteritis activity by delayed contrast-enhanced magnetic resonance imaging. *Int J Cardiol* 2012;155:262-267.
154. Uthman IW, Chaaban H. The use of sildenafil in pediatric Takayasu arteritis. *Clin Rheumatol* 2006;25:550.
155. Datskovskii BM, et al. Case of Kussmaul-Maier disease. *Vestn Dermatol Venerol* 1983;40-41.
156. Kussmaul A, Maier K. Über eine nicht bisher beschriebene eigenthümliche arterienerkrankung, die mit Morbus Brightii und rapid fortschreitender allgemeiner Muskellähmung einhergeht. *Dtsch Arch Med* 1866;1:484.
157. Lie JT. Illustrated histopathologic classification criteria for selected vasculitis syndromes. American College of Rheumatology Subcommittee on Classification of Vasculitis. *Arthritis Rheum* 1990;33:1074-1087.
158. Ozen S, et al. Diagnostic criteria for polyarteritis nodosa in childhood. *J Pediatr* 1992;120:206-209.
159. Moskowitz RW, Baggenstoss AH, Slocumb CH. Histopathologic Classification of Periarthritis Nodosa: A Study of 56 Cases Confirmed at Necropsy. *Proc Staff Meet Mayo Clin* 1963;38:345-357.
160. Tasdemir I, et al. Spontaneous perirenal haematoma secondary to polyarteritis nodosa. *Br J Urol* 1988;62:219-222.
161. Pettigrew HD, Teuber SS, Gerishwin ME. Polyarteritis nodosa. *Compr Ther* 2007;33:144-149.
162. Ozen S, et al. Juvenile polyarteritis: results of a multicenter survey of 110 children. *J Pediatr* 2004;145:517-522.
163. Brogan PA, et al. Renal angiography in children with polyarteritis nodosa. *Pediatr Nephrol* 2002;17:277-283.
164. Fink CW. Polyarteritis and other diseases with necrotizing vasculitis in childhood. *Arthritis Rheum* 1977;20:378-384.
165. Magilavy DB, et al. A syndrome of childhood polyarteritis. *J Pediatr* 1977;91:25-30.
166. Naumann-Bartsch N, et al. Childhood polyarteritis nodosa in autoimmune lymphoproliferative syndrome. *Pediatrics* 2010;125:e169-e173.
167. Maeda M, et al. Clinical observation of 14 cases of childhood polyarteritis nodosa in Japan. *Acta Paediatr Jpn* 1997;39:277-279.
168. Allen HD, et al. *Heart Disease in Infants, Children, and Adolescents*. 6th ed. New York, NY: Lippincott Williams & Wilkins, 2001.
169. Gunal N, et al. Cardiac involvement in childhood polyarteritis nodosa. *Int J Cardiol* 1997;60:257-262.
170. Glikson M, et al. Polyarteritis nodosa and familial Mediterranean fever: a report of 2 cases and review of the literature. *J Rheumatol* 1989;16: 536-539.
171. Ozen S, et al. Polyarteritis nodosa in patients with Familial Mediterranean Fever (FMF): a concomitant disease or a feature of FMF? *Semin Arthritis Rheum* 2001;30:281-287.
172. Bosacki C, et al. The association of polyarteritis nodosa and familial Mediterranean fever. *Presse Med* 2003;32:24-26.
173. Trepo CG, et al. The role of circulating hepatitis B antigen/antibody immune complexes in the pathogenesis of vascular and hepatic manifestations in polyarteritis nodosa. *J Clin Pathol* 1974;27:863-868.
174. Guillevin L, et al. Polyarteritis nodosa related to hepatitis B virus. A retrospective study of 66 patients. *Ann Med Interne (Paris)* 1992;143:63-74.
175. Samuels J, et al. Familial Mediterranean fever at the millennium. Clinical spectrum, ancient mutations, and a survey of 100 American referrals to the National Institutes of Health. *Medicine (Baltimore)* 1998;77:268-297.
176. Sachs D, et al. Polyarteritis nodosa and familial Mediterranean fever. *Br J Rheumatol* 1987;26:139-141.
177. Pechere MC, Helfer, Laurence FL. Periodic disease and periarteritis nodosa in the same patient: coincidence?. *Schweiz Med Wochenschr* 1991;121:1166-1168.
178. Guillevin, L, et al. The Five-Factor Score revisited: assessment of prognosis of systemic necrotizing vasculitides based on the French Vasculitis Study Group (FVSG) cohort. *Medicine (Baltimore)* 2011;90:19-27.
179. Gayraud M, et al. Long-term followup of polyarteritis nodosa, microscopic polyangiitis, and Churg-Strauss syndrome: analysis of four prospective trials including 278 patients. *Arthritis Rheum* 2001;44:666-675.
180. Khan SA, et al. Outcome of patients with small-vessel vasculitis admitted to a medical ICU. *Chest* 2007;131:972-976.
181. Engel DG, et al. Fatal infantile polyarteritis nodosa with predominant central nervous system involvement. *Stroke* 1995;26:699-701.
182. Landing BH, Larson EJ. Are infantile periarteritis nodosa with coronary artery involvement and fatal mucocutaneous lymph node syndrome the same? Comparison of 20 patients from North America with patients from Hawaii and Japan. *Pediatrics* 1977;59:651-662.
183. Munro AR, et al. Fatal late onset necrotizing enterocolitis in a term infant: Atypical Kawasaki disease or polyarteritis nodosa of infancy? *J Paediatr Child Health* 2003;39:555-557.
184. Edwin P, Scott, Rotondo CC. Periarteritis Nodosa: Report of Two Cases, One Complicated by Intrapericardial Hemorrhage. *J Pediatr* 1944;25:306.
185. Jacob L, Rothstein, Sara Welt. Periarteritis Nodosa in Infancy and in Childhood: Report of Two Cases With Necropsy Observations; Abstracts of Cases in the Literature. *Am J Dis Child* 1933;45:1277.
186. Wilmer HA. Two cases of periarteritis nodosa occurring in the first month of life. *Bull Johns Hopkins Hosp* 1945;77:275-286.
187. Pickard CM, Owen JG, Dammin G. Aneurysms of the coronary arteries due to polyarteritis nodosa occurring in an infant: report of a case with coronary artery thrombosis and myocardial infarction. *J Lab Clin Med* 1947;32:1513.

188. Sinclair W Jr, Nitsch. Polyarteritis nodosa of the coronary arteries; report of a case in an infant with rupture of an aneurysm and intrapericardial hemorrhage. *Am Heart J* 1949;38:898-904.
189. Stryker WA. Coronary Occlusive Disease in Infants and Children. *Am J Dis Child* 1946;71:280.
190. Munro-Faure H. Necrotizing arteritis of the coronary vessels in infancy; case report and review of the literature. *Pediatrics* 1959;23:914-926.
191. Schmidt WA. Use of imaging studies in the diagnosis of vasculitis. *Curr Rheumatol Rep* 2004;6:203-211.
192. Basoglu T, et al. Tc-99m DMSA renal scan in polyarteritis nodosa with bilateral intraparenchymal renal artery aneurysms. *Clin Nucl Med* 1999;24:201-202.
193. Kobayashi H, et al. Cardiac magnetic resonance imaging in polyarteritis nodosa. *J Rheumatol* 2010;37:2427-2429.
194. Ozen S, et al. Juvenile polyarteritis: results of a multicenter survey of 110 children. *J Pediatr* 2004;145:517-522.
195. Cassidy J, et al. *Textbook of Pediatric Rheumatology*. 6th ed. New York, NY: Saunders, 2010.
196. Brogan PA, Dillon MJ. Endothelial microparticles and the diagnosis of the vasculitides. *Intern Med* 2004;43:1115-1119.
197. Erdbruegger U, et al. Diagnostic role of endothelial microparticles in vasculitis. *Rheumatology* 2008;47:1820-1825.
198. Kumpers P, et al. Circulating angiopoietin-2 is a marker and potential mediator of endothelial cell detachment in ANCA-associated vasculitis with renal involvement. *Nephrol Dial Transplant* 2009;24:1845-1850.
199. Haubitz M, Woywodt A. Circulating endothelial cells and vasculitis. *Int Med* 2004;43:660-667.
200. Brogan PA, Dillon MJ. The use of immunosuppressive and cytotoxic drugs in non-malignant disease. *Arch Dis Child* 2000;83:259-264.
201. Leib ES, Restivo C, Paulus HE. Immunosuppressive and corticosteroid therapy of polyarteritis nodosa. *Am J Med* 1979;67:941-947.
202. Jayne D. Current attitudes to the therapy of vasculitis. *Kidney Blood Press Res* 2003;26:231-239.
203. Dillon MJ. Vasculitis treatment—new therapeutic approaches. *Eur J Pediatr* 2006;165:351-357.
204. Jayne D, et al. A randomized trial of maintenance therapy for vasculitis associated with antineutrophil cytoplasmic autoantibodies. *N Engl J Med* 2003;349:36-44.
205. Altmeyer P, Seifarth D, Bacharach-Buhles M. High dosage intravenous immunoglobulin (IVIG) therapy in therapy-refractory ANCA-negative, necrotizing vasculitis. *Hautarzt* 1999;50:853-858.
206. Jayne DR, et al. Intravenous immunoglobulin for ANCA-associated systemic vasculitis with persistent disease activity. *QJM* 2000;93:433-439.
207. Richter C, et al. Treatment of anti-neutrophil cytoplasmic antibody (ANCA)-associated systemic vasculitis with high-dose intravenous immunoglobulin. *Clin Exp Immunol* 1995;101:2-7.
208. Lockwood CM. New treatment strategies for systemic vasculitis: the role of intravenous immune globulin therapy. *Clin Exp Immunol* 1996;104:77-82.
209. Wright E, Dillon MJ, Tullus K. Childhood vasculitis and plasma exchange. *Eur J Pediatr* 2007;166:145-151.
210. Jolles S, et al. Atypical C-ANCA following high dose intravenous immunoglobulin. *J Clin Pathol* 1999;52:177-180.
211. Al-Bishri J, le Riche N, Pope JE. Refractory polyarteritis nodosa successfully treated with infliximab. *J Rheumatol* 2005;32:1371-1373.
212. Bartolucci P, et al. Efficacy of the anti-TNF-alpha antibody infliximab against refractory systemic vasculitides: an open pilot study on 10 patients. *Rheumatology* 2002;41:1126-1132.
213. Ribeiro E, et al. Rituximab Efficacy during a Refractory Polyarteritis Nodosa Flare. *Case Report Med* 2009;2009:738293.
214. Keogh KA, et al. Induction of remission by B lymphocyte depletion in eleven patients with refractory antineutrophil cytoplasmic antibody-associated vasculitis. *Arthritis Rheum* 2005;52:262-268.
215. Sonomoto K, et al. A case of polyarteritis nodosa successfully treated by rituximab. *Nihon Rinsho Meneki Gakkai kaishi* 2008;31:119-123.
216. Wedderburn LR, et al. Autologous stem cell transplantation for paediatric-onset polyarteritis nodosa: changes in autoimmune phenotype in the context of reduced diversity of the T- and B-cell repertoires, and evidence for reversion from the CD45RO(+) to RA(+) phenotype. *Rheumatology* 2001;40:1299-1307.
217. Tyndall A. Hematopoietic stem cell transplantation in rheumatic diseases other than systemic sclerosis and systemic lupus erythematosus. *J Rheumatol* 1997;48:94-97.
218. Tyndall A, Gratwohl A. Hemopoietic blood and marrow transplants in the treatment of severe autoimmune disease. *Curr Opin Hematol* 1997;4:390-394.
219. Tyndall A, Gratwohl A. Blood and marrow stem cell transplants in autoimmune disease. A consensus report written on behalf of the European League Against Rheumatism (EULAR) and the European Group for Blood and Marrow Transplantation (EBMT). *Rheumatology (Oxford)* 1997;36:390-392.
220. Guillevin L, et al. Short-term corticosteroids then lamivudine and plasma exchanges to treat hepatitis B virus-related polyarteritis nodosa. *Arthritis Rheum* 2004;51:482-487.
221. Takeshita S, et al. Hepatitis B-related polyarteritis nodosa presenting necrotizing vasculitis in the hepatobiliary system successfully treated with lamivudine, plasmapheresis and glucocorticoid. *Intern Med* 2006;45:145-149.
222. MacLachlan D, et al. Successful treatment of hepatitis B-associated polyarteritis nodosa with a combination of lamivudine and conventional immunosuppressive therapy: a case report. *Rheumatology* 2000;39:106-108.
223. Guillevin L, et al. Treatment of polyarteritis nodosa related to hepatitis B virus with short term steroid therapy associated with antiviral agents and plasma exchanges. A prospective trial in 33 patients. *J Rheumatol* 1993;20:289-298.
224. Dilsen N. History and development of Behcet's disease. *Rev Rhum Engl Ed* 1996. 63:512-519.
225. Mahr A, et al. Population-based prevalence study of Behcet's disease: differences by ethnic origin and low variation by age at immigration. *Arthritis Rheum* 2008;58:3951-3959.
226. Shang Y, et al. The clinical feature of Behcet's disease in Northeastern China. *Yonsei Med J* 2009;50:630-636.
227. Cassidy J, et al. *Behcet's disease in Textbook of Pediatric Rheumatology*. New York, NY: Saunders, 2010.
228. Koné-Paut I, et al. Clinical features of Behcet's disease in children: an international collaborative study of 86 cases. *J Pediatr* 1998;132:721-725.
229. Karincoglu Y, et al. Demographic and clinical properties of juvenile-onset Behcet's disease: A controlled multicenter study. *J Am Acad Dermatol* 2008;58:579-584.
230. Atzeni F, et al. Behcet's disease and cardiovascular involvement. *Lupus* 2005. 14:723-726.
231. Bang D, et al. Epidemiological and clinical features of Behcet's disease in Korea. *Yonsei Med J* 1997;38:428-436.
232. Zouboulis CC, et al. Epidemiological features of Adamantiades-Behcet's disease in Germany and in Europe. *Yonsei Med J* 1997;38:411-422.
233. Krause I, et al. Childhood Behcet's disease: clinical features and comparison with adult-onset disease. *Rheumatology* 1999;38:457-462.
234. Davatchi F, et al. Behcet's disease in Iran: analysis of 6500 cases. *Int J Rheum Dis* 2010;13:367-373.
235. Durrani K, Papaliodis GN. The genetics of Adamantiades-Behcet's disease. *Semin Ophthalmol* 2008;23:73-79.
236. Ahn JK, Park YG. Human leukocyte antigen B27 and B51 double-positive Behcet uveitis. *Arch Ophthalmol* 2007;125:1375-1380.
237. Abdolhadi N, et al. HLA-B27 in Behcet's Disease, analysis of 5567 patients, in 13th International Conference and 5th Patients' Convention on Behcet's Disease 2008, Rheumatology Research Center; Articles 2008: Iran.
238. Schwartz T, et al. Behcet's disease in Familial Mediterranean fever: characterization of the association between the two diseases. *Semin Arthritis Rheum* 2000;29:286-295.
239. Atagunduz P, Ergun T, Direskeneli H. MEFV mutations are increased in Behcet's disease (BD) and are associated with vascular involvement. *Clin Exp Rheumatol* 2003;21:S35-S37.
240. Rabinovich E, et al. Common FMF alleles may predispose to development of Behcet's disease with increased risk for venous thrombosis. *Scand J Rheumatol* 2007;36:48-52.
241. Gurgun C, et al. Cardiovascular involvement in Behcet's disease. *Jpn Heart J* 2002;43:389-398.
242. Kim DK, et al. Clinical analysis of 40 cases of childhood-onset Behcet's disease. *Pediatr Dermatol* 1994;11:95-101.
243. San Luis Miranda R, et al. Right ventricular thrombus and pulmonary artery aneurysms in Behcet's disease. Report of one case. *Arch Cardiol Mex* 2007;77:130-136.
244. Adams EE, et al. Cardiac tumor in juvenile onset Behcet's disease: case report and review of the literature. *Pediatr Cardiol* 2010;31:277-279.
245. Cook AL, et al. Giant aneurysm of the left anterior descending coronary artery in a pediatric patient with Behcet's disease. *Pediatr Cardiol* 2010;31:700-702.
246. El Houari T, et al. Management of Behcet disease with multiple complications. *Hellenic J Cardiol* 2009;50:420-422.
247. Hollander SA, et al. Behcet's disease and heart transplantation: a word of caution. *J Heart Lung Transplant* 2010;29:1306-1308.
248. Zhuang J, et al. Acute myocardial infarction and ascending aortic aneurysm in a child with Behcet's disease. *Turk J Pediatr* 2008;50:81-85.
249. Karaca NE, et al. Juvenile dermatomyositis with a rare and remarkable complication: sinus bradycardia. *Rheumatol Int* 2006;27:179-182.
250. Lundberg LE. The heart in dermatomyositis and polymyositis. *Rheumatology* 2006;45:18-21.
251. Sato S, et al. Autoantibodies to a 140-kd polypeptide, CADM-140, in Japanese patients with clinically amyopathic dermatomyositis. *Arthritis Rheum* 2005;52:1571-1576.
252. Sato S, Kuwana M. Clinically amyopathic dermatomyositis. *Curr Opin Rheumatol* 2010;22:639-643.
253. Sultan SM, et al. Outcome in patients with idiopathic inflammatory myositis: morbidity and mortality. *Rheumatology* 2002;41:22-26.
254. Danko K, et al. Long-term survival of patients with idiopathic inflammatory myopathies according to clinical features: a longitudinal study of 162 cases. *Medicine(Baltimore)* 2004;83:35-42.
255. Yoshi A, et al. [Cardiac involvement in polymyositis and dermatomyositis (PM-DM) (author's transl)]. *Nihon Naika Gakkai zasshi* 1980;69:535-540.
256. Oka M, Raasakka T. Cardiac involvement in polymyositis. *Scand J Rheumatol* 1978;7:203-208.
257. Younes M, et al. [Polymyositis with antisynthetase syndrome and cardiac involvement]. *Rev Med Interne* 2005;26:673-675.

258. Haupt HM, Hutchins GM. The heart and cardiac conduction system in polymyositis-dermatomyositis: a clinicopathologic study of 16 autopsied patients. *Am J Cardiol* 1982;50:998–1006.
259. Denbow CE, et al. Cardiac involvement in polymyositis: a clinicopathologic study of 20 autopsied patients. *Arthritis Rheum* 1979;22:1088–1092.
260. Hochberg MC, Feldman D, Stevens, MB. Adult onset polymyositis/dermatomyositis: an analysis of clinical and laboratory features and survival in 76 patients with a review of the literature. *Semin Arthritis Rheum* 1986;15:168–178.
261. Benveniste O, et al. Correlation of anti-signal recognition particle autoantibody levels with creatine kinase activity in patients with necrotizing myopathy. *Arthritis Rheum* 2011;63:1961–1971.
262. Hengstman GJ, et al. Anti-signal recognition particle autoantibodies: marker of a necrotizing myopathy. *Ann Rheum Dis* 2006;65:1635–1638.
263. Constantin T, et al. National registry of patients with juvenile idiopathic inflammatory myopathies in Hungary—clinical characteristics and disease course of 44 patients with juvenile dermatomyositis. *Autoimmunity* 2006;39:223–232.
264. Schwartz T, et al. Cardiac dysfunction in juvenile dermatomyositis: a case-control study. *Ann Rheum Dis* 2011;70:766–771.
265. Coyle K, et al. Metabolic abnormalities and cardiovascular risk factors in children with myositis. *J Pediatr* 2009;155:882–887.
266. Heine J. Über ein eigenartiges Krankheitsbild von deiffuser Sklerosis der haut und innerer organe. *Virchows Arch* 1926;262–271.
267. Weiss EA. Scleroderma heart disease: with a consideration of certain other visceral manifestations. *Arch Intern Med* 1943;71:749–776.
268. Zulian F, Martini G. Childhood systemic sclerosis. *Curr Opin Rheum* 2007;19:592–597.
269. Rosenkranz ME, et al. Systemic and localized scleroderma in children: current and future treatment options. *Paediatr Drugs* 2006;8:85–97.
270. Scalapino K, et al. Childhood onset systemic sclerosis: classification, clinical and serologic features, and survival in comparison with adult onset disease. *J Rheumatol* 2006;33:1004–1013.
271. Foeldvari I. Systemic sclerosis in childhood. *Rheumatology* 2006;45:28–29.
272. de Macedo PA, Shinjo SK, Goldenstein-Schainberg C. Juvenile scleroderma. *Acta Reumatol Port* 2008;33:289–297.
273. Athreya BH, Juvenile scleroderma. *Curr Opin Rheumatol* 2002;14:553–561.
274. Martini G, et al. Systemic sclerosis in childhood: clinical and immunologic features of 153 patients in an international database. *Arthritis Rheum* 2006;54:3971–3978.
275. Leitenberger JJ, et al. Distinct autoimmune syndromes in morphea: a review of 245 adult and pediatric cases. *Arch Dermatol* 2009; 145: 545–550.
276. Zulian F, et al. Localized scleroderma in childhood is not just a skin disease. *Arthritis Rheum* 2005;52:2873–2881.
277. Zannin ME, et al. Ocular involvement in children with localised scleroderma: a multi-centre study. *Br J Ophthalmol* 2007;91:1311–1314.
278. Quartier P, et al. Severe cardiac involvement in children with systemic sclerosis and myositis. *J Rheumatol* 2002;29:1767–1773.
279. Follansbee WP, Zerbe TR, Medsger, TA, Jr. Cardiac and skeletal muscle disease in systemic sclerosis (scleroderma): a high risk association. *Am Heart J* 1993;125:194–203.
280. Champion HC. The heart in scleroderma. *Rheum Dis Clin North Am* 2008;34:181–90.
281. Purice S, et al. Cardiac involvement in progressive systemic sclerosis and polymyositis: a comparative study in 116 patients. *Med Int* 1989;27: 209–213.
282. Bulkley BH, et al. Myocardial lesions of progressive systemic sclerosis. A cause of cardiac dysfunction. *Circulation* 1976;53:483–490.
283. Deswal A, Follansbee WP. Cardiac involvement in scleroderma. *Rheum Dis Clin North Am* 1996;22:841–860.
284. Follansbee WP. The cardiovascular manifestations of systemic sclerosis (scleroderma). *Curr Probl Cardiol* 1986;11:241–298.
285. Follansbee WP, et al. A controlled clinicopathologic study of myocardial fibrosis in systemic sclerosis (scleroderma). *J Rheumatol* 1990;17:656–662.
286. Leinwand I. Generalized scleroderma; report with autopsy findings. *Ann Intern Med* 1951;34:226–238.
287. Leinwand I, Duryee AW, Richter MN. Scleroderma; based on a study of over 150 cases. *Ann Intern Med* 1954;41:1003–1041.
288. Alexander EL, et al. Reversible cold-induced abnormalities in myocardial perfusion and function in systemic sclerosis. *Ann Intern Med* 1986;105:661–668.
289. Gustafsson R, et al. Cold-induced reversible myocardial ischaemia in systemic sclerosis. *Lancet* 1989;2:475–479.
290. Follansbee WP, et al. Physiologic abnormalities of cardiac function in progressive systemic sclerosis with diffuse scleroderma. *N Engl J Med* 1984;310:142–148.
291. Kahan A, et al. Pharmacodynamic effect of dipyridamole on thallium-201 myocardial perfusion in progressive systemic sclerosis with diffuse scleroderma. *Ann Rheum Dis* 1986;45:718–725.
292. Kahan A, et al. Nicardipine improves myocardial perfusion in systemic sclerosis. *J Rheumatol* 1988;15:1395–1400.
293. Kahan A, et al. Nifedipine and thallium-201 myocardial perfusion in progressive systemic sclerosis. *N Engl J Med* 1986;314:1397–1402.
294. Kahan A, et al. Decreased coronary reserve in primary scleroderma myocardial disease. *Arthritis Rheum* 1985;28:637–646.
295. Bernstein M, Konzelman FW, Sidlick DM. Boeck's sarcoid: report of a case with visceral involvement. *Arch Intern Med* 1929;4:721–734.
296. Sohn IS. Cardiac sarcoidosis: oldies but not goodies. *Korean Circ J* 2011;41:296–298.
297. Paule P, et al. Diagnosis of cardiac sarcoidosis and follow-up of 24 consecutive patients. *Revue Med Interne* 2004;25:357–362.
298. Habersberger J, Manins V, Taylor AJ. Cardiac sarcoidosis. *Intern Med J* 2008;38:270–277.
299. Matsui Y, et al. Clinicopathological study of fatal myocardial sarcoidosis. *Ann N Y Acad Sci* 1976;278:455–469.
300. Matsui Y, Iwai K, Tachibana T. Clinicopathological study on fatal myocardial sarcoidosis. *Ann NY Acad Sci* 1976;278:455–469.
301. Hoffmann AL, Milman N, Byg KE. Childhood sarcoidosis in Denmark 1979–1994: incidence, clinical features and laboratory results at presentation in 48 children. *Acta Paediatr* 2004;93:30–36.
302. Duke C, Rosenthal E. Sudden death caused by cardiac sarcoidosis in childhood. *J Cardiovasc Electrophysiol* 2002;13:939–942.
303. Iwai K, et al. Racial difference in cardiac sarcoidosis incidence observed at autopsy. *Sarcoidosis* 1994;11:26–31.
304. Gideon NM, Mannino DM. Sarcoidosis mortality in the United States 1979–1991: an analysis of multiple-cause mortality data. *Am J Med* 1996;100:423–427.
305. Virmani R, Bures JC, Roberts WC. Cardiac sarcoidosis; a major cause of sudden death in young individuals. *Chest* 1980;77:423–428.
306. Schulte W, et al. Cardiac Involvement in Sarcoidosis. European Respiratory Monograph. Wakefield, UK: ERS Journals Ltd, 2005.
307. Mitropoulos FA, et al. Cardiac sarcoidosis. *Thorac Cardiovasc Surg* 2009;57:187–190.
308. Syed J, Myers R. Sarcoid heart disease. *Can J Cardiol* 2004;20:89–93.
309. Shetty AK, Stopa AR, Gedalia A. Low-dose methotrexate as a steroid-sparing agent in a child with Takayasu's arteritis. *Clin Exp Rheumatol* 1998; 16:335–336.
310. Silverman, KJ, Hutchins GM, Bulkley BH. Cardiac sarcoid: a clinicopathologic study of 84 unselected patients with systemic sarcoidosis. *Circulation* 1978;58:1204–1211.
311. Iannuzzi MC, Rybicki BA, Teirstein AS. Sarcoidosis. *N Engl J Med* 2007;357:2153–2165.
312. Sekiguchi M, et al. Cardiac sarcoidosis: diagnostic, prognostic, and therapeutic considerations. *Cardiovasc Drugs* 1996;10:495–510.
313. Roberts W, McAllister H, Ferrans V. Sarcoidosis of the heart: a clinicopathologic study of 35 necropsy patients (group 1) and review of 78 previously described necropsy patients (group 11). *Am J Med* 1977;63:86–108.
314. Divakara Menon SM, Chemello D, Morillo CA. Sarcoidosis: yet another masquerader the cardiologist/electrophysiologist has to fight with. *Indian Pacing Electrophysiol J* 2010;10:479–485.
315. Schaedel H, et al. Sarcoid heart disease—results of follow-up investigations. *Eur Heart J* 1991;12:26–27.
316. Mehta D, et al. Cardiac involvement in patients with sarcoidosis: diagnostic and prognostic value of outpatient testing. *Chest* 2008;133: 1426–1435.
317. Sun BJ, et al. Prevalence of echocardiographic features suggesting cardiac sarcoidosis in patients with pacemaker or implantable cardiac defibrillator. *Korean Circ J* 2011; 41:313–320.
318. Uemura A, et al. Relationship between basal thinning of the interventricular septum and atrioventricular block in patients with cardiac sarcoidosis. *Sarcoidosis Vasc Diffuse Lung Dis* 2005;22:63–65.
319. Hunold P, et al. Myocardial late enhancement in contrast-enhanced cardiac MRI: distinction between infarction scar and non-infarction-related disease. *AJR Am J Roentgenol* 2005;184:1420–1426.
320. Uemura A, et al. Histologic diagnostic rate of cardiac sarcoidosis: evaluation of endomyocardial biopsies. *Am Heart J* 1999;138:299–302.
321. Smedema, JP, et al. Evaluation of the accuracy of gadolinium-enhanced cardiovascular magnetic resonance in the diagnosis of cardiac sarcoidosis. *J Am Coll Cardiol* 2005;45:1683–1690.
322. Paz HL, et al. The automated implantable cardiac defibrillator. Prophylaxis in cardiac sarcoidosis. *Chest* 1994;106:1603–1607.
323. Kim JS, et al. Cardiac sarcoidosis. *Am Heart J* 2009;157:9–21.
324. Baughman RP, Sharma OP, Lynch JP III. Sarcoidosis: is therapy effective? *Semin Respir Infect* 1998;13:255–273.
325. Lynch JP 3rd, Sharma OP, Baughman RP. Extrapulmonary sarcoidosis. *Semin Respir Infect* 1998;13:229–254.
326. Furushima H, et al. Ventricular tachyarrhythmia associated with cardiac sarcoidosis: its mechanisms and outcome. *Clin Cardiol* 2004;27:217–222.
327. Tahara N, et al. Heterogeneous myocardial FDG uptake and the disease activity in cardiac sarcoidosis. *JACC Cardiovasc Imaging* 2010;3: 1219–1228.

Jonathan N. Johnson ■ Frank Cetta

NORMAL ANATOMY AND PHYSIOLOGY

The pericardium is composed of two principal layers, the visceral pericardium and the parietal pericardium. The visceral pericardium, or epicardium, is a single serous layer covering the surface of the heart and proximal great vessels (Fig. 62.1). The parietal pericardium consists of three layers. The innermost layer is a serous layer, continuous with the serous visceral pericardium. The space between the visceral serous and parietal serous layers is the pericardial space, and it contains a small amount of serous fluid for lubrication (<20 to 30 mL in adults, less in children). The middle layer of the parietal pericardium is fibrous, while the outer layer is collagenous connective tissue. The pericardium gets its arterial blood supply from the descending aorta and internal mammary artery, and its innervation from the phrenic and vagus nerves. Within the thoracic cavity, it is bordered anteriorly by the sternum, inferiorly by the diaphragm and a portion of the inferior vena cava, and posteriorly by the esophagus, aorta, pulmonary veins, and thoracic vertebrae (1,2).

The pericardium provides mechanical protection to the heart from the spread of neoplastic, infectious, and inflammatory diseases from adjacent structures. The presence of a small amount of fluid in the pericardial space allows for free movement of the heart throughout the cardiac cycle. The pericardium limits acute distension of the heart and therefore limits end-diastolic volume. It permits diastolic coupling of the two ventricles, whereby filling pressure abnormalities of one ventricle affect the other. Slow progressive accumulation of fluid within the pericardium is tolerated by stretching and growth of the parietal pericardium; however, rapid accumulation of even a small amount of fluid is tolerated poorly (3).

ACUTE PERICARDITIS

Symptoms

Acute pericarditis may present with precordial or substernal chest pain. The pain is described as squeezing, sharp, or dull and characteristically is worse in the supine position. The patient will prefer to sit upright leaning forward and may refuse to lie down to be examined. The pain worsens with inspiration, coughing, and with movement (4,5). Younger children may present with atypical symptoms. Respiratory distress is uncommon unless tamponade or pulmonary disease is present. Rarely, abdominal pain can result from hepatic distension in patients with quickly accumulating effusions. Fever may be present.

Physical Examination

The pathognomonic physical finding in patients with acute pericarditis is a friction rub. This is a high-frequency, scratching or

sandpaper-like sound caused by friction between the inflamed pericardial surfaces. The rub can be heard throughout the cardiac cycle. However, it may be intermittent. It often is heard best at the left sternal border or the apex. The rub is loudest when the heart is closest to the chest wall, such as when the patient leans forward, kneels, and/or inspires (6,7). Absence of a friction rub does not exclude pericarditis, particularly in patients with large effusions. In patients with large effusions or tamponade, the heart sounds may be muffled.

Cardiac Tamponade

Cardiac tamponade occurs when the heart is compressed by a fluid-filled pericardium. This causes restriction of ventricular and atrial filling and decreased cardiac output (8). Tamponade results from a sudden increase in pericardial fluid volume or from progressive increase in volume beyond the point of potential pericardial distension. On examination, tamponade is characterized by Beck's triad, which includes (a) distant heart sounds, (b) hypotension, and (c) elevated central venous pressure with jugular venous distension (9). Patients will have tachycardia, tachypnea, and a narrow pulse pressure with pulsus paradoxus. During the initial stages of tamponade, cardiac output is preserved by increased ejection fraction and heart rate. As these physiologic mechanisms are unable to maintain cardiac output, the patient will become unstable as systemic vascular resistance increases to maintain systemic blood pressure. This will cause the pulse pressure to narrow, with compromised systemic perfusion. Ultimately, decreased coronary perfusion pressure will result in decreased myocardial function, cardiac output, and blood pressure (8,9).

Pulsus paradoxus is defined as a decrease in systolic blood pressure of >10 mm Hg during inspiration. Normally during inspiration, systolic blood pressure decreases by 4 to 6 mm Hg due to decreased intrathoracic pressure and increased capacity of the pulmonary venous bed. With cardiac tamponade, the left ventricular (LV) diastolic volume is restricted by increased pericardial pressure, decreased pulmonary venous return, and shifting of the interventricular septum. Clinically, to determine the presence of pulsus paradoxus, the patient should be supine. A blood pressure cuff is inflated until the radial pulse is not palpable. With slow release of pressure, one should listen for the initial Korotkoff sounds. With inspiration, the Korotkoff sounds disappear, particularly in the presence of pulsus paradoxus. Cuff pressure should be slowly released until the Korotkoff sounds are heard throughout the respiratory cycle. The difference in pressure between the first Korotkoff sound and when it is heard with each heartbeat is the pulsus. If the pressure difference exceeds 10 mm Hg, pulsus paradoxus is present (10).

During inspiration in normal patients, intrathoracic pressure decreases with an increase in venous return to the right atrium. In patients with cardiac tamponade, however, expansion of

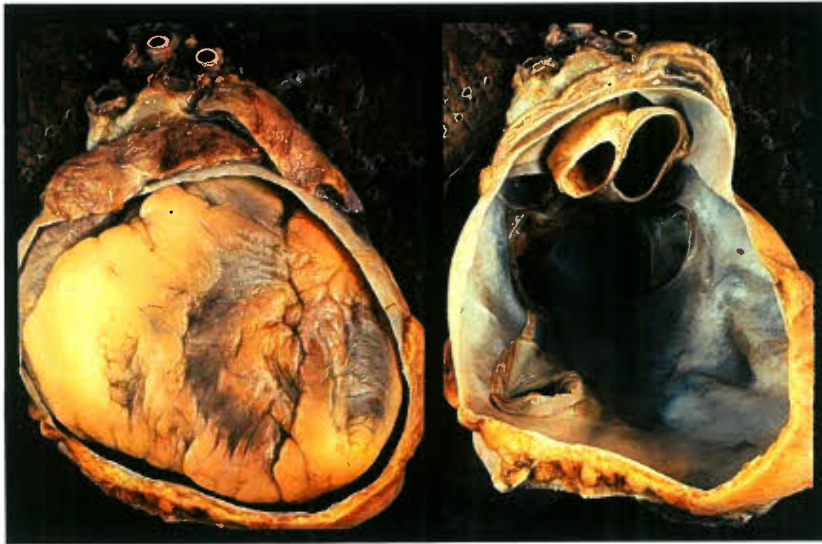


Figure 62.1. Heart specimen, showing the heart within the pericardial cavity (left) and the bilayered pericardium with the heart removed (right). (Courtesy of Dr. William D. Edwards, Division of Anatomic Pathology, Mayo Clinic, Rochester, MN.)

the right atrium is limited by pericardial pressure. Thus, during inspiration, there may be a paradoxical increase in central venous pressure. This is evident by Kussmaul's sign; a rise in observed jugular venous pressure during inspiration (3).

Chest Radiography

The absence of cardiomegaly by chest radiography does not exclude pericarditis or pericardial effusion. Tamponade can occur in patients with a normal-appearing cardiac silhouette. With progressively increasing effusion, the cardiac silhouette may assume a triangular or "water-bottle" shape, with normal pulmonary vascular markings (Fig. 62.2). Patients with chronic pericarditis may have calcification of the pericardium (Fig. 62.3). The remainder of the chest radiograph may suggest potential causes of the pericarditis, including tuberculosis, pneumonia, or neoplastic disease (4,5).

Electrocardiography

The electrocardiographic changes in patients with pericarditis are secondary to direct inflammation of the epi/myocardium or pressure exerted against the epicardium by pericardial fluid. Acute pericarditis is the most frequent cause of ST elevation in children. Low QRS voltages occur in all leads in the presence of large pericardial effusions or chronic pericarditis. Electrical

alternans, a cyclical variation of the QRS amplitude, may occur secondary to the pendular motion of the heart with a large pericardial effusion.

Four stages of electrocardiographic changes have been reported in patients with pericarditis (11). Stage 1 consists of ST-segment elevation in the lateral/inferior leads (I, II, aVF, aVL, V4-V6) (Fig. 62.4). Reciprocal ST-segment depression may be present in leads aVR and V1. PR interval depression can occur if atrial tissue is inflamed. In stage 2, the ST segment normalizes, and T-wave amplitude diminishes. In stage 3, the ST segment remains normal, but the T-waves become inverted in the lateral/inferior leads (aVF, aVL, V4-V6). Stage 4 is characterized by the relative normalization of the ECG, although some T-wave changes may persist (5,12).

Echocardiography

Echocardiography is the primary imaging methodology used for the diagnosis of pericardial effusions, which appear as an echo-free space around the heart (13). Fibrinous strands may be noted in the pericardial space (Fig. 62.5). Thrombus, adhesions, or metastases also may be noted. Echocardiography also is helpful in detecting other structural and myocardial causes of cardiomegaly (14).

With the patient in the supine position, a small effusion most commonly is seen posteriorly and may be detectable only in systole. A tiny space in systole that is not evident in diastole is normal. An effusion that is present during both systole and diastole is abnormal (15). As the volume of the effusion increases, fluid may be detected both anterior and posterior to the heart (Fig. 62.6). With large effusions, the heart may swing to and fro within the pericardial space. This swinging movement can be seen by M-mode echocardiography (Fig. 62.7). The earliest sign of hemodynamic impairment in cardiac tamponade is collapse of the right ventricular (RV) free wall in early to mid-diastole (Fig. 62.8) (16). The right atrial free wall may appear indented late in diastole (Fig. 62.9). Inferior vena cava dilation without normal inspiratory variation and abnormal ventricular septal motion also may occur. Thrombus may occur in the pericardial space and suggests a hemopericardium.

Normally, during inspiration, the intrapericardial and the intrathoracic pressures decrease equally. Thus, the left atrial and LV diastolic pressures and the pulmonary capillary wedge pressure decrease equally during inspiration. How-

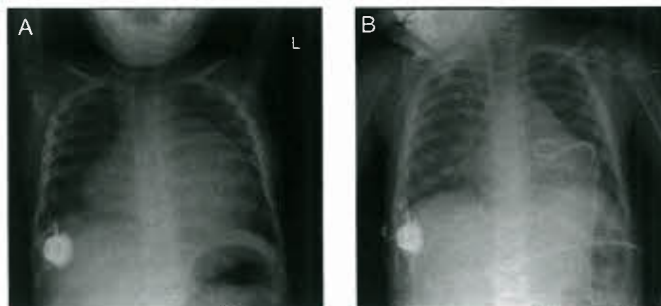


Figure 62.2. A: Chest radiograph of a 2-year-old girl who presented with tachypnea. The patient required an emergent pericardiocentesis, after which (B) her cardiothymic silhouette had markedly decreased in size.

Figure 62.3. Chest radiograph of an adult with chronic pericarditis and resultant calcification of the pericardial space. (Courtesy of Dr. William D. Edwards, Division of Anatomic Pathology, Mayo Clinic, Rochester, MN.)

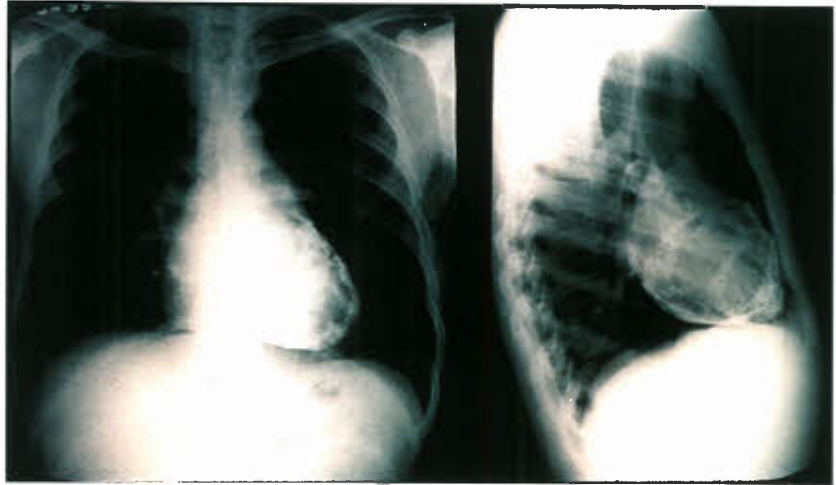


Figure 62.4. Electrocardiogram of a 17-year-old male 2 days after surgical repair of an atrial septal defect. Note the diffuse ST-segment changes including ST-segment elevation in the lateral and inferior leads.

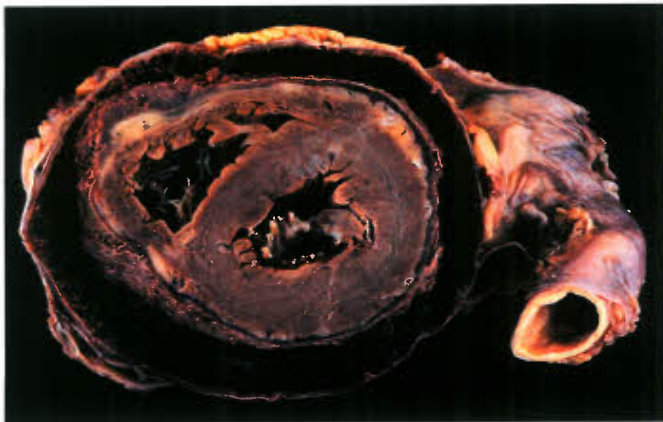
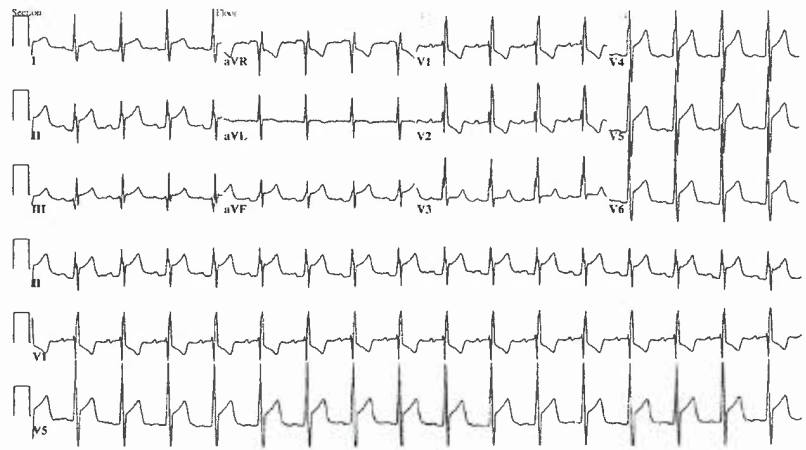


Figure 62.5. Heart specimen, showing the heart within the pericardial space with a large effusion. Fibrinous stranding can be seen within the pericardial space. (Courtesy of Dr. William D. Edwards, Division of Anatomic Pathology, Mayo Clinic, Rochester, MN.)



Figure 62.6. Parasternal long-axis echo image showing a large pericardial effusion (asterisk). LV, left ventricle; RV, right ventricle; Ao, aorta.

ever in tamponade, during inspiration, the intrathoracic pressure declines to a greater degree than the intrapericardial pressure. Thus, the gradient between the pulmonary capillary wedge pressure and LV diastolic pressures decreases with inspiration. Therefore, in cardiac tamponade, there is an exaggerated decrease in the mitral inflow velocity (E velocity) and velocity-time integral by at least 30%, with a

relatively increased atrial component during inspiration (A velocity) (Fig. 62.10A). Conversely, there is an exaggerated increase in tricuspid inflow velocity (tricuspid E velocity) and the velocity-time integral by at least 70% during inspiration (17,18). The aortic and pulmonary outflow changes mirror those of their respective atrioventricular valves (Fig. 62.10B).

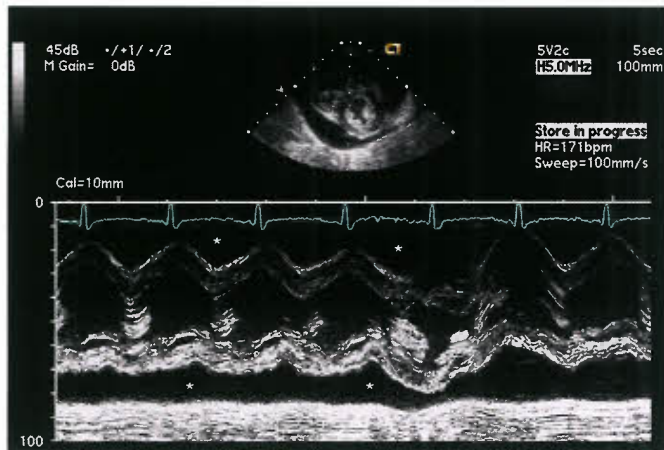


Figure 62.7. M-mode echo image showing a large pericardial effusion (*asterisk*) anterior and posterior to the heart. Note the swinging motion of the heart evident in the M-mode signal.

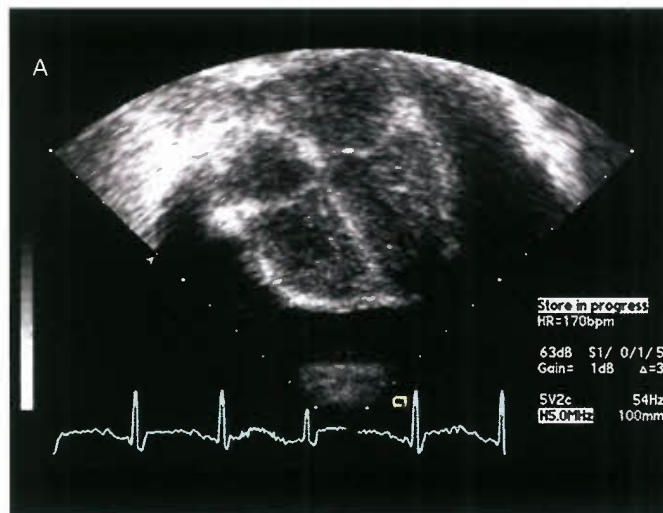


Figure 62.8. RV collapse in early diastole in a patient with tamponade. Note that in the left image in systole (A), the full four-chamber view is noted, while in the right image in diastole (B), the RV free wall is compressed.



Figure 62.9. Right atrial collapse (*arrow*) in late diastole in a patient with tamponade. (Courtesy of Dr. Malek El-Yaman, West Virginia University Children's Hospital, Morgantown, WV.)

Cardiac Catheterization

With large accumulations of pericardial fluid, diastolic pressures rise in all four chambers and ultimately equalize (19). RV and pulmonary artery pressures may be elevated. Pulsus paradoxus can be seen on femoral artery pressure tracing (10). In patients with constrictive physiology, due to the equalization of the LV and RV end-diastolic pressures, the characteristic “square root” sign may be present on the LV pressure tracing (Fig. 62.11).

Other Imaging Modalities

Magnetic resonance imaging (MRI) or computed tomography (CT) can be useful if constrictive pericarditis is suspected. Active pericardial inflammation (a treatable cause of constriction) and hemodynamic evidence of constriction may be apparent using MRI. MRI is helpful in characterizing pericardial masses and congenital anomalies of the pericardium, such as absence of the pericardium and pericardial cysts (20).

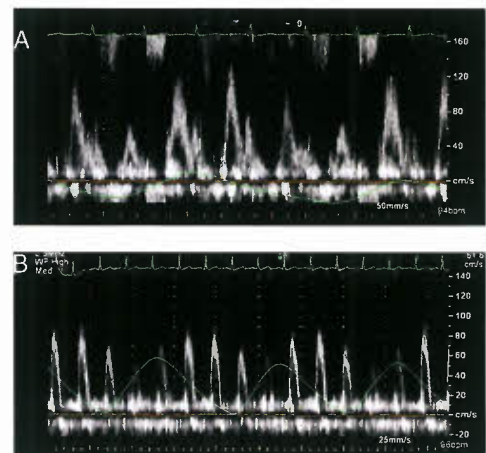


Figure 62.10. Doppler echocardiographic patterns seen in an adolescent patient with a large pericardial effusion and tamponade physiology, including (A) mitral inflow pulse-wave Doppler and (B) abdominal aorta pulse-wave Doppler signals. Note the marked respiratory variation (respirometer below Doppler tracing in each figure) in peak velocities of both LV filling and aortic antegrade flow.

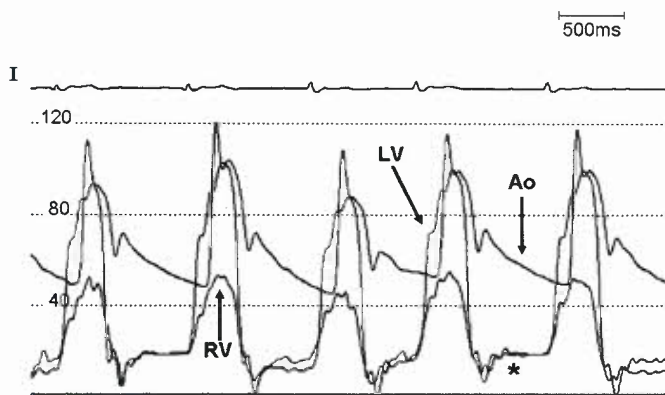


Figure 62.11. Cardiac catheterization tracing of a patient with physiology consistent with constriction. Note the “square root sign” (asterisk) secondary to equalization of LVEDP and RVEDP. LV, left ventricle; RV, right ventricle; Ao, aorta.

Management of Tamponade

After diagnosing cardiac tamponade, one should administer IV fluid immediately to increase diastolic filling pressure temporarily in order to stabilize the patient (21). Medications that decrease systemic arterial blood pressure such as vasodilators and diuretics should be avoided. Indications for pericardiocentesis include low cardiac output, hypotension, pulsus paradoxus >10 mm Hg, suspected bacterial pericarditis, pericardial effusions in immunocompromised hosts, or for diagnostic purposes when the etiology is unclear (22,23).

Pericardiocentesis should be performed in a monitored setting. The patient should be placed in a 30-degree head-up position and adequately sedated. Echocardiographic guidance allows for accuracy in entering the pericardial space usually from an apical approach, but is unnecessary in emergent situations (23). One can perform an agitated saline injection to confirm the location of the needle in the pericardial space. In the majority of patients, a drainage catheter should be placed for at least 48 hours to detect and drain recurrent effusions (22). Potential complications of pericardiocentesis include hemopericardium, pneumothorax, arrhythmias, myocardial puncture, coronary artery, aorta or internal mammary artery injury, and death (23,24).

Pericardial fluid should be analyzed for cell content, glucose concentration, protein concentrations, Gram stain, acid-fast bacilli stain, cultures (bacterial, viral, and fungal), and microscopic analysis (25). Specific bacterial or viral-specific antigens may be assessed using polymerase chain reaction (PCR) studies and latex agglutination studies. High triglyceride levels are diagnostic of chylopericardium. Adenosine deaminase activity levels can be measured to assist in the diagnosis of tuberculous pericarditis (26).

If the effusion is purulent, it may be too thick to adequately drain or it is loculated within the pericardium. In this case, surgical drainage will be necessary, and a subtotal pericardiectomy or pericardial window should be performed (27–29).

ETIOLOGY

Viral Pericarditis

The most common etiology of pericarditis in the pediatric population is viral. The most common viral causes of pericarditis are listed in Table 62.1. Coxsackievirus is the most common

TABLE 62.1 Pericarditis—Potential Viral Causes

Enterovirus (primarily Coxsackie B)	Measles
Adenovirus	Cytomegalovirus (CMV)
Influenza virus (A and B)	Respiratory syncytial virus (RSV)
Rubella	Herpes simplex
Mumps	Hepatitis B
Epstein-Barr virus (EBV)	HIV

viral cause of pericarditis in children (30). Patients often present 10 to 14 days after an upper respiratory or gastrointestinal infection, with precordial chest pain, fever, and a friction rub. Some patients present with abdominal pain. Patients with viral pericarditis generally are less toxic appearing than those patients with bacterial pericarditis. However, patients with viral pericarditis may appear toxic when there is associated myocarditis. Tamponade is rare in patients with viral myocarditis; however, patients should be monitored closely after initial diagnosis.

If collected, pericardial fluid usually is serous or serosanguineous, and displays lymphocyte predominance, although neutrophils may be common in the early stages of the illness. Viral cultures can be obtained from pericardial fluid, the nasopharynx, or the stool. PCR studies often are useful in determining a specific viral cause (31,32).

Specific treatment for viral pericarditis is symptomatic, including bedrest and oral nonsteroidal anti-inflammatory drugs (NSAIDs). If NSAIDs are unsuccessful, steroids may be considered once bacterial causes have been excluded. The use of colchicine with aspirin as first-line combination therapy decreases the likelihood of recurrence in adults. However, colchicine has not been well studied in the pediatric population (33). Resolution occurs in days to weeks, with complete resolution usually in <6 weeks. Relapse occurs in a small subset of patients, typically improving with reinstitution of NSAIDs or steroids. Constrictive pericarditis rarely occurs as a late complication of viral pericarditis.

Bacterial Pericarditis

Bacterial pericarditis is a serious, life-threatening disease. It presents most frequently in patients under 2 years of age (34). Patients present with symptoms of fever, chest pain, friction rub, and muffled heart sounds, but may be in shock on presentation. In addition, patients have dyspnea, tachypnea, and tachycardia out of proportion to the fever. Bacterial pericarditis can result from hematogenous dissemination or direct contact. The lung is the most common origin of dissemination, particularly when the agent is *Staphylococcus aureus*, *Haemophilus influenzae*, and *Streptococcus pneumoniae*. Septic arthritis, osteomyelitis, meningitis, or soft tissue infection also may be the source for hematogenous dissemination (34–37).

In bacterial pericarditis, the pericardial fluid demonstrates a marked predominance of neutrophils, and cultures typically are positive for the causative organism. Latex agglutination studies of the pericardial fluid, serum, or urine may be helpful if antibiotics have been given prior to obtaining a sample of pericardial fluid. Potential bacterial causes of pericarditis are listed in Table 62.2. *Staphylococcus aureus* is the most common bacterium isolated, accounting for half of the cases of bacterial pericarditis (34). Also, it is the most common cause of postoperative bacterial pericarditis (i.e., occurring within

TABLE 62.2 Pericarditis—Potential Bacterial Causes

<i>Staphylococcus aureus</i>	<i>Chlamydia psittaci</i>
<i>Haemophilus influenzae</i>	<i>Nocardia asteroides</i>
<i>Streptococcus pneumoniae</i>	<i>Brucella</i>
Other <i>Streptococci</i> species	<i>Yersinia</i>
<i>Neisseria meningitidis</i>	<i>Salmonella</i>
<i>Neisseria gonorrhoeae</i>	<i>Actinomyces</i>
<i>Campylobacter fetus</i>	<i>Mycobacterium tuberculosis</i>
<i>Pseudomonas aeruginosa</i>	<i>Escherichia coli</i>
<i>Mycoplasma pneumoniae</i>	<i>Listeria monocytogenes</i>
<i>Mycoplasma hominis</i>	<i>Pasteurella multocida</i>
<i>Legionella</i>	<i>Klebsiella</i>
<i>Francisella tularensis</i>	<i>Anaerobes</i>

3 months of a cardiac operation) (38). Anaerobic bacteria should be considered in patients with concurrent lung abscess, abdominal infection, or a history of blunt chest trauma.

Importantly, antibiotics alone are not sufficient to treat bacterial pericarditis. All patients require percutaneous or surgical drainage of the pericardial cavity. If the purulent pericardial fluid cannot be aspirated percutaneously, a surgically created window or pericardiectomy will be required (29). Streptokinase administered in the pericardium may improve drainage (39,40). Broad-spectrum antibiotics are mandatory and initially should be directed toward the most common organisms (*Staphylococcus aureus* and *Haemophilus influenzae*). Initial treatment should include an intravenous penicillinase-resistant penicillin (nafcillin or oxacillin) or vancomycin in patients at risk for methicillin-resistant *Staphylococcus aureus*, as well as a third-generation cephalosporin (ceftriaxone, cefotaxime) (34,38,41). An aminoglycoside may be added for immunocompromised patients. Specific therapy can be tailored once specific culture/sensitivity results are known. Patients with bacterial pericarditis should be treated for at least 3 to 4 weeks with intravenous antibiotics.

Survival for patients with bacterial pericarditis currently is >90% (39,41). Risk factors for poor outcome include young age at diagnosis, septicemia, tamponade, delay in diagnosis, inadequate drainage, concurrent myocarditis, and a staphylococcal etiology (37,39,42). Constrictive pericarditis can be a late complication (36,39), most commonly associated with *Staphylococcus aureus*, *Haemophilus influenzae*, or *Streptococcus pneumoniae* infections.

Tuberculous Pericarditis

Once common throughout the world, *Mycobacterium tuberculosis* pericarditis now occurs most frequently only in developing nations. The typical onset is insidious with symptoms of low-grade fever, night sweats, weight loss, malaise, dyspnea, and chest pain. The presentation may be complicated by subacute pericardial tamponade. Tuberculous pericarditis often occurs due to direct extension of miliary tuberculosis or lymphatic spread into the pericardium. Hematogenous spread may occur without evidence of pulmonary infiltrates. Most patients have a positive Mantoux skin test.

The pericardial fluid, when aspirated, is serosanguineous or hemorrhagic with lymphocyte predominance. Acid-fast bacilli

may be seen on auramine-rhodamine fluorescent-stained smears (43). Pericardial biopsy is useful to provide histologic confirmation. Pericardial fluid adenosine deaminase levels are diagnostic for tuberculous pericarditis if >50 U/L (26,43,44). Mycobacterium cultures may take up to 6 weeks to grow; thus, treatment should be initiated before confirmation of diagnosis.

Multidrug therapy is essential due to the risk of drug-resistant tuberculosis. A treatment regime of rifampicin, isoniazid, pyrazinamide, and ethambutol for at least 2 months, followed by isoniazid and rifampicin for another 4 months is highly effective (43). One or two months of steroid therapy may be useful to reduce inflammation and increase pericardial fluid resorption (45). Early in the course of the disease, pericardiectomy is difficult due to the presence of diffuse inflammatory and caseous material. Some investigators recommend delaying pericardiectomy for at least 6 weeks, although this remains controversial (43,46). Tuberculosis is a common cause of chronic pericardial effusion, and constrictive pericarditis may develop after recovery. Worldwide, tuberculous pericarditis is one of the leading causes of constrictive pericarditis (43).

HIV and Other Infections

Pericardial effusions are common in patients with human immunodeficiency virus (HIV) and are present in up to 25% of children with HIV infection (47–49). Children with HIV rarely develop tamponade. Pericardial fluid cultures typically are negative. Immunocompromised patients, including patients with HIV, are at risk for rarer causes of pericarditis, including parasitic and fungal causes (Table 62.3). In developing nations, concurrent infection with tuberculosis and HIV is common. The presence of HIV is a significant risk factor for developing tuberculous pericarditis (43).

Other Causes of Pericarditis and Pericardial Effusion

Renal Failure

Pericarditis occurs in 10% of patients with chronic renal failure (50,51). It is more common in patients with concurrent systemic lupus erythematosus (SLE), or drug-induced in those receiving hydralazine for hypertension. Most pericardial effusions will resolve with efficient dialysis (51). The pericardial fluid typically is serous. Care should be taken with heparinization in these patients, as a pericardial hemorrhage can occur with resultant tamponade. NSAIDs can be given for chest pain, but do not affect the size of the effusion. Pericardiocentesis should be performed for the usual indications, including patients suspected of having bacterial pericarditis and in those with hemodynamic compromise. If the effusion fails to resolve with dialysis, or if constriction develops, pericardiectomy may be necessary (51).

TABLE 62.3 Pericarditis—Other Infectious Causes

Fungal	<i>Candida</i> , <i>Aspergillus</i> , <i>Blastomyces</i> , <i>Coccidioides</i> , <i>Histoplasma</i> , <i>Cryptococcus</i>
Parasitic	<i>Entamoeba histolytica</i> , <i>Echinococcus</i>
Protozoal	<i>Toxoplasma gondii</i>
Rickettsial	Typhus, Q fever
Spirochetal	Syphilis, leptospirosis

TABLE 62.4 Drug-Induced Pericarditis

Cromolyn Sodium	Isoniazid
Cyclophosphamide	Methysergide
Cyclosporine	Penicillin
Dactinomycin	Phenytoin
Doxorubicin	Procainamide
Hydralazine	

Kawasaki Disease

During the acute phase of Kawasaki disease, one-third of patients have a pericardial effusion, which typically resolves within 2 weeks. Effusions related to this inflammatory process do not commonly progress to tamponade, but this has been reported (52,53).

Drug-Induced Pericarditis

Drug-induced pericarditis may occur in patients treated with the medications listed in Table 62.4. The most common offenders are hydralazine, isoniazid, procainamide, and phenytoin. Antinuclear antibodies often are elevated in these patients. Effusions due to a lupus-like effect rarely progress to tamponade (54). Treatment includes discontinuing the offending drugs and initiation of NSAIDs. Patients with hypersensitivity reactions to penicillin and cromolyn sodium in association with pericardial effusion have been reported (55,56).

Hypothyroidism

The hypothyroid patient with a pericardial effusion most commonly is asymptomatic. It occurs in up to 80% of patients with myxedema, but is rare in patients with only mild hypothyroidism (57). Cardiac tamponade is exceedingly uncommon due to the slow accumulation of fluid (57). Patients present with paradoxical bradycardia, unlike others with pericardial effusions who usually have tachycardia. If pericardiocentesis is required, the fluid contains elevated protein and mucopolysaccharides (58). Most effusions will resolve gradually after initiation of thyroid hormone replacement therapy.

Chylopericardium

Chylous pericardial effusion may occur in patients following congenital heart surgery, particularly after trauma to the thoracic duct or in patients with elevated central venous pressures (59,60). Concurrent chylous pleural effusion may be present. Chylopericardium can occur in patients with mediastinal masses that obstruct lymphatic drainage, and in association with cystic hygromas, radiation therapy, or pancreatitis. It rarely may be idiopathic. The pericardial fluid obtained is milky-colored, with elevated triglyceride and protein levels. Patients should be given a low-fat or median-chain triglyceride diet, initiated after a period of parenteral nutrition without oral intake to allow resolution of the chylous effusion. Persistent chylous effusions can be treated by thoracic duct ligation. Some patients may require palliation with a pericardial window, pericardiectomy, or placement of a pericardioperitoneal or pleuroperitoneal shunt (59,60). Successful use of intravenous octreotide has been reported in some patients with chronic chylous pleural effusions (61).

Trauma

Blunt and penetrating cardiac trauma may result in hemorrhagic pericardial effusion. In cases of trauma, the usual Beck's triad of symptoms (distant heart sounds, hypotension, and jugular venous distension) rarely occurs, and echocardiography is diagnostic (9). All symptomatic patients require emergency pericardiocentesis. Iatrogenic hemopericardium also can occur during placement of central venous lines and invasive cardiac procedures. A pneumopericardium may be present in patients after an esophageal rupture (Fig. 62.12).

Neoplastic Disease

Primary tumors of the pericardium are rare. Metastatic disease is more common. Primary neoplasms include lymphoma, malignant teratoma, mesothelioma, and angiosarcoma. Potentially metastatic tumors include Hodgkin disease, non-Hodgkin lymphoma, leukemia, malignant melanoma, Wilms tumor, neuroblastoma, Kaposi sarcoma, and bone/soft tissue sarcomas (62–65). Nonmalignant congenital intrapericardial lesions may occur, including pericardial cysts, extralobar pulmonary sequestration, cystic lymphangioma, bronchogenic cysts, and pericardial teratomas (66–70). Teratomas can be large and cause hydrops fetalis in the fetus (71). Surgical excision of these large tumors, when possible, is curative (67).

Pericardial effusions often occur in patients with malignancies, independent of the primary tumor, due to infectious causes or metastatic invasion of pericardial lymphatics. Pericarditis can occur as a complication of certain chemotherapy agents, listed in Table 62.4. Diagnosis of the cause of a malignant effusion can be made using cytologic analysis and culture of pericardial fluid (72).

Patients who have received mediastinal irradiation are at increased risk of pericardial involvement after chemotherapy. Up to 5% of patients receiving mediastinal irradiation will develop pericarditis, typically from 2 months to 2 years after treatment (73). The patient may present with only mild symptoms or may progress to fulminant constrictive pericarditis.

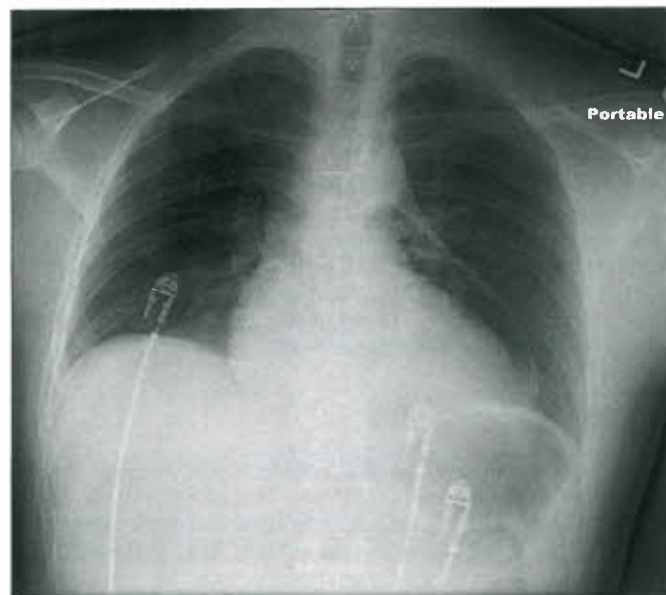


Figure 62.12. Chest radiograph of an adolescent patient who presented with chest pain after an esophagogastroduodenoscopy procedure. Perforation of the esophagus had occurred, with resultant pneumopericardium evident. (Courtesy of Dr. Malek El-Yaman, West Virginia University Children's Hospital, Morgantown, WV.)

(74). Most cases improve with treatment with NSAIDs, but pericardiectomy may be necessary for recurrent effusions (75). Steroids are required in some patients (76).

Postpericardiotomy Syndrome

Postpericardiotomy syndrome usually occurs at least 1 week after intracardiac or pericardial surgery. Because there is pericardial and pleural inflammation, these patients frequently have pleuritic chest pain. It has been estimated to occur in up to 30% of patients following surgery (77,78). Postpericardiotomy syndrome typically occurs as a single episode, although it can recur weeks to years later. Children younger than 2 years old rarely are affected (79). Postpericardiotomy syndrome may produce irritability, malaise, decreased appetite, and arthralgias. Physical examination will reveal a friction rub and tachycardia. The patient may have signs of fluid retention. Cardiac tamponade is rare, but can occur (80).

The cause of postpericardiotomy syndrome remains speculative. The most likely etiology however is that of an autoimmune reaction (81,82). Postpericardiotomy syndrome can occur after blunt cardiac trauma, pacemaker lead placement, and in Dressler's syndrome (postmyocardial infarction syndrome) (83). While postpericardiotomy syndrome may occur after any cardiac operation, it is most frequent after repair of atrial septal defects, ventricular septal defects, and Tetralogy of Fallot (77). It occurs in up to 50% of pediatric patients after cardiac transplantation (84). Serum laboratory evaluation may reveal nonspecific inflammatory markers, including elevated erythrocyte sedimentation rate or C-reactive protein, and an elevated white blood cell count. Echocardiography may reveal an effusion, which typically reaches its maximal size by the 10th postoperative day (77).

Postpericardiotomy syndrome typically is benign and self-limited. Treatment includes diuretics for fluid retention and NSAIDs. Pericardiocentesis may be needed for symptomatic effusions (85). Aspirin is the primary anti-inflammatory medication recommended, in doses as high as 30 to 75 mg/kg/d in four divided doses for 4 to 6 weeks. As postpericardiotomy syndrome resolves, the drug is then tapered (85,86). In patients refractory to NSAIDs, or in those with large effusions, prednisone (2 mg/kg/d, maximum dose 60 mg daily, for 1 week with a 4-week taper) can be effective (87). Patients with recurrent effusions may require pericardiocentesis or pericardiectomy (88,89).

Autoimmune and Connective Tissue Diseases

Pericarditis and pericardial effusions occur in many autoimmune and connective tissue diseases, including SLE, juvenile rheumatoid arthritis, dermatomyositis, periarteritis nodosa, mixed connective tissue diseases, Wegener granulomatosis, Takayasu arteritis, and the spondyloarthropathies. It has been estimated that 25% of pediatric patients with SLE develop pericarditis (90). This usually is treated with oral NSAIDs, but

potentially could require pericardiocentesis if hemodynamic compromise develops (91). Pericarditis occurs in 10% of patients with juvenile rheumatoid arthritis at the time of diagnosis. This usually is treated effectively with oral NSAIDs. Short courses of steroids hasten resolution of symptoms (92). Patients with acute rheumatic fever rarely will develop pericarditis (50). Pericardial effusions in patients with acute rheumatic fever respond well to NSAIDs.

Recurrent and Chronic Pericarditis

Pericarditis *recurs* when the underlying disease relapses, or when an effusion reaccumulates after discontinuation of previously effective medical therapy (4,93). This occurs most frequently in patients with postpericardiotomy syndrome, juvenile rheumatoid arthritis, or SLE (94,95). Treatment strategies include reinstitution of NSAIDs, colchicine, or oral steroids. Patients have been treated successfully with immune modulators including azathioprine and cyclophosphamide (95). Pericardiectomy should be reserved for the patient with multiple recurrences.

Chronic pericarditis is defined as pericardial inflammation lasting >3 months. Similar treatments can be used for symptomatic patients, including NSAIDs, steroids, and percutaneous or surgical drainage of the effusion when necessary (94,96). Intravenous immunoglobulin has been reported to be effective in some patients with chronic pericarditis (97).

Congenital Abnormalities of the Pericardium

Absence of the Pericardium

Complete or partial absence of the pericardium is rare. Most cases are identified incidentally at autopsy or surgery. Most commonly, partial absence of the pericardium is left sided (98,99). Up to one-third of patients have an associated cardiac defect or pulmonary anomaly, including bicuspid aortic valve, atrial septal defect, patent ductus arteriosus, tetralogy of Fallot, pulmonary sequestration, or bronchogenic cyst (98). Although usually asymptomatic, patients can present with nonspecific symptoms such as dyspnea, light-headedness, and chest pain. Rarely, sudden death occurs due to herniation of the left atrium, left atrial appendage, or right atrium through the defect (99). Compression of a coronary artery and torsion of the great vessels also may occur.

The apical impulse may be shifted leftward. Chest radiography reveals a leftward shift of the cardiac silhouette. The diagnosis is not typically made by echocardiography, although unusual scanning windows, cardiac hypermobility, and abnormal ventricular motion may be present (100). The entire cardiac structure is shifted to the left; thus, the RV cavity may appear enlarged from the standard parasternal windows (15). CT and MRI are diagnostic (Fig. 62.13) (20). Surgical repair is indicated for patients with cardiac chamber herniation, or

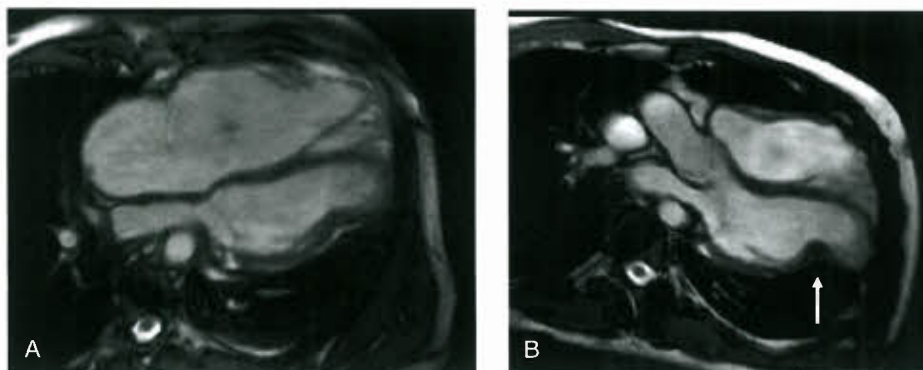


Figure 62.13. Cardiac MRI sequences in an adolescent patient demonstrating partial absence of the pericardium. Note the marked displacement of the heart into the left hemithorax. While the herniation of the apical LV wall is more subtle in this four-chamber view in systole (A), it becomes more apparent in the LV outflow-tract view in late diastole (B). (Courtesy of Dr. Malek El-Yaman, West Virginia University Children's Hospital, Morgantown, WV.)



Figure 62.14. Chest radiography (A) and CT scans (B, C) of a patient with a coarctation of the aorta and incidentally discovered pericardial cyst (asterisk).

in patients with a small defect if future herniation is possible (99). This can be performed either by patch closure of the defect, or by enlargement of the defect to prevent incarceration of the herniated tissue. Patients with complete absence of the pericardium usually are asymptomatic and require no treatment (98).

Pericardial Cysts

Pericardial cysts are congenital anomalies resulting from failure of fetal lacunae to coalesce into the pericardial coelom (101). Patients usually are asymptomatic. The cysts often are discovered incidentally on chest x-ray (Fig. 62.14A). A cyst can become infected or cause bronchial compression, and the patient may have chest pain, dyspnea, or cough (102,103). Due to the benign nature of pericardial cysts, usually no treatment is required. Sometimes cysts present as previously unknown masses in the thoracic cavity, and infection or neoplasm must be excluded (104). Cysts may appear as echo-free spaces adjacent to the heart. CT or MRI, in conjunction with a normal history and clinical exam, can confirm the diagnosis of a pericardial cyst (Fig. 62.14B,C) (20).

CONSTRICTIVE PERICARDITIS

Constrictive pericarditis is characterized by a thickened and fibrotic pericardium that restricts ventricular filling (Fig. 62.15). While focal constriction has been reported, the constrictive process usually involves the entire pericardium. Constrictive pericarditis can develop as an idiopathic process, but most commonly represents the end stage of various forms of pericarditis (105,106). Worldwide, tuberculous pericarditis is the most common cause of constrictive pericarditis (43).

With constriction, diastolic expansion of the ventricles is limited causing hemodynamic compromise. Early diastolic filling will be normal, with limited mid and late diastolic filling. Ventricular systolic function generally is normal. Pulmonary wedge and central venous pressures are increased due to elevated ventricular filling pressures (107). Patients may have dyspnea, fatigue, exercise intolerance, or syncope. Hepatomegaly, splenomegaly, jugular venous distension, edema, or ascites may occur. Auscultation may reveal a diastolic filling sound corresponding to abrupt cessation of ventricular filling ("precordial knock") (105,108). Chest radiography may be normal or may display pericardial calcification in 25% of patients (Fig. 62.3) (15). The electrocardiogram often is non-specific, but may demonstrate low-voltage QRS complexes and ST-segment of T-wave abnormalities.

Echocardiography shows paradoxical septal motion with a septal "bounce." The "bounce" refers to the septum shifting leftward with increased RV filling during inspiration, and then shifting back rightward with expiration due to improved LV filling. The superior and inferior vena cavae may be dilated due to elevated ventricular diastolic and central venous pressures. Subcostal imaging may demonstrate "diaphragmatic tethering," where the diaphragm is pulled toward the heart with each ventricular contraction. Doppler echocardiography demonstrates marked respiratory variation of both left- and right-sided flows (Fig. 62.16) (109). With inspiration, there is an exaggerated decrease in the mitral inflow velocity (mitral E velocity) and an exaggerated increase in tricuspid inflow velocity (tricuspid E velocity) (109). Conversely, in expiration, there is an exaggerated increase in mitral inflow velocity and an exaggerated decrease in tricuspid inflow velocity.

CT and MRI may reveal pericardial thickening and/or calcification (20). Cardiac catheterization demonstrates equalization of LV and RV end-diastolic pressures, left and right mean atrial pressures, and the mean pulmonary capillary wedge pressure. The "square root sign" refers to the early diastolic pressure decrease followed by a plateau on LV and RV pressure tracings, and results from rapid early diastolic filling with abrupt cessation (Fig. 62.12). The definitive treatment for constrictive pericarditis is radical pericardiectomy (96,108).



Figure 62.15. Severe constrictive pericarditis. Note the markedly thickened pericardium in this ventricular short-axis slice. (Courtesy of Dr. William D. Edwards, Division of Anatomic Pathology, Mayo Clinic, Rochester, MN.)

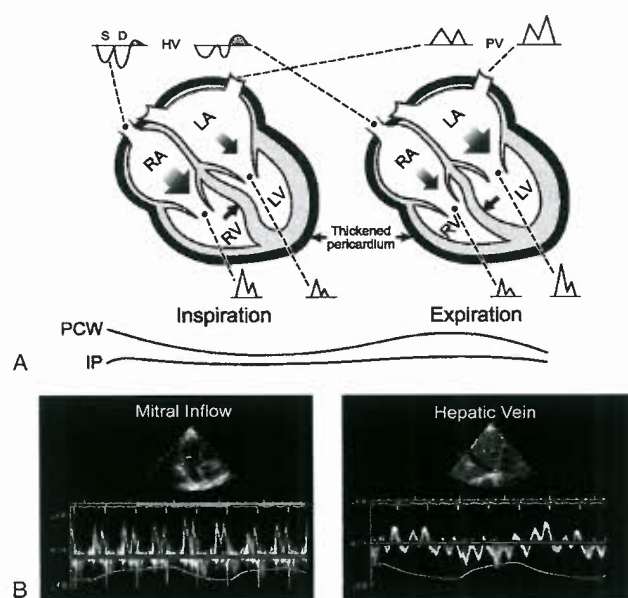


Figure 62.16. Hemodynamic filling patterns in constriction. These diagrams illustrate a patient with constrictive pericarditis and the corresponding Doppler echocardiographic patterns with inspiration and expiration. Note the (A) respiratory variation in ventricular filling and the corresponding Doppler features of mitral and tricuspid valve inflow and pulmonary vein (PV) and hepatic vein (HV) flow. B: Typical mitral inflow and hepatic vein pulsed-wave Doppler recordings in constriction. Inspiration starts with the upward deflection of the respirometer tracing, while expiration starts with the downward deflection of the tracing. Note the decrease in mitral inflow E velocity with inspiration, and increase with the onset of expiration (*left frame*). In hepatic vein flow, there is a prominent diastolic flow reversal with expiration. (Adapted from Oh JK. *The Echo Manual*, 3rd ed. Philadelphia, PA: Lippincott Williams & Wilkins, 2006.)

Differentiating Between Constrictive Pericarditis and Restrictive Cardiomyopathy

Restrictive cardiomyopathy commonly is an infiltrative process and includes amyloidosis, hemochromatosis, endomyocardial fibrosis, and eosinophilic cardiomyopathy. It may be idiopathic (110,111). Restrictive cardiomyopathy is characterized by markedly abnormal diastolic function with preserved systolic function.

The differentiation between constrictive pericarditis and restrictive cardiomyopathy often is difficult (107,112–114). Echocardiographic measurements of diastolic function in children often are confounded by factors including preload, heart rate, age, and body size (115). Differentiating between constriction and restriction is critical, since the definitive treatments for these disorders are markedly disparate (pericardiectomy vs. cardiac transplant) (Table 62.5).

Cardiac catheterization can be useful in differentiating constriction from restriction (Fig. 62.17) (107). In constrictive pericarditis, there is an inspiratory increase in the area of the RV pressure curve compared with expiration. The area of the LV pressure curve decreases during inspiration as compared with expiration. Conversely, in restrictive cardiomyopathy, there is an inspiratory decrease in the area of the RV pressure curve as compared with expiration. The area of the LV pressure curve is unchanged during inspiration as compared with expiration. Talreja et al. (107) have described a catheterization-based calculation called the *systolic area index*, which is obtained by taking the ratio of the area under the RV pressure curve to the area under the LV pressure curve in inspiration versus expiration (calculated as $(RV_{insp}/LV_{insp})/(RV_{exp}/LV_{exp})$) (Fig. 62.17). A systolic area index value >1.1 was 97% sensitive and 100% specific for diagnosing constrictive pericarditis. This study only evaluated adult patients and requires validation in a pediatric cohort.

Echocardiographic differentiation between constriction and restriction includes the factors listed in Table 62.5 and those depicted graphically in Figure 62.18. The characteristic

TABLE 62.5

Distinguishing Constrictive Pericarditis and Restrictive Cardiomyopathy

Finding	Constriction	Restriction
History of Cardiac Surgery	Common	Uncommon
Echo: Septal “bounce”	Common	Typically absent
Echo: Atrial size	Normal/mildly enlarged	Significantly enlarged
Echo: Systolic function	Typically normal	Normal or mildly decreased
Echo: Wall thickness	Normal	Normal or increased
Echo: Doppler changes with inspiration/expiration	Significant and common	Rare
CT: Pericardial thickening	Common	Typically absent
Cath: RVSP	<50 mm Hg	>50 mm Hg
Cath: LVEDP – RVEDP	<4 mm Hg	>4 mm Hg
Cath: Wedge pressure – RA pressure	<4 mm Hg	>4 mm Hg
Cath: RVEDP/RVSP	>0.33	<0.3
Cath: Systolic area index	>1.1	<1.1

RVSP, right ventricular systolic pressure; RVEDP, right ventricular end-diastolic pressure; LVEDP, left ventricular end-diastolic pressure; RA, right atrium.

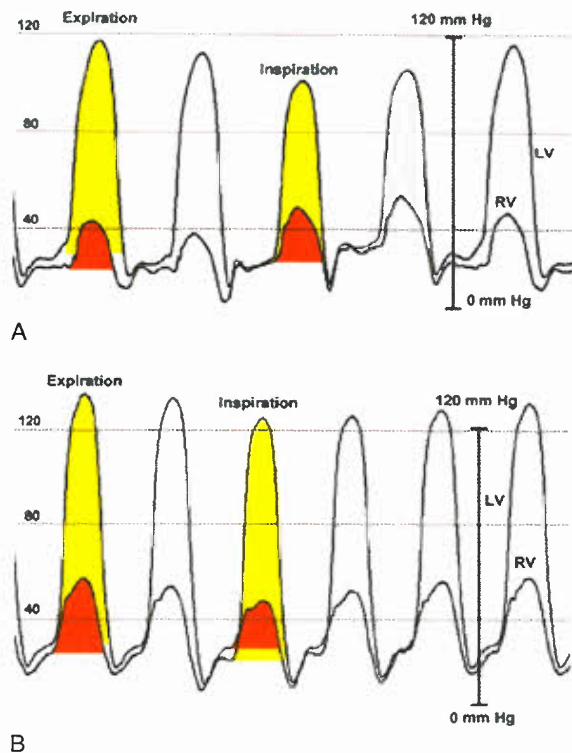


Figure 62.17. Catheterization tracings in constrictive physiology (A) and restrictive cardiomyopathy (B). Note that both patients have early rapid filling with elevation and equalization of the left ventricular (LV) and right ventricular (RV) pressures at end expiration. In constrictive pericarditis, there is an inspiratory increase in the area of the RV pressure curve (orange shaded area) compared with expiration. The area of the LV pressure curve (yellow shaded area) decreases during inspiration as compared with expiration. Conversely, in restrictive cardiomyopathy, there is an inspiratory decrease in the area of the RV pressure curve (orange shaded area) as compared with expiration. The area of the LV pressure curve (yellow shaded area) is unchanged during inspiration as compared with expiration. (Reprinted from Talreja DR, Nishimura RA, Oh JK, et al. Constrictive pericarditis in the modern era. *J Am Coll Cardiol* 2008;51:317, with permission from Elsevier).

septal “bounce” occurs more commonly in constriction, while severe atrial enlargement is more typically observed in restriction. Doppler velocities, including mitral inflow, hepatic venous flow, tricuspid inflow, and pulmonary venous inflow, are affected by respiration in constriction. There may be a relatively normal peak mitral valve E velocity during expiration in constriction or restriction. These mitral valve signals can be differentiated by the respiratory variation that occurs in constriction (increased E velocity during expiration), and the short deceleration time (DT) that occurs in restriction. Normally, hepatic vein Doppler waveforms will demonstrate larger systolic and diastolic forward flow waves compared to small systolic flow reversal and diastolic flow reversal waves. In constriction, decreased LV filling on inspiration allows for increased RV filling, causing hepatic vein diastolic forward flow to increase. In expiration, hepatic vein diastolic forward flow decreases, and significant flow reversals in diastole may occur. Thus, in patients with constriction, the flow may appear normal with inspiration, while marked diastolic reversals will be seen with expiration (Fig. 62.18). Conversely, in restriction, marked reversals in the hepatic veins occur with inspiration, and may occur in both systole and diastole. Mitral, tricuspid, and pulmonary vein velocities rarely are affected by respiration in patients with pure restriction. Importantly, the

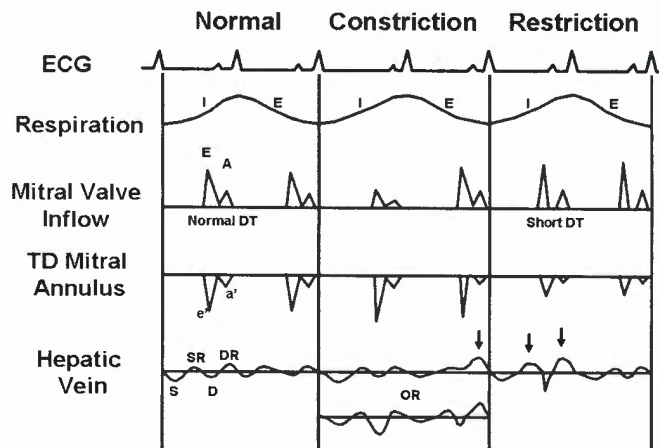


Figure 62.18. Diagram of Doppler velocities from mitral inflow (MV), mitral annulus velocity, and hepatic vein (HV), and the ECG and respirometer recordings indicating inspiration (I) and expiration (E). Note the relatively similar peak mitral valve E velocity in normal, constriction, and restriction in expiration. The striking difference is the respiratory variation seen in constriction, with increased E velocity during expiration, and the short deceleration time (DT) seen in restriction. Patients with constriction will have normal or even increased tissue Doppler (TD) early diastolic mitral annulus (e') velocities, compared to patients with restriction, whose e' velocities are markedly blunted, typically below 8 cm/s. Examining hepatic vein flow, the normal patient will have larger systolic (S) and diastolic (D) flow waves compared to tiny insignificant systolic flow reversal (SR) and diastolic flow reversal (DR) waves. In patients with constriction, marked diastolic reversals will be seen with expiration (arrow), while the flow may appear normal with inspiration. Conversely, in restriction, marked reversals in the hepatic veins are typically seen with inspiration, and may occur in both systole and diastole (arrows). (Modified from Oh JK. *The Echo Manual*, 3rd ed. Philadelphia, PA: Lippincott Williams & Wilkins, 2006.)

diastolic flow reversals seen on expiration in constriction may not be evident in patients with tachycardia or atrial fibrillation. In these situations, augmented systolic reversals actually may be seen on expiration instead of prominent diastolic reversals.

Tissue Doppler imaging can be helpful in the differentiation of constriction and restriction (Fig. 62.18). In normal pediatric subjects beyond infancy, the early diastolic septal mitral annulus velocity (e') should be between 9 and 16 cm/s. In constriction, the e' velocity is normal or even increased as compared to normal. In restriction, the e' velocity often is <8 cm/s (similar to other cardiomyopathies) (15,116). In normal hearts, the lateral mitral annulus e' velocity is greater than the septal mitral annulus e' velocity. But, in constriction, the septal mitral annulus e' velocity can be greater than or equal to the lateral mitral annulus e' velocity, a paradoxical finding called *mitral annulus reversal* (117). This reversal of mitral annulus velocities is not seen in patients with restrictive cardiomyopathy.

Special Circumstances

Ventilator-Dependent Patient

During normal breathing, there is a decrease in intrathoracic pressure with inspiration and an increase with expiration. During positive pressure mechanical ventilation, the intrathoracic pressure changes are opposite those that occur with spontaneous breathing. Mechanical inflation of the lungs causes an

increase in intrathoracic pressure (118). As a result, the prominent Doppler respiratory variation in patients with constrictive pericarditis reverses during positive pressure ventilation, with mitral and pulmonary vein inflow velocities increasing during inspiration and decreasing in expiration (119).

Single-Ventricle Patient

The diagnosis of constriction in patients with single ventricle can be difficult. The traditional echocardiographic and catheter based methods rely on assessment of interventricular hemodynamics. With single ventricle patients, symptoms of dyspnea, fatigue, or exercise intolerance may be present, along with signs of venous congestion such as hepatomegaly, splenomegaly, jugular venous distension, and edema even in the absence of constriction. Evaluation of pericardial thickness by CT or MRI may provide the only specific findings for constriction. Constriction may cause protein-losing enteropathy after Fontan operation (120). It is important to consider constriction as a potential etiology in a patient after Fontan operation who presents with new-onset protein-losing enteropathy, since pericardiectomy could be curative (121).

ACKNOWLEDGMENTS

The authors would like to thank Dr. Philip Young, MD and Dr. Patrick O'Leary, MD for their assistance with this chapter.

REFERENCES

- Spodick DH. Macrophysiology, microphysiology, and anatomy of the pericardium: a synopsis. *Am Heart J* 1992;124:1046-1051.
- Ishihara T, Ferrans VJ, Jones M, et al. Histologic and ultrastructural features of normal human parietal pericardium. *Am J Cardiol* 1980;46:744-753.
- Shabetai R, Fowler NO, Guntheroth WG. The hemodynamics of cardiac tamponade and constrictive pericarditis. *Am J Cardiol* 1970;26:480-489.
- Troughton RW, Asher CR, Klein AL. Pericarditis. *Lancet* 2004;363:717-727.
- Lange RA, Hillis LD. Clinical practice: acute pericarditis. *N Engl J Med* 2004;351:2195-2202.
- Dressler W. Effect of respiration on the pericardial friction rub. *Am J Cardiol* 1961;7:130-131.
- Holldack K, Heller A, Groth W. The pericardial friction rub in the phonocardiogram. *Am J Cardiol* 1959;4:351-355.
- Farringer JL Jr, Carr D. Cardiac tamponade. *Ann Surg* 1955;141:437-442.
- Jacob S, Sebastian JC, Cherian PK, et al. Pericardial effusion impending tamponade: a look beyond Beck's triad. *Am J Emerg Med* 2009;27:216-219.
- Golinko RJ, Kaplann N, Rudolph AM. The mechanism of pulsus paradoxus during acute pericardial tamponade. *J Clin Invest* 1963;42:249-257.
- Spodick DH. The electrocardiogram in acute pericarditis. In: Spodick DH, ed. *Acute Pericarditis*. New York, NY: Grune & Stratton, 1959:17.
- Maisch B, Seferovic PM, Ristic AD, et al. Guidelines on the diagnosis and management of pericardial diseases executive summary; the Task force on the diagnosis and management of pericardial diseases of the European society of cardiology. *Eur Heart J* 2004;25:587-610.
- Pepi M, Muratori M. Echocardiography in the diagnosis and management of pericardial disease. *J Cardiovasc Med (Hagerstown)* 2006;7:533-544.
- Berger M, Bobak L, Jelveh M, et al. Pericardial effusion diagnosed by echocardiography. Clinical and electrocardiographic findings in 171 patients. *Chest* 1978;74:174-179.
- Grogan M, Oh JK. Pericardial disorders. In: Eidem BW, Cetia F, O'Leary PW, eds. *Echocardiography in Pediatric and Adult Congenital Heart Disease*. Philadelphia, PA: Lippincott Williams & Wilkins, 2010.
- Fowler NO. Cardiac tamponade: a clinical or an echocardiographic diagnosis? *Circulation* 1993;87:1738-1741.
- Leeman DE, Levine MJ, Come PC. Doppler echocardiography in cardiac tamponade: exaggerated respiratory variation in transvalvular blood flow velocity integrals. *J Am Coll Cardiol* 1988;11:572-578.
- Vignola PA, Pohost GM, Curfman GD, et al. Correlation of echocardiographic and clinical findings in patients with pericardial effusion. *Am J Cardiol* 1976;37:701-707.
- Myers RB, Spodick DH. Constrictive pericarditis: clinical and pathophysiological characteristics. *Am Heart J* 1999;138:219-232.
- Wang ZJ, Reddy GP, Gotway MB, et al. CT and MR imaging of pericardial disease. *Radiographics* 2003;23:S167-S180.
- Cooper FW, Stead EA, Warren JV. The beneficial effect of intravenous infusions in acute pericardial tamponade. *Ann Surg* 1944;120:822-825.
- Tsang TS, El-Najdawi EK, Seward JB, et al. Percutaneous echocardiographically guided pericardiocentesis in pediatric patients: evaluation of safety and efficacy. *J Am Soc Echocardiogr* 1998;11:1072-1077.
- Callahan JA, Seward JB, Nishimura RA, et al. Two-dimensional echocardiographically guided pericardiocentesis: experience in 117 consecutive patients. *Am J Cardiol* 1985;55:476-479.
- Kopecky SL, Callahan JA, Tajik AJ, et al. Percutaneous pericardial catheter drainage: report of 42 consecutive cases. *Am J Cardiol* 1986;58:633-635.
- Ben-Horin S, Shinfeld A, Kachel E, et al. The composition of normal pericardial fluid and its implications for diagnosing pericardial effusions. *Am J Med* 2005;118:636-640.
- Martinez-Vazquez JM, Ribera E, Ocana I, et al. Adenosine deaminase activity in tuberculous pericarditis. *Thorax* 1986;41:888-889.
- Levin BH, Aaron BL. The subxiphoid pericardial window. *Surg Gynecol Obstet* 1982;155:804-806.
- Picardi EJ, Bedingfield J, Statz M, et al. Laparoscopic pericardial window. *Surg Laparosc Endosc* 1997;7:320-323.
- Piehl J, Pluth JR, Schaff HV, et al. Surgical management of effusive pericardial disease: influence of extent of pericardial resection on clinical course. *J Thorac Cardiovasc Surg* 1985;90:506-516.
- Fujioka S, Koide H, Kitaura Y, et al. Molecular detection and differentiation of enteroviruses in endomyocardial biopsies and pericardial effusions from dilated cardiomyopathy and myocarditis. *Am Heart J* 1996;131:760-765.
- Shimizu C, Rambaud C, Cheron G, et al. Molecular identification of viruses in sudden infant death associated with myocarditis and pericarditis. *Pediatr Infect Dis J* 1995;14:584-588.
- Satoh T, Kojima M, Ohshima K. Demonstration of the Epstein-Barr genome by the polymerase chain reaction and in situ hybridisation in a patient with viral pericarditis. *Br Heart J* 1993;69:563-564.
- Imazio M, Bobbio M, Cecchi E, et al. Colchicine in addition to conventional therapy for acute pericarditis: results of the COLchicine for acute Pericarditis (COPE) trial. *Circulation* 2005;112:2012-2016.
- Feldman WE. Bacterial etiology and mortality of purulent pericarditis in pediatric patients: review of 162 cases. *Am J Dis Child* 1979;133:641-644.
- Wyller F, Knusli D, Rutishauser M, et al. Pericarditis purulenta in children. *Helv Paediatr Acta* 1977;32:135-140.
- Roodpeyma S, Sadeghian N. Acute pericarditis in childhood: a 10-year experience. *Pediatr Cardiol* 2000;21:363-367.
- Cakir O, Gurkan F, Balci AE, et al. Purulent pericarditis in childhood: ten years of experience. *J Pediatr Surg* 2002;37:1404-1408.
- Pinsky W, Friedman R, Jubelirer D, et al. Infectious pericarditis. In: Feigin RD, Cherry JD, eds. *Textbook of Pediatric Infectious Diseases*. Philadelphia, PA: WB Saunders, 1992:377.
- Pankuweit S, Ristic AD, Seferovic PM, et al. Bacterial pericarditis: diagnosis and management. *Am J Cardiovasc Drugs* 2005;5:103-112.
- Ustunsoy H, Celkan MA, Sivrikov MC, et al. Intrapericardial fibrinolytic therapy in purulent pericarditis. *Eur J Cardiothorac Surg* 2002;22:373-376.
- Dupuis C, Gronnier P, Kachaner J, et al. Bacterial pericarditis in infancy and childhood. *Am J Cardiol* 1994;74:807-809.
- Van Reken D, Strauss A, Hernandez A, et al. Infectious pericarditis in children. *J Pediatr* 1974;85:165-169.
- Mayosi BM, Burgess LJ, Doubell AF. Tuberculous pericarditis. *Circulation* 2005;112:3608-3616.
- Arroyo M, Soberman JE. Adenosine deaminase in the diagnosis of tuberculous pericardial effusion. *Am J Med Sci* 2008;335:227-229.
- Ntsekhe M, Wiysonge C, Volmink JA, et al. Adjuvant corticosteroids for tuberculous pericarditis: promising, but not proven. *QJM* 2003;96:593-599.
- Bozbuga N, Erentug V, Eren E, et al. Pericardiectomy for chronic constrictive tuberculous pericarditis: risks and predictors of survival. *Tex Heart Inst J* 2003;30:180-185.
- Lipshultz SE, Chanock S, Sanders SP, et al. Cardiovascular manifestations of human immunodeficiency virus infection in infants and children. *Am J Cardiol* 1989;63:1489-1497.
- Starc TJ, Lipshultz SE, Kaplan S, et al. Cardiac complications in children with human immunodeficiency virus infection: pediatric pulmonary and cardiac complications of vertically transmitted HIV infection (P2C2 HIV) Study Group, National Heart, Lung, and Blood Institute. *Pediatrics* 1999;104:e14.
- Mast HL, Haller JO, Schiller MS, et al. Pericardial effusion and its relationship to cardiac disease in children with acquired immunodeficiency syndrome. *Pediatr Radiol* 1992;22:548-551.
- Persellin ST, Ramirez G, Moatamed F. Immunopathology of rheumatic pericarditis. *Arthritis Rheum* 1982;25:1054-1058.
- Renfrew R, Buselmeier TJ, Kjellstrand CM. Pericarditis and renal failure. *Annu Rev Med* 1980;31:345-360.
- Ozdogu H, Boga C. Fatal cardiac tamponade in a patient with Kawasaki disease. *Heart Lung* 2005;34:257-259.
- Newburger JW, Takahashi M, Gerber MA, et al. Diagnosis, treatment, and long-term management of Kawasaki disease: a statement for health professionals from the Committee on Rheumatic Fever, Endocarditis and Kawasaki Disease, Council on Cardiovascular Disease in the Young, American Heart Association. *Circulation* 2004;110:2747-2771.

54. Rheuban KS. Pericarditis. *Curr Treat Options Cardiovasc Med* 2005;7:419-427.
55. Schoenwetter AH, Siber EN. Penicillin hypersensitivity, Acute pericarditis, and eosinophilia. *JAMA* 1965;191:672-673.
56. Slater EE. Cardiac tamponade and peripheral eosinophilia in a patient receiving cromolyn sodium. *Chest* 1978;73:878-879.
57. Chou SL, Chern CH, How CK, et al. A rare case of massive pericardial effusion secondary to hypothyroidism. *J Emerg Med* 2005;28:293-296.
58. Manolis AS, Variale P, Ostrowski RM. Hypothyroid cardiac tamponade. *Arch Intern Med* 1987;147:1167-1169.
59. Campbell RM, Benson LN, Williams WW, et al. Chylopericardium after cardiac operations in children. *Ann Thorac Surg* 2001;72:193-196.
60. Kanemoto S, Abe M, Ikeda A, et al. Recurrent symptomatic chylopericardium after cardiac surgery in a child. *Pediatr Cardiol* 2008;29:683-685.
61. Helin RD, Angeles ST, Bhat R. Octreotide therapy for chylothorax in infants and children: a brief review. *Pediatr Crit Care Med* 2006;7:576-579.
62. McAllister HA Jr. Primary tumors and cysts of the heart and pericardium. *Curr Probl Cardiol* 1979;4:1-51.
63. Almeda FQ, Adler S, Rosenson RS. Metastatic tumor infiltration of the pericardium masquerading as pericardial tamponade. *Am J Med* 2001;111:504-505.
64. Lam KY, Dickens P, Chan AC. Tumors of the heart: a 20-year experience with a review of 12,485 consecutive autopsies. *Arch Pathol Lab Med* 1993;117:1027-1031.
65. Thurber DL, Edwards JE, Achor RW. Secondary malignant tumors of the pericardium. *Circulation* 1962;26:228-241.
66. de Vreede I, Bilardo CM, van Rijn RR, et al. Intrapericardial extralobar pulmonary sequestration presenting as a prenatal intrathoracic mass. *Pediatr Cardiol* 2008;29:980-982.
67. Pratt JW, Cohen DM, Murabagani KH, et al. Neonatal intrapericardial teratomas: clinical and surgical considerations. *Cardiol Young* 2000;10:27-31.
68. Snyder SN. Massive pericardial coelomic cyst: diagnostic features and unusual presentation. *Chest* 1977;71:100-102.
69. Buyers RA, Emery FB. Pericardial celomic cysts; review of the literature and report of a case. *Arch Surg* 1950;60:1002-1005.
70. Kavunkal AM, Ramkumar J, Gangahanumiah S, et al. Isolated mediastinal cystic lymphangioma in a child. *J Thorac Cardiovasc Surg* 2007;134:1596-1597.
71. Rheuban KS, McDaniel NL, Feldman PS, et al. Intrapericardial teratoma causing nonimmune hydrops fetalis and pericardial tamponade: a case report. *Pediatr Cardiol* 1991;12:54-56.
72. Posner MR, Cohen GI, Skarin AT. Pericardial disease in patients with cancer: the differentiation of malignant from idiopathic and radiation-induced pericarditis. *Am J Med* 1981;71:407-413.
73. Carmel RJ, Kaplan HS. Mantle irradiation in Hodgkin's disease: an analysis of technique, tumor eradication, and complications. *Cancer* 1976;37:2813-2825.
74. Lee PJ, Mallik R. Cardiovascular effects of radiation therapy: practical approach to radiation therapy-induced heart disease. *Cardiol Rev* 2005;13:80-86.
75. Morton DL, Glancy DL, Joseph WL, et al. Management of patients with radiation-induced pericarditis with effusion: a note on the development of aortic regurgitation in two of them. *Chest* 1973;64:291-297.
76. Biran S. Corticosteroids in radiation-induced pericarditis. *Chest* 1978;74:96-98.
77. Clapp SK, Garson A Jr, Gutgesell HP, et al. Postoperative pericardial effusion and its relation to postpericardiotomy syndrome. *Pediatrics* 1980;66:585-588.
78. Hammel CL, Lyons WS. Postpericardiotomy syndrome. *Am J Dis Child* 1962;104:385-390.
79. Engle MA, Zabriskie JB, Senterfit LB, et al. Viral illness and the postpericardiotomy syndrome: a prospective study in children. *Circulation* 1980;62:1151-1158.
80. Scarfone RJ, Donoghue AJ, Alessandrini EA. Cardiac tamponade complicating postpericardiotomy syndrome. *Pediatr Emerg Care* 2003;19:268-271.
81. Maisch B, Berg PA, Kochsiek K. Clinical significance of immunopathological findings in patients with post-pericardiotomy syndrome. I: relevance of antibody pattern. *Clin Exp Immunol* 1979;38:189-197.
82. Mason TG, Neal WA, DiBartolomeo AG. Elevated antinuclear antibody titers and the postpericardiotomy syndrome. *J Pediatr* 1990;116:403-404.
83. Dressler W. A post-myocardial infarction syndrome; preliminary report of a complication resembling idiopathic, recurrent, benign pericarditis. *J Am Med Assoc* 1956;160:1379-1383.
84. Cabalka AK, Rosenblatt HM, Towbin JA, et al. Postpericardiotomy syndrome in pediatric heart transplant recipients: immunologic characteristics. *Tex Heart Inst J* 1995;22:170-176.
85. Engle MA, Zabriskie JB, Senterfit LB, et al. Postpericardiotomy syndrome: a new look at an old condition. *Mod Concepts Cardiovasc Dis* 1975;44:59-64.
86. Lessof MH. Postcardiotomy syndrome: pathogenesis and management. *Hosp Pract* 1976;11:81-86.
87. Wilson NJ, Webber SA, Patterson MW, et al. Double-blind placebo-controlled trial of corticosteroids in children with postpericardiotomy syndrome. *Pediatr Cardiol* 1994;15:62-65.
88. McCabe JC, Engle MA, Ebert PA. Chronic pericardial effusion requiring pericardiectomy in the postpericardiotomy syndrome. *J Thorac Cardiovasc Surg* 1974;67:814-817.
89. Maisch B, Ristic AD. Practical aspects of the management of pericardial disease. *Heart* 2003;89:1096-1103.
90. Yeh TT, Yang YH, Lin YT, et al. Cardiopulmonary involvement in pediatric systemic lupus erythematosus: a twenty-year retrospective analysis. *J Microbiol Immunol Infect* 2007;40:525-531.
91. Brigden W, Bywaters EG, Lessof MH, et al. The heart in systemic lupus erythematosus. *Br Heart J* 1960;22:1-16.
92. Yancey CL, Dougherty RA, Cohlman BA, et al. Pericarditis and cardiac tamponade in juvenile rheumatoid arthritis. *Pediatrics* 1981;68:369-373.
93. Shabetai R. Recurrent pericarditis: recent advances and remaining questions. *Circulation* 2005;112:1921-1923.
94. Imazio M, Demicheli B, Parrini I, et al. Management, risk factors, and outcomes in recurrent pericarditis. *Am J Cardiol* 2005;96:736-739.
95. Maisch B. Recurrent pericarditis: mysterious or not so mysterious? *Eur Heart J* 2005;26:631-633.
96. Thompson JL, Burkhart HM, Dearani JA, et al. Pericardiectomy for pericarditis in the pediatric population. *Ann Thorac Surg* 2009;88:1546-1550.
97. Peterlana D, Puccetti A, Simeoni S, et al. Efficacy of intravenous immunoglobulin in chronic idiopathic pericarditis: report of four cases. *Clin Rheumatol* 2005;24:18-21.
98. Abbas AE, Appleton CP, Liu PT, et al. Congenital absence of the pericardium: case presentation and review of literature. *Int J Cardiol* 2005;98:21-25.
99. Gatzoulis MA, Munk MD, Merchant N, et al. Isolated congenital absence of the pericardium: clinical presentation, diagnosis, and management. *Ann Thorac Surg* 2000;69:1209-1215.
100. Connolly HM, Click RL, Schattenberg TT, et al. Congenital absence of the pericardium: echocardiography as a diagnostic tool. *J Am Soc Echocardiogr* 1995;8:87-92.
101. Le Roux BT. Pericardial coelomic cysts. *Thorax* 1959;14:27-35.
102. Satur CM, Hsin MK, Dussek JE. Giant pericardial cysts. *Ann Thorac Surg* 1996;61:208-210.
103. Elamin WF, Hannan K. Pericardial cyst: an unusual cause of pneumonia. *Cases J* 2008;1:26.
104. Imazio M, Demicheli B, Parrini I, et al. Relation of acute pericardial disease to malignancy. *Am J Cardiol* 2005;95:1393-1394.
105. Strauss AW, Santa-Maria M, Goldring D. Constrictive pericarditis in children. *Am J Dis Child* 1975;129:822-826.
106. Schewefer M, Aschenbach R, Heidemann J, et al. Constrictive pericarditis, still a diagnostic challenge: comprehensive review of clinical management. *Eur J Cardiothorac Surg* 2009;36:502-510.
107. Talreja DR, Nishimura RA, Oh JK, et al. Constrictive pericarditis in the modern era: novel criteria for diagnosis in the cardiac catheterization laboratory. *J Am Coll Cardiol* 2008;51:315-319.
108. Chen CA, Lin MT, Wu ET, et al. Clinical manifestations and outcomes of constrictive pericarditis in children. *J Formos Med Assoc* 2005;104:402-407.
109. Oh JK, Hatle LK, Seward JB, et al. Diagnostic role of Doppler echocardiography in constrictive pericarditis. *J Am Coll Cardiol* 1994;23:154-162.
110. Ammash NM, Seward JB, Bailey KR, et al. Clinical profile and outcome of idiopathic restrictive cardiomyopathy. *Circulation* 2000;101:2490-2496.
111. Cetta F, O'Leary PW, Seward JB, et al. Idiopathic restrictive cardiomyopathy in childhood: diagnostic features and clinical course. *Mayo Clin Proc* 1995;70:634-640.
112. Nishimura RA. Constrictive pericarditis in the modern era: a diagnostic dilemma. *Heart* 2001;86:619-623.
113. Hatle LK, Appleton CP, Popp RL. Differentiation of constrictive pericarditis and restrictive cardiomyopathy by Doppler echocardiography. *Circulation* 1989;79:357-370.
114. Goldstein JA. Cardiac tamponade, constrictive pericarditis, and restrictive cardiomyopathy. *Curr Probl Cardiol* 2004;29:503-567.
115. O'Leary PW, Durongpisitkul K, Cordes TM, et al. Diastolic ventricular function in children: a Doppler echocardiographic study establishing normal values and predictors of increased ventricular end-diastolic pressure. *Mayo Clin Proc* 1998;73:616-628.
116. Ha JW, Ommen SR, Tajik AJ, et al. Differentiation of constrictive pericarditis from restrictive cardiomyopathy using mitral annular velocity by tissue Doppler echocardiography. *Am J Cardiol* 2004;94:316-319.
117. Reuss CS, Wilansky SM, Lester SJ, et al. Using mitral 'annulus reversus' to diagnose constrictive pericarditis. *Eur J Echocardiogr* 2009;10:372-375.
118. Santamore WP, Heckman JL, Bove AA. Cardiovascular changes from expiration to inspiration during IPPV. *Am J Physiol* 1983;245:H307-H312.
119. Abdalla IA, Murray RD, Awad HE, et al. Reversal of the pattern of respiratory variation of Doppler inflow velocities in constrictive pericarditis during mechanical ventilation. *J Am Soc Echocardiogr* 2000;13:827-831.
120. Petersen VR, Hastrup J. Protein-losing enteropathy in constrictive pericarditis. *Acta Med Scand* 1963;173:401-410.
121. Muller C, Globits S, Glogar D, et al. Constrictive pericarditis without typical haemodynamic changes as a cause of oedema formation due to protein-losing enteropathy. *Eur Heart J* 1991;12:1140-1143.

Michael Gewitz ■ Kathryn A. Taubert

Infective endocarditis (IE) is a disease that is associated with considerable morbidity and mortality and remains a dreaded complication of structural heart disease. Although relatively rare in children, this cardiac infection with protean manifestations continues to have a disproportionate influence on clinical practice. Reported mortality rates are much lower now than in the preantibiotic era; however, overall morbidity and expense burden of prolonged and often intense medical and surgical therapies remain formidable.

Major advances in understanding this disease process have been made over the years. Additionally, the development and refinement of echocardiographic techniques have contributed to better diagnosis and management of endocarditis. Increasingly precise clinical criteria for the diagnosis of IE have been established (1,2) that assist physicians in making a better objective assessment of the varied clinical manifestations of this disease process.

DEFINITION

IE is a microbial infection of the endocardial (endothelial) surface of the heart. Native or prosthetic heart valves are the most frequently involved sites. Endocarditis also can involve septal defects, the mural endocardium, or intravascular foreign devices such as intracardiac patches, surgically constructed shunts, and intravenous catheters. Infective endarteritis is a similar clinical illness involving arteries, including the ductus arteriosus, the great vessels, aneurysms, or arteriovenous shunts.

At one time, endocarditis was classified as acute or subacute, but the recent tendency has been to avoid this terminology. It is preferable to describe the disease based on the etiologic agent involved. Low-virulence organisms such as α -hemolytic streptococci, enterococci, or coagulase-negative staphylococci usually cause a prolonged subacute form of the illness. On the other hand, *Staphylococcus aureus* and other pyogenic bacteria, such as *Streptococcus pneumoniae* or β -hemolytic streptococci, are usually associated with a more virulent or acute clinical illness.

EPIDEMIOLOGY

The epidemiology of heart disease in children has changed during the past several decades as has the epidemiology of IE itself. While it is difficult to get exact incidence data for IE because it is not a notifiable disease, the incidence is believed to have increased since the mid-1900s. The reported U.S. incidence from the early 1980s was approximately 1 in 1,280 (3). In a review of several published studies between 1986 and 1995, the estimated incidence in children overall was 0.3 per 100,000 children per year with a mortality of 11.6% (4).

The apparent increase in the incidence of IE in children reflects increased survival of patients with cardiovascular disease, paralleling advances in surgical and medical approaches to congenital heart disease (CHD) during the past several decades as well as to aggressive treatment regimens in neonatal and pediatric intensive care units. Whereas rheumatic heart disease was a major underlying cardiac condition in U.S. children with endocarditis until the 1970s, it has become an unusual underlying cardiac condition in more recent years. This is not true in developing countries, where endocarditis remains an important complicating factor in individuals with rheumatic heart disease.

CHD conditions, such as ventricular septal defect, patent ductus arteriosus, aortic valve abnormalities, and tetralogy of Fallot, are now the more common underlying conditions. An increasing proportion of children with IE have had previous corrective or palliative surgery for CHD, with or without implanted vascular grafts, patches, or prosthetic cardiac valves (5), and various reports have indicated that 50% to 70% of children with CHD have had previous cardiac surgery (3,6–9).

In neonatal IE, most cases occur in structurally normal hearts. Although relatively uncommon, increasing numbers of cases of neonatal IE have been reported since the 1970s. This reflects marked increases in cardiovascular interventions (surgical and nonsurgical) in newborns and young infants with concomitant increased use of prosthetic intravascular devices and insertion of long-term indwelling central venous catheters (5).

Patients with underlying cardiovascular disease may develop endocarditis at any age—in childhood, adolescence, or adulthood. In a pooled series of 723 children with congenital heart defects who developed endocarditis, the defects most frequently associated with IE were ventricular septal defect, tetralogy of Fallot, and aortic stenosis (6). Two recent, important reviews have characterized these epidemiologic changes succinctly. Yoshinaga et al. (10) identified increasing morbidity and mortality from IE in infants with CHD under 1 year of age. Rosenthal et al. (11) also found that it is younger children with CHD, especially those who have undergone surgical treatment, who constitute increasing number of IE patients as compared to earlier health care eras.

MICROORGANISMS

Most cases of endocarditis are caused by a relatively small number of microorganisms (Table 63.1). Experimental data and clinical observations indicate that some bacteria are more commonly associated with endocarditis than others. One of the most logical and intriguing explanations relates to bacterial adherence. Following careful *in vitro* studies, Gould et al. (12) found that bacteria most frequently responsible for endocarditis (e.g., viridans streptococci) display a propensity for

TABLE 63.1

Etiologic Agents of Infective Endocarditis in Infants and Children

Agent	Frequency
Streptococci	
α -Hemolytic	Most common
β -Hemolytic	Uncommon
Enterococci	Rare
Pneumococci	Rare
Others	Uncommon
Staphylococci	
<i>S. aureus</i>	Second most common
Coagulase negative	Uncommon, but increasing
Gram-negative agents	
Enterics	Rare
<i>Pseudomonas</i> species	Rare
HACEK ^a	Rare
<i>Neisseria</i> species	Rare
Fungi	
<i>Candida</i> species	Uncommon
Others	Rare

^a*Haemophilus, Actinobacillus, Cardiobacterium, Eikenella, Kingella.*

adherence to canine or human valves. In contrast, gram-negative organisms, seldom responsible for endocarditis, adhere rather poorly in this *in vitro* system.

Gram-positive cocci account for about 90% of recoverable bacteria in adult patients. Viridans group streptococci are responsible for most cases of endocarditis in all age groups in developing countries where, as a predisposing condition, rheumatic heart disease is prevalent. Staphylococci (*S. aureus* and coagulase-negative staphylococci) may account for more cases than do viridans group streptococci in developed countries where health care-associated infections are becoming more prevalent (13).

Similar trends have been noted in the pediatric age group (5,6,9,14). One study examined the prevalence of IE among children with *S. aureus* bacteremia. The prevalence of definite IE was approximately 12%, and definite or possible IE was 20%. Most of these children developed bacteremia from an infected intravascular device (15). Overall, enterococcal endocarditis occurs much less frequently in children than in adults.

Gram-negative organisms cause <10% of the endocarditis in children. However, neonates, immunocompromised patients, and injection drug users (IDUs) are at an increased risk for Gram-negative bacterial endocarditis. Among the fastidious Gram-negative bacilli of the HACEK group (*Haemophilus parainfluenzae*, *H. aphrophilus*, *H. paraphrophilus*, *H. influenzae*, *Actinobacillus actinomycetemcomitans*, *Cardiobacterium hominis*, *Eikenella corrodens*, *Kingella kingae*, and *K. denitrificans*), *Haemophilus* species are more common than the others in children, frequently affect previously damaged valves, and cause a subacute course of endocarditis. Rarely, *Neisseria gonorrhoeae* can cause endocarditis, presenting as an acute illness and affecting previously normal valves. Commonly, valvular destruction results from this organism.

In IDUs, other organisms isolated include *S. aureus* and occasionally *Candida* or other fungal species.

In instances of prosthetic valve endocarditis, the infective organisms differ depending on whether endocarditis occurs early (<2 to 3 months after surgical procedure) or late. Prosthetic valve endocarditis frequently is caused by *S. aureus* or coagulase-negative staphylococci. These infections often are implanted at the time of surgery and are seen ≤ 60 days after cardiac surgery, but coagulase-negative staphylococci may be present as late as 1 year after surgery.

Anaerobic organisms rarely cause endocarditis in children. Some individuals with the clinical picture of endocarditis, but with sterile routine blood cultures, may be infected with anaerobic organisms, which are not readily recovered by the usual culture methods in the clinical laboratory.

Fungal endocarditis is relatively unusual in children although it is one of the most feared forms of endocarditis. Complications, especially embolization, are frequent. *Candida* species are the most common organisms recovered; *Aspergillus* species, *Torulopsis glabrata*, and some other fungi (*Histoplasma*, *Coccidioides*, *Cryptococcus*) also have been reported. Fungal endocarditis is often noted in narcotic addicts or after cardiac surgery, but it also occurs in immunocompromised individuals and in neonates. In neonates, this infection may be a complication of intensive care measures, including hyperalimentation fluid infusion, use of broad-spectrum antibiotics for a prolonged time, and extended use of indwelling venous catheters. The mortality rate from fungal endocarditis is high, even with intensive medical and surgical therapy (5,14).

Approximately 5% to 10% of patients with endocarditis have negative blood cultures. A diagnosis of culture-negative endocarditis is made when a patient has clinical and/or echocardiographic evidence of IE but persistently negative blood cultures. The most common causes of culture-negative IE are current or recent antibiotic therapy or infection caused by a fastidious organism that grows poorly *in vitro* (5). Many of these individuals demonstrate subsequent proof of endocarditis, either in the operating room or at necropsy. Consultation with the clinical microbiologist is invaluable in looking for unusual and fastidious organisms. The clinician should carefully evaluate such cases for the possibility of other diseases. For example, IE can be confused with other causes of postoperative fever (e.g., postpericardiotomy syndrome) and may be appropriately included in the differential diagnoses of collagen vascular diseases or even certain oncologic diseases presenting in childhood.

PATHOGENESIS

Several independent factors and events are requisites for the development of IE. A pre-existing congenital or acquired lesion of the heart or great vessels is usually present, although in some instances, such as in IDUs and in patients with intravenous catheters, endocarditis may develop in the absence of cardiovascular structural abnormalities. The sequence of events resulting in endocarditis includes damage to the endothelium, formation of nonbacterial thrombotic endocarditis (NBTE) on the surface of the damaged endothelium, occurrence of a transient bacteremia, adherence of these bacteria to the NBTE, and subsequent proliferation of the bacteria within a vegetation.

Careful clinical and pathologic studies of endocarditis have defined the underlying structural cardiac or great vessel abnormalities that are the most frequent sites of infection. The risk of endocarditis varies for different underlying conditions (Table 63.2). A review of available reports by Steckelberg and Wilson (16) suggests that the incidence of endocarditis in the general population is approximately 5 cases per 100,000

TABLE 63.2 **Relative Risk of Endocarditis for Various Cardiovascular and Underlying Conditions**

High Risk

Prosthetic valves
Previous episode of endocarditis
Complex cyanotic CHD (e.g., single-ventricle states, transposition of the great arteries, tetralogy of Fallot)
Surgically constructed systemic artery-to-pulmonary artery shunts
Injection drug use
Indwelling central venous catheters

Moderate Risk

Uncorrected patent ductus arteriosus
Uncorrected ventricular septal defect
Uncorrected atrial septal defect (other than secundum)
Bicuspid aortic valve
Mitral valve prolapse with regurgitation
Rheumatic mitral or aortic valve disease
Other acquired valvar diseases
Hypertrophic cardiomyopathy

person-years. In high-risk groups, the incidence is substantially higher (300 to 2,160 cases per 100,000 person-years). The incidence in the moderate-risk groups ranges from 50 to 440 cases per 100,000 person-years.

Virtually all vegetations occur in areas where there is a pressure gradient with resulting turbulence of blood flow. Turbulent blood flow produced by certain types of congenital or acquired heart disease, such as flow from a high- to low-pressure chamber or across a narrowed orifice (e.g., where a jet through a small ventricular septal defect hits the right ventricular wall) traumatizes the endothelium. The sites of high-velocity jets where most IE vegetations occur are most often on the atrial side of the atrioventricular valves and the ventricular side of the semilunar valves. Intact cardiac endothelium is a poor stimulator of blood coagulation and is weakly receptive to bacterial attachment, whereas damaged or denuded endothelium is a potent inducer of thrombogenesis. Thrombogenesis at such a site results in the deposition of sterile clumps of platelets, fibrin, and occasionally red blood cells and the formation of NBTE. This provides an environment to which bacteria can adhere and eventually form an infected vegetation. NBTE also can be produced in children with indwelling intravenous catheters positioned in the right side of the heart. Such catheters may traumatize the endocardium or valvular endothelium, exposing the subendothelial collagen. Much has been learned about the pathogenesis of the developing site of infection by study in experimental animals of NBTE. Use of a polyethylene catheter in the rabbit model yielded important information. Very shortly after the vascular endothelium is injured by the catheter, platelets and fibrin will adhere to the site of injury. This meshwork continues to grow with further accumulation of platelets and fibrin; very few leukocytes are involved. Following the initial deposition of platelets and fibrin, thrombus formation occurs. Certain bacteria such as staphylococci and streptococci, commonly implicated in endocarditis, are potent

stimuli of platelet aggregation. In addition, the lysosomal granules of platelets may release hydrolytic enzymes or other active proteins that may potentiate the process.

Experimental studies have shown that circulating microorganisms are entrapped within this meshwork, becoming the nidus of infection. This usually occurs distal to the pressure gradient. The exception to this is valvular aortic stenosis, where the site of the vegetation is usually on the ventricular side of the aortic valve. A possible explanation for this finding is that in almost all instances of aortic stenosis there is at least some degree of aortic insufficiency. The ability of various microorganisms to adhere to specific sites determines the location of the infection. Mediators of bacterial adherence serve as virulence factors in the pathogenesis of IE. Numerous bacterial surface components present in streptococci, staphylococci, and enterococci have been shown in animal models of endocarditis to function as critical adhesions. Bacteria adhering to the vegetation stimulate further deposition of fibrin and platelets on their surface. Within this secluded focus, the buried microorganisms multiply rapidly.

The original site of infection subsequently changes in character. This change depends on several factors, including the microorganism involved. In endocarditis caused by α -hemolytic streptococci, the large colonies of bacteria become encased in an organizing mass of fibrin. The fibrin barrier has a direct effect on two important factors in the defense against infection: the prevention of the invasion by phagocytic leukocytes and the difficulty in penetration of the vegetation by antimicrobial agents. For reasons that are not fully appreciated, this type of vegetation formation does not frequently occur with some of the more virulent bacteria, such as *S. aureus*, where the infection rapidly destroys the valve or invades the myocardium with subsequent abscess formation.

There have been substantial gains within the past several years in the understanding of the pathogenesis of endocarditis largely because of the availability of newer molecular biologic techniques. These techniques have allowed the examination of individual virulence factors of Gram-positive cocci and the investigation of important host-cell interactions with microorganisms. Several specific surface structures of staphylococci, streptococci, and enterococci have been identified as markers of virulence (17). Mucosal surfaces are populated by endogenous bacteria. Transient bacteremia can be induced by trauma to a mucosal surface during various dental, oral, and surgical procedures; however, spontaneous bacteremia may also occur (16). The bacteremia associated with various tissue manipulations, including dental and surgical procedures, has been carefully studied. Spontaneous bacteremia also has been noted to occur after tooth brushing, chewing hard foods, or other daily events. Many dental procedures have been associated with bacteremia, particularly procedures known to induce gingival or mucosal bleeding. Transient bacteremia caused by viridans group streptococci and other oral microflora following tooth extraction may reach 80%. In experimental animals, large doses of bacteria are generally needed to induce endocarditis. In humans, it is likely that the dose in spontaneous bacteremia may be too small to lead to implantation of bacteria on cardiac lesions, but this concept is not evidence-based.

Following successful medical therapy, the cardiac lesions of endocarditis usually heal, although important residua can remain. Experimental studies in rabbits suggest that the resolution process includes endothelialization of the affected surface; phagocytosis of bacterial debris, sometimes with calcification; and subsequent organization by fibroblasts. Resulting hemodynamic abnormalities depend on the site of infection, the specific damage caused by the active vegetation, and the size and location of the abscess.

The immediate consequences of endocarditis, including vegetation formation, hemodynamic alterations, and the clinical syndrome, are only part of an evolving complex disease entity.

Distal manifestations of the disease in the past were considered to be the results of embolic phenomena. It is now recognized that additional mechanisms are involved in the pathogenesis of endocarditis that lead to peripheral manifestations. Many important extracardiac findings in endocarditis are related to immunologic mechanisms. Rheumatoid factor is present for 6 weeks or longer in sera of about half of the patients with endocarditis. This is considered to be due to a gradual hyperimmunization of the host. Rheumatoid factor is more frequently found in patients with endocarditis related to α -hemolytic streptococci or coagulase-negative staphylococci (low-virulence organisms) than in those caused by *S. aureus* (more virulent organisms). There is also correlation of the duration of infection with the presence of this antiglobulin. Rheumatoid factor tends to disappear from the sera with successful therapy. Immunologic mechanisms also underlie other clinical manifestations of the disease including the skin, subcutaneous tissues, and eye findings noted below (Clinical Features).

Another immunologic consequence of endocarditis is the development of circulating immune complexes in the sera of patients. This is due to extended exposure to foreign antigen, and these immune complexes disappear after successful antimicrobial therapy. Although deposition of immune complexes in renal parenchyma can occur, their precise role in pathogenesis has not been fully defined. The nephritis seen in patients with endocarditis may manifest itself microscopically as either focal or diffuse glomerulonephritis. In the focal lesion, there is often segmental fibrinoid necrosis of isolated lobules of the glomerular tuft. In the more diffuse form, there is marked cellular proliferation with interstitial round cell infiltrates. Immunofluorescence studies show granular deposits in the glomerular basement membrane and mesangium, usually associated with complement and immunoglobulin G (IgG) deposits, although IgA, IgM, and fibrinogen also have been demonstrated. Urinalysis results may be normal, but hematuria, cylindruria, and pyuria have been reported. Compromise of renal function may occur and appears to be more common in adults than in children. In addition to immune mechanisms, the kidney is an extracardiac site frequently affected in patients with endocarditis because of microscopic and macroscopic emboli of pathologic lesions. Many emboli are reportedly sterile. However, abscess formation also has been reported following septic embolization to the kidney. Abscess formation in other vital organs occurs as well (see below) and is involved in the pathogenesis of many of the life threatening sequelae of active IE.

CLINICAL FEATURES

Most clinical manifestations and complications of endocarditis are directly related to hemodynamic and structural changes caused by the local infection, to embolization from vegetations, or to immunologic reactions by the host. Bacteremia itself can also cause clinical findings such as fever and systemic toxicity. Endocarditis simulates a wide variety of disorders, including other infectious diseases, malignancies, and connective tissue diseases. It should be part of the differential diagnosis of any unusual or febrile illness in patients with underlying heart disease. If the diagnosis is not made promptly, the disease may escape detection until the process is far advanced with irreparable damage.

The clinical features differ, in part, depending on the primary infection site. Findings also may be different in children compared with adults. Most cases of endocarditis in adults are valvar, but endocarditis in children with congenital heart lesions may often involve other structures such as mural endocardium, patent ductus arteriosus, arteries or other vascular sites such as conduits or surgical shunts.

Endocarditis involving the left side of the heart frequently results in peripheral embolization, leading to ischemia, infarction, or mycotic aneurysms. In these cases, specific clinical findings depend on the localization of the emboli. In children, embolization from the right heart may be no less frequent, but such emboli, if small, are not as easily appreciated clinically because of filtration by the lungs. However, large pulmonary emboli may complicate endocarditis of the tricuspid valve.

Table 63.3 lists clinical findings and usual laboratory findings seen in patients with endocarditis. Fever is the most common finding in all patients with endocarditis, with the exception of neonates, and can vary depending on the infecting organism. When hemolytic streptococci are the causative agents, for example, fever is often low grade, reaching a maximum of 39°C. In contrast, endocarditis caused by *S. aureus* is frequently associated with high, spiking temperature elevations of $\geq 40^\circ\text{C}$.

Children with “subacute” endocarditis usually display slowly progressive nonspecific symptoms, including myalgias, arthralgias, headache, and general malaise. Fever may be relapsing and low grade. There is often a marked diminution in appetite. In contrast, with the acute form of endocarditis a toxic course is the rule with high fever, systemic debilitation, and more overt hemodynamic changes on presentation.

With diligent auscultation, new or changing murmurs are often heard. Since it may be difficult to recognize changes in a patient who has a pre-existing murmur, serial auscultation is essential. This will assist not only with diagnosis but also with management. For example, increased intensity of the diastolic murmur of aortic insufficiency should alert the examiner to the possibility of progressive aortic valvar deterioration,

TABLE 63.3

Clinical and Laboratory Findings in Patients with Endocarditis

Finding	Frequency ^a
Clinical	
Fever	+++
Nonspecific symptoms (myalgia, arthralgia, headache, malaise)	++
Heart murmur (new or changing)	++
Heart failure	++
Petechiae	++
Embolic phenomena	++
Splenomegaly	++
Neurologic findings	++
Osler nodes, Janeway lesions, Roth spots, splinter hemorrhages	+
Laboratory	
Positive blood culture (off antibiotics)	+++
Elevated acute-phase reactants	+++
Anemia	++
Hematuria	++
Presence of rheumatoid factor	++
Leukocytosis	++

^a+++ very common; ++, in most cases; +, infrequent; +, rare.

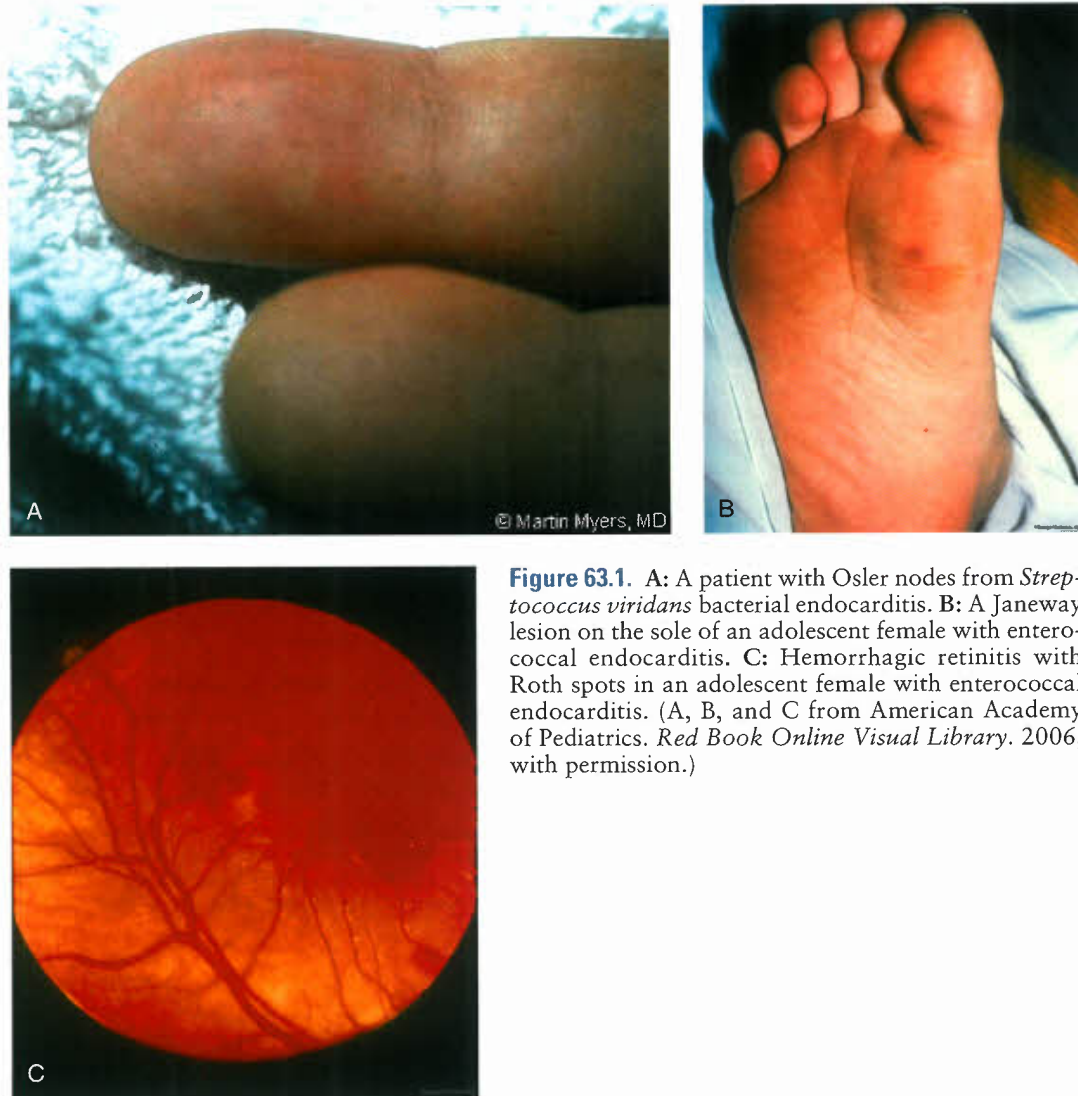


Figure 63.1. A: A patient with Osler nodes from *Streptococcus viridans* bacterial endocarditis. B: A Janeway lesion on the sole of an adolescent female with enterococcal endocarditis. C: Hemorrhagic retinitis with Roth spots in an adolescent female with enterococcal endocarditis. (A, B, and C from American Academy of Pediatrics. *Red Book Online Visual Library*. 2006, with permission.)

which can lead to worsening left ventricular dysfunction, heart failure, and to the possible need for early valve replacement. Similarly, diminution of a continuous murmur in a cyanotic child with a prosthetic systemic-to-pulmonary shunt may be a sign of endocarditic involvement of the graft. Extracardiac findings can include splenomegaly, which may be seen in most instances when the disease has been present for weeks or months. Neurologic findings are present in about 20% of children with endocarditis and may simulate the picture of an abscess, an infarct, or aseptic meningitis. Renal abnormalities, including proteinuria, hematuria, and leukocyturia, can occur in the presence of emboli or in association with endocarditis-related immune complex deposition, as noted previously. The classically described signs such as small, tender, raised lesions on the pads of the fingers and toes (Osler nodes, Fig. 63.1A); small, nontender, flat erythematous lesions on the palms or soles (Janeway lesions, Fig. 63.1B); retinal hemorrhages with a central white spot (Roth spots, Fig. 63.1C); and splinter hemorrhages can also occur but are relatively rare in children.

Neonates represent a unique group in that many may have relatively few specific symptoms. In those newborns who are symptomatic, systemic hypotension, clinical signs compatible with generalized sepsis, or focal neurologic findings from central nervous system embolization may be clues to the development of endocarditis. Neonates appear particularly prone to

peripheral septic embolization and the development of satellite infections including meningitis and osteomyelitis.

LABORATORY DIAGNOSIS

The blood culture is the most valuable aid in making the diagnosis of endocarditis. Although a positive blood culture in a child with underlying or predisposing cardiac disease or a history of previous endocarditis does not necessarily indicate endocarditis, it is imperative that the diagnosis be considered in such a patient.

It is not possible to specify the exact number of cultures that should be obtained in each situation. The collection of three separate sets of blood cultures, each from a separate venipuncture over a 24-hour period, is adequate in most cases. In patients in whom the diagnosis of endocarditis is highly suspect, and the clinical situation is changing, arbitrary therapy should be considered after blood cultures have been obtained over an appropriate time period. In some situations, however, making careful observations and obtaining more blood cultures before initiating antibiotic therapy are appropriate.

Since the bacteremia in patients with IE is usually continuous, it is not necessary to obtain blood cultures only upon a

temperature elevation. The volume of blood to be collected is another consideration, particularly in instances where there is a likely low magnitude of bacteremia. Usually 20 to 30 mL of blood are collected from an adult patient, but this is not possible in a small child. Thus, 1 to 3 mL in infants and young children and 5 to 7 mL in older children are adequate, depending on the blood culture detection system (5). It is rare for IE to be caused by anaerobic bacteria; therefore, the emphasis is usually on inoculating blood into bottles designed for aerobic incubation. Usually, three blood cultures are obtained by separate venipunctures on the first day, and if there is no growth by the second day of incubation, two more may be obtained. It is usually not necessary to obtain more than five blood cultures over 2 days unless the patient received prior antibiotic therapy.

Other laboratory tests are not specific for confirming the diagnosis of endocarditis (Table 63.3), but they may be helpful in the management and follow-up of patients with this infection. Acute-phase reactants are commonly elevated. Initially, it is possible to find that the erythrocyte sedimentation rate (ESR) is only minimally elevated. As the disease progresses, the ESR will usually increase. It may remain elevated for some time even after documented bacteriologic cure. About half of the patients with endocarditis may have detectable rheumatoid factor or immune complexes in their sera. Anemia is common and may be hemolytic or may represent the anemia of chronic disease. It should be noted that chronic low-grade hemolysis also may be caused by a prosthetic valve in the absence of IE. Microscopic or macroscopic hematuria represents either renal embolization or immune complex related nephritis. Extreme leukocytosis is not a consistent finding and is more common in acute IE. In some situations, tests for the presence of antibodies to specific bacterial antigens are helpful. For example, antibodies against teichoic acid and against the cell wall peptidoglycan in severe staphylococcal infection may be present.

ECHOCARDIOGRAPHY

Two-dimensional echocardiography has become the principal diagnostic method in cases of suspected IE with sensitivities in children reported to be >80% (18). Neither sensitivity nor specificity of echocardiography is 100%. Therefore, a negative echocardiogram does not always rule out endocarditis. Transthoracic echocardiography (TTE) generally is more helpful in children with normal cardiac anatomy or with isolated valvar abnormalities and septal defects than it is in children with complex congenital anomalies (7). Echocardiographic examination is often definitive in patients destined for surgery.

Although data from adults indicate that transesophageal echocardiography (TEE) is superior to TTE for identification of vegetations (19), similar information in children is not available. Nevertheless, even in children, TEE adds to the ability to diagnose paravalvular leakage and complications such as dehiscence in prosthetic valve endocarditis as it does in older patients (20). Also, TEE is considered useful to assess the development of complications of left ventricular outflow tract IE and may be especially helpful in children who have had multiple surgeries for complex congenital cardiac disease or in others with limitations of TTE ultrasound windows such as children with chronic lung diseases or congenital chest wall deformities.

Echocardiography is particularly important as part of the serial evaluation of a patient with IE after the initial diagnosis. Select echocardiographic findings can indicate the likelihood of progressive complications including the need for operative intervention (Table 63.4) (21). Serial assessment of cardiovascular performance by echo can also be important to guide clinical decision making. Figure 63.2 demonstrates 2-D echocardiographic examples of both left and right heart IE.

TABLE

63.4

Echocardiographic Features Suggesting Potential Need for Surgical Intervention

Vegetation

Persistent vegetation after systemic embolization:

Anterior mitral leaflet vegetation, particularly with size >10 mm^a

One or more embolic events during first 2 wk of antimicrobial therapy^a

Two or more embolic events during or after antimicrobial therapy^a

Increase in vegetation size after 4 wk of antimicrobial therapy^{a,b}

Valvular dysfunction

Acute aortic or mitral insufficiency with signs of ventricular failure^b

Heart failure unresponsive to medical therapy^b

Valve perforation or rupture^b

Perivalvular extension

Valvular dehiscence, rupture, or fistula^b

New heart block^b

Large abscess, or extension of abscess despite appropriate antimicrobial therapy^b

^aSurgery may be required because of risk of embolization.

^bSurgery may be required because of heart failure or failure of medical therapy. From Bayer et al. Diagnosis and management of infective endocarditis and its complications. *Circulation* 1998;98:2936–2948, with permission.

DIAGNOSTIC CRITERIA

The diagnosis of IE can be straightforward in patients with classic manifestations including bacteremia (or fungemia), active valvulitis, peripheral emboli, and immunologic vascular phenomena. In many patients, however, classic peripheral manifestations may be few or absent, particularly in newborns, young infants, patients with acute-onset IE, and cases of right-sided endocarditis. Acute IE may evolve too quickly for immunologic vascular phenomena to develop, which are more characteristic of subacute IE.

Variability in the clinical presentation of IE requires diagnostic criteria that are both sensitive for disease detection and specific for its exclusion across all forms of the disease. A diagnostic strategy was developed (the Duke criteria) that uses a combination of clinical, microbiologic, pathologic, and echocardiographic findings (1). These criteria stratified patients with suspected IE into three categories: “definite” cases, identified either clinically or pathologically (IE proved at surgery or autopsy), “possible” cases (not meeting the criteria for definite IE), and “rejected” cases (those with no pathologic evidence of IE at autopsy or surgery; rapid resolution of the clinical syndrome with either no treatment or short-term antibiotic therapy; or a firm alternative diagnosis). In the mid-to-late 1990s, the criteria were validated in geographically and clinically diverse groups including children (22,23). Several refinements in the Duke criteria have been made recently to both the major and minor criteria (2). These so-called modified Duke criteria have been shown to be more sensitive in diagnosing IE in children than the original Duke criteria (24). The modified Duke criteria are shown in Table 63.5.

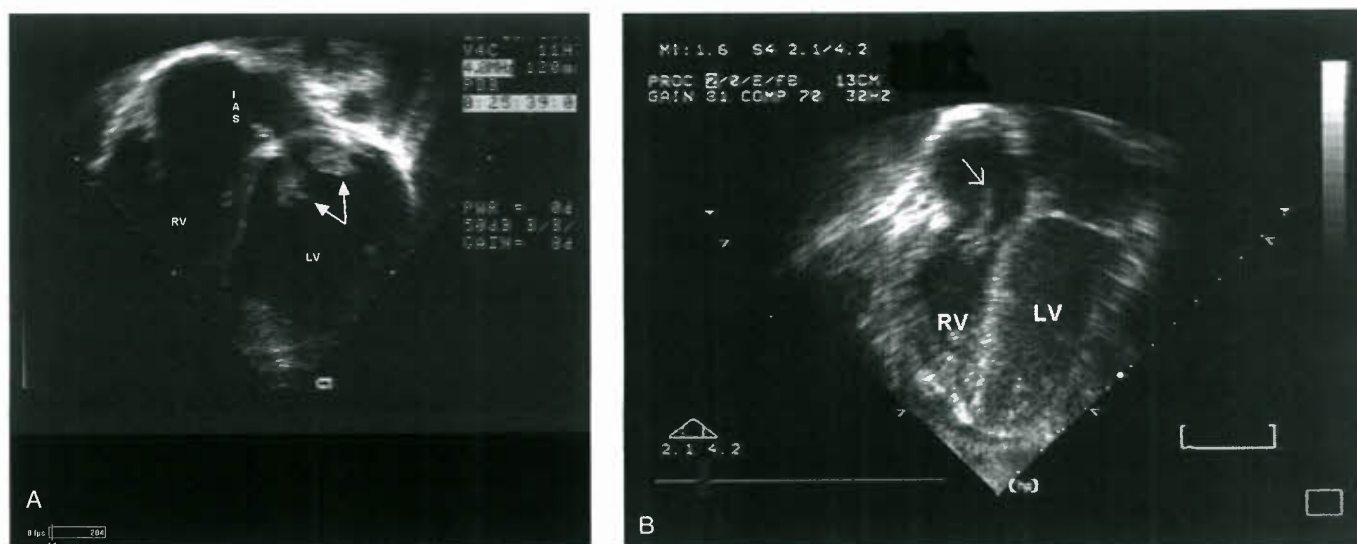


Figure 63.2. A: Mitral valve vegetations (arrows) in preteen patient with low-grade, persistent fever, weight loss, and malaise. Blood cultures grew α -hemolytic streptococci. Prior history of abnormal mitral valve known. IAS, intra-atrial septum; LV, left ventricle; RV, right ventricle. B: Right heart endocarditis involving vegetations on tricuspid valve (arrow) in a neonate. Blood cultures grew coagulase-negative staphylococci.

ANTIMICROBIAL THERAPY

General Principles

Complete eradication of the infecting microorganism in a vegetation usually requires several weeks of antibiotic therapy. Prolonged therapy is usually necessary for several reasons.

Within vegetations, organisms are embedded within the fibrin-platelet matrix and exist in very high concentrations. Additionally, there are relatively low rates of bacterial metabolism and cell division, which result in decreased susceptibility to beta-lactam and other cell wall-active antibiotics.

Bactericidal, rather than bacteriostatic, antibiotics should be chosen whenever possible to decrease the possibility of

TABLE 63.5A Definition of Infective Endocarditis According to the Modified Duke Criteria

Definite infective endocarditis (IE):

1. Pathologic criteria:

- A. Microorganisms demonstrated by culture or histologic examination of a vegetation, a vegetation that has embolized, or an intracardiac abscess specimen; or
- B. Pathologic lesions; vegetation or intracardiac abscess confirmed by histologic examination showing active endocarditis

2. Clinical criteria (see Table 63.5B):

- A. Two major criteria; or
- B. One major criterion and three minor criteria; or
- C. Five minor criteria

Possible IE:

- 1. **One major criterion and one minor criterion; or**
- 2. **Three minor criteria**

Rejected IE:

- 1. Firm alternative diagnosis explaining evidence of IE; or
- 2. Resolution of IE syndrome with antibiotic therapy for ≤ 4 d; or
- 3. No pathologic evidence of IE at surgery or autopsy, with antibiotic therapy for ≤ 4 d; or
- 4. Does not meet criteria for possible IE as above

From Li JS, Sexton DJ, Mick N, et al. Proposed modifications to the Duke criteria for the diagnosis of infective endocarditis. *Clin Infect Dis* 2000;30:633–638, with permission. Modifications shown in boldface.

TABLE 63.5B

Definition of Terms Used in the Modified Duke Criteria for the Diagnosis of Infective Endocarditis**Major Criteria**

1. Blood culture positive for IE
 - A. Typical microorganisms consistent with IE from two separate blood cultures:
 - i. Viridans streptococci, *Streptococcus bovis*, HACEK group, *S. aureus*; or
 - ii. Community-acquired enterococci in the absence of a primary focus; or
 - B. Microorganisms consistent with IE from persistently positive blood cultures defined as follows:
 - i. At least two positive cultures of blood samples drawn >12 h apart; or
 - ii. All of three or a majority of ≥four separate cultures of blood (with first and last sample drawn ≥1 h apart)
 - C. **Single positive blood culture for *Coxiella burnetii* or anti-phase-1 IgG antibody titer >1:800**
2. Evidence of endocardial involvement
 - A. Echocardiogram positive for IE (**TEE recommended for patients with prosthetic valves, rated at least “possible IE” by clinical criteria, or complicated IE [paravalvular abscess]; TTE as first test in other patients**) defined as follows:
 - i. Oscillating intracardiac mass on valve or supporting structures, in the path of regurgitant jets, or on implanted material in the absence of an alternative anatomic explanation; or
 - ii. Abscess; or
 - iii. New partial dehiscence of prosthetic valve
 - B. New valvular regurgitation (worsening or changing or pre-existing murmur not sufficient)

Minor Criteria

1. Predisposition, predisposing heart condition, or injection drug use
2. Fever, temperature >38°C
3. Vascular phenomena, major arterial emboli, septic pulmonary infarcts, mycotic aneurysm, intracranial hemorrhage, conjunctival hemorrhages, and Janeway lesions
4. Immunologic phenomena: glomerulonephritis, Osler nodes, Roth spots, and rheumatoid factor
5. Microbiologic evidence: positive blood culture, but does not meet a major criterion as noted above^a or serologic evidence of active infection with organism consistent with IE
6. **Echocardiographic minor criteria eliminated**

^aExcludes single positive cultures for coagulase-negative staphylococci and organisms that do not cause endocarditis.

HACEK, *Haemophilus parainfluenzae*, *H. aphrophilus*, *H. paraphrophilus*, *H. influenzae*, *Actinobacillus actinomycetemcomitans*, *Cardiobacterium hominis*, *Eikenella corrodens*, *Kingella kingae*, and *K. denitrificans*; TEE, transesophageal echocardiography; TTE, transthoracic echocardiography.

From Li JS, Sexton DJ, Mick N, et al. Proposed modifications to the Duke criteria for the diagnosis of infective endocarditis. *Clin Infect Dis* 2000;30:633–638, with permission. Modifications shown in boldface.

treatment failures or relapses. Parenterally administered antibiotics are recommended because of the desirability of achieving high blood levels of the agents. In small children, intravenous antibiotics are preferred over intramuscular agents because of their small muscle mass. Use of heparin lock devices or indwelling catheters for intravenous therapy in older children and adults facilitates ambulation and activity. Outpatient (home) therapy can be considered in selected patients after initial treatment in the hospital and after confirming that these patients are hemodynamically stable and afebrile, have negative blood cultures, and are not at high risk for complications. Patient and parent compliance with the medical plan is important, and frequent monitoring by a home health provider is essential. There should also be easy access to a hospital for prompt reevaluation by an experienced physician should complications develop. When combinations of antibiotics are used, they can be tested in the laboratory for synergistic bactericidal activity, such as demonstrated by the combination of penicillin G with gentamicin against enterococci or α -hemolytic streptococci.

Documentation of cessation of bacteremia should be sought early in therapy as a means of measuring the adequacy of the

antibiotic regimen. Serum peak and trough antibiotic levels should be monitored when potentially toxic antibiotics (e.g., aminoglycosides) are used. This will ensure that levels are adequate and have not reached a toxic range. The clinician should still be alert to signs of toxicity even if serum levels remain within the generally accepted limits. All patients with endocarditis require close follow-up. Obtaining occasional blood cultures during the first 6 to 8 weeks after cessation of treatment is important because most relapses occur during this period.

The role of cardiovascular surgery in the therapy of endocarditis is determined by the site of infection and by the clinical course, especially the hemodynamic status of the patient. Decisions for surgical intervention must be individualized. Indications for surgery that are usually agreed upon include major or recurrent embolic events, persistent infection, and progressive cardiac failure (21,25), especially when the aortic or mitral valves are involved. Medical management alone of progressive valvar damage and resulting heart failure is dangerous. A decision to operate based on hemodynamic deterioration should not be delayed solely because the full course of antibiotic therapy has not been completed.

TABLE 63.6 Therapy of Native Valve Endocarditis Caused by Streptococci**Highly penicillin-susceptible viridans group streptococci and *streptococcus bovis* (MIC ≤ 0.12 $\mu\text{g/mL}$)**

Regimen	Dosage ^a	Route	Duration, weeks
Aqueous crystalline penicillin G sodium	200,000 U/kg per 24 h	IV in 4–6 equally divided doses	4
Or			
Ceftriaxone sodium	100 mg/kg per 24 h	IV/IM in 1 dose	4
Aqueous crystalline penicillin G sodium	200,000 U/kg per 24 h	IV in 4–6 equally divided doses	2 ^b
Or			
Ceftriaxone sodium	100 mg/kg per 24 h	IV/IM in 1 dose	2
Plus			
Gentamicin sulfate ^c	3 mg/kg per 24 h	IV/IM in 3 equally divided doses	2
Vancomycin hydrochloride ^d	40 mg/kg per 24 h	IV in 2–3 equally divided doses	4

Strains of viridans group streptococci and *S. bovis* relatively resistant to penicillin (MIC >0.12 to ≤ 0.5 $\mu\text{g/mL}$)

Regimen	Dosage ^a	Route	Duration, weeks
Aqueous crystalline penicillin G sodium	300,000 U/kg per 24 h	IV in 4–6 equally divided doses	4
Or			
Ceftriaxone sodium	100 mg/kg per 24 h	IV/IM in 1 dose	4
Plus			
Gentamicin sulfate ^c	3 mg/kg per 24 h	IV/IM in 3 equally divided doses	2
Vancomycin hydrochloride ^d	40 mg/kg 24 h	IV in 2 or 3 equally divided doses	4

Streptococci with MIC >0.5 $\mu\text{g/mL}$ as well as for enterococcal endocarditis caused by strains susceptible to penicillin, gentamicin, and vancomycin

Regimen	Dosage ^a	Route	Duration, weeks
Ampicillin sodium	300 mg/kg per 24 h	IV in 4–6 equally divided doses	4–6
Or			
Aqueous crystalline penicillin G sodium	300,000 U/kg per 24 h	IV in 4–6 equally divided doses	4–6
Plus			
Gentamicin sulfate ^c	3 mg/kg per 24 h	IV/IM in 3 equally divided doses	4–6
Vancomycin hydrochloride ^d	40 mg/kg per 24 h	IV in 2 or 3 equally divided doses	6
Plus			
Gentamicin sulfate ^c	3 mg/kg per 24 h	IV/IM in 3 equally divided doses	6

^aDosages recommended are for patients with normal renal and hepatic function. Maximum dosages per 24 h: penicillin, 18 million units; ceftriaxone, 2 g; gentamicin, 240 mg. Pediatric dose should not exceed that of a normal adult.

^bTwo-week regimen not intended for patients with known cardiac or extracardiac abscess, impaired renal function, symptoms of infection >3 mo in duration, impaired eighth cranial nerve function

^cDosage of gentamicin should be adjusted to achieve peak serum concentration of 3–4 $\mu\text{g/mL}$ and a trough concentration of <1 $\mu\text{g/mL}$ when 3 divided doses are used. Patients with a creatinine clearance of <50 mL/min should be treated in consultation with an infectious diseases specialist. Other potentially nephrotoxic drugs should be used with caution in patients receiving gentamicin therapy.

^dVancomycin therapy recommended only for patients unable to tolerate penicillin, ampicillin or ceftriaxone. Dosage should be adjusted to obtain peak (1 h after infusion completed) serum concentration of 30–45 $\mu\text{g/mL}$ and a trough concentration range of 10–15 $\mu\text{g/mL}$. Vancomycin dosages should be infused over at least a 1 h period to reduce risk of histamine-release “red man” syndrome.

MIC, minimal inhibitory concentration.

A detailed set of recommendations for antibiotic treatment of IE has been made by both the American Heart Association (AHA) (5,13) and the European Society of Cardiology (ESC) (26). Tables 63.6 and 63.7 are modified from these recommendations.

Streptococcal Endocarditis

Table 63.6 presents recommended treatment regimens for endocarditis caused by streptococci. Highly penicillin-susceptible streptococci have a minimal inhibitory concentration (MIC) to

TABLE 63.7 Therapy for Endocarditis Caused by Staphylococci in the Absence of Prosthetic Materials

Regimen	Dosage ^a	Route	Duration
Oxacillin-susceptible strains			
Nafcillin or oxacillin ^b	200 mg/kg per 24 h	IV in 4–6 equally divided doses	6 wk
With			
Optional addition of gentamicin sulfate ^c	3 mg/kg per 24 h	IV/IM in 3 equally divided doses	3–5 d
For penicillin-allergic (nonanaphylactoid type) patients:			
Cefazolin	100 mg/kg per 24 h	IV in 3 equally divided doses	6 wk
With			
Optional addition of gentamicin sulfate	3 mg/kg per 24 h	IV/IM in 3 equally divided doses	3–5 d
Oxacillin-resistant strains			
Vancomycin ^d	40 mg/kg per 24 h	IV in 2 or 3 equally divided doses	6 wk

^aDosages recommended are for patients with normal renal function. Pediatric dose should not exceed that of a normal adult.

^bPenicillin G 300,000 U/kg per 24 h IV in 4–6 equally divided doses may be used in place of nafcillin or oxacillin if strain is penicillin susceptible (minimum inhibitory concentration $\leq 0.1 \mu\text{g/mL}$) and does not produce β -lactamase.

^cGentamicin should be administered in close temporal proximity to vancomycin, nafcillin, or oxacillin dosing.

^dFor specific dosing adjustment and issues concerning vancomycin, see Table 65.6 footnotes.

penicillin ($<0.12 \mu\text{g/mL}$ [micrograms/mL]). They are the most common organisms causing endocarditis in children. The vast majority of these organisms is the viridans group (α -hemolytic streptococci); the rest are *S. bovis* (a nonenterococcal penicillin-susceptible group D *Streptococcus*) or β -hemolytic streptococci. For patients who are not penicillin allergic, intravenous aqueous crystalline penicillin G for 4 weeks is associated with high cure rates. This regimen is preferred for patients with impaired renal function or for those who are at risk of aminoglycoside toxicity. Ampicillin is an alternative to penicillin and has been used when penicillin is not available because of supply deficiencies. Ceftriaxone sodium given intravenously (IV) or intramuscularly (IM) daily for 4 weeks is also an acceptable regimen and is more commonly used today in the outpatient setting due to ease of dosing. Unacceptably high relapse rates occur when intravenous penicillin is used alone for 2 weeks.

A 2-week course of therapy with either penicillin or ceftriaxone combined with gentamicin has become increasingly popular and results in high cure rates in adults (13). This regimen is recommended for uncomplicated cases of native valve IE caused by highly penicillin-susceptible viridans group streptococci or *S. bovis* in patients at low risk for adverse events caused by gentamicin therapy. It should not be used for patients who have any of the following clinical features: endocarditis of >3 months' duration, prosthetic valve infection, shock or decreased perfusion, extracardiac foci of infection, mycotic aneurysm or cerebritis, renal failure, vestibular dysfunction, or presence of a vegetation visible by echocardiography. Reported relapse rates have been very low, and there are considerable savings associated with a shortened hospital stay. Experience with the 2-week regimen in children is limited, but it appears promising (with limited information).

Strains of viridans group streptococci and *S. bovis* with an MIC for penicillin of $>0.12 \mu\text{g/mL}$ and $\leq 0.5 \mu\text{g/mL}$ are referred to as relatively resistant strains. They are occasionally recovered from pediatric patients with endocarditis. These patients are best treated with 4 weeks of penicillin or ceftriaxone combined with 2 weeks of gentamicin.

Patients with IE caused by streptococci with an MIC $>0.5 \mu\text{g/mL}$ should be treated with ampicillin or aqueous crystalline

penicillin G plus gentamicin for 4 to 6 weeks. This regimen is also used for treating *Abiotrophia defectiva* and *Granulicatella* species (formerly known as nutritionally variant streptococci) and *Gemella* species. It is also used for enterococcal endocarditis susceptible to penicillin, gentamicin, and vancomycin. Enterococci uncommonly cause endocarditis in pediatric patients.

Patients allergic to penicillin (or ampicillin) frequently can be desensitized to enable treatment with these agents of choice. An effective alternative regimen when neither penicillin nor ceftriaxone can be used safely is intravenous vancomycin. For all streptococci with a penicillin MIC of $\leq 0.5 \mu\text{g/mL}$, 4 weeks of vancomycin therapy appears adequate. For more resistant streptococci (penicillin MIC of $>0.5 \mu\text{g/mL}$), treatment for 6 weeks of vancomycin (which may be combined with gentamicin) is recommended. Patients receiving these regimens should be closely monitored for renal toxicity and ototoxicity.

IE caused by *S. pneumoniae*, *S. pyogenes*, and group B, C, and G streptococci is relatively uncommon. There are few published reports of large series of cases evaluating therapeutic regimens for endocarditis caused by these microorganisms in patients of any age. Recent AHA recommendations review this aspect of the problem in more detail (13).

Staphylococcal Endocarditis

Table 65.7 presents recommended treatment regimens for endocarditis caused by staphylococci. Staphylococci are coagulase-positive (*S. aureus*) or coagulase-negative (*S. epidermidis* and various other species). Only a few *S. aureus* strains are penicillin susceptible because of production of enzymes called beta-lactamases. Therefore, antibiotic therapy must include a penicillinase-resistant penicillin (e.g., nafcillin or oxacillin) administered IV for 6 weeks. Addition of gentamicin for the first 3 to 5 days is optional. However, gentamicin's clinical benefit has not been formally demonstrated and it is associated with increased toxicity, so it should be used cautiously. Cefazolin may be used rather than nafcillin or oxacillin in patients with nonanaphylactoid-type penicillin allergy.

There are increasing rates of oxacillin resistance in hospital as well as community settings. Furthermore, recovery of

clinical *S. aureus* isolates highly resistant to vancomycin (27) has complicated the treatment of *S. aureus* endocarditis. The cyclic lipopeptide antibiotic daptomycin has been approved for *S. aureus* bacteremia and right-sided IE. Data on its use for endocarditis treatment in children are still somewhat limited. The reader is referred to guidelines from the Infectious Diseases Society of America for more information (28).

In nonaddicts, *S. aureus* endocarditis primarily involves the left side of the heart and is associated with mortality rates as high as 25% to 40%. *S. aureus* endocarditis in IDUs often involves the tricuspid valve. Cure rates for right-sided *S. aureus* endocarditis in IDUs are high (>85%) and may be achieved with relatively short courses of treatment (13).

Rifampin is effective against most staphylococci, but when it is used alone, resistance quickly develops. Routine use of rifampin is not recommended for treatment of native valve staphylococcal endocarditis.

Some coagulase-negative staphylococci and *S. aureus* strains are resistant to penicillin G and to penicillinase-resistant penicillins. Although in vitro evaluations may suggest that cephalosporins are effective, these organisms are indeed resistant to cephalosporins. They should not be used as therapeutic agents. Oxacillin-resistant staphylococci should be treated with vancomycin. In the penicillin-allergic individual who cannot be desensitized, intravenous vancomycin administered for 6 weeks is the drug of choice.

Gram-Negative Bacterial Endocarditis

Gram-negative bacteria that most often cause IE in children are the HACEK group of fastidious coccobacilli (*Haemophilus parainfluenzae*, *H. aphrophilus*, *H. paraphrophilus*, *H. influenzae*, *Actinobacillus actinomycetemcomitans*, *Cardiobacterium hominis*, *Eikenella corrodens*, *Kingella kingae*, and *K. denitrificans*). These microorganisms grow slowly in standard blood culture media, and recovery may require prolonged incubation. Typically, only a small portion of the blood culture bottles in patients with HACEK endocarditis demonstrate growth. In cases in which blood cultures are initially negative, the microbiology laboratory should be asked to retain blood cultures for at least 2 weeks in all patients suspected of having IE. Bacteremia caused by HACEK microorganisms in the absence of an obvious focus of infection is highly suggestive of endocarditis even in the absence of typical physical findings.

Infections with these organisms should be treated for 4 weeks with ceftriaxone or another appropriate third- or fourth-generation cephalosporin or ampicillin/sulbactam. In adults, ciprofloxacin is recommended in patients unable to tolerate cephalosporins or ampicillin. Fluoroquinolones are generally not recommended for patients younger than 18 years old, and an infectious disease consultation should be sought if this drug is considered.

IE caused by aerobic enteric organisms such as *Escherichia coli*, *Pseudomonas aeruginosa*, or *Serratia marcescens* is occasionally seen. Many such patients are IDUs, although occasionally a postoperative cardiac patient, an immunocompromised patient, or a neonate may develop endocarditis with one of these organisms. Therapy must be individualized and guided by in vitro antimicrobial susceptibility testing. Most experience has been with an extended-spectrum penicillin or a cephalosporin such as cefotaxime or ceftazidime together with an aminoglycoside such as gentamicin or amikacin. Therapy for at least 6 weeks is recommended. Cardiac surgery in combination with a prolonged course of antibiotic therapy is often necessary (13,29).

Gonococcal endocarditis, although rare and very aggressive, can be treated successfully with high-dose penicillin if the organism is penicillin susceptible. For penicillin-resistant organisms, an appropriate third-generation cephalosporin (such as cefotaxime or ceftriaxone) is recommended.

Fungal Endocarditis

Fungal endocarditis is a relatively new syndrome and is often a complication of medical and surgical advances. Its incidence in children is reported to have increased significantly in recent years (14). The prognosis is poor, with high mortality and morbidity. Fungal endocarditis can occur in immunocompromised patients (including preterm infants), IDUs, patients on broad-spectrum antibiotics for a prolonged period of time, and patients who have cardiovascular devices such as prosthetic cardiac valves or central venous catheters. About two-thirds of the cases of fungal endocarditis are due to *Candida* species (30). Despite aggressive combined medical and surgical interventions, mortality rates for fungal endocarditis remain unacceptably high. The survival rate for patients with mold-related endocarditis is <20%. Treatment of fungal endocarditis with antifungal agents alone is almost always unsuccessful, particularly in older patients. Amphotericin B is the most often recommended medical treatment option although the new echinocandin antifungal drug caspofungin is a viable alternative (30). Surgical replacement of the infected valve (native or prosthetic) and excision of infected tissue are usually required in conjunction with antifungal agents. Surgery is probably best performed after 1 to 2 weeks of medical therapy if the patient's hemodynamic status permits, but earlier if there is evidence of embolic phenomena. Antifungal therapy is then usually given for 6 weeks. Suppressive treatment with oral azoles is often maintained long term and sometimes for life. (For more detailed treatment options, the reader is referred to reference (30).)

Culture-Negative Endocarditis

Blood cultures can be negative in ≤20% of cases of endocarditis. This failure to culture the causative microorganism can be the result of inadequate microbiologic techniques, infection with highly fastidious bacteria or nonbacterial pathogens, or previous administration of antimicrobial agents before blood cultures were obtained (the latter of which is most common in the United States). Administration of antibiotics to patients before blood cultures are obtained reduces the recovery rate of bacteria by 35% to 40% (13). The antimicrobial susceptibility of the organism and the duration and nature of previous antimicrobial therapy together determine the length of time that blood cultures will remain negative. Patients with blood cultures that are initially negative after the patient has received only a few days of antibiotic therapy may still develop positive blood cultures after several subsequent days without antibiotics. The blood cultures of patients who receive longer courses of high-dose bactericidal antimicrobials may remain negative for weeks. Selection of the most appropriate medical therapy for patients with culture-negative endocarditis is difficult. The AHA and the ESC guidelines discuss various therapy recommendations for culture-negative IE (13,26).

Prosthetic Valve Endocarditis

Antibiotic therapy for patients with infected prosthetic heart valves must be appropriate for the specific infecting agent. Duration of therapy is usually 6 weeks or longer. Prosthetic valve infections owing to highly penicillin-susceptible streptococci (MIC ≤0.12 µg/mL) should be treated with 6 weeks of penicillin or ceftriaxone with or without gentamicin for the first 2 weeks. Infections caused by relatively or highly penicillin-resistant streptococci or enterococci should be treated as above except that gentamicin for 6 weeks should be combined with the penicillin or ceftriaxone. For penicillin-allergic patients who cannot be desensitized, vancomycin is recommended.

Staphylococcal endocarditis in the presence of a foreign body such as a prosthetic valve or graft should be treated with nafcillin or oxacillin (for an oxacillin-susceptible organism) plus both gentamicin and rifampin or vancomycin (for a methicillin-resistant organism). The aminoglycoside can be stopped after 2 weeks, but the other agents are continued for ≥ 6 weeks of therapy. In this situation, cardiac surgery is often required because of paravalvular abscess formation and difficulty eradicating the infection from the prosthetic material.

Therapy for other causes of prosthetic valve endocarditis is based on the results of in vitro MIC and minimal bactericidal concentration (MBC) tests and in vitro evaluation of antimicrobial synergy. Various regimens are discussed by the AHA (13).

Experience in adults with prosthetic valve endocarditis has emphasized that early surgical replacement of the infected valve may reduce the excessively high mortality rate associated with such infections. The timing of surgical removal and replacement of an infected prosthetic valve must be individualized. Some experts recommend that most or all patients with staphylococcal infection or prosthetic valve infection early after implantation should undergo valve replacement. Indications for operative intervention include significant valvular obstruction, progressive heart failure secondary to valvular insufficiency or dehiscence, fungal endocarditis, persistently positive blood cultures after appropriate antibiotics for 10 to 14 days, bacteriologic relapse after an appropriate course of therapy, and recurrent major emboli. Less definite indications for surgery include a single major embolus, echocardiographic demonstration of a large vegetation, and extension of infection to an annular abscess or a myocardial abscess.

Anticoagulation therapy during the treatment of IE remains controversial. A previous AHA statement (21) has noted the relative contraindication to anticoagulation during treatment of native valve IE in view of the confirmed risk for cerebral hemorrhage in these patients, particularly with left heart lesions. Conversely, most authorities agree that for prosthetic valve endocarditis, and for others with IE who already are on anticoagulation for other reasons, maintenance of anticoagulation is appropriate. This sentiment was confirmed as a preferred approach in a large survey of cardiologists and infectious disease specialists published in 2005 (31).

PREVENTION

Prophylaxis

Because of the high rates of morbidity and mortality associated with IE, any measure that can prevent the disease is desirable. Endocarditis can often be prevented by repairing the underlying cardiac defect or reducing the likelihood of bacteremia. In fact, the AHA has published recommendations for antibiotic regimens to be used before certain dental and surgical procedures for IE prevention since the mid-1950s (32). However, there has never been a prospective study in patients with underlying structural cardiac disease to determine definitively whether prophylactic antibiotics provide protection against development of IE during bacteremia-inducing procedures. Additionally, most instances of IE are not attributable to an antecedent invasive procedure but more likely result from routine activities of daily activities (chewing, toothbrushing, etc.). Within the past few years, some groups, including the AHA in 2007 (32), the UK's National Institute for Health and Clinical Excellence (NICE) in 2008 (33), and the ESC in 2009 (26), have reexamined the evidence underlying the antibiotic prophylaxis recommendations. These groups have significantly restricted the recommendations for who should receive routine prophylaxis (AHA and ESC) or have eliminated routine prophylaxis entirely (NICE). All three

organizations recognize that there are groups of individuals at increased risk of IE, including most with unrepaired congenital cardiac defects, acquired valvular heart disease with stenosis or regurgitation, a prosthetic cardiac valve or other prosthetic material, and/or a history of previous IE.

The AHA now limits prophylaxis recommendations to patients with "cardiac conditions associated with the highest risk of adverse outcome from IE" (Table 63.8), whereas the ESC limits its recommendations to "patients with the highest risk of IE." The patient groups are the same under either definition with the exception that the AHA includes cardiac transplant recipients who develop valvulopathy while the ESC does not include this group of patients in their recommendations.

For the above patient groups, both the AHA and ESC limit prophylaxis to dental procedures that involve manipulation of gingival tissue or the periapical region of teeth or perforation of the oral mucosa. They also list situations for which prophylaxis is not appropriate, such as routine anesthetic injections through noninfected tissue, taking dental radiographs, placement of removable prosthodontic or orthodontic appliances, adjustment of orthodontic appliances, placement of orthodontic brackets, or shedding of deciduous teeth and bleeding from trauma to the lips or oral mucosa. None of the three groups recommend routine prophylaxis for most procedures involving the upper or lower respiratory tract, upper or lower gastrointestinal (GI) tract, or genitourinary (GU) tract. A question sometimes arises concerning tattooing or body piercing in patients who have CHD. While these procedures should be discouraged, and if undertaken they should be performed under sterile conditions, antibiotic prophylaxis for the prevention of endocarditis is not recommended.

The recommended prophylactic regimens are given in Table 63.9 and are those from the AHA (32). The antibiotic should be administered as a single dose 30 to 60 minutes before the procedure. Amoxicillin is the drug of choice for children who can take oral medications and who are not allergic to

TABLE 63.8

Cardiac Conditions Associated with the Highest Risk of Adverse Outcome from Endocarditis for Which Prophylaxis with Dental Procedures is Recommended

Prosthetic cardiac valve

Previous IE

Congenital heart disease (CHD)^a

Unrepaired cyanotic CHD, including palliative shunts and conduits

Completely repaired congenital heart defect with prosthetic material or device, whether placed by surgery or by catheter intervention, during the first 6 mo after the procedure^b

Repaired CHD with residual defects at the site or adjacent to the site of a prosthetic patch or prosthetic device (which inhibit endothelialization)

Cardiac transplantation recipients who develop cardiac valvulopathy

^aExcept for the conditions listed above, antibiotic prophylaxis is no longer recommended for any other form of CHD.

^bProphylaxis is recommended because endothelialization of prosthetic material occurs within 6 mo after the procedure.

TABLE 63.9 Prophylactic Regimens for Dental, Oral, or Respiratory Tract, Procedures

	Agent	Regimen (single dose 30–60 min before procedure)
Standard oral prophylaxis	Amoxicillin	50 mg/kg PO (maximum 2 g)
Unable to take oral medications	Ampicillin	50 mg/kg IM or IV (maximum 2 g)
	Or	
	Cefazolin or ceftriaxone	50 mg/kg IM or IV (maximum 1 g)
Penicillin allergic–oral regimen	Clindamycin	20 mg/kg PO (maximum 600 mg)
	Or	
	Cephalexin ^a	50 mg/kg PO (maximum 2 g)
	Or	
	Azithromycin or clarithromycin	15 mg/kg PO (maximum 500 mg)
Penicillin allergic and unable to take oral medication	Clindamycin	20 mg/kg IV (maximum 600 mg)
	Or	
	Cefazolin ^a	50 mg/kg IM or IV (maximum 1 g)

^aCephalosporins should not be used in individuals with immediate-type hypersensitivity reaction (urticaria, angioedema, or anaphylaxis) to penicillins.

penicillins. If a patient is already taking an antibiotic when he or she has a procedure that requires IE prophylaxis, an antibiotic from a different class should be chosen for prophylaxis rather than increasing the dose of the current antibiotic.

If any patient included by AHA or ESC in Table 63.8 (highest risk of adverse outcome/highest risk group) is undergoing a respiratory tract procedure to treat an established infection, the antibiotic regimen administered to them should contain an agent that covers organisms that cause IE. Similarly, if a patient is undergoing a GI or a GU tract procedure where there is an established infection, or for those who receive antimicrobial therapy to prevent wound infection or sepsis associated with a GI or GU procedure, the patient should receive a regimen that includes an agent effective against enterococci.

The risk of acquiring endocarditis may change after surgical or other reparative procedures. This risk could go down (e.g., successful closure of atrial septal defect or ventricular septal defect), not change (e.g., placement of palliative shunts/conduits), or could go up (e.g., replacement of a native cardiac valve with a prosthetic valve). Patients/parents should be reminded that a child's need for antibiotic prophylaxis could change as they evolve through various treatment programs.

Finally, the new AHA recommendations note that poor dental hygiene and periodontal or periapical dental infections may produce bacteremia themselves even in the absence of dental or oral procedures. The guidelines emphasize the importance of maintenance of good oral health as an important factor in preventing endocarditis in susceptible individuals. Clinicians are urged to educate their patients/parents in this regard and to frequently remind them of this need.

REFERENCES

- Durack DT, Lukes AS, Bright DK. New criteria for diagnosis of infective endocarditis: utilization of specific echocardiographic findings. *Am J Med* 1994;96:200–209.
- Li JS, Sexton DJ, Mick N, et al. Proposed modifications to the Duke criteria for the diagnosis of infective endocarditis. *Clin Infect Dis* 2000;30:633–638.
- Van Hare GF, Ben-Shacher G, Liebman J, et al. Infective endocarditis in infants and children during the past 10 years: a decade of change. *Am Heart J* 1984;107:1235–1240.
- Caviness AC, Cantor SB, Allen CH, et al. A cost-effectiveness analysis of bacterial endocarditis prophylaxis for febrile children who have cardiac lesions and undergo urinary catheterization in the emergency in the emergency department. *Pediatrics* 2004;113:1291–1296.
- Ferrieri P, Gewitz MH, Gerber MA, et al. Unique features of infective endocarditis in childhood. *Circulation* 2002;105:2115–2127.
- Berkowitz FE. *Infective Endocarditis in Childhood*. St. Louis, MO: CV Mosby, 1995:961–986.
- Saiman L, Prince A, Gersony WM. Pediatric infective endocarditis in the modern era. *J Pediatr* 1993;122:847–853.
- Martin JM, Neches WH, Wald ER. Infective endocarditis: 35 years of experience at a children's hospital. *Clin Infect Dis* 1997;24:669–675.
- Coward K, Tucker N, Darville T. Infective endocarditis in Arkansas children from 1990 through 2002. *Pediatr Infect Dis J* 2003;22:1048–1052.
- Yoshinaga M, Niwa K, Niwa A, et al. Risk factors for in-patient mortality during infective endocarditis in patients with congenital heart disease. *Am J Cardiol* 2008;101:114–118.
- Rosenthal L, Feja K, Levasseur S, et al. The changing epidemiology of pediatric endocarditis at a children's hospital over seven decades. *Pediatr Cardiol* 2010;31:813–820.
- Gould K, Ramirez-Ronda CH, Holmes RK, et al. Adherence of bacteria to heart valves in vitro. *J Clin Invest* 1975;56:1364–1370.
- Baddour LM, Wilson WR, Bayer AS, et al. Infective endocarditis: diagnosis, antimicrobial therapy, and management of complications. *Circulation* 2005;111:e394–e434.
- Tissieres P, Jaeggi ET, Beghetti M, et al. Increase in fungal endocarditis in children. *Infection* 2005;33:267–272.
- Valente AM, Jain R, Scheurer M, et al. Frequency of infective endocarditis among infants and children with *Staphylococcus aureus* bacteremia. *Pediatrics* 2005;115:15–19.
- Steckelberg JM, Wilson WR. Risk factors for infective endocarditis. *Infect Dis Clin North Am* 1993;7:9–19.
- Baddour LM, Sullam PM, Bayer AS. The pathogenesis of infective endocarditis. In: Sussman M, ed. *Molecular Medical Microbiology*. San Diego, CA: Academic Press, 2001:999–1020.
- Kavey RE, Frank DM, Byrum CJ, et al. Two-dimensional echocardiographic assessment of infective endocarditis in children. *Am J Dis Child* 1983;137:851–856.
- Fowler VG Jr, Li J, Coery GR, et al. Role of echocardiography in evaluation of patients with *Staphylococcus aureus* bacteremia: experience in 103 patients. *J Am Coll Cardiol* 1997;30:1072–1078.
- Barbour SI, Louie EK, O'Keefe JP. Penetration of the atrioventricular septum by spread of infection from aortic valve endocarditis: early diagnosis by transesophageal echocardiography and implications for surgical management. *Am Heart J* 1996;132:1287–1289.
- Bayer A, Bolger AF, Taubert K, et al. Diagnosis and management of infective endocarditis and its complications. *Circulation* 1998;98:2936–2948.

22. Del Pont JM, De Cicco LT, Vartaliis C, et al. Infective endocarditis in children: clinical analysis and evaluation of two diagnostic criteria. *Pediatr Infect Dis J* 1995;14:1079-1086.
23. Stockhelm JA, Chadwick EG, Kessler S, et al. Are the Duke criteria superior to the Beth Israel Criteria for the diagnosis of infective endocarditis in children? *Clin Infect Dis* 1998;27:1451-1456.
24. Tissieres P, Gervais A, Beghetti M, et al. Value and limitations of the von Reyn, Duke, and modified Duke criteria for the diagnosis of infective endocarditis in children. *Pediatrics* 2003;112:e467-e471.
25. Citak M, Rees A, Mavroudis C. Surgical management of infective endocarditis in children. *Ann Thorac Surg* 1992;54:755-760.
26. Habib G, Hoen B, Tornos P, et al. Guidelines on the prevention, diagnosis, and treatment of infective endocarditis (new version 2009). The task force on the prevention, diagnosis and treatment of infective endocarditis of the European Society of Cardiology (ESC). *Eur Heart J* 2009;30:2369-2413.
27. Pfeltz RF, Wilkinson BJ. The escalating challenge of vancomycin resistance in *Staphylococcus aureus*. *Curr Drug Targets Infect Disord* 2004;4:273-294.
28. Liu C, Bayer A, Cosgrove SE, et al. Clinical Practice Guidelines by the Infectious Diseases Society of America for the treatment of methicillin-resistant *Staphylococcus aureus* infections in adults and children. *Clin Infect Dis* 2011;52:1-38.
29. Bashore TM, Cabell C, Fowler V Jr. Update on infective endocarditis. *Curr Probl Cardiol* 2006;31:274-352.
30. Varghese G, Sobel J. Fungal endocarditis. *Curr Infect Dis Reports* 2008;10:275-279.
31. Kamalakannan D, Beeai M, Gardin J et al. Anticoagulation in IE: a survey of infectious disease specialists and cardiologists. *Infect Dis Clin Prac* 2005;13:122-126.
32. Wilson W, Taubert KA, Gewitz M, et al. Prevention of infective endocarditis. Guidelines from the American Heart Association. *Circulation* 2007;116:1736-1754.
33. Richey R, Wray D, Stokes T. Prophylaxis against infective endocarditis. Summary of the NICE (National Institute for Clinical Excellence) guidance. *Br Med J* 2008;336:770-771.

Ali N. Zaidi ■ Curt J. Daniels

Although chest pain is common in patients presenting to pediatric cardiology clinics, myocardial ischemia is rarely ever the etiology. The list of etiologies leading to myocardial ischemia is potentially long, and each diagnosis for the most part is uncommon. Myocardial ischemia must always be considered in any patient who presents with chest pain or has a known diagnosis that could lead to ischemia, that is, Kawasaki disease (KD). The consequences of not considering this diagnosis can be devastating. Unfortunately, many patients who suffer an ischemic episode do not present until after a myocardial event. This group of rare patients must undergo a rapid evaluation that leads to definitive therapy. The patient who presents with symptoms of chest pain before an event or in the middle of an event is the focus of this particular chapter. An algorithm based upon a detailed history, exam, and appropriate diagnostic testing should lead to the correct diagnosis and the ability to include or exclude myocardial ischemia from the differential diagnosis. For the purposes of this chapter, we do not review atherosclerotic coronary artery disease (CAD) as this is covered elsewhere (see Chapter 71).

DEFINITION

Myocardial ischemia is an imbalance between myocardial oxygen supply and demand. Left untreated, it results in angina pectoris, myocardial stunning, myocardial hibernation, or under the most severe instances, acute coronary syndromes such as myocardial infarctions.

From a supply standpoint, a reduction or decrease in coronary blood flow due to spasm or obstruction leads to low flow ischemia of the myocardium and eventually to an acute coronary syndrome or myocardial infarction. Also, coronary blood flow may be normal but myocardial oxygen supply reduced in cases of severe hypoxia. Cyanotic heart disease, severe anemia, and hemoglobinopathies all have the potential for significant hypoxia leading to myocardial ischemia.

On the demand side, an increase in myocardial oxygen demand, that is, exercise, may lead to ischemia if there is a limitation on a supply that under normal or steady-state conditions is adequate but is not sufficient during times of increased demand. Although this mechanism of ischemia may lead to an acute coronary syndrome, more commonly, patients suffer chronic chest pain during times of increased demand.

Therefore, in our pediatric population and adults with CHD, chest pain often stems from a benign etiology, but, rarely, it may portend imminent catastrophe. In this patient population, the diagnoses leading to ischemia must fall under these two broad categories to cause myocardial ischemia.

HISTORY

For the patient who presents with chest pain, a detailed history provides the most important information to include or exclude myocardial ischemia from the differential diagnosis. Myocardial ischemia causing chest pain has typical characteristics that, when present, requires further investigation. Chest pain is more likely ischemic in origin when it is associated with:

- Exertion more than at rest
- Dyspnea
- Diaphoresis
- Syncope

and is characterized as:

- Substernal pressure or burning rather than pain
- Pressure that radiates to neck or arm
- Fairly reproducible with similar activity
- Short lived; 2 to 10 minutes as opposed to hours

Other important historical features include how the pain is relieved. If a patient is able to continue to run and play and the pain goes away despite continuing activity, myocardial ischemia is less likely.

Excluding atherosclerotic CAD, where hypertension, diabetes, tobacco use, and hyperlipidemia are important risk factors, prior medical history tends not to be helpful in evaluating other causes except in KD. Patients diagnosed with KD should be extensively interviewed and old records obtained regarding history of treatment, echocardiogram results, and follow-up studies. Patients should also be screened for prior febrile illnesses that may have been mistaken for KD. A family history should screen for Marfan syndrome, other aortopathies, and hypertrophic cardiomyopathy. A prior surgical history where the coronary arteries were manipulated or reimplanted is important in a patient with typical ischemic chest pain. The surgical reports pertaining to the procedure and how the coronary arteries were either reimplanted or manipulated are important to the current care of the patient and future testing that would need to be done.

DIFFERENTIAL DIAGNOSIS

The etiologies for nonatherosclerotic CAD and myocardial ischemia remain rare and for the most part difficult to diagnose, require a high index of suspicion, and often involve advanced imaging studies. Most of the diagnoses are covered in other areas of this textbook and are detailed in those

chapters. This group of diagnoses can be divided into those involving the coronary arteries directly and those that involve the myocardium leading to myocardial ischemia.

Related to the Coronary Arteries

- Anomalous coronary arteries
 - Left main coronary artery from the pulmonary artery
 - Left main coronary artery from the right coronary cusp
 - Right coronary artery from the left coronary cusp
- Coronary artery fistula
- Coronary artery spasm
- Thromboembolic or embolic CAD
- Kawasaki disease
- Coronary artery dissection
- Ostial CAD s/p reimplantation
 - D-TGA arterial switch
 - Aortic root replacement
 - Ross procedure
- Intramyocardial bridging
- Atresia of the left coronary artery orifice

Related to the Myocardium (Supply/Demand Mismatch)

- Hypertrophic cardiomyopathy
- Severe aortic stenosis
- Dilated cardiomyopathy
- Tachycardia in the face of limited coronary blood flow

Other

- Severe hypoxia or cyanosis

EXAMINATION

The cardiovascular examination in a patient with concerns for myocardial ischemia may be completely normal. Important cardiovascular findings in specific disease states include

- Dynamic systolic ejection murmur consistent with hypertrophic obstructive cardiomyopathy. Nonobstructive patients may not have a left ventricular outflow tract murmur with dynamic maneuvers but carry the same risk for ischemia.

- Continuous murmur along the left or right lower sternal border consistent with a coronary fistula or anomalous left main coronary artery from the pulmonary artery (LCAPA).
- Patients with dilated cardiomyopathy and heart failure will have signs of elevated jugular venous pressure, third or fourth heart sound, holosystolic murmur of mitral regurgitation, peripheral edema, and hepatic enlargement.
- Harsh systolic ejection murmur of hemodynamically significant aortic stenosis.

ELECTROCARDIOGRAM

The electrocardiogram (ECG) remains the most important diagnostic test in the evaluation for myocardial ischemia. Many factors are involved in the interpretation of the ECG; age, autonomic tone, heart rate, race, gender, and body habitus. Standing, hyperventilating, and performing a Valsalva maneuver can all have an effect on ST segments with small degrees of ST depression or T wave inversions just from body position or maneuvers. Pellicia et al. (1) described abnormal ECGs in 40% of Olympic athletes who had structurally normal hearts.

When the ECG is being performed to evaluate myocardial ischemia, the ECG should be obtained during episodes of chest pain, when possible, or shortly thereafter. The presence of an old ECG or an ECG obtained when the patient did not have chest pain for comparison is crucial when trying to decide whether dynamic ST changes are present, therefore consistent with myocardial ischemia. The ECG findings depend on several major factors as follows:

- Duration of myocardial ischemia
- Presence of prior bundle branch block (BBB) or WPW (pre-excitation), paced rhythm that could alter the ECG findings of myocardial ischemia
- The extent of the myocardial ischemia—subendocardial, transmural
- Location of the myocardial ischemia; i.e., anterior, posterior

Duration, location, and extent of myocardial ischemia will determine the changes seen on ECG. Whether the ischemia is subendocardial or transmural will affect the ST changes and the interpretation of the ECG (Fig. 64.1). When acute transmural ischemia occurs, tall peaked T waves with ST elevation are produced from epicardial injury representing the ischemic zone at risk of myocardial injury. The location that represents

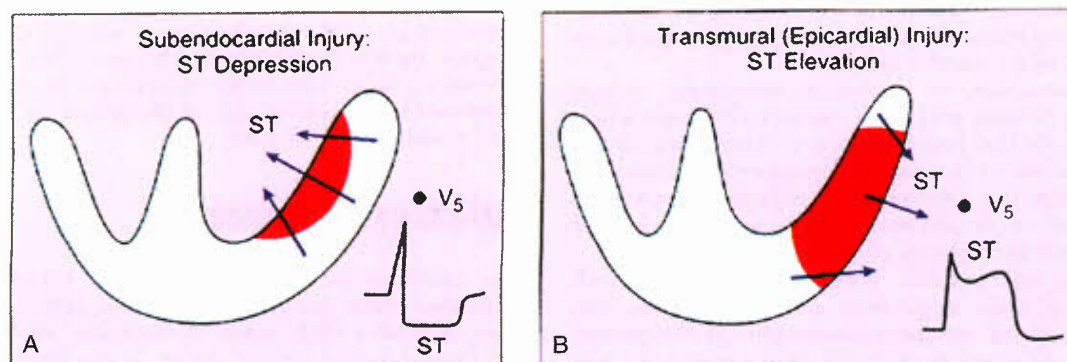


Figure 64.1. A: Represents subendocardial ischemia with the direction of injury toward the inner surface of the heart and therefore away from the surface chest leads. The injury current leads to ST depression. B: Represents transmural or epicardial injury with the injury current going toward the chest leads and therefore upright ST elevation. (Reprinted from Mirvis DM, Goldberger AL. *Electrocardiography*. In: Zipes DP, Libby P, Bonov TO, et al., eds. *Braunwald's Heart Disease*. 7th ed. Philadelphia, PA: Elsevier Saunders, 2005, with permission from Elsevier.)

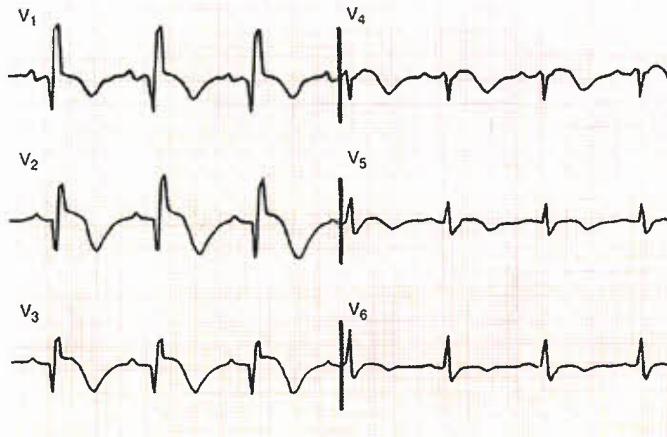


Figure 64.2. Right bundle branch block (RBBB) with acute anterior myocardial infarction. There are Q waves in the right-sided precordial leads and ST elevation in leads V1-V6. (Reprinted from Mirvis DM and Goldberger AL. *Electrocardiography*. In: Zipes DP, Libby P, Bonov TO, et al., eds. *Braunwald's Heart Disease*. 7th ed. Philadelphia, PA: Elsevier Saunders, 2005, with permission from Elsevier.)

the ischemic zone is represented by the placement of the surface ECG:

- Inferior—leads II, III, aVF
- Anterior—V2-V6
- Anterior-septal—V1-V3
- Lateral—I, aVL
- Posterior—leads V1 and V2 with tall R waves and ST depression, usually accompanied by ischemic changes in the inferior leads.

With subendocardial ischemia, the ischemic zone is toward the inner ventricular layer (subendocardium) and the overlying precordial leads demonstrate ST depression. Subendocardial ischemia is the common pattern for patients experiencing chronic chest pain secondary to ischemia. Abnormal base-

line ECG with preexisting ST or T wave change, prior BBB or evidence of preexcitation can limit the typical findings of myocardial ischemia (Figs. 64.2 and 64.3) and make the interpretation of myocardial ischemia more difficult, if not impossible, without other diagnostic tools.

For pediatric and adolescent patients in particular, normal variants and other disease states may mimic ischemic ST changes and need to be differentiated from true ischemic ST changes. Repolarization changes, pericardial disease, digitalis effect, and electrolyte abnormalities may all be associated with ST changes (Figs. 64.4–64.7).

A completely negative ECG at the time of ongoing chest pain is extremely predictive of nonischemic chest pain. The risk of an acute myocardial event is <2% among patients with no prior history for CAD presenting with a negative ECG at the time of chest pain (2). Therefore, differentiating between ischemic and nonischemic ST changes is crucial in the evaluation of chest pain.

BIOMARKERS OF MYOCARDIAL INJURY

When myocardial injury occurs, enzymes from the myocardium are released approximately 2 hours later and can be detected by various assays. Cardiac troponin T and I and creatine kinase MB isoenzyme (CK-MB) are all important biomarkers of myocardial injury and, when elevated, signify myocardial damage with good sensitivity and specificity (3,4). After injury occurs, these enzymes will rise within 2 hours, and may continue to rise for several hours. By 12 hours, the CK-MB will begin to decrease and by 24 hours the sensitivity of the troponins remains high whereas the CK-MB sensitivity diminishes (5) (Fig. 64.8). The CK-MB false positives are possible due to trace amounts of CK-MB in skeletal muscle. Therefore, damage to skeletal muscle on a large scale may increase the amount of CK-MB in the blood stream. Additionally, cardiac enzymes may be elevated with perimyocarditis due to inflammatory changes to the myocardium.

Troponins I and T are more specific than CK-MB for myocardial injury. However, since the troponin assays are able to detect what is felt to be very small degrees of myocardial

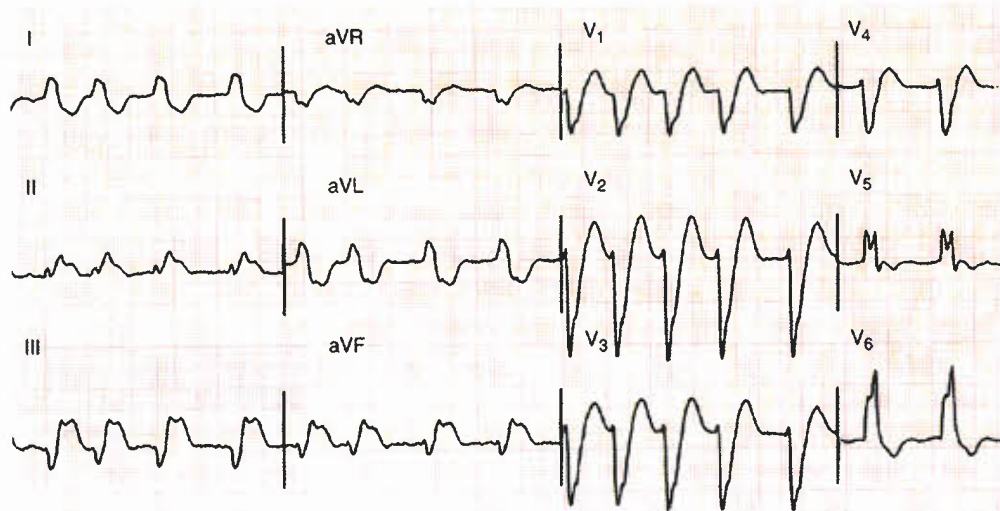
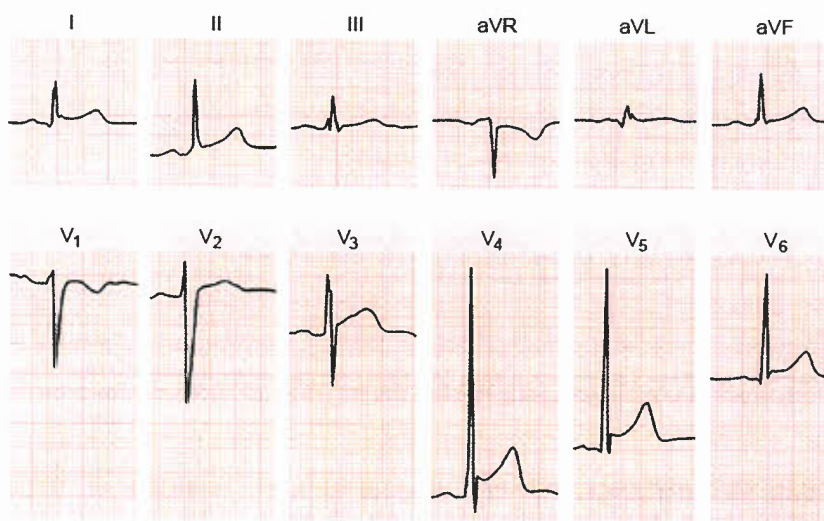


Figure 64.3. LBBB with acute inferior myocardial infarction. There is ST elevation in the inferior leads II, III, aVF. The patient is in atrial fibrillation. (Reprinted from Mirvis DM, Goldberger AL. *Electrocardiography*. In: Zipes DP, Libby P, Bonov TO, et al., eds. *Braunwald's Heart Disease*. 7th ed. Philadelphia, PA: Elsevier Saunders, 2005, with permission from Elsevier.)

Figure 64.4. Normal variant repolarization abnormality. There is J-point elevation mostly seen in lead V4. There are no reciprocal ST depression and no PR depression to distinguish this from acute myocardial infarction and pericarditis, respectively. (Reprinted from Goldberger AL. *Myocardial Infarction: Electrocardiographic Differential Diagnosis*. 4th ed. St Louis, MO: Mosby-Year Book, 1991, with permission from Elsevier.)



damage, in all cases, this may not be due to CAD. Myocarditis, pericardial disease, and trauma may all yield a positive troponin result. Therefore, the context in which the assay is performed may be equally important to the interpretation of the result.

There is increased sensitivity and specificity of the biomarkers for myocardial when serial assays are performed and when they are performed several hours after the onset of chest pain. Depending on the timing of the study, a single CK-MB and troponin I drawn early after the onset of chest pain may have a sensitivity of only 34% and 40%, respectively, whereas serial assays and assays drawn late (>12 hours) after the onset of chest pain have sensitivities that approach 90% (6).

A typical approach to the patient who presents with chest pain and the concern for myocardial injury would be to draw CK-MB and troponin cardiac enzymes at presentation. If positive, there is a high likelihood of myocardial damage and appropriate therapy should be initiated, if not already started

based upon other data. If the initial study is negative, and there remains a high likelihood that the chest pain represents myocardial ischemia, serial enzymes should be performed over the next 24 hours. Important in the use of cardiac biomarkers is the recommendation that patients with a very low probability for myocardial ischemia should not undergo cardiac enzyme testing because of the possibility for a false-positive result leading to unnecessary testing (7).

CARDIAC IMAGING AND STRESS TESTING

Two-dimensional transthoracic Doppler echocardiography (TTE) is an important diagnostic study when directed based upon history, exam, and ECG findings. The utility in a patient with no risk factors for myocardial ischemia, a normal exam, and normal ECG is far less helpful. From the list of potential

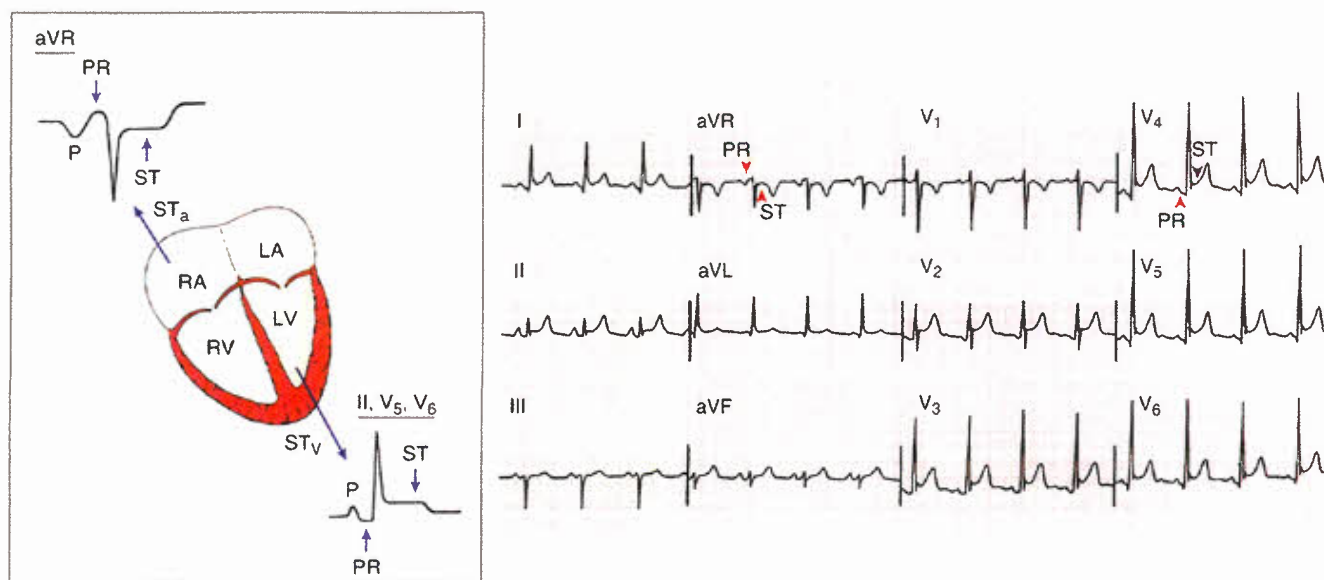


Figure 64.5. Acute pericarditis. PR depression represents reciprocal atrial inflammatory changes in all leads except AVr where there is PR elevation as the vector of injury is directed upward and to the right. Ventricular injury current is directed down and leftward leading to ST elevation in most leads except AVr. (Reprinted from Goldberger AL. *Myocardial Infarction: Electrocardiographic Differential Diagnosis*. 4th ed. St Louis, MO: Mosby-Year Book, 1991, with permission from Elsevier.)

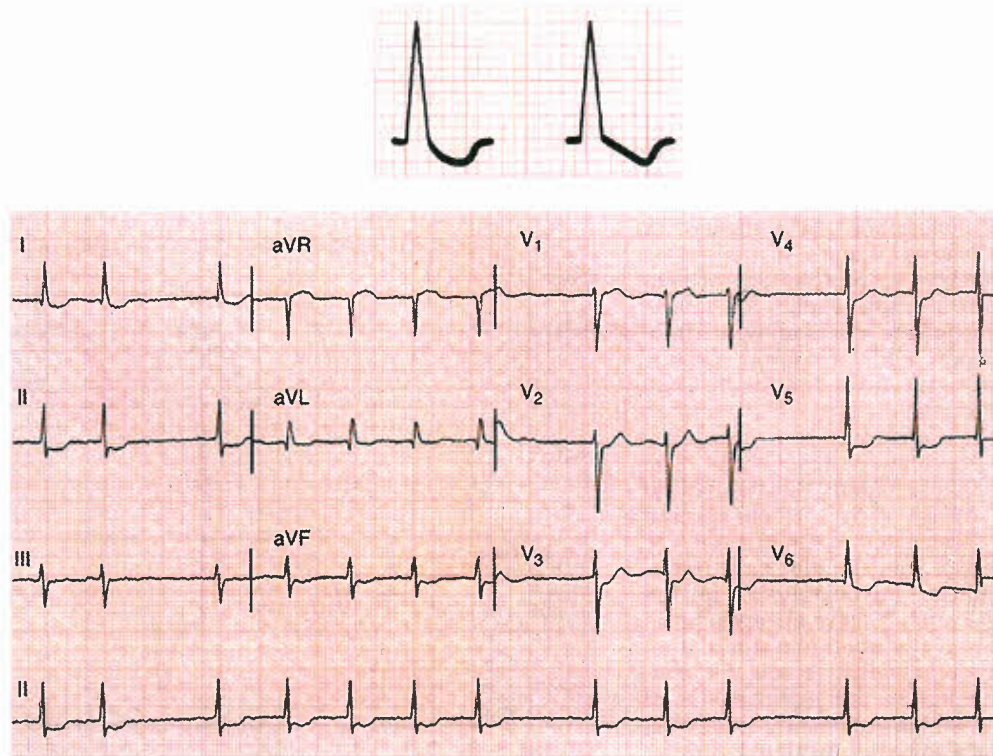


Figure 64.6. Digitalis effect (top) and digitalis toxicity (bottom). The typical ST segments have a scooped-out appearance. With digitalis toxicity (bottom), arrhythmias are common. In this case, the underlying rhythm is atrial fibrillation. The group beating is consistent with junctional tachycardia typical for digitalis toxicity. (Reprinted from Goldberger AL. *Clinical Electrocardiography: A Simplified Approach*. 4th ed. St Louis, MO: Mosby-Year Book, 1991, with permission from Elsevier.)

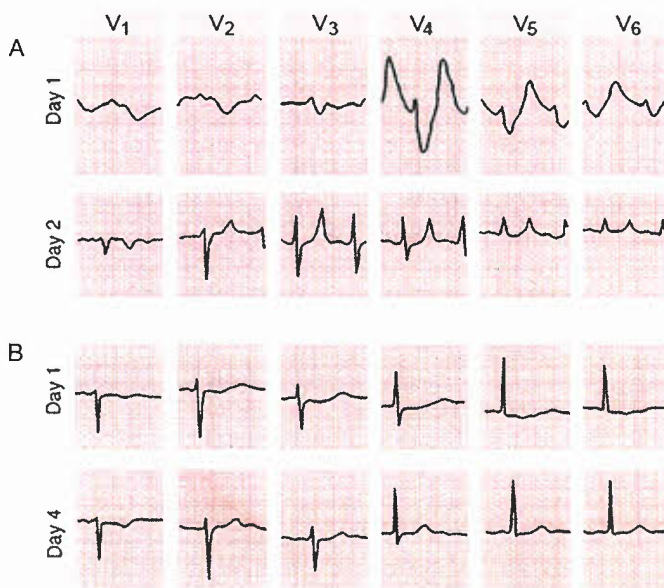


Figure 64.7. ECG changes associated with hyperkalemia (A) and hypokalemia (B). Day 1 (A) represents high serum levels of potassium with no recognizable P waves and prolonged QRS. On Day 2, the potassium level has decreased, and the P waves return and QRS becomes more narrowed. The T waves are tented consistent with hyperkalemia and must be recognized versus ischemic T waves. Day 1 (B) with low levels of serum potassium, the T and U waves have merged, and by Day 4 as the potassium approaches normal, the ECG normalizes. (Reprinted from Mirvis DM, Goldberger AL. *Electrocardiography*. In: Zipes DP, Libby P, Bonov TO, et al., eds. *Braunwald's Heart Disease*. 7th ed. Philadelphia, PA: Elsevier Saunders, 2005, with permission from Elsevier.)

causes of myocardial ischemia, TTE will accurately diagnose the following:

- Hypertrophic cardiomyopathy
- Severe aortic stenosis
- Dilated cardiomyopathy

In some cases TTE may provide clues to the diagnosis, but in many of these diagnoses, the echocardiogram may appear completely normal.

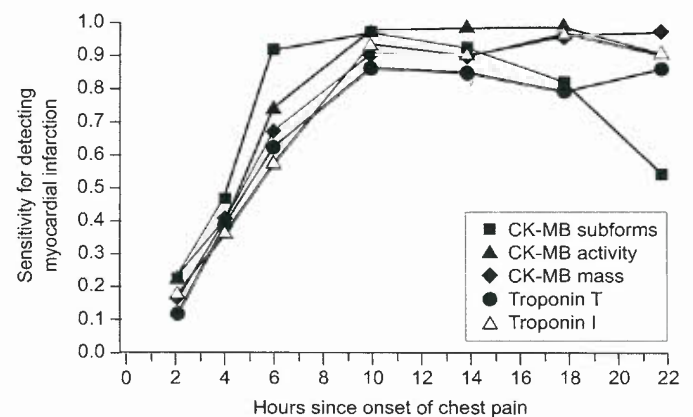


Figure 64.8. Sensitivity of markers of myocardial ischemia according to length of time from onset of chest pain. CK-MB, creatine kinase MB isoenzyme. (From Zimmerman J, Fromm R, Meyer D, et al. Diagnostic marker cooperative study for the diagnosis of myocardial infarction. *Circulation* 1999;99:1671, with permission.)

- Anomalous left main coronary artery from the pulmonary artery
 - Diastolic color flow within the ventricular septum representing coronary collateral circulation
 - Retrograde flow into the left main coronary artery
 - Mitral regurgitation with a structurally normal mitral valve (ischemic mitral regurgitation secondary to papillary muscle dysfunction)
 - Segmental left ventricular systolic dysfunction
- Coronary artery fistula
 - Diastolic color flow in the chamber receiving the coronary fistula, that is, right atrium
 - Enlarged right atrium and right ventricle if significant left-to-right shunt.
- Kawasaki disease
 - Coronary aneurysms

Cardiac MRI (CMR) and CT are the tests of choice when evaluating for anomalous coronary arteries, coronary fistulae, coronary aneurysm and ostial CAD following coronary reimplantation.

The main objective of stress testing for myocardial ischemia is to unmask the mismatch between myocardial oxygen demand and myocardial perfusion. At rest, the supply of myocardial

blood flow may be sufficient compared to the myocardial oxygen demand. However, with exertion, and increased demand, the amount of supply, i.e. myocardial perfusion may be inadequate and therefore ischemia is induced. Stress-induced ischemia may be detected by:

- ECG changes (ST depression)
- Segmental wall motion abnormality by echocardiography or CMR
- Perfusion defect by nuclear imaging or CMR

The role of stress testing in this population is less well defined. For the most part, stress testing is most sensitive and specific when the heart is structurally normal heart at rest, defined as a normal ECG with normal myocardial perfusion and wall motion at baseline. Therefore, a change in myocardial perfusion with stress will more clearly define the differences between normal and abnormal. In patients with a structurally abnormal heart (hypertrophic cardiomyopathy) or abnormal ECG (left bundle branch block [LBBB]), the ability to detect true myocardial ischemia with stress becomes much less accurate.

Additionally, when the diagnosis is nonatherosclerotic fixed CAD, a negative stress test may not clearly define the

TABLE 64.1

Strengths and Weaknesses of Various Stress Testing Techniques for Detecting Myocardial Ischemia

Technique	Strengths	Limitations
Exercise ECG	Low cost, short duration High sensitivity in three-vessel or left main CAD Provides useful prognostic information (e.g., ischemia at low workload)	Suboptimal sensitivity Low detection rate of one-vessel disease Nondiagnostic with abnormal baseline ECG Need to achieve $\geq 85\%$ of maximum heart rate for maximizing accuracy
Exercise or pharmacologic nuclear perfusion imaging	Higher sensitivity and specificity than exercise ECG Studies can be performed in almost all patients Quantitative image analysis	Suboptimal specificity because of artifacts Long procedure time when rest and stress both performed Higher cost than exercise ECG Radiation exposure Poor-quality images in obese patients
Exercise or pharmacologic stress echocardiography	Higher sensitivity and specificity than exercise ECG Comparable value with dobutamine stress Short time to complex examination Identification of coexisting structural cardiac abnormalities (e.g., valvular disease) Relatively lower cost than other techniques No radiation	Decreased sensitivity for detection of one-vessel disease Inability to image all of the left ventricle in some patients Highly operator dependent for image analysis No quantitative image analysis Poor acoustic window in some patients (e.g., chronic obstructive lung disease) Infarct zone ischemia less well detected
Magnetic resonance imaging (MRI)	High spatial resolution MRI coronary angiography promising Visualizing of subendocardial perfusion Pharmacologic stress procedure short No radiation	Inability to image patients with metal devices Difficult to image in setting of irregular heart rhythm <i>Motion artifact in absence of good breath-hold and respiratory gating</i> Coronary motion No large clinical studies yet published
Cardiac CT	Noninvasive coronary angiography to rule out significant coronary stenosis	Radiation exposure Cardiac motion artifacts Beta-blockers often required to reduce heart rate to < 60 beats/min Artifacts caused by coronary motion Prolonged breath-holding for scanner with < 16 -slice/s Images not generated in real time

TABLE 64.2 Causes of Myocardial Ischemia in Nonatherosclerotic CAD

Diagnosis	Treatment
Anomalous coronary arteries	Surgical repair with reimplantation or coronary bypass
Coronary spasm	Medical therapy with CCB, β B, Nitrates
Kawasaki disease	Medical therapy with β B, antiplatelets, anticoagulation, PCI
HCM	Medical therapy with β B, associated with intramyocardial bridging which may require myocardial release or coronary bypass
Aortic stenosis	Surgical replacement of the aortic valve, some may be candidates for balloon valvuloplasty
Coronary artery fistula	Transcatheter occlusion of fistula vs. surgical ligation
Thromboembolic CAD	Anticoagulation
Ostial CAD s/p reimplantation	Surgical repair of the ostium vs. coronary bypass

CCB, calcium channel blockers; β B, beta-blockers; PCI, percutaneous coronary intervention; HCM, hypertrophic cardiomyopathy.

risk of ischemia. Patients with anomalous CAD may exercise and participate in highly competitive sports with no symptoms of ischemia, but may still have intermittent ischemia that is unpredictable placing them at risk for sudden cardiac death. Stress testing in the population is frequently normal. Basso et al. (8) reviewed the clinical profile of young competitive athletes who suffered sudden cardiac death and at autopsy were found to have anomalous coronary arteries with origin of the coronary artery from the wrong sinus. They found that 6 of the 27 patients had premonitory stress testing, and that in all cases, the stress study was normal, including stress ECG and echo wall motion (2/2).

Therefore, the following patients in whom a high index of suspicion still exists after initial work up would benefit most from stress testing:

- Those with structurally normal heart
- Those who are able to cooperate with stress testing, whether medically or exercise induced

There remain many different types of stress testing to detect myocardial ischemia. Each test has strengths and weaknesses that depend not only on the test itself and imaging technique but also institutional experience. There are some institutions that clearly favor nuclear stress testing to echocardiography, or vice versa, and therefore become more proficient in one technique compared to another. A list of various techniques to detect myocardial ischemia are now available, each with their own set of strengths and weaknesses (Table 64.1).

TREATMENT

When patients present with myocardial ischemia from nonatherosclerotic CAD and ongoing chest pain, the immediate therapeutic interventions involve reducing myocardial oxygen demand with β -blocker therapy, antiplatelet agents, diagnostic testing to delineate the cause, and finally definitive treatment. Those with a history of KD presenting with chest pain and ischemic ECG changes are treated similar to typical acute myocardial infarction patients with thrombolytic therapy versus immediate cardiac catheterization and percutaneous coronary intervention. Other diagnoses such as anomalous CAD will require surgical intervention for definitive therapy. (see Chapter 32) (see Table 64.2)

SUMMARY

Myocardial ischemia remains rare in the pediatric population and in those with CHD. Historical features of myocardial ischemia are important to elucidate. With typical symptoms for ischemic chest pain, a high index of suspicion should dictate further testing. Definitive diagnostic testing with echocardiography, CMR and CT testing should confirm the diagnosis for the majority of those with a cause for myocardial ischemia. Cardiac catheterization should be performed when chest pain c/w ischemia is ongoing and when other diagnostic testing fails to find a cause for myocardial ischemia. General therapies include antiplatelet agents and reducing myocardial oxygen demand with β -blocker therapy. Definitive therapy is based upon the structural or functional abnormalities leading to myocardial ischemia and may involve additional medical therapies, catheter-based intervention or surgical repair.

REFERENCES

1. Pellicia A, Maron BJ, Culasso F, et al. Clinical significance of abnormal electrocardiogram patterns in trained athletes. *Circulation* 2000;102:278.
2. Lee TH, Goldman L. Evaluation of the patient with acute chest pain. *N Engl J Med* 2000;342:1187.
3. Antman EM, Tanasijevic MJ, Thompson B, et al. Cardiac specific troponin T levels to predict the risk of mortality in patients with acute coronary syndromes. *N Engl J Med* 1996;335:1342.
4. Polanczyk CA, Johnson PA, Cook EF, et al. A proposed strategy for utilization of CK-MB and Troponin I in the evaluation of acute chest pain. *Am J Cardiol* 1999;83:1175.
5. Zimmerman J, Fromm R, Meyer D, et al. Diagnostic marker cooperative study for the diagnosis of myocardial infarction. *Circulation* 1999;99:1671.
6. Brogan GX, Hollander JE, McCluskey CF, et al. Evaluation of a new assay for cardiac troponin I vs creatine kinase MB for the diagnosis of acute myocardial infarction. Biomarkers for acute myocardial infarction study group. *Acad Emerg Med* 1997;4:6.
7. Brunwald E, Antman EM, Beasley JW, et al. ACC/AHA 2002 guideline update for the management of patients with unstable angina and non-ST segment elevation myocardial infarction: summary article. A report of the American College of Cardiology/American Heart Association Task Force on Practice Guidelines (Committee on the management of patients with unstable angina). *Circulation* 2002;106:1893.
8. Basso C, Maron BJ, Corrado D, et al. Clinical profile of congenital coronary artery anomalies with origin from the wrong sinus leading to sudden cardiac death in young competitive athletes. *J Am Coll Cardiol* 2000;35:1493.

Robert E. Shaddy ■ Francesco Parisi

Pediatric heart transplantation has been practiced for over 25 years. With the advent of the T-cell activation inhibitors such as cyclosporine, heart transplant success rates for pediatric and adult patients have improved to the point that the initially restricted ages and indications have expanded considerably. Infant heart transplantation has been performed for over 20 years (1), and infants, children, and adolescents with complex cardiac anatomic lesions are now routinely successfully transplanted (2–4). There have been additional immunosuppressant pharmacologic agents discovered since cyclosporine, and novel new agents are in investigational stages. The increasing experience and newer drugs promise even better long-term results. Currently, the half-life (50% still alive) for children transplanted in the early 1980s is approximately 11 to 18 years (4). Decades-long survival seems likely (5).

Over 300 heart transplant procedures are performed annually in pediatric patients in the United States. Many more infants and children and adolescents could benefit from heart transplantation each year. The rate-limiting step to making heart transplantation more widely available is donor availability. Matching of appropriate donors to recipients is a more complicated problem in pediatrics with fewer recipients awaiting transplant at any given time compared to adults. Thus, the logistics of matching the size, blood type, and location of donor and recipient are logistically more complex.

Organ transplantation in the United States is sanctioned by congressional mandate through the National Organ Transplant Act (NOTA). NOTA created the framework for the Organ Procurement and Transplant Network (OPTN). The contractor for the OPTN is the United Network for Organ Sharing (UNOS). The process of organ donor identification is required for all hospitals, and the management of organ donors is by government-regulated local agencies called OPOs (Organ Procurement Organizations). The decision to donate organs remains a voluntary process involving donor and family wishes. The current UNOS allocation algorithm has three status categories based on medical urgency. These categories are status IA, IB, and II. Status IA is for the sickest patients needing an urgent transplantation for survival. Waiting mortality is 17% to 25% for status I patients and remains a significant problem in all age groups (6,7). Even within the sickest pediatric wait-list group (status 1A), there is large variability in outcomes, with those requiring extracorporeal membrane oxygenation (ECMO) having the highest wait-list mortality (7,8). The synchronization of recipient need, donor availability, consent for organ donation, and finally organ transplantation is a modern medical miracle that represents the ultimate in human sharing.

At present, 1-year survival in excess of 85% and 5-year survival >70% can be expected following pediatric heart transplantation (Fig. 65.1). Catch-up growth and hemodynamic rehabilitation to normal childhood functional status is likely. The quality of life can be normal. Heart transplantation remains the only hope for children with lethal cardiomyopathy,

some forms of complex congenital heart disease, and some infants and children with failed surgical interventions. This chapter discusses the indications for heart transplantation, various phases of the transplant process (preoperative, early postoperative, and late), the immunosuppressive drugs, the role of heart and lung transplantation, and the issue of retransplantation.

PRETRANSPLANT EVALUATION

A large amount of historical, anatomic, hemodynamic, metabolic, immunologic, and psychosocial information is required before deciding whether or not a child is an acceptable transplant candidate (9) (Table 65.1). A comprehensive history and physical examination is mandatory, including age, height, weight, and body surface area. Since pediatric heart donors are matched with recipient size, accurate measurements of the recipient are critical and need to be continually updated in those patients who wait long periods of time and undergo changes in their height or weight. Cardiac diagnoses, including all previous surgeries, must be meticulously delineated, with particular attention to venous and arterial connections, since the surgeon will need this information in order to devise a surgical plan in those with complex congenital heart disease with abnormal connections. The use of extended donor heart and vessel retrieval and creative intraoperative techniques has resulted in successful orthotopic heart transplantation in children with abnormal situs and/or significant systemic and pulmonary venous anomalies (2,10). Immunization status should be determined, and if incomplete prior to listing for transplant, immunizations may be given as indicated by age (11,12). A history of malignancy, once considered to be an absolute contraindication to transplantation, may not preclude transplantation in selected patients (13,14). A thorough laboratory evaluation is necessary to determine liver and kidney function since severe, irreversible liver or kidney dysfunction would generally exclude the child from consideration for heart transplantation, although some centers may consider multiple organ transplants. An equally extensive infectious disease evaluation is necessary to exclude active infection, to determine potential latent infections such as cytomegalovirus (CMV) or Epstein-Barr virus (EBV), and to provide baseline data on susceptibilities that can be followed serially after transplant. An accurate and documented blood type is critical since this is usually the main compatibility factor used for donor/recipient matching.

Evaluation of the immune system is an important part of the pretransplant evaluation. Although it is common to check recipient and donor human leukocyte antigen (HLA) status, this information is not normally part of the decision-making process when determining donor suitability. Retrospective studies have suggested that HLA compatibility is rare but may lessen rejection and improve graft survival in heart

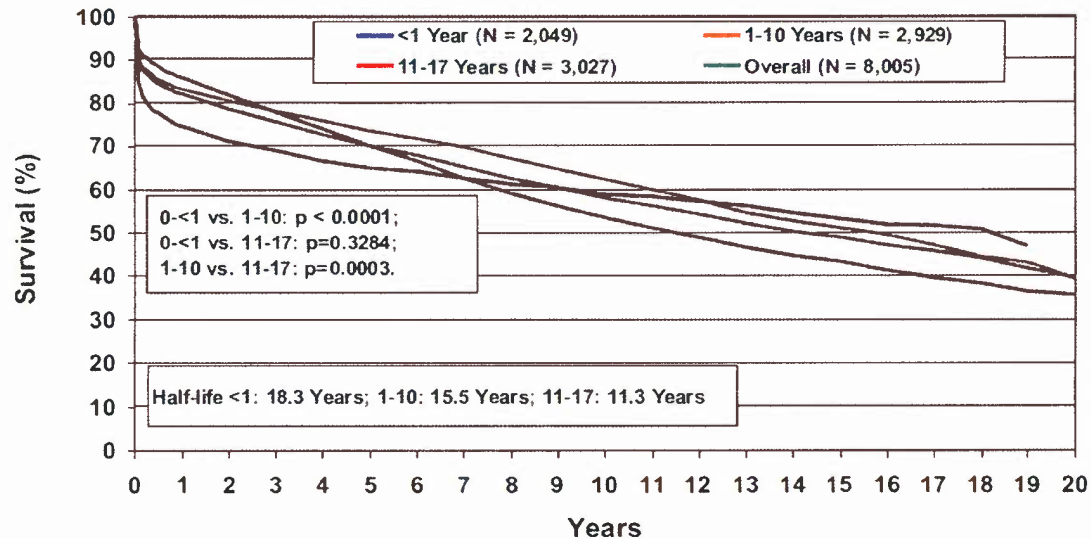


Figure 65.1. Actuarial survival for pediatric heart transplants performed January 1982 through June 2008. (From Kirk R, Edwards LB, Kucheryavaya AY, et al. The Registry of the International Society for Heart and Lung Transplantation: thirteenth official pediatric heart transplantation report—2010. *J Heart Lung Transplant* 2010;29:1119–1128, with permission.)

transplantation (15). In part due to the constraints of cold ischemic time (usually a maximum of about 4 hours) and the ongoing organ donor shortage, prospective HLA matching is not routinely utilized in heart transplantation. Panel reactive antibodies (PRA), a laboratory measure of preformed anti-HLA antibodies, are assayed to determine whether the recipient has any circulating anti-HLA antibodies. Recipients with circulating donor-specific anti-HLA antibodies before transplant have decreased graft survival when compared to those without these antibodies (16,17). Patients with a significantly elevated PRA before transplantation have traditionally undergone a prospective crossmatch between donor and recipient before acceptance of a donor organ (18–20). However, this can severely limit the donor pool available to a recipient and increases mortality waiting for transplant in those awaiting a compatible donor (16,20). Because of the significant difficulties associated with finding a compatible crossmatch in patients with elevated PRAs, multiple treatment modalities, including intravenous immunoglobulin, plasmapheresis, cyclophosphamide, and rituximab, have been utilized with variable degrees of success to try to decrease the PRA of highly sensitized patients (21–23). In sensitized adult patients awaiting renal transplant, rituximab has been shown to decrease HLA-antibody levels and thus expand the available donor pool for a HLA-compatible transplant (24). At the current time, there are conflicting data regarding the utility of the proteasome inhibitor, bortezomib, as an agent to reduce pretransplant donor-specific antibody (25,26).

With the exception of some infants with unoperated congenital heart disease (e.g., hypoplastic left heart syndrome [HLHS]), most children will require a cardiac catheterization before heart transplantation. Cardiac catheterization and angiography should be performed as part of the pretransplant evaluation by someone experienced in the diagnosis and treatment of pediatric cardiovascular disease and heart transplantation. Especially in patients with complex congenital heart disease, hemodynamic and anatomic assessments are critical for appropriate pretransplant evaluation. In addition to precise anatomic and hemodynamic definition, it is necessary to determine whether other pharmacologic, catheter interventional, or surgical options may be necessary prior to transplantation. Patients with univentricular physiology, particularly those who have undergone multiple palliative procedures, are

a unique group of patients whose pretransplant evaluation can be very complicated. For example, children after the Fontan operation may have many complications such as dysrhythmias, protein-losing enteropathy, cirrhosis, and/or low cardiac output that may bring them to transplant consideration.

Assessment of pulmonary artery anatomy, pressures and, when possible, pulmonary vascular resistance is critically important in the pretransplant evaluation of most children being assessed for heart transplantation. Severe, fixed elevation of the pulmonary vascular resistance is a contraindication to orthotopic heart transplantation because of concerns of acute posttransplant donor right ventricular failure. Both elevated transpulmonary pressure gradient and elevated pulmonary vascular resistance have been identified as risk factors for early mortality after heart transplantation (27). However, a previous multi-institutional analysis of risk factors for mortality in children >1 year of age at the time of transplantation did not find elevated pulmonary vascular resistance to be a risk factor (28). The current selection criteria for pediatric orthotopic heart transplant recipients exclude those patients with significantly elevated nonreactive pulmonary vascular resistance (3,9). In these patients who are denied orthotopic heart transplantation, other options such as heterotopic heart transplantation, heart/lung transplantation, or lung transplantation with repair of the congenital heart defect may be considered (29–31). Accurate evaluation of the degree of pulmonary hypertension may not be possible in those patients with either discontinuous pulmonary arteries or multiple sources of pulmonary blood flow, or in those with multiple branch pulmonary artery stenoses. Several agents have been shown to have both acute and chronic beneficial effects in lowering transpulmonary gradients and pulmonary artery pressures in adults and children. Response to these agents, including intravenous nitroglycerin, nitroprusside, prostaglandin E₁, dobutamine, enoximone, milrinone, in addition to inhaled nitric oxide, has been shown to predict outcome after heart transplantation (32–36). Mechanical circulatory support can also be considered in refractory cases (37). Children with restrictive cardiomyopathy appear to be at higher risk for development and rapid progression of significant pulmonary hypertension and thus require careful monitoring and possibly early consideration for heart transplantation (38,39).

Assessment of anatomy and function by a complete Doppler echocardiogram is a necessary part of the pretransplant evaluation.

TABLE 65.1 Routine Pretransplant Evaluation**Comprehensive history and physical examination, including:**

- Age, height, weight, body surface area
- Diagnoses
- Past medical history
- Medications
- Allergies
- Immunization record

Laboratory data

- Liver and kidney function tests
- Urinalysis
- Glomerular filtration rate
- Prothrombin time/partial thromboplastin time
- Complete blood count and differential
- PPD skin test
- Serologies for human immunodeficiency virus, hepatitis, cytomegalovirus, Epstein–Barr virus, *Toxoplasmosis gondii*, syphilis
- ABO type
- Panel reactive antibody

Consultation with dental service, or other services as indicated

- Cardiopulmonary data
- Cardiac catheterization and angiography
- Echocardiogram
- Radionuclide angiography
- Endomyocardial biopsy
- Electrocardiogram
- Chest radiograph
- Pulmonary function tests
- Vo₂ max

Psychosocial evaluation

- Possible relocation
- Long-term supportive care
- Parental substance abuse
- History of neglect or abuse

Cardiac magnetic resonance imaging may also be beneficial for defining anatomy and physiology. Radionuclide angiography may be superior to echocardiography in terms of quantitating the degree of systemic ventricular dysfunction. Endomyocardial biopsy may be indicated in certain instances, for example, to exclude active myocarditis or myocardial infiltrative diseases. Electrocardiograms and 24-hour continuous ambulatory electrocardiograms may be important in determining underlying rhythm, evidence of ischemia or previous infarction, and abnormal rhythms or intervals. A chest radiograph may be very useful for measuring the degree of recipient cardiomegaly to help in determining size limitations in potential donors. In older children, pulmonary function tests may be important, especially if there is any concern of chronic lung disease. In those who can cooperate, measurement of maximal O₂ consumption may be very useful for quantifying the degree of cardiorespiratory compromise the patient is experiencing. A significantly reduced maximal O₂ consumption <50% of that predicted for age may be considered evidence of compromise that should at least lead to consideration of heart transplantation as a therapeutic option (9,40). This diagnostic test may be much less useful in those children with heart failure who have undergone

the Fontan operation, since a significant number of patients in this group is unable to achieve maximal aerobic exercise capacity (41).

Psychosocial evaluation is a critical part of the pretransplant evaluation. A stable family support system that is emotionally and intellectually able to provide medications and posttransplant care is crucial to the success of the heart transplant. In many instances, it is necessary for the family to relocate to be in close proximity to the transplant center for the entire waiting period before transplantation and for 3 to 6 months after the transplant. This often provides additional stressors to the family. It is uncommon to have an absolute psychosocial contraindication to pediatric heart transplantation. However, a family history of noncompliance, substance abuse, or child abuse or neglect may be a relative contraindication to transplantation. In some instances in which the patient's parents have been determined to be incapable of handling the responsibility of caring for the child before and after transplantation, it has been necessary for a relative to take over those responsibilities (11). Financial needs and resources can vary considerably and should be thoroughly evaluated.

PRETRANSPLANT MANAGEMENT

Once a patient is under consideration for transplantation, every effort must be made to stabilize or improve the patient's clinical status. Since the waiting time for donors is unpredictable, patients may wait for long periods of time, during which time ongoing pharmacologic, catheter interventional, and occasional surgical treatments must be used as needed. Patients may deteriorate rapidly while waiting for a suitable donor, in which case, more invasive measures may be necessary to bridge the patient to transplantation.

The epidemiology of infant heart transplantation has changed through the years as the results for staged repair have improved and donor resources have remained stagnant. Heart transplantation, because of donor limitations, became consigned as primary therapy to those very few infants deemed unsuitable for staged reconstruction. Primary transplantation has remained available in some centers as a parental choice, and as the only solution for the occasional young infant with profound cardiomyopathic disease and inoperable complex congenital heart disease, including some tumors. Infants awaiting heart transplantation with ductal-dependent lesions (e.g., HLHS variants or other ductal-dependent lesions without good surgical options), are critically ill, chronically instrumented, and usually in an intensive care setting while they await transplantation (42,43). Since waiting times for donors has increased at many institutions, there are increased challenges and problems associated with keeping these infants stable, sometimes for several months, before a suitable donor becomes available (44,45). Initial efforts must be directed toward opening and maintaining patency of the ductus arteriosus through the use of continuous infusion of prostaglandin E₁. Once unrestricted ductal patency is achieved, therapy must be directed toward maintaining adequate systemic blood flow, sometimes through pharmacologic manipulation of the pulmonary vasculature (46,47). Some infants with HLHS and other ductal-dependent lesions have undergone percutaneous or surgical stenting of the ductus arteriosus in order to maintain ductal patency (48,49). The development of the so-called hybrid procedures has allowed surgical bilateral branch pulmonary artery banding and transcatheter stenting of the ductus arteriosus in place of a Norwood procedure (50). If necessary, heart transplantation after the hybrid procedure can be performed with acceptable results (51). Up to 50% of infants with HLHS may develop a critical restriction at the atrial septal defect level. These infants have excessive cyanosis and hemodynamic instability and

represent a high-risk group of infants who can be stabilized with interventional catheter procedures (52).

Heart transplantation has become a possible alternative to a high-risk Fontan operation in a strategy of staged palliation for single ventricle physiology. Heart transplantation should be considered as an alternative to Fontan completion in the decision-making algorithm for high-risk Fontan candidates, since rescue heart transplantation after early Fontan failure is associated with poor outcomes (53–58).

Patients with end-stage biventricular congenital heart disease represent a complex group for heart transplantation and require careful evaluation and management to ensure optimal perioperative and long-term outcomes. The vast majority of patients with biventricular congenital heart disease have undergone prior cardiac surgical procedures. Indications for transplantation in this subgroup are primarily progressive refractory heart failure following prior cardiac surgical reconstructive procedures. Contraindications to transplantation mimic those for other forms of end-stage heart disease (9,59,60).

Patients with heart failure secondary to ventricular dysfunction represent a significant proportion of children who are referred for heart transplantation. The natural history of dilated cardiomyopathy in children is quite variable; thus the optimal therapy for dilated cardiomyopathy and timing for transplantation in these children is unknown. Large, multicenter, randomized studies in adults with chronic heart failure have shown a significant improvement in left ventricular performance, symptoms, and survival in patients receiving angiotensin-converting enzyme (ACE) inhibitors and beta-blockers such as carvedilol or metoprolol when compared with placebo controls (61–64). Addition of beta-blockers to chronic heart failure therapy in some children (particularly those with a systemic left ventricle) may improve ventricular function, symptoms, and survival, thus delaying or even precluding the need for transplantation (65–68). ECMO has been used successfully in children as a bridge to transplantation, but remains problematic due to complications such as sepsis, bleeding, and neurologic injury (8,69–72). Options for mechanical support in children include miniaturized intra-aortic balloon pumps, ECMO, centrifugal pumps, and, more recently, both pulsatile ventricular assist devices (VADs) and axial flow devices (see Chapter 21). ECMO remains the most common form of mechanical support available and is the best option for acute decompensation. ECMO provides total cardiopulmonary support, can be relatively quickly accomplished, and allows the flexibility of peripheral and central cannulation (73,74). ECMO pumps, however, achieve nonpulsatile flow, and the circuit is complex. The incidence of bleeding and infectious complications is very high, and neurologic impairment with extended use is also common. ECMO also restricts patients' mobility, impairing physical rehabilitation. VADs have potential advantages over ECMO as a mechanical bridge (70). Pulsatile pumping may result in better tissue perfusion and specifically provides better recruitment of the microcirculation of the brain, lungs, and kidneys during extracorporeal circulation. In addition to improving a patient's hemodynamic status and reversing end-organ dysfunction, VADs can be partially or fully implanted and allow for physical rehabilitation to improve the patient's overall condition and likelihood for successful transplantation. Biventricular VAD support can effectively be used in small children as a bridge to heart transplantation and can be accomplished with low mortality and morbidity. Biventricular VAD support may offer an additional means to reverse extremely elevated pulmonary vascular resistance (37,75–79). However, the persistent high rate of morbidity emphasizes the importance of optimizing the decision-making process and, particularly, the timing of implantation. Patients with congenital heart disease and end-stage heart failure currently have a

limited number of options for long-term mechanical circulatory support. In recent years, significant advances have been made, and more devices are under development with some having already reached preclinical trials (80). Over the next few years, continued improvements in the field of pediatric mechanical circulatory support are expected, including the addition of new pediatric VADs, new magnetically levitated centrifugal pumps, and new low-pressure-drop hollow-fiber membrane oxygenators for ECMO.

DONOR ISSUES

Because of the ongoing donor shortage for pediatric heart transplantation, transplant cardiologists have made great efforts to maximize donor usage. Although optimal donors have normal cardiac anatomy and function, ideal size and blood type match, and minimal cold ischemic time, many successful pediatric heart donors are used that do not meet these ideal criteria (1). Some degree of both systolic and diastolic dysfunction in the donor heart can be tolerated (1,81). Studies have shown successful pediatric heart transplant outcomes after donor ischemic times as long as 8 hours, with no significant differences in outcomes between those with donor ischemic times >8 hours and those with donor ischemic times ≤90 minutes (82). Although the mechanism is unclear, the use of advanced-age donor hearts (>40 years of age) for appropriately sized teenage recipients carries a significantly higher 1-year posttransplant mortality than use of younger donor hearts (83).

The incidence of sudden infant death syndrome (SIDS) has decreased over the last 15 years (58). Still, SIDS is the third leading cause of death for infants with an estimated annual incidence in the United States of 0.54 per 1,000 live births. There has been no difference in clinical outcome between infants transplanted with a donor who died from SIDS compared to donors who died of other causes (1,84). Recently, the proportion of transplanted infant donor hearts where donor cause of death was SIDS has increased from just over 4% in 2000–2002 to nearly 9% in 2006–2008. This is possibly due to transplant centers' increasing confidence with the use of SIDS donors. Most recently, there is increased interest and investigation into the use of non-heart-beating heart donors after cardiocirculatory death as an additional source of donors for both adults and children (85,86). Increasing the number of donors remains an important goal to ensure that sick patients in need of transplant have that opportunity.

ABO INCOMPATIBLE HEART TRANSPLANTATION

The need for matching donors and recipients can lead to donor hearts that are not used and recipients who die waiting. Blood group matching is considered critical for heart transplantation. Since infants usually lack preformed blood group antibodies (isohemagglutinins), ABO incompatible heart transplants have been successfully performed in infants <1 year old, and occasionally older patients (87,88). Cardiac transplantation in infancy using ABO incompatible donors in the appropriate setting has now become an established protocol in many centers around the world. Those infants who received an ABO incompatible graft usually (but not always) fail to develop antibodies against the incompatible blood group epitope from the donor, while making antibodies normally to other incompatible blood groups (88,89). For example, a recipient whose

blood type is O and receives a heart from a B donor will later make antibody to blood group A but usually not to blood group B. This observation has been used as an example of B cell tolerance (90). This type of approach has resulted in improved wait-time survival of infants in some studies, but not in all studies (91,92). This difference may reflect the fact that donor hearts are still offered to ABO-compatible recipients before ABO-incompatible recipients in the UNOS system in the United States, but not in other systems. The 10-year outcomes of infants receiving ABO-incompatible heart transplants are virtually identical to ABO-compatible heart transplants (89). Thus, there appears to be no contraindication to listing all infants with low isohemagglutinin titers for ABO-incompatible heart transplant.

POSTOPERATIVE MANAGEMENT

General Considerations

The postoperative course after heart transplantation can be complicated by numerous unique issues. Potential complications relate both to the donor and the recipient. Myocardial injury and cause of death, donor versus recipient size, donor heart ischemic time, blood and tissue compatibility, infectious status of both donor and recipient, recipient diagnosis, and recipient clinical and psychosocial conditions may affect myocardial performance and postoperative course.

The effects of brain injury and death on myocardial performance have been investigated (81,93). The process of brain death leads to myocardial dysfunction and is often due to multiple factors: brain death itself may cause myocardial dysfunction; the donor cause of death (sepsis, trauma, etc.) can directly depress myocardial contractility; and the high catecholamine environment of stress or the pharmacologic support of the donor can lead to receptor downregulation. Although no specific correlation with survival has been demonstrated, it is common for many centers to accept some degree of donor heart systolic or diastolic dysfunction, either or both of which are often reversible after transplantation. Donor ischemic times in pediatric heart transplantation have been reported by many centers to increase the postoperative need for inotropic support but to not be a risk factor for 1-year mortality (82,94).

As described above, ABO-incompatible heart transplants have been successful in the 1st year of life before the onset of isohemagglutinin production. This practice requires particular attention to postoperative management including specific immunosuppression and transfusion protocols (87–89). In the adolescent age group, the number of patients with congenital heart disease who become transplant candidates after a long surgical and blood transfusion history is increasing. These patients represent an increasingly HLA-sensitized heart transplant population who require special consideration and often require pre- and postoperative immunomodulatory treatment (16,23,95). Many strategies have been tried to reduce this allosensitization before transplantation in order to optimize the opportunity for finding and transplanting an HLA cross-match-compatible organ. These strategies have included plasmapheresis, a procedure that involves extracorporeal removal and replacement of the entire plasma volume (containing antibodies as well as other proteins such as coagulation factors). Plasmapheresis requires placement of a large bore dual lumen catheter in a large central vein. This is often challenging in young children due to size of blood vessels, lack or minimal vascular access because of venous occlusions from previous catheters, and/or systemic venous anomalies. Exchange transfusions are often performed in children who are too small for vascular catheter placement and plasmapheresis. Additional

strategies include immunosuppressant medications (such as cyclophosphamide), intravenous immune globulin (IVIG), rituximab, or some combination of these (23,96,97). It has been known for decades that the presence of circulating anti-HLA antibodies before transplantation is associated with increased risk of rejection, graft vasculopathy, graft dysfunction, and death after transplantation (16,98–100). Injury to the graft may be acute with hemodynamic dysfunction or more chronic manifesting as chronic rejection or graft vasculopathy. Donor specific anti-HLA antibodies may be preformed due to allosensitization prior to transplant, or develop *de novo* at any time following transplant. The *de novo* development of anti-HLA antibodies after heart transplantation correlates with decreased long-term survival (101). Patients with *de novo* antibodies appearing more than 1 year following transplantation have the poorest survival (102).

Patients with congenital heart disease present unique perioperative problems related to their specific morphology, previous surgical procedures, and reconstructive surgery. Heart transplantation in children with an anatomic or physiologic single lung has been successfully performed, but pulmonary artery reconstruction increases risk for mortality (103–105). Heart transplantation for structural congenital heart disease with single ventricle physiology is associated with substantial early mortality, and transplantation after the acutely failing Fontan may be prohibitively risky (53). Fontan status remains a risk factor of mortality after heart transplantation with an expected 5-year survival barely approaching 70%, with particularly increased risk in those with evidence of pulmonary vascular disease (106). Tailoring of immunosuppressive therapy is a crucial issue in these patients since they are often immunocompromised from their failing Fontan physiology with protein loss, liver dysfunction, and low cardiac output. Heart transplantation outcomes for patients after the Fontan operation are better in those who require heart transplantation owing to ventricular dysfunction (rather than those with preserved ventricular function and failing Fontan circuit) and those without significant comorbidities such as hepatic cirrhosis or chronic malnutrition (57). Protein-losing enteropathy is a severe complication of Fontan physiology but can be improved by heart transplantation (55,58,107). Moreover, the long-term fate of protein-losing enteropathy after heart transplantation has not been completely elucidated, and recurrence of protein-losing enteropathy after heart transplantation has been reported.

Practical Considerations

Adequate monitoring of the postoperative heart transplant patient is essential. Recently published guidelines from the International Society for Heart and Lung Transplantation (ISHLT) for the perioperative monitoring of both adult and pediatric heart transplant recipients are detailed in Table 65.2 (108). Of these, standard pediatric monitoring would include all except assessment of pulmonary arterial wedge pressure and cardiac output via invasive catheters owing to concerns of catheter size and maintaining appropriate catheter position, especially in smaller recipients. However, continuous, direct measurement of pulmonary artery pressures is often monitored in pediatric patients, particularly those with elevated pretransplant pulmonary arterial pressures. Perioperative hemodynamic instability can be present and can be a result of multiple causes including graft reperfusion injury, inflammatory response after cardiopulmonary bypass, elevated pulmonary vascular resistance, and labile fluid status. Most patients can be supported with catecholamine infusions after transplant surgery and often benefit from an elevated heart rate to compensate for diastolic filling abnormalities. Temporary pacing is also used. Milrinone is often used to reduce pulmonary

TABLE 65.2

ISHLT Guidelines for Post-Heart Transplant Monitoring

Postoperative 12-lead ECG	Invasive arterial pressure monitoring
Right atrial or central venous pressure monitoring	Left atrial or pulmonary artery wedge pressure monitoring
Intermittent measures of cardiac output	Arterial oxygen saturation monitoring
Intraoperative transesophageal echocardiogram	Continuous assessment of urinary output

and systemic vascular resistance and potentially provides a non-adrenergic-receptor-dependent form of inotropic support. The donor right ventricle is not “prepared” to deal with elevation in pulmonary vascular resistances, and thus some degree of right ventricular failure is common and usually lasts for several days. Many agents, such as prostaglandins, prostacyclin, nitroprusside, inhaled nitric oxide, and others have been proven to be effective in these patients (36). In rare instances, right heart failure may be so severe that ECMO is required to support the circulation. Hemodynamic parameters, such as right-sided filling pressures and functional right ventricular assessment with echocardiography can be used to follow the course of right ventricular recovery and direct appropriate weaning from supportive measures. A preventive therapy with selective vasodilators as well as the availability of mechanical assist devices during and after heart transplantation can reduce deleterious effects of both transitional pulmonary hypertension and primary graft failure (109).

The early posttransplant period (<30 days) is the most hazardous. Primary graft failure and early morbidity are largely explained by recipient issues that increase perioperative risk (110). Review of the ISHLT Scientific Registry details several major risk factors for 1-year mortality (4):

1. Congenital diagnosis, on ECMO (relative risk: 2.86)
2. Congenital diagnosis, no ECMO (relative risk: 2.02)
3. Retransplantation (relative risk: 1.96)
4. Year of transplant: 1996–1997 versus 2002–2003 (relative risk: 1.68)
5. Year of transplant: 1998–1999 versus 2002–2003 (relative risk: 1.49)
6. On dialysis (relative risk: 1.66)
7. On ventilator (relative risk: 1.54)
8. Panel reactive antibody >10% (relative risk: 1.36)

Postoperative bleeding can be significant in children following heart transplantation. Causes are multifactorial and include previous congenital heart surgery necessitating extensive dissection, cardiopulmonary bypass, multiple suture lines, pretransplant heparinization for VAD or ECMO support, and poor preoperative nutritional status. Platelet and fresh frozen plasma infusions should be used as necessary to control hemorrhage, and recombinant factor VII may be useful for refractory bleeding. Volume resuscitation including packed red blood cells (preferably leukocyte-reduced and CMV negative) may be necessary, but should be administered with caution given the potential increased risk for alloimmunization from transfused leukocytes, which may express non-donor-matched HLA antigens. Patients with refractory hemorrhage or those demonstrating clinical evidence of cardiac tamponade should be surgically explored.

Acute renal failure occurs postoperatively in 3% to 10% of transplant recipients (111). Hemodialysis may be necessary for refractory fluid overload and oliguria in the presence of a rising serum creatinine. Multidisciplinary team management including nephrology consultation is often useful in this circumstance. Patients often develop systemic hypertension in the immediate postoperative period. This can be secondary to baroreflex-mediated hypertension, catecholamine dysregulation from low cardiac output before transplant, significant pre-existing renal injury, and newly initiated immunosuppressive medications such as corticosteroids or calcineurin inhibitors. Nitroprusside, calcium-channel blockers, ACE inhibitors, or a combination of these usually provides adequate blood pressure control. Recipient/donor size mismatching can also influence postoperative course. “Big heart syndrome” results when the donor size is significantly larger than the recipient. In the early transplant period, donor/recipient weight ratio mismatches of >2.0 may result in systemic hypertension syndrome with associated central nervous system symptoms including seizures and coma. Treatment consists of antihypertensive medication titration to achieve a normal blood pressure for age. An inappropriately small donor heart size has been associated with increased mortality, and a donor/recipient weight ratio <1 has been reported as a significant predictor of fatal postoperative heart failure (112). Postoperative pericardial effusions develop in 9% to 21% of adult recipients (113,114). The incidence in pediatric patients is unknown but is likely similar to adults and may, in part, be related to an increased pericardial volume created after a dilated heart is replaced with normal-sized heart that fills with fluid. Unless the effusion is hemodynamically compromising or there is a strong suspicion of an infectious etiology, the effusion usually does not require surgical or percutaneous drainage and can be monitored serially by echocardiography. Posttransplant sinus node dysfunction is common with a reported prevalence as high as 44% (115) and is likely related to myocardial ischemia and surgical manipulation. The ISHLT guidelines recommend pharmacologic treatment or pacing to maintain an adequate heart rate.

Immunosuppression is started in the perioperative period. Some institutions begin calcineurin inhibitors (cyclosporine or tacrolimus) just before the transplant operation. High-dose corticosteroids are given intraoperatively and continued for a brief period of time, after which they can be discontinued or decreased to a low-dose maintenance regimen. Additional immunosuppressive medications may be given postoperatively in the form of polyclonal antibodies directed toward multiple T-cell epitopes (antithymocyte globulin), or either chimeric or humanized monoclonal antibodies directed toward the interleukin 2 (IL-2) activation pathway (CD25) (116,117). Despite its success in achieving these goals, the universal use of induction therapy has been nonetheless limited due to mixed reports that it may have increased the risk for infection and posttransplant lymphoproliferative disease (PTLD), and there is no consistent evidence that it improves outcomes. Recent data suggest that induction strategies can be implemented without increasing early infection or PTLD risk (118). Other maintenance immunosuppressants include azathioprine or mycophenolate mofetil (MMF), and in a few selected cases, sirolimus.

Over the last 12 years, the incidence of rejection in the 1st year after pediatric heart transplant has decreased from about 60% to just over 40% (119). The peak hazard, or instantaneous risk, for rejection is around 1 to 2 months after transplantation (120). Older age at transplantation represents a risk for first rejection and a risk for an increased number of episodes of rejection within the first 6 months after transplantation. Infections occur in up to 25% of pediatric recipients during the early postoperative period, and 60% of these infections are bacterial (121). The most common bacterial pathogens reported are *Staphylococcus*, *Pseudomonas*, and *Enterobacter*.

cloacae (122). Bloodstream and pulmonary infections are most common, followed by urinary tract and surgical site infections (123,124). The ISHLT guidelines recommend perioperative antibiotic prophylaxis against skin flora, particularly *Staphylococcus aureus*, and, if donor infection is confirmed, additional targeted therapy against the potentially transmissible donor organism should be strongly considered.

Rejection: Diagnosis and Treatment

Institutional preference usually dictates whether endomyocardial biopsy or echocardiography is used as the primary rejection surveillance tool. Because of the inconvenience, greater technical challenges, and possible increased morbidity of biopsy in smaller children, there has been much interest in evaluating the role of echocardiography in children undergoing transplantation (125–131). Many quantitative echocardiographic parameters have been investigated, including various measures of systolic and diastolic function, changes in left ventricular wall thickness and mass, and development of mitral regurgitation or pericardial effusion. Doppler studies and tissue characterization have also been evaluated. Despite this interest, the controversy over the role of echocardiography is far from resolved. Furthermore, if endomyocardial biopsy is still considered the gold standard for diagnosing allograft rejection after heart transplantation (132–135), the value of routine surveillance biopsies is also controversial in children. In fact, many centers have discontinued routine surveillance biopsies after the 1st or 2nd year from transplantation. Many centers perform routine endomyocardial biopsy on infants significantly less frequently or not at all, instead depending on physical exam and echocardiogram to aid in diagnosis, and reserve biopsy only for clinical indications (136). With any clinical deterioration in the early postoperative period, evaluation of and treatment for rejection as the potential cause should be considered.

The need for noninvasive diagnosis of rejection has stimulated the ongoing search for biohumoral markers, such as B-type natriuretic peptide. The clinical relevance is still to be defined for all these markers (137–140).

Clinical evaluation of rejection is important but can be misleading, particularly in pediatric patients in whom infectious issues can mimic the presentation of rejection. The characteristic infiltration of the donor heart by lymphocytes leads to the diagnosis of rejection on endomyocardial biopsy (141). Histologically, cardiac allograft rejection and lymphocytic myocarditis can be very similar. There have been reports of positive viral genome in heart transplant endomyocardial biopsy specimens, suggesting viral myocarditis, in addition to improved outcomes in these patients if treated with IVIG for presumed myocarditis (142,143). Arrhythmias also may be a marker for rejection. The surface electrocardiogram may suggest atrial flutter or atrioventricular dissociation, but this observation may be attributed to the fact that the recipient atrial tissue contracts independently of the donor atrial tissue, and there may be two P waves present on the surface electrocardiogram that are not synchronous.

The vast majority of initial rejection episodes can be successfully reversed by high-dose corticosteroids alone or in conjunction with anti-T-cell antibodies. Corticosteroids as either intravenous methylprednisolone (10 to 30 mg/kg every 12 hours) or oral prednisone are the first line in rejection therapy. Humoral or antibody-mediated rejection (AMR) results from an antibody-mediated response to mismatched human leukocyte antigens present within the donor myocardium and vascular endothelium, and the number of mismatches may influence the speed and degree of rejection (144). Pathologically, this form is characterized by a lack of significant cellular

rejection on endomyocardial biopsy with characteristic histologic and/or immunohistochemical findings (145,146). It is often accompanied by left ventricular dysfunction and detection of donor-specific antibodies in the recipient serum. Treatment of AMR following heart transplant is focused on elimination of circulating antibodies, inhibition of circulating antibodies, suppression of B cells, plasma cell depletion, and/or complement inhibition, in addition to support of graft function, which is often impaired due to immune-mediated injury (147–149). Attempts to remove antibody are most commonly performed with plasmapheresis. Sedation may be required for catheter placement, which has risks if the patient is experiencing hemodynamic compromise from AMR. Fluid shifts, calcium and other electrolyte flux, and systemic reactions to blood products used for plasma replacement are other risks related to plasmapheresis and/or exchange transfusion. Immune apheresis (immunoadsorption) is an emerging modality to specifically remove circulating antibodies and immune complexes. Plasmapheresis is often accompanied by the use of high-dose IVIG for immunomodulation to block anti-HLA antibody activity and inhibit complement, as well as corticosteroids to further attenuate the negative effect of circulating antibodies. Therapies to specifically target B cells are often incorporated into treatment for AMR. Rituximab is a chimeric murine/human anti-CD20 monoclonal antibody that is utilized to deplete B cells and interfere with antigen-presenting cell activity to attempt to reduce the risk of recurrent AMR. While most reports have shown utility in treating AMR, all are small case series with different response rates and treatment protocols, combining various doses of rituximab with IVIG, steroid, and plasmapheresis. Serious infections are a notable side effect observed with rituximab therapy. Cyclophosphamide and MMF have also been used to directly suppress B-cell population. New therapies are constantly being sought since the current methods are not universally successful.

Immunosuppressive Medications

The class of drugs that inhibit T-cell activation are still the mainstay of immunosuppressive therapy. Cyclosporine was the first drug of this class to reach clinical utility in the early 1980s and in effect began the modern era of solid organ transplantation. Cyclosporine can be given initially intravenously in a dose of 0.03 to 0.1 mg/kg/h. When oral medications can be tolerated, the usual starting dose is approximately three times the intravenous dose or 2 to 6 mg/kg/day divided every 12 hours in older children, although higher doses are usually required in infants. Trough blood levels of cyclosporine must be monitored to insure efficacy and avoid toxicity. The therapeutic range for blood levels for the active compound, cyclosporine A, range from 100 to 350 ng/mL. Higher blood levels are usually maintained early after transplant, and tapered based on time posttransplant and clinical course. The bioavailability of cyclosporine is variable particularly in children, although the microemulsion preparations have improved bioavailability (150). Studies comparing cyclosporine with tacrolimus have suggested no definitive benefit of tacrolimus over cyclosporine in terms of reducing the incidence of rejection, although tacrolimus is now more widely used in pediatric heart transplantation than cyclosporine (4,151,152).

Tacrolimus acts at a different site in the IL-2 activation pathway of lymphocytes. Like cyclosporine it can be given intravenously. When given orally the starting dose is usually 0.05 to 0.1 mg/kg/day divided twice daily. Trough blood levels must be monitored. The usual therapeutic range is 5 to 15 ng/mL. The third agent in this class (T-cell activation inhibitors) is rapamycin (sirolimus). Sirolimus acts at a more distal site (target of rapamycin receptor) in the lymphocyte activation

cascade by blocking transcription of activation genes. Early experience with this medication as adjunctive or replacement therapy for calcineurin inhibitors have been promising (153,154). Sirolimus can inhibit smooth muscle proliferation and may have another advantage by inhibiting the process of cardiac allograft vasculopathy (CAV) (155). The dosing and monitoring of sirolimus in pediatric patients is not well defined. The usual starting dose is 1 to 2 mg/m²/day with levels of 5 to 15 ng/mL at present in heart transplant (156). Sirolimus is most often used in combination with a calcineurin inhibitor. However, sirolimus appears to be less nephrotoxic over the long term and has been successfully used as the sole T-cell activation inhibitor at a later stage in liver, renal, and most recently heart transplant recipients (157). Use in pediatric heart transplantation has been growing and has been positive for allowing reduction in calcineurin dose and in stabilizing and/or improving renal function (154,156). Everolimus is an inhibitor of the p70 S6 kinase, arresting the cell cycle of lymphocytes and vascular smooth muscle in the G1 phase, with additional immunosuppressive actions of IL-2 and IL-15-mediated T- and B-cell proliferation (158,159). Experience with everolimus in pediatric heart transplantation is limited.

Drug and food interactions are common with immunosuppressive agents. They should be carefully evaluated when starting new drugs, including even antibiotics or foods such as grapefruit.

Antiproliferative Agents

Historically, the most commonly used agent to block immune cell proliferation has been azathioprine. It is a nonselective inhibitor causing nonspecific bone marrow suppression. The usual dose is 1 to 2 mg/kg/day as a single daily dose and drug effect is monitored by the white blood count. The white blood count is usually maintained at >4,000/mL. Mycophenolic acid in the form of MMF inhibits the *de novo* pathway for purine synthesis. Since lymphocytes lack the salvage pathway, MMF can selectively block lymphocyte proliferation without the side effects of nonspecific bone marrow suppression. The improved selectivity compared to azathioprine may provide more effective immunosuppression (160). Because of these benefits, MMF has replaced azathioprine in most pediatric heart transplant protocols (4). Comparative studies in adult heart transplantation indicate an efficacy benefit for MMF over azathioprine (161). The usual starting dose of MMF in children is 600 mg/m², but absorption varies widely and higher doses may be required. In adults and adolescents, the dose of MMF is 3 g/day divided twice daily. The value of blood levels is controversial. The effective blood level for mycophenolic acid has been reported as 3 to 7 ng/mL (108). Methotrexate and cyclophosphamide have also been used in transplant recipients as adjunctive therapy for chronic or recurrent rejection (162,163).

Nonspecific Immunosuppression

Corticosteroids are potent immunosuppressive agents and are the first line of rejection therapy. Many centers also use corticosteroids as part of routine immunosuppression. In pediatric patients, the side effects of corticosteroids have encouraged most programs to attempt to discontinue routine oral steroids (164,165). The favorable experience in pediatric heart transplant with a corticosteroid-free maintenance protocol has led to its use with other pediatric solid organ transplant recipients. For significant rejection, methylprednisolone is usually given in a dose of 10 to 30 mg/kg every 12 hours intravenously for six to eight doses. A tapering dose may then be used to return

to usual maintenance oral doses of prednisone or discontinued depending on the policy of each individual program. The dose for maintenance of oral prednisone is in the range of 0.1 to 1 mg/kg/day.

All the current immunosuppressive medications do not lead to tolerance in humans, although they can lead to tolerance in experimental models. The transplanted graft must work for many decades in pediatric recipients. In order to reduce the burden of immunosuppressive drugs, the drive to develop tolerizing protocols for infants and children is pressing.

Late Follow-Up

The number of pediatric heart transplants performed worldwide markedly increased in the late 1980s and has since plateaued (4). The 5- to 10-year survival after pediatric heart transplantation can be achieved with good quality of life, although long-term concerns remain regarding rejection, infection, CAV, and complications of chronic immunosuppression, including malignancy, hypertension, renal insufficiency, as well as compliance with therapy (166). Since 1982, more than 8,500 pediatric heart transplantations have been successfully completed around the world (4). Of these 8,500, 24% were infant heart transplantations. The median survival time period for adolescents undergoing heart transplantation was 11.3 years and for infant heart transplantation was 18.3 years. These data indicate that the majority of the transplant recipients are surviving into their late adolescence and early adulthood. Given the improved health outcomes of the pediatric transplant recipients, research attention has begun to focus on growth, development (cognitive and psychosocial), and quality of life. Data from the Registry of the ISHLT also shows a different late survival for young child and adolescent recipients: When looking at conditional survival (i.e., subsequent survival for recipients who survived at least 1 year after transplant), both infants (age <1 year) and children (age 1 to 10 years) show a significantly lower risk of late mortality than adolescents (age 11 to 17 years). The median conditional graft half-life was >19 years for childhood recipients, and 15.2 years for adolescent recipients. In addition to immunologic factors that may provide an advantage for transplantation in the 1st year of life (167), reduced compliance to therapies in adolescent age patients may play a key role in determining these results. Many centers have reported that incomplete adherence with immunosuppressive therapy is the leading cause of late death in the adolescents (168). Reduced compliance to therapies in adolescent patients may play a key role in determining these results. Adherence is an important topic of investigation, particularly with adolescent transplant recipients, because of the negative impact it can have on their health status and mortality (169). Adolescent transplant recipients appear to be at particular risk for nonadherence for multiple reasons. First, the adolescent time period itself is a risk factor for nonadherence due to increased need during this period to fit in with their peer group and suppress any qualities that make them appear different (170). Additionally, body image becomes very important during this period as it is associated with peer acceptance, and the negative impact immunosuppressant therapy has on physical appearance may cause adolescents, especially girls, to stop taking the medication (170). Third, parents may expect adolescents to be more responsible for their own medical management and provide less supervision than they would with younger children (171). Fourth, there are data from pediatric cancer and the adult transplant literature that suggest patients become less adherent to medical regimen over time, which connotes increased rates for adolescence, given that many of them were transplanted as infants or younger children (172,173). Finally, the normal stressors that occur during adolescence can

interact with the stressors that are a result of the chronic illness to create psychological distress, which also increases the risk of nonadherence. The pediatric heart transplant recipient's ability to transition from childhood into a happy and productive adult life can be significantly affected by his or her cognitive abilities, learning experiences, sense of self, and emotions. Overall, the existing literature suggests that transplant recipients present with impairments in cognitive, academic, and neuropsychological functioning. While more information is available regarding pediatric transplant recipients' neurodevelopmental functioning, there are still limitations to the current understanding since few of the studies examined functioning beyond childhood. Attention to these factors is an important part of caring for these children. In this section, we discuss some of the important facets of long-term follow-up of pediatric heart transplant recipients, including routine health care maintenance issues and potential complications that may occur.

Health Care Maintenance

Vaccination is an important therapeutic approach to minimize infectious complications due to vaccine-preventable pathogens in organ transplant recipients (174). Nevertheless, vaccinations are commonly underused, and prospective randomized studies on their efficacy in transplant recipients are rare. Physicians should aim at complete vaccination coverage of both the patient and household contacts before transplantation, and vaccination should be performed as early as possible in the course of the underlying disease. Moreover, particular attention should be paid for complete vaccination of health care workers. All inactivated vaccines may be safely administered in transplant recipients, whereas most live vaccines are strictly contraindicated or should only be administered after a careful risk/benefit assessment. It is recommended to administer live vaccines such as measles, mumps, rubella (MMR) and varicella vaccine prior to transplantation (12). While MMR is the most effective after a year of age when maternal antibody has waned, it can be administered as early as 6 months of age for pediatric patients who may require transplantation. If transplantation has still not occurred by the time the baby is a year of age, the dose can be repeated. The second dose of MMR can be administered as soon as 4 weeks later. A minimum of 4 weeks between live-virus vaccine administration and transplantation is suggested. For patients who are incompletely vaccinated or unvaccinated prior to transplant, consultation with an infectious diseases specialist is recommended. While data regarding timing of vaccines after transplantation have not been fully evaluated, most centers restart vaccination at approximately 3 to 6 months after transplantation, when baseline immunosuppression levels are attained.

As vaccine-specific protective immunity may wane more rapidly on initiation of immunosuppressive drug therapy, a monitoring of specific immunity may help to identify patients who have lost protective immunity and may benefit from booster immunizations. If booster immunizations or primary vaccinations are applied after transplantation, they should be started at approximately 6 months posttransplantation to increase efficacy.

Generally, to reduce the risk of morbidity and mortality from these preventable diseases, it is important that physicians caring for pediatric transplant recipients update the immunization status of their patients. As with all children, pediatric heart transplant recipients can have fevers and require prompt evaluation for these. Fortunately, most acute febrile illnesses in these patients are not serious and can be managed safely in an outpatient setting (175).

Quality of Life and Rehabilitation

Children have very good quality of life and rehabilitation after heart transplantation. Key pediatric issues after transplantation include psychosocial support for patients and families with regard to school, growth, development, and future expectations (176). Heart transplantation in children aged 5 to 18 years seems to be associated with an ongoing deficit in parent-perceived physical health status (177). Most children grow at a normal rate after transplantation, showing normal onset and progression of puberty. However, catch-up growth may not be observed. This seems related to the types of heart disease, the age at transplantation, and the immunosuppressive regimen (178–180). Most children and adolescents have the capacity for healthy cognitive and psychological functioning after heart transplantation. Nevertheless, approximately 20% of pediatric heart recipients have abnormal neurologic examinations and 25% have emotional adjustment difficulties (181). Adolescent poor compliance or noncompliance represents part of these difficulties. Late rejection, associated with poor outcome, is often associated with nonadherence and adolescent age (169). Older children return to school and a more normal lifestyle after transplantation and express an improvement in the quality of their lives. Rehabilitation of the pediatric heart transplant recipient depends on the age of the patient and the degree of illness before and after transplantation. In contrast to the experience with adult heart transplant recipients, pediatric heart transplant recipients generally enjoy near-normal exercise capacity with low-normal oxygen consumption and just mildly reduced workload. Younger age at transplant is associated with greater exercise capacity (oxygen consumption). The persistence of some chronotropic incompetence may contribute to the lesser exercise capacity (182). Heart rate, systolic blood pressure response, and oxygen consumption all demonstrate significant incremental improvements with time after heart transplant, possibly providing supportive evidence for reinnervation of the allograft in many patients. In serial studies, deterioration in percent-predicted maximal oxygen consumption has been associated with a need for retransplantation owing to CAV. The utility of serial routine graded exercise tests in pediatric heart transplant recipients warrants further study, especially for its role in the detection of CAV (183). Exercise should be encouraged in this population. Benefits include improved blood glucose control, increase in bone density, and potential psychological enrichment. Return to age-appropriate activities including a physical education class can be achieved in the majority of patients within the first 6 months after transplantation (184). Patients with neurologic deficits may require special treatment programs.

Arrhythmias and Heart Rate Response

Significant arrhythmias after transplantation are relatively uncommon and when they occur may be indicative of graft problems such as rejection. Onset of supraventricular and ventricular tachyarrhythmias always raise concern of rejection (185), although pediatric heart transplant recipients appear to be more prone to tachyarrhythmias than adult heart transplant recipients, and they are not always associated with rejection (186). Ventricular arrhythmias also may be indicative of CAV. Symptomatic sinus bradycardia and heart block after transplantation requiring pacemaker placement have been described in a small percentage of children (187). Heart rate response to exercise and heart rate recovery after exercise in pediatric heart transplant recipients are consistent with autonomic denervation after transplant and suggestive of late autonomic reinnervation of these hearts (188). Previous studies in adults have demonstrated that parasympathetic reinnervation

is rather infrequent after heart transplant and occurs in only 5% to 10% of recipients (189). Sympathetic reinnervation occurs much more frequently, however, and has been described using both invasive and noninvasive approaches in adults (190). These include (a) measurement of norepinephrine levels from coronary sinus and heart rate response after intracoronary injection of tyramine; (b) kinetics after intravenous infusion of radiolabeled norepinephrine that includes coronary sinus catheterization; (c) histologic evidence of nerve endings on endomyocardial biopsy tissues using special staining; (d) scintigraphic techniques such as single-photon emission computerized tomography or positron emission tomography imaging using radioisotopes; and (e) heart-rate variability studies (191–194). A study in neonatal heart transplant recipients at 9.5 ± 2.3 years after their transplant reported higher peak heart rate and better exercise performance compared with reports in other cohorts of pediatric (nonneonatal) heart transplant recipients (182).

Late Rejection

One of the most important factors in reducing the risk of and morbidity from rejection is to maintain regular and frequent routine office visits for all pediatric heart transplant patients. Evidence of rejection in infants and small children ranges from no symptoms to a wide variety of nonspecific symptoms including tachycardia, tachypnea, lethargy, irritability, and poor feeding. Physical signs are similar to those in adults, including jugular venous distention, organomegaly, new murmur, and gallop rhythm. Children who have no rejection in the 1st year after transplant may be at lower risk for hemodynamically compromising rejection late after transplantation. Also “biopsy-negative” rejection—at times presenting with severe left ventricular dysfunction and negative cellular or immunohistochemical abnormality on biopsy—can occur late after transplantation. These patients can improve with augmented immunosuppression including plasmapheresis, cyclophosphamide, antilymphocyte therapy, and agents suppressing antibody production, but their long-term outcome remain guarded (195). Either cellular rejection or AMR can present as recurrent or refractory. In these cases, treatment strategies can include several immunosuppressant combinations and total lymphoid irradiation (196). Generally, late rejection can be an ominous sign and may be predictive of graft loss. Episodes of late rejection with or without hemodynamic compromise always raise the concern of noncompliance.

Infection

Pediatric heart transplant recipients are at risk for serious and opportunistic infections, including bacterial, viral (especially CMV), and protozoal (*Pneumocystis*) infections, particularly in the first 6 months after heart transplantation when immunosuppression is greatest. Because of the significant postoperative risk of infection, many centers use some form of prophylaxis against fungal (nystatin), CMV (acyclovir or ganciclovir in recipients who receive organs from CMV-positive donors), and/or protozoal (trimethoprim/sulfamethoxazole) infections, although exact indication and duration of prophylaxis are unknown (108). The Pediatric Heart Transplant Study reported the time-related risk of “serious” infection and death in a large pediatric heart transplant population from 22 participating centers in the United States (121). The most common types of infections were bacterial in 60%, followed by CMV (18%), other viral infections (13%), fungal (7%), and protozoal (2%). The peak hazard for bacterial and fungal infections was in the 1st month after transplantation, whereas the peak hazard for viral infection was in the 2nd month after

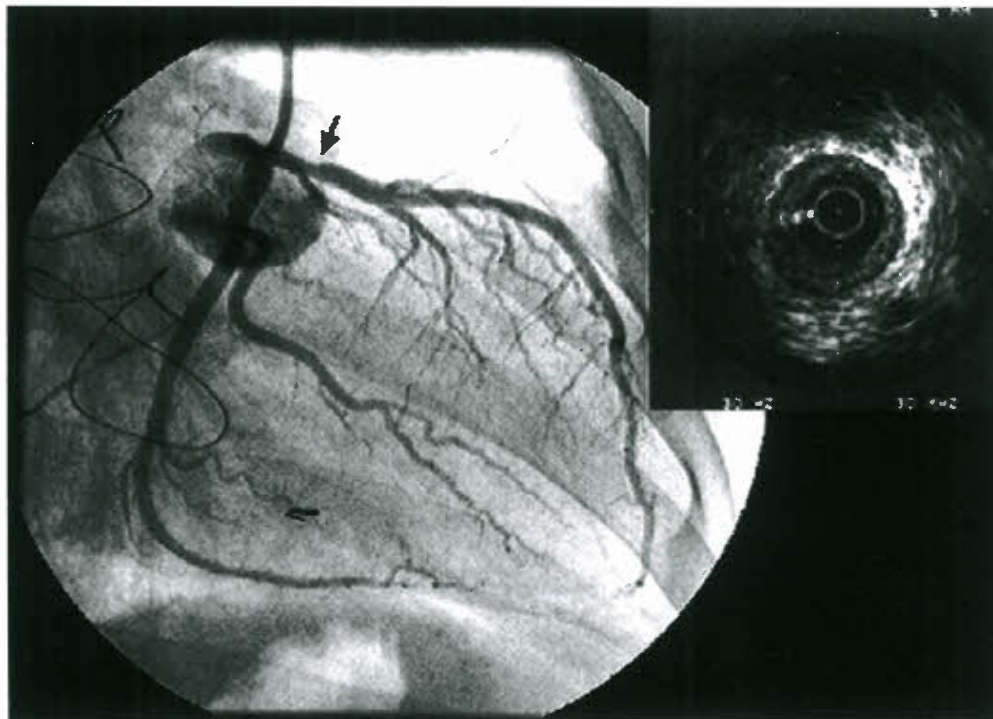
transplantation, with the most common virus being CMV. Availability of ganciclovir and the development of assays for rapid diagnosis of active infection, such as the polymerase chain reaction (PCR) detection of viral genome, have reduced the risk of CMV disease. In contrast to adults in whom previous CMV exposure is common, fewer pediatric donors and recipients are CMV seropositive (CMV+), thus increasing the risk of CMV posttransplant infection in pediatric recipients. Often this infection consists of benign viremia and does not lead to clinically relevant disease. Because CMV disease can occur early after transplant and the perioperative morbidity can be significant, prophylactic and preemptive strategies to minimize or prevent CMV infection/disease have been developed. Prophylaxis consists of intravenous ganciclovir or oral valganciclovir initiated in the early postoperative period with a goal of preventing CMV infection. Preemptive therapy consists of close monitoring of recipient CMV status, either by quantitative PCR or CMV antigenemia, and initiating treatment when a previously CMV-negative patient becomes CMV-positive thereby minimizing transition of infection into significant CMV disease. Prophylaxis with intravenous ganciclovir, oral valganciclovir, or CMV immunoglobulin is commonly used by pediatric transplant centers for CMV-mismatched patients and has a survival benefit over nonprophylaxis. The recent ISHLT guidelines recommend initiating treatment with oral or intravenous ganciclovir or valganciclovir for CMV+ or CMV-mismatched pediatric recipients (108).

Identification of viral genome in the myocardium of pediatric transplant recipients, particularly if untreated with IVIG, appears to be predictive of adverse clinical events, including CAV and graft loss (142,143). The risk of all types of infections is very low by 6 months after transplant, but a low risk persists indefinitely. Exposure to pets is controversial, but most centers recommend avoidance of cat feces because of the risk of toxoplasmosis and avoidance of reptiles because of the risk of *Salmonella*. Although infective endocarditis is a rare complication after heart transplantation, most centers recommend endocarditis prophylaxis long-term after heart transplantation before dental, upper respiratory, gastrointestinal, and genitourinary tract procedures that are likely to cause bacteremia.

Malignancy, Epstein-Barr Virus Infection, and Posttransplant Lymphoproliferative Disorders

Increased risk of malignancy is a well-recognized complication after organ transplantation. In pediatrics, the vast majority are lymphoproliferative disorders and are often associated with primary infection with EBV (197,198). In contrast to adults, PTLTD is the major malignancy in pediatric patients after solid organ transplantation, while other neoplasms are rare. The incidence of PTLTD increases during the year after transplantation and varies between the different types of organ transplantation; high incidence has been reported for the thoracic organs and intestine (5% to 40%), whereas the incidence in kidney and liver transplant patients (1% to 10%) is lower (199). The pathology of early onset disease is usually polymorphic, whereas late expression, usually beyond 3 years, is often monomorphic and lymphomatous (120,197). First-line treatment remains the reduction of immunosuppression with variable clinical response (198). Monomorphic disease may require treatment with conventional chemotherapeutic agents. Since the vast majority of lymphoproliferative disorders are of recipient B-cell origin after heart transplantation, the use of the chimeric anti-CD20 monoclonal antibody, rituximab, has been successful (198). The development of quantitative EBV PCR on peripheral blood samples represents a useful technique for diagnosing and monitoring viral loads, but it is still unclear how to use this information to guide patient care (200,201).

FIGURE 65.2. Selected posttransplantation left coronary angiogram demonstrating proximal left anterior descending (LAD) lesion that appeared minimal by angiography but demonstrated prominent intimal thickening on intravascular ultrasonography (inset).



Another novel approach is cellular immunotherapy, whereby the patient is given infusion of EBV-specific cytotoxic T-cells (198). Reports of malignant neoplasia other than lymphoma are rare in transplanted children. These include squamous cell carcinomas and other skin cancers. Therefore, children should be advised to avoid excessive sun exposure and use sunscreen.

Chronic Rejection and Cardiac Allograft Vasculopathy

Cardiac allograft vasculopathy (CAV) is the major factor limiting long-term survival after pediatric heart transplantation. CAV is manifested pathologically by a diffuse and accelerated form of coronary disease consisting of myointimal proliferation that is concentric and involves the entire length of the vessel, including intramyocardial branches. Eventually, luminal occlusion occurs. There may also be a pronounced inflammatory component (202). The cause(s) of CAV has been an area of intense research for decades, and is still not ideally defined. Most investigators agree that CAV is primarily an immune-mediated disease, and thus can be considered a major manifestation of chronic rejection (203). Immunologic events interact with nonimmunologic risk factors, such as donor age, hypertension, and graft ischemia/reperfusion injury, in addition to recipient hypertension, hyperlipidemia, obesity, diabetes, smoking, race, and gender (204). CMV infection after transplantation also has been associated with the development of CAV. The final common pathway of these mechanisms is endothelial activation, a prothrombotic environment, and endothelial damage with subsequent diffuse intimal proliferation. Major risk factors for development of disease in children are older recipient and donor age, and two or more episodes of rejection in the 1st year (205), in addition to late rejection episodes and late pacemaker requirement (206). Patients suffering from severe late rejection or presenting with symptoms of high-grade atrioventricular block must be monitored

aggressively and should be evaluated closely for the presence or development of CAV.

The incidence of CAV in children is less than that in adults (66% of pediatric patients are CAV-free at 10 years after transplant), but recipient age has been significantly related to freedom from CAV; infants and younger recipients (<10 years old) have lower risk of CAV than adolescents (4). It is possible that pediatric recipients have less CAV than adults because of less persisting donor factors or because of less nonimmune risk factors. However, the actual incidence of CAV in children is probably being underestimated because of the lack of reliable methods for diagnosing and monitoring the disease. Because the cardiac allograft is not innervated, angina is an uncommon presenting symptom of CAV. Clinical symptoms, when present, are generally limited to congestive heart failure with allograft dysfunction, silent myocardial infarction, or sudden death. Coronary angiography is still the first modality for diagnosing CAV, although it is well-appreciated that this modality underestimates the incidence and severity of disease. Dobutamine stress echocardiography is a safe, noninvasive technique that may be useful in diagnosing and following CAV in children (207). Intravascular ultrasound provides an additional modality for detecting CAV also in pediatric heart recipients, but is not always predictive of outcomes (208–210) (Fig. 65.3). More recently, intracoronary Doppler flow measurement of coronary flow reserve (CFR) with adenosine is a good indicator of endothelium-independent vasodilator response in children after heart transplantation and may be performed with reasonable safety in pediatric heart transplant recipients. Reduced CFR after systemic or intracoronary application of adenosine is associated similarly with CAV based on biopsy and coronary angiography, which might be important in future studies for establishing a noninvasive diagnostic tool for CAV in children (211). The ideal management of CAV is unknown; intervention or surgical management has had limited utility while medical management has been disappointing. As stated earlier in this chapter, both sirolimus and everolimus have potential for preventing and/or treating CAV

(155,158,212). Coronary interventional procedures can be used in pediatric heart transplant recipients for palliation of CAV (213,214). Medical treatment has primarily been directed toward attempts to decrease the progression of the disease by using preventive measures and manipulation of immunosuppression (203). A reduction in the incidence of CAV has been found after treatment with statins in adult patients (215). In pediatric patients, pravastatin and atorvastatin have been found safe and effective to reduce total cholesterol and low-density lipoprotein, and retrospective studies suggest a benefit on reducing the incidence of CAV in children (216–218). Long-term studies are required to evaluate the effect of statins on the incidence of CAV and on growing organs. For this reason they must be used with caution particularly in young patients. Minimizing the use of steroids and tailoring immunosuppression to protocols with tacrolimus may be beneficial over cyclosporine or sirolimus in maintaining better lipid profiles. Whether statins, and in particular pravastatin, affect progression of CAV or aid in its prevention in children has not yet been conclusively proven (219). Nevertheless, the clinical use of statins is now common in most pediatric heart transplant centers. Unfortunately, the mainstay of therapy for established, severe CAV remains retransplantation.

Complications of Immunosuppression

Because two of the main functions of the immune system are fighting infection and tumor surveillance, all immunosuppressants put the patient at risk for infection and malignancy. Additionally, individual immunosuppressant medications have significant adverse effects, even when properly used in appropriate doses. Hypertension is a common complication after transplantation and may represent in part an adverse effect of cyclosporine or tacrolimus, particularly when used in combination with corticosteroids. The multifactorial etiology of hypertension in this population means that blood pressure control is often difficult to attain, and further research is essential if we are to optimize our management and limit the impact of complications (220). Catastrophic neurologic complications have resulted from severe postoperative hypertension and require urgent treatment. Chronic hypertension appears to be less prevalent in pediatric heart transplant recipients than in adults, but it is still a problem requiring treatment, even in centers using a steroid-sparing maintenance immunosuppressive protocol. Antihypertensive therapy in these children should be similar to that used for adults, including calcium channel blockers, angiotensin-converting enzyme inhibitors, and/or angiotensin-receptor blockers (108).

Neurotoxicity is another recognized complication of cyclosporine, occurring in as many as 10% to 25% of patients, with a peak in the early postoperative period. Symptoms include tremors, restlessness, dysesthesias of the palms and soles, seizures, and altered mental status. Cyclosporine and tacrolimus (calcineurin inhibitors) may cause acute and chronic renal insufficiency and monitoring for renal insufficiency in children should be lifelong. Renal insufficiency increases over time in pediatric heart transplant recipients. African American race, younger age at transplant, longer duration of listing, high level of calcineurin inhibitors, and renal insufficiency at 6 months after transplant are important risk factors for renal insufficiency at 5 years after transplant (221). These patients should be followed carefully with early referral to a pediatric nephrologist if they develop evidence of renal insufficiency. Individual susceptibility, including transforming growth factor β_1 gene polymorphism, could play a role in the long-term outcome of renal function in patients with calcineurin inhibitor-based immunosuppression (222). Strategies to minimize long-term exposure to calcineurin inhibitors may reduce the

prevalence of renal insufficiency in this vulnerable population (223,224). These strategies include dosage reduction of calcineurin inhibitors and the use of antiproliferative agents like sirolimus and everolimus (154,225,226).

A high prevalence of lipoprotein abnormalities has been described among pediatric heart transplant recipients (227). Again, the use of cyclosporine and steroids has been associated with this disorder. Therefore, the increasing use of lipid-lowering agents also in pediatric patients appears justified. Posttransplant diabetes mellitus is present in approximately 2% of pediatric recipients with cyclosporine-based immunosuppression, but in 8% of recipients with tacrolimus-based immunosuppression (228, 229). Diabetes may be related to reversible insulin resistance. Tacrolimus levels, HLA-DR mismatch, and older age at transplant may predispose to posttransplant diabetes. Gastrointestinal complications can also occur during the follow-up of pediatric heart transplant recipients. They include cholelithiasis, intestinal pneumatosis, and colitis (230–232). Sirolimus reportedly has less nephrotoxicity than cyclosporine or tacrolimus but has been associated with severe stomatitis and frequent elevations in cholesterol and lipid profiles (233). Sirolimus has growth factor antagonist properties and may cause marrow suppression particularly when used in combination with other agents that can suppress the marrow such as tacrolimus or MMF.

Miscellaneous

Infants with HLHS who undergo heart transplantation require extended reconstruction of their aortic arch. Of these, as many as 20% will develop coarctation of the aorta that may require treatment. Although surgical repair may be necessary in complex obstructive lesions, balloon coarctation angioplasty is a safe and effective treatment in most situations (234) (see Chapter 13). Severe tricuspid regurgitation secondary to valve damage from endomyocardial biopsies is an uncommon but potentially hemodynamically significant complication. Attempts to minimize the number of biopsies, careful placement of the biopsy catheter, or the use of a long sheath may reduce the incidence of this complication. Anemia is highly prevalent in children after heart transplantation. The etiology of this uncertain, but usually is not secondary to iron deficiency (235).

Retransplantation

Experience with pediatric heart retransplantation is limited. Nevertheless, in the most recent summary of the Registry of the ISHLT, the number of patients undergoing retransplantation has increased to 6% for recipients between 11 and 17 years of age (4). The most common indications for retransplantation are CAV, followed by acute rejection, chronic rejection, and intraoperative donor organ failure. Elective retransplantation can be performed with acceptable mortality. Intermediate outcome is similar to that of children undergoing primary heart transplantation (236,237). When retransplantation is performed in the setting of early primary graft failure, the results are quite poor and many investigators consider retransplantation in this setting inappropriate (237,238). Encouragingly, the outcomes following retransplantation after a long intertransplant interval are equivalent to the outcomes following primary transplant (236). The medical and pharmacologic issues after retransplant mimic those following primary transplant.

Heterotopic and Heart–Lung Transplantation

Experience with heterotopic heart transplantation in children is limited. The main indications for this procedure are primarily the presence of fixed high pulmonary vascular resistance

that precludes orthotopic heart transplantation, although some consider availability of an undersized donor or expectation of a certain degree of recipient heart recovery to be indications as well. One- and five-year actuarial survival rates have been reported to be as high as 83% and 66%, respectively. Thus, in selected patients, heterotopic heart transplantation may be considered an alternative, particularly when pulmonary vascular resistance is excessively high for orthotopic heart transplantation. Another alternative in this situation is heart–lung transplantation. The volume of pediatric heart–lung transplantation decreased significantly in the 2000s both in frequency and in survival rates (239,240). Thus, the ongoing role of this procedure in the management of irreversible pediatric cardiopulmonary disease remains uncertain. In general, the poor late survival after heart–lung transplant tracks the poor late survival seen after lung transplant alone. Another alternative that has met with some success in the setting of excessively high, fixed pulmonary vascular resistance in those patients with unrepaired congenital heart lesions is the performance of single-lung transplantation and repair of the congenital heart lesion (30).

REFERENCES

1. Boucek MM, Kanakriyeh MS, Mathis CM, et al. Cardiac transplantation in infancy: donors and recipients. Loma Linda University Pediatric Heart Transplant Group [see comments]. *J Pediatr* 1990;116:171–176.
2. Mayer JE Jr. Cardiac transplantation for neonates with hypoplastic left heart syndrome [editorial; comment]. *Ann Thorac Surg* 1990;50:864–865.
3. Webber SA, Fricker FJ, Michaels M, et al. Orthotopic heart transplantation in children with congenital heart disease. *Ann Thorac Surg* 1994;58:1664–1669.
4. Kirk R, Edwards LB, Kucheryavaya AY, et al. The Registry of the International Society for Heart and Lung Transplantation: thirteenth official pediatric heart transplantation report—2010. *J Heart Lung Transplant* 2010;29:1119–1128.
5. Ross M, Kouretas P, Gamberg P, et al. Ten- and 20-year survivors of pediatric orthotopic heart transplantation. *J Heart Lung Transplant* 2006;25:261–270.
6. McGiffin DC, Naftel DC, Kirklin JK, et al. Predicting outcome after listing for heart transplantation in children: comparison of Kaplan-Meier and parametric competing risk analysis. Pediatric Heart Transplant Study Group. *J Heart Lung Transplant* 1997;16:713–722.
7. Almond CS, Thiagarajan RR, Piercey GE, et al. Waiting list mortality among children listed for heart transplantation in the United States. *Circulation* 2009;119:717–727.
8. Almond CS, Singh TP, Gauvreau K, et al. Extracorporeal membrane oxygenation for bridge to heart transplantation among children in the United States: analysis of data from the organ procurement and transplant network and extracorporeal life support organization registry. *Circulation* 2011;123:2975–2984.
9. Canter CE, Shaddy RE, Bernstein D, et al. Indications for heart transplantation in pediatric heart disease: a scientific statement from the American Heart Association Council on Cardiovascular Disease in the Young; the Councils on Clinical Cardiology, Cardiovascular Nursing, and Cardiovascular Surgery and Anesthesia; and the Quality of Care and Outcomes Research Interdisciplinary Working Group. *Circulation* 2007;115:658–676.
10. Chartrand C, Dumont L, Stanley P. Pediatric cardiac transplantation. *Transplant Proc* 1989;21:3349–3350.
11. Addonizio LJ. Cardiac transplantation in the pediatric patient. *Prog Cardiovasc Dis* 1990;33:19–34.
12. Verma A, Wade JJ. Immunization issues before and after solid organ transplantation in children. *Pediatr Transplant* 2006;10:536–548.
13. Levitt G, Bunch K, Rogers CA, et al. Cardiac transplantation in childhood cancer survivors in Great Britain. *Eur J Cancer* 1996;32A:826–830.
14. Cimato TR, Jessup M. Recipient selection in cardiac transplantation: contraindications and risk factors for mortality. *J Heart Lung Transplant* 2002;21:1161–1173.
15. Opelz G, Wujciak T. The influence of HLA compatibility on graft survival after heart transplantation. The Collaborative Transplant Study [see comments]. *N Engl J Med* 1994;330:816–819.
16. Holt DB, Lublin DM, Phelan DL, et al. Mortality and morbidity in pre-sensitized pediatric heart transplant recipients with a positive donor crossmatch utilizing peri-operative plasmapheresis and cytolytic therapy. *J Heart Lung Transplant* 2007;26:876–882.
17. Rossano JW, Morales DL, Zafar F, et al. Impact of antibodies against human leukocyte antigens on long-term outcome in pediatric heart transplant patients: an analysis of the United Network for Organ Sharing database. *J Thorac Cardiovasc Surg* 2010;140:694–699, 699 e1–e2.
18. Jacobs JP, Quintessenza JA, Boucek RJ, et al. Pediatric cardiac transplantation in children with high panel reactive antibody. *Ann Thorac Surg* 2004;78:1703–1709.
19. Smith JD, Danskin AJ, Laylor RM, et al. The effect of panel reactive antibodies and the donor specific crossmatch on graft survival after heart and heart–lung transplantation. *Transpl Immunol* 1993;1:60–65.
20. Feingold B, Bowman P, Zeevi A, et al. Survival in allosensitized children after listing for cardiac transplantation. *J Heart Lung Transplant* 2007;26:565–571.
21. Tyan DB, Li VA, Czer L, et al. Intravenous immunoglobulin suppression of HLA alloantibody in highly sensitized transplant candidates and transplantation with a histoincompatible organ. *Transplantation* 1994;57:553–562.
22. McIntyre JA, Higgins N, Britton R, et al. Utilization of intravenous immunoglobulin to ameliorate alloantibodies in a highly sensitized patient with a cardiac assist device awaiting heart transplantation. Fluorescence-activated cell sorter analysis. *Transplantation* 1996;62:691–693.
23. Shaddy RE, Fuller TC. The sensitized pediatric heart transplant candidate: causes, consequences, and treatment options. *Pediatr Transplant* 2005;9:208–214.
24. Vo AA, Lukovsky M, Toyoda M, et al. Rituximab and intravenous immune globulin for desensitization during renal transplantation. *N Engl J Med* 2008;359:242–251.
25. Hartono C, Lubetzky M, Aull MJ, et al. Use of bortezomib for prevention and treatment of rejection in sensitized patients. *Clin Transpl* 2009;499–503.
26. Sberro-Soussan R, Zuber J, Suberbielle-Boissel C, et al. Bortezomib as the sole post-renal transplantation desensitization agent does not decrease donor-specific anti-HLA antibodies. *Am J Transplant* 2010;10:681–686.
27. Kirklin JK, Naftel DC, Kirklin JW, et al. Pulmonary vascular resistance and the risk of heart transplantation. *J Heart Transplant* 1988;7:331–336.
28. Shaddy RE, Naftel DC, Kirklin JK, et al. Outcome of cardiac transplantation in children. Survival in a contemporary multi-institutional experience. Pediatric Heart Transplant Study. *Circulation* 1996;94:II69–II73.
29. Khaghani A, Santini F, Dyke CM, et al. Heterotopic cardiac transplantation in infants and children [see comments]. *J Thorac Cardiovasc Surg* 1997;113:1042–1048; discussion 1048–1049.
30. Spray TL, Mallory GB, Canter CE, et al. Pediatric lung transplantation for pulmonary hypertension and congenital heart disease. *Ann Thorac Surg* 1992;54:216–223; discussion 224–225.
31. Webber SA, McCurry K, Zeevi A. Heart and lung transplantation in children. *Lancet* 2006;368:53–69.
32. Murali S, Uretsky BF, Armitage JM, et al. Utility of prostaglandin E1 in the pretransplantation evaluation of heart failure patients with significant pulmonary hypertension [see comments]. *J Heart Lung Transplant* 1992;11:716–723.
33. Zales VR, Pahl E, Backer CL, et al. Pharmacologic reduction of pretransplantation pulmonary vascular resistance predicts outcome after pediatric heart transplantation. *J Heart Lung Transplant* 1993;12:965–972; discussion 972–973.
34. Gajarski RJ, Towbin JA, Bricker JT, et al. Intermediate follow-up of pediatric heart transplant recipients with elevated pulmonary vascular resistance index. *J Am Coll Cardiol* 1994;23:1682–1687.
35. Kieler-Jensen N, Lundin S, Ricksten SE. Vasodilator therapy after heart transplantation: effects of inhaled nitric oxide and intravenous prostacyclin, prostaglandin E1, and sodium nitroprusside. *J Heart Lung Transplant* 1995;14:436–443.
36. Shaddy RE. Pulmonary hypertension in pediatric heart transplantation. *Prog Pediatr Cardiol* 2000;11:131–136.
37. Gandhi SK, Grady RM, Huddleston CB, et al. Beyond Berlin: heart transplantation in the “untransplantable”. *J Thorac Cardiovasc Surg* 2008;136:529–531.
38. Denfield SW, Webber SA. Restrictive cardiomyopathy in childhood. *Heart Fail Clin* 2010;6:445–452, viii.
39. Fenton MJ, Chubb H, McMahon AM, et al. Heart and heart–lung transplantation for idiopathic restrictive cardiomyopathy in children. *Heart* 2006;92:85–89.
40. Das BB, Taylor AL, Boucek MM, et al. Exercise capacity in pediatric heart transplant candidates: is there any role for the 14 ml/kg/min guideline? *Pediatr Cardiol* 2006;27:226–229.
41. Paridon SM, Mitchell PD, Colan SD, et al. A cross-sectional study of exercise performance during the first 2 decades of life after the Fontan operation. *J Am Coll Cardiol* 2008;52:99–107.
42. Boucek RJ Jr, Chrisant MR. Cardiac transplantation for hypoplastic left heart syndrome. *Cardiol Young* 2004;14:83–87.
43. Chrisant MR, Naftel DC, Drummond-Webb J, et al. Fate of infants with hypoplastic left heart syndrome listed for cardiac transplantation: a multicenter study. *J Heart Lung Transplant* 2005;24:576–582.
44. Sable CA, Shaddy RE, Suddaby EC, et al. Impact of prolonged waiting times of neonates awaiting heart transplantation. *J Perinatol* 1997;17:481–488.
45. Mitchell MB, Campbell DN, Clarke DR, et al. Infant heart transplantation: improved intermediate results. *J Thorac Cardiovasc Surg* 1998;116:242–252.
46. Day RW, Tani LY, Minich LL, et al. Congenital heart disease with ductal-dependent systemic perfusion: Doppler ultrasonography flow velocities are

- altered by changes in the fraction of inspired oxygen. *J Heart Lung Transplant* 1995;14:718–725.
47. Bourke KD, Sondheimer HM, Ivy DD, et al. Improved pretransplant management of infants with hypoplastic left heart syndrome enables discharge to home while waiting for transplantation. *Pediatr Cardiol* 2003;24:538–543.
 48. Ruiz CE, Gamra H, Zhang HP, et al. Brief report: stenting of the ductus arteriosus as a bridge to cardiac transplantation in infants with the hypoplastic left-heart syndrome. *N Engl J Med* 1993;328:1605–1608.
 49. Boucek MM, Mashburn C, Chan KC. Catheter-based interventional palliation for hypoplastic left heart syndrome. *Semin Thorac Cardiovasc Surg Pediatr Card Surg Annu* 2005;72–77.
 50. Galantowicz M, Cheatham JP, Phillips A, et al. Hybrid approach for hypoplastic left heart syndrome: intermediate results after the learning curve. *Ann Thorac Surg* 2008;85:2063–2070; discussion 2070–2071.
 51. Sebastian VA, Guleserian KJ, Leonard SR, et al. Heart transplantation techniques after hybrid single-ventricle palliation. *J Card Surg* 2010;25:596–600.
 52. Canter CE, Moorehead S, Huddleston CB, et al. Restrictive atrial septal communication as a determinant of outcome of cardiac transplantation for hypoplastic left heart syndrome. *Circulation* 1993;88:II456–II460.
 53. Michielon G, Parisi F, Squitieri C, et al. Orthotopic heart transplantation for congenital heart disease: an alternative for high-risk fontan candidates? *Circulation* 2003;108:II140–II149.
 54. Michielon G, Parisi F, Di Carlo D, et al. Orthotopic heart transplantation for failing single ventricle physiology. *Eur J Cardiothorac Surg* 2003;24:502–510; discussion 510.
 55. Jayakumar KA, Addonizio LJ, Kichuk-Christant MR, et al. Cardiac transplantation after the Fontan or Glenn procedure. *J Am Coll Cardiol* 2004;44:2065–2072.
 56. Bernstein D, Naftel D, Chin C, et al. Outcome of listing for cardiac transplantation for failed Fontan: a multi-institutional study. *Circulation* 2006;114:273–280.
 57. Griffiths ER, Kaza AK, Wyler von Ballmoos MC, et al. Evaluating failing Fontans for heart transplantation: predictors of death. *Ann Thorac Surg* 2009;88:558–563; discussion 563–564.
 58. Brancaccio G, Carotti A, D'Argenio P, et al. Protein-losing enteropathy after Fontan surgery: resolution after cardiac transplantation. *J Heart Lung Transplant* 2003;22:484–486.
 59. Lamour JM, Kanter KR, Naftel DC, et al. The effect of age, diagnosis, and previous surgery in children and adults undergoing heart transplantation for congenital heart disease. *J Am Coll Cardiol* 2009;54:160–165.
 60. Simmonds J, Burch M, Dawkins H, et al. Heart transplantation after congenital heart surgery: improving results and future goals. *Eur J Cardiothorac Surg* 2008;34:313–317.
 61. Bristow MR, Gilbert EM, Abraham WT, et al. Carvedilol produces dose-related improvements in left ventricular function and survival in subjects with chronic heart failure. MOCHA Investigators. *Circulation* 1996;94:2807–2816.
 62. Packer M, Colucci WS, Sackner-Bernstein JD, et al. Double-blind, placebo-controlled study of the effects of carvedilol in patients with moderate to severe heart failure. The PRECISE Trial. Prospective Randomized Evaluation of Carvedilol on Symptoms and Exercise [see comments]. *Circulation* 1996;94:2793–2799.
 63. Effect of metoprolol CR/XL in chronic heart failure: Metoprolol CR/XL Randomised Intervention Trial in Congestive Heart Failure (MERIT-HF). *Lancet* 1999;353:2001–2007.
 64. Packer M, Fowler MB, Roecker EB, et al. Effect of carvedilol on the morbidity of patients with severe chronic heart failure: results of the carvedilol prospective randomized cumulative survival (COPERNICUS) study. *Circulation* 2002;106:2194–2199.
 65. Azeka E, Franchini Ramirez JA, Valler C, et al. Delisting of infants and children from the heart transplantation waiting list after carvedilol treatment. *J Am Coll Cardiol* 2002;40:2034–2038.
 66. Rusconi P, Gomez-Marín O, Rossique-Gonzalez M, et al. Carvedilol in children with cardiomyopathy: 3-year experience at a single institution. *J Heart Lung Transplant* 2004;23:832–838.
 67. Blume ED, Canter CE, Spicer R, et al. Prospective single-arm protocol of carvedilol in children with ventricular dysfunction. *Pediatr Cardiol* 2006;27:336–342.
 68. Shaddy RE, Boucek MM, Hsu DT, et al. Carvedilol for children and adolescents with heart failure: a randomized controlled trial. *JAMA* 2007;298:1171–1179.
 69. Gajarski RJ, Mosca RS, Ohye RG, et al. Use of extracorporeal life support as a bridge to pediatric cardiac transplantation. *J Heart Lung Transplant* 2003;22:28–34.
 70. Blume ED, Naftel DC, Bastardi HJ, et al. Outcomes of children bridged to heart transplantation with ventricular assist devices: a multi-institutional study. *Circulation* 2006;113:2313–2319.
 71. Ibrahim AE, Duncan BW, Blume ED, et al. Long-term follow-up of pediatric cardiac patients requiring mechanical circulatory support. *Ann Thorac Surg* 2000;69:186–192.
 72. Duncan BW. Mechanical circulatory support for infants and children with cardiac disease. *Ann Thorac Surg* 2002;73:1670–1677.
 73. Kirshbom PM, Bridges ND, Myung RJ, et al. Use of extracorporeal membrane oxygenation in pediatric thoracic organ transplantation. *J Thorac Cardiovasc Surg* 2002;123:130–136.
 74. Hetzer R, Loebe M, Potapov EV, et al. Circulatory support with pneumatic paracorporeal ventricular assist device in infants and children. *Ann Thorac Surg* 1998;66:1498–1506.
 75. Gandhi SK, Huddleston CB, Balzer DT, et al. Biventricular assist devices as a bridge to heart transplantation in small children. *Circulation* 2008;118:S89–S93.
 76. Malaisrie SC, Pelletier MP, Yun JJ, et al. Pneumatic paracorporeal ventricular assist device in infants and children: initial Stanford experience. *J Heart Lung Transplant* 2008;27:173–177.
 77. Garcia-Guereta L, Cabo J, de la Oliva P, et al. Ventricular assist device application with the intermediate use of a membrane oxygenator as a bridge to pediatric heart transplantation. *J Heart Lung Transplant* 2009;28:740–742.
 78. Haddad H, Elabbassi W, Moustafa S, et al. Left ventricular assist devices as bridge to heart transplantation in congestive heart failure with pulmonary hypertension. *ASAIO J* 2005;51:456–460.
 79. Brancaccio G, Amodeo A, Ricci Z, et al. Mechanical assist device as a bridge to heart transplantation in children less than 10 kilograms. *Ann Thorac Surg* 2010;90:58–62.
 80. Potapov EV, Stiller B, Hetzer R. Ventricular assist devices in children: current achievements and future perspectives. *Pediatr Transplant* 2007;11:241–255.
 81. Paul JJ, Tani LY, Shaddy RE, et al. Spectrum of left ventricular dysfunction in potential pediatric heart transplant donors. *J Heart Lung Transplant* 2003;22:548–552.
 82. Scheule AM, Zimmerman GJ, Johnston JK, et al. Duration of graft cold ischemia does not affect outcomes in pediatric heart transplant recipients. *Circulation* 2002;106:II163–II167.
 83. Chin C, Miller J, Robbins R, et al. The use of advanced-age donor hearts adversely affects survival in pediatric heart transplantation. *Pediatr Transplant* 1999;3:309–314.
 84. Silva JN, Canter CE, Singh TP, et al. Outcomes of heart transplantation using donor hearts from infants with sudden infant death syndrome. *J Heart Lung Transplant* 2010;29:1226–1230.
 85. Singhal AK, Abrams JD, Mohara J, et al. Potential suitability for transplantation of hearts from human non-heart-beating donors: data review from the Gift of Life Donor Program. *J Heart Lung Transplant* 2005;24:1657–1664.
 86. Boucek MM, Mashburn C, Dunn SM, et al. Pediatric heart transplantation after declaration of cardiocirculatory death. *N Engl J Med* 2008;359:709–714.
 87. West LJ, Pollock-Barziv SM, Dipchand AI, et al. ABO-incompatible heart transplantation in infants. *N Engl J Med* 2001;344:793–800.
 88. Roche SL, Burch M, O'Sullivan J, et al. Multicenter experience of ABO-incompatible pediatric cardiac transplantation. *Am J Transplant* 2008;8:208–215.
 89. Dipchand AI, Pollock BarZiv SM, Manlhiot C, et al. Equivalent outcomes for pediatric heart transplantation recipients: ABO-blood group incompatible versus ABO-compatible. *Am J Transplant* 2010;10:389–397.
 90. Fan X, Ang A, Pollock-Barziv SM, et al. Donor-specific B-cell tolerance after ABO-incompatible infant heart transplantation. *Nat Med* 2004;10:1227–1233.
 91. West LJ, Karamlou T, Dipchand AI, et al. Impact on outcomes after listing and transplantation, of a strategy to accept ABO blood group-incompatible donor hearts for neonates and infants. *J Thorac Cardiovasc Surg* 2006;131:455–461.
 92. Everitt MD, Donaldson AE, Casper TC, et al. Effect of ABO-incompatible listing on infant heart transplant waitlist outcomes: analysis of the United Network for Organ Sharing (UNOS) database. *J Heart Lung Transplant* 2009;28:1254–1260.
 93. Odum J, Laks H, Banerji A, et al. Does duration of donor brain injury affect outcome after orthotopic pediatric heart transplantation? *J Thorac Cardiovasc Surg* 2005;130:187–193.
 94. Morgan JA, John R, Park Y, et al. Successful outcome with extended allograft ischemic time in pediatric heart transplantation. *J Heart Lung Transplant* 2005;24:58–62.
 95. Pollock-Barziv SM, den Hollander N, Ngan BY, et al. Pediatric heart transplantation in human leukocyte antigen sensitized patients: evolving management and assessment of intermediate-term outcomes in a high-risk population. *Circulation* 2007;116:I172–I178.
 96. Kobashigawa J, Mehra M, West L, et al. Report from a consensus conference on the sensitized patient awaiting heart transplantation. *J Heart Lung Transplant* 2009;28:213–225.
 97. Kobashigawa JA, Patel JK, Kittleson MM, et al. The long-term outcome of treated sensitized patients who undergo heart transplantation. *Clin Transplant* 2011;25:E61–E67.
 98. Rose EA, Pepino P, Barr ML, et al. Relation of HLA antibodies and graft atherosclerosis in human cardiac allograft recipients. *J Heart Lung Transplant* 1992;11:S120–S123.
 99. Itescu S, Tung TC, Burke EM, et al. Preformed IgG antibodies against major histocompatibility complex class II antigens are major risk factors for high-grade cellular rejection in recipients of heart transplantation. *Circulation* 1998;98:786–793.
 100. Michaels PJ, Espejo ML, Kobashigawa J, et al. Humoral rejection in cardiac transplantation: risk factors, hemodynamic consequences and

- relationship to transplant coronary artery disease. *J Heart Lung Transplant* 2003;22:58–69.
101. Tambur AR, Pamboukian SV, Costanzo MR, et al. The presence of HLA-directed antibodies after heart transplantation is associated with poor allograft outcome. *Transplantation* 2005;80:1019–1025.
 102. Ho EK, Vlad G, Vasilescu ER, et al. Pre- and posttransplantation allosensitization in heart allograft recipients: major impact of de novo alloantibody production on allograft survival. *Hum Immunol* 2010;72:5–10.
 103. Chen JM, Davies RR, Mital SR, et al. Trends and outcomes in transplantation for complex congenital heart disease: 1984 to 2004. *Ann Thorac Surg* 2004;78:1352–1361; discussion 1352–1361.
 104. Groetzner J, Reichart B, Roemer U, et al. Cardiac transplantation in pediatric patients: fifteen-year experience of a single center. *Ann Thorac Surg* 2005;79:53–60; discussion 61.
 105. Lamour JM, Hsu DT, Quaegebeur JM, et al. Heart transplantation to a physiologic single lung in patients with congenital heart disease. *J Heart Lung Transplant* 2004;23:948–53.
 106. Mitchell MB, Campbell DN, Ivy D, et al. Evidence of pulmonary vascular disease after heart transplantation for Fontan circulation failure. *J Thorac Cardiovasc Surg* 2004;128:693–702.
 107. Gamba A, Merlo M, Fiocchi R, et al. Heart transplantation in patients with previous Fontan operations. *J Thorac Cardiovasc Surg* 2004;127:555–562.
 108. Costanzo MR, Dipchand A, Starling R, et al. The International Society of Heart and Lung Transplantation Guidelines for the care of heart transplant recipients. *J Heart Lung Transplant* 2010;29:914–956.
 109. Schindler E, Muller M, Akinturk H, et al. Perioperative management in pediatric heart transplantation from 1988 to 2001: anesthetic experience in a single center. *Pediatr Transplant* 2004;8:237–242.
 110. Huang J, Trinkaus K, Huddleston CB, et al. Risk factors for primary graft failure after pediatric cardiac transplantation: importance of recipient and donor characteristics. *J Heart Lung Transplant* 2004;23:716–722.
 111. Rubel JR, Milford EL, McKay DB, et al. Renal insufficiency and end-stage renal disease in the heart transplant population. *J Heart Lung Transplant* 2004;23:289–300.
 112. Tamisier D, Vouhe P, Le Bidois J, et al. Donor-recipient size matching in pediatric heart transplantation: a word of caution about small grafts. *J Heart Lung Transplant* 1996;15:190–195.
 113. Quin JA, Tauriainen MP, Huber LM, et al. Predictors of pericardial effusion after orthotopic heart transplantation. *J Thorac Cardiovasc Surg* 2002;124:979–983.
 114. Hauptman PJ, Couper GS, Aranki SF, et al. Pericardial effusions after cardiac transplantation. *J Am Coll Cardiol* 1994;23:1625–1629.
 115. Heinz G, Hirschl M, Buxbaum P, et al. Sinus node dysfunction after orthotopic cardiac transplantation: postoperative incidence and long-term implications. *Pacing Clin Electrophysiol* 1992;15:731–737.
 116. Boucek MM, Pietra B, Sondheimer H, et al. Anti-T-cell-antibody prophylaxis in children: success with a novel combination strategy of mycophenolate mofetil and antithymocyte serum. *Transplant Proc* 1997;29:165–205.
 117. Di Filippo S. Anti-IL-2 receptor antibody vs polyclonal anti-lymphocyte antibody as induction therapy in pediatric transplantation. *Pediatr Transplantation* 2005;9:373–380.
 118. Gajarski RJ, Blume ED, Urschel S, et al. Infection and malignancy after pediatric heart transplantation: the role of induction therapy. *J Heart Lung Transplant* 2011;30:299–308.
 119. Gossett JG, Canter CE, Zheng J, et al. Decline in rejection in the first year after pediatric cardiac transplantation: a multi-institutional study. *J Heart Lung Transplant* 2010;29:625–632.
 120. Webber SA. The current state of, and future prospects for, cardiac transplantation in children. *Cardiol Young* 2003;13:64–83.
 121. Schowengerdt KO, Naftel DC, Seib PM, et al. Infection after pediatric heart transplantation: results of a multi-institutional study. The Pediatric Heart Transplant Study Group. *J Heart Lung Transplant* 1997;16:1207–1216.
 122. Mattner F, Fischer S, Weissbrodt H, et al. Post-operative nosocomial infections after lung and heart transplantation. *J Heart Lung Transplant* 2007;26:241–249.
 123. Schaenman JM, Rosso F, Austin JM, et al. Trends in invasive disease due to Candida species following heart and lung transplantation. *Transpl Infect Dis* 2009;11:112–121.
 124. Munoz R, Bouza E. Fungal infections in patients undergoing solid organ transplantation. *Enferm Infect Microbiol Clin* 1997;15:34–50.
 125. Kimball TR, Semler DC, Witt SA, et al. Noninvasive markers for acute heart transplant rejection in children with the use of automatic border detection. *J Am Soc Echocardiogr* 1997;10:964–972.
 126. Boucek MM, Mathis CM, Boucek RJ Jr, et al. Prospective evaluation of echocardiography for primary rejection surveillance after infant heart transplantation: comparison with endomyocardial biopsy. *J Heart Lung Transplant* 1994;13:66–73.
 127. Asante-Korang A, Fickey M, Boucek MM, et al. Diastolic performance assessed by tissue Doppler after pediatric heart transplantation. *J Heart Lung Transplant* 2004;23:865–872.
 128. Levi DS, DeConde AS, Fishbein MC, et al. The yield of surveillance endomyocardial biopsies as a screen for cellular rejection in pediatric heart transplant patients. *Pediatr Transplant* 2004;8:22–28.
 129. Boucek RJ Jr, Boucek MM, Asante-Korang A. Advances in methods for surveillance of rejection. *Cardiol Young* 2004;14:93–96.
 130. Mooradian SJ, Goldberg CS, Crowley DC, et al. Evaluation of a noninvasive index of global ventricular function to predict rejection after pediatric cardiac transplantation. *Am J Cardiol* 2000;86:358–360.
 131. Estep JD, Shah DJ, Nagueh SF, et al. The role of multimodality cardiac imaging in the transplanted heart. *JACC Cardiovasc Imaging* 2009;2:1126–40.
 132. Chin C, Naftel DC, Singh TP, et al. Risk factors for recurrent rejection in pediatric heart transplantation: a multicenter experience. *J Heart Lung Transplant* 2004;23:178–185.
 133. Wagner K, Oliver MC, Boyle GJ, et al. Endomyocardial biopsy in pediatric heart transplant recipients: a useful exercise? (Analysis of 1,169 biopsies). *Pediatr Transplant* 2000;4:186–192.
 134. Kirklin JK. Is biopsy-proven cellular rejection an important clinical consideration in heart transplantation? *Curr Opin Cardiol* 2005;20:127–131.
 135. Rosenthal DN, Chin C, Nishimura K, et al. Identifying cardiac transplant rejection in children: diagnostic utility of echocardiography, right heart catheterization and endomyocardial biopsy data. *J Heart Lung Transplant* 2004;23:323–329.
 136. Putzer GJ, Cooper D, Keehn C, et al. An improved echocardiographic rejection-surveillance strategy following pediatric heart transplantation. *J Heart Lung Transplant* 2000;19:1166–1174.
 137. Lindblade CL, Chun DS, Darragh RK, et al. Value of plasma B-type natriuretic peptide as a marker for rejection in pediatric heart transplant recipients. *Am J Cardiol* 2005;95:909–111.
 138. Shaw SM, Williams SG. Is brain natriuretic peptide clinically useful after cardiac transplantation? *J Heart Lung Transplant* 2006;25:1396–1401.
 139. Rossano JW, Denfield SW, Kim JJ, et al. B-type natriuretic peptide is a sensitive screening test for acute rejection in pediatric heart transplant patients. *J Heart Lung Transplant* 2008;27:649–654.
 140. Geiger M, Harake D, Halnon N, et al. Screening for rejection in symptomatic pediatric heart transplant recipients: the sensitivity of BNP. *Pediatr Transplant* 2008;12:563–569.
 141. Winters GL, Marboe CC, Billingham ME. The International Society for Heart and Lung Transplantation grading system for heart transplant biopsy specimens: clarification and commentary. *J Heart Lung Transplant* 1998;17:754–760.
 142. Shirali GS, Ni J, Chinnock RE, et al. Association of viral genome with graft loss in children after cardiac transplantation. *N Engl J Med* 2001;344:1498–1503.
 143. Moulik M, Breinholt JP, Dreyer WJ, et al. Viral endomyocardial infection is an independent predictor and potentially treatable risk factor for graft loss and coronary vasculopathy in pediatric cardiac transplant recipients. *J Am Coll Cardiol* 2010;56:582–592.
 144. Dodd DA CJ, Dipchand AI, eds. *Acute Rejection: Natural History, Risk Factors, Surveillance, and Treatment*. Philadelphia, PA: Elsevier, 2007.
 145. Kfoury AG, Hammond ME. Controversies in defining cardiac antibody-mediated rejection: need for updated criteria. *J Heart Lung Transplant* 2010;29:389–394.
 146. Berry GJ, Angelini A, Burke MM, et al. The ISHLT working formulation for pathologic diagnosis of antibody-mediated rejection in heart transplantation: evolution and current status (2005–2011). *J Heart Lung Transplant* 2011;30:601–611.
 147. Kfoury AG, Renlund DG, Snow GL, et al. A clinical correlation study of severity of antibody-mediated rejection and cardiovascular mortality in heart transplantation. *J Heart Lung Transplant* 2009;28:51–57.
 148. Takemoto SK, Zeevi A, Feng S, et al. National conference to assess antibody-mediated rejection in solid organ transplantation. *Am J Transplant* 2004;4:1033–1041.
 149. Flechner SM, Fatica R, Askar M, et al. The role of proteasome inhibition with bortezomib in the treatment of antibody-mediated rejection after kidney-only or kidney-combined organ transplantation. *Transplantation* 2010;90:1486–1492.
 150. Barone G, Chang CT, Choc MG Jr, et al. The pharmacokinetics of a micro-emulsion formulation of cyclosporine in primary renal allograft recipients. The Neoral Study Group. *Transplantation* 1996;61:875–880.
 151. Reichart B, Meiser B, Vigano M, et al. European Multicenter Tacrolimus (FK506) Heart Pilot Study: one-year results–European Tacrolimus Multicenter Heart Study Group. *J Heart Lung Transplant* 1998;17:775–781.
 152. Pollock-Barziv SM, Dipchand AI, McCrindle BW, et al. Randomized clinical trial of tacrolimus- vs cyclosporine-based immunosuppression in pediatric heart transplantation: preliminary results at 15-month follow-up. *J Heart Lung Transplant* 2005;24:190–194.
 153. Keogh A, Richardson M, Ruygrok P, et al. Sirolimus in de novo heart transplant recipients reduces acute rejection and prevents coronary artery disease at 2 years: a randomized clinical trial. *Circulation* 2004;110:2694–2700.
 154. Lobach NE, Pollock-Barziv SM, West LJ, et al. Sirolimus immunosuppression in pediatric heart transplant recipients: a single-center experience. *J Heart Lung Transplant* 2005;24:184–189.
 155. Gregory CR. Immunosuppressive approaches to the prevention of graft vascular disease. *Transplant Proc* 1998;30:878–880.
 156. Matthews K, Gossett J, Kappelle PV, et al. Indications, tolerance and complications of a sirolimus and calcineurin inhibitor immunosuppression

- regimen: intermediate experience in pediatric heart transplantation recipients. *Pediatr Transplant* 2010;14:402-408.
157. Raichlin E, Chandrasekaran K, Kremers WK, et al. Sirolimus as primary immunosuppressant reduces left ventricular mass and improves diastolic function of the cardiac allograft. *Transplantation* 2008;86:1395-1400.
 158. Rothenburger M, Zuckermann A, Bara C, et al. Recommendations for the use of everolimus (Certican) in heart transplantation: results from the second German-Austrian Certican Consensus Conference. *J Heart Lung Transplant* 2007;26:305-311.
 159. Engelen MA, Amler S, Welp H, et al. Prospective study of everolimus with calcineurin inhibitor-free immunosuppression in maintenance heart transplant patients: results at 2 years. *Transplantation* 2011;91:1159-1165.
 160. Kobashigawa J, Miller L, Renlund D, et al. A randomized active-controlled trial of mycophenolate mofetil in heart transplant recipients. Mycophenolate Mofetil Investigators. *Transplantation* 1998;66:507-515.
 161. Eisen HJ, Kobashigawa J, Keogh A, et al. Three-year results of a randomized, double-blind, controlled trial of mycophenolate mofetil versus azathioprine in cardiac transplant recipients. *J Heart Lung Transplant* 2005;24:517-525.
 162. Ross HJ, Gullestad L, Pak J, et al. Methotrexate or total lymphoid irradiation for treatment of persistent or recurrent allograft cellular rejection: a comparative study. *J Heart Lung Transplant* 1997;16:179-189.
 163. Shaddy RE, Bullock EA, Tani LY, et al. Methotrexate therapy in pediatric heart transplantation as treatment of recurrent mild to moderate acute cellular rejection. *J Heart Lung Transplant* 1994;13:1009-1013.
 164. Boucek Jr RJ, Boucek MM. Pediatric heart transplantation. *Curr Opin Pediatr* 2002;14:611-619.
 165. Singh TP, Faber C, Blume ED, et al. Safety and early outcomes using a corticosteroid-avoidance immunosuppression protocol in pediatric heart transplant recipients. *J Heart Lung Transplant* 2010;29:517-522.
 166. Sigfusson G, Fricker FJ, Bernstein D, et al. Long-term survivors of pediatric heart transplantation: a multicenter report of sixty-eight children who have survived longer than five years [see comments]. *J Pediatr* 1997;130:862-871.
 167. Ibrahim JE, Sweet SC, Flippin M, et al. Rejection is reduced in thoracic organ recipients when transplanted in the first year of life. *J Heart Lung Transplant* 2002;21:311-318.
 168. Kaufman M, Shemesh E, Benton T. The adolescent transplant recipient. *Pediatr Clin North Am* 2010;57:575-592.
 169. Ringewald JM, Gidding SS, Crawford SE, et al. Nonadherence is associated with late rejection in pediatric heart transplant recipients. *J Pediatr* 2001;139:75-78.
 170. Griffin KJ, Elkin TD. Non-adherence in pediatric transplantation: a review of the existing literature. *Pediatr Transplant* 2001;5:246-249.
 171. Serrano-Ikkos E, Lask B, Whitehead B, et al. Incomplete adherence after pediatric heart and heart-lung transplantation. *J Heart Lung Transplant* 1998;17:1177-1183.
 172. Tebbi CK, Cummings KM, Zevon MA, et al. Compliance of pediatric and adolescent cancer patients. *Cancer* 1986;58:1179-1184.
 173. Grady KL, Russell KM, Srinivasan S, et al. Patient compliance with annual diagnostic testing after heart transplantation. *Transplant Proc* 1993;25:2978-2980.
 174. Sester M, Gartner BC, Girndt M, et al. Vaccination of the solid organ transplant recipient. *Transplant Rev (Orlando)* 2008;22:274-284.
 175. Crandall WV, Norlin C, Bullock EA, et al. Etiology and outcome of outpatient fevers in pediatric heart transplant patients. *Clin Pediatr (Phila)* 1996;35:437-442.
 176. Kichuk-Christians MR. Children are not small adults: some differences between pediatric and adult cardiac transplantation. *Curr Opin Cardiol* 2002;17:152-159.
 177. Hirshfeld AB, Kahle AL, Clark BJ III, et al. Parent-reported health status after pediatric thoracic organ transplant. *J Heart Lung Transplant* 2004;23:1111-1118.
 178. de Broux E, Huot CH, Chartrand S, et al. Growth after pediatric heart transplantation. *Transplant Proc* 2001;33:1735-1737.
 179. Hathout EH, Chinnock RE. Growth after heart transplantation. *Pediatr Transplant* 2004;8:97-100.
 180. Cohen A, Addonizio LJ, Softness B, et al. Growth and skeletal maturation after pediatric cardiac transplantation. *Pediatr Transplant* 2004;8:126-135.
 181. DeMaso DR, Douglas Kelley S, Bastardi H, et al. The longitudinal impact of psychological functioning, medical severity, and family functioning in pediatric heart transplantation. *J Heart Lung Transplant* 2004;23:473-480.
 182. Abarbanell G, Mulla N, Chinnock R, et al. Exercise assessment in infants after cardiac transplantation. *J Heart Lung Transplant* 2004;23:1334-1338.
 183. Dipchand AI, Manlhiot C, Russell JL, et al. Exercise capacity improves with time in pediatric heart transplant recipients. *J Heart Lung Transplant* 2009;28:585-590.
 184. Fricker F. Should physical activity and/or competitive sports be curtailed in pediatric heart transplant recipients? *Pediatr Transplantation* 2002;6:267-269.
 185. Collins KK, Thiagarajan RR, Chin C, et al. Atrial tachyarrhythmias and permanent pacing after pediatric heart transplantation. *J Heart Lung Transplant* 2003;22:1126-1133.
 186. LaPage MJ, Rhee EK, Canter CE. Tachyarrhythmias after pediatric heart transplantation. *J Heart Lung Transplant* 2010;29:273-277.
 187. Chinnock RE, Torres VI, Jutzy RV, et al. Cardiac pacemakers in pediatric heart transplant recipients: incidence, indications, and associated factors. Pediatric Heart Transplant Group- Loma Linda. *Pacing Clin Electrophysiol* 1996;19:26-30.
 188. Singh TP, Gauvreau K, Rhodes J, et al. Longitudinal changes in heart rate recovery after maximal exercise in pediatric heart transplant recipients: evidence of autonomic re-innervation? *J Heart Lung Transplant* 2007;26:1306-1312.
 189. Ramaekers D, Ector H, Vanhaecke J, et al. Heart rate variability after cardiac transplantation in humans. *Pacing Clin Electrophysiol* 1996;19:2112-2119.
 190. Gallego-Page JC, Segovia J, Alonso-Pulpon L, et al. Re-innervation after heart transplantation: a multidisciplinary study. *J Heart Lung Transplant* 2004;23:674-682.
 191. Bengel FM, Ueberfuhr P, Ziegler SI, et al. Serial assessment of sympathetic reinnervation after orthotopic heart transplantation. A longitudinal study using PET and C-11 hydroxyephedrine. *Circulation* 1999;99:1866-1871.
 192. Wilson RF, Johnson TH, Haider GC, et al. Sympathetic reinnervation of the sinus node and exercise hemodynamics after cardiac transplantation. *Circulation* 2000;101:2727-2733.
 193. De Marco T, Dae M, Yuen-Green MS, et al. Iodine-123 metaiodobenzylguanidine scintigraphic assessment of the transplanted human heart: evidence for late reinnervation. *J Am Coll Cardiol* 1995;25:927-931.
 194. Schwaiblmair M, von Scheidt W, Ueberfuhr P, et al. Functional significance of cardiac reinnervation in heart transplant recipients. *J Heart Lung Transplant* 1999;18:838-845.
 195. Pahl E, Crawford SE, Cohn RA, et al. Reversal of severe late left ventricular failure after pediatric heart transplantation and possible role of plasmapheresis. *Am J Cardiol* 2000;85:735-739.
 196. Asano M, Gundry SR, Razzouk AJ, et al. Total lymphoid irradiation for refractory rejection in pediatric heart transplantation. *Ann Thorac Surg* 2002;74:1979-1985.
 197. Webber SA, Naftel DC, Fricker FJ, et al. Lymphoproliferative disorders after paediatric heart transplantation: a multi-institutional study. *Lancet* 2006;367:233-239.
 198. Evens AM, Roy R, Sterrenberg D, et al. Post-transplantation lymphoproliferative disorders: diagnosis, prognosis, and current approaches to therapy. *Curr Oncol Rep* 2010;12:383-394.
 199. Schubert S, Abdul-Khalik H, Lehmkuhl HB, et al. Diagnosis and treatment of post-transplantation lymphoproliferative disorder in pediatric heart transplant patients. *Pediatr Transplant* 2009;13:54-62.
 200. Benden C, Aurora P, Burch M, et al. Monitoring of Epstein-Barr viral load in pediatric heart and lung transplant recipients by real-time polymerase chain reaction. *J Heart Lung Transplant* 2005;24:2103-2138.
 201. Bingle MA, Feingold B, Miller SA, et al. Chronic high Epstein-Barr viral load state and risk for late-onset posttransplant lymphoproliferative disease/lymphoma in children. *Am J Transplant* 2008;8:442-445.
 202. Billingham ME. Histopathology of graft coronary disease. *J Heart Lung Transplant* 1992;11:S38-S44.
 203. Zimmer RJ, Lee MS. Transplant coronary artery disease. *JACC Cardiovasc Interv* 2010;3:367-377.
 204. Costanzo MR, Naftel DC, Pritzker MR, et al. Heart transplant coronary artery disease detected by coronary angiography: a multiinstitutional study of preoperative donor and recipient risk factors. Cardiac Transplant Research Database. *J Heart Lung Transplant* 1998;17:744-753.
 205. Pahl E, Naftel DC, Kuhn MA, et al. The impact and outcome of transplant coronary artery disease in a pediatric population: a 9-year multi-institutional study. *J Heart Lung Transplant* 2005;24:645-651.
 206. Webber SA, Naftel DC, Parker J, et al. Late rejection episodes more than 1 year after pediatric heart transplantation: risk factors and outcomes. *J Heart Lung Transplant* 2003;22:869-75.
 207. Dipchand AI, Bharat W, Manlhiot C, et al. A prospective study of dobutamine stress echocardiography for the assessment of cardiac allograft vasculopathy in pediatric heart transplant recipients. *Pediatr Transplant* 2008;12:570-576.
 208. Kuhn MA, Jutzy KR, Deming DD, et al. The medium-term findings in coronary arteries by intravascular ultrasound in infants and children after heart transplantation. *J Am Coll Cardiol* 2000;36:250-254.
 209. Costello JM, Wax DF, Binns HJ, et al. A comparison of intravascular ultrasound with coronary angiography for evaluation of transplant coronary disease in pediatric heart transplant recipients. *J Heart Lung Transplant* 2003;22:44-49.
 210. Nicolas RT, Kort HW, Balzer DT, et al. Surveillance for transplant coronary artery disease in infant, child and adolescent heart transplant recipients: an intravascular ultrasound study. *J Heart Lung Transplant* 2006;25:921-927.
 211. Schubert S, Abdul-Khalik H, Wellenhofer E, et al. Coronary flow reserve measurement detects transplant coronary artery disease in pediatric heart transplant patients. *J Heart Lung Transplant* 2008;27:514-521.
 212. Delgado JF, Manito N, Segovia J, et al. The use of proliferation signal inhibitors in the prevention and treatment of allograft vasculopathy in heart transplantation. *Transplant Rev (Orlando)* 2009;23:69-79.
 213. Shaddy RE, Revenaugh JA, Orsmond GS, et al. Coronary interventional procedures in pediatric heart transplant recipients with cardiac allograft vasculopathy. *Am J Cardiol* 2000;85:1370-1372.

214. Sachdeva R, Seib PM, Frazier EA. Percutaneous coronary intervention using drug-eluting stents in pediatric heart transplant recipients. *Pediatr Transplant* 2009;13:1014–1019.
215. Kobashigawa JA, Moriguchi JD, Laks H, et al. Ten-year follow-up of a randomized trial of pravastatin in heart transplant patients. *J Heart Lung Transplant* 2005;24:1736–1740.
216. Chin C, Gamberg P, Miller J, et al. Efficacy and safety of atorvastatin after pediatric heart transplantation. *J Heart Lung Transplant* 2002;21:1213–1217.
217. Penson MG, Fricker FJ, Thompson JR, et al. Safety and efficacy of pravastatin therapy for the prevention of hyperlipidemia in pediatric and adolescent cardiac transplant recipients. *J Heart Lung Transplant* 2001;20:611–618.
218. Chin C, Lukito SS, Shek J, et al. Prevention of pediatric graft coronary artery disease: atorvastatin. *Pediatr Transplant* 2008;12:442–446.
219. Pahl E. Statins in the prevention of transplant coronary artery disease: in pediatric heart recipients. *Pediatr Transplant* 2007;11:459–460.
220. Roche SL, O'Sullivan JJ, Kantor PF. Hypertension after pediatric cardiac transplantation: detection, etiology, implications and management. *Pediatr Transplant* 2010;14:159–168.
221. Sachdeva R, Blaszk RT, Ainley KA, et al. Determinants of renal function in pediatric heart transplant recipients: long-term follow-up study. *J Heart Lung Transplant* 2007;26:108–113.
222. Di Filippo S, Zeevi A, McDade KK, et al. Impact of TGFbeta1 gene polymorphisms on late renal function in pediatric heart transplantation. *Hum Immunol* 2005;66:133–139.
223. Alonso EM. Long-term renal function in pediatric liver and heart recipients. *Pediatr Transplant* 2004;8:381–385.
224. Boyer O, Le Bidois J, Dechaux M, et al. Improvement of renal function in pediatric heart transplant recipients treated with low-dose calcineurin inhibitor and mycophenolate mofetil. *Transplantation* 2005;79:1405–1410.
225. Groetzner J, Kaczmarek I, Meiser B, et al. Sirolimus and mycophenolate mofetil as calcineurin inhibitor-free immunosuppression in a cardiac transplant patient with chronic renal failure. *J Heart Lung Transplant* 2004;23:770–773.
226. Hymes LC, Warshaw BL. Five-year experience using sirolimus-based, calcineurin inhibitor-free immunosuppression in pediatric renal transplantation. *Pediatr Transplant* 2011;15:437–441.
227. Chin C, Rosenthal D, Bernstein D. Lipoprotein abnormalities are highly prevalent in pediatric heart transplant recipients. *Pediatr Transplant* 2000;4:193–199.
228. Paolillo JA, Boyle GJ, Law YM, et al. Posttransplant diabetes mellitus in pediatric thoracic organ recipients receiving tacrolimus-based immunosuppression. *Transplantation* 2001;71:252–256.
229. Hathout EH, Chinnoek RE, Johnston JK, et al. Pediatric post-transplant diabetes: data from a large cohort of pediatric heart-transplant recipients. *Am J Transplant* 2003;3:994–998.
230. Rakhit A, Nurko S, Gauvreau K, et al. Gastrointestinal complications after pediatric cardiac transplantation. *J Heart Lung Transplant* 2002;21:751–759.
231. Sakopoulos AG, Gundry S, Razzouk AJ, et al. Cholelithiasis in infant and pediatric heart transplant patients. *Pediatr Transplant* 2002;6:231–234.
232. Fleenor JT, Hoffman TM, Bush DM, et al. Pneumatosis intestinalis after pediatric thoracic organ transplantation. *Pediatrics* 2002;109:E78–E88.
233. Chueh SC, Kahan BD. Dyslipidemia in renal transplant recipients treated with a sirolimus and cyclosporine-based immunosuppressive regimen: incidence, risk factors, progression, and prognosis. *Transplantation* 2003;76:375–382.
234. Shirali GS, Cephus CE, Kuhn MA, et al. Posttransplant recoarctation of the aorta: a twelve year experience. *J Am Coll Cardiol* 1998;32:509–514.
235. Embleton ND, O'Sullivan JJ, Hamilton JR, et al. High prevalence of anemia after cardiac transplantation in children. *Transplantation* 1997;64:1590–1594.
236. Kanter KR, Vincent RN, Berg AM, et al. Cardiac retransplantation in children. *Ann Thorac Surg* 2004;78:644–649; discussion 644–649.
237. Johnson MR, Aaronson KD, Canter CE, et al. Heart retransplantation. *Am J Transplant* 2007;7:2075–2081.
238. Mahle WT, Vincent RN, Kanter KR. Cardiac retransplantation in childhood: analysis of data from the United Network for Organ Sharing. *J Thorac Cardiovasc Surg* 2005;130:542–546.
239. Boucek MM, Edwards LB, Keck BM, et al. Registry of the International Society for Heart and Lung Transplantation: eighth official pediatric report—2005. *J Heart Lung Transplant* 2005;24:968–982.
240. Aurora P, Edwards LB, Kucheryavaya AY, et al. The Registry of the International Society for Heart and Lung Transplantation: thirteenth official pediatric lung and heart-lung transplantation report—2010. *J Heart Lung Transplant* 2010;29:1129–1141.

SECTION

VIII

Pulmonary Vascular Disease

CHAPTER

66

Pathophysiology of Pulmonary Hypertension

Marlene Rabinovitch

This chapter addresses the pathophysiologic mechanisms leading to pulmonary hypertension associated with congenital heart defects and other disease-related or idiopathic processes. Our evolving knowledge of fundamental mechanisms has led to new and improved treatments and holds great promise for the development of future therapies.

HEART DEFECTS WITH INCREASED PULMONARY BLOOD FLOW

High-Flow Congenital Heart Defects and Pulmonary Hypertension

As early as 1935, Brenner (1) observed different types of pulmonary vascular lesions in patients with congenital heart defects. A variety of physiologic factors appeared to contribute to the severity and rate at which vascular disease developed in patients with congenital heart defects (Table 66.1). In 1958, Heath and Edwards (2) suggested that there was a progression of structural changes (grades I through VI) (Fig. 66.1). Grades I and II, medial hypertrophy and intimal hyperplasia, respectively, were considered mild and probably reversible. Grades III and IV were, respectively, lumen occlusion from intimal hyperplasia and early to advanced arterial dilation. Grade III was thought to be, at best, partially reversible, but grade IV, irreversible. Grades V and VI were considered terminal changes, grade V being angiomatoid formation, and grade VI fibrinoid necrosis. The latter changes were identified most frequently in older children. Structural changes that predicted severe and fixed elevation in pulmonary vascular resistance were therefore more difficult to establish in infants and young children, although it was recognized that certain lesions, such as transposition of the great arteries with intact septum, but especially with a large ventricular septal defect (VSD) or a patent ductus arteriosus, were at high

risk. Curiously, there have been reports of late progression of pulmonary vascular disease in infants with transposition of the great arteries even after successful and timely surgical correction. Infants with a large VSD, especially an atrioventricular septal defect, also developed pulmonary vascular disease in early infancy; in the latter group, there were advanced changes observed even within the first 6 months of life. Patients with cyanotic heart defects who had large, surgically created systemic-to-pulmonary artery shunts were also at risk for pulmonary vascular disease. Several investigators tried to quantify the degree of medial hypertrophy, but their measurements did not correlate closely with the preoperative level of pulmonary vascular resistance or with its change postoperatively (3).

Structural Remodeling and Growth

Beginning in 1965, a new and quantitative method of analysis of the pulmonary vascular bed was developed that was particularly applicable to the study of infants and young children because it incorporated features of altered growth of the pulmonary circulation. This method was based upon extensive studies carried out using a technique of radiopaque barium–gelatin arterial injection of a postmortem lung specimen. It was observed from the postmortem arteriograms that the vessels are prominent in the newborn, whereas in the adult they are obscured by a dense background haze produced by the addition of many small intraacinar arteries not present at birth (4). On microscopic examination, three features of normal remodeling and growth of the pulmonary vascular bed were established (5). With increasing age, muscle is observed in arteries located more peripherally within the acinus. At first, nonmuscular arteries become partially muscular, and later they become fully muscularized. At birth, the muscularized arteries are thick walled, but within a few days, the smallest muscular arteries dilate and their walls thin to adult levels. When infants are 4 months of age,

TABLE 66.1

Factors Determining the Development of Pulmonary Vascular Disease in Patients with Common Varieties of Congenital Heart Disease

	Major Factors					Minor Factors		PVD
	$\uparrow P_{PA}$	$\uparrow P_{PV}$	$\uparrow Q_{PA}$	$\uparrow PO_{2PA}$	$\downarrow PO_{2SA}$	$\downarrow pH_{SA}$	Hematocrit \uparrow	
ASD, secundum	—	—	+	+	—	—	—	Unlikely
ASD, primum	—	±	+	+	—	—	—	Possible
TAPVC	+	+	+	+	±	±	±	Highly probable
Large VSD	+	±	+	+	—	—	—	Probable
With mitral disease	+	+	+	+	—	—	—	Virtually certain
TF	—	—	—	—	+	+	+	Unlikely until late
With Potts	+	±	+	+	±	—	±	Probable
TGA	±	±	+	+	+	±	+	Virtually certain
With VSD	+	+	+	+	+	±	+	Certain

ASD, atrial septal defect; TAPVC, total anomalous pulmonary venous connection; PVD, pulmonary vascular disease; P, pressure; PV, pulmonary vein; Q, flow; PA, pulmonary artery; SA, systemic artery; P_{PA} , mean pulmonary artery pressure; P_{PV} , mean pulmonary venous pressure; PO_{2PA} , oxygen pressure in pulmonary artery; PO_{2SA} , oxygen pressure in systemic artery; pH_{SA} , pH in systemic artery; Q_{PA} , flow in pulmonary artery. +, present; —, absent; ±, may or may not be present; TF, tetralogy of Fallot; VSD, ventricular septal defect; TGA, transposition of the great arteries.

Adapted from Nadas AS, Fyler DF. *Pediatric Cardiology*. Philadelphia, PA: WB Saunders, 1972:68.

this process has included the largest muscular pulmonary arteries and is complete. Arteries grow both in number and size, and they grow most rapidly in infancy. Although alveoli also proliferate, the ratio of alveoli to arteries actually decreases from the newborn value of 20:1 to the value of 8:1, which is achieved first in early childhood and which persists (Fig. 66.2).

Morphometric analysis of the lungs of patients with congenital heart defects reveals disturbed growth and remodeling of the pulmonary vascular bed (Table 66.2) (6). On postmortem arteriograms from infants with VSD, the axial arteries were dilated at the hilum but narrowed peripherally. On microscopic examination of the pulmonary vascular bed, muscle had extended precociously into normally nonmuscular peripheral arteries, regression of the perinatal musculature had

not occurred, and there was additional medial hypertrophy. Also, the peripheral arteries had not grown normally in that they were small and few. Alveolar differentiation and multiplication, however, were normal. Because there were no regional variations in the lung, it was feasible to apply the morphometric technique to analysis of lung biopsy tissue in assessing abnormal muscularity and evaluating arterial size and number (7).

Lung Biopsy

Lung biopsy studies indicated that the severity of altered growth and development of the pulmonary vascular bed correlated with the hemodynamic state. Three progressively severe

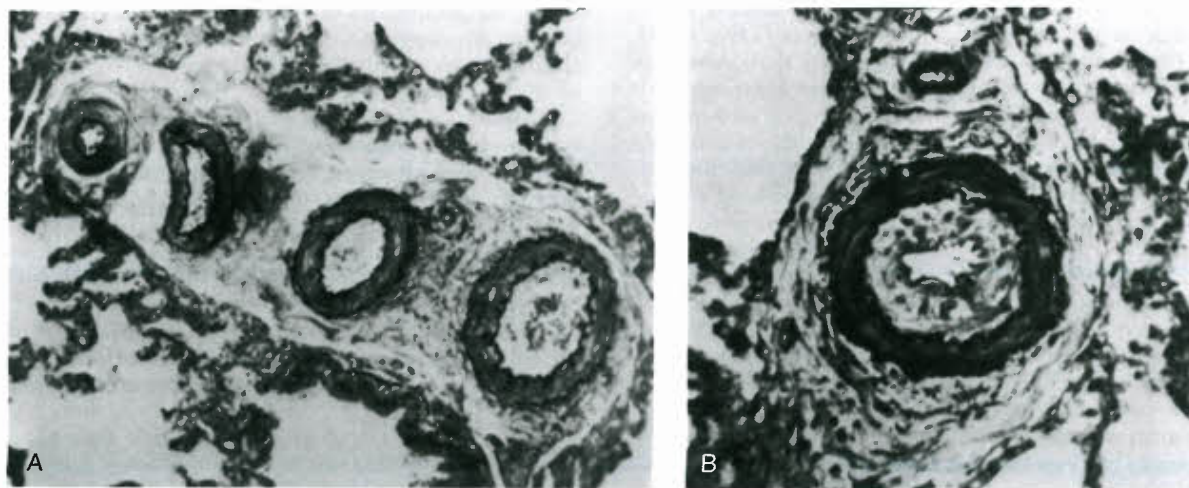


Figure 66.1. Heath-Edwards classification of pulmonary vascular changes. A: Grade I: medial hypertrophy. Elastin–van Gieson stain (EVG), original magnification, $\times 150$. B: Grade II: cellular intimal proliferation in an abnormally muscular artery. EVG, original magnification, $\times 250$.

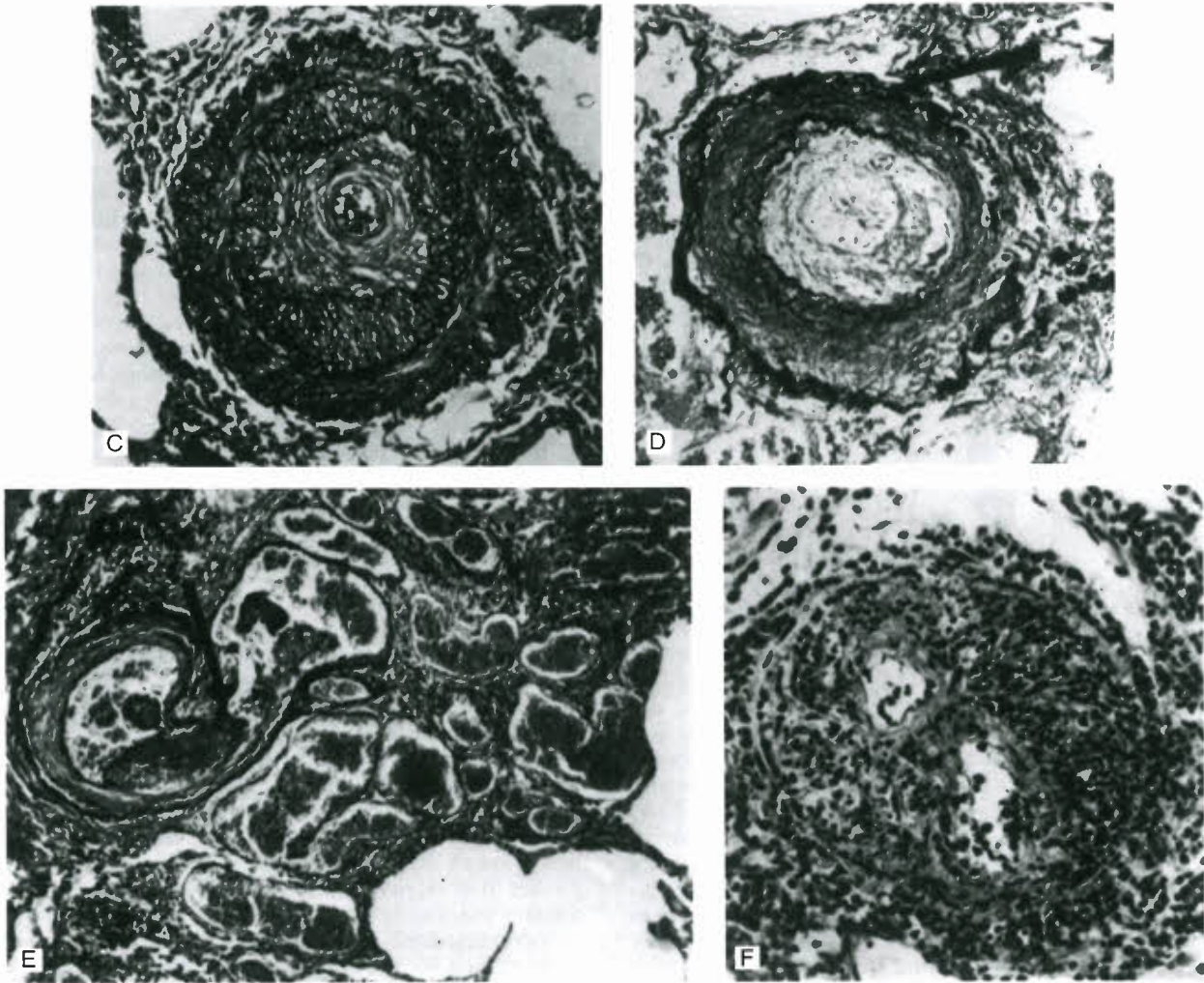


Figure 66.1. (Continued) C: Grade III: occlusive changes. Medium is thickened as a result of fasciculi of longitudinal muscle, and vessel is all but occluded by fibroelastic tissue. EVG, original magnification, $\times 150$. D: Grade IV: dilation. Vessel is dilated, and medium is abnormally thin (arrow). Lumen is occluded by fibrous tissue. EVG, original magnification, $\times 150$. E: Grade V: plexiform lesion. There is cellular intimal proliferation (arrow); clustered around are numerous thin-walled vessels that terminate as capillaries in the alveolar wall. EVG, original magnification, $\times 95$. F: Grade VI: acute necrotizing arteritis. A severe reactive inflammatory exudate is seen through all layers of the vessel. Hematoxylin eosin stain, original magnification, $\times 250$. (From Wagenvoort CA, Heath D, Edwards JE. *The Pathology of the Pulmonary Vasculature*. Springfield, IL: Charles C. Thomas, 1964, with permission.)

stages are seen. With grade A, there is abnormal extension of muscle into small peripheral arteries, or, in addition, there is a mild increase in wall thickness of the normally muscular arteries (<1.5 times normal). These patients have increased pulmonary blood flow and increased pulse pressure but normal mean pulmonary artery pressure. Meyrick and Reid (8) showed from ultrastructural studies of lung biopsy tissue that this change is due to precocious differentiation to mature smooth muscle cells (SMCs) of the pericyte in the nonmuscular region of the artery and the intermediate cell in the partially muscular region. Because arteries become more muscular as they increase in size, it is tempting to speculate that, in the altered hemodynamic setting of chronic high flow and high pressure, “stretch” is the stimulus for SMC differentiation from precursor cells.

With grade B, as in grade A, there is increased extension of muscle, but, in addition, there is more severe medial hypertrophy of normally muscular arteries. When medial-wall thickness

is >1.5 but <2 times normal (mild grade B), pulmonary hypertension is usually present; when medial wall thickness is more than twice normal (severe grade B), pulmonary hypertension is invariably present and usually the pressure value is greater than half that of the systemic level. The medial thickness is due to hypertrophy as well as hyperplasia of preexisting SMCs and also to an increase in the intercellular connective tissue proteins.

With grade C, in addition to the findings of severe grade B, arterial concentration and usually artery size are reduced. Patients with these changes usually have a pulmonary vascular resistance of $>3.5 \text{ U}\cdot\text{m}^2$. When the artery number is less than half of normal (severe grade C), pulmonary vascular resistance values are often in excess of $6 \text{ U}\cdot\text{m}^2$. The basis for grade C is likely the failure of new vessels to grow normally, although some loss of arteries also may occur. Morphometric grades A and B are refinements of Heath-Edwards grade I; grade C is a new feature that also appears to be of important functional

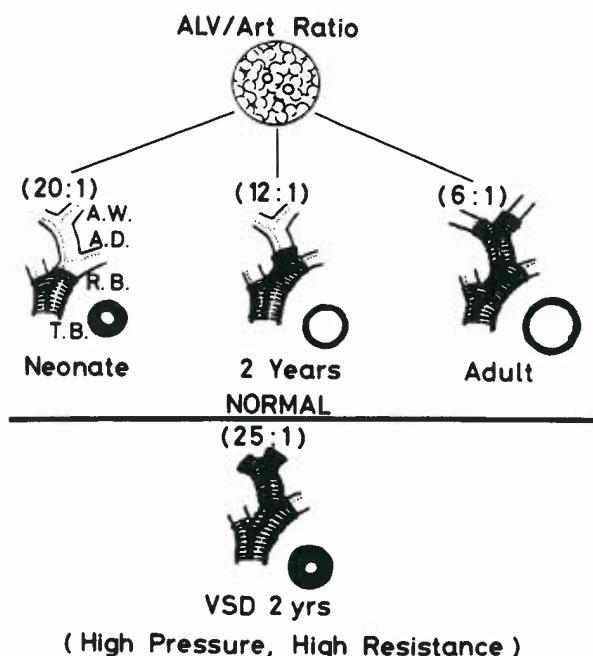


Figure 66.2. Schema showing peripheral pulmonary arterial development through morphometric changes: extension of muscle into peripheral arteries, percent wall thickness, and artery number (alveolar–arterial ratio) as they relate to age. **Upper panel:** Normal development. **Bottom panel:** Abnormalities in all three features in a 2-year-old child with a hypertensive VSD. T.B., artery accompanying a terminal bronchiolus; R.B., artery accompanying a respiratory bronchiolus; A.D., artery accompanying an alveolar duct; A.W., artery accompanying an alveolar wall; ALV/Art, alveolar–arterial ratio. (From Rabinovitch M, Haworth SG, Castaneda AR, et al. Lung biopsy in congenital heart disease: a morphometric approach to pulmonary vascular disease. *Circulation* 1978;58:1107–1122, with permission.)

significance. Grade C may be found with Heath-Edwards grade I, is common with grade II, and is invariable with grade III. In fact, when grade III is seen, arterial concentration is generally half of normal or less.

Whether and to what extent abnormal growth and structural remodeling of the pulmonary vascular bed are permanent and result in persistent pulmonary hypertension can be determined best by correlating these features with

postoperative hemodynamic studies. We correlated the quantitative features of abnormal growth and remodeling of the pulmonary arteries and the qualitative changes described by Heath and Edwards with the hemodynamic behavior of the pulmonary circulation in the immediate postoperative period in the intensive care unit 1 day after repair and at the time of routine cardiac catheterization study 1 year later (9). Patients with grade A or mild grade B changes have normal pulmonary artery pressures in the early postoperative period or only a minimal degree of elevation. Most patients with more severe medial hypertrophy (i.e., severe grade B and Heath-Edwards I) have elevated values. The pulmonary hypertension is frequently labile and almost always can be controlled. The mechanism and treatment are discussed in the next section. Both the presence and the severity of pulmonary hypertension in the early postoperative period are increasingly predictable when there are more advanced changes on lung biopsy, that is, reduced artery number (grade C) and intimal hyperplasia (Heath-Edwards II and III) (Fig. 66.3).

One year after repair, however, patients operated on within the first 8 months of life tend to have normal pulmonary hemodynamics regardless of the severity of vascular changes on lung biopsy, as do all patients with severe grade B (Heath-Edwards I) abnormalities, regardless of their age at repair. Patients surgically corrected between 9 months and 2 years of life with grade C and Heath-Edwards II or III structural changes may have persistent elevation in pulmonary vascular resistance. This appears inevitable in patients operated on after the age of 2 years (Fig. 66.3).

Quantitative techniques have been applied successfully to the analysis of lung biopsy tissue prepared by frozen section to help the surgeon decide between a palliative and corrective procedure when preoperative hemodynamic data are borderline or difficult to obtain or to interpret. The ability to predict from biopsy tissue whether even mild elevation in pulmonary vascular resistance will be present postoperatively is of increasing importance, particularly in the consideration of patients for a Fontan procedure. Patients with tricuspid atresia who have had previous systemic-to-pulmonary artery shunts and those with single-ventricle and previous pulmonary artery bands are particular problems. We currently consider a biopsy showing severe grade C (less than half the normal number of arteries) and grade III or greater changes in 20% of vessels to indicate severe vascular disease that is unlikely to regress postoperatively and may preclude a successful result from closure of a VSD; severe grade B, medial wall thickness greater than twice normal, or grade II changes in any vessel may preclude a favorable result from a Fontan procedure. Even minor vascular changes on lung biopsy tissue (mild grade B)

TABLE 66.2 Structural Features Quantified in Congenital Heart Defects

Congenital Heart Defect	Artery Size	Artery No.	Extension of Muscle	Medial Wall Thickness
VSD	↓	↓	↑	↑
Hypoplastic left heart	N	↑	↑	↑
CA	N	N	↑	↑
TAPVC	N	N	↑	↑
TF	↓	N or ↑	N	↓ or ↑
PA	↓	↓	N	↓

VSD, ventricular septal defect; TF, tetralogy of Fallot; TAPVC, total anomalous pulmonary venous connection; CA, common AV canal; PA, pulmonary atresia; ↑, increased, above normal; ↓, decreased, below normal; N, normal.

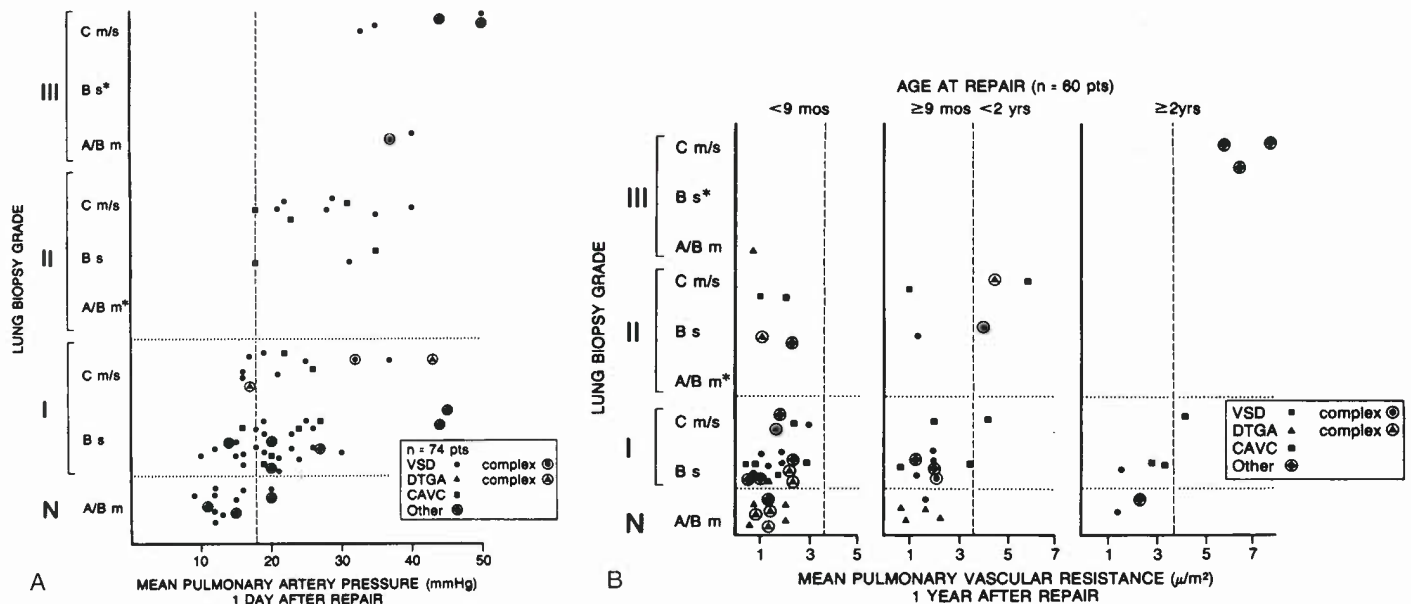


Figure 66.3. A: Lung biopsy grade is correlated with mean pulmonary arterial pressure recorded the day after surgical repair. The dashed vertical lines separate the normal from the abnormally elevated pressure values, and the dotted horizontal lines separate the biopsy grades. Note that with the more severe Heath-Edwards changes on lung biopsy tissue, there is a trend toward a greater proportion of patients with elevated pulmonary arterial pressures and higher values. A, B, C, morphometric grades; m, mild, s, severe. N, I, II, III, Heath-Edwards grades; n, normal; *, no patients in this group; VSD, ventricular septal defect; DTGA, D-transposition of the great arteries; complete atrioventricular septal defect; (AVSD) complex, associated abnormality. B: Graph correlating lung biopsy grade with pulmonary vascular resistance 1 year after cardiac repair. Patients who underwent repair within the first 8 months of life, but not those operated on later, had normal pulmonary vascular resistance regardless of the severity of their structural changes. (From Rabinovitch M, Keane JP, Norwood WI, et al. Vascular structure in lung biopsy tissue correlated with pulmonary hemodynamic findings after repair of congenital heart defects. *Circulation* 1984;69:655–667, with permission.)

are associated with increased morbidity after the Fontan procedure, gauged by prolonged hospitalization, as a result of the need for increased ventilator support and drainage from chest tubes (unpublished observations).

Wedge Angiography

Techniques of wedge angiography have been developed to assess preoperatively the structural state of the pulmonary vascular bed. Changes that can be evaluated quantitatively, such as sparsity of arborization of the pulmonary tree, abrupt termination, tortuosity and narrowing of small arteries, and reduced background capillary filling, generally reflect advanced changes in the preacinar arteries of at least Heath-Edwards grade III severity. A technique has been described that allows quantitative assessment of abnormalities in a pulmonary wedge angiogram (10). An end-hole balloon catheter is directed to the origin of the axial artery of the posterior basal segment of the right lower lobe; the balloon is inflated, contrast material is injected, and the injection is filmed on biplane cineangiography. The rate of tapering of the arteries is assessed by measuring the length of a segment over which the lumen diameter narrows from 2.5 to 1.5 mm. More abrupt arterial tapering is suggestive of more severe changes in the intraacinar arteries, assessed both morphometrically and by the Heath-Edwards classification (Table 66.3 and Fig. 66.4).

Further studies revealed that there are several pitfalls and limitations in the interpretation of the pulmonary wedge angiogram. Pulmonary stenosis or previous placement of a pulmonary artery band, owing to poststenotic dilation, will give the impression of rapid tapering. With advanced vascular

disease, there is sometimes such extensive intimal hyperplasia that the vessel appears narrowed all the way from the hilum so that abrupt tapering is no longer apparent. In this situation, however, the background haze is absent and the pulmonary circulation time is usually prolonged. Technical abnormalities also can result in difficulties in interpretation. If the injection of contrast fails to fill the vessels all the way out to the pleura, the background will appear dark, and if the balloon does not completely occlude the vessel, the false impression of a dense background will be created owing to filling of capillaries and veins. Assessment of the circulation time depends on the exclusion of pulmonary vein stenosis and intrapulmonary shunting.

Intravascular ultrasound could be investigated to estimate the severity of pulmonary vascular disease at least in proximal vessels. Optical coherence tomography is a new technique that can resolve neointimal lesions in very small arteries and may hold greater promise, but has just recently been applied clinically to assess coronary stent stenosis (11).

Reactive Pulmonary Circulation

A major challenge in pediatric cardiology is to understand and control the reactive pulmonary circulation, which can be particularly problematic in the early postoperative period. The pulmonary hypertensive crisis, as it has been called, is thought to result from interaction of a hypertrophied and perhaps hypercontractile circulation with an injured vascular endothelium, with platelets and leukocytes that were exposed to postcardiopulmonary bypass and hypothermia and may more easily degranulate and release potent vasoconstrictor agents, particularly thromboxanes and leukotrienes. In recent

TABLE 66.3

Correlation of the Pathology, Physiology, and Angiogram in Pulmonary Vascular Disease

Grade	Pathology	Physiology			Wedge Angiogram
		Q_p	P_{PA}	R_p	
A	Abnormal extension of muscle into small arteries; ± mild medial hypertrophy	↑	N	N	Show tapering of axial arteries
B	"A" plus severe medial hypertrophy	↑	↑	N	Abrupt tapering
C	"B" plus artery, number, and size	± ↑	↑	↑	Very abrupt tapering

Q_p , pulmonary blood flow; P_{PA} , mean pulmonary artery pressure; R_p , pulmonary vascular resistance; N, normal; The symbols are: ↑ increased; ±, may or may not be increased; ↓, decreased.

studies, increased density of neuroepithelial bodies has been observed in the airways of patients at risk for this complication (12). The neuroendocrine cells, which are also oxygen sensors, contain bombesin and serotonin, agents known to be potent vasoconstrictors. There is also an increase in vasoconstrictor neuropeptide-containing nerves (13) (Fig. 66.5). Because most of the pulmonary hypertensive crises occur while weaning patients from the ventilator, it is tempting to speculate that swings in airway pressure might lead to degranulation of the neuroepithelial cells and release of the vasoconstrictor substances. Moreover, we have observed a striking

decrease in lung compliance accompanying the pulmonary hypertensive crisis.

In ultrastructural lung-biopsy studies in patients with congenital heart defects and pulmonary hypertension, alterations in endothelial cells support endothelial dysfunction as a cause of heightened pulmonary vascular reactivity and also relate endothelial dysfunction to the pathogenesis of progressive pulmonary vascular disease. On scanning electron microscopy, the endothelial surface of normal thin-walled pulmonary arteries has a "corduroy-like" appearance in that the cells form narrow, even ridges. In contrast, the endothelial

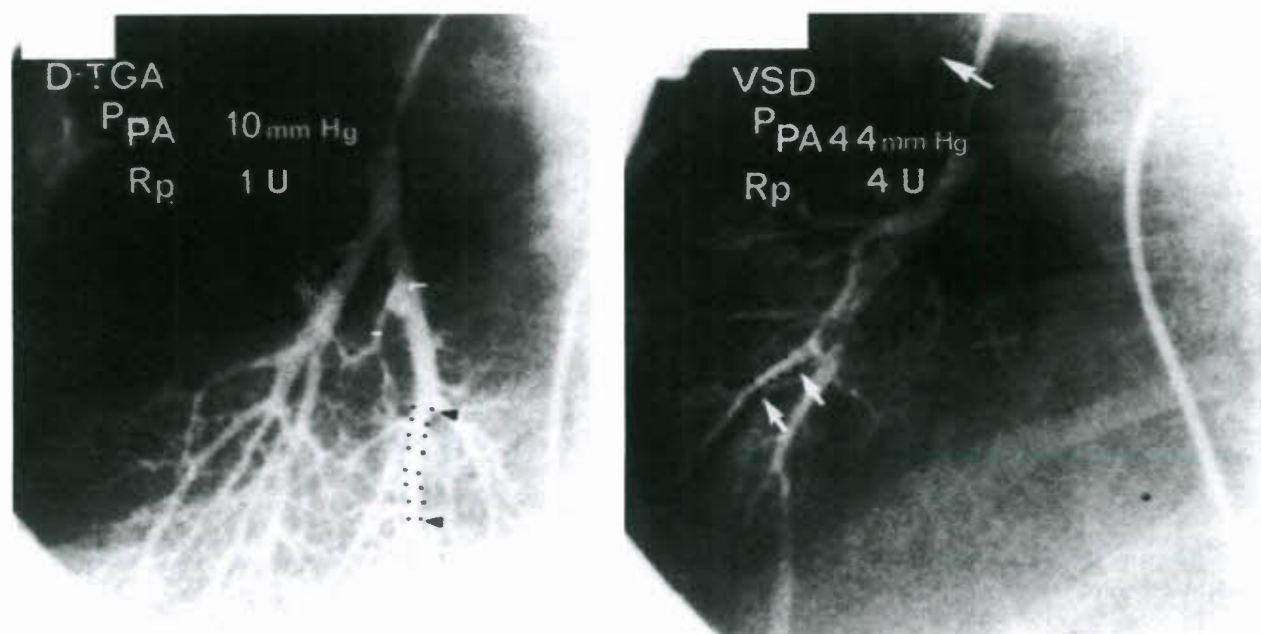


Figure 66.4. Left: A wedge angiogram shows slow tapering of the axial artery in a child with dTGA and normal pulmonary artery pressure (P_{pa}) and resistance (R_p). Approximate segment length between 2.5 and 1.5 mm internal diameter is marked off (arrows). Right: A wedge angiogram in a child with a VSD shows rapid tapering of the artery when there is increased P_{pa} and R_p . An approximate segment length between 2.5 and 1.5 mm internal diameter is marked off (arrows). Large arrow denotes takeoff to the right pulmonary artery. (From Rabinovitch M, Reid L. Quantitative structural analysis of the pulmonary vascular bed in congenital heart defects. In: Engle MA, ed. *Cardiovascular Clinics: Pediatric Cardiovascular Disease*. Philadelphia, PA: FA Davis, 1981, with permission.)

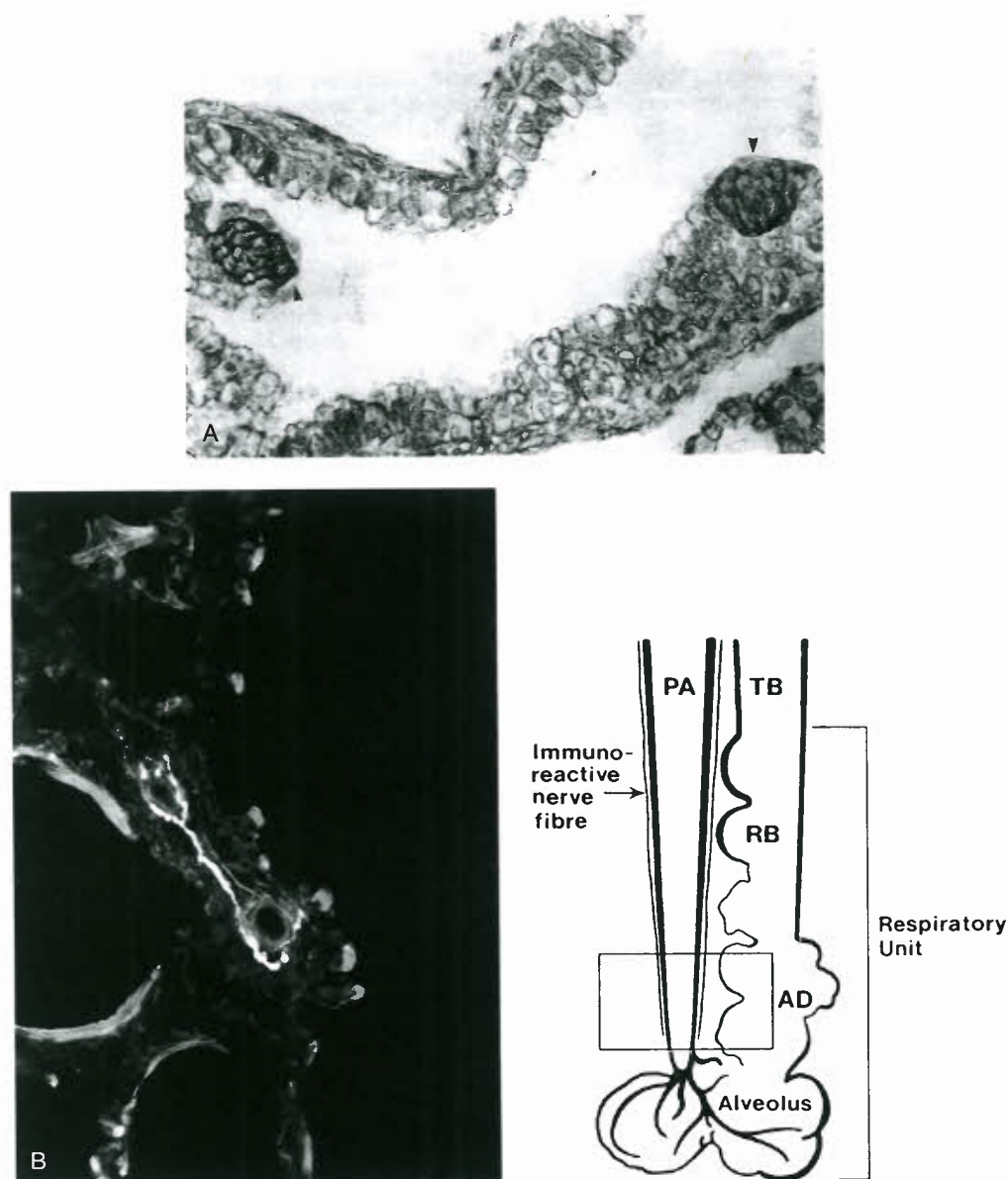


Figure 66.5. A: Neuroepithelial bodies (arrowheads) are seen as dark-staining regions (immunoreactive for serotonin) in airway of a newborn infant. (kindly supplied by E. Cutz.). B: Tyrosine hydroxylase immunoreactive perivascular nerve fibers (arrow) at the adventitial-medial border of an alveolar duct artery in a child aged 2 1/2. Scale bar = 50 μ m. Diagram on the right shows terminal bronchiolus (TB) and airways of respiratory unit accompanied by an innervated pulmonary artery (PA). RB, respiratory bronchiolus; AD, alveolar duct. Square indicates area shown in (B). (From Allen K, Wharton J, Polak J, et al. A study of nerves containing peptides in the pulmonary vasculature of healthy infants and children and of those with pulmonary hypertension. *Br Heart J* 1989;62:353–360, with permission.)

surface of hypertensive thick-walled pulmonary arteries has a “cable-like” texture in that the cells form deep, twisted ridges. The hypertensive endothelium may be predisposed to interact abnormally with marginating blood elements, such as platelets and leukocytes. This might result in the release of pulmonary vasoconstrictor substances and smooth muscle mitogens (14).

On transmission electron microscopy, the endothelium appeared to show heightened metabolic activity with an increased rough endoplasmic reticulum. The subendothelium of the muscular arteries is also abnormal in that there appears to be degradation and neosynthesis of the internal elastic lamina. This observation provided an important clue related to the discovery of heightened elastolytic activity in

the vessel wall associated with the initiation and progression of pulmonary vascular disease. Further studies were designed to try to identify what the products of increased endothelial metabolism might be. We hypothesized that, because endothelial cells produce von Willebrand factor (vWF, factor VIII), an increase in this protein may cause platelet adhesion, formation of microthrombi, and may result in the release of pulmonary vasoconstrictor substances and smooth muscle mitogens. Using an immunoperoxidase stain for factor VIII, hypertensive pulmonary arteries stained densely, whereas nonhypertensive vessels did not. Circulating levels of the factor VIII molecule, both the antigenic component (VIII:Ag) and the biologic, assessed as ristocetin-induced platelet

agglutination (VIII:rist) were measured. Although VIII:Ag levels were significantly higher in patients with congenital heart defects and elevated pulmonary artery pressure than in those with normal pressure, only a few patients showed a concomitant elevation in biologic activity. This finding indicated that the molecule being secreted was lacking in biologic activity; indeed, further biochemical analysis of the factor VIII molecule showed lack of the high-molecular-weight components (15).

Under conditions that aggravate the endothelial dysfunction (e.g., cardiopulmonary bypass), vWF biologic activity was markedly increased (16). This could account for the development of platelet fibrin microthrombi in the postoperative period and for abnormal release of vasoactive compounds causing increased vascular reactivity. Various regimens have been adopted to anticipate and manage postoperative increased pulmonary vascular reactivity that include monitoring of pulmonary artery and left atrial pressures, institution of nitric oxide (NO) therapy, and the institution of phosphodiesterase inhibitors such as sildenafil, if therapy is needed beyond the intensive care unit.

There is now convincing evidence that impaired production of NO appears at an early time point in patients with congenital heart defects (17). There also is evidence that production of the vasoconstrictor endothelin also might be increased in patients with pulmonary hypertension and congenital heart defects (18).

Almost all patients with high-flow congenital heart defects who are operated upon in a timely fashion, show a fall in pulmonary artery pressure and return to normal resting hemodynamics indicating resolution and regression of pulmonary hypertensive structural changes. This is supported by experimental studies carried out by our group and others as well as by anecdotal reports of resolution of severe pulmonary vascular disease in the remaining lung after single lung transplant. There are, however, a few patients who maintain a high level of pulmonary vascular resistance and are refractory to vasodilator therapy despite what appear to be mild vascular changes on light microscopy (medial hypertrophy), and others who develop rapidly progressive pulmonary vascular disease despite early diagnosis and timely intervention. For these patients, the prognosis may be not much better than for those with unexplained pulmonary hypertension (19).

Therapies for the patient with Eisenmenger syndrome have included chronic oxygen, anticoagulants, and palliative surgical procedures, including atrial septal defect creation and intravenous prostacyclin as well as, more recently, aerosolized, nebulized, or oral prostacyclin. In some cases, these measures have improved the quality of life and in others they have served as a bridge to a heart-lung transplant or surgical correction along with single- or double-lung transplant, including living donors. More recent addition of sildenafil and endothelin receptor blockers in this group of patients awaits the results of clinical trials, but is discussed later in this chapter, and in the subsequent chapter, with regard to patients with primary pulmonary hypertension.

Pathophysiology Based Upon Further Pathologic Assessments

Recent immunohistochemical studies have been carried out in lung-biopsy tissue from patients with congenital heart defects to elucidate mechanisms that are directly related to enhanced proliferation and migration of cells in the neointima with characteristics of SMCs. There is a progressive increase in the deposition of two matrix glycoproteins, tenascin, and fibronectin, in the media and neointima (Fig. 66.6). We previously related the increased expression of tenascin to vascular SMCs

and fibroblasts. Fibronectin has been related to increased migration of smooth muscle-like cells in the context of neointimal formation. There is evidence from other studies that the neointimal lesions are associated with increased expression of transforming growth factor beta and procollagen in addition to fibronectin (20). It is also proposed that endothelial cell proliferation and a form of angiogenesis are observed with plexiform lesions. The plexiform lesions in pulmonary hypertension appear to be derived from different clonal populations of endothelial cells compared with those observed in primary pulmonary hypertension where a single clone is usually found (21). More recently, we described an increase in the expression of the calcium binding protein S100A4/Mts1 in advanced lesions from patients with congenital heart defects causing pulmonary arterial hypertension (PAH) as well as idiopathic PAH (Fig. 66.7) (22). S100A4/Mts1 stimulates vascular SMC migration and proliferation, is produced in response to serotonin stimulation (23), and is enhanced when there is increased activity of the serotonin transporter (SERT). This is in keeping with studies indicating that a polymorphism causing increased activity of the SERT is highly prevalent in patients with PAH (24).

Experimental Studies Simulating High Flow and Pressure

In experimental studies, an aortopulmonary shunt surgically created in a growing piglet results in a progressive increase in pulmonary artery pressure associated with the development of structural changes similar to those seen in the clinical setting. Creation of large aortopulmonary shunts in dogs, particularly into a single pulmonary artery, resulted in more rapidly progressive pulmonary vascular changes. There are several other experimental models of high-flow congenital heart defects such as in sheep or calves after an aortopulmonary lobar anastomosis. In utero placement of an aortopulmonary shunt most faithfully reproduces the changes that might be expected to occur in the newborn with a left-to-right shunt when the pulmonary vascular resistance falls. In this model, the initial response to high flow induced from the time of birth experimentally appears to be angiogenic with high levels of vascular endothelial growth factor (VEGF) and its receptors, but later in association with the decrease in VEGF and decline in arterial number, the resistance becomes elevated (25).

Takedown of the shunts during the period of rapid lung growth resulted in regression of both structural changes and pulmonary hypertension (26). Regression of medial hypertrophy and muscularization of distal vessels has been shown in experimental studies following pressure off-loading (27). There are many common features linking the cellular and molecular pathophysiology of pulmonary vascular disease, regardless of etiology, that we have linked to elevated elastase activity and this subject is discussed at the end of the chapter.

HEART DEFECTS WITH INCREASED PULMONARY VENOUS PRESSURE

Vascular Changes

Although advanced pulmonary vascular disease is less likely to occur early in patients with congenital heart defects related to increased pulmonary venous pressure, Collins-Nakai et al. (28) reported greater than Heath-Edwards grade III changes in the majority of older children in their series with congenital mitral stenosis. In patients with total anomalous pulmonary venous connection, abnormal muscularization of the

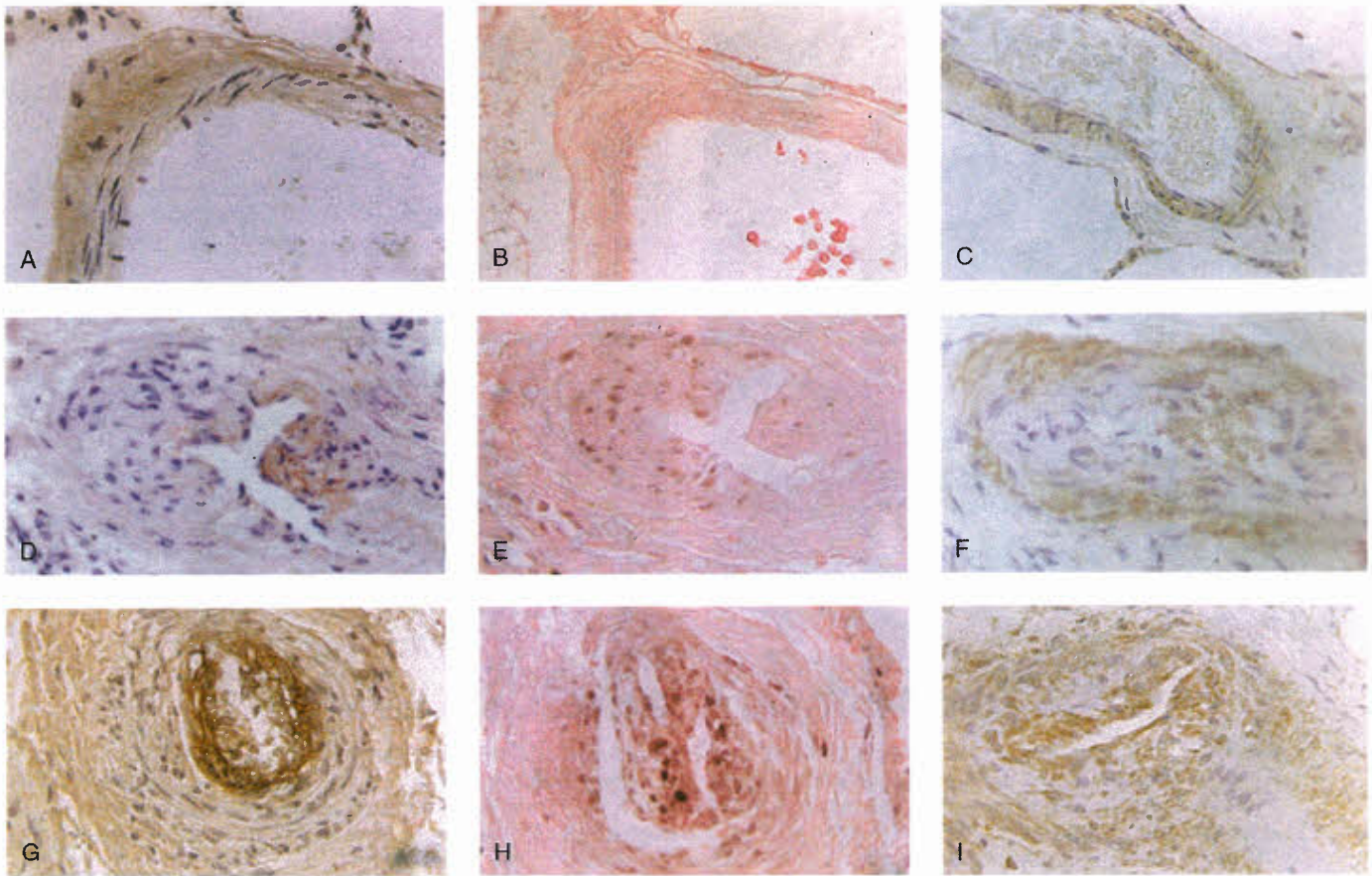


Figure 66.6. Representative photomicrographs showing immunoperoxidase staining for tenascin-C (TN) (A,D,G), proliferating cell nuclear antigen (PCNA) (B,E,H), and epidermal growth factor (EGF) (C,F,I) in graded lung biopsy tissue sections. A–C: Vessel showing a typical grade IA lesion; D–F: Vessel showing a typical grade IC lesion; G–I: vessel showing a typical grade IIIC lesion. In low-grade lesions (A), modest TN immunostaining was evident in the adventitia. With medial hypertrophy, TN immunoreactivity became more prominent in the periendothelium (D), with the most intense immunostaining being apparent within the neointima of high-grade lesions showing occlusive neointimal formation (G). In the lowest grade of lesion, PCNA was negative (B), despite foci of EGF in the media. With medial hypertrophy, PCNA was expressed in the media (E), together with foci of EGF (F). With the development of higher-grade occlusive lesions, TN (G), PCNA (H), and EGF (I) co-localized to the neointimal cell layers. Note that TN and PCNA staining was performed on serial sections, whereas EGF detection was carried out on similar vessels within the same biopsy. Original magnification, $\times 40$. (From Jones PL, Cowan KN, Rabinovitch M. Progressive pulmonary vascular disease is characterized by a proliferative response related to deposition of tenascin-C and is preceded by subendothelial accumulation of fibronectin. *Am J Pathol* 1997;150:1349–1360, with permission.)

small arteries and veins was observed from birth, and more severe structural changes (i.e., Heath-Edwards grade III) were described in infants as young as 1 month of age. In infants with hypoplastic left heart syndrome, there is such severe medial hypertrophy of the small arteries and veins from birth that it must have developed in utero (29). In both adults and children with rheumatic mitral stenosis, Wagenvoort and Wagenvoort (30) observed increased medial-wall thickness of the pulmonary arteries.

In postmortem arteriograms of infants and children with congenital heart defects and elevated pulmonary venous pressure, the axial pulmonary arteries have a reduced lumen diameter throughout their lengths. On microscopic examination of the lung, there is severe extension of muscle into peripheral intraacinar arteries, which are normally nonmuscular, and failure of regression of the fetal musculature of the normally muscular arteries. The vessels, however, appear normal sized and are normal or slightly increased in number. The presence of pulmonary vascular changes in defects with high pulmonary

venous pressure and the capacity for these abnormalities to regress with improvement in hemodynamics may be relevant because the Norwood and other various staged surgical procedure for the treatment of hypoplastic left heart syndrome ultimately depend on the success of a bidirectional cavopulmonary shunt and a right atrial-to-pulmonary artery anastomosis or tunnel.

Experimental Studies

Pulmonary venous hypertension has been created experimentally by banding the pulmonary veins or by elevating left atrial pressure. LaBourene et al. (31) banded the pulmonary veins in newborn piglets and studied the pathophysiology of progressive pulmonary venous obstruction. After 1 week, they observed no change in pulmonary hemodynamics, but there was a striking decrease in compliance of the pulmonary veins. By 3 weeks, there was PAH without elevation in

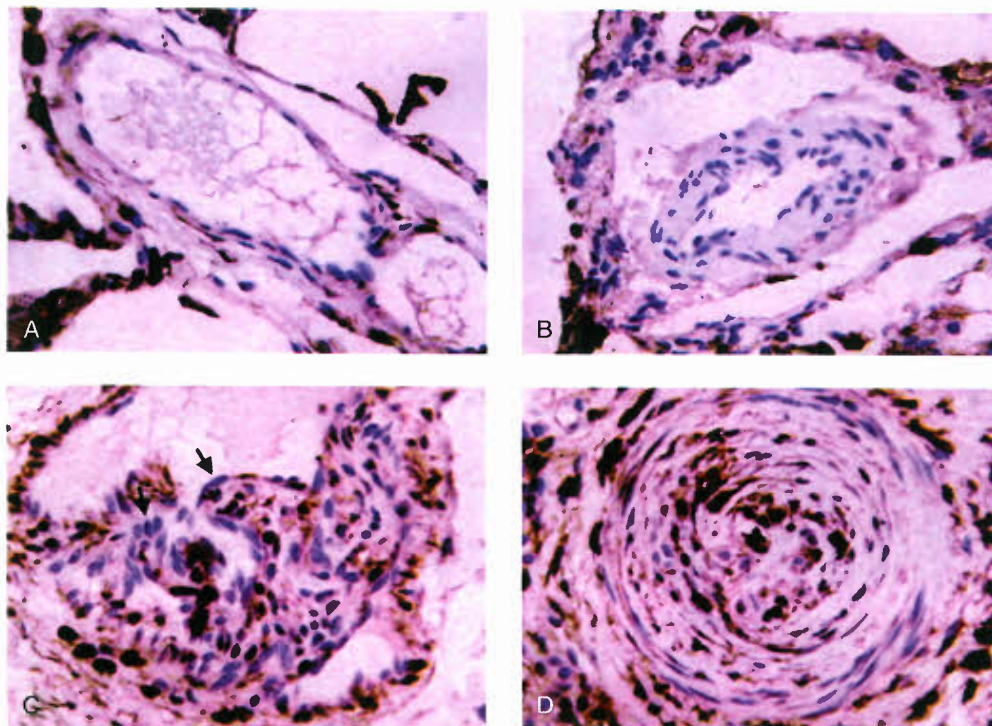


Figure 66.7. Representative photomicrographs of human lung biopsy tissue after immunoperoxidase staining for S100A4/Mts1. **A:** Vessel from patient graded 0-IB showing normal pulmonary artery with no immunodetectable S100A4/Mts1. **B:** Vessel showing a typical grade IB lesion with severe medial hypertrophy but without immunoreactivity for S100A4/Mts1. **C:** An artery from a patient with grade IVC disease with occlusive neointimal proliferation and strong positive staining for S100A4/Mts1 particularly in the intima compared to the media of the vessel. S100A4/Mts1 was not detected in all cells and appears to be localized in a subpopulation of intimal cells. **D:** A plexogenic lesion from a patient with grade IVC disease with staining of the SMCs and sparing of the endothelial cells (arrows). Immunoreactivity for S100A4/Mts1 was present in the lung parenchyma at a similar level in all grades of pulmonary vascular disease. Original magnification, $\times 40$. (Reproduced from Greenway S, van Suylen RJ, Du Marchie Sarvaas G, et al. S100A4/Mts1 produces murine pulmonary artery changes resembling plexogenic arteriopathy and is increased in human plexogenic arteriopathy. *Am J Pathol* 2004;164:253–262, with permission.)

pulmonary venous pressure. By 6 weeks, further progression of pulmonary hypertension was associated with elevated pulmonary venous pressure (Fig. 66.8). At 1 week, ultrastructural changes in the veins occurred that consisted of fragmentation of elastin and a phenotypic switch in medial SMCs in which they appeared to be more synthetic and migrating toward the subendothelium (Fig. 66.8). By 3 weeks, pulmonary venous hypertension developed and there was already evidence of intimal proliferation. By 6 weeks, there was an increase in collagen in the walls of the pulmonary veins. This study suggested that pulmonary hypertension may be the first sign of pulmonary venous obstruction and that elevation of pulmonary venous pressure is associated with considerable structural remodeling.

HEART DEFECTS WITH DECREASED PULMONARY BLOOD FLOW

Structural Features

In patients with congenital heart defects causing low pulmonary blood flow, hypoplasia of the pulmonary arterial musculature is observed, and in those in whom the hematocrit is particularly elevated, thromboemboli can occur. The creation

of systemic-to-pulmonary artery shunts may improve the hypoplasia, but secondary to abnormally high flow and pressure, medial hypertrophy and intimal hyperplasia also could ensue. Studies suggest that the potential for growth of the central pulmonary arteries is correlated with the proportion of elastin in the media, and the same may be true for the intrapulmonary vessels (32).

On postmortem arteriograms in patients with decreased pulmonary blood flow, the axial arteries are abnormally narrow in lumen diameter (33). The background haze also may be reduced, as in patients with pulmonary atresia and intact ventricular septum. On microscopic examination of the lung from patients with pulmonary atresia and intact ventricular septum, the intraacinar pulmonary arteries are abnormally thin walled, small, and few in number. In patients with tetralogy of Fallot, these vessels are normal or decreased in muscularity, normal in number, and small (34). Alveolar development is impaired in patients with decreased pulmonary blood flow, and this is reflected mostly by a reduction in alveolar number. Patients with tetralogy of Fallot and associated pulmonary atresia form a special subgroup in which the relative distribution of central pulmonary arteries and aortopulmonary collaterals determines peripheral pulmonary vascular structure. In patients with tricuspid atresia, the structural state of the pulmonary vascular bed is variable, depending on whether pulmonary blood flow is increased or decreased.

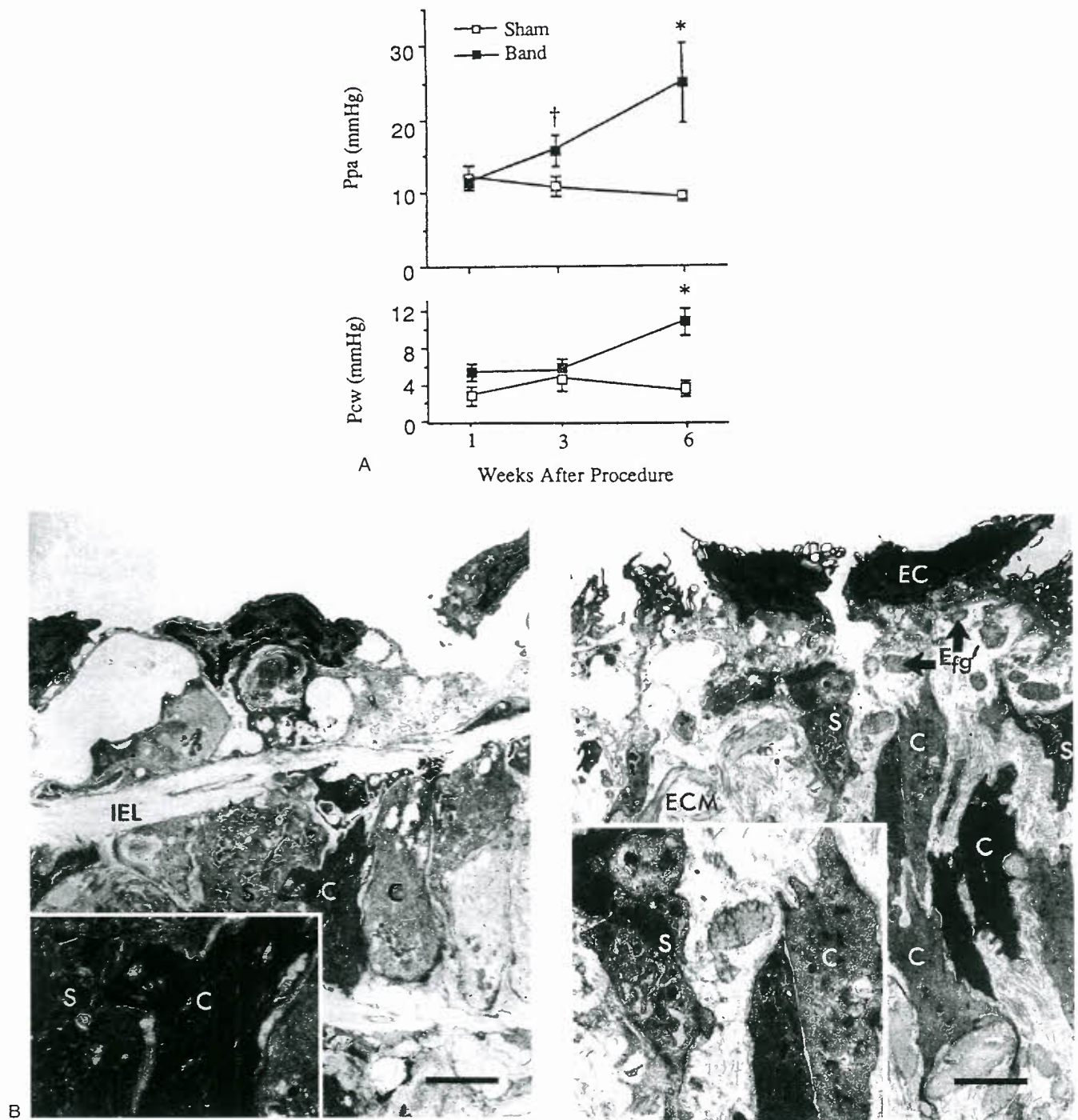


Figure 66.8. A: Pulmonary artery pressure (Ppa, upper panel) and pulmonary capillary wedge pressure (Pcw, lower panel) in banded and sham-operated piglets at 1, 3, and 6 weeks after banding. Values are averages of mean \pm SEM (n = six piglets per group at each time point). At 1 week, there was no change. At 3 weeks, there was a significant increase in Ppa, which preceded the further rise in Ppa, at 6 weeks ($*p < 0.01$; $^{\dagger}p < 0.05$). B: Transmission electron photomicrographs of representative pulmonary veins (PVs) from banded (right panel) and sham-operated (left panel) piglets at 3 weeks after banding (original magnification, $\times 14,131$) (inset original magnification, $\times 28,263$). Both pulmonary veins show apparent injury and lifting of endothelial cells and subendothelial spaces as a result of poor preservation during handling. Sham-operated PV displays on intact internal elastic lamina (IEL) and predominantly contractile-appearing SMCs (c) in media. In contrast, PV from banded piglet depicts complete breakdown of IEL into elastin fragments (Efg), a thickened subendothelium composed of collagen, extracellular matrix (ECM), and SMCs that appear to have migrated in from media, many of which have a synthetic-appearing phenotype (S) exemplified by a large amount of endoplasmic reticulum and a corresponding paucity of contractile filaments. C and S SMCs are better appreciated in insets. (Bar = 1 μ m). (From LaBourene JI, Coles J, Johnson DJ, et al. Alterations in elastin and collagen related to the mechanism of progressive pulmonary venous obstruction in a piglet model. *Circ Res* 1990;66:438–456, with permission.)

Experimental Studies

Levin et al. (35) created low pulmonary blood flow by banding the main pulmonary artery of fetal lambs. The changes in the lung that resulted consisted of diffuse hypoplasia of the musculature of the peripheral pulmonary vessels; those identified were small in caliber and few. Haworth et al. (36) ligated the left pulmonary artery in newborn piglets and demonstrated normal development of the intraacinar arteries owing to extensive anastomoses with bronchial arteries, but in the preacinar vessels, there was occlusive fibrosis of the lumen.

HYPOXIA-INDUCED PULMONARY VASCULAR DISEASE

Hypoxia and Pulmonary Vasoconstriction

The pulmonary hypertension that occurs in response to acute hypoxia is usually mild and rapidly reversible. Hultgren et al. (37) demonstrated an 18% increase in pulmonary artery pressure in men brought suddenly from sea level to high altitude (7,800 feet). There is much variability in individual response to hypoxia; some people hyperventilate and become mildly alkalotic, hardly increasing their pulmonary artery pressure at all, whereas others develop severe pulmonary hypertension with high-altitude pulmonary edema. Several theories have been proposed to explain high-altitude pulmonary edema. Endothelial swelling of small arteries occurs in some areas of the lung and causes high resistance, which results in diversion of excessive flow through small vessels, causing edema. Defective fibrinolysis with formation of microemboli has been reported, as has inadequate diuresis (38). Abnormal endothelial metabolism of factor VIII has also been described. There is increased circulating antigenic activity without increased biologic activity, suggesting that the high-molecular-weight components of the molecule may be associated with platelet microaggregates (39). Some studies suggest that high-altitude pulmonary edema may have an immune basis because it is associated with major histocompatibility complex HLA-DR6 and HLA-DQ4. The subset with pulmonary hypertension is associated with HLA-DR6 (40). The combination of acetazolamide, NO, and oxygen treatment has been successful in alleviating the symptoms of high-altitude pulmonary edema, and acetazolamide is also effective in preventing this complication.

Experimental Studies of Acute Hypoxia

Micropuncture has shown that both the small arteries and veins contribute to the acute hypoxic vasoconstrictor response. Studies by Hales et al. (41) suggested that prostaglandins mitigate the response to hypoxia, but the studies showed that the response to endothelial-derived relaxing factor is impaired. Recent reports revealed that with hypoxic vasoconstriction there is inhibition of a Ca^{2+} -activated depolarizing potassium channel. With chronic hypoxia, this channel may become activated as a relaxing mechanism.

The relationship between acute hypoxic vasoconstriction, the sustained pulmonary hypertension, and structural changes in the pulmonary vascular bed induced by chronic hypoxia is not known. Experimental studies of unilaterally banding the pulmonary artery in chronically hypoxic rats support the hypothesis that some structural changes in hypoxia are influenced by an alteration in the hemodynamics of the pulmonary circulation and others are more direct effects of hypoxia per se (42). The direct effect of hypoxia

is associated with increased ornithine decarboxylase activity, an enzyme implicated in structural remodeling of pulmonary arteries (43).

CHRONIC HYPOXIA

Clinical Features of Chronic Hypoxia

In persons who live at high altitudes, there is chronic elevation in pulmonary artery pressure that is frequently reversible at least under conditions of rest with administration of oxygen or return to sea level (44). In a study by Arias-Stella and Saldana (45), postmortem lung tissue from persons who had been living at high altitudes was compared with that obtained from sea-level dwellers. Structural changes were found in the vessels in the high altitude lung specimens; the peripheral arteries were more muscular than normal and had decreased lumen diameters.

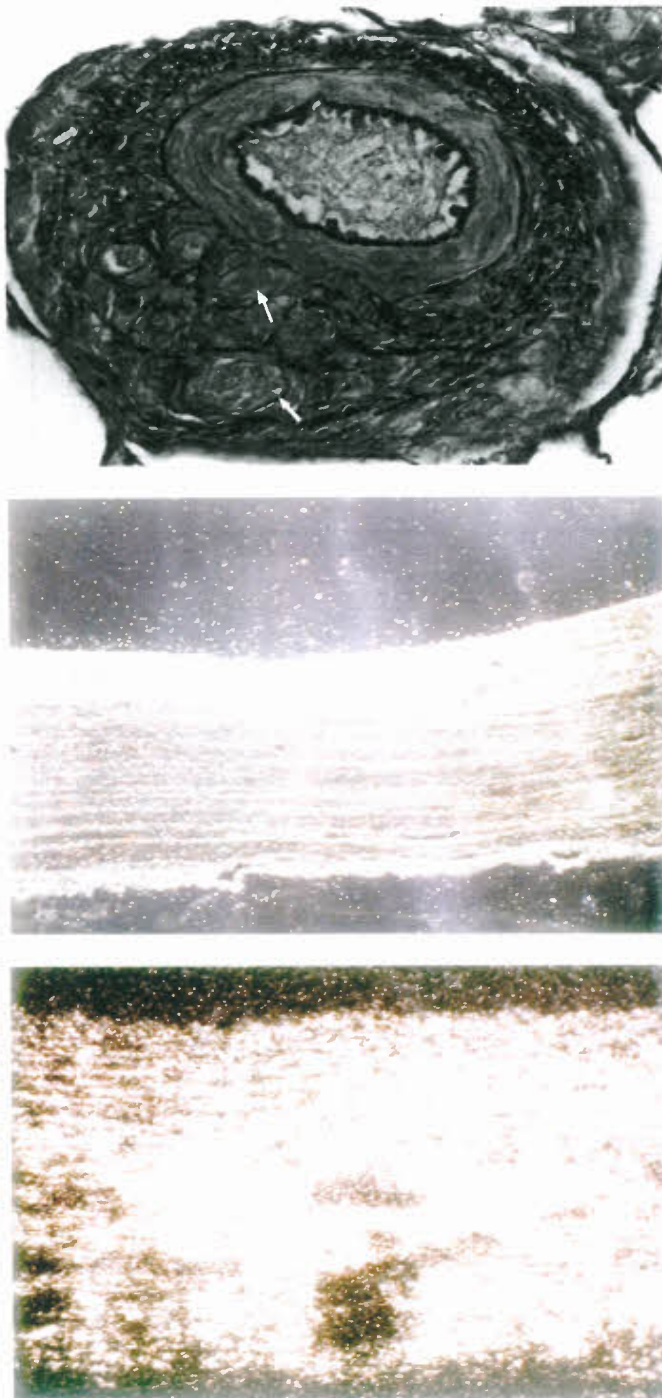
Children living in Denver (elevation 5,200 feet) have slightly higher mean pulmonary artery pressures than sea-level dwellers, and children living in Morococha, Peru (elevation 14,900 feet) have mean pulmonary artery pressures that are twice as high. Moreover, in the high-altitude residents, mean pulmonary artery pressure more than doubles with exercise, whereas it increases by only 50% in sea-level dwellers.

Experimental Studies

In animal studies, Tucker et al. (46) observed that the degree of reactivity to hypoxia or the level of pulmonary hypertension varied among different species according to the amount of smooth muscle in the pulmonary vascular bed. In the rat, the hemodynamic and structural responses of the pulmonary vascular bed to chronic hypoxia were studied. After just 3 days of chronic hypoxia, a sustained elevation in pulmonary artery pressure and resistance was measured even after the rats were kept in room air for several hours. This finding coincides with the time that structural changes in the pulmonary vascular bed appear, in particular, the extension of muscle into peripheral arteries that are normally nonmuscular. Over the ensuing 2 weeks of hypoxia, mean pulmonary artery pressure progressively rises to double control values (47). This increase is accompanied by right ventricular hypertrophy, further extension of muscle into peripheral arteries, medial hypertrophy of normally muscular arteries, and reduction in arterial related to alveolar concentration. In the large preacinar pulmonary arteries, the adventitia is thickened as the result of an increase in the number of fibroblasts and collagen, and the media is also thicker as a result of hypertrophy of SMCs and accumulation of collagen, elastin, and other extracellular matrix components such as tenascin.

Relative hyporesponsiveness to hypoxia of the female animal has been observed in a number of species. During recovery from chronic hypoxia, mean pulmonary artery pressure returned to near normal in rats exposed as adults but remained 50% above normal in animals exposed during infancy, correlating with more severe residual vascular abnormalities. Ultrastructural and biochemical studies in the rat have shown that regression of smooth muscle hypertrophy following return to room air is accompanied by an increase in the amount of elastin and collagen in the vessel wall (48). Thus, the vessel, although less muscular, is enclosed in a tight sheath, which may interfere with its compliance and its ability to grow. In studies by Kerr et al. (49), inhibition of collagen synthesis decreased chronic hypoxic pulmonary hypertension and vascular changes.

Stenmark et al. (50) took newborn calves to a simulated high altitude of 4,300 m and observed severe pulmonary hypertension with right-to-left shunting owing to the rapid development of suprasystemic levels of pulmonary artery pressure. There was striking medial hypertrophy and remarkable proliferation of a dense adventitial sheath, which, in large vessels, was sometimes seen to exhibit neovascularization (Fig. 66.9). Further studies showed striking synthesis of elastin in the pulmonary arteries of these neonatal calves. Most recent studies have implicated fibrocytes as key contributors to the remodeling of the pulmonary vasculature. It is believed that these “stem cells” that have characteristics of both fibroblasts and leukocytes (51) migrate into the vessel wall through the angiomata located in the expanding adventitia (52) (Fig. 66.10)



and there is also a population of stem cells in the adventitia that may expand under conditions of hypoxia (53). There is also evidence in this model that epigenetic factors may be controlling the expression of proinflammatory cytokines in the fibroblasts in this model and that the inflammatory response is critical to the evolution of the disease (54).

Studies in transgenic mice suggest that genetic factors might modulate the response to chronic hypoxia. For example, in the absence of hemoxygenase 1, there is reduced production of NO and its associated vasodilatory effects (55). Prostacyclin synthetase overexpression is protective against the hemodynamic and vascular changes of pulmonary hypertension (56). Serotonin has been implicated in the increased vasoreactivity of the fawn-hooded rat (57), and there is attenuated severity of pulmonary vascular disease in mice lacking the SERT gene (58). Overexpression of the SERT worsens hypoxia-induced pulmonary hypertension (59) as does haploinsufficiency of *bone morphogenetic protein receptor 2* (*Bmpr2*) (60) or dominant negative *Bmpr2* (61), although in both cases the degree of structural remodeling is relatively unimpressive. Haploinsufficiency of *Bmpr2* in cultured SMCs and in transgenic mice makes them more sensitive to the proliferative effects of serotonin (62). Epigenetic factors also appear to control signaling via *Bmpr2* (63) as well as reduced expression of the free radical scavenger superoxide dismutase seen in the fawn-hooded rat with pulmonary hypertension (64).

We have shown that mice overexpressing the calcium binding protein S100A4/Mts1 have mild pulmonary hypertension under room air conditions. Values are increased over control mice in hypoxia but the remodeling response also appears to be mitigated. We related this to increased production of fibulin-5 and thickening of the elastic laminae (65). Thus overexpression of genes that might worsen hypoxia-induced pulmonary hypertension appears to invoke compensatory mechanisms that protect against the remodeling response. Understanding why these compensatory mechanisms fail may be critical in appreciating why some patients develop rapidly progressive pulmonary hypertension.

Numerous studies have attempted to show how acute vasoconstriction or a direct hypoxic “injury” initiates the structural changes observed in the pulmonary arteries. There is convincing evidence that the high endothelin levels are causally related to hypoxic vasoconstriction and the subsequent initiation of vascular changes. In some studies, chronic hypoxia appears to decrease endothelial nitric oxide synthase (eNOS). Strategies proven effective in the treatment of chronic hypoxic pulmonary hypertension in rats include inhibition of 5-lipoxygenase activating protein as

Figure 66.9. An artery from the lung of a 2-week-old calf raised at a simulated altitude of 4,300 m from birth. Pulmonary artery systolic pressure was 100 mm Hg. There is marked medial hypertrophy and adventitial thickening with neovascularization (arrow). Elastic tissue stain, original magnification, $\times 400$. (Kindly supplied by K. Stenmark.) (top). In situ hybridization localization of tropoelastin mRNA in control and hypertensive vessels from neonatal calves. White staining over areas indicates tropoelastin mRNA labeling. In normotensive vessels (middle), labeled cells (35S-labeled T66-T7) were confined to the inner media. Minimal signal is noted in the outer vessel wall. In vessels from hypertensive animals (14 days of hypoxia) (bottom), intense autoradiographic signal was observed throughout the media, albeit in a patchy distribution. (From Prosser IW, Stenmark K, et al. Regional heterogeneity of elastin and collagen gene expression in intralobar arteries in response to hypoxic pulmonary hypertension as demonstrated by in situ hybridization. *Am J Pathol* 1989;135:1073–1088, with permission.)

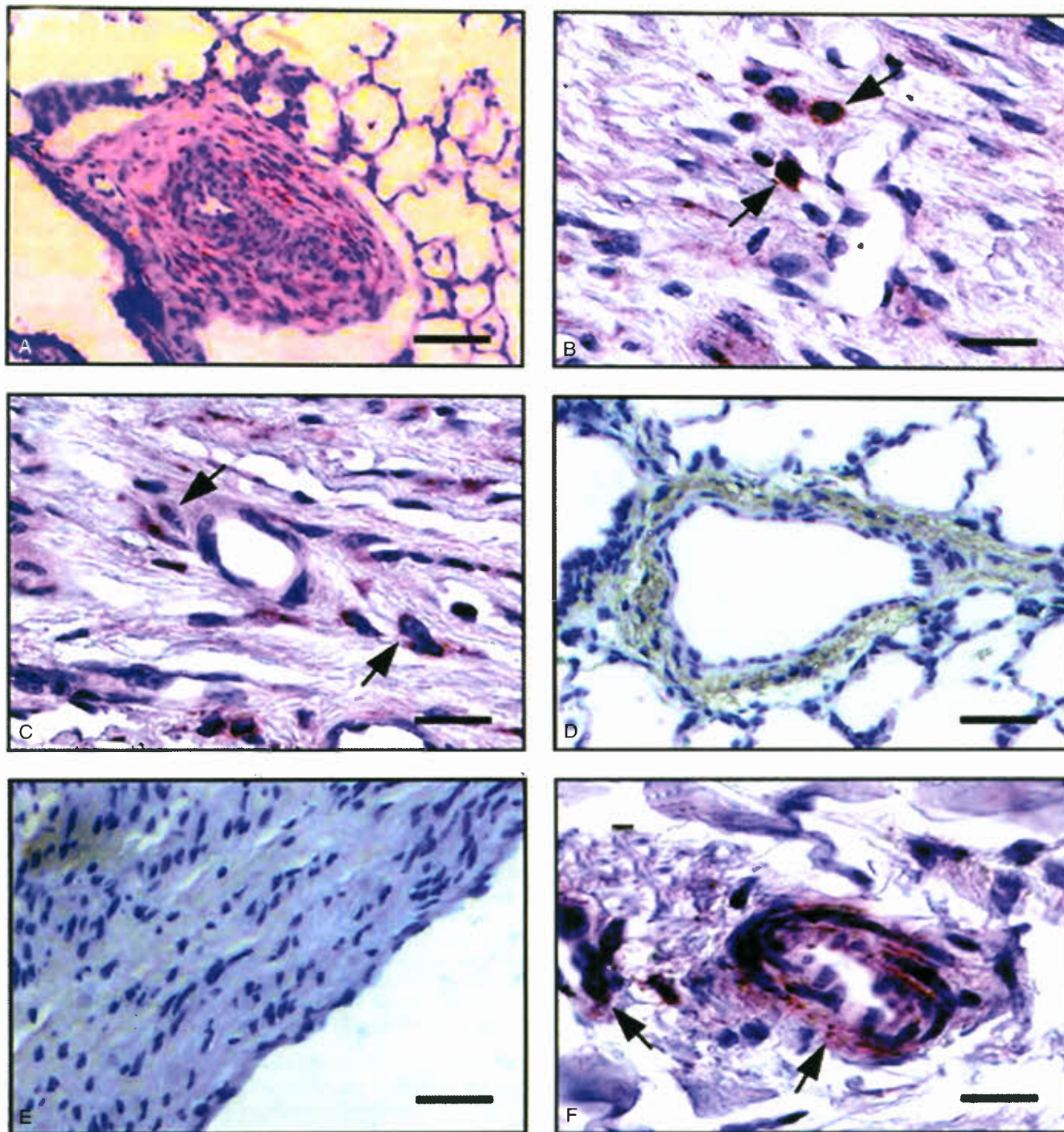


Figure 66.10. Immunohistochemistry (brown peroxidase signal) revealed a greater number of *c-kit*⁺ cells (arrows) in the vessel wall of distal (A) and proximal (B and C) arteries from hypoxic animals compared with control animals. The *c-kit*⁺ cells (arrows) are localized contiguous to vasa vasorum in proximal vessels (B and C) and continuous to and within the vessel wall of vasa located in the adventitia (F). Scale Bar represents 100 μ m in A, D, and E, and 50 μ m in B, C and F. (Reproduced from Davie NJ, Crossno JT Jr, Frid MG, et al. 2004. Hypoxia-induced pulmonary artery adventitial remodeling and neovascularization: contribution of progenitor cells. *Am J Physiol Lung Cell Mol Physiol* 286:L668–L678, with permission).

well as inhibition of cyclic 3'-5'-guanosinemonophosphate-specific phosphodiesterase, and continuous infusion of NO. In other studies, activation of voltage-gated K channels (Kv2.1) by gene transfer or a metabolic activator inhibited chronic hypoxic pulmonary hypertension (66,67). Serine elastase inhibitors also effectively reduce chronic hypoxia-induced pulmonary hypertension and associated vascular remodeling (68). In addition, experimental studies suggest

that vascular smooth muscle growth inhibitors may be useful in preventing vascular disease. Heparin infusion will decrease the severity of hypoxia-induced vascular changes, presumably by decreasing smooth muscle hyperplasia. Most recently, rho kinase inhibitors have proven effective when administered even by inhalation, in preventing pulmonary hypertension and structural changes associated with chronic hypoxia (69–72).

LUNG DISEASE

Several factors may contribute to the pulmonary hypertension that commonly but not invariably accompanies severe parenchymal lung disease: the level of hypoxia and polycythemia, the degree of endothelial injury and subsequent imbalance in vasoactive mediators and vascular reactivity, the level of pulmonary venous pressure secondary to dysfunction of the hypoxemic left ventricle, and the nature and severity of the structural damage to the pulmonary arteries. Treatment of the lung disease will decrease the level of pulmonary artery pressure by eliminating the contributing causes and by allowing some regression of the structural changes. The latter, however, ultimately determines the level of pulmonary hypertension and the rate of development of right-sided heart failure.

Obstructive Lung Disease

In children, unlike in the adult population, obstructive lung disorders such as asthma are only rarely associated with the development of pulmonary hypertension. In patients with cystic fibrosis, however, cor pulmonale is common. When right ventricular hypertrophy and failure are observed, they generally reflect the degree of abnormal structural remodeling of the pulmonary vascular bed. The severity of the arterial changes tend to be patchy, reflecting the nature of the lung disease, but the venous changes are more uniform suggesting that they result from left atrial hypertension secondary to the left ventricular dysfunction.

Restrictive lung disease may occur in childhood from a variety of causes, and pulmonary hypertension is a common complication. Examples of such restrictive lung disorders are diffuse interstitial fibrosis (Hamman-Rich syndrome), bronchopulmonary dysplasia, radiation fibrosis and chemotherapy toxicity, infiltrative lung tumors, and collagen vascular disease. In the latter, pulmonary vasculitis may be important etiologically and is discussed separately. Reversal of the pulmonary hypertension generally depends on the ability to affect the course of the interstitial lung disease. Few structural studies have been done in patients with restrictive lung disorders. It has been proposed that, secondary to fibrosis of the alveolar septa, the loss of small alveolar wall arteries results in an increase in pulmonary vascular resistance, and as a secondary response there is hypertrophy of normally muscular arteries. In a study of the lungs from premature infants in whom bronchopulmonary dysplasia was a complication of severe respiratory distress syndrome, Rendas et al. (73) observed that, although the preacinar arteries had dilated appropriately, there was extension of muscle into normally nonmuscular peripheral arteries, which might explain the persistent pulmonary hypertension in these patients. In addition, although the number of peripheral arteries relative to alveoli was normal, the marked reduction in alveolar number suggested an absolute decrease in the cross-sectional area of the pulmonary vascular bed.

UPPER AIRWAY OBSTRUCTION

Severe upper airway obstruction from a variety of causes (Fig. 66.11 and Table 66.4) may be complicated by the development of pulmonary hypertension. In each case, the hypertension is not always a direct result of the degree of airway obstruction but seems to depend also on whether there is a central component, such as diminished ventilatory drive or general neuromuscular pharyngeal dysfunction. Many patients with upper airway obstruction have worsening of their symptoms with sleep; this worsening may be mechanical, such as

positioning of the head or it may be the result of a central mechanism. Although removal of the airway obstruction often results in prompt return to normal pulmonary artery pressure and resolution of heart failure, these symptoms can persist for some time perhaps because of slow regression of hypoxia-induced structural changes in the pulmonary vascular bed or persistent impairment of ventilatory drive.

The Pickwickian syndrome described in adults, consisting of hypersomnolence and obesity associated with pulmonary hypertension, also has been reported in children (Table 66.4). The obesity, through increased work of breathing, stresses the respiratory control system, and depending on its inherent sensitivity, hypoventilation may result, causing further retention and hypoxia, which contribute to the lethargy and cor pulmonale (Fig. 66.11). Mental retardation is often but not invariably associated with this syndrome. Damage to the respiratory center, either as a primary disorder (Ondine's curse) or secondary to trauma or other neurologic disease, also may result in cor pulmonale as a result of chronic intermittent hypoxia and hypercarbia. Although the pulmonary hypertension of sleep apnea in adults is in large part attributable to airway obstruction, in children, it is often the manifestation of an abnormal central mechanism. Increasing attention to the "metabolic syndrome" and systemic vascular disease has prompted us to investigate insulin resistance, which occurs with obesity and is also related to the development or progression of pulmonary hypertension (74).

Structural studies of the lung at postmortem have been carried out in patients with hypoventilation caused by damage to the respiratory center and in children with sudden infant death syndrome. In the former group, the degree of medial hypertrophy was compatible with hypoxia-induced pulmonary hypertension. Severe extension of muscle into peripheral arteries was observed in one-third of all patients with sudden infant death syndrome and in all "near-miss" infants in whom apnea was documented and who later died suddenly.

DISORDERS OF THE CHEST WALL

Neuromuscular disorders affecting the chest wall, such as Duchenne muscular dystrophy, poliomyelitis, Werdnig-Hoffman disease, and diseases affecting the vertebrae and rib cage, such as scoliosis, may so impair ventilation as to cause pulmonary hypertension. In patients with scoliosis, the heart and lungs have been studied at postmortem using morphometric techniques. Mild right ventricular hypertrophy has been described in association with medial hypertrophy of normally muscular arteries, increased extension of muscle into peripheral arteries, and reduced arterial number, changes ordinarily found in association with chronic hypoxia-induced pulmonary hypertension. Reduction in arterial number has been found both in patients with lobes having a reduced alveolar number and in those with a normal alveolar number.

PERSISTENT PULMONARY HYPERTENSION OF THE NEWBORN

Persistent pulmonary hypertension of the newborn (PPHN) may result from one of three causes: underdevelopment of the lung and pulmonary vascular bed as seen in congenital diaphragmatic hernia, maladaptation of the pulmonary vascular bed to extrauterine life as a result of postnatal stress, and maldevelopment of the pulmonary vasculature (e.g., alveolar capillary dysplasia) (Figs. 66.12 and 66.13).

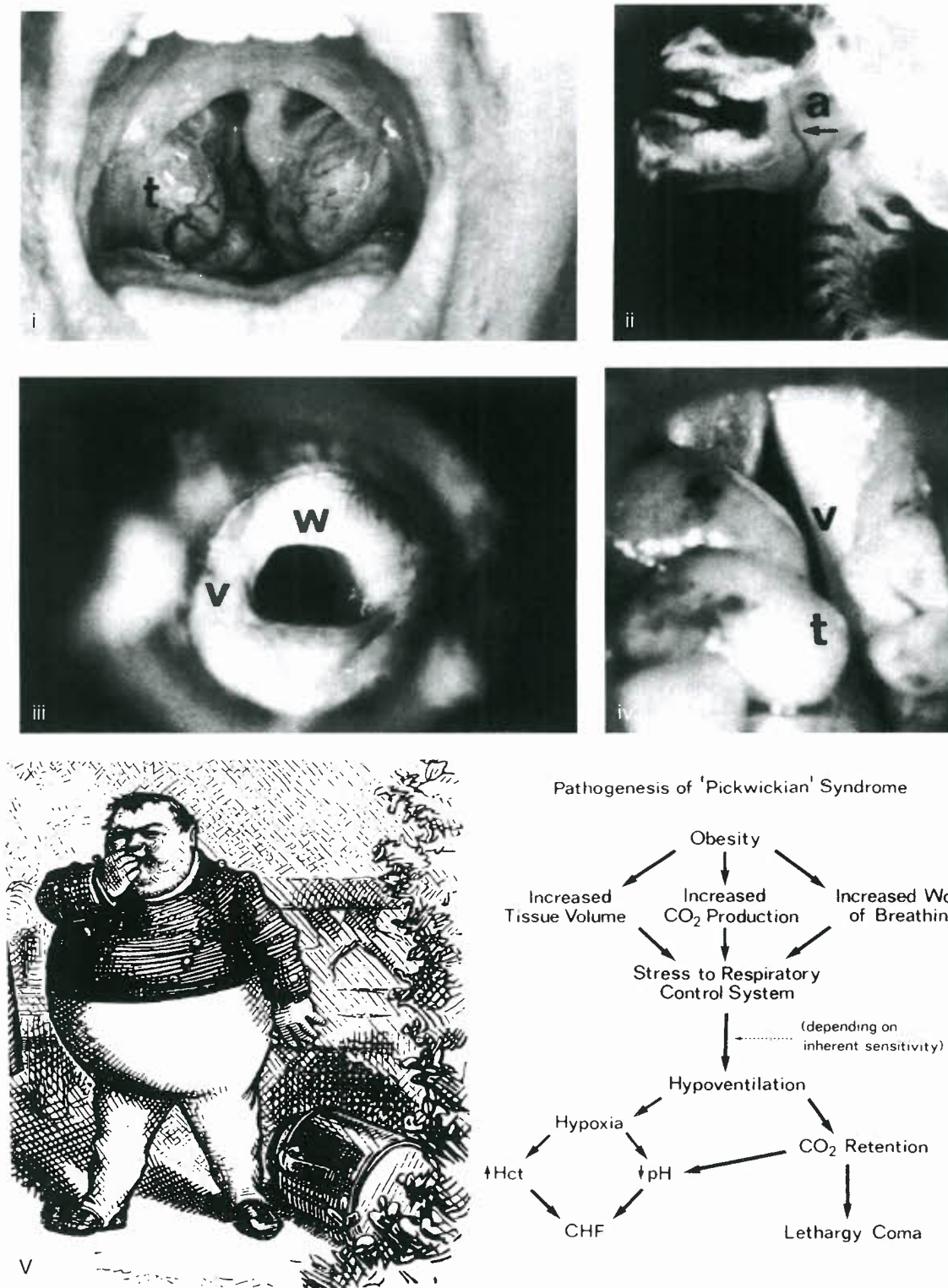


Figure 66.11. Top: Four different causes of upper airway obstruction. i: Hypertrophied tonsils (t). ii: X-ray of head and neck demonstrating compression of nasopharynx (arrow) by hypertrophied adenoids (a). iii: Glottic web (w) adjacent to vocal cord (v). iv: Lingual tonsils (t). v: bottom left: Thomas Nast's drawing of the fat boy in "The Pickwick Papers" from an American edition of the Posthumous Papers of the Pickwick Club, London, 1837; New York, 1873. Bottom right: A schema of the pathogenesis of the pulmonary hypertension in the Pickwickian syndrome. (Modified from Auchincloss JH, Gilbert R. The cardiorespiratory syndrome related to obesity: clinical manifestations and pathologic physiology. *Prog Cardiovasc Dis* 1959;1:413.)

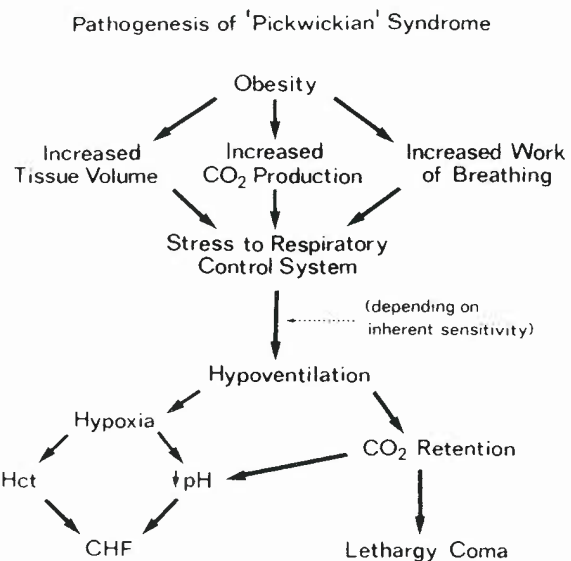


TABLE 66.4 Causes of Upper-Airway Obstruction in Children

Hypertrophied tonsils and/or adenoids
Laryngotracheomalacia
Subglottic stenosis secondary to congenital web or posttraumatic
Micrognathia with glossoptosis (e.g., Pierre-Robin)
Crouzon disease
Hurler disease (macroglossia)
Ankylosis of the temporomandibular joint
Craniovertebral anomaly
Laryngeal tumors or cysts
Post cleft palate repair

Development of the Normal Perinatal Pulmonary Vasculature

Current studies are addressing factors that regulate the fetal growth and development of the pulmonary vasculature, such

as matrix molecules (fibronectin and tenascin), and growth factors including VEGF, fibroblast growth factor, transforming growth factor, bone morphogenetic proteins, and Wnts. The balance between proteases such as elastase and matrix metalloproteinases and antiproteases controls the response to growth factors in two ways. Proteolytic enzymes release growth factors from the extracellular matrix and they also influence the production of matrix molecules that interact with cells and can promote or repress the activation of growth factor receptors.

Vasoactive molecules also regulate pulmonary vascular development; for example, endothelin production is associated with cell proliferation, and NO and prostacyclin are associated with the suppression of cell growth. Transcription factors are being identified that control vascular SMC differentiation and the programming of constellations of genes involved in pulmonary vascular morphogenesis.

The mediators responsible for maintaining the increased pulmonary vascular tone in the constricted fetal circulation and for the normal fall in pulmonary vascular resistance in the newborn have been the subject of much study, both experimentally and clinically. Studies by Wang and Cocceani (75) in isolated peripheral pulmonary arteries from fetal and neonatal lambs showed that endothelin is a powerful vasoconstrictor and may be responsible for the increase in pulmonary vascular resistance in the fetus, but this may depend also on the availability of specific receptors and on basal tone. Endothelin is released by endothelial cells in culture when subjected to

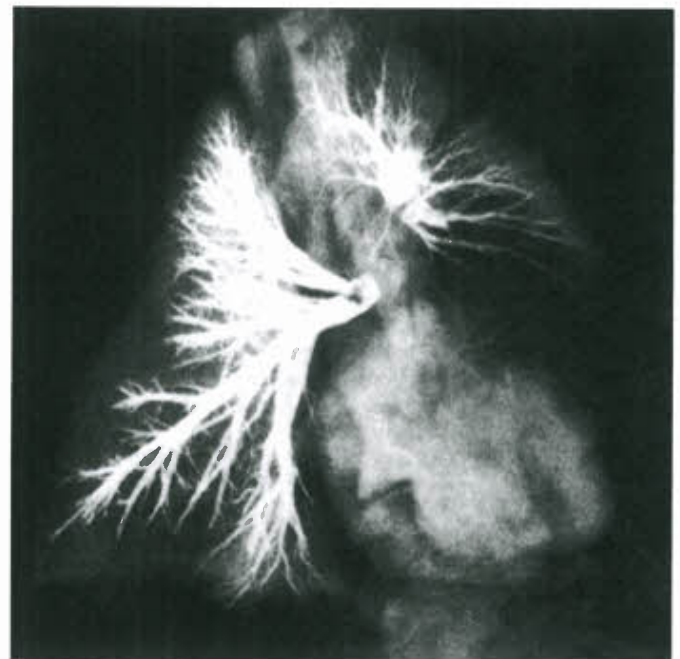
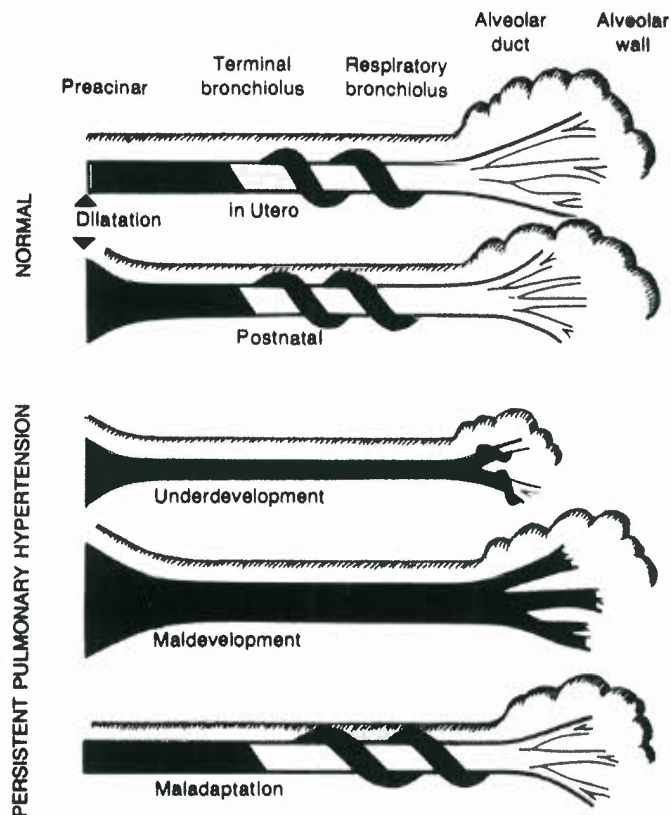


Figure 66.12. Left: Schema showing normal arterial dilation during transition from fetal to neonatal circulation. When the lung is underdeveloped, the vascular bed is hypoplastic and abnormally muscular. When it is maldeveloped, the vascular bed is abnormally muscular; when it is maladapted, it has not dilated appropriately at birth. Right: Arteriogram showing a small right lung with a distorted and even smaller left lung. Arteries in both lungs are reduced in size and number. (From Kitagawa M, Hislop A, Boyden EA, et al. Lung hypoplasia in congenital diaphragmatic hernia: a quantitative study of airway, artery, and alveolar development. *J Surg* 1971;58:342–346, with permission.)

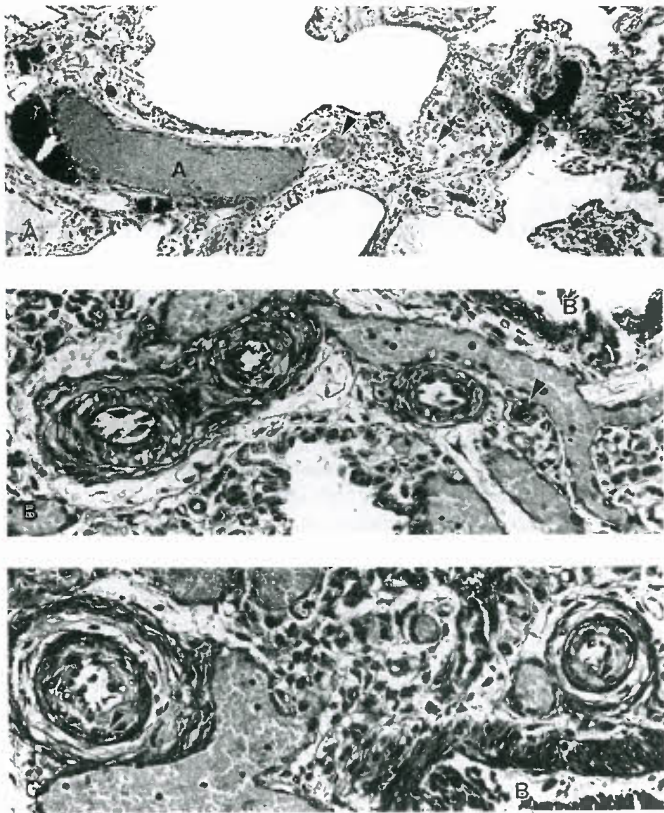


Figure 66.13. Lung micrographs from the left (A) and right (B,C) lungs of an infant with alveolar capillary dysplasia. A: Barium distends the lumen of a preacinar artery (A) but does not enter the anomalous vein to the left of the artery. Intraacinar arterial branches that contain barium are identified (arrowheads), but intraacinar veins and venules are distended with red cells, presumably forced ahead of the barium by the postmortem angiogram. Airspaces are lined by cuboidal epithelium, and no luminal capillaries are seen, all vessels lying centrally in the airspace walls. Hematoxylin and eosin, original magnification, $\times 90$. B: Intraacinar pulmonary arteries showing medial muscular thickening that forms a continuous layer, even in the smallest branch (arrowhead), which is 20 mm in external diameter. Media is demarcated by external and internal elastic laminae, stained black in this elastic stain. A bronchiole is identified (B). Elastic-van Gieson, original magnification, $\times 220$. C: Intraacinar arteries, the smaller measuring 60 μm in external diameter, with concentric intimal fibrosis; the latter is overlaid by arrowheads that mark the internal elastic laminae. The media is narrow in these branches, but the lumen (containing festooned endothelial cells) is the same size as in the similar-sized arteries seen in B. Elastic-van Gieson, original magnification, $\times 220$. (From Cullinane C, Cox PN, Silver MM. Persistent pulmonary hypertension of the newborn due to alveolar capillary dysplasia. *Pediatr Pathol* 1992;12:499–514, with permission.)

hypoxia. Dilator prostaglandins partially influence the fall in pulmonary vascular resistance because indomethacin retards but does not prevent the decrease observed with oxygen. Current thinking suggests that vasodilation of the newborn pulmonary circulation may be the result of increased production of NO (76) and repression of potassium channels (77). Studies by Belik et al. (78) also suggested that the mechanical properties of fetal pulmonary vascular SMCs differ from those of the neonate.

Underdevelopment of the Lung

Underdevelopment of the lung parenchyma and associated pulmonary vasculature is associated with congenital diaphragmatic hernia, hypoplastic or dysplastic lungs, scimitar syndrome, and oligohydramnios secondary to renal agenesis and dysplasia. Pulmonary hypoplasia is also a feature of prematurity, absence of the phrenic nerve, asphyxiating thoracic dystrophy, rhesus isoimmunization, and, experimentally, amniocentesis and smoking.

Pulmonary hypertension and right-to-left shunting from birth will result from hypoplasia of the pulmonary vascular bed (Fig. 66.12). Heightened pulmonary vascular resistance can be attributed to the impaired gas exchange (hypoxia, hypercarbia) in addition to the structural changes in the vessels. In infants with congenital diaphragmatic hernia, reversal of pulmonary hypertension has been achieved by using vasodilators, extracorporeal membrane oxygenation (ECMO) or high-frequency oscillation, and NO alone or in combination with phosphodiesterase inhibitors. Some infants with hypoplastic lungs that had been refractory to NO prior to ECMO demonstrated a beneficial effect of NO after ECMO. The expectation is that the reduction in pulmonary artery resistance will stimulate regression of vascular changes and maturation in growth of the pulmonary arteries. There is recent evidence that endothelin receptor blockade may be a useful strategy in congenital diaphragmatic hernia (79). In some cases, however, the lung hypoplasia might be excessive and stimulation of growth of distal arteries and alveoli may be inadequate. Dysplasias of the lung associated with PPHN, such as alveolar capillary dysplasia (Fig. 66.13), which may be familial in nature, are currently so refractory to treatment that a biopsy probably should be done to guide clinical management.

Experimental studies carried out in newborn lambs and rabbits have shown that heparin can stimulate remodeling of the pulmonary circulation. Accelerated maturation of the pulmonary circulation was achieved by inducing an increase in the number of peripheral pulmonary arteries relative to alveoli. Clinical data show that this therapeutic strategy might prove useful in inducing the growth of peripheral arteries, thereby reducing pulmonary vascular resistance (80). Most impressive is the use of NO to experimentally stimulate angiogenesis and growth of distal vessels as well as alveoli (81,82). This has also been achieved with recombinant VEGF (83) and an activator of soluble guanylate cyclase (84). More recently, bone marrow progenitor cells and mesenchymal progenitor cells or even conditioned medium have been used to stimulate growth of vessels and alveoli (85–87) (Fig. 66.14).

Maladaptation of the Pulmonary Vascular Bed

Perinatal stress, for example, hemorrhage, hypoglycemia, aspiration, or hypoxia may result in failure of dilation of normally muscular vessels and left ventricular dysfunction, both contributing to persistent pulmonary hypertension. Structural studies of the lung at postmortem in fatal cases of meconium aspiration suggest that there were antecedent pulmonary vascular abnormalities that exacerbated the postnatal pulmonary hypertension. The most striking feature is the presence of muscle in arteries that are small and peripheral in location and normally nonmuscular. The use of inhaled NO in clinical studies and L-arginine in experimental studies and strategies to maximize dilator effects attributable to cyclic guanosine monophosphate (GMP) by inhibiting phosphodiesterases with agents such as sildenafil have proven effective in lowering pulmonary artery pressure. Because GMP-increased production of endothelin may underlie the pathophysiology, the use of endothelin receptor blockade or endothelial converting enzyme

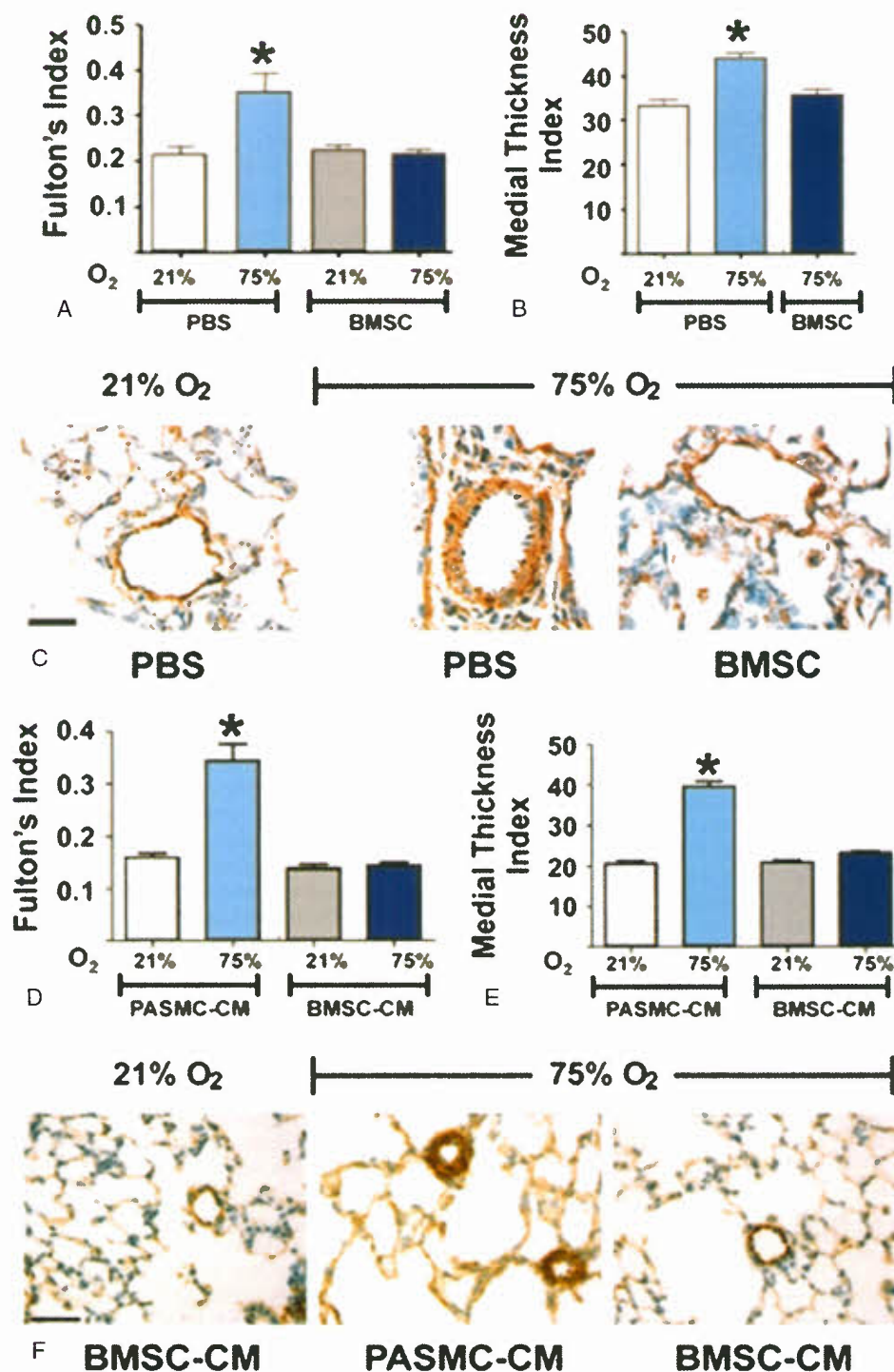


Figure 66.14. Either bone marrow stromal cell (BMSC) or BMSC-conditioned media (CM) treatment prevents vascular changes associated with pulmonary hypertension in hyperoxia-induced lung injury. **A:** Hyperoxia-exposed, phosphate-buffered saline (PBS)-treated newborn mice develop significant right ventricular hypertrophy that is significantly reduced by BMSC treatment. Data are expressed as mean \pm SEM ($n = 10$ to 12 animals per group). $*p < 0.001$, compared with the two normoxia groups and the hyperoxia group that received BMSC. **B:** BMSC treatment significantly reduced the medial wall thickness as compared with the hyperoxia group that received PBS treatment. Data are expressed as mean \pm SEM. $*p < 0.001$, compared with normoxia and the hyperoxia group that received BMSC. **C:** Representative pulmonary arterioles immunostained for α -smooth muscle actin, displaying a thickened smooth muscle layer in hyperoxia-exposed mouse lungs as compared with normoxic controls, and absence of muscularization on BMSC treatment. **D:** Similar to BMSC treatment, BMSC-CM treatment significantly reduced right ventricular hypertrophy in hyperoxia-exposed animals, and **(E)** significantly reduced medial wall thickness as compared with the hyperoxia group that received pulmonary artery SMC-CM. Data are expressed as mean \pm SEM ($n = 16$ to 18 animals per group). $*p < 0.0001$ versus normoxic groups or BMSC-CM treated groups. **F:** Representative small pulmonary arterioles, as in **(C)**. Solid bar scale represents $100 \mu\text{m}$ and all the panels are under the same magnification. (From Aslam M, Baveja R, Liang OD, et al. Bone marrow stromal cells attenuate lung injury in a murine model of neonatal chronic lung disease. *Am J Respir Crit Care Med* 2009;180:1122–1130 with permission.)

inhibition may prove beneficial, especially if specificity could be controlled to maximize dilatory activity. That is, endothelin A receptors and endothelin B constrictor (as opposed to endothelin B dilator) receptors should be targeted.

Maldevelopment of the Pulmonary Vascular Bed

Newborns in whom there is no apparent reason for persistent pulmonary hypertension are the most perplexing of all. Clinical studies suggested in some cases a relationship between maternal ingestion of prostaglandin synthase inhibitors and subsequent persistent pulmonary hypertension. In a study of infants with PPHN reduced expression of the gene for eNOS was reported (88).

Chronic hypoxia in pregnant guinea pigs and in pregnant rats will produce structural changes in the pulmonary vascular bed of the newborn. In lambs, the clinical syndrome has been produced by administration of a cytokine associated with inflammation, that is, tumor necrosis factor alpha. Relatively short periods of hypoxia in the fetal lamb will result in sustained elevation of pulmonary artery pressure and structural changes in the pulmonary arteries. In utero ligation of the ductus arteriosus simulates the structural changes and the initial hemodynamic profile of persistent pulmonary hypertension. In this model, increased lung preproendothelin and decreased (endothelin B) ETB receptors were observed (89). These features have been reported in the same experimental model in association with reduced expression of NO synthase. In addition, there is an elevation of cyclic GMP phosphodiesterase activity that would potentiate the effects of reduced NO. In this model, phosphodiesterase inhibitors have proven effective in reducing pulmonary hypertension. Endothelin receptor blockade has also been used to successfully treat an experimental model of pulmonary hypertension associated with prematurity (90). Structural changes in the contractile apparatus of the hypertensive pulmonary arteries, such as the reduction in myosin light-chain phosphatase, also could influence the response to vasodilators. There are promising studies in lambs using antioxidant (superoxide dismutase) along with NO in neonatal lambs with persistent pulmonary hypertension (91).

THROMBOEMBOLIC DISEASES

Clinical Features

Diagnosing thromboemboli as a cause of pulmonary hypertension requires a high index of suspicion in patients who have disorders in which the former are likely to occur (Table 66.5 and Fig. 66.15). For example, thromboemboli frequently occur in children who have ventriculoatrial shunts for hydrocephalus because of either clots dislodging from the end of the catheter or an abnormal fibrinolytic reaction of cerebrospinal fluid within the lung. Children with sickle cell anemia may develop pulmonary thromboses and infarctions. In endogenous areas, ova emboli due to schistosomiasis have been described. Fat emboli may occur secondary to trauma and also in association with collagen vascular disease. Tumor emboli may carry metastatic disease from the kidneys or other abdominal organs, or they may be present in association with infiltrative carcinomatous disease of the lung. Thromboembolic pulmonary hypertension is also associated with tumor chemotherapy. Deep vein thrombosis is also seen in children as a source of pulmonary emboli. Right-sided endocarditis and right atrial myxoma also may be sources of emboli. In the newborn and young infant, pulmonary thrombosis may be associated with sepsis

TABLE 66.5

Causes of Thromboembolic Disease in Children

Ventriculoatrial shunts for hydrocephalus
Fat emboli (posttraumatic or with collagen vascular disease)
Sickle cell anemia
Tumor emboli
Ova emboli (schistosomiasis)
Thrombosis in other vascular structures (secondary to immobilization)
Sepsis and/or dehydration
Right-sided endocarditis
Right atrial myxoma

and dehydration and portal or renal vein thrombosis, and it is seen with nephrotic syndrome. Thromboembolic pulmonary hypertension also can be associated with steroids. There is little direct evidence that oral contraceptives alone will cause the development of pulmonary vascular disease in women, but these compounds probably should be avoided, particularly in susceptible women, such as those with congenital heart defects and pulmonary hypertension. Diagnosis of the nature and severity of embolic phenomena can be established by chest radiography and lung scans, although occasionally angiography is necessary, and there have been advances in treatment by thromboendarterectomy (92). There are two factors that probably contribute to the pulmonary hypertension of thromboembolic disease: first, the structural damage and occlusive changes within the large and small arteries; and, second, the concomitant release of vasoactive substances, particularly from degenerating platelets, serotonin, or thromboxane.

The nature of the pulmonary vascular abnormalities in thromboembolic disorders has not been studied extensively in children, but findings can be expected to be similar to those described in adults. In postmortem pulmonary arteriograms of adult patients, some vessels show evidence of thrombi (seen as filling defects), and filling of the peripheral distribution of these vessels with contrast material is scant. Other areas of the lung, however, appear normal. Upon microscopic examination of the abnormally filled areas, fibrous intimal hyperplasia is observed, mostly eccentric in nature, in both the preacinar and peripheral intraacinar arteries. Some vessels show evidence of having been completely occluded and later recanalized. Microscopic examination of areas that appear normal on the arteriogram show intraacinar pulmonary arteries that are increased both in size and concentration, suggesting compensatory dilation and recruitment. Throughout the lung, there may be medial hypertrophy of muscular arteries, but this probably depends on the duration of the disease and the severity of pulmonary hypertension.

SICKLE CELL DISEASE AND OTHER HEMOGLOBINOPATHIES

There has been increasing recent attention given to the complication of pulmonary hypertension in patients with sickle cell disease (93) and other hemoglobinopathies such as thalassemia. This complication is now recognized as a significant risk factor for death (94). The cause goes beyond thromboemboli

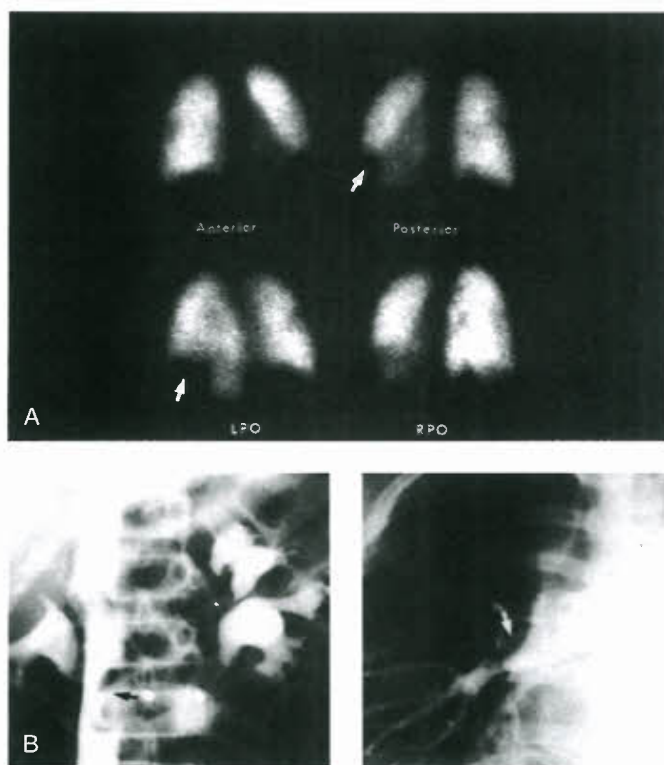


Figure 66.15. A: Lung perfusion scan performed after injection of technetium-99m macroaggregated albumen in a teenage boy who, after an orthopedic procedure, developed deep vein thromboses and pulmonary emboli. The latter are visualized as filling defects (arrows). LPO, left posterior oblique; RPO, right posterior oblique; B: Venous angiogram (left) shows site of tumor (infiltrative reticulum cell sarcoma) in inferior vena cava. Right ventricular cineangiogram (right) demonstrates large embolus from same tumor in right pulmonary artery.

and appears to relate to hemolysis-induced endothelial dysfunction and subsequent dysregulation of arginine metabolism and reduced NO bioavailability. Initial results of studies using sildenafil to treat chronic pulmonary hypertension appear promising (95). New studies suggest a potential benefit of nitrite therapy in this disorder (96).

PORTAL HYPERTENSION

Severe liver disease producing cirrhosis and intrahepatic portal hypertension, as well as portal vein thrombosis producing extrahepatic portal hypertension have been associated with the development of pulmonary hypertension (97). Severe structural changes, consisting of medial hypertrophy, occlusive cellular intimal hyperplasia, plexiform lesions, and dilation complexes occur in the peripheral pulmonary arteries. It has therefore been postulated that the “toxic liver” is unable to degrade a certain vasoconstrictor substance that then circulates through the lung in high concentration causing structural damage to the vessels. In some patients with liver disease, however, there is generalized vasodilation of the vessels in the lung (98). In other patients, anastomoses develop between pulmonary and hepatic arteries (99). Thus, the pulmonary vascular response (both structural and hemodynamic) in individual patients with liver disease may differ greatly. Severe pulmonary hypertension should not be considered a contraindication to

liver transplantation because regression of the hemodynamic abnormality has been described. Recently portopulmonary hypertension has been linked to a polymorphism in S100A4 (100), a gene we linked to experimental pulmonary hypertension discussed later in this chapter.

GRANULOMATOUS AND COLLAGEN VASCULAR DISEASES AND IMMUNE/INFECTIOUS DISEASES

Pulmonary hypertension may occur either in adults or in children with sarcoidosis. This seems to be due to the presence of obstructive granulomas within the pulmonary arteries. Pulmonary hypertension also may occur in association with collagen vascular disease, such as scleroderma, and the CREST syndrome (calcinosis, Raynaud's phenomenon, esophageal dysfunction, sclerodactyly, telangiectasia) and more rarely in association with systemic lupus erythematosus, rheumatoid arthritis, Takayasu arteritis, polymyositis, and dermatomyositis. While the pathologic features of PAH include thromboemboli, particularly in association with the antiphospholipid syndrome (101) an immune/inflammatory vasculitis appears to be the initiating event. The prevailing hypothesis is that there is endothelial injury coupled to an immune defect and this leads to a peri- and intravascular inflammatory response that causes vascular lesions that lead to progressive PAH. In addition to high circulating levels of endothelin-1 (indicative of an endothelial injury), there is increased production of autoantibodies that reflect the immune compromise. Activating antibodies to platelet-derived growth factor (PDGF) receptor (102) could explain the proliferative response of SMCs causing vascular lesions. In an allergic model of PAH, an IL-13-mediated increase in a resistin-like molecule was observed and this protein can induce SMC proliferation (103).

The results of therapy, including intravenous prostacyclin, have not appreciably improved long-term survival in the subset of patients with PAH in association with systemic sclerosis. These patients appear to deteriorate with lower levels of pulmonary artery pressure and resistance, perhaps because of intrinsic abnormalities in the right ventricle or related to increased stiffness of the conduit pulmonary arteries (104).

Inflammation has been linked to the development of PAH, and both the chemokine receptor CX3CR1 and the chemokine fractalkine appear to be elevated (105). Severe PAH has been associated with acquired immunodeficiency syndrome, even in the absence of lung parenchymal disease (106), and has been reproduced experimentally (107). Moreover, the development of PAH in the subset of patients with human immunodeficiency virus (HIV) infection may be a function of the immunogenetic background (i.e., human leukocyte antigen class II alleles) (108). More recently, a link has been made between expression of human herpesvirus 8 associated with Kaposi sarcoma and idiopathic PAH (109), although this association has not been confirmed in all populations studied.

It appears that the Kaposi sarcoma virus can stimulate lysosomal-mediated degradation of BMPR2 (110), the receptor that is mutated and dysfunctional in patients with idiopathic pulmonary hypertension. This receptor normally protects the pulmonary vasculature, as is discussed later in the chapter. The HIV-nef gene has been implicated in plexogenic pulmonary vascular lesions associated with PAH in HIV-infected patients and Simian immunodeficiency virus-infected nonhuman primates (111).

Recently, we have reported that the mouse that overexpresses S100A4/Mts1 develops extensive and severe neointimal lesions following injection of the gamma murine herpes

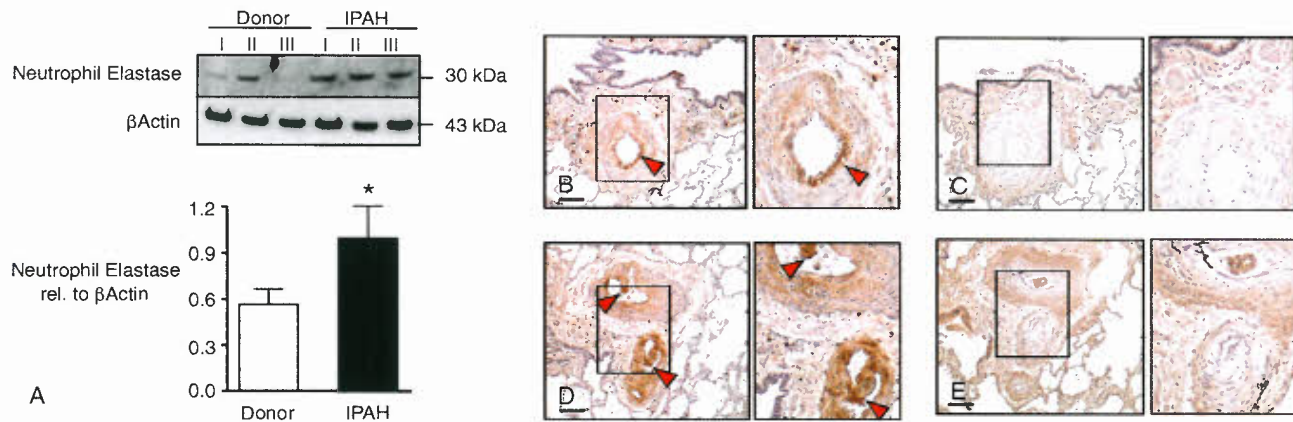


Figure 66.16. Heightened neutrophil elastase expression in cultured pulmonary artery SMCs is localized to neointimal lesions in lungs from patients with idiopathic pulmonary artery hypertension (IPAH). **A:** Western immunoblots on top and relative densitometry on the bottom comparing neutrophil elastase relative to β -actin in cultured pulmonary artery SMCs isolated from three IPAH patients versus three unused donor lungs as controls. Bars represent mean of $n = 3$ per group, with $*p < 0.05$ determined by t -test. Representative immunohistochemistry from one of five IPAH and one of four control lungs. Cells strongly expressing neutrophil elastase are apparent in the subendothelium and media of pulmonary arteries with neointimal or plexiform lesions in the IPAH lung (B,D). Little immunoreactivity for neutrophil elastase was apparent in the pulmonary arteries in the control donor lung (F). Background immunoreactivity is apparent using IgG as a control (C,E). Arrowheads point to regions of intense immunoreactivity. Marked areas are shown with twofold higher magnification, on the right. Scale bars, 100 μ m (B–F). (From Kim YM, Haghighat L, Spiekerkoetter E, et al. Neutrophil elastase is produced by pulmonary artery smooth muscle cells and is linked to neointimal lesions. *Am J Pathol* 2011;179:1560–1572, with permission.)

virus-68 (the murine homologue of human herpesvirus-8). This is associated with an elevated elastase activity that we have now identified as neutrophil elastase produced by pulmonary artery SMCs. In this model, we identified high levels of neutrophil elastase in SMCs and also observed high levels of this enzyme in the vessels from patients with pulmonary hypertension (Fig. 66.16) (112).

The high incidence of PAH in areas of the world endemic for schistosomiasis has resulted in a number of experimental studies addressing pathogenesis and pathobiology of this complication. About 10% of patients with schistosomiasis will develop portal hypertension and 10% of those (1% total) will have PAH. Chronic infection with the high-dose cercariae resulted in extensive lung vascular remodeling and PAH (113) (Fig. 66.17).

Allergic responses to ovalbumin or to aspergillus (114) can result in extensive vascular remodeling although in this model of disease, as in the S100A4 overexpressing mice inoculated with virus, elevation in right ventricular systolic pressure is not observed. A Th2 immune response characterizes both the ovalbumin and the cercariae models but not the viral model of pulmonary vascular remodeling. In mice lacking prostaglandin synthase, induction of allergic inflammation with the house dust mite induces intense pulmonary vascular remodeling; changes that are reversed by administration of prostaglandin E2.

A recent study has shown that in the model of PAH in which loss of arteries is induced by the combination of injection of an inhibitor of VEGF and hypoxia, depletion of T cell subsets actually worsens the pathology (115). This adverse response has been attributed to unbalanced B cell activity resulting from impaired regulatory T cell (Treg) production (116).

In patients with idiopathic pulmonary artery hypertension (IPAH), there is a pronounced inflammatory response, heightened circulating levels of cytokines and their receptors, stromal-derived factor-1 and monocyte chemoattractant protein (MCP)-1, as well as fractalkine (105), and its cognate receptor, which are associated with heightened SMC proliferation. Also intriguing are recent studies suggesting that heightened expression of the transcription factor NFATc2 that is associated with inflammatory cells may underlie PAH. Increased nuclear NFATc2 is observed in T cells from IPAH patients and in pulmonary vascular lesions, and this can lead to repression of Kv 1.5 channel expression. NFATc2 can be inhibited by a small molecule and its nuclear translocation can be suppressed by cyclosporine. These agents can also attenuate experimentally induced PAH (117).

DRUGS AND TOXINS

Clinical Studies

The ingestion of substances associated with PAH include amphetamine, as well as the fenfluramine compounds, for example, dexfenfluramine, a serotonin antagonist (118). These agents resemble epinephrine in their chemical structure, suppress appetite, and cause symptoms of right-sided heart failure in 10% of patients within 6 to 12 months of initial administration. Microscopic changes in the lung are similar to those in patients with end-stage pulmonary vascular disease, regardless of etiology (i.e., medial hypertrophy and intimal fibroelastosis, including the presence of plexiform and dilation lesions).

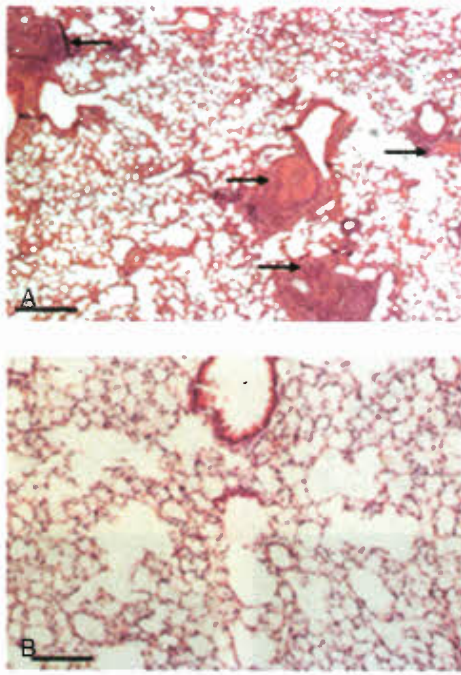


Figure 66.17. Representative photomicrographs ($\times 100$ magnification) of lung sections. **A:** Mice infected with *Schistosoma mansoni* for 25 weeks with eggs in the lung; numerous grossly remodeled vessels can be seen (arrows indicate remodeled vessels). **B:** In mice infected with *S. mansoni* for 25 weeks and treated with praziquantel for the final 8 weeks, no grossly remodeled vessels can be seen. Sections were stained with hematoxylin and eosin. Bar represents 10 μm . (From Crosby A, Jones FM, Kolosionek E, et al. Praziquantel reverses pulmonary hypertension and vascular remodeling in murine schistosomiasis. *Am J Respir Crit Care Med* 2011;184:467–473, with permission.)

Pathophysiologic studies have also suggested that there are similarities to primary PAH in terms of monoclonal expansion of endothelial cell populations (119). As previously mentioned, our studies have linked serotonin to increased production and secretion of S100A4/Mts1, a gene associated with advanced clinical and experimental PAH (22,23).

The toxic oils, such as rapeseed oil, have been implicated in the development of malignant PAH (120). Ingestion of pyrrolizidine alkaloids, such as bush tea, causes hepatic veno-occlusive disease, and a similar compound, monocrotaline, when ingested by animals, causes severe pulmonary vascular disease (121).

Experimental Studies

Rats that ingest the toxin monocrotaline develop pulmonary arterial changes that can be correlated with hemodynamic evidence of progressive PAH with increased pulmonary vascular resistance (122–127). Initially, there is an increase in cardiac output associated with extension of muscle into peripheral arteries that are normally nonmuscular. After a few weeks, when there is an increase in pulmonary artery pressure, medial hypertrophy of normally muscular arteries is apparent. After 3 weeks, when an increase in pulmonary vascular resistance occurs secondary to both a further rise in pulmonary artery pressure and a drop in cardiac output, there is a reduction in the number of peripheral pulmonary arteries, and “ghost,” or disappearing, vessels can be seen.

Ultrastructural studies have shown injury to the vascular endothelium within several hours of monocrotaline

injection; inflammatory cells and edema are apparent after 1 week. Studies carried out in our laboratory comparing the response to monocrotaline in neonatal, infant, and adult rats suggested that, in the neonate, transient inflammation causes a severe decrease in alveolar number. The development of vascular changes is similar in the three groups. In the infant rat, however, the abnormalities regress between 2 and 4 weeks after injection, whereas in the adult animal, they progress (122). Our studies showed that increased elastase activity not only initiated but also contributed to the progression of the vascular changes. Similar to pulmonary hypertension secondary to chronic hypoxia, there is an early increase in enzymatic activity only 2 days after injection of the toxin, but there is also a further increase in elastase activity observed with malignant progression of the disease in adult rats. Furthermore, we demonstrated that elastase inhibitors are effective in reducing the pulmonary hypertension and vascular changes (125). We have also shown that elastase inhibitors can effectively reverse the pulmonary hypertension that results from monocrotaline toxicity with values similar to those in control animals that did not receive this toxin (128) (Figs. 66.18 and 66.19). Reversibility of disease was associated with coordinated apoptosis and caspase-mediated degradation of the excess extracellular matrix (129) with regeneration of normal endothelial channels and precapillary vessels.

Based upon subsequent knowledge that the effect of elastase was critical in maintaining survival signals through epidermal growth factor receptors (EGFRs) (130), we recently blocked EGFR (131). In these studies, we were able to show reversal of progressive PAH that was sustained even 1 month after cessation of treatment. More recently, the use of a PDGF receptor blocker to reverse PAH in this experimental model (132) has prompted a case report showing the successful use of imatinib in a patient with advanced pulmonary vascular disease (133). This report has prompted several clinical trials using imatinib in patients with PAH, with the published data suggesting potential efficacy in those with the most severe disease (134).

Others have used eNOS gene therapy in association with endothelial progenitor cell administration (Fig. 66.20) (135,136), gene therapy with survivin (137) (Fig. 66.21), angiopoietin-1 (138), inhibition of the SERT (139), adrenomedullin (140), and the rho kinase inhibitor, fasudil (141). Recently, gene replacement therapy with the Bmpr2 has shown similar efficacy to that seen in the hypoxia model (142). Potassium channel dysfunction is implicated in the pathogenesis of pulmonary vascular disease (143), and gene therapy restoring K channel function has been used effectively to suppress pulmonary vascular disease (67) but this has not been tested to reverse the process.

Recently, this group has shown abnormal metabolism linked to inflammation in pulmonary hypertension and important novel therapeutic targets linked to reversing a fatty acid oxidation defect (144). An important link between altered metabolism and inflammation underlies the propensity of mice (145,146) and highlights the role of mitochondrial dysfunction as pivotal to the pathology (147) (Fig. 66.22). Mice with insulin resistance develop pulmonary hypertension (148) and there is a high incidence of metabolic syndrome in women with idiopathic pulmonary hypertension (74). Mice with loss of peroxisome proliferator-activated receptor- γ (PPAR γ) in endothelial (149) or in SMCs (150) have spontaneous pulmonary hypertension and this can be rescued by adding back a apelin, a downstream target of PPAR γ gene regulation (151).

Other experimental models of chronic inflammation, such as repeated injections of endotoxin, and tumor necrosis factor also have been associated with the development of pulmonary vascular changes. In models of chronic air

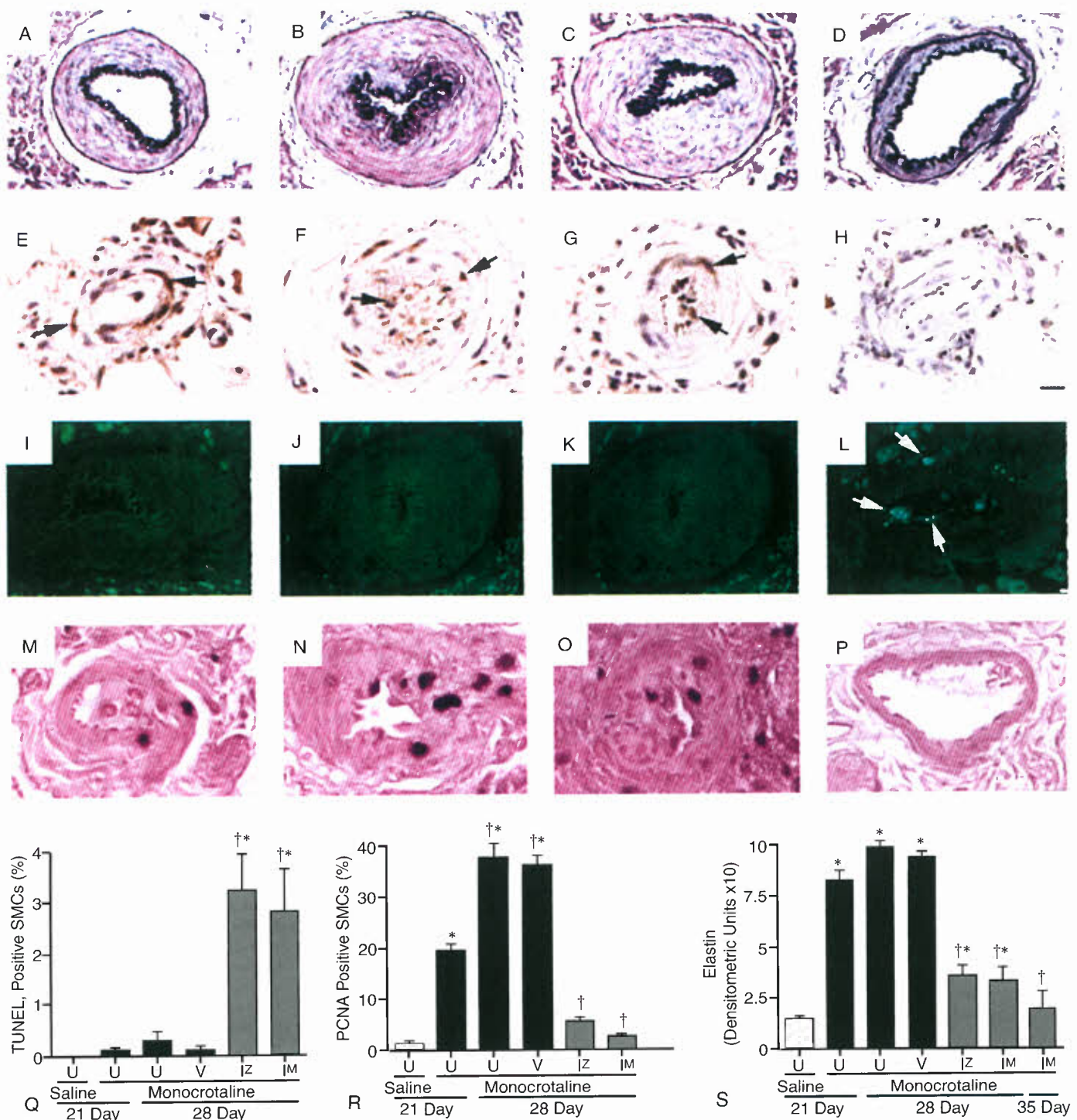


Figure 66.18. Cellular mechanism responsible for reversal of pulmonary artery muscularity. Elastase inhibition arrests tenascin-C accumulation and proliferation and induces apoptosis and loss of extracellular matrix (such as elastin). A–P: Days refer to time after injection of monocrotaline: A,E,I,M, day 21; B,F,J,N, day 28; C,G,K,O, day 28; D,H,L,P, day 28. A–D: Saline-perfused pulmonary arteries stained with Movat pentachrome stain. E–H: Pulmonary arteries after tenascin-C immunohistochemistry. Arrows indicate positive brown peroxidase staining. I–L: In situ TUNEL assays identifying apoptosis. Arrows indicate TUNEL-positive vascular cells. M–P: Proliferating vascular cells, shown by immunohistochemistry for proliferating cell nuclear antigen (PCNA); dark nuclei are PCNA-positive cells. Q,R: Percent of smooth muscle cells (SMCs) that are TUNEL positive (Q) or PCNA positive (R). S: Densitometric quantification of elastin I, inhibitor treated (IZ, ZD0892; IM M249314); TUNEL, in situ DNA nick end labeling; u, untreated; v, vehicle treated. Graphed data represent mean \pm standard error of the mean of $n = 4$; scale bars represent $5 \mu\text{m}$; *, $p < 0.05$, compared with †, $p < 0.05$, compared with results on day 21 in rats treated with monocrotaline. (Reproduced from Cowan KN, Heilbut A, Humpl T, et al. Complete reversal of fatal pulmonary hypertension in rats by a serine elastase inhibitor. *Nat Med* 200;6:698–702, with permission.)

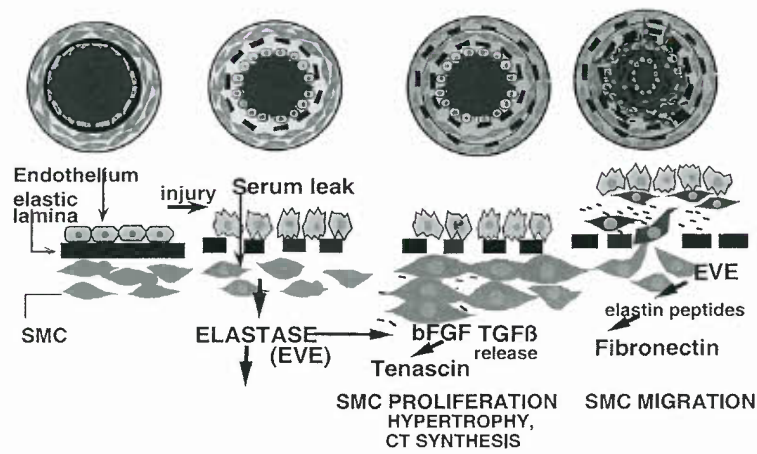


Figure 66.19. We have speculated how a stimulus could induce activity of an elastolytic enzyme and how this might stimulate the remodeling process. The process of progressive pulmonary hypertension involves a series of switches in the smooth-muscle cell (SMC) phenotype (i.e., differentiation of muscle from nonmuscle precursor cells, SMC hypertrophy, proliferation accounting for medial hypertrophy, and SMC migration resulting in neo-intimal formation). In response to a stimulus, such as high flow and pressure, the first “casualty” is the endothelial cell. As a result of structural and functional alterations in endothelial cells, some of the barrier function would be lost, allowing a leak into the subendothelium of a serum factor normally excluded from this region. The serum factor could induce activity of an endogenous vascular elastase (EVE). This enzyme released from precursor or mature SMCs would activate growth factors normally stored in the extracellular matrix in an inactive form, such as basic fibroblast growth factor (bFGF) and transforming growth factor(TGF)- β , which are known to induce smooth muscle hypertrophy and proliferation and increases in connective tissue protein (e.g., collagen and elastin) synthesis. Growth factors also induce tenascin, a matrix glycoprotein that amplifies the proliferative response as described in the text. This results in the differentiation of precursor cells to mature smooth muscle related to the muscularization of normally nonmuscular small peripheral arteries. In the muscular arteries, the release of growth factors would result in hypertrophy of the vessel wall. Continued elastase activity would cause migration of SMCs in several ways. The elastin peptides or degradation products of elastin can stimulate fibronectin, a glycoprotein that is pivotal in altering SMC shape and switches them from the contractile to motile phenotype.

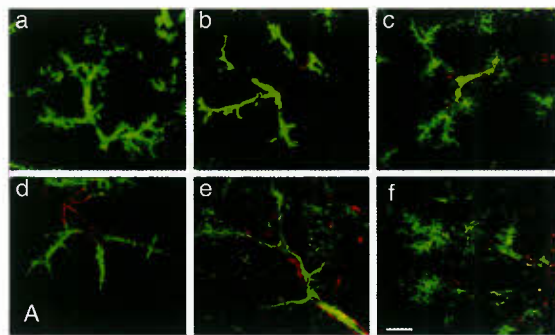
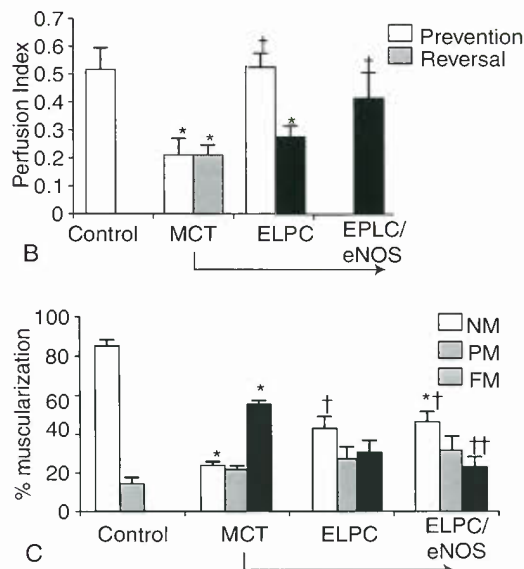


Figure 66.20. Representative confocal projection images of lung sections perfused with fluorescent microspheres (green) suspended in agarose (i.e., fluorescent microangiography) and immunostained for alpha smooth muscle actin (red). A: Normal filling of the microvasculature was observed in control rats (a), whereas rats treated with monocrotaline (MCT) showed a marked loss of microvascular perfusion and widespread precapillary occlusion 21 days (b) and 35 (d) days after MCT injection. In the prevention model, animals receiving endothelial-like progenitor cells (ELPCs) displayed improved microvascular perfusion and preserved continuity of the distal vasculature (c). In the reversal model, eNOS-transduced ELPCs dramatically improved the appearance of the pulmonary microvasculature (f), whereas progenitor cells alone resulted in more modest increases in perfusion and little noticeable reduction in arteriolar muscularization (e), calibration bars=100 μ m. In the prevention model, animals receiving ELPCs displayed improved microvascular perfusion (B) and preserved continuity of the distal vasculature (C), and similar findings were observed in the reversal model. NM, nonmuscular; PM, partially muscular; FM, fully muscular. (Reproduced from Zhao YD, Courtman DW, Deng Y, et al. Rescue of monocrotaline-induced pulmonary arterial hypertension using bone marrow-derived endothelial-like progenitor cells: efficacy of combined cell and eNOS gene therapy in established disease. *Circ Res* 2005;96:442–450, with permission.)



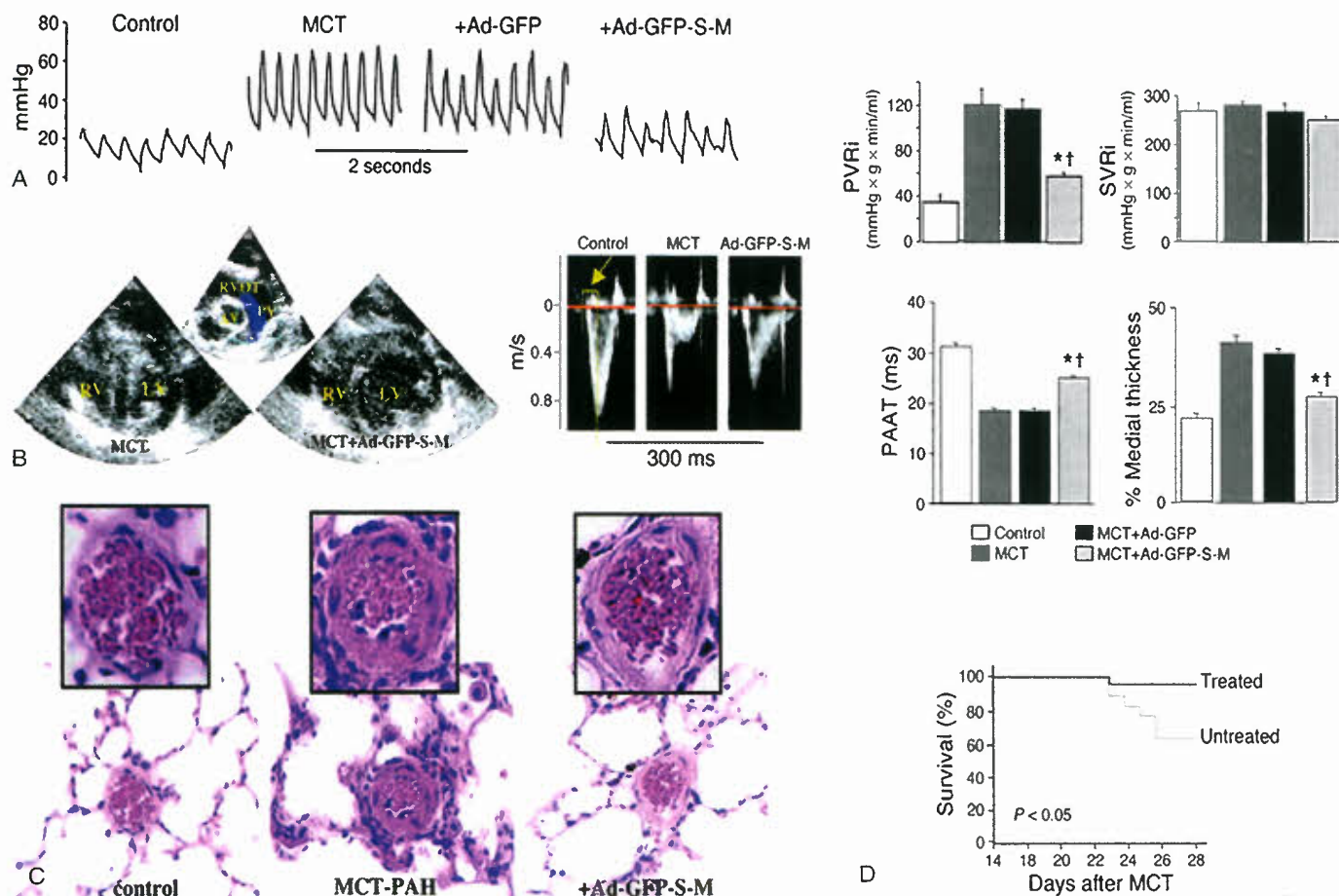


Figure 66.21. Gene therapy of rat monocrotaline-pulmonary artery hypertension (MCT-PAH) with adenovirus-green fluorescent protein survivin-mutant (Ad-GFP-S-M) improves hemodynamics, reduces remodeling of the pulmonary artery (PA) resistance, and prolongs survival. **A:** Representative high-fidelity PA pressure tracings and mean data show that Ad-GFP-S-M, but not Ad-GFP, therapy reduces PA pressure and pulmonary vascular resistance index (PVRi), without altering systemic hemodynamics. SVRi, systemic vascular resistance index. **B,C:** Ad-GFP-S-M, but not Ad-GFP, reduces right ventricle (RV) thickness measured in parasternal short axis and preserves the normal round shape of the left ventricle (LV). Similarly, Ad-GFP-S-M reduces pulmonary artery acceleration time (PAAT). Resistance PA remodeling, as measured by percent medial thickness, is reduced by treatment with Ad-GFP-S-M. RVOT, RV outflow tract; AV, aortic valve; PV, pulmonary valve. Magnification in (C), ×40. **D:** Targeting survivin with inhaled gene therapy in MCT-PAH significantly prolongs survival within the study period. * $p < 0.05$ versus MCT; † $p < 0.05$ versus Ad-GFP. (Reproduced from McMurtry MS, Archer SL, Altieri DC, et al. Gene therapy targeting survivin selectively induces pulmonary vascular apoptosis and reverses pulmonary arterial hypertension. *J Clin Invest* 2005;115:1479–1491, with permission.)

embolization and thoracic irradiation, in which pulmonary hypertension and vascular changes are produced, endothelial injury is the common observation, as it is in the monocrotaline model.

IDIOPATHIC PULMONARY HYPERTENSION

After all known causes of pulmonary hypertension have been ruled out, the diagnosis becomes that of idiopathic pulmonary hypertension. This unexplained disease, in which a structural abnormality is always found either in the arteries or in the veins, occurs both in children and adults and sometimes with a familial tendency (152–154). By the time the patient becomes symptomatic, the disease is usually advanced; in the absence of treatment, it is usually rapidly progressive and invariably fatal, although rare cases of spontaneous regression have been reported. The preponderance of affected females ranges in

some studies from a ratio of 4:1 to 2:1. In general, there is an inverse relationship between the age of onset of symptoms and the duration of illness until death. Children are most frequently diagnosed in infancy and in the absence of treatment may die within a year.

Recent attention has been directed to the genetics of this disease. Studies by Loyd et al. (155) have shown that there is genetic anticipation with the disease occurring earlier in subsequent generations and a preponderance of affected females at birth, suggesting that in the male there may be fetal wastage. In young children, the pathobiology suggests failure of the neonatal vasculature to open and a striking reduction in arterial number (156). In older children, intimal hyperplasia and occlusive changes are found in the pulmonary arteries as well as plexiform lesions. In adults, in addition to the latter changes, “ghost” arteries also have been reported. An electron microscopic study (157), performed on a lung biopsy of an adult patient, showed severe endothelial injury, which was speculated to be the initial

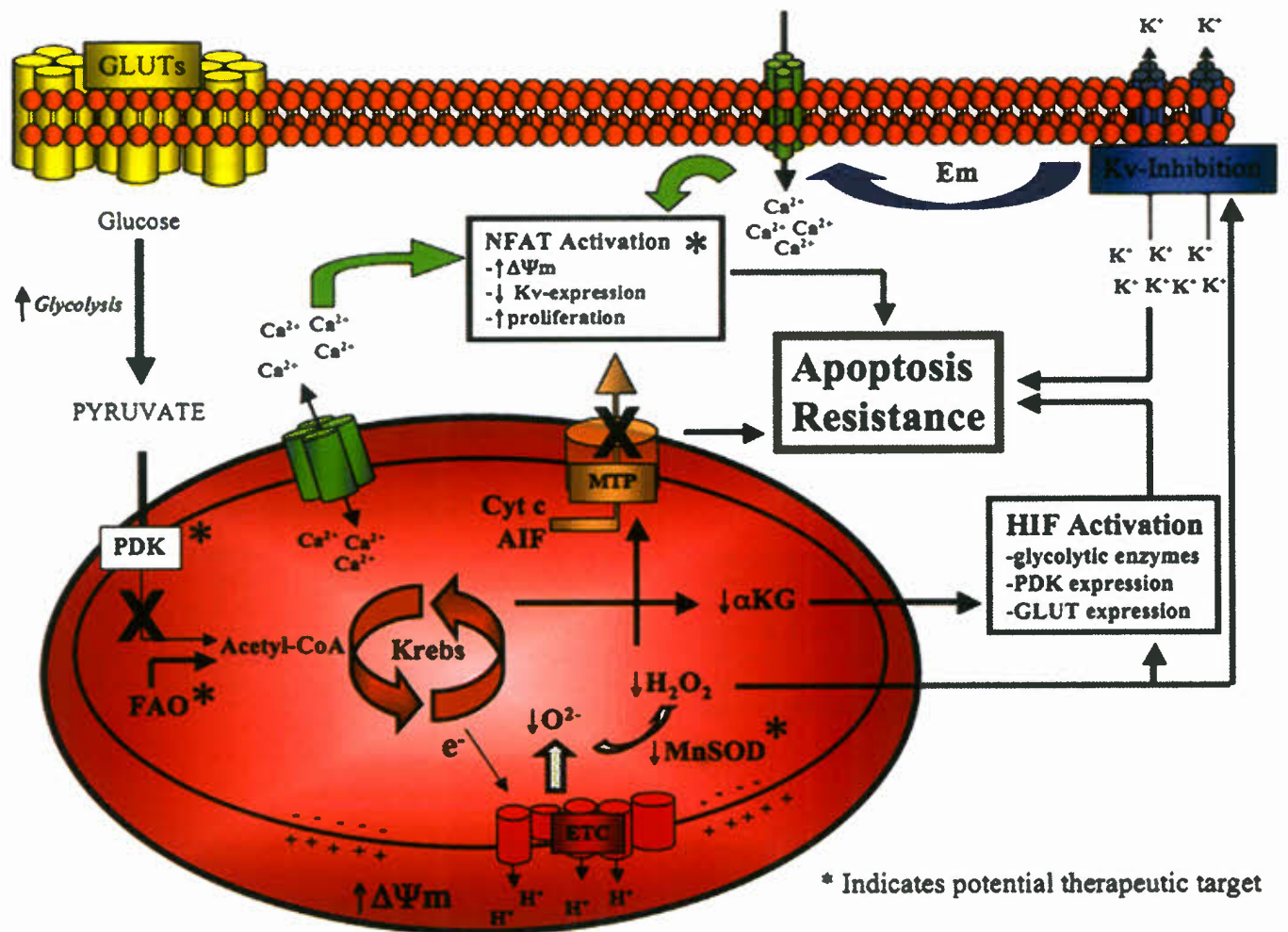


Figure 66.22. Metabolic hypothesis of pulmonary arterial hypertension (PAH). PAH pulmonary artery SMC mitochondria have decreased pyruvate influx, hyperpolarized mitochondria and reduced Krebs cycle activity, and mitochondrial-reactive oxygen species (ROS) (free radical) production. Hyperpolarized mitochondria and suppressed mROS close the mitochondrial transport pore (MTP), “trapping” cytochrome c, and apoptosis-inducing factor (AIF) in the matrix, resulting in resistance to apoptosis. This also results in closure of redox-sensitive Kv channels and influx of intracellular Ca^{2+} resulting in contraction and proliferation. Increased Ca^{2+} activates transcription factors (HIF and NFAT) that further suppress apoptosis and potentiate proliferative response. This whole mechanism initiated by hyperpolarization of mitochondria can be reversed by the inhibition of pyruvate dehydrogenase kinase (PDK), by dichloroacetate (DCA) thereby activating pyruvate dehydrogenase (PDH). In addition, inhibition of fatty acid oxidation (FAO) indirectly activates PDH (via the Randle cycle), thus mimicking DCA, also reversing PAH. *Denotes potential additional targets for therapy predicted by this mitochondria-centric model of PAH pathogenesis. (From Dromparis P, Sutendra G, Michelakis ED. The role of mitochondria in pulmonary vascular remodeling. *J Mol Med (Berl)* 2010;88:1003–1010, with permission.)

site of damage. In some patients, defective vWF (158) and fibrinolysis (159) have been described. Additional features include thickening of the pulmonary adventitia and venous hypertrophy as well as endothelial cell hyperplasia (160). Immunohistochemical changes include increased expression of TGF- β , matrix proteins, and macrophages (161), as well as the molecules observed with advanced lesions in congenital heart defect patients, that is, fibronectin, tenascin C, and S100A4/Mts1.

In the venous form of unexplained pulmonary hypertension, the clinical presentation is somewhat different from the arterial in that orthopnea is a characteristic feature and changes suggesting pulmonary edema are apparent on the chest radiograph, despite a normal pulmonary wedge pressure. Structural abnormalities in the lung are most striking in both large and small veins and consist of loose, fibrous intimal hyperplasia

with dilated lymphatics. There is also evidence that pulmonary venous occlusive disease might occur in utero. A number of factors affect the prognosis in idiopathic pulmonary hypertension such as insulin resistance in female patients (74) and iron deficiency associated with elevated hepcidin levels (162) (Fig. 66.23).

A mutation in the gene for *Bmpr2* is associated with 60% of familial cases of PAH (152–154), but the penetrance is only about 20%. That is, 80% of family members who carry the mutation will never develop PAH. Moreover, mutations in *Bmpr2* have been described in 20% of sporadic cases of PAH (163,164). In addition, other BMP-TGF beta receptor family members such as ALK1 and endoglin that were first identified as mutated in hemorrhagic telangiectasia are also occasionally mutated in patients with PAH (165,166). Focusing additional evidence on this family of receptors, a microsatellite instability

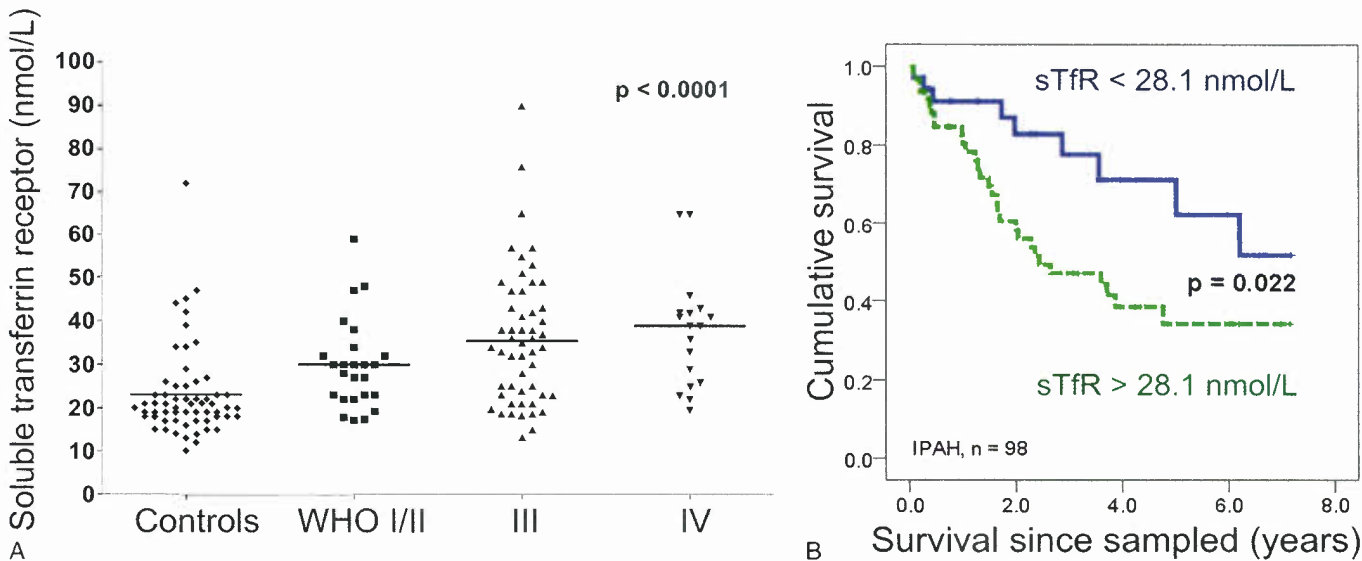


Figure 66.23. Serum transferrin receptor levels and idiopathic pulmonary arterial hypertension (IPAH). **A:** Distribution of soluble transferrin receptor (sTfR) levels according to World Health Organization (WHO) functional class in patients with IPAH and in healthy controls. *p* value relates to Kruskal-Wallis ANOVA. **B:** Kaplan-Meier survival estimates stratified by sTfR level below (blue solid line) or above (green dashed line) the predefined upper limit of the normal range, 28.1 nmol/L. (From Rhodes CJ, Howard LS, Busbridge M, et al. Iron deficiency and raised hepcidin in idiopathic pulmonary arterial hypertension: clinical prevalence, outcomes, and mechanistic insights. *J Am Coll Cardiol* 2011;58:300–309, with premission.)

in the TGF- β receptor II, resulting in its reduced expression and function, is observed in patients with IPAH (167). Recent studies have linked the penetrance of pulmonary hypertension in affected family members to the expression of *Bmpr2* from the normal allele (168). A host of new studies also implicate estrogen metabolism (169) and estrogen receptor expression (170) to the female predisposition to pulmonary hypertension. Although the penetrance is low, the functional link between mutations in *Bmpr2* and PAH is reinforced by the fact that independent of a mutation in *Bmpr2*, IPAH patients have reduced *Bmpr2* protein expression as do, to some extent, patients with secondary PAH. The functional consequence of reduced or absent *Bmpr2* in endothelial or SMCs is related to the pathologic features observed in PAH and discussed below. Impaired downstream signaling has been described in association with a variety of *Bmpr2* mutations (171,172), and there is also a newly described mutation in pSmad 8 in a patient with IPAH. A few studies have specifically addressed the transcription factors and genes that are subsequently upregulated or suppressed as a result of impaired *Bmpr2* signaling. We have shown in SMCs that BMPs can induce PPAR γ transcriptional activity to induce apoE, a suppressor of SMC proliferation (150). These studies showed that the main function of *Bmpr2* signaling is to suppress the proliferative response of SMCs when there is stimulation by growth factors that are induced under conditions of vascular injury. In endothelial cells, in contrast to SMCs, BMPs induce a complex between PPAR γ and β -catenin to regulate genes like apelin that have important protective paracrine and autocrine effects (151). BMPs suppress apoptosis of endothelial cells in response to injury and are proangiogenic, indicating that they may play an important role in repairing damaged microvessels. Apelin, in addition to being a factor that improves endothelial survival, can also suppress SMC proliferation, vasodilate, and improve cardiac function (173). Interactions between the *Bmpr2* signaling pathway and the Notch signaling pathway led investigators to determine that

Investigative and Other Potential Treatments for Pulmonary Hypertension	
TABLE 66.6	
Novel Therapeutic Strategies for Pulmonary Arterial Hypertension	
Elastase inhibition	
Kv channel openers (DCA)	
Malonyl coenzyme decarboxylase inhibitor	
TRP channel suppressor	
Dominant negative surviving	
*Statins	
VIP	
*PPAR γ agonists	
*Growth factor inhibitors (anti-PDGF, EGF)	
Adrenomedullin	
*Rho kinase inhibition	
*Endothelial progenitor cells engineered with eNOS	
Cyclosporine and rapamycin	
Apelin	
Gamma secretase inhibitors	

This is a summary schema that outlines processes that are current and future targets of therapy. Those with asterisk are in trial for PAH, those in green are in trial for other indications, and those in blue are in clinical use for other indications. Modified from Robinovitch M. Molecular pathogenesis of pulmonary arterial hypertension. *J Clin Invest* 2008;118:2372–2379.

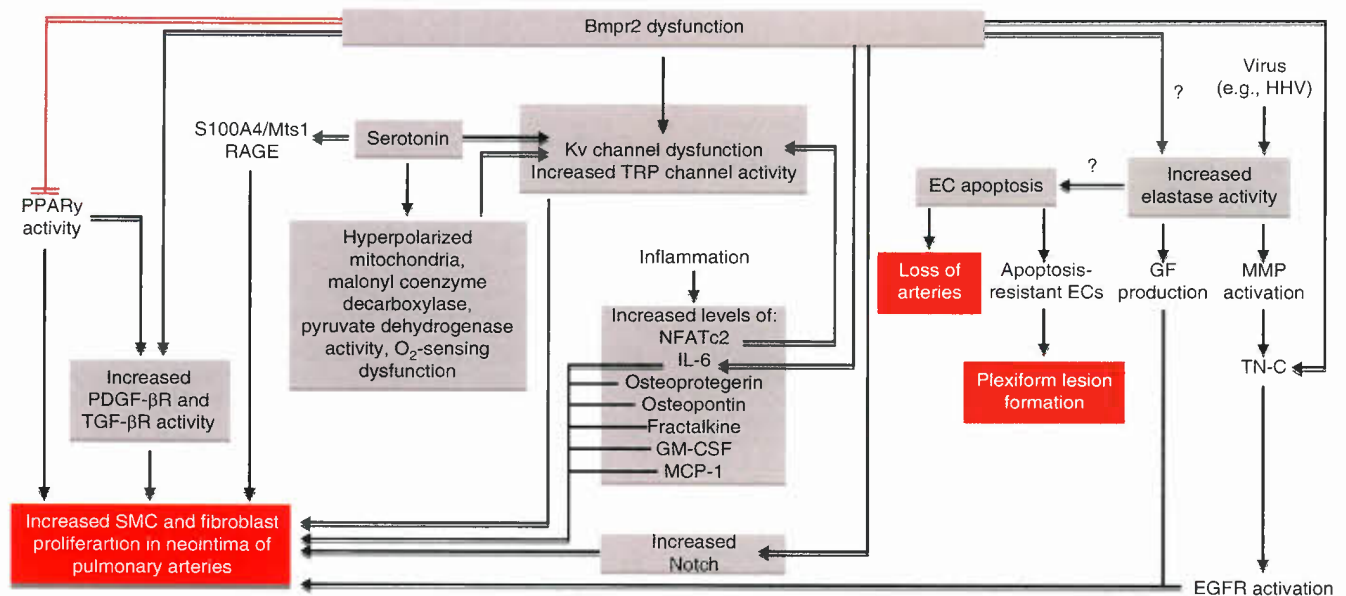


Figure 66.24. Schema outlining factors that converge in the molecular pathogenesis of PAH and how these may interact with *Bmpr2* dysfunction, a known genetic defect associated with PAH. This schema focuses on factors causing increased SMC and fibroblast proliferation as well as apoptosis of endothelial cells, causing an initial reduction in vessel number, followed by proliferation of apoptosis-resistant endothelial cells (ECs) in plexiform lesions. It shows multiple levels of interaction, with numerous factors related as described in the text. For example, serotonin stimulates both PDGF-mediated and S100A4/Mts1-mediated SMC and fibroblast proliferation and it also reduces Kv channel function, as does hyperpolarized mitochondria. *Bmpr2* dysfunction causes Kv channel dysfunction and enhances transient receptor potential Ca^{2+} (TRP) channel activity, which increases intracellular calcium levels, and may (as reflected by question mark) induce elastase activity. Viruses of the herpes family can induce elastase activity. Elastase, via activation of matrix metalloproteinases (MMPs) and tenascin C (TN-C), upregulates growth factor (GF) receptors such as epidermal GF receptors (EGFRs) and also triggers release of growth factors such as EGF from the extracellular matrix, all of which leads to SMC proliferation. *Bmpr2* dysfunction can also increase the mitogenic activity of PDGF activity, increase SMC proliferation by suppressing peroxisome proliferator-activated receptor (PPAR) γ , and increase transforming growth factor (TGF)- β activity. *Bmpr2* dysfunction can enhance inflammation via osteoprotegerin and interleukin (IL)-6. The transcription factor, nuclear factor of activated T cells (NFAT)c2 can suppress Kv channel function. Other inflammatory mediators such as fractalkine and mast cell proteinase (MCP)-1 can, in addition to osteoprotegerin and IL-6, increase SMC proliferation. *Bmpr2* dysfunction can lead to EC apoptosis, as can elastase activity. EC apoptosis may predispose to the development of apoptosis-resistant ECs in plexiform lesions. Loss of *Bmpr2* also activates Notch signaling that induces SMC proliferation. (Modified from Rabinovitch M. Molecular pathogenesis of pulmonary arterial hypertension. *J Clin Invest* 2008;118:2372–2379.)

in PAH there is an increase in activity of Notch. The cleavage of Notch following its interaction with a receptor on the SMC surface leads to the internalization of the Notch intracellular domain that serves as a transcription factor to induce genes that cause SMC proliferation (174). Blockade of gamma secretase, the enzyme that cleaves Notch, resulted in prevention and regression of experimental PAH.

SUMMARY

The experimental studies point to intersecting and highly interrelated pathways that underlie the pathobiology of pulmonary hypertension (Fig. 66.24). They suggest potential new therapies, some of which are already finding their way into clinical practice, as delineated in Table 66.6.

FUTURE DIRECTIONS

Further insights into the pathophysiology of PAH will come from genomic studies in which extensive sequencing will likely

reveal additional genetic variants associated with this disease. Epigenetic studies are currently being undertaken to address whether changes in chromatin remodeling will help explain why the lung is a target organ and how environmental factors perturb the genome and can lead to further alterations in expression of a rare variant or in the genes that interact with this rare variant. A number of studies using experimental models of pulmonary hypertension point to compelling changes in methylation (175) that silence genes such as eNOS (176) or superoxide dismutase (64) or that confer a proinflammatory signature on fibroblasts (177) from patients with pulmonary hypertension. Regulation of *Bmpr2* signaling also can be under epigenetic control (63).

High throughput gene expression and proteomic studies are also revealing changes that reflect specific pathways that are perturbed and how environmental exposures and immune defects can interact with a vulnerable vasculature. Intense focus on aberrations in immune mechanisms ranging from disturbances in T cell subsets to autoantibody production will be important in understanding all forms of PAH. The more we learn about specific pathways, the better equipped we will be to develop new treatments for pulmonary hypertension.

REFERENCES

- Brenner O. Pathology of the vessels of the pulmonary circulation: part 1. *Arch Intern Med* 1935;56:211.
- Heath D, Edwards J. The pathology of hypertensive pulmonary vascular disease. *Circulation* 1958;18:533-547.
- Ferencz C. Transposition of the great vessels: pathologic considerations based upon a study of the lungs. *Circulation* 1966;33:232-241.
- Elliot FM, Reid L. Some new facts about the pulmonary artery and its branching pattern. *Clin Radiol* 1965;6:193-198.
- Hislop A, Reid L. Pulmonary arterial development during childhood: branching pattern and structure. *Thorax* 1990;28:129-135.
- Haworth SG. Pulmonary vascular disease in different types of congenital heart disease: implications for interpretation of lung biopsy findings in early childhood. *Br Heart J* 1984;52:557-571.
- Haworth SG, Reid L. A morphometric study of regional variation in lung structure in infants with pulmonary hypertension and congenital heart defect: a justification of lung biopsy. *Br Heart J* 1978;40:825-831.
- Meyrick B, Reid L. Ultrastructural findings in lung biopsy material from children with congenital heart defects. *Am J Pathol* 1980;101:527-537.
- Rabinovitch M, Keane JF, Norwood WI, et al. Vascular structure in lung tissue obtained at biopsy correlated with pulmonary hemodynamic findings after repair of congenital heart defects. *Circulation* 1984;69:655-667.
- Rabinovitch M, Keane JF, Fellows KE, et al. Quantitative analysis of the pulmonary wedge angiogram in congenital heart defects: correlation with hemodynamic data and morphometric findings in lung biopsy tissue. *Circulation* 1981;63:152-164.
- Regar E, Lighthart J, Bruining N, et al. The diagnostic value of intracoronary optical coherence tomography. *Herz* 2011;36:417-429.
- Cutz E, Chan W, Wong V, et al. Pulmonary neuroendocrine cells in normal human lung and in pulmonary hypertension. *Lab Invest* 1986;54:14A.
- Allen KM, Wharton J, Polak JM, et al. A study of nerves containing peptides in the pulmonary vasculature of healthy infants and children and of those with pulmonary hypertension. *Br Heart J* 1989;62:353-360.
- Rabinovitch M, Bothwell T, Hayakawa BN, et al. Pulmonary artery endothelial abnormalities in patients with congenital heart defects and pulmonary hypertension: a correlation of light with scanning electron microscopy and transmission electron microscopy. *Lab Invest* 1986;55:632-653.
- Rabinovitch M, Andrew M, Thom H, et al. Abnormal endothelial factor VIII associated with pulmonary hypertension and congenital heart defects. *Circulation* 1987;76:1043-1052.
- Turner-Gomes SO, Andrew M, Coles J, et al. Abnormalities in von Willebrand factor and antithrombin III after cardiopulmonary bypass operations for congenital heart disease. *Thorac Cardiovasc Surg* 1992;103:87-97.
- Celermajer DS, Cullen S, Deanfield JE. Impairment of endothelium-dependent pulmonary artery relaxation in children with congenital heart disease and abnormal pulmonary hemodynamics. *Circulation* 1993;87:440-446.
- Chang H, Wu GJ, Wang SM, et al. Plasma endothelin levels and surgically correctable pulmonary hypertension. *Ann Thorac Surg* 1993;55:450-458.
- Houde C, Bohn DJ, Freedom RM, et al. Profile of paediatric patients with pulmonary hypertension judged by responsiveness to vasodilators. *Br Heart J* 1993;70:461-468.
- Botney MD, Bahadori L, Gold LI. Vascular remodeling in primary pulmonary hypertension. Potential role for transforming growth factor- β . *Am J Pathol* 1994;144:286-295.
- Lee SD, Shroyer KR, Markham NE, et al. Monoclonal endothelial cell proliferation is present in primary but not secondary pulmonary hypertension. *J Clin Invest* 1998;101:927-934.
- Greenway S, van Suylen RJ, Du Marchie Sarvaas G, et al. S100A4/Mts1 produces murine pulmonary artery changes resembling plexogenic arteriopathy and is increased in human plexogenic arteriopathy. *Am J Pathol* 2004;164:253-262.
- Lawrie A, Spiekerkoetter E, Martinez EC, et al. Interdependent serotonin transporter and receptor pathways regulate s100a4/mts1, a gene associated with pulmonary vascular disease. *Circ Res* 2005;97:227-235.
- Eddahibi S, Chaouat A, Morrell N, et al. Polymorphism of the serotonin transporter gene and pulmonary hypertension in chronic obstructive pulmonary disease. *Circulation* 2003;108:1839-1844.
- Mata-Greenwood E, Meyrick B, Steinhorn RH, et al. Alterations in TGF- β 1 expression in lambs with increased pulmonary blood flow and pulmonary hypertension. *Am J Physiol Lung Cell Mol Physiol* 2003;285:L209-L221.
- Rendas A, Reid L. Pulmonary vasculature after correction of aortopulmonary shunts. *J Thorac Cardiovasc Surg* 1983;85:911-916.
- O'Blenes S, Fischer S, McIntyre B, et al. Hemodynamic unloading leads to regression of pulmonary vascular disease in rats. *J Thorac Cardiovasc Surg* 2000;121:279-289.
- Collins-Nakai RL, Rosenthal A, Castaneda AR, et al. Congenital mitral stenosis: a review of 20 years of experience. *Circulation* 1977;56:1039-1047.
- Haworth SG, Reid L. Quantitative structural study of pulmonary circulation on the newborn with aortic atresia, stenosis or coarctation. *Thorax* 1977;32:121-128.
- Wagenvoort CA, Wagenvoort N. Smooth muscle content and pulmonary arterial media in pulmonary venous hypertension as compared to other forms of pulmonary hypertension. *Chest* 1982;81:581-585.
- LaBourene JI, Coles JG, Johnson DJ, et al. Alterations in elastin and collagen related to the mechanism of progressive pulmonary venous obstruction in a piglet model. A hemodynamic, ultrastructural, and biochemical study. *Circ Res* 1990;66:438-456.
- Rosenberg HC, Williams WG, Trusler GA, et al. Structural composition of central pulmonary arteries. Growth potential following surgical shunts. *J Thorac Cardiovasc Surg* 1987;94:498-503.
- Haworth SG, Macartney FJ. Growth and development of pulmonary circulation in pulmonary atresia with ventricular septal defect and major aortopulmonary collateral arteries. *Br Heart* 1980;44:14-24.
- Rabinovitch M, Herrera-deLeon V, Castaneda AR, et al. Growth and development of the pulmonary vascular bed in patients with tetralogy of Fallot with or without pulmonary atresia. *Circulation* 1981;64:1234-1249.
- Levin DL, Heymann MA, Rudolph AM. Morphological development of the pulmonary vascular bed in experimental pulmonary stenosis. *Circulation* 1979;59:179-182.
- Haworth SG, de Leval M, McCartney FJ. Hypoperfusion and hyperperfusion in the immature lung: Pulmonary arterial development following ligation of the left pulmonary artery in the newborn pig. *J Thorac Cardiovasc Surg* 1981;82:281-292.
- Hultgren HN, Kelly J, Miller H. Pulmonary circulation in acclimatized man at high altitude. *J Appl Physiol* 1965;20:233-238.
- Grover RF. Speculations on the pathogenesis of high-altitude pulmonary edema. *Adv Cardiol* 1980;27:1-5.
- O'Broovich HM, Andrew M, Gray GW, et al. Hypoxia alters blood coagulation during acute decompression in humans. *J Appl Physiol* 1984;56:66-670.
- Hanaoka M, Kubo K, Yamazaki Y, et al. Association of high-altitude pulmonary edema with the major histocompatibility complex. *Circulation* 1998;97:1124-1208.
- Hales CA, Rouse ET, Slate JL. Influence of aspirin and indomethacin on variability of alveolar hypoxic vasoconstriction. *J Appl Physiol* 1978;45:33-39.
- Rabinovitch M, Konstam MA, Gamble WJ, et al. Changes in pulmonary blood flow affect vascular response to chronic hypoxia in rats. *Circ Res* 1983;52:432-441.
- Haven CA, Olson JW, Arcot SS, et al. Polyamine transport and ornithine decarboxylase activity in hypoxic pulmonary artery smooth muscle cells. *Am J Resp Cell Mol Biol* 1992;7:286-292.
- Grove RF, Vogel JH, Voigt GC, et al. Reversal of high altitude pulmonary hypertension. *Am J Cardiol* 1966;18:928-932.
- Arias-Stella J, Saldana M. The terminal portion of the pulmonary arterial tree in people native to high altitude. *Circulation* 1963;28:915-925.
- Tucker A, McMurtry IF, Reeves JT, et al. Lung vascular smooth muscle as a determinant of pulmonary hypertension at high altitude. *Am J Physiol* 1975;228:762-767.
- Rabinovitch M, Gamble W, Nadas AS, et al. Rat pulmonary circulation after chronic hypoxia: hemodynamic and structural features. *Am J Physiol* 1979;236:H818-H827.
- Meyrick B, Reid L. Endothelial and subintimal changes in rat hilar pulmonary artery during recovery from hypoxia. *Lab Invest* 1980;42:603-615.
- Kerr JS, Riley DJ, Frank MM. Reduction of chronic hypoxic pulmonary hypertension in the rat by beta-aminopropionitrile. *J Appl Physiol* 1984;57:1760-1766.
- Stenmark KR, Fasules J, Hyde DM, et al. Severe pulmonary hypertension and arterial adventitial changes in newborn calves at 4,300 m. *J Appl Physiol* 1987;62:821-830.
- Stenmark KR, Davie NJ, Reeves JT, et al. Hypoxia, leukocytes, and the pulmonary circulation. *J Appl Physiol* 2005;98:715-721.
- Davie NJ, Crossno JT Jr, Frid MG, et al. Hypoxia-induced pulmonary artery adventitial remodeling and neovascularization: contribution of progenitor cells. *Am J Physiol Lung Cell Mol Physiol* 2004;286:L668-L678.
- Passman JN, Dong XR, Wu SP, et al. A sonic hedgehog signaling domain in the arterial adventitia supports resident Sca1+ smooth muscle progenitor cells. *Proc Natl Acad Sci U S A* 2008;105:9349-9354.
- Li M, Riddle SR, Frid MG, et al. Stenmark. Emergence of fibroblasts with a proinflammatory epigenetically altered phenotype in severe hypoxic pulmonary hypertension. *J Immunol* 2011;187:2711-2722.
- Yet SF, Perrella MA, Layne MD, et al. Hypoxia induces severe right ventricular dilatation and infarction in heme oxygenase-1 null mice. *J Clin Invest* 1999;103:R23-R29.
- Geraci M, Gao B, Shepherd DC, et al. Pulmonary prostacyclin synthase overexpression in transgenic mice protects against development of hypoxic pulmonary hypertension. *J Clin Invest* 1999;103:1509-1515.
- Le Cras TD, Kim DH, Markham NE, et al. Early abnormalities of pulmonary vascular development in the Fawn-Hooded rat raised at Denver's altitude. *Am J Physiol Lung Cell Mol Physiol* 2000;279:L283-L291.
- Eddahibi S, Hanoun N, Lanfumey L, et al. Attenuated hypoxic pulmonary hypertension in mice lacking the 5-hydroxytryptamine transporter gene. *J Clin Invest* 2000;105:1555-1562.
- MacLean MR, Deuchar GA, Hicks MN, et al. Overexpression of the 5-hydroxytryptamine transporter gene: effect on pulmonary hemodynamics and hypoxia-induced pulmonary hypertension. *Circulation* 2004;109:2150-2155.
- Beppu H, Ichinose F, Kawai N, et al. BMPR-II heterozygous mice have mild pulmonary hypertension and an impaired pulmonary vascular remodeling response to prolonged hypoxia. *Am J Physiol Lung Cell Mol Physiol* 2004;287:L1241-L1247.

61. West J, Fagan K, Steudel W, et al. Pulmonary hypertension in transgenic mice expressing a dominant-negative *bmprii* gene in smooth muscle. *Circ Res* 2004;94:1109–1114.
62. Long L, MacLean MR, Jeffery TK, et al. Serotonin increases susceptibility to pulmonary hypertension in BMPR2-deficient mice. *Circ Res* 2006;98:818–827.
63. Wu X, Chang MS, Mitsialis SA, et al. Hypoxia regulates bone morphogenetic protein signaling through C-terminal-binding protein 1. *Circ Res* 2006;99:240–247.
64. Archer SL, Marsboom G, Kim GH, et al. Epigenetic attenuation of mitochondrial superoxide dismutase 2 in pulmonary arterial hypertension: a basis for excessive cell proliferation and a new therapeutic target. *Circulation* 2010;121:2661–2671.
65. Merklinger SL, Wagner RA, Spiekerkoetter E, et al. Increased fibulin-5 and elastin in S100A4/Mts1 mice with pulmonary hypertension. *Circ Res* 2005;97:596–604.
66. Michelakis ED, Dyck JR, McMurtry MS, et al. Gene transfer and metabolic modulators as new therapies for pulmonary hypertension. Increasing expression and activity of potassium channels in rat and human models. *Adv Exp Med Biol* 2001;502:401–418.
67. Michelakis ED, McMurtry MS, Wu XC, et al. Dichloroacetate, a metabolic modulator, prevents and reverses chronic hypoxic pulmonary hypertension in rats: role of increased expression and activity of voltage-gated potassium channels. *Circulation* 2002;105:244–250.
68. Maruyama K, Ye CL, Woo M, et al. Chronic hypoxic pulmonary hypertension in rats and increased elastolytic activity. *Am J Physiol* 1991;261:H1716–H1726.
69. Fagan KA, Oka M, Bauer NR, et al. Attenuation of acute hypoxic pulmonary vasoconstriction and hypoxic pulmonary hypertension in mice by inhibition of Rho-kinase. *Am J Physiol Lung Cell Mol Physiol* 2004;287:L656–L664.
70. Nagaoka T, Fagan KA, Gebb SA, et al. Inhaled Rho kinase inhibitors are potent and selective vasodilators in rat pulmonary hypertension. *Am J Respir Crit Care Med* 2005;171:494–499.
71. Stenmark KR, McMurtry IF. Vascular remodeling versus vasoconstriction in chronic hypoxic pulmonary hypertension: a time for reappraisal? *Circ Res* 2005;97:5–8.
72. Hyvelin JM, Howell K, Nichol A, et al. Inhibition of Rho-kinase attenuates hypoxia-induced angiogenesis in the pulmonary circulation. *Circ Res* 2005;97:185–191.
73. Rendas A, Brown ER, Avery ME, et al. Prematurity, hypoplasia of the pulmonary vascular bed, and hypertension: fatal outcome in a ten-month-old infant. *Am Rev Respir Dis* 1980;121:873–880.
74. Zamanian RT, Hansmann G, Snook S, et al. Insulin resistance in pulmonary arterial hypertension. *Eur Respir J* 2009;33:318–324.
75. Wang Y, Cocceani F. Isolated pulmonary resistance vessels from fetal lambs. Contractile behavior and responses to indomethacin and endothelin-1. *Circ Res* 1992;71:320–330.
76. Fineman JR, Chang R, Soifer SJ. EDRF inhibition augments pulmonary hypertension in intact newborn lambs. *Am J Physiol* 1992;262:H1365–H1371.
77. Chang JK, Moore P, Fineman JR, et al. K⁺ channel pulmonary vasodilation in fetal lambs: Role of endothelium-derived nitric oxide. *J Appl Physiol* 1992;73:188–194.
78. Belik J, Halayko, Rao K, et al. Pulmonary vascular smooth muscle: biochemical and mechanical changes. *J Appl Physiol* 1991;71:1129–1135.
79. Keller RL, Tacy TA, Hendricks-Munoz K, et al. Congenital diaphragmatic hernia: endothelin-1, pulmonary hypertension, and disease severity. *Am J Respir Crit Care Med* 2010;182:555–561.
80. Atz A, Wessel D. Inhaled nitric oxide and heparin for infantile primary pulmonary hypertension. *Lancet* 1998;351:1701.
81. Balasubramaniam V, Maxey AM, Fouty BW, et al. Nitric oxide augments fetal pulmonary artery endothelial cell angiogenesis in vitro. *Am J Physiol Lung Cell Mol Physiol* 2006;290:L1111–L1116.
82. Balasubramaniam V, Maxey AM, Morgan DB, et al. Inhaled NO restores lung structure in eNOS-deficient mice recovering from neonatal hypoxia. *Am J Physiol Lung Cell Mol Physiol* 2006;291:L119–L127.
83. Kunig AM, Balasubramaniam V, Markham NE, et al. Recombinant human VEGF treatment enhances alveolarization after hyperoxic lung injury in neonatal rats. *Am J Physiol Lung Cell Mol Physiol* 2005;289:L529–L535.
84. Deruelle P, Balasubramaniam V, Kunig AM, et al. BAY 41-2272, a direct activator of soluble guanylate cyclase, reduces right ventricular hypertrophy and prevents pulmonary vascular remodeling during chronic hypoxia in neonatal rats. *Biol Neonate* 2006;90:135–144.
85. Aslam M, Baveja R, Liang OD, et al. Bone marrow stromal cells attenuate lung injury in a murine model of neonatal chronic lung disease. *Am J Respir Crit Care Med* 2009;180:1122–1130.
86. Balasubramaniam V, Ryan SL, Seedorf GJ, et al. Bone marrow-derived angiogenic cells restore lung alveolar and vascular structure after neonatal hyperoxia in infant mice. *Am J Physiol Lung Cell Mol Physiol* 2010;298:L315–L323.
87. van Haaften T, Byrne R, Bonnet S, et al. Airway delivery of mesenchymal stem cells prevents arrested alveolar growth in neonatal lung injury in rats. *Am J Respir Crit Care Med* 2009;180:1131–1142.
88. Villanueva M, Zaher F, Svinarich D, et al. Decreased gene expression of endothelial nitric oxide synthase in newborns with persistent pulmonary hypertension. *Pediatr Res* 1998;44:338–343.
89. Fratz S, Meyrick B, Ovadia B, et al. Chronic endothelin A receptor blockade in lambs with increased pulmonary blood flow and pressure. *Am J Physiol Lung Cell Mol Physiol* 2004;287:L592–L597.
90. Ivy D, Parker T, Kinsella J, et al. Endothelin A receptor blockade decreases pulmonary vascular resistance in premature lambs with hyaline membrane disease. *Pediatr Res* 1998;44:175–180.
91. Farrow KN, Lakshminrusimha S, Czech L, et al. SOD and inhaled nitric oxide normalize phosphodiesterase 5 expression and activity in neonatal lambs with persistent pulmonary hypertension. *Am J Physiol Lung Cell Mol Physiol* 2010;299:L109–L116.
92. Moser KM, Daily PO, Peterson K, et al. Thromboendarterectomy for chronic, major-vessel thromboembolic pulmonary hypertension. Immediate and long-term results in 42 patients. *Ann Intern Med* 1987;107:560–565.
93. Rother RP, Bell L, Hillmen P, et al. The clinical sequelae of intravascular hemolysis and extracellular plasma hemoglobin: a novel mechanism of human disease. *JAMA* 2005;293:1653–1662.
94. Gladwin MT, Sachdev V, Jison ML, et al. Pulmonary hypertension as a risk factor for death in patients with sickle cell disease. *N Engl J Med* 2004;350:886–895.
95. Machado RF, Martyr S, Kato GJ, et al. Sildenafil therapy in patients with sickle cell disease and pulmonary hypertension. *Br J Haematol* 2005;130:445–453.
96. Kato GJ, Gladwin MT. Evolution of novel small-molecule therapeutics targeting sickle cell vasculopathy. *JAMA* 2008;300:2638–2646.
97. Edwards BS, Weir EK, Edwards WD, et al. Coexistent pulmonary and portal hypertension: morphologic and clinical features. *J Am Coll Cardiol* 1987;10:1233–1238.
98. Williams A, Trewby P, Williams R, et al. Structural alterations to the pulmonary circulation in fulminant hepatic failure. *Thorax* 1979;34:447–453.
99. Stanley NN, Williams AJ, Dewar CA, et al. Hypoxia and hydrothoraces in a case of liver cirrhosis: correlation of physiological, radiographic, scintigraphic, and pathological findings. *Thorax* 1977;32:457–471.
100. Peng T, Zamanian R, Krowka MJ, et al. Plasma levels of S100A4 in portopulmonary hypertension. *Biomarkers* 2009;14:156–160.
101. Sandoval J, Amigo MC, Barragan R, et al. Primary antiphospholipid syndrome presenting as chronic thromboembolic pulmonary hypertension. Treatment with thromboendarterectomy. *J Rheumatol* 1996;23:772–775.
102. Baroni SS, Santillo M, Bevilacqua F, et al. Stimulatory autoantibodies to the PDGFR receptor in systemic sclerosis. *N Engl J Med* 2006;354:2667–2676.
103. Angelini DJ, Su Q, Yamaji-Kegan K, et al. Resistin-like molecule-beta in scleroderma-associated pulmonary hypertension. *Am J Respir Cell Mol Biol* 2009;41:553–561.
104. Chung L, Liu J, Parsons L, et al. Characterization of connective tissue disease-associated pulmonary arterial hypertension from REVEAL: identifying systemic sclerosis as a unique phenotype. *Chest* 2010;138:1383–1394.
105. Balabanian K, Foussat A, Dorfmueller P, et al. CX(3)C chemokine fractalkine in pulmonary arterial hypertension. *Am J Respir Crit Care Med* 2002;165:1419–1425.
106. Rhodes J, Schiller MS, Montoya CH, et al. Severe pulmonary hypertension without significant pulmonary parenchymal disease in a pediatric patient with acquired immunodeficiency syndrome. *Clin Pediatr* 1992;31:629–631.
107. Gillespie MN, Hartsfield CL, O'Connor WN, et al. Pulmonary hypertension in a murine model of the acquired immunodeficiency syndrome. *Am J Respir Crit Care Med* 1994;150:194–199.
108. Morse JH, Barst RJ, Itescu S, et al. Primary pulmonary hypertension in HIV infection: an outcome determined by particular HLA class II alleles. *Am J Respir Crit Care Med* 1996;153:1299–1301.
109. Cool CD, Rai PR, Yeager ME, et al. Expression of human herpesvirus 8 in primary pulmonary hypertension. *N Engl J Med* 2003;349:1113–1122.
110. Durrington HJ, Upton PD, Hoer S, et al. Identification of a lysosomal pathway regulating degradation of the bone morphogenetic protein receptor type II. *J Biol Chem* 2010;285:37641–37649.
111. Sehgal PB, Mukhopadhyay S, Patel K, et al. Golgi dysfunction is a common feature in idiopathic human pulmonary hypertension and vascular lesions in SHIV-nef-infected macaques. *Am J Physiol Lung Cell Mol Physiol* 2009;297:L729–L737.
112. Kim YM, Haghighat L, Spiekerkoetter E, et al. Neutrophil elastase is produced by pulmonary artery smooth muscle cells and is linked to neointimal lesions. *Am J Pathol* 2011;179:1560–1572.
113. Crosby A, Jones FM, Kolosionek E, et al. Praziquantel reverses pulmonary hypertension and vascular remodeling in murine schistosomiasis. *Am J Respir Crit Care Med* 2011;184:467–473.
114. Daley E, Emson C, Guignabert C, et al. Pulmonary arterial remodeling induced by a Th2 immune response. *J Exp Med* 2008;205:361–372.
115. Tarasviciene-Stewart L, Nicolls MR, Kraskauskas D, et al. Absence of T cells confers increased pulmonary arterial hypertension and vascular remodeling. *Am J Respir Crit Care Med* 2007;175:1280–1289.
116. Tamosiuniene R, Tian W, Dhillon G, et al. Regulatory T cells limit vascular endothelial injury and prevent pulmonary hypertension. *Circ Res* 2011;109:867–879.
117. Bonnet S, Rochefort G, Sutendra G, et al. The nuclear factor of activated T cells in pulmonary arterial hypertension can be therapeutically targeted. *Proc Natl Acad Sci U S A* 2007;104:11418–11423.
118. Abenheim L, Moride Y, Brenot F, et al. Appetite-suppressant drugs and the risk of primary pulmonary hypertension. International Primary Pulmonary Hypertension Study Group. *N Engl J Med* 1996;335:609–616.
119. Tuder R, Radisavljevic Z, Shroyer K, et al. Monoclonal endothelial cells in appetite suppressant-associated pulmonary hypertension. *Am J Respir Crit Care Med* 1998;158:1999–2001.

120. James TN. The toxic oil syndrome. *Clin Cardiol* 1994;17:463–470.
121. Meyrick B, Gamble W, Reid L. Development of Crotalaria pulmonary hypertension: hemodynamic and structural study. *Am J Physiol* 1980;239:H692–H702.
122. Todd L, Mullen M, Olley P, et al. Pulmonary toxicity of monocrotaline differs at critical periods of lung development. *Pediatr Res* 1985;19:731–737.
123. Todorovich-Hunter L, Ranger P, Johnson D, et al. Altered elastin and collagen synthesis associated with progressive pulmonary hypertension induced by monocrotaline. A Biochemical and ultrastructural study. *Lab Invest* 1988;58:184–195.
124. Todorovich-Hunter L, Dodo H, Ye C, et al. Increased pulmonary artery elastolytic activity in adult rats with monocrotaline-induced progressive hypertensive pulmonary vascular disease compared with infant rats with nonprogressive disease. *Am Rev Respir Dis* 1992;146:213–223.
125. Ye C, Rabinovitch M. Inhibition of elastolysis by SC-37698 reduces development and progression of monocrotaline pulmonary hypertension. *Am J Physiol* 1991;261:H1255–H1267.
126. Zhu L, Wigle D, Hinek A, et al. The endogenous vascular elastase that governs development and progression of monocrotaline-induced pulmonary hypertension in rats is a novel enzyme related to the serine proteinase adipsin. *J Clin Invest* 1994;94:1163–1171.
127. Rosenberg HC, Rabinovitch M. Endothelial injury and vascular reactivity in monocrotaline pulmonary hypertension. *Am J Physiol* 1988;255:H1484–H1491.
128. Cowan KN, Heilbut A, Humpl T, et al. Complete reversal of fatal pulmonary hypertension in rats by a serine elastase inhibitor. *Nat Med* 2000;6:698–702.
129. Cowan KN, Leung WC, Mar C, et al. Caspases from apoptotic myocytes degrade extracellular matrix: a novel remodeling paradigm. *Faseb J* 2005;19:1848–1850.
130. Jones P, Crack J, Rabinovitch M. Regulation of tenascin-C, a vascular smooth muscle cell survival factor that interacts with the $\alpha v\beta 3$ integrin to promote epidermal growth factor receptor phosphorylation and growth. *J Cell Biol* 1997;139:279–293.
131. Merklinger SL, Jones PL, Martinez EC, et al. Epidermal growth factor receptor blockade mediates smooth muscle cell apoptosis and improves survival in rats with pulmonary hypertension. *Circulation* 2005;112:423–431.
132. Schermuly RT, Dony E, Ghofrani HA, et al. Reversal of experimental pulmonary hypertension by PDGF inhibition. *J Clin Invest* 2005;115:2811–2821.
133. Ghofrani HA, Seeger W, Grimminger F. Imatinib for the treatment of pulmonary arterial hypertension. *N Engl J Med* 2005;353:1412–1413.
134. Ghofrani HA, Morrell NW, Hoepfer MM, et al. Imatinib in pulmonary arterial hypertension patients with inadequate response to established therapy. *Am J Respir Crit Care Med* 2010;182:1171–1177.
135. Zhao L, Wang K, Ferrara N, et al. Vascular endothelial growth factor coordinates proper development of lung epithelium and vasculature. *Mech Dev* 2005;122:877–886.
136. Zhao YD, Courtman DW, Deng Y, et al. Rescue of monocrotaline-induced pulmonary arterial hypertension using bone marrow-derived endothelial-like progenitor cells: efficacy of combined cell and eNOS gene therapy in established disease. *Circ Res* 2005;96:442–450.
137. McMurtry MS, Archer SL, Altieri DC, et al. Gene therapy targeting survivin selectively induces pulmonary vascular apoptosis and reverses pulmonary arterial hypertension. *J Clin Invest* 2005;115:1479–1491.
138. Zhao YD, Campbell AI, Robb M, et al. Protective role of angiopoietin-1 in experimental pulmonary hypertension. *Circ Res* 2003;92:984–991.
139. Marcos E, Adnot S, Pham MH, et al. Serotonin transporter inhibitors protect against hypoxic pulmonary hypertension. *Am J Respir Crit Care Med* 2003;168:487–493.
140. Nagaya N, Mori H, Murakami S, et al. Adrenomedullin: angiogenesis and gene therapy. *Am J Physiol Regul Integr Comp Physiol* 2005;288:R1432–R1437.
141. Abe K, Shimokawa H, Morikawa K, et al. Long-term treatment with a Rho-kinase inhibitor improves monocrotaline-induced fatal pulmonary hypertension in rats. *Circ Res* 2004;94:385–393.
142. Reynolds AM, Xia W, Holmes MD, et al. Bone morphogenetic protein type 2 receptor gene therapy attenuates hypoxic pulmonary hypertension. *Am J Physiol Lung Cell Mol Physiol* 2007;292:L1182–L1192.
143. Weir EK, Reeve HL, Johnson G, et al. A role for potassium channels in smooth muscle cells and platelets in the etiology of primary pulmonary hypertension. *Chest* 1998;114:S200–S204.
144. Sutendra G, Bonnet S, Rochefort G, et al. Fatty acid oxidation and malonyl-CoA decarboxylase in the vascular remodeling of pulmonary hypertension. *Sci Transl Med* 2010;2:44a58.
145. Sutendra G, Dromparis P, Bonnet S, et al. Pyruvate dehydrogenase inhibition by the inflammatory cytokine TNF α contributes to the pathogenesis of pulmonary arterial hypertension. *J Mol Med (Berl)* 2011;89:771–783.
146. Sutendra G, Dromparis P, Wright P, et al. The role of Nogo and the mitochondria-endoplasmic reticulum unit in pulmonary hypertension. *Sci Transl Med* 2011;3:88ra55.
147. Dromparis P, Sutendra G, Michelakis ED. The role of mitochondria in pulmonary vascular remodeling. *J Mol Med (Berl)* 2010;88:1003–1010.
148. Hansmann G, Wagner RA, Schellong S, et al. Pulmonary arterial hypertension is linked to insulin resistance and reversed by peroxisome proliferator-activated receptor- γ activation. *Circulation* 2007;115:1275–1284.
149. Guignabert C, Alvira CM, Alastalo TP, et al. Tie2-mediated loss of peroxisome proliferator-activated receptor- γ in mice causes PDGF receptor- β -dependent pulmonary arterial muscularization. *Am J Physiol Lung Cell Mol Physiol* 2009;297:L1082–L1090.
150. Hansmann G, de Jesus Perez VA, Alastalo TP, et al. An antiproliferative BMP-2/PPAR γ /apoE axis in human and murine SMCs and its role in pulmonary hypertension. *J Clin Invest* 2008;118:1846–1857.
151. Alastalo TP, Li M, de Jesus Perez V, et al. Disruption of PPAR γ /beta-catenin-mediated regulation of apelin impairs BMP-induced mouse and human pulmonary arterial EC survival. *J Clin Invest* 2011;121:3735–3746.
152. Nichols W, Koller D, Slovis B, et al. Localization of the gene for familial primary pulmonary hypertension to chromosome 2q31-32. *Nat Genet* 1997;15:277–280.
153. Lane KB, Machado RD, Pauculo MW, et al. Heterozygous germline mutations in BMPR2, encoding a TGF- β receptor, cause familial primary pulmonary hypertension. *Nat Genet* 2000;26:81–84.
154. Deng Z, Morse JH, Slager SL, et al. Familial primary pulmonary hypertension (gene PPH1) is caused by mutations in the bone morphogenetic protein receptor-II gene. *Am J Hum Genet* 2000;67:737–744.
155. Loyd JE, Butler MG, Foroud TM, et al. Genetic anticipation and abnormal gender ratio at birth in familial primary pulmonary hypertension. *Am J Respir Crit Care Med* 1995;152:93–97.
156. Robertson B. Idiopathic pulmonary hypertension in infancy and childhood. Microangiographic and histological observations in five cases. *Acta Pathol Microbiol Scand [A]* 1971;79:217–227.
157. Meyrick B, Clarke SW, Symons C, et al. Primary pulmonary hypertension: a case report including electronmicroscopic study. *Br J Dis Chest* 1974;68:11–20.
158. Geggel RL, Carvalho AC, Hoyer LW, et al. von Willebrand factor abnormalities in primary pulmonary hypertension. *Am Rev Respir Dis* 1987;135:294–299.
159. Tubbs RR, Levin RD, Shirey EK, et al. Fibrinolysis in familial pulmonary hypertension. *Am J Clin Pathol* 1979;71:384–387.
160. Chazova I, Loyd JE, Zhdanov VS, et al. Pulmonary artery adventitial changes and venous involvement in primary pulmonary hypertension. *Am J Pathol* 1995;146:389–397.
161. Liptay MJ, Parks WC, Mecham RP, et al. Neointimal macrophages colocalize with extracellular matrix gene expression in human atherosclerotic pulmonary arteries. *J Clin Invest* 1993;91:588–594.
162. Rhodes CJ, Howard LS, Busbridge M, et al. Iron deficiency and raised hepcidin in idiopathic pulmonary arterial hypertension: clinical prevalence, outcomes, and mechanistic insights. *J Am Coll Cardiol* 2011;58:300–309.
163. Machado R, Pauculo M, Thomson J, et al. BMP2 haploinsufficiency as the inherited molecular mechanism for primary pulmonary hypertension. *Am J Hum Genet* 2001;68:92–102.
164. Thomson JR, Machado RD, Pauculo MW, et al. Sporadic primary pulmonary hypertension is associated with germline mutations of the gene encoding BMPR-II, a receptor member of the TGF- β family. *J Med Genet* 2000;37:741–745.
165. Harrison RE, Flanagan JA, Sankelo M, et al. Molecular and functional analysis identifies ALK-1 as the predominant cause of pulmonary hypertension related to hereditary haemorrhagic telangiectasia. *J Med Genet* 2006;40:865–871.
166. Chaouat A, Coulet F, Favre C, et al. Endoglin germline mutation in a patient with hereditary haemorrhagic telangiectasia and dexfenfluramine associated pulmonary arterial hypertension. *Thorax* 2004;59:446–448.
167. Yeager ME, Halley GR, Golpon HA, et al. Microsatellite instability of endothelial cell growth and apoptosis genes within plexiform lesions in primary pulmonary hypertension. *Circ Res* 2001;88:E2–E11.
168. Hamid R, Cogan JD, Hedges LK, et al. Penetrance of pulmonary arterial hypertension is modulated by the expression of normal BMPR2 allele. *Hum Mutat* 2009;30:649–654.
169. Austin ED, Cogan JD, West JD, et al. Alterations in estrogen metabolism: Implications for higher penetrance of FPAH in females. *Eur Respir J* 2009;34:1093–1099.
170. Umar S, Iorga A, Matori H, et al. Estrogen rescues pre-existing severe pulmonary hypertension in rats. *Am J Respir Crit Care Med* 2011;184:715–723.
171. Nishihara A, Watabe T, Imamura T, et al. Functional heterogeneity of bone morphogenetic protein receptor-II mutants found in patients with primary pulmonary hypertension. *Mol Biol Cell* 2002;13:3055–3063.
172. Rudarakanchana N, Flanagan JA, Chen H, et al. Functional analysis of bone morphogenetic protein type II receptor mutations underlying primary pulmonary hypertension. *Hum Mol Genet* 2002;11:1517–1525.
173. Japp AG, Cruden NL, Barnes G, et al. Acute cardiovascular effects of apelin in humans: potential role in patients with chronic heart failure. *Circulation* 2010;121:1818–1827.
174. Li X, Zhang X, Leathers R, et al. Notch3 signaling promotes the development of pulmonary arterial hypertension. *Nat Med* 2009;15:1289–1297.
175. Rexhaj E, Bloch J, Jayet PY, et al. Fetal programming of pulmonary vascular dysfunction in mice: role of epigenetic mechanisms. *Am J Physiol Heart Circ Physiol* 2011;301:H247–H252.
176. Xu XF, Ma XL, Shen Z, et al. Epigenetic regulation of the endothelial nitric oxide synthase gene in persistent pulmonary hypertension of the newborn rat. *J Hypertens* 2010;28:2227–2235.
177. Li P, Oparil S, Sun JZ, et al. Fibroblast growth factor mediates hypoxia-induced endothelin—a receptor expression in lung artery smooth muscle cells. *J Appl Physiol* 2003;95:643–651;discussion 863.

Clinical Management of Pediatric Pulmonary Arterial Hypertension

D. Dunbar Ivy

Pulmonary hypertension (PH) is an important cause of morbidity and mortality in pediatric patients (1,2). PH is defined as an elevation of pulmonary artery pressure (PAP) due to any cause. Pulmonary arterial hypertension (PAH) is defined as a specific type of PH caused by pulmonary vascular disease of the precapillary arterioles in the absence of other causes. Advances in understanding the pathobiology of PAH have led to novel therapies; however, there remains no cure for some forms of PAH, such as idiopathic pulmonary arterial hypertension (IPAH) (3). Evaluation and treatment for known causes of PH is crucial as the best strategy for treatment includes treatment of any underlying disorders. The selection of appropriate therapies for PH is complex and must be carefully done according to the etiology and determination of pulmonary vasoreactivity at cardiac catheterization.

DIAGNOSIS AND CLASSIFICATION

PH is no longer classified as primary or secondary. Currently, diseases are grouped according to similar pathology, pathophysiology, and treatment. A revision of the World Health Organization (WHO) classification, including most of the forms of PH encountered in children, was proposed at the WHO Dana Point meeting in 2008 (Table 67.1) (4); however, this classification was not designed specifically for children. Group 1 is defined as PAH. This form of PH is due to pulmonary vascular disease of the precapillary arterioles in the absence of other causes (such as left heart disease—Group 2). PAH is defined as a mean PAP ≥ 25 mm Hg at rest, with a normal pulmonary capillary wedge pressure (≤ 15 mm Hg) and increased pulmonary vascular resistance (PVR) index (≥ 3 Wood units \times m²) (4). A recent article reviews the clinical presentation of children with PH and outlines the difficulties of classifying pediatric PH according to this classification (5). In particular, the adult classification does not include abnormalities of alveolar growth and development nor does it account for many of the syndromes seen in pediatric practice, such as Down syndrome. Patients with PAH and congenital heart disease (CHD) are a heterogeneous population, with a range of vascular disease: some patients have a right-to-left central shunt (Eisenmenger syndrome), others have a residual shunt and severe PAH but are not cyanotic, some patients with a small shunt may have severe PAH and are more similar to IPAH, and finally it is well known that PAH may persist and progress despite corrective cardiac surgery (Table 67.2) (4). PAH may be idiopathic (IPAH) or heritable (HPAH) with no underlying cause, or associated with a specific disease (associated PAH). Mutations of the bone morphogenetic protein receptor, type 2 (BMPR2) gene are the most common genetic abnormalities known to cause HPAH. Most studies in children have focused on PAH associated with CHD (Table 67.3) and IPAH (6–8). IPAH is a diagnosis of exclusion and thus

is defined as PAH unexplained by other causes. An extensive evaluation to rule out secondary causes must be performed before a patient can be diagnosed with IPAH. Persistent pulmonary hypertension of the newborn (PPHN) is the most common cause of PH in the neonatal period, and is most often reversible. PH associated with left heart disease is defined as Group 2 PH. In these disorders, the main cause of PH is an elevation of left heart pressure due to impaired relaxation (diastolic dysfunction) or an anatomic lesion that leads to high left atrial pressure (such as mitral stenosis). Group 3 PH, or PH associated with lung disease or hypoxemia, is separated from Group 1 as treatment of the lung disorder may result in normalization of PAP. PH associated with chronic lung diseases, such as bronchopulmonary dysplasia (BPD) or congenital diaphragmatic hernia (CDH) is increasingly recognized as an important cause of PH in the infant and child. Group 4 PH, or PH associated with chronic thromboembolic disease, is a rare cause of PH in children, but is still important to recognize and treat as therapy may be curative. Group 5 consists of miscellaneous disorders that do not fit well into Groups 1 to 4.

Due to the difficulties of applying the Dana Point Classification to children, a working group of the Pulmonary Vascular Research Institute developed a unique pediatric classification (Table 67.4) (9). This classification recognizes the concepts of perinatal maladaptation, maldevelopment, and pulmonary hypoplasia as important contributors to pediatric PH disease. This classification is not meant to be a guide for therapy. Many children presenting with PH have complex heterogeneous disease consisting of prematurity, a chromosomal or genetic anomaly, a congenital cardiac defect, chronic aspiration, and sleep-disordered breathing. In this classification, PH in children is defined as in adults for a biventricular circulation, but PH in the setting of single ventricle physiology is defined as a PVR index >3.0 Wood units \times m² or a transpulmonary gradient (TPG) >6 mm Hg (9).

CLINICAL PRESENTATION

Symptoms of PH in children are frequently misleading and the diagnosis may be unrecognized for some time. A high degree of suspicion should be the rule and PH should be suspected in any child with undue shortness of breath, tiredness, or a syncopal episode. In patients with asthma who do not respond appropriately to medical therapy, PH should be considered in the differential diagnosis. Other clinical symptoms may include seizures, hemoptysis, chest pain, dizziness, syncope, arrhythmias, or in advanced disease, symptoms of right heart failure, for example, facial edema. For IPAH patients or those with CHD who have undergone complete surgical repair with elevated PVR, syncope or hypoxic seizures can occur. Thus, children are sometimes misdiagnosed with a seizure disorder prior to making the diagnosis of PH. In contrast, syncope is a rare presenting symptom in patients with Eisenmenger syndrome.

TABLE 67.1

Updated WHO Clinical Classification of Pulmonary Hypertension (Dana Point, 2008)

1 Pulmonary arterial hypertension

- 1.1 Idiopathic
- 1.2 Heritable
 - 1.2.1 *BMPR2*
 - 1.2.2 *ALK1*, endoglin (with or without hereditary hemorrhagic telangiectasia)
 - 1.2.3 Unknown
- 1.3 Drug- and toxin-induced
- 1.4 Associated with (APAH)
 - 1.4.1 Connective tissue diseases
 - 1.4.2 HIV infection
 - 1.4.3 Portal hypertension
 - 1.4.4 Congenital heart disease
 - 1.4.5 Schistosomiasis
 - 1.4.6 Chronic hemolytic anemia
- 1.5 Persistent PH of the newborn

1' PVOD and/or PCH

2 PH due to left heart disease

- 2.1 Systolic dysfunction
- 2.2 Diastolic dysfunction
- 2.3 Valvular disease

3 PH due to lung diseases and/or hypoxemia

- 3.1 Chronic obstructive pulmonary disease
- 3.2 Interstitial lung disease
- 3.3 Other pulmonary diseases with mixed restrictive and obstructive pattern
- 3.4 Sleep-disordered breathing
- 3.5 Alveolar hypoventilation disorders
- 3.6 Chronic exposure to high altitudes
- 3.7 Developmental abnormalities

4 Chronic thromboembolic PH

5 PH with unclear and/or multifactorial mechanisms

- 5.1 Hematologic disorders: myeloproliferative disorders, splenectomy
- 5.2 Systemic disorders: sarcoidosis, pulmonary Langerhans cell histiocytosis, lymphangioleiomyomatosis, neurofibromatosis, vasculitis
- 5.3 Metabolic disorders: glycogen storage disease, Gaucher disease, thyroid disorders
- 5.4 Others: tumoral obstruction, fibrosing mediastinitis, chronic renal failure on dialysis

ALK1, activin receptor-like kinase 1 gene; APAH, associated pulmonary arterial hypertension; *BMPR2*, bone morphogenetic protein receptor, type 2; HIV, human immunodeficiency virus; WHO, World Health Organization.

Reprinted from Simonneau G, Robbins IM, Beghetti M, et al. Updated clinical classification of pulmonary hypertension. *J Am Coll Cardiol* 2009;54:S43–S54, with permission from Elsevier.

TABLE 67.2

Clinical Classification of Congenital Systemic-to-Pulmonary Shunts associated with Pulmonary arterial Hypertension

■ Eisenmenger syndrome

Includes all systemic-to-pulmonary shunts due to large defects, leading to a severe increase of PVR and resulting in a reversed (pulmonary-to-systemic) or bidirectional shunt. Cyanosis, erythrocytosis, and multiple organs involvement are present.

■ PAH associated with systemic-to-pulmonary shunts

In these patients with moderate-to-large septal defects the increase of PVR is mild to moderate, systemic-to-pulmonary shunt is still largely prevalent and no cyanosis is present at rest.

■ PAH with small septal defects

In these cases with small defects (usually VSDs <1 cm and ASD <2 cm of effective diameter assessed by echo) the clinical picture is very similar to idiopathic PAH.

■ PAH after corrective cardiac surgery

In these cases, CHD has been corrected but PAH either is still present immediately after surgery or has recurred several months or years after surgery in the absence of significant immediate postoperative residual lesions.

Reprinted from Simonneau G, Robbins IM, Beghetti M, et al. Updated clinical classification of pulmonary hypertension. *J Am Coll Cardiol* 2009;54:S43–S54, with permission from Elsevier.

SIGNS AND SYMPTOMS

The physical signs of PAH include a single and loud P2 without respiratory variation, right ventricular lift, and hepatomegaly with peripheral edema in the case of heart failure. In cases of severe disease, the P2 may be palpable. A diastolic murmur of pulmonary insufficiency, a holosystolic murmur of tricuspid regurgitation, or gallop rhythm may be audible. In infants, symptoms are less specific and may involve poor appetite, failure to thrive, lethargy, diaphoresis, tachypnea, tachycardia, and irritability (10–12).

EVALUATION

Because of the many diseases associated with PH, a methodical and comprehensive evaluation is important. The most successful strategy in treatment of PH is the correction of an underlying abnormality, rather than addition of vasodilator therapy. A diagnostic algorithm is shown in Figure 67.1 (13). Special situations may predispose to the development of PAH. As an example, children living at high altitude and presenting with high-altitude pulmonary edema (HAPE) should be screened for PH (14). In addition, children with biliary atresia, cavernous transformation of the portal vein, primary sclerosing cholangitis, or cryptogenic cirrhosis, may have portopulmonary hypertension (PPHTN) with an associated high mortality (15,16).

CHEST RADIOGRAPHY

The enlargement of the central pulmonary artery and/or right ventricle (RV) on chest radiography suggests the presence of

TABLE 67.3 Cardiac Lesions associated with Pulmonary Hypertension

Left-to-right shunts	<ul style="list-style-type: none"> ■ Ventricular septal defect ■ Atrioventricular septal (canal) defect ■ Patent ductus arteriosus ■ Atrial septal defect ■ Aortopulmonary window
Increased pulmonary venous pressure	<ul style="list-style-type: none"> ■ Cardiomyopathy ■ Coarctation of the aorta (left ventricular diastolic dysfunction) ■ Hypoplastic left heart syndrome ■ Shone complex ■ Mitral stenosis ■ Supravalvar mitral ring ■ Cor triatriatum ■ Pulmonary vein stenosis ■ Total anomalous pulmonary venous return ■ Left ventricular outflow tract obstruction
Single ventricle	<ul style="list-style-type: none"> ■ Norwood/Damus Stansel Kaye ■ Cavopulmonary anastomosis (Glenn) ■ Fontan procedure
Cyanotic heart disease	<ul style="list-style-type: none"> ■ Transposition of the great arteries ■ Truncus arteriosus ■ Tetralogy of Fallot (pulmonary atresia/VSD) ■ Univentricular heart (high flow with/without restrictive atrial septum)
Anomalies of the pulmonary artery or pulmonary vein	<ul style="list-style-type: none"> ■ Origin of a pulmonary artery from the aorta ■ Isolated pulmonary artery of ductal origin-unilateral “absence” of a pulmonary artery ■ Scimitar syndrome
Palliative shunting operations	<ul style="list-style-type: none"> ■ Waterston anastomosis ■ Potts anastomosis ■ Blalock-Taussig anastomosis

VSD, ventricular septal defect.

From Ivy DD, Saji B. A new era in medical management of severe pediatric pulmonary arterial hypertension. *Pediatr Cardiol Cardiac Surgery* 2010;26:206–218, with permission.

PAH. Prominence of the main pulmonary arteries is apparent in most patients with IPAH. The chest radiograph may show variable peripheral lung fields, depending on the amount of pulmonary blood flow. As pulmonary blood flow decreases as a result of increasing PVR, the lung fields become progressively oligemic. Chest radiography findings may be useful to uncover secondary causes of PH: pulmonary venous congestion may suggest pulmonary veno-occlusive disease (PVOD) or pulmonary capillary hemangiomatosis (PCH), hyperinflation or kyphosis are signs of restrictive lung disease, and asymmetry of the enlarged central pulmonary arteries may

TABLE 67.4 Pulmonary Vascular Research Institute Classification of Pediatric Pulmonary Hypertensive Vascular Disease (Panama 2011)

1. Prenatal or developmental pulmonary vascular disease
2. Perinatal pulmonary vascular maladaptation
3. Pediatric cardiovascular disease
4. Bronchopulmonary dysplasia
5. Pediatric lung diseases
6. Multifactorial pulmonary vascular disease in congenital malformation syndromes
7. Isolated pediatric PAH
8. Pediatric thromboembolic disease
9. Pediatric hypobaric hypoxic exposure
10. Pulmonary vascular disease associated with other system disorders

From Del Cerro MJ, Abman SH, Diaz G, et al. A consensus approach to the classification of pediatric pulmonary hypertensive vascular disease: report from the PVRI pediatric taskforce, Panama 2011. *Pulm Circ* 2011;1:286–298, with permission.

warrant investigation of chronic thromboembolic disease or PPHTN (12,17,18). Asymmetric lung volumes may suggest either pulmonary arterial or pulmonary venous abnormalities. A unilateral small lung may be seen in unilateral “absence” of a pulmonary artery, scimitar syndrome, or unilateral congenital absence of pulmonary veins.

ELECTROCARDIOGRAPHY

Electrocardiography (ECG) is often the first test to suggest PH by showing RV hypertrophy and right atrial enlargement. Evidence of RV hypertrophy on ECG is present in most but not all children with PH. ECG findings include a qR complex in lead V1 or V3R regardless of voltage. An upright T wave in V1 is indicative of RV hypertrophy from 7 days to 7 years. However, some studies have suggested that the specificity (69%) and positive predictive value (67%) of EKG is low in children with an echocardiographic diagnosis of PH (19). However, the sensitivity is likely higher, especially in combination with a complete physical examination.

ECHOCARDIOGRAPHY

Echocardiography is the most useful noninvasive screening tool to evaluate patients with a clinical suspicion of PAH, and can diagnose almost all congenital heart disease. (20,21). The echocardiogram documents RV size and function, left ventricular systolic and diastolic function, morphology and function of valves, and the presence of pericardial effusion or a patent foramen ovale. Doppler ultrasound can be used noninvasively to estimate the pulmonary artery systolic pressure (PASP). PASP can be determined by measuring the peak systolic pressure gradient from the RV to the right atrium and calculated using the Bernoulli equation ($4v^2$, where v is the maximum velocity of the TR jet measured by continuous wave Doppler and added to the estimated right atrial pressure)

(Fig. 67.2). One must be aware that using the tricuspid regurgitant jet velocity as an estimate of PASP can over or underestimate the PAP and thus other features of the echocardiogram are essential to support the diagnosis of PH (22). A qualitative assessment of RV function is also important. This is often challenging due to the geometry of the RV, which is more complex to analyze than the left ventricle. Several measures are available to attempt to quantify the degree of RV dysfunction including the Tei index, (myocardial performance index), RV ejection fraction, RV fractional area change, and the tricuspid annular plane systolic excursion (TAPSE) (23–29). Normal values for TAPSE in children have recently been published and should serve as a reference for children with PH (26). Pulmonic valve insufficiency is frequently seen, and characteristics of the pulmonic regurgitant flow velocity or changes in the systolic flow velocity profile across the pulmonic valve also can be used to estimate noninvasively the pulmonary artery diastolic pressure and the mean PAP (30). The presence of a pericardial effusion is rare in children, but when present, suggests a poor prognosis (27,31). As PH progresses and RV function worsens, the systolic portion of the cardiac cycle lengthens leading to an increase in the systolic:diastolic (S:D) ratio. The S:D ratio is higher in PH patients than in controls (1.38 ± 0.61 vs. 0.72 ± 0.16 , $p < 0.001$), and is associated with worse echocardiographic RV fractional area change, worse catheterization hemodynamics, shorter 6-minute walk distance (6MWD), and worse clinical outcomes independent of PVR or pressures (32).

Recent interest has grown in the area of measurement of total RV afterload by measurement of input vascular impedance. Impedance incorporates the sum of total compliance and resistance of the vascular bed (33–36). Currently, measurement

of impedance requires invasive pressure measurements in addition to measurement of Doppler flow. A recent manuscript on adults with PH showed that a measure of capacitance (stroke volume / pulse pressure) was a better predictor of survival than measurement of PVR (37,38). In children, pulmonary vascular input impedance has recently been shown to be feasible and predict clinical outcomes better than PVR in children with PAH (39).

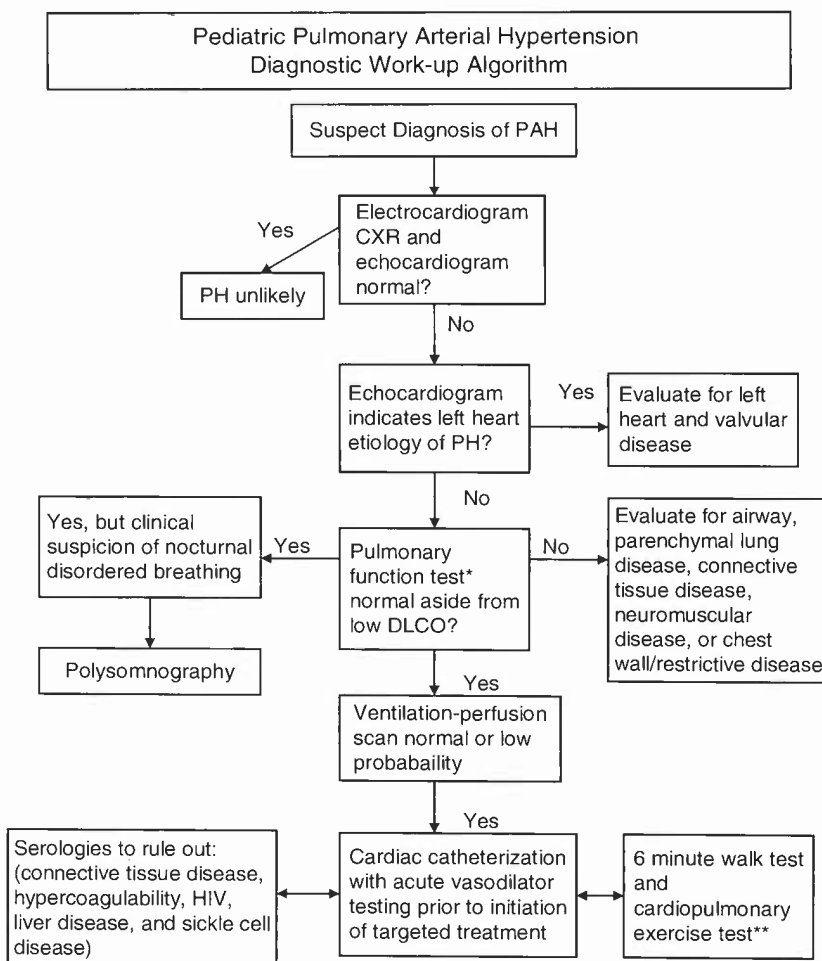
CARDIAC MAGNETIC RESONANCE IMAGING

Cardiac magnetic resonance imaging (MRI) provides exact measurements of heart function and blood flow and is used with increasing frequency to evaluate patients with PAH (40–46). Cardiac MRI provides valuable information without radiation on RV volumes, mass, left ventricular septal bowing, cardiac index, and the presence of delayed contrast enhancement. Most young children require anesthesia for this procedure, which is an important consideration.

EXERCISE CAPACITY

Cardiopulmonary exercise testing (CPET) using cycle ergometry or 6-minute walk testing has been shown to correlate with disease severity and prognosis, and is helpful in assessing responses to clinical treatments. Recently published data showed that children can safely undergo CPET and the peak

Figure 67.1. Pediatric PAH diagnostic workup algorithm. *If unable to obtain a reliable test in a young child and there is a high index of suspicion for underlying lung disease, the patient may require further lung imaging, such as high resolution CT scan. **Children older than 7 years of age can usually perform reliably to assess exercise tolerance and capacity in conjunction with diagnostic workup. (Reprinted from Rosenzweig EB, Feinstein JA, Humpl T, et al. Pulmonary arterial hypertension in children: Diagnostic work up and challenges. *Prog Pediat Cardiol* 2009;27:7–11, with permission from Elsevier.)



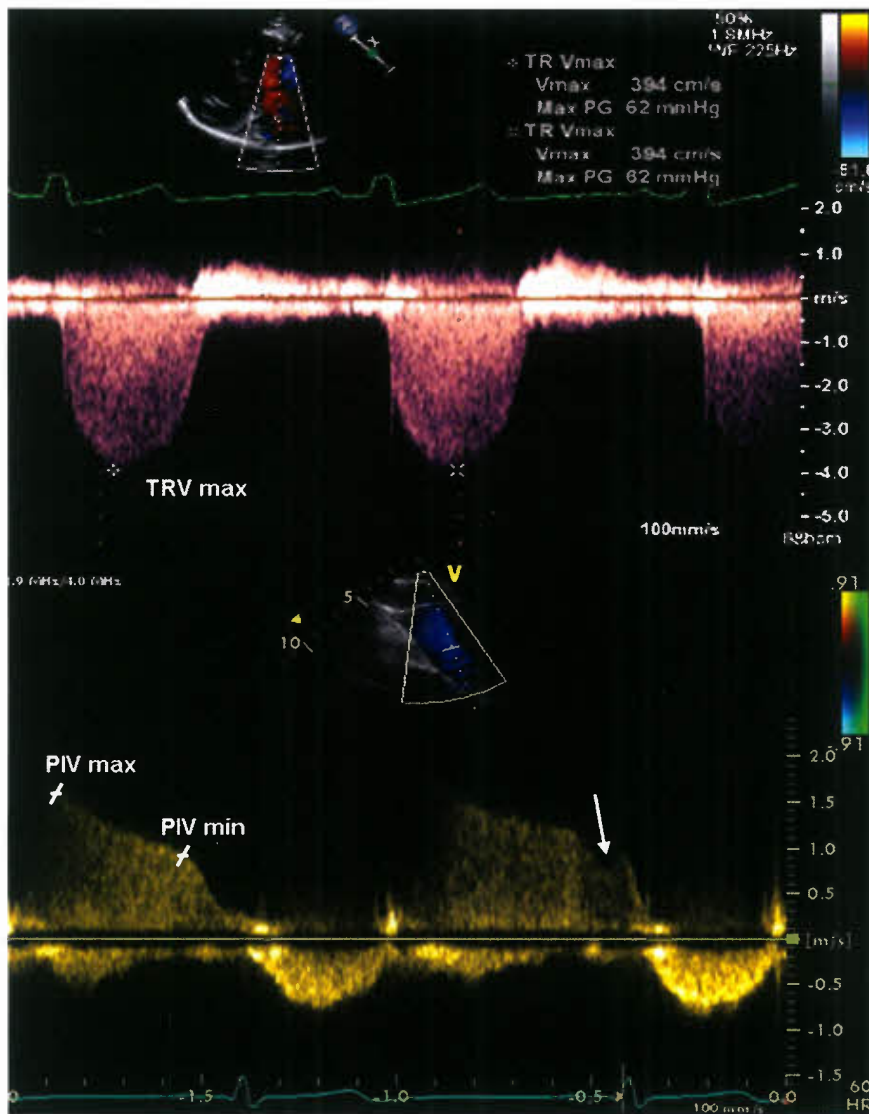


Figure 67.2. Echocardiographic evaluation of PH. Spectral Doppler images of TR, demonstrating an optimal Doppler envelope to obtain the maximal TR velocity (top image), and of pulmonary insufficiency (bottom image). The left marker represents the peak early diastolic velocity and the right marker represents the end diastolic velocity of the pulmonary insufficiency Doppler curve. The arrow represents the end-diastolic “shoulder” of the pulmonary insufficiency jet. V(TR) max, tricuspid regurgitation peak velocity; V(PR) max, pulmonary insufficiency peak velocity; v(PR) min, pulmonary insufficiency end-diastolic velocity. (From Tissot C, Ivy DD. Echocardiographic evaluation of pulmonary hypertension. In: Beghetti M, ed. *Pediatric Pulmonary Hypertension*. Munich, Germany: Elsevier Urban & Fischer; 2011, with permission.)

oxygen consumption is strongly correlated to disease severity (47–49). A recent study of maximal CPET using cycle ergometry in children with PH concluded that the study could be performed safely in pediatric patients with PH, with the exception of patients with severe limitation who were excluded from exercise testing. ST-segment depression was graded as mild (19%) or moderate (1.5%). There were no significant adverse events, such as syncope, chest pain, or dizziness, and the study was stopped for fatigue in 53% of patients, leg fatigue in 23%, dyspnea in 21%, and miscellaneous reasons in 3% (49).

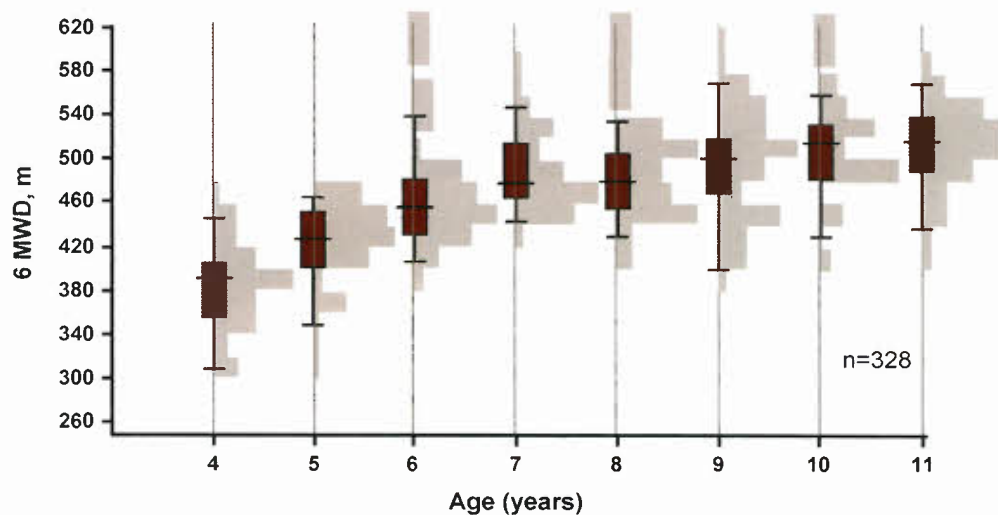
Six-minute walk test (6MWT) is a submaximal test shown to have a strong independent association with mortality among adults with IPAH (50–55); however, children often have less right heart failure for a given elevation of PAP leading to a further distance walked. A recent study compared CPET with 6MWT. Peak oxygen consumption and oxygen consumption at anaerobic threshold showed correlation with 6MWT distance ($r = 0.49$; $p = 0.001$ and $r = 0.40$, $p = 0.01$, respectively), while an inverse correlation was found between measures of ventilatory efficiency (VE/VCO_2) at anaerobic threshold and 6MWT distance ($r = -0.43$; $p = 0.005$). The 6MWT reflected maximal exercise capacity in children with a 6MWT distance below

300 m, but correlation was poor above 300 m (54). Normal values for 6MWD for children have recently been published (51–53,55) (Fig. 67.3).

CARDIAC CATHETERIZATION

PAH must be confirmed by catheterization, and acute pulmonary vasoreactivity testing should be performed to determine appropriate therapy. It is uncertain if the same definition of vasoreactivity should be applied for adults and children (see Therapy section). An anesthesiologist experienced in the management of PH should be present during the cardiac catheterization, as sedation may pose a significant risk to the patient with PAH. A skilled specialist with experience doing cardiac catheterizations on children with PAH should perform the procedure. Patients with suprasystemic PH pose particular risk (56,57). During the catheterization, baseline measures including right atrial pressure, PAP, systemic arterial pressure, mixed venous and systemic arterial saturation, cardiac index, pulmonary capillary wedge pressure, PVR, systemic vascular resistance (SVR), and PVR/SVR ratio should be obtained in addition to evaluation of shunts when there is a suspicion of

Figure 67.3. The distance walked in 6 minutes by different age groups in normal children. Data are shown as histograms and box-and-whiskers plots illustrating the median, 25th and 75th percentile as well as 5th and 95th percentile. (From Lammers AE, Hislop AA, Flynn Y, et al. The 6-minute walk test: normal values for children of 4–11 years of age. *Arch Dis Child* 2008;93:464–468, with permission.)



6MWD, six-minute walk distance

a systemic-to-pulmonary communication (58). Measurements must be obtained when the patient is closest to his/her usual hemodynamic and metabolic state and with a normal pH. Particular care is necessary at the time of catheterization to exclude additional intracardiac as well as extracardiac defects and to measure left ventricular filling pressure accurately to rule out postcapillary PH. Acute vasodilator testing is essential at the baseline diagnostic catheterization to assist in determining the optimal therapeutic regimen, and is described in a subsequent section.

LABORATORY ASSESSMENT

A comprehensive serologic evaluation looking for other systemic conditions that might lead to PAH and warrant additional treatment is performed (Table 67.5). Approximately, 5% to 20% of children with idiopathic disease may have an elevation of antinuclear antibodies as well as evidence of hypothyroidism or hyperthyroidism suggesting an autoimmune association (59–62). Furthermore, children should be screened for evidence of a hypercoagulable state as some may have an underlying coagulopathy such as antiphospholipid antibody syndrome or a lupus anticoagulant. The evaluation should include a liver ultrasound in cases suspected of having portopulmonary hypertension. A chest CT scan is important in the evaluation of the child with suspected IPAH to be certain that there is no underlying interstitial lung disease. CT scan of the chest may also be very helpful in evaluation for pulmonary capillary hemangiomatosis or veno-occlusive disease. HIV and sickle cell testing should be routinely performed in those patients at risk. If there is a family history of PH or early/sudden death, one could offer genetic testing for a BMPR2 mutation as well.

VENTILATION–PERFUSION SCINTIGRAPHY

Ventilation–perfusion lung scanning is mandatory in patients in whom IPAH is suspected to exclude chronic thromboembolic disease as a cause of the elevated PAP. Although thromboembolic disease is rare in children, it is one of the few diseases that can be cured with appropriate therapy including pulmonary

thromboendarterectomy. A normal or low-probability lung scan essentially rules out thromboembolic disease as the cause of the PH. Patients with IPAH will frequently have a patchy appearance to the perfusion scan.

PULMONARY FUNCTION TESTING/NOCTURNAL OXIMETRY

Evaluation for obstructive or restrictive lung disease should be performed as part of the evaluation of children with PH. Abnormalities of pulmonary function may be present in PAH patients particularly in the more advanced stages of the disease. A mild restrictive lung defect is seen in 20% to 50% of patients with IPAH. The presence of moderate or severe restrictive or obstructive physiologic defects should suggest another diagnosis. Mild reduction in the diffusion capacity is seen in most patients with IPAH. Severe hypoxemia is not usually present unless there is either intracardiac shunting via a patent foramen ovale or an open congenital heart defect in patients with Eisenmenger syndrome or severely depressed cardiac output with resultant mixed venous hypoxemia in both conditions. Nocturnal oximetry should be performed as a screening test for obstructive sleep apnea (OSA) or sleep-disordered breathing if there is a suspicion of OSA, for example, in a child with enlarged tonsils or adenoids and history of snoring. Sleep-disordered breathing may cause mild PH, which may resolve with nighttime continuous positive airway pressure.

EVALUATION OF REFLUX AND ASPIRATION

In the young child, reflux and aspiration may worsen PH. Many children with genetic syndromes, and in particular Down syndrome, routinely have aspiration. Silent aspiration is of particular concern, as these children do not always cough during aspiration events. Modified barium swallow study and measurement of reflux with a pH probe are important studies in the evaluation of these patients. In general, treatment of reflux and aspiration should precede treatment with pulmonary vasodilators.

TABLE 67.5 Lab Analyses for Pulmonary Arterial Hypertension Workup

CBC, urinalysis, Chem-20 including liver function profile, BNP/NT-proBNP

Coagulation studies:

- Factor VIII
- Lupus anticoagulant
- Protein C
- Protein S
- Factor II, V, VII
- Factor V Leiden
- Beta-2 Glycoprotein Antibodies
- Cardiolipin IgG, IgM Ab
- Antithrombin III
- Prothrombin mutation
- Platelet function assay

HIV test

Hepatitis profile

Thyroid function tests

CTD workup:

- Lupus anticoagulant
- ESR
- ANA
- Anti-DNA
- Anticardiolipin antibodies
- CH50 complement and components
- Special ANAs
- Anticentromere
- Rheumatoid factor

Consider *BMPR2* genetic testing

Ag, antigen; ANA, antinuclear antibodies; BNP, brain natriuretic peptide; CBC, complete blood counts; CH50, total serum hemolytic component; ESR, erythrocyte sedimentation rate; HIV, human immunodeficiency virus; HLA, human leukocyte antigen; *BMPR2*, bone-morphogenetic protein receptor 2.

Reprinted from Rosenzweig EB, Feinstein J, Humpl T, et al. Pulmonary arterial hypertension in children: diagnostic work-up and challenges. *Progress Pediatr Cardiol* 2009;27:7–11, with permission from Elsevier.

BIOMARKERS

Interest in biomarkers has grown in the last several years. In adults, b-type natriuretic peptide (BNP) is a useful tool to assess mortality risk, progression of the disease, and response to therapy (63). Recent studies in children have begun to identify usefulness of BNP or N-terminal pro BNP (NT-proBNP) (64–66). BNP correlates positively with functional status in children with PAH, and values above 130 pg/mL are associated with increased risk of death or need for transplantation (65). Furthermore, change in BNP measurements over time correlates with the change in the hemodynamic and echocardiographic parameters of children with PAH, with a BNP value >180 pg/mL predicting a decreased survival rate in a more recent study (Fig. 67.4). The change in BNP level in a specific patient over time was shown to be more helpful in determining risk or

hemodynamic response to therapy than the average BNP value in a pediatric PAH population (64). NT-proBNP, uric acid, or norepinephrine levels have also been shown to correlate with outcome in children with PAH (66). When using a cutoff value of NT-proBNP of 1,664 pg/mL, sensitivity and specificity for predicting mortality was 100% and 94%, respectively (66).

LUNG BIOPSY AND WEDGE ANGIOGRAPHY

Lung biopsy is not used as part of the routine workup of PH given the relatively high risk of the procedure in children with PH. Performance of a lung biopsy has played a major role in understanding PH associated with CHD as is described in Chapter 66, and may help guide surgical management in select cases (67–71). In a series of children with CHD and PH assessed 1 year after repair, Rabinovitch et al. (71) compared pulmonary hemodynamics and morphometric changes. Hemodynamics normalized in all children repaired before 9 months of age, regardless of severity of the preoperative Heath-Edwards, morphometric, or hemodynamic changes. In contrast, in children with severe preoperative changes at lung biopsy (grade C morphometric, Heath-Edwards III), PAP and PVR remained significantly elevated if they were repaired after 2 years of age (71). The Heath-Edwards changes are heterogeneous, making absolute determination of being inoperable difficult (72).

Lung biopsy is indicated if there is a suspicion of another diagnosis that would be treated differently such as PVOD or PCH. Likewise, an increasing number of patients are being diagnosed with interstitial lung disease associated with PH. Examples include surfactant protein deficiency, such as ATP-binding cassette transporter A3 (ABCA3) deficiency, or capillaritis (73–76). These patients often do not respond to treatments currently available for PAH and thus need a definitive diagnosis for lung transplant listing. The evaluation of PH by lung biopsy is further described in Chapter 66.

Wedge angiography may provide clues to the severity of pulmonary vascular disease (70,77,78). Abnormalities of capillary blush are seen with mild elevation of PVR and may progress to the appearance of a “tree in winter” as disease progresses.

IMPORTANT CAUSES OF PH IN CHILDREN

Idiopathic Pulmonary Arterial Hypertension

PAH was first described by Dresdale in 1951 as a sporadic disease known as PPH. Subsequently, in 1954, Dresdale reported the familial transmission of PPH. PPH, currently named IPAH, is characterized by progressive and sustained elevations of PAP without a defined etiology. IPAH is a rare disease, which occurs most frequently in young adult females (79). While generally developing in the adult population, pediatric IPAH is well reported, and carried a dismal prognosis in a cohort from the National Institutes of Health, with a median survival of only 10 months in individuals <16 years old (80). Evaluation for IPAH in the pediatric age group is similar to that outlined for adults and is a diagnosis of exclusion, but increased scrutiny for the possibility of CHD is appropriate, and acute pulmonary vasoreactivity may be more common in children (81–84). Certain comorbidities, such as thyroid disease, an elevated antinuclear antibody, and lower airways obstruction are seen in children with IPAH (60,62,85).

Heritable—Familial Pulmonary Artery Hypertension

Between 6% and 12% of cases of IPAH may be familial in origin with an autosomal dominant pattern of inheritance (86).

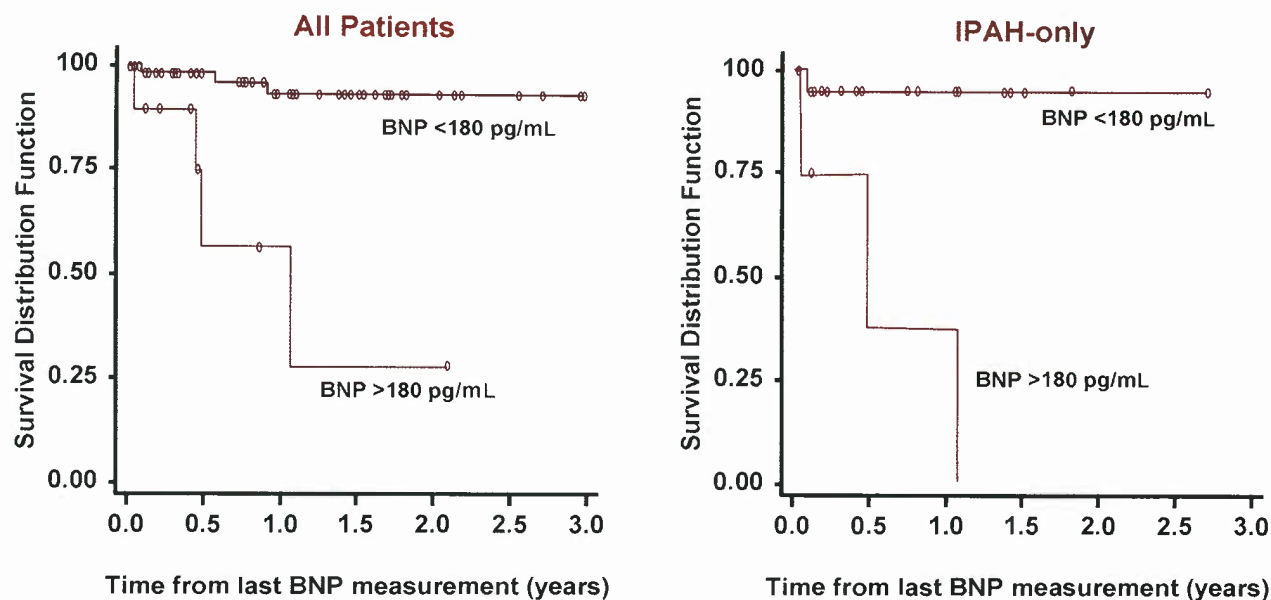


Figure 67.4. Kaplan-Meier survival curves for children with IPAH and PAH associated with CHD. Survival curves are shown for all patients (left) and for the subgroup of IPAH patients (right) categorized with either BNP >180 pg/mL or <180 pg/mL. (From Bernus A, Wagner BD, Accurso F, et al. Brain natriuretic peptide levels in managing pediatric patients with pulmonary arterial hypertension. *Chest* 2009;135:745–751. Reproduced with permission from the American College of Chest Physicians.)

BMPR2 mutations present on chromosome 2 q31-32 have been identified in children and adults with IPAH and familial PAH (87–91). This genetic mutation in the TGF- β receptor family has been found in patients with familial PAH (50% to 70%) (87,89) and sporadic PAH (15% to 26%) (90). Currently, about 300 mutations in the *BMPR2* gene have been discovered (92). The pattern of inheritance in children with *BMPR2* mutations is the same as adults with an autosomal dominant pattern with reduced penetrance. Reduced penetrance implies that generations of mutation-carrying persons may not express the disease. Only 20% of individuals with a known *BMPR2* mutation will develop clinical PAH. HPAH may also be characterized as “genetic anticipation,” in which HPAH presented progressively earlier with subsequent generations. In families, it may be the child who presents first with severe disease, and then further evaluation of first-degree relatives reveals milder disease in the parents or grandparents (93).

The bone morphogenetic proteins (BMPs) are members of the TGF- β superfamily of receptors. BMPs play an important role in the development of the lungs, bone, and cartilage. BMP binds to the *BMPR1* receptor leading to heterodimerization with the *BMPR2* receptor. Activation of the receptor leads to phosphorylation of a series of cytoplasmic mediators, such as the SMAD proteins. In the BMP cascade, SMAD proteins 1/5/8 complex with SMAD 4 for translocation to the nucleus leading to target gene expression and inhibit cell growth and induction of apoptosis (Fig. 67.5) (87,94–103). A similar cascade is present for TGF- β signaling. It has been proposed that a second hit leads to a further decrease in BMP signaling and thus an imbalance/increase in proproliferative TGF- β signaling. Most forms of PAH are associated with abnormal *BMPR2* signaling, even if a defined mutation is not found.

BMPR2 mutations have been evaluated in several pediatric series with inconsistent results. Grunig et al. (88) found no *BMPR2* mutations or deletions in 13 children with IPAH. However, in a study by Harrison et al. (104), 22% of children with IPAH or PH associated with CHD had activin-like kinase type-1 (ALK-1) or *BMPR2* mutations. *BMPR2* mutations were found in only 6% of a mixed cohort of adults and children with

PAH and CHD (105). More recently, a study by Rosenzweig et al. (106) evaluated whether children and adults with PAH had a positive response to acute vasodilator testing. In this study, the authors found that *BMPR2* mutation-positive children appeared less likely to respond to acute vasodilator testing than mutation-negative children. Furthermore, these children had lower mixed venous oxygen saturation and cardiac index than those without a *BMPR2* mutation. These findings are similar to those by Elliott et al. (107) who reported that IPAH and FPAH adult patients with *BMPR2* mutations are less likely to respond to acute vasodilator testing than *BMPR2* mutation-negative patients. Recently, Sztrymf et al. (108) reported that patients with a *BMPR2* mutation presented at an earlier age, developed more severe disease, and died earlier. Mutations in other members of the TGF- β family, such as ALK-1 or endoglin have also been described as leading to PH in children (92,94,98,109,110).

The variable clinical expression with reduced penetrance makes genetic counseling difficult. As there is reduced penetrance, only 20% of carriers will develop the disease. A negative *BMPR2* testing result may be reassuring for a family member with a known *BMPR2* mutation. If negative, a family member's risk falls from 1 in 10 to that of the general population, which is about 1 in 1,000,000. It is mandatory that genetic testing be performed in conjunction with experienced genetic counselors before and after the test results (87).

Other genetic loci may also play important roles. Studies have suggested an important role of the serotonin transporter gene in some adults with PAH (111,112), and a study in children found that homozygosity for the long variant of the serotonin transporter gene was highly associated with IPAH in children (113).

Connective Tissue Disease

PAH complicates the course of some patients with connective tissue disease (CTD). The recent WHO classification recognizes PAH associated with CTD in Group 1 PAH, and CTD as one of the most common forms of PAH in adults. It is estimated that almost 30% of adult cases of PAH are associated with CTD, many with systemic sclerosis (114). Among these

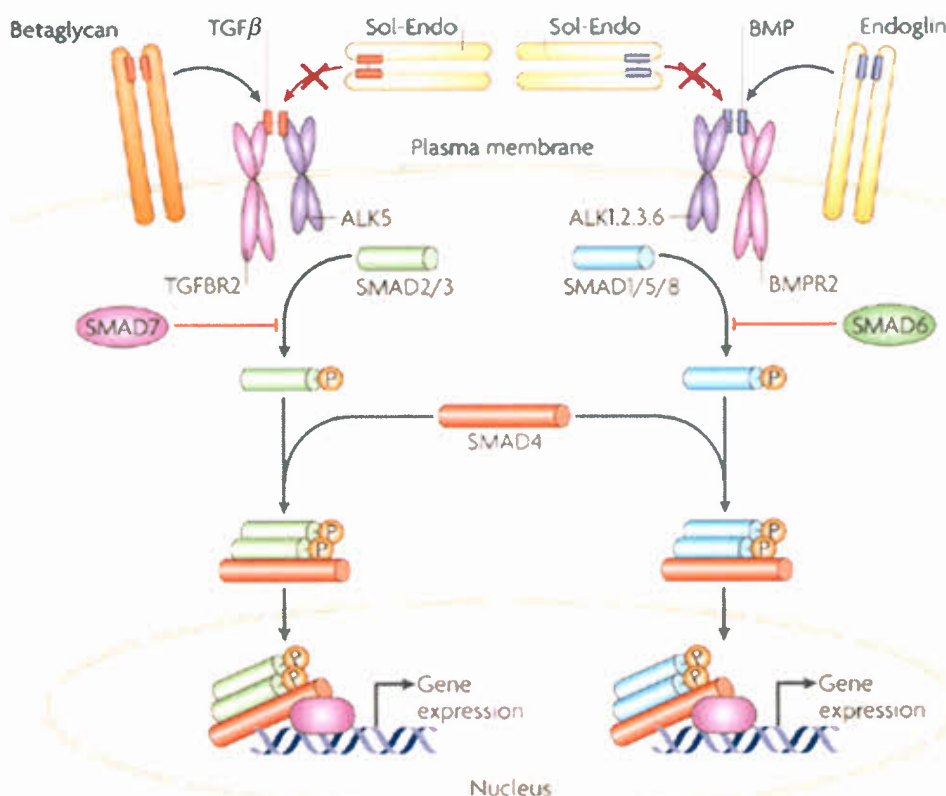


Figure 67.5. Abnormalities of signaling by the transforming growth factor- β . TGF- β superfamily members play a major role in heritable PH. TGF- β can be divided into two main intracellular pathways according to the SMAD mediators: either SMAD2/3 or SMAD1/5/8. Members of the TGF- β family bind to specific Ser/Thr kinase type II and type I receptors; in most cells, TGF signals via TGFBR2 and ALK5 (also known as TGF receptor-1; TGFBR1), and BMPs signal via the BMP type II receptor (BMPR2) and ALK1, ALK2, ALK3, and ALK6. Activated type I receptors induce the phosphorylation of specific receptor-regulated (R-) SMADs, which are the intracellular effectors of TGF- β family members. In most cell types, TGF- β induces SMAD2/3 phosphorylation and BMPs induce SMAD1/5/8 phosphorylation. Activated R-SMADs form heteromeric complexes with SMAD4 that accumulate in the nucleus, where they regulate the expression of target genes. The imbalance of decreased BMPR2 signaling and increased TGF- β signaling leads to a proliferative state in PH. (From ten Dijke P, Arthur HM. Extracellular control of TGFbeta signaling in vascular development and disease. *Nat Rev Mol Cell Biol* 2007;8:857–869, with permission.)

patients, PAH is often multifactorial, including pulmonary fibrosis-related CTD and thrombosis associated with vasculitis and/or thrombophilia. PAH associated with CTD is also a major risk factor for death in these patients. Recently, various pulmonary vasodilator therapies have improved the prognosis for patients with PAH associated with CTD. Previous studies have shown that epoprostenol increases exercise capacity compared with conventional therapy in patients with PAH associated with systemic sclerosis (115) and improves hemodynamics and exercise capacity in patients with systemic lupus erythematosus (116). Pulmonary vasodilators have been used in these patients with some success. Management of the underlying CTD is crucial for successful management of the child with PAH and CTD (117).

Congenital Heart Disease

A variety of congenital cardiac lesions can cause PH (10) (Table 67.3). The age and type of lesion strongly contribute to the risk of developing irreversible pulmonary vascular disease. Early surgery has markedly decreased the development of late PAH and the propensity for postoperative pulmonary hypertensive crises. In general, patients with a ventricular septal defect (VSD) or patent ductus arteriosus (PDA) do not develop

irreversible pulmonary vascular changes before 2 years of age. Most centers perform early surgical repair in the first months of age to decrease the likelihood of pulmonary vascular disease. Without appropriate surgery an estimated 50% of patients with a large nonrestrictive VSD will develop Eisenmenger syndrome (118). Patients with an atrial septal defect (ASD) are less likely to develop severe PAH, and this usually occurs in the third to fifth decade. Infants with an ASD or VSD with concomitant chronic lung disease are at an increased risk for the early development of severe pulmonary vascular disease. In one study of infants with BPD who underwent cardiac surgery for the repair of CHD, 25% of those who died had PAH (119). In the Euro Heart survey of adults with CHD, 882 patients with a secundum ASD were identified. Hemodynamics was worse in nonoperated patients than the patients whose defects had been closed. In moderate or large defects, when not operated, clinical parameters tended to worsen with time. In adults with small ASDs, the patients did well and an operation was not necessarily indicated (120). Eisenmenger syndrome in adults with an ASD was rare and occurred in 15 of 896 patients in a different analysis of the data (121). The risk of PAH with a sinus venosus ASD is likely higher than that of a secundum ASD (122,123). Of the 1,877 patients in the survey, there were 710 with a VSD; the defect was closed

in 275, open without Eisenmenger syndrome in 352, and open with Eisenmenger syndrome in 83. Patients with cyanotic congenital cardiac lesions such as transposition of the great arteries, truncus arteriosus, and univentricular heart with high flow are more likely to develop rapid irreversible pulmonary vascular disease. Palliative shunting operations for certain cardiac anomalies designed to increase pulmonary blood flow also may lead to the subsequent development of PH.

Operability

In the child with CHD and pulmonary vascular disease, determination of baseline hemodynamics and reactivity to vasodilators is crucial for successful short-term and long-term outcome (69,71,124–133). A recent manuscript has extensively reviewed this topic (125). One of the most important factors in long-term survival and freedom from pulmonary vascular disease is the age at which surgery is performed. In 1984, Rabinovitch et al. (71) stated “early corrective surgery is the best safeguard against the persistence or progression of structural changes in the pulmonary vascular bed.” In their series, all children repaired before 9 months of age, regardless of severity of the preoperative Heath-Edwards, morphometric, or hemodynamic changes had normal PAP one year after surgery. Rabinovitch et al. (71) also noted that certain lesions, such as d-transposition of the great arteries, complete atrioventricular septal defect, and truncus arteriosus are more prone to the early development of severe pulmonary vascular changes than others (69,130). In general, surgery of the child with CHD is recommended before 2 years of age (134–136), but most centers will perform complete repair of the majority of lesions within the first months of life.

Cardiac catheterization aids in determination of PVR, pulmonary-to-SVR ratio (Rp/Rs), and pulmonary-to-systemic blood flow. However, several issues arise in the determination of hemodynamics in these patients. Viswanathan and Kumar (127) have described that the assessment of preoperative PVR and pulmonary vascular reactivity in the patient with CHD is difficult and is prone to error. Hemodynamic evaluation of these patients is a “snapshot” that may not represent the usual state of the patient. These studies are frequently performed under general anesthesia, which frequently leads to a lower systemic blood pressure than the precatheterization condition (58). Furthermore, the determination of oxygen consumption in children with CHD is problematic (137,138). Oxygen consumption is frequently estimated since direct measurement of oxygen consumption in intubated patients is not readily available due to lack of an FDA-approved device. The LaFarge equation introduces significant overestimation of oxygen consumption in ventilated patients with CHD of all ages, particularly in children younger than 3 years (137,138). Estimation rather than measurement of PaO_2 in the pulmonary veins leads to overestimation of pulmonary blood flow, and subsequently underestimation of the PVR. In patients with single-ventricle anatomy and physiology, additional problems arise. In patients with a bidirectional cavopulmonary anastomosis, the PAP is measured with less than a full cardiac output, thus the pressure after Fontan completion may not be similar. Furthermore, aortopulmonary collaterals are frequent in the single-ventricle patient leading to underestimation of pulmonary blood flow by catheterization. Patients with CHD may also have various degrees of pulmonary vein disease leading to inability to accurately measure PVR. This problem, in addition to the low cardiac output seen in pretransplant evaluation makes assessment of PVR in the pretransplant evaluation particularly difficult (139).

Although many studies have evaluated hemodynamics to determine operability, the precise values that best correlate with early and late outcome remain unclear. Many of these studies are not directly comparable due to differences in sedation and

the use of measured or assumed oxygen consumption. The first Natural History Study of VSD found that no child repaired under 2 years of age, regardless of Rp/Rs had an elevated Rp/Rs 4 to 8 years after surgery (136). Haneda et al. (135) reported similar findings. In 1982, Lock evaluated the pulmonary vascular response to oxygen in 25 children with large VSDs and elevated PVR. A positive preoperative response to oxygen, defined as a fall in the Rp/Rs of 30%, did not correlate with either operative survival or late Rp/Rs (140). In adult patients with an isolated ASD, Steele retrospectively evaluated patients with a total PVR $>7 \text{ U} \times \text{m}^2$. Total pulmonary resistance (TPR) (defined as mean PAP/pulmonary flow index) had the highest correlation with survival of the hemodynamic parameters measured. Of 18 surgically treated patients at 10-year follow-up, only 1 of 14 with TPR of $<15 \text{ U} \times \text{m}^2$, compared with three of four with TPR of $>15 \text{ U} \times \text{m}^2$ had died (122). Bush and colleagues in 1988 measured PVR and evaluated lung biopsies in 14 children with PH and CHD. Patients with a lowest PVR of $>6 \text{ U} \times \text{m}^2$ had a poor prognosis whatever their lung morphology, and some patients with Heath-Edwards grade I or II still had a high PVR. Other vasodilators, such as isoproterenol, were used in a study of 87 children and young adults with VSD. When resting PVR was $\leq 7.9 \text{ U} \times \text{m}^2$, it always decreased with isoproterenol and no postoperative problems were experienced in 21 patients (141). In 1991, Moller et al. (142) evaluated 290 patients who underwent closure of a VSD from 1954 to 1960. Death occurred in 59 patients, with higher mortality rates in those operated on after the age of 5 years, those with PVR $>7 \text{ U} \times \text{m}^2$, and those with complete heart block (Fig. 67.6) (142). More recently, Berner studied 13 children aged 6 months to 16 years with a baseline PVR of $>6 \text{ U} \times \text{m}^2$ and Rp/Rs of >0.3 at catheterization with inhaled nitric oxide (NO). Six of seven with a fall in PVR and Rp/Rs $>10\%$ and a value of Rp/Rs <0.3 survived (143). Inhaled NO, 80 ppm with oxygen, was studied by Atz et al. (144), and they showed that a response of 20% or more reduction in PVR was seen in 22/25 patients with NO+oxygen compared with 16/25 in oxygen alone. Of the 71 patients studied, 10 underwent surgery. In these patients, baseline PVR in room air was $12.9 \pm 1.9 \text{ U} \times \text{m}^2$ that decreased to $4.1 \pm 1.9 \text{ U} \times \text{m}^2$ in NO (144). In a collaborative study of 10 institutions, 124 patients with CHD were studied under conditions of room air, oxygen, and NO (145). Seventy four of these underwent surgery and 12 died or

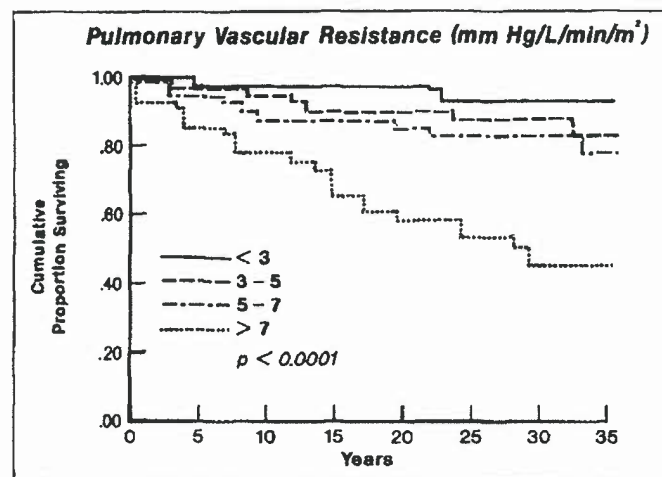


Figure 67.6. VSD after surgery. Life table analysis of 168 patients divided into categories according to level of PVR before surgery. (From Moller JH, Patton C, Varco RL, et al. Late results (30 to 35 years) after operative closure of isolated ventricular septal defect from 1954 to 1960. *Am J Cardiol* 1991;68:1491–1497, with permission.)

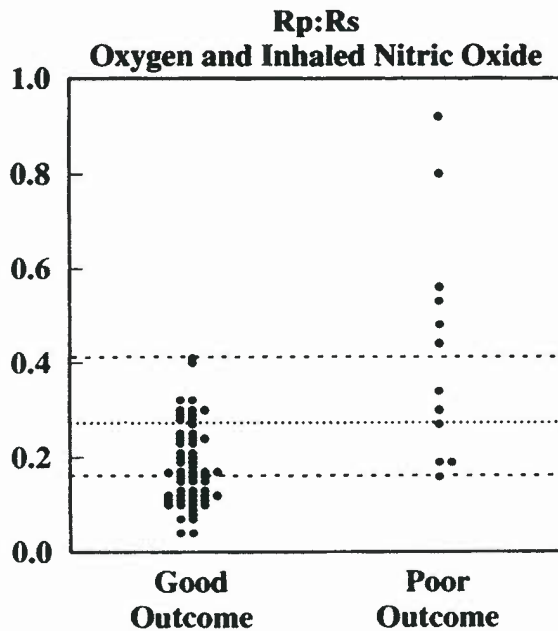


Figure 67.7. Rp:Rs during preoperative testing according to outcome following surgery. In a combination of oxygen and nitric oxide, the lowest value of Rp:Rs that was associated with a poor outcome secondary to PH was 0.16. The highest value of Rp:Rs that was associated with a good outcome was 0.41. An optimal balance in sensitivity and specificity correlated with an Rp:Rs < 0.27 in a combination of oxygen and nitric oxide as criteria for operability. Rp, pulmonary vascular resistance index; Rs, systemic vascular resistance index. (From Balzer DT, Kort HW, Day RW, et al. Inhaled nitric oxide as a preoperative test (INOP test I): the INOP Test Study Group. *Circulation* 2002;106:176–181, with permission.)

developed right heart failure. When Rp/Rs of <0.33 was used as the criterion, sensitivity (64% vs. 97%) and accuracy (68% vs. 90%) were increased by using inhaled NO (iNO) in combination with oxygen compared with oxygen alone (Fig. 67.7). When iNO plus oxygen was used, the lowest value of Rp/Rs that was associated with a poor outcome was 0.16. The highest value of Rp/Rs that was associated with a good outcome was 0.41 (Fig. 66.7) (145). Most recently, Kannan et al. (146) in 2003 described long-term follow-up of 38 patients with an unrestricted VSD and elevated PVR $>6.9 \text{ U} \times \text{m}^2$ operated on at a median age 7.5 years (range, 6 months to 27 years), from 1985 to 1996 in India. Preoperative PVR, ratio of pulmonary blood flow to systemic blood flow, and Rp/Rs were 7.63 ± 1.8 Wood units, 1.9 ± 0.48 , and 0.41 ± 0.12 , respectively. Thirty patients (79%) had a good outcome and were asymptomatic at a mean follow-up of 8.7 years, with significant reduction in PAP. Eight patients (21%) had a poor outcome, but there was no significant difference regarding hemodynamic parameters at baseline between those who had a good outcome and those who did not (146). Importantly, Kumar et al. recommend a holistic approach that combines clinical, noninvasive, and invasive data to make a decision regarding operability in this challenging group of patients with shunt lesions and elevated PVR (127,147). This approach and an algorithm have recently been described by Lopes (147). Patients who are under 2 years of age with evidence of pulmonary overcirculation and exclusive left-to-right shunting by echo do not necessarily need to undergo cardiac catheterization prior to surgery. Those patients who are older and have desaturation or bidirectional shunting may benefit from vasodilator testing to stratify risk (Fig. 67.8). Several studies suggest that a baseline PVR or lowest PVR <7 to $8 \text{ Wood units} \times \text{m}^2$

predicts a good outcome, (125,141,142,148) although there are reports of good surgical outcomes with higher PVR. The role of longer-term “treatment and repair” or a period of pulmonary artery banding is less well defined but is intriguing (149).

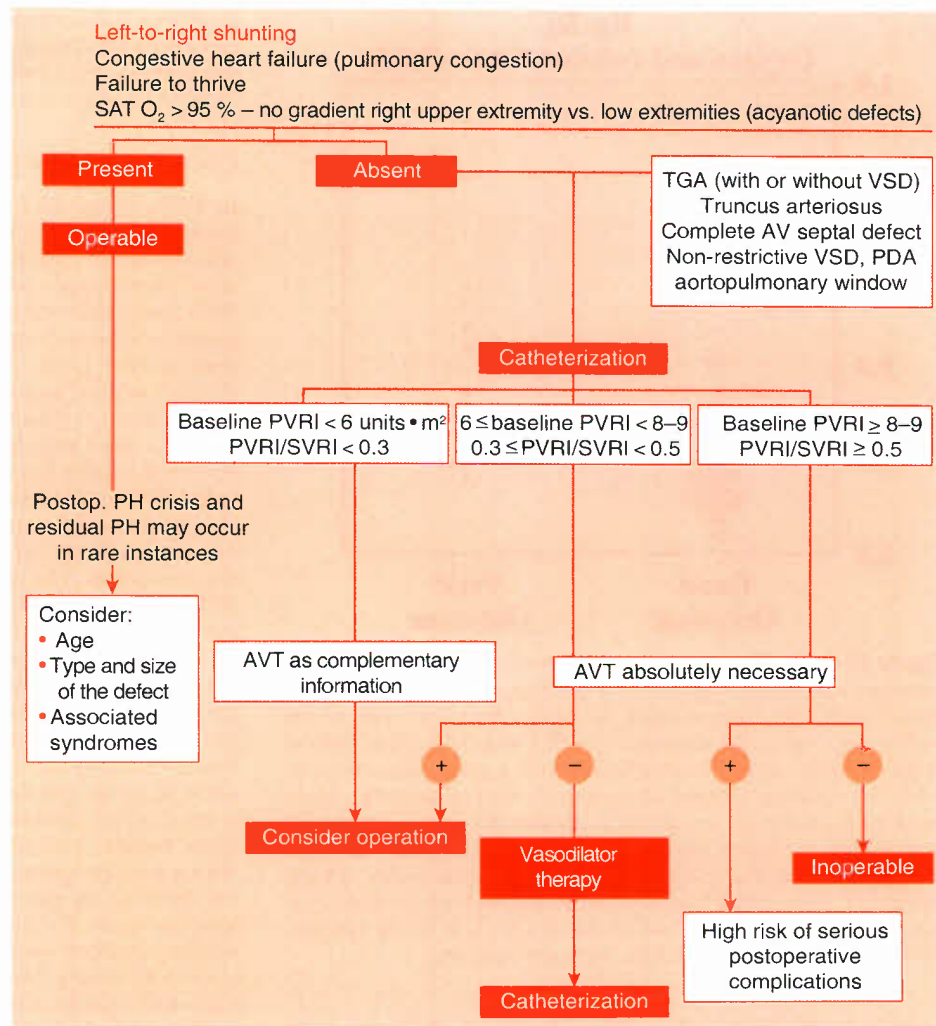
Eisenmenger Syndrome

In 1897, Viktor Eisenmenger described a 32-year-old cyanotic patient who died of massive hemoptysis and whose postmortem showed a VSD. Subsequently, Paul Wood, in 1958 used the term Eisenmenger complex to define the condition of a large VSD associated with increased PAP and PVR causing bidirectional or reversed (right-to-left) shunting and systemic oxygen desaturation (150). Currently, the term “Eisenmenger syndrome” is used more broadly to describe PH with a reversed central shunt (150–156). In general, the term Eisenmenger syndrome is used mainly for shunts distal to the tricuspid valve, but some studies have included patients with a large ASD. Elevated PVR and bidirectional or right-to-left shunting through a systemic-to-pulmonary connection, such as a VSD, PDA, univentricular heart, or aortopulmonary window, characterizes the syndrome. The most common lesions being VSD (33%), ASD (30%), and PDA (14%) in one series (157). The shunt is initially left-to-right, but as the underlying condition continues to increase PVR, there is a reversal of the shunt to a right-to-left configuration, leading to cyanosis and erythrocytosis. Some patients who are diagnosed with Eisenmenger syndrome do not have a prior history of congestive heart failure suggesting that PVR never fell to normal levels in the perinatal period. In general, the prognosis of patients with Eisenmenger syndrome is much better than for patients with IPAH, but syncope, right-heart failure, and severe hypoxemia are similarly associated with a poor prognosis. The RV plays a critical role in determining survival. In general, patients with Eisenmenger syndrome have favorable RV function until the later stages of the disease, whereas patients with late repair of CHD who develop PAH tend to do poorly. Morbidity in Eisenmenger syndrome is common and includes hemoptysis, pulmonary thromboembolism, stroke, and cerebral abscess. An increased risk of death has been shown to be related to noncardiac surgery with general anesthesia. Maternal mortality is estimated at 50% during the course of the pregnancy. Patients with complex heart disease and Eisenmenger syndrome tend to have earlier clinical deterioration and death compared to those with Eisenmenger syndrome related to an ASD, VSD, or PDA (158–160).

Red blood cell depletion may be utilized in Eisenmenger syndrome to provide temporary relief of major hyperviscosity symptoms or to improve perioperative hemostasis, but should not routinely be performed as this leads to increased stiffness of the red blood cell (161). Treatment of iron deficiency and routine monitoring of hemoglobin level are key elements of treatment and may improve exercise tolerance. Noncardiac operations on Eisenmenger patients are associated with a high mortality rate and should be managed by a multidisciplinary team experienced in the care of patients with this condition. Nocturnal oxygen therapy in Eisenmenger syndrome does not appear to alter long-term outcome (162).

Therapy for Eisenmenger syndrome has evolved over the last decade (163–165). The Bosentan Randomized Trial of Endothelin (ET) Antagonist Therapy-5 (BREATHE-5) was a 16-week, multicenter, randomized, double-blind, placebo-controlled study evaluating the effect of bosentan, a dual ET receptor antagonist (ERA), on systemic pulse oximetry (primary safety end point) and PVR (primary efficacy end point) in patients with WHO functional class III Eisenmenger syndrome. The placebo-corrected effect on systemic pulse oximetry was 1.0% (95% confidence interval, -0.7 to 2.8), demonstrating that bosentan did not worsen oxygen saturation. Compared with placebo, bosentan reduced PVR

Figure 67.8. An algorithm of preoperative evaluation and management of pediatric patients with congenital cardiac shunts. Proposed criteria for a pulmonary vasodilator response to be considered as positive: $\geq 20\%$ decrease in PVRI and Rp/Rs ratio from baseline, with respective final (lowest) values of <6 Wood units \times m^2 and <0.3 . Criteria for patient assignment to palliative surgery are not suggested. The routine is not applicable to complex conditions such as the absence of a subpulmonary ventricle (candidates to cavopulmonary anastomoses). AVT, acute pulmonary vasoreactivity test; PDA, patent ductus arteriosus; PVRI, pulmonary vascular resistance index; SVRI, systemic vascular resistance index; TGA, transposition of great arteries; VSD, ventricular septal defect. (From Lopes A. Pre-operative pulmonary hypertension in congenital heart disease and aspects of Eisenmenger's syndrome in children. In: Beghetti M, ed. *Pediatric Pulmonary Hypertension*. Munich, Germany: Elsevier Urban & Fischer, 2011, with permission.)



and mean PAP and increased exercise capacity by 53.1 m (164). Patients with Eisenmenger syndrome due to an ASD or VSD were equally likely to improve (166). In a separate study, in children on bosentan a progressive decline in exercise capacity was observed from 1-year follow-up, whereas in the adults, improvement lasted longer (167). A recent retrospective study evaluated the use of advanced therapies (ATs), such as type 5 phosphodiesterase (PDE-5) inhibitors, prostanooids or ERAs, in 229 patients (aged 34.5 ± 12.6 years). The majority had complex anatomy, and 53.7% were in New York Heart Association class \geq III at baseline assessment. Sixty-eight patients either were on AT or had AT initiated during follow-up. During a median follow-up of 4.0 years, 52 patients died, only two of them while on AT. Patients on AT were at a significantly lower risk of death by propensity score regression adjustment (C statistic = 0.80; hazard ratio, 0.16; 95% confidence interval, 0.04 to 0.71; $p = 0.015$) (Fig. 67.9) (165). ATs should be considered when other causes of functional limitation, such as iron deficiency, have been first addressed (168).

HEPATOPULMONARY SYNDROME AND PORTOPULMONARY HYPERTENSION

Hepatopulmonary syndrome (HPS) and PPHTN are distinct pulmonary vascular complications of hepatic and extrahepatic portal hypertension (169–172). HPS is defined as dilated

pulmonary capillaries and precapillary arteriovenous malformations resulting in intrapulmonary vascular shunting, ventilation–perfusion mismatching, and chronic hypoxemia in the setting of liver disease or portal hypertension. PPHTN is defined as PAH with an elevated mean PAP and increased PVR caused by a pulmonary arteriopathy in the setting of portal hypertension and in the absence of underlying cardiopulmonary disease (171,173). PPHTN and HPS are estimated to occur in 2% to 10% and 4% to 29%, respectively, of adults with cirrhosis (174). Both PPHTN and HPS are associated with increased morbidity and mortality and are significant risk factors for requiring orthotopic liver transplantation (OLT) (175,176). However, resolution of both disorders is possible after successful OLT (175,176). PPHTN and HPS have been reported in children with portal hypertension from both cirrhosis and congenital or acquired portal vein abnormalities; however, the incidence of these complications in children is unknown (15,16). An autopsy study of children with portal hypertension found 5.2% of cases with severe PH. All were females in late childhood or adolescence with idiopathic portal hypertension (177).

The pathogenesis of PPHTN and HPS remains unknown. Proposed theories suggest that these disorders result from a combination of hyperdynamic circulation, increased cardiac output, sheer injury to vascular walls, and an imbalance of circulating vasoactive peptides (178,179). Abnormal hepatic synthesis of vasoactive peptides, such as ET-1, or impaired hepatic metabolism of intestinally derived endotoxins, cytokines, and neurohormones may result in these substances reaching the pulmonary vascular bed via portosystemic shunting, directly altering

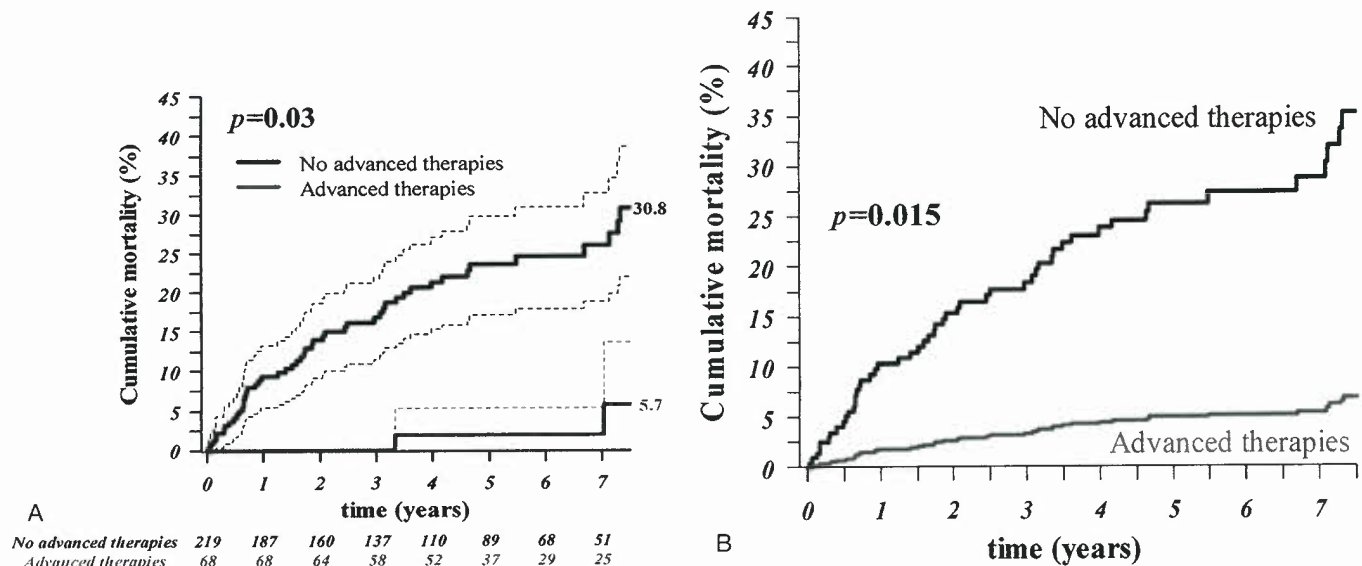


Figure 67.9. A: Unadjusted survival rate curves (with 95% CIs) by treatment with ATs in adults with Eisenmenger syndrome AT ($n = 287$). P value refers to Cox model. B: Adjusted survival rate curves, based on the propensity score-adjusted Cox model, of patients within the third propensity score quartile, with and without advanced therapy. (From Dimopoulos K, Inuzuka R, Goletto S, et al. Improved survival among patients with Eisenmenger syndrome receiving advanced therapy for pulmonary arterial hypertension. *Circulation* 2010;121:20–25, with permission.)

vessel tone or leading to pulmonary vascular inflammation and remodeling. Recent studies have highlighted the potential role of vascular endothelial growth factor and hypoxia inducible factor in the development of vascular dilation and arteriovenous malformations (180–184). The resulting pathology is strikingly different in these two disorders with vasodilation of pulmonary arterioles and capillaries causing arteriovenous shunting in HPS and intimal fibrosis with endothelial and smooth muscle cell proliferation leading to increased PVR in PPHTN.

Patients with elevated RV systolic pressure estimated by echocardiography should undergo confirmatory right heart catheterization (175,176). In children, a dilated pulmonary artery on chest radiograph and loud second heart sound are suggestive of PH, whereas the EKG is not uniformly abnormal (15). In children, the initial clinical presentation is subtle with the initial presentation rarely being death from a pulmonary hypertensive crisis (185).

PPHTN is frequently resistant to many first-line medications. If the diagnosis of PPHTN is made early prior to the development of irreversible pulmonary vasculopathy, then liver transplantation can be successfully performed and may reverse the process of PPHTN. Similar to adults, few patients with PPHTN respond to calcium channel blocker therapy. In more severe cases treatment with epoprostenol is used, in addition to other targeted PAH agents (15,174,176).

HUMAN IMMUNODEFICIENCY VIRUS

Since the first description by Kim et al. (186), the association between PAH and HIV infection has been well established; there are multiple reports for adult patients (187,188) whereas little is known about the incidence, clinical outcome, and therapy options for children (189,190). Most children with HIV are infected in the perinatal period (191). Pongprot et al. (190) detected PH in 41% of their highly selected cohort of HIV-infected children. The pathogenesis of HIV-PAH is not completely understood. It has been hypothesized that the

HIV infection may damage the cells by stimulating the host to release proinflammatory cytokines, growth factors, or ET-1 that would result in PAH (192). HIV Nef, an accessory HIV protein, may play a role in the development of PH. The prognosis of HIV-PAH is limited but seems to improve in adults with highly active antiretroviral therapy (HAART). However, the efficacy of HAART in patients with HIV-related PAH in general and, in the pediatric population more specifically, is still uncertain (188,193).

HEMOGLOBINOPATHIES

PH is a known complication of many hereditary hemolytic anemias including sickle-cell disease, thalassemia, and spherocytosis (194). Echocardiographic studies have estimated an incidence of PAH in 20% to 30% of patients with sickle-cell disease screened (195,196). Furthermore, recent studies have shown that up to 75% of adults with sickle-cell disease may have physiologic evidence of PH at the time of death. Gladwin et al. (195) studied 195 adults with sickle-cell disease and found a 32% prevalence of PH. The mortality of those with PH was 40% at 45 months whereas mortality was only 2% at 45 months in those without PH. PH was defined as a Doppler-derived tricuspid regurgitation (TR) velocity of >2.5 m/s. A mild elevation of RV systolic pressure carried a >10 -fold risk of death in adults with PH. Data in children with sickle cell disease are lacking, but recent studies have begun to evaluate the prevalence and risk factors for PH (194,197–201).

In a study by Pashankar et al. (196), screening echocardiograms were performed in children over 6 years of age with homozygous SS or thalassemia. When using a definition of PH as a PASP >30 mm Hg, corresponding to a peak of TR velocity ≥ 2.5 m/s, 30% of patients had elevated TR jet velocity ≥ 2.5 m/s. Furthermore, one-third of these patients had TR >3 m/s. Almost all patients with an elevated TR jet velocity had hemoglobin homozygous SS disease. Factors associated with elevated PAP included a high reticulocyte count, low oxygen saturation,

and a high platelet count. Interestingly, neither the incidences of acute chest syndrome, hydroxyurea therapy, blood transfusion, or stroke, nor hemoglobin and bilirubin levels between patients with and without elevated PAP were different. Furthermore, in patients with an elevated TR velocity, transcranial Doppler examinations were normal (196). Further study by Pashankar et al. (202) followed patients with echocardiographic evidence of PAH. Those with a TR velocity $>3\text{m/s}$ were offered treatment with hydroxyurea; a normalization of TR velocity was seen in 8 of 19 patients treated with hydroxyurea.

In children as well as adults with sickle cell disease, PH is likely due to multifactorial causes such as left ventricular diastolic dysfunction and/or thromboembolic disease due to hypercoagulability (203,204). Frequently, patients with an elevated TR velocity have elevated cardiac output and normal PVR at catheterization. However, it is important to note that viscosity, that is, hemoglobin, may affect PVR, and viscosity is rarely considered in the calculation of PVR (205). Intravascular hemolysis may lead to release of hemoglobin, which reacts with and destroys NO (206) (Fig. 67.10). Likewise, arginase released from the erythrocyte degrades arginine and thus further reduces NO formation through arginine (197,206). Xanthine oxidase may also lead to a decrease in NO. This reduced NO bioavailability leads to a cascade of other events that further exacerbates PH and includes an increase in ET, an increase in activation of adhesion molecules, and activation of platelets (207). Due

to abnormalities of NO, sildenafil is being studied as a potential therapy for treatment of PAH associated with sickle cell disease (208,209). However, caution is needed. The National Heart, Lung, and Blood Institute of the National Institutes of Health stopped a recent clinical trial testing sildenafil treatment for PH in adults with sickle cell disease nearly one year early due to safety concerns. Compared to participants on placebo, participants taking sildenafil were significantly more likely to have serious medical problems, such as sickle cell crises (NIH News, July 28, 2009).

PULMONARY CAPILLARY HEMANGIOMATOSIS AND PULMONARY VENO-OCCLUSIVE DISEASE

PCH and pulmonary veno-occlusive disease (PVOD) both are characterized by precapillary PAH and are included in WHO classification group 1 (210–215). These disorders differ in that treatment of these disorders may differ from many of the other WHO group 1 diagnoses, and thus are in a separate category in the new WHO classification. In particular, vasodilators may worsen pulmonary edema in PCH and PVOD (212,216). Furthermore, these two disorders may be difficult to diagnose and are frequently found at autopsy (217). Both PVOD and PCH are characterized by widespread vascular obstruction at either the alveolar capillary bed (PCH) or the pulmonary venules and

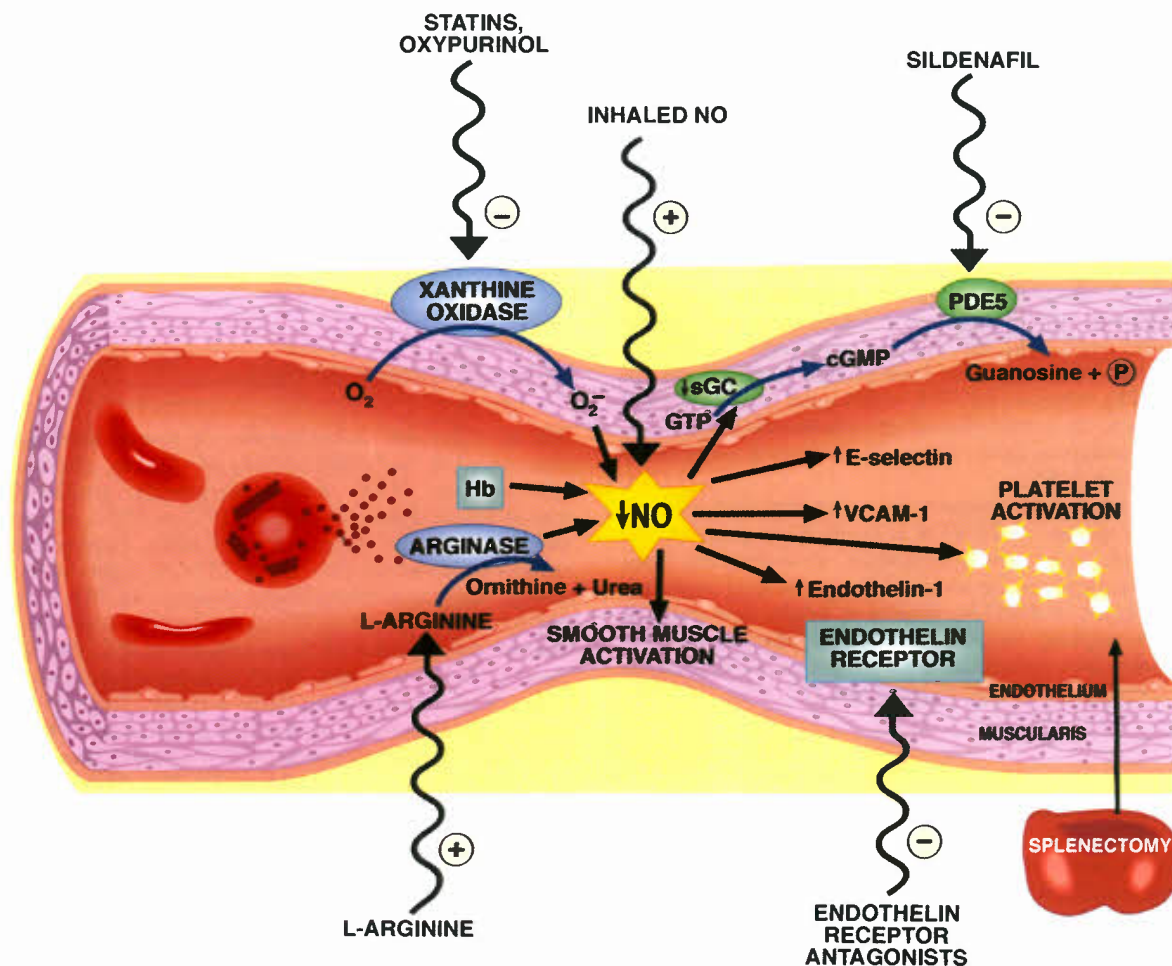


Figure 67.10. Mechanisms of pulmonary vascular dysfunction in hemoglobinopathies. (From Gladwin MT, Kato GJ. Cardiopulmonary complications of sickle cell disease: role of nitric oxide and hemolytic anemia. *Hematology Am Soc Hematol Educ Program* 2005:51–57, with permission.)

small veins (PVOD) (214,215). Treatment of either PVOD or PCH has been frequently unsuccessful and may require lung or heart/lung transplantation. In both disorders, the definitive diagnosis is usually made by surgical lung biopsy. Clues to the diagnosis of PVOD and PCH may lie in underlying pulmonary edema on chest radiograph and these findings may worsen with the initiation of either oxygen or inhaled NO. Characteristic findings may be seen on a chest CT scan and include central pulmonary artery prominence with widespread interlobular septa in the case of PVOD as well as ground-glass opacities. In PCH, the chest radiograph demonstrates enlarged central pulmonary arteries as well as a reticulonodular or micronodular areas of opacity, which may be seen on chest radiograph but are more prominent on the chest CT (215). Likewise, in both of these disorders pulmonary arteriograms may appear normal, particularly if the PVOD is microvascular in nature and not associated with larger vessel pulmonary vein disease. However, PVOD is rare in the spectrum of pulmonary vein abnormalities usually seen in children. In both disorders, PAP is elevated, and may be suprasystemic in patients with PVOD. Likewise, the pulmonary capillary wedge pressure is frequently normal in both disorders.

Clinical experience has shown that potent vasodilators (including continuous intravenous prostacyclin [PGI₂] and calcium channel blockers) induce florid and even fatal pulmonary edema in patients with either PVOD or PCH. To exclude unsuspected radiologic evidence of PVOD or PCH, it is currently suggested that patients with presumed IPAH should undergo a high-resolution CT examination before initiation of vasodilator therapy. Therapy for these disorders is limited and is not uniformly effective. Lung transplantation is the only curative option. However, trials of anticoagulation and steroids have been attempted in children with PVOD with mixed results. Due to the findings of myofibroblasts seen in patients with pulmonary vein disorders investigators have attempted use of chemotherapeutic agents with mixed results (218). In general, vasodilator therapy is unsuccessful, frequently contraindicated, and may worsen the patient status (108). In the case of PCH, experimental therapies have included alpha interferon (219), doxycycline (220), or possibly platelet-derived growth factor (PDGF) antagonists.

LEFT HEART DISEASE

Pulmonary venous hypertension may be caused by increased pressure anywhere between the pulmonary veins within the lung and the left ventricle. Adatia et al. (221) have recently reviewed left heart disease in children. Left heart disease in adults is common, particularly in the later part of life and is mainly due to left ventricular diastolic dysfunction. However, in children, structural heart disease, such as in Shone's complex or borderline small left ventricular physiology, is the most common. In addition, congenital and acquired cardiomyopathies are common causes of left heart disease and PH.

Paul Wood described three important mechanisms in the pathophysiology of PH secondary to mitral stenosis, which can be applied to most forms of PH due to left heart disease (222–225). First, there is a passive increase in PAP as downstream pressure increases to maintain left-sided preload and cardiac output. The pulmonary artery diastolic pressure is similar to the left atrial and left ventricular end diastolic pressure (LVEDP) in the absence of structural mitral disease. Therefore, the TPG and PVR are low (TPG <10 mm Hg, PVR <2.5 to 5 Wood units \times m²). Second, there is reflex vasoconstriction of the pulmonary arteries or veins or both. The diastolic PAP will be higher than the left atrial or LVEDP. Vasodilators, such as NO, will decrease the pulmonary artery diastolic pressure

to equal LVEDP (Fig. 67.11). The TPG will be >10 mm Hg and PVR >2.5 to 5 Wood units \times m². The use of pulmonary vasodilators in the setting of pulmonary vein disease, mitral stenosis, or an elevation of LVEDP may lead to pulmonary edema (128, 226–228). Reflex vasoconstriction is protective in some circumstances as described by Paul Wood, who observed that patients with mitral stenosis and elevated PVR had few symptoms of pulmonary edema (222). Third, there may be fixed pulmonary artery or vein obstruction. If there is fixed pulmonary vascular disease, there will be little or no change in pulmonary artery hemodynamics in response to inhaled NO. Frequently, a combination of all three mechanisms contributes to PH (221).

Pulmonary vein disease is a particularly vexing problem. Despite surgical, medical, and catheter-based attempts, often these therapies are ineffective with recurrence of disease and no cure (229–235). “Sutureless” repair of pulmonary vein stenosis after repair of total anomalous pulmonary venous return is more likely to be successful than in native pulmonary vein disease (236–239). Jenkins et al. (231) have described the expression of endothelial and smooth muscle cell markers in children with pulmonary vein stenosis. They noted strong staining of smooth muscle markers and receptor tyrosine kinases (RTK), such as PDGF receptor-alpha and -beta, fibroblast growth factor receptor (FGFR), and vascular endothelial growth factor VEGFR-2, suggesting that these cells are myofibroblast like (233). Studies are underway to target the RTK pathway.

RESPIRATORY DISEASE

Parenchymal lung disease is an important cause of PH in many patients. Complications include hypoxic pulmonary vasoconstriction causing increased PAP and can lead to RV hypertrophy and failure. RV function is usually preserved until disease is advanced. In most cases, correction of hypoxia can lead to reversal of PH. However, the development of cor pulmonale carries a poorer prognosis for reversibility.

Treatment of cor pulmonale depends on the precise etiology of lung disease, as well as disease severity. Nocturnal oxygen administration may alleviate hypoxia, typically without causing hypercapnia. Disorders of respiratory mechanics may also lead to hypoxia and the development of PH, as can BPD (240). More recent studies have suggested that abnormalities of the pulmonary vasculature may be a primary rather than secondary cause of abnormal alveolarization in BPD (241,242).

Of the chronic lung diseases associated with pediatric PH, BPD is the most common (243). BPD is described as chronic lung disease of infancy that generally occurs in prematurely born infants who have been treated with mechanical ventilation and oxygen therapy for acute respiratory distress syndrome. Northway and colleagues in 1967 defined BPD by the presence of persistent respiratory signs and symptoms, the need for supplemental oxygen to treat hypoxemia, and an abnormal chest radiograph at 36 weeks postmenstrual age. The introduction of prenatal steroid use, surfactant therapy, new ventilator strategies, and aggressive management of the PDA changed the clinical course and outcomes of premature newborns. This “new BPD” often develops in extremely low gestational age newborns who may have required minimal or even no ventilator support and low inspired oxygen concentrations. Despite these changes in the course of the premature infant, PH in BPD continues to contribute to significant morbidity and mortality. In premature infants (<32 weeks of gestation) with BPD who were diagnosed as having PAH at a median age of 4.8 months, Khemani et al. (244) found that the mean PAP was 43 ± 8 mm Hg and the PVR was 9.9 ± 2.8 Wood units. Survival rates were $64\% \pm 8\%$ at 6 months and $53\% \pm 11\%$ at 2 years after

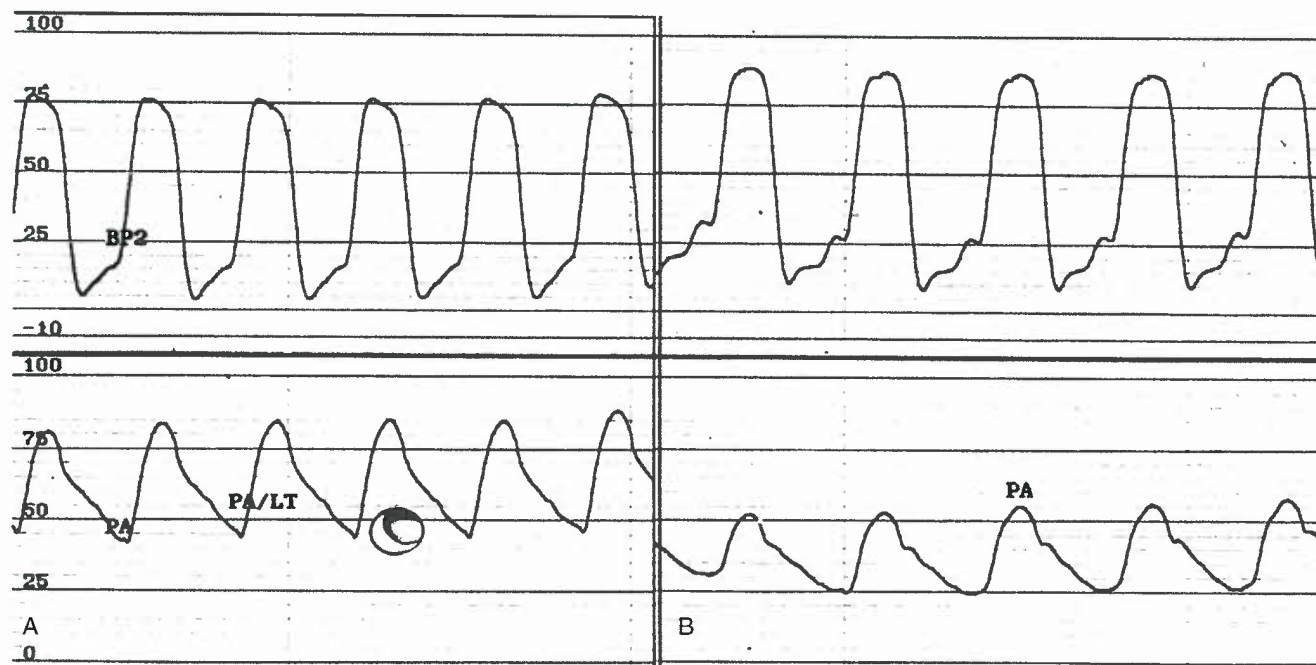


Figure 67.11. An example of reflex pulmonary vasoconstriction in a 5-year-old patient with restrictive cardiomyopathy. A: Simultaneous PAP (85/45 mm Hg) and LVED pressure (23 mm Hg) at baseline. B: After inhaled NO abolishes the vasoconstrictive element the simultaneous PAP (55/25 mm Hg) and LVED pressure (25 mm Hg). (Reprinted from Adatia I, Kulik T, Mullen M. Pulmonary venous hypertension or pulmonary hypertension due to left heart disease. *Prog Pediatr Cardiol* 2009;27:35–42, with permission from Elsevier.)

diagnosis of PAH (Fig. 67.12). PAH and small birth weight for gestational age were associated with worse survival rates. Among 26 survivors PAH was improved in 89%.

Before vasodilator therapy is started, a complete evaluation of all causes of lung disease and its associated comorbidities should be done (245). This includes an extensive evaluation

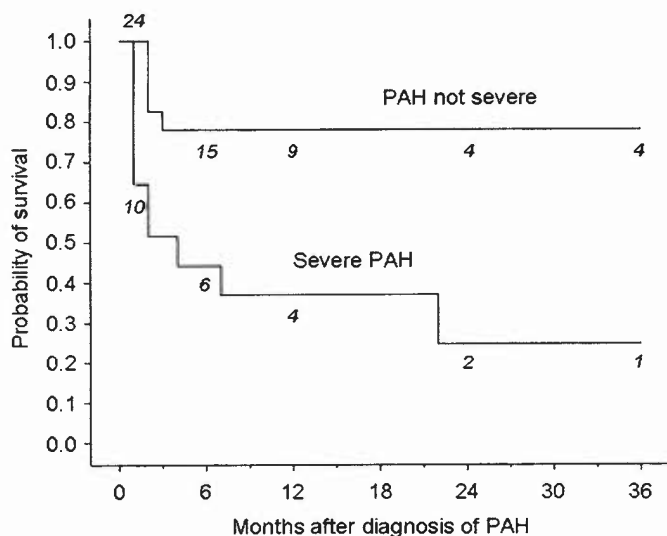


Figure 67.12. Kaplan-Meier graph demonstrating the probability of survival from the time of diagnosis of PAH for patients with BPD and PAH in patients with severe PAH at any time ($n = 18$) and those with less-than-severe PAH ($n = 24$). (Reproduced with permission from Khemani E, McElhinney DB, Rhein L, et al. Pulmonary artery hypertension in formerly premature infants with bronchopulmonary dysplasia: clinical features and outcomes in the surfactant era. *Pediatrics* 2007;120:1260–1269, Copyright © 2007 by the AAP.)

for chronic reflux and aspiration, structural airway abnormalities (such as tonsillar and adenoidal hypertrophy, vocal cord paralysis, subglottic stenosis, and tracheomalacia), and assessments of bronchoreactivity (243). Cardiac catheterization is recommended for patients with BPD who: (a) have persistent signs of severe cardiorespiratory disease or clinical deterioration not directly related to airways disease, (b) are suspected of having significant PH despite optimal management of their lung disease and associated morbidities, (c) are candidates for chronic PH drug therapy, or (d) have unexplained, recurrent pulmonary edema. The goals of cardiac catheterization are to assess the severity of PH; exclude or document the severity of associated anatomic cardiac lesions; define the presence of systemic–pulmonary collateral vessels, pulmonary venous obstruction, or left heart dysfunction (246); and to assess pulmonary vascular reactivity in patients who fail to respond to oxygen therapy alone (243). Pulmonary vein stenosis is common in children with BPD and PH (229). Management of children with pulmonary vein stenosis is difficult as catheter-based intervention or surgery has shown poor long-term results and overall survival is poor with the 2-year survival rate from diagnosis of 43% (229). Left ventricular diastolic dysfunction may complicate the course of the infant with BPD with cardiac catheterization being required for certain diagnosis (246).

Patients with CDH are at risk for PH, which can develop at any phase of the disease (247–251). In addition to lung hypoplasia, patients with CDH may develop pulmonary artery or pulmonary vein stenosis (250). Infants with CDH and poor outcome have higher plasma ET-1 levels and severity of PH than infants with better outcomes (249).

THROMBOEMBOLIC DISEASE

Chronic thromboembolic disease as a cause of PH in children is rare, but an accurate diagnosis is essential for treatment

(252,253). Predisposing factors include antiphospholipid antibody syndrome, bacterial endocarditis, and ventriculoatrial shunt for the treatment of hydrocephalus. Likewise, the use of oral contraceptive agents may cause hypercoagulability, leading to pulmonary thromboembolic phenomena.

The diagnosis of chronic thromboembolic PH in children requires a high index of suspicion, as well as evaluation by ventilation perfusion, CT scanning, or angiography. In adults with chronic thromboembolic PH, surgically accessible disease, and no severe comorbidities, pulmonary thromboendarterectomy has been demonstrated to improve survival and quality of life (254). A similar approach should be considered for children who develop this condition despite the relative paucity of data on this procedure in the pediatric age group.

PHARMACOLOGIC THERAPY OF PULMONARY ARTERIAL HYPERTENSION

Based on known mechanisms of action, three classes of drugs have been extensively studied for the treatment of PAH: prostanooids (epoprostenol, treprostinil, iloprost, beraprost), ERAs (bosentan, ambrisentan), and type 5 phosphodiesterase (PDE-5) inhibitors (sildenafil, tadalafil) (Fig. 67.13). Without therapy, and sometimes despite appropriate surgical correction of congenital cardiac lesions, PAH progresses at a variable rate. As

vasoconstriction is an important component in the development of medial hypertrophy, vasodilators are frequently used to decrease PAP, improve cardiac output, and potentially reverse some of the pulmonary vascular changes noted in the lung. The long-term strategy for the treatment of PH in children (Fig. 67.14) (255) is similar to adults (Fig. 67.15), except that it is difficult to place young children in the WHO classification. Therapy in adults is evidence based whereas in children it is based on experience. Targeted PH therapy has empirically improved survival in most forms of PAH (Fig. 67.16A), except that severe PH after complete repair of CHD continues to have a worse prognosis (Fig. 67.16B).

Before commencing vasodilator therapy for chronic PAH, vasodilator responsiveness should be assessed in the cardiac catheterization unit. A positive response is defined by assessing the change in hemodynamic parameters to vasodilators. The younger the child at the time of testing, the greater the likelihood of acute pulmonary vasodilation in response to vasoreactivity testing (81,144,256). Many oral and inhaled vasodilators have been used for testing of vasodilator responsiveness (129,143,144,256–261).

CONVENTIONAL THERAPY

Conventional therapy in patients used to treat RV failure is frequently used in PAH in children. Digoxin is used in the presence of RV failure, although there are no clear-cut data in

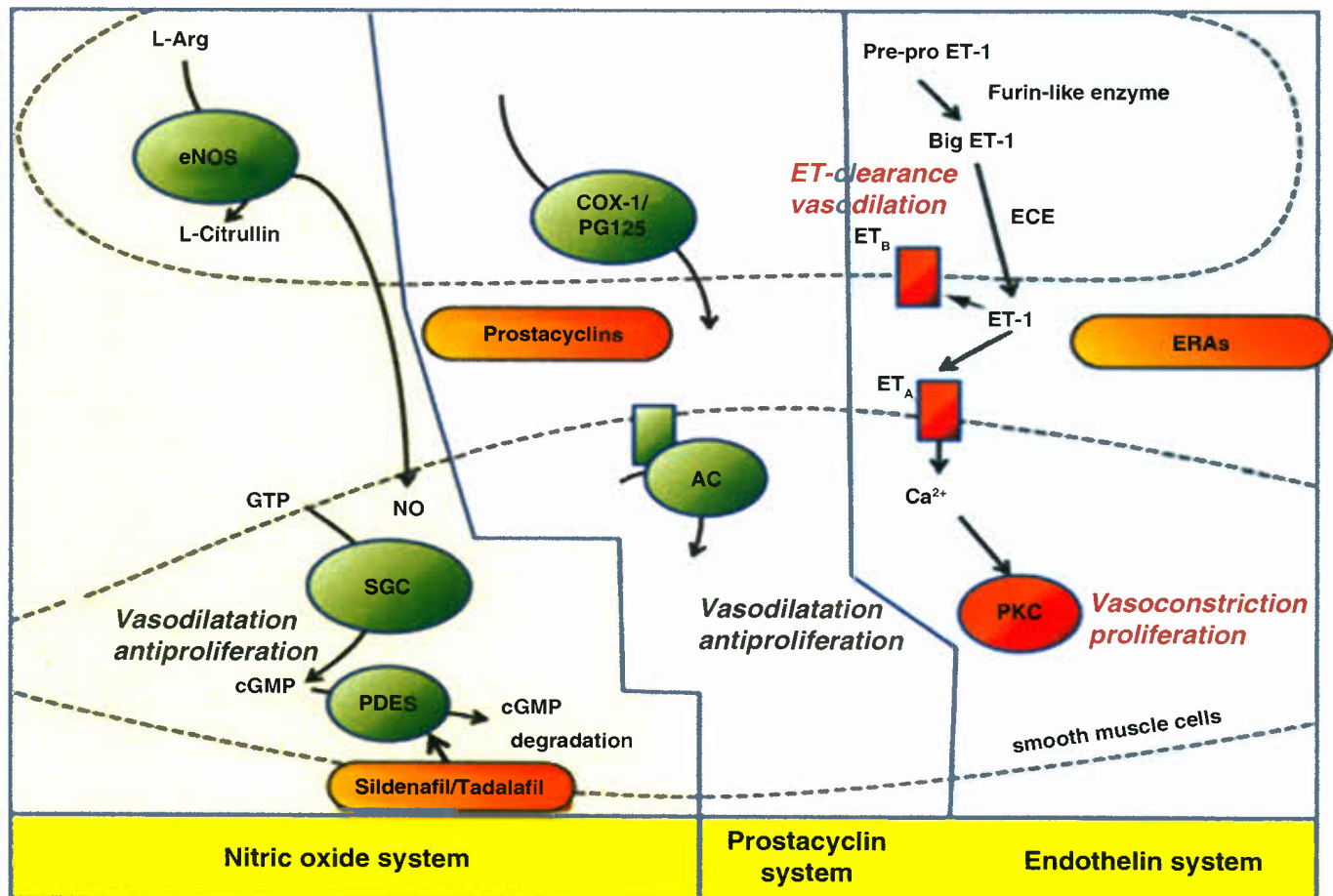


Figure 67.13. The nitric oxide, prostacyclin, and endothelin system signaling pathways and targets for therapy in PH. (From Diller GP, Baumgartner H. Pulmonary arterial hypertension in adults with congenital heart disease. *Int J Clin Pract Suppl* 2010;13–24, with permission.)

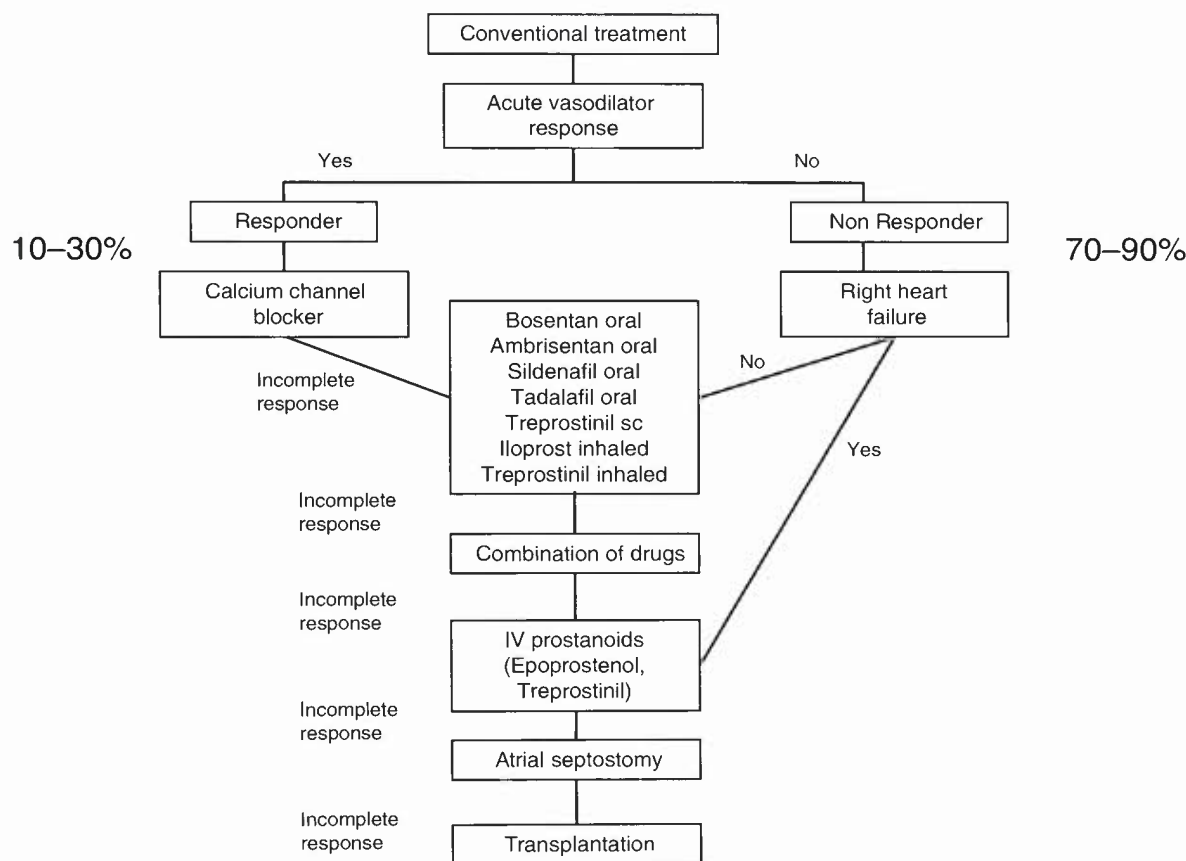


Figure 67.14. Treatment algorithm in children with severe PAH. (Reprinted from Tissot C, Ivy DD, Beghetti M. Medical therapy for pediatric pulmonary arterial hypertension. *J Pediatr* 2010;157:528–532, with permission from Elsevier.)

children (262). Diuretics are used to treat peripheral edema or ascites in the presence of right heart failure; however, excessive diuresis should be avoided. Careful attention to respiratory tract infections is required as this may worsen alveolar hypoxia, and routine influenza vaccination is recommended. The use of decongestants with pseudoephedrine or other stimulant-type medications is discouraged as these have been associated with PAH (263). In children who require the use of oral contraceptive agents either for prevention of pregnancy or for regulation of menses, we recommend agents that have no estrogen content. Pulse oximetry and polysomnography are indicated and chronic hypoxemia or nighttime desaturation is aggressively treated. However, oxygen therapy is not used as a mainstay of therapy in children with normal daytime saturations.

ANTICOAGULATION

In retrospective trials in adults with IPAH, the use of warfarin has been associated with improved survival. Although the use of chronic anticoagulation has not been studied widely in children, it is usually recommended in IPAH, and particularly in those with an indwelling central catheter. During treatment with warfarin the aim is to maintain an INR between 1.5 and 2.0. The use of anticoagulation in patients with Eisenmenger syndrome or other forms of PH is controversial and the potential risks and benefits of anticoagulation in this setting must be carefully weighed.

VASOREACTIVITY TESTING

As in adults, cardiac catheterization with acute vasodilator testing is essential prior to selecting targeted therapy in children. Cardiac catheterization carries a greater risk in those children with baseline suprasystemic PAP (Odds Ratio = 8.1, $p = 0.02$) (56,57). As in adults, a short-acting vasodilator is used, such as inhaled NO (144,264,265). The conventional pediatric definition of a response to acute vasodilator testing for determination of suitability for calcium channel blockade is a 20% fall in mean PAP and PVR to a vasodilator agent with no change or an increase in cardiac output (82). Note that this is not the definition for operability (see above Operability). Because patients treated with calcium channel blockers began to fail this therapy, Sitbon et al. (266) established more stringent criteria for defining acute vasoreactivity in adults. Their definition mandated a fall in mean PAP >10 mm Hg to <40 mmHg to predict long-term response to calcium channel blocker therapy. Although more strict criteria are used in children, this has not been adequately studied in this population. Recent data have shown that 7% to 35% of children with IPAH and 6% of those with APAH are responders to acute vasodilator testing (267).

CALCIUM CHANNEL BLOCKERS

The use of calcium channel blockers to evaluate vasoreactivity has significant potential risks, as these drugs can cause a decrease in cardiac output or a marked drop in systemic

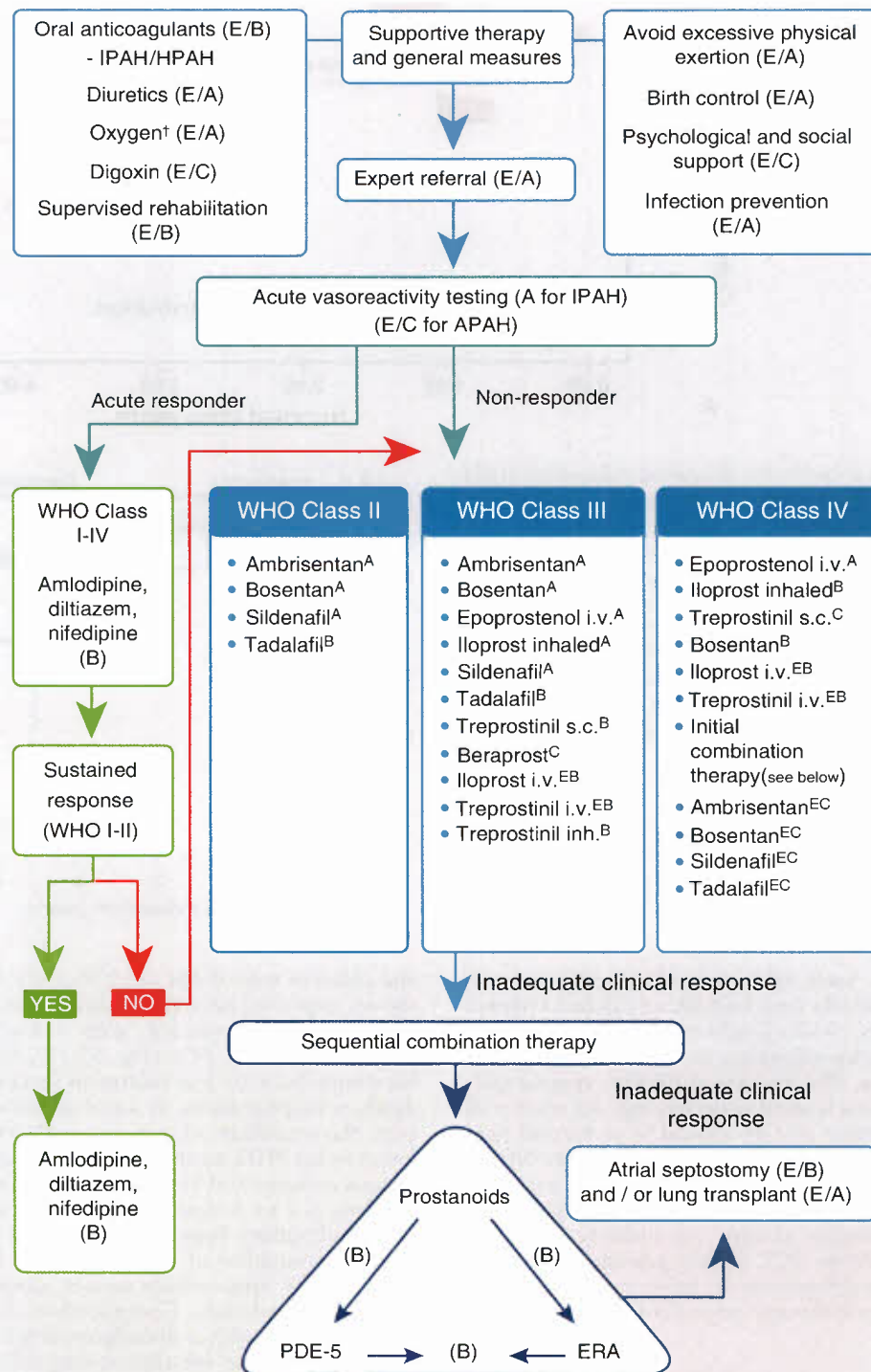


Figure 67.15. Treatment algorithm in adults with severe PAH. In: *Pulmonary Arterial Hypertension GUIDELINES Pocketcard™*. APAH, associated pulmonary arterial hypertension; ERA, endothelin receptor antagonist; HPAH, heritable pulmonary arterial hypertension; IPAH, idiopathic pulmonary arterial hypertension; IV, intravenous; PAH, pulmonary arterial hypertension; PDE-5, phosphodiesterase type 5; SC, subcutaneous; WHO, World Health Organization. (Adapted from Barst RJ, Gibbs JSR, Ghofrani HA, et al. Updated evidence-based treatment algorithm in pulmonary arterial hypertension. *JACC* 2009;54:S78–S84.)

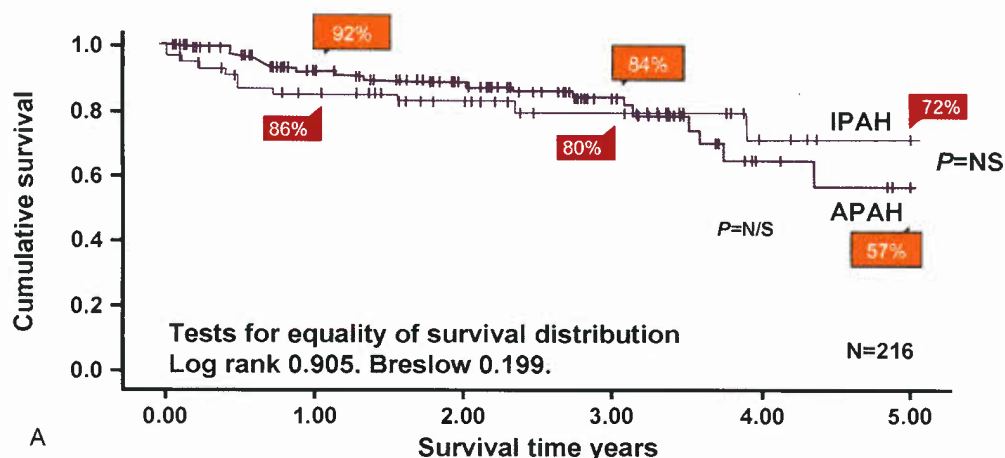
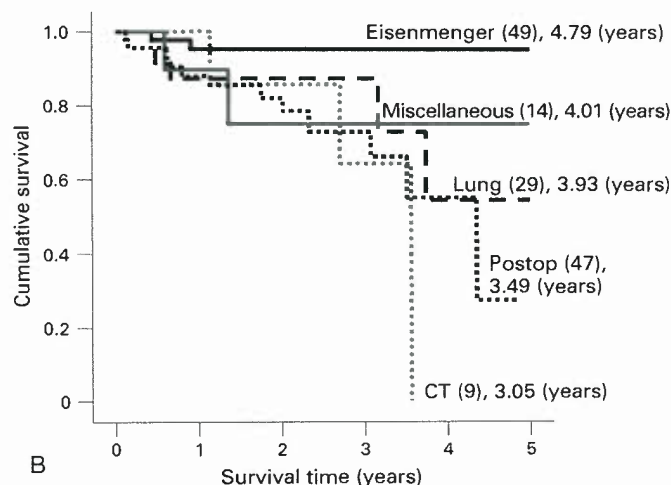


Figure 67.16. A: Survival curves for idiopathic pulmonary arterial hypertension (IPAH) and associated pulmonary arterial hypertension (APAH) cases censored for time in the study and for transplantation. There was no significant difference between the two groups. B: Survival curves for the subgroups within the APAH group. The number in each group (*brackets*) and the predicted survival out of a possible 5 years are shown. (Reproduced from Haworth SG, Hislop AA. Treatment and survival in children with pulmonary arterial hypertension: the UK Pulmonary Hypertension Service for Children 2001–2006. *Heart* 2009;95:312–317, with permission from BMJ Publishing Group Ltd.)



blood pressure (252). Such deleterious effects may be prolonged due to the relatively long half-life of calcium channel blockers. Consequently, elevated right atrial pressure and low cardiac output are contraindications to acute or chronic calcium channel blockade. The number of patients treated with calcium channel blockers is steadily decreasing. An acute trial of calcium channel blocker therapy should be performed only in those patients who are acutely responsive to either NO or PGI₂. Likewise, patients who do not have an acute vasodilatory response to short-acting agents and who are then placed on calcium channel blocker therapy are unlikely to benefit from this form of therapy (82). Eighty percent of children with severe PH are nonresponsive to acute vasodilator testing, and therefore require therapy other than calcium channel blockers.

PROSTACYCLINS

Adults with IPAH and children with CHD demonstrate an imbalance in the biosynthesis of thromboxane A₂ and PGI₂ (268). Likewise, adults and children with severe PH show diminished PGI₂ synthase expression in the lung vasculature (269). PGI₂ and PGI₂ analogues stimulate the cyclic-AMP pathway to increase pulmonary vasodilation. Intravenous PGI₂ was first used in the 1980s and continues to be the standard for treatment of severe PH with right heart failure. Epoprostenol was FDA approved in 1995. PGI₂ administered over the long term, utilizing intravenous epoprostenol, has shown to improve survival and quality of life in adults

and children with IPAH (82,270–272). Barst et al. (82) have shown improved survival in children treated with long-term intravenous epoprostenol, with a 4-year survival rate for treated children of 94% (Fig. 67.17), whilst Yung et al. (84) have reported a 10-year treatment success rate (freedom from death, transplantation, or atrial septostomy) of 37%. However, the treatment of patients with PGI₂ is cumbersome. Intravenous PGI₂ must be infused 24-hours/day via a central venous catheter and kept cold with ice packs; the half-life of the drug is 2 to 5 minutes, placing the patient at risk for an acute pulmonary hypertensive crisis if there is an accidental discontinuation of the medication. In addition, the side effects of the drug include nausea, diarrhea, jaw pain, bone pain, and headaches. Complications like line sepsis, local infection, and catheter dislodgement are not unusual and can be responsible for life-threatening rebound PH (273,274). Recently, the use of specific closed hub systems has been described in children to decrease the risk of catheter-related infection (275). Some children with an exceptional response to intravenous epoprostenol may wean from intravenous to oral therapy (47,276). Inhaled PGI₂ has been used in the critical care setting (277). A generic form of epoprostenol has been developed as well as a form that is stable at room temperature.

The PGI₂ analog treprostinil was approved by the FDA, initially for subcutaneous use (2002), and more recently for intravenous administration (2004) and inhaled administration (2009). Subcutaneous treprostinil allows patients to remain free of central venous catheters, and recent data have shown long-term efficacy in adults with PAH (278). Treprostinil has also been given in the intravenous form. Intravenous

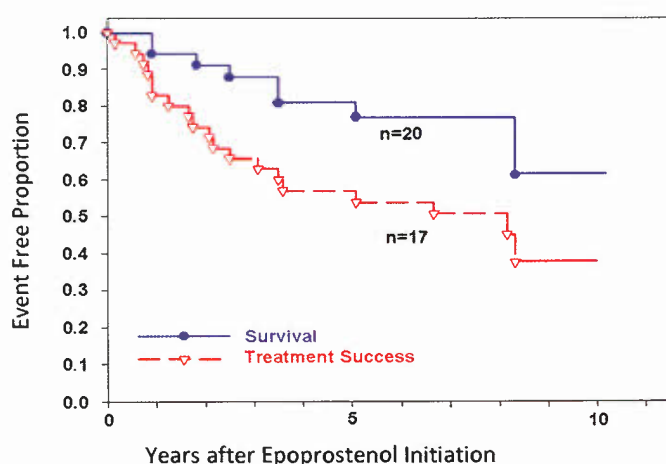


Figure 67.17. Kaplan-Meier curves for survival and treatment success in children with IPAH who received epoprostenol ($n = 35$). Survival rates at 1, 3, 5, and 10 years were 94%, 88%, 81%, and 61%, respectively; treatment success rates at 1, 3, 5, and 10 years were 83%, 66%, 57%, and 37%, respectively. (From Yung, D, Widlitz AC, Rosenzweig EB, et al. Outcomes in children with idiopathic pulmonary arterial hypertension. *Circulation* 2004;110:660–665, with permission.)

treprostinil requires central line access and continuous infusion, but is easier for families to mix, and has a half-life of 4 hours. Intravenous treprostinil has fewer side effects than intravenous epoprostenol, but there are no studies comparing efficacy (279). In its subcutaneous form, discomfort at the infusion site is common and represents a limiting factor. However, a recent study of subcutaneous treprostinil in young children showed promise with tolerable side effects (280). Treprostinil has also been studied in an inhaled form (281) and studies are being performed in children.

An inhaled PGI₂ analog iloprost, received approval for the treatment of PAH in the United States in 2004. This medication is administered by nebulization 6 to 9 times a day. Iloprost requires patient cooperation with the treatment administration lasting 10 to 15 minutes, which is difficult for young children (256,282,283). The advantage of an inhaled PGI₂ is that it can cause selective pulmonary vasodilation without affecting systemic blood pressure. Additionally, inhaled PGI₂ analogues can improve gas exchange and intrapulmonary shunt in cases of impaired ventilation/perfusion by redistributing pulmonary blood flow from nonventilated to ventilated, aerosol-accessible lung regions (283,284). In children with CHD and PAH, inhaled iloprost may be as effective in lowering PAP and PVR as inhaled NO, and thus may be useful in evaluation of acute vasoreactivity (283). Inhaled iloprost has also been studied in combination with bosentan and sildenafil, among others (285–287).

Beraprost is an orally active PGI₂ analog with a half-life of 35 to 40 minutes. While beneficial effects have been noted in short-term trials, these may be attenuated with prolonged treatment (288,289). Data in children are scarce and beraprost is not available in the US or Europe but is used in Japan (288). Long-acting beraprost has recently been approved for adult PAH in Japan (289).

ENDOTHELIN

Another target for treatment of PH is the vasoconstrictor peptide ET(290). The ETs are a family of isopeptides consisting of ET-1, ET-2, and ET-3. ET-1 is a potent vasoactive peptide

produced primarily in the vascular endothelial cell, but also may be produced by smooth muscle cells. Two receptor subtypes, ET_A and ET_B, mediate the activity of ET-1. ET_A and ET_B receptors on vascular smooth muscle mediate vasoconstriction, whereas ET_B receptors on endothelial cells cause release of NO and PGI₂, and act as clearance receptors for circulating ET-1. ET-1 expression is increased in the pulmonary arteries of patients with PH (291–293). Bosentan, a dual ERA, lowers PAP and PVR, and improves exercise tolerance in adults with PAH (294). These results can also be extrapolated to children (8,47,264,295,296,297). In children with PAH related to CHD or IPAH, bosentan lowers PAP and PVR, and is well tolerated (295,298). Elevated hepatic aminotransferase levels occur in approximately 11% of adults and 3% of children treated with bosentan. In a 12-week study of children with IPAH or PAH related to CHD, bosentan was well tolerated and lowered PAP and PVR (295). A retrospective study of 86 children on bosentan for a median exposure of 14 months with and without concomitant therapy found that bosentan provided a sustained clinical and hemodynamic improvement and was overall well tolerated, with 2-year survival estimates of 91% (8). Follow-up of these patients at 4 years revealed that the Kaplan-Meier estimate of disease progression in patients while on bosentan was 54% with a survival estimate of 82%. At end of data collection, 25 patients (29%) remained on bosentan. (299). Nevertheless, in a study including both children and adults with PAH and systemic-to-pulmonary shunt, bosentan therapy was shown to produce short-term improvement in WHO functional class and 6MWT distance (167). There was a progressive decline in the beneficial effect of bosentan after 1 year, with a more pronounced decline in the children, who tended to have more severe disease at baseline (167). The safety of bosentan therapy in children with PAH has been recently reported by Beghetti et al. (6). Elevated transaminase levels were reported in 2.7% of children compared with 7.8% of patients aged ≥12 years, and the overall discontinuation rate from bosentan was 14% in children compared with 28% in patients aged ≥12 years. In a Japanese cohort, bosentan pharmacokinetics was not altered by sildenafil (300). Bosentan has been studied in Eisenmenger syndrome in a placebo-controlled trial in patients (see Eisenmenger syndrome). Bosentan was well tolerated and improved exercise capacity and hemodynamics without compromising peripheral oxygen saturation (164). A specific pediatric formulation has been recently approved in Europe (301).

Selective ET_A receptor blockade is also possible using ambrisentan or sitaxsentan, ERAs with high oral bioavailability and a long duration of action, and high specificity for the ET_A receptor. Selective ET_A receptor blockade may benefit patients with PAH by blocking the vasoconstrictor effects of ET_A receptors while maintaining the vasodilator/clearance functions of ET_B receptors. Sitaxsentan given orally for 12 weeks improved exercise capacity and cardiopulmonary hemodynamics in patients with PAH that was idiopathic or related to CTD or CHD (302–304). However, sitaxsentan was removed from the market due to concerns of adverse effects on the liver. Ambrisentan, an ERA that is selective for the ET_A receptor was approved by the FDA in June of 2007. Adults showed significant improvements in 6MWT distance and significant delay in clinical worsening on ambrisentan. The incidence of elevated hepatic aminotransferase levels was 2.8% and was similar to the placebo group (306). In a retrospective study, 38 pediatric PAH patients treated with ambrisentan were evaluated (305). Fifteen of 38 patients were switched from bosentan to ambrisentan. The remaining 23 children were treated with ambrisentan as an add-on therapy due to disease progression. In both transition and add-on cases, mean pulmonary artery pressure significantly improved, and World Health Organization functional class improved in 31% of

patients during the follow-up period (median, range; 20, 4-44 months). Although 5 patients (13%) discontinued ambrisentan due to severe headache, lack of clinical efficacy, or near syncope, no patients had aminotransferase abnormalities and there were no deaths after initiation of ambrisentan during follow-up (305). Recently, monthly liver function testing for ambrisentan was removed from the FDA label, but most centers still perform routine monitoring. Studies in children are underway. A novel dual ERA, macitentan, is currently under study.

PHOSPHODIESTERASE INHIBITORS

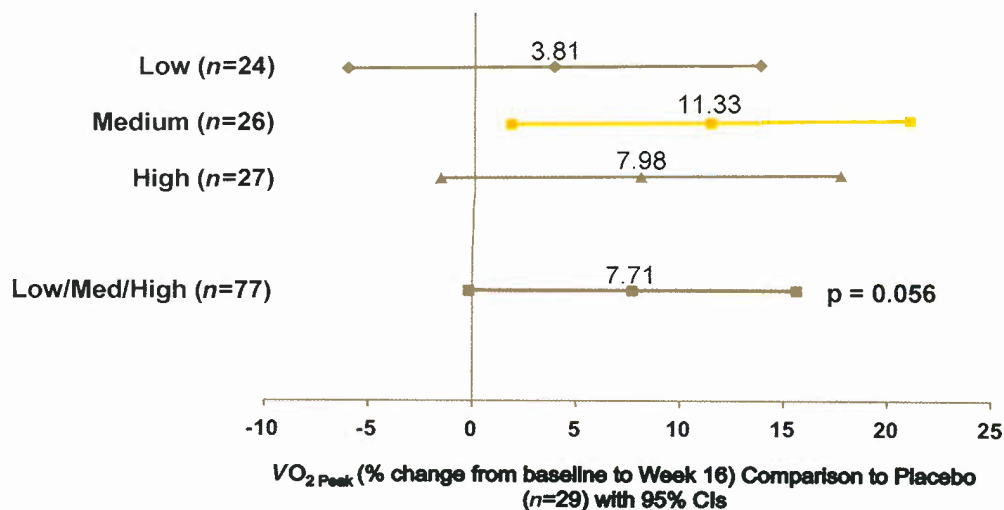
Phosphodiesterase type 5 (PDE-5) inhibitors block the degradative action of PDE5 on cyclic GMP in the smooth muscle cells, (307,308), and specific PDE-5 inhibitors, such as sildenafil, (309-314) or tadalafil promote an increase in cGMP levels and thus promote pulmonary vasodilation and remodeling (Fig. 67.13). Sildenafil is as effective a pulmonary vasodilator as inhaled NO and may be preferred because it does not increase pulmonary capillary wedge pressure in patients with an increased wedge pressure at baseline. Sildenafil may also be useful in the setting of inhaled NO therapy withdrawal (315,316,317) in postoperative PH (318), or in the presence of PH related to chronic lung disease (286). Sildenafil was initially studied in 14 children with PAH. During sildenafil therapy, the mean 6MWT distance increased from 278 ± 114 to 443 ± 107 m over 6 months ($p = 0.02$), and at 12 months, the distance walked was 432 ± 156 m ($p = 0.005$). A plateau was reached between 6 and 12 months ($p = 0.48$). Mean PAP and PVR fell (319). In a small study of children with IPAH and PH associated with CHD, sildenafil improved oxyhemoglobin saturation and exercise capacity without significant side effects (313). In children with PAH associated with chronic lung disease, sildenafil has been shown to improve hemodynamics in 88% of patients, was well tolerated, and did not worsen oxyhemoglobin saturation (320). A study of sildenafil in Japanese children has also suggested safety and efficacy (321). In a 16-week, randomized, double-blind study (STARTS-1) the effects of oral sildenafil in pediatric PAH were studied (322). Children ($n = 235$) with PAH (aged 1 to 17 years; ≥ 8 kg) received low-, medium-, or high-dose sildenafil or placebo orally 3 times daily. The primary comparison was percent change in peak oxygen consumption (pVO_2) for the three sildenafil doses combined from baseline to week 16; exercise testing was performed only in children

able to exercise reliably. Secondary endpoints, including mean PAP, PVR, and functional class, were assessed in all enrolled patients, including those unable to reliably exercise. The estimated mean \pm standard error percentage change in pVO_2 for the low, medium and high doses combined versus placebo was $7.7\% \pm 4.0\%$ (95% CI, -0.2% to 15.6% ; $p = 0.056$). Peak VO_2 , functional capacity, mean PAP, and PVR improved with the medium- and high-dose groups compared to placebo, whilst the low dose was ineffective (Fig. 67.18). Upper respiratory tract infections, pyrexia, and vomiting occurred more often with sildenafil than placebo (322). A long-term extension study included children continued on sildenafil monotherapy. At three years, an increase in mortality was noted in the high-dose group and the data safety monitoring board requested to decrease the dose of any child receiving high dose. Deaths in the extension study were related to etiology and baseline disease severity. The majority of deaths occurred in patients with IPAH/FPAH. Of patients who died, most had baseline values above median values for PVRI, mean pulmonary artery pressure, and right atrial pressure. Sildenafil is approved for use in children with PAH in Europe: 10 mg t.i.d. in patients up to 20 kg, and 20 mg t.i.d. in heavier patients, but sildenafil is not approved for children with PAH in the U.S.

Intravenous sildenafil has been shown to potentiate the increase in cGMP in response to NO in children with increased PVR related to CHD or in the postoperative state. Nevertheless, sildenafil infusion has been associated with increased intrapulmonary shunting and augmentation of hypoxemia related to ventilation/perfusion mismatch in the postoperative CHD patient (323,324). However, a recent study of intravenous sildenafil has shown improvement in oxygenation index in PPHN in patients treated with or without inhaled NO (325).

Other PDE-5 inhibitors, such as tadalafil have been recently studied leading to FDA approval in 2009, but studies in children are lacking. Tadalafil is also a selective PDE-5 inhibitor with a longer duration of action than sildenafil. A recent study demonstrated clinical safety and efficacy of tadalafil therapy in 33 pediatric patients with PAH (326). In this study, 29 of 33 patients were switched from sildenafil to tadalafil. The average dose of sildenafil and tadalafil were 3.4 ± 1.1 mg/kg/day and 1.0 ± 0.4 mg/kg/day, respectively. In 14 of 29 children transitioned from sildenafil to tadalafil, repeat cardiac catheterization showed statistically significant improvements in mean pulmonary arterial pressure (53.2 ± 18.3 mmHg versus 47.4 ± 13.7 mmHg, $p < 0.05$) and pulmonary vascular resistance index (12.2 ± 7.0 units \times m 2 versus 10.6 ± 7.2 units \times m 2 , $p < 0.05$) (326). In adults with severe PAH, tadalafil

Figure 67.18. Placebo-adjusted percent change in $\text{VO}_{2\text{ Peak}}$ by cardiopulmonary exercise after 16 weeks of sildenafil or placebo in a randomized, double-blind, placebo-controlled, dose-ranging study of oral sildenafil citrate in treatment-naïve children with PAH. (From Barst RJ, Ivy DD, Gaitan G, et al. A randomized, double-blind, placebo-controlled, dose-ranging study of oral sildenafil citrate in treatment-naïve children with pulmonary arterial hypertension. *Circulation* 2012;125:324-34, with permission.)



26. Koestenberger M, Ravekes W, Everett AD, et al. Right ventricular function in infants, children and adolescents: Reference values of the tricuspid annular plane systolic excursion (TAPSE) in 640 healthy patients and calculation of z score values. *J Am Soc Echocardiogr* 2009;22:715–719.
27. Raymond RJ, Hinderliter AL, Willis PW, et al. Echocardiographic predictors of adverse outcomes in primary pulmonary hypertension. *J Am Coll Cardiol* 2002;39:1214–1219.
28. Tei C, Dujardin KS, Hodge DO, et al. Doppler echocardiographic index for assessment of global right ventricular function. *J Am Soc Echocardiogr* 1996;9:838–847.
29. Dyer KL, Pauliks LB, Das B, et al. Use of myocardial performance index in pediatric patients with idiopathic pulmonary arterial hypertension. *J Am Soc Echocardiogr* 2006;19:21–27.
30. Masuyama T, Kodama K, Kitabatake A, et al. Continuous-wave doppler echocardiographic detection of pulmonary regurgitation and its application to noninvasive estimation of pulmonary artery pressure. *Circulation* 1986;74:484–492.
31. Benza RL, Miller DP, Gomberg-Maitland M, et al. Predicting survival in pulmonary arterial hypertension: insights from the registry to evaluate early and long-term pulmonary arterial hypertension disease management (REVEAL). *Circulation* 2010;122:164–172.
32. Alkon J, Humpl T, Manlihot C, et al. Usefulness of the right ventricular systolic to diastolic duration ratio to predict functional capacity and survival in children with pulmonary arterial hypertension. *Am J Cardiol* 2010;106:430–436.
33. Weinberg CE, Hertzberg JR, Ivy DD, et al. Extraction of pulmonary vascular compliance, pulmonary vascular resistance, and right ventricular work from single-pressure and doppler flow measurements in children with pulmonary hypertension: a new method for evaluating reactivity: in vitro and clinical studies. *Circulation* 2004;110:2609–2617.
34. Dyer K, Lanning C, Das B, et al. Noninvasive doppler tissue measurement of pulmonary artery compliance in children with pulmonary hypertension. *J Am Soc Echocardiogr* 2006;19:403–412.
35. Hunter KS, Lee PF, Lanning CJ, et al. Pulmonary vascular input impedance is a combined measure of pulmonary vascular resistance and stiffness and predicts clinical outcomes better than pulmonary vascular resistance alone in pediatric patients with pulmonary hypertension. *Am Heart J* 2008;155:166–174.
36. Lankhaar JW, Westerhof N, Faes TJ, et al. Quantification of right ventricular afterload in patients with and without pulmonary hypertension. *Am J Physiol Heart Circ Physiol* 2006;291:H1731–1737.
37. Mahapatra S, Nishimura RA, Oh JK, et al. The prognostic value of pulmonary vascular capacitance determined by doppler echocardiography in patients with pulmonary arterial hypertension. *J Am Soc Echocardiogr* 2006;19:1045–1050.
38. Mahapatra S, Nishimura RA, Sorajja P, et al. Relationship of pulmonary arterial capacitance and mortality in idiopathic pulmonary arterial hypertension. *J Am Coll Cardiol* 2006;47:799–803.
39. Hunter KS, Gross JK, Lanning CJ, et al. Noninvasive methods for determining pulmonary vascular function in children with pulmonary arterial hypertension: Application of a mechanical oscillator model. *Congenit Heart Dis* 2008;3:106–116.
40. Alunni JP, Degano B, Arnaud C, et al. Cardiac MRI in pulmonary artery hypertension: correlations between morphological and functional parameters and invasive measurements. *Eur Radiol* 2010;20:1149–1159.
41. Apfel HD, Shen Z, Gopal AS, et al. Quantitative three dimensional echocardiography in patients with pulmonary hypertension and compressed left ventricles: comparison with cross sectional echocardiography and magnetic resonance imaging. *Heart* 1996;76:350–354.
42. Benza R, Biederman R, Murali S, et al. Role of cardiac magnetic resonance imaging in the management of patients with pulmonary arterial hypertension. *J Am Coll Cardiol* 2008;52:1683–1692.
43. Biederman RW. Cardiovascular magnetic resonance imaging as applied to patients with pulmonary arterial hypertension. *Int J Clin Pract Suppl* 2009;162:20–35.
44. Bouchard A, Higgins CB, Byrd BF III, et al. Magnetic resonance imaging in pulmonary arterial hypertension. *Am J Cardiol* 1985;56:938–942.
45. Didier D, Higgins CB. Estimation of pulmonary vascular resistance by MRI in patients with congenital cardiovascular shunt lesions. *Am J Roentgenol* 1986;146:919–924.
46. Vogel-Claussen J, Skrok J, Shehata ML, et al. Right and left ventricular myocardial perfusion reserves correlate with right ventricular function and pulmonary hemodynamics in patients with pulmonary arterial hypertension. *Radiology* 2011;258:119–127.
47. Ivy DD, Doran A, Claussen L, et al. Weaning and discontinuation of epoprostenol in children with idiopathic pulmonary arterial hypertension receiving concomitant bosentan. *Am J Cardiol* 2004;93:943–946.
48. Yetman AT, Taylor AL, Doran A, et al. Utility of cardiopulmonary stress testing in assessing disease severity in children with pulmonary arterial hypertension. *Am J Cardiol* 2005;95:697–699.
49. Smith G, Reyes JT, Russell JL, et al. Safety of maximal in pediatric patients with pulmonary hypertension. *Chest* 2009;135:1209–1214.
50. Takken T. Six-minute walk test is a poor predictor of maximum oxygen uptake in children. *Acta Paediatr* 2010;99:958–959.
51. Lesser DJ, Fleming MM, Maher CA, et al. Does the 6-min walk test correlate with the exercise stress test in children? *Pediatr Pulmonol* 2010;45:135–140.
52. Li AM, Yin J, Au JT, et al. Standard reference for the six-minute-walk test in healthy children aged 7 to 16 years. *Am J Respir Crit Care Med* 2007;176:174–180.
53. Geiger R, Straszak A, Trembl B, et al. Six-minute walk test in children and adolescents. *J Pediatr* 2007;150:395–399.
54. Lammers AE, Diller GP, Odenaall D, et al. Comparison of 6-min walk test distance and cardiopulmonary exercise test performance in children with pulmonary hypertension. *Arch Dis Childhood* 2011;96:141–147.
55. Lammers AE, Hislop AA, Flynn Y, et al. The 6-minute walk test: normal values for children of 4–11 years of age. *Arch Dis Childhood* 2008;93:464–468.
56. Carmosino MJ, Friesen RH, Doran A, et al. Perioperative complications in children with pulmonary hypertension undergoing noncardiac surgery or cardiac catheterization. *Anesth Analg* 2007;104:521–527.
57. Friesen RH, Williams GD. Anesthetic management of children with pulmonary arterial hypertension. *Paediatr Anaesth* 2008;18:208–216.
58. Hill KD, Lim DS, Everett AD, et al. Assessment of pulmonary hypertension in the pediatric catheterization laboratory: current insights from the MAGIC registry. *Catheter Cardiovasc Interv* 2010;76:865–873.
59. Barst RJ, Flaster ER, Menon A, et al. Evidence for the association of unexplained pulmonary hypertension in children with the major histocompatibility complex. *Circulation* 1992;85:249–258.
60. Ferris A, Jacobs T, Widlitz A, et al. Pulmonary arterial hypertension and thyroid disease. *Chest* 2001;120:1980–1981.
61. Roberts KE, Barst RJ, McElroy JJ, et al. Bone morphogenetic protein receptor 2 mutations in adults and children with idiopathic pulmonary arterial hypertension: Association with thyroid disease. *Chest* 2005;128:S618.
62. Satoh M, Aso K, Nakayama T, et al. Autoimmune thyroid disease in children and adolescents with idiopathic pulmonary arterial hypertension. *Circ J* 2010;74:371–374.
63. Nagaya N, Nishikimi T, Uematsu M, et al. Plasma brain natriuretic peptide as a prognostic indicator in patients with primary pulmonary hypertension. *Circulation* 2000;102:865–870.
64. Bernus A, Wagner BD, Accurso F, et al. Brain natriuretic peptide levels in managing pediatric patients with pulmonary arterial hypertension. *Chest* 2009;135:745–751.
65. Lammers AE, Hislop AA, Haworth SG. Prognostic value of b-type natriuretic peptide in children with pulmonary hypertension. *Int J Cardiol* 2009;135:21–26.
66. Van Albada ME, Loot FG, Fokkema R, et al. Biological serum markers in the management of pediatric pulmonary arterial hypertension. *Pediatr Res* 2008;63:321–327.
67. Haworth SG. Pathophysiological and metabolic manifestations of pulmonary vascular disease in children. *Herz* 1992;17:254–261.
68. Heath D, Smith P, Gosney J, et al. The pathology of the early and late stages of primary pulmonary hypertension. *Br Heart J* 1987;58:204–213.
69. Juanea E, Haworth SG. Pulmonary vascular disease in children with truncus arteriosus. *Am J Cardiol* 1984;54:1314–1320.
70. Rabinovitch M, Haworth SG. Balloon occlusion pulmonary wedge angiography and lung biopsy assessment in the child with a congenital cardiac defect. *Cardiol Young* 2009;19:13–15.
71. Rabinovitch M, Keane JF, Norwood WI, et al. Vascular structure in lung tissue obtained at biopsy correlated with pulmonary hemodynamic findings after repair of congenital heart defects. *Circulation* 1984;69:655–667.
72. Epting CL, Wolfe RR, Abman SH, et al. Reversal of pulmonary hypertension associated with plexiform lesions in congenital heart disease: a case report. *Pediatr Cardiol* 2002;23:182–185.
73. Gower WA, Wert SE, Ginsberg JS, et al. Fatal familial lung disease caused by ABCA3 deficiency without identified ABCA3 mutations. *J pediatr* 2010;157:62–68.
74. Hamvas A. Evaluation and management of inherited disorders of surfactant metabolism. *Chin Med J (Engl)* 2010;123:2943–2947.
75. Szczawinska-Poplonyk A, Breborowicz A, Langfort R. Interstitial lung disease associated with surfactant protein b and c deficiencies. *Pneumonol Alergol Pol* 2010;78:224–228.
76. Van Moersel CH, van Oosterhout MF, Barlo NP, et al. Surfactant protein c mutations are the basis of a significant portion of adult familial pulmonary fibrosis in a dutch cohort. *Am J Respir Crit Care Med* 2010;182:1419–1425.
77. Ivy DD, Neish SR, Knudson OA, et al. Intravascular ultrasonic characteristics and vasoreactivity of the pulmonary vasculature in children with pulmonary hypertension. *Am J Cardiol* 1998;81:740–748.
78. Nihill MR MD. Magnification pulmonary wedge angiography in the evaluation of children with congenital heart disease and pulmonary hypertension. *Circulation* 1978;58:1094–1106.
79. Humbert M, Sitbon O, Simonneau G. Treatment of pulmonary arterial hypertension. *N Engl J Med* 2004;351:1425–1436.
80. D'Alonzo GE, Barst RJ, Ayres SM, et al. Survival in patients with primary pulmonary hypertension. Results from a national prospective registry. *Ann Intern Med* 1991;115:343–349.
81. Barst RJ. Pharmacologically induced pulmonary vasodilatation in children and young adults with primary pulmonary hypertension. *Chest* 1986;89:497–503.
82. Barst RJ, Maislin G, Fishman AP. Vasodilator therapy for primary pulmonary hypertension in children. *Circulation* 1999;99:1197–1208.
83. Moledina S, Hislop AA, Foster H, et al. Childhood idiopathic pulmonary arterial hypertension: a national cohort study. *Heart* 2010;96:1401–1406.

84. Yung D, Widlitz AC, Rosenzweig EB, et al. Outcomes in children with idiopathic pulmonary arterial hypertension. *Circulation* 2004;110:660–665.
85. Rastogi D, Ngai P, Barst RJ, et al. Lower airway obstruction, bronchial hyperresponsiveness, and primary pulmonary hypertension in children. *Pediatr Pulmonol* 2004;37:50–55.
86. Loyd JE, Butler MG, Foroud TM, et al. Genetic anticipation and abnormal gender ratio at birth in familial primary pulmonary hypertension. *Am J Respir Crit Care Med* 1995;152:93–97.
87. Austin ED, Loyd JE, Phillips JA III. Genetics of pulmonary arterial hypertension. *Semin Respir Crit Care Med* 2009;30:386–398.
88. Grunig E, Koehler R, Miltenberger-Miltenyi G, et al. Primary pulmonary hypertension in children may have a different genetic background than in adults. *Pediatr Res* 2004;56:571–578.
89. Newman JH, Wheeler L, Lane KB, et al. Mutation in the gene for bone morphogenetic protein receptor II as a cause of primary pulmonary hypertension in a large kindred. *N Engl J Med* 2001;345:319–324.
90. Thomson JR, Machado RD, Pauculo MW, et al. Sporadic primary pulmonary hypertension is associated with germline mutations of the gene encoding BMPR-II, a receptor member of the TGF-beta family. *J Med Genet* 2000;37:741–745.
91. Trembath RC, Harrison R. Insights into the genetic and molecular basis of primary pulmonary hypertension. *Pediatr Res* 2003;53:883–888.
92. Fujiwara M, Yagi H, Matsuoka R, et al. Implications of mutations of activin receptor-like kinase 1 gene (ALK1) in addition to bone morphogenetic protein receptor II gene (BMPR2) in children with pulmonary arterial hypertension. *Circ J* 2008;72:127–133.
93. Loyd JE, Slovis B, Phillips JA III, et al. The presence of genetic anticipation suggests that the molecular basis of familial primary pulmonary hypertension may be trinucleotide repeat expansion. *Chest* 1997;111:825–835.
94. Abdalla SA, Gallione CJ, Barst RJ, et al. Primary pulmonary hypertension in families with hereditary haemorrhagic telangiectasia. *Eur Respir J* 2004;23:373–377.
95. Aldred MA, Comhair SA, Varella-Garcia M, et al. Somatic chromosome abnormalities in the lungs of patients with pulmonary arterial hypertension. *Am J Respir Crit Care Med* 2010;182:1153–1160.
96. Consortium TIP, Lane KB, Machado RD, et al. Heterozygous germline mutations in BMPR2, encoding a TGF-beta receptor cause familial primary pulmonary hypertension. *Nat Genet* 2000;26:81–84.
97. Deng Z, Morse JH, Slager SL, et al. Familial primary pulmonary hypertension (gene PPH1) is caused by mutations in the bone morphogenetic protein receptor-II gene. *Am J Hum Genet* 2000;67:737–744.
98. Girerd B, Montani D, Coulet F, et al. Clinical outcomes of pulmonary arterial hypertension in patients carrying an acvr11 (alk1) mutation. *Am J Respir Crit Care Med* 2010;181:851–861.
99. Lane KB, Machado RD, Pauculo MW, et al. Heterozygous germline mutations in BMPR2, encoding a TGF-beta receptor, cause familial primary pulmonary hypertension. The international PPH consortium. *Nat Genet* 2000;26:81–84.
100. Machado RD, Pauculo MW, Thomson JR, et al. BMPR2 haploinsufficiency as the inherited molecular mechanism for primary pulmonary hypertension. *Am J Hum Genet* 2001;68:92–102.
101. West J. Cross talk between SMAD, MAPK, and actin in the etiology of pulmonary arterial hypertension. *Adv Exp Med Biol* 2010;661:265–278.
102. Upton PD, Morrell NW. TGF-beta and BMPR-II pharmacology—implications for pulmonary vascular diseases. *Curr Opin Pharmacol* 2009;9:274–280.
103. Newman JH, Phillips JA III, Loyd JE. Narrative review: the enigma of pulmonary arterial hypertension: new insights from genetic studies. *Ann Intern Med* 2008;148:278–283.
104. Harrison RE, Berger R, Haworth SG, et al. Transforming growth factor-beta receptor mutations and pulmonary arterial hypertension in childhood. *Circulation* 2005;111:435–441.
105. Roberts KE, McElroy JJ, Wong WP, et al. BMPR2 mutations in pulmonary arterial hypertension with congenital heart disease. *Eur Respir J* 2004;24:371–374.
106. Rosenzweig EB, Morse JH, Knowles JA, et al. Clinical implications of determining BMPR2 mutation status in a large cohort of children and adults with pulmonary arterial hypertension. *J Heart Lung Transplant* 2008;27:668–674.
107. Elliott CG, Glissmeyer EW, Havlena GT, et al. Relationship of BMPR2 mutations to vasoreactivity in pulmonary arterial hypertension. *Circulation* 2006;113:2509–2515.
108. Strymf B, Coulet F, Girerd B, et al. Clinical outcomes of pulmonary arterial hypertension in carriers of BMPR2 mutation. *Am J Respir Crit Care Med* 2008;177:1377–1383.
109. Harrison RE, Flanagan JA, Sankelo M, et al. Molecular and functional analysis identifies ALK-1 as the predominant cause of pulmonary hypertension related to hereditary haemorrhagic telangiectasia. *J Med Genet* 2003;40:865–871.
110. Smoot LB, Obler D, McElhinney DB, et al. Clinical features of pulmonary arterial hypertension in young people with an ALK1 mutation and hereditary haemorrhagic telangiectasia. *Arch Dis Child* 2009;94:506–511.
111. Eddahibi S, Adnot S. The serotonin pathway in pulmonary hypertension. *Arch Mal Coeur Vaiss* 2006;99:621–625.
112. Eddahibi S, Humbert M, Fadel E, et al. Serotonin transporter overexpression is responsible for pulmonary artery smooth muscle hyperplasia in primary pulmonary hypertension. *J Clin Invest* 2001;108:1141–1150.
113. Willers ED, Newman JH, Loyd JE, et al. Serotonin transporter polymorphisms in familial and idiopathic pulmonary arterial hypertension. *Am J Respir Crit Care Med* 2006;173:798–802.
114. Mukerjee D, St George D, Coleiro B, et al. Prevalence and outcome in systemic sclerosis associated pulmonary arterial hypertension: application of a registry approach. *Ann Rheum Dis* 2003;62:1088–1093.
115. Badesch DB, Tapson VF, McGoon MD, et al. Continuous intravenous epoprostenol for pulmonary hypertension due to the scleroderma spectrum of disease. A randomized, controlled trial. *Ann Intern Med* 2000;132:425–434.
116. Robbins IM, Gaine SP, Schilz R, et al. Epoprostenol for treatment of pulmonary hypertension in patients with systemic lupus erythematosus. *Chest* 2000;117:14–18.
117. Takatsuki S, Soep JB, Calderbank M, et al. Connective tissue disease presenting with signs and symptoms of pulmonary hypertension in children. *Pediatr Cardiol* 2011;32:828–833.
118. Kidd L, Driscoll DJ, Gersony WM, et al. Second natural history study of congenital heart defects. Results of treatment of patients with ventricular septal defects. *Circulation* 1993;87:138–151.
119. McMahon CJ, Penny DJ, Nelson DP, et al. Preterm infants with congenital heart disease and bronchopulmonary dysplasia: postoperative course and outcome after cardiac surgery. *Pediatrics* 2005;116:423–430.
120. Engelfriet P, Meijboom F, Boersma E, et al. Repaired and open atrial septal defects type II in adulthood: an epidemiological study of a large European cohort. *Int J Cardiol* 2008;126:379–385.
121. Engelfriet PM, Duffels MG, Moller T, et al. Pulmonary arterial hypertension in adults born with a heart septal defect: the Euro heart survey on adult congenital heart disease. *Heart* 2007;93:682–687.
122. Steele PM, Fuster V, Cohen M, et al. Isolated atrial septal defect with pulmonary vascular obstructive disease—long-term follow-up and prediction of outcome after surgical correction. *Circulation* 1987;76:1037–1042.
123. Vogel M, Berger F, Kramer A, et al. Incidence of secondary pulmonary hypertension in adults with atrial septal or sinus venosus defects. *Heart* 1999;82:30–33.
124. Beghetti M, Adatia I. Inhaled nitric oxide and congenital cardiac disease. *Cardiol Young* 2001;11:142–152.
125. Giglia TM, Humpl T. Preoperative pulmonary hemodynamics and assessment of operability: is there a pulmonary vascular resistance that precludes cardiac operation? *Pediatr Crit Care Med* 2010;11:S57–S69.
126. Morris K, Beghetti M, Petros A, et al. Comparison of hyperventilation and inhaled nitric oxide for pulmonary hypertension after repair of congenital heart disease. *Crit Care Med* 2000;28:2974–2978.
127. Viswanathan S, Kumar RK. Assessment of operability of congenital cardiac shunts with increased pulmonary vascular resistance. *Catheter Cardiovasc Interv* 2008;71:665–670.
128. Wessel DL, Adatia I. Clinical applications of inhaled nitric oxide in children with pulmonary hypertension. *Adv Pharmacol* 1995;34:475–504.
129. Wessel DL, Adatia I, Giglia TM, et al. Use of inhaled nitric oxide and acetylcholine in the evaluation of pulmonary hypertension and endothelial function after cardiopulmonary bypass. *Circulation* 1993;88:2128–2138.
130. Haworth SG. Pulmonary vascular bed in children with complete atrioventricular septal defect: relation between structural and hemodynamic abnormalities. *Am J Cardiol* 1986;57:833–839.
131. Beghetti M, Tissot C. Pulmonary arterial hypertension and congenital heart disease: targeted therapies and operability. *J Thorac Cardiovasc Surg* 2009;138:785–786.
132. Hoffman JI, Rudolph AM, Heymann MA. Pulmonary vascular disease with congenital heart lesions: pathologic features and causes. *Circulation* 1981;64:873–877.
133. Lopes AA, O'Leary PW. Measurement, interpretation and use of haemodynamic parameters in pulmonary hypertension associated with congenital cardiac disease. *Cardiol Young* 2009;19:431–435.
134. Blackstone EH, Kirklin JW, Bradley EL, et al. Optimal age and results in repair of large ventricular septal defects. *J Thor Cardiovasc Surg* 1976;72:661–679.
135. Haneda K, Sato N, Togo T, et al. Late results after correction of ventricular septal defect with severe pulmonary hypertension. *Tohoku J Exp Med* 1994;174:41–48.
136. Weidman WH, Blount SG Jr, DuShane JW, et al. Clinical course in ventricular septal defect. *Circulation* 1977;56:156–169.
137. Li J, Bush A, Schulze-Neick I, et al. Measured versus estimated oxygen consumption in ventilated patients with congenital heart disease: the validity of predictive equations. *Crit Care Med* 2003;31:1235–1240.
138. Rutledge J, Bush A, Shekerdemian L, et al. Validity of the LaFarge equation for estimation of oxygen consumption in ventilated children with congenital heart disease younger than 3 years—a revisit. *Am Heart J* 2010;160:109–114.
139. Shaddy R. Pulmonary hypertension in pediatric heart transplantation. *Prog Pediatr Cardiol* 2002;11:131–136.
140. Lock JE, Einzig S, Bass JL, et al. The pulmonary vascular response to oxygen and its influence on operative results in children with ventricular septal defect. *J Thorac Cardiovasc Surg* 1982;3:41–46.
141. Neutze JM, Ishikawa T, Clarkson PM, et al. Assessment and follow-up of patients with ventricular septal defect and elevated pulmonary vascular resistance. *Am J Cardiol* 1989;63:327–331.
142. Moller JH, Patton C, Varco RL, et al. Late results (30 to 35 years) after operative closure of isolated ventricular septal defect from 1954 to 1960. *Am J Cardiol* 1991;68:1491–1497.

143. Berner M, Beghetti M, Spahr-Schopfer I, et al. Inhaled nitric oxide to test the vasodilator capacity of the pulmonary vascular bed in children with long-standing pulmonary hypertension and congenital heart disease. *Am J Cardiol* 1996;77:532-535.
144. Atz AM, Adatia I, Lock JE, et al. Combined effects of nitric oxide and oxygen during acute pulmonary vasodilator testing. *J Am Coll Cardiol* 1999;33:813-819.
145. Balzer DT, Kort HW, Day RW, et al. Inhaled nitric oxide as a preoperative test (INOP test I): The INOP test study group. *Circulation* 2002;106:176-181.
146. Kannan BR, Sivasankaran S, Tharakan JA, et al. Long-term outcome of patients operated for large ventricular septal defects with increased pulmonary vascular resistance. *Indian Heart J* 2003;55:161-166.
147. Lopes A. Pre-operative pulmonary hypertension in congenital heart disease and aspects of Eisenmenger's syndrome in children. In: Beghetti MEA, ed. *Pediatric Pulmonary Hypertension*. Munich, Germany: Elsevier Urban & Fischer, 2011.
148. Bush A, Busst CM, Haworth SG, et al. Correlations of lung morphology, pulmonary vascular resistance, and outcome in children with congenital heart disease. *Br Heart J* 1988;59:480-485.
149. Dimopoulos K, Peset A, Gatzoulis MA. Evaluating operability in adults with congenital heart disease and the role of pretreatment with targeted pulmonary arterial hypertension therapy. *Int J Cardiol* 2008;129:163-171.
150. Wood P. The Eisenmenger syndrome or pulmonary hypertension with reversed central shunt. *Br Med J* 1958;2:701-709.
151. Berman EB, Barst RJ. Eisenmenger's syndrome: current management. *Prog Cardiovasc Dis* 2002;45:129-138.
152. Beghetti M, Galie N. Eisenmenger syndrome a clinical perspective in a new therapeutic era of pulmonary arterial hypertension. *J Am Coll Cardiol* 2009;53:733-740.
153. Hopkins WE, Ochoa LL, Richardson GW, et al. Comparison of the hemodynamics and survival of adults with severe primary pulmonary hypertension or Eisenmenger syndrome. *J Heart Lung Transplant* 1996;15:100-105.
154. Vongpatanasin W, Brickner ME, Hillis LD, et al. The Eisenmenger syndrome in adults. *Ann Intern Med* 1998;128:745-755.
155. Rosenzweig EB, Barst RJ. Pulmonary arterial hypertension in children: a medical update. *Curr Opin Pediatr* 2008;20:288-293.
156. Kumar RK, Sandoval J. Advanced pulmonary vascular disease: the Eisenmenger syndrome. *Cardiol Young* 2009;19:622-626.
157. Saha A, Balakrishnan KG, Jaiswal PK, et al. Prognosis for patients with Eisenmenger syndrome of various aetiology. *Int J Cardiol* 1994;45:199-207.
158. Daliento L, Somerville J, Presbitero P, et al. Eisenmenger syndrome. Factors relating to deterioration and death. *Eur Heart J* 1998;19:1845-1855.
159. Cantor WJ, Harrison DA, Moussadji JS, et al. Determinants of survival and length of survival in adults with Eisenmenger syndrome. *Am J Cardiol* 1999;84:677-681.
160. Niwa K, Perloff JK, Kaplan S, et al. Eisenmenger syndrome in adults: ventricular septal defect, truncus arteriosus, univentricular heart. *J Am Coll Cardiol* 1999;34:223-232.
161. Perloff JK, Marelli AJ, Miner PD. Risk of stroke in adults with cyanotic congenital heart disease. *Circulation* 1993;87:1954-1959.
162. Sandoval J, Aguirre JS, Pulido T, et al. Nocturnal oxygen therapy in patients with the Eisenmenger syndrome. *Am J Resp Critic Care Med* 2001;164:1682-1687.
163. Mukhopadhyay S, Sharma M, Ramakrishnan S, et al. Phosphodiesterase-5 inhibitor in Eisenmenger syndrome: a preliminary observational study. *Circulation* 2006;114:1807-1810.
164. Galie N, Beghetti M, Gatzoulis MA, et al. Bosentan therapy in patients with Eisenmenger syndrome: A multicenter, double-blind, randomized, placebo-controlled study. *Circulation* 2006;114:48-54.
165. Dimopoulos K, Inuzuka R, Goletto S, et al. Improved survival among patients with Eisenmenger syndrome receiving advanced therapy for pulmonary arterial hypertension. *Circulation* 2010;121:20-25.
166. Berger RM, Beghetti M, Galie N, et al. Atrial septal defects versus ventricular arterial hypertension related to Eisenmenger's syndrome: a subgroup analysis. *Int J Cardiol* 2010;144:373-378.
167. Van Loon RL, Hoendermis ES, Duffels MG, et al. Long-term effect of bosentan in adults versus children with pulmonary arterial hypertension associated with systemic-to-pulmonary shunt: does the beneficial effect persist? *Am Heart J* 2007;154:776-782.
168. Dimopoulos K, Giannakoulas G, Wort SJ, et al. Pulmonary arterial hypertension in adults with congenital heart disease: distinct differences from other causes of pulmonary arterial hypertension and management implications. *Curr Opin Cardiol* 2008;23:545-554.
169. Krowka MJ. Hepatopulmonary syndrome and portopulmonary hypertension: Implications for liver transplantation. *Clin Chest Med* 2005;26:587-597.
170. Krowka MJ, Plevak D. The distinct concepts and implications of hepatopulmonary syndrome and portopulmonary hypertension. *Crit Care Med* 2005;33:470.
171. Rodriguez-Roisin R, Krowka MJ, Herve P, et al. Highlights of the ERS task force on pulmonary-hepatic vascular disorders. *J Hepatol* 2005;42:924-927.
172. Swanson KL, Wiesner RH, Krowka MJ. Natural history of hepatopulmonary syndrome: Impact of liver transplantation. *Hepatology* 2005;41:1122-1129.
173. Krowka MJ. Many faces of portopulmonary hypertension. *J Pediatr* 2005;147:3-4.
174. Hoepfer MM, Krowka MJ, Strassburg CP. Portopulmonary hypertension and hepatopulmonary syndrome. *Lancet* 2004;363:1461-1468.
175. Swanson KL, Krowka MJ. Screen for portopulmonary hypertension, especially in liver transplant candidates. *Cleve Clin J Med* 2008;75:121-122, 125-130, 133 passim.
176. Swanson KL, Wiesner RH, Nyberg SL, et al. Survival in portopulmonary hypertension: Mayo clinic experience categorized by treatment subgroups. *Am J Transplant* 2008;8:2445-2453.
177. Ridaura-Sanz C, Mejia-Hernandez C, Lopez-Corella E. Portopulmonary hypertension in children. A study in pediatric autopsies. *Arch Med Res* 2009;40:635-639.
178. Ling Y, Zhang J, Luo B, et al. The role of endothelin-1 and the endothelin b receptor in the pathogenesis of hepatopulmonary syndrome in the rat. *Hepatology* 2004;39:1593-1602.
179. Luo B, Liu L, Tang L, et al. ET-1 and TNF-alpha in HPS: analysis in prehepatic portal hypertension and biliary and nonbiliary cirrhosis in rats. *Am J Physiol Gastrointest Liver Physiol* 2004;286:G294-G303.
180. Dodge-Khatami A, Sreeram N, de Mol BA, et al. Systemic plasma vascular endothelial growth factor levels as a marker for increased angiogenesis during the single ventricle surgical pathway. *Interact Cardiovasc Thorac Surg* 2003;2:458-461.
181. Mumtaz MA, Fraga CH, Nicholls CM, et al. Increased expression of vascular endothelial growth factor messenger RNA in lungs of rats after cavopulmonary anastomosis. *J Thorac Cardiovasc Surg* 2005;129:209-210.
182. Ootaki Y, Yamaguchi M, Yoshimura N, et al. Vascular endothelial growth factor in children with congenital heart disease. *Ann Thorac Surg* 2003;75:1523-1526.
183. Malhotra SP, Reddy VM, Thelitz S, et al. The role of oxidative stress in the development of pulmonary arteriovenous malformations after cavopulmonary anastomosis. *J Thorac Cardiovasc Surg* 2002;124:479-485.
184. Starnes SL, Duncan BW, Kneebone JM, et al. Angiogenic proteins in the lungs of children after cavopulmonary anastomosis. *J Thorac Cardiovasc Surg* 2001;122:518-523.
185. Weber MA, Ashworth MT, Sebire NJ. Portopulmonary hypertension in childhood presenting as sudden death. *Pediatr Dev Pathol* 2006;9:65-71.
186. Kim HC, Nahum K, Raska K, Jr, et al. Natural history of acquired immunodeficiency syndrome in hemophilic patients. *Am J Hematol* 1987;24:169-176.
187. Polos PG, Wolfe D, Harley RA, et al. Pulmonary hypertension and human immunodeficiency virus infection. Two reports and a review of the literature. *Chest* 1992;101:474-478.
188. Zuber JP, Calmy A, Evison JM, et al. Pulmonary arterial hypertension related to HIV infection: Improved hemodynamics and survival associated with antiretroviral therapy. *Clin Infect Dis* 2004;38:1178-1185.
189. Diogenes MS, Succi RC, Machado DM, et al. Cardiac longitudinal study of children perinatally exposed to human immunodeficiency virus type 1. *Arq Bras Cardiol* 2005;85:233-240.
190. Pongprot Y, Sittiwangkul R, Silvilairat S, et al. Cardiac manifestations in HIV-infected Thai children. *Ann Trop Paediatr* 2004;24:153-159.
191. McDonald CL, Kaltman JR. Cardiovascular disease in adult and pediatric HIV/AIDS. *J Am Coll Cardiol* 2009;54:1185-1188.
192. Humbert M. Mediators involved in HIV-related pulmonary arterial hypertension. *AIDS* 2008;22:S41-S47.
193. Barbaro G, Lucchini A, Pellicelli AM, et al. Highly active antiretroviral therapy compared with HAART and bosentan in combination in patients with HIV-associated pulmonary hypertension. *Heart* 2006;92:1164-1166.
194. Zuckerman WA, Rosenzweig EB. Pulmonary hypertension in children with sickle cell disease. *Expert Rev Respir Med* 2011;5:233-243.
195. Gladwin MT, Sachdev V, Jison ML, et al. Pulmonary hypertension as a risk factor for death in patients with sickle cell disease. *N Engl J Med* 2004;350:886-895.
196. Pashankar FD, Carbonella J, Bazy-Asaad A, et al. Prevalence and risk factors of elevated pulmonary artery pressures in children with sickle cell disease. *Pediatrics* 2008;121:777-782.
197. Villavicencio K, Ivy D, Cole L, et al. Symptomatic pulmonary hypertension in a child with sickle cell disease. *J Pediatr* 2008;152:879-881.
198. Nelson SC, Adade BB, McDonough EA, et al. High prevalence of pulmonary hypertension in children with sickle cell disease. *J Pediatr Hematol Oncol* 2007;29:334-337.
199. Onyekwere OC, Campbell A, Teshome M, et al. Pulmonary hypertension in children and adolescents with sickle cell disease. *Pediatr Cardiol* 2008;29:309-312.
200. Sedrak A, Rao SP, Miller ST, et al. A prospective appraisal of pulmonary hypertension in children with sickle cell disease. *J Pediatr Hematol Oncol* 2009;31:97-100.
201. Suell MN, Bezold LI, Okcu MF, et al. Increased pulmonary artery pressures among adolescents with sickle cell disease. *J Pediatr Hematol Oncol* 2005;27:654-658.
202. Pashankar FD, Carbonella J, Bazy-Asaad A, et al. Longitudinal follow up of elevated pulmonary artery pressures in children with sickle cell disease. *Br J Haematol* 2009;144:736-741.

203. Adejebi MO, Cespedes J, Allen K, et al. Pulmonary thrombotic arteriopathy in patients with sickle cell disease. *Arch Pathol Lab Med* 2001;125:1436-1441.
204. Sachdev V, Machado RF, Shizukuda Y, et al. Diastolic dysfunction is an independent risk factor for death in patients with sickle cell disease. *J Am Coll Cardiol* 2007;49:472-479.
205. Hoffman JI. Pulmonary vascular resistance and viscosity: the forgotten factor. *Pediatr Cardiol* 2011;32:557-561.
206. Morris CR. Mechanisms of vasculopathy in sickle cell disease and thalassemia. *Hematology Am Soc Hematol Educ Program* 2008:177-185.
207. Kato GJ, Martyr S, Blackwelder WC, et al. Levels of soluble endothelium-derived adhesion molecules in patients with sickle cell disease are associated with pulmonary hypertension, organ dysfunction, and mortality. *Br J Haematol* 2005;130:943-953.
208. Bunn HF, Nathan DG, Dover GJ, et al. Pulmonary hypertension and nitric oxide depletion in sickle cell disease. *Blood* 2010;116:687-692.
209. Gladwin MT, Barst RJ, Castro OL, et al. Pulmonary hypertension and NO in sickle cell. *Blood* 2010;116:852-854.
210. Montani D, Jais X, Price LC, et al. Cautious use of epoprostenol therapy is a safe bridge to lung transplantation in pulmonary veno-occlusive disease. *Eur Respir J* 2009;34:1348-1356.
211. Montani D, Price LC, Dorfmueller P, et al. Pulmonary veno-occlusive disease. *Eur Respir J* 2009;33:189-200.
212. Humbert M, Maitre S, Capron F, et al. Pulmonary edema complicating continuous intravenous prostacyclin in pulmonary capillary hemangiomatosis. *Am J Resp Crit Care Med* 1998;157:1681-1685.
213. Kawut SM, Assaad AM, Arcasoy SM, et al. Pulmonary capillary hemangiomatosis: results of gene expression analysis. *Chest* 2005;128:575S-576S.
214. Lantuejoul S, Sheppard MN, Corrin B, et al. Pulmonary veno-occlusive disease and pulmonary capillary hemangiomatosis: a clinicopathologic study of 35 cases. *Am J Surg Pathol* 2006;30:850-857.
215. Frazier AA, Franks TJ, Mohammed TL, et al. From the archives of the AFIP: pulmonary veno-occlusive disease and pulmonary capillary hemangiomatosis. *Radiographics* 2007;27:867-882.
216. Gugnani MK, Pierson C, Vanderheide R, et al. Pulmonary edema complicating prostacyclin therapy in pulmonary hypertension associated with scleroderma: a case of pulmonary capillary hemangiomatosis. *Arthritis Rheum* 2000;43:699-703.
217. Harch S, Whitford H, McLean C. Failure of medical therapy in pulmonary arterial hypertension. Is there an alternative diagnosis? *Chest* 2009;135:1462-1469.
218. Overbeek MJ, van Nieuw Amerongen GP, Boonstra A, et al. Possible role of imatinib in clinical pulmonary veno-occlusive disease. *Eur Respir J* 2008;32:232-235.
219. White CW, Wolf SJ, Korones DN, et al. Treatment of childhood angiomatous diseases with recombinant interferon alfa-2a. *J Pediatr* 1991;118:59-66.
220. Ginns LC, Roberts DH, Mark EJ, et al. Pulmonary capillary hemangiomatosis with atypical endotheliomatosis: Successful antiangiogenic therapy with doxycycline. *Chest* 2003;124:2017-2022.
221. Adatia I, Kulik T, Mullen M. Pulmonary venous hypertension or pulmonary hypertension due to left heart disease. *Prog Pediatr Cardiol* 2009;27:35-42.
222. Wood P. An appreciation of mitral stenosis: II. Investigations and results. *Br Med J* 1954;1:1113-1124.
223. Wood P. An appreciation of mitral stenosis. I. Clinical features. *Br Med J* 1954;1:1051-1063.
224. Wood P. Pulmonary hypertension with special reference to the vasoconstrictive factor. *Br Heart J* 1958;20:557-570.
225. Wood P, Besterman EM, Towers MK, et al. The effect of acetylcholine on pulmonary vascular resistance and left atrial pressure in mitral stenosis. *Br Heart J* 1957;19:279-286.
226. Adatia I, Perry S, Landzberg M, et al. Inhaled nitric oxide and hemodynamic evaluation of patients with pulmonary hypertension before transplantation. *J Am Coll Cardiol* 1995;25:1656-1664.
227. Bocchi EA, Bacal F, Auler Junior JO, et al. Inhaled nitric oxide leading to pulmonary edema in stable severe heart failure. *Am J Cardiol* 1994;74:70-72.
228. Loh E, Stamler JS, Hare JM, et al. Cardiovascular effects of inhaled nitric oxide in patients with left ventricular dysfunction. *Circulation* 1994;90:2780-2785.
229. Drossner DM, Kim DW, Maher KO, et al. Pulmonary vein stenosis: prematurity and associated conditions. *Pediatrics* 2008;122:e656-e661.
230. Holcomb RG, Tyson RW, Ivy DD, et al. Congenital pulmonary venous stenosis presenting as persistent pulmonary hypertension of the newborn. *Pediatr Pulmonol* 1999;28:301-306.
231. Jenkins KJ, Sanders SP, Orav EJ, et al. Individual pulmonary vein size and survival in infants with totally anomalous pulmonary venous connection. *J Am Coll Cardiol* 1993;22:201-206.
232. Peng LF, Lock JE, Nugent AW, et al. Comparison of conventional and cutting balloon angioplasty for congenital and postoperative pulmonary vein stenosis in infants and young children. *Catheter Cardiovasc Interv* 2010;75:1084-1090.
233. Riedlinger WF, Juraszek AL, Jenkins KJ, et al. Pulmonary vein stenosis: Expression of receptor tyrosine kinases by lesional cells. *Cardiovasc Pathol* 2006;15:91-99.
234. Sadr IM, Tan PE, Kieran MW, et al. Mechanism of pulmonary vein stenosis in infants with normally connected veins. *Am J Cardiol* 2000;86:577-579, A510.
235. Shuhaiber J, Rehman M, Jenkins K, et al. The role of surgical therapy for pulmonary vein atresia in childhood. *Pediatr Cardiol* 2011;32:639-645.
236. Lacour-Gayet F. Surgery for pulmonary venous obstruction after repair of total anomalous pulmonary venous return. *Semin Thorac Cardiovasc Surg Pediatr Card Surg Annu* 2006:45-50.
237. Lacour-Gayet F, Rey C, Planché C. Pulmonary vein stenosis. Description of a sutureless surgical procedure using the pericardium in situ. *Archives des Maladies du Cœur et des Vaisseaux* 1996;89:633-636.
238. Lacour-Gayet F, Zoghbi J, Serraf AE, et al. Surgical management of progressive pulmonary venous obstruction after repair of total anomalous pulmonary venous connection. *J Thorac Cardiovasc Surg* 1999;117:679-687.
239. Serraf A, Bruniaux J, Lacour-Gayet F, et al. Obstruction of total anomalous pulmonary venous drainage. Factors influencing improvement in surgical results. *Archives des maladies du cœur et des vaisseaux* 1990;83:643-646.
240. Parker TA, Abman SH. The pulmonary circulation in bronchopulmonary dysplasia. *Semin Neonatol* 2003;8:51-62.
241. Thebaud B. Angiogenesis in lung development, injury and repair: implications for chronic lung disease of prematurity. *Neonatology* 2007;91:291-297.
242. Thebaud B, Abman SH. Bronchopulmonary dysplasia: where have all the vessels gone? Roles of angiogenic growth factors in chronic lung disease. *Am J Respir Crit Care Med* 2007;175:978-985.
243. Mourani PM, Mullen M, Abman SH. Pulmonary hypertension in bronchopulmonary dysplasia. *Progress in Pediatric Cardiology* 2009;27:43-48.
244. Khemani E, McElhinney DB, Rhein L, et al. Pulmonary artery hypertension in formerly premature infants with bronchopulmonary dysplasia: clinical features and outcomes in the surfactant era. *Pediatrics* 2007;120:1260-1269.
245. Kulik TJ, Rhein LM, Mullen MP. Pulmonary arterial hypertension in infants with chronic lung disease: will we ever understand it? *J Pediatr* 2010;157:186-190.
246. Mourani PM, Ivy DD, Rosenberg AA, et al. Left ventricular diastolic dysfunction in bronchopulmonary dysplasia. *J Pediatr* 2008;152:291-293.
247. Keller RL. Antenatal and postnatal lung and vascular anatomic and functional studies in congenital diaphragmatic hernia: implications for clinical management. *Am J Med Genet C Semin Med Genet* 2007;145C:184-200.
248. Keller RL, Moore P, Teitel D, et al. Abnormal vascular tone in infants and children with lung hypoplasia: findings from cardiac catheterization and the response to chronic therapy. *Pediatr Crit Care Med* 2006;7:589-594.
249. Keller RL, Tacy TA, Hendricks-Munoz K, et al. Congenital diaphragmatic hernia: Endothelin-1, pulmonary hypertension, and disease severity. *Am J Respir Crit Care Med* 2010;182:555-561.
250. Kinsella JP, Ivy DD, Abman SH. Pulmonary vasodilator therapy in congenital diaphragmatic hernia: acute, late, and chronic pulmonary hypertension. *Semin Perinatol* 2005;29:123-128.
251. Thebaud B, Tibboel D. Pulmonary hypertension associated with congenital diaphragmatic hernia. *Cardiol Young* 2009;19:49-53.
252. Barst RJ. Recent advances in the treatment of pediatric pulmonary artery hypertension. *Pediatr Clin North Am* 1999;46:331-345.
253. Rashid A, Ivy D. Severe paediatric pulmonary hypertension: new management strategies. *Arch Dis Child* 2005;90:92-98.
254. Auger WR CR, Kerr KM, et al. Evaluation of patients with suspected chronic thromboembolic pulmonary hypertension. *Semin Thorac Cardiovasc Surg* 1999;11:179-190.
255. Tissot C, Ivy DD, Beghetti M. Medical therapy for pediatric pulmonary arterial hypertension. *J Pediatr* 2010;157:528-532.
256. Rimensberger PC, Spahr-Schopfer I, Berner M, et al. Inhaled nitric oxide versus aerosolized iloprost in secondary pulmonary hypertension in children with congenital heart disease: vasodilator capacity and cellular mechanisms. *Circulation* 2001;103:544-548.
257. Pepke-Zaba J HT, Dinh-Xaun AT, et al. Inhaled nitric oxide as a cause of selective pulmonary vasodilatation in pulmonary hypertension. *Lancet* 1991;338:1173-1174.
258. Ivy DD, Kinsella JP, Wolfe RR, et al. Atrial natriuretic peptide and nitric oxide in children with pulmonary hypertension after surgical repair of congenital heart disease. *Am J Cardiol* 1996;77:102-105.
259. Ivy DD, Ziegler JW, Kinsella JP, et al. Hemodynamic effects of dipyridamole and inhaled nitric oxide in pediatric patients with pulmonary hypertension. *Chest* 1998;114:175.
260. Atz AM WD. Inhaled nitric oxide in the neonate with cardiac disease. *Semin Perinatol* 1997;21:441-455.
261. Roberts JD, Jr, Lang P, Bigatello LM, et al. Inhaled nitric oxide in congenital heart disease. *Circulation* 1993;87:447-453.
262. Rich S SM, Dodin E, et al. The short-term effects of digoxin in patients with right ventricular dysfunction from pulmonary hypertension. *Chest* 1998;114:787-792.
263. Barst RJ, Abenheim L. Fatal pulmonary arterial hypertension associated with phenylpropanolamine exposure. *Heart* 2004;90:e42.
264. Beghetti M. Current treatment options in children with pulmonary arterial hypertension and experiences with oral bosentan. *Eur J Clin Invest* 2006;36:16-24.
265. Barst RJ, Agnoletti G, Fraisse A, et al. Vasodilator testing with nitric oxide and/or oxygen in pediatric pulmonary hypertension. *Pediatr Cardiol* 2010;31:598-606.
266. Sitbon O, Humbert M, Jais X, et al. Long-term response to calcium channel blockers in idiopathic pulmonary arterial hypertension. *Circulation* 2005;111:3105-3111.

267. Haworth SG. The management of pulmonary hypertension in children. *Arch Dis Child* 2008;93:620–625.
268. Adatia I, Barrow SE, Stratton PD, et al. Thromboxane a₂ and prostacyclin biosynthesis in children and adolescents with pulmonary vascular disease. *Circulation* 1993;88:2117–2122.
269. Tuder RM, Cool CD, Geraci MW, et al. Prostacyclin synthase expression is decreased in lungs from patients with severe pulmonary hypertension. *Am J Respir Crit Care Med* 1999;159:1925–1932.
270. Barst RJ, Rubin LJ, McGoon MD, et al. Survival in primary pulmonary hypertension with long-term continuous intravenous prostacyclin. *Ann Intern Med* 1994;121:409–415.
271. Nakayama T, Shimada H, Takatsuki S, et al. Efficacy and limitations of continuous intravenous epoprostenol therapy for idiopathic pulmonary arterial hypertension in Japanese children. *Circ J* 2007;71:1785–1790.
272. Saji T, Nakayama T, Ishikita T, et al. Current status and future prospect of prostacyclin therapy for pulmonary hypertension—intravenous, subcutaneous, inhaled and oral PGI₂ derivatives. *Nippon Rinsho* 2001;59:1132–1138.
273. Doran A, Harris S, Goetz B. Advances in prostanoid infusion therapy for pulmonary arterial hypertension. *J Infus Nurs* 2008;31:336–345.
274. Doran AK, Ivy DD, Barst RJ, et al. Guidelines for the prevention of central venous catheter-related blood stream infections with prostanoid therapy for pulmonary arterial hypertension. *Int J Clin Pract Suppl* 2008;160:5–9.
275. Ivy DD, Calderbank M, Wagner BD, et al. Closed-hub systems with protected connections and the reduction of risk of catheter-related blood-stream infection in pediatric patients receiving intravenous prostanoid therapy for pulmonary hypertension. *Infect Control Hosp Epidemiol* 2009;30:823–829.
276. Melnick L, Barst RJ, Rowan CA, et al. Effectiveness of transition from intravenous epoprostenol to oral/inhaled targeted pulmonary arterial hypertension therapy in pediatric idiopathic and familial pulmonary arterial hypertension. *Am J Cardiol* 2010;105:1485–1489.
277. Ivy DD. Prostacyclin in the intensive care setting. *Pediatr Crit Care Med* 2010;11:S41–S45.
278. Barst RJ, Galie N, Naeije R, et al. Long-term outcome in pulmonary arterial hypertension patients treated with subcutaneous treprostinil. *Eur Respir J* 2006;28:1195–1203.
279. Ivy DD, Claussen L, Doran A. Transition of stable pediatric patients with pulmonary arterial hypertension from intravenous epoprostenol to intravenous treprostinil. *Am J Cardiol* 2007;99:696–698.
280. Levy M, Celermajor DS, Bourges-Petit E, et al. Add-on therapy with subcutaneous treprostinil for refractory pediatric pulmonary hypertension. *J Pediatr* 2011;158:584–588.
281. Voswinckel R, Enke B, Reichenberger F, et al. Favorable effects of inhaled treprostinil in severe pulmonary hypertension: results from randomized controlled pilot studies. *J Am Coll Cardiol* 2006;48:1672–1681.
282. Olschewski H, Simonneau G, Galie N, et al. Inhaled iloprost for severe pulmonary hypertension. *N Engl J Med* 2002;347:322–329.
283. Beghetti M, Berner M, Rimensberger PC. Long term inhalation of iloprost in a child with primary pulmonary hypertension: an alternative to continuous infusion. *Heart* 2001;86:E10.
284. Hallioglu O, Dilber E, Celiker A. Comparison of acute hemodynamic effects of aerosolized and intravenous iloprost in secondary pulmonary hypertension in children with congenital heart disease. *Am J Cardiol* 2003;92:1007–1009.
285. McLaughlin VV, Oudiz RJ, Frost A, et al. Randomized study of adding inhaled iloprost to existing bosentan in pulmonary arterial hypertension. *Am J Respir Crit Care Med* 2006;174:1257–1263.
286. Ghofrani HA, Wiedemann R, Rose F, et al. Sildenafil for treatment of lung fibrosis and pulmonary hypertension: A randomised controlled trial. *Lancet* 2002;360:895–900.
287. Ghofrani HA, Rose F, Schermuly RT, et al. Oral sildenafil as long-term adjunct therapy to inhaled iloprost in severe pulmonary arterial hypertension. *J Am Coll Cardiol* 2003;42:158–164.
288. Saji T, Ozawa Y, Ishikita T, et al. Short-term hemodynamic effect of a new oral PGI₂ analogue, beraprost, in primary and secondary pulmonary hypertension. *Am J Cardiol* 1996;78:244–247.
289. Kunieda T, Nakanishi N, Matsubara H, et al. Effects of long-acting beraprost sodium (trk-100st) in Japanese patients with pulmonary arterial hypertension. *Int Heart J* 2009;50:513–529.
290. Rubin LJ, Roux S. Bosentan: a dual endothelin receptor antagonist. *Expert Opin Investig Drugs* 2002;11:991–1002.
291. Beghetti M, Black SM, Fineman JR. Endothelin-1 in congenital heart disease. *Pediatr Res* 2005;57:16R–20R.
292. Giaid A, Yanagisawa M, Langleben D, et al. Expression of endothelin-1 in the lungs of patients with pulmonary hypertension. *N Engl J Med* 1993;328:1732–1739.
293. Lutz J, Gorenflo M, Habighorst M, et al. Endothelin-1- and endothelin-receptors in lung biopsies of patients with pulmonary hypertension due to congenital heart disease. *Clin Chem Lab Med* 1999;37:423–428.
294. Rubin LJ, Badesch DB, Barst RJ, et al. Bosentan therapy for pulmonary arterial hypertension. *N Engl J Med* 2002;346:896–903.
295. Barst RJ, Ivy D, Dingemans J, et al. Pharmacokinetics, safety, and efficacy of bosentan in pediatric patients with pulmonary arterial hypertension. *Clin Pharmacol Ther* 2003;73:372–382.
296. Simpson CM, Penny DJ, Cochrane AD, et al. Preliminary experience with bosentan as initial therapy in childhood idiopathic pulmonary arterial hypertension. *J Heart Lung Transplant* 2006;25:469–473.
297. Maiya S, Hislop AA, Flynn Y, et al. Response to bosentan in children with pulmonary hypertension. *Heart* 2006;92:664–670.
298. Sibon O, Beghetti M, Petit J, et al. Bosentan for the treatment of pulmonary arterial hypertension associated with congenital heart defects. *Eur J Clin Invest* 2006;36:25–31.
299. Ivy DD, Rosenzweig EB, Lemarie JC, et al. Long-term outcomes in children with pulmonary arterial hypertension treated with bosentan in real-world clinical settings. *Am J Cardiol* 2010;106:1332–1338.
300. Taguchi M, Ichida F, Hirono K, et al. Pharmacokinetics of bosentan in routinely treated Japanese pediatric patients with pulmonary arterial hypertension. *Drug Metab Pharmacokinet* 2011;26:280–287.
301. Beghetti M, Haworth SG, Bonnet D, et al. Pharmacokinetic and clinical profile of a novel formulation of bosentan in children with pulmonary arterial hypertension: the FUTURE-1 study. *Br J Clin Pharmacol* 2009;68:948–955.
302. Barst RJ, Langleben D, Badesch D, et al. Treatment of pulmonary arterial hypertension with the selective endothelin-a receptor antagonist sitaxsentan. *J Am Coll Cardiol* 2006;47:2049–2056.
303. Barst RJ, Rich S, Widlitz A, et al. Clinical efficacy of sitaxsentan, an endothelin-a receptor antagonist, in patients with pulmonary arterial hypertension: open-label pilot study. *Chest* 2002;121:1860–1868.
304. Barst RJ, Langleben D, Frost A, et al. Sitaxsentan therapy for pulmonary arterial hypertension. *Am J Respir Crit Care Med* 2004;169:441–447.
305. Takatsuki S, Rosenzweig EB, et al. Clinical safety and efficacy of ambrisentan therapy in children with pulmonary arterial hypertension. *Pediatr Pulmonol* (in press).
306. Galie N, Badesch D, Oudiz R, et al. Ambrisentan therapy for pulmonary arterial hypertension. *J Am Coll Cardiol* 2005;46:529–535.
307. Cohen AH, Hanson K, Morris K, et al. Inhibition of cyclic 3'-5'-guanosine monophosphate-specific phosphodiesterase selectively vasodilates the pulmonary circulation in chronically hypoxic rats. *J Clin Invest* 1996;97:172–179.
308. Hanson KA, Ziegler JW, Rybalkin SD, et al. Chronic pulmonary hypertension increases fetal lung cgmp phosphodiesterase activity. *Am J Physiol* 1998;275:L931–L941.
309. Prasad S, Wilkinson J, Gatzoulis MA. Sildenafil in primary pulmonary hypertension. *N Engl J Med* 2000;343:1342.
310. Kumar S. Indian doctor in protest after using viagra to save “blue babies”. *BMJ* 2002;325:181.
311. Michelakis ED, Tymchak W, Noga M, et al. Long-term treatment with oral sildenafil is safe and improves functional capacity and hemodynamics in patients with pulmonary arterial hypertension. *Circulation* 2003;108:2066–2069.
312. Abrams D, Schulze-Neick I, Magee AG. Sildenafil as a selective pulmonary vasodilator in childhood primary pulmonary hypertension. *Heart* 2000;84:E4.
313. Karatza AA, Bush A, Magee AG. Safety and efficacy of sildenafil therapy in children with pulmonary hypertension. *Int J Cardiol* 2005;100:267–273.
314. Galie N, Ghofrani HA, Torbicki A, et al. Sildenafil citrate therapy for pulmonary arterial hypertension. *N Engl J Med* 2005;353:2148–2157.
315. Ivy DD, Kinsella JP, Ziegler JW, et al. Dipyridamole attenuates rebound pulmonary hypertension after inhaled nitric oxide withdrawal in postoperative congenital heart disease. *J Thorac Cardiovasc Surg* 1998;115:875–882.
316. Atz AM, Wessel DL. Sildenafil ameliorates effects of inhaled nitric oxide withdrawal. *Anesthesiology* 1999;91:307–310.
317. Namachivayam P, Theilen U, Burt WW, et al. Sildenafil prevents rebound pulmonary hypertension after withdrawal of nitric oxide in children. *Am J Respir Crit Care Med* 2006;174:1042–1047.
318. Atz AM, Fairbrother DL, Uber WE, et al. Sildenafil augments the effect of inhaled nitric oxide for postoperative pulmonary hypertensive crisis. *J Thorac Cardiovasc Surg* 2002;124:628–629.
319. Humpl T, Reyes JT, Holtby H, et al. Beneficial effect of oral sildenafil therapy on childhood pulmonary arterial hypertension: twelve-month clinical trial of a single-drug, open-label, pilot study. *Circulation* 2005;111:3274–3280.
320. Mourani PM, Sontag MK, Ivy DD, et al. Effects of long-term sildenafil treatment for pulmonary hypertension in infants with chronic lung disease. *J Pediatr* 2009;154:379–384.
321. Satoh T, Saji T, Watanabe H, et al. A phase III, multicenter, collaborative, open-label clinical trial of sildenafil in Japanese patients with pulmonary arterial hypertension. *Circ J* 2011;75:677–682.
322. Barst RJ, Ivy DD, Gaitan G, et al. A randomized, double-blind, placebo-controlled, dose-ranging study of oral sildenafil citrate in treatment-naïve children with pulmonary arterial hypertension. *Circulation* 2012;125:324–34.
323. Schulze-Neick I, Hartenstein P, Li J, et al. Intravenous sildenafil is a potent pulmonary vasodilator in children with congenital heart disease. *Circulation* 2003;108:II167–II173.
324. Stocker C, Penny DJ, Brizard CP, et al. Intravenous sildenafil and inhaled nitric oxide: a randomised trial in infants after cardiac surgery. *Int Care Med* 2003;29:1996–2003.

325. Steinhorn RH, Kinsella JP, Pierce C, et al. Intravenous sildenafil in the treatment of neonates with persistent pulmonary hypertension. *J Pediatr* 2009;155:841–847.
326. Takatsuki S, Calderbank M, Ivy DD. Initial experience with tadalafil in pediatric pulmonary arterial hypertension. *Pediatr Cardiol*. 2013;33(5):683–8.
327. Bendayan D, Shitrit D, Kramer MR. Combination therapy with prostacyclin and tadalafil for severe pulmonary arterial hypertension: a pilot study. *Respirology* 2008;13:916–918.
328. Galie N, Brundage BH, Ghofrani HA, et al. Tadalafil therapy for pulmonary arterial hypertension. *Circulation* 2009;119:2894–2903.
329. Rosenzweig EB. Tadalafil for the treatment of pulmonary arterial hypertension. *Expert Opin Pharmacother* 2010;11:127–132.
330. Barst RJ, Oudiz RJ, Beardsworth A, et al. Tadalafil monotherapy and as add-on to background bosentan in patients with pulmonary arterial hypertension. *J Heart Lung Transplant* 2011;30:632–643.
331. Jing ZC, Yu ZX, Shen JY, et al. Vardenafil in pulmonary arterial hypertension: A randomized, double-blind, placebo-controlled study. *Am J Resp Critic Care Med* 2011;183:1723–1729.
332. Humbert M, Barst RJ, Robbins IM, et al. Combination of bosentan with epoprostenol in pulmonary arterial hypertension: Breathe-2. *Eur Respir J* 2004;24:353–359.
333. Simonneau G, Rubin LJ, Galie N, et al. Addition of sildenafil to long-term intravenous epoprostenol therapy in patients with pulmonary arterial hypertension: a randomized trial. *Ann Intern Med* 2008;149:521–530.
334. Hoeper MM, Markevych I, Spiekerkoetter E, et al. Goal-oriented treatment and combination therapy for pulmonary arterial hypertension. *Eur Respir J* 2005;26:858–863.
335. Micheletti A, Hislop AA, Lammers A, et al. Role of atrial septostomy in the treatment of children with pulmonary arterial hypertension. *Heart* 2006;92:969–972.
336. Sandoval J, Gaspar J, Pulido T, et al. Graded balloon dilation atrial septostomy in severe primary pulmonary hypertension. A therapeutic alternative for patients nonresponsive to vasodilator treatment. *J Am Coll Cardiol* 1998;32:297–304.
337. Blanc J, Vouhe P, Bonnet D. Potts shunt in patients with pulmonary hypertension. *N Engl J Med* 2004;350:623.
338. Labombarda F, Maragnes P, Dupont-Chauvet P, et al. Potts anastomosis for children with idiopathic pulmonary hypertension. *Pediatr Cardiol* 2009;30:1143–1145.
339. Gaynor JW, Bridges ND, Clark BJ, et al. Update on lung transplantation in children. *Curr Opin Pediatr* 1998;10:256–261.
340. Aurora P, Edwards LB, Kucheryavaya AY, et al. Registry of the international society for heart and lung transplantation: thirteenth official pediatric heart transplantation report—2010. *J Heart Lung Transplant* 2010;29:1129–1141.
341. Goldstein BS, Sweet SC, Mao J, et al. Lung transplantation in children with idiopathic pulmonary arterial hypertension: an 18-year experience. *J Heart Lung Transplant* 2011;30:1148–1152.
342. Hanna B, Conrad C. Lung transplantation for pediatric pulmonary hypertension. *Prog Pediatr Cardiol* 2009;27:49–55.
343. Dewachter L, Dewachter C, Naeije R. New therapies for pulmonary arterial hypertension: an update on current bench to bedside translation. *Expert Opin Investig Drugs* 2010;19:469–488.
344. Schermuly RT, Dony E, Ghofrani HA, et al. Reversal of experimental pulmonary hypertension by PDGF inhibition. *J Clin Invest* 2005;115:2811–2821.
345. Ghofrani HA, Morrell NW, Hoeper MM, et al. Imatinib in pulmonary arterial hypertension patients with inadequate response to established therapy. *Am J Resp Critic Care Med* 2010;182:1171–1177.
346. Ghofrani HA, Seeger W, Grimminger F. Imatinib for the treatment of pulmonary arterial hypertension. *N Engl J Med* 2005;353:1412–1413.
347. Girgis RE, Mozammel S, Champion HC, et al. Regression of chronic hypoxic pulmonary hypertension by simvastatin. *Am J Physiol Lung Cell Mol Physiol* 2007;292:L1105–L1110.
348. Kao PN. Simvastatin treatment of pulmonary hypertension: an observational case series. *Chest* 2005;127:1446–1452.
349. Kawut SM, Bagiella E, Lederer DJ, et al. Randomized clinical trial of aspirin and simvastatin for pulmonary arterial hypertension: ASA-STAT. *Circulation* 2011;123(25):2985–93.
350. Zhao YD, Courtman DW, Deng Y, et al. Rescue of monocrotaline-induced pulmonary arterial hypertension using bone marrow-derived endothelial-like progenitor cells: efficacy of combined cell and eNOS gene therapy in established disease. *Circ Res* 2005;96:442–450.
351. Stewart DJ, Zhao YD, Courtman DW. Cell therapy for pulmonary hypertension: what is the true potential of endothelial progenitor cells? *Circulation* 2004;109:e172–e173.
352. Satoh KMD, Fukumoto Y, Shimokawa H. Rho-kinase: important new therapeutic target in cardiovascular diseases. *Am J Physiol Heart Circ Physiol* 2011;301:H287–H297.
353. Fujita H, Fukumoto Y, Saji K, et al. Acute vasodilator effects of inhaled fasudil, a specific Rho-kinase inhibitor, in patients with pulmonary arterial hypertension. *Heart Vessels* 2010;25:144–149.
354. Li F, Xia W, Yuan S, Sun R. Acute inhibition of Rho-kinase attenuates pulmonary hypertension in patients with congenital heart disease. *Pediatr Cardiol* 2009;30:363–366.
355. Oka M, Homma N, Taraseviciene-Stewart L, et al. Rho kinase-mediated vasoconstriction is important in severe occlusive pulmonary arterial hypertension in rats. *Circ Res* 2007;100:923–929.
356. Ishikura K, Yamada N, Ito M, et al. Beneficial acute effects of Rho-kinase inhibitor in patients with pulmonary arterial hypertension. *Circ J* 2006;70:174–178.
357. Fukumoto Y, Matoba T, Ito A, et al. Acute vasodilator effects of a rho-kinase inhibitor, fasudil, in patients with severe pulmonary hypertension. *Heart* 2005;91:391–392.
358. Belik J. Riociguat, an oral soluble guanylate cyclase stimulator for the treatment of pulmonary hypertension. *Curr Opin Investig Drugs* 2009;10:971–979.
359. Ghofrani HA, Hoeper MM, Halank M, et al. Riociguat for chronic thromboembolic pulmonary hypertension and pulmonary arterial hypertension: a phase II study. *Eur Respir J* 2010;36:792–799.
360. Grimminger F, Weimann G, Frey R, et al. First acute haemodynamic study of soluble guanylate cyclase stimulator riociguat in pulmonary hypertension. *Eur Respir J* 2009;33:785–792.
361. Schermuly RT, Janssen W, Weissmann N, et al. Riociguat for the treatment of pulmonary hypertension. *Expert Opin Investig Drugs* 2011;20:567–576.
362. Morrison K, Ernst R, Hess P, et al. Selexipag: a selective prostacyclin receptor agonist that does not affect rat gastric function. *J Pharmacol Exp Ther* 2010;335:249–255.
363. Sidharta PN, van Giersbergen PL, Halabi A, et al. Macitentan: entry-into-humans study with a new endothelin receptor antagonist. *Eur J Clin Pharmacol* 2011;67:977–984.
364. Iglarz M, Binkert C, Morrison K, et al. Pharmacology of macitentan, an orally active tissue-targeting dual endothelin receptor antagonist. *J Pharmacol Exp Ther* 2008;327:736–745.

SECTION

IX

The Young Adult with Congenital Heart Disease

CHAPTER

68

The Adolescent and Adult with Congenital Heart Disease

Ali N. Zaidi ■ Curt J. Daniels

In the United States, there are approximately 1 million adults with congenital heart disease (CHD), with 20,000 new patients reaching adolescence each year (Fig. 68.1). With earlier pediatric and fetal diagnoses and improved medical, surgical and ICU care, it is now expected that 90% of patients born with CHD will survive to adulthood, and therefore, the number of adult congenital heart disease (ACHD) patients will continue to rise (Fig. 68.2). In fact, it is now estimated that there are more adults living with CHD than children (1) (Fig. 68.3).

Marelli et al. (2) estimated the prevalence of CHD from 1985 to 2000 for children and adults and also found a shift in the population living with CHD to those >18 years of age (Fig. 68.4). Therefore, with further improvements in diagnostic and therapeutic options, the population of adults with CHD will only continue to increase.

Many patients with simple lesions who have undergone total corrective surgery will have few if any hemodynamic residua requiring infrequent evaluation and treatment (e.g., atrial septal defects [ASD], ventricular septal defects [VSDs], patent ductus arteriosus [PDA], and mild pulmonary stenosis).

Patients with more complex lesions, or complications that stem from less complex lesions, such as residual shunts, valvular disease, ventricular dysfunction, and arrhythmias require more frequent evaluation, medical treatment, and consideration for further surgical or catheter-based interventions. As we continue to learn about surgically altered CHDs, some “routine” patients will have previously unrecognized problems. For other adults, surgical approaches of the past and their long-term complications (e.g., D-TGA s/p Mustard or Senning Atrial Repair) will eventually become obsolete and replaced by new complications of present day surgical repair.

The success of pediatric cardiology and CHD surgery is tempered by the long-term complications in adult patients that

may involve every subspecialty within the field of cardiology (Fig. 68.5). By far, the most concerning of these long-term complications is sudden cardiac death (SCD) (3) (Fig. 68.6).

The cardiologist who deals with these patients must therefore be familiar with congenital heart lesions in their uncomplicated state and be aware of appropriate testing and follow-up. Most importantly, they must also provide expert care for both natural and unnatural (surgical) consequences and be qualified to evaluate and treat residual lesions, arrhythmias, and heart failure, and manage high-risk pregnancies in this growing population.

Advanced diagnostic testing with cardiac MRI (CMR) has expanded our ability to evaluate complex CHD with greater clarity, allowing accurate assessment of systemic ventricular function and great vessel anatomy, evaluation of systemic or pulmonary venous baffles and valvular heart disease, and to look for myocardial scar burden with delayed gadolinium techniques. CMR has changed our approach to the ACHD patient shifting the indication for cardiac catheterization from diagnostic to therapeutic. The need for angiography to evaluate ventricular function, aortic arch stenosis or aneurysm, and branch pulmonary artery (PA) stenosis is now rarely necessary, and CMR provides the diagnostic platform for directed catheter-based intervention.

Therefore, ACHD clinics are seeing more patients because of improved survival, are performing more noninvasive diagnostic studies based on the presence of symptoms or using screening tools, and are ultimately treating more patients with catheter-based or surgical intervention. At The Adolescent and Adult Congenital Heart Disease Program at The Nationwide Children’s Hospital and The Ohio State University, we have experienced an exponential rise in all areas of clinical care attesting to the expanding population and the need for ongoing appropriate care for this population (Fig. 68.7).

Figure 68.1. Expanding population of adults with congenital heart disease (CHD) by year.

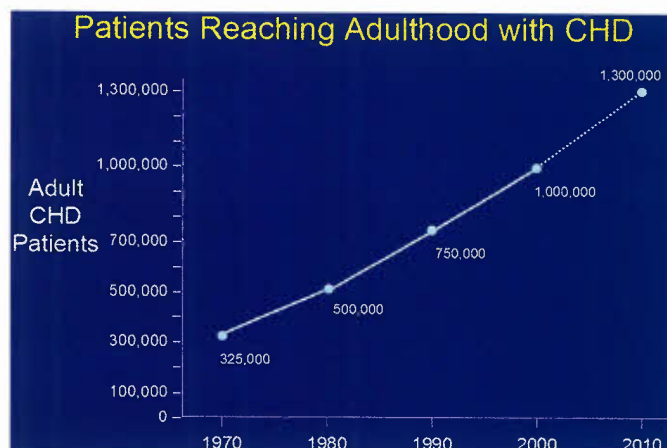


Figure 68.2. Factors leading to the expanding population of adults with congenital heart disease (CHD).

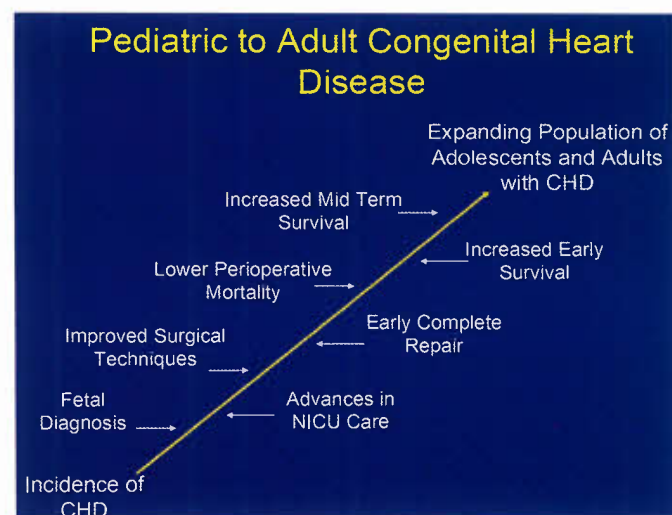
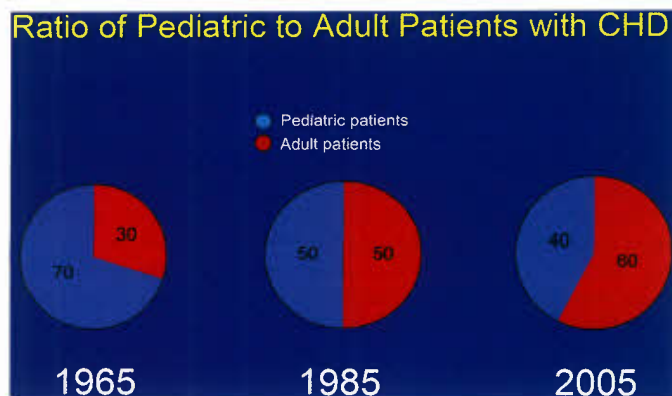


Figure 68.3. Estimated ratio of pediatric to adult patients with congenital heart disease (CHD).



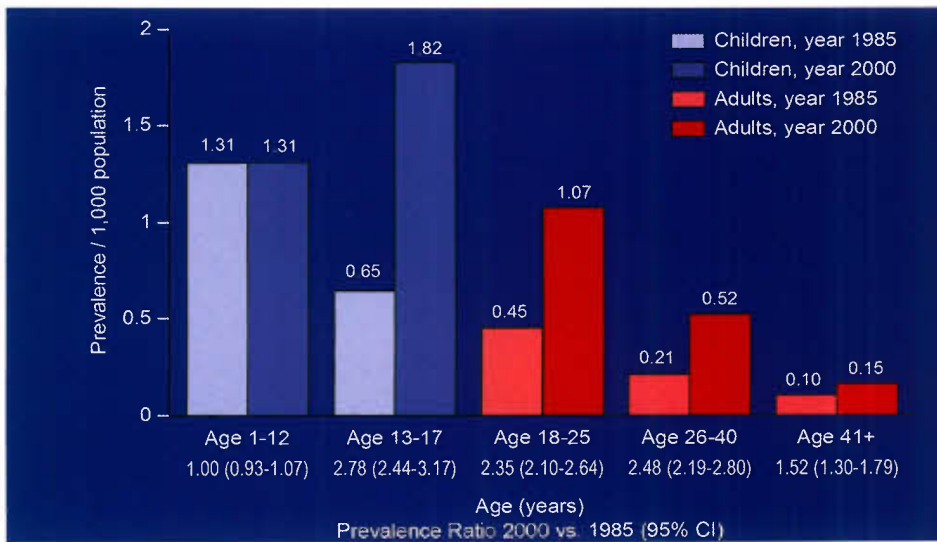


Figure 68.4. Change in prevalence of congenital heart disease (CHD) from 1985 to 2000 among patients of different age-groups. The highest increase in prevalence has occurred in the 13 to 17 year age group followed by the 18 to 40-year-old group.

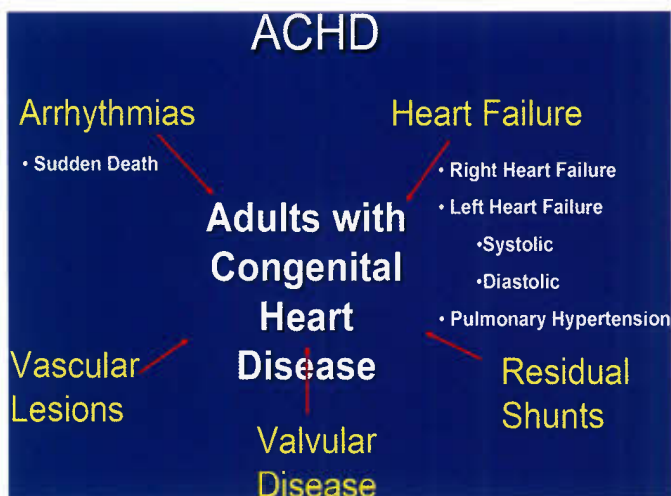


Figure 68.5. Long-term complications and residual cardiac abnormalities facing adult congenital heart disease (ACHD).

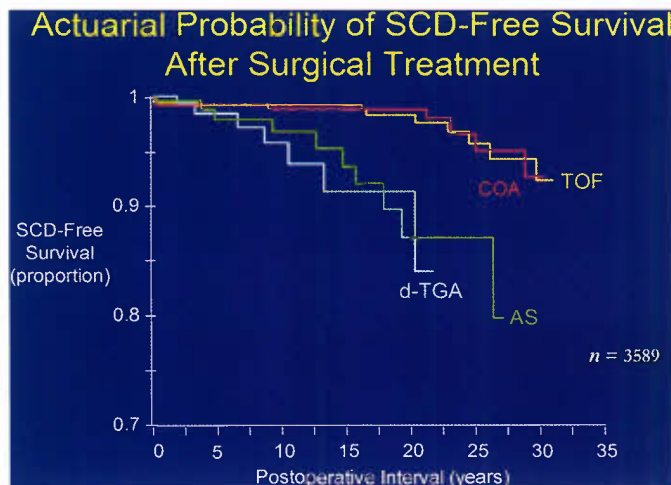
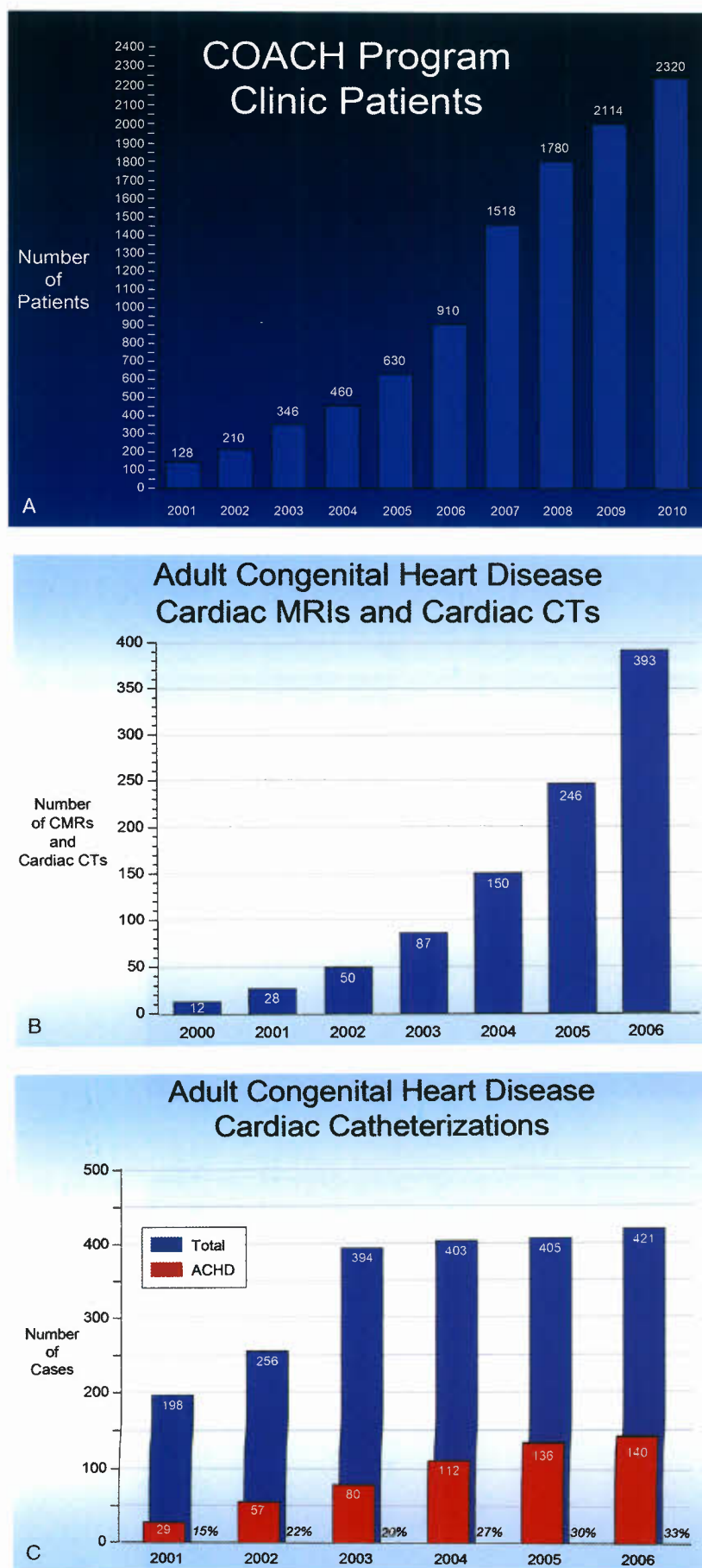


Figure 68.6. Risk of sudden cardiac death (SCD) versus years following operative repair for CHD. TOF, tetralogy of Fallot; COA, coarctation of the aorta; AS, aortic stenosis; d-TGA, D-transposition of the great arteries.

Figure 68.7. (A) ACHD clinic, (B) CMR/CT and (C) cardiac catheterization volume since 2000 at The Columbus Ohio Adult Congenital Heart Disease (COACHD) Program at the Nationwide Children's Hospital and The Ohio State University.



Successful ACHD programs employ a multidisciplinary team approach that includes a director having completed specialized training in ACHD cardiology (both adult cardiovascular disease and pediatric cardiology), along with experts in CMR, interventional cardiology, heart failure/cardiac transplant, electrophysiology, cardiothoracic surgery, and midlevel practitioners (advanced practice nurses). There are only a few dedicated ACHD experts currently, due to the need for both CHD experience and adult medicine training.

The following sections review the most common CHD lesions presenting in adulthood with or without prior repair, and the long-term complications, diagnostic workup, and therapeutic options that are deemed necessary.

LEFT-SIDED LESIONS

Bicuspid Aortic Valve

The congenitally bicuspid aortic valve (BAV) is the most common congenital malformation occurring in approximately 2% of the general population (4). It is the most common cause of isolated valvular aortic stenosis (AS) in adults, with a male to female ratio of 3:1 (5). The BAV may be functionally normal with no significant pressure gradient across the valve and with no more than trace valvular aortic regurgitation (AR). However, thickening and focal calcification of the bicuspid valve can be detected as early as in the second decade of life (6). The most common presenting sign or symptom in a young adult is often the detection of a systolic ejection murmur and usually an ejection click. However, depending on the severity of valvular disease, patients with AS or aortic insufficiency may present with exercise intolerance, dyspnea on exertion, or atypical chest pain with the peak incidence of symptoms (angina, syncope, or heart failure) developing with advancing years.

Those without significant AS (usually defined as a gradient <25 mm Hg) and less than mild aortic insufficiency only require regular follow-up. However, over time, the lesion often progresses due to fibrocalcific stenosis with almost 75% of patients requiring eventual surgery (7). The joint study on the Natural History of Congenital Heart Defects followed 473 patients with aortic valve disease at a mean of 20 years (8). Only 20% of those with an initial peak to peak gradient <25 mm Hg at catheterization had a subsequent intervention. However, in those with a gradient >50 mm Hg, arrhythmias, sudden death, endocarditis, syncope, and angina occurred at a rate of 1.2% per year.

The risk factors that lead to the development of AS in patients with BAVs are variable and have been poorly defined, often thought to be related to valvular characteristics. Beppu et al. (9) performed an echocardiographic study evaluating 75 patients (15 to 76 years of age) with a BAV and found that aortic valve sclerosis began around the second decade of life and aortic calcification started in the fourth decade. Aortic valve pressure gradient increased approximately 18 mm Hg each decade, concomitant with valve sclerosis. Patients with anteroposterior (as opposed to right-left) and eccentric (vs. symmetric) valve leaflets had a faster rate of progression with an aortic valve pressure gradient increase averaging 27 mm Hg per decade.

Treatment modalities include percutaneous balloon valvuloplasty that should be considered in a select population with significant aortic stenosis—usually defined as a peak gradient ≥ 60 mm Hg or ≥ 50 mm Hg in a symptomatic patient (10). In a large collaborative registry involving 606 patients, the peak to peak gradient was reduced by a mean of 60% (11). However, this procedure should be considered palliative

and these patients require serial follow-up (12). Pulmonary autograft aortic valve replacement (AVR) (Ross procedure) has a role and for some is the surgical procedure of choice, especially in the adolescent and young adult with significant aortic valve disease. With a successful operation, long-term anticoagulation is not indicated and therefore the patient may not need to be restricted from most activities. The long-term follow-up of this population is promising but particular attention must include assessment of the neo-aortic valve, the neo-aorta, and also the new pulmonary homograft, as it may progressively stenose (13,14). Mid- to long-term results of the Ross procedure have shown excellent results; however, with longer follow-up patients can develop neo-aortic valvular regurgitation and dilation of the neo-aortic root (15,16). Patients with neo-aortic regurgitation and/or neo-aortic root dilation need routine follow-up with serial imaging using echocardiography, CMR, or computed tomography (CT). Whether a patient following the Ross procedure is safe to compete in contact or highly competitive sports is yet to be determined.

BAVs can be associated with other cardiovascular anomalies, the most common of which is coarctation of the aorta (COA). Less common and often previously treated lesions include atrial or VSDs and PDA. Aortic root dilation may develop in some patients with a BAV. Interestingly, some studies provide support to the theory that the BAV is partly a single developmental anomaly affecting the aortic root that eventually leads to aortic root dilation. Two lines of evidence support this theory. First of all, autopsy studies have demonstrated a 5 to 10 times increase in the incidence of aortic dissection compared to patients with trileaflet aortic valves. This occurred without aortic stenosis, aortic coarctation, or hypertension (17,18). Second, Warren et al. (19) in children and Hahn et al. (20) in adults showed that the aortic root was enlarged in patients with a BAV without AS as compared to age- and sex-matched controls. These associations have led to the theory that congenital abnormalities of the aortic valve and the aorta may reflect a common developmental defect. It is also postulated that increased risk of aortic disease in patients with BAVs (including those that function normally) is mediated by coexisting defects in the aortic media by fragmentation of elastic fibers, loss of smooth muscle cells, and increase in collagen (21,22).

Therefore, those with a BAV but without significant aortic valve stenosis or regurgitation require only routine assessment for aortic root enlargement. Echocardiography may be utilized to screen and follow the aortic root, but may not provide adequate imaging beyond the first few centimeters above the sinuses of Valsalva and therefore potentially miss significant enlargement in the distal ascending aorta. CMR as a screening tool is often necessary to evaluate the entire aortic root from the valve annulus to the take off of the great vessels (Fig. 68.8). According to current guidelines, serial evaluation of a patient with a BAV and dilated ascending aorta (>4 cm) with echocardiography, CMR, or CT is recommended on a yearly basis, and first-degree relatives of all patients with a BAV should be screened with echocardiography (23). Since 2007, the need for antibiotic prophylaxis for patients with BAVs prior to dental or surgical procedures is not considered necessary (24).

Surgery is recommended to repair the aortic root or replace the ascending aorta in patients with BAVs if the diameter of the aortic root or ascending aorta is >5 cm, if the rate of increase in diameter is 0.5 cm per year or more, or if patients are undergoing AVR due to severe AS or AR, when the diameter of the aortic root or ascending aorta exceeds 4.5 cm (23). Borger et al. (24) found that the 15-year freedom from aortic root complications (replacement, dissection) following AVR was 86%, 81%, and 43% for aortic diameters of <40 mm, 41 to 44 mm, and >45 mm, respectively at the time of AVR.

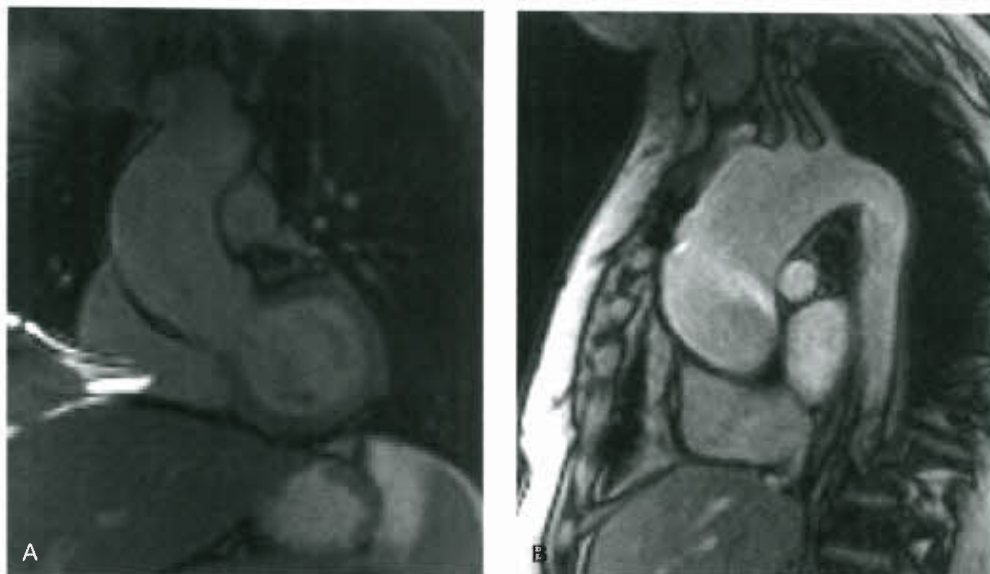


Figure 68.8. Cardiovascular magnetic resonance imaging (CMR). A: 26-year-old with BAV with no aortic stenosis/aortic valve insufficiency, CMR demonstrates aortic root enlargement measuring 4.7 cm at the widest diameter mid ascending aorta. B: A 32-year-old with BAV, mild AS, and large ascending aortic aneurysm measuring 5.2 cm with the widest diameter just proximal to the take off of the right innominate artery. Echocardiographic maximal diameter just above sinuses of valsalva was 4.0 cm, therefore underestimating the maximal diameter of the ascending aorta.

Aortic Valve Regurgitation

Aortic valve regurgitation is usually a manifestation of a congenitally abnormal aortic valve, subaortic obstruction damaging the aortic valve, aortic cusp prolapse through a supulmonic VSD, or aortic root dilation from connective tissue disorder. For most, chronic aortic valve regurgitation is well tolerated for a number of years, with slow progression but can ultimately lead to left ventricular dilation and dysfunction. Such patients are often asymptomatic for decades, until they have symptoms suggestive of left heart failure (dyspnea with exertion, angina, or syncope). The volume load that affects the left ventricle (LV) leads to a series of compensatory myocardial remodeling that lead to left ventricular dilation. Often, these changes can be reversed using appropriate pharmacologic therapy; however, ultimately patients with significant aortic valve regurgitation and dilated LVs may require AVR. Patients with severe AR can be treated with vasodilator therapies to alleviate the volume load on the LV (when AVR is not recommended) or to improve the hemodynamic profile and provide symptomatic relief for patients with severe heart failure and severe LV dysfunction (23).

The appropriate timing of AVR for aortic valve regurgitation is partially based on the development of symptoms. Symptomatic adults (with angina, syncope, or dyspnea with exertion) with chronic severe AR should undergo AVR. Asymptomatic patients with chronic severe AR with LV systolic dysfunction (ejection fraction [EF] <0.50) or with progressive LV enlargement (end-diastolic dimension greater than four standard deviations above normal) should receive aortic valve repair or replacement (23).

The presence of LV systolic dysfunction (left ventricular ejection fraction <0.5) indicates that the patient may be entering a decompensated stage. Such patients should not only undergo intense medical treatment including the use of vasodilators and diuretics to eliminate the congestive state but should also undergo a thorough evaluation and be considered for AVR.

Subaortic Stenosis

Subvalvar AS encompasses a variety of lesions that can occur alone or in combination. These include a thin membrane (the most common lesion), thick fibromuscular ridge, diffuse tunnel-like obstruction, abnormal mitral valve attachments, and occasionally, accessory endocardial cushion tissue.

In the majority of patients, obstruction is caused by a discrete membrane or a thick fibromuscular ridge that is attached to the ventricular septum or completely encircles the left ventricular outflow tract. Diffuse, “tunnel-like” narrowing of the left ventricular outflow tract is rare and is characterized by marked myocardial hypertrophy and, often, aortic annular hypoplasia.

Patients with mild to moderate obstruction often remain asymptomatic for several years and are often not identified until later in life. Significant subaortic obstruction is associated with left ventricular hypertrophy (LVH), and often with aortic valvular regurgitation leading to operative repair. In contrast to valvar AS, subvalvar AS does not respond to balloon dilation. Definitive therapy consists of surgical correction using simple membrane removal, extensive ring resection with or without myomectomy, or the Konno procedure. Patients with discrete membrane or fibromuscular ridge usually would have undergone surgery by adulthood; however, these lesions have a tendency for regrowth and concomitant aortic valve disease (25). A large retrospective study of 75 patients after surgical resection found a recurrence rate of 16% at 5 years and 30% at 10 years. A higher preoperative gradient (>40 mm Hg), higher postoperative gradient (>10 mm Hg), and younger age at surgery were predictors for recurrence (26). Additionally, the need for aortic valve repair and the progressive aortic insufficiency occurred less often in those with a lower preoperative gradient. This finding has led some to recommend early repair of fixed subaortic obstruction prior to the development of high-gradient or aortic valve disease (26).

Lupinetti et al. was able to demonstrate a significantly lower recurrence of subaortic obstruction requiring reoperation when membrane excision was combined with myectomy as opposed to membrane excision alone (4% vs. 25% over a mean of 4.5 and 5.2 years, respectively). However, there was a slightly higher incidence of postoperative heart block in the myectomy group (27).

With or without surgical intervention, AR may develop many years after the initial diagnosis. Therefore, patients with subaortic stenosis should have periodic evaluation. Unoperated adults with mild to moderate gradients without significant LVH and trace AR should be followed periodically. Surgery for prevention of AR in such patients is not indicated at this time; however, the presence of AR is frequently used as a surrogate marker for surgical intervention.

Coarctation of the Aorta

COA is usually a postoperative concern in adults. Previously undiagnosed adults with native coarctation are rare. Most adult patients are asymptomatic, unless they have severe hypertension leading to headaches, epistaxis, heart failure, and/or aortic dissection.

Unfortunately, despite adequate childhood surgery, patients are at risk for several concern-causing long-term complications:

1. Systemic hypertension
2. Recoarctation
3. Aortic aneurysm and dissection
4. SCD

A long-term follow-up study of patients repaired in childhood or adolescence demonstrated a significantly reduced long-term survival—mean age of death being 38 years (28). Patients died from, in decreasing order, coronary artery disease, congestive heart failure, sudden death, cerebral vascular accidents, and ruptured aortic aneurysms. Silka et al. (3) found the risk of SCD following COA repair to be 25 times greater than expected 20 years from repair.

Systemic Hypertension

Systemic hypertension is one of the major long-term problems following repair of COA. Although the blood pressure (BP) typically falls after successful repair, persistent or recurrent hypertension and disproportionate systolic hypertension with exercise are not uncommon.

Multiple studies have found a significant incidence of systemic hypertension either at rest or with exercise following repair (29–32). When combining resting BP, ambulatory BP monitoring, and exercise testing, systemic hypertension has been reported in as many as 70% of patients following coarctation repair (33). Hypertension may occur irrespective of the age at surgery or the presence of a residual gradient. Patients who had delayed initial repair often have residual hypertension despite surgical or transcatheter intervention. When hypertension is detected at rest, recoarctation must be excluded by physical exam (brachial/femoral pulse delay, arm/leg BP gradient), Doppler echocardiography, and/or CMR or Cardiac CT imaging. Recoarctation should be evaluated for transcatheter therapy (stent, angioplasty)—see ACHD interventional therapy section.

If there is no evidence of recoarctation, then medical management for hypertension is indicated. Once resting BP is normal, assessment of activity-related hypertension is performed with a 24-hour ambulatory BP monitor or in athletes, an exercise study should be done to determine peak systolic BP at maximal exercise.

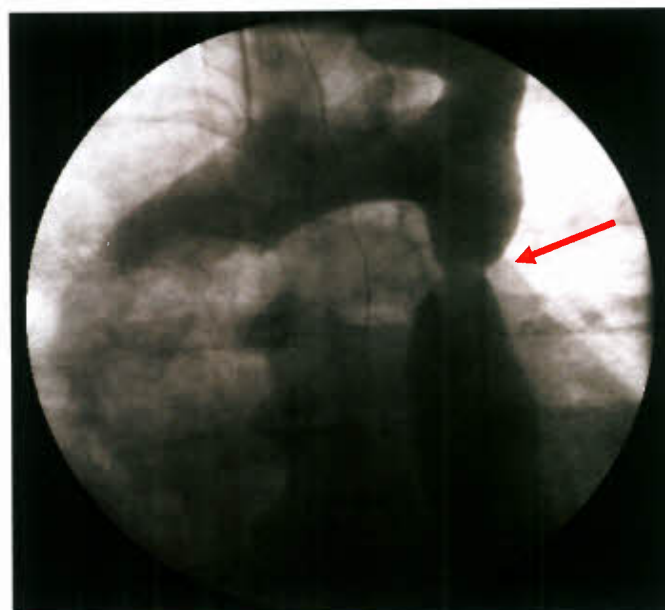


Figure 68.9. A 39-year-old with COA s/p end-to-end anastomosis presents with hypertension and found to have recoarctation, (see arrow) subsequently relieved with transcatheter stent therapy.

Recoarctation

Recurrent recoarctation refers to restenosis after an initially successful intervention. Often the major findings that suggest that a patient has developed recoarctation are resting hypertension and headaches, though some patients can be asymptomatic. Recoarctation occur less often in older patients (34,35). Recoarctation can be based on anatomic narrowing, arm/leg BP gradient, evidence of hypertension, or a combination of these factors (Fig. 68.9). Most patients with recoarctation will undergo transcatheter therapy to relieve the aortic obstruction (see section ACHD interventional therapy).

Discrete coarctation in older children and adults is treated with percutaneous balloon angioplasty, often with stent therapy (36). Indications for percutaneous interventions for recurrent discrete coarctation include a peak to peak gradient of at least 20 mm Hg (36). Eicken et al. (37) reported that despite successful stent therapy, the patient may still demonstrate systemic hypertension requiring medical therapy once again attesting to the intrinsic abnormality associated with COA.

Aortic Aneurysm/Pseudoaneurysm

An aortic aneurysm may develop following surgery or balloon dilation of native coarctation, typically at the site of prior repair. Development of aortic aneurysm and rupture may occur years after successful repair of COA (38–41). This finding can occur without recurrent coarctation and despite relief of systemic hypertension (Fig. 68.10). For the majority of patients, aneurysm repair requires surgical intervention with resection of the aneurysm and graft placement. Unfortunately, there are no criteria to guide the timing of aortic aneurysm repair in this population.

Pseudoaneurysms at the COA repair site are an area of weakening with outpouching of the adventitial thin layer of the aorta usually along the suture line. Pseudoaneurysms are at a higher risk for rupture and should be considered

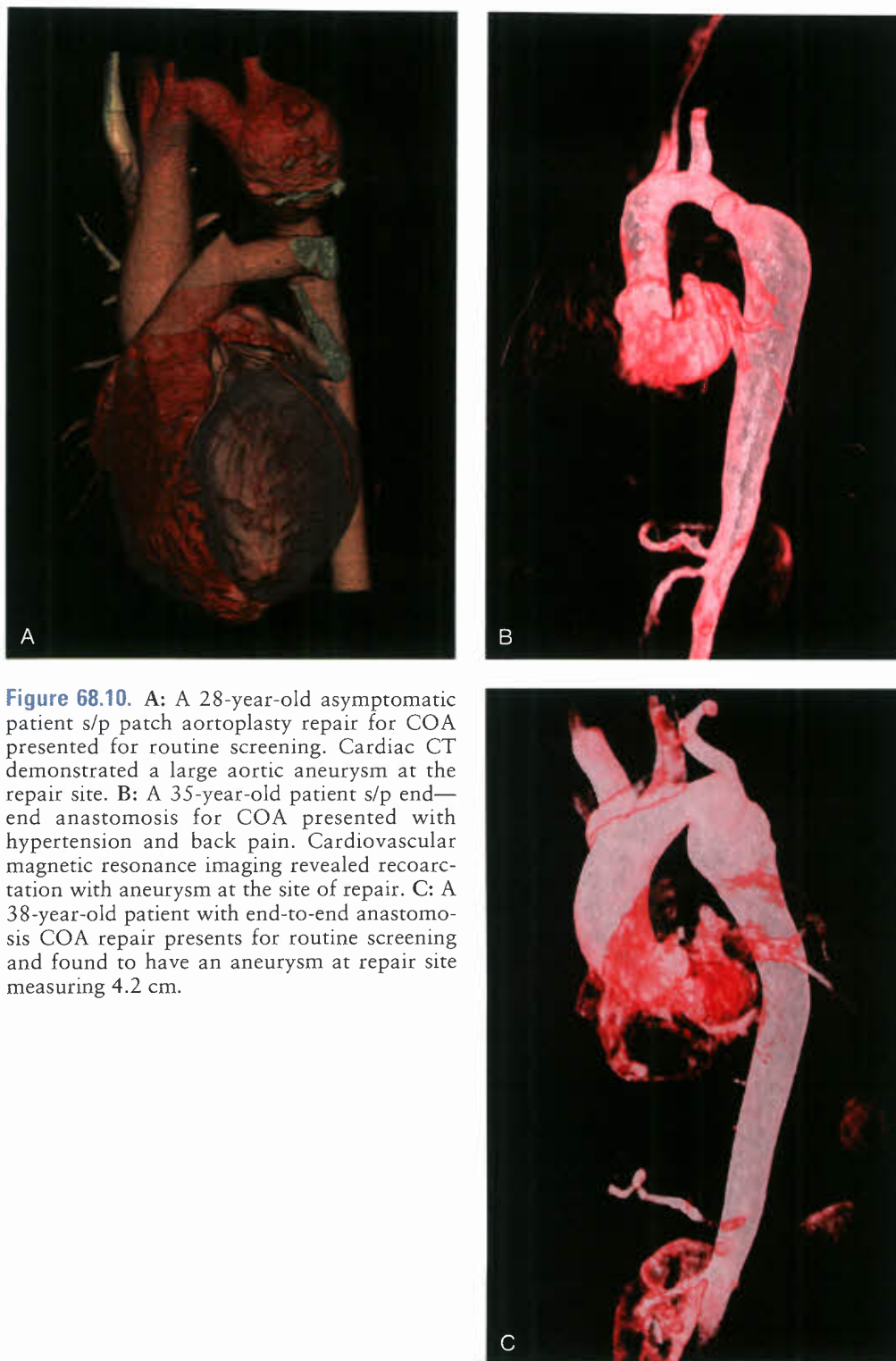


Figure 68.10. A: A 28-year-old asymptomatic patient s/p patch aortoplasty repair for COA presented for routine screening. Cardiac CT demonstrated a large aortic aneurysm at the repair site. B: A 35-year-old patient s/p end—end anastomosis for COA presented with hypertension and back pain. Cardiovascular magnetic resonance imaging revealed recoarctation with aneurysm at the site of repair. C: A 38-year-old patient with end-to-end anastomosis COA repair presents for routine screening and found to have an aneurysm at repair site measuring 4.2 cm.

for repair at the time of diagnosis. Either surgical repair or in select cases, excluding the aneurysm with a covered stent should be employed to remove the risk of pseudoaneurysm rupture (Fig. 68.11).

Although risk factors for postrepair aneurysms have been identified, including a later age at initial repair and the use of patch angioplasty, there are no clear risk factors for the higher incidence of hypertension and aortic dissection following coarctation repair. However, a growing body of evidence demonstrates that there is an intrinsic abnormality of aortic

function that persists despite adequate repair (42). Patients with repaired coarctation can rarely also develop aneurysms of the ascending aorta, which are often associated with BAVs (43–46). A stiff or less distensible aorta has been described with essential hypertension, coronary artery disease, and Marfan syndrome and may be the underlying mechanism contributing to the late abnormalities associated with repaired COA (43).

Documenting the type of repair performed is important in the evaluation of this population. Most underwent patch aortoplasty, resection of the coarctation with end-to-end

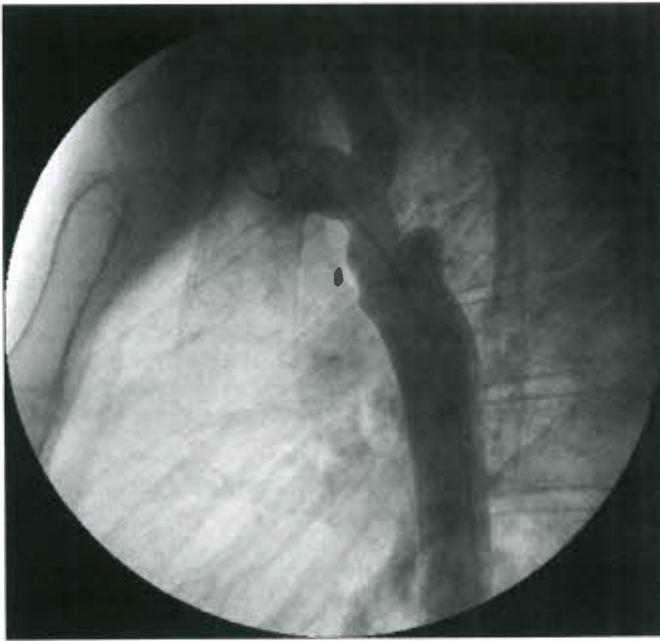


Figure 68.11. Aortogram from a 26-year-old patient with COA s/p end-to-end anastomosis found upon routine screening to have a small pseudoaneurysm and recoarctation at the repair site. The aneurysm was excluded and the obstruction relieved with a covered stent.

anastomosis, or subclavian flap repair. However, a small percent may have undergone bypass tube grafting around the coarctation segment. A clear understanding of the type of repair will aid in the diagnosis of complications and help guide timing as to when follow-up studies are necessary (Fig. 68.12). Therrien et al. (47) demonstrated that the most cost-effective



Figure 68.12. Cardiac CT in a 26-year-old patient with COA s/p ascending aorta to descending aorta tube graft.

evaluation for adults with repaired COA includes a clinical visit (thorough history and physical examination) and CMR to rule out aortic aneurysm and recoarctation.

Adult patients with previous coarctation repair should be followed serially for evidence of hypertension, both at rest and with ambulatory monitoring, and should be carefully assessed for recoarctation, aortic aneurysms, aortopathy, and progressive valvular disease especially in those with concomitant aortic or mitral valve abnormalities.

LEFT-TO-RIGHT SHUNTING LESIONS

Adults may present either with repaired or unrepaired hemodynamically significant shunt lesions including VSDs, atrioventricular septal defects (AVSDs), ASDs, PDA, in rare cases aorticopulmonary window, and arteriovenous (including coronary) fistulae. Those with shunt lesions repaired at a young age (VSD, AVSD, PDA < 1 year) are unlikely to develop pulmonary vascular disease. Large shunts either left unrepaired as a child or found incidentally as an adult will inevitably lead to elevated pulmonary vascular resistance and Eisenmenger syndrome (ES).

Ventricular and Atrioventricular Septal Defects

Adult patients with VSDs or AVSDs associated with high pulmonary resistance (especially if operated later than 1 year of age) can develop increasing pulmonary vascular obstructive disease (PVOD) (48–51). Associated concerns include residual shunts, aortic valve regurgitation, arrhythmias, including complete heart block requiring a pacemaker, PA deformity or acquired pulmonary valve stenosis (PVS) from previously placed pulmonary arterial bands, and residual atrioventricular (AV) valve regurgitation in the AVSD group. The varied constellation of symptoms can often make their clinical presentation, natural history, and treatment quite variable and make treatment options challenging.

Many patients who have a VSD do not undergo repair because the VSD is anatomically small, closing, or hemodynamically insignificant. This applies particularly to perimembranous defects where septal aneurysmal tissue can partially occlude the defect and to some smaller muscular defects. On the other hand, false security might exist when a subpulmonic defect seems to be getting smaller. In these patients, an aortic cusp can prolapse and partially or completely occlude the defect. In these patients, early operation is necessary to help protect the integrity of aortic valve coaptation.

Though it is rare to find an adult patient who would benefit from isolated VSD closure, thorough clinical, echocardiographic assessment and at times invasive hemodynamic evaluation are important in the evaluation of these patients to determine the most appropriate timing of surgical or percutaneous VSD repair, to prevent the development of irreversible PVOD, preserve the integrity of the aortic valve, and protect LV size and function. In unrepaired adults, either the VSD is small and restrictive and therefore closure would not be indicated, or at the other extreme, the defect is large enough to have caused PVOD and closure would subsequently be considered harmful.

Though surgical repair is first line for most VSDs, transcatheter device VSD closure is a treatment option for isolated uncomplicated muscular VSDs and for certain membranous VSDs, but only in very selected patients with suitable anatomy. The technical success rate of transcatheter closure of selected muscular and membranous VSDs is high and the mortality rate is low (52). Hijazi et al. reported 10-year results of percutaneous closure in adult congenital and acquired (non-post-infarct) VSDs using different types of Amplatzer occluder devices. The patients ranged in age from 18 to 84 years with a median age of

34 years. Indications for closure included symptoms related to significant shunt (dyspnea on exertion), unexplained deterioration of LV function and/or LV dilation, recurrent endocarditis, and concerns for pulmonary hypertension (PH). They showed that the procedure was both safe (two minor procedural complications) and very effective in eliminating intracardiac shunts, showing improvement in LV size after closure (53).

Long-term survival is excellent for patients with small restrictive VSD, normal ventricular function, and normal PA pressures but is limited for those with Eisenmenger complex.

Atrial Septal Defect

ASDs are the most common congenital lesion in adults after BAV. Although the defect is often asymptomatic until adulthood, potential complications of an undetected ASD include right ventricular failure, atrial arrhythmias, paradoxical embolization leading to a cerebrovascular accident or transient ischemic attacks, cerebral abscess, and PH that can become irreversible and lead to right-to-left shunting (ES). Most smaller ASDs close spontaneously in infants; however, spontaneous closure is unusual in older children and adults. Patients with ASDs are often operated before adulthood. Rarely, patients will go undetected until a high school sports physical examination or following an incidental chest film that is interpreted as abnormal. Exercise intolerance, fatigue, dyspnea, overt heart failure, and paradoxical embolization are manifestations of symptomatic ASDs in adults that warrant defect closure. Most patients do well in the long term after successful surgical closure and remain symptom free, though rare atrial arrhythmias or sick sinus syndrome can occur (54).

Murphy et al. (55) demonstrated that the age at operation and the PA pressure influences survival after ASD repair. Patients repaired <25 years of age have similar long-term survival compared to controls. However, patients ≥25 years old and those with PA systolic pressure ≥40 mm Hg at repair have a lower long-term survival apparently due to late cardiac failure, stroke, and atrial fibrillation (Fig. 68.13). The

postoperative ASD patients should be followed, albeit infrequently, with periodic examinations, electrocardiography, and occasional 24-hour ambulatory monitoring.

Percutaneous device closure is an alternative to surgical closure in patients with ostium secundum ASDs that have appropriate anatomic characteristics. The United States Food and Drug Administration's Center for Devices and Radiological Health has approved two devices for percutaneous ASD closure (56,57): the Amplatzer Septal Occluder and the CardioSEAL Septal Occlusion System. The indications for transcatheter device closure are the same as surgical closure (see interventional cardiac catheterization, Chapter 13) except that device closure with Amplatzer atrial septal occluder (ASO) is only indicated for secundum ASDs up to a maximum device size of 38 mm. Patients with sinus venosus or primum ASDs and any patient with an anomalous pulmonary venous return should have surgical repair.

Congenital Heart Disease, Pulmonary Hypertension, and Eisenmenger Syndrome

Significant left-to-right shunts unrepaired or those repaired at a later age may develop PH. Defects or complexes lesions at risk to develop PH include

1. L-R shunting defects—ASD, VSD, AVSD, PDA AP window
2. Single ventricle complexes—double-outlet right ventricle, double-inlet left ventricle
3. Transposition of the great arteries
4. Truncus arteriosus

In a large ACHD registry of over 5,000 patients from the Netherlands, the overall incidence of PH was 4.2%, 6% in those with only a septal defect, and 10% in those with a high-risk lesion for PH (categories above) (58,59) (Fig. 68.14). Of those with a septal defect and PH, 58% met the definition of ES. VSD was the most common diagnosis in the group with septal defects and PH; however, AVSD had the highest prevalence at 41% (Fig. 68.15).

ASD Long-Term Survival; Age and Main Pulmonary Artery Pressure at Operation

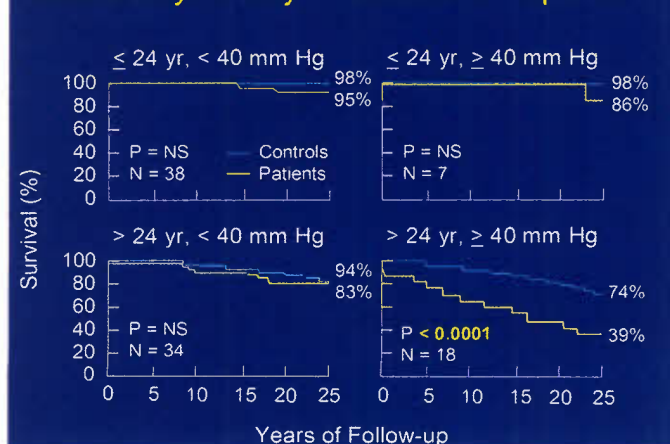


Figure 68.13. Survival curves for atrial septal defect (ASD) patients based upon age at surgical repair (≤ or >24 years of age) and pulmonary artery (PA) systolic pressure at the time of repair (< or ≥40 mm Hg). Survival was significantly diminished only with a combination of age 24 years and PA systolic pressure >40 mm Hg (Eicken A, Pensl U, Sebening W, et al. The fate of systemic blood pressure in patients after effectively stented coarctation. *Eur Heart J* 2006;27:1100–1105).

Prevalence of Pulmonary Hypertension in the Main Diagnostic Groups

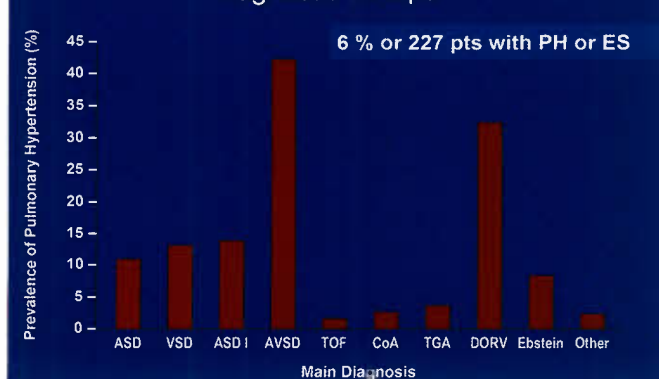


Figure 68.14. Prevalence of pulmonary hypertension (PH) in the main diagnostic categories from the CONCOR project. ASD, atrial septal defect; VSD, ventricular septal defect; ASD I, Primum atrial septal defect; AVSD, atrioventricular septal defect; TOF, tetralogy of Fallot; CoA, coarctation of the aorta; DORV, double-outlet right ventricle. (From Vander Velde ET, Vriend JW, Mannens MM, et al. CONCOR, an initiative towards a national registry and DNA-bank of patients with congenital heart disease in the Netherlands: Rationale, design, and first results. *Eur J Epidemiol* 2005;20:549–557, with permission.)

Total Number of Patients ($n = 1824$) per Type of Septal Defect in the CONCOR Registry

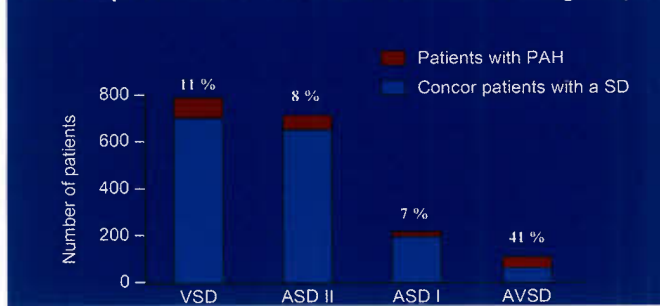


Figure 68.15. Total number of patients from the CONCOR project with septal defects and those with PH. VSD is the most common septal defect with PH and AVSD has the highest prevalence. VSD, ventricular septal defect; ASD II, secundum atrial septal defect; ASD I, primum atrial septal defect; AVSD, atrio-ventricular septal defect. (From Duffels MG, Engelfriet PM, Berger RM, et al. Pulmonary arterial hypertension in congenital heart disease: an epidemiologic perspective from a Dutch registry. *Int J Cardiol* 2006;120:198–204, with permission.)

Eisenmenger Syndrome

ES consists of systemic-to-pulmonary cardiovascular communication, pulmonary arterial disease, and cyanosis. The development of pulmonary arterial disease is a consequence of increased pulmonary blood flow and pressure and requires exclusion of other causes of PH. The diagnosis requires the presence of underlying CHD, though in some cases the diagnosis is not established until adulthood. With the advent and subsequent advancement of surgical management of CHD, the incidence of ES has declined, though it is not negligible. The overall incidence of ES is not known.

In the Netherlands study, 1% of all of the patients registered through their ACHD clinic and 58% of those with a septal defect and PH had ES (55). The development of ES is based upon the size and location of the left-to-right shunt. From the second natural history study of patients with VSD, 3% of those with a small to moderate defect (≤ 1.5 cm in diameter) will develop ES. However, with a large VSD (>1.5 cm), nearly 50% will develop ES (60). From the time of PH diagnosis, ES survival is longer than those with the idiopathic PH and patients commonly survive into the third or fourth decade of life with ES. Patients with ES carry a survival rate of 80% at 10 years, 77% at 15 years, and 42% at 25 years. Poorer survival has been associated with syncope, elevated right heart filling pressures, and lower systemic saturations ($<85\%$) (61–63).

ES patients are at risk for multiple medical problems including polycythemia, coagulopathy, especially platelet consumption, brain abscess, cerebral microemboli, hemoptysis, gout, and renal dysfunction (64). These patients should be routinely seen by centers with CHD–pulmonary artery hypertension (PAH)-trained physicians. The evaluation should include comprehensive assessment of their functional capacity, measurement of their hemoglobin, platelet count, iron studies, creatinine, and uric acid. Digital oximetry, both with and without supplemental oxygen therapy and oxygen-responsive hypoxemia should be investigated and they warrant expedited evaluation and treatment of underlying arrhythmias (65).

Other situations that are associated with a markedly increased risk in patients with ES include pregnancy, volume depletion, isometric exercise, high altitude (including air travel), and endocardial pacing. Meticulous care of intravenous

(IV) lines is required to avoid the risk of air emboli. Pregnancy in patients with ES is associated with significant morbidity and mortality and is contraindicated. The reported rate of maternal mortality in patients with ES is between 30% and 50%, with pregnancy continuing to be prohibitive in such patients despite the advances in medical therapies (6666). Gatzoulis et al. (67) reported that the overall maternal mortality was lower compared with data from a previous era (25% vs. 38%), with 17% mortality in patients with idiopathic PAH, 28% in those with CHD–PAH, and 33% in patients with other causes for PH.

Symptomatic patients with PVOD may benefit from phlebotomy and non-red cell colloid replacement. Patients should be carefully monitored during the procedure. This procedure repeated periodically carries the risk of hypotension and even death, especially if fluid shifts during the phlebotomy procedure are abrupt. Therefore, phlebotomy should only be approached as a therapy when there are significant symptoms felt to clearly be due to polycythemia and hyperviscosity rather than polycythemia alone. Symptoms include worsening dyspnea and hemoptysis. In select patients, presurgical phlebotomy may be beneficial to reduce bleeding diathesis risk (64).

Particular care must be taken not to deplete the iron stores in these patients. A patient with Eisenmenger complex who has several phlebotomies and has a hemoglobin of 18 g/dL, but who has microcytosis has iron deficiency polycythemia. These patients are at higher risk for cerebral vascular accidents. The Mayo clinic reviewed the course of 162 cyanotic CHD patients ≥ 18 years of age over an 8-year period and found that 29 cerebrovascular events had occurred in 22 patients (13.6%) (68). Risk factors for the development of a cerebrovascular event included hypertension, atrial fibrillation, a history of phlebotomy, and microcytosis. Microcytosis was the strongest predictor for a cerebrovascular event. Judicious iron replacement with frequent monitoring of the hemoglobin level and mean corpuscular volume is necessary.

In the last decade, medical therapy for ES has become an important consideration to improve exercise capacity and as a bridge to lung or heart/lung transplantation. Bosentan (a dual endothelin receptor antagonist), epoprostenol (a prostacyclin [PC]), and sildenafil (a phosphodiesterase-5 inhibitor) have been evaluated in limited numbers of patients with ES. In the only randomized controlled trial dedicated to end-stage PAH–CHD, bosentan significantly reduced pulmonary vascular resistance and significantly increased 6-minute walk distance without compromising peripheral oxygen saturation in patients with ES. These data suggest that targeted therapies are beneficial in the PAH–CHD population, and warrant further research (69). More recently, Zuckerman et al. (70) showed that in a small cohort of patients with ES, ambrisentan (endothelin receptor antagonist) was safe and was associated with increasing exercise capacity.

In a short-term study, Fernandes et al. demonstrated significant improvement in exercise capacity and hemodynamics with IV PC use. ES patients ($n = 8$, mean age 37 years) underwent hemodynamic assessment and 6-minute walk test at baseline and at 3 months following initiation of IV PC. The median pulmonary valve replacement (PVR) for the group decreased from 41 to 21 U/m², $Qp:Qs$ ratio shifted more leftward from 0.55 to 0.75:1, systemic saturation improved from 69% to 85%, and the 6-minute walk distance improved from 68 to 375 yards (Fig. 68.16) (71). Galie et al. (72) randomized 54 ES patients to either placebo ($n = 17$) or to the endothelin receptor antagonist Bosentan ($n = 37$). After 16 weeks, Bosentan patients demonstrated a significant reduction in PVR and mean PA pressure and an improvement in exercise capacity compared to the placebo patients. Adriaenssens and colleagues found a significant delay in need for transplant when patients were treated with advanced medical therapy (IV PC or endothelin receptor antagonist) compared to those

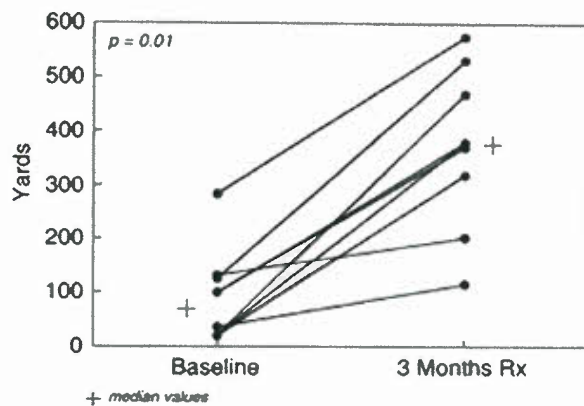


Figure 68.16. Eisenmenger patients who underwent baseline and 3-month follow-up 6-minute walk test after initiation of IV PC therapy. There was a significant improvement in exercise capacity by 6-minute walk test.

without PH-specific medications, 7.8 ± 1.0 versus 3.4 ± 0.9 years, respectively (Fig. 68.17) (73).

Therefore, ES patients should be considered for PH-specific medications either to improve exercise tolerance or as a bridge to transplant. Whether survival is improved with PH-specific medication is more difficult to determine.

Heart and lung transplantation or lung transplantation with intracardiac repair are treatment options in Eisenmenger patients. Transplantation should be reserved for severely symptomatic patients (74,75). The survival of ES patients who undergo lung or heart/lung transplantation in some studies was less than that of idiopathic PH, but in other studies the survival was similar to those with idiopathic PH or pulmonary fibrosis. In general, the 5-year survival is approximately 55%, 10 year 35%, and 15 year 20% (76,77).

Therefore, there are options for the ES patient that were not previously available or readily considered. General guidelines include the following:

1. Confirm the anatomy and determine that no surgical intervention is necessary, for example, anecdotal cases exist where an adult with tetralogy of Fallot (TOF) was misdiagnosed as having ES should be completely repaired.

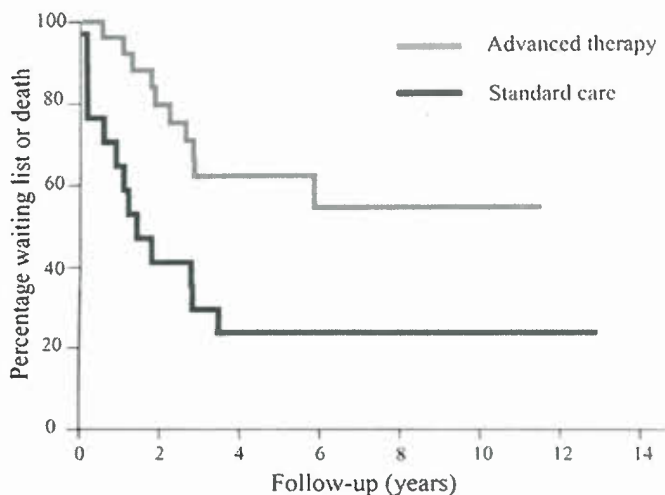


Figure 68.17. Kaplan-Meier curves for waiting on transplant list or death versus time on either standard medical therapy or advanced therapy with PC or endothelin receptor antagonist. Log rank test $p = 0.0062$.

2. Maintain adequate hydration.
3. Provide oxygen therapy at night especially in case of documented worsening nocturnal systemic saturations.
4. Phelbotomy only in select cases where hyperviscosity is the etiology of the symptoms. Replace blood volume with adequate intravenous colloid solution in a monitored environment.
5. Discuss and recommend permanent sterilization in women.
6. Consider PH-specific medications (e.g., endothelin receptor antagonists, IV PC therapies), particularly for those with declining functional status.
7. In select patients consider lung or heart/lung transplantation.

Patent Ductus Arteriosus

PDA is one of the few lesions that can be considered cured by operation, and unless rare complications of “recanalization” have occurred, these patients can be discharged from further cardiac reevaluation.

PDA closure is recommended for patients with a significant left-to-right shunt who are symptomatic, have evidence of left-sided volume overload (i.e., left atrial or ventricular enlargement), or have reversible pulmonary arterial hypertension (PAH) (66,78). PDA closure is not recommended for patients with severe and/or irreversible PAH, since closure in such patients does not improve survival and often right-to-left shunting is needed to maintain adequate cardiac output, especially during episodes of increased pulmonary vascular resistance (78). Most clinically relevant PDAs are closed (pharmacologically, surgically, or via percutaneous intervention) during either infancy or early childhood. The rare patient who is not diagnosed with a PDA until adulthood should have preoperative hemodynamic cardiac catheterization before being considered for closure. Some may have low-flow shunts due to PVOD, and this must be established before treatment.

In the older patient, an additional consideration is the potential for significant pulmonary vascular disease and PAH. However, it is not always clear which patient with PAH will benefit from PDA occlusion. Careful consideration for PDA closure must be given to patients with PAH. Patients with documented patent ductus arteriosus with pulmonary vascular resistance >6 Wood units/ m^2 when breathing 100% oxygen are usually not considered suitable candidates for correction of their shunt (78).

The anatomy of PDA in the adult is remarkable for the presence of calcification and general tissue friability in the area of the aortic isthmus and PA, which makes surgical manipulation in the adult more hazardous than in the child. Thus, surgery even for a small ductus in the adult, carries a serious risk because the calcified ductal wall can tear during ligation (66,79). Thus, these procedures should take place in a center where an experienced surgeon and team can deal with such patients. Adults with PDA are better suited for percutaneous closure with either an occlusion device or coils because of high success and few complications, and is now considered to be the treatment of choice, especially in the patient with comorbidities (80).

OTHER VALVE ABNORMALITIES

Mitral Valve Prolapse

Mitral valve prolapse (MVP) is the most common cause of primary mitral regurgitation (MR) in developed countries. Since symptoms are nonspecific, the diagnosis of MVP is usually suspected on physical examination and confirmed by echocardiography. MVP is often encountered for the first time in adolescence or early adulthood. Because it is a clinical diagnosis with Doppler echocardiographic corroboration (if necessary), careful dynamic

auscultation of the patient in various positions, especially when standing after squatting, is important (see Chapter 5).

MVP has had many names, including click/murmur syndrome, myxomatous mitral valve disease, floppy valve syndrome, and Barlow's syndrome. It is classified as primary, secondary, or functional based upon the anatomic or physiologic defects responsible for the abnormal leaflet motion. If the prolapse valve is not due to a floppy valve in association with a connective tissue disorder, then the degree of prolapse usually does not progress until the patient is older, with most patients remaining asymptomatic. MVP can be associated with chest pain, palpitations, dizziness, numbness, or tingling but these symptoms are usually benign and only require careful history, examination, electrocardiography, and occasionally 24-hour ambulatory monitoring (81). Reinforcement by inquiry may make the patient more symptomatic than is necessary. However, even asymptomatic patients, especially young women, can suffer sudden death when no other pathologically proven cause can be found (82,83). The exact incidence of sudden death associated with MVP is unknown. Furthermore, since atrial and ventricular arrhythmias are common in the general population, it is not clearly established that the incidence of arrhythmias and SCD are in fact increased in patients with MVP. It has been postulated that the incidence of arrhythmias may be higher in patients with MVP who have at least moderate MR (84).

It is important to always perform dynamic auscultation. The classic murmur of MVP is accentuated by standing and Valsalva maneuver (earlier systolic click and longer murmur) and diminished with squatting (later systolic click(s) and shorter murmur).

The symptomatic relief of patients with MVP may require both general and pharmacologic measures. Reassurance about the benign nature of the disorder is often adequate to reduce the severity of symptoms in many patients. Many patients also appear to benefit from a change in lifestyle, including aerobic exercise training, the avoidance of stimulants (caffeine), alcohol, undue fatigue, and a reduction in stress. Beta-blockers may be helpful in patients with MVP who present with hyperadrenergic state including tachycardia, palpitations, or nervousness but there have been no large-scale randomized trials to prove their benefit in this cohort of patients (85).

Though most patients do not need surgical therapies, MVP associated with severe MR can be treated with repair or surgical replacement of the mitral valve. Repair of the mitral valve is always preferable to replacement and should be performed by surgeons who are skilled in the procedure (22).

Pulmonary Valve Stenosis

Almost all cases of valvular pulmonic stenosis are congenital in origin, and most cases occur as an isolated lesion. Acquired cases are encountered less commonly but may be caused by the carcinoid syndrome, rheumatic fever (in which case pulmonic stenosis is always associated with other valve abnormalities), or stenosis of a bioprosthetic valve or valved conduit. Mild or moderate PVS is not a progressively obstructive lesion. Most patients who have had severe PVS would have had either balloon valvuloplasty or operation and should have little to no outflow obstruction by the time they reach adolescence.

Earing and colleagues at the Mayo clinic reviewed the long-term outcome after surgical repair for PVS (86). Fifty-three patients (mean age at follow-up 43 ± 15 years) who underwent surgical treatment for PVS from 1951 to 1982 were reviewed 33 years (range 18 to 51 years) later. At follow-up, 53% had reintervention with PVR for pulmonary insufficiency (PI) being the most common operation. Atrial and ventricular arrhythmias were common (38%).

The rare undetected or untreated adolescent or adult patient with significant PVS may still require intervention. The

initial diagnostic modality of choice remains a transthoracic echocardiogram in patients with isolated pulmonary valvar stenosis. The role of diagnostic cardiac catheterization is now only indicated in patients if the Doppler peak jet velocity is >3 m/s (estimated peak gradient >36 mm Hg), and balloon dilation can be performed if indicated (22). The high success and low complication rates, along with favorable long-term hemodynamic and clinical results, have resulted in pulmonary balloon valvotomy becoming the treatment of choice for patients with moderate to severe pulmonic stenosis. It is recommended in symptomatic patients with a right ventricle (RV)-to-PA gradient >30 mm Hg, or in asymptomatic patients with a RV-to-PA gradient greater than 40 mm Hg at catheterization (22). Pulmonary balloon valvuloplasty is effective with good mid-term results similar to surgical valvulotomy (see Chapters 13 and 40). Whether treated or not, those with right ventricular outflow gradients (and normal cardiac output) <50 mm Hg can expect a normal lifespan and no symptoms (87,88).

Cyanotic Congenital Defects

Adults with CHD anatomy associated with cyanosis would nearly always have had some type of prior operation. These operations may have been palliative, such as systemic artery-PA shunts or systemic vein-PA shunts, or they might have undergone definitive procedures, such as closure of VSD and opening of the right ventricular outflow as in TOF.

Although many patients who had systemic-to-PA anastomoses have sufficient pulmonary blood flow to achieve reasonable systemic arterial oxygen saturation, some patients with palliative shunts have developed PVOD, possibly related to a high-flow-high-pressure stimulus. This particularly applies to those who had the now-seldom-used Potts or Waterston central shunts. The latter was frequently associated with distortion and even obstruction of the right PA at the site of anastomosis (Fig. 68.18). These patients still have obligatory intracardiac right-to-left shunting, and air or clots

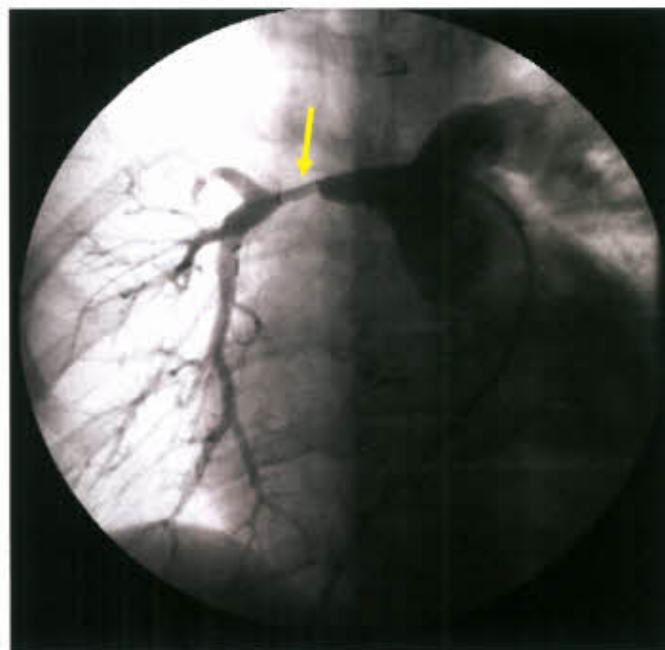


Figure 68.18. Right PA angiogram in a 26-year-old patient with rTOF s/p palliative Waterston shunt. Angiogram demonstrates discrete right PA stenosis (arrow) and hypoplastic secondary and tertiary branch vessels. Patient underwent successful angioplasty and stent therapy.

from intravenously placed lines can embolize paradoxically, leading to brain, renal, or cardiac infarction. Additionally, the group of patients with cyanotic CHD and palliative systemic artery-PA shunts is at the highest risk for endocarditis (89).

Tetralogy of Fallot

The majority of young adults with TOF would have undergone complete repair. It is important during the patient evaluation to obtain a detailed history of prior surgical procedures. Depending on the degree of pulmonary outflow obstruction, size of the pulmonary arteries, presence of branch pulmonary stenosis, and coronary anatomy, a variety of techniques might have been utilized to complete the repair. A prior systemic to PA shunt (i.e., Blalock-Thomas-Taussig, Waterston, Potts) has the potential to cause elevated pulmonary vascular resistance and distortion of the branch pulmonary arteries (Fig. 68.18). This appears especially true for the patients with a prior Waterston shunt or Potts operation. Murphy et al. (90) found a significant decrease in survival after complete repair for patients with a prior Waterston shunt or Potts operation compared to those with Blalock-Thomas-Taussig shunt. This occurred presumably from progressive PVOD as a consequence of high pulmonary blood flow from a larger size shunt. Improving surgical techniques have now made a single intracardiac repair the procedure of choice in most centers rather than a staged approach.

Patients with TOF and pulmonary valve atresia, or anomalous left anterior descending coronary artery from the right coronary artery would have had a prosthetic or homograft conduit, with or without a valve placed between the RV and the PA. These conduits can develop endothelial overgrowth and the valves can stiffen, both causing progressive obstruction to the neo-right ventricular outflow area (91,92). These patients should be periodically reevaluated for development of obstruction that may be treated by balloon dilation transcatheter valve replacement or by operative conduit replacement.

The most typical adult with TOF would have undergone complete repair (rTOF), with VSD patch closure, pulmonary valvectomy, transannular patch, and possibly subpulmonic infundibulectomy. Long-term complications of surgically repaired patients with TOF include

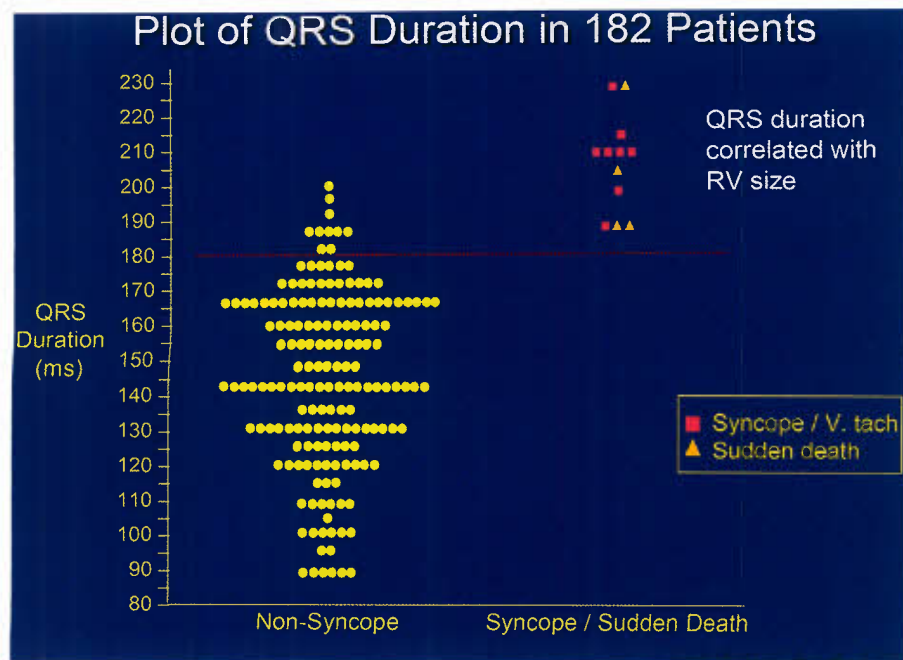
- chronic pulmonary regurgitation leading to right ventricular enlargement,
- residual right ventricular outflow tract (RVOT) obstruction,
- RV wall motion abnormalities with progressive RV dysfunction,
- supraventricular and ventricular arrhythmias including ventricular tachycardia (VT) (usually monomorphic) and
- the risk for SCD

Both atrial and ventricular tachyarrhythmias are common after repair of TOF. Several studies have demonstrated the prevalence of sustained episodes of tachyarrhythmias several years after intracardiac repair. In older rTOF patients, 34% develop symptomatic atrial or supraventricular tachycardias (SVTs), 8.5% develop high-grade VT, with an increasing number of implantable defibrillators being used due to a sudden-death estimate of 2% per decade. Thus, an estimated 50,000 adults with repaired ToF will require electrophysiology follow-up with 100 sudden deaths per year nationally (93). In a series of 242 patients, 29 (12%) developed sustained episodes of atrial tachyarrhythmia at a mean of 16 years after repair, while in another series, 29 of 793 (4%) had sustained atrial flutter or atrial fibrillation at a mean of 21 years after repair (94).

Therefore, life-threatening ventricular arrhythmias remain the greatest concern for the adult with rTOF. The incidence may be as high as 10%, and until the past decade, there were no consistently identifiable risk factors to consider which patients were at risk (95–99).

Gatzoulis et al. in 1995 provided the first clues to a potential etiology for ventricular arrhythmias in rTOF. They reviewed the clinical data on 178 adult survivors with rTOF (mean follow-up 21.4 years). Nine patients were found to have sustained ventricular arrhythmias and four patients had postoperative SCD. Holter monitor data, electrocardiograms (ECGs), chest x-rays (CXRs), and Doppler echocardiographic data were included in the analysis comparing those with versus without sustained ventricular arrhythmias/SCD. They found that QRS duration ≥ 180 ms was 100% sensitive to predict sustained ventricular arrhythmias and SCD, and that QRS duration correlated with RV size (100) (Fig. 68.19).

Figure 68.19. Plot of QRS duration in 182 patients. Those with syncope and VT (squares) and sudden death (triangles). QRS duration ≥ 180 ms was 100% sensitive in predicting sustained VT and syncope. (From Gatzoulis MA, Till JA, Sommerville J, et al. Mechanoelectrical interaction in tetralogy of Fallot; QRS prolongation relates to right ventricular size and predicts malignant ventricular arrhythmias and sudden death. *Circulation* 1995;92:231–237, with permission.)



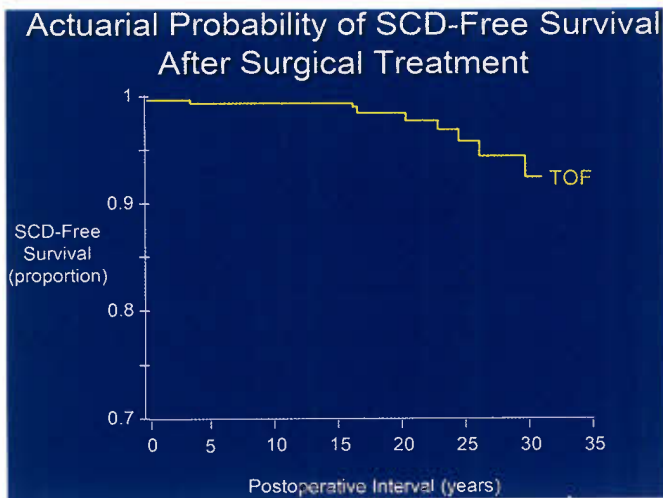


Figure 68.20. Actuarial probability of sudden cardiac death-free survival after surgical treatment of tetralogy of Fallot. (From Silka MJ, Hardy BG, Menashe VD, et al. A population based prospective evaluation of risk of sudden cardiac death after operation for common congenital heart defects. *J Am Coll Cardiol* 1998;32:245–251, with permission.)

Over the next few years, there was an emergence of data suggesting that the SCD risk in rTOF was a time-related risk factor that accelerated after 20 to 25 years after surgical repair. Silka et al. demonstrated that the risk of developing SCD in rTOF was close to 100 times greater than the general population and the risk became apparent 20 years after repair (Fig. 68.20). Nollert et al. (101) found that the risk for SCD was 0.27% per year for the first 25 years post repair but accelerated to 0.94% per year after 25 years ($p = 0.003$) (Fig. 68.21).

Long-term postoperative PI with progressive RV enlargement and dysfunction were the anatomic and physiologic correlates that began to explain the time-related risk of SCD and the relationship between RV size and QRS duration. PI leads

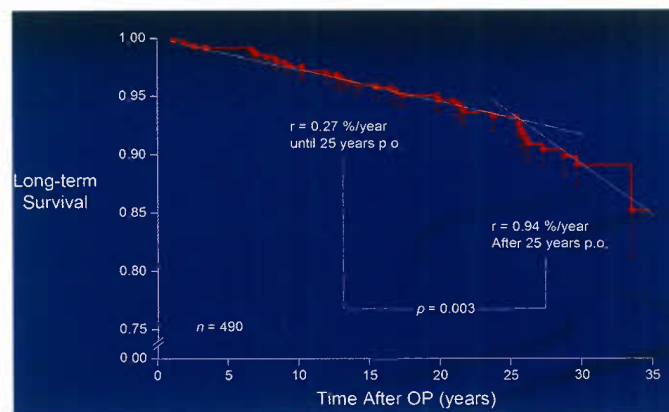


Figure 68.21. Long-term survival after correction of tetralogy of Fallot. All patients who died within the 1st year after correction were excluded for calculation of long-term survival. The curve shows two different phases that are distinct. The early, low-risk phase lasts 25 years; thereafter, the risk increases significantly. Mortality risk (r) per year, as a linearized number, is calculated for each phase. (From Nollert G, Fischlein T, Bouterwek S, et al. Long-term survival of patients with repair of tetralogy of Fallot: 36-year followup of 490 survivors of the first year after surgical repair. *J Am Coll Cardiol* 1997;30:1374–1383, with permission.)

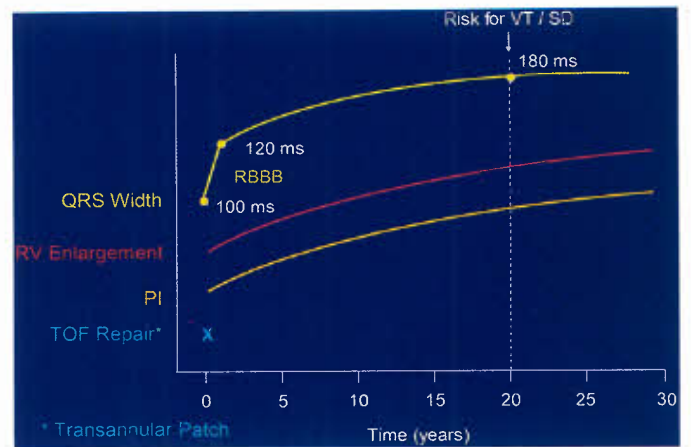


Figure 68.22. Proposed relationship between PI, RV size, and QRS duration over time following TOF repair. Risk of SCD related to duration of 180 ms. PI, Pulmonary insufficiency; RV, right ventricle; RBBB, right bundle branch block.

to progressive RV enlargement and eventually RV systolic dysfunction. The QRS, although widened from a right bundle branch block pattern since repair, lengthens with time to eventually reach the risk-related duration of 180 ms (Fig. 68.22).

Ventricular tachyarrhythmias, including sustained monomorphic VT and SCD, can occur early after surgery or years after intracardiac repair of TOF. The risk factors associated with ventricular tachyarrhythmias and SCD appear multifactorial in origin consisting of several clinical risk factors including older age at repair, male sex, severe heart failure as assessed by New York Heart Association (NYHA) classification, and repair via a right ventriculotomy rather than atriotomy (102).

With the recognition of PI as the culprit hemodynamic lesion in rTOF, many studies have evaluated the outcome following PVR, investigating the change in functional class, RV size and function, and the risk for VT and SCD. Prior studies have demonstrated that following PVR, NYHA functional class improves (103) (Fig. 68.23).

Over the years, echocardiography has provided useful information in the diagnosis and long-term management of patients

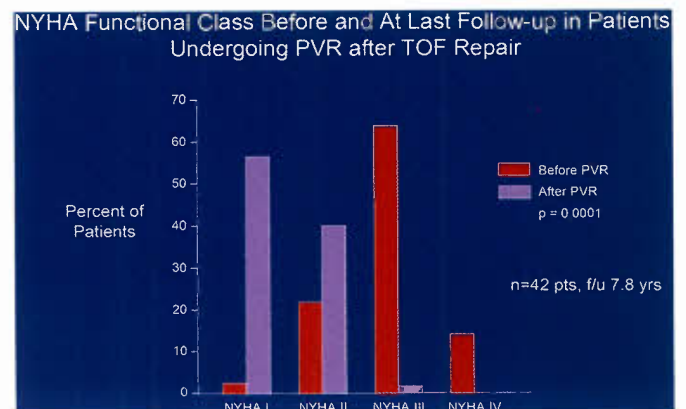


Figure 68.23. Bar graph demonstrating New York Heart Association (NYHA) functional class pre and post-pulmonary valve replacement for PI in repaired tetralogy of Fallot. Functional class of patients was improved significantly; preoperatively, 76% of patients were in NYHA class III-IV, and after pulmonary valve replacement, 97% of surviving patients were in class I-II ($p = 0.0001$).

with rTOF; however, advances in CMR have provided accurate and reproducible measurements of the RV size and function and can now be used to predict major adverse clinical outcomes late after TOF repair. CMR has already demonstrated that there is a threshold of right ventricular dilation beyond which restoration of normal right ventricular systolic function cannot be achieved with pulmonary valve replacement, leading to appropriate risk stratification and therapeutic interventions. Knauth et al. determined independent predictors for major adverse clinical outcomes (death, sustained VT, and worsening NYHA functional class to III or IV) late after rTOF. They found that 20.5% adverse outcomes occurred over a median follow-up period of 4.7 years. Predictors for poor outcome included late repair (≥ 6 years old), increased RV end-diastolic volume, reduced RV and LV ejection fraction, and longer QRS duration. Additionally, there was 100% sensitivity for adverse clinical outcome when the RV end systolic volume was ≥ 45 mL/m², and 96% specificity when the right ventricular ejection fraction (RVEF) $< 30\%$ (104).

RV volume decreases following PVR for severe PI. Vliegen et al. (105) demonstrated with CMR that the RV end-diastolic and systolic indexed volumes decreased following PVR. However, RVEF did not significantly change (Fig. 68.24). Therrien et al. also evaluated RV size and function following PVR for PI in rTOF. She and her colleagues demonstrated that when the RVEF was $\geq 40\%$ pre-PVR, 50% maintained an RVEF $\geq 40\%$ at follow-up, compared to those with preoperative EF $< 40\%$, where only 13% were able to achieve an EF $> 40\%$ at follow-up (106).

Therefore, the exact timing of when to perform PVR in adult patients with rTOF continues to evolve. Timing is a balance between removing the regurgitant volume and therefore improving RV size and possibly improving or maintaining systolic function, and eventual valve failure and need for reintervention following PVR. Geva recommended PVR when regurgitant fraction $\geq 25\%$ (moderate to severe insufficiency) and at least two of the following objective criteria in asymptomatic patients were observed:

RV end-diastolic volume index >150 mL/m² or Z-score >4

- RV end-systolic volume index >80 mL/m²
- RVEF $< 47\%$
- LV ejection fraction $< 55\%$
- Large RVOT aneurysm

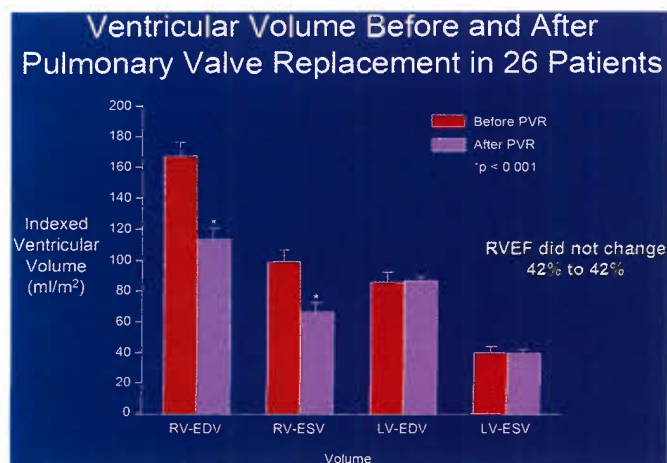


Figure 68.24. Ventricular volumes before and after pulmonary valve replacement in 26 patients. Note the significant decrease of right ventricular volumes in contrast to the unchanged left ventricular volumes. (From Vliegen HW, Van Straten A, de Roos A, et al. Magnetic resonance imaging to assess the hemodynamic effects of pulmonary valve replacement in adults late after repair of tetralogy of Fallot. *Circulation* 2002;106:1703–1707, with permission.)

- QRS duration >140 ms
- Sustained tachyarrhythmia related to right heart volume load
- RVOT obstruction with RV systolic pressure $\geq 2/3$ systemic
- Severe branch PA stenosis not amenable to transcatheter therapy
- \geq Moderate tricuspid regurgitation (TR)
- Residual left-to-right shunts with pulmonary-to-systemic flow ratio ≥ 1.5
- Severe AR
- Severe aortic dilatation (diameter ≥ 5 cm)

PVR was indicated in symptomatic patients with rTOF fulfilling ≥ 1 of the quantitative criteria detailed above (107).

Though surgical PVR had remained the procedure of choice for several years, the first successful human percutaneous pulmonary valve implant was performed by Bonhoeffer et al. (108) in a patient in 2000. Since there have been significant advances in transcatheter therapies directed toward PVR (see Chapter 13), with encouraging success rates. Initial studies have demonstrated marked improvements in right ventricular pressure, RVOT gradient, pulmonary regurgitation, and MRI-defined ventricular indices as well as pulmonary regurgitation, and improvement in both subjective and objective exercise capacity (109).

Finally, does the risk for VT/SCD improve following PVR? Therrien et al. evaluated ECG changes and risk for VT and SCD following PVR for severe PI in rTOF. Seventy patients with a mean age of 28.2 years underwent PVR with follow-up at a mean of 4.7 years. They found that the QRS duration stabilized but did not decrease, and the incidence of monomorphic VT decreased from 22% to 9%. Nine patients underwent intraoperative cryoablation for VT and at 5 years follow-up had 100% freedom from recurrent VT whereas the nonablation group had only a 68% freedom from VT (110).

Still, despite the advances in CMR to better define RV size and function along with the severity of PI, the data on QRS duration, and the success achieved with PVR, clinicians evaluating and treating those with rTOF continue to struggle with risk stratification for SCD of rTOF patients. Khairy et al. through a multicenter trial found that programmed ventricular stimulation predicted those who subsequently developed VT and SCD. Both inducible monomorphic VT, relative risk of 5.0, and polymorphic VT, relative risk of 12.9, predicted future clinical VT and SCD (111) (Fig. 68.25).

PI leading to RV enlargement and systolic dysfunction continues to be the most common problem facing this population and evidence suggests that this leads to QRS prolongation and risk for SCD. Programmed stimulation may also help to differentiate those at risk and PVR along with VT mapping. Intraoperative cryoablation seems to provide the best risk reduction for SCD. As risk factors for SCD in rTOF become reproducible and agreed upon, the next era will evaluate those who would benefit from primary prevention with intracardiac cardioverter defibrillators.

Although VT and SCD continue as the most worrisome of long-term issues for the rTOF patient, other problems may arise including

1. Atrial arrhythmias; almost one third of those with rTOF develop atrial fibrillation, flutter, or SVT (112).
2. Branch PA stenosis; there are no consensus guidelines on the indication to intervene upon branch PA stenosis in rTOF. Balloon angioplasty and/or stenting of a branch PA may be considered when the RV pressure is $>50\%$ of the systemic level or at lower pressure when there is RV dysfunction. Transcatheter interventions may also be considered when there is unbalanced pulmonary blood flow or otherwise unexplained dyspnea with severe vascular stenosis (66). Anatomic narrowings of the PAs are common

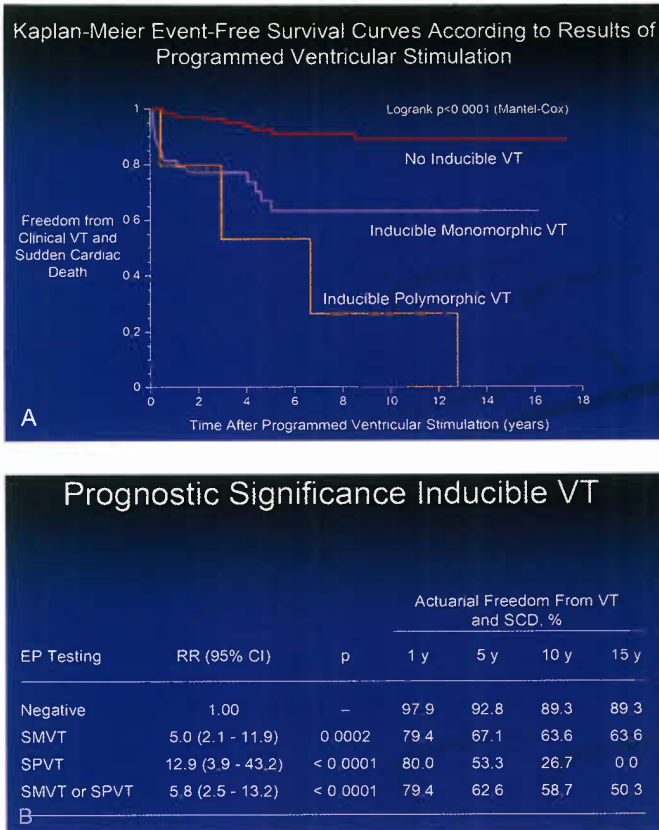


Figure 68.25. A: Kaplan-Meier curve of event-free survival according to results of programmed ventricular stimulation. B: EP indicates electrophysiologic; SMVT, sustained monomorphic VT; and SPVT, sustained polymorphic VT.

(Fig. 68.26) in this patient population; however, the indication to proceed with transcatheter or surgical repair is currently unknown.

3. Aortic root dilation; more recently it has been found that adults with rTOF have significant aortic root dilation that appears to be related to abnormal aortic wall structure. Tan et al. found that the aortic root diameter was greater than expected and that intrinsic aortic wall abnormalities exist from infancy into adulthood. This therefore suggests a potential cause and effect relationship leading to aortic root dilation (113) (Fig. 68.27). Recently, case reports for the first time have described aortic root dissection in patients with rTOF and severe aortic root enlargement (114).

In summary, the pathophysiology of rTOF is complex and the patient carries several cardiovascular concerns into adulthood that are unique to their anatomy and often their surgical repair. Over time, the risks of ventricular dilation and dysfunction, exercise intolerance, heart failure, arrhythmias, and risk for sudden death increase, though overall the long-term outcome of patients after TOF repair is excellent, with estimated 20-year survival rates of over 90%. Patients should be followed on a routine basis with CMR for RV size and function, degree of PI, branch PA stenosis, and aortic root size. Routine ambulatory monitoring and ECGs should also be performed. Eventually, with improvements in both diagnostic and percutaneous intervention capabilities, patients requiring PVR with even differing RVOT morphologies may become candidates for transcatheter PVR (115).

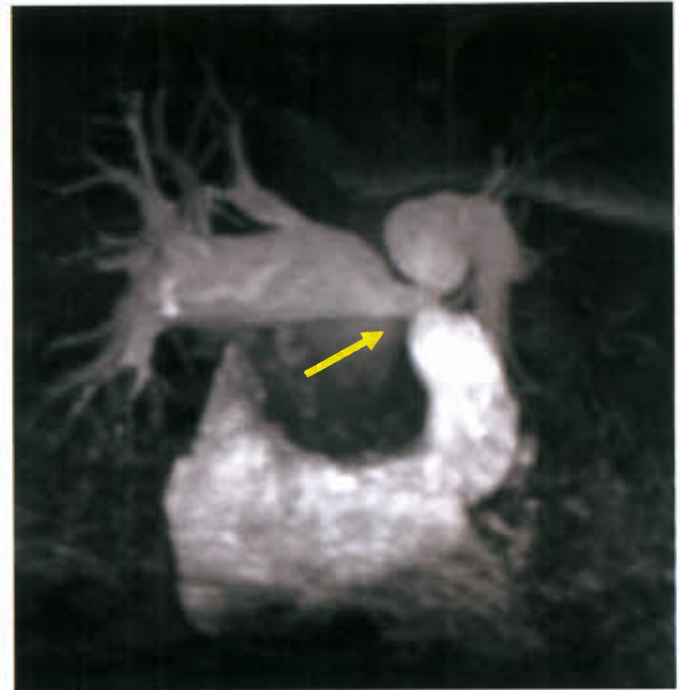


Figure 68.26. CMR demonstrating severe proximal right and left PA stenosis (arrow).

D-Transposition of the Great Arteries

The hallmark of D-transposition of the great arteries (TGA) is ventriculoarterial discordance, in which the aorta arises from the RV and the PA arises from the LV. The atrial switch repair was first described by Senning in 1959 and later by Mustard in 1964 to route the systemic venous blood flow (“baffled”) to the mitral valve and the “pulmonary” LV, and the pulmonary venous blood flow is routed to the tricuspid valve (TV) and the “systemic” RV. A postoperative population of patients who have undergone atrial switch (Mustard, Senning) procedures for D-TGA has emerged over the years. The majority of such patients will do well for a number of years but with time, they are at risk for a number of concerning problems.

1. Arrhythmias—atrial and ventricular tachyarrhythmias, heart block
2. Baffle obstruction—systemic and pulmonary venous obstruction
3. Systemic (right) ventricular failure
4. Systemic (tricuspid) AV valve regurgitation,
5. SCD.

Arrhythmias

Patients who have undergone an atrial switch operation (e.g., Mustard or Senning operations) are rarely exclusively in sinus rhythm a decade after repair, suffering from either atrial or ventricular arrhythmias. There is little doubt that these arrhythmias relate directly to the extensive suture lines created during atrial baffling, because the problem has largely disappeared in patients who were managed with the later arterial switch operation (ASO) (116). The overall incidence of arrhythmias in the population of D-TGA s/p atrial switch is not known but appears in most studies to be one of the highest-risk lesions/repairs leading to clinically significant arrhythmias. In a large Dutch registry of over 5,000 ACHD

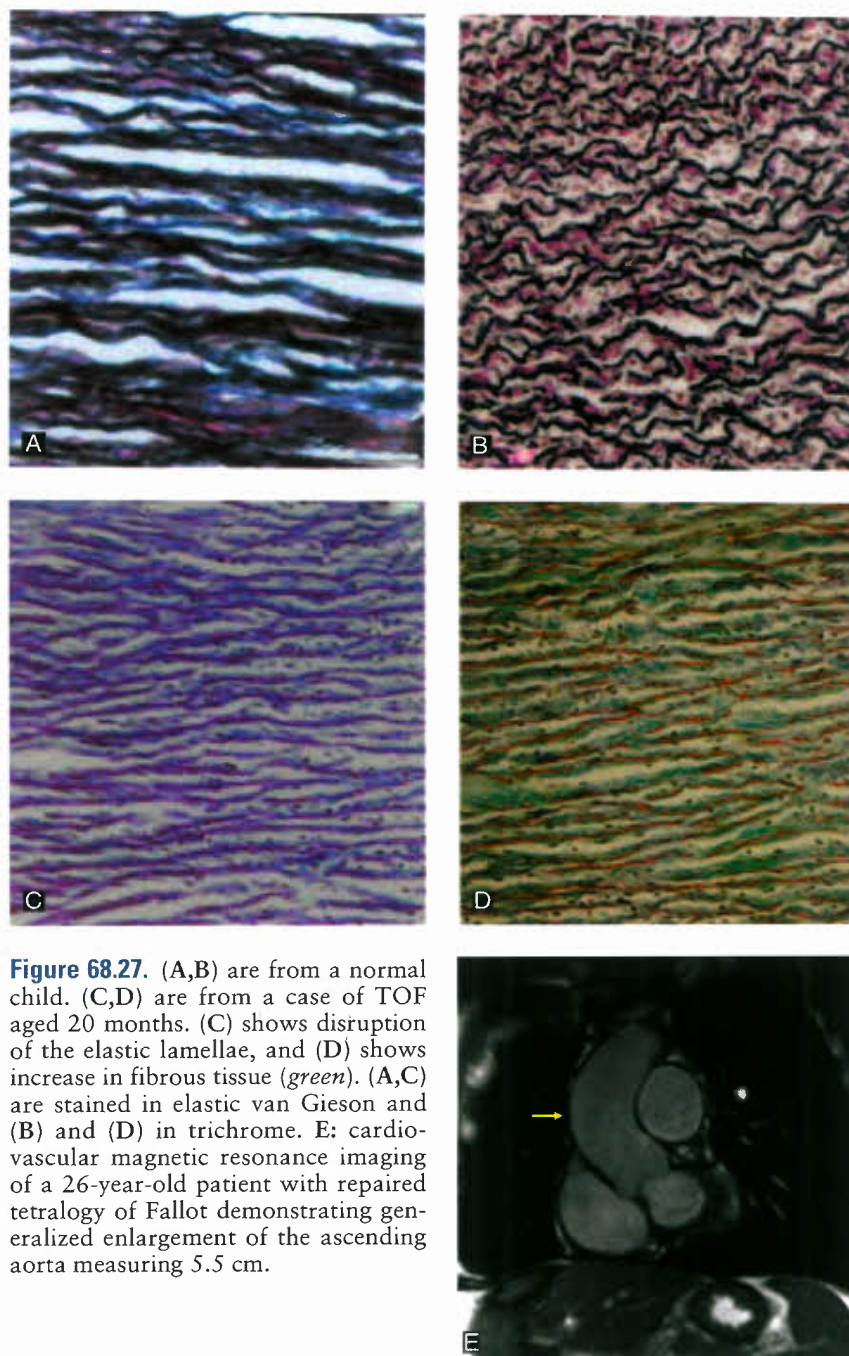


Figure 68.27. (A,B) are from a normal child. (C,D) are from a case of TOF aged 20 months. (C) shows disruption of the elastic lamellae, and (D) shows increase in fibrous tissue (*green*). (A,C) are stained in elastic van Gieson and (B) and (D) in trichrome. E: cardiovascular magnetic resonance imaging of a 26-year-old patient with repaired tetralogy of Fallot demonstrating generalized enlargement of the ascending aorta measuring 5.5 cm.

patients, D-TGA/atrial switch patients had a 35% prevalence of atrial arrhythmias (second only to single-ventricle patients) and 7% prevalence of ventricular arrhythmias (second only to TOF) (54). Gelatt et al. found a 14% incidence of atrial flutter and only 40% in sinus rhythm after 20 years, whereas Wilson et al. found a higher incidence of losing sinus rhythm over time with only 18% in sinus rhythm 15 years after repair (117–119) (Fig. 68.28).

SCD is the most common cause of late mortality in patients with TGA and atrial switch (Mustard or Senning) with an actuarial incidence approaching 10%, 20 years after surgery (3). Unfortunately, SCD remains the most concerning unpredictable event in the post-atrial switch D-TGA patient; however, identifying a high-risk group has been difficult. Main associated features are severe systemic ventricular dysfunction and history of

atrial tachyarrhythmias. Importantly, supraventricular arrhythmias often precede or coexist with VT, suggesting that they are important triggers for fatal events (119–123). Multiple studies have demonstrated this higher than expected incidence of SCD with no consistent risk factors (3,117). Some studies suggest that atrial arrhythmias are the culprit arrhythmia leading to SCD (124). Silka et al. (3) found that the risk for SCD with D-TGA/atrial switch began shortly after repair as opposed to other CHD lesions, such as TOF, where the risk is not significantly realized until 15 to 20 years postrepair (Fig. 68.29).

Ultimately, many patients will require pacemaker therapy as a result of sinus node dysfunction or symptomatic bradycardia. However, a thorough anatomic assessment for residual baffle leaks and/or obstruction should be performed prior to pacemaker lead placement. Transvenous intracardiac lead

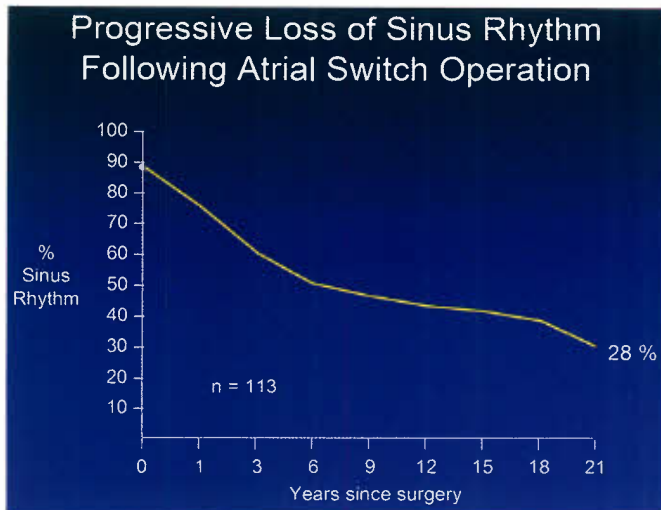


Figure 68.28. Cumulative actuarial curves showing loss of sinus rhythm.

placement and obtaining adequate thresholds can be difficult in these patients and require knowledge of complex CHD anatomy (Fig. 68.30) (Chapter 13).

Tachyarrhythmias can be treated with either radiofrequency ablation or antiarrhythmic therapy. Because of the apparent sick sinus syndrome associated with this lesion, caution must be exercised when utilizing antiarrhythmic medications. Radiofrequency ablation in this population is challenging, secondary to the complex anatomy, multiple areas of scar, and large amounts of patch material. The success of ablation for tachyarrhythmias is approximately 70%, therefore less than expected for those with normal anatomy (125). The indication for implantable cardioverter defibrillator therapy remains secondary prevention.

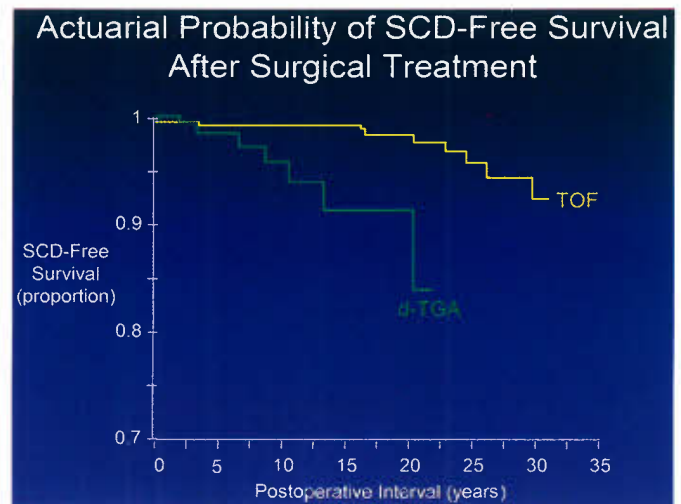


Figure 68.29. Actuarial probability of sudden cardiac death (SCD)-free survival after surgical treatment of tetralogy of Fallot (TOF) and D-transposition (D-TGA). Note the early accumulation of SCD following repair for D-TGA as compared to the risk with TOF occurring 20 to 25 years after repair.

Baffle Obstruction and Leaks

Baffle obstruction is an infrequent but serious complication following the atrial switch repair. Systemic venous obstruction is much more common after the Mustard compared to the Senning operation. When encountered, it commonly involves the superior vena cava (SVC) rather than the inferior vena cava (IVC), though both may be clinically silent and though significant stenosis in either can present with either SVC syndrome in the former and hepatic congestion and/or cirrhosis with edema in the latter. Wilson et al. (119) discovered baffle obstruction requiring

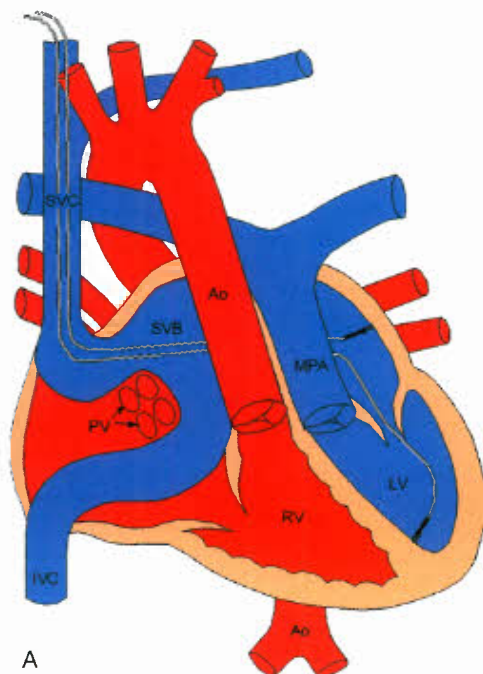


Figure 68.30. Pacemaker therapy for D-transposition/atrial switch. **A:** Atrial lead must travel from the superior vena cava through the systemic venous baffle to the remnant left atrium/atrial appendage. The ventricular lead continues across the mitral valve and is fixed within the left ventricle. **B:** Chest radiograph showing final positioning of the pacemaker leads.

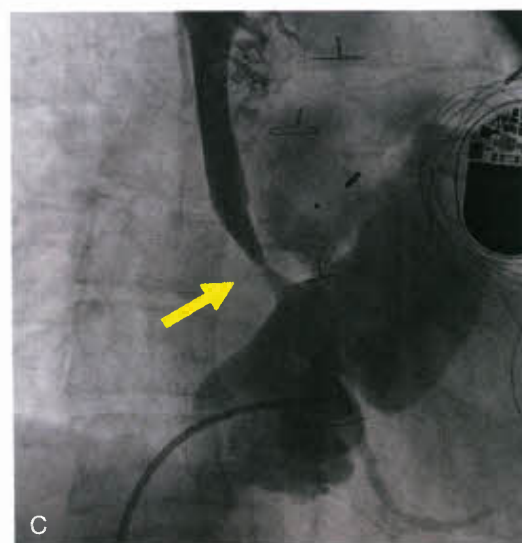
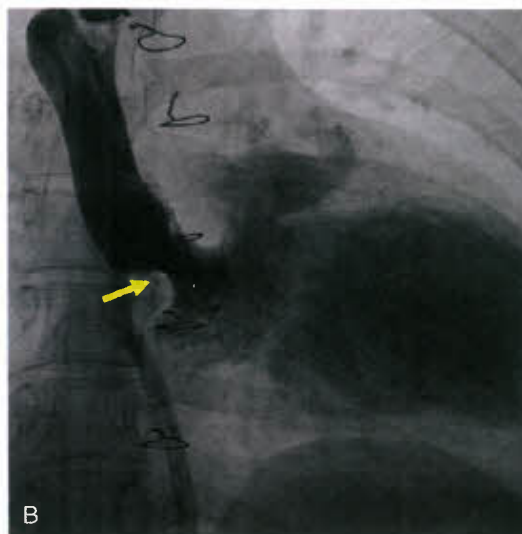
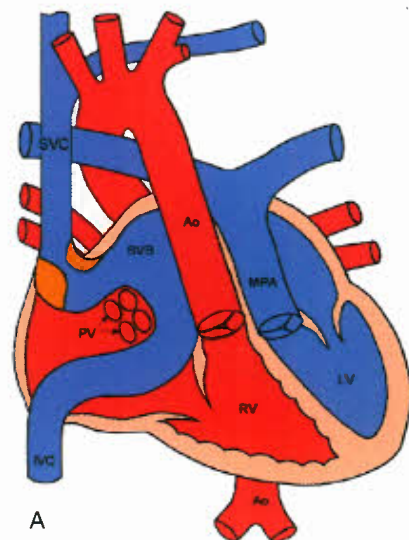


Figure 68.31. Systemic venous baffle obstruction in D-transposition/atrial switch. **A:** Diagram demonstrating the typical location of systemic venous baffle obstruction. **B:** Moderate narrowing typically seen in this population. **C:** Severe obstruction of the SVC as it enters the systemic venous baffle.

reoperation in 6/113 (5%) patients. In an additional 5%, sudden death was related to baffle obstruction following the Mustard operation. In this long-term study spanning 28 years, there were 19 deaths overall and 50% were related to baffle obstruction. Other studies have not found this association. Nevertheless, how to define baffle obstruction is open for debate. Most will have narrowing at the junction between the SVC and the systemic venous baffle as it bends anteriorly and leftward (Fig. 68.31).

Doppler echocardiography, particularly transesophageal imaging, may detect obstruction; however, limitations still exist. CMR has become the gold standard for the evaluation of baffle obstruction (see Chapter 10). The indication for relief of obstruction is not clear. Whether intervention should be based upon one or several factors is not known.

1. Percent narrowing compared to normal SVC
2. Pressure gradient
3. Symptoms (extremely rare), or
4. Planned intervention such as placing pacing wires across the narrowed segment.

Clearly, placing pacing wires across the narrowed segment will increase the likelihood of causing complete obstruction (Fig. 68.32). Percutaneous delivery of balloon expandable stents have been deployed for systemic venous baffle obstruction and found to be safe and effective in limited follow-up

(126,127). General guidelines for SVC baffle obstruction include the following:

- Angiography of the SVC prior to placing pacing wires across the systemic venous baffle. If there is significant narrowing (>50% normal SVC, pressure gradient by cardiac catheterization, systemic venous collaterals secondary to obstruction), SVC stent therapy should be performed prior to placing pacing wires. (see Chapter 13)
- Patients with SVC syndrome (upper extremity/body edema) should undergo cardiac catheterization and stent therapy.
- Patients with mild narrowing without hemodynamic gradient with no need for pacing wires can be observed.

Pulmonary venous baffle obstruction may also occur but less frequently. It is rare after both the Senning and Mustard procedures, but is a serious complication that may lead to PH requiring prompt attention. Transesophageal Doppler echocardiography or CMR will confirm the diagnosis (Fig. 68.33). Although balloon angioplasty can be performed, long-term complete relief is achieved with surgical repair.

BAFFLE LEAKS

Small leaks through the baffle are common but in our experience are rarely seen by transthoracic echocardiography

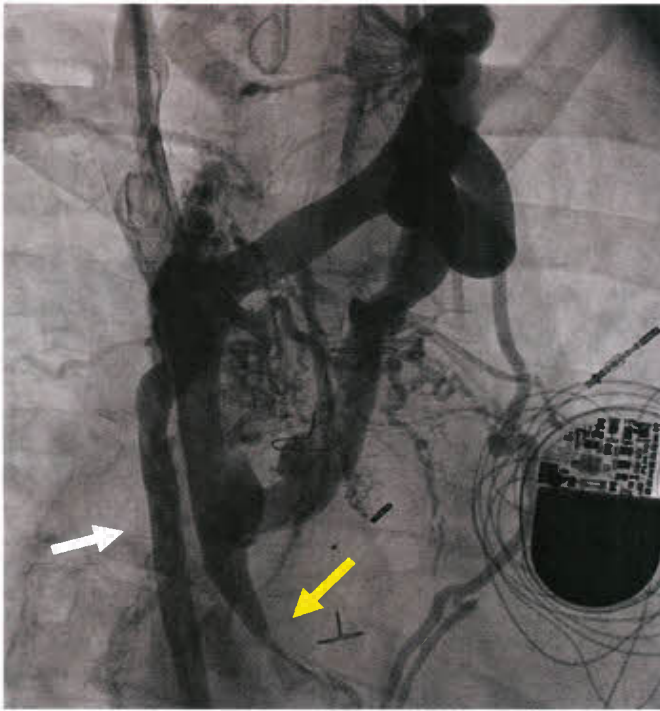


Figure 68.32. A 28-year-old patient with D-transposition/atrial switch s/p pacer placement now with essentially complete baffle obstruction (yellow arrow). Azygous runoff (white arrow) and multiple venous collaterals are present. The leads have been extracted. The patient underwent successful stent placement and the pacemaker leads were replaced.

(Fig. 68.34). Transesophageal echocardiography with bubble contrast will usually detect leaks from the SVC limb into the systemic venous baffle but may miss leaks around the inferior limb. These are more common than obstruction with an increased frequency in the Mustard population. They are usually small and hemodynamically insignificant but can pose a risk of paradoxical embolus or a cerebrovascular accident in the setting of tachyarrhythmias or transvenous pacemaker leads. Angiography from the SVC and IVC is the most sensitive imaging modality to detect small baffle leaks. Small leaks are hemodynamically insignificant and only pose a thromboembolic risk increased by pacing wires through the baffle, atrial arrhythmias, and atrial enlargement. In a multicenter study, Khairy et al. (128) found that transvenous pacing wires incur a greater than twofold increased risk of thromboembolic neurologic events with intracardiac shunts and that aspirin and coumadin did not provide protection.

Percutaneous baffle leak device closure is preferable over open heart surgery and cardiopulmonary bypass (127) (Fig. 68.35) (Chapter 13). Percutaneous closure should be considered when there is/are

- a significant left-to-right shunt with hemodynamic compromise
- systemic desaturation either at rest or with exercise (not related to PH)
- transvenous pacing wires either already in place or to be placed in the future and
- tricuspid valve regurgitation

Systemic AV valve (TV) regurgitation is present in most adult patients. On occasion, the TV maybe intrinsically abnormal, but more commonly the TR is secondary to annular dilation from

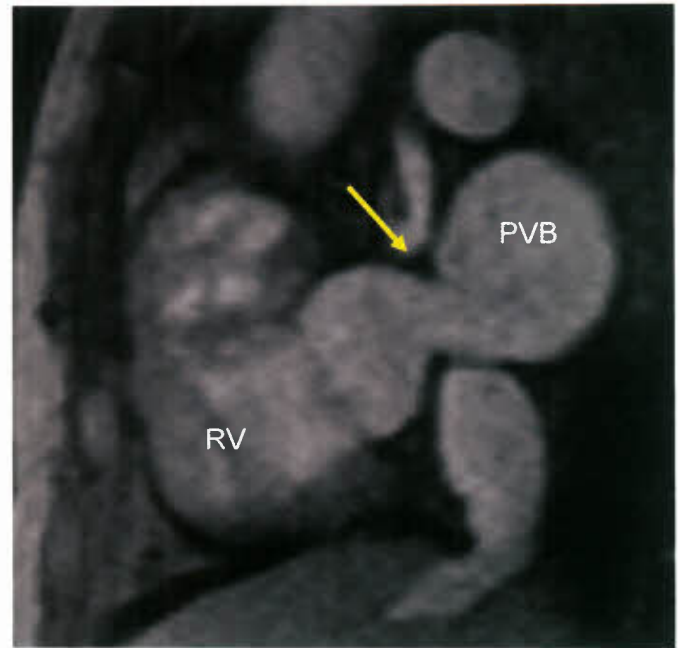


Figure 68.33. A 34-year-old patient with D-transposition/atrial switch presents with dyspnea on exertion. CMR demonstrates pulmonary venous baffle (PVB) obstruction (yellow arrow). RV, right ventricle.

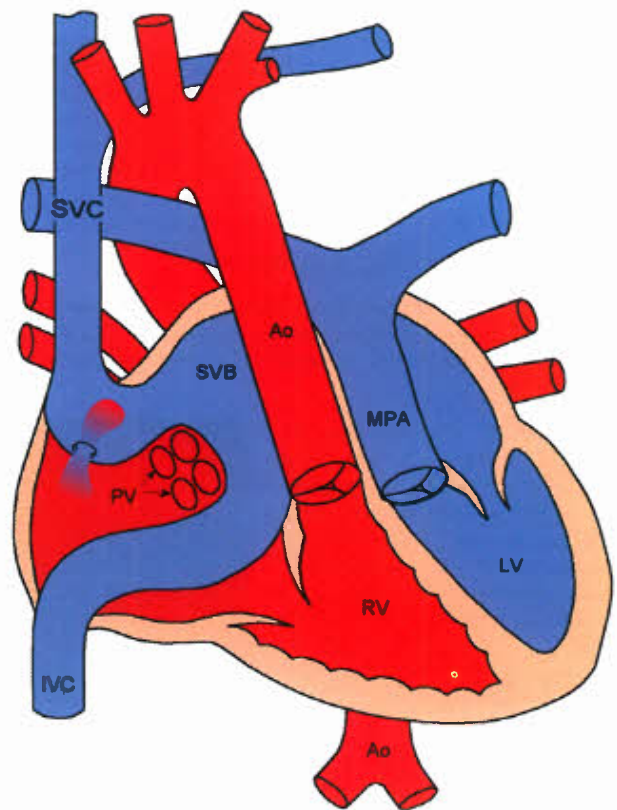


Figure 68.34. D-transposition/atrial switch with a baffle leak. Ao, aorta; MPA, main pulmonary artery; SVC, superior vena cava; SVB, systemic venous baffle; IVC, inferior vena cava; PV, pulmonary veins; LV, left ventricle; RV, right ventricle.

Figure 68.35. Superior vena cava angiogram lateral projection in a 32-year-old patient with D-transposition s/p Mustard operation presents with cyanosis. **A:** demonstrates a large baffle leak (arrows) as contrast enters the pulmonary venous chamber. **B:** Now s/p NuMed Covered Cheatham Platinum stent to exclude the large baffle leak and relieve mild baffle stenosis. Pacemaker wires were extracted and then replaced following stent placement.



right ventricular enlargement. Mild to moderate TR is usually well tolerated. However, TV repair and/or replacement should be considered for those with severe TR to prevent worsening right ventricular function. In a single institutional study of 58 patients at a mean of 14 years following the Mustard operation, 60% had moderate and 2% had severe TR determined by Doppler echocardiography (129). Although the relationship between RV myocardial function and TR is not well defined, significant TR will exacerbate already impaired ventricular function and may contribute to exercise-related symptoms. Valvular repair should be considered when other cardiac surgery is being performed or in cases of severe TR in the face of right ventricular systolic dysfunction. Moons et al. (130) described the long-term outcome of patients who underwent Mustard or Senning repair for TGA in 339 patients in Belgium. TV regurgitation was shown to be positively correlated with worsening systemic ventricular function. Most patients had only trivial to mild TR (65.2%), 27.5% had moderate regurgitation, and 7.4% had severe regurgitation. Surgical TV replacement was performed in four patients and annuloplasty in one. Severe regurgitation was more prevalent in the Senning (9.2%) than the Mustard (3.2%) cohort (130).

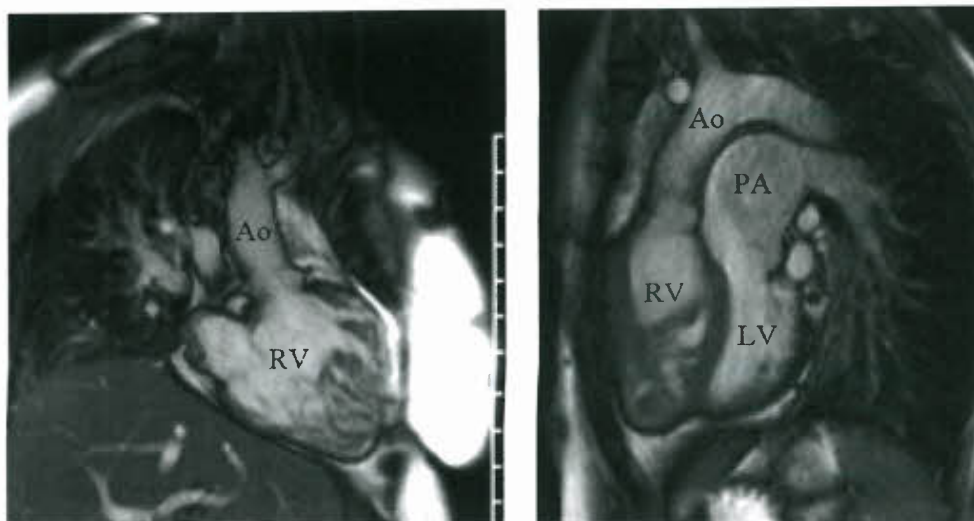
Systemic (Right) Ventricular Dysfunction

Progressive right ventricular enlargement and worsening systolic function after atrial switch operations can develop, often resulting from the systemic workload placed on the

morphologic RV. Right ventricular dysfunction will occur in approximately 15% of patients by the second to third decade of life (119,131). In contrast, clinical right ventricular failure is unusual occurring in only 2% of patients up to the third decade of life and rarely is the cause of death. Ross-Hesselink et al. performed a prospective study of young adults to evaluate systemic right ventricular function 25 years after repair. Initially, patients demonstrated good right ventricular function. However, over half (61%) demonstrated moderate-to-severe dysfunction after 25 years of follow-up (132). Although applying heart failure pharmacologic regimens to those with a systemic RVs and systolic dysfunction seems reasonable and intuitive, there are no convincing data to support this practice. Most patients are typically placed on ACE inhibitors for afterload reduction and it would seem that the possible benefit to risk ratio favors this practice. However, studies have not proven that ACE inhibitors do in fact provide benefit in exercise ability or right ventricular indices (133). Caution must be used with beta-blocker therapy in this population because of the risk for heart block in the face of conduction system disease.

Echocardiography provides a qualitative assessment of RV function but lacks details of accurate volume assessment and EF to follow patients long term. Tissue Doppler evaluation may provide important information regarding RV diastolic function and contractility. CMR has now become the gold standard for the evaluation of right ventricular size and function (Fig. 68.36) (96,134).

Figure 68.36. Cardiovascular magnetic resonance imaging (CMR) of a 32-year-old patient with D-transposition/Mustard. CMR has become the gold standard to assess right ventricular size and function. Ao, aorta; LV, left ventricle; PA, pulmonary artery.



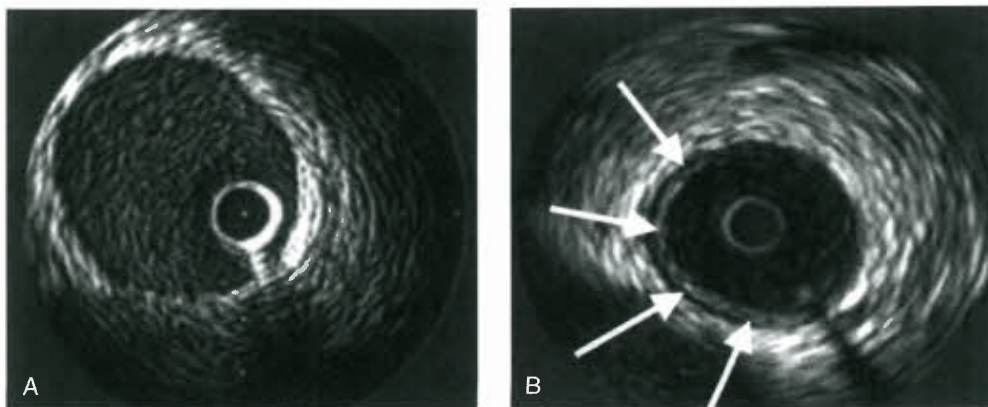


Figure 68.37. Intracoronary ultrasound image of a normal coronary artery segment (A) and anterior descending segment (B) with intimal proliferation comprising 180° of the vessel circumference (arrows indicate intimal thickening).

Late-Stage Ventricular Failure

In patients who develop late systemic ventricular failure after atrial switch, surgical intervention with either cardiac transplantation or anatomic correction (arterial switch) should be considered. To achieve successful ASO it requires “training” of the LV. PA banding is performed to train the LV and create LVH prior to arterial switch. With PA banding, the ventricular septum may shift toward the RV and decrease the tricuspid regurgitant volume by improving leaflet coaptation (135). Although this staged surgery has been successfully performed at a few centers (136,137), adult patients have significant problems progressing to the second stage after banding. Poirier et al. (138) found that in a series of 35 patients, 10 failed LV training and was common in those >12 years old.

Arterial Switch for D-TGA

ASO, originally performed in 1975, has become the standard corrective procedure for patients with D-TGA who do not have significant left ventricular outflow obstruction (139). Excellent long-term outcomes after ASO of >95% survival at 20 years following discharge have been reported from several centers (140,141).

In the next decade, a number of adults who survived neonatal arterial switch will reach adolescence and young adulthood. Theoretically, patients should do well with successful surgery; however, the long-term effects of this operation are not known. The former pulmonary valve (the neo-aortic valve) is not symmetrically formed in transposition (142), and its long-term competency will require ongoing assessment. The coronary arteries that were reimplanted in the infant may or may not be normal in the future.

Exercise electrocardiography (with subsequent confirmation at cardiac catheterization) has identified obstructive coronary ostial disease in a small percent of patients (143). Patients with myocardial ischemia after the arterial switch may not experience typical angina due to denervation of the heart as the great arteries are transected (144). It is also not known how coronary disease in such patients may accelerate in the future and whether they should be treated with antiplatelet or lipid-lowering agents. Additionally, we still do not know the best imaging modality to follow these patients. These patients will more than likely require serial evaluations with stress imaging (echocardiography, nuclear or CMR) for coronary obstructive disease and ischemia. There have been reported cases of myocardial ischemia and even infarction status post the ASO (145).

Hutter et al. (146) from the Netherlands reviewed the long-term outcome of children undergoing arterial switch for D-TGA. Outcomes of 151 patients demonstrated pulmonary

stenosis as the most common cause for reintervention, and there were two late deaths (PH and coronary artery disease with ventricular fibrillation). Sixty-one patients underwent coronary angiography and four patients had significant coronary pathology: occluded left anterior descending coronary artery in two, occluded right coronary artery in one, and stenosis of the right coronary in one (146). Pedra et al. (147) reviewed 20 asymptomatic arterial switch patients for coronary artery disease with intravascular ultrasound. Almost 90% of the vessels imaged had some degree of coronary atherosclerosis with 30% being severe (147) (Fig. 68.37).

In conclusion, despite close medical and cardiac supervision, sudden death occurs in approximately 7% of patients (118,119) following atrial switch. To date, no specific risk factors have been identified that consistently predict a higher incidence of sudden death in this population. Specific attention to arrhythmias, both supraventricular and ventricular, the need for pacemaker therapy, right ventricular function, TV regurgitation, and baffle obstruction is necessary for optimal follow-up. Therefore, the young adult with D-TGA status-post surgical repair requires careful and thorough evaluation with detailed knowledge of the past medical, surgical, and transcatheter therapies. Routine testing should include a detailed history and examination, ECG, ambulatory Holter monitor, cardiopulmonary exercise testing, and noninvasive imaging with CMR, CCT, or echocardiography (if CMR not available or is contraindicated).

Congenitally Corrected Transposition of the Great Arteries

The natural history of patients with congenitally corrected transposition of the great arteries (ccTGA) is largely dictated by the function of the systemic RV and by the presence or absence of associated abnormalities. Patients with ccTGA may not present for diagnosis until adolescence or adulthood. However, the majority of patients will have associated abnormalities—VSD (70%), pulmonary and subpulmonary stenosis (40%), abnormalities of the systemic (tricuspid) valve (90%), and complete heart block (2% per year)—that may permit early diagnosis.

In the largest single-institution study to date, Connelly et al. reported the clinical findings in 52 adult patients with ccTGA. Thirteen (25%) of the patients died at a mean age of 38 years. The most common causes of death were progressive heart failure and sudden death accounting for 70% of the mortality in this series. Arrhythmias were common with almost 50% of the patients requiring pacemaker therapy for complete heart block, and 38% of patients demonstrated atrial arrhythmias (atrial fibrillation, atrial flutter, and SVT). Moderately severe and severe systemic (tricuspid) valve regurgitation developed in 26% of the survivors. Surgical intervention was necessary

in 70% of patients. Systemic (right) ventricular function was reduced compared to controls (43% vs. 58%) and did not augment with exercise (148). The combination of poor ventricular function and systemic AV valve regurgitation appears to be a marker of poor outcome.

Patients with ccTGA have a 2% per annum risk of developing complete heart block. There is also a risk of tachyarrhythmias, both reentry type arrhythmias related to the abnormal conducting system anatomy or to accessory pathways and atrial and VTs that may all contribute to worsening systemic ventricular function. In the context of the systemic RV, chronic ventricular pacing may further negatively impact its long-term ventricular function (149).

SYSTEMIC VENTRICULAR FAILURE IN CONGENITALLY CORRECTED

TRANSPOSITION OF THE GREAT ARTERIES

Many patients do very well with a systemic RV with uncomplicated ccTGA into early adulthood; however, the rarity of this condition limits experience at a single center. A multicenter retrospective study by Graham et al. demonstrated that the time-related progressive decline in systemic ventricular function risk factors for progression included associated defects and prior open heart surgeries. In this study, one-third of patients without associated lesions developed heart failure by the fifth decade, and two-thirds of patients developed heart failure by 45 years of age when associated defects were present (150).

Such patients, though often asymptomatic, need to have objective evaluation of their functional capacity. This was highlighted by Fredriksen et al. publishing their results of cardiopulmonary exercise testing in a group of 41 adult patients from Toronto. They showed a notably reduced maximal oxygen uptake of 22 mL/kg/min in the 19 to 29 year age group and 21 mL/kg/min in the 30 to 39 year age group (both were approximately half that of normal controls). In the 40 to 55 year age group this significantly dropped to 11 mL/kg/min. The reasons for this are multifactorial, but important factors include impaired ventricular function, limited chronotropic response to exercise, and abnormal lung function, particularly in patients who had previous surgery (151).

Systemic AV valve regurgitation plays a significant role in worsening systemic ventricular function (152). Similar to the approach for MR and left ventricular systolic dysfunction, the TV should be considered for repair or replacement when ventricular function worsens in the face of moderate or severe regurgitation, rather than waiting for a decline in functional status. Late referrals for TV replacement may predict a poor surgical outcome. Beauchesne et al. demonstrated that preoperative RVEF was the only marker for poor survival. Therefore, TV replacement must be considered early when there is severe regurgitation with either RV systolic dysfunction and/or heart failure symptoms (153).

Systemic AV valve replacement is not without risk but can be performed with acceptable outcomes. At the Mayo clinic, 40 patients underwent systemic AV valve replacement for severe regurgitation. The preoperative RVEF was 20% to 60% (mean 48%). In-house mortality was 10% and another eight patients died during follow-up. Overall survival was 78% at 5 years and 61% at 10 years. Systemic ventricular failure was the cause of death for all patients in this series. Survivorship correlated with preoperative RVEF > 44%, therefore emphasizing the need for early systemic AV valve replacement in this population (154).

The double switch operation remains an option for those who develop systemic ventricular failure as an alternative to cardiac transplant. The procedure restores the LV to the systemic position and therefore the physiology and the

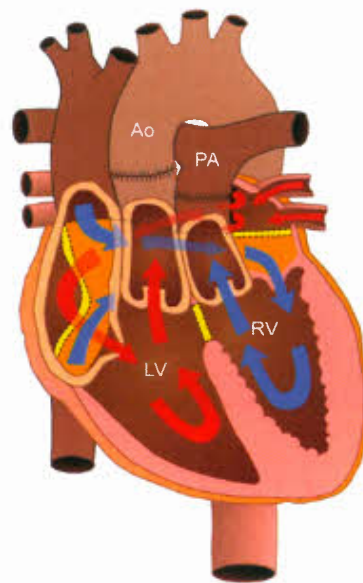


Figure 68.38. Congenitally corrected transposition of the great arteries and heart diagram following double switch procedure. Initial pulmonary artery banding is not shown. This is followed by atrial switch and arterial switch so that the physiology is correct and the systemic circulation is supported by the morphologic left ventricle. RV, right ventricle; LV, left ventricle; RV, right ventricle; Ao, aorta; PA, pulmonary artery.

anatomy are corrected. The LV must be “trained” to handle the systemic circulation by banding the PA, raising LV pressure, and promoting hypertrophy. This would also be the appropriate surgical opportunity to repair or replace the systemic AV valve. Once the LV is prepared and functioning at systemic circulation, a combined atrial switch and an ASO is performed (Fig. 68.38). Therefore, the venous return through the baffle is directed to the anatomically and physiologically correct ventricle and the ventricular–arterial concordance is completed with the arterial switch. Langley et al. described the outcome in a cohort of 54 children and adults (mean age 3.2 years) with ccTGA undergoing the double switch procedure. The surgical mortality was 5.6% and there were two late deaths. Of those with preoperative advanced TR, two died early, two died late, and one underwent transplant (155). Despite these results, LV dysfunction is more common in older patients, and the incidence of atrial arrhythmias would statistically increase following atrial baffle. Overall comparison with long-term data of aggressive heart failure management, cardiac transplantation, and double switch operation is necessary to determine the best approach in the adult patient.

In conclusion, patients with ccTGA represent a rare and complex group for whom outcomes have traditionally been largely dependent on function of the systemic RV. Although this lesion may seem fairly benign in the asymptomatic adult patient, clearly, survival is limited and multiple associated abnormalities may occur requiring close medical supervision. Adult patients should undergo routine exams, ECG, 24-hour ambulatory monitoring, and an assessment for valvular disease. The evaluation of systemic ventricular function can be difficult due the geometry of the RV. Similar to D-TGA, echocardiography may provide qualitative assessment of RV size and function; however, accurate assessment of RV volumes and EF is best assessed with CMR (Fig. 68.39) (156). Those with pacemakers need radionuclide angiography (104) or cardiac CT (157).

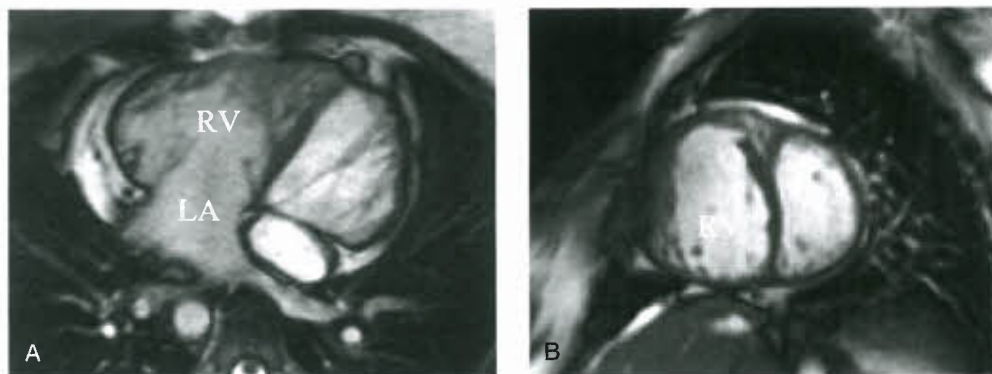


Figure 68.39. Cardiovascular magnetic resonance imaging of a 36-year-old patient with congenitally corrected transposition of the great arteries. **A:** Four-chamber view, note the left atrium to the enlarged right ventricle (RV) supporting systemic circulation. **B:** Sagittal two chamber view showing an enlarged systemic RV.

SINGLE VENTRICLE

Many complex cardiac malformations are characterized by the existence of only one functional ventricle, which has to maintain both systemic and the pulmonary circulations. Single-ventricle anatomy and surgical options are detailed elsewhere (see Chapter 52).

Unrepaired young adult patients with a univentricular heart have a poor prognosis. In a series of unoperated patients with various forms of univentricular anatomy, ($n = 83$), 70% died before 16 years of age with left ventricular anatomy, and 50% died 4 years after the diagnosis when the RV was the systemic ventricle. In this study, the most common causes of death were arrhythmogenic, heart failure, and SCD (158). Anatomic and physiologic factors that support extended survival in the unoperated univentricular heart include (159)

- Double inlet LV with transposed great vessels
- Pulmonary stenosis
- Normal LV systolic function and
- \leq mild AV valve regurgitation

Cyanotic Adult

Multiple medical problems occur as a result of chronic cyanosis. These are both a factor of chronic hypoxia to vital organs and hyperviscosity. The hematologic manifestations include thrombocytopenia, erythrocytosis, thromboemboli, iron deficiency, and bleeding complications. It seems paradoxical that cyanotic patients may suffer thromboembolic events but develop bleeding issues as well. Embolic events are from derangements in the coagulation pathway whereas bleeding diatheses are secondary to platelet dysfunction and thrombocytopenia (68). Thus, there is no agreement as to whether cyanotic patients should receive antiplatelet agents or systemic anticoagulation. The decision to initiate aspirin or coumadin therapy is individually based and many times driven by a documented thromboembolic event or discontinued after a clinically significant bleeding episode, for example, hemoptysis.

Patients may develop hyperuricemia from decreased absorption of uric acid and may lead to gout, urate nephropathy, and nephrolithiasis. Renal disease is also common from hypoperfusion and chronic hypoxia. Neurologic events include cerebral abscesses, hemorrhage, and thromboemboli from right-to-left intracardiac shunting. Therefore, air filters should always be placed on intravenous lines to prevent paradoxical air embolization. Hyperviscosity symptoms from polycythemia occur at various levels of hematocrit, with no level being an exact cut-off for symptoms. Symptoms may include headache, dizziness, fatigue, dyspnea, mental status changes, and paresthesias. Symptoms may be exacerbated at lower levels of hematocrit when iron deficiency is present. In this case, iron replacement is recommended (160).

The Fontan Patient

The Fontan operation places the systemic and pulmonary circulation in series, and is the treatment of choice for patients with a univentricular heart, resulting in near normalization of arterial saturation, and removal of the chronic volume overload. Patients who have undergone the Fontan procedure have now entered their fourth decade of life. In such patients, both the benefits and long-term sequelae associated with this palliation are often seen. Several late complications include arrhythmias, heart failure, exercise intolerance, ventricular dysfunction, thromboembolic complications, hepatic dysfunction, protein losing enteropathy (PLE), and worsening cyanosis (161).

The Fontan circulation is dependent upon some degree of systemic venous hypertension at the expense of pulmonary hypoperfusion. This hemodynamic derangement, along with multiple prior surgeries, extensive suture lines and intracardiac scarring, chronic cyanosis for a period of time, all contribute to potential complications in the adult patient that are listed below.

- Arrhythmias
- Thromboemboli from enlarged hypocontractile right atrium in classic Fontan circuit (Fig. 68.40). Paradoxical emboli are possible with residual right-to-left shunts.
- Protein losing enteropathy



Figure 68.40. Transesophageal echocardiogram of the right atrium (RA) in a 23-year-old patient with tricuspid atresia, s/p classic Fontan procedure. Image demonstrates an enlarged RA with a clot (arrow) attached to the wall of the RA. Note the heavy spontaneous contrast. The patient had persistent atrial arrhythmias and heart failure symptoms and subsequently underwent EC Fontan revision.

- Hepatic dysfunction
- Pulmonary vein compression
- Cyanosis
- Systemic venous collaterals
- Pulmonary arteriovenous malformations (AVMs)

Arrhythmias

After Fontan completion, arrhythmias can result from multiple etiologies including dysfunction of the sinus node, increased atrial pressure, and the presence of suture lines and scars with the incidence of atrial tachy- and bradyarrhythmias increasing with time. Data from the Netherlands found atrial arrhythmias in 50% of their adult Fontan patients (162). In this population, atrial arrhythmias were frequently resistant. The mechanism for most are in the form of a macro-reentry circuit, many of which are multiple and complex. Radiofrequency ablative techniques are successful in >80%; however, recurrence is common and may be as high as 30% to 45% over the subsequent 6 to 12 months (163).

When atrial arrhythmias are detected, a complete hemodynamic evaluation for obstruction within the Fontan circuit should be pursued. The classic Fontan patient with “failing Fontan” criteria will tend to have a severely enlarged right atrium contributing to the medically resistant atrial arrhythmias and is frequently the indication for Fontan revision.

Previously, the incidence or presumed risk factors for SCD in patients with Fontan surgery has not been clearly defined. Khairy et al. (164) evaluated 261 Fontan patients to better define determinants of mortality in univentricular patients. Although the etiology appeared multifactorial, arrhythmias were likely responsible for the majority of sudden deaths (9.2%) when there was no other obvious cause. Other factors contributing to late deaths in this population included heart failure and thromboembolic complications.

Finally, completion of the extracardiac Fontan procedure (e.g., total cavopulmonary connection) for single ventricles avoids extensive suture lines in the right atrium, thereby reducing scarring and higher pressures that lead to intra-atrial reentry tachycardia and sinus node dysfunction. Extracardiac (EC) conduits and lateral tunnel (LT) Fontans are preferred today, and the Fontan conversion procedure (converting prior atriopulmonary Fontans to the EC or LT type) can be performed to reduce arrhythmia and thromboembolic events (93).

Thromboembolic Complications

Thromboembolic complications are a common source of morbidity with multiple clotting abnormalities reported in such patients, including decreased levels of protein C, protein S, and antithrombin III. Recently, clinical predictors for thromboembolic death included a lack of antiplatelet therapy or anticoagulant therapy and clinically diagnosed intracardiac thrombus. Though it is still unclear if all univentricular patients with Fontan palliation should receive antiplatelet or anticoagulation therapies, it is now recommended to give warfarin for patients who have a documented atrial shunt, atrial thrombus, atrial arrhythmias, or a thromboembolic event (36). Most centers will provide either antiplatelet or anticoagulation therapy to patients whom they consider at increased risk (164).

Protein-Losing Enteropathy

The presence of generalized edema, ascites, chronic pleural effusions, and diarrhea in an adult Fontan patient is highly suggestive of the diagnosis of protein-losing enteropathy. PLE

occurs in 3.7% of those with Fontan operation. The loss of a significant amount of protein via the gastrointestinal tract leads to symptoms of peripheral edema, fatigue, pleural and pericardial effusions, ascites, and chronic diarrhea (165). The etiology is not known but thought to be secondary to elevated systemic venous pressures. Other risk factors contributing to PLE include longer cardiopulmonary bypass times, heterotaxy syndrome, and ventricular anatomy other than a morphologic LV (166,167). Unfortunately, PLE bodes for a poor prognosis, with a 5-year survival of only 50% (165). There is no gold standard therapy as multiple case reports and small studies have described varying degrees of success. Current treatment strategies have included a high protein diet, afterload reduction therapy, inotropic agents, heparin, albumin infusion, octreotide, prednisone, and creation of an atrial fenestration (165,167).

Hepatic Complications Post-Fontan Surgery

In addition to the cardiac and hemodynamic disadvantages of Fontan circulation, there is a growing body of literature that has demonstrated that hepatic abnormalities may occur after the Fontan operation. These include coagulation disorders, cholestasis, liver fibrosis, and hepatomegaly with or without ascites (168,169). Baek et al. performed a cross-sectional study of 139 Fontan patients who underwent cardiac CT scans out of a total of 204 patients who had undergone the Fontan procedure between 1986 and 2003. Mean age was 19.0 ± 6.3 years and mean elapsed time since the initial Fontan operation was 11.5 ± 4.7 years. Fifty-seven patients had hepatic complications, including liver cirrhosis (25.9%), thrombocytopenia (7.2%), hyperbilirubinemia (20.9%), and hepatic masses (2.9%). Hepatic complications were significantly associated with ventricular dysfunction, absence of fenestration, thrombus in the Fontan tract, sinus node dysfunction, and tachyarrhythmia. Moreover, hepatic complications were correlated with the duration of Fontan circulation. Thus, the hepatic condition of patients who undergo the Fontan procedure should be regularly evaluated including non-invasive hepatic fibrosis markers and imaging modalities (170).

Cyanosis

Typically, systemic oxygen saturation in Fontan patient should exceed 94%. Etiologies for cyanosis include

- Residual surgically created fenestration
- Pulmonary arteriovenous malformations
- Systemic venous collaterals
- Baffle leaks—area where the Fontan circuit was sutured to native tissue

When cyanosis is found, some residual fenestrations may be seen with transesophageal echocardiography especially with echo contrast studies. Pulmonary AVMs, systemic venous collaterals, and most baffle leaks require angiography to make an accurate diagnosis. During catheterization direct agitated saline contrast to each PA along with transesophageal echocardiography can detect small vessel AVMs. Most causes of cyanosis can be treated with transcatheter device therapy (Fig. 68.41). In our practice, it is recommended that any patient who has Fontan circuit and cyanosis should undergo a diagnostic (often resulting in a therapeutic) cardiac catheterization. Cyanosis should be evaluated not only at rest but also with exertion.

Fontan Revision

The Fontan revision should be considered in those with a failing Fontan. This would include those with congestive

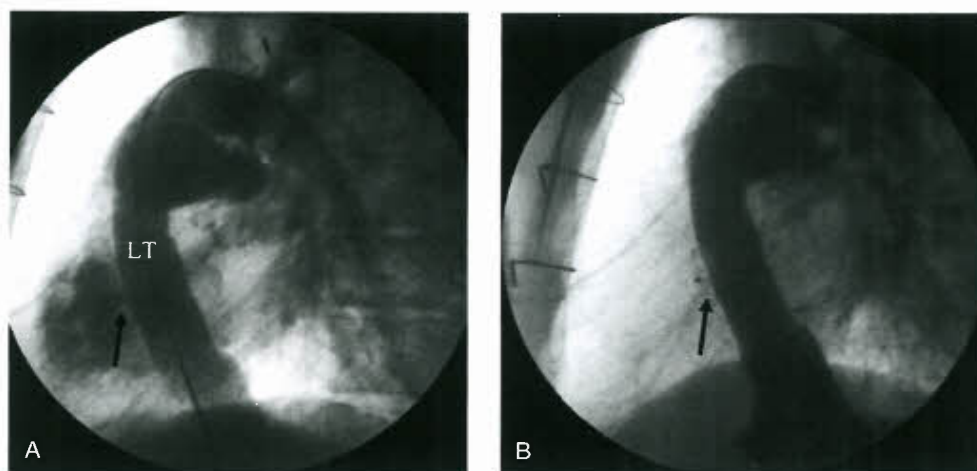


Figure 68.41. Lateral tunnel (LT) angiogram of a 33-year-old patient with tricuspid atresia s/p LT Fontan with fenestration. Patient presented to clinic with systemic saturation of 83%. **A:** demonstrates large residual shunt through the fenestration. **B:** LT angiogram following closure with a 18 mm Amplatzer septal occluder. A second defect was closure by the IVC. Saturation improved to 93%.

heart failure (dyspnea on exertion), recurrent and resistant atrial arrhythmias, persistent thromboemboli from low flow state, and poor kinetic energy through the Fontan circuit (Fig. 68.42). Surgery involves debulking of the enlarged right atrium, removal of any atrial thrombi, excision of right atrial scar tissue, epicardial pacemaker implantation, placement of an EC Gortex conduit from the IVC to the right PA SVC junction (EC Fontan), modified right atrial Maze procedure, and if documented atrial fibrillation, then left atrial Maze as well. The purpose of this revision is to improve cardiac output, reduce atrial arrhythmias, and prevent thrombus formation (171) (Fig. 68.43). Reported perioperative mortality rates for Fontan revision range from 2.4% to 6.7% with short-term follow-up revealing recurrent atrial arrhythmias in 13% to 30% (171–173). If recurrent atrial arrhythmias occur, vascular access for radiofrequency ablation is now more complicated with an EC circuit and requires transbaffle puncture.



Figure 68.42. Cardiovascular magnetic resonance imaging of a 23-year-old patient with a classic Fontan and symptoms of shortness of breath, and persistent atrial arrhythmias. The right atrium is enlarged with poor forward flow through the Fontan. The patient underwent Fontan revision.

Managing a univentricular patient remains a challenge, from the rare unoperated patient to those with failing Fontan circuits. Ultimately, the Fontan operation is a palliative procedure with resultant unique single-ventricle physiology with a high incidence of long-term complications. Adult patients with univentricular hearts and the Fontan physiology require careful, close, and routine follow-up.

Evaluation should be with specialized ACHD clinics including a detailed history and physical examination with particular emphasis on the type of prior surgical repairs, ECG, thorough noninvasive imaging (CMR, echocardiography, cardiac CT), and ambulatory Holter monitoring.

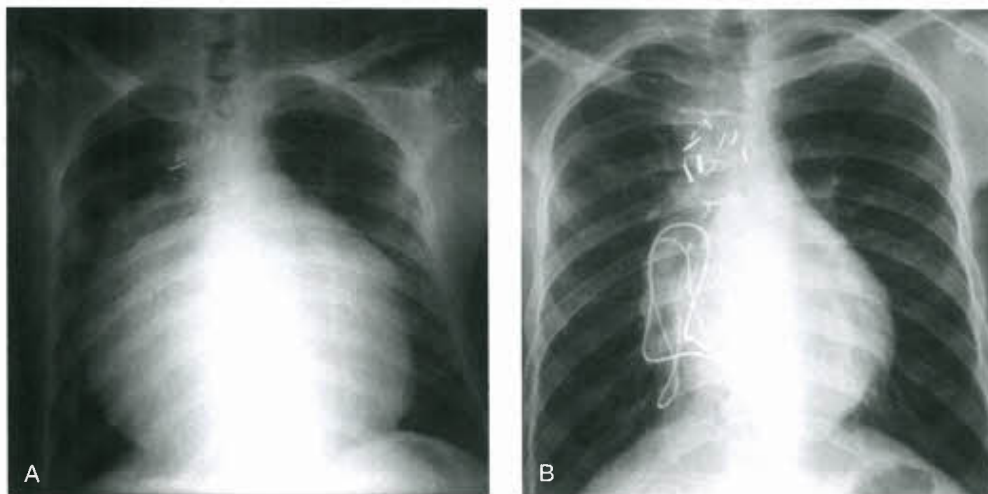
UNIQUENESS OF AN ADOLESCENT AND YOUNG ADULT CARDIAC CLINIC

When the adolescent or adult is evaluated, the office setting, staffing, ambience, and style of evaluation are different from the setting for newborns and toddlers. If treated in the same manner as used for young patients, this population will seek other resources. The clinic should be held separately from that for younger patients, and its setting should be geared toward the age of the patient population.

Depending on the patient's age and maturity, parents may or may not accompany the patient to the office visit. Some patients will come with their spouses and some will even bring their own children. Since many are young adults, unless the patient's development level prohibits understanding, the practitioner should deal with the patient privately as well as with those who accompany the patient. The adolescent and adult should understand that the cardiologist is willing to discuss certain issues in privacy and that these discussions are confidential. By this age, these patients should share in or primarily decide their courses of therapy and behaviors. "Weaning" the young adult from parental decision making is one of the real challenges facing patients as they reach adulthood.

Rather disturbing is the discovery that the same patient who was evaluated annually by a pediatric cardiologist saw a cardiologist only every 10 years after reaching the age of 21 (174). This indicates that a better and more accessible system must be provided to these patients. Because of lack of training and interest, some pediatric cardiologists, who are the best trained to understand most of the defects encountered in this population, do not care to be involved in the care of this age-group. Some internal medicine cardiologists have had minimal exposure to CHD during their training or experience

Figure 68.43. A: Chest radiograph of a 28-year-old patient with classic Fontan for tricuspid atresia with a severely enlarged cardiac silhouette mainly from the enlarged right atrium. B: Following Fontan revision the heart size is significantly decreased. Note epicardial pacing wires.



and are now expected to manage even the most complex of these patients. In fact, internal medicine cardiology training only requires 6 hours of CHD lectures to be board eligible for internal medicine cardiovascular boards (175).

The best present answer for adequate care of this population is a specialized ACHD clinic. Staffing adolescent and adult cardiac clinic varies from institution to institution. It usually includes a team of interested and experienced pediatric cardiologists, internal medicine cardiologists, cardiac surgeons experienced in dealing with congenital heart defects, nurse clinicians, and, occasionally, social workers. The milieu should include trainees from both pediatric and internal medicine disciplines so that a more coordinated effort can be secured for the future. The reality is that there are very few pediatric cardiologists compared with the number of internal medicine cardiologists, and that the transition of many of these patients to adult cardiologists is inevitable. Those providing care must be trained and have the ability to care for this unique population. More recently, internal medicine/pediatric-trained individuals are seeking specialized ACHD training and some have completed both internal medicine and pediatric cardiology training programs with the intent to care for this population.

Consultative access to obstetricians and gynecologists, psychiatrists, endocrinologists, nephrologists, hematologists, rheumatologists, pulmonologists, anesthesiologists, and pathologists, all with an understanding of CHDs and their impacts on this population, is most desirable (176).

Sources of general health care for the adolescent and adult can include pediatricians, most of whom discontinue care when the patient is 21 years old, internists, family practitioners, adolescent health specialists, athletic trainers, and student health center staff, including physicians and nurses. In many cases, the extent of their care may be no more than episodic emergency room visits. The physician trained in internal medicine–pediatrics residency may be the ideal primary care resource for these young people. When the patient has an identified primary provider, that person should be informed about, and frequently augment, recommendations that the clinic team offers to the patient.

In addition to assisting their parents through a sophisticated understanding of their heart problems, the practitioner in the ACHD clinic is expected to help the patient manage lifestyle issues. These include sexuality (including contraception, pregnancy, and evaluation of offspring), education and employability, insurability, and exercise and athletics (177,178).

The ongoing management of this complex patient population can often be challenging in the subset of patients with ACHD who have multiple physical and/or mental disabilities. It is not uncommon for adults with CHD to be living with their parents or to have complex psychosocial needs. Continuity of care may also be compromised by noncompliance in the presence of minimal or no symptoms or with the denial phase, which is common during adolescence. Finally, patients may be lost to follow-up when they move for education or work-related reasons (177,178).

The ACHD population is growing and for the foreseeable future will continue to grow. The estimated number of adults living with CHD is now greater than the estimated population of children with CHD. However, our resources, training, specialized care, research, and clinical trials in this field do not approach other subspecialty areas in cardiology. Although the prognosis for patients with CHD is improving, significant cardiovascular problems persist and limitations to long-term survival still exist. Recurrent vascular lesions, residual shunts, ventricular dysfunction, heart failure, PH, cyanosis, valvular disease, and SCD are unfortunate but realistic problems for the ACHD population. New research, specialized training and care, and legislative help are all necessary to improve the lives of those adults living with CHD.

REFERENCES

1. Williams R, Pearson G, Barst R, et al. Report of the national heart, lung and blood institute working group on research in adult congenital heart disease. *J Am Coll Cardiol* 2006;47:701–707.
2. Marelli A, Mackie A, Ionescu-Ittu R, et al. Congenital heart disease in the general population: changing prevalence and age distribution. *Circulation* 2007;115:163–172.
3. Silka MJ, Hardy BG, Menashe VD, et al. A population based prospective evaluation of risk of sudden cardiac death after operation for common congenital heart defects. *J Am Coll Cardiol* 1998;32:245–251.
4. Roberts WC. The congenitally bicuspid aortic valve. A study of 85 autopsy cases. *Am J Cardiol* 1970;26:72–83.
5. Roberts WC, Ko JM. Frequency by decades of unicuspid, bicuspid, and tricuspid aortic valves in adults having isolated aortic valve replacement for aortic stenosis, with or without associated aortic regurgitation. *Circulation* 2005;111:920–925.
6. Fenoglio JJ Jr, McAllister HA Jr, DeCastro CM, et al. Congenital bicuspid aortic valve after age 20. *Am J Cardiol* 1977;39:164.
7. Lewin MB, Otto CM. The bicuspid aortic valve: adverse outcomes from infancy to old age. *Circulation* 2005;111:832.
8. Gersony WM, Hayes CJ, Driscoll DJ, et al. Second natural history study of congenital heart defects: of life of patients with aortic stenosis, pulmonary stenosis or ventricular septal defect. *Circulation* 1993;87:152–165.

9. Beppu S, Suzuki S, Matsuda H, et al. Rapidity of progression of aortic stenosis in patients with congenital bicuspid aortic valves. *Am J Cardiol* 1993;71:322–327.
10. Bonow RO, Carabello B, De Leon AC, et al. ACC/AHA guidelines for the management of patients with valvular heart disease. *J Am Coll Cardiol* 1998;32:1486–1588.
11. McCrindle BW. Independent predictors of immediate results of percutaneous balloon aortic valvotomy in children: Valvuloplasty and angioplasty of congenital anomalies (VACA) registry investigators. *Am J Cardiol* 1996;77:286–293.
12. Lock JE. The adult with congenital heart disease: cardiac catheterization as a therapeutic intervention. *J Am Coll Cardiol* 1991;18:330–331.
13. Kouchoukos NT, Davila-Roman VG, Spray TL, et al. Replacement of the aortic root with the pulmonary autograft in children and young adults with aortic—valve disease. *NEJM* 1994;330:1–6.
14. Chambers JC, Somerville J, Stone S, et al. Pulmonary autograft procedure for aortic valve disease. Long-term results of the pioneer series. *Circulation* 1997;96:2206–2214.
15. Pasquali SK, Cohen MS, Shera D, et al. The relationship between neo-aortic root dilation, insufficiency, and reintervention following the Ross procedure in infants, children, and young adults. *J Am Coll Cardiol* 2007;49:1806–1812.
16. Kouchoukos NT, Masetti P, Nickerson NJ, et al. The Ross procedure: long-term clinical and echocardiographic follow-up. *Ann Thorac Surg* 2004;78:773–781.
17. Larson EW, Edwards WD. Risk Factors for aortic dissection: a necropsy study of 161 cases. *Am J Cardiol* 1984;53:849–855.
18. Roberts CS, Roberts WC. Dissection of the aorta associated with congenital malformation of the aortic valve. *J Am Coll Cardiol* 1991;17:712–716.
19. Warren AE, Boyd ML, O'Connell, et al. Dilation of the ascending aorta in pediatric patients with bicuspid aortic valve; frequency, rate of progression, and risk factors. *Heart* 2006;92:1496–1500.
20. Hahn RT, Roman MJ, Mogtader AH, et al. Association of aortic dilation with regurgitant, stenotic and functionally normal bicuspid aortic valves. *J Am Coll Cardiol* 1992;19:283–288.
21. Fedak PW, de Sa MP, Verma S, et al. Vascular matrix remodeling in patients with bicuspid aortic valve malformations: implications for aortic dilatation. *J Thorac Cardiovasc Surg* 2003;126:797–806.
22. Nataatmadja M, West M, West J, et al. Abnormal extracellular matrix protein transport associated with increased apoptosis of vascular smooth muscle cells in marfan syndrome and bicuspid aortic valve thoracic aortic aneurysm. *Circulation* 2003;108:II329–II334.
23. Bonow RO, Carabello BA, Chatterjee K, et al. 2008 focused update incorporated into the ACC/AHA 2006 guidelines for the management of patients with valvular heart disease: a report of the American College of Cardiology/American Heart Association Task Force on Practice Guidelines (Writing Committee to revise the 1998 guidelines for the management of patients with valvular heart disease). Endorsed by the Society of Cardiovascular Anesthesiologists, Society for Cardiovascular Angiography and Interventions, and Society of Thoracic Surgeons. American College of Cardiology/American Heart Association Task Force on Practice Guidelines. *J Am Coll Cardiol*. 2008 23;52:e1–e142.
24. Borger MA, Preston M, Ivanov J, et al. Should the ascending aorta be replaced more frequently in patient with bicuspid aortic valve disease? *J Thorac Cardiovasc Surg* 2004;128:677.
25. Stellin G, Mazzucco A, Bortolotti U, et al. Late results after resection of discrete and tunnel subaortic stenosis. *Eur J Cardiothorac Surg* 1989;3:235–239.
26. Brauner R, Laks H, Drinkwater DC, et al. Benefits of early surgical repair in fixed subaortic stenosis. *J Am Coll Cardiol* 1997;30:1835–1842.
27. Lupinetti FM, Pridjian AK, Callow LB, et al. Optimum treatment of discrete subaortic stenosis. *Ann Thorac Surg* 1992;54:467–471.
28. Cohen M, Fuster V, Steele PM, et al. Coarctation of the aorta: long-term follow-up and prediction of outcome after surgical correction. *Circulation* 1989;80:840–845.
29. James FW, Kaplan S. Systolic hypertension during submaximal exercise after correction of coarctation of the aorta. *Circulation* 1974;50:II27–II33.
30. Balderston SM, Daberkow E, Clarke DR, et al. Maximal voluntary exercise variables in children with postoperative coarctation of the aorta. *J Am Coll Cardiol* 1992;19:154–158.
31. Vigano M, Ressler L, Gaeta R. Long-term follow-up after repair of coarctation of the aorta in adults. *Ann Thorac Surg* 1997;63:1825–1834.
32. Leandro J, Smallhorn JF, Benson L, et al. Ambulatory blood pressure monitoring and left ventricular mass and function after successful surgical repair of coarctation of the aorta. *J Am Coll Cardiol* 1992;20:197–204.
33. Kaemmerer H, Oelert F, Bahlmann J, et al. Arterial hypertension in adults after surgical treatment of aortic coarctation. *Thorac Cardiovasc Surg* 1998;46:121–125.
34. Choy M, Rocchini AP, Beekman RH, et al. Paradoxical hypertension after repair of coarctation of the aorta in children: balloon angioplasty versus surgical repair. *Circulation* 1987;75:1186.
35. Fawzy ME, Awad M, Hassan W, et al. Long-term outcome (up to 15 years) of balloon angioplasty of discrete native coarctation of the aorta in adolescents and adults. *J Am Coll Cardiol* 2004;43:1062.
36. Harrison DA, McLaughlin PR, Lazzam C, et al. Endovascular stents in the management of coarctation of the aorta in the adolescent and adult: one year follow up. *Heart* 2001;85:561.
37. Eicken A, Pensl U, Sebening W, et al. The fate of systemic blood pressure in patients after effectively stented coarctation. *Eur Heart J* 2006;27:1100–1105.
38. White CW, Zoller RP. Left aortic dissection following repair of coarctation of the aorta. *Chest* 1973;63:573–577.
39. Lindsay J Jr, Rosenberg J, Ross JW, et al. Anuloaortic ectasia as a late complication following repair of coarctation of the aorta. *Vasc Surg* 1986;20:288–292.
40. Maron BJ, Humphries JO, Rowe RD, et al. Prognosis of surgically corrected coarctation of the aorta. *Circulation* 1973;47:119–126.
41. Fortang K, Rostad H, Sorland S, et al. Late sudden death after surgical correction of coarctation of the aorta. *Acta Med Scand* 1979;206:375–379.
42. Brili S, Dernelis J, Aggeli C, et al. Aortic elastic properties in patients after repaired coarctation of the aorta. *Am J Cardiol* 1998;82:1140–1143.
43. Hirata K, Triposkiadis F, Sparks E, et al. The Marfan syndrome: abnormal elastic properties. *J Am Coll Cardiol* 1991;18:57–63.
44. Yuan SM, Raanani E. Late complications of coarctation of the aorta. *Cardiol J* 2008;15:517–524.
45. Tsai SF, Trivedi M, Boettner B, et al. Usefulness of screening cardiovascular magnetic resonance imaging to detect aortic abnormalities after repair of coarctation of the aorta. *Am J Cardiol* 2011;107:297–301.
46. Krieger EV, Stout K. The adult with repaired coarctation of the aorta. *Heart* 2010;96:1676–1681.
47. Therrien J, Thorne SA, Wright A, et al. Repaired coarctation: a “cost-effective” approach to identify complications in adults. *J Am Coll Cardiol* 2000;35:997–1002.
48. Kidd L, Driscoll DJ, Gersony WM, et al. Second natural history study of congenital heart defects: results of treatment of patients with ventricular septal defects. *Circulation* 1993;87:138–151.
49. Allen HD, Anderson RC, Noren GR, et al. Post-operative follow-up of patients with ventricular septal defects. *Circulation* 1974;50:465–471.
50. Moller JH, Anderson RC. 1000 consecutive children with a cardiac malformation with 26 to 37 year follow-up. *Am J Cardiol* 1992;70:661–667.
51. Moller JH, Patton C, Varco RL, et al. Late results (30 to 35 years) after operative closure of isolated ventricular septal defect from 1954 to 1960. *Am J Cardiol* 1991;68:1491–1497.
52. Carminati M, Butera G, Chessa M, et al. Transcatheter closure of congenital ventricular septal defects: results of the European Registry. *Eur Heart J* 2007;28:2361.
53. Al-Kashkari W, Balan P, Kavinsky CJ, et al. Percutaneous device closure of congenital and iatrogenic ventricular septal defects in adult patients. *Catheter Cardiovasc Interv* 2011;77:260–267.
54. Meijboom F, Hess J, Szatmari A, et al. Long-term follow-up (9 to 20 years) after surgical closure of atrial septal defect at a young age. *Am J Cardiol* 1993;72:1431–1434.
55. Murphy JG, Gersh BJ, McGoon MD, et al. Long-term outcome after surgical repair of isolated atrial septal defect. *N Engl J Med* 1990;323:1645–1650.
56. Schwetz BA. From the Food and Drug Administration. *JAMA* 2002;287:578.
57. Masura J, Gavora P, Podnar T. Long-term outcome of transcatheter secundum-type atrial septal defect closure using Amplatzer septal occluders. *J Am Coll Cardiol* 2005;45:505.
58. Vander Velde ET, Vriend JW, Mannens MM, et al. CONCOR, an initiative towards a national registry and DNA-bank of patients with congenital heart disease in the Netherlands: rationale, design, and first results. *Eur J Epidemiol* 2005;20:549–557.
59. Duffels MG, Engelfriet PM, Berger RM, et al. Pulmonary arterial hypertension in congenital heart disease: an epidemiologic perspective from a Dutch registry. *Int J Cardiol* 2007;120:198–204.
60. Kidd L, Driscoll DJ, Gersony WM, et al. Second natural history study of congenital heart defects. Results of treatment of patients with ventricular septal defects. *Circulation* 1993;87:138–151.
61. Saha A, Balakrishnan KG, Jaiswal PK, et al. Prognosis for patient with Eisenmenger syndrome of various aetiology. *Int J Cardiol* 1994;45:199–207.
62. Vongpatanasin W, Brickner ME, Hillis LD, et al. The Eisenmenger syndrome in Adults. *Ann Intern Med* 1998;128:745–755.
63. Hopkins WE, Ochoa LL, Richardson GW, et al. Comparison of the hemodynamics and survival of adults with severe primary pulmonary hypertension or Eisenmenger syndrome. *J Heart Lung Transplant* 1996;15:100–105.
64. Perloff JK, Rosove MH, Child JS, et al. Adults with cyanotic congenital heart disease: hematologic management. *Ann Intern Med* 1988;109:406–413.
65. Drenthen W, Pieper PG, Roos-Hesselink JW, et al. Outcomes of pregnancy in women with congenital heart disease: a literature review. *J Am Coll Cardiol* 2007;49:2303.
66. Warnes CA, Williams RG, Bashore TM, et al. ACC/AHA 2008 Guidelines for the Management of Adults with Congenital Heart Disease: a report of the American College of Cardiology/American Heart Association Task Force on Practice Guidelines (writing committee to develop guidelines on the management of adults with congenital heart disease). *Circulation* 2008;118:e714.
67. Bédard E, Dimopoulos K, Gatzoulis MA. Has there been any progress made on pregnancy outcomes among women with pulmonary arterial hypertension? *Eur Heart J* 2009;30:256.
68. Ammash N, Warnes CA. Cerebrovascular events in adult patients with cyanotic congenital heart disease. *J Am Coll Cardiol* 1996;28:768–762.

69. Gatzoulis MA, Alonso-Gonzalez R, Beghetti M. Pulmonary arterial hypertension in paediatric and adult patients with congenital heart disease. *Eur Respir Rev* 2009;18:154–161.
70. Zuckerman WA, Leaderer D, Rowan CA, et al. Ambrisentan for pulmonary arterial hypertension due to congenital heart disease. *Am J Cardiol* 2011;107:1381–1385.
71. Fernandes SM, Newburger JW, Lang P, et al. Usefulness of epoprostenol therapy in the severely ill adolescent/adult with Eisenmenger physiology. *Am J Cardiol* 2003;91:632–635.
72. Galie N, Gatzoulis MA, Granton J, et al. Bosentan therapy in patients with Eisenmenger syndrome: a multicenter, double-blind, randomized, placebo—controlled study. *Circulation* 2006;114:48–54.
73. Adriaenssens T, Delcroix M, Van Deyk K, et al. Advanced therapy may delay the need for transplantation in patients with the Eisenmenger syndrome. *Eur Heart J* 2006;27:1472–1477.
74. Görler H, Strüder M, Ballmann M, et al. Lung and heart-lung transplantation in children and adolescents: a long-term single-center experience. *J Heart Lung Transplant* 2009;28:243–248.
75. Waddell TK, Bennett L, Kennedy R, et al. Heart-lung or lung transplantation for Eisenmenger syndrome. *J Heart Lung Transplant* 2002;21:731.
76. De Perrot M, Chaparro C, McRae K, et al. Twenty-year experience of lung transplantation at a single center: Influence of recipient diagnosis on long-term survival. *J Thoracic Cardiovasc Surg* 2004;127:1493–1501.
77. Burton CM, Milman N, Carlson J, et al. The Copenhagen National Lung Transplant Group: survival after single lung, double lung, and heart-lung transplantation. *J Heart Lung Transplant* 2005;24:1834–1843.
78. Rigby ML. Closure of a large patent ductus arteriosus in adults: first do no harm. *Heart* 2007;93:417.
79. Celermajer DS, Sholler GF, Hughes CF, et al. Persistent ductus arteriosus in adults. A review of surgical experience with 25 patients. *Med J Aust* 1991;155:233–236.
80. Ing FF, Mullins CE, Road M, et al. Transcatheter closure of the PDA in adults using Gianturco coils. *Clin Card* 1996;19:875–879.
81. Daniels CJ, Franklin WH. Common cardiac diseases in adolescence. *Pediatr Clin North Am* 1997;44:1591–1601.
82. Fontana ME, Sparks EA, Boudoulas H, et al. Mitral valve prolapse and the mitral valve prolapse syndrome. *Curr Prob Cardiol* 1991;16:311–375.
83. Dollar AL, Roberts WC. Morphologic comparison of patients with mitral valve prolapse who died suddenly with patients who died from severe valvular dysfunction or other conditions. *J Am Coll Cardiol* 1991;17:921–931.
84. Turker Y, Ozaydin M, Acar G, et al. Predictors of ventricular arrhythmias in patients with mitral valve prolapse. *Int J Cardiovasc Imaging* 2010;26:139–145.
85. Desai PA, Tafreshi J, Pai RG. Beta-blocker therapy for valvular disorders. *J Heart Valve Dis* 2011;20:241–253.
86. Earing MG, Connolly HM, Dearani JA, et al. Long-term follow-up of patients after surgical treatment for isolated pulmonary valve stenosis. *Mayo ClinicProc* 2005;80:871–876.
87. McCrindle BW. Independent predictors of long-term results after balloon pulmonary valvuloplasty. Valvuloplasty and angioplasty of congenital anomalies (VACA) registry investigators. *Circulation* 1994;89:1751–1759.
88. Hayes CJ, Gersony WM, Driscoll DJ, et al. Second natural history study of congenital heart defects: results of treatment of patients with pulmonary valvular stenosis. *Circulation* 1993;87:128–137.
89. Kaplan EL. Infective endocarditis in the pediatric age group: an overview. In: Kaplan EL, Taranta AV, eds. *Infective Endocarditis: An American Heart Association symposium*. Dallas: American Heart Association, 1977:51–54.
90. Murphy JG, Gersh BJ, Mair DD, et al. Long-term outcome in patients undergoing surgical repair of Tetralogy of Fallot. *NEJM* 1993;329:593–599.
91. Kloevekorn WP, Meisner H, Paek SU, et al. Long-term results after right ventricular outflow tract reconstruction with porcine bioprosthetic conduits. *J Card Surg* 1991;6:624–626.
92. Danielson GK, Downing TP, Schaff HV, et al. Replacement of obstructed extracardiac conduits with autogenous tissue reconstructions. *J Thorac Cardiovasc Surg* 1987;93:555–559.
93. Lam W, Friedman RA. Electrophysiology issues in adult congenital heart disease. *Methodist Debakey Cardiovasc J* 2011;7:13–17.
94. Gatzoulis MA, Balaji S, Webber SA, et al. Risk factors for arrhythmia and sudden cardiac death late after repair of tetralogy of Fallot: a multicentre study. *Lancet* 2000;356:975–981.
95. Attenhofer Jost CH, Connolly HM, Burkhardt HM, et al. Tetralogy of fallot repair in patients 40 years or older. *Mayo Clin Proc* 2010;85:1090–1094.
96. Rosing DR, Borer JS, Kent KM, et al. Long-term hemodynamic and electrocardiographic assessment following operative repair of tetralogy of Fallot. *Circulation* 1978;58:1209–1217.
97. Deanfield JE, McKenna WJ, Halliday-Smith KA. Detection of late arrhythmia and conduction disturbance after correction of tetralogy of Fallot. *Br Heart J* 1980;44:248–253.
98. Garson A, Nihill MR, McNamara DG, et al. Status of the adult and adolescent after repair of tetralogy of Fallot. *Circulation* 1979;59:1232–1240.
99. Le Gloan L, Khairy P. Management of arrhythmias in patients with tetralogy of Fallot. *Curr Opin Cardiol* 2011;26:60–65.
100. Gatzoulis MA, Till JA, Sommerville J, et al. Mechano-electrical interaction in tetralogy of Fallot; QRS prolongation relates to right ventricular size and predicts malignant ventricular arrhythmias and sudden death. *Circulation* 1995;92:231–237.
101. Nollert G, Fischlein T, Bouterwek S, et al. Long-term survival of patients with repair of tetralogy of Fallot: 36-year follow-up of 490 survivors of the first year after surgical repair. *J Am Coll Cardiol* 1997;30:1374–1383.
102. Nollert GD, Däbritz SH, Schmoeckel M, et al. Risk factors for sudden death after repair of tetralogy of Fallot. *Ann Thorac Surg* 2003;76:1901–195.
103. Discipil B, Dearani JA, Puga FJ, et al. Late Pulmonary valve replacement after repair of tetralogy of Fallot. *J Thorac Cardiovasc Surg* 2001;121:344–351.
104. Knauth AL, Gauvreau K, Powell AJ, et al. Ventricular size and function assessed by Cardiac MRI predict major adverse clinical outcomes late after tetralogy of Fallot repair. *Heart* 2008;94:211–216.
105. Vliegen HW, Van Straten A, de Roos A, et al. Magnetic resonance imaging to assess the hemodynamic effects of pulmonary valve replacement in adults late after repair of tetralogy of fallot. *Circulation* 2002;106:1703–1707.
106. Therrien J, Siu SC, McLaughlin PR, et al. Pulmonary valve replacement in adults late after repair of tetralogy of Fallot: are we operating too late? *J Am Coll Cardiol* 2000;36:1670–1675.
107. Geva T. Repaired tetralogy of Fallot: the roles of cardiovascular magnetic resonance in evaluating pathophysiology and for pulmonary valve replacement decision support. *J Cardiovasc Magn Reson* 2011;13:9.
108. Bonhoeffer P, Boudjemline Y, Saliba Z, et al. Percutaneous replacement of pulmonary valve in a right-ventricle to pulmonary-artery prosthetic conduit with valve dysfunction. *Lancet* 2000;356:1403–1405.
109. Khambadkone S, Coats L, Taylor A, et al. Percutaneous pulmonary valve implantation in humans: results in 59 consecutive patients. *Circulation* 2005;112:1189–1197.
110. Therrien J, Siu SC, Harris L, et al. Impact of pulmonary valve replacement on arrhythmia propensity late after repair of tetralogy of Fallot. *Circulation* 2001;103:2489–2494.
111. Khairy P, Landzberg MJ, Gatzoulis MA, et al. Value of programmed ventricular stimulation after tetralogy of Fallot repair: a multicenter study. *Circulation* 2004;109:1994–2000.
112. Roos-Hesselink J, Perloth MG, McGhie J, et al. Atrial arrhythmias in adults after repair of tetralogy of Fallot; correlations with clinical, exercise, and echocardiographic findings. *Circulation* 1995;91:2214–2219.
113. Tan JL, Davlouros PA, McCarthy KP, et al. Intrinsic histological abnormalities of aortic root and ascending aorta in tetralogy of Fallot: evidence of causative mechanism for aortic dilatation and aortopathy. *Circulation* 2005;112:961–968.
114. Rath VK, Doyle M, Williams RB, et al. Massive aortic aneurysm and dissection in repaired tetralogy of Fallot; diagnosis by cardiovascular magnetic resonance imaging. *Int J Cardiology* 2005;101:169–170.
115. Khambadkone S. Percutaneous implantation of the pulmonary and aortic valves: indications and limitations. *J Cardiovasc Med* 2007;8:57–161.
116. Flinn CJ, Wolff GS, Dick M II, et al. Cardiac rhythm after the Mustard operation for complete transposition of the great arteries. *N Engl J Med* 1984;310:1635–1638.
117. Gelatt M, Hamilton RM, McCrindle BW, et al. Arrhythmia and mortality after the Mustard procedure: a 30-year single-center experience. *J Am Coll Cardiol* 1997;29:194–201.
118. Helbing WA, Hansen B, Ottenkamp J, et al. Long-term results of atrial correction for transposition of the great arteries. Comparison of Mustard and Senning operation. *J Thorac Cardiovasc Surg* 1994;108:363–372.
119. Wilson NJ, Clarkson PM, Barratt-Boyes BG, et al. Long-term outcome after the Mustard repair for simple transposition of the great arteries. *J Am Coll Cardiol* 1998;32:758–765.
120. Janousek J, Paul T, Luhmer I, et al. Atrial baffle procedures for complete transposition of the great arteries: natural course of sinus node dysfunction and risk factors for dysrhythmias and sudden death. *Z Kardiol* 1994;83:933–938.
121. Kammeraad JA, van Deurzen CH, Sreeram N, et al. Predictors of sudden cardiac death after Mustard or Senning repair for transposition of the great arteries. *J Am Coll Cardiol* 2004;44:1095–1102.
122. Schwerzmann M, Salehian O, Harris L, et al. Ventricular arrhythmias and sudden death in adults after a Mustard operation for transposition of the great arteries. *Eur Heart J* 2009;30:1873–1879.
123. Khairy P, Harris L, Landzberg MJ, et al. Sudden death and defibrillators in transposition of the great arteries with intra-atrial baffles: a multicenter study. *Circ Arrhythm Electrophysiol* 2008;1:250–257.
124. Kammeraad JA, van Deurzen CH, Sreeram N, et al. Predictors of sudden cardiac death after Mustard or Senning repair for transposition of the great arteries. *J Am Coll Cardiol* 2004;44:1095–1102.
125. Kanter RJ, Papagiannis J, Carboni MP, et al. Radiofrequency catheter ablation of supraventricular tachycardia substrates after mustard and senning operations for d-transposition of the great arteries. *J Am Coll Cardiol* 2000;35:428–441.
126. Bu'Lock FA, Tometzki AJ, Kitchiner DJ, et al. Balloon expandable stents for systemic venous pathway stenosis late after Mustard's operation. *Heart* 1998;79:225–229.

127. Daehnert I, Hennig B, Wiener M, et al. Interventions in leaks and obstructions of the interatrial baffle late after Mustard and Senning correction for transposition of the great arteries. *Cathet Cardiovasc Interv* 2005;66:400-407.
128. Khairy P, Lanzberg MJ, Gatzoulis MA, et al. Epicardial versus endocardial pacing and thromboembolic events investigators. Transvenous pacing leads and systemic thromboemboli in patients with intracardiac shunts: a multicenter study. *Circulation* 2006;113:2391-2397.
129. Meijboom F, Szatmari A, Deckers JW, et al. Long-term follow-up (10 to 17 years) after Mustard repair for transposition of the great arteries. *J Thorac Cardiovasc Surg* 1996;111:1158-1168.
130. Moons P, Gewillig M, Sluysmans T, et al. Long term outcome up to 30 years after the Mustard or Senning operation: a nationwide multicentre study in Belgium. *Heart* 2004;90:307-313.
131. Hurwitz RA, Caldwell RL, Girod DA, et al. Right ventricular systolic function in adolescents and young adults after Mustard operation for transposition of the great arteries. *Am J Cardiol* 1996;77:294-297.
132. Roos-Hesselink JW, Meijboom FJ, Spitaels SE, et al. Decline in ventricular function and clinical condition after Mustard repair for transposition of the great arteries (a prospective study of 22-29 years). *Eur Heart J* 2004;25:1264-1270.
133. Hechter SJ, Fredriksen PM, Liu P, et al. Angiotensin-converting enzyme inhibitors in adults after the Mustard procedure. *Am J Cardiol* 2001;87:660-663.
134. Lorenz CH, Walker ES, Graham TP Jr, et al. Right ventricular performance and mass by use of cine MRI late after atrial repair of transposition of the great arteries. *Circulation* 1995;92:II233-II239.
135. Van Son JA, Reddy VM, Silverman NH, et al. Regression of tricuspid regurgitation after two-stage arterial switch operation for failing systemic ventricle after atrial inversion operation. *J Thorac Cardiovasc Surg* 1996;111:42-47.
136. Palalino MA, Stellin G, Brawn WJ, et al. Arterial switch operation after left ventricular retraining in the adult. *Ann Thorac Surg* 2000;70:1753.
137. Chang AC, Wernovsky G, Wessel DL, et al. Surgical management of late right ventricular failure after Mustard or Senning repair. *Circulation* 1992;86:II40-II44.
138. Poirier NC, Yu JH, Brizard CP, et al. Long-term results of left ventricular reconditioning and anatomic correction for systemic right ventricular dysfunction after atrial switch procedures. *J Thorac Cardiovasc Surg* 2004;127:975-981.
139. Jatene AD, Fontes VF, Paulista PP, et al. Anatomic correction of transposition of the great vessels. *J Thorac Cardiovasc Surg* 1976;72:364.
140. Hutter PA, Krieb DL, Mantel SF, et al. Twenty-five years' experience with the arterial switch operation. *Thorac Cardiovasc Surg* 2002;124:790.
141. Tobler D, Williams WG, Jegatheeswaran A, et al. Cardiac outcomes in young adult survivors of the arterial switch operation for transposition of the great arteries. *J Am Coll Cardiol* 2010;56:58.
142. Kovalchin JP, Allen HD, Cassidy SC, et al. Pulmonary valve eccentricity in d-transposition of the great arteries: implication for arterial switch operation. *Am J Cardiol* 1994;73:186-190.
143. Massin M, Hovels-Gurich H, Dabritz S, et al. Results of the Bruce treadmill test in children after arterial switch operation for simple transposition of the great arteries. *Am J Cardiol* 1998;81:56-60.
144. Skinner J, Hornung T, Rumball E. Transposition of the great arteries: from fetus to adult. *Heart* 2008;94:1227-1235.
145. Legendre A, Losay J, Touchot-Kone A, et al. Coronary events after arterial switch operation for transposition of the great arteries. *Circulation* 2003;108:II-186-II-190.
146. Hutter PA, Krieb DL, Mantel SF, et al. Twenty-five years experience with the arterial switch operation. *J Thorac Cardiovasc Surg* 2002;124:790-797.
147. Pedra SR, Pedra CA, Abizaid AA, et al. Intracoronary ultrasound assessment late after the arterial switch operation for transposition of the great arteries. *J Am Coll Cardiol* 2005;45:2061-2068.
148. Connelly MS, Liu PP, Williams WG, et al. Congenitally corrected transposition of the great arteries in the adult: functional status and complications. *J Am Coll Cardiol* 1996;27:1238-1243.
149. Hornung TS, Calder L. Congenitally corrected transposition of the great arteries. *Heart* 2010;96:1154-1161.
150. Graham TP Jr, Bernard YD, Mellen BG, et al. Long-term outcome in congenitally corrected transposition of the great arteries: a multi-institutional study. *JACC* 2000;36:255.
151. Fredriksen PM, Chen A, Veldtman G, et al. Exercise capacity in adult patients with congenitally corrected transposition of the great arteries. *Heart* 2001;85:191-195.
152. Prieto LR, Hordof AJ, Secic M, et al. Progressive disease in patients with congenitally corrected transposition of the great arteries. *Circulation* 1998;98:997-1005.
153. Beauchesne LM, Warnes CA, Connolly HM, et al. Outcome of the unoperated adult who presents with congenitally corrected transposition of the great arteries. *J Am Coll Cardiol* 2002;40:285-290.
154. Van Son JA, Danielson GK, Huhta JC, et al. Late results of systemic atrioventricular valve replacement in corrected transposition. *J Thorac Cardiovasc Surg* 1995;109:642.
155. Langley SM, Winlaw DS, Stumper O, et al. Midterm results after restoration of the morphologically left ventricle to the systemic circulation in patients with congenitally corrected transposition of the great arteries. *J Thorac Cardiovasc Surg* 2003;125:1229.
156. Dodge-Khatami A, Tulevski II, Bennink GB, et al. Comparable systemic ventricular function in healthy adults and patients with unoperated congenitally corrected transposition using MRI dobutamine stress testing. *Ann Thorac Surg* 2002;73:1759-1764.
157. Raman SV, Cook SC, McCarthy B, et al. Usefulness of multidetector row computed tomography to quantify right ventricular size and function in adults with either tetralogy of Fallot or transposition of the great arteries. *Am J Cardiol* 2005;95:683.
158. Moodie DS, Ritter DG, Tajik AJ, et al. Long-term follow-up in the unoperated univentricular heart. *Am J Cardiol* 1984;53:1124.
159. Ammass NM, Warnes CA. Survival into adulthood of patients with unoperated single ventricle. *Am J Cardiol* 1996;77:542.
160. Oechslin E. Hematological management of the cyanotic adult with congenital heart disease. *Int J Cardiol* 2004;97:109-115.
161. Khairy P, Poirier N, Mercier LA. Univentricular heart. *Circulation* 2007;115:800-812.
162. van den Bosch AE, Roos-Hesselink JW, Van Domburg R, et al. Long-term outcome and quality of life in adult patients after the Fontan operation. *Am J Cardiol* 2004;93:1141-1145.
163. Kannankeril PJ, Anderson ME, Rottman JN, et al. Frequency of late recurrence of intra-atrial reentry tachycardia after radiofrequency catheter ablation in patients with congenital heart disease. *Am J Cardiol* 2003;92:879.
164. Khairy P, Fernandes SM, Mayer JE, et al. Long-term survival, modes of death, and predictors of mortality in patients with Fontan surgery. *Circulation* 2008;117:85-92.
165. Mertens L, Hagler DJ, Sauer U, et al. Protein-losing enteropathy after the Fontan operation: an international multicenter study. PLE study group. *J Thorac Cardiovasc Surg* 1998;115:1063.
166. Powell AJ, Gauvreau K, Jenkins KJ, et al. Perioperative risk factors for development of protein-losing enteropathy following a Fontan procedure. *Am J Cardiol* 2001;88:1206.
167. Meadows J, Jenkins K. Protein-losing enteropathy: integrating a new disease paradigm into recommendations for prevention and treatment. *Cardiol Young* 2011;21:363-377.
168. Kendall TJ, Stedman B, Hacking N, et al. Hepatic fibrosis and cirrhosis in the Fontan circulation: a detailed morphological study. *J Clin Pathol* 2008;61:504-508.
169. Camposilvan S, Milanese O, Stellin G, et al. Liver and cardiac function in the long term after Fontan operation. *Ann Thorac Surg* 2008;86:177-182.
170. Baek JS, Bae EJ, Ko JS, et al. Late hepatic complications after Fontan operation; non-invasive markers of hepatic fibrosis and risk factors. *Heart* 2010;96:1750-1755.
171. Mavroudis C, Deal BJ, Backer CL. The beneficial effects of total cavopulmonary conversion and arrhythmia surgery for the failed Fontan. *Semin Thorac Cardiovasc Surg Pediatr Card Surg Annu* 2002;5:12-24.
172. Dearani JA, Mavroudis C, Quintessenza J, et al. Surgical advances in the treatment of adults with congenital heart disease. *Curr Opin Pediatr* 2009;21:565-572.
173. Setty SP, Finucane K, Skinner JR, et al. Extracardiac conduit with a limited maze procedure for the failing Fontan with atrial tachycardias. *Ann Thorac Surg* 2002;74:1992-1997.
174. Gersony WM, Hayes CJ, Driscoll DJ, et al. Second natural history study of congenital heart defects: quality of life of patients with aortic stenosis, pulmonary stenosis or ventricular septal defect. *Circulation* 1993;87:152-165.
175. Skorton DJ, Cheitlin MD, Freed MD, et al. Guidelines for training in adult cardiovascular medicine. COCATS. Task Force 9: training in the care of adult patients with congenital heart disease. *J Am Coll Cardiol* 1995;25:31-33.
176. Somerville J, Webb GD, Skorton DJ, et al. Characteristics of the special care facilities for adults with congenital heart disease. *J Am Coll Cardiol* 1991;18:315-318.
177. Allen HD, Franklin WH. Lifestyle issues. In: Gessner IH, Victorica BE, eds. *Pediatric Cardiology: A Problem Oriented Approach*. Philadelphia, PA: WB Saunders, 1993:269-277.
178. Seal R. Adult congenital heart disease. *Paediatr Anaesth* 2011;21:615-622.

Pregnancy in Young Women with Congenital Heart Disease

Candice K. Silversides ■ Jack M. Colman ■ Samuel C. Siu

In general, pregnancy is well tolerated in women with congenital heart disease. However, misconceptions are common. Discussions regarding contraception and pregnancy should begin once adolescent women reach an age when they may become sexually active. Optimal management includes a complete cardiac assessment prior to conception. This assessment should include a full review of the underlying cardiac lesion and prior surgical procedures, determination of the risk of pregnancy, and development of plans for cardiac interventions prior to pregnancy when indicated. Because the severity of a low-risk condition may be misinterpreted or given undue importance, even women with low-risk cardiac lesions often benefit from preconception counseling. All women need to understand which types of contraception are appropriate and safe. Unfortunately, among women with congenital heart disease preconception counseling is often not provided and knowledge of risks of contraception and pregnancy is often suboptimal (1–3).

Many issues need to be addressed in women with heart disease contemplating or undergoing pregnancy, including the risks for the mother and the baby, possible adverse effects of medication used during pregnancy, maternal long-term prognosis, and the risk of recurrence of cardiac disease in offspring (Table 69.1). The cardiologist plays a critical role by providing and/or ensuring informed education of the patient, her partner, and her caregivers.

PHYSIOLOGIC CHANGES DURING PREGNANCY

Maintenance of adequate oxygen delivery to maternal peripheral tissues as well as to the fetus is achieved through changes in maternal circulating blood volume, red cell mass, peripheral vascular compliance and resistance, heart rate, and cardiac output (Fig. 69.1) (4). These adaptive changes are usually well tolerated by women without heart disease; however, in some women with heart disease such changes result in cardiac decompensation. As well, preexisting heart disease may first be revealed during pregnancy when the heart is challenged by an increased hemodynamic burden.

Blood volume increases during pregnancy; the increase begins as early as the sixth week of gestation and peaks at an average of 50% more than the prepregnant state by the end of the second trimester (5,6) though individual increases range between 20% and 100% above prepregnant blood volume (7). Blood volume plateaus in the third trimester (8). Red cell mass increases during pregnancy to as much as 40% above prepregnancy levels (6,9). A “physiologic anemia of pregnancy” is seen because the increase in plasma volume is proportionately greater than the increase in red blood cell mass. In addition, there are increased levels of clotting factors and decreased fibrinolytic activity (10), both acting to promote the

hypercoagulability that underlies the increased risk for thromboembolism during pregnancy.

Systemic (peripheral) vascular resistance decreases beginning in the fifth week of gestation. This mediates a decrease in systemic arterial pressure that begins in the first trimester and reaches its nadir in midpregnancy, after which blood pressure stabilizes (11,12). After the 32nd week of gestation, the systemic vascular resistance slowly increases until term, accompanied by recovery of systemic arterial pressure, which ultimately reaches or exceeds prepregnancy levels. Placental blood flow increases until about the 25th week of gestation and then remains unchanged. Renal blood flow also increases, accompanied by a 50% increase in glomerular filtration rate (13). Increased blood flow to the hands and feet, nasal passages, and breasts results in warm erythematous extremities, nasal congestion, and breast engorgement, respectively. The impact of pregnancy on coronary blood flow has not been studied.

Cardiac output increases during pregnancy as a result of increases in both heart rate and stroke volume. Most of the early increase in cardiac output is a result of progressive increase in stroke volume, whereas later in pregnancy the heart rate effect becomes more important because the stroke volume stabilizes while the heart rate continues to rise (11,14). The mean heart rate increases to approximately 10 to 20 beats above prepregnancy levels by term. Increase in cardiac output begins as early as the fifth week of gestation, reaches its zenith near the end of the second trimester, typically after the 24th week of gestation and then plateaus till term at 30% to 50% above prepregnancy levels (11,15–17). Pregnant women with underlying cardiac disease have been shown to have lower cardiac output than pregnant women with normal cardiac function (18). Cardiac output can fall acutely if the inferior vena cava is compressed by the gravid uterus in the supine position, a phenomenon that can be reversed by assuming the left lateral decubitus position. Although increases in left ventricular ejection fraction during pregnancy have been reported by some, (11,16) other studies have not demonstrated this finding (17,19,20). Ejection fraction is sensitive to loading conditions, so the differences may be related to uncontrolled variation in preload or afterload among studies.

During labor and delivery pain, anxiety and uterine contractions result in tachycardia, hypertension, and further increases in cardiac output, sometimes provoking cardiac decompensation in women with heart disease. During labor, there is a 10% increase in cardiac output beyond the prelabor level, mediated by increases in heart rate and stroke volume, augmented by a further increase of 7% to 15% in response to each uterine contraction, with maximal augmentation noted during the second stage of labor (21). Immediately following delivery, cardiac output may transiently increase to as much as 80% above prelabor values due to relief of inferior vena cava compression and autotransfusion from the placenta, but

TABLE 69.1

Women of Childbearing Age with Cardiac Disease: Approach to Contraception and Pregnancy**Contraception**

- Patient education regarding contraception options

Preconception

- Preconceptual counseling should begin in adolescence
- All women with heart disease should receive preconception counseling including women with simple cardiac lesions in whom reassurance about the safety of pregnancy is an appropriate aspect of counseling
- Maternal cardiac risk of pregnancy should be assessed
- Long-term prognosis of the mother should be considered
- Fetal and neonatal risks during pregnancy should be assessed
- The safety of medication use during pregnancy should be determined
- The risk of transmission of congenital heart disease to offspring (including a formal clinical genetics assessment when appropriate) should be determined

Pregnancy

- For intermediate and high-risk patients, assessment by a multidisciplinary team including cardiologists and obstetricians knowledgeable in management of high-risk pregnancy should occur early in the pregnancy
- The patient should be advised of antepartum follow-up requirements
- Individualized antepartum management issues should be addressed
- Women with congenital heart disease or who are spouses of men with congenital heart disease should be offered fetal echocardiography
- Peripartum plans should be established and conveyed to all appropriate caregivers
- Intrapartum and postpartum management issues specific to each individual should be addressed

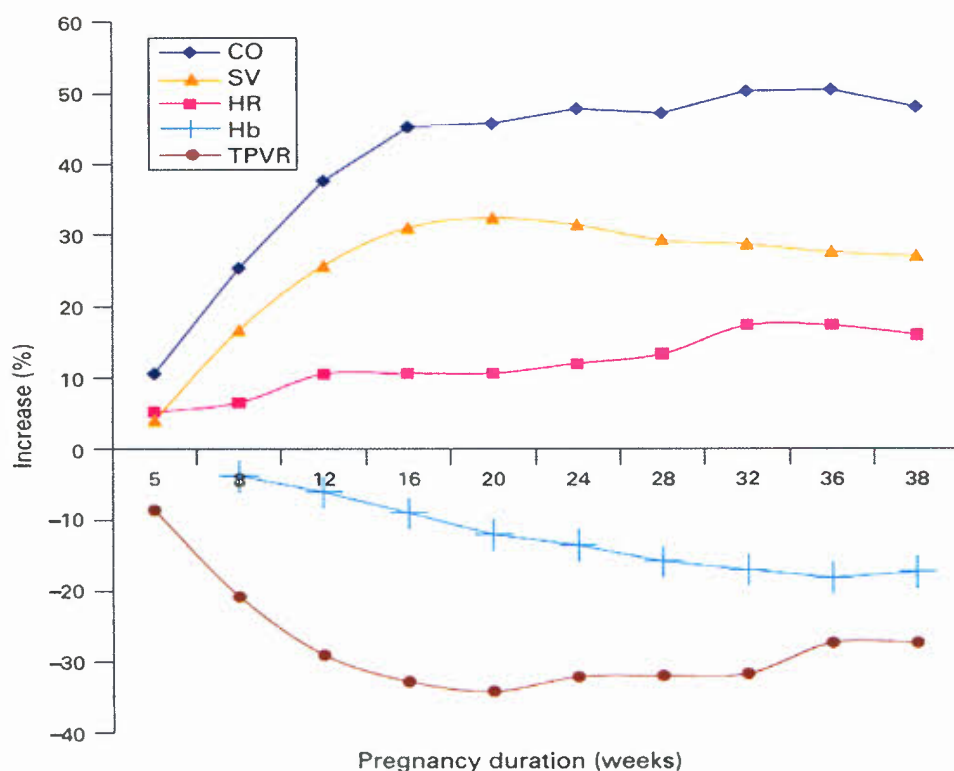


Figure 69.1. Hemodynamic changes during pregnancy. Changes in cardiac output (CO), stroke volume (SV), total peripheral vascular resistance (TPVR), heart rate (HR), and hemoglobin concentration (Hb) during pregnancy. (From Karamermer Y, Roos-Hesselink JW. Pregnancy and adult congenital heart disease. *Expert Rev Cardiovasc Ther* 2007;5:859–869, with permission.)

output returns to prelabor levels by approximately 1 hour postpartum. Thereafter, the hemodynamic changes that developed during pregnancy return toward baseline values; most of the changes resolve early after delivery, although complete resolution of all measureable pregnancy-associated effects may take as long as 6 months (22).

CARDIAC FINDINGS IN NORMAL PREGNANCY

Fatigue, dyspnea, light-headedness, and palpitations are normal symptoms associated with pregnancy but overlap with symptoms of cardiac decompensation. The hemodynamic changes of pregnancy are responsible for corresponding changes in the physical examination that can mimic cardiac disease. They include displacement of the apical impulse, prominence of the jugular venous pulsation, wide splitting of the first and second heart sounds, soft systolic flow murmurs, and continuous murmurs. Sinus tachycardia and premature atrial or ventricular ectopic beats may also increase in frequency during normal pregnancy and do not necessarily reflect cardiac decompensation or any cardiac disease. This overlap of signs and symptoms may make diagnosis of cardiac decompensation during pregnancy challenging; brain natriuretic peptide can be a useful test to adjudicate the basis for symptoms and signs when a benign basis is not certain (23).

On the 12-lead electrocardiogram during normal pregnancy, there may be a leftward shift in the frontal axis, T-wave inversion in lead II, and ST-segment depression. Echocardiographic studies during normal pregnancy show that dimensions of all four cardiac chambers increase and there is an increase in left ventricular wall thickness and mass (16,22,24,25). Increases in transvalvular flow velocities are seen (26). Mitral, tricuspid, and pulmonic annular diameters increase and may result in increasing degrees of mitral, tricuspid, and pulmonic regurgitation, respectively (27).

ASSESSMENT OF PREGNANCY RISK IN WOMEN WITH CONGENITAL HEART DISEASE: GENERAL CONCEPTS AND GLOBAL EVALUATION

Women with cardiac disease are at increased risk of developing adverse maternal cardiac events during pregnancy (28). Maternal cardiac risk can usually be predicted after a complete cardiovascular history and physical examination, a 12-lead electrocardiogram, a transthoracic echocardiogram, and arterial oxygen saturation when indicated. Echocardiography is safe during pregnancy. Prepregnancy exercise testing, specifically focusing on measures of heart rate responsiveness to exercise, may aid risk stratification (29).

Early studies showed that poor maternal functional class and cyanosis are associated with adverse maternal cardiac events (30,31). Subsequently, a prospective multicenter study addressed global risk assessment of pregnant women with congenital and acquired heart disease and identified poor functional status (NYHA > II) or cyanosis, systemic (subaortic, "left") ventricular systolic dysfunction, left heart obstruction, and history of cardiac events prior to pregnancy (arrhythmia, stroke, or pulmonary edema) as independent predictors of maternal cardiac events during pregnancy. Based on these predictors, women can be classified into low (0 predictor), intermediate (1 predictor), or high (>1 predictor) risk categories. The study showed that women in low, intermediate, and high-risk categories have, respectively, a 5%, 25%, or >75% chance of

developing an adverse cardiac event during pregnancy (Table 69.2) (Fig. 69.2) (32). This risk score, sometimes referred to as the CARPREG score, has been validated by other groups (33). Additional risk predictors have also been suggested. A single-center retrospective study that validated the CARPREG index in a population limited to congenital heart disease reported also that subpulmonary ventricular dysfunction and/or severe pulmonic regurgitation were additional independent risk factors for adverse maternal outcomes (33). The ZAHARA investigators carried out a large multicenter retrospective review of outcomes in pregnant women, also limited to congenital heart disease ($n = 1,302$ pregnancies in 714 women) and derived a more complex weighted risk score that included additional factors such as mechanical valve replacement and moderate or severe subaortic (systemic) or subpulmonary atrioventricular valve regurgitation (34).

Any global risk index should be used in conjunction with lesion-specific risk estimates, since certain intermediate or high-risk lesions may not have been represented in the population from which the global risk index was derived. For example, women with Marfan syndrome and dilated aortic roots, with Eisenmenger syndrome, or with a Fontan circulation were underrepresented in the derivation sets. Therefore, their known pregnancy-associated risks will not be reliably predicted by the global risk scores. Figure 69.3 shows pooled estimates of maternal and fetal and/or neonatal risks in women with congenital heart disease, stratified by lesion, derived primarily from retrospective single-center studies. Additional described factors that increase pregnancy risk include the presence of a prosthetic valve or conduit (especially if associated with abnormal prosthetic valve function), occurrence of an obstetric complication such as preeclampsia, and use of anticoagulants or teratogenic drugs. Some of these matters are elaborated further in sections that follow. In comprehensive assessment of maternal risk, it is helpful to integrate a global risk index with contemporary lesion-specific and other markers of risk. When there is discordance between the global and the lesion-specific estimates of risk, the higher-risk estimate should drive the care plan to avoid false reassurance.

In addition to increased risk of adverse maternal cardiac events, women with cardiac disease are at increased risk for adverse fetal and neonatal complications, which include fetal or neonatal death, premature birth and its associated complications (respiratory distress syndrome, intraventricular hemorrhage), or small-for-gestational-age birth weight neonates (28,35) (Fig. 69.4). Maternal cardiac risk factors for adverse fetal and neonatal outcomes have been identified (Table 69.2) (32). The risk of neonatal complications is further increased if there are concomitant maternal noncardiac (obstetrical and other) risk factors (Table 69.2) (Fig. 69.5). Finally, there is cardiac-lesion-specific variation in the risk for adverse obstetric outcomes during pregnancy (Fig. 69.3) (35).

Women with an intermediate to high risk of adverse maternal cardiac events during pregnancy or those at increased risk for fetal and neonatal complications should be considered for enhanced multidisciplinary surveillance in specialized high-risk cardiac and obstetric programs where these are available. As well, the impact of maternal heart disease on the probability of adverse obstetric outcomes should be considered when evaluating the need for enhanced intensity of obstetric oversight of pregnancy.

Hemodynamic and hormonal changes of pregnancy may continue to impact maternal outcomes late after pregnancy (36–40). For example, adverse cardiac events late after pregnancy occurred more often in women who had had adverse cardiac events during pregnancy (38) (Fig. 69.6). At this time, the full extent and mechanisms of the late effects of pregnancy on the heart are poorly understood.

TABLE 69.2

Risk Factors for Adverse Maternal Cardiac and Fetal/Neonatal Events During Pregnancy in Women with Heart Disease

Adverse Event	Risk Factor
Maternal cardiac adverse event ^a	■ Poor functional class (NYHA Class III or IV) or cyanosis
	■ Systemic ventricular ejection fraction <40%
	■ Left heart obstruction (mitral valve area <2 cm ² , aortic valve area <1.5 cm ² , or peak left ventricular outflow tract gradient >30 mm Hg)
	■ Cardiac event (sustained or symptomatic arrhythmias requiring treatment, stroke, pulmonary edema) prior to pregnancy
	■ Subpulmonic ventricular dysfunction
	■ Significant pulmonary regurgitation
	■ Mechanical heart valves
	■ Moderate or severe subaortic or subpulmonary atrioventricular valve regurgitation
	■ Known lesion-specific risk
Fetal and/or neonatal adverse event ^b	■ Poor maternal functional class (NYHA Class III or IV) or cyanosis
	■ Maternal left heart obstruction (defined above)
	■ Maternal age <20 or >35 years
	■ Obstetric risk factors ^c
	■ Multiple gestation
	■ Smoking during pregnancy
	■ Anticoagulant therapy
	■ Known lesion-specific risk

The risk factors highlighted in red are components of the CARPREG risk index: the risk of a maternal cardiac adverse event with zero risk factors present is <5%, with one risk factor present is 25%, and with more than one risk factor present is 75% (32).

Additional risk factors identified from subsequent studies on pregnancy risk (33,34).

^aMaternal cardiac adverse events include pulmonary edema, arrhythmia, stroke, or death.

^bFetal/neonatal adverse events include premature birth, small-for-gestational age birth weight, respiratory distress syndrome, intraventricular hemorrhage, or fetal or neonatal death.

^cHistory of premature delivery or rupture of membranes, incompetent cervix, or caesarean section; or intrauterine growth retardation, antepartum bleeding >12 weeks gestation, febrile illness, or uterine/placental abnormalities during present pregnancy.

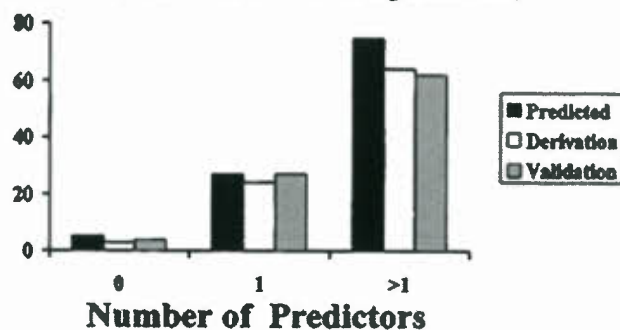
Cardiac Event Rate (% Pregnancies)

Figure 69.2. Frequency of adverse maternal cardiac events in pregnancy as predicted by the CARPREG risk index. Frequency of primary maternal cardiac events, as predicted by the CARPREG risk index (32), and observed in derivation and validation groups, expressed as a function of the number of predictors (x axis). (From Siu SC, Sermer M, Colman JM, et al. Prospective multicenter study of pregnancy outcomes in women with heart disease. *Circulation* 2001;104:515–521, with permission.)

LESION-SPECIFIC RISKS AND OUTCOMES

Pooled estimates of the frequency of adverse pregnancy outcomes (maternal cardiac, fetal, neonatal, and obstetric), stratified according to type of congenital heart disease, are presented in Figure 69.3 (35). Pregnancy outcomes stratified solely by diagnosis can be helpful, but in addition, it is important to consider the specific surgical history, the history of prior cardiac events, the functional status of the woman, and ventricular and valve function, since individual variation in these factors may influence risk over and above the risk imparted by diagnosis alone.

Cardiac shunts. Women with uncorrected left-to-right shunts, including secundum atrial septal defect (ASD), ventricular septal defect (VSD), and patent ductus arteriosus (PDA) are at low risk for adverse maternal cardiac events during pregnancy, in part because the pregnancy-associated fall in peripheral vascular resistance mitigates the effect of volume overload on the ventricle (30,32,41–44). Potential complications include atrial arrhythmias and heart failure, particularly if the shunt is large. In women with ASD or patent foramen ovale, there is a potential for paradoxical embolization if systemic vasodilation and/or elevation of pulmonary resistance

result in transient right-to-left shunting. Atrioventricular septal defects (AVSDs) are more complex, and pregnancy may be less well tolerated. In one study of 62 pregnancies (29 women) in women with AVSD, cardiac complications including persistent NYHA functional class deterioration, arrhythmias, and heart failure were reported to be 23%, 19%, and 2%, respectively (45). If cardiac shunts are associated with pulmonary hypertension, risk is dominated by the impact of the elevated pulmonary vascular resistance, which is discussed elsewhere in this chapter.

Right ventricular outflow tract obstruction. If pulmonic stenosis is mild or has been previously corrected surgically or by valvuloplasty, it is typically well tolerated during pregnancy (32,41,46). In severe pulmonic stenosis, the increase in preload associated with pregnancy may not be tolerated and may result in atrial arrhythmias or right heart failure. Thus, correction of severe pulmonic stenosis prior to pregnancy should be considered. If decompensation develops during pregnancy, balloon valvuloplasty can be carried out if initial medical therapy proves insufficient (47). Although one group

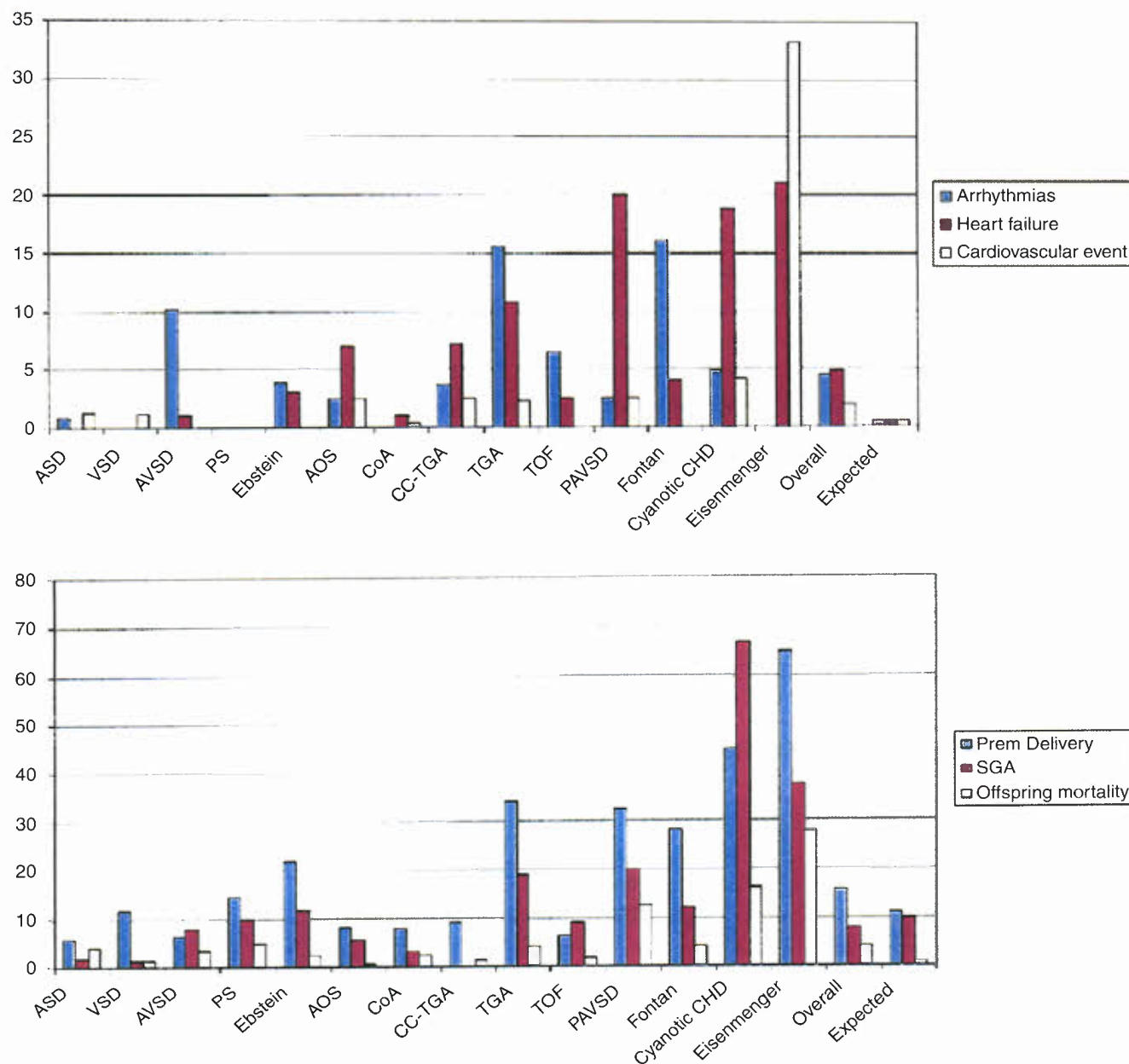


Figure 69.3. Estimates of maternal cardiac, fetal and neonatal, and obstetric outcomes during pregnancy in women with congenital heart disease. AOS, aortic stenosis; ASD, atrial septal defect; AVSD, atrioventricular septal defect; ccTGA, congenitally corrected transposition of the great arteries; CoA, aortic coarctation; Ebstein, Ebstein anomaly; Eisenmenger, Eisenmenger syndrome; Fontan, patients after Fontan repair; PAVSD, pulmonary atresia with ventricular septal defects; PS, pulmonary valve stenosis; TGA, complete transposition of the great arteries; TOF, tetralogy of Fallot; VSD, ventricular septal defect; TEC, thromboembolic complication; SGA, small for gestational age. (From Drenthen W, Pieper PG, Roos-Hesselink JW, et al. Outcome of pregnancy in women with congenital heart disease: a literature review. *J Am Coll Cardiol* 2007;49:2303–2311, with permission.)

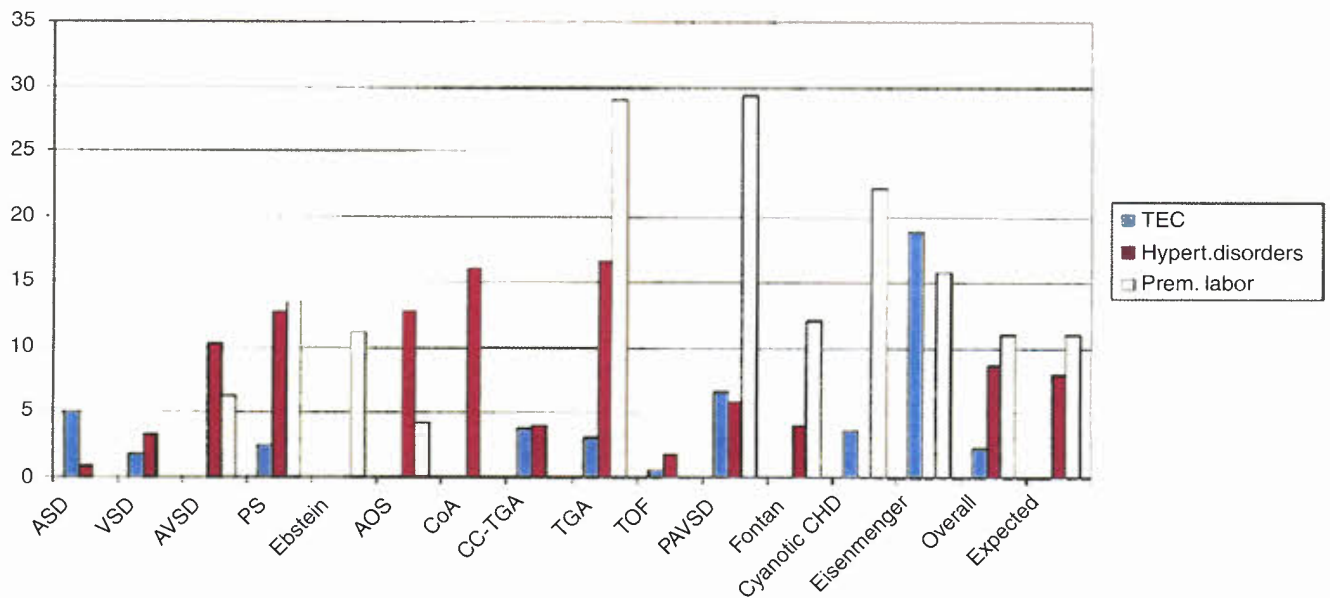


Figure 69.3. (Continued)

has reported high rates of obstetric and fetal complications in women with pulmonary stenosis (48), this differs from experience reported elsewhere (32,41,46).

Tetralogy of Fallot. Most women with tetralogy of Fallot would have undergone surgical correction with closure of the VSD and relief of right ventricular outflow tract obstruction. After repair, women may be left with residual shunts, right ventricular outflow tract obstruction, pulmonary regurgitation, right ventricular dilation or dysfunction, and atrial or ventricular arrhythmias. In general, pregnancy is well tolerated, but risk of complications is increased in presence of such residual and surgical sequelae. In one series, maternal complications

including symptomatic right heart failure, arrhythmias, or both occurred in 12% of pregnancies (49), though other studies have reported lower adverse event rates (50–52). Adverse maternal cardiac events have been reported in association with maternal cardiac factors (left ventricular dysfunction, severe pulmonary hypertension, severe pulmonic regurgitation with right ventricular dysfunction, or right ventricular outflow tract obstruction) and obstetric risk factors (twin pregnancies) (50,51).

Following biventricular repair for double outlet right ventricle a low risk for adverse maternal cardiac complications was reported in one series; however, the risk of fetal, neonatal, and obstetric complications was increased (53).

Event rate (% pregnancies)

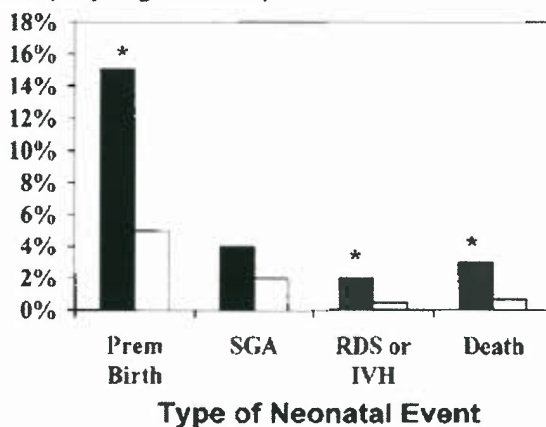


Figure 69.4. Rate of fetal and/or neonatal adverse events in 302 consecutive women with heart disease and 572 controls. Event rates in heart disease (black bars) and controls (white bars) subdivided into specific type of neonatal complication. Prem birth indicated birth at <37 weeks gestation; SGA small-for-gestational-age birth weight; RDS or IVH respiratory distress syndrome or intraventricular hemorrhage; and death, fetal, or neonatal death. (From Siu SC, Colman JM, Sorensen S, et al. Adverse neonatal and cardiac outcomes are more common in pregnant women with cardiac disease. *Circulation* 2002;105:2179–2184, with permission.)

Neonatal event rate (% pregnancies)

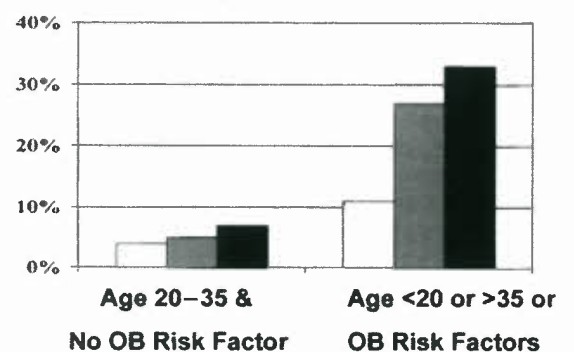


Figure 69.5. Frequency of fetal and/or neonatal complications according to presence and risk profile of cardiac lesion and the presence of maternal high-risk obstetric characteristics. High-risk obstetric characteristics include smoking, use of anticoagulation, multiple gestations, and maternal age. Control group is represented by empty bars. Heart disease group with neither left heart obstruction nor poor functional class/cyanosis is represented by grey bars. Heart disease group with left heart obstruction or poor functional class/cyanosis is represented by black bars. (From Siu SC, Colman JM, Sorensen S, et al. Adverse neonatal and cardiac outcomes are more common in pregnant women with cardiac disease. *Circulation* 2002;105:2179–2184, with permission.)

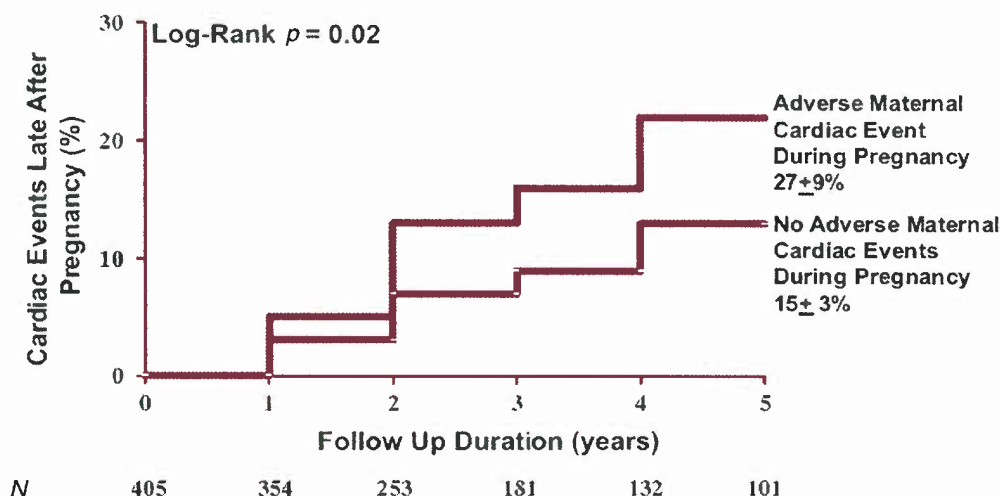


Figure 69.6. Incidence of adverse cardiac events late after pregnancy according to the presence or absence of pregnancy-related adverse cardiac events. Time 0 = date of delivery. (From Balint OH, Siu SC, Mason J, et al. Cardiac outcomes after pregnancy in women with congenital heart disease. *Heart* 2010;96:1656–1661, with permission.)

Left ventricular outflow tract obstruction. Significant left ventricular outflow tract obstruction most commonly occurs as a result of aortic stenosis due to bicuspid aortic valve disease and limits the ability of the heart to increase cardiac output. Abnormal elevation of left ventricular filling pressures may also occur. The hypertrophied, noncompliant ventricle is more sensitive to a fall in preload. During pregnancy, all of these factors contribute to an increased propensity to heart failure, ischemia, or hypotension. Bicuspid aortic disease is commonly associated with ascending aortopathy and sometimes with coarctation of the aorta, which confer additional risks during pregnancy. Maternal mortality is not as high as once described (54,35). However, women with significant aortic stenosis continue to be at risk for heart failure, arrhythmias, and angina (46,54–56). We recently reported that assessment of ventricular torsion, a novel echocardiographic parameter, may provide additional insights into why some women with aortic stenosis deteriorate during pregnancy and has the potential to be an additional risk stratifier (57). Women with symptomatic aortic stenosis should undergo correction prior to pregnancy (58). Asymptomatic women with mild to moderate aortic stenosis typically do well. Management of asymptomatic women with severe aortic stenosis is more controversial and careful risk stratification prior to pregnancy is required. In select women, aortic valvuloplasty may provide short-term palliation prior to a planned pregnancy. In general, we do not advocate prophylactic surgery in women with severe asymptomatic aortic stenosis who otherwise would not be candidates for valve surgery if pregnancy were not a consideration. Palliation by balloon valvuloplasty can be accomplished during pregnancy if necessary and when anatomy allows (59). Pregnancy may increase the risk of cardiac events late after pregnancy; for example, women with aortic stenosis who had had a pregnancy were more likely to require aortic valve replacement than a matched control group of women who had not been pregnant (40,55).

Aortic dissection has been reported in women with bicuspid aortic valve and aortopathy although overall risk is likely lower than in women with aortopathy associated with Marfan syndrome (60). The approach to the aortopathy associated with bicuspid aortic valve at our center is to offer empiric beta-blockade and serial echocardiographic assessment during pregnancy.

Coarctation of the aorta. In the current era, most women with coarctation of the aorta would have undergone repair

prior to pregnancy. Even when there is no residual coarctation, persistent or recurrent systemic hypertension may manifest after repair. Significant coarctation of the aorta impedes delivery of blood to the arterial tree distal to the coarctation site; during pregnancy this may impact on the placental circulation. Upper body hypertension and concomitant aortic valve disease pose additional risks. Maternal mortality has been reported, but this is rare in contemporary series (61,62). Women with Turner syndrome are at higher risk such that most experts advise against pregnancy in the presence of aortopathy of any sort (63), and some recommend against pregnancy even with a normal aorta, though it may be technically feasible with the assistance of reproductive technology, and occasionally spontaneously. Women with repaired coarctation are at increased risk for pregnancy-induced hypertension and preeclampsia (32,41,64). The risk of hypertension is highest in women with unrepaired coarctation in proportion to the degree of residual gradient (61,62). Miscarriages are common (62). Control of upper body hypertension during pregnancy may result in hypotension distal to the coarctation site with potential adverse impact on oxygen delivery to the fetus. Intrauterine growth restriction and premature labor are more common in women with unrepaired coarctation.

Marfan syndrome. In Marfan syndrome, increased cardiac output, hypervolemia, and the hormonal milieu of pregnancy contribute to increased risk of aortic dilation and dissection. Women with smaller aortic root dimensions are at lower risk for aortic complications than those with dilated aortic roots (>40 mm) or prior aortic root surgery (65,66). Favorable pregnancy outcomes were reported in a series of 33 women with aortic root size <45 mm prior to pregnancy (36). On the other hand, a European consensus document estimates that 1% of women with aortic diameters <40 mm and no significant aortic or mitral regurgitation will develop dissection or other serious maternal cardiac complication and that 10% of women with an aortic diameter more than 40 mm will develop dissection (67). Unfortunately, prophylactic root replacement prior to pregnancy or the presence of a normal-sized aortic root does not guarantee a safe pregnancy as it is possible for dissection to occur in an aorta that appears “normal” by imaging or in the segment distal to a prior repair (66). Patients with significant aortic root dilation should receive preconception counseling. If seen first only in early pregnancy they should be offered termination. For women with Marfan syndrome whose aortic

size is normal, counseling should incorporate discussion of the increasing risk with increasing maternal age, and explain that if pregnancy is contemplated it is best achieved at a younger age. Women with Marfan syndrome have a 50% chance of transmitting the syndrome to offspring. In addition, they are at increased risk for fetal, neonatal, and obstetric complications, the most common of which is preterm delivery due to premature rupture of membranes and cervical incompetence (68). Fetal and neonatal mortality of 7% has been reported (68).

Ebstein anomaly. There is substantial variability in the clinical phenotype of Ebstein anomaly, and the ability of the heart to tolerate a pregnancy varies according to the severity of the disease. Women with milder anatomic variations who are acyanotic can expect to have an uncomplicated pregnancy, whereas women with severe Ebstein anomaly may be unable to tolerate the increased preload and cardiac output of pregnancy and as a consequence are at risk for functional deterioration, right heart failure, and arrhythmia (69). In the largest published pregnancy series, no serious maternal cardiac complications (maternal death, congestive heart failure, arrhythmias, stroke) were reported; however, there was an increased risk of fetal loss, prematurity, and congenital heart disease in the offspring (70). Women with interatrial shunts may demonstrate reversal to or increase in right-to-left shunting, hence increasing cyanosis during pregnancy, and are at high risk for complications as a consequence.

Transposition of the great arteries. Women with complete transposition of the great arteries would have undergone an atrial switch operation (Mustard or Senning procedure), an arterial switch operation (Jatene procedure), or, less commonly, a Rastelli repair. Late complications after atrial switch operations include sinus node dysfunction, atrial arrhythmias, systemic ventricular dysfunction, and systemic atrioventricular valve regurgitation, all of which may contribute to complications during pregnancy, including, rarely, maternal death (32,71–73). Arrhythmias are the most common cardiac complication during pregnancy. In the largest published series they occurred in 22% of pregnancies (73), more commonly in women with a history of prior arrhythmias. The same series reported a high incidence of obstetric complications and mortality in the offspring (73). Other complications seen during pregnancy include heart failure and deterioration in cardiac function (71,72). Pregnancy has been associated with progressive subaortic right ventricular dilation (31%) and deterioration in subaortic right ventricular function (25%) determined by qualitative echocardiographic assessment (37).

Women treated with the Jatene operation are now reaching childbearing age, but reported experience during pregnancy is limited. Successful pregnancy outcomes have been described; however, complications including valve thrombosis in a woman with a mechanical valve and ventricular arrhythmia have been reported (74,75).

Congenitally corrected transposition of the great arteries can be associated with systemic ventricular dysfunction and systemic atrioventricular valve regurgitation. Associated lesions are common, especially VSD, pulmonary stenosis, or complete heart block. Potential problems in pregnancy include heart failure as a result of a dysfunctional subaortic (systemic) right ventricle and/or increased subaortic (tricuspid) atrioventricular valve regurgitation, atrial arrhythmias, atrioventricular block, and late sequelae from prior surgical interventions (e.g., dysfunction of a right ventricular to pulmonary artery conduit). In the two largest published series, no maternal mortality was reported; (76,77) however, approximately 25% of women developed adverse cardiac events during pregnancy including heart failure, endocarditis, stroke, or myocardial infarction (77).

Fontan circulation. The Fontan operation for functionally single ventricle palliates the condition by directing right atrial

or caval blood into the pulmonary artery, generally with no subpulmonary ventricle in the circuit. Although the operation improves cyanosis and volume overload of the subaortic (systemic) ventricle, the ability of the heart to increased cardiac output is limited. In addition, scarring and remodeling of the atria contribute to atrial arrhythmias and atrial thrombi. The largest series of pregnancies in a selected group of high-functioning women after Fontan operation reported good maternal outcomes with no maternal mortality (78). Supraventricular tachycardia, atrial fibrillation, and deterioration of NYHA functional class did occur (78,79). The reasonably good reported maternal cardiac outcomes were likely the result of preconceptual counseling and careful patient selection, as most or all the patients reported had a favorable clinical profile. Fetal and neonatal adverse outcomes remain common with only 45% of pregnancies resulting in live births in one series (78). The incidence of first trimester miscarriage is high.

Cyanotic heart disease. Women with cyanotic congenital heart disease are at substantial risk for pregnancy-associated adverse events, in proportion to the degree of maternal hypoxemia and cyanosis. In the largest series ($n = 96$ pregnancies) adverse maternal cardiac events occurred in 32% of pregnancies and included one death from endocarditis after delivery. Other adverse cardiac events included heart failure, arrhythmias, pulmonary artery thrombosis, and cerebral infarction. Prematurity was common, occurring in 37% of pregnancies. There was a low live birth rate, 43% overall; if the maternal oxygen saturation was $\leq 85\%$, the live birth rate was only 12% (80).

In women with Eisenmenger syndrome, pregnancy-associated decrease in afterload facilitates increase in right-to-left intracardiac shunting, leading to increasing hypoxemia and cyanosis. There is a high maternal mortality ($\sim 30\%$ per pregnancy) (81–83). Women with Eisenmenger syndrome are particularly sensitive to the volume depletion and hypotension that can occur during labor and delivery. Deaths are most likely to occur within the first few weeks postpartum. Preconceptual counseling should advise against pregnancy. Termination of pregnancy should be offered to such patients if counseled early in pregnancy. High maternal mortality during pregnancy is reported in women with pulmonary hypertension from other causes and recommendations regarding preconceptual counseling and pregnancy termination are similar to those for Eisenmenger syndrome. In the event that pregnancy continues, the use of pulmonary vasodilators is being increasingly reported and may be beneficial in reducing pulmonary artery pressures (83,84). One series of 11 pregnancies in women with pulmonary hypertension managed by an experienced team and treated with pulmonary vasodilators reported no maternal deaths (84). Adverse fetal events are common. Perinatal mortality, most of which was associated with prematurity, has been reported at 28% (81).

Prosthetic heart valves. Risks of complications during pregnancy in women with prosthetic valves are dependent on the type of valve and its position, the baseline function of the prosthesis, and the type of anticoagulant used. Women with normally functioning bioprosthetic valves often tolerate pregnancy well. Although there had been concern that degeneration of bioprosthetic or homograft valves may be accelerated by pregnancy, this has not been confirmed in all studies (85–87). Women with pulmonary autograft aortic valve replacement (Ross procedure) are reported to do well during pregnancy (88,89). Although mechanical valves have excellent durability, women with mechanical valve prostheses are at increased risk for thromboembolic events, primarily valve thrombosis, which is seen in 4% to 9% of pregnancies depending on the study and the anticoagulant regime, and maternal bleeding secondary to anticoagulation, seen in 2.5% of pregnancies (58,90,91). Warfarin embryopathy has been reported to be

less frequent in pregnant women who can be therapeutically controlled on ≤ 5 mg of warfarin per day (92,93).

TRANSMISSION OF CARDIAC DISEASE TO OFFSPRING

The risk of recurrence of congenital heart disease in offspring should be discussed prior to pregnancy when opportunity exists. Estimating recurrence risk is complex and should factor in the type of cardiac defect of the parent(s), other patient characteristics, and the presence of congenital heart disease in other family members (94). Formal clinical genetic counseling is often helpful and should be offered. In patients with congenital heart disease who do not have specific genetic syndromes, the recurrence risk of congenital heart disease to offspring is approximately 3% to 5% (95,96). Some studies have suggested higher rates of transmission if the affected parent is the mother rather than the father (96,97), though others have found no such difference (98). Parental left heart obstructive lesions are associated with higher rates of transmission (13% to 18%) (96). Autosomal dominant conditions such as Noonan syndrome (99), Williams syndrome (100), Holt-Oram syndrome (101), Marfan syndrome, or 22q11.2 deletion syndrome confer a 50% risk of recurrence in an offspring. The presence of congenital heart disease in a family member of the mother or father should raise the possibility of a familial or autosomal dominant form of inheritance. Preconception use of multivitamins containing folic acid has been shown to decrease the incidence of congenital defects and should be encouraged (102). A fetal echocardiogram is indicated when a parent has congenital heart disease to assess the fetus for congenital cardiac anomalies. After delivery, pediatric cardiac assessment should be offered as it has incremental diagnostic utility for detection of congenital heart disease in the offspring of women with congenital heart disease (103).

MANAGEMENT ISSUES DURING PREGNANCY

Risk assessment and management of pregnant women with congenital cardiac disease is addressed to some extent in comprehensive adult congenital heart disease guidelines from the American Heart Association/American College of Cardiology (104), the Canadian Cardiovascular Society (105–109), and the European Society of Cardiology (110). The European Society of Cardiology also published a specific expert consensus document on management of cardiovascular diseases during pregnancy in 2003 (67).

Preconception Issues

Preconceptual counseling should be offered to all women with cardiac disease contemplating pregnancy. Counseling should include assessment of the maternal risk of pregnancy and the effects of the maternal cardiac condition on fetal outcomes. The risks and benefits of drug therapy need to take into account the health and safety of the mother and of the fetus. Exposure to teratogens such as alcohol, hydantoin, lithium, retinoic acid, valproic acid, and warfarin is associated with cardiovascular defects in offspring; therefore, use of such agents should be terminated prior to conception if possible. Drug dosing and frequency of administration of continued medication may need adjustment in pregnancy because of changes in volume of distribution, glomerular filtration rate, and hepatic metabolism.

In circumstances where maternal life expectancy may be limited, the issue of long-term prognosis should be addressed to allow women and their families to make informed decisions regarding pregnancy. Such a discussion should also include consideration of possible effects of pregnancy on progression of maternal heart disease and of need for earlier cardiac intervention. However, uncertainties regarding the effect of pregnancy on late maternal prognosis need to be acknowledged, as very little data are available in this regard (37,40).

Antepartum Issues

Women with heart disease who are at low risk for complications can typically be managed in local obstetric units. Conversely, women who are at intermediate or high risk for complications should receive care in a high-risk obstetrics unit from a multidisciplinary team including obstetricians, cardiologists, anesthesiologists, pediatricians, and others as indicated. Regardless of the perceived risk level, all pregnant women with heart disease not previously evaluated should be offered a consultation with an experienced cardiologist and obstetrician, ideally in an interdisciplinary program where maternal cardiac, obstetrical, and fetal issues can be addressed by appropriate specialists.

The optimal frequency of cardiac follow-up during pregnancy in women with heart disease needs to be individualized. In general, an early assessment (first trimester) is useful to establish the baseline and to initiate planning. Peak cardiac output occurs near the end of the second trimester so assessment at this time allows for cardiac evaluation at a point at which maximal hemodynamic stress is evident. A third trimester visit around the end of the eighth month ensures that the patient is stable prior to delivery. Women who are symptomatic and those at higher risk need to be seen more frequently.

Echocardiography is the cardiac imaging modality of choice during pregnancy. We perform transthoracic echocardiography during the baseline antenatal visit as part of risk stratification. We will often repeat the echocardiographic examination at the time of the late second-trimester assessment particularly in patients who are at risk of deterioration as a result of the hemodynamic burden associated with advancing pregnancy. Cardiac magnetic resonance imaging (MRI) can be used during pregnancy when necessary. If possible, MRI should be performed after the first trimester because the effect of MRI on early fetal development has not been well studied. Gadolinium, the commonly used MRI contrast agent, crosses the placenta and is contraindicated during pregnancy. Potential fetal risks of MRI include the effects of heat, noise, and the magnetic field on the developing fetus (111). Ionizing radiation (computed tomography, cardiac catheterization, nuclear imaging) should be avoided during pregnancy unless there are no alternatives. However, when clearly indicated, x-ray procedures such as coronary arteriography should not be withheld. Modification of technique (e.g., radial artery approach for coronary arteriography, abdominal shielding) can minimize fetal radiation exposure (112).

Ambulatory ECG monitoring is often useful in women with symptomatic palpitations to diagnosis arrhythmia, determine arrhythmia burden and monitor the effect of therapy. Because benign palpitations are common, symptom–rhythm correlation provided by ambulatory monitoring may relieve unnecessary concern and may avoid inappropriate therapy.

Management of Heart Failure

Women with limited cardiac reserve are at risk of developing heart failure as a consequence of the increased hemodynamic burden of pregnancy. Other causes of deterioration of

cardiac status such as gestational hypertension, hyperthyroidism, and anemia should be considered as well. In women with symptomatic heart failure, activity limitation may be helpful. Acute heart failure should be treated with oxygen, diuretics, and afterload-reducing agents such as hydralazine. Nitroprusside may be toxic to the fetus and should be avoided. For women with preexisting systemic ventricular dysfunction, beta-blockers can be used in pregnancy, but women need to be informed of potential fetal and neonatal risks. Digoxin is safe in pregnancy. Angiotensin-converting enzyme inhibitors and angiotensin receptor blockers are associated with birth defects and should be avoided (113,114).

Management of Arrhythmias

The hemodynamic and hormonal changes of pregnancy may provoke or exacerbate arrhythmias. Women with a history of arrhythmias are at increased risk for adverse maternal cardiac events during pregnancy, including arrhythmia recurrences (41). Recurrence of arrhythmias during pregnancy is associated with an increase in adverse fetal and neonatal events (115). However, pharmacologic therapies may have undesirable effects on the developing fetus or neonate and so should be reserved for patients with significant symptoms or when sustained episodes result in hemodynamic compromise or intolerable symptomatology. Hemodynamically significant arrhythmias should be treated promptly, but teratogenic drugs should be avoided when possible.

In women with paroxysmal supraventricular tachycardia, including atrioventricular nodal reentrant tachycardia and atrioventricular reentrant tachycardia, beta-blockers can be used for arrhythmia prophylaxis. The treatment of an acute exacerbation of tachycardia in the pregnant woman is generally similar to that in the nonpregnant patient. Intravenous adenosine or beta-blockers can be used for acute management of supraventricular arrhythmias (116,117). Amiodarone is a FDA class D drug and is relatively contraindicated because it may impair neonatal thyroid function (118,119). Cardioversion is considered safe, although there is a theoretical risk of inducing fetal tachyarrhythmias (117).

There are many causes of ventricular tachycardia. During pregnancy, prophylactic therapy for ventricular tachycardia should be tailored according to the underlying condition. For instance, women with catecholamine-sensitive ventricular tachycardia are best treated with beta-blockers. Women with ventricular tachycardia in the setting of congenital heart disease will likely require antiarrhythmic therapy, but choice of medication needs to be individualized. Intravenous procainamide, sotalol, amiodarone, or beta-blocker can be used for acute management (120).

Bradyarrhythmias are less common during pregnancy. Pacemakers and implantable cardioverter-defibrillators are safe during pregnancy (121). Management of arrhythmias during pregnancy and safety profiles of antiarrhythmic medications can be found elsewhere (122).

Management of Anticoagulation

Pregnancy is associated with changes in clotting factors and fibrinolysis that increase the risk of thrombosis and thromboembolism. Consequently, optimized anticoagulation therapy is of utmost importance, especially for women with mechanical heart valves. The specific type of anticoagulant used during pregnancy must be carefully individualized. Options include warfarin, unfractionated heparin, low-molecular-weight heparin (LMWH), and adjunctive aspirin. Risks and benefits of various anticoagulant regimens should be discussed with the patient. High-risk women, such as those with early generation

mechanical heart valves (e.g., Starr-Edwards and Bjork-Shiley valves), have a greater risk of thromboembolic events, and consequently, anticoagulant regimens need to be more aggressive (123,124). In a systematic review of studies examining anticoagulation regimens and pregnancy outcomes in women with prosthetic heart valves, the pooled maternal mortality was 2.9% (91). The use of oral vitamin K antagonists (e.g., warfarin) throughout pregnancy was associated with the lowest rate of thrombosis, 3.9%. The substitution of unfractionated heparin between week 6 and week 12 gestational age only was associated with a 9.2% risk of valve thrombosis, whereas the use of unfractionated heparin throughout pregnancy carried a much higher 33.3% risk of valve thrombosis. The main concern regarding use of warfarin is its potential for embryopathy; however, there is evidence that a daily warfarin dose of ≤ 5 mg (assuming therapeutic anticoagulation can be achieved with such a dose) may not be teratogenic (92). When the mother takes warfarin, fetal intracranial bleeding is a risk throughout pregnancy and particularly during vaginal delivery. Thus warfarin should be replaced by heparin at least 2 weeks prior to labor (58). Adjusted-dose subcutaneous unfractionated heparin does not cross the placenta and has no teratogenic effects, but maintenance of therapeutic anticoagulation is difficult. Use of heparin may result in maternal thrombocytopenia and osteoporosis. LMWH is easier to administer and appears to be a satisfactory, though not risk-free, alternative to adjusted-dose unfractionated heparin (125–128).

Guidelines for the use of anticoagulants during pregnancy in women with mechanical valves have been offered by the American Heart Association/American College of Cardiology (129), the American College of Chest Physicians (124), and the European Society of Cardiology (130). Differences exist among the guidelines. For instance, the American College of Chest Physicians guideline includes as a treatment option the use of LMWH throughout pregnancy whereas the European Society of Cardiology guidelines do not recommend LMWH. Some experts suggest an alternative approach based on a modification of the guidelines to include further stratification based on risk of thrombosis (123). However, all current recommendations are based on case series and expert opinion as there are no data available from randomized trials. Our current approach includes offering women with mechanical valves LMWH as an alternative anticoagulation strategy to continued use of warfarin. For women at high thromboembolic risk (those with older style valves, more than one mechanical valve, prior thromboembolic events), we suggest adjunctive aspirin. Anticoagulation in pregnancy is often best managed in a specialized thrombosis clinic. At our center, all women are seen by a hematologist associated with the thrombosis clinic, are counseled in regard to the advantages and risks associated with various regimens, and are asked to sign a written consent acknowledging that they are aware of the issues and agree to the treatment chosen. It is clear that no specific strategy can fully mitigate the risk of pregnancy for women who require anticoagulation, particularly those with mechanical valves.

High-Risk Conditions

Women with cyanotic cardiac lesions (30) or symptomatic obstructive lesions (58) should be referred for repair prior to conception when possible. If a woman with Eisenmenger syndrome does not accept advice to terminate, or presents late in pregnancy, early hospitalization may be required along with supplemental oxygen and possibly empiric anticoagulation. Pulmonary vasodilators have been used in pregnant women with pulmonary hypertension including those with Eisenmenger

syndrome (83,84). However, some commonly used pulmonary vasodilators such as the endothelin receptor blockers cannot be used during pregnancy because of teratogenicity.

The risk in Marfan syndrome increases in proportion to aortic root size and is very high when aorta is already enlarged prior to pregnancy. Surveillance during pregnancy should include echocardiograms approximately every 6 weeks up to 6 months postpartum to monitor the size of the aortic root. Prophylactic beta-blockade is indicated in patients with Marfan syndrome. We recommend continuation of such therapy throughout pregnancy and thereafter. In patients not previously so treated we do recommend at our initial encounter that beta-blocker be started and continued (131).

Cardiac Surgery During Pregnancy

Cardiovascular surgery during pregnancy is associated with significant maternal and fetal mortality of approximately 6% and 14% to 30%, respectively, and should be avoided when possible (132,133). Fetal risk is increased in part by provocation of uterine contractions in association with extracorporeal circulation. Maternal hypotension and consequent placental hypoperfusion contribute as well, these factors conspiring to promote fetal hypoperfusion, hypoxia, and bradycardia. Fetal mortality at maternal cardiac surgery has been reported to vary with factors such as maternal age >35 years, maternal functional class, reoperation, emergency surgery, the type of myocardial protection, and anoxic time (134). To minimize fetal risks, tailored anesthetic and bypass techniques can be used during cardiac surgery (135). In some circumstances, cardiac surgery can be combined with elective caesarean delivery immediately before bypass.

MANAGEMENT ISSUES DURING LABOR AND DELIVERY

In our center, caesarean delivery is favored only in women who have aortic dissection or Marfan syndrome with dilated aortic root or if there has been a failure to switch from warfarin to heparin at least 2 weeks prior to labor. In essentially all other circumstances, vaginal delivery is preferred in the absence of obstetric contraindication. At our institutions, rates of caesarean deliveries in women with heart disease are the same as those in women without heart disease (136). Preterm induction of labor is rarely indicated. There is an association between antepartum adverse cardiac events and premature labor and delivery (41). Induction of labor is generally safe in women with heart disease (137). Subcutaneous administration of unfractionated heparin should be discontinued at least 12 hours prior to induction of labor or reversed with protamine if spontaneous labor develops. LMWH cannot be reversed with protamine and needs to be discontinued earlier or switched to unfractionated heparin for the last stage of pregnancy. Epidural anesthesia with adequate volume preloading is the anesthetic technique of choice. Epidural fentanyl, which does not lower peripheral vascular resistance, is particularly advantageous in cyanotic patients with shunt lesions or in patients with significant aortic stenosis. Air and particulate filters should be placed in all intravenous lines in women with intracardiac shunts. The use of invasive hemodynamic monitoring during labor and delivery must be individualized. For instance, intra-arterial monitoring and central venous pressure monitoring may be used in cases where there are concerns about the interpretation and deleterious effects of a sudden drop in systemic blood pressure (e.g., patients with severe aortic stenosis, pulmonary

hypertension, severe systemic ventricular systolic dysfunction, or preload-dependent physiology such as seen after a Fontan operation). Pulmonary artery catheters are utilized only in the extremely rare situations where the information sought is not available otherwise and warrant the risk of the procedure. At our institution, there has been a major decline in the use of arterial lines and use of pulmonary artery catheter for labor and delivery (136). Labor can be conducted in the left lateral decubitus position to attenuate hemodynamic fluctuations associated with uterine contractions in the supine position. Forceps or vacuum extraction will reduce need for maternal expulsive efforts during the latter part of the second stage of labor. The 2007 American Heart Association Prevention of Infective Endocarditis guideline do not suggest endocarditis prophylaxis for uncomplicated vaginal deliveries (138). The 2008 American Heart Association/American College of Cardiology Guideline for the Management of Adults With Congenital Heart Disease states that there is no consensus on endocarditis prophylaxis at the time of delivery and suggests that it may be used in the same high-risk groups for which antibiotic prophylaxis should be administered prior to dental procedures (139).

The hemodynamic changes of labor and delivery often do not return to baseline levels for many days after delivery; therefore, high-risk women may require additional monitoring postpartum. The mortality risk persists for at least a week in women with Eisenmenger syndrome who therefore require extended postpartum observation.

CONTRACEPTION

Contraception planning is important and age-appropriate counseling should begin in early adolescence. Choice of contraceptive method needs to be individualized and should take into account patient safety specifically regarding thromboembolic risk, patient preference, efficacy, and the consequences of contraceptive failure (140,141). Studies pertaining to risk in women with congenital heart disease are not available so contraceptive safety is extrapolated from safety profiles determined in women without heart disease. Recommendations for the use of estrogen-containing contraceptives in women with heart disease are shown in Table 69.3 (140). Low-estrogen oral contraceptives are highly effective, but should be used only in women with a low to moderate thrombotic risk. Estrogen-containing contraceptive therapy is also contraindicated in women with thromboembolic disease, undiagnosed abnormal genital bleeding, acute liver disease, liver tumors, or known or suspected breast carcinoma. For patients with higher thromboembolic risk, progestin-only contraceptive pills ("mini-pill") or other progesterone-containing contraceptives such as long-acting medroxyprogesterone acetate injection (Depo-Provera™) or levonorgestrel implant (Norplant™) may be suitable options. Barrier methods have few complications, but are associated with high failure rates compared to other forms of contraception, hence unsuitable as the sole method if pregnancy is to be avoided. Intrauterine devices, such as Mirena™ levonorgestrel-releasing intrauterine device, are best suited for women in monogamous relationships after childbearing years because of the risk of pelvic inflammatory disease. Sterilization may be considered in select cases when the risk of pregnancy is prohibitive or childbearing has been completed. In the absence of systematic data examining contraception in women with congenital heart disease, the above recommendations and Table 69.3 represent a starting point for discussion. If a woman is not in a low-risk group, consultation with a gynecologist with expertise in caring for women with heart disease is advised.

TABLE 69.3

Risk Classification for the Use of Combined Hormonal Contraceptive in Women with Congenital Heart Disease

WHO 1 Always useable Condition with no restriction for the use of the contraceptive method	WHO 2 Broadly useable Condition where the advantages of the method generally outweigh the theoretical or proven risks	WHO 3 Caution in use Condition where the theoretical or proven risks usually outweigh the advantages of using the method	WHO 4 Do not use Condition that represents an unacceptable health risk if the contraceptive method is used
<ul style="list-style-type: none"> ■ Mitral valve prolapse with trivial mitral regurgitation ■ Bicuspid aortic valve with normal function ■ Mild pulmonary stenosis ■ Repaired coarctation with no hypertension or aneurysm ■ Simple congenital lesions successfully repaired in childhood and with no sequelae (atrial or ventricular septal defect, PDA or total anomalous pulmonary venous drainage) 	<ul style="list-style-type: none"> ■ Most arrhythmias other than atrial fibrillation or flutter ■ Uncomplicated mild native mitral and aortic valve disease ■ Tissue prosthetic valve lacking any of the features noted in WHO 3 or 4 columns ■ Surgically corrected congenital heart disease lacking any of the features noted in WHO 3 or 4 columns ■ Small left-to-right shunts not reversible with physiologic maneuvers (i.e., small VSD, small PDA) ■ Hypertrophic cardiomyopathy lacking any WHO III or IV features ■ Past cardiomyopathy, fully recovered, including peripartum cardiomyopathy ■ Uncomplicated Marfan 	<ul style="list-style-type: none"> ■ Atrial fibrillation or flutter even on warfarin ■ Bileaflet mechanical valve even on warfarin ■ ASD with left-to-right shunt that may reverse with physiologic stress (i.e., Valsalva maneuver) ■ Repaired coarctation with aneurysm and/or hypertension ■ Previous thromboembolism 	<ul style="list-style-type: none"> ■ Atrial fibrillation or flutter, if not anticoagulated ■ Bjork Shiley or Starr Edwards valve even if taking warfarin ■ Fontan circulation even if on warfarin ■ Cyanotic heart disease ■ Pulmonary arteriovenous malformation ■ Prior left ventricular dysfunction from any cause (i.e., dilated cardiomyopathy) (LVEF <30%) ■ Coronary artery disease ■ Coronary arteritis (i.e., Kawasaki disease with coronary involvement)

WHO—World Health Organization contraception classification.

Modified from Thorne S, MacGregor A, Nelson-Piercy C. Risks of contraception and pregnancy in heart disease. *Heart* 2006;92:1520–1525, with permission.

REFERENCES

- Kovacs AH, Harrison JL, Colman JM, et al. Pregnancy and contraception in congenital heart disease: what women are not told. *J Am Coll Cardiol* 2008;52:577–578.
- Vigl M, Kaemmerer M, Seifert-Klauss V, et al. Contraception in women with congenital heart disease. *Am J Cardiol* 2010;106:1317–1321.
- Curtis SL, Marsden-Williams J, Sullivan C, et al. Current trends in the management of heart disease in pregnancy. *Int J Cardiol* 2009;133:62–69.
- Karamermer Y, Roos-Hesselink JW. Pregnancy and adult congenital heart disease. *Expert Rev Cardiovasc Ther* 2007;5:859–869.
- Lind T. Hematologic system. *Maternal Physiology*. Washington, DC: CREOG 25, 1985:7–40.
- Pirani BB, Campbell DM, MacGillivray I. Plasma volume in normal first pregnancy. *J Obstet Gynaecol Br Commonw* 1973;80:884–887.
- Pritchard JA, Rowland RC. Blood volume changes in pregnancy and the puerperium. iii. whole body and large vessel hematocrits in pregnant and nonpregnant women. *Am J Obstet Gynecol* 1964;88:391–395.
- Lund CJ, Donovan JC. Blood volume during pregnancy. Significance of plasma and red cell volumes. *Am J Obstet Gynecol* 1967;98:394–403.
- Taylor DJ, Lind T. Red cell mass during and after normal pregnancy. *Br J Obstet Gynaecol* 1979;86:364–370.
- Barbour LA, Pickard J. Controversies in thromboembolic disease during pregnancy: a critical review. *Obstet Gynecol* 1995;86:621–633.
- Robson SC, Hunter S, Boys RJ, et al. Serial study of factors influencing changes in cardiac output during human pregnancy. *Am J Physiol* 1989;256:H1060–H1065.
- Duvekot JJ, Cheriex EC, Pieters FA, et al. Early pregnancy changes in hemodynamics and volume homeostasis are consecutive adjustments triggered by a primary fall in systemic vascular tone. *Am J Obstet Gynecol* 1993;169:1382–1392.
- Davison JM, Dunlop W. Renal hemodynamics and tubular function in normal human pregnancy. *Kidney Int* 1980;18:152–161.
- Mabie WC, DiSessa TG, Crocker LG, et al. A longitudinal study of cardiac output in normal human pregnancy. *Am J Obstet Gynecol* 1994;170:849–856.
- Clark SL, Cotton DB, Lee W, et al. Central hemodynamic assessment of normal term pregnancy. *Am J Obstet Gynecol* 1989;161:1439–1442.
- Rubler S, Damani PM, Pinto ER. Cardiac size and performance during pregnancy estimated with echocardiography. *Am J Cardiol* 1977;40:534–540.
- Katz R, Karliner JS, Resnik R. Effects of a natural volume overload state (pregnancy) on left ventricular performance in normal human subjects. *Circulation* 1978;58:434–441.
- Ueland K, Novy MJ, Metcalfe J. Hemodynamic responses of patients with heart disease to pregnancy and exercise. *Am J Obstet Gynecol* 1972;113:47–59.
- Mashini JS, Albazzaz SJ, Fadel HE, et al. Serial noninvasive evaluation of cardiovascular hemodynamics during pregnancy. *Am J Obstet Gynecol* 1987;156:1208–1213.
- Geva T, Mauer MB, Striker L, et al. Effects of physiologic load of pregnancy on left ventricular contractility and remodeling. *Am Heart J* 1997;133:53–59.
- Robson SC, Dunlop W, Boys RJ, et al. Cardiac output during labour. *Br Med J (Clin Res Ed)* 1987;295:1169–1172.
- Robson SC, Hunter S, Moore M, et al. Haemodynamic changes during the puerperium: a Doppler and M-mode echocardiographic study. *Br J Obstet Gynaecol* 1987;94:1028–1039.

23. Tanous D, Siu SC, Mason J, et al. B-type natriuretic peptide in pregnant women with heart disease. *J Am Coll Cardiol* 2010;56:1247-1253.
24. Campos O. Doppler echocardiography during pregnancy. *Echocardiography* 1996;13:135-146.
25. Mone SM, Sanders SP, Colan SD. Control mechanisms for physiological hypertrophy of pregnancy. *Circulation* 1996;94:667-672.
26. McLennan FM, Hailes NE, Rawles JM. Stroke and minute distance in pregnancy: a longitudinal study using Doppler ultrasound. *Br J Obstet Gynaecol* 1987;94:499-506.
27. Campos O, Andrade JL, Bocanegra J, et al. Physiologic multivalvular regurgitation during pregnancy: a longitudinal Doppler echocardiographic study. *Int J Cardiol* 1993;40:265-272.
28. Siu SC, Colman JM, Sorensen S, et al. Adverse neonatal and cardiac outcomes are more common in pregnant women with cardiac disease. *Circulation* 2002;105:2179-2184.
29. Lui GK, Silversides CK, Khairy P, et al. Heart rate response during exercise and pregnancy outcome in women with congenital heart disease. *Circulation* 2010;123:242-248.
30. Shime J, Mocarski EJ, Hastings D, et al. Congenital heart disease in pregnancy: short- and long-term implications. *Am J Obstet Gynecol* 1987;156:313-322.
31. Whittemore R, Hobbins JC, Engle MA. Pregnancy and its outcome in women with and without surgical treatment of congenital heart disease. *Am J Cardiol* 1982;50:641-651.
32. Siu SC, Sermer M, Colman JM, et al. Prospective multicenter study of pregnancy outcomes in women with heart disease. *Circulation* 2001;104:515-521.
33. Khairy P, Ouyang DW, Fernandes SM, et al. Pregnancy outcomes in women with congenital heart disease. *Circulation* 2006;113:517-524.
34. Drenthen W, Boersma E, Balci A, et al. Predictors of pregnancy complications in women with congenital heart disease. *Eur Heart J* 2010;31:2124-2132.
35. Drenthen W, Pieper PG, Roos-Hesselink JW, et al. Outcome of pregnancy in women with congenital heart disease: a literature review. *J Am Coll Cardiol* 2007;49:2303-2311.
36. Meijboom LJ, Vos FE, Timmermans J, et al. Pregnancy and aortic root growth in the Marfan syndrome: a prospective study. *Eur Heart J* 2005;26:914-920.
37. Guedes A, Mercier LA, Leduc L, et al. Impact of pregnancy on the systemic right ventricle after a Mustard operation for transposition of the great arteries. *J Am Coll Cardiol* 2004;44:433-437.
38. Balint OH, Siu SC, Mason J, et al. Cardiac outcomes after pregnancy in women with congenital heart disease. *Heart* 2010;96:1656-1661.
39. Uebing A, Arvanitis P, Li W, et al. Effect of pregnancy on clinical status and ventricular function in women with heart disease. *Int J Cardiol* 2010;139:50-59.
40. Tzemos N, Silversides CK, Colman JM, et al. Late cardiac outcomes after pregnancy in women with congenital aortic stenosis. *Am Heart J* 2009;157:474-480.
41. Siu SC, Sermer M, Harrison DA, et al. Risk and predictors for pregnancy-related complications in women with heart disease. *Circulation* 1997;96:2789-2794.
42. Zuber M, Gautschi N, Oechslin E, et al. Outcome of pregnancy in women with congenital shunt lesions. *Heart* 1999;81:271-275.
43. Actis Dato GM, Rinaudo P, Revelli A, et al. Atrial septal defect and pregnancy: a retrospective analysis of obstetrical outcome before and after surgical correction. *Minerva Cardioangiologica* 1998;46:63-68.
44. Yap SC, Drenthen W, Pieper PG, et al. Pregnancy outcome in women with repaired versus unrepaired isolated ventricular septal defect. *BJOG* 2010;117:683-689.
45. Drenthen W, Pieper PG, van der Tuuk K, et al. Cardiac complications relating to pregnancy and recurrence of disease in the offspring of women with atrioventricular septal defects. *Eur Heart J* 2005;26:2581-2587.
46. Hameed A, Karaalp IS, Tummala PP, et al. The effect of valvular heart disease on maternal and fetal outcome of pregnancy. *J Am Coll Cardiol* 2001;37:893-899.
47. Presbitero P, Prever SB, Brusca A. Interventional cardiology in pregnancy. *Eur Heart J* 1996;17:182-188.
48. Drenthen W, Pieper PG, Roos-Hesselink JW, et al. Non-cardiac complications during pregnancy in women with isolated congenital pulmonary valvular stenosis. *Heart* 2006;92:1838-1843.
49. Meijer JM, Pieper PG, Drenthen W, et al. Pregnancy, fertility, and recurrence risk in corrected tetralogy of Fallot. *Heart* 2005;91:801-805.
50. Veldtman GR, Connolly HM, Grogan M, et al. Outcomes of pregnancy in women with tetralogy of Fallot. *J Am Coll Cardiol* 2004;44:174-180.
51. Greutmann M, Von Klempener K, Brooks R, et al. Pregnancy outcome in women with congenital heart disease and residual haemodynamic lesions of the right ventricular outflow tract. *Eur Heart J* 2010;31:1764-1770.
52. Balci A, Drenthen W, Mulder BJ, et al. Pregnancy in women with corrected tetralogy of Fallot: occurrence and predictors of adverse events. *Am Heart J* 2010;161:307-313.
53. Drenthen W, Pieper PG, van der Tuuk K, et al. Fertility, pregnancy and delivery in women after biventricular repair for double outlet right ventricle. *Cardiology* 2008;109:105-109.
54. Lao TT, Sermer M, MaGee L, et al. Congenital aortic stenosis and pregnancy—a reappraisal. *Am J Obstet Gynecol* 1993;169:540-545.
55. Silversides CK, Colman JM, Sermer M, et al. Early and intermediate-term outcomes of pregnancy with congenital aortic stenosis. *Am J Cardiol* 2003;91:1386-1389.
56. Yap SC, Drenthen W, Pieper PG, et al. Risk of complications during pregnancy in women with congenital aortic stenosis. *Int J Cardiol* 2008;126:240-246.
57. Tzemos N, Silversides CK, Carasso S, et al. Effect of pregnancy on left ventricular motion (twist) in women with aortic stenosis. *Am J Cardiol* 2008;101:870-873.
58. Bonow RO, Carabello B, de Leon AC, Jr, et al. Guidelines for the management of patients with valvular heart disease: executive summary. A report of the American College of Cardiology/American Heart Association Task Force on Practice Guidelines (Committee on Management of Patients with Valvular Heart Disease). *Circulation* 1998;98:1949-1984.
59. Lao TT, Adelman AG, Sermer M, et al. Balloon valvuloplasty for congenital aortic stenosis in pregnancy. *Br J Obstet Gynaecol* 1993;100:1141-1142.
60. Immer FF, Bansi AG, Immer-Bansi AS, et al. Aortic dissection in pregnancy: analysis of risk factors and outcome. *Ann Thorac Surg* 2003;76:309-314.
61. Beauchesne LM, Connolly HM, Ammash NM, et al. Coarctation of the aorta: outcome of pregnancy. *J Am Coll Cardiol* 2001;38:1728-1733.
62. Vriend JW, Drenthen W, Pieper PG, et al. Outcome of pregnancy in patients after repair of aortic coarctation. *Eur Heart J* 2005;26:2173-2178.
63. Practice committee of American Society for Reproductive Medicine. Increased maternal cardiovascular mortality associated with pregnancy in women with Turner syndrome. *Fertil Steril* 2008;90:S185-S186.
64. Krieger EV, Landzberg MJ, Economy KE, et al. Comparison of risk of hypertensive complications of pregnancy among women with versus without coarctation of the aorta. *Am J Cardiol* 2011;107:1529-1534.
65. Rossiter JP, Repke JT, Morales AJ, et al. A prospective longitudinal evaluation of pregnancy in the Marfan syndrome. *Am J Obstet Gynecol* 1995;173:1599-1606.
66. McDermott CD, Sermer M, Siu SC, et al. Aortic dissection complicating pregnancy following prophylactic aortic root replacement in a woman with Marfan syndrome. *Int J Cardiol* 2007;120:427-430.
67. Task force on the Management of Cardiovascular Diseases During Pregnancy of the European Society of Cardiology. Expert consensus document on management of cardiovascular diseases during pregnancy. *Eur Heart J* 2003;24:761-781.
68. Meijboom LJ, Drenthen W, Pieper PG, et al. Obstetric complications in Marfan syndrome. *Int J Cardiol* 2006;110:53-59.
69. Chopra S, Suri V, Aggarwal N, et al. Ebstein's anomaly in pregnancy: maternal and neonatal outcomes. *J Obstet Gynaecol Res* 2010;36:278-283.
70. Connolly HM, Warnes CA. Ebstein's anomaly: outcome of pregnancy. *J Am Coll Cardiol* 1994;23:1194-1198.
71. Clarkson PM, Wilson NJ, Neutze JM, et al. Outcome of pregnancy after the Mustard operation for transposition of the great arteries with intact ventricular septum. *J Am Coll Cardiol* 1994;24:190-193.
72. Genoni M, Jenni R, Hoerstrup SP, et al. Pregnancy after atrial repair for transposition of the great arteries. *Heart* 1999;81:276-277.
73. Drenthen W, Pieper PG, Ploeg M, et al. Risk of complications during pregnancy after Senning or Mustard (atrial) repair of complete transposition of the great arteries. *Eur Heart J* 2005;26:2588-2595.
74. Ploeg M, Drenthen W, van Dijk A, et al. Successful pregnancy after an arterial switch procedure for complete transposition of the great arteries. *BJOG* 2006;113:243-244.
75. Tobler D, Fernandes SM, Wald RM, et al. Pregnancy outcomes in women with transposition of the great arteries and arterial switch operation. *Am J Cardiol* 2010;106:417-420.
76. Connolly HM, Grogan M, Warnes CA. Pregnancy among women with congenitally corrected transposition of great arteries. *J Am Coll Cardiol* 1999;33:1692-1695.
77. Therrien J, Barnes I, Somerville J. Outcome of pregnancy in patients with congenitally corrected transposition of the great arteries. *Am J Cardiol* 1999;84:820-824.
78. Canobbio MM, Mair DD, van der Velde M, et al. Pregnancy outcomes after the Fontan repair. *J Am Coll Cardiol* 1996;28:763-767.
79. Drenthen W, Pieper PG, Roos-Hesselink JW, et al. Pregnancy and delivery in women after Fontan palliation. *Heart* 2006;92:1290-1294.
80. Presbitero P, Somerville J, Stone S, et al. Pregnancy in cyanotic congenital heart disease. Outcome of mother and fetus. *Circulation* 1994;89:2673-2676.
81. Gleicher N, Midwall J, Hochberger D, et al. Eisenmenger's syndrome and pregnancy. *Obstet Gynecol Surv* 1979;34:721-741.
82. Weiss BM, Zemp L, Seifert B, et al. Outcome of pulmonary vascular disease in pregnancy: a systematic overview from 1978 through 1996. *J Am Coll Cardiol* 1998;31:1650-1657.
83. Bedard E, Dimopoulos K, Gatzoulis MA. Has there been any progress made on pregnancy outcomes among women with pulmonary arterial hypertension? *Eur Heart J* 2009;30:256-265.
84. Kiely DG, Condliffe R, Webster V, et al. Improved survival in pregnancy and pulmonary hypertension using a multiprofessional approach. *BJOG* 2010;117:565-574.
85. North RA, Sadler L, Stewart AW, et al. Long-term survival and valve-related complications in young women with cardiac valve replacements. *Circulation* 1999;99:2669-2676.
86. Avila WS, Rossi EG, Grinberg M, et al. Influence of pregnancy after bio-prosthetic valve replacement in young women: a prospective five-year study. *J Heart Valve Dis* 2002;11:864-869.

87. Jamieson WR, Miller DC, Akins CW, et al. Pregnancy and bioprostheses: influence on structural valve deterioration. *Ann Thorac Surg* 1995;60:S282–S286; discussion S287.
88. Dore A, Somerville J. Pregnancy in patients with pulmonary autograft valve replacement. *Eur Heart J* 1997;18:1659–1662.
89. Yap SC, Drenth W, Pieper PG, et al. Outcome of pregnancy in women after pulmonary autograft valve replacement for congenital aortic valve disease. *J Heart Valve Dis* 2007;16:398–403.
90. Elkayam U. Pregnancy through a prosthetic heart valve. *J Am Coll Cardiol* 1999;33:1642–1645.
91. Chan WS, Anand S, Ginsberg JS. Anticoagulation of pregnant women with mechanical heart valves: a systematic review of the literature. *Arch Intern Med* 2000;160:191–196.
92. Vitale N, De Feo M, De Santo LS, et al. Dose-dependent fetal complications of warfarin in pregnant women with mechanical heart valves. *J Am Coll Cardiol* 1999;33:1637–1641.
93. De Santo LS, Romano G, Della Corte A, et al. Mitral mechanical replacement in young rheumatic women: analysis of long-term survival, valve-related complications, and pregnancy outcomes over a 3707-patient-year follow-up. *J Thorac Cardiovasc Surg* 2005;130:13–19.
94. Burchill L, Greenway S, Silversides CK, et al. Genetic counseling in the adult with congenital heart disease: what is the role? *Curr Cardiol Rep* 2011;13:347–355.
95. Burn J, Brennan P, Little J, et al. Recurrence risks in offspring of adults with major heart defects: results from first cohort of British collaborative study. *Lancet* 1998;351:311–316.
96. Nora JJ, Nora AH. Maternal transmission of congenital heart diseases: new recurrence risk figures and the questions of cytoplasmic inheritance and vulnerability to teratogens. *Am J Cardiol* 1987;59:459–463.
97. Ferencz C, Boughman JA, Neill CA, et al. Congenital cardiovascular malformations: questions on inheritance. Baltimore-Washington Infant Study Group. *J Am Coll Cardiol* 1989;14:756–763.
98. Whittemore R, Wells JA, Castellsague X. A second-generation study of 427 probands with congenital heart defects and their 837 children. *J Am Coll Cardiol* 1994;23:1459–1467.
99. Collins E, Turner G. The Noonan syndrome—a review of the clinical and genetic features of 27 cases. *J Pediatr* 1973;83:941–950.
100. Ensing GJ, Schmidt MA, Hagler DJ, et al. Spectrum of findings in a family with nonsyndromic autosomal dominant supravalvular aortic stenosis: a Doppler echocardiographic study. *J Am Coll Cardiol* 1989;13:413–419.
101. Smith AT, Sack GH Jr, Taylor GJ. Holt-Oram syndrome. *J Pediatr* 1979;95:538–543.
102. Czeizel AE. Reduction of urinary tract and cardiovascular defects by periconceptional multivitamin supplementation. *Am J Med Genet* 1996;62:179–183.
103. Thangaroopan M, Wald RM, Silversides CK, et al. Incremental diagnostic yield of pediatric cardiac assessment after fetal echocardiography in the offspring of women with congenital heart disease: a prospective study. *Pediatrics* 2008;121:e660–e665.
104. Warnes CA, Williams RG, Bashore TM, et al. ACC/AHA 2008 Guidelines for the Management of Adults with Congenital Heart Disease: Executive Summary: a report of the American College of Cardiology/American Heart Association Task Force on Practice Guidelines (writing committee to develop guidelines for the management of adults with congenital heart disease). *Circulation* 2008;118:2395–2451.
105. Silversides CK, Marelli A, Beaulac L, et al. Canadian Cardiovascular Society 2009 Consensus Conference on the management of adults with congenital heart disease: executive summary. *Can J Cardiol* 2010;26:143–150.
106. Marelli A, Beaulac L, Mital S, et al. Canadian Cardiovascular Society 2009 Consensus Conference on the management of adults with congenital heart disease: introduction. *Can J Cardiol* 2010;26:e65–e69.
107. Silversides CK, Dore A, Poirier N, et al. Canadian Cardiovascular Society 2009 Consensus Conference on the management of adults with congenital heart disease: shunt lesions. *Can J Cardiol* 2010;26:e70–e79.
108. Silversides CK, Kiess M, Beaulac L, et al. Canadian Cardiovascular Society 2009 Consensus Conference on the management of adults with congenital heart disease: outflow tract obstruction, coarctation of the aorta, tetralogy of Fallot, Ebstein anomaly and Marfan's syndrome. *Can J Cardiol* 2010;26:e80–e97.
109. Silversides CK, Salehian O, Oechslin E, et al. Canadian Cardiovascular Society 2009 Consensus Conference on the management of adults with congenital heart disease: complex congenital cardiac lesions. *Can J Cardiol* 2010;26:e98–e117.
110. Baumgartner H, Bonhoeffer P, De Groot NM, et al. ESC Guidelines for the management of grown-up congenital heart disease (new version 2010). *Eur Heart J* 2010;31:2915–2957.
111. De Wilde JP, Rivers AW, Price DL. A review of the current use of magnetic resonance imaging in pregnancy and safety implications for the fetus. *Prog Biophys Mol Biol* 2005;87:335–353.
112. NCRP Report No. 91. *Medical Radiation Exposure of Pregnant and Potentially Pregnant Women*. Washington, DC: National Commission on Radiation Protection, 1977.
113. Shotan A, Widerhorn J, Hurst A, et al. Risks of angiotensin-converting enzyme inhibition during pregnancy: experimental and clinical evidence, potential mechanisms, and recommendations for use. *Am J Med* 1994;96:451–456.
114. Cooper WO, Hernandez-Diaz S, Arbogast PG, et al. Major congenital malformations after first-trimester exposure to ACE inhibitors. *N Engl J Med* 2006;354:2443–2451.
115. Silversides CK, Harris L, Haber K, et al. Recurrence rates of arrhythmias during pregnancy in women with previous tachyarrhythmia and impact on fetal and neonatal outcomes. *Am J Cardiol* 2006;97:1206–1212.
116. Fuster V, Ryden LE, Asinger RW, et al. ACC/AHA/ESC Guidelines for the management of patients with atrial fibrillation: executive summary a report of the American College of Cardiology/American Heart Association Task Force on Practice Guidelines and the European Society of Cardiology Committee for Practice Guidelines and Policy Conferences (Committee to Develop Guidelines for the Management of Patients With Atrial Fibrillation) Developed in Collaboration With the North American Society of Pacing and Electrophysiology. *Circulation* 2001;104:2118–2150.
117. Blomstrom-Lundqvist C, Scheinman MM, Alpert EM, et al. ACC/AHA/ESC guidelines for the management of patients with supraventricular arrhythmias—executive summary: a report of the American College of Cardiology/American Heart Association Task Force on Practice Guidelines and the European Society of Cardiology Committee for Practice Guidelines (Writing Committee to Develop Guidelines for the Management of Patients With Supraventricular Arrhythmias). *Circulation* 2003;108:1871–1909.
118. Magee LA, Downar E, Sermer M, et al. Pregnancy outcome after gestational exposure to amiodarone in Canada. *Am J Obstet Gynecol* 1995;172:1307–1311.
119. Bartalena L, Bogazzi F, Braverman LE, et al. Effects of amiodarone administration during pregnancy on neonatal thyroid function and subsequent neurodevelopment. *J Endocrinol Invest* 2001;24:116–130.
120. Guidelines 2000 for Cardiopulmonary Resuscitation and Emergency Cardiovascular Care. Part 6: Advanced Cardiovascular life support: section 7: algorithm approach to ACLS emergencies: section 7A: principles and practice of ACLS. The American Heart Association in collaboration with the International Liaison Committee on Resuscitation. *Circulation* 2000;102:1136–1139.
121. Natale A, Davidson T, Geiger MJ, et al. Implantable cardioverter-defibrillators and pregnancy: a safe combination? *Circulation* 1997;96:2808–2812.
122. Laksman Z, Harris L, Silversides CK. Cardiac arrhythmias during pregnancy: a clinical approach. *Fetal Matern Med Rev* 2011;22:123–143.
123. Elkayam U, Bitar F. Valvular heart disease and pregnancy: part II: prosthetic valves. *J Am Coll Cardiol* 2005;46:403–410.
124. Bates SM, Greer IA, Hirsh J, et al. Use of antithrombotic agents during pregnancy: the Seventh ACCP Conference on Antithrombotic and Thrombolytic Therapy. *Chest* 2004;126:627S–644S.
125. Yinon Y, Siu SC, Warshafsky C, et al. Use of low molecular weight heparin in pregnant women with mechanical heart valves. *Am J Cardiol* 2009;104:1259–1263.
126. McLintock C, McCowan LM, North RA. Maternal complications and pregnancy outcome in women with mechanical prosthetic heart valves treated with enoxaparin. *BJOG* 2009;116:1585–1592.
127. Abildgaard U, Sandset PM, Hammerstrom J, et al. Management of pregnant women with mechanical heart valve prosthesis: thromboprophylaxis with low molecular weight heparin. *Thromb Res* 2009;124:262–267.
128. Quinn J, Von Klemperer K, Brooks R, et al. Use of high intensity adjusted dose low molecular weight heparin in women with mechanical heart valves during pregnancy: a single-center experience. *Haematologica* 2009;94:1608–1612.
129. Bonow RO, Carabello BA, Kanu C, et al. ACC/AHA 2006 guidelines for the management of patients with valvular heart disease: a report of the American College of Cardiology/American Heart Association Task Force on Practice Guidelines (writing committee to revise the 1998 Guidelines for the Management of Patients With Valvular Heart Disease): developed in collaboration with the Society of Cardiovascular Anesthesiologists: endorsed by the Society for Cardiovascular Angiography and Interventions and the Society of Thoracic Surgeons. *Circulation* 2006;114:e84–e231.
130. Vahanian A, Baumgartner H, Bax J, et al. Guidelines on the management of valvular heart disease: The Task Force on the Management of Valvular Heart Disease of the European Society of Cardiology. *Eur Heart J* 2007;28:230–268.
131. Shores J, Berger KR, Murphy EA, et al. Progression of aortic dilatation and the benefit of long-term beta-adrenergic blockade in Marfan's syndrome. *N Engl J Med* 1994;330:1335–1341.
132. Weiss BM, von Segesser LK, Alon E, et al. Outcome of cardiovascular surgery and pregnancy: a systematic review of the period 1984–1996. *Am J Obstet Gynecol* 1998;179:1643–1653.
133. John AS, Gurley F, Schaff HV, et al. Cardiopulmonary bypass during pregnancy. *Ann Thorac Surg* 2011;91:1191–1196.
134. Arnoni RT, Arnoni AS, Bonini RC, et al. Risk factors associated with cardiac surgery during pregnancy. *Ann Thorac Surg* 2003;76:1605–1608.
135. Jamieson WR, Cartier PC, Allard M, et al. Surgical management of valvular heart disease 2004. *Can J Cardiol* 2004;20:7E–120E.
136. Goldszmidt E, Macarthur A, Silversides C, et al. Anesthetic management of a consecutive cohort of women with heart disease for labor and delivery. *Int J Obstet Anesth* 2010;19:266–272.
137. Oron G, Hirsch R, Ben-Haroush A, et al. Pregnancy outcome in women with heart disease undergoing induction of labour. *BJOG* 2004;111:669–675.

138. Wilson W, Taubert KA, Gewitz M, et al. Prevention of infective endocarditis: guidelines from the American Heart Association: a guideline from the American Heart Association Rheumatic Fever, Endocarditis, and Kawasaki Disease Committee, Council on Cardiovascular Disease in the Young, and the Council on Clinical Cardiology, Council on Cardiovascular Surgery and Anesthesia, and the Quality of Care and Outcomes Research Interdisciplinary Working Group. *Circulation* 2007;116:1736–1754.
139. Warnes CA, Williams RG, Bashore TM, et al. ACC/AHA 2008 Guidelines for the Management of Adults with Congenital Heart Disease: a report of the American College of Cardiology/American Heart Association Task Force on Practice Guidelines (writing committee to develop guidelines on the management of adults with congenital heart disease). *Circulation* 2008;118:e714–e833.
140. Thorne S, MacGregor A, Nelson-Piercy C. Risks of contraception and pregnancy in heart disease. *Heart* 2006;92:1520–1525.
141. Silversides CK, Sermer M, Siu SC. Choosing the best contraceptive method for the adult with congenital heart disease. *Curr Cardiol Rep* 2009;11:298–305.

Other Special Problems and Issues

Chest Pain in Children and Adolescents

Jonathan N. Johnson ■ David J. Driscoll

Chest pain is a common presenting symptom in children and adolescents. In prospective studies, it has been shown to occur at a rate of 0.25% to 0.6% of visits both in the outpatient setting and the emergency department (1–3). Chest pain accounts for 650,000 physician visits per year in patients 10 to 21 years of age (4). Awareness of both cardiovascular disease and the risk of sudden cardiac death has increased both in media and in national education programs. In fact, >50% of adolescents with a history of chest pain report significant fear of cardiac pathology (5). Fortunately, chest pain in children and adolescents is rarely cardiac in nature; cardiac causes typically account for fewer than 5% of chest pain cases in published studies (Table 70.1) (1–3). The mean age of children and adolescents who complain of chest pain is 11 to 14 years, but chest pain can occur in children as young as 4 years of age (1,6). Chest pain is equally common in males and females, although certain etiologies may have a sex-specific predilection.

The relative frequencies of types of chest pain have been reported by several investigators and are summarized in Table 70.2, and are described below. The most common source of chest pain in children and adolescents is the musculoskeletal structures of the chest wall (1,2,4–9).

MUSCULOSKELETAL/CHEST-WALL PAIN

Costochondritis

Costochondritis is a common cause of musculoskeletal chest-wall pain, particularly in adolescent patients (10). The onset of the pain may be preceded by a respiratory illness, although the exact etiology is unknown. The pain typically involves two to four contiguous costochondral or costosternal junctions, between the second and fifth costal cartilages (1,10). The joints are not inflamed, and there is no swelling of the joints. The pain is most commonly unilateral and may affect the left side more frequently than the right. The patient will complain of a sharp pain lasting from several seconds to several minutes, which is exacerbated by deep breathing. Direct palpation of

the affected joint(s) will reproduce the pain. The patient may describe a “burning” sensation for a few minutes after deep palpation. It is important to apply sufficient pressure during this palpation, as light touch may not reproduce the pain. Costochondritis is typically self-limited (11). Treatment consists of reassurance and rest from athletic or strenuous activities, and occasionally may require the use of nonsteroidal anti-inflammatory medications, at least in the acute phase.

Tietze Syndrome

Tietze syndrome involves the inflammation of a single costochondral junction (12). While this syndrome has been reported in children and even infants, it remains relatively uncommon in childhood (12). The affected joint will be swollen and tender to palpation, and may be warm to the touch. Its etiology is unknown. The pain is typically self-limited, lasting anywhere from a few weeks to a few months. When necessary, nonsteroidal anti-inflammatory medications can be used.

Idiopathic Chest-Wall Pain

Nonspecific (idiopathic) chest-wall pain is the most common type of chest pain in children and adolescents (Table 70.2). The pain is described as sharp, lasting several seconds to several minutes. The pain often is exacerbated by deep breathing, and may occur during exercise or while at rest. It is most often located in the center of the chest or just below the breast. Sometimes, squeezing the chest cage or gently pressing on the sternum can reproduce the pain. More frequently, the pain cannot be reproduced by palpating and pushing on various chest structures, but the costochondral and costosternal joints are not tender. There are no associated symptoms, but patients may feel anxious while experiencing the pain (13). Most patients are able to continue activities despite the pain. Children with idiopathic chest pain tend to have longer courses than children with other etiologies and may have intermittent chest pain for many months (16,14). A thoughtful explanation of the cause and benign nature of the pain frequently is enough to reassure the patient with idiopathic chest-wall pain.

TABLE 70.1 Differential Diagnosis of Chest Pain in Children and Adolescents*Cardiac*

Anomalous coronary artery
 Kawasaki disease
 Coronary vasospasm/compression)
 Cocaine abuse
 Supraventricular tachycardia
 Ventricular tachycardia
 Pericarditis
 Myocarditis
 Hypertrophic cardiomyopathy
 Aortic or Pulmonary stenosis
 Aortic dissection

Pulmonary

Asthma/Reactive airway disease
 Pneumonia
 Pneumothorax
 Pneumomediastinum
 Pulmonary embolism
 Chronic cough

Psychogenic

Hyperventilation
 Anxiety

Gastrointestinal

Gastroesophageal reflux
 Esophagitis
 Gastritis
 Foreign body ingestion

Musculoskeletal

Chest-wall trauma
 Rib fracture
 Muscle strain
 Costochondritis
 Precordial catch syndrome
 Slipping rib syndrome
 Hypersensitive xiphoid syndrome
 Tietze syndrome

Other

Herpes zoster
 Sickle cell disease
 Pleurodynia
 Pleural effusion
 Thoracic malignancy/masses
 Breast tenderness
 Idiopathic chest-wall pain

Precordial Catch Syndrome

Precordial catch syndrome is a brief (several seconds), sharp, stabbing pain occurring in healthy children, most commonly in patients between 6 and 12 years of age (15). The pain typically is located below the left breast or at the lower left sternal border (15,16). It frequently is pleuritic in nature, worsening with deep inspiration. It also may worsen when the patient bends forward. The pain can be so sharp that the patient will breathe shallowly for several seconds. It can occur at rest or with exercise. When it occurs during exercise, the patient may have to stop and breathe shallowly until the pain subsides. The patient is able to resume activities immediately after pain resolution. The physical examination typically is unremarkable. The etiology is unknown. Treatment typically is unnecessary and ineffective, due to the random nature of the pain (15).

Slipping-Rib Syndrome

Slipping-rib syndrome involves the 8th, 9th, and 10th ribs, which do not attach directly to the sternum (17,18). Instead, they attach to each other via dense fibrous tissue. In many cases, there is a history of trauma to the area, which results in disruption of these intercostal connections. This can result in rib laxity, pressure on intercostal nerves, and a “popping” sensation (19). Subsequently, any form of activity that causes these tissues to move (coughing, athletics, stretching) will produce or worsen the characteristic intense aching pain (17). The characteristic exam finding in slipping-rib syndrome is the “hooking maneuver.” This is performed by the examiner putting his or her fingers under the inferior rib margin and pulling anteriorly. This action will reproduce the pain and may produce a clicking or popping sound (17). Treatment options for slipping rib syndrome primarily include rest and

nonsteroidal anti-inflammatory medications. In difficult cases, local anesthetic blocks can be performed. Surgical resection of the specific cartilages can be performed but should be reserved only for severe cases (17,18).

Hypersensitive Xiphoid Syndrome

Hypersensitive xiphoid syndrome is a rare form of chest pain in children (20). Patients may present with sternal pain that can radiate to the shoulders, back, arms, or precordium. In these patients, gentle digital pressure on the xiphoid process will reproduce the pain. Treatment is typically unnecessary.

Trauma and Muscle Strain

Chest pain often can be caused by traumatic injury to the chest wall, particularly in athletes. The history of prior trauma is suggestive, and typically the pain is reproducible with palpation of the affected area of the chest. The pain often is worsened with positioning or activities involving the specific muscle and bony tissues (13). For simple muscle strains, nonsteroidal anti-inflammatory medications are typically effective. The examiner must be aware that significant trauma can produce a myocardial contusion and possibly a hemopericardium (see Chapter 23), both of which can cause chest pain. Significant trauma requires full evaluation for potential bony and visceral injuries.

OTHER NONCARDIAC CAUSES OF CHEST PAIN

Although musculoskeletal chest-wall pain is the most common cause of chest pain in children and adolescents, there are many

TABLE 70.2 Percentage Distribution of Causes of Chest Pain in Children and Adolescents

Cause of pain	Reference No.						
	(1)	(2)	(3)	(5)	(6)	(8)	(9) (21)
Idiopathic		28	12	46	21	55	13
Musculoskeletal	45	15	28	13	15		16
Costochondritis	23	10		16	9	2	9
Asthma		4			7	3	12 64
Psychogenic			5		9		9
Trauma		4	15	3	9		7
Respiratory	12.5	6	19		10		11
Pneumonia		2			4		6
Hyperventilation				23			
Cardiac disease			1		4	6	4
Mitral prolapse				1			
Arrhythmia		3					
Gastrointestinal		7		3	4	2	3
Sickle cell disease					2		3
Breast-related				6			
Functional		17					
Miscellaneous	10	4	20	2	9	31	6

other, less common, causes of chest pain. These include the following.

Pulmonary

Asthma and exercise-induced asthma are well-known causes of chest pain in children and adolescents. Laboratory evidence of asthma has been detected in up to 73% of children evaluated for chest pain, although this is likely an overrepresentation (21). Nonetheless, reactive airway disease should be considered in patients with chest pain, particularly if there is a history of asthma, eczema, allergies, shortness of breath with exercise, exercise-associated chest pain, exertional cough, wheezing, or a family history of asthma. Chest pain in patients with asthma most likely is secondary to cough, chest-wall muscle strain, or dyspnea/hyperinflation (19). Exertional asthma can be treated with inhaled bronchodilators prior to initiation of activities.

Pneumonia can be a cause of chest pain, particularly if there is pleural or diaphragmatic irritation (19). Additionally, pleural effusions or localized empyemas may produce localized chest pain. In addition to pneumonia/pneumonitis, infection of the large airways may cause chest pain, including bronchitis and tracheitis. These patients often present with other concurrent typical symptoms to help clarify the diagnosis. Finally, the physician should ask of any possible ingestion history, as the presence of a foreign body in the airway may produce dyspnea and chest pain.

Pulmonary embolism is extremely rare in children (22). However, it requires consideration in patients presenting with chest pain who have a history of clotting disorders, venous thromboembolism, Klippel-Trenaunay syndrome, concurrent

malignancy, recent surgery, or who are taking oral contraceptive medications.

Herpes Zoster

Herpes zoster can produce intense localized sharp chest pain. The pain is caused by an intercostal neuralgia and may present before the appearance of the characteristic skin eruption. Worsening of the pain may occur with movement and deep breathing. The pain typically resolves with healing of the skin lesions; however, postherpetic neuralgia may persist and be quite painful. In these cases, neuromodulating pain medications like gabapentin may be helpful. Local anesthetic blocks can be performed in severe cases.

Sickle Cell Disease

Patients with sickle cell disease can develop a vaso-occlusive crisis that includes chest pain ("acute chest syndrome") and an infiltrate on chest radiography. The pain can be secondary to several processes, including infarction of bony structures, intercostal muscles, and lung tissue from microvascular occlusion. A patient suspected to have acute chest syndrome should be evaluated emergently (23).

Pericarditis

Pericarditis, whether due to an infectious etiology or a noninfectious inflammatory cause, is associated with chest pain. The pain associated with pericarditis is generally more severe than that of benign forms of chest-wall pain. Children may describe

the pain as squeezing, sharp, or dull. It may be intensified by lying down. Patients often will sit with a forward lean, which alleviates the pain. The pain is worse with inspiration, coughing, and movement (24).

The pathognomonic physical finding is a friction rub: a high-frequency, scratching/sandpaper-like sound caused by friction between the inflamed pericardial surfaces. It is best heard at the left sternal border or apex and is loudest when the heart is closest to the chest wall (when the patient leans forward, kneels, and inspires). Muffled heart sounds suggest the presence of a large pericardial effusion (24). Pericarditis is associated with typical electrocardiographic findings of generalized ST-segment elevation. Echocardiography may be helpful in diagnosis (see Chapter 62).

Gastrointestinal

Gastrointestinal disorders are a common cause of chest pain, particularly in adolescents and adults. The most common causes are esophagitis (reflux, pill related, and eosinophilic) and gastritis. Symptoms often are difficult to discern from cardiac or chest-wall pain. Pain associated with food ingestion or associated with dysphagia may indicate a gastrointestinal cause (19).

Pneumothorax/Pneumomediastinum

Among patients with chest pain, pneumothorax or pneumomediastinum are uncommon; however, these conditions are always associated with chest pain (25). Small air collections may be difficult to detect by clinical examination. The abrupt onset of severe chest pain should alert the clinician to this potential diagnosis. Particular consideration for a pneumothorax should be given to patients with Marfan syndrome who develop sudden-onset chest pain or dyspnea. Chest radiography is diagnostic.

Psychogenic

Chest pain secondary to psychogenic etiologies is a diagnosis of exclusion, requiring a full evaluation for potential life-threatening causes. It has a higher incidence in teenagers, particularly in females. There often is a trigger for the onset of the pain, including recent psychologic and emotional stress, or recent diagnosis of another organic disease. Psychogenic chest pain is more common in patients with a family history of cardiac disease (26). The physical examination is normal. Treatment is difficult, and includes extensive reassurance and treatment/counseling for their underlying psychiatric concerns.

Anxiety-related hyperventilation also can cause chest pain. Physiologically, this occurs secondary to respiratory alkalosis and subsequent coronary artery vasoconstriction (27). Treatment involves referral to a physiotherapist, who can help the patient learn specific breathing techniques to prevent the dysfunctional breathing patterns.

CARDIAC CAUSES OF CHEST PAIN

In a population of children and adolescents with chest pain, the proportion with a cardiac origin for the chest pain is extremely low. Some cardiac conditions, however, are associated with chest pain. These include obstructive hypertrophic cardiomyopathy, aortic stenosis, pericarditis, arrhythmias, coronary insufficiency, dissecting aortic aneurysm (especially in patients with Marfan syndrome), and mitral valve prolapse.

Causes of coronary insufficiency in children include Kawasaki disease, Williams syndrome, anomalous origin of the coronary arteries, and coronary arteriovenous and coronary cameral fistulae. These conditions are reviewed in other chapters of this textbook. Additionally, it is critical to ask about recent medication and drug intake, particularly substances that may induce coronary vasospasm.

Even in a population with these conditions, chest pain is an uncommon presenting symptom. It is important to identify patients who are at high risk for these conditions through historical information and characteristics of the pain so that appropriate diagnostic and therapeutic steps can be taken. A recent study reported the experience at the busy outpatient clinics at Children's Hospital Boston of patients aged 7 to 21 years. In a 10-year period, only 41 patients with an initial presentation of chest pain were ultimately determined to have a cardiac cause (28). Only 32 of these were considered to have serious cardiac pathology. Patients with coronary anomalies and chest pain are far more likely to present to an outpatient clinic, while patients with chest pain secondary to myocarditis, pericarditis, or pulmonary embolism are more likely to present to an emergency department or inpatient setting (28).

MEDICAL EVALUATION

The evaluation of chest pain requires a thorough history and careful physical examination (1,13). The family history should be explored for premature forms of heart or lung disease and instances of premature death. Particular inquiry should be made as to a family history of unexplained drownings, car accidents, syncope, and sudden infant death syndrome (SIDS). In addition, it may be helpful to know whether other family members have chest pain, such as a parent or grandparent who experiences angina.

In the majority of cases, the cause of the pain will be apparent after the history and physical examination. Most patients will not have a serious underlying medical problem, but the patient and the patient's family may think they do (5). A thorough and thoughtful history and physical examination are important in reassuring the patient and family that there is no serious problem. The examination should include a full heart, lung, extremity, and abdominal exam. It is important to palpate the costochondral joints and other areas of the chest to try to elicit localized tenderness.

Few patients truly have angina. If, however, a history of angina is elicited, appropriate testing will be needed. A history of chest pain associated with presyncope, syncope, sweating, nausea, palpitations, cyanosis, or dyspnea should make raise suspicion of a potentially serious underlying cause of the chest pain. Additionally, a history of chest pain with exercise should be evaluated further. A strong family history of sudden death, aortic dissection, or cardiomyopathy also may prompt further evaluation despite an equivocal personal history.

In the vast majority of cases of chest pain in children, only a history and physical examination are necessary and additional tests are not particularly helpful (1,2,28). In the unusual circumstance where cardiac disease is strongly suspected, several investigations may be performed. An electrocardiogram may be performed to assess for heritable arrhythmia disorders including preexcitation. Chest radiography can assess for heart size, effusions, and pulmonary processes. An echocardiogram can be performed to assess for structural heart disease, cardiomyopathy, and coronary anomalies. Exercise stress testing can assess for exercise-induced ST-segment changes, exercise-induced arrhythmias or ectopy, and overall cardiovascular conditioning.

TREATMENT

The specific treatment of chest pain depends on the underlying cause. For most patients with musculoskeletal causes of chest pain, an explanation of the cause of the pain and its benign nature frequently is enough to reassure the patient and their family. The goal in these discussions is to reduce the anxiety associated with the pain, allowing the patient to tolerate the pain better with less fear. Children with noncardiac chest pain have been reported to have more symptoms of anxiety as compared to children with cardiac causes of chest pain (29). The use of medication is usually unnecessary for the majority of causes of chest-wall pain. If necessary, mild doses of non-steroidal anti-inflammatory medications are often sufficient. If history and physical examination suggest a cardiac cause, appropriate consultation and evaluation should be sought.

OUTCOME

The long-term outcome of chest pain in children is generally very good. Driscoll et al. (1) found resolution of chest pain in 58% of patients when questioned 4 weeks to 2 years after initial evaluation of their chest pain. Lam et al. (30) reported that almost half (49%) of patients had recurrence of their chest pain. However, 12 of 26 patients with recurrent chest pain had pain only occasionally on follow-up. Selbst et al. (9) reported 6-month follow-up on 149 patients who had presented with chest pain. They noted that the initial diagnosis was changed in 34% of the patients on follow-up, typically indicating a nonorganic cause of the chest pain. A new organic cause was found in only 12/149 (8%) patients. Only one child was found to have evidence of cardiac pathology, mitral valve prolapse. The pain resolved in 57% of patients. Pain lasting longer than 6 months is more likely due to an idiopathic or psychogenic etiology (1,2).

REFERENCES

1. Driscoll DJ, Glicklich LB, Gallen WJ. Chest pain in children: a prospective study. *Pediatrics* 1976;57:648–651.
2. Selbst SM. Chest pain in children. *Pediatrics* 1985;75:1068–1070.
3. Rowe BH, Dulberg CS, Peterson RG, et al. Characteristics of children presenting with chest pain to a pediatric emergency department. *CMAJ* 1990;143:388–394.
4. Epstein SE, Gerber LH, Borer JS. Chest wall syndrome. A common cause of unexplained cardiac pain. *JAMA* 1979;241:2793–2797.
5. Pantell RH, Goodman BW Jr. Adolescent chest pain: a prospective study. *Pediatrics* 1983;71:881–887.
6. Selbst SM, Ruddy RM, Clark BJ, et al. Pediatric chest pain: a prospective study. *Pediatrics* 1988;82:319–323.
7. Coleman WL. Recurrent chest pain in children. *Pediatr Clin North Am* 1984;31:1007–1026.
8. Fyfe DA, Moodie DS. Chest pain in pediatric patients presenting to a cardiac clinic. *Clin Pediatr (Phila)* 1984;23:321–324.
9. Selbst SM, Ruddy R, Clark BJ. Chest pain in children. Follow-up of patients previously reported. *Clin Pediatr (Phila)* 1990;29:374–377.
10. Brown RT. Costochondritis in adolescents. *J Adolesc Health Care* 1981;1:198–201.
11. Brown RT, Jamil K. Costochondritis in adolescents. A follow-up study. *Clin Pediatr (Phila)* 1993;32:499–500.
12. Mukamel M, Kornreich L, Horev G, et al. Tietze's syndrome in children and infants. *J Pediatr* 1997;131:774–775.
13. Cava JR, Sayger PL. Chest pain in children and adolescents. *Pediatr Clin North Am* 2004;51:1553–1568, viii.
14. Gokhale J, Selbst SM. Chest pain and chest wall deformity. *Pediatr Clin North Am* 2009;56:49–65, x.
15. Gumbiner CH. Precordial catch syndrome. *South Med J* 2003;96:38–41.
16. Miller AJ, Texidor TA. Precordial catch, a neglected syndrome of precordial pain. *JAMA* 1955;159:1364–1365.
17. Porter GE. Slipping rib syndrome: an infrequently recognized entity in children: a report of three cases and review of the literature. *Pediatrics* 1985;76:810–813.
18. Mooney DP, Shorter NA. Slipping rib syndrome in childhood. *J Pediatr Surg* 1997;32:1081–1082.
19. Ives A, Daubeney PE, Balfour-Lynn IM. Recurrent chest pain in the well child. *Arch Dis Child* 2010;95:649–654.
20. Lipkin M, Fulton LA, Wolfson EA. The syndrome of the hypersensitive xiphoid. *N Engl J Med* 1955;253:591–597.
21. Wiens L, Sabath R, Ewing L, et al. Chest pain in otherwise healthy children and adolescents is frequently caused by exercise-induced asthma. *Pediatrics* 1992;90:350–353.
22. Stein PD, Kayali F, Olson RE. Incidence of venous thromboembolism in infants and children: data from the National Hospital Discharge Survey. *J Pediatr* 2004;145:563–565.
23. Vichinsky EP, Styles LA, Colangelo LH, et al. Acute chest syndrome in sickle cell disease: clinical presentation and course. Cooperative Study of Sickle Cell Disease. *Blood* 1997;89:1787–1792.
24. Lange RA, Hillis LD. Clinical practice. Acute pericarditis. *N Engl J Med* 2004;351:2195–2202.
25. Sahn SA, Heffner JE. Spontaneous pneumothorax. *N Engl J Med* 2000;342:868–874.
26. Pillay AL, Lalloo M. Psychogenic pain disorder in children. *S Afr Med J* 1989;76:195–196.
27. Neill WA, Hattenhauer M. Impairment of myocardial O₂ supply due to hyperventilation. *Circulation* 1975;52:854–858.
28. Kane DA, Fulton DR, Saleeb S, et al. Needles in hay: chest pain as the presenting symptom in children with serious underlying cardiac pathology. *Congenit Heart Dis* 2010;5:366–373.
29. Lipsitz JD, Masia-Warner C, Apfel H, et al. Anxiety and depressive symptoms and anxiety sensitivity in youngsters with noncardiac chest pain and benign heart murmurs. *J Pediatr Psychol* 2004;29:607–612.
30. Lam JC, Tobias JD. Follow-up survey of children and adolescents with chest pain. *South Med J* 2001;94:921–924.

Stephen R. Daniels

ATHEROSCLEROSIS

Coronary artery disease and stroke are the most common causes of morbidity and mortality in developed countries. The breakdown of the prevalence of different cardiovascular diseases in the United States is presented in Figure 71.1. It can be seen that coronary heart disease and stroke constitute 68% of cardiovascular diseases in the United States with coronary heart disease accounting for 51% alone.

Clearly, this is an important public health problem. In the past, atherosclerosis has been viewed as a problem of adults and not a focus in the pediatric age range. This is because the clinical manifestations of atherosclerosis are often not observed until middle age. However, there is increasing evidence that the process of atherosclerosis begins in childhood and is progressive throughout life.

Atherosclerosis results from deposits of lipid and cholesterol in the intima of the arterial wall. The earliest abnormality is thought to be the fatty streak (Fig. 71.2). This is an accumulation of lipid-filled macrophages within the intima (1). These lesions are flat and do not obstruct the arterial lumen. The natural history of these lesions is that some progress to raised plaques. This is a result of continued lipid accumulation and a proliferation of macrophages and smooth muscle cells (2). In this lesion, smooth muscle-type cells form a fibrous cap over a deposition of necrotic debris, cholesterol crystals, and ultimately calcification within the arterial wall. It is these raised lesions that result in a myocardial infarction because of either their increasing size and obstruction of the arterial lumen or their rupture, which results in the release of thrombogenic substances from the necrotic core. It has been noted that the fibrous plaques tend to develop at the anatomic site where fatty streaks are formed in children (3). Plaques generally tend to develop in the coronary arteries prior to their appearance in the cerebral arteries.

The early stages of the atherosclerotic process are asymptomatic. The best understanding of this process has come from a series of pathology studies. The earliest pathology studies were performed during the Korean War and the war in Vietnam (4,5). The results of these studies were somewhat surprising in that young and healthy males were found to have both fatty streaks and raised lesions. Although these early pathology studies documented the presence of atherosclerosis, they did not establish the risk factors for the early stages of this process. This information would come from subsequent studies.

There has been substantial epidemiologic research on the risk factors for cardiovascular disease development in adults. Longitudinal studies such as the Framingham study have measured potential risk factors and followed subjects to the development of cardiovascular disease. In fact, investigators have proposed >200 potential risk factors for the development of coronary artery disease. Most of these proposed risk factors have come from cross-sectional correlation studies. However, establishing a causal relationship is substantially more

difficult. This requires multiple studies including some with a longitudinal design with follow-up to the cardiovascular end point. It has also been difficult to establish the independence of a particular risk factor because often associations exist among risk factors. After decades of research, a group of risk factors, often referred to as the traditional risk factors, has been established. These risk factors are presented in Table 71.1. As can be seen, some of the risk factors are potentially modifiable and others are not. Table 71.2 lists novel factors that have strong consideration but are not yet considered established as independent risk factors.

The risk factors for the early aspects of the process of atherosclerosis have been determined by the more recent pathology studies including the Bogalusa study and the Pathobiological Determinants of Atherosclerosis in Youth (PDAY) study. The PDAY study was a multicenter investigation of individuals aged 15 to 34 years who died of accidental causes and suicide unrelated to the known presence of cardiovascular disease (6,7). The investigators performed autopsies to evaluate the extent of atherosclerosis in the aorta and coronary arteries. They used various indicators of risk factor status obtainable at the time of autopsy to define risk. They found that the traditional risk factors, including dyslipidemia, blood pressure elevation, and obesity, were associated with the presence of fatty streaks and of fibrous plaques.

The Bogalusa study investigators were able to obtain autopsies in individuals who had been participants in a school-based risk factor study, were followed longitudinally, and died of accidental causes (8,9). The investigators in the Bogalusa study found that the percent of the surface of the arteries covered with fatty streaks and fibrous plaques increased with increasing age at the time of death. They also found that the extent of coverage of the arteries (aorta and coronary arteries) was associated with elevation of total cholesterol, low-density lipoprotein cholesterol (LDL-C), triglycerides, blood pressure, and body mass index (BMI) during the school-age surveys. A low high-density lipoprotein cholesterol (HDL-C) was also associated with a greater extent of coverage of the arterial surface with fatty streaks and fibrous plaques. An additional important finding was that the prevalence of atherosclerosis increased with an increasing number of risk factors present. This was particularly true for fibrous plaques in the coronary arteries where the presence of three or four risk factors was associated with 7% coverage and the presence of one or two risk factors was associated with 1% and 2% coverage, respectively (9).

Imaging

One factor that has made the study of atherosclerosis difficult is the lack of noninvasive tools to image the early atherosclerotic lesions. In adults, computed tomography (CT) scanning has been used to detect the presence of calcium in the coronary arteries. The presence of calcium deposits has been associated

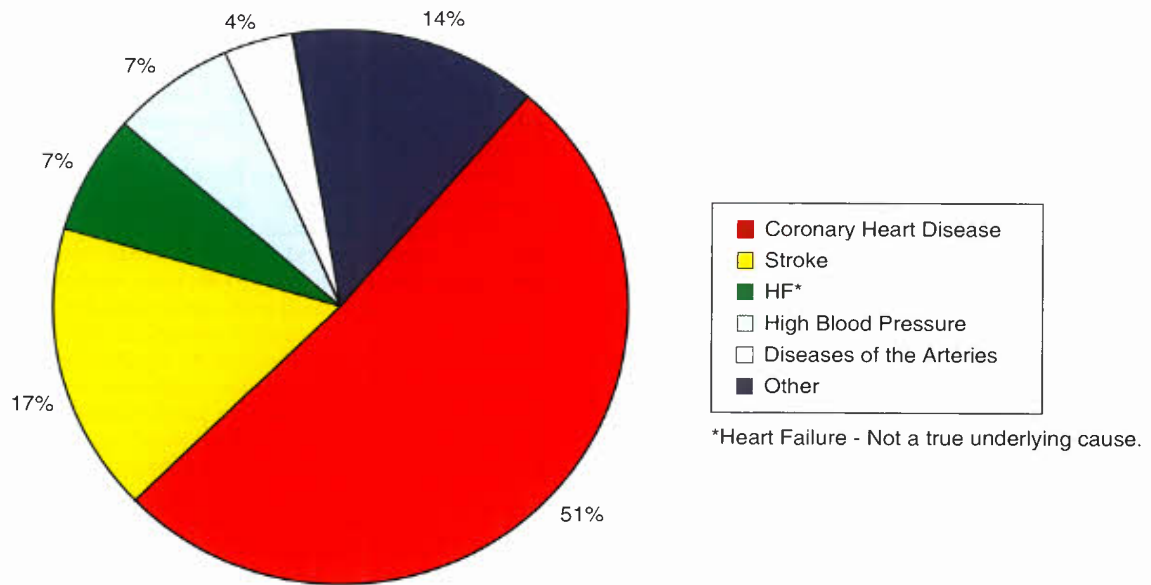


Figure 71.1. Prevalence of cardiovascular disease in the United States. (From Lloyd-Jones D, Adams RJ, Brown TM, et al. Heart Disease and Stroke Statistics—2010 Update: A Report From the American Heart Association. *Circulation* 2010;121:e46–e215, with permission.)

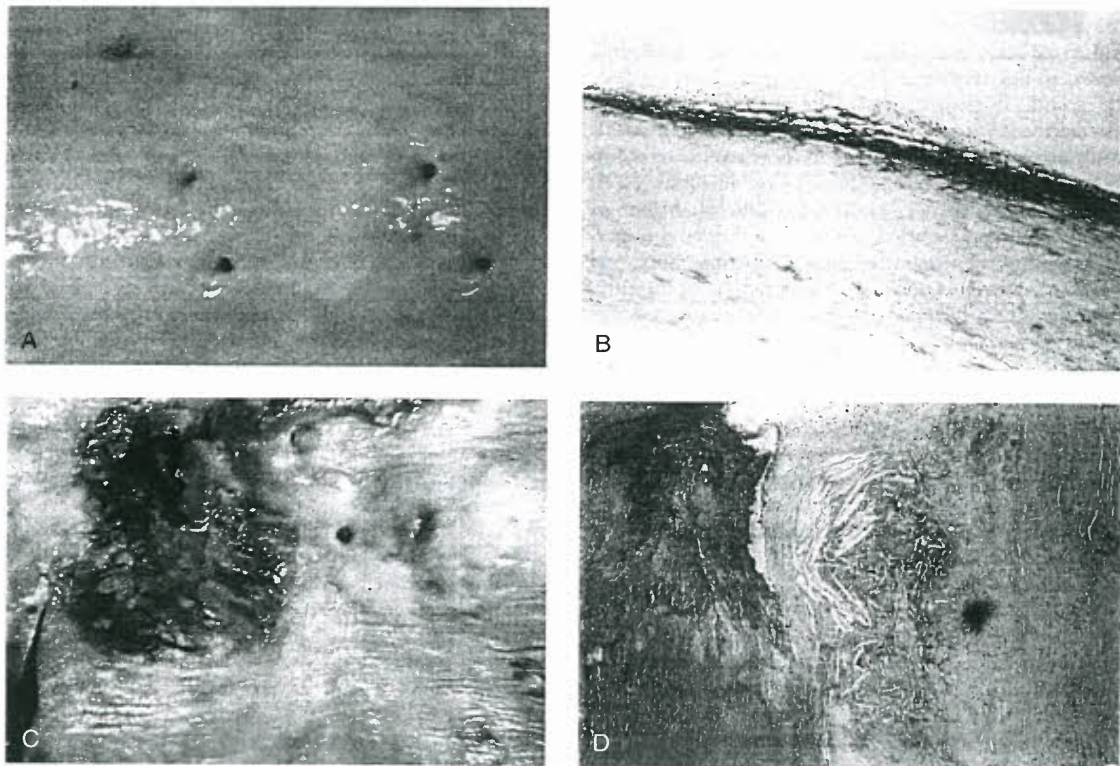


Figure 71.2. A: Gross anatomic specimen of the abdominal aorta. Fatty streaks, the earliest evidence for atherosclerosis, are seen as white strands through the tissue. B: Photomicrograph (original magnification $\times 0$) of fatty streak using Sudan black stain. The vacuolization is caused by the fat globules of the lesion. C: Gross anatomic specimen of the origin of the left coronary artery. A complex lesion (plaque) of calcium, fibrous tissue, and fat fills the vessel. D: Photomicrograph (original magnification, $\times 100$) of coronary artery plaque using hematoxylin and eosin stain. This complex raised lesion shows erosion of the endothelium, clot, and cholesterol clefts. (Photographs courtesy of Margaret Grimes, M.D., Medical College of Virginia/Virginia Commonwealth University.)

TABLE 71.1 Established Risk Factors for Coronary Artery Disease*Nonmodifiable*

Age
Sex male > female
Family history

Modifiable

Dyslipidemia
Blood pressure elevation
Diabetes mellitus
Cigarette smoking
Obesity/metabolic syndrome
Coagulation factors

with increased risk for adverse cardiovascular disease outcomes (10). Fewer studies have evaluated this issue in young subjects. Investigators from the Muscatine Study used electron beam CT to evaluate young adults who had participated in a longitudinal epidemiologic study of cardiovascular risk factors as children (11). The subjects were younger than 35 years of age. The prevalence of coronary artery calcium was 31% in men and 10% in women.

The investigators also evaluated the extent to which risk factors were associated with the presence of coronary artery calcium. They found that the risk factors measured most recently were the strongest predictors including systolic blood pressure, BMI, LDL-C, and HDL-C. However, weight in childhood and BMI, diastolic blood pressure, and cholesterol in young adulthood were also associated with increased risk of calcium in the coronary arteries (11).

Gidding et al. (12) studied a group of adolescents and young adults aged 11 to 23 years with heterozygous familial hypercholesterolemia. They found that 7 of 29 subjects had coronary artery calcium. Calcium was more likely to be present when obesity and cholesterol elevation were both present.

Magnetic resonance imaging (MRI) may also be used to evaluate the atherosclerotic process. It has been used to evaluate the presence of atherosclerotic plaques and supraaortic stenosis in young patients with homozygous familial hypercholesterolemia (13). Studies in adults have also demonstrated that high-resolution multicontrast MRI can be used to evaluate whether arterial plaque is unstable and subject to

rupture (14). This is important as other noninvasive methods have been unable to characterize this progression of atherosclerosis. This method allows the fibrous cap to be distinguished from the lipid core. It is not currently known if MRI will be useful in following the evolution of fatty streaks to fibrous plaques.

Ultrasound methodology has also been used to evaluate the presence of atherosclerosis. In adults, the measurement of the carotid artery intima-media thickness (IMT) has gained acceptance as a useful method in epidemiologic studies to evaluate atherosclerosis. In adults, it has been shown that increased carotid IMT is associated with cardiovascular risk factors (15) and with incident myocardial infarction (16) and stroke (17). However, in a meta-analysis of 41 randomized clinical trials, Costanzo et al. (18) found that regression or slowed progression of carotid IMT induced by cardiovascular drug therapies in adults does not reflect reduction of cardiovascular events. Fewer studies have used ultrasound to evaluate carotid IMT in children and adolescents. Davis et al. (19) studied the young adult Muscatine population aged 33 to 42. These were individuals who had participated in the school surveys when they were younger. In males, childhood total cholesterol and triglycerides were higher in those with elevated carotid IMT. In females, childhood weight, BMI, total cholesterol, and triglycerides were higher in those with high carotid IMT. The Young Finns study had a similar design (20). In multivariable models adjusting for age and sex, they found that childhood LDL-C, systolic blood pressure, BMI, and cigarette smoking were associated with increased carotid IMT in young adulthood. Sanchez et al. (21) performed a study of high school students. They found relationships between LDL-C, HDL-C, systolic blood pressure, diastolic blood pressure, and BMI with carotid artery IMT. Other studies have also found that children with elevated cholesterol levels have significantly elevated carotid artery IMT compared with controls (22). Sorof et al. (23) evaluated 32 children with hypertension. They found a significant association between carotid artery IMT and left ventricular mass after adjustment for age, sex, and BMI. In those patients with hypertension and increased carotid artery IMT, the prevalence of left ventricular hypertrophy was 89% compared with 25% in those with normal carotid artery IMT. Jarvisalo et al. (24) reported a significant association between C-reactive protein (CRP), which is a marker of inflammation, and carotid artery IMT. They also found an association between elevated CRP and impaired brachial artery flow-mediated dilation, which is a measure of endothelial function.

Juonala et al. (25) studied the relationship of cardiovascular risk factors measured in childhood with carotid IMT in adulthood in four large cohort studies: the Cardiovascular Risk in Young Finns Study, the Childhood Determinants of Adult Health Study, the Bogalusa Heart Study, and the Muscatine Study. They found significant relationships between childhood risk factors and adult carotid IMT that were dependent on the age at which childhood risk factors were measured. These data demonstrated that risk factor measurements obtained at age 9 years or older are predictive of subclinical atherosclerosis in adulthood.

Thus, it does appear that evaluation of the carotid arteries using ultrasound is a useful marker of preclinical atherosclerosis in children and adolescents (26). This method is currently used only in the research setting, but as it is studied in more detail, it may also ultimately be useful as a clinical test. In the meantime, other modalities are being investigated and may prove useful in the future.

Risk Factors for Atherosclerosis

Several risk factors have been established as being important in the development of atherosclerosis and ultimately in

TABLE 71.2 Possible Risk Factors for Atherosclerosis and Coronary Artery Disease

Inflammation
Elevated CRP
Socioeconomic status
Ethnicity
Physical activity/physical fitness
Diet

the occurrence of myocardial infarction and cerebrovascular disease. Dyslipidemia and hypertension are reviewed in detail in Sections “Lipids and Lipoproteins” and “Hypertension”. Other risk factors are discussed here briefly.

Diabetes

Diabetes is well established as a major risk factor for cardiovascular disease in adults (27). In the past, most pediatric patients with diabetes had type 1 diabetes mellitus. This was different from the experience with adults in whom the prevalence of type 2 diabetes mellitus was much higher. However, with the increasing prevalence and severity of obesity in the pediatric population, the prevalence of type 2 diabetes has increased dramatically (28). This is of critical importance from the standpoint of cardiovascular disease development. In adults, type 2 diabetes is responsible for more cases of renal failure and peripheral vascular disease than any other disease process (29). The risk of cardiovascular disease in patients with diabetes is increased by as much as fivefold compared with individuals without diabetes (30). It has been estimated that 70% of adult patients with type 2 diabetes die of cardiovascular disease (31), and the 10-year mortality rate for patients with type 2 diabetes is approximately 10 times higher than in a nondiabetic comparison group, with most deaths occurring as a result of coronary artery disease (32).

The predisposition to cardiovascular disease in patients with diabetes cannot be overemphasized. This is underscored by the recommendations of the American Diabetes Association (33) and the National Cholesterol Education Program (NCEP) (34), which consider the presence of diabetes to be a coronary artery disease risk equivalent. This means that patients with diabetes should be treated with the same aggressive approach to risk factor management that would be recommended in a patient who already has established coronary artery disease or who has had a myocardial infarction.

The risk status for cardiovascular disease in adolescents with type 2 diabetes is not well understood. However, if the progression of atherosclerosis is similar to that seen in adults, it can be anticipated that these patients may develop clinically apparent cardiovascular disease as early as their late thirties and early forties. Unfortunately, because so little is known about the progression of cardiovascular disease in young patients with type 2 diabetes, it is difficult to make evidence-based decisions regarding the optimum clinical strategies to prevent cardiovascular disease.

Some results regarding the relationship of diabetes and cardiovascular abnormalities have begun to emerge. Shah et al. (35) evaluated cardiac structure and function in adolescents with type 2 diabetes and those with obesity alone. They found that adolescents with obesity and with obesity-related type 2 diabetes had changes in cardiac geometry consistent with cardiac remodeling. Both groups also had decreased diastolic function when compared to lean controls with the greatest decrease in those with type 2 diabetes.

Urbina et al. (36) reported increased arterial stiffness, a marker for the development of atherosclerosis, in both adolescents with obesity and those with type 2 diabetes mellitus after controlling for other risk factors. Wadwa et al. (37) studied adolescents with type 1 and type 2 diabetes mellitus. They found that youth with type 2 diabetes had increased arterial stiffness compared to those with type 1 diabetes. In their study, increased central adiposity and blood pressure were associated with increased arterial stiffness independent of the type of diabetes. Urbina et al. (38) studied carotid IMT and stiffness in relation to obesity and type 2 diabetes and found that abnormalities in carotid thickness and stiffness are only partially explained by traditional cardiovascular risk factors. This suggests that more

research is needed to understand additional factors that may be related to this process. Shah et al. (39) reported that longer duration of diabetes and poorer glycemic control both have an independent association with carotid IMT in adolescents with type 2 diabetes. These results emphasize the need for improved blood glucose control to prevent the progression of cardiovascular disease in patients with type 2 diabetes.

Additional research will be needed to better define the optimum clinical approaches to young patients with type 2 diabetes. Nevertheless, it is important to manage the diabetes with appropriate weight management and blood glucose control methods. It is also important to evaluate cardiovascular risk factors in patients with diabetes and treat those risk factors when present.

Cigarette Smoking

Cigarette smoking is a major independent risk factor for cardiovascular disease (40). Although prevention of cigarette smoking is of the greatest importance, it has also been shown that cessation of smoking can provide a benefit by reducing risk of cardiovascular and lung disease. Investigators from the Multiple Risk Factor Intervention Trial (MRFIT) have reported that cessation of smoking will reduce the risk of the development of cardiovascular disease (41). This reduction of risk begins in the first year after cessation and continues to further reduction as long as 3 years after cessation.

In adolescents, atherosclerotic lesions have been seen with increased prevalence in cigarette smokers as young as 15 years of age. In addition, LDL-C is increased and HDL-C is decreased in adolescent smokers compared with their non-smoking counterparts (42). Chronic cigarette smoking may lead to injury of the endothelium, which serves as the nidus for the development of atherosclerosis. It has been estimated that of smoking-related deaths, cardiovascular disease is involved in over one-third, and this process often begins early in life (43).

Most individuals who become regular smokers initiate cigarette smoking in childhood and adolescence. Overall, approximately one of five high school students becomes a regular smoker. Many adolescents, while experimenting with smoking, believe that they can control their use of cigarettes. Unfortunately, this is not the case as many cannot quit smoking and continue to smoke on a regular basis. During the period from 1997 to 2003, overall smoking prevalence declined in high school students from >27% to 22% (44). Unfortunately, the prevalence of smoking in girls has increased over time, so now the prevalence is closer to equal for boys and girls (45). In 2009, the prevalence of cigarette smoking in adolescent high school students was 17.2% overall, 19.6% for adolescents boys, and 14.8% for girls (46). The major influences on initiation of smoking appear to be parents and peers smoking regularly (47,48). It has been shown that parent discussion of smoking, rules against smoking, and punishment for use of cigarettes all have a beneficial effect on decreasing adolescent smoking (48,49). Of greatest importance is that adolescents are significantly less likely to initiate smoking when parents quit smoking (50). Studies have also demonstrated an inverse association between physical activity and smoking, suggesting that an increased level of physical activity may protect against smoking initiation (51). These epidemiologic study results suggest important approaches to the prevention of the onset of cigarette smoking. Efforts of prevention should begin in elementary and middle school students because many children are already experimenting with cigarette smoking by age 10 years (52).

Exposure to environmental tobacco smoke may also be associated with increased risk of cardiovascular disease. Moskowitz et al. (53) reported lower HDL-C in boys exposed to environmental tobacco smoke compared with

those who were not exposed. Weitzman et al. (54) reported a dose-response relationship between exposure to tobacco smoke measured by serum cotinine and presence of the metabolic syndrome in 12- to 19-year-olds in the National Health and Nutrition Examination Survey III (NHANES III). In this population-based cohort, the prevalence of metabolic syndrome was 1.2% for nonexposed, 5.4% for those exposed to environmental tobacco smoke, and 8.7% for active smokers (54). The prevalence of metabolic syndrome for overweight adolescents was 19.6 for those exposed to environmental tobacco smoke and 23.6 for active smokers. These results emphasize that elimination of cigarette smoking in the household may have a dual benefit by directly reducing cardiovascular risk and by decreasing the risk for initiating active smoking. One of the most striking public health results comes from studies that show that banning smoking in public places, such as restaurants and bars, resulted in a dramatic decline in cardiovascular disease mortality (55,56). These results suggest that exposure to environmental tobacco smoke has a substantial deleterious effect.

Obesity/Metabolic Syndrome

The prevalence of overweight in children has more than tripled from 1980 to 2006. The prevalence nationally is approximately 17% for both children and adolescents (57). This increase in prevalence of overweight or obesity appears to be occurring worldwide.

The Muscatine and Bogalusa studies have shown that obesity in childhood and adolescence is associated with several risk factors for cardiovascular disease including atherogenic dyslipidemia (elevated triglycerides and low HDL-C), hypertension, left ventricular hypertrophy, atherosclerosis, and obstructive sleep apnea (9,58,59). When a child or adolescent is evaluated for overweight, it is important that assessment of cardiovascular risk factors be included as part of the evaluation.

Children and adolescents should be evaluated for overweight by calculating the BMI. This should then be compared with age- and sex-specific percentiles. Obesity is defined as a BMI ≥ 95 th percentile. BMI between the 85th and 95th percentiles is considered overweight (60). Treatment of overweight is difficult but can be accomplished by behavioral, pharmacologic, and surgical approaches (61–64). The U.S. Preventive Services Task Force has performed a systematic review of pediatric weight management programs (65). They concluded that the available research supports at least short-term benefits of comprehensive medium- to high-intensity behavioral interventions in obese children and adolescents. They also found no adverse impact of comprehensive weight management programs.

Barlow et al. (66) have presented recommendations for prevention, assessment, and treatment of obesity in children and adolescents. These recommendations include a graded approach to weight management depending on the level of BMI and the presence of comorbid conditions, such as diabetes, hypertension, dyslipidemia, obstructive sleep apnea, and nonalcoholic fatty liver disease.

An important consideration with obesity is the metabolic syndrome. This is a clustering of risk factors for diabetes and cardiovascular disease that is frequently observed in patients who are overweight, particularly with an increased central distribution of fat (67). Factors that are often included in the metabolic syndrome are listed in Table 71.3. Many definitions of the metabolic syndrome have been proposed for clinical use in adults. There have also been proposed definitions for children and adolescents. Most investigators have chosen to adopt a schema similar to that used in adults but have used age- and sex-specific percentiles to define clinical cutpoints

TABLE 71.3

Factors Considered Part of the Metabolic Syndrome

Obesity (particularly central obesity)

Atherogenic dyslipidemia

↓ Triglycerides

↑ HDL-C

Hypertension

Hyperinsulinemia

Impaired glucose metabolism

Inflammation

Prothrombotic factors

(68–70). However, investigators have chosen a wide range of cutpoints. This often results in a discontinuity between the child/adolescent definition and the adult definition. As might be expected, the choice of different risk factors and different cutpoints results in very different estimates of the prevalence of metabolic syndrome. One approach has been to use the variables in the metabolic syndrome complex as continuous variables rather than defining cutpoints (71). A particular concern about the metabolic syndrome is that it appears not to be a stable diagnosis throughout adolescence with some individuals gaining the diagnosis and others losing it over time (72). Further research is necessary to determine the optimum definition of the metabolic syndrome (73). Nevertheless, clinicians should be well aware of the clustering of cardiovascular risk factors that occurs with obesity. These factors should be evaluated in the child with obesity, and the risk factors should be treated when abnormalities are found.

Physical Activity

Strong et al. (74) have evaluated the effects of physical activity on health in school-aged youth. They identified a number of cardiovascular health issues that are related to diminished physical activity. Cardiovascular fitness has been identified as a risk factor for cardiovascular disease in adults (75). Physical fitness probably has both genetic and environmental influences. Strong et al. (74) identified several correlational studies indicating an association between low levels of vigorous physical activity and low levels of cardiovascular fitness. Experimental studies showed that exercise training can improve cardiovascular fitness in children 8 years of age and older. Generally, the successful programs included continuous vigorous exercise for >30 minutes per session at a minimum of 3 days per week.

Epidemiologic studies in children have generally shown a weak association between the level of physical activity and lipids and lipoproteins. The strongest associations are usually seen with HDL-C (74). The results of studies evaluating the relationship of cardiovascular fitness to lipids and lipoproteins mostly do not show a significant correlation. Intervention studies show a weak but beneficial effect primarily in improvement of triglyceride and HDL-C concentrations, usually in the context of improvement of BMI. One of the reasons for inconsistent results is the fact that different studies used different levels of intensity of physical activity with different frequencies of exercise episodes and different durations of treatment. From the available data, it appears that a minimum of 40 minutes of activity per day 5 days per week for 4 months is required to result in lower triglyceride and increased HDL-C levels (74).

Isometric or resistance exercise may also have a benefit in raising HDL-C levels. Goldberg et al. (76) found decreased LDL-C and increased HDL-C in adolescent boys who underwent a 9-week resistance exercise training program. These improvements were not related to changes in weight or adiposity.

There is no clear association between exercise and lower blood pressure in children with normal blood pressure (74). On the other hand, in adolescents with hypertension, aerobic activity programs of 12 to 32 weeks' duration have been shown to have a blood pressure-lowering effect. Strength training appears to have little effect on blood pressure in children with hypertension.

These results suggest that children and adolescents with essential hypertension should be encouraged to engage in aerobic activity on a regular basis. It is necessary to continue the physical activity to maintain the beneficial effect. An important aspect of the impact of physical activity is that it is also useful in management of overweight. Because many cardiovascular risk factors cluster with overweight, improvement in BMI is an important mechanism of action for increased physical activity. It has been shown that programs of moderate intensity lasting 30 to 60 minutes per episode with three to seven episodes per week can lead to a reduction in both total body and visceral adiposity in children and adolescents (74). Thus, it is clear that there are numerous beneficial effects to increasing the level of physical activity in children. This may also establish better exercise habits that will last into adulthood.

Summary

There has been increasing interest in the improvement of cardiovascular health (77). There is evidence that individuals who are able to maintain low-risk status with optimum levels of cardiovascular disease risk factors through childhood, adolescence, and adulthood to age 50 have a very low lifetime risk of cardiovascular disease (78). This puts the focus on primordial prevention, which is the prevention of development of risk factors in the first place. Unfortunately, currently the prevalence of ideal cardiovascular health is quite low. Bambs et al. (79) evaluated cardiovascular health in a cohort of 1,933 individuals (mean age 59 years, 44% African American, 66% women). They found that only 0.1% met the criteria of seven risk factor

and behavioral components. Less than 10% met ≥ 5 of these components. Thus, the prevalence of ideal cardiovascular health is currently quite low in a community-based sample of middle-aged adults. While there are genetic factors involved, there are clearly behavioral and lifestyle factors that are quite important. It is increasingly clear that pediatricians, family physicians, and pediatric cardiologists must play a critical role in developing and maintaining cardiovascular health. It is also clear that achievement of this will pay great dividends.

Atherosclerosis is a slow but progressive process that begins in childhood and progresses throughout adolescence and into adulthood. There are numerous risk factors for atherosclerosis in children, which generally parallel the risk factors in adults. Pediatricians and pediatric cardiologists should take an integrated approach to the prevention of cardiovascular disease and atherosclerosis (80,81). This type of approach will be necessary for reducing death and disability from cardiovascular disease, which is the major cause of death in the United States.

LIPIDS AND LIPOPROTEINS

Lipids are organic compounds that are not soluble in water but are soluble in organic solvents. Plasma lipids are transported by lipoproteins. This combination of lipids (including cholesterol triglycerides and phospholipids) and protein (called apolipoproteins) allows the lipid component to become soluble in water and blood. Lipids are important components of cell membranes and also serve as building blocks for some hormones.

The principal apolipoproteins are A-1, A-II, B-100, and C-II. Apolipoproteins have several functions. First, they bind with specific receptor sites in cells. They also are cofactors for enzymes involved in lipid metabolism such as lecithin cholesterol acyltransferase and lipoprotein lipase. Third, they function as structural protein for the biosynthesis and secretion of plasma lipoproteins. For example, Apo A-1 has been proposed as an important structural protein for the biosynthesis of HDL.

There are four major classes of lipoproteins including chylomicrons, very low density lipoproteins (VLDLs), low-density lipoproteins (LDLs), and high-density lipoproteins (HDLs) (Table 71.4).

TABLE 71.4 Lipids, Lipoproteins, and Apolipoproteins

Lipoprotein	Apolipoprotein	Source	Lipid Constituents	Factors that Influence Levels
Chylomicrons	Apo B-48 Apo A-1 Apo II Apo IV	Intestine	Exogenous triglycerides	Genetic Estrogen use, diabetes, alcohol, hypertriglyceridemia
VLDL	Apo B-100 Apo C-1 Apo C-II Apo C-III	Liver	Endogenous triglycerides, phospholipids	Genetic Excess carbohydrate, alcohol, or calories
LDL	Apo B-100	Breakdown of VLDL	Esterified cholesterol, triglycerides	Genetic Male sex, diabetes, LDL-receptor defects, intake of saturated fat and cholesterol
HDL	Apo A-1 Apo A-II Apo C-II Apo E	Liver and intestine breakdown of VLDL	Cholesterol, phospholipids	Genetic Low levels: male sex, diabetes, obesity, uremia, use of androgens or progestins, smoking; high levels: physical activity, alcohol intake

VLDL, very low density lipoprotein; LDL, low-density lipoprotein; HDL, high-density lipoprotein.

Chylomicrons are triglyceride-rich particles produced by the intestine. They are the largest lipoprotein. Their primary function is to transport cholesterol and triglycerides from the diet to sites for metabolism or storage (82). Chylomicrons are usually not present during fasting and normally are rapidly cleared after a meal. The clearance occurs as a result of lipoprotein lipase, which creates remnants of chylomicrons. These remnants are thought to be atherogenic and are cleared by the liver.

VLDL particles are also relatively large particles. VLDL is produced by the liver. VLDL transports triglycerides and cholesterol, which is endogenously synthesized, to the periphery (83).

LDL is the major carrier of cholesterol to peripheral tissues. LDL is made up of 45% cholesterol. LDL particles are found in atherosclerotic plaque and are associated with increased risk of cardiovascular disease (84). In particular, small dense LDL particles are considered especially atherogenic. LDL particles are recognized by specific receptors on the cell wall. When LDL particles bind to the receptor on the cell wall, they are then internalized into the cell. It has been estimated that approximately 75% of LDL particles are removed by binding with receptors, whereas the remaining particles are removed by macrophages (Fig. 71.3).

HDLs can be produced in several ways. They can be produced by the liver and the gastrointestinal tract. HDL particles are also produced by catabolism of chylomicrons and VLDL particles. HDL particles are also thought to be heterogeneous. HDL₂ is the subfraction that is thought to be most protective against atherosclerosis (85).

Normal Levels of Lipids and Lipoproteins

Normal values and distribution for plasma lipids and lipoproteins in American children have been published (86). These values have generally been used in subsequent guidelines to characterize children from a clinical perspective. These values are presented in Table 71.5.

Overall, total and LDL-C are lower in males than in females for most age groups. In children 5 to 10 years of age, HDL-C is lower in girls than in boys. It can be seen that HDL levels then gradually increase in girls and decrease in boys. The changes in concentration of lipids and lipoproteins during puberty can be important from a clinical perspective (87). LDL-C often declines during this period by as much as 10% to 20%. This means that some adolescents may experience a decline from an abnormal value to normal for a period of time. However, in the latter part of puberty, the LDL-C begins to rise and often continues to rise through adulthood.

The decline in HDL-C for males during puberty has been shown to extend into the adult ages. In young adults, HDL-C levels are approximately 10 mg/dL higher in women compared with men (88).

Epidemiology

Longitudinal studies such as the Framingham study and the MRFIT study have shown that the level of cholesterol in the blood is an important and independent predictor of coronary heart disease (89,90). It has been estimated that for each 1% increase in cholesterol, there is an approximately 3% increase in risk of cardiovascular disease (91). Studies have also consistently shown that higher levels of HDL-C are associated with a lower risk of cardiovascular disease (92).

There are international differences in levels of plasma cholesterol. In general, there are genetic and environmental influences on plasma cholesterol levels. The nutritional component most related to these differences appears to be the intake of saturated fat. In countries where intake of saturated fat in the diet is low, the blood total cholesterol levels are also low and the incidence of coronary heart disease is low (93).

Lipids and lipoproteins have been demonstrated to track over time. Tracking is an epidemiologic concept in which an individual retains their ranking with respect to their peers over time. For cholesterol, this means that, if tracking is present, a child with an elevated LDL-C will be more likely to become an adult with elevated LDL-C. Conversely, children with low levels relative to their peers will remain low over time. Epidemiologic studies of children and adolescents have shown that cholesterol levels do track, but that rank order is not maintained as consistently as it is for height and weight (94,95). In a separate analysis of the data from the Muscatine Study, Lauer et al. (96) evaluated factors that affect the relationship between cholesterol levels in childhood and adulthood. They found that cholesterol levels during childhood were important, but that obesity development, cigarette smoking, and the use of oral contraceptives in women had deleterious effects on cholesterol levels in adulthood.

Magnussen et al. (97) evaluated longitudinal data from the Childhood Determinants of Adult Health Study in which children in Australia were followed from 1985 until follow-up as young adults in 2004. They found that lifestyle changes that occur between youth and adulthood influence whether an individual maintains, loses, or develops high-risk blood lipid and lipoprotein levels in adulthood. The factors that are most important are excess weight gain, physical inactivity, and cigarette smoking.

Figure 71.3. Sequential steps in the LDL pathway in cultured mammalian cells. Vertical arrows suggest regulatory effects. HMG-CoA, β -hydroxy- β -methylglutaryl-coenzyme A; ACAT, acyl-CoA:cholesterol acetyltransferase. (From Brown MS, Goldstein JL. Receptor-mediated endocytosis: insights from the lipoprotein receptor system. *Proc Natl Acad Sci U S A* 1979;76:3330–3337, with permission.)

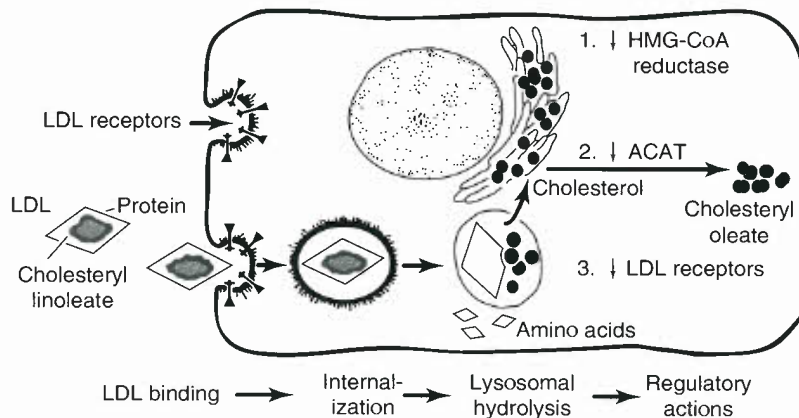


TABLE 71.5 Lipid and Lipoprotein Distributions in Children Aged 5 to 19 Years

Age (y)	Males							Females						
	Total Cholesterol (percentiles)							Total Cholesterol (percentiles)						
	5	10	25	50	75	90	95	5	10	25	50	75	90	95
5–9	125	131	141	153	168	183	189	131	135	150	164	177	189	197
10–14	124	132	144	161	173	191	204	125	131	142	159	171	191	205
15–19	118	123	135	152	168	183	191	119	126	140	157	176	198	208
	Triglyceride							Triglyceride						
	5	10	25	50	75	90	95	5	10	25	50	75	90	95
5–9	28	34	39	48	58	70	85	32	37	45	57	74	103	120
10–14	33	37	46	58	74	94	111	39	44	53	68	85	104	120
15–19	38	43	53	68	88	125	143	36	40	52	64	85	112	126
	LDL Cholesterol							LDL Cholesterol						
	5	10	25	50	75	90	95	5	10	25	50	75	90	95
5–9	63	69	80	90	103	117	129	68	73	88	98	115	125	140
10–14	64	73	82	94	109	123	133	68	73	81	94	110	126	136
15–19	62	68	80	93	109	123	130	59	73	78	93	110	129	137
	HDL Cholesterol							HDL Cholesterol						
	5	10	25	50	75	90	95	5	10	25	50	75	90	95
5–9	38	43	49	55	64	70	75	36	38	48	52	60	67	73
10–14	37	40	46	55	61	71	74	37	40	45	52	58	64	70
15–19	30	34	39	46	52	59	63	35	38	43	51	61	68	74

LDL, low-density lipoprotein; HDL, high-density lipoprotein.

Adapted from Tamir I, Heiss G, Glueck CJ, et al. Lipid and lipoprotein distributions in white children ages 6–19 yr. The Lipid Research Clinics Program Prevalence Study. *J Chronic Dis* 1981;34:27–39, with permission from Elsevier.

Factors Causing Dyslipidemia

Genetic

Lipid synthesis and metabolism is quite complex. Because there are numerous steps in the processes, they are vulnerable to genetic abnormalities that lead to dyslipidemia.

The most important and well-understood genetic abnormality is familial hypercholesterolemia. Brown and Goldstein (98) have described the LDL-C receptors that are associated with familial hypercholesterolemia. They have now described numerous mutations of the genes for the LDL receptor, which is a membrane glycoprotein. The most common LDL-C receptor gene mutations often result in a situation where the LDL receptor protein is produced only in small amounts. Other mutations result in the synthesis of precursors of the receptor that are not converted to the complex endoglycosidase H-resistant form. In these mutations, the receptors remain in the endoplasmic reticulum and are not available on the cell surface. A third type of mutation results in receptors that are expressed on the cell surface, but are unable to bind effectively with LDL-C. A fourth kind of mutation results in receptors that are on the cell surface and can bind with LDL-C but are unable to undergo receptor-mediated endocytosis (99). There is also a less common gain of function mutation in PCSK 9 that results in the rapid disposal of receptors, making them less accessible to bind with LDL-C (100). These mutations all result in the phenotype of elevation of plasma LDL-C.

Genetic abnormalities causing dyslipidemia are important to understand because they increase understanding of underlying mechanisms, and the prevalence for these disorders is relatively high. The prevalence of the homozygous form of familial hypercholesterolemia is 1 in 1,000,000. The prevalence of the heterozygous form of familial hypercholesterolemia is 1 in 500 (101). In some populations, the heterozygous form is as

common as 1 in 300. The heterozygous state is generally fully expressed in the pediatric age range, and it is characterized by total and LDL cholesterol levels of approximately 300 and 240 mg/dL, respectively. These levels may fall somewhat during pubertal maturation. Children and adolescents with the homozygous form of familial hypercholesterolemia have total and LDL cholesterol in the range of 600 to 1,000 mg/dL and 450 to 850 mg/dL, respectively. Homozygous patients develop planar xanthomas (orange-colored skin lesions found on extensor surfaces) by the age of 5 years and develop coronary artery disease between the ages of 10 and 20 years. Patients with homozygous familial hypercholesterolemia often also develop aortic stenosis (102). Patients with the heterozygous form rarely have xanthomas in adolescence. However, they are at risk for coronary artery disease between ages 30 and 50 years. Among individuals who have had a myocardial infarction prior to age 60 years, approximately 5% have the heterozygous form of familial hypercholesterolemia (103).

There are also genetic abnormalities that lead to low HDL-C. These may be due to a primary abnormality in the metabolism of HDL and its major apolipoprotein Apo A-1. This is a heterogeneous group of abnormalities that result in low HDL-C but may or may not lead to premature coronary artery disease (104).

There are also genetic abnormalities that lead to elevation of triglycerides. Familial hypertriglyceridemia is an autosomal dominant disorder but is often not expressed until adulthood (105). The development of obesity, however, can speed its expression. Lipoprotein lipase deficiency is a rare disorder that results in hypertriglyceridemia and can be a cause of pancreatitis and neurologic symptoms (106). The most important aspect of treatment of elevation of triglycerides is very aggressive restriction of dietary fat (107). This is because the level of chylomicrons is very dependent on the intake of total fat in the diet.

Familial combined hyperlipidemia includes the phenotype of elevated plasma LDL-C and triglyceride levels. It has a dominant genetic pattern. It is found in 1% of the adult population and in 10% of survivors of premature coronary artery disease. Children with parents who have familial combined hyperlipidemia may have elevated triglycerides and LDL-C (108). However, the levels of LDL-C are usually lower than in children with heterozygous familial hypercholesterolemia. The specific genetic abnormalities for familial combined hyperlipidemia have not been determined, but it is currently thought to result from multiple genes.

Lipoprotein (a) is a protein that is homologous to plasminogen. It consists of an LDL molecule with its Apo B-100 linked with a disulfide bridge to Apo (a). Higher levels of Lp (a) are associated with increased risk of cardiovascular disease in adults (109). Plasma levels of Lp (a) are inversely associated with the molecular weight of the Apo (a) component (110). Isoforms of Lp (a) are genetically determined. This means that levels of Lp (a) in the plasma are also largely inherited. Generally, levels of Lp (a) >30 mg/dL are associated with increased risk of coronary artery disease and stroke. Because of the homology between Lp (a) and plasminogen, there has been a question of whether increased levels of Lp (a) may also be associated with increased thrombosis. A study in children showed increased risk of thrombosis associated with increased Lp (a) (111). High levels of Lp (a) can be expressed in childhood and adolescence (112).

From a clinical perspective, it is quite difficult to lower LP (a). The only effective pharmacologic treatment is with nicotinic acid, which is difficult for most children and adolescents to tolerate. However, because of the increased risk of atherosclerotic cardiovascular disease associated with increased concentrations of LP (a), it is appropriate to use a more aggressive approach to lower LDL-C, when LP (a) concentrations are elevated.

Diet

Another major factor that influences plasma cholesterol is diet. This has been studied more extensively in adults than in children but seems to have similar effects across ages. The major dietary components that affect plasma cholesterol levels are fat and cholesterol. In particular, it is the amount of saturated fat in the diet that is associated with the level of plasma cholesterol. Saturated fat and cholesterol come primarily from animal-based foods. In addition, there are some plant-based oils that are high in saturated fat, such as palm oil.

It is these relationships that ultimately form the basis for nonpharmacologic treatment of cholesterol elevation. In animal models, those fed with increased levels of saturated fat and cholesterol had increased levels of plasma cholesterol and increased risk of atherosclerosis development (113).

Furthermore, reduction of dietary fat and cholesterol has been shown to result in lower plasma cholesterol concentrations and resolution of atherosclerotic plaque (114).

Secondary Causes of Cholesterol Elevation

There are several secondary causes of dyslipidemia. Selected causes and their underlying mechanisms are presented in Table 71.6. In addition to those listed, liver disease and obstructive jaundice, infection, and obesity are important secondary causes of abnormal cholesterol levels.

Abnormalities of lipids and lipoproteins are seen in both type 1 and type 2 diabetes. When control of diabetes is poor, triglycerides and LDL-C are often increased and HDL-C is decreased. Improved control of diabetes with intensive management of blood glucose can result in improved plasma lipids and lipoproteins (115–117).

Hypothyroidism is associated with increased triglycerides and LDL-C. HDL-C may also be decreased with hypothyroidism. Although it is usually possible to diagnose hypothyroidism by clinical signs and symptoms, occasionally the diagnosis is made because an abnormal fasting lipid profile is found. Appropriate treatment of hypothyroidism results in improvement of abnormal lipids and lipoproteins.

The nephrotic syndrome is a common secondary cause of dyslipidemia in children. Nephrotic syndrome is characterized by proteinuria, hypoalbuminemia, edema, and hypercholesterolemia. Generally, LDL-C is elevated. There may also be hypertriglyceridemia. In this condition, the liver responds to low albumin in the blood by increasing protein synthesis. This includes increased synthesis of the apolipoproteins. This increase in hepatic cholesterol synthesis leads to a down-regulation of LDL receptors in the liver, which in turn leads to a reduced rate of removal of LDL-C from the circulation (118). Usually, the length of exposure to increased LDL-C is short because nephrotic syndrome is easily recognized, is treated, and resolves. This may mean that the impact on the risk of atherosclerosis is low; however, the LDL-C level may be quite high prior to treatment (119).

Patients with chronic renal insufficiency are at high risk for cardiovascular disease (120). The dyslipidemia most commonly seen with chronic renal failure is elevation of triglycerides and a low HDL-C. This may be as prevalent as 30% (121). These abnormalities may contribute to the increased risk of cardiovascular disease seen in patients with chronic renal insufficiency. The hypertriglyceridemia of uremia results from deficiency of lipoprotein lipase or hepatic lipase. Treatment of patients with chronic renal insufficiency should include dietary changes to lower intake of saturated fat, cholesterol, and simple sugars. Increased physical activity may also be helpful in increasing HDL-C.

TABLE 71.6 Selected Secondary Causes of Dyslipoproteinemia

Disease	Elevated Lipoprotein	Mechanism
Type 1 diabetes mellitus	Triglycerides	Defective lipolysis of VLDL owing to inhibition of lipoprotein lipase and hepatic lipase
Type 2 diabetes mellitus	Triglycerides	Overproduction and defective lipolysis of VLDL triglycerides
Hypothyroidism	LDL, triglycerides	Suppression of LDL-receptor activity, overproduction of VLDL
Nephrotic syndrome	LDL, triglycerides	Overproduction of VLDL

VLDL, very low density lipoprotein; LDL, low-density lipoprotein.

Secondary dyslipidemia can result from taking certain medications. For example, estrogen- and progestin-containing contraceptives can result in elevation of triglycerides. Retinoic acid results in elevation of triglycerides in some patients. Anabolic steroids can cause increased LDL-C and lower HDL-C (122).

Acute and chronic infections can result in dyslipidemia. The causative organism and the chronicity of infection determine which lipid or lipoprotein is altered and to what extent (123). Gidding et al. (124) reported that HDL-C and apolipoprotein A-1 were significantly reduced after a recent viral infection in school-aged children. This means that a lipid profile should generally not be measured within 2 weeks of an acute infections.

Metabolic Syndrome

Obesity has been associated with a cluster of risk factors for cardiovascular disease called the metabolic syndrome (73,125). The metabolic syndrome includes increased waist circumference and atherogenic dyslipidemia that consists of elevated triglycerides and low HDL-C. Patients with the metabolic syndrome often also have insulin resistance. This is characterized by high circulating levels of insulin while fasting. There are a number of definitions for use in the clinical setting for diagnosis of the metabolic syndrome in children as well as adults. The prevalence of metabolic syndrome appears to be increasing in children and adolescents as the prevalence and severity of obesity is increasing (126).

The primary clinical approach to treating the metabolic syndrome is improvement in weight through changes in diet and physical activity. It has been shown that with weight management, the components of the metabolic syndrome, including atherogenic dyslipidemia, improve (127).

Clinical Recommendations

Guidelines from the NCEP for Children and Adolescents were first published in 1992 (128). These have been updated since that time, as a substantial amount of research has been done in screening and treatment of dyslipidemia in children (81,129). However, the overall framework presented in the original guidelines remains useful. These guidelines present both a population and an individual approach. The population approach addresses the diet and levels of physical activity that would result

in a healthy lifestyle for all children. The individual approach addresses the recommended guidelines for the identification and treatment of children and adolescents who are at the highest level of risk. This approach provides a more aggressive strategy for changes in diet than the population approach. The individual approach has been updated by the National Heart Lung and Blood Institute in a new set of evidence-based guidelines (81).

Population Approach

The overall goal of this approach is to improve the health of the pediatric population. If the recommended diet was adopted broadly, this would result in a lower prevalence of obesity and a lowering of the population mean for total and LDL cholesterol. It has been suggested by Rose (130) that a small shift in the population mean of a risk factor will result in substantially fewer individuals in the high-risk range. In addition, if lower levels of LDL-C are maintained from childhood into adolescence and adulthood, then it is likely that this would result in lower risk over time for this childhood population.

Diet

The United States Department Agriculture (USDA) guidelines provide diet recommendations for all children (131,132). The proposed diet for young children is somewhat different because infants and young children require a higher level of saturated fat and cholesterol in their diet to support development of the central nervous system. The first 2 years of life is a time when myelination of nerves is occurring. This process requires increased dietary fat intake. However, for children for whom there is a concern about obesity or an increased risk of cardiovascular disease, it is prudent to consider a lower saturated fat diet starting at 12 months of age. This may start with the introduction of lower fat milk at that time (130). This recommendation is supported by the results of the Special Turku Coronary Risk Factors Intervention Project (133). In this randomized controlled clinical trial, children were randomized to either a lower saturated fat diet or a routine higher fat diet at 6 months of age or at weaning. The participants of this study have been followed into their teenage years. There were no adverse effects of the lower saturated fat diet while there were beneficial effects on blood cholesterol (134). For older children, the USDA recommends a diet low in saturated fat and cholesterol (Table 71.7). There is evidence that this type

TABLE 71.7 Population Dietary Recommendations for Children and Adolescents

- Adequate nutrition should be achieved by eating a wide variety of foods low in saturated fat and cholesterol.
- Total caloric intake should be sufficient to support normal growth and development and maintain a desirable body weight.
- Saturated fatty acids should provide <10% of total calories.
- Total fat should provide an average of no >30% and no <20% of total calories.
- Polyunsaturated fatty acids should provide ≤10% of total calories.
- Children should consume <300 mg of cholesterol per day.
- Children should consume ≥5 daily servings of fruits and vegetables.
- Children should consume 6 to 11 daily servings of whole-grain and other grain products.
- Children should consume adequate amounts of dietary fiber (child's age + 5 g/d).

Based on the NCEP, USDA Dietary Guidelines, and The American Heart Recommendations.

Daniels SR, et al. NHLBI guidelines for evaluation, prevention and treatment of atherosclerotic cardiovascular disease in children and adolescents. *Pediatrics* 2011 ;128:S213–S256.

of diet will lower cholesterol levels in children and adolescents without having an adverse effect on growth and development (135,136).

The optimum percentages for dietary intake of macronutrients to reduce LDL-C the most and support normal growth and development are not known. It should also be emphasized that the recommendation of 25% to 30% of calories from fat is not necessarily a daily recommendation but should be a recommendation as an average over several days. This recognizes that daily intake may vary substantially for children based on whether they are in school and where and when they eat (129). Children and adolescents should generally not go below a level of fat intake that is 20% of calories. The purpose of this is to avoid over restriction of fat intake by parents, which could lead to failure to grow and thrive (137).

The population-based diet can also be effective for children with borderline elevation of LDL-C. The population diet can result in a lowering of LDL-C by 3% to 10% (138). Usually, it is necessary for patients to be on the diet for 3 to 6 months to adequately assess its effect.

To achieve the dietary recommendations, 5 to 6 oz/d of lean meats and 24 to 32 oz/d of low-fat dairy products are recommended. Lean cuts of meat include ground or lean meats that have had fat trimmed. Skin should be removed from poultry products. All types of fresh or frozen unbreaded fish are acceptable. Choices for dairy include low-fat or nonfat milk, yogurt, and cottage cheese. Cheeses that contain <6 g of fat/oz (<2 g/oz for the more-restrictive diet with <7% of calories from saturated fat) are acceptable. Eggs should be limited to <2 to 4 per week (131,132).

The largest portion of the child's diet should be made up of whole grains, cereals, fruits, and vegetables. Most of these food choices are high in fiber and low in saturated fat and cholesterol.

One concern with cereals and fruit juices is the intake of increased amounts of simple sugars. This may result in increased levels of plasma triglycerides (139). Other obvious sources of simple sugars are soft drinks and snack foods. Lower-fat and lower-sugar options for snacks include pretzels, graham crackers, and vanilla wafer cookies. Fruit should also be recommended as a healthful snack.

Another issue for the diet of children is the food they eat at school. For those who participate in the school lunch program, it is estimated that nearly 60% of children in the United States eat 25% to 30% of their saturated fat and cholesterol intake at that meal (128). However, schools increasingly offer additional competitive food items as part of their school lunch program. These foods are often higher in fat, saturated fat, cholesterol, and sugar and may be more attractive to children, leading to their increased selection and decreased selection of more nutrient-dense foods.

The population approach to cardiovascular health promotion also includes recommendations for physical activity. Although the optimum level of intensity is not known, increasing the duration and frequency of physical activity and decreasing sedentary time will allow children more flexibility in their diet. For example, the USDA has established recommendations for discretionary calories for children. These are "extra" calories that might be included in the diet once a healthful diet has been consumed and still maintain acceptable energy balance (131,132). The number of discretionary calories increases with age and with the level of physical activity. It is likely that many children are not getting the optimum amount of physical activity and are spending too much time on sedentary pursuits. The American Academy of Pediatrics has recommended no more than 2 h/d be spent on sedentary activities, including television viewing, computer time, and playing video games (140). This means that many children should have only 150 to 300 discretionary calories each day.

One factor that must be considered in implementing the population approach for both diet and physical activity is the role of socioeconomic status (141). Low-income families may have more barriers to purchasing healthful foods. Supermarkets in the inner city may be less convenient and may have lower availability of fresh fruits and vegetables. There are also concerns about neighborhood safety and the lack of opportunities for physical activity including organized sport or unsupervised free-time games.

Implementation of the population-based approach to cholesterol lowering requires the input and cooperation of a number of types of institutions. The government must be involved in improved food labeling and oversight of food assistance programs. Schools must be involved by creating an improved environment for both eating and physical activity. Health professionals should serve as resources for their communities and schools as they develop educational and other risk-reduction programs. In addition, the media can be helpful in the promotion of a healthful diet and increased levels of physical activity.

Individual Approach

The individual approach is directed at identifying children and adolescents who are at higher risk of future cardiovascular disease and treating them to lower their risk. This approach is probably most important from the standpoint of the pediatrician and the pediatric cardiologist. It is this approach that is focused in the physician's office.

Identification

To initiate the individual high-risk strategy, it is necessary to identify those children who are at higher risk of cardiovascular disease. This approach is directed at identifying children who are likely to have genetic dyslipidemias, who are at highest risk.

In adults, the Framingham risk score has been used to stratify risk (125). The use of this score is dependent on all adults having their risk factors including cholesterol measured on a regular basis. These values can then be used in an equation to estimate risk of a cardiovascular event over the next 10 years. Unfortunately, the data are not available to use a similar approach for children and adolescents. To construct a similar risk score for children would require large-scale longitudinal studies with complete follow-up in which risk factor levels are measured in childhood and subjects are followed until the occurrence of cardiovascular end points in adulthood. In fact, it is unlikely that such data will be available. This means that a different strategy will be needed to identify children at high risk.

The NCEP pediatric panel originally recommended a targeted approach to screening using the family history of cardiovascular disease or cholesterol elevation as the indicator for evaluation (128). However, since publication of the original NCEP guidelines, several studies have been performed to evaluate this approach (142–146). In general, these investigations have found that from 35% to 46% of adolescents would have cholesterol measurements based on their family history. These studies have also shown that many children with elevated cholesterol will be missed using a screening approach based on their family history. It is likely that this approach will miss 30% to 60% of pediatric patients with elevated cholesterol (147–149).

Difficulties with using the family history as a trigger for screening include that the family history may be incomplete or inaccurate. The family history would be more useful if all parents and grandparents knew their cholesterol levels, but, unfortunately, this is often not the case. In addition, parents (and sometimes grandparents) of younger children are often too young themselves to have reached the age when they are at greatest risk for a myocardial infarction or a stroke (149).

These problems with a targeted approach to screening have led to the recommendation of universal screening of all children at 9 to 11 years of age (81). In addition, children aged 2 years or older should have a lipid profile if they have a family history of premature cardiovascular disease (prior to age 55 in men or age 65 in women) or of dyslipidemia or with other cardiovascular disease risk factors, such as diabetes, hypertension, or obesity (81).

For universal screening, it is acceptable to use either a fasting lipid profile or a nonfasting non-HDL-C (total cholesterol—HDL-C). If the non-HDL-C is elevated, it should be confirmed with a fasting lipid profile. The focus of universal screening is to identify children with substantial elevation of LDL-C, usually as a result of a genetic dyslipidemia. However, it may also be useful to identify children with elevated triglycerides or a low HDL-C.

The recommended cutpoints for total, LDL, and non-HDL cholesterol are presented in Table 71.8. These cutpoints are used for children and adolescents aged 2 to 18 years. This use across a broad age range is recommended despite the fact that there is considerable variation of cholesterol with age during growth and development. This is especially true during the period of puberty (150–152). Total and LDL cholesterol tend to decline during puberty, meaning that some adolescents will appear normal when, in fact, they will have elevated levels after puberty. However, it has been shown that the proposed single cutpoints work well in practice (153).

The NHLBI has recommended that triglycerides >150 mg/dL and HDL-C <40 mg/dL be considered abnormal for children and adolescents (81).

Use of the Cutpoints

The NHLBI recommends that children and adolescents whose total and LDL cholesterol levels are in the elevated range be considered for treatment (81). Initially, this treatment should focus on improved diet with lower saturated fat and cholesterol. For treatment with pharmacologic agents, they suggest that patients be 8 years of age or older and have even higher levels of LDL-C as would be seen in a genetic form of dyslipidemia. The recommended levels for treatment with pharmacologic agents are presented in Table 71.9. The goal for treatment is to lower the LDL-C to <130 mg/dL, which would be lower than the 95th percentile for pediatric patients.

Treatment

The mainstay of all treatment for dyslipidemia is alteration of lifestyle including diet and the level of physical activity. The initial approach is to use the population-based diet, but to do so more aggressively and with the aid of a dietitian. Dietitians

can be helpful both in providing education about the fat and cholesterol content of foods and in providing behavioral strategies that improve the likelihood that the recommended diet will be adopted by the family and the pediatric patient. Parents can promote improvement in diet by making healthful foods available in the home and restricting the availability of foods that are high in energy density, fat, saturated fat, cholesterol, and simple sugars (154). Research has supported the concept that children will choose to eat foods that are available (155,156). It is important for children to try new foods multiple times to develop familiarity with and ultimately have a preference for these foods. Starting with these foods early in life is also helpful. A minimum of 8 to 10 exposures to new foods may be required before preference for these foods increases and is established (157,158).

For children with greater elevation of LDL-C, a more aggressive approach to diet than the population approach is needed. For these children and adolescents, the NHLBI recommends a diet with <7% of total calories from saturated fat and <200 mg/d of cholesterol. This more-restrictive diet often requires support from a dietitian to accomplish and can result in additional lowering of LDL-C by 4% to 14% (159,160).

Studies have shown that diet therapy is both safe and effective. The Dietary Intervention Study in Children (DISC) is probably the best study regarding this concept. In this investigation, children aged 8 to 10 years with elevated LDL-C were randomly assigned to an intervention group or a usual care group. The intervention group received behavioral intervention focused on adherence to a Step 2 Diet. This involved sessions with the family from 4 to 12 times per year over a 3-year period (161). LDL-C decreased by 15.4 mg/dL in the intervention group and 11.9 mg/dL in the control group. It is encouraging that a 7-year follow-up showed that the intervention effect was maintained and that growth and development continued to be normal in the intervention group (161).

Other studies have supported the results from the DISC study in a clinic setting (162,163). This emphasizes the concept that these changes can be made in practice in a safe and effective manner.

Increasing dietary fiber may also be useful in cholesterol lowering (164). Plant stanol and sterol esters have also been used. These compounds reduce cholesterol absorption from the gastrointestinal tract. Plasma cholesterol reduction of 7% to 15% has been reported using these compounds in a spread (165,166).

Pharmacologic Treatment

There are three main classes of medication used in the treatment of elevated LDL-C in children (167). These are listed in Table 71.10.

TABLE 71.8 Cutpoints for Total and LDL Cholesterol Levels in Children and Adolescents

Category	Percentile	Total Cholesterol (mg/dL)	LDL-C (mg/dL)	Non-HDL-C (mg/dL)
Acceptable	<75th	<170	<110	<120
Borderline	75th–95th	170–199	110–129	120–144
Elevated	>95th	>200	>130	>130

Adapted from Daniels SR, et al. NHLBI guidelines for evaluation, prevention and treatment of atherosclerotic cardiovascular disease in children and adolescents. *Pediatrics* 2011 ;128:S213–S256.

TABLE 71.9 Recommended Values for Pharmacologic Treatment of Children and Adolescents Aged 10 and Older

Patient Characteristics	Recommended Cutpoints
1. No other risk factors for CVD	LDL-C is persistently >190 mg/dL despite diet therapy
2. Other risk factors present including obesity, hypertension, diabetes, cigarette smoking, or positive family history of premature CVD	LDL-C is persistently >160 despite diet therapy

CVD, cardiovascular disease; LDL-C, low-density lipoprotein cholesterol.

Bile Acid Binding Agents. These medications are attractive because they have been available for a long time, are operative in the gastrointestinal tract, and are not absorbed systemically. In addition, their side effects are limited to gastrointestinal discomfort. These side effects can be minimized with increased

intake of water and fiber. Unfortunately, adherence with these medications is often limited because they are difficult for children to take. The powder forms are gritty and must be mixed with juice or water. Even with this mixture, they are difficult to take. The tablet forms are more palatable, but the tablets are

TABLE 71.10 Pharmacologic Intervention for Dyslipidemia in Children

Class	Dose	Side Effects
<i>Bile acid sequestrant</i>		
Colestipol Provided as granules or tablets	1 packet or 1 level scoopful of flavored granules contains 5 g of colestipol hydrochloride. Also comes as tablets; 1–4 tablets/d.	Limited to GI symptoms: constipation, bloating, abdominal cramping. May bind with other medication
Cholestyramine Provided as powder; 1 package contains 4 g	Dose is related not to the weight of the child but to levels of total and LDL cholesterol. Should be started on the lowest dose, 1 package (4 g) and then dosage may be increased over time to daily, 4 packages/d for those most severely affected.	GI symptoms
Colesevelam	Doses of 375-mg capsules/d and 625-mg tablet/d.	GI symptoms
<i>Cholesterol absorption blocker</i>		
Ezetimibe The long-term safety and effectiveness have not been established in children and adolescents	10-mg tablets. The dose recommended is 1 tablet/d.	GI symptoms, liver enzyme elevation, skeletal muscle effects, including myopathy and rhabdomyolysis
<i>HMG-CoA reductase inhibitors</i>		
Atorvastatin	Available in 10-, 20-, 40-, and 80-mg tablets.	Patients on statins should be advised of the risk of myopathy. If muscle pains occur, measurement of CK should be obtained. With increasing doses, liver dysfunction may occur. Measurement of liver function should be obtained prior to drug use and again 6–12 wk after initial therapy or initiation of higher doses and periodically thereafter (e.g., q3mo). May be teratogenic; control advised for use in adolescent females.
Simvastatin The long-term safety and efficacy have not been established in children. In adolescent males, it has been shown to be safe and effective.	Available in 5-, 10-, 20-, 40-, and 80-mg tablets. Dosage is started low and increased as required to lower LDL-C.	

GI, gastrointestinal; LDL, low-density lipoprotein; CK, creatine kinase.

large and difficult for some children to swallow (168–170). If used appropriately, bile acid binding agents can lower LDL-C from 13% to 20% (168–170). The reduction is seen in addition to the cholesterol-lowering effect of diet.

Colesevelam is another medication in the bile acid binding class of medications. The safety and efficacy of colesevelam has been evaluated in a clinical trial of pediatric patients with heterozygous familial hypercholesterolemia (171). They found that colesevelam lowered LDL-C by 6.3% to 12.5% compared to placebo. There were no important adverse effects, and adherence to the medication regimen was good.

Inhibitors of Cholesterol Absorption. Ezetimibe works by blocking cholesterol absorption in the gastrointestinal tract. It is FDA approved for adults, but has not been extensively studied in pediatric patients. Ezetimibe has been shown to reduce LDL-C levels by approximately 20% in adults (172). In adults, ezetimibe is used primarily in combination with statins to achieve additional cholesterol lowering. Because it comes in a single-dose level and because it has so few side effects and is easier to take than bile acid binding agents, it may be attractive as an initial agent for cholesterol lowering in pediatric patients.

HMG-CoA Reductase Inhibitors. HMG-CoA (β -hydroxy- β -methylglutaryl-coenzyme A) medications are usually referred to as statins. These medications competitively inhibit mevalonate synthesis by HMG-CoA reductase. This process is essential for biosynthesis of cholesterol in the liver. In studies of adults, these medications have been shown to be effective in both lowering plasma LDL-C and prevention of cardiovascular end points. This appears to be true of both primary prevention (prevention of an initial myocardial infarction) and secondary prevention (prevention of subsequent myocardial infarctions) (173–175).

A Cochrane review of the use of statins in primary prevention of cardiovascular disease has been published (176). They evaluated 14 randomized controlled clinical trials including more than 34,000 participants. All-cause mortality was reduced by the use of statins, as was combined fatal and nonfatal CVD endpoints, including revascularization. There was no evidence of important adverse events. However, there was some concern about selective reporting of outcomes. There is also some concern about the cost-effectiveness of statins for primary prevention of cardiovascular disease. This may be improved by the availability of cheaper generic forms of statin medication.

Several studies have been performed to evaluate the safety and efficacy of statins in children and adolescents (167,177–183). These studies, although not long-term investigations, have shown effective lowering of LDL-C with minimal side effects and no adverse effect on growth and development.

There have also been studies of statins that have evaluated vascular structure and function as endpoints. De Jongh et al. (181) studied simvastatin and found that after 28 weeks, flow-mediated dilation assessed by vascular ultrasound of the brachial artery was improved to normal levels in patients treated with 40 mg simvastatin compared to no improvement in the placebo group. Wiegman et al. (183) assessed carotid IMT in a clinical trial of pravastatin in children with familial hypercholesterolemia. Participants in the placebo group showed progression of carotid-intima media thickness over 2 years, suggesting progression of atherosclerosis. Those treated with pravastatin demonstrated regression of carotid IMT.

Children and adolescents who are treated with medication for hypercholesterolemia should be started on a low dose of medication with upward titration based on the LDL-C concentrations. Increasing the dose can further lower cholesterol but may also be associated with an increased risk of side effects.

The side effects of statin agents are an increase in hepatic transaminases and elevation of creatine kinase. Statins have also been associated with myositis, which can progress to rhabdomyolysis. If symptoms of abnormal muscle aches or

cramps are present, then creatine kinase should be measured and the medication should be discontinued.

Another concern regarding the use of statins in adolescent females is the potential for these medications to be teratogenic. Women taking statins should use reliable contraception if they are sexually active. Pregnancies should be planned and the medication discontinued prior to pregnancy and through delivery and the duration of breast-feeding. These agents should be used with caution in adolescent females.

A recent meta-analysis of adult patients taking statins has demonstrated a small but measurable increase in risk of type 2 diabetes mellitus in those taking statins, particularly at higher doses (184). While there are potential side effects of statins, they are relatively rare and, on balance, it is clear that the benefits of substantial LDL-C reduction, reduction of inflammation (185), and lowering the risk of adverse cardiovascular disease endpoints outweigh the risks.

Summary

It is clear that cholesterol elevation can contribute to the development of cardiovascular disease owing to atherosclerosis. This means that it is important to identify children and adolescents who are at high risk because of elevated LDL-C. Once such pediatric patients are identified, appropriate dietary treatment should be implemented. When dietary treatment is insufficient, then pharmacologic therapy should be considered in those patients who continue to have substantial elevation of their LDL-C.

HYPERTENSION

Epidemiology

Blood pressure elevation is established as an important risk factor for the development of cardiovascular disease in adults. In the Framingham study, elevated blood pressure is associated with increased incidence of myocardial infarction, cerebrovascular disease, left ventricular hypertrophy, and congestive heart failure (186). A 10-mm Hg increase in systolic blood pressure is associated with a 20% increase in risk of cardiovascular events in adults aged 35 to 64 years (187).

There are numerous potential causes of blood pressure elevation. The most common cause of hypertension in both children and adults is primary hypertension. The mechanism of primary hypertension is not known. It clusters in families, so presumably it has a genetic cause. Primary hypertension may have a heterogeneous cause as some individuals with hypertension have increased sensitivity to salt in the diet, whereas others may have increased activity of the renin-angiotensin-aldosterone system, and still others have increased activity of the sympathetic nervous system. Secondary hypertension is also heterogeneous and may occur as a result of renal parenchymal disease, coarctation of the aorta, renal artery stenosis, and other underlying disease entities.

In adults, it is estimated that 92% to 95% of cases of hypertension are due to essential hypertension (188). Essential hypertension is also the most common form of hypertension in children and adolescents with as many as 90% to 95% of cases without an identifiable cause in primary care clinic-based and population-based studies (189,190).

High blood pressure in children and adolescents is based on percentile values as opposed to a single cutpoint, which is used for adults. For pediatric patients, the 95th percentile based on previous large epidemiologic studies is used to define high blood pressure. For hypertension, the blood pressure must be

elevated persistently over time. The prevalence of hypertension has been previously estimated to be 1% to 3% for children and adolescents (191). More recent estimates have placed the prevalence at approximately 5% (192–194). It appears that average blood pressure may be increasing across the pediatric population over time. Muntner et al. (195) have shown that average blood pressures are higher in more recent national surveys compared with previous surveys. In a multivariable analysis, they also showed that this increase was at least in part owing to population increases in BMI.

Body weight or BMI is the strongest determinant of blood pressure in children. Rosner et al. (196) found that the odds of elevated blood pressure were significantly higher for children in the upper decile compared with the lower decile of BMI. Paradis et al. (197) found that the mean BMI for subjects with elevated systolic blood pressure was 4 to 6 kg/m² higher than in subjects with systolic blood pressure <25th percentile. Sorof et al. (192) found that the strongest determinant of hypertension in a study of school-aged children was BMI. They found that the prevalence of elevated blood pressure after three sequential measurements was 11% for children with BMI > 95th percentile compared with 2% in those with BMI < 5th percentile. These results emphasize that abnormal weight gain and obesity are pivotal factors in blood pressure elevation in children and adolescents (198).

Birth Weight and Blood Pressure

Barker (199) has proposed that birth weight is an important determinant of blood pressure elevation later in life. He hypothesized that infants born with low birth weight owing to fetal undernutrition would have decreased renal mass and changes in vascular structure and function and that these abnormalities would predispose to future hypertension.

Law et al. (200) evaluated this relationship in young adults. They found that lower birth weight and greater weight gain between age 1 and 5 years were correlated with higher blood pressure at age 22. However, not all studies have found this association. Matthes et al. (201) did not find a difference in systolic blood pressure of adolescents with low birth weight compared with those with normal birth weight.

Tracking

In general, there is a continuous rise in blood pressure from infancy through adolescence. However, at any age, there is a wide distribution of blood pressure for both systolic and diastolic blood pressure. The concept of tracking refers to the tendency for individuals to maintain their rank order compared with their peers over time. This means that those with higher blood pressures at one age would also tend to be higher later in life. This would also indicate that those individuals would be at higher risk for cardiovascular disease morbidity and mortality later in life.

Longitudinal studies have shown that blood pressures do tend to track over time for children and adolescents (202,203). Although tracking of blood pressure is reasonably good from an epidemiologic standpoint, there is also substantial variability of blood pressure over time. The prediction of blood pressure at a later age is not as accurate as is the prediction of height from measurements at a younger age (204). However, Cook et al. (205) have shown that the ability to predict future blood pressure level is improved when multiple measurements are taken over several years during childhood.

It has been shown that much of the variability in blood pressure results from variability in weight and BMI, as well as growth (206). In the Muscatine Study, in addition to the current level of blood pressure, changes in weight and adiposity were the most important predictors of future blood pressure (203).

As with cholesterol, the fact that tracking exists for blood pressure over time does not ensure that children who are

destined to have hypertension in adulthood can be readily identified. Results from the Bogalusa study show that of the adults with hypertension, >40% had been in the top 20% in the distribution of blood pressure during childhood (202). Children who maintain a relatively high level of blood pressure over time are, on average, taller, have greater adiposity, and have greater bone age and more advanced pubertal development than their peers (206,207). Data from the Muscatine Study show that of young adults with high systolic blood pressure, 45% had at least one systolic blood pressure measurement in childhood that was >90th percentile and that of adults with elevated diastolic blood pressure, 40% had a diastolic blood pressure elevated during childhood (203).

This raises some question regarding the utility of blood pressure screening in children and adolescents. Wang et al. (208) evaluated the long-term effectiveness and cost-effectiveness of three approaches to managing elevated blood pressure in adolescents. The approaches were (a) no intervention, (b) screen and treat, and (c) population-wide strategies to lower the entire blood pressure distribution. They found that routine screening is moderately effective, but population-based strategies could also be cost-effective for early cardiovascular disease prevention. They recommended that both strategies be implemented in parallel.

Target Organ Effects

Hypertension is associated with increased risk for cardiovascular disease in adults, and treatment of hypertension results in decreased risk over time (209). Elevated blood pressure is also a component of the metabolic syndrome, which is associated with increased risk of cardiovascular disease in adults (73,210). It has been less clear whether hypertension in childhood is related to the development of cardiovascular disease. It has been well known that severe blood pressure elevation, often owing to a secondary cause of hypertension, can result in cerebrovascular disease, hypertensive encephalopathy, congestive heart failure, and even death (195–199). It has been less clear whether milder forms of hypertension including primary hypertension are associated with cardiovascular disease.

The Bogalusa Study and PDAY study have shown that blood pressure elevation is related to the presence of fatty streaks and fibrous plaques in the aorta and coronary arteries (216,217). This means that systemic blood pressure elevation plays an important role in the early stages of the development of atherosclerosis.

Blood pressure elevation has also been associated with increased left ventricular mass in children and adolescents (218–220). This is important because left ventricular hypertrophy has been established as an independent risk factor for cardiovascular disease in adults (221,222). Daniels et al. (218) reported that 55% of pediatric patients with essential hypertension had left ventricular mass index >90th percentile for normal children and 8% had left ventricular mass above the cutpoint of 51 g/m^{2.7} that has been associated with a fourfold increase in adverse cardiovascular events in adults with primary hypertension (222). Studies have used ultrasound to evaluate the carotid artery IMT as a noninvasive surrogate marker of atherosclerosis. Some studies have found an association between blood pressure elevation and increased carotid IMT (223), whereas others have not (224). This is an area that will require further study.

Data are now emerging on the effects of treatment of hypertension on left ventricular mass and other target organ abnormalities. Litwin et al. assessed the effects of 12 months of nonpharmacologic and pharmacologic intervention on left ventricular mass index, left ventricular hypertrophy, and carotid IMT (225). They found that average left ventricular mass index decreased (38.5 ± 10.7 vs. 35.2 ± 7.5 g/m^{2.7}), the prevalence of

left ventricular hypertrophy decreased (46.5% vs. 31.4%), and there was a decrease in carotid IMT (0.44 ± 0.05 vs. 0.42 ± 0.04 mm). All of the results were statistically significant ($p < 0.001$). These are encouraging results that suggest that standard management of hypertension can lead to regression of target organ abnormalities in children with hypertension.

In adults, hypertension is associated with decreased performance on objective physical and cognitive function, even in the absence of subjective symptoms (226). The underlying mechanisms of those relationships have not been clear. Hajjar et al. investigated the association between hypertension and impairment of mobility, cognition, and mood. They also performed brain MRI to evaluate potential abnormalities (227). They found that hypertension increases the risk of concurrent impairments in mobility, cognition, and mood, which were associated with increased disability and mortality. These associations were partly mediated by microvascular injury (white matter hyperintensities) of the brain.

There have also been studies of the potential association between blood pressure elevation and neurocognitive abnormalities in pediatric patients. Lande et al. (228) found that there was an association between elevated blood pressure and decreased cognitive function in school-aged children and adolescents, using data from the NHANES III. Children with elevated systolic blood pressure had lower average scores for digit span, block design, and mathematics compared to children with normal blood pressure. Adams et al. (229) reported that the prevalence of learning disabili-

ties was higher in children with primary hypertension compared to those without hypertension. Lande et al. (230) reported that parental ratings of their child's executive function improved after 12 months of antihypertensive treatment. Taken together, these results emphasize the broad range of target organ abnormalities that can be associated with hypertension in children and adolescents. They also emphasize that treatment of elevated blood pressure can result in improvements in neurocognitive and cardiovascular function.

For most children, blood pressure elevation is not associated with any adverse symptoms. Therefore, most children and their families cannot recognize that blood pressure is elevated. This is why accurately obtained blood pressure measurements are recommended in the clinical setting as part of well child care. This is also why additional testing such as echocardiography is recommended in pediatric patients who are identified with blood pressure elevation, to determine if the blood pressure elevation is having an adverse effect on target organs.

Normal Blood Pressure

Tables for normal blood pressure have been developed from combining data from large epidemiologic studies of blood pressure in children. These values are presented in Tables 71.11 and 71.12. These blood pressures represent values measured in the sitting position using auscultation. It

TABLE 71.11 Blood Pressure Levels for Girls by Age and Height Percentile

Age (y)	BP Percentile ↓	Systolic BP (mm Hg)							Diastolic BP (mm Hg)						
		Percentile of Height							Percentile of Height						
		5th	10th	25th	50th	75th	90th	95th	5th	10th	25th	50th	75th	90th	95th
1	50th	80	81	83	85	87	88	89	34	35	36	37	38	39	39
	90th	94	95	97	99	100	102	103	49	50	51	52	53	53	54
	95th	98	99	101	103	104	106	106	54	54	55	56	57	58	58
	99th	105	106	108	110	112	113	114	61	62	63	64	65	66	66
2	50th	84	85	87	88	90	92	92	39	40	41	42	43	44	44
	90th	97	99	100	102	104	105	106	54	55	56	57	58	58	59
	95th	101	102	104	106	108	109	110	59	59	60	61	62	63	63
	99th	109	110	111	113	115	117	117	66	67	68	69	70	71	71
3	50th	86	87	89	91	93	94	95	44	44	45	46	47	48	48
	90th	100	101	103	105	107	108	109	59	59	60	61	62	63	68
	95th	104	105	107	109	110	112	113	63	63	64	65	66	67	67
	99th	111	112	114	116	118	119	120	71	71	72	73	74	75	75
4	50th	88	89	91	93	95	96	97	47	48	49	50	51	51	52
	90th	102	103	105	107	109	110	111	62	63	64	65	66	66	67
	95th	106	107	109	111	112	114	115	66	67	68	69	70	71	71
	99th	113	114	116	118	120	121	122	74	75	76	77	78	78	79
5	50th	90	91	93	95	96	98	98	50	51	52	53	54	55	55
	90th	104	105	106	108	110	111	112	65	66	67	68	69	69	70
	95th	108	109	110	112	114	115	116	69	70	71	72	73	74	74
	99th	115	116	118	120	121	123	123	77	78	79	80	81	81	82
6	50th	91	92	94	96	98	99	100	53	53	54	55	56	57	57
	90th	105	106	108	110	111	113	113	68	68	69	70	71	72	72
	95th	109	110	112	114	115	117	117	72	72	73	74	75	76	76
	99th	116	117	119	121	123	124	125	80	80	81	82	83	84	84

(continued)

TABLE 71.11 Blood Pressure Levels for Girls by Age and Height Percentile (Continued)

Age (y)	BP Percentile ↓	Systolic BP (mm Hg)							Diastolic BP (mm Hg)						
		Percentile of Height							Percentile of Height						
		5th	10th	25th	50th	75th	90th	95th	5th	10th	25th	50th	75th	90th	95th
7	50th	92	94	95	97	99	100	101	55	55	56	57	58	59	59
	90th	106	107	109	111	113	114	115	70	70	71	72	73	74	74
	95th	110	111	113	115	117	118	119	74	74	75	76	77	78	78
	99th	117	118	120	122	124	125	126	82	82	83	84	85	86	86
8	50th	94	95	97	99	100	102	102	56	57	58	59	60	60	61
	90th	107	109	110	112	114	115	116	71	72	72	73	74	75	76
	95th	111	112	114	116	118	119	120	75	76	77	78	79	79	80
	99th	119	120	122	123	125	127	127	83	84	85	86	87	87	88
9	50th	95	96	98	100	102	103	104	57	58	59	60	61	61	62
	90th	109	110	112	114	115	117	118	72	73	74	75	76	76	77
	95th	113	114	116	118	119	121	121	76	77	78	79	80	81	81
	99th	120	121	123	125	127	128	129	84	85	86	87	88	88	89
10	50th	97	98	100	102	103	105	106	58	59	60	61	61	62	63
	90th	111	112	114	115	117	119	119	73	73	74	75	76	77	78
	95th	115	116	117	119	121	122	123	77	78	79	80	81	81	82
	99th	122	123	125	127	128	130	130	85	86	86	88	88	89	90
11	50th	99	100	102	104	105	107	107	59	59	60	61	62	63	63
	90th	113	114	115	117	119	120	121	74	74	75	76	77	78	78
	95th	117	118	119	121	123	124	125	78	78	79	80	81	82	82
	99th	124	125	127	129	130	132	132	86	86	87	88	89	90	90
12	50th	101	102	104	106	108	109	110	59	60	61	62	63	63	64
	90th	115	116	118	120	121	123	123	74	75	75	76	77	78	79
	95th	119	120	122	123	125	127	127	78	79	80	81	82	82	83
	99th	126	127	129	131	133	134	135	86	87	88	89	90	90	91
13	50th	104	105	106	108	110	111	112	60	60	61	62	63	64	64
	90th	117	118	120	122	124	125	126	75	75	76	77	78	79	79
	95th	121	122	124	126	128	129	130	79	79	80	81	82	83	83
	99th	128	130	131	133	135	136	137	87	87	88	89	90	91	91
14	50th	106	107	109	111	113	114	115	60	61	62	63	64	65	65
	90th	120	121	123	125	126	128	128	75	76	77	78	79	79	80
	95th	124	125	127	128	130	132	132	80	80	81	82	83	84	84
	99th	131	132	134	136	138	139	140	87	88	89	90	91	92	92
15	50th	109	110	112	113	115	117	117	61	62	63	64	65	66	66
	90th	122	124	125	127	129	130	131	76	77	78	79	80	80	81
	95th	126	127	129	131	133	134	135	81	81	82	83	84	85	85
	99th	134	135	136	138	140	142	142	88	89	90	91	92	93	93
16	50th	111	112	114	116	118	119	120	63	63	64	65	66	67	67
	90th	125	126	128	130	131	133	134	78	78	79	80	81	82	82
	95th	129	130	132	134	135	137	137	82	83	83	84	85	86	87
	99th	136	137	139	141	143	144	145	90	90	91	92	93	94	94
17	50th	114	115	116	118	120	121	122	65	66	66	67	68	69	70
	90th	127	128	130	132	134	135	136	80	80	81	82	83	84	84
	95th	131	132	134	136	138	139	140	84	85	86	87	87	88	89
	99th	139	140	141	143	145	146	147	92	93	93	94	95	96	97

BP, blood pressure.

Reproduced with permission from Falkner B, Daniels SR, Flynn JT, et al. The fourth report on the diagnosis, evaluation and treatment of high blood pressure in children and adolescents. *Pediatrics* 2004;114:555–576, Copyright © 2004 by the AAP.

TABLE 71.12 Blood Pressure Levels for Boys by Age and Height Percentile

Age (y)	BP Percentile ↓	Systolic BP (mm Hg)							Diastolic BP (mm Hg)						
		Percentile of Height							Percentile of Height						
		5th	10th	25th	50th	75th	90th	95th	5th	10th	25th	50th	75th	90th	95th
1	50th	80	81	83	85	87	88	89	34	35	36	37	38	39	39
	90th	94	95	97	99	100	102	103	49	50	51	52	53	53	54
	95th	98	99	101	103	104	106	106	54	54	55	56	57	58	58
	99th	105	106	108	110	112	113	114	61	62	63	64	65	66	66
2	50th	84	85	87	88	90	92	92	39	40	41	42	43	44	44
	90th	97	99	100	102	104	105	106	54	55	56	57	58	58	59
	95th	101	102	104	106	108	109	110	59	59	60	61	62	63	63
	99th	109	110	111	113	115	117	117	66	67	68	69	70	71	71
3	50th	86	87	89	91	93	94	95	44	44	45	46	47	48	48
	90th	100	101	103	105	107	108	109	59	59	60	61	62	63	63
	95th	104	105	107	109	110	112	113	63	63	64	65	66	67	67
	99th	111	112	114	116	118	119	120	71	71	72	73	74	75	75
4	50th	88	89	91	93	95	96	97	47	48	49	50	51	51	52
	90th	102	103	105	107	109	110	111	62	63	64	65	66	66	67
	95th	106	107	109	111	112	114	115	66	67	68	69	70	71	71
	99th	113	114	116	118	120	121	122	74	75	76	77	78	78	79
5	50th	90	91	93	95	96	98	98	50	51	52	53	54	55	55
	90th	104	105	106	108	110	111	112	65	66	67	68	69	69	70
	95th	108	109	110	112	114	115	116	69	70	71	72	73	74	74
	99th	115	116	118	120	121	123	123	77	78	79	80	81	81	82
6	50th	91	92	94	96	98	99	100	53	53	54	55	56	57	57
	90th	105	106	108	110	111	113	113	68	68	69	70	71	72	72
	95th	109	110	112	114	115	117	117	72	72	73	74	75	76	76
	99th	116	117	119	121	123	124	125	80	80	81	82	83	84	84
7	50th	92	94	95	97	99	100	101	55	55	56	57	58	59	59
	90th	106	107	109	111	113	114	115	70	70	71	72	73	74	74
	95th	110	111	113	115	117	118	119	74	74	75	76	77	78	78
	99th	117	118	120	122	124	125	126	82	82	83	84	85	86	86
8	50th	94	95	97	99	100	102	102	56	57	58	59	60	60	61
	90th	107	109	110	112	114	115	116	71	72	72	73	74	75	76
	95th	111	112	114	116	118	119	120	75	76	77	78	79	79	80
	99th	119	120	122	123	125	127	127	83	84	85	86	87	87	88
9	50th	95	96	98	100	102	103	104	57	58	59	60	61	61	62
	90th	109	110	112	114	115	117	118	72	73	74	75	76	76	77
	95th	113	114	116	118	119	121	121	76	77	78	79	80	81	81
	99th	120	121	123	125	127	128	129	84	85	86	87	88	88	89
10	50th	97	98	100	102	103	105	106	58	59	60	61	61	62	63
	90th	111	112	114	115	117	119	119	73	73	74	75	76	77	78
	95th	115	116	117	119	121	122	123	77	78	79	80	81	81	82
	99th	122	123	125	127	128	130	130	85	86	86	88	88	89	90
11	50th	99	100	102	104	105	107	107	59	59	60	61	62	63	63
	90th	113	114	115	117	119	120	121	74	74	75	76	77	78	78
	95th	117	118	119	121	123	124	125	78	78	79	80	81	82	82
	99th	124	125	127	129	130	132	132	86	86	87	88	89	90	90
12	50th	101	102	104	106	108	109	110	59	60	61	62	63	63	64
	90th	115	116	118	120	121	123	123	74	75	75	76	77	78	79
	95th	119	120	122	123	125	127	127	78	79	80	81	82	82	83
	99th	126	127	129	131	133	134	135	86	87	88	89	90	90	91

(continued)

TABLE 71.12 Blood Pressure Levels for Boys by Age and Height Percentile (Continued)

Age (y)	BP Percentile ↓	Systolic BP (mm Hg)							Diastolic BP (mm Hg)						
		Percentile of Height							Percentile of Height						
		5th	10th	25th	50th	75th	90th	95th	5th	10th	25th	50th	75th	90th	95th
13	50th	104	105	106	108	110	111	112	60	60	61	62	63	64	64
	90th	117	118	120	122	124	125	126	75	75	76	77	78	79	79
	95th	121	122	124	126	128	129	130	79	79	80	81	82	83	83
	99th	128	130	131	133	135	136	137	87	87	88	89	90	91	91
14	50th	106	107	109	111	113	114	115	60	61	62	63	64	65	65
	90th	120	121	123	125	126	128	128	75	76	77	78	79	79	80
	95th	124	125	127	128	130	132	132	80	80	81	82	83	84	84
	99th	131	132	134	136	138	139	140	87	88	89	90	91	92	92
15	50th	109	110	112	113	115	117	117	61	62	63	64	65	66	66
	90th	122	124	125	127	129	130	131	76	77	78	79	80	80	81
	95th	126	127	129	131	133	134	135	81	81	82	83	84	85	85
	99th	134	135	136	138	140	142	142	88	89	90	91	92	93	93
16	50th	111	112	114	116	118	119	120	63	63	64	65	66	67	67
	90th	125	126	128	130	131	133	134	78	78	79	80	81	82	82
	95th	129	130	132	134	135	137	137	82	83	83	84	85	86	87
	99th	136	137	139	141	143	144	145	90	90	91	92	93	94	94
17	50th	114	115	116	118	120	121	122	65	66	66	67	68	69	70
	90th	127	128	130	132	134	135	136	80	80	81	82	83	84	84
	95th	131	132	134	136	138	139	140	84	85	86	87	87	88	89
	99th	139	140	141	143	145	146	147	92	93	93	94	95	96	97

The 90th percentile is 1.28 SD, the 95th percentile is 1.645 SD, and the 99th percentile is 2.326 SD over the mean.

Reproduced with permission from National High Blood Pressure Education Program Working Group on High Blood Pressure in Children and Adolescents. The fourth report on the diagnosis, evaluation and treatment of high blood pressure in children and adolescents. *Pediatrics* 2004;114:555–576, Copyright © 2004 by the AAP.

can be seen from these tables that blood pressure generally increases with age. Blood pressure also increases with height, which is why height percentiles are included in the tables as a way of classifying blood pressure elevation. There is also a strong correlation between BMI and blood pressure. However, this is believed to be a pathologic relationship, so weight or BMI are not considered in determining normal blood pressure, and it is not considered normal for children who are overweight to have higher blood pressure. Separate tables are presented for males and females as blood pressure in males is somewhat higher than for females. This difference by sex increases with age. It has been shown that after accounting for the correlates of blood pressure such as body size, ethnic differences in blood pressure are minimal in childhood and adolescence.

Normal values for blood pressure during the first year of life are presented in Figure 71.4. These values are for the supine position and measured with an oscillometric type of device.

Ambulatory Blood Pressure

Blood pressure has traditionally been measured with the patient resting quietly in a sitting position. This approach to measurement has been very useful both in the research and clinical setting for both children and adults. Nevertheless, it is clear that this does not reflect the variability of blood pressure seen normally during the day and night. Blood pressures measured in the clinic setting may also be subject to the white coat effect. This is a well-recognized circumstance in which

some individuals experience an elevation in blood pressure, not seen in other environments, when they are in the doctor's office.

Ambulatory blood pressure monitoring is a procedure in which a patient wears a portable blood pressure measuring device over a 24-hour period (231,232). This method has been increasingly used in adults and pediatric patients to provide a better characterization of blood pressure. It allows for calculation of mean day and mean night time blood pressure and also the frequency with which blood pressure exceeds the upper limit of normal. Normal standards for ambulatory blood pressures have been published and are available for clinical use (233,234). Ambulatory blood pressure measurements have been shown to be associated with the presence of target organ abnormalities and may be more sensitive than casual blood pressure measurements in indicating risk (231).

Ambulatory blood pressure monitoring is also useful in the evaluation of white coat hypertension. In this case, blood pressure measurements in the clinic setting are persistently elevated, whereas 24-hour ambulatory blood pressure measurements are normal. When white coat hypertension is present, the use of ambulatory monitoring may spare the patient from more intensive treatment. Children with white coat hypertension should not be considered completely normal; however, blood pressure reactivity to stressful stimuli may be a marker for future hypertension (225).

Another aspect of 24-hour ambulatory blood pressure monitoring that may be useful is the normal decline in blood

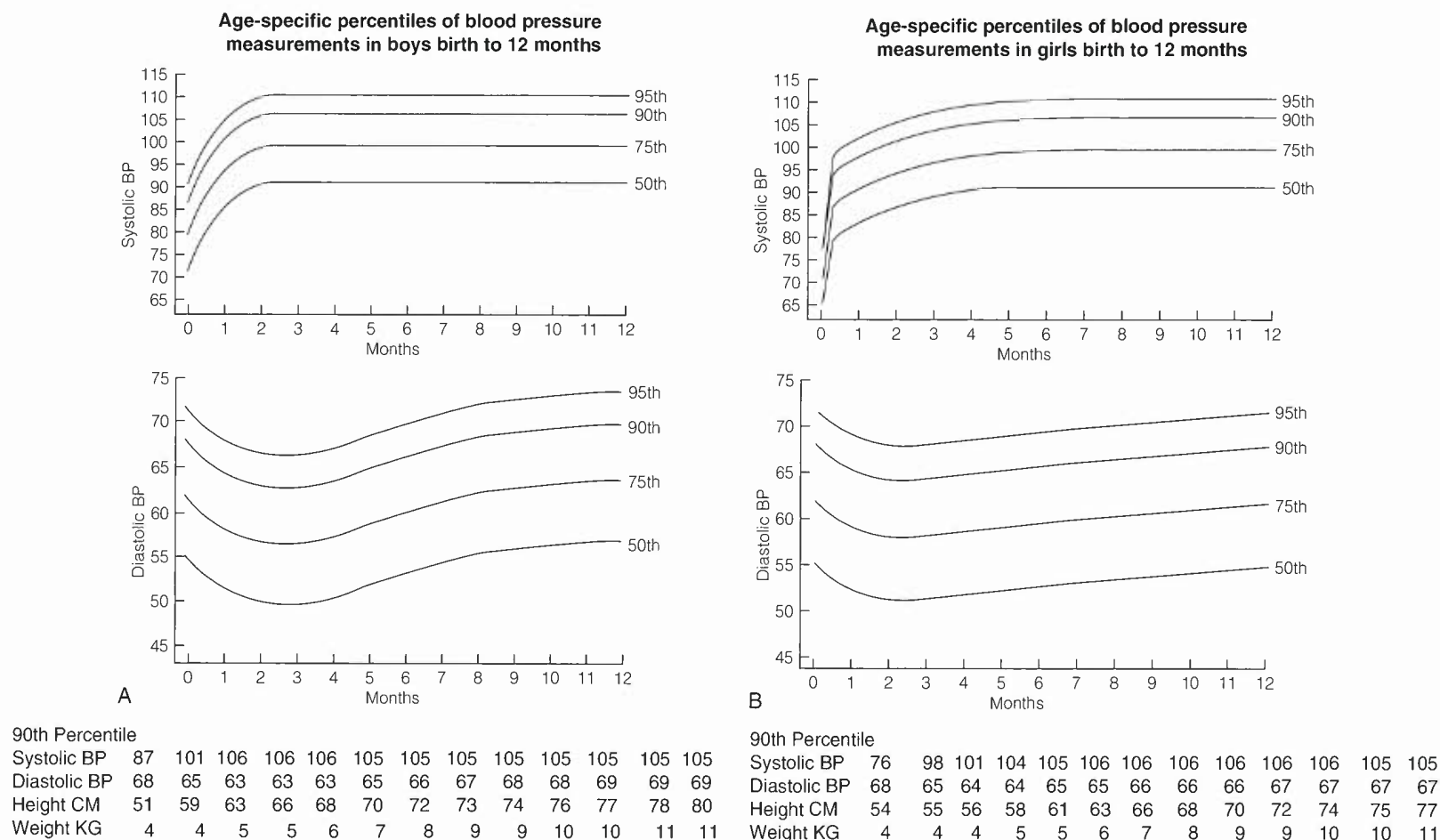


Figure 71.4. Age-specific percentiles for blood pressure in boys (A) and girls (B) from birth to 12 months of age. BP, blood pressure. (Reproduced with permission from Task Force on Blood Pressure Control in Children. National Heart, Lung, and Blood Institute, Bethesda, Maryland. Report of the Second Task Force on Blood Pressure Control in Children—1987. *Pediatrics* 1987;79:1–25, Copyright © 1987 by the AAP.)

pressure observed at night during sleep. This is often referred to as “dipping” of blood pressure. The normal nocturnal decline in blood pressure is approximately 10%. Nondipping has been associated with higher future blood pressure, increased risk of target organ disease, and some secondary forms of hypertension (236,237).

For pediatric patients with hypertension, 24-hour ambulatory blood pressure monitoring may be useful (232). However, its use requires specialized equipment and trained staff for appropriate application and interpretation of the results.

Definition of Hypertension

In adults, a single set of values is used to define hypertension at any age (209). In children, this would be problematic because blood pressure increases with age as children grow normally. This has led to the definition of hypertension based on percentiles that has been proposed by the National High Blood Pressure Education Program (238). These definitions are presented in Table 71.13. For the diagnosis of hypertension to be established, it is necessary for blood pressure to be elevated (≥ 95 th percentile) on a persistent basis over three separate occasions. The level of blood pressure on the first measurement dictates when the patient should return for repeat blood pressure measurements. Confirming an elevated blood pressure measurement is important because higher blood pressure tends to fall on subsequent visits and may not be persistently elevated. On the other hand, severe blood pressure elevation requires more acute, diagnostic, and therapeutic action.

Measurement of Blood Pressure

For appropriate interpretation of blood pressure, it is important that it be measured appropriately. Unfortunately, in many clinical settings, blood pressure measurements may not be taken at all, and when they are taken, the techniques used may not be appropriate. Even when blood pressure is measured appropriately, it is often not interpreted correctly. Hansen et al. (239) evaluated the frequency of undiagnosed prehypertension and hypertension in a large academic urban medical system with an electronic medical record. They found that prehypertension and hypertension were frequently undiagnosed. This was especially true for younger children without obesity or other cardiovascular risk factors. A greater number

of elevated blood pressures and blood pressure readings in the range of stage 2 hypertension were associated with increased recognition and diagnosis. Training in blood pressure measurement and interpretation for nurses and physicians is often minimal.

Neonates

The optimum method for measurement of blood pressure is the indwelling arterial catheter. In ill neonates, an umbilical artery or radial artery catheter is often in place (240). An alternative method is the oscillometric monitor. These devices have been shown to correlate reasonably well with intra-arterial measurements under controlled circumstances such as during anesthesia (241). However, in the clinical setting, such devices have been shown to vary significantly from auscultation (242). In addition, oscillometric devices may differ from each other (243).

Blood pressures obtained using oscillometric devices are useful when blood pressure is monitored over time and the trend in blood pressure is of particular interest. Blood pressure should be measured in the arm because blood pressure in the leg may be higher than that in the arm (244). Normal standards are not available for blood pressure measured in the leg. Routine blood pressure measurement is not recommended for normal neonates or infants. Blood pressure should be measured in the presence of other medical conditions where hypertension might be expected, such as renal disease or congenital heart disease (Table 71.14).

Older Children and Adolescents

Children aged 3 years and older should have their blood pressure measured in the clinical setting at least annually. It is recommended that blood pressures be obtained with auscultation. The right arm is preferred for blood pressure measurement with the patient seated quietly and the arm at heart level (238). Blood pressure should be measured at all well child and ill visits for children older than age 3 years through adolescence.

The size of the blood pressure cuff bladder is quite important for accurate blood pressure measurement. The use of a blood pressure cuff that is too small will result in a falsely elevated blood pressure recording. The width of the cuff should be at least 40% of the arm circumference at the point midway between the olecranon and the acromion. The length of the bladder should be between 80% and 100% of the circumference of the arm so that it encircles the arm appropriately (245). Therefore, the bladder width-to-length ratio should be

TABLE 71.13 Classification of Hypertension in Children and Adolescents

	SBP or DBP Percentile ^a	Frequency of BP Measurement
Normal	<90th	Recheck at next scheduled physical examination.
Prehypertension	90th to <95th or if BP exceeds 120/80 mm Hg even if below 90th percentile up to <95th percentile ^b	Recheck in 6 mo.
Stage 1 hypertension	95th percentile to the 99th percentile plus 5 mm Hg	Recheck in 1–2 wk or sooner if the patient is symptomatic; if persistently elevated on two additional occasions, evaluate or refer to source of care within 1 mo.
Stage 2 hypertension	>99th percentile plus 5 mm Hg	Evaluate or refer to source of care within 1 wk or immediately if the patient is symptomatic.

^aFor sex, age, and height measured on at least three separate occasions; if systolic and diastolic categories are different, categorize by the higher value.

^bThis occurs typically at 12 years of age for SBP and for DBP.

SBP, systolic blood pressure; DBP, diastolic blood pressure.

TABLE 71.14

Conditions for Which Neonates and Infants Should Have Measurement of Blood Pressure

- Prematurity neonatal complications
- Congenital heart disease
- Renal disease or urologic malformation
- Evidence of elevated intracranial pressure
- Treatment with drugs that raise blood pressure

at least 1:2. In clinical practice, if a cuff is too small, then the next largest should be chosen until the cuff that is the most appropriate size is identified.

The Korotkoff phases are auscultated and used to determine systolic and diastolic blood pressure. The onset of tapping sounds (phase 1) is the point used for systolic blood pressure and the disappearance of sound (phase 5) is used for the diastolic blood pressure. When sounds can be heard to 0 mm Hg, then the onset of the phase 4, or muffing of sound, should be used to determine the diastolic blood pressure.

The mercury sphygmomanometer is the optimum device for measurement of blood pressure. However, because of environmental concerns about mercury, many hospitals have removed mercury manometers from the clinical setting. An appropriate alternative is the aneroid device, which is a mechanical device that is calibrated against the mercury column. In general, automated oscillometric devices are not recommended for routine measurement of blood pressure in children and adolescents. If an automated oscillometric device is used and elevated blood pressure is identified, this should be confirmed using a mercury manometer or aneroid device (238).

Etiology of Hypertension

There is a number of potential causes of hypertension. The likelihood of finding a secondary form of hypertension varies with the age of the child, the degree of blood pressure elevation, and the presence of hypertension in family members. This means that for a younger child, with greater elevation of blood pressure and little or no family history of hypertension, consideration should be given to possible secondary causes. For the adolescent with mild elevation of blood pressure, over-

weight, and a strong family history of hypertension, primary or essential hypertension is most likely.

Neonatal Hypertension

In neonates with blood pressure elevation, an evaluation for secondary causes should usually be performed. The causes of hypertension in the neonate include renal parenchymal disease and renovascular, cardiovascular, endocrine, pharmacologic, and neoplastic disorders. Other causes include bronchopulmonary dysplasia and increased intracranial pressure (246–248).

The evaluation of potential secondary causes in this age group includes measurement of blood pressure in all four extremities to rule out coarctation of the aorta. The history of umbilical artery catheterization may suggest vascular trauma and renal artery stenosis. Usually, a careful history and physical examination will provide clues to the possible cause of hypertension.

For most patients, few laboratory tests are needed. It is important to assess renal function with a blood urea nitrogen (BUN) and creatinine and to evaluate a urine specimen to investigate the presence of renal parenchymal disease.

A chest radiograph and echocardiogram may be useful if signs and symptoms of congestive heart failure are present. Ultrasound of the genitourinary tract is important when renal or urologic abnormalities are suspected. For infants with very high blood pressure for which no cause can be readily identified, an evaluation of possible renal artery stenosis may be indicated.

Children and Adolescents

For older children, the likelihood of secondary hypertension is diminished, but it still may be present. In general, the history and physical examination are most useful in the identification of possible secondary causes. The standard evaluation for children with persistent elevation of blood pressure is presented in Table 71.15. Findings on history that may suggest other causes of hypertension are presented in Table 71.16. Physical examination findings that may suggest secondary forms of blood pressure elevation are presented in Table 71.17. Based on history and physical findings, additional laboratory tests may be performed to evaluate the possibility of an underlying cause for the blood pressure elevation.

Evaluation of Target Organ Abnormalities

Echocardiography is recommended as the main tool for clinical evaluation of target organ abnormalities. Left ventricular mass can be calculated from standard echocardiographic

TABLE 71.15

Standard Clinical Evaluation of Children and Adolescents with Hypertension

Study or Procedure	Purpose
<i>Evaluation for identifiable causes</i>	
History, including sleep history, family history, risk factors, diet, and habits such as smoking and drinking alcohol; physical examination	History and physical examination help focus subsequent evaluation
BUN, creatinine, electrolytes, urinalysis, and urine culture	Rule out renal disease and chronic pyelonephritis
CBC	Rule out anemia, consistent with chronic renal disease
Renal ultrasound	Rule out scar, congenital anomaly, or disparate renal size

BUN, blood urea nitrogen; CBC, complete blood count.

Reproduced with permission from Falkner B, Daniels SR, Flynn JT, et al. The fourth report on the diagnosis, evaluation and treatment of high blood pressure in children and adolescents. *Pediatrics* 2004;114:555–576, Copyright © 2004 by the AAP.

TABLE 71.16 Historical Information that May Suggest Primary or Secondary Hypertension

Information	Relevance
Family history of hypertension, preeclampsia, toxemia, renal disease, tumors	Important in essential hypertension, inherited renal disease, and some endocrine diseases (e.g., familial pheochromocytoma with multiple endocrine adenopathy II)
Neonatal history	Use of umbilical artery catheter suggests need to evaluate renal vasculature and kidneys
Headaches, dizziness, epistaxis, visual problems	Nonspecific symptomatology, usually not etiologically helpful
Abdominal pain, dysuria, frequency, nocturia, enuresis	May suggest underlying renal disease
Joint pains/swelling, facial or peripheral edema	Suggest connective tissue disease and/or other forms of nephritis
Weight loss, failure to gain weight with good appetite, sweating, flushing, fevers, palpitations	In combination, symptoms suggest pheochromocytoma
Muscle cramps, weakness, constipation	May suggest hypokalemia and hyperaldosteronism
Age of onset of menarche, sexual development	May be helpful in suggesting endocrine causes
Ingestion of prescription and over-the-counter drugs, contraceptives, illicit drugs	Drug-induced hypertension

Reproduced with permission from Falkner B, Daniels SR, Flynn JT, et al. The fourth report on the diagnosis, evaluation and treatment of high blood pressure in children and adolescents. *Pediatrics* 2004;114:555–576, Copyright © 2004 by the AAP.

measurements including the left ventricular end-diastolic dimension (LVED), the intraventricular septal thickness (IVS), and the thickness of the left ventricular posterior wall (LVPW). From these measurements, the method of Devereux et al. (249) can be used to calculate left ventricular mass:

LV mass (g) = 0.80

$$\left[1.04 (\text{IVS} + \text{LVED} + \text{LVPW})^3 - (\text{LVED})^3 \right] + 0.6$$

The size of the left ventricle is very dependent on body size and in particular lean body mass (250). This means that the determination of left ventricular mass should be indexed or standardized to allow for comparisons with normal standards. The recommended approach to indexing is to use the height to the power of 2.7. This method comes close to accounting for the patient's lean body mass and excludes any effect that obesity may have on blood pressure. Obesity may have a pathologic effect resulting in elevation of left ventricular mass (251). A conservative cut-point for determining elevation of left ventricular mass index is 51 g/m^{2.7}. This is >99th percentile for normal children and adolescents and is a level that is associated with increased cardiovascular morbidity and mortality in adults with hypertension (222).

Other methods for evaluation of target organ effects such as ultrasound evaluation of the carotid arteries or evaluation of the urine for microalbuminuria are not currently recommended in children and adolescents. Ophthalmologic examination of the retinal vessels may be useful in identifying children and adolescents with retinal vascular changes, which may reflect abnormal changes in other vascular beds.

It is often useful to evaluate children for comorbid conditions that may increase the risk of cardiovascular disease and may be associated with hypertension. This includes a fasting lipid profile and glucose to identify potential metabolic abnormalities that may be part of the metabolic syndrome. In children with a history of snoring, irregular breathing during sleep, and daytime sleepiness, a polysomnogram may be indicated to

evaluate the possibility of obstructive sleep apnea. In the older child and adolescent, a history of alcohol or drug abuse may suggest the utility of a drug screen.

Treatment of Hypertension

An overall approach to the evaluation and treatment of hypertension in children and adolescents recommended by the National Heart Lung and Blood Institute is presented in Figure 71.5A and B.

In general, the initial approach to treatment includes therapeutic changes to lifestyle. If patients are overweight, this should include aggressive weight management. It is when lifestyle changes have been shown to be insufficient and blood pressure remains elevated that more aggressive treatment with pharmacologic agents is instituted.

Lifestyle Modification

There is good evidence in adults that modification of lifestyle focused on changing diet and physical activity can have a beneficial effect on blood pressure. There is increasing evidence that this is true for children as well.

Diet. From the standpoint of diet, overweight, excess intake of salt and alcohol, and low intake of potassium have all been associated with blood pressure elevation (252). However, whether these dietary factors also make good targets for treatment is less clear.

Numerous clinical trials have been conducted to evaluate the relationship of weight loss to blood pressure. Almost all have shown that weight loss or improvement in BMI is related to lower blood pressure in adults. In a meta-analysis, the mean reduction in blood pressure for a weight loss of 5.1 kg was 4.4 mm Hg for systolic blood pressure and 3.6 mm Hg for diastolic blood pressure (253).

In children and adolescents, much of the observed primary hypertension is at least in part related to overweight. With the increasing prevalence and severity of childhood obesity, weight management is an increasing aspect of the nonpharmacologic

TABLE 71.17 Examples of Physical Examination Findings Suggestive of Secondary Hypertension

	Finding	Possible Cause
Vital signs	Tachycardia	Hyperthyroidism, pheochromocytoma, neuroblastoma, primary hypertension
	Decreased lower-extremity pulses; drop in BP from upper to lower extremities	Coarctation of the aorta
Eyes	Retinal changes	Severe hypertension, more likely to be associated with secondary hypertension
Ear, nose, and throat (ENT)	Adenotonsillar hypertrophy	Suggests association with sleep-disordered breathing (sleep apnea), snoring
Height/weight	Growth retardation	Chronic renal failure
	Obesity (high BMI)	Primary hypertension
	Truncal obesity	Cushing syndrome, insulin resistance syndrome
Head and neck	Moon facies	Cushing syndrome
	Elfin facies	Williams syndrome
	Webbed neck	Turner syndrome (coarctation of the aorta)
	Thyromegaly	Hyperthyroidism
Skin	Episodic pallor, flushing, diaphoresis	Pheochromocytoma
	Acne, hirsutism, striae	Cushing syndrome, anabolic steroid abuse
	Café au lait spots	Neurofibromatosis
	Adenoma sebaceum	Tuberous sclerosis
	Malar rash	Systemic lupus erythematosus
	Acanthosis nigricans	Type 2 diabetes
Chest	Widely spaced nipples	Turner syndrome
	Systolic heart murmur	Coarctation of the aorta
	Friction rub	Systemic lupus erythematosus (pericarditis), collagen-vascular disease, end-stage renal disease with uremia
	Apical heave	Left ventricular hypertrophy/chronic hypertension
Abdomen	Mass	Wilms tumor, neuroblastoma, pheochromocytoma
	Epigastric/flank bruit	Renal artery stenosis
	Palpable kidneys	Polycystic kidney disease, hydronephrosis, multicystic-dysplastic kidney
Genitalia	Ambiguous/virilization	Adrenal hyperplasia
Extremities	Joint swelling	Systemic lupus erythematosus, collagen vascular disease
	Muscle weakness	Hyperaldosteronism, Liddle syndrome

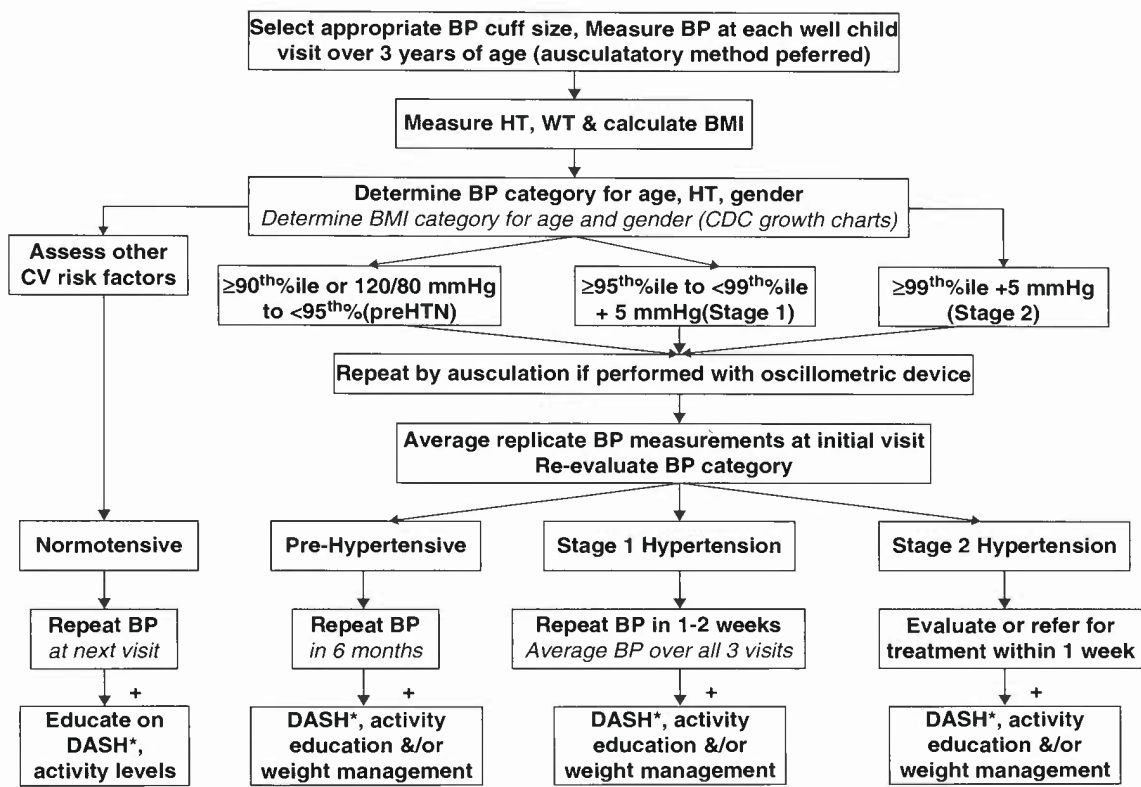
BP, blood pressure; BMI, body mass index.

Reproduced with permission from Falkner B, Daniels SR, Flynn JT, et al. The fourth report on the diagnosis, evaluation and treatment of high blood pressure in children and adolescents. *Pediatrics* 2004;114:555–576, Copyright © 2004 by the AAP.

management of hypertension (254). Intervention studies involving weight loss in children with blood pressure elevation have demonstrated beneficial results (255–257). This is also true for clinic-based studies of weight reduction (258). In addition, lipid profiles and insulin sensitivity improve after weight loss (257,258). This means that there is improvement in the main components of the metabolic syndrome. In pediatric studies where an 8% to 10% reduction in BMI is obtained, reduction in blood pressure ranges from 8 to 16 mm Hg (255–258). An important question is whether these benefits are maintained with stabilization of weight. This is an important area

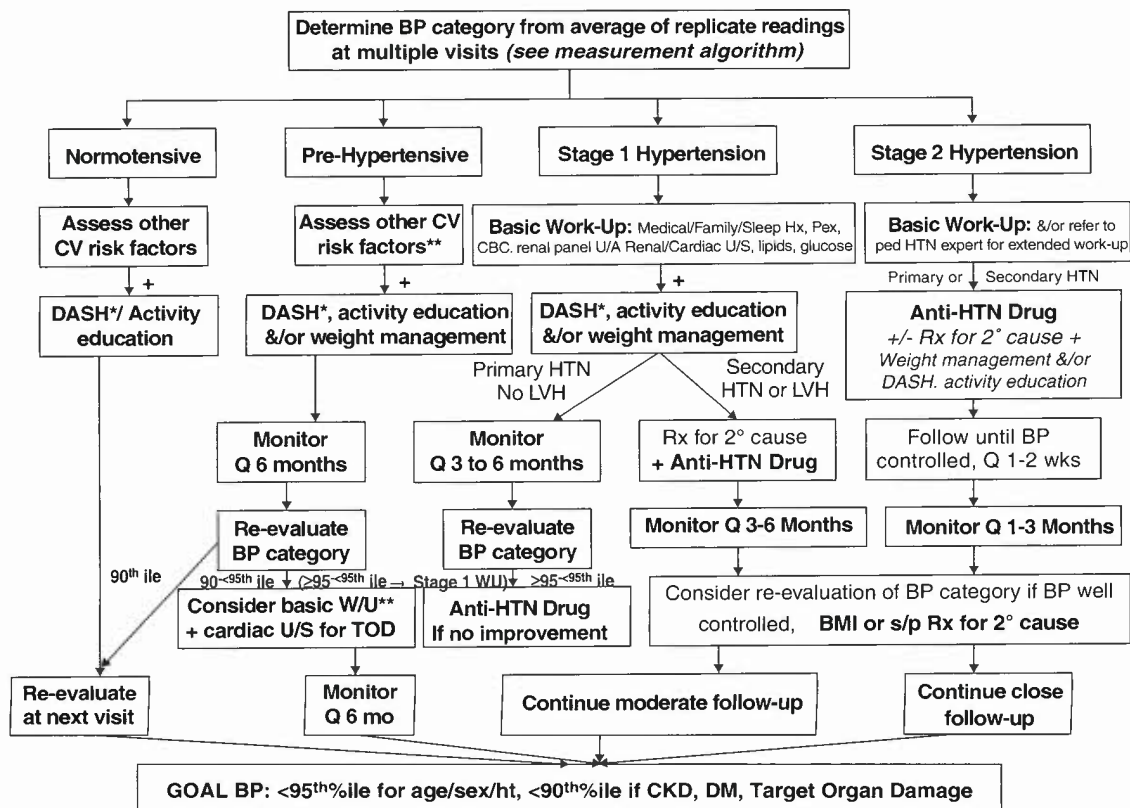
for future research. Because treatment of obesity and maintenance of weight loss are difficult, it is important to focus on prevention of abnormal weight gain in pediatric patients. It is clear that additional increases in BMI through the pediatric age range will have a deleterious effect on future blood pressure no matter what the baseline blood pressure had been (203).

The intake of dietary salt has also been a concern, and reduction of salt intake has been proposed as an important therapeutic modality. Many randomized controlled clinical trials have been performed in adults. In a meta-analysis, a median reduction of urinary sodium of approximately 1.8 g/d



*DASH = Institute DASH Pattern Diet

A



*DASH = Institute DASH Pattern Diet

**Work up for target organ damage (TOD)/LVH if obese of (+) for other CV risk factors

B

Figure 71.5. A: Blood pressure measurement and categorization. B: Blood pressure management by category. Evaluation and management of children and adolescents with hypertension. BMI, body mass index; BP, blood pressure; Rx, prescription; Q, every. (Adapted from Daniels et al. National Heart Lung and Blood Institute Guidelines for Integrated Cardiovascular Risk Reduction in Children and Adolescents. *Pediatrics* 2011 [in press]).

lowered systolic blood pressure by 5.0 mm Hg and diastolic blood pressure by 2.7 mm Hg on average in individuals with hypertension (259). Sodium restriction has also been demonstrated to lower blood pressure when used as an adjunct to antihypertensive medication (260). In addition, sodium restriction can prevent the development of hypertension over time (261). Bibbins-Domingo et al. (262) used the Coronary Heart Disease Policy Model to quantify the potential benefits of population-wide reductions of dietary salt of up to 3 g (1,200 mg of sodium) per day. They found that modest reductions of dietary salt would result in saving 194,000 to 392,000 quality-adjusted life-years and \$10 to \$24 billion in health care costs annually. These reductions are similar to the benefits of reduction in tobacco use, obesity, and cholesterol levels.

One issue that complicates the relationship between dietary salt intake and blood pressure is that the relationship is heterogeneous across individuals. Some individuals appear to be more sensitive to salt in the diet and have a greater increase in blood pressure when exposed to it than others (263). However, this does not appear to be a dichotomous response; instead, it is probably a graded one with varying degrees of sensitivity to salt in the diet (264). In general, the effects of sodium reduction appear to be more pronounced in African American patients (265). Unfortunately, a simple approach to assessment of the degree of sensitivity to sodium is not available for use in the clinical setting.

Infancy may be an important period in relation to dietary sodium. Hofman et al. (266) conducted a randomized trial of sodium reduction in infants. They found a small but statistically significant reduction in blood pressure at 6 months of age. This difference was diminished at 1 year of age after the intervention had ceased. However, a follow-up study was done when the subjects reached age 15. The low-sodium group had significantly lower blood pressure than the normal-sodium group, despite the fact that the intervention had not been continued through childhood (267).

There have been few studies of restriction of dietary sodium in pediatric patients with hypertension (268–271). These studies have yielded conflicting results, with some showing an effect and others showing no effect (267). This may be in part due to the heterogeneity of response to dietary sodium and the inability to identify individuals who are more salt sensitive. It may also be due to difficulty in adherence to a low-salt diet.

Other micronutrients such as potassium and calcium have been studied in children. However, the results of these studies have not demonstrated a strong and consistent enough effect for them to be recommended as targets for therapeutic intervention. Studies have documented a dose-dependent effect of alcohol intake on blood pressure (272). A meta-analysis of studies on adults shows that a median reduction of alcohol consumption of 76% resulted in a reduction in systolic blood pressure by 3.3 mm Hg and diastolic blood pressure by 2.0 mm Hg (273). Although alcohol intake has not been studied extensively in adolescents, it is a potential cause of hypertension. In patients who are identified with alcohol abuse, cessation of intake may provide important improvement in blood pressure.

More recently, studies in adults have focused on dietary patterns rather than specific micronutrients. The best studied diet in adults is the DASH (dietary approaches to stop hypertension) diet. This diet includes increased intake of fruits and vegetables, low-fat dairy products, whole grains, poultry, fish, and nuts. The diet reduces intake of red meat, sweets, and sugar-containing beverages. This diet has been shown to significantly reduce blood pressure in men, women, whites, and African Americans with hypertension (274–277). Of interest is that it has also been shown to reduce blood pressure in adults without hypertension (277). In individuals with hypertension, the diet resulted in a decrease of 11.6 mm Hg for systolic blood pressure and 5.3 mm Hg for diastolic blood pressure.

In adults, the DASH diet has been shown to be safe, effective, and broadly applicable across populations. There have been some studies of the DASH diet in children and adolescents with hypertension. Couch et al. (278) found that the DASH diet resulted in a greater decrease in systolic blood pressure z-scores from baseline to a posttreatment assessment at 3 months compared to hypertensive adolescents who received standard diet restrictions. There was also a trend for a greater reduction in diastolic blood pressure z-scores for the hypertensive adolescents randomly assigned to the DASH diet. The National High Blood Pressure Education Program and the National Heart Lung and Blood Institute(s) have proposed that the use of a DASH eating plan would be appropriate for patients with hypertension in this age range (238).

Physical Activity. Regular physical activity may also be a useful component of therapeutic lifestyle changes to treat hypertension in children. There are many beneficial effects of physical activity including its utility for weight management (278). Whether physical activity has an independent effect on blood pressure is less clear. A meta-analysis of 12 randomized trials in children and adolescents demonstrated that increased physical activity leads to a small reduction in blood pressure (279). However, this decrease in blood pressure was not statistically significant. Nevertheless, it appears that the benefits of increased physical activity and decreased sedentary time outweigh any risks. The National High Blood Pressure Education Program has recommended increased and regular physical activity (30 to 60 min/d of moderate physical activity on most days) as part of the therapeutic lifestyle approach to treatment in children and adolescents (238).

A clinical issue that may arise is the competitive athlete who has hypertension. In general, athletes with mild-to-moderate elevation of blood pressure (prehypertension and stage 1 hypertension) who have no evidence of target organ abnormalities should be allowed to continue in competition (280). It is important for these patients to have ongoing monitoring of their blood pressure (every 1 to 3 months). Athletes with stage 2 hypertension or with evidence of target organ abnormalities should be evaluated more extensively. In these patients, it is prudent to discontinue competitive sports until better control of blood pressure has been achieved.

The role of exercise testing in the evaluation of athletes who have hypertension is controversial. Blood pressures recorded during testing may differ from blood pressures during actual competition (281). In addition, different sports require different amounts of aerobic and isometric activity. In general, resistance exercises such as weight lifting are associated with a higher acute rise in blood pressure during the event. When hypertension and other cardiovascular diseases are present concomitantly, the eligibility for competitive sports will depend on the type and severity of heart disease as well as the level of blood pressure. Careful assessment of the types of activity involved in both conditioning/practice and in competition will allow a more rational decision regarding the level of restriction.

Pharmacologic Treatment of Hypertension

It is well established that treatment of hypertension in adults is associated with a reduction in cardiovascular disease morbidity and mortality (282,283). The evidence base to support pharmacologic treatment of hypertension in children and adolescents is less well developed. However, there have been an increasing number of clinical trials in pediatric patients. These have been primarily short-term studies and have focused on the ability of pharmacologic agents to lower blood pressure as well as the evaluation of safety.

The indications for use of antihypertensive agents are presented in Table 71.18. The decision to use antihypertensive medication is best made on a patient-by-patient basis taking a

TABLE 71.18

Indications for Treatment with Antihypertensive Medications

- Symptomatic hypertension
- Secondary hypertension
- Stage 2 hypertension
- Hypertension (stage 1 or 2) with established target organ damage
- Hypertension (stage 1 or 2) with the presence of other risk factors for cardiovascular disease
- Persistent hypertension (stage 1 or 2) despite implementation of therapeutic lifestyle changes

number of factors into account including clinical features and the acceptance of antihypertensive medication by the family. However, the more severe the blood pressure elevation, the more urgent the use of blood pressure lowering with medication will be.

The therapeutic goal for children and adolescents with hypertension is to lower the blood pressure below the 95th percentile for age and height percentile. However, for some children, such as those with diabetes or chronic renal disease, a more aggressive goal is appropriate. These patients should have blood pressure lowered below the 90th percentile for age, sex, and height as they are thought to be at highest risk for cardiovascular disease over time.

The available medications for routine treatment of hypertension in pediatric patients are listed in Table 71.19. As can

TABLE 71.19

Antihypertensive Drugs for Outpatient Management of Hypertension in Children 1–17 Years Old^a

Class	Drug	Dose ^b	Dosing Interval	Comments ^c
Angiotensin-converting enzyme (ACE) inhibitor	Benazepril	Initial: 0.2 mg/kg/d up to 10 mg/d Maximum: 0.6 mg/kg/d up to 40 mg/d	qd	1. All ACE inhibitors are contraindicated in pregnancy; females of childbearing age should use reliable contraception.
	Captopril	Initial: 0.3–0.5 mg/kg/dose Maximum: 6 mg/kg/d	tid	2. Check serum potassium, creatinine periodically to monitor for hyperkalemia and azotemia.
	Enalapril	Initial: 0.08 mg/kg/d up to 5 mg/d Maximum: 0.6 mg/kg/d up to 40 mg/d	qd–bid	3. Cough and angioedema are reportedly less common with newer members of this class than with captopril.
	Fosinopril	Children >50 kg: Initial: 5–10 mg/d Maximum: 40 mg/d	qd	4. Benazepril, enalapril, and lisinopril labels contain information on the preparation of a suspension; captopril may also be compounded into a suspension.
	Lisinopril	Initial: 0.07 mg/kg/d up to 5 mg/d Maximum: 0.6 mg/kg/d up to 40 mg/d	qd	5. FDA approval for ACE inhibitors with pediatric labeling is limited to children ≥6 y if age and to children with creatinine clearance ≥30 mL/min/1.73 m ² .
	Quinapril	Initial: 5–10 mg/d Maximum: 80 mg/d	qd	
Angiotensin-receptor blocker	Irbesartan	6–12 y: 75–150 mg/d ≥13 y: 150–300 mg/d	qd	1. All ARBs are contraindicated in pregnancy; females of childbearing age should use reliable contraception.
	Losartan	Initial: 0.7 mg/kg/d up to 50 mg/d Maximum: 1.4 mg/kg/d up to 100 mg/d	qd	2. Check serum potassium, creatinine periodically to monitor for hyperkalemia and azotemia. 3. Losartan label contains information on the preparation if a suspension. 4. FDA approval for ARBs is limited to children with creatinine clearance ≥30 mL/min/1.73 m ² .
α- and β-blocker	Labetalol	Initial: 1–3 mg/kg/d Maximum: 10–12 mg/kg/d up to 1,200 mg/d	bid	1. Asthma and overt heart failure are contraindications. 2. Heart rate is dose limiting. 3. May impair athletic performance. 4. Should not be used in insulin-dependent diabetics.

TABLE 71.19

Antihypertensive Drugs for Outpatient Management of Hypertension in Children 1–17 Years Old^a (Continued)

Class	Drug	Dose ^b	Dosing Interval	Comments ^c
β -blocker	Atenolol	Initial: 0.5–1 mg/kg/d Maximum: 2 mg/kg/d up to 100 mg/d	qd–bid	1. Noncardioselective agents (propranolol) are contraindicated in asthma and heart failure.
	Bisoprolol/ HCTZ	Initial: 2.5/6.25 mg/d Maximum: 10/6.25 mg/d	qd	2. Heart rate is dose limiting.
	Metoprolol	Initial: 1–2 mg/kg/d Maximum: 6 mg/kg/d up to 200 mg/d	bid	3. May impair athletic performance.
	Propranolol	Initial: 1–2 mg/kg/d Maximum: 4 mg/kg/d up to 640 mg/d	bid–tid	4. Should not be used in insulin-dependent diabetics. 5. A sustained-release formulation of propranolol is available that is dosed once daily.
Calcium channel blocker	Amlodipine	Children 6–17 y: 2.5–5 mg once daily	qd	1. Amlodipine can be compounded into a stable extemporaneous suspension. 2. May cause tachycardia.
Central α -agonist	Clonidine	Children ≥ 12 y: Initial: 0.2 mg/d Maximum: 2.4 mg/d	bid	1. May cause dry mouth and/or sedation. 2. Transdermal preparation also available. 3. Sudden cessation of therapy can lead to severe rebound hypertension.
Diuretic	HCTZ	Initial: 1 mg/kg/d Maximum: 3 mg/kg/d up to 50 mg/d	qd	1. All patients treated with diuretics should have electrolytes monitored shortly after initiating therapy and periodically thereafter.
	Chlorthalidone	Initial: 0.3 mg/kg/d Maximum: 2 mg/kg/d up to 50 mg/d	qd	2. Useful as add-on therapy in patients being treated with drugs from other drug classes.
	Furosemide	Initial: 0.5–2.0 mg/kg/dose Maximum: 6 mg/kg/d	qd–bid	3. Potassium-sparing diuretics (spironolactone, triamterene, amiloride) may cause severe hyperkalemia, especially if given with ACE inhibitor or ARB.
	Spironolactone	Initial: 1 mg/kg/d Maximum: 3.3 mg/kg/d up to 100 mg/d	qd–bid	4. Furosemide is labeled only for treatment of edema but may be useful as add-on therapy in children with resistance hypertension, particularly in children with renal disease.
	Triamterene	Initial: 1–2 mg/kg/d Maximum: 3–4 mg/kg/d up to 300 mg/d	Bid	5. Chlorthalidone may precipitate azotemia in patients with renal diseases and should be used with caution in those with severe renal impairment.
	Amiloride	Initial: 0.4–0.625 mg/kg/d Maximum: 20 mg/d	qd	
Vasodilator	Hydralazine	Initial: 0.75 mg/kg/d Maximum: 0.75 mg/kg/d	qid	1. Tachycardia and fluid retention can occur. 2. Hydralazine can cause a lupus-like syndrome in slow acetylators.
	Minoxidil	Children < 12 y: Initial: 0.2 mg/kg/d Maximum: 50 mg/kg/d Children ≥ 12 y: Initial: 5 mg/d Maximum: 100 mg/d	qd–tid	3. Prolonged use of minoxidil can cause hypertrichosis. 4. Minoxidil is usually reserved for patients with hypertension resistant to multiple drugs.

^aIncludes drugs with prior pediatric experience or recently completed clinical trials.^bThe maximum recommended adult dose should not be exceeded in routine clinical practice.^cComments apply to all members of each drug class except where otherwise stated.

ACE, angiotensin-converting enzyme; qd, once daily; bid, twice daily; FDA, Federal Drug Administration; ARB, angiotensin-receptor blocker; HCTZ, hydrochlorothiazide; tid, three times daily; qid, four times daily.

be seen, several classes of antihypertensive medications are available for use. In adults, the Antihypertensive and Lipid Lowering Heart Attack Trial (ALLHAT) study compared different classes of antihypertensive medications (285). The results of that study support the preferential use of diuretics and β -adrenergic blockers as first-line agents in the treatment of hypertension. However, subsequent research has called those results into question. Pediatric trials have not focused on comparing different classes of agents in the treatment of hypertension. This means there is little or no evidence base to drive the decision regarding an initial agent in children. However, the choice of certain classes of medication is appropriate for some subsets of patients. For example, angiotensin-converting enzyme (ACE) inhibitors or angiotensin-receptor blockers are recommended for patients with diabetes or proteinuric renal disease. There is one study that found that these medications can be teratogenic when used in the first trimester of pregnancy (286). A more recent analysis using a large population-based case-control study found that women who reported the use of any antihypertensive medication during pregnancy were at increased risk of having certain cardiovascular malformations. Because the association was not specific for ACE inhibitors or for the first trimester of pregnancy, this suggests the possibility that hypertension itself may be an important factor for congenital abnormalities of the cardiovascular system. In any case, exposure to ACE inhibitors during the second and third trimester is well known to be associated with fetopathy (287). So, the use of these medications in adolescent females should be approached with caution regarding potential pregnancy. Beta-adrenergic blocking agents may be helpful in patients with comorbid migraine headaches.

The approach to treatment in children and adolescents includes starting a low dose of the initial medication. Blood pressure should be monitored and the dose increased until the goal blood pressure is achieved, or intolerable side effects occur. If the first choice of medication is not as effective as desired, a medication from another class may be substituted. Again, the recommended approach is to start with

a low dose and titrate upward until appropriate blood pressure control is achieved. Sometimes it is necessary to add a second agent from another class to the first medication to achieve desired blood pressure lowering. It is useful to consider combining drugs from classes with complementary mechanisms of action (238). In adults, the use of multiple antihypertensive medications to achieve goal blood pressure is increasingly recommended, sometimes even as first-line therapy (288).

In addition to longitudinal follow-up of blood pressure in the clinic, it is important to follow patients for side effects associated with the class of medication being used. It is also important to monitor for target organ changes over time.

Treatment of Severe Hypertension

Severe hypertension may occur in children and adolescents. These patients will have stage 2 hypertension and some may have blood pressure substantially >99th percentile for age, sex, and height percentile. These children frequently have a secondary underlying cause of their hypertension. This is a situation that requires prompt evaluation and treatment. The pharmacologic agents that are useful in the treatment of severe hypertension are presented in Table 71.20. Pediatric patients may also present with hypertensive emergencies. In this situation, the hypertension is often accompanied by hypertensive encephalopathy and possibly seizures. Such emergencies should be treated with an intravenous infusion that can produce a controlled reduction in blood pressure. It is recommended that the blood pressure be lowered by $\leq 25\%$ in the first 8 hours with normalization over a 24- to 48-hour period (289,290).

Hypertensive urgencies occur with less elevation of blood pressure and less serious symptoms, which may include severe headache and vomiting. Children with a hypertensive urgency can be treated with either oral or intravenous antihypertensive agents depending on the level of blood pressure and symptoms present.

TABLE 71.20 Antihypertensive Drugs for Management of Severe Hypertension in Children

Most Useful				
Drug	Class	Recommended Dose	Route	Comments
Esmolol	β -Blocker	100–500 $\mu\text{g/kg/min}$	IV infusion	Very short acting; constant infusion preferred. May cause profound bradycardia. Produced modest reductions in BP in a pediatric clinical trial.
Hydralazine	Vasodilator	0.2–0.6 mg/kg/dose	IV, IM	Should be given q4h when given IV bolus. Recommended dose is lower than FDA label.
Labetalol	α - and β -blocker	Bolus: 0.2–1.0 mg/kg/dose up to 40	IV bolus or infusion	Asthma and overt heart failure are relative contraindications.
Nicardipine	Calcium channel blocker	1–3 $\mu\text{g/kg/min}$	IV infusion	May cause reflex tachycardia.
Sodium nitroprusside	Vasodilator	0.53–10 $\mu\text{g/kg/min}$	IV infusion	Monitor cyanide levels with prolonged (>72 h) use or in renal failure; or coadminister with sodium thiosulfate.

IV, intravenous; BP, blood pressure; IM, intramuscular.

Summary

Hypertension is an important clinical entity in children and adolescents that may be associated with early atherosclerosis and other target organ disease. Recognition of hypertension usually requires blood pressure measurements on a regular basis during well and ill visits. Blood pressure elevation is often accompanied by obesity and other risk factors for cardiovascular disease. Treatment of hypertension requires a stepwise approach, usually starting with therapeutic lifestyle changes and progressing to pharmacologic treatment as needed. For most patients, the goal should be to lower blood pressure below the 95th percentile for age, sex, and height percentile.

REFERENCES

1. Strydom HC, Chandler AB, Dinsmore RE, et al. A definition of advanced types of atherosclerotic lesions and histological classification of atherosclerosis. A report from the Committee on Vascular Lesions of the Council on Arteriosclerosis, American Heart Association. *Arterioscler Thromb Vasc Biol* 1995;15:1512-1531.
2. Glagov S, Guyton JR, Insull W Jr, et al. A definition of initial, fatty streak, and intermediate lesions of atherosclerosis. A report from the Committee on Vascular Lesions of the Council on Arteriosclerosis, American Heart Association. *Circulation* 1994;89:2462-2478.
3. Ross R. The pathogenesis of atherosclerosis—an update. *New Engl J Med* 1986;314:488-500.
4. Enos WF, Holmes RH, Beyer J. Coronary disease among United States soldiers killed in action in Korea; preliminary report. *J Am Med Assoc* 1953;552:1090-1093.
5. McNamara JJ, Molot MA, Strempel JF, et al. Coronary artery disease in combat casualties in Vietnam. *JAMA* 1971;216:1185-1187.
6. Relationship of atherosclerosis in young men to serum lipoprotein cholesterol concentrations and smoking. A preliminary report from the Pathobiological Determinants of Atherosclerosis in Youth (PDAY) Research Group. *JAMA* 1990;264:3018-3024.
7. McGill HC Jr, McMahan CA, Zieske AW, et al. Effects of nonlipid risk factors on atherosclerosis in youth with a favorable lipoprotein profile. *Circulation* 2001;111:1546-1550.
8. Newman WP, Freedman DS, Voors AW, et al. Relation of serum lipoprotein levels and systolic blood pressure to early atherosclerosis. The Bogalusa Heart Study. *New Engl J Med* 1986;314:138-144.
9. Berenson GS, Srinivasan SR, Bao W, et al. Association between multiple cardiovascular risk factors and atherosclerosis in children and young adults. The Bogalusa Heart Study. *New Engl J Med* 1998;338:1650-1656.
10. Keelan PC, Bielak LF, Ashai K, et al. Long-term prognostic value of coronary calcification detected by electron-beam computed tomography in patients undergoing coronary angiography. *Circulation* 2001;104:412-417.
11. Mahoney LT, Burns TL, Stanford W, et al. Coronary risk factors measured in childhood and young adult life are associated with coronary artery calcification in young adults: The Muscatine Study. *J Am Coll Cardiol* 1996;27:277-284.
12. Gidding SS, Bookstein LC, Chomka EV. Usefulness of electron beam tomography in adolescents and young adults with heterozygous familial hypercholesterolemia. *Circulation* 1998;98:2580-2583.
13. Summers RM, Andrasko-Bourgeois J, Feuerstein IM, et al. Evaluation of the aortic root by MRI: Insights from patients with homozygous familial hypercholesterolemia. *Circulation* 1998;98:509-518.
14. Hatsukami TS, Ross R, Polissar NL, et al. Visualization of fibrous cap thickness and rupture in human atherosclerotic carotid plaque in vivo with high-resolution magnetic resonance imaging. *Circulation* 2000;102:959-964.
15. Chambless LE, Folsom AR, Evans GW. Risk factors for progression of common carotid atherosclerosis: the atherosclerosis risk in communities study, 1987-1998. *Am J Epidemiol* 2002;155:38-47.
16. O'Leary DH, Polak JF, Kronmal RA, et al. Carotid-artery intima and media thickness as a risk factor for myocardial infarction and stroke in older adults. *New Engl J Med* 1999;340:14-22.
17. Chambless LE, Folsom AR, Clegg LX, et al. Carotid wall thickness is predictive of incident clinical stroke. *Am J Epidemiol* 2000;151:478-487.
18. Costanzo P, Perrone-Filardi P, Vassallo E, et al. Does carotid intima-media thickness regression predict reduction of cardiovascular events? A meta-analysis of 41 randomized trials. *J Am Coll Cardiol* 2010;56:2006-2020.
19. Davis PH, Dawson JD, Riley WA, et al. Carotid intimal-medial thickness is related to cardiovascular risk factors measured from childhood through middle age. *Circulation* 2001;104:2815-2819.
20. Raitakari OT, Juonala M, Kahonen M, et al. Cardiovascular risk factors in childhood and carotid artery intima-media thickness in adulthood: the Cardiovascular Risk in Young Finns Study. *JAMA* 2003;290:2277-2283.
21. Sanchez A, Barth JD, Zhang L. The carotid artery wall thickness in teenagers is related to their diet and the typical risk factors of heart disease among adults. *Atherosclerosis* 2000;152:265-266.
22. Tonstad S, Jokimsen O, Stensland-Bugge E, et al. Risk factors related to carotid intima-media thickness and plaque in children with familial hypercholesterolemia and control subjects. *Arterioscl Thromb Vasc Biol* 1996;16:984-991.
23. Sorof JM, Alexandrov AV, Cardwell G, et al. Carotid artery intimal-medial thickness and left ventricular hypertrophy in children with elevated blood pressure. *Pediatrics* 2003;111:61-66.
24. Jarvisalo MJ, Harmoinen A, Hakanen M, et al. Elevated serum C-reactive protein levels and early arterial changes in healthy children. *Arterioscl Thromb Vasc Biol* 2002;22:1323-1328.
25. Juonala M, Magnussen CG, Venn A, et al. Influence of age on associations between childhood risk factors and carotid intima-media thickness in adulthood. *Circulation* 2010;122:2514-2520.
26. Jarvisalo MJ, Jartti L, Nanto-Salonen K, et al. Increased aortic intima-media thickness. A marker of preclinical atherosclerosis in high-risk children. *Circulation* 2001;104:2943-2947.
27. Grundy SM, Garber A, Goldberg R, et al. Prevention Conference VI: Diabetes and Cardiovascular Disease: Writing Group IV: Lifestyle and medical management of risk factors. *Circulation* 2002;105:e153-e158.
28. Pinhas-Hamiel O, Dolan LM, Daniels SR, et al. Increased incidence of non-insulin-dependent diabetes mellitus among adolescents. *J Pediatr* 1996;128:608-615.
29. Nathan DM. Initial management of glycemia in type 2 diabetes mellitus. *New Engl J Med* 2002;347:1342-1349.
30. Kannel WB, McGee DL. Diabetes and cardiovascular disease: the Framingham Study. *JAMA* 1979;241:2035-2038.
31. Panzram G. Mortality and survival in type 2 (non-insulin-dependent) diabetes mellitus. *Diabetologia* 1987;30:123-131.
32. Palumbo PJ, Elveback LR, Chu CP, et al. Diabetes mellitus: incidence, prevalence, survivorship, and cause of death in Rochester, Minnesota, 1945-1970. *Diabetes* 1976;24:566-573.
33. American Diabetes Association. Management of dyslipidemia in adults with diabetes. *Diabetes Care* 2002;24:S74-S77.
34. Executive Summary on the Third Report on the National Cholesterol Education Program (NCEP) Expert Panel on Detection, Evaluation and Treatment of High Blood Cholesterol in Adults (Adult Treatment Panel III). *JAMA* 2001;285:2486-2497.
35. Shah AS, Khoury PR, Dolan LM, et al. The effects of obesity and type 2 diabetes mellitus on cardiac structure and function in adolescents and young adults. *Diabetologia* 2011;54:722-730.
36. Urbina EM, Kimball TR, Khoury PR, et al. Increased arterial stiffness is found in adolescents with obesity or obesity-related type 2 diabetes mellitus. *J Hypertens* 2010;28:1692-1698.
37. Wadwa RP, Urbina EM, Anderson AM, et al.; SEARCH Study Group. Measures of arterial stiffness in youth with type 2 and the 2 diabetes: the SEARCH for diabetes in youth study. *Diabetes Care* 2010;33:881-886.
38. Urbina EM, Kimball TR, McCoy CE, et al. Youth with obesity and obesity-related type 2 diabetes mellitus demonstrate abnormalities in carotid structure and function. *Circulation* 2009;119:2913-2919. [Epub 2010 Jan 12.]
39. Shah AS, Dolan LM, Kimball TR, et al. Influence of duration of diabetes, glycemic control, and traditional cardiovascular risk factors on early atherosclerotic vascular changes in adolescents and young adults with type 2 diabetes mellitus. *J Clin Endocrinol Metab* 2009;94:3740-3745. [Epub 2009 Sep 1.]
40. Gidding SS, Schydlower M. Active and passive tobacco exposure: a serious pediatric health problem. *Pediatrics* 1994;94:750-751.
41. Ockene JK, Kuller LH, Svendsen KH, et al. The relationship of smoking cessation to coronary heart disease and lung cancer in the Multiple Risk Factor Intervention Trial (MRFIT). *Am J Public Health* 1990;80:954-958.
42. U.S. Department of Health and Human Services. *The Health Consequences of Smoking: A Report of the Surgeon General*. Atlanta, Georgia: U.S. Department of Health and Human Services, Public Health Service, Centers for Disease Control and Prevention, National Center for Chronic Disease Prevention and Health Promotion, Office on Smoking and Health, 2004.
43. Centers for Disease Control and Prevention (CDC). Annual smoking-attributable mortality, years of potential life lost, and economic costs—United States, 1995-1999. *MMWR Morb Mortal Wkly Rep* 2002;51:300-303.
44. Centers for Disease Control and Prevention. Youth risk behavior surveillance—United States, 2003. *MMWR Morb Mortal Wkly Rep* 2004;53:1-100.
45. Centers for Disease Control and Prevention. Tobacco use among middle school and high school students—United States, 2002. *MMWR Morb Mortal Wkly Rep* 2003;52:1096-1098.
46. Centers for Disease Control and Prevention. Tobacco use among middle school and high school students—United States, 2000-2009. *MMWR Morb Mortal Wkly Rep* 2010;59:1063-1068. [accessed March 11, 2011.]
47. Gritz ER, Prokhorov AV, Hudmon KS, et al. Cigarette smoking in a multiethnic population of youth: methods and baseline findings. *Prev Med* 1998;27:265-284.
48. Jackson C, Henriksen L. Do as I say: parent smoking, antismoking socialization and smoking onset in children. *Addict Behav* 1997;22:107-114.
49. Chassin L, Presson CC, Todd M, et al. Maternal socialization of adolescent smoking: the intergenerational transmission of parenting and smoking. *Dev Psychol* 1998;34:1189-1201.

50. Farkas AJ, Distefan JM, Choi WS, et al. Does parental smoking cessation discourage adolescent smoking? *Prev Med* 1999;28:213–218.
51. Winnail S, Valois R, McKeown R, et al. Relationship between physical activity level and cigarette, smokeless tobacco, and marijuana use among public high school adolescents. *J School Health* 1995;65:438–442.
52. Williams CL, Hayman LL, Daniels SR, et al. Cardiovascular health in childhood: a statement for health professionals from the Committee on Atherosclerosis, Hypertension and Obesity in the Young (AHOY) of the Council on Cardiovascular Disease in the Young. American Heart Association. *Circulation* 2002;106:143–160.
53. Moskowitz WB, Mosteller M, Schieken RM, et al. Lipoprotein and oxygen transport alterations in passive smoking preadolescent children: The MCV Twin Study. *Circulation* 1990;81:586–592.
54. Weitzman M, Cook S, Auinger P, et al. Tobacco smoke exposure is associated with the metabolic syndrome in adolescents. *Circulation* 2005;112:862–869.
55. Meyers DG, Neuberger JS. Cardiovascular effect of bans on smoking in public places. *Am J Cardiol* 2008;102:1421–1424.
56. Glantz S. Meta-analysis of the effects of smokefree laws on acute myocardial infarction: an update. *Prev Med* 2008;47:452–453.
57. Ogden CL, Carroll MD, Flegal KM. High body mass index for age among US children and adolescents, 2003–2006. *JAMA* 2008;299:2401–2405.
58. Lauer RM, Lee J, Clarke WR. Factors affecting the relationship between childhood and adult cholesterol levels: the Muscatine Study. *Pediatrics* 1988;82:309–318.
59. Lauer RM, Clarke WR. Childhood risk factors for high adult blood pressure: the Muscatine Study. *Pediatrics* 1987;84:633–641.
60. Daniels SR, Arnett DK, Eckel RH, et al. Overweight in children and adolescents. *Circulation* 2005;111:1999–2012.
61. Yanovski JA, Yanovski SZ. Treatment of pediatric and adolescent obesity. *JAMA* 2003;289:1851–1853.
62. Kirk S, Zeller M, Claytor R, et al. The relationship of health outcomes to improvement in BMI in children and adolescents. *Obes Res* 2005;13:876–882.
63. Yanovski SZ. Pharmacotherapy for obesity—promise and uncertainty. *New Engl J Med* 2005;353:2187–2189.
64. Inge TH, Krebs NF, Garcia VF, et al. Bariatric surgery for severely overweight adolescent: concerns and recommendations. *Pediatrics* 2004;114:217–223.
65. Whitlock EP, O'Connor EA, Williams SB, et al. Effectiveness of weight management interventions in children: a targeted systematic review for the USPSTF. *Pediatrics* 2010;125:e396–e418.
66. Barlow SE; Expert Committee. Expert committee recommendations regarding the prevention, assessment and treatment of child and adolescent overweight and obesity: summary report. *Pediatrics* 2007;120:S164–S192.
67. Grundy SM, Cleeman JI, Daniels SR, et al. Diagnosis and management of the metabolic syndrome: an American Heart Association/National Heart, Lung and Blood Institute Scientific Statement. *Circulation* 2005;112:2735–2752.
68. Cook S, Weitzman N, Auinger P, et al. Prevalence of a metabolic syndrome phenotype in adolescents: findings from the Third National Health and Nutrition Examination Survey, 1988–1994. *Arch Pediatr Adolesc Med* 2003;157:821–827.
69. Weiss R, Dziura J, Burgert TS, et al. Obesity and the metabolic syndrome in children and adolescents. *New Engl J Med* 2004;350:2362–2374.
70. Duncan GE, Li SM, Zhou X-H. Prevalence and trends of a metabolic syndrome phenotype among U.S. adolescents, 1999–2000. *Diabetes Care* 2004;27:2438–2443.
71. Eisenmann JC. On the use of a continuous metabolic syndrome score in pediatric research. *Cardiovasc Diabetol* 2008;7:17.
72. Goodman E, Daniels SR, Meigs JB, et al. Instability in the diagnosis of metabolic syndrome in adolescents. *Circulation* 2007;115:2316–2322.
73. Steinberger J, Daniels SR, Eckel RH, et al. Progress and challenges in metabolic syndrome in children and adolescents. A scientific statement from the American Heart Association Atherosclerosis, Hypertension, and Obesity in the Young; Council on Cardiovascular Nursing; and Council on Nutrition, Physical Activity and Metabolism. *Circulation* 2009;119:628–647.
74. Strong WB, Malina RM, Blimkie CJ, et al. Evidence based physical activity for school-age youth. *J Pediatr* 2005;146:732–737.
75. Peter RK, Cady LD, Bischoff DP, et al. Physical fitness and subsequent myocardial infarction in healthy workers. *JAMA* 1983;249:3052–3056.
76. Goldberg L, Elliot DL, Schutz RW, et al. Changes in lipid and lipoprotein levels after weight training. *JAMA* 1984;252:504–506.
77. Lloyd-Jones DM, Hong Y, Labarthe D, et al. Defining and setting national goals for cardiovascular health promotion and disease reduction: the American Heart Association's strategic impact goal through 2020 and beyond. *Circulation* 2010;121:586–613.
78. Lloyd-Jones DM, Leip EP, Larson MG, et al. Prediction of lifetime risk for cardiovascular disease by risk factor burden at 50 years of age. *Circulation* 2006;113:791–798.
79. Bambs C, Kip KE, Dinga A, et al. Low prevalence of “ideal cardiovascular health” in a community-based population. *Circulation* 2011;123:850–857.
80. Kavey RE, Daniels SR, Lauer RM, et al. American Heart Association guideline for primary prevention of atherosclerotic cardiovascular disease beginning in childhood. *Circulation* 2003;107:1562–1566.
81. Daniels SR, et al. NHLBI guidelines for evaluation, prevention and treatment of atherosclerotic cardiovascular disease in children and adolescents. *Pediatrics* 2011;128:S213–S256.
82. Schaefer EJ, Levy RI. Pathogenesis and management of lipoprotein disorders. *New Engl J Med* 1985;312:1300–1310.
83. Gotto AM, Pownall HR, Havel RJ. Introduction to the plasma lipoproteins. *Methods Enzymol* 1986;128:3.
84. Austin MA, Breslow JL, Hennekens CH, et al. Low-density lipoprotein subclass patterns and risk for myocardial infarction. *JAMA* 1988;260:1917–1921.
85. Miller NE. Association of high density lipoprotein subclasses and apolipoprotein with ischemic heart disease and coronary atherosclerosis. *Am Heart J* 1987;113:589.
86. Tamir I, Heiss G, Glueck CJ, et al. Lipid and lipoprotein distributions in white children ages 6–19 yrs: the Lipid Research Clinics Program Prevalence Study. *J Chronic Dis* 1981;34:27–39.
87. Jolliffe CJ, Janssen I. Distribution of lipoproteins by age and gender in adolescents. *Circulation* 2006;114:1056–1062.
88. Expert Panel on Detection, Evaluation and Treatment of High Blood Cholesterol in Adults. Executive summary of the Third Report of the National Cholesterol Education Program (NCEP) Expert Panel on Detection, Evaluation, and Treatment of High Blood Cholesterol in Adults (Adult Treatment Panel III). *JAMA* 2001;285:2486–2497.
89. Multiple Risk Factor Intervention Trial Research Group. Mortality Rates After 10.5 years for Participants in the Multiple Risk Factor Intervention Trial: Findings related to a priori hypotheses of the trial. *JAMA* 1990;263:3151.
90. Castelli WP, Garrison RJ, Wilson WF, et al. Incidence of coronary heart disease and lipoprotein cholesterol levels. The Framingham Study. *JAMA* 1986;256:2835–2838.
91. Davis CE, Rifkind BM, Brenner H, et al. A single cholesterol measurement underestimates the risk for coronary heart disease. An empirical example from the Lipid Research Clinics Mortality Follow-up Study. *JAMA* 1990;264:3044–3046.
92. Gordon DJ, Rifkind BM. High-density lipoprotein: the clinical implications of recent studies. *New Engl J Med* 1989;321:1311–1316.
93. Knudsen JR, West CE, Katan MB, et al. Total cholesterol and high density lipoprotein cholesterol levels in populations differing in fat and carbohydrate intake. *Arteriosclerosis* 1987;7:612–619.
94. Freedman DS, Shear CL, Srinivasan SR, et al. Tracking of serum lipids and lipoproteins in children over an 8-year period: the Bogalusa Heart Study. *Prev Med* 1985;14:203–216.
95. Clarke WR, Schrott HG, Leaverton PE, et al. Tracking of blood lipids and blood pressures in school age children: the Muscatine Study. *Circulation* 1978;58:626–634.
96. Lauer RM, Lee J, Clarke WR. Factors affecting the relationship between childhood and adult cholesterol levels: the Muscatine Study. *Pediatrics* 1988;82:309–318.
97. Magnusson CG, Thomson R, Cleland VJ, et al. Factors affecting the stability of blood lipid and lipoprotein levels from youth to adulthood: evidence from the Childhood Determinants of Adult Health Study. *Arch Pediatr Adolesc Med* 2011;165:68–76.
98. Brown MS, Goldstein JL. A receptor-mediated pathway for cholesterol homeostasis. *Science* 1986;232:34–47.
99. Goldstein JL, Brown MS, Anderson RG, et al. Receptor-mediated endocytosis: Concepts emerging from the LDL receptor system. *Annu Rev Cell Biol* 1985;1:1–39.
100. Kwiterovich PO Jr. Recognition and management of dyslipidemia in children and adolescents. *J Clin Endocrinol Metab* 2008;93:4200–4209.
101. Goldberg AC, Hopkins PN, Toth P, et al. Familial hypercholesterolemia: screening, diagnosis and management of pediatric and adult patients clinical guidance from the National Lipid Association Expert Panel on Familial Hypercholesterolemia. *J Clin Lipidol* 2011;5:S1–S8.
102. Kwiterovich PO Jr. Diagnosis and management of familial dyslipoproteinemia in children and adolescents. *Pediatr Clin Am* 1990;37:1489–1523.
103. Berg K. Genetics of coronary heart disease and its risk factors. *Prog Clin Biol Res* 1985;177:351–374.
104. Yamakawa-Kobayashi K, Yanagi H, Fukayama H, et al. Frequent occurrence of hypoalphalipoproteinemia due to mutant apolipoprotein A-I gene in the population: a population based study. *Hum Mol Genet* 1999;8:331–336.
105. Clauss SB, Kwiterovich PO. Genetic disorders of lipoprotein transport in children. *Prog Pediatr Cardiol* 2003;17:123–133.
106. Brunzell JD. Familial lipoprotein lipase deficiency and other cause of chylomicronemia syndrome. In: Scriver CR, Beaudet AL, Sly WS, et al., eds. *The Molecular Basis of Inherited Disease*. New York, NY: McGraw-Hill, 1987:1165.
107. Feoli-Fonseca JC, Levy E, Godard M, et al. Familial lipoprotein lipase deficiency in infancy: clinical, biochemical and molecular study. *J Pediatr* 1998;133:417–423.
108. Cortner JA, Coates PM, Gallaher PR. Prevalence and expression of familial combined hyperlipidemia in childhood. *J Pediatr* 1990;116:514–519.
109. Berg K, Dahlen G, Borresen AL. Lp (a) phenotypes, other lipoprotein parameters, and a family of coronary heart disease in middle-aged males. *Clin Genet* 1979;16:347–352.
110. Suzuki K, Kuriyama M, Saito T, et al. Plasma lipoprotein (a) levels and expression of the apolipoprotein (a) gene are dependent on the nucleotide polymorphisms in its 5'-flanking region. *J Clin Invest* 1997;99:1361–1366.

111. Nowak-Gottl U, Debus O, Findeisen M, et al. Lipoprotein (a): Its role in childhood thromboembolism. *Pediatrics* 1997;99:E11.
112. Utermann G, Menzel HJ, Kraft HG, et al. Lp (a) glycoprotein phenotype: Inheritance and relation to Lp (a) lipoprotein concentrations in plasma. *J Clin Invest* 1987;80:458.
113. Clarkson TB, Lofland HB Jr, Bullock BC, et al. Genetic control of plasma cholesterol: studies on squirrel monkeys. *Arch Pathol* 1971;92:37-45.
114. Clarkson TB, Bond MG, Bullock BC, et al. A study of atherosclerosis regression in Macaca mulatta. IV: changes in coronary arteries from animals with atherosclerosis induced for 19 months and then regressed for 24 to 48 months at plasma cholesterol concentrations of 300 or 200 mg/dL. *Exp Mol Pathol* 1981;34:345-68.
115. Rosenstock J, Strowig S, Cercone S, et al. Reduction in cardiovascular risk factors with intensive diabetes treatments in insulin-dependent diabetes mellitus. *Diabetes Care* 1987;10:729-734.
116. Kershner A, Daniels SR, Imperatore G, et al. Lipid abnormalities are prevalent in youth with type 1 and type 2 diabetes: The Search for Diabetes in Youth Study. *J Pediatr* 2006;149:314-319.
117. Pettit DB, Imperatore G, Palla SL, et al.; for the SEARCH for Diabetes in Youth Study Group. Serum lipids and glucose control. *Arch Pediatr Adolesc Med* 2007;161:159-165.
118. Grundy SM. Management of hyperlipidemia of kidney disease. *Kidney Int* 1990;37:847-853.
119. Joven J, Villabona C, Vilella E, et al. Abnormalities of lipoprotein metabolism in patients with the nephrotic syndrome. *New Engl J Med* 1990;323:579-584.
120. Lindner A, Charra B, Sherrard DJ, et al. Accelerated atherosclerosis in prolonged maintenance hemodialysis. *New Engl J Med* 1974;290:697-701.
121. Yoshimura N, Ohmori Y, Tsuji T, et al. Effect of pravastatin on renal transplant recipients treated with cyclosporine—4-year follow up. *Transplantation Proc* 1994;26:2652-2633.
122. Hazzard WR, Haffner SM, Kushwaha RS, et al. Preliminary report: kinetic studies on the modulation of high-density lipoprotein, apolipoprotein, and subfraction metabolism by sex steroids in a post-menopausal woman. *Metabolism* 1984;33:779-784.
123. Gallin JL, Kaye D, O'Leary WM. Serum lipids in infection. *New Engl J Med* 1969;281:1081-1086.
124. Gidding SS, Stone NJ, Bookstein LC, et al. Month to month variability of lipids, lipoproteins and apolipoprotein and the impact of acute infection in adolescents. *J Pediatr* 1998;133:242-246.
125. Expert Panel on Detection Evaluation, and Treatment of High Blood Cholesterol in Adults. Executive summary of the third report of the National Cholesterol Education Program (NCEP) expert panel on detection, evaluation and treatment of high blood cholesterol in adults (Adult Treatment Panel III). *JAMA* 2001;285:2508-2509.
126. Sinha R, Fisch G, Teague B, et al. Prevalence of impaired glucose tolerance among children and adolescents with marked obesity. *New Engl J Med* 2002;346:802-810.
127. Kirk S, Zeller M, Claytor R, et al. The relationship of health outcomes to improvement in body mass index in children and adolescents. *Obesity Res* 2005;13:876-882.
128. American Academy of Pediatrics. National Cholesterol Education Program: Report of the Expert Panel on Blood Cholesterol Levels in Children and Adolescents. *Pediatrics* 1992;89:525-584.
129. Daniels SR, Greer FR; Committee on Nutrition. Lipid screening and cardiovascular health in childhood. *Pediatrics* 2008;122:198-208.
130. Rose G. Sick individuals and sick populations. *Int J Epidemiol* 1985;14:32-38.
131. U.S. Department of Agriculture and U.S. Department of Health and Human Services. Dietary guidelines for America, 2010. 7th ed. December 2010: Washington DC, U.S. Government Printing Office.
132. Dietary Guidelines Advisory Committee, U.S. Department of Agriculture and U.S. Department of Health and Human Services. 2010 report of the dietary guidelines advisory committee on the dietary guidelines for America, 2010, to the Secretary of Agriculture and the Secretary of Health and Human Services.
133. Simell O, Niinikoski H, Rönnemaa T, et al. Special Turku Coronary Risk Factor Intervention Project for Babies (STRIP). *Am J Clin Nutr* 2000;72:1316s-1331s.
134. Niinikoski H, Iagstrom H, Jokinen E, et al. Impact of repeated dietary counseling between infancy and 14 years of age on dietary intakes and serum lipids and lipoproteins: the STRIP study. *Circulation* 2007;116:1032-1040.
135. DISC Collaborative Research Group. The efficacy and safety of lowering dietary intake of total fat, saturated fat, and cholesterol in children with elevated LDL cholesterol: The Dietary Intervention Study in Children (DISC). *JAMA* 1995;273:1429-1435.
136. Salo P, Viikari M, Hamalainen M, et al. Serum cholesterol ester fatty acids in 7- and 13-month-old children in a prospective randomized trial of a low-saturated fat, low-cholesterol diet: The STRIP baby project. *Special Turku Coronary Risk Factor Intervention Project for Children. Acta Paediatr* 1999;88:505-512.
137. Lifshitz F, Moses N. Growth failure. A complication of dietary treatment of hypercholesterolemia. *Am J Dis Child* 1989;143:537-542.
138. Tershakovec AM, Shannon BM, Achterberg CL, et al. One year follow-up of nutrition education for hypercholesterolemia in children. *Am J Public Health* 1998;88:258-261.
139. Nicklas TA, Baranowski T, Baranowski JC, et al. Family and child-care provider influences on preschool children's fruit, juice and vegetable consumption. *Nutr Rev* 2001;59:224-235.
140. Epstein LH, Paluch RA, Gordy CC, et al. Decreasing sedentary behaviors in treating pediatric obesity. *Arch Pediatr Adolesc Med* 2000;154:220-226.
141. Emmons L. Food procurement and the nutritional adequacy of diets in low-income families. *J Am Diet Assoc* 1986;86:1684-1693.
142. Dennison BA, Jenkins PL, Pearson TA. Challenges to implementing the current pediatric cholesterol screening guidelines into practice. *Pediatrics* 1994;94:296-302.
143. Rifai N, Neufeld E, Ahlstrom P, et al. Failure of current guidelines for cholesterol screening in urban African-American adolescents. *Pediatrics* 1996;98:383-388.
144. Rastam L, Hannan PJ, Luepker RV, et al. Seasonal variation in plasma cholesterol distributions: Implications for screening and referral. *Am J Prev Med* 1992;8:360-366.
145. Williams RR, Hunt SC, Barlow GK, et al. Prevention of familial cardiovascular disease by screening for family history and lipids in youths. *Clin Chem* 1992;38:1555-1560.
146. Bachman RP, Schoen EJ, Stemberge A, et al. Compliance with childhood cholesterol screening among members of a prepaid health plan. *Am J Dis Child* 1993;147:382-385.
147. Resnicow K, Cross D, Lacosse J, et al. Evaluation of a school-site cardiovascular risk factor screening intervention. *Prev Med* 1993;22:838-856.
148. Boulton TJ. The validity of screening for hypercholesterolemia at different ages from 2 to 17 years. *Aust N Z J Med* 1979;9:542-546.
149. Ritchie SK, Murphy ECS, Ice C, et al. Universal versus targeted blood cholesterol screening among youth: the CARDIAC Project. *Pediatrics* 2010;126:260-265.
150. Dennison BA, Kikuchi DA, Srinivasan SR, et al. Serum total cholesterol screening for detection of elevated low-density lipoprotein in children and adolescents: the Bogalusa Heart Study. *Pediatrics* 1990;85:472-479.
151. Labarthe DR, Dai S, Fulton J. Cholesterol screening in children: insights from Project HeartBeat! and NHANES III. *Prog Pediatr Cardiol* 2003;17:159-168.
152. Morrison J. A longitudinal evaluation of the NCEP-Peds guidelines for elevated total and LDL-cholesterol in adolescent girls and boys. *Prog Pediatr Cardiol* 2003;17:159-168.
153. Magnussen CG, Raitakari OT, Thomson R, et al. Utility of currently recommended pediatric dyslipidemia classifications in predicting dyslipidemia in adulthood: evidence from the Childhood Determinants of Adult Health (CDAH) Study, Cardiovascular Risk in Young Finns Study, and Bogalusa Heart Study. *Circulation* 2008;117:32-42.
154. Kavey RE, Daniels SR, Lauer RM, et al.; American Heart Association. American Heart Association guidelines for primary prevention of atherosclerotic cardiovascular disease beginning in childhood. *J Pediatr* 2003;142:368-372.
155. Cullen KW, Bartholomew LK, Parcel GS, et al. Measuring stage of change for fruit and vegetable consumption in 9- to 12-year-old girls. *J Behav Med* 1998;21:241-254.
156. Birch LL. Development of food preferences. *Annu Rev Nutr* 1993;19:41-62.
157. Birch LL. Children's preferences for high-fat foods. *Nutr Rev* 1992;50:249-255.
158. Birch LL, McGhee L, Shoba BC. What kind of exposure reduces children's food neophobia? *Appetite* 1987;9:171-178.
159. Miettus-Snyder M, Baker AL, Neufeld EJ, et al. Effects of nutritional counseling on lipoprotein levels in pediatric lipid clinic. *Am J Dis Child* 1993;147:378-381.
160. Alexandrov AA, Maslennikova GY, Kulikov SM, et al. Primary prevention of cardiovascular disease: 3-year intervention results in boys of 12 years of age. *Prev Med* 1992;21:53-62.
161. Obarzanek E, Kimm SY, Barton BA, et al.; DISC Collaborative Research Group. Long-term safety and efficacy of a cholesterol-lowering diet in children with elevated low-density lipoprotein cholesterol: seven-year results of the Dietary Intervention Study in Children. *Pediatrics* 2001;107:256-264.
162. Jacobson MS, Tomopoulos S, Williams CL, et al. Normal growth in high-risk hyperlipidemic children and adolescents with dietary intervention. *Prev Med* 1998;27:775-780.
163. Kuehl KS, Cockerham JT, Hitchings M, et al. Effective control of hypercholesterolemia in children with dietary intervention based in pediatric practice. *Prev Med* 1993;22:154-166.
164. Davidson MH, Dugan LD, Burns JH, et al. A psyllium-enriched cereal for the treatment of hypercholesterolemia in children: a controlled, double-blind, crossover study. *The Am J Nutr* 1996;63:96-102.
165. Tammi A, Rönnemaa T, Gylling H, et al. Plant stanol ester margarine lowers serum total and low-density lipoprotein cholesterol concentrations of healthy children: the STRIP project. *Special Turku Coronary Risk Factors Intervention Project. J Pediatr* 2000;136:503-510.
166. Gylling H, Siimes MA, Miettinen TA. Sitostanol ester margarine in dietary treatment of children with familial hypercholesterolemia. *J Lipid Res* 1995;36:1807-1812.
167. McCrindle BW, Urbina EM, Dennison BA, et al. Drug therapy of high risk lipid abnormalities in children and adolescents: A scientific statement from the American Heart Association Atherosclerosis, Hypertension and Obesity in Youth Committee, Council of Cardiovascular Disease in the Young with the Council on Cardiovascular Nursing. *Circulation* 2007;115:1948-1967.

168. Tonstad S, Sivertsen M, Aksnes L, et al. Low dose colestipol in adolescents with familial hypercholesterolemia. *Arch Dis Child* 1996;74:157-160.
169. Tonstad S, Knudtzon J, Sivertsen M, et al. Efficacy and safety of cholestyramine therapy in peripubertal and prepubertal children with familial hypercholesterolemia. *J Pediatr* 1996;129:42-49.
170. McCrindle BW, O'Neill MB, Cullen-Dean G, et al. Acceptability and compliance with two forms of cholestyramine in the treatment of hypercholesterolemia in children: a randomized, crossover trial. *J Pediatr* 1997;130:266-273.
171. Stein EA, Marais AD, Szamosi T, et al. Colesevelam hydrochloride: efficacy and safety in pediatric subjects with heterozygous familial hypercholesterolemia. *J Pediatr* 2010;156:231-6.e1-e3. [Epub 2009 Oct 31.]
172. Gagne C, Gaudet D, Bruckert E. Efficacy and safety of ezetimibe coadministered with atorvastatin or simvastatin in patients with homozygous familial hypercholesterolemia. *Circulation* 2002;105:2469-2475.
173. Smith SC. Review of recent clinical trials of lipid lowering in coronary artery disease. *Am J Cardiol* 1997;80:10H-13H.
174. Shepherd J. Preventing coronary artery disease in the West of Scotland: implications for primary prevention. *Am J Cardiol* 1998;82:57T-59T.
175. Pederson TR. Coronary artery disease: the Scandinavian Simvastatin Survival Study experience. *Am J Cardiol* 1998;82:53T-56T.
176. Taylor F, Ward K, Moore THM, et al. Statins for the primary prevention of cardiovascular disease. *Cochrane Database Syst Rev* 2011, Issue 1. Art No. CD004816.
177. Firth JC, Marais AD, Byrnes P, et al. Fluvastatin in heterozygous familial hypercholesterolaemia. *Cardiol Young* 2000;10:35.
178. Ducobu J, Brasseur D, Chaudron JM, et al. Simvastatin use in children. *Lancet* 1992;339:1488.
179. Knipscheer HC, Boelen CC, Kastelein JJ, et al. Short-term efficacy and safety of pravastatin in 72 children with familial hypercholesterolaemia. *Pediatr Res* 1996;39:867-871.
180. Lambert M, Lupien PJ, Gagne C, et al. Treatment of familial hypercholesterolaemia in children and adolescents: effect of lovastatin. *Pediatrics* 1996;97:619-628.
181. de Jongh S, Ose L, Szamosi T, et al.; Simvastatin in Children Study Group. Efficacy and safety of statin therapy in children with familial hypercholesterolaemia: a randomized, double-blind, placebo-controlled trial with Simvastatin. *Circulation* 2002;106:2231-2237.
182. McCrindle BW, Ose L, Marais AD. Efficacy and safety of atorvastatin in children and adolescents with familial hypercholesterolaemia or severe hyperlipidemia: a multicenter, randomized, placebo-controlled trial. *J Pediatr* 2003;143:74-80.
183. Wiegman A, Hutten BA, de Groot E, et al. Efficacy and safety of statin therapy in children with familial hypercholesterolaemia: a randomized controlled trial. *JAMA* 2004;292:331-337.
184. Waters DD, Ho JE, Demicco DA, et al. Predictors of new-onset diabetes in patients treated with atorvastatin results from 3 large randomized clinical trials. *J Am Coll Cardiol* 2011;57:1535-1545.
185. Mizuno Y, Jacob RF, Mason RP. Inflammation and the development of atherosclerosis: effects of lipid-lowering therapy. *J Atheroscler Thromb* 2011;18:351-358.
186. MacMahon S, Peto R, Cutler J, et al. Blood pressure, stroke and coronary heart disease. I. Prolonged differences in blood pressure—prospective observational studies corrected for the regression dilution bias. *Lancet* 1990;335:765-774.
187. Kannel WB. Hypertension: epidemiological appraisal. In: Robinson K, ed. *Preventive Cardiology: A Guide for Clinical Practice*. Armonk, NY: Futura Publishing, 1998:1-14.
188. Sinclair AM, Isles CG, Brown I, et al. Secondary hypertension in a blood pressure clinic. *Arch Intern Med* 1987;147:1289-1293.
189. Londe S. Causes of hypertension in the young. *Pediatr Clin North Am* 1978;25:55-65.
190. Rames LK, Clark WR, Connor WE, et al. Normal blood pressure and the evaluation of sustained blood pressure elevation in childhood: the Muscatine Study. *Pediatrics* 1978;61:245-251.
191. Sinaiko AR, Gomez-Marin O, Prineas RJ. Prevalence of "significant" hypertension in junior high school-aged children: the Children and Adolescent Blood Pressure Program. *J Pediatr* 1989;114:664-669.
192. Sorof J, Lai D, Turner J, et al. Overweight, ethnicity, and the prevalence of hypertension in school-aged children. *Pediatrics* 2004;113:475-482.
193. McNiece KL, Poffenbarger TS, Turner JL, et al. Prevalence of hypertension and pre-hypertension among adolescents. *J Pediatr* 2007;150:640-644.e1.
194. Din-Dzietham R, Liu Y, Bielo MV, et al. High blood pressure trends in children and adolescents in national surveys, 1963 to 2002. *Circulation* 2007;116:1488-1496.
195. Muntner P, He J, Cutler JA, et al. Trends in blood pressure among children and adolescents. *JAMA* 2004;291:2109-2113.
196. Rosner B, Prineas R, Daniels SR, et al. Blood pressure differences between blacks and whites in relation to body size among US children and adolescents. *Am J Epidemiol* 2000;151:1007-1019.
197. Paradis G, Lambert M, O'Laughlin J, et al. Blood pressure and adiposity in children and adolescents. *Circulation* 2004;110:1832-1838.
198. Sorof J, Daniels SR. Obesity hypertension in children. A problem of epidemic proportions. *Hypertension* 2002;40:441-447.
199. Barker D. The fetal origins of hypertension. *J Hypertens Suppl* 1996;14:117S-120S.
200. Law CM, Shiell AW, Newsome CA, et al. Fetal, infant, and childhood growth and adult blood pressure: a longitudinal study from birth to 22 years of age. *Circulation* 2002;105:1088-1092.
201. Matthes JW, Lewis PA, Davies DP, et al. Relation between birth weight at term and systolic blood pressure in adolescence. *BMJ* 1994;308:1074-1077.
202. Bao W, Threefoot SA, Srinivasan SR, et al. Essential hypertension predicted by tracking of blood pressure during childhood: the Bogalusa Heart Study. *Am J Hypertens* 1995;8:657-665.
203. Lauer RM, Clarke WR. Childhood risk factors for high adults' blood pressure: the Muscatine Study. *Pediatrics* 1989;84:633-641.
204. Clarke WR, Schrott H, Leaverton PE, et al. Tracking of blood lipids and blood pressure in children: the Muscatine Study. *Circulation* 1978;62:626-634.
205. Cook NR, Gillman MW, Rosner BA, et al. Combining annual blood pressure measurements in childhood to improve prediction of young adult blood pressure. *Stat Med* 2000;19:2625-2640.
206. Lauer RM, Anderson AR, Beaglehole R, et al. Factors related to tracking of blood pressure in children: U.S. National Center for Health Statistics Health Examination Surveys Cycles II and III. *Hypertension* 1984;6:307-314.
207. Daniels SR, McMahon RP, Obarzanek E, et al. Longitudinal correlates of change in blood pressure in adolescent girls. *Hypertension* 1998;31:97-103.
208. Wang YC, Cheung AM, Bibbins-Domingo K, et al. Effectiveness and cost-effectiveness of blood pressure screening in adolescents in the United States. *J Pediatr* 2011;158:257-264.
209. Chobanian AV, Bakris GL, Black HR, et al.; National Heart, Lung, and Blood Institute Joint National Committee on Prevention, Detection, Evaluation, and Treatment of High Blood Pressure; National High Blood Pressure Education Program Coordinating Committee. The Seventh Report of the Joint National Committee on Prevention, Detection, Evaluation and Treatment of High Blood Pressure: The JNC 7 report. *JAMA* 2003;289:2560-2572.
210. Grundy SM, Cleeman JI, Daniels SR, et al.; American Heart Association; National Heart, Lung, and Blood Institute. Diagnosis and management of the metabolic syndrome: an American Heart Association/National Heart, Lung, and Blood Institute Scientific Statement. *Circulation* 2005;112:2735-2752.
211. Still JL, Cottom DG. Severe hypertension in childhood. *Arch Dis Child* 1967;42:34-39.
212. Gill DG, Mendes da Costa B, Cameron JS, et al. Analysis of 100 children with severe and persistent hypertension. *Arch Dis Child* 1976;51:951-956.
213. Trompeter RS, Smith RL, Hoare RD, et al. Neurological complication of arterial hypertension. *Arch Dis Child* 1982;57:913-917.
214. Watson AR, Balfe JW, Hardy BE. Renovascular hypertension in childhood: a changing perspective in management. *J Pediatr* 1985;106:366-372.
215. Daniels SR, Loggie JMH, McEnery PT, et al. Clinical spectrum of intrinsic renovascular hypertension in children. *Pediatrics* 1987;80:698-704.
216. Berenson GS, Srinivasan SR, Bao W, et al. Association between multiple cardiovascular risk factors and atherosclerosis in children and young adults. The Bogalusa Heart Study. *New Engl J Med* 1998;338:1650-1656.
217. McGill HC Jr, McMahan CA, Zieske AW, et al. Effects of nonlipid risk factors on atherosclerosis in youth with a favorable lipoprotein profile. *Circulation* 2001;103:1546-1550.
218. Daniels SR, Loggie JMH, Khoury P, et al. Left ventricular geometry and severe left ventricular hypertrophy in children and adolescents with essential hypertension. *Circulation* 1998;97:1907-1911.
219. Hanevold C, Waller J, Daniels S, et al. International Pediatric Hypertension Association. The effects of obesity, gender, and ethnic group on left ventricular hypertrophy and geometry in hypertensive children: a collaborative study of the International Pediatric Hypertension Association. *Pediatrics* 2004;113:328-333.
220. Sorof JM, Alexandrov AV, Cardwell G, et al. Carotid artery intimal-medial thickness and left ventricular hypertrophy in children with elevated blood pressure. *Pediatrics* 2003;111:61-66.
221. Levy D, Garrison RJ, Savage DD, et al. Prognostic implications of echocardiographically determined left ventricular mass in the Framingham Study. *New Engl J Med* 1990;322:1561-1566.
222. deSimone G, Devereux RG, Daniels SR, et al. Effect of growth on variability of left ventricular mass: Assessment of allometric signals in adults and children and their capacity to predict cardiovascular risk. *J Am Coll Cardiol* 1995;25:1056-1062.
223. Jarvisalo MJ, Jartti L, Nanto-Salonen K, et al. Increased aortic intima-media thickness: A marker of preclinical atherosclerosis in high risk children. *Circulation* 2001;104:2943-2947.
224. Davis PH, Dawson JD, Riley WA, et al. Carotid intimal-medial thickness is related to cardiovascular risk factors measured from childhood through middle age. *Circulation* 2001;104:2815-2819.
225. Litwin M, Niemirska A, Sladowska-Kozłowska J, et al. Regression of target organ damage in children and adolescents with primary hypertension. *Pediatr Nephrol* 2010;25:2489-2499.
226. Hajjar I, Lackland DT, Cupples LA, Lipsitz LA. Association between concurrent and remote blood pressure and disability in older adults. *Hypertension* 2007;50:1026-1032.

227. Hajjar I, Quach L, Yang F, et al. Hypertension, white matter hyperintensities, and concurrent impairments in mobility, cognition and mood: the Cardiovascular Health Study. *Circulation* 2011;123:858–865.
228. Lande MB, Kaczorowski JM, Auinger P, et al. Elevated blood pressure and decreased cognitive function among school-age children and adolescents in the United States. *J Pediatr* 2003;143:720–724.
229. Adams HR, Szilagyi PG, Gebhardt L, et al. Learning and attention problems among children with pediatric primary hypertension. *Pediatrics* 2010;126:e1425–e1429. [Epub 2010 Nov. 8.]
230. Lande MB, Adams H, Falkner B, et al. Parental assessment of executive function and internalizing and externalizing behavior in primary hypertension after anti-hypertensive therapy. *J Pediatr* 2010;157:114–9. [Epub 2010 Mar 15.]
231. Lurbe E, Sorof JM, Daniels SR. Clinical and research aspects of ambulatory blood pressure monitoring in children. *J Pediatr* 2004;144:7–16.
232. Urbina E, Alpert B, Flynn J, et al. Ambulatory blood pressure monitoring in children and adolescents: recommendations for standard assessment: a scientific statement from the American Heart Association Atherosclerosis, Hypertension and Obesity in Youth Committee of the Council on Cardiovascular Disease in the Young and the Council for High Blood Pressure. *Hypertension* 2008;52:433–451.
233. Soergel M, Kirschstein M, Busch C, et al. Oscillometric twenty-four hour ambulatory blood pressure values in healthy children and adolescents: a multi-center trial including 1141 subject. *J Pediatr* 1997;130:178–184.
234. Lurbe E, Cremades B, Torro I, et al. Reference values of ambulatory blood pressure in children and adolescents. *Am J Hypertens* 2000;13:265A.
235. Verhaaren HA, Schieken RM, Schwartz P, et al. Cardiovascular reactivity in isometric exercise and mental arithmetic in children. *J Appl Physiol* 1994;76:146–150.
236. Lurbe E, Redon J, Passual JM, et al. Altered blood pressure during sleep in normotensive subject with type 1 diabetes. *Hypertension* 1993;21:227–235.
237. Parati G, Di Rienzo M, Ulian L, et al. Clinical relevance of blood pressure variability. *J Hypertens* 1998;16:S25–S33.
238. Falkner B, Daniels SR, Flynn JT, et al. The fourth report on the diagnosis, evaluation and treatment of high blood pressure in children and adolescents. *Pediatrics* 2004;114:555–576.
239. Hansen ML, Gunn PW, Kaelber DC. Underdiagnosis of hypertension in children and adolescents. *JAMA* 2007;298:874–879.
240. Elliot SJ, Hansen TN. Neonatal hypertension. In: Long WA, ed. *Fetal and Neonatal Cardiology*. Philadelphia, PA: WB Saunders, 1990:492–498.
241. Low JA, Panagiotopoulos C, Smith JT, et al. Validity of newborn oscillometric blood pressure. *Clin Invest Med* 1995;18:163–167.
242. Park MK, Menard SM. Normative oscillometric blood pressure values in the first 5 years of life in an office setting. *Am J Dis Child* 1989;143:860–864.
243. Kaufmann MA, Pargger H, Drop LJ. Oscillometric blood pressure measurements by different devices are not interchangeable. *Anesth Analg* 1996;82:377–381.
244. Crapanzano MS, Strong WB, Newman IR, et al. Calf blood pressure: clinical implications and correlations with arm blood pressure in infants and young children. *Pediatrics* 1996;97:220–224.
245. Pickering TG, Hall JE, Appel LJ, et al. Recommendations for blood pressure measurement in humans and experimental animals: Part 1: Blood pressure measurement in humans: A statement for professionals from the Subcommittee of Professional and Public Education of the American Heart Association Council on High Blood Pressure Research. *Circulation* 2005;111:697–716.
246. Blowey DL, Warady BL, Alon U. Hypertension in the neonatal period. *Child Nephrol Urol* 1992;12:113–118.
247. Adelman R. Long-term follow-up of neonatal renovascular hypertension. *Pediatr Nephrol* 1987;1:35–41.
248. Alagappan A, Malloy MH. Systemic hypertension in very low-birth weight infants with bronchopulmonary dysplasia: incidence and risk factors. *Am J Perinatol* 1998;15:3–8.
249. Devereux RB, Alonso DR, Lutas EM, et al. Echocardiographic assessment of left ventricular hypertrophy: comparison to necropsy findings. *Am Coll Cardiol* 1986;57:450–458.
250. Daniels SR, Kimball TR, Morrison JA, et al. Effect of lean body mass, fat mass, blood pressure, and sexual maturation on left ventricular mass in children and adolescents: statistical, biological, and clinical significance. *Circulation* 1995;92:3249–3254.
251. de Simone G, Daniels SR, Devereux RB, et al. Left ventricular mass and body size in normotensive children and adults: assessment of allometric relations and impact of overweight. *J Am Coll Cardiol* 1992;20:1251–1260.
252. Dyer A, Elliott P, Chee D, et al. Urinary biochemical markers of dietary intake in the INTERSALT study. *Am J Clin Nutr* 1997;66:1246s–1253s.
253. Neter JE, Stam BE, Kok FJ, et al. Influence of weight reduction on blood pressure: a meta-analysis of randomized controlled trials. *Hypertension* 2003;42:878–884.
254. Daniels SR, Arnett DK, Eckel RH, et al. Overweight in children and adolescents: pathophysiology, consequences, prevention, and treatment. *Circulation* 2005;111:1999–2012.
255. Figueroa-Colon R, Franklin FA, Lee JY, et al. Comparison of two hypocaloric diets in obese children. *Am J Dis Child* 1993;147:160–166.
256. Gallistl S, Sudi KM, Aigner R, et al. Changes in serum interleukin-6 concentrations in obese children and adolescents during a weight reduction program. *Int J Obes Relat Metab Disord* 2001;25:1640–1643.
257. Reinehr T, Andler W. Changes in the atherogenic risk factor profile according to degree of weight loss. *Arch Dis Child* 2004;89:419–422.
258. Kirk S, Zeller M, Claytor R, et al. The relationship of health outcomes to improvement in body mass index in children and adolescents. *Obes Res* 2005;13:876–882.
259. He FJ, MacGregor GA. Effect of modest salt reduction on blood pressure: a meta-analysis of randomized trials. Implications for public health. *J Hum Hypertens* 2002;16:761–770.
260. Appel LJ, Espeland MA, Easter L, et al. Effects of reduced sodium intake on hypertension control in older individuals: results from the Trial of Nonpharmacologic Interventions in the Elderly (TONE). *Arch Intern Med* 2001;161:685–693.
261. Effects of weight loss and sodium reduction intervention on blood pressure and hypertension incidence in overweight people with high-normal blood pressure. The Trials of Hypertension Prevention, Phase II. The Trials of Hypertension Prevention Collaborative Research Group. *Arch Intern Med* 1997;157:657–667.
262. Bibbins-Domingo K, Chertow GM, Coxson PG, et al. Projected effect of dietary salt reductions on future cardiovascular disease. *N Engl J Med* 2010;362:590–599.
263. Weinberger MH, Miller JZ, Luft FC, et al. Definitions and characteristics of sodium sensitivity and blood pressure resistance. *Hypertension* 1986;8:II127–II134.
264. Obarzanek E, Proschan MA, Vollmer WM, et al. Individual blood pressure responses to changes in salt intake: results from the DASH-Sodium trial. *Hypertension* 2003;42:459–467.
265. He FJ, Markandu ND, MacGregor GA. Importance of the renin system for determining blood pressure fall with acute salt restriction in hypertensive and normotensive whites. *Hypertension* 2001;38:321–325.
266. Hofman A, Hazebroek A, Valkenburg HA. A randomized trial of sodium intake and blood pressure in newborn infants. *JAMA* 1983;250:370–373.
267. Geleijnse JM, Hofman A, Witteman JC, et al. Long-term effects of neonatal sodium restriction on blood pressure. *Hypertension* 1997;29:913–917.
268. Simons-Morton DS, Obarzanek E. Diet and blood pressure in children and adolescents. *Pediatr Nephrol* 1997;11:244–249.
269. Sinaiko AR, Gomez-Marín O, Prineas RJ. Effect of low sodium diet or potassium supplementation on adolescent blood pressure. *Hypertension* 1993;21:989–994.
270. Gillum RF, Elmer PJ, Prineas RJ, et al. Changing sodium intake in children: the Minneapolis Children's Blood Pressure Study. *Hypertension* 1981;3:698–703.
271. Howe PRC, Jureidini KF, Smith RM. Sodium and blood pressure in children: a short-term dietary intervention study. *Proc Nutr Soc* 1985;10:121–124.
272. Klatsky AL, Friedman GD, Siegel AB, et al. Alcohol consumption and blood pressure Kaiser-Permanente Multiphasic Health Examination data. *New Engl J Med* 1977;296:1194–1200.
273. Xin X, He J, Frontini MG, et al. Effects of alcohol reduction on blood pressure: a meta-analysis of randomized controlled trials. *Hypertension* 2001;38:1112–1117.
274. Sacks FM, Svetkey LP, Vollmer WM, et al.; DASH-Sodium Collaborative Research Group. Effects on blood pressure of reduced dietary sodium and the dietary approaches to stop hypertension (DASH) diet. DASH-Sodium Collaborative Research Group. *New Engl J Med* 2001;344:3–10.
275. Appel LJ, Moore TJ, Obarzanek E, et al. A clinical trial of the effects of dietary patterns on blood pressure. DASH Collaborative Research Group. *New Engl J Med* 1997;336:1117–1124.
276. Appel LJ, Sacks FM, Carey VJ, et al.; OmniHeart Collaborative Research Group. Effects of protein, monounsaturated fat, and carbohydrate intake on blood pressure and serum lipids: Results of the OmniHeart randomized trial. *JAMA* 2005;294:2455–2464.
277. Svetkey LP, Simons-Morton D, Vollmer WM, et al. Effects of dietary patterns on blood pressure: Subgroup analysis of the Dietary Approaches to Stop Hypertension (DASH) randomized clinical trial. *Arch Intern Med* 1999;159:285–293.
278. Couch SC, Saelens BE, Levin L, et al. The efficacy of a clinic-based behavioral nutrition intervention emphasizing a DASH-type diet for adolescents with elevated blood pressure. *J Pediatr* 2008;152:494–501. [Epub 2007 Nov 5.]
279. Strong WB, Malina RM, Blimkie CJ, et al. Evidence based physical activity for school-age youth. *J Pediatr* 2005;146:732–737.
280. Kelley GA, Kelley KS, Tran ZV. The effects of exercise on resting blood pressure in children and adolescents: a meta-analysis of randomized controlled trials. *Prev Cardiol* 2003;6:8–16.
281. Demorest RA, Washington RL; Council on Sports Medicine and Fitness. Athletic participation by children and adolescents who have systemic hypertension. *Pediatrics* 2010;125:1287–1294.
282. Palatini P, Mos L, Mormino P, et al. Intra-arterial blood pressure monitoring in the evaluation of the hypertensive athlete. *Eur Heart J* 1990;11:348–354.
283. Veterans Administration Cooperative Study Group on Antihypertensive Agents. Effects of treatment on morbidity in hypertension. Results in patients with diastolic blood pressures averaging 115 through 129 mm Hg. *JAMA* 1967;202:116–122.

284. Neaton, JD, Grimm RH Jr, Prineas RJ, et al. Treatment of Mild Hypertension Study. Final results. *JAMA* 1993;270:713–724.
285. ALLHAT Officers and Coordinators for the ALLHAT Collaborative Research Group. Major outcomes in high-risk hypertensive patients randomized to angiotensin-converting enzyme inhibitor or calcium channel blocker vs. diuretic: The Antihypertensive and Lipid-Lowering Treatment to Prevent Heart Attack Trial (ALLHAT). *JAMA* 2002;288:2981–2997.
286. Cooper WO, Hernandez-Diaz S, Arbogast PG, et al. Major congenital malformations after first-trimester exposure to ACE inhibitors. *N Engl J Med* 2006;354:2443–2451.
287. Quan A. Fetopathy associated with exposure to angiotensin converting enzyme inhibitors and angiotensin receptor antagonists. *Early Hum Dev* 2006;82:23–28.
288. Brook RD, Weder AB. Initial hypertension treatment: one combination fits most? *J Am Soc Hypertens* 2011;5:66–75.
289. Adelman RD, Coppo R, Dillon MJ. The emergency management of severe hypertension. *Pediatr Nephrol* 2000;14:422–427.
290. Vaughan CJ, Delanty N. Hypertensive emergencies. *Lancet* 2000;356:411–417.

Gerald R. Marx ■ Adrian M. Moran

HISTORY OF CARDIAC TUMORS

Columbus, a noted pathologist, recorded the first description of a cardiac tumor in 1562 (1). Subsequently, the first report of a cardiac tumor diagnosed in a living patient occurred in 1934, when the presence of myocardial involvement was inferred in a patient with metastatic disease and an abnormal electrocardiogram (ECG) (2). In 1942, surgical resection of two cardiac tumors was reported; both operations culminated in perioperative deaths (3,4). The first successful excision of a cardiac tumor, an atrial myxoma, was performed in 1955 (5).

Despite this rather long history, primary cardiac tumors were, and continue to be, quite rare, especially in the pediatric age group. Their atypical clinical presentation had often prevented timely diagnosis, with discovery at autopsy (6–8). Recent advances in noninvasive diagnosis and surgical management have resulted in marked improvement in recognition, survival, and long-term prognosis.

Most primary cardiac tumors in the pediatric age group are benign. These benign primary cardiac tumors maintain the potential for serious illness related to their conspicuous location. Furthermore, certain primary cardiac tumors can be associated with generalized systemic illness or peripheral emboli. Fewer than 10% of these primary tumors are malignant (6–8). Secondary tumors are also infrequent (7,8). Secondary tumor involvement continues to be quite rare in the pediatric age group although it is encountered more commonly than primary tumors in adults. Secondary tumors usually involve both the myocardium and pericardium. Primary pericardial tumors are also uncommon but again are important because early diagnosis and surgical intervention may be lifesaving.

INCIDENCE

The incidence of cardiac tumors has been difficult to ascertain. Prior data have been limited to autopsy series, case reports, and reviews from large pediatric centers. Based on general autopsy series from patients of all ages, cardiac tumors had a reported incidence from 0.002% to 0.03% (8,9). Autopsy studies in children reported an incidence from 0.027% to 0.08% (6). The earliest reports, with the advent of echocardiography, reported an incidence of primary cardiac tumors of 0.0017% to 0.003%, using the number of hospital admissions as the common denominator (10,11). Using a similar database in a more recent era, 1980 to 1995, the reported incidence of primary cardiac tumors in fetuses to patients 18 years of age evaluated for heart disease at a large pediatric center had increased to 0.2% (12). The incidence of primary cardiac tumors, using the number of echocardiograms at a single pediatric institution from 1981 to 1997 as the denominator, had an incidence of 0.08% (13). In a seven-center collaborative

study of 14,000 fetal echocardiograms, the incidence of primary cardiac tumors was 0.05% (14).

In an attempt to evaluate the incidence of primary cardiac tumors in pediatric patients, a retrospective review was performed between 1980 and 1998 using a computerized cardiology database at Boston Children's Hospital. The incidence was based on a review of all first-time echocardiographic diagnoses of primary cardiac tumors in pediatric patients, which included fetal studies, newborns, infants, children, and adolescents. The denominator of the incidence was all first-time echocardiograms performed during the same time period. The rationale for choosing an echocardiography database implied that most, if not all, pediatric patients with significant murmurs, hemodynamic compromise, dysrhythmias, and associated systemic emboli or unexplained systemic illness seen at Boston Children's Hospital would have undergone echocardiographic evaluation. The computerized pathology registry databases recorded during the same time interval were searched to determine whether any patients had had surgery or whether there had been a sudden death or incidental findings of a primary cardiac tumor that were not included in the echocardiography database. Only one additional patient was found. Hence, using the echocardiography database, 67 primary cardiac tumors were found in review of 38,952 studies, for an incidence of 0.17%. This is similar to the incidence of 0.2% reported in a similar manner during a concurrent time period at the Hospital for Sick Children, Toronto, Ontario (12). The incidence of 0.17% was also similar to 0.14% (14) reported in a multicenter review of fetal echocardiograms. Despite some of the inherent difficulties with these computations, this incidence does present interesting and important new information. The incidence of primary cardiac tumors in the pediatric age group appears to have increased nearly 10-fold. Moreover, this increased incidence is based on echocardiographic recognition of tumors in living patients, not on autopsy findings. This new incidence suggests that one or two new primary cardiac tumors will be detected for every 1,000 first-time pediatric echocardiograms.

Previous autopsy reports have reported that the most common primary cardiac tumors were rhabdomyomas (45%), fibromas (25%), myxomas (10%), intrapericardial teratomas (10%), and hemangiomas (5%) (7,8). The most common tumors in newborns and infants were rhabdomyomas, fibromas, and intrapericardial teratomas. In older children and adolescents, myxomas, rhabdomyomas, and fibromas predominated. Using the recent computerized databases of echocardiography, surgery, pathology, catheterization, magnetic resonance imaging (MRI), and computerized axial tomography, the frequencies of primary cardiac tumors were evaluated at Boston Children's Hospital from 1980 to 2005 (Table 72.1). A total of 129 tumors were found with frequencies as follows: rhabdomyomas (60.5%), myxomas (13.9%), fibromas (7.8%), pericardial teratomas (1.6%), others (7.0%), nonspecified (5.4%), and metastatic dissemination (3.9%)

TABLE 72.1

Frequencies of Cardiac Tumors at Boston Children's Hospital from 1980 to 2005

Tumor	Age at Diagnosis			Total
	<1 Mo	<1 Yr	>1 Yr	
Rhabdomyoma	32	17	29	78 (60.5%)
Myxoma	2	1	15	18 (13.9%)
Fibroma	1	4	5	10 (7.8%)
PT	2	0	0	2 (1.6%)
Other	2	1	6	9 (7.0%)
NS	1	1	5	7 (5.4%)
Mets	0	0	5	5 (3.9%)
Total	40 ^a	24	65	129

PT, pericardial teratoma; NS, not specified; Mets, metastatic cardiac tumor.

^aDiagnosed in utero.

From Steven Colan, M.D., Department of Cardiology, Children's Hospital, Harvard Medical School, unpublished data, with permission.

(Table 72.1). "Others" included three hemangiomas, a mass related to excessive eustachian valve tissue, cardiac calcification, blood cyst of the tricuspid valve, neurofibroma in a patient with neurofibromatosis, hypereosinophilia in a patient with Loeffler syndrome, and one Purkinje cell tumor. Five patients had metastatic tumor dissemination to the heart. Their primary diagnoses included rhabdomyosarcoma, hepatoblastoma, Ewing sarcoma, testicular carcinoma, and malignant melanoma. Three of the five presented with symptoms related to tumor pulmonary emboli. The increased relative incidence of rhabdomyomas seems related to the increased diagnosis of tuberous sclerosis and surveillance echocardiography in patients with known or suspected tuberous sclerosis at a specialized tertiary medical center.

In this Boston Children's hospital experience, in patients diagnosed younger than 1 month of age, (including fetal studies), rhabdomyomas were most often diagnosed (80%), followed by myxomas (5%), pericardial teratomas (5.0%), fibromas (2.5%), others (5.0%), and nonspecified (2.5%) (Table 72.1). All seven of the tumors diagnosed in utero were rhabdomyomas, and six of these patients were subsequently diagnosed with tuberous sclerosis. In a seven-center retrospective review of 14,000 fetal echocardiograms, 19 patients had tumors for a fetal incidence of 0.14% (14). Seventeen of the 19 (89%) were rhabdomyomas and 10 (54%) had tuberous sclerosis. The other tumors included a fibroma and atrial hemangioma. In a similar multicenter retrospective review of patients diagnosed either in utero or at younger than 1 month of age, 84 of 94 patients with cardiac tumors had rhabdomyomas (89%); 80% of these patients had tuberous sclerosis (15).

In patients older than 1 year of age diagnosed at Boston Children's Hospital, rhabdomyomas were diagnosed in 45%, myxomas 23%, fibromas 8%, other 9%, nonspecified 7%, and metastatic dissemination 7% (Table 72.1). The ages of those patients diagnosed with metastatic tumor involvement ranged from 6 to 15 years of age. The median age of presentation for all myxomas was 7 years. The relative increased incidence of myxomas in recent years seems in part attributable to earlier referral and subsequent echocardiographic diagnosis. The increased detection of secondary tumor involvement in the pediatric age group most probably relates to increased awareness and early referral for echocardiographic evaluation.

DIAGNOSTIC PROCEDURES

Electrocardiogram and Chest Roentgenogram

Early studies reported abnormalities on chest roentgenograms in 80% of patients with cardiac tumors (16). Findings including cardiomegaly, abnormal cardiac silhouette, and calcification are nonspecific. Only 47% of patients with primary cardiac tumors have abnormal ECGs. However, in patients with known tumor involvement, the ECG can show S-T segment abnormalities or strain, and ventricular hypertrophy. Additionally, dysrhythmias may be the presenting mode of presentation of cardiac tumors in pediatric patients of all ages. Some have ECG evidence of pre-excitation.

Echocardiography

More than two decades of collective experience have established 2-D Doppler echocardiography as the primary diagnostic procedure for the evaluation of cardiac tumors in pediatric patients (10–43). Two-dimensional Doppler echocardiography is expedient, noninvasive, and accurate. The anatomic and hemodynamic abnormalities can be determined quickly, and critically ill patients can be sent for surgical intervention. More stable patients can be monitored serially by using this noninvasive technique. Echocardiography is also useful for the follow-up of patients after surgical removal of the tumor (44). Two-dimensional echocardiography may aid in tumor differentiation (45,46). Strain and strain rate Doppler tissue imaging has been applied to differentiate tumors based on inherent properties of tissue deformation (47). Transesophageal echocardiography (TEE) provides precise delineation of cardiac tumors and can be used intraoperatively to guide surgical management (48–54). In adults, TEE has been reported to provide improved determination of tumor attachment sites as well as the extent of myocardial/pericardial involvement (54).

Recent developments in matrix array 3-D echocardiography allow timely analysis of tumor volume (Fig. 72.1A–C). The spatial relationship of tumors to other cardiac structures, including atrioventricular and semilunar valves, and inflow

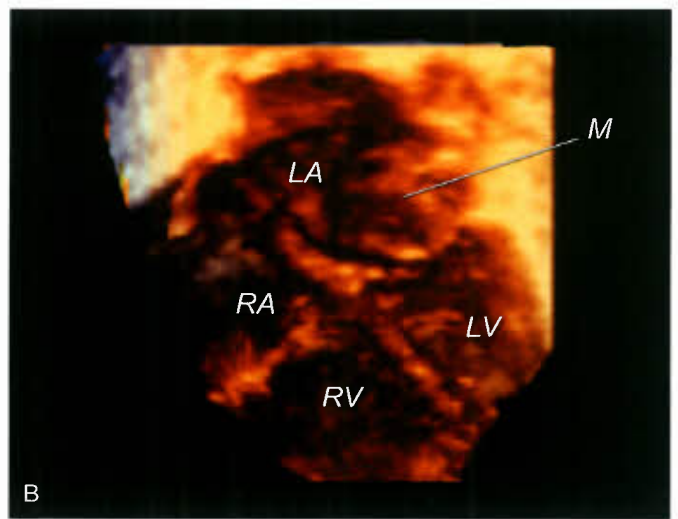
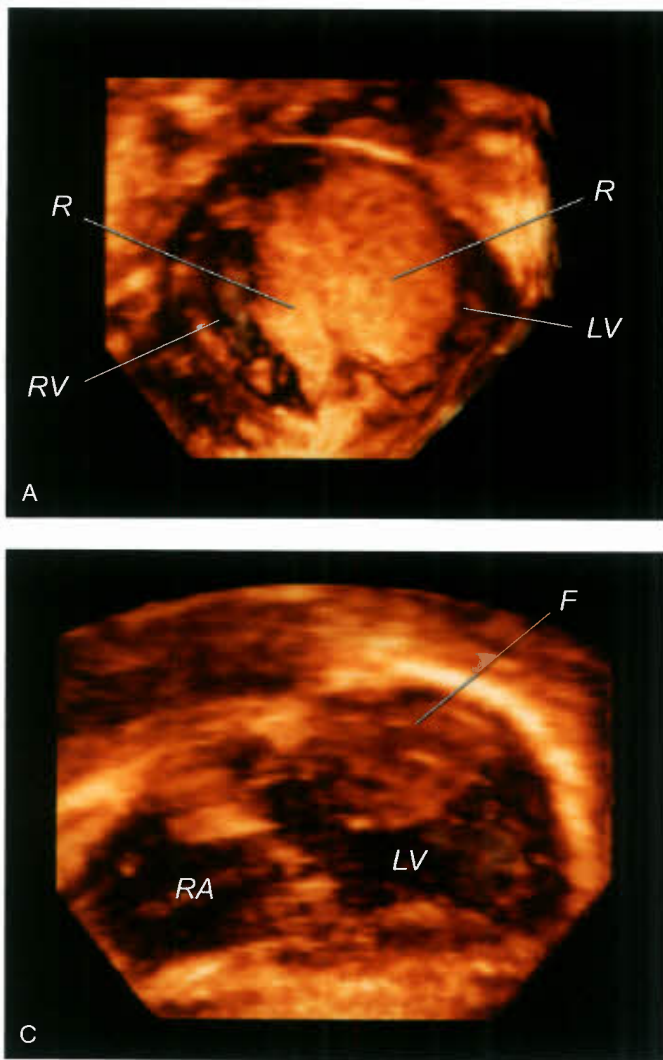
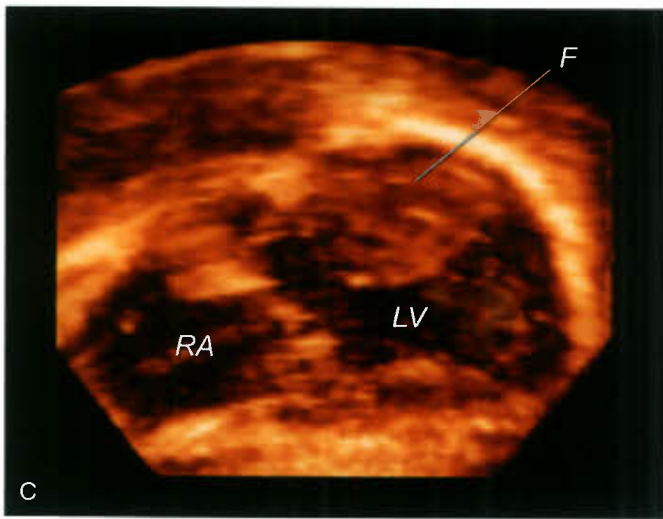


FIGURE 72.1. Three-dimensional echocardiograms using a matrix array transducer. **A:** Large right and left ventricular rhabdomyomas (R) in a newborn. **B:** Round, multilobulated left atrial myxoma (M) in a 2-year-old child. **C:** Large left ventricular fibroma (F) in a 4-year-old boy. LA, left atrium; LV, left ventricle; RA, right atrium; RV, right ventricle.



and outflow tracts can readily be appreciated with 3-D echocardiography (55,56).

Magnetic Resonance Imaging

MRI also shows the location, number, and size of cardiac tumors in the pediatric age group (28,57–72). MRI is also important in the clinical management of secondary tissues because it can visualize mediastinal and other intrathoracic sites (64). Spin-echo MR images provide high-resolution images to enhance delineation of the specific pathology of intracavitary, valvar, myocardial, pericardial, and juxtacardiac masses (Fig. 72.2A). Cine MR provides dynamic imaging techniques to provide additional hemodynamic information (65). MRI can be particularly helpful in visualization of spatial relation of the tumor mass to the coronary arteries, which has been helpful in guiding surgical management. Recent technologic advances in MRI use a combination of sequences that allow differentiation of tumor from myocardium (67) and differentiation of the type of tumor (Fig. 72.2B) (68–72). This MRI technology has been applied to differentiate vascular tumors such as cardiac hemangiomas from rhabdomyomas and fibromas. This differentiation is important in that certain vascular hemangiomas may resolve with either steroid or interferon administration (68,71). In comparative studies, 2-D echocardiography appears to have greater sensitivity than MRI for the detection of intramural (28) and intracavitary cardiac tumors (59); however, MRI has been superior in

detection of apical tumors (59). In a recent multicenter experience of several pediatric centers, 97% of the tumor cases were correctly diagnosed by comprehensive MRI exams (73).

Angiography

Invasive angiography also has been used to diagnose cardiac tumors. This modality provides indirect and nonspecific findings of intracavitary filling defects or cavity obliteration by large intramural tumors. Pressure measurements can be obtained with catheterization, with the inherent risk of placing a catheter near or across a friable tumor. Tissue diagnosis can be attempted by biopsy technique, with the risk of embolizing tumor fragments (43).

RHABDOMYOMAS

Rhabdomyomas constitute 45% to 80% of all primary cardiac tumors in the pediatric age group (7–13) (Table 72.1). They are considered the most common primary cardiac tumor in this age group (7–13). These tumors can be diagnosed in the prenatal period but are most frequently diagnosed in the newborn infant (73–79). Occurrences of sudden death in pediatric patients of all ages, including stillbirths, have been attributed to cardiac rhabdomyomas (74–81).

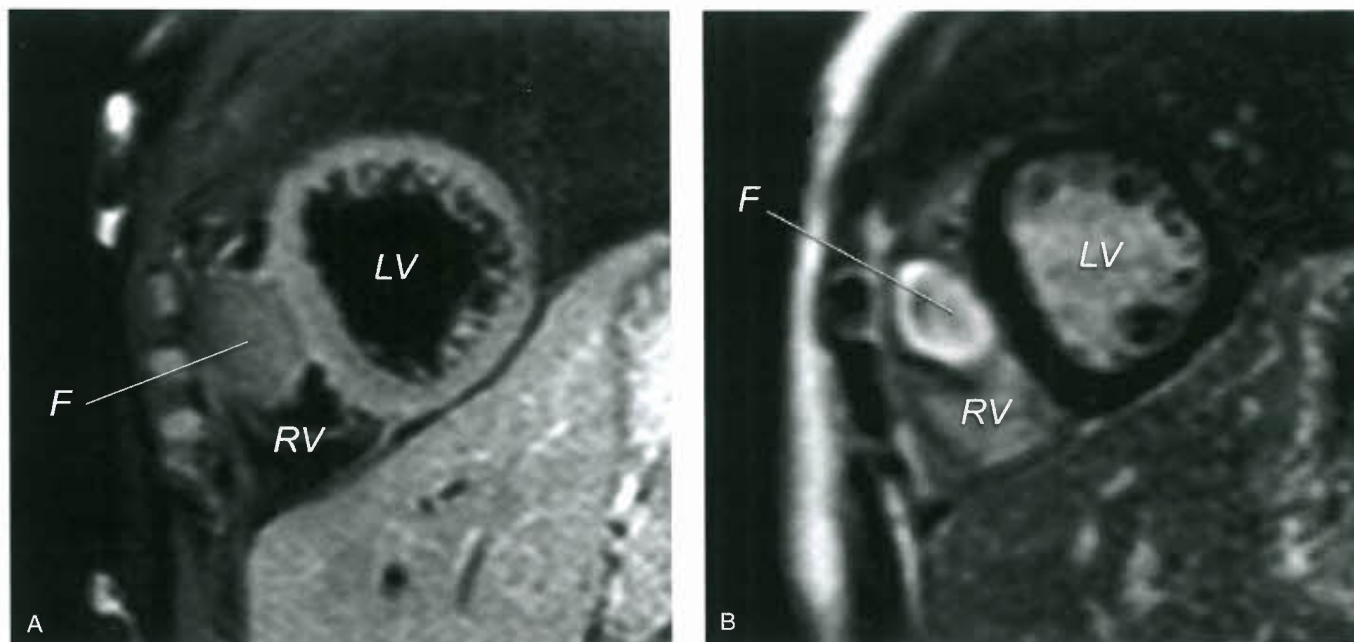


FIGURE 72.2. A: Spin-echo MRI from a child with a large right ventricular fibroma (F). B: Gadolinium-enhanced MRI, from same child, demonstrating uptake within tumor mass. This uptake indicates fibrous tissue, consistent with a cardiac fibroma. LV, left ventricle; RV, right ventricle. (Courtesy of Tal Geva, M.D., Department of Cardiology, Children's Hospital, Harvard Medical School, Boston, MA.)

In general, rhabdomyomas are multiple, well-circumscribed, noncapsulated, white or gray-white intramural or intracavitary nodules that can occur anywhere within the heart (8,20,21,24,74,77–80), most commonly involving the ventricles (82). Although intramural, these large tumors can encroach on the intracavitary space. Other tumors occur as intracavitary pedunculated masses, or attached by a broad base to the endocardial surface (80–83). Cardiac rhabdomyomas occur as single intramural or intracavitary masses in 10% of patients (8,80,84). Histologically, rhabdomyomas contain large vacuolated cells filled with glycogen (Fig. 72.3). Typical spider cells are seen with eccentric nuclei, granular cytoplasm, and thin

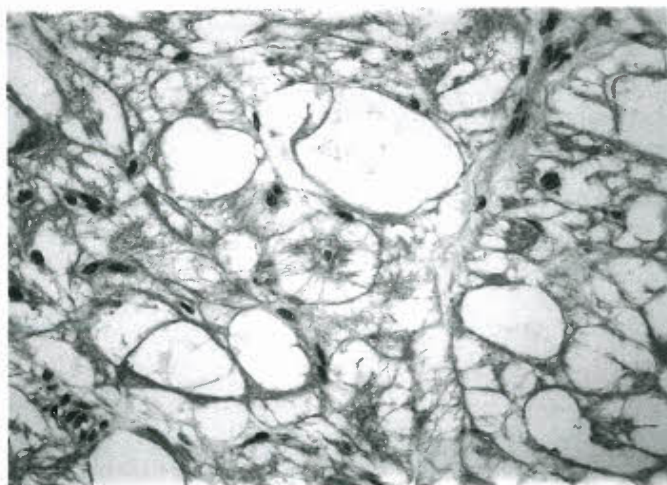


FIGURE 72.3. Rhabdomyoma. Photomicrograph showing cells with clear cytoplasm, vacuolization, and an occasional spider cell (center). (Hematoxylin and eosin stain.) (Courtesy of Peter Paul, MB, BCh, Department of Pathology, Children's Hospital, Harvard Medical School, Boston, MA.)

cytoplasmic extensions projecting toward the cell membrane (80). Rhabdomyomas often are classified as hamartomas, with an inability of cells to undergo mitotic division (80,85).

A rare form of cardiomyopathy, rhabdomyositis, has been described. Tumor nodules are not grossly apparent; microscopically, however, the cardiac muscle fibers and conduction system are diffusely involved with rhabdomyomatous histologic changes (86,87). Recurrent atrial tachycardia and sudden death from intractable ventricular tachycardia have been attributed to rhabdomyositis (86,87).

The clinical findings of cardiac rhabdomyomas are related to the number, position, and size of the tumors. Large intramural or intracavitary rhabdomyomas may obstruct the intracavitary space or the orifice of the atrioventricular or semilunar valves (21,73–77). Extensive cardiac involvement has been associated with diminished myocardial function (18,41,73,77,80). Direct compression of the conduction system can result in serious dysrhythmias (27,37,64,73–84). Rhabdomyomas have been diagnosed by 2-D echocardiography in the fetus (27,75,88–94) (Fig. 72.4). Such prenatal detection has been made while screening fetal dysrhythmias, nonimmune hydrops, decreased fetal growth, and familial tuberous sclerosis (27,75–79,88–94). Postnatally, patients may present without obvious clinical findings, despite extensive cardiac involvement (6,7,40,73,84). Others may have only a murmur of valvular obstructive disease (41,74,77).

Newborns and infants with large rhabdomyomas are often critically ill and present with respiratory distress, congestive heart failure, and low cardiac output (18,73–81). Rhabdomyomas may simulate hypoplastic left heart syndrome when tumors obliterate the left ventricular cavity and severely obstruct blood flow across the mitral or aortic valves (73,95–97). Cardiomyopathy has been diagnosed in newborns and infants with extensive myocardial infiltration (18,41,77). Single pedunculated tumors have been associated with subaortic stenosis (39,41,96–98).

Right atrial or right ventricular rhabdomyomas can cause low cardiac output and signs and symptoms of right-sided

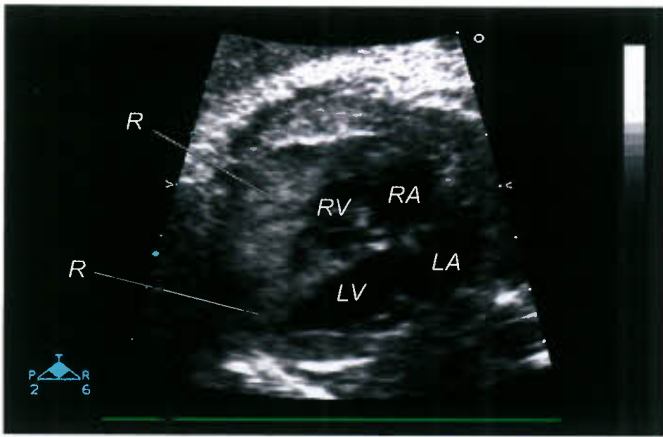


FIGURE 72.4. Two-dimensional fetal echocardiogram at 22 weeks' gestation, demonstrating right and left ventricular rhabdomyomas (R). In utero, a brain MRI scan showed intracranial masses, and at birth the baby was diagnosed as having tuberous sclerosis. LA, left atrium; LV, left ventricle; RA, right atrium; RV, right ventricle.

heart failure (74). Extreme cyanosis can occur when tumors obstruct the tricuspid valve or right ventricular outflow tract, resulting in right-to-left atrial shunting (20,39,41,74,77). Single obstructive pedunculated rhabdomyomas may simulate tricuspid atresia, tetralogy of Fallot, or critical valvar pulmonic stenosis of the newborn (83). The clinical presentation may be even more confusing when rhabdomyomas coexist with significant congenital heart defects (99,100).

Abnormal ECG findings include left-axis deviation, atrial enlargement, ventricular hypertrophy, and ST-T wave abnormalities consistent with ischemia and/or strain (18,73–74,77). These abnormal ECG findings are also indicative of extensive intramural infiltration. Involvement of the conduction system can be inferred from baseline ECGs that manifest bundle branch block (73,74,77), pre-excitation (25,37,39,73,77), or first- through third-degree atrioventricular block (6,22,27,73–75,77,81). Sudden death has been attributed to arrhythmias in pediatric patients of all ages (18,19,27,74–81). These arrhythmias may be a result of either severe hemodynamic compromise or contiguous location of tumors to the conduction

system. All major rhythm disturbances have been reported, including sinus bradycardia, atrial and ventricular tachycardias, and first- through third-degree atrioventricular block. In a more recent large review of 106 patients with rhabdomyomas, 17 (16%) had significant arrhythmias (101). Six percent had ventricular tachycardia and 10% had manifest pre-excitation. In most cases, the rhythm disturbances seemed to resolve with natural tumor regression. When necessary, surgical excision and/or radiofrequency catheter ablation therapy was effective (101).

The chest radiograph may appear normal in older patients with cardiac rhabdomyomas. Occasionally, the only abnormal finding may be distortion of the cardiac silhouette, especially when the rhabdomyomas extend to the epicardium. The chest radiograph, however, often shows cardiomegaly and pulmonary edema in the critically ill neonate and infant (7,18,39,73–77).

The 2-D and 3-D echocardiographic characteristics of cardiac rhabdomyomas are highly echogenic, multiple, well-circumscribed intramural or intracavitary nodules occurring anywhere within the heart (Figs. 72.1A and 72.5) (21,37,40,46,84,87–90,101,102). Rhabdomyomas also may be visualized as either single pedunculated intracavitary or intramural masses (39,40,41,76,84,95,101–103). Rhabdomyomas have a homogeneous, echo-bright, finely speckled pattern (101). In contrast, intracardiac thrombi, myxomas, and hemangiomas have circumscribed echolucent areas as a result of hemorrhage formation. Moreover, rhabdomyomas do not have interspersed, distinct, echogenic regions consistent with calcification or fibrosis. Rhabdomyomas rarely have an associated pericardial effusion (20). Fetal rhabdomyomas are readily diagnosed in utero (Fig. 72.4), and in recent multicenter studies, the in utero incidence of rhabdomyomas was as high as 88% (14) and 89% (15), respectively. Multiple tumors are highly indicative of rhabdomyomas both in the fetus and neonate (14,15,78,79). Fetal rhabdomyomas have been reported to grow in utero ≤ 32 weeks' gestation and then regress in size (79).

Cardiac rhabdomyomas are closely associated with the syndrome of tuberous sclerosis. Tuberous sclerosis is a complex disorder that is transmitted as an autosomal dominant trait of variable expression (104–113). The incidence of tuberous sclerosis has been reported to be 1 in 6,000; two-thirds of cases are sporadic resulting from mutation (79). In an autopsy series, 31% of patients with tuberous sclerosis were reported to have had rhabdomyomas (80). Fifty percent

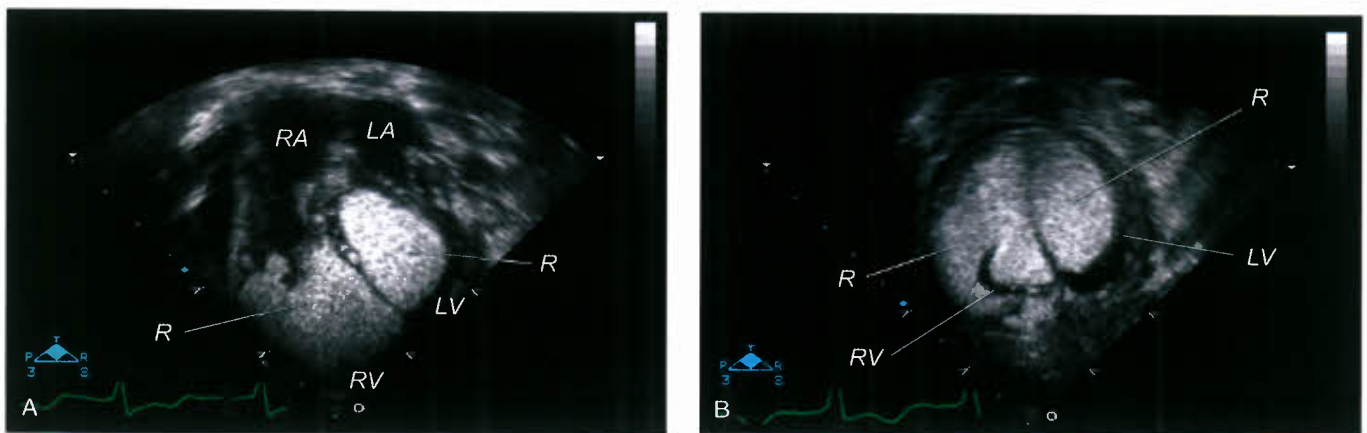


FIGURE 72.5. Two-dimensional echocardiogram in a newborn infant demonstrating very large right and left ventricular rhabdomyomas (R). The patient was diagnosed with tuberous sclerosis. Despite the large tumors, surgery was not undertaken, and the tumors regressed by 2 years of age. A: Four-chamber view showing extensive right and left ventricular tumors. B: Orthogonal short-axis views demonstrating the extensive tumor mass. Ao, aorta; LA, left atrium; LV, left ventricle; RA, right atrium; RV, right ventricle.

of patients with tuberous sclerosis had echocardiographic evidence of tumor involvement (14,84). More recent studies indicate a higher incidence of patients with rhabdomyomas having tuberous sclerosis. Fetal studies indicate that 52% to 79% of all fetuses with cardiac tumors have tuberous sclerosis (14,15,78). The incidence of tuberous sclerosis is as high as 59% to 80% in patients with confirmed fetal rhabdomyomas. Although not invariably, multiple rhabdomyomas are more consistent with the diagnosis of tuberous sclerosis than a singular tumor, with one report indicating that in the fetus or newborn with multiple ventricular tumors, 95% had tuberous sclerosis (15). However, in the latter report, 23% of fetuses or neonates with a singular tumor had tuberous sclerosis as well. In the fetus and neonate, MRI imaging can demonstrate the association of cerebral nodules, establishing the diagnosis of tuberous sclerosis in these patients. The clinical importance of the association between tuberous sclerosis and cardiac rhabdomyomas is evident in a report indicating that 1 in 40 patients with tuberous sclerosis may die as a direct result of cardiac rhabdomyomas (106).

In addition to cardiac involvement, tuberous sclerosis can affect almost all organ systems, including the brain, kidney, pancreas, retina, and skin (104,105,107–109). Therefore, clinical manifestations of tuberous sclerosis may not be clinically apparent in mildly affected patients (107,108,112). Even in severely affected patients, clinical manifestations such as Shagreen patches, adenoma sebaceum, seizures, and mental retardation may not become evident until later in life (105,107–112). Despite the variability in clinical presentation, a family history of tuberous sclerosis or evidence of other organ system involvement may aid in establishing the diagnosis. This is especially germane to the neonate who presents with an intracardiac mass. Neonates with tuberous sclerosis, however, may have no manifestations of this syndrome other than cardiac tumors (77,88,92,93,108). Furthermore, a negative family history does not preclude the diagnosis since $\leq 50\%$ of cases of tuberous sclerosis may be spontaneous mutations. Recent advances in genetic testing may elucidate more fully the inheritance of tuberous sclerosis. To date, two loci associated with tuberous sclerosis have been identified on chromosome 9q34 (TSC1-hamartin gene) and 16p13.3 (TSC2-tuberin gene) (111,112). These loci code for proteins, hamartin and tuberin, that have a tumor-suppressor function (113).

Prostaglandin E_1 (PGE_1), by maintaining patency of the ductus arteriosus, may help stabilize critically ill newborns in whom cardiac rhabdomyomas cause severe right or left ventricular obstruction. Prompt surgical excision is indicated for life-threatening hemodynamic compromise or arrhythmias (37,38,74,77) and is required in $\leq 23\%$ of patient series (95). Partial excision may provide significant relief of inflow or outflow tract obstruction when attempts at complete resection would severely damage the remaining myocardium (18,20,41). The Ross procedure has been proposed when the aortic valve is severely compromised (114). Surgical intervention may be highly successful, without compromising either myocardial or valvular function, in patients with single intracavitary rhabdomyomas (39,83,97,98). Medical treatment has been successful for the treatment of severe dysrhythmias, especially as the tumor resolves. Others have reported successful radiofrequency ablation therapy in select patients with rhabdomyomas and supraventricular tachycardia (115). However, even very large rhabdomyomas may significantly regress in size or disappear completely without intervention (21,37,38,88,98). Unoperated patients may have minimal cardiac signs or symptoms several years later (88). Therefore, the presence of rhabdomyomas alone, without life-threatening hemodynamic instability or arrhythmias, should not be an absolute indication for surgery (17,18,37,38,88,98).

FIBROMAS

Fibromas are generally reported as the second most common primary cardiac tumor in the pediatric age group (1,7,8,12). However, in a more recent review of the Boston Children's Hospital database from 1980 to 2005, fibromas were the third most common tumor (8%) (Table 72.1). Although fibromas have recently been reported in utero (13,14) and in patients younger than 1 month of age (33–36,116–119), they are found much less commonly than rhabdomyomas in this age group. In the recent review at Boston Children's Hospital, fibromas were the second most common tumors (17%) in patients diagnosed between 1 month and 1 year of age (Table 72.1). These primary tumors are rarely seen in older children, adolescents, or young adults. Sudden death has been attributed to cardiac fibromas in pediatric patients of all ages (30,119,120). To date, no distinct genetic inheritance or familial predisposition has been associated with cardiac fibromas. These tumors have been associated with Gorlin syndrome, which includes multiple nevoid basal cell carcinomas, cysts of the jaw, and diffuse skeletal abnormalities (121).

Cardiac fibromas are predominantly single, white, firm, nonencapsulated, intramural tumors that involve the left ventricular free wall or interventricular septum (31,36,116–120,122). These tumors often are located at the left ventricular apex. Less frequently, fibromas can be multiple and invade the right ventricular free wall, atrial septum, or atrial free wall (31,34–36,118,119). Extensive intramural fibromas can encroach and obliterate the intracavitary space (34–36,118,119,122). Although rare, intracavitary fibromas have been reported (34–36,118,119,122), occurring either as a single pedunculated mass (36) or attached by a broad base to the endocardium (33). Both the mitral and tricuspid valve leaflets can be entangled within the tumor mass, causing significant valvar regurgitation (33,34). Similar to rhabdomyomas, fibromas also can be associated with congenital heart defects (89). Cardiac fibromas have been reported to increase in size both prenatally and postnatally (12,13). Histologically, cardiac fibromas consist of fibroblasts, collagen fibers, and minimal elastic tissue (31,32,34,116,119,122) (Fig. 72.6). Occasionally, calcium can be interspersed within the tumor (32,113).

Clinical manifestations of cardiac fibromas are dependent also on the size and location of the tumor. Extremely large

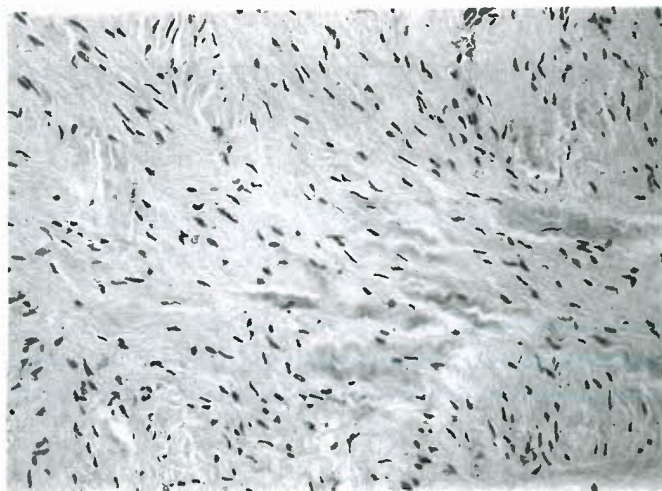


FIGURE 72.6. Fibroma. Photomicrograph showing spindle-shaped fibroblasts and deposition of wavy collagen. (Hematoxylin and eosin stain.) (Courtesy of Peter Faul, MB, BCh, Department of Pathology, Children's Hospital, Harvard Medical School, Boston, MA.)

intramural tumors can encroach the intracavitary space, causing subaortic and subpulmonic obstruction (122). Pedunculated fibromas have been reported to mimic subaortic stenosis (119). Newborns and infants can present with severe congestive heart failure and low cardiac output (33,34,12,123), simulating hypoplastic left heart syndrome (31). Neonates with right-sided fibromas can present with cyanosis and right-sided heart failure, similar to critical pulmonary stenosis or pulmonary atresia (36). Older pediatric patients can have a nonspecific murmur without clinically apparent disease (31,32,76,118,124–126). In this older age group, cardiac fibromas are diagnosed during the evaluation of an incidental abnormality on chest roentgenogram.

As in rhabdomyomas, the ECG is important in the evaluation of pediatric patients with cardiac fibromas. Baseline studies show abnormalities consistent with extensive intramural involvement, including partial to complete bundle branch block and delayed progression of the terminal R wave (118,120,122). The ECG may show QRS axis deviation, atrial enlargement, or ventricular hypertrophy (31–34,116,120,122). Similar to rhabdomyomas, cardiac fibromas invariably have ST-T wave abnormalities consistent with strain or ischemia (31–35,120,122–125,127). These changes have been reported to revert to normal after successful surgery (31,35). Life-threatening arrhythmias can be the primary mode of presentation (31,32,119,123). These arrhythmias include complete atrioventricular block, ventricular tachycardia, and, rarely, supraventricular tachycardia. The diagnosis of a cardiac fibroma often is not established until autopsy, with arrhythmia the presumed cause of death (120). In a recent single institution review of 25 patients with fibromas, 16 (64%) had ventricular tachycardia; two presented with ventricular fibrillation and cardiac arrest (101). Thirteen of sixteen had complete or partial tumor resection and ventricular tachycardia was eliminated in all cases (101).

The chest radiograph may show slight (32,34) or severe cardiomegaly and pulmonary edema (33–36,120–122). Older asymptomatic patients can have nonspecific findings such as an irregular protuberance of the heart border or calcifications within the cardiac silhouette (31,32,35,116,120,125,127).

On 2-D and 3-D echocardiography (Figs. 72.1C and 72.7A,B), cardiac fibromas are seen as a single, bright, intramural, echogenic mass within the interventricular septum or the left ventricular free wall (18,31–33,127). Right ventricular fibromas also have been visualized by this technique (35,36). Multiple fibromas (32,34,119) and calcification within the tumor mass (32,119) have also been reported on pathologic

specimens. Similar to rhabdomyomas, fibromas are rarely associated with significant pericardial effusions. Fibromas may be differentiated from rhabdomyomas by the presence of calcification and cystic degeneration. These tumors may also be differentiated from rhabdomyomas by echocardiographic strain imaging, with fibromas not being compressed during the cardiac cycle (47). These two tumors may also be differentiated by multiple-sequence MRI (68,69) (Fig. 72.2A,B). Fibromas have an inhomogeneous hypointense signal on spin-echo sequences. With gadolinium delayed contrast magnetic resonance angiography, the central signal is again hypointense, with a strong hyperintense shell region (68,69). MRI has also aided in surgical planning to delineate the relationship of the tumor mass to coronary artery anatomy. Fibromas and certain rhabdomyomas may have similar appearances. When surgery is not imminent, complete evaluation for tuberous sclerosis is warranted. Rhabdomyomas may decrease significantly in size or disappear, whereas cardiac fibromas have not been reported to become smaller.

To stabilize the newborn with severe right or left ventricular obstruction, PGE_1 may be used (36). Prompt surgical excision should be undertaken in patients with significant hemodynamic compromise or life-threatening dysrhythmias. Successful removal of large intramural (31,35,36,116,120, 127,124,126–129) and intracavitary pedunculated tumors (117) has been reported in pediatric patients of all ages, with absence of disease reported up to several years later (126–129). In patients with severe tumor involvement, subtotal excision has shown good long tumor survival (128). However, patients with very extensive tumor involvement have undergone cardiac transplantation (129).

MYXOMAS

Myxomas constitute about 50% of primary cardiac tumors in patients of all ages (8,85,130,131). Most often, these tumors are diagnosed in the third to sixth decades of life. Prior autopsy studies in pediatric patients had reported that myxomas constituted 6% of primary cardiac tumors (2). In a more recent echocardiographic-based survey from a single institution from 1981 to 1997, 1 of 22 primary cardiac tumors (4.5%) was a myxoma (17). From 1980 to 1995, 27,640 patients from the fetus to 18 years of age were evaluated at a single center for cardiac disease. Fifty-six patients had a primary tumor; none had a cardiac myxoma (12). This is quite different than the

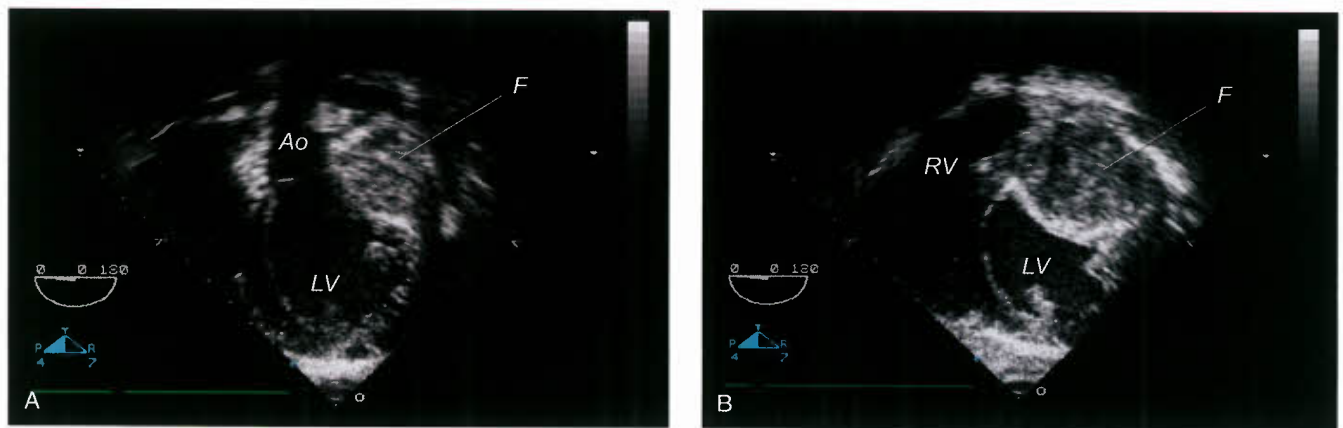


FIGURE 72.7. Two-dimensional echocardiogram in a 2-year-old child with a large left ventricular fibroma (F). A: Long-axis plane showing homogenous encapsulated intramural mass extending from the left ventricular posterior wall into the cavity. B: Corresponding orthogonal short-axis plane in same patient. Ao, aorta; LV, left ventricle; RV, right ventricle.

review of the computer database at Boston Children's Hospital, in which 18 of 129 (14%) primary cardiac tumors were myxomas (Table 72.1). In patients older than 1 year, 15 of 65 (23%) primary cardiac tumors were myxomas.

When these tumors occur in neonates and young infants, they often mimic congenital heart disease (132–135). In older children and adolescents, myxomas have manifestations that can lead to severe morbidity and unexpected mortality. Their presentation is often enigmatic because of vague constitutional findings (130,131,136,137). Early diagnosis and prompt surgical intervention can avoid profound illness and death in these patients.

Cardiac myxomas are single left atrial tumors in about 75% and single right atrial tumors in about 25% of patients (124,131,136). Myxomas are generally friable, pedunculated, gelatinous, yellowish brown to red lobular tumors (130,131). These tumors may be calcified (130,131,136,138), with a higher incidence of calcification in right-sided tumors (130,132,133,136,138). The tumor pedicle usually is attached to the fossa ovalis. Rarely, the tumor pedicle is attached to other segments of the atrial septum, atrial free wall, or mitral valve leaflets (131,134,137,139,140). Myxomas can occur as biatrial tumors attached to the fossa ovalis (138,141,142) or as left atrial tumors protruding through the foramen ovale and filling the right atrium (143). These tumors can occur as single right or left ventricular myxomas (130,131,135,144,145) or, infrequently, as multiple myxomas occupying different areas of the same heart (130,136,145).

Histologically, these benign tumors are composed of cords and strands of cells in a pale, paucicellular myxoid background (Fig. 72.8). Multiple small blood vessels, lymphocytes, and histiocytes are seen (130,131). Malignant myxomas are rare and are differentiated by increased mitotic activity and pleomorphism (139,146–148). However, the malignant potential may not be determined by histologic findings alone, (146,147,149). Other characteristics of malignant predisposition include local invasion at the primary site, regrowth of the tumor at the original site or different location, and development of peripheral aneurysms (139,146,147). In $\leq 40\%$ of patients who experience recurrence, the tumor exhibits an abnormal DNA ploidy pattern (150); however, some pathologists doubt the existence of malignant cardiac myxomas (2), suggesting they instead represent misinterpretation of sarcomas (151–154).

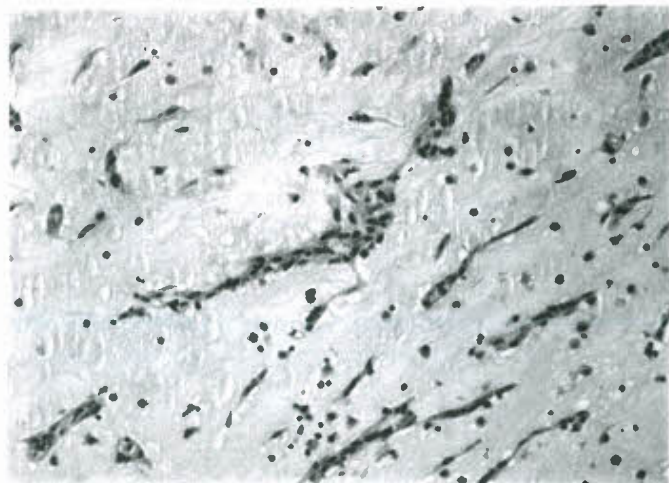


FIGURE 72.8. Atrial myxoma. Photomicrograph showing cords and strands of cells in a pale paucicellular myxoid background. (Hematoxylin and eosin stain.) (Courtesy of Peter Faul, MB, BCh, Department of Pathology, Children's Hospital, Harvard Medical School, Boston, MA.)

Myxomas present with a classic triad of symptoms, including cardiac obstruction, emboli, and systemic illness (130,131,136,137,142). Patients are rarely asymptomatic (155,156). The vague and unusual signs and symptoms of cardiac myxomas often have led to delayed diagnosis or misdiagnosis in children and adolescents (137).

About 80% of pediatric patients present with symptoms of valvular obstruction (137). Atrial tumors create mitral or tricuspid valve stenosis by a to-and-fro motion through the valves (130,131). Typically, these large pedunculated tumors advance through and obstruct the atrioventricular valve during diastole and are expelled retrogradely into the atrium during systole. Large left atrial myxomas obstruct pulmonary venous inflow and flow across the mitral valve, resulting in signs and symptoms of pulmonary edema, pulmonary arterial hypertension, and low cardiac output (130,131,155). Ventricular ischemia and dysfunction may develop when cardiac output is significantly impeded (137). Right-sided heart failure and low cardiac output occur when right atrial tumors impede systemic venous inflow and obstruct flow across the tricuspid valve (130–134). Myxomas may mimic neonatal cyanotic heart disease when obstructive right-sided tumors cause right-to-left shunting at the atrial level (132–135). Sudden death has been reported when large tumors completely obstruct either the mitral or tricuspid valve (132,133). Atrial tumors also can cause atrioventricular valve insufficiency (155). Large calcified tumors have been associated with complete valve destruction (136).

Semilunar valve obstruction can occur when large myxomas are inferiorly positioned within the atrium and are attached to a long tumor pedicle (156). This allows atrial tumors to prolapse through the atrioventricular valve and ventricular outflow tract, resulting in diastolic semilunar valve stenosis. Pedunculated ventricular myxomas (157) also can cause systolic aortic or pulmonary outflow tract obstruction (28,135,136,156,158).

Auscultatory findings of left atrial myxomas are consistent with atrioventricular valve stenosis and insufficiency (130, 131,136). A middiastolic murmur and low-pitched tumor plop are characteristic findings (130,131,159); however, absence of the murmur may occur with severe obstruction (119). Right atrial tumors have nonspecific systolic and diastolic murmurs mimicking the Ebstein anomaly or tricuspid valve stenosis and regurgitation (130–134). Symptoms and physical findings are often positional (130,131,136,137). When atrial myxomas obstruct the atrioventricular valves, the patient may experience dyspnea, dizziness, or syncope when sitting or standing, with alleviation of symptoms on lying down. In the neonate, positional symptoms consist of feeding difficulty and irritability while sitting (134). When tumors obstruct the semilunar valves, patients experienced symptoms while bending forward or lying down, with relief of symptoms when standing (157).

Peripheral emboli occur in $>70\%$ of pediatric patients with myxomas (137), including newborns in whom embolization has been reported to have occurred in utero (132). Emboli are related to fragmentation of tumor substance or embolization of thrombi adherent to the tumor external surface (131,160). As expected, left-sided tumors are associated with systemic (161) and right-sided tumors with pulmonary arterial embolization (132,134). Bilateral atrial myxomas have been reported to cause both pulmonary and systemic arterial emboli (142), and right-sided tumors have been associated with paradoxical emboli in patients with atrial septal communications (132,134). Systemic embolization can occlude coronary, pancreatic, thyroid, adrenal, renal, splenic, cerebral, and extremity arteries, resulting in infarction of corresponding tissue (85,142,155,160).

Symptoms related to peripheral emboli may not become apparent until months to years after removal of the primary myxoma (139,142,146,160). This temporal delay has been

attributed to recurrence of nonmalignant myxomas at the same or other cardiac sites (139). The potential for recurrence appears to be associated with inadequate resection (162–165) or totipotent multicentricity (166). Peripheral arterial aneurysms also have been diagnosed years after initial embolic events. Small embolic myxoma fragments may continue to grow, undergo malignant transformation, and invade and replace the medial arterial wall, resulting in aneurysm formation (130,142,146,160).

Constitutional symptoms, the third major component of the clinical triad, occur in $\leq 65\%$ of pediatric patients with myxomas (137). Persistent fever, malaise, weight loss, arthralgias, and myalgias may be present months before tumor diagnosis (130,131,136,137,140,161,167). Laboratory studies show anemia, thrombocytopenia, elevated sedimentation rate, and elevated gamma globulins. Patients have been diagnosed as having acute rheumatic fever, chronic rheumatic carditis, subacute bacterial endocarditis, septicemia, myocarditis, and other collagen vascular disorders (134–140,159,161,167–169). These constitutional findings have been attributed to a diffuse immunologic response to the primary tumor or to tumor emboli (130,134). Recent reports suggested that these systemic abnormalities are secondary to secretion of interleukin-6 and frequently resolve with tumor resection (169–171). Interleukin-6 is associated with the synthesis of several proteins that contribute to the acute-phase response and corresponding constitutional signs and symptoms (172).

Depending on the size and site of the cardiac myxoma, the ECG can demonstrate atrial enlargement or ventricular hypertrophy (130,131,136,137). Right ventricular hypertrophy may be due to pulmonary valvar obstruction, pulmonary arterial hypertension secondary to pulmonary emboli, or pulmonary venous hypertension from left atrial tumors (131). Ischemic ECG changes can occur with tumor embolization to the coronary arteries (160) or with severe obstruction and diminished cardiac output (137,159,160). Bundle branch block, repolarization abnormalities, or severe conduction abnormalities, commonly seen with intramural rhabdomyomas and fibromas, are rarely seen with myxomas.

The chest radiograph may be normal (134,144) or may demonstrate cardiomegaly with pulmonary edema (130,131,134,136). Right-sided myxomas show right atrial and right ventricular enlargement (144,156). Tumor calcification also can be seen (130,131,136). Unlike with rhabdomyomas or fibromas, irregular contour of the heart border is rarely visualized.

The mainstay in the diagnosis of cardiac myxomas is 2-D Doppler echocardiography (130,138,144,156,158,161,173,174). In a retrospective review, myxomas were diagnosed in 37% of patients before, and in 90% of patients after, the advent of echocardiography (175). The virtual pathognomonic finding of an atrial myxoma is that of a large pedunculated tumor mass traversing through the atrioventricular valve in a to-and-fro motion (Figs. 72.1B and 72.9). In some patients, however, the tumor may not appear to prolapse into the ventricle either as a result of a short pedicle or because of its large size (158,173). Single ventricular (158), biatrial (138), and simultaneous atrial and ventricular myxomas (144) have been diagnosed accurately by this technique. Semilunar valve obstruction (135,158) has been corroborated by Doppler technique. Similar to rhabdomyomas and fibromas, pericardial effusions have not been reported with atrial myxomas.

Cardiac myxomas should be removed on diagnosis. Surgical results have been excellent (130,131,136,137), with resolution of associated symptoms (130,136,176). Surgery includes wide resection at the point of attachment of the pedicle to the heart. Since attachment most commonly occurs at the fossa ovalis, removal of large segments of the atrial septum is often done. Careful examination of the entire heart is

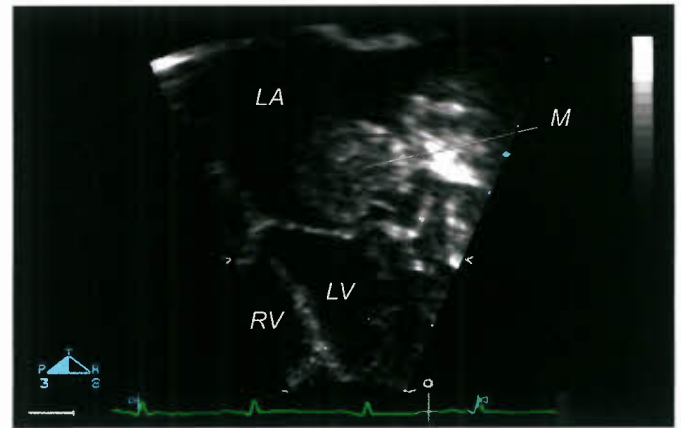


FIGURE 72.9. Two-dimensional echocardiogram in a 2-year-old child with a left atrial myxoma (M). LA, left atrium; LV, left ventricle; RV, right ventricle.

necessary to remove concurrent sites of myxomatous tissue. The use of echocardiography to facilitate a surgical approach has been proposed (177) by preoperatively defining tumor size, location, point of attachment, and presence of concurrent site involvement. Patients require continual reevaluation for recurrence of disease and for later development of peripheral arterial aneurysms (130,136,139,142,146,160,175). The approximate incidence of recurrence is 4% to 7% in most large series (162,164,178,179).

Familial occurrence of cardiac myxomas is well established (130,131,136,137,180,181) and accounts for 7% of all myxomas. Cardiac myxomas often are seen in children and adolescents with multiple lentigines syndromes (157) and may be associated with nonneoplastic endocrine abnormalities (Fig. 72.10). Acronyms have been proposed, including LAMB (lentigines, atrial myxoma, mucocutaneous myxoma, and blue nevi) and NAME (nevi, atrial myxoma, myxoid neurofibroma, and ephelides) syndromes. Recent nosology aggregates these conditions under the broader category of Carney complex, which consists of (a) myxomas in other locations (breast or skin), (b) spotty pigmentation (lentigines, pigmented nevi, or both), and (c) endocrine overactivity (pituitary adenoma, primary pigmented nodular adrenocortical disease, or testicular tumors). The precise gene defects remain unknown (182); however, certain investigators have mapped these syndromes to two loci, on chromosome 2p (183) and chromosome 17q (184).



FIGURE 72.10. Facial picture of patient with multiple lentigines.

INTRAPERICARDIAL TERATOMAS

Despite their rare occurrence, intrapericardial teratomas constitute another major subgroup of primary pediatric cardiac tumors (14,73,183) (Table 72.1). These tumors are diagnosed in the fetus or newborn infant. These rare tumors previously were associated with a high mortality rate (185–189). More recently, increased survival is emerging as a result of earlier diagnosis and improvements in surgical care (129,185). Intrapericardial tumors are seldom malignant or recurrent; therefore, surgery is considered curative for such life-threatening illness.

Intrapericardial teratomas are single, encapsulated, grayish tan, bosselated tumors attached to the base of the heart (189–191). These tumors contain multiple cysts within a yellow mucoid stroma (192). Often a broad-based stalk or narrow pedicle firmly attaches the tumor to the root of the aorta or pulmonary artery (185,188,189). The tumor capsule itself can be firmly attached to the aorta (186–200) or to pulmonary artery adventitia (187,189,191,197,200). The tumor has been reported to adjoin the superior vena cava (191), right atrium (187,189,191), right ventricle, left atrium, and left ventricle (189). The tumor blood supply usually emanates as nutrient vessels from the aortic vasa vasorum (187,189,197,198). Single blood vessels from the vicinity of the coronary arteries (190) or multiple small blood vessels from the superior mediastinum also may supply the tumor (191).

Intrapericardial teratomas may be three to four times the size of the newborn or infant heart (186,189,199); however, the tumor may be relatively small in asymptomatic older children and adolescents. Critically ill newborns and babies almost always have a large pericardial effusion (188,189,197). Obstruction and compression of the heart develop due to an essentially solid tumor mass contained within a restrictive fibrous pericardium (188,189,198). In newborns and infants, the tumor is most frequently right sided, attached to the ascending aorta, and wedged between the aorta and superior vena cava (187,188,195–200). These right-sided tumors rotate the heart, on a vertical axis, to the left and posteriorly (189,192,198). They have a propensity to severely obstruct the superior vena cava, pulmonary artery, and ascending aorta. The tumors also may compress the right atrium and right ventricle (186–189,200–203). Less frequently, the tumor is left-sided, attached to the aorta, overlying the left atrium and left ventricle (189,192,198). Left-sided intrapericardial teratomas rotate the heart anteriorly and to the right (189,192,198). Rarely, the tumor is located posteriorly behind the aorta (192). Intrapericardial teratomas also can occur concomitantly with other congenital heart defects (189,190).

Intracardiac teratomas occur even less frequently than intrapericardial teratomas (201). To date, they have been found predominantly on the right side of the heart. These intracardiac teratomas cause findings similar to those for the intramural and intracavitary tumors described above. Intracardiac teratomas are rarely malignant in young infants and children (201,202).

Intrapericardial teratomas consist of tissue derived from all three embryonic germinal layers (Fig. 72.11) (185–199). Mesodermal tissue includes smooth and striated muscle, hyaline, and elastic cartilage. Endodermal tissue consists of respiratory bronchial, pancreatic, intestinal, and salivary glands; ectodermal neuroepithelial structures include choroid plexus and eyes. Intrapericardial teratomas are rarely malignant, particularly in infants and newborns (185,188,192,195).

Intrapericardial bronchogenic cysts have the same gross appearance and clinical manifestations as intrapericardial teratomas (187,192,194,195,199). These two intrapericardial tumors can be differentiated only by histologic examination. Intrapericardial bronchogenic cysts consist predominantly of

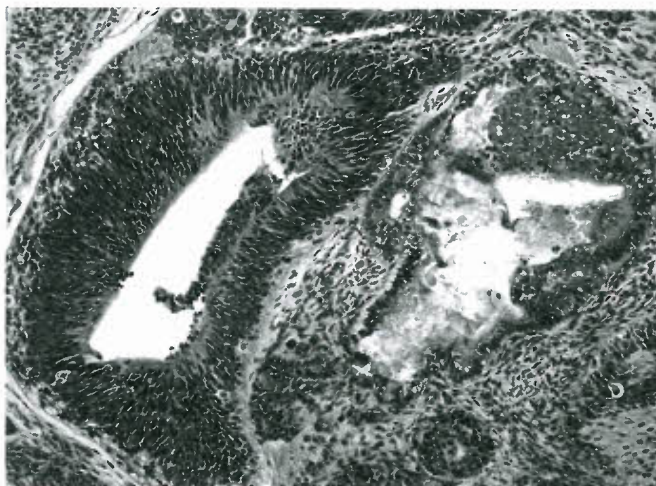


FIGURE 72.11. Photomicrograph of pericardial teratoma showing primitive neural tissue including ependymal type rosette (left aspect of photograph) and immature glands and stroma, with foci of endodermal sinus tumor. (Hematoxylin and eosin stain.) (Courtesy of Harry Kozakewich, M.D., Department of Pathology, Children's Hospital, Harvard Medical School, Boston, MA.)

respiratory and gastrointestinal tissue. They do not have the neuronal tissue elements that can be found in intrapericardial teratomas (187,192,194). The true incidence of intrapericardial teratomas remains somewhat unclear because earlier reports may have included intrapericardial bronchogenic cysts (187,192).

Half of all intrapericardial teratomas are diagnosed in newborns and infants younger than 1 month of age and two-thirds in infants younger than 1 year of age (192,198). In recent reviews from Boston Children's Hospital (Table 72.1) and other centers (13,14), all intrapericardial teratomas were diagnosed in infants younger than 1 year of age. Critically ill newborns and infants have a distinct clinical presentation consisting of respiratory distress, pericardial effusion, and direct cardiac compression by the tumor mass as well as cardiac tamponade (185–199). Nonimmune fetal hydrops has been attributed to intrapericardial teratomas (186). Direct compression of pulmonary parenchyma may contribute to the extreme respiratory distress in the newborn or infant (187,191,198,199). Sudden deaths occurred in two-thirds of pediatric patients who had intrapericardial teratomas (188). These events were attributed to acute rupture of cysts into the pericardial space with sudden tamponade (203), severe encroachment by the tumor on the heart and great vessels (188,191), and infectious pericarditis (191).

Signs and symptoms of severe disease may not be apparent in the rare situation in which an infant does not have an associated significant pericardial effusion (189,192,198). Patients older than 3 months of age are usually asymptomatic or have findings of a chronic pericardial effusion (189,192,198). Intrapericardial teratomas can be diagnosed in the asymptomatic older child during evaluation of an abnormal chest radiograph or as an incidental finding at autopsy (189,192,198).

Heart sounds are distant or muffled, murmurs are inaudible, and the precordial impulse conspicuous for its absence in the newborn or infant who has impending tamponade (185,189,192,196,199). The patient may have marked hepatomegaly and diminished peripheral pulses (185,192,198). Stenotic murmurs may be heard when the tumor mass compresses cardiac chambers or great vessels (195,198). The newborn may present with cyanosis from compression of the

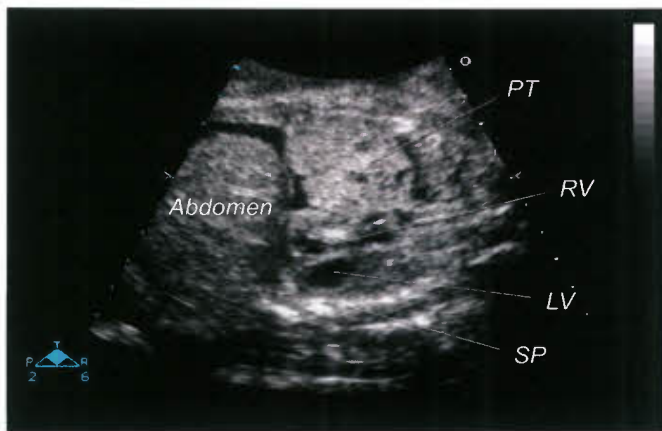


FIGURE 72.12. Fetal echocardiogram showing massive heterogeneous intrapericardial mass attached to the right atrium and aorta. Histology confirmed this mass to be a pericardial teratoma (PT) (see Fig. 72.11). LV, left ventricle; RV, right ventricle; SP, spine.

pulmonary parenchyma (185,199) or from right-to-left atrial shunting (195).

Low-voltage QRS complexes are often seen (185,186, 189,192,198). Arrhythmias, ST-T wave abnormalities, and intraventricular conduction delays are notably absent. In critically ill patients, a markedly enlarged cardiac silhouette is seen on chest radiographs (185–199). Calcifications may also be visualized on radiographic studies (189,199,200). Irregularity of the cardiac silhouette may be the only abnormal finding in older asymptomatic patients (192).

Pericardiocentesis is nondiagnostic except for the absence of a bloody effusion (189). A hemorrhagic effusion almost always is associated with a malignant cardiac or pericardial tumor (189). Recurrence of the pericardial effusion invariably occurs if the tumor is not removed (189,191).

Intrapericardial teratomas have been visualized by 2-D echocardiography in the fetus, neonate, and infant (13,185–187,192,193,196–198,200) (Figs. 72.12 and 72.13). The tumor appears as a single, nonhomogeneous, lobular, intrapericardial mass (Fig. 72.11) (185,187,191,196–198,200). Pericardial effusion is almost always present in the neonate

and infant. Cystic formations appear as echolucent areas, calcifications as echogenic foci (185,187,196). Attachment of the pedicle to the aorta can be visualized, and compression of the great vessels and intracardiac chambers may occur (187,193,196–200). Neonates and infants have been operated on the basis of echocardiography alone (185,187, 196,202). MRI has been applied to the differentiation of intrapericardial teratomas from bronchogenic cysts (201).

Early noninvasive diagnosis, surgical removal of the intrapericardial teratoma, and decompression of the pericardial effusion result in high survival rates, even in critically ill neonates and infants. In utero recognition allows prompt postnatal surgical intervention before significant cardiopulmonary distress develops (197). Surgery in older asymptomatic patients is indicated because of the propensity of these tumors to cause sudden death (185,187–189,191,195) or to undergo rare but known malignant degeneration (185,198). Careful dissection is necessary to remove a tumor that is adherent to the external surface of the heart or coronary arteries (187,189,191) and to remove the tumor pedicle from the aorta or pulmonary artery (187,191,192,198,199). Successful long-term results have been reported following surgery (129,185–187,192,198,199).

OTHER PRIMARY BENIGN MYOCARDIAL TUMORS

Cardiac hemangiomas are another more common benign tumor in this age group (7,204–206). In the review of 129 primary cardiac tumors at Boston Children's Hospital, three (2.3%) were hemangiomas. These tumors are almost always single and can occupy the epicardial, intramural, or intracavitary space (206). Hemangiomas are polypoid or sessile, often with central areas of necrosis and calcification (17,62,205). They often are associated with nonhemorrhagic pericardial effusions. These tumors consist of large blood vessels and small vascular channels interdigitating within the myocardium (17,205). On echocardiography, these vascular channels appear as large echolucent areas (17,204,205). Angiography has been used to demonstrate the highly vascular nature of these tumors (17,62,204). Recently, MRI has also been used to differentiate the highly vascular nature of cardiac vascular tumors (68,70,71), particularly with rapid enhancement on first-pass gadolinium scanning. The importance of

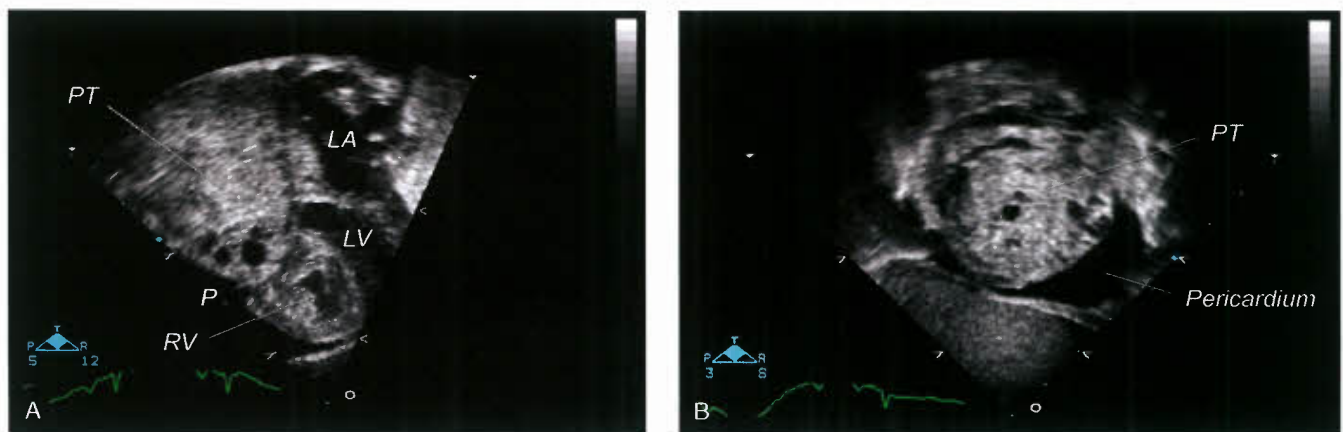


FIGURE 72.13. Huge intrapericardial teratoma (P) in a newborn infant. A: Four-chamber view showing the heterogeneous mass with multiple vacuoles at the region of the right atrium, within the pericardial space. B: Orthogonal short-axis views showing the large tumor mass in the pericardium. LA, left atrium; LV, left ventricle; PT, pericardial teratoma; RV, right ventricle.

tissue differentiation has been emphasized in that congenital hemangiomas may regress in size with interferon or steroid administration (71). The variability in clinical course may be related to the variability in histology (71). Some patients have been reported as being well 4 years following diagnosis (204). Sudden death has also been reported (1,85,206). Surgical intervention has been successful in removal of singular intracavitary tumors (17,204,205). Cardiac transplantation has been considered in some patients who had severe invasion of the myocardium (17).

Other examples of rare primary benign cardiac tumors include papillary tumors (207), accessory endocardial cushion tissue (208), cardiac lipomas (72,209–211), and fibroelastomas (212). These tumors have been associated with a myriad of cardiac signs and symptoms ranging from minimal disease to systemic embolization to near-death episodes. MRI has been able to differentiate cardiac lipomas from other tumor masses (68,72).

PRIMARY MALIGNANT MYOCARDIAL TUMORS

Malignant myocardial tumors constitute <10% of primary cardiac tumors in pediatric patients (7,8,63). These malignant tumors include fibrosarcoma, angiosarcoma, lymphosarcoma, giant cell sarcoma, fibromyxosarcoma, leiomyosarcoma, neurogenic sarcoma, rhabdomyosarcoma, and undifferentiated sarcoma (43). Some pathologists argue that the imprecise terminology applied to these tumors has been a general source of confusion (148). Moreover, the histologic differentiation of benign from malignant tumors may be subtle (146).

Angiosarcoma is the most frequent primary malignant cardiac tumor (213–216). These tumors most often involve the right atrium and pericardium. Patients present with cardiac tamponade, right-sided heart failure, and superior vena caval obstruction. Pericardial effusions are hemorrhagic; metastatic involvement of the liver, lungs, and central nervous system is common. Despite early noninvasive diagnosis and surgical and chemotherapeutic interventions, the outlook remains poor.

Cardiac sarcomas are rare in patients of all ages. In a National Sarcoma Registry database, 0.4% were thoracic sarcomas, with only one case of cardiac sarcoma reported (217). Although rare in pediatrics, primary cardiac sarcomas have been diagnosed in infants as young as 3 months of age (43). These tumors usually involve the right side of the heart (43,218–221) and often are located primarily in the pulmonary artery (219). Poorly differentiated sarcomas can infiltrate the right atrium and right ventricle, extend to the pericardium, and encroach on the atrial and ventricular cavities (43). Surgical removal of these tumors has been attempted (43,219) with a low survival rate and with both local and distant recurrence (43,219,222). Often, the tumor is so invasive that surgical removal is impossible. Metastases to the lung and mediastinum often occur, and prognosis is poor (43,218,219). Certain nonresectable sarcomas, without evidence of distant metastasis, have been approached by cardiac transplantation (222–230). The role of transplantation in the management of such patients is unclear.

SECONDARY CARDIAC TUMORS

Secondary cardiac tumors more frequently are observed than primary tumors. The most common secondary tumors in pediatric patients are non-Hodgkin lymphoma, leukemia, and neuroblastoma (7,63).

Non-Hodgkin lymphoma is becoming more prevalent, with occurrence seen in immunosuppressed patients who are infected with Epstein-Barr virus (231). Occurrence is 0.2% and 1.2% in the 1st year in renal and cardiac transplant recipients, respectively, with rates of 0.04% and 0.30% per year, respectively, for kidney and cardiac transplant patients thereafter (232). In the cardiac transplant patients who develop non-Hodgkin lymphoma, the incidence of direct cardiac involvement is 18% (233). Cardiac involvement from non-Hodgkin lymphoma can present with pericardial effusions, arrhythmias, and congestive heart failure (234,235). Marked ST-T wave abnormalities, low-voltage QRS complexes, and infarct patterns are seen (234,235). Two-dimensional echocardiography shows significant ventricular wall thickening and dyskinesis (234). The myocardium has echo-bright areas alternating with echolucent areas. This is consistent with autopsy findings of large areas of necrosis and hemorrhage alternating with myocardium and solid tumor (234,235).

Direct extension from the inferior vena cava to the right atrium can occur in patients with Wilms tumor, renal myosarcoma, leiomyoma, and leiomyosarcoma (236–239). Patients with Wilms tumor can have symptoms of right heart obstruction or failure before presenting signs and symptoms of an abdominal mass or hematuria (238). Ultrasound can demonstrate a tumor extending proximal to the iliac arteries, continuing up the inferior vena cava to the right atrium (237,238). Large atrial tumors can prolapse into the left atrium through an atrial septal communication (239). Atrial Wilms tumors can mimic atrial myxomas by their to-and-fro motion across atrioventricular valves (239).

Malignant pericardial tumors are usually metastatic (8,85,157). Rarely, primary intrapericardial tumors do occur (235). Metastatic tumors directly invade the pericardium and often are associated with hemorrhagic effusions. These tumors can invade the myocardium but rarely invade the intracavitary space (235).

REFERENCES

1. Columbus M. *De Re Anatomica*. Paris, France: Libr XV, 1562.
2. Beck C. An intrapericardial teratoma and a tumor of the heart: both removed intraoperatively. *Ann Surg* 1942;116:161–174.
3. Goldberg H, Glenn F, Dotter C, et al. Myxoma of the left atrium: diagnosis made during life with operative and post-mortem findings. *Circulation* 1952;6:762–767.
4. Van Trigt P, Sabiston D. Tumors of the heart. In: Sabiston D, Spencer F, eds. *Surgery of the Chest*. 6th ed. Philadelphia, PA: WB Saunders, 1995:2069–2086.
5. Chirverman WR Jr. Clarence Crafoord and the first successful resection of a cardiac myxoma. *Ann Thorac Surg* 1992;54:997–998.
6. Nadas AS, Ellison RC. Cardiac tumors in infancy. *Am J Cardiol* 1968;21:363–366.
7. Chan HS, Sonley MJ, Moes CAF, et al. Primary and secondary tumors of childhood involving the heart, pericardium and great vessels: a report of 75 cases and review of the literature. *Cancer* 1985;56:825–836.
8. McAllister HA Jr. Primary tumors of the heart and pericardium. *Pathol Annu* 1979;14:325–355.
9. Silverman NA. Primary cardiac tumors. *Ann Surg* 1980;191:127–138.
10. Ludomirsky A. Cardiac tumors. In: Garson A, Bricker JT, Fisher D, et al., eds. *The Science and Practice of Pediatric Cardiology*. 2nd ed. Philadelphia, PA: Lippincott Williams & Wilkins, 1997:1885–1893.
11. Fowler R, Keith J. Cardiac tumors. In: Keith J, Rowe R, Vlad P, eds. *Heart Disease in Infancy and Childhood*. 3rd ed. New York, NY: Macmillan, 1978.
12. Freedom RM, Lee KJ, Macdonald C, et al. Selected aspects of cardiac tumors in infancy and childhood. *Pediatr Cardiol* 2000;21:299–316.
13. Sallee D, Spector ML, van Heeckeren DW, et al. Primary pediatric cardiac tumors: a 17 year experience. *Cardiol Young* 1999;9:155–162.
14. Holley DG, Martin GR, Brenner JJ, et al. Diagnosis and management of fetal cardiac tumors: a multicenter experience and review of published reports. *J Am Coll Cardiol* 1995;26:516–520.
15. Tworetzky W, McElhinney DB, Margossian R. Association between cardiac tumors and tubular sclerosis in the fetus and neonate. *Am J Cardiol* 2003;92:487–489.

16. Bogren HG, DeMaria AN, Mason DT. Imaging procedures in the detection of cardiac tumors, with emphasis on echocardiography: a review. *Cardiovasc Intervent Radiol* 1980;3:107-125.
17. Scully RE, Mark EJ, McNeely BU. Case records of the Massachusetts General Hospital: weekly clinicopathological exercises. *N Engl J Med* 1983;308:206-214.
18. Bini RM, Westaby S, Barger LM Jr, et al. Investigation and management of primary cardiac tumors in infants and children. *J Am Coll Cardiol* 1983;2:351-357.
19. Kiény R, de Geeter B, Kretz JG, et al. Cardiac tumors in infancy: recent aspects. *Thorac Cardiovasc Surg* 1983;31:169-171.
20. Arciniegas E, Hakimi M, Farooki ZQ, et al. Primary cardiac tumors in children. *Surgery* 1980;79:582-591.
21. Marx GR, Bierman FZ, Matthews E, et al. Two-dimensional echocardiographic diagnosis of intracardiac masses in infancy. *J Am Coll Cardiol* 1984;3:827-832.
22. Duncan WJ, Rowe RD, Freedom RM, et al. Space-occupying lesions of the myocardium: role of two-dimensional echocardiography in detection of cardiac tumors in children. *Am Heart J* 1982;104:780-785.
23. Rees AH, Solinger RE, Elbl F, et al. Two-dimensional echocardiographic assessment of intracardiac masses in infants and children. *South Med J* 1991;84:587-590.
24. Sharritt GP, Lacson AG, Cornet G, et al. Echocardiography of intracardiac filling defects in infants and children. *Pediatr Cardiol* 1986;7:189-194.
25. Biancaniello TM, Meyer RA, Gaum WE, et al. Primary benign intramural ventricular tumors in children: Pre- and postoperative electrocardiographic, echocardiographic, and angiographic evaluation. *Am Heart J* 1982;103:852-857.
26. Bricker JT, Murphy DJ Jr. Atrial alternans. *Am Heart J* 1990;119: 412-414.
27. Birnbaum SE, McGahan JP, Janos GG, et al. Fetal tachycardia and intramural cardiac tumors. *J Am Coll Cardiol* 1985;6:1358-1361.
28. Rienmüller R, Lloret JL, Tiling R, et al. MR imaging of pediatric cardiac tumors previously diagnosed by echocardiography. *J Comput Assist Tomogr* 1989;13:621-626.
29. Riggs T, Paul MH, DeLeon S, et al. Two-dimensional echocardiography in evaluation of right atrial masses: five cases in pediatric patients. *Am J Cardiol* 1991;68:961-966.
30. Fitzpatrick PG, Nancarrow NC, Harris JP, et al. Two-dimensional echocardiographic identification of multiple cardiac tumors in a newborn. *Ultrasound Med Biol* 1982;8:695-699.
31. Brown IW, McGoldrick JP, Robles A, et al. Left ventricular fibroma: echocardiographic diagnosis and successful surgical excision in three cases. *J Cardiovasc Surg* 1990;31:536-540.
32. Filiatrault M, Bieland MJ, Neilson KA, et al. Cardiac fibroma presenting with clinically significant arrhythmias in infancy. *Pediatr Cardiol* 1991;12:118-120.
33. Kutayli F, Malouf J, Slim M, et al. Cardiac fibroma with tumor involvement of the mitral valve: diagnosis by cross-sectional echocardiography. *Eur Heart J* 1988;9:563-566.
34. Gonzalez-Crussi F, Eberts TJ, Mirkin DL. Congenital fibrous hamartoma of the heart. *Arch Pathol Lab Med* 1978;102:491-493.
35. Tahernia AC, Bricker JT, Ott DA. Intracardiac fibroma in an asymptomatic infant. *Clin Cardiol* 1990;13:506-512.
36. Marin-Garcia J, Fitch CW, Shenfeldt RE. Primary right ventricular tumor (fibroma) simulating cyanotic heart disease in a newborn. *J Am Coll Cardiol* 1984;3:868-871.
37. Farooki ZQ, Ross RD, Paridon SM, et al. Spontaneous regression of cardiac rhabdomyoma. *Am J Cardiol* 1991;67:897-899.
38. Alkalay AL, Ferry DA, Lin B, et al. Spontaneous regression of cardiac rhabdomyoma in tuberous sclerosis. *Clin Pediatr* 1987;26:532-535.
39. Fischer DR, Beerman LB, Park SC, et al. Diagnosis of intracardiac rhabdomyoma by two-dimensional echocardiography. *Am J Cardiol* 1984;53:978-997.
40. Diamant S, Sharaz J, Holtzman WD, et al. Echocardiographic diagnosis of cardiac tumors in symptomatic tuberous sclerosis patients. *Clin Pediatr* 1983;22:297-299.
41. Foster ED, Spooner EW, Farina MA, et al. Cardiac rhabdomyoma in the neonate: surgical management. *Ann Thorac Surg* 1984;37:249-253.
42. Villafane J, Saltz M, Kaiser G, et al. A rare right atrial tumor presenting with cyanosis in a newborn. *Am Heart J* 1987;113:1036-1038.
43. Ludomirsky A, Vargo TA, Murphy DJ, et al. Intracardiac undifferentiated sarcoma in infancy. *J Am Coll Cardiol* 1985;6:1362-1364.
44. Fyke FED, Seard JB, Edwards WD, et al. Primary cardiac tumors: experience with 30 consecutive patients since the introduction of two-dimensional echocardiography. *J Am Coll Cardiol* 1985;5:1465-1473.
45. Green SE, Joynt LF, Fitzgerald PJ, et al. In vivo ultrasonic tissue characterization of human intracardiac masses. *Am J Cardiol* 1983;51:231-236.
46. Allan LD, Joseph MC, Tynan M. Clinical value of echocardiographic colour image processing in two cases of primary cardiac tumour. *Br Heart J* 1983;49:154-156.
47. Ganame J, D'hooge J, Mertens L. Different deformation patterns in intracardiac tumors. *Eur J Echocardiogr* 2005;6:461-464.
48. Rittoo D, Cotter L. Detection of a small left atrial myxoma: value and limitations of four imaging modalities. *J Am Soc Echocardiogr* 1997;10:874-876.
49. DiFlo T, Cantelmo NL, Haudenschild CC, et al. Atrial myxoma with remote metastasis: case report and review of the literature. *Surgery* 1992;111: 352-356.
50. Samdarshi TE, Mahan EF 3rd, Nanda NC, et al. Transesophageal echocardiographic diagnosis of multicentric left ventricular myxomas mimicking a left atrial tumor. *J Thorac Cardiovasc Surg* 1992;103:471-474.
51. Obeid AI, Marvasti M, Parker F, et al. Comparison of transthoracic and transesophageal echocardiography in diagnosis of left atrial myxoma. *Am J Cardiol* 1989;63:1006-1008.
52. Engberding R, Daniel WG, Erbel R, et al. Diagnosis of heart tumours by transesophageal echocardiography: a multicentre study in 154 patients. European Cooperative Study Group. *Eur Heart J* 1993;14:1223-1228.
53. Brown AS, Why H, Monaghan MJ. Value of multiplane transesophageal echocardiography in recurrent atrial myxoma. *Br Heart J* 1994;71:540.
54. Geibel A, Kasper W, Keck A, et al. Diagnosis, localization and evaluation of malignancy of heart and mediastinal tumors by conventional and transesophageal echocardiography. *Acta Cardiologica* 1996;51:395-408.
55. Wang XF, Li ZA, Cheng TO, et al. Clinical application of three-dimensional transesophageal echocardiography. *Am Heart J* 1994;128:380-388.
56. Borges AC, Witt C, Bartel T, et al. Preoperative two- and three-dimensional transesophageal echocardiographic assessment of heart tumors. *Ann Thorac Surg* 1996;61:1163-1167.
57. Boxer RA, LaCorte MA, Singh S, et al. Diagnosis of cardiac tumors in infants by magnetic resonance imaging. *Am J Cardiol* 1985;56:831-832.
58. Rienmüller R, Tiling R. Evaluation of paracardiac and intracardiac masses in children. *Semin Ultrasound CT MR* 1990;11:246-250.
59. Shiraishi H, Yanagisawa M, Kuramatsu T, et al. Cardiac tumour in a neonate with tuberous sclerosis: echocardiographic demonstration and magnetic resonance imaging. *Eur J Pediatr* 1988;148:50-52.
60. Magherini A, Bartolozzi C, Petacchi D. Magnetic resonance and echocardiography in the investigation of cardiac tumour in an infant. *Int J Cardiol* 1988;18:263-266.
61. Niwa K, Tashima K, Terai M, et al. Contrast-enhanced magnetic resonance imaging of cardiac tumors in children. *Am Heart J* 1989;118:424-425.
62. Braverman RM, Lipshultz SE, McCarten KM, et al. Pediatric case of the day. *Radiographics* 1991;11:932-934.
63. Ensing GJ, Driscoll DJ, Smithson WA. Left atrial mass 16 years after radiation therapy for mediastinal neuroblastoma. *Pediatr Cardiol* 1987;8:271-274.
64. Lund JT, Ehman RL, Julsrud PR, et al. Cardiac masses: assessment by MR imaging. *AJR Am J Roentgenol* 1989;152:469-473.
65. Link KM, Lesko NM. MR evaluation of cardiac/juxtacardiac masses. *Top Magn Reson Imaging* 1995;7:232-245.
66. Matsuoka H, Hamada M, Honda T, et al. Morphologic and histologic characterization of cardiac myxomas by magnetic resonance imaging. *Angiology* 1996;47:693-698.
67. Bouton S, Yang A, McCrindle BW, et al. Differentiation of tumor from viable myocardium using cardiac tagging with MR imaging. *J Comput Assist Tomogr* 1991;15:676-678.
68. Kiaffas M, Powell AJ, Geva T. Magnetic resonance imaging evaluation of cardiac tumor characteristics in infants and children. *Am J Cardiol* 2002;89:1229-1233.
69. De Cobelli F, Esposito A, Mellone R, et al. Late enhancement of a left ventricular cardiac fibroma assessed with gadolinium-enhanced cardiovascular magnetic resonance. *Circulation* 2005;112:e242-e243.
70. Moniotte S, Geva T, Perez-Antonio A, et al. Cardiac hemangioma. *Circulation* 2005;112:e103-e104.
71. Mackie AS, Kozakewich HP, Geva T, et al. Vascular tumors of the heart in infants and children: case series and review of the literature. *Pediatr Cardiol* 2005;26:344-349.
72. Friedberg M, Chang I, Silverman HN, et al. Near sudden death from cardiac lipoma in an adolescent. *Circulation* 2006;113:778-779.
73. Van der Hauwaert LG. Cardiac tumours in infancy and childhood. *Br Heart J* 1971;33:125-132.
74. Allen HD, Blieden L, Stone FM, et al. Echocardiographic demonstration of a right ventricular tumor in a neonate. *J Pediatr* 1974;84:854.
75. Deeg KH, Voigt HJ, Hofbeck M, et al. Prenatal ultrasound diagnosis of multiple cardiac rhabdomyomas. *Pediatr Radiol* 1990;20:291-292.
76. Simopoulos AP, Breslow A. Tuberous sclerosis in the newborn. *Am J Dis Child* 1983;3:313-316.
77. Shaher RM, Mintzer J, Farina M, et al. Clinical presentation of rhabdomyoma of the heart in infancy and childhood. *Am J Cardiol* 1972;30:95-103.
78. Bader RS, Chitayat D, Kelly E, et al. Fetal rhabdomyomas: prenatal diagnosis, clinical outcome, and incidence of associated tuberous sclerosis complex. *J Pediatr* 2003;143:620-624.
79. Isaacs H. Fetal and neonatal cardiac tumors. *Pediatr Cardiol* 2004;25:252-273.
80. Fenoglio JJ Jr, McAllister HA Jr, Ferrans VJ. Cardiac rhabdomyoma: a clinicopathologic and electron microscopic study. *Am J Cardiol* 1976;38:241-250.
81. Yamashita H, Nagaoka H, Matsushita R, et al. Cardiac rhabdomyoma associated with tuberous sclerosis: an autopsy case of newborn infant died of cardiac failure. *Acta Pathol Jpn* 1987;37:645-653.
82. Kirk JW, ed. *Cardiac Surgery*. Edinburgh, UK: Harcourt Publishers, 1992:1627-1653.
83. Mahoney L, Schieken RM, Doty D. Cardiac rhabdomyoma simulating pulmonary stenosis. *Cathet Cardiovasc Diagn* 1979;5:385-388.
84. Bass JL, Brenningstall GN, Swaiman KF. Echocardiographic incidence of cardiac rhabdomyoma in tuberous sclerosis. *Am J Cardiol* 1985;55:1379-1382.
85. Prichard RW. Tumors of the heart: review of the subject and report of one hundred and fifty cases. *AMA Arch Pathol* 1951;75:98-128.

86. Shrivastava S, Jacks JJ, White RS, et al. Diffuse rhabdomyomatous of the heart. *Arch Pathol Lab Med* 1977;101:78-80.
87. Gotlib AI, Chan M, Palmer WH, et al. Ventricular preexcitation syndrome: accessory left atrioventricular connection and rhabdomyomatous myocardial fibers. *Arch Pathol Lab Med* 1977;101:486-489.
88. Smythe JF, Dyck JD, Smallhorn JF, et al. Natural history of cardiac rhabdomyoma in infancy and childhood. *Am J Cardiol* 1990;66:1247-1249.
89. Journel H, Roussey M, Plais MH, et al. Prenatal diagnosis of familial tuberous sclerosis following detection of cardiac rhabdomyoma by ultrasound. *Prenat Diagn* 1986;6:283-289.
90. Guereta LG, Burgueros M, Elorza MD, et al. Cardiac rhabdomyoma presenting as fetal hydrops. *Pediatr Cardiol* 1986;7:171-174.
91. Watanabe T, Hojo Y, Kozaki T, et al. Hypoplastic left heart syndrome with rhabdomyoma of the left ventricle. *Pediatr Cardiol* 1991;12:121-122.
92. Harding CO, Pagon RA. Incidence of tuberous sclerosis in patients with cardiac rhabdomyoma. *Am J Med Genet* 1990;37:443-446.
93. Platt LD, Devore GR, Horenstein J, et al. Prenatal diagnosis of tuberous sclerosis: the use of fetal echocardiography. *Prenat Diagn* 1987;7:407-411.
94. Gresser CD, Shime J, Rakowski H, et al. Fetal cardiac tumor: a prenatal echocardiographic marker for tuberous sclerosis. *Am J Obstet Gynecol* 1987;156:689-690.
95. Black MD, Kadletz M, Smallhorn JF, et al. Cardiac rhabdomyomas and obstructive left heart disease: histologically but not functionally benign. *Ann Thorac Surg* 1998;65:1388-1390.
96. Rees AH, Elbl FE, Minhas KV, et al. Echocardiographic evidence of left ventricular tumor in a neonate. *Chest* 1978;73:433-435.
97. Howanitz EP, Teske DW, Qualman SJ, et al. Pedunculated left ventricular rhabdomyoma. *Ann Thorac Surg* 1986;41:443-444.
98. Spooner EW, Farina MA, Shaher RM, et al. Left ventricular rhabdomyoma causing subaortic stenosis: the two-dimensional echocardiographic appearance. *Pediatr Cardiol* 1982;2:67-71.
99. Russell GA, Dhasmana JP, Berry PJ, et al. Coexistent cardiac tumours and malformations of the heart. *Int J Cardiol* 1989;22:89-98.
100. Matsuoka Y, Nakati T, Kawaguchi K, et al. Disappearance of a cardiac rhabdomyoma complicating congenital mitral regurgitation as observed by serial two-dimensional echocardiography. *Pediatr Cardiol* 1990;11:98-101.
101. Bhandari AK, Nanda NC, Hicks DG. Two-dimensional echocardiography of intracardiac masses: echo pattern—histopathology correlation. *Ultrasound Med Biol* 1982;8:673-680.
102. Diamant S, Sharaz J, Holtzman M, et al. Echocardiographic diagnosis of cardiac tumors in symptomatic tuberous sclerosis patients. *Clin Pediatr* 1983;22:297-299.
103. Duncan WJ. Left ventricular rhabdomyoma. *Pediatr Cardiol* 1983;4:170-171.
104. Gomez MR. Varieties of expression of tuberous sclerosis. *Neurofibromatosis* 1988;1:330-338.
105. Wilding G, Green HL, Longo DL, et al. Tumors of the heart and pericardium. *Cancer Treat Rev* 1988;15:165-181.
106. Shepherd CW, Gomez MR, Lie JT, et al. Causes of death in patients with tuberous sclerosis. *Mayo Clin Proc* 1991;66:792-796.
107. Arens R, Feingold M. Denouement and discussion. *Am J Dis Child* 1988;142:1083-1084.
108. Fryer AE, Connor JM, Povey S, et al. Evidence that the gene for tuberous sclerosis is on chromosome 9. *Lancet* 1987;1:659-662.
109. Williams R, Taylor D. Tuberous sclerosis. *Lancet Surv Ophthalmol* 1983;30:143-154.
110. Baraitser M, Patton MA. Reduced penetrance in tuberous sclerosis. *J Med Genet* 1985;22:29-31.
111. Haines JL, Short MP, Kwiatkowski DJ, et al. Localization of one gene for tuberous sclerosis within 9q32-9q34, and further evidence for heterogeneity. *Am J Hum Genet* 1991;49:764-772.
112. Van Oppen ACC, Breslau-Siderius EJ, Stoutenbeek PH, et al. A fetal cystic neck mass associated with maternal tuberous sclerosis: case report and literature review. *Prenat Diagn* 1991;2:915-920.
113. Franz DN. Diagnosis and management of tuberous sclerosis complex. *Sem Pediatr Neurol* 1998;5:253-268.
114. Giamberti A, Giannico S, Squitieri C, et al. Neonatal pulmonary autograft implantation for cardiac tumor involving aortic valve. *Ann Thorac Surg* 1995;59:1219-1221.
115. Emmel M, Sreeram N, Brockmeier K. Radiofrequency catheter ablation of symptomatic neonatal rhabdomyoma. *Cardiol Young* 2006;16:97-98.
116. Feldman PS, Meyer MW. Fibroelastic hamartoma (fibroma) of the heart. *Cancer* 1976;38:314-323.
117. Oliva PB, Breckinridge JC, Johnson ML, et al. Left ventricular outflow obstruction produced by a pedunculated fibroma in a newborn: clinical, angiographic, echocardiographic and surgical observations. *Chest* 1978;74:S90-S93.
118. Abend M, Tirosh E, Grishkan A, et al. Congenital cardiac fibroma: an unusual presentation. *Eur J Pediatr* 1982;139:207-209.
119. Fernando SSE. Cardiac fibroma (fibrous hamartoma) of infancy: two case reports. *Pathology* 1979;11:111-117.
120. Williams WG, Trusler GA, et al. Left ventricular myocardial fibroma: a case report and review of cardiac tumors in children. *J Pediatr Surg* 1972;7:324-328.
121. Jones KL, Wolf PL, Jensen P, et al. The Gorlin syndrome: a genetically determined disorder associated with cardiac tumor. *Am Heart J* 1986;111:1013-1015.
122. Folger GM Jr, Peters HJ. Nodular fibroelastosis (fibroelastic hamartoma): a tumorous malformation of the heart. *Am J Cardiol* 1968;21:420-427.
123. Etches PC, Gribbin B, Gunning AJ. Echocardiographic diagnosis and successful removal of cardiac fibroma in 4-year old child. *Br Heart J* 1980;43:360-362.
124. Osano M, Yashiro K, Oikawa T, et al. Intramural fibroma of the heart: a case report. *Pediatrics* 1969;43:605-608.
125. Schwartz J, Saldivar V, Fermin T, et al. Interventricular fibroma and cystic renal dysplasia in a newborn. *Pediatr Pathol* 1984;2:187-195.
126. Yamaguchi M, Hosokawa Y, Ohashi H, et al. Cardiac fibroma. Long-term fate after excision. *J Thorac Cardiovasc Surg* 1992;103:140-145.
127. Takahashi K, Imamura Y, Ochi T, et al. Echocardiographic demonstration of an asymptomatic patient with left ventricular fibroma. *Am J Cardiol* 1984;53:981-982.
128. Cho J, Danielson G, Puga FJ. Surgical resection of ventricular cardiac fibromas: early and late results. *Ann Thorac Surg* 2003;76:1929-1934.
129. Beghetti M, Gow RM, Haney I, et al. Pediatric primary benign cardiac tumors: a 15-year review. *Am Heart J* 1997;134:1107-1114.
130. Talley JD, Wenger NK. Atrial myxoma: overview, recognition, and management. *Compr Ther* 1987;13:12-18.
131. Zitnik RS, Giuliani ER. Clinical recognition of atrial myxoma. *Am Heart J* 1970;80:689-700.
132. Dianzumba SS, Char G. Large calcified right atrial myxoma in a newborn: rare cause of neonatal death. *Br Heart J* 1982;48:177-179.
133. Hals J, Ek J, Sandnes K. Cardiac myxoma as the cause of death in an infant. *Acta Paediatr Scand* 1990;79:999-1000.
134. Sanyal SK, de Leuchtenberg N, Rojas RH, et al. Right atrial myxoma in infancy and childhood. *Am J Cardiol* 1967;20:263-269.
135. Balsara RK, Pelias AJ. Myxoma of right ventricle presenting as pulmonic stenosis in a neonate. *Chest* 1983;83:145-146.
136. Crawford FA Jr, Selby JH Jr, Watson D, et al. Unusual aspects of atrial myxoma. *Ann Surg* 1978;188:240-244.
137. Steinke WE, Perry LW, Gold HR, et al. Left atrial myxoma in a child. *Pediatrics* 1972;49:580-589.
138. Bhat PS, Subramanyan R, Venkitachalam CG, et al. Biatial myxomas: a case report. *Indian Heart J* 1984;36:75-77.
139. Markel ML, Armstrong WF, Waller BF, et al. Left atrial myxoma with multicentric recurrence and evidence of metastases. *Am Heart J* 1986;111:409-413.
140. Kaminsky ME, Ehlers KH, Engle ME, et al. Atrial myxoma mimicking a collagen disorder. *Chest* 1979;75:93-95.
141. Fitterer JD, Spicer MJ, Nelson WP. Echocardiographic demonstration of bilateral atrial myxomas. *Chest* 1976;70:282-284.
142. Leonhardt ETG, Kullenberg KPG. Bilateral atrial myxomas with multiple arterial aneurysms—a syndrome mimicking polyarteritis nodosa. *Am J Med* 1977;62:792-794.
143. Cumming GR, Finkel K. Intracardiac myxoma involving the right and left atria in a young patient. *J Pediatr* 1961;58:559-567.
144. Abramowitz R, Majdan JF, Plzak LF, et al. Two-dimensional echocardiographic diagnosis of separate myxomas of both the left atrium and left ventricle. *Am J Cardiol* 1984;53:379-380.
145. Chandraratna PAN, San Pedro S, Elkins RC, et al. Echocardiographic, angiographic, and surgical correlations in right ventricular myxoma simulating valvar pulmonic stenosis. *Circulation* 1977;55:619-622.
146. Attum AA, Johnson GS, Masri Z, et al. Malignant clinical behavior of cardiac myxomas and "myxoid imitators." *Ann Thorac Surg* 1987;44:217-222.
147. Carter D, Bibro MC, Touloukian RJ. Benign clinical behavior of immature mediastinal teratoma in infancy and childhood: report of two cases and review of the literature. *Cancer* 1982;49:398-402.
148. Mahar LJ, Lie JT, Groover RV, et al. Primary cardiac myxosarcoma in a child. *Mayo Clin Proc* 1979;54:261-266.
149. Atherton DJ, Pitcher DW, Wells RS, et al. A syndrome of various cutaneous pigmented lesions, myxoid neurofibromata and atrial myxoma: the NAME syndrome. *Br J Dermatol* 1980;103:421-429.
150. McCarthy PM, Schaff HV, Winkler HZ, et al. Deoxyribonucleic acid ploidy pattern of cardiac myxomas. Another predictor of biologically unusual myxomas. *J Thorac Cardiovasc Surg* 1989;98:1083-1086.
151. Burke A, Virmani R. More on cardiac myxomas. *New Engl J Med* 1996;335:1462-1463.
152. Goldstein DJ, Oz MC, Michler RE. Radical excisional therapy and total cardiac transplantation for recurrent atrial myxoma. *Ann Thorac Surg* 1995;60:1105-1107.
153. Cleveland DC, Westaby S, Karp RB. Treatment of intra-atrial cardiac tumors. *JAMA* 1983;249:2799-2802.
154. Alkhulaifi AM, Horner S, Pugsley WB, et al. Recurrent left atrial myxoma. *Cardiovasc Surg* 1994;2:232-236.
155. Goodwin JF, Lond MD. Diagnosis of left atrial myxoma. *Lancet* 1963;1:464-468.
156. Roudaut R, Pouget P, Videau P, et al. Right atrial myxoma in an asymptomatic child: echocardiographic diagnosis. *Eur Heart J* 1980;1:453-459.
157. Robertson R. Primary cardiac tumours: surgical treatment. *Am J Surg* 1957;94:183-193.

158. Liu HY, Panidis I, Soffer J, et al. Echocardiographic diagnosis of intracardiac myxomas: present status. *Chest* 1983;84:62–67.
159. Neches WH, Park SC, Lenox CC, et al. Left atrial myxoma: clinical presentation suggesting acute myocarditis. *JAMA* 1974;229:1906–1907.
160. New PFJ, Price DL, Carter B. Cerebral angiography in cardiac myxoma: correlation of angiographic and histopathological findings. *Radiology* 1970;96:335–345.
161. Oetgen WJ, Umfrid RP III, Hamilton KM, et al. Two-dimensional echocardiography in the diagnosis of left atrial myxoma in a child. *South Med J* 1982;75:1125–1127.
162. Gray IR, Williams WG. Recurring cardiac myxoma. *Br Heart J* 1985;53:645–649.
163. Nakata S, Nakano S, Mitsuda N, et al. Recurrent left atrial myxoma in a patient with a twin fetus pregnancy. *Jpn Circ J* 1996;60:130–132.
164. Kabbani SS, Jokhadar M, Meada R, et al. Atrial myxoma: report of 24 operations using the biatrial approach. *Ann Thorac Surg* 1994;58:483–487; discussion 487–488.
165. Castells E, Ferran V, Octavio de Toledo MC, et al. Cardiac myxomas: surgical treatment, long-term results and recurrence. *J Cardiovasc Surg* 1993;34:49–53.
166. Jugdutt BI, Rossall RE, Sterns LP. An unusual case of recurrent left atrial myxoma. *Can Med Assoc J* 1975;112:1099–1100.
167. McWhirter WR, Tetteh-Lartey EV. A case of atrial myxoma. *Br Heart J* 1974;36:839–840.
168. Daubenton JD, Human DG, Hassoulas J, et al. Left atrial myxoma in a 13-month-old infant. *S Afr Med J* 1985;68:261–262.
169. Soeparwata R, Poeml P, Schmid C, et al. Interleukin-6 plasma levels and tumor size in cardiac myxoma. *J Thorac Cardiovasc Surg* 1996;112:1675–1657.
170. Kanda T, Umeyama S, Sasaki A, et al. Interleukin-6 and cardiac myxoma. *Am J Cardiol* 1994;74:965–967.
171. Parisis JT, Mentzikof D, Georgopoulou M, et al. Correlation of interleukin-6 gene expression to immunologic features in patients with cardiac myxomas. *J Interferon Cytokine Res* 1996;16:589–593.
172. Abbas AK, Lichtman AH, Pober JS, eds. *Cytokines, Cellular and Molecular Immunology*. 2nd ed. Philadelphia, PA: WB Saunders, 1994:250–251 (Chapter 12).
173. Salcedo EE, Adams KV, Lever HM, et al. Echocardiographic findings in 25 patients with left atrial myxoma. *J Am Coll Cardiol* 1983;1:1162–1166.
174. Sicart M, Roudaut R, d'Agata P, et al. The contribution of bidimensional echocardiography in the diagnosis of cardiac tumours: based on 25 observed cases. *Eur J Radiol* 1981;1:241–244.
175. St John Sutton MG, Mercier LA, Giuliani ER, et al. Atrial myxomas: a review of clinical experience in 40 patients. *Mayo Clin Proc* 1980;55:371–376.
176. Park JM, Garcia RR, Patrick JK, et al. Right atrial myxoma with a nonembolic intestinal manifestation. *Pediatr Cardiol* 1990;11:164–166.
177. Chitwood W. Atrial myxoma: report of 24 operations using the biatrial approach (invited commentary). *Ann Thorac Surg* 1994;58:487–488.
178. Sellke FW, Lemmer JH Jr, Vandenberg BF, et al. Surgical treatment of cardiac myxomas: long-term results. *Ann Thorac Surg* 1990;50:557–561.
179. Actis Dato GM, De Benedictis M, Actis Dato A Jr, et al. Long-term follow-up of cardiac myxomas (7–31 years). *J Cardiovasc Surg* 1993;34:141–143.
180. Siltanen P, Tuuteri L, Norio R, et al. Atrial myxoma in a family. *Am J Cardiol* 1976;38:252–256.
181. McCarthy PM, Piehler JM, Schaff HV, et al. The significance of multiple, recurrent, and “complex” cardiac myxomas. *J Thorac Cardiovasc Surg* 1986;91:389–396.
182. Basson CT, MacRae CA, Korf B, et al. Genetic heterogeneity of familial atrial myxoma syndromes (Carney complex). *Am J Cardiol* 1997;79:994–995.
183. Stratakis CA, Carney JA, Lin JP, et al. Carney complex, a familial multiple neoplasia and lentiginosis syndrome. Analysis of 11 kindreds and linkage to the short arm of chromosome 2. *J Clin Invest* 1996;97:699–705.
184. Casey M, Mah C, Merliss AD, et al. Identification of a novel genetic locus for familial cardiac myxomas and Carney complex. *Circulation* 1998;98:2560–2566.
185. Aguzzino L, Vosa C, Arciprete P, et al. Intrapericardial teratoma in the newborn: review of literature and report of successful surgery in infant with intrapericardial teratoma. *Int J Cardiol* 1984;5:21–28.
186. Banfield F, Dick M II, Behrendt DM, et al. Intrapericardial teratoma: a new and treatable cause of hydrops fetalis. *Am J Dis Child* 1980;134:1174–1175.
187. Weber HS, Kleinman CS, Hellenbrand WE, et al. Development of a benign intrapericardial tumor between 20 and 40 weeks of gestation. *Pediatr Cardiol* 1988;9:153–156.
188. White JJ, Kaback MM, Haller JA Jr. Diagnosis and excision of an intrapericardial teratoma in an infant. *J Thorac Cardiovasc Surg* 1968;55:704–710.
189. Reynolds JL, Donahue JK, Pearce CW. Intrapericardial teratoma: a cause of acute pericardial effusion in infancy. *Pediatrics* 1969;43:71–78.
190. MacDonald S, Fay JE, Lynn RB. Intrapericardial teratoma: a continuing challenge. *Can J Surg* 1983;26:81–82.
191. Lintermans JP, Schoevaertds JC, Fiasse L, et al. Intrapericardial teratoma: a curable cause of cardiac tamponade in infancy. *Clin Pediatr* 1973;12:316–318.
192. Deenadayalu RP, Tuuri D, Dewall RA, et al. Intrapericardial teratoma and bronchogenic cyst. *J Thorac Cardiovasc Surg* 1974;67:945–952.
193. Seguin JR, Coulon PL, Perez M, et al. Echocardiographic diagnosis of an intrapericardial teratoma in infancy. *Am Heart J* 1987;113:1239–1240.
194. Ow EP, Suarez CR, Subramanian R, et al. Diagnosis of intrapericardial tumor in an infant by two-dimensional echocardiography. *Pediatr Cardiol* 1986;6:223–225.
195. Farooki ZQ, Hakimi M, Arciniegas E, et al. Echocardiographic features in a case of intrapericardial teratoma. *J Clin Ultrasound* 1978;6:108–110.
196. Farooki ZQ, Arciniegas E, Hakimi M, et al. Real-time echocardiographic features of intrapericardial teratoma. *J Clin Ultrasound* 1982;10:125–128.
197. De Geeter B, Kretz JG, Nisand I, et al. Intrapericardial teratoma in a newborn infant: use of fetal echocardiography. *Ann Thorac Surg* 1983;35:664–666.
198. Arciniegas E, Hakimi M, Farooki ZQ, et al. Intrapericardial teratoma in infancy. *J Thorac Cardiovasc Surg* 1980;79:306–311.
199. Legnani FA, Corwin RD. Intrapericardial teratoma: report of a case. *Am Heart J* 1963;65:674–677.
200. Cyr DR, Guntheroth WG, Nyberg DA, et al. Prenatal diagnosis of an intrapericardial teratoma: a cause for nonimmune hydrops. *J Ultrasound Med* 1988;7:87–90.
201. Costas C, Williams RL, Fortune RL. Intracardiac teratoma in an infant. *Pediatr Cardiol* 1986;7:179–181.
202. Solomon RD. Malignant teratoma of the heart: report of case with necropsy. *AMA Arch Path* 1951;52:561–568.
203. Marsten JL, Cooper AG, Ankeney JL. Acute cardiac tamponade due to perforation of a benign mediastinal teratoma into the pericardial sac. Review of cardiovascular manifestations of mediastinal teratomas. *J Thorac Cardiovasc Surg* 1966;51:700–707.
204. Grenadier E, Margulis T, Palant A, et al. Huge cavernous hemangioma of the heart: a completely evaluated case report and review of the literature. *Am Heart J* 1989;117:479–481.
205. Franciosi RA, Gay RM, Ah-Tye P. Vascular hamartoma of the heart in a child. *Am Heart J* 1970;79:676–682.
206. Tabry I, Nassar VH, Rizk G, et al. Cavernous hemangioma of the heart: case report and a review of the literature. *J Thorac Cardiovasc Surg* 1975;69:415–420.
207. Anderson KR, Fiddler GI, Lie JT. Congenital papillary tumor of the tricuspid valve: an unusual cause of right ventricular outflow obstruction in a neonate with trisomy E. *Mayo Clin Proc* 1977;52:665–669.
208. Furuta N, Luhmer I, Hetzer R, et al. Abnormal accessory mitral leaflet simulating left ventricular outflow tract tumor. *Thorac Cardiovasc Surg* 1983;31:249–253.
209. Harada K, Seki I, Kobayashi H, et al. Lipoma of the heart in a child: clinical, echocardiographic, angiographic, and pathological features. *Jpn Heart J* 1980;21:903–910.
210. Barberger-Gateau P, Paquet M, Desaulniers D, et al. Fibrolipoma of the mitral valve in a child: clinical and echocardiographic features. *Circulation* 1978;58:955–958.
211. Behnam R, Williams G, Gerlis L, et al. Lipoma of the mitral valve and papillary muscle. *Am J Cardiol* 1983;51:1459–1460.
212. Sridhar AV, Bullock F, Hickey MS. Papillary fibroelastoma of the tricuspid valve presenting as a neonatal pulmonary hemorrhage. *Acta Paediatr* 2004;93:1254–1265.
213. Marni E, Pedroni E, Magrini U, et al. Angiosarcoma of the heart: report of a case in a 9-year-old boy. *Pediatr Oncol* 1983;11:336–338.
214. Lin T, Stech J, Eckert W, et al. Pericardial angiosarcoma simulating pericardial effusion by echocardiography. *Chest* 1978;73:881–883.
215. Tse R, Frank M. Angiosarcoma of the heart: first reported case in an adolescent. *Angiology* 1971;22:147–152.
216. Wakely P. Angiosarcoma of the heart in an adolescent: a light and electron microscopic and immunohistochemical study. *Arch Pathol Lab Med* 1987;111:472–475.
217. Andrassy RJ, Wiener ES, Raney RB, et al. Thoracic sarcomas in children. *Ann Surg* 1998;227:170–173.
218. Caralis D, Kennedy H, Bailey I, et al. Primary right cardiac tumor: detection by echocardiographic and radioisotopic studies. *Chest* 1980;77:100–102.
219. Farooki Z, Chang C-H, Jackson W, et al. Primary pulmonary artery sarcoma in two children. *Pediatr Cardiol* 1988;9:243–251.
220. Schmaltz A, Apitz J. Primary rhabdomyosarcoma of the heart. *Pediatr Cardiol* 1982;2:73–75.
221. Sholler G, Hawker R, Nunn G, et al. Primary left ventricular rhabdomyosarcoma in a child: noninvasive assessment and successful resection of a rare tumor. *J Thorac Cardiovasc Surg* 1987;93:465–472.
222. Babatasi G, Massetti M, Agostini D, et al. Recurrent left-sided heart leiomyosarcoma: should heart transplantation be legitimate? *J Heart Lung Transplant* 1998;17:1133–1138.
223. Aravot DJ, Banner NR, Madden B, et al. Primary cardiac tumours—is there a place for cardiac transplantation? *Eur J Cardiothorac Surg* 1989;3:521–524.
224. Jamieson SW, Gaudiani VA, Reitz BA, et al. Operative treatment of an unresectable tumor of the left ventricle. *J Thorac Cardiovasc Surg* 1981;81:797–799.
225. Siebenmann R, Jenni R, Makek M, et al. Primary synovial sarcoma of the heart treated by heart transplantation [letter]. *J Thorac Cardiovasc Surg* 1990;99:567–568.
226. Crespo MG, Pulpon LA, Pradas G, et al. Heart transplantation for cardiac angiosarcoma: should its indication be questioned? *J Heart Lung Transplant* 1993;12:527–530.

227. Takach TJ, Reul GJ, Ott DA, et al. Primary cardiac tumors in infants and children: Immediate and long-term operative results. *Ann Thorac Surg* 1996;62:559-564.
228. Armitage JM, Kormos RL, Griffith BP, et al. Heart transplantation in patients with malignant disease. *J Heart Transplant* 1990;9:627-629; discussion 630.
229. Baay P, Karwande SV, Kushner JP, et al. Successful treatment of a cardiac angiosarcoma with combined modality therapy. *J Heart Lung Transplant* 1994;13:923-925.
230. Cooley D, Reardon M, Frazier O, et al. Human cardiac explantation and autotransplantation: application in a patient with a large cardiac pheochromocytoma. *Tex Heart Inst J* 1985;12:171-176.
231. Purtilo DT, Strobach RS, Okano M, et al. Epstein-Barr virus-associated lymphoproliferative disorders. *Lab Invest* 1992;67:5-23.
232. Opelz G, Henderson H. Incidence of non-Hodgkin lymphoma in kidney and heart transplant recipients. *Lancet* 1993;342:1514-1516.
233. Penn I. The changing pattern of post-transplant malignancies. *Transplant Proc* 1991;23:1101-1103.
234. Zuppiroli A, Cecchi F, Ciaccheri M, et al. Two-dimensional echocardiographic findings in a case of massive cardiac involvement by malignant lymphoma. *Acta Cardiol* 1985;40:485-492.
235. Anclamo N, King T, Mills N, et al. Lymphoma with large intracavitary metastasis to the heart: report of a case. *J CardioVasc Surg* 1976;17:136-139.
236. Aytac A, Tuncali T, Tinaztepe K, et al. Metastatic Wilms' tumor in the right atrium propagated through the inferior vena cava. *Vasc Surg* 1976;10:268-274.
237. Kolmannskog S, Moe P, Besigye E, et al. Wilms tumor with extension to the right atrium. *Med Pediatr Oncol* 1979;6:313-316.
238. Luck S, DeLeon S, Shkolnik A, et al. Intracardiac Wilms tumor: diagnosis and management. *J Pediatr Surg* 1982;17:551-554.
239. Farooki Z, Green E, Arciniegas E. Echocardiographic pattern of right atrial tumour motion. *Br Heart J* 1976;38:580-583.

Robert E. Shaddy ■ Lloyd Y. Tani

Hear failure in children is a very heterogeneous syndrome with multiple possible causes and treatments. This chapter reviews the causes of heart failure in children and discusses the management of chronic heart failure. Acute heart failure is addressed elsewhere in this book.

ETIOLOGY OF CHRONIC HEART FAILURE IN CHILDREN

Accurate determination of the cause of heart failure in children is critical to both prognosis and optimal treatment. In children, it is useful to consider the various causes of heart failure by age. Although not absolute, this classification provides a useful framework from which to approach children with suspected or known heart failure. In the following discussion, causes are considered in two broad age categories: (a) neonates and infants and (b) children and adolescents (Table 73.1). Most of the entities included in this section are discussed in greater detail elsewhere in this textbook. Causes of heart failure in the fetus include structural heart disease, arrhythmias, and myocardial dysfunction, and are discussed in Chapter 27 (Fetal Echocardiography and Fetal Cardiology).

NEONATES AND INFANTS

Heart failure in neonates and infants can occur due to a variety of causes including structural heart disease, myocardial dysfunction, arrhythmias, and metabolic abnormalities. Congenital structural anomalies can be broadly classified as volume overload lesions, pressure overload lesions, and complex lesions that often involve a combination of pressure and volume overload.

Heart failure that presents at birth may be due to asphyxia-related myocardial dysfunction, hypoglycemia or hypocalcemia, sepsis, anemia or polycythemia, myocarditis, arrhythmias (supraventricular tachycardia, congenital complete heart block), a sizable atrioventricular malformation, or severe tricuspid regurgitation (asphyxia-related papillary muscle dysfunction, Ebstein anomaly, tricuspid valve dysplasia) (1).

Pressure overload lesions presenting in neonates include left heart obstructive lesions such as critical aortic valve stenosis, coarctation of the aorta or interrupted aortic arch, and the spectrum of left heart hypoplasia. Neonates with these anomalies depend on the ductus arteriosus to provide systemic blood flow and typically present between 2 days and 2 weeks of age, coincident with ductal constriction and closure. The combination of compromised cardiac output and ventricular dysfunction results in tachypnea, poor pulses, poor perfusion,

pallor, feeding difficulty, and sometimes circulatory collapse and shock.

Many volume overload lesions present in infancy and include significant left-to-right shunts (ventricular septal defect, atrioventricular septal defect, patent ductus arteriosus, truncus arteriosus, aortopulmonary window, forms of single ventricle without obstruction to pulmonary flow, pulmonary atresia with ventricular septal defect and large aortopulmonary collaterals, and total anomalous pulmonary venous return without obstruction). In such cases, pulmonary flow increases as pulmonary vascular resistance drops, resulting in pulmonary overcirculation and, in some cases, decreased systemic blood flow (2). An additional factor contributing to the increasing left-to-right shunt in this age group is the physiologic fall in hemoglobin (3).

Complex structural anomalies may combine pressure and volume overload, in some cases resulting in a combination of heart failure and cyanosis. Detailed descriptions of the anatomic subtypes with their physiologic and hemodynamic consequences are presented in other chapters. Broadly, this group of lesions includes variable combinations of ventricular hypoplasia (including functionally single left or right ventricles), atrioventricular valve dysfunction, critical obstruction to systemic flow, obstruction to pulmonary venous drainage or systemic ventricular inflow, and intracardiac shunting. As neonatal cardiac surgery has evolved, more neonates, infants, and young children who have undergone palliative or corrective cardiac surgery are at risk for heart failure owing to residual abnormalities including residual shunts, systemic outflow tract obstruction, myocardial dysfunction, significant semilunar or atrioventricular valve regurgitation, pulmonary venous or systemic ventricular inflow obstruction, and/or rhythm disturbances.

Ventricular dysfunction in young children can occur due to a number of causes. A relatively uncommon form of congenital heart disease that presents at 1 to 2 months of age is anomalous origin of the left coronary artery from the pulmonary artery (4,5). As pulmonary vascular resistance drops, antegrade perfusion of the left coronary artery from the pulmonary artery also drops, resulting in myocardial ischemia and dysfunction. Babies with this anomaly present with fussiness, irritability, poor feeding, including crying and pallor after eating (angina), tachypnea, diaphoresis, and, in some cases, cardiovascular shock. Although uncommon, this diagnosis must be considered in any infant presenting with left ventricular dysfunction and heart failure (6,7). Ventricular dysfunction occurring in the setting of myocarditis or related to various forms of cardiomyopathy (CM) (dilated, hypertrophic, or restrictive) may present with heart failure in this time period (7–10). Sustained supraventricular tachycardia may result in acquired ventricular dysfunction and heart failure (11,12). Noncardiac causes such as renal failure or sepsis may also result in low cardiac output and heart failure (1). These entities are described in detail in other chapters.

TABLE 73.1 Etiology of Chronic Heart Failure**Neonates and infants**

- Structural heart disease
 - Pressure overload
 - Severe/critical aortic stenosis
 - Aortic arch obstruction (coarctation or interruption)
 - Volume overload
 - Left-to-right shunt
 - Ventricular septal defect
 - Atrioventricular septal defect
 - Patent ductus arteriosus
 - Truncus arteriosus
 - Aortopulmonary window
 - Large aortopulmonary collaterals
- Valvular dysfunction
 - Atrioventricular valve insufficiency (post-op atrioventricular canal, Ebstein anomaly)
 - Semilunar valve insufficiency
 - Aortic insufficiency after valvotomy
 - Truncal valve regurgitation
 - Tetralogy with absent pulmonary valve
- Complex
 - Single ventricle (obstruction to systemic ventricular outflow, obstruction to ventricular inflow or pulmonary venous return)
- Myocardial dysfunction
 - Ischemia
 - Anomalous left coronary artery from the pulmonary artery
 - Asphyxia-related ventricular dysfunction
- Cardiomyopathy
 - Myocarditis
 - Primary
 - Secondary (arrhythmia, renal, hypothyroid, hypoglycemia, sepsis, etc.)
- Postoperative ventricular dysfunction

Children and adolescents

- Unoperated structural heart disease

- Left heart failure
 - Increase in mitral regurgitation
 - Increase in aortic regurgitation
 - Progressive aortic outflow obstruction
- Right heart failure
 - Ebstein anomaly
 - Eisenmenger syndrome
- Rhythm disturbances
- Postoperative structural heart disease
 - Left heart failure
 - Myocardial dysfunction (ischemia, fibrosis, systemic single or right ventricle)
 - Volume overload (residual shunt, valve regurgitation)
 - Pressure overload (residual and/or progressive aortic outflow obstruction)
 - Right heart failure
 - Ventricular dysfunction
 - Pressure overload (residual outflow obstruction, pulmonary hypertension)
 - Volume overload (pulmonary or tricuspid insufficiency)
 - Rhythm disturbances
- Structurally normal heart
 - Cardiomyopathy (primary)
 - Dilated
 - Hypertrophic
 - Restrictive
 - Cardiomyopathy (secondary)
 - Infectious or inflammatory (myocarditis, endocarditis)
 - Ischemia (Kawasaki disease, other forms of coronary artery disease)
 - Chronic volume overload (acquired valve dysfunction, rheumatic heart disease)
 - Chronic arrhythmia
 - Toxins (anthracyclines, radiation)
 - Muscular dystrophy
 - Metabolic

CHILDHOOD OR ADOLESCENCE**Unoperated Structural Heart Disease**

Although presentation with heart failure because of unoperated congenital heart disease is uncommon beyond the first few months of life in developed countries, it is more common in developing countries with poor access to health care. Thus, it is useful to subdivide heart failure in this age group into left versus right heart failure (Table 73.1).

Left heart failure may occur in patients with structural heart disease and severe atrioventricular valve (i.e., atrioventricular septal defects or the tricuspid valve in congenitally corrected transposition) (13,14) or aortic insufficiency (i.e., ventricular septal defect–associated aortic valve prolapse) (15,16). Although progression of valve regurgitation may occur spontaneously over time, infective endocarditis is an important etiology of altered valvular function in this group of patients (17). Less commonly, patients with either progressive or undiagnosed severe left ventricular outflow obstruction may present with heart failure due to ventricular dysfunction (18).

An important cause of right heart failure in this group of patients is Ebstein anomaly of the tricuspid valve with an increase in the degree of tricuspid regurgitation with or without associated arrhythmias (19,20). Severe elevation of pulmonary vascular resistance associated with an intracardiac or great vessel shunt (Eisenmenger syndrome) may be associated with right ventricular dysfunction, tricuspid and/or pulmonary regurgitation, and right heart failure (21).

POSTOPERATIVE STRUCTURAL HEART DISEASE

More common is the patient who has undergone previous intervention (transcatheter or surgical) for structural heart disease. Such patients may develop left or right heart failure due to ventricular dysfunction, valve disease, residual shunts, and/or rhythm abnormalities (13,22).

Left heart failure may occur in the postoperative patient with ventricular dysfunction, a residual left-to-right shunt, outflow tract obstruction, or valve regurgitation (various combinations of these may coexist in any given patient). Examples include (a) aortic stenosis and/or insufficiency after previous

valvotomy (23–25), (b) truncal valve stenosis and/or regurgitation after repair (25,26), and (c) severe atrioventricular valve regurgitation after atrioventricular septal defect repair (27,28). Patients with a systemic morphologic right ventricle (D-transposition of great arteries after atrial baffle or congenitally corrected transposition of great arteries after repair) are at risk for ventricular dysfunction, tricuspid (systemic atrioventricular valve) regurgitation, and arrhythmias that may result in heart failure (29–36).

Right ventricular hypertension owing to pulmonary hypertension (37) or residual pulmonary outflow obstruction (native or conduit) (38) may progress after initial intervention and result in right heart failure. Right heart failure may also occur after previous intervention owing to significant pulmonary insufficiency, such as may occur after surgery for tetralogy of Fallot (39–41).

Patients who have undergone a Fontan procedure for single ventricle physiology represent another group at high risk for developing ventricular dysfunction, arrhythmias, and heart failure (33,42–46).

As stated previously, patients after catheter or surgical intervention for structural heart disease may develop either acute or chronic rhythm disturbances that may result in heart failure (44,47–49). Ventricular dyssynchrony can cause ventricular dysfunction and heart failure, with resynchronization therapy and optimization of atrioventricular delay emerging as an effective treatment modality in select patients (50–54).

STRUCTURALLY NORMAL HEART AND ACQUIRED HEART DISEASE

Acquired heart disease is a common cause of heart failure in this age group compared to younger children. Kawasaki disease (55) (KD) is the most common cause of acquired heart disease in children in the United States (56). Children younger than 5 years are most commonly affected (median 2 years). KD is a panvasculitis, and most of the morbidity and mortality in affected patients is due to coronary artery aneurysms and associated complications (57,58). Children may present with heart failure in the acute phase of KD due to myocarditis and myocardial dysfunction (59). Less commonly, pericarditis or valvulitis during the acute illness may contribute to clinical heart failure. Those who develop coronary sequelae may develop acute or chronic heart failure secondary to myocardial ischemia resulting in myocardial dysfunction with or without associated valve regurgitation (58).

Worldwide, rheumatic fever with carditis leading to rheumatic heart disease is the most common cause of acquired heart disease in children and young adults (60–62). Although classically described as pancarditis, the important abnormality in acute rheumatic carditis is valve dysfunction (mitral and/or aortic regurgitation); myocardial dysfunction does not occur (63,64). In 15% to 47% of cases of acute carditis, the valve regurgitation is severe enough to result in heart failure (65,66). The incidence of heart failure is even higher if recurrences are considered (67). Chronic rheumatic heart disease consists of variable combinations of mitral regurgitation/stenosis and aortic regurgitation/stenosis. The right heart is uncommonly involved. Heart failure may result from significant, progressive valve dysfunction (61,68,69). Less commonly, left ventricular dysfunction may develop secondary to chronic severe volume overload if significant mitral and/or aortic regurgitation are present. Although rheumatic mitral stenosis severe enough to result in symptomatic heart failure may occur in the first two decades of life in developing countries (70), chronic rheumatic heart disease with mitral stenosis

in the United States typically presents in the fourth to fifth decade of life (61,71).

Patients in this age group may also develop heart failure secondary to infective endocarditis. Such endocarditis usually occur in patients with underlying structural heart disease, but may occur in those with a normal heart especially with other risk factors (indwelling catheters, history of intravenous drug abuse, and staphylococcal bacteremia) (72,73).

Myocardial dysfunction owing to a wide range of causes may result in clinical heart failure in children and adolescents. Several infectious agents have been reported to cause myocarditis (most commonly enterovirus, adenovirus, and parvovirus) (7,9,74,75). In other cases, myocarditis may occur as part of a generalized inflammatory process, such as occurs with KD or connective tissue disease (76–78). Dilated CM may be a primary disorder or may occur secondary to myocarditis, coronary artery disease, or cancer treatment (anthracyclines and/or radiation) (79–85). A dilated cardiomyopathy may occur with a variety of storage diseases, mitochondrial disorders, or in association with myopathies (muscular dystrophy) (9). An increasing number of cardiomyopathies are being recognized as familial (86,87). Although less common than the dilated form, hypertrophic, restrictive, and left ventricular noncompaction cardiomyopathies may result in clinical heart failure, due to systolic and/or diastolic dysfunction (88–90). Although less common than in the neonate and infant, tachyarrhythmia-related (supraventricular tachycardia or atrial flutter) heart failure in children and adolescents has also been reported (91).

Other causes of heart failure in children and adolescents are worth noting. Patients with Marfan syndrome with mitral valve prolapse may develop heart failure if the mitral valve becomes progressively insufficient or aortic regurgitation progresses because of the progressive aortic root dilation (92). Sickle cell disease may be associated with myocardial ischemia or infarction (93). Renal dysfunction with systemic hypertension and fluid overload may result in left ventricular dysfunction (94,95). Conversely, primary or secondary (chronic lung disease or obstructive airways disease) pulmonary hypertension may result in right heart failure (96–98).

BIOMARKERS IN CHILDREN WITH HEART FAILURE

Biomarkers have been found to be valuable for diagnosis, prognosis, and monitoring response to therapy in patients with heart failure (99). The most established heart failure biomarkers are the natriuretic peptides (NPs). Four different NPs have been identified: (a) atrial natriuretic peptide (ANP), primarily released from the atria; (b) B-type natriuretic peptide (BNP), primarily released from the ventricles, (c) C-type natriuretic peptide (CNP), released from and acts on the vascular endothelium; and (d) D-type natriuretic peptide (DNP), isolated from ventricular myocardium (99–101). BNP was originally called brain natriuretic peptide because it was isolated from porcine brain. Subsequent studies showed BNP to be primarily released from ventricular myocytes. Both ANP and BNP can be produced by either the atria or the ventricles under pathologic hemodynamic conditions. Increased wall stress related to increased preload, increased afterload, or impaired systolic or diastolic ventricular function results in the synthesis of pre-pro-B-type NP (pre-proBNP). This is subsequently cleaved to proBNP, and then is further cleaved to the biologically active 32-amino-acid polypeptide (BNP) and an inactive aminoterminal fragment, N-terminal pro-BNP (NT-proBNP). The NPs have actions aimed at protecting the cardiovascular system from volume overload. BNP

results in smooth muscle relaxation with improved myocardial relaxation and vasodilation of the systemic, pulmonary, and coronary vascular beds. In addition, in the kidneys, the NPs result in diuresis and natriuresis. Further, the NPs inhibit the renin-angiotensin-aldosterone system, play a role in blunting the sympathetic nervous system, and inhibit endothelin release (contributing to vasodilation, diuresis, and natriuresis (99,100,102). Despite the fact that BNP and NT-proBNP are secreted in equal amounts and have levels that move concordantly in most clinical scenarios, it is important to note that the levels are not interchangeable. The half-lives are different, approximately 20 minutes for BNP and 1 and 2 hours for NT-proBNP in adults. The majority of young, healthy adults have BNP levels <25 pg/mL and NT-proBNP levels <70 pg/mL (99,101).

In adults, the serum levels of NPs (BNP and NT-proBNP) have been shown to be valuable in a number of clinical settings: (a) differentiating heart failure from pulmonary disease as the etiology for acute dyspnea, (b) increasing with diastolic dysfunction, (c) increasing with heart failure exacerbations, (d) increasing and having prognostic value in coronary artery disease, (e) increasing in the setting of pulmonary embolism, pulmonary hypertension, and chronic obstructive pulmonary disease, (f) increasing in high-output states (sepsis, cirrhosis, and hyperthyroidism), and (g) predicting subsequent events in patients with known heart failure (99,101,102).

From studies in adults, NP levels are known to vary with age, gender, obesity, renal disease, and other conditions. In pediatrics, it is important to note the striking variation of NP levels with age. BNP levels are higher at birth, peaking at 1 to 2 days of age, and then decreasing during the following days of life (103). In addition, the method and type of assay used can influence NP plasma values. Studies have reported on normal ranges of NPs during infancy and childhood (104–108). Serum concentrations of BNP and NT-proBNP suggestive of cardiac disease in children are shown in Table 73.2. Other studies have evaluated NPs in children in a variety of clinical settings, and there are a number of excellent reviews available (100,109–111). Table 73.3 lists the types of clinical settings, and Table 73.4 attempts to list selected studies, including cutoffs for use in the evaluation and management of patients.

TABLE 73.2 Serum Concentrations of BNP and NT-proBNP Suggestive of Cardiac Disease in Children

Age	NT-proBNP ^a (pg/mL)	Age	BNP ^b (pg/mL)
0–2 d	■ 12,000	0–2 d	■ 750
3–11 d	■ 6,000	3–7 d	■ 480
1 mo–1 y	■ 650	2 wk–10 y	■ 45
1–2 y	■ 400		
2–6 y	■ 300		
6–18 y	■ 160		

BNP, B-type (brain) natriuretic peptide; NT-proBNP, N-terminal pro-BNP.

^aOn the basis of the 95th percentile in healthy infants and children (104).

^bOn the basis of the 97.5 percentile in healthy infants and children (105).

From Lenz AM. Natriuretic peptides in children: physiology and clinical utility. *Curr Opin Pediatr* 2011;23:452–459, with permission.

TABLE 73.3 Clinical Utility of Natriuretic Peptide Levels in Children

Differentiating lung disease from heart disease
Identifying heart disease in children
Children with known heart failure
Use in neonates
Persistent pulmonary hypertension of the newborn
Congenital diaphragmatic hernia
Patent ductus arteriosus (prematures)
Children with known congenital heart disease
Postoperative congenital heart disease
Anthracycline-treated children
Children after heart transplant
Children with pulmonary hypertension
Other conditions: Kawasaki disease, hypertrophic cardiomyopathy, end-stage renal disease, sepsis, after severe neurologic injury

Differentiating Lung Disease from Heart Disease

Both BNP and NT-proBNP have been found to be valuable for distinguishing between cardiac and pulmonary causes of respiratory distress in neonates and children. Significantly, higher BNP and NT-proBNP levels have been found in patients with heart failure than in those with lung disease (112–115).

Identifying Heart Disease in Children

Two studies have shown BNP to be valuable in children being evaluated for possible heart disease. In both studies, BNP was significantly higher in children with newly diagnosed significant heart disease than in children without significant heart disease (116,117).

Children with Known Heart Failure

From the data available, evaluation of BNP appears to be helpful for assessing prognosis and monitoring children with known heart failure. From two similar studies of children with chronic left ventricular dysfunction, BNP levels >~290 to 300 pg/mL predicted adverse events (death, hospitalization, listing for transplant) (118,119). A post-hoc analysis of patients with symptomatic systolic ventricular dysfunction from the carvedilol trial found elevated BNP of value in identifying patients at increased risk for HF event within 1 year (120). Studies of children with decompensated heart failure admitted to the intensive care unit found elevated BNP to be predictive of readmission or death (121) and serial BNP measurements to be of value in identifying patients who may need mechanical circulatory support (122).

Use in Neonates

Although levels are known to be higher in neonates, measurement of NPs may be of value in a few specific clinical scenarios. BNP has been shown to be higher in neonates with

TABLE 73.4 Natriuretic Peptides in the Evaluation and Management of Children

Condition	Age Range	N	NP	Cutoffs	Endpoints	Change in Risk	Reference
Patients with respiratory difficulty: differentiate HF and lung disease	1–36 mo	48	NT-proBNP	2,940 pg/mL	HF vs. lung disease	100% accurate	(113)
	Infants and children	49	BNP	40 pg/mL	HF vs. lung disease	84% accurate, 91% sens, 77% spec	(112)
	1 mo–17.5 y	76	NT-proBNP	727 pg/mL	HF vs. lung disease	97% accurate, 100% sens, 94% spec	(115)
Patients with possible heart disease	36 wk gestational age–19 y	100	BNP	170 pg/mL (neonates <7 d) 41 pg/mL (older patients)	Diagnosis of significant structural or functional heart disease	Neonates: 94% sens, 73% spec, 91% PPV Older: 87% sens, 70% spec, 77% PPV	(116)
	2 d–17.5 y	33	BNP	100 pg/mL	Diagnosis of critical heart disease (requiring admission to ICU)	100% sens, 98% spec	(117)
Outpatients with LV dysfunction	2 mo–21 y	53	BNP	300 pg/mL	Adverse events (cardiac death, hospitalization for cardiac reason, listing for transplant)	93% sens, 95% spec, 88% PPV, 97% NPV	(118)
	3 wk–16.6 y	92 (48 patients)	BNP	290 pg/mL	Adverse outcome (death, listing for transplant)	80% sens, 87% spec	(119)
Patients with HF admitted to ICU	2 d–21 y	82	BNP	760 pg/mL	Adverse outcome at 60 d after discharge (readmission or death)	74% sens, 93% spec	(121)
Premature babies	25–34 wk gestational age	66	BNP	1,110 pg/mL	Clinically significant and echocardiographically large PDA	100% sens, 95% spec	(126)
	30 wk (mean gestational age)	31	BNP	1,805 pg/mL	Lack of response of PDA to indomethacin	88% sens, 87% spec	(128)
Children with symptomatic HF	Age <18 y	138	BNP	140 pg/mL	Adverse event (hospitalization for worse HF, transplant, death)	71% sens, 63% spec	(120)
Children with CHD	1–37.5 y	62	BNP	40 pg/mL	Ventricular dysfunction	85% sens, 81% spec, 92% PPV, 68% NPV	(129)
Postoperative CHD	1 d–15.5 y	51	BNP (12 h postoperative)	540 pg/mL	Mechanical ventilation >48 h	89% sens, 83% spec	(138)
				815 pg/mL	Low cardiac output within 48 h	88% sens, 90% spec	
Children after heart transplant	10.5 y (median)	560 biopsies (86 patients)	BNP	100 pg/mL	Acute rejection, ISHLT ≥3A (biopsy)	For patients >1 y posttransplant, 96% sens, 99% NPV	(147)
	2 mo–20 y	53	BNP	700 pg/mL	Acute rejection, ISHLT ≥3A (biopsy)	100% sens, 92% spec, 100% NPV	(148)
	14–15 y (mean)	53	BNP	250 pg/mL	Death or retransplant in ensuing 90 d	Not given	(149)

BNP, B-type natriuretic peptide; CHD, congenital heart disease; HF, heart failure; NPV, negative predictive value; NT-proBNP, N-terminal B-type natriuretic peptide; PDA, patent ductus arteriosus; PPV, positive predictive value; sens, sensitivity; spec, specificity.

persistent pulmonary hypertension of the newborn (compared to babies with respiratory disease without elevated pulmonary pressures and babies without respiratory disease) (123). In neonates with congenital diaphragmatic hernia, elevated NT-proBNP correlated with pulmonary artery pressure and was associated with worse prognosis (124). In preterm neonates, elevated BNP is associated with a hemodynamically significant patent ductus arteriosus and may be valuable in predicting the need for medical or surgical intervention (125–128).

Children with Congenital Heart Disease

In the setting of congenital heart disease, BNP is increased in patients with ventricular dysfunction and may be predictive of subsequent events (129,130). In addition, BNP has been shown to correlate with the degree of shunting, right ventricular systolic pressure and pulmonary artery pressure, and pulmonary vascular resistance (131). Significant pulmonary insufficiency occurs after repair of some forms of congenital heart disease (most commonly tetralogy of Fallot), resulting in right heart volume overload and associated risk for right ventricular dysfunction, heart failure, and arrhythmias. In adolescents after repair of tetralogy of Fallot, NPs correlate with right ventricular hemodynamics and dilation (132,133). NPs have been reported to be of value for diagnosing heart failure in children with single ventricle physiology (134,135) and for identifying patients at risk for poor outcome (136), but a recent study suggests that routine measurement of NPs is not warranted in patients after the Fontan procedure (137). There is also suggestion that NPs may be useful in risk stratification of adults with CHD.

Postoperative Congenital Heart Disease

An elevated 12-hour postoperative BNP is associated with duration of mechanical ventilation and predictive of low cardiac output state (138). Another study found 24-hour postoperative BNP levels that are higher than preoperative levels to be associated with low cardiac output syndrome, more days of mechanical ventilation, and was predictive of poor postoperative outcome (139). Postoperative BNP has also been found to be associated with clinical heart failure scores in patients with single ventricle physiology (at various stages of palliation) (140), predictive of outcome in patients undergoing bidirectional cavopulmonary or total cavopulmonary connection for single ventricle (135), and NT-proBNP correlates with clinical heart failure in patients after the Fontan procedure (141). In pediatric patients requiring extracorporeal support following cardiac surgery, NPs may be useful in weaning (142), and an increase in BNP during a trial off of support is predictive of outcome (need for unplanned operation and survival) (143).

Anthracycline-Treated Children

Studies have shown BNP to be elevated in children with ventricular dysfunction late after treatment with anthracyclines and may have a role in the follow-up of these patients (144–146).

Children After Heart Transplant

Elevated or rising BNP levels in children after heart transplantation have been found to be valuable as a screening test for rejection (147,148) and for identifying patients at increased risk of death or retransplant (149,150).

Children with Pulmonary Hypertension

In children with pulmonary hypertension, a rising BNP correlates with hemodynamic and echocardiographic changes, and an elevated BNP is associated with decreased survival (151). In a different study of children with pulmonary hypertension, NT-proBNP correlated with functional class and 6-minute walking distance and was predictive of mortality (152).

Other Conditions

In addition to the scenarios described above, measurement of NPs may be valuable in other conditions. BNP and NT-proBNP were found to be a useful marker for the myocarditis of KD and may have value in differentiating KD from a viral illness (153). A recent study reported an association between BNP and development of coronary artery lesions (154). BNP levels have been reported to correlate with noninvasive parameters of disease severity in children with hypertrophic cardiomyopathy, including diastolic dysfunction (155). BNP levels may be elevated in patients with end-stage renal disease, independent of heart dysfunction. Nonetheless, even in this population, BNP levels may be predictive of ventricular dysfunction, cardiac events, and survival (156). NT-proBNP levels should be interpreted cautiously in children with sepsis since patients with normal ventricular function may have elevated NT-proBNP levels (157). Finally, in patients with severe central nervous system injury who progress to brain death, mechanisms other than myocardial performance appear to regulate BNP levels (elevated despite normal function and ultimately good outcome after use as a donor heart for transplant), limiting the value of these levels in this patient population (158).

TREATMENT OF CHRONIC HEART FAILURE

One could argue that the term “heart failure” is somewhat of a misnomer for the clinical syndrome of large left-to-right shunt with pulmonary overcirculation. However, many of the same neurohormonal abnormalities are present in these patients that are present in patients with congestive heart failure owing to systemic ventricular dysfunction. Patients with large left-to-right shunts are tachypneic, tachycardic, and diaphoretic. They have elevations in plasma norepinephrine and aldosterone levels (159,160). However, the treatment of this clinical syndrome usually entails surgical correction of the underlying anatomic problem.

Treatment strategies utilized in the management of chronic heart failure owing to systemic ventricular dysfunction in children have been almost entirely derived from large multicenter, randomized, placebo-controlled trials in adults with heart failure due to left ventricular systolic dysfunction. Some of these studies are restricted to adults with either ischemic cardiomyopathy or only nonischemic (dilated) cardiomyopathy (161), although most studies include adults with both ischemic and nonischemic cardiomyopathy. Even in those adults with nonischemic CM, there are significant comorbidities not seen in children with heart failure, such as diabetes and hypertension, that make extrapolation of treatment strategies from these adults to children with dilated CM problematic (162). Within the limitations of extrapolating data from adult studies of this kind, pediatric cardiologists have adapted many of the treatments that are currently recommended for adults with heart failure owing to left ventricular systolic dysfunction (163). This section reviews the current evidence base for the treatment of chronic heart failure in children in addition to current recommendations based on small case series and published anecdotal experience.

Once a child has been diagnosed with chronic heart failure, therapeutic strategies are directed toward the underlying cause of the heart failure. In patients with “heart failure” due to left-to-right shunt (e.g., ventricular septal defects, single ventricle without pulmonary stenosis) and resultant pulmonary overcirculation, surgical intervention is currently the treatment of choice in virtually every situation. If, for some reason, surgery is not an option (e.g., small size of the patient, no surgical options available), there are some potential medical interventions that may improve symptoms. These include diuretics, angiotensin-converting enzyme (ACE) inhibitors, and possibly beta-adrenergic receptor (beta) blockers. Diuretics are the mainstay of therapy in this situation through their ability to reduce pulmonary edema and systemic congestion (see below). There is some evidence that ACE inhibitors may be beneficial through their ability to reduce systemic vascular resistance in preference to pulmonary vascular resistance and thus reduce pulmonary blood flow (164–166). There is also evidence that beta-blockade with propranolol may be beneficial to infants in this situation. Bucchorn et al. have demonstrated that propranolol can reduce heart rate, respiratory rate, and heart failure symptoms as well as improve growth in infants with heart failure owing to large left-to-right shunts (160,167,168).

In children with heart failure caused by isolated systemic ventricular systolic dysfunction, there are usually no good surgical options short of heart transplantation. Thus, it is incumbent on the pediatric cardiologist to maximize medical therapy and avoid or delay heart transplantation in as many children as possible. Unfortunately, there is very little evidence base from which to derive guidance for which medications are best in which situations and at which dosages. For older children with dilated cardiomyopathy, it may be reasonable to extrapolate from some of the larger trials in adults with nonischemic cardiomyopathy. In children with heart failure with congenital heart disease and possibly a systemic ventricle that is not a left ventricle, it is much less clear how appropriate it is to extrapolate from these adult studies. We present here what is known about the use of medications and devices in the treatment of adults with chronic heart failure. Where possible, we also present existing data in children.

DIURETICS

With the exception of aldosterone antagonists, conventional diuretics used in the treatment of heart failure consist of agents that block specific ion transport proteins in tubular cells and thereby inhibit the reabsorption of solutes (169). Although diuretics have never been shown to improve survival in heart

failure, they are considered to be essential to the treatment of fluid overload in patients with heart failure. They relieve symptoms of heart failure and decrease systemic and pulmonary vascular pressures (170). A recent multicenter study in adults demonstrated that there were no significant differences in patients’ global assessment of symptoms or in the change in renal function when diuretic therapy was administered by bolus as compared with continuous infusion or at a high dose as compared with a low dose (171). Some patients with heart failure do not require diuretics, but the majority of symptomatic patients with heart failure will require some diuretic therapy. Table 73.5 summarizes some commonly used oral diuretics in children. These non-potassium-sparing diuretics have potential adverse consequences even while reducing systemic and pulmonary venous congestion. They have been shown to activate the renin-angiotensin-aldosterone system and the sympathetic nervous system (172), in addition to adversely affecting renal function. For this and other reasons, some have advocated using ultrafiltration in adults with heart failure and fluid overload, rather than treatment with diuretics (173). In infants, diuretics cause an increase in plasma renin levels in those with large left-to-right shunts (160). Some patients with heart failure can develop resistance to loop diuretics. Possible reasons for this include noncompliance, simultaneous use of nonsteroidal anti-inflammatory drugs, and diminished renal natriuretic effect owing to compensatory hypertrophy and hyperplasia of epithelial cells of the distal convoluted tubule leading to increased reabsorption of sodium (174). Once noncompliance has been excluded, one should try higher doses and more frequent administration of loop diuretics and possibly add a thiazide diuretic. The thiazide diuretic, metolazone, administered in conjunction with a loop diuretic can be uniquely successful in effecting diuresis in edematous or diuretic-resistant patients (175).

Although spironolactone and eplerenone are potassium-sparing diuretics, their beneficial effects in heart failure are probably less related to their diuretic effects than other effects. Plasma aldosterone levels can reach as much as 20 times normal in adults with heart failure, both because of increased production and decreased rate of hepatic clearance (176). In addition to its effects on salt and water homeostasis, aldosterone has multiple other effects including decreased endothelial vasomotor reactivity and increased myocardial fibrosis (177). Two studies have demonstrated that aldosterone antagonists, spironolactone and eplerenone, both reduce mortality and hospitalization in adults with heart failure when compared to placebo (178,179). In the latter study, there was a significantly increased risk of hyperkalemia and a significantly decreased risk of hypokalemia in patients treated with eplerenone compared to placebo (179). The list of potential mechanisms by

TABLE 73.5 Commonly Used Oral Diuretics in Pediatrics

Drug	Class	Action	Dose	Interval	Maximum Daily Oral Dose
Furosemide	Loop	Inhibit Na ⁺ Cl ⁻ K ⁺ cotransport, ascending loop of Henle	0.5–2 mg/kg/dose	bid—qid	600 mg
Bumetanide	Loop	Same as above	0.015–0.1 mg/kg/dose	qd—bid	10 mg
Chlorothiazide	Thiazide	Inhibit Na ⁺ Cl ⁻ cotransport, distal tubule	10–20 mg/kg/dose	bid	2,000 mg
Hydrochlorothiazide	Thiazide	Same as above	1–2 mg/kg/dose	bid	200 mg
Metolazone (as Zaroxolyn)	Thiazide	Same as above	0.2–0.4 mg/kg/24 h	qd—bid	20 mg

TABLE 73.6 Summary of Landmark Enalapril Trials in Adult Heart Failure

Study	Patient Population	ACE Inhibitor	Treatment Duration	Outcome
CONSENSUS	NYHA IV (<i>n</i> = 253)	Enalapril vs. placebo	1 d–20 mo	Decreased mortality; decreased HF
SOLVD treatment	NYHA II and III (<i>n</i> = 2,569)	Enalapril vs. placebo	22–55 mo	Decreased mortality; decreased HF
V-HeFT II	NYHA II and III (<i>n</i> = 804)	Enalapril vs. hydralazine, isosorbide	0.5–5.7 y	Decreased mortality; decreased sudden death

HF, heart failure; NYHA, New York Heart Association.

which aldosterone antagonism benefits patients with heart failure continues to grow (180). There is increasing evidence that aldosterone antagonists may be beneficial in all stages of symptomatic heart failure, including those with mild symptoms (181).

DIGOXIN

The main mechanism of action of digoxin is to inhibit the sodium–potassium ATPase pump in the myocardium. This promotes sodium–calcium exchange and increases intracellular calcium and thus contractility. Digoxin also has beneficial modulating effects in the neurohormonal system: improvement in baroreceptor function, increased vagal tone, sympathoinhibitory effects, decreased circulating norepinephrine levels, and possibly aldosterone antagonistic effects (182). In adults with heart failure owing to left ventricular systolic dysfunction, digoxin is currently indicated only in those patients with symptoms or a history of symptoms (163). The Digitalis Investigators Group (DIG) trial showed no differences in mortality in those treated with digoxin and those treated with placebo over a 3-year period, although there were significantly fewer cardiovascular hospitalizations in the digoxin-treated group (183). The Randomized Assessment of Digoxin on Inhibitors of Angiotensin Converting Enzyme (RADIANCE) trial demonstrated that patients withdrawn from digoxin had significantly worsened heart failure symptoms and exercise tolerance (184). In another digoxin-withdrawal trial, the Prospective Randomized study of Ventricular failure and the Efficacy of Digoxin (PROVED) trial, patients with heart failure who received digoxin had a lower incidence of worsening heart failure and hospitalizations for heart failure, a higher left ventricular ejection fraction (LVEF), and better treadmill exercise time than patients who received placebo (185). Optimal dosing of digoxin is still a matter of debate. Post-hoc analyses of the DIG trial examined mortality as a function of serum digoxin concentrations and found that higher serum digoxin concentrations were associated with a higher mortality, suggesting a possible benefit from lower serum digoxin concentrations in patients with heart failure (186,187).

The role of digoxin in children with chronic heart failure is even less clear. Some studies have suggested a benefit from digoxin in children with heart failure owing to large left-to-right shunt, whereas others have not (188,189). One study suggests that digoxin may actually adversely affect this clinical situation by causing an acute increase in pulmonary blood flow and left atrial pressure (190). In the setting of decreased

systemic ventricular systolic function, no data are available in children to guide therapy; thus one must consider cautiously extrapolating from adult heart failure studies as described above.

ANGIOTENSIN-CONVERTING ENZYME INHIBITORS

ACE inhibitors are currently recommended for the treatment of asymptomatic and symptomatic adults with decreased left ventricular systolic function (191). ACE, which is the same as kininase II, is a bivalent dipeptidyl carboxyl metalloproteinase present as a membrane-bound form in endothelial cells, in epithelial or neuroepithelial cells, in the brain, and as a soluble form in blood and numerous bodily fluids (192). ACE inhibitors have favorable effects on hemodynamics in patients with heart failure due to systolic dysfunction through their ability to reduce afterload, preload, and systolic wall stress, with a resultant increase in cardiac output without an increase in heart rate. Several studies in adults with left ventricular systolic dysfunction have shown that ACE inhibitors improve survival and symptoms in adults with symptomatic heart failure and improve survival in adults with asymptomatic heart failure (193–196) (Table 73.6). Although the optimal dosing of ACE inhibitors in adults is not well defined, there is some evidence that, in the absence of side effects, intermediate or higher doses may be more beneficial than lower doses (197,198). As stated above, there is some evidence from non-randomized studies in children that ACE inhibitors may benefit some children with large left-to-right shunts (164–166). However, there are few reports of ACE inhibitors benefiting children with heart failure due to systemic ventricular systolic dysfunction (199,200). The first randomized, placebo-controlled trial of ACE inhibitors in children with heart disease was performed in 18 patients after the Fontan operation who were randomized to either placebo or enalapril (201). There was no difference between groups using the primary endpoint of exercise capacity after 10 weeks of therapy. Furthermore, the mean percent change in the cardiac index from rest to maximal exercise was significantly *decreased* in the enalapril group compared to the placebo group. However, these patients were not in heart failure at the time of the study, and exercise capacity has been shown to be problematic as a primary endpoint in heart failure trials (202,203). Thompson et al. performed a prospective comparison of 36 children undergoing a Glenn procedure at two different hospitals, 18 of whom received perioperative

enalapril and 18 who did not (204). They found that there was a shorter duration and amount of pleural drainage in those who received enalapril compared to those who did not. A recently completed placebo-controlled, randomized trial found that administration of enalapril to infants with single-ventricle physiology in the first year of life does not improve somatic growth, ventricular function, or heart failure severity (205).

ANGIOTENSIN RECEPTOR BLOCKERS

Angiotensin II receptor blockers (ARBs) directly block the effects of angiotensin II at the receptor level. There are theoretical advantages of ARBs over ACE inhibitors. For instance, ARBs do not increase bradykinin levels as ACE inhibitors do, an effect that is responsible for the common adverse effect of cough seen with ACE inhibitors. One of the first studies comparing an ACE inhibitor (captopril) with an ARB (losartan), the Evaluation of Losartan in the Elderly (ELITE) trial, showed no difference in the primary endpoint (heart failure hospitalizations) in elderly patients with heart failure, but an unexpected statistically significant improvement in survival with losartan (206). However, the follow-up study, ELITE II, failed to show a significant survival benefit from ARBs over ACE inhibitors (207). In the Valsartan in Heart Failure Trial (ValHeFT), the ARB valsartan or placebo was added to therapy including digoxin, diuretics, ACE inhibitors, and beta-blockers. The addition of valsartan had no effect on all cause mortality but provided a 13% reduction in combined morbidity and mortality (208). On the basis of these and other studies, the use of ARBs is currently only recommended for patients with heart failure who are unable to tolerate ACE inhibitors. The little data available on the use of ARBs in children are primarily limited to its use in pediatric hypertension (209–212).

BETA-ADRENERGIC RECEPTOR BLOCKERS

Before Waagstein et al. first described the successful use of beta-blockers in a small group of adults with heart failure, these medications were thought to be contraindicated in patients with heart failure (213). Many small studies throughout the 1980s and early 1990s suggested a benefit of beta-blockers in adults with heart failure (214–217). However, it was not until 1996 that two studies demonstrated a significant benefit of beta-blockers in adults with heart failure with regard to symptoms, left ventricular systolic function, and survival (202,203).

There are many proposed mechanisms through which beta-blockers improve left ventricular function, symptoms, and survival in patients with heart failure (218). Although different beta-blockers may have different effects in patients

with heart failure, the available data support the hypothesis that the primary mechanism of action of beta-blocking agents in chronic heart failure is to prevent and reverse adrenergically mediated intrinsic myocardial dysfunction and remodeling (219). On a cellular level, sustained cardiac adrenergic activation results in desensitization of beta-adrenergic signal transduction mechanisms and direct damage to cardiac myocytes (219). Clinically, this results in ventricular dysfunction and remodeling (chamber dilation and assumption of a more spherical shape) and ultimately the development of heart failure. Various other mechanisms of action have been proposed for the beneficial effects of beta-blockers in heart failure, including upregulation of beta-adrenergic receptors. Failing human hearts have decreased catecholamine sensitivity and beta-adrenergic receptor density, suggesting that regulation of beta-adrenergic receptors may be an important variable in heart failure (220). However, upregulation of beta receptors must not be a major mechanism of action of beta-blockers since some beta-blockers that are efficacious in the treatment of heart failure, such as metoprolol, upregulate beta-receptors, whereas others that are at least as efficacious, such as carvedilol, do not upregulate beta-receptor density (221). Other potential mechanisms of the beneficial effects of beta-blockers in heart failure include decreased stimulation of other neuro-hormonal systems, antiarrhythmic effects, coronary vasodilation, negative chronotropic effects, antioxidant effects, and improved myocardial energetics (222). Individual beta-blockers may also have unique properties that may be beneficial in heart failure. For instance, carvedilol and several of its metabolites are potent antioxidants that may inhibit catecholamine toxicity through the ability of catecholamines to generate oxygen free radicals in the myocardium (223).

Heart failure trials in adults have shown that both metoprolol and bisoprolol improve symptoms and survival in adults with mild-to-moderate heart failure (224,225), and that carvedilol improves symptoms and survival in adults with severe heart failure (226). These trials are summarized in Table 73.7. Based on this evidence, beta-blockers are currently recommended treatment for symptomatic or asymptomatic left ventricular dysfunction in adults (191). Both metoprolol and carvedilol are currently recommended for the treatment of chronic heart failure in adults. Several studies have now shown an advantage of carvedilol over metoprolol (227).

Many small nonrandomized reports of beta-blockers in children with heart failure had suggested possible benefit in this group (228–230). The Pediatric Carvedilol trial was a multicenter, placebo-controlled, double-blind, parallel-group study that randomized 161 children with symptomatic heart failure secondary to systemic ventricular dysfunction to receive either placebo, lower dose, or higher dose carvedilol on top of background heart failure medications (231). The primary endpoint was a composite measure of clinical heart failure outcomes, and patients were determined to have a response to therapy

TABLE 73.7 Summary of Landmark Beta-Blocker Trials in Adult Heart Failure

Study (Year)	Beta-Blocker	# Pts/NYHA Class	Endpoint	Survival Benefit
Mocha (1996)	Carvedilol	345/NYHA 1–3	Submaximal exercise	Dose-dependent survival
U.S. Coreg (1996)	Carvedilol	1094/NYHA 1–3	Submaximal exercise	67%
MERIT-HF (1999)	Metoprolol	3,991/NYHA 1–3	All-cause mortality	35%
CIBIS-II (1999)	Bisoprolol	2,647/NYHA 1–3	All-cause mortality	29%
COPERNICUS (2001)	Carvedilol	2,289/Severe HF	All-cause mortality	35%

of worsened, improved, or unchanged. The study showed a surprisingly high rate of improvement in the placebo group (56%) and failed to show any difference between placebo and carvedilol on the primary outcome. However, a prespecified analysis of the improved versus not improved outcome showed a significant interaction between study drug and ventricular morphology, suggesting a possible differential effect of the treatment between patients with a systemic left ventricle (beneficial trend) and those whose systemic ventricle was not a left ventricle (nonbeneficial trend) ($p < 0.02$). Post-hoc analyses of this study found that in children with moderately symptomatic heart failure, BNP levels ≥ 140 pg/mL, age > 2 years, and abnormal echocardiographic myocardial performance indices identified subjects at higher risk for worse outcome (232,233).

DEVICE THERAPY FOR HEART FAILURE

Two major advances in the treatment of heart failure and prevention of sudden death are the use of devices in adults: cardiac resynchronization therapy (CRT) and implantable cardioverters/defibrillators (ICDs). Studies in adults have shown that CRT can improve symptoms, exercise tolerance, quality of life, echocardiographic indices of left ventricular performance, and survival in adults with heart failure and interventricular conduction delays (234–236). CRT is now recommended for adults with symptomatic heart failure and electrical dyssynchrony manifested as an interventricular conduction delay. There is evidence that selected patients without electrical dyssynchrony (e.g., those with a normal QRS duration) may, however, have mechanical dyssynchrony that may benefit from biventricular pacing and resynchronization therapy. It may be possible to identify such patients by using tissue Doppler imaging or other such techniques (237,238). These techniques are becoming increasingly validated in children (239). There are few data regarding the use and indications of CRT in children. One study in seven children with congenital heart disease and a right bundle branch block pattern found that resynchronization therapy resulted in small, but statistically significant, acute improvements in cardiac output and right ventricular dp/dt (50). Standard right ventricular pacing without careful manipulation of the atrioventricular interval may be insufficient to shorten the QRS duration in patients with tetralogy of Fallot and right bundle branch block (240). Experience with the use of CRT in children with systemic ventricular dysfunction and heart failure is modest, but increasing. A recent single-center experience with CRT in 60 consecutive children demonstrated benefit in the majority of patients, although there were significant challenges associated with implantation (53). However, the heterogeneous patient population, technical limitations from patient size, vascular access issues, and unique forms of ventricular dyssynchrony make it difficult to determine risks and benefits of this procedure in children (54,241).

Patients succumb to heart failure from either pump failure or from sudden death. Although the mode of sudden death is often not known, it is speculated that a many of these deaths are due to tachyarrhythmias, particularly ventricular tachycardia and ventricular fibrillation (242). Because of this, multiple prospective, randomized trials have assessed the utility of ICDs in patients with heart failure. The Antiarrhythmics Versus Implantable Defibrillator (AVID) trial and the Canadian Implantable Defibrillator Study (CIDS) demonstrated that ICDs produced approximately a 30% reduction in relative risk of sudden cardiac death in adults with a history of malignant ventricular arrhythmias (243,244). After demonstrating possible benefit of ICDs in secondary prevention of sudden cardiac death, the next step was to see if this therapy could be applied to primary prevention. The Multicenter Automatic Defibrillator Implantation Trial (MADIT) (245), the

Multicenter Unsustained Tachycardia Trial (MUSTT) (246), and MADIT II (245) all showed mortality benefit from ICDs in adults with coronary artery disease and reduced LVEF. The Comparison of Medical Therapy, Pacing, and Defibrillation in Chronic Heart Failure (COMPANION) study for the first time demonstrated survival benefit of CRT and combined device (biventricular pacemaker with defibrillator capacity) therapy in heart failure (247). Similarly, the MIRACLE ICD trial demonstrated that combined CRT and ICD therapy in adults with left ventricular systolic dysfunction, moderate-to-severe heart failure, and prolonged QRS duration resulted in improved quality of life, functional status, and exercise capacity when compared to placebo (235). Finally, the SCD-HeFT trial demonstrated a clear survival benefit in adults treated with an ICD, when compared to either placebo or amiodarone (248). The incidence of sudden death in children with heart failure appears to be significantly less than that seen in adults with heart failure (249,250). Although still controversial, there are guidelines for the use of ICDs in children, some of which has been extrapolated from adult trials (251,252).

Despite all of these available therapies, there is still significant concern that current transplant-free survival is not significantly better than in previous eras when the only therapies available were digoxin and diuretics (253). The possible reasons for this remain elusive, but clearly provide stimulus for continued research into the differences between adult and pediatric heart failure and into finding new pharmacologic therapies for children with heart failure.

REFERENCES

- Kothari SS. Congestive heart failure: diagnosis and management. *Indian Pediatr* 1996;33:571–580.
- Scott DJ, Rigby ML, Miller GA, et al. The presentation of symptomatic heart disease in infancy based on 10 years' experience (1973–82). Implications for the provision of services. *Br Heart J* 1984;52:248–257.
- Lister G, Hellenbrand WE, Kleinman CS, et al. Physiologic effects of increasing hemoglobin concentration in left-to-right shunting in infants with ventricular septal defects. *N Engl J Med* 1982;306:502–506.
- Backer CL, Stout MJ, Zales VR, et al. Anomalous origin of the left coronary artery. A twenty-year review of surgical management. *J Thorac Cardiovasc Surg* 1992;103:1049–1057; discussion 1049–1057.
- Wesselhoeft H, Fawcett JS, Johnson AL. Anomalous origin of the left coronary artery from the pulmonary trunk. Its clinical spectrum, pathology, and pathophysiology, based on a review of 140 cases with seven further cases. *Circulation* 1968;38:403–425.
- Prabhu SS, Dalvi BV. Treatable cardiomyopathies. *Indian J Pediatr* 2000;67:S7–S10.
- Burch M. Heart failure in the young. *Heart* 2002;88:198–202.
- Jefferies JL, Towbin JA. Dilated cardiomyopathy. *Lancet* 2010;375:752–762.
- Gajarski RJ, Towbin JA. Recent advances in the etiology, diagnosis, and treatment of myocarditis and cardiomyopathies in children. *Curr Opin Pediatr* 1995;7:587–594.
- Waber LJ, Valle D, Neill C, et al. Carnitine deficiency presenting as familial cardiomyopathy: a treatable defect in carnitine transport. *J Pediatr* 1982;101:700–705.
- Packer DL, Bardy GH, Worley SJ, et al. Tachycardia-induced cardiomyopathy: a reversible form of left ventricular dysfunction. *Am J Cardiol* 1986;57:563–570.
- Berger S, Dubin AM. Arrhythmogenic forms of heart failure in children. *Heart Fail Clin* 2010;6:471–481, viii.
- Artman M, Parrish MD, Graham TP Jr. Congestive heart failure in childhood and adolescence: recognition and management. *Am Heart J* 1983;105:471–480.
- Bjarke BB, Kidd BS. Proceedings: congenitally corrected transposition of the great arteries: a clinical study of 101 cases. *Br Heart J* 1976;38:535.
- Nadas AS, Thilenius OG, Lafarge CG, et al. Ventricular septal defect with aortic regurgitation: medical and pathologic aspects. *Circulation* 1964;29:862–873.
- Kostolny M, Schreiber C, von Arnim V, et al. Timing of repair in ventricular septal defect with aortic insufficiency. *Thorac Cardiovasc Surg* 2006;54:512–515.
- Ferrieri P, Gewitz MH, Gerber MA, et al. Unique features of infective endocarditis in childhood. *Circulation* 2002;105:2115–2126.
- Jindal RC, Saxena A, Kothari SS, et al. Congenital severe aortic stenosis with congestive heart failure in late childhood and adolescence: effect on left ventricular function after balloon valvuloplasty. [see comments.] *Cathet Cardiovasc Interv* 2000;51:168–172.

19. Paranon S, Acar P. Ebstein's anomaly of the tricuspid valve: from fetus to adult: congenital heart disease. *Heart* 2008;94:237-243.
20. Celermajer DS, Bull C, Till JA, et al. Ebstein's anomaly: presentation and outcome from fetus to adult. *J Am Coll Cardiol* 1994;23:170-176.
21. Daliento L, Somerville J, Presbitero P, et al. Eisenmenger syndrome. Factors relating to deterioration and death. *Eur Heart J* 1998;19:1845-1855.
22. Kantor PF, Redington AN. Pathophysiology and management of heart failure in repaired congenital heart disease. *Heart Fail Clin* 2010;6:497-06, ix.
23. Lambert V, Obreja D, Losay J, et al. Long-term results after valvotomy for congenital aortic valvar stenosis in children. *Cardiol Young* 2000;10:590-596.
24. Bacha EA, McElhinney DB, Guleserian KJ, et al. Surgical aortic valvuloplasty in children and adolescents with aortic regurgitation: acute and intermediate effects on aortic valve function and left ventricular dimensions. *J Thorac Cardiovasc Surg* 2008;135:552-559, 559.e551-553.
25. Hawkins JA, Kouretas PC, Holubkov R, et al. Intermediate-term results of repair for aortic, neo-aortic, and truncal valve insufficiency in children. *J Thorac Cardiovasc Surg* 2007;133:1311-1317.
26. Reddy VM, Hanley F. Late results of repair of truncus arteriosus. *Semin Thorac Cardiovasc Surg Pediatr Card Surg Annu* 1998;1:139-146.
27. Boening A, Scheewe J, Heine K, et al. Long-term results after surgical correction of atrioventricular septal defects. *Eur J Cardiothorac Surg* 2002;22:167-173.
28. Permut LC, Mehta V. Late results and reoperation after repair of complete and partial atrioventricular canal defect. *Semin Thorac Cardiovasc Surg* 1997;9:44-54.
29. Williams WG, McCrindle BW, Ashburn DA, et al. Outcomes of 829 neonates with complete transposition of the great arteries 12-17 years after repair. *Eur J Cardiothorac Surg* 2003;24:1-9; discussion 9-10.
30. Wells WJ, Blackstone E. Intermediate outcome after Mustard and Senning procedures: a study by the Congenital Heart Surgeons Society. *Semin Thorac Cardiovasc Surg Pediatr Card Surg Annu* 2000;3:186-197.
31. Carrel T, Pfammatter JP. Complete transposition of the great arteries: surgical concepts for patients with systemic right ventricular failure following intraatrial repair. *Thorac Cardiovasc Surg* 2000;48:224-227.
32. Hucin B, Voriskova M, Hruda J, et al. Late complications and quality of life after atrial correction of transposition of the great arteries in 12 to 18 year follow-up. *J Cardiovasc Surg (Torino)* 2000;41:233-239.
33. Piran S, Veldtman G, Siu S, et al. Heart failure and ventricular dysfunction in patients with single or systemic right ventricles. *Circulation* 2002;105:1189-1194.
34. Dyer K, Graham TP. Congenitally corrected transposition of the great arteries: current treatment options. *Curr Treat Options Cardiovasc Med* 2003;5:399-407.
35. Graham TP Jr, Bernard YD, Mellen BG, et al. Long-term outcome in congenitally corrected transposition of the great arteries: a multi-institutional study. *J Am Coll Cardiol* 2000;36:255-261.
36. Oechslin E, Jenni R. 40 years after the first atrial switch procedure in patients with transposition of the great arteries: long-term results in Toronto and Zurich. *Thorac Cardiovasc Surg* 2000;48:233-237.
37. Ivy D. Diagnosis and treatment of severe pediatric pulmonary hypertension. *Cardiol Rev* 2001;9:227-237.
38. Dearani JA, Danielson GK, Puga FJ, et al. Late follow-up of 1095 patients undergoing operation for complex congenital heart disease utilizing pulmonary ventricle to pulmonary artery conduits. *Ann Thorac Surg* 2003;75:399-410; discussion 410-391.
39. Ilbawi MN, Idriss FS, DeLeon SY, et al. Factors that exaggerate the deleterious effects of pulmonary insufficiency on the right ventricle after tetralogy repair. Surgical implications. *J Thorac Cardiovasc Surg* 1987;93:36-44.
40. Discigil B, Dearani JA, Puga FJ, et al. Late pulmonary valve replacement after repair of tetralogy of Fallot. *J Thorac Cardiovasc Surg* 2001;121:344-351.
41. Lim C, Lee JY, Kim WH, et al. Early replacement of pulmonary valve after repair of tetralogy: is it really beneficial? *Eur J Cardiothorac Surg* 2004;25:728-734.
42. Mital S, Addonizio LJ, Lamour JM, et al. Outcome of children with end-stage congenital heart disease waiting for cardiac transplantation. *J Heart Lung Transplant* 2003;22:147-153.
43. Gentles TL, Gauvreau K, Mayer JE Jr, et al. Functional outcome after the Fontan operation: factors influencing late morbidity. *J Thorac Cardiovasc Surg* 1997;114:392-403; discussion 404-395.
44. Weipert J, Noebauer C, Schreiber C, et al. Occurrence and management of atrial arrhythmia after long-term Fontan circulation. *J Thorac Cardiovasc Surg* 2004;127:457-464.
45. Mavroudis C, Backer CL, Deal BJ, et al. Total cavopulmonary conversion and maze procedure for patients with failure of the Fontan operation. *J Thorac Cardiovasc Surg* 2001;122:863-871.
46. Jenkins PC, Chinnock RE, Jenkins KJ, et al. Decreased exercise performance with age in children with hypoplastic left heart syndrome. *J Pediatr* 2008;152:507-512.
47. Weinstein S, Cua C, Chan D, et al. Outcome of symptomatic patients undergoing extracardiac Fontan conversion and cryoablation. *J Thorac Cardiovasc Surg* 2003;126:529-536.
48. Puley G, Siu S, Connelly M, et al. Arrhythmia and survival in patients >18 years of age after the mustard procedure for complete transposition of the great arteries. *Am J Cardiol* 1999;83:1080-1084.
49. Walsh EP. Arrhythmias in patients with congenital heart disease. *Card Electrophysiol Rev* 2002;6:422-430.
50. Dubin AM, Feinstein JA, Reddy VM, et al. Electrical resynchronization: a novel therapy for the failing right ventricle. *Circulation* 2003;107:2287-2289.
51. Roofthoof MT, Blom NA, Rijlaarsdam ME, et al. Resynchronization therapy after congenital heart surgery to improve left ventricular function. *Pacing Clin Electrophysiol* 2003;26:2042-2044.
52. Janousek J, Tomek V, Chaloupecky V, et al. Dilated cardiomyopathy associated with dual-chamber pacing in infants: improvement through either left ventricular cardiac resynchronization or programming the pacemaker off allowing intrinsic normal conduction. *J Cardiovasc Electrophysiol* 2004;15:470-474.
53. Cecchin F, Frangini PA, Brown DW, et al. Cardiac resynchronization therapy (and multisite pacing) in pediatrics and congenital heart disease: five years experience in a single institution. *J Cardiovasc Electrophysiol* 2009;20:58-65.
54. Greene EA, Berul CI. Pacing treatment for dilated cardiomyopathy: optimization of resynchronization pacing in pediatrics. *Curr Opin Cardiol* 2010;25:95-101.
55. Kawasaki T, Kosaki F, Okawa S, et al. A new infantile acute febrile mucocutaneous lymph node syndrome (MLNS) prevailing in Japan. *Pediatrics* 1974;54:271-276.
56. Newburger JW, Takahashi M, Gerber MA, et al. Diagnosis, treatment, and long-term management of Kawasaki disease: a statement for health professionals from the Committee on Rheumatic Fever, Endocarditis and Kawasaki Disease, Council on Cardiovascular Disease in the Young, American Heart Association. *Circulation* 2004;110:2747-2771.
57. Fujiwara H, Hamashima Y. Pathology of the heart in Kawasaki disease. *Pediatrics* 1978;61:100-107.
58. Kato H, Sugimura T, Akagi T, et al. Long-term consequences of Kawasaki disease. A 10- to 21-year follow-up study of 594 patients. *Circulation* 1996;94:1379-1385.
59. Moran AM, Newburger JW, Sanders SP, et al. Abnormal myocardial mechanics in Kawasaki disease: rapid response to gamma-globulin. *Am Heart J* 2000;139:217-223.
60. Strategy for controlling rheumatic fever/rheumatic heart disease, with emphasis on primary prevention: memorandum from a joint WHO/ISFC meeting. *Bull World Health Organ* 1995;73:583-587.
61. Rheumatic fever and rheumatic heart disease. *World Health Organ Tech Rep Ser* 2004;923:1-122, back cover.
62. Olivier C. Rheumatic fever—is it still a problem? *J Antimicrob Chemother* 2000;45(suppl):13-21.
63. Barlow JB, Marcus RH, Pocock WA, et al. Mechanisms and management of heart failure in active rheumatic carditis. *S Afr Med J* 1990;78:181-186.
64. Essop MR, Wisenbaugh T, Sareli P. Evidence against a myocardial factor as the cause of left ventricular dilation in active rheumatic carditis. *J Am Coll Cardiol* 1993;22:826-829.
65. Veasy LG, Tani LY, Hill HR. Persistence of acute rheumatic fever in the intermountain area of the United States. [see comments.]. *J Pediatr* 1994;124:9-16.
66. Veasy LG, Wiedmeier SE, Orsmond GS, et al. Resurgence of acute rheumatic fever in the intermountain area of the United States. *N Engl J Med* 1987;316:421-427.
67. Ravisha MS, Tullu MS, Kamat JR. Rheumatic fever and rheumatic heart disease: clinical profile of 550 cases in India. *Arch Med Res* 2003;34:382-387.
68. Saxena A. Rheumatic fever and long-term sequelae in children. 2002;4:309-319.
69. Chopra P, Bhatia ML. Chronic rheumatic heart disease in India: a reappraisal of pathologic changes. *J Heart Valve Dis* 1992;1:92-101.
70. Agarwal BL. Juvenile mitral stenosis in developing countries: problems and challenge. *J Assoc Physicians India* 1986;34:141-144.
71. Vasan RS, Selvaraj N. Natural history of acute rheumatic fever. In: Narula J, Virmani R, Reddy KS, et al., eds. *Rheumatic Fever*. Washington, DC: American Registry of Pathology, 1999: 347-358.
72. Ferrieri P, Gewitz MH, Gerber MA, et al. Unique features of infective endocarditis in childhood. *Pediatrics* 2002;109:931-943.
73. Baltimore RS. Infective endocarditis in children. *Pediatr Infect Dis J* 1992;11:907-912.
74. Levi D, Alejos J. Diagnosis and treatment of pediatric viral myocarditis. *Curr Opin Cardiol* 2001;16:77-83.
75. Bowles NE, Bowles KR, Towbin JA. Viral genomic detection and outcome in myocarditis. *Heart Fail Clin* 2005;1:407-417.
76. Michels H. Course of mixed connective tissue disease in children. *Ann Med* 1997;29:359-364.
77. Dutschmann L, Ferreira C, De Sousa G, et al. [Cardiac manifestations of connective tissue diseases]. *Acta Med Port* 1989;2:103-110.
78. Caeiro F, Michielson FM, Bernstein R, et al. Systemic lupus erythematosus in childhood. *Ann Rheum Dis* 1981;40:325-331.
79. Kasper EK, Agema WR, Hutchins GM, et al. The causes of dilated cardiomyopathy: a clinicopathologic review of 673 consecutive patients. *J Am Coll Cardiol* 1994;23:586-590.
80. Adams MJ, Lipshultz SE, Schwartz C, et al. Radiation-associated cardiovascular disease: manifestations and management. *Semin Radiat Oncol* 2003;13:346-356.
81. Krischer JP, Epstein S, Cuthbertson DD, et al. Clinical cardiotoxicity following anthracycline treatment for childhood cancer: the Pediatric Oncology Group experience. *J Clin Oncol* 1997;15:1544-1552.

82. Goorin AM, Chauvenet AR, Perez-Atayde AR, et al. Initial congestive heart failure, six to ten years after doxorubicin chemotherapy for childhood cancer. *J Pediatr* 1990;116:144-147.
83. Lipshultz SE, Colan SD, Gelber RD, et al. Late cardiac effects of doxorubicin therapy for acute lymphoblastic leukemia in childhood. *N Engl J Med* 1991;324:808-815.
84. Lipshultz SE, Alvarez JA, Scully RE. Anthracycline associated cardiotoxicity in survivors of childhood cancer. *Heart* 2008;94:525-533.
85. Heidenreich PA, Kapoor JR. Radiation induced heart disease: systemic disorders in heart disease. *Heart* 2009;95:252-258.
86. Michels VV, Driscoll DJ, Miller FA, et al. Progression of familial and non-familial dilated cardiomyopathy: long term follow up. *Heart* 2003;89:757-761.
87. Michels VV, Olson TM, Miller FA, et al. Frequency of development of idiopathic dilated cardiomyopathy among relatives of patients with idiopathic dilated cardiomyopathy. *Am J Cardiol* 2003;91:1389-1392.
88. Maron BJ. Hypertrophic cardiomyopathy in childhood. *Pediatr Clin North Am* 2004;51:1305-1346.
89. Weller RJ, Weintraub R, Addonizio LJ, et al. Outcome of idiopathic restrictive cardiomyopathy in children. *Am J Cardiol* 2002;90:501-506.
90. Ichida F. Left ventricular noncompaction. *Circ J* 2009;73:19-26.
91. Horenstein MS, Saarel E, Dick M, et al. Reversible symptomatic dilated cardiomyopathy in older children and young adolescents due to primary non-sinus supraventricular tachyarrhythmias. *Pediatr Cardiol* 2003;24:274-279.
92. Figueiredo S, Martins E, Lima MR, et al. Cardiovascular manifestations in Marfan syndrome. *Rev Port Cardiol* 2001;20:1203-1218.
93. de Montalembert M, Maunoury C, Acar P, et al. Myocardial ischaemia in children with sickle cell disease. *Arch Dis Child* 2004;89:359-362.
94. Morris KP, Skinner JR, Wren C, et al. Cardiac abnormalities in end stage renal failure and anaemia. *Arch Dis Child* 1993;68:637-643.
95. Scharer K, Schmidt KG, Soergel M. Cardiac function and structure in patients with chronic renal failure. *Pediatr Nephrol* 1999;13:951-965.
96. Stern RC, Borkat G, Hirschfeld SS, et al. Heart failure in cystic fibrosis. Treatment and prognosis of cor pulmonale with failure of the right side of the heart. *Am J Dis Child* 1980;134:267-272.
97. Perkin RM, Anas NG. Pulmonary hypertension in pediatric patients. *J Pediatr* 1984;105:511-522.
98. Blum RH, McGowan FX Jr. Chronic upper airway obstruction and cardiac dysfunction: anatomy, pathophysiology and anesthetic implications. *Paediatr Anaesth* 2004;14:75-83.
99. Taub PR, Gabbai-Saldade P, Maisel A. Biomarkers of heart failure. *Congest Heart Fail* 2010;16(suppl 1):S19-S24.
100. Tobias JD. B-type natriuretic peptide: diagnostic and therapeutic applications in infants and children. *J Intensive Care Med* 2011;26:183-195.
101. Daniels LB, Maisel AS. Natriuretic peptides. *J Am Coll Cardiol* 2007;50:2357-2368.
102. Palazzuoli A, Gallotta M, Quatrini I, et al. Natriuretic peptides (BNP and NT-proBNP): measurement and relevance in heart failure. *Vasc Health Risk Manag* 2010;6:411-418.
103. Koch A, Singer H. Normal values of B type natriuretic peptide in infants, children, and adolescents. *Heart* 2003;89:875-878.
104. Nir A, Lindinger A, Rauh M, et al. NT-pro-B-type natriuretic peptide in infants and children: reference values based on combined data from four studies. *Pediatr Cardiol* 2009;30:3-8.
105. Cantinotti M, Storti S, Crocetti M, et al. Decision levels for plasma B-type natriuretic peptide assay to diagnose significant cardiovascular disease in children. *J Am Coll Cardiol* 2010;55:1166-1167; author reply 1167.
106. Cantinotti M, Storti S, Parti MS, et al. Reference intervals for brain natriuretic peptide in healthy newborns and infants measured with an automated immunoassay platform. *Clin Chem Lab Med* 2010;48:697-700.
107. Das BB, Raj S, Solinger R. Natriuretic peptides in cardiovascular diseases of fetus, infants and children. *Cardiovasc Hematol Agents Med Chem* 2009;7:43-51.
108. Yoshibayashi M, Kamiya T, Saito Y, et al. Plasma brain natriuretic peptide concentrations in healthy children from birth to adolescence: marked and rapid increase after birth. *Eur J Endocrinol* 1995;133:207-209.
109. Das BB. Plasma B-type natriuretic peptides in children with cardiovascular diseases. *Pediatr Cardiol* 2010;31:1135-1145.
110. Favilli S, Frenos S, Lasagni D, et al. The use of B-type natriuretic peptide in paediatric patients: a review of literature. *J Cardiovasc Med (Hagerstown)* 2009;10:298-302.
111. Smith J, Goetze JP, Andersen CB, et al. Practical application of natriuretic peptides in paediatric cardiology. *Cardiol Young* 2010;20:353-363.
112. Koulouri S, Acherman RJ, Wong PC, et al. Utility of B-type natriuretic peptide in differentiating congestive heart failure from lung disease in pediatric patients with respiratory distress. *Pediatr Cardiol* 2004;25:341-346.
113. Cohen S, Springer C, Avital A, et al. Amino-terminal pro-brain-type natriuretic peptide: heart or lung disease in pediatric respiratory distress? *Pediatrics* 2005;115:1347-1350.
114. Ko HK, Lee JH, Choi BM, et al. Utility of the rapid B-type natriuretic peptide assay for detection of cardiovascular problems in newborn infants with respiratory difficulties. *Neonatology* 2008;94:16-21.
115. Sezgin Evim M, Ucar B, Kilic Z, et al. The value of serum N-terminal pro-brain natriuretic peptide levels in the differential diagnosis and follow-up of congestive cardiac failure and respiratory distress due to pulmonary aetiologies in infants and children. *Cardiol Young* 2010;20:495-504.
116. Law YM, Hoyer AW, Reller MD, et al. Accuracy of plasma B-type natriuretic peptide to diagnose significant cardiovascular disease in children: the Better Not Pout Children Study. *J Am Coll Cardiol* 2009;54:1467-1475.
117. Maher KO, Reed H, Cuadrado A, et al. B-type natriuretic peptide in the emergency diagnosis of critical heart disease in children. *Pediatrics* 2008;121:e1484-e1488.
118. Price JF, Thomas AK, Grenier M, et al. B-type natriuretic peptide predicts adverse cardiovascular events in pediatric outpatients with chronic left ventricular systolic dysfunction. *Circulation* 2006;114:1063-1069.
119. Mangat J, Carter C, Riley G, et al. The clinical utility of brain natriuretic peptide in paediatric left ventricular failure. *Eur J Heart Fail* 2009;11:48-52.
120. Auerbach SR, Richmond ME, Lamour JM, et al. BNP levels predict outcome in pediatric heart failure patients: post hoc analysis of the Pediatric Carvedilol Trial. *Circ Heart Fail* 2010;3:606-611.
121. Tan LH, Jefferies JL, Liang JF, et al. Concentrations of brain natriuretic peptide in the plasma predicts outcomes of treatment of children with decompensated heart failure admitted to the Intensive Care unit. *Cardiol Young* 2007;17:397-406.
122. Wong DT, George K, Wilson J, et al. Effectiveness of serial increases in amino-terminal pro-B-type natriuretic peptide levels to indicate the need for mechanical circulatory support in children with acute decompensated heart failure. *Am J Cardiol* 2011;107:573-578.
123. Reynolds EW, Ellington JG, Vranicar M, et al. Brain-type natriuretic peptide in the diagnosis and management of persistent pulmonary hypertension of the newborn. *Pediatrics* 2004;114:1297-1304.
124. Baptista MJ, Rocha G, Clemente F, et al. N-terminal-pro-B type natriuretic peptide as a useful tool to evaluate pulmonary hypertension and cardiac function in CDH infants. *Neonatology* 2008;94:22-30.
125. Puddy VF, Amirmansour C, Williams AF, et al. Plasma brain natriuretic peptide as a predictor of haemodynamically significant patent ductus arteriosus in preterm infants. *Clin Sci (Lond)* 2002;103:75-77.
126. Choi BM, Lee KH, Eun BL, et al. Utility of rapid B-type natriuretic peptide assay for diagnosis of symptomatic patent ductus arteriosus in preterm infants. *Pediatrics* 2005;115:e255-e261.
127. Sanjeev S, Pettersen M, Lua J, et al. Role of plasma B-type natriuretic peptide in screening for hemodynamically significant patent ductus arteriosus in preterm neonates. *J Perinatol* 2005;25:709-713.
128. Hsu JH, Yang SN, Chen HL, et al. B-type natriuretic peptide predicts responses to indomethacin in premature neonates with patent ductus arteriosus. *J Pediatr* 2010;157:79-84.
129. Law YM, Keller BB, Feingold BM, et al. Usefulness of plasma B-type natriuretic peptide to identify ventricular dysfunction in pediatric and adult patients with congenital heart disease. *Am J Cardiol* 2005;95:474-478.
130. Koch A, Zink S, Singer H. B-type natriuretic peptide in paediatric patients with congenital heart disease. *Eur Heart J* 2006;27:861-866.
131. Cowley CG, Bradley JD, Shaddy RE. B-type natriuretic peptide levels in congenital heart disease. *Pediatr Cardiol* 2004;25:336-340.
132. Cheung EW, Lam WW, Chiu CS, et al. Plasma brain natriuretic peptide levels, right ventricular volume overload and exercise capacity in adolescents after surgical repair of tetralogy of Fallot. *Int J Cardiol* 2007;121:155-162.
133. Khositseth A, Manop J, Khowsathit P, et al. N-terminal pro-brain natriuretic peptide as a marker in follow-up patients with tetralogy of Fallot after total correction. *Pediatr Cardiol* 2007;28:333-338.
134. Law YM, Ettedgui J, Beerman L, et al. Comparison of plasma B-type natriuretic peptide levels in single ventricle patients with systemic ventricle heart failure versus isolated cavopulmonary failure. *Am J Cardiol* 2006;98:520-524.
135. Hsu JH, Oishi PE, Keller RL, et al. Perioperative B-type natriuretic peptide levels predict outcome after bidirectional cavopulmonary anastomosis and total cavopulmonary connection. *J Thorac Cardiovasc Surg* 2008;135:746-753.
136. Inuzuka R, Tatebe S, Wakiguchi S, et al. B-type natriuretic peptide at the early stage of univentricular circulation reflects inadequate adaptation to volume overload. *Int J Cardiol* Mar 11, 2011 (Epub ahead of print).
137. Atz AM, Zak V, Breitbart RE, et al. Factors associated with serum brain natriuretic peptide levels after the Fontan procedure. *Congenit Heart Dis* 2011;6:313-321.
138. Shih CY, Sapru A, Oishi P, et al. Alterations in plasma B-type natriuretic peptide levels after repair of congenital heart defects: a potential perioperative marker. *J Thorac Cardiovasc Surg* 2006;131:632-638.
139. Hsu JH, Keller RL, Chikovani O, et al. B-type natriuretic peptide levels predict outcome after neonatal cardiac surgery. *J Thorac Cardiovasc Surg* 2007;134:939-945.
140. Shah A, Feraco AM, Harmon C, et al. Usefulness of various plasma biomarkers for diagnosis of heart failure in children with single ventricle physiology. *Am J Cardiol* 2009;104:1280-1284.
141. Lechner E, Gitter R, Mair R, et al. Amino-terminal brain natriuretic peptide levels in children and adolescents after Fontan operation correlate with congestive heart failure. *Pediatr Cardiol* 2008;29:901-905.
142. Heise G, Lemmer J, Weng Y, et al. Biomarker responses during mid-term mechanical cardiac support in children. *J Heart Lung Transplant* 2008;27:150-157.
143. Chikovani O, Hsu JH, Keller R, et al. B-type natriuretic peptide levels predict outcomes for children on extracorporeal life support after cardiac surgery. *J Thorac Cardiovasc Surg* 2007;134:1179-1187.

144. Aggarwal S, Pettersen MD, Bhambhani K, et al. B-type natriuretic peptide as a marker for cardiac dysfunction in anthracycline-treated children. *Pediatr Blood Cancer* 2007;49:812–816.
145. Hayakawa H, Komada Y, Hirayama M, et al. Plasma levels of natriuretic peptides in relation to doxorubicin-induced cardiotoxicity and cardiac function in children with cancer. *Med Pediatr Oncol* 2001;37:4–9.
146. Pinarli FG, Oguz A, Tunaoglu FS, et al. Late cardiac evaluation of children with solid tumors after anthracycline chemotherapy. *Pediatr Blood Cancer* 2005;44:370–377.
147. Rossano JW, Denfield SW, Kim JJ, et al. B-type natriuretic peptide is a sensitive screening test for acute rejection in pediatric heart transplant patients. *J Heart Lung Transplant* 2008;27:649–654.
148. Geiger M, Harake D, Halnon N, et al. Screening for rejection in symptomatic pediatric heart transplant recipients: the sensitivity of BNP. *Pediatr Transplant* 2008;12:563–569.
149. Bramlet M, Moore R, Murphy D, et al. Increase of B-type natriuretic peptide from baseline increases the risk of death or retransplant in pediatric cardiac transplant patients, midterm results. *Congenit Heart Dis* 2007;2:297–302.
150. Rossano JW, Denfield SW, Kim JJ, et al. B-type natriuretic peptide levels late after transplant predict graft survival in pediatric heart transplant patients. *J Heart Lung Transplant* 2009;28:385–386.
151. Bernus A, Wagner BD, Accurso F, et al. Brain natriuretic peptide levels in managing pediatric patients with pulmonary arterial hypertension. *Chest* 2009;135:745–751.
152. Van Albada ME, Loot FG, Fokkema R, et al. Biological serum markers in the management of pediatric pulmonary arterial hypertension. *Pediatr Res* 2008;63:321–327.
153. Kawamura T, Wago M, Kawaguchi H, et al. Plasma brain natriuretic peptide concentrations in patients with Kawasaki disease. *Pediatr Int* 2000;42:241–248.
154. Kaneko K, Yoshimura K, Ohashi A, et al. Prediction of the risk of coronary arterial lesions in Kawasaki disease by brain natriuretic peptide. *Pediatr Cardiol* 2011;32:1106–1109.
155. Kaski JP, Tome-Esteban MT, Mead-Regan S, et al. B-type natriuretic peptide predicts disease severity in children with hypertrophic cardiomyopathy. *Heart* 2008;94:1307–1311.
156. Ouali S, Bougmiza I, Abroug S, et al. Relationship of brain natriuretic peptide concentrations to left ventricular function and adverse outcomes in children with end-stage renal disease undergoing hemodialysis. *Pediatr Cardiol* 2011;32:568–577.
157. Fried I, Bar-Oz B, Algur N, et al. Comparison of N-terminal pro-B-type natriuretic peptide levels in critically ill children with sepsis versus acute left ventricular dysfunction. *Pediatrics* 2006;118:e1165–e1168.
158. Lieppman K, Kramer-Clark L, Tobias JD. Plasma B-type natriuretic peptide monitoring to evaluate cardiovascular function prior to organ procurement in patients with brain death. *Paediatr Anaesth* 2008;18:852–856.
159. Ross RD, Daniels SR, Schwartz DC, et al. Plasma norepinephrine levels in infants and children with congestive heart failure. *Am J Cardiol* 1987;59:911–914.
160. Buchhorn R, Hulpke-Wette M, Hilgers R, et al. Propranolol treatment of congestive heart failure in infants with congenital heart disease: The CHF-PRO-INFANT Trial. Congestive heart failure in infants treated with propranolol. *Int J Cardiol* 2001;79:167–173.
161. Waagstein F, Bristow MR, Swedberg K, et al. Beneficial effects of metoprolol in idiopathic dilated cardiomyopathy. Metoprolol in Dilated Cardiomyopathy (MDC) Trial Study Group. *Lancet* 1993;342:1441–1446.
162. Krum H, Gilbert RE. Demographics and concomitant disorders in heart failure. *Lancet* 2003;362:147–158.
163. Hunt SA, Abraham WT, Chin MH, et al. ACC/AHA 2005 guideline update for the diagnosis and management of chronic heart failure in the adult—summary Article A report of the American College of Cardiology/American Heart Association Task Force on Practice Guidelines (Writing Committee to Update the 2001 Guidelines for the Evaluation and Management of Heart Failure). *J Am Coll Cardiol* 2005;46:1116–1143.
164. Shaddy RE, Teitel DF, Brett C. Short-term hemodynamic effects of captopril in infants with congestive heart failure. *Am J Dis Child* 1988;142:100–105.
165. Montigny M, Davignon A, Fouron JC, et al. Captopril in infants for congestive heart failure secondary to a large ventricular left-to-right shunt. *Am J Cardiol* 1989;63:631–633.
166. Boucek MM, Chang RL. Effects of captopril on the distribution of left ventricular output with ventricular septal defect. *Pediatr Res* 1988;24:499–503.
167. Buchhorn R, Bartmus D, Siekmeyer W, et al. Beta-blocker therapy of severe congestive heart failure in infants with left to right shunts. *Am J Cardiol* 1998;81:1366–1368.
168. Buchhorn R, Ross RD, Hulpke-Wette M, et al. Effectiveness of low dose captopril versus propranolol therapy in infants with severe congestive heart failure due to left-to-right shunts. *Int J Cardiol* 2000;76:227–233.
169. Costello-Boerrigter LC, Boerrigter G, Burnett JC, Jr. Revisiting salt and water retention: new diuretics, aquaretics, and natriuretics. *Med Clin North Am* 2003;87:475–491.
170. Taylor SH. Diuretic therapy in congestive heart failure. *Cardiol Rev* 2000;8:104–114.
171. Felker GM, Lee KL, Bull DA, et al. Diuretic strategies in patients with acute decompensated heart failure. *N Engl J Med* 2011;364:797–805.
172. Francis GS, Benedict C, Johnstone DE, et al. Comparison of neuroendocrine activation in patients with left ventricular dysfunction with and without congestive heart failure. A substudy of the Studies of Left Ventricular Dysfunction (SOLVD). *Circulation* 1990;82:1724–1729.
173. Costanzo MR, Guglin ME, Saltzberg MT, et al. Ultrafiltration versus intravenous diuretics for patients hospitalized for acute decompensated heart failure. *J Am Coll Cardiol* 2007;49:675–683.
174. De Bruyne LK. Mechanisms and management of diuretic resistance in congestive heart failure. *Postgrad Med J* 2003;79:268–271.
175. Sica DA. Metolazone and its role in edema management. *Congest Heart Fail* 2003;9:100–105.
176. Jessup M. Aldosterone blockade and heart failure. *N Engl J Med* 2003;348:1380–1382.
177. Weber KT. Aldosterone in congestive heart failure. *N Engl J Med* 2001;345:1689–1697.
178. Pitt B, Zannad F, Remme WJ, et al. The effect of spironolactone on morbidity and mortality in patients with severe heart failure. Randomized Aldactone Evaluation Study Investigators. *N Engl J Med* 1999;341:709–717.
179. Pitt B, Remme W, Zannad F, et al. Eplerenone, a selective aldosterone blocker, in patients with left ventricular dysfunction after myocardial infarction. *N Engl J Med* 2003;348:1309–1321.
180. Ezekowitz JA, McAlister FA. Aldosterone blockade and left ventricular dysfunction: a systematic review of randomized clinical trials. *Eur Heart J* 2009;30:469–477.
181. Zannad F, McMurray JJ, Krum H, et al. Eplerenone in patients with systolic heart failure and mild symptoms. *N Engl J Med* 2011;364:11–21.
182. Gheorghiadu M, Adams KF Jr, Colucci WS. Digoxin in the management of cardiovascular disorders. *Circulation* 2004;109:2959–2964.
183. The effect of digoxin on mortality and morbidity in patients with heart failure. The Digitalis Investigation Group. *N Engl J Med* 1997;336:525–533.
184. Packer M, Gheorghiadu M, Young JB, et al. Withdrawal of digoxin from patients with chronic heart failure treated with angiotensin-converting-enzyme inhibitors. RADIANCE Study. *N Engl J Med* 1993;329:1–7.
185. Uretsky BF, Young JB, Shahidi FE, et al. Randomized study assessing the effect of digoxin withdrawal in patients with mild to moderate chronic congestive heart failure: results of the PROVED trial. PROVED Investigative Group. *J Am Coll Cardiol* 1993;22:955–962.
186. Rathore SS, Curtis JP, Wang Y, et al. Association of serum digoxin concentration and outcomes in patients with heart failure. *JAMA* 2003;289:871–878.
187. Adams KF Jr, Patterson JH, Gattis WA, et al. Relationship of serum digoxin concentration to mortality and morbidity in women in the digitalis investigation group trial: a retrospective analysis. *J Am Coll Cardiol* 2005;46:497–504.
188. Kimball TR, Daniels SR, Meyer RA, et al. Effect of digoxin on contractility and symptoms in infants with a large ventricular septal defect. *Am J Cardiol* 1991;68:1377–1382.
189. Redington AN, Carvalho JS, Shinebourne EA. Does digoxin have a place in the treatment of the child with congenital heart disease? *Cardiovasc Drugs Ther* 1989;3:21–24.
190. Seguchi M, Nakazawa M, Momma K. Further evidence suggesting a limited role of digitalis in infants with circulatory congestion secondary to large ventricular septal defect. *Am J Cardiol* 1999;83:1408–1411, A1408.
191. Hunt SA, Baker DW, Chin MH, et al. ACC/AHA Guidelines for the Evaluation and Management of Chronic Heart Failure in the Adult: Executive Summary A Report of the American College of Cardiology/American Heart Association Task Force on Practice Guidelines (Committee to Revise the 1995 Guidelines for the Evaluation and Management of Heart Failure): Developed in Collaboration With the International Society for Heart and Lung Transplantation; Endorsed by the Heart Failure Society of America. *Circulation* 2001;104:2996–3007.
192. Brown NJ, Vaughan DE. Angiotensin-converting enzyme inhibitors. *Circulation* 1998;97:1411–1420.
193. Garg R, Yusuf S. Overview of randomized trials of angiotensin-converting enzyme inhibitors on mortality and morbidity in patients with heart failure. Collaborative Group on ACE Inhibitor Trials. *JAMA* 1995;273:1450–1456.
194. Effects of enalapril on mortality in severe congestive heart failure. Results of the Cooperative North Scandinavian Enalapril Survival Study (CONSENSUS). The CONSENSUS Trial Study Group. *N Engl J Med* 1987;316:1429–1435.
195. Effect of enalapril on survival in patients with reduced left ventricular ejection fractions and congestive heart failure. The SOLVD Investigators. *N Engl J Med* 1991;325:293–302.
196. Cohn JN, Johnson G, Ziesche S, et al. A comparison of enalapril with hydralazine-isosorbide dinitrate in the treatment of chronic congestive heart failure. *N Engl J Med* 1991;325:303–310.
197. Packer M, Poole-Wilson PA, Armstrong PW, et al. Comparative effects of low and high doses of the angiotensin-converting enzyme inhibitor, lisinopril, on morbidity and mortality in chronic heart failure. ATLAS Study Group. *Circulation* 1999;100:2312–2318.
198. van Veldhuisen DJ, Genth-Zotz S, Brouwer J, et al. High- versus low-dose ACE inhibition in chronic heart failure: a double-blind, placebo-controlled study of imidapril. *J Am Coll Cardiol* 1998;32:1811–1818.
199. Bengur AR, Beekman RH, Rocchini AP, et al. Acute hemodynamic effects of captopril in children with a congestive or restrictive cardiomyopathy. *Circulation* 1991;83:523–527.

200. Lewis AB, Chabot M. The effect of treatment with angiotensin-converting enzyme inhibitors on survival of pediatric patients with dilated cardiomyopathy. *Pediatr Cardiol* 1993;14:9-12.
201. Kouatli AA, Garcia JA, Zellers TM, et al. Enalapril does not enhance exercise capacity in patients after Fontan procedure. *Circulation* 1997;96:1507-1512.
202. Bristow MR, Gilbert EM, Abraham WT, et al. Carvedilol produces dose-related improvements in left ventricular function and survival in subjects with chronic heart failure. MOCHA Investigators. *Circulation* 1996;94:2807-2816.
203. Packer M, Bristow MR, Cohn JN, et al. The effect of carvedilol on morbidity and mortality in patients with chronic heart failure. U.S. Carvedilol Heart Failure Study Group [see comments]. *N Engl J Med* 1996;334:1349-1355.
204. Thompson LD, McElhinney DB, Culbertson CB, et al. Perioperative administration of angiotensin converting enzyme inhibitors decreases the severity and duration of pleural effusions following bidirectional cavopulmonary anastomosis. *Cardiol Young* 2001;11:195-200.
205. Hsu DT, Zak V, Mahony L, et al. Enalapril in infants with single ventricle: results of a multicenter randomized trial. *Circulation* 2010;122:333-340.
206. Pitt B, Segal R, Martinez FA, et al. Randomised trial of losartan versus captopril in patients over 65 with heart failure (Evaluation of Losartan in the Elderly Study, ELITE). *Lancet* 1997;349:747-752.
207. Pitt B, Poole-Wilson PA, Segal R, et al. Effect of losartan compared with captopril on mortality in patients with symptomatic heart failure: randomised trial—the Losartan Heart Failure Survival Study ELITE II. *Lancet* 2000;355:1582-1587.
208. Cohn JN, Tognoni G. A randomized trial of the angiotensin-receptor blocker valsartan in chronic heart failure. *N Engl J Med* 2001;345:1667-1675.
209. Friedman AL. Approach to the treatment of hypertension in children. *Heart Dis* 2002;4:47-50.
210. Marino MR, Vachharajani NN. Pharmacokinetics of irbesartan are not altered in special populations. *J Cardiovasc Pharmacol* 2002;40:112-122.
211. Hilgers KF, Dotsch J, Rascher W, et al. Treatment strategies in patients with chronic renal disease: ACE inhibitors, angiotensin receptor antagonists, or both? *Pediatr Nephrol* 2004;19:956-961.
212. Schaefer F, van de Walle J, Zurowska A, et al. Efficacy, safety and pharmacokinetics of candesartan cilexetil in hypertensive children from 1 to less than 6 years of age. *J Hypertens* 2010;28:1083-1090.
213. Waagstein F, Hjalmarson A, Varnauskas E, et al. Effect of chronic beta-adrenergic receptor blockade in congestive cardiomyopathy. *Br Heart J* 1975;37:1022-1036.
214. Swedberg K, Hjalmarson A, Waagstein F, et al. Beneficial effects of long-term beta-blockade in congestive cardiomyopathy. *Br Heart J* 1980;44:117-133.
215. Waagstein F, Hjalmarson A, Swedberg K, et al. Beta-blockers in dilated cardiomyopathies: they work. *Eur Heart J* 1983;4(suppl A):173-178.
216. Eichhorn EJ, Bedotto JB, Malloy CR, et al. Effect of beta-adrenergic blockade on myocardial function and energetics in congestive heart failure. Improvements in hemodynamic, contractile, and diastolic performance with bucindolol [see comments]. *Circulation* 1990;82:473-483.
217. Gilbert EM, O'Connell JB, Bristow MR. Therapy of idiopathic dilated cardiomyopathy with chronic beta-adrenergic blockade. *Heart Vessels Suppl* 1991;6:29-39.
218. Sackner-Bernstein JD, Mancini DM. Rationale for treatment of patients with chronic heart failure with adrenergic blockade. *JAMA* 1995;274:1462-1467.
219. Bristow MR. Mechanism of action of beta-blocking agents in heart failure. *Am J Cardiol* 1997;80:26L-40L.
220. Bristow MR, Ginsburg R, Minobe W, et al. Decreased catecholamine sensitivity and beta-adrenergic-receptor density in failing human hearts. *N Engl J Med* 1982;307:205-211.
221. Gilbert EM, Abraham WT, Olsen S, et al. Comparative hemodynamic, left ventricular functional, and antiadrenergic effects of chronic treatment with metoprolol versus carvedilol in the failing heart. *Circulation* 1996;94:2817-2825.
222. Eichhorn EJ, Heesch CM, Barnett JH, et al. Effect of metoprolol on myocardial function and energetics in patients with nonischemic dilated cardiomyopathy: a randomized, double-blind, placebo-controlled study. *J Am Coll Cardiol* 1994;24:1310-1320.
223. Feuerstein GZ, Bril A, Ruffolo JR Jr. Protective effects of carvedilol in the myocardium. *Am J Cardiol* 1997;80:41L-45L.
224. Effect of metoprolol CR/XL in chronic heart failure: Metoprolol CR/XL Randomised Intervention Trial in Congestive Heart Failure (MERIT-HF). *Lancet* 1999;353:2001-2007.
225. The Cardiac Insufficiency Bisoprolol Study II (CIBIS-II): a randomised trial. *Lancet* 1999;353:9-13.
226. Packer M, Fowler MB, Roecker EB, et al. Effect of carvedilol on the morbidity of patients with severe chronic heart failure: results of the carvedilol prospective randomized cumulative survival (COPERNICUS) study. *Circulation* 2002;106:2194-2199.
227. Poole-Wilson PA, Swedberg K, Cleland JG, et al. Comparison of carvedilol and metoprolol on clinical outcomes in patients with chronic heart failure in the Carvedilol Or Metoprolol European Trial (COMET): randomised controlled trial. *Lancet* 2003;362:7-13.
228. Blume ED, Canter CE, Spicer R, et al. Prospective single-arm protocol of carvedilol in children with ventricular dysfunction. *Pediatr Cardiol* 2006;27:336-342.
229. Rusconi P, Gomez-Marín O, Rossique-Gonzalez M, et al. Carvedilol in children with cardiomyopathy: 3-year experience at a single institution. *J Heart Lung Transplant* 2004;23:832-838.
230. Foerster SR, Canter CE. Pediatric heart failure therapy with beta-adrenoceptor antagonists. *Paediatr Drugs* 2008;10:125-134.
231. Shaddy RE, Boucek MM, Hsu DT, et al. Carvedilol for children and adolescents with heart failure: a randomized controlled trial. *JAMA* 2007;298:1171-1179.
232. Auerbach SR, Richmond ME, Lamour JM, et al. BNP levels predict outcome in pediatric heart failure patients: post hoc analysis of the Pediatric Carvedilol Trial. *Circ Heart Fail* 2010;3:606-611.
233. Petko C, Minich LL, Everitt MD, et al. Echocardiographic evaluation of children with systemic ventricular dysfunction treated with carvedilol. *Pediatr Cardiol* 2010;31:780-784.
234. Abraham WT, Fisher WG, Smith AL, et al. Cardiac resynchronization in chronic heart failure. *N Engl J Med* 2002;346:1845-1853.
235. Young JB, Abraham WT, Smith AL, et al. Combined cardiac resynchronization and implantable cardioversion defibrillation in advanced chronic heart failure: the MIRACLE ICD Trial. *JAMA* 2003;289:2685-2694.
236. Cleland JG, Daubert JC, Erdmann E, et al. The effect of cardiac resynchronization on morbidity and mortality in heart failure. *N Engl J Med* 2005;352:1539-1549.
237. Yu CM, Chau E, Sanderson JE, et al. Tissue Doppler echocardiographic evidence of reverse remodeling and improved synchronicity by simultaneously delaying regional contraction after biventricular pacing therapy in heart failure. *Circulation* 2002;105:438-445.
238. Gorcsan J, 3rd, Kanzaki H, Bazaz R, et al. Usefulness of echocardiographic tissue synchronization imaging to predict acute response to cardiac resynchronization therapy. *Am J Cardiol* 2004;93:1178-1181.
239. Friedberg MK, Silverman NH, Dubin AM, et al. Mechanical dyssynchrony in children with systolic dysfunction secondary to cardiomyopathy: a Doppler tissue and vector velocity imaging study. *J Am Soc Echocardiogr* 2007;20:756-763.
240. Stephenson EA, Cecchin F, Alexander ME, et al. Relation of right ventricular pacing in tetralogy of Fallot to electrical resynchronization. *Am J Cardiol* 2004;93:1449-1452, A1412.
241. Khairy P, Fournier A, Thibault B, et al. Cardiac resynchronization therapy in congenital heart disease. *Int J Cardiol* 2006;4:711-720.
242. Josephson M, Wellens HJ. Implantable defibrillators and sudden cardiac death. *Circulation* 2004;109:2685-2691.
243. A comparison of antiarrhythmic-drug therapy with implantable defibrillators in patients resuscitated from near-fatal ventricular arrhythmias. The Antiarrhythmics versus Implantable Defibrillators (AVID) Investigators. *N Engl J Med* 1997;337:1576-1583.
244. Connolly SJ, Gent M, Roberts RS, et al. Canadian implantable defibrillator study (CIDS): a randomized trial of the implantable cardioverter defibrillator against amiodarone. *Circulation* 2000;101:1297-1302.
245. Moss AJ, Zareba W, Hall WJ, et al. Prophylactic implantation of a defibrillator in patients with myocardial infarction and reduced ejection fraction. *N Engl J Med* 2002;346:877-883.
246. Buxton AE, Lee KL, Fisher JD, et al. A randomized study of the prevention of sudden death in patients with coronary artery disease. Multicenter Unsustained Tachycardia Trial Investigators. *N Engl J Med* 1999;341:1882-1890.
247. Salukhe TV, Francis DP, Sutton R. Comparison of medical therapy, pacing and defibrillation in heart failure (COMPANION) trial terminated early; combined biventricular pacemaker-defibrillators reduce all-cause mortality and hospitalization. *Int J Cardiol* 2003;87:119-120.
248. Bardy GH, Lee KL, Mark DB, et al. Amiodarone or an implantable cardioverter-defibrillator for congestive heart failure. *N Engl J Med* 2005;352:225-237.
249. Rhee EK, Canter CE, Basile S, et al. Sudden death prior to pediatric heart transplantation: would implantable defibrillators improve outcome? *J Heart Lung Transplant* 2007;26:447-452.
250. Dimas VV, Denfield SW, Friedman RA, et al. Frequency of cardiac death in children with idiopathic dilated cardiomyopathy. *Am J Cardiol* 2009;104:1574-1577.
251. Walsh EP. Practical aspects of implantable defibrillator therapy in patients with congenital heart disease. *Pacing Clin Electrophysiol* 2008;31(suppl 1):S38-S40.
252. Silka MJ, Bar-Cohen Y. Should patients with congenital heart disease and a systemic ventricular ejection fraction less than 30% undergo prophylactic implantation of an ICD? Patients with congenital heart disease and a systemic ventricular ejection fraction less than 30% should undergo prophylactic implantation of an implantable cardioverter defibrillator. *Circ Arrhythm Electrophysiol* 2008;1:298-306.
253. Kantor PF, Abraham JR, Dipchand AI, et al. The impact of changing medical therapy on transplantation-free survival in pediatric dilated cardiomyopathy. *J Am Coll Cardiol* 2010;55:1377-1384.

Neurodevelopmental Outcomes after Heart Surgery in Children

Caren S. Goldberg ■ Jane W. Newburger

The survival of children with congenital heart disease has improved dramatically over the past four decades; indeed the number of adults with congenital heart disease is now believed to exceed the number of children (1,2). As mortality has declined, neurologic and developmental morbidities in survivors have come increasingly into focus. Poor school performance and the resultant need of educational support across the developmental span from kindergarten through 12th grade may have considerable personal and societal costs. Furthermore, the increasing number of adults with congenital heart disease has highlighted the consequences of neurodevelopmental impairments for employability and mental health (3). Neurodevelopmental disabilities can derive from innate or genetic factors; from aberrant fetal circulation; from the physiology and sequelae of congenital heart disease itself (e.g., chronic severe cyanosis, failure to thrive, cardiac arrests secondary to arrhythmia); or from the procedures, such as cardiac catheterization or cardiac surgery, used to treat congenital heart disease. Particularly in congenital heart disease, it can be difficult to separate developmental outcomes for particular diagnoses and their genetic underpinnings from consequences of surgical and transcatheter procedures used in their management. It is likely that central nervous system effects of congenital heart disease are cumulative and affected by the complex interaction of genetic, preoperative, intraoperative, and postoperative factors (4,5). In this chapter, we review variables that contribute to neurodevelopmental outcomes in children after heart surgery and summarize findings related to long-term neurodevelopmental outcomes for more common, complex congenital heart malformations.

GENETIC ABNORMALITIES

Chromosomal abnormalities may cause both congenital heart defects and abnormalities of central nervous system structure and function. Examples include chromosomal disorders (e.g., trisomy 13, 18, or 21), microdeletions (e.g., velocardiofacial syndrome secondary to 22q11 microdeletion), or mutations (e.g., Williams syndrome, Alagille syndrome, or CHARGE syndrome). The genetic causes of other syndromes with congenital anomalies, such as VATER syndrome, are unknown. Children with genetic syndromes have much worse neurodevelopmental outcome than those without recognizable syndromes (6). Furthermore, it is suspected that genetic factors may underlie delayed development without other explanation even in some patients without a recognizable constellation of congenital abnormalities.

Specific types of congenital heart defects may be associated with different chromosomal abnormalities with varying molecular pathways that impact central nervous system structure and function. For example, tetralogy of Fallot (TOF) can be associated with mutation or deletion of several different

genes (NKX2.5, JAG1, TBX5, TBX1, and FOXC2) and with several clinical syndromes, such as velocardiofacial syndrome or trisomy 21 (7,8). Three genes known thus far to cause TOF (i.e., TBX5, NKX2.5, and JAG1) have been found in the brain as well as the heart (<http://www.ncbi.nlm.nih.gov>, UniGene). JAG1, mutated in Alagille syndrome, encodes a ligand for the notch intercellular signaling pathway of tremendous importance in brain development (9–13), and 16% of patients with Alagille syndrome have mental retardation (14). In TOF patients without other features of Alagille syndrome, polymorphisms in JAG1 may be associated with both cardiac and neurocognitive phenotypes.

Mutations causing congenital heart defects may be associated with specific neurodevelopmental profiles. For example, although the clinical phenotype associated with 22q11 microdeletion is variable (15), a reasonably consistent neurodevelopmental profile has emerged. Intelligence quotient (IQ) can range from profound mental retardation (16) to average range (17–21), with the prevalence of learning disabilities approaching 100% (18). In adults with velocardiofacial syndrome, specific deficits have been reported in visual-spatial ability, problem solving and planning (executive functions), abstract social thinking, and attentiveness (20,22,23). Studies in children report that verbal IQ tends to exceed performance IQ, with velocardiofacial syndrome patients displaying relative strengths in rote verbal knowledge and memory and relative weaknesses in visual-spatial and perceptual skills and mathematical abilities (24,25). Finally, the 22q11 microdeletion is associated with increased psychiatric risk (16,20,25–28). In adults with 22q11 microdeletion, the prevalence of late-onset psychosis, most commonly schizophrenia and schizoaffective disorders, is 10% to 20% (18,29,30). With advances in research on genetic causes of congenital heart disease, it is likely that an increasing number of genetic abnormalities will be linked to neurologic and developmental outcomes in congenital heart disease patients.

BRAIN ANATOMY, PATHOLOGY, AND NEUROIMAGING

Cerebral dysgenesis has been reported in autopsy series to occur in 10% to 29% of children with congenital heart disease and may include such features as microdysgenesis, incomplete operculization, microcephaly, and agenesis of the corpus callosum (5,31–34). The incidence varies by lesion and is particularly high in hypoplastic left heart syndrome (HLHS) (31–33,35). The cause of cerebral dysgenesis may be related to genetic factors or to abnormalities of fetal cerebrovascular flow dynamics caused by particular congenital heart defects. For example, fetuses with HLHS, whose cerebral perfusion is supplied retrogradely through the ductus arteriosus, as well as those with hypoplastic right heart syndrome and other

congenital defects, have been shown to have cerebrovascular resistance that is lower than normal (36,37).

Fetuses with congenital heart disease and with low cerebral-to-placental resistance ratios (<1) have smaller head circumferences than normal (37). Multiple studies have demonstrated an association of smaller brains and congenital heart disease (37–40). Recently, Limperopoulos et al. (39) performed brain magnetic resonance imaging (MRI) on third-trimester fetuses with a variety of congenital cardiac malformations and found that compared to fetuses with normal cardiac anatomy, with adjustment for gestational age and weight, those with cardiac malformations had smaller brain volumes and impairment of neuroaxonal development and metabolism. In addition, work by Schaer et al. (40) supports the interaction of hemodynamic consequences of congenital heart disease with genetic background on neurologic development. These investigators performed MRI on 53 patients with 22q11.2 deletion and found that compared to healthy controls, cerebral volume was 6.9% less; yet in those patients with 22q11.2 deletion and associated congenital heart disease that required cardiac surgery, cerebral volume reduction was 16.9% (40).

In addition to cerebral dysgenesis, infarction may be seen on histopathologic examination of the brains of infants and children with congenital heart disease. Thromboembolic events related to cardiac catheterization, cardiac surgery, or endocarditis may cause focal infarction. Decreased cerebral perfusion, related to hypotension, hypoperfusion, or cardiac arrest, is associated with a diffuse pattern of cerebral injury (41). Kinney et al. (42) analyzed the neuropathology of 38 infants who died after undergoing reparative or palliative cardiac surgery. Although a spectrum of gray matter lesions was evident, cerebral white matter damage, composed of either periventricular leukomalacia or diffuse white matter gliosis, was the most significant finding. Neonates were more likely than infants to have periventricular leukoencephalopathy, reflecting the vulnerability of the immature (premyelinating) white matter to hypoxic-ischemic injury. Otherwise, the timing and type of surgery were unrelated to the pattern and severity of overall brain injury.

Brain MRI allows the opportunity to evaluate brain structure and pathology in living patients, both preoperatively and postoperatively. In the preoperative period, McConnell et al. (43) found that one-third of infants undergoing cardiac surgery had ventriculomegaly and enlargement of subarachnoid spaces consistent with cerebral atrophy. The Total Maturation Scoring System developed by Childs to measure brain maturation in premature infants incorporates information related to myelination, cortical infolding, glial cell migration bands, and presence of germinal matrix tissue (44). Licht et al. (45) using this score found neonates with HLHS and dextro-transposition of the great arteries (D-TGA) to have structural immaturity of the brain, on average delayed by 1 month (45), compared to healthy neonates. Utilizing this same measurement of brain maturation, Andropoulos et al. (46) demonstrated that postoperative neurologic injury as measured by MRI was greater in newborns undergoing cardiac surgery with less mature brain development. Mahle et al. (47) reported that among 24 infants undergoing cardiac surgery, preoperative MRI revealed periventricular leukoencephalopathy in 16% and infarct in 8%. Moreover, preoperative cerebral lactate peaks were elevated in more than half of infants evaluated by magnetic resonance spectroscopy. In the early postoperative period, 48% of infants had new periventricular leukoencephalopathy, 19% had new infarcts, and 33% had new parenchymal hemorrhage. Interestingly, on late postoperative MRI, performed in 17 infants, all previously detected periventricular leukoencephalopathy had resolved. However, cerebral atrophy was detected in two, old infarct in one, and new infarct in one subject. Similarly, Galli et al. (48) detected periventricular leukoencephalopathy

in 54% of neonates and 4% of infants who underwent brain MRIs in the period between 6 and 14 days following open heart surgery. While the predictive value of MRI findings on longer term developmental outcome remains unclear, evidence is accumulating that preoperative brain abnormalities, as well as brain injury suffered in the intraoperative and postoperative periods, contribute to neurodevelopmental sequelae in children with congenital heart disease.

PERIOPERATIVE RISK FACTORS

Most prospective studies of central nervous system protection and injury have focused on risk factors related to open heart surgery and the perioperative period. The intense attention to perioperative risk factors is likely related to the ability of investigators to study the brain during this high-risk period, which includes planned brain ischemia-reperfusion injury with use of hypothermic cardiopulmonary bypass and total circulatory arrest techniques. Furthermore, perioperative management strategies can be tested in randomized clinical trials.

Perioperative Monitoring Approaches

As investigators have sought to optimize neurodevelopmental outcomes by modifying surgical and medical perioperative approaches, a limiting factor has been identification of early predictive markers of longer term developmental outcomes. To date, MRI has been performed primarily in a research setting. However, some centers have adopted perioperative monitoring strategies that can include continuous electroencephalogram, near-infrared spectroscopy, and/or transcranial Doppler ultrasound (46,49,50). Clinical adoption of these monitoring techniques has outpaced establishment of definitive evidence of clinical benefit. However, recently, Kussman et al. (51) found that among infants undergoing cardiac operation for biventricular repair, decreased cerebral oxygen delivery as measured by near-infrared spectroscopy during the perioperative period was associated with lower scores on the Psychomotor Development Index (PDI) and increased abnormalities found at brain MRI. Further study of this technique, other perioperative monitoring approaches, and additional potential early markers are needed to better understand how late outcomes can be predicted in newborns and infants undergoing cardiac surgery. Nonetheless, a great deal has been learned since the 1990s related to perioperative risk factors of central nervous system insults for children with congenital heart disease.

Intraoperative Support Techniques

Repair of congenital heart disease requires the use of cardiopulmonary bypass, in which blood is exposed to artificial surfaces. This, in turn, causes a massive systemic inflammatory response, with induction of proinflammatory cytokines, chemokines, and endotoxin, as well as activation of the complement system, leukocytes, and the endothelium (52). Furthermore, cardiopulmonary bypass is accompanied by risks of gaseous and particulate embolism, macroemboli, and hypoperfusion resulting in diffuse ischemia/reperfusion injury (53).

During the most complex cardiac operations in the neonate, vital organ support is accomplished using deep hypothermia with low-flow continuous cardiopulmonary bypass (low-flow bypass) and/or deep hypothermic circulatory arrest (DHCA) (54–56). These techniques are often used sequentially in the same patient. Hypothermia is the principal technique used to protect vital organs during use of low-flow bypass or DHCA (57). Its effects are derived, in part, from a reduction in

metabolic activity, reflected in reduced oxygen consumption. Additional mechanisms of hypothermic protection of the brain and other organs during ischemia include preservation of intracellular stores of high-energy phosphates and of high intracellular pH, as well as protection against reperfusion injury including the no-reflow phenomenon, calcium influx, and free radical damage (57).

Circulatory arrest has been widely used since the 1960s in centers with expertise in infant open-heart surgery. This technique has advantages for the surgeon of absence of perfusion cannulae and of blood from the operative field, though it is thought to increase the risk for neurologic insult. In recent years, regional (antegrade) cerebral perfusion has been advocated to avoid exposure to DHCA (58,59) during neonatal aortic arch reconstruction. However, one single-center randomized trial did not show any benefit of regional cerebral perfusion, compared to DHCA, as a method of vital organ support during the Norwood operation with respect to developmental outcomes before Stage II surgery or at 1 year of age, (60). In addition, using MRI, Dent and colleagues found that the rate of new periventricular leukomalacia in the postoperative period was not reduced by the use of regional cerebral perfusion, compared to historical controls who underwent Norwood operation with a DHCA-only strategy (61).

When evaluated as a continuous variable, longer duration of total circulatory arrest has been associated with increased risk of seizures, choreoathetosis, release of brain isoenzymes, and developmental delay (21,62–71), though in some studies, duration of circulatory arrest has not been a significant predictor of outcome (60,73). The absence of an effect may be related, in part, to a narrow range of circulatory arrest times, small sample sizes, or overwhelming effects of other risk factors for adverse outcome, such as underlying genetic abnormalities or severe hemodynamic instability in the preoperative or postoperative period. However, Wypij et al. (74) analyzed the relationship of duration of total circulatory arrest to neurodevelopmental outcomes at age 8 years in infants with D-TGA who underwent the arterial switch operation in the neonatal period or early infancy. The relationship of duration of circulatory arrest to various developmental outcomes was nonlinear. Developmental scores did not decline until the duration of total DHCA exceeded a threshold of approximately 41 minutes (95% one-sided lower confidence limit of 32 minutes) (74). A universally “safe” duration of total circulatory arrest cannot be determined, however, because of its potential interaction with patient factors, such as age, and a host of other perfusion variables that affect outcomes. In addition to duration of total circulation arrest (74), these include the depth of hypothermia (75), the rate and duration of core cooling (76), acid–base management during core cooling (77,78), and the degree of hemodilution (79).

The level of cerebral blood flow during cardiopulmonary bypass is affected by arterial carbon dioxide tension (PCO_2) (77,80). In the *alpha-stat* strategy of pH management, arterial PCO_2 is not corrected for the patient’s temperature during hypothermic cardiopulmonary bypass. Thus, patients are relatively alkalotic during hypothermia. In contrast, in the *pH-stat* strategy, CO_2 is added to the bypass circuit to maintain a pH of 7.40 at the patient’s hypothermic temperature. Because higher arterial PCO_2 is associated with greater cerebral blood flow, the *pH-stat* strategy may provide better brain protection during the periods of global brain hypoperfusion that occur during use of hypothermic cardiopulmonary bypass techniques (77,78,81).

Hemodilution during hypothermic cardiopulmonary bypass has also been studied with respect to its effects on brain injury during infant heart surgery. At the profoundly low temperatures (15°C to 18°C) used during infant and neonatal cardiac surgery, hypothermia increases the viscosity of blood and red

blood cell aggregation (82), potentially increasing the risk of microvascular occlusion. Hemodilution has been used to counter these risks (83) and has been shown to increase cerebral blood flow (84), but could reduce the oxygen-carrying capacity of blood. Furthermore, because hypothermia induces a leftward shift of oxyhemoglobin dissociation, hemodilution has the potential to limit oxygen delivery to the central nervous system (83). In a randomized single-center clinical trial of hemodilution strategy in infants undergoing reparative open heart surgery using hypothermic bypass techniques, low hematocrit (20%) at the onset of low-flow bypass was shown to be a risk factor for adverse neurodevelopmental outcome, specifically lower PDI score, at age 1 year (79). A subsequent trial showed no differences in neurodevelopmental outcome at 1 year with hemodilution within the range of 25% to 35% (85).

It is likely that factors such as hematocrit, temperature, pH strategy, and duration of circulatory arrest or very reduced flow interact in their effects on the central nervous system (86,87). For example, the reduced oxygen-carrying capacity of a low hematocrit during cardiopulmonary bypass can be compensated for by the use of the *pH stat* strategy, or by increasing flow rate, reducing duration of circulatory arrest, or reducing temperature.

Preoperative Factors and Host Susceptibility

Host susceptibility is likely to affect the response of the central nervous system to cardiopulmonary bypass and perioperative events (88). Preoperative patient characteristics such as low Apgar scores at 5 minutes, younger gestational age, lower birth weight, and other attributes have been independent risk factors for adverse neurodevelopmental outcome in clinical trials (79,89). Furthermore, response to cardiac surgery may be mediated by genetic polymorphisms in the pathways affected by exposure to cardiopulmonary bypass, including inflammation, thrombosis, vascular reactivity, and oxidative stress (90). Indeed, it is most likely that the effects of bypass on individual patients are mediated by many different genetic polymorphisms in the domains of inflammation, coagulation, and response to ischemia/reperfusion injury.

The influence of genetic polymorphisms on postoperative morbidity has been extensively studied among adults undergoing open heart surgery (91–94). For example, among adults, worse postoperative bleeding is more common among those with polymorphisms in genes coding for coagulation proteins and platelet glycoproteins (95), and postoperative thrombotic complications have been associated with gene polymorphisms in fibrinogen and angiotensin-converting enzyme (96). Postoperative stroke has been found to be more common among patients with genetic variants for C-reactive protein (CRP) and interleukin-6 (IL-6) (97).

Gaynor et al. (98) have studied the effect of *APOE* genotype on neurodevelopmental outcomes in infants after cardiac surgery. The *APOE* $\epsilon 2$ allele was an independent risk factor for worse PDI scores in multivariable regression adjusting for preoperative and postoperative covariates. Indeed, children with the *APOE* $\epsilon 2$ allele had PDI scores that were approximately one-half standard deviation (SD) lower than those with other genotypes. Of note, although an IQ deficit of approximately 0.5 SD is unlikely to be clinically significant for an individual child, when it represents a mean decline in a population its implications are substantial (99). The effect of *APOE* genotype was seen across the spectrum of children with and without genetic syndromes. The adverse effect of *APOE* $\epsilon 2$ allele is most likely related to decreased neuroresiliency and impaired neuronal repair after central nervous system injury. Interestingly, this finding underscores that children and adults may differ with respect to the effects of particular genotypes.

In contrast to infants, adults carrying the APOE ϵ 4 allele who undergo open heart surgery have increased levels of biochemical markers of brain injury (100,101) and a greater rate of postoperative cognitive decline (102,103).

Postoperative Factors

Various risk factors for brain injury occur in the postoperative period. Low cardiac output syndrome is common in the first 24 to 48 hours following repair of complex congenital heart disease (104,105). Hemodynamic instability and low cardiac output syndrome may be especially damaging to the vulnerable central nervous system of the neonate who has just undergone cardiac surgery using deep hypothermic cardiopulmonary bypass techniques. Hypoxic-ischemic insult related to hypothermic cardiopulmonary bypass techniques disrupts the integrity of cerebral vasoregulatory systems in the early postoperative period, and autoregulation of cerebral blood flow is impaired (106–109). Persistence of such disturbances in cerebrovascular control renders the brain vulnerable to subsequent insults, such as hypotension or hypoxia. Galli et al. (48) reported that hypotension and hypoxemia are independent risk factors for periventricular leukomalacia, and found such injury to occur in 50% of neonates undergoing open heart surgery.

General measures of postoperative course complexity also have been associated with later neurodevelopmental outcome. In the Boston Circulatory Arrest Study, children with D-TGA with longer ICU and hospital stays during their arterial switch operation scored worse on tests of cognitive function at age 8 years. Indeed, mean IQ scores among those in the first and fourth quartiles of length of stay differed by one-half SD. Similarly, Limperopoulos et al. (4) studied a more diverse population and found that longer ICU and hospital lengths of stay were independent predictors of worse scores at age 1 to 3 years on various developmental measures. The adverse effect of longer hospitalization on neurodevelopmental outcome reflects multiple contributory factors that prolong recovery.

The hormonal milieu after cardiac surgery might influence the central nervous system. For example, sick euthyroid syndrome is common among infants and children following open heart surgery, and the degree of thyroid suppression appears to be greatest after the most complex operations (110–119). Even transiently low thyroid levels may adversely impact brain development. In cohort studies, preterm infants with transiently low thyroid levels in the first weeks of life have been found to have later abnormalities of neurologic and developmental function, including higher risks of cerebral palsy (120) and learning disabilities (121). Furthermore, transient hypothyroxinemia of prematurity has been noted to be an independent risk factor for cerebral white matter damage (120,122). The causes of thyroid hormone suppression after cardiopulmonary bypass, likely multifactorial, may include hypothermia, hemodilution, and use of medications (e.g., corticosteroids, catecholamines, dopamine) or topical iodinated antiseptic solutions (123–126).

The association of longer hospital length of stay and worse neurodevelopmental outcome may also be mediated by the inflammatory response. Inflammation can precipitate autoregulatory disturbance and microvascular ischemia and cause neonatal cerebral white matter damage (127,128). Circulating proinflammatory cytokines and chemokines, induced by the massive inflammatory effects of cardiopulmonary bypass and subsequently by postoperative events, could be associated with late brain structural and functional abnormalities.

In contrast to the multitude of studies on the effects of intraoperative management strategies, few prospective trials have tested the efficacy of interventions related to postoperative risk factors on later neurodevelopmental outcome.

OTHER CAUSES OF NEUROLOGIC MORBIDITY

Cardiac catheterization in children has been associated with neurologic complications at a reported incidence of 0.38%; the most frequent sequelae are seizures and stroke (129). Similar to cardiac surgery, cardiac catheterization may be associated with cerebral embolism or hypoxic/ischemic injury secondary to hypoperfusion. In addition, contrast toxicity may be a cause of seizures after cardiac catheterization (130). Catheter interventions may increase the associated risk of cerebrovascular injury for some patient groups. McQuillen et al. (131) performed brain MRI on newborns with D-TGA prior to cardiac surgery and found that 12 of 19 patients who required balloon atrial septostomy, compared to 0 of 10 newborns who did not require balloon atrial septostomy, had evidence of focal or multifocal brain injury. However, other groups have not found balloon atrial septostomy to be associated either with evidence of cerebrovascular accident by MRI (132,133) or with clinical stroke (134) in children with D-TGA.

Although procedures such as open heart surgery or cardiac catheterization are most commonly associated with embolic stroke in children with congenital heart disease, embolic strokes can also occur from intracardiac thrombi that form in the setting of arrhythmia (e.g., atrial fibrillation), poor left ventricular function, and left-sided prosthetic valves. Furthermore, paradoxical emboli may travel from the systemic circulation (e.g., systemic veins, right-sided cardiac structures, or venous catheters) through an intracardiac communication to the brain. Patients with venous hypertension and polycythemia are at increased risk for cerebral venous thrombosis. Risk of cerebrovascular accidents may also increase in the setting of relative anemia in patients with cyanotic heart disease and increased blood viscosity (135).

Infections in the heart or brain may cause neurologic morbidity among children with congenital heart disease. Most common among these is the occurrence of infective endocarditis, with its risk of septic or nonseptic emboli and of mycotic aneurysms (136, 137, 142). Even in the current era, congenital heart disease is the most common predisposing cause of brain abscess (138). Brain abscess is especially common in individuals with cyanotic heart disease, with the incidence inversely related to oxygen saturation (139–144). Because of the high morbidity and mortality of brain abscess, this diagnosis should be pursued with contrast-enhanced computed tomography or brain MRI in patients with cyanotic heart disease and suggestive clinical features, such as headache, seizures, fever, and findings on neurologic examination.

LONG-TERM NEURODEVELOPMENTAL OUTCOME

Compared with the normal population, children who have undergone repair or palliation of congenital heart defects have significantly lower IQ scores, inferior achievement testing, and worse gross and fine motor function and coordination. Many require special services because of their higher frequencies of learning disabilities and of speech, language, and behavioral abnormalities (4,72,145–150). Visual-spatial skills are an area of relative weakness among children with congenital heart disease (148–151). On a measure of functional independence 1 to 3 years after surgery, Limperopoulos et al. (148) reported that only 21% of congenital heart disease survivors scored within the age-appropriate range, 40% had difficulty performing activities of daily living, and 53% had poor socialization skills. Compared with children with acyanotic heart disease or no heart disease, children with cyanotic congenital heart

disease have lower IQs and poorer perceptual and gross motor function (152–154). Furthermore, longer duration of significant cyanosis is associated with a greater decline in cognitive ability (154–160). In general, outcomes after repair of simple lesions, such as atrial septal defects, are similar to those in the normal population, whereas developmental outcomes appear to be worse after biventricular repair of more complex lesions (5,146,159,160–163), though the specific causative factors and the role of cardiopulmonary bypass remain unclear (160). Adverse developmental outcome is most common among those with various forms of single ventricle (72,145,166).

Outcomes in Diagnostic Groups

Congenital heart disease comprises rare and diverse disorders, and most studies of development in children with congenital heart disease include patients with heterogeneous lesions. However, children in a few diagnostic groups have been studied in greater detail, and these are briefly reviewed.

D-Transposition of the Great Arteries

Patients with D-TGA have been studied in great detail in the Boston Circulatory Arrest Study, a randomized trial of predominant total circulatory arrest versus low-flow cardiopulmonary bypass for vital organ support during the arterial switch operation in the neonatal period and early infancy. Patients were followed perioperatively and at ages 1, 4, 8, and 16 years. (89,104,147,164–168,186). By age 1 year, 23% of children had a possible or definite abnormality on brain MRI examination, although the frequency was not related to treatment assignment or duration of circulatory arrest. MRI abnormalities were diffuse in 16 children, focal/multifocal in 20, and developmental (incidental) in 3. At 2.5 years of age, the circulatory arrest group had slower expressive language development and, at 4 years, had lower fine and gross motor scores as well as more speech/language abnormalities and oromotor apraxia. Children in both treatment groups, however, had higher rates of neurodevelopmental problems than would be expected in a normal population. At age 4 years, for instance, the mean Full-Scale IQ was approximately 0.5 SD below the expected population mean; both groups had marked difficulties on tests of expressive language, visual-spatial, and visual-motor skills; and 24% met diagnostic criteria for oromotor apraxia (147).

By age 8 years, when the children had begun primary school and were being challenged to acquire academic skills (e.g., reading, mathematics), the practical implications of the deficits noted at earlier evaluations could be determined with greater certainty (90). Performance in both motor function and visual-spatial skills was especially weak. Other areas of weakness included working memory, hypothesis generation and testing, vigilance and sustained attention, and higher-order language skills. These problem areas contributed to difficulty with executive function, that is, the ability to organize, implement, and modify plans (169). As a group, the cohort had difficulty integrating details into a coherent whole and in higher-order abstract thinking. For example, most children could read individual words without undue difficulty, but many had difficulty reading connected discourse for meaning. Similarly, the children scored well in basic arithmetic but had difficulty solving math problems. The neurodevelopmental characteristics of children with D-TGA were typical of non-verbal learning disability (170).

Other investigators have also reported that children with D-TGA have neurodevelopmental performance below that in the normative population. Ellerbeck et al. (151) reported that children with D-TGA were more likely to have abnormal neurologic examination findings and learning disabilities

than either the general population or their siblings. Similarly, Karl et al. (171) found that, on later follow-up, patients with D-TGA who underwent the arterial switch operation had a higher likelihood of abnormalities on neurologic exam, lower IQ, more motor impairment, and more speech and expressive language problems than a normal control group. In a Congenital Heart Surgeon's Society study of children who underwent repair of D-TGA between 1985 and 1988 at 24 centers, parents reported learning disabilities in 31% of children, behavioral disorders in 13%, hyperactivity in 12%, and cerebral palsy in 3%. Risk factors for adverse outcomes included institution, longer circulatory arrest time, postoperative seizures, and use of a repair other than the arterial switch operation (172).

Tetralogy of Fallot

Although TOF is one of the most common forms of congenital heart disease, data on associated neurodevelopmental deficits are more limited than for D-TGA. Shampaine et al. (173) studied, at a mean age of 30 years, 21 patients with TOF who underwent surgical repair at a mean age of 8.7 years. Their mean IQ in adulthood was 93.4, with an SD of 15.6. Personality assessment revealed reduced scores on adaptability and leadership scales, as well as higher scores on harm avoidance. The patients were described, in summary, as low average in intellectual development, and characterized by anxiety and dependency (173). Other early studies by Ferencz (174) and Garson et al. (175) also suggested increased psychosocial morbidity among TOF patients. In more recent studies, patients with TOF have been included in samples with heterogeneous forms of congenital heart disease (176). In one study in which analyses were stratified, the TOF group was reported to have a mean IQ of 100 (177). The validity of this observation is limited, however, by the exclusion from the study sample of "... children who had any postoperative complication likely to affect development ... [and] children known to have any preoperative intellectual handicaps." Clarkson et al. (65) found that the mean IQ of 17 patients with TOF (88.5) was lower than the mean IQs of any of the other diagnosis groups (ventricular septal defect, D-TGA, total anomalous pulmonary venous return, atrioventricular septal defect, other), which ranged from 90.6 to 102.4. Neurodevelopmental outcome of patients with TOF is thought to be influenced by the presence of an underlying genetic abnormality (e.g., 22q11 microdeletion, Alagille syndrome).

Single Ventricle

Children with single ventricle are at highest risk for adverse developmental sequelae. This group often has prolonged cyanosis, congestive heart failure, multiple cardiac catheterizations, and a series of operations culminating with Fontan palliation. They also are likely to have disturbances of cerebral flow in utero, cerebral dysgenesis, and genetic or associated congenital abnormalities. Neonates with HLHS and other duct-dependent forms of single ventricle may have unstable preoperative hemodynamics and lower cerebral oxygen saturation levels than patients with other forms of congenital heart disease. In addition, infants with HLHS and other forms of single right ventricle undergoing the Norwood procedure have relatively long periods of DHCA and are especially subject to postoperative hemodynamic instability.

In a small series, Uzark et al. (64) studied 32 children following the Fontan procedure. Mean IQ was 97.5 ± 12.1 , and visual motor integration was a particular area of weakness. Use of total circulatory arrest as part of the Norwood procedure tended to be a risk factor for adverse outcome. Wernovsky et al. (145) measured ability and achievement in

a cohort of geographically selected survivors whose Fontan procedure was performed in the 1970s and 1980s. Subjects were a median of 11 years of age at testing and 6 years after surgery. Median Full-Scale IQ was 95.7 ± 17.4 , significantly lower than that in the normal population; 8% of patients scored in the mentally retarded range (<70). In multivariable analyses adjusting for social class, lower IQ was associated with the use of circulatory arrest and with the anatomic diagnosis of HLHS or "Other" complex forms of single ventricle, and marginally with prior placement of a pulmonary artery band. Mean composite achievement score was 91.6 ± 15.4 , much worse than normal and relatively worse than IQ scores, suggesting the presence of learning disabilities. Independent risk factors for worse achievement included the diagnosis of HLHS and "Other" complex single ventricle, or prior use of total circulatory arrest, as well as with reoperation using cardiopulmonary bypass within 30 days after the Fontan procedure. In a more contemporary series of neurodevelopmental outcome after the Fontan procedure, Goldberg et al. (178) found a mean Full-Scale IQ score of 101.4 ± 5.4 . Those with HLHS scored significantly lower (93.8 ± 7.3) than those without HLHS, and additional risk factors for worse neurodevelopmental outcome included lower socioeconomic status, longer duration of circulatory arrest, and occurrence of perioperative seizures.

Indeed, children with HLHS appear to have the highest risk of neurodevelopmental disabilities of any form of congenital heart disease (72,73,178–182). Mahle et al. (72) performed neurocognitive testing on a local group of school-aged survivors of Fontan procedure repaired at Children's Hospital of Philadelphia before 1992. Among 28 children, 18% were mentally retarded, 14% had learning disabilities, 17% had cerebral palsy, and 13% had microcephaly; most children had attention deficit and hyperactivity disorder. Risk factors for worse neurodevelopmental outcome included seizures (lower Full-Scale, Verbal, and Performance IQ scores) and longer bypass time (Performance IQ and achievement in math and reading). Neither social class nor duration of total circulatory arrest was an independent risk factor in this small series, perhaps because the variation attributable to socioeconomic factors was overwhelmed by other medical factors, and the duration of circulatory arrest had a narrow range. The Single Ventricle Reconstruction Trial, conducted through the Pediatric Heart Network, was designed primarily to compare outcomes of children with HLHS randomized to a right ventricle to pulmonary artery shunt to outcomes of participants randomized to a Blalock-Thomas-Taussig shunt (181). Long-term follow-up of this large multicenter cohort enrolled in the Single Ventricle Reconstruction Trial promises to lead to further insights about factors associated with impaired neurodevelopmental outcomes for this high-risk patient group.

Children with HLHS may also be treated with a primary cardiac transplant strategy. Ikle et al. (182) studied developmental outcome of HLHS patients undergoing cardiac transplantation as a primary management strategy. Median Full-Scale IQ was almost 1 SD below average in the normal population. A more recent prospective, multicenter study compared the neurodevelopmental outcomes of school-aged children (mean age 12.4 ± 2.5 years) with HLHS managed by primary heart transplantation compared with staged palliation (73). Among the 47 children who completed testing, 26 had undergone the Norwood procedure and 21, cardiac transplantation. The mean Full-Scale IQ for the cohort was 1 SD below normal (i.e., 86 ± 14), and surgical strategy was not significantly associated with any developmental outcome. As has been noted in other studies, a prolonged initial hospitalization stay was a risk factor for adverse neurodevelopmental outcomes.

Psychosocial Function and Academic Ability and Achievement

Quality of life has been studied in several populations of children and adolescents with congenital heart disease (183–186). Using the Child Health Questionnaire (CHQ)-50, parents of 8-year-old children with D-TGA in the Boston Circulatory Arrest Study rated their children similarly to parents of normative samples with respect to overall physical and psychosocial health (186). However, within the D-TGA group, measures of academic ability and achievement emerged as the most significant correlates of psychosocial functioning. Specifically, worse Psychosocial Summary scores were associated with lower Full-Scale, Verbal, and Performance IQ scores, as well as with worse academic achievement. Indeed, psychosocial health in this population was lower than in patients with juvenile rheumatoid arthritis or asthma, but higher than those among children with attention deficit hyperactivity disorder (ADHD). These data are consistent with the association of learning disabilities with psychosocial dysfunction in the general population (187).

Culbert et al. (188) studied 306 of 708 adolescents who underwent repair of D-TGA between 1985 and 1988 at 24 centers and included children who had undergone arterial switch, atrial switch, and Rastelli repairs. The CHQ-87 instrument was completed by each child. Patients with D-TGA scored higher than the normative population except in self-esteem. Use of the arterial switch operation was associated with higher scores than atrial or Rastelli repairs. Thus, adolescents with D-TGA in this series did not view themselves in a fashion suggesting low psychosocial functioning. Of note, parents of these adolescents did not complete a general health status instrument in this study.

General health status was also assessed by parents of 6- to 18-year-old patients who had undergone the Fontan operation using the CHQ-50 instrument (189,190). Both physical and psychosocial health scores were lower in Fontan patients than among normal children or other populations of cardiac children except for those with pacemakers and automatic internal defibrillators. It seems likely that low scores in the Fontan group are related to their many medical morbidities and lower cognitive function. Worse psychosocial health was associated with the parent's report of current presence of problems with behavior, learning, anxiety, attention, and depression, as well as with lower family income.

The recent development of quality of life measures that are cardiac specific (191,192) will be valuable as we aim to identify modifiable variables to improve quality of life for children with congenital heart disease. Using these measures, children with more severe congenital heart disease have rated their physical and psychosocial quality of life lower than children with milder heart disease (191,192).

Mental Health

Rates of psychosocial dysfunction, particularly depression and panic disorder, have been reported to be elevated in long-term follow-up studies of patients with congenital heart disease (193–195). Many adolescents meet some but not all DSM (*Diagnostic and Statistical Manual of Mental Disorders*) criteria (196–198), and many adolescents with congenital heart disease report low self-esteem (199). These data are consistent with reports that American youth who have a chronic physical illness bear a disproportionate burden of psychiatric comorbidities, particularly depression (200–204). Among adolescents with other forms of physical illness, depression has been associated with higher health care utilization, poorer medical outcome, heightened functional impairment, decreased quality of life, and increased mortality (205–208).

CONCLUSION

In summary, neurologic and developmental sequelae have a major impact on the lives of children with congenital heart disease and their families, sometimes eclipsing the heart disease itself. Children with most diagnoses requiring open heart surgery should be presumed to be at risk, and pediatric cardiologists should incorporate neurodevelopmental surveillance in their routine care of the child with congenital heart disease. Because cognitive disabilities and poor school performance are associated with lower psychosocial health and self-esteem, appropriate interventions should be initiated promptly as problems are detected. In addition, families should be counseled to anticipate issues that may arise in school performance. Recognizing the significant risk to development associated with complex congenital heart disease, there is growing enthusiasm for routine screening for developmental delays and behavioral abnormalities to provide earlier recognition of neurocognitive problems and therefore earlier referral for appropriate interventions. In the future, it is hoped that the prevalence of neurologic and developmental disabilities may be further diminished through advances in engineering and bioengineering, pharmacogenomics, and perioperative care.

REFERENCES

- Marelli AJ, Mackie AS, Ionescu R, et al. Congenital heart disease in the general population: changing prevalence and age distribution. *Circulation* 2007;115:163–172.
- Williams RG, Pearson GD, Barst RJ, et al. Report of the National Heart, Lung, and Blood Institute Working Group on research in adult congenital heart disease. *J Am Coll Cardiol* 2006;47:701–707.
- Webb GD, Williams RG. Care of the adult with congenital heart disease: introduction. *J Am Coll Cardiol* 2001;37:1166.
- Limperopoulos C, Majnemer A, Shevell MI, et al. Predictors of developmental disabilities after open heart surgery in young children with congenital heart defects. *J Pediatr* 2002;141:51–58.
- Wernovsky G. Current insights regarding neurological and developmental abnormalities in children and young adults with complex congenital cardiac disease. *Cardiol Young* 2006;16(Suppl):92–104.
- Kaltman JR, Jarvik GP, Bernbaum J, et al. Neurodevelopmental outcome after early repair of a ventricular septal defect with or without aortic arch obstruction. *J Thorac Cardiovasc Surg* 2006;131:792–798.
- Fokstuen S, Arbenz U, Artan S, et al. 22q11.2 deletions in a series of patients with non-selective congenital heart defects: incidence, type of defects and parental origin. *Clin Genet* 1998;53:63–69.
- Goldmuntz E, Clark BJ, Mitchell LE, et al. Frequency of 22q11 deletions in patients with conotruncal defects. *J Am Coll Cardiol* 1998;32:492–498.
- Cohen JD, Perlstein WM, Braver TS, et al. Temporal dynamics of brain activation during a working memory task. *Nature* 1997;386:603–607.
- Gaiano N, Fishell G. The role of notch in promoting glial and neural stem cell fates. *Annu Rev Neurosci* 2002;25:471–490.
- Whitford KL, Dijkhuizen P, Polleux F, et al. Molecular control of cortical dendrite development. *Annu Rev Neurosci* 2002;25:127–149.
- Pasini A, Wilkinson DG. Stabilizing the regionalisation of the developing vertebrate central nervous system. *Bioessays* 2002;24:427–438.
- Brennan K, Gardner P. Notching up another pathway. *Bioessays* 2002;24:405–410.
- Alagille D, Estrada A, Hadchouel M, et al. Syndromic paucity of interlobular bile ducts (Alagille syndrome or arteriohepatic dysplasia): review of 80 cases. *J Pediatr* 1987;110:195–200.
- Ryan AK, Goodship JA, Wilson DJ, et al. Spectrum of clinical features associated with interstitial chromosome 22q11 deletions: a European collaborative study. *J Med Genet* 1997;34:798–804.
- Kozma C. On cognitive variability in velocardiofacial syndrome: profound mental retardation and autism. *Am J Med Genet* 1998;81:269–270.
- Swillen A, Devriendt K, Legius E, et al. Intelligence and psychosocial adjustment in velocardiofacial syndrome: a study of 37 children and adolescents with VCFs. *J Med Genet* 1997;34:453–458.
- Thomas JA, Graham JM Jr. Chromosomes 22q11 deletion syndrome: an update and review for the primary pediatrician. *Clin Pediatr (Phila)* 1997;36:253–266.
- Moss EM, Batshaw ML, Solot CB, et al. Psychoeducational profile of the 22q11.2 microdeletion: a complex pattern. *J Pediatr* 1999;134:193–198.
- Niklasson L, Rasmussen P, Oskarsdottir S, et al. Chromosome 22q11 deletion syndrome (CATCH 22): neuropsychiatric and neuropsychological aspects. *Dev Med Child Neurol* 2002;44:44–50.
- Forbess JM, Visconti KJ, Hancock-Friesen C, et al. Neurodevelopmental outcome after congenital heart surgery: results from an institutional registry. *Circulation* 2002;106:195–1102.
- Henry JC, van Amelsvoort T, Morris RG, et al. An investigation of the neuropsychological profile in adults with velo-cardio-facial syndrome (VCFs). *Neuropsychologia* 2002;40:471–478.
- Goldberg R, Motzkin B, Marion R, et al. Velo-cardio-facial syndrome: a review of 120 patients. *Am J Med Genet* 1993;45:313–319.
- Kok LL, Solman RT. Velocardiofacial syndrome: learning difficulties and intervention. *J Med Genet* 1995;32:612–618.
- Swillen A, Vogels A, Devriendt K, et al. Chromosome 22q11 deletion syndrome: update and review of the clinical features, cognitive-behavioral spectrum, and psychiatric complications. *Am J Med Genet* 2000;97:128–135.
- Papoulos DF, Faedda GL, Veit S, et al. Bipolar spectrum disorders in patients diagnosed with velo-cardio-facial syndrome: does a hemizygous deletion of chromosome 22q11 result in bipolar affective disorder? *Am J Psychiatry* 1996;153:1541–1547.
- Yan W, Jacobsen LK, Krasnewich DM, et al. Chromosome 22q11.2 interstitial deletions among childhood-onset schizophrenics and “multidimensionally impaired.” *Am J Med Genet* 1998;81:41–43.
- Usiskin SI, Nicolson R, Krasnewich DM, et al. Velocardiofacial syndrome in childhood-onset schizophrenia. *J Am Acad Child Adolesc Psychiatry* 1999;38:1536–1543.
- Gothelf D, Frisch A, Munitz H, et al. Velocardiofacial manifestations and microdeletions in schizophrenic inpatients. *Am J Med Genet* 1997;72:455–461.
- Murphy KC, Jones LA, Owen MJ. High rates of schizophrenia in adults with velo-cardio-facial syndrome. *Arch Gen Psychiatry* 1999;56:940–945.
- Glauser TA, Rorke LB, Weinberg PM, et al. Acquired neuropathologic lesions associated with the hypoplastic left heart syndrome. *Pediatrics* 1990;85:991–1000.
- Jones M. Anomalies of the brain and congenital heart disease: a study of 52 necropsy cases. *Pediatr Pathol* 1991;11:721–736.
- Terplan KL. Brain changes in newborns, infants and children with congenital heart disease in association with cardiac surgery. *J Neurol* 1976;212:225–236.
- Limperopoulos C, Majnemer A, Shevell MI, et al. Neurodevelopmental status of newborns and infants with congenital heart defects before and after open heart surgery. *J Pediatr* 2000;137:638–645.
- Clancy RR, McGaurn SA, Goin JE, et al. Allopurinol neurocardiac protection trial in infants undergoing heart surgery using deep hypothermic circulatory arrest. *Pediatrics* 2001;108:61–70.
- Kaltman JR, Di H, Tian Z, et al. Impact of congenital heart disease on cerebrovascular blood flow dynamics in the fetus. *Ultrasound Obstet Gynecol* 2005;25:32–36.
- Donofrio MT, Bremer YA, Schieken RM, et al. Autoregulation of cerebral blood flow in fetuses with congenital heart disease: the brain sparing effect. *Pediatr Cardiol* 2003;24:436–443.
- Hinton RB, Andelfinger G, Sekar P, et al. Prenatal head growth and white matter injury in hypoplastic left heart syndrome. *Pediatric Research* 2008;64:364–369.
- Limperopoulos C, Tworetzky W, McElhinney, et al. Brain volume and metabolism in fetuses with congenital heart disease: evaluation with quantitative magnetic resonance imaging and spectroscopy. *Circulation* 2010;121:26–33.
- Schaer M, Glaser B, Ottet MC, et al. Regional cortical volumes and congenital heart disease: a MRI study in 22q11.2 deletion syndrome. *J Neurodev Disord* 2010;2:224–234.
- Terplan KL. Patterns of brain damage in infants and children with congenital heart disease: association with catheterization and surgical procedures. *Am J Dis Child* 1973;125:175–185.
- Kinney HC, Panigrahy A, Newburger JW, et al. Hypoxic-ischemic brain injury in infants with congenital heart disease dying after cardiac surgery. *Acta Neuropathol (Berl)* 2005;110:563–578.
- McConnell JR, Fleming WH, Chu WK, et al. Magnetic resonance imaging of the brain in infants and children before and after cardiac surgery. A prospective study. *Am J Dis Child* 1990;144:374–378.
- Childs AM, Ramenghi LA, Cornette L, et al. Cerebral maturation in premature infants: quantitative assessment using MR imaging. *AJNR Am J Neuroradiol* 2001;22:1577–1582.
- Licht DJ, Shera DM, Clancy RR, et al. Brain maturation is delayed in infants with complex congenital heart defects. *J Thorac Cardiovasc Surg* 2009;137:529–536.
- Andropoulos DB, Hunter JV, Nelson DP, et al. Brain immaturity is associated with brain injury before and after neonatal cardiac surgery with high-flow bypass and cerebral oxygenation monitoring. *J Thorac Cardiovasc Surg* 2010;139:543–556.
- Mahle WT, Tavani F, Zimmerman RA, et al. An MRI study of neurological injury before and after congenital heart surgery. *Circulation* 2002;106:1109–1114.
- Galli KK, Zimmerman RA, Jarvik GP, et al. Periventricular leukomalacia is common after neonatal cardiac surgery. *J Thorac Cardiovasc Surg* 2004;127:692–704.

49. Su XW, Undar A. Brain protection during pediatric cardiopulmonary bypass. *Artif Organs* 2010;34:E91-E102.
50. Tweddell JS, Ghanayem NS, Hoffman GM. Pro: NIRS is "standard of care" for postoperative management. *Semin Thorac Cardiovasc Surg Pediatr Card Surg Annu* 2010;13:44-50.
51. Kussman BD, Wypij D, Laussen PC, et al. Relationship of intraoperative cerebral oxygen saturation to neurodevelopmental outcome and brain magnetic resonance imaging at 1 year of age in infants undergoing biventricular repair. *Circulation* 2010;122:245-254.
52. Levy JH, Tanaka KA. Inflammatory response to cardiopulmonary bypass. *Ann Thorac Surg* 2003;75:S715-S720.
53. Jonas RA. The effect of extracorporeal life support on the brain: cardiopulmonary bypass. *Semin Perinatol* 2005;29:51-57.
54. Weiss M, Piwnicka A, Lenfant C, et al. Deep hypothermia with total circulatory arrest. *Trans Am Soc Artif Intern Organs* 1960;6:227-239.
55. Kirklin JW, Dawson B, Devloo RA, et al. Open intracardiac operations: use of circulatory arrest during hypothermia induced by blood cooling. *Ann Surg* 1961;154:769-775.
56. Colditz I, Zwahlen R, Dewald B, et al. In vivo inflammatory activity of neutrophil-activating factor, a novel chemotactic peptide derived from human monocytes. *Am J Pathol* 1989;134:755-760.
57. Hickey PR, Andersen NP. Deep hypothermic circulatory arrest: a review of pathophysiology and clinical experience as a basis for anesthetic management. *J Cardiothorac Anesth* 1987;1:137-155.
58. Pigula FA, Nemoto EM, Griffith BP, et al. Regional low-flow perfusion provides cerebral circulatory support during neonatal arch reconstruction. *J Thorac Cardiovasc Surg* 2000;119:331-339.
59. McDonald MJ, Hanley FL, Reddy VM. Arch reconstruction without circulatory arrest: current clinical applications and results of therapy. *Semin Thorac Cardiovasc Surg Pediatr Card Surg Annu* 2002;5:95-103.
60. Goldberg CS, Bove EL, Devaney EJ, et al. A randomized clinical trial of regional cerebral perfusion versus deep hypothermic circulatory arrest: outcomes for infants with functional single ventricle. *J Thorac Cardiovasc Surg* 2007;133:880-887.
61. Dent CL, Spaeth JP, Jones BV, et al. Brain magnetic resonance imaging abnormalities after the Norwood procedure using regional cerebral perfusion. *J Thorac Cardiovasc Surg* 2005;130:1523-1530.
62. Oates RK, Simpson JM, Turnbull JAB, et al. The relationship between intelligence and duration of circulatory arrest with deep hypothermia. *J Thorac Cardiovasc Surg* 1995;110:786-792.
63. Wells FC, Coghill S, Caplan HL, et al. Duration of circulatory arrest does influence the psychological development of children after cardiac operation in early life. *J Thorac Cardiovasc Surg* 1983;86:823-831.
64. Uzark KC, Lincoln A, Lamberti JJ, et al. Neurodevelopmental outcomes in children with Fontan repair of functional single ventricle. *Pediatrics* 1998;101:4.
65. Clarkson PM, MacArthur BA, Barratt-Boyes BG, et al. Developmental progress after cardiac surgery in infancy using hypothermia and circulatory arrest. *Circulation* 1980;62:855-861.
66. Subramanian S, Vlad P, Fischer L, et al. Sequelae of profound hypothermia and circulatory arrest in the corrective treatment of congenital heart disease in infants and small children. In: Kidd BSL, Rowe RD, eds. *The Child with Congenital Heart Disease at Surgery*. Mt. Kisco, NY: Futura Publishing, 1976:421-431.
67. Haka-Ikse K, Blackwood MJA, Steward DJ. Psychomotor development of infants and children after profound hypothermia during surgery for congenital heart disease. *Dev Med Child Neurol* 1978;20:62-70.
68. Messmer BJ, Schallberger U, Gattiker R, et al. Psychomotor and intellectual development after deep hypothermia and circulatory arrest in early infancy. *J Thorac Cardiovasc Surg* 1976;72:495-502.
69. Stevenson J, Stone E, Dillard D, et al. Intellectual development of children subjected to prolonged circulatory arrest during hypothermic open heart surgery in infancy. *Circulation* 1974;49:54-59.
70. Wright JS, Hicks RG, Newman DC. Deep hypothermic arrest: observations on later development in children. *J Thorac Cardiovasc Surg* 1979;77:466-468.
71. Dickinson D, Sambrooks J. Intellectual performance in children after circulatory arrest with profound hypothermia in infancy. *Arch Dis Child* 1979;54:1-6.
72. Mahle WT, Clancy RR, Moss EM, et al. Neurodevelopmental outcome and lifestyle assessment in school-aged and adolescent children with hypoplastic left heart syndrome. *Pediatrics* 2000;105:1082-1089.
73. Mahle WT, Visconti KJ, Freier MC, et al. Relationship of surgical approach to neurodevelopmental outcomes in hypoplastic left heart syndrome. *Pediatrics* 2006;117:e90-e97.
74. Wypij D, Newburger JW, Rappaport LA, et al. The effect of duration of deep hypothermic circulatory arrest in infant heart surgery on late neurodevelopment: the Boston Circulatory Arrest Trial. *J Thorac Cardiovasc Surg* 2003;126:1397-1403.
75. Schell RM, Stanley T, Croughwell N, et al. Temperature during cardiopulmonary bypass and neuropsychologic outcome. *Anesthesiology* 1992;77:A119.
76. Bellinger DC, Wernovsky G, Rappaport LA, et al. Cognitive development of children following early repair of transposition of the great arteries using deep hypothermic circulatory arrest. *Pediatrics* 1991;87:701-707.
77. du Plessis AJ, Jonas RA, Wypij D, et al. Perioperative effects of alpha-stat versus pH-stat strategies for deep hypothermic cardiopulmonary bypass in infants. *J Thorac Cardiovasc Surg* 1997;114:991-1001.
78. Bellinger DC, Wypij D, du Plessis AJ, et al. Developmental and neurologic effects of alpha-stat versus pH-stat strategies for deep hypothermic cardiopulmonary bypass in infants [see comments]. *J Thorac Cardiovasc Surg* 2001;121:374-383. Erratum in *J Thorac Cardiovasc Surg* 2001;121:893.
79. Jonas RA, Wypij D, Roth SJ, et al. The influence of hemodilution on outcome after hypothermic cardiopulmonary bypass: results of a randomized trial in infants. *J Thorac Cardiovasc Surg* 2003;126:1765-1774.
80. Burrows F. Con: pH-stat management of blood gases is preferable to alpha-stat in patients undergoing brain cooling for cardiac surgery. *J Cardiothorac Vasc Anesth* 1995;9:219-221.
81. Duebener LF, Hagino I, Sakamoto T, et al. Effects of pH management during deep hypothermic bypass on cerebral microcirculation: alpha-stat versus pH-stat. *Circulation* 2002;106:1103-1108.
82. Cooper MM, Elliott M. Haemodilution. In: Jonas RA, Elliott MJ, eds. *Cardiopulmonary Bypass in Neonates, Infants, and Young Children*. Oxford, UK: Butterworth-Heinemann, 1994:91.
83. Neptune WB, Bougas JA, Panico FG. Open heart surgery without the need for donor blood priming in the pump oxygenator. *N Engl J Med* 1960;263:111-115.
84. Sungurtekin H, Cook DJ, Orszulak TA, et al. Cerebral response to hemodilution during hypothermic cardiopulmonary bypass in adults. *Anesth Analg* 1999;89:1078-1083.
85. Newburger JW, Jonas RA, Soul J, et al. Randomized trial of hematocrit 25% versus 35% during hypothermic cardiopulmonary bypass in infant heart surgery. *J Thorac Cardiovasc Surg* 2008;135:347-354.
86. Sakamoto T, Zurakowski D, Duebener LF, et al. Interaction of temperature with hematocrit level and pH determines safe duration of hypothermic circulatory arrest. *J Thorac Cardiovasc Surg* 2004;128:220-232.
87. Anttila V, Hagino I, Zurakowski D, et al. Specific bypass conditions determine safe minimum flow rate. *Ann Thorac Surg* 2005;80:1460-1467.
88. Gaynor JW, Wernovsky G, Jarvik GP, et al. Patient characteristics are important determinants of neurodevelopmental outcome at one year of age after neonatal and infant cardiac surgery. *J Thorac Cardiovascular Surg* 2007;133:1344-1353.
89. Bellinger DC, Wypij D, duPlessis AJ, et al. Neurodevelopmental status at eight years in children with dextro-transposition of the great arteries: the Boston Circulatory Arrest Trial. *J Thorac Cardiovasc Surg* 2003;126:1385-1396.
90. Podgoreanu MV, Schwinn DA. New paradigms in cardiovascular medicine: emerging technologies and practices: perioperative genomics. *J Am Coll Cardiol* 2005;46:1965-1977.
91. Schroeder S, Borger N, Wrigge H, et al. A tumor necrosis factor gene polymorphism influences the inflammatory response after cardiac operation. *Ann Thorac Surg* 2003;75:534-537.
92. Tomasdottir H, Hjartarson H, Riksten A, et al. Tumor necrosis factor gene polymorphism is associated with enhanced systemic inflammatory response and increased cardiopulmonary morbidity after cardiac surgery. *Anesth Analg* 2003;97:944-949, table of contents.
93. Brull DJ, Montgomery HE, Sanders J, et al. Interleukin-6 gene -174g>c and -572g>c promoter polymorphisms are strong predictors of plasma interleukin-6 levels after coronary artery bypass surgery. *Arterioscler Thromb Vasc Biol* 2001;21:1458-1463.
94. Stafford-Smith M, Podgoreanu M, Swaminathan M, et al. Association of genetic polymorphisms with risk of renal injury after coronary bypass graft surgery. *Am J Kidney Dis* 2005;45:519-530.
95. Welsby IJ, Podgoreanu MV, Phillips-Bute B, et al. Genetic factors contribute to bleeding after cardiac surgery. *J Thromb Haemost* 2005;3:1206-1212.
96. Ozbek N, Atac FB, Yildirim SV, et al. Analysis of prothrombotic mutations and polymorphisms in children who developed thrombosis in the perioperative period of congenital cardiac surgery. *Cardiol Young* 2005;15:19-25.
97. Grocott HP, White WD, Morris RW, et al. Genetic polymorphisms and the risk of stroke after cardiac surgery. *Stroke* 2005;36:1854-1858.
98. Gaynor JW, Gerdes M, Zackai EH, et al. Apolipoprotein E genotype and neurodevelopmental sequelae of infant cardiac surgery. *J Thorac Cardiovasc Surg* 2003;126:1736-1745.
99. Bellinger DC. Perspectives on incorporating human neurobehavioral end points in risk assessments. *Risk Anal* 2002;22:487-498.
100. Grocott HP, Newman MF, El Moalem H, et al. Apolipoprotein E genotype differentially influences the proinflammatory and anti-inflammatory response to cardiopulmonary bypass. *J Thorac Cardiovasc Surg* 2001;122:622-623.
101. Drabe N, Zund G, Grunenfelder J, et al. Genetic predisposition in patients undergoing cardiopulmonary bypass surgery is associated with an increase of inflammatory cytokines. *Eur J Cardiothorac Surg* 2001;20:609-613.
102. Lelis RG, Krieger JE, Pereira AC, et al. Apolipoprotein E4 genotype increases the risk of postoperative cognitive dysfunction in patients undergoing coronary artery bypass graft surgery. *J Cardiovasc Surg (Torino)* 2006;47:451-456.
103. Tardiff B, Newman M, Saunders A, et al. Apolipoprotein E allele frequency in patients with cognitive deficits following cardiopulmonary bypass. *Circulation* 1994;90(Suppl):201.

104. Wernovsky G, Wypij D, Jonas RA, et al. Postoperative course and hemodynamic profile after the arterial switch operation in neonates and infants: a comparison of low-flow cardiopulmonary bypass versus circulatory arrest. *Circulation* 1995;92:2226–2235.
105. Hoffman TM, Wernovsky G, Atz AM, et al. Efficacy and safety of milrinone in preventing low cardiac output syndrome in infants and children after corrective surgery for congenital heart disease. *Circulation* 2003;107:996–1002.
106. Lou H. The “lost autoregulation hypothesis” and brain lesions in the newborn—an update. *Brain Dev* 1988;10:143–146.
107. Bassan H, Gauvreau K, Newburger JW, et al. Identification of pressure passive cerebral perfusion and its mediators after infant cardiac surgery. *Pediatr Res* 2005;57:35–41.
108. Greeley WJ, Ungerleider RM, Smith LR, et al. The effects of deep hypothermic cardiopulmonary bypass and total circulatory arrest on cerebral blood flow in infants and children. *J Thorac Cardiovasc Surg* 1989;97:737–745.
109. Greeley WJ, Bracey VA, Ungerleider RM, et al. Recovery of cerebral metabolism and mitochondrial oxidation state is delayed after hypothermic circulatory arrest. *Circulation* 1991;84(Suppl):III400–III406.
110. Saatvedt K, Lindberg H, Geiran OR, et al. Thyroid function during and after cardiopulmonary bypass in children. *Acta Anaesthesiol Scand* 1998;42:1100–1103.
111. Ririe DG, Butterworth JF, Hines M, et al. Effects of cardiopulmonary bypass and deep hypothermic circulatory arrest on the thyroid axis during and after repair of congenital heart defects: preservation by deep hypothermia? *Anesth Analg* 1998;87:543–548.
112. Murzi B, Iervasi G, Masini S, et al. Thyroid hormones homeostasis in pediatric patients during and after cardiopulmonary bypass. *Ann Thorac Surg* 1995;59:481–485.
113. Bettendorf M, Schmidt KG, Tiefenbacher U, et al. Transient secondary hypothyroidism in children after cardiac surgery. *Pediatr Res* 1997;41:375–379.
114. Allen DB, Dietrich KA, Zimmerman JJ. Thyroid hormone metabolism and level of illness severity in pediatric cardiac surgery patients. *J Pediatr* 1989;114:59–62.
115. Belgorosky A, Weller G, Chaler E, et al. Evaluation of serum total thyroxine and triiodothyronine and their serum fractions in nonthyroidal illness secondary to congenital heart disease: studies before and after surgery. *J Endocrinol Invest* 1993;16:499–503.
116. Mainwaring RD, Lamberti JJ, Carter TL Jr, et al. Reduction in triiodothyronine levels following modified Fontan procedure. *J Card Surg* 1994;9:322–331.
117. Mainwaring RD, Capparelli E, Schell K, et al. Pharmacokinetic evaluation of triiodothyronine supplementation in children after modified Fontan procedure. *Circulation* 2000;101:1423–1429.
118. Mainwaring RD, Lamberti JJ, Billman GF, et al. Suppression of the pituitary thyroid axis after cardiopulmonary bypass in the neonate. *Ann Thorac Surg* 1994;58:1078–1082.
119. Mainwaring RD, Healy RM, Meier FA, et al. Reduction in levels of triiodothyronine following the first stage of the Norwood reconstruction for hypoplastic left heart syndrome. *Cardiol Young* 2001;11:295–300.
120. Reuss ML, Paneth N, Pinto-Martin JA, et al. The relation of transient hypothyroxinemia in preterm infants to neurologic development at two years of age. *N Engl J Med* 1996;334:821–827.
121. Den Ouden AL, Kok JH, Verkerk PH, et al. The relation between neonatal thyroxine levels and neurodevelopmental outcome at age 5 and 9 years in a national cohort of very preterm and/or very low birth weight infants. *Pediatr Res* 1996;39:142–145.
122. Leviton A, Paneth N, Reuss ML, et al. Hypothyroxinemia of prematurity and the risk of cerebral white matter damage. *J Pediatr* 1999;134:706–711.
123. Nussey S, Whitehead S. *Endocrinology. An Integrated Approach*. World Wide Web. Oxford, UK: Bios Scientific Publishers Ltd., 2001.
124. Brogan TV, Bratton SL, Lynn AM. Thyroid function in infants following cardiac surgery: comparative effects of iodinated and noniodinated topical antiseptics. *Crit Care Med* 1997;25:1583–1587.
125. Van den BG, de Zegher F, Lauwers P. Dopamine and the sick euthyroid syndrome in critical illness. *Clin Endocrinol (Oxf)* 1994;41:731–737.
126. Van den BG, de Zegher F, Lauwers P. Dopamine suppresses pituitary function in infants and children. *Crit Care Med* 1994;22:1747–1753.
127. Berger R, Garnier Y, Jensen A. Perinatal brain damage: underlying mechanisms and neuroprotective strategies. *J Soc Gynecol Invest* 2002;9:319–328.
128. Leviton A, Dammann O. Coagulation, inflammation, and the risk of neonatal white matter damage. *Pediatr Res* 2004;55:541–545.
129. Liu XY, Wong V, Leung M. Neurologic complications due to catheterization. *Pediatr Neurol* 2001;24:270–275.
130. Torvik A, Walday P. Neurotoxicity of water-soluble contrast media. *Acta Radiol Suppl* 1995;399:221–229.
131. McQuillen PS, Hamrick SEG, Perez M, et al. Balloon atrial septostomy is associated with preoperative stroke in neonates with transposition of the great arteries. *Circulation* 2006;113:280–285.
132. Beca J, Gunn J, Coleman L, et al. Pre-operative brain injury in newborn infants with transposition of the great arteries occurs at rates similar to other complex congenital heart disease and is not related to balloon atrial septostomy. *J Am Coll Cardiol* 2009;53:1807–1811.
133. Petit CJ, Rome JJ, Wernovsky G, et al. preoperative brain injury in transposition of the great arteries is associated with oxygenation and time to surgery, not balloon atrial septostomy. *Circulation* 2009;119:709–716.
134. Applegate SE, Lim DS. Incidence of stroke in patients with d-transposition of the great arteries that undergo balloon atrial septostomy in the University Healthsystem Consortium Clinical Data Base/resource manager. *Catheter Cardiovasc Interv* 2010;76:129–131.
135. Cottrill CM, Kaplan S. Cerebral vascular accidents in cyanotic congenital heart disease. *Am J Dis Child* 1973;125:484–487.
136. Ferrieri P, Gewitz MH, Gerber MA, et al. Unique features of infective endocarditis in childhood. *Circulation* 2002;105:2115–2126.
137. Baddour LM, Wilson WR, Bayer AS, et al. Infective endocarditis: diagnosis, antimicrobial therapy, and management of complications: a statement for healthcare professionals from the Committee on Rheumatic Fever, Endocarditis, and Kawasaki Disease, Council on Cardiovascular Disease in the Young, and the Councils on Clinical Cardiology, Stroke, and Cardiovascular Surgery and Anesthesia, American Heart Association: endorsed by the Infectious Diseases Society of America. *Circulation* 2005;111:e394–e434.
138. Goodkin HP, Harper MB, Pomeroy SL. Intracerebral abscess in children: historical trends at Children's Hospital Boston. *Pediatrics* 2004;113:1765–1770.
139. Shu-yuan Y. Brain abscess associated with congenital heart disease. *Surg Neurol* 1989;31:129–132.
140. Aebi C, Kaufmann F, Schaad U. Brain abscess in childhood: long-term experiences. *Eur J Pediatr* 1991;150:282–286.
141. Ciurea AV, Stoica F, Vasilescu G, et al. Neurosurgical management of brain abscesses in children. *Childs Nerv Syst* 1999;15:309–317.
142. Nielsen H, Gyldensted C, Harmsen A. Cerebral abscess. Aetiology and pathogenesis, symptoms, diagnosis and treatment. *Acta Neurol Scand* 1982;65:609.
143. Samson DS, Clark K. A current review of brain abscess. *Am J Med* 1973;54:201–210.
144. Scheld MW, Winn RH. Brain abscess. In: Mandell GL, Douglas RG, Bennett JE, eds. *Principles and Practice of Infectious Diseases*. New York, NY: John Wiley & Sons, 1985:585–591.
145. Wernovsky G, Stiles KM, Gauvreau K, et al. Cognitive development after the Fontan operation. *Circulation* 2000;102:883–889.
146. Mahle WT, Wernovsky G. Long-term developmental outcome of children with complex congenital heart disease. *Clin Perinatol* 2001;28:235–247.
147. Bellinger DC, Wypij D, Kuban CK, et al. Developmental and neurologic status of children at 4 years of age after heart surgery with hypothermic circulatory arrest or low-flow cardiopulmonary bypass. *Circulation* 1999;100:526–532.
148. Limperopoulos C, Majnemer A, Shevell MI, et al. Functional limitations in young children with congenital heart defects after cardiac surgery. *Pediatrics* 2001;108:1325–1331.
149. Forbess JM, Visconti KJ, Bellinger DC, et al. Neurodevelopmental outcomes after biventricular repair of congenital heart defects. *J Thorac Cardiovasc Surg* 2002;123:631–639.
150. Bellinger DC, Jonas RA, Rappaport LA, et al. Developmental and neurologic status of children after heart surgery with hypothermic circulatory arrest or low-flow cardiopulmonary bypass. *N Engl J Med* 1995;332:549–555.
151. Ellerbeck KA, Smith ML, Holden EW, et al. Neurodevelopmental outcomes in children surviving d-transposition of the great arteries. *J Dev Behav Pediatr* 1998;19:335–341.
152. Samango-Sprouse C, Suddaby EC. Developmental concerns in children with congenital heart disease. *Curr Opin Cardiol* 1997;12:91–98.
153. Tindall S, Rothermel RR, Delamater A, et al. Neuropsychological abilities of children with cardiac disease treated with extracorporeal membrane oxygenation. *Dev Neuropsychol* 1999;16:101–115.
154. Wright M, Nolan T. Impact of cyanotic heart disease on school performance. *Arch Dis Child* 1994;71:64–70.
155. Linde LM, Rasof B, Dunn OJ. Mental development in congenital heart disease. *J Pediatr* 1967;71:198–203.
156. Linde LM, Rasof B, Dunn OJ. Longitudinal studies of intellectual and behavioral development in children with congenital heart disease. *Acta Paediatr Scand* 1970;59:169–176.
157. Phornphutkul C, Rosenthal A, Nadas AS, et al. Cerebrovascular accidents in infants and children with cyanotic congenital heart disease. *Am J Cardiol* 1973;32:329–334.
158. Newburger JW, Silbert AR, Buckley LP, et al. Cognitive function and duration of hypoxemia in children with transposition of the great arteries. *N Engl J Med* 1984;310:1495–1499.
159. O'Dougherty M, Wright FS, Gormczy N, et al. Later competence and adaptation in infants who survive severe heart defects. *Child Dev* 1983;54:1129–1142.
160. Silbert A, Wolff PH, Mayer B, et al. Cyanotic heart disease and psychological development. *Pediatrics* 1969;43:192–200.
161. Visconti KJ, Bichell DP, Jonas RA, et al. Developmental outcome after surgical versus interventional closure of secundum atrial septal defect in children. *Circulation* 1999;100(Suppl):II145–II150.
162. Stavinoha PL, Fixler DE, Mahony L. Cardiopulmonary bypass to repair an atrial septal defect does not affect cognitive function in children. *Circulation* 2003;107(21):2722–2725.

163. Quartermain MD, Ittenbach RF, Flynn TB, et al. Neuropsychological status in children after repair of acyanotic congenital heart disease. *Pediatrics* 2010;126:e351–e359.
164. Bellinger DC, Wypij D, Rivkin MJ, et al. Adolescents with d-transposition of the great arteries corrected with the arterial switch procedure: neuropsychological assessment and structural brain imaging. *Circulation* 2011;124:1361–1369.
165. Newburger JW, Jonas RA, Wernovsky G, et al. A comparison of the perioperative neurologic effects of hypothermic circulatory arrest versus low-flow cardiopulmonary bypass in infant heart surgery. *N Engl J Med* 1993;329:1057–1064.
166. Williams DL, Gelijs AC, Moskowitz AJ, et al. Hypoplastic left heart syndrome: valuing the survival. *J Thorac Cardiovasc Surg* 2000;119:720–731.
167. Ovadia R, Hemphill L, Winner K, et al. Just pretend: participation in symbolic talk by children with histories of early corrective heart surgery. *Appl Psycholinguistics* 2000;21:321–340.
168. Hemphill L, Uccelli P, Winner K, et al. Narrative discourse in young children with histories of early corrective heart surgery. *J Speech Lang Hear Res* 2002;45:318–331.
169. Lezak M. *Neuropsychological Assessment*. 2nd ed. New York, NY: Oxford University Press, 1995.
170. Harnadek MC, Rourke BP. Principal identifying features of the syndrome of nonverbal learning disabilities in children. *J Learn Disabil* 1994;27:144–154.
171. Karl TR, Hall S, Ford G, et al. Arterial switch with full-flow cardiopulmonary bypass and limited circulatory arrest: neurodevelopmental outcome. *J Thorac Cardiovasc Surg* 2004;127:213–222.
172. Williams WG, McCrindle BW, Ashburn DA, et al. Outcomes of 829 neonates with complete transposition of the great arteries 12–17 years after repair. *Eur J Cardiothorac Surg* 2003;24:1–9.
173. Shampaine EL, Nadelman L, Rosenthal A, et al. Longitudinal psychological assessment in tetralogy of Fallot. *Pediatr Cardiol* 1989;10:135–140.
174. Ferencz C. The quality of life of the adolescent cardiac patient. *Postgrad Med* 1974;56:67–73.
175. Garson A Jr, Williams RB Jr, Reckless J. Long-term follow-up of patients with tetralogy of Fallot: physical health and psychopathology. *J Pediatr* 1974;85:429–433.
176. Kramer HH, Awiszus D, Sterzel U, et al. Development of personality and intelligence in children with congenital heart disease. *J Child Psychol Psychiatry* 1989;30:299–308.
177. Oates RK, Simpson JM, Cartmill TB, et al. Intellectual function and age of repair in cyanotic congenital heart disease. *Arch Dis Child* 1995;72:298–301.
178. Goldberg CS, Schwartz EM, Brunberg JA, et al. Neurodevelopmental outcome of patients after the Fontan operation: a comparison between children with hypoplastic left heart syndrome and other functional single ventricle lesions. *J Pediatr* 2000;137:646–652.
179. Rogers BT, Msall ME, Buck GM, et al. Neurodevelopmental outcome of infants with hypoplastic left heart syndrome. *J Pediatr* 1995;126:496–498.
180. Kern JH, Hinton VJ, Nereo NE, et al. Early developmental outcome after the Norwood procedure for hypoplastic left heart syndrome. *Pediatrics* 1998;102:1148–1152.
181. Ohye RG, Gaynor JW, Ghanayem NS, et al. Design and rationale of a randomized trial comparing the Blalock-Taussig and right ventricle to pulmonary artery shunts in the Norwood procedure. *J Thorac Cardiovasc Surg* 2008;136:968–975.
182. Ikle L, Hale K, Fashaw L, et al. Developmental outcome of patients with hypoplastic left heart syndrome treated with heart transplantation. *J Pediatr* 2003;142:20–25.
183. Landgraf JM, Abetz LN. Functional status and well-being of children representing three cultural groups: initial self-reports using the CHQ-CF87. *Psychol Health* 1997;12:839–854.
184. Landgraf JM, Abetz L. Measuring health outcomes in pediatric populations: issues in psychometrics and application. In: Spilker B, ed. *Quality of Life and Pharmacoeconomics in Clinical Trials*. New York, NY: Raven Press, 1996.
185. Landgraf JM, Abetz L, Ware JE Jr. *Child Health Questionnaire (CHQ)*. 1st ed. Boston, MA: The Health Institute, New England Medical Center, 1996.
186. Dunbar-Masterson C, Wypij D, Bellinger DC, et al. General health status of children with D-transposition of the great arteries after the arterial switch operation. *Circulation* 2001;104(Suppl):I138–I142.
187. Greenham SL. Learning disabilities and psychosocial adjustment: a critical review. *Child Neuropsychol* 1999;5:171–196.
188. Culbert EL, Ashburn DA, Cullen-Dean G, et al. Quality of life of children after repair of transposition of the great arteries. *Circulation* 2003;108:857–862.
189. McCrindle BW, Williams RV, Mitchell PD, et al. Relationship of patient and medical characteristics to health status in children and adolescents after the Fontan procedure. *Circulation* 2006;113:1123–1129.
190. Sleeper LA, Anderson P, Hsu DT, et al. Design of a large cross-sectional study to facilitate future clinical trials in children with the Fontan palliation. *Am Heart J* 2006;152:427–433.
191. Uzark K, Jones K, Slusher J, et al. Quality of life in children with heart disease as perceived by children and parents. *Pediatrics* 2008;121:e1060–e1067.
192. Marino BS, Tomlinson RS, Wernovsky G, et al. Validation of the pediatric cardiac quality of life inventory. *Pediatrics* 2010;126:498–508.
193. Bjornstad PG, Spurkland ILH. The impact of severe congenital heart disease on physical and psychosocial functioning in adolescents. *Cardiol Young* 2002;5:56–62.
194. Spurkland I, Bjornstad PG, Lindberg H, et al. Mental health and psychosocial functioning in adolescents with congenital heart disease: a comparison between adolescents born with severe heart defect and atrial septal defect. *Acta Paediatr* 1993;82:71–76.
195. Utens EM, Verhulst FC, Meijboom FJ, et al. Behavioural and emotional problems in children and adolescents with congenital heart disease. *Psychol Med* 1993;23:415–424.
196. Brandhagen DJ, Feldt RH, Williams DE. Long-term psychologic implications of congenital heart disease: a 25-year follow-up [see comments]. *Mayo Clin Proc* 1991;66:474–479.
197. Bromberg JI, Beasley PJ, D'Angelo EJ, et al. Depression and anxiety in adults with congenital heart disease: a pilot study. *Heart Lung* 2003;32:105–110.
198. Horner T, Liberthson R, Jellinek MS. Psychosocial profile of adults with complex congenital heart disease. *Mayo Clin Proc* 2000;75:31–36.
199. Salzer-Muhar U, Herle M, Floquet P, et al. Self-concept in male and female adolescents with congenital heart disease. *Clin Pediatr* 2002;41:17–24.
200. Bennett D. Depression among children with chronic medical problems: a meta-analysis. *J Pediatr Psychol* 1994;19:149–169.
201. Burke P, Elliott M. Depression in pediatric chronic illness. A diathesis-stress model. *Psychosomatics* 1999;40:5–17.
202. Fleming J, Offord D. Epidemiology of childhood depressive disorders: a critical review. *J Am Acad Child Adolesc Psychiatry* 1990;29:571–580.
203. Knapp P, Harris E. Consultation liaison in child psychiatry: a review of the past ten years. Part II: research on treatment approaches and outcome. *J Am Acad Child Adolesc Psychiatry* 1998;37:139–146.
204. Newacheck PW, McManus MA, Fox HB. Prevalence and impact of chronic illness among adolescents. *Am J Dis Child* 1991;145:1367–1373.
205. DeGroot M, Jacobson A, Samson J, et al. Glycemic control and major depression in patients with type I and type II diabetes mellitus. *J Psychosom Res* 1999;46:425–435.
206. Engstrom I. Mental health and psychological functioning in children and adolescents with inflammatory bowel disease: a comparison with children having other chronic illnesses and with healthy children. *J Child Psychol Psychiatry* 1992;33:563–582.
207. Kovacs M, Mukerji P, Drash A, et al. Biomedical and psychiatric risk factors for retinopathy among children with IDDM. *Diabetes Care* 1995;18:1592–1599.
208. Marcus MD, Wing RR, Guare J, et al. Lifetime prevalence of major depression and its effect on treatment outcome in obese type II diabetic patients. *Diabetes Care* 1992;15:25.

Hematologic Aspects of Pediatric and Adolescent Heart Disease: Bleeding, Clotting, and Blood Component Abnormalities

Therese M. Giglia ■ Char Witmer

The cardiovascular system is both the conduit and the propeller of the circulating blood, and as such, a mandatory codependence exists between these two organ systems. As expected, perturbations in one system result in alterations in the other and vice versa. The purpose of this chapter is to describe the cardiovascular effects of hematologic derangements on the normal heart as well as the hematologic problems seen in children and adolescents with congenital and acquired heart disease. The chapter begins with an overview of basic principles of hematology in the developing child and progresses to discussions of abnormalities in individual blood components and bleeding and how each affects the normal heart as well as the heart of the child and adolescent with congenital and acquired heart disease. Since thrombosis is becoming more commonly recognized as a major source of morbidity and at times mortality in children with heart disease, the chapter ends with a detailed discussion of thrombosis in pediatric heart disease including a description of anticoagulants, antiplatelet agents, and thrombolytic therapy commonly used in children with these disorders.

BASIC PRINCIPLES OF HEMATOLOGY

Red Blood Cells

Red blood cells (RBC) are nonnucleated biconcave discs whose major cellular component is hemoglobin (Hb), an oxygen transport protein. Erythropoietin, a hematopoietic growth factor produced in the kidney, is the major regulator of red cell production. A normal red cell life span is approximately 120 days. Normal developmental factors influence Hb values in children including age, gender, and sexual maturity necessitating the need for age-appropriate reference values.

Hb production begins early in gestation and undergoes a series of transitions. Hb is formed by two pairs of identical subunits called globin chains. Fetal erythropoiesis consists of an orderly evolution through a series of different Hbs. All forms of Hb are made up of a combination of two α -like globin proteins (α or ξ) and two β -like globin proteins (β , δ , γ , or ϵ). In the embryo, the predominant Hbs include Gower 1 ($\xi_2\epsilon_2$), Gower 2 ($\alpha_2\epsilon_2$), and Portland ($\xi_2\gamma_2$). In the fetus, there is a transition to fetal Hb ($\alpha_2\gamma_2$). After birth, there is a final switch to adult Hb ($\alpha_2\beta_2$).

At birth, neonates have a mean Hb of 15.9 g/dL (± 1.86) and an elevated mean corpuscular volume (MCV) of 110 fL (± 5) (1). After birth, red cell production quickly decreases likely

secondary to the abrupt increase in oxygen concentration. The half-life of neonatal red cells is shorter (average 23.3 days) than in adults and is even shorter in premature infants (average 16.6 days) (2). The Hb naturally decreases over the first 2 to 3 months of life (physiologic nadir) and then slowly increases in the fourth to sixth month of life. Throughout childhood, there is a mild increase in the mean Hb. In males during puberty, as the Tanner stage increases, the Hb increases. There is no relationship between Hb and Tanner stage in females.

White Blood Cells

White blood cells (WBC) play an integral role in the immune system. There are five types of WBC including neutrophils, eosinophils, basophils, lymphocytes, and macrophages/monocytes. Individual WBC percentages have limited clinical utility; instead, absolute counts should always be considered. The WBC reference range will vary with age. In general, newborns have a higher total WBC (mean 18.1 k/ μ L) that will quickly decrease over the first week of life. Lymphocyte predominance is seen from 2 weeks to approximately 5 years of age, then neutrophils become predominant.

Hemostasis

Platelets are small anucleated cell particles that are made in the bone marrow via fragmentation of megakaryocytes; production is mediated via thrombopoietin. Platelets circulate for approximately 7 to 10 days and are subsequently removed via the reticuloendothelial system. By 18 weeks of gestation, the plasma platelet concentration reaches the adult range of 150 to 450 k/ μ L. At birth, neonates have the same platelet count range and volume as adults. Data regarding platelet function in neonates demonstrate hyporeactivity to some agonists and hyperreactivity to others (1). Platelets play an integral role in hemostasis.

Hemostasis refers to the coordinated process that stops bleeding at the site of vascular injury through the formation of an impermeable platelet and fibrin plug. Hemostasis is achieved through the following three main mechanisms:

- Vascular constriction
- Primary platelet plug formation (primary hemostasis)
- Clot propagation through fibrin formation (secondary hemostasis)

Vascular constriction decreases blood flow at the site of injury. Platelets adhere to the exposed subendothelium, through

von Willebrand factor (vWF) tethering, forming an initial platelet plug. Simultaneously, coagulation is initiated by the exposure of tissue factor. Tissue factor binds and activates FVII that activates the coagulation cascade, resulting in a small thrombin burst. This small thrombin burst stimulates further platelet activation and the activation of coagulation on the platelet surface. On this increased platelet surface, a large amount of thrombin is formed that is sufficient to convert fibrinogen to fibrin leading to stable clot formation. To limit clot formation at the site of injury, activated procoagulant proteins are inhibited by anticoagulant proteins (protein C, S, antithrombin, thrombomodulin, heparin cofactor II, and tissue factor pathway inhibitor). Clot degradation is initiated by the fibrinolytic system (plasminogen, tissue plasminogen activator, and urokinase plasminogen activator). This is a finely balanced system, and a derangement at any level can result in a tendency for bleeding or a prothrombotic state.

In the neonate, these hemostatic processes are in place but in different concentrations than adults. In normal postnatal development, many values normalize by 6 months of age, although changes can still be seen throughout childhood (3,4). Understanding the difference in neonatal values is imperative when interpreting coagulation studies to ensure the correct diagnosis of either a bleeding or clotting disorder. It also has direct implications for the use of specific hemostatic interventions in a neonate (i.e., unfractionated or low molecular weight heparin (LMWH) therapy).

Coagulation proteins do not cross the placenta and are independently synthesized by the fetus; most are present by 10 weeks of gestation and gradually increase with gestational age (5,6). In a neonate, the following procoagulant proteins are decreased including the vitamin K–dependent factors (II, VII, IX, and X) and the contact pathway factors (XI, XII, prekallikrein, and high molecular weight kininogen) (4,6,7). This results in a prolonged prothrombin time (PT) and partial thromboplastin time (PTT) when compared to normal adult values. Conversely, neonates have increased plasma vWF levels and elevated levels of circulating ultra-large von Willebrand multimers (8,9). Similar to the procoagulant factors, the inhibitors of coagulation are also decreased. The anticoagulant proteins including protein C, S, antithrombin, heparin cofactor II, and tissue factor pathway inhibitor are decreased, resulting in a slower rate of thrombin inhibition (4,6,7,10). The fibrinolytic system is also depressed secondary to a unique neonatal glycoform of plasminogen that is inefficiently converted to plasmin (11). Neonates will have markedly elevated D-dimer values at birth lasting up to 3 days (7,10).

HEMATOLOGIC DISORDERS

Special Consideration of Hematologic Disorders in Congenital Heart Disease

Adolescents and children with congenital and acquired heart disease are at increased risk for hematologic abnormalities including red cell anomalies, bleeding, and thrombosis. The following sections discuss individual hematologic disorders describing the effects on the normal heart and in addition paying attention to particular concerns regarding the child and adolescent with congenital heart disease (CHD).

Disorders of Red Blood Cells

Anemia

Anemia is defined as a decrease in Hb that is two standard deviations below the mean value for age. Physiologically, anemia can be divided into three main categories: decreased or ineffective RBC production, increased RBC destruction, or blood loss. The etiology of an anemia can be determined using a morphologic approach based on the red cell MCV. The initial approach to anemia should include a thorough history, physical exam, complete blood count (CBC) with differential, reticulocyte count, and review of the peripheral smear.

The differential for a *microcytic anemia* is rather narrow and includes acquired and congenital causes. The most common acquired cause in pediatrics is iron deficiency. Premature infants are at increased risk for iron deficiency secondary to decreased in utero iron absorption, decreased birth weight, and concurrent anemia. Toddlers commonly have dietary-induced iron deficiency when there is excess milk intake combined with poor solid food intake. The congenital causes for a microcytic anemia include β - or α -thalassemia trait, other forms of thalassemia, sickle cell combined with thalassemia, or anemia of chronic disease. Table 75.1 provides a summary of laboratory values to help differentiate between the common causes of a microcytic anemia. An Hb electrophoresis helps in diagnosing other forms of thalassemia and sickle cell disease (SCD).

A *normocytic anemia* has a much broader differential than a microcytic anemia. Figure 75.1 provides a flow diagram for the approach to a normocytic anemia. The reticulocyte count should be used to further classify the anemia into two broad categories of increased or decreased red cell turnover.

TABLE 75.1 Laboratory Evaluation for a Microcytic Anemia

Test	Iron Deficiency	Anemia of Chronic Disease	α -Thalassemia Trait	β -Thalassemia Trait
Serum ferritin	↓Low	Normal to ↑high	Normal	Normal
Serum iron	↓Low	↓Low	Normal	Normal
TIBC	↑High	↓Low	Normal	Normal
Transferrin saturation	↓Low	↓Low	Normal	Normal
MCV	↓Microcytic	Micro- or normocytic	↓Microcytic	↓Microcytic
RDW	↑Increased	↑Increased	Normal	Normal
Hemoglobin electrophoresis	Normal	Normal	Normal *Hemoglobin Barts on newborn screen	↑Elevated hemoglobin A2 and/or F

TIBC, total iron binding capacity; MCV, mean corpuscular volume; RDW, red cell distribution width.

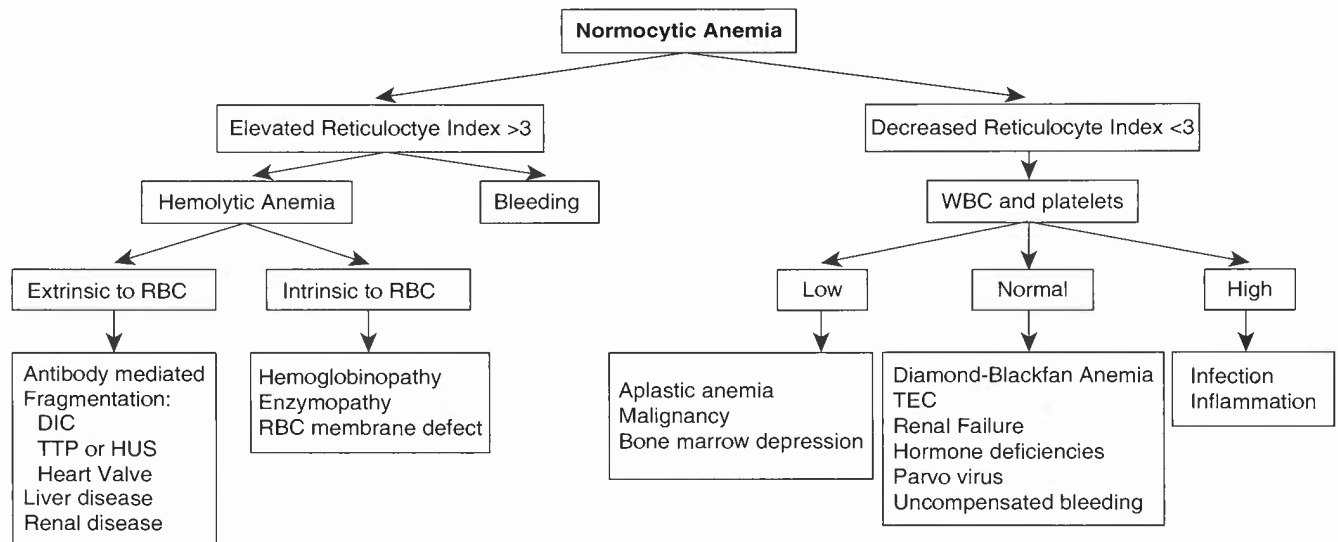


Figure 75.1. The differential for a normocytic anemia.

The reticulocyte count needs to be adjusted for the degree of anemia to determine if it is truly elevated. A reticulocyte index (RI) can be calculated as

$$\frac{\text{Patient's hematocrit}}{\text{Normal hematocrit}} \times \text{Patient's reticulocyte count.}$$

An RI > 3 indicates increased red cell turnover and an RI < 3 indicates decreased red cell turnover. In patients with an elevated RI, it is important to differentiate between bleeding versus red cell destruction (*hemolysis*). Laboratory markers of hemolysis include an increased lactate dehydrogenase (LDH), elevated indirect bilirubin, elevated aspartate aminotransferase (AST) with a concomitant normal alanine transaminase (ALT), or a decreased haptoglobin.

Patients with congenital or acquired are at increased risk for developing an *acquired hemolytic anemia* from an increase in shear forces most commonly seen in patients with prosthetic valves. These patients will develop an anemia with an elevated RI. Review of the peripheral smear will show red cell fragments that will have evidence of intravascular hemolysis with a decreased haptoglobin, increased LDH, and hemoglobinuria. Other markers of hemolysis including indirect bilirubin or AST may or may not be elevated.

Macrocytic anemia is much less common in pediatrics. The differential includes vitamin B₁₂ or folate deficiency, hypothyroidism, bone marrow failure, significant reticulocytosis, liver disease, or medications. Common medications that can increase the MCV include hydroxyurea, zidovudine, or chemotherapeutic agents. In the neonatal period, infants normally have an increased MCV. In Down syndrome, an increased MCV is common in up to two-thirds of patients (12).

Anemia and RBC transfusion in children and adolescents with CHD: Since children and adolescents with cyanotic heart disease have higher Hb levels commensurate with their desaturation and higher than age-matched controls without cyanotic heart disease, assessment of anemia is more challenging. Recognition of this discrepancy is imperative to being able to diagnose anemia in patients with CHD. Paying attention to a particular patient's baseline values and a change over time will be more informative than age-matched normal values.

Children with cyanotic defects are commonly transfused to an Hb >14 g/dL especially postoperatively or during periods of hemodynamic instability to increase their oxygen-carrying

capacity and optimize oxygen delivery. The rationale of this strategy is that a compromised cyanotic patient has limited ability to increase cardiac output to compensate for a low systemic oxygen delivery (13–15). Although a common practice, there is a paucity of data on the optimal Hb concentration and transfusion strategies in these patients. A recent, single-center, prospective, randomized, controlled clinical trial compared a restrictive Hb strategy (mean Hb 11 g/dL, mean RBC transfusions 0.43) to a liberal strategy (mean Hb 13.9 g/dL, mean RBC transfusions 2.1) in children during the first 48 hours after bidirectional cavopulmonary or Fontan operation (16). No differences were found in mean or peak arterial lactate, arteriovenous or arteriocerebral oxygen content, or clinical outcomes. This question warrants further investigation.

Red Blood Cell Disorders with Particular Cardiac Manifestations

SCD and thalassemia are two congenital red cell disorders with well-defined cardiovascular complications. SCD is a group of *inherited hemoglobinopathies* that are the result of abnormal Hb production. It is a multisystem disease characterized by a chronic hemolytic anemia and vaso-occlusive complications resulting in episodes of acute illness and a chronic progression to end-organ damage. SCD is an autosomal recessive condition. The most common form of SCD is homozygous SS. Other variants of SCD are the result of other Hb variants combined with Hb S (i.e., SC, S-β⁰ thalassemia or S-β⁺ thalassemia). More than 100,000 Americans are affected with SCD. The carrier rate in African Americans is approximately 8% (1 in 12).

In Hb S, an amino acid substitution in the β-globin gene from glutamic acid to valine ultimately leads to the polymerization of Hb S molecules, causing the red cell "sickling" effect with resultant vascular occlusion and hemolytic anemia. SCD was once seen as a disease where the morbidity and mortality were directly related to vascular occlusion but it is now evident that chronic hemolysis significantly contributes to the development of endothelial dysfunction and vasculopathy. With intravascular hemolysis, there is a release of free Hb that generates reactive oxygen species that are potent scavengers of nitric oxide (17). There is also a release of arginase that decreases nitric oxide bioavailability. Nitric oxide has several key roles in endothelial function including as a regulator of vasodilator tone and inhibitor of platelet and hemostatic

activation (18–20). SCD confers a state of nitric oxide resistance, and human and animal studies have provided evidence that a reduction in nitric oxide is associated with vasoconstriction, decreased blood flow, platelet activation, and end-organ injury (21).

Cardiac involvement in SCD is quite common and is primarily the result of a chronic anemia with a compensatory increased cardiac output. In general, the heart is usually enlarged and a systolic ejection murmur is found in most patients. Fifty percent of pediatric patients will have electrocardiographic findings of left ventricular (LV) hypertrophy (22). The steady-state blood pressure in patients with SCD is lower than that in age-, race-, and gender-matched controls (23). This finding is likely related to the steady-state anemia as well as renal losses of sodium and water. While vaso-occlusion is a common occurrence in SCD, myocardial infarction is quite rare although infarction of LV papillary muscles with mitral regurgitation has been reported (22,24,25). Autopsy studies show that atherosclerosis is also uncommon in this patient population (24).

Pulmonary hypertension (PH) is a common complication in adult patients with SCD with a reported prevalence of 6% to 32% and has been associated with significant morbidity and mortality (26,27). Studies with a higher prevalence of PH only used echocardiographic assessments of pulmonary artery systolic pressure with a cutoff tricuspid regurgitant (TR) jet velocity of 2.5 m/s. A recent prospective study in adult patients with SCD utilized right heart catheterization to confirm the echocardiographic findings. They reported a prevalence of elevated TR jet velocity of 27% (consistent with prior studies) but right heart catheterization confirmed PH in only 6% of subjects (27). Studies addressing PH in pediatric patients with SCD are limited but have not demonstrated the increased morbidity and mortality seen in adults (28–32). The prevalence of elevated TR velocities is similar in children as in adults; however, the significance of the findings and implications for prognosis remain unclear. Further pediatric studies that follow patients into adulthood are required.

The etiology of PH in patients with SCD is likely multifactorial. Hemolysis is believed to play a key role in the development of PH through endothelial dysfunction. Other chronic hemolytic disorders have an increased incidence of PH including thalassemia, hereditary spherocytosis, and paroxysmal nocturnal hemoglobinuria. Other contributing factors in SCD may include chronic hypoxia, chronic thromboembolism, in situ thrombosis, parenchymal and vascular injury from sequestration of sickled erythrocytes, chronic liver disease, iron overload, and asplenia (33).

Patients with SCD who undergo surgery are at increased risk for morbidity and mortality (34–36). Specific morbidities include acute chest syndrome, SCD, cerebrovascular accidents, and infections. These risks are likely secondary to the underlying anemia from SCD, a propensity for microvasculature occlusion from sickled red cells, and asplenia. Improved outcomes have been reported in patients who received preoperative transfusions to a goal Hb level of 10 g/dL (which decreases the percent S and improves the patient's baseline anemia), hydration, and aggressive intra- and postoperative monitoring (37,38). The patient's hemodynamic status, that is, the effect of volume overload on a left-to-right shunt or ventricular dysfunction, will need to be considered. If a patient with SCD requires cardiac surgery or prolonged sedation for a cardiac procedure, a pediatric hematologist should be involved to work with the cardiologist/intensivist and cardiac anesthesiologist to determine the appropriate pre- and postoperative management.

Thalassemia syndromes are a group of inherited anemias resulting from defects in the production of Hb. Thalassemia is classified according to the globin chain that is underproduced,

either α (α -thalassemia) or β (β -thalassemia) globin. A decrease in the production of either an α - or β -globin chain results in an excess of free globin chains that precipitate in the red cell and cause RBC membrane damage. The end result is anemia from RBC hemolysis and ineffective erythropoiesis in the bone marrow. α -Thalassemia is more commonly found in Southeast Asia, whereas β -thalassemia is more common in Mediterranean countries.

There are two α -globin genes located on chromosome 16. α -Thalassemias are usually the result of gene deletions. The severity of disease is related to the number of gene deletions present. One gene deletion is termed a silent carrier and has no hematologic manifestations. A two-gene deletion is termed α -thalassemia trait; the patient has a mild microcytic hypochromic anemia but is otherwise well with a normal Hb electrophoresis. A three-gene deletion results in Hb H disease. Hb H is composed of tetramers of β -globin. Patients with Hb H disease have a moderate microcytic hemolytic anemia and are not transfusion dependent. The Hb electrophoresis will demonstrate the presence of Hb H. The presence of a four-gene deletion is termed hydrops fetalis and results in severe anemia in the fetus with intrauterine death.

There is one β -globin gene located on chromosome 11. Point mutations are the most common type of genetic mutation in β -thalassemia. β -Thalassemia trait occurs when only one gene is affected, resulting in a mild microcytic anemia. Hb electrophoresis shows increased Hb A2 and/or Hb F levels. In contrast, the inheritance of two affected β -globin genes results in a broad spectrum of clinical disease. Severity is determined by the residual amount of β -globin synthesis. The clinical phenotype ranges from transfusion dependence (β -thalassemia major) to a moderate anemia that does not necessitate chronic transfusions (β -thalassemia intermedia).

Treatment of β -thalassemia major consists of either lifelong chronic red cell transfusions or bone marrow transplant. Chronic red cell transfusions correct the anemia and suppress ineffective erythropoiesis. Transfusions are typically given every 3 to 4 weeks with target nadir Hb of 9 to 10 g/dL. Unfortunately, a direct consequence of chronic transfusions is iron overload with excessive iron deposition in the liver, heart, and endocrine organs.

Currently, heart failure is the most common cause of death in patients with β -thalassemia major. Most of these deaths are attributable to cardiac iron overload (39,40). The most common cardiac abnormality in patients with heart failure from iron overload is a biventricular dilated cardiomyopathy, and severe right ventricular cardiomyopathy is evident in advanced disease (41). Iron deposition is greatest in the ventricular walls and less in the atria and the conduction system. Cardiomyocytes are also sensitive to oxidative damage from non-transferrin-bound iron. Pericarditis was common prior to the use of chelation therapy but appears to be decreasing in frequency (42). Paroxysmal atrial fibrillation is common and is typically associated with myocardial dysfunction; restoration of sinus rhythm does not usually reverse the cardiomyopathy (42). Currently, iron loading in the heart can be measured using MRI T2* technology, >20 ms indicates no significant iron loading, 10 to 19 ms indicates mild-to-moderate iron loading, and <10 ms indicates severe cardiac iron loading (43).

Iron overload is currently treated with chelation. First-line chelators currently in use in the United States include deferoxamine, which is given as a 12-hour infusion intravenously or subcutaneously or deferasirox, an oral medication given once daily. Recently, deferiprone was approved as a second-line oral chelator in the United States. An escalation in chelation therapy is imperative for patients with significant cardiac iron loading. Recent studies have demonstrated that deferiprone in combination with an additional chelator has improved cardiac

iron removal versus monotherapy (44–46). Patients can experience a reversal of the iron-induced cardiomyopathy with intensive chelation (42).

Polycythemia

Polycythemia is defined as an increase in red cell volume, especially the Hb or hematocrit is two standard deviations above the mean value for age. Polycythemia can be classified by the response of erythroid progenitors to cytokines (i.e., erythropoietin) (47). In primary polycythemia, erythroid progenitors exhibit an excessive response to cytokines secondary to an inherited or acquired genetic mutation (i.e., polycythemia vera or erythropoietin receptor mutations). Secondary polycythemia is characterized by a normal response of the erythroid progenitors to elevated levels of cytokines. Secondary polycythemia is usually the result of a physiologic response to chronic hypoxia (i.e., cyanotic CHD or sleep apnea), autonomous erythropoietin production (tumor secretion), or exogenous erythropoietin administration. Rarely, secondary polycythemia can be due to Hb variants with an altered affinity for oxygen or genetic mutations that result in disordered hypoxic sensing.

Disorders of White Blood Cells

Two genetic disorders, Barth Syndrome and 22q11.2 deletion syndrome, have both CHD and white cell disorders. Barth syndrome is an X-linked recessive mitochondrial disorder that is characterized by a dilated cardiomyopathy with endocardial fibroelastosis, skeletal myopathy, growth retardation, neutropenia, and organic aciduria (48,49). It is secondary to mutations in the TAZ gene that is responsible for remodeling the mitochondrial phospholipid: cardiolipin (50). The etiology of neutropenia in Barth syndrome is unclear at this time. Treatment can include granulocyte colony-stimulating factor to prevent severe neutropenia. Chromosome 22q11.2 deletion syndrome encompasses a heterogeneous group of disorders. The most common phenotypic features include conotruncal cardiac malformations, immunologic dysfunction, developmental delay, and palate deformities (51). Immunologic dysfunction is the result of thymic aplasia or hypoplasia resulting in a variable T-cell deficiency with a resultant increase in infections and autoimmune disease (52). Decreased regulatory T cells may play a role in the increased incidence of autoimmune disorders (52,53). Autoimmune disease can include acquired cytopenias (54,55).

Disorders of Hemostasis Associated with Bleeding

Hemostatic derangements complicated with bleeding are very common in pediatric patients with CHD. The holy grail of hemostatic testing would be one test that is rapidly available and adequately reports on all components of hemostasis. Unfortunately, this test does not exist, leaving clinicians with a series of coagulation tests that reflect various aspects of hemostasis.

Hemostatic testing: The PT and PTT serve as screening tests for procoagulant factor deficiencies. The PT and PTT do not provide a global picture of hemostasis. Proper specimen handling is imperative for coagulation assays. Heparin contamination of a specimen is the most common reason for a prolonged PTT in a hospitalized patient. Heparinase can be used to remove heparin from a specimen. Coagulation assays are also sensitive to the plasma-to-citrate ratio in the specimen tube. Underfilling of the specimen tube will falsely prolong the coagulation assays. Patients with significant polycythemia (hematocrit > 55%) can also have an altered plasma-to-citrate

ratio and will have falsely prolonged coagulation assays. A special specimen tube with a decreased amount of citrate should be used for patients with significant polycythemia. This is of particular concern when using the prothrombin time/international normalized ratio (PT/INR) to adjust warfarin dosing in cyanotic/polycythemic patients. Factor deficiencies that can cause an isolated prolonged PTT include either a deficiency in factor VIII, IX, XI, XII, prekallikrein or high molecular weight kininogen. An isolated prolonged PT is secondary to factor VII deficiency. Prolongation in both the PT and PTT can be seen in the setting of factor II, V, X, or fibrinogen deficiency.

For monitoring unfractionated heparin (uFH) therapy, the PTT is commonly used as a surrogate marker of heparin activity. For therapeutic heparin, the PTT is titrated to 1.5 to 3 times control. There are limitations to the PTT, especially it is affected by variables other than heparin including an elevated factor VIII, fibrinogen, or a Lupus anticoagulant. For example, when the FVIII level is >250%, the PTT is significantly shortened and will no longer reflect the heparin effect. (Factor VIII is an acute phase reactant and can be elevated in inflammatory states.) For a direct measure of heparin activity, the uFH anti-Xa level can be used with a recommended therapeutic range of 0.35 to 0.7 U/mL (note this is different from the LMWH anti-Xa-recommended therapeutic range of 0.5 to 1 U/mL).

The **activated clotting time (ACT)** is used to monitor higher heparin doses given to patients undergoing cardiac surgery with cardiopulmonary bypass (CPB), cardiac catheterization, or extracorporeal membrane oxygenation (ECMO). The ACT is a whole blood clotting time that is simple to perform with a rapid turnaround time. It is more sensitive to a wider range of heparin doses than the PTT. The limitations to this assay are that it is imprecise, proper specimen handling and timing are imperative, it is affected by the same variables that can prolong the PTT assay, and it is affected by the platelet count.

Fibrinogen is the final procoagulant protein in the coagulation pathway. It is converted by thrombin into fibrin. Fibrin is then cross-linked by factor XIII to make a stable clot. In the setting of a bleeding patient, it is imperative that the fibrinogen level is maximized to ensure adequate hemostasis. The **thrombin time** measures the conversion of fibrinogen to fibrin and is affected by quantitative or qualitative abnormalities of fibrinogen, the presence of thrombin inhibitors, and fibrinogen degradation products. Heparin contamination of the specimen can prolong the thrombin time.

For an assessment of primary hemostasis, a **platelet count** indicates the number of platelets that are available but does not provide any information regarding platelet function. At this time, there is a limited availability to rapidly assess platelet function. The **bleeding time** assesses platelet and capillary function but this technique is patient and operator dependent and has fallen out of favor (56). It is insensitive to mild platelet defects and does not consistently predict a bleeding tendency (57). The **platelet function analyzer (PFA-100)** is an in vitro screen for platelet function (57). The PFA-100 is prolonged in the setting of anemia or thrombocytopenia and is insensitive to mild platelet aggregation defects; it has also fallen out of favor as a screening test.

Thromboelastography (TEG) is a whole blood point-of-care assay that provides a real-time graph of clot formation and stability. Values measured include *R* (time necessary for initial clot formation), *K* (clot kinetics), α (rate of clot formation), maximum amplitude (maximum strength of the clot), and A-60 to maximum amplitude ratio (fibrinolysis). TEG has been utilized in pediatric CPB and in patients with LV assist devices (58–60).

Platelet mapping assay is a modification of the standard TEG and is used clinically to assess the effectiveness of antiplatelet medications. This assay utilizes whole blood that is heparinized to suppress thrombin generation, then known

platelet agonists are added to the sample to assess platelet activation. This assay is currently utilized most commonly in patients with a LV heart device to monitor antiplatelet therapy.

Acquired von Willebrand Disease

There is an increasing awareness of acquired von Willebrand disease (vWD) in patients with cardiovascular disorders. vWF is a procoagulant protein that has two important roles in hemostasis: it facilitates the binding of platelets to the site of vascular injury and it is the carrier protein for the coagulant protein FVIII. vWF is initially secreted as a large multimeric protein that is further proteolyzed by ADAMTS-13 into variable sizes of multimers. The distribution in the size of these multimers is imperative for hemostatic balance. For example, a bleeding tendency is seen with decreased vWF multimer size and a prothrombotic tendency is found when there is a persistence of ultra-large vWF multimers.

Most of the data on acquired vWD have focused on patients with aortic stenosis and with LV assist devices (61,62). There have been reports in neonates with patent ductus arteriosus, endocarditis, dysfunctional valve prosthesis, septal defects, and mitral valve prolapse (63,64). The pathophysiology of acquired vWD in cardiovascular disorders is likely multifactorial but thought to be secondary to lesions that result in increased shear stress. Increased shear stress results in the mechanical destruction of the larger vWF multimers and causes platelet activation that leads to the absorption of larger vWF multimers. Clinically, these patients will experience an increase in mucocutaneous bleeding and they could be at increased risk of hemorrhage with surgical procedures.

Laboratory findings in patients with cardiovascular disorders and acquired vWD reveal an abnormal multimer vWF distribution with a specific loss of the high molecular weight multimers. Commonly, the vWF antigen and activity are normal to increased. Routine coagulation testing PT/INR, PTT, and platelet count will be normal. Definitive treatment of acquired vWD would be to correct the underlying cardiac abnormality but this may not always be plausible (65). Other treatment modalities would include desmopressin (DDAVP) that facilitates the release of endogenous stores vWF, although the response rate is low (10%) in this setting (64). An alternative therapy would be the use of plasma-derived vWF replacement product (64,66). Treatment would only be necessary to treat active bleeding that does not resolve with local measures or prior to a significant hemostatic challenge to prevent excessive bleeding.

Platelet Disorders

Platelet disorders are either inherited or acquired. Congenital platelet disorders are very rare in the general population. Bernard-Soulier syndrome, a congenital platelet disorder, should be considered when caring for patients with 22q11.2 deletion syndrome. Bernard-Soulier syndrome is an autosomal recessive platelet disorder. The mutation is in the platelet GP 1b/IX complex that binds platelets to vWF. Children with 22q11.2 deletion syndrome can be heterozygotes for the Bernard-Soulier mutation given the proximity of the gene encoding the GP 1b/IX complex (67). Heterozygotes for this condition are clinically normal but may have mild thrombocytopenia and minor platelet function abnormalities (67). Patient with 22q11.2 deletion syndromes also have an increased prevalence of immune thrombocytopenia (ITP) (68,69).

In patients with cyanotic CHD, there is an inverse relationship between the platelet count and the degree of cyanosis. The lower the systemic arterial oxygen saturation, the higher will be the compensatory polycythemia. These physiologic changes are associated with a lower platelet count (70,71). Typically,

the thrombocytopenia is not severe and the platelet count will be $>50,000/\mu\text{L}$. The thrombocytopenia can improve with phlebotomy especially when the hematocrit is $>65\%$ (72). The etiology of thrombocytopenia in cyanotic CHD with polycythemia is unclear at this time.

Drug exposure is a common reason for acquired platelet dysfunction or thrombocytopenia. Antiplatelet medications are commonly used in patients with CHD to prevent thrombotic complications; these are discussed below. Numerous drugs have been implicated in causing thrombocytopenia. The more commonly used drugs include antibiotics (penicillins, or sulfa-containing antibiotics), antiepileptics (phenytoin, valproate, carbamazepine), H₂ agonists (cimetidine or ranitidine), thiazide diuretics, and furosemide. In general, thrombocytopenia will resolve with removal of the offending drug. A special circumstance of drug-induced thrombocytopenia is heparin-induced thrombocytopenia (HIT).

HEPARIN-INDUCED THROMBOCYTOPENIA

HIT is the result of antibodies that are formed against the heparin-PF4 complex that exists on platelets (73). It is proposed that the binding of antibodies to this platelet complex results in increased platelet reactivity and thus a prothrombotic state (73). This disorder is characterized by thrombocytopenia and resultant arterial and/or venous thrombosis that can be catastrophic. In adults, the prevalence of HIT is estimated to be 1% to 5% of patients exposed to heparin and untreated HIT has a mortality of 20% to 30% (74). The incidence of HIT in the pediatric population is not clearly defined but appears to be less than adults with a reported range of 0% to 2.3% (75–78). Higher risk pediatric groups include patients undergoing CPB (79).

The diagnosis of HIT is based on clinical criteria. Multiple scoring systems have been developed and validated in adults but not in pediatric patients (80–82). Classically, HIT is characterized by symptoms appearing 5 to 10 days post-heparin exposure with a 50% fall in the platelet count (rarely is the platelet count $<50,000/\mu\text{L}$) and there can be venous or arterial thrombosis. Laboratory testing can be supportive in making the diagnosis and includes ELISA for the heparin-P4 antibodies and the serotonin-releasing assay. The ELISA are readily available with a fast turnaround time. This test is highly sensitive but has a significant false positive rate. The ELISA is most helpful in ruling out the diagnosis with a negative assay. The serotonin-releasing assay is highly specific and sensitive; it measures platelet reactivity in the presence of the patient's plasma. Unfortunately, it is only performed in a few highly specialized laboratories so is not readily available for most clinicians.

The treatment of HIT includes the removal of all heparin from the patient including avoidance of LMWH. Anticoagulation should be initiated with a non-heparin anticoagulant such as a direct thrombin inhibitor (i.e., bivalirudin or argatroban). In this setting, warfarin should never be initiated by itself due to an increased risk of skin necrosis and further thrombotic events. Warfarin can be initiated once the platelet count has normalized and overlapped with the nonheparin anticoagulant until the INR is therapeutic.

Additional causes of acquired thrombocytopenia in pediatric patients with CHD include sequestration and consumptive causes. The spleen normally contains 30% of the platelet mass, and in the setting of an enlarged spleen, it can trap a larger portion of platelets with resultant thrombocytopenia. In patients with CHD, specific consumptive causes of thrombocytopenia include CPB and artificial heart valves or grafts. Other causes of consumption not necessarily specific to patients with CHD include the use of ECMO, the presence of disseminated intravascular coagulation, thrombotic thrombocytopenic purpura,

hemolytic uremic syndrome, hemophagocytic lymphocytic histiocytosis, HIV, or immune destruction of platelets.

IMMUNE THROMBOCYTOPENIA

ITP is an immune-mediated destruction of platelets generated by the presence of IgG autoantibodies. These antibodies coat the surface of the platelets and these platelets are cleared through the Fc γ receptors in the spleen. In childhood, ITP is considered a benign self-limited disorder; 80% of patients spontaneously resolve within 6 months with only a small percentage (<20%) developing chronic ITP. Treatment can include observation combined with thrombocytopenic precautions or the use of immune-modulating therapies like immune globulin or steroids. In the neonate, immune destruction of platelets can be secondary to a mismatch between the fetal and maternal platelets, termed neonatal alloimmune thrombocytopenia. The mother develops antibodies against antigens on the fetal platelet surface that were inherited from the father. These antibodies cross in the placenta, coat the fetal platelets, and result in significant thrombocytopenia. Thrombocytopenia can also be the result of decreased production that can be found in aplastic anemia, myelodysplastic syndrome, infiltrative marrow processes (i.e., leukemia), or nutritional deficiency states.

THROMBOCYTOSIS

Thrombocytosis is defined as an increase in the platelet count that is two standard deviations above the mean value for age. Thrombocytosis can be primary or secondary. Primary causes include myeloproliferative disorders that are either inherited (essential thrombocythemia) or acquired (polycythemia vera, leukemia, or myelodysplastic syndrome). Secondary causes are the result of underlying inflammation (infection, rheumatologic disorders, or inflammatory bowel disease), hematologic disorders (hemolytic anemia or iron deficiency), drugs (vinca alkaloids or corticosteroids), or decreased splenic pooling in the setting of asplenia.

CPB, ECMO, and Ventricular Assist Devices

Postoperative Bleeding after CPB

Postoperative bleeding is a common complication in pediatric patients undergoing CPB and is associated with increased morbidity and mortality (83,84). CPB is a nonphysiologic state and the passage of blood through the artificial circuit results in the activation of the coagulation, fibrinolytic, and inflammatory systems. The coagulation system is activated through the contact pathway and ultimately results in the formation of fibrin. With fibrin deposition within the CPB circuit, there is platelet adherence and activation. Prematurely activated platelets are no longer available for hemostasis.

Post-CPB bleeding is more common in pediatric patients than in adults. Clinical factors associated with postoperative bleeding include younger age (<1 year), lower weight (<8 kg), cyanosis, prolonged circuit, and deep hypothermia times (85–87). One major contributing factor is the degree of hemodilution that occurs in pediatric patients with the institution of cardiac bypass. This is secondary to the large discrepancy between a pediatric patient's blood volume and the circuit volume. An adult patient experiences approximately 25% hemodilution with the institution of bypass, while a pediatric patient can experience up to 60% of hemodilution (88). This dilution is further exacerbated by developmental hemostasis in neonates who, at baseline, already have lower procoagulant and anticoagulant proteins (4).

To prevent postoperative CPB bleeding, multiple approaches have been utilized including adequate anticoagulation during CPB, modified ultrafiltration, adequate reversal of

anticoagulation post-CPB, transfusion of blood components, and antifibrinolytics (88). High-dose heparin is used during CPB to prevent thrombosis of the circuit. Heparin exerts its anticoagulant effect through the binding of antithrombin. Neonates developmentally have lower antithrombin levels that can contribute to a variable heparin effect. There are also significant issues with monitoring heparin therapy during CPB in pediatric patients. It has been shown in children that the ACT values do not correlate with heparin levels. Specifically, the ACT overestimates the heparin effect because it is prolonged by other variables including hemodilution and hypothermia (88–90). Adequate reversal of heparin with protamine is dependent on knowing the correct heparin concentration. Too little protamine means heparin is still circulating or excessive unbound protamine has anticoagulant properties (91,92). Hyperfibrinolysis is also an important mechanism that leads to post-CPB bleeding (93,94). All three antifibrinolytic therapies (aprotinin, tranexamic acid, and aminocaproic acid) have been shown to decrease post-CPB hemorrhage (95). Aprotinin was removed from the US market in 2008 because of its association with renal failure and death in adult recipients (95,96). Despite the use of these therapies, hemorrhage following CPB remains a frequent occurrence.

MANAGEMENT OF POSTOPERATIVE BLEEDING

Although some bleeding from indwelling mediastinal drains is expected after cardiac surgery, the rate of bleeding should decrease as each postoperative hour goes by. Excessive bleeding is a clinical concern that warrants immediate attention and constant vigilance. In the immediate postoperative period, bleeding of <5 mL/kg/h is often associated with minor abnormalities in coagulation status. Red cell transfusion may be necessary to correct a postoperative anemia but blood component administration is rarely necessary. Bleeding 5 to 10 mL/kg/h should prompt notification of the cardiothoracic surgeon and continued evaluation of the patient at the bedside. Any abnormalities in coagulation parameters should be corrected. Blood loss must be balanced by RBC transfusion. The patient must be closely monitored for persistence or an increase in the rate of bleeding that may signal the presence of a surgical bleeding site or may be the result of loss of coagulation factors secondary to the ongoing hemorrhage. Bleeding of >10 mL/kg/h that persists or increases will likely result in hemodynamic compromise if not abated. The cardiothoracic surgeon should decide whether reexploration is needed to exclude a bleeding site or to remove thrombus that may be perpetuating further bleeding. The cardiac intensivist must exclude concomitant hemothorax and/or hemothorax (often heralded by tachycardia, hypotension, desaturation, and/or tamponade physiology) while keeping up with the blood loss (RBC transfusion) and coagulopathy (blood component replacement). Even when the decision is made to go back to the operating room, the bedside medical team must continue to be vigilant with RBC, volume, and blood component replacement as indicated by hemodynamic parameters and laboratory data.

Recombinant factor VIIa (rFVIIa, eptacog alfa (activated), NovoSeven, Novo Nordisk Pharmaceuticals Inc., Princeton, NJ) is currently utilized as an off-label hemostatic agent in the management of postoperative CPB bleeding. It is an analogue of the naturally occurring procoagulant factor VII and induces hemostasis by binding to exposed tissue factor at the site of endothelial injury and stimulating thrombin formation (97,98). Current studies indicate that children and adults with cardiovascular disease account for a large proportion of off-label rFVIIa use (99,100).

There are concerns regarding the thrombotic potential of rFVIIa and this concern is further heightened in pediatric patients with CHD because of a known increased incidence of thrombosis (101). Current evidence to support

off-label use of rFVIIa in CPB in children is limited. Only one pediatric randomized clinical trial of rFVIIa in CPB has been conducted and it was found that there was no benefit to the prophylactic use of rFVIIa among 82 infants undergoing surgery for correction of CHD (102). The primary end point, time to chest closure, was actually prolonged in the treatment group. No difference was noted in the secondary end points of surgical blood loss or use of blood products (102). A recent systematic review regarding the off-label use of rFVIIa in pediatric cardiac surgery reviewed 29 studies that included a total of 169 patients (103). The authors concluded that there is no supporting evidence to use rFVIIa prior to cardiac surgery to prevent bleeding. Randomized clinical trials should be performed that utilize appropriate clinical outcomes to address the use of rFVIIa to treat bleeding after cardiac surgery. Therapeutic options for postoperative bleeding are listed in Table 75.2.

ECMO and Ventricular Assist Devices

Patients on ECMO or who have ventricular assist devices are at increased risk for both bleeding and thrombotic complications. Similar to CPB, both processes have the passage of blood through an artificial circuit resulting in activation of coagulation. Anticoagulation remains the mainstay to prevent thrombotic outcomes. In ECMO, uFH is commonly used for anticoagulation. In patients with a ventricular assist device, one type of anticoagulation (uFH, LMWH, or warfarin) is combined with antiplatelet therapy.

Thrombosis

Thrombosis in Children and Adolescents with Congenital and Acquired Heart Disease

Thrombosis has long been recognized as a clinical problem to the clinician caring for adolescents and children with congenital and acquired heart disease. Much work has focused on the diagnosis, treatment, and prevention of thromboses in Kawasaki disease (104–107) and to a lesser extent on the thrombotic complications associated with cardiac catheterization (108–111) or cardiomyopathies (112,113). The prevention and management of thromboses related to prosthetic valves (114), arrhythmias (115,116), and PH (117,118) in children has largely been extrapolated from the adult literature. For the past decade, the single ventricle population has been identified as a particularly high-risk population for thrombosis and their potentially devastating sequelae (119–128).

Overall, there is a paucity of information on the true scope of thrombotic complications in children and adolescents with heart disease. Two retrospective studies reviewed thrombotic incidence and risk factors in cardiovascular surgical populations. Early limited work by Giglia et al. in 2001 (129) reported a 3.6% incidence of clinically evident thrombi from a survey of pediatric cardiovascular patients over a 9-year period (1,940 total operations). Mean time from operation was 2.6 months; mean time from operation was 21 days. Deep venous thromboses associated with indwelling central lines were the most common. Of those with thrombi, 20.8% were felt to have died as a direct result of the thrombus. In 43.4%, the diagnosis was felt to have been delayed, and in 17.0%, it was not made until autopsy. A recent retrospective review by Manlhiot et al. (130) of 1,542 pediatric cardiothoracic operations at a single center reported an 11% incidence of clinically evident as well as silent thrombi identified by testing ordered by the attending physician. Factors associated with increased odds of thrombi were age <31 days, baseline oxygen saturation <85%, previous thrombosis, heart transplantation, use of deep hypothermic circulatory arrest, longer cumulative time

with central lines, and postoperative use of ECMO. Serious complications occurred in 28% of patients with thrombi and were associated with thrombus location (intrathoracic, the highest risk), symptoms, and partial/full occlusion. Thrombosis was associated with a longer ICU and hospital stay, and a higher odds ratio of cardiac arrest, catheter reintervention, reoperation, and mortality. Much work is still needed in the area of diagnosis and treatment and most importantly in defining risk factors so that these potential life-threatening complications can be prevented.

The Propensity for Thrombosis in Adolescents and Children with Congenital and Acquired Heart Disease

Congenital and acquired heart disease put adolescents and children at risk for thrombosis mainly because the triad of risk factors for thrombosis initially described by Virchow (131) in 1856 is often at play. These factors are (a) stasis of blood flow, (b) hypercoagulability, and (c) endothelial injury. However, the risk for thrombosis in pediatric heart disease warrants an expansion of Virchow's triad. Turbulent blood flow across abnormal cardiac structures, that is, stenotic valves, can lead directly to platelet activation (132), making "altered blood flow" more applicable to pediatric heart disease than "static blood flow" alone. In addition, advances in cardiothoracic surgery have introduced CPB, which is well associated with thrombotic risks, as well as the use of other nonendothelial surfaces, such as prosthetic valves, graft materials, and indwelling catheters, that are in and of themselves thrombogenic. Also, recent work has found children with CHD to have a higher incidence of coagulation abnormalities than children without CHD; this includes children with acyanotic heart disease as well as the more widely studied single ventricle population (121,122,125,126,133–138). Therefore, risk factors for thrombus in adolescents and children with heart disease should be expanded to include:

1. Hypercoagulability:

Coagulation abnormalities have been identified to include altered coagulation protein levels, decrease endogenous inhibitors of coagulation, and decreased fibrinolytic proteins among others. Such coagulopathies were first identified in children and adolescents with a Fontan circulation but more recently have been found in children through all stages of single-ventricle palliation and also in children with acyanotic and acquired heart disease (121,122,125,126,133–138). Table 75.3 lists the thrombophilia evaluation. The thrombophilia evaluation can assist the clinician in determining a patient's recurrent risk for thrombosis and the appropriate duration of therapy.

2. Altered blood flow

- a. **Stasis:** may occur in dilated heart chambers as well as in dilated native or prosthetic outflow tracts. These areas of stasis serve as a nidus for thrombus formation.
- b. **Turbulent flow:** is a flow across stenotic native or prosthetic heart valves, stents, and/or obstructed outflow tracts with increased sheer stress that can result in platelet activation independent of endothelial damage (139).
- c. **Endothelial disruption:** occurs from turbulent flow on endothelial surfaces as well as vessel wall endothelial damage from insertion and persistence of central lines and catheters. Endothelial injury, as discussed previously, exposes tissue factor and subendothelial collagen-stimulating platelet aggregation and coagulation at the site of injury. Note, platelets can also be activated by other mechanisms in addition to endothelial injury such as from cytokines release during inflammation (139–141).

TABLE 75.2 Therapeutic Options for Postoperative Bleeding

Product	Mechanism	Dose	Indication	Side Effects
Fresh frozen plasma	Contains all clotting, anticoagulant, and fibrinolytic proteins	10–15 mL/kg	Bleeding associated with a coagulopathy (multiple factor deficiencies)	Allergic reaction Fever Volume overload TRALI (rare)
Cryoprecipitate	Fibrinogen (Also contains factor VIII, vWF, and factor XIII)	1–2 U (bags)/10 kg	Bleeding associated with a fibrinogen deficiency	Allergic reaction Fever TRALI (rare)
Platelets	Platelets	<35 kg 10 mL/kg >35 kg 1 SDP (with a maximum volume of 15 mL/kg)	Bleeding from thrombocytopenia	Allergic reaction Fever Volume overload TRALI (rare)
Aminocaproic acid	Synthetic lysine analogue that inhibits plasmin. Prevents fibrinolysis	100 mg/kg Q6 hours (maximum daily dose 30 g)	Bleeding associated with excessive fibrinolysis	Nausea/emesis Abdominal pain Dizziness Thrombosis
DDAVP **Off-label use**	Synthetic analogue of DDAVP, increases factor VIII and vWF levels and activates platelets	0.3 µg/kg q12 hours <i>Tachyphylaxis (no longer has a hemostatic effect) after 3–4 doses</i>	Severe bleeding resistant to maximized component therapy. <i>Suggest a hematology consult</i>	Hypotension tachycardia Free water retention with an associated risk of hyponatremia Thrombosis
Prothrombin complex concentrates (PCC) **Off-label use**	Contains factors II, VII, IX, and X (some PCCs also contain protein C and S)	No RCTs in this setting to guide dosing 20–25 IU/kg	Severe bleeding resistant to maximized component therapy. <i>Suggest a hematology consult</i>	Plasma-derived product Allergic reaction Thrombosis
rFVIIa **Off-label use**	Analogue of the naturally occurring procoagulant factor VII. Induces hemostasis by binding to exposed tissue factor at the site of endothelial injury and stimulating thrombin formation	No RCTs in this clinical setting to guide dosing. Wide dose ranges have been reported (17–200 µg/kg) Lower doses are advisable 40–60 µg/kg	Severe bleeding resistant to component therapy. *Suggest a hematology consult	Allergic reaction Thrombosis

SDP, single donor, apheresis platelet product; RCT, randomized clinical trials; TRALI, Transfusion-related acute lung injury.

TABLE 75.3 The Thrombophilia Evaluation**Protein C deficiency****Protein S deficiency****Antithrombin deficiency****Factor V Leiden Gene mutation****Prothrombin gene mutation****Lipoprotein (a)****Homocysteine****Factor VIII****Evaluation for the presence of antiphospholipid antibodies:***Dilute Russel viper venom time (DRVVT)**Anti-beta-2glycoprotein antibodies (immunoglobulin G and M)**Anticardiolipin antibodies (immunoglobulin G and M)*

d. **Prosthetic materials:** may result in turbulent flow that activates platelets. Activated platelets will adhere to these “abnormal” artificial vascular surfaces, that is, ECMO surface, prosthetic valves, and intravascular stents. Again activated platelets and an abnormal vascular service may result in pathologic thrombus (125–127,142).

- **Mechanical support:** including CPB, ECMO, and ventricular assist devices have thrombotic risk potential despite systemic anticoagulation. The procoagulant state may extend beyond the time of decannulation (143). Interestingly, all of the above-mentioned risk factors including coagulation abnormalities, altered blood flow, endothelial damage, and abnormal vascular surfaces are operative.

3. Inflammation and bloodstream infection:

Tissue factor has been documented to become accessible via activated monocytes or endothelial cells when stimulated by sepsis or through cytokine production during inflammation (140,142). In recent clinical studies, sepsis was associated with increased thrombus formation especially in the presence of an indwelling central venous catheter (144–146).

Consequence of Significant Thrombi in Adolescents and Children with Cyanotic Heart Disease

Adolescents and children with cyanotic heart disease are at particular risk of devastating complications from both venous as well as arterial thrombi. Whereas stroke, limb compromise, and pulmonary emboli are the major risks in patients with separated circulations, patients with CHD have additional life-threatening risks, namely the following:

1. Occlusion of systemic-to-pulmonary shunts or Fontan circuits are both lethal without immediate intervention.
2. Postcatheterization arterial or venous thrombotic occlusions may make performance of further essential diagnostic and/or therapeutic cardiac catheterizations difficult to impossible.
3. Occlusion of large veins of the upper body may make it impossible for a single-ventricle patient to go on to a bidirectional cavopulmonary anastomosis or to a Fontan palliation, rendering transplant the only long-term option.

Common Thrombotic Complications in Congenital Heart Disease

Table 75.4 lists the commonly used antiplatelet, anticoagulant, and thrombolytic therapies and includes mechanisms of actions, pharmacokinetics, dosing, monitoring, and reversal.

EARLY POSTOPERATIVE THROMBOSES

Patients in the early postoperative period may be at particular risk for thrombotic events secondary to effects of CPB (see discussion), use of indwelling central lines, immobilization, pleural effusions, low cardiac output, and/or intravascular depletion. There is evidence that sepsis may further increase the thrombotic risk (144,145).

The presentation of perioperative thrombi may be insidious, for example, low-grade fever and/or thrombocytopenia from platelet consumption in the thrombus. The diagnosis may be equally elusive since thrombi may be missed by routine imaging (echocardiography or ultrasound) unless there is a high degree of suspicion and vigilance in imaging. Areas notorious for difficult-to-image thrombi are Fontan baffles/conduits and right ventricular outflow tract patches/conduits, both of which are often seated anteriorly, limiting noninvasive imaging.

Although, to date, there are no established guidelines to minimize the risk of early postoperative thrombi, it appears prudent to

- recognize the potential triggers of thrombosis (younger age, baseline oxygen saturation <85%, previous thrombosis, heart transplantation, use of deep hypothermic circulatory arrest, longer cumulative time with central lines, postoperative use of ECMO, immobilization, pleural effusions, low cardiac output, intravascular depletion, polycythemia, or sepsis)
- minimize these risk factors whenever possible (i.e., assess the need for central lines daily and removal central lines as early as possible, avoid intravascular depletion)
- recognize the signs of perioperative thromboses (limb edema, ascites, pleural effusions, superior vena cava [SVC] syndrome, unexplained desaturation, i.e., from pulmonary emboli)
- always be suspicious of thrombi in high-risk patients and proceed to imaging studies as clinically indicated.

The efficacy of prophylactic heparin to prevent central venous line (CVL)-associated thrombi in children has not been established. The PROTEKT trial (147) did not find a benefit to using LMWH in preventing CVL-associated thrombi in a general pediatric population. More recently, low-dose, continuous infusion of uFH was not protective in infants after cardiac surgery (148). It is unclear, however, whether subgroups exist where such prophylaxis may be beneficial (i.e., CVL in the SVC or inferior vena cava [IVC] in children who anticipate a cavopulmonary anastomosis procedure in the future, children with CVL and concomitant bacteremia, or children with prior thrombi or other hypercoagulable risk factors).

SINGLE VENTRICLE POPULATION

Children at each stage of single-ventricle palliation are potentially at increased risk for thrombotic complications.

Aortopulmonary Shunts Thrombosis: Prevention and Treatment

An aortopulmonary shunt is often required in infants with cyanotic CHD either as palliation to a two-ventricle repair (i.e., in Tetralogy of Fallot) or as part of a staged single-ventricle palliation as in the Norwood procedure for hypoplastic left heart syndrome. Risk factors for shunt thrombosis include dehydration, pleural effusions, shunt distortion, and

TABLE 75.4 Common Antiplatelet, Anticoagulant, and Thrombolytic Therapies Utilized in Pediatric Patients with CHD

Drug Name	Mechanism of Action	Pharmacokinetics	Dosing	Therapeutic Monitoring	Reversal
ASA	Irreversibly acetylates cyclo-oxygenase impairing platelet prostaglandin metabolism and synthesis of thromboxane	Half-life 15–20 min Rapidly absorbed in proximal GI tract. Platelet inhibition achieved in 60 min	Low dose: 1–5 mg/kg/d	None	Platelet transfusion
Dipyridamole	Inhibits phosphodiesterase enzymes that break down cAMP and block the platelet uptake of adenosine	Half-life 10 h Elimination primarily through biliary excretion	2–5 mg/kg divided every 6–8 h	None	Platelet transfusion
Clopidogrel	Irreversibly inhibits ADP-induced platelet aggregation	Half-life 8 h Requires hepatic activation Platelet inhibition within 2 h of oral dose	0.2 mg/kg/d	None	Platelet transfusion
uFH	Binds to antithrombin and potentiates anticoagulant activity 1,000-fold. The heparin/AT complex inactivates factors IIa (thrombin), Xa, XIa, and XIIa	Half-life 0.5–2.5 h	Age <12 mo Bolus 75 U/kg 28 U/kg/h Age > 1 y–12 y Bolus 75 U/kg 20 U/kg/h Age >12 y Bolus 80 U/kg 18 U/kg/h	Titrate dose by PTT or anti-Xa level PTT: 1.5–3 times control uFH anti-Xa level: 0.35–0.7 U/mL	Protamine sulfate
LMWH (i.e., enoxaparin)	Binds to AT and potentiates anticoagulant activity. Same inhibition as uFH but has a reduced inhibitory activity against factor IIa (thrombin) relative to factor Xa	Half-life 3–6 h Renal clearance	Enoxaparin dosing Age <2 mo 1.5 mg/kg q12 h Age >2 mo 1 mg/kg q12 h	Titrate dose by LMWH anti-Xa peak level: 0.5–1 U/mL (drawn 4 h after the second or third dose)	Protamine sulfate (only a partial reversal, 70%)
Bivalirudin	Inhibition of factor IIa (thrombin) by reversibly binding the active catalytic and substrate binding site	Half-life 25 min Renal clearance is 20%	Bolus: 0.125 mg/kg Maintenance: 0.125 mg/kg/h	Titrate dose by PTT PTT: 1.5–3 times control	None
Argatroban	Inhibition of factor IIa (thrombin) by reversibly binding the active catalytic site	Half-life 45 min Metabolized in liver	0.75–1 µg/kg/min	Titrate dose by PTT PTT: 1.5–3 times control	None
Warfarin	Interferes with the cyclic conversion of vitamin K through the inhibition of vitamin K epoxide reductase. There is a resultant decrease in the posttranslational γ-carboxylation of vitamin K–dependent clotting factors II, VII, IX, and X as well as anticoagulant protein C and S	Half-life 20–60 h	No loading dose: Age 2–10 y 0.09 mg/kg/d Age >12 y 0.08 mg/kg/d	Titrate dose by INR INR: 2.0–3.0	Vitamin K Fresh frozen plasma
Tissue plasminogen activator (tPA)	Converts plasminogen to plasmin. Plasmin cleaves fibrin leading to clot dissolution	Half-life 5 min	Systemic thrombolysis: Low dose: 0.03–0.06 mg/kg/h (max 2 mg/h) High dose: 0.1–0.6 mg/kg/h (max 50 mg/h) <i>Reassess at 6 h</i>	Monitor closely for bleeding. Follow CBC, PT, PTT, fibrinogen, D-dimer every 4–8 h while on the infusion An elevated D-dimer and drop in fibrinogen is indicative of a lytic state	None

AT, antithrombin; PTT, partial thromboplastin time; PT, prothrombin time; INR, international normalized ratio; CBC, complete blood cell count.

bloodstream infection. Complete or near-complete thrombosis of an aortopulmonary shunt is a medical emergency requiring prompt recognition, diagnosis, and treatment.

Most centers recommend the following:

- Systemic anticoagulation via immediate administration of an intravenous bolus of uFH (50 to 100 U/kg) followed by a continuous heparin infusion.
- Maneuvers to increase systemic blood pressure thereby increasing shunt flow (phenylephrine, epinephrine)
- Maximize oxygen delivery and minimize oxygen consumption (intubation, mechanical ventilation, muscle paralysis)

Definitive diagnosis is usually made angiographically. Occlusion or near-occlusion must be treated expeditiously with intravascular stenting, manual shunt manipulation, or shunt revisions. ECMO may be necessary for stabilization or resuscitation. Systemic thrombolytic therapy is usually not used in aortopulmonary shunt occlusion since it may complicate subsequent emergent catheterization and/or surgery.

Partial shunt thrombosis presents with unexplained O₂ saturations lower than baseline without another etiology. An angiogram is usually recommended for confirmation since concomitant balloon dilation may be helpful for nonocclusive thrombus and stent placement for distortion or kinking at the insertion site. (149,150)

Low-dose aspirin (ASA) has become the standard of care for chronic prophylaxis in infants with aortopulmonary shunts. In 2005, Wells et al. (151) examined 155 polytetrafluoroethylene shunts at elective takedown and reported 21% with >50% luminal narrowing. Li et al. (152) in 2007 reported the results of a multicenter study that evaluated 1-year postoperative rates of death, shunt thrombosis, and early stage II operation in 1,004 infants. Around 80% received ASA. Event rates were 38% for the composite end point, 26% for death, and 12% for shunt thrombosis. Excluding early postoperative mortality, patients receiving ASA had a lower risk of shunt thrombosis and death compared with those not receiving ASA. Adding clopidogrel to chronic low-dose ASA did not reduce overall mortality or shunt-related morbidity in an early report (153). Despite chronic ASA therapy, shunt-related morbidity and mortality remains high. Investigation into alternative means of thrombosis prevention in these high-risk populations is warranted.

Bidirectional Glenn Anastomosis

Few data are currently available regarding the overall incidence and risk factors for thrombotic complications after a bidirectional cavopulmonary anastomosis beyond the early postoperative period. Certain high-risk groups have been identified and include patients with bilateral SVC (low flow in the interconnecting pulmonary artery segment) (154), a blind-ending pulmonary artery stump (155), and interrupted inferior vena cava with azygous continuation to the SVC (resultant Kawashima palliation). (120) Although Odegard et al. (134,156) have documented coagulation abnormalities in children post-stage II and pre-Fontan, there are no clear recommendations for chronic anticoagulation in children after the bidirectional Glenn anastomosis or hemi-Fontan operation. Antiplatelet therapy may be reasonable although prospective data are lacking. A few centers are advocating prophylactic anticoagulation. Clearly more work is needed in this area. At any stage in the single ventricle pathway, certain factors, in addition to those mentioned above, may put a patient at increased risk for thrombosis including flow stasis, ventricular dysfunction, previous thrombosis, protein-losing enteropathy, prolonged pleural effusions, arrhythmias, prolonged immobilization, and/or an abnormal thrombophilia profile. Initiation of prophylactic anticoagulation therapy or increasing the magnitude

of antithrombotic therapy (from antiplatelet to anticoagulant) may warrant consideration in such circumstances.

Fontan

There has been much interest over the past 20 to 30 years in thrombosis after the Fontan operation (123,124,127,157–164). The incidence of thrombotic complications after the Fontan operation has been reported to be 3% to 33% overall (1.4 to 3.6 for stroke) depending on the population studied, the time from the Fontan procedure, the method of thrombosis detection, the location of the thrombus investigated (i.e., pulmonary embolus vs. cerebral vascular event), or whether the study investigated clinically evident or silent thrombi. Although these reviews are an important source of observational data, their heterogeneous designs limit the ability to draw conclusions from which practice guidelines can be generated. The following observations, however, can be made:

- There appear to be two peaks in the incidence of thrombotic complications post-Fontan: early (3 to 6 months postoperatively) and late (5 to 10 years after the Fontan) (159,161,165).
- Thrombi have been identified in systemic venous atrium, pulmonary venous atrium, hypoplastic ventricle, ligated pulmonary artery stump, extracardiac, lateral tunnel and aortopulmonary pathways, silent pulmonary emboli, and thrombi in conjunction with HIT.
- Identified risk factors for thrombosis include flow stasis, ventricular dysfunction, arrhythmias, bilateral bidirectional cavopulmonary anastomoses, hypoplastic cardiac chambers with flow stasis, presence of a blind ended pulmonary artery stump, Kawashima connection, history of previous thrombosis, protein-losing enteropathy, prolonged pleural effusions, and prolonged immobilization.

There are limited retrospective reviews on the use of prophylactic anticoagulation after the Fontan operation. Seipelt et al. (161) in 2002 concluded that warfarin was indicated in patients post-Fontan. Jacobs et al. (123) also in 2002 concluded that ASA was sufficient prophylaxis although his patient population was limited to young children in the early post-Fontan years. Kaulitz et al. (127) in 2008 presented a retrospective review of a strategy that adjusted antithrombotic therapy depending on the development of prothrombotic risk factors over time.

The only published clinical trial to date was reported by Monagle et al. (128) in 2011. In this multicenter, randomized trial of primary prophylactic anticoagulation after the Fontan operation, patients were randomized to receive for 2 years either warfarin (started within 24 hours of uFH lead-in of 10 to 20 U/kg/h, target INR 2.0 to 3.0) or ASA (5 mg/kg/day) started as soon as they were able to tolerate oral intake. Transthoracic and transesophageal echocardiograms were performed at 3 and 24 months post-Fontan. There was no difference in thrombus detection between the two groups; thrombi were identified in 24% of those receiving warfarin and 21% of those receiving ASA. All thrombi were venous, 72% were detected on routine echocardiogram, and 28% were associated with clinical signs/symptoms. Seven of the 25 patients had thrombi in multiple locations; 20 within the Fontan connection; 4 within the pulmonary arteries; 7 within other venous sites. For those receiving warfarin, the mean INR at the time of thrombus detection was 2.2. At routine surveillance, 41% were below target INR and 14% above. Thrombi were detected by transthoracic echo in 52% and by transesophageal echo in 84%. Thrombi were generally treated with uFH (one patient required a thrombolytic agent). Thrombosis recurred in 28% despite an increase in the level of anticoagulation after the initial thrombotic event. Two patients required operation,

one a complicated Fontan revision followed by multiorgan failure and death (ASA group) and the other a Fontan take-down after initial thrombosis (warfarin group). Although there was no difference in the incidence of thrombi in the warfarin versus ASA group, the incidence of thrombi in both groups was unacceptably high. In addition, the study further points out the difficulty with warfarin administration in young children with 41% below target INR at routine surveillance further emphasizing the need for alternative therapies to both warfarin and ASA. It is important to realize, however, that this study only evaluated patients during the first 2 years after the Fontan. The second peak in thrombosis risk (5 to 10 years post-Fontan) warrants rigorous investigation as well.

Conclusions that can be drawn from the currently available data regarding monitoring and prophylaxis of the Fontan patient:

- Since the risk for thrombotic complications may change over time, repeated clinical screening for changes in anatomic and hemodynamic risk factors appears indicated.
- Close monitoring for thrombosis with periodic transthoracic echocardiography with focused attention to the identification of thrombi should be a part of routine of post-Fontan care. Additional imaging modalities (transesophageal echo, CT, computed tomography angiography (CTA), MRI, nuclear medicine lung perfusion scan, and venography/angiography) may be useful in patients with thrombosis suspected clinically or in whom transthoracic images are suboptimal.
- There is growing evidence that certain patients are “repeated clotters” and their propensity to thrombosis may warrant a higher level of surveillance and possibly a higher level of prophylaxis (128).
- Antiplatelet therapy for prophylactic long-term anticoagulation appears reasonable after the Fontan operation.
- An increase in the magnitude of antithrombotic therapy (change in medication from antiplatelet to anticoagulant or higher target levels) may be warranted if anatomic and/or hemodynamic risk factors become present.
- Further identification of risk factors, patients at particular individual risk (“clotters”), alternative agents, as well as alternative management strategies are essential.

PROSTHETIC VALVES

Prosthetic valves are used in both the atrioventricular and semilunar valve positions in children and adolescents with both congenital and acquired heart disease. This differs from adults with non-CHD where right-sided valve replacement is very uncommon. Two classes of valves are available: mechanical and bioprosthetic. Bioprosthetic valves, also referred to as “tissue valves,” are allografts or xenografts (bovine or porcine). Mechanical valves have a higher durability but require systemic anticoagulation, with a higher degree of anticoagulation theoretically required on the right side of the heart secondary to the lower pressures and the lower flow velocities. Long-term systemic anticoagulation is usually not required with bioprosthetic valves although they are less durable than mechanical valves with rapid deterioration in children especially in the aortic and mitral positions. Bioprosthetic valves, however, are more durable on the right side compared with the left side of the heart. Based on the above observations, mechanical valves are usually used in the mitral position and bioprosthetic valves on the pulmonary side. Since systemic anticoagulation with a vitamin K antagonist (VKA), most commonly warfarin, is difficult especially in young children, a few centers are attempting bioprosthetic valves in the mitral position in the hope that medium-term anticoagulation will not be necessary and the valve may last long enough until upsizing is needed at an older age when a mechanical valve may be more feasible.

Despite prescribed anticoagulation with warfarin, patients with mechanical valves are still at increased risk for both bleeding and clotting. A single, prospective, multicenter study of children <5 years of age at mitral valve replacement with a mechanical prosthesis (average follow-up 6.2 years, no time to event analysis) reported thrombotic events in 3% and stroke in 2% (target and achieved INRs were not reported) (166). The risk for thrombotic complications is less with mechanical aortic valves. Several retrospective studies in pediatric patients report the risk of thrombotic complications as 0% to 1.3% per patient per year and the risk of bleeding as 0% to 2.3% per patient per year (167–178). Tricuspid valve replacement is rare with Ebstein anomaly the most common indication and bioprosthetic valves most commonly employed. Mechanical valves are rarely used in the tricuspid position, and when they are used, an increased level of anticoagulation has been recommended because of the decreased flow velocity. Although reports are limited and mainly in adults, the risk of thrombosis appears to be high despite anticoagulation. One study reported a 2.9% per patient per year risk of valve thrombosis despite target INR of 2.0 to 3.0 (179). Another study in adult patients only reported a 15.4% incidence of tricuspid valve thrombosis despite a target INR of 2.5 to 3.5 with a mean follow-up of 7.9 years (180).

Bioprosthetic valves in the pulmonary position have a low risk for thrombosis and essentially no risk for systemic embolization. There are no data to support systemic anticoagulation for a bioprosthetic valve in the pulmonary position. As discussed above, tricuspid valve replacement is rare, with Ebstein anomaly being the most common indication. Although bioprosthetic valves are more commonly used in this situation, reports from a large experience at the Mayo Clinic recommend anticoagulation with a VKA for 3 to 6 months postoperatively (target INR 2.0 to 3.0) and lifelong with ASA (181–183).

Since there is a paucity of data on the efficacy and safety of anticoagulation strategies for prosthetic valves in children and adolescents, most centers and experts in the field follow the guidelines established for adults by the American College of Cardiology and the American Heart Association revised in 2008 (114,184) and those of the American College of Chest Physicians published that same year (185). Prophylactic anticoagulation guidelines for adults with prosthetic aortic and mitral valves are outlined in Table 75.5. Although not common practice in pediatrics, these guidelines recommend low-dose ASA in addition to therapeutic warfarin for patients with mechanical valves and for those with bioprosthetic valves who have risk factors. Warfarin is currently the mainstay of prophylactic therapy for mechanical valves, although stable, long-term anticoagulation is difficult especially in children because several medications are taken concomitantly and certain food may enhance or diminish the anticoagulant effect. In addition, the anticoagulant effect may be altered by intercurrent illness. Although enoxaparin (a LMWH) is an attractive alternative because of its ease in monitoring, to date, its use in prophylaxis for mechanical valves has been limited as an adjunct to bridge therapy when warfarin is stopped for an invasive procedure (184,186) and in pregnant women secondary to the teratogenic potential of warfarin (186–189).

Complete or near complete thrombosis of a prosthetic valve is a medical emergency, although small thrombi may result in no signs or symptoms. Infants are generally at higher risk of prosthetic valve thrombosis because of the smaller size of the prosthesis further complicated by the difficulties in achieving stable anticoagulation with warfarin therapy. Partial valve occlusion should be suspected in children with signs of low cardiac output, respiratory distress, hepatomegaly, pleural effusions, and/or pulmonary edema. Transesophageal echocardiography may reveal an increased inflow gradient across the valve and decreased leaflet mobility. Thrombi may be more

TABLE 75.5

Recommendations for Antithrombotic Therapy in Patients with Prosthetic Heart Valves

	ASA (75–100 mg)	Warfarin (INR 2.0–3.0)	Warfarin (INR 2.5–3.5)	No Warfarin
Mechanical prosthetic valves				
AVR—low risk				
<3 mo	Class I	Class I	Class IIa	
>3 mo	Class I	Class I		
AVR—high risk	Class I		Class I	
MVR	Class I		Class I	
Biological prosthetic valves				
AVR—low risk				
<3 mo	Class I	Class IIa		Class IIb
>3 mo	Class I			Class IIa
AVR—high risk	Class I	Class I		
MVR—low risk				
<3 mo	Class I	Class IIa		
>3 mo	Class I			Class IIa
MVR—high risk	Class I	Class I		

Depending on patients' clinical status, antithrombotic therapy must be individualized (see special situations in text). In patients receiving warfarin, ASA is recommended in virtually all situations. Risk factors: atrial fibrillation, left ventricular dysfunction, previous thromboembolism, and hypercoagulable condition. INR should be maintained between 2.5 and 3.5 for aortic disc valves and Starr-Edwards valves.

Modified from McAnulty JH, Rahimtoola SH. Antithrombotic therapy in valvular heart disease. In: Schlant R, Alexander RW, eds. *Hurst's The Heart*. New York, NY: McGraw-Hill, 1998:1867–1874(934).

AVR, aortic valve replacement; MVR, mitral valve replacement.

easily visualized with transesophageal echocardiography. Fluoroscopy is often used to evaluate valve motion and may be diagnostic as well. Therapy depends on the extent of the thrombus (clot burden) and the compromise to the patient. Small, nonobstructive thrombi are often managed with an increase in anticoagulation, close monitoring, and reevaluation. Thrombolytic therapy and/or operative exploration (thrombectomy or valve replacement) are required for larger thrombi resulting in hemodynamic compromise. Results of thrombolytic therapy in children mirror those in adults with an approximate 75% success rate and 25% incidence of complications including bleeding, thromboembolism, reoperation, and death (190–197). Management guidelines for valve thrombosis in children are taken from the adult experience and the reader is referred to the American College of Cardiology/American Heart Association Guidelines for Management of Patients with Valvular Heart Disease (114,184) and the American College of Chest Physicians Evidence-Based Clinical Practice Guidelines (8th Edition) (185,198).

ARRHYTHMIAS

Concerns for thrombosis in children with arrhythmias focus on three areas: atrial arrhythmias especially intra-atrial reentrant tachycardia/atrial flutter/atrial fibrillation, pacemakers/internal cardiac defibrillators, and electrophysiologic studies/catheter ablation procedures. Comprehensive practice guidelines for atrial fibrillation in adults were published in 2006 as a joint effort of the American College of Cardiology, American Heart Association, and the European Society of Cardiology (115). An extensive literature exists regarding arrhythmia and

pacemaker-related thrombosis in both adults and children and is beyond the scope of this chapter.

ACQUIRED HEART DISEASE

The two acquired heart diseases with known increased thrombotic risk are coronary involvement associated with Kawasaki disease and cardiomyopathy/myocarditis.

Kawasaki Disease

During the inflammatory phase of Kawasaki disease, two processes increase the risk of thrombus formation: vasculitis-induced endothelial injury to the coronary arteries and an increase in platelet quantity and activation. Later in the course, if coronary aneurysms form, especially giant coronary aneurysms 8 mm or greater, there is an increased risk of thrombus formation within the aneurysms secondary to low coronary blood flow velocities and relative stasis in addition to the endothelial injury and activated platelets. This risk is highest in the first 6 months of the disease. An extensive literature exists on the pathogenesis and natural history of Kawasaki disease and the diagnosis and management of thrombotic complications and is beyond the scope of this chapter (see Chapter 59). Recommendations for thrombosis prevention are outlined in the American Heart Association 2004 scientific statement, "Diagnosis, Treatment, and Long-term Management of Kawasaki disease: a Statement for Health Professionals from the Committee on Rheumatic Fever, Endocarditis and Kawasaki Disease, Council on Cardiovascular Disease in the Young, American Heart Association" (104) as well as in the 2008 American College of Chest Physicians

Evidence-Based Clinical Practice Guidelines, Antithrombotic Therapy in Infants and Children (199).

Cardiomyopathy/Myocarditis

Children and adolescents with cardiomyopathy including myocarditis are at risk for intracavitary thrombus formation secondary to stasis, regional wall motion abnormalities, endothelial dysfunction, and/or arrhythmias. The LV is the most common site although thrombi have been documented in the atria, right ventricle, systemic, and pulmonary vessels. Prevalence has been reported from 14% to 16% in moderate-sized pediatric series and thrombi have been identified in patients despite systemic prophylactic anticoagulation (112,113,200–204). Data are limited from which to generate management guidelines regarding antithrombotic prophylaxis, diagnosis, and treatment in the pediatric population. Limited guidelines are outlined in 2008 American College of Chest Physicians Evidence-Based Clinical Practice Guidelines, Antithrombotic Therapy in Infants and Children (199).

Cardiac Catheterization

The risk for thrombotic complications associated with cardiac catheterization is a known concern in pediatric cardiology that has generated a substantial literature and is beyond the scope of this chapter (see Chapters 12 and 13). The areas of major interest are thromboprophylaxis during diagnostic and interventional cardiac catheterization, postprocedure prophylaxis for intravascularly placed stents and occlusion devices, and management of catheterization-related vascular thrombosis.

Bridging Therapy

The question frequently arises concerning the discontinuation of anticoagulation in the event of an upcoming invasive procedure (operation, dental work, catheterization). Two factors should be considered: (a) the risk of thrombus during cessation of anticoagulation and (b) the potential of bleeding during the procedure (i.e., at what level of anticoagulation is the provider comfortable that the risk of bleeding will be acceptable). The options are as follows:

- Perform the procedure without interruption in anticoagulation. (Usually employed when the risk of bleeding is low.)
- Stop the warfarin 48 to 72 hours before the procedure (INR anticipated to fall to about 1.5). Restart the warfarin within 24 hours of the procedure without a heparin bridge. (Usually employed when the risk of thrombosis is low.)
- Stop the warfarin typically 48 hours before the procedure. Begin UFH when the INR falls below 2.0 and discontinue it 4 to 6 hours before the procedure. Restart heparin after the operation as soon as the risk of bleeding is determined to be low. Restart the warfarin and continue the heparin until target INR is reached. (Usually employed when the risk of thrombosis is high and the risk of bleeding during the procedure is also high.)

Guidelines for the management of warfarin during invasive procedures in *adults with prosthetic valves* is well established (184). Guidelines for the management of anticoagulation during invasive procedures in children with prosthetic valves as well as those anticoagulated for other reasons and with other agents (i.e., LMWH) have been extrapolated from these adult valve guidelines.

In an emergency situation when there is no time to wait for the INR to fall, the adult guidelines state that it is reasonable to give FFP prior to an invasive procedure in patients with a *mechanical valve* (class IIa, level of evidence B). These guidelines state that high-dose vitamin K should not be given to patients with a mechanical valve since a hypercoagulable state may be potentiated (class III, level of evidence B) (184,205).

Thrombolytic Therapy in Children and Adolescents with Heart Disease

Local and systemic thrombolytic therapy has been used extensively in children and adolescents with heart disease and thrombotic complications.

The strongest indication for thrombolytic therapy includes either a life- or limb-threatening thrombotic event. Significant bleeding (including intracranial hemorrhage) and thromboembolism are known complications of thrombolysis. The highest risk of bleeding from thrombolytic therapy is seen in preterm infants. When possible, the expertise of a pediatric hematologist should be sought. Contraindications to thrombolytic therapy need to be considered including active bleeding, an inability to maintain the platelet count $>75,000/\mu\text{L}$ or fibrinogen $>100\text{ mg/dL}$, a major surgery or site of hemorrhage within 7 to 10 days, seizures within 48 hours, central nervous system surgery/ischemia/trauma/hemorrhage within 30 days, preterm infant <32 weeks, or uncontrolled hypertension. While these contraindications are neither absolute nor evidence-based for every individual, the relative risks of thrombolytic therapy should be weighed against the potential benefits.

When instituting thrombolytic therapy, baseline laboratory values should be obtained (CBC, PT, PTT, fibrinogen, and D-dimer) prior to therapy and followed every 4 to 6 hours during therapy. An increase in the D-dimer and a drop in the fibrinogen level are indicative of a “lytic” state. To minimize the risk of bleeding, if the fibrinogen level drops below 100 mg/dL , consider either holding thrombolytic therapy or infusing cryoprecipitate as an external source of fibrinogen. The platelet count should be kept $>75,000/\mu\text{L}$. A head ultrasound should be obtained in all infants prior to thrombolytic therapy and FFP infusion should be considered to increase the infant’s plasminogen level (normally decreased in infants) to ensure the effectiveness of the thrombolytic therapy. Tissue plasminogen activator is currently the only thrombolytic agent available; Table 75.4 provides further information regarding mechanism of action and dosing. Concomitant low-dose heparin is often employed.

Future Directions

The Manuscript Oversight Committee of the American Heart Association has approved preparation of a scientific statement by an expert panel on the prevention and treatment of thrombosis in children and adults with CHD and in children with acquired heart disease (in review) (206). This statement includes an extensive review of thrombotic concerns in children and adolescents with single ventricle anatomy, prosthetic valves, arrhythmias, cardiac catheterization, and acquired heart disease (Kawasaki disease and cardiomyopathy/myocarditis) and includes graded recommendations based on currently available data. It is the anticipation of the writing group that this work will serve as a springboard for the much needed research on the etiology, risk factors, prevention, and treatment of thromboses in children and adolescents with heart disease.

REFERENCES

- Orkin SH, Fisher DE, Thomas Look A, et al. *Nathan and Oski's Hematology of Infancy and Childhood*. Philadelphia, PA: Saunders Elsevier, 2009.
- Pearson HA. Life-span of the fetal red blood cell. *J Pediatr* 1967;70:166–171.
- Andrew M, Vegh P, Johnston M, et al. Maturation of the hemostatic system during childhood. *Blood* 1992;80:1998–2005.
- Andrew M, Paes B, Milner R, et al. Development of the human coagulation system in the full-term infant. *Blood* 1987;70:165–172.

5. Monagle P, Massicotte P. Developmental haemostasis: secondary haemostasis. *Semin Fetal Neonatal Med* 2011;16:294–300.
6. Andrew M, Paes B, Milner R, et al. Development of the human coagulation system in the healthy premature infant. *Blood* 1988;72:1651–1657.
7. Monagle P, Barnes C, Ignjatovic V, et al. Developmental haemostasis. Impact for clinical haemostasis laboratories. *Thromb Haemost* 2006;95:362–372.
8. Katz JA, Moake JL, McPherson PD, et al. Relationship between human development and disappearance of unusually large von Willebrand factor multimers from plasma. *Blood* 1989;73:1851–1858.
9. Weinstein MJ, Blanchard R, Moake JL, et al. Fetal and neonatal von Willebrand factor (vWF) is unusually large and similar to the vWF in patients with thrombotic thrombocytopenic purpura. *Br J Haematol* 1989;72:68–72.
10. Tay SP, Cheong SK, Boo NY. Circulating tissue factor, tissue factor pathway inhibitor and D-dimer in umbilical cord blood of normal term neonates and adult plasma. *Blood Coagul Fibrinolysis* 2003;14:125–129.
11. Edelberg JM, Enghild JJ, Pizzo SV, et al. Neonatal plasminogen displays altered cell surface binding and activation kinetics. Correlation with increased glycosylation of the protein. *J Clin Invest* 1990;86:107–112.
12. Dixon N, Kishnani PS, Zimmerman S. Clinical manifestations of hematologic and oncologic disorders in patients with Down syndrome. *Am J Med Genet C Semin Med Genet* 2006;142C:149–157.
13. Ibsen LS, Underleider RM. Perioperative management for patients with congenital heart disease: a multidisciplinary approach. In: Nicols D, Underleider RM, Spevak PJ, et al, eds. *Critical Heart Disease in Infants and Children*. St. Louis, MO: Mosby, 2006:561–578.
14. Armano R, Gauvin F, Ducruet T, et al. Determinants of red blood cell transfusions in a pediatric critical care unit: a prospective, descriptive epidemiological study. *Crit Care Med* 2005;33:2637–2644.
15. Desmer L, Lacroix J. Transfusion in pediatrics. *Crit Care Clin* 2004;20:299–311.
16. Cholette JM, Mamikonian L, Alfieri GM, et al. Aspirin resistance following pediatric cardiac surgery. *Thromb Res* 2010;126:200–206.
17. Reiter CD, Wang X, Tanus-Santos JE, et al. Cell-free hemoglobin limits nitric oxide bioavailability in sickle-cell disease. *Nat Med* 2002;8:1383–1389.
18. Furchgott RF, Zawadzki JV. The obligatory role of endothelial cells in the relaxation of arterial smooth muscle by acetylcholine. *Nature* 1980;288:373–376.
19. Jin RC, Voetsch B, Loscalzo J. Endogenous mechanisms of inhibition of platelet function. *Microcirculation* 2005;12:247–258.
20. Space SL, Lane PA, Pickett CK, et al. Nitric oxide attenuates normal and sickle red blood cell adherence to pulmonary endothelium. *Am J Hematol* 2000;63:200–204.
21. Rother RP, Bell L, Hillmen P, et al. The clinical sequelae of intravascular hemolysis and extracellular plasma hemoglobin: a novel mechanism of human disease. *JAMA* 2005;293:1653–1662.
22. Shubin H, Kaufman R, Shapiro M, et al. Cardiovascular findings in children with sickle cell anemia. *Am J Cardiol* 1960;6:875.
23. Pegelow CH, Colangelo L, Steinberg M, et al. Natural history of blood pressure in sickle cell disease: risks for stroke and death associated with relative hypertension in sickle cell anemia. *Am J Med* 1997;102:171–177.
24. Barrett O Jr, Saunders DE Jr, McFarland DE, et al. Myocardial infarction in sickle cell anemia. *Am J Hematol* 1984;16:139–147.
25. Drossner DM, Hirsh DA, Sturm JJ, et al. Cardiac disease in pediatric patients presenting to a pediatric ED with chest pain. *Am J Emerg Med* 2011;29:632–638.
26. Gladwin MT, Sachdev V, Jison ML, et al. Pulmonary hypertension as a risk factor for death in patients with sickle cell disease. *N Engl J Med* 2004;350:886–895.
27. Parent F, Bachir D, Inamo J, et al. A hemodynamic study of pulmonary hypertension in sickle cell disease. *N Engl J Med* 2011;365:44–53.
28. Onyekwere OC, Campbell A, Teshome M, et al. Pulmonary hypertension in children and adolescents with sickle cell disease. *Pediatr Cardiol* 2008;29:309–312.
29. Colombatti R, Maschietto N, Varotto E, et al. Pulmonary hypertension in sickle cell disease children under 10 years of age. *Br J Haematol* 2010;150:601–609.
30. Pashankar FD, Carbonella J, Bazzy-Asaad A, et al. Prevalence and risk factors of elevated pulmonary artery pressures in children with sickle cell disease. *Pediatrics* 2008;121:777–782.
31. Ambrusko SJ, Gunawardena S, Sakara A, et al. Elevation of tricuspid regurgitant jet velocity, a marker for pulmonary hypertension in children with sickle cell disease. *Pediatr Blood Cancer* 2006;47:907–913.
32. Suell MN, Bezold LI, Okcu MF, et al. Increased pulmonary artery pressures among adolescents with sickle cell disease. *J Pediatr Hematol Oncol* 2005;27:654–658.
33. Machado RF, Gladwin MT. Chronic sickle cell lung disease: new insights into the diagnosis, pathogenesis and treatment of pulmonary hypertension. *Br J Haematol* 2005;129:449–464.
34. Janik J, Seeler RA. Perioperative management in children with sickle hemoglobinopathy. *J Pediatr Surg* 1980;15:117–120.
35. Gibson J. Anesthesia for sickle cell diseases and other hemoglobinopathies. *Semin Anesthesia* 1987;IV:27–35.
36. Esseltine DW, Baxter MR, Bevan JC. Sickle cell states and the anaesthetist. *Can J Anaesth* 1988;35:385–403.
37. Vichinsky EP, Haberkern CM, Neumayr L, et al. A comparison of conservative and aggressive transfusion regimens in the perioperative management of sickle cell disease. The Preoperative Transfusion in Sickle Cell Disease Study Group. *N Engl J Med* 1995;333:206–213.
38. Koshy M, Weiner SJ, Miller ST, et al. Surgery and anesthesia in sickle cell disease. Cooperative Study of Sickle Cell Diseases. *Blood* 1995;86:3676–3684.
39. Borgna-Pignatti C, Cappellini MD, De Stefano P, et al. Survival and complications in thalassemia. *Ann N Y Acad Sci* 2005;1054:40–47.
40. Zurlo MG, De Stefano P, Borgna-Pignatti C, et al. Survival and causes of death in thalassemia major. *Lancet* 1989;2:27–30.
41. Hahalis G, Manolis AS, Apostolopoulos D, et al. Right ventricular cardiomyopathy in beta-thalassemia major. *Eur Heart J* 2002;23:147–156.
42. Hahalis G, Alexopoulos D, Kremastinos DT, et al. Heart failure in beta-thalassemia syndromes: a decade of progress. *Am J Med* 2005;118:957–967.
43. Anderson LJ, Holden S, Davis B, et al. Cardiovascular T2-star (T2*) magnetic resonance for the early diagnosis of myocardial iron overload. *Eur Heart J* 2001;22:2171–2179.
44. Pennell DJ, Berdoukas V, Karagiorga M, et al. Randomized controlled trial of deferiprone or deferoxamine in beta-thalassemia major patients with asymptomatic myocardial siderosis. *Blood* 2006;107:3738–3744.
45. Origa R, Bina P, Agus A, et al. Combined therapy with deferiprone and desferrioxamine in thalassemia major. *Haematologica* 2005;90:1309–1314.
46. Tanner MA, Galanello R, Dessi C, et al. A randomized, placebo-controlled, double-blind trial of the effect of combined therapy with deferoxamine and deferiprone on myocardial iron in thalassemia major using cardiovascular magnetic resonance. *Circulation* 2007;115:1876–1884.
47. Prechal JT. Classification and molecular biology of polycythemia (erythrocytoses) and thrombocytosis. *Hematol Oncol Clin North Am* 2003;17:1151–1158, vi.
48. Barth PG, Scholte HR, Berden JA, et al. An X-linked mitochondrial disease affecting cardiac muscle, skeletal muscle and neutrophil leucocytes. *J Neurol Sci* 1983;62:327–355.
49. Barth PG, Wanders RJ, Vreken P. X-linked cardioskeletal myopathy and neutropenia (Barth syndrome)-MIM 302060. *J Pediatr* 1999;135:273–276.
50. Houtkooper RH, Turkenburg M, Poll-The BT, et al. The enigmatic role of tafazzin in cardiolipin metabolism. *Biochim Biophys Acta* 2009;1788:2003–2014.
51. McDonald-McGinn DM, Sullivan KE. Chromosome 22q11.2 deletion syndrome (DiGeorge syndrome/velocardiofacial syndrome). *Medicine (Baltimore)* 2011;90:1–18.
52. McLean-Tooke A, Barge D, Spickett GP, et al. Immunologic defects in 22q11.2 deletion syndrome. *J Allergy Clin Immunol* 2008;122:362–367, 7 e1–e4.
53. Sullivan KE, McDonald-McGinn D, Zackai EH. CD4(+) CD25(+) T-cell production in healthy humans and in patients with thymic hypoplasia. *Clin Diagn Lab Immunol* 2002;9:1129–1131.
54. Kratz CP, Niehues T, Lyding S, et al. Evans syndrome in a patient with chromosome 22q11.2 deletion syndrome: a case report. *Pediatr Hematol Oncol* 2003;20:167–172.
55. Davies JK, Telfer P, Cavenagh JD, et al. Autoimmune cytopenias in the 22q11.2 deletion syndrome. *Clin Lab Haematol* 2003;25:195–197.
56. Lippi G, Favaloro EJ, Franchini M, et al. Milestones and perspectives in coagulation and hemostasis. *Semin Thromb Hemost* 2009;35:9–22.
57. Harrison P. The role of PFA-100 testing in the investigation and management of haemostatic defects in children and adults. *Br J Haematol* 2005;130:3–10.
58. Romlin BS, Wahlander H, Berggren H, et al. Intraoperative thromboelastometry is associated with reduced transfusion prevalence in pediatric cardiac surgery. *Anesth Analg* 2011;112:30–36.
59. Moganandram S, Hunt BJ, Sykes K, et al. The relationship among thromboelastography, hemostatic variables, and bleeding after cardiopulmonary bypass surgery in children. *Anesth Analg* 2010;110:995–1002.
60. Miller BE, Guzzetta NA, Tosone SR, et al. Rapid evaluation of coagulopathies after cardiopulmonary bypass in children using modified thromboelastography. *Anesth Analg* 2000;90:1324–1330.
61. Vincentelli A, Susen S, Le Tourneau T, et al. Acquired von Willebrand syndrome in aortic stenosis. *N Engl J Med* 2003;349:343–349.
62. Tiede A, Priesack J, Werwitzke S, et al. Diagnostic workup of patients with acquired von Willebrand syndrome: a retrospective single-centre cohort study. *J Thromb Haemost* 2008;8:569–576.
63. Rauch R, Budde U, Koch A, et al. Acquired von Willebrand syndrome in children with patent ductus arteriosus. *Heart* 2002;88:87–88.
64. Federici AB, Rand JH, Bucciarelli P, et al. Acquired von Willebrand syndrome: data from an international registry. *Thromb Haemost* 2000;84:345–349.
65. Anderson RP, McGrath K, Street A. Reversal of aortic stenosis, bleeding gastrointestinal angiodysplasia, and von Willebrand syndrome by aortic valve replacement. *Lancet* 1996;347:689–690.
66. Tiede A, Rand JH, Budde U, et al. How I treat the acquired von Willebrand syndrome. *Blood* 2011;117:6777–6785.
67. Lawrence S, McDonald-McGinn DM, Zackai E, et al. Thrombocytopenia in patients with chromosome 22q11.2 deletion syndrome. *J Pediatr* 2003;143:277–278.
68. Duke SG, McGuire WF Jr, Jewett T, et al. Velocardiofacial syndrome: incidence of immune cytopenias. *Arch Otolaryngol Head Neck Surg* 2000;126:1141–1145.

69. Jawad AF, McDonald-McGinn DM, Zackai E, et al. Immunologic features of chromosome 22q11.2 deletion syndrome (DiGeorge syndrome/velocardiofacial syndrome). *J Pediatr* 2001;139:715-723.
70. Lill MC, Perloff JK, Child JS. Pathogenesis of thrombocytopenia in cyanotic congenital heart disease. *Am J Cardiol* 2006;98:254-258.
71. Horigome H, Hiramatsu Y, Shigeta O, et al. Overproduction of platelet microparticles in cyanotic congenital heart disease with polycythemia. *J Am Coll Cardiol* 2002;39:1072-1077.
72. Maurer HM, McCue CM, Robertson LW, et al. Correction of platelet dysfunction and bleeding in cyanotic congenital heart disease by simple red cell volume reduction. *Am J Cardiol* 1975;35:831-835.
73. Warkentin TE, Hayward CP, Boshkov LK, et al. Sera from patients with heparin-induced thrombocytopenia generate platelet-derived microparticles with procoagulant activity: an explanation for the thrombotic complications of heparin-induced thrombocytopenia. *Blood* 1994;84:3691-3699.
74. Ahmed I, Majeed A, Powell R. Heparin induced thrombocytopenia: diagnosis and management update. *Postgrad Med J* 2007;83:575-582.
75. Klenner AF, Fusch C, Rakow A, et al. Benefit and risk of heparin for maintaining peripheral venous catheters in neonates: a placebo-controlled trial. *J Pediatr* 2003;143:741-745.
76. Newall F, Barnes C, Ignjatovic V, et al. Heparin-induced thrombocytopenia in children. *J Paediatr Child Health* 2003;39:289-292.
77. Schmugge M, Risch L, Huber AR, et al. Heparin-induced thrombocytopenia-associated thrombosis in pediatric intensive care patients. *Pediatrics* 2002;109:E10.
78. Spadone D, Clark F, James E, et al. Heparin-induced thrombocytopenia in the newborn. *J Vasc Surg* 1992;15:306-311; discussion 11-22.
79. Risch L, Huber AR, Schmugge M. Diagnosis and treatment of heparin-induced thrombocytopenia in neonates and children. *Thromb Res* 2006;118:123-135.
80. Cuker A, Arepally G, Crowther MA, et al. The HIT Expert Probability (HEP) Score: a novel pre-test probability model for heparin-induced thrombocytopenia based on broad expert opinion. *J Thromb Haemost* 2010;8:2642-2650.
81. Lo GK, Juhl D, Warkentin TE, et al. Evaluation of pretest clinical score (4 T's) for the diagnosis of heparin-induced thrombocytopenia in two clinical settings. *J Thromb Haemost* 2006;4:759-765.
82. Lillo-Le Louet A, Bourouyrie P, Alhenc-Gelas M, et al. Diagnostic score for heparin-induced thrombocytopenia after cardiopulmonary bypass. *J Thromb Haemost* 2004;2:1882-1888.
83. Petaja J, Lundstrom U, Leijala M, et al. Bleeding and use of blood products after heart operations in infants. *J Thorac Cardiovasc Surg* 1995;109:524-529.
84. Chambers LA, Cohen DM, Davis JT. Transfusion patterns in pediatric open heart surgery. *Transfusion* 1996;36:150-154.
85. Williams GD, Bratton SL, Ramamoorthy C. Factors associated with blood loss and blood product transfusions: a multivariate analysis in children after open-heart surgery. *Anesth Analg* 1999;89:57-64.
86. Miller BE, Mochizuki T, Levy JH, et al. Predicting and treating coagulopathies after cardiopulmonary bypass in children. *Anesth Analg* 1997;85:1196-1202.
87. Oliver WC Jr, Beynen FM, Nuttall GA, et al. Blood loss in infants and children for open heart operations: albumin 5% versus fresh-frozen plasma in the prime. *Ann Thorac Surg* 2003;75:1506-1512.
88. Eaton MP, Iannoli EM. Coagulation considerations for infants and children undergoing cardiopulmonary bypass. *Paediatr Anaesth* 2011;21:31-42.
89. Chan AK, Leaker M, Burrows FA, et al. Coagulation and fibrinolytic profile of paediatric patients undergoing cardiopulmonary bypass. *Thromb Haemost* 1997;77:270-277.
90. Culliford AT, Gitel SN, Starr N, et al. Lack of correlation between activated clotting time and plasma heparin during cardiopulmonary bypass. *Ann Surg* 1981;193:105-111.
91. Griffin MJ, Rinder HM, Smith BR, et al. The effects of heparin, protamine, and heparin/protamine reversal on platelet function under conditions of arterial shear stress. *Anesth Analg* 2001;93:20-27.
92. Lindblad B, Wakefield TW, Whitehouse WM Jr, et al. The effect of protamine sulfate on platelet function. *Scand J Thorac Cardiovasc Surg* 1988;22:55-59.
93. Paramo JA, Rifon J, Llorens R, et al. Intra- and postoperative fibrinolysis in patients undergoing cardiopulmonary bypass surgery. *Haemostasis* 1991;21:58-64.
94. Ray MJ, Marsh NA, Hawson GA. Relationship of fibrinolysis and platelet function to bleeding after cardiopulmonary bypass. *Blood Coagul Fibrinolysis* 1994;5:679-685.
95. Schouten ES, van de Pol AC, Schouten AN, et al. The effect of aprotinin, tranexamic acid, and aminocaproic acid on blood loss and use of blood products in major pediatric surgery: a meta-analysis. *Pediatr Crit Care Med* 2009;10:182-190.
96. Pasquali SK, Hall M, Li JS, et al. Safety of aprotinin in congenital heart operations: results from a large multicenter database. *Ann Thorac Surg* 2010;90:14-21.
97. Hoffman M, Monroe DM III. A cell-based model of hemostasis. *Thromb Haemost* 2001;85:958-965.
98. Roberts HR, Monroe DM, White GC. The use of recombinant factor VIIa in the treatment of bleeding disorders. *Blood* 2004;104:3858-3864.
99. Witmer CM, Huang YS, Lynch K, et al. Off-label recombinant factor VIIa use and thrombosis in children: a multi-center cohort study. *J Pediatr* 2011;158:820-825 e1.
100. Logan AC, Yank V, Stafford RS. Off-label use of recombinant factor VIIa in U.S. hospitals: analysis of hospital records. *Ann Intern Med* 2011;154:516-522.
101. Monagle P. Thrombosis in pediatric cardiac patients. *Semin Thromb Hemost* 2003;29:547-555.
102. Ekerdt H, Brizard C, Evers R, et al. Elective administration in infants of low-dose recombinant activated factor VII (rFVIIa) in cardiopulmonary bypass surgery for congenital heart disease does not shorten time to chest closure or reduce blood loss and need for transfusions: a randomized, double-blind, parallel group, placebo-controlled study of rFVIIa and standard haemostatic replacement therapy versus standard haemostatic replacement therapy. *Blood Coagul Fibrinolysis* 2006;17:389-395.
103. Warren OJ, Rogers PL, Watret AL, et al. Defining the role of recombinant activated factor VII in pediatric cardiac surgery: where should we go from here? *Pediatr Crit Care Med* 2009.
104. Newburger JW, Takahashi M, Gerber MA, et al. Diagnosis, treatment, and long-term management of Kawasaki disease: a statement for health professionals from the Committee on Rheumatic Fever, Endocarditis and Kawasaki Disease, Council on Cardiovascular Disease in the Young, American Heart Association. *Circulation* 2004;110:2747-2771.
105. Sugahara Y, Ishii M, Muta H, et al. Warfarin therapy for giant aneurysm prevents myocardial infarction in Kawasaki disease. *Pediatr Cardiol* 2008;29:398-401.
106. Manlihot C, Brandao LR, Somji Z, et al. Long-term anticoagulation in Kawasaki disease: initial use of low molecular weight heparin is a viable option for patients with severe coronary artery abnormalities. *Pediatr Cardiol* 2010;31:834-842.
107. Manlihot C, Millar K, Golding F, et al. Improved classification of coronary artery abnormalities based only on coronary artery z-scores after Kawasaki disease. *Pediatr Cardiol* 2010;31:242-249.
108. Mehta R, Lee KJ, Chaturvedi R, et al. Complications of pediatric cardiac catheterization: a review in the current era. *Catheter Cardiovasc Interv* 2008;72:278-285.
109. Ing FF, Fagan TE, Grifka RG, et al. Reconstruction of stenotic or occluded iliofemoral veins and inferior vena cava using intravascular stents: reestablishing access for future cardiac catheterization and cardiac surgery. *J Am Coll Cardiol* 2001;37:251-257.
110. Agnoletti G, Bonnet C, Boudjemline Y, et al. Complications of paediatric interventional catheterisation: an analysis of risk factors. *Cardiol Young* 2005;15:402-408.
111. Balaguru D, Dilawar M, Ruff P, et al. Early and late results of thrombolytic therapy using tissue-type plasminogen activator to restore arterial pulse after cardiac catheterization in infants and small children. *Am J Cardiol* 2003;91:908-910.
112. McCrindle BW, Karamlou T, Wong H, et al. Presentation, management and outcomes of thrombosis for children with cardiomyopathy. *Can J Cardiol* 2006;22:685-690.
113. John JB, Cron SG, Kung GC, et al. Intracardiac thrombi in pediatric patients: presentation profiles and clinical outcomes. *Pediatr Cardiol* 2007;28:213-220.
114. Bonow RO, Carabello BA, Kanu C, et al. ACC/AHA 2006 guidelines for the management of patients with valvular heart disease: a report of the American College of Cardiology/American Heart Association Task Force on Practice Guidelines (writing committee to revise the 1998 Guidelines for the Management of Patients With Valvular Heart Disease): developed in collaboration with the Society of Cardiovascular Anesthesiologists: endorsed by the Society for Cardiovascular Angiography and Interventions and the Society of Thoracic Surgeons. *Circulation* 2006;114:e24-e231.
115. Fuster V, Ryden LE, Cannom DS, et al. ACC/AHA/ESC 2006 Guidelines for the Management of Patients with Atrial Fibrillation: a report of the American College of Cardiology/American Heart Association Task Force on Practice Guidelines and the European Society of Cardiology Committee for Practice Guidelines (Writing Committee to Revise the 2001 Guidelines for the Management of Patients With Atrial Fibrillation): developed in collaboration with the European Heart Rhythm Association and the Heart Rhythm Society. *Circulation* 2006;114:e257-e354.
116. Connolly SJ, Pogue J, Hart RG, et al. Effect of clopidogrel added to aspirin in patients with atrial fibrillation. *N Engl J Med* 2009;360:2066-2078.
117. Frank H, Mlczoch J, Huber K, et al. The effect of anticoagulant therapy in primary and anorectic drug-induced pulmonary hypertension. *Chest* 1997;112:714-721.
118. McLaughlin VV, Archer SL, Badesch DB, et al. ACCF/AHA 2009 expert consensus document on pulmonary hypertension: a report of the American College of Cardiology Foundation Task Force on Expert Consensus Documents and the American Heart Association: developed in collaboration with the American College of Chest Physicians, American Thoracic Society, Inc., and the Pulmonary Hypertension Association. *Circulation* 2009;119:2250-2294.
119. Monagle P, Andrew M. Coagulation abnormalities after Fontan procedures. *J Thorac Cardiovasc Surg* 1998;115:732-733.
120. Monagle P, Karl TR. Thromboembolic problems after the Fontan operation. *Semin Thorac Cardiovasc Surg Pediatr Card Surg Annu* 2002;5:36-47.
121. Odegard KC, McGowan FX Jr, Zurakowski D, et al. Procoagulant and anticoagulant factor abnormalities following the Fontan procedure: increased factor VIII may predispose to thrombosis. *J Thorac Cardiovasc Surg* 2003;125:1260-1267.

122. Cromme-Dijkhuis AH, Hess J, Hahlen K, et al. Specific sequelae after Fontan operation at mid- and long-term follow-up. Arrhythmia, liver dysfunction, and coagulation disorders. *J Thorac Cardiovasc Surg* 1993;106:1126-1132.
123. Jacobs ML, Pourmoghadam KK, Geary EM, et al. Fontan's operation: is aspirin enough? Is coumadin too much? *Ann Thorac Surg* 2002;73:64-68.
124. Jahangiri M, Ross DB, Redington AN, et al. Thromboembolism after the Fontan procedure and its modifications. *Ann Thorac Surg* 1994;58:1409-1413; discussion 13-14.
125. Jahangiri M, Kreutzer J, Zurakowski D, et al. Evaluation of hemostatic and coagulation factor abnormalities in patients undergoing the Fontan operation. *J Thorac Cardiovasc Surg* 2000;120:778-782.
126. Jahangiri M, Shore D, Kakkar V, et al. Coagulation factor abnormalities after the Fontan procedure and its modifications. *J Thorac Cardiovasc Surg* 1997;113:989-992; discussion 92-93.
127. Kaulitz R, Ziemer G, Rauch R, et al. Prophylaxis of thromboembolic complications after the Fontan operation (total cavopulmonary anastomosis). *J Thorac Cardiovasc Surg* 2005;129:569-575.
128. Monagle P, Cochrane A, Roberts R, et al. A multicenter, randomized trial comparing heparin/warfarin and acetylsalicylic acid as primary thromboprophylaxis for 2 years after the Fontan procedure in children. *J Am Coll Cardiol* 2011;58:645-651.
129. Giglia TM, Sell JE, Chamberlain RS, et al. Thrombotic Complications in a Pediatric Cardiovascular Surgery Population: a Nine-Year Experience. *J Am Coll Cardiol* 2001;37:465A.
130. Manlhiot C, Menjak IB, Brandao LR, et al. Risk, clinical features, and outcomes of thrombosis associated with pediatric cardiac surgery. *Circulation* 2011;124:1511-1519.
131. Virchow R LK. Thrombose und Embolie. Gefässentzündung und septische Infektion. *Gesammelte Abhandlungen zur wissenschaftlichen Medicin*. Frankfurt am Main: Von Meidinger & Sohn, 1856.
132. Waniewski J, Kurowska W, Mizerski JK, et al. The effects of graft geometry on the patency of a systemic-to-pulmonary shunt: a computational fluid dynamics study. *Artif Organs* 2005;29:642-650.
133. Odegard KC, Zurakowski D, DiNardo JA, et al. Prospective longitudinal study of coagulation profiles in children with hypoplastic left heart syndrome from stage I through Fontan completion. *J Thorac Cardiovasc Surg* 2009;137:934-941.
134. Odegard KC, McGowan FX Jr, Zurakowski D, et al. Coagulation factor abnormalities in patients with single-ventricle physiology immediately prior to the Fontan procedure. *Ann Thorac Surg* 2002;73:1770-1777.
135. van Nieuwenhuizen RC, Peters M, Lubbers LJ, et al. Abnormalities in liver function and coagulation profile following the Fontan procedure. *Heart* 1999;82:40-46.
136. Odegard KC, Zurakowski D, Hornykewycz S, et al. Evaluation of the coagulation system in children with two-ventricle congenital heart disease. *Ann Thorac Surg* 2007;83:1797-1803.
137. Nowak-Gottl U, Kothhoff S, Hagemeyer E, et al. Interaction of fibrinolysis and prothrombotic risk factors in neonates, infants and children with and without thromboembolism and underlying cardiac disease: a prospective study. *Thromb Res* 2001;103:93-101.
138. Alioglu B, Avci Z, Tokel K, et al. Thrombosis in children with cardiac pathology: analysis of acquired and inherited risk factors. *Blood Coagul Fibrinolysis* 2008;19:294-304.
139. Savage B, Saldivar E, Ruggeri ZM. Initiation of platelet adhesion by arrest onto fibrinogen or translocation on von Willebrand factor. *Cell* 1996;84:289-297.
140. Mann KG. Thrombin formation. *Chest* 2003;124:4S-10S.
141. Michelson AD, Barnard MR, Hechtman HB, et al. In vivo tracking of platelets: circulating degranulated platelets rapidly lose surface P-selectin but continue to circulate and function. *Proc Natl Acad Sci U S A* 1996;93:11877-11882.
142. Mann KG. Thrombin: can't live without it; probably die from it. *Chest* 2003;124:1S-3S.
143. Jagers JJ, Neal MC, Smith PK, et al. Infant cardiopulmonary bypass: a procoagulant state. *Ann Thorac Surg* 1999;68:513-520.
144. Randolph AG, Cook DJ, Gonzales CA, et al. Benefit of heparin in peripheral venous and arterial catheters: systematic review and meta-analysis of randomised controlled trials. *BMJ* 1998;316:969-975.
145. Thornburg CD, Smith PB, Smithwick ML, et al. Association between thrombosis and bloodstream infection in neonates with peripherally inserted catheters. *Thromb Res* 2008;122:782-785.
146. O'Connor MJ, Ravishanker C, Ballweg JA, et al. Early systemic-to-pulmonary artery shunt intervention in neonates with congenital heart disease. *J Thorac Cardiovasc Surg* 2011;142:106-112.
147. Massicotte P, Julian JA, Gent M, et al. An open-label randomized controlled trial of low molecular weight heparin for the prevention of central venous line-related thrombotic complications in children: the PRO-TEKT trial. *Thromb Res* 2003;109:101-118.
148. Schroeder AR, Axelrod DM, Silverman NH, et al. A continuous heparin infusion does not prevent catheter-related thrombosis in infants after cardiac surgery. *Pediatr Crit Care Med* 2010;11:489-495.
149. Gillespie MJ, Rome JJ. Transcatheter treatment for systemic-to-pulmonary artery shunt obstruction in infants and children. *Catheter Cardiovasc Interv* 2008;71:928-935.
150. Petit CJ, Gillespie MJ, Kreutzer J, et al. Endovascular stents for relief of cyanosis in single-ventricle patients with shunt or conduit-dependent pulmonary blood flow. *Catheter Cardiovasc Interv* 2006;68:280-286.
151. Wells WJ, Yu RJ, Batra AS, et al. Obstruction in modified Blalock shunts: a quantitative analysis with clinical correlation. *Ann Thorac Surg* 2005;79:2072-2076.
152. Li JS, Yow E, Berezny KY, et al. Clinical outcomes of palliative surgery including a systemic-to-pulmonary artery shunt in infants with cyanotic congenital heart disease: does aspirin make a difference? *Circulation* 2007;116:293-297.
153. Wessel DL, Berger F, Li JS, et al. Abstract 19459: A Randomized Trial of Clopidogrel to Reduce Mortality and Shunt-Related Morbidity in Infants Palliated with a Systemic to Pulmonary Artery Shunt. *Circulation* 2010;122(21_MeetingAbstracts): A19459.
154. Iyer GK, Van Arsdell GS, Dicke FP, et al. Are bilateral superior vena cavae a risk factor for single ventricle palliation? *Ann Thorac Surg* 2000;70:711-716.
155. Yie K, Lee CH, Kim SJ. Thrombi in the main pulmonary artery stump after a fontan operation. *Pediatr Cardiol* 2008;29:870-871.
156. Odegard KC, McGowan FX Jr, DiNardo JA, et al. Coagulation abnormalities in patients with single-ventricle physiology precede the Fontan procedure. *J Thorac Cardiovasc Surg* 2002;123:459-465.
157. du Plessis AJ, Chang AC, Wessel DL, et al. Cerebrovascular accidents following the Fontan operation. *Pediatr Neurol* 1995;12:230-236.
158. Day RW, Boyer RS, Tait VF, et al. Factors associated with stroke following the Fontan procedure. *Pediatr Cardiol* 1995;16:270-275.
159. Rosenthal DN, Friedman AH, Kleinman CS, et al. Thromboembolic complications after Fontan operations. *Circulation* 1995;92:II287-293.
160. Barker PC, Nowak C, King K, et al. Risk factors for cerebrovascular events following fontan palliation in patients with a functional single ventricle. *Am J Cardiol* 2005;96:587-591.
161. Seipelt RG, Franke A, Vazquez-Jimenez JF, et al. Thromboembolic complications after Fontan procedures: comparison of different therapeutic approaches. *Ann Thorac Surg* 2002;74:556-562.
162. Bailing G, Vogt M, Kaemmerer H, et al. Intracardiac thrombus formation after the Fontan operation. *J Thorac Cardiovasc Surg* 2000;119:745-752.
163. Varma C, Warr MR, Hendler AL, et al. Prevalence of "silent" pulmonary emboli in adults after the Fontan operation. *J Am Coll Cardiol* 2003;41:2252-2258.
164. Porcelli R, Moskowitz BC, Cetta F, et al. Heparin-induced thrombocytopenia with associated thrombosis in children after the Fontan operation: report of two cases. *Tex Heart Inst J* 2003;30:58-61.
165. Coon PD, Rychik J, Novello RT, et al. Thrombus formation after the Fontan operation. *Ann Thorac Surg* 2001;71:1990-1994.
166. Caldaroni CA, Raghuveer G, Hills CB, et al. Long-term survival after mitral valve replacement in children aged <5 years: a multi-institutional study. *Circulation* 2001;104:1143-1147.
167. Arnold R, Ley-Zaporozhan J, Ley S, et al. Outcome after mechanical aortic valve replacement in children and young adults. *Ann Thorac Surg* 2008;85:604-610.
168. Sachweh JS, Tiete AR, Muhler EG, et al. Mechanical aortic and mitral valve replacement in infants and children. *Thorac Cardiovasc Surg* 2007;55:156-62.
169. Tiete AR, Sachweh JS, Groetzner J, et al. Systemic mechanical heart valve replacement in children under 16 years of age. *Clin Res Cardiol* 2006;95:281-288.
170. Larsen SH, Houliand K, Hansen OK, et al. Medium-term follow-up of mechanical valves inserted in children. *Cardiol Young* 2006;16:579-585.
171. Shanmugam G, MacArthur K, Pollock J. Mechanical aortic valve replacement: long-term outcomes in children. *J Heart Valve Dis* 2005;14:166-171.
172. Alexiou C, McDonald A, Langley SM, et al. Aortic valve replacement in children: are mechanical prostheses a good option? *Eur J Cardiothorac Surg* 2000;17:125-133.
173. Mazzitelli D, Guenther T, Schreiber C, et al. Aortic valve replacement in children: are we on the right track? *Eur J Cardiothorac Surg* 1998;13:565-571.
174. Champsaur G, Robin J, Tronc F, et al. Mechanical valve in aortic position is a valid option in children and adolescents. *Eur J Cardiothorac Surg* 1997;11:117-122.
175. Abid F, Abid A, Fekih M, et al. Aortic valve replacement in children under 16 years of age with congenital or rheumatic valvular disease. A study of 64 cases. *J Cardiovasc Surg (Torino)* 1992;33:265-271.
176. Solymar L, Rao PS, Mardini MK, et al. Prosthetic valves in children and adolescents. *Am Heart J* 1991;121:557-568.
177. Stewart S, Cianciotta D, Alexson C, et al. The long-term risk of warfarin sodium therapy and the incidence of thromboembolism in children after prosthetic cardiac valve replacement. *J Thorac Cardiovasc Surg* 1987;93:551-554.
178. Schaff HV, Danielson GK, DiDonato RM, et al. Late results after Starr-Edwards valve replacement in children. *J Thorac Cardiovasc Surg* 1984;88:583-589.
179. Kawano H, Oda T, Fukunaga S, et al. Tricuspid valve replacement with the St. Jude Medical valve: 19 years of experience. *Eur J Cardiothorac Surg* 2000;18:565-569.
180. Kang CH, Ahn H, Kim KH, et al. Long-term result of 1144 CarboMedics mechanical valve implantations. *Ann Thorac Surg* 2005;79:1939-1944.
181. Kizilhan HT, Theodoro DA, Warnes CA, et al. Late results of bioprosthetic tricuspid valve replacement in Ebstein's anomaly. *Ann Thorac Surg* 1998;66:1539-1545.

182. Brown ML, Dearani JA, Danielson GK, et al. The outcomes of operations for 539 patients with Ebstein anomaly. *J Thorac Cardiovasc Surg* 2008;135:1120–1136, 1136.e1–e7.
183. Brown ML, Dearani JA, Danielson GK, et al. Comparison of the outcome of porcine bioprosthetic versus mechanical prosthetic replacement of the tricuspid valve in the Ebstein anomaly. *Am J Cardiol* 2009;103:555–561.
184. Bonow RO, Carabello BA, Chatterjee K, et al. 2008 focused update incorporated into the ACC/AHA 2006 guidelines for the management of patients with valvular heart disease: a report of the American College of Cardiology/American Heart Association Task Force on Practice Guidelines (Writing Committee to revise the 1998 guidelines for the management of patients with valvular heart disease). Endorsed by the Society of Cardiovascular Anesthesiologists, Society for Cardiovascular Angiography and Interventions, and Society of Thoracic Surgeons. *J Am Coll Cardiol* 2008;52:e1–e142.
185. Salem DN, O'Gara PT, Madias C, et al. Valvular and structural heart disease: American College of Chest Physicians Evidence-Based Clinical Practice Guidelines (8th Edition). *Chest* 2008;133:593S–629S.
186. Seshadri N, Goldhaber SZ, Elkayam U, et al. The clinical challenge of bridging anticoagulation with low-molecular-weight heparin in patients with mechanical prosthetic heart valves: an evidence-based comparative review focusing on anticoagulation options in pregnant and nonpregnant patients. *Am Heart J* 2005;150:27–34.
187. Saeed CR, Frank JB, Pravin M, et al. A prospective trial showing the safety of adjusted-dose enoxaparin for thromboprophylaxis of pregnant women with mechanical prosthetic heart valves. *Clin Appl Thromb Hemost* 2011;17:313–319.
188. McLintock C, McCowan LM, North RA. Maternal complications and pregnancy outcome in women with mechanical prosthetic heart valves treated with enoxaparin. *BJOG* 2009;116:1585–1592.
189. Groce JB, 3rd. "Bridging" therapy with low molecular weight heparin in pregnant patients and patients with mechanical prosthetic heart valves. *J Thromb Thrombolysis* 2003;16:79–82.
190. Kogon B, Kirshbom PH, Forbess JM, et al. Thrombolytic therapy for prosthetic valve thrombosis in children: two case reports and review of the literature. *J Thorac Cardiovasc Surg* 2004;127:1519–1522.
191. Munclinger MJ, Patel JJ, Mitha AS. Thrombolysis of thrombosed St. Jude Medical prosthetic valves: rethrombosis—a sign of tissue ingrowth. *J Thorac Cardiovasc Surg* 1998;115:248–249.
192. Seltzer SM, Reed MD, Siwik ES. Intra-atrial tissue plasminogen activator infusion for prosthetic valve thrombosis. *Catheter Cardiovasc Interv* 2006;67:139–141.
193. Bolz D, Kuhne T, Jivraj R, et al. Thrombolysis of prosthetic tricuspid valve thrombosis with human recombinant tissue plasminogen activator in an adolescent. *Pediatr Cardiol* 2000;21:397–400.
194. Fyfe DA, Taylor AB, Kline CH, et al. Doppler echocardiographic evaluation of streptokinase lysis of thrombosed right-sided St. Jude Medical valves in patients with congenital heart defects. *Am Heart J* 1991;121:1156–1160.
195. Joyce LD, Boucek M, McGough EC. Urokinase therapy for thrombosis of tricuspid prosthetic valve. *J Thorac Cardiovasc Surg* 1983;85:935–937.
196. Newall F, Browne M, Savoia H, et al. Assessing the outcome of systemic tissue plasminogen activator for the management of venous and arterial thrombosis in pediatrics. *J Pediatr Hematol Oncol* 2007;29:269–273.
197. Serpi M, Schmidt KG, Kreuz W, et al. Thrombolysis of prosthetic heart valve thrombosis using recombinant tissue plasminogen activator (rt-PA) in infancy and childhood. *Z Kardiol* 2001;90:191–196.
198. Sun JC, Davidson MJ, Lamy A, et al. Antithrombotic management of patients with prosthetic heart valves: current evidence and future trends. *Lancet* 2009;374:565–576.
199. Monagle P, Chalmers E, Chan A, et al. Antithrombotic therapy in neonates and children: American College of Chest Physicians Evidence-Based Clinical Practice Guidelines (8th Edition). *Chest* 2008;133:887S–968S.
200. Gunthard J, Stocker F, Bolz D, et al. Dilated cardiomyopathy and thromboembolism. *Eur J Pediatr* 1997;156:3–6.
201. Chang YC, Wu JM, Wu MH, et al. Left ventricular thrombi in children with dilated cardiomyopathy. *J Formos Med Assoc* 1995;94:469–473.
202. Hsu DT, Addonizio LJ, Hordof AJ, et al. Acute pulmonary embolism in pediatric patients awaiting heart transplantation. *J Am Coll Cardiol* 1991;17:1621–1625.
203. Ozkutlu S, Ozbarlas N, Ozme S, et al. Intracardiac thrombosis diagnosed by echocardiography in childhood: predisposing and etiological factors. *Int J Cardiol* 1993;40:251–256.
204. Ahnert AM, Freudenberger RS. What do we know about anticoagulation in patients with heart failure? *Curr Opin Cardiol* 2008;23:228–232.
205. ACC. ACC/AHA Task Force on Practice Guidelines. 2003.
206. Giglia TM, Massicotte MP, Bauman ME, Barst R, Erickson C, Feltes T, Foster E, Hinoki K, Ichord R, Kreutzer J, McCrindle B, Newburger J, Tabbutt S, Todd J, Tweddell J, Webb C. Prevention and treatment of thrombosis in children and adults with congenital heart disease and in children with acquired heart disease. *Circulation* 2012; in press.

Evaluation of Quality of Life in Children and Adolescents with Congenital and Acquired Heart Disease

Bradley S. Marino

Ultimately, the goals of pediatric research and clinical care are to maximize health and minimize symptomatology, disability, and dysfunction that may impact the lives of children with acute and chronic disease processes. Over the last several decades, new surgical techniques and advances in cardiopulmonary bypass, intensive care, interventional cardiac catheterization, noninvasive imaging, and medical therapies have significantly lowered neonatal mortality rates for children with the most complex congenital heart disease (CHD) (e.g., hypoplastic left heart disease) to <10% (1). In addition, cardiac-related mortality in patients with congenital and acquired heart disease has diminished significantly during the first two decades of life (2,3). Although survival rates vary by disease complexity, long-term survival (>20 years) rates for children with heart disease are estimated to be 95% for simple CHD, 90% for moderate CHD, and 80% for complex CHD in the current era (3).

Despite these advances, however, survivors suffer from morbidity resulting from their circulatory abnormalities and the medical and surgical therapies they have received. These morbidities significantly impact the child's neurodevelopmental (4–6), psychosocial (7–9), and physical (10–12) functioning and diminish their quality of life (QOL) (Fig. 76.1). Given the high incidence of functional impairment in the pediatric cardiac population, there has been a paradigm shift in clinical research from short-term mortality prevention to long-term morbidity assessment. As a result, outcome assessment focusing on QOL has become increasingly important in this high-risk population.

QOL may be described as a child's ability to function in situational contexts (family, school, and peer) and derive personal satisfaction from doing so (13–15). The multidimensional construct of QOL is thought to include three essential domains: physical health status and physical functioning, psychological status, and social functioning (Fig. 76.2) (13–15). QOL measurement provides a comprehensive description of an individual's health, may result in the identification of physical, functional, and psychosocial dysfunction, and is a critical component of the evaluation of long-term outcomes of chronic conditions and disease-specific therapies.

This paper delineates health measurement definitions including QOL and health-related QOL (HRQOL), identifies inherent difficulties in HRQOL measurement in the pediatric heart disease population, and discusses salient aspects of HRQOL instrument evaluation. In addition, it describes existing generic and disease-specific HRQOL measures that may be used to assess HRQOL in the pediatric heart disease population, what research on HRQOL in the pediatric heart disease population has shown, and the extent to which HRQOL evaluations are being fully utilized in clinical practice. Finally, a research and clinical agenda is proposed to harness the potential applications of HRQOL assessment.

HEALTH MEASUREMENT DEFINITIONS: QOL AND HRQOL

There are many ways to define “health.” While the differences in meaning between various attributes of health may be subtle, the differences are important and have significant implications as to how clinical and research data are interpreted and findings incorporated into how we care for children with chronic disease. *Health* has been defined by the World Health Organization as “a state of complete physical, mental, and social well-being and not merely the absence of disease or infirmity” (16). Indeed it was this initial definition of health that gave rise to the concept of QOL. *Health status*, which impacts QOL, may be thought of as a child's level of wellness versus illness, describing the impact of physiologic dysfunction, symptom burden, and/or level of illness control. Alternatively, *functional status* is defined as an individual's ability to perform activities of daily living, meet basic needs, fulfill roles, and maintain health and well-being within the context of various life situations (17). Functional status is often affected by health status and has a significant impact on QOL. However, it is HRQOL, a more specific description of QOL, which is the most relevant construct relative to clinical and research data assessing outcomes and the provision of comprehensive clinical care of children and adolescents with chronic illness or injury (18). *HRQOL* is defined as the influence of a specific illness, medical therapy, or health services policy on the ability of the patient to both function in and derive personal satisfaction from various physical, psychological, and social life contexts (19). For the purposes of this manuscript all references to QOL, hereafter, refer specifically to HRQOL.

Evaluating HRQOL is important because it allows for better communication among patients, parents, and health care providers; prioritization of problems based partially on patient and/or parent preference; the monitoring of changes over time or in response to a specific therapy; and screening for other significant physical and psychosocial problems (20). HRQOL measurement has emerged as a high priority not only for patients and their families and medical caregivers but also for the National Institutes of Health (NIH), Food and Drug Administration (FDA), and insurance providers (21). The NIH's Patient-Reported Outcomes Measurement Information System, part of the NIH Roadmap, is a multi-million dollar effort devoted in part to improving HRQOL (22–27). The FDA recognized the importance of such patient-reported outcomes by issuing guidance to industry on the use of such outcomes in clinical trials in support of medical product claims (28). A better understanding of the perceptions of HRQOL among patients with heart disease and their parents and health care providers may improve treatment and patient outcome (29,30) and enhance the ability to perform important

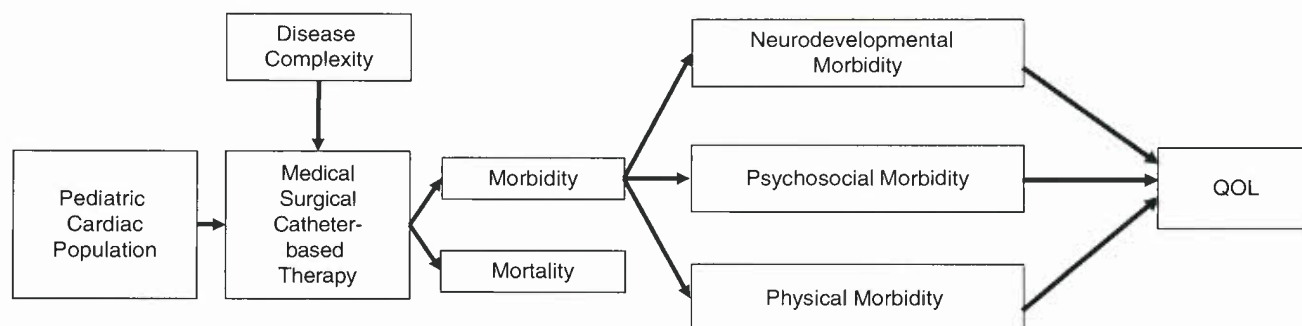


Figure 76.1. The relationship between heart disease-related morbidity factors and QOL. (From Marino BS, Uzark K, Ittenbach I, et al. Evaluation of quality of life in children with heart disease. *Prog Ped Cardiol* 2010;29:131–138, with permission.)

prospective cross-sectional, cohort, and randomized clinical trials to improve patient outcome. Despite the known advantages, assessment of HRQOL in the pediatric cardiac population is lacking.

Measurement of HRQOL in patients with congenital and acquired heart disease has been limited over the last 25 years. Moons et al. (31) noted that only 1 in 70 outcome studies published between 1980 and 2003 that purported to assess HRQOL in pediatric cardiac patients actually measured the patients' perceived HRQOL. In addition, more than half of the 70 articles did not meet any of the ten critical appraisal criteria for HRQOL research studies advocated by Gill and Feinstein in JAMA in 1994 (32). The lack of rigorous research on HRQOL in the pediatric heart disease population is not surprising given the inherent difficulties of measuring HRQOL in this population.

INHERENT DIFFICULTIES OF HRQOL EVALUATION IN THE PEDIATRIC HEART DISEASE POPULATION

HRQOL assessment in the pediatric population is challenging due to the wide age range and the changing developmental capabilities of the patients as they age. HRQOL assessment in the pediatric cardiac population is further complicated by the

variety of congenital and acquired diseases, varying levels of severity, the array of therapeutic modalities that may be utilized to treat the patient (medical, surgical, and interventional), and the spectrum of outcomes. Similar to other pediatric chronic diseases, there may be variation in the perceived impact of heart disease on HRQOL, since many of the patients have always had heart disease (as in CHD) while others have been diagnosed with heart disease at an age when they were aware of the acute change in their health status (as in acquired heart disease).

Patient–family interactions are critical in QOL assessment, and the role of proxy reporting (parent/guardian) and cross informant variance is often debated (33). It has been extensively documented that HRQOL measurement in children with chronic health conditions and healthy children provided by proxy respondents is not equivalent to that reported by the child (34,35). These findings indicate that proxy reports cannot be substituted for child self-reports (36) and evaluations of pediatric cardiac patients' perspectives regarding treatment outcome should be included in pediatric clinical care and clinical trials given the documented differences between child and proxy reports. While pediatric patient self-report should be considered the standard for measuring patient-perceived HRQOL (37), there may be situations when the child is too young, too cognitively impaired, or too ill to complete an HRQOL instrument, and proxy reporting may be required. Further, it is typically parents' perceptions of their child's HRQOL that influences health care use (38,39). Ideally, parent and child QOL instruments that measure the perspectives of both the child and proxy reporter with the same constructs and parallel items to make comparisons between self and proxy reports more informative and useful should be chosen (40). As noted by Moons et al. (31) most research studies assessing HRQOL in children with heart disease have only assessed proxy reporters (parents/guardians) and ignored the HRQOL perceptions of the child. Studies of the cognitive development in children, psychometric studies on pediatric QOL measures that have included child self-reporting, and cognitive interviewing studies on children's abilities to respond to questionnaires indicate that self-reports from children over 7 years of age are reliable and valid (41). Both patients and their parents provide important information, even though they may vary or even disagree significantly with one another. It may be that understanding the differences in perception of HRQOL between patients, their parent/guardians, and medical caregivers is more important and informative than perceived agreement (30).

In addition to assessment issues related to the pediatric population in general and the pediatric heart disease population specifically, issues related to cultural and demographic variables (culture, race, ethnicity, income) affect HRQOL assessment in both pediatric and adult respondents. Culture, race, ethnicity, and income have critical influences on HRQOL measurement relative to the values that are attributed to various

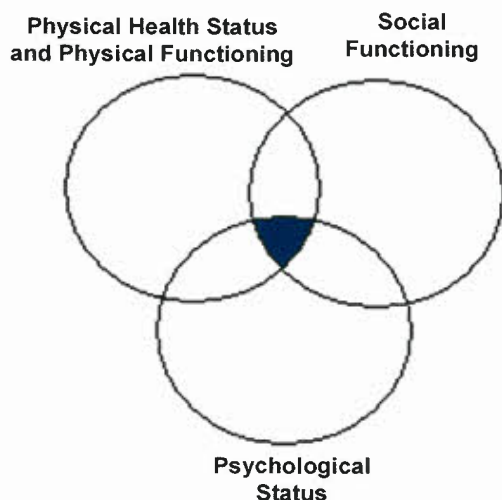


Figure 76.2. Definition of quality of life. (From Marino BS, Uzark K, Ittenbach I, Drotar D. Evaluation of quality of life in children with heart disease. *Prog Ped Cardiol* 2010;29:131–138, with permission.)

health states by children and their parents, the language in which health is described by children and their families, and the perceived functional impact of symptoms and changes in health states (42).

HRQOL INSTRUMENT EVALUATION

When measuring HRQOL, it is important to be clear on whether the goal of the application is to assess HRQOL, functional status, or both. These measures of health are distinct constructs and are often confused with each other; note prior definitions. When assessing either HRQOL or functional status for research and clinical application, specific aspects of instrument selection (Tables 76.1 and 76.2), validation (Table 76.3), and availability (Table 76.4) must be considered.

When selecting an instrument, it is important to note the instrument type, the specific construct that will be assessed, desired respondent type(s), patient and proxy reporter age range(s), and the domains to be assessed (Table 76.1). When selecting a specific form from within an instrument grouping, the number of items in the tool and the average completion time should be considered as it may impact the feasibility of completing the research project or clinical application (Table 76.2).

Both generic and disease-specific instruments exist that may be used to measure HRQOL or functional status in the pediatric heart disease population (43–49). Whether generic or disease specific, the “ideal” QOL measure will have a patient self-reporting mechanism with parent/guardian proxy reporting and a wide age range, be easily self-administered in a reasonable timeframe, and have an array of relevant constructs to describe and measure HRQOL or functional status. Generic HRQOL or functional status measures assess these constructs in both healthy children and in children with chronic disease. They may be used to compare various chronic disease groups or chronic disease groups and healthy controls. Disease-specific instruments assess HRQOL in a particular condition or disease, may be more comprehensive for a specific disease, and may be a better discriminator of differences between subgroups within a disease category. Disease-specific pediatric cardiac HRQOL instruments may provide new, critical information on the outcome of present and future interventional catheterization and cardiac surgical procedures in the short and long term and may be utilized for randomized clinical trials for cardiovascular drugs and new technologies and interventions. In addition, a disease-specific pediatric cardiac HRQOL instrument may define changes in HRQOL over time (evaluative tool), predict future changes in HRQOL (prognostic tool), and signal new problems or issues that might not be noted by traditional biologic markers (diagnostic tool).

Assessing prior validation data on a given HRQOL or functional status instrument is central to the instrument evaluation process (Table 76.3). When assessing validation of a given instrument, four specific questions relative to the psychometric properties of the instrument should be asked: (a) *Has the instrument been shown to be reliable in the patient population being studied?*, (b) *Has the instrument been shown to be internally valid in the patient population being studied?*, (c) *Has the instrument been shown to be externally valid in the patient population to be studied?*, (d) *If the study is assessing change over time or the impact of an intervention, has the instrument been shown to be responsive in the patient population to be studied?*

All psychometric instruments must be shown to be reliable before validity and responsiveness may be considered (50). An “unreliable instrument” cannot be deemed valid or responsive. Demonstrating reliability involves assessing score “reproducibility” through internal consistency measurement (Cronbach α)

and comparing scores on the same patient at two distinct points in time with an appropriate interval between them to minimize recall bias (test–retest reliability). Validity testing of a psychometric scale is an ongoing, evidence-based process that assesses the degree of confidence that one should have in inferences made about a test taker based on their score. Assessing validity is often divided into the domains of “internal” and “external” construct validity (51–53). “Internal validity” (50–52,54) may be thought of as an assessment of content validity and structural validity, which includes assessment of the theoretical conceptualization of the respective instrument; the clarity, relevance, and representativeness of the item content; and tool construction. In contrast, establishing “external validity” requires demonstrating convergent and discriminant construct validity and “generalizability” (51,52,55). “Generalizability” may be defined as the ability of a tool to provide valid and reliable information when utilized in different geographic regions and patient populations (52). Generalizable tools allow researchers to have confidence that data collected from multiple sites and regions are comparable. Substantiation of the “generalizability” part of external validity enables a HRQOL instrument to be used for clinical applications and multicenter research that may serve as a platform for future multisite cross-sectional and prospective studies using HRQOL as an outcome. Responsiveness describes the ability of the HRQOL or functional status instrument to be sensitive to change in score after intervention or if there is meaningful change in score over time (50). Having a responsive instrument allows the investigator to note differences in HRQOL based on a specific intervention or treatment strategy, which is critical to assessing all potential interventions in a given disease population. In addition, a responsive tool will allow the clinician or researcher to see changes in HRQOL over time as a patient’s health status or functional status worsens. Having a responsive instrument is critical to any interventional agenda or follow-up program for any given chronic disease population.

EXISTING GENERIC AND DISEASE-SPECIFIC HRQOL MEASURES THAT MAY BE USED TO ASSESS HRQOL IN THE PEDIATRIC HEART DISEASE POPULATION

Both the PedsQL 4.0 Cores scales, a generic HRQOL measure, and the Child Health Questionnaire (CHQ), a generic functional status measure, have patient and proxy reporting, wide age range, and may be administered in a reasonable timeframe. In addition, these commercially available tools have been shown to be reliable and internally and externally valid, and responsive in the United States and many other countries after language translation (Tables 76.1 through 76.4) (43,44). Five disease-specific pediatric cardiac HRQOL instruments have been previously described (45–49). The CHD-TNO/AZL Adult QOL (CHD-TAAQOL) questionnaire is a disease-specific instrument that assesses HRQOL in young adults with CHD (45). The PedsQL 3.0 Cardiac Module (46), Congenital Heart Adolescent and Teenager Questionnaire (CHAT) (47), ConQOL (48), and Pediatric Cardiac Quality-of-Life Inventory (PCQLI) (49) measure HRQOL in the pediatric cardiac population. Instrument availability (form specific authorization requirements, user costs, and available language translations) are shown in Table 76.4. The PedsQL 3.0 Cardiac Module (46), created and validated by Uzark et al. at a single site, was a critical and important step forward in the objective assessment of HRQOL in children with heart disease. The PedsQL 3.0 Cardiac Module has been shown to be reliable, internally and externally valid. The 27-item PedsQL Cardiac Module encompasses six Scales: Heart Problems and Treatment;

TABLE 76.1 Instrument Selection: Constructs, Respondent Types, and Domains

Instrument Type	Instrument	Construct Measured	Respondent Type	Age Range (years)	Domain(s)
Generic	CHQ (43)	Functional status	Self-report Proxy report ^a	10–18 5–18	Physical functioning, Role/Social emotional, Role/social behavioral, Role/social physical, Bodily pain, General behavior, Mental health, Self-esteem, General health perceptions, Change in health, Family activities, Family cohesiveness, Parental impact-time, Parental impact-emotional ^b
	PedsQL 4.0 General Core Scales (33)	HRQOL	Self-report Proxy report	5–7, 8–12, 13–18, 19–25 2–4, 5–7, 8–12, 13–18	Physical, Emotional, Social, School ^c
	CHAT (47)	HRQOL	Self-report	11–18	Physical symptoms, Physical limitations, Limitations of physical education at school, Social limitations, External pressures, Concerns (general, social, educational, physical, total)
Disease-Specific (CHD)	ConQol (48)	HRQOL	Self-report	8–11, 12–16	Symptoms, Activities, Relationships, Coping and control ^d
	CHD-TAAQOL (45)	HRQOL	Self-report	17–32	Symptoms, Impact cardiac surveillance, Worries
	PCQLI (49)	HRQOL	Self-report Proxy report	8–12, 13–18 8–12, 13–18	Disease impact (physical) Psychosocial impact
	PedsQL 3.0 Cardiac Module (46)	HRQOL	Self-report Proxy report	5–7 ^e , 8–12, 13–18 2–4, 5–7, 8–12, 13–18	Heart problems (symptoms) Treatment (barriers) Perceived physical appearance Treatment anxiety Cognitive problems Communication

^aProxy reports are for parents, guardians, or primary home care providers of patients.

^bThe CHQ domain lists include both those for the patient and proxy reporter. Domain differences between patient and proxy report forms include the Parental Impact-Time, and Parental Impact-Emotional domains may only be found in the proxy form; the domains Role/Social-Emotional and Role/Social-Behavioral from the self report form are combined into one domain, Role/Social Emotional/Behavior in the proxy form; the listed domains except for Change in Health, Family Activities, and Family Cohesiveness create the Physical and Psychosocial summary scores for the Proxy Report Forms (CHQ-PF50 and CHQ-PF28) only.

^cThe Physical domain makes up the Physical Health Summary Score, while the Emotional, Social, and School domains make up the Psychosocial Summary Score.

^dFor adolescents 12–16 years old only.

^eReliability of the PedsQL 3.0 Cardiac Module Young Child self-report Form for ages 5–7 years has not been established (ranged from 0.35 to 0.83).

CHAT, Congenital Heart Adolescent and Teenage questionnaire; CHQ, Child Health Questionnaire; PCQLI, Pediatric Cardiac Quality of Life Inventory; PedsQL, Pediatric Quality of Life Inventory 4.0; UK, United Kingdom; USA, United States of America.

From Marino BS, Uzark K, Ittenbach I, Drotar D. Evaluation of quality of life in children with heart disease. *Prog Ped Cardiol* 2010;29:131–138, with permission.

TABLE 76.2 Instrument Selection: Forms

Instrument Type	Instrument	Name	Respondent Type/ Age Range [years]	Items (#)	Completion Time (minutes)
Generic	CHQ	CHQ-CF87	Child/adolescent [10–18]	87	25
		CHQ-PF50	Parent proxy [5–18]	50	15
		CHQ-PF28	Parent proxy [5–18]	28	10
	PedsQL 4.0 General Core Scales	Young Child Report	Young child [5–7]	23	10
		Child Report	Child [8–12]		
		Teen Report	Teen [13–18]		
		Young Adult Report	Young adult [19–25]		
		Parent of Toddler Report	Parent proxy [2–4]	23	10
		Parent of Young Child Report	Parent proxy [5–7]		
		Parent of Child Report	Parent proxy [8–12]		
		Parent of Teen Report	Parent proxy [13–18]		
Disease-Specific (CHD)	CHAT	CHAT Questionnaire	Adolescent [11–18]	53	20–30
	ConQol	ConQol 8-11	Child [8–11]	29	10
		ConQol 12-16	Adolescent [12–16]	35	10
	CHD-TAAQOL	CHD-TAAQOL Questionnaire	Young adult [17–32]	26	10
Disease-Specific (HD)	PCQLI	Child Form	Child [8–12]	24	10
		Adolescent Form	Adolescent [13–18]	30	10
		Parent of Child Form	Parent proxy [8–12]	24	10
	PedsQL 3.0 Cardiac Module	Parent of Adolescent Form	Parent proxy [13–18]	30	10
		Young Child Report	Young child [5–7]	27	10
		Child Report	Child [8–12]		
		Adolescent Report	Adolescent [13–18]		
		Parent of Toddler Report	Parent proxy [2–4]	27	10
		Parent of Young Child Report	Parent proxy [5–7]		
		Parent of Child Report	Parent proxy [8–12]		
		Parent of Teen Report	Parent proxy [13–18]		

CHAT, Congenital Heart Adolescent and Teenage questionnaire; CHQ, Child Health Questionnaire; PCQLI, Pediatric Cardiac Quality-of-Life Inventory; PedsQL, Pediatric Quality-of-Life Inventory 4.0; UK, United Kingdom; USA, United States of America.

From Marino BS, Uzark K, Ittenbach I, et al., Evaluation of quality of life in children with heart disease. *Prog Ped Cardiol* 2010;29:131–138, with permission.

Treatment II, Perceived Physical Appearance, Treatment Anxiety, Cognitive Problems, and Communication (46,56). The PedsQL 3.0 Cardiac Module has not yet been shown to be generalizable to other geographic regions or demographic populations in the United States. The CHAT and ConQol questionnaires have important limitations that include intended for use in heart disease patients with CHD only (47,48), narrow age range (47,48), lack of parent proxy reporting (48), no generalizability data to support broad applicability to other geographic regions or demographics within the United States (47,48), and/or an inadequate ability to discriminate among various types of cardiovascular disease across a wide age range (48). The PCQLI is the most recently published disease-specific instrument. Similar to the PedsQL 3.0 Cardiac Module, it has a patient self-reporting mechanism with parent/guardian proxy reporting, wide age range, is easily self-administered in a reasonable time frame, and has an array of relevant constructs to describe and measure HRQOL in the pediatric heart disease population. The PCQLI is the only disease-specific measure that has been tested in a multicenter trial and shown to be

reliable, valid, and generalizable in the United States (57,58). The ConQol and PedsQL 3.0 Cardiac Module can distinguish among disease severity subgroups but only within select subsets of a study population (age, respondent type) (46,48). In contrast, PCQLI Total and subscale scores (Disease Impact and Psychosocial Impact) differentiate between CHD severity subgroups irrespective of age category, score examined, or respondent type (40). From a research perspective, this is an important development that will facilitate cross-sectional and prospective studies of HRQOL in clinically important subgroups in the pediatric heart disease population. It is important to note that none of the five disease-specific instruments have been shown to be responsive in the United States.

In summary, whether selecting a measurement tool for research or clinical application it is critical to define the specific hypothesis or what clinical information is desired and then match the hypothesis/clinical data requirement to potential instruments based on the constructs assessed in the specific instrument, the respondents desired, and the feasibility of utilization. It is important to use age-appropriate measures

TABLE 76.3 Instrument Validation: Reliability, Validity, and Responsiveness

Instrument Type	Instrument	Reliability	Internal Validity	External Validity		
				Construct Validity	Generalizability	Responsiveness
Generic	CHQ	USA ^a	USA ^a	USA ^a	USA ^a	USA ^a
	PedsQL 4.0 General Core Scales	USA ^b	USA ^b	USA ^b	USA ^b	USA ^b
Disease-Specific (CHD)	CHAT	Canada	Canada	Canada	—	—
	ConQol	UK, Canada	UK, Canada	UK, Canada	—	—
	CHD-TAAQOL	Netherlands	Netherlands	Netherlands	—	—
Disease-Specific (HD)	PCQLI	USA (49,57), UK (81)	USA (49,57), UK (81)	USA (49,57), UK (81)	USA (57,76)	—
	PedsQL 3.0 Cardiac Module	USA	USA	USA	—	—

^aThe CHQ has been translated and validated in multiple languages and countries. Only the original is listed here for clarity. Please see www.healthactchq.com for an exhaustive list.

^bThe PedsQL has been translated and validated in multiple languages and countries. Only the original is listed here for clarity. Please see www.pedsq.org for an exhaustive list.

CHAT, Congenital Heart Adolescent and Teenage questionnaire; CHQ, Child Health Questionnaire; PCQLI, Pediatric Cardiac Quality of Life Inventory; PedsQL, Pediatric Quality of Life Inventory 4.0; UK, United Kingdom; USA, United States of America.

From Marino BS, Uzark K, Ittenbach I, et al. Evaluation of quality of life in children with heart disease. *Progr Ped Cardiol* 2010;29:131–138, with permission.

that reflect the maturity and the cognitive development of the desired respondents. It is vital that the instrument being considered for measurement be reliable, valid, and responsive in the patient population being considered. The instrument needs to have been shown to be responsive if assessing change in score over time or after intervention in the population being studied. It is important to collect data from both patient *and* parent/guardian proxy respondents to identify the full HRQOL impact on the patient, parent, and family. Finally, it is important to use both a disease-specific and generic measure, to allow discrimination between subgroups and comparison with other chronic disease groups and/or healthy children.

RESEARCH ON HRQOL IN PEDIATRIC PATIENTS WITH HEART DISEASE: WHAT IS KNOWN

HRQOL Studies in the General Congenital Health Disease Population

Most early outcome studies in patients with CHD described mortality and morbidity or health status, including anatomic or hemodynamic outcome, electrophysiologic sequelae, and/or exercise capacity following surgical interventions or included “QOL” parameters such as marital status, number of offspring,

TABLE 76.4 Instrument Availability: Authorization, Cost, and Languages

Instrument Type	Instrument	Authorization	Cost	Language(s)
Generic	CHQ	Licensure	Licensing fee	English (USA) ^a
	PedsQL 4.0 General Core Scales	User agreement	None/licensing fee	English (USA) ^b
Disease-Specific (CHD)	CHAT	None required	None required	English
	ConQol	None required	None	English (UK)
	CHD-TAAQOL	NA	NA	English, Dutch
Disease-Specific (HD)	PCQLI		None	English (USA, UK)
	PedsQL 3.0 Cardiac Module	User agreement User agreement	None/licensing fee	English (USA)

^aThe CHQ has been translated in multiple languages. Only the original is listed here for clarity. Please see www.healthact.com for an exhaustive list.

^bThe PedsQL has been translated and validated in multiple languages and countries. Only the original is listed here for clarity. Please see www.pedsq.org for an exhaustive list. CHAT, Congenital Heart Adolescent and Teenage questionnaire; CHQ, Child Health Questionnaire; NA, information not available; PCQLI, Pediatric Cardiac Quality-of-Life Inventory; PedsQL, Pediatric Quality-of-Life Inventory 4.0; UK, United Kingdom; USA, United States of America.

From Marino BS, Uzark K, Ittenbach I, et al. Evaluation of quality of life in children with heart disease. *Progr Ped Cardiol* 2010;29:131–138, with permission.

employment status, or educational attainment in adults with CHD (59). More recent studies have recognized the multidimensional nature of HRQOL and have included not only physical health status and physical functioning but also psychological status and social functioning. Unfortunately, there are only a few studies that have evaluated the patient's self-perceptions of HRQOL.

Health Status and Functional Status in the Heart Disease Population

In children with CHD as young as one to three years, Limpopoulos et al reported a high incidence of functional limitations including difficulties in socialization skills (11). Walker et al. (60) evaluated functional status in children attending a cardiology clinic, utilizing the CHQ (CHQ PF-50) to describe the physical and psychosocial health status by parent-proxy report. The sample of children seen in the out-patient cardiology clinic was reported to have worse physical functioning, general health perception, assessment of family activities, and parental emotional impact, as well as more anxiety problems and learning problems. Majnemer et al. (61) used the CHQ PF-50 as well as the Child Behavior Checklist and the Parenting Stress Index in describing well-being in children 5 years of age following open heart surgery in infancy. Mean scores on the CHQ were in the normal range; however, parents

more often reported problems related to anxiety, attention, developmental delays, and learning. The child's psychosocial health status was significantly correlated with parental stress. Both of the later studies acknowledge parental responses are likely to be influenced by their hopes and expectations for their child and how well they are coping as a family. This is consistent with one of the earliest studies of the emotional adjustment of children with CHD by DeMaso and colleagues, (62) who found that approximately 33% of the variability in the child's adjustment was accounted for by maternal perceptions, while medical severity accounted for <3% of the variability.

HRQOL in the Heart Disease Population

Self-reported HRQOL related to physical health, psychosocial health, social functioning, and school functioning for children with CHD is reduced compared to healthy children (Fig. 76.3A,B) (56,57,63,64). Mussatto et al. (64) found that the greatest negative impact on HRQOL was reported in the areas of social and educational functioning, despite the perception that CHD primarily has physical effects. In a large single-center study of HRQOL in children with heart disease, Uzark et al (56) evaluated both parent proxy and self-reported perceptions utilizing the PedsQL 4.0 Core scales. As perceived by parents, worse physical and psychosocial HRQOL is related

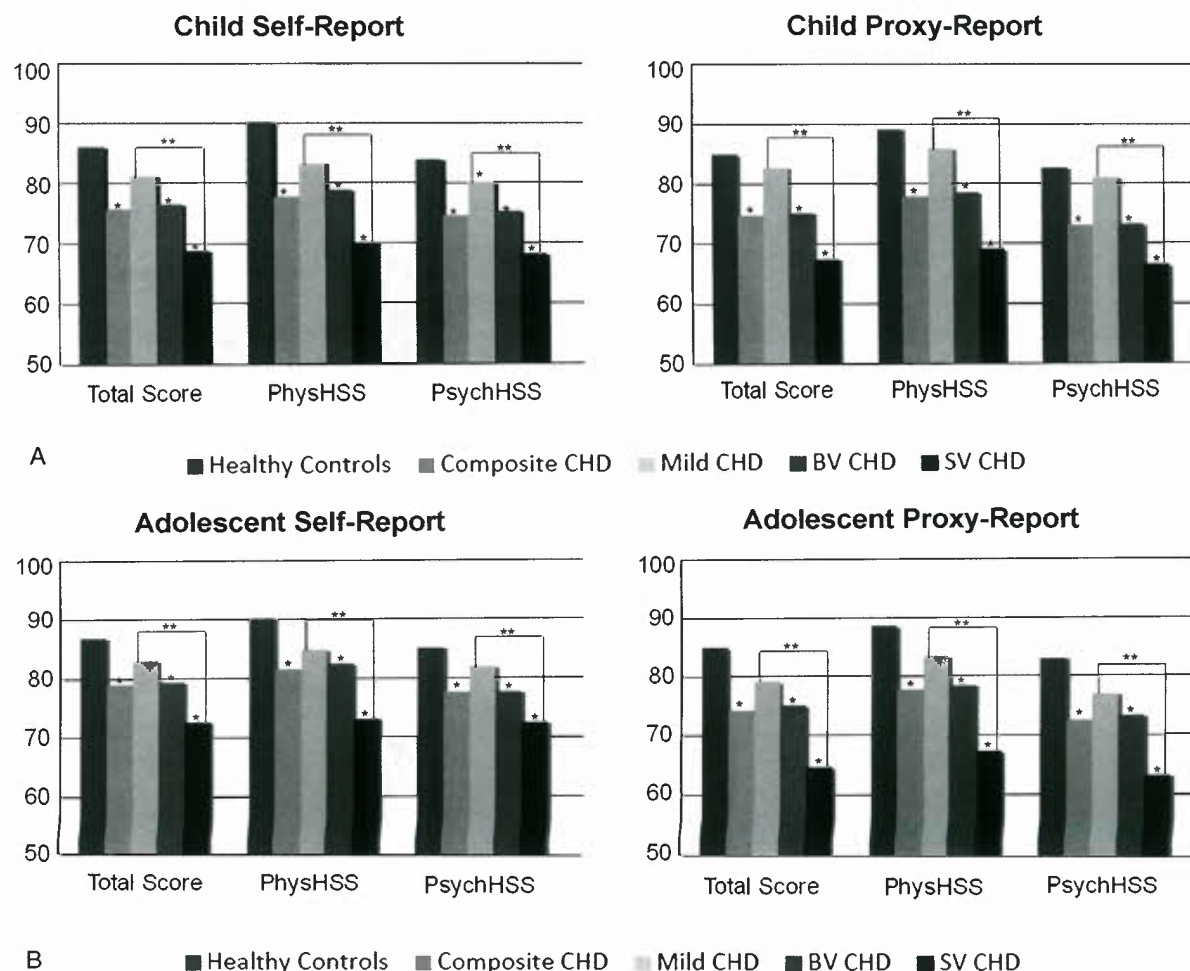


Figure 76.3. A: PedsQL generic HRQOL measure—Child. B: Adolescents with CHD have lower PedsQL scores than healthy controls. Lower PCQLI scores are associated with increasing severity of CHD in children and adolescents. *Significant difference when compared to healthy controls, determined by t-test. **Significant difference among disease severity categories, determined by one-way analysis of variance. (From Marino BS, Tomlinson R, Wernovsky G, et al. Validation of the pediatric cardiac quality of life inventory. *Pediatrics* 2010;126:498–508, with permission.)

to the severity of heart disease. While most children with heart disease reported good overall HRQOL, 20% of the children with heart disease reported significantly impaired psychosocial HRQOL, including children with mild or repaired heart disease. A recent systematic review of studies assessing psychological adjustment and HRQOL in children and adolescents following open heart surgery for CHD (63) concluded that studies on self-reported psychological adjustment indicate a good outcome; however, according to their parents, a considerable proportion of children experienced psychological maladjustment, which was related to severity of CHD and developmental delay.

The largest multicenter study assessing HRQOL in the United States utilizing a reliable, valid, and generalizable disease-specific HRQOL measure including both child and adolescent self-report and parent/guardian-proxy report was performed by Marino et al. in the PCQLI Validation Study (40). In this study 1,605 patient–parent pairs (3,210 total respondents) participated from seven geographically diverse centers in the United States. In this study, heart disease patients with both CHD (68% of the cohort) and acquired heart disease (32% of the cohort) were included. This study showed that lower patient and parent-reported HRQOL scores were associated with higher disease severity (Fig. 76.4) and increased medical care utilization (Fig. 76.5), poorer patient self-perception and competency, and increased behavioral and emotional problems in the pediatric heart disease population (Table 76.5). PCQLI scores (Total, Disease Impact, and Psychosocial Impact) differed significantly among disease severity subgroups (mild CHD, biventricular CHD s/p surgical repair or palliation, and single ventricle CHD s/p Fontan completion) (Fig. 76.4). Mild CHD was defined as CHD that had not required surgical or catheter-based intervention. Furthermore, patients in the repaired biventricular subgroup had significantly lower PCQLI Total and subscale scores than patients in the mild subgroup, and patients in the palliated single-ventricle subgroup had significantly lower PCQLI Total and subscale scores than patients in both the repaired biventricular and mild CHD subgroups (Fig. 76.4). These results were reproducible across all age categories and respondent types and are consistent with

widespread clinical observations that increased disease severity is associated with a lower HRQOL. Increased number of cardiac surgeries, cardiac-related hospital admissions, and doctor visits in the last 12 months were associated with lower PCQLI Total score (Fig. 76.5). These results were consistent across all four forms (Child Form, Parent of Child Form, Adolescent Form, and Parent of Adolescent Form). Worse PCQLI Total score was significantly correlated with lower Global Self-Worth score on the Self Perception Profile for Children and Adolescents for both age groups (Table 76.5). A statistically significant positive correlation was noted between the PCQLI Total score and Achenbach (Youth Self Report and Child Behavior Checklist) Total Competency score, and statistically significant inverse correlations existed between PCQLI Total score and both the Achenbach Internalizing Problems summary scale score and DSM-IV Oriented Scale scores (Affective Disorder, Anxiety Disorder, Somatic Disorder, Attention Deficit Hyperactivity Disorder) for all groups (Table 76.5) (40).

Interestingly, there was significant variation noted in the specific diagnosis and procedural groups (Table 76.6) for acyanotic two-ventricle (e.g., aortic stenosis), cyanotic two-ventricle (e.g., tetralogy of Fallot) and the palliated single-ventricle Fontan populations (40). While each specific population group segregated into a particular HRQOL score range (aortic stenosis—80s; tetralogy of Fallot—70s; and Fontan—60s) based on the underlying disease severity and the medical, catheter-based, and surgical therapy required, there were complex single-ventricle Fontan patients who had HRQOL scores as high as aortic stenosis patients who had not undergone intervention and aortic stenosis patients who had undergone intervention who had HRQOL scores that were worse than the typical Fontan. These data suggest that there are resilience and depressant factors that increase or decrease each individual patient's arc of HRQOL over time (Fig. 76.6). Understanding broad resilience and depressant factors across the entire heart disease population and/or resilience and depressant factors important for specific diagnosis or procedural groups will create opportunities to prevent the development of lower HRQOL or treat heart disease patients with lower HRQOL to improve it.

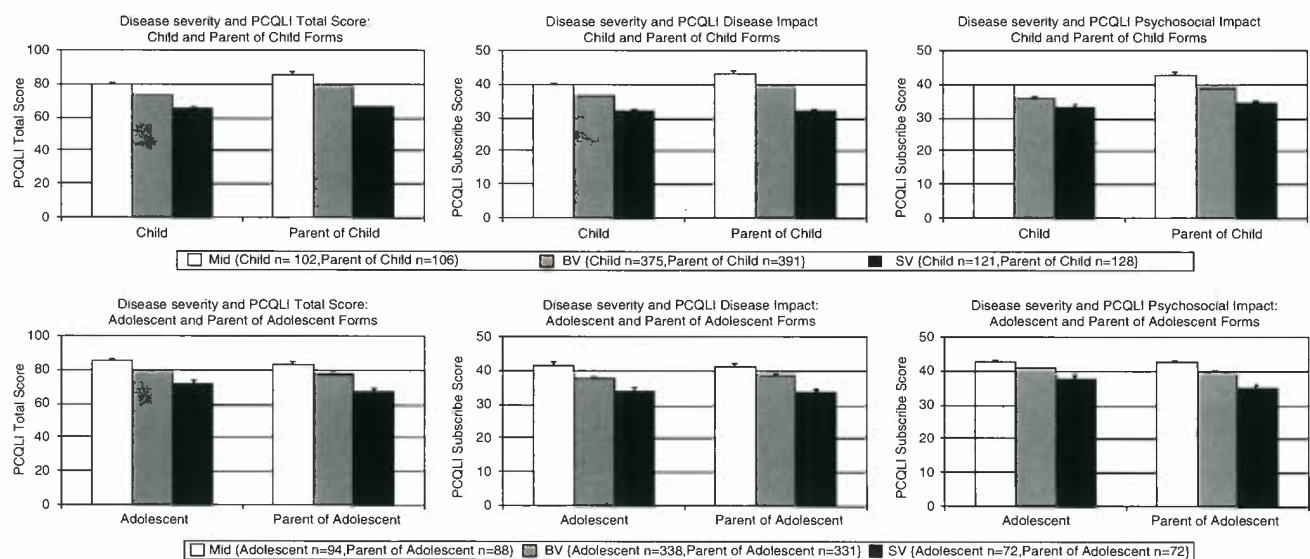


Figure 76.4. Association of severity of congenital HD with PCQLI scores. Values are expressed as means, with error bars representing SEMs. All three-way ($p < 0.001$) and two-way ($p \leq 0.036$) comparisons were statistically significant. BV indicates repaired biventricular HD subgroup; SV, palliated single-ventricle subgroup; mild, mild HD subgroup. (From Marino BS, Tomlinson R, Wernovsky G, et al. Validation of the pediatric cardiac quality of life inventory. *Pediatrics* 2010;126:498–508, with permission.)

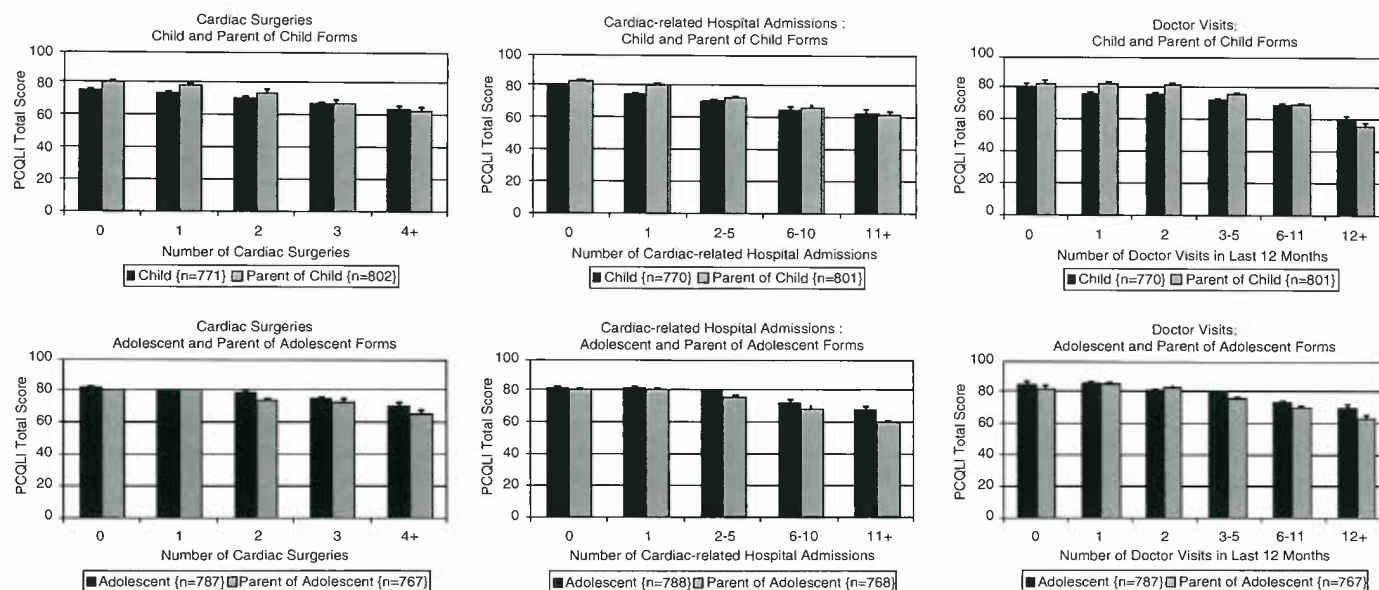


Figure 76.5. Lower PCQLI scores are associated with increasing medical care utilization in children and adolescents. Variation of PCQLI total scores with medical care utilization factors. Values are expressed as means, with error bars representing SEMs. All comparisons were significant ($p < 0.001$). (From Marino BS, Tomlinson R, Wernovsky G, et al. Validation of the pediatric cardiac quality of life inventory. *Pediatrics* 2010;126:498–508, with permission.)

HRQOL Studies in Specific Heart Disease Subgroups

HRQOL and functional status have also been studied in some specific patient subgroups with heart disease. In children with transposition of the great arteries (TGA), Culbert et al. (65) from the Congenital Heart Surgeons Society assessed

functional status using the CHQ-CF87 completed by 306 children 11 to 15 years after TGA repair. Health status was perceived as excellent when compared with published normative data and was better after arterial switch operation (ASO) than after atrial switch operation. Dunbar-Masterson et al. (66) who used the parent version of the CHQ also found that at 8 years

TABLE 76.5

PCQLI Total Score Correlates with Self-Perception, Competency, and Behavioral and Emotional Problems

Instrument	Domain	Respondent Group	Correlation Coefficient
SPPC/SPPA	Global self worth	Child	0.49
		Adolescent	0.40
Achenbach	Total competence scale (activity, social, school)	Child/parent	0.31/0.33
		Adolescent/parent	0.31/0.38
	Internalizing problem (anxious/depressed, Withdrawn/depressed, somatic complaints)	Child/parent	–0.52/–0.51
		Adolescent/parent	–0.51/–0.51
Achenbach (DSM)	Affective disorder	Child/parent	–0.55/–0.47
		Adolescent/parent	–0.49/–0.51
	Anxiety Disorder	Child/parent	–0.38/–0.44
		Adolescent/parent	–0.37/–0.39
	Somatic problems	Child/parent	–0.34/–0.34
		Adolescent/parent	–0.36/–0.36
	ADHD	Child/parent	–0.33/–0.33
		Adolescent/parent	–0.25/–0.34

All comparisons significant <0.0001 .

From Marino BS, Tomlinson R, Wernovsky G, et al. Validation of the Pediatric Cardiac Quality of Life Inventory. *Pediatrics* 2010;126:498–508, with permission.

TABLE 76.6

Variation in PCQLI Scores (Median and Range) Within Specific CHD Diagnosis and Procedural Groups

	PCQLI Median Total Score (Range)			
	Child	Parent of Child	Adolescent	Parent of Adolescent
AS (<i>n</i> = 75)	86.2 (51.9, 100)	86.8 (54.1, 100)	89.5 (65.1, 97.8)	85.2 (40.8, 99.3)
TOF (<i>n</i> = 125)	75.6 (48.7, 100)	78.6 (43.5, 100)	79.6 (39.6, 99.3)	78.7 (33.5, 100)
Fontan (<i>n</i> = 219)	64.4 (32.2, 99.1)	66.1 (30.7, 100)	70.5 (39.6, 100)	69.7 (26.0, 98.5)

AS, Aortic Stenosis; TOF, Tetralogy of Fallot.

From Marino BS, Tomlinson R, Wernovsky G, et al. Validation of the Pediatric Cardiac Quality of Life Inventory. *Pediatrics* 2010;126:498–508, with permission.

of age, children had an overall physical and psychosocial health status after the ASO similar to that of the general population. It was also noted that lower IQ and academic achievement were associated with worse psychosocial health status. Hovels-Gurich et al. (67) reported that children with TGA who had undergone neonatal ASO had parent-reported behavioral impairment at age 8 to 14 years with normal self-reported HRQOL.

Brosig et al. (68) compared psychosocial outcomes between preschool-aged survivors who underwent ASO for TGA and Fontan palliation for hypoplastic left heart syndrome (HLHS). By parent report, HRQOL scores in both CHD subgroups did not differ from healthy controls. Parents of children with HLHS reported more negative impact of the child's illness on the family and more parenting stress than parents of children with TGA. Children with HLHS had higher rates of attention and externalizing behavior problems than children with TGA. In a large study of Fontan survivors (69) 6 to 18 years of age, parents reported CHQ functional status summary scores that were significantly lower than the US population for Physical Functioning and Psychosocial Functioning. Parent-reported patient conditions, including behavior, learning, anxiety, attention problems, and depression explained the greatest amount of variation in the Psychosocial Functioning scores.

In a study by DeMaso et al. (70) HRQOL has been assessed in children and adolescents with implantable cardioverter-defibrillators. While the parent-reported psychosocial summary scores for children with defibrillators were not significantly different from the normative U.S. sample, the domains of social emotional behavioral roles, self-esteem, and the emotional impact of their child's health on themselves were all significantly lower than the normative sample. A recent multicenter study by Czosek et al. (71) compared HRQOL scores between pediatric device patients and healthy controls, and determined the key drivers of HRQOL in pediatric device patients. The study included 173 patient–parent pairs (40 implantable cardiac

defibrillators [ICD]/133 pacemaker; 50% CHD; 50% male; median age 13 [8 to 18] years). Compared to healthy controls, both patients and parents reported significantly lower PedsQL Total scores. ICD patients had significantly lower PCQLI Total scores than pacemaker patients. CHD patients had significantly lower PCQLI Total score than non-CHD patients. The key drivers of patient HRQOL were presence of ICD, CHD, and worse self-perception. For parent proxy reporters, patient HRQOL was driven by internalizing behavioral problems (anxiety, depression, and somatization). Interestingly, activity restrictions and device complications did not impact HRQOL. Whether these factors can be mitigated through the use of psychological interventions needs to be assessed.

Finally, in the pediatric heart transplant population, using the Children's Global Assessment Scale, 27% of children 6.1 to 12.9 years after transplant had emotional adjustment difficulties (72) and there was a significant correlation between emotional adjustment and family functioning. Wray et al. (73) also found that a significant number of pediatric heart transplant recipients (>33%) had increased behavior problems and diminished social competence, especially in children with a pretransplant diagnosis of CHD in comparison to children with cardiomyopathy pretransplant.

Predictors of HRQOL in the Pediatric Heart Disease Population

Neurodevelopmental Predictors of HRQOL in the Pediatric Heart Disease Population

Few studies have investigated the impact of neurodevelopmental outcome on HRQOL in the pediatric CHD population. For children with TGA, Dunbar-Masterson et al found that lower full-scale IQ (intelligence) and lower performance in reading and math (academic achievement) were associated with lower parent-reported psychosocial HRQOL scores at eight years of age (66). Williams et al. (74) found that children with Fontan palliation for HLHS displayed significant delays in communication and motor skills and lower parent-reported psychosocial HRQOL scores. Of note, both of these studies used a generic QOL instrument to measure psychosocial QOL, which may not be as sensitive or accurate as a disease-specific instrument (75). In addition, neither study measured patient-perceived HRQOL or specifically assessed the association between neuropsychological impairments and patient-perceived HRQOL. Parent-reported and self-reported HRQOL are both important since perception of HRQOL differs between patients and parents (30,56).

The cardiac-specific module of the PedsQL includes a cognitive problems subscale and a communication subscale (44,46). Using the PedsQL cardiac-specific module, Uzark et al. (56)

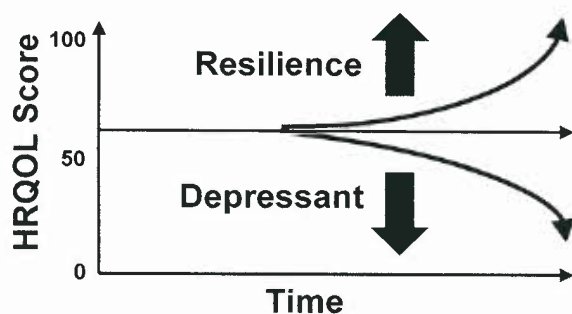


Figure 76.6. Patient independent arc of HRQOL: resilience versus depressant factors.

found that children with severe cardiovascular disease have lower parent-reported and self-reported HRQOL scores on the cognitive problems subscale and lower parent-reported HRQOL scores on the communications subscale than children with less severe cardiovascular disease. Recently, Marino et al. (76) demonstrated that worse executive functioning, gross motor ability, and mood (presence of anxiety and depression) significantly predicted lower PCQLI score after controlling for patient demographics and important clinical covariates. Executive functioning, gross motor ability, and mood accounted for up to 50% of the variance in patient and parent-reported HRQOL scores. These factors appear to be key drivers of HRQOL in complex CHD survivors and may be targets for future intervention (76).

Psychosocial Predictors of HRQOL in the Pediatric Heart Disease Population

While multiple studies have shown that there is psychosocial dysfunction in the pediatric heart disease population, few studies have assessed association between psychosocial predictors in the individual or family environment and HRQOL (56,57,69,77–79). A recent multicenter multinational study in the United States and England completed by Marino and colleagues explored the relationships between heart disease complexity, HRQOL, and psychosocial morbidity factors. Eight hundred and fifteen patient–parent pairs participated in the study with a mean patient age of 12.5 ± 1.5 years. The study assessed the mediating impact of specific psychosocial morbidity factors (family functioning and parental stress, and patient and parent posttraumatic stress and trait anxiety) on the association between heart disease complexity and lower HRQOL. High complexity was associated with a lower PCQLI Psychosocial Impact subscale score. Higher parental stress, posttraumatic stress, and trait anxiety scores were associated with a lower PCQLI Psychosocial Impact subscale score. The association between high complexity and lower PCQLI PI score was mediated by worse parental stress, posttraumatic stress, and trait anxiety (Total Correlation [direct and indirect effects] = -0.21 to -0.46 ; $p < 0.001$) for both patients and parents. Interventions on these psychosocial morbidities may improve QOL (80).

SUMMARY

Many studies of HRQOL in children with CHD have been limited by small sample size, have often relied on parental proxy report of the child's HRQOL, reported health status or observed functional status, or focused on a single dimension of HRQOL. Recent instrument development has allowed multidimensional, self-report of HRQOL, essential to development of interventions to improve HRQOL. Further research is needed to discover links between specific aspects of neurodevelopmental and psychosocial morbidity factors and HRQOL to identify developmental delays and psychosocial issues that may be improved through intervention. By characterizing the relationship between disease complexity, neurodevelopmental and psychosocial morbidity and HRQOL, physicians and caregivers will be able to change the medical care delivery system to significantly improve the lives of children with CHD and ensure their future success.

CLINICAL IMPLEMENTATION (IS HRQOL EVALUATION UTILIZED IN CLINICAL PRACTICE?)

The importance and utility of HRQOL assessment with reliable, valid, generalizable, and responsive instruments in the

pediatric heart disease population is centered on the fact that they provide a means to improve patient HRQOL outcomes through (a) the improvement of comprehensive follow-up of the pediatric heart disease population (surveillance and screening), (b) the identification of at-risk patients (risk stratification of heart disease subpopulations), (c) the identification of modifiable risk factors to prevent adverse outcomes (prevention), and (d) the design of interventions for children with poor outcomes (treatment planning). Early identification of neurodevelopmental impairments in academic achievement, language, visual construction and perception, attention, processing speed, memory, executive functioning, fine and gross motor skills, and/or attention deficit hyperactivity disorder (ADHD) in these children may allow the clinical care team to stratify populations and improve HRQOL outcomes through targeted intervention for at-risk children. Given some of the early data on the utility of physical rehabilitation in patients with CHD and diminished exercise capacity, physical functioning and HRQOL may be improved through rehabilitation or medical or device-based (pacemaker) therapies. In addition, early identification of psychosocial functioning issues in the child and/or family (posttraumatic stress, trait anxiety, depression, coping, family functioning, and parental stress) may allow risk stratification and the incorporation of targeted interventions to prevent or treat psychological or social morbidity. Unfortunately, the clinical evaluation of neurodevelopmental impairments and physical and psychosocial morbidity on HRQOL in children with heart disease has not become a standard component of care and much is to be learned. The clinical utility of current instruments is largely unknown.

Multiple barriers exist to incorporating HRQOL assessment into the clinical environment (19). Pediatricians and cardiologists (medical home providers) have ever-increasing demands on their time and the utilization of HRQOL instruments for surveillance and screening will only occur if administration, scoring, and interpretation of measures are simple and are easily integrated into the clinical practice setting in “real-time” as part of the “paper” or electronic medical record. In addition, practitioners will only incorporate HRQOL assessment into their clinical care if there is compelling evidence that surveillance, screening, referral, evaluation, and intervention are efficient, cost-effective, and make a difference in patient-specific HRQOL outcomes. One of the biggest barriers to incorporation is the lack of knowledge among practitioners of the theoretical benefits to HRQOL assessment. Only through clinical research studies focusing on harnessing the potential of HRQOL assessment will these barriers begin to fall.

RESEARCH AGENDA (WHAT IS NEEDED IN HRQOL RESEARCH IN PEDIATRIC HEART DISEASE PATIENTS?)

1. Future HRQOL research should focus on the associations of specific morbidities/phenotypes in the pediatric heart disease population and HRQOL to determine candidate factors for interventional studies for *prevention* and *treatment*. Specifically, further research is needed to discover links between neurodevelopmental, psychosocial, and physical morbidity factors and HRQOL to identify specific functional deficits that may be prevented or mitigated through intervention.
2. Both patient and parent respondents need to be evaluated in HRQOL research to learn more about similarities and differences between patient and parent respondents. These patterns will inform clinical applications on how best to assess HRQOL in patients and their parent/guardians and

inform how future screening and interventions programs may improve HRQOL.

3. It must be demonstrated that HRQOL assessment in the clinical setting will ultimately result in clinically meaningful changes in HRQOL and/or functional status. Specifically, it must be demonstrated that (a) it is feasible to collect HRQOL data in “real-time” in the clinical setting and that patients may be stratified into low- and high-risk groups for neurodevelopmental, physical, and psychosocial dysfunction, (b) it is feasible to refer patients with lower HRQOL scores stratified into a high-risk category into interventions, and (c) interventions in a high-risk group will result in clinically meaningful changes in HRQOL.
4. A responsive instrument is required and fundamental for the field to pursue an interventional agenda that will improve current clinical practice. Efforts should be made to demonstrate responsiveness in disease-specific measures shown to be reliable, valid, and generalizable in the United States. Once responsiveness has been demonstrated, this HRQOL tool should be considered for inclusion in all randomized clinical or interventional drug, device, or surgical treatment trials, where appropriate.
5. New HRQOL instruments should be developed for aging cohorts of pediatric heart disease patients (young adults and adults) in the United States as there is a rapidly growing population of Adult with CHD (ACHD population) in transition with changing HRQOL assessment needs. HRQOL instruments for adults with heart disease are intended for patients with heart disease due to hypertension or coronary ischemia. A combination of an adult generic HRQOL measure and an ACHD disease-specific HRQOL measure will provide the necessary tools to provide critical information on this unique and growing population.

CLINICAL AGENDA (WHAT IS NEEDED TO HARNESS THE POTENTIAL OF HRQOL ASSESSMENT FOR CLINICAL USE IN PEDIATRIC HEART DISEASE PATIENTS?)

1. Begin incorporating HRQOL evaluation into the clinic visit to take full advantage of the current advances in HRQOL measurement.
2. Strive to make all HRQOL evaluations conducted in clinical settings “research quality” (or at least create standard evaluation protocols) so that the field may benefit from reliable, valid, and potentially generalizable clinical information. There is so much variability in the way evaluations are presently conducted that it makes it difficult to generalize any data collected at any particular site or clinical setting across settings and/or populations.
3. Once it has been demonstrated that HRQOL assessment may be used for neurodevelopmental, psychosocial, and physical morbidity risk stratification, HRQOL assessment should be performed in all out-patient clinic visits as part of a formal standardized surveillance and screening program to allow for referral, intervention, and follow-up.

CONCLUSION

Over the last several decades mortality rates for children with heart disease have fallen. However, survivors may have neurodevelopmental, psychosocial, and physical morbidities that lower HRQOL. Although HRQOL assessment in this high-risk population has been lacking due to inherent issues in

HRQOL assessment in the pediatric heart disease population, advances have been made in HRQOL measurement with new reliable, valid, and generalizable measures. These questionnaires may be utilized to rapidly improve HRQOL research and obtain critical information that may be translated into the clinical domain. Rigorous characterization of the relationship between neurodevelopmental, psychosocial, and physical morbidity factors and HRQOL will identify specific factors amenable to intervention and allow clinicians to modify the medical care delivery system to significantly improve the lives of children with CHD and promote their future success. Formal screening and intervention programs based on HRQOL assessment will allow clinicians to intervene in the case of those children with significant deficits with the greatest potential to improve HRQOL.

FINANCIAL DISCLOSURE/CONFLICTS OF INTEREST

There are no financial relationships or conflicts of interest to disclose relevant to this manuscript.

REFERENCES

1. Tweddell JS, Hoffman GM, Mussatto KA, et al. Improved survival of patients undergoing palliation of hypoplastic left heart syndrome: lessons learned from 115 consecutive patients. *Circulation* 2002;106:182–189.
2. Mahle WT, Spray TL, Wernovsky G, et al. Survival after reconstructive surgery for hypoplastic left heart syndrome: A 15-year experience from a single institution. *Circulation* 2000;102:III136–III141.
3. Warnes CA, Liberthson R, Danielson GK, et al. Task force 1: the changing profile of congenital heart disease in adult life. *J Am Coll Cardiol* 2001;37:1170–1175.
4. Mahle WT, Clancy RR, Moss EM, et al. Neurodevelopmental outcome and lifestyle assessment in school-aged and adolescent children with hypoplastic left heart syndrome. *Pediatrics* 2000;105:1082–1089.
5. Wernovsky G, Stiles KM, Gauvreau K, et al. Cognitive development after the Fontan operation. *Circulation* 2000;102:883–889.
6. Bellinger DC, Wypij D, duPlessis AJ, et al. Neurodevelopmental status at eight years in children with dextro-transposition of the great arteries: the Boston Circulatory Arrest Trial. *J Thorac Cardiovasc Surg* 2003;126:1385–1396.
7. Wray J and Sensky T. How does the intervention of cardiac surgery affect the self-perception of children with congenital heart disease? *Child Care Health Dev* 1998;24:57–72.
8. Casey FA, Sykes DH, Craig BG, et al. Behavioral adjustment of children with surgically palliated complex congenital heart disease. *J Pediatr Psychol* 1996;21:335–352.
9. Davis CC, Brown RT, Bakeman R, et al. Psychological adaptation and adjustment of mothers of children with congenital heart disease: stress, coping, and family functioning. *J Pediatr Psychol* 1998;23:219–228.
10. Mahle WT, McBride MG, and Paridon SM. Exercise performance after the arterial switch operation for D-transposition of the great arteries. *Am J Cardiol* 2001;87:753–758.
11. Limperopoulos C, Majnemer A, Shevell MI, et al. Functional limitations in young children with congenital heart defects after cardiac surgery. *Pediatrics* 2001;108:1325–1331.
12. Paridon SM, Mitchell PD, Colan SD, et al. A cross-sectional study of exercise performance during the first 2 decades of life after the Fontan operation. *J Am Coll Cardiol* 2008;52:99–107.
13. Ware JE, Jr. Methodology in behavioral and psychosocial cancer research. Conceptualizing disease impact and treatment outcomes. *Cancer* 1984;53:2316–2326.
14. Aaronson NK. Quality of life: what is it? How should it be measured? *Oncology (Williston Park)* 1988;2:69–76.
15. Drotar D. Measuring Child Health: Scientific Questions, Challenges, and Recommendations. *Ambulatory Pediatrics* 2004;4:353–357.
16. World Health Organization. Preamble to the Constitution of the World Health Organization as adopted by the International Health Conference, New York, 19–22 June 1946; signed on 22 July 1946 by the representatives of 61 States (Official Records of the World Health Organization, no. 2, p. 100) and entered into force on 7 April 1948.
17. Stein REK, Jessop DJ. Functional Status II(R): a Measure of Child Health Status. *Med Care* 1990;28:1041–1055.

18. U.S. Department of Health and Human Services FDA Center for Drug Evaluation and Research, U.S. Department of Health and Human Services FDA Center for Biologics Evaluation and Research, and U.S. Department of Health and Human Services FDA Center for Devices and Radiological Health. *Guidance For Industry: Patient-Reported Outcome Measures: Use in Medical Product Development to Support Labeling Claims*. 2006: 1–20.
19. Drotar D. *Measuring Health-Related Quality of Life in Children and Adolescents*. Mahwah, NJ: Lawrence Erlbaum Associates, Publishers, 1998.
20. Higginson IJ, Carr AJ. Measuring quality of life: using quality of life measures in the clinical setting. *BMJ* 2001;322:1297–1300.
21. Lee CP, Chertow GM, Zenios SA. An empiric estimate of the value of life: updating the renal dialysis cost-effectiveness standard. *Value Health* 2009;12:80–87.
22. Cella D, Riley W, Stone A, et al. The Patient-Reported Outcomes Measurement Information System (PROMIS) developed and tested its first wave of adult self-reported health outcome item banks: 2005–2008. *J Clin Epidemiol* 2010;63:1179–1194.
23. Hahn E, DeVellis R, Bode R, et al. Measuring social health in The Patient-Reported Outcomes Measurement Information System (PROMIS): item bank development and testing. *Qual Life Res* 2010;19:1035–1044.
24. Hays R, Bjorner J, Revicki D, et al. Development of physical and mental health summary scores from the Patient-Reported Outcomes Measurement Information System (PROMIS) global items. *Qual Life Res* 2009;18:873–880.
25. Irwin DE, Varni JM, Yeatts K, et al. Cognitive interviewing methodology in the development of a pediatric item bank: a Patient Reported Outcomes Measurement Information System (PROMIS) study. *Health Qual Life Outcomes* 2009;7:3.
26. Rothrock NE, Hays RD, Spritzer K, et al. Relative to the general US population, chronic diseases are associated with poorer health-related quality of life as measured by the Patient-Reported Outcomes Measurement Information System (PROMIS). *J Clin Epidemiol* 2010;63:1195–1204.
27. Ware JE. The Patient-Reported Outcomes Measurement Information System (PROMIS) seeks to improve and standardize measures of five generic health-related QOL domains. *Pediatric Reported Outcomes Newsletter* 2007;38:1–3.
28. U.S. Department of Health and Human Services Food and Drug Administration, Center for Drug Evaluation and Research (CDER), Center for Biologics Evaluation and Research (CBER), and Center for Devices and Radiological Health (CDRH). *Guidance for Industry: Patient-Reported Outcome Measures: Use in Medical Product Development to Support Labeling Claims*. 2009:1–43.
29. Janse AJ, Uiterwaal CS, Gemke RJ, et al. A difference in perception of quality of life in chronically ill children was found between parents and pediatricians. *J Clin Epidemiol* 2005;58:495–502.
30. Marino BS, Tomlinson RS, Drotar D, et al. Quality-of-life concerns differ among patients, parents, and medical providers in children and adolescents with congenital and acquired heart disease. *Pediatrics* 2009;123:e708–e715.
31. Moons P, Van Deyk K, Budts W, et al. Caliber of quality-of-life assessments in congenital heart disease: a plea for more conceptual and methodological rigor. *Arch Pediatr Adolesc Med* 2004;158:1062–1069.
32. Gill TM, Feinstein AR. A critical appraisal of the quality of quality-of-life measurements. *JAMA* 1994;272:619–626.
33. Varni JW. The Pediatric Cancer Quality of Life Inventory (PCQL). I. Instrument development, descriptive statistics, and cross-informant variance. *J Behavior Med* 1998;21:179–204.
34. Eiser C, Morse R. Can parents rate their child's health-related quality of life? Results of a systematic review. *Qual Life Res* 2001;10:347–357.
35. Upton P, Lawford J, Eiser C. Parent-child agreement across child health-related quality of life instruments: a review of the literature. *Qual Life Res* 2008;17:895–913.
36. Theunissen NCM, Vogels TGC, Koopman HM, et al. The proxy problem: child report versus parent report in health-related quality of life research. *Qual Life Res* 1998;7:387–397.
37. Varni JW, Limbers CA, Burwinkle TM. How young can children reliably and validly self-report their health-related quality of life? An analysis of 8,591 children across age subgroups with the PedsQL 4.0 Generic Core Scales. *Health Qual Life Outcomes* 2007;5:1–13.
38. Campo JV, Comer DM, Jansen-McWilliams L, et al. Recurrent pain, emotional distress, and health service use in childhood. *J Pediatrics* 2002;141:76–83.
39. Janicke DM, Finney JW, Riley AW. Children's health care use: a prospective investigation of factors related to care-seeking. *Med Care* 2001;39:990–1001.
40. Creameens J, Eiser C, Blades M. Characteristics of health-related self-report measures for children aged three to eight years: a review of the literature. *Qual Life Res* 2006;15:739–754.
41. Riley AW. Evidence that school-age children can self-report on their health. *Ambul Pediatr* 2004;4:371–376.
42. Olson LM, Lara M, Pat Frintner M. Measuring health status and quality of life for US children: relationship to race, ethnicity, and income status. *Ambul Pediatr* 2004;4:377–386.
43. Landgraf JM, Abetz L, Ware JE. *The Child Health Questionnaire (CHQ): A User's Manual*. Boston, BA: The Health Institute, New England Medical Center, 1996.
44. Varni JW, Seid M, Rode CA. The PedsQL: measurement model for the pediatric quality of life inventory. *Med Care* 1999;37:126–139.
45. Kamphuis M, Zwinderman KH, Vogels T, et al. A cardiac-specific health-related quality of life module for young adults with congenital heart disease: development and validation. *Qual Life Res* 2004;13:735–745.
46. Uzark K, Jones K, Burwinkle TM, et al. The Pediatric Quality of Life Inventory in children with heart disease. *Prog Ped Cardiol* 2003;18:141–149.
47. Kendall L, Lewin RJ, Parsons JM, et al. Factors associated with self-perceived state of health in adolescents with congenital cardiac disease attending paediatric cardiology clinics. *Cardiol Young* 2001;11:431–438.
48. Macran S, Birks Y, Parsons J, et al. The development of a new measure of quality of life for children with congenital cardiac disease. *Cardiol Young* 2006;16:165–172.
49. Marino BS, Shera D, Wernovsky G, et al. The development of the pediatric cardiac quality of life inventory: a quality of life measure for children and adolescents with heart disease. *Qual Life Res* 2008;17:613–626.
50. Streiner DL, Norman GR. *Health Measurement Scales*. New York, NY: Oxford University Press, 1995.
51. Koot HM, Wallander JL. *Quality of Life in Child and Adolescent Illness: Concepts, Methods And Findings*. New York, NY: Brunner-Routledge, 2001.
52. Messick S. Validity of psychological assessment: validation of inferences from persons' responses and performances as scientific inquiry into score meaning. *American Psychologist* 1995;50:741–749.
53. Clark LA, Watson D. Constructing validity: basic issues in objective scale development. *Psychol Assess* 1995;7:309–319.
54. Lohr KN. Assessing health status and quality-of-life instruments: attributes and review criteria. *Qual Life Res* 2002;11:193–205.
55. Thorndike RM, Thorndike-Christ T. *Measurement and Evaluation in Psychology and Education*. Boston, MA: Pearson, 2010.
56. Uzark K, Jones K, Slusher J, et al. Quality of life in children with heart disease as perceived by children and parents. *Pediatrics* 2008;121:e1060–e1067.
57. Marino BS, Tomlinson R, Wernovsky G, et al. Validation of the pediatric cardiac quality of life inventory. *Pediatrics* 2010;126:498–508.
58. Marino BS, Drotar D, Cassidy A, et al. External validity of the pediatric cardiac quality of life inventory. *Qual Life Res* 2011;20:205–214.
59. Gersony WM, Hayes CJ, Driscoll DJ, et al. Second natural history study of congenital heart defects. Quality of life of patients with aortic stenosis, pulmonary stenosis, or ventricular septal defect. *Circulation* 1993;87:152–165.
60. Walker RE, Gauvreau K, Jenkins KJ. Health-related quality of life in children attending a cardiology clinic. *Pediatr Cardiol* 2004;25:40–48.
61. Majnemer A, Limperopoulos C, Shevell M, et al. Health and well-being of children with congenital cardiac malformations, and their families, following open-heart surgery. *Cardiol Young* 2006;16:157–164.
62. DeMaso DR, Campis LK, Wypij D, et al. The impact of maternal perceptions and medical severity on the adjustment of children with congenital heart disease. *J Pediatr Psychol* 1991;16:137–149.
63. Latal B. Psychological adjustment and quality of life in children and adolescents following open-heart surgery for congenital heart disease: a systematic review. *BMC Pediatr* 2009;9:6.
64. Mussatto K, Tweddell J. Quality of life following surgery for congenital cardiac malformations in neonates and infants. *Cardiol Young* 2005;15:174–178.
65. Culbert EL, Ashburn DA, Cullen-Dean G, et al. Quality of life of children after repair of transposition of the great arteries. *Circulation* 2003;108:857–862.
66. Dunbar-Masterson C, Wypij D, Belling DC, et al. General health status of children with D-transposition of the great arteries after the arterial switch operation. *Circulation* 2001;104:1138–1142.
67. Hovels-Gurich HH, Konrad K, Wiesner M, et al. Long term behavioural outcome after neonatal arterial switch operation for transposition of the great arteries. *Arch Dis Child* 2002;87:506–510.
68. Brosig CL, Mussatto KA, Kuhn EM, et al. Psychosocial outcomes for pre-school children and families after surgery for complex congenital heart disease. *Pediatr Cardiol* 2007;28:255–262.
69. McCrindle BW, Williams RV, Mitchell PD, et al. Relationship of patient and medical characteristics to health status in children and adolescents after the Fontan procedure. *Circulation* 2006;113:1123–1129.
70. DeMaso DR, Lauretti A, Spieth L, et al. Psychosocial factors and quality of life in children and adolescents with implantable cardioverter-defibrillators. *Am J Cardiol* 2004;93:582–587.
71. Czosek J, Bonney WJ, Mah D, et al. Impact of cardiac devices on the quality of life in pediatric patients and parents. *Circulation* 2011;124:A10016.
72. DeMaso DR, Douglas Kelley S, Bastardi H, et al. The longitudinal impact of psychological functioning, medical severity, and family functioning in pediatric heart transplantation. *J Heart Lung Transplant* 2004;23:473–480.
73. Wray J and Radley-Smith R. Longitudinal assessment of psychological functioning in children after heart or heart-lung transplantation. *J Heart Lung Transplant* 2006;25:345–352.
74. Williams DL, Gelijs AC, Moskowitz AJ, et al. Hypoplastic left heart syndrome: valuing the survival. *J Thorac Cardiovasc Surg* 2000;119:720–731.
75. Drotar D, Stancin T, Dworkin PH, et al. Selecting developmental surveillance and screening tools. *Pediatr Rev* 2008;29:e52–e58.
76. Marino BS, Beebe D, Cassidy A, et al. Executive functioning, gross motor ability and mood are key drivers of poorer quality of life in child and adolescent survivors with complex congenital heart disease. *J Am Coll Cardiol* 2011;57:421.

77. American Academy of Pediatrics Committee on Children With Disabilities and Committee on Psychosocial Aspects of Child and Family Health: Psychosocial risks of chronic health conditions in childhood and adolescence. *Pediatrics* 1993;92:876–878.
78. Spijkerboer A, Utens E, Bogers A, et al. Long-term behavioural and emotional problems in four cardiac diagnostic groups of children and adolescents after invasive treatment for congenital heart disease. *Int J Cardiol* 2008;125:66–73.
79. Spurkland I, Bjørnstad PG, Lindberg H, et al. Mental health and psychosocial functioning in adolescents with congenital heart disease. A comparison between adolescents born with severe heart defect and atrial septal defect. *Acta Paediatrica* 1993;82:71–76.
80. Marino BS, Cassidy AEC, Drotar D, et al. Psychosocial morbidity factors mediate the relationship between heart disease complexity and lower quality of life (Submitted for national presentation at the 61th Scientific Sessions of the American College of Cardiology, Chicago, IL, 2012).
81. Wray J, Brown K, Franklin R, et al. The pediatric cardiac quality of life inventory: testing a new disease specific quality of life measure in the UK. *Arch Dis Child* 2010;95:A74.

Anthony Y. Lee ■ Thomas Taghon ■ Richard Eugene McClead, Jr., ■ Terrance Davis ■ Richard J. Brilli

INTRODUCTION

Much of the science of quality, safety, and continuous quality improvement (QI) comes from fields outside of medicine such as nuclear power and commercial aviation. Some quality-related terminology may not be part of the usual lexicon of pediatric cardiologists, or they may not be familiar with the specific definitions. To avoid confusion and put some of these terms in the clinical context of the heart center, the following is a brief list of definitions:

Quality: The degree to which health services for individuals and populations increase the likelihood of desired health outcomes and are consistent with current professional knowledge (1). Thus, quality is about outcomes: how successful are we in treating a certain type of cardiac defect? How accurately can we diagnose it?

Patient Safety: Freedom from accidental injury (2), or avoidance, prevention, and amelioration of adverse outcomes or injuries from the processes of health care (3). This is different from employee's safety only in point of view. The practices that maximize patient safety will also maximize employee safety.

Adverse Event: An injury that is caused by medical management, not the patient's disease (2). Not all adverse events are preventable. Not all untoward outcomes are the result of adverse events. An untoward outcome in the absence of medical mismanagement may not be preventable.

Medical Error: An event where a planned action is not carried out or carried out incorrectly—an "error of execution" or an event that happened because of a faulty plan—an "error of planning." (2,4) James Reason (4) further dissects the anatomy of medical errors into slips, lapses, and fumbles. A *slip* is when individuals do something they are not supposed to do, a *lapse* is when they don't do something they are supposed to do, and a *fumble* is when a normally well-executed task is simply bungled.

Swiss Cheese Phenomenon: Another concept popularized by Reason is that most significant adverse events are not the result of a single medical error. They are the result of a series of failures of the barriers (usually policies and procedures) that were intended to protect the patient. Each barrier is represented as a slice of cheese. The barriers are not perfect, and the holes in the Swiss cheese represent areas where the barrier could be breached. For an error to reach the patient and cause harm, all the holes in the various layers of Swiss cheese must line up.

QI work requires a change in the mindset for many clinician scientists. QI in health care consists of systematic, data-guided activities designed to bring about immediate positive changes. QI tools are used as deliberate actions guided by data that reflect the effects of those actions. QI is an overarching ongoing process to improve the outcomes of health

care delivery and as such is different than more traditional research that is aimed at answering a specific question over a discrete time (5). Further, most clinician scientists are trained in the traditional model of research (randomized trials with treatment groups and control groups) wherein an intervention is introduced while controlling for all or most other variables and then examining the result. Often a comparative group is monitored that did not receive the intervention. QI work, on the other hand, seeks to monitor the system in real time, introduce interventions, and monitor for how the system responds and then introduce further interventions until a desired and measurable outcome is achieved. QI does not attempt to control system variables as interventions are introduced. Understanding complex system interactions rather than controlling them distinguishes QI from intervention-based research trials.

This chapter is intended to guide the cardiology specialist through an overview of quality- and safety-related principles. We have chosen to use a clinical case scenario that caused significant harm to a patient to illustrate QI concepts and tools. The case is based upon a cardiac intensive care unit (ICU)-related medical error but could have happened in the pediatric ICU or even in a general care unit.

CASE STUDY

TJ was a 4-year-old female patient with truncus arteriosus who was admitted for replacement of an obstructive right ventricle to pulmonary artery conduit.

The surgery was routine, but postoperatively the chest tube output was high and bloody. Her hemoglobin level dropped from 10.5 to 7.0 g/dL over the first 4 hours postoperatively. Tachycardia developed, and in response, the attending physician ordered 1 unit of packed red blood cells and fresh frozen plasma to be given as soon as possible for this blood type O negative patient.

Meanwhile, a new patient arrived from another hospital and was being placed on extracorporeal membrane oxygenation (ECMO). The ECMO team had ordered 2 units of packed red blood cells (A positive) as well as fresh frozen plasma and platelets.

TJ's chest bleeding was not decreasing, so preparations were made to take her back to the operating room to explore for a bleeding site. Her blood pressure was beginning to drop, and the critical care physician asked for the blood to be delivered to the ICU "stat." Shortly thereafter, the blood bank technician appeared in the ICU with blood in hand for the ECMO patient, but was unfamiliar with the physical layout of the unit. TJ's nurse saw the blood bank technician looking in the door to ask for directions, and assumed that blood was what had just been ordered for TJ. The nurse signaled the technician into the room and received the blood. TJ's blood pressure was dropping rapidly, so the decision had been made

to not take the patient to the OR, but to explore her chest in the pediatric intensive care unit (PICU). As the surgeon was donning gown and gloves, he indicated an urgency to get the blood running quickly, so the blood was hung and a rapid infusion was started.

Within 5 minutes, as the chest was being prepped, TJ's urine turned red. She had worsening hypotension and increased bleeding. An acute hemolytic transfusion reaction was confirmed when the donor blood was identified as the A positive blood intended for the ECMO patient down the hall. The transfusion was immediately discontinued. Steroids and mannitol were given while the exploration was under way. The transfusion was reinstituted when the correct O negative blood originally intended for TJ arrived. A source of active bleeding was found and surgically corrected, but diffuse oozing continued. Serum potassium rose over the next 2 hours to 7.5 mEq/L along with the development of anuria. Despite an infusion of insulin and glucose, mannitol, intravenous hydration, Kayexalate enemas, and intravenous calcium, cardiac arrest ensued from which the patient could not be resuscitated.

A serious safety event was declared, and a root cause analysis (RCA) was carried out.

Root Cause Analysis—A Road to Resolution: What Happened and Why

TJ's Case: The wrong blood was given to TJ. A subsequent cause analysis of the event revealed: (a) the perceived urgency of blood administration was used by the nurse as a reason to "skip" the double check that should occur prior to all blood product administration (an "individual failure"); and (b) the hospital and blood bank did not have a clear and well-known double check policy (with consequences for policy violation) prior to all medication and blood product administration (a "system failure.")

RCA is a framework used in industry and recently applied to health care that is utilized retrospectively to determine system and individual causes of adverse events. In 1996, the Joint

Commission mandated that an RCA be done on all reportable sentinel events including "mismatched blood administration with transfusion reaction," yet the literature to date supporting the effectiveness of RCA is limited. In 1998, the Veteran's Administration (VA) National Center for Patient Safety (NCPS) was established. Bagian et al. (6) transformed the VA system of cause analysis by implementing a frontline staff-driven process that emphasized searching for system vulnerabilities with actionable solutions and de-emphasizing the less actionable human error root causes. Recently, Percarpio et al. (7) examined the evidence that RCA improved patient safety. From among 38 references, 11 case studies used clinical or process outcome measures to assess RCA effectiveness, described corrective actions, and outlined improved clinical outcomes subsequent to the RCA. Examples of improved outcomes included reduced mortality following various surgical procedures, reduced numbers of patient falls, and improved liver transplant graft survival. However, no pediatric studies were reported.

There are multiple templates used to complete an RCA, with all involving a description of the event with a timeline, identification of causal events, and suggested corrective actions (7,8). Causal factors are often broken into subcategories such as patient factors, caregiver factors, team factors, and technology or environmental factors (8). Asking the question, "why?" five times has been used to help identify all the contributing factors associated with an adverse event (9). The responses obtained to these "why" questions are used to help create a cause-and-effect diagram. This cause-and-effect diagram or "fishbone diagram" can also be used to help map the process and better categorize root causes. The main categories of factors contributing to the event are listed in the various "branches." Within each major branch, smaller branches may be added describing the deeper issues within each category (Fig. 77.1). Percarpio et al. also include "measures to track improvement" and "baseline with follow-up data" to the aforementioned RCA framework.

There are several limitations associated with how most RCA work is completed. Many resources are required by frontline staff and hospital leaders with limited evidence that the RCA process improves patient safety or quality. Primary limitations

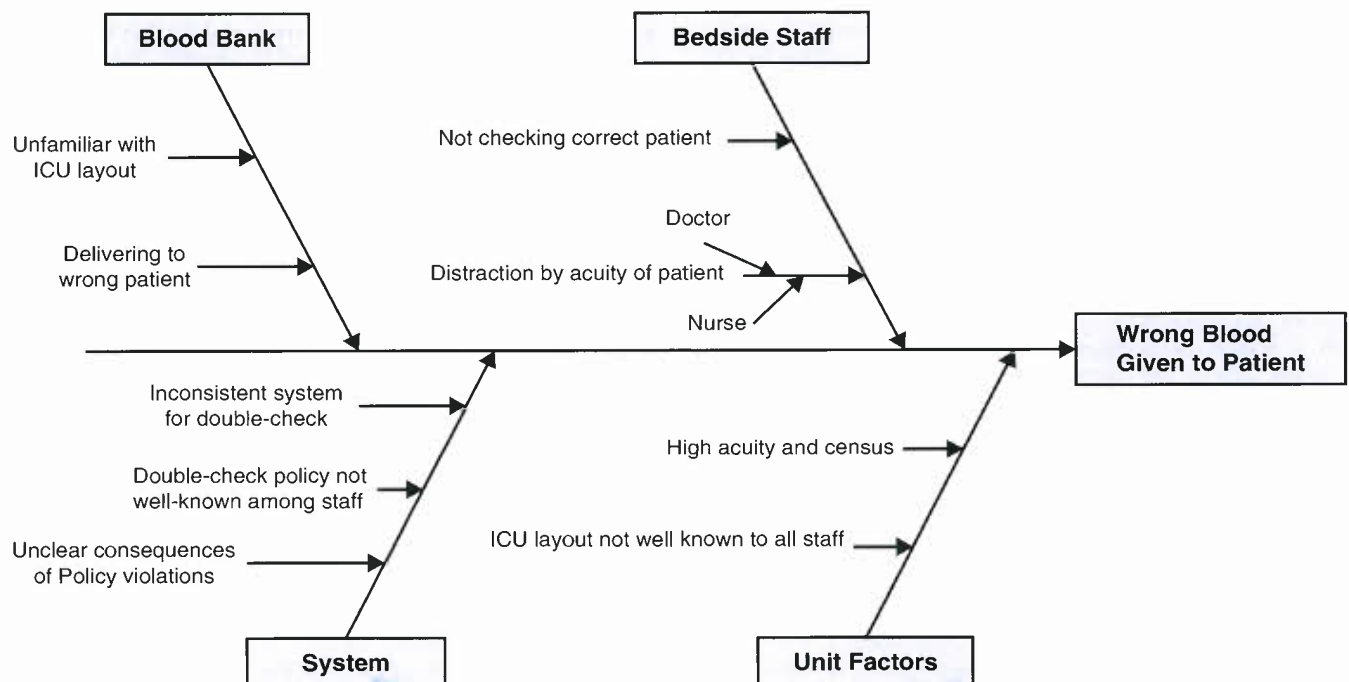


Figure 77.1. Cause-and-effect (fishbone) diagram for the TJ's case.

are more related to the implementation of the RCA process and include: (a) narrow scope (limiting the findings to only the event in question rather than generalizing to other areas of the hospital system); (b) lack of reliable implementation of the identified corrective actions and follow-up to ensure the corrective actions are sustained; (c) too much focus on the individual human error (punitive culture) and less on the larger system that enabled the individual to fail; and (d) hindsight bias by the RCA team because the RCA, by definition, is conducted after the event has occurred.

In contrast to the retrospective RCA approach, the Healthcare Failure Modes and Effects Analysis (HFMEA) method utilizes a prospective approach to adverse event analysis. By anticipating where problems may occur or proactively analyzing high-risk processes before they are implemented, hospitals may use the HFMEA process to prevent adverse events, rather than reacting to an event that has already occurred. A commonly used HFMEA template was designed by the VA NCPS and involves five steps to assess a health care process: (a) identifying the topic, (b) forming of a multidisciplinary team, (c) creating a graphical description of the process, (d) performing a hazard analysis, and (e) developing actions and identifying outcome measures (10). The hazard analysis (step d) is an essential part of the HFMEA process and uses a mathematical scoring system to prioritize risk and potential errors (failure modes) in the process being evaluated. Scoring takes into account the probability of the failure actually happening as well as the consequences of the failure if it did occur. Failure modes with high scores get prioritized to develop a mitigation strategy and action plan to be followed if the failure happens. Recently, Ashley et al. (11) have questioned the reliability of the mathematical scoring systems in use today that result in very different prioritization recommendations for the failure modes. They suggest that a consensus scoring system should be developed to mitigate this possibility.

Our organization and a few other US pediatric hospitals have collaborated with Healthcare Performance Improvement, LLC, to implement a robust RCA process as part of a larger high reliability strategy to improve safety and quality outcomes. RCAs are triggered by serious harm events, near-miss harm events, or Joint Commission "sentinel events." Joint Commission sentinel events are "an unexpected occurrence involving death or serious physical or psychological injury, or the risk thereof." (12) Sentinel events are identified by the outcome without consideration for preventability or whether there was a variation from expected care practices that caused the event. In contrast, a serious harm event starts with a deviation from best practice that results in serious harm. Therefore, a serious harm event includes both the causal process and the untoward outcome.

The RCA model we are using involves a careful reconstruction of the timeline describing the sequence of actions preceding and following the harm event. The timeline description requires interviews with all staff involved in the event along with a review of pertinent policies and procedures. Inappropriate actions are identified when there is deviation from expected practice or local or national policies/guidelines. The timeline and possible inappropriate actions are discussed by an RCA team composed of individuals who are *not* involved in the harm event but are knowledgeable of the patient care processes that failed. The RCA team is led by an executive sponsor whose role is to help the RCA team when or if they reach system barriers that require executive interventions. Root causes, once identified, are discussed by the RCA team and corrective actions are codified. The root causes are categorized into system or individual failure modes. There are multiple subcategories within the larger system or individual failure groupings. This subcategorization is intended to make it easier to find common causes for adverse events, even if the

specifics of the various events are disparate. Individuals who possess the authority to implement the corrective actions are identified, and a timeline for implementation is established. An expected date of completion is recorded and follow-up by QI staff takes place to ensure that the corrective actions have been implemented and are sustained.

TJ's Case: TJ received the wrong blood. **System failures included the following:** The hospital did not have a clear, consistent method and policy for double-checking blood products. Additionally, the expectations and potential consequences of violating a double check were not clearly understood by all staff members. **Individual failures included the following:** The nurse did not perform a double check prior to blood administration to ensure that the blood was intended for her patient, although she knew the double check was necessary. The blood bank technician did not confirm delivering the blood product to the correct patient bed. **System corrective measures included the following:** Establish a hospital-wide policy regarding how blood products are ordered and delivered to the patient. Require a mandatory double check of blood products (as well as high-risk medications) by all staff members. Provide education to staff members regarding this policy as well as provide background to why it was established. **Individual corrective measures include:** Provide coaching to the nurse involved as she chose to take an unacceptable risk, but has no prior history of safety issues. Provide required education and increased supervision of this nurse and blood bank technician.

When Individuals Fail

There are several individual failures that may have contributed to the preventable harm suffered by TJ. The care provider likely realized that a double check of the blood transfusion was required. However, because the environment in the ICU was hectic and the patient was unstable and deteriorating rapidly, this important step was omitted. Health care has often promoted a "culture of blame" when individuals fail. "Who messed up?" is often the first question when patient harm occurs. Individuals are blamed for errors when hospital leadership fails to recognize the influence and impact of a "flawed" system on individual performance. How was the system designed to "help the individual fail?" The "blame culture" leads to decreased reporting of errors and further impairs the ability of leaders and frontline staff to identify and fix system-related issues. Nevertheless, it is easier to blame someone and resort to familiar solutions such as "counseling, disciplinary action, enforcing rules, or developing new rules" rather than finding the root cause of systemic problems. Reason's "Swiss Cheese Model" outlines how systems have flaws (holes in the cheese) that when lined up appropriately will make it easier for the individual failure (an error) to reach the patient and ultimately lead to a patient being harmed (Fig. 77.2) (13). Providers and patients become the victims of systems that are inadequately designed to prevent or reduce human error. Punishing the individual will not reduce the error rate. In fact, in an environment of blame, staff members are less likely to report errors or near-miss errors. James Reason has been quoted as saying, when an individual forgets (a slip), there is little value in "putting a carcass on the wall" to demonstrate that the problem is fixed (14).

Nevertheless, sometimes individuals who make mistakes leading to patient harm should be held accountable for their individual failures. A healthy safety environment is one that balances the "blame-free culture" with fairness regarding personal accountability. The term "just culture" has been used to describe this cultural balance (15,16). A "just culture" environment is not totally blame-free, but rather a culture in which the process for evaluating errors is clear, transparent, and carefully separates blame-worthy from blame-less acts. In

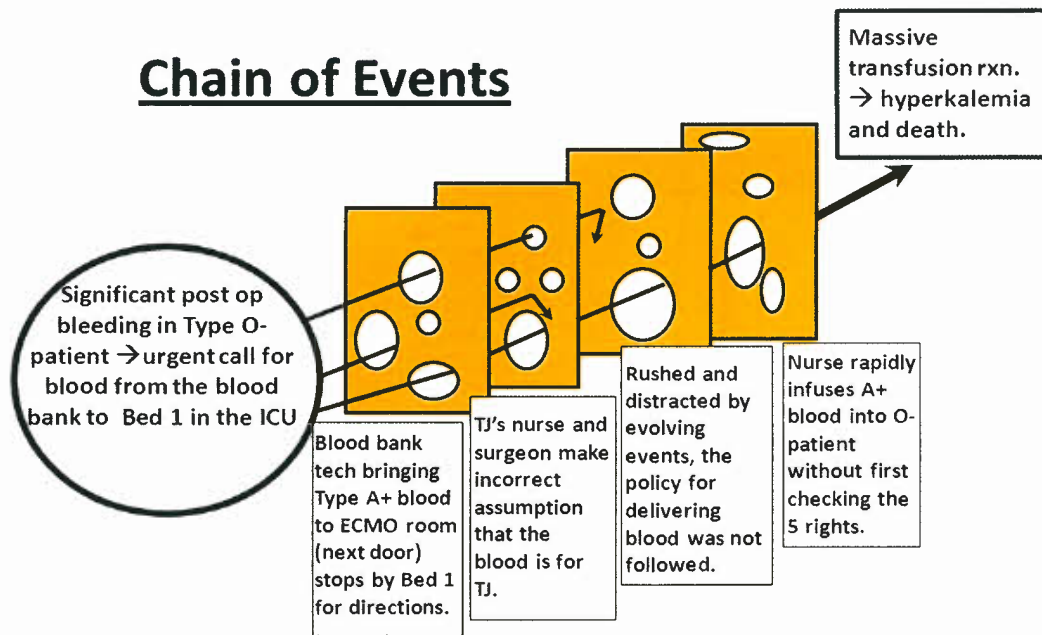


Figure 77.2. Chain of events passing through corresponding holes in layers of defense (Swiss Cheese Model). (Concept adapted from J Reason. *Managing the Risks of Organizational Accidents*, 1997 by Healthcare Performance Improvement, LLC © with permission.)

this case scenario, blaming the individual and removing the employee likely will not prevent a similar episode from occurring by another employee. The system must be constructed to make it easier for employees working in the high-stress ICU environment to stop and think prior to proceeding with a safety critical act (e.g., double-checking patient records prior to blood administration). Since “just culture” does not imply “blame-free,” determining culpability is essential. James Reason (17) provides an algorithm for assessing individual culpability associated with unsafe acts, which is consistent with a just culture. Through a series of questions, leaders can assess individual culpability: Were the actions and consequences intended? Is there a medical condition (e.g., substance abuse or chronic illness) involved? Did the individual knowingly violate a safe operating procedure that was readily available to and understandable by the individual? Would others in the same circumstances do the same thing? Does this person have a history of unsafe acts? Based on the answers to these questions, stages of diminishing culpability can be assigned ranging from criminal negligence to blameless error (Fig. 77.3).

The Improvement Team—Aim, Key Drivers, and Interventions Developed by the Team

Multiple methodologies have been described to fix failing systems including the Model for Improvement, Six-Sigma DMAIC, Lean Improvement, and the Seven-Step Problem-Solving model (18). These methodologies have many similarities and use many of the same tools to implement change. One of the most widely used methodologies in health care is the Model for Improvement. This method “attempts to balance the rewards from taking action with the wisdom of careful study before taking action” (18). The Model for Improvement starts with three questions (Fig. 77.4):

1. “What are we trying to accomplish?” Define your improvement project in the form of a specific aim that states what you intend to improve, by how much, by when, in what

population, and for how long. The specific aim should be concise, measurable, and achievable. This is most likely to happen when your specific aim includes SMART elements. That is, it should be Specific, Measurable, Attainable, Relevant, and Timely (see below).

2. “How will you know that a change is an improvement?” If the system that requires improvement is relatively simple, the improvement should be obvious. That may not be the case for more complex systems. Choosing the right metric(s) is critical to the success of the improvement project.
3. “What changes can we make that will result in improvement?” Ideas for improvement can come from a variety of sources such as peer-reviewed literature, a detailed analysis of internal data or identification of best practices used by other organizations or industries. Often, improvement ideas can be generated by QI teams through group process activities such as brainstorming, nominal group technique, process mapping, the development of a fishbone diagram, or the use of tally sheets.

Through an iterative Plan-Do-Study-Act (PDSA) process, improvement ideas become “tests of change” that are developed (Plan), implemented (Do), monitored (Study), and interpreted (Act). Plan: Each “test of change” is based on a prediction that improvement will occur. Each PDSA cycle tests that prediction and learning is acquired. Other factors that should be considered in determining the size of the first PDSA include: (a) the readiness of the system for change, (b) the probability the proposed system change will work, and (c) the consequences to the system if the proposed system change fails. The less ready the system, the lower the probability the change will work, and the greater the risk if the change fails, then the smaller the first PDSA should be. Do: Carry out your plan on the limited scale that you planned and see what happens. Study: Study the effect of the “test of change” on the process being changed. The data derived from each “test of change” generate new knowledge or learning and influence the next test of change. Act: After interpreting the results of the first cycle, determine next steps. It is this learning that fuels

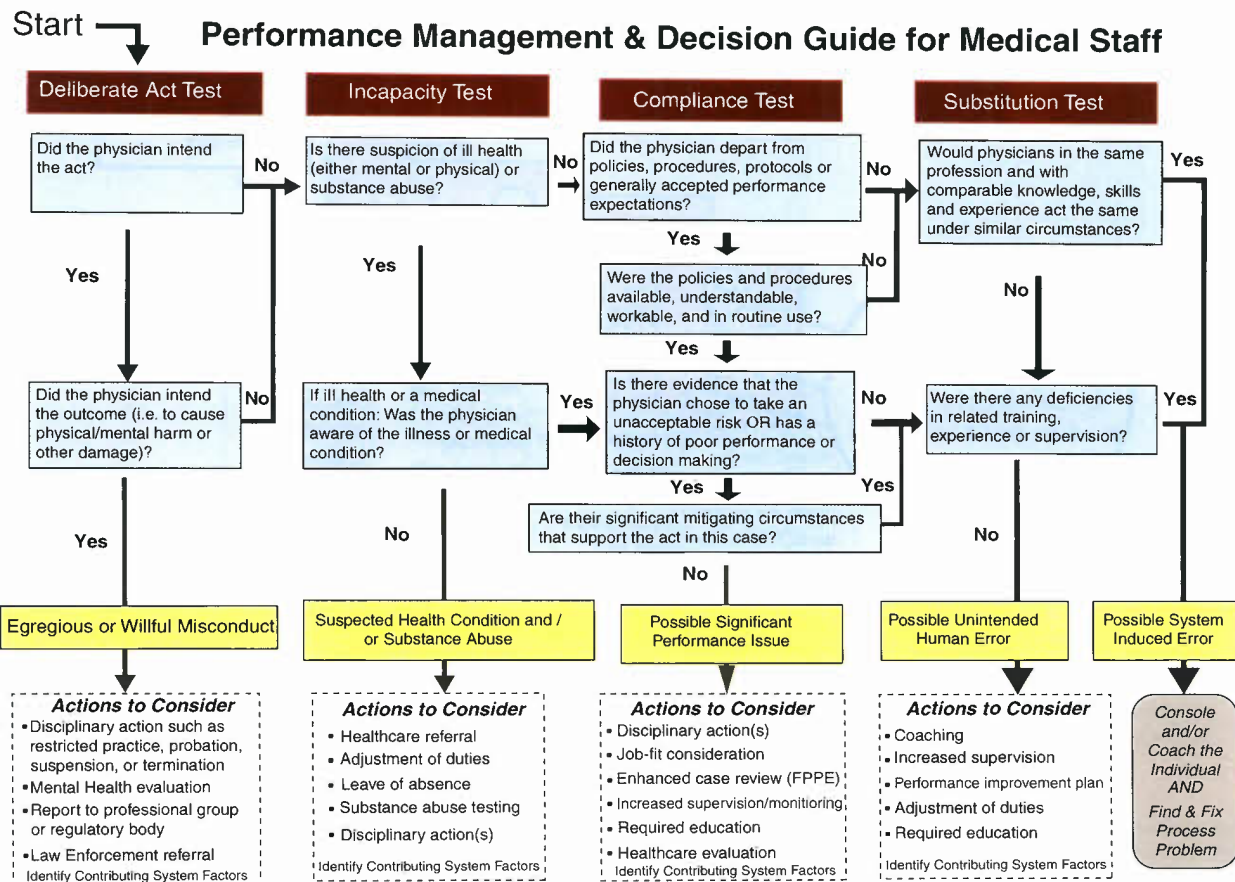


Figure 77.3. Accountability grid—just culture. (Concept adapted from J Reason *Managing the Risks of Organizational Accidents*, 1997 by Healthcare Performance Improvement, LLC ©.)

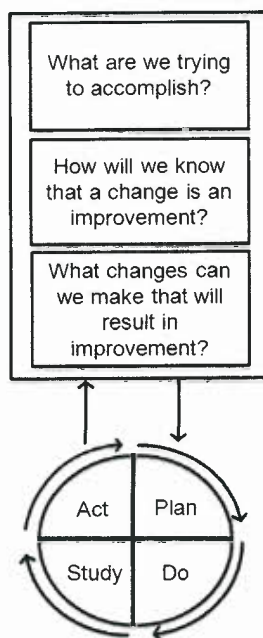


Figure 77.4. The model for improvement. (Adapted from Berwick DM. A primer on leading the improvement of systems. *BMJ* 1996;312:619–622.)

the action that initiates the next PDSA cycle. The PDSA process is repeated incorporating the learning from the previous cycles. Because all improvement involves change, but not all change is improvement, PDSAs should usually start on a small scale with just a few patients or staff. Some improvement ideas are not successful, and must be abandoned. As the confidence in the “test of change” improves with each cycle, the size of the PDSA cycles can be “scaled up involving more staff or patients” until the new process becomes the norm.

Specific Aim and Key Driver Diagram

The aim and key driver diagram is a tool used to organize the quality team’s theories of improvement. It is intended to focus and target the work of the team. In TJ’s case, a team was charged with creating a reliable process to guarantee the use of a “double check” prior to the administration of blood products. They organized their team by developing a well-defined aim statement, key drivers, and interventions necessary to reach the stated aim.

SMART aims must be *specific*. What is the goal? What is to be achieved? Importantly, an improvement aim must be designed to improve only one thing. SMART aim statements are *measurable*. An increase or decrease in the measure will be directly associated with the desired change in the process being changed. SMART aims are *actionable*. The team empowered to improve a failed process must be able to impact the process and overcome any barriers to improve-

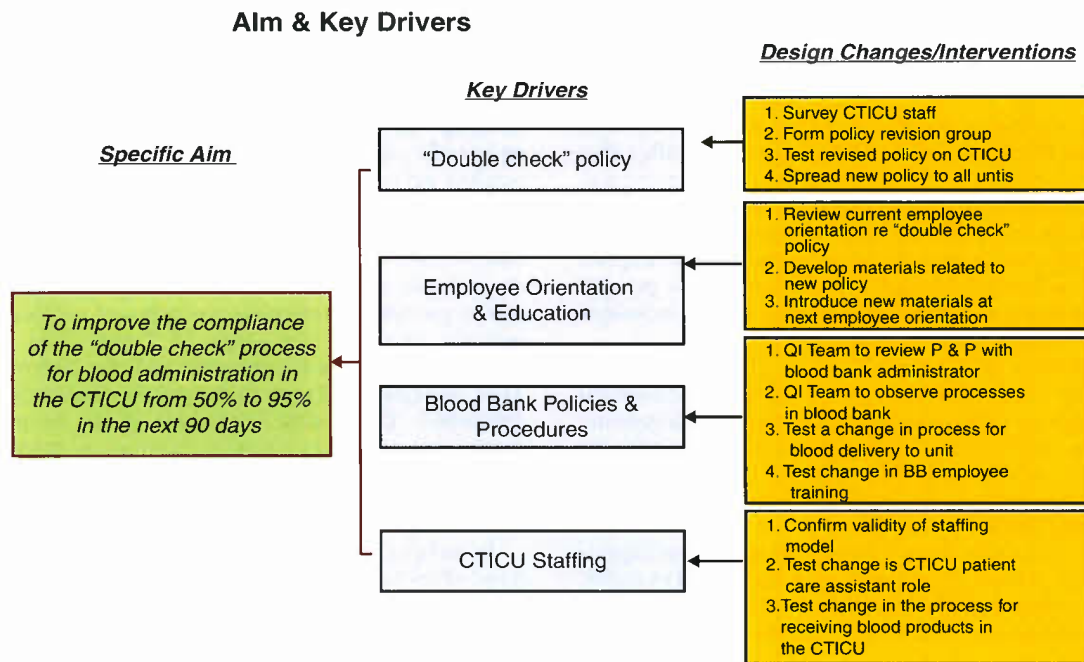


Figure 77.5. Key driver diagram—increase compliance with the “double check process” for blood administration.

ment. SMART aims are *realistic* in that there must be a reasonable expectation that the aim can be achieved. A realistic aim statement often requires that it be “bounded” or narrowly focused. The team may limit their improvement work to a single unit, patient care service, or a defined patient population. By doing so, the team can test changes on a small scale prior to spreading the improvement ideas to other areas or patient populations. Finally, a SMART aim must be *timely*. The improvement aim must have a target date by which it will be completed. If that date is more than 6 months from the beginning of the improvement work, interim milestones of improvement should be set. While all elements of a SMART aim are important, the two that often lack clarity are the elements of measurability and timeliness. Poorly constructed aim statements speak of improving failed processes, but do not define how much improvement is expected and by when the improvement is expected. During his 2004 IHI Key Note address, Don Berwick, former President and CEO of the Institute for Healthcare Improvement stated this concept well, “Some is not a number, soon is not a time.”

TJ’s Case: A team was codified to examine and put in place reliable processes to prevent a similar occurrence from happening. Specifically, the process had to ensure that “double checks” were consistently done prior to any blood product administration. The team developed the following SMART aim statement (Fig. 77.5): To improve the compliance of the “double check” process for blood administration in the ICU from 50% to 95% within the next 90 days. This aim statement presumes that the process for a correct “double check” is already known and that a baseline compliance rate of 50% had been established through a preliminary audit of the process in the ICU.

Key drivers are those factors that the team believes will impact the failed process and bring about improvement. The key drivers can often be identified from the RCA process, or a “cause-and-effect” or “fishbone” diagram. Sometimes, a key driver can be found in the mapping of the failed process. In the case of the failed “double check” process for blood administration, key drivers might be (a) the “double check” policy, (b) employee orientation/education, (c) blood bank policies and procedures, and (d) staffing in the PICU.

Each key driver is associated with “interventions” that, if implemented, should influence the key driver in order to drive toward achieving the specific aim. The interventions are the “tests of change” that form the basis of PDSA cycles. For example in TJ’s case, hospital employees may not interpret the “double check” policy the same way. An intervention for this key driver could be an informal survey of PICU staff to determine ambiguities or potential misunderstandings in the “double check” policy. If ambiguities are discovered, a second intervention would include reviewing the policy with a multidisciplinary team to broaden input and reduce ambiguities. A third intervention might include a test by ICU staff to make sure the policy is clear, can be implemented without problems, and compliance with the policy can be measured. Once this is done, a fourth intervention is to implement the policy throughout the organization. A sample of aim and key driver diagram for the failed “double check” process for blood administration in the PICU is shown in Figure 77.5.

Teams

A successful QI project begins with establishing a team whose members understand their roles, responsibilities, and expectations (19). An ideal improvement team should include individuals who “work in, own, supply, have knowledge of, or receive benefits from the work process” to be improved. Team members share the responsibility of the improvement work both in and outside the team meetings and should represent a cross-section of the organization that utilizes the process to be improved. Some team members will have very specific roles.

Every team must have a leader. In general, the team leader is the person who owns the process. The leader coordinates and directs the improvement work as the team studies the process and develops “tests of change” that might lead to improvement. The leader is not a passive team member. The team leader should have the authority to effect change or be empowered to break down barriers that the team may encounter. The leader contributes ideas, participates in data interpretation, and facilitates team decision making.

An improvement team needs a recorder. This role need not be the same person for every improvement team meeting, but the team leader should clearly identify who should serve as the recorder for each meeting. The recorder's responsibilities include logging significant content in such a way that all team members can see the information. This can be done with a flip-chart or from typed notes recorded from a laptop and projected. Visual display of team discussions enhances team meeting efficiency. A QI facilitator may be a team consultant bringing the knowledge of QI tools and techniques to the content experts about the process being discussed. The facilitator may provide "just-in-time" training to teach the use of a QI tool or technique that is required as part of the improvement process.

Finally, a QI team must have a sponsor. The sponsor is the executive leader who is the champion for the improvement project. While not an active member of the improvement team, the sponsor has a critical role. The sponsor makes sure that the right people are on the team. The sponsor resolves conflicts and any barriers to success. The sponsor secures resources for the team to do its work.

For projects that cross many boundaries within an organization or hospital, a team charter may be a useful tool to codify the scope and authority of the improvement team. The charter should outline the project's focus and reasons for the effort. It should define the expected outcomes and measures that will be used to define success or failure. The charter should address the project scope (including boundary limits) and define the sponsor, team leader, facilitator and team members, the project start date, and end date.

TJ's Case: Recommendations for immediate change to the process were made to correct individual and system-related failure within hours of the event. The RCA committee also recommended that a QI team be established. The QI team was to review the process in greater detail, identify additional safety measures, monitor the performance of the process over time, and report quarterly to the hospital's Quality Improvement and Safety Committee. As the process of blood product delivery to the various ICUs was different from that of the medical-surgical units, the recommendation directed the committee to limit (bound) their scope to the ICUs.

The medical director for QI was assigned the responsibility for establishing the QI team and serving as its sponsor. The chief of the blood bank was asked to lead the team, and the

QI coordinator for the intensive care services was asked to facilitate the team. Team representatives included the medical and nursing representatives for the neonatal, pediatric, cardiac, surgical, and bone marrow transplant units. At the first meeting, the QI team developed its charter and determined its specific aim. A flowchart for the current process of blood product delivery to the ICUs was developed and failure points were determined. A historical review of serious safety events related to blood product administration was conducted, and a Pareto chart of different error types was developed. A Pareto chart displays types of errors by frequency so that attention can be put on the relatively few types of errors that cause the majority of events (e.g., Figs. 77.7 and 77.8). A cause-and-effect diagram was constructed and the "whys" for failures were determined. From this analysis, four key drivers were developed. These were (a) failure of the hospital's "double check" process, (b) inadequate training and orientation of new employees, (c) confusion regarding hospital policies and procedures, and (d) inadequate staffing of the cardiac ICU during times of high census (e.g., Fig. 77.5).

In subsequent meetings, the QI team developed interventions (PDSAs), which they thought would impact the key drivers such that the process would be improved. One of the interventions tested was the use of a checklist when blood products arrive in the ICUs. The cardiac ICU team representatives were asked to trial a checklist and report back to the QI team regarding the checklist effectiveness at the next weekly QI team meeting (Fig. 77.6).

Bundles and Checklists

In 2005, Resar et al. (20) described a novel approach to QI in which three to five evidence-based best practices are "bundled" together and implemented as "one" in order to achieve a desired improvement outcome. "Bundles" afford health care providers the opportunity to deliver care more reliably and safely to patients undergoing treatments that have inherent risks, such as assisted ventilation and central line placement and management (21). When "bundles" are used reliably, outcomes improve (22–24).

Checklists can be used to remind the health care team of steps in a clinical practice process. The checklist can also be

Figure 77.6. Sample checklist trialed as PDSA by the ICU team.

Checklist for Blood Product Delivery to an ICU	
PDSA #1: Handoff of Blood Products from Blood Bank Technician to Certified ICU Clinician will utilize three-way communication	
<input type="checkbox"/>	Blood Bank Technician (<i>Initials</i>) delivers blood product to ICU
<input type="checkbox"/>	Blood technician reads product identification information to certified clinician (<i>Initials</i>): patient name, medical record number, blood product identification number, blood type
<input type="checkbox"/>	Certified clinician confirms each product identification element matches the blood product order form by immediate read back of each element
<input type="checkbox"/>	Blood Bank Technician acknowledges that the information stated by the certified clinician is correct by stating "Check".
<input type="checkbox"/>	When all identifying elements have been stated, read-back, and acknowledged correctly, then Blood Bank Technician will hand the blood product to the certified clinician

used to measure compliance with each step in the process. Checklists may represent best practices or may be “good ideas” that seem to be appropriate steps to follow in clinical care processes. Usually multiple individuals are responsible for completing different elements of the checklist, but no one person is accountable for completion of all the elements on the checklist. The use of a surgical safety checklist in the operating room time-out process prior to the beginning of an operation has been associated with significant improvement in surgical outcomes (25,26). Similarly, the daily goals sheet is a checklist used in many ICUs to remind the clinical team to cover all essential clinical care related items during daily rounds (27,28).

Data Drive Change—Don’t Let Data Paralyze the Team

TJ’s Case: The wrong blood was given to TJ. A Pareto chart analysis of medication errors at the hospital revealed that administration errors were the most common (Fig. 77.7) followed by prescribing and then dispensing errors. Within administration errors, the most common errors were failure to complete a “double check” prior to medication administration. This analysis, using Pareto’s methodology, suggests a hospital-wide problem that is most commonly due to errors associated with medication administration. A focused corrective effort, across the entire hospital, addressing reliable medication administration (including blood administration), may yield valuable results more quickly than simultaneously targeting all aspects of medication delivery.

When broken down into its component steps, the process of blood administration is complicated and without an organizing framework, it may be difficult to identify the most important steps that need intervention(s). A Pareto chart using the *Pareto principle*, or 80–20 rule can be used to focus the team’s work. This principle is based on the work of Vilfredo Pareto and states that approximately 80% of problems are due to 20% of the reasons for them (30). Identification of the most

common flaws (top 20%) in the blood administration system can be accomplished by convening frontline staff involved in blood administration and developing a process map for blood administration. They can begin by asking, “where do the problems occur?” The answers can be recorded by using a simple tally sheet to vote for the steps in the process that are most problematic. From these data, a histogram can be constructed, sometimes referred to as a “Pareto chart.” Figure 77.8 is an example of a second Pareto chart depicting feedback from frontline clinicians regarding problematic components of the process of blood product administration in the cardiac ICU. Improvement steps, designed as PDSA cycles of change, can then focus the QI efforts to those areas most likely to improve the process. For example, in Figure 77.8, clinicians identified availability of a “second check RN” to cross-check blood products as an essential and often problematic step. This information can be utilized by the improvement team to plan the first PDSA cycle of change. Similarly, fishbone diagrams, frequency distribution plots, or scatter plots can be utilized to identify and stratify steps in any process that are likely to result in improvement. (For a detailed discussion of data analysis tools, see reference (31)).

An aim (outcome) in QI work must be measurable, and data are used to quantify the results of such work. QI teams can leverage data to identify components of a process or system that have significant variation requiring targeted interventions. This can contribute to the design of tests of change. Finally, data can be used to measure compliance with interventions intended to sustain change. Data are essential to effect change, but the acquisition and interpretation of data must enhance the process of change not paralyze it. This section outlines the use of data to facilitate change.

A comprehensive discussion of statistical process control and Shewhart control charts is beyond the scope of this chapter; however, the brief summary that follows introduces the reader to important concepts in data interpretation that are

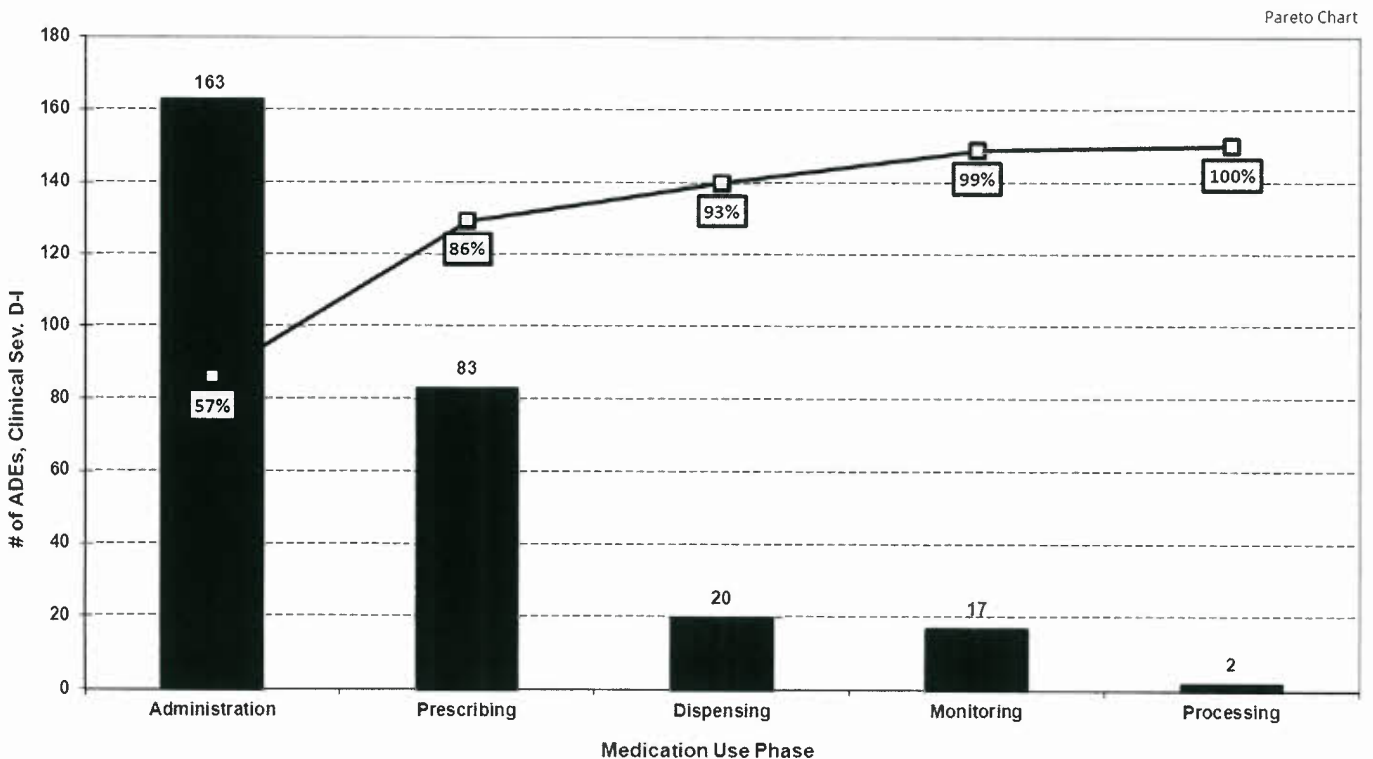


Figure 77.7. Pareto chart—distribution of adverse drug events by phases of medication use—clinical severity D-I; Jan-Dec 2010.

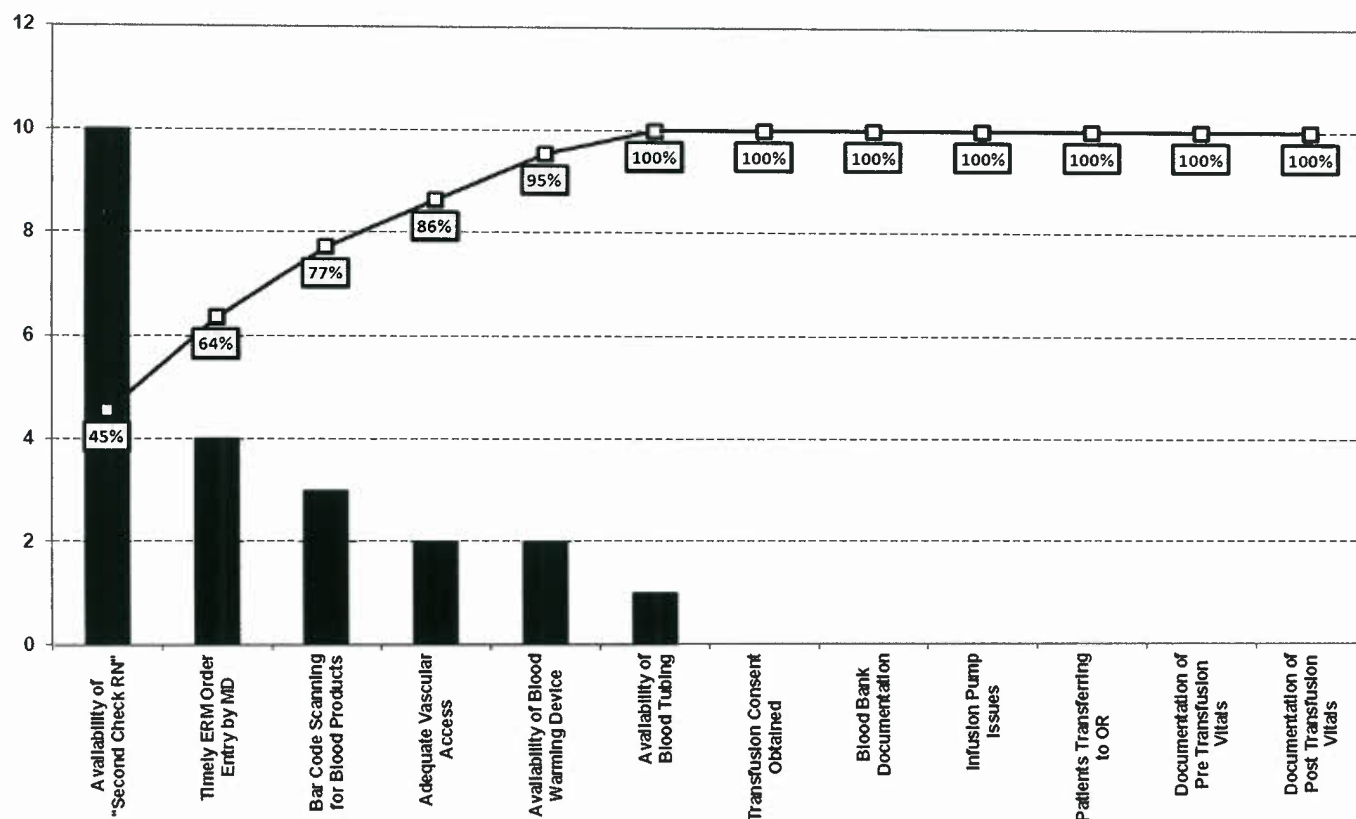


Figure 77.8. Blood product administration—histogram of improvement opportunities.

useful to direct QI changes (18,32). There is always variation within systems. Data may vary minute to minute, week to week, or month to month. Common cause variation (chance cause) is variation that is inherent within a system and affects all those working in the system and all outcomes from the system. An example is the variation in heart rate (± 5 BPM) around a mean normal rate of 100 BPM. Special cause variation (assignable cause) is not inherent to the system and arises when special or unique circumstances arise that perturb the system. A child, for example, develops fever and the heart rate can increase dramatically to 170 or 180 BPM. This special cause increase in heart rate deserves investigation to ascertain what perturbed the system to generate such an outlier in heart rate. Systems in control (common cause variation) do not need interventions if the data are in the goal range. Failure to recognize common cause variation as normal and acceptable can lead to wasted resources and attempts to tamper with a stable process delivering acceptable results. In fact, "tampering" with such in control systems may create unintended consequences that push the system out of control. In contrast, systems with special cause variation need interventions (e.g., PDSA targeted at the special cause) to investigate and eliminate the special cause. In its most simple form, special cause data points are 3-sigma (standard deviations) above or below the center line (mean) of normally distributed data (Fig. 77.9). The special cause data point depicted in Figure 77.9 might be the heart rate of 180 as noted in the case above. The fundamental value of depicting data in the control chart format is to identify systems that require additional interventions (e.g., a fever evaluation) or that have improved or worsened as a result of interventions. Process control charts are said to be the "voice of the process" and are powerful tools to identify significant change in response to either a test or some unknown variable that has been introduced into a previously stable process (33).

There are many types of statistical process control charts. The type of data that is being analyzed will determine the best control chart to use to display the variation in a manner that is helpful to QI work. Data may be continuous (variable quantitative measurements) or attributed (counts or classification of qualitative data, e.g., number of errors or pass/fail items). Figure 77.10 outlines the type of control chart that should be used depending upon the type of data. A more in-depth discussion of control charts and their interpretation can be found in *The Improvement Guide* (18).

TJ's Case: Data were used to focus the efforts of the improvement team's work. Specifically, the RCA team constructed a process map for the ordering, delivering, and verification that the correct blood is administered to the correct patient and to examine which parts of the process required change. The team also developed a blood product administration checklist that was to be completed prior to administering blood products in the cardiac ICU. The team wanted to confirm that the checklist was being consistently used. They gathered data by analyzing information from the completed blood administration checklist (Fig. 77.6). A control chart was used to monitor progress in the completion of all elements of the checklist (Fig. 77.11). If the "test of change" is real improvement, then further observation over time will show that the variability of the system has been reset and only common cause variability will be exhibited going forward. At this point, the system is once again stable and predictable with high compliance in the use of the checklist.

Statistical process control data analysis is a powerful tool to maximize the efficiency and effectiveness of process improvement teams. These kinds of charts may, however, allow the teams working on improvement to forget that the elimination of all errors that cause harm is the goal in health care, however difficult that might be to achieve. In our organization, the drive to zero is measured by "numbers of patients harmed" and even if a system is "in control," the goal remains zero defects

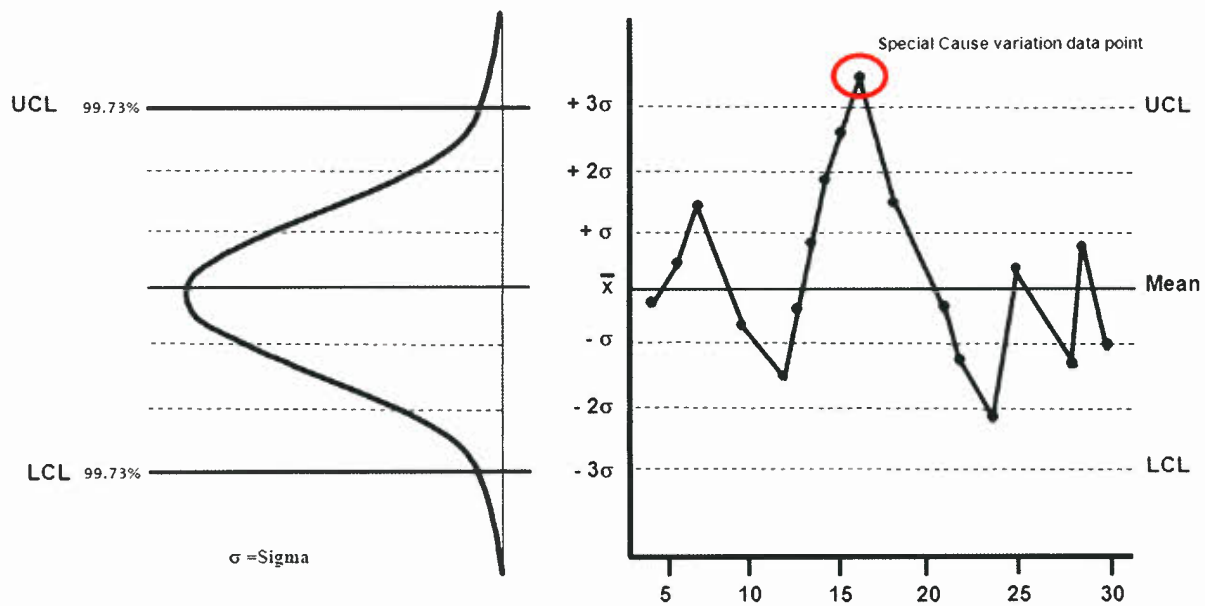


Figure 77.9. Control chart with special cause variation.

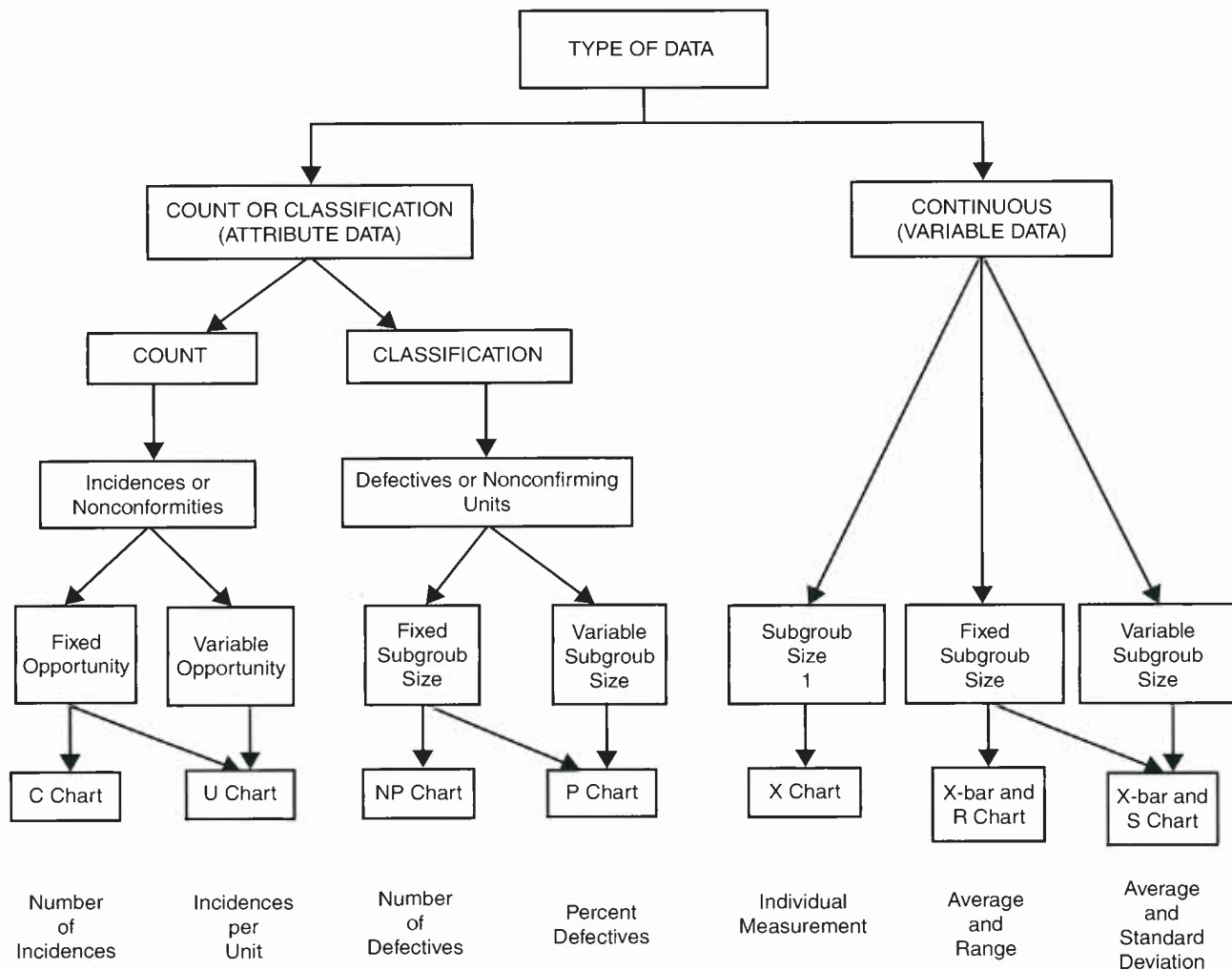


Figure 77.10. How to choose a control chart. (Adapted from Langley GJ, Moen RD, Nolan KM, et al., eds. *The improvement guide: a practical approach to enhancing organizational performance*. 2nd ed. San Francisco, CA: Jossey-Bass, 2009.)

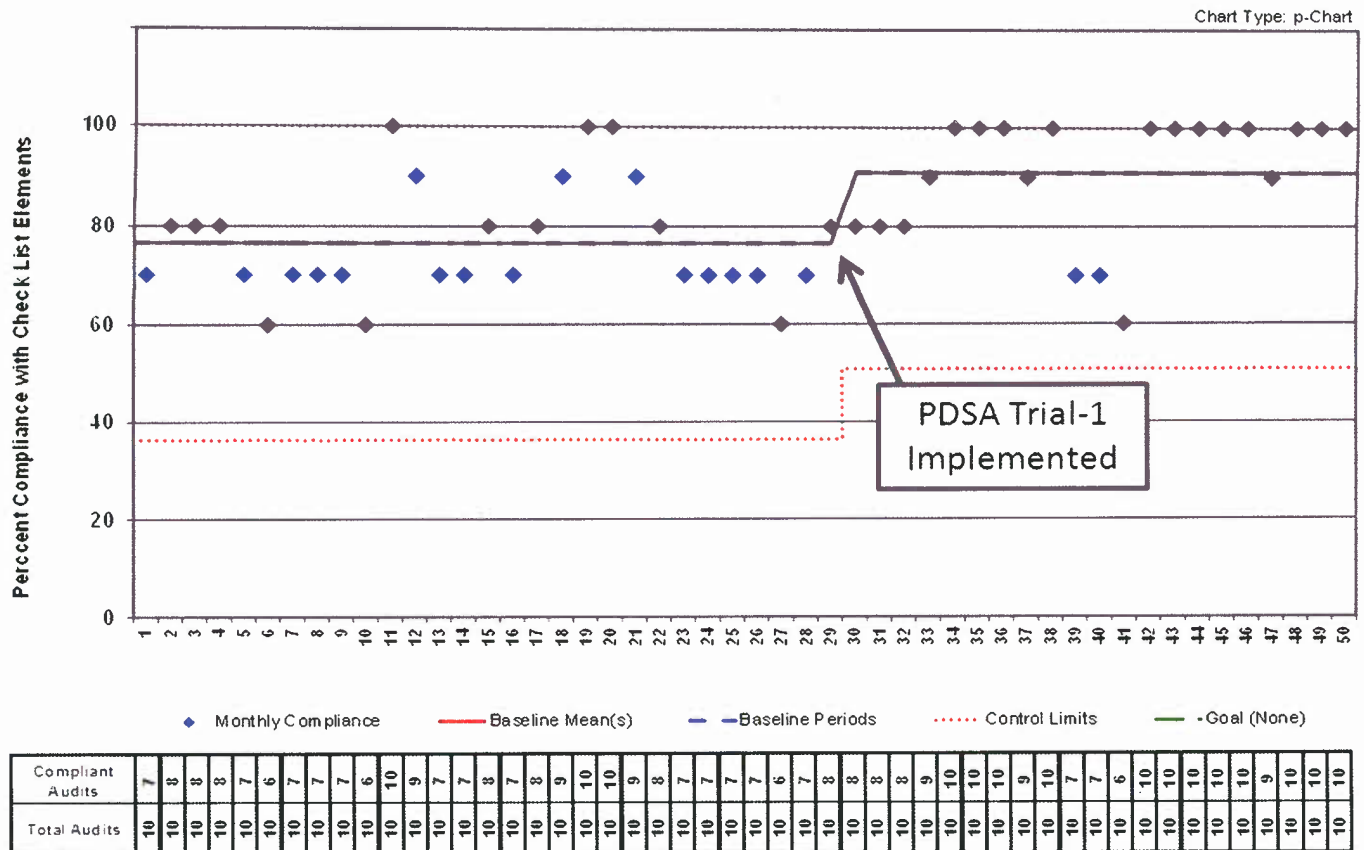


Figure 77.11. Annotated p-chart measuring cardiac ICU compliance with components of the 10-point pre-blood administration checklist. The system is stable through patient number 30, with average checklist compliance at 76%. A PDSA cycle based on feedback from frontline staff resulted in a shift to 92% compliance. The new system is also stable but delivers improved performance.

(errors) (34). For example, a process control chart depicting the incidence of adverse transfusion reactions per 1,000 units transfused could be created and used as the metric to monitor blood administration errors. This graph is likely to show that transfusion reactions are uncommon and represent common cause variation, and while regrettable, the rate of transfusion reactions does not achieve special cause variation. It is our view, however, that an approach to data analysis that utilizes rates of harm event and the total number of harm events is the best combination to achieve a motivated workforce to work to achieve zero preventable harm.

High Reliability—Do What You Say and Say What You Mean

Systems Thinking

“Every system is perfectly designed to achieve the results it gets.” This statement, attributed to Paul Batalden, MD of Dartmouth School of Medicine (35), is an often quoted QI axiom. Stated another way, Albert Einstein said, “continuing to do the same thing over and over again and expecting a different result is insanity” (36). Thus, if one expects to achieve different results, the system must be changed.

An understanding of how a hospital or health care network is an integrated system with multiple interrelated and interdependent parts is an essential concept associated with QI. James Reason (17) defined a system as a set of interdependent elements interacting to achieve a common aim. Those

interdependent elements may interact to achieve a desirable aim or an undesirable one. As improvement teams or individual practitioners work to achieve the best possible outcomes, understanding the interdependency of the various processes that comprise the delivery of health care is critical. For example, if “first OR case start times” are predictably delayed and the entire OR schedule is disrupted, only a process redesign can change the outcomes. In the case of TJ, if there is a problem with the process of blood administration and the desired outcome is to make that delivery process a highly reliable error-free process, then only a study of all the interdependent parts (the system) will lead to optimal system performance and the desired outcome.

Human Factors That Contribute to Error

Human factors science is a multidisciplinary field that combines the expertise of psychologists, engineers, industrial designers, statisticians, and others. It concerns the understanding of human capability and the application and integration of this knowledge to system design. A human factor is a physical or cognitive characteristic that influences how people interact with systems. For example, in 2006, the FDA issued a recall of an infusion pump with a sensitive keypad for setting infusion rates. The sensitive pad sometimes produced a “key bounce” that resulted in a number to be entered twice when it was only intended to be entered once. Hurried nurses who failed to catch the error through pump programming verification were prone to make 10-fold errors in the infusion rates. Human factors such as fatigue, stress, external distractions, and personal issues are likely to blame (though the device itself may also

be poorly designed). The interaction between technology and humans is of particular importance in the high-tech hospital environment, particularly the ICU. At various safety critical moments (e.g., high-tech device interfaces with human being), it is important to recognize when human factors may impair performance. This has been called situational awareness. Situational awareness is “the perception of the elements in the environment within a volume of time and space, the comprehension of their meaning, and the projection of the status in the near future” (37). A lack of situational awareness is one of the individual failure modes, and is a common root cause of errors during safety critical functions such as blood product administration. Endsley (37) further emphasizes the importance of distinguishing situational awareness that is a “state of knowledge” from situational assessment that is the process by which that “state of knowledge” is attained and operationalized. Certainly, health care workers cannot avoid performing safety critical acts, and those same workers cannot avoid the burden of human factors. However, it is possible to modify human behaviors to recognize when human factors are at play and practice simple safety practices to aid performance. One such practice is the *STAR* technique that can be used prior to performing any safety critical function. For example, before administering an intravenous medication, the health care worker can Stop for a moment. Think about the critical act about to be performed (right patient, right dose, etc.) prior to performing the Act. Then, immediately Review what was just done. Were all elements performed correctly? The *STAR* technique is a useful tool to enhance situational assessment that facilitates better situational awareness. If the *STAR* technique had been used by the ICU nurse prior to starting TJ’s blood transfusion, it is quite possible that the error would have been prevented.

Creating High Reliability Organizations

Unexpected events are common, and high reliability organizations (HROs) are structured to anticipate and react to the unexpected. HROs recognize lapses early, learn why they occurred, and respond to mitigate the minor lapses before they result in catastrophic failure. HROs are always mindful of what is happening within and to their systems. In a way, HROs engage in a form of “institutional situation awareness.” Weick and Sutcliffe (38) have described the characteristics of HROs. Those characteristics are now being explored and more fully integrated into the health care environment. HRO characteristics include the following:

1. Preoccupation with failure, to track small lapses as if they were symptoms of a system about to fail catastrophically
2. Resisting oversimplification, seeing a more complete and nuanced picture of complex systems that are riddled with the unstable, unknowable, and unpredictable.
3. Remaining sensitive to operations and to relationships; realizing that frontline staff have knowledge that leaders lack, and staff willingness to report that knowledge is key to identifying the small failures before they become catastrophic.
4. Maintaining capabilities for resilience such that, while not error-free, HROs are not disabled by their errors. They keep errors small and utilize workarounds that allow the system to keep functioning.
5. Deferring to expertise and taking advantage of changing locations of expertise. HROs are culturally diverse, lack rigid hierarchies, and drive decision-making down to the frontline staff. Authority migrates to the person with the most expertise, not necessarily the most experience.

HROs learn both from successes and failures. It is often the failures that derive the greatest learning. Weick and Sutcliffe (38) further state that the two perceived enemies of HROs are

“complacency and hubris.” Health care organizations often have too much of both.

If the ICU in which TJ was hospitalized was part of an HRO, a different outcome would be expected. While staffing issues are always a factor in busy, high-acuity ICUs, an ICU in an HRO hospital would have had processes in place to address the likelihood that multiple, critically ill patients might require blood administration at the same time. A standardized hand-off of the blood product from the blood delivering personnel to the ICU staff would exist. A clearly understood process for “double-checking” the blood received against the order placed and TJ’s identification band would have been used. A redundant system of “double checking” using bar coded information that linked the blood unit “bag tag,” the order for blood product, and TJ’s identification band would exist. Finally, immediately prior to initiating the blood administration, TJ’s nurse would have stopped and thought about the safety critical nature of blood administration (*STAR*) prior to connecting the blood. The nurse would have confirmed that the right unit of blood was about to be administered to TJ. Each of these steps would have required no more than a few additional seconds of staff time. In an ICU in an HRO hospital, the entire episode would have occurred as part of routine patient care and no one would think to do otherwise.

Culture—an Essential Ingredient

Although not a tightly defined scientific concept, the role of culture is widely recognized as an important part of the fabric of any health care organization. Hospital mission and vision statements are rigorously crafted and widely recited by employees throughout the organization; however, the culture of an organization is not so easily defined. The way people behave at 3:00AM when nobody else is watching is what really defines an organization’s culture. In the middle of the night, does the nurse always check two patient identifiers when giving medications to a patient with whom she is very familiar?

TJ’s Case: TJ was rapidly decompensating and TJ’s physician and nurse were rushed, worried, and in a hurry to get the blood product administered quickly. Because of those distractions, they skipped an essential double check to ensure this was the correct blood for the correct patient. The consequences of by-passing this step is clear. It is likely that, when not rushed, this standard step is virtually always done by these two clinicians. When rushed and distracted, individuals may forget essential steps unless those steps are “habit” or a forcing step is in place that cannot be by-passed. If these two individuals are the only ICU staff who would make this mistake in this setting, then these are individual failures. However, if in this ICU, clinicians often use shortcuts when stressed, then the ICU has a culture of noncompliance, which if unaddressed will lead to recurrent errors, in particular during safety critical processes.

A safety culture does not occur spontaneously. Zohar (39) summarized organizational characteristics of companies with low accident rates. The most important factors included: (a) successful safety program with strong leadership commitment, (b) safety training for all the workforce, (c) a senior official as a safety officer, and (c) safety promoted through guidance and reinforcement instead of admonition. Health care professionals have begun to recognize the importance of having a strong safety culture as a method to improve quality and safety (40,41); however, controversy remains regarding how to measure and quantify the benefits. Measuring improvement in safety culture is a process measure that may reflect improved actual safety; however, the more important metric would be to correlate improved safety climate with improved clinical outcomes.

Tools that measure safety and teamwork culture within a health care system are increasingly accepted as valid metrics that reflect the climate of opinion among various professional groups. While a variety of survey tools are available, two tools commonly in use are the Safety Attitudes Questionnaire (SAQ) and the Agency for Healthcare Research and Quality (AHRQ) Hospital Survey on Patient Safety Culture. The SAQ is a proprietary survey currently administered by Pascal Metrics (42). Several versions of the SAQ exist and focus upon ambulatory, inpatient, or emergency departments. The survey examines multiple domains including teamwork, safety, job satisfaction, stress recognition, working conditions, and perceptions of unit and hospital management. Studies have demonstrated a link between the SAQ safety and teamwork climate and clinical outcomes. In a large cohort of ICUs, high scores (e.g., >80% on a 100% scale) were associated with lower rates of complications such as bloodstream infections and scores below 60% were associated with higher infection rates (43). Recent papers describe the use of SAQ survey results to both assess and improve the safety environment in various health care settings (44–46). Using the results of the SAQ, Sexton et al. (47) documented the ability of a comprehensive unit-based patient safety program to change the teamwork and safety climates in ICUs across an entire state. The SAQ results can also demonstrate disparate perceptions about safety and teamwork climates between different professional groups within the same ICU (48,49). The other widely used cultural survey is the AHRQ Hospital Survey on Patient Safety Culture. The survey was first released for public use in 2004 and is available for use online (50), free of charge. The survey measures 12 areas or composites of patient safety culture including communications openness, feedback and communication about error, handoffs and transitions, teamwork across units, and others. Over 900 hospitals currently use this survey and the aggregate results are available for benchmarking between hospitals (51). As with the SAQ, the AHRQ scores can be broken down by specific unit and/or by caregiver type. Early studies attempting to link the AHRQ Hospital Survey with clinical outcomes showed mixed results (52–56). Some of the discrepancies among the studies may be related to the use of the AHRQ Patient Safety Indicators (AHRQ PSI) as the outcome measure. The database from which the AHRQ PSIs are generated is the Healthcare Cost and Utilization Project (HCUP). HCUP catalogs inpatient discharge data from 44 participating states. Multiple data elements are extracted, and severity adjustment is done using APR-DRGs and co-morbidity groupings. Each PSI is a rate, with the numerator being the number of cases with an outcome of interest (e.g., Central venous catheter-related bloodstream infection (CLABSI)) and the denominator is the population at risk (e.g., number of patients with a central venous line during that time period). Currently, 18 PSIs include CLABSI, death in low mortality DRGs, postoperative sepsis, pressure ulcers, and 14 other indicators. The AHRQ PSI is an administrative database and published studies outline its limitations including (a) insufficient clinical detail and risk adjustment and (b) its dependency upon the accuracy of documentation and coding and caution against using it as a definitive outcome metric (57–59). However, recently, Mardon et al. (60) examined data from 179 hospitals and using refined and updated PSIs found that a positive patient safety culture was associated with fewer adverse events in hospitals. Indeed, the preponderance of evidence suggests that improved safety culture is associated with less patient harm, no matter what survey tool is used.

Hospitals focused on transformational change to achieve improved safety-related outcomes will be focused not only on cultural change but also will have active QI teams focused on strategic projects such as reducing bloodstream infections, pressure ulcers, and adverse drug events (e.g., blood administration errors); both are essential. The health care drive to

eliminate harm and improve quality and safety will occur only in hospitals with strong safety and teamwork climates. Such hospitals will have environments where (a) an error or a near-miss error is viewed as opportunity to improve, and leadership takes the opportunity to find the commensurate system solutions; (b) all personnel feel responsible for not only their work but for that of their partner; and (c) all team members are comfortable speaking up when a team member (even a senior one) is getting ready to make an error. These characteristics can only enhance the likelihood of success of the focused teams mentioned previously. Future research using cultural assessment surveys may help distinguish the relative importance of each.

REFERENCES

1. Lohr KN. *Medicare: a strategy for quality assurance*. Washington, DC: National Academy Press, 1990.
2. Kohn LT, Corrigan JM, Donaldson MS, eds. *To err is human. Building a safer health system*. Washington, DC: National Academy Press, 2000.
3. Cooper JB, Gaba DM, Liang B, et al. National patient safety foundation agenda for research and development in patient safety. *MedGenMed* 2000;2:e38.
4. Reason J. *Human Error*. Cambridge, UK: Cambridge University Press, 1990.
5. Margolis P, Provost L, Schoettler P, et al. Quality improvement, clinical research, and quality improvement research—opportunities for integration. *Pediatr Clin North Am* 2009;56:831–834.
6. Bagian J, Gosbee J, Lee C, et al. The Veterans Affairs root cause analysis system in action. *Jt Comm J Qual Improv* 2002;28:531–545.
7. Percarpio K, Watts V, Weeks W. The effectiveness of root cause analysis: what does the literature tell us? *Jt Comm J Qual Patient Saf* 2008;34:391–398.
8. Pronovost P, Holzmueller C, Martinez E, et al. A practical tool to learn from defects in patient care. *Jt Comm J Qual Patient Saf* 2006;32:102–108.
9. Ono T. *Toyota Production System: beyond large-scale production*. Cambridge, MA: Productivity Press, 1988.
10. DeRosier J, Stalhandske E, Bagian J, et al. Using health care Failure Mode and Effect Analysis: the VA National Center for Patient Safety's prospective risk analysis system. *Jt Comm J Qual Improv* 2002;28:248–267.
11. Ashley L, Armitage G. Failure mode and effects analysis: an empirical comparison of failure modes scoring procedures. *J Patient Saf* 2010;6:210–215.
12. Joint Commission: Sentinel Event Available at: http://www.jointcommission.org/sentinel_event.aspx. Accessed August 29, 2011.
13. Reason J. Human error: models and management. *BMJ* 2000;320:768–770.
14. Pettker C, Funai E. Getting it right when things go wrong. *JAMA* 2010;303:977–978.
15. Marx D. *Patient safety and the "just culture": a primer for health care executives*. New York, NY: Columbia University, 2001.
16. Wachter R, Pronovost P. Balancing "no blame" with accountability in patient safety. *N Engl J Med* 2009;361:1401–1406.
17. Reason J. *Managing the risks of organizational accidents*. Burlington, VT: Ashgate Publishing, 2004.
18. Langley GJ, Moen RD, Nolan KM, et al., eds. *The improvement guide: a practical approach to enhancing organizational performance*. 2nd ed. San Francisco, CA: Jossey-Bass, 2009.
19. Scholes PR, Joiner BL, Streibel BJ. *The team handbook*. 3rd ed. Madison, WI: Oriel, 2003; 2–1–32.
20. Resar R, Pronovost P, Haraden C, et al. Using a bundle approach to improve ventilator care processes and reduce ventilator-associated pneumonia. *Jt Comm J Qual Patient Saf* 2005;31:243–248.
21. Raising the bar with bundles: Treating patients with an all-or-nothing standard. *Jt Comm Perspect Patient Saf* 2006;n6:5–6.
22. Wheeler DS, Giaccone MJ, Hutchinson N, et al. A hospital-wide quality improvement collaborative to reduce catheter-associated bloodstream infections. *Pediatrics* 2011;128:e995–e1007.
23. Miller M, Griswold M, Harris M, et al. Decreasing PICU catheter-associated bloodstream infections: NACHRI's Quality Transformation Efforts. *Pediatrics* 2010;125:206–213.
24. Bigham M, Amato R, Bondurant P, et al. Ventilator-associated pneumonia in the pediatric intensive care unit: characterizing the problem and implementing a sustainable solution. *J Pediatr* 2009;154:582–587.
25. Haynes AB, Weiser TG, Berry WR, et al. A surgical safety checklist to reduce morbidity and mortality in a global Population. *N Engl J Med* 2009;360:491–499.
26. deVries EN, Prins HA, Crolla R, et al. Effect of a comprehensive surgical safety system on patient outcomes. *N Engl J Med* 2010;363:1928–1937.
27. Pronovost P, Berenholtz S, Dorman T, et al. Improving communication in the ICU using daily goals. *J Crit Care* 2003;18:71–75.
28. Schwartz JM, Nelson KL, Saliski, et al. The daily goals communication sheet: a simple and novel tool for improved communication and care. *Jt Comm J Qual Patient Saf* 2008;34:608–613.

29. Berwick DM. A primer on leading the improvement of systems. *BMJ* 1996;312:619–622.
30. Mahajan P. Quality in pediatric emergency medicine: a learning curve and a curveball. *Clin Pediatr Emerg Med* 2011;12:80–90.
31. Provost L, Murray S. *The data guide-learning from data to improve health-care*. Austin, TX: Associates in Process Improvement and Corporate Transformation Concepts, 2010.
32. Shewhart W. *Economic control of quality of manufactured product*. New York, NY: Van Nostrand, 1931.
33. Wheeler DJ. *Understanding variation*. 2nd ed. Knoxville, TN: SPC Press, 2000.
34. Brilli R, McClelland R, Davis T, et al. The preventable harm index: an effective motivator to facilitate the drive to zero. *J Pediatr* 2010;157:681–683.
35. Carr S. "A quotation with a life of its own." Patient Safety and quality healthcare. July/Aug 2008 [Editor's Notebook] Available at: <http://www.psqh.com/julaug08/editor.html>. Accessed October 2, 2011.
36. This quotation is commonly attributed to Albert Einstein; however, its true origins are obscure.
37. Endsley MR. Toward a theory of situation awareness in dynamic systems. *Hum Factors* 1995;37:32–64.
38. Weick KE, Sutcliffe KM. *Managing the unexpected*. San Francisco, CA: Jossey-Bass Publishing, 2001.
39. Zohar D. Safety climate in industrial organizations: theoretical and applied implications. *J Appl Psychol* 1980;65:96–102.
40. Pronovost PJ, Weast B, Holzmüller CG, et al. Evaluation of the culture of safety: survey of clinicians and managers in an academic medical center. *Qual Saf Health Care* 2003;12:405–410.
41. Sexton JB, Thomas EJ, Helmreich RL. Error, stress, and teamwork in medicine and aviation: cross sectional surveys. *BMJ* 2000;320:745–749.
42. Pascal Metrics Inc., 3050 K Street, NW, Washington, DC, 20007, USA.
43. Pronovost PJ, Berenholtz SM, Goeschel C, et al. Improving patient safety in intensive care units in Michigan. *J Crit Care* 2008;23:207–221.
44. Halligan M, Zecevic A. Safety culture in healthcare: a review of concepts, dimensions, measures and progress. *BMJ Qual Saf* 2011;20:338–343.
45. Huang DT, Clermont G, Kong L, et al. Intensive care unit safety culture and outcomes: a US multicenter study. *Int J Qual Health Care* 2010;22:151–161.
46. Pettker CM, Thung SF, Norwitz ER, et al. Impact of a comprehensive patient safety strategy on obstetric adverse events. *Am J Obstet Gynecol* 2009;200:492.e1–e8.
47. Sexton JB, Berenholtz SM, Goeschel CA, et al. Assessing and improving safety climate in a large cohort of intensive care units. *Crit Care Med* 2011;39:934–939.
48. Relihan E, Glynn S, Daly D, et al. Measuring and benchmarking safety culture: application of the safety attitudes questionnaire to an acute medical admissions unit. *Ir J Med Sci* 2009;178:433–439.
49. Huang DT, Clermont G, Sexton JB, et al. Perceptions of safety culture vary across intensive care units of a single institution. *Crit Care Med* 2007;35:165–176.
50. Agency for Healthcare Research and Quality. Patient Safety Surveys. Available at: <http://ahrq.gov/qual/patientsafetyculture/>
51. Sorra J, Famolaro T, Dyer N, et al. Hospital survey on patient safety culture: 2010 user comparative database report. (Prepared by Westat, Rockville, MD under contract No. HHSA290200710024C). Rockville, MD: Agency for Healthcare Research and Quality; February 2010. AHRQ Publication No. 10-0026.
52. Singer S, Lin S, Falwal A, et al. Relationship of safety climate and safety performance in hospitals. *Health Serv Res* 2009;44:399–421.
53. Pronovost P, Weast B, Rosenstein B, et al. Implementing and validating a comprehensive unit-based safety program. *J Patient Saf* 2005;1:33–40.
54. Hoffman DA, Mark BA. An investigation of the relationship between safety climate and medication errors as well as other nurse and patient outcomes. *Pers Psychol* 2006;59:847–869.
55. Mark BA, Hughes LC, Belyea M, et al. Exploring organizational context and structure as predictors of medication errors and patient falls. *J Patient Saf* 2008;4:66–77.
56. Weingart SN, Farbstein K, Davis RB, et al. Using a multihospital survey to examine the safety culture. *Jt Comm J Qual Saf* 2004;30:125–132.
57. Sedman A, Harris M, Schulz K, et al. Relevance of the Agency for Healthcare Research and Quality Patient Safety Indicators for Children's Hospitals. *Pediatrics* 2005;115:135–145.
58. Bahl V, Thompson MA, Kau T, et al. Do the AHRQ Patient Safety Indicators flag conditions that are present at the time of hospital admission? *Med Care* 2008;46:516–522.
59. Kaafarani HM, Borzecki AM, Itani K, et al. Validity of selected Patient Safety Indicators: opportunities and concerns. *J Am Coll Surg* 2011;212:924–934.
60. Mardon RE, Khanna K, Sorra J, et al. Exploring relationships between hospital patient safety culture and adverse events. *J Patient Saf* 2010;6:226–232.

Design, Execution, and Appraisal of Clinical Trials

Brian W. McCrindle

WHAT IS EVIDENCE-BASED MEDICINE AND WHY ARE CLINICAL TRIALS SO RELEVANT TO THAT PRACTICE?

Definition and Practice of Evidence-based Medicine

The practice of evidence-based medicine occurs when clinical decision making involves the incorporation of the best available research evidence together with the clinician's expertise and consideration of local or individual circumstances and the patient's preferences regarding therapies and outcomes. An additional step involves tracking, appraisal, and updating of the process. As a result, the practice is not based solely on research evidence, and should not be viewed as a directive or "cook book" approach. The sequence of steps in the practice of evidence-based clinical decision making is outlined in Table 78.1.

Both Absence and Proliferation of Evidence

The important necessary first step includes a search for applicable research evidence to inform the clinical question at hand and a critical appraisal of that evidence and subsequent synthesis. Given the exponential expansion of both available evidence (i.e., the medical literature and proliferation of journals) and the ease of means to access it (i.e., searchable databases like PubMed, proliferation of open access journals), clinicians in search of answers are often faced with having to sift through hundreds or thousands of individual articles. The task often seems very daunting, and so one may resort to expert opinion or review articles (often just another form of expert opinion) or to the claims of industry. This is actually largely what many patients are doing, making their own decisions on the basis of what they are exposed to in the media or what they are told by other lay people. The popular "news" media are fraught with errors in both reporting the facts and their interpretation, are prone to sensationalism, and in the obligation to provide balanced viewpoints often resort to inclusion of dissenting unsupported opinions from the fringes of reason. An unregulated claim extolling the curative wonders of an alternative or complementary health product of unproven effectiveness or safety may carry more weight than the best evidence-based recommendation from their health care provider. Together with rising health care costs and stories regarding conflicts of interest and sometimes conflicting study results, many patients have become suspicious of the health care system and abandon therapies that are of proven benefit based on best evidence, sometimes to the detriment of their own health or that of others.

Evidence and Clinical Trials

In order to provide the best possible care to their patients and to expertly and convincingly counsel them about that

care, clinicians need to be expert users and appraisers of research evidence. One needs to be able to efficiently sift through the evidence and then be able to appraise the quality of that evidence before deciding how much weight to give it in terms of clinical decision making. One is looking to find evidence that is applicable to the clinical scenario and answerable question at hand, but of sufficient quality such that one can be confident that the findings are valid and reliable or as close to the truth as one can get. Clinical trials, by the nature of their design, execution, and systematic approach to appraisal, provide the greatest potential for freedom from biases that result in deviations from the truth and, thus, represent or contribute to the highest levels of evidence. This is why clinical trials have a greater impact within systems for developing and reporting clinical practice guidelines or recommendations. Clinical trials are assigned the highest grades in terms of quality of evidence and have the greatest influence in informing the strength of recommendations, as noted in Table 78.2 (1).

HOW DO CLINICAL TRIALS ACHIEVE A HIGH GRADE OF EVIDENCE?

Well-designed and well-executed randomized clinical trials achieve a high grade of evidence for several reasons, as noted in Table 78.3.

Causality

Clinical trials provide the best evidence that any differences in the comparison of outcomes being assessed are a direct result of differences in the interventions being compared (or comparison to nonintervention or standard of care). Clinical trials provide strong evidence for defining causality and can determine the efficacy (how well it works in a research or controlled setting), effectiveness (how well it works in clinical practice), and safety of an intervention. There are several criteria for defining causality, as noted in Table 78.4. Many of these criteria are explicitly satisfied by clinical trials, and hence clinical trials provide the best evidence that an intervention either directly or indirectly (through reduction or elimination of intermediate causal factors) is the cause of observed differences in outcomes. The design and execution of clinical trials attempt to minimize confounding factors that may influence the outcomes of interest, with the observed effects then being confidently attributable to the interventions being compared. This is achieved by random allocation of study subjects, blinding of study assignment as far as possible, standardization of interventions and tracking of any cointerventions or crossovers, continuous accounting for all study subjects, and standardization of all assessments and interpretations of outcomes.

TABLE 78.1 Steps in the Practice of Evidence-Based Clinical Decision Making

1. Begin the process with a clinical scenario of immediate relevance, and specify the need for information as a well-thought-out and answerable question.
2. Obtain the best available research evidence, usually by executing an informed and efficient search strategy of the published literature.
3. Filter the results of the search by critically appraising the most relevant articles through assessment of methods and results in terms of their validity, the magnitude, and reliability of the reported effect, and their applicability and relevance to the clinical scenario at hand.
4. In addition to the appraised evidence, take into account the unique aspects of the clinical scenario in terms of the individual patient's pathophysiology, social and cultural milieu, and preferences and values.
5. Take into account your own, your colleagues', and your settings' particular experiences and resources, that is, those aspects that make up "clinical expertise."
6. From this integration and synthesis of the appraised evidence, together with the unique aspects of the clinical scenario, make the best-informed clinical decision.
7. Record, track, and update the results of the preceding process. Assess the process itself, and strive for greater efficiency and benefit when applying it to future clinical scenarios.

Bias can be further detected and minimized during the data analysis, with statistical adjustment for any unbalances in potentially confounding factors.

Randomization

The process of randomization, or random assignment of subjects to the study interventions, is a key feature of clinical trials that minimizes bias. In order for the intervention groups to be compared fairly, they must be as similar as possible regarding all characteristics and management other than the intervention to which they were assigned. In clinical practice, patients do not receive interventions at random, but usually variably based on three aspects (best research evidence, clinical expertise, patient preferences) defining evidence-based decision making. When examining the data derived from such clinical practice in a case-series review, those patients who receive one intervention versus another will likely differ regarding some characteristics that will influence the outcomes, rendering the direct comparison of outcomes unfair due to selection bias. This differential influence on outcome can be directly causal, or may have a mediating relation between the intervention and outcome, such as confounding or interaction. Random assignment of subjects helps to minimize bias from confounding by producing groups of subjects whereby baseline characteristics are similarly randomly present between groups, not only those that were measured, but also those that were not measured. Any subsequent differences between groups after random assignment should be due to chance or random error. The degree to which this achieves equivalency of the groups depends on how many subjects are being randomized, with the larger the number of subjects randomized, the smaller the likelihood that a random unbalance will be present. The success of random assignment can be tested at the end of recruitment by comparing measured baseline characteristics between groups and identifying potentially influential differences.

Prospective and Concurrent Data Collection

All clinical trials are prospective by design, whereby the main exposure, the intervention, is applied and then the subjects are

followed forward in time with assessments for the outcomes. Also, all clinical trials rely on data collection that occurs in the present or concurrent data collection as the subjects progress through the study period. This prospective and concurrent data collection allows a higher quality of data to be acquired, versus the use of secondary data such as the clinical record that characterizes the majority of observational studies. Standard definitions and measurement procedures can be applied. Central measurement and interpretation can occur in core laboratories. For more subjective measurements or outcomes, expert and independent adjudication panels can be used. Blinding is important, whereby the subjects, the study personnel and investigators, and those analyzing the data have no knowledge of the randomized assignment of the subject and which intervention was received. Blinding minimizes biases from confounding due to cointerventions. Cointerventions might occur in the application of the intervention, implementation of the protocol, application and interpretation of the measurements, and the attribution of causal relationships to adverse events. Well-meaning study personnel and investigators may provide different subjective interpretations of assessments if they know the intervention the subject was assigned. Subjects have been known to differentially report adverse events while on inert placebo if they believed that they were receiving the active study drug. Thus, clinical trials, through concurrent data collection and blinding, allow a high degree of quality control over the data collection and further opportunities to minimize random and systematic errors.

Appraisal and Regulation

The methodology of clinical trials is fairly prescribed and regimented; errors in the design, execution, or analysis are often readily detectable. If the methods and results are described in sufficient detail, the appraisal of the validity, reliability, quality, and applicability of the findings is possible. Appraisal can inform assignment of a quality and strength grade to the evidence provided by a clinical trial. Standardized reporting of clinical trials has been adopted and required by most prominent scientific journals, which facilitate appraisal. The CONSORT (Consolidated Standards of Reporting Trials; www.consort-statement.org) Statement to

TABLE 78.2 System for Grading the Quality of Evidence and the Strength of Recommendations**EVIDENCE QUALITY FOR GRADES OF EVIDENCE:**

Grade	Evidence
A	Well-designed randomized, controlled trials or diagnostic studies performed on a population similar to the guideline's target population
B	Randomized, controlled trials or diagnostic studies with minor limitations; genetic natural history studies; overwhelmingly consistent evidence from observational studies
C	Observational studies (case-control and cohort design)
D	Expert opinion, case reports, or reasoning from first principles (bench research or animal studies)

GUIDELINE DEFINITIONS FOR EVIDENCE-BASED STATEMENTS:

Statement Type	Definition	Implication
Strong recommendation	The reporter(s) believe that the benefits of the recommended approach clearly exceed the harms and that the quality of the supporting evidence is excellent (grade A or B). In some clearly defined circumstances, strong recommendations may be made on the basis of lesser evidence when high-quality evidence is impossible to obtain and the anticipated benefits clearly outweigh the harms.	Clinicians should follow a strong recommendation unless a clear and compelling rationale for an alternative approach is present.
Recommendation	The reporter(s) feel that the benefits exceed the harms but the quality of the evidence is not as strong (grade B or C). In some clearly defined circumstances, strong recommendations may be made on the basis of lesser evidence when high-quality evidence is impossible to obtain and the anticipated benefits clearly outweigh the harms.	Clinicians should generally follow a recommendation but remain alert to new information and sensitive to patient preferences.
Option	Either the quality of the evidence that exists is suspect (grade D) or well-performed studies (grade A, B or C) show little clear advantage to one approach versus another.	Clinicians should be flexible in their decision making regarding appropriate practice, although they may set boundaries on alternatives; patient preference should have a substantial influencing role.
No recommendation	There is both a lack of pertinent evidence (grade D) and an unclear balance between benefits and harms.	Clinicians should feel little constraint in their decision making and be alert to new published evidence that clarifies the balance of benefit versus harm; patient preference should have a substantial influencing role.

Adapted from American Academy of Pediatrics, Steering Committee on Quality Improvement and Management. Classifying recommendations for clinical practice guidelines. *Pediatrics* 2004;114:874–877.

TABLE 78.3 Advantages of Randomized Clinical Trials

- They provide the best evidence that the intervention being studied is causally related to the outcomes of interest.
- The process of randomization minimizes patient selection bias.
- The prospective and concurrent nature of the data collection allows further minimization of bias through blinding, standardization, and quality control of measurements.
- The design, execution, and reporting for clinical trials allow standardization and more detailed and accurate critical appraisal than observational study designs.

which many journals adhere ensures that those aspects that inform critical appraisal are clearly described during reporting (2,3). These guidelines are also now being used by investigators in the planning of clinical trials, and some funding sources require protocols to be submitted in a CONSORT format. Since clinical trials have a more influential contribution to recommendations and evidence-based clinical care, they are subject to more regulation. Institutional ethics boards may have more explicit criteria by which they assess and approve clinical trials. Regulatory agencies may also be involved, such as the U.S. Food and Drug Administration.

WHY ARE THERE NOT MORE CLINICAL TRIALS?

While clinical trials provide the best evidence, there are challenges that preclude many trials from being performed.

TABLE

78.4

Criteria for Defining Causality in Relationships between Interventions and Outcomes

- Is the relationship biologically plausible in terms of the current state of knowledge regarding pathophysiology?
- Is the relationship strong?
- Is the temporal relationship correct? (i.e., Does the intervention precede the development of the outcome or condition?)
- Is there evidence for a dose–response relationship between the intervention and outcome?
- Is the relationship specific for the intervention and outcomes of interest?
- Is the relationship consistent across variations in study populations, settings and investigators, and design?
- Is the relationship free of known and potential confounding?
- Is the relationship free of systematic and random measurement error?
- If an intervention is successful in reducing or eliminating a particular risk factor or causal mechanism for an outcome, does this then alter the outcome in a consistent and predicted manner?

Resource Requirements and Conflicts of Interest

The execution of clinical trials often requires a lot of resources, and almost invariably cannot be performed without some external funding. Often, this funding may come, wholly or in part, from industry. The relationship with industry brings up issues of real and perceived conflicts of interest, when the industry sponsor or partners have a financial interest in the results of the trial. This may also be true of nonindustry funding sources.

Equipoise and Execution

The logistics of designing and executing a clinical trial are often greater than those of performing an observational study. Equipoise must exist at the beginning and throughout the study period, meaning that the investigators must be convinced that there is insufficient evidence regarding the superiority or equivalency of one intervention over another or standard of care, otherwise it would be unethical to withhold the superior intervention from subjects. Investigators must agree to follow a common protocol, that measurements must be performed to a given standard, and that every effort is made to ensure that data collection is complete and subjects are not lost to follow-up. Often additional quality control measures are necessary, including data coordinating centers, data coordinators, core laboratories, and data and safety monitoring boards (DSMBs).

Feasibility

A major factor that keeps many important clinical trials from being performed is lack of feasibility. This is most often

because there are insufficient participating subjects. This may be as a result of the clinical condition being rare with few available potential subjects, necessary but restrictive inclusion and exclusion criteria limiting the number of eligible subjects, poor recruitment or consent rates, or the outcomes being tracked are rare or take exceedingly long to become manifest. Another feature about clinical trials that informs feasibility is that one can only study a limited number of interventions, usually only two or three, within any given single trial.

Failure of Assumptions

Clinical trials are risky endeavors. One usually begins with a hypothesis, around which assumptions are made based on available preliminary trials, observational studies, extrapolations, or educated guesses. These assumptions inform how much of a differential effect on a primary outcome attributable to the interventions being studied might be expected or clinically sufficient, and how much variation or error there might be around that effect. Often, well-designed clinical trials fail because these assumptions were incorrect. When a clinical trial shows an effect that is less than anticipated from the hypothesis and often not statistically significant but still potentially of clinical relevance, or the variation around the effect is such that one cannot be confident that one has excluded a clinically relevant effect, then the results of the trial fall into a “no man’s land,” being neither definitively positive or definitively negative.

Publication Bias

The results of negative and inconclusive clinical trials are less likely to be published and contribute to the body of evidence. The absence of these trials from the published evidence leads to an unbalance toward trials with positive results, the so-called “publication bias.” The current requirement for clinical trials to be registered with a cataloging service within the public domain before starting recruitment is an attempt by journal editors to prevent this bias, as well as to make participation in clinical trials more widely available to potential subjects (4).

Specialty-specific Challenges

There are a number of challenges regarding clinical trials specific to pediatric and congenital cardiology and cardiovascular surgery, as outlined in Table 78.5. One of the major advances in overcoming some of these obstacles was the funding and formation in 2001 of the Pediatric Heart Network by the U.S. National Institutes of Health, National Heart, Lung and Blood Institute (5). The Pediatric Heart Network is a consortium of leading North American pediatric cardiology programs, together with a data coordinating center, aimed at performing multi-institutional studies, and has successfully completed some landmark clinical trials(6–9).

DESIGN ISSUES FOR CLINICAL TRIALS

Both the design and execution of a clinical trial can have a strong influence on the degree to which the findings from the completed study represent the truth in terms of the answer to the research question (Fig. 78.1). Errors in the design and execution may compromise the degree to which the findings have validity, reliability, and generalizability. Errors in the execution can influence the degree to which the findings from

TABLE 78.6 Phases of Clinical Trials

Phase I Usually an uncontrolled study
Determine dosage and administration of the intervention associated with safety
Evaluate short-term safety and tolerability of the intervention
Provide preliminary data on efficacy
Phase II Smaller scale controlled study
Refine optimal dose and administration associated with potential efficacy
Determine common short-term adverse effects and risks
Provide further data to inform feasibility and design of larger efficacy trials
Phase III Randomized clinical trial
Determine clinical efficacy or effectiveness and safety parameters
Phase IV Usually long-term surveillance or specific clinical trials
Determine efficacy and effectiveness regarding long-term outcomes
Determine long-term safety and track rare adverse events
Investigate the intervention in more specific populations, such as children

intervention and determining feasibility, to more definitive determinations of efficacy, effectiveness, and safety. Each phase provides preliminary data and evidence to inform the next phase, creating a body of evidence that will eventually inform recommendations and evidence-based clinical decision making. These phases are particularly applicable to interventions involving investigational new drugs and devices, and proceed in a defined sequence, as noted in Table 78.6. The aims of each phase are different, and inform the choice of approach and study design. Given that large scale efficacy and effectiveness trials are risky endeavors, these phases help to ensure that sufficient rationale and preliminary data inform their design and execution.

Phase I studies are usually the bridge from experiments in animal models to human subjects. For drugs, these studies are usually conducted with healthy volunteers, although they may be conducted with patients to whom the drug may be of benefit or for whom conventional therapies have failed. Phase I studies are usually not randomized or controlled (no comparison group), are small in scale, and are aimed at determining short-term safety and tolerability, dosing (including the maximally tolerated dose and toxicity) and administration through pharmacodynamic and pharmacokinetic testing, and preliminary results regarding effectiveness.

Phase II studies are based on the results from phase I studies, and are aimed at determining whether or not the intervention will have an effect on the outcomes of interest in the population to whom the intervention will be applied in clinical practice. Usually these are smaller randomized and controlled clinical trials, and the primary outcomes may be more mechanistic in nature. Phase II studies also may lead to refinements in dosing and administration, and determine short-term adverse effects and risks beyond those noted in the Phase I preliminary studies. Phase II studies will help to determine feasibility and to provide important information about assumptions around the hypothesis that will be tested in Phase III studies.

Phase III studies are aimed at providing robust evidence for clinical efficacy or effectiveness, while further specifying safety. These studies are meant to satisfy regulatory requirements for industry prior to marketing a drug or device, and are used to inform clinical recommendations and evidence-based practice. Phase III studies are rigorous randomized controlled clinical trials with large numbers of subjects, and tend to have a shorter intervention or follow-up period than would be used in clinical practice. These trials are powered to detect a clinically meaningful impact on an outcome that is immediately relevant to the patient, such as mortality, symptomatic morbidity, and functional health or quality of life. These outcomes are much harder to study in children and congenital heart patients, where the outcomes occurring are less frequent, occur over a longer period of time, or are less well-conceptualized.

Phase IV studies are long-term studies or surveillances conducted after the drug or device has received regulatory approval and is being marketed. They are aimed at monitoring the incidence of adverse events, particularly those that are rare, and to determine long-term effectiveness and safety. Phase IV studies are usually registries, although they may include clinical trials, particularly if they are aimed at determining efficacy, effectiveness, and safety for more specific indications or in more specialized populations (such as children or congenital heart patients) than in the Phase III trials.

Questions, Hypotheses, and Aims

The conceptualization of all clinical trials begins with a question. The specification of that question is founded on a sound knowledge base and preliminary evidence that leads one to a specific and focused area of controversy or uncertainty. A focused question will define the study population, the intervention and comparison, and the primary outcome for the clinical trial. The process of specification of the question forms the rationale for the clinical trial that is proposed.

The rationale informs the background/preliminary studies section of study protocols and the introduction section of manuscripts. The rationale is not merely an exhaustive literature review, but should represent a synthesis, and like any good story, should have a climax and a point. A well-conceived background to a proposal also represents the starting point for the discussion section of a manuscript once the study results are determined. In outlining these sections, one usually begins by defining the broad topic area, and then honing down to the specific area of controversy or uncertainty. The rationale is provided from both the published literature and preliminary work by the investigators. The rationale is based on the identification of deficiencies in previous studies, conflicting or paradoxical results, gaps in knowledge, or gaps in evidence. The rationale should lead directly to a statement of the research question (stated as a question), which leads to a statement of the primary aim of the trial (the question rephrased as an action item).

The relevance and significance of the question being pursued is another important aspect of the rationale. It defines the importance of the question, which is dependent on the importance of a truthful answer. Put simply, the potential answer must pass the “So what?” test. There are many dimensions to relevance and significance, which can be qualitatively or quantitatively supported. The answer may provide evidence leading to further lines of inquiry, may impact the care of patients, leading to reductions in disease burden or risk, or improvements in patient level outcomes, or may inform clinical recommendations, guidelines, or health policy. The answer should be both interesting and novel.

A *hypothesis* is the best guess as to what the answer to the study question might be. It should ideally be based on knowledge of the published literature and preliminary work and, hence, be an informed guess. The hypothesis should be specified at the same time that one poses the study question, which should be before any data are collected. It should also be detailed and specific to the study subjects, the intervention, and the direction and magnitude of effect on the primary outcome. Hypotheses should similarly be prespecified for each secondary research question. For the purposes of sample size estimation and inferential statistical testing, the hypotheses must be restated in a different manner, to be discussed in a later section of this chapter.

Study aims represent the main and secondary study questions, but are rephrased as an action item. As such, they are like mission statements, which define the direction or design of the clinical trial. The primary study aim should include the defining characteristic of the study population, the intervention and comparison being studied, and the primary outcome (the main or most important outcome). The design of the trial should be specific to achieve this primary aim. Sample size calculations to estimate the number of subjects required are based on the primary aim and an associated hypothesis, together with statistical considerations specifying the risk tolerance for random errors. Secondary aims are usually structured around subgroup comparisons, other types of outcomes, and mechanistic explorations. Secondary aims and hypotheses should be relevant to the primary aim, but provide a greater degree of breadth and depth to the study, which can increase the relevance and significance of a trial. One does not usually hinge sample size calculations on these secondary aims and hypotheses, but one can calculate the degree of power that may be available to test the hypotheses reliably.

Primary and secondary outcomes should be clearly specified and justified and relate directly to the study aims and underlying research questions. In the design phase of clinical trial development, much consideration is usually given to choosing the primary outcome. Preference is usually given to outcomes that are of direct relevance to the patient, with mortality being the outcome of utmost importance. Other relevant outcomes might be morbidities that impact on patient well-being, risk of intervention or further reintervention, and, more recently, assessments of functional health status or health-related quality of life. A hypothesis regarding the differential impact of the study interventions on the primary outcome informs the sample size calculations specifying the number of subjects required. Secondary outcomes are outcomes of interest that may be related to the primary outcome, either by association or informing a mechanistic relationship. The most common secondary outcomes are measures of adverse effects or events, pathophysiologic parameters, or health care system factors, such as utilization or costs.

Interventions and Clinical Trial Designs

The choice of intervention(s) and comparison should be evident from specification of the research question and primary aim, as well as the phase of investigations as described previously. All aspects of the intervention and its application (what, how, when, where, who) should be considered and exactly specified in advance. In pediatric trials, particular attention should be given to dosing and formulation, and to monitoring for adverse effects. The strategy for ensuring and monitoring of compliance should be detailed. The specification of the interventions should be such that they can be replicated and applied in further studies, adapted to different populations and scenarios, or implemented in clinical practice. These details should be provided in the study protocol, the manual of

operations, and in any subsequent publication of the methods and/or the results of the trial.

Choice of the comparison group can be a key factor in the design of clinical trials. If aspects of the application of the intervention are likely to be influencers of outcomes or to unblind the allocation assignment, then precautions should be taken to have as many aspects as possible replicated identically for the comparison. This may include identical formulation and application of study drug and placebo, or the use of sham procedures. Often, particularly for pediatric patients, the undue burden of taking placebo or undergoing sham procedures cannot be supported due to ethical concerns. Additionally, there may be ethical concerns if there is a reasonable standard of care or alternative that may be withheld. These considerations become key drivers in the design of clinical trials in pediatrics.

The approach or perspective of the clinical trial is linked to the primary aims. Some clinical trials aim to determine if one intervention is better or safer than either usual or standard care, placebo or nonintervention, or an alternative study intervention (superiority trial). While the majority of clinical trials are undertaken with the hypothesis that the intervention of interest will be shown to be better (a one-tailed approach), statistical testing of that hypothesis is conventionally performed with a supposition that the intervention of interest may also be shown to be worse (a two-tailed approach). The two-tailed approach underlies inferential statistical testing, but it also has merit in that many interventions supported by observational studies and preliminary data are subsequently shown to be either equivalent or inferior to their comparison in a large-scale phase III trial. Alternatively and less frequently, some clinical trials aim to determine whether one intervention is no better or worse than either usual care or an alternative study intervention (non-inferiority or equivalence trial). These trials are relevant when a new intervention has advantages over an established or alternative intervention (reduced costs, greater availability, improved feasibility, better tolerance, and acceptability) but there is a need to establish that outcomes will be at least equivalent and noninferior. The threshold for defining noninferior depends on the advantages of the new intervention, and there may be a trade-off for accepting some decrease in efficacy.

Simple randomized clinical trial, also called parallel group design, is the most common clinical trial design. It is characterized by subjects being recruited and randomized concurrently to only one of either an intervention or comparison, and followed concurrently to a specified single study end point. This design is the easiest to implement and to critically appraise, and is also somewhat flexible. It is limited in that it only allows one to study the relative effect of one intervention at a time.

Crossover clinical trials are a variation of the parallel group design whereby subjects are first randomized to either the intervention or comparison for a specified period of time, and then reassigned to the opposite of the initial allocation for a second specified period of time. It allows each subject to receive both intervention and comparison in randomized order. It is often used when the number of study subjects is limited and when the outcomes occur over a relatively short period of time. It allows both within group and between group comparisons, with each subject acting as their own control or comparison, which also helps to minimize bias and allows for paired analyses. Besides increased logistical issues, one of the major limitations of this design is the problem of dropouts, since the subjects are followed longer, have increased exposure to adverse effects, and may not wish to continue with a second period of possible placebo or a less-desirable alternative. Another limitation is the potential for carryover effects, whereby the effects of the initial intervention continue to operate over the second period to influence outcomes. One method

to help prevent carryover effects is to have an appropriate washout period between study periods, although this may be ineffective and further lengthen the study and contribute to dropout. Both of these limitations complicate the analysis and interpretation of the trial results.

A *factorial design* allows the study of more than one intervention together (interaction) as well as separately (independent). The least complex factorial design randomizes subjects to one of four groups—neither intervention (comparison), both interventions, and each intervention separately—and is called a 2×2 factorial design. This design can be efficient in determining both the individual and combined benefits of interventions, including synergy, but also carries the risk of unexpected adverse effects from the combination. Factorial design trials require larger numbers of subjects and have greater logistical issues, and the analysis and interpretation can be complex.

Study Subjects

The degree to which the study subjects enrolled and completing the trial are representative, meaning similar in characteristics and response, of all applicable patients depends on specific aspects of how those subjects were chosen, recruited, and maintained as participants in the trial. These aspects can have important impacts on the validity of the results and their generalizability, and are outlined in Table 78.7.

Definition of the study population begins with examination of the aims and hypotheses of the clinical trial. One wishes to infer that the results of the trial for those subjects studied will be representative of the truth if the trial had been performed in the universe of potential subjects, or the target population. It is usually given that one cannot study absolutely everyone, but one can study those potential subjects who can be identified and approached by the investigators, or the accessible population. Of the accessible population, some subjects cannot be contacted, will prove not appropriate for study, may decline to participate or may start but not complete their participation, and represent the actual study subjects. The degree to which,

at each stage, the subjects are similar to the target population will inform the validity of inferences based on the results from the actual study subjects.

Inclusion and exclusion criteria are defined to refine specification of the accessible population that may be recruited for study participation. Inclusion criteria are the defining characteristics specific to the target population applicable to the study aims. They usually include demographic characteristics (age, sex), clinical characteristics (anatomy, diagnoses, morbidities, procedures), accessibility characteristics (geography, settings), and the time period. Exclusion criteria are characteristics that may influence participation (language barriers, anticipated poor compliance or follow-up, cognitive or physical limitations), applicability or safety of the study interventions (contraindications), or unduly influence outcomes (associated conditions or treatments). Each criterion should be exactly and objectively defined as far as possible. There must be an appropriate balance between being too general and too overly restrictive, balancing generalizability with feasibility.

Sampling strategies may sometimes be necessary when the number of accessible and potentially eligible subjects exceeds the number of subjects required, but one wishes to minimize selection bias. Convenience sampling is most liable to potential bias, and involves selecting subjects who are the most accessible, such as enrolling subjects as they present from routinely scheduled clinic visits. Systematic sampling involves having a system to select subjects, such as enrolling no more than four subjects per week from the surgical list. Simple random sampling involves creating a list of all accessible subjects and then selecting subjects at random until the desired number is achieved, and is the method most likely to minimize selection bias. Random sampling can be stratified by dividing the accessible subjects into defined subgroups, and then sampling within those subgroups, and may be used when the investigators wish to examine the differential effects of the study interventions. If used, any sampling strategy must be exactly specified and tamperproof.

Study Measurements

In any clinical trial, a large amount of data will be collected at various time points throughout the study and for various purposes. Each individual piece of information will play different and sometimes multiple roles in helping to define truth in the results and inform the interpretation and appraisal of the evidence emerging from the clinical trial. The purpose and measurement properties of every variable should be justified and specified in the design of the trial. Each variable can be specified according to several different classifications, as outlined in Table 78.8.

The purpose or rationale provides the justification for inclusion of each measurement or variable. Measurements can be used to characterize the study subjects for description, and should include data collection that verifies inclusion and exclusion criteria. Particularly for procedural study interventions, data should be collected about the execution of the intervention and both concomitant and subsequent management. Outcome variables can be assessed prior to randomization, to either ensure study subjects are free of the outcome or to provide a baseline measure against which subsequent change is assessed. Variables that can confound the relationship between the study interventions and outcomes should be assessed. Confounding occurs when the relationship between the intervention and the outcome is actually due to another factor that is not associated with the intervention. In clinical trials, randomization minimizes the chance of confounding by balancing these factors between intervention and comparison groups. Variables that may interact with the

TABLE 78.7 Defining and Selecting the Study Subjects

- Identify the characteristics of the population to which you would wish to apply the results of the completed trial.
- Identify the population of subjects that are available and accessible for potential recruitment.
- Define the inclusion and exclusion criteria that will specify eligibility for participation.
- If the number of available subjects exceeds the number required, identify an appropriate sampling strategy.
- Define the recruitment and consenting strategy.
- Define strategies for minimizing dropouts and loss to follow-up.
- During execution of the trial, carefully track subject numbers, any available subject-level information, and reasons for exclusion, failed recruitment or consent, and subject loss.
- During data analysis, explore available information to detect any differences or potential bias between participants and nonparticipants at various stages of selecting, enrolling, and studying the subjects.

TABLE 78.8

Characteristics of Study Measurements or Variables

- Purpose or rationale for the measurements or variables
 - study subject characterization
 - study intervention characterization
 - outcome variables
 - potential confounding variables
 - potential interaction variables
- Nature of the measurements
 - Time-related events
 - cross-sectional measures
 - repeated or serial measures
 - qualitative assessment
- Timing of the measurements during study execution
 - at baseline before randomization
 - during study execution
 - at study period endpoint
- Properties of the measurements
 - validity and systematic error
 - reliability and random error
 - level of measurement
 - nominal
 - ordinal
 - interval
 - ratio

study interventions in influencing outcomes should also be considered. In clinical trials, this is the rationale justifying prespecified subgroup analyses, whereby the investigators are determining if the effect of the intervention on the outcome is modified by the presence of other factors. Usually, subgroup analyses in clinical trials are considered exploratory and hypothesis generating, and are often not sufficiently powered to be definitive.

The nature of the measurements, particularly of the outcome variables, influences how sample size should be calculated and how the data will need to be handled during data analysis. Most primary outcomes in clinical trials will be events that are associated with a variable period of time, such as death, morbidities, or procedures. Survival or timed-event analyses are required. Some outcomes are measured after a specific period of time after randomization and study intervention, where the final measurement is cross-sectional in nature. Intervention group comparisons are made at that time point, but may be adjusted for baseline assessment or other potential confounders in multivariable regression analyses. Some outcomes are made repeatedly throughout the period of observation, usually at prespecified time points, and one is interested in determining the difference in trends between groups. Repeated measures or longitudinal regression analysis techniques are required. Less frequently, the outcome of interest is of a qualitative nature, such as responses from a structured interview. Techniques for identifying themes within transcripts of these interviews can be used, and the themes compared between groups.

The timing of measurements during study execution is an important consideration, and is linked to the rationale for that measurement. Some data are collected at baseline and then repeatedly during study execution, and are usually secondary outcome measures such as adverse effects. Other data may be collected only at baseline, such as descriptive or potential confounding variables, or only at study endpoint, such as outcome measures.

Various properties of the measurement need to be considered when planning the measurements and defining what data are to be collected and in what format. An important property is the validity of the measure, or the degree to which the measure is an accurate reflection of the concept of what one is trying to measure. This is particularly of importance when one is trying to measure concepts that are more subjective in nature, such as functional health status or symptom severity. The greater the degree of subjectivity of a measurement, the greater is the risk of systematic error. To some extent, systematic error is a component reflected in intraobserver and interobserver variability. Another property is reliability, or the degree to which you get the same result if you measure the same thing in the same way on the same subject or specimen. Reliability is influenced by random error as well as systematic error. Both systematic and random errors can be reduced with increased quality control over performance and interpretation of the measurements.

Level of measurement is another property that influences sample size calculations and data analysis techniques. Some measures are nominal in nature, meaning that the values are in discrete, unordered, and mutually exclusive categories. An example would be type of device placed for transcatheter atrial septal defect closure. Some measures are ordinal in nature, with the values also in nominal categories but with a non-quantifiable gradient relationship between them. An example might be grading of aortic regurgitation as none, mild, moderate, and severe. Continuous interval variables are those whose values are more infinite and have a quantifiable gradient. An example might be weight or temperature. Ratio variables are continuous variables that vary over a discrete range defined by a denominator, such as percent oxygen saturation. In general, using continuous measures can reduce sample size requirements, and allow determination and specification of dose-response relationships between variables.

Randomization

In clinical practice, patients receive interventions based on specific characteristics, which may include clinical variables, practice variables, and patient and provider preferences. Some of these characteristics influence outcomes, independent of or in interaction with the intervention received. This introduces error when comparing outcomes after interventions. Ideally, one would like to be assured that any differences in outcomes were solely attributable to the interventions being compared. Differences in baseline characteristics can be minimized if the subjects are randomly allocated to intervention groups, hence eliminating selection bias. Random allocation gives the best chance that baseline differences will be minimized, including differences in both measured and unmeasured characteristics. The greater the number of subjects randomized, the greater the likelihood that there will be few important differences in characteristics between the groups. One can also test the success of randomization, by comparing the measured baseline characteristics between assigned intervention groups and by looking for both potentially relevant and statistically significant differences. In analyses of outcome comparisons, one has the opportunity for applying statistical adjustment for any or all baseline characteristics.

TABLE 78.9 Requirements for Valid Randomization

- Ensure that the generation of the allocation schedule is truly random by using random number tables or computer algorithms.
- Ensure the sequence is not predictable, but that the method can be replicated.
- Have the process of generation of the allocation schedule performed and maintained independently from those implementing the study.
- Ensure that the allocation schedule is tamperproof, and that assignment is masked to the subjects and study personnel until the intervention is to be applied or started.
- Allocation of assignment should only be made or unmasked after subject eligibility has been confirmed, consent obtained, baseline measures completed, and at the time the intervention is to be applied or started.
- Ongoing masking or blinding of assignment for subjects, study personnel, and those performing data analyses should be in place, as appropriate for the specific study, and be tamperproof.
- Ensure that the assignment process is clearly documented and tracked for quality control.

Valid randomization can only be achieved if it is performed and applied properly, as noted in Table 78.9. This is achieved when allocation is truly random and when it is tamperproof.

Variations of randomization can be employed for specific purposes, as noted in Table 78.10. Most large trials employ simple randomization, as the large number of subjects minimizes

the chance of random imbalances in characteristics between groups. Use of blocks with simple randomization ensures that the number of subjects in each group is equal at the start of the intervention throughout the study. Cluster randomization is used when subjects fall into natural groups where there might be contamination between individuals within the groups if they were to receive different interventions, such as an educational or behavioral intervention. Some randomization variations are employed to ensure that there are no chance differences between groups regarding specific baseline characteristics that have an important influence on the outcomes, and included stratified randomization and pair matching.

Controversial variations of randomization include unequal allocation and adaptive randomization. Unequal allocation entails allocating more subjects to one group than another, usually in a specific ratio other than 1:1, creating groups of unequal sizes. It may be used to evaluate multiple treatment groups against a single control group, with relatively larger numbers allocated to control. Increased allocation to an intervention group may be desired to detect rare outcomes and adverse effects specific to that intervention. It may be used to increase recruitment when it is known that subjects have a greater chance of being allocated to a desirable intervention. Conversely, it may be used to limit allocation to an intervention that is expensive or of limited availability. This type of allocation reduces statistical power, complicates consent, and remains controversial as to validity. Adaptive randomization entails changing the probability of allocation for the next subject based on the characteristics of those subjects previously randomized. This can be used as the allocation proceeds to correct for imbalances regarding baseline characteristics (covariate adaptive) or differences in group sizes (treatment adaptive). It may also be used to preferentially assign subjects to the “best” intervention based on the outcomes of preceding subjects, allowing more subjects to be given the potentially beneficial intervention, or fewer subjects to be given a potentially harmful or ineffective intervention. Adaptive allocation requires continuous tracking of characteristics and outcomes,

TABLE 78.10 Types of Randomization

	Method	Advantages	Challenges
Simple randomization	Allocating subjects independently, sequentially, and randomly to intervention groups with no consideration as to previous allocations	Simple, efficient, sufficient for large trials	May result in imbalances in numbers and characteristics when applied in small trials
Block randomization	Simple randomization with the subjects being allocated within blocks of a specified but preferably random size	Ensures an equal number of subjects in each group at the end of allocation of each block	Use of fixed block sizes may allow for prediction of sequential assignments
Cluster randomization	Subjects allocated as clusters, with groupings based on specific characteristics, e.g., families, schools, clinics, communities	Reduces contamination bias between individuals in the same cluster, as they all receive the same intervention	Applicable only to large trials and must be sufficient clusters; analyses must consider inter- and intracluster variation and effects
Stratified randomization	Block randomization according to potentially influential baseline characteristics where equal allocation must be assured	Ensures there is no imbalance between groups regarding the specific influential baseline characteristic	Increases complexity; can only practically have no more than one to three stratifying variables
Pair matching	Subjects are paired at baseline according to matching characteristics, and then the individuals in the pair are randomly assigned to the intervention groups	Ensures there is no imbalance between groups regarding those characteristics used to match subjects	More potential subjects needed to make good matches; increases complexity; requires analysis of pairs

often precludes effective blinding, and reduces statistical power and validity.

Cointerventions and Blinding

A significant factor that may alter, or confound, the results of a clinical trial is cointervention, a phenomenon that occurs when potentially outcome-altering interventions (other than the study intervention) are administered to some subjects, but are not specified in the study protocol. Cointerventions may be introduced into the study intentionally or unintentionally, and are often allocated to subjects by nonrandom means. For example, if investigators believe the study intervention to be effective, they may (consciously or unconsciously) give compensatory care to those not receiving the intervention in the control group. Conversely, subjects in the study intervention group may take extra steps to supplement or augment any intervention effect, to increase the likelihood of an anticipated outcome. Such behavior results in uneven distribution of cointervention across trial groups, and subsequent confounding of the trial outcome.

Ascertainment or reporting bias is another important confounding behavior in clinical trials, wherein study investigators or subjects may have an altered perception or reporting of outcomes due to knowledge of the subject's group assignment. For example, an investigator may become more likely to seek and declare a positive outcome measure when aware of a subject's assignment to the study intervention group.

Blinding or masking can minimize both cointervention and ascertainment bias in clinical trials. When blinding, either the study subjects, investigators, or both are made unaware of the intervention assignments until the end of the trial, as outlined in Table 78.11. Triple blinding adds blinding to any data analyses, whereby those performing or reviewing interim and final analyses for either safety or for efficacy are unaware of the meaning of the groups, that is, the groups are labeled A and B. Regardless of the degree of blinding of subjects and investigators, any individual charged with measuring the primary outcome of a trial should always be blinded to the greatest extent possible. This includes any laboratory personnel analyzing study samples, as well as clinical staff charged with interpreting any data susceptible to significant interobserver variability, as outlined in Table 78.12.

Use of placebo systems can facilitate blinding. Placebos are an inert or sham intervention designed to mimic the study intervention in all but biologic effect, and would be administered to the control or comparison group of a clinical trial. Placebo controls serve to make the study interventions indistinguishable to both subjects and investigators, maintaining blindness to individual group assignments. Placebos should, therefore, be matched to the study intervention in as many dimensions as possible. In certain cases, placebo use may be restricted by ethical or logistical limitations, forcing the trial

TABLE 78.11 Types of Blinding in Clinical Trials

■ Unblinded	Both subjects and investigators are aware of group assignments. Sometimes necessitated by logistical and ethical constraints. Most susceptible to cointervention and ascertainment bias.
■ Single-blinded	Only the subjects are unaware of the group assignments.
■ Double-blinded	Both subjects and investigators are unaware of assignments. Gold standard of clinical trial designs. Least susceptible to cointervention and ascertainment bias.

to follow a single-blind or unblinded design, as outlined in Table 78.13.

Unblinding of a subject's intervention assignment may be necessary in certain emergency circumstances, such as the presence of a severe adverse effect or some unrelated emergency requiring intervention that may interact with their study intervention. Since such circumstances often evolve suddenly, safety measures should be put in place to allow for quick and accurate unblinding in the case of such an event. Such measures might include distribution of a 24-hour emergency telephone number to all subjects through which their care providers may access immediate unblinding. The decision to break blinding to any extent directly impacts the validity of any trial results, and should only be considered when deemed essential by the subject's treating care provider. Where possible, the level of unblinding should be kept to a minimum. One can often unblind to the treating care provider without disclosure to the subject or investigators.

Success of blinding throughout a trial can be evaluated at the end of a study by a simple survey, asking subjects and investigators to make guesses on group assignments. If >50% of guesses are correct for either subjects or investigators, then the blindness of the study may have been compromised.

Sample Size and Power

A pivotal component of clinical trial design is an estimation of the number of completing study subjects needed in order to reliably achieve the study aim and confidently answer

TABLE 78.12 Influence of Outcome Type on Blindness of Study Design

Outcome Type	Definition	Example	Implications
Subjective	Ascertainment requires a subjective judgment on the part of an observer.	Outcome determined by diagnosis based on interpretation of echocardiography.	High risk of ascertainment bias. Trial should be blinded to the greatest possible extent.
Nonsubjective or binary	Ascertainment does not require a subjective judgment.	Mortality as a study end point.	Low risk of ascertainment bias. Full blinding may not be strongly required, but the highest feasible degree of blinding is recommended.

TABLE 78.13 Limitations on Placebo Use in Clinical Trials**Ethical Limitations****Studies investigating severe conditions**

Withholding of active intervention through placebo use may pose unacceptable risk to subject safety.

Studies evaluating surgical interventions

Performance of sham surgeries on the control group may be unethical, due to high risk and invasiveness.

Consent issues

Subjects must be made fully aware of the likelihood of assignment to placebo, which may not be feasible with certain types of interventions.

Logistical Limitations**Difficulty in intervention matching**

Due to properties of the active intervention; for example:

Distinct color, taste, or smell

High risk of distinct side effects

Highly specific administration procedure

the research question. If too few subjects are studied the possibility of erroneous conclusions is increased; if too many subjects are studied there is greater cost and loss of efficiency. The required number of subjects who completed participation in the trial and had valid outcome assessment is a subset of the subjects who were enrolled and allocated to the study interventions, which is a subset of accessible subjects who were deemed potentially eligible, which is a subset of the target population to whom one wishes to generalize the trial results. One would like to be confident that one can infer that the results of the study as performed in the participating subjects is a reasonable reflection of the results had the study been performed perfectly with the entire target population, and hence, are the truth.

The calculation of sample size is always based on a number of assumptions, and must, therefore, be viewed as an estimation. The necessary components to calculate sample size are hypotheses that include an estimation regarding an anticipated and clinically relevant effect size and its variation, and specification of tolerance limits for making potentially erroneous conclusions, as outlined in Table 78.14.

The null hypothesis is derived from the research hypothesis but states that there will be no difference in the primary outcome between the study intervention and comparison groups. The null hypothesis forms the basis for formal statistical testing, and in superiority trials, the goal is to reject this hypothesis with a certain level of confidence that a clinically relevant difference is likely. In inferiority trials, the goal is to accept this hypothesis with a certain level of confidence that a clinically relevant difference is unlikely.

The alternative hypothesis is the converse of the null hypothesis, stating that a difference or effect will be present. The alternative hypothesis is accepted if the observed results favor rejection of the null hypothesis. The alternative hypothesis can be stated such that the effect will only be in one direction, either a benefit or decrement, which is referred to as a one-sided hypothesis. The convention is to simply state the alternative hypothesis such that an effect exists, but that it could be in either direction, which is referred to as a two-tailed hypothesis.

The effect size and its variation are a further specification of the alternative hypothesis. The specification of the primary outcome, effect size, and variation are the most challenging components of designing a clinical trial, since they may lead to sample size estimates that render a trial not feasible or relevant, or lead to results that are subject to error and inconclusive. The estimation of effect size and variation should be based on as much relevant information as is possible. This can come

from the published literature, and from smaller pilot trials or observational studies. Ideally, one should specify an effect size that has clinical significance or importance. For superiority trials, clinical importance is defined as the minimum effect size in the direction of benefit attributable to the study intervention that would justify preference for that intervention in clinical practice. For inferiority trials, clinical importance is defined as the minimum effect size in the direction of lack of benefit that would justify abandoning the intervention as an alternative in clinical practice.

TABLE 78.14 Requirements for Estimating Sample Size

- State a null hypothesis specifying no difference in primary outcome between the study intervention and comparison groups.
- State an alternative hypothesis specifying that there will be a difference in the primary outcome between groups.
- Specify whether the expected difference in the primary outcome can be in one direction only (one-sided) or can be in either direction (two-sided).
- Specify the magnitude of the expected difference or effect size, and estimate the degree of variation or random error around that difference.
- Specify the tolerance (alpha) for incorrectly concluding, based on the observed results of the study, that there is a relevant effect size when in truth there is none (type I error—erroneously reject the null hypothesis).
- Specify the tolerance (beta) for incorrectly concluding, based on the observed results, that there is no relevant effect size when in truth one is present (type II error—erroneously accept the null hypothesis).
- Specify the method for calculation of sample size, based on the statistical test, to be applied for comparison of study groups according to the nature and level of measurement of the primary outcome.

The tolerance for erroneously rejecting or accepting the null hypothesis based on the observed study results also informs sample size estimation. A type I error entails incorrectly rejecting the null hypothesis and concluding that a significant difference or effect exists based on the results in the observed sample, when in truth, in the target population there is no effect or difference. This is also referred to as a false positive. The tolerance for making this error based on probability theory and random chance is referred to as alpha. In general, the convention is to accept a 5% chance of making this error, or specifying an alpha of 0.05. Alpha is also referred to as the level of statistical significance, and is analogous to the *p*-value of inferential statistical testing. A type II error entails incorrectly accepting the null hypothesis and concluding that there is no significant difference or effect when in truth one exists. This is also referred to as a false negative. The tolerance for making this type of error is also based on random chance and referred to as beta. In general, the convention is to accept a 5% to 20% chance of making this error, or specifying a beta of 0.05 to 0.20. The flip side of beta is power, or 1-beta, which is the probability of correctly rejecting the null hypothesis based on the observed results and concluding that an effect equal to

or greater than that observed in the study actually is truly present in the target population. Power calculations take on importance when considering anticipated effects on secondary outcomes and related hypotheses, or when the observed results regarding effect on the primary outcome are less than hypothesized or the variation is greater, and one lacks the confidence to reject the null hypothesis.

The method of calculation of sample size is specified by the number of study groups and the nature and level of measurement of the primary outcome that determines the probability distribution for testing. This determines the statistical test to be applied when comparing the primary outcome between study groups. An example of a worked calculation of sample size from a specific study is outlined in Table 78.15, based on a clinical trial of thromboprophylaxis in Fontan patients (10). Formulas and tables for estimating sample size and calculating power are available in many textbooks, and online calculators are available on many websites. For complex study designs and outcomes, including time-related events, longitudinal data, or multivariable regression, consultation with a statistician is usually required. Being able to specify the requirements outlined in Table 78.14 will greatly facilitate the statistician in choosing the appropriate methods for calculation.

TABLE 78.15 Worked Example of Sample Size Calculation

Scenario: A 2-year open-label randomized clinical trial was performed on patients undergoing Fontan procedure. Patients were randomized after Fontan procedure completion to either low dose acetylsalicylic acid (ASA) or a heparin lead-in followed by warfarin to maintain an international normalized ratio (INR) between 2.0 and 3.0. The primary outcome was the presence of thrombosis or occurrence of a thrombosis-related event occurring over a 2-year period, with scheduled transesophageal echocardiography performed at 3 months and 2 years after randomization and all outcomes being adjudicated.

Sample size parameters:

Null hypothesis: There will be no difference between treatment groups regarding the 2-year incidence of thrombosis/events.

Alternative hypothesis: There will be a difference between treatment groups (two-sided hypothesis).

Effect size: The incidence will be 25% in the ASA group and 10% in the warfarin group, based on a systematic review of published observational studies. A 15% absolute difference was judged to be the minimal clinically important benefit that would justify the inconvenience and risks of warfarin.

Alpha: 0.05.

Beta: 0.20.

Statistical test: Kaplan-Meier timed-event analysis would be used to determine the freedom from thrombosis/event at 2 years for each group, which would, for simplicity of sample size calculation, then be compared using Chi-square.

The calculation:

The formula for estimation of the total sample size *N* (both groups combined) is:

$$N = \frac{[z_{\alpha} \times \sqrt{P(1-P)(1/q_1 + 1/q_2)} + z_{\beta} \times \sqrt{P_1(1-P_1)(1/q_1) + P_2(1-P_2)(1/q_2)}]^2}{(P_1 - P_2)^2}$$

Where

P_1 = incidence in the warfarin group = 0.10

P_2 = incidence in the ASA group = 0.25

q_1 = proportion allocated to the warfarin group = 0.50

q_2 = proportion allocated to the ASA group = 0.50

$P = q_1P_1 + q_2P_2$

z_{α} = the standard normal deviate for alpha (0.05), two-sided = 1.96

z_{β} = the standard normal deviate for beta (0.20) = 0.84

sqrt = square root

Based on this formula and the specified parameters, *N* would be 224, or 112 subjects per group. (Recruitment is then inflated based on estimated dropouts and loss to follow-up)

EXECUTION ISSUES FOR CLINICAL TRIALS

Nearly all of the issues relevant to the execution of the clinical trial protocol can be minimized in the planning and design stages. However, not all issues can be anticipated or prevented, and ongoing quality control and monitoring are required throughout the execution of the protocol. In addition, the trial must be conducted in compliance with good clinical practice. All study personnel should be trained in the ethical conduct of clinical research, privacy and confidentiality policy, and best practices involving tracking and documentation. The Clinical Trials Networks through the Duke Clinical Research Institute provides information and online training in best practices (www.ctnbestpractices.org).

Operationalization

Implementation of a clinical trial begins with obtaining the necessary administrative and ethics board approvals, and ensuring the trial is registered prior to any recruitment. The protocol should be expanded into an operations manual, which outlines in detail the standard operating procedures (SOPs) for rigorous execution of the trial (Table 78.16). Discussions with study personnel should document roles and responsibilities and accountability, together with completion of training in study procedures. Discussions should also occur with clinical staff who might care for study subjects or identify potential subjects for recruitment. Data collection forms and procedures should be finalized, with detailed data definitions. During the conduct of the trial, any amendments to the protocol should be tracked, together with the reasons and approvals. Any deviations from study procedures should also be documented and tracked. Procedures for adverse event monitoring, documentation, classification, attribution, and reporting should be specified. Periodic study site audits may be planned to ensure compliance with SOPs, complete and accurate documentation and reporting, and to troubleshoot local challenges such as low recruitment or consent rates or excessive loss to follow-up.

Recruitment

Recruitment strategies should be tailored to the individual circumstances of the clinical trial and the nature and characteristics of the accessible population. Well-designed clinical trials can fail or be considerably weakened if the desired number of subjects as specified in the sample size estimation are not recruited and retained until study completion. The study

quickly becomes underpowered in its ability to detect confidently the hypothesized outcome difference or effect size. If the number of accessible subjects is excessively large, then successful recruitment of sufficient study subjects is made more feasible. This is enhanced if the accessible subjects are easy to identify and to contact or approach. Recruitment strategies can be enhanced by piloting recruitment procedures and approach related to the specific trial. Barriers to study recruitment and retention for which strategies should be considered to address them are outlined in Table 78.17.

The identification and approach of potential subjects can be made more or less challenging depending on the nature of

TABLE 78.17 Potential Barriers to Subject Recruitment and Retention

Related to the subjects

- Long wait times and inconvenient scheduling
- Uncomfortable with the uncertainty associated with a trial, particularly randomization
- Misperceptions about research and misinformation about clinical treatments or tests
- Unrealistic understanding of the nature and level of required participation
- Other factors, such as disease status (particularly the presence of symptoms or a poor prognosis), very young or very old age (perceived vulnerability), level of education, social circumstances, language barriers

Related to the investigator

- Inability to integrate and balance roles as caregiver and investigator
- Lack of time or sufficient resources
- Presence of competing interests
- Confusion regarding responsibilities
- Underestimation of workload for study execution, including administration

Related to the study protocol

- Lack of equipoise for the study interventions
- Lack of support for the study aims and design
- Complicated and overly tight eligibility criteria
- Complex study procedures that are difficult to follow
- Long studies and studies with frequent visit schedules
- Studies with excessive monitoring or complex dosing/titration schedules
- Interventions associated with poor subject compliance

Other barriers

- Requirement for excessive documentation and reporting
- Administrative and regulatory barriers
- Insufficient financial support or resources
- Overly intrusive monitoring and audit procedures and schedules
- Poor relationship with lead investigators, study sponsors, clinical research organization

TABLE 78.16 Sample Topics Detailed in the Trial Operations Manual

- Description of the patient population to be studied
- Recruitment, enrollment, and consenting procedures
- Standardized definitions of all study parameters and measurements
- SOPs for all trial functions
- Responsibilities of study personnel
- Standardized solutions to any foreseeable issues that may arise, such as emergency unblinding
- Data collection forms and study instruments

the accessible population. Studies recruiting from the general population present more challenges than those studies where recruitment can occur in settings where potential subjects are put in close proximity with investigators, such as clinical settings where regular care is provided for patients with specific characteristics consistent with study subject inclusion criteria. Initial contact can be indirect, such as through advertising or media or mail-outs, where the obligation is then on to the subject to contact the investigators for more information or to volunteer. For clinical populations, the potential subjects are usually known and can be identified from patient lists and databases. Initial contact should come with the permission and involvement of the patient's responsible care provider, usually by a letter of introduction or a face-to-face introduction on the part of that provider on behalf of the investigators and study personnel. Subjects must not be coerced or inappropriately enticed into participation, and have complete freedom to decline with no impact on their relationship or care provided by their treating providers.

Enrollment begins by providing simple yet complete explanations for the reason for the study, the nature of the study intervention and comparison, and the schedule and type of study measurements. Subjects must understand the concept of randomization and protocolized follow-up, and should also have equipoise for the study interventions. They also must be completely informed of all potential benefits and risks or inconveniences associated with participation. Enrollment is facilitated if the study is simple and short with few study visits, study measures are focused and not obtrusive, and there are perceived benefits for the subject, such as an enhanced feeling of altruism, access to new treatments and more specialized tests, access to treatment and care without costs, costs of participation are reimbursed and incentives are provided, and the patient has the potential to benefit from improved outcomes.

Tracking and documentation of recruitment and enrollment is very important. At each step, moving from the accessible population down to subjects enrolled, minimal data collection regarding characteristics can allow one to look for participation bias. One must enumerate the number and, if possible, characteristics of the accessible population. This can be achieved through census statistics or patient databases, and through minimal data collection at the time of approach. Screening logs should be kept. The number of subjects approached and screened should be tracked, and of those the number of subjects who both meet inclusion criteria or have exclusion criteria should be enumerated. Reasons for exclusions should be tracked. For those declining enrollment, the reasons should be specified and tracked. For eligible subjects agreeing to participate, the consenting process should be transparent and documented, and consent obtained by study personnel with no or minimal perceived conflicts of interest. The care providers for subjects who consent to participate should be notified and informed of procedures for reporting adverse effects and concomitant conditions and treatments.

Retention

The success of a study is dependent on the number of subjects who complete participation and have measurement of study outcomes. For various reasons, which must be tracked and documented, subjects will either terminate their further participation (dropouts) or will be lost and unable to be contacted (loss to follow-up). In planning for recruitment, extra subjects above those specified by the sample size calculations should be recruited in order to account for an estimated proportion of dropouts and loss to follow-up and to maintain study power. If dropout and loss to follow-up occur differently in the study groups being compared, this can unbalance

the groups both regarding numbers and characteristics, which can then introduce bias. Dropouts can occur when subjects decline to return for study visits, change eligibility, develop adverse effects, no longer require ongoing treatment, change their accessibility, or simply decide to withdraw from further participation. Loss to follow-up occurs when the subject can no longer be contacted, which may represent an intentional subject withdrawal or may be due to death, relocation, or unreported changes in contact information.

Strategies to maximize retention and completion should be considered in the study design phase and incorporated into trial operations. Dropouts can be minimized by keeping participation short and simple and minimizing inconveniences, establishing supportive relationships with study personnel and addressing all concerns, creating an appealing and organized environment for study visits and measurements, covering any participation-related costs, and providing feedback where possible. Loss to follow-up can be minimized by collecting as much contact information as feasible at the time of recruitment, including alternative means of contact and contact information of family or friends and care providers. Additional sources of information can be used to trace lost subjects with whom direct contact has been lost.

Crossover and Compliance

Sometime subjects may not receive or be compliant with the assigned study intervention. Crossovers occur when a subject randomized and assigned to a study intervention either receives nothing or receives the alternative or comparison intervention, and vice versa. In essence, the subject is changing study groups. Crossovers can occur during the initial application of the intervention, when criteria are unexpectedly noted that preclude or contraindicate that intervention. It occurs when the subject experiences adverse effects and discontinues treatment or pursues alternative treatment, and when the clinical condition changes such that the study intervention is no longer applicable or continued treatment is unethical. Crossover does not preclude ongoing participation in the study and completion of study measurements and outcomes assessments, as these subjects do not necessarily drop out. However, they do complicate comparison of study groups. The convention is to analyze crossovers according to their original assignment, referred to as an intention to treat analysis. This has the potential to minimize observed effect size, but it maintains freedom from allocation bias achieved by randomization. Alternatively, statistical adjustments can be made to minimize confounding.

Compliance with study interventions can also minimize the observed effect size. This includes subject compliance and discontinuations that may be as a result of discretion of the treating care providers. Strategies to monitor compliance, such as overdispensing and then counting returned medication, compliance logs, or devices that record when medication is accessed, or indicative testing of blood levels or treatment effect should be incorporated into study procedures. Compliance should be tracked, and the reasons for noncompliance recorded, as well as action taken. Frequent reminders and feedback regarding compliance can be useful. Episodes of both temporary and permanent discontinuation of study interventions should be minimized and prevented by frequent contact with both subjects and treating care providers. Decisions regarding discontinuations should be discussed with study personnel. Discontinuations should be tracked and reasons documented. Again, the convention in analysis is to analyze subjects according to initial study assignment, or by intention to treat. Additional analyses are often performed to compare groups according to intervention actually received,

or with adjustments for compliance and discontinuations. These analyses should be viewed as secondary, since biases may be introduced, but they can be supportive of results from the primary intention to treat analysis.

Quality Control

Quality control is an important aspect of clinical trial execution, putting place methods for standardizing and monitoring the implementation of a trial in an effort to preserve the study's internal validity. Careful quality control can help to avoid incidences of inaccurate or imprecise data collection, missing data, or data falsification, all of which are likely to introduce error in the study results and undermine the strength of any conclusions drawn. The larger a clinical trial, the greater the importance of quality control—increasing numbers of investigators and primary sites of data collection introduce mounting opportunity for error and inconsistency in study implementation.

Standardization is one of the primary means of implementing quality control in clinical trials. Standardization measures are often implemented before the start of a study, and function to minimize variation in and absence of data through the systematization of study methods and practices. Study aspects often standardized include measurement procedures, working lab and clinical definitions, and data collection, storage, and analysis protocols. The most fundamental tool available for the standardization of a clinical trial is the operations manual, essentially an expanded protocol precisely detailing important methods to be used in implementing the study (Table 78.16). The operations manual is meant to be readily available to all study personnel for the entire duration of the study, and consulted when any protocol uncertainties arise. Training and certifying all study personnel in proficiency for all study procedures is also a useful means of implementing standardization. Training and certification helps to reduce the inter- and intraobserver variability in any study measurements, as well as ensure clear understanding of all study protocols and definitions for all study personnel. Regular performance reviews of study personnel and whole trial centers help to maintain standardization measures throughout the duration of the trial, by auditing data collection and evaluating adherence to protocol as outlined in the operations manual. Such reviews are especially important in longer-term trials, where it may be difficult to maintain the rigor of standardization methods long after the study has begun.

Adjudication is an especially important quality control measure where considerable variability may exist between investigators with respect to the ascertainment and reporting of events (Table 78.18). Particularly with outcomes requiring a complex and/or subjective judgment, adjudication plays a key role in confirming the reproducibility and reliability of any study findings. Several methods exist for standardizing

and controlling the adjudication process. Quality control by repeated adjudication involves the replication of a given outcome measurement or diagnosis by multiple observers, and comparison of the individual results to assess the interobserver reliability. The implications of repeated adjudication vary depending on the type of outcome being ascertained. For nonnumerical outcomes, such as attribution of cause of death, comparison of multiple judgments helps assess the interobserver reliability of the measure and the most likely correct outcome. A high degree of disagreement between observers may indicate a high level of error and/or bias in the adjudication process, and require that the outcome be subject to further assessment before a final decision is made. In the adjudication of a numerical outcome, multiple measurements can be averaged to reduce the variation in the reading.

Central adjudication committees or core labs are a robust method of quality control in the adjudication process. A core lab is a centralized data collection and interpretation system, which acts to ensure that standardization is strictly maintained throughout the processes of outcome adjudication, reporting, and analysis. Core labs may take one of two forms in clinical trials: that of a physical laboratory site centralizing all lab-dependent data analysis, or that of an auxiliary review center charged with verifying outcomes adjudicated and reported by individual trial centers (Table 78.19). Both types of core labs are able to guarantee a high degree of standardization of the adjudication process, since only a small number of individuals are responsible for either all study adjudication, or the verification of each reported outcome within a strict set of criteria. Although more costly, time and labor-intensive than repeated adjudication, core labs are a preferred method of standardization in clinical trials, especially those involving multiple separate study centers.

Data and Safety Monitoring

Data monitoring describes the process of screening and analyzing data as they accumulate over the course of a trial. It is primarily a method of quality control, serving to detect and correct important discrepancies such as absent, imprecise, or falsified data. Such discrepancies may be inevitable, due to forces such as patient noncooperation and error introduced by trial staff or equipment. By allowing preliminary results analysis of incoming data, data monitoring also plays a role in aspects of study planning and administration, such as verification and adaptation of the study's working hypothesis and assessment of possible safety issues (Table 78.20).

Quality control of the data collection process can involve multiple strategies of data monitoring. Some may be performed by study personnel concurrent to data collection and database entry, such as minimization of the lag time between data collection and database entry, manual data checks, and double data entry. Other monitoring procedures may be initiated before a block of data collection has begun, or carried out on working databases after data entry is complete. Such methods include duplicate analysis testing of the data collection process, or software checks for absent, incorrect, or falsified fields in a working database (Table 78.21).

Data editing is the process of correcting errors or absences in data as detected by data monitoring. In order to avoid undermining the integrity of the data collection process, any data editing procedures must be standardized in the operations manual before the start of the study, and clearly documented when performed.

Trial monitoring for safety and efficacy should be conducted by allowing preliminary or interim analyses of subject characteristics and safety and efficacy outcomes to be performed as data are being collected. Such analyses may help

TABLE 78.18

Sources of Intra- and Interobserver Variability in Outcome Adjudication

- Multiple, complex or subjective decisions involved in the adjudication process
- Large numbers of possible decision results
- Lack of attention to decision-making protocols in the adjudication process
- Errors or omissions in available data

TABLE 78.19 Alternate Forms of Core Labs in Standardization

Type of Core Lab	Description	Role in Standardization
Centralized laboratory	Physical, standardized lab site.	Allows all adjudication to be performed by a handful of individuals under highly standardized conditions.
	Staffed by a small number of highly trained, fully blinded technicians.	Drastically reduces intra- and interobserver variability in outcome reporting.
	Receives collected data from separate trial center(s), is responsible for final adjudication and analysis of all outcomes.	
Quality Assurance (QA) Center	Supporting trial review center.	Allows a small number of individuals to verify all reported outcomes, based on highly standardized criteria.
	Staffed by a panel of expert reviewers.	
	Responsible for verifying outcomes adjudicated and reported by individual trial centers, by ensuring each decision meets a specific set of protocol-specified criteria.	Ensures final outcome results are unaffected by variability in adjudication at individual study centers.
	May also fill other roles in quality control, such as organizing and monitoring adjudication procedures, undertaking performance reviews, and coordinating training and certification of study center staff.	
	Most often employed in multicenter trials.	

to detect emerging data trends and relationships, allowing formulation and adaptation of working hypotheses and adjustments to sample size as the trial progresses. Interim analyses should be specified in advance and lead to adjustment in initial sample size estimation.

An *independent DSMB* should be formed, and should assume responsibility for ensuring compliance with the study protocol and procedures, monitor recruitment and study timelines, assure quality control, and to review any interim analysis performed as part of data monitoring. The activities of the DSMB should be carried out independently from the investigators of a study, to avoid any conflict of interest that may arise in determining and reporting significant interim results. Having interim analyses performed and reviewed by an independent body also carries the benefit of maintaining any investigator blindness in a trial, since results analysis and review may require knowledge of treatment assignments. Bodies responsible for performing this analysis may be a preappointed, independent review committee, or simply the institutional review board of a single-center study.

The decision to prematurely stop a study before completion is informed by data monitoring and interim analyses, which may identify exceptional information that may warrant stopping a study, such as clear excessive benefit or harm related to the study intervention (Table 78.22). The decision to prematurely stop a study in response to interim results is a critical one, with serious repercussions if miscalculated. For example, failing to stop a study under necessitating circumstances can have severe ethical implications, by either exposing subjects to unacceptable harm or preventing public access to an excessively beneficial treatment. Conversely, unnecessarily stopping a study can be very costly in terms of wasted resources, and may invalidate any useful results emerging before the study was stopped. Therefore, careful consideration and weighing of all possible risks and benefits must be done by qualified individuals before the decision to prematurely stop a study is made (Table 78.23). Ideally, thresholds of benefit or risk should be prespecified in advance of any interim analysis, preferably in the design or operationalization stages of trial development. These thresholds should be of greater magnitude

TABLE 78.20 Purposes of Data Monitoring

Quality Control of Data Collection

- i. Detection of missing data from final database.
- ii. Discovery and correction of inaccurate or imprecise data.
- iii. Prevention of falsification of data.

Administrative and Planning Purposes

- Performance of preliminary analyses, for:
- i. Generation or modification of working hypotheses.
 - ii. Assessment of safety.
 - iii. Assessment of excessive risks or benefits that may warrant early stopping of the trial.

TABLE 78.21 Strategies of Data Monitoring

Strategy	Timing of Implementation	Description	Purpose
Timely data entry	Concurrent with data collection and entry	Minimization of lag time between data collection and entry into database.	Minimizes data entry errors, since data are fresh, still have clear context. Allows efficient completion of any missing or incorrect fields, since data source was recently available.
Manual data checks	Concurrent with data collection and entry	Staff review of data for obvious errors before and after entry into database.	Allows efficient verification of overall accuracy and completeness of data. Minimizes data entry errors.
Double data entry	Concurrent with data collection and entry	Independent entry of data by two separate individuals, comparison of the resulting databases for discrepancies.	Minimizes data entry errors. Verifies the overall accuracy data entry.
Duplicate analysis	Before data collection begins	Intermittent study processing of known, blinded standards alongside patient samples.	Provides quality control information on the data collection and entry processes.
Software checks	After data entry is completed	Computerized queries to detect missing or unreasonable values in a working database.	Allows detection and correction of data discrepancies after database entry is complete.

than the effect sizes hypothesized for primary and secondary outcomes, and when statistical testing is applied to determine the level of confidence in the observed effect, a more rigorous (i.e., smaller) p -value should be specified.

ANALYSIS ISSUES FOR CLINICAL TRIALS

Data analysis is the process whereby the data collected are used to test the study hypotheses and to answer the study questions. Hence, a data analysis plan must not just be a specification of

statistical tests to be applied, but a description of the means by which results are described and associations determined, with the primary association of interest in a clinical trial being that of the study interventions with the primary and secondary outcomes. The data analysis should also detail plans for further specifying these associations, either by adjustment or subgroup analyses to determine the effects of confounding and interaction. Clinical trials datasets also provide excellent observational data for exploring associations and hypothesis generation, other than with the study interventions. These analyses should also be planned and specified. The analysis plan together with the nature and distribution of variables being used are the determinants of the statistical methods to be applied. The data analysis plan is a key component that should be clearly specified in the design phase of the clinical trial, although modifications may be required when data analysis actually proceeds. These modifications should be justified and documented.

TABLE 78.22 Exceptional Circumstances Warranting Stopping a Study

Serious Adverse Risk of Treatment	Excessive Benefit of Treatment
<ul style="list-style-type: none"> ■ Preliminary analysis demonstrates that treatment poses a serious risk of adverse side effects to patients. ■ Unethical to continue to administer study—all patients should be withdrawn from active treatment. ■ Treatment should not be administered further to new subjects. 	<ul style="list-style-type: none"> ■ Preliminary analysis demonstrates a clear and excessive benefit associated with the experimental treatment. ■ Unethical to withhold an excessively beneficial—study should be stopped to expedite availability of treatment to public.

Data Management, Cleaning, and Descriptive Statistics

Investigators frequently underestimate the amount of effort required to prepare a dataset for analysis. However, the

TABLE 78.23 Factors to be Considered in the Decision to Stop a Study

- Reliability of the interim results in question.
- Follow-up period required for adequate assessment of the effects of the intervention.
- Relative weight of risks and benefits of the intervention to subjects, future patients.

quality control and data-monitoring procedures described previously and implemented during the study execution should minimize many data problems. The first step in the preparation of a dataset for analysis is to ensure completion of all data entry. Quality checks should be in place. Descriptive statistics including frequencies and distributions are then performed for every variable. The number and proportion of missing values should be determined, and efforts made to determine those values. Each variable should be examined for values that are out of range, with verification if they represent true outlier values or are data errors. In addition, values that are miscoded should be corrected. Care should be taken for verifying conditional variables, which are variables the values for which are linked to another variable. For example, duration of circulatory arrest should not have a value if the subject did not have a period of circulatory arrest. The process of data cleaning and verification, and the determination of descriptive statistics should generate a high degree of familiarity with the quantity, quality, and limitations of the available data in order to inform performance of the data analysis plan.

Test of Randomization

While randomization should minimize unbalancing regarding subject characteristics, it does not guarantee that random or systematic differences that may be influential in a comparison of outcomes are not present. Unbalancing, or incomplete randomization, may be a chance occurrence or represent flaws or deviations in the randomization procedure and assignment. One can test the randomization procedures that were employed to verify the randomness and to ensure that the system does not have any inherent bias or predictability. One can also audit the randomization procedures and their implementation, looking for documentation of deviations and their reason.

A *comparison of baseline characteristics* between study groups, the first comparison in the analysis of a clinical trial, and usually the first table in a published report, is a test of the randomization. It should be recognized that one can only detect unbalancing of characteristics that were measured. However, effective randomization should minimize unbalancing for both measured and unmeasured characteristics. The frequencies or distribution of values for each variable within each group should be calculated and compared. Statistical testing can be applied, which can identify those differences that represent deviations from balancing that may not be attributable to chance occurrence. However, one should give more relevance to the magnitude of actual differences than to p -values. Usually, one is comparing across many baseline characteristics, and hence some p -values will meet the threshold for statistical significance on the basis of chance alone as a result of multiple comparisons. Thus, the presence of some unbalancing does not necessarily point to a flaw in randomization procedures. In addition, p -values are highly dependent on the number of subjects and the variation in distribution, in addition to the magnitude of differences. If there is a large number of subjects, small differences have a high likelihood of achieving a significant p -value, yet not be relevant indicators of bias. If there is a small number of subjects, large differences may not be statistically significant, yet impart bias in the comparison of outcomes. One should also look for patterns among the differences in characteristics, particularly among characteristics that may be associated with one another, which may further indicate important unbalancing.

Statistical adjustment for unbalancing can be applied during comparisons of outcomes. This should be performed after the unadjusted intention-to-treat analysis. One can use multivari-

able regression techniques to adjust for baseline characteristics that were significantly different, either statistically or by magnitude, as noted during the test of randomization. This adjustment can be more formally performed by calculation and adjustment or matching for propensity score. A propensity score represents the probability or propensity that a given subject, based on their measured baseline characteristics, was randomized to a particular study intervention group, and can provide simultaneous adjustment for multiple characteristics. The propensity score is calculated from a multivariable logistic regression model with assignment as the dichotomous dependent variable, and relevant baseline characteristics as independent variables. The ensuing regression equation can be solved for individual subjects to give the probability of assignment. The propensity score can then be used either as an adjustment variable when comparing outcomes, or subjects can be matched between groups regarding propensity score, and matched pair analyses applied.

Outcomes Comparisons

The foremost comparison of outcomes between study groups should be an unadjusted comparison based on an intention-to-treat analysis. Intention-to-treat analysis preserves the random allocation that minimizes bias. Subjects are analyzed according to the original group allocation, regardless of crossover, coin-tervention, dropout, noncompliance or other deviations from the study protocol. This is the most valid type of analysis, although if deviations are great, it can minimize the observed effect size.

Statistical testing is applied to comparisons in order to determine the chance probability of observing the magnitude of difference between groups if the null hypothesis is actually true and there indeed is no true difference. This probably is the p -value, and by convention one usually sets the level of statistical significance at a $p < 0.05$, meaning that there is a <5% chance that the observed difference is a random error. The type of statistical test employed to determine the p -value depends on the number of groups and the nature and distribution of the outcome variable.

Measures of effect of study interventions are important for expressing the magnitude of effect and in interpreting its relevance or importance. Of primary interest is the absolute effect, or the direction and magnitude of the difference in the outcome between study groups. One usually calculates this as the effect in the study intervention group minus the effect in the comparison group. Of secondary interest is the relative effect. One usually calculates this as the absolute effect divided by the effect in the comparison group, expressed as a percentage. One applies statistical testing and calculates confidence intervals around the absolute effect, which then inform the interpretation of the observed effect. One can also calculate power, or the probability of correctly rejecting the null hypothesis (no effect) and avoiding a type II error. Power is of more importance when the results of the study are inconclusive based on confidence, or when there are important differences in the magnitude, and sometimes direction as well, of the observed effect versus the hypothesized effect. Table 78.24 outlines a worked example of clinical trial results based on the trial previously described in Table 78.15.

Confidence intervals are similar in nature to p -values, but much more informative. Based on the observed effect and its variation, and influenced by the number of subjects studied, a confidence interval is the range of possible effect sizes over which one can be reasonably (usually 95%) confident that true effect lies. Confidence intervals that include

TABLE 78.24 Worked Example of Effect Measures and Interpretation

Scenario: The clinical trial of thromboprophylaxis in patients after Fontan procedure outlined in Table 78.15 is performed. However, due to slow recruitment and lack of funding, the trial is prematurely stopped short of the intended sample size of 112 subjects per group, with 111 total subjects randomized, 57 to ASA, and 54 to warfarin. At 2 years after randomization, an intention-to-treat analysis of Kaplan-Meier estimates of the primary outcome of thrombosis or thrombosis-related event showed a period prevalence of 14% for the ASA group (8/57) and 24% for the warfarin group (13/54).

Absolute effect: $0.24 - 0.14 = +0.10$. For every 100 patients treated with warfarin, 10 additional patients would have thrombosis/event over the number who would have had thrombosis/event had they been treated with ASA (baseline or comparison risk).

Relative effect: $(0.24 - 0.14)/0.14 = +0.71$. Warfarin is associated with a 71% relative increase in thrombosis/events over treatment with ASA.

p-value: 0.18. There is an 18% probability (two-tailed) of observing an absolute of effect of +0.10 by chance if the truth is that there is no effect.

95% confidence interval around the observed absolute effect: -0.06 to $+0.24$. The confidence interval includes 0, meaning that one can be 95% sure that the truth may reasonably be no effect. If one assumes that an absolute reduction in thrombosis/events of -0.15 over ASA would be the minimal clinically important effect to justify preference for warfarin, then the lower limit of the confidence interval of -0.06 excludes this effect, meaning that one can be 95% sure that a clinically important benefit of warfarin does not in truth exist. If one also assumes that an absolute increase in thrombosis/events of 0.15 associated with warfarin compared to ASA would be the minimal clinically important harm to justify a recommendation not to use warfarin, then the upper limit of the confidence interval of $+0.24$ includes this effect, meaning that one can be 95% sure that a clinically important harm does in truth exist.

Power: 0.20. Based on the observed findings and the number of subjects studied, there is only 20% chance of correctly rejecting the null hypothesis or avoiding a type II error, that is, concluding that there is no differential effect of warfarin compared to ASA when in truth there is no effect.

Interpretation: One can be confident that there is no clinically important reduction in thrombosis/events with warfarin thromboprophylaxis over ASA. However, one cannot be confident that there is in truth no difference, and in fact, one can be reasonably confident that warfarin is in truth associated with a clinically important increase over ASA in the risk of thrombosis/events. However, the study did not include a nontreatment group, so one cannot be certain that warfarin is not of benefit, just that it appears to be of less benefit compared to ASA. The results must be viewed in light of some limitations, including a high and disproportionate prevalence of crossovers, dropouts, out of therapeutic target range and study drug discontinuations, a high prevalence of deviations from the study protocol, as well as the limited power reflective of the lower than expected number of enrolled and randomized subjects.

Of note: The analysis depicted was matched exactly to the analysis as specified in the sample size calculations. However, for the reported trial, given the number of dropouts and, hence, censored observations and the late performance of protocol transesophageal echocardiography beyond the 2-year study endpoint, log rank testing was performed on the entire stratified Kaplan-Meier curve, with no significant difference noted (p -value 0.45). There was also a convergence after 2 years of the incidence of thrombosis/events between groups. The hazard ratio for outcome for warfarin versus ASA was 1.35, indicating a 1.35 times greater risk of outcome with warfarin. The 95% confidence interval was 0.62 to 3.00, which includes a hazard ratio of 1 (no difference, but includes an upper limit of 3.00, or a three times greater risk of outcome with warfarin versus ASA. This risk would probably be deemed above a minimum clinically important threshold for harm.

an effect size indicative of no difference lead one to conclude that one cannot be confident that the observed effect size is not a random error and that the null hypothesis cannot be rejected. If that same confidence interval also includes an effect size that would meet minimal thresholds for a clinically relevant benefit or harm, then the study results are inconclusive, with a relevant effect size being neither confidently proven nor disproven. This scenario occurs most frequently when observed effects sizes are less than what was hypothesized or variation was greater, or the number of subjects studied is insufficient to give the needed power to detect or be confident that the observed effect represents the truth. Ideally, one wishes to have a confidence interval around the observed effect size that excludes no difference and for which the lower limit is not below the minimal threshold of clinical importance.

Deviations from intention-to-treat analysis of outcomes can be of importance when the results of the intention-to-treat analysis are inconclusive or differ significantly from what was

hypothesized. These deviations may introduce bias, since they sometimes depart from randomized assignment, but may be more clinically meaningful. The most common deviation is to perform comparisons based on intervention actually received. This type of analysis may be more meaningful if there are a lot of crossovers. Another deviation is to incorporate measures of compliance with study interventions into the analysis, or to analyze only outcomes occurring before any study intervention discontinuation or dropout. Adjustment, matching, and propensity scores can be used in analyses to statistically adjust for any potential bias in random allocation, or to minimize potential bias from important confounders. Analysis can be conducted to look for differential effect within prespecified subgroups of subjects, or to look for characteristics that interact with the study interventions in their effect on outcomes. The results of these types of analyses are given less weight, and are usually viewed as exploratory or hypothesis generating. Nonetheless, they enrich the information derived from a clinical trial.

REPORTING AND APPRAISAL ISSUES FOR CLINICAL TRIALS

Since clinical trials have a well-defined and structured methodology, usually flaws and deviations are readily apparent. However, consideration of those flaws and deviations, which represent potential bias, is only possible if all aspects of the design and execution of the trial are completely disclosed and the results are presented in sufficient detail, together with a balanced interpretation that includes discussion of the study limitations and the generalizability of the findings. Clinical trials are given the highest weight in systematic reviews and clinical practice guidelines, and are the sole contributors to the majority of meta-analyses. This is predicated on the fact that clinical trials provide the highest quality of evidence based on having the greatest possibility of absence or minimization of bias. The usefulness of a clinical trial report is dependent on the degree to which the study and results can be critically appraised, which is dependent on complete reporting and transparency.

The *CONSORT Group* (Consolidated Standard of Reporting Trials; www.consort-statement.org) is a group of international clinical trials experts, statisticians, journal editors, and authorities from industry, as well as some members from the Cochrane Collaboration (www.cochrane.org). The Group has defined guidelines for standardized reporting of clinical trials, which have been adopted as a reporting requirement by most of the leading medical journals. The CONSORT Flow Diagram (Fig. 78.2) shows how the tracking of subjects

from enrollment, through allocation, follow-up, and analysis should be depicted, together with reasons for any deviations. This figure should be the first figure in any report of a clinical trial. The CONSORT Group also provides a CONSORT Statement consisting of a 25-item checklist (Fig. 78.3), together with an explanation and elaboration document to be used in conjunction with the checklist. Many journals now require that the completed checklist be submitted together with the manuscript draft.

Transparency in clinical trial reporting is also achieved by ensuring that the trial was registered prior to the start of any subject recruitment. The name of the trial registry, the date of registration and the registration number should be reported. The report must also include details regarding institutional research ethics board review and approval, and the process for obtaining consent for participation and how it was tracked. The report may detail how compliance with privacy policies was ensured and maintained. All sources of funding and other support must be disclosed, as well as any other potential conflicts of interest on the part of investigators and authors, such as stock ownership or financial interest, consultancy, and honoraria. Provisions should be specified for making the full protocol for the clinical trial available. Assurances must be provided that all authors had full access to the study data and had taken full responsibility for the reported results, had participated sufficiently in the generation of the trial report or manuscript, and approve of any version and its disposition.

Critical appraisal of reports of clinical trials is made easier when the information specified in the CONSORT Statement checklist is clearly provided. Critical appraisal is usually aimed

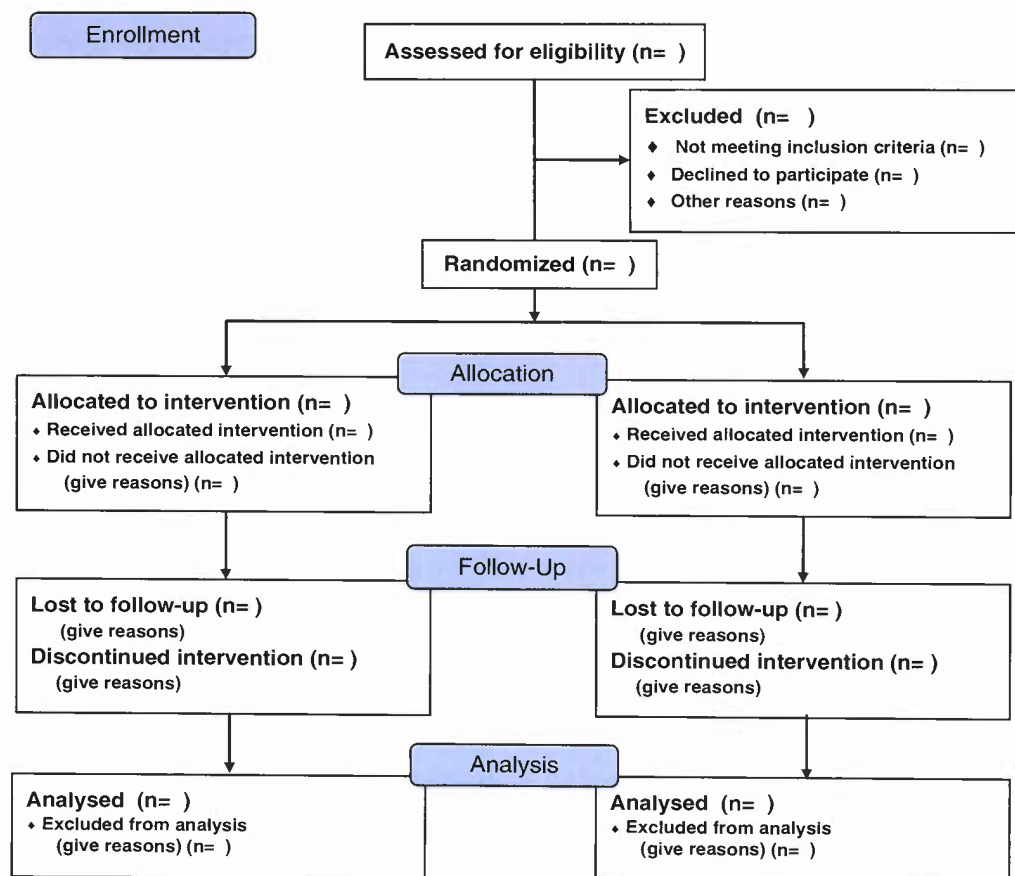


Figure 78.2. CONSORT flow diagram for reporting of subject accrual and retention.



CONSORT 2010 checklist of information to include when reporting a randomised trial*

Section/Topic	Item No	Checklist item	Reported on page No
Title and abstract			
	1a	Identification as a randomised trial in the title	_____
	1b	Structured summary of trial design, methods, results, and conclusions (for specific guidance see CONSORT for abstracts)	_____
Introduction			
Background and objectives	2a	Scientific background and explanation of rationale	_____
	2b	Specific objectives or hypotheses	_____
Methods			
Trial design	3a	Description of trial design (such as parallel, factorial) including allocation ratio	_____
	3b	Important changes to methods after trial commencement (such as eligibility criteria), with reasons	_____
Participants	4a	Eligibility criteria for participants	_____
	4b	Settings and locations where the data were collected	_____
Interventions	5	The interventions for each group with sufficient details to allow replication, including how and when they were actually administered	_____
Outcomes	6a	Completely defined pre-specified primary and secondary outcome measures, including how and when they were assessed	_____
	6b	Any changes to trial outcomes after the trial commenced, with reasons	_____
Sample size	7a	How sample size was determined	_____
	7b	When applicable, explanation of any interim analyses and stopping guidelines	_____
Randomisation:			
Sequence generation	8a	Method used to generate the random allocation sequence	_____
	8b	Type of randomisation; details of any restriction (such as blocking and block size)	_____
Allocation concealment mechanism	9	Mechanism used to implement the random allocation sequence (such as sequentially numbered containers), describing any steps taken to conceal the sequence until interventions were assigned	_____
Implementation	10	Who generated the random allocation sequence, who enrolled participants, and who assigned participants to interventions	_____
Blinding	11a	If done, who was blinded after assignment to interventions (for example, participants, care providers, those	_____

Figure 78.3. CONSORT checklist for reporting of clinical trials. (*Continued*)

		assessing outcomes) and how	
	11b	If relevant, description of the similarity of interventions	
Statistical methods	12a	Statistical methods used to compare groups for primary and secondary outcomes	
	12b	Methods for additional analyses, such as subgroup analyses and adjusted analyses	
Results			
Participant flow (a diagram is strongly recommended)	13a	For each group, the numbers of participants who were randomly assigned, received intended treatment, and were analysed for the primary outcome	
	13b	For each group, losses and exclusions after randomisation, together with reasons	
Recruitment	14a	Dates defining the periods of recruitment and follow-up	
	14b	Why the trial ended or was stopped	
Baseline data	15	A table showing baseline demographic and clinical characteristics for each group	
Numbers analysed	16	For each group, number of participants (denominator) included in each analysis and whether the analysis was by original assigned groups	
Outcomes and estimation	17a	For each primary and secondary outcome, results for each group, and the estimated effect size and its precision (such as 95% confidence interval)	
	17b	For binary outcomes, presentation of both absolute and relative effect sizes is recommended	
Ancillary analyses	18	Results of any other analyses performed, including subgroup analyses and adjusted analyses, distinguishing pre-specified from exploratory	
Harms	19	All important harms or unintended effects in each group (for specific guidance see CONSORT for harms)	
Discussion			
Limitations	20	Trial limitations, addressing sources of potential bias, imprecision, and, if relevant, multiplicity of analyses	
Generalisability	21	Generalisability (external validity, applicability) of the trial findings	
Interpretation	22	Interpretation consistent with results, balancing benefits and harms, and considering other relevant evidence	
Other information			
Registration	23	Registration number and name of trial registry	
Protocol	24	Where the full trial protocol can be accessed, if available	
Funding	25	Sources of funding and other support (such as supply of drugs), role of funders	

*We strongly recommend reading this statement in conjunction with the CONSORT 2010 Explanation and Elaboration for important clarifications on all the items. If relevant, we also recommend reading CONSORT extensions for cluster randomised trials, non-inferiority and equivalence trials, non-pharmacological treatments, herbal interventions, and pragmatic trials. Additional extensions are forthcoming: for those and for up to date references relevant to this checklist, see www.consort-statement.org.

Figure 78.3. (Continued)

TABLE 78.25 Critical Appraisal of Clinical Trials

1. Is the study well designed and executed such that the results are likely to be free of bias, and therefore representative of the truth?
 - a. Was treatment assignment randomized? If so,
 - i. is the randomization strategy specified?
 - ii. was it tamper-proof?
 - iii. was it successful, in that baseline characteristics are comparable between comparison groups?
 - b. Are all of the study subjects accounted for throughout the study, and analyzed according to their initial assignment?
 - c. Were the groups treated equally in all other respects besides the study maneuver?
 - d. Are the primary and secondary outcomes relevant and sufficient?
 - e. Was the study period sufficiently long for the outcomes to occur?
 - f. Was the study maneuver, assessments, and data analysis blinded to the initial assignment?
 - g. Is there a stated hypothesis, and are sample size calculations provided?
2. What are the results, and is the analysis and presentation in a format that allows assessment of the magnitude and reliability of treatment effects?
 - a. What are the magnitudes of the treatment effects?
 - i. Absolute effects
 - ii. Relative effects
 - b. How reliable are the estimates of the treatment effects?
 - i. Are standard errors or confidence intervals provided?
 - ii. Are power calculations provided for nonsignificant differences?
3. Are the results relevant and applicable to the clinical scenario at hand?
 - a. Are inclusion and exclusion criteria described in sufficient detail?
 - b. Is the treatment described in sufficient detail to enable implementation?
 - i. Is the treatment feasible in the clinical scenario?
 - c. Is any information provided that would allow further specification of the treatment effects to the characteristics of an individual patient?
 - i. What are the benefits and harms for the specific patient?
 - d. What are the values and preferences for the specific patient?

at determining the strength of the evidence that a specific study provides, and whether the findings are relevant to a meta-analysis, clinical guideline, or to one's own clinical practice. Key questions for appraisal are outlined in Table 78.25. Appraisal of a trial begins with an assessment of the validity of the trial, primarily through appraisal of the study design and execution. The next step is an assessment of the results, their statistical and clinical significance, and their reliability. The balance of benefits versus risks should be evident and considered. The final step is an assessment as to the applicability of the study findings to the clinical scenario at hand. Further information and resources regarding critical appraisal and the practice of evidence-based medicine can be found through The Journal of the American Medical Association (www.jamaevidence.com), which had previously published some of the first User's Guides to critical appraisal of the medical literature (11,12).

The standard of clinical care is not solely determined by the results of a single clinical trial, but a well-designed and executed clinical trial with clinically important results can influence the

standard of care. Further criteria to consider are outlined in Table 78.26.

ACKNOWLEDGMENTS

The chapter author would like to acknowledge the outstanding and invaluable contributions of Elizabeth Niedra in the preparation of this chapter.

RECOMMENDED RESOURCES

This chapter provides an overview of the value, design, execution, analysis, reporting, and appraisal of clinical trials. For more detailed information, a list of excellent textbooks is provided. Additional resources can increasingly be found online.

TABLE 78.26 Criteria to Consider Before Adopting a New Intervention as the Standard of Care

- There is a sound rationale for the therapy based on current knowledge of physiology and pathophysiology in the specific population to which the therapy is to be applied.
- It is feasible for the therapy to be more widely applied in the clinical setting.
- The best quality evidence exists that the therapy has a beneficial effect on the primary outcomes of interest.
- The full spectrum of beneficial and adverse effects of the therapy is known.
- Factors that influence the effects of the therapy in the clinical setting have been identified.
- The best quality evidence exists that the therapy compares favorably to currently applied therapies.
- Patients' preferences for the therapy are favorable. The therapy can be applied in a cost-effective and efficient manner in the clinical setting. The practical limitations for widespread delivery of the therapy are minimal.

Reprinted from McCrindle BW. Optimizing outcomes through clinical research and evidence-based clinical decision-making. *Prog Pediatr Cardiol* 2005;20:55–64, with permission from Elsevier.

1. Gallin JI, Ognibene FP, eds. *Principles and Practice of Clinical Research*. 2nd ed. Burlington, MA: Elsevier, 2007.
2. Hulley SB, Cummings SR, Browner WS, et al. *Designing Clinical Research*. 3rd ed. Philadelphia, PA: Lippincott Williams & Wilkins, 2007.
3. Meinert CL. *Clinical Trials: design, Conduct and Analysis*. New York, NY: Oxford University Press, 1986.
4. Friedman LM, Furberg CD, DeMets DL. *Fundamentals of Clinical Trials*. 4th ed. St. Louis, MO: Mosby, 2010.
5. Chow SC, Liu JP. *Design and Analysis of Clinical Trials*. 2nd ed. Hoboken, NJ: Wiley-Interscience, 2004.
6. Elwood M. *Critical Appraisal of Epidemiological Studies and Clinical Trials*. 3rd ed. New York, NY: Oxford University Press, 2007.
7. Cleophas TJ, Zwinderman AH, Cleophas TF. *Statistics Applied to Clinical Trials*. Dordrecht, The Netherlands: Kluwer Academic Publishers, 2000.

5. Mahony L, Sleeper LA, Anderson PA, et al. The pediatric heart network: a primer for the conduct of multicenter studies in children with congenital and acquired heart disease. *Pediatr Cardiol* 2006;27:191–198.
6. Newburger JW, Sleeper LA, McCrindle BW, et al. Randomized trial of pulsed corticosteroid therapy for primary treatment of kawasaki disease. *N Engl J Med* 2007;356:663–675.
7. Hsu DT, Mital S, Ravishankar C, et al. Rationale and design of a trial of angiotensin-converting enzyme inhibition in infants with single ventricle. *Am Heart J* 2009;157:37–45.
8. Hsu DT, Zak V, Mahony L, et al. Enalapril in infants with single ventricle: results of a multicenter randomized trial. *Circulation* 2010;122:333–340.
9. Ohye RG, Gaynor JW, Ghanayem NS, et al. Design and rationale of a randomized trial comparing the blalock-taussig and right ventricle-pulmonary artery shunts in the norwood procedure. *J Thorac Cardiovasc Surg* 2008;136:968–975.
10. Monagle P, Cochrane A, Roberts R, et al. A multicenter, randomized trial comparing heparin/warfarin and acetylsalicylic acid as primary thromboprophylaxis for 2 years after the fontan procedure in children. *J Am Coll Cardiol* 2011;58:645–651.
11. Guyatt GH, Sackett DL, Cook DJ. Users' guides to the medical literature. II. How to use an article about therapy or prevention. A. Are the results of the study valid? Evidence-based medicine working group. *JAMA* 1993;270:2598–2601.
12. Guyatt GH, Sackett DL, Cook DJ. Users' guides to the medical literature. II. How to use an article about therapy or prevention. B. What were the results and will they help me in caring for my patients? Evidence-based medicine working group. *JAMA* 1994;271:59–63.

REFERENCES

1. Steering Committee on Quality Improvement and Management. Classifying recommendations for clinical practice guidelines. *Pediatrics* 2004;114:874–877.
2. Schulz KF, Altman DG, Moher D. Consort 2010 statement: updated guidelines for reporting parallel group randomised trials. *BMJ* 2010;340:c332.
3. Moher D, Hopewell S, Schulz KF, et al. Consort 2010 explanation and elaboration: updated guidelines for reporting parallel group randomised trials. *BMJ* 2010;340:c869.
4. De Angelis C, Drazen JM, Frizelle FA, et al. Clinical trial registration: a statement from the international committee of medical journal editors. *N Engl J Med* 2004;351:1250–1251.

Michael Artman ■ Gregory L. Kearns

The use of drugs for patient treatment carries a single therapeutic imperative, namely, selecting the best drug and administering it in a dosing regimen that is predictive of efficacy and safety. While a “one size fits all” approach to drug dosing in adults is the norm, pediatrics represents the exception whereby development requires that drug dosing be individualized. A safe, therapeutic drug regimen for children must account for the impact of ontogeny and other factors that contribute to variability in the exposure–response relationship.

Human development represents a continuum of biologic events that includes somatic growth, neurobehavioral development, and eventual reproduction. During the process of maturation over the first 15 years of life, profound physiologic changes occur in a variety of processes that can alter both drug disposition and action (1). Moreover, during the first 2 years of life, many of these changes are dynamic and their association with body size can be nonlinear—a situation that precludes the use of fixed (i.e., age-independent) drug dosing regimens and, in some instances, the application of simple allometric scaling to predict age-appropriate drug dose. Therefore, safe and effective drug therapy for children requires a fundamental and integrative understanding of how ontogeny contributes to the other factors (e.g., genetic constitution, the role of environment, the impact of concomitant disease and its treatment) capable of influencing both drug disposition and action and thereby, the relationship between drug dose, concentration, effect, and efficacy. Such considerations collectively represent the essence of pediatric clinical pharmacology. A sound understanding of basic pharmacology principles is necessary for facilitating individualization of drug treatment in infants, children, and adolescents.

Over the past 30 years, pediatric clinical pharmacology has evolved from an area of research emphasis/focus within pediatrics to a subdiscipline of clinical pharmacology with demonstrated therapeutic importance to the medical care of pediatric patients. The large amount of knowledge generated in the field of pediatric clinical pharmacology during this time precludes the presentation of a comprehensive, content-based review or treatise in this chapter. Rather, it is our intention to provide the reader with a “primer” on pediatric clinical pharmacology and, in particular, its relationship to the practice of pediatric cardiology through a presentation of fundamental principles and their illustration using relevant therapeutic examples. We also present summary information pertaining to the clinical pharmacology of drugs commonly used in pediatric cardiology. Collectively, this will equip the reader with a solid foundation for further inquiry and also provide a fundamental, conceptual framework upon which sound therapeutic decision making in pediatric cardiology can be based.

COMMON DEFINITIONS OF TERMS IN CLINICAL PHARMACOLOGY

As is the case with many disciplines, clinical pharmacology has its own lexicon, an understanding of which is fundamental to the clinical application of its principles to therapeutic decision making. The following paragraphs represent a glossary of common terms in clinical pharmacology, each of which is accompanied by a conceptual summary derived from information contained in a recent textbook (2).

Absolute bioavailability (F) is the fraction of a drug dose administered by an extravascular route that is absorbed into the systemic circulation. It is determined within a given individual by comparing the area under the plasma concentration with time curve (area under the curve; AUC) following an oral dose of the drug to that resulting from an intravenous dose (where bioavailability is generally 100% given that no absorption occurs).

Relative bioavailability is similarly determined by comparing the AUC following extravascular administration of a “test” formulation and a “reference” drug formulation (e.g., comparing the AUC from an extemporaneously formulated liquid to that from a marketed oral solid dosage form of a given drug).

Absorption of drugs describes the process of drug uptake from a site of extravascular administration (e.g., oral, intramuscular, subcutaneous, intraperitoneal, intraosseous, and intratracheal) into the systemic circulation. The majority of drug absorption occurs via passive diffusion, although for some compounds, carrier-mediated and/or active transport (e.g., via a transporter such as P-glycoprotein) can occur. Because a drug must generally exist in a true solution to be absorbed, liberation of the active drug from a drug product (e.g., release of a calcium channel blocker from a sustained-release dose formulation) can be a rate-limiting event for absorption. Drug absorption is most accurately conceptualized by considering both rate (e.g., absorption half-life, time to peak concentration) and extent (e.g., bioavailability), either of which can be influenced by biopharmaceutical (e.g., drug formulation), physicochemical (e.g., pH, solubility, hydro- and lipophilicity, protein binding, and complexation characteristics with food or drugs), and physiologic factors (e.g., barrier integrity, motility, volume and pH of body fluids at absorptive site, protein-binding capacity, and degradation/biotransformation potential).

Area under the curve (AUC) is a concentration- and time-dependent parameter that reflects systemic exposure to a drug. Mathematically, AUC represents the integral of blood levels of drug over time from zero to either a predetermined post-dose time point (i.e., $AUC_{0 \rightarrow t(x)}$) or extrapolated to infinity (i.e., $AUC_{0 \rightarrow \infty}$), which is done by using the apparent terminal elimination rate constant (similarly calculated from the observed plasma concentration vs. time plot) (Fig. 79.1).

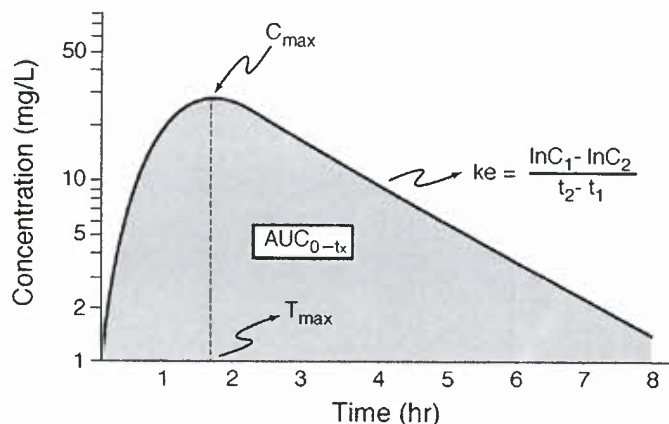


Figure 79.1. Representative plasma concentration versus time curve. Illustrated are commonly referenced pharmacokinetic parameters including AUC, area under the curve; C_{\max} , maximal plasma drug concentration; k_e , the apparent first-order elimination rate constant; and T_{\max} , the time to achieve apparent peak plasma concentrations. (Reprinted from Abdel-Rahman SM and Kearns GL. The pharmacokinetic-pharmacodynamic interface: determinants of anti-infective drug action and efficacy in pediatrics. In: Feigin RD, Cherry JD, Demmler-Harrison GJ, et al., eds. *Feigin and Cherry's Textbook of Pediatric Infectious Disease*. 6th ed. Philadelphia, PA: Saunders-Elsevier, 2009:3158, with permission from Elsevier.)

Bioequivalence of a drug product reflects an assessment of whether one drug formulation (e.g., a generic drug) produces a rate and extent of absorption that is comparable to that of the reference formulation. It assumes that effect and toxicity profiles of the two drugs will be virtually identical if the systemic exposures (as determined from AUC) are comparable. The determination of bioequivalence as defined in current regulatory guidelines is purely pharmacokinetic in nature in that it does not involve a relative assessment of drug effect from a given drug product and/or dose.

Clearance (CL) of a drug is conceptually represented by the volume of blood from which a certain amount of unmetabolized drug is removed (i.e., cleared) per unit time by all pathways capable of drug removal (e.g., renal, hepatic, biliary, pulmonary). Clearance is generally represented as either total body (or plasma) clearance, renal clearance (CL_{ren}), or nonrenal clearance (CL_{nr}). The calculation of CL is made from knowledge of the AUC and for CL_{ren} , from knowing the total amount of drug excreted unchanged in the urine over a 24 or more hour period. For drugs administered by any extravascular route, CL yields an “apparent” value (e.g., CL/F) that must be corrected for the extent of absolute bioavailability. Finally, it should be noted that CL can be influenced by *ex vivo* procedures (e.g., extracorporeal membrane oxygenation, dialysis [hemodialysis, peritoneal dialysis, continuous hemofiltration with dialysis]).

Disposition refers to the collective processes of drug absorption, distribution, metabolism, and excretion/elimination, all of which occur simultaneously after drug administration as opposed to being discrete events. Pharmacokinetic behavior for a given drug is a common surrogate for disposition in that the concentration versus time profile for a given drug is determined by the aforementioned processes.

Elimination half-life ($T_{1/2}$) is defined as the time following drug absorption required for blood or plasma drug concentrations to be reduced by 50%. It is calculated from the apparent elimination rate constant (k_e), which is the slope of the apparent drug elimination phase from blood/plasma (Fig. 79.1). While $T_{1/2}$ is frequently considered as a “surrogate” for CL,

it should be noted that it is dependent both upon CL and the apparent volume of distribution. Practically, $T_{1/2}$ is an important pharmacokinetic parameter in that it can be used to predict when steady-state drug concentrations are attained (e.g., steady state reached at a time equal to four to five times the $T_{1/2}$ following the initiation of drug treatment or a change in dose/dosing regimen) or alternatively, when a drug should be eliminated from the body (e.g., 75% elimination in a period equal to three times $T_{1/2}$).

Peak concentration (C_{\max}) represents the highest concentration of drug attained in a particular biologic fluid following the administration of a drug dose. As illustrated in Figure 79.1, C_{\max} occurs at a corresponding postdose time (T_{\max}) that temporally reflects the time required for drug absorption following a dose administered by an extravascular route.

Pharmacodynamics of a drug reflects a relationship between drug exposure (i.e., concentration), time, and drug effect (both intensity and duration). Simply stated, pharmacodynamics is a reflection of what a given drug/dose does to the body and the association of the effect(s) with time of drug administration. In the context of clinical pharmacology, pharmacodynamics refers to the exposure–response (i.e., concentration–effect) relationship for a given drug.

Pharmacokinetics reflects a quantitative approach used to describe the movement of a drug throughout the body and also, concentrations (or amounts) of drug that reside in a given body space (e.g., fluid spaces and tissue). Pharmacokinetics is conceptualized by considering those characteristics that are the determinants of drug disposition.

Pharmacogenetics can be defined as the study or clinical testing of variations of specific genes that impact upon either the pharmacokinetics or pharmacodynamics of a given drug. In contrast, **pharmacogenomics** represents a focus on events at the level of the genome (e.g., gene–gene interaction) and how, in an integrated context, genetic constitution contributes to the variability in the exposure–response relationship.

Presystemic clearance (first-pass effect) occurs when a drug is either catabolized (e.g., through chemical degradation) or metabolized before it reaches the systemic circulation. Examples associated with oral drug administration include the pH-sensitive degradation of specific drugs in the stomach, drug biotransformation by enterocytes, enteral drug translocation by transporters, and enterohepatic drug recirculation. Presystemic drug clearance can also occur *ex vivo* (e.g., drug degradation and/or adsorption to tubing associated with cardiopulmonary bypass, extracorporeal membrane oxygenation). Drugs subject to first-pass effect (a classic example is propranolol) generally have a reduced rate and/or extent of relative bioavailability when compared to that achieved with parenteral administration.

Protein binding results when a drug combines with plasma, extracellular proteins, or tissue proteins to form a reversible drug–protein complex. In general, drug–protein binding is usually nonspecific and depends on the drug’s affinity for the protein molecule (i.e., binding site), the number of protein-binding sites, and the drug and protein concentration. With few exceptions, drugs that are bound to proteins are pharmacologically inactive and cannot be readily metabolized and/or excreted. Protein and/or tissue drug binding can also influence both the apparent volume of distribution and elimination $T_{1/2}$ of drugs that are extensively (i.e., >70%) bound, as well as their concentration–effect profiles (e.g., extent of plasma protein binding for amiodarone = 93% to 97%, sildenafil = 96%, and warfarin = 99%).

Steady state reflects a level of drug accumulation in blood and tissue upon multiple dosing when the rates of input (i.e., the amount of drug placed into the systemic circulation) and output (i.e., drug clearance) are at equilibrium. When drugs are given at fixed doses and dosing intervals, the steady-state

concentrations in blood or plasma fluctuate between a maximum (C_{\max}) and minimum (C_{\min}) within a given dose interval. The interdose values of C_{\max} and C_{\min} should be identical provided that dose size, method of drug administration, dosing interval, and/or drug pharmacokinetics do not change between doses. In general, the pharmacokinetics of a drug at steady state provides the most accurate means to assess drug effect(s) given that a proportional equilibrium between drug concentrations in the plasma and those at the effector sites(s) (i.e., receptors) should exist.

Therapeutic range represents a range of plasma drug concentrations (i.e., systemic exposure) associated with desirable therapeutic effect(s) and absent or minimal adverse effects. It may be influenced by factors that can modulate pharmacodynamics (e.g., age, disease, concomitant drugs, environmental exposures). The **therapeutic index** for a given drug reflects the relationship between the systemic exposure associated with desirable effects and that associated with the production of adverse effects. For drugs with a narrow therapeutic index such as digoxin, the difference between the systemic exposure (plasma levels) associated with therapeutic and adverse effects is small.

Trough drug concentrations (C_{\min}) represent those in plasma that occur immediately prior to a scheduled dose for drugs that are administered in repeated dosing regimens. The interdose excursion between C_{\max} and C_{\min} is a reflection of systemic drug exposure and in some instances, is associated with a “target” dosing strategy (e.g., cases in which a specific plasma drug concentration or AUC is associated with a desired pharmacodynamic effect).

Volume of distribution (VD) (apparent volume of distribution) represents a hypothetical volume of body fluid that would be required to dissolve the total amount of drug at the same concentration as that found in the blood. For drugs that do not distribute extensively or associate with great affinity to proteins and/or tissue, the VD may dimensionally correspond to a physiologic/anatomic body spaces (e.g., $VD < 0.1$ L/kg ~ intravascular space, 0.1 to 0.3 L/kg ~ extracellular space, 0.6 to 0.7 L/kg ~ total body water space). An apparent $VD > 1$ L/kg is suggestive of drugs with significant tissue binding (e.g., digoxin) that can influence its residence time in the body. Following extravascular drug administration, the apparent VD is impacted by the extent of drug absorbed (i.e., VD/F). In those instances where a drug has incomplete absorption, it may underestimate the true value of the VD.

THE EXPOSURE–RESPONSE RELATIONSHIP

Drug action results only when an exposure (both extent and duration of) occurs that is sufficient to translate a drug–receptor interaction into a physiologic response. Thus, the exposure–response relationship for a given drug represents an interface between pharmacokinetics and pharmacodynamics that can be conceptualized by simultaneous consideration of two profiles: (a) plasma concentration versus time (Figs. 79.1 and 79.2) and (b) plasma concentration versus effect (Fig. 79.2).

In the vast majority of instances, the relationship between drug concentration and effect is not linear. As illustrated in Figure 79.2 in the absence of drug in the body (i.e., at a concentration of zero), there is no discernable drug effect (E_0). Following drug administration, the concentration (both in the plasma and by inference, also at the receptor) increases as does the effect; first in an apparent linear fashion (at low drug concentrations) followed by a nonlinear increase in effect to an asymptotic point that reflects the maximal effect (E_{\max}) after which further increases in drug concentration are not associated with an increase in the desired drug effect. The drug

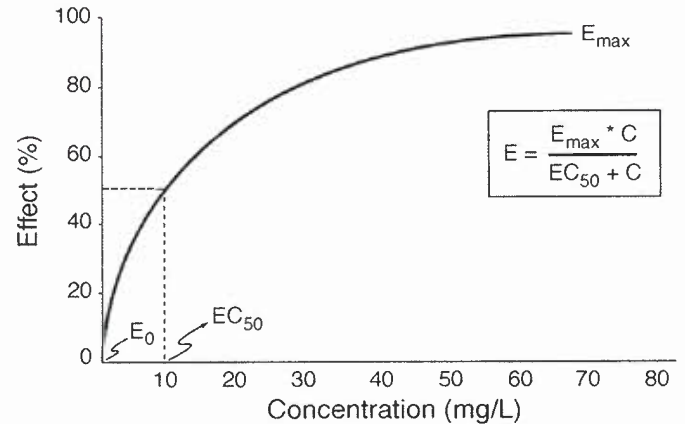


Figure 79.2. Representative nonlinear concentration (C) versus effect profile. Illustrated are E_{\max} , maximal effect; E_0 , the baseline effect associated with the absence of drug concentration; and EC_{50} , the concentration which is associated with an observed effect that is 50% of E_{\max} . (Reprinted from Abdel-Rahman SM, Kearns GL. The pharmacokinetic–pharmacodynamic interface: determinants of anti-infective drug action and efficacy in pediatrics. In: Feigin RD, Cherry JD, Demmler-Harrison GJ, et al., eds. *Feigin and Cherry's Textbook of Pediatric Infectious Disease*. 6th ed. Philadelphia, PA: Saunders-Elsevier, 2009:3158, with permission from Elsevier.)

concentration corresponding to 50% of the maximal effect is defined as the EC_{50} (Fig. 79.2); a pharmacodynamic term reflective of drug potency that is used to compare concentration–effect relationships between individuals and in some instances, between drugs in a given drug class. With rare exception, both E_{\max} and EC_{50} are rarely determined during therapeutic drug administration but rather are calculated pharmacodynamic parameters from research aimed at characterizing the dose–concentration–effect relationship.

With few exceptions, it is rarely possible to measure drug concentrations at or near the receptor. Therefore, it is necessary to utilize a surrogate measurement (e.g., direct measurement of blood pressure, blood glucose, electrocardiogram, echocardiography) to assess exposure–response relationships. In most instances, a change in a given surrogate measurement is examined in association with the plasma drug concentration versus time curve to assess pharmacodynamic properties. For drugs whose pharmacokinetic properties are best described by first-order (as opposed to zero- or mixed-order) processes, a semi-logarithmic plot of plasma drug concentration versus time data for an agent given by an extravascular route of administration (e.g., intramuscular, subcutaneous, intracasternal, intraperitoneal, peroral, transmucosal, transdermal, rectal) produces a pattern depicted by Figure 79.1. The ascending portion of this curve represents a time during which the liberation of a drug from its formulation, dissolution of the drug in a biologic fluid (e.g., gastric or intestinal fluid), and absorption of a drug are rate limiting relative to its elimination. After the time where maximal plasma concentrations (C_{\max}) are observed, the plasma concentration decreases as metabolism and elimination become rate limiting; the terminal portion of this segment of the plasma concentration versus time curve being representative of drug elimination from the body. Finally, the AUC can be determined by integrating the plasma concentration data over time.

By being able to characterize the pharmacokinetics of a specific drug, the clinician can use the data to individualize drug dosing regimens so as to compensate for factors that can influence pharmacokinetics (e.g., development, disease, concomitant treatment). For drugs where a therapeutic plasma

concentration range and/or “target” systemic exposure (i.e., AUC) is known, *a priori* knowledge of pharmacokinetic parameters for a given patient can facilitate the selection of a drug dosing regimen and thereby, optimize therapeutic response (e.g., cyclosporine, tacrolimus) (3). When linked with information regarding the pharmacodynamic behavior of a drug and the status of the patient (e.g., age, organ function, disease state, concomitant medications), the application of pharmacokinetics affords the practitioner the ability to exercise therapeutic decision making by enabling the selection of

a drug and dosing regimen that has the greatest likelihood of producing both efficacy and safety.

DEVELOPMENTAL PHARMACOKINETICS

For well over three decades, it has been known that physiologic changes that occur during human development produce alterations in drug disposition. As illustrated in Figure 79.3,

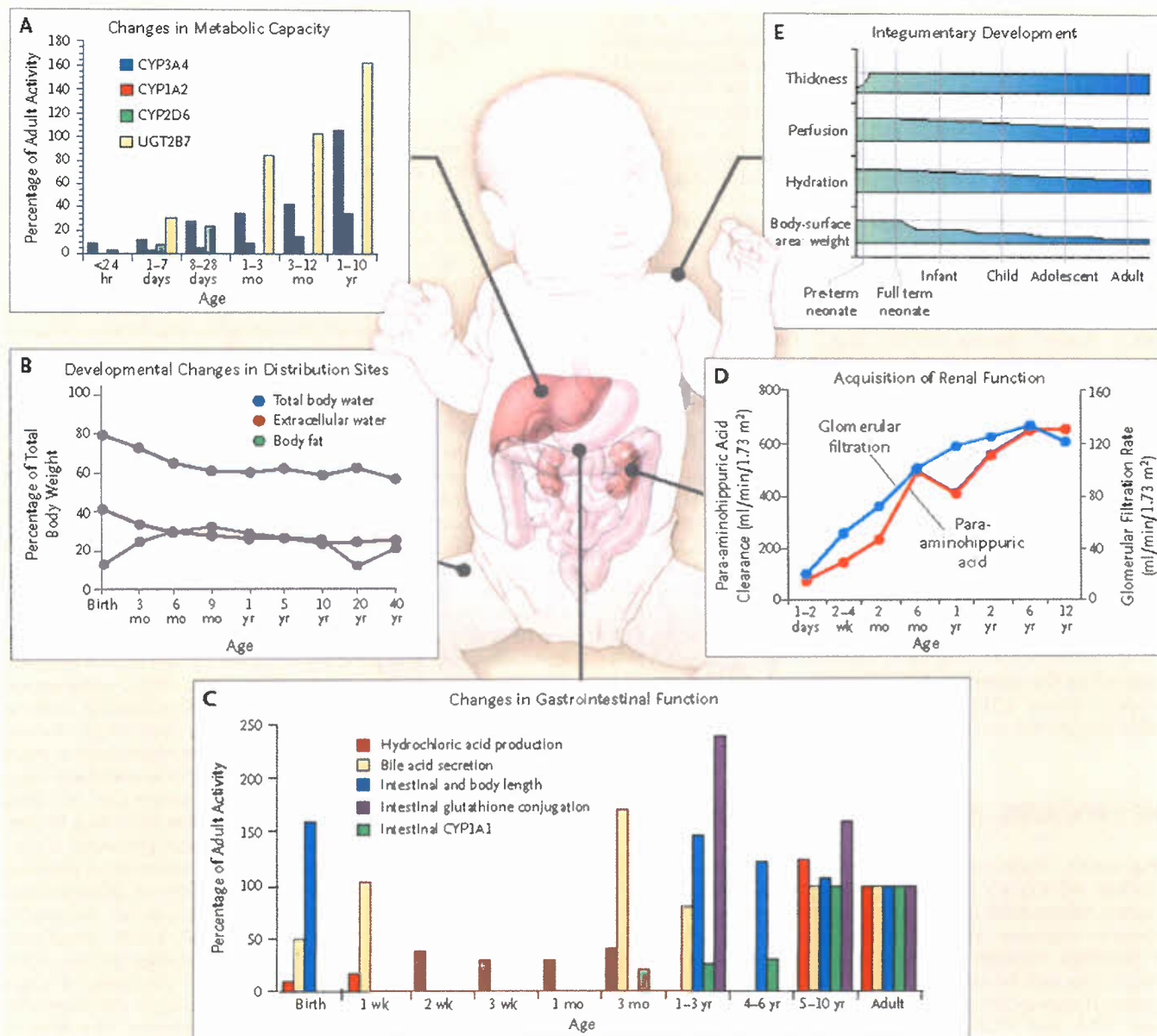


Figure 79.3. Developmental changes in physiologic factors that influence drug disposition in infants, children, and adolescents. **Panel A** illustrates age-dependent activity (relative to adult values) for important Phase I and Phase II enzymes responsible for drug biotransformation. **Panel B** illustrates developmental differences in body composition that can influence the apparent volume of distribution for drugs. **Panel C** illustrates the ontogeny of factors pertaining to gastrointestinal physiologic function, one or more of which can influence either the rate and/or extent of drug absorption. **Panel D** illustrates the acquisition of renal function (both glomerular filtration rate and active tubular secretory capacity reflected by para-aminohippuric acid clearance, a validated biomarker) during development. **Panel E** illustrates the impact of development on aspects of the integumentary system that collectively can modulate the systemic absorption of drugs applied to the skin. (From Kearns GL, Abdel-Rahman SM, Alander SW, et al. Developmental pharmacology—drug disposition, action and therapy in infants and children. *N Engl J Med* 2003;349:1157–1167, Copyright © 2003 Massachusetts Medical Society. Reprinted with permission from Massachusetts Medical Society.)

maturation can produce, especially in early life, dramatic physiologic changes that impact drug absorption, distribution, metabolism, and excretion. Accumulated information supports that many of these changes are indeed predictable (4) and consequently, they can be used to inform the design of pediatric clinical trials through the use of modeling and simulation and also, to clinically individualize drug treatment for a given patient based on known or expected pharmacokinetic behavior of a given drug (5). An example of therapeutic utility of pharmacokinetic-based optimization of drug treatment has been recently illustrated in the provision of antiretroviral therapy in children (6).

For the clinical application of such data, it is important for the clinician to have a conceptual understanding of how development influences both drug disposition and effect. In the following paragraphs, we provide a summary of developmental pharmacokinetics, much of which has been excerpted (with permission) from recent works (1,7,8) published by one of the coauthors (G.L.K.). These publications can be referred to for reference to citations in the primary literature upon which the following summaries are based.

Drug Absorption

Absorption of drugs administered by extravascular routes occurs largely via passive diffusion. At certain anatomical sites where drug transport proteins are expressed, absorption can occur via active transport or facilitated diffusion. In addition to physiologic changes that occur during development, the concomitant presence of certain disease states (e.g., inflammatory bowel disease, diarrhea) can produce changes in either the rate or extent of drug absorption. A summary of important

factors that can influence drug absorption in neonates, infants, and children is provided in Table 79.1.

Oral Absorption

As is the case in adults, most therapeutic drugs administered in the outpatient setting are given by the oral route. During development, maturational changes of gastric, intestinal, and biliary tract function (Fig. 79.3, panel C) occur and either singly or collectively can impact the rate and extent of drug absorption.

Given that most orally administered drugs have the physicochemical property of being either a weak acid or weak base, pH within the gastrointestinal tract can influence the amount of potentially absorbable drug (i.e., the un-ionized moiety existing in a true solution) available. As illustrated in Figure 79.3 (panel C), gastric hydrochloric acid production changes as a function of age. Gastric pH changes significantly throughout development with the highest values occurring during the neonatal period. In the fully mature neonate, the gastric pH ranges from 6 to 8 at birth and drops to 2 to 3 within a few hours of birth. However, after the first 24 hours of postnatal life, the gastric pH increases due to the immaturity of the parietal cells and gradually reaches expected adult values (e.g., gastric pH 2 to 3) by approximately 2 to 3 years of age. As a result of these developmental differences, the bioavailability of acid-labile drugs (e.g., penicillin, ampicillin) is increased (relative to older children and adults) in neonates and young infants, whereas the absorption of weak organic acids is decreased. For drugs with a relatively narrow therapeutic index (e.g., phenytoin), the ontogeny of gastric pH can produce significant age-associated alterations in bioavailability that may necessitate more frequent alterations in drug dosing regimens required to achieve therapeutic plasma levels.

TABLE 79.1

Summary of Important Factors that Influence Drug Absorption in Neonates, Infants, and Children

	Neonates	Infants	Children
<i>Physiologic alteration</i>			
Gastric emptying time	Irregular	Increased slightly	Increased
Gastric pH	>5	4–2	Adult pattern
Intestinal motility	Reduced	Increased	Slightly increased
Intestinal surface area	Reduced	Near adult	Adult pattern
Microbial colonization	Reduced	Near adult	Adult pattern
Biliary function	Immature	Near adult	Adult pattern
Muscular blood flow	Reduced	Increased	Adult pattern
Skin permeability	Increased	Increased	Near adult pattern
<i>Possible pharmacokinetic consequences</i>			
Oral absorption	Erratic—reduced	↑ rate	Near adult pattern
IM absorption	Variable	Increased	Adult pattern
Percutaneous absorption	Increased	Increased	Near adult pattern
Rectal absorption	Very efficient	Efficient	Near adult pattern
Presystemic clearance	< adult	> adult	> adult (↑ rate)

Direction of alteration given relative to expected normal adult patterns.

Reprinted from Ritschel WA, Kearns GL. Definitions and nomenclature. In: Ritschel WA, Kearns GL, eds. *Handbook of Basic Pharmacokinetics... Including Clinical Applications*, 7th ed. Washington, DC: American Pharmacists Association, 2009:1–10; Table 24.1, with permission.

During development, one of the most important physiologic changes capable of altering the rate of drug absorption resides with gastrointestinal motility. During early infancy, gastric emptying time is prolonged, which can delay delivery of orally administered drugs to the small intestine where the majority of absorption takes place. By 6 to 8 months of age, gastrointestinal transit times may be shorter than those observed for older children and adults; a situation which can significantly influence both the rate and extent of bioavailability of drugs with limited water solubility (e.g., phenytoin, carbamazepine) by reducing residence time at the absorptive sites in the small intestine. Lastly, immature biliary function in neonates and young infants in the first few months of life has the potential for reducing the extent of oral bioavailability of lipophilic drugs that are dependent upon bile acids for their solubility in the small intestine (e.g., fat-soluble vitamins).

Developmental differences in the activity of intestinal drug-metabolizing enzymes (e.g., CYP3A4/5, CYP1A, *N*-acetyltransferase, xanthine oxidase, and glutathione-*S*-transferase) and efflux transporters (e.g., P-glycoprotein or MDR1) can markedly alter the bioavailability of some orally administered drugs. While the patterns of ontogeny for these enzymes and transporters are not concordant, the majority appear to have adult expression within the first 6 to 12 months of postnatal life at which time the influence of development on their activity as a determinant of bioavailability would be expected to be minimal.

Extravascular Drug Absorption

As is the case with oral drug absorption, development can influence the bioavailability of drugs administered by other extravascular routes (e.g., subcutaneous, intramuscular, introsseous, intratracheal, intraperitoneal, rectal, dermal) largely as a result of changes in regional blood flow and tissue composition (Table 79.1). In the neonate, muscular blood flow is reduced in the first few days of life, as is the relative efficiency of muscular contractions. Furthermore, neonates and young infants have greatly reduced muscle mass (compared to older infants and children) and increased percentage of water per unit of muscle mass. Collectively, these developmental changes can produce variable and delayed rates of absorption of drugs given by the intramuscular route.

In contrast, mucosal (rectal and buccal) and dermal permeability in the neonate and young infant is increased and thus may result in enhanced absorption by these routes. In the case of transdermal drug absorption, a more highly perfused and hydrated stratum corneum (Fig. 79.3, panel E) facilitates drug absorption in the neonate and very young infant. In addition, the ratio of body surface area to body weight is greater in infants and children as compared to adults. Collectively, these developmental differences may predispose infants and young children in the first 8 to 12 months of life to increased exposure and risk for toxicity for drugs/chemicals placed on the skin (e.g., silver sulfadiazine, topical corticosteroids, benzocaine, diphenhydramine, isopropyl alcohol).

Normal developmental differences in drug absorption from almost all extravascular routes of administration can influence the dose–plasma concentration relationship in a manner sufficient to alter pharmacodynamics. Disease states that affect the integrity of the physiologic barriers that drugs given by extravascular routes must traverse prior to their translocation to the vascular space must be considered, as they can influence both the rate and extent of drug absorption. Finally, with regard to extravascular drug administration, it must be recognized that the onset of drug effect is directly dependent upon the route of administration. For example, the onset of effect for most drugs given intravenously is, in most cases, virtually instantaneous. This is contrasted with drugs given by inhalation (onset ~ 2 to 3 minutes), sublingual administration (onset ~ 3 to 5 minutes), intramuscular injection

(onset ~ 10 to 20 minutes), subcutaneous injection (onset ~ 15 to 30 minutes), rectal (onset ~ 30 minutes), oral (onset ~ 30 to 90 minutes), and transdermal (onset ~ minutes to hours) routes.

Drug Distribution

Drug distribution is influenced by a variety of factors including drug-specific physicochemical properties, tissue composition (e.g., water, fat, and lean muscle content) and perfusion, the role of drug transporters, blood/tissue protein binding, blood, and the pH of blood and tissue fluids. To a great degree, changes in drug distribution during development are associated with changes in body composition and the quantity of plasma proteins capable of drug binding. As well, certain disease states (e.g., ascites, dehydration, burn injuries involving large surface area, sepsis with capillary leak syndrome) can influence body water compartment sizes and thereby, the distribution of drugs with an apparent volume of distribution less than or equal to the total body water space (i.e., 0.6 L/kg).

As illustrated in Figure 79.3 (panel B), neonates and young infants have significantly higher total body water and extracellular water spaces than older infants and children. The reduction in relative total body water occurs rapidly during the first year of life, and by 12 years, adult values (i.e., ~60% of lean muscle mass) are attained. In contrast, the percentage of intracellular water as a function of body mass remains stable from the first months of life through adulthood. For drugs that are primarily distributed to a space that approximates the extracellular fluid pool and are not highly bound to plasma proteins (e.g., aminoglycoside antibiotics), their weight-adjusted apparent volumes of distribution (i.e., L/kg) are larger (e.g., approximately 0.4 to 0.6 L/kg in neonates and infants vs. 0.2 to 0.3 L/kg in adults), which necessitates the administration of higher weight-adjusted (mg/kg) doses in order to attain target plasma (blood) levels.

Despite the relatively low body fat content in the neonate (~16%, Fig. 79.3, panel B), the developing central nervous system (CNS) has a relatively high lipid content in early life; a condition with implications for the distribution of lipophilic drugs capable of acting in the CNS. The body fat percentage tends to increase up to about 10 years of age and then changes composition with respect to puberty and sex. In normal children and adolescents with age-appropriate body habitus, changes in body composition beyond the first 3 months of life do not appear to produce profound developmental differences in drug disposition. This does not appear to be the case for obese children in whom increased body fat appears to require adjustment in the normal age-appropriate dosing regimen for several drugs (e.g., aminoglycosides, carbamazepine, phenytoin, benzodiazepines, digoxin, lithium, opiates) (9).

Of the circulating proteins in plasma, albumin (which preferentially binds weak acids) and α_1 -acid glycoprotein (which preferentially binds weak bases) are quantitatively the most important for drug binding. As summarized in Table 79.2, the concentration of these proteins changes over development with low concentrations in the neonate and young infant (~80% of adult), increasing to adult values by approximately 1 year of age. A similar pattern of maturation is observed with α_1 -acid glycoprotein where neonatal plasma concentrations are approximately three times lower than in maternal plasma and attain adult values by approximately 1 year of age. Additionally, specific conditions (e.g., malnutrition, protein-losing enteropathy, nephrotic syndrome, large burn injuries, extravascular translocation of proteins, sepsis, acidosis, protracted hyperglycemia, chronic renal failure with uremia) can reduce the absolute concentration of drug-binding proteins and in some instances (e.g., acidosis, glycation of albumin associated with chronic hyperglycemia, carbamylation of albumin associated with uremia), the binding affinity of a given drug

TABLE 79.2

Ontogenic Influences of Plasma Drug–Protein Binding and Drug Distribution

	Neonates	Infants	Children
<i>Physiologic alteration</i>			
Plasma albumin concentration	Reduced	Near normal	Near adult pattern
Fetal albumin concentration	Present	Absent	Absent
Total protein concentration	Reduced	Decreased	Near adult pattern
Total globulin concentration	Reduced	Decreased	Near adult pattern
Serum bilirubin	Increased	Normal	Normal adult pattern
Serum free fatty acids	Increased	Normal	Normal adult pattern
Blood pH	7.1–7.3	7.4 (normal)	7.4 (normal)
Adipose tissue	Scarce (↑ CNS)	Reduced	Generally reduced
Total body water	Increased	Increased	Near adult pattern
Extracellular water	Increased	Increased	Near adult pattern
Endogenous maternal substances (ligands)	Present	Absent	Absent
<i>Possible pharmacokinetic consequences</i>			
Free drug fraction	Increased	Increased	Slightly increased
<i>Apparent volume of distribution</i>			
Hydrophilic drugs	Increased	Increased	Slightly increased
Hydrophobic drugs	Reduced	Reduced	Slightly decreased
Tissue/plasma ratio	Increased	Increased	Slightly increased

Direction of alteration given relative to expected normal adult patterns.

Reprinted from Ritschel WA and Kearns GL. *Handbook of Basic Pharmacokinetics*. 7th ed. Washington, DC: American Pharmacists Association, 2009, with permission.

for a protein. Binding affinity for acidic drugs is also reduced in the neonate as a consequence of the higher concentrations of fetal albumin (which has a lower binding capacity) and endogenous substances (e.g., bilirubin) that can compete with drugs for albumin binding sites. For example, circulating fetal albumin in the neonate has significantly reduced binding affinity for acid drugs such as phenytoin that is extensively (~94% to 98%) bound to albumin in adults as compared to 80% to 85% in the neonate. The resultant six- to eightfold difference in the free fraction can result in CNS adverse effects in the neonate when total plasma phenytoin concentrations are within the generally accepted “therapeutic range” (10 to 20 mg/L), thereby influencing the pharmacodynamics of this agent.

Drug transporters, such as P-glycoprotein, MDR1, and MDR2 (multidrug resistance 1 or 2), can also influence drug distribution. These drug transporters can markedly influence the extent to which drugs cross membranes in the body and whether drugs can penetrate or are secreted from the target sites. While there are limited data on the ontogeny of drug transport proteins, available information demonstrates their presence as early as 22 weeks’ gestation and low levels in the neonatal period that rapidly increase to adult values by 1 to 2 years of age.

Drug Metabolism

Metabolism reflects the biotransformation of an endogenous or exogenous molecule by one or more enzymes to moieties that generally are more polar (hydrophilic) and thereby, more

easily eliminated via excretion, secretion, and/or exhalation. While in many cases, drug metabolism results in pharmacologic inactivation of a drug, there are instances where it can either contribute to or be a determinant of drug action. The former situation is illustrated by drugs that have pharmacologically active metabolites (e.g., metabolism of amitriptyline to nortriptyline, codeine to morphine) and the latter, by the example of prodrugs where an inactive moiety is biotransformed to an active agent (e.g., enalaprilat). It should be noted that metabolic activation for some drugs has been identified as a mechanism underlying toxicity (e.g., acetaminophen-associated hepatotoxicity; Stevens-Johnson syndrome associated with sulfonamides, phenytoin, and carbamazepine; halothane-associated hepatitis).

Quantitatively, the most important organ responsible for drug biotransformation is the liver. However, drug-metabolizing enzymes (e.g., phosphatases, esterases) also exist in the blood, brain, lung, small intestine, adrenal glands, kidney, and skin. Drug metabolism has historically been conceptualized as occurring via two general classes of enzymatic processes: **Phase I**, or nonsynthetic reactions (e.g., oxidation, reduction, hydrolysis, hydroxylation) and **Phase II**, or synthetic (e.g., glycine, glucuronide, glutathione, sulfate conjugation) reactions. It is important to note that in many instances, Phase I and Phase II reactions can occur sequentially (e.g., hydroxylation of drug molecule followed by glucuronidation of the primary metabolite) as most all therapeutic drugs are polyfunctional substrates for a variety of drug-metabolizing enzymes. At birth, the concentration of drug-oxidizing enzymes in fetal liver (corrected

for liver weight) appears similar to that in adult liver. However, the activity of these oxidizing enzyme systems is reduced, which results in slow clearance (and prolonged elimination) of many drugs. Finally, as illustrated by Figure 79.3 (panel A), both Phase I and II drug-metabolizing enzymes have an ontogenic profile that generally is reflective of maturation over a period of months to years with different enzymes having specific developmental trajectories. For example, alcohol dehydrogenase (ADH1C) is expressed at extremely low levels in the fetus but increases dramatically in the first 1 to 2 years after birth. In contrast, CYP3A7, a cytochrome P450 (CYP450) responsible for the biotransformation of the endogenous substrate dihydroepiandrosterone sulfate (DHEA-S), is expressed at the highest level during the first trimester, whereas its activity at 1 to 2 years of age is virtually absent in most individuals. Finally, one of the isoforms of sulfotransferase (SULT1A1) is expressed at relatively constant levels during gestation and postnatal life (10).

The impact of ontogeny on the activity of human drug-metabolizing enzymes has been the topic of several reviews (11–13). Of the many enzymes capable of metabolizing drugs and other small molecules, the CYP450 supergene family is quantitatively the most important. Specific CYP450 isoforms (and prototypical drug substrates) responsible for the majority of drug metabolism in humans include CYP1A2 (caffeine), CYP2C9 (warfarin, losartan, phenytoin), CYP2C19 (proton pump inhibitors, clopidogrel), CYP2D6 (codeine, tamoxifen), CYP2E1 (ethanol), CYP3A5 (tacrolimus), and CYP3A4 (midazolam, cyclosporine).

Compared to Phase I drug-metabolizing enzymes, the impact of development on the activity of Phase II enzymes is not as well characterized. However, studies to date indicate that in general, Phase II enzyme activities are decreased in the newborn and increase in childhood. For example, conjugation of compounds metabolized by UDP-glucuronosyltransferase (UGT) isoforms (e.g., morphine, bilirubin, and chloramphenicol) illustrates reduced metabolic capacity at birth that in turn can dramatically reduce drug plasma clearance (e.g., the gray baby syndrome tragedy associated with excessive systemic exposure to chloramphenicol following the administration of “normal” pediatric doses to neonates and young infants). Development of metabolic competence for most Phase II drug-metabolizing enzymes occurs rapidly during the first year of life and for selected enzymes can exceed adult values by 3 to 4 years of age (12). As illustrated by data for human glucuronosyltransferases (14), the impact of ontogeny on drug-metabolizing enzyme activity can be isoform specific. For example, the activity of the UGT isoforms responsible for acetaminophen metabolism (UGT1A1 and UGT1A9) is markedly reduced in neonates and infants, and as a result, conjugation of the drug metabolites is primarily dependent upon glutathione transferase and sulfotransferase isoforms. As infants develop, UGT activity increases and by the first year of life, these enzymes become the most quantitatively important for acetaminophen metabolism. A similar developmental profile exists for morphine, a drug whose metabolism is largely dependent upon two polymorphically expressed UGT isoforms, UGT2B7 and UGT1A1 (15).

Many drug-metabolizing enzymes represent the products of genes that in some instances, are polymorphically expressed, with the variant alleles often conveying reduced and/or absent activity. A notable exception is exemplified by the CYP2C19*17 allele that appears to convey increased catalytic activity to the enzyme (16). Similarly, polymorphic expression of genes responsible for regulation of specific drug transporter proteins also exists. Together with drug-metabolizing enzymes, their activities are often the rate-limiting event for metabolic clearance of a drug from the body and, in some instances, for drug action. Thus, genetic polymorphisms can influence both the pharmacokinetics and pharmacodynamics of drugs.

The potential clinical importance of genetic polymorphisms for a drug-metabolizing enzyme has been recently illustrated by a comprehensive review published by Swen et al. (17) that discusses CYP2D6 phenotype and its relevance to the therapeutic use of flecainide, metoprolol, and propafenone. As illustrated by Table 79.3, differences in the pharmacokinetics of these drugs associated with CYP2D6 phenotype (i.e., poor-metabolizer, intermediate metabolizer, or ultrarapid metabolizer; each conveyed by specific allelic variants of the CYP2D6 gene) must be considered in the selection of a dosing regimen so as to prevent either therapeutic failure (e.g., subtherapeutic systemic exposure resulting from a “normal” dose given to an individual with rapid drug clearance consequent to having an ultrarapid CYP2D6 metabolizer phenotype) or therapeutic misadventure (e.g., increased systemic exposure associated with drug toxicity in individuals having a poor-metabolizer CYP2D6 phenotype). A recent review published by Visscher et al. (18) also highlights the importance of polymorphic expression of genes responsible for the expression of drug-metabolizing enzymes, transporters, and receptors. As summarized in Table 79.4 with the example of warfarin, allelic variants of the enzyme primarily responsible for its metabolism (i.e., CYP2C9) and also for its mechanism of action (i.e., VKORC1 or vitamin K epoxide reductase) require therapeutic dose adjustment in order to prevent excessive coagulation. In contrast, the example of clopidogrel illustrates that polymorphic expression of both the primary drug-metabolizing enzyme (i.e., CYP2C19) and the efflux transporter ABCB1 (also called MDR1 or P-glycoprotein) serve as determinants of therapeutic dosing regimens. Finally, the importance of genetic polymorphism on pharmacodynamics is well illustrated by the β -adrenergic receptor blockers where variant alleles of the β -receptor are associated with either an improved response to therapy or, alternatively, an increased likelihood of adverse events that are dependent upon a specific genotype.

In addition to their importance in removing drugs from the body, it is important to recognize that both drug-metabolizing enzymes and transporters that exist predominantly in the small intestine and both their polymorphic and ontogenic expression can alter the absolute bioavailability of drugs. Like drug-metabolizing enzymes, the activity of intestinal drug transporters (MDR1 or P-glycoprotein) is low at birth (relative to adults) and increases throughout the first 2 years of life (19). Given that the activity of most drug-metabolizing enzymes is markedly reduced in the neonate, the extent of bioavailability of drugs that are substrates for drug-metabolizing enzymes (e.g., CYP3A4, CYP3A5) and transporters (ABCB1) in the small intestine would be expected to be increased during the first weeks of life. Presystemic clearance (also described as first-pass effect) would increase as the functional capacity of these proteins increases, with the potential for reducing the bioavailability of drugs given by the oral route. Unfortunately, very few bioavailability studies are conducted in infants and children; thus, assumptions regarding the impact of ontogeny on presystemic drug clearance must be made based on the known developmental profiles and pharmacogenomics for the drug-metabolizing enzymes and transporters involved (20). Thus, estimates of how presystemic clearance may influence drug bioavailability derived from adult studies cannot be accurately applied to extrapolate how a drug dose given by the oral route may need to be age-adjusted for a neonate or infant.

Table 79.5 summarizes the physiologic alterations during development that contribute to drug metabolism and also their potential pharmacokinetic consequences. However, with regard to predicting the impact of development on drug metabolism, it is the isoform-specific ontogenic profile for each enzyme and transporter involved that must be considered in deducing how developmental differences *per se* can effect drug clearance as a determinant of the exposure–response relationship.

TABLE 79.3

Examples of Cardiovascular Drugs where Polymorphic Gene Expression of CYP2D6 in Adults Supports Modification of Dosing Regimen

Drug	Genotype or Phenotype	Level of Evidence	Clinical Relevance	Impact on Dosing Recommendations
Flecainide	PM	Good from controlled studies	Minor clinical effect	Reduce dose by 50%, record ECG, monitor plasma concentration
	IM	—	—	Reduce dose by 25%, record ECG, monitor plasma concentration
	UM	—	—	Record ECG, monitor plasma concentration
Metoprolol	PM	Good from controlled studies	Long-standing, significant implications	Production of heart failure. Select alternative drug or reduce dose by 75% and monitor for drug-associated adverse events
	IM	Good from controlled studies	Short lived with mild implications	Actively monitor for drug-associated adverse events
	UM	Good from controlled studies	Long-standing, significant implications	Heart failure due to subtherapeutic exposure. Select alternative drug or titrate to maximum of 250% of the normal dose
Propafenone	PM	Good from controlled studies	Long-standing, significant implications	Reduce dose by 70%, record ECG and monitor plasma concentrations
	IM	Moderate from published studies	Moderate clinical effect	Insufficient data to allow for dose calculation. Record ECG and adjust dose to plasma concentration or select alternative drug
	UM	Moderate from published studies	Minor clinical effect	Insufficient data to allow for dose calculation. Record ECG and adjust dose to plasma concentration or select alternative drug

PM, poor metabolizer; IM, intermediate metabolizer; and UM, ultrarapid metabolizer.

Adapted from Swen JJ, Nijenhuis M, de Boer A, et al. Pharmacogenetics: from bench to byte—an update of guidelines. *Clin Pharmacol Ther* 2011;89:662–673, where evidence level and clinical relevance for specific examples are further defined and references to applicable primary literature are provided.

TABLE 79.4

Overview of Drug-Metabolizing Enzyme and Transporter Gene Variants and their Association with Cardiovascular Drug Response

Drug (class)	Gene	Variants	Effect(s)
Warfarin	<i>CYP2C9</i>	*2	Decreased enzyme activity, reduced daily dose requirement
	<i>CYP2C9</i>	*3	Markedly reduced enzyme activity, reduced daily dose requirement
	<i>VKORC1</i>	–1639G>A	Reduced gene expression, increased drug susceptibility, need for reduced dose requirement
Clopidogrel	<i>CYP2C19</i>	*2	Decreased enzyme activity, increased dose requirement, reduced drug response
	<i>CYP2C19</i>	*3	Decreased enzyme activity, increased dose requirement
	<i>CYP2C19</i>	*4	Decreased enzyme activity, increased dose requirement
	<i>CYP2C19</i>	*5	Decreased enzyme activity, increased dose requirement
	<i>ABCB1</i>	3435C>T	Reduced plasma levels of active metabolites, increased dose requirement
β-Blockers	<i>ADRB1</i>	Ser49Gly	Improved drug response in Gly49 carriers
	<i>ADRB1</i>	Arg389Gly	Improved response in Arg/Arg homozygotes
	<i>ADRB2</i>	Gly16Arg and Gln27Glu	Increased risk of adverse outcomes in Gly16/Gln27 haplotype carriers
	<i>ADRA2C</i>	Deletion of amino acids 322–325	Improved response to metoprolol in deletion carriers when combined with <i>ADRB1</i> Arg/Arg phenotype

CYP refers to specific cytochrome P450 isoforms; ABCB1 refers to P-glycoprotein; ADRB1 and ADRB2 refer to the β-1 and β-2 adrenergic receptor, respectively, and ADRA2C refers to the α-2c-adrenergic receptor.

Adapted from Visscher H, Amstutz U, Sistonen J, et al. Pharmacogenomics of cardiovascular drugs and adverse effects in paediatrics. *J Cardiovasc Pharmacol* 2011; epub ahead of print (April 2011).

TABLE 79.5 Drug Metabolism in the Neonate, Infant, and Child

	Neonates	Infants	Children
<i>Physiologic alteration</i>			
Liver/body weight ratio	Increased	Increased	Slightly increased
Cytochrome P450 activity	Reduced	Increased	Slightly increased
Blood esterase activity	Reduced	Normal (by 12 mo)	Adult pattern
Hepatic blood flow	Reduced	Increased	Near adult pattern
Phase II enzyme activity	Reduced	Increased	Near adult pattern
<i>Possible pharmacokinetic consequences</i>			
Metabolic rates	Reduced	Increased	Near adult pattern ^a
Presystemic clearance	Reduced	Increased	Near adult pattern
Total body clearance	Reduced	Increased	Near adult pattern ^a
Inducibility of drug-metabolizing enzymes	More evident	Slightly increased	Near adult pattern ^a

Direction of alteration given relative to expected normal adult patterns. ^aDenotes assumption of adult pattern of activity after the conclusion of puberty. The activity of all drug-metabolizing enzymes is generally higher before versus after puberty.

Reprinted with permission from Ritschel WA and Kearns GL. *Handbook of Basic Pharmacokinetics*. 7th ed. Washington, DC: American Pharmacists Association, 2009.

Renal Drug Elimination

The kidney is the primary organ responsible for the excretion of drugs and their metabolites. The development of renal function begins during early fetal development and is complete by early childhood (Fig. 79.3, panel D). From a developmental perspective, renal function is highly dependent on gestational age and postnatal adaptations. Renal function begins to mature early during fetal organogenesis and is complete by early childhood. Increases in glomerular filtration rate (GFR) result from both nephrogenesis, a process that is completed by 36 weeks of

gestation, and changes in renal and intrarenal blood flow (21). GFRs vary widely among different postconceptional ages and range from approximately 2 to 4 mL/min/1.73 m² in term neonates to a low of 0.6 to 0.8 mL/min/1.73 m² in preterm neonates. The GFR increases rapidly during the first 2 weeks of life and then more slowly until adult values are reached by 8 to 12 months of postnatal age (22,23). Development impacts not only GFR but also tubular secretion, which is immature at birth and reaches adult capacity during the first year of life (Fig. 79.3, panel D).

Developmental changes that occur in renal function are better characterized than any other organ system (Table 79.6).

TABLE 79.6 Renal Function in the Neonate, Infant, and Child

	Neonates	Infants	Children
<i>Physiologic alteration</i>			
Kidney/body weight ratio	Increased	Increased	Near adult values
Glomerular filtration rate	Reduced	Normal (by 12 mo)	Normal adult values
Active tubular secretion	Reduced	Near normal	Normal adult values ^a
Active tubular reabsorption	Reduced	Near normal	Normal adult values
Proteins present in urine	Present	Low to absent	Normally absent
Urinary acidification capacity	Low	Normal (by 1 mo)	Normal adult activity
Urine output (mL/h/kg)	3–6	2–4	1–3
Urine concentrating capacity	Reduced	Near normal	Normal adult values
<i>Possible pharmacokinetic consequences</i>			
Active drug excretion	Reduced	Near normal	Normal adult pattern
Passive drug excretion	Reduced to increased	Increased	Normal adult pattern
Excretion of basic drugs	Increased	Increased	Near normal

Direction of alteration given relative to expected normal adult patterns.

^aDenotes slight increase in excretion rate for basic compounds.

Reprinted from Ritschel WA and Kearns GL. *Handbook of Basic Pharmacokinetics*. 7th ed. Washington, DC: American Pharmacists Association, 2009, with permission.

For drugs that have substantial renal clearance, kidney function serves as a major determinant of age-specific drug dosing regimens. Failure to account for the ontogeny of renal function and adjust dosing regimens accordingly can result in a degree of systemic exposure that can increase the risk of drug-associated adverse events. A well-characterized example resides with digoxin. Consequent to its predominant renal elimination, the plasma clearance of digoxin is markedly reduced in the neonate and young infant, and only approaches adult values when both GFR and active tubular secretory capacity mature (Fig. 79.3, panel D) (24). Failure to adjust the dose and dosing interval for digoxin to compensate for developmentally associated differences in its plasma clearance can produce significant toxicity, especially given the low therapeutic index for this drug (25). Another example resides with gentamicin where a starting dosage interval of 12 hours in infants of any gestational age or a starting dosage interval of 24 hours for infants of <30 weeks' gestational age has been shown to lead to serum gentamicin trough levels in the toxic range (26). It is also important to note that use of some medications concomitantly (i.e., betamethasone and indomethacin) may cause alteration of the normal pattern of renal maturation in the neonate (27). Therefore, both maturation and effects of treatment with regard to renal function are important considerations when determining appropriate drug treatments in neonates and infants.

DEVELOPMENTAL PHARMACODYNAMICS

When one considers the impact of development on the exposure–response relationship for a given drug, it is important to realize that these do not simply occur consequent to pharmacokinetic differences (e.g., increased systemic drug exposure resulting from age-associated reduced drug clearance). As recently reviewed by Mulla (28), development can influence pharmacodynamics through consequences of maturational changes in drug receptor number, receptor affinity, receptor density, signal transduction, or alterations in the intracellular milieu necessary for the creation of a pharmacologic effect. For example, a previous study performed using lymphocytes harvested from pediatric patients from infancy through adolescence demonstrated a markedly enhanced sensitivity to the effects of cyclosporine (i.e., significant reduction in EC_{50}) in infants as compared to older children and adults (29). A more recent study of sotalol pharmacodynamics in children with supraventricular tachycardia (30) demonstrated that neonates had a higher sensitivity toward drug-associated QTc interval prolongation, which in turn supported the use of a lower starting dose for the drug as compared to older infants and children. In addition to desired therapeutic drug effects, age-dependent pharmacodynamics are illustrated through the consideration of several well-known clinical adverse drug reactions. For example, the susceptibility to metoclopramide-associated movement disorders (e.g., dystonias, bradykinetic reactions) is much higher in infants <2 years of age and diminishes with maturation into the second decade of life (28). Similarly, ontogenic profiles appear to be operative for valproic acid-associated hepatotoxicity (31), midazolam-associated sedation (32), and warfarin sensitivity (33,34), all of which are examples where age-associated differences in drug response appear independent of pharmacokinetic alterations.

As also reviewed by Mulla (28), much of the data concerning developmental pharmacodynamics are derived from animal studies. However, there are instances where human and animal correlates have been established. Examples include differences in gamma-aminobutyric acid type A ($GABA_A$) receptor density associated with paradoxical seizures evoked by antiepileptic drugs in children and increased sensitivity to immunosuppressant drugs associated with maturational

changes in the immune system. The paucity of developmental pharmacodynamic information in humans resides with a relative absence of validated, functional biomarkers capable of quantitating differences in drug action that are suitable for longitudinal use across the spectrum of human development. Finally, it is important to recognize that perceived developmental differences in both pharmacokinetics and pharmacodynamics can be influenced by the concomitant expression of disease whereby observations made during the “well” state can be very different from those during both acute (e.g., multiorgan system disease associated with sepsis) and chronic phases of a given illness (e.g., vascular endothelial changes associated with long-standing diabetes and sickle cell disease).

DEVELOPMENTAL PHARMACOGENOMICS

Developmental pharmacogenomics represents the intersection of normal human development and genetic constitution as determinants of drug disposition and/or action. In healthy adults, the interpretation of genotype–phenotype relationships is largely two dimensional given that the genotype is “fixed” (with the exception of epigenetic events) and absent external modifiers (e.g., concomitant disease and/or drug treatment), the expression of phenotype is invariant. This is not the case in the developing human where ontogeny of processes governing either pharmacokinetics (e.g., drug-metabolizing enzymes, transporters) or pharmacodynamics (e.g., receptor expression, signal transduction) can add a third dimension in the interpretation of the genotype–phenotype relationship. As recently denoted by Neville et al. (35), the impact of ontogeny on the genotype–phenotype relationships for drug-metabolizing enzymes, transporters, and/or receptor expression has in most cases not been explored experimentally across the continuum of development or reduced to age- and genotype-specific treatment guidelines for pediatric patients. In instances where these relationships have been evaluated, pharmacologic probe substrates (i.e., drugs whose biotransformation occurs preferentially by a given enzyme) have been used and pharmacokinetic data (either clearance or elimination rate) have been employed as a surrogate to assess the impact of development on the activity of one or more drug-metabolizing enzymes (14,36,37). Despite the fact that the U.S. Food and Drug Administration has included pharmacogenetic data (predominantly derived from adult studies) in the approved product labels for approximately 10% of drugs sold in the United States (38), the clinical utility of these data in pediatric therapeutic decision making can be quite limited. Specifically, understanding the developmental trajectory for the functional activity of genes as well as the developmental context in which the gene(s) of interest is/are operating is of paramount importance when considering the predictive nature of genotype related to either drug disposition or action, both therapeutic and adverse (39).

As intimated above, when genotype and phenotype are concordant, genotype can theoretically be used to predict the activity of a drug-metabolizing enzyme or transporter (i.e., the phenotype). This has been demonstrated for CYP2D6 where an “activity score” predictive of enzyme activity was constructed following consideration of over 25 different allelic variants and their functional consequences (40). The potential clinical utility involved with the use of genotype-derived activity scores for a specific drug metabolism is when the score can be demonstrated to be a reliable predictive biomarker of drug clearance.

As denoted previously, maturation of metabolic capacity for a given drug-metabolizing enzyme or transporter has a specific developmental trajectory with functional maturity (i.e., that observed in healthy adults) generally attained within the first decade of life (4). In those instances where the enzyme

of interest is functionally mature (i.e., a metabolic capacity observed in a healthy adult), concordance of genotype and phenotype can enable the use of allometric scaling to predict drug clearance and age-appropriate drug dose based on weight throughout the pediatric age spectrum. However, as recently denoted by Holford (41), predictive accuracy of allometric scaling is compromised during periods of development where the activities of pathways responsible for drug clearance (e.g., enzymes, transporters, renal elimination processes) are immature. The extension of this principle to the arena of developmental pharmacogenomics is exemplified by periods of life where the maturation of drug clearance pathways/mechanisms demonstrates genotype–phenotype discordance. This is illustrated by data for pantoprazole, a proton pump inhibitor that, in both adults and children, is predominantly metabolized by the polymorphically expressed enzyme, CYP2C19 (16).

Figure 79.4 illustrates apparent plasma clearance (CL/F) data for pantoprazole from a population of neonates (both preterm and term) (42), children, and adolescents (43) with a clinical diagnosis of gastroesophageal reflux disease. Examination of the CL/F data for infants from this study with a postnatal age of <5 weeks showed no difference in the parameter between one patient with a CYP2C19 genotype predictive of a poor-metabolizer phenotype and those with a CYP2C19 genotype corresponding to an extensive-metabolizer phenotype. Beyond a postnatal age of 5 weeks, the pantoprazole CL/F values increase commensurate with previously reported maturational profiles for CYP2C19 (44) and as a result, concordance between CYP2C19 genotype and phenotype occurs. Thus, as reflected by this example, genotyping results for CYP2C19 obtained during the first month of life would not be expected to be predictive of the clearance of drugs that are substrates for this enzyme until such time that genotype and phenotype were concordant.

Finally, it should be recognized that during development, maturation of functional capacity for drug-metabolizing

enzymes (or transporters) is not the only “event” capable of modulating the genotype–phenotype relationship. Relevant examples include the potential impact of diet as reflected by the previously reported differential effect of breast milk versus formula feeding on the developmental acquisition of CYP1A2 activity (36) and the potential of therapeutic drugs to alter the activity of a drug-metabolizing enzyme (e.g., induction of CYP3A4/5 by rifampin and inhibition of the enzyme(s) by erythromycin or azole antifungal agents).

CARDIOVASCULAR DRUGS

It is beyond the scope of this chapter to provide an exhaustive detailed description of every drug used to treat every conceivable cardiovascular condition. Instead, we provide an overview of the general classifications and mechanisms of action of the most commonly used cardiovascular drugs in the pediatric population. Information regarding drug dosing is available in standard references (45). More disease-specific drug information and additional details are available in accompanying chapters dealing with cardiac transplantation, arrhythmias, heart failure, myocarditis, hypertension, and hyperlipidemias.

CARDIAC GLYCOSIDES

Digoxin

Digoxin is the cardiac glycoside recommended for use in children (46). The primary cellular mechanism of action of digoxin is inhibition of sarcolemmal Na⁺–K⁺ ATPase activity, resulting in a slight increase in intracellular sodium concentration. This change in sodium concentration affects sodium–calcium

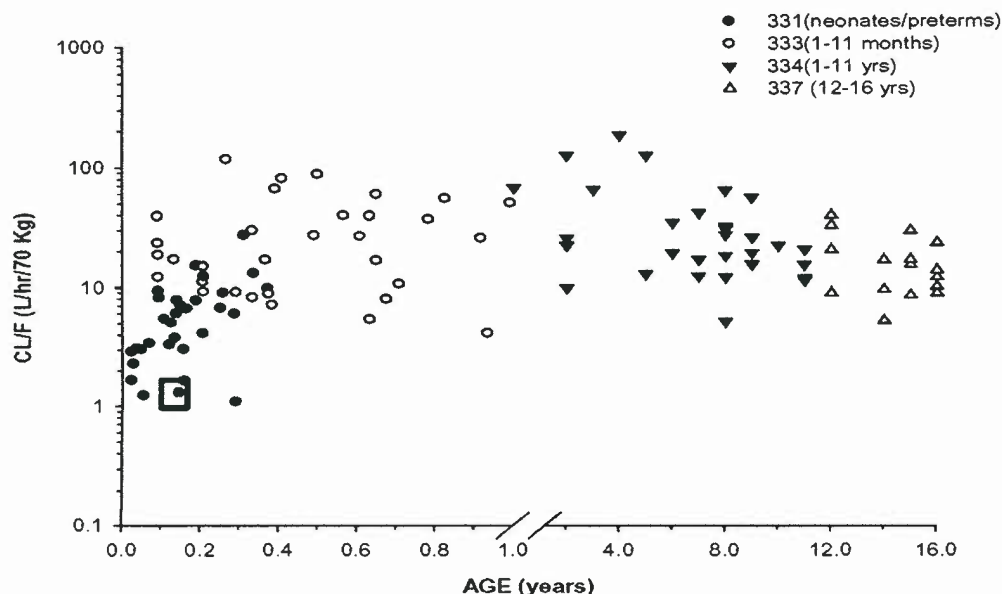


Figure 79.4. Association with age on the apparent plasma clearance (CL/F) of pantoprazole. Composite data were derived from four registration studies of the drug (Pantoprazole Study Numbers 331, 333, 334, and 337) conducted by the innovator company (Wyeth Pharmaceuticals Radnor, PA). The data reflect the ontogeny of CYP2C19, the cytochrome P450 isoform primarily responsible for pantoprazole metabolism. The circle illustrated within the square box represents one subject that had a CYP2C19 genotype predictive of a poor-metabolizer phenotype. This is denoted to illustrate that during the first months of life, CYP2C19 genotype–phenotype discordance (i.e., developmentally associated reductions of enzyme activity in patients with a CYP2C19 genotype predictive of an extensive metabolizer phenotype) is expected.

exchange activity, which subsequently increases intracellular calcium concentration and contractility. However, the increase in contractility is modest and may be imperceptible in the nonfailing heart. In addition to this direct myocardial effect, digoxin slows cardiac conduction and heart rate and alters the neurohormonal milieu in patients with heart failure.

Digoxin is readily absorbed from the gastrointestinal tract, and peak serum levels occur approximately 30 to 90 minutes after an oral dose. Because digoxin has a large apparent volume of distribution, therapy may be initiated with a loading dose. The loading dose (digitalization dose) is generally divided over 12 to 24 hours (half total loading dose initially, one-fourth 6 to 12 hours later, and one-fourth 12 to 24 hours after the initial dose). Administration of a loading dose is associated with a higher incidence of toxic effects, especially in newborns. Furthermore, digoxin is rarely (if ever) required in an emergency so it is reasonable in most cases to begin maintenance dose therapy without a loading dose. Digoxin is excreted by the kidneys with a half-life that changes with age. The half-life is approximately 20 hours in infants and 40 hours in older children, changes associated with developmental increases in renal function. The clearance of digoxin is directly related to renal function, and the dosage must be adjusted in patients with impaired renal function and in premature infants. Consequent to its long elimination half-life, digoxin may be given once daily in infants and children.

In patients with normal renal function and who receive age-appropriate maintenance doses of digoxin, routine monitoring of serum digoxin levels is not necessary. In addition, the presence of endogenous digoxin-like immunoreactive substances in infants may confound interpretation of serum digoxin concentrations performed by certain analytical methods in newborns. If drug concentration monitoring is performed, trough serum concentrations (as opposed to peak levels) should be used to guide adjustments in therapy. Because of the lack of relationship between higher serum levels and a greater therapeutic effect, the target serum digoxin levels should range between 1 and 2 ng/mL. The major indication for obtaining a serum digoxin concentration is in cases of known or suspected digoxin toxicity. This occurs most commonly in cases of accidental overdose and in complicated patients with renal failure and/or those taking medications that may interfere with digoxin clearance.

The primary indication for digoxin therapy in children is heart failure with systemic ventricular dysfunction. However, no randomized, prospective, controlled clinical trials of digoxin have been performed in this population. Therapeutic recommendations are therefore based largely on inferences drawn from adult studies and animal experiments. The use of digoxin in infants with a large left-to-right shunt is controversial. Most infants with intracardiac left-to-right shunts have apparently normal systolic ventricular function and likely do not benefit from a positive inotropic agent. Manipulation of loading conditions with diuretics is a more rational approach and should be used initially. However, some patients may benefit from the reduction in heart rate mediated by digoxin. Digoxin exerts important neurohormonal modulating effects in adult patients with congestive heart failure which may be of benefit, even in the absence of measurable objective changes in cardiac function. The neurohormonal effects of digoxin have not been adequately studied in infants and children.

Digoxin has a narrow therapeutic index and consequently, a high potential for producing toxicity. Common signs and symptoms of systemic toxicity in adults (anorexia, vomiting, visual disturbances, and CNS disturbances) may be difficult to recognize in infants. Digoxin toxicity should be suspected in any infant receiving the drug who presents with apathy toward feeding or feeding intolerance. Drugs that may predispose to digoxin toxicity include diuretics (hypokalemia)

and amiodarone (reduced elimination of digoxin). Cardiac toxicity in infants often results in second- or third-degree atrioventricular block with resulting bradycardia, but almost any type of arrhythmia can be produced by digoxin toxicity. Prolongation of the PR interval is an expected digoxin effect and is not a sign of toxicity. Treatment of acute digoxin toxicity requires hemodynamic and ECG monitoring, temporary cardiac pacing if necessary, normalization of serum potassium levels, and antiarrhythmic drug therapy. In cases of life-threatening arrhythmias, specific Fab antibody fragments should be administered intravenously.

ADRENERGIC AGONISTS

The cardiac and vascular responses to adrenergic agonists are mediated by specific receptors (47,48). Although grossly oversimplified, the heart contains mainly β_1 -, the lungs β_2 -, and the vasculature both β_2 - and α -adrenergic receptors. Stimulation of β_1 -adrenergic receptors in the mature heart increases rate, contractility, relaxation, and conduction. These events are mediated by G-protein-coupled stimulation of adenylyl cyclase, generation of cAMP, activation of cAMP-dependent protein kinase, and phosphorylation of key regulatory proteins involved in intramyocellular calcium regulation. Stimulation of β_2 -adrenergic receptors in the lungs produces bronchodilation and modest pulmonary vasodilation. Systemic vasoconstriction results from activation of α -adrenergic receptors. In contrast to most of the vascular bed, skeletal muscle vasculature contains β_2 -adrenergic receptors that promote vasodilation when activated. Dopaminergic receptors in the splanchnic and renal vascular beds produce vasodilation in response to dopaminergic agonists.

Maturation changes in the receptor-effector and signal transduction pathways result in age-related variability in responsiveness to adrenergic agonists (49–51). Loading conditions, volume status, and responsiveness of the peripheral vasculature can also influence the responses to these agents, especially in critically ill infants and children. Adrenergic agonists undergo rapid biotransformation and consequent to their very short elimination half-life, are administered by continuous intravenous infusion. The dose (infusion rate) must be carefully titrated with appropriate clinical and hemodynamic monitoring. Comparison of the relative effects on β -, α -, and dopaminergic receptor subtypes for various drugs is presented in Table 79.7.

TABLE 79.7 Effects of Agonists on Adrenergic Receptor Subtypes

Drug	Predominant Agonistic Effects
Dopamine	$\beta_1 = DA_1 > \alpha$
Dobutamine	β_1
Epinephrine	$\beta_1 = \beta_2 = \alpha$
Fenoldopam	DA_1
Phenylephrine	α
Norepinephrine	$\beta_1 = \alpha$
Isoproterenol	$\beta_1 = \beta_2$

Reprinted with permission of The McGraw-Hill Companies. Artman M, Mahony L, Teitel DF. *Neonatal Cardiology*. 2nd ed. New York, NY: McGraw-Hill Medical, 2011:239; Table 12.6 Ref. (90).

Dopamine

Dopamine is an endogenous precursor of norepinephrine with direct cardiac β_1 -adrenergic agonist effects. In addition, dopamine indirectly stimulates β_1 -receptors by promoting the release of norepinephrine from presynaptic sympathetic nerve terminals within the myocardium. Unlike the other related catecholamines, dopamine exhibits specific dopaminergic receptor agonism (dopamine DA_1 receptor agonist). Dopamine has little or no effect on β_2 -adrenergic receptors, but at higher concentrations, it stimulates α_1 -adrenergic receptors. At low to moderate doses, the major action of dopamine is to increase contractility (β_1 -effect) and to dilate the renal vascular bed (DA_1 effect). At higher rates of infusion, α_1 -receptor stimulation (vasoconstriction) becomes more pronounced and the renal vasodilating effect is overcome.

Dopamine has gained considerable popularity for use in the acutely ill infant or child with cardiac dysfunction from any etiology (52–54). Low to moderate doses are thought to incur an additional advantage by increasing renal blood flow and maintaining urine output, although this has not been conclusively proven. At conventional doses, dopamine has little effect on pulmonary vascular resistance. High rates of infusion may increase systemic vascular resistance, induce sinus tachycardia, and provoke arrhythmias and, in critically ill patients with circulatory insufficiency, can result in peripheral gangrene. The clearance of dopamine is reduced in the presence of significant hepatic and/or renal compromise and the drug is not chemically stable when mixed with alkaline solutions.

Fenoldopam

Like dopamine, fenoldopam is a selective DA_1 agonist, but in contrast, fenoldopam is more potent than dopamine and does not stimulate α - or β -adrenergic receptors at conventional dosages. This pharmacologic profile results in dilation of the renal and splanchnic beds, increased renal blood flow and glomerular filtration rate, and diuresis. Fenoldopam is used primarily for treating hypertension in adults, but some centers have used intravenous fenoldopam in infants and children in an effort to promote diuresis (55,56). Potential advantages of fenoldopam include rapid titration and few side effects beyond excessive hypotension. However, the limited published results in oliguric infants immediately after cardiac surgery do not provide compelling evidence for a dramatic benefit from fenoldopam infusion. Additional prospective studies are needed to determine the role of fenoldopam in the management of acutely ill infants and children with heart disease.

Dobutamine

Dobutamine is a racemic mixture with complex actions involving α - and β -adrenergic receptors. The net response to conventional dosages in adult patients is that of β_1 -agonism with relatively little effect on β_2 -receptors, α -receptors, or DA_1 receptors. The usual pharmacodynamic response to dobutamine in children is an increase in contractility and cardiac output with minimal effects on pulmonary vascular resistance or heart rate. Systemic vascular resistance may decline because of improved cardiac output. In contrast to dopamine, dobutamine does not dilate the renal vascular bed. Dobutamine is often selected in situations for which the primary goal of therapy is to improve ventricular contractility (48,53).

Dobutamine may be administered as a single drug or as an adjunct to the infusion of other agents. Wide variability in drug clearance and in hemodynamic responses requires individual titration of dobutamine therapy, especially in infants. As the dosage increases, dobutamine may adversely increase heart

rate and myocardial oxygen demand. However, it appears to be less arrhythmogenic than the other sympathomimetic amines.

Epinephrine

Epinephrine is produced by the adrenal medulla and has extremely potent effects on α - and β -adrenergic receptors. At low concentrations, the predominant effects include increased heart rate, contractility, and systolic blood pressure due to β_1 -adrenergic stimulation. As the dose increases, diastolic blood pressure may decline slightly due to β_2 -adrenergic effects in the peripheral vasculature. At higher doses, α -adrenergic effects become prominent and pronounced vasoconstriction occurs.

The major indication for epinephrine is cardiovascular collapse associated with low cardiac output that is refractory to dopamine and/or dobutamine (47,48). Epinephrine must be infused cautiously with careful hemodynamic monitoring. The initial infusion rate should be at the lower end of the recommended dosage and then gradually increased as needed. The major life-threatening toxic effect of epinephrine is the induction of ventricular arrhythmias. Epinephrine increases myocardial oxygen requirements because of its prominent inotropic and chronotropic effects. High doses may produce myocardial ischemia, especially in cases involving either coronary artery anomalies or significant ventricular hypertrophy. Tissue ischemia can occur because of peripheral vasoconstriction, especially with high rates of infusion.

Norepinephrine

Norepinephrine has β_1 - and α -adrenergic agonist effects, but in contrast to epinephrine and isoproterenol, it does not stimulate β_2 -receptors (at conventional concentrations). Infusion of norepinephrine increases systolic and diastolic blood pressure, systemic vascular resistance, and contractility. Heart rate is largely unaffected. The prominent α -adrenergic effects of norepinephrine result in systemic vasoconstriction and reduced renal perfusion leading to reductions in urine output.

Norepinephrine is rarely used as a positive inotropic agent because of significant elevation of systemic vascular resistance, reduction in renal blood flow, and increased myocardial oxygen demand. Norepinephrine may be useful in gravely ill patients with cardiovascular collapse associated with profound peripheral vasodilation, such as hyperdynamic septic shock. Some infants exhibit little vascular tone following cardiopulmonary bypass surgery and norepinephrine may be helpful temporarily in supporting the systemic blood pressure. Adverse effects of norepinephrine include arrhythmias and tissue ischemia secondary to extreme vasoconstriction.

Isoproterenol

Isoproterenol is a synthetic catecholamine with potent non-selective β -adrenergic agonism and no significant effect on α -adrenergic receptors (47). Isoproterenol increases cardiac contractility and heart rate (β_1 -effect) and reduces systemic vascular resistance due to dilation of skeletal muscle, renal, and splanchnic beds (β_2 -effect). The drug is a potent bronchodilator and thus, may be particularly beneficial in patients with pulmonary disease and bronchoconstriction.

Bradycardia caused by atrioventricular block or sinus node dysfunction is probably the most common indication for isoproterenol in young infants. These patients may be managed temporarily by infusing isoproterenol until pacing can be instituted (either a temporary pacing catheter or a permanent

pacemaker). Although isoproterenol increases myocardial contractility and therefore increases cardiac output, this agent causes a much greater increase in heart rate than other adrenergic drugs. Since many infants with low cardiac output are already tachycardic, isoproterenol is used rarely.

Phenylephrine

Phenylephrine stimulates α_1 -adrenergic receptors and has relatively little effect on other adrenergic receptors. The hemodynamic effects of phenylephrine are related primarily to vasoconstriction and increased systemic vascular resistance. There may be a reflex decrease in heart rate. Administration of phenylephrine is indicated in conditions such as septic shock where the primary goal of therapy is to promote vasoconstriction. Phenylephrine has been used acutely during hypercyanotic episodes in patients with tetralogy of Fallot to increase systemic resistance, reduce the right-to-left shunt, increase pulmonary blood flow, and thereby improve systemic oxygenation.

PHOSPHODIESTERASE INHIBITORS

A family of phosphodiesterase enzymes with distinct activities and subcellular distributions controls the degradation of intracellular cAMP (and cGMP). Drugs that selectively inhibit cAMP phosphodiesterase activity increase the activation of protein kinase A, resulting in a positive inotropic effect in mature myocardium. Maturation of the phosphodiesterase system in human myocardium has not been characterized, but virtually every immature mammalian species studied exhibits little or no positive inotropic response to cAMP-specific phosphodiesterase inhibitors such as milrinone (41). Despite these observations, milrinone has gained widespread usage in the pre- and postoperative management of infants and children with ventricular dysfunction (48,57–59). However, whether the apparently beneficial hemodynamic responses are primarily due to increased contractility or to pulmonary and systemic vasodilation remains unclear.

Milrinone

Milrinone is a relatively selective inhibitor of type 3 cAMP-phosphodiesterase that is used in the postoperative period following cardiac surgery and in children with low cardiac output and ventricular dysfunction. Milrinone has lower clearance in infants than in older children and the dose must be adjusted accordingly. Milrinone is generally well tolerated and is not arrhythmogenic. Side effects include hypotension due to vasodilation (especially at higher doses) and thrombocytopenia.

CALCIUM-SENSITIZING AGENTS

Positive inotropic drugs that act via the cAMP–protein kinase A pathway (e.g., β_1 -adrenergic agonists, type 3 phosphodiesterase inhibitors) have side effects and inherent limitations that may be avoided by drugs that increase the sensitivity of the myofilaments to calcium. Many calcium-sensitizing agents have been developed but the drug that appears to hold the most promise is levosimendan (48,60–62). Levosimendan binds to troponin C and improves the efficiency of contraction without a requisite increase in either cAMP or intracellular calcium. Although not yet approved by the Food and Drug Administration, studies in adults suggest that levosimendan may be of

value as an adjunct or alternative to conventional inotropic agents in patients with refractory heart failure and systolic dysfunction. The published experience with levosimendan in children is quite limited and additional studies are necessary to determine the safety and efficacy in pediatric patients with depressed cardiac function.

DIURETICS

Diuretics remain a mainstay of therapy for heart failure and hypertension (59,63). However, diuretics do not improve the neurohormonal alterations that contribute to the heart failure syndrome. Aggressive diuresis can actually promote activation of the sympathetic nervous system and the renin–angiotensin–aldosterone system. Hypovolemia, decreased renal blood flow, reduced glomerular filtration rate, or sodium depletion may reduce diuretic efficacy. Given the array of drugs available, it is helpful to classify diuretics according to their predominant site of action within the nephron (see below). Relative potency and adverse effects vary among the different classes.

Loop Diuretics

These agents are potent diuretics and have been widely used in children for a variety of indications. The most commonly used drug is furosemide, but ethacrynic acid and bumetanide are also available. Loop diuretics inhibit chloride–sodium–potassium cotransport in the thick ascending limb of the loop of Henle. This reduces reabsorption of chloride, sodium, and potassium and increases net excretion of free water.

Furosemide

Furosemide increases renal blood flow, enhances renin release, and reduces renal vascular resistance. It has diuretic and non-diuretic pulmonary effects and appears to reduce pulmonary transvascular fluid filtration. The primary indications for furosemide in children with heart disease include acute and chronic management of congestive circulatory states and diuresis following cardiac surgery. Furosemide may be administered orally or intravenously. The drug is primarily excreted unchanged by the kidneys and the dosage must be adjusted in renal failure or in infants with immature renal function. Consequent to developmentally associated reductions in glomerular filtration rate, the plasma elimination half-life of furosemide in preterm infants is approximately 20 hours, as compared with 8 hours in term infants and 1 hour in adults. Likewise, the plasma clearance of furosemide is reduced in all patients with significant reductions in renal function; a scenario that also can lead to reduced diuretic response.

Adverse effects of furosemide include excessive contraction of extracellular volume, electrolyte imbalances, and ototoxicity. The risk of ototoxicity increases if renal dysfunction is present or if other ototoxic medications are administered concomitantly (such as aminoglycosides). Hyponatremia in older patients with congestive heart failure is generally due to excess total body water. However, in premature and term newborn infants with limited sodium intake, chronic or excessive use of furosemide may promote excessive sodium excretion and contribute to hyponatremia. Hypokalemia is a relatively common side effect of therapy with loop diuretics, and serum potassium should be monitored, especially in the acute care setting. Potassium supplementation is often required in the perioperative period for infants with significant congenital heart disease. Hypochloremic metabolic alkalosis is a common occurrence with furosemide therapy and if severe, chloride

supplementation is required. Hypocalcemia and hypomagnesemia are usually not significant clinically, but one must be alert to these potential complications, especially in the immediate postoperative period.

Ethacrynic Acid

Ethacrynic acid is occasionally used acutely in the management of patients with significant or refractory volume overload. Generally, ethacrynic acid is reserved for use in children who do not respond adequately to furosemide. The indications and toxic effects of ethacrynic acid are otherwise comparable to those described for furosemide.

Bumetanide

Bumetanide is generally reserved for use in patients who have not responded adequately to conventional diuretic regimens. Bumetanide can be administered orally or intravenously. In contrast to furosemide, bumetanide is partially metabolized in the liver with approximately 50% excreted unchanged in the urine. Thus, the dosage may need to be reduced in patients with clinically significant hepatic and/or renal dysfunction. The indications and potential complications are similar to those described for furosemide.

Thiazide Diuretics

Thiazides inhibit sodium and chloride transport in the distal convoluted tubule of the nephron. Thiazide diuretics have been available for many years and there is broad experience with these agents. Hydrochlorothiazide and chlorothiazide are the primary drugs in this class used in children with cardiovascular disease. They are close structural analogs with similar mechanism of action, diuretic efficacy, and side effects. The main differences relate to dosage, absorption, and excretion. Following oral administration, a diuretic effect is generally noted within 60 minutes and may persist as long as 12 to 24 hours. Hydrochlorothiazide is more potent than chlorothiazide. A thiazide diuretic is generally used for outpatient management of a chronically congested circulatory state, but may also be useful in the inpatient setting for patients with more advanced heart failure. In this situation, they may be used in combination with a loop diuretic and/or a potassium-sparing agent. Adverse effects of thiazides include hypokalemia, hyperuricemia, and hypercalcemia. Nonrenal effects of thiazide diuretics that have been described in older patients and adults include carbohydrate intolerance and adverse effects on plasma cholesterol and triglycerides. The extent and implications of potential disturbances in cholesterol, lipoproteins, and triglycerides have not been determined in young children.

Metolazone

Metolazone is a sulfonamide derivative that blocks sodium reabsorption in the distal and proximal convoluted tubule. It exhibits several thiazide properties although it does not have a classic thiazide structure. In general, metolazone is reserved for short-term treatment of edematous states that are resistant to conventional therapy with loop diuretics or thiazides. The combination of metolazone and furosemide can be synergistic and promote marked diuresis (with associated electrolyte loss). Metolazone is given orally once a day or every other day. The major adverse effects of metolazone include significant volume depletion and severe electrolyte disturbances.

Potassium-Sparing Diuretics

Spironolactone is the prodrug of canrenone, and therefore, bioactivation is required for drug action. The drug competitively inhibits aldosterone at the distal tubule and thus reduces potassium loss in the urine. The diuretic effect of spironolactone is relatively weak compared with the loop or thiazide diuretics. In most cases, it is used in combination with either furosemide or hydrochlorothiazide predominantly for its potassium-sparing effects. The major adverse effect of spironolactone is hyperkalemia, which, in most patients, is not a significant problem in the absence of excessive potassium intake (e.g., when coadministered with a potassium supplement), renal dysfunction, or hepatic dysfunction. Caution is required if spironolactone is used in combination with an angiotensin-converting enzyme (ACE) inhibitor because of the propensity for hyperkalemia. Similarly, if coadministration of a potassium supplement is necessary, serum potassium levels should be monitored carefully.

VASODILATORS

Many vasodilators are available that encompass a broad spectrum of mechanisms, primary sites of action, efficacy, and toxicity (59,64,65). The major indications for the use of vasodilators in children with heart disease are impaired ventricular function, pulmonary hypertension, aortic valve regurgitation, and systemic hypertension. The selection of a specific drug depends upon the primary goal of therapy, underlying or associated conditions, and whether or not the treatment is acute or chronic in nature. One approach to classifying vasodilators groups the drug classes according to their major mechanism of action (Table 79.8). Knowledge of the mechanism of action of a given drug provides a framework for understanding the pharmacology and therapeutic applications. Another method is to group drugs according to their predominant site of action (predominately venous, arteriolar, or balanced; Table 79.8). Depending on the therapeutic goals, one may select an agent that has predominant effects on venous capacitance, arteriolar resistance, or both.

Nitric Oxide–Modifying Drugs

Relaxation of vascular smooth muscle by drugs in this class is mediated by nitric oxide. Nitric oxide activates guanylyl

TABLE 79.8 Vasodilator Mechanisms and Sites of Action

Predominant Mechanism	Drug Examples	Predominant Site of Action
Nitrovasodilator	Nitroglycerin	Venous
Calcium channel antagonist	Nifedipine	Arteriolar
ACE inhibitor	Captopril	Mixed
Angiotensin receptor blocker	Losartan	Mixed
Natriuretic peptide	Nesiritide	Mixed

Reprinted with permission of The McGraw-Hill Companies. Artman M, Mahony L, Teitel DF. *Neonatal Cardiology*. 2nd ed. New York, NY: McGraw-Hill Medical, 2011:239; Table 12.6 Ref. (90).

cyclase, resulting in increased formation of cGMP in vascular smooth muscle cells and activation of cGMP-dependent protein kinase. The net effect is relaxation of vascular smooth muscle.

Nitroglycerin

Nitroglycerin relaxes smooth muscle in the cardiovascular, respiratory, and gastrointestinal systems. At the usual therapeutic concentrations, the predominant site of action is the venous vascular bed. Nitroglycerin therefore acts principally to increase venous capacitance, promoting a reduction in atrial and ventricular filling pressures. Nitroglycerin has been largely replaced by other agents, but is sometimes administered after cardiac surgery. At low doses, there is little effect on systemic vascular resistance, systemic arterial pressure, or heart rate. However, higher doses can produce arteriolar dilation with hypotension and reflex tachycardia. Nitroglycerin is rapidly metabolized in the liver and must be given by continuous infusion. Nitroglycerin is a potent vasodilator that must be used with appropriate hemodynamic monitoring. Patients with decreased intravascular volume (low preload) may respond adversely to nitroglycerin because a further decline in filling pressure may significantly reduce cardiac output. Overdose causes hypotension and tachycardia, which respond quickly to a reduction in dose or cessation of the infusion.

Nitroprusside

Nitroprusside is an extremely potent vasodilator that reduces systemic and pulmonary vascular resistance and increases venous capacitance. It is used for treating hypertensive emergencies consequent to its potency, rapid onset of action, and titratable effects. Nitroprusside is occasionally administered to pediatric cardiac surgical patients in the immediate postoperative period. In addition, it may be effective acutely in children with left ventricular dysfunction and low cardiac output. With proper monitoring and dosing, nitroprusside appears to be safe and effective in neonates.

Nitroprusside is rapidly metabolized to thiocyanate and cyanide. While the precise relationships between cyanide or thiocyanate concentrations in plasma or red blood cells and clinical toxicity are not entirely clear, potential toxicity should be considered in patients with renal dysfunction who are receiving prolonged infusions of nitroprusside. Because of the rapid onset of action and rapid metabolism, the desired hemodynamic effect can be achieved by careful dose titration. The major adverse effects of nitroprusside are a direct extension of its powerful vasodilator activity. Careful hemodynamic monitoring is imperative in order to avoid significant hypotension. Due to limited stability and photodegradation, nitroprusside solutions must be freshly prepared before use and protected from light.

Pulmonary Vasodilators

Nitric Oxide

Nitric oxide is a gas that is administered via inhalation. This agent produces pulmonary vasodilation without affecting the systemic vasculature. Nitric oxide plays a central role in the management of infants with persistent pulmonary hypertension of the newborn (66,67). This agent is also beneficial in the perioperative period for infants and children with pulmonary arterial hypertension associated with congenital heart disease (48). Assessment of the response includes evaluation of systemic oxygenation and pulmonary artery pressure.

Echocardiography may be helpful in assessing pulmonary artery pressure noninvasively. Methemoglobin levels should be monitored regularly in patients receiving high concentrations or prolonged therapy.

Sildenafil

Sildenafil is a potent and selective inhibitor of cyclic nucleotide phosphodiesterase type 5, the predominant isoform involved in degradation of cGMP in the lung vasculature. Inhibition of this phosphodiesterase results in pulmonary vasodilation and will also increase the efficacy of inhaled nitric oxide (48,68,69). Sildenafil can be administered enterally, intravenously, or as an aerosol but most of the published experience in infants and children has been with the oral and intravenous forms. Orally administered sildenafil has been shown to be effective in treating persistent pulmonary hypertension in newborns and is well tolerated. However, given the lack of a proprietary liquid formulation of the drug, the potential exists for alterations in the oral bioavailability of sildenafil as a result of improperly constructed extemporaneous formulations. The primary use of sildenafil in children with cardiac disease is for patients with acute or chronic pulmonary hypertension following cardiac surgery. It has also been used in older children and adolescents with primary pulmonary hypertension.

α -Adrenergic Receptor Antagonists

Phentolamine

Phentolamine is a competitive nonselective antagonist of α -adrenergic receptors that blocks α_1 - and α_2 -receptors. Blockade of presynaptic α_2 -adrenergic receptors may contribute to the tachycardia and arrhythmias that occur at high doses of phentolamine. Administration of phentolamine to patients with low cardiac output produces a decrease in systemic vascular resistance with a resultant increase in cardiac output. Although phentolamine is classified as a mixed vasodilator, the effects on venous capacitance are minimal compared with other mixed vasodilators. Phentolamine reduces pulmonary vascular resistance and pulmonary arterial pressure. Experience with phentolamine in children is limited to short-term intravenous administration. In general, phentolamine is effective and well tolerated in infants and children. Adverse effects include significant sinus tachycardia, arrhythmias, and excessive hypotension.

Calcium Channel Antagonists

Calcium channel antagonists block the opening of calcium channels in vascular smooth muscle, thereby promoting vasodilation. However, these drugs also block L-type calcium channels in the heart. Newborns are more sensitive to the negative inotropic effects of calcium channel blockers than are older children, and intravenous administration of calcium channel blockers in infants has been associated with cardiovascular collapse. These drugs must be avoided or used with extreme caution in neonates and infants.

Calcium channel antagonists are categorized into three major chemical classes: phenylalkylamines (e.g., verapamil), dihydropyridines (e.g., nifedipine), and benzothiazepines (e.g., diltiazem). Drugs of the dihydropyridine class exhibit the most pronounced vasodilation and should be selected if that is the primary goal of therapy. Most of the published pediatric experience with dihydropyridines is limited to nifedipine, but the clinically important differences among the various drugs in this chemical class are slight. In young infants, nifedipine is used primarily to treat pulmonary hypertension associated

with bronchopulmonary dysplasia. Oral verapamil is occasionally used in older infants with arrhythmias or hypertrophic cardiomyopathy.

Angiotensin-Converting Enzyme (ACE) Inhibitors

ACE inhibitors play a central role in the management of systemic hypertension and congestive heart failure in adults. However, relatively few randomized prospective clinical trials have been performed using ACE inhibitors in infants and children. Despite the relative paucity of information from well-controlled clinical trials, anecdotal reports, case series, and clinical experience suggest that the ACE inhibitors have beneficial effects in children with hypertension and heart failure, especially in the short term (64,70,71).

The result of inhibiting ACE is reduced conversion of angiotensin I to angiotensin II, a potent vasoconstrictor. In addition, ACE inhibitors reduce the degradation of vasodilatory bradykinins and diminish production of aldosterone. Hemodynamic effects of ACE inhibitors include a reduction in systemic vascular resistance and systemic blood pressure. Long-term studies of ACE inhibitors in adults with heart failure demonstrate significant improvements in survival, reduction in hospitalizations, and improvements in quality of life. The beneficial effects and safety profile of ACE inhibitors have prompted the recommendation that these drugs be prescribed for asymptomatic adults with documented left ventricular dysfunction.

Several ACE inhibitors are commercially available in the United States. These drugs are similar with regard to their mechanism of action but differ slightly in their metabolism and pharmacokinetics. Most of the published experience in children is with captopril, enalapril, and lisinopril.

Captopril

Captopril (as with all ACE inhibitors) is a mixed or balanced vasodilator that reduces systemic vascular resistance and increases venous capacitance. In children with congestive heart failure, these effects result in increased cardiac output and a reduction in cardiac filling pressures. Pulmonary vascular resistance generally declines and heart rate is usually minimally affected. Mild-to-moderate diuresis may occur because of increased renal blood flow and reduced aldosterone formation. Captopril is administered orally and peak plasma concentrations generally occur 1 to 2 hours after a single oral dose. Its plasma elimination half-life is relatively rapid with values ranging between 2 and 3 hours. Approximately 50% is excreted in the urine unchanged, and thus, captopril plasma clearance is reduced in patients with impaired renal function.

Captopril is used for the treatment of systemic hypertension and congestive heart failure in infants, children, and adolescents. It is generally well tolerated, but significant hypotension may occur in volume-depleted patients or in patients with extremely high basal renin activity. When starting captopril therapy for congestive heart failure in neonates and young infants, a low first dose is given and blood pressure should be monitored. If the drug is well tolerated, then the dosage can be escalated over a few days.

Adverse effects include neutropenia and proteinuria, especially in children with underlying renal disease. Less serious reactions include rash, taste impairment, and minor gastrointestinal disturbances. A dry nonproductive cough is a well-described feature of ACE inhibitor therapy in adults, but this does not seem to be a major problem in children. In general, potassium supplements and potassium-sparing diuretics should not be administered concomitantly to patients receiving captopril because of the risk of hyperkalemia. All ACE

inhibitors are contraindicated in pregnancy because of the association with fetal demise and major congenital malformations. Thus, captopril must be used with appropriate caution in adolescent females and should be immediately discontinued if pregnancy occurs.

Enalapril and Lisinopril

The mechanism of action, hemodynamics, and clinical indications for enalapril and lisinopril are similar to those described above for captopril. These drugs have a slower onset of action and longer half-life than captopril. Enalapril and lisinopril can be administered once daily, which may improve compliance compared to captopril. Enalapril is a prodrug that must be de-esterified to form the active agent, enalaprilat. Enalaprilat is commercially available for parenteral administration. The overall incidence of side effects due to enalapril and lisinopril appears to be lower than that reported for captopril.

Angiotensin Receptor Blockers

Angiotensin (AT) receptors exist as distinct subtypes that couple AT with specific intracellular responses. Because local tissue production of AT may occur that is not ACE-dependent, more complete local inhibition of the AT pathway can theoretically be achieved by direct blockade of AT receptors. Several selective AT₁ receptor blockers are commercially available and have been studied in adults with heart failure and/or hypertension (72). The prototype is losartan. Experience with these agents in infants and children is limited at present. However, based on theoretical considerations and results obtained from clinical trials in adults, these agents may prove to be useful in the pediatric population.

In addition to blocking AT₁ receptors, losartan also blocks transforming growth factor (TGF- β) activity. This effect has been shown experimentally to be beneficial in animal models of muscular dystrophy and connective tissue disorders (73,74). Use of these agents in pediatric patients with connective tissue disease such as Marfan and Loeys-Dietz syndromes and Duchenne muscular dystrophy is a subject of current investigation.

ALDOSTERONE RECEPTOR ANTAGONISTS

Activation of the renin-angiotensin system with increased synthesis of aldosterone is a hallmark of the heart failure syndrome. Aldosterone plays an important role in promoting the abnormal collagen production and interstitial fibrosis that occurs in chronic heart failure. Therapy with an ACE inhibitor blocks angiotensin II formation and reduces aldosterone production. However, aldosterone synthesis may "escape" despite the appropriate use of an ACE inhibitor (72). An escape of aldosterone production in adult patients is associated with sodium retention, potassium and magnesium loss, excessive myocardial collagen production, ventricular hypertrophy, myocardial norepinephrine release, endothelial dysfunction, and a decrease in serum high-density lipoprotein cholesterol. Administration of aldosterone antagonists, such as spironolactone or eplerenone, to adult patients with heart failure treated with conventional therapy results in increased diuresis and symptomatic improvement (72,75). Spironolactone has been used for years as a potassium-sparing diuretic in infants and children with heart failure, but it has not been extensively studied in this

patient population. Whether additional benefit is derived from inhibiting the other effects of aldosterone in pediatric patients remains to be determined.

HORMONES

Nesiritide

Nesiritide is a recombinant B-type natriuretic peptide that has been studied in adults with heart failure. It is administered intravenously and produces vasodilation, increases glomerular filtration rate, inhibits renal sodium reabsorption, and promotes diuresis. Despite considerable investigation in the adult population, the role and efficacy of nesiritide is controversial. Several studies in children suggest nesiritide may increase urine output and reduce levels of neurohormonal markers of heart failure. Some centers use nesiritide acutely for infants with low cardiac output following cardiac surgery and for infants with severely depressed cardiac function due to cardiomyopathy (48,76,77). Additional studies are needed to determine the safety and efficacy of nesiritide in pediatric patients with heart disease.

Thyroxine and Triiodothyronine

Thyroid hormone secretion is reduced in critically ill adults and children following cardiac surgery. These changes in thyroid hormone levels are referred to as “non-thyroidal illness syndrome” and generally have not been thought to represent true hypothyroidism. However, this concept is controversial and some authorities suggest that these patients may have acquired true central hypothyroidism as a consequence of their critical illness or surgical procedure. Some centers administer either thyroxine or triiodothyronine in the postoperative period if thyroid-stimulating hormone is elevated, circulating thyroid hormone levels are reduced, and the child has evidence of low cardiac output (78). However, relatively little published information exists regarding the safety, efficacy, and long-term effects of thyroid hormone administration to children in the early postcardiac surgery period. Additional studies are required to determine if thyroid hormone therapy has a beneficial role in this setting.

Vasopressin

Vasopressin is a potent vasoconstrictor that acts directly on the vasculature via V1 receptors and indirectly by potentiating the vasoconstrictor effects of catecholamines. Cardiopulmonary bypass produces a systemic inflammatory response that can result in low cardiac output and vasodilatory shock. The first line of therapy in this setting is infusion of catecholamines such as dopamine or norepinephrine. However, shock persists in some infants and children despite maximal supportive therapy. This clinical syndrome mimics that seen in patients with septic shock, which has been associated with depressed levels of vasopressin in adults and children. In contrast to catecholamines, the responses to vasopressin are preserved in the presence of acidosis or hypoxia. Based on results from studies demonstrating a beneficial effect of vasopressin infusion in patients with vasodilatory septic shock, several investigators have administered vasopressin to infants with vasodilatory shock following cardiopulmonary bypass (79,80). In general, the reported results are favorable and it appears that vasopressin can be an effective adjunct to more conventional therapy in this setting. However, additional

studies are required to more fully define the indications, safety, and efficacy of vasopressin treatment in children with heart disease.

β -ADRENERGIC RECEPTOR BLOCKERS

β -Blockers can be classified as first generation, nonselective for β_1 - and β_2 -blockade (e.g., propranolol); second generation with relative selectivity for β_1 -receptors (e.g., metoprolol and atenolol); and third generation drugs (selective or nonselective; e.g., carvedilol, and nebivolol). Furthermore, individual drugs differ with regard to the degree of important ancillary properties such as α -adrenergic receptor blockade, antioxidant activity, and intrinsic sympathomimetic activity (81,82). Because of these important differences, the various β -blockers are not interchangeable. Published experience in pediatric patients is limited and therapy for children is derived from adult experiences. The most commonly used β -blockers in infants are propranolol and esmolol. These drugs are also used in older children and adolescents, but in these older age groups, drugs such as metoprolol, atenolol, and carvedilol are also used.

Propranolol

Propranolol was the first commercially available β -adrenergic blocker in the United States, and consequently, this is the drug in this class with the most widely published experience in pediatrics. Propranolol is available for oral or intravenous administration, but if intravenous β -blocker therapy is necessary, the short-acting β -adrenergic blocker, esmolol (see below) should be used because of the risk of hypotension and bradycardia from the intravenous administration of propranolol.

Propranolol is used in infants for management of supraventricular tachycardia, some forms of ventricular arrhythmias, treatment of long QT syndromes, and hypertrophic cardiomyopathy. In the past, it was sometimes used in an attempt to reduce the frequency and severity of hypercyanotic episodes in infants with tetralogy of Fallot. Presently, most patients undergo surgical correction or palliation if hypercyanotic episodes occur. However, some infants with critical pulmonary stenosis may benefit from a short course of propranolol after relief of pulmonary valve stenosis until the infundibular hypertrophy improves.

Propranolol is well absorbed after an oral dose, although it undergoes extensive first-pass hepatic metabolism that reduces the bioavailability to approximately 30% to 40%. Class-dependent effects of β -adrenergic blockers include depression of contractility, atrioventricular block, bronchospasm, and sleep disturbances. Propranolol should be avoided if possible in infants with significant pulmonary disease because of the propensity for bronchoconstriction. While the chronic use of propranolol in infants appears to be safe and well tolerated, infants are at risk for developing hypoglycemia if their oral intake is restricted because of other illnesses or other conditions. Blood glucose should be monitored in infants receiving propranolol (or other β -adrenergic receptor blockers) who are unable to feed normally.

Esmolol

Esmolol is a β_1 -selective adrenergic blocker with a short plasma half-life (~5 to 10 minutes). The indications and precautions for esmolol are similar to those described above for propranolol. The major difference is that because of its rapid plasma clearance (and short elimination half-life), esmolol is administered by continuous intravenous infusion that can be easily titrated.

Generally, esmolol is used for short periods of time in acute care settings (i.e., cardiac catheterization laboratory, postoperative recovery unit, and neonatal intensive care nursery).

Metoprolol and Atenolol

Metoprolol and atenolol are relatively selective for β_1 -adrenergic receptors (this selectivity is lost at higher concentrations). Metoprolol is more lipid soluble than atenolol and has greater passage across the blood-brain barrier as compared to atenolol. Consequently, metoprolol may have greater CNS effects (dizziness, depression, sleep disturbances) than atenolol. Although fewer CNS effects occur with atenolol, the clinical implications in neonates and young infants are unclear. Metoprolol is metabolized more rapidly than atenolol and has a shorter plasma elimination half-life. Extended release preparations of metoprolol are available but are difficult to use in infants and small children consequent to inflexibility in the dosage form to permit weight-based (i.e., mg/kg) dosing. Atenolol has the advantage of requiring only once or twice daily administration because of a longer elimination half-life (8 to 10 hours). Flexibility in oral dosing of atenolol for young infants and children can be achieved via the extemporaneous formulation of a liquid preparation.

Carvedilol

Carvedilol is a third-generation β -adrenergic receptor blocker that blocks β_1 -, β_2 -, and α_1 -adrenergic receptors. In addition, it exhibits antioxidant, anti-inflammatory, and antiapoptotic activities. Results from a randomized controlled trial of carvedilol therapy in children with heart failure failed to show a beneficial effect of the drug on a composite measure of heart failure outcomes (83). However, event rates were lower than expected, the study population was heterogeneous, and the trial may have been underpowered. Furthermore, the improvement rate among placebo-treated patients was higher than predicted, and trough carvedilol concentrations in the blood were lower than expected (based on adult studies). Additionally, the high proportion of infants and toddlers may have impacted the overall results as this age group tends to have higher spontaneous improvement rates. Additional studies are necessary to define the potential role of carvedilol (and other β -adrenergic receptor blockers) in managing children with heart failure.

PROSTAGLANDIN E_1

Prostaglandin E_1 (PGE_1) is used to dilate the ductus arteriosus in newborns dependent upon a patent ductus arteriosus to maintain either pulmonary or systemic blood flow or to improve mixing (e.g., d-transposition of the great arteries). The common indications for PGE_1 therapy include pulmonary atresia, critical pulmonary stenosis, transposition of the great arteries, coarctation of the aorta, interrupted aortic arch, critical aortic stenosis, and hypoplastic left heart syndrome. Administration of PGE_1 should be strongly considered very early in the management of infants in whom a ductus-dependent cardiac defect is considered as part of the differential diagnosis, especially for infants with possible congenital heart disease born at a center without tertiary care cardiac services. In these cases, it is advisable to begin PGE_1 therapy before transport and continue the infusion until definitive delineation of the cardiac status can be accomplished. Early treatment can be lifesaving and conversely, withholding therapy can be disastrous if the ductus arteriosus closes in a patient with a ductus-dependent defect. Although not entirely benign, the potential benefits of PGE_1 administration outweigh its risks in this condition.

PGE_1 has a short half-life and must be given by continuous intravascular infusion. Because these infants are critically dependent upon the infusion for maintaining ductus patency, a reliable intravenous line is essential. Thus, the use of a central venous (umbilical venous) catheter is recommended whenever possible. Although the intravenous route is preferred, it can be given via an umbilical arterial catheter. The short elimination half-life of PGE_1 also results in rapid termination of effect when infusions are discontinued in infants found not to have ductus-dependent heart lesions. In addition to relaxing the ductus arteriosus, PGE_1 dilates the systemic and pulmonary vascular beds and may thereby cause hypotension. If the blood pressure falls, reduction of the rate of infusion is generally sufficient to restore the blood pressure. Another potentially serious adverse effect is apnea. Administration of a high dose or an inadvertent bolus of PGE_1 will likely induce apnea. Thus, whenever PGE_1 is administered, personnel and equipment necessary to support ventilation must be available. Infusion pumps with a continuous action should be used and the intravenous line containing the drug must not be flushed. Additional side effects include fever, irritability, edema, and cutaneous flushing.

ANTIARRHYTHMIC DRUGS

In contrast to older children and adults in whom catheter ablation has decreased the need for pharmacologic management of arrhythmias, drug therapy remains important in infants and young children because of the technical difficulties associated with ablation and device placement in this age group. Pharmacokinetics differ in infants compared to older children, and developmental changes in ion channels and the autonomic nervous system affect the responses to these agents. Despite these considerations, there is a paucity of information in young children from prospective trials and therapeutic approaches are extrapolated from studies in adults. Several antiarrhythmic agents are available, but only the most commonly used drugs in the pediatric population are presented in this chapter. Additional information on antiarrhythmic drugs is available in Chapter 18.

Children receiving antiarrhythmic agents must be monitored carefully because many of these agents have variable potential to produce arrhythmias (i.e., proarrhythmic effects) other than those being treated. Serial ECG examinations are helpful in evaluating changes in response to various agents that may be proarrhythmic. For those agents with defined serum concentration-effect profiles, therapeutic drug monitoring is recommended during their use to facilitate safe and effective treatment. It should be noted that while proarrhythmic effects are likely to occur soon after initiation of treatment, late effects for most drugs have been reported. The Vaughan Williams classification of antiarrhythmic medications describes antiarrhythmic actions and is used traditionally (84). However, the therapeutic utility of this classification scheme is somewhat limited from a clinical standpoint because several drugs have more than one effect, antiarrhythmic actions do not always correlate with efficacy, and some useful agents such as adenosine do not fit into this classification (85).

Class I Agents

A common feature of Class I antiarrhythmic agents is blockade of sodium channels. These drugs are further subclassified on the basis of other electrophysiologic effects.

Class IA (Procainamide)

The IA drugs decrease the upstroke velocity of the action potential by blocking sodium channels. This slows conduction

time in the atrial and ventricular muscle cells, His-Purkinje cells, and accessory atrioventricular pathways and decreases automaticity. These agents also block potassium channels. The PR interval is prolonged, the QRS duration is increased, and the QTc interval is prolonged. These agents are contraindicated in patients with long QT syndrome and should not be used with other drugs such as amiodarone that also prolong the QTc interval. While oral administration is common for chronic use of procainamide in adults, the drug is usually administered by the intravenous route in pediatric patients with careful monitoring of infusion-related hypotension. Procainamide can also cause mild depression of myocardial contractile function. The drug is also biotransformed via the polymorphically expressed enzyme *N*-acetyltransferase to *N*-acetylprocainamide (NAPA), an active moiety with Class III properties. The risk of proarrhythmia, especially *torsade de pointes*, is moderate and not related to serum drug concentrations.

Class IB (Lidocaine, Mexiletine, Phenytoin)

These drugs shorten action potential duration and the refractory period primarily in Purkinje fibers and in ventricular myocytes producing a decrease in automaticity. Cells in the sinoatrial and atrioventricular nodes and autonomic tone are minimally affected. The ECG may show a slight decrease in the QTc interval. Proarrhythmic effects are relatively uncommon with these agents. Lidocaine, the prototypical agent of this class, is given intravenously. High plasma concentrations are associated with depressed myocardial function and toxicity often causes drowsiness, disorientation, muscle twitching, and seizures. Mexiletine is available for oral administration and is used in some forms of congenital long QT syndrome because of its effects on sodium channels. Phenytoin is used rarely and is generally restricted to the treatment of ventricular arrhythmias associated with toxicity from digoxin and tricyclic antidepressant agents.

Class IC (Flecainide, Propafenone)

These agents markedly decrease the upstroke velocity of the action potential and decrease conduction. The PR interval is prolonged and QRS duration increases. Flecainide is a particularly effective inhibitor of abnormal automaticity and reentry within atrial and ventricular muscle and in accessory atrioventricular pathways. It has been used successfully to treat various arrhythmias including supraventricular tachycardia, persistent junctional reciprocating tachycardia, and ventricular tachycardia. The relatively high incidence of proarrhythmia, especially *torsade de pointes*, limits the use of flecainide in patients with structural heart disease. Flecainide is useful for treating infants with supraventricular tachycardia and structurally normal hearts who do not respond to β -adrenergic blocking agents and digoxin.

Propafenone blocks sodium channels but also has β -blocking effects and is a weak calcium channel antagonist. It is effective in controlling reentrant and automatic tachycardias but should be used with caution in patients with structural heart disease because of the risk of proarrhythmia.

Class II (Propranolol, Atenolol, Esmolol)

Drugs in this class are β -adrenergic blocking agents and have been discussed above in this chapter. These drugs indirectly decrease automaticity and slow atrioventricular conduction by virtue of blocking the effects of catecholamines. The slowing of AV conduction and suppression of premature beats that may initiate a reentrant circuit explain the efficacy of these agents in treating reentrant tachycardias.

Class III (Amiodarone, Sotalol)

Class III drugs block potassium channels and prolong the plateau of the action potential, but action potential upstroke velocity is not affected.

Amiodarone has broad and complex pharmacologic effects (86). In addition to blocking potassium channels, it also inhibits sodium and calcium channels. Action potential duration is increased and the effective refractory period is prolonged in atrial and ventricular muscle, Purkinje fibers, and accessory AV pathways. Amiodarone also has α - and β -blocking properties but does not depress myocardial function despite its decreasing automaticity. Changes in the ECG include sinus slowing, prolongation of the PR interval, minimal widening of the QRS complex, and prolongation of the QTc interval. Proarrhythmic responses are infrequent. Amiodarone has the potential to produce adverse reactions in multiple systems that include corneal microdeposits, hyper- or hypothyroidism, pulmonary interstitial fibrosis, hepatitis, peripheral neuropathy, and a slate-blue discoloration of the skin. These adverse reactions seem to be less common in pediatric patients than in adults. Baseline hepatic, renal, and thyroid function tests, ophthalmologic examination, and pulmonary function tests should be obtained before starting long-term therapy and then repeated every 6 months as long as the patient is taking amiodarone. Amiodarone can be administered intravenously for the acute management of a variety of arrhythmias in pediatric patients (86,87) and by this route, may cause hypotension. Amiodarone interacts with digoxin, phenytoin, and warfarin and the doses of these medications should be appropriately decreased and closely monitored when amiodarone is coadministered. Dronedarone is a newer derivative of amiodarone that appears to have a more favorable safety profile (88), but this drug remains to be studied in the pediatric population.

Sotalol is a nonselective β -adrenergic blocking agent at low doses but shows Class III activity at higher doses. The QTc interval increases in a dose-dependent manner. *Torsade de pointes* occurs in up to 10% of pediatric patients, usually within a few days of starting therapy. Close monitoring of the QTc interval on the ECG is recommended. Sotalol should not be administered with other drugs such as procainamide that also prolong the QTc interval.

Class IV (Calcium Channel Blockers)

Calcium channel antagonists are reviewed above in this chapter. Calcium channel blockers prolong refractoriness and conduction time. Dihydropyridines have much less effect on electrophysiologic properties and are not used for treating arrhythmias. Phenylalkylamines (e.g., verapamil) and benzothiazepines (e.g., diltiazem) are effective in managing supraventricular tachycardia and some forms of ventricular tachycardia, such as that originating from the right ventricular outflow tract. Administration of intravenous verapamil is contraindicated in patients <1 year of age because of the risk of precipitating cardiovascular collapse.

Digoxin

As denoted previously in this chapter, digoxin decreases action potential duration and effective refractory period. Additionally, digoxin increases vagal tone causing slowing of sinus node rate and decreased atrioventricular node conduction. The ECG shows sinus slowing, prolongation of the PR interval, mild depression of the ST segment, and mild flattening of T waves.

Digoxin is used primarily for its effect to inhibit atrioventricular conduction and is therefore used to decrease the rate

of ventricular response in atrial fibrillation, ectopic atrial tachycardia, and other refractory supraventricular tachycardias. Digoxin is also effective in all reentrant arrhythmias in which the atrioventricular node is involved in the reentrant circuit. However, digoxin should not be used on an outpatient basis in patients with Wolff-Parkinson-White syndrome because it may shorten the effective refractory period of the accessory pathway and thus allow very rapid ventricular response rates in patients with atrial fibrillation or flutter.

Adenosine

Adenosine is an endogenous nucleoside that is considered as first-line medical therapy to terminate supraventricular tachycardia by blocking conduction through the atrioventricular node (89). Adenosine has a very short elimination half-life and thus, it is administered as a rapid intravenous bolus injection. This will convert most reentrant tachycardias to sinus rhythm. The most common reason for failure of adenosine to convert a patient to sinus rhythm is probably poor administration technique (not given as a rapid bolus). If adenosine is not effective after three doses or it is effective but the tachycardia recurs immediately, there is no reason to continue repeating the dose. If adenosine does not terminate tachycardia, other modalities should be considered because the tachycardia may not involve the atrioventricular node. Adenosine administration may be diagnostic in that the transient induction of atrioventricular block allows flutter waves or P waves consistent with ectopic atrial tachycardia to be seen more easily on the ECG.

CONCLUSIONS

The effective pharmacotherapy of cardiac disease and disorders in pediatric patients requires not only drug selection based on the pharmacologic properties of a given drug but also consideration of how ontogeny can influence both the drug's pharmacokinetics and pharmacodynamics. While data pertaining to drug action in adults can be used to predict drug action in an infant or child, this may not be true for drug disposition given that the maturation of multiple pathways that contribute to drug clearance may not develop in synchrony. Employing the "tools" of clinical pharmacology such as therapeutic drug monitoring (i.e., to assess dose-concentration-effect relationships) and pharmacogenetics (i.e., to predict, based on genotype-phenotype relationships, increased likelihood for sub- or suprathreshold response with conventional drug dosing regimens) can do much to improve the safety and efficacy of cardiovascular drug treatment in pediatric patients.

REFERENCES

- Neville KA. Pediatric pharmacokinetics. In: Ritschel WA, Kearns GL, eds. *Handbook of Basic Pharmacokinetics...Including Clinical Applications*. 7th ed. Washington, DC: American Pharmacists Association, 2009: 263-278.
- Ritschel WA, Kearns GL. Definitions and nomenclature. In: Ritschel WA, Kearns GL, eds. *Handbook of Basic Pharmacokinetics...Including Clinical Applications*. 7th ed. Washington, DC: American Pharmacists Association, 2009:1-10.
- Zhao W, Fakhoury M, Jacqz-Aigrain E. Developmental pharmacogenetics of immunosuppressants in pediatric organ transplantation. *Ther Drug Monit* 2010;32:688-699.
- Kearns GL, Abdel-Rahman SM, Alander SW, et al. Developmental pharmacology—drug disposition, action, and therapy in infants and children. *N Engl J Med* 2003;349:1157-1167.
- Johnson TN, Rostami-Hodjegan A. Resurgence in the use of physiologically based pharmacokinetic models in pediatric clinical pharmacology: parallel shift in incorporating the knowledge of biological elements and increased applicability to drug development and clinical practice. *Pediatr Anesth* 2011;21:291-301.
- Neely MN, Rakhmanina NY. Pharmacokinetic optimization of antiretroviral therapy in children and adolescents. *Clin Pharmacokinet* 2011;50:143-189.
- Neville KA, Blake MJ, Reed MD, et al. Pediatric pharmacology. In: Waldman SA, Terzic A, eds. *Pharmacology and Therapeutics: Principles to Practice*. Philadelphia, PA: Saunders-Elsevier, 2010:239-250.
- Lowry JA, Jones BL, Sandritter T, et al. Principles of drug therapy. In: Kliegman RM, Stanton B, St. Geme J, Schor N, Behrman RE, eds. *Nelson Textbook of Pediatrics*. 19th ed. Philadelphia, PA: Saunders-Elsevier, 2011 (published June 2011).
- Kendrick JG, Carr RR, Ensom MHH. Pharmacokinetics and drug dosing in obese children. *J Pediatr Pharmacol Ther* 2010;15:94-109.
- Hines RN. The ontogeny of drug metabolism enzymes and implications for adverse effects. *Pharmacol Ther* 2008;118:250-267.
- Hines RN, McCarver DG. The ontogeny of human drug-metabolizing enzymes: phase I oxidative enzymes. *J Pharmacol Exp Ther* 2002;300:355-360.
- McCarver DG, Hines RN. The ontogeny of human drug-metabolizing enzymes: phase II conjugation enzymes and regulatory mechanisms. *J Pharmacol Exp Ther* 2002;300:361-366.
- Hines RN. Ontogeny of human hepatic cytochromes P450. *J Biochem Mol Toxicol* 2007;21:169-175.
- Strassburg CP, Strassburg A, Kneip S, et al. Developmental aspects of human hepatic glucuronidation in young children and adults. *Gut* 2002;50:259-265.
- Knibbe CA, Kerkels EH, van den Anker JN, et al. Morphine glucuronidation in preterm neonates, infants, and children younger than 3 years. *Clin Pharmacokinet* 2009;48:371-385.
- Kearns GL, Leeder JS, Gaedigk A. Impact of the CYP2C19*17 allele on the pharmacokinetics of omeprazole and pantoprazole in children: evidence for a differential effect. *Drug Metab Dispos* 2010;38:894-897.
- Swen JJ, Nijenhuis M, de Boer A, et al. Pharmacogenetics: from bench to byte—an update of guidelines. *Clin Pharmacol Ther* 2011;89:662-673.
- Visscher H, Amstutz U, Sistonen J, et al. Pharmacogenomics of cardiovascular drugs and adverse effects in paediatrics. *J Cardiovasc Pharmacol* 2011; epub ahead of print (April 2011).
- Johnson TN, Thomson M. Intestinal metabolism and transport of drugs in children: the effects of age and disease. *J Pediatr Gastroenterol Nutr* 2008;47:3-10.
- Johnson TN, Rostami-Hodjegan A. Resurgence in the use of physiologically based pharmacokinetic models in pediatric clinical pharmacology: parallel shift in incorporating the knowledge of biological elements and increased applicability to drug development and clinical practice. *Pediatr Anesth* 2011;21:291-301.
- Robillard J, Fuillery E, Petershack J. Renal function during fetal life. In: Barratt TM, Avner ED, Harmon WE, eds. *Pediatric Nephrology*. Baltimore, MD: Lippincott Williams & Wilkins, 1999:21-37.
- Arant BS Jr. Developmental patterns of renal functional maturation compared in the human neonate. *J Pediatr* 1978;92:705-712.
- van den Anker JN, Schoemaker RC, Hop WC, et al. Ceftazidime pharmacokinetics in preterm infants: effects of renal function and gestational age. *Clin Pharmacol Ther* 1995;58:650-659.
- Steinberg C, Notterman DA. Pharmacokinetics of cardiovascular drugs in children. Inotropes and vasopressors. *Clin Pharmacokinet* 1994;27:345-367.
- Wells TG, Young RA, Kearns GL. Age-related differences in digoxin toxicity and its treatment. *Drug Saf* 1992;7:135-151.
- Davies MW, Cartwright DW. Gentamicin dosage intervals in neonates: longer dosage interval—less toxicity. *J Paediatr Child Health* 1998;34:577-580.
- van den Anker JN, Hop WC, de Groot R, et al. Effects of prenatal exposure to betamethasone and indomethacin on the glomerular filtration rate in the preterm infant. *Pediatr Res* 1994;36:578-581.
- Mulla H. Understanding developmental pharmacodynamics: importance for drug development and clinical practice. *Pediatr Drugs* 2010;12:223-233.
- Marshall JD, Kearns GL. Developmental pharmacodynamics of cyclosporine. *Clin Pharmacol Ther* 1999;66:66-75.
- Laer S, Elshoff J-P, Meibohm B, et al. Development of a safe and effective pediatric dosing regimen for sotalol based on population pharmacokinetics and pharmacodynamics in children with supraventricular tachycardia. *Pediatr Cardiol* 2005;46:1322-1330.
- Bryant AE, Dreifuss FD. Valproic acid hepatic fatalities. III. U.S. experience since 1986. *Neurology* 1996;46:465-469.
- deWildt SN, de Hoog M, Vinks AA, et al. Pharmacodynamics of midazolam in pediatric intensive care patient. *Ther Drug Monit* 2005;27:98-102.
- Massicotte P, Leaker M, Marzinotto V, et al. Enhanced thrombin regulation during warfarin therapy in children compared to adults. *Thromb Haemost* 1998;80:570-574.
- Takahashi H, Ishikawa S, Nomoto S, et al. Developmental changes in pharmacokinetics and pharmacodynamics of warfarin enantiomers in Japanese children. *Clin Pharmacol Ther* 2000;68:541-555.
- Neville KA, Becker ML, Goldman JL, et al. Developmental pharmacogenomics. *Pediatr Anesth* 2011;21:255-265.

36. Blake MJ, Abdel-Rahman SM, Pearce RE, et al. Effect of diet on the development of drug metabolism by cytochrome P-450 enzymes in healthy infants. *Pediatr Res* 2006;60:717–723.
37. Blake MJ, Gaedigk AG, Pearce RE, et al. Ontogeny of dextromethorphan O- and N-demethylation in the first year of life. *Clin Pharmacol Ther* 2007;81:510–516.
38. <http://www.fda.gov/Drugs/ScienceResearch/ResearchAreas/Pharmacogenetics/ucm083378.htm>; accessed 14 December 2010
39. Becker ML, Leeder JS. Identifying genomic and developmental causes of adverse drug reactions in children. *Pharmacogenomics* 2010;11:1591–1602.
40. Gaedigk A, Simon SD, Pearce RE, et al. The CYP2D6 activity score: translating genotype information into a qualitative measure of phenotype. *Clin Pharmacol Ther* 2008;83:234–242.
41. Holford N. Dosing in children. *Clin Pharmacol Ther* 2010;87:367–370.
42. Ward RM, Tammara B, Sullivan SE, et al. Single-dose, multiple-dose and population pharmacokinetics of pantoprazole in neonates and preterm infants with a clinical diagnosis of gastroesophageal reflux disease (GERD). *Eur J Clin Pharmacol* 2010;66:555–561.
43. Ward RM, Kearns GL, Tammara B, et al. A multi-center, randomized, open-label, pharmacokinetics and safety study of pantoprazole tablets in children and adolescents aged 6 through 16 years of age with gastroesophageal reflux disease. *J Clin Pharmacol* 2011;51:876–887.
44. Koukouritaki SB, Manro JR, Marsh SA, et al. Developmental expression of human hepatic CYP2C9 and CYP2C19. *J Pharmacol Exp Ther* 2004;308:965–974.
45. Taketomo CK, Hodding JH, Kraus DM. *Pediatric Dosage Handbook*. 17th ed. Hudson, OH: Lexi-Comp, Inc., 2010.
46. Hougren TJ. Digitalis use in children: an uncertain future. *Prog Pediatr Cardiol* 2000;12:37–43.
47. Latifi S, Lidsky K, Blumer JL. Pharmacology of inotropic agents in infants and children. *Prog Pediatr Cardiol* 2000;12:57–79.
48. Shekerdemian L. Perioperative manipulation of the circulation in children with congenital heart disease. *Heart* 2009;95:1286–1296.
49. Artman M. *Developmental Changes in Myocardial Inotropic Responsiveness*. Austin, TX: R. G. Landes Company, 1994.
50. Kuznetsov V, Pak E, Robinson RB, et al. β_2 -Adrenergic receptor actions in neonatal and adult rat ventricular myocytes. *Circ Res* 1995;76:40–52.
51. Collis L, Srivastava S, Coetzee WA, et al. β_2 -adrenergic receptor agonists stimulate L-type calcium current independent of PKA in newborn rabbit ventricular myocytes. *Am J Physiol Heart Circ Physiol* 2007;293:H2826–H2835.
52. Zaritsky A, Chernow B. Use of catecholamines in pediatrics. *J Pediatr* 1984;105:341–350.
53. Ward RM, Lugo RA. Cardiovascular drugs for the newborn. *Clin Perinatol* 2005;32:979–997.
54. Evans JR, Short BL, Van Meurs K, et al. Cardiovascular support in preterm infants. *Clin Ther* 2006;28:1366–1384.
55. Costello JM, Thiagarajan RR, Dionne RE, et al. Initial experience with fenoldopam after cardiac surgery in neonates with an insufficient response to conventional diuretics. *Pediatr Crit Care Med* 2006;7:28–33.
56. Ricci Z, Stazi GV, Di Chiara L, et al. Fenoldopam in newborn patients undergoing cardiopulmonary bypass: controlled clinical trial. *Interact Cardiovasc Thorac Surg* 2008;7:1049–1053.
57. Chang AC, Atz AM, Wernovsky G, et al. Milrinone: systemic and pulmonary hemodynamic effects in neonates after cardiac surgery. *Crit Care Med* 1995;23:1907–1914.
58. Hoffman TM, Wernovsky G, Atz AM, et al. Prophylactic intravenous use of milrinone after cardiac operation in pediatrics (PRIMACORP) study. *Am Heart J* 2002;143:15–21.
59. Rosenthal D, Chrisant MRK, Edens E, et al. International society for heart and lung transplantation: practice guidelines for management of heart failure in children. *J Heart Lung Transplant* 2004;23:1313–1333.
60. Turanlahti M, Boldt T, Palkama T, et al. Pharmacokinetics of levosimendan in pediatric patients evaluated for cardiac surgery. *Pediatr Crit Care Med* 2004;5:457–462.
61. Egan JR, Clarke AJB, Williams S, et al. Levosimendan for low cardiac output: a pediatric experience. *J Intensive Care Med* 2006;21:183–187.
62. Namachivayam P, Crossland DS, Butt WW, et al. Early experience with levosimendan in children with ventricular dysfunction. *Pediatr Crit Care Med* 2006;7:445–448.
63. Lowrie L. Diuretic therapy of heart failure in infants and children. *Prog Pediatr Cardiol* 2000;12:45–55.
64. Grenier MA, Fioravanti J, Truesdell SC, et al. Angiotensin-converting enzyme inhibitor therapy for ventricular dysfunction in infants, children and adolescents: a review. *Prog Pediatr Cardiol* 2000;12:91–111.
65. Balaguru D, Auslender M. Vasodilators in the treatment of pediatric heart failure. *Prog Pediatr Cardiol* 2000;12:81–90.
66. Neonatal Inhaled Nitric Oxide Study Group. Inhaled nitric oxide in full-term and nearly full-term infants with hypoxic respiratory failure. *N Engl J Med* 1997;336:597–604.
67. Clark RH, Kueser TJ, Walker MW, et al. Low-dose nitric oxide therapy for persistent pulmonary hypertension of the newborn. *N Engl J Med* 2000;342:469–474.
68. Steinhorn RH, Kinsella JP, Pierce C, et al. Intravenous sildenafil in the treatment of neonates with persistent pulmonary hypertension. *J Pediatr* 2009;155:841–847.
69. Baquero H, Soliz A, Neira F, et al. Oral sildenafil in infants with persistent pulmonary hypertension of the newborn: a pilot randomized blinded study. *Pediatrics* 2006;117:1077–1083.
70. Balaguru D, Artman M, Auslender M. Management of heart failure in children. *Curr Probl Pediatr* 2000;30:5–30.
71. Shaddy R, Wernovsky G, eds. *Pediatric Heart Failure*. Boca Raton, FL: Taylor & Francis Group, 2005.
72. Vijayaraghavan K, Deedwania P. Renin-angiotensin-aldosterone blockade for cardiovascular disease prevention. *Cardiol Clin* 2011;29:137–156.
73. Spurney CE, Sali A, Guerron AD, et al. Losartan decreases cardiac muscle fibrosis and improves cardiac function in dystrophin-deficient mdx mice. *J Cardiovasc Pharmacol Ther* 2011;16:87–95.
74. Holm TM, Habashi JR, Doyle JJ, et al. Noncanonical TGF β signaling contributes to aortic aneurysm progression in Marfan syndrome mice. *Science* 2011;332:358–361.
75. Jacob MS, Tang HW. Aldosterone-receptor antagonists in heart failure: insights after EMPHASIS-HF. *Curr Heart Fail Rep* 2011;8:7–13.
76. Mahle WT, Cuadrado AR, Kirshbom PM, et al. Nesiritide in infants and children with congestive heart failure. *Pediatr Crit Care Med* 2005;6:543–546.
77. Jeffries JL, Denfield SW, Price JF, et al. A prospective evaluation of nesiritide in the treatment of pediatric heart failure. *Pediatr Cardiol* 2006;27:402–407.
78. Shih JL, Agus MSD. Thyroid function in the critically ill newborn and child. *Curr Opin Pediatr* 2009;21:536–540.
79. Lechner E, Hofer A, Mair R, et al. Arginine-vasopressin in neonates with vasodilatory shock after cardiopulmonary bypass. *Eur J Pediatr* 2007;166:1221–1227.
80. Jerath N, Frndova H, McCrindle BW, et al. Clinical impact of vasopressin infusion on hemodynamics, liver and renal function in pediatric patients. *Intensive Care Med* 2008;34:1274–1280.
81. Lopez-Sendon J, Swedberg K, McMurray J, et al. Task force on beta-blockers of the European Society of Cardiology. Expert consensus document on beta-adrenergic receptor blockers. *Eur Heart J* 2004;25:1342–1362.
82. Weir MR. β -blockers in the treatment of hypertension: are there clinically relevant differences? *Postgrad Med* 2009;121:90–98.
83. Shaddy RE, Boucek MM, Hsu DT, et al. Carvedilol for children and adolescents with heart failure: a randomized controlled trial. *JAMA* 2007;298:1171–1179.
84. Vaughn Williams EM. Classifying antiarrhythmic actions: by facts or speculation. *J Clin Pharmacol* 1992;32:964–977.
85. Members of the Sicilian Gambit. New approaches to antiarrhythmic therapy: emerging therapeutic applications of the cell biology of cardiac arrhythmias. *Cardiovasc Res* 2001;52:345–360.
86. Lane RD, Nguyen K-T, Niemann JT, et al. Amiodarone for the emergency care of children. *Pediatr Emerg Care* 2010;26:382–393.
87. Saul JP, Scott WA, Brown S, et al. Intravenous amiodarone for incessant tachyarrhythmias in children: a randomized, double-blind, antiarrhythmic drug trial. *Circulation* 2005;112:3470–3477.
88. Oyetayo OO, Rogers CE, Hofmann PO. Dronedarone: a new antiarrhythmic agent. *Pharmacotherapy* 2010;30:904–915.
89. Manole MD, Saladino RA. Emergency department management of the pediatric patient with supraventricular tachycardia. *Pediatr Emerg Care* 2007;23:176–185.
90. Artman M, Mahony L, Teitel DF. *Neonatal Cardiology*, 2nd ed. New York, NY: McGraw-Hill Companies, Inc., 2011.

INDEX

Note: Page numbers followed by “f” refer to figures; page numbers followed by “t” refer to tables.

A

- Abdomen
 - child assessment and, 91
 - visceral anatomy, 1197f
- Abdominal aorta
 - anatomic specimen, atherosclerosis, 1515f
 - truncus arteriosus, 994
- Abdominal pain, RF and, 1314
- Abdominal situs (Sidedness), 36, 37f, 38f
 - Down syndrome, 706
 - morphology, 146, 147f
 - transducer and cardiac position, 145, 146f
- Abdominal situs ambiguus, 1195
 - with asplenia, 1195
 - liver and, 1195
 - midline apex of heart, 34
 - treatment, 1211–1212
- Abdominal situs solitus, 1195
 - of atria, 1182f
 - dextrocardia and, 1195
 - subcostal transverse view, 146f
- Abernethy malformation, agitated saline contrast and, 164
- Aberrant right subclavian artery, 760–763, 761f, 762f
 - diagnosis and management, 762–763
 - embryology, 761–762, 761f, 762f
- Ablation, 419f, 424–426, 425f
 - catheter manipulation, 421
 - catheter projections for, 406f
 - 3-D mapping systems, 405
 - left cardiac sympathetic denervation, 395
 - sedation and anesthesia, 401
 - WPW syndrome, 417
- Ablation catheter, manipulation, 421
- Abnormal left aortic arch, 760–766
- Abnormal origin of right coronary artery from inappropriate sinus, 747–748
 - pathology and clinical features, 748–749
- Abnormal systemic venous connection, 840–861
- Abnormal vascular communications, closure of, 327–329
- ABO-incompatible heart transplantation, 1387–1388
- Absence of pulmonary artery, unilateral, 996
- Absent ductus venosus, 856, 856f
- Absent pulmonary valve, PDA, 731–732
- Absent right superior vena cava, in visceroatrial situs solitus, 849–850
- Absolute bioavailability (F), 1661
- Absorption, drugs, 1661
- Accelerated ventricular rhythm, 453, 453f
- Accessory pathway-mediated tachycardia, 444–446, 445f
- Accessory pathways
 - elimination, results, 418
 - location of, PJRT and, 448
 - Mahaim fibers, 448
 - mapping, 421
 - WPW syndrome, 446–447
- ACE inhibitors (Angiotensin-converting enzyme inhibitors), 479, 1678
 - acquired heart disease, childhood/adolescence, 1567, 1571
 - clinical trial, children with heart failure, 1572
 - congenital aortic stenosis, 1033
 - DCM and, 1243
 - decrease LV systolic function, 1572
 - Duchenne muscular dystrophy, 1279–1283
 - HLHS, 1080
 - hypertension, 1542
 - during pregnancy, 601
 - RCM and, 1274
 - RV dysfunction, arterial switch for d-TGA, 1484
- Acetylcholine (ACH), parasympathetic activity, 63–64
- Acetylene helium rebreathing techniques, cardiac output, measurement techniques, 129–131, 130f
- ACH. *See* Acetylcholine
- ACHD. *See* Adult congenital heart disease
- Acoustic impedance, ultrasound and, 135
- Acquired AV block, bundle branch block and, 466
- Acquired coronary disease, SCD and, 110–113
- Acquired heart disease
 - childhood/adolescence, 1565–1567
 - primary referral diagnosis, 208t
- Acquired hemolytic anemia, 1591
- “Acquired” pulmonary arterial malformations, 792–794
- Acrocyanosis
 - cyanosis and clubbing, 86
 - infants and, heart disease and, 82–83
- ACS. *See* Antenatal corticosteroid
- ACT. *See* Activated clotting time
- ACTA-2 gene mutation
 - bicuspid aortic valve, 804
- Actin
 - microfilaments and, 56–57, 57f
- Action potential durations (APDs), 364
- Action potentials, ventricular specialized conduction system, newborn v. adult dog, 367f
- Activated clotting time (ACT), balloon aortic valvuloplasty and, 317
- Activities of daily living, 94
 - aortic coarctation, 102
 - aortic stenosis, 100
 - atherosclerotic CAD, 111–112
 - bicuspid aortic valve, 101
 - congenital coronary anomalies, 110
 - congenitally corrected transposition of the great arteries, 106
 - D-transposition of the great arteries, 105
 - Ebstein anomaly, 104
 - heart transplantation, 109
 - hypertrophic cardiomyopathy, 112
 - Kawasaki disease, 111
 - pulmonary hypertension, 108
 - pulmonary stenosis, 102
 - shunt lesion, 99
 - single ventricle physiology, 106
 - systemic hypertension, 113
 - tetralogy of fallot, 104
- Activity restriction, congenital heart disease and, 94
- Acute carditis, surgery, 1321
- Acute hypoxia, experimental studies of, 1412
- Acute hypoxic vasoconstriction, pulmonary hypertension, 1412
- Acute Kawasaki disease, treatment, 1296–1297
- Acute pericarditis, 1350–1354, 1351f, 1352f, 1353f, 1354f
- Acute rheumatic carditis
 - medical management, 1320
 - treatment, 1319, 1319f
- Acute rheumatic fever, medical management, 1310f, 1320–1321
- Acute transmural ischemia, 1378
- Acute vasodilator drug testing, response to, 1440
- Acyanotic heart disease, 1582
- Acyclovir, CMV and, 1393
- Adenine nucleotide translocator (ANT), 1258
- Adenosine, 458–459, 1682
 - fetal pulmonary vascular resistance, 74
- Adenosine triphosphate (ATP)
 - electron transport chain enzyme defects, DNA and, 1228
 - fetal pulmonary vascular resistance, 74
 - intracardiac study and, 407
 - myosin and, 57–58
 - sarcolemma and, 54–55
- Adenovirus
 - genes of, 1260, 1260f
 - myocarditis, 1247
 - positive v. negative, PCR, 1247f
- Adjudication, quality control implementation in clinical trial, 1651, 1651t
- Adjunctive therapies, HLHS and, 1073
- ADO. *See* Amplatzer duct occluder
- Adolescent and young adult cardiac clinic, 1489–1490
- Adolescents
 - aorta and, 19
 - cardiovascular disease, 1517
 - chest pain, 1509–1512
 - percentage distribution, 1511t
 - drug disposition in, developmental changes, 1664f
 - myocarditis and, clinical manifestations in, 1248
 - patient history, 83–84
- Adrenal insufficiency
 - PCICU, 522
- Adult congenital heart disease (ACHD), 1463, 1464f
 - cardiac catheterization volume, 1466f
 - complications and cardiac abnormalities, 1465f
 - MRI/CT volume, 1466f
 - pediatric to, 1463, 1464f
- Aerobic power, 119–121
- Afterload, 66
 - reduction, HLHS and, 1076
 - systolic function and, 64
- Afterload-reducing agents
 - RCM and, 1274
- Agency for Healthcare Research and Quality (AHRQ), 1634
- Agitated saline contrast echocardiography
 - principle, 164
 - right-to-left intrapulmonary shunt and, 164
 - technique and indications for, 164
- Air trapping, CHD and, 247
- Airway
 - management, 502–506
 - resistance, pulmonary edema and, 477
 - suctioning, infant and, 504
- Airway malacia, CHD and, 253, 254f
- Alagille's syndrome, 618, 622t, 630–631, 630f, 928, 1579
- Alcohol
 - blood pressure and, 1539
 - congenital heart defects and, 602
 - pregnancy and, 1502
- Alcohol septal ablation, HCM and, 1232
- Aliasing, 138
 - VEC MRI, 223
- ALLHAT study, hypertension, 1542
- Allograft rejection, pediatric heart transplantation, 1390
- α-Adrenergic receptor antagonists, 1677
- α-ANP. *See* Alpha-atrial natriuretic peptide
- Alpha-adrenergic agonists
 - peripheral circulation, 78
- Alpha-adrenergic blockade, Qp/Qs, 1076, 1078
- Alpha-atrial natriuretic peptide (α-ANP), 1238, 1281
- Alpha-MHC gene, 58
- Alpha-stat strategy, cardiopulmonary bypass, 532

- Alternating electrical current, fatality and, 557–558
- Alveolar capillary dysplasia, lung micrographs, 1418, 1418f
- Ambiguous atrioventricular connections, 44
- Ambulatory blood pressure, monitoring, 1532
- Ambulatory Holter monitoring
- athletic screening and
 - arrhythmias, 110
 - cardiomyopathy, 113
 - ccTGA, 106
 - Ebstein anomaly, 104
 - pulmonary stenosis, 102
 - single ventricle physiology, 106
- Amikacin, gram-negative bacterial endocarditis, 1373
- ϵ -Aminocaproic acid (EACA), excessive fibrinolysis and, 509, 535
- Amiodarone, 1681
- arrhythmias, 456–458, 499
 - catecholamine-sensitive ventricular tachycardia, pregnancy and, 1503
 - junctional ectopic tachycardia, 430
 - during pregnancy, arrhythmias, 1503
 - sudden cardiac death, 1230
- A-mode ultrasound, MIT and, 134
- Amoxicillin, endocarditis, 1324
- AMP-activated protein kinase (PRKAG2), HCM and, 1225
- Amphotericin B, fungal endocarditis, 1373
- Ampicillin
- gram-negative bacterial endocarditis, 1373
 - streptococcal endocarditis, 1372, 1373
- Amplatzer
- atrial septal occluder, ASD closure and, 1472
 - cribriform septal occluder, multifenestrated ASDs and, 290
 - membranous VSD occluder, 289, 290f, 291
 - muscular VSD occluder, 291
 - vascular plug, congenital cardiac lesions and, 291
- Amplatzer duct occluder (ADO), 290f, 291–292
- Amplatzer patent foramen ovale occluder (PFO occluder), 289, 290f
- Amplatzer septal occluder (ASO)
- ASD closure, 318–321
 - closure of Fontan's fenestration and, 322, 327f
 - secundum ASDs closure, 684–685
 - septal defects occlusion, 289, 290, 290f
- Amrinone, 1242
- Amyl nitrite, myocardial contractility, 1224
- ANA test. *See* Antinuclear antibody
- Anaerobic organisms, endocarditis and, 1364, 1364t
- Anaerobic threshold, 120–121
- Analgesia, 516–518
- Anatomic correction, without coronary translocation, arterial switch, 1128–1132
- Anatomic injury, blunt cardiac injury, 552–553, 553t
- Anatomy, segmental approach, echocardiographic examination, 144–153
- Anemia
- acquired hemolytic, 1591
 - cardiac catheterization and, 285
 - with CHD, 1591
 - cyanotic adult, 1487
 - ejection murmurs and, 90
 - hemolysis, 1591
 - laboratory testing, 1590, 1590t
 - macrocytic, 1591
 - microcytic, 1590
 - normocytic, 1590–1591, 1591f
 - TGA and, 1113
- Anesthesia
- cardiac catheterization and, 258–259
 - CMR and, 208, 210, 210f
 - Duchenne muscular dystrophy, 1279
 - stage 1 palliation, HLHS and, 1075–1076
- Aneuploidy, 625–626
- Aneurysm(s). *See also* specific i.e. Ventricular aneurysm
- coarctation of the aorta, 805
 - complication of PDA, 732
 - Kawasaki disease, 110
 - of sinus of Valsalva, 755–756
- ANF. *See* Atrial natriuretic factor
- Angina, HCM, 1227
- Angiocardiography
- anomalous muscle bundles, 927
 - ccTGA and, 1155–1156, 1155f
 - isolated valvar pulmonary stenosis, 919–920, 919f
 - PAPVC, 821
 - PA-VSD and, 963–965
 - peripheral pulmonary arterial stenosis, 930
 - pulmonary atresia and intact ventricular septum, 948, 950f–952f
 - TGA and, 116–118
 - truncus arteriosus, 995–996
- Angiogenesis, coronary development, 61
- Angiogram, coarctation of aorta, 1047f, 1050–1051
- Angiography, 727
- aberrant right subclavian artery, 762
 - absent right superior vena cava, in viscerotransposition, 850, 850f
 - basic concepts of, 273
 - cardiac catheterization and, 258–286
 - cardiac tumors, 1551
 - common atrium, 699
 - complete atrioventricular septal defect, 705–706
 - double-lumen aortic arch, 782
 - PDA, 733–734
 - pulmonary arteriovenous malformations, 793
 - sinus of Valsalva aneurysms, 755–756
 - specific techniques, 279–283
 - subvalvular aortic stenosis, 1037f
 - systemic arterial malformations, 790
 - univentricular atrioventricular connection, 1189–1192
- Angiosarcoma, 1560
- Angiotensin II, postnatal peripheral circulation and, 76
- Angiotensin-converting enzyme inhibitors. *See* ACE inhibitors
- Angiotensin-receptor blockers (ARBs), 1678
- aortic root dilation, 802
 - diabetes and, hypertension, 1542
 - heart failure and, 1573
- Angled-tip catheters, balloon valvuloplasty, 920
- Animal models
- DNA mutations and, 560
 - fetal sheep study, 649
 - high frequency ultrasound, 167
 - isolated valvar pulmonary stenosis, 913
 - valve development, 569
- Animal research
- CMR and, 210, 219, 227
 - research echocardiography and, 166–167, 166f
 - valve development, 569
- Annular dilation, valvular aortic stenosis and, 1025
- Annular overriding, 48, 48f, 50
- Anomalies of aortic arch, CMR and, 230–233
- Anomalous coronaries, imaging, 974
- Anomalous incorporation of common pulmonary vein into left atrium, 812
- Anomalous left coronary artery from pulmonary artery, 749–752, 751f
- angiography, 751
 - cardiac catheterization, 751
 - clinical features, 750, 818
 - electrocardiography, 750
 - natural history, 751
 - noninvasive imaging, 751
 - pathology, 750
 - pathophysiology, 749–750, 751f
 - treatment, 751–752
 - TTE and, 1382
- Anomalous mitral arcade, 1008, 1009f
- Anomalous muscle bundles, 925
- physiology, 926
 - right ventricular obstruction, 925–927, 925–928, 926f, 927f
- Anomalous origin of left coronary arterial branches, from right sinus of Valsalva, 747, 748f
- Anomalous origin of pulmonary artery from ascending aorta, 786
- from right pulmonary artery, 786–787
 - imaging, 787f
- Anomalous origin of right coronary arterial branches, from left sinus of Valsalva, 747, 748f, 749f
- Anomalous pulmonary venous connection, 809
- clinical features, 818–819
- Anomalous pulmonary venous drainage to right atrium, heart and lungs, 811f
- Anomalous termination of umbilical veins, and absent ductus venosus, 858–859, 859f
- Anomalous venous channel, pulmonary venous drainage and, 822–833
- Anomalous venous vessels, microscopic anatomy, 827
- Antedromic SVT, 445, 445f
- Antegrade catheter, patent ductus arteriosus, 284, 284f
- Antegrade volumes, Doppler, 142
- Antenatal corticosteroid (ACS) administration, 475
- Antepartum, heart disease and, 1497t, 1502
- Anterior bridging leaflet, complete atrioventricular septal defect, 702f
- Anterior cardinal veins, 843f
- Anterior mitral leaflet prolapse, RF heart disease and, 1313f
- Anthracyclines, RCM and, 1269
- Antiarrhythmic drugs, 1680–1682
- DCM and, 1244
 - fetus, 664
 - intracardiac study and, 415
 - QT interval, 384
 - transesophageal electrophysiologic study, 415
- Antibiotic prophylaxis
- asplenia syndrome and, 1212
 - pulmonary arterial stenosis, 935
 - prosthetic valve endocarditis, 1373–1374
 - therapy
 - vegetation formation, IE and, 1365
- Anticoagulation
- pulmonary arterial hypertension (PAH), 1450
 - therapy
 - IE and, 1374
 - during pregnancy, management, 1503
 - prosthetic heart valves, pregnancy outcomes, 1503
- Anticoagulation clinics, INR and, 1450
- Antidepressants, congenital heart defects and, 601
- Antiepileptic drugs, congenital heart defects and, 600
- Antihypertensive drugs
- hypertension in children, 1540t–1541t
 - indications for, 1540t
 - severe hypertension, 1542, 1542t
- Anti-inflammatory therapy
- acute KD, 1297
 - acute RF, 1320
 - acute rheumatic fever, 1310t, 1320
 - arthritis, 1311
 - aspirin, 1296
- Antimicrobial prophylaxis, asplenia syndrome and, 1212
- Antimicrobial therapy, IE and, 1369–1371
- Antinuclear antibody (ANA) test, 1331, 1439
- Antioxidants, cardiopulmonary bypass, 532
- Antiphospholipid antibody test, SLE and, 1337
- Antiplatelet drugs, arterial thrombosis, 1599t, 1601
- Aorta, 41. *See also* Ascending aorta
- anatomy, 19–20
 - divisions of, 19, 19f
 - echocardiography, 147, 147f
 - imaging views, 279, 279f
 - position, 1196, 1197f
 - pressure tracings, 1026f
 - transesophageal echocardiography, 154
- Aortic anastomosis, postoperative measurements, 1135, 1135f
- Aortic aneurysm
- CMR and, 233, 234f
 - COA and, 1469–1471
 - coarctation repair, 1057, 1057f, 1058f

- Aortic annular dimension, assessment, 152
- Aortic arch, 19–20, 730f
 suprasternal notch view, HLHS on, 1067, 1068f
 tetralogy of Fallot, 974
 univentricular atrioventricular connection, 1192
- Aortic arch anomalies, 758–796
 anatomical classifications, 758–796
 clinical classification, 759–760
 diagnostic methods, 759
 embryology, 758–759
 22q11 deletion syndrome, 627–628
 TGA and, 1148
- Aortic arch arteries, development, cardiac neural crest, 567, 567f
- Aortic arch hypoplasia
 in PCICU, 513
 transposition type DORV, 1165
- Aortic arch system, anomalies of, 786–788
- Aortic atresia, HLHS and, 1063
- Aortic balloon dilation, balloon aortic valvuloplasty and, 299
- Aortic balloon valvuloplasty, congenital heart disease, prenatal treatment of, 656
- Aortic coarctation
 exercise and, 101–102
 postangioplasty, MDCT and, 255f
 severity evaluation, 232f
- Aortic dissection
 coarctation repair, 1057
 pregnancy and, 1500, 1504
- Aortic insufficiency
 PDA, 732
 truncus arteriosus, 999
- Aortic insufficiency jet, Doppler, 140
- Aortic regurgitant murmurs, 89
 rheumatic carditis, 1311
- Aortic regurgitation, 1035
 balloon aortic valvuloplasty and, 297, 299
 chronic rheumatic heart disease, 1316–1317
 rheumatic carditis, 1311–1312
 subvalvular aortic stenosis, 1036–1038
- Aortic root
 anomalies, structural heart disease, 746–756
 dilation
 bicuspid aortic valve, 1467
 Turner syndrome, 626
 Tetralogy of Fallot, 984
- Aortic sac, 567
- Aortic sinuses, nomenclature of, 1100, 1101f
- Aortic stenosis, 1023–1039
 chronic rheumatic heart disease, 1318
 congenitally bicuspid aortic valve, 1467
 exercise test, 100
 left ventricle and, 14, 15
 maternal risk and, 1500
 with patent mitral valve, HLHS and, 1063, 1063f
 response to exercise, 100
- Aortic valve
 anatomy, 1024f
 CHD and, 572
 commissure, 17
 disease
 coarctation repair, 1057
 joint study, 1467
 LAO views, 275, 277f
 normal, 1024, 1024f
 pulmonary atresia and intact ventricular septum, 941
 RAO views, 275, 277f, 278f
 regurgitation, 1467
 truncus arteriosus, 992
 replacement, 1033
 BAV and, 1467
 truncus arteriosus correction and, 999f
- Aortic valve areas
 calculation of, congenital aortic stenosis, 1030, 1031f
 Gorlin formula, 272, 272t
- Aortic valve atresia, TGA and, 1148
- Aortic valve flow (AVF)
 calculation of, congenital aortic stenosis, 1031
 Gorlin formula, 272t
- Aortic valve insufficiency, 185
- Aortic-left ventricular tunnel, 754–755, 754f
- Aorticopulmonary window, truncus arteriosus *v.*, 996
- Aortogram, PDA and, 325
- Aortography
 cardiac catheterization, 948
 great vessel injury, 555
 patent ductus arteriosus occlusion, 326
 pulmonary atresia and intact ventricular septum, 948
- Aortopathy, in congenital heart disease, 801, 801f
- Aortopulmonary collaterals, 153
 obstructed pulmonary flow and, 283–285, 284f–285f
 tetralogy of Fallot, 974
- Aortopulmonary shunt
 pulmonary artery pressure, 1408
 thrombosis, 1598, 1600
 tricuspid atresia, 879
- Aortopulmonary window, 740–743
 cardiac catheterization, 741
 clinical features, 741
 diagnosis, 741, 743
 ECG features, 741
 echocardiographic feature, 741, 742f
 pathology, 740–741, 741f
 radiologic features, 741
 treatment of, 743
 truncus arteriosus, 994
- Apgar scores, preoperative patient and, 1581
- Apical direction, 33–34
- Apical four-chamber view, ECG, 1066, 1067f
- Apical window, 140
- APOE genotype, 1581
- Apolipoproteins, 1519t
 functions, 1519
 nephrotic syndrome, 1522
- Apoptosis
 cardiac development, 62
 myocarditis and, 1259–1260
- Aprotinin, cardiopulmonary bypass, 532, 535
- Arch coarctation, 153
- Arch hypoplasia, 153
 complete TGA and, 1106
 Pediatric Cardiac Intensive Care, 513
 transposition type DORV, 1165
- Arch interruption, 153
- Area under the curve (AUC), 1661, 1662f
- Arrhythmias, 1602. *See also* specific *i.e.*
 Ventricular arrhythmias
 cardiac catheterization, 285
 CCTGA, 1485–1486
 d-TGA, 1479–1481
 Fontan and, HLHS, 1086
 Fontan patient and, 1487–1488
 intrapericardial teratomas, 1559
 modified Fontan operation, 880
 myocarditis, 1262–1263
 in PCICU
 diagnosis, 499, 499f
 etiology and incidence, 498–499
 prevention and treatment, 499–500, 500t
 during pregnancy, management, 1503
 pulmonary stenosis and, 923
 rhabdomyomas and, 1553
 SCD and exercise, 113
 surgical treatment, 908
 TAPVC, postoperative course, 832–833
 treatment, 456–460
- Arrhythmic drugs, transesophageal electrophysiologic study, 290
- Arrhythmogenic right ventricular cardiomyopathy (ARVC)
 pre-athletic screening, 97
 SCD, in youth, 389, 390f
- Arterial access, cardiac catheterization and, 259
- Arterial blood gases
 TGA and, 1109
- Arterial blood oxygen saturation, oximetry and, 131
- Arterial blood pressure
 blood flow, 69, 654, 666f
- Arterial carbon dioxide tension (PCO₂), 1581
- Arterial desaturation, exercise, 127
- Arterial mean pressures, pulmonary atresia and intact ventricular septum, 947
- Arterial pulses, coarctation of aorta, 1048
- Arterial saturation (SaO₂), 1069
 range of, 1069f
- Arterial shunt, pulmonary atresia and intact ventricular septum, 951, 952
- Arterial switch operation (ASO), 805–806, 1128–1135. *See also* Neonatal arterial switch repair
 anatomic challenges, 1128f, 1131
 baffle obstructions and, d-TGA, 1481–1484
 cardiac malpositions, 1208
 d-transposition of great arteries, 1479
 effects of exercise, 104, 105
 results and sequelae of, 1132–1135
 supravulvar narrowing, 1132, 1135f
 surgical technique of, 1129f–1131f
 TGA/LVOTO, 1132
- Arterial-venous oxygen saturation, cardiac catheterization and, 262
- Arteriovenous communication, PDA, 731
- Arteriovenous malformations (AVMs), 90
- Arteriovenous saturations, parallel circulation and, 1065f, 1069
- Arthritis, RF, 1310, 1310t
- Artifact
 ECG and, 129
 pressure measurements and, 263
- Atrioventricular valve, size and function
 As low as reasonably achievable (ALARA) protocol, 249–250
- Ascending aorta
 HLHS and, 1063
 positions of, 43, 44f
 pulse pressure in, 263
- Ascending aortic aneurysms, truncus arteriosus, 991
- Aschoff nodule, RF and, 1306
- Aspirin
 acute rheumatic fever, 1310t, 1320–1321
- Asplenia, 36, 38f, 1205–1207, 1207f
 isomerism and, 34
 liver and, 1195
 TAPVC, 823
- Asplenia syndrome, 1196
 septicemia and, 1212
- Asthma, 1511
 chest pain, 1509
- Asystole, lightning-related injury, 558
- Atenolol, 457, 1680
 HCM and, 1229
- Atherosclerosis, 1514–1519
 abdominal aorta, anatomic specimen, 1515f
 blood pressure and, 1528
 imaging, 1514, 1515
 possible risk factors, 1516t
 risk factors, 1516–1519
- Atherosclerotic coronary artery disease
 exercise and SCD, 111–112
- Athletes
 ECG and, 386
 heart, 1227, 1227f
 valvuloplasty, 100, 104
- Athletic screening
 diagnostic testing, 95–98
- Athletics
 congenital cardiovascular disease, 93
- Atresia
 of common pulmonary vein, 833
 of coronary ostium, 752
 of right atrial ostium of coronary sinus, 860
 treatment and prognosis, 833
 univentricular atrioventricular connection, 1175
- Atria, 39, 40f
 abdominal situs solitus, 1182f
 comparison, 8f, 9–10, 10t
 positions of, 42
 venous return and, 146–149
- Atrial appendages
 anatomy, 1200f
- Atrial arrhythmias
 ASD, 685–686
 TAPVC, postoperative course, 833
- Atrial chambers
 fetal cardiovascular system and, 656
 normal, 646
- Atrial dilation, ASD, 9

- Atrial ectopic tachycardia (AET), 448–449
- Atrial fibrillation, 429–430, 450–451, 451f
chronic rheumatic heart disease, 1316
heart disease, 429–430
WPW, 447, 447f
- Atrial flutter
heart disease, 429–430
neonatal, 450, 451f
- Atrial hypertrophy, 377, 377f
- Atrial myxomas, 1556
pathognomonic finding, 1557
- Atrial natriuretic factor (ANF), 350
- Atrial natriuretic peptide (ANP), 76, 1567
- Atrial refractory period, 416
- Atrial rhythm, bradycardias, 662
- Atrial septal anatomy, subcostal view, HLHS on, 1066–1067, 1068f
- Atrial septal aneurysm (ASA), 687
- Atrial septal defects (ASD)
atrial dilation, 9
closure
in infancy, 319, 323
results, 319–321, 324f, 325f
CMR and, 229
echocardiogram and, 162, 163f
electrocardiographic/electrophysiologic features, 677–678
GATA4 mutation, 635
genetic and environmental risk factors, 672–673
genetic causes, 570–571
incidence, 672
isolated valvar pulmonary stenosis, 916
natural history of, 683
NKX2.5 gene, 635
pathogenesis and anatomic features, 672–673, 673f–676f
PA-VSD and, 961
physical examination, 677
response to exercise, 99, 683
survival curves, 1472, 1472f
TGA and, 1121–1122
transcatheter closure of, 316–322
transcatheter devices for, 289
valvar pulmonary stenosis *v.*, 920
- Atrial septostomy, 1454–1455
- Atrial septum, 8–9, 8f
Doppler, 142
echocardiogram and, 147–148, 162
pulmonary atresia and intact ventricular septum, 940–941
TEE, 162
transcatheter device, transesophageal echocardiography, 162, 163f
- Atrial situs, 1210, 1211f
abnormalities, 1196–1200, 1199t
cardiac malpositions, 1202–1203
- Atrial switch operation
inferior vena caval obstruction, 1123, 1127f, 1128f
Mustard technique, 1123, 1124, 1125f
postoperative
CMR of, 215, 236–237, 237f
results and sequelae of, 1122–1128
Senning repair, 1122, 1124f
sinus rhythm, 1479
- Atrial tachycardia
rhabdomyositis and, 1552
- Atrial transposition, fetal heart, 647, 650f
- Atrioventricular block
complete, 463–465, 463f
fetus, 657, 661
first degree, 462, 462f
myocarditis, 1248, 1249f
NKX2.5 gene
second-degree, 462–463, 463f
- Atrioventricular canal defect, coarctation of aorta, 1044
- Atrioventricular (AV) conduction, 377, 1201
atrial septal defects, 672–673
disorders, 461–466
- Atrioventricular conduction system (ACS), 354–357, 357f–360f
- Atrioventricular connections
50% rule and, 1178 f
- cardiac malpositions, echocardiographic feature, 1198t, 1210, 1213f
echocardiography and, 145t, 149–150
modes of, 44, 46f
normal *v.* discordant, 1200–1201
univentricular atrioventricular connection, cineangiography, 1176–1178
- Atrioventricular discordance
TGA and, 1147
- Atrioventricular (AV) node
anatomy, 441, 442f
modification, 426–428, 428f
- Atrioventricular override, ccTGA and, 1152
- Atrioventricular septal defect (AVSD), 1471–1472
anatomic features, 691, 692f, 692t
demographics, 691
3-dimensional echocardiography, 161f
Down syndrome, 625
embryogenesis, 691–692, 693f–694f
exercise and, 99
imaging, 277, 278f
maternal risk and, 1498
in PCICU, 513
surgical repair, 691
Tetralogy of Fallot, 976
trisomy 21 and, 617
- Atrioventricular septum (AVS)
left-right asymmetry and, 565–567, 567f
- Atrioventricular (AV) straddling, 1201
- Atrioventricular valve(s), 10–12, 1181f
abnormalities, 1179f
antegrade Doppler, 142
atrioventricular valve insufficiency, 188
ccTGA and, 1150
insufficiency, 188
mitral/ tricuspid stenosis, 187–188, 187f
morphology, 39–40, 40f
quantitative morphometric evaluation, 186–187, 186f, 187f
septal structures, 149
- Atropine
intracardiac study and, 408
- Attention deficit hyperactivity disorder (ADHD), 1618
- Auscultation, 88
coarctation of aorta, 1049
dynamic, 91
equipment for, 85
isolated valvar pulmonary stenosis, 920, 920f
- Austin-Flint murmur, 90
- Autoimmune myocarditis, nitric oxide expression and, 1258
- Autoimmunity, myocarditis, 1258
- Automaticity, tachyarrhythmia, 441
- Autonomic nervous system, E-C coupling, 63
- Autopsy, tricuspid stenosis, 886
- Autopsy-negative sudden unexplained death, 391
- Autoregulation
cerebral blood flow and, postnatal peripheral circulation, 77
postnatal peripheral circulation, 76–77
- AV nodal physiology, 367
- AV ring bundles, 348
- Axial resolution, SPL and, 135–136, 136f
- Axial-flow VAD, for children, 540
- Axis deviation, 377–378
- Azathioprine, pediatric heart transplantation, 1389, 1391
- Azithromycin, endocarditis, 1322
- Azygos veins
interrupted IVC and, 855, 855f
normal development, 842f, 843–844, 845f
- B**
- Back, child assessment and, 91
- Bacteremia, IE and, 1365
- Bacterial endocarditis
ASD, 686
coarctation repair, 1057
prophylaxis
congenital aortic stenosis, 1039
supravalvular aortic stenosis, 1039
pulmonary valve stenosis, 924
- Bacterial myocarditis, 1255
- Bacterial pericarditis, 1354–1355, 1355t
- Bactericidal antibiotic therapy, vegetation formation, IE and, 1369–1370
- Baffles operation, TGA and, 1121
- Baffle leaks
arterial switch operation, 1483f
device closure, 1483, 1484f
transthoracic echocardiography, 1482, 1483f
- Baffle obstructions
d-TGA, 1483f
- Balke treadmill protocol, 128t
- Balloon angioplasty
coarctation and, 304–305
coarctation of aorta, 1054
for native coarctation, 1054
peripheral pulmonary arterial stenosis, 932–933
complications, 933
primary stenting *v.* coarctation and, 305
recurrent postoperative coarctation, 1053
right ventricular angiogram, 932, 933f
supravalvular pulmonary stenosis, 1132
- Balloon atrial septostomy (BAS), 294–295, 295, 296f
follow-up study, 1121–1122, 1121f
pulmonary atresia and intact ventricular septum, 947
TAPVC, 831
TGA, 1116, 1116f, 1118–1119
- Balloon catheter
LSVC, 279, 281f
- Balloon dilation
supravalvular aortic stenosis, 1039
- Balloon mitral valvuloplasty (BMVP), 295, 303
- Balloon valvuloplasty
aortic stenosis, 100
aortic valve disease, 1467
chronic rheumatic mitral stenosis, 1321
congenital aortic stenosis, 1034
pulmonary valve stenosis, 102
RE, 1320
technique, pulmonary stenosis and, 920–925, 921f
- Balloon-annulus ratio, 921
- Balloon-expandable intravascular stents
baffle obstructions and, 1482
complications, 934
peripheral pulmonary arterial stenosis, 933–935, 934f
ventricular-to-aortic pressure ratio, 934
- Balloon-in-balloon (BIB) catheter, 289
- Balloon-occlusion angiography, systemic venous drainage, 279, 281f
- Balloon-occlusion aortogram, antegrade catheter, 284, 285f
- Barrier methods, CHD and, 1504
- Barth syndrome, 1593
- Basal lamina, 53
- Base-apex of heart
axis, 33–34, 33f, 34f
ventricles and, 42
- Baseline drift, pressure measurements and, 263
- Basement membrane, cardiac fibroblasts, 53
- Basis of Aliasing equation, 138, 139f
- Basis of Image Generation equation, echocardiography and, 135, 135f
- Basis of Image Resolution equation
part I, 135–136, 136f
part II, 136–137, 136f
- Basis of Temporal Resolution equation, 137, 137f
- Baylis radiofrequency puncture generator, perforation of atretic pulmonary valve and, 301, 302
- B-cell alloantigen, GAS pharyngitis, 1306
- Becker muscular dystrophy (BMD), 1260, 1283–1284
anesthesia, 1279
Duchenne muscular dystrophy, 1279
- Beck's triad, cardiac tamponade, 553
- Bedrest, viral pericarditis, 1354
- Benzathine penicillin G
rheumatic fever, 1323, 1323t
streptococcal pharyngitis, 1322, 1323t
- Benzodiazepine
afterload reduction and, HLHS and, 1076
- Berlin heart VAD, 540

- Bernard-Soulier syndrome, 1594
 Bernoulli effect, heart murmurs and, 89
 Bernoulli equation, 138–139
 congenital aortic stenosis, 1029
 Beta adrenergic antagonists, 497
 Beta blockade with propranolol, acquired heart disease, childhood/adolescence, 1571
 Beta-adrenergic agonists, 1078
 HCM and, 1229
 peripheral circulation, 78
 β -adrenergic receptor blockers, 1679–1680
 Beta-blockade
 aortic root dilation, 802
 BAV disease, 804
 Beta-blockers (Beta-adrenergic receptor blockers)
 catecholamine-sensitive ventricular tachycardia, pregnancy and, 1503
 DCM, 1243
 hypertension, 1542
 myocardial contractility, 1224
 pediatric heart failure and, 1573–1574
 RCM and, 1274
 trial studying, 1573, 1573t
 Beta-mimetic agents, pregnant women, 666
 Beta-myosin heavy chain, HCM and, 1224
 Bethesda conference report
 aortic stenosis, 100
 atherosclerotic CAD, 112
 atrial septal defect, 99
 heart transplantation, 109
 Kawasaki disease, 111
 Bicuspid aortic valve (BAV)
 ACTA-2 gene mutation, 804
 aortic dilation, 804
 aortic root dilation, 1467
 CMR, 1468f
 diagnosis, 804
 eNOs deficiency, 804
 FBN1 synthesis defect, 803–804
 histologic abnormalities, 803, 803f
 Notch homolog 1 gene, 804
 prevalence, 802
 therapy, 804
 Bicuspid aortic valves, exercise and, 101
 Bidirectional cavopulmonary connection, in PCICU, 513–514, 514f, 514t
 Bidirectional cavopulmonary shunt, univentricular atrioventricular connection, 1193
 Bidirectional Glenn
 anastomosis, tricuspid atresia, 884
 shunt, HLHS, 1082, 1082f
 tricuspid atresia, 882
 Bidirectional glenn anastomosis, 1600
 Bifascicular block, QRS complex, 380, 380f
 Bilateral conal relationship, 151
 Bilateral inferior venae cavae, 856, 856f
 Bilateral persistence of subarterial conus, double-outlet RV, 151
 Bilateral superior venae cavae
 with normal drainage to right atrium, 845–853
 with unroofed coronary sinus
 clinical manifestations, 848–849
 diagnostic features, 849
 Bilateral trilobed lungs, 36
 Bilaterally deficient subarterial conus, 151
 Bile acid binding agents, elevated LDL cholesterol and, 1526–1527
 Bioequivalence, drug, 1662
 Biologic materials, CMR and, 210
 Biomarkers
 in children, heart failure, 1567–1570
 anthracycline treatment, 1570
 BNP and NT-proBNP, cardiac disease, 1568t
 congenital heart disease, 1570
 evaluation and management of, 1568, 1570t
 heart transplant, 1570
 natriuretic peptide level, children, 1567, 1568t
 pulmonary hypertension, 1570
 PDA, 727
 Biplane fluoroscopy, intracardiac technique, 421
 Biplane Simpson's method, echocardiography, 172–173, 173f
 Bipolar recording system, transesophageal technique, 412, 413f
 Births
 central circulation, 69
 history, 84
 pulmonary atresia and intact ventricular septum, 949
 transitional circulation, 72
 valves of sinus venosus and, 860
 vascular resistance, 73f
 weight, blood pressure and, 1528
 Bisoprolol, heart failure and, 1573
 Biventricular circulation, rehabilitation of branch pulmonary artery stenosis, 307–308
 Biventricular heart, imaging of, 274–277, 276f
 Biventricular hypertrophy (BVH), 382–383
 truncus arteriosus, 992
 Biventricular pacing, 468
 Blade atrial septostomy, 295, 296f
 Blade catheters, 295
 Blade septostomy, 295
 Blalock-Hanlon operation
 TGA and, 1121, 1122f
 Blalock-Thomas-Taussig shunt, 87
 Bernoulli equation, 139
 PA-VSD and, 962
 TOF, 1476–1479
 tricuspid atresia, 879
 Blinding, clinical trial, 1646
 Blood
 cultures
 endocarditis and, 1364
 IE and, 1367
 oxygen in, 266–267, 267f
 Blood cysts, 10
 Blood flow
 analysis, VEC MRI sequence and, 223–225
 atrioventricular valves, 10
 changes at birth, 73f
 coronary development, 62
 measurements, VEC MRI
 accuracy of, 225
 clinical applications, 225–226, 226f
 physical determinants of, 69, 655
 placental circulation, 654, 655f
 Blood oxygen concentration, cerebral blood flow, postnatal peripheral circulation, 77
 Blood pressure
 birth weight and, 1528
 boys
 age and height percentile, 1531t–1532t
 age specific, 1533f
 cuff bladder, adolescents, 1534
 elevation, 1527
 exercise and, 129, 129f
 girls, age specific, 1533f
 measurement, 85, 1534
 cardiovascular response to exercise, 123–124, 123f, 124f
 normal, 1529, 1529t–1532t
 first year of life, 1534t
 supravalvular aortic stenosis, 1038
 values, classification of, 1529, 1534t
 Blood stream, in PCICU, 522
 Blood volume, pregnancy, 1494
 Blunt trauma
 brachiocephalic arteries, 555
 cardiac, 552–556
 mechanisms of, 552, 553t
 types of, 552–553, 553t
 chest, heart valve injury and, 555
 Bmp2, cardiac valve and, 568
 BMPR2 mutation, PAH, 1439–1440
 BNP levels decrease, term and preterm infant, 727
 Body mass index (BMI)
 blood pressure and, 1528
 hypertension, 1537
 obesity in childhood, 1518
 Body surface area (BSA), 172
 Body surface mapping, 373–374
 Body weight, VO_2 max and, 120
 Bogalusa study
 atherosclerosis, 1514
 hypertension, target organ effects, 1528–1529
 obesity in childhood, 1518
 Bohr equation, 118–119, 129
 Bone morphogenetic proteins (BMPs), 1440
 Bonhoeffer-Medtronic valve, 288
 Brachial pulses, assessment, 87
 Brachiocephalic arteries
 bifurcation, echocardiography, 153, 153f
 blunt trauma and, 555
 persistent fifth aortic arch, 782
 Bradycardias
 atrioventricular block, 461–465
 bundle branch block, 465–466, 466f
 complete AV block and, 662
 d-TGA, 1480
 fetus, 662
 sinus, 460–461, 460f
 sinus node dysfunction, 461, 461t
 Bradykinin, fetal pulmonary vascular resistance, 74
 Brain abscesses, TGA and, 1113
 Brain anatomy, pathology and neuroimaging, 1579–1580
 Brain injury/death
 cardiopulmonary bypass, postoperative factors, 1582
 pediatric heart transplantation, 1388
 Branch pulmonary artery
 assessment, 152
 banding, HLHS and, 1075
 PAPVC and, 829
 multiplane TEE, 156f
 stenosis, arterial switch operation, 1132
 Branch vessels, echocardiography, 153, 153f
 Breath-by-breath measurement, ventilatory indices, 121
 Breathing patterns
 child inspection, 86
 infants and, heart disease and, 83
 Bridge to cardiac transplantation
 ECMO and, 534, 536
 VADs and, 540
 Bridge to recovery, pediatric ECMO, 535
 “Bright blood” imaging, CMR and, 213–214, 214f
 Brockenbrough needle, radiofrequency energy ν , 296–297
 Bronchial anatomy, normal, 1199, 1200f
 Bronchomalacia, CHD and, 247
 Bronchopulmonary collateral circulation, TGA and, 1107–1109
 Bronchopulmonary dysplasia (BPD), 1447–1448, 1448f
 in premature infants, prevention of, 475
 Bruce treadmill protocol, 127–128, 128t
 Brugada syndrome, 55, 396–397, 397f
 athletic screening and, 95
 Bruits, 89
 B-type natriuretic peptide (BNP), 498, 727, 1281, 1567
 Bulk flow, SV and, 124
 Bumetanide, 1243, 1676
 Bundle branch block (BBB), 465–466, 466f
 myocardial ischemia, 1378, 1379f
 QRS and, 378
 Burns, lightning-related injury, 558, 558t
 Busulfan, RCM and, 1269
 Buttoned device, 323
 C
 Ca^{2+} regulation, sarcoplasmic reticulum, 55–56, 56f
 Ca^{2+} channels, cardiac action potential, 55, 55f
 Cadherin, cell-cell interactions, 60
 Caffeine
 congenital heart defects and, 602
 intracardiac study and, 283
 Calcification
 valvular aortic stenosis and, 1023–1024
 Calcified human valves, 572
 Calcium, 492t, 494
 blood pressure and, 1539
 mature heart and, 56
 Na + Ca^{2+} , 55
 Calcium binding, troponin C, 57, 57f
 Calcium channel antagonists, 1677–1678
 Calcium channel blockers, 458, 1681
 pulmonary arterial hypertension (PAH), 1450, 1452
 RCM and, 1274

- Calcium imbalance, 385
- Calcium pump activity
 - dephosphorylated phospholamban, 56, 56f
- Calcium-induced calcium release, 62
- Calibration error, marker catheter, 274
- Calsequestrin, 62
- Camera, biventricular heart, 274
- cAMP (Cyclic adenosine monophosphate)
 - pulmonary vascular resistance, 73
- Capillary refill time, child assessment and, 87
- Captopril, 1243, 1678
- Carbon dioxide (CO₂), 1070
 - cerebral blood flow, postnatal peripheral circulation, 77
 - production, ventilation measurements, 131
- Carbon dioxide (CO₂) rebreathing, cardiac output, measurement techniques, 129
- Carcinoid disease of bowel, pulmonary stenosis and, 920
- Cardiac action potential, 55, 55f
- Cardiac anatomy, 1–30
- Cardiac anomalies, TAPVD and, 826
- Cardiac apex, transducer and, 145, 146f
- Cardiac arrest, 522
- Cardiac base, 17–18, 17f
- Cardiac base-apex axis, cardiac malpositions, 1195, 1196f, 1197f, 1210–1211
- Cardiac catheterization, 727, 733–734
 - angiography and, 258–286
 - anomalous left coronary artery from pulmonary artery, 751
 - anomalous muscle bundles, 926–927
 - aortopulmonary window, 741
 - atries of common pulmonary vein, 833
 - with balloon atrial septostomy, TGA and, 1113f, 1114–1116, 1116f
 - ccTGA and, 1154–1155
 - in children, complications, 410
 - coarctation of aorta, 1050–1051
 - common atrium, 699
 - complete atrioventricular septal defect, 705–706
 - complications, 285
 - congenital aortic stenosis, 1030–1031
 - cor triatriatum, 836
 - DCM, 1241–1242
 - Ebstein's anomaly, 896
 - ECMO and, 536, 537
 - hemodynamics of, isolated valvar pulmonary stenosis, 918–919
 - HLHS, 1084
 - imperforate valve, 947f
 - indications for, 258
 - isolated valvar pulmonary stenosis, 918
 - neurologic morbidity, 1582
 - partial atrioventricular septal defect, 699
 - PA-VSD and, 963–965
 - pericardial disease, 1353, 1354f
 - peripheral pulmonary arterial stenosis, 930–931, 930f
 - pulmonary arterial hypertension, 1437–1438
 - pulmonary arteriovenous malformations, 793
 - pulmonary atresia and intact ventricular septum, 946–948
 - RCM, 1272–1273, 1272f
 - RF and, 1315–1316
 - sinus of Valsalva aneurysms, 755–756
 - stenosis of individual pulmonary veins, 836
 - systemic arterial malformations, 790
 - techniques for, 258
 - therapeutic, 288–343
 - thrombosis, 1603
 - tricuspid atresia, 881–882
 - truncus arteriosus, 995–996
 - ventricular septal defects, 717–719, 718f
- Cardiac catheterization volume, ACHD, 1466f
- Cardiac chambers, morphogenesis of, 563–564, 563f
- Cardiac channelopathies
 - autosomal dominant long QT syndrome, 391–395
 - autosomal recessive LQTS, 395
 - Brugada syndrome, 396–397, 397f
 - catecholaminergic polymorphic ventricular tachycardia, 396
 - electrocardiographic features of, 391, 392f
 - SCD and exercise, 113
 - short QT syndrome, 395–396
- Cardiac computed tomography
 - CHD and
 - children with, 247–256
 - conclusions, 255
 - contrast enhancement, 248, 249f
 - indications for, 251–255
 - methods and technique, 247–251
 - sedation, 247–248
 - TTE and, 1382
- Cardiac concussion (Commotio cordis)
 - cardiac contusion *v.*, features differentiating, 553t
- Cardiac conduction system
 - anatomy, 349f
 - functional maturation development (*See* Functional maturation development)
- Cardiac contusion, cardiac concussion *v.*, features differentiating, 553t
- Cardiac crescent, 350
- Cardiac defects, teratogens, maternal exposure, 84, 84t
- Cardiac development
 - biology, 560
 - molecular determinants, 560–573
- Cardiac dilation, DCM and, 1235
- Cardiac diseases
 - congenital infections, 84
 - fetal risk and, 1496, 1497t
 - maternal long-term prognosis, pregnancy and, 1502
 - maternal risk and, 1496, 1497t
 - in offspring, 1502
 - women of childbearing age, 1495t
- Cardiac dysrhythmias
 - alternating electrical current, 557
 - RF energy, 955
- Cardiac electrophysiology, 362, 364f
 - electrical impulse, atrial myocardium, 363–364, 366f, 367f
 - heart pacemaking, 362–363, 365f
 - maturing AV conduction system, 364–367
 - VCS, developmental aspects, 367, 367f
- Cardiac embryogenesis, atrial septation and
- Cardiac examination
 - in infants, isolated valvar pulmonary stenosis, 916
 - normal pregnancy, 1496
- Cardiac fibroblast, extracellular matrix and, 52–53, 54f
- Cardiac gating, MRI and, 207–208, 210f, 211f
- Cardiac genetic pathways, 560
- Cardiac glycosides, 1672–1673
- Cardiac hemangiomas, 1559
- Cardiac herniation, 553
- Cardiac history, DMD and, 1279
- Cardiac hypertrophy, 1235
- Cardiac imaging, RF and, 1316
- Cardiac index, cardiac catheterization and, 262, 262f
- Cardiac intensive care, pediatric, 483–639
- Cardiac intervention, in premature neonate, 479–480
- Cardiac lesions, specific, genetics of, 636
- Cardiac lipomas, 1560
- Cardiac looping, 1200, 1201f
 - left-right asymmetry and, 565–567, 566f
- Cardiac malformations, adult consequences, 572
- Cardiac malpositions
 - Echocardiographic features, 1208–1211
 - segmental approach, 1208–1211
 - treatment, 1211–1212
- Cardiac mechanical support therapies, pediatrics, 530–543
- Cardiac morphogenesis
 - complex regulation, 565–570
 - left-right signaling and, 566f
 - region-specific, pathways regulating, 563f
- Cardiac MRI (Magnetic resonance imaging). *See also* Magnetic resonance imaging
 - CHD and, 1463
 - congenital aortic stenosis, 1030, 1030f
 - pulmonary artery stenosis, 1478, 1479f
 - TTE and, 1382
- Cardiac myocytes
 - cell-extracellular matrix interactions, 58, 59f
 - development and maturation, gap junction, 61
 - myocardial growth and remodeling, 62
 - Na⁺- and Ca²⁺-ATPases and exchangers, 54–55
 - plasma membrane, 54
 - sarcomere, 56, 57f
 - sarcoplasmic reticulum, 55–56, 56f
 - thick filaments, 57–58
 - thin filaments, 56–57, 57f
 - titin, 58
 - T-tubules, 56
 - Z-disks, 58
- Cardiac neural crest, aortic arch and, 567, 567f
- Cardiac outflow tract
 - chronic rheumatic heart disease, 1316–1319
 - regulation, 567–568, 567f
- Cardiac output, 93
 - antepartum issues, 1495t, 1506
 - cardiac catheterization and, 267–268, 267f, 268f, 269t
 - congenital aortic stenosis, 1031
 - determinants of, 489–490, 490f
 - exercise, 121, 121f
 - HLHS, 1069
 - isolated valvar pulmonary stenosis, 919
 - MRI and, 225, 226
 - myxomas, 1556
 - oxygen uptake *v.*, 121f
 - pregnancy, 1494
 - thermodilution, 487–488, 487t–488t
- Cardiac pathology, DMD and, 1279
- Cardiac patient, genetics evaluation and, 636–637
- Cardiac perforation, 285–286
- Cardiac precursors, transcriptional regulation of, 562–564, 563f
- Cardiac resynchronization therapy (CRT), 468, 1574
 - DCM and, 1244
- Cardiac rhythm
 - and conduction disorders, 441–469
 - ECG and, 378
- Cardiac rupture, 554
- Cardiac sarcoma, 1560
- Cardiac segments
 - anatomic features of, 1199t
 - connections of, 43–44, 46f–51f, 48, 50
 - positions of, 42–43, 43f–45f
 - right-sided *v.* left sided, comparison, 10t
 - segmental diagnosis and, 1195–1196
- Cardiac situs (Sidedness), 34, 35f
- Cardiac sounds, TAPVC, without pulmonary venous obstruction, 828
- Cardiac specimens, 1–30
 - examination of, 25–26, 28, 30
 - photography of, 28, 30
- Cardiac stem cell, regenerative approaches and, 572–573, 573f
- Cardiac surgeon, cardiac interventionalists, collaboration of, 336
- Cardiac surgery
 - IE and, 1373
 - during pregnancy, 1504
- Cardiac tamponade
 - pericardiocentesis, 1354
 - pulsus paradoxus, 1350
 - stab wound, 556
- Cardiac transplantation, 516
 - Ebstein's anomaly, 898–899
- Cardiac trauma, 552–558
- Cardiac troponin T, myocardial injury, 1379
- Cardiac tumors, 1549–1560
 - diagnostic procedures, 1550–1551
 - history of, 1549
 - incidence, 1549–1550
- Cardiac valve, formation, 568–570, 568f–570f
- Cardiac veins, anatomy, 746–747, 748f
- Cardio-cerebral-pulmonary circulation, 514f
- Cardiology databases, PICCU, 485
- Cardiomegaly
 - cyanotic neonate, 946t
- Cardiomyocyte differentiation
 - epigenetic factors
 - microRNA regulation
- Cardiomyocyte precursors, origin of

- Cardiomyopathy
 ECMO and, 536
 muscular dystrophy, 1284
 PCICU, 523
 pre-athletic screening, 97
 VADs and, 538
 Cardiopulmonary bypass (CPB), 530–533
 cerebral blood flow and, 1581
 children and, 530–531
 hypothermic circulatory arrest, in infants, 531
 left atrial drainage of right superior vena cava, 851
 management, HLHS and, 1076–1078
 MCSDs
 perioperative risk factors, 1580–1582
 postoperative bleeding, 1595–1596
 Cardiopulmonary exercise testing (CPET), PAH, 1436–1437
 Cardiopulmonary interactions, 476–477
 congenital heart disease, 547
 left heart, 548
 normal circulation, 546–547, 547f
 right heart, abnormal, 547–548, 548f
 Cardiopulmonary resuscitation (CPR)
 defibrillation, 460
 pediatric ECMO, 536–537
 Cardiorespiratory disease, postmortem arteriogram, 1410
 CardioSEAL septal occlusion system, 289, 321, 323
 Cardiothoracic ratio, 1, 2f
 Cardiovascular anatomy
 assessment, CMR and, 213
 SSFP and, 214
 Cardiovascular anomalies, classification and terminology, 32–51
 Cardiovascular diseases
 cigarette smoking, 1517–1518
 diabetes mellitus, 1517
 Cardiovascular drugs, 1672
 Cardiovascular examination, 86
 Cardiovascular function, pressure-volume loops and, 65–66
 Cardiovascular Profile Score, fetal heart and, 654f
 Cardiovascular reflexes, physiology of shock and, HLHS and, 1068–1069
 Cardiovascular system, 486–489
 Cardioversion, 459–460
 Carditis
 acquired heart disease, 1567
 RF and, 1311–1313
 Carey Coombs murmur, rheumatic carditis, 1313
 Carina, pulmonary situs, 1199
 Carney complex, myxomas, 1557
 Carnitine deficiency, DCM and, 1244
 Carotid pulse, HCM, 1226
 Cartesian system, axis deviation and, 378, 378f
 Carvedilol, 457, 1680
 heart failure and, 1573, 1574
 PRIMACORP, 1244
 CATCH 22, 759
 Catecholamine(s)
 cerebral blood flow, postnatal peripheral circulation, 77
 DCM, 1243
 infusions
 pediatric heart transplantation and, 1388
 peripheral circulation, 78
 Catecholaminergic polymorphic ventricular tachycardia (CPVT), 396
 Catecholamine-sensitive ventricular tachycardia, treatment, pregnancy and, 1503
 Catheter
 angiography and, 261, 261f
 manipulation, cardiac catheterization and, 261–262
 obstruction, artifact and, 263
 placement
 catheterization laboratory, intracardiac technique, 403, 403f
 transesophageal technique, 411–416, 412f, 413f, 414f, 416t
 Catheter ablation
 atrial flutter and fibrillation, 429
 3-D mapping technology, 407
 direct current, 418
 Ebstein's anomaly, 899
 ectopic atrial tachycardia, 428, 429
 electrode catheters, 405
 manipulation, 421
 permanent form of junctional reciprocating tachycardia, 426
 right anterior septal pathways, 423, 424f
 supraventricular arrhythmias, 448
 tachycardia-induced cardiomyopathy, 455
 Catheter device closure
 infants, children, and adults, treatment of PDA, 737, 738f, 740f
 preterm infant, treatment of PDA, 736, 737f
 Catheter embolization therapy, bronchopulmonary collateral circulation, TGA and, 1107, 1108f
 Catheter entrapment, artifact and, 263
 Catheter "flying" artifact and, 263
 Catheter-induced atrioventricular block, 285
 Catheter-induced damping, 308
 Catheterization laboratory (Cath lab)
 costs, 343
 intracardiac shunt and, 269
 PCICU and, 522–523
 personnel exposure, radiation dose, 274
 Catheterization of umbilical vein, anomalous termination of umbilical veins, and absent ductus venosus, 858
 Catheter-related infection
 in PCICU, 522
 Catheters, electrode, 405, 406f
 Causality, clinical trials, 1636–1637, 1639t
 Ceftriaxone
 gram-negative bacterial endocarditis, 1373
 streptococcal endocarditis, 1372
 Cell adhesion molecules (CAMs)
 dilated cardiomyopathy and, 1258–1259
 myocarditis and, 1259
 Cell-cell interactions
 cadherin, 60
 desmin, 60
 desmosomes, 60
 intercalated discs, 60
 Cell-extracellular matrix interactions
 costameres, 59
 Cell-mediated immunity, myocarditis, 1257
 Central cyanosis
 infants and, heart disease and, 82–83
 Central nervous system (CNS)
 balloon atrial septostomy, 1113
 genetic abnormalities, 1579
 hormonal milieu, 1582
 TGA and, 1112–1113
 Central palpation, 87–88
 Central pulmonary arteries
 angiography, 279, 280f
 hypoplastic, 965, 965f
 PA-VSD and, 960, 961, 964, 965f
 spin echo, 235
 Central shunts, fetal circulation, 69–70, 70f
 Central venous catheter-related bloodstream infection (CLABSI), 1634
 Central venous circulation, 69–71
 return, pattern of, 70, 71f
 Central venous oxygen saturation (ScvO₂), 486
 Central venous stent implantations, results, 312
 Centrifugal assist pump, 537–538
 circulation support and, 537–538
 Cephalosporin
 gram-negative bacterial endocarditis, 1373
 streptococcal pharyngitis, 1322, 1323t
 Cerebral atrophy, CHD and, 1580
 Cerebral blood flow
 cardiopulmonary bypass, 1582
 Cerebral circulation
 postnatal peripheral circulation, 77–78
 Cerebral dysgenesis, fetal cerebrovascular flow, 1579
 Cerebral protection, cardiopulmonary bypass, 532–533
 Cerebral saturation, Norwood palliation, HLHS and, 1078f
 Cerebrovascular accidents
 coarctation repair, 1057
 TGA and, 1113
 Cervical aortic arch, 778
 Cesarean delivery, congenital heart disease, 651, 653
 Chamber morphogenesis, epigenetic factors, 563, 563f
 Chaotic atrial tachycardia, 449, 450t
 CHARGE syndrome, 622t, 633–634, 634f
 CHD7 gene, 633
 Cheatham Platinum stent, 293–294, 293t
 Chest
 child inspection, 87–88
 heart position in
 location in, 33
 orientation of, 33–34, 33f–34f
 palpation of, 1509
 Chest cage pain, types of, 1509
 Chest impact, blunt cardiac injury, 552
 Chest pain
 adolescents, 83, 1509–1512
 percentage distribution, 1511t
 cardiac causes, 1512
 children, 1509–1512
 percentage distribution, 1512t
 CK-MB and troponin I, 1381f
 medical evaluation, 1512
 myocardial ischemia, 1377–1378
 treatment and outcome, 1513
 Chest radiography
 bilateral superior venae cavae, with unroofed coronary sinus, 849
 ccTGA and, 1150, 1150f
 chronic rheumatic heart disease, 1316–1317
 coarctation of aorta, 1049, 1049f
 Ebstein's anomaly, 894, 896f
 fibromas, 1555
 HLHS, 1066
 mitral valve prolapse, 1017–1018
 myocarditis, 1248, 1250f
 pericardial disease, 1351, 1351f, 1352f
 peripheral pulmonary arterial stenosis, 930
 pulmonary arterial hypertension (PAH), 1434–1435
 rhabdomyomas and, 1553
 truncus arteriosus, 993–994, 993f
 Chest roentgenogram
 anomalous origin of pulmonary artery from ascending aorta, 787
 anomalous pulmonary venous connection, 819
 innominate artery compression of trachea, 787–788
 TGA and, 1113–1114, 1113f
 Chest wall
 disorders of, 1415
 pain, 1509
 Chest X-ray, ASD, 678, 678f
 Chirality, 1200, 1201f
 Cholesterol
 arterial wall, 1514
 elevation, secondary causes, 1522–1523
 level, coronary heart disease and, 1520
 Choral hydrate, CMR and, 208
 Chorea
 RF, 1309t, 1311
 Chromosomal deletion, 627
 Chromosome 21, 617, 625
 Chromosome 7, peripheral pulmonary arterial stenosis and, 928
 Chromosome abnormality syndromes
 CHDs and, 619t–621t
 genetic syndromes, 1579
 Chromosome 22q11.2 deletion syndrome, 759, 1593
 Chromosome 7q11.23, Williams-Beuren syndrome, 628
 Chronic cyanosis, 1488
 Chronic heart failure, 1565–1570
 biomarker, 1567–1570
 in children, etiology of, 1565–1574
 etiology of, 1566t
 neonates and infants, 1565
 Chronic hypoxia, 1412–1414
 clinical features, 1412
 experimental studies, 1412–1414
 Chronic pericarditis
 cardiac trauma and, 553

- Chronic renal insufficiency, cardiovascular disease and, 1522
- Chronic rheumatic heart disease, 1316–1319, 1567
- HF in, 1320
 - medical management, 1319*t*, 1320–1321
 - surgery, 1321–1322
 - treatment, 1319, 1319*t*
- Chronic rheumatic mitral stenosis, intervention indications, 1322
- Chronotropes, 494
- Chylomicrons, 1520
- Chylopericardium
- pericardial effusion, 1356
- Cigarette smoking
- cardiovascular disease, 1517–1518
 - congenital heart defects and, 602
- Cine MRI
- congenitally absent right pulmonary artery, 235*f*
 - flow velocity, 224*f*
 - SSFP and, 214
 - ventricular function and, 214
- Cineangiography
- radiation dose, 273
- Circular shunt, pulmonary atresia and intact ventricular septum, 955
- Circulation
- physiology, 69–80
 - components of, 69, 653, 656
 - general, 69, 660
 - regulation, exercise, 124
 - transitional, 473
- Circulatory arrest, low flow bypass, neonate and, 1580
- Circulatory management, SvO₂, 1079, 1079*t*
- Circumferential end-systolic wall stress
- calculation, 166, 166*f*
 - midwall shortening *v.*,
- Clarithromycin, endocarditis, 1324
- Class Ia agents
- arrhythmias, 456
- Class Ib agents, 456
- Class Ic drugs, 456
- Class III drugs, 457–458
- Class IV agents, 458
- Claustrophobia, CMR and, 208
- Clear zone, atrioventricular valves, 10
- Clearance (CL), drug, 1662
- Cleft mitral valve, 1009–1010, 1009*f*, 1010*f*
- Clindamycin, endocarditis, 1273, 1324
- Clinical manifestations
- pulmonary arteriovenous malformations, 792–793
 - systemic arterial malformations, 790
- Clinical risk marker, HCM, 1228–1229, 1229*f*, 1230*f*
- Clinical studies
- Alagille syndrome, 630
 - diet, hypertension and, 1536–1537, 1539
 - HLHS outcomes, 1086–1088
 - myocardial viability, CMR and, 227–228
 - pulmonary atresia and intact ventricular septum, 948–953
 - research echocardiography and, 166–167, 166*f*
- Clinical trials
- advantages of, 1638*t*
 - analysis issues for
 - data management, 1653–1654
 - descriptive statistics, 1654
 - outcomes comparisons, 1654–1655, 1655*t*
 - test of randomization, 1654 - appraisal and regulation, 1637–1638
 - causality, 1636–1637, 1639*t*
 - conflicts of interest, 1639
 - critical appraisal of, 1656, 1659, 1659*t*
 - data collection, 1637
 - design issues for
 - clinical trial phases, 1640–1641, 1641*t*
 - cointerventions and blinding, 1646, 1646*t*, 1647*t*
 - hypothesis, 1642
 - interventions and clinical trial designs, 1642–1643
 - question, 1641 - randomization, 1644–1646, 1645*t*
 - sample size and power, 1646–1648, 1647*t*, 1648*t*
 - study aims, 1642
 - study measurements, 1643–1644, 1644*t*
 - study subjects, 1643, 1643*t*
 - validity, 1639, 1640*f*
- equipoise and execution, 1639
- execution issues for
- crossover and compliance, 1650–1651
 - data and safety monitoring, 1651–1653, 1652*t*, 1653*t*
 - operationalization, 1649, 1649*t*
 - quality control, 1651, 1651*t*, 1652*t*
 - recruitment strategies, 1649–1650, 1649*t*
 - retention, 1650
 - failure of assumptions, 1639
 - feasibility, 1639
 - publication bias, 1639
 - randomization, 1637
 - reporting and appraisal issues for, 1656–1659
 - resource requirements, 1639
 - specialty-specific challenges, 1639, 1640*t*
- Closure of Fontan fenestration, 322, 327*f*
- Cloves syndrome, 864
- Clubbing
- child's general appearance, 86
- CMR (Cardiac magnetic resonance)
- antepartum issues, 1502
 - BAV and, 1468*f*
 - clinical applications for
 - examples, 229–241 - congenital heart disease, indication for, 207, 208*t*
 - d-TGA/Mustard, 1484
 - myocardial ischemia, 226–227, 227*f*
 - pre-examination planning, 212–213
 - sedation and monitoring, 208, 210, 210*f*
- CNP (C-type natriuretic peptide), postnatal peripheral circulation, 76
- Coarctation
- in childhood repair, prognosis, 1056–1057, 1056*t*
 - iliac rupture, 305, 306*f*
 - recurrent postoperative, angioplasty for, 1054–1055
 - transcatheter management of, 304–307
- Coarctation of aorta (COA), 805, 1044–1058, 1045*f*, 1469–1471
- clinical features, 1048–1051
 - CMR and, 230–231
 - complete TGA and, 1106
 - complications, 1469
 - diagnosis of infant, 1048
 - effects of exercise, 101–102
 - embryology, 1046–1047
 - extracardiac vascular anomalies with, 1045
 - fetal hemodynamics, 1047–1048
 - Gd-enhanced 3-D MRA, 231, 232*f*
 - maternal risk and, 1500
 - MRI and, 230
 - pathology, 1044–1045
 - presentation in infancy and childhood, treatment, 1051
 - prevalence and etiology, 1044
 - recoarctation rates, 1469, 1469*f*
 - repair, 1469
 - repair in childhood, prognosis, 1056*t*
 - simultaneous pressure recordings, 1047*f*
 - surgical repair, 1052–1053, 1052*f*, 1053*f*
 - treatment, 1051–1056
 - tricuspid atresia, 877
- Coarctation stenting, 1055–1056, 1055*f*
- Coaxial catheter, perforation of atretic pulmonary valve and, 301–302
- Coffin-Lowry syndrome, 1268
- Coil migration, 326–327
- Coil occlusion of arterial duct, technique, 325
- Colesevelam, elevated LDL cholesterol and, 1527
- Collagen
- DCM and, 1235
- Collagen network, myocardium, 52, 54*f*
- Collateral arteries, PA-VSD and, 960, 962, 965*f*
- Color-flow Doppler, 141–143, 144*f*
- congenital aortic stenosis, 1027–1030
 - coronary sinus diverticulum, 854
 - tricuspid atresia, 880
 - truncus arteriosus, 994, 994*f*
- Color-flow imaging, ASD
- Combined inotropic and vasodilator support, 1242–1243
- COMET trial, heart failure and, 1573
- Commissure, 11
- Common atrioventricular valve, 40
- leaflets of, 149, 149*f*
- Common atrium, 39, 699
- Common brachiocephalic trunk, 760
- Common cardiac chambers and, 38
- Common outlet connection, great arteries and, 47*f*, 48
- Common ventricle, 41
- Common-inlet atrioventricular connections, 1176, 1176*f*
- Complete atrioventricular block (CAVB), 463–464, 463*f*
- bradycardia, 662, 663*f*
 - fetus, 662
 - in infants, children, young adults, 465
- Complete atrioventricular septal defect
- cardiac catheterization and angiography, 705–706
 - clinical course, 706
 - clinical manifestations, 700, 702
 - Down syndrome, 706
 - echocardiography, 702–703
 - electrocardiography, 705
 - intermediate defect, 706
 - pathology, 700
 - radiography, 705
 - Rastelli classification, 700, 702*t*
 - surgical treatment, 707
- Complete cartilaginous tracheal rings, anomalous origin of left pulmonary artery from right pulmonary artery, 787
- Complete cavopulmonary anastomosis, tricuspid atresia, 884
- Complete transposition of great arteries (Complete TGA), 753, 753*f*, 1097, 1098*f*
- corrected, 754
- Completion Fontan, stage 3, 1082–1083, 1083*f*
- Complex heart disease, echocardiogram, segmental diagnosis and, 1195–1196, 1198*t*
- Compression, digital echocardiography, 165–166
- Conal septal malalignment, fetal heart, 647
- Conal septum, truncus arteriosus, 990
- CONCOR project, septal defects an, 1472*f*
- Concordance, 44
- Conduction abnormalities
- athletic screening and, 105
- Conduction disturbances, muscular dystrophy, 1280
- Conduction system
- morphogenesis, 571–572
- Conduction tissue
- specialized, ccTGA and, 1149
 - truncus arteriosus, 992
- Conduit failure, truncus arteriosus repair, 1000*f*
- Congenital aortic arch anomalies, 778
- Congenital aortic stenosis, 1023–1039
- in children, guidelines
 - long-term outcome, 1033
 - medical management, 1322
 - natural history, 1031
 - symptoms and physical examination, 1026
 - treatment, 1031–1033
- Congenital bicuspid aortic valve, aortic regurgitation, 101
- Congenital cardiac defects, cardiac outflow tract, 567–568
- Congenital cardiac lesions
- Amplatzer vascular plug for, 292
 - balloon aortic valvuloplasty and, 297, 298*f*
- Congenital cardiac malformations, 730–731, 990
- treatment, 1211–1212
- Congenital coronary anomalies, response to exercise, 109–110
- Congenital heart defects
- anatomic features of, 560
 - decreased pulmonary blood flow, 1410–1412
 - epidemiology
 - and prevention of, 577–611

- risk and causes, 595–602
 - familial risks, 621, 623
 - genetic abnormalities and, 1579
 - genetics of, 617–639
 - 22q11 deletion syndrome, 627–628
 - repair, long-term neurodevelopmental outcome, 1582–1583
 - risk factors and prevention, 597–602
 - screening tools, 609, 610f
 - vascular disease in, 1401, 1402f, 1402t
- Congenital heart disease (CHD), 430. *See also*
 - Adult congenital heart disease
 - adolescents and adults, 1463–1490
 - adult *v.* pediatric, 1463, 1464f
 - adult with, PCICU, 523
 - aortic root abnormalities, 799–806, 880t
 - associated anomalies, 651–653
 - balloon-expandable intravascular stents, 934
 - cardiac CT, children with, 247–256
 - cardiopulmonary interactions
 - catheter-based techniques, 288
 - childhood/adolescence, 1566
 - clinical agenda, 1619
 - CMR
 - safety and, 210–212, 212t
 - echocardiography, 247
 - in gestation, 664
 - health-related QOL (HRQOL), 1608
 - definitions, 1608–1609
 - generic, disease-specific measurement, 1610, 1612
 - instrument availability, 1613f, 10610
 - instrument selection, 1610, 1611t, 1612t
 - instrument validation, 1610, 1613f
 - neurodevelopmental predictors, 1617–1618
 - outcomes, 1618
 - pediatric heart disease population, 1609–1610
 - psychosocial predictors, 1618
 - specific heart disease subgroups, 1616–1617
 - hematologic disorders in, 1590
 - infants, 1565
 - intrauterine fetal demise, 657, 661f
 - m-mode echocardiography, 134
 - neonates, 657, 1565
 - operative repair, SCD risk, 1465f
 - pediatric heart transplantation, 1384
 - pharmacologic therapy for, 490–498
 - pregnancy and, physiology and management, 1494–1505
 - prenatal evolution of, 656
 - prenatal screening, 645–647, 649f
 - prenatal treatment of, 656–657
 - prevalence, 1465f
 - primary referral diagnosis, 208t
 - psychosocial function and, academic ability/function, 1584
 - pulmonary stenosis and, 920
 - quality of life (QOL), 1060f, 1608
 - right-left heart interactions, 548–550
 - functional interactions, 550
 - geometric interactions, 550, 550f
 - screening for, 645–647, 645f, 646f
 - surgery
 - long-term neurodevelopmental outcome, 1582–1583
 - outcomes, specific diagnostic groups, 1583–1584
 - truncus arteriosus, 993
 - visceral situs, 1196–1197
- Congenital heart lesions, angled views, 274
- Congenital heart malformations, 560, 572
 - diagnosed in utero, 652, 658f
 - HCM, 1228, 1229f
- Congenital hemangiomas, vascular anomalies, 865–866, 866f
- Congenital infections, cardiac diseases and, 84
- Congenital mitral stenosis
 - balloon valvuloplasty, 297, 298f
- Congenital mitral valve stenosis
 - incidence of, 1003
 - management and prognosis of
 - balloon *v.* surgical management, 1018–1019
 - medical management, 1018
 - mitral valve replacement, 1019–1020
- Congenital pericardial defects, 1212–1214
 - types of, 1214
- Congenital rubella, 935
- Congenital tricuspid stenosis, 885–886
 - balloon valve dilation, 303
- Congenitally absent right pulmonary artery, cine MRI, 235, 235f
- Congenitally bicuspid aortic valve, 1467
- Congenitally corrected transposition of great arteries (ccTGA), 1147, 1148f, 1485–1486, 1486f
 - associated lesions, 1148, 1148f
 - conventional surgery and outcomes, 1156
 - exercise and, 105–106
 - maternal risk and, 1501
 - morphology, 1147–1148
 - natural history and management, 1156
- Congenitally malformed hearts, 368, 368f
- Congestive cardiomyopathy
 - clinical picture and treatment, 1242
 - natural history of, in children, 1244
- Congestive heart failure
 - atrial septal defects and
 - ccTGA and, 1149
 - children and, coarctation of aorta and, 1048
 - feeding history, infants and, 82
 - neuroendocrine abnormalities, 1281
 - research echocardiography and, 166–167, 166f
 - severe, univentricular atrioventricular connection, 1185
- Connective tissues, human heart, 54f
- Conotruncal Anomaly Face Syndrome, 621t, 627
- Conotruncal septum, formation, 567
- Conotruncal syndrome, DiGeorge syndrome and, 651
- Consolidated Standards of Reporting Trials (CONSORT), 1637–1638, 1656, 1656f, 1657t–1658t
- Constitutional symptoms, myxomas, 1557
- Constrictive pericarditis (CP), 196
 - characterized by, 1358, 1358f
 - echocardiography, 1358
 - hemodynamic filling patterns, 1358, 1358f
 - RCM *v.*, 1273, 1273t
 - RCM *vs.*, 1359–1360, 1359t, 1360f
 - single-ventricle patient, 1361
 - ventilator-dependent patient, 1360–1361
- Continuous murmurs, 89f, 91
- Continuous positive airway pressure (CPAP), 475, 727
- Continuous-wave Doppler
 - cardiac catheterization, coarctation of aorta, 1050, 1051f
 - univentricular atrioventricular connection, 1185
- Contraception
 - CHD and, 1504
 - statins and, 1527
 - Tetralogy of Fallot, 985
 - women of childbearing age, 1495t
- Contractile reserve, pharmacologic stress and, 157, 158
- Contractility, 65f, 66
- Contrast agents, 164, 165
 - PA-VSD and, 964–965
 - pulmonary angiography, 279–282, 282f
- Contrast echocardiography, 164–165
 - ASD, 679
- Contrast enhancement, MDCT and, 248, 249f
- Contrast media
 - angiography and, 273
 - catheters, 261f, 273
- Contrast-enhanced MRA, 215
- Controlled ventilation, CT imaging and, 248, 248f
- Conus artery, Tetralogy of Fallot, 753–54
- Conventional therapy
 - pulmonary arterial hypertension (PAH), 1449–1450
- Cooled-tip radiofrequency, 420
- Copy number variants (CNVs), TOF, 970
- Cor triatriatum, 833–836, 835f
 - anatomic classification, 834, 834t, 835f
 - clinical manifestations, 835
 - dexter, 834
 - differential diagnosis, 836
 - imaging, 836
 - microscopic anatomy, 834
 - physiology, 835
 - prognosis, 836
 - sinister, 834
- Coronary anomalies
 - PA-VSD and, 961
 - rare, 752
 - response to exercise, 109–110, 110t
 - structural heart disease, absence of, 747–752
- Coronary arteries, MDCT, 253, 255f
- Coronary artery
 - anatomy, 746, 747f
 - ccTGA and, 1148–1149
 - pulmonary atresia and intact ventricular septum, surgical strategies for, 953t
 - ccTGA and, 1150f
 - congenital heart defects, patterns with, 753–754
 - echocardiography, 201–202
 - growth of, arterial switch operation and, 1132, 1138
 - HCM and, 1229, 1230f
 - imaging, 215, 217f
 - myocardial ischemia, 1378
 - pulmonary atresia and intact ventricular septum, 944–945
 - stenosis, 946
 - supravalvular aortic stenosis, 1039
 - tetralogy of Fallot, 974
 - TGA, 1099, 1102f
 - trauma and, 556
 - truncus arteriosus, 991–992
- Coronary artery disease (CAD), 1514
 - established risk factors, 1516t
 - possible risk factors, 1516t
 - prevalence of, 1515f
- Coronary artery intimal-medial thickness (IMT), 1516
- Coronary atresia, 752
- Coronary heart disease, blood cholesterol level, 1520
- Coronary ostium, truncus arteriosus, 992
- Coronary perfusion, echocardiography, 202
- Coronary root anomalies, structural heart disease, 747–752
- Coronary sinus, 7, 38, 746
 - anomalies of, 853–855, 853f
 - LSVC and, 846, 846f
 - normal development, 840–841
 - ASD, 685
 - diverticulum, 854
 - orifice atresia, 854, 854f
 - pulmonary atresia and intact ventricular septum, 940–941
- Coronary vascular anomalies
 - anatomy, 746–747
 - embryology, 746
- Coronary vascular endothelium, origin, 571
- Coronary vasculature, 61–62
- Coronary vessel formation, origin, 571
- Coronary-cameral fistula, 944
- Cortical blood flow
 - in young, 79
- Corticosteroids
 - pregnant women and, 666
- Costameres, 59
- Costochondritis, 1509
- CPAP (Continuous positive airway pressure)
 - left heart failure, 548
- CPK-MB isoenzyme
 - myocardial contusions, 554
 - myocardial infarction, electrical injury and, 557
- Cranial angulation, arteries and, 275
- C-reactive protein, 1516
- Creatine kinase MB isoenzyme (CK-MB), myocardial injury, 1381f
- Cre-lox technologies, mammalian heart development, 561–562, 562f
- Criss-cross atrioventricular connections, 1201
- Crista supraventricularis (Supraventricular crest), 13–14
- Crossover clinical trials, 1642–1643
- Cryopreserved homograft tissue, truncus arteriosus, 998, 998f

- Cryotherapy, electrophysiologic therapeutic catheterization, 420
- Crystalloid pump, cardiopulmonary bypass, 532
- CT (Computed tomography)
- aortic dilation, 802, 803f
 - congenital aortic stenosis, 1026, 1027f
 - peripheral pulmonary arterial stenosis, 930–932
 - pulmonary stenosis, 102
- CT angiography (CTA), 247
- CT angiography (Computed tomography angiography), coarctation of aorta, 1049–1050, 1050f
- CT scan
- patent ductus arteriosus (PDA), 734
- C-type natriuretic peptide (CNP), 1567
- Culture-negative endocarditis, 1373
- Current magnitude, lightning-related injury, 558
- Cutting balloons, 295
- Cyanosis, 730, 1110
- atries of common pulmonary vein, 833
 - bilateral superior venae cavae, with unroofed coronary sinus, 849
 - child's general appearance, 86
 - Ebstein's anomaly, 893
 - Fontan operation, 1487–1488
 - HLHS and, 1067
 - infants and, heart disease and, 82–83
 - inferior vena cava drainage to left atrium, 857
 - isolated valvar pulmonary stenosis, 913, 914
 - left atrial drainage of right superior vena cava, 850
 - PAPVC, 818
 - patent ductus arteriosus, 730
 - PA-VSD and, 961
 - pulmonary atresia and intact ventricular septum, 945
 - rhabdomyoma and, 1553
 - TGA and, 1111
 - tricuspid atresia, 878
 - truncus arteriosus, 993
 - univentricular atrioventricular connection, 1185, 1193
- Cyanotic adult, 1487
- Cyanotic cardiac lesions, pregnancy and, 1503
- Cyanotic congenital heart defects, 1475–1476, 1475f
- Cyanotic congenital heart disease, maternal risk and, 1501
- Cyanotic neonate, differential diagnosis, 946t
- Cycle ergometers, types of, 127
- Cyclosporine, pediatric heart transplantation, 1391
- Cysts, intrapericardial teratomas, 1558
- Cytokine response, stage 1 palliation, HLHS and, 1075
- Cytokines
- myocarditis and, 1258–1259
- Cytolysis, myocarditis, 1256
- Cytomegalovirus (CMV)
- immunopathogenesis of, 1255
- Cytoskeletal proteins, thick filaments and, 57–58
- Cytoskeleton, and extracellular matrix, 59
- D**
- Dallas criteria, myocarditis, 1250
- Damus-Kaye-Stansel technique, 1139
- TGA and, 1138–1139
- DASH diet, hypertension, 1539
- Deep hypothermic circulatory arrest (DHCA), 531, 532
- neonate and, 1580
- Defect closure devices, transesophageal echocardiography, 154
- Defibrillation, 459–460
- Deletion-Duplication syndromes, 626–630
- Delivery, prenatal cardiac diagnosis and, 653
- Dephosphorylated phospholamban, calcium pump activity and, 56, 56f
- Depression of right ventricular function, atrial switch repair, 1125
- Desmin
- cell-cell interactions, 60
 - restrictive cardiomyopathies, 1268
- Desmoglein, 60
- Desmoplakin, 60
- Desmosomes, cell-cell interactions, 60
- Devereux method of calculation, left ventricular mass, 1536
- Device therapy, for heart failure, 1574
- Dextrocardia
- categories, 145
 - with situs inversus and atrioventricular and ventriculoatrial discordance, with right anterior aorta, 1204, 1206f
 - with situs inversus and inverted normally related great arteries, 1202f, 1204–1205
 - with situs inversus, atrioventricular concordance and ventriculoatrial discordance with left anterior aorta, 1204, 1205f
 - with situs solitus, 1195
 - types of, 1195
- Dextroversion, 145
- d-globulin, myocarditis, 1263
- Diabetes mellitus. *See also* specific i.e. insulin dependent diabetes
- angiotensin receptor blockers, hypertension, 1542
 - atherosclerosis, 1517
 - congenital heart defects and, 597, 599
- Diagnosis and procedural groups, HRQOL, 1615, 1617f
- Diagnostic tests
- myocarditis, 1248–1254
- Diaphoresis
- infants and, heart disease and, 83
- Diastole, 57, 57f, 188
- Diastolic dysfunction
- HCM and, 1224
- Diastolic function
- MRI and, 222–223
- Diastolic murmurs, 90
- chronic rheumatic heart disease, 1316
 - univentricular atrioventricular connection, 1185
- Diastolic pressure time index (DPTI), 1025
- Diastolic tricuspid flow murmur, 819
- Diastolic ventricular function
- color M-mode, 192, 193f
 - deformation imaging, 192–193, 193f
 - Doppler diastolic assessment, 189
 - Doppler myocardial velocity assessment, 191, 191f
 - echocardiographic diastolic function, 193–194
 - echocardiographic evaluation, 189
 - during exercise, 196
 - left atrial volume estimation, 191–192, 192f
 - physiology of, 188–189, 188f, 189f
 - pulmonary venous doppler flow analysis, 190–191, 190f
 - transmitral doppler flow evaluation, 189, 190f
- Diazepam
- electrophysiologic studies, intracardiac technique, 403
- DICOM (Digital Imaging and Communications in Medicine standard), digital echocardiography, 166
- Diet
- dyslipidemia, 1522
 - in children, 1523
 - hypertension and, 1536–1537, 1539
 - individual approach, 1524–1525
 - population approach, 1523, 1523t
- Dietary Intervention Study in Children (DISC), 1525
- Dietary patterns, hypertension, 1539
- Dietary salt, blood pressure and, 1539
- Dietitians, dyslipidemia, 1525
- Differential diagnosis
- pulmonary arteriovenous malformations, 793
 - systemic arterial malformations, 790
- Differential lung perfusion, MRI and, 225
- DIG trial (Digitalis Investigators Group), digoxin, 1572
- DiGeorge syndrome, 627–628, 759
- conotruncal syndrome, 651
 - interrupted aortic arch, 991
 - SHF transcriptional regulation, 563
- DiGeorge/velocardiofacial syndrome (DGS/VCFS) genetics and, 959
- Digital archiving, research echocardiography and, 165–166
- Digital echocardiography, 165
- Digital stethoscope, auscultation and, 85
- Digoxin, 458, 1672–1673, 1681–1682
- DCM, 1243
 - duchenne muscular dystrophy, 1281
 - HLHS, 1080
 - hypokalemia and, 385
 - pediatric acquired heart disease, 1572
 - during pregnancy, arrhythmias, 1503
 - RCM and, 1274
 - rheumatic carditis, 1320
- Digoxin-withdrawal trial, 1572
- Dilated cardiomyopathy
- CAMs, 1259
 - childhood/adolescence, 1567
 - genes, 1236–1238, 1237t, 1239f
 - mitral regurgitation in, 1241, 1242f
- Dilated congestive cardiomyopathy (DCM), 1235–1244
- causes of, 1235, 1236t
 - clinical features and treatment, 1240–1244
 - history, 1240
 - etiology and pathogenesis, 1235–1240
 - long-term sequelae, 1260–1261
- Dilation of peripheral arteries, 304
- Dilation of systemic veins, technique, 311
- Dimple deformity, 927
- Diphtheria myocarditis, 1255
- Discordance, 44
- Disposition, drug, 1662
- Distal vascular system BP measurement, systolic blood pressure measurement v, 129, 129f
- Diuretic therapy, 1675–1676. *See also* specific i.e. Non-potassium-sparing diuretics
- acquired heart disease, childhood/adolescence, 1571–1572, 1571t
 - DCM, 1244
 - Duchenne muscular dystrophy, 1281
 - HCM and, 1230
 - HLHS, 1073, 1080
 - hypertension, 1542
 - myocarditis, 1262
 - RCM and, 1274
 - rheumatic carditis, 1320
- Dizziness
- tachyarrhythmia, 443–444
- D-loop, chirality and, 1201, 1201f
- DNA
- mutations, Zebrafish, 560
 - myocarditis, 1257
 - sequencing, HCM and, 1224
- Dobutamine, 492t, 493, 1673t, 1674
- DCM, 1243
 - stress, 158, 159, 160f
- Dobutamine stress CMR (DSMR)
- myocardial ischemia, 226
- Dobutamine stress echocardiogram (DSE), 160f
- myocardial ischemia, 226
- Dofetilide, 458
- Donor(s)
- cardiac transplantation, HLHS, 1086
 - pediatric heart transplantation and, 1387
- Donor right ventricle, pediatric heart transplantation, 1389
- Donor/recipient matching, 1384
- Dopamine, 492t, 493, 1673t, 1674
- Doppler assessment, history of, 134
- Doppler, C., ultrasound and, 137
- Doppler continuity equation, 141
- Doppler echocardiography
- ASD, 678–679, 679f
 - coarctation of aorta, 1050
 - congenital aortic stenosis, 1027–1030, 1027f, 1028f, 1036
 - DCM and, 1241, 1242f
 - DMD and, 1280–1281
 - isolated valvar pulmonary stenosis, 917–918, 918f
 - optimizing, 140–141, 143f
 - pediatric patient and, 140
 - RF and, 1314–1315
 - systolic regurgitation, 946
 - TGA and, 1111

- Doppler equation, 137–138
Doppler flow mapping, LSV and, 846–847, 847f
Doppler spectral envelopes, 140
Doppler study, two-dimensional echocardiogram, 728
Doppler tissue imaging, 138
Doppler ultrasound imaging, 138
Doppler velocity, echocardiography, 179, 179f
Doppler-derived peak, isolated valvar pulmonary stenosis, 917, 918f
Dorsal ventral polarity, primitive heart tube and, 565
Double aortic arch, 778–782, 779f–782f
 with atretic left arch, 781f
Double balloon technique
 systemic blood pressure and, 300
Double chambered right ventricle, 925–928, 926f, 927f, 928
Double conus, 14
Double inlet LV with left-sided subaortic hypoplastic RV, 1182–1183, 1182f
Double inversion recovery, CMR and, 213
Double outlet connection
 great arteries and, 44, 47f
Double outlet right ventricle (DORV), 754, 1214, 1214f
 adult with, 1173, 1173t
 aortogram of, 1134f
 bilateral persistence of subarterial conus, 151
 clinical features and pathophysiology, 1163
 definition, 1161
 doubly committed VSD, 1167, 1169f
 embryology and, 566
 incidence, 1161
 morphology, 1161–1163
 noncommitted VSD, 1167, 1169f
 PA-VSD *v.*, 965
 reintervention and reoperation, 1172–1173
 surgical repair, 1167, 1169
 anatomic determinants, 1169–1170, 1169t
 clinical outcomes, 1171–1172
 timing of, 1170, 1170t
 types of, 1170–1171, 1171f, 1172f
 tetralogy type, 1163–1164, 1164f
 transposition type, 1164–1165, 1166f–1168f
 truncus arteriosus *v.*, 996
 VSD type, 1165
 with subpulmonary VSD, 1097
Double outlet ventricle, fetal heart, 647
Double-chambered right ventricle
 course and prognosis, 928
Double-inlet left ventricle (DILV), 40, 46f, 754, 1179, 1180f, 1183
 with hypoplastic left ventricle, 1179f
Double-inlet ventricle
 embryonic ventricular looping, 1178f
 with indeterminate morphology, 1182–1183, 1182f
 mixed morphology, 1183, 1188f
Double-lumen aortic arch, 782, 782f
 angiography, 783
Double-orifice left atrioventricular valve, 708, 1010, 1011f
Double-outlet right atrium, 699
Double-switch repair, ccTGA and, 1157, 1157f
 outcomes for, 1157–1158
Doubly committed VSD, DORV, 1167, 1169f
Down syndrome, 651, 706, 970
 CHDs and, 625, 625f
 Mitral papillary muscle, echogenic focus, 651, 654f
Dronedrone, 458
Drugs, 1503. *See also* specific *i.e.* midazolam dosing
 absorption, 1665–1666, 1665t
 distribution, 1666–1667, 1667t
 metabolism, 1667–1669, 1669t, 1670t
 pediatric hypertension, 1540, 1540t–1541t
 and toxins
 clinical studies, 1422–1423
 experimental studies, 1423, 1426
 transesophageal electrophysiologic study, 415
DSM criteria (Diagnostic and Statistical Manual of Mental Disorders criteria), CHD, 1584
d-Transposition of great arteries (d-TGA), 1479–1486
 arterial switch, 1485
 atrial switch with baffle leak, 1485f
 coarctation of aorta, 1045
 exercise and, 104–105
 neurodevelopmental outcomes, 1583
 tricuspid atresia, 878
D-type natriuretic peptide (DNP), 1567
Duchenne carrier, 1239, 1283
Duchenne muscular dystrophy (DMD), 1260, 1279–1283
 anesthesia, 1279
 electrocardiogram, 1279f, 1280
 M-mode tracing, 1280f
 MRI, 1278f
 neuroendocrine abnormalities, 1281
 therapy, 1281–1283
Ductal patency
 HLHS and, 1072
 pulmonary atresia and intact ventricular septum, 948
Ductal-dependent lesions, pediatric heart transplantation and, 1386
Ductus ampulla/ductus bump, chest roentgenogram, 724, 725f
Ductus arteriosus (Ductal artery), 42, 766
 HLHS, 1065
 PA-VSD and, 961
 postnatal closure of, 71
Ductus venosus
 anomalies of, 858–860
 normal development, 843, 844f
 umbilical-placental circulation, 71
 waveforms, fetus and, 654, 655f
Dye injection of umbilical vein, anomalous termination of umbilical veins, and absent ductus venosus, 859
Dynamic exercise
 hemodynamic responses to, 93
 ventricular septal defects and, 99
Dynamic subvalvar obstruction, isolated valvar pulmonary stenosis, 913, 914f
Dyslipidemia
 in children, clinical recommendations, 1523–1527
 factors causing, 1521–1523
 secondary causes, 1522–1523
 treatment, 1525–1527
 pharmacologic, 1525–1527
Dyslipoproteinemia, secondary causes, 1522t
Dysplasia
 mitral valve, 1006–1007, 1006f, 1007f
Dysplastic pulmonary valves
 pulmonary valvuloplasty, 921
 surgical valvotomy, 923
Dysplastic tricuspid valve, transplantation, 953–954
Dyspnea
 atriasis of common pulmonary vein, 833
 Ebstein's anomaly, 893
 on exertion
 d-TGA, 1483f
 peripheral pulmonary arterial stenosis, 928
 HCM, 1230
Dysrhythmias
 lightning-related injury, 558
 postoperative, atrial switch repair, 1128–1132, 1130t
Dystrobrein, 60
Dystrophic myotonia type 1 (DM1), 1277
Dystrophica myotonica-protein kinase (DMPK), 1277
Dystrophin
 glycoprotein complex, 59–60
 muscular dystrophy and, 59
Dystrophin gene, Duchenne muscular dystrophy, 1239–1240, 1284
Dystrophinopathies, 1278–1285
E
Early diastolic murmurs, 89f, 90
Early repolarization, 384, 385f
Ebstein's anomaly, 150, 159, 947, 956, 1169
 cardiac defects, 891–892
 children and adults, 899–908
 classifications, 890
 clinical presentation, 892–894
 congenital TV regurgitation, 909–910
 diagnostic evaluation, 894–897
 exercise and, 104
 functional outcome after surgery, 909
 genetic factors, 890–891
 history of, 889, 890f
 maternal risk and, 1501
 natural history, 897
 neonatal
 biventricular repair, 897–898, 901f
 cardiac transplantation, 898–899
 right ventricular exclusion, 898, 901f
 pathologic anatomy, 889–890
 pathophysiology, 892
 persistent valves of sinus venosus, 861
 pregnancy and, 908–909
 prevalence, 889
 right coronary artery, 889
 right ventricle, 889–890, 893f
 transplantation, 953
 tricuspid valve, 889, 890f
 valvar pulmonary stenosis *v.*, 920
Ebstein's-like anomaly
 mitral valve, 1010
ECG (Electrocardiography)
 anomalous left coronary artery from pulmonary artery, 750
 anomalous pulmonary venous connection, 819
 aortopulmonary window, 741
 athletic screening and, 96–98
 ccTGA and, 1149–1150
 coarctation of aorta, 1049
 congenital aortic stenosis, 1026
 DCM and, 1240
 developmental changes, 385–386
 DILV and, 1183
 DMD and, 1279f, 1280
 Ebstein's anomaly, 894, 896, 897f, 898f
 fibromas, 1555
 guidelines and indication, 387
 HCM, 1227
 history of, 372
 HLHS, 1066–1067, 1066f, 1067f, 1069f
 HR, 128–129
 isolated valvar pulmonary stenosis, 916, 916f
 myocardial contusions, 554
 myocarditis, 1248–1249, 1250f, 1251f
 mitral valve prolapse, 1017, 1018f
 myxomas, 1557
 normal, 372–387
 PA-VSD and, 962
 pediatric, reading, 375, 375t
 pericarditis, 1351, 1352f
 principles and technical considerations, 372–375
 pulmonary arterial hypertension (PAH), 1435
 pulmonary arteriovenous malformations, 793
 pulmonary atresia and intact ventricular septum, 945, 945t
 RCM, 1271–1272
 RF and, 1314
 right heart catheterization and, 263–265, 264f, 264t
 subvalvular aortic stenosis, 1036, 1037f
 TGA and, 1113
 tricuspid atresia, 879–880, 879f, 880f
 truncus arteriosus, 993
 univentricular atrioventricular connection, 1185–1189
 ventricular septal defects, 715
 waveforms of, 372, 373f
ECG gating (Electrocardiographic gating)
 MDCT and, 250–251, 251f
 MRI and, 208
ECG-triggered SSFP cine
 aortic aneurysm, 233
 ventricular function and, 215
Echocardiographic windows, to heart, 139
Echocardiography, 134–168. *See also* Two-dimensional echocardiogram; specific *i.e.* intracardiac echocardiography
 aberrant right subclavian artery, 763

- Echocardiography (*Continued*)
 absent right superior vena cava, in viscerotrial situs solitus, 850, 850f
 anomalous origin of left pulmonary artery from right pulmonary artery, 787
 antepartum issues, 1502
 ASD
 athletic screening and, 97
 atresia of common pulmonary vein, 833
 atrioventricular delay, 198
 bilateral superior venae cavae, with unroofed coronary sinus, 849
 cardiac anatomy, segmental approach, 144–153
 cardiac tumors, 1550–1551
 ccTGA and, 1150–1554, 1151f, 1152f, 1153f, 1154f
 chamber dimensions and cardiac structures, 172
 CHD and, 247
 chronic rheumatic heart disease, 1313f, 1316
 coarctation of aorta, 1050, 1050f
 congenital aortic stenosis, 1027–1030, 1027f, 1036
 cor triatriatum, 813f, 836
 coronary artery, 201–202
 double aortic arch, 782
 Ebstein's anomaly, 896, 898t
 fibromas, 1555, 1555f
 history, 134
 IE and, 1368, 1368t
 interrupted aortic arch, 784
 interventricular dyssynchrony, 198, 198f
 intraventricular dyssynchrony, 198–201
 left ventricle, 172–174
 left ventricular mass, 174
 malposition of septum primum, 815f
 myocardial contusions, 554
 myocarditis, 1248–1249, 1250f, 1251f
 patent ductus arteriosus (PDA), 732, 733f
 PA-VSD and, 962–963
 in PCICU, 486
 pericardial disease, 1351–1352, 1351f, 1353f
 pulmonary arterial hypertension (PAH), 1435–1436, 1437f
 pulmonary arteriovenous malformations, 793
 pulmonary atresia and intact ventricular septum, 945–946, 946f–950f
 RCM, 1271–1272, 1272f
 RF, 1313f, 1314–1315
 rhabdomyoma and, 1553
 right ventricle, 174, 175f
 stenosis of individual pulmonary veins, 837
 supravalvular aortic stenosis, 1039
 systemic arterial alformations, 790
 systolic ventricular function
 ejection fraction, 177
 fiber to pump level, 175, 176f
 myocardial function, 175
 VCF-end-systolic wall stress relationship, 177–178
 ventricular function, Doppler Indices of, 178–182
 tricuspid atresia, 880, 881f
 truncus arteriosus, 994–995, 994f
 truncus arteriosus repair, 1000f
 univentricular atrioventricular connection, 1176f, 1179f, 1185–1189, 1186f, 1187f, 1188f, 1189f, 1190f
 univentricular heart, 175
 valve function, assessment of
 atrioventricular size and function, 186–188
 diastolic ventricular function, 188–194
 semilunar valves and great vessels, 182–186
 ventricular synchrony, 197
 ventricular septal defects, 715, 715f–717f, 717
 wall motion, MI and, 1383
 Echo-Doppler studies, muscular dystrophies, 1278
 Ectopia cordis, 1195, 1214–1215
 Ectopic atrial tachycardia, 428, 429f
 Ectopic heart, 33
 Edema
 adolescents, 84
 Edward syndrome, 970
 Edwards diagrams, aortic arch anomalies, embryology, 758–759, 759f
 Effective pulmonary flow (Qep), shunts and, 269–270
 Effective systemic flow (Qes), 269, 269t
 Einthoven, W., ECG, 372
 Eisenmenger syndrome (ES), 1443–1444, 1445f, 1473–1474
 exercise and, 107–108
 labor and delivery, 1504
 maternal risk and, 1501
 therapies, 1408
 Ejection clicks, 88–89
 Ejection fraction (EF), 121, 160
 Ejection murmurs, 89f, 90
 Elastic fibers, 52
 Elastin
 arteriopathy, supravalvular aortic stenosis, 1039, 1039f
 gene mutations, 628, 629
 peripheral pulmonary arterial stenosis and, 928
 vasculopathy, supravalvular aortic stenosis, 1039
 Electrical dyssynchrony, cardiac
 resynchronization therapy, 1574
 Electrical impulse, atrial myocardium, 363–364, 366f, 367f
 Electrical injury, 557–558
 severity of, factors affecting, 557t
 Electricity, man-made, injury from, 557, 557t
 Electrode catheters, 405, 406f
 Electrogram recording, 403f
 Electron beam CT scanners, CHD, 251
 Electronic medical record (EMR), PCICU, 485
 Electrophysiologic studies, 401
 intracardiac technique, 401–411
 planning, 401
 Electrophysiology (EP) cardiac laboratory
 components of, 403f, 405
 Elimination half-life ($T_{1/2}$), 1662
 ELITE trial, ARB, 1573
 Ellis-van Creveld syndrome, 623t
 Embolism, cardiac catheterization, 285
 Embolization coils, 292
 Embryo
 cardiac neural crest cell migration, 567–568, 567f
 embryocardiac precursors, 561–562
 human
 valves of sinus venosus and, 860, 861f
 venous systems in, 840–845, 841f
 pulmonary venous anomalies, 809–816
 Embryology
 aberrant right subclavian artery, 761–762, 761f, 762f
 atrial septal defects and
 heart, 561–562, 562f
 Embryonic ventricular looping, double-inlet ventricles, 1178f
 Emergency department
 lightning-related injury, 558
 penetrating cardiac wounds, 556
 Emery-Dreifuss muscular dystrophy (EDMD), 1284
 restrictive cardiomyopathies, 1268
 Emotional preparation, electrophysiologic studies, intracardiac technique, 401
 Enalapril, 1678
 End-diastolic pressure-volume curve, 65, 65f
 End-diastolic volume (EDV)
 exercise and, 121, 122
 End-hole artifact, 263
 End-inspiratory lung volume (LVEDV),
 exercise, 127
 Endocardial fibroelastosis, HLHS and, 1064
 Endocardial visualization, contrast agents and, 165
 Endocarditis
 childhood/adolescence, 1567
 coarctation repair, 1057
 prophylaxis, 1322–1323
 pulmonary arterial stenosis, 935
 PVS, 1475
 RF and, 1307
 risk of, cardiovascular conditions, 1364, 1365t
 Tetralogy of Fallot, 984
 Endomyocardial biopsy
 myocarditis, 1250, 1253f
 RCM, 1272–1273
 Endomyocardial fibrosis (EMF), 1268–1269
 Endomysium, collagen network, 52
 Endothelial function, postnatal peripheral circulation, 76
 Endothelial injury, cardiopulmonary bypass, 532
 Endothelial nitric oxide synthase (eNOS) deficiency, BAV, 804
 Endothelial progenitor cells (EPCs), 1455
 Endothelin
 pulmonary arterial hypertension (PAH), 1453
 Endothelin-1 (ET-1), fetal pulmonary vascular resistance, 73–74
 Endothelium-derived nitric oxide (EDNO), fetal pulmonary vascular resistance, 72, 74
 Endovascular stents, 292–293
 cutting balloon angioplasty *vs.*, 310, 314f
 End-systolic elastance (Ees), 66
 End-systolic pressure-volume relationship, 65f, 66
 End-systolic stress, calculation, 219
 End-systolic volume (ESV), exercise and, 121
 End-systolic wall stress (ESWS)
 166, 166f
 End-tidal CO₂ (ETCO₂), 486
 End-to-end anastomosis, COA and, 1469, 1469f
 Energy, 118–119
 sources, 418–421
 transfer, 135, 135f
 Environment
 PA-VSD and, 959
 RF and, 1304–1305
 Environmental exposures
 CHD, 617, 618t
 Enzymes, myocardial injury, 1379
 Epicardial mapping, catheterization laboratory, intracardiac technique, 405
 Epicardium, 3
 Epidural anesthesia, labor and delivery, 1504
 Epilepsy
 congenital heart defects and, 600
 Epimysium, collagen network, 52
 Epinephrine, 492t, 493, 1078, 1673t, 1674
 DCM, 1243
 intracardiac study and, 407
 stage 1 palliation, HLHS and, 1076
 Epistaxis, RF and, 1314
 Epithelial to mesenchymal transition (EMT), 61
 atrioventricular canal and, 568
 Eplerenone, acquired heart disease, childhood/adolescence, 1571
 Epstein-Barr virus (EBV)
 apoptosis and, 1247
 pediatric heart transplantation, 1393–1394
 Equilibrium radionuclide angiography, DMD and, 1281
 Equipment, transesophageal technique, 412–415, 413f, 414f
 Ergometers, types of, 127
 Ergotamine, RCM and, 1269
 Erythema marginatum, RF and, 1309t, 1314
 Esmolol, 457, 1679–1680
 Esophageal atresia, surgery and, 767
 Esophageal electrocardiography, 374
 Esophageal intubation, transesophageal echocardiography, 154
 Esophagitis, chest pain, 1510
 Ethacrynic acid, 1676
 Eustachian valve, 147f, 856
 EVC2 genes, 613t
 Excitation-contraction coupling, 62–63
 contraction portion, 63
 embryonic myocytes, 63
 “excitation” component, 62–63
 myofilament Ca²⁺ sensitivity, 63
 regulation of
 intrinsic regulation, 63–64
 structural changes, 64
 Exercise
 cardiac responses to, 121–125
 coarctation in childhood repair, 1056t
 congenital aortic stenosis, 1031–1033

- contractile reserve and, 158–159
 echocardiogram, 158
 isolated valvar pulmonary stenosis, 919
 performance, determinants of
 physiology, 118–121
 protocols, 127–128, 128t
 QT interval, 384
 regulation of circulation during, 124
 tachyarrhythmia, 4
 testing, 118–132
 athletic screening and, 93–113
 congenital aortic stenosis, 1027
 hypertension, 1539
 methodology, 127–128
 types of, 118
 ventilatory response to, 125–127
- Exercise tidal volume
 cardiac output and, 130
- Exercise tolerance
 tricuspid atresia, 885
- External topography, 4, 4f–5f
- Extracardiac malformations of fetus, congenital
 heart disease and, 651
- Extracellular matrix (ECM), 52, 561
 composition of, 52
 connections to, 58–61
 cytoskeleton and, 59
 remodeling, DCM and, 1235–1236
- Extracorporeal membrane oxygenation (ECMO), 1622
 cardiopulmonary bypass, 535
 circuit guidelines, 537
 contraindications, 536
 indications for, 533, 535–536
 pediatrics
 survival, cardiac procedure and
 technical considerations, 536–537
 VADs *v.*, 536
 ventricular assist devices, 1596
- Extrasystoles
 fetal cardiac rhythm, 660
- Ezetimibe, cholesterol absorption and, 1527
- F**
- Facioscapulohumeral muscular dystrophy, 1284
- Factorial clinical trial, 1643
- Familial CHD syndrome, 637
- Familial dilated cardiomyopathy, 1236
- Familial heterotaxy, 1195
- Familial risks, CHDs and, 621, 623
- Family
 history, 84
 DCM, 1236
 pediatric heart transplantation, 1386
 preparation, electrophysiologic studies, intra-
 cardiac technique, 401
 support, pediatric heart transplantation,
 1386
- Family-centered care, PICU, 485
- Fast imaging employing steady state acquisition
 (FIESTA), 214
- Fast spin echo (FSE)
 CMR and, 213
 TOF and, 236
 vascular rings, 233–234, 234f
- FDA (Federal Drug Administration), CMR and,
 210, 211
- Feasibility, clinical trials, 1639
- Feeding
 history, cardiac diseases and, infants and, 82
 intestinal circulation response, postnatal
 peripheral circulation and, 80
- Femoral artery pressure, electrophysiologic stud-
 ies, intracardiac technique, 403
- Femoral vessels, approach to, cardiac catheteriza-
 tion and, 259–260
- Fenestration of atrial septum, fetus and, 656
- Fenoldopam, 497, 1673t, 1674
- Fentanyl
 CMR and, 208
 labor and delivery, 1504
 stage 1 palliation, HLHS and, 1076
- Fetal aortic balloon valvuloplasty, HLHS and,
 1062
- Fetal bradycardia, treatment, 656–657
- Fetal capillary hemodynamics, postnatal *v.*
 schematic, 653f
- Fetal cardiac arrhythmias
 analysis of, 663, 664f
 therapy for, 664–666, 665f
- Fetal cardiology
 fetal echocardiography and, 645t, 649t,
 657–660, 658t
 historical perspective of, 644–645
- Fetal cardiovascular performance, echocardi-
 ographic assessment, 647–651,
 651f, 652f
- Fetal cardiovascular system
 atrial chamber, 646, 653f
 human, 644
- Fetal cerebrovascular flow, cerebral dysgenesis,
 1579
- Fetal circulation, 69–70, 70f, 71f, 72
 TGA and, 1109
- Fetal congenital complete atrioventricular block,
 464–465
- Fetal congenital heart disease, Doppler, 657
- Fetal echocardiography
 current role, 649t, 657–660, 658t–660t
 fetal cardiology and, 645–647, 645f, 646f
 HLHS and, 1061–1062, 1062f
 indications for, 645
 patent ductus arteriosus (PDA), 725, 725f
 pericardial teratomas, 1559f
 pulmonary atresia and intact ventricular
 septum, 939
 truncus arteriosus, 995
- Fetal flow pathways, 647
- Fetal heart
 four chamber anatomy, 645, 645f
 abnormalities, 646, 646f
 normal, 646
 hypoxic pulmonary vasoconstriction, 72
 long axis views, 647, 650f
 pulmonary venous obstruction, 654, 655f
- Fetal life
 ductus arteriosus, 20
 IVC blood and, 856
 physiologic pulmonary hypertension and, 18
 valve of fossa ovalis and, 8
- Fetal rhabdomyomas, 1553
- Fetal right ventricular output, isolated valvar
 pulmonary stenosis, 914, 914f
- Fetal risk
 antepartum issues, 1502
 cardiac diseases, 1496, 1497t
- Fetal tachyarrhythmias, analysis and treatment,
 663–664, 665f
- Fetal tachycardia
 hydrops fetalis and, 662
- Fetoscopy, fetus and, 656
- Fetus
 antenatal surveillance of, techniques for, 654
 antiarrhythmic therapy and, 663
 blood cysts, 10
 cardiac defect and, 625
 great arteries, 18
 M-mode echocardiographic studies, 647, 651f
 regional blood flow analysis and, 654–656,
 655f
- Fever
 congenital heart defects and, 599
- Fibrillin-1 (FBN1) gene mutations, 799
- Fibrinoid necrosis, 1401
- Fibroblast growth factor (FGF), coronary
 development, 61
- Fibroelastosis, 943, 944f
- Fibroma, 1554–1555, 1555f
 incidence, 1550, 1550t
 spin echo MRI, 1552f
- Fibronectin, 52
- Fibrosis, valvular aortic stenosis and, 1025
- Fick equation, 1107, 1108
 cardiac output and, 267, 267f, 268f, 269t
 cardiac output measurement, 118–119
 congenital aortic stenosis, 1030
 Fick equation, 1039, 1041f, 1049
 single-ventricle parallel circulation, HLHS
 and, 1069–1070
- Fiedler myocarditis, 1255
- First degree atrioventricular block, 462, 462f
- First heart sound (S1), 88
 coarctation of aorta, 1049
 peripheral pulmonary arterial stenosis, 915
- First trimester fetal nuchal thickness, 651
- First-pass effect, 1662
- First-pass myocardial perfusion CMR,
 myocardial ischemia, 226–227, 227f
- FISH analysis, genetic testing, 638
- Fistula, 944
 coronary artery, 1382
- Fitness, repetitive exercise and, 124–125
- Flecainide, 457, 1681
 fetus, 661, 668t
- Flipper coil, 291, 292
- Flu
 congenital heart defects and, 599
- Fluorescence in situ hybridization (FSH), 618, 970
- Fluoroscopy, radiation dose, 273
- Folic acid, congenital heart defects and, 603
- Fontan, 1600–1601
- Fontan completion, 514–515
- Fontan leak, agitated saline contrast and, 164
- Fontan operation, 1487–1488, 1489f. *See also*
 Modified Fontan operation
 arrhythmias, 1487–1488
 cardiac catheterization, HLHS, 1084
 cyanosis, 1487–1488
 effects of exercise, 106
 HLHS, 1084
 maternal risk and, 1501
 mortality, HLHS, 1084
 protein-losing enteropathy, 1487
 tricuspid atresia, 883
 univentricular atrioventricular connection, 1185
- Fontan palliation, CMR, 215, 240–241
- Fontan-type palliation, ccTGA and, 1156
- Foramen ovale, 8–9
- Force-frequency relationship, 157
- Foreign bodies, retrieval of, 329–331, 331f
- Four-chamber view
 ccTGA and, 1150f, 1151f, 1152f
 HLHS, 1066, 1067f
 ventricular function, 215, 218f
- Framingham Heart Study, 1520, 1527
 atherosclerosis, 1514
 research echocardiography and, 166
- Frank system, 373
- Frank-Starling mechanism, 723
- Freeze-frame ultrasound image, digital echocardi-
 ography, 165
- Friction rubs, 87
- Fryns syndrome, 624t, 634
- Functional maturation development
 atrioventricular conduction system, 354–357,
 357f–360f
 AV plane, fibrous insulation, 357–358, 361f
 cardiac electrophysiology, 362, 364f
 electrical impulse, atrial myocardium,
 363–364, 366f, 367f
 heart pacemaking, 362–363, 365f
 maturing AV conduction system, 364–367
 VCS, developmental aspects, 367, 367f
 congenitally malformed hearts, 368, 368f
 mammalian heart, building plan, 350–352,
 350f–352f
 postnatal heart, conduction tissues
 recognition, 348–350, 349f
 sinus node
 heart beat initiation, 352, 353f
 SN development, 353–354, 354f, 355f, 356f
 ventricular conduction network, 359–361,
 362f, 363f
- Fungal endocarditis, 1364
- Furosemide, 1675–1676
 DCM, 1243
 drugs and, 1243
 pediatric acquired heart disease, 1571
- G**
- G proteins, extracellular matrix, 54
- Gadolinium delayed contrast MRA, fibromas,
 1555
- Gadolinium-enhanced 3-D MRA
 aortic segments and, 233, 234f
 aortopulmonary collateral vessels, 236, 237f

- Gadolinium-enhanced (*Continued*)
left pulmonary artery sling, 234, 234f
maximal intensity projection, 229, 230f
PDA and, 230
pulmonary venous anomaly, 236, 236f
scimitar syndrome, 217f
secundum ASDs and, 229
severe aortic coarctation, 231, 232f
TOF and, 236, 237f
- Gap junctions, 366
- cell-cell interactions, 60–61
- Gas exchange
fetal circulation, 72
- Gastroesophageal reflux, chest pain, 1510
- Gastrointestinal system, 479
chest pain, 1510
postnatal peripheral circulation, 80
- GATA4 transcription factor, 563, 571, 635–636
- Gender
cardiomyopathies and, 1267
ECG and, 387–388
- Gene expression, DCM and, 1236
- Gene mapping
22q11.2 deletion syndrome, 627–628
- General anesthesia
CMR and, 208, 210
electrophysiologic studies, intracardiac technique, 401–402
- Generic, disease-specific measurement, HRQOL, 1610, 1612, 1613t, 1614f
- Genetic(s). *See also* Molecular genetics
abnormalities
CNS, 1579
congenital heart defects, 1579
CHDs, 617–639
dyslipidemia, 1521–1523
evaluation, and counseling, 636–638
HCM and, 1224–1226
mutation, peripheral pulmonary arterial stenosis and, 928
myxomas, 1557
PA-VSD and, 959
polymorphisms, cardiac surgery and, 1581
restrictive cardiomyopathies, 1267–1268
syndromes, 1579
HLHS and, 1061
mutations in single genes, 630–634
testing, 617–618
pregnancy termination and, 651
- Genetic cardiomyopathy, 1239
- Genetic heterogeneity, 624t, 630
- Gentamicin
gram-negative bacterial endocarditis, 1373
streptococcal endocarditis, 1372
- Gestation
congenital heart disease, 664
HLHS and, 1062
human, mouse embryo *u.*, 561
postnatal peripheral circulation, 78
venous channels, 842f, 843
- Giant cell myocarditis, 1255
- Gianturco coils, 291, 325, 328
abnormal vascular communications, 328
- Gianturco-Grifka vascular occlusion device (GGVOD)
canine model, 292
- Glenn shunt, 18
tricuspid atresia, 883, 884f
univentricular atrioventricular connection, 1191, 1193
- Global risk assessment, pregnancy, maternal/fetal risk, 1496–1497, 1497t
- Glomerular filtration, neonates and, 78–79
- Glomerular filtration rate (GFR), 479
- Glycemic control, 520, 522
- Gorlin formula, aortic valve areas, 272, 272t
- Gorlin method, congenital aortic stenosis, 1030
- Gower sign, DMD and, 1279
- Gradient echo MRI
central pulmonary arteries, 235
- Gram negative organisms, IE and, 1364
- Gram positive cocci, IE and, 1364, 1364t
- Gram-negative bacterial endocarditis, 1373
- Gram-negative organisms, IE and, 1364, 1364t
- Great arteries, 41–42, 42f, 1211
position of, 43, 44f, 45f
- Great artery connections, segmental approach, 1202, 1202f
- Great veins, 6–7
pulmonary atresia and intact ventricular septum, 940–941
- Great vessel(s)
echocardiography, 151–152
injury, 555
relationship of, echocardiography, 151–152
- Group A streptococcus (GAS)
pharyngitis, 1303
migratory polyarthritis, 1310
RF and, 1303
- Growth and development, toddlers and pre-schoolers, 83
- Growth parameters, 86
- Gunshot wounds, 556
- H
- HACEK group, IE and, 1364, 1364t
- Hamartomas, 1552
- Hand2
expression, 563, 565
SHF transcriptional regulation, 563
- Hand1, SHF transcriptional regulation, 563
- Haploinsufficiency of short stature homeobox (SHOX), Turner syndrome, 626
- Harmonic phase imaging (HARP), 221
- Haycock formula, 172
- Health status and functional status
pediatric heart disease population, HROOL, 1614
- Healthcare Cost and Utilization Project (HCUP), 1634
- Healthcare Failure Modes and Effects Analysis (HFMEA), 1624
- Health-related QOL (HRQOL)
congenital heart disease (CHD), 1608
generic, disease-specific measurement, 1610, 1612, 1613t
health status and functional status, 1614
instrument availability, 1613f, 10610
instrument selection, 1610, 1611t, 1612t
instrument validation, 1610, 1613f
neurodevelopmental predictors, 1617–1618
pediatric heart disease population, 1609–1610
psychosocial predictors, 1618
specific heart disease subgroups, 1616–1617
- Heart. *See also* Fetal heart
anomalous connection and, 809
blunt cardiac injury, 552
cell types, 52, 53f
cellular constituents, 52, 53f
contraction, 57
imaging planes, 140, 140f
intrapericardial teratomas, 1550t, 1558–1559
mammalian development, 562, 562f
muscular dystrophy and, 1277–1278
normal, 1195, 1196f
position, 33–34
pulmonary veins development and, 809, 810f
sarcolemmal reticulum, 57
segments of, 1196
size and position, 1–2, 2f
weight, 1
- Heart beat initiation, 352, 353f
- Heart block, ccTGA and, 1150
- Heart center, safety and quality, 1622–1634
blame culture, 1624
bundles and checklists, 1628–1629
chest bleeding, 1622–1623
criminal negligence to blameless error, 1625, 1626f
culture, 1633–1634
data drive change, 1629–1632, 1629f, 1630f, 1631f
double check process, 1626, 1627f
ECMO, 1622
essential ingredient, 1633–1634
high reliability, 1632–1633
individual failures, 1624–1625, 1625f
just culture, 1624–1625, 1626f
key driver diagram, 1627, 1627f
RCA, 1623–1624, 1623f
SAQ, 1634
SMART aims, 1626–1627, 1627f
Swiss Cheese phenomenon, 1622
model, 1624, 1625f
team improvement, 1625–1626
- Heart defects
decreased pulmonary blood flow, 1410–1412
with increased pulmonary blood flow, 1401–1408
increased pulmonary venous pressure, 1408–1410
- Heart disease
adults and, 561
antepartum issues, 1495t, 1502
identification, 1568
- Heart failure
children, 1568
atrial natriuretic peptide (ANP), 1567
B-type natriuretic peptide (BNP), 1567
C-type natriuretic peptide (CNP), 1567
D-type natriuretic peptide (DNP), 1567
Ebstein's anomaly, 893
HCM, 1224
medical management, 1320
PA-VSD and, 965
during pregnancy, management, 1052–1053
TGA and, 1112
- Heart fields, morphogenesis of, 561–562
- Heart murmurs
classification of, 89–91
HCM, 1224
intensity of, 89
neonatal period and, 83
timing of, 89, 89f
tricuspid atresia, 879
- Heart opacification, contrast agents and, 164
- Heart pacemaking, 362–363, 365f
- Heart rate (HR), 85
ECG and, 128–129, 375
exercise, 121–122, 121f, 122f
- Heart sounds, 88
DMD and, 1279
intrapericardial teratomas, 1558
truncus arteriosus, 993
- Heart surgery
neurodevelopmental morbidities and, in children, 1579–1585
- Heart transplantation, 908. *See also* National Organ Transplant Act
acquired heart disease, childhood/adolescence, 1571
DCM and, 1244
exercise and, 108–109
HLHS, 1086, 1584
pediatric, morbidity, 1384
RCM and, 1275
univentricular atrioventricular connection, 1193
- Heart tube
extracellular matrix and, 561
formation, SHF cells, 568
outer curvature, 565
rightward looping, 562
- Heart valves. *See also specific i.e.* Mitral valves
injury, 555
- Heath-Edwards classification
of pulmonary vascular changes, 1402f
- HELEX septal occluder, 291, 321, 322
- Hemangiomas, 794–796, 1559
incidence, 1550, 1550t
- Hematocrit
cardiopulmonary bypass, 532
cerebral blood flow, postnatal peripheral circulation, 78
CNS and, 1581
- Hematologic disorders, 1590–1603
- Hematology
principles of, 1589–1590
- Hemiazygos veins, normal development, 843–844, 845f
- Hemiparesis, TGA and, 1113
- Hemodynamic data, cardiac catheterization and, 262, 262f
- Hemoglobinopathy, 1420–1421
pulmonary arterial hypertension, 1445–1446, 1446f

- Hemolysis, 1591
 Hemopericardium, 556, 557
 Hemostasis, 1589–1590
 disorders of, bleeding
 acquired von Willebrand Disease, 1594
 activated clotting time (ACT), 1593
 fibrinogen, 1593
 hemostatic testing, 1593
 platelet count, 1593
 platelet disorders, 1594–1595
 platelet mapping assay, 1593–1594
 thromboelastography (TEG), 1593
 Heparin
 electrophysiologic studies, intracardiac technique, 404–405
 labor and delivery, 1504
 pregnancy and, 1503
 Heparin binding (HB)-EGF, 570
 Heparin-induced thrombocytopenia, 1594–1595
 Hepatic circulations
 normal development, 844f
 postnatal peripheral circulation, 80
 Hepatic venous access, cardiac catheterization and, 260–261
 Hepatopulmonary syndrome, 164, 1444–1445
 Heterodimeric dystroglycan, 60
 Heterotaxy, 624t, 634, 1195
 interrupted IVC and, 855, 855f
 High frequency ultrasound
 animal studies, 167
 intracardiac echocardiography, 162
 High reliability, heart center, safety and quality
 human factors, 1632–1633
 systems thinking, 1632
 High reliability organizations (HROs), 1633
 High-altitude pulmonary edema (HAPE), 1434
 High-density lipoprotein (HDL), 1514
 cardiovascular disease, 1520
 Higher end-inspiratory lung volume (higher LV-EDV), 127
 High-torque wires, balloon valvuloplasty, 920
 High-voltage electrical injury, lightning-related
 injury *v.*, 557–558, 558t
 His bundle electrogram (HBE), 406
 HIV (Human immunodeficiency virus)
 apoptosis and, 1247
 infantile cardiomyopathy and, 84
 HLA alloantibodies, pediatric heart transplantation, 1384
 Holmes heart, 1181f
 Holter monitor
 muscular dystrophies, 1278
 RCM, 1275
 Holt-Oram syndrome
 CHDs, 622t, 631
 TBXS and, 571
 Homozygous familial hypercholesterolemia, 1521
 MRI, 1516
 Hormonal milieu, cardiac surgery and, 1582
 Hosmer-Lemeshow's goodness of fit, cardiac catheterization in children, 284, 410
 Hospital length of stay, neurodevelopmental outcome and, 1582
 Host immune response, RF and, 1305, 1306
 Host susceptibility, CNS and, 1581–1582
 24-hour ambulatory electrocardiography, 374
 Howell-Jolly bodies, abdominal situs and, 36
 Human embryonic life developmental stages, 351t
 Human factors, heart center, safety and quality, 1632–1633
 Human Genome Project, disease genes and, 618
 Human immunodeficiency virus (HIV)
 pericardial effusions, 1355, 1355t
 pulmonary arterial hypertension, 1445
 Humanitarian device exemption (HDE), transcatheter devices, 288
 Hunter and Hurler diseases, 1228
 Hybrid cardiac catheterization, 336–342, 336f–342f
 Hybrid stage II procedure, 338, 338f
 Hydantoin, pregnancy and, 1502
 Hydrogen protons (1H), MRI and, 207
 Hydrops fetalis
 fetal heart and, 645f
 fetal tachycardia, 662
 Hypercyanotic episode
 cardiac catheterization, 286
 Hypereosinophilic syndrome/Löffler endocarditis, 1269
 Hyperkalemia
 T-waves and, 385
 Hypersensitive Xiphoid syndrome, 1510
 Hypertension, 1527–1543
 in adolescents
 classification of, 1534, 1534t
 clinical evaluation, 1535t
 in children
 antihypertensive drugs, 1542t
 classification of, 1534, 1534t
 clinical evaluation, 1535t
 etiologic, 1535
 measurement in children, 1532, 1534
 pharmacologic treatment, 1539–1540, 1542
 treatment, 1536–1542
 Hypertensive right ventricle, angiocardiology, 948, 950f–952f
 Hyperthermia
 congenital heart defects and, 599
 Hypertriglyceridemia of uremia, 1522
 Hypertrophic cardiomyopathy (HCM), 1217–1232
 athletes heart *v.*, 1227, 1227f
 athletic screening and, 97
 children with, SCD risk, 1228–1229, 1229f, 1230f
 clinical features, 1226–1227
 definition and nomenclature, 1217
 exercise and SCD, 112
 families, clinical screening strategies, 1226, 1226t
 histopathology, 1218–1222
 in infants, diabetic mothers, 477–478
 medical management, 1229–1230
 algorithm for, 1229, 1231f
 morphology, 1218–1222
 pathophysiology, 1222–1224
 phenotype, 1218, 1222f
 preparticipation screening for, 1227–1228
 prevalence, 1217–1218
 pulmonary stenosis and, 920
 SCD, in youth, 389, 390f
 surgery and alternatives, 1231–1232
 troponin I mutations, 1267
 TTE and, 1383t
 wall motion abnormalities, 159
 Hyperuricemia, cyanotic adult, 1487
 Hypnotic drugs, 1078
 Hypoalbuminemia, protein-losing enteropathy and, HLHS, 1085
 Hypocarbica, pulmonary atresia and intact ventricular septum, 945, 945t
 Hypokalemia, 385
 Hypoplasia
 of arch, truncus arteriosus, 991
 of main pulmonary artery, arterial switch operation, 1135
 mitral valve, 1006–1007, 1006f, 1007f
 of right ventricle, 1180f, 1181
 tricuspid valve annulus, 150
 Hypoplastic left heart syndrome (HLHS), 305, 336–339, 337f, 570, 1061–1089
 anatomy and, 1063–1064
 coarctation of aorta, 1045
 epidemiology and genetics, 1061
 family studies of, 621
 fetal development, 1061–1062
 fetus, 646
 HRQOL, 1617
 hybrid stage I, 337f, 338
 MRI, 239f
 neonate, preoperative preparation, 1072–1074
 in PICU, 510–511, 510f, 511f
 pediatric heart transplantation, 1386
 postoperative management, 1080
 presentation and diagnosis, 1064–1067
 single ventricle, 1583–1584
 spectrum of, 1063
 stage 2 palliation, interstage management, 1080–1082
 stage 1 palliation, postoperative management, 1080
 venous oximetry, 486
 with ventricular septal defect, forms of, 1064
 Hypoplastic left ventricle, 1179f
 Hypoplastic right heart syndrome, persistent
 valves of sinus venosus, 860
 Hypoplastic tripartite right ventricle with pulmonary atresia, 954f
 Hypoplastic ventricle, 41
 Hypothermia
 cardiopulmonary bypass, 532–533
 HLHS and, 1076
 Hypothermic circulatory arrest (DHCA), 1077
 in infants, CPB and, 531, 532
 Hypothyroidism
 PICU, 522
 pericardial effusion, 1356
 triglycerides and, 1522
 Hypotonia, Down syndrome, 625
 Hypovolemia, cardiac tamponade, 556
 Hypovolemic-septic shock, stress response, 1068
 Hypoxemia
 late Fontan and, HLHS, 1085
 TGA and, 1112
 univentricular atrioventricular connection, 1185
 Hypoxia
 pulmonary atresia and intact ventricular septum, 945, 947
 pulmonary vasoconstriction, 1412
 Hypoxia-induced pulmonary vascular disease, 1412
 Hypoxic patient, HLHS and, 1018, 1073
 Hypoxic pulmonary vasoconstriction, fetal heart and, 72
 I
 ICD device (Implantable cardioverter-defibrillator), 466, 468, 1574
 indications for, 468t
 ventricular tachycardia, pregnancy and, 1503
 Idiopathic chest pain, 1509
 Idiopathic dilation of main pulmonary artery, valvar pulmonary stenosis *v.*, 920
 Idiopathic pulmonary arterial hypertension (IPAH)
 congenital heart disease, 1441
 connective tissue disease, 1440–1441
 eisenmenger syndrome, 1443–1444, 1445f
 heritable-familial pulmonary, 1439–1440, 1441f
 operability, 1442–1443, 1442f, 1443f, 1444f
 Idiopathic pulmonary hypertension, 1426–1429
 Illicit drugs, cardiac diseases and, 84
 Image artifacts, CMR and, 212, 212t
 Imaging. *See also* specific *i.e.* MRI
 anomalous left coronary artery from pulmonary artery, 751
 atherosclerosis, 1514, 1515
 DMD and, 1280, 1280f
 double aortic arch, 779, 782
 fetal risks and, 1502
 LSVC and, 846–847, 847f
 muscular dystrophies, 1278
 pulmonary arteriovenous malformations, 793
 systemic arterial malformations, 790, 791f
 Imatinib, novel therapy of PAH, 1455
 Immune system
 pediatric heart transplantation, 1395
 RF and, 1305
 Immune thrombocytopenia, 1595
 Immunosuppression
 pediatric heart transplantation, 1395
 Immunosuppressive agents
 myocarditis, 1263
 Impedance cardiography, 131
 Imperforate valve, cardiac catheterization and, 947f
 Implantable axial-flow device, 540
 Implantable loop recorder, tachyarrhythmia, 444
 Implanted metallic objects, CMR and, 211–212
 In situ hybridization, myocarditis, 1253
 Inability to wean, pediatric ECMO, 535
 Incomplete? Right bundle branch block, QRS complex, 378–379
 Incremental cycle ergometer protocol, 128
 Indeterminate atrial morphology, 39

- Individual approach, diet and, dyslipidemia in children, 1524–1525, 1525*t*
- Induced pulmonary insufficiency, 924–925
pulmonary valve replacement for, 924–925
- Inducible nitric oxide synthase (iNOS), myocarditis, 1259
- Infantile aortic stenosis, symptoms, 1026
- Infantile cardiomyopathy, HIV and, 84
- Infantile hemangiomas (IHs), 864, 865*t*
angiography, 866, 869*f*
MRI of, 866, 868*f*
ultrasonography of, 866, 867*f*
vascular anomalies, 865, 865*f*
- Infants. *See also* Preterm infant
atrial septal defects
clinical features
physiology of
blood cysts, 10
blood pressure measurements, conditions for, 1535*t*
cardiac examination, isolated valvar pulmonary stenosis, 916
ccTGA and, 1149
cervical aortic arch, 778
CMR, 210, 211*f*
coarctation of aorta, 1045, 1049
drug disposition in, developmental changes, 1664*f*
florid tricuspid regurgitation, 939
intrapercardial teratomas, 1558
isolated valvar pulmonary stenosis, 914
LV hypertrophy, 729
patient history, 82–83
preterm
physiology, 473–480
pulmonary flow murmur, 92
QRS complex, 386
rhabdomyoma and, 1552
right ventricular hypoplasia, pulmonary atresia and intact ventricular septum, 949
Toronto transseptal catheter, 297
treatment of PDA, 738–739, 738*f*
truncus arteriosus, 993, 996–997, 998*f*
- Infarction, CHD and, 1580
- Infection
chest pain, 1511
neurologic morbidity, 1582
- Infectious agents, myocarditis, childhood/adolescence, 1567
- Infectious diseases, pediatric heart transplantation, 1392
- Infective endocarditis (IE), 1363–1375
antimicrobial therapy
general principles of, 1369–1371
clinical features, 1366–1367
laboratory features and, 1366, 1366*t*
diagnostic criteria, 1368
echocardiography
surgical intervention, 1368
epidemiology, 1363
laboratory features and, 1367–1368
micro-organisms, 1363–1364, 1364*t*
mitral valve vegetations, 1369*f*
modified Duke criteria, 1368
pathogenesis, 1364–1366, 1364*t*
prophylaxis, 1374–1375, 1375*t*
- Inferior vena cava (Inferior caval vein), 7, 38
anomalies of, 855–858
drainage to left atrium, 856–858, 857*f*
echocardiogram and, 146*f*, 147
normal development, 841–843, 844*f*, 845, 846*f*
obstruction, atrial switch repair, 1123, 1124, 1127*f*, 1128*f*
return, fetus and, 70, 71*f*
sinus venosus defects, subcostal sagittal view, 146*f*, 147
- Infiltrative myopathies, 1228, 1269
- Inflammatory response
cardiopulmonary bypass, 532
HLHS and, 1067, 1068
- Inhaled nitric oxide, 496–497
- Inhibitors of cholesterol absorption, 1527
- In-hospital cardiac arrest, pediatric ECMO, 535–536
- Injection drug users, IE and, 1364, 1364*t*
- Injury. *See also* Coronary artery; Electrical injury; Myocardial injury
heart valves, 555
intra-abdominal injury, 556
lightning, 557–558
- Innocent murmurs, 91–92
- Innominate artery compression of trachea, 787–788, 788*f*
- Inotropes, 492*t*, 493–494,
HLHS and, 1073
myocarditis, 1262
- Inoue balloon, 303, 304*f*
- Inspired gases, HLHS and, 1073
- Instrument availability, HRQOL, 1613*f*, 10610
- Instrument selection, HRQOL, 1610, 1611*t*, 1612*t*
- Instrument validation, HRQOL, 1610, 1613*f*, 1613*t*
- Insulin-dependent diabetes, PA-VSD and, 959
- Intact ventricular septum (IVS), and pulmonary atresia and, 939–956
- Integrins, extracellular matrix, 59
- Intelligence quota (IQ) scores, 1582
CHD repair, 1582
d-TGA outcome and, 1583
heart surgery in children and, 1579
HLHS, 1583
TOF and, 1583
- Interarterial communication, 813
- Interatrial septum, pulmonary venous drainage and, 826
- Intercalated discs, cell-cell interactions, 60
- Interferon, myocarditis, 1263
- Intermediate AVSD, 691
- Intermediate filament, myocyte and, 64
- Internal jugular vein, approaches to, cardiac catheterization and, 260
- Internal mammary artery bypass grafting, supra-valvular aortic stenosis, 1039
- Interrupted aortic arch, 783–786
complete TGA and, 1106
diagnosis and management, 784–786
DiGeorge syndrome, 991
embryology, 784
types, 785
- Interrupted aortic arch type B, 22q11 deletion syndrome, 627
- Interrupted inferior vena cava (Interrupted IVC), 148*f*, 855, 855*f*
- Interstage death, risk factors, HLHS, 1080
- Interstage monitoring program, HLHS, 1080–1081
- Interstitial edema, fetal heart and, 649
- Interventional armamentarium, 289–294
- Interventricular conduction delay, cardiac resynchronization therapy, 1574
- Interventricular dyssynchrony
echocardiography, 198, 198*f*
- Intestinal circulation, feeding and, postnatal peripheral circulation and, 80
- Intestinal obstruction, anomalous termination of umbilical veins, and absent ductus venosus, 859
- Intra-abdominal injury, penetrating injury, 556
- Intra-aortic balloon pump (IABP)
children and, 537
circulation support and, 537
pediatric circulation support and, 537–538
- Intra-atrial baffle repair, 1126*f*
- Intra-atrial communications, 294–297
- Intraatrial reentrant tachycardia (IART), 430, 451–452, 452*f*
- Intracardiac echocardiography (ICE),
transcatheter closure of atrial septal defects, 290
- Intracardiac echocardiography, ASD, 681
- Intracardiac electrograms
display and recording, 405, 419
- Intracardiac electrophysiologic study, pacing protocols, 410*t*
- Intracardiac shunt
contrast agents and, 164
derived hemodynamic variables and, 266
qualitative assessment of, 270–271
quantitative assessment of, 269–270
- Intracardiac techniques
comparison of, 416–417, 417*t*
electrophysiologic studies, 405, 416–417
- Intracardiac teratomas, 1558
- Intracardiac tumors, pulmonary stenosis and, 920
- Intracellular calcium signaling, calsequestrin, 62
- Intramural coronary arteries, abnormal, HCM and, 1218, 1219
- Intrapercardial bronchogenic cysts, 1558
- Intrapercardial teratomas, 1550*t*, 1558–1559
incidence, 1550, 1550*t*
- Intrapulmonary shunts, microbubbles in heart and, 164
- Intrauterine antitachyarrhythmic therapy, 664–666
- Intrauterine devices, CHD and, 1504
- Intrauterine fetal demise
congenital heart disease and, 657, 661*t*
- Intravenous agents
intracardiac study and, 407
- Intravenous contrast injection, CT, 248
- Intraventricular dyssynchrony
deformation imaging, 199, 200*f*
mechanical dyssynchrony in children, 199–200
M-mode, 198
three-dimensional echocardiography, 199, 200*f*
tissue doppler imaging, 198–199
- Intrinsic regulation, E-C coupling
cardiac force-frequency relationship, 63
Frank-Starling relationship, 63
sympathetic innervation, 63–64
thyroid hormone, 64
- Ionizing radiation
children, CT protocols, 247
CT *v.* MRI, 247
- Isolated dextrocardia
with AV and ventriculoarterial discordance and left anterior aorta-corrected TGA, 1202–1203, 1204*f*, 1205*f*
with AV concordance and normally related great arteries, 1202
- Isolated tricuspid stenosis, 885
- Isolated valvular pulmonary stenosis, 913–920
differential diagnosis, 920
embryology and pathology, 913, 914*f*
manifestations of, 914–920, 915*f*
physiology, 914, 915*f*
- Isomerism, 34
- Isometric exercise, 118
blood pressure, 124
coarctation of aorta, 102
HDL and, 1519
ventricular septal defects and, 99
- Isoproterenol, 492*t*, 494, 1673*t*, 1674–1675
DCM, 1243
intracardiac study and, 407
myocardial contractility, 1224
- Isotonic exercise, 118
blood pressure, 123, 124
oxygen consumption and, 93
- Isotropic 3-dimensional steady-state free precession MRI, 215, 216*f*
- Ivemark syndrome, 1196
- J
- Jacobsen syndrome, 1023
- JAG1 gene mutation
tetralogy of Fallot, 636
- Jagged 1, Alagille syndrome, 630–631
- James protocol, cycle testing, 128, 128*t*
- Judkins right coronary guide catheters, 319
- Jugular venous approach, Fenestrations and, 322
- Jugular venous pulsations, isolated valvar pulmonary stenosis, 916, 916*f*
- Junctional ectopic tachycardia (JET), 430–431, 449–450, 450*f*
- Juxtaposition of the atrial appendages, tricuspid atresia, 877
- K
- K⁺ channels, cardiac action potential, 55, 55*f*
- Kabuki syndrome, 633

- Kaplan-Meier survival curve, 1440f
 ES, 1473–1474, 1474f
 programmed stimulation, 1478
- Kaposiform hemangioendotheliomas (KHEs), 864
- Kartagener syndrome, 634
- Karyotype, 617
- Karyotypic abnormalities, CHD and, 651
- Kawasaki disease (KD), 1240, 1377
 activities of daily living, 111
 aneurysm(s), 110
 Bethesda conference report, 111
 cardiac MRI, 226
 exercise and SCD, 110–111
 MDE and, 228f
 myocardial infarction, 385
 pericarditis, 1356
 TTE and, 1382
- Kearns-Sayre syndrome, 1228
- Kidney, neonates and, 78–79
- Knott-Craig Approach, Ebstein's anomaly, 897–898, 901f
- Konno procedure, subvalvular aortic stenosis, 1038
- Korotkoff sounds, 85, 1535
- KRAS mutations, Noonan syndrome, 633
- Kuhne classification system, tricuspid atresia, 877
- Kussmaul's sign, 1351
- L**
- Labor and delivery
 CHD and, 1494
 management issues, 1504
- Laid-back aortogram, 1118, 1118f, 1119f
- Large collateral arteries, truncus arteriosus *v.*, 996
- Large ductus arteriosus, persistent patency in, infants, children, and adults, 729–730
- Late diastolic murmurs, 89f, 91
- Late systolic murmurs, 89f, 90
- Lateral resolution, 136, 136f
- Lateral thoracotomies, PA-VSD and, 966, 967f
- Late-stage ventricular failure, arterial switch for, d-TGA, 1485
- Latex allergy, cardiac catheterization, 286
- LCOS. *See* Low cardiac output syndrome
- LDL. *See* Low-density lipoprotein
- Leaflets
 atrioventricular valves, 11, 11f
 isolated valvar pulmonary stenosis, 913
 thickening, chronic rheumatic heart disease, 1316
 valvular aortic stenosis and, 1024
- Lecompte maneuver, 1141
- Left anterior descending coronary artery from pulmonary artery, 752
- Left anterior Hemiblock, QRS complex, 260, 379–380
- Left aortic arch, 758
 with cervical origin of right subclavian artery, 765–766, 765f
 with isolated subclavian artery, 765
 normal, 760, 761f
 and variants, 760
 with retroesophageal diverticulum of Kommerell, 763, 763f
 with right descending aorta and right ductus diagnosis and management, 764–765
 embryology, 764–765, 764f
 with right descending aorta and right ductus, 764–765, 764f
- Left atrial appendage, 146, 147f
- Left atrial dilation, 9
- Left atrial drainage of right superior vena cava, 850–851, 851f
- Left atrial free wall, 9
- Left atrial (LA) pressure, 723
- Left atrial septal structure, 146, 147f
- Left atrioventricular (AV) valve, 40
 ccTGA and, 1151
- Left atrium, 9, 39
 microscopic anatomy, 827
 pulmonary atresia and intact ventricular septum, 941
- Left bundle branch block (LBBB), QRS complex, 379, 379f
- Left circumflex coronary artery from pulmonary artery, 752
- Left coronary artery, 731
- Left heart
 cardiopulmonary interactions and, 548
 catheterization, 265, 265f
 desaturation, oxygen and, 271
 hemodynamics, right heart hemodynamics *v.*, 546, 547f
 pulmonary arterial hypertension, 1447
 waveforms, left heart catheterization, 265, 265f
- Left innominate vein (LIV), left pulmonary veins, 817
- Left posterior Hemiblock, QRS complex, 380
- Left pulmonary artery sling, spin echo and, 234
- Left pulmonary veins (LPVs)
 to inferior vena cava, 817
 to left innominate vein, 817–818
 PAPVC, 817f
- Left subclavian flap aortoplasty, coarctation repair, 1057
- Left superior vena cava (LSVC), 846
 venogram of, 849
 view, 146, 148f
- Left ventricle (LV), 14–15, 15f, 41, 150–151
 diastolic function
 pseudonormal diastolic dysfunction, 194–195
 restrictive physiology, 195–196
 stage I diastolic dysfunction, 194, 194f, 195f
 echocardiography
 2-D and 3-D techniques, 172–174, 173f, 174f
 left ventricular mass, 174
 M-mode measurements, 172, 173f
 three-dimensional echocardiography, 174, 174f
 two-dimensional measurement, 172, 173f
 effects on RV, 549, 549f
 free wall, 147, 147f
 hypertrophy and, 1218
 mass, 1382
 Devereux method of calculation, 1536
 preparation, TGA with low left ventricular pressure, 1138–1139
 pressure tracings, 1026f
 pulmonary atresia and intact ventricular septum, 941
 tetralogy of fallot, 983–984
- Left ventricle outflow-aortic complex, HLHS and, 1063
- Left ventricle with normally related great arteries (A-1 single ventricle), 1180, 1181f
- Left ventricular angiography, pulmonary atresia and intact ventricular septum, 948, 950f–952f
- Left ventricular angiography, coarctation of aorta, 1051
- Left ventricular cavity hypoplasia, HLHS and, 1063
- Left ventricular diastolic dysfunction, coarctation of aorta and, 1048
- Left ventricular function
 after primary arterial switch, indices of, 1139f
 ASD, 686
- Left ventricular hypertrophy (LVH), 381–382, 381f
 age *v.* patient proportion, 1228, 1229f
 HCM and, 1222
 morphology, 1218
 valvular aortic stenosis and, 1025
- Left Ventricular Hypoplasia, 708
- Left ventricular mass
 echocardiography, 174
- Left ventricular outflow tract (LVOT), 1106
 fetal cardiovascular system and, 646, 653f
 stenosis, echocardiogram, 1114
- Left ventricular outflow tract obstruction (LVOTO), 1141–1142
 fetal intervention and, 1062–1063
 HCM, 1222–1224, 1223f
 HLHS, 1064
 maternal risk and, 1500
 TGA, 1097, 1099f, 1101, 1104f, 1141–1142
- Left ventricular outflow, valvular aortic stenosis, 1036
- Left ventricular pressure-volume loop, 65
- Left ventricular subendocardial ischemia, valvular aortic stenosis, 746, 1025
- Left ventricular wall segments, 220f
- Left ventriculogram, 283, 283f
- Left vertebral artery, separate origin of, 760, 761f
- Left-right asymmetry, cardiac looping, 565–567, 566f
- Left-sided lesions, 1467–1471, 1468–1471
- Left-sided obstructive defects, family studies of, 621
- Left-sided obstructive lesions, 516
 aortic coarctation, 101–102
 aortic stenosis, 100
 bicuspid aortic valves, 101
- Left-to-right shunts
 in infancy
 bilateral superior venae cavae, with unroofed coronary sinus, 848
 lesions, 100–102, 1471–1474
 maternal risk and, 1497–1498
 PH, 1472
 quantitative assessment of, 269–270
 TGA and, 1106
- Leftward juxtaposition of atrial appendages, TGA and, 1106
- Leisure activity, 94–95
- Lentigines, myxomas, 1557, 1557f
- LEOPARD syndrome, 622t, 633
- Leukemia, 1560
- Leukocytosis, acute IE and, 1368
- Levodardia, 145, 1195, 1207
 pulmonary atresia and intact ventricular septum, 939
 subcostal coronal views, 146f
- Levonorgestrel, CHD and, 1504
- Levoposition, balloon atrial septostomy, 1116
- Levosimendan, 497–498, 1243
- Lidocaine, 457, 1681
- Lifestyle modification, hypertension and, 1536
- Lightning-related injury, 557–558
 high-voltage electrical injury *v.*, 557–558, 558t
- Limb reduction, 651
- Limb-Girdle muscular dystrophies, 1285–1286
- Limbus of fossa ovalis, morphologic right atrium and, 39
- Linkage analyses, Holt-Oram syndrome, 631
- Lipid deposit, arterial wall, 1514
- Lipids, 1519–1521, 1519t
 distribution in children, 1521t
 normal levels, 1520
 physical activity, 1518
- Lipoproteins, 1519–1521, 1519t
 classes of, 1519
 distribution in children, 1521t
 normal levels, 1520
 physical activity and, 1518
- Lisinopril, 1243, 1678
- Lithium
 congenital heart defects and, 600–601
 pregnancy and, 1502
- Lithium dilution cardiac output (LiDCO), 488
- Liver
 abdominal situs ambiguus, 1195
 abdominal situs and, 36, 37f
 child assessment and, 91
 interrupted IVC and, 855, 855f
 mass, asplenia, 1195, 1197f
 postnatal peripheral circulation, 80
 VLDL and, 1520
- L-loop, chirality and, 1200, 1201f
- LMNA gene, 1277
- LMWH. *See* Low-molecular weight heparin
- Long QT syndrome (LQTS), autopsy-negative SUD, 391
- Long-axis view, ccTGA and, 1152f
- Loop diuretics, 1675–1676
- Loop of Henle, drugs and, 1243
- Low birth weight (LBW) infants, 484, 523
- Low cardiac output syndrome (LCOS)
 clinical findings in, 489t
 prevention and management of, 489–498
 pulmonary atresia and intact ventricular septum, 948

- Low-density lipoprotein (LDL), 1514, 1520
cutpoints for, children and adolescents, 1525t
1525t
receptor mutations, 1521
sequential steps in, 1520f
- Lower body cyanosis
infants and, heart disease and, 82–83
- Lower end-expiratory lung volume,
exercise, 127
- Low-estrogen oral contraceptives, CHD and,
1504
- Low-flow deep hypothermic bypass, 531
- Low-molecular weight heparin (LMWH)
HLHS, 1080
pregnancy and, 1503
- Lown-Ganong-Levine syndrome, 380–381
- Low-voltage QRS complexes, 383
- LPVs. *See* Left pulmonary veins
- LSVC. *See* Persistent left superior vena cava
- Lung(s)
biopsy
grades of, 1403–1404
pulmonary arterial hypertension, 1439
pulmonary vascular bed, 1402–1405,
1405f
development, 474–475
inflation, pulmonary vascular resistance and,
546, 547f
microscopic anatomy, 827
transplantation, stenosis of individual
pulmonary veins, 836
underdevelopment of, 1418
- Lung disease
differentiate, heart failure, 1568
obstructive, 1415
- Lutembacher syndrome, 674
- LVH. *See* Left ventricular hypertrophy
- LVOTO. *See* Left ventricular outflow tract
obstruction
- Lymphatic malformations, 872–873
- M
- Macrophages, LDL and, 1520, 1520f
- MADIT II trial, 1574
- Magnesium
arrhythmias, 459
imbalance, 385
- Mahaim fiber, 448
- Mahaim's pathway, 380
- Mahaim-type reentry tachycardia, 358
- Main pulmonary artery
echocardiography, 152
obstruction, univentricular atrioventricular
connection, 1185
positions of, 42, 43, 44f
- Major aortopulmonary collateral arteries
(MAPCAs), PA-VSD and, 966
- Malaligned atrial septum, 699
- Malalignment, 48, 48f–50f
- Malformation syndrome
genetic syndromes, 623
mutations in single gene, 630–634
- Malformed hearts
aortic position of, 43
history, 32
- Malignant myxomas, 1556
- Malignant pericardial tumors, metastases and,
1560
- Malposition of septum primum, 815–816, 815f
imaging, 815f
PAPVD and, 815
- MAPCAs. *See* Multiple aortopulmonary col-
laterals
- Marfan syndrome (FBN1), 618, 1470
aortic regurgitation, 101
childhood/adolescence, 1567
CMR and, 233
congenital aortic stenosis, 1033
3-D flow vector mapping, 226, 226f
labor and delivery, 1504
maternal risk and, 1500–1501
pregnancy and, 1504
- Marfan syndrome (MFS)
diagnosis, 799, 800t, 801, 801f, 802f
FBN1 mutations, 799
therapy, 802, 803f
transforming growth factor beta, 799
- Marker catheter, calibration error and, 274
- Maternal diabetes
congenital heart defects, 597
fetus and newborn infant, 477
PA-VSD and, 959
truncus arteriosus, 990
- Maternal environmental exposure, teratogens
and, cardiac defects, 84, 84t
- Maternal hypoxemia, 78
- Maternal mortality, CHD and, 1500
- Maternal phenylketonuria (PKU)
congenital heart defects, 599
PA-VSD and, 959
- Maternal risk, cardiac diseases, 1496
- Maternal-Fetal Medicine community, 657, 666
- Matrix array three-dimensional echocardiog-
raphy, tumor volume analysis, 1550,
1551f
- Maturing AV conduction system, 364–367
- Max LD stents, 305f, 306, 306f, 315
- Maximal aerobic power, determinants of,
119–121, 120f
- Maximum oxygen uptake (VO₂ max)
age in children v., 120f
in children, by ethnic group, 120
- Maximum ventilation volume (MVV), exercise,
126–127
- McFee system, 373
- MCSDs. *See* Mechanical circulatory support
devices
- MDCT (Multidetector computed tomography)
electrocardiograph gating and, 251, 251f
future directions, 255
- 8-MDCT scanner, 252f
- 64-MDCT scanner, 249f, 251
- Mean Aortic valve gradient, 272
- Mean modal velocity, 141
- Mechanical circulatory support devices
(MCSDs). *See also* Pediatric circulatory
support systems
duration of support, 540
HLHS and, 1079–1080
infants and children, indications for, 535t
long-term, for children, 538–543
pediatrics, 530
short term, 530–538
- Mechanical interventions, RF, 1325
- Mechanical stimulation, cardiac fibroblasts,
52–53
- Mediastinal radiation, RCM and, 1269
- Mediastinum, 1–2, 2f
heart position in, 1–2, 33
- Medroxyprogesterone acetate, CHD and, 1504
- Medullary blood flow, 78, 79
- Mega LD stents, 312, 315f
- Membranous septum, cardiac base and, 17
- Mendelian genes, syndromes due to, 634–636
- Mental health, CHD, 1584
- Mental retardation
intelligence quotient, 1579
Williams-Beuren syndrome (7q11 deletion),
628–629
- Mercurial agents, RCM and, 1269
- Mercury sphygmomanometer, 1535
- Mesenchyme cells, 567, 568
- Mesocardia, 1195, 1207, 1211
- Metabolic syndrome, 1518t
cardiovascular disease, 1518
obesity and, 1523
- Metallic implants, Fontan palliation, CMR and,
241
- Methysergide, RCM and, 1269
- Metolazone, 1676
- Metoprolol, 1680
HCM and, 1229
heart failure and, 1573, 1574
- Mexiletine, 457, 1681
- MFS. *See* Marfan syndrome
- MI. *See* Myocardial ischemia
- Microbubble “cloud,” contrast echocardiogra-
phy, 164
- Microcytic anemia, 1590
- MicroMed DeBakey VAD *Child*, 540
- Micro-organisms, IE, 1363–1364, 1364t
- MicroRNA (miRNA) regulation, cardiomyocyte
differentiation, 564–565, 564f
- Microtubules, myocyte and, 64
- Microwave, electrophysiologic therapeutic cath-
eterization, 420
- Midazolam
CMR and, 208
electrophysiologic studies, intracardiac tech-
nique, 403
- Middiastolic murmurs, 89f, 90–91
- Midline apex of heart, situs ambiguus, 33–34
- Migratory polyarthritis, GAS infection, 1309t,
1310
- Mild valvar pulmonary stenosis, 920, 923
- Milrinone, 492t, 493–494, 1675
DCM, 1242
HLHS and, 1073
pediatric heart transplantation, 1386,
1388–1389
- Mini Tyshak balloons, 300
- Minimum anesthetic concentration (MAC), stage
1 palliation, HLHS and, 1075–1076
- Minute ventilation, ventilation measurements,
131
- Minute volume, 132
- Miracle ICD trial, 1574
- Mirror-image dextrocardia, 145
- Mirror-image right arch, 766–767, 767f
diagnosis and management, 767
embryology, 767
- Miscarriages, cardiac defect and, 625
- Mitochondrial DNA, Kearns-Sayre syndrome
and, 1228
- Mitochondrial metabolism, 58
- Mitral annulus, 1004–1005, 1004f
- Mitral annulus reversus, 1360
- Mitral arcade, 1008, 1009f
- Mitral atresia, 41, 827
- Mitral regurgitation
ASD, 686
assessment of
dominant pulsed Doppler E profile, 1015,
1015f
left atrial and left ventricular size, 1014,
1014f
pulmonary venous Doppler pattern, 1015,
1015f
vena contracta size, 1013–1014
congenital
management and prognosis of, 1020
Doppler assessment, 1015
- Mitral stenosis, 187–188, 187f
chronic rheumatic, 1322
chronic rheumatic heart disease, 1268, 1269f,
1317, 1318f
heart murmurs, 90–91
- Mitral valve(s), 12, 39–40, 1148
abnormalities, 1106
approaching
chronic rheumatic mitral stenosis, 1316
cleft mitral valve, 1009–1010, 1009f, 1010f
in corrected transposition, 1010, 1012f
development, 1003
dilation, 303, 304f
disease, coarctation repair, 1057
Doppler spectral profile, 143f
double-orifice, 1010, 1011f
dysplasia and hypoplasia, 1006–1007, 1006f,
1007f
Ebstein's-like anomaly, 1010
echocardiography, 150
flow, Gorlin equation for, 272t
HCM, 1218
hemodynamic assessment of, 1013, 1014f
leaflets and supporting apparatus, 1005–1006,
1005f
mitral arcade, 1008, 1009f
morphology and function, 1003
parachute, 1010
straddling of, 1010–1011, 1012f–1013f, 1013
supravalvular mitral stenosis, 1008, 1008f
TEE, 154, 156f
TGA and, 1098, 1098f
tricuspid valves v., 39–40
- Mitral valve Doppler spectral profile, peak veloc-
ity trace, modal velocity trace v., 143f

- Mitral valve prolapse (MVP), 1474–1475
 clinical presentation of
 electrocardiography, 1017, 1018f
 hemodynamic evaluation, 1018
 magnetic resonance imaging, 1018
 physical findings of, 1017
 radiography, 1017–1018
 echocardiographic assessment, 150, 1016f, 1017
 IE, 1365t
 management and prognosis of, 1020
 mitral annulus, 1015–1016, 1016f
 MMVP1 and MMVP2, 1017
 mural leaflet, 1017
 pediatric population, 1015
 valvar pulmonary stenosis *u.*, 920
 Mitral valve replacement (MVR), 1019–1020
 Mitral valvular regurgitation (MVR)
 chronic rheumatic heart disease, 1316
 rheumatic carditis, 1311–1312, 1313
 MLC2. *See* Myosin light chain
 M-mode calculation, LV mass, 166f
 M-mode echocardiography, 644
 congenital heart disease and, 134
 Moderate ductus arteriosus, persistent patency
 in, infants, children, and adults, 729
 Moderate pulmonary valve stenosis, course and
 prognosis, 924
 Modified Blalock-Thomson-Taussig shunt
 pulmonary angiography, 279–280, 282, 282f
 Modified Fontan operation, 879, 880, 885
 Molecular diagnostics, myocarditis, 1253–1254
 Molecular genetics, 1061
 Molecular pathways regulating sinus node development, 354f
 Monitoring
 CMR and, 208, 210, 210f
 Monoclonal antibodies, pediatric heart transplantation, 1389
 Monopril, DCM and, 1243
 Morphologic right atrium, limbus of fossa ovalis
 and, 39
 Morphologic tricuspid valve, lesions of, ccTGA
 and, 1148
 Mortality. *See also* Survival
 anomalous left coronary artery from pulmonary artery, 749–752
 cardiac catheterization, 285
 in children, 411
 cardiac transplantation, HLHS, 1086
 DCM and, 1235
 Fontan operation, HLHS, 1084
 HCM, 1223f, 1228
 HLHS and, 1062, 1063
 PA-VSD and, 966, 967f
 penetrating cardiac wounds, 556
 TAPVC
 surgery for, 831
 tricuspid atresia, 885
 Mortality rate
 arterial switch operation, 1132
 ccTGA and, outcomes for, 1158
 coarctation of aorta, surgical repair, 1052
 Mosaicism, 625, 626
 Motion artifact, CMR and, 208, 210
 Motion Picture Expert Group method (MPEG)
 method, digital echocardiography,
 165–166
 Motor vehicle crash, blunt cardiac injury, 552
 Mouse
 echocardiography, 166, 166f
 embryo, human gestation *u.*, 561
 MPI. *See* Myocardial performance index
 MRA (Magnetic resonance angiogram)
 LSVC and, 847, 848f
 peripheral pulmonary arterial stenosis, 931
 TAPVC, 829
 truncus arteriosus repair, 1000f
 MRI (Magnetic resonance imaging). *See also*
 Cardiac MRI
 absent right superior vena cava, in vis-
 ceroatrial situs solitus, 850, 850f
 anomalous muscle bundles, 927
 anomalous pulmonary venous connection,
 820–821
 aortic dilation, 802, 803f
 atherosclerosis, 1516
 bicuspid aortic valve, 804
 cardiac tumors, 1551, 1552f
 ccTGA and, 1154, 1154f, 1155f
 CHD and, 1580
 coarctation of aorta, 1049–1050
 contraindications for, 212
 cor triatriatum, 836
 diastolic function, 222–223
 Duchenne muscular dystrophy, 1281, 1281f
 Ebstein's anomaly, 897, 899f, 900f
 intrapericardial teratomas, 1559
 MDCT *u.*, 255
 mitral valve prolapse, 1018
 pericardial disease, 1353
 peripheral pulmonary arterial stenosis,
 930–932
 pulmonary arterial hypertension, 1436
 stenosis of individual pulmonary veins, 837
 TAPVC, 829
 techniques, 207–208, 209f–210f
 truncus arteriosus, 966f, 996
 truncus arteriosus repair, 1000f
 Turner syndrome, 626
 ventricular septal defects, 717
 Multi Track system, 303
 Multifenestrated atrial septum, Amplatzer cribriform
 septal occluder and, 319, 322f
 Multifocal atrial tachycardia, 449, 450t
 Multiple aortopulmonary collaterals (MAPCAs),
 516
 Multiple lentiginos syndrome, pulmonary stenosis
 and, 920
 Multisystem organ dysfunction, HLHS and, 1080
 Multi-Track catheter, 300
 Mumps virus vaccine, 1264
 Murmurs. *See also specific i.e. innocent murmurs*
 coarctation of aorta, 1049
 isolated valvar pulmonary stenosis, 915
 myxomas, 1556
 peripheral pulmonary arterial stenosis, 935
 rheumatic carditis, 1311
 truncus arteriosus, 993
 Muscatine studies, 1520, 1528
 obesity in childhood, 1518
 Muscle bundles, left ventricle and, 14
 Muscle strain, chest pain and, 1510
 Muscular dystrophy
 assessment tools, 1278
 cardiomyopathy and, 1277
 with clinical cardiac disease, 1277–1278
 dystrophin and
 heart in, 1277–1285
 Muscular septal defects device closure, 323–325
 Mustard procedure, 1122, 1125f, 1479
 baffle obstructions and, 1481
 banding, 1157–1158
 ccTGA and, 1157, 1157f
 pulmonary venous atrial morphology, 1126f
 Senning repair *u.*, 1122–1128
 superior vena caval pathway obstruction,
 1123, 1127f
 TGA, 104, 1098, 1143
 tricuspid valve regurgitation, 1483
 MUSTT trial, 1574
 Mutations, disease-related, 618
 MVP. *See* Mitral valve prolapse
 Mycophenolate mofetil (MMF), pediatric heart
 transplantation, 1389
 Myocardial architecture
 electrophysiologic impulses and, 1218
 MRI and, 228, 228f
 Myocardial bridges, 752–753
 Myocardial contraction
 interventions for, 1224
 mature heart and, 52
 systolic function and, 65
 Myocardial contusions, 553–554
 autopsy-proven, history of, 554
 complications, 554
 Myocardial dysfunction, 1567
 brain death, 1388
 childhood/adolescence, 1567
 heart rate and respiratory rate, 85
 isoproterenol, 494
 neonates and infants, 1565
 Myocardial fibrosis, valvular aortic stenosis and,
 1025
 Myocardial function, 62–63
 assessment, CMR, 219
 development of, 52–66, 649
 rhabdomyositis and, 1552
 Myocardial infarction
 CPK-MB isoenzyme, 557
 family history, 84
 HMG-CoA reductase inhibitors, 1527
 Kawasaki disease, 385
 myocardial viability, 227
 Myocardial injury
 biomarkers of, 1379–1380
 Myocardial ischemia (MI), 855, 1377–1383
 alternating electrical current, 557
 cardiac imaging and, stress testing and,
 1380–1383
 children and, 385
 CMR and, 226–227, 227f
 differential diagnosis, 1377–1378
 dobutamine stress CMR, 226
 electrocardiogram (ECG), 1378–1379
 examination, 1379
 HCM and, 1224
 history, 1377
 pulmonary atresia and intact ventricular
 septum, 953
 small vessel disease, 1218
 stress testing, 1380–1383
 summary, 1383
 treatment, 1383
 Myocardial necrosis, lightning-related injury, 558
 Myocardial performance index (MPI), 178, 178f
 Myocardial perfusion
 cardiac MRI and, 226–228
 contrast agents, 165
 stress echocardiogram, 158
 Myocardial strain, analysis of, 221, 222f, 223f
 Myocardial stress, analysis of, 221, 222f, 223f
 Myocardial structure, development and function
 of, 52–66
 Myocardial tagging, ventricular mechanics and,
 221, 222f
 Myocardial viability, CMR and, 227–228, 228f
 Myocarditis, 385, 1247–1264
 CAMs, 1259
 causes of, 1247, 1248t
 noninfectious etiologic agents, 1247, 1249t
 nonviral, 1247, 1248t
 viral, 1247, 1248t
 clinical manifestations of, 1247–1248, 1249f
 cytokines and, 1258–1259
 diagnostic tests, 1248–1254
 differential diagnosis, 1254
 ECMO and, 536
 etiology and epidemiology, 1247
 infectious agents, childhood/adolescence, 1567
 left ventricle and, 15
 pathology, gross and microscopic findings,
 1254–1255
 pathophysiology of, 1254, 1257f
 PICU, 523
 pediatric heart transplantation, 1390
 RF and, 1259, 1307
 risk factors, 1256
 treatment, 1221–1222, 1262–1264
 viral cause/effect relationship, 1261–1262
 Myocardium
 fetal sheep study, 649
 MRI and, 228, 229f
 myocardial ischemia, 1378
 Myocellular hypertrophy, and death, DCM and,
 1235
 Myocytes (Cardiac muscle cells), 1218, 1221f
 DCM and, 1235
 extracellular matrix, 58–61
 membrane systems, 54–58
 myocardial structure and, 54–58
 Myofilaments, calcium and, 63
 Myosin, 57–58
 Myosin heavy chain (MHC), 58
 mutations in, 571
 Myosin light chain (MLC), 58
 Myosin-binding protein C, 58
 HCM and, 1224

- Myotonic muscular dystrophy, 1277, 1284
 Myxomas, 1550*t*, 1555–1557
 histology, 1556*f*
 incidence, 1550, 1550*t*
 two-dimensional echocardiogram, 1557*f*
- N**
 Na⁺/Ca²⁺ exchanger (NCX1), 55
 Na⁺ channels, cardiac action potential, 55, 55*f*
 N-acetylprocainamide (NAPA), 456
 Nadolol, 457, 1229
 HCM and, 1229
 NAFAT. *See* Nonautomatic focal atrial tachycardia
 Nafcillin, Staphylococcal endocarditis, 1372
 Na⁺/K⁺-ATPase activity, ionic gradient, 54–55
 NAME syndromes, myxomas, 1557
 NAPA. *See* N-acetylprocainamide
 Narrow complex tachycardia, 444, 445*t*
 National Center for Patient Safety (NCPS), 1623
 National Cholesterol Education Program (NCEP), 1523, 1524
 bile acid binding agents and, 1526–1527
 National High Blood Pressure Education blood pressure values, 1529, 1535*t*
 hypertension, adolescents and children with, 1538*f*
 physical activity, 1539
 National Organ Transplant Act (NOTA), pediatric heart transplantation, 1384
 Native coarctation, angioplasty for, 1054, 1054*f*
 Natural history
 pulmonary arteriovenous malformations, 793
 systemic arterial malformations, 791–792
 Natural killer cells, myocarditis, 1256
 Nausea
 amiodarone therapy, 458
 NBTE. *See* Nonbacterial thrombotic endocarditis
 NCEP. *See* National Cholesterol Education Program
 NCX1. *See* Na⁺/Ca²⁺ exchanger
 Near-infrared spectroscopy (NIRS)
 brain and somatic tissue oxygenation, 486–487
 tissue oxygen status, 1071–1072, 1072*f*
 NEC. *See* Necrotizing enterocolitis
 Neck, cervical aortic arch, 778
 embryology, 778, 779*f*
 Neck veins, child inspection, 86
 Necropsy
 HCM and, 1218
 Necrotizing enterocolitis (NEC), 479
 Negative-pressure ventilation (NPV), effects of, 548, 548*f*
Neisseria gonorrhoeae, IE and, 1364
 Neoaortic regurgitation, arterial switch operation and, 1136
 Neoaortic root
 dilation, 1136, 1136*f*
 echocardiograph, 1135, 1135*f*, 1136*f*
 Neonatal anatomic correction, TGA and, 1137*f*
 Neonatal arterial switch repair, 1120–1120
 Neonatal atrial flutter, 450, 451*f*
 Neonatal human hearts, 349*f*
 Neonatal hyperbilirubinemia, fetal tachycardia, 662
 Neonatal one-stage arterial repair, 1132
 Neonatal period
 DMD and, 1279
 murmurs and, 82–83
 risk during pregnancy, cardiac diseases and, 1496, 1497*t*
 Neonate(s)
 balloon valvuloplasty, 920, 920*f*
 pulmonary stenosis and, 921
 blood pressure, 1534
 congenital heart disease, 644–667
 fibromas, 1555
 great arteries, 18
 HLHS and, preoperative preparation, 1072–1073
 hypertension etiology, 1535
 IE, 1367
 64-MDCT scanner, 254
 pulmonary valvuloplasty, 921
 pump flow rates, 531
 right ventricular-to-coronary artery connections, 946
 ventricular tachycardia in, 454, 454*f*
 Nerve growth factor (NGF), E-C coupling, 63
 Nesiritide, 498, 1679
 Nester coils, 291
 Neural crest disruption, SHF development, 568
 Neuro fibromatosis, pulmonary stenosis and, 920
 Neuroblastoma, 1560
 Neurodevelopment(al)
 fetus, 656
 morbidity, after heart surgery, 1579–1585
 outcomes, HLHS, 1086–1088
 Neurodevelopmental predictors, HROOL, 1617–1618
 Neuroendocrine cells, reactive pulmonary circulation, 1406
 Neurofibroma, 1550, 1550*t*
 Neurohormonal response, stage 1 palliation, HLHS and, 1075
 Neurologic morbidity, causes, 1582
 Neurorepellants, E-C coupling, 63
 New England Regional Infant Cardiac Program, pulmonary atresia and intact ventricular septum, 939
 New York Heart Association, functional classification, TOF and, 1477
 Newborn
 acute myocarditis, mortality, 1263
 atrial flutter, 450
 intrapericardial teratomas, 1558, 1559*f*
 myocarditis and, clinical manifestations in, 1247
 patient history, 82–83
 pulmonary atresia and intact ventricular septum, 945
 rhabdomyoma and, 1552
 thoracic ectopia, 1215*f*
 tricuspid atresia, 878
 Newton-meter, 118
 NF1 mutations, 569
 Nicardipine, 497
 Nit-Occlud PDA occlusion system, 292, 292*f*
 Nitric oxide, 1676–1677
 reactive pulmonary circulation, 1408
 Nitric oxide (NO)
 expression
 autoimmune myocarditis, 1258
 Nitric oxide-cGMP pathway (NO-cGMP)
 fetal heart and, 73, 73*f*
 perinatal pulmonary circulation, 73, 73*f*
 Nitroglycerin, 492*t*, 495, 1677
 Nitroprusside, 1677
 SVR and, 1078
 NKX2.5 gene, CHDs and, 635
 NO-cGMP. *See* Nitric oxide-cGMP pathway
 Nocturnal oximetry
 obstructive sleep apnea (OSA), 1438
 Nomenclature, heart and, 32
 Nonatherosclerotic coronary artery disease, MI, 1383*t*
 Nonautomatic focal atrial tachycardia (NAFAT), 449
 Nonbacterial thrombotic endocarditis (NBTE), 1365
 Noncommitted VSD, DORV, 1167, 1169*f*
 Noncompaction cardiomyopathy, 360
 SCD and exercise, 113
 Nondipping, ambulatory blood pressure, 1534
 Non-ECG-triggered Gd-enhanced 3-D MRA, secundum ASDs and, 215, 217*f*
 Non-Hodgkin lymphoma, 1560
 Non-potassium-sparing diuretics, acquired heart, 1571
 Nonsteroidal anti-inflammatory drugs (NSAIDs)
 PDA, 724
 viral pericarditis, 1354, 1354*t*
 Noonan syndrome, 569, 622*t*, 631–633, 632*f*, 913, 930, 935
 pulmonary stenosis and, 920, 928, 930, 932
 Norepinephrine, 494–495, 1673*t*, 1674
 Norepinephrine, E-C coupling, 63
 Normocytic anemia, 1590–1591, 1591*f*
 Norwood procedure, 1141
 coarctation of aorta, 1053
 HLHS and, 1064, 1072*f*
 NOTCH 1 gene
 mutations, 636
 valve disease and, 570
 valvular aortic stenosis, 1023
 Notch homolog 1 (NOTCH1) gene
 bicuspid aortic valve, 804
 NOTCH signaling pathway, Alagille syndrome, 631
 Nuchal fold, congenital heart disease and, 651
 NuMED
 CP stent, 306
 sizing balloon, 318–319
 Nutrition
 HLHS, 1081–1082
 Nykanen RF perforation wire, perforation of atretic pulmonary valve and, 301
- O**
 Obesity
 cardiovascular disease, 1518
 congenital heart defects and, 601
 metabolic syndrome, 1523
 Obstructed pulmonary flow, aortopulmonary collateral vessels, 283–285, 284*f*–285*f*
 Obstructive lung disease, 1415
 Occlusion of septal defects, transcatheter devices for, 289
 Occlusion of vascular structures, devices for, 291
 Ohm's law, 557
 blood flow, 69
 pulmonary vascular resistance, 271
 Oligemic lungs, cyanotic neonate, 946*t*
 Omphalomesenteric veins, normal development, 844*f*
 Open commissurotomy, chronic rheumatic mitral stenosis, 1274, 1322
 Open heart surgery, perioperative risk factors, 1580–1582
 intraoperative support techniques, 1580–1581
 postoperative factor, 1582
 preoperative factors/host susceptibility, 1581–1582
 Opioids, stage 1 palliation, HLHS and, 1075
 OPTN. *See* Organ Procurement and Transplant Network
 Organ Procurement and Transplant Network (OPTN), 1384
 Organ procurement organizations (OPOs), 1384
 Organ transplantation, 1384. *See also* specific i.e. Heart transplantation
 pretransplant status, VAD, 538
 Organic pulmonary atresia, transplantation, 953
 Origin of left coronary artery from inappropriate sinus, abnormal, 748–749
 Oromotor apraxia, d-TGA outcome and, 1583
 Orthodromic SVT, 445, 445*f*
 OSA. *See* Obstructive sleep apnea
 Ostium primum atrial septal defects, 816
 Obstructive sleep apnea (OSA)
 nocturnal oximetry, 1438
 Overdilation, endovascular stents, 294
 Overriding aortic valves
 ventriculoarterial connections and, 48, 50*f*
 Overriding atrioventricular valves, 50, 50*f*–51*f*
 Overriding semilunar valves, 48, 49*f*
 Overriding valves, 48, 48*f*–51*f*
 Oximeters, cardiac catheterization and, 266
 Oximetry
 arterial blood oxygen saturation and, 127
 PAPVC and, 821
 TAPVC, with pulmonary venous obstruction, 831
 ventilation measurements, 131
 Oxygen (O₂)
 in blood, 266–267, 267*f*
 cardiopulmonary bypass, 532
 Oxygen consumption (VO₂), 1069
 HLHS and, 1080
 hypnotic drugs and, 1078
 measurement methods, 257–258, 257*f*, 258*f*
 workload v., 119*f*
 Oxygen delivery (DO₂), 1080
 determinants of, 489–490, 490*f*

- HLHS and, 1068, 1080
 Oxygen flux, in single-ventricle parallel circulation, HLHS and, 1069–1070
 Oxygen saturation
 cardiac catheterization and, 266–267
 HLHS, 1583
 tricuspid atresia, 881
 Oxygen uptake
 cardiac output *v.*, 121*f*
 ventilation measurements, 131, 132
- P**
 P wave, pacemaker, 375, 377
 PAC. *See* Premature atrial contractions
 Pacemaker, 466–467
 atrial switch repair, 1127
 d-TGA, 1483*f*
 origin of, 375, 377
 pediatric population, indications, 467*t*
 Pacemaker channel expression, 365*f*
 PAH. *See* Pulmonary arterial hypertension
 Palliative atrial switch repairs, TGA and pulmonary vascular obstructive disease, 1143
 Palliative procedures, tetralogy of Fallot, 978–979
 Palliative therapy
 TGA and, 1119
 univentricular atrioventricular connection, 1192
 Palmaz P308 stents, 294
 Palpation of precordium, coarctation of aorta, 1048
 Palpitations, 87–88
 Ebstein's anomaly, 893
 older children, abnormal heartbeat, 83
 "Pancaked" ventricle, 1099*f*, 1117
 Pancarditis, acquired heart disease, 1567
 PANDAS (Pediatric autoimmune neuropsychiatric disorders associated with streptococcal infections), Sydenham chorea, 1311
 Panel reactive antibodies (PRA), pediatric heart transplantation, 1385
 Pansystolic crescendo-decrescendo murmur
 anomalous muscle bundles, 926
 pulmonary atresia and intact ventricular septum, 945
 Papillary muscle, mitral valve, 1005*f*, 1006
 Papillary muscles, 11
 Papillary tumors, 1560
 Parachute deformity, 708
 Parachute mitral valve, 1010
 Paradoxical embolization
 Ebstein's anomaly, 893
 Parallel circulation
 arteriovenous saturations in, 1067–1068, 1070*t*
 HLHS and, 1067–1068
 monitoring, 1070–1072, 1072*f*, 1073*f*
 Parasternal window, 139, 140
 Parenteral nutrition, HLHS and, 1073
 Parents, prenatal diagnosis and, 651, 652
 Parietal band, 13–14
 Parietal pericardium, 2–3, 3*f*
 Parkes Weber syndrome, 864
 Paroxysmal atrial fibrillation, 363
 Partial anomalous pulmonary venous connection (PAPVC), 809, 811–813, 816–822, 816*f*, 831
 anatomy, 816–818
 associated cardiac defects and syndromes, 819
 with atrial septal defect, 818
 connection to umbilicovitaline system, 826
 to coronary sinus, 822
 surgical treatment, 821
 differential diagnosis, 821
 to inferior vena cava, surgical treatment, 822
 with intact atrial septum, 818
 to left cardinal system, 825
 of left pulmonary veins, 817
 of left pulmonary veins to innominate vein, surgical treatment, 822
 physiology of, 818
 prognosis
 postoperative course, 822
 untreated, 822
 to right azygos vein, 824
 to right superior vena cava, 824
 sites of, 818
 treatment, 821
 Partial atrioventricular septal defect
 angiography, 699
 cardiac catheterization, 699
 clinical manifestations, 692–693
 common atrium, 699
 double-outlet right atrium, 699
 echocardiography, 693, 695, 697, 699
 electrocardiography and electrophysiology, 699
 pathology, 692, 694*f*–695*f*
 radiography, 699
 surgical treatment, 707
 Partial exchange transfusion, cardiac catheterization and, 258
 Partial venous return repair, TGA and, 1121
 Patau syndrome, 970
 Patch enlargement of coronary ostial stenosis, supravalvular aortic stenosis, 1039
 Patent ductus arteriosus (PDA), 325–326, 722–723, 1110, 1474
 anatomy, 722
 aneurysm/calcification, 732, 732*f*
 aortic insufficiency, 732
 arteriovenous communication, 731
 clinical differential diagnosis, 731–732
 clinical features, 725
 CMR and, 230, 231*f*
 congenital cardiac malformations, 730–731
 diagnostic testing
 angiography, 733–734, 734*f*
 cardiac catheterization, 733–734
 CT scan, 734, 736*f*
 echocardiography, 732, 733*f*
 MRI, 734, 736*f*
 Down syndrome, 625, 637*t*
 endarteritis, 732
 exercise and, 99
 incidence, 473–474
 left coronary artery, 731
 maternal risk and, 1497
 NSAIDs, 724
 PA-VSD, 877, 961–962
 peripheral pulmonary stenosis, 732
 persistent patency
 infants, children, and adults, 728–730, 728*f*
 premature infants, 725–728
 physiology, 474, 722–724
 delayed closure, infant, 724, 725*f*
 fetus role, 722
 left-to-right shunt, 723–724
 patency, 723
 postnatal closure, 722–723
 premature closure *in utero*, 724–725
 pulmonary circulation and lungs effect, 724
 posterior–anterior chest roentgenogram, 728, 728*f*
 pulmonary atresia, 732
 pulmonary valve, 731–732
 Q and taller R wave, 729
 ruptured sinus of valsalva, 731
 total anomalous pulmonary venous connection, 731
 treatment approach, 474
 truncus arteriosus, 732
 truncus arteriosus *v.*, 996
 venous hum, 731
 ventricular septal defect, 732
 Patent foramen ovale (PFO), 687–688, 687*f*
 atrial dilation, 687, 687*f*
 embryology and, 673, 673*f*
 HLHS and, 1064
 PA-VSD and, 961
 Patent mitral valve, HLHS and, 1008, 1062
- Patient**
 education, electrophysiologic studies, intracardiac technique, 401
 preparation
 catheterization laboratory, intracardiac technique, 403, 403*f*
 CMR and, 210, 211*f*
 procedure room, transesophageal technique, 411–412
 Patient-reported outcomes measurement information system, 1608
 Pattern of inheritance, CHD and, 621
 PA-VSD. *See* Pulmonary atresia with ventricular septal defect
 PCICU. *See* Pediatric Cardiac Intensive Care Unit
 PCQLI. *See* Pediatric cardiac quality-of-life inventory
 PDA. *See* Patent ductus arteriosus
 PDA aneurysm, treatment of, 731*f*
 PDA occluding device, VSDs and, 323
 PDAY study (Pathobiological Determinants of Atherosclerosis in Youth), atherosclerosis, 1514
 PDI. *See* Psychomotor Development Index
 PDSA. *See* Plan-Do-Study-Act
 Peak concentration (C_{max}), 1662, 1662*f*
 Peak systolic pressure, left ventricle and, 265
 Peak work capacity, 119
 Pectinate muscles, 7–8
 Pediatric Cardiac Intensive Care Unit (PCICU)
 cardiac OR and catheterization laboratory, 484
 central nervous system issues, 516–518
 continuous quality improvement, 484–485, 485*f*
 CPR and ECPRI IN, 522
 endocrine issues, 522
 family-centered care, 485
 infection in, 522
 multidisciplinary team approach to, 484
 patient safety, 484–485
 renal dysfunction in, 518–520
 Pediatric cardiac quality-of-life inventory (PCQLI), 1615, 1616*t*, 1617*t*
 higher disease severity score, 1615*f*, 1616*f*
 score variation, 1617*f*
 Pediatric cardiology programs 645, 647
 Pediatric circulatory support systems
 children
 anatomic differences in, 530
 physiologic differences in, 530
 Pediatric echocardiography laboratory, digital echocardiography, 166
 Pediatric ECMO, 533–537
 Pediatric heart disease population, HROOL, 1609–1610, 1616*f*
 health status and functional status, 1614
 neurodevelopmental predictors, 1617–1618
 psychosocial predictors, 1618
 Pediatric Heart Transplant Study, pediatric heart transplantation, 1393
 Pediatric heart transplantation
 morbidity, 1389
 myocarditis, 1390
 postoperative management, 1388–1396
 pretransplant evaluation, 1384–1386
 pretransplant management, 1386–1387
 risk factors, post-transplantation, 1393
 Pediatric hypertension, medications, 1540, 1540*t*–1541*t*
 Pediatric RIFLE (pRIFLE), 519, 519*f*
 Pedunculated fibromas, 1555
 Peel operation, truncus arteriosus, 998, 999*f*
 Penetrance, DCM and, 1236
 Penetrating injury, intra-abdominal injury, 556
 Penetrating wounds, cardiac injury and, 556–557
 Penicillin
 RF and, 1303
 staphylococcal endocarditis, 1372
 Penicillin and sulfa-allergic patients, rheumatic fever, 1323, 1323*t*
 Penicillin G with gentamicin, IE and, 1370
 Penicillin-allergic patients
 streptococcal endocarditis, 1372
 streptococcal pharyngitis, 1322, 1323*t*
 Percussion, role of, 91
 Perforation of atretic pulmonary valve, 301–303
 Pericardial cysts, 1358, 1358*f*
 Pericardial defects, 1212–1214
 Pericardial diseases, 1350–1361
 Pericardial effusion
 autoimmune and connective tissue diseases, 1357
 miscellaneous causes, 1355–1357
 neoplastic disease, 1356–1357
 trauma, 1350–1351, 1351*f*

- Pericardial effusions
 blunt chest trauma and, 553, 554
 intrapericardial teratomas, 1557
- Pericardial injury, 553
- Pericardial lacerations, thoracotomy and, 553
- Pericardial reflection, 3–4, 3f
- Pericardial teratomas, 1558f
 fetal ECG, 1559f
- Pericardiectomy, pericardiac lacerations, 553
- Pericardiocentesis
 acute pericarditis, 1354
 intrapericardial teratomas, 1559
- Pericarditis
 autoimmune and connective tissue diseases, 1357
 bacterial, 1354–1355, 1355t
 cardiac catheterization, 1353, 1354f
 cardiac tamponade, 1350–1351
 chest pain, 1511–1512
 chest radiography, 1351, 1351f, 1352f
 chylopericardium, 1356
 constrictive, 196, 1358–1361
 drug-induced, 1356, 1356t
 echocardiography, 1351–1352, 1351f, 1353f
 electrocardiography, 1351, 1352f
 HIV, 1355, 1355t
 hypothyroidism, 1356
 Kawasaki disease, 1356
 MRI, 1353
 physical examination, 1350
 postpericardiotomy syndrome, 1357
 recurrent and chronic, 1357
 renal failure, 1355
 RF and, 1306
 ST-segment, 384
 symptoms, 1350
 tuberculous, 1355
 viral, 1354, 1354t
- Pericardium, 2–4
 absence of, 1357–1358, 1357f
 anatomy and physiology of, 1350, 1351f
 MRI and, 228
- Perimembranous ventricular septal defects
 device closure, technique, 289
 22q11 deletion syndrome, 627, 628
- Perimysium, collagen network, 52
- Peripheral circulation, postnatal peripheral circulation and, 78
- Peripheral emboli, myxomas, 1556
- Peripheral gating, MRI and, 208, 209f
- Peripheral pulmonary arteries
 PA-VSD and, 964
- Peripheral pulmonary stenosis (PPS)
 classification of, 928, 928f
 differential diagnosis, 932
 embryology and pathology, 928
 with intact ventricular septum, 928
 manifestations of, 929–932
 murmur, 92
 physiology, 929
 valvar pulmonary stenosis *v.*, 928
- Peripheral pulmonary stenosis, PDA, 732
- Peripheral pulses
 PA-VSD and, 962
 truncus arteriosus, 993
- Peripheral vascular injury, cardiac catheterization, 286
- Periprosthetic leaks, 331
- Perlecan, 54
- Permanent implanted pacing, atrial switch repair, 1127
- Permanent junctional reciprocating tachycardia (PJRT), 448, 448f
- Persistent eustachian valve, 860
- Persistent left superior vena cava (LSVC), 817
 anatomy, 846
 clinical manifestations, 846, 846f
 diagnostic features, 846–848
 echocardiographic features, 847f
 HLHS and, 1064
 tricuspid atresia, 877
- Persistent pulmonary hypertension of the newborn (PPHN)
 normal perinatal pulmonary vasculature, 1417–1418
 underdevelopment of the lung, 1418
- Persistent valves of sinus venosus, 860–861
- PET (Position emission tomography), myocardial ischemia, HCM and, 1224
- PFO. *See* Patent foramen ovale
- pH strategy, cardiopulmonary bypass, 532–533, 1581
- Pharmacodynamics, 1662
 developmental, 1671
- Pharmacogenetics, 1662
- Pharmacogenomics
 developmental, 1671–1672
- Pharmacokinetics, 1662
 developmental
 drug absorption, 1665–1666, 1665t
 drug distribution, 1666–1667, 1667t
 drug metabolism, 1667–1669, 1669t, 1670t
 physiologic factors, drug disposition, 1664–1665, 1664f
 renal drug elimination, 1670–1671, 1670t
- Pharmacologic stress
 blood flow measurements, 225–226
 contractile reserve and, 157
 postoperative atrial switch, CMR of, 237
- Pharmacologic treatment, arrhythmias, 459f
- Pharmacology
 adrenergic agonists, 1673–1675, 1673t
 aldosterone receptor antagonists, 1678–1679
 antiarrhythmic drugs, 1680–1682
 beta-adrenergic receptor blockers, 1679–1680
 calcium-sensitizing agents, 1675
 cardiac glycosides, 1672–1673
 cardiovascular drugs, 1672
 definition, 1661–1663
 developmental pharmacodynamics, 1671
 developmental pharmacogenomics, 1671–1672
 developmental pharmacokinetics, 1664–1671
 diuretics, 1675–1676
 exposure-response relationship, 1663–1664, 1663f
 hormones, 1679
 pediatrics, 1661
 phosphodiesterase inhibitors, 1675
 prostaglandin E1, 1690
 vasodilators, 1676–1678, 1676t
- Phase-velocity cine, blood flow, 224f
- Phase-velocity cine MRI, myocardial stress, 221, 222f
- Phenoxybenzamine, 1078
 afterload reduction and, HLHS and, 1076, 1076f
 SaO₂ relationship and, 1076, 1076f
 SVO₂-blood pressure relationship, 1076, 1077f
- Phenoxymethylpenicillin
 rheumatic fever, 1322, 1323t
 streptococcal pharyngitis, 1322, 1323t
- Phentolamine, 1677
- Phenylephrine, 492t, 495, 1673t, 1675
 myocardial contractility, 1224
- Phenylketonuria (PKU)
 maternal, 599
 congenital heart defects, 599
 PA-VSD and, 959
- Phenytoin, 1681
- Phosphocreatine (PCr)-ATP system, 118
- Phosphodiesterase inhibitors, 1675
 DCM, 1242
- Phosphodiesterase inhibitors, PAH
 combination therapy
 atrial septostomy, 1454–1455
 transplantation, 1455
 VO₂ peak, cardiopulmonary exercise, 1454, 1454f
- Phospholamban, immature heart, 56
- Photosensitivity
 amiodarone toxicity, 457–458
- Physical activity
 cardiovascular disease, 1518–1519
 congenital heart disease, 95
 dyslipidemia, 1525
 exercise and, 93–95
 hypertension, 1539
 types
 activities of Daily Living, 94
 competitive sports, 95
 leisure and recreational sports, 94–95
- Physical examination, 1270
 athletic screening and, 82–92, 96f
 chest pain, 1512
 coarctation of aorta, 1048–1049
 DCM and, 1240
 DMD and, 1279
 Ebstein's anomaly, 894
 HCM, 1226
 neonate, HLHS, 1065–1066
 PA-VSD and, 962
 truncus arteriosus, 993
- Physical health status and physical function, QOL, 1610f
- PiCCO. *See* Pulse contour analysis
 cardiac output
- PISA. *See* Proximal isovelocity surface area
- “Pistol shot” sounds, 87
- PJRT. *See* Permanent junctional reciprocating tachycardia
- Placental circulation, blood flow, 654, 655f
- Placental vascular resistance, 654
- Plakoglobin, 60
- Planar xanthomas, 1521
- Plan-Do-Study-Act (PDSA), 1625
- Platelet function analyzer (PFA-100), 1593
- Platelets, 1589–1590
 disorders of
 Bernard-Soulier syndrome, 1594
 heparin-induced thrombocytopenia, 1594–1595
 immune thrombocytopenia, 1595
 thrombocytosis, 1595
- PLE. *See* Protein-losing enteropathy
- Plication, 908
- Pneumococcal conjugate vaccine, asplenia syndrome and, 1212
- Pneumothorax, chest pain, 1512
- Poiseuille's law, pulmonary vascular resistance, 271
- Polyarthritis, and fever, causes, 1310, 1310t
- Polyclonal antibodies, pediatric heart transplantation, 1389
- Polycythemia, 1593
 cyanotic adult, 1487
 TGA and, 1113
- Polyhydramnios, 651
- Polymerase chain reaction (PCR)
 mumps virus, 1253
- Polysplenia, 34
 bilateral superior venae cavae, with unroofed coronary sinus, 848
 cardiac situs, 34
 inferior vena cava, 38
 interrupted IVC and, 855, 855f
 PAPVD and, 819
- Polysplenia syndrome, 1207, 1209, 1209f
 abdominal situs and, 36
- Polysplenia syndrome and dextrocardia, 1207
- Population-based diet
 dyslipidemia, 1523
 dyslipidemia in children, 1523, 1523t
- Portal hypertension, 1421
- Portal vein, normal development, 844–845, 844f
- Portal venous blood, hepatic circulations, postnatal peripheral circulation and, 80
- Portal-systemic encephalopathy, postnatal persistence of ductus venosus, 860
- Portopulmonary hypertension (PPHTN), 1434, 1444–1445
- Postcardiotomy, pediatric ECMO, 535, 535t
- Posterior aortic sinus, 9, 17
- Posterior cardinal veins, 843f
- Posterior mural leaflet, echocardiography, 150
- Posterior sinus of Valsalva, coronary arterial branches from, 748
- Post-myocardial infarction VSD, 289
- Postnatal circulation, 70–71
- Postnatal heart, conduction tissues recognition, 348–350, 349f
- Postnatal persistence of ductus venosus, 860
- Postoperative pulmonary insufficiency, dysplastic pulmonary valves, 921
- Postoperative structural heart disease, childhood/adolescence, 1566

- Postpericardiotomy syndrome, 1357
 Postpericardiotomy syndrome, ASD, 685
 Poststreptococcal reactive arthritis, 1311
 Postural orthostatic tachycardia syndrome (POTS), 124
 Potassium
 blood pressure and, 1539
 Potassium channels, sarcolemma and, 55
 Potassium imbalance, T-waves and, 385
 Potassium-sparing diuretics, 1676
 POTS. *See* Postural orthostatic tachycardia syndrome
 Potts operation, Tetralogy of Fallot, 1476
 Potts shunt, tricuspid atresia, 883
 PPHN. *See* Persistent pulmonary hypertension of the newborn
 PPS. *See* Peripheral pulmonary stenosis
 Pre-athletic participation screening
 economic consequence of, 98
 electrocardiogram analysis, 97–98
 sudden cardiac death
 American Heart Association, 96, 96f
 electrocardiogram screening, benefits, 96–97
 incidence of, 95
 screening purpose, 96
 Precapillary arteries, near-term fetus and, 72
 Preconception counseling
 cardiac disease, 1502
 maternal risk and, 1502
 Pre-contraception counseling, women of childbearing age, 1495t
 Precordial activity, palpation of, 87
 Precordial catch syndrome, 1510
 Pre-excitation, 380, 432
 Preexcitation syndromes, 432, 435–436
 Pregnancy
 cardiac surgery, 1504
 CMR and, 211
 corticosteroid, 666
 high-risk conditions, 1503–1504
 management issues, 1502–1504
 PA-VSD and, 967
 physiologic changes during, 1494–1496
 physiology and management, CHD and, 1494–1505
 Tetralogy of Fallot, 985
 women of childbearing age, 1495t
 Pregnancy termination
 fetal congenital heart disease, compassionate care in, 657, 659t, 660t
 genetic testing, 644
 pulmonary atresia and intact ventricular septum, 939, 955
 Preload
 altered, fetus and, 654
 contraction and, 66
 drugs and, 1235
 Premarket approval (PMA), transcatheter devices, 289
 Premature atrial contractions (PAC), 455–456, 455f
 Premature ventricular contraction (PVC), 456
 Premedication, cardiac catheterization and, 258–259
 Prenatal cardiac diagnosis
 delivery planning and, 653, 654, 655f
 parents and, 653
 TAPVC, 829
 Prenatal care
 history, 84
 screening CHD, 645–647, 649f
 Pressure measurements, cardiac catheterization and, 262–263
 Pressure tracing, cardiac catheterization, RCM, 1230, 1230f, 1272, 1272f
 Pressure-volume loops, cardiovascular function and, 65–66
 Presystemic clearance (first-pass effect), 1662
 Presystolic murmurs, 89f, 91
 Preterm infant
 BNP levels, 727
 ECG and, 386
 physiology, 473–480
 treatment of PDA, 734, 736–737, 737f
 Prevalence
 pulmonary arteriovenous malformations, 792
 systemic arterial alformations, 789
 Preventive therapy, Duchenne muscular dystrophy, 1281
 PRIMACORP trial
 carvedilol, 1242
 Primary benign myocardial tumors, 1560
 Primary cardiac tumors, frequency of, Boston Childrens Hospital, 1549, 1550, 1550t
 Primary graft failure, pediatric heart transplantation, 1388
 Primary heart field, 561, 562
 Primary hypertension, historical information suggesting, 1536t
 Primary infundibular stenosis, 925
 Primary malignant myocardial tumors, 1560
 Primary stenting, balloon angioplasty v. coarctation and, 305
 Probe manipulation, transesophageal echocardiography, 154, 154f
 Procainamide, 456, 1680–1681
 catecholamine-sensitive ventricular tachycardia, pregnancy and, 1503
 intracardiac study and, 407
 Procedure room, patient preparation in, transesophageal technique, 411–412
 Propafenone, 1681
 Prophylactic antiplatelet therapy, HLHS, 1080
 Prophylactic closure, preterm infant, treatment of PDA, 737
 Propofol
 CMR and, 208
 electrophysiologic studies, intracardiac technique, 408
 Propranolol, 457, 1679
 fetus, 661
 HCM and, 1229
 intracardiac study and, 410
 Prostacyclin
 pulmonary arterial hypertension (PAH), 1422–1453, 1452f
 pulmonary vascular resistance, 72, 73
 Prostaglandin
 pulmonary atresia and intact ventricular septum, 945, 947, 948, 955
 Prostaglandin E1, 1110, 1690
 balloon valvuloplasty, 922
 HLHS and, 1072–1073
 neonatal arterial switch repair and, 1120–1121
 newborns, rhabdomyomas and, 1554
 TGA, 1103
 Prostaglandins, 496
 Prosthetic heart valves
 anticoagulation therapy, pregnancy outcomes, 1503
 IE and, 1364
 maternal risk and, 1501–1502
 pulmonary valve replacement, 924
 Prosthetic patch aortoplasty, coarctation of aorta, 1052, 1053f
 Prosthetic reconstruction, thoracic ectopia cordis, 1215
 Prosthetic valve endocarditis
 infectious organisms, 1354r, 1364
 Prosthetic valve, staphylococcal endocarditis, 1374
 Protein binding, 1662
 Protein-losing enteropathy (PLE)
 fontan operation, 1487
 late Fontan and, HLHS, 1085
 Proteins, Z-disk, 58
 PROVED trial, digoxin and, 1572
 Proximal isovelocity surface area (PISA)
 mitral regurgitation, 1015
 Proximal thoracic aorta, stenosis, 1044, 1045f
 Pseudoaneurysms
 COA repair site and, 1469–1471, 1470f
 Pseudoprolopse, 1313f, 1316
 Pseudotruncus arteriosus, 991
 Psychological testing, TGA and, 1113
 Psychomotor Development Index (PDI), 1580
 Psychosocial evaluation, pediatric heart transplantation, 1386
 Psychosocial predictors, HROOL, 1618
 PTPN11 gene, Noonan syndrome, 632
 Publication bias, clinical trials, 1639
 Pulmonary arterial hypertension (PAH)
 after birth, 18, 19f
 anticoagulation, 1450
 biomarkers, 1438–1439, 1440f
 calcium channel blockers, 1450, 1452
 cardiac catheterization, 1437–1438
 cardiac lesions, 1433, 1435t
 chest radiography, 1434–1435
 clinical evaluation
 diagnostic algorithm, 1434, 1436f
 high-altitude pulmonary edema (HAPE), 1434
 portopulmonary hypertension (PPHTN), 1434
 clinical presentation, 1433
 coarctation of aorta and, 1048
 congenital systemic-to-pulmonary shunts, 1433, 1434t
 conventional therapy, 1449–1450
 definition, 1433
 echocardiography, 1435–1436, 1437f
 electrocardiography, 1435
 endothelin, 1453
 exercise capacity, 1436–1437
 hemoglobinopathy, 1445–1446, 1446f
 hepatopulmonary syndrome, 1444–1445
 human immunodeficiency virus, 1445
 laboratory assessment, 1438, 1439t
 left heart disease, 1447
 lung biopsy, 1439
 magnetic resonance imaging, 1436
 nocturnal oximetry, 1438
 novel therapy of, 1455–1456
 pediatric pulmonary hypertensive vascular disease, 1433, 1435t
 pH, idiopathic pulmonary arterial hypertension, 1439–1444
 pharmacologic therapy of
 drug classes of, 1449, 1449f
 survival curves, IPAHA, 1449, 1452f
 treatment algorithm in adults, 1449, 1451f
 treatment algorithm in children, 1449, 1450f
 phosphodiesterase inhibitors, 1453–1455
 portopulmonary hypertension, 1444–1445
 prostacyclins, 1422–1453, 1452f
 pulmonary capillary hemangiomatosis, 1446–1447
 pulmonary function testing, 1438
 PVOD, 1446–1447
 reflux and aspiration evaluation, 1438
 respiratory disease, 1447–1448, 1448f
 serotonin transporter, 1408
 signs and symptoms, 1434
 thromboembolic disease, 1448–1449
 vasoreactivity testing, 1450
 ventilation–perfusion scintigraphy, 1438
 wedge angiography, 1439
 World Health Organization (WHO) classification, 1433, 1434t
 Pulmonary arteries, 18–19, 18f, 19f
 all coronary arteries from, syndrome of, 752
 anomalies, CHD and, 235, 235f
 banding, 1138
 TGA and, 1138
 catheters
 labor and delivery, 1504
 imaging of, 279, 279f
 MDCT, 251, 252f, 537
 PA-VSD and, 959, 960f
 pediatric heart transplantation, 1386
 truncus arteriosus, 991
 univentricular atrioventricular connection, 1192–1193
 Pulmonary arteriovenous fistula (AVF)
 univentricular atrioventricular connection, 1191–1192
 Pulmonary arteriovenous malformations, 792–794, 792f
 angiography, 793
 cardiac catheterization, 793
 clinical manifestations, 792–793
 differential diagnosis, 793
 echocardiography, 793
 electrocardiography, 793

- Pulmonary arteriovenous malformations
(*Continued*)
imaging, 793
natural history, 793
pathology, 792
prevalence, 792
radiography, 793
treatment, 793
- Pulmonary artery, 42
banding
tricuspid atresia, 880
Tetralogy of Fallot, 974
- Pulmonary artery catheter monitoring, hemodynamic formulae, 487*t*
- Pulmonary artery pressures
altitude, 1412
banded piglet, 1411*f*
birth, 72, 73*f*
chronic rheumatic heart disease, 1317
experimental studies, 1408
- Pulmonary artery sling, CT, 254*f*
- Pulmonary artery stenosis
cardiac MRI, 1478, 1479*f*
- Pulmonary artery wedge pressure, right heart catheterization and, 265
- Pulmonary atresia, 42, 48, 516
fetal heart, 656
hypoplasia of individual pulmonary veins, 837
mirror-image right arch, 766
Tetralogy of Fallot, 974
truncus arteriosus *v.*, 996
valvar pulmonary stenosis *v.*, 920
- Pulmonary atresia, PDA, 732
- Pulmonary atresia with intact ventricular septum (PA-IVS), 939–956
abnormal coronary artery anatomy, surgical strategies for, 953*t*
clinical features, 945–948
differential diagnosis, 945*t*
echocardiographic features, 945–946, 946*f*–950*f*
electrocardiographic features, 945, 945*t*
epidemiology, 939
morphogenesis, 939–940
neonates and, 302, 302*f*
pathology and physiology, 940–945
transcatheter techniques, 954–955
treatment, 948–955
- Pulmonary atresia with ventricular septal defect (PA-VSD), 959–967
differential diagnosis, 965
embryology, 959–960
environmental factors, 959
genetics and, 959
natural history, 965–966
pathology, 960–965
preoperative aortogram, 966*f*
treatment, 966–967
- Pulmonary balloon valvuloplasty
indications, 923
PVS, 1475
- Pulmonary blood flow
abnormal distribution of, TGA and, 1109*f*
angiocardiology, 882
heart defect and, 1401, 1402*f*–1403*f*, 1402*t*
physiology, 818
pulmonary atresia and intact ventricular septum, 946
tricuspid atresia, 877
- Pulmonary blood supply mapping, PA-VSD and, 965
- Pulmonary capillary hemangiomatosis
pulmonary arterial hypertension (PAH), 1446–1447
- Pulmonary circulation
fetal circulation, 72
fetus and, 72
morphologic development, 71–74
pulmonary atresia and intact ventricular septum, 941–942, 948
structural remodeling and growth, 1401–1402, 1404*f*, 1404*t*
TGA and, 1106–1111
transitional circulation, 72, 73*f*
univentricular atrioventricular connection, 1191–1192
- Pulmonary fibrosis
amiodarone therapy, 458
- Pulmonary flow murmur
of childhood, 92
of infancy, 92
- Pulmonary function testing, 1438
- Pulmonary homograft, 1467
- Pulmonary hypertension, 475
biomarker in children, heart failure, 1570
exercise and, 107–108
granulomatous and collagen vascular diseases and immune/infectious diseases, 1421–1422, 1423*f*
high-flow congenital heart defects, 1401
left-to-right shunts and, 1472
of newborn, 1415–1420
patent ductus arteriosus (PDA), 723
pathophysiology of, 1401–1429
in PICCU
diagnosis, 501–502, 502*f*
etiologies, 500–501
treatment, 502
pediatric heart transplantation, 1386
treatment of PDA, 739–740
- Pulmonary hypertension (PH)
atrial septal defects in infancy
atrioventricular septal defects and, 99
rheumatic carditis, 1312
stress echocardiography, 159
- Pulmonary hypertension, ASD, 685
- Pulmonary hypertensive crisis, 1405
- Pulmonary infection
in PICCU, 522
- Pulmonary insufficiency
rTOE, 1476
transcatheter valve therapy, 341*f*
- Pulmonary isomerism, 36, 37*f*
- Pulmonary out flow murmur, 819
- Pulmonary outflow tract obstruction
ccTGA and, 1148
DILV and, 1181*f*
- Pulmonary regurgitant murmurs, 92
- Pulmonary regurgitation, 150
fetus and, 654, 655*f*
MRI and, 236, 237*f*
tetralogy of Fallot, 980–981
- Pulmonary resistance
truncus arteriosus, 993
- Pulmonary situs (Sidedness), 34, 36, 36*f*, 37*f*, 1199
- Pulmonary stenosis
exercise and, 102, 103*t*
- Pulmonary stenosis (PS), 913–935
course and prognosis, 927–928
with intact ventricular septum, embryology and pathology, 928–929
maternal risk and, 1501
with systemic diseases, 920–925
truncus arteriosus *v.*, 996, 997
- Pulmonary valve
pulmonary atresia and intact ventricular septum, 940, 940*f*
replacement
indications, 924–925
ventricular volumes, 1478, 1478*f*
- Pulmonary valve dysplasia, 913, 914*f*
- Pulmonary valve leaflets
Tetralogy of Fallot, 975–976, 975*f*
- Pulmonary valve regurgitation, 185–186, 186*f*
- Pulmonary valve replacement
monitoring after, 984
Tetralogy of Fallot, 983
timing of, 984
- Pulmonary valve stenosis (PVS), 1475
echocardiography, 152
fetal cardiovascular system and, 646
GATA4 mutation, 635
- Pulmonary valvotomy
indications, 923
- Pulmonary valvuloplasty
children, 922
complications from, 922
- Pulmonary vascular bed
analysis of, 1401–1402
factors affecting, 546
maladaptation of, 1418, 1420
maldevelopment of, 1420
structural remodeling and growth, 1401–1402, 1404*f*, 1404*t*
- Pulmonary vascular disease
atrial septal defects and
cardiac catheterization, 286
reactive pulmonary circulation, 1405–1408
TGA and, 1110–1111, 1111*f*
- Pulmonary vascular lesions, 1401
- Pulmonary vascular obstruction, atrial switch repair, 1131
- Pulmonary vascular obstructive disease (PVOD), 1471
truncus arteriosus, 996–997
- Pulmonary vascular resistance (PVR)
afterload reduction and, HLHS and, 1076
cardiac catheterization and, 258
fetus and, 72
HLHS, 1065, 1073
physiologic regulation of, 72–74
postnatal central circulation, 70–71
Qp/Qs, 1073
surgery and, 1068
TGA and pulmonary vascular obstructive disease, 1143
- Pulmonary vasodilators, 1677
- Pulmonary vein(s), 7, 38–39
abnormal numbers of, 809
development of, 809
echocardiography and, 148–149
MDCT, 251, 252*f*
- Pulmonary vein stenoses
stenting of, 310, 314*f*
transcatheter interventions, 310–311, 314*f*
- Pulmonary vein wedge angiography, 282–283, 283*f*
- Pulmonary veno-occlusive disease (PVOD), 1446–1447
- Pulmonary venous anomalies, 809–838
CMR and, 235–236, 236*f*
embryology, 809–816
embryonic classification of, 809, 811*t*
- Pulmonary venous connections, 1207
- Pulmonary venous doppler flow analysis, 190–191, 190*f*
- Pulmonary venous drainage, site of obstruction, 826
- Pulmonary venous hypertension, experimental studies, 1409–1410
- Pulmonary venous obstruction
atresia of common pulmonary vein, 833
atrial switch repair, 1124, 1127*f*
baffle, 1482, 1483*f*
fetal heart, 654, 655*f*
TAPVC, postoperative course, 832
- Pulmonary-to-systemic flow ratio (Qp/Qs), 1069, 1074
CMR and, 229
- Pulsatile masses, cervical aortic arch, 778
- Pulsatile VAD pump
mechanics of, 541*f*
pediatrics, 540–541
troubleshooting algorithm, 541, 542*t*
- Pulse contour analysis cardiac output (PiCCO), 488–489
- Pulse oximetry screening, 85
- Pulse pressure, ascending aorta and, 265
- Pulse rate, assessment, 87
- Pulsed Doppler assessment
mitral regurgitation, 1015
- Pulsed wave Doppler, 143
flow analysis, fetal heart, 647
mitral valve velocities, 143*f*
- Pulsed wave Doppler flow analysis, fetal heart, third trimester pregnancy, 647
- Pulsus paradoxus, cardiac tamponade, 1350
- Pump failure, heart failure and, 1574
- Pump flow rates, neonates and, 531
- Purkinje fibers, 348–350, 349*f*
- Purkinje fibers, functions of, 52
- PVC. *See* Premature ventricular contraction
- PVOD. *See* Pulmonary vascular obstructive disease
- PVR. *See* Pulmonary vascular resistance
- PVS. *See* Pulmonary valve stenosis

- Q
 22q11.2 microdeletion syndrome, 970
 Q waves, 381, 381f
 ccTGA and, 1149, 1150
 DMD and, 1279, 1280f
 QRS axis
 ECG and, 377–378
 isolated valvar pulmonary stenosis, 916, 916f
 tricuspid atresia, 879
 QRS complex, 1248
 age-related transitions, 385
 intrapericardial teratomas, 1559
 myocarditis, 1208, 1210f, 1248, 1251f
 tachyarrhythmia, 444
 QRS duration
 sudden death and, 1476f
 ventricular tachycardias, 1476f
 QRS vectorcardiogram, 373
 QT interval, ventricular repolarization, 384
 Quadrivalent meningococcal vaccine, 1212
 Quality of life (QOL)
 evaluation, 1608–1619
 HLHS, 1086–1088
 Quinapril, DCM and, 1243
- R
 Race, ECG and, 386–387
 RADI Pressure Wire, 308
 RADIANCE trial, digoxin, 1572
 Radiation, dose and exposure, angiography and, 273
 Radiation protection, CT, 249–250, 250f
 Radiofrequency catheter ablation
 cardiac dysrhythmias and, 955
 Radiofrequency, electrophysiologic therapeutic catheterization, 417f, 418–420
 cooled-tip, 420
 Radiofrequency (RF) perforation of pulmonary valve plate, 301–303
 Radiographic source, biventricular heart, 274–277, 276f, 277f, 278f
 Radiography. *See also* Chest radiography
 cor triatriatum, 836
 isolated valvar pulmonary stenosis, 916, 917f
 PA-VSD and, 962
 peripheral pulmonary arterial stenosis, 930
 pulmonary arteriovenous malformations, 793
 pulmonary atresia and intact ventricular septum, 945, 945t
 stenosis of individual pulmonary veins, 837
 TAPVC, with pulmonary venous obstruction, 831
 truncus arteriosus, 993–994
 Radiology
 coarctation of aorta, 1049, 1049f
 congenital aortic stenosis, 1026
 univentricular atrioventricular connection, 1189
 RADIUS trial, 647
 RAIV. *See* Retroaortic innominate vein
 Ramp protocol, 118, 128
 Ranitidine, 456
 Rapamycin, pediatric heart transplantation, 1390
 Rapidly involuting congenital hemangioma (RICH), 864
 ras/MAPK pathway, Noonan syndrome, 631
 Rastelli classification, 700, 702t
 Rastelli operation, TGA/VSD, 1140, 1141f
 RBCs. *See* Red blood cells
 RCM. *See* Restrictive cardiomyopathy
 Reactive pulmonary circulation, 1405–1408
 Real-time CMR, MRI and, 208
 Real-time 3-D imaging, 159
 Recanalization of obstructed superior vena cava
 Recoarctation rates, COA and, 1469, 1469f
 Recording apparatus, transesophageal technique, 412
 Recording speed, 406f
 Recording/stimulation technique, transesophageal technique, 405–410, 412–415
 Recreational sports, 94–95
 Red blood cell control, postnatal peripheral circulation, 76
 Red blood cells (RBCs)
 hematologic disorders and, 1590–1593
 normal development of, 1589
 Reentry mechanism, tachyarrhythmia, 441, 442f
 Regional blood flow analysis, fetus, 654–655
 Regional flow, MRI and, 225
 Regional oxygen saturation (rSO₂), 486
 Regional vascular beds, postnatal peripheral circulation, 77
 Regional wall motion, analysis of, 220, 220f, 221f
 Regurgitant volume, 139
 Rehabilitation of branch pulmonary artery stenosis
 Relative bioavailability, 1661
 Relaxation
 diastolic, 65, 65f
 Renal circulations, postnatal peripheral circulation, 78–79
 Renal failure
 pericarditis, 1355
 Renal replacement therapy, 519–520
 Renal system, 479
 Renin-angiotensin system, 78, 79
 Reoperation
 ccTGA and, 1156
 supravalvular pulmonary stenosis, 1133
 Research echocardiography, 166–167, 166f
 Resistance exercise, HDL and, 1519
 Resistant pulmonary artery stenosis, balloon angioplasty, 933
 Respiratory compensation point, exercise, 121, 126
 Respiratory distress syndrome, 725
 Respiratory examination, 86
 Respiratory gating, MRI and, 207–208, 210f, 211f
 Respiratory motion, MRI and, 207–208
 Respiratory navigator, 210f
 Respiratory physiology, 475–476
 Respiratory rate, 85
 Respiratory rate (RR), ventilation measurements, 131
 Respiratory support, HLHS and, 1073
 Respiratory syncytial virus (RSV), 478
 congenital mitral valve stenosis, 1018
 Restenosis
 pulmonary stenosis and, 923
 pulmonary vein stenoses and, 310–311
 systemic vein stenoses, 311–312
 Restrictive cardiomyopathy (RCM), 1267–1275
 clinical presentation, 1270
 CP *v.*, 1273, 1273t
 diagnostic studies, 1270–1273
 differential diagnosis, 1273–1274
 epidemiology, 1267
 etiologic, 1268–1269
 management, 1274–1275
 pathology, 1270, 1270f
 pathophysiology and clinical presentation, 1270
 prognosis, for children, 1274
 Restrictive fetal ventricular myocardium, 652f
 Retinal vascular change, evaluation, 1536
 Retinoic acid
 congeners, 599–600
 maternal exposure, tetralogy of Fallot, 617
 PA-VSD and, 959
 pregnancy and, 1502
 Retroaortic innominate vein (RAIV), 852–853, 852f
 Retrograde ascending aortogram, 263
 Retrograde catheter, angiography and, 263
 REV (*Réparation à l'étage ventriculaire*), Rastelli operation *v.*, 1140
 Reynolds number, heart murmurs and, 89
 RF. *See* Rheumatic fever
 Rhabdomyomas, 1550t, 1551–1554, 1552f
 incidence, 1550, 1550t, 1551
 Rhabdomyomas in utero, fetal echocardiogram, 1552f, 1553f
 Rhabdomyositis, 1552
 RHD. *See* Rheumatic heart disease
 Rheumatic aortic valve stenosis, 1318
 Rheumatic carditis
 natural history, 1306
 Rheumatic fever (RF)
 acquired heart disease, 1567
 clinical manifestations, diagnosis and evaluation, 1308, 1308t, 1309t, 1310t
 crude death rates from, 1303, 1304f
 environment and, 1304–1305
 epidemiology, 1303–1305
 pathogenesis, 1257–1260
 pathology, 1306–1307
 primary prophylaxis, 1322–1323, 1323t
 RHD and, 1303–1325
 secondary prophylaxis after, 1323–1324, 1323t
 Rheumatic heart disease (RHD)
 RF and, 1303–1325
 Rheumatic mitral stenosis, 1317
 Rheumatic tricuspid valve disease
 chronic rheumatic heart disease, 1321
 surgical approach, 1322
 Rho-Kinase inhibitor, PAH, 1456
 Rifampin
 Staphylococcal endocarditis, 1373
 Right anterior oblique views (RAO views)
 aortic valve, 275
 left ventricle, 275
 Right aortic arch, 758, 766–778
 with brachiocephalic branching, truncus arteriosus, 991
 with isolation of contralateral arch vessel, 776–778, 776f, 777f
 with left descending aorta
 and aberrant left subclavian artery, 774f
 and left ductus arteriosus, 772–774, 773f, 7734f
 with retroesophageal diverticulum of Kommerell, 769–772, 770f, 771f
 diagnosis and management, 771–772
 embryology, 771
 with retroesophageal innominate artery, 775–776, 775f
 with retroesophageal left subclavian artery, 767–769, 768f
 tricuspid atresia, 877
 Right aortic sinus
 free wall and, 9
 Right atrial appendage, sagittal view, 146, 147f
 Right atrial flap, 860
 Right atrial free wall, 7–8, 8f
 Right atrial isomerism with asplenia, fetal heart, 651, 654
 Right atrial sail, 860
 Right atrial spinnaker, 860
 Right atrial windsock, 860
 Right atrioventricular valves, 40
 Right atrium, 7–9
 septal structures of, 146
 tricuspid atresia and, 860, 861f, 877, 878f
 Right bundle branch block (RBBB), QRS complex, 378–379
 Right cardiac isomerism, 34, 35f
 Right coronary artery
 Ebstein's anomaly, 889, 892f
 from pulmonary artery, 752
 Right heart
 abnormal, cardiopulmonary interactions, 547–548, 548f
 catheterization, 263–265, 264f, 264t
 disease, chronic rheumatic heart disease, 1318–1319
 hemodynamics, left heart hemodynamics *v.*, 546, 547f
 obstructive lesions, fetal flow pathways, 647
 waveforms, right heart catheterization and, 263–265, 264f, 264t
 Right parasternal window, 139, 140f
 Right pulmonary artery, flow waveforms, fetus and, 647, 655f
 Right pulmonary veins
 to inferior vena cava, 817
 to superior vena cava, 816
 Right reduction atrioplasty, 908
 Right sided heart failure, rhabdomyomas and, 1555
 Right superior vena cava (RSVC)
 echocardiogram, 146, 148f
 normal development, 840–841
 Right upper pulmonary vein
 transducer sweeping, 148

- Right venous valve
pulmonary atresia and intact ventricular septum, 940–941
remnants of, normal, 861f
- Right ventricle (RV), 10t, 13–14, 14f, 41, 150
angiogram, 275, 276
atrial switch repair, 1128–1132
atrialized, 908
Ebstein's anomaly, 889–890, 893f
echocardiography, 174, 175f
doppler assessment of, 196, 197f
fractional area change, 181, 181f
tricuspid annular planar systolic excursion, 181, 181f
effects on LV, 549
exclusion of, 548
isolated valvar pulmonary stenosis, 913
PA-VSD and, 960, 960f
pulmonary atresia and intact ventricular septum, 941, 942f, 943f
tetralogy of fallot, 980–981, 981f
- Right ventricle (RV) angiogram, truncus arteriosus repair, 1000f
- Right ventricular contractile performance, reduced, 547
- Right ventricular diastolic dysfunction
Tetralogy of Fallot, 982–983
- Right ventricular diastolic function
abnormal, 547–548, 548f
- Right ventricular dysfunction
arterial switch for d-TGA, 1484
ccTGA and, 1156–1157
- Right ventricular ejection fraction, atrial switch repair, 1107f, 1124
- Right ventricular failure, following physiologic correction, surgery for, 1142
- Right ventricular function
contrast agents, 165
four-chamber view, 1066, 1067f
- Right ventricular hypertrophy (RVH), 382, 382f
PA-VSD and, 962
- Right ventricular hypoplasia
infants, pulmonary atresia and intact ventricular septum, 949
- Right ventricular outflow tract (RVOT)
anomalous muscle bundles and, 925–927, 926f
obstruction
anomalous muscle bundles and, 925–928, 926f
- Right ventricular outflow tract obstruction, 860–861, 973–974, 973f
- Right ventricular overload, adverse effects, 548
- Right ventricular pressure tracing, right heart catheterization and, 264
- Right ventricular pressure-volume relationship, 546, 547f
- Right ventricular volumes, 3-dimensional echocardiography, 160
- Right ventricular wall segments, 220, 221f
- Right ventricular-dependent coronary artery circulation, 944–945, 945t
- Right ventricular-to-coronary artery connections, neonates, 944
- Right-left heart interactions
congenital heart disease, 550
- Right-sided obstructive lesions, 516
congenitally corrected transposition of the great arteries, 105–106
D-transposition of the great arteries, 104–105
Ebstein's Anomaly, 104
Eisenmenger syndrome, 107–108
heart transplantation, 108–109
pulmonary hypertension, 107–108
pulmonary stenosis, 102, 103t
single ventricle physiology, 106
Tetralogy of Fallot, 103–104
- Right-to-left shunts
agitated saline contrast and, 164
quantitative assessment of, 270–271
- Root cause analysis (RCA), 1623
cause-and-effect, 1623, 1623f
HFMEA, 1624
individual failures, 1624
liver transplant graft survival, 1623
process implementation, 1624
sentinel events, 1624
system failures, 1624
- Ross procedure
aortic valve disease, 1467
rhabdomyomas and, 1554
- Ross/Konno procedure, subvalvular aortic stenosis, 1038
- RSV. *See* Respiratory syncytial virus
- RSVC. *See* Right superior vena cava
- Rubella
cardiac diseases and, 84
congenital heart defects and, 599
- Ruptured sinus of valsalva, PDA, 731, 755
- RVH. *See* Right ventricular hypertrophy
- RVOT. *See* Right ventricular outflow tract
- R-wave amplitude, RVH and, 382
- Ryanodine, relaxation and, 62
- S**
- S1. *See* First heart sound (S1)
- S2. *See* Second heart sound (S2)
- S3. *See* Third heart sound
- S. aureus* bacteremia, IE and, 1364
- Sarcoplasmic reticulum, calcium, 55–56, 56f
- Safety attitudes questionnaire (SAQ), 1634
- Safety, CMR and, 210–212, 212t
- Sagittal views, atrial septum, 147
- SAM. *See* Systolic anterior motion
- SaO2. *See* Arterial saturation
- Sarcoglycans, isoforms of, 60
- Sarcolemma, myocardial structure and, 54
- Sarcomere
cytoskeletal proteins, 56, 57f
protein composition, 56, 57f
schematic diagram, 57f
- Sarcoplasmic reticulum (SERCA-2), 55–56, 56, 56f, 157
calcium release channels, 56, 56f
- Scalar electrocardiogram, 372–373
interpretation, 372
- SCD. *See* Sudden cardiac death
- Scimitar syndrome, 817, 818, 821f
- SCN5A gene mutations, 55
- S1-coincident murmurs, 89f, 90
- Scoliosis, 91, 651
- Screening obstetric ultrasound, HLHS, 1064
- SCV. *See* Superior vena cava
- Second heart field, 350
- Second heart sound (S2), 88
ccTGA and, 1149
coarctation of aorta, 1049
HLHS, 1066
isolated valvar pulmonary stenosis, 915
peripheral pulmonary arterial stenosis, 915–916
pulmonary atresia and intact ventricular septum, 945
- Second Natural History Study, pulmonary stenosis and, 923
- Secondary cardiac tumors, 1560
- Secondary heart field (SHF) cells
mammalian heart development, 562, 562f
regulation of, 562, 563f
- Secondary hypertension
historical information suggesting, 1536t
physical examination findings, 1537t
- Second-degree atrioventricular block, 462–463, 463f
- Secundum atrial septal defects
imaging, 229, 230f
maternal risk and, 1497–1498
- Sedation
cardiac catheterization, 258–259
cardiac CT, 247–248
CMR and, 208, 210, 210f
electrophysiologic studies, intracardiac technique, 401–403
transesophageal electrophysiologic study, 403
- Segmental analysis
cardiac malpositions and, 1208
complex heart disease, echocardiogram, 1196, 1198t
- Segmental ventricular wall motion, analysis of, 220, 220f, 221f
- Segmented k-space fast gradient recalled echo (fast GRE) sequence, 214
- Selective coronary arteriography, indications for, 283, 283f–284f
- Self-gating, MRI and, 208
- Semaphorin 3a (Sema 3a), E-C coupling, 63
- Semilunar valves, 15–18, 16f, 41
angiocardigram, 1116, 1117f
comparison of, 17–18
and great vessels
aortic valve insufficiency, 185
pulmonary valve regurgitation, 185–186, 186f
quantitative anatomic assessment of, 182–183
semilunar valve stenosis, 183–184, 184f
valve areas calculation, 184–185
obstruction, myxomas, 1556
stenosis, 183–184, 184f
- Senning repair, 1122, 1124f, 1479
ccTGA and, outcomes for, 1158
Mustard repair *v.*, 1122–1128
TGA and, 1098
transposition of great arteries, 104
- SENSE technology (Sensitivity encoding technology), ventricular function and, 215
- Septal band, 13f, 14
- Septal bulge, in TGA, 1098, 1098f
- Septal convexity, pulmonary atresia and intact ventricular septum, 941
- Septal defects
CONCOR project, 1472f
human, genetics of, 570–571
landmarks for, 14, 14f
- Septal disruptions, 554–555
- Septal malalignment, 48, 48f
- Septal myectomy, HCM and, 1231
- Septicemia, asplenia syndrome, 1212
- Septum primum flap, rupture, balloon atrial septostomy, 1118
- Sequential segmental analysis, 32–33
- SERCA-2. *See* Sarcoplasmic reticulum
- Series circulation, monitoring, 1070–1072, 1070f
- 7q11 deletion. *See* Williams-Beuren syndrome
- Severe aortic coarctation, Gd-enhanced 3-D MRA, 231, 232f
- Severe aortic stenosis, TTE and, 1378
- Severe hypertension, treatment, 1542
- Sheath placement, catheterization laboratory, intracardiac technique, 403–405, 404f
- SHF. *See* Secondary heart field
- Shone syndrome, 1045
- Short-axis plane, ventricular function, 215, 217, 218f
- Shortening fraction, 159
- Shortest preexcited RR interval (SPERRI), 447
- SHP-2 gene, Noonan syndrome, 632, 633
- Shunt lesion
atrial septal defect, 99
atrioventricular septal defect, 99
competitive sports, 99–100
leisure activities and activities of daily living, 99
patent ductus arteriosus, 99
pre-athletic participation screening, 99
ventricular septal defect, 99
- Shunts. *See also* specific *i.e.* Aortopulmonary shunts
lesions, CMR and, 229–230
pulmonary atresia and intact ventricular septum, 956
tricuspid atresia, 883
- Sickle cell anemia, 1420–1421
cardiac manifestations, 1591–1592
chest pain and, 1511
- Sideris "buttoned device," 685
- SIDS. *See* Sudden infant death syndrome
- Signal void, 231f
- Signal-averaged electrocardiography, 374
- Signaling cascades, mutations in, 568
- Sildenafil, 496, 1677
- Simple valvotomy, dysplastic pulmonary valves, 923
- Simultaneous left ventricular and aortic pressure tracings, 1029f
- Simultaneous surface electrocardiographic leads, transesophageal technique, 413, 413f

- Single coronary artery, 747–748, 750f
complete transposition of great arteries, 753, 753f
echocardiogram, 749
- Single nucleotide polymorphisms (SNPs)
chromosomal deletions/duplications, 629
- Single outlet connection, great arteries and, 44, 47f
- Single photon emission computed tomography (SPECT), 219
- Single ventricle, 1177f, 1184, 1487–1489
aortopulmonary shunts thrombosis, 1598, 1600
bidirectional glenn anastomosis, 1600
CMR
before stage I palliation, 238
before stage II palliation, 238–239, 239f–240f
fontan, 1600–1601
neurodevelopmental outcomes, 1583–1584
parallel circulation, HLHS and, 1069–1070
physiology, exercise and, 106
- Single-inlet right ventricle with left atrioventricular valve atresia, echocardiogram, 1186, 1190f
- Single-nephron phenomenon, postnatal peripheral circulation and, 79
- Sinotubular junction, supraaortic stenosis, 1038–1039
- Sinus arrhythmia, 444
- Sinus bradycardia, 460–461, 460f
atrial switch repair, 1127
- Sinus node, 441
development, 353–354, 354f, 355f, 356f
heart beat initiation, 352, 353f
PA-VSD and, 961
- Sinus node dysfunction, 460–461, 460f, 461, 461t
- Sinus of Valsalva aneurysms, 755–756
anatomy and physiology, 755
- Sinus rhythm
atrial switch operation and, 1481f
- Sinus venosus
ASD, 685
defects, 813–815, 813f, 814f, 850
echocardiogram, 813f
embryology, 840, 841f
- Situs inversus totalis, 1207
- Six-minute walk test (6MWT), PAH, 1437, 1438f
- Sjögren syndrome, 662
- Slipping rib syndrome, 1510
- Small vessel disease, myocardial ischemia, 1218
- Smyd1 chromatin remodeling protein (Bop), 563
- SNPs. *See* Single nucleotide polymorphisms
- Sodium channel blocker, 457
- Sodium nitroprusside, 495–496
- Sodium-potassium pump, sarcolemma and, 55
- Somatic growth, HLHS, 1081–1082
- SOS1, Noonan syndrome, 632, 633
- Sotalol, 458, 1681
catecholamine-sensitive ventricular tachycardia, pregnancy and, 1503
fetus, 661
- Sox 9, mitral valve development, 1003
- “Spade deformity,” HCM, 1218
- Spatial modulation of magnetization (SPAMM)
myocardial tagging, 221
- Spatial pulse length (SPL), axial resolution and, 136, 136f
- Spatial relationships, 3-D imaging, 140
- Speckle tracking imaging, echocardiography, 180, 180f
- SPECT. *See* Single photon emission computed tomography
- SPERRI. *See* Shortest preexcited RR interval
- Spironolactone, 1676
acquired heart disease, childhood/adolescence, 1571
DCM, 1243
- Splanchnic circulation, postnatal peripheral circulation and, 79–80
- Spleen
child assessment and, 91
postnatal peripheral circulation, 79–80
- Splenic anomalies, 34, 1196
- Spontaneous abortion, Turner syndrome, 626
- Sports
classification of, 94–95
competitive, 95
aortic coarctation, 102
aortic stenosis, 100–101
atherosclerotic CAD, 112
atrioventricular septal defect, 99–100
congenital coronary anomalies, 110
congenitally corrected transposition of the great arteries, 106
d-transposition of the great arteries, 105
Ebstein's anomaly, 104
heart transplantation, 109
hypertrophic cardiomyopathy, 112
Kawasaki disease, 111
pediatric cardiomyopathy, 113
pulmonary stenosis, 102
single ventricle physiology, 106
systemic hypertension, 113
tetralogy of fallot, 104
screening, and participation, 93–113
- SPTI. *See* Systolic pressure time index
- SR Ca 2+-ATPase (SERCA2a), 56
- SSFP. *See* Steady-state free precession
- ST segment, 384
abnormalities affecting, 384–385
myocardial ischemia, 1378, 1381f
- Stab wound, cardiac tamponade and, 556
- Staged palliation
cardiac transplantation, HLHS, 1088
HLHS, PVR and, 1074–1088
- Standardization, quality control implementation in clinical trial, 1651
- Staphylococcal endocarditis, 1372–1373
prosthetic valve and, 1374
- Staphylococcus*
acute pericarditis, 1354–1355
- STARFlex septal occlusion system, 321
- Starling's law, stroke volume and, 63
- Starnes approach, Ebstein's anomaly, 898, 901f
- Static 3-D imaging, 159
- Static magnetic fields, CMR and, 207
- Statins (HMG-CoA reductase inhibitors), cholesterol and, 1527
- Statins, novel therapy of PAH, 1455
- Steady-state free precession (SSFP)
ECG triggered, 214, 214f
TOF and, 236, 237f
VCG triggered, 214
- Stenosis
anatomy, 837
of common pulmonary vein, 833
of coronary ostium, 752
of individual pulmonary veins, 836–837
manifestations, 837
treatment, 836
- Stenotic connections, pulmonary veins and, 809
- Stent(s). *See also* specific i.e. Endovascular stents
biodegradable, 935
implantation
complications, 935
placement, MDCT, 255, 255f, 256f
re-dilation, 935
therapy, COA and, 1469
- Sternal closure, HLHS and, 1080
- Steroids
acute rheumatic fever, 1308, 1308f
cardiopulmonary bypass, 532
- Stethoscope, auscultation and, 85
- Stillborn fetuses, cardiac defect and, 625
- Still's murmur, 92
- Stimulator system, transesophageal technique, 413
- Stimulus current, transesophageal technique, 413
- Stoke-Adams episodes, atrial switch repair, 1127
- Stomach
abdominal situs and, 36, 37f
visceral situs, 1196, 1196f
- Storage, digital echocardiography, 165
- Storage diseases, 617, 1269
- Straddling valves, 50, 50f, 51f, 1177, 1178f
double-inlet right ventricle and, 1183
- Straight back syndrome, valvar pulmonary stenosis *v.*, 920
- Straight wire, cardiac catheterization and, 328
- Strain, echocardiography, 179–180, 180f
- Streptococcal endocarditis, 1364, 1372
- Streptococcal infection
arthritis and, 1305
RF and, 1308
- Streptococcal pharyngitis
primary prophylaxis, 1322–1323, 1323t
secondary prophylaxis, 1323–1324, 1323t
- Stress
renal cortical blood flow, 79–80
stage 1 palliation, HLHS and, 1076
testing, MI and, 1380–1383
- Stress CMR. *See* Dobutamine stress CMR; Stress echocardiography
- Stress echocardiography, 156–157
MI and, 1382t
technical aspects, 158
wall motion abnormalities, 158–159
- Strip-chart recorder, transesophageal technique, 412–413, 413f
- Stroke, 1514
- Stroke volume (SV)
equation, 131
exercise and, 106, 122–123, 122f
mitral regurgitation, 1015
Starling's law and, 63
- Structural heart disease, 747–752
- ST-segment
lightning-related injury, 558
- ST-T waveforms, intrapericardial teratomas, 1559
- Subaortic conus, identifying, 151
- Subaortic gradient
HCM and, 1224
LV wall thickness and, 1227, 1227f
- Subaortic membrane, imaging, 379f
- Subaortic obstruction, 1179, 1180f
- Subaortic stenosis, 708–709, 1468–1469
- Subclavian artery anomaly, 759
- Subclavian flap aortoplasty, coarctation of aorta, 1053, 1053f
- Subclavian steal syndrome, 778
coarctation repair, 1057
- Subclavian vein, approach to, cardiac catheterization and, 260
- Subcostal coronal views, atrial septum, 147
- Subcostal view
ccTGA and, 1152f, 1153f
ECG, HLHS on, 1066–1067, 1068f
- Subcostal window, 139
- Subcutaneous nodules, RF and, 1308, 1308t
- Subendocardial ischemia, 1378f, 1379
- Subpulmonary conus, 151
- Subpulmonary obstruction, 1117
TGA/VSD and, 1105f
- Subtotal cor triatriatum, 834, 835f
- Subvalvular aortic stenosis, 1035–1038
long term outcome, 1038
natural history, 1036
pathology, 1035
physiology, 1035
prevalence and etiology, 1035
treatment, 1036–1038
- Sudden cardiac death (SCD), 1463, 1574
athletes, 1227
in athletes
acquired coronary disease, 110–113
congenital coronary artery abnormalities, 109–110
CHD operative repair, 1465f
epidemiology of, in youth, 389–390, 390f
infantile deaths, 389
LV wall thickness and, 1229
postmortem examination, 389
pulmonary atresia and intact ventricular septum, 956
RCM and, 1274
rhabdomyositis and, 1552
right coronary artery from pulmonary artery, 752
risk assessment for, 1228–1229
rTOF, 1478
single coronary artery, 747
TOF, 1476, 1477, 1477f
in youth, prevalence and causes, 389–390

- Sudden death, 1230
 aortic stenosis, 100–101
 athletic participation and, 95–97
 incidence of, 95
 in infancy, myocarditis, 1255
- Sudden infant death syndrome (SIDS), 389, 1218
 HCM and, 1228
- Sudden unexpected death (SUD)
 atrial switch repair, 1129
- Superior cavopulmonary connection, HLHS,
 1082, 1082f
- Superior vena cava (SVC), 6–7, 6f, 38, 145
 anomalies of, 845–853
 d-TGA, 1485
 pathway obstruction, Mustard repair and,
 1123, 1127f
- Supply/demand mismatch, 1378
- Suprasternal long-axis view, HLHS, 1067, 1068f
- Suprasternal notch view
 HLHS on, 1067, 1069f
- Suprasternal notch window, 139, 140
- Supravalvar stenosing ring, ccTGA and, 1152
- Supravalve mitral stenosis, 1008, 1008f
- Supravalvular aortic stenosis, 1038–1039
 arterial switch operation, 1133, 1133f, 1134f
 clinical features, diagnostic method and,
 1038–1039
 long-term outcome, 1039
 natural history, 1039
 pathology, 1038
 physiology, 1038
 prevalence and etiology, 1038
 treatment, 1039
- Supravalvular narrowing, arterial switch opera-
 tion, 1132, 1133f
- Supravalvular pulmonary stenosis, arterial switch
 operation, 1133
- Supraventricular tachycardia (SVT), 444, 445t
 treatment of, 448
- Surfactant administration, in premature infants,
 475
- Surgery. *See also* specific i.e. Open heart surgery
 acute carditis, 1321
 alternatives to, HCM and, 1232
 anomalous left coronary artery from pulmo-
 nary artery, 751
 anomalous muscle bundles, 927
 chronic rheumatic heart disease, 1321–1322
 congenital pericardial defects, 1212–1214
 coronary artery anatomy, abnormal, pul-
 monary atresia and intact ventricular
 septum, 953t
 HCM and, 1190, 1231–1232
 HLHS, PVR and, 1068
 inferior vena cava drainage to left atrium, 858
 interrupted aortic arch, 783
 myxomas, 1557
 PA-VSD and, 966–967, 967f
 pulmonary arterial stenosis, complications,
 934–935, 935f
 resection, cor triatriatum, 836
 rheumatic carditis, 1314
 right aortic arch with retroesophageal diver-
 ticulum of Kommerell, 767
 right coronary artery from pulmonary artery,
 752
 RV failure, following physiologic correction,
 1142–1143
 stage 1 palliation, HLHS and, 1074–1075,
 1075f
 supravalvular aortic stenosis, 1039
 survival, 1579
 TGA, 1122–1143
 TGA and pulmonary vascular obstructive
 disease, 1143
 TGA/LVOTO, 1140–1143
 thoracic ectopia cordis, 1215
 tricuspid atresia, 882–885
 truncus arteriosus, 997–100, 998f, 1000f
 univentricular atrioventricular connection,
 1193–1194
- Surgical closure
 infants, children, and adults, treatment of
 PDA, 739
 preterm infant, treatment of PDA, 736
- Surgical commissurotomy, 303
- Surgical dissection of umbilical vein, anomalous
 termination of umbilical veins, and
 absent ductus venosus, 859
- Survival. *See also* Kaplan-Meier survival curve
 curves, ASD, 1472, 1472f
 ECMO cannulation, neonates, 533, 533t
 ES and, 1473–1474
 PA-VSD and, 966, 967f
 pediatric heart transplantation, 1384
 rTOF, 1477f
 transposition of great arteries, 1097, 1098f
 VAD implant and
- SV. *See* Stroke volume
- SVB. *See* Systemic venous baffle
- SvO₂. *See* Systemic venous saturation
- SVR. *See* Systemic vascular resistance
- SVT. *See* Supraventricular tachycardia
- Sweeping technique
 heart imaging planes, 139–140, 140f
- Swiss Cheese phenomenon,
 heart center, safety and quality, 1622
- Sydenham chorea, 1309f, 1311
- Sympathetic innervation, E-C coupling, 63–64
- Sympathetic nervous system
 neurotransmitters of, 63
- Syncope
 adolescents, 83–84
- Syndromes. *See also* specific i.e. Down
 syndrome
 peripheral pulmonary arterial stenosis and,
 935
- Syringe, pulmonary angiography, 283, 283f
- Systemic arterial malformations, 789–792
 angiography, 790
 cardiac catheterization, 790
 differential diagnosis, 790
 echocardiography, 790
 imaging, 790, 791f
 natural history, 791–792
 pathology and pathogenesis, 789–790
 physiology and clinical manifestations, 790
 prevalence, 789
 treatment, 791–792
 ultrasound, 790
- Systemic arterial desaturation
 tricuspid atresia, 879
- Systemic arterial pressure, pregnancy, 1494
- Systemic atrioventricular valve regurgitation,
 1157f
- Systemic blood pressure, double balloon tech-
 nique
- Systemic circulation, univentricular atrioventricu-
 lar connection, 1193
- Systemic diseases, pulmonary stenosis and,
 920–925
- Systemic hypertension
 COA, 1469
 SCD and exercise, 113
- Systemic inflammatory response, cardiopulmo-
 nary bypass, 532
- Systemic oxygen delivery
 HLHS, 1069–1072
 Qp/Qs, 1069, 1071
- Systemic right ventricle, maternal risk
 and, 1501
- Systemic vascular resistance (SVR)
 equation, 269t, 271
 pregnancy, 1494
 Qp/Qs, 1071
- Systemic vein stenoses, transcatheter
 management, 31–32
- Systemic veins
 cardiac CT, 251
 echocardiogram and, 146–147
- Systemic venous anomalies
 CMR and, 235–236, 236f
 treatment, 1207
- Systemic venous baffle (SVB)
 d-TGA, 1483
- Systemic venous drainage, balloon-occlusion
 angiography, 269
- Systemic venous return, HLHS and, 1064
- Systemic venous saturation (SvO₂)
 circulatory management and, 1069, 1070t
- Systemic ventricular dysfunction, childhood/
 adolescence, 1567
- Systemic ventricular failure, in CCTGA, 1486,
 1486f
- Systemic-pulmonary anastomosis, TGA and,
 1122
- Systemic/pulmonary (s/p) patch aortoplasty,
 COA and, 1470, 1470f
- Systemic-to-pulmonary artery shunt
 HLHS and, 1074, 1075
 pulmonary artery banding, 1140
- Systemic-to-pulmonary artery shunts, 512–513
- Systemic-to-pulmonary collateral arteries,
 PA-VSD and, 964, 965f
- Systems thinking, heart center, safety and quality,
 1632
- Systolic anterior motion (SAM)
 mitral valve, 1229f
 of mitral valve, HCM, 1218
- Systolic arterial hypertension, coarctation of
 aorta and, 1048
- Systolic blood pressure
 coarctation of aorta, 1048
 isolated valvar pulmonary stenosis, 919
- Systolic crescendo-decrescendo systolic ejection
 murmur, congenital aortic stenosis,
 1026
- Systolic ejection murmur
 congenitally bicuspid aortic valve, 1467
 HCM and, 1226
 peripheral pulmonary arterial stenosis, 929
- Systolic function
 determinants of, 65
 developmental aspects of, 65
- Systolic murmurs, 89
 cyanotic neonate, 946t
 HCM, 1226
 isolated valvar pulmonary stenosis, 916, 916f
 peripheral pulmonary arterial stenosis, 932
 supravalvular aortic stenosis, 1038
- Systolic pressure time index (SPTI), 1025, 1026f
- Systolic regurgitant flow
 Doppler echocardiography, 946
- Systolic thrill
 isolated valvar pulmonary stenosis, 916
 univentricular atrioventricular connection,
 1185
- T
- T3. *See* Triiodothyronine
- T waves, 384
 abnormalities affecting, 384–385
 age-related transitions, 386
 myocardial ischemia, 1378, 1379
 tricuspid atresia, 879, 880f
- Tachyarrhythmia. *See* Tachycardia
- Tachycardia
 atrial ectopic, 448–449
 atrial fibrillation, 450–451, 451f
 atrial flutter, 450, 451f
 atrial switch repair, 1127
 basic mechanisms, 441, 442f, 443
 cardiomyopathy, 455
 chaotic atrial, 449, 450t
 characterization of, 444
 d-TGA, 1481
 ECG evaluation, 443–444, 443f
 intraatrial reentrant, 451–452, 452f
 junctional ectopic, 449–450, 450f
 Mahaim fiber, 448
 narrow complex tachycardia, 444, 445t
 nonautomatic focal atrial, 449
 normal resting heart rates, pediatric patients,
 443, 443t
 permanent junctional reciprocating tachycar-
 dia, 448, 448f
 premature atrial contractions, 455–456, 455f
 premature ventricular contraction, 456
 prophylaxis, during pregnancy, 1503
 sinus arrhythmia, 444
 unidirectional retrograde accessory pathway,
 448
 ventricular tachycardia, 453–454, 453f–455f
 wide complex, 452–453, 452f, 453f
 Wolff-Parkinson-White syndrome, 446–448
- Tachypnea
 complete AVSD, 700

- partial atrioventricular septal defect, 692
 pulmonary atresia and intact ventricular septum, 945
 TAPVC without pulmonary venous obstruction, 828
- Tamponade**
 cardiac rupture, 504
 chest radiography, 1351, 1351f
- TAPSE.** *See* Tricuspid annular planar systolic excursion
- TAPVC.** *See* Total anomalous pulmonary venous connection
- Target organ abnormalities, evaluation of,** 1535–1536
- Taussig-Bing anomaly,** 1097, 1101, 1104f
 Damus-Kaye-Stansel technique, 1139
 surgical arterial switch and, 1132
- Taussig-Bing double outlet right ventricle, coarctation of aorta,** 1045
- TBX2, cardiac valve and,** 568
- TBX5 mutations,** 631
- TBX1 transcription factor**
 22q11 deletion syndrome, 970
 DiGeorge syndrome, 563
- T-cell(s)**
 activation inhibitors, pediatric heart transplantation, 1390
 myocarditis, 1256
- TDI.** *See* Tissue Doppler imaging
- Team improvement, heart center, safety and quality,** 1627–1628, 1627f, 1628f, 1629f, 1630f
 model, 1625, 1626f
 seven step problem solving model, 1625
 Six-Sigma DMAIC, 1625
 SPDSA, 1625–1626
- TED.** *See* Thromboembolic disease
- TEE.** *See* Transesophageal echocardiography
- Temporal resolution,** 137, 137f
- Temporary pacing, CICU,** 500
- Tenascin-C**
 perinatal pulmonary vasculature, 1417
 photomicrographs, 1409f
- Tendinous cords, leaflets and,** 10
- Teratogens**
 maternal exposure, cardiac defects, 84, 84t
 pregnancy and, 1502
- Terminal transferase labeling, apoptosis,** 1259
- Terminology, diversity of,** 32
- Tetralogy of Fallot (TOF), 708, 748f, 749f,** 753–754, 781, 804–805, 1476–1479
 activities of daily living, 104
 aortic arch, 974
 aortic root, 984
 aortopulmonary collaterals, 974
 atrioventricular septal defect, 976
 competitive sports, 104
 contraception, 985
 conus artery, 753–54
 coronary artery, 974
 endocarditis, 984
 JAG1 gene mutation, 636
 left ventricle, 983–984
 palliative procedures, 978–979
 percutaneous palliation, 978
 Potts operation, 1476
 pregnancy, 985
 pulmonary artery, 974
 pulmonary atresia, 974
 pulmonary regurgitation, 980–981
 pulmonary valve leaflets, 975–976, 975f
 pulmonary valve replacement, 983
 22q11 deletion syndrome, 627
 retinoic acid, maternal exposure, 617
 right ventricle, 980–981, 981f
 right ventricular diastolic dysfunction, 982–983
 right-sided obstructive lesions, 103–104
- Tetralogy of Fallot repair (rTOF), 1476**
 long-term problems for, 1478–1479
 New York Heart Association functional classification, 1477f
 QRS duration over time, 1477f
- Tetralogy type DORV, 1163–1164, 1164f**
 adult with, 1173
- TGA.** *See* Transposition of great arteries
- TGFβ.** *See* Transforming growth factor beta
- Thalassemia syndromes,** 1592–1593
- Thalidomide,** 599–600
- Thermomodulation method, oxygen consumption,** 268
- Thiazide diuretics,** 1676
- Thick filaments**
 cardiac myocytes, 57–58
 myosin, 57–58
- Third degree atrioventricular (AV) block,** 463–464, 463–465, 463f
- Third heart sound (S3), 88**
 HLHS, 1066
- Thoracic aortic aneurysm and dissection (TAAD) disease, ACTA-2 gene mutation,** 804
- Thoracic ectopia cordis**
 newborn and, 1215f
 treatment, 1215
- Thoracic impedance, stroke volume and,** 131
- Thoracic roentgenography, DCM and,** 1241, 1241f
- Thoracic sarcomas,** 1560
- Thoracoabdominal ectopia cordis, congenital heart disease and,** 1215
- Thoracocervical ectopia cordis,** 1214, 1214f
- Thoracotomy, 87, 557**
 pericardiac lacerations, 553
- Thorax, heart position in,** 33
- Three-dimensional CT angiogram, coarctation of aorta,** 1049, 1050f
- Three-dimensional echocardiography, 159–162**
 ASD, 681, 682f
 ccTGA and, 1154, 1154f
 rhabdomyomas and, 1553
- Three-dimensional magnetic resonance angiography, coronary arteries and,** 215
- Three-dimensional mapping**
 abnormal flow patterns, 226, 226f
 intracardiac electrograms, 421, 422f
- Thrills.** *See also* Systolic thrill
 anomalous muscle bundles, 926
 child assessment and, 87
 pulmonary atresia and intact ventricular septum, 945
- Thrombocytosis,** 1595
- Thromboembolic disease (TED), 1448–1449**
 CHD and, 1580
 clinical features, 1420
- Thromboembolism, 1085–1086**
- Thrombosis, 1522**
 bridging therapy, 1603
 in children and adolescents, 1596
 congenital heart disease
 altered blood flow, 1596
 antiplatelet, anticoagulant, and thrombolytic therapies, 1598, 1599t
 arrhythmias, 1602
 cardiac catheterization, 1603
 cardiomyopathy/myocarditis, 1603
 early postoperative thromboses, 1598
 hypercoagulability, 1596
 inflammation and bloodstream infection, 1598
 Kawasaki disease, 1602–1603
 prosthetic valves, 1601–1602, 1602t
 single ventricle population, 1598, 1600–1601
 in cyanotic heart disease, 1598
 during pregnancy, management, 1503
 therapy in children and adolescents, 1603
- Thrombosis clinic, anticoagulation therapy, pregnancy,** 1503
- Thrombus**
 formation, endocarditis, 1365
 right atrial enlargement and, 8
 TEE, 159f
- THs.** *See* Thyroid hormones
- Thyroid dysfunction**
 amiodarone therapy, 458
- Thyroid hormones (THs), 58**
 E–C coupling, 64
- Thyroxine,** 1679
- Tidal volume (VT), 125**
 exercise and, 125
 ventilation measurements, 131
- Tietze syndrome,** 1509
- Tissue, characteristics of, MRI and,** 228–229, 229f
- Tissue Doppler imaging (TDI), 189**
- Tissue oxygen status, monitoring,** 1071
- Titin,** 57f, 58
- TNF.** *See* Tumor necrosis factor
- Toddlers**
 CMR and, 207
 patient history, 83
- Toronto transseptal catheter, infants and,** 296–297
- Torsades de pointes,** 454, 455f
- Total anomalous pulmonary venous connection (TAPVC), 809, 811, 816, 818, 819,** 821–836, 838f
v. anatomic site comparison, 825f
 anatomy, 823–826
 chest radiogram, 817f, 819
 to coronary sinus, surgical technique, 825
 genetics and epidemiology, 823
 to left innominate vein, surgical technique, 825
 manifestations of, 828
 with obstruction, microscopic anatomy, 827
 PDA, 731
 postoperative course, 832
 prognosis
 postoperative course, 832
 untreated, 832
 with pulmonary venous obstruction, 827, 830
 clinical features, 830–831
 differential diagnosis, 831
 physiology, 827
 surgical treatment, 831–832
 without obstruction, microscopic anatomy, 827
 without pulmonary venous obstruction, 828, 830f
 clinical features, 827
 microscopic anatomy, 827
- Total anomalous pulmonary venous return,** 512
- Total cavopulmonary anastomosis, tricuspid atresia,** 885
- Total systemic vascular resistance (SVR) equation for, HLHS and,** 1068
- Totipotential aortic arch, embryology,** 759f, 760
- Trabeculations, ventricular myocardium,** 1180, 1181f
- Tracheomalacia,** 247, 787
- Tracking, lipids,** 1520
- Transcatheter closure**
 of fenestrations, 322–323
 of VSDs, 289
- Transcatheter device, transesophageal echocardiography,** 155
- Transcatheter occlusion of persistent ductus arteriosus,** 325–327
- Transcatheter procedures**
 pulmonary atresia and intact ventricular septum, 954–955
 pulmonary vein stenoses and, 310–311
 rehabilitation of branch pulmonary artery stenosis, 307–310
- Transcatheter stent therapy, complex arch stenting,** 305
- Transcription factors**
 cardiac precursors, 562–570
 coronary development, 572
 SHF regulation, 562–563
- Transducer position, Doppler echocardiography,** 140
- Transesophageal atrial pacing**
 protocols, 410t
 transesophageal technique, 403f, 405
- Transesophageal echocardiography (TEE), 153–156**
 approach, 154
 ASD, 679, 682f
 cardiac tumors, 1550
 ccTGA and, 1154
 congenital aortic stenosis, 1029
 imaging planes, 155f
 intraoperative, 154
 ventricular septal defects, 717, 718f

- Transesophageal electrophysiologic study
complications, 410–411
drug administration, 403
education and emotional preparation, 401
objectives of, 416–417
pacing protocols for, 410*t*
- Transesophageal recordings, 412, 414*f*
unipolar *v.* bipolar, 415*f*
- Transesophageal techniques
catheter placement, 403–405, 404*f*
comparison of, 416–417, 417*t*
- Transforming growth factor beta (TGFβ), 799
- Transient bacteremia, endocarditis, 1365
- Transitional AVSD, 691
- Transitional circulation, 473
birth, 72
TGA and, 1110
- Transmitral doppler flow evaluation, 189, 190*f*
- Transparency, clinical trial reporting, 1656
- Transplant rejection, PICU, 523
- Transposed great arteries, tricuspid atresia, 878–879
- Transposition complexes, terminology, 44
- Transposition of great arteries (TGA), 1097–1143, 1098
angiogram, 1119
arterial repair, 1122
with associated right ventricular outflow tract obstruction, surgery for, 1141–1142
balloon atrial septostomy, 1114, 1116*f*
cardiac segments, 1098, 1098*f*
clinical manifestations, 1111–1119
CMR of, 236–238
coarctation of aorta, 1045
coexisting anomalies, 1101–1106
coronary artery distribution, 1099, 1102*f*
coronary patterns, frequency distribution of, 1103*f*
echocardiographic features, 1115*f*
maternal risk and, 1501
effects of exercise, 104–105
HRQOL, 1616
infants and, surgical options, 1122–1143
intracirculatory mixing, 1107*f*, 1116–1107
with IVS, 1097, 1098*f*, 1106, 1106, 1107*f*, 1107*f*, 1113–1114, 1113–1116
angiogram, 1119
echocardiographic features, 1115*f*
prostaglandin E1, 1120–1121
without associated outflow tract obstruction, 1122–1128
with large VSD, 1113
with low left ventricular pressure, surgery for, 1138–1139
with LVOTO, 1097, 1098*f*, 1101–1103, 1103, 1104*f*
preoperative *v.* postoperative, 1142*f*
surgery for, 1140–1143
morphogenesis and etiology, 1098, 1098*f*
neoaortic dysfunction
arterial switch operation, 805–806
echocardiographic assessment, 806
histologic abnormalities, 806
prevalence of, 805
nomenclature, 1097
oxygen saturation, 1116
PA-VSD *v.*, 965
with PDA, 1097
physiologic-clinical classification, 1112*t*
physiology, 1106–1111
with pulmonary blood flow
and large intercirculatory shunt, 1112
and small intercirculatory shunt, 1112
pulmonary vascular obstructive disease and restricted pulmonary blood flow, 1112
surgery for, 1143
restricted pulmonary blood flow, 1112
with situs solitus of atria and viscera, 1097
surgical arterial switch and, 1131
surgical repair, electrophysiologic consequences of, 1130*t*
treatment, 1119–1122
with VSD, 1097, 1101, 1103*f*, 1104*f*
- Transposition type DORV, 1164–1165, 1166*f*–1168*f*
survival, 1173
- Transpulmonary contrast echocardiography, 164–165
- Transpulmonary resection, TGA/IVS, 1140
- Transseptal puncture, 295–297
- Transtelephonic event recording, 374–375
- Transthoracic echocardiography (TTE)
IE and, 1368
MI and, 1380
- Transverse arch, HLHS, 1067, 1068*f*
- Transverse tubule system, 56
- Trauma, chest pain and, 1510
- Traumatic cardiac tamponade, 553
- Traumatic pericarditis, 553
- Triangle of Koch, 9, 24
- Triatriatum dextrum, 860
- Tricuspid annular planar systolic excursion (TAPSE), 181, 181*f*
pulmonary arterial hypertension, 1436
- Tricuspid atresia, 44, 46*f*, 516, 877–885
classification of, 877, 878*f*
ECG features, 879–880, 879*f*, 880*f*
pathology of, 877, 878*f*
persistent valves of sinus venosus, 860
prognosis, 885
RA, 877, 878*f*
treatment, 882–885
truncus arteriosus *v.*, 996
- Tricuspid regurgitation, 1156
atrial switch repair, 1124
ccTGA and, 1157
Mustard operation and, 1484
pulmonary atresia and intact ventricular septum, 945
- Tricuspid stenosis, 885–886
- Tricuspid valve (TV), 10*t*, 11–12, 11*f*, 149–150
anatomy, four-chamber view, 1066, 1067*f*
angiocardiology, 1116–1118
anomalies, 1103, 1105
pulmonary atresia and intact ventricular septum, 942*f*
ccTGA and, 1154
dilation, 303
disease of, 877
displasia, HLHS and, 1064
Ebstein's anomaly, 516, 889, 890*f*, 891*f*, 892*f*
Broussais approach, 902
cone reconstruction, 902
da Silva approach, 900, 902, 904*f*
Danielson repair, 900, 903*f*
history, 900
ventriculization, 902
HLHS and, 1064
insufficiency, 886
mitral valves *v.*, 39–40
morphology, 39
obstruction, 861
pulmonary atresia and intact ventricular septum, 941, 942*f*, 946
replacement, 903, 906–907
surgery, 1142
- Triggered activity, tachyarrhythmia, 441
- Triglycerides
genetics and, 1521
hypothyroidism and, 1522
- Triiodothyronine, 1679
- Trimethadione, PA-VSD and, 959
- Triphosphate nick end labeling (TUNEL), 1259, 1259*f*
- Trisomy 18, 619, 625–626, 657
- Trisomy 21
atrioventricular septal defects, 625
fetus and, 651
tetralogy of Fallot, 617
- Tropomyosin, 57, 57*f*
- Troponin, 1267
complex, 56–57
- Troponin C
calcium binding, 57, 57*f*
- Troponin I, 57
myocardial injury, 1381*f*
- Troponin T, 56–57
- Troponin-tropomyosin complex interaction, actin filament, 57, 57*f*
- Trough drug concentrations (C min), 1663
- True fast imaging with steady precession (TrueFISP), 214
- Truncal valve
dysfunction, 100
incompetence, 994
truncus arteriosus, 991
- Truncus arteriosus (Common truncal artery), 42, 150, 153, 512, 754, 990–1001
anomalies associated with, 993
classification system, 990, 992*f*
differential diagnosis, 996–997
embryology, 990
long-term issues, 1001
manifestations of, 993–996, 996*f*
natural history and treatment, 997
pathology, 990–993, 991*f*
PDA, 732
22q11 deletion syndrome, 627
- Trypanosoma cruzi*, myocarditis, 1255
- TSE. *See* Turbo spin echo
- TTE. *See* Transthoracic echocardiography
- T-tubules, 56
- T-type voltage-gated calcium channel, 362
- Tuberculous pericarditis, 1355
- Tuberous sclerosis syndrome, cardiac rhabdomyoma, manifestations of, 1553
- Tumor necrosis factor (TNF), 1258
- Tumor volume analysis, matrix array three-dimensional echocardiography, 1550, 1551*f*
- TUNEL. *See* Triphosphate nick end labeling
- Turbo spin echo (TSE)
abdominal coarctation, 232*f*
central pulmonary arteries, 235
CMR and, 213
with double inversion recovery, 234, 234*f*
fibroma, 1552*f*
hemangioma, 214*f*
left pulmonary artery sling, 234
pericardial teratoma, 228*f*
- Turner syndrome, 657, 819, 1023
CHD, 618
coarctation repair, 1057
women, 626
- 22q11 deletion syndrome
mutations and, 1579
testing, 627–628
tetralogy of Fallot, 627
- Two-chamber plane, ventricular function, 215, 218*f*
- Two-dimensional echocardiogram
anomalous muscle bundles, 926, 926*f*
cardiac tumors, 1550
coarctation of aorta, 1050, 1050*f*
doppler study, 728
fibroma, 1555*f*
HLHS and, 1061–1062, 1062*f*, 1066
IE and, 1368
isolated valvar pulmonary stenosis, 916–917, 918*f*
myxomas, 1557*f*
physics of, 134–139
RCM, 1271, 1272*f*
rhabdomyomas and, 1553, 1553*f*
TGA and, 1110
truncus arteriosus, 994–995, 994*f*
- Type B interrupted aortic arch, 8-month child, 248*f*
- Type IV collagen, 54
- U
U waves, 384
abnormalities affecting, 384–385
- UHL anomaly, 886–887
associated anomalies, 911
clinical presentation, 910
differential diagnosis, 911
history, 910
pathology, 910
prevalence, 910
treatment, 911
- Ultrafiltration, 1078
- Ultrasonography, 759
- Ultrasound
atherosclerosis, 1516
systemic arterial abnormalities, 790

- Umbilical artery, recording of, normal fetus, 655
 Umbilical catheters
 in newborns, congenital heart disease, 479
 Umbilical veins
 ductus venosus, 458, 459f
 recording of, normal fetus, 654
 Umbilical venous access, cardiac catheterization and, 260
 Umbilical-placental circulation
 postnatal central circulation, 71
 postnatal peripheral circulation and, 78
 Unblinding, clinical trial, 1646
 Unfractionated heparin, pregnancy and, 1503
 Unifocalization procedures, PA-VSD and, 966, 966f
 Unipolar recording system, transesophageal technique, 412, 413f, 415f
 Unipolar transesophageal simultaneous recordings, transesophageal technique, 412, 415f
 United Network for Organ Sharing (UNOS) allocation algorithm, 1384
 Univentricular atrioventricular connection, 44, 1175–1194
 anomalies having, 1177, 1178f
 cardiac catheterization, 1189–1192
 clinical features, 1185
 echocardiogram, 1176 f, 1179f, 1185–1189, 1186 f, 1187 f, 1188 f, 1189 f, 1190f
 electrocardiographic features, 1185–1189
 embryology, 1178f
 goals of, 1189
 radiologic features, 1189
 treatment, 1192–1194
 Univentricular heart, 175, 182. *See also* Double-inlet left ventricle
 Unoperated structural heart disease, childhood/adolescence, 1566
 Unroofed coronary sinus, coronary sinus defect and, 853–854, 853f
 Upper airway obstruction, 1415, 1416f, 1417f, 1417t
 Upper body cyanosis, infants and, heart disease and, 82–83
 Upper limb abnormalities, Holt-Oram syndrome, 631
 Upper septum abnormalities, 15
 Urinary infection, 522
- V**
 Vaccination, myocarditis, 1222, 1263–1264
 VACTERL association, 634–635
 VAD. *See* Ventricular assist device
 Valid randomization, 1645, 1645t
 Valproic acid, pregnancy and, 1502
 Valsalva maneuver
 foramen ovale and, 9
 HCM, 1226
 myocardial contractility, 1224
 Valvar pulmonary stenosis, 923–924, 923–925
 Valve areas
 calculation of, 272t
 pressure gradient across, 272
 Valve remodeling, EGF signaling and, 569
 Valves of sinus venosus, embryology of, 860, 861f
 Valvotomy
 balloon valvuloplasty *v.*, 923
 congenital aortic stenosis, 1031–1033
 Valvular aortic stenosis, 1024, 1024f
 embryology and pathology, 1024–1025
 in infancy
 clinical features, 1033–1034
 evaluation and management, 1034–1035, 1034f
 physiology, 1025–1026
 prevalence and etiology, 1023–1024
 Valvular obstruction, myxomas, 1556
 Valvular regurgitation
 ccTGA and, 1152
 rheumatic carditis, 1311–1312
 Valvuloplasty
 aortic stenosis, 100
 congenital mitral valve stenosis, 1019
 pulmonary valve stenosis, 102
- Valvuloplasty catheter, partially inflated, 920, 920f, 921f
 Van Praagh Classification System, 32
 truncus arteriosus, 990, 992f
 Vancomycin
 staphylococcal endocarditis, 1373
 streptococcal endocarditis, 1372
 Variant repolarization, myocardial injury and, 1380f
 Vascular access, cardiac catheterization and, 259
 Vascular anomalies, 788–789
 Alagille syndrome, 631
 classification, 789, 789t
 classification of, 864
 coarctation repair, 1057, 1057f, 1058f
 embryology and genetics, 864
 embryology and pathogenesis, 788–789
 imaging of, 866–867
 management of, 867
 Mulliken and Glowacki classification of, 864
 vascular tumors, 865–867
 Vascular endothelial growth factor (VEGF), 788
 coronary development, 61
 pulmonary artery pressures, 1408
 Vascular interstitial cells (VIC), ECM, 569
 Vascular malformations, 794–796
 capillary malformations, 873
 fast-flow vascular malformations, 873–874, 976
 imaging of, 873
 lymphatic malformations, 872–873
 venous malformations, 867–868, 870f (*see also* Venous malformations)
 Vascular resistance
 cardiac catheterization and, 271–272
 changes at birth, 72, 73f
 Vascular response, hypnotic drugs and, 1078
 Vascular rings, 253, 253f, 759–760, 760t, 760t
 aortic arch anomalies, 759
 double aortic arch, 778–782
 mirror-image right arch, 766–767, 767f, 768f, 769f
 MRI, 233–234, 234f
 turbo spin echo, 234, 234f
 Vascular sheaths, 424
 Vasculitis, RF and, 1307
 Vasculogenesis, 61
 distal coronary development, 571
 Vasoactive medications, HLHS and, 1076
 Vasoconstrictor neuropeptide-containing nerves
 reactive pulmonary circulation, 1406, 1407f
 Vasoconstrictors, 494–495
 Vasodilating drugs
 cardiopulmonary bypass, 532
 pediatric heart transplantation, 1394
 Vasodilators, 492t, 495–497, 1676–1678, 1676t
 Vasopressin, 495, 1679
 cerebral blood flow, postnatal peripheral circulation, 76
 kidney and, 79
 Vasoreactivity testing, pulmonary arterial hypertension, 1450
 VAT. *See* Ventilatory anaerobic threshold
 VATER association, 624t, 634–635, 1579
 Vaughan-Williams classification
 action potential changes, 456f
 chaotic atrial tachycardia, 449, 450t
 VCS. *See* Ventricular conduction system
 VEC MRI sequence, blood flow analysis, 223–225
 Vectorcardiography, 373
 Vegetation formation
 antibiotic therapy, IE and, 1365
 endocarditis, 1365
 Velocardiofacial syndrome, 621t, 627–628
 Velocity-time integral (VTI), 131
 Vena caval injury, trauma and, 556
 Venoarterial extracorporeal membrane oxygenator (ECMO), HLHS and, 1079
 Venoatrial connections, 44
 Venous collateral vessels, angiogram, 279, 281f
 Venous connections
 cardiac malpositions, 1210
 univentricular atrioventricular connection, 1189
- Venous drainage, LSCV, 279
 Venous hum murmur, 92
 Venous hum, PDA, 731
 Venous malformations
 congenital phlebectasia, 868, 871f
 histological features of, 867
 intralesional venography, 868, 871f
 localized intravascular coagulation, 868
 macrocytic lymphatic malformation, 868, 872f
 MRI of, 867, 870f
 sclerotherapy, 868, 871f
 treatment of
 compression stocking for, 869
 extralesional extravasation, sclerosant, 871, 875f
 sclerotherapy, 869–870
 Venous murmurs, 92
 Venous oximetry, intravascular oxyhemoglobin monitoring, 486
 Venous systems, embryology, 840–845
 Venous valves, pulmonary atresia and intact ventricular septum, 940–941
 Ventilation measurements, 131–132
 Ventilation-perfusion scintigraphy
 pulmonary arterial hypertension (PAH), 1438
 Ventilatory anaerobic threshold (VAT), 120–121
 Ventilatory threshold (VT), 120–121
 Ventricle repair, 907–908
 Ventricles, 40–41, 40f, 1089
 anatomy, 1211
 base-apex characteristics, 4
 comparison of, 13f, 15
 general features, 4
 positions of, 42–43, 43f
 Ventricular aneurysm, 504
 MRI and, 228
 posttraumatic, 555
 Ventricular aneurysmectomy, ventricular aneurysm, 555
 Ventricular arrhythmias
 athletic screening and, 103, 104
 rTOE, 1476
 Ventricular assist device (VAD)
 adverse events, 539, 539t
 clinical criteria for, 538–539, 538f, 539f
 extracorporeal membrane oxygenation (ECMO), 1596
 implant in children, by era, 539–540, 540f, 541f
 implant, survival and, 539f
 pediatric patients, short-term VADs *v.* chronic pulsatile device, 539t
 pediatrics, 538–542
 Ventricular chambers, fetal cardiovascular system and, 645f, 646
 Ventricular conduction network, 359–361, 362f, 363f
 Ventricular conduction system (VCS)
 developmental aspects, 367, 367f
 Ventricular depolarization, 376f, 377
 Ventricular diastole, 188
 Ventricular dysfunction, late Fontan and, HLHS, 1085
 Ventricular failure, DMD and, 1279
 Ventricular fibrosis, 981–982
 Ventricular function
 quantitative evaluation, steps in, 215, 217–219
 SSFP and, 215, 218, 219
 Ventricular ischemia, myxomas, 1556
 Ventricular mass, in children, blood pressure and, 1528
 Ventricular morphology, 41
 myocardial, 1180, 1181 f
 univentricular atrioventricular connection, 1190–1191, 1192f
 Ventricular myocardium, morphology, 1190–1191, 1192f
 Ventricular out flow tracts (OFTs), 349
 Ventricular outflow
 tracts, fetal cardiovascular system and, 650f
 Ventricular outlet septum, malalignment defects of, 1117
 Ventricular output
 preferential pattern of, 70, 70f

- Ventricular pacing, 500
- Ventricular pressure, isolated valvar pulmonary stenosis, 913, 914f
- Ventricular pressure-volume relationships, right *v.* left, 546, 547f
- Ventricular rate, 375
- Ventricular repolarization, 384
- Ventricular septal defect
in PCICU, 513
response to exercise, 99
- Ventricular septal defect (VSD), 926, 1114, 1401, 1471–1472
angiocardiology, 882
ccTGA and, 1148, 1152
chest radiography, 715
clinical outcomes and prognosis, 720
CMR and, 229
coarctation repair, 1057
differential diagnosis, 719
Ebstein's anomaly, 890–891
echocardiography and, 162, 715, 715f–717f, 717, 1114–1116
electrocardiography and, 715
fetal heart, 647, 650f
GATA4 mutation, 635
imaging of, 229, 231f
interrupted aortic arch, 784
magnetic resonance imaging, 717
maternal risk and, 1497–1498
medical therapy, 719
mirror-image right arch, 766
pathology, 713–714
PDA, 732
physical examination, 715
physiology, 714
prevalence, 713
surgical therapy, 719–720
tricuspid atresia, 877, 878f
truncus arteriosus, 990
univentricular atrioventricular connection, 1177
- Ventricular septal myotomy-myectomy operation (Morrow procedure), 1231
- Ventricular septation, univentricular atrioventricular connection, 1193
- Ventricular septum, 14, 14f
echocardiography, 150
hypertrophy and, 1217
TGA and, 1098, 1098f
- Ventricular situs
abnormalities, 1197–1200
morphology, 1201
- Ventricular synchrony
echocardiography, 197
- Ventricular tachycardia(s), 431, 453–454, 453f–455f
Duchenne muscular dystrophy, 1284
myocarditis, 1208, 1210f, 1249, 1251f
rTOF, 1478
- Ventricular transesophageal pacing, 414–415
- Ventricular volumes, 160
- CMR, accuracy/reproducibility/reference values, 219
determining, error sources, 219
image analysis and, 217–218, 218f
- Ventricular-great artery connections, 1211
univentricular atrioventricular connection, 1189–1190, 1192f
- Ventricular-great artery discordance, subaortic obstruction, 1179, 1180f
- Ventricular-to-aortic pressure ratio, balloon-expandable intravascular stents, 934
- Ventricular-vascular coupling, normal fetus, 655
- Ventricular-ventricular interactions, 182, 550
tetralogy of fallot, 983–984
- Ventricles, anatomy, 1211
- Ventriculoarterial connections, 44, 47f, 151
- Ventriculocoronary artery communication, persistent valves of sinus venosus, 860
- Ventriculography, 265
- Verapamil
HCM and, 1229
intracardiac study and, 410
- Very low density lipoprotein particles (VLDL), 1520
- Viral genome, myocarditis, 1253–1254
- Viral pericarditis, 1354, 1354t
- Viral studies, myocarditis, 1250–1253
- Viruses, apoptosis and, 1259
- Visceral heterotaxy, PAPVD and, 819
- Visceral heterotaxy with asplenia, bilateral superior venae cavae, with unroofed coronary sinus, 848
- Visceral pericardium (Epicardium), 3, 571
- Visceral situs (Sidedness), 34, 35f–37f, 36, 1195, 1197f
abnormalities, 1196–1200, 1198t
cardiac malpositions, echocardiographic features, 1197f, 1208–1210, 1208f, 1209f, 1210f
- Visceral situs ambiguous, 1210, 1210f
- Visceral situs inversus, 1208, 1209f
- Visceral-atrial situs, 1195, 1197f
- Vital signs
assessment, 85
congenital aortic stenosis, 1026
- Vitamin A, congenital heart defects and, 603
- VLDL. *See* Very low density lipoprotein particles
- Volume of distribution (VD) (apparent volume of distribution), 1663
- von Willebrand Disease (vWD), 1594
- von Willebrand factor (vWF) tethering, 1589–1590
- VSD. *See* Ventricular septal defect
- V-slope method, pediatrics and, 121
- VT. *See* Tidal volume; Ventilatory threshold
- VTI. *See* Velocity-time integral
- mitral valve prolapse, 1020
- pregnancy and, 1502, 1504
- Waterston operation, Tetralogy of Fallot, 1476
- Waterston shunt
tricuspid atresia, 883
- WBCs. *See* White blood cells
- Wedge angiography, 1405, 1406f, 1406t
pulmonary arterial hypertension (PAH), 1439
- Weight loss, hypertension and, 1536
- Wenckebach's periodicity, 366
- Werdnig-Hoffman disease, 1415
- White blood cells (WBCs)
disorders of, 1593
normal development of, 1589
- WHO (World Health Organization)
cardiomyopathies and, 1267
Doppler echocardiography, RF and, 1314
- Wide complex tachycardia, 452–453, 452f, 453f
- Williams syndrome, 620t, 628–629, 628f, 933, 1579
balloon angioplasty, 934
peripheral pulmonary arterial stenosis and, 928
peripheral pulmonary arterial stenosis *v.* 932
- Williams-Beuren syndrome (7q11 deletion), 628–629
- Wolff-Parkinson-White pattern, 374
- Wolff-Parkinson-White syndrome (WPW syndrome), 358, 446–448, 1271
ablation, 417
accessory pathways, 446–447
atrial fibrillation, 447, 447f
risk stratification, 447–448, 447f
- Wood unit, 271
- Work, 118–119, 119f
HR *v.*, in children, 121f, 122
- Workload, oxygen consumption *v.*, 119f
- X
- X chromosome, 1277–1278
Turner syndrome, 626
- X-linkage, BAV, 804
- X-linked cardiomyopathy, Duchenne muscular dystrophy, 1284
- X-linked recessive inheritance, Kartagener syndrome and, 634
- Y
- Yin-Yang relationship, 137
- Z
- Z-disk
myocyte and, 58
- Zebrafish, DNA mutations and, 560
- Zinc-finger transcription factor, 567
- Zink finger protein 9 gene (ZNF9), 1277
- ZNF9. *See* Zink finger protein 9 gene
- Z-scores, echocardiography, 172
- W
- Warfarin therapy
chronic rheumatic heart disease, 1319t, 1320